ICCES 2019

PROCEEDINGS

of the

4th International Conference on Communication and Electronics Systems (ICCES 2019)

17-19, July 2019

Technical Sponsors

IEEE

PPG Institute of Technology

ICCES 2019

PROCEEDINGS

of the

4th International Conference on Communication and Electronics Systems (ICCES 2019)

17-19, July 2019

Technical Sponsors

IEEE

PPG Institute of Technology

MESSAGE FROM THE CHAIRMAN

On behalf of the organizing committee, it is a pleasure for me to welcome you to the IEEE International Conference on Communication and Electronics Systems (ICCES 2019). The overwhelming response to our call-for-papers indicates the popularity of this conference and confirms that IEEE has become the world-wide forum for all aspects of science and technology in the field of information and Communication related topics.

In the long history of IEEE Conferences, it has provided a venue for researchers to address the new technology and findings, as well as to exchange recent research results. I hope that the presentations and special sessions will be valuable resources in your professional, research and educational activities whether you are a researcher, or a practicing professional.

The conference is intended to involve various research areas, including Communication Systems, Computer and Networks, VLSI Design, Medical Imaging, Signal Processing and Image Processing.The conference theme focuses on the new innovative technology in the field of Communication, Electronics Systems.

Finally, I thank all conference participants for making ICCES 2019 success, and hope that you have an enjoyable and fruitful stay in Coimbatore.

Dr.L.P.Thangavelu, M.S., FAIS, FIAGES, FICS
Founder-Chairman,
PPG Group of Institutions.

MESSAGE FROM THE CORRESPONDENT

It is a great honor and pleasure to welcome you to the IEEE International Conference on Communication and Electronics Systems (ICCES 2019) organized on 17-19 July 2019. We sincerely thank all members of the Organizing Committee for their long term enthusiasm in organizing the conference and we are very grateful to all the authors who created the scientific program of the 4th International Conference on Communication and Electronics Systems (ICCES 2019).

Finally, I would like to extend our thanks to the sponsors, who decided to join us at this important event.

We heartily welcome professors, scientists, experts and students from all countries to 4th International Conference on Communication and Electronics Systems (ICCES 2019) and we wishyou a pleasant experience in Coimbatore.

Tat. Shanti Thangavelu
Correspondent
PPG Group of Institutions.

MESSAGE FROM THE PRINCIPAL

It is an immense pleasure to welcome you all to the 4th International Conference on Communication and Electronics Systems (ICCES 2019). I am sure that the participants of this conference will return immensely enriched with knowledge and gain more confidence.

With the evolution of new technology, there is a stiff competition in this challenging world. To meet these challenges, one has to constantly and updates oneself in a Particular field to survive and to become successful. It is necessary to be keen towards the latest technology in their related fields and conference is one such way that helps to meet different people across the country and exchange their ideas. These experiences create innovative ideas among budding engineers. We are amazed to see a great response from various institutions across the globe and I am sure that this will develop the team spirit and leadership qualities among our students.

Hearty congratulations to the organizing committee. Wishing the delegates a fruitful deliberations and happy stay during ICCES-2019.

Dr.R.Prakasam, B.E (Hons),
M.E., Ph.D., F.I.E. C.Engg, M.I.S.T.E., PRINCIPAL,
PPG Institute of Technology.

MESSAGE FROM THE CONFERENCE CHAIR

It is my great pleasure to welcome you to the IEEE International Conference Communication and Electronics Systems (ICCES 2019) which takes place in Coimbatore, Tamil Nadu on July 17-19, 2019. It has been a real honor and privilege to serve as the Conference Chair on the conference.

I am sure that his conference will provide a cross-disciplinary venue for researchers and practitioners to address the rich space of Communication and Electronics System. The Conference spans two days and includes two Keynote Address followed by two days of main conference. The presentations and planned social events will provide ample opportunities for discussions, debate, and exchange of ideas and information among conference participants.

I would like to express our appreciation to the Technical Program Chair, for his valuable contribution in assembling the high quality conference program. We also thank the Chairs. A conference of this size relies on the contributions of many volunteers, and we would like to acknowledge the efforts of our conference judges and their invaluable help in the review process. We are also grateful to all the authors who trusted the conference with their work.

Dr.V.Bindhu,
Professor and Head,
ECE, PPG Institute of Technology,
Coimbatore, India.

4th International Conference on Communication and Electronics Systems

(ICCES 2019)

Table of Contents

S.No	Title/ Authors Name	Page. No
1	Fog Computing: An Enhanced Performance Analysis Emulation Framework for IoT with Load Balancing Smart Gateway Architecture Bikash Sarma, Gajender Kumar, R. Kumar, Themrichon Tuithung	1
2	Energy Efficient Spectrum Access Design for Cognitive Radio Wireless Sensor Network Professor Ruksar Fatima, Shaik humera tauseef, Rohina khanam	6
3	Object Detection and Tracking using Zernike Moment Samidha Girish Vengurlekar, Dipti Jadhav, Swapnil Shinde	12
4	Design of a miniaturised and novel DGS-based UWB antenna Ria Benny, P. Mythili	18
5	Low Power Hardware Based Real Time Music System and Digital Data Transmission Using FPGA Sudip Mondal, R. K. Sharma	21
6	Design of GMII Transparent Interface Based on Ethernet IEEE 802.3 Standard Rajat Kumar Maheshwari, T. N. Sasamal	24
7	Design of Efficient 2-4 Modified Mixed Logic Design Decoder Rohit Kumar Arya, Sonali Agrawal	29
8	HYBRID KEY GENERATION FOR RSA AND ECC E.VIDHYA, S.SIVABALAN, R.RATHIPRIYA	35
9	An Efficient Trusted Graph Based Approach for Inferring Trust in Epinions Network Debdutta Dey, Awadhesh Kumar Singh	41
10	AES Arduino Handshake for Unattackable Data Processing Gourav Saini, Dr. R.K Sharma	46
11	To evolve a predictive model for Dengue incidence using meteorological and geo spatial data N V Ganapathi Raju, P Gopala Krishna, Katapally Manognya, G S S Raj Kiran, Palakodeti Rohit, K Likhith	51
12	Pedestrian Detection Using Deep Learning Ponugumati Pavani, Kodali Bhavana, Duvvaki Venkatesh, Suneetha Manne	60

S.No	Title/ Authors Name	Page. No
13	Fast Error Correction for Header Flit in NoC V.Taraka Sai Srinatha Reddy, G.Hema Sekhar Reddy, K.Jeshmitha Reddy, M.Vinodhini	66
14	RCSA scheme with Rayleigh Fading Effect in massive-MIMO system Umesha G B, Dr M N Shanmukha Swamy	71
15	Implementation and Analysis of Adaptive Odd-Even Routing in Booksim 2.0 Simulator Jaswanth Marri, Sunder Manishankar, D. Radha, Minal Moharir	77
16	Analysis of Load Balancing Algorithms in Software Defined Networking Himanshi Babbar, Shalli Rani	85
17	A Multicasting Approach for Path Establishment in Vehicular Ad hoc Networks Abhander Chaudhary, Rakesh Kumar	91
18	Developing Augmented Reality Application for All-in-one Interface Card Rashmi M, S.G Raghavendra Prasad	97
19	Design of low power SR-flip-flop with on/off (ONOFIC) implementation Masood Ahmad Malik, Vijay Kumar Sharma	102
20	Design of 6T FinFET SRAM cell at 7nm Umayia Mushtaq, Vijay Kumar Sharma	105
21	Evaluation of Data Efficacy in Privacy-aware Computing Geetha P, Dr. Chandrakant Naikodi, Dr. Suresh L.	110
22	Saturation Optimization and Extrinsic Timing Analysis for Optically Controlled GFET S.Chakraborty, K.Bhowmick, N.S. Murty	116
23	Advanced Military Helmet aided with Wireless Live Video Transmission, Sensor Integration and Augmented Reality Headset Sandeep Jalui, Tushar Hait , Tulika Hathi , Soumes Ghosh	124
24	A Comparative Analysis of 8-bit Novel Adder Architecture Design using Traditional CMOS and m-GDI technique Gautam Nayan	129
25	Threshold driven Dual Cluster Head clustering protocol Navajyoti Nath, Biswanath Dey	137
26	Change Detection in Land use-Land cover using Convolutional Neural Network Sahithi Samudrala, Suhail Mohammad, Mekala Pranvitha nand, Radhesyam Vaddi	142
27	Efficient Resource Allocation Model For D2D Communication Under Overlapping Area of Multiple Cellular Cell Professor Ruksar Fatima, Rohina khanam, Shaik humera tauseef	146
28	IoT Based Automatic Attendance System Dharani Devi, Devi.A, Piriyyadarisani.V	152

S.No	Title/ Authors Name	Page. No
29	Gesture and Speech Recognizing Helper Bot Kailash Gogineni, Akhil Chitreddy, Anirudh Vattikuti, Dr. Natarajan P	156
30	Cost Efficient Subtractor Designs in QCA Marshal Raj, Lakshminarayanan Gopalakrishnan	162
31	FLOOD FORECASTING BY USING MACHINE LEARNING Amitkumar Baburao Ranit, Dr. P. V. Durge	167
32	Performance analysis of Transformer – Less UPFC Shaikh Mohammed Tauseef, S. M. Kulkarni	171
33	The Decomposition methods in Synthetic Aperture Radar Polarimetry Plasin Francis Dias, R. M. Banakar	175
34	Energy Aware Virtual Machine Consolidation for Load Balancing in Virtualized Environment Bishwabara Panda, Suresh Chandra Moharana, Himansu Das, Manoj Kumar Mishra	181
35	Design and Verification of Analog Integrated Circuits Using Free or Open source EDA Tools Guruprasad, Kumara Shama	187
36	Weighted Pseudorandom Based Deterministic Bist for Fault Testing and Self-Healing G.Bhavani, K. Jamal, B.Veera Reddy	193
37	Road Crack Detection and Segmentation for Autonomous Driving Geetika Aggarwal, Sarika Jain	199
38	Enhanced Secrecy Capacity under Eavesdropping Attack in Multi-Traffic Industrial WSN A.Chandra Shaker	204
39	Hybrid Algorithms for Moving Vehicle Plate Recognition System Shreyas S Bagi, Harshith C H, Santosh Tuppad, Dinu V, Dr. R Srikantaswamy	210
40	DIGICERT: A Secured Digital Certificate Application using Blockchain through Smart Contracts Ms. R.Poorni, Mr. M.Lakshmanan, Ms. S. Bhuvaneswari	216
41	Semantic Segmentation of Satellite Images Using Deep Learning(Deep Learning Technique for Semantic Segmentation of Satellite Images) Mohammad Yousuf Saifi, Dr. Jimmy Singla, Nikita	222
42	Real Time Virtual Human Hand Using Leap Motion Controller R. Satheeshkumar, Dr. R. Arivoli	228
43	Wireless IoT based Solution for Women Safety in Rural Areas Rahul Paknikar, Shrey Shah, Dr. Prachi Gharpure	234
44	Implementation of Power Quality Enhancement using Hybrid Series Active Filter VANITA NAKADE, SANGITA PATIL	240

S.No	Title/ Authors Name	Page. No
45	Neural Differential Equations for Face Recognition Gadicherla Sameer, Gogineni Manasa	244
46	TWO-DIMENSIONAL ECG SIGNAL COMPRESSION BASED ON REGION OF INTEREST USING PCA ANEESH K N, DARSHAN SINGH S, M H ABHISHEK, Dr. SHREEKANTH T	250
47	Library - A Face Recognition and QR Code Technology based Smart Library System Dhaval Bagal, Pallavi Saindane	255
48	Image Representation based on quantum Computation and their Application : Milestone Ontogeny Sanjay Singh, Ashish Mani, Rashmi Jain	261
49	Translating Artificial Intelligence into Healthcare: Diabetic Retinopathy Detection Reaya Grewal, Avleen Kaur Malhi, Palika Chopra	269
50	Single Phase AC-DC Cascaded Boost-SEPIC (CBS) Converter for Improved Power Quality at High Duty Cycle Mohammad Dehan Rahman, Md Saif Kabir, Md Nazaf Rabbi, Mohammad Abir Hassan Sarker, Dr. Golam Sarowar	275
51	Saturable Absorbers for Mode-Locking of Lasers Operating at Ultraviolet Wavelengths Akshayaa Venkatesh, Janani MV, Arya M Hari, R.Kumar, Dhanalakshmi Samiappan, Venkatesh Chakravartula, Junaid M Laskar	281
52	Level management in connected water reservoirs employing curve fitting based PID control scheme Mohit kumar, Dr. Sathans	286
53	Nonlinear Model Predictive Controller for the Real-Time control of Fast Dynamic System Mrs. Supriya P. Diwan, Dr.(Mrs.)Shraddha S. Deshpande	290
54	PANCHENDRIYA: A Multi-sensing framework through Wireless Sensor Networks for Advanced Border Surveillance and Human Intruder Detection Arjun D, Indukala P K, K A Unnikrishna Menon	296
55	Disparity Map Estimation Using Combined Cost Measure Deepa, Jyothi K	300
56	Object Detection and Gesture Control of Four-Wheel Mobile Robot M. Jain, M. Sehgal, Y. Kalra, P. Jain , N. Aggarwal, R.Singh, D. Kumar, T. K. Bera	304
57	Robust Hybrid Image and Audio Watermarking Using Cyclic Codes and Arnold Transform Bhavneet Sharma, Mayank Dave	310

S.No	Title/ Authors Name	Page. No
58	ANALYSIS OF BOOST CONVERTERS FOR PV AND WIND IN A HYBRID MICROGRID RAJALAKSHMI MENON, GOMATHY S, Lakshmipriya K J	317
59	Various Data Deduplication Techniques of Primary Storage D.Viji, Dr.S.Revathy	323
60	LAND COVER CHANGE DETECTION BASED ON SATELLITE IMAGES USING DEEP STACKING NETWORKS Deepa Palanisamy, Radha Senthilkumar	329
61	Influence of trip complexity on optimal driving based Energy Management System of Electric Vehicle Mousumi Khanra, Arup Kr Nandi	335
62	Load Flow Analysis for Smart Grid With Renewable Energy Resources Shaikh Mohammad Aamir, Dr. P. M. Joshi	341
63	Mathematical analysis of RNN and LSTM for Malicious URL detection M. Arivukarasi, A. Antonidoss,	345
64	Performance Enhancement of OFDM System Using Modified PTS (MOPTS) PAPR Reduction Algorithm Prabal Gupta, H. Pal Thethi	350
65	Evaluating Visual Performance of Multi-object Scene Reconstruction using Triangulation from Airborne Geo-spatial Point Clouds Swati RajeshKumar Maurya, Ganesh M. Magar	358
66	Network Traffic Optimization in Hadoop MapReduce through Pre-shuffling D C VINUTHA, G T RAJU	364
67	Intelligent Edge Security with Dynamic Task Offloading in Fog Environment Albin Mathew, Namboodiri E I Deepu, Dr. Maya Mohan	368
68	Selection of Optimal Renewable Energy Resources in Uncertain Environment Using ARAS-Z Methodology Nisha Rathore, M.P.Singh	374
69	Secure Defense Mechanism against Data Leakage and Distributed Denial of Service Attacks in Software Defined Networks P. Mohana Priya	379
70	A Machine Learning Approach for URL Based Web Phishing Using Fuzzy Logic as Classifier Happy Chapla, Riddhi Kotak	384
71	Power Analysis of 2-bit Array Multiplier using Adiabatic Logic Jacob Savio, Rekha Bhandarkar	390
72	Safety and Driver Assistance in VANETs: An Experimental Approach for V2V C. Suganthi Evangeline, Vinoth Babu Kumaravelu, Atul Joshi	398

S.No	Title/ Authors Name	Page. No
73	Design and Implementation of Automatic Miniature Indoor Plant Cultivator Using Artificial Environment Akhila S, Shriya Nithyan, Sowmya C, Priya B. K	404
74	A Network Intrusion Detection Approach Using Variant of Convolution Neural Network Ashish Kumar Verma, Dr.Praveen Kaushik, Gourav Shrivastava	410
75	Analysis of Bi-directional DC-DC Buck-Boost Quadratic Converter for Energy Storage Devices Neeti Dubey, Ashok kumar Sharma	418
76	Building a Cloud Solution for Energy Management using Raspberry Pi Laxmi Khichadi, Siva Ganesh Kumar, Dr. Nagamani K.	423
77	Test Pattern Generation to Detect Single Stuck- at Faults for Combinational Circuits Using ZBDD Antony Thomas, J. P. Anita	428
78	Design and performance analysis of WDM optical Communication system with EDFA-DCF and FBG for dispersion compensation using 8x5 Gbps data rate Nirmala Mahawar, Ajay Khunteta	432
79	Collaborative Filtering based Recommender System using Regression and Grey Wolf Optimization Algorithm for Sparse Data Sneha V., Shrinidhi K.R., Sunitha R. S., Dr.Mydhili K. Nair.	437
80	Automatic Evaluation of Short Answers Using Deep Neural Networks Barsha Sharma , Chandni Agarwal , Deep Shikha , Udit Kr. Chakraborty	443
81	Performance Analysis Of Inter-satellite Optical Wireless Communication System Using WDM(Comparison of BER and Q-factor in an Is-OWC system using WDM with different modulation techniques) Shubhneet Kaur, Ameeta Seehra	449
82	A Metaheuristic-based Emotional ANN (EmNN) Approach for Rainfall-runoff Modeling Bishwajit Roy, Maheshwari Prasad Singh	455
83	Reconfigurable Warped Digital Filter Architecture for Hearing Aid Kaustubh Banninthaya K., Niranjan N., Risla Fathima P., Pranav Kumar M. P., Dr. Ipsita Biswas Mahapatra	460
84	SUPPRESSION OF CROSS POLARIZATION WITH VARIOUS GEOMETRIES OF DGS IN THE DESIGN OF MICROSTRIP PATCH ANTENNA B Naveen reddy,M Hema dharani,S Pavithra,A Sivapradhayni, Mekaladevi V	465
85	Enhancing Security of AES Using Key Dependent Dynamic Sbox Yashvir Singh Chauhan, T.N. Sasasmal	469

S.No	Title/ Authors Name	Page. No
86	Performance Analysis Of Full Duplex MIMO Fiber-Optical Wireless Communication (OWC) System Bhumika Narang, Dr. Baljeet Kaur, Prof.Harminder Kaur	475
87	AUTOMATED RAINWATER HARVESTING SYSTEM(IoT-AIS: Internet of things for Automated Irrigation System) Dr. C Kishor Kumar Reddy, P R Anisha, Rajashekar shastry, Dr. B V Ramana Murthy, Dr. Vuppu Padmakar	480
88	File I/O Performance Analysis of ZFS & BTRFS over iSCSI on a Storage Pool of Flash Drives Devyani Gurjar, Satish S. Kumbhar	485
89	An effective security protocol for GDS (group Data sharing) in Healthcare Cloud Environment Uma Hombal, Dr. R. B. Dayananda	489
90	Obstacle Detection Using Sensor Based System For An Four Wheeled Autonomous Electric Robot Miss. Shusmita M. Rathod, Mrs. S.K. Apte	494
91	Synchronization of Distributed Photovoltaic Generation with an Active network using Phase Locked Loop technique Mr. Syed Noorul Faraz, Prof. S. V. Murkute	499
92	Luenberger observer based sensorless speed control of induction motor with Fuzzy tuned PID controller Vaibhav S. Virkar, Sushil S. Karvekar	504
93	Energy Monitoring of Curing Pumps Using PLC and SCADA Sahil Desouza, Roshwyn De Melo, Shreyas Aigal, Ketan Dessai, Duane Dsilva, Flavia Leitao, Mohini Naik	510
94	Security of Cloud Storage based on Extended Hill Cipher and Homomorphic Encryption Bablu Kumar Das, Ritu Garg	516
95	Yaw stability of 4WS with variable steering ratio strategy using inertial delay control based sliding mode control Tushar Khanke, Sushant Chaudhari, Shrivijay Phadke, Pramod Shendge	522
96	Pneumatic Controlled Smart Arecanut Plucking Robot with Raspberry Pi S Kushal Gowda, Prathima K R, Yashaswini L, Rakesh M D, T R Sateesh Kumar	528
97	Implementation of digital lattice filter using Schur Polynomial Sneha Sivaramakrishnan , Swathika Shanmugam, B. Bala Tripura Sundari	534
98	Energy Efficient Coverage and Sensor Localization for Scheduling Miss.Sujata Dhumal, Prof.B.S.Shetty	538
99	An Improvement in Performance and Computational Cost of ANN Based Wind Speed Prediction System Shashank Sinha, S. Tiwari	543

S.No	Title/ Authors Name	Page. No
100	An Improved Inverter Control for Grid-Connected PV System Varun Kumar Mahawar, S. Tiwari	548
101	Design of Low Power FinFET Based Adiabatic Logic Circuits in 18nm Technology Apoorva Raghunandan, Shilpa D R	553
102	A Compact Four Port UWB-MIMO Antenna With Notch Band Characteristics And High Isolation Preeti Pannu, Devendra Kumar Sharma	558
103	Wireless Power Transfer For Third Harmonics With the Improved Input Power factor Akhila E. M, Suhara E. M	563
104	Diagnosing Insomnia Using Single Channel EEG Signal N Purushotham Raju, Venkatesh U, Sudha Yadav	570
105	Identifying fake user using FRUI, Content and Profile based Algorithm Ms. Rohini N Khedkar, Prof. Sujata Bhairnallykar, Prof. Vaishali Jadhav	574
106	Fuzzy based Technique for Nodes Coverage with Load Balancing Data collection using Multiple Conflicting Factors Anjali, Nidhi, Kumkum Dubey, Prince Rajpoot, Amit Kumar Singh, Ajeet Kumar	578
107	Power Balanced Efficient Clustering Algorithm for WSN Prince Rajpoot, Pragya Dwivedi, Kumkum Dubey	584
108	Different Input Impedance Matching Circuits for Cascode Common Source LNA with Inductive Degeneration Topology in 45nm CMOS Technology Malti Bansal , Diksha Singh	589
109	Cascode Common Source LNA with Inductive Degeneration Topology utilizing Different Output Matching Circuits in 45nm CMOS Technology Malti Bansal , Diksha Singh	594
110	An Enhanced Cluster Head Technique for Energy Consumption in DataFusion E.Brumancia, S.Justin Samuel, A.Sivasangari, Vishwanthi Suvetha.R, Sandhiya.M	599
111	Advanced Wheelchair Movement System Using Facial Gestures For Aiding Human With Tetraplegia Condition Dr.P.V.Ramaraju, K. JaideepSai Narayan, G. Naga Raju	605
112	An Effective Data Normalization Strategy for Academic Datasets using Log Values V.Sathya Durga, Thangakumar Jeyaprakash	609
113	Saliency Guided Image Super-Resolution using PSO and MLP based Interpolation in Wavelet Domain Sheetal Shivagunde, Mantosh Biswas	612

S.No	Title/ Authors Name	Page. No
114	Change Detection in Vegetation Cover Using Deep Learning Yamini Katta, Nomitha Datla, Sowmya Sri Kilaru, Dr. T. Anuradha	620
115	Design of quadrature error correction loop for communication Bhagyashri D.Kale, Dr.U.S.Ghodeswar	625
116	Critical Path Delay Improvement in Logic Circuit Operated at Subthreshold Region Limbasiya Mohit Dhirubhai, Kirti S. Pande	632
117	SISA : A secret-sharing scheme application for cloud environment Rohit B. Chilwant, Taral S. Sarvagod, Kunal R. Kumbhar, Prathmesh N. Gunjgur, Dr. Amarsinh V. Vidhate	637
118	Performance Evaluation and Analysis of various Network Security tools Sinchana K, Sinchana C, Gururaj H L, Sunil Kumar B R,	643
119	DESIGN AND SIMULATION OF VARIOUS STRUCTURES OF UNIMORPH PIEZOELECTRIC CANTILEVER FOR ENERGY HARVESTING(CONSTRUCTION AND SIMULATION OF VARIOUS STRUCTURES OF UNIMORPH PIEZOELECTRIC CANTILEVER FOR ENERGY HARVEST) Newton Rai, Nagaraj M J, Amogh.M.Morey, V Shantha	650
120	Design of laboratory model for demonstration of solid state transformer for smart grid applications Smita anil sonawale, Dr.P.M.Joshi	655
121	Design and Implementation of Ramp ADC using 45.nm Technology Sowjanya, Sunitha Lasrado	660
122	Intrusion Detection System Based RPL Attack Detection Techniques and Countermeasures in IoT: A Comparison P.S.Nandhini, B.M.Mehtre	665
123	Integer Wavelet Transform and Arnold Transform based image steganography with cryptanalysis Rima V G, Lakshmi V S	672
124	Smart Security, Food and Environment Monitoring System for Cows using Microcontroller Aritro Roy Arko, Saadat Hasan Khan, Md Saiful Islam	678
125	Coupling Between Automatic Generation Control And Automatic Voltage Regulator While Considering Generation Rate Constraint Of Two Areas Omer Elmukhtar, Jianhua Zhang	684
126	A Dynamic Coordinator Election Algorithm in Cognitive Radio Networks Shailendra Kumar, Mahendra Kumar Murmu	689
127	A Multi-Hop Low Duty Cycle MAC protocol for Wireless Sensor Networks Kumar Debasis, M. P. Singh, Rajat Gupta	695
128	Genetic Algorithm : An Approach on Optimization Immanuel Savio D, Udit Kr. Chakraborty	700

S.No	Title/ Authors Name	Page. No
129	Heterogeneous LEACH protocol with sink node protection in a wireless sensor network Miss. Bhagyshree Pawde, Prof. Bharathi Shetty	708
130	A Review: Parameter Reduction Methods in Soft Set Theory Priyanka D. Lanjewar, B. F. Momin	714
131	INTELLIGENT SYSTEM FOR IDENTIFYING DYSCALCULIA A. Devi, Dr. G. Kavya	722
132	A Detailed survey on Virtual Network Embedding Aqsa Hashmi, C.P Gupta	729
133	Modified 802.11b for Co-operative Ad-hoc Networks Gayathri G, Usha Padma, Jhanavi B S, T Yathin Sai	737
134	A NOVEL FUZZY CONTROLLED INTERLEAVED SEPIC POWER FACTOR PREREGULATOR WITH REDUCED RIPPLES Lakshmipriya K J, Dr.Jeno Paul, Rajalakshmi Menon	743
135	A Modern Cardiac Monitoring System Based on Wireless Sensing for Human Health Care Rosmy John, Dr. Sajith Vijayaraghavan, Dr. Pradeep R	750
136	Mobile Application for Storage and Retrieval of e-learning videos Using Hadoop Jyoti Parsola, Durgaprasad Gangodkar, Ankush Mittal	757
137	QoS Based Optimal Resource Allocation in Service Composition for Heterogeneous Devices Y V Dongre, R B Ingle,	762
138	Faults in CMOS IC's and Their Mitigation Techniques: Review Sameeksha Munjal, Prof. Gurpurneet Kaur, Dr. Sandeep Singh Gill	767
139	Full Fledged Automated Fruit Farm Ganaraj Borkar, Pramesh, Budkuley, Gourav Kanekar , Prannoy Caeiro, Parth Ghaware , Flavia Leitao, Vidhya D.S.	773
140	Efficient load Balancing algorithm analysis in Cloud Computing SONU SAHU, MANISH PANDEY	778
141	Fast and Accurate Traffic Sign Recognition for Self Driving Cars using RetinaNet based Detector Shehan P Rajendran, Linu Shine, Pradeep R, Sajith Vijayaraghavan	783
142	Asymmetric Multilevel Inverter Induction Motor Drive for Fuel Cell Based Electrical Vehicles Sumit Kumar, Yash Pal	790
143	SURVEILLANCE SYSTEM FOR DEAD ZONE Ayushi Kandoi, Pradyumna Hegade, Utkarsh Goel, Venkata Harshavardhan Reddy Allu, Dhanalakshmi Samiappan, R. Kumar	795
144	A noval methodology for tumor detection in MRI images Ishrat jan, Giridhar Reddy Bojja, Er Harish Kumar Dogra	801

S.No	Title/ Authors Name	Page. No
145	Disaster Prediction System using Convolution Neural Network Purva Mohan Padmawar, Talat Zakirhusen Sayyed, Ashutosh Sudam Shinde, Shubham Kalidas Shinde, Prof.Kavita Moholkar	807
146	QoS Evaluation of VANET Routing Protocol B.S. Yelure, S.P. Sonavane	812
147	Things-to-Cloud (T2C): A Protocol Based Nine Layered Architecture ND Patel, BM Mehtre	818
148	Formulation of Aggregate Key in cloud by Cipher Text storage Reduction for data Outsourcing in healthcare K.Ketzial Jebaseeli, Dr.V.G.Rani	827
149	Swarm Optimization techniques using Attribute assortment and Clustering for Machine Learning Classifiers Vadivu.T, Sumathi.B	833
150	Image Segmentation using Convolutional Neural Network for Image Annotation S. B. Nemade, S. P. Sonavane	837
151	Behaviour of Distance Relay under Faults in presence of Static Synchronous Series Compensator Priti Sathe, Pranita Chavan, Dhananjay Borse	843
152	Modeling of Carbon Nanotube Field-Effect Transistor and Evaluation of an Inverter Circuit Guru Prasath C, Rakshita Vishali V, Sabarrish S, Khevin Nair, B Bala Tripura Sundari	848
153	Analysis on Machine Learning Algorithms and Neural Networks for Demand Forecasting of Anti- Aircraft Missile Spare Parts Nikita Pawar, Prof. Bhavana Tiple	853
154	Classification of tumors in brain MRI images with hybrid of global and local DWT features using SVM Sanjay Kumar C K, Dr. H. D. Phaneendra	859
155	Secure and Efficient Session Initiation Protocol Authentication Scheme for VoIP Communications B. B. Gupta, Varun Prajapati	865
156	Fully Connected Convolutional Network with Laplacian Filter For Salt Segmentation In Seismic Images Jasdeep Singh, Tarandeep Singh, Munish Rattan	871
157	A survey on effective data computation in inter cloud environment Makrand Samvatsar, Priyesh Kanungo	876
158	Infrared Vision for Fog Detection System to Improve Road Visibility Jatin Talwar, Dr. Love Kumar, Dr. Gurmohan Singh	881

S.No	Title/ Authors Name	Page. No
159	2x2 Circular Patch Antenna Array at 2.4 GHz for WSN Applications Shravan G. S, Hemanth Kumar N. G, L. Sai Suhas, Vinay S, Girish Kumar N. G.	886
160	A Comparative Analysis of Matrix Based Key Management Schemes For Wireless Sensor Network Rishabh Kamal, Priyanka Ahlawat	891
161	Document Management using Artificial Neural Network Kaustubh Pimparkar, Rahul Lulla, Pratik Rathod, V Anirudh, Suruchi G Dedgaonkar	896
162	Memory Optimizing Algorithms for Data Acquisition in Electric Drive of Hybrid Electric Vehicles Gopika Rajan, Vinoth Ramalingam	900
163	Capacitor Switching Logic with Efficient MPPT Scheme for Multi Input Sepic Converter in Solar Powered Systems Sanoj Kumar Roy S., Shiny G	904
164	Fog Computing for Smart Cities Chintam Muni Kanaka Sri Shalini, Y. Mohana Roopa, J. Sirisha Devi	910
165	Iot Applications In Smart Cities Sunitha Cheepurishetti, Y. Mohana Roopa	916
166	AGRI SUCCOR: Mobile Application for Agriculture Mrs. J. Jayachitra, M. Madhu, S.D. Shaik Mohammed Faruk	920
167	Object detection using Adaptive Thresholding, Sobel Operator and Morphological Operations in Underwater Images Akshita Saini, Mantosh Biswas	924
168	A Study on Label TSH, T3, T4U, TT4, FTI in Hyperthyroidism and Hypothyroidism using Machine Learning Techniques Afzal Hussain Shahid, Maheshwari Prasad Singh, Rahul Kumar Raj , Rashmi Suman, Drakhshan Jawaid, Muqtadir Alam	929
169	Fusion of QuickBird Imagery Using Multi-Resolution Analysis Based Algorithms Vaibhav R. Pandit, Dr. R. J. Bhiwani	933
170	A Modified Block Based Biometric Fragile Watermark Technique Feni Patel, Chirag Paunwala, Aarohi Vora	941
171	Data Deduplication with Encrypted Big Data Management in Cloud Computing Nahlah Aslam K.P., Dr. Swaraj K.P.	946
172	Controller Area Network (CAN-Bus) Packet Filtering Firewall – A Survey Sahana Y P, Ajey Gotkhindikar, Shailendra Kumar Tiwari	952
173	Intelligent Storage Device for Commoners Swarnali Dey, Amrita Dutta, Madhusmita Mishra, Subhabrata Banerjee	959

S.No	Title/ Authors Name	Page. No
174	Dynamic Branch Prediction for Embedded System Applications Subramanya G. Nayak	965
175	Performance Analysis of PV & Fuel cell based Grid Integrated Power System Kuldeep Singh Rathode, Santosh Kr Sharma, Surbhi Shringi	969
176	ECG MONITORING SYSTEM USING AD8232 SENSOR Anitha S Prasad, Kavanashree N	975
177	A Low-Noise Front-End Amplifier with 15 dB Gain Operating at 100-120 GHz in 65 nm CMOS Technique Rajendra Chikkanagouda, Cyril Prasanna Raj P.,	980
178	Automated Segmentation Technique for Detection of Myocardial Contours in Cardiac MRI Sushmitha. R, Dr. Arbind Kumar Gupta, Mrs. Chandrakala B M	984
179	Proposal of smart home resource management for waste reduction and sustainability using AI and ML Naveen Ananda Kumar J, Srija Chimmani	990
180	Improved IIR tracking by fusion of centroid estimation processing with IMM filter V S N Murthy A, Chandrakanth V, P V R R Bhogendra Rao, Ramakalyan Ayyagari	996
181	A Novel Encryption Algorithm based on DNA Cryptography A.Vikram, S.Kalaivani, G.Gopinath	1001
182	Design and Analysis of Slotted Ground Rectangular Patch Antenna for Worldwide Interoperability for Microwave Access,Wireless Local Area Network,Ultra Wideband and X-Band Applications Anjaneyulu Katuru, Mahesh Dronadula	1007
183	Fusion Methods & Applications – A Survey Freceena Francis, Dr. Maya Mohan	1013
184	Swheel: Low-Cost Smart Wheelchair with Wireless Control Tushar Agarwal, Shloka Bhalgat, Chirag Khandhar, Bhumika Khetan	1018
185	Internet of Things (IoT) enabled Sustainable Home Automation along with Security using Solar Energy Swetha Amit, Anitha Sarah Koshy, Samprita S, Shwetali Joshi, Ranjitha N	1023
186	Ultra Wide Band Symmetric Slots Antenna for Wearable Applications Swetha Amit, T R Ramya, Vandana S, Pooja C R	1027
187	An AI and ML driven approach for Smart Kitchen to enhance Restaurant like Cooking at Home Naveen Ananda Kumar J, Shubashree S	1031
188	An Approach to Secure Data Transmission Through the Use of Cryptography and Steganography Dr Manjula Shenoy K, Seema Gulam Shaikh	1036

S.No	Title/ Authors Name	Page. No
189	Detection and Tracking of Anxiety Related Diseases for Autism Spectrum Disorder Using ECG Abhirami A , Sudheesh P	1041
190	A proposed model of a Smart Faucet Naveen Ananda Kumar J, Shivani Suresh	1050
191	SMART AID FOR VISUALLY CHALLENGED PEOPLE Rohit P, Ranganatha Gowda S J, Imran Quadri, Vinay Prasad M S, Krishna Raju D R	1053
192	An Examination System Automation Using Natural Language Processing Indrashis Das, Bharat Sharma, Siddharth S. Rautaray, Bhubaneswar	1059
193	Performance Analysis of Hybrid Transformer-less PFC boost Converter Prerna Saxena, Ashok Kumar Sharma, Lata Gidwani, Mohit Sharma	1065
194	Tree based node verification key management scheme for wireless sensor networks B Srinivas, N Rukma Rekha, Subbarao Y.V	1071
195	Depth Analysis Using Stereo Vision Mr. Nitin Borhade, Mr. Vijay Kunjir, Prof. Mrs. Vandana Jirafe, Mr. Nandan Andhare	1077
196	Design and Development of Hybrid Powertrain for Motorcycles Kandi Suyash, Ghadge Tejraj, Jadhav Vasudev, Dhaygude Akshay, Mursal Siddique, Kharade Mahesh	1083
197	Performance Evaluation of Power over Ethernet in an Ethernet Switch Laxmi Khichadi, Dr. Nagamani K.	1088
198	An Improved Vivaldi Antenna Design for Through-Wall Radar Imaging Rajashree R Menon, Sultana Najeeb, Swetha N Prabhu, Treesa Angel George, Anila Kuriakose	1093
199	A Survey on Privacy Preserving Schemes in Cloud Computing Mr. Sunilkumar, Mr.A.H. Shanthakumara,	1098
200	Optimization Of Vehicle Using Monitoring Systems Sasvanth Narayan R, Loganathan V, Prateek Lakkar, Suganthan B	1105
201	Design & Development Of AgriculturalRobot Using PLC & IoT Safin Khan, Atul Ingale, Akshara Buchake, Swaraj Ahire, Prof.Jitendra Gaikwad	1110
202	A Effective Content Based Image Retrieval Using Dot Diffusion Block Truncation Coding Admile Nandkumar Sushen, Dr.Anup S.Vibhute	1116
203	Comparative Analysis of DC-DC Converters for Tracking MPP for Roof-Top PV Power Systems with and without Partial Shading Condition Kamalesh Tripathy, S. Gupta	1122

S.No	Title/ Authors Name	Page. No
204	Fault Detection and Classification scheme using KNN for AC/HVDC Transmission Lines Supriya Naik, Dr. Ebha Koley	1128
205	Heart Disease Predictions Using Numerous Classification Techniques and Dynamic LSTM Model Aishwarya Mishra, Dayashankar Singh	1134
206	A Hybrid Apporach to Improve Full Coverage in Wireless Sensor Networks Amandeep Kaur Sohal, Dr. Ajay Kumar Sharma, Dr. Neetu Sood	1140
207	Power Efficient e-Bike with Terrain Adaptive Intelligence D. S. H. Abhilash , Iqbal Wani, Kiran Joseph, Rashmi Jha, Haneesh K. M.	1146
208	Designing Of Beach Rescue Drone Using GPS And Zigbee Technologies Sreedevi Nair, Gloria Rodrigues, Cheryl Dsouza, Shirin Bellary and Velliza Gonsalves	1152
209	Offline Mobile Application for Train Time Prediction Ramesh R , Divya G, Anaswara Jayan , Sonam V Maju, Rosemary Varghese	1157
210	AN AMALGAMATION OF FIREFLY ALGORITHM AND WiMAX REFINING BER AND SNR Garima Behl, Dalveer Kaur	1162
211	A deep learning approach for the classification of diseased plant leaf images Siddharth Singh Chouhan, Ajay Kaul, Uday Pratap Singh	1166
212	Cooperative Routing in MANETs Using Trust Inference Framework Fiza Firdose, Dr. Shankaraiah	1171
213	Performance analysis of three phase integrated generation of SOFC (solid oxide fuel cell), PV (photovoltaic), with IC MPPT (maximum power point tracking) Controller Kritika Sharma, Dr. Seema Agrawal, Dr. R.K. Somani, Pankaj Kumar	1177
214	Emotion Recognition Using Feature-level Fusion of Facial Expressions and Body Gestures Tanya Keshari, Suja Palaniswamy	1182
215	A Hybrid Cloud Approach for Efficient Data Storage and Security Sandeep HR, Dr. Thangam S	1188
216	Smart Sugar Cane Grower Inquiry and Plotting Using Android Application Apoorv Kansal, Pradeep Kumar	1193
217	Landslide detection system using computer vision approach and Raspberry Pi Praveen Kumar Mishra, Sunil Dhar, M K Kalra	1199

S.No	Title/ Authors Name	Page. No
218	A Survey of Recent Advances in Crowd Density Estimation using Image Processing Komal R Ahuja, Nadir N. Charniya	1205
219	Smart City Management System using IoT with Deep Learning Shubham Jain , Aman Jatain , Shalini Bhaskar	1212
220	Microcontroller rooted collaborative functioning system in Vehicles P. Tarun, T. Pradeep Chandra, G. Anil Kumar, Sudha Yadav	1220
221	A Review on Various Inter Cluster Multi-hop Routing Protocols in Wireless Sensor Network Sanjeev Kumar, Dheeraj Kumar Sharma	1228
222	Design of Microstrip Bandpass Filter Based on Genetic Optimization Navin Baaskar E V, Harshini R, Poornima T, Natarajamani S	1234
223	Support Vector machines based gender detection by using Gait Energy image Projections Hema M, K Esther Rachel	1237
224	Design of Knee Exoskeleton using Electromyography Sensor P. Jain, G. Himanshu, M. Bhupendra, Y. Dharmendra,V. Aditya, D. Kumar, T. K. Bera	1243
225	Designing of Microcontroller based Energy Meter (Smart Energy Meter) for Energy Preserving K. V. Jyothi Prakash, Chethana N S, Fariya Tamkeen, Kala C S, Kavya N R	1249
226	FLOOD AND EARTHQUAKE DETECTION AND RESCUE USING IOT TECHNOLOGY Venita Babu, Dr.Vishnu Rajan	1253
227	Feature Selection based Classification of Spams Using Fuzzy Support Vector Machine Lovely Bansal, Dr. Nirupama Tiwari	1258
228	Analytical Study of PV Array with 3-Phase 3- Level Z-source inverter and VSI inverter Kailash Baindara,Seema Agrawal,Tanushree Samaria, Mahendra Lalwani	1264
229	Voice Activity Detection Using Novel Teager Energy Based Band Spectral Entropy Raveesh Hegde, R. Muralishankar	1269
230	AGRI SUCCOR : Mobile Application for Agriculture Mrs. J. Jayachitra, M. Madhu , S.D. Shaik Mohammed Faruk	1276
231	A Survey on Energy Efficient Routing Protocol for IoT Based Precision Agriculture T. Aishwarya Lakshmi, Balaji Hariharan, Rekha P	1280
232	Beamforming Based Underwater Wireless Optical Communication Systems Sajmath P. K., Renjith V. Ravi	1285

S.No	Title/ Authors Name	Page. No
233	Improving GPS based distance measurement accuracy using Machine Learning: an empirical study Rishish Kumar Naik, Binoy B. Nair	1290
234	Design and development of fuel level measurement technique for automotive application Mr. Kiran Patil, Prof. Dr. C. Y. Patil, Mr. Sujit Barhate	1296
235	A Card Emulation Technique based Secure Framework for Internet of Things (IoTs) Applications B. B. Gupta, Shaifali Narayan	1300
236	Software Defined Networking (SDN) based Secure Integrated Framework against Distributed Denial of Service (DDoS) Attack in Cloud Environment Dr. B. B. Gupta, Chhavi Chaturvedi	1306
237	Modeling and Simulation of gird connected hybrid power system integrated with solar PV/Wind and controlled by Voltage Regulator Vandana Chaudhary, Annapurna Bhargava, Swati Bhasin	1312
238	Analysis of Z-Source Based Single Stage Three-Port Converter for PV Renewable Energy System Mohit Sharma, Dr. Ashok Kumar Sharma, Anshul Gautam, Dolly Murodia, Prerna Saxena	1317
239	Direction of Arrival and Channel Estimation using Machine Learning for Multiple Input Multiple Output System Sruthi Ravindran, Dr. Renu Jose	1323
240	FPGA Implementation of 8-bit SSA Multiplier for designing OFDM Transceiver Mallapareddi Sagar, Ganapathi Hegde	1327
241	Location Module for 5G Base Station to Support Mobility Management of Drones Nithin P S, Sai Shibu N B, Sree Lakshmi S, Seshaiah Ponnekanti	1332
242	Comparison between Hybrid AMI and Duobinary– VLC (Visible light Communication) using WDM (Wavelength Division Multiplexing)–PI (Polarization interleaving) Transmission System Chetna Verma, Chetan Selwal	1337
243	Remote Vehicle Data Logging system for Off Highway Mining Equipment's Hifza shaima, Yashwanth S D, E K Ratna Kanth	1342
244	Interference in Large Scale wireless networks: A Case Study with LoRa (Long Range WiFi) and LTE (Long Term Evolution) Adwitiya Mukhopadhyay, Ashish Sunil Thomas, Rekha Ramakrishna Hegde	1348

S.No	Title/ Authors Name	Page. No
245	Implementation On High-Performance Quasi-Z-Source Series Resonant DC To DC Converter for Photovoltaic Module Level Power Electronics Applications Tejashri S .Wable, V. M.. Panchade	1354
246	MODIFIED BUCK BOOST CONVERTER WITH REDUCED CURRENT RIPPLE USING DELTA TO STAR IMPEDANCE NETWORK SANJU B, Dr.JENO PAUL, SREEHARI S, REJOICE THOMAS PAUL, KRISHNAPRIYA VINOD	1358
247	Prediction of Bug Severity by Classification of Bug Reports Sarbjeet Kaur, Maitreyee Dutta	1365
248	Data Modelling for Thing Prediction in Station-of- Things Environment Soumya Saha, Tejashree S. Bhave, Manisha J. Nene	1372
249	Performance Analysis of Immense Preference Data Forwarding (IPDF) Scheme incorporated with Constructive Time Slot Allocation in IEEE 802.15.4 for Wireless Body Area Networks Sindhuja Banu.S, Dr. Baskaran.K	1378
250	Automated Library System Using Robotic Arm K. V. Jyothi Prakash, K M T Tejaswi Kumar, K Punyadeep, Kamsala Ravi Theja, Gopala Krushna	1386
251	Controllability Intelligence of Lightning Protection System due to 110kV Transmission line Mohammed Abdaldaim Ibrahim, Lin Li, Ping Wang	1391
252	Analysis of Single Phase Pulse Width Modulation (PWM) AC to AC Step-Up Converter Based on SC Structure Priyanka Nehra, Ashok Kumar Sharma	1397
253	Deep learning based Customized Model for Features Extraction Akshya Reghunath, Shalini Vanaja Nair, Jalpa Shah	1402
254	Non Orthogonal Multiple Access in Cooperative Relay Sharing with Randomly Deployed Users Dr. Ankur Bansal, Avinav Joshi	1408
255	Building Detection from LiDAR Point Cloud Data Mayura N P, Veni S	1412
256	Eye Movement Based Cursor Control and Home Automation for Disabled People Sharon Mathew, Sreeshma A, Theresa Anitta Jaison, Varsha Pradeep, S Santhi Jabarani	1418
257	STAVI : Smart Travelling Application for the Visually Impaired Prerana V, S Tejaswini, Jasmine Manandhar, Santhosh T K, Pushpa S K, Manjunath T N	1423
258	Location Based Cluster Head Selection for Wireless Sensor Networks Rudramurthy V C, Dr. R Aparna	1429

S.No	Title/ Authors Name	Page. No
259	Analysis of Single-Stage Boost Inverter for Renewable Energy Generation System(REGS) in Discontinuous Conduction Mode(DCM) Dolly Murodia, Dr. Ashok Kumar Sharma, Sawan Singh	1434
260	Gain Enhancement of Compact UWB Antenna Using Planar Reflector Mahadu A. Trimukhe, B. G. Hogade	1440
261	A novel systematic approach for Residential Smart Grid Naveen Ananda Kumar J, Shubashree S	1443
262	Survey on Classification Techniques Applied to Intrusion Detection System and its Comparative Analysis Ritumbhra Uikey, Dr. Manasi Gyanchandani	1447
263	An Efficient Approach for Multiclass Student Performance Prediction based upon Machine Learning Abhinav Jain, Shano Solanki	1453
264	Extracting Primitive Tasks from Procedural Videos using Machine Learning Amulya Shivanath, Dr.Sumana M	1459
265	Design of Beam Steering Antenna for ISM Band III Using Corporate Feed Network Amit Abhishek, Ankur Utsav, Ritesh Kr. Badhai, P. Suraj	1464
266	A DECODER-MUX BASED ARBITER PHYSICAL UNCLONABLE FUNCTIONS FOR LOW COST SECURITY APPLICATIONS Anil Kumar.Kurra, Usha Rani.Nelakuditi	1469
267	Memory Optimizing Algorithms for Data Acquisition in Electric Drive of Hybrid Electric Vehicles Gopika Rajan, Vinoth Ramalingam	1474
268	Real-Time Vehicular Traffic Analysis using Big Data Processing and IoT based Devices for Future Policy Predictions in Smart Transportation Ramesh R, Divya G, Dr. M A Dorairangaswamy, Unnikrishnan K N, Aleena Joseph, Asha Vijayakumar, Arun Mani	1478
269	Reliable Machine Learning Approach to Predict Patient Satisfaction for Optimal Decision Making and Quality Health Care G.Sabarmathi, Dr.R.Chinnaiyan	1485
270	Application of Tree Data Structures for Improving Energy Efficiency & Life Time Of Wireless Sensor Networks(WSN): A Critical Study of the State-of-the-Art and Feasibillity For Further Research Pranesh, Santhosh L Deshpande	1490
271	A Survey of Privacy Leakage and Security Vulnerabilities in the Internet of Things Amit Kumar Tyagi, Deepti Goyal	1496

S.No	Title/ Authors Name	Page. No
272	A Performance analysis of Medical Image Transmission Based on Compression and Parallelism Sree Vasulu	1504
273	Lane-Finding Based on Structure Analysis of Lane and Computer Vision Shashank Gupta, Divakar Yadav	1511
274	A Distributed Minimum Spanning Tree Based on all Best Swap Edges in CRN Deepak Rohilla, Mahendra Kumar Murmu	1518
275	A Robust Code for MBU Correction Till 5-Bit Error K. Sai Karan, N. Srikanth, Sonali Agrawal	1522
276	Enhanced Security through Cloud-Fog Integration Rose K Johney, Elizabeth Shelry, K R Remesh Babu	1528
277	Remote Controlled Car using Smartphone Accelerometer Varsha Vishwa Kiran, S Santhanalakshmi	1534
278	Centralized System For Emergency Vehicle Passing With Authentication L.Megalan Leo, Karthik Tummala, R.Pradeep Kumar Raju	1541
279	IOT BASED PEST CONTROLLING SYSTEM FOR SMART AGRICULTURE P.Uva Darshni, P.Uva Dharini, S.Monisha, K.Saranya	1546
280	Performance comparison of adaptive filters used for Acoustic Echo cancellation application under double talk scenario S Radhika, A Chandrasekar	1550
281	Raspberry-Pi based Smart Power Monitoring system Abhay Kshirsagar, Narendra Walawalkar, Harish Yadav, Shrutisneha Prasad, Prajakta Paranjape,	1556
282	Implementation of Non isolated DC DC Boost Converter based on Inductor for DC Microgrid Application Vishwesh Anand Sahasrabudhe, S.Y.Gadgune, Viraj Savakhande	1562
283	An Effective Content Based Image Retrieval Using Dot Diffusion Block Truncation Coding Admile Nandkumar Sushen, Dr.Anup S.Vibhute	1567
284	An Intelligent System for Phishing Attack Detection and Prevention Megha N, K R Remesh Babu, Elizabeth Sherly	1573
285	Deep Learning Based Classification Algorithm For Detection Of Diabetic Disease Pavithra C M, Dr Shankaraiah, Dr Srikanth T	1579
286	Implementation of IEEE 802.11p in Fixed Vehicle-to-Vehicle Communication System using NS3 Simulator Amanpreet Singh Saini, 1Sarthak Agarwal, Snehal Agrawal, Srishti Agarwal, Umme Kulsum	1585

S.No	Title/ Authors Name	Page. No
287	Augmenting Vehicular Network with Software Defined Internet-of Vehicles Paradigm Sanjai Pathak, Ashish Mani, Mayank Sharma, Amlan Chatterjee	1589
288	Spike Correlations and Synchrony Affects the Information Encoding of Neurons Manjusha Nair, Richard Laji, Reshma Mohan	1595
289	Real time Facial Expression Recognition using Grid of Local Binary Pattern and Histogram of Gradients and Genetic Algorithm on Raspberry Pi ARISTON RODRIGUES, KIRAN TALELE	1601
290	Conformal Reflector Backed Printed Dipole Antenna For Directional UAV Communications Prashant Ravindra, Ravishankar B. N. , Samudra Dasgupta , Selvanayaki K	1608
291	An Ensemble-Based Feature Selection and Classification of Gene Expression using Support Vector Machine, K-Nearest Neighbor, Decision Tree Anu J Nair, Maheeshma KM, Kavitha K R, Rizwana Rasheed, Aiswarya LS	1613
292	A Survey on IoT Based Agricultural Crop Growth Monitoring and Quality Control Jayvant Devare, Neha Hajare	1619
293	Simulink Model of Controlling Fuel Cell Powered Direct Current Motor with Comparative Performance Analysis Md. Moontasir Rashid, Md. Niaz Morshedul Haque, Tasneema Akhtar, Md. Sayem Miah	1626
294	A Cloud Resource Scheduling Framework for big data stream and analytics in Cloud Environment K. Manivannane, Dr. M. Chidambaram	1633
295	Secondary User As An Opportunistic Relay Based Path Selection Network Using Fuzzy Logic In Cognitive Radio Network Vasundhara, Avtar singh buttar	1638
296	Analysis of the Electric field of the 1200kv power transmission line using the Finite Element Method Akibaehmad A. Arora, Anuradha S. Deshpande	1643
297	Comparative analysis of Cuk converter with proportional integral controller & proportional resonant controller Tejal Dinesh Patil, D. S. More	1649
298	An Approach for Analysis and Prediction of CKD using Deep Learning Architecture Navaneeth Bhaskar, Suchetha M	1655
299	A Novel Approach to Aggregate and Secure Data in Wireless Sensor Networks Harsha K.M, Divya James	1660

S.No	Title/ Authors Name	Page. No
300	Analysing the learning style of an individual and suggesting field of study using Machine Learning techniques Ananthu S Kuttattu, Gokul G S, Hari Prasad, Jijith Murali, Lekshmi S Nair	1666
301	Comparative Analysis of Texture Features and Deep Learning Method for Real-time Indoor Object Recognition Jayakanth K	1671
302	Matlab And Arduino Based Real Time Face Detection And Tracking System Mr. V. Prakasam, Mr. P. Sandeep	1678
303	PERFORMANCE MEASURES FOR PASSBAND DIGITAL TRANSMISSION TECHNIQUES OVER AWGN CHANNEL Parag Jain, Meha Shrivastava	1683
304	Solving fuzzy clustering problem using fuzzy bacterial colony optimization K.VIJAYAKUMARI, Dr. V. BABY DEEPA	1689
305	Local Grid Connected Microgrid Musters with PV System along POC of BESS Sandeep Verma, Dr. Annapurna Bhargava, Swati Bhasin, Vandana Chaudhary	1694
306	Modelling and Analysis of Gigahertz Transverse Electromagnetic Mode (GTEM) Cell Prachi Kotwal, Gyanendra Verma, Dr. P. K. Katti	1703
307	Credit Card Fraud Detection Using Various Classification and Sampling Techniques: A Comparative Study J. V. V. Sriram Sasank, G. Ram sahith, K.Abhinav, Meena Belwal	1708
308	Dynamic Load Shedding Management for Optimizing Power Distrubution Karthik S, Devaraj BN,Keshav Kashyap A, B T Venkatesh Murthy	1714
309	An Efficient Reconfigurable FIR Filter for Dynamic Filter order variation Bandreddi Ray Srinivasa Rao, Bala Tripura Sundari B	1719
310	Sparse based Dimensionality Reduction for Big Data Management: SDN Perspective Miss. Rajnandani Pawar, Prof. Vinod Jadhav	1724
311	Hardware Implementation of VANET Communication based Collision Warning System Rakesh.G, Meena Belwal	1729
312	FPGA Based Emulator Design of a DC Motor Rama D, Ananthan T	1734
313	A software Based Network simulation model For Internet Service Providers Miss. Shrutika Mahale, Prof. Vinod Jadhav	1739

S.No	Title/ Authors Name	Page. No
314	A Grid-Connected Single Step High Gain Buck-Boost Inverter Using Fuzzy Maximum Power Point Tracking Saurabh Shripad Dixit, Dr. D. R. Patil	1744
315	PROFICIENT RESOURCE ALLOCATION TO SECONDARY USER USING NATURE INSPIRED TECHNIQUE IN COGNITIVE RADIO NETWORK Ridhima, Avtar Singh Buttar	1750
316	Enhancement of UAV Performance Through Xbee Based Telemetry System Design Chidura Bhanu Teja, Heena Sharma	1757
317	A Slotted Compact Antipodal Vivaldi Antenna(CAVA) for UWB Applications Harish Ravichandran , Jayakrishnan V M, Sethuraman N Rao	1761
318	K Medoids Based Clustering Algorithm with Minimum Spanning Tree in Wireless Sensor Network Shaffali Jain, Prof. Nitesh Bharot	1766
319	Detection of Zinc Mineralization in North India using Hyperspectral Image Processing Aravinth J., Biplab Nath, Siva Subramanian M., Rohit V.S.S. Bulusu and Monish P.	1772
320	Analysis and Control of Hybrid Boost Converter with Simultaneous DC and AC Outputs Akshay Laxman Pujari, D. S. More	1777
321	An enhanced approach for movie review analysis using deep learning techniques Aswathi Sajeevan, Lakshmi K S	1783
322	IMPROVING MEAN OPINION SCORE (MOS) OF VoIP IN WiMAX SYSTEM BY USING AN EFFICIENT TECHNIQUE Misha, Dalveer Kaur	1790
323	Whale Optimization Algorithm Based Cognitive Radio System Design for Internet of Things Kiranjot Kaur, Munish Rattan, Manjeet Singh Patterh	1795
324	AUTOMATED MAPPING OF SERVICE LEVEL AGREEMENTS TO APPLICATION PROGRAMMING INTERFACES OF DIFFERENT CLOUD SERVICE PROVIDERS Aishwarya S Pattar, B K Srinivas	1802
325	Control and Management of Autonomous Power between Standalone DC Microgrids Prasad Subhash Kirtane, Dr. A. D. Shendge	1806
326	Delay Minimization by Offloading in Fog Computing Shahid Sultan Hajam, Dr. Shabir Ahmad Sofi, Zahoor Ahmad Najar	1811

S.No	Title/ Authors Name	Page. No
327	Designing a help system including website mobile application along with secured locker as a communication medium for students Dr.Thangam Palaniswamy, Ruba Al-Ghamdi, Ayshah Banabilah, Mawaddah Kuddah, Nesren Attiah	1816
328	Core Control System Of An Autonomous Electric Vehicle Adeeba Fazal Pathan, Prof. Mahantesh P. Mattada	1823
329	Power Quality Improvement Using Unified Power Quality Conditioner with Distribution Generation Sachin Baliram Shahapure, Ramchandra P. Hasabe	1829
330	Security for IOT devices using Blockchain Sri Harshini Popuri, Y Mohana Roopa	1836
331	GENETIC ALGORITHM BASED TUNING OF NONFRAGILE AND ROBUST PI CONTROLLER FOR PSFB DC-DC CONVERTER Aswathi Divakar, Dr. Jeevamma Jacob	1841
332	Adaptive Tracking Technique for Communication Cost Reduction in Wireless Sensor Network Krishna Tulasi M.S, Sudheesh .P	1847
333	STAR – DELTA STARTER USING STATIC SWITCHES WITH ARDUINO MICROCONTROLLER AS A BASE DRIVE CIRCUIT Shubham Sonawadekar, Shivprasad Desai	1853
334	Performance Evaluation of Network Layer Routing Protocols on Wireless Sensor Networks Amitkumar V. Jha, Bhargav Appasani, Abu Nasar Ghazali	1857
335	The PI Controllers and its optimal tuning for Load Frequency Control (LFC) of Hybrid Hydro-thermal Power Systems Amitkumar V. Jha, Deepak Kumar Gupta, Bhargav Appasani	1861
336	A SURVEY ON MESSAGE QUEUING TELEMETRY TRANSPORT (MQTT) PROTOCOL OF INTERNET OF THINGS (IOT) Lokesh A R, Shashidhar R	1866
337	A Review on tumor segmentation techniques for Magnetic Resonance Images R.Sakthi prabha, Dr.M.Vadivel	1871
338	Load Frequency Control for Multi-Area Power System using Fuzzy Logic Controller Himanshu Yadav, D. K. Sambariya	1878
339	Analysis of Techniques for Correcting Power Factor of AC-DC Converters Prerna Saxena, Lata Gidwani, Ashok Kumar Sharma	1884
340	INTELLIGENT PUBLIC RATION DISTRIBUTION SYSTEM (IPRDS) Vaisakh A.K, Ganesh K.V, Sooraj Suresh, Linoy Vincent, Thobias P T, Dr.Indhu.P.Nair	1889

S.No	Title/ Authors Name	Page. No
341	Reliable Constrained Application Protocol to Sense and Avoid attacks in WSN for IoT Devices Divya.R, Dr.R.Chinnaiyan	1893
342	Radiation Data Acquisition System Using Wireless Communication Reshma Ramanan. M, G.Shekar, Sreelatha. P, Pradeepkumar. P	1897
343	Integrated Cloud based Smart Home with Automation and Remote controllability Aravind Hanumanthaiah, Arjun D, Liya M L, Chandni Arun, Athira Gopinath	1903
344	Mutispectral brain Magnetic Resonance Imaging denoising using non-local means with statistical nearest neighbor Utkarsha I. Jondhale, Prof. Rachna S. Potpelwar	1908
345	Word Based Statistical Machine Translation Neeha Ashraf, Manzoor Ahmad	1914
346	A Hybrid Approach to Improve Full Coverage in Wireless Sensor Networks Amandeep Kaur Sohal, Dr. Ajay K. Sharma, Dr. Neetu Sood,	1919
347	Performance Analysis of Switched-Boost DC to DC Converter for Distributed Generation system Deepanshu Gautam, Ashok kumar sharma, Jyoti Shukla, Neeti Dubey, Priyanka Nehra	1925
348	Regenerative Model for Electric Vehicle Application Aniket A. Manjare, Vishal M. Patil, Mandar M. Bhalekar, Promod R. Ubare	1931
349	Design of smart Monitor for automobiles using FPGA based Data Logger Merugu Bhavani, Dharmavaram Asha Devi	1935
350	FPGA Implementation of segmented feature fusion in MRI images using wavelet S.SREEKRISHNA YADAV, VIKAS MITTAL	1941
351	FDDS: An Integrated Conceptual FDDS Framework for DDS Based Middleware Mukesh Kumar, Awadhesh Kumar Singh	1947
352	Classification System for Lung Cancer Nodule Using Machine Learning Technique and Ct Images Baskar.S, Mohamed shakeel, K.P.Sridhar, Kanimozhi R	1952
353	Analysis and Design of Precision Time Protocol System Based on IEEE1588 Standards Priyanshu Pandey, Bhanu Pratap, Radhey Shyam Pandey	1958
354	Implementation of FreeRTOS based Precision Time Protocol (PTP) application as per IEEE1588v2 standards for Xilinx Zynq UltraScale Plus MPSoC devices Priyanshu Pandey, Bhanu Pratap, Radhey Shyam Pandey	1963

S.No	Title/ Authors Name	Page. No
355	Miniaturized Cupcake Fractal Patch Antenna for Biomedical Applications Anita Garhwal, Badrul Hisham Ahmad, Pushpendra Singh, Mohd Riduan Ahmad, Sanyog Rawat, Kanad Ray, Anirban Bandyopadhyay	1969
356	Bi-directional Methodology for Literature Extraction from PubMed Abstracts using Web Scrapper and Web Crawler Koras. S, Mannem.Venkatarao Rao, V. Bhuvaneswari	1973
357	IoT Visibility Issues and securing using Deep Neural Networks Moinak Bhattacharya, Dr. R. Annie Uthra, Rounak Datta, Arindam Chakraborty	1979
358	Autocorrelation based Chordiogram Image Descriptor for Image Retrieval A.Saravanan, S.Sathiamoorthy	1985
359	Multimodal Data Security Framework Using Steganography Approaches Sarang Parikh, Sanjay H A, K. Aditya Shastry, Amith K K	1992
360	Investigations on Steel as Low Cost Substrate for Low Frequency Patch Antenna Lakshmi K K, Sabarish Narayanan B	1998
361	Design and Implementation of Encoder and Decoder for Cyclic Redundancy Check Arpita Sahu, Dr. R. S. Gamad, Dr. P. P. Bansod	2002
362	Analysis of Various Security Techniques of Internet of Things Chandni Krish, Dr.Rakesh Kumar	2007
363	Design and Development of IOT Based SMART water distribution network for Residential areas Chetan S. Patel, Prof. Jitendra A. Gaikwad	2014
364	Standalone PV System Integrated with Hysteresis Current Controlled Inverter using MPPT Techniques Saurav Sahoo, Saroj Kumar Mishra, Jayanta Kumar Sahu	2019
365	IoT Enabled Smart Industrial Pollution Monitoring and Control System Using Raspberry Pi with BLYNK Server S.Ramalingam, K.Baskaran, D.Kalaiarasan	2025
366	ENHANCED RANKING OF WEBSITES BASED ON CREDIBILITY EVALUATION Subbulakshmi. S, Gopika. A, Lincy Thomson	2030
367	Design and Simulation of Two Stage Sample and Hold Circuit with Low Power using Current Controlled Conveyor Vivek Kumar Jain, Prof. D. S. Ajnar, Prof. P. K. Jain	2036
368	A Knowledge Interchange Format (KIF) for Robots in Cloud Dhruba Ningombam, Tejbanta Singh Chingtham, Mrinal Kanti Ghose	2041
369	Energy-Delay Based Route Request Scheme for Load Balanced Routing in Wireless Mesh Networks Keerthi D S, Shobha Rani A, T G Basavaraju	2047

S.No	Title/ Authors Name	Page. No
370	Driver Fatigue Detection Based On Eye State Recognition Using Convolutional Neural Network Sharan S S, Viji R, Pradeep R, Sajith V	2052
371	Power quality enhancement using unified power flow controller in grid connected hybrid PV/Wind system Vandana Chaudhary, Annapurna Bhargava, Sandeep Verma	2059
372	Speed Optimization of the AES Algorithm Using Pipeline Hardware Architecture Dheeraj Punia, Dr. Brahmjit Singh	2065
373	Analysis of Coupled Inductor Based Buck-Boost Single Phase PWM AC to AC Converter Priyanka Nehra, Ashok Kumar Sharma, Dolly Murodia, Deepanshu Gautam	2070
374	Classification of Retinal Diseases using Transfer Learning Approach Amrit Das, Rohan Giri, Gunjan Chourasia, A. Anilet Bala	2075
375	DESIGN AND IMPLEMENTATION OF VINCULUM BINARY CODED DECIMAL MULTIPLIERS USING VINCULUM BINARY CODED DECIMAL COMPRESSORS G.Sreelakshmi, Dr. Kaleem Fatima, Dr.B.K.Madhavi	2080
376	BVLCs and BDIPs in Covariance Descriptor with a Statistical Measure of Divergence for Image Retrieval M. Bennet Rajesh, S.Sathiamoorthy	2086
377	Content Based Medical Image Retrieval Using Multi-Trend Structure Descriptor and Fuzzy k-NN Classifier M.Natarajan, S.Sathiamoorthy	2092
378	Co-occurrence of Edges and Valleys for Content Based Image retrieval M. Bennet Rajesh, S.Sathiamoorthy	2098
379	Wavelet based Chordiogram ImageDescriptor for Image Retrieval A.Saravanan, S.Sathiamoorthy	2104
380	Wavelet Based Multi-Trend Structure Descriptor for Effective Image Retrieval M.Natarajan, S.Sathiamoorthy	2111
381	Ambipolar supression in L-shaped Tunnel Field Effect Transistor using dielectric pockets Sonakshi Beniwal, Gaurav Saini	2118
382	Use Of Electroencephalogram Signal and Screening Test For Detecting Cognitive Ability Of Person Amruta Koli, Prof. Shridevi Karande	2123
383	Impact of Imperfect Channel State Information on Downlink Sum-Rate of Two user mmWave Non Orthogonal Multiple Access Sumathi S., Arpita Thakre	2129

S.No	Title/ Authors Name	Page. No
384	Long-Short term Memory based Channel Prediction for SISO System Draksham Madhubabu, Arpita Thakre	2135
385	CPW fed Antenna for Dual Band Applications with Loop Ground Plane Anu Suresh, Sreedevi K. Menon	2140
386	A unified Convolutional Neural Network framework for intelligent decision making related to navigation Khyati Marwah, Dr. Jogeshwar Singh Sohal	2144
387	Speckle Noise Reduction Using Fuzzy Logic in Ultrasound Images Azrah Rubanee, Harish Kumar Dogra, Giridhar Reddy Bojja	2149
388	Plants Leaf Segmentation using Bacterial Foraging Optimization algorithm Siddharth Singh Chouhan, Ajay Kaul, Uday Pratap Singh	2156
389	Optimization of Advanced Encryption Standard Algorithm (AES) on Field Programmable Gate Array (FPGA) Mr. Neelesh Jain, Mr. D. S. Ajnar, Mr. P. K. Jain	2162
390	A Proposal of smart hospital management using hybrid Cloud, IoT, ML, and AI Naveen Ananda Kumar J, Shivani Suresh,	2167
391	Dual Band Monopole Antenna with a Stepped Ground Plane Sooraj Muralidharan, Sreedevi K. Menon	2171
392	Cooperative Hybrid Automatic Repeat Request Based on the Number of Retransmissions Arpitha R, Chaithra B R and Usha Padma	2176
393	Symptom Based Health Prediction using Data Mining Vijaya Shetty S, Karthik G A, M Ashwin	2181
394	Design of Electrostatic Energy Harvesting Pre charge Circuit Apoorva Raghunandan, Shilpa D R	2187
395	DESIGN AND IMPLEMENTATION OF NOVEL ECG ACQUISITION SYSTEM J.Dharneeshkar, Dr.V.Vanitha	2192
396	Facial Expression Recognition using Convolutional Neural Network and SoftMax function on Captured Images Ashish Deopa, Abhishek Sinha, Aditya Prakash, Rupesh Kumar Sinha	2197
397	Analysis of Horizontal Grounding Electrode in Transmission Line Approach Koppakula Nagarjuna, K Chandrasekaran	2204
398	Data Leakage Detection by Adaptive Weighted Graph Walk Model Manoj kumar M N, M B Nirmala	2210

Proceedings of the Fourth International Conference on Communication and Electronics Systems (ICCES 2019)
IEEE Conference Record # 45898; IEEE Xplore ISBN: 978-1-7281-1261-9

Fog Computing: An Enhanced Performance Analysis Emulation Framework for IoT with Load Balancing Smart Gateway Architecture

Bikash Sarma
Department of CSE,
National Institute of Technology Nagaland
Chumukedima, Dimapur,
Nagaland, India
bikash.sarma2010@gmail.com

Gajender Kumar
Department of CSE,
National Institute of Technology Nagaland
Chumukedima, Dimapur,
Nagaland, India
gk201719nit@gmail.com

R. Kumar
Department of EIE,
National Institute of Technology Nagaland
Chumukedima, Dimapur,
Nagaland, India
rajagopal.kumar4@gmail.com

Themrichon Tuithung
Department of CSE,
National Institute of Technology Nagaland
Chumukedima, Dimapur,
Nagaland, India
t_tuithung@yahoo.com

***Abstract*—** With the exponential progress of IoT applications in last few years, a huge amount of data is being collected and stored every day and thus an enhanced and mature solution is very much necessary to knob these data. Usually cloud is utilized as the processing and storing unit of an IoT system. Cloud is deliberated to be the best solution for emerging IoT solutions with its diversified facilities. To tackle the massy amount of data that is being pumped everyday throughout the network, Fog computing is an effective solution which can trim and pre-process the data before forwarding it to cloud where Fog resides near the IoT application. Unlike cloud, Fog may not have high computing facilities but it can perform better in case of time sensitive application with moderate processing. Based on the recent trend smart gateway-based Fog-Cloud solutions are gaining more popularities compared with the other related solutions. In this paper, we have extensively discussed about a load balancing based smart gateway with Fog and Cloud environment where an analysis of load balancing environment with regards to processing delay and network delay is performed. Subsequently we have compared different scenarios with and without load balancing algorithm in the projected architecture.

***Keywords*—**IoT; Fog Computing; Smart Gateway; Load balancing; Cloud Computing

I. INTRODUCTION

Technology is developing rapidly and devices are becoming smart in day to day culture due to which the trend of IoT has taken a high rise in the world of applications in recent times. Ordinarily IoT paradigm is considered as a group of interconnected real-world small things, with storage and process constraint, distributed in nature and delivers good performance. Usually in IoT, devices like home appliances, process automation, life saving devices, smart devices and other related types are connected with Cloud for processing and storing the data generated over the period of intervals. The average growth of the connected devices has reached much higher due to which in 2020, it might reach nearer to 6.58 devices per person [1]. As a result, the data traffic in the network will be amplified enormously which may shape problems for latency sensitive and real time applications. Latency sensitive applications are typically restricted with strict response time. Even if the client gets response beyond the bounded time, the response will be considered as null and void. There are many ways latency may occur but in case of IoT, processing and network latency is mostly contemplated. Though network latency typically depends on the size of the data, distance it has covered and the medium it has to travel which also depends on the number of devices it has to travel across as each one conceivably checks and alters the header of the packet. Similarly a processing latency depends on the processing capacity as well as on the number of jobs waiting to get processed in the server.

Until fog computing was popularized by CISCO in the year 2012[2], cloud was one of the traditional tools to support Internet of Things (IoT). Cloud has a representative part in today's growth of IoT though is not precisely a group of interconnected devices rather an information and knowledge providing mechanism from the data it collected by sensing the environment. The data collected via IoT devices are sent to the cloud for central access and processing. The characteristics such as ease of access and scalability of cloud make it more comprehensive with IoT. As devices in IoT are collecting bulk

amount of data every day and it is gradually increasing, a scalable storage along with processing is necessary that can further be extended as per demand. With the help of those collected data many business models are being designed and established mechanism are used to find out certain patterns while designing such business models which require extendable and high processing where cloud is trending. Apart from that, the concept of pay-as-used makes cloud convenient for the IoT users, in spite of such infrastructure and facilities of cloud, fog is getting acceptance but of course cannot be replaced as they complement each other [3].

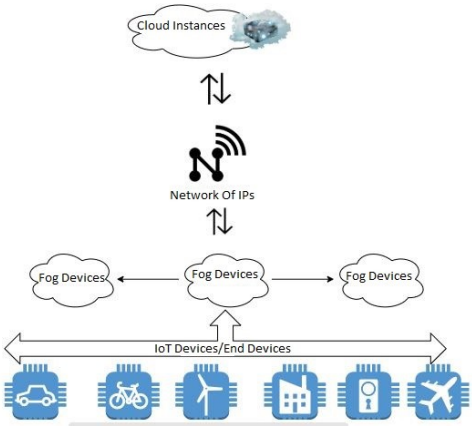

Fig 1: IoT with Fog and Cloud Environment

In this research work we have analyzed the Fog with smart gateway-based load balancing scenario in an emulation framework and in the remaining part of this paper we have discussed about the Fog computing in section II, related works in section III. In section IV and V, we have explained about the framework setup and output of the emulation. Finally, we conclude the paper in section VI with future work.

II. FOG COMPUTING

Fog computing is a platform that can compute, store and provide network services between the IoT nodes and the Cloud computing data centers, but it is not exactly positioned at the edge of the network [4]. It extends the typical Cloud environment providing better result in many applications where Fog is a type of distributed computing method that facilitates application of low latency services [5]. Fog Computing used to work on network ends instead of hosting and working from a centralized server or cloud and in most of the fog devices, computation is performed when necessary and also storage facilities is available for a while [6]. However, for the cloud, real-time interaction with IoT devices is such a task which is not possible because of its high latency [5], [7], [8]. Fog reside near the IoT devices due to that there is no latency issue but obviously it creates a problem of low processing power as it does not consist of any high computing configuration. Usually Fog nodes are available in the private network of the IoT system which exists in the local network makes Fog nodes and its communication much more secure than the Cloud. Fog and Edge computing are not only analogous with respect to their proximity with the source of the data but also both remain different paradigms at one point. In edge computing the processing power is in the device itself whereas in fog computing the processing power is in the network where the Fog nodes are interconnected. Moreover edge computing does not depend on the gateway but in Fog computing gateway is the key component which transmits the data from the edge nodes to the Fog. A typical IoT system architecture is shown in Figure 1 where all the IoT devices are connected with cloud through different IP networks crossing Fog layer.

III. RELATED WORK

Fog is trending towards the mainstream of Information technology. Many researchers are putting their effort for the nourishment of Fog and upbringing it to future level. In an automated system, Fog can be used in traffic light management system and with the help of image processing technique, emergency vehicle like ambulance can be identified. Further the conjugative smart traffic lights can change their status considering the current traffic as these smart traffic lights can communicate with each neighboring one and build a green corridor for emergency vehicle [4]. Smart meters are also a stimulating device which intelligently decide the other input power source which can be solar or wind, based on certain parameters like cost, availability as well as demand [9] and can also be implemented within the area of Fog. An intelligent home control system [10] is a type of intelligent system which works with the help of an android phone working as a special gateway instead of ordinary gateway that will observe and predict the behavior of the user and automatically power off the devices that will not be available for use due to which the wastage of energy can be minimized. In Smart e-Health Gateway [11], a health monitoring system has been elaborated and implemented with the help of Fog Computing where an immediate and automated medical instruction was derived on the basis of sensors data fitted on patient body. Further an implementation for an in-home EWS system was improvised to which patient may get different services and environment that is feasibly accepted medically. However to reduce the unnecessary data uploading to network, a smart gateway based communication was discussed in Fog Computing [12] where they suggest that the data can be pre-processed before uploading to the core network which may reduce the over burden to the cloud data centers. Here the gateway namely smart gateway, signifies a responsibility for data filtering and trimming as suggested in a design shown in Figure 2.

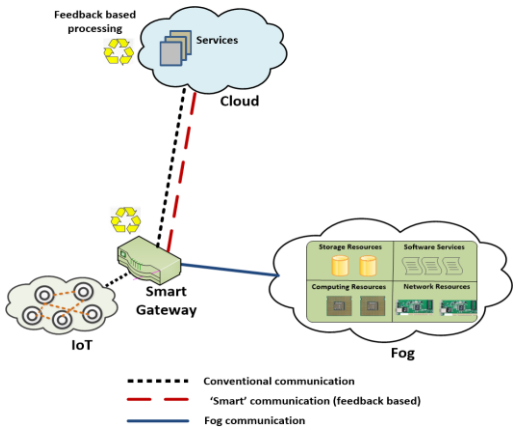

Fig 2: Smart Gateway with Fog computing/Smart network [11]

Many directions were discussed in most of the research papers of Fog and Cloud Computing but here we proposed the and verified the following approches appropriately to get better comparison with respect to network delay and processing delay.

1. IoT with Cloud alone situation
2. IoT with Fog alone Situation, Fog consisting of one node.
3. IoT with Fog alone Situation, Fog consists of multiple node.
4. IoT with Fog, Cloud and Smart Gateway based load balancing situation, Fog consists of multiple nodes.

In the last approach, a smart gateway will be used as load balancer between Fog and Cloud which usually perform the operation of data filtering before forwarding it to Cloud. A load balancing algorithm will be implemented in the same gateway which will route data to get executed. Sending all data to Cloud may increase the network latency and at the same time executing everything in Fog may overload the Fog servers. To achieve high computing (in Cloud) and less network latency (in Fog), launching a load balancer (smart gateway) between Cloud and Fog might be prolific direction. Hence in the following section a discussion about all the analysis with an emulation framework is mentioned systematically.

IV. INITIAL SETUP

Various simulators are available to simulate fog but since there was not much upgradation to those utilized in early stages, analyzing the Fog in a different scenario was equipped in this research work. A design implemented here is emulated framework where real gateway, real cloud, real fog nodes were adopted but simulated sensor data are utilized. Sensor nodes are contrived in such a way that it will send data in a continuous manner to the gateway.

For building the cloud environment, in this work the help of Google Cloud Computing Engine (VM instance) was availed. Creation of a cloud VM instance of 4 vCPUs, 15 GB Memory and on the other hand, for Fog environment Raspberry-Pi board with quad-core ARM Cortex A53 processor and 1 GB Memory were chosen accordingly. Raspberry-Pi was selected as a computing unit with less processing power and memory which matches the Fog server requirements. As gateway is a key part of the entire system and it has a lot of decision making along with pre-processing work with a chosen desktop machine as smart gateway with 8 GB RAM and core i7 processor. Secondly a system with i5 processor and 4 GB RAM was selected as a generator of sensor nodes from which N number of sensor nodes can be created and each of these can send the required amount of data as sensor data to the gateway. For the experimentation of the work the decision of using 10 sensor nodes was approximated which will send a constant data of 7kb size in every second of interval. Utilizing the concepts of multithreading, gateway will handle all 10 virtual sensor nodes in isolation along with the programming part carried out with the help of python programming language and python 2.17 compiler. To simulate the processing part in cloud and Fog, a mathematical calculation was put under a loop for certain number of iterations and the server was made busy as if they are busy with processing of the data sent via gateway. The processing time was calculated at the Fog/Cloud side and the calculated results are reverted back as reply and at the same time a round trip time is also been calculated in the gateway. By continuing the round trip time in this work a discussion about time constraint applications is carried out expecting the responses in real time and by subtracting the processing time from the round trip time the network delay was calculated.

V. RESULTS AND DISCUSSION

Once the execution of framework starts, sensor generator generates 10 sensor nodes and each of them will pump the file to the gateway. The gateway will forward the data to its destination with respect to the multiple scenarios. Whenever the framework is kept in run mode, it will record 10000 number of entries which can be increased or decreased as per the demand of the user.

A. IoT with Cloud alone situation(Case 1)

Here the gateway forwards the sensor data to the cloud server directly though gateway has no extra burden other than simply forwarding the received data to cloud server. Hence a simple gateway is enough to take care of this situation. Following are the results obtained after the execution.

Table 1: Delay details for Case 1

Network Delay	Processing Delay	Total Delay
0.674784167	0.015158118	0.689942285

B. IoT with Fog alone Situation, Fog consist of one node(Case 2)

Based on the scenario, replacement of the cloud server with one fog server has been executed. Usually Fog does not consist of only one node but to get more experimental results Fog was considered. Here also the gateway working is similar to cloud alone situation. Following are the results obtained after the execution.

Table 2: Delay details for Case 2

Network Delay	Processing Delay	Total Delay
0.539716318	0.559499568	1.099215885

C. IoT with Fog alone situation, Fog consist of multiple node (Case 3)

Considering multiple Fog nodes, the gateway used in this scenario should be smart enough to handle all the nodes simultaneously. Hence a smart gateway with a simple Round-robin load balancing algorithm was used which forwards the data to all the fog nodes periodically. Results obtained in this experiment are as follows.

Table 3: Delay details for Case 3

Network Delay	Processing Delay	Total Delay
0.172555609	0.441512057	0.614067666

D. IoT with Fog, Cloud and smart gateway based load balancing situation, Fog consist of multiple nodes (Case 4)

To experience the power of cloud processing and Fog proximity, this scenario is experimented. The same smart gateway with Round-robin load balancing algorithm is used to route the data. Results achieved for this experiment is as follows.

Table 4: Delay details for Case 4

Network Delay	Processing Delay	Total Delay
0.208520656	0.302323014	0.51084367

All the experimented results summary is as shown in Figure 3. With no doubt about the performance of cloud, overall response time was pushed back by the network delay (Case 1). If the network delay can be reduced, the system may work much better.

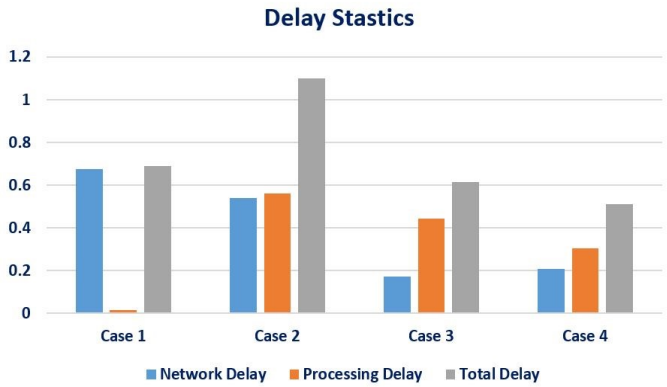

Fig 3: Delay statistics of all the Cases

Therefore by replacing the cloud server with a Fog node will decrease the network delay as the Fog node resides near the gateway. But as per the results obtained, replacing cloud server with one Fog node will not solve the issue because the processing time it takes is much higher than the cloud that increases the overall delay (Case 2). As Fog nodes do not possess high computing configuration it cannot handle more requests, because of which the overall network delay will not deliver much impressive output. With the addition of more Fog nodes in the Fog group can specify some exciting results i.e. as the number increase in Fog group, the load on the individual Fog nodes decreased which reduced the total delay (Case 3). Based on the work carried out, the smart gateway with load balancing mechanism plays an important role to balance the traffic and route all of those(data) carefully among Cloud and Fog servers. The achieved results after combining Cloud and Fog together has proved as the best one as per Case 4 mentioned above. All the Fog nodes and Cloud takes the load of individual request equally and yields more performance where Fog nodes contributes with less network delay and Cloud provide high computing. In figure 3, Case 4 shows less network delay then Case 1 where only Cloud is used and more processing delay as Fog is incorporated with less processing speed but still produced minimum total delay. During experiment the smart gateway is not used as a simple data trimmer or data forwarder instead it worked as a data traffic load balancing hardware. Even though a simple Round-robin load balancing algorithm is used in case 4 but still it has produce the best result among all the case considered in the experiment with minimum total delay. Hence the key part of the entire experiment is smart load balancer where a load balancing algorithm is used in a gateway which is connected to all the sensor nodes to intelligently route the traffic between Cloud and Fog.

VI. CONCLUSION AND FUTURE WORK

As per the research work conducted here many researchers introduced a smart gateway with the facility of pre-processing and data trimming before sending it to Cloud in literature. But here a conclusion has been drawn by which it is not necessary that smart gateway has to do data trimming and pre-processing every time instead this device can be used as smart load balancer. Thus data trimming and pre-processing shows an importance of work and it has a very good impact on overall performance though some file/data needs to be sent in its original size without trimming. In few multiple cases, smart gateway can be used as a smart load balancer. In future, researchers or scientists can introduce different load balancing algorithms to implement in the smart gateway which suite their respective applications and as the smart gateway is capable, the overall performance of Fog and Cloud can be improved with sophisticated and standard load balancing algorithms.

REFERENCES

[1] M. Aazam, S. Zeadally, K. A. Harras, "Offloading in fog computing for IoT: Review enabling technologies and research opportunities", Future Gener. Comput. Syst., vol. 4, no. 57, pp. 278-289, 2018.

[2] R. Mahmud, R. Kotagiri, R. Buyya, "Fog Computing: A Taxonomy Survey and Future Directions", Singapore:Springer, pp. 103-130, 2018.

[3] M. Etemad, M. Aazam, M. St-Hilaire, "Using DEVS for modeling and simulating a fog computing environment", 2017 International Conference on Computing Networking and Communications (ICNC), pp. 849-854, Jan 2017.

[4] F. Bonomi, R. Milito, J. Zhu, S. Addepalli, "Fog computing and its role in the Internet of Things", Proc. 1st Edition MCC Workshop Mobile Cloud Comput., pp. 13-16, 2012.

[5] J. Li, T. Zhang, J. Jin, Y. Yang, D. Yuan, L. Gao, "Latency estimation for fog-based Internet of Things", Proc. 27th Int. Telecommun. Netw. Appl. Conf. (ITNAC), pp. 1-6, Nov. 2017.

[6] R. Naha et al., "Fog computing: Survey of trends architectures requirements and research directions", IEEE Access, vol. 6, pp. 47980-48009, 2018.

[7] M. R. Mahmud, F. Koch, R. Buyya, "Cloud-fog interoperability in IoT-enabled healthcare solutions", Proc. Int. Conf. Distrib. Comput. Netw., pp. 1-10, 2018.

[8] S. Yi, Z. Hao, Z. Qin, Q. Li, "Fog computing: Platform and applications", Proc. 3rd IEEE Workshop Hot Topics Web Syst. Technol. (HotWeb), pp. 73-78, 2015.

[9] C. Wei, Z. M. Fadlullah, N. Kato and I. Stojmenovic, "On Optimally Reducing Power Loss in Micro-grids With Power Storage Devices," Selected Areas in Communications, IEEE Journal on, vol. 32, no. 7, pp. 1361-1370, 2014.

[10] J. Bian, D. Fan, and J. Zhang. "The new intelligent home control system based on the dynamic and intelligent gateway". In Proceedings of the International Conference on Broadband Network and Multimedia Technology, pp 526–530, 2011.

[11] A. M. Rahmani et al., "Exploiting smart E-health gateways at the edge of healthcare Internet-of-Things: A fog computing approach", Future Gener. Comput. Syst., vol. 78, pp. 641-658, Jan. 2018.

[12] M. Aazam, E. N. Huh, "Fog computing and smart gateway based communication for cloud of things", Proc. IEEE Conf. FiCloud, pp. 464-470, Aug. 2014.

Proceedings of the Fourth International Conference on Communication and Electronics Systems (ICCES 2019)
IEEE Conference Record # 45898; IEEE Xplore ISBN: 978-1-7281-1261-9

Energy Efficient Spectrum Access Design for Cognitive Radio Wireless Sensor Network

Professor Ruksar Fatima
Head of the Department
Computer science and engineering,
Khaja Bandanawaz college of engineering ,gulbarga
Email- ruksarf@gmail.com

Shaik humera tauseef
PHD scholar,
khaja Bandanawaz college of engineering, gulbarga
Email-humera1919@rediffmail.com

Rohina khanam
PHD scholar,
Khaja Bandanawaz college of engineering, gulbarga
Email-rohina1119@rediffmail.com

***Abstract*— Wireless sensor networks (WSN) considered to play an important part in Internet of Things (IoT). The increased wireless access device makes spectrum access challenging. Cognitive radio (CR) plays an eminent mechanism to address this issues by enabling sensor device to opportunistically access licensed spectrums. However, energy constraint of sensor device to provide cognitive capability such as channel switching, channel sensing and opportunistic access requires careful planning for enhancing energy efficiency of CR-WSN. For enabling WSN with cognitive capability to provision IOT requires efficient spectrum access and medium access control (MAC) design. The exiting spectrum access model incurs energy overhead and induces higher collision due to interference among contending user and very limited work is carried out considering multi-channel CR-WSN network. As a result, they are not efficient in utilizing spectrum. For overcoming research challenges, this work present an energy efficient spectrum access (EESA) model for multi-channel mobile CR-WSN. Experiment outcome shows EESA attain significant performance over exiting model in terms of throughput and energy efficiency. The EESA utilize spectrum more efficiently considering multi-channel mobile CR-WSN.**

Keywords*— Cognitive radio network, Dynamic spectrum access, energy efficiency, multi-channel.

I. INTRODUCTION

WSN device that are employed in perilous place where charging the sensor is highly improbable, at such places, these WSN are self -possessed and made up of the smallest sensor device available. Since the sensor device is less expensive, this property of the device has made the enormous growth in the IoT, where they are connected to the internet for various purpose and application [1], [2] such as IoT and Big-Data. These application needs the huge amount of data, LLS (Low Latency Service) delivery along with low energy dissipation, it also requires the availability of higher spectrum [3], hierarchical structure. Moreover, the frequency channel with 2.4GHZ is with the several application. These application includes Wi-Fi and Bluetooth, also the 5G network is expected to arrive in nearby future. The latest generation of the network needs the ESA (Efficient Spectrum Access) design.

For the future IoT technology which is based on the cognitive network, CRN (Cognitive Radio Network) [4] may be considered to address the accessing of spectrum. The model of CIoT provides enhanced intelligence to obtain the efficient DS (Data Sensing) and analysis [5] mainly for WSN. Improvised as well as the smartest version of MAC is used for absolute incorporation of CIoT in WSN. Moreover, also for the absolute incorporation cognition in the spectrum needs to be addressed. The spectrum utilizes the on and off scenario and they are intended to congested on the particular sections of spectrum. The several cases of real SS (Spectrum Scarcity) [6] and artificial makes it mandatory for needs of efficient spectrum uses. Fig1 shows the architectural design of CR-WSN (Cognitive Radio-WSN).

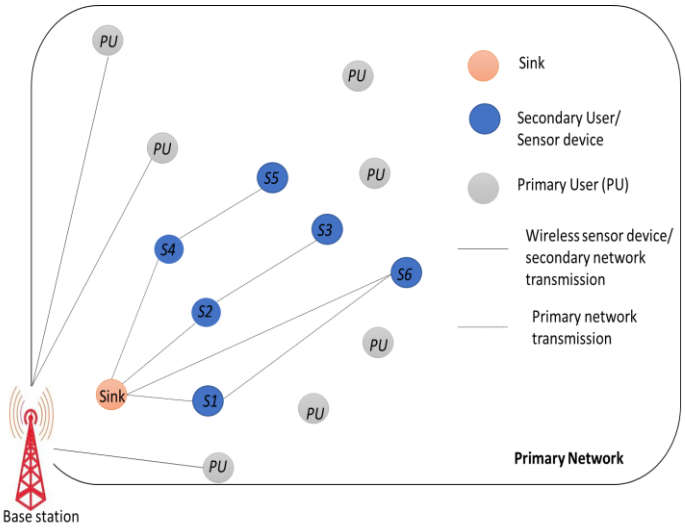

Fig. 1. Architecture of CR-WSN

Effective spectrum access design are required to attain efficient throughput for dynamic CIoT applications [7], [8], and [9]. The wireless network is getting more crowded and complicated. As a result, it is problematic in obtaining network information for cognitive user. Further, the fifth generation network is expected to offer ultra-low power and super-efficient spectrum access design to cater large density of users with low jitter, delay and restricted bandwidth which will be a challenging

task for existing crowded spectrum. Spectrum inefficiency can be overcome by using Opportunistic Spectrum Access (OSA) mechanism which is also denoted as Dynamic Spectrum Access (DSA) mechanism. Opportunistic spectrum access is considered to be key component of cognitive radio where wireless device can sense, learn and adapt. Though cognitive radio wireless sensor network aid in enhancing IoT network performance and user requirement. However, sensor devices incurs energy overhead to perform spectrum sensing and spectrum sharing [10] for attaining good QoS and high throughput requirement [11] of applications [8]. These real-time application [12] requires distributed channel access [13] considering unknown network information. Such methods was modelled for single cognitive radio user in [14] and for multi-user in [15]. However, considering multi-user scenario it induces collision in network due to interference [16] among user and some user are selfish in nature in CR-WSN. To reduce collision, priority access [17], random access [18], and fair resource allocation [19] model has been presented. However, these model are limited to provide only one channel at a time to a cognitive user. As a result, if a selected medium is busy then, that subscriber needs to wait another slot and if another channel is free at that time the spectrum is wasted.

For allocating and utilizing bandwidth or spectrum more efficiently game theory model is been adopted by various existing research [20], [21] and [22]. However, these model are designed considering single channel, static secondary network, and homogenous environment. In [23] presented a spectrum access model adopting game theory model and [24] presented a distributed spectrum access model adopting Markov model considering mobile secondary network and multi-channel environment. However, [23] failed to attain existence of Nash equilibrium and [23], [24] incurs channel switching overhead due to interference when mobility speed is increased. To overcome the research challenges, this paper presents an Energy efficient Spectrum Access (EESA) model for multi-channel mobile cognitive radio wireless sensor network.

The research contribution as follows

- This work presented a energy efficient spectrum access model considering both spatial and temporal information for multi-channel mobile CR-WSN. As per our knowledge no prior work as considered spectrum access model considering multi-channel mobile CR-WSN.
- EESA attain significant performance in terms of throughput and energy efficiency.
- EESA model brings good tradeoff between minimizing energy, maximizing throughput and utilizing spectrum efficiently.

The rest of the paper is organized as follows. In section II the Energy Efficient Spectrum Access (EESA) model for multi-channel mobile cognitive radio wireless sensor network is presented. In penultimate section experimental study is carried out. The conclusion and future work is described in last section.

II. ENERGY EFFICIENT SPECTRUM ACCESS DESIGN FOR COGNITIVE RADIO WIRELESS SENSOR NETWORK

This work present a novel Distributed and Efficient Channel Access (DECA) model for Multi-Channel Mobile Cognitive Radio Network. The DECA channel access model is designed considering both spatial distribution and temporal channel usage pattern of primary network considering mobile cognitive radio network. For attaining efficient spectrum/channel access model firstly, this work presents a system model for multi-channel mobile CR-WSN. Secondly, the channel accessibility model for multi-channel mobile CR-WSN is presented.

a) System network for CR-WSN:

Let considers there are set of primary network such as cellular network base station. Let consider set of secondary network as sensor node that has fitted with cognitive radio equipment which can resourcefully access the licensed band of primary network in an opportunistic manner. Let us assume that there are non-empty set of L licensed frequency slots that can be resourcefully accessed by sensor device in an opportunistic manner. Further, this work considers heterogeneous sensor i.e., the sensor device are mobile in nature. The channel accessibility for sensor device is affected due to mobility of sensor device and channel usage pattern of primary user. The channel accessibility status for sensor device can be described as the time period length in which channel is not accessible or accessible for a particular sensor device. The accessibility of channel j, $j \in L$, for a sensor device is described as temporal channel utilization behavior and spatial distribution of primary users that functions on j, as well as mobile nature of sensor device. Further, this work considers a grid-like topology where vertical segment M_W and horizontal segment M_I is identical.

Further, the **spatial distribution of primary user** that function on common channel j are generally distributed across topology segments. The distance among two adjacent primary users in vertical is depicted as $M_{QW,j}$and horizontal constructions is depicted as $M_{QI,j}$. The communication range of primary user on channel j is depicted as S_j. This work approximate the coverage area of primary user by a square area with side length $2S_j$, where $S_j < \min(M_{QW,j}, M_{QI,j})$ to evade overlapping coverage section of primary users (note: generally the approximated coverage area is greater than the actual coverage to avoid interference affecting primary communication).

Similarly, the **temporal channel utilizatio**n of primary users that functions on common channel j is designed as a discontinuous busy (i.e., the primary user is active in communication) and idle (i.e., the primary user does not communities) process. Further, to avoid interference among primary network during communication, this work does not permits sensor device in same coverage area to use same channel. The length of idle/busy session is designed as an exponential arbitrary functional with variables $\beta_{\mathbb{b}}/\beta_{\mathbb{i}}$,that is.,

$U_{\mathbb{b}} \sim e(\beta_{\mathbb{b}}, j)$ and $U_{\mathbb{i}} \sim e(\beta_{\mathbb{i}}, j)$	(1)

where $Y \sim U_{\mathbb{b},j} \sim e(\beta)$ depicts that functional Y follows exponential distribution with respect to variable β. The ideal condition likelihood that a primary transmitter on channel j is active is expressed as follows

$$\alpha_{\mathbb{i},j} = \beta_{\mathbb{b},j}/\beta_{\mathbb{i},j} + \beta_{\mathbb{b},j} \quad (2)$$

Similarly, the ideal condition likelihood that a primary transmitter on channel j is inactive is expressed as follows

$$\alpha_{\mathbb{b},j} = 1 - \alpha_{\mathbb{i},j} \quad (3)$$

Further, this work considers **mobile CR-WSN**. The sensor nodes moves at constant speed w and each sensor nodes can communicate with each other within its coverage region. The sensor can move in different direction such top, down, left, and right with different likelihood $\mathbb{L}_{\mathbb{t}}$, $\mathbb{L}_{\mathbb{d}}$, $\mathbb{L}_{\mathbb{l}}$, and $\mathbb{L}_{\mathbb{r}}$ respectively. It holds that $\mathbb{L}_{\mathbb{t}} + \mathbb{L}_{\mathbb{d}} + \mathbb{L}_{\mathbb{l}} + \mathbb{L}_{\mathbb{r}} = 1$. The sensor nodes changes its direction when it reaches end of region/network.

b) Energy model for data transmission in CR-WSN:

The energy dissipation of senor device in CR-WSN is mainly characterized by following things such as channel sensing, channel switching, packet transitions and packet reception. Let P_S denotes the energy dissipation of sensor devices for performing sensing on licensed channel, which is considered to be static and fixed across different available channels. Further, the sensor device consumes energy for configuring radio and switching to a new channel. Thus, we represent P_C as parameter to depict energy dissipation for performing channel switching. The spectrum sensing period S_k and for S_k, the packet communication energy dissipation $P_{k,u}$ is evaluated based on energy model [25] as follows

$$P_{k,u} = \left(E_k + E_{k,d}\right) * u_{k,y}, \quad (4)$$

where E_k is the communication power, $E_{k,d}$ is the circuit power at S_k and $u_{k,y}$ is the packet communication session period. Further, using model presented in [26], $E_{k,d}$ can be computed as follows

$$E_{k,d} = \beta_k + \left(\frac{1}{\delta} - 1\right) * E_k, \quad (5)$$

where β_k is a communication power coreponding elemnt with respt to power incurred by the circuit, and δ is described by drain efficiency the modulation scheme and radio frequency power amplifier [29], [30]. Therefore, the energy dissipation of packet transmission at S_k is computed as follows

$$E_{k,u} = \frac{1}{\delta} * E_k * u_{k,y} + \beta_k * u_{k,y} = \frac{1}{\delta}\left(E_k + \beta_{d,k}\right) * u_{k,y} \quad (6)$$

where $\beta_{d,k} = \delta * \beta_k$ is described as the identical circuit power dissipation for packet communication. the energy dissipation for packet reception is proportional tp the packet that a sensor device obtains [27]. If S_k obtains m bits packets, the energy dissipation is computed as

$$P_{k,o} = P_c * m \quad (7)$$

where P_c is the circuit power for packet reception.

c) Channel access model for CR-WSN:

This work consider channel information status to enhance the QoS performance and bandwidth utilization for secondary user considering mobile CR-WSN. Here we estimate the channel accessibility status of channel j considering both temporal channel utilization characteristic and spatial distribution. It is considered that primary network operates at same channel belongs to same class of network and possess same temporal channel utilization characteristics and spatial distribution. Therefore, he transition amount among the state in Markov model can be estimated by mean segment of the region of primary user coverage on channel j as follows

$$\varphi_j = \frac{4S_j^2}{M_{q,j}^2}. \quad (8)$$

Therefore, the mean segment of region where channel j is accessible at an instance of time is expressed as follows

$$\omega_j = \left(1 - \varphi_j\right) + \varphi_j \alpha_{\mathbb{i},j} = 1 - \varphi_j \alpha_{\mathbb{b},j}. \quad (9)$$

The proposed channel accessibility model for multi-channel bring good trade-off between maximizing energy efficiency, throughput and utilizing spectrum efficiently which is experimentally proven in next section below.

III. SIMULATION RESULT AND ANNALYSIS

This section present performance evaluation of proposed EESA over exiting model [20], [23], and [24]. The performance is evaluated in terms of throughput and energy efficiency considering varied sensor devices and mobility speed of sensor device. The proposed EESA and exiting model is implemented using C# programing language and Dot Net framework 4.5 and above. The experiment are conducted on windows 10 home single language edition, Intel Pentium I-5 class processor, 12 GB RAM with 4 GB dedicated CUDA enabled GPU. The parameter used for experiment analysis is described in Table I.

TABLE I. SIMULATION PARAMETER CONSIDERED

Network Parameter	Value
Wireless sensor network size	100m * 100m
Number of wireless sensor device	20, 30, 40 & 60
Initial energy of sensor device	1.0 joules
Energy consumption for data reception P_c	5 nj/bit
Circuit power $\beta_{d,k}$ [25]	5 mW
Power amplifier efficiency δ [25]	0.9
Per-device energy dissipation for channel Switching P_C [29]	10^{-5} J
Per-energy energy dissipation for sensing a licensed channel P_S [28]	$1.31*10^{-4}$ J
Modulation scheme	16-QAM
Mobility of devices	4, 6, 8 cycle per frame

Coding rate	3/4
Bandwidth	18 Mbps
Number of Frequency Channels	5
Time slots	12 µs
Message information size	27 bytes
MAC used	EESA

a) Throughput performance evaluation considering varied mobility speed of wireless sensor device and varied wireless sensor device:

This section presents throughput performance evaluation considering varied mobility speed of wireless sensor network and varied wireless sensor device. For varied sensor device case, the sensor device is varied as 20, 40 and 60 and is moving with fixed mobility speed of 3 cycle per frame, with one control channel and 4 data channel and experiment are conducted. The outcome of experimented is graphically represented in Fig. 2. Experiment outcome shows EESA improves throughout performance by 41.21%, 28.33%, and 28.45% over exiting model considering 20, 40, and 60 wireless sensor device, respectively. An average energy efficiency performance improvement of 32.62% is attained by EESA over existing model considering varied wireless sensor device. Further, for varied mobility speed of sensor device case, the senor device mobility speed is varied as 4 (highest mobility speed), 6 and 8 (least mobility speed) cycle per frame, senor device is fixed to 30, with one control channel and 4 data channel and experiment are conducted. The outcome of experiment is graphically represented in Fig. 3. Experiment outcome shows EESA improves energy efficiency performance by 65.11%, 52.22%, and 24.74% over exiting model considering 4, 6, and 8 cycle per frame, respectively. An average energy efficiency performance improvement of 47.35% is attained by EESA over existing model. From, Fig 4 and 5, it can be seen as sensor device and mobility speed of sensor device is increased the overall network performance is affected for both existing and proposed. However, the proposed model attain significant performance than exiting model considering varied sensor device and mobility speed of wireless sensor device shows adaptiveness of EESA considering multi-channel mobile CR-WSN.

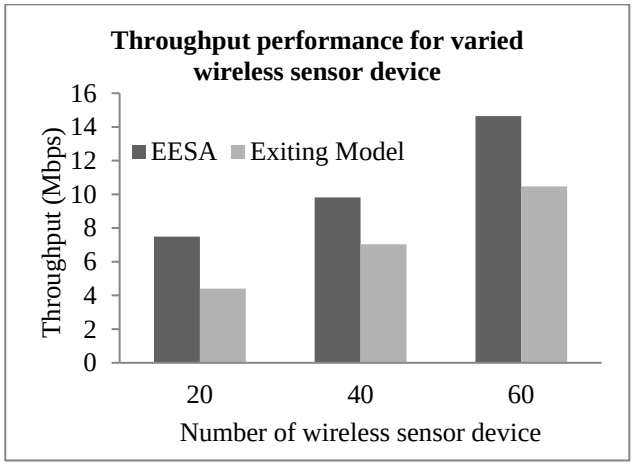

Fig. 2. Throughput performance considering varied wireless sensor device

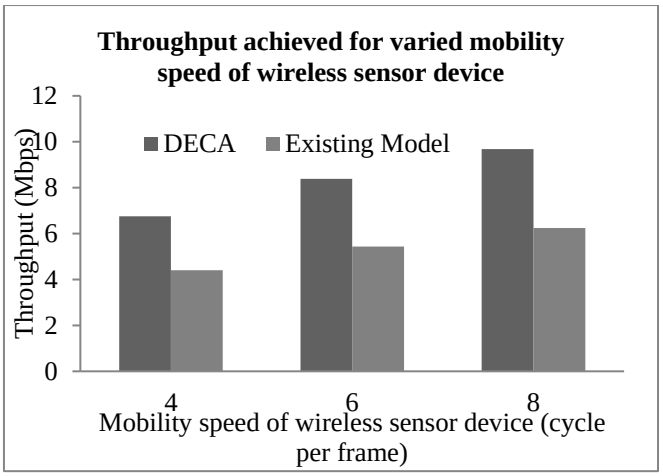

Fig. 3. Throughput performance considering varied mobility speed of wireless sensor device

b) Energy efficiency performance evaluation considering varied mobility speed of wireless sensor device and varied wireless sensor device:

This section presents energy efficiency performance evaluation considering varied mobility speed of wireless sensor network and varied wireless sensor device. For varied sensor device case, the sensor device is varied as 20, 40 and 60 and is moving with fixed mobility speed of 3 cycle per frame, with one control channel and 4 data channel and experiment are conducted. The outcome of experimented is graphically represented in Fig. 2. Experiment outcome shows EESA improves energy efficiency performance by 48.53%, 52.55%, and 54.513% over exiting model considering 20, 40, and 60 wireless sensor device, respectively. An average energy efficiency performance improvement of 51.86% is attained by EESA over existing model considering varied wireless sensor device. Further, for varied mobility speed of sensor device case, the senor device mobility speed is varied as 4 (highest mobility speed), 6 and 8 (least mobility speed) cycle per frame, senor device is fixed to 30, with one control channel and 4 data channel and experiment are conducted. The outcome of experiment is graphically represented in Fig. 3. Experiment outcome shows EESA improves throughout performance by 34.83%, 35.15%, and 35.52% over exiting model considering 4, 6, and 8 cycle per frame, respectively. An average throughput performance improvement of 35.96% is attained by EESA over existing model. From, Fig 2 and 3, it can be seen as sensor device and mobility speed of sensor device is increased the overall energy efficiency performance is affected for both existing and proposed. However, the proposed model attain significant performance than exiting model considering varied sensor device and mobility speed of wireless sensor device shows adaptiveness of EESA considering multi-channel mobile CR-WSN.

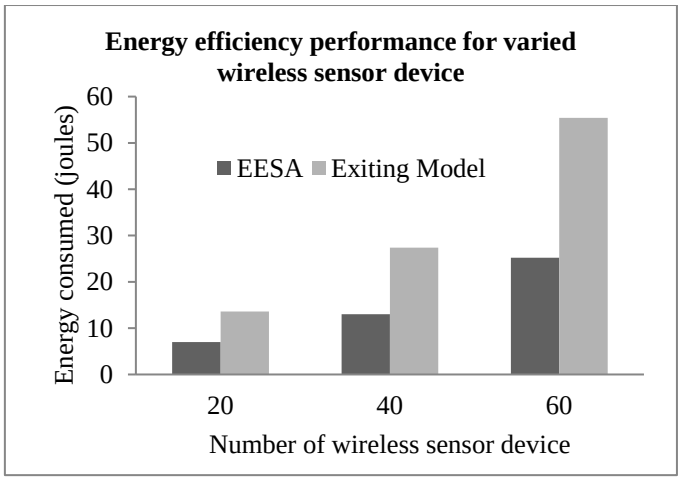

Fig. 3. Energy efficiency performance considering varied wireless sensor device

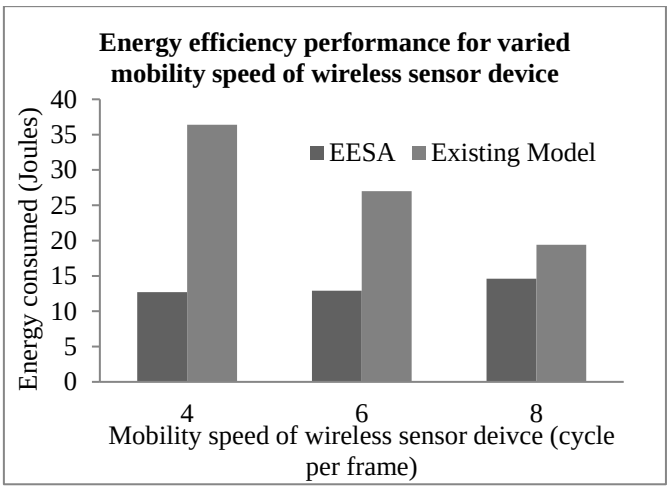

Fig. 5. Energy efficiency performance considering varied mobility speed of wireless sensor device

IV. CONCLUSION

This work conducted extensive survey and identified that the exiting spectrum access model suffers from energy overhead and spectrum utilization inefficiency issues. This paper overcome these issues and presented an energy efficient spectrum access model of multi-channel and mobile cognitive radio network. EESA used both temporal and spatial information for obtaining channel accessibility status for contending device. The EESA model addresses interference issues among contending device. Thus aided in maximizing throughput and minimizing energy overhead. Experiment are conducted to evaluate performance of EESA over exiting model. The result shows EESA attain significant performance over exiting model in terms of throughput and energy efficiency. The outcome shows EESA attain an average throughput performance improvement of 37.4% over existing model considering varied mobility speed of wireless sensor device and varied wireless sensor device. Further, EESA attain an average energy efficiency performance improvement of 48.8% over existing model considering varied mobility speed of wireless sensor device and varied wireless sensor device. The overall result attained shows, the EESA minimize energy consumption, maximize throughput and utilize spectrum more efficiently considering multi-channel mobile CR-WSN. The future work would consider performance evaluation considering varied network parameter and enhancing channel access model.

REFERENCES

[1] Lin Y, Yang J, Lv Z, et al. A self-assessment stereo capture model applicable to the internet of things[J]. Sensors, 15(8): 20925-20944, 2015.

[2] Yang J, He S, Lin Y, et al. Multimedia cloud transmission and storage system based on internet of things[J]. Multimedia Tools and Applications, 2015: 1-16, 2015.

[3] Naranjo, Paola G. Vinueza, et al. "P-SEP: a prolong stable election routing algorithm for energy-limited heterogeneous fog-supported wireless sensor networks." The Journal of Supercomputing: 1-23, 2016.

[4] N. Li, M. Xiao and L. K. Rasmussen, "Spectrum Sharing with Network Coding for Multiple Cognitive Users," in IEEE Internet of Things Journal. doi: 10.1109/JIOT.2017.2728626, 2017.

[5] A. Aijaz and A. H. Aghvami, "Cognitive machine-to-machine communications for Internet-of-Things: A protocol stack perspective," IEEE Internet Things J., vol. 2, no. 2, pp. 103–112, Apr. 2015.

[6] T. M. Chiwewe and G. P. Hancke, "Fast Convergence Cooperative Dynamic Spectrum Access for Cognitive Radio Networks," in IEEE Transactions on Industrial Informatics. doi: 10.1109/TII.2017.2783973, 2017.

[7] Yang J, Chen B, Zhou J, et al. A low-power and portable biomedical device for respiratory monitoring with a stable power source[J]. Sensors, 15(8): 19618-19632, 2015.

[8] Maghsudi S, Stanczak S. Hybrid Centralized-Distributed Resource Allocation for Device-to-Device Communication Underlaying Cellular Networks[J]. IEEE Transactions on Vehicular Technology, 1, 2016.

[9] D. Jiang, Y. Wang, C. Yao, et al. An effective dynamic spectrum access algorithm for multi-hop cognitive wireless networks[J]. Computer Networks, June 19, 2015, 84(19): 1-16, 2015.

[10] S. Aslam, W. Ejaz and M. Ibnkahla, "Energy and Spectral Efficient Cognitive Radio Sensor Networks for Internet of Things," in IEEE Internet of Things Journal. doi: 10.1109/JIOT.2018.2837354.

[11] W. Ejaz, G. A. Shah, H. S. Kim et al., "Energy and throughput efficient cooperative spectrum sensing in cognitive radio sensor networks," Transactions on Emerging Telecommunications Technologies, vol. 26, no. 7, pp. 1019–1030, Jul. 2015.

[12] S. Sodagari, "Real-Time Scheduling for Cognitive Radio Networks," in IEEE Systems Journal. doi: 10.1109/JSYST.2017.2771328, 2018.

[13] C. Xin, P. Paul, M. Song and Q. Gu, "On Dynamic Spectrum Allocation in Geo-location Spectrum Sharing Systems," in IEEE Transactions on Mobile Computing. doi: 10.1109/TMC.2018.2848250, 2018.

[14] Myrvoll, T.A and Hakegard, J.E. "Dynamic Spectrum Access in Realistic Environments Using Reinforcement Learning," International Symposium on Communications and Information Technologies (ISCIT), pp. 465-470, 2012.

[15] Yuhua Xu; Jinlong Wang; Qihui Wu; Anpalagan, A.; Yu-Dong Yao. "Opportunistic Spectrum Access in Unknown Dynamic Environment: A Game-Theoretic Stochastic Learning Solution," IEEE Trans. Wireless Communications, pp. 1380-1391, 2012.

[16] Z. Du, Q. Wu, B. Jiang, Y. Xu and Z. Qin, "Interference-Aware Spectrum Access Self-Organization: A Weighted Graph Game Perspective," in IEEE Systems Journal. doi: 10.1109/JSYST.2017.2765345, 2018.

[17] A. Anandkumar, N. Michael, A. Tang, and A. Swami, "Distributed algorithms for learning and cognitive medium access with logarithmic regret," IEEE J. Sel. Areas Commun. on Advances in Cognitive Radio Networking for Communications, vol. 29, pp. 731–745, 2011.

[18] S. Vakili, K. Liu, and Q. Zhao, "Deterministic sequencing of exploration and exploitation for multi-armed bandit problems," IEEE J. Sel. Topics Signal Process., vol. 59, no. 3, pp. 1902–1916, 2013.

[19] Y. Gai and B. Krishnamachari, “Decentralized online learning algorithms for opportunistic spectrum access,” in Proc. IEEE Global Commun. Conf. (GLOBECOM), pp. 1–6, 2011.

[20] Y. Xu, Q. Wu, J. Wang, L. Shen and A. Anpalagan, "Robust Multiuser Sequential Channel Sensing and Access in Dynamic Cognitive Radio Networks: Potential Games and Stochastic Learning," in IEEE Transactions on Vehicular Technology, vol. 64, no. 8, pp. 3594-3607, Aug. 2015.

[21] F. Zhou, N. C. Beaulieu, J. Cheng, Z. Chu and Y. Wang, "Robust Max–Min Fairness Resource Allocation in Sensing-Based Wideband Cognitive Radio With SWIPT: Imperfect Channel Sensing," in IEEE Systems Journal. doi: 10.1109/JSYST.2017.2698502, 2017.

[22] H. Jang, S. Y. Yun, J. Shin and Y. Yi, "Game Theoretic Perspective of Optimal CSMA," in IEEE Transactions on Wireless Communications, vol. 17, no. 1, pp. 194-209, Jan. 2018. doi: 10.1109/TWC.2017.2764081, 2018.

[23] Y. Lu and A. Duel-Hallen, "A Sensing Contribution-Based Two-Layer Game for Channel Selection and Spectrum Access in Cognitive Radio Ad-hoc Networks," in IEEE Transactions on Wireless Communications, vol. 17, no. 6, pp. 3631-3640, June 2018.

[24] B. Dappuri and T. G. Venkatesh, "Design and Performance Analysis of Multichannel MAC Protocol for Cognitive WLAN," in IEEE Transactions on Vehicular Technology, vol. 67, no. 6, pp. 5317-5330, 2018.

[25] T. Shu, M. Krunz, and S. Vrudhula, “Joint optimization of transmit power-time and bit energy efficiency in cdma wireless sensor networks,” IEEE Trans. Wireless Commun., vol. 5, no. 11, pp. 3109–3118, 2006.

[26] S. Cui, A. J. Goldsmith, and A. Bahai, “Energy-constrained modulation optimization,” IEEE Trans. Wireless Commun., vol. 4, no. 5, pp. 2349–2360, 2005.

[27] J. Ren, Y. Zhang, K. Zhang, A. Liu, J. Chen, and X. Shen, “Lifetime and energy hole evolution analysis in data-gathering wireless sensor networks,” IEEE Trans. Industrial Info., 2015, published online on Mar. 9, 2015.

[28] M. Timmers, S. Pollin, A. Dejonghe, L. Van der Perre, and F. Catthoor, “A distributed multichannel mac protocol for multihop cognitive radio networks,” IEEE Trans. Vehicular Tech., vol. 59, no. 1, pp. 446–459, 2010.

[29] S. Bayhan and F. Alagoz, “Scheduling in centralized cognitive radio networks for energy efficiency,” IEEE Trans. Vehicular Tech., vol. 62, no. 2, pp. 582–595, 2013.

Proceedings of the Fourth International Conference on Communication and Electronics Systems (ICCES 2019)
IEEE Conference Record # 45898; IEEE Xplore ISBN: 978-1-7281-1261-9

Object Detection and Tracking using Zernike Moment

Samidha Girish Vengurlekar
Student,
Department of Information Technology,
RAIT, Nerul
Navi Mumbai-400706
samidhavengurlekar03@gmail.com

Dipti Jadhav
Assistant Professor,
Department of Information Technology,
RAIT, Nerul
Navi Mumbai-400706
dipti.jadhav@rait.ac.in

Swapnil Shinde
Assistant Professor,
Department of Information Technology,
RAIT, Nerul
Navi Mumbai-400706
swapnil.shinde@rait.ac.in

Abstract: **In this paper, the cameras capture lot of information that can be highly used in detecting and tracking objects in motion. Though it is challenging, object detection is used to detect object either in each frame or when it first comes in the video. Various methods like frame difference, background subtraction, optical flow can be used for detection. The highest objective of this is to contribute the human operators which help in detecting and tracking doubtful or uncommon actions in the video sequence. The visual observation system needs fast and strong approaches of detecting and tracking the moving objects. Moving objects were detected using canny edge method positively. Moments of different order were extracted using Zernike moments techniques. Analysis was done on all the Zernike moments from z00 to z88. The results show that the number of unique motion in the video and number of unique motion detected by the system is equal with accuracy of 100%.**

Keywords: Canny edge detection, Niblacks Algorithm, Object Tracking Sharpening filter, Zernike Moment.

I. INTRODUCTION

Image processing is amongst the peak explored fields. Surveillance systems are mainly utilized for safety purpose, and also many other necessities. Object tracking as well as object detection are the key phases. Various methods are being used for these phases. To automate the system and for reliability, researches are also done to a high extent. [1]. Object detecting and tracking are amongst the greatest jobs which are challenged which a surveillance system has to achieve so that important events and doubtful actions can be defined, and automatically explain and get the video data [2]. In an object tracking, an object is something which plays a vital role for the analysis done later. Objects are characterized based on shapes and forms [3]. Using a data in a single frame is a common approach to detect an object. To lesser the quantity of untrue detections, a temporary data is included from sequences of frames which are used by the approaches to detect an object [3]. Video Summarization generates the detailed information of the videos which covers extreme data that helps to understand the information in the video in an improved way. Video summarization techniques are of two types viz. Static Video summarization and Dynamic Video Summarization [4]. Summarization of static video basically includes selected key frames [5]. Also includes a group of key frames which is in the original video and there is no constraint with the sequence and time factors. Most methodologies contain the visual characteristics figured from video frames. A worth video abstraction helps the user to extract immense information regarding the aimed video sequence in a given time limit or sufficient data in less amount of time. The produced summarization can provide individuals in navigating big video files and in getting the judgments more powerfully related to selection consuming, sharing, or deleting information [4].

II. LITERATURE SURVEY

Authors have presented a system which is integrated for the abstraction of video which is object based [6]. Their contributions and features for the proposed methodology are as follows. • Effectiveness • Online processing• Open framework. Motion, color, special relationship, text and speech are certain features to describe an object. A research done for every feature should be led in order to discover important characteristics. Authors have proposed an algorithm which uses Kalman filters for segmentation as well as detecting an object [7]. For the purpose of prediction and filtering Algorithm, Kalman filter is used. Those extra situation is involved in this dynamic structure is to catch the error which are between the real and estimated position of the ball

which is done using filter. The model, the Authors have proposed is an Adaptive background subtraction [8]. For the purpose of object tracking and detection, this model is used to obtain best detection values using a stationary camera. In filtering process color and other characteristics are considered beneficial for both models viz.1. Generative Model 2. Discriminate Model. To improve the accuracy rate of the tracked objects, proposed model makes use of the tracking levels and reduce the computational difficulty for both indoor as well as outdoor dataset. It makes the use of illumination variant for dynamic variations tracking in the entire background. Authors have proposed a fast as well as accurate technique for detecting and tracking the objects which are moving [9]. The proposed technique has good performance of the detection amongst various objects present in the scenario and it is also non-sensitive to moving objects. In addition, the technique accurately evaluates the quantity of moving objects in each and every frame, which is appropriate for the scenarios where this data is unavailable or it is hard to get. The proposed technique works with feature points and also the time of execution is low than the others and its usage of memory is also very less, as all the frame doesn't go under the process. The Proposed method describes that as compared to 2 frames technique in which problem is regarding holes; there background subtraction gave the good results [10]. When comparison is done with existing and proposed, better estimation of the detected object is given by the background subtraction, proposed technique. The proposed system showed accurate and broader foreground as compared to existing background as well as 2 frame method and reduced the holes problem efficiently. In this paper, authors have discussed a widespread study of object detection as well as tracking approaches [11]. A detailed discussion over advantages and disadvantages of existing approaches of object detection, classification as well as tracking has been done. The method, background subtraction is determined to be the easiest technique which gave the detailed description about the object when comparison is done to frame difference along with the optical flow detecting approaches. Authors of [16] have proposed a video summarization technique based on SURF and its optimization. Video summarization technique based on color and texture features is proposed in [15].

III. COMPARATIVE ANALYSIS

The detailed comparison of different object detection and tracking techniques are given in the Table 3.1

Table 3.1: Comparative analysis of object detection and tracking techniques

Sr. No	Name of the Paper	Techniques Used	Advantages
1	Object-Based video Abstraction for video Surveillance system [6].	Canny edge detection method.	• Efficiency • Effectiveness • Online processing • Open framework.
2	Moving object tracking using Kalman filter [7].	Kalman Filter	• For security system , it is used for the navigation. • Best for prediction and filtering • Availability of high quality
3	A Novel approach on object detection and tracking using adaptive background subtraction method [8].	Gaussian, Adaptive Background Subtraction.	• Recognition rate for bending, running and walking is excellent.
4	Motion-based moving object detection and tracking using Automatic K-means [9].	Automatic K-means, Shi and Tomasi algorithm, Lucas-Kanade method, K-means algorithm.	• The performance for detection is good. • Accurately estimation of moving objects. • It has less execution time.
5	Optimized dynamic background subtraction technique for moving object detection and tracking [10].	Three Frame difference, Background subtraction	• Background subtraction technique is way much better when compared to two frames technique. • It gives the better estimation of the objects which are detected. • Shows accurate and wider foreground.

6	A survey on Moving Object Tracking Using Image Processing [11].	Frame Difference, Background Subtraction, Optical Flow	• Performs well in the static background. • Low memory requirement. • Produces complete movement information

IV. PROPOSED METHODOLOGY

The proposed system includes obtaining of videos of .avi and .mp4 formats. The video is full of information and can be used for the further processing. The bulk of data we get from the videos contains noise and redundant information so the images or the frames which are extracted need an enhancement.

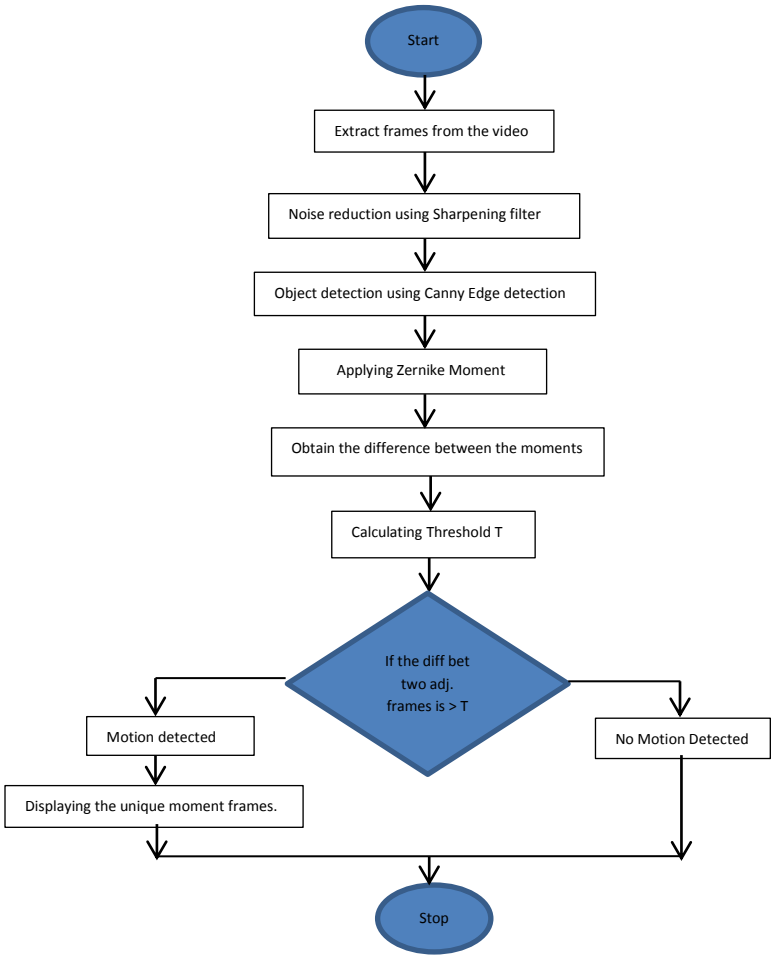

Fig 4.1. Proposed system diagram

Enhancement can be done in various ways like color illumination, noise removing, removing blur from the blurred images etc. In the proposed system removal of noise and blur frames is performed using Sharpening filter to get the enhanced images or frames. After the noise removal the main aim is to detect the object on which we need to do the tracking of its movements. The canny edge detection method is used to identify the object from the frames which will just keep the object on focus. Then the next step is to track the object for which object features are extracted by using Zernike moments for better results. Once the object is tracked then the main focus is to track the unique moments of that tracked object. Figure 4.1 explains the proposed system. The detailed description about the proposed system is as follows:

Step1: Extract frames from the video: The proposed system includes obtaining of videos of .avi and .mp4 formats. Frames of the video are extracted and are stored for the further processing task.

Step 2: Noise reduction using sharpens filter: imsharp filter sharpens the image with the help of unsharp masking concept. Sharpness is essentially the distinct between various colors. A quick changeover from black to white appears sharp. A steady transition from black to gray to white appears blurry. Sharpening images growths the contrast along the edges where variety of colors meet. There is confusion with the name of this filter but an unsharp filter is an operator used to sharpen an image. Fig 4.2 shows the original and sharpen image.

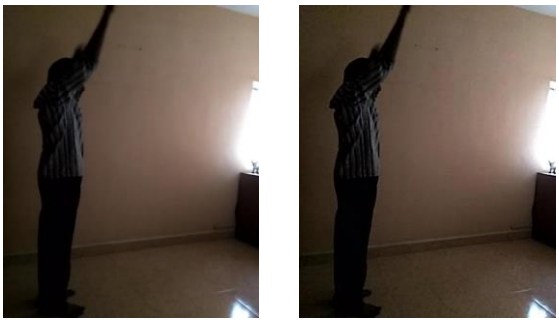

Original Image Sharpen Image

Fig 4.2: Original image Sharpen image (For image no: 115)

Step 3: Object detection using Canny Edge detection: The performance criteria that the canny detector aims at are as follows:

1. Detection should be good
2. Good localization
3. Single edge should have only one response.

The steps of canny edge detection algorithm are as follows:

1. Gaussian filter helps to make the input image smooth.

2. Perform calculation of Gradient magnitude and phase of the filtered images.

3. Gradient Magnitude image is further used for applying non maxima suppression.

4. Apply two thresholds and perform connectivity to obtain the edges and link them. [12]
Fig 4.3 shows the original and canny edge detected image.

Original Image Canny Edge detected

Fig 4.3: Original image and canny edge detected image (For image no: 115)

Step 4: Applying Zernike moment: Moments defines the numeric amounts at certain distance from a reference point/axis. They are the scalar quantities which are used to describe a function and to obtain its features. It is broadly used for the description of shape. Hence, we can say that moments are used to extract the features [13] [14]. This concept was introduced in 1934 by Zernike. Zernike moments are representation of the image properties with negligible redundancy and information overlapping between them. Thus they can be utilized to extract features from the images. Zernike put forward a combination of complex polynomials which forms a complete orthogonal set over the interior of unit circle. For moment computation the origin is considered as the center of the given image and pixel co-ordinates mapping is done in the range of circle with unit distance. The pixels lying outside the unit distance circle are ignored at the time of computation. Hence Zernike moments are invariant under rotation. If all moments of a function f(x, y) up to order Nmax are known, then it is possible to reconstruct discrete function f(x, y) , whose moment matches to those of original function f(x, y) up to order Nmax [13].
Advantages of Zernike moments:
• Simple rotation invariance. • Higher accuracy for detailed shapes. • No redundancy. • Better at reconstruction.
Step 5: Obtain the difference between the moments: Initially the difference between two-two frames will be calculated. Assume there are 300 frames, so 299 differencing values will be calculated. Then the average of the same will be calculated. Sum of all the difference values will be divided by the total number. The result got is the mean.

Step 6: Calculating Threshold T:
Threshold is calculated with formula, niblack's algorithm:
$T(x, y) = m(x, y) + k^* \delta(x, y)$
Where $m(x, y)$ = local mean, $\delta(x, y)$ = standard deviation of the pixels which is inside the local window and K = bias. Default value of K is set as 0.5; $m(x, y)$ and $\delta(x, y)$ adjust the value of the threshold according to the contrast present in the local neighbourhood of the pixel. The k controls the adaptation levels by varying the value of threshold. Any value of frame differences higher than the threshold has unique motion in that frame. Then those frames are stored as uniquely detected motion.

V. EXPERIMENTAL RESULTS:

The Proposed method is implemented in MATLAB R2013a version.

Video details:
Name: walk3.flv
Size: 5310KB
Duration: 17 seconds
Total number of frames: 526

According to the analysis done on the video using all the Zernike moments right from z00 to z88, we have found that z75 and z55 are the two Zernike moments which gave the excellent results. These two moments have captured the small unique details from the extracted frames, which helps to find out what exactly happened in the entire video instead of going through the whole video.

The unique detected frames of Zernike moments Z55,Z60,Z75,Z77 and Z82 is shown in Fig 5.1, 5.2, 5.3, 5.4 and 5.5 respectively.

Z55

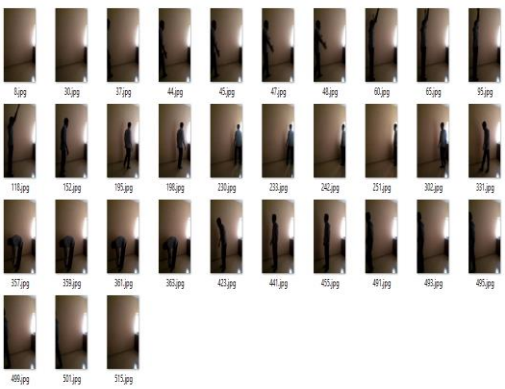

Fig 5.1: Uniquely Detected Frames of Zernike Moment z55

Z60

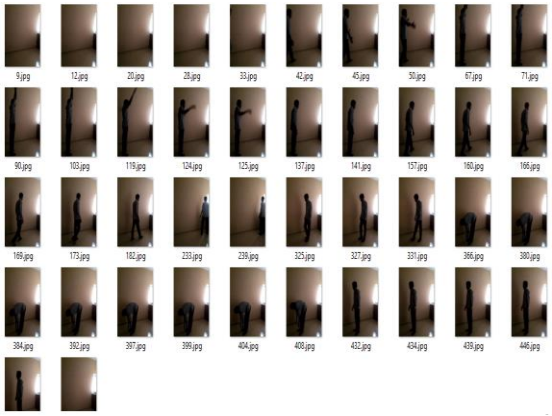

Fig 5.2: Uniquely Detected Frames of Zernike Moment z60

Z75

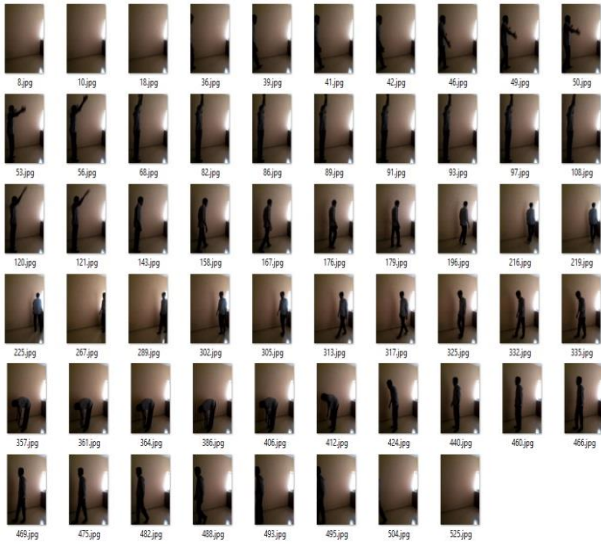

Fig 5.3: Uniquely Detected Frames of Zernike Moment z75

Z77

Fig 5.4: Uniquely Detected Frames of Zernike Moment z77

Z82

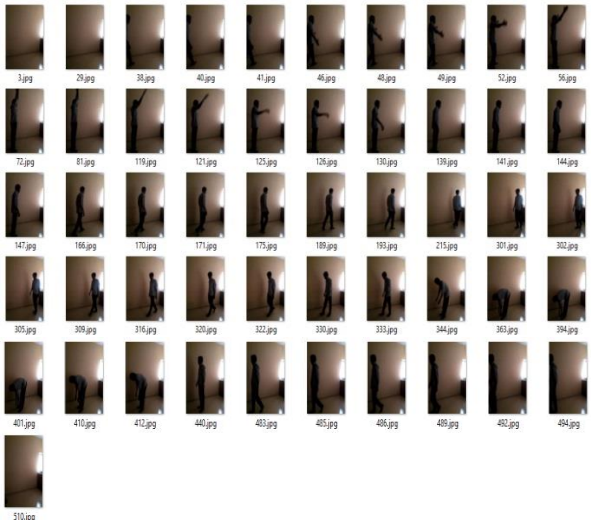

Fig 5.5: Uniquely Detected Frames of Zernike Moment z82

The total number of frames, unique frames detected and accuracy of the Zernike moments Z55,Z60,Z75,Z77 and Z82 is given in table 5.1

Table 5.1: Analysis of Zernike Moments, total number of frames, unique frames detected and accuracy.

Zernike Moment	Total no of frames	Unique frames	Accuracy
Z55	526	33	100
Z60	526	42	80
Z75	526	58	100
Z77	526	28	90
Z82	526	51	90

VI. PERFORMANCE ANALYSIS

6.1 Subjective Performance Analysis:

The Performance for the above mentioned Zernike moments were analysed by different types of audiences. The testing was done on it by different people and the analysis was done accordingly. As the audiences changes the way to the testing procedure changes. It was evaluated by other students, faculties, etc. The evaluator might rate the testing on each subjective criterion using a scale that ranges from poor to excellent. Subjective Performance Analysis for Zernike Moments is shown in Table 6.1.

Table 6.1: Subjective Performance Analysis

Zernike Moment	Poor	Good	Excellent
Z55	1	4	5
Z60	4	4	2
Z75	2	3	5
Z77	3	3	4
Z82	3	4	3

VII. CONCLUSION

The main idea of the work is to detect unique motion of the objects to trace any doubtful or unusual behavior. The study shows that the videos are taken by static cameras. That video is properly converted to the frames. As frames may contain some noise that is reduced using sharpen filter. Object detection plays an important role so the procedure should be done in such a manner that the object is properly extracted. This is done using canny edge detection algorithm successfully. Using Zernike moment the object tracking is done. Analysis was done with all the Zernike moments from z00 to z88. After the analysis, z55 and z75 gave the excellent results with 100% of accuracy.

References

[1] Asad Abdul Malik, Amaad Khalil, Hameed Ullah Khan,Object Detection and Tracking using Background Subtraction and Connected Component Labeling , International Journal of Computer Applications, August 2013.

[2] Alper Yilmaz, Omar Javed, and Mubarak Shah, Object tracking: A survey, ACM Computing Surveys (CSUR), 2006.

[3] Henry Schneider man and Takeo Kanade,Object Detection Using the Statistics of Parts , USA.

[4] Tinumol Sebastian, Jiby J. Puthiyidam , A Survey on Video Summarization Techniques,International Journal of Computer Applications (0975 – 8887) , Volume 132 – No.13, December 2015.

[5] Yingbo Li, Bernard Merialdo, Mickael Rouvier, Georges Linares,Static and Dynamic Video Summaries,Proceedings of 19th International Conference on Multimedia 2011, Scottsdale, Arizona, USA, November 28–December 1 2011.

[6] Changick Kim,Object-Based Video Abstraction for Video Surveillance Systems, IEEE Transactions on Circuits and Systems for Video Technology, December 2002.

[7] Mr. Pramod R. Gunjal, Miss. Bhagyashri R. Gunjal, Mr. Haribhau A. Shinde, Mr.Swapnil M. Vanam , Mr. Sachin S. Aher, Moving Object Tracking using Kalman Filter,International Conference On Advances in Communication and Computing Technology (ICACCT) Amrutvahini College of Engineering, Sangamner, Ahmednagar, Feb 8-9, 2018.

[8] Kandavalli Michael Angelo,A novel approach on object detection and tracking using adaptive background subtraction method, Proceedings of the Second International Conference on Computing Methodologies and Communication (ICCMC 2018) IEEE Conference.

[9] Arghavan Keivani , Jules-Raymond Tapamo , Farzad Ghayoor,Motion-based Moving Object Detection and Tracking using Automatic K-means , IEEE Africon Proceedings,2017.

[10] Rahul Dutt Sharma, Shubh Lakshmi Agrwal, Sandeep K Gupta, Anil Prajapati, Optimized dynamic background subtraction technique for moving object detection and tracking, International Conference on Telecommunication and Networks, 2017.

[11] S. R. Balaji, Dr. . S. Karthikeyan, A Survey on Moving Object Tracking Using Image Processing, 11th International Conference on Intelligent Systems and Control (ISCO),2017.

[12] Swapnil R. Shinde, Dr. Sudeep D. Thepade, Gender Classification with KNN by Extraction of Haar Wavelet Features from Canny Shape Fingerprints, International Conference on Information Processing(ICIP), 2015.

[13] Shilpa Bane, Prof. D.R. Pawar, Survey on Feature Extraction methods in Object Recognition, International Journal of Computer Science and Information Technologies, 2014.

[14] Zhihu Huang, Jinsong Leng Edith,Analysis of Hu's Moment Invariants on Image Scaling and Rotation, Edith Cowan University, 2010.

[15] Pooja Tarare, Dipti Jadhav, A novel video summarization technique using weighted combination of color and texture feature, International Conference on Applied and Theoretical Computing and Communication Technology (iCATccT),2015.

[16] Dipti Jadhav, Udhav Bhosle, SURF based video summarization Conference on Communication and Signal Processing (ICCSP), 2017.

Proceedings of the Fourth International Conference on Communication and Electronics Systems (ICCES 2019)
IEEE Conference Record # 45898; IEEE Xplore ISBN: 978-1-7281-1261-9

Design of a miniaturised and novel DGS-based UWB antenna

***Abstract*—A novel and compact microstrip antenna with a slot designed in the shape of alphabet-I and a Defective Ground Structure (DGS) has been designed for UWB (Ultra Wide Band) and X-band applications. The dimensions of the designed antenna is 19 mm x 29 mm x 1.6 mm. The antenna was imprinted on FR4 material having relative permittivity of 4.4. Simulations were carried out using HFSS software and thereafter measurements of the fabricated prototype were done to validate the results. The reflection coefficient obtained covers both the UWB and X-bands extending upto 15.14 GHz. The radiation pattern is seen to be stable over the above mentioned band. This antenna with such a large band is designed with an aim to be put to use in microwave imaging experiments.**

***Index Terms*—antenna, ultrawideband, defected ground structure, microwave imaging.**

I. Introduction

In the year 2002, the Federal Communication commission (FCC) assigned the frequencies from 3.1 GHz to 10.6 Ghz as the UWB band for carrying out commercial communication. [1]. Since then active research efforts have been involved in developing more and more compact and low cost UWB antennas over time. The challenge faced by the designers is maintaining the large impedance bandwidth from 3.1-10.6 GHz along with a stable radiation pattern in the comptele frequency band [2].

Recently, UWB antennas are widely being applied in medical imaging using microwaves, such as in radar-based detection of bone anomolies, pulmonary edema, breast tumour, brain stroke etc. The antenna reported in this paper was designed to be integrated into a microwave imaging experimental setup. The antenna can act as transmitters to illuminate the model under study and also collect the scattered signals (occupying a large range of frequencies) coming from breast models to aid in a more accurate reconstruction [3].

Researchers across the globe have documented different (UWB) antennas which have microstrip feed or coplanar waveguide (printed) feed [4-7]. These antennas have various structures of the patch, have different shapes of slots, have complete ground on the bottom side or various levels of defected ground geometries; while others have been etched on substrates with varying ranges of dielectric constant (eg. Rogers substrate) [8-13].

In this article, a compact microstrip fed antenna with an I-shaped slot and a defected ground working in the UWB and X-bands (8-12 GHz) is presented. This DGS design with a semi-circular slot was instrumental in extending the bandwidth upto 15.14 GHz. This reported design was developed in HFSS software and was also verified using CST simulation studio. The fabricated antenna was placed in the anechoic chamber and tested with the Vector Network Analyzer (VNA) Agilent-PNAE8362B.

The paper has been arranged as follows. Section II explains in detail about the structure of the designed antenna complete with the dimensions of the cuts and slots made to the patch and ground planes.. Section III reports the results obtained during the testing of this antenna after fabrication against the simulated results. Finally, Section IV concludes the paper.

II. Antenna Design

The patch and ground schematic of the reported antenna has been depicted in Fig. 1 (a) and (b). The dimensions of the antenna and its slots have been listed in Table I. This novel structure was modeled using the HFSS platform to obtain the desired radiation characteristics. Thereafter, the antenna was etched on an FR4 substrate material which is prevalently employed in antenna fabrications. The FR4 material possesses dielectric constant of 4.4, loss tangent of 0.02 and comes with a height of 1.6mm.

Patch has an I-shaped slot to obtain the desired return loss in the UWB band. A hexagonal shaped patch of copper has been placed inside a circle of radius 5.7mm at the centre of the patch to attain better radiation patterns. The dimensions of the various cuts and slots of the patch at the top and near the feed end have been optimized through parametric analysis.

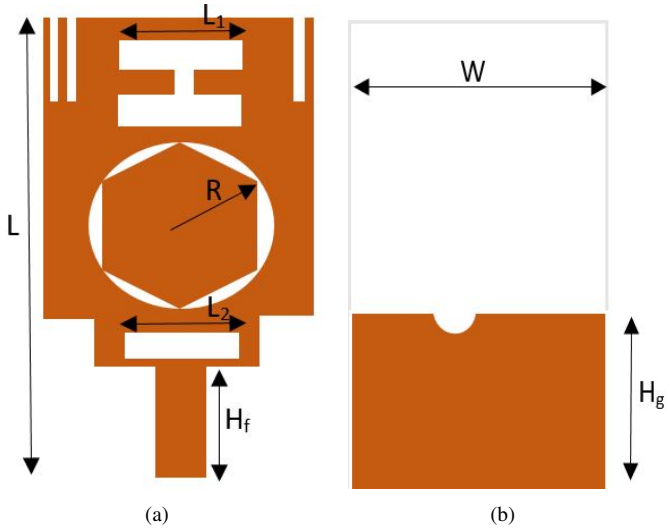

Fig. 1. Schematic diagram of the designed antenna showing the (a) top patch and (b) the ground.

The ground plane does not occupy the entire bottom side of this micro strip antenna. The ground plane has been modified to arrive at a DGS structure extending only upto a height of 5.8mm. A semicircular slot of radius 1.3mm has been etched out of this ground at the top. The DGS structure aided in attaining the large bandwidth as reported.

TABLE I
ANTENNA PARAMETERS

Parameter	***Value in mm***
L	29
W	19
L_1	9
L_2	8
R	5.7
H_f	7
H_g	5.8

III. RESULTS AND DISCUSSION

The return loss simulations showed that the antenna had an impedence bandwidth extending from 3.05 to 14.5 GHz covering the UWB as well as the X-band and extending further. To verify the simulated results, the fabricated antenna was tested in the laboratory using the PNAE8362B network analyzer that could measure upto 20 GHZ. The measurements of return loss obtained validated the antenna's simulated results as clearly depicted in Fig. 2. It can be seen that the resonances of the fabricated antenna fall at 3.6 GHz, 4.9 GHz, 7.4 GHz, 8.3GHz, 9.6 GHz, 11.8 GHz and 13.9 GHz. The connector losses and fabrication errors may be the reason for this slight shift.

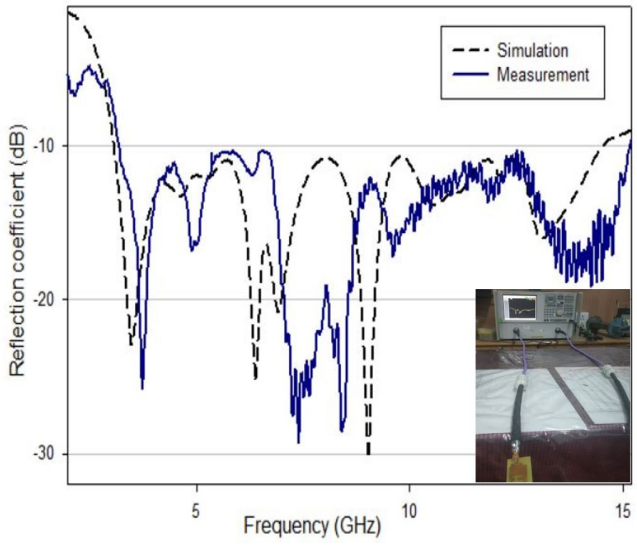

Fig. 2. The return loss of the antenna and the measurement setup in the inset

The return loss alone is not enough for judging the versatility of any antenna. Additionally, an omnidirectional radiation pattern that is stable throughout the proposed band is also required. Hence, the radiation pattern analysis was carried out for the antenna in the desired range of frequencies. The pattern is observed to have a desired nature in the entire band. The E-field and H-field radiation pattern plots have been shown in Fig. 3 (a-c) for 4GHz, 8GHz and 10GHz. It is observed that the pattern is more ideal at the lower frequencies and keep on taking more and more distorted shapes at higher frequencies.

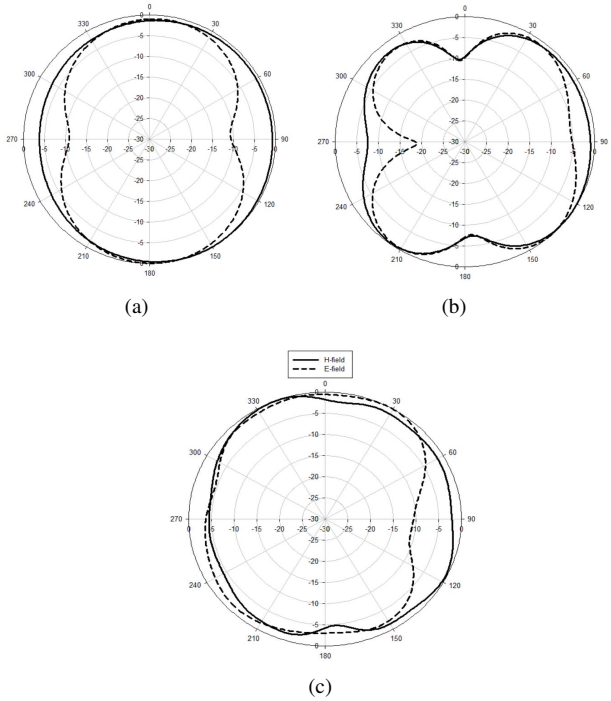

(a) (b)

(c)

Fig. 3. E-field and H-field radiation pattern obtained at (a) 4GHz, (b) 8GHz and (c) 10GHz.

To know the advantage of the designed novel antenna reported in this paper over other state-of-art antennas present in the literature, a comparative analysis is carried out and illustrated in Table II below. Compactness in antenna size has been achieved with the dimensions of 19 x 29 sq.mm. Additionally, it may be noted that a very large bandwidth extending upto 15.14 GHz has been maintained with such compact antenna dimensions.

TABLE II
COMPARISON TABLE

Reference	***Size*** (mm^2)	***Band (GHz)***
Sharma et al. [4]	34 x 34	3-12
AnilKumar et al. [5]	25 x 30	3.1-10.15
Rahman et al. [8]	30 x 18	$2.9 - 10.7$
Bukkawar et al. [9]	34 x 38	2.80-12
Safia et al. [10]	34 x 32.5	3.1-10.9
Ali et al. [11]	28 x 28	3.50-15.1
Yeo et al. [12]	30 x 30	$3.02 - 11.04$
Yeo et al. [13]	30 x 32	2.99-10.87
Proposed antenna	19 x 29	$3.1 - 15.14$

IV. Conclusion

A novel ultrawideband antenna capable of operating in the UWB and X-bands was designed and fabricated. The antenna has a compact size of 19mm x 29 mm x 1.6 mm operating over a band of 3.1 to 15.14 GHz. The antenna has been developed to be included in a microwave imaging setup to illuminate the object under study and to collect the signals scattered off this object for further reconstruction and analysis for breast tumour detection.

Acknowledgment

The authors express their gratitude to Professor P. Mohanan of Department of Electronics, Cochin University of Science and Technology, Cochin for his guidance and also for permitting to carry out the measurements of the fabricated antenna in Centre for Research in Electromagnetics and antennas (CREMA) lab.

References

[1] Federal Communications Commission, “FCC report and order on ultra wideband technology,” Washington DC, 2002.
[2] C A Balanis, “Antenna Theory, Analysis and Design, Wiley, USA,2005.
[3] T. A. Anjit, R. Benny, N. Soumya, S. Shilpa and P. Mythili, “Application of Compressive sensing for brain stroke microwave imaging,” Antennas and Propagation Symposium APSYM 2018, pp. 1-4, Cochin, Kerala, December 3-5, 2018.
[4] V. Sharma, K. G. Jangid, D. Bhatnagar, S. Yadav and M. M. Sharma, “A Compact CPW Fed Modified Circular Patch Antenna with Stub for UWB Applications,” International Conference on Signal Propagation and Computer Technology (ICSPCT 2014), pp. 214-217, Ajmer, India, August, 2014.
[5] C. V. AnilKumar, S. Damodaran and B. Paul, “A Printed Antenna with Circular Cut for Bandwidth Enhancement,” IEEE TENCON, pp. 1-3, Macau SAR, China, November, 2015.
[6] P. Cherian and P. Mythili, “A Stopband Control Technique for Conversion of CPW-Fed Wideband Antenna to UWB,” Progress In Electromagnetics Research Letters, vol. 67, pp. 131-137, 2017.
[7] N. Anveshkumar and A. S. Gandhi, “Design and Performance Analysis of a Modified Circular Planar Monopole UWB Antenna,” International Conference on Computing Communication and Networking Technologies (ICCCNT), pp. 1-5, Delhi, India, 2017.
[8] M. N. Rahman, M. T. Islam, M. Z. Mahmud, S. Kibria and M. Samsuzzaman, “Broken-heart shaped microstrip patch antenna design for ultrawideband applications,” Microw Opt Technol Lett., vol. 59, pp. 2324-2330, 2017.
[9] S. Bukkawar and V. Ahmed,“Omnidirectional and Directional Fractal UWB Monopole Antenna,” International Conference on Nascent Technologies in the Engineering Field (ICNTE-2017), pp. 1-4, Navi Mumbai, India, 2017.
[10] O. A. Safia and G. V. Eleftheriades, “A New Gosper Island Fractal UWB Monopole Antenna with Enhanced Bandwidth Characteristics,” IEEE International Symposium on Antennas and Propagation & USNC/URSI National Radio Science Meeting, pp. 1043-1044, Boston, USA, 2018.
[11] T. Ali, B. K. Subhash and R. C. Biradar,“Miniaturized Decagonal Sierpinski UWB Fractal Antenna,” Progress In Electromagnetics Research C, Vol. 84, pp. 161-174, 2018.
[12] J. Yeo, J. Lee and Y. Cho,“Miniaturized Stepped Open Slot Antenna for UWB Applications,” APS-URSI, pp. 1271-1272, Boston, USA, 2018.
[13] J. Yeo, “Miniaturized UWB Stepped Open-Slot Antenna,” Progress In Electromagnetics Research Letters, vol. 78, pp. 119-127, 2018.

Proceedings of the Fourth International Conference on Communication and Electronics Systems (ICCES 2019)
IEEE Conference Record # 45898; IEEE Xplore ISBN: 978-1-7281-1261-9

Low Power Hardware Based Real Time Music System and Digital Data Transmission Using FPGA

Sudip Mondal[1]
School of VLSI Design and Embedded system
National Institute of Technology
Kurukshetra, Haryana
[1]mondalsudip44@gmail.com

R. K. Sharma[2]
School of VLSI Design and Embedded system
National Institute of Technology
Kurukshetra, Haryana
[2] mail2drrks@gmail.com

Abstract—**This paper presents implementation of FPGA based low power music system and digital data transmission in real time environment. The proposed system consists of a music source, voltage divider, JXADC Pmod, Artix-7 Processor, DDR2 memory and Mono Audio Out. Music source provides analog input using auxiliary wire to the JXADC port. The music data is sampled at 44.1KHz using JXADC and output is taken from the headphone jack using PWM. JXADC port requires bias voltage of 0.5volt that is made available from on-board 1volt rail found on J14. A divider circuit is used to obtain 0.5volt out of 1.0volt input. Nexys4 DDR board is used for designing the algorithm of real time music system. Algorithm is designed using Verilog on Vivado 2018.3 Design Suite. In this process XADC's consumes 0.002W of total power 1.198W. The music system provides an excellent music data to the audio out pin J8 in real time.**

Keywords— FPGA (Field Programmable Gate Array), JXADC Pmod (Analog to Digital Converter Peripheral module), PWM (Pulse Width Modulation), DDR2 memory (Double Data Rate 2 RAM).

I. INTRODUCTION

Rapid progress of digital and multimedia technology, real time music data has been used in many remote locations like analog to digital transmission, Bluetooth transmission or by wired transmission [1]. In the recent days, digital audio data transmission is very important in digital electronics world [2]. The digital audio processing in real time made a vital role [3], where low power processing take place. The digital Audio data processing done in three steps [4], at first, the analog audio data process through the Pmod XADC port for converting the data in analog to digital format. Secondly, the digital formatted data can be transmitted in remote location from FPGA [5], that is very first process in terms of other devices. Thirdly, we can transmit the data by wires in digital format that's also been converted to analog formatted data by using of PWM on J8 pin on Nexys4 DDR board [6]. The basic advantages of Artix-7 processor is control. Artix-7 processor gives highest performance in per watt fabric, data processing and integration in a cost sensitive FPGA. Featuring the micro-blaze soft processor and 128MiB DDR2 support, the family is perfect for power-sensitive applications including low-end wireless communication, software-defined radio and machine vision cameras [7].

The goal of this paper is to introduce a novel low power-based music framework utilizing rough string-coordinating circuits for diminishing the computational time [8]. Field programmable gate arrays (FPGA) based design is appropriate instead of using application specific design. The FPGA procedures have similar computational speed to that of ASIC strategies. In addition, in light of their reconfigurable capacity, the FPGA gadgets give lower cost to changing circuits. This is very useful at the point of data transmission management. In the FPGA, signal processing is done by serially. So, minimum power management is also restored here.

This paper is separated in 5 Section and individual Section as follows, Introduction is discussed in section I and Section II describes the system design as block design format for real time music system. In the Section III low power-based design analyzed using proper implementation design and in Section IV the implementation design has been programmed on Nexys4 DDR FPGA board and simulation result has been discussed. In the last Section V result has been concluded and mentions the future scope.

II. SYSTEM DESIGN

Low power hardware-based music system is a data processing system in real time [9]. The music data processes from an external input sources and we can get the output at the mono audio output port. At the same time, this digital music data can be simultaneously sent through wired channel [10], Bluetooth or wireless transmission at any remote location [11]. The core design of music System block diagram is shown in Fig.1.The whole design act as an audio data processing system. The music or audio data fed to the JXADC by an auxiliary input cable and converted to the digital audio data. Which processed by the main process controller. Hence, digital data ready for transmission from FPGA to the remote location at the same time. Digital data transmission can be done by wire or wireless medium by using proper channel [12]. Digital data easily played at the mono audio output port through the head phone jack at J8 pin. Because of PWM the digital data converted to the analog format simultaneously. In this process the voice quality has been improved at the low power consumption level.

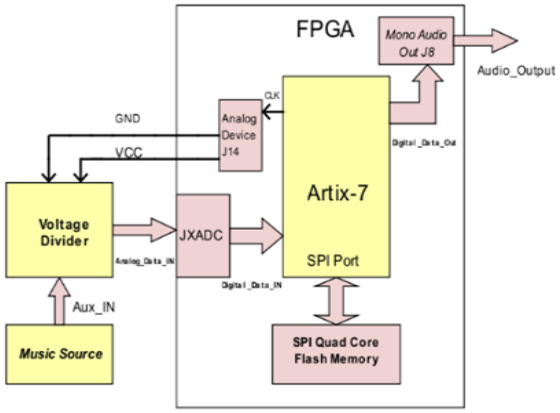

Fig.1. Block Diagram of Real Time Music System using FPGA

In the above block design in order to have a reliable transmission of data following blocks such as Music Source, Voltage Divider, JXADC and Mono audio output plays a crucial role. The analog data is transmitted at 0.5v after passing through the Voltage Divider from the Music Source. Analog to digital conversion is done by JXADC and after processing the data from Artix-7 processor the digital data out fed to the Audio out port. The Mono Audio Port plays a vital role for Noise cancellation and Pulse Width Modulation (PWM) and output is taken from the same port.

III. POWER ANALYSIS

The entire process is strongly able to manage a low power analysis. The implementation design is most effective in low power application [13]. In music system the maximum power is consumed up to 1.218 W. After implementing the design algorithm in Nexys4 DDR board, we have been analyzed the total on chip power is 1.198W shown in Fig.2. and the XADCs consumed the minimum power reason of using a voltage divider after the music source shown in Fig.3. The static and dynamic power is also derived from constraints files, simulation files or vector analysis. The static power of the device depends on the process, voltage and temperature. In this design the device static power is 9% of total on-chip power and the rest of the power is dynamic power i.e. 91% of total on-chip power, describes in fig.2.

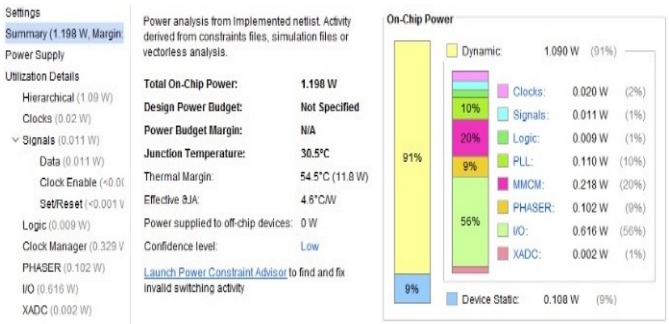

Fig.2. Power Analysis of Real Time Music System

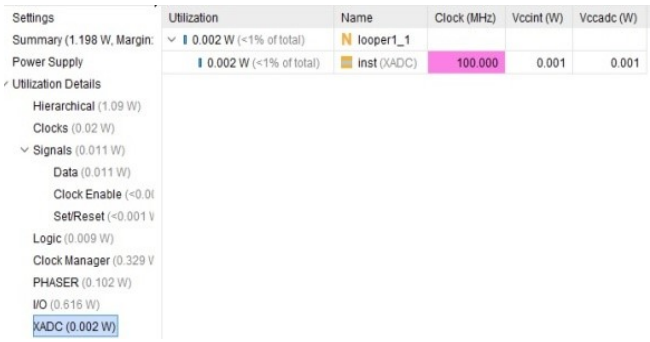

Fig.3. Minimum Power supply to the XADC Port of Real Time Music System

IV. RESULT

The prospective architecture is synthesized using VHDL in Vivado 2018.3 Design Suite. The design has been implemented on Nexys4 DDR (Xilinx part number XC7A100T-1CSG324C) FPGA kits. On board JXADC (Analog to Digital converter Pmod) that is next to the Pmod of JA. MIC is used to acquire the voice data from outsides and that data has been converted to the digital format by the on-board JXADC that is interfaces through the processor to the MONO AUDIO OUT (J8) pin. The real music system is implemented using FPGA at low power level. The RTL level schematic design and Simulation result of music system has been shown in Fig.4. and Fig.5. The hardware implementation design of low power based real time music system is depicted in Fig.6. where the music data is continuously playing in the audio port using a headphone jack at J8 pin.

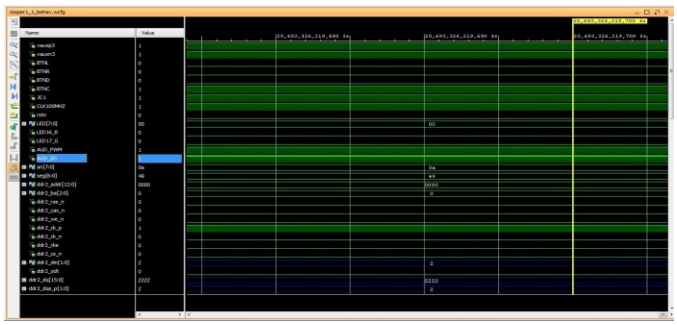

Fig.4. The simulation result of Real Time Music System

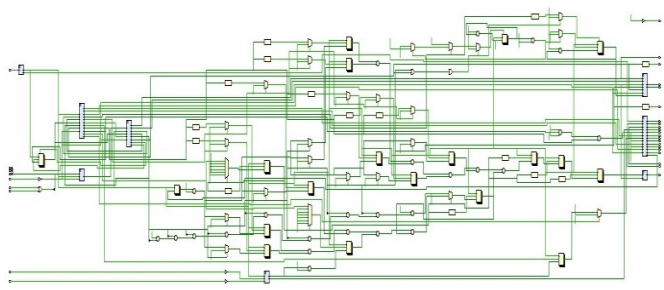

Fig.5. The RTL design of real time low power-based Real Time Music system

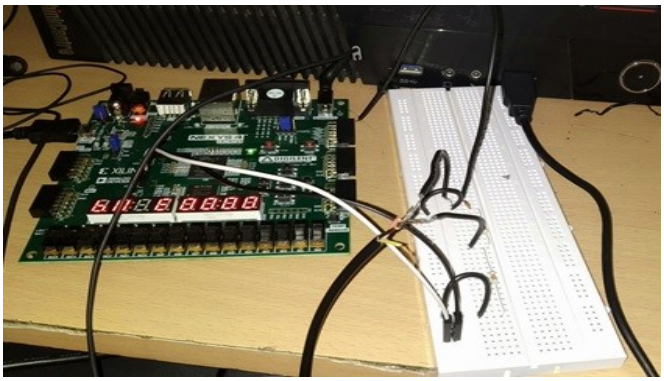

Fig.6. The hardware implemented design of low power based Real Time Music System

V. CONCLUSION

In this paper, low power level based real time music system hardware has been implemented on Nexys4 DDR board. First, the Auxiliary input analog data fed to XADC port by using a bias voltage with the help of voltage divider circuit shown in Fig.6. Then entire design has been synthesized on Vivado design suite 2018.3 and implemented on Nexys4 DDR board successfully and ensures superb voice quality on real time music system. Wherever low power is maintained in music system, we can use this type of approach and digital data transmission from the FPGA in real time produce a great advantage to manage the data at any remote location area where digital audio data is essential. In the future of work, the current approach and implementation design will improve by adding some extra interfaces for conventional real time music system.

ACKNOWLDGEMENT

This work is a part of SMDP-C2SD project under (Under MeitY). The authors acknowledge the technical and EAA tools support. Further optimization is required then it's may be possible to done on FPGA for sophisticated application. we are very thankful to the ministry for providing constant support.

REFRENCES

[1] D. L. Kuhite and M. S. Madankar, "Wireless audio transmission system for real-time applications — A review," *2017 International Conference on Inventive Systems and Control (ICISC)*, Coimbatore, 2017, pp. 1-5.doi: 10.1109/ICISC.2017.8068680

[2] C. Scott and W. Butler, "Real-Time Data Transmission System," in *IRE Transactions on Communications Systems*, vol. 7, no. 3, pp. 201-205, September 1959. doi: 10.1109/TCOM.1959.1097565

[3] Ou, C., Yeh, C., Su, Y., Hwang, W., & Chen, J. (2008). FPGA Implementation of Content-Based Music Retrieval Systems. *2008 International Conference on Embedded Software and Systems Symposia*. doi: 10.1109/icess.symposia.2008.25

[4] Zhang, J., Ning, G., & Zhang, S. (2015). Design of audio signal processing and display system based on SoC. *2015 4th International Conference on Computer Science and Network Technology (ICCSNT)*. doi:10.1109/iccsnt.2015.7490868

[5] J. Rusia, A. Naugarhiya, S. Majumder, S. Majumdar, B. Acharya and S. Verma, "RF based wireless data transmission between two FPGAs," 2016 International Conference on ICT in Business Industry & Government (ICTBIG), Indore, 2016, pp. 1-6. doi: 10.1109/ICTBIG.2016.7892643

[6] H. Peng and Y. Nie, "Design of serial communication interface based on FPGA," 2011 IEEE International Conference on Computer Science and Automation Engineering, Shanghai, 2011, pp. 410-414.doi: 10.1109/CSAE.2011.5952879

[7] Proceedings of the 2005 3rd Workshop on Embedded Systems for Real-Time Multimedia (IEEE Cat. No.05EX1149). (2005). *3rd Workshop on Embedded Systems for Real-Time Multimedia, 2005.*doi:10.1109/estmed.2005.1518044

[8] Hu, Y., & Loizou, P. C. (2008). Evaluation of Objective Quality Measures for Speech Enhancement. *IEEE Transactions on Audio, Speech, and Language Processing,16*(1), 229-238. doi:10.1109/tasl.2007.911054

[9] Hoffbeck, J. P., & Sugiyama, M. M. (2013). Real-time FM radio for teaching DSP and communication systems. *2013 IEEE Frontiers in Education Conference (FIE)*. doi:10.1109/fie.2013.6684995

[10] R. V. Cox, C. A. Kamm, L. R. Rabiner, J. Schroeter and J. G. Wilpon, "Speech and language processing for next-millennium communications services," in Proceedings of the IEEE, vol. 88, no. 8, pp. 1314-1337, Aug. 2000. doi: 10.1109/5.880086

[11] Lee, Y., & Fathia, R. N. (2016). Interactive music visualization for music player using processing. *2016 22nd International Conference on Virtual System & Multimedia (VSMM)*. doi:10.1109/vsmm.2016.7863205

[12] Poudereux, P., Hernandez, A., Cruz-Roldan, F., & Mateos, R. (2018). FPGA-Based Architecture for Medium Access Techniques in Broadband PLC. *IEEE Access,6*, 9534-9542. doi:10.1109/access.2018.2808371

[13] L. Puglia, M. Vigliar and G. Raiconi, "Real-Time Low-Power FPGA Architecture for Stereo Vision," in IEEE Transactions on Circuits and Systems II: Express Briefs, vol. 64, no. 11, pp. 1307-1311, Nov. 2017. doi: 10.1109/TCSII.2017.2691675

Proceedings of the Fourth International Conference on Communication and Electronics Systems (ICCES 2019)
IEEE Conference Record # 45898; IEEE Xplore ISBN: 978-1-7281-1261-9

Design of GMII Transparent Interface Based on Ethernet IEEE 802.3 Standard

Rajat Kumar Maheshwari
School of VLSI Design & Embedded Systems
National Institute of Technology
Kurukshetra, India
rajat_31711222@nitkkr.ac.in

T. N. Sasamal
Department of ECE
National Institute of Technology
Kurukshetra, India
tnsasamal.ece@nitkkr.ac.in

***Abstract*—Today applications those work above Ethernet or Fast Ethernet will operate similarly well on Gigabit Ethernet. The redesigned system will convey undeniably more the application traffic. In this paper, Ethernet IEEE 802.3 Standard based interface design system in Verilog-HDL has been designed. This GMII interface recognizes Ethernet Frame Protocol and works at 1Gbps speed. The interface configuration has been simulated, later on it has been synthesized and implemented. The interface works on 125 MHz frequency. With the designing of this interface, Total On-Chip power as Static and Dynamic power, Slice logic, LUT as logic parameters are analysed. Furthermore, the implementation result is verified.**

Keywords—Ethernet, GMII interface, Ethernet MAC, OSI reference model.

I. INTRODUCTION

The development of data innovation including progression of data communications is quickly expanding. This open door impacts a significant improvement in other's life aspects. Without a doubt, the development of data innovation itself impacts likewise on innovation advancement of planning and executing hardware-based framework [1]. Usage of web, treated as one medium or arrangement of information correspondences, results numerous points of interest, for example, information security, far reaching network, fast of information transmission, and solid information trade component.

However, the execution of web arranges which will be utilized is unquestionably affected by gadgets or gear utilized inside the system [2]. The gear which will be utilized can be viewed as from the physical viewpoint, for example the equipment viewpoint. Conventions which will be utilized for information interchanges are additionally considered as imperative piece of executing the web organize.

Moreover, Advances in VLSI innovation have additionally pushed joining to the point where it is presently conceivable to structure and execution a system controller and microchip on single chip, which is known as SoC (System-on-chip) [3]. The Gigabit Ethernet innovation is an augmentation of the 10Mbps and 100Mbps Ethernet standard. Gigabit Ethernet gives an information data transfer capacity of 1000Mbps while keeping up full similarity with the introduced base of more than 70 million Ethernet hubs [4].

Gigabit Ethernet includes both full-duplex and half-duplex working modes. Gigabit Ethernet underpins arrange the board, existing applications, and the system working frameworks, which requires insignificant expectation to absorb information for Ethernet organize clients and directors [5]. These hazard minimization and speculation conservation angles are make Gigabit Ethernet excessively appealing.

The principle point of planning the Header and Trailer of Ethernet frame is isolated and remerged by the module which an interface module. The planning module will be an equipment based coordinated framework structured utilizing Verilog-HDL which may taking care of data relating correspondence conventions or principles which are utilized. The module interfacing procedure will be centred around the interfacing of Data-link-layer (Layer 2) and Physical Layer (Layer 1) in the view of the Ethernet convention IEEE 802.3 for picked the availability of Ethernet 1Gbps.

Fig. 1.1 gives an outline of IEEE 802.3 Gigabit Ethernet layer tends to the MAC and PHY layers of ISO model.

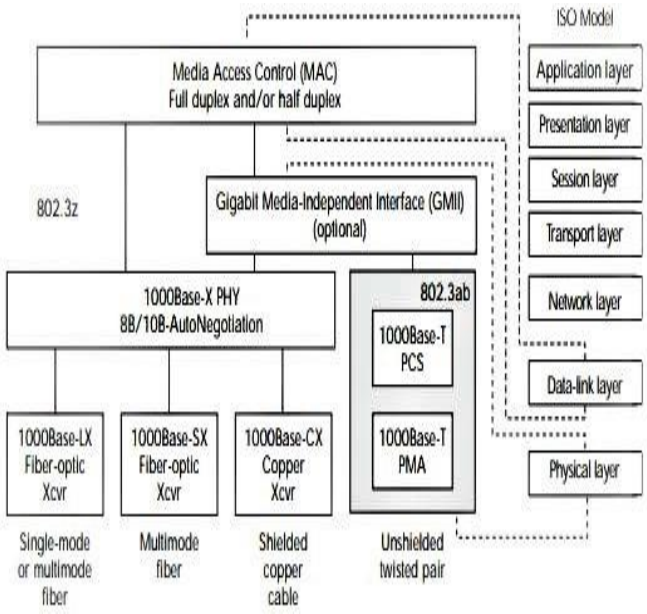

Fig. 1.1. Gigabit Ethernet layer graph tends to the MAC and PHY layers of the ISO model [7]

II. BACKGROUND

There are a few aspects or parts of communication conventions. These conventions are mainly centred to principal idea of Ethernet IEEE 802.3.

A. Introduction to OSI

A certain device manufactured by different manufactures need to follow consistent standards to able to communicate properly. This shows the development of certain reference models and network models, while network models set a standard as to how data communication or information transfer over a network.

The reference models divide the functions of network into layers. The two most popular reference models are OSI reference model and TCP/IP reference model. Open Systems Interconnection (OSI) provide standardization for protocols to be used in different seven layers [6]. The OSI reference model's every single layer act based on protocol of definitive type to communicate to peer layer of another node or system. Ethernet is perturbed with physical and data link layers of OSI reference model.

The Layer 1 (Physical layer) is responsible for converting the data from the form in which it is represented in data link layer to the form in which it is transmitted over the raw bits i.e. physical medium. Physical layer provides the hardware required to send and receive information over the physical medium [7]. This hardware contains clock synchronizer, signal encoders, line drivers, etc. It also defines the mechanical, electrical, and timing specifications for these devices that enable transfer of data over the communication channel. It also includes pin voltages, line impedances, cabling specifications like cabling distance, cabling type etc.

Data link layer is responsible for peer to peer or node to node communication within a network. The main function of data link layer is to convert the incoming data into frames, while other functions are include addressing, error control, control of access to shared medium and flow control [8]. Each frame contains its destination and source addresses which allows the identification of the sending and receiving stations respectively on the network. The corresponding OSI reference model and its Layer 2 architecture shown in below Fig. 2.1.

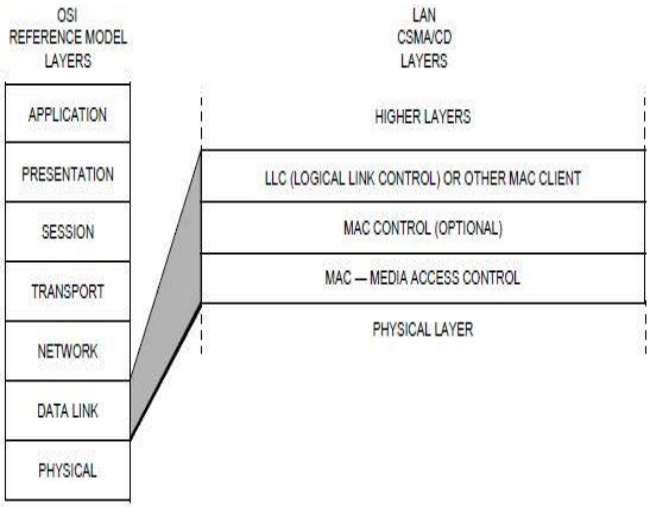

Fig. 2.1. OSI reference model and architectural positioning of Layer 2 [2]

B. Ethernet Frame Format

The heart of the Ethernet communication system is the Ethernet frame. The network hardware constitutes of the Ethernet interfaces, physical media cables move Ethernet frames between computers network or stations. In Ethernet frame the bits are formed up in specified fields. The basic Ethernet frame format is shown below Fig 2.2.

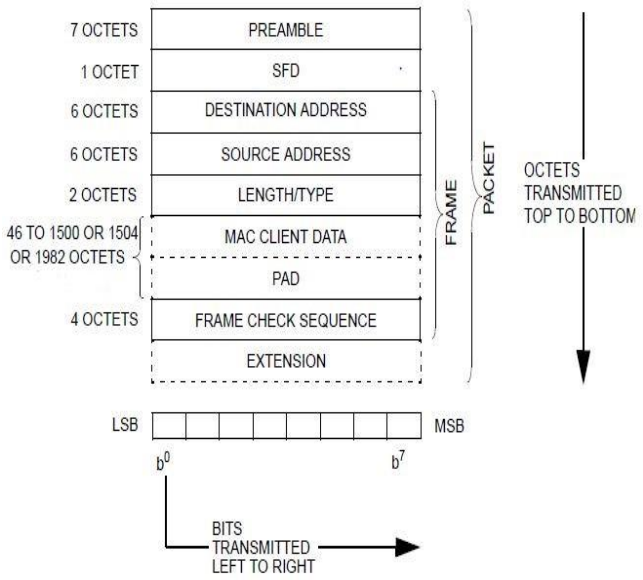

Fig. 2.2. Basic Ethernet Frame Format [5]

C. Ethernet Media Access Control

The Data link layer is partitioned into 2-Sub-layers namely the Logical Link Control sub-layer (LLC) and the Media Access Control sub-layer (MAC). The Logical Link Control sub-layer works as alliance between physical layer and the higher layer of protocol. The Media Access Control sub-layer adopts LLC to different media access technologies and physical medium. The main functions of the LLC sub-layer are flow control and multiplexing the protocol fields transmitted over the MAC sub-layer while transmitting and decoding them while receiving [9].

All Protocol signals are created which are required by the MAC module and its separate FIFO supportive buffers, according to the Host interface [10].

- The Transmitter control module, which originates frames is consisted by the Transmitter.
- The Destination address field, the Source address field and the Length/Type field of frame which is originate in transmit control module is included in the MAC address viper.
- A Cyclic Redundancy Code (CRC) generator is comprised in the transmitter to create the necessary CRC bits which is attached as the Frame Check Sequence (FCS).
- The Receiver control module, which decapsulates the protocol fields of frame is consisted by the Receiver.
- A checker of CRC is responsible to check lapses in frame transmission.

- The checker of MAC address is responsible for MAC address fields checking. It additionally checks for broadcast or multicast frames address.

The Ethernet Media Access Control (MAC) architecture shown in below Fig 2.3 consists of the Transmitter module and the Receiver module.

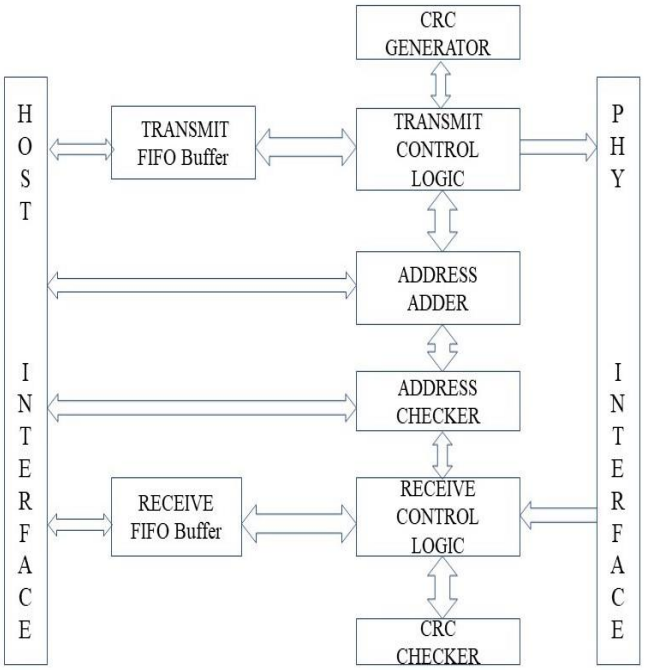

Fig. 2.3. MAC Implementation Block Diagram

III. THE DESIGN AND ITS SIMULATION

For the designing of this interface and advancement, the essential idea of configuration stream as following: the underlying advance of this reasonable structuring is started with characterizing the for the most part structure detail. The idea of configuration stream of this structured framework and advancement completed as the framework satisfied the significant criteria seen from its distinguishing identification process.

A. Design Specification

The initial step of design is started with characterizing about design specification. The plan worries on information interfacing which created from ethernet controller. Information unquestionably came about because of controller are 8-bit [11]. Information treatment of this plan isn't totally centred around the information originated from Ethernet PHY. The information is real information that complying with Ethernet frame protocol i.e. IEEE 802.3 Ethernet Standard.

Besides, this structure isn't totally executed for 10Mbps of Ethernet availability [12]. In any case, this structure is actualized dependent on strategy for 1Gbps of Ethernet connectivity.

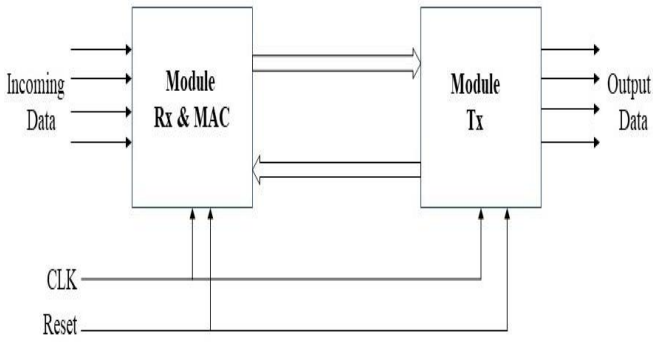

Fig. 3.1. Main Modules of Interfacing System

B. Functionality of the Designed Interface

The planned framework comprises of two primary modules to be specific, the Transmitter (Tx) and the Receiver (Rx). The Transmitter (Tx) as the primary module is arranged at host/PC, and the other module is arranged as the Receiver (Rx) at host/PC. However, the principal module and second module are capricious.

The interface framework outline is delineated in above Fig 3.1. Each unit has its own particular usefulness. The usefulness of every unit can be characterized as:

- **Module Rx-MAC,** which forms the approaching information, which will at that point recognize the Ethernet frame presence and complying with the MAC IEEE 802.3 convention inside the approaching information coursing through framework interface. In receive module the clock provided by PHY device (125MHz) is connected to MAC clock, rx_clk.
- **Module Tx,** which processes to control the gearbox information out from the interfacing framework. The gearbox information out is identified with MAC bits (Eight - bits). In transmit module standard programmable PHY devices operating in 1000Mbps mode generate a 125MHz clock.

Below Fig 3.2 shows the RTL view diagram of main module of interfacing design system, which consist of Rx and Tx-modules respectively.

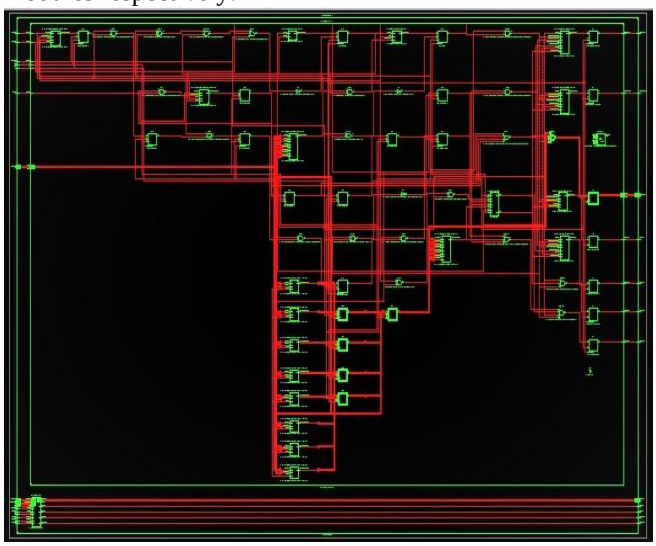

Fig. 3.2. RTL view diagram of design interfacing system

C. Design Simulation

The design system simulation was performed utilizing Xilinx ISE 14.7 and Vivado HLS 2016.2. The ISE Design Suite 14.7 was utilized to simulate the Verilog based interface plan framework. Inside the simulation, each module of incorporated plan framework will be gotten to dependent on usefulness and time imperative.

The PHY device expects a 125MHz clock from MAC system function in gigabit mode. Due to the MAC system function does not generate a clock output, an outside clock module is acquainted with drive the 125MHz clock to PHY devices and MAC system function. During the transmission MAC control signal selects GMII, which subsequently drives the MAC GMII to PHY interface.

In the Fig 3.3, recognition of substantial Ethernet frame is appeared, and yellow circle depicts the frame Preamble field which is responsible for clock synchronization. And red circle indicates the Payload or MAC client data field of Ethernet frame. MAC client data can be 46 to 1500 Bytes for Data frame, and those Ethernet frame contains Payload (> 1536 bytes) consider as Type frame. In indigo circle indicates the Inter Frame Gap (IFG) between the two consecutive frames. According to IEEE 802.3 Ethernet standard IFG should be 12 Bytes in normal communication transmission, most importantly IFG is decided by PHY device. As per IEEE 802.3 Ethernet standard minimum value of IFG can be 5 Bytes.

Fig. 3.3. Detection of different field of Ethernet Frame

Ethernet frame has dispatched to beneficiary module to one occasionally and analysed for recreation confirmation of casing. As indicated by Fig 3.4, at whatever point the FCS sent to beneficiary, the module RX-MAC looks at the FCS to other assertion FCS come about by checking the information section of Ethernet frame. In below Fig 3.4, red circle indicates FCS field match to receiver module side and transmitter module side. In Ethernet frame FCS field can be 4 bytes at before end of frame i.e. tx_en = 0.

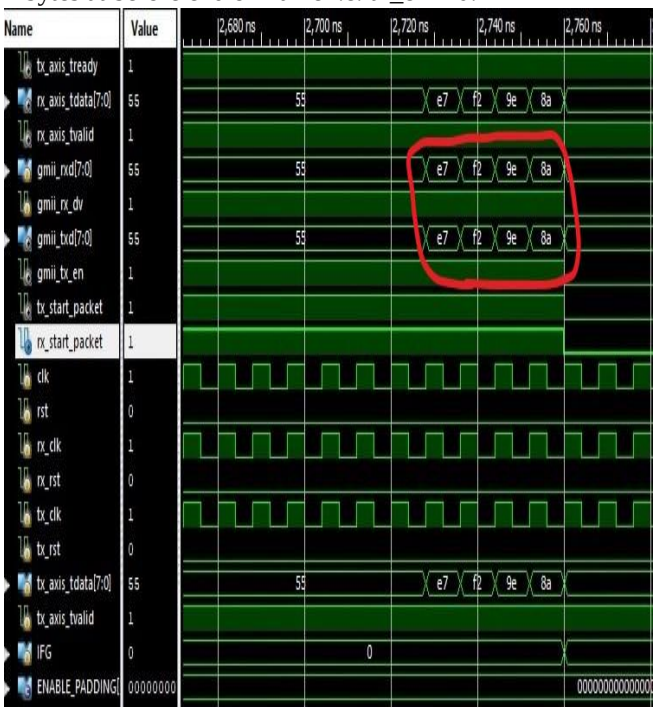

Fig. 3.4. Detection of FCS with no error

IV. VERIFICATION PROCESS

Verification procedure of our interface configuration is the procedure executed at whatever point the information embedded to interfacing plan framework. Verification process depends on a few stages which are characterized as pursues as:

- The first 7 bytes of Ethernet frame, will consider to Preamble field identification and to recognize next byte will consider as Start of Frame Delimiter (SFD).
- Address field identification, at any time the preamble field and SFD identifiaction process has been done, the next six bytes will occupy as Destination address field, and further next six bytes will consider as Source address field.
- The other stage is related to identification of the tagged frame, it will occupy next four bytes if frame is tagged and occupy next 2 bytes for Length/Type field. In case of untagged frame it will occupy 2 bytes only.
- After the identification of Length/Type field, MAC client data field starts, it can be 46 to 1500 bytes in case of Data frame. And in Jumbo Ethernet frame can carry up to 9000 bytes Payload.
- Last four bytes (before Inter frame gap) of Ethernet frame will consider as Frame Check Sequence (FCS).

Below Fig 4.1 shows the Verification process of Ethernet frame FSM. It shows the distinct fields detection of Ethernet frame.

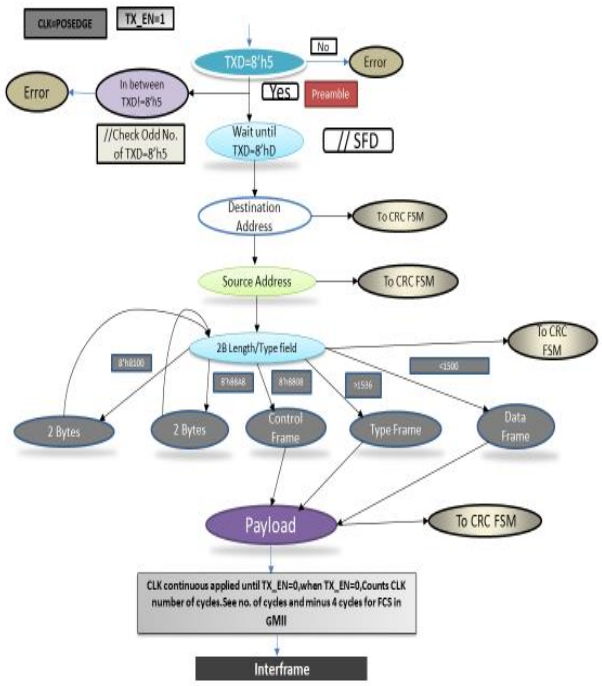

Fig. 4.1. Verification process FSM of Ethernet frame

V. CONCLUSION

In this report, a straightforward interface configuration dependent on Ethernet convention has been designed. The configuration of this interface is open or straightforward to physical media for information correspondence. To plan this interface, it is required 297 Slice logic, 136 LUT as logic and based on sysnthesis result, the Total On-Chip power 2.738W in which Dynamic 2.636W and rest Device static 0.102W is used. The Ethernet casing of IEEE 802.3 Protocol is recognized by this interface, which also comprises of Rx-module and Tx - module. The interface's design functionality has been verified by indicated its Verification process that it works appropriately as it also can recognize 802.3 Ethernet Frame.

REFERENCES

[1] Silitonga, A., & Hutabarat, M. (2015). An emulation of transparent interface design based on TCP/IP implemented onto FPGA of an Altera Nios® Board. *2015 9th International Conference on Telecommunication Systems Services and Applications (TSSA)*. doi:10.1109/tssa.2015.7440432

[2] IEEE Std 802.3TM-2008, "Carrier Sense multiple access with Collision Detection(CSMA/CD) Access Method and Physical Layer Specifications".

[3] Frazier, H. (1998). The 802.3z Gigabit Ethernet Standard. *IEEE Network,12*(3), 6-7. doi:10.1109/65.690946

[4] Gad, V. (2012). Implementation of Gigabit Ethernet Standard using FPGA. *International Journal of Mobile Network Communications & Telematics*,*2*(4), 31-44. doi:10.5121/ijmnct.2012.2404

[5] IEEE Standard for Ethernet. (n.d.). doi:10.1109/ieeestd.2016.7428776

[6] Prathima, N. (2013) et al,"*Design and FPGA Prototyping of embedded Ethernet Controller",International Journal of Engineering Research and Applications (IJERA)* Vol 3. Issue 3,May-June.

[7] Frazier, H., & Johnson, H. (1999). Gigabit Ethernet: From 100 to 1,000 Mbps. *IEEE Internet Computing*,*3*(1), 24-31. doi:10.1109/4236.747317

[8] Talledo, J. P. (2005, February). Design and implementation of an ethernet frame analyzer for high speed networks. In *15th International Conference on Electronics, Communications and Computers (CONIELECOMP'05)* (pp. 171-176). IEEE.

[9] Duan, M., & Han, H. (2011, July). Research and implementation of Gigabit Ethernet full line rate. In *Proceedings of 2011 Cross Strait Quad-Regional Radio Science and Wireless Technology Conference* (Vol. 1, pp. 736-738). IEEE.

[10] Metcalfe, R. M., & Boggs, D. R. (1976). Ethernet: Distributed packet switching for local computer networks. *Communications of the ACM*, *19*(7), 395-404.

[11] Zamora, J. M., Corrales, P. R., & Perez, J. S. (2003, November). Design of a parametrizable low cost Ethernet MAC core for SoC solutions. In *Proceedings. 2003 International Symposium on System-on-Chip (IEEE Cat. No. 03EX748)* (pp. 139-142). IEEE.

[12] Hadzic, I. (2001). Hierarchical MAC address space in public Ethernet networks. In *GLOBECOM'01. IEEE Global Telecommunications Conference (Cat. No. 01CH37270)* (Vol. 3, pp. 1563-1569). IEEE.

Proceedings of the Fourth International Conference on Communication and Electronics Systems (ICCES 2019)
IEEE Conference Record # 45898; IEEE Xplore ISBN: 978-1-7281-1261-9

Design of Efficient 2-4 Modified Mixed Logic Design Decoder

Rohit Kumar Arya, Sonali Agrawal
Department of Electronics & Communication Engineering
Amrita School of Engineering, Bengaluru
Amrita Vishwa Vidyapeetham
India

***Abstract*— This paper proposes a Modified-Mixed Logic Design (MMLD) for the decoders, which comprises full swing Gate diffusion input (GDI) technique, conventional complementary metal oxide semiconductor (CMOS) and Dual value logic (DVL). Two modernized topologies: 14T and 15T decoders are designed for minimizing power dissipation and propagation delay respectively. Each traditional and inverting decoder is enforced in every case. Compared to the conventional CMOS logic, the proposed decoder gives full swing with reduced count of the transistors. The spread of Cadence (Virtuoso) simulation at 45nm is used for implementing this proposed mixed logic decoder at different frequencies with different various supply voltages, which shows reduction in power dissipation & propagation delay as compared to typical CMOS and existing mixed logic design.**

Keywords—Modified Mixed Logic Design (MMLD), Full swing GDI, DVL.

I. INTRODUCTION

The primary issue in modern technology world is power reduction. The low-power [1] designs are of great importance among all electronics domains like Integrated Circuits, System on Chip (SoC), DSPs, Digital Phase Locked Loop [2] and Very Large-Scale Integration (VLSI) and in many different domains [3].

The design of the systems is becoming increasingly compact in today's world as the technology is developing so rapidly. Even though the circuits are not compact in some systems; there is still a need for less power consumption. There is a huge demand of applications that consume less power and are smaller in area.

Static CMOS network consists of one pull-up and one pull-down network and it gives good output driving capabilities [4] together. There are different CMOS technologies to design any circuit like PTL, TGL etc.

Pass transistor logic (PTL) was initiated during late 20th century, whose main motive was to deliver a good backup to conventional CMOS design in the sense of power, area and delay [5]-[7]. The major difference in the design is that, in PTL all the terminals that are presented can work as inputs.

Transmission gate logic (TGL) is a parallel bidirectional switch composed of NMOS and PMOS transistor. With the help of TG logic, implementation of complex designs can be easily done with a smaller number of transistors [8].

Further the paper is sectioned as follows: Brief understanding of Decoder circuit designed by using normal CMOS logic and mixed logic is given in section II. The modified mixed logic design is explained in section III. Relative simulation results and performance analysis among different designs is discussed in section IV. Section V provides application of proposed decoder and finally section VI tells about the conclusion and future scopes.

II. OVERVIEW OF DECODER CIRCUITS

Decoder is used to convert the data (which is available in coded format) from one format to another. So, we can say that a decoder translates a set of input data signals as their outputs into an equal decimal code. In other words, decoder is mainly a circuit that changes an obtained code into a group of signals. N-digit binary information is being translated into 2^n unique data lines in basic decoder circuit.

A. 2-4 Decoder using conventional CMOS logic

A decoder of size 2-4 produces four outputs from D0 to D3, where A & B are two inputs. Based on the combination of inputs, at a time only one output is set to one, while the remaining outputs are set to zero. On the other hand, an inverting decoder of size 2-4 also produces four complementary outputs from I0 to I3 in which based on the combination of inputs, one of the outputs is made to zero and all the remaining outputs are made to one.

The truth table of 2-4 Non-Inverting and inverting decoders are shown in Table I and II respectively.

TABLE I
TRUTH TABLE OF THE 2–4 DECODER

A	B	D_0	D_1	D_2	D_3
0	0	**1**	0	0	0
0	1	0	**1**	0	0
1	0	0	0	**1**	0
1	1	0	0	0	**1**

TABLE II
TRUTH TABLE OF THE INVERTING 2–4 DECODER

A	B	I_0	I_1	I_2	I_3
0	0	**0**	1	1	1
0	1	1	**0**	1	1
1	0	1	1	**0**	1
1	1	1	1	1	**0**

A 2-4 non-inverting decoder requires four NOR logic and two inverter logic as depicted in Fig. 1(a). On the other hand, a 2-4 inverting decoder is implemented with four Nand logic and two inverter logic as depicted in Fig. 1(b).

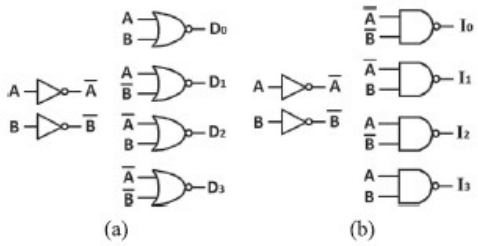

Fig. 1. 2-4 Decoder (a) Non-inverting decoder (b) Inverting decoder.

B. 2-4 Decoder using mixed logic design

Mixed logic [9] design comprises of transmission gate logic (TGL), conventional CMOS logic and dual value logic (DVL).

DVL is a type of Pass Transistor Logic (PTL). Actually, in PTL, two types of styles are present: Those using only NMOS transistors such as CPL and those using both NMOS & PMOS transistors, such as DPL and DVL [7]. But the logic which is taken here is DVL, because it eliminates the extra branches which are available in DPL and also it will sustain the full swing of DPL [10].

With the help of transmission gate logic and dual value logic AND & OR gates can be easily implemented [8], therefore it is used in decoders. To implement non-inverting decoder, take two inputs A and B. D0 & D2 outputs are designed with the help of DVL gates [7], where signal A is working as propagating signal. D1 & D3 outputs are done with TGL gates as shown in Fig. 2(a). Whereas to implement inverting decoder outputs I0 & I2 are done with TGL gates and outputs I1 & I3 are done with DVL gates as shown in Fig. 2(b).

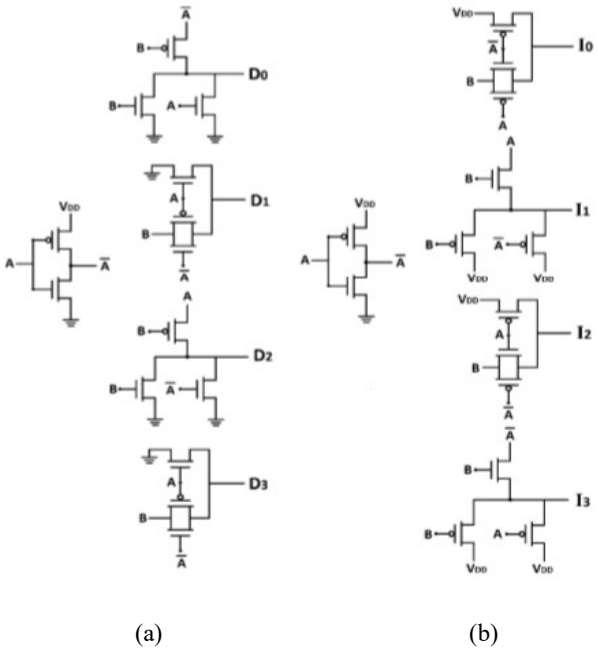

Fig. 2. 2-4 decoders. (a) Non-inverting. (b) Inverting.

III. MODIFIED MIXED LOGIC DESIGNS

In modified mixed logic design the transmission gate part of decoder, used in existing mixed logic decoder, is replaced by full swing GDI technique. AND and OR gates can be accurately done by using full swing GDI logic technique and DVL. Hence a decoder can be designed by using GDI and DVL with conventional CMOS inverter. Full swings GDI based AND/OR gates [11]-[12] and DVL based two input AND/OR gates are shown in Fig. 3(a), (b), (c) and (d) respectively.

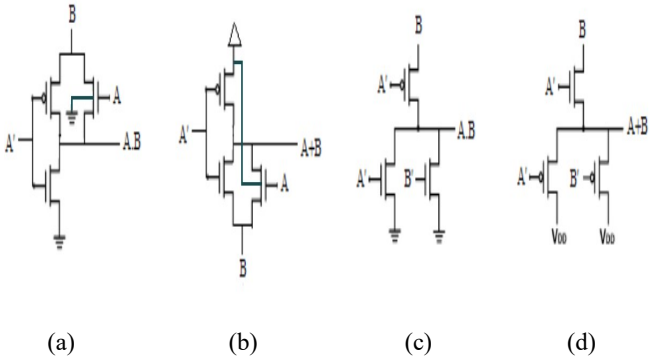

Fig. 3. AND/OR gates with three transistors (a) GDI based AND Logic. (b) GDI based OR logic. (c) DVL based AND logic. (d) DVL based OR logic.

As indicated in Fig. 3, two gate inputs A & B are labeled. In full swing GDI based AND/OR gates, input A is controlling all the three transistor's gate terminals, whereas in case of DVL based AND/OR gates input A is connected to the gate terminals of two transistors, while input B is controlling the gate terminal of one transistor and it is also working as propagating signal.

While designing any gates with the help of these techniques, always the concern is that never use complementary input signal as propagating signal because it adds inverter in the propagation path, which will contribute more in delay.

A. 2-4 Low-Power Decoder using 14-Transistor Topology

A 2-4 inverting decoder is designed with the proposed modified mixed logic design. Let us take two inputs A & B, where D0 & D2 outputs, of decoder, are designed with the help of DVL gates, where A is working as propagating signal. D1 & D3 outputs are done with the help of full swing GDI based AND gates and inverter is implemented with the help of conventional CMOS logic. Resulting in 2-4 non-inverting decoder using 14-transistors contains 9 NMOS and 5 PMOS as shown in Fig. 4.

Maintain the same procedure to design 2-4 inverting decoder with 14-transistor topology, where I0 & I2 outputs are designed with full swing GDI based OR gates and I1 & I3 outputs are done with DVL gates. This resulting 2-4 inverting decoder using 14-transistors contains 5 NMOS and 9 PMOS as shown in Fig.5.

The two introduced topologies are called "2-4 LP" and "2-4 LPI", with "LP" being "Low Power" and "I" being "Inverting".

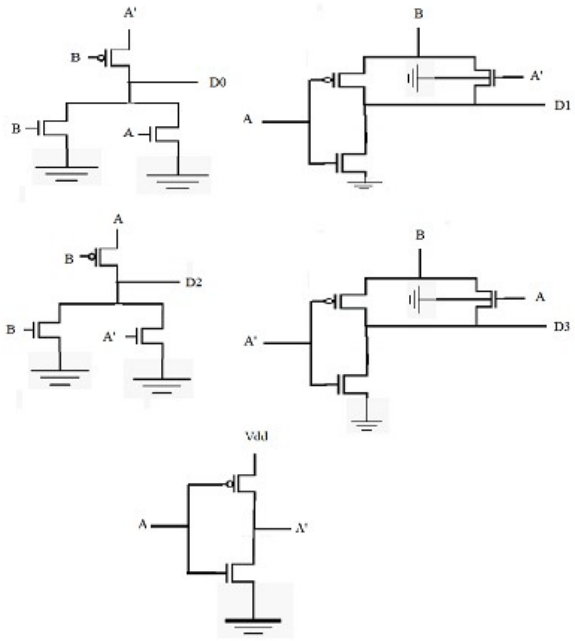

Fig. 4. 2-4 LP non-inverting decoder using 14-T.

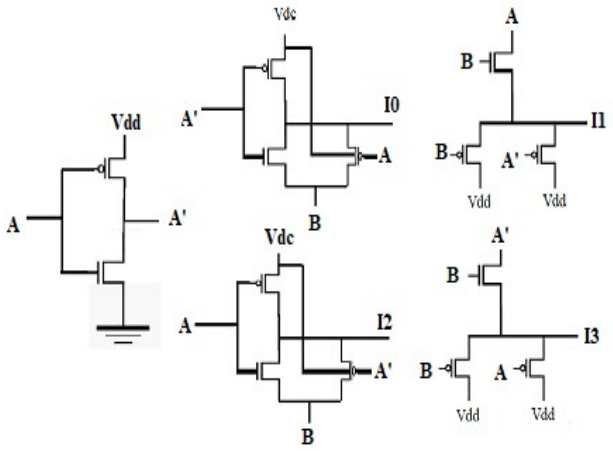

Fig. 5. 2-4 LP inverting decoders using 14-T.

B. *2-4 High-Performance Decoder using 15-Transistor Toplogy*

The low-power 14-T topologies have a disadvantage with respect to the delay, which is resulting by taking signal A (which is in complement form) in the act of propagating signal for D0 and I3 outputs. An inverter is used to complement the signal A which increases delay in that path.

In spite of that, D0 and I3 outputs can be accurately implemented with static CMOS. D0 output can be designed with CMOS based NOR gate and I3 output can be done with CMOS based NAND gate. Since, one extra transistor is added in both non-inverting and inverting cases, transistor count is increased by one. So, new 15-transistor topology reduces the delay, but power is increased little bit. A 2-4 non-inverting and inverting decoder using 15-T topology contain 9 NMOS & 6 PMOS and 6 NMOS & 9 PMOS respectively as shown in Fig. 6 and Fig. 7.

The two introduced topologies are called “2-4 HP” and “2-4 HPI”, with “HP” being “High-Performance” and “I” being “Inverting”.

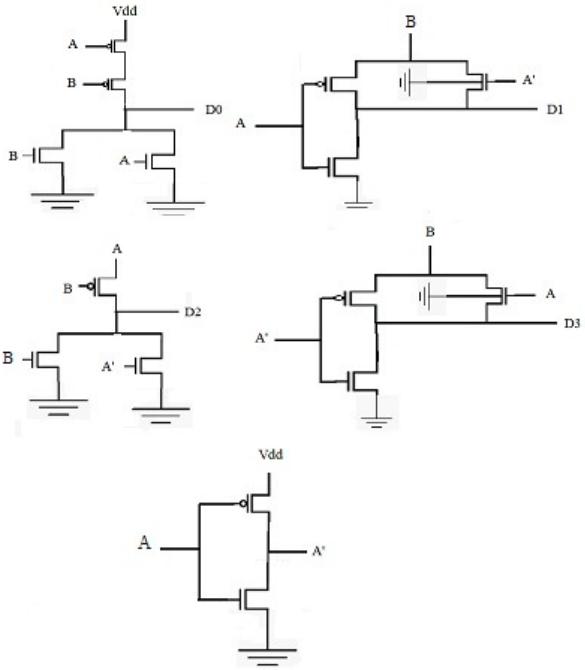

Fig. 6. 2-4 HP non-inverting decoders using 15-T.

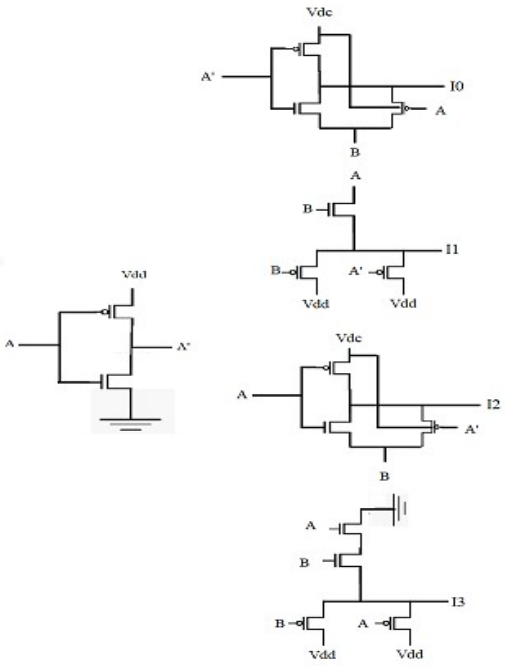

Fig. 7. 2-4 HPI inverting decoders using 15-T.

IV. Simulation Results & Performance Analysis

A. Simulation Results

A range of Cadence Virtuoso based simulation is performed for comparing modified mixed logic based 2-4 decoder with existing mixed logic and conventional CMOS based decoders. All circuits are designed in 45nm technology to get the reliable outputs. All designs are analyzed at different frequencies (0.5GHz, 1GHz, and 2GHz) and voltage (0.8V, 1V, 1.2 V). A capacitance of 0.2fF is connected to all outputs as a load. Input/output waveforms of non-inverting and inverting decoders using proposed method are depicted in Fig. 8 and Fig. 9 respectively.

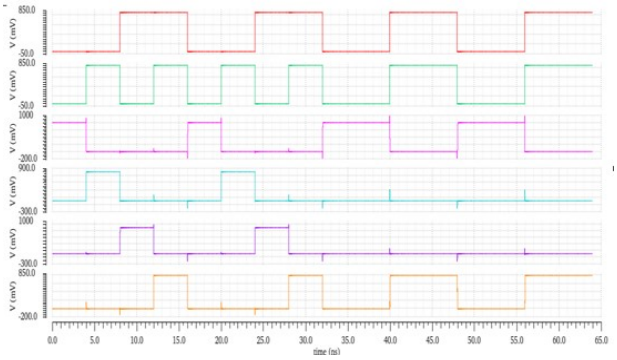

Fig. 8. I/O waveforms of proposed 2-4 non-inverting decoder.

B. Performance Analysis

The parameters taken for the analysis are: Power dissipation and Propagation delay. Various performance analyses are given in Table III, IV, V and VI for power dissipation and propagation delay. Each proposed design technique is compared with existing mixed logic technique [9] and conventional CMOS logic technique. Proper bit sequences are taken as input of the design to maintain all feasible transitions. In this analysis both power and delay are calculated by using Cadence Virtuoso tool. Power is obtained in Nanowatts. For the delay, maximum value that occurs from all input/output combinations is taken and measured in Picoseconds.

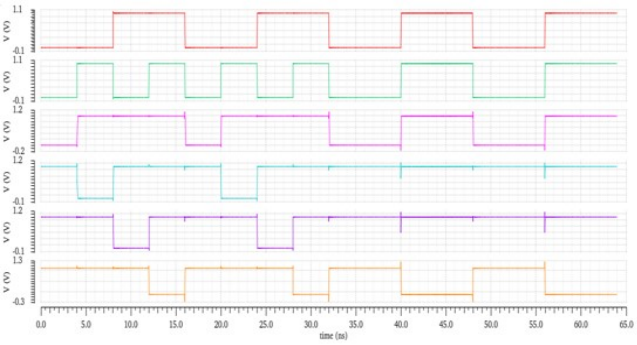

Fig. 9. I/O waveforms of proposed 2-4 inverting decoder.

TABLE III

POWER DISSIPATION FOR 2-4 DECODERS (IN NANOWATTS)

2-4 Decoder	500 MHz			1 GHz			2 GHz		
	0.8 V	***1 V***	***1.2 V***	***0.8 V***	***1 V***	***1.2 V***	***0.8 V***	***1 V***	***1.2 V***
CMOS	559.5	903.4	1313	1165	1899	2780	2330	3798	5560
MIXED LOGIC LP [9]	252.3	409.8	597.9	538.9	878.6	1286	1078	1757	2570
PROPOSED LOGIC LP	218.0	350.8	508.2	435.7	701.2	1016	871.2	1402	2030
MIXED LOGIC HP [9]	252.8	411.3	600.7	540.1	881.9	1292	1080	1764	2583
PROPOSED LOGIC HP	218.3	352.0	510.7	436.5	703.8	1021	873	1408	2041
CMOS INVERTING	560.6	904.7	1315	1167	1901	2783	2334	3802	5566
MIXED LOGIC LPI [9]	281.5	458.4	670.6	595.5	973.5	1428	1190	1945	2854
PROPOSED LOGIC LPI	247.3	398.7	577.7	493.1	795.6	1155	990.2	1589	2309
MIXED LOGIC HPI [9]	281.5	458.6	670.6	595.8	974.1	1429	1192	1947	2858
PROPOSED LOGIC HPI	247.2	399.5	578.2	494.9	794.8	1149	991.1	1592	2317

TABLE IV

PROPAGATION DELAY FOR 2-4 DECODERS (IN PICOSECONDS)

2-4 DECODER	0.8 V	1 V	1.2 V
CMOS	42.36	37.00	36.21
MIXED LOGIC LP [9]	23.50	21.22	16.62
PROPOSED LOGIC LP	23.50	21.23	16.61
MIXED LOGIC HP [9]	20.90	18.65	14.60
PROPOSED LOGIC HP	20.92	18.65	14.59
CMOS INVERTING	56.56	29.51	29.03
MIXED LOGIC LPI [9]	13.58	6.834	5.035
PROPOSED LOGIC LPI	13.34	6.707	5.046
MIXED LOGIC HPI [9]	12.75	6.33	4.78
PROPOSED LOGIC HPI	12.73	6.30	4.75

The parameters considered in this analysis are: Power dissipation and Propagation delay. According to obtained results, for 2-4 non-inverting decoder, proposed modified mixed logic design (MMLD) 2-4 LP gives 62.41% and 18.18% reduced power dissipation compared to CMOS and mixed logic based 2-4 LP respectively. On the other hand, proposed MMLD 2-4 HP gives 62.88% and 18.16% reduced power dissipation compared to CMOS and mixed logic based 2-4 HP respectively.

For 2-4 inverting decoder, Proposed MMLD 2-4 LPI gives 57.39% and 16.41% reduced power dissipation compared to CMOS and mixed logic based 2-4 LPI respectively. On the other hand, proposed mixed logic 2-4 HPI gives 57.36% and 16.39% reduced power dissipation compared to CMOS and mixed logic based 2-4 HPI respectively.

Regarding delay, for 2-4 non-inverting decoders: proposed MMLD 2-4 LP gives 47.06% less delay than CMOS and gives almost same delay as mixed logic 2-4LP. Similarly proposed mixed logic 2-4 HP gives 53.3% less delay than CMOS and presents almost same delay as mixed logic 2-4 HP.

For 2-4 inverting decoder: Proposed MMLD 2-4 LPI gives 78.76% less delay than CMOS and presents almost same delay as mixed logic 2-4 LPI. On the other hand, proposed mixed logic 2-4 HPI gives 79.92% less delay than CMOS and presents almost same delay as mixed logic 2-4 HPI.

Percentage of power reduction for non-inverting and inverting decoder based on proposed mixed logic design and mixed logic design [9] with respect to conventional CMOS is shown in Fig. 10. It is indicating that as voltage increases percentage of reduction also increases but delay is almost same in both the cases.

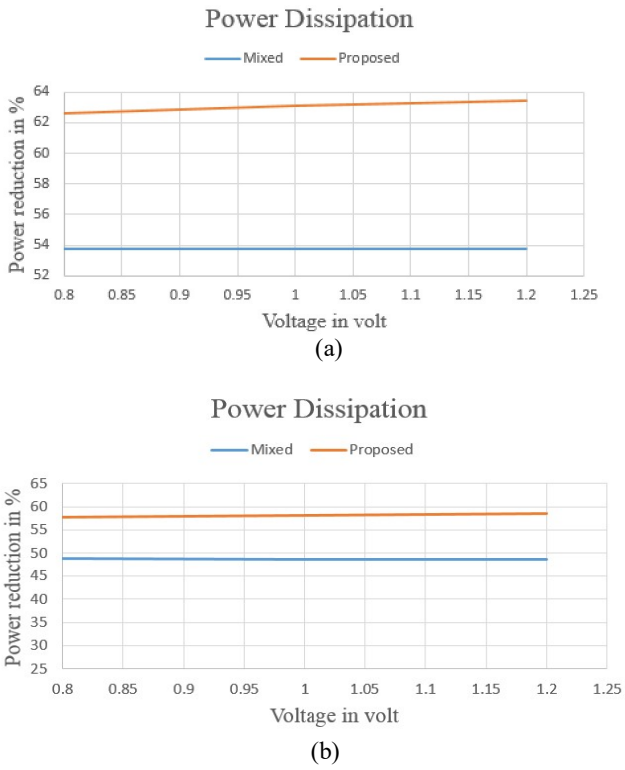

Fig. 10. Percentage of power reduction with respect to CMOS with different supply voltages (a) 2-4 non-inverting decoder. (b) 2-4 inverting decoder.

V. APPLICATION OF DECODERS

In digital systems full adder is a fundamental block [13], which adds three binary numbers of one bit, two operands and a bit of carry. Here, full adder contains two 2-4 decoder and three OR gates as shown in Fig. 11.

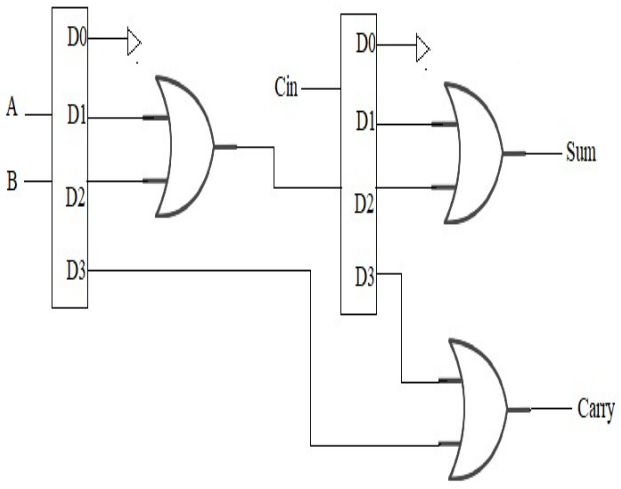

Fig. 11. Schematic of Full Adder.

Here full adder is designed with modified mixed logic decoder (MMLD) technique and compared with full adder using existing mixed logic-based decoder & conventional CMOS based full adder. The obtained results for power and delay are given in the table V and VI. Full adder based on MMLD taking less power and delay as compared to existing mixed logic and CMOS based full adder.

TABLE V

POWER DISSIPATION FOR FULL ADDER (IN NANOWATTS)

Full Adder (FA)	**0.8 V**	**1 V**	**1.2 V**
CMOS BASED FA	11300	30300	57000
MIXED LOGIC BASED FA	10930	29310	55210
PROPOSED MIXED LOGIC BASED FA	9793	26300	49560

TABLE VI

PROPAGARTION DELAY FOR FULL ADDER (IN PICOSENCODS)

Full Adder (FA)	**0.8 V**	**1 V**	**1.2 V**
CMOS BASED FA	193.3	94.11	77.82
MIXED LOGIC BASED FA	171.9	92.09	67.17
PROPOSED MIXED LOGIC BASED FA	101.5	81.37	64.62

For full adder, proposed full adder gives 13.29% and 10.33% less power dissipation than conventional CMOS and existing mixed logic based full adder respectively. Regarding delay proposed full adder gives 25.99% and 6.26% less delay than CMOS based full adder and mixed logic based full adder respectively.

VI. CONCLUSION AND FUTURE SCOPE

This paper proposed a modified mixed logic design for different styles of 2-4 decoders and implemented a full adder using proposed decoder. The analysis concludes that proposed 2-4 decoder (both non-inverting and inverting) consumes less power compared to existing mixed logic [9] and conventional CMOS based 2-4 decoders. On the other hand, proposed 2-4 decoders consumes less delay compared to conventional CMOS based 2-4 decoder but gives almost same delay as mixed logic based 2-4 decoders.

Full adder designed and implemented with modified mixed logic design consumes less power and delay compared to existing mixed logic decoder based and CMOS based full adders.

Decoders which are presented here deals only with binary number. Future research can design the decoders that will deal with BCD and Excess-3 codes.

REFERENCES

[1] N. Sowjith, K. Sandeep, S., Sumanth, M., and S. Agrawal, “Low power VLSI architecture for combined FMO/Manchester encoder for reusability and FMO/Manchester codecs”, IEEE International Conference on Computational Intelligence and Computing Research, ICCIC 2016.

[2] Bissa P.R., Pande K.S., “All Digital Phase Locked Loop for Low Frequency Applications”, International Conference on Advances in Computing Communications and Informatics,ICACCI 2018.

[3] Mathew , Krishnamurthy ,Anders, Hsu and Borkar, “Advanced circuits techniques for high-performance microprocessor and low power DSPs”, Proceedings of the IEEE Dallas/CAS Workshop on Implementation of high-performance circuits, pp. 1-45, September 2004.

[4] R. Zimmermann and W. Fichtner, “Low-power logic styles: CMOS versus pass-transistor logic,” IEEE Journal on Solid State Circuits, vol. 32, no. 7, pp. 1079–1090, Jul. 1997.

[5] Arun Pratap Singh Rathod ; Praveen Lakhera ; A. K. Baliga ; Poornima Mittal ; Brijesh Kumar, “Performance comparison of pass transistor and CMOS logic configuration based de-multiplexers,” International Conference on Computing, communication & automation, pp. 1433-1437, 2015.

[6] V. G. Oklobdzija and B. Duchene, “Synthesis of high-speed pass-tarnsistor logic,” IEEE Transactions on Circuits and Systems II: Analog and Digital Signal Processing, vol. 44, pp. 974-976, 1997.

[7] V. G. Oklobdzija and B. Duchene, “Pass-transistor dual value logic for low-power CMOS,” International Symposium on VLSI Technology, pp. 341–344, 1995.

[8] X. Wu, “Theory of transmission switches and its application to design of CMOS digital circuits,” International Journal on Circuit Theory and Appllications, vol. 20, no. 4, pp. 349–356, 1992.

[9] D. Balobas and N. Konofaos “Design of Low Power, High Performance 2-4 and 4-16 Mixed Logic Line Decoders” IEEE transaction on circuits and system –II :express briefs, VOL. 64, NO.2, February 2017.

[10] D.Markovi´c, B.Nikoli´c, and V.G.Oklobdžija, “A general method in synthesis of pass-transistor circuits”, Microelectron. Journal, vol. 31, pp. 991–998, 2000.

[11] Prabhu E. and Mangalam, H., “Power Optimized Vedic Parallel MAC Unit: GDI Technique”, Asian Journal of Information Technology, vol. 15, no. 16, pp. 2954-2957, 2016.

[12] Mohan Shoba, Rangaswamy Nakkeeran, “GDI based full adders for energy efficient arithmetic applications”, International Journal on Engineering Science and Technology, pp. 485-496, 2016.

[13] Simma Ranjitha, Pasumarthy Srikanth, “ Design of decoders using mixed logic for various applications”, International Journal of Engineering and Advanced Technology (IJEAT), pp. 43-47, July 2017.

Proceedings of the Fourth International Conference on Communication and Electronics Systems (ICCES 2019)
IEEE Conference Record # 45898; IEEE Xplore ISBN: 978-1-7281-1261-9

HYBRID KEY GENERATION FOR RSA AND ECC

E.VIDHYA,
Ph.D Research Scholar,
Department of Computer Science,
Periyar University,
Salem,India.
vidhya11tamilarasi@gmail.com

S.SIVABALAN
Ph.D Research Scholar,
Department of Computer Science,
Periyar University,
Salem,India.
sivabalan1990s@gmail.com

R.RATHIPRIYA,
Assistant Professor,
Department of Computer Science,
Periyar University,
Salem,India.
rathipriyar@gmail.com

***Abstract*--The Rivest, Shamir, and Adleman (RSA) is one of the most important types of the Asymmetric cryptography. In RSA the key size is bigger when compared to the algorithms in cryptography. The keys are generated with any two prime numbers. The unauthorized person can easily get the keys with a Greatest Common Divisor(GCD) Attack. This is one of the main drawbacks of RSA cryptography. The Elliptic Curve Cryptography (ECC) is also Asymmetric cryptography with a small key size. The proposed work is to overcome the drawback of the GCD Attack in RSA. The RSA private and public key can be combined with an ECC private and public key by using an Exclusive OR(XOR) and the new hybrid private and public key are generated. The RSA encryption can be done with a new hybrid public key. The RSA decryption can be done with a new hybrid private key. The advantages of the proposed work is the creation of three levels of key for cryptography to avoid the GCD attack in RSA. The key strength is higher when compared to the simple key generation of RSA algorithm.**

***Keywords--* RSA algorithm, ECC algorithm.**

I. INTRODUCTION

A. RSA Cryptography

The RSA algorithm is invented by Rivest, Shamir, and Adleman in 1977 [9], [10]. RSA is Public-Key cryptography. RSA has three phases first one is the key generation, Second is the Encryption and the third one is a Decryption. The key generation algorithm is to generate two keys that are private key and public key. The public key is used to encrypt the message and send to a public channel, this key is enabled anyone can access the public key. Another one is a private key, this is used to decrypt the message. This is only accessible by an authenticated person. The private key is also known as a secret key.[3]. Figure (1) shows the RSA encryption and decryption process.

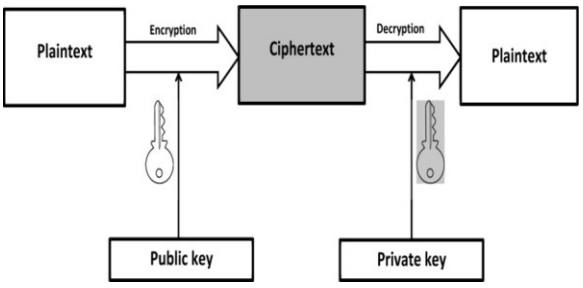

Figure 1. RSA Encryption and Decryption

B. Elliptic Curve Cryptography [ECC]

Elliptic Curve Cryptography is one of the public key encryption. ECC is difficult because it fully depends on the mathematical background. The problems of ECC can be solved using a discrete logarithm problem. [1]. The discrete logarithm problem is used to solve the problem of calculating the points which are moved from one point to another point in the ECC. In ECC, the process of encryption and decryption can be done by three processes. First one is an abelian group, the second one is an elliptic curve over the real numbers and the last one is the elliptic curve defined over a finite field.

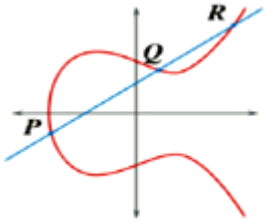

Figure 2. Basic Elliptic Curve Cryptography

The elliptic curve can be generated by using a binary curve. The Fig (2) is drawn based on the equation (1)[4] is

$$y^2 = x^3 + ax + b \qquad (1)$$

In equation (1), x and y are the standard variables which are used to define the function and 'a' and 'b' are the constant coefficient [5] which is used to define the curve. The discriminate form of elliptic curve is

$$\Delta = 4a^3 + 27b^2 \neq 0 \quad (2)$$

Equation (2), is used to assign the operation of elliptic curve. The operations are [2] point addition, point multiplication and point doubling.
The finite field is one of the important concepts in the ECC. Main use of the finite field is to define the limited points on the curve. The points are represented in x-axis which is defined as an 'p' which is also called as an modulo value. The point 'p' is defined the operation of ecc based on the discriminate form. [12]. The modulo value is also used to define the key size of ECC. The parameters are

P : finite field.
a,b : curve coefficients.
G : generator point based on operation of curve.
N : order of G.
H : divide the total points on the curve.

Table 1 : Key length of Different Algorithms

SYMMETRIC KEY LENGTH	RSA KEY LENGTH	ECC KEY LENGTH
80	1024	160
112	2048	224
128	3072	256
192	7680	384
256	15360	512

Table 1. represent the comparison of the key length of the symmetric, RSA and ECC. The symmetric key length is start from 80 bits and end with an 256 bits. The RSA key length is stratr from 1024 bits and end with an 15360 bits and the ECC key length is start from 160 bits and end with 512 bits.

II. RELATED WORK

This section is to provide the general overview of related works in the field of RSA and ECC cryptography. In particular, for those works are survey and received in detailed of RSA cryptography and ECC cryptography are listed below.

Author Name	Cryptography	Description	Remarks
Ansah Jeelani Zargar, Mehreen Manzoor, Taha Mukhtar	ECC cryptography	Making a essential relationship between the techniques explaining why ECC is better than any other cryptographic techniques recent to it.	Use of elliptical curve cryptography for given that the data security in high-level more or less all low power devices
F. Amounas and E. H. El Kinani	Elliptic Curve Cryptography, Discrete Logarithm, Cryptosystem	The ECC algorithm gives a strong point against crypto analysis and the work can be compared with standard algorithms like Rivest-Shamir-Adleman algorithm (RSA).	In the ECC the use of data sequence will given better result in this hold.
Anoop MS	Elliptic Curve Cryptography.	The basics of prime and binary field arithmetic	The polynomial reduction in binary field to run much faster than the modular reduction in prime field.
Avi Kak	Elliptic Curve Cryptography	The basics of Elliptic Curve Cryptography	Fully understand about the ECC in mathematical formate
Sriram Vajapeyam	Shannon's Entropy	Uses of Shannon entropy and how to measure the entropy value for text and image data.	Shannon's Entropy is used to calculate the lower-bound on number of actual bits required to store or transmit information
Joseph H. Silverman	Elliptic Curve Cryptography	Deatiled describtion on Elliptic curve cryptography	Fully describtion of ecc with an advantages and disadvantages

Joseph H. Silverman	Elliptic Curve Cryptography	Deatiled describtion on Elliptic curve cryptography	Fully describtion of ecc with an advantages and disadvantages
Ankush Sharma, Jyoti Attri, Aarti Devi & Pratibha Sharma	RSA, ElGamal cryptograaphy	comparison of the rsa and elgamal algorithms has been completed on the basis of security and time consumption for encryption and decryption.	ElGamal algorithm is more secure as compared to RSA algorithm
Fanyu Kong, Jia Yu, and Lei Wu	RSA, Key generation algorithm	The algorithm leak enough secret information and then everybody can recover the factorization of the RSA modulus *N* in polynomial time.	Generate the rsa key as strength.
M. Preetha, M. Nithya	RSA Algorithm	Public key algorithm RSA and enhanced RSA are compared analysis is made on time based on execution time.	It is used for encryption of long messages without employing the hybrid and symmetric encryption.
Wang	Information & Entropy.	How the entropy is worked and given with an simple example.	Calculate the entropy with an large data.
Kefa Rabah	RSA Algorithm	RSA Key generation are implementated in JCE provider	Compare to any other provider it gives some of the best result
H.J. Shiu, K.L. Ng, J.F. Fang, R.C.T. Lee, C.H. Huang.	Complementary pair, Data recovery	The data hiding methods crated based on the properties of DNA sequences. The three methods are: the Insertion Method, the Complementary Pair Method and the Substitution Method.	For all image media schemes and text message, the three methods are easy to implement and hard to detect
Mansi Rathi1, Shreyas Bhaskare, Tejas Kale, Niral Shah, Naveen Vaswani	DNA Cryptography, DNA Sequencing	This technique encrypt the data in a very complex and it prove it is very efficient algorithm with high accuracy	Implementing the DNA sequencing to the cipher text it will enable the cipher text to get strong encrypted and it can be also used for banking applications to encrypt the vital data of the customer such as the account number or pin or password.

From the above study, it has been observed that most of the work are carried out to compare the performance of RSA with ECC . But in this work, the hybridation of RSA key with ECC key a strong key with a less information gain and with an less execution time. Limitations in the above study, the GCD attack is to taken for the proposed work.

III. METHODS

Method 1: RSA Cryptography

Algorithm 1-1 RSA Key generation.
Input: Two Prime Numbers.   ***Output: Generate Public key and Private key.***
Step 1: Select the two large prime numbers as p and q where p is not equal q [bits are 512 bits].   **Step 2:** Calculate the modulo value represented as N , N=p*q   **Step 3:** Calculate the N with an phi value

$\phi(N)=(p-1)*(q-1)$.
Step 4: Select the integer of 'e'
'e' value must in small integer which is relatively prime to an $\phi(N)$ and not equal to 1.
Where $1<e<\phi(N)$.
Step 5: Compute Greatest Common Division[gcd]
$gcd(e, \phi(N))=1$.
Step 6: Calculate d, which is an multiplicative inverse of e modulo $\phi(N)$
$e*d=1 \bmod \phi(N)$, where $0 \le d \le N$.
Step 7: Return Public Key pair (e, N).
Step 8: Return Private Key pair (d, N).

In algorithm 1-1 [3] RSA Key generation, the public and the private key pairs are generated based on the large prime numbers which is given by users. The key bits are given as an 512 bits based on the bits the two prime numbers are generated the product of two primes 'p' and 'q' are stored in the variable ' N'. The phi value is find for an variable N. select an e which is lesser then the phi of N. find the GCD of e, phi of N. calculate the value of d . the private key is created with an two values 'e' and 'N'. The private key is created with an 'd' and 'N'.

Algorithm 1-2 RSA Encryption.
Input : Plaintext
Output : Cipher text
Step 1: Enter the plaintext as M.
Step 2: Encrypt the plaintext M with an public key pair (e, N).
$C=M^e \bmod N$, Where $0 \le M \le N$.
Step 3: Return the Cipher text C.

In algorithm 1-2 RSA Encryption, [6],[8] the plaintext is represented as 'M' which is encrypted with an public key pair (e,N) and stored in an variable 'C' which is represented an cipher text.

Algorithm 1-3 RSA Decryption
Input : *Cipher text*
Output : *Plaintext*
Step 1: Enter the cipher text as C.
Step 2: Decrypt the cipher text C with an private key pair (d, N).
$M=C^d \bmod N$, Where $0 \le M \le N$.
Step 3: Return the plaintext M.

In algorithm 1-2 RSA Decryption, [9],[10],[11] the cipher text 'C' is decrypted with an private key pair (d,N) and generate an plain text as 'M'. The original text is decrypted by the user.

Method 2: Elliptic Curve Cryptography

Algorithm 2-1 Elliptic Curve key generation
Input : Parameters
Output: User A And User B Public key
Step 1: Input the parameters as a, b and q,
Where q is a prime with an integer of the form 2^m.
Step 2: Compute the generator G as a point on the curve whose order is larger value as n.
Step 3: Select the Public key as n_A.
$n_A<n$, where A is an User A
Step 4 : select the Public key as n_B.
$n_B<n$, where B is an User B
Step 5: Calculate the Public key P_A
$P_A=n_A*G$, where A is an User A
Step 6: Calculate the Public key P_B
$P_B=n_B*G$, where B is an User B
Step 7: Return Public Key P_A.
Step 8: Return Public Key P_B.

In algorithm 2-1 Elliptic Curve Key Generation,[12] Input the parameters are 'a','b' and 'q' where 'q' is an prime number the points on the curve has been generated as 'G' which order is larger the n. [15] The public key of user A is selected and represented as n_A which less than 'n'. The public key of user B is selected which is represented as n_B which is less than 'n'. The public key of user B has been calculated with product of n_B and 'G'. which is stored in P_B. The public key of user A has been calculated with product of n_A and 'G' which is stored in P_B. The private key of user A is represented as P_A and the public key of user B has been represented as an P_B.

Algorithm 2-2 Elliptic Curve Secret key
Input : *Public key of User A and Public Key User B.*
Output: *Secret key k.*
Step 1: Calculate the Secret key of User A.
$K_A=n_{A*}P_B$.
Step 2: Calculate the Secret key of User B.
$K_B=n_{B*}P_A$.
Step 3 : Return Secret key of user A.
Step 4: Return Secret key of user B.

In algorithm 2-2 Elliptic curve Secret key, the input of user A and user B public key. Calculate the secret key of User A with the product of selected user A publick key n_A and with an user an calculated public key P_A. Calculate the secret key of User B with the product of selected user A public key n_B and with an user an calculated public key P_B.

A. Exclusive OR

Exclusive OR is one of the logical operation. The inputs of binary numbers are same the output is false(0). The inputs of the binary numbers are differ it returns true(1).

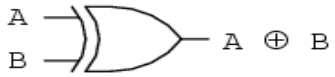

Figure 3. Exclusive OR

IV. PROPOSED WORK

In proposed work, the RSA public key and the private key are combined with an Elliptic Curve secret key and

public key using an exclusive OR and generate a new key pair based on the new key pair the data are encrypted and decrypted using an RSA encryption and decryption process. The proposed work is mainly concentrating on generating a strong key pair for the encryption and decryption.

A. Proposed Work Flow For Key Generation, Encrypt And Decrypt Process

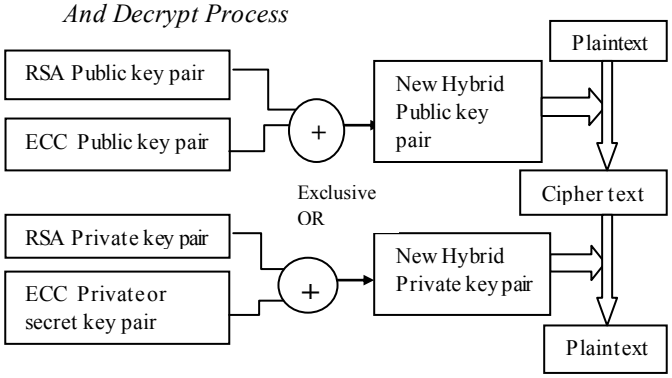

Figure 4. key generation, encryption and decryption process.

Figure 3. RSA public key is exclusiveOR with an ECC public key and generates a new public key. Like a RSA , private key is exclusive or with an ECC private key and generate a new private key. The plaintext is given for an encryption process the new public key is used to encrypt the plaintext and generate a cipher text. The cipher text is to decrypt by using a new private key and the plaintext is generated.

B. Proposed Algorithm For Key Generation, Encrypt And Decrypt Process.

Algorithm3-1: New Key generation
Input: RSA public and private key, ECC public and private key. *Output: New public and private key.*
Step1: Input an RSA public key pair as n and e. **Step 2 :**Input an ECC public key pair as P_A and P_B. **Step 3 :** ExclusiveOR with an Step1 and Step 2 and generate new hybrid public key pair. **Step 4 :** Input an RSA Private key pair as d and n. **Step 5:** Input an ECC private key pair as K_A and K_B. **Step 6:** ExclusiveOR with an Step4 and Step 5 and generate new hybrid private key pair. **Step 7:** Return New hybrid public key pair . **Step 8:** Return New hybrid private key pair.

In algorithm 3-1, The input parameters are RSA public key and private key, ECC public key and private key. The RSA public key can be XOR with an ECC public key and the new hybrid public key pair is created. the RSA private key can be XOR with an ECC private key and the new hybrid private key is created.

Algorithm3-2 Encryption
Input: RSA public and private key, ECC public and private key. *Output: New public and private key.*
Step1: Input an RSA public key pair as n and e. **Step 2 :**Input an ECC public key pair as P_A and P_B. **Step 3 :** ExclusiveOR with an Step1 and Step 2 and generate new hybrid public key pair. **Step 4 :** Input an RSA Private key pair as d and n. **Step 5:** Input an ECC private key pair as K_A and K_B. **Step 6:** ExclusiveOR with an Step4 and Step 5 and generate new hybrid private key pair. **Step 7:** Return New hybrid public key pair . **Step 8:** Return New hybrid private key pair.

In algorithm 3-2, the input parameters are plain text and the new hybrid public key. The plaintext can be encrypted with an new hybrid public key and return an cipher text which is represented as a variable 'cip'.

Algorithm 3-3 Decryption
Input : Cipher text as cip and New hybrid Private key *Output : Plaintext.*
Step 1: Enter the cipher text as cip. Step 2: Decrypt the cipher text cip with an new private key pair (d1, N1). $M1=C1^{d1} \bmod N1$, Where $0 \le M1 \le N1$ Step 3: Return the plaintext M1.

In algorithm 3-3, the input parameters are cipher text and the private key. The cipher ext can be decrypted with an new hybrid private key and return an plaintext as 'M'.

V. RESULT AND DISCUSSION

A. Information Entropy

Information entropy is defined as the amount of information in a variable, that variable has been providing the basic theory around the notation of information. It can be simply defined in terms of the probabilistic model. [13],[14]. It means that the modules which have many possible rearrangements then the system has high entropy, and the system has very few rearrangements, then the system has low entropy.

The Shannon entropy equation (3) is used to estimate the average minimum number of bits needed to encode a string of symbols, based on the frequency of the symbols.

$$H(X)= -\sum_{i=1}^{n} P(x_i)\log_b P(x_i) \qquad (3)$$

Where P is Probability of given symbol, b is the base of the logarithm.

Table 2 Information entropy values of cipher text.

FILE SIZE	INFORMATION ENTROPY	
	RSA	RSA-ECC
1kb	3.060	2.726
20kb	3.044	2.743
25kb	3.165	2.990
54kb	2.962	2.845
14mb	3.338	3.116

In table 2, the information entropy value for different file size is given. The first column is represented as file size. The file size is given as 1kb,20kb,25kb,54kb and 14 mb. The information entropy value are calculated for each of the file size separately for the algorithms RSA and RSA-ECC. Compare the entropy value of two algorithm. The proposed algorithm of RSA-ECC gives an better result compared to RSA algorithm. The figure 4, shows the graphical representation of the table 2 values.

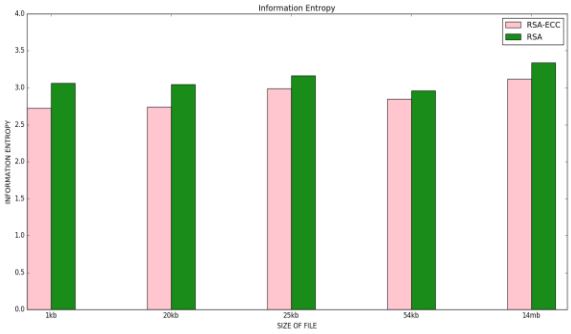

Figure 5. Information entropy values of cipher text.

Table 3 Execution time of the algorithms.

File Size	Execution time in milliseconds(m/s)	
	RSA	RSA-ECC
10kb	3.7	3.5
20kb	4.1	2.7
25kb	7.5	6.8
54kb	11.0	9.8
14mb	244	240

In table 3 the execution time is calculated with an milliseconds. The first column is filesize from 10kb,20kb,25kb,54kb and 14 mb. The execution time is calculated and compared the two algorithms RSA and RSA-ECC with this comparison the ECC-RSA is given an less execution time when compared to RSA algorithm. The figure 5. represented the execution time values in graphical representation.

Figure 6. Execution time of the algorithms

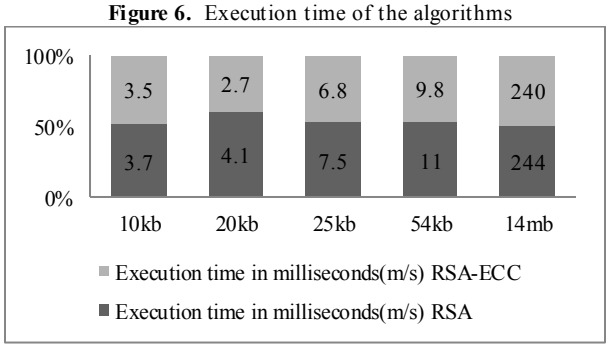

VI. CONCLUSION

The GCD attack is one of the disadvantage in the RSA algorithm. To overcome this problem, the proposed work is to combine the RSA key and the ECC key using an Exclusive OR and create an new hybrid key. The encryption and decryption can be done with an new hybrid private key and new hybrid public key. The hybrid key giving an secured key. The key strength can be measured by using an information entropy. In the result the proposed algorithm giving an high entropy when compared to an RSA algorithm. The proposed work has been created with an three levels of key but in future to increases the key levels and give an high secured level.

REFERENCES

[1] Amounas, F., & Elkinani, H. E. (2012). ECC Encryption and Decrytion with a Data Sequence. *Applied mathematical sciences , 6*.
[2] An Introduction to the theory of elliptic curve.
[3] Ankush sharma, J. D. Implementation and analysis of RSA and Elgamal algorithm . *Asian journal of Advanced Basic Sciences* .
[4] Avikak. Elliptic Curve Cryptography And Digital Rights Management. *Computer and network Security* .
[5] Biggs, N. L. Elliptic curve Cryptography. *An Introduction to information communication and cryptography*
[6] Chenghuai Lu, A. L.. Implementation of fast RSA key generation on smart cards. *ACM* .
[7] Entropy (information theory).
[8] Fanyu Kong, j. Y. Security Analysis of an RSA key generation algorithm with a large private key. *Springer* .
[9] Goshwe, N. Y. (2013). Data encryption and decryption using Rsa algorithm in a network environment. *International Journal of computer science and network security , 13* (7).
[10] M.Nithya, M. a. (2013). A Study and performance Analysis of RSA Algorithm. *International Journal of Computer Science and Mobile computation , 2* (6).
[11] Rabah, K. (2006). Implementing secure RSA cryptosystems using your own cryptograaphic JCE Provider. *Journal of Applied Sciences , 6* (3).
[12] S, A. M. Elliptic Curve Cryptography. *An Implementation tutorial* .
[13] Vajapeyam, S. (2014, March). Understanding Shannon's Entropy metric for Information.
[14] Wang. Information & Entropy.
[15] zargar, A. J., & Manzeor, m. (2017). Encryption/Decryption using elliptic curve cryptography. *International journal of Advanced Research in computer science. , 8* (1).

Proceedings of the Fourth International Conference on Communication and Electronics Systems (ICCES 2019)
IEEE Conference Record # 45898; IEEE Xplore ISBN: 978-1-7281-1261-9

An Efficient Trusted Graph Based Approach for Inferring Trust in Epinions Network

Debdutta Dey
Department of Computer Engineering
National Institute of Technology, Kurukshetra
Haryana, India
iamdebdutta11@gmail.com

Awadhesh Kumar Singh
Department of Computer Engineering
National Institute of Technology, Kurukshetra
Haryana, India
aksinreck@gmail.com

***Abstract*—**The social network has acquired popularity due to cheap availability of wireless connectivity and portable devices. It links people with common interests and provides platform to share information. However, the information shared over social network demands high level of trust and privacy. The paper presents a trusted graph based trust inference approach for measuring trustworthiness of an user. The effectiveness of the proposed approach has been assessed on real online social network dataset, Epinions and the same has been contrasted with recently published algorithms.

Keywords—Epinions; Online social network; Trust Evaluation; Trusted Graph

I. INTRODUCTION

A social network can be represented as a connected graph. Each node of the connected graph represents entity which can be any individual, group, organization or government agency and edges represent interdependencies among nodes. Recently, the popularity of online social network is witnessing a rapid increase due to its user friendly characteristic. Moreover, SN provides a platform that allows users to share and exchange information.

In the last decade, the evolution of networking technology has boosted up the acceptance of social networks like Facebook, LinkedIn among common users. However, many challenges like community detection, spam detection, availability of dynamic dataset, security issues, trust evaluation of users, are putting a stop to its wider acceptance. Since a SN consists of large number of users, an user may not be familiar with many of them. As an outcome, information breaching may occur. Thus determining trustworthiness of an user becomes very frequent problem faced by every SN user. Hence, trust plays a significant role in social network. In this paper, we have proposed an efficient approach to evaluate trustworthiness of an user. Our motivation is to provide an environment where users can share their thoughts, opinions and experiences in a transparent path without worries about privacy and dread of being judged [12]. "Trust in a person is a commitment to an action, based on a belief that the future actions of that person will lead to a good outcome (Golbeck [1])". In our real life, trust is being calculated cumulatively. For an example, if a person A wants to know how much he should trust another person B, he will consult with his friends first. If they don't have any knowledge about B, they may ask their friends and so on.

Trust can be of two types, direct and indirect or transitive trust. In Fig 1, we can see that A trusts neighbor node P directly, as there is direct edge between A and P .On the other hand, A trusts B indirectly, via a trusted path (A,P,Q,B) or (A,R,B). Direct trust can be easily derived based on the direct communication experience of two users, while indirect trust is usually evaluated based on other relevant users' interaction experiences in the social network [2]. There are different approaches available to evaluate indirect trust like Subjective logic based, Traditional mathematics tools based, AI information learning based, Graph based [3]. We have focused on trusted graph based approach in this work. Trusted graph is a directed acyclic graph(DAG) which includes a trustor, a trustee, recommenders and trust relationship among them [4]. Fig 1. is an example of trusted graph. Trustor is a node having no edge pointing to itself like A here and a trustee implies a node having no edge pointing from itself, node B is an example. Each edge of the DAG let (i,j) is associated with a values, which signifies how much I trusts neighbor node j. A trusted graph may have multiple paths between a trustor and a trustee, each of the paths is called as trusted path.

Several attempts have been done on modeling trust inference system based on trusted graph. Golbeck [1] proposes TidalTrust to generate a recommendation about the trust degree of an user according to another one based on trusted paths. Breadth-first search from the trustor to the trustee generates the trusted paths and only the shortest and strongest paths are being considered in TidalTrust. Due to considering only shortest paths, many important information may be neglected.

RN-Trust algorithm has been proposed by Taherian et. al. [5] to evaluate trust value from a trustor to trustee by modeling trust network as a resistive network. Each trust relationship between two nodes in graph has been represented by a resistor, so that the trust value would be more for less resistance value of resistor. Multiple paths between two nodes are combined using parallel circuit rule. RN-Trust considered all paths rather than only shortest paths, for trust inference. Main drawbacks of RN-Trust includes that there are no maximum path length limit and no threshold for the trust values between intermediary nodes. However, the weakest trust values causes decrease in inferred trust value.

Most of the graph based trust models pre-assume that a small trusted graph already available. But generating small trusted graph from large social network is very challenging task. Jiang et. al. [6] first proposed SWTrust to overcome this challenge. Along with the theory of "weak ties" [7] , it uses user's active domain information to assign trust value, which is more objective than explicit trust ratings. SWTrust constructs a small trusted graph by considering all paths between trustor and trustee with path length constraint as well as trust threshold. In this work, authors have performed eight trust prediction strategies which comprise three key factors of trust propagation functions (Min and Multiply), trust aggregation functions (Max and Weighted Average), and if all paths or only shortest paths are considered. Experimental results show that Weighted average function performs best to measure most accurate trust value. But in some scenarios, taking average of inferred trust values for all paths decreases the quality of inferred trust value as it weighs up the opinions of malicious nodes.

Sana et. al.[8] modeled TISoN to evaluate trust in social network. They proposed two algorithms for this model, first one is TPS (Trust Path Searching) and second one is TIM (Trust Inference Measuring) . TPS prioritizes neighbors based on the direct trust degrees and chooses trusted paths with path length constraint. TIM measures trust by constructing a trust network. TISoN depends on direct trust matrix. Thus lacking the advantage of constructing trust value from user's domain knowledge like SWTrust [6].

GFTrust [9] is another latest trusted graph based trust inference algorithm that uses SWTrust algorithm for generating small trusted graph and then uses generalized network flow concept to evaluate trust rating between two indirectly connected nodes or users. In this work Jiang et. al. [9] overcomes trust aggregation issue of social network.

In this paper, we propose an efficient trusted graph based approach for inferring trust for Epinions network. Our work includes SWTrust [6] framework to generate small trusted graph using user's domain related information as well as trust inference scheme used by Sana et. al. [8] for evaluation of trust between two indirectly connected users. We incorporate SWTrust framework to overcome the challenge of generating small trusted graph from a large social network dataset like Epinions. Then, we have implemented the approach used by Sana et. al. to calculate trust for increasing quality of the trust value. Finally efficiency of the proposed scheme has been estimated on Epinions network data set and comparative analysis has been performed with SWTrust [6] and GFTrust [9].

The remainder of this paper is organized as follows: In Section II, we will review the SWTrust framework. In Section III, we go through trust inference scheme used by Sana et. al.[8]. In Section IV, we discuss in details about our proposed approach. In Section V, we conduct experiments on Epinions dataset and give experimental result. Lastly, In Section VI, we conclude this paper.

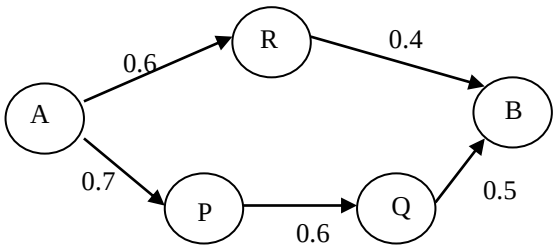

Fig 1: Trusted graph between A and B.

II. SWTrust Framework: Review

In this section we provide brief review of SWTrust framework. This framework has been architected with three key steps:

A. Preprocessing of an online social network (PSN):

The PSN starts with preprocessing of large online dataset to collect all domain related information related to every user and beside that domain information of topic (reason to know trustee by the trustor) has also noted. Jiang et. al. [6] Consider that every recommender or friend must be related to the topic and the target. Following that according to the theory of "weak ties" user domain based trusted acquaintance chain has been discovered. Thus Depending on social distance all the neighbors of an user has been categorized into three types e.g. local neighbors, longer neighbors and longest neighbors. Then neighbors in each category have been sorted conforming to their priority in descending order. Jiang uses referral trust to decide priority of a neighbor node with respect to a node.

"Referral trust" is ability to recommend a good target (i.e. trustee). If (i,j) is an edge in trusted graph, then referral trust is priority of selecting neighbor j as the next hop by i. Assuming that user i has full information of the active domains (domains in which user has participated) of his neighbor j, topic (reason to know trustee by the trustor) and target, below is the mathematical expression for calculating referral trust of neighbor j by user i.

$$p(i,j)=\frac{\lambda 1*x(j)+\lambda 2*y(j)}{^{\circ}D_{topic}+^{\circ}D_{target}}$$

$^{\circ}D_{topic}$: denotes total number of active domains of topic

$^{\circ}D_{target}$: denotes total number of active domains of target

λ1, λ2 belongs to [0,1]. x(j) denotes number of common domains between j and topic and y(j) denotes number of common domains between j and target.

Finally, next hop neighbors have been chosen uniformly from the three categories to build trust acquaintance chain.

B. Building the trust network (BTN):

Two methods of breadth-first search have been provided to construct a trust network from source to sink or trustor and trustee. First one is centralized BFS for small scale social networks and second one is distributed BFS, suitable for large scale online social networks. Max path length constraint has been used to maintain efficiency.

C. Generation of trusted graph (GTG):

GTG process includes deletion of paths in previously generated trust network having path length more than max path length constraint. Any path holding referral trust of any edge of it less than defined trust threshold has also been omitted. GTG has been performed in centralized server, resulting set of trusted paths. Thus a trusted graph between given trustor and trustee can be generated.

III. TRUST INFERENCE SCHEME

Sana et. al. [8] proposed trust inference between trustor and trustee using two interdependent methods:
i) trust propagation from trustor to the direct neighbor of trustee via a trusted path and ii) trust aggregation from trustor to trustee.

A. *Trust Propagation:*

A propagation function has been presented to calculate strength s_p of each trusted path p. Following function for s_p uses PathAverage, PathVariance and PathWeight as three factors:

$$s_p=\alpha t_p+\beta(1-\upsilon_p)+\gamma w_p$$

•PathAverage: t_p symbolizes average of direct trust values between n path nodes of a trusted path. They assumed that high trust rating values of mediator friends increase the quality of trust calculation.

$$t_p=\frac{1}{n}\sum_{i=1}^{n}t_i$$

•PathVariance: υ_p signifies path variance that is how much n trust values of a path is deviated from its average path trust. As per their assumption, friends with close trust ratings maintain accuracy of trust calculation.

$$\upsilon_p=\frac{1}{|n|}\sum_{i=1}^{|n|}(t_i-t_p)^2$$

•PathWeight: Path weight has been symbolized as w_p. It denotes fraction between shortest trusted path length, |n'| and current trusted path length, |n|. Any path having length tends to shortest one enhances accuracy of calculation.

$$w_p=\frac{|n'|}{|n|}$$

Let, p is a trusted path that having last intermediary node a_{pn}. a_{pn} has direct trust rating of trustee o, $t(a_{pn}->o)$. Then, multiplying path strength s_p of path p to $t(a_{pn}->o)$ gives inferred trust value of path p from trustor to trustee.

B. Trust Aggregation:

Sana et. al. have used four trust aggregation functions to aggregate trust values of all trusted paths from trustor to trustee. Those methods are as follows:

•Mean aggregation method: Assuming that a trustor s has n numbers of trusted paths between itself and trustee o, path strength of each path is s_{pi} and direct trust rating in the middle of last intermediary node of each path and o is $t(a_{pi}->o)$, where i varies from 1 to n, aggregated trust value of node o to trustor s can be calculated as:

$$t(s->o)=\frac{\sum_{i=1}^{|PATHS|}s_{pi}\times t\,(a_{pi}->o)}{|PATHS|}$$

•Mult aggregation method: Mult aggregation method calculates aggregated trust similarly. Following is the aggregation function:

$$t(s->o)=\prod_{i=1}^{|PATHS|}s_{pi}\times t(a_{pi}->o)$$

•Min aggregation method: This method chooses trusted path with minimum path strength and multiply its path strength with direct trust between corresponding last intermediary node and trustee o to get the final aggregated trust.

$$t(s->o)=s_{pk}\times t(a_{pk}->o)$$
$$s_{pk}=\min(s_{pi}),\ i\in[1,|PATHS|]$$

•Max aggregation method: Like min aggregation method, this method calculates aggregated trust considering trusted path max path strength.

$$t(s->o)=s_{pk}\times t(a_{pk}->o)$$

$$S_{pk} = \max\left(S_{pi}\right), i \in \left[1, |PATHS|\right]$$

In this paper, we have used max aggregation method as it performs best for the accurate result calculation.

IV. Proposed Approach

We have used SWTrust [6] framework to generate small trusted network from large social network dataset. Calculated referral trust values have been considered as trust values for the edges of the generated trusted graph. This helps transforming trust value of edge to be in continuous range of [0,1]. After that Sana et. al. Trust inference approach has been applied on the trusted graph to find the final trustworthiness of the trustee to the trustor.

Epinions [10] is a dataset where users can express their opinion about another users and also can rate any article written by another author. Epinions dataset consists of three files. First file contains user's trust or distrust relationships. Trust is marked as 1 and distrust as -1. We have not considered distrust for our approach. All information related to article like article Id, writer of the article, domain of the article are stored in second file. Third file caches ratings of articles and other additional details.

We have modeled our approach as following:

1. Preprocessing of Epinions dataset to gather domain information of users and articles.
2. Performing PSN step to build up user domain based trusted acquaintance chain.
3. Building trust network using max path length constraint.
4. Trusted graph generation of Epinions.
5. For each path of the generated trusted graph path strength has been calculated implementing method used by Sana et. al.[8].
6. Finally, max aggregation method has been applied to calculate aggregated trust value of all the trusted paths between the trustor and the trustee.

By following the above steps , the calculated final trust value can be directly taken as trust score of target or trustee according to the source or trustor without any normalization.

V. Experiment and Result

Published dataset of Epinions has been used for our experiment. As mentioned before, this network provides platform for users to rate opinion of another users as well as the articles written by another users in a scale of 1 to 10.

Our process starts with preprocessing of dataset to gather all domain related information of each user and article written by user. Then three key steps of SWTrust [6] have been applied on the dataset to generate the trusted graph. Referral trusts are used to assign trust rating of the edges of the generated trusted graph. After that trust aggregation of trusted graph has been performed as per the method used by Sana et. al. [8] to get final trust score of the trustee to the trustor.

We have used leave one out, a standard evaluation technique by Kohavi [11], for our experimental analysis. For this we have masked direct edge between two nodes lets s and o of the trusted graph, and calculated trust score implementing different algorithms using trusted graph. After that, a comparison has been performed between the masked trust value and the calculated trust value for performance evaluation.

We have consider trust prediction accuracy as evaluation metric. Accuracy has been measured by calculating mean absolute error (MAE). Let, there are T numbers of total test pairs of trustor s and trustee o and among these total numbers of predictable (at least one trusted path exists between s and o) trustor-trustee pairs is N. MAE can be calculated as: $MAE = \sum(t_r - t_p)/ N$, where t_r denotes masked trust value or real trust value and t_p denotes predicted trust value.

In Table I we have provided a comparative accuracy analysis of our proposed method, SWTrust [6] and GFTrust [9] . According to Jiang [9] GFTrust performs best with polynomial leakage function. Hence, we have used same leakage function for GFTrust in our experiment. We have assumed trust threshold value as 0.4.

From the comparative analysis it can be observed that our method produces less mean error in comparison with that of SWTrust and GFTrust. As mentioned above, comparative analysis has been performed by considering multiple numbers of test pairs of trustor and trustee. So, smaller value of mean absolute error indicates that in most of the test scenarios our method predicts most accurate trust value than both SWTrust and GFTrust. Hence, it can be concluded that our proposed method performs efficiently for inferring trust in Epinions network.

TABLE I. COMPARATIVE ANALYSIS OF ACCURACY

Method	Mean Absolute Error
SWTrust	0.14
GFTrust	0.49
Proposed method	0.02

VI. Conclusion and Future Scope

With rapid increase in acceptance of social network, trust related issues are becoming more important among online service provider and common users. In this paper, an effective trusted graph based trust inference approach has been proposed for Epinions . Our approach overcomes challenge of generating small trusted graph from large dataset. Thus helps to perform trust aggregation method more efficiently over a small trusted graph. It also does not depend on direct trust matrix rather uses domain knowledge to generate quality trust ratings. Experiments are carried out over Epinions dataset to justify its efficiency. As imminent work, trust calculation method can be dynamic and more powerful to reflect updated trust between nodes in online social network in real-time.

REFERENCES

[1] J. Golbeck, “Computing and applying trust in web-based social networks,” PhD thesis,Dept. Comput. Sci., College Park, Md,Univ. Of Maryland, 2005.

[2] C. Mao, C. Xu and Q. He, “A cost-effective algorithm for inferring the trust between two individuals in social networks”, in Knowledge-Based Systems, vol. 164, pp. 122-138, 2019.

[3] W. Jiang, G. Wang, M. Z. A. Bhuiyan, and J. Wu, “Understanding Graph-Based Trust Evaluation in Online Social Networks:Methodologies and Challenges”, in ACM Comput. Surv., volume 49, pp.10:1–10:35, 2016.

[4] G. Wang and J. Wu, “FlowTrust: Trust inference with network flows,”Frontiers Comput. Sci. China, vol. 5, no. 2, pp. 181–194, 2011.

[5] M. Taherian, M. Amini, and R. Jalili, “Trust inference in web-based social networks using resistive networks”, in Proceedings of the 3rd International Conference on Internet and Web Applications and Services (ICIW). pp.233–238,2008.

[6] W. Jiang, G. Wang, and J. Wu, “Generating trusted graphs for trust evaluation in online social networks,” Future Generation Comput. Syst.,vol. 31, pp. 48–58, 2014.

[7] M. Granovetter, “The strength of weak ties: a network theory revisited”,Sociological Theory 1 (1983) 201–233.

[8] S. Hamdi, A. L. Gancarski AL, A. Bouzeghoub, S. B. Yahia,” TISoN: Trust inference in trust-oriented social networks”, ACM Transactions on Information Systems (TOIS)., vol.34(3), no. 17,2016.

[9] W. Jiang, J. Wu,and G. Wang,”Trust Evaluation in Online Social Networks Using Generalized Network Flow”,IEEE Transactions on Computers,vol. 65,no. 3,pp.952-963,2016.

[10] P. Massa, P. Avesani, “Trust metrics on controversial users: balancing between tyranny of the majority and echo chambers”, International Journal on Semantic Web and Information Systems , vol. 3, pp. 39–64,2007.

[11] R.Kohavi, "A study of cross-validation and bootstrap for accuracy estimation and model selection", in Proc. 14th Int. Joint Conf. Artif.Intell.,1995,pp.1137-1143.

[12] W. Sherchan, S. Nepal, and C. Paris, “A survey of trust in social networks,” ACM Comput. Surveys, vol. 45, no. 4, pp. 47:1–47:33,2013.

Proceedings of the Fourth International Conference on Communication and Electronics Systems (ICCES 2019)
IEEE Conference Record # 45898; IEEE Xplore ISBN: 978-1-7281-1261-9

AES Arduino Handshake for Unattackable Data Processing

Gourav Saini[1]
School of VLSI Design and Embedded Engineering
National Institute of Technology
Kurukshetra-136119, Haryana, India
Email:[1] imgouravsaini@gmail.com

Dr. R.K Sharma[2]
School of VLSI Design and Embedded Engineering
National Institute of Technology
Kurukshetra-136119, Haryana, India
Email: [2]Mail2drrks@gmail.com

***Abstract*— Arduino are used worldwide in different hardware applications ranges from industrial applications to private uses. In, this application information could be scrutinized by unauthorized individual, which could progress into a security rupture and information burglary. From now on to set up a protected and dependable communication, the methodology ought to be to verify information utilizing explicit encryption methodology. Executing AES on programming isn't gainful, as the Arduino has less memory space, low handling rate and has more Power consumption and less utilization of AES libraries. These limitations can be overwhelmed by the utilization of AES-128-bit core as Hardware approach. This paper has tended to every one of these limitations and proposed a novel methodology of Data processing Model Using "AES-128" on Hardware core working on 200MHZ. The Arduino and AES-128 core handshake with one another utilizing the SPI protocol with max recurrence of 16Mbps. For the exhibit Purpose a ".txt" document is sent from PC to Arduino through AES core and this Encrypted information is shown on the LCD.**

Keywords—Advanced Encrypt Standard (AES), Serial Peripheral interface (SPI), Arduino

I. INTRODUCTION

Data communication done by Arduino UNO in Home automation [1] clarifies how Arduino implanted System can Communicate with another gadgets Device. Information sent from sender side to recipient side must be sufficiently secure so as to keep away from abuse. Min-KYU [2] Choi referenced one method for secure information correspondence by utilizing Encryption strategy.

With expanding tendency towards data security there was even more inclination as to security concern which goes as blockage between hackers and the critical data. Parcel of Encryption standard are being used beginning from Asymmetric model to Symmetric model incorporate AES which replaced older DES. Already AES was incorporating into Software approach. In these cutting-edge ERA, our objective is likewise concentrating on Low resources utilize Increase of Speed and Low Power utilization. To satisfy necessities, we move from AES on software approach to AES on hardware. To think about this, we are utilizing customized AES on Hardware Implemented on NEXYS 4 DDR Kit, their interface with Arduino through SPI protocol. The encrypted data further used in so many applications on Real time basics in industries.

Along these lines, this Paper concentrated on giving a novel methodology on Data Communication between Arduino and FPGA occurs and its interface with a Customized AES for the better speed and less resources use. The Paper separate into 5 sections and each Section is clarified as Section (I) An Introduction part, Section (II) Gives an Overview on different Issues in AES as Software library inside Arduino. In Section (III) AES execution on Hardware, at that point Section (IV) Highlights System Design and Implementation, Finally the Conclusion in section (V).

II AES AS S/W LIBRARIES ON ARDUINO

A noteworthy concern utilizing Arduino in Personal Security Device (PSD) is its restricted memory. The significant distinction between a broadly useful PC and the Arduino microcontroller is sheer measure of accessible memory. The Arduino UNO we are utilizing have just 32K bytes of Flash Memory, SRAM having size 2KBand 1K bytes of EEPROM. That is multiple times less physical memory than a Low-end PC. It prompts the issue of actualized any Encryption Library inside Arduino memory.

AES encryption for 128 bit requires 10 rounds of processing and for 192-bit keys require 12 rounds. For processing of each round include a single-byte based substitution step, a Row-wise permutation step, a column-wise mixing step, and

the addition of the round key. The encryption process will require some memory to store the temporary results and final encrypted results that goes in flash. Key will be in the EEPROM. If we reasonably add AES as software libraries it doesn't give enough room for other applications. Alternatively, if we use AES on Hardware, we diminish this problem to a certain extent.

Currently several hardware implementations of AES have been designed and published. There are, many design choices are encountered during hardware implementation of AES. In reality, these choices are limited to its application and budget. For performance point of view, major decision lies in trade-off between area and speed. To consider all these, we are Customized our AES that uses less resources and provide high speed. The complete AES-128-bit core is explained in section (III).

III. AES IMPLENTATION ON HARDWARE

AES 128-bit is written in Verilog language. The design is Complete 128-bit mode which is synthesized and verified. The design contain both encrypt/decrypt and key scheduler inside it and both the input and output are connected to SPI protocol for taking DATA through Arduino and Vice-versa.

The LUT put together usage of AES calculation with respect to FPGA is a customary methodology. It is basic and simple to execute the ideal usefulness. When it is integrated, it extensively possesses a less amount of area on FPGA. Inside our AES block, we have top level AES controller for control both encryption and decryption and with the help of MUX any one of between shift row, mix column and Plain text data is selected.

A. AES ARCHITECTURE FLOW

It's a 2-stage pipeline approach and takes 10 rounds to complete, the input data is 128 bits with each round requiring 1 cycle to complete. The AES architecture Flow is shown in Fig3.1.

A. Sub Byte

It is non-linear transformation where byte is replaced with a value in Sbox. The Sbox is predetermined for using it in the algorithm.

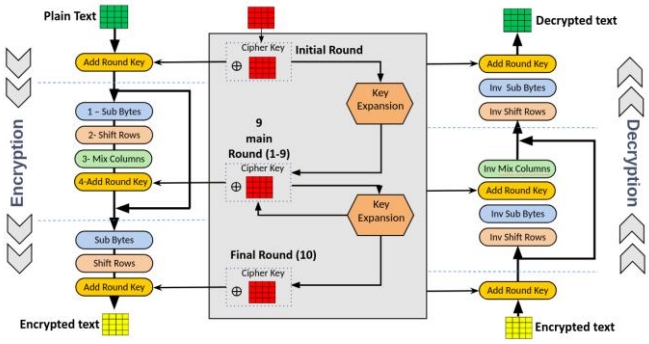

Fig 3.1. AES architecture Flow

B. Shift Rows

In shift Rows transformation, row of each state is cylindrically shifted left with different offset. First Rows is kept as it is and second row shifted by one byte and third row by two and finally the fourth row is shifted by three bytes left.

C. Mix Column Transformation

Mix column transformation is based on Galois field multiplication. Where each byte is replaced with particular value calculated. Each multiplication value is calculated using logic shown below.

$$S'(x) = a(x) \otimes S(x)$$
$$a(x) = \{03\} \times x3 \oplus \{01\} \times x2 \oplus \{01\} \times x \oplus \{02\}$$

Where x represents Galois field representation and xored gate for used.

D. Add Round key

The matrix of 16 bytes are consider as 128 bits and xored to 128 bits of the round key. If last round is this then output is 128 bits Encrypted output. Otherwise these 128 bits again going to the similar round considering 16 bytes.

The Data Flow path of both encryption and decryption is shown in Fig 3.2. Here in the 13 cycle's encryption completed and is obtained our data through 128-bit data out pins and Arduino for further processing.

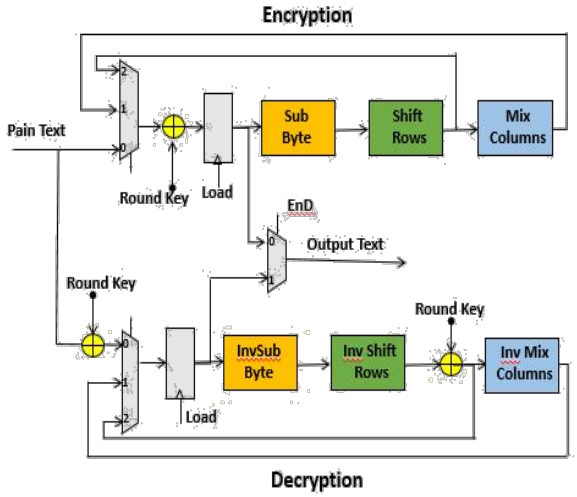

Fig 3.2. Data Flow path of AES 128-bit core

The complete block diagram and design hierarchy of AES block part at each level is shown in Fig 3.3 and fig 3.4

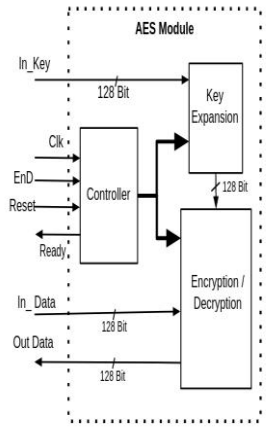

Interface signals of AES-128 core

S.No.	I/O Pin	Data Width	Direction	Description
1	Start	1 bit	Input	When it is true, Core will load input data and key, start encryption/decryption.
2	Reset	1 bit	Input	Reset the Core
3	EnD	1 bit	Input	Select mode, if it is false then Encryption , true then Decryption
4	In_Data	128 bit	Input	Input Data
5	In_key	128 bit	Input	Input Key
6	Clk	1 bit	Input	Clock
7	Out_data	128 bit	Output	Output Data
8	Ready	1 bit	Output	Encryption/Decryption is Over

Fig 3.3 Block Diagram of 128-bit AES core

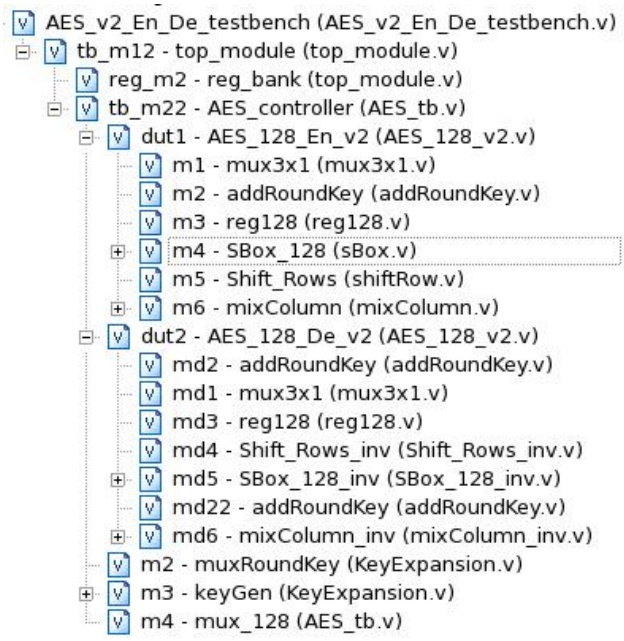

Fig 3. 4 Hierarchy view of AES Verilog code

IV. Proposed Appraoch and Experimental Setup

A. Proposed Approach

Firstly, we have taken data from PC in .txt format as input and then processed it through Arduino and converted it into bit format and then sending each bit data through SPI protocol working on 16MHZ to AES core implemented inside FPGA. After the Encryption is done data is send back to Arduino through SPI protocol. The communication of Data from PC to Arduino and FPGA to Arduino are monitored using Real Term serial analyser.

Arduino is programmed in Arduino IDE and the Pins declaration and EEROM to store the key value inside it first are shown below. Top level shows 5 main signals that are used for sending and receiving both data and clk.

```
#include <EEPROM.h>
#include <SPI.h>
int i = 0, j = 0;
int data_out = 17, data_in = 18, clk = 19, KEY = 12, SSEL =
16; int flag = 1;
//int time delay = 100;
int main_data[128];
void setup() {
Serial.begin(9600);
// start the SPI
 library: SPI.begin();
SPI.setBitOrder(MSBFIRST);
 //initalize the data ready and chip select
pins: pinMode(data_in,INPUT);
pinMode(data_out,OUTPUT);
pinMode(SSEL,OUTPUT);
pinMode(KEY,OUTPUT);
pinMode(clk,OUTPUT);
digitalWrite(SSEL,HIGH);
for (int i = 0; i < 128; i = i + 32) {
EEPROM.write(i,1);    //00000001
 EEPROM.write(i+8,2); //00000010
 EEPROM.write(i+16,3); //00000011
EEPROM.write(i+24,4); //00000100
}
}
```

B. SPI Protocol

The Serial peripheral interface, is a Synchronous Serial data communication protocol, used in sending data for short distance communication. It operates on frequency 16 MHz

provided by Arduino. The various signals used are described below.

1.) SCK: Clock signal
2.) MOSI: Master out slave in line
3.) MISO: Master In slave out line
4.) SS: Slave selection

C. *Experimental setup*

For realizing the design, we are using Arduino Uno and Nexys4DDR FPGA kit. It is a Digital circuit development platform based on Artix 7 FPGA from Xilinx having part no XC7A100T-1CSG324C.With its large, high capacity, it is suitable for Implementing AES.

In this implementation, for demonstration purpose we use "Hello_NITKKR" as input and encrypt data is shown on LCD as in Fig 4.1 AES as working on 200MHZ and it communicates with Arduino Through SPI working on 16MHZ, clock is provided by Arduino through Pin 19.

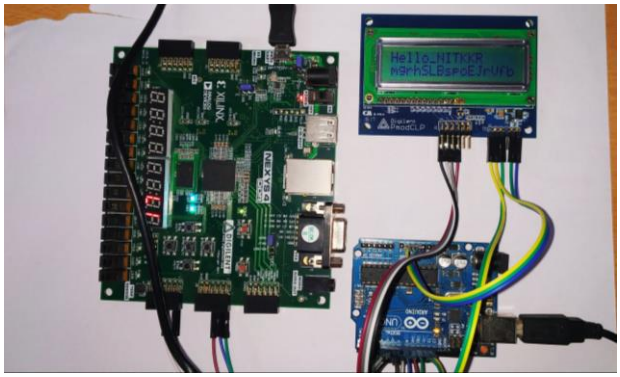

Fig 4.1. Experimental Setup

V.) EXPERIMENTAL RESULTS AND DISCUSSIONS

The AES utilize less resources and it provide high performance due to pipeline approach. The AES design utilize 389FF and 860 LUT. The top-level module of our project2 is shown below in Fig 5.1. It contains two SPI protocol modules, one for sending the data from Arduino to FPGA and second one for receiving the data back to Arduino from FPGA. Inside it we implemented our AES 128-bit core.

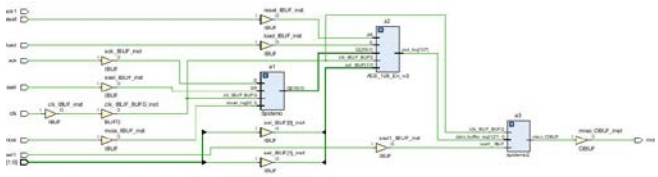

Fig 5.1. Top Level module

The Fig 5.2shows the resource utilization in our design which shows how less resources are used and how efficient that approach is.

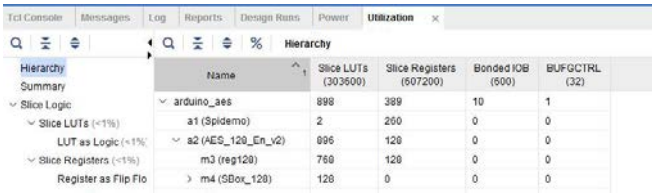

Fig 5.2. Resources utilization

The Fig 5.3 shows the Simulation result of design system i.e. AES output, here we are taking input from testbench and from the Encryption and Decryption Modules are instantiated inside our Top-level Module. The encryption module simulation results are verified.

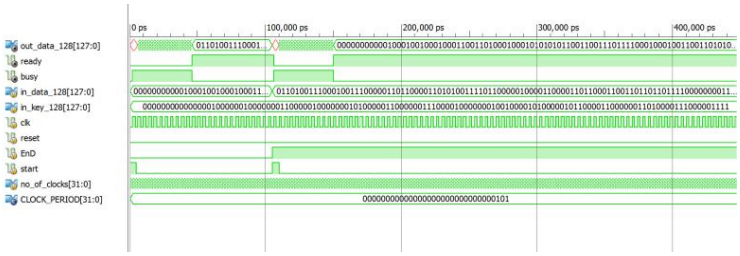

Fig 5.3 AES Encryption Module Waveform

VI.) CONCLUSION

This paper implemented the AES Core interface with Arduino as Hardware approach to provide sufficient space for Arduino to perform other functionality. While securing our data and dealing with data and control issues using SPI protocol, this interface provides an efficient speed performance and require least resources as 389 FF's and 860 LUTs used inside our FPGA. Further We can use this in Securable Arduino Applications where Security is also a major concern.

VII.) ACKNOLWLEDGMENT

This work is a part of SMDP-C2SD project under (Under MeitY). The authors acknowledge Dr. R.K Sharma and the technical and EDA tools provided in VLSI design lab.

REFERENCES

[1] Chandramohan, J., et al. "Intelligent smart home automation and security system using Arduino and Wi-fi." *International Journal of Engineering And Computer Science (IJECS)* 6.3 (2017): 20694-20698.

[2] Choi, Min-kyu, et al. "Wireless network security: Vulnerabilities, threats and countermeasures." *International Journal of Multimedia and Ubiquitous Engineering* 3.3 (2008): 77-86.

[3] Urien, P. An innovative security architecture for low cost low power IoT devices based on secure elements: A four quarters security architecture. In *2018 15th "IEEE Annual Consumer Communications & Networking Conference" (CCNC)* (pp. 1-2). IEEE. (2018, January)

[4] Pournaghshband, Vahab, Majid Sarrafzadeh, and Peter Reiher. "Securing legacy mobile medical devices." *International Conference on Wireless Mobile Communication and Healthcare*. Springer, Berlin, Heidelberg, 2012.

[5] Win, S. Z. Z., Htun, Z. M. M., & Tun, H. M). Smart security system for home appliances control based on internet of things. *International journal of scientific & technology research*, *5*(06), 102-107. . (2016).

[6] Prof. (Dr.) Khanna SamratVivekanand Omprakash., *"WIRELESS HOME SECURITY SYSTEM WITH MOBILE", IJAET*, Vol. 2, Dec. (2011).

[7] Kumar, Yogesh, and Prashant Purohit. "Hardware Implementation of Advanced Encryption Standard." *2010 International Conference on Computational Intelligence and Communication Networks*. IEEE, (2010).

[8] Jonwal, Sheetal U., and Pratibha P. Shingare. "Advanced Encryption Standard (AES) implementation on FPGA with hardware in loop." *2017 International Conference on Trends in Electronics and Informatics (ICEI)*. IEEE, (2017).

[9] Kamble, A., & Bhutad, S. (2018, January). Survey on Internet of Things (IoT) security issues & solutions. In *2018 2nd International Conference on Inventive Systems and Control (ICISC)* (pp. 307-312). IEEE.

[10] Kumar, J. S., & Mahalakshmi, C. Implementation of pipelined hardware architecture for AES algorithm using FPGA. In *2014 International Conference on Communication and Network Technologies* (pp. 260-264). IEEE. (2014, December).

[11] Ismat, T. *Comparative analysis of AES algorithms and implementation of AES in Arduino* (Doctoral dissertation, BRAC University). (2015).

[12] Fayed, M., El-Kharashi, M. W., & Gebali, F. (2006, December). A high-speed, fully-pipelined VLSI architecture for real-time AES. In *2006 ITI 4th International Conference on Information & Communications Technology* IEEE (pp. 1-2).

Proceedings of the Fourth International Conference on Communication and Electronics Systems (ICCES 2019)
IEEE Conference Record # 45898; IEEE Xplore ISBN: 978-1-7281-1261-9

To Evolve a Predictive Model for Dengue Incidence using Meteorological and Geo Spatial Data

N V Ganapathi Raju[1], P Gopala Krishna[2], Katapally Manognya[3], G S S Raj Kiran[4], Palakodeti Rohit[5], K Likhith[6]

Department of Information Technology, GRIET, Hyderabad, Telangana, India

Email: [1]nvgraju@griet.ac.in, [2] gopalakrishna@griet.ac.in, [3]manognya.katapally@gmail.com, [4]gssrajkiran@gmail.com, [5]rohitpalakodeti@gmail.com, [6]likhithkeetha@gmail.com

Abstract: Dengue is a mosquito-borne, fatal viral disease expanding as a global problem. Three climate factors effect dengue fever namely temperature, rainfall, and humidity, they are critical to mosquito survival, reproduction, and development and can influence mosquito presence and abundance. A Predictive model for the dengue incidence and its prevalence has been proposed by considering Kerala state's Dengue data. In prediction module the algorithm predicts the number of dengue cases that might occur in that month. In meteorological analysis the relationship between humidity, temperature, rainfall and dengue cases was studied. The machine learning algorithms employed for the prediction were Linear Regression, SVR and Kernel Ridge. Comparative study been done on meteorological and geo spatial analysis on the data. The parameters taken into consideration for geo-spatial analysis were district's distance from the equator, shortest distance from the nearest seashore and percentage of forest cover in district, altitude of the district.

Keywords: dengue fever, regression algorithms, meteorological and geo spatial analysis

I. Introduction

Dengue has emerged as one of the most important mosquito-borne, fatal viral disease, apparently expanding as a global health problem [1]. Dengue is rampant in urban poor areas, suburbs and the countryside. It is also very common in more affluent neighborhoods in tropical and subtropical countries [2]. Dengue is transmitted through mosquitoes namely Aedes aegypti and Aedes albopictus. The primary vector of dengue, Aedes aegypti, is ordinarily found between 35°N and 35°S. The whole tropical area including America, Asia and Africa is prone to dengue, and highly populated countries like India, Indonesia, Brazil, and China have the greatest burden of share.

An estimated 3.6 billion people are at risk for dengue, with 50 million infections per year occurring across 100 countries globally [1]. India has also been witnessed an increase in the incident of dengue fever. Kerala state has been recording a greater number of Dengue fever cases over the years. Kerala has seen 1304 dengue cases in year 2011, 4056 in the year 2012, 7938 in the year 2013, 2548 in the year 2014, 4114 in the year 2015, 7218 in the year 2016, 21993 in the year 2017 and 4083 in the year 2018.

The algorithms which were used for classification are support vector classifier, logistic regression, naïve bayes, out of which support vector classifier performed best scoring an accuracy of 92.85% with precision, recall and f1-measure being 0.93,0.93 and 0.92 respectively.

For regression linear regression, support vector regressor were used. As our data was non-linear in nature linear regression didn't perform well by just scoring an accuracy of 48.49% with mean absolute error and mean percentage error being 190.04535 and -0.69568688 respectively. Support vector regressor performed extremely well by fitting a polynomial curve and scoring an accuracy of 90.63% with mean absolute error and mean percentage error being 103.48891 and -0.38543662.

In geo-spatial analysis the geographical parameters of the districts like distance from sea shore, distance from equator, altitude and percentage of forest cover were studied and conclusions were drawn in terms of how the variance of their parameters is affecting the dengue cases.

II. Background Study

In this study, the Author [3] adopted Naïve Bayes and Multi-regression to understand the relation between meteorological parameters and the occurrence of Dengue epidemic, also used k-means clustering to identify areas with similar spreading patterns.

In this study, the Author [4] focused on the extrinsic incubation period (EIP) and its changeability in different climatic zones of India. The results suggested that temperature is important for the virus to develop in different climatic regions and may be useful in understanding spatio-temporal variations in dengue risk.

In this study, the Author [5] collected the monthly mosquito larval survey data of Thailand from January to December 2010 and the results suggested that Aedes larvae were found more in rainy reasons compared to any other season.

In this study, the Author [6] used a methodology involving geospatial analysis. The Dengue cases from 2011 to 2014 were used as inputs for the analysis. The results suggested that a relationship exists between the climatic conditions and dengue occurrence.

III. Methodology

The methodology of the paper consists of the following steps:

A. Data Collection

1. Epidemiological data

From January 2011 to December 2018 except the year 2017 was obtained from the Directorate of Health Services, Government of Kerala [7]. The number of confirmed cases registered were taken into consideration and studied.

2. Metrological Data

The Barometrical data, of Kerala state from January 2011 to December 2018 was obtained from worldweatheronline website [8] as on 27th January 2018. The data included Behavior of monthly rainfall, temperature and relative humidity values.

B. Data Preprocessing

1. Data Normalization

Before applying the algorithms, various preprocessing techniques were applied to the data. The data was normalized using StandardScaler from sklearn.preprocessing package. The weather parameters such as humidity, rainfall and temperature were scaled in such a manner that their mean and standard deviation were -1 and 1 respectively [9].

2. Correlation Analysis

There is good amount of correlation between the rainfall and dengue cases occurring in a month. 0.63 was the correlation coefficient. Also, there was fair bit of correlation between humidity and dengue cases occurring in a month 0.52. And there is a negative correlation of -0.20 between the temperature and the dengue cases occurring per month. The pointbiserialr correlation between month and dengue cases is 0.12 [10].

3. Feature Selection

Temperature was dropped from the data-set before training the regression models for the reason being that average monthly temperature throughout the state of Kerala doesn't change drastically [11].

4. Cross-Validation

For regression the data-set was divided into training and testing data-sets. 80% (67 rows) of the data were given for training and the remaining data 20% (17 rows) were given for testing [12].

5. Choosing the best hyper parameters

Algorithm model ( )
{
$Param_1$ _combinations:= [val_1,..... val_n];
$Param_2$ _combinations:= [val_2,.....val_n];

```
.
.
Param_n _combinations:= [val_1,..... val_n];
error:=100000
for i_1 in param_1 _combinations do
{
for i_2 in param_2 _combinations do
{
.
.
for i_n in param_n_combinations do
{
model=algorithm(param_1=i_1, param_2= i_2,..... paramn=i_n);
model.fit(x_train,y_train);
if error>mean_squared_error(model.predict(x_test),y_test):do
{
error= mean_squared_error(model.predict(x_test),y_test);
print (i_1, i_2,....., i_n);
}
}
}
}
}
```

This logic was implemented in order to extract the ideal set of hyper parameters of each algorithm (except Linear Regression) which can extract maximum performance from the model and generate least mean_squared_error. In the above algorithm the $param_1$_combinations,$param_2$_combinations,…..,para m_n_combinations are the lists which contain the various values which when taken together generate a combination of hyper parameters with which the machine learning algorithm is trained.

In the above algorithm error which is initialized with 1000000 is later updated with latest maximum accuracy value. When the trained model is generating higher accuracy score then the till now highest acc then we are updating the existing error with new minimum error and printing the combination of parameters which are giving the best results. In this way the best parameters for SVR and Kernel Ridge were chosen.

6. *Model Generation*

Regression: To predict the number of dengue cases that might occur in a month from 2011 to 2018 except 2017 based on the weather parameters and data of Kerala

- Linear regression and Support vector regressor were used for this purpose.
- The parameters of support vector regressor were tweaked and adjusted in order to extract peak performance from the algorithm.

IV. Results and Discussion

The paper is implemented on Python programming on Anaconda 3.4 distribution. The dataset consists of humidity, rainfall, temperature and month. The paper uses supervised machine learning algorithms for predicting dengue cases of Kerala state of South India.

A. *As a predictive task*

Fig 1 to Fig 7 depicts index values of all records in dataset on x-axis and respective dengue cases on y-axis.

1. *Linear Regression:*

LinearRegression(copy_X=True, fit_intercept=True, n_jobs=1, normalize=False)

The Data was non-linear in nature and as a result Linear Regression algorithm didn't really fare well and gave us an accuracy of 47.49%.

The MAE (Mean-Absolute-Error) is 190.0453500344 8942.

The MSE (Mean-Squared-Error) is 87781.036833493 05.

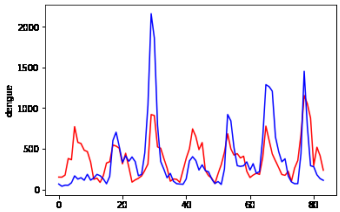

Fig 1 it is clearly visible that the model couldn't catch up to the sudden spikes during June and July in few cases.

The model is underestimating the values while testing. This is mainly accounted to the sudden spikes in the number of dengue cases in months of July and august which is the general trend in the state of Kerala as we have seen.

The coefficients of the features in linear regression decision curve- humidity, month, and rainfall were 62.60707993, -21.97886451, and 189.90310392. 376. 6528045066428 is the intercept of the fit equation.

Prediction = 62.60707993 (humidity) -21.97886451 (month) + 189.90310392 (rainfall) + 376.6528045066 428.

This clearly throws light on how different features ar e affecting the model. The dengue cases clearly depe nd on the amount of rainfall as it has the highest valu ed coefficient 182.90 followed by 62.60 of the feature humidity.

2. Support Vector Regressor:

support vector regressor with rbf kernel didn't really perform well as it is clearly visible in the below graph. The model specifically failed in fitting a curve which can take a sharp curve during the months of May, June and July. Accuracy of the model was 7%.

SVR(C=50.0, cache_size=200, coef0=0.0, degree=1. 0, epsilon=0.001, gamma=1.0, kernel='rbf', max_iter =-1, shrinking=True, tol=0.001, verbose=False)

MAE (Mean-Absolute-Error) is 180.6120357544998 9.
MSE (Mean-Squared-Error) is 153681.21744890077.

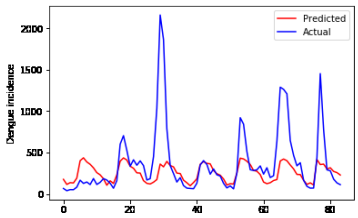

Fig 2 the model predicted very badly during the mont hs which had recorded very high dengue incidences.

SVR(C=50.0, cache_size=200, coef0=0.0, degree= 1.0, epsilon=10.0, gamma=1.0, kernel='linear', max_i ter=-1, shrinking=True, tol=0.001, verbose= F alse)

The model with linear kernel performed better than rbf kernel but when compared to polynomial kernel d idn't perform well. It scored an accuracy of 32.4%.

The MAE (Mean Absolute Error) is 177.9041777855 6534.
The MSE (Mean-Squared-Error) is 112893.94413108 726.

The linear kernel fitted a curve of decision curve with coefficients of the feature's humidity, month, and rai nfall being 3.20686362, 1.88293777, and 2.9 7340883. The intercept of the equation is 253.902288 14.

Prediction = 3.20686362 (humidity) + 1.88293777 (month) + 2.97340883(rainfall) + 253.90228814.

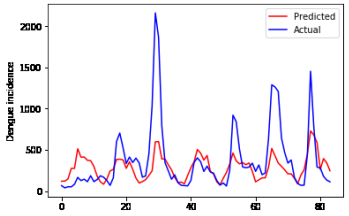

Fig 3 The model with linear kernel performed better when compared to rbf kernel but still is not the ideal kernel for prediction.

The Support vector regressor with polynomial kernel outperformed both rbf and linear kernels by a mile as it scored an accuracy of 90.63%.

SVR(C=50.0, cache_size=200, coef0=0.0, degree=4.0, epsilon=0.1, gamma=1.0, kernel='poly', max_iter=-1, shrinking=True, tol=0.001, verbose=False)

The MAE (Mean-Absolute-Error) is 103.4889107277 9048.
The MSE (Mean-Squared-Error) is 15635.611625347 123.

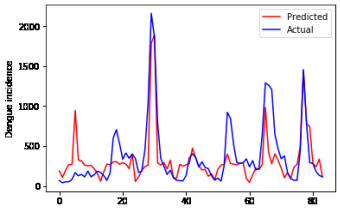

The model with polynomial kernel performed very w ell even during the sudden spikes in dengue incidence s during the months of June and July.

3. Kernel Ridge

3.1 Linear

The R^2 of the model on training with the model with linear kernel is -0.27. The negative value of the R^2 coefficient indicates that the model predicts values lesser than the mean of the target value distribution.

KernelRidge (alpha=1.0, coef0=1, degree=1, gamma =1e-06, kernel='linear',kernel_params=None)

The MSE (Mean-Squared-Error) of the model is 213211.95906435975
The MAE (Mean-Absolute-Error) of the model is 366.5700603704342

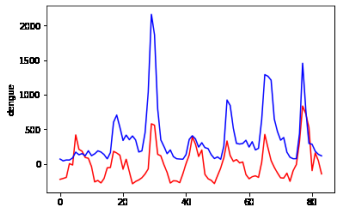

Fig 5 the linear kernel of Kernel Ridge performed the worst among all the kernels of SVR and Kernel Ridg e. It not only predicted way off the target during the J une and July but also during the non-monsoon month s during which the dengue incidences are very less.

3.2 poly

Kernel Ridge with polynomial kernel performed best among all the kernels of Kernel Ridge. The R^2 coefficient of the model is 0.87.

KernelRidge (alpha=100.0, coef0=1, degree=5, gam ma=1.0, kernel='poly',kernel_params=None)
The MSE (Mean-Squared-Error) of the model is 2008 9.045130779024
The MAE (Mean-Absolute-Error) of the model is 108 .96932376142536

The curve was well fit and when compared to the oth er two kernels of the Kernel Ridge.

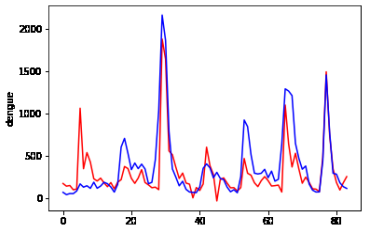

Fig 6 the polynomial kernel of Kernel Ridge performed second best among all the models. It performed decently during the sudden spikes in dengue incidences.

3.3 Rbf

Kernel Ridge with rbf performed better than the linear and rbf kernels of the SVR's rbf and linear kernels. The R^2 of 0.58.

KernelRidge (alpha=1e-05, coef0=1, degree=1, gam ma=0.001, kernel='rbf', kernel_params=None)

The MSE (Mean-Squared-Error) of the model is 6883 6.23541726012
The MAE (Mean-Absolute-Error) of the model is 158 .31175149670418

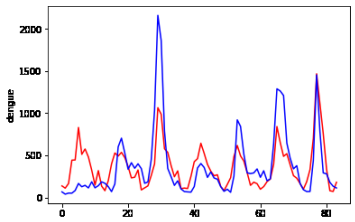

Fig 7 the rbf kernel of the Kernel Ridge performed better than the rbf kernel of the SVR but it is not the ideal model for predicting the dengue incidence.

B. Meteorological Analysis

Here humidity and rainfall refer to the monthly averages of the respective parameters. In fig 8 the red dots indicate the scenarios in which the dengue cases occurring in a month were more than 400. The blue dots indicate the scenarios in which the dengue cases occurring in a month were less than or equal to 400.

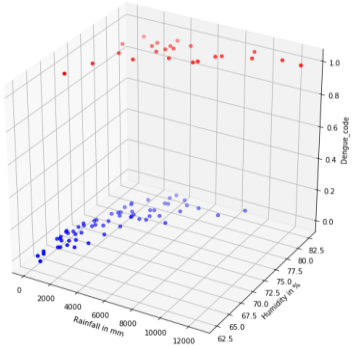

Fig 8 is a 3-Dimensional plot to understand the relationship between humidity, rainfall and the magnitude of dengue epidemic occurrence.

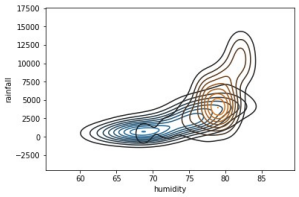

Fig 9 is KDE plot indicates the ranges of values in which majority of points belonging to a class label are existing. In this figure the blue spirals indicate the existence of scenarios with dengue cases less than 400 (n<=400) and the orange spirals indicate the existence of scenarios where the dengue cases are

greater than 400 (n>400). The more densely are the spirals indicates that a greater number of points of a particular class label are occurring in that particular region.

In the case of the blue points, they are generally occurring when humidity is varying between 66 % - 75%. At the same time the rainfall is varying in between as low as 63mm-8000mm. But the density of blue points decreases as both rainfall and humidity increase. More number of blue points can be observed when the humidity is in between 66% - 72% and rainfall is in between 63mm-2500mm.

In the case of red points, they are mostly occurring when the humidity is in the high 70's (77%-82%) or higher and when the rainfall is range 2500mm – 5500mm.

By this analysis it can be concluded that the ideal conditions for aedes aegypti to breed would be humidity 77% - 82% and rainfall 2500mm – 5500mm.

1. Study on effect on dengue cases changes in meteorological parameters throughout the time period from 2011-2018 (except 2017)

In the state of Kerala generally the dengue cases rapidly increase after the month April as Kerala experiences an early monsoon when compared to the rest of the India. Monsoon in Kerala starts right in the end of May. This is when things start to change.

The fig 10 and fig 11 depict the monthly variation of humidity, temperature, rainfall and dengue cases in terms of percentages with respect to previous month.

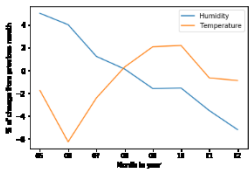

Fig 10

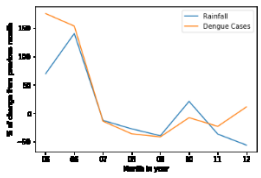

Fig 11

The mean-humidity increases by 5.02% and mean-rainfall increases by 69.49% and a -1.74 % decrease in mean-temperature from April to May and as a result dengue cases increase by 175%.

While going from May to June mean-humidity increases by 4.02% and mean-rainfall increases by 140.14% and mean-temperature falls by -6.26% which lead to an increase of 153% in dengue cases when compared to May.

And then going from June to July mean- humidity increases slightly by 1.23% and mean-rainfall decreases by -12.38% and mean- temperature decreases by -2.41% as a result dengue cases decrease -13.18%. This is expected as June in Kerala has highest mean rainfall and dengue cases.

This trend continues till September and from there on the dengue cases tend to decrease as time passes.

Figs 12 to 15 depict the variation of monthly mean values of humidity, temperature, rainfall and dengue cases with respect to their respective mean values.

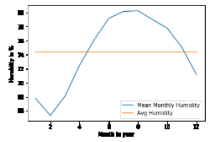

Fig 12

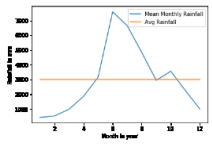

Fig 13

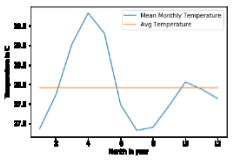

Fig 14

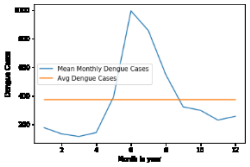

Fig 15

It is clearly visible that whenever there is a rise in dengue cases there is also rise in mean- humidity and mean-rainfall, while there is a descent in mean-temperature.

C. Geo Spatial Analysis:

To study and understand the relationship between geospatial parameters and the dengue cases in the state of Kerala:

- The data considered for this study was the cumulative data of dengue cases district wise taken from the year 2011-2018(except 2017)

- Study was done on how the variation of geospatial parameter like distance from the seashore and distance from the equator of a district affected the dengue cases recorded in that particular district in the time period of 2011-2018(except 2017).
- Study was done on how the variation of geospatial parameters like percentage of forest cover and altitude of a particular district affected the number of dengue cases recorded in the time period of 2011-2018(except 2017).

In the fig 16 and fig 17 dark green points represent the districts which recorded total dengue cases in the range 0 – 1000, dark blue points represent districts which recorded total dengue cases in the range 1001 – 2000, light blue points represent districts which recorded total dengue cases in the range 2001 – 3000, light green points represent districts which recorded total dengue cases in range 3000 – and above from 2011 – 2018.

1. *Distance from nearest sea-shore vs distance from equator:*

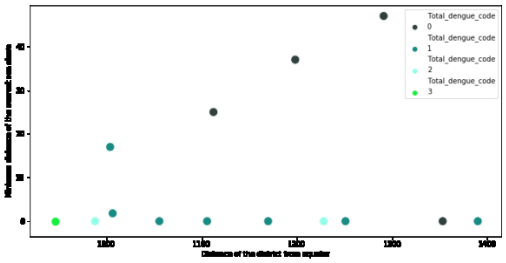

In the fig 16 Idukki (1112.3,25), Palakkad (1198.30,37), Wayanad (1291.23,47), Kannur (1353.30,0), Pahtanamthitta (1003.73,17), Kottayam (1006.35,1.8), Alappuzha (1055.45,0), Ernakulam (1105.61,0), Thrissur (1169.77,0), Kozhikode (1251.07,0), Kasargode (1390.19,0), Kollam (987.85,0), Malappuram (1228.20,0) and Thiruvananthapuram (945.86,0).

Fig 16 depicts the relationship between distance from equator and Minimum distance from the nearest seashore.

The general trend here is as both the distance from the coast and equator increase the dengue cases count is taking a hit. The only light green point which is Thiruvananthapuram is a coastal district and also it is the closest district to the equator of the earth 945.86 km and it recorded 12000+ dengue cases. The districts of Wayanad, Palakkad, and Idukki are 47.5 km, 37.5 km, 25 km away from their nearest sea shores. Also, their distances from equator of the earth are 1291.23 km, 1198.30 km, 1112.3 km respective. All the three districts are far ideal range from both the parameters as a result they recorded very a smaller number of dengue cases during 2011 – 2018 which are as low as 571, 893, 770 cases respectively.

There is one outlier in this graph which happens to be Malappuram. Though its distance from equator is as high as 1228.20 km it still was able to generate high number of dengue cases due to the following reasons, It is a coastal district, Also it is the most populated district of Kerala with 41,12,920 and also a high population density of 1158 people per sq. km. Due to high population and population density there is a good scope for the dengue epidemic to spread among more people as a single aedes mosquito carrying can inject the virus into many people.

2. *Altitude of district vs % area occupied by forest in district:*

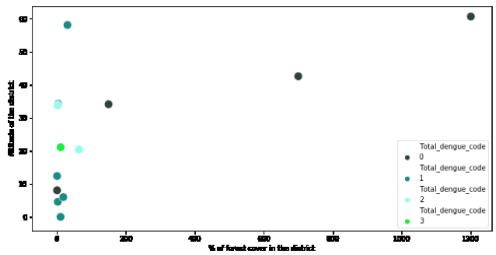

In the fig 17 Idukki (1200,60.62), Palakkad (150,34.09), Wayanad (700,42.56), Kannur (1.02,8.06), Pahtanamthitta (31,58.05), Kottayam (3,4.57), Alappuzha (11,0.004), Ernakulam (4,34.41), Thrissur (2.83,33.73), Kozhikode (1,12.39), Kasargode (19,5.99), Kollam (3,33.74), Malappuram (64,20.39) and Thiruvananthapuram(10,21.16).

Fig 17 depicts the relationship between altitude of the district and percentage of forest cover in district.

The general trend here is as the altitude increases the dengue cases are decreasing. But when it comes to percentage of forest cover districts like Thiruvananthapuram, Kollam, and Malappuram

which recorded very high dengue cases are having forest cover in range of 20% - 33%. In the remaining scenarios where the forest cover is below 20% or above 33% the dengue cases took a hit. Districts like Alappuzha, Kottayam, Kasaragod, Kannur, Kozhikode which are having percentage of forest cover less than 20% as a result they have recorded lower number of dengue cases. Whereas the districts like Pahtanamthitta, Wayanad, and Idukki are having percentage of forest cover greater than 33% and even they recorded a smaller number of dengue cases.

Even though the district of Palakkad has the percentage of forest cover near to 33% it recorded a smaller number of dengue cases because it has higher altitude when compared to other districts in that range. The districts Ernakulum and Thrissur despite having very low altitude and forest cover percentage lying in the range of 20% - 33% failed to record higher number of dengue cases due to their distance from the equator of the earth being seemingly high.

The districts Wayanad and Idukki have recorded least number of dengue cases when compared with other districts of Kerala; this is due to them being at a higher altitude of 700m and 1200m respectively. Also their percentage 42.56% and 60.62% of forest cover respectively are above the ideal range which is 20% - 33%. As altitude increases the average temperature of the district decreases, this effect the survival of aedes aegypti as they are most likely to survive in high 20's which is around 28 to 30 degrees Celsius. The average temperatures of Wayanad and Idukki are 24.25 and 25.55 degrees Celsius respectively. Also, as the forest cover increases this generally leads to decrease in population of a particular district as people generally tend to live civilizations away from forests. If the forest is occupying the majority of the district's area, then it is most likely that the population and population density of the district decrease. Generally, when there is less population density the scope for dengue spreading decreases. It is observed that the districts Wayanad, Idukki and Pahtanamthitta are having forest covers of 42.56%, 60.62% and 58.05% having very low population of 817,420, 11,08,974 and 11,97,412 respectively , these are lower than the average population of a district of Kerala which is 23,86,147. Also, their population densities are lower 383, 254 and 453 respectively compared with the average population density of a district of Kerala which is 911.

V. Conclusion

The SVR algorithm with polynomial kernel performed the best among all the algorithms. But apart from the polynomial kernel of the SVR the remaining two kernels rbf and linear didn't perform as well as the rbf and linear kernel of Kernel Ridge algorithm. Both Kernel Ridge and SVR use l2 regularization but they use different loss function. The SVR uses epsilon intensive loss function whereas the Kernel Ridge uses squared loss function. Linear Regression didn't perform up to the mark. This is expected as the nature of the data is non-linear. In the meteorological analysis the findings suggest that the ideal conditions for occurring of high number of dengue incidences the average monthly humidity should be in range 77%-82% and average monthly rainfall should be in range 2500mm-5500mm. Also, the variation of average monthly humidity is affecting the occurrence of dengue incidences to higher extent when compared to what variation of average monthly rainfall. The findings found in geo-spatial analysis were that as the distance of the district from the equator increased the occurrence of dengue incidences decreased. Also as the distance from the nearest sea-shore increased the occurrence of dengue incidences decreased. The ideal amount of forest cover to be present in the district in order to record higher dengue incidences is 20%-33% area in total area of the district. As the altitude increased the prevalence of dengue incidences decreased in the state of Kerala.

References

[1]. Das, Sushmita, et al. "Impediments of reporting dengue cases in India." *Journal of infection and public health* 10.5 (2017): 494-498.

[2]. Dengue control, WHO, https://www.who.int/denguecontrol/disease/en/, Accessed: 20- jan- 2019].

[3]. https://www.currentscience.ac.in/Volumes/114/11/2281.pdf

[4]. Mutheneni, Srinivasa Rao, et al. "Dengue burden in India: recent trends and importance of climatic parameters." *Emerging microbes & infections* 6.1 (2017): 1-10.

[5]. Wongkoon, S., M. Jaroensutasinee, and K. Jaroensutasinee. "Distribution, seasonal variation & dengue transmission prediction in Sisaket, Thailand."

The Indian journal of medical research 138.3 (2013): 347.

[6]. Jonna Sara V, Soman B, "Dengue Fever and Climate Analysis in Thiruvananthapuram, Proceedings of IRF International Conference, 2nd August 2015, Jaipur, India, ISBN: 978-93-85465-67-3

[7]. Directorate of Public Health, http://dhs.kerala.gov.in/index.php/publichealth.html

[8]. WorldWeather, https://www.worldweatheronline.com/

[9]. https://scikitlearn.org/stable/modules/generated/sklearn.preprocessing.StandardScaler.html

[10]. https://docs.scipy.org/doc/scipy0.14.0/reference/generated/scipy.stats.pointbiserialr.html

[11]. https://towardsdatascience.com/feature-selection-correlation-and-p-value-da8921bfb3cf

[12]. https://scikitlearn.org/0.16/modules/generated/sklearn.cross_validation.train_test_split.html

Proceedings of the Fourth International Conference on Communication and Electronics Systems (ICCES 2019)
IEEE Conference Record # 45898; IEEE Xplore ISBN: 978-1-7281-1261-9

Pedestrian Detection Using Deep Learning

Ponugumati Pavani
Department of Information Technology
V.R.Siddhartha Engineering College
Kanuru, Vijayawada-7
pavani.p1998@gmail.com

Kodali Bhavana
Department of Information Technology
V.R.Siddhartha Engineering College
Kanuru, Vijayawada-7
kbhavana56@gmail.com

Duvvaki Venkatesh
Department of Information Technology
V.R.Siddhartha Engineering College
Kanuru, Vijayawada-7
duvvakivenkatesh4@gmail.com

Suneetha Manne
Professor and Head, Department of Information Technology
V.R.Siddhartha Engineering College
Kanuru, Vijayawada-7
suneethamanne74@gmail.com

***Abstract*— This paper makes a specialty of the utility of Convolutional Neural Networks for pedestrian detection. This is important for self riding vehicles. Work in this area become based on function based totally methods for a while earlier than convolutional neural networks have been implemented to it. On this work, a convolutional neural network based totally pedestrian detection pipeline become installation the use of the AlexNet and ResNet algorithms. Those had been trained on a subset of the Caltech Pedestrian Database and then tested on another subset of the database. It changed into determined that both the methodologies executed pretty nicely in detecting pedestrians from the specified photos. But the outcomes seemed a bit too constructive due to the small dataset used to check the consequences. Exams on the complete dataset is required to verify whether or not the methodology works well.**

Keywords*— *Convolutional Neural Networks; pedestrian detection; AlexNet; ResNet;

I. INTRODUCTION

Object detection has been an essential and challenging a part of laptop imaginative and prescient issues. It is a vital component of many regions which includes robotics, autonomous systems, protection systems, and unmanned aerial automobiles. Pedestrian detection, is a sub-part of item detection wherein the aim is to take both a frame (an picture) or video and stumble on the presence of human beings (human beings) in the picture. This has been a subject of studies over the last few years as it is an crucial factor of self sufficient/self- using vehicles. It can also be used as a protection feature for present motors to come across pedestrians and warn the driver, as well as in security structures like site visitors cameras. For this paintings we cognizance on detection in frames/pictures. Moreover even as sensible structures require real time detection, we do no longer attempt to speed up the test/detection mechanism. As a result the problem input reduces to a hard and fast of images containing or now not containing pedestrians, which are fed into the pedestrian detection pipeline (defined underneath) containing a convolutional neural community. The neural network is needed to offer a bounding container indicating the presence of a pedestrian. As a sliding window technique (defined below) is used for photo subsampling, the CNN gets a hard and fast of cropped images and the output is a class declaring whether the cropped photo contains a pedestrian or now not. The submit-processing strategies use this output to compute the bounding containers.

II. RELATED WORK

To start with function primarily based strategies were implemented to this hassle. With the resurgence of convolutional neural networks, those were carried out to the trouble as well. Function-based strategies Supervised and unsupervised studying techniques have been applied to this trouble. The paintings of Rowley[6] which carried out neural networks for facial detection become a first step on this course with the point of interest on function primarily based detection. The work via Viola and Jones[7] among 2001 and 2003 was a first-rate milestone in pedestrian/item detection. They used an crucial photograph representation and a new feature detection/mastering set of rules based on AdaBoost. This become accompanied by means of the work of Dalal and Triggs[5] on Histograms of oriented Gradients (HOG) for human detection which ended in addition enhancements to

feature primarily based prediction and pedestrian detection systems. Those have been followed by using improvements to the characteristic based methods with the intention to improve characteristic-based totally detection. However maximum of these techniques used function-based totally detection coupled with SVM regression methods to carry out pedestrian detection. The overview papers by using dollar et al. In 2009[2] and 2012[4] summarize the different function based techniques in detail and examine their performance on the Caltech pedestrian database[3].

III. Proposed Method

A. Convolutional Neural Networks

However since 2012, convolutional neural networks have revolutionized the sphere of laptop imaginative and prescient and photograph detection. Architectures like AlexNet[12] and GoogleNet[13] reduced the mistakes within the picture internet project by using report degrees. This has caused a sizable shift inside the method of the network with convolutional neural networks being applied effectively to a huge wide variety of vision and photograph classification issues. Due to the fact convolutional neural nets are a brand new idea, their software to pedestrian detection systems remains in its infancy. The paintings by means of Tome et al.[1] in 2015 applied CNNs to this problem. The work checked out the overall performance of different area concept and function extraction methods coupled with a CNN. Each the AlexNet and the GoogleNet architectures have been studied. Different paintings inside the same time frame consists of the work by using Fukui et al.[10], Sermanet et al.[8] and Angelova et al.[9] . Some of these procedures perform a feature extraction from the image and then use CNNs for classification. A distinctive approach turned into observed within the thesis of Molin, D [11] where the community takes within the complete photo as an enter (in preference to a characteristic) and generates the chance of a pedestrian at the photo pixels (at a place) as the output. The method whilst giving results just like present methods changed into a shift from present methods discovered. R-CNN based totally pipeline turned into recently correctly applied to this problem[17].

B. Methods

Solving the pedestrian detection problem requires the putting in place of a pedestrian detection pipeline as shown in parent 1. The pipeline contains a vicinity concept technique, a function extraction pipeline and a place classifier. In the case while an R-CNN method is used (no longer here), the vicinity concept and the feature extraction techniques are part of the R-CNN.

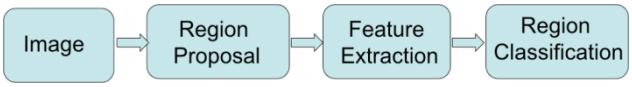

Fig.1 Pedestrian Detection Pipeline

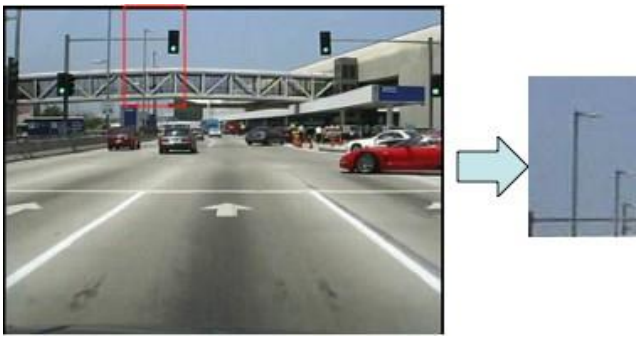

Fig.2 Sliding window approach

For area idea, a sliding window technique is followed right here. At some point of this technique, sections of the snap shots (sub pics) , which could have special sizes/component ratios are extracted from the picture. As shown in figure 2 where the purple phase/window is extracted as a feature. Those are then fed into characteristic extractor. The sliding window approach is used each at some point of schooling and take a look at runs within the same style. The characteristic extractor for earlier implementations turned into a simple HOG like function detector. For this technique the convolutional neural network (CNN) is used as a characteristic extractor. The cropped photo from the sliding window detector is surpassed directly to convolutional neural community. Inside the education runs, the photograph is preprocessed by first scaling the image (that is smaller). For maximum of the cases, the sliding window detector is ready to go back photographs of size 96x48. Those are scaled to required length of the CNN (224 x 224) inputs. The images are then normalized (subtracting a mean and scaling with the aid of a well known deviation). Education is then completed on those photographs in batches of 32. CNN architectures are attempted as characteristic extractors, AlexNet[12] and a 18 layer ResNet[14]. The AlexNet architecture has been applied to the trouble in present literature but no cases of the ResNet being implemented to the hassle were found via the author. As a consequence reading how well the ResNet performs at the hassle as compared to the other architectures changed into seen to be an interesting problem.

In education mode, once the set of the scaled and normalized photos are passed to the CNN (each architectures), it is skilled

in batch mode (32 photos/batch) the usage of a Nesterov momentum based SGD method. The presence of the bounding containers within the scaled photograph for the training snap shots is handed on to the CNN for training. At some point of the take a look at opinions, the photographs are handed to the CNN which classifies it as magnificence zero or magnificence 1 and those magnificence values are extracted out of the pipeline. These may be used to test the check accuracy of the CNN.

The AlexNet version is a 8 layer CNN containing five convolutional layers and 3 fully connected layers. It is a distinctly simple however pretty powerful version that turned into attempted for its simplicity and its effectiveness. The info of the version are defined in Reference.

The ResNet is a fairly complex CNN with many layers. An 18 layer network is used for this paintings although a good deal large layers were used for other packages. The simple concept of the ResNet (Residual network) is that unlike previous architectures, the community additionally has connections between neurons 2 layers aside. As a result the trade layers acquire statistics from neurons that aren't simply within the preceding layer permitting the features in that layer to be laid low with greater neurons and layer with feature sets. Information of the technique are described in Reference.

The closing step of the pipeline is a category pipeline is the classifier. For the contemporary examine, the classification hassle is stored simple with two training, man or woman detected (elegance zero), individual now not detected (class 1). But, a more complicated problem with lessons together with vehicles detected, and so on. Can be solved using the identical method with the aid of converting the final fully linked of the CNNs. The softmax classifier is used right here. The components for the loss is proven in Equation 1 (taken shape the CS231N notes)[18] wherein Li is the loss associated with sample i, and fyi is the elegance score of the magnificence y for pattern i

$$L_i = -\log\left(\frac{e^{f_{yi}}}{\sum_j e^{f_j}}\right) \quad \text{- Equation 1}$$

Furthermore, those can be used for in addition publish processing. The sub pics may be regrouped into their figure photos and based at the magnificence detected, the bounding container may be created inside the picture. Furthermore, these can be used to generate other evaluation/checking out metrics, which includes the ones distinctive inside the paper through dollar et al[2,4].

The pedestrian detection pipeline is setup in Torch7[19] the use of current implementation in torch which have been changed to in shape into the pipeline. Python scripts were used for pre and submit processing. The overall CNN testing and education framework was obtained by using modifying the ResNet implementation on github through facebook [15,16]. This implementation carries the resent along with and interface to load/preprocess pix, educate using sgd and run take a look at opinions. This framework turned into tailored to allow different networks (AlexNet obtained from the paintings of Soumith[20,who installation a fixed of ConvNet benchmarks on github) to be plugged in and incorporated with the pedestrian detection pipeline. Post-processing modules were introduced to permit extraction of the check/assessment results for further publish processing.

C. Dataset and Features

The Caltech Pedestrian Database[3] containing approximately 250,000 frames (60x480) with 350,000 bounding containers is used to attain education and take a look at statistics. This is a well known take a look at for the pedestrian detection hassle. The dataset is described in element in the paper by dollar et al[2,4]. Samples from the database are proven in parent 3. As shown some of the photograph incorporate a single pedestrian, some incorporate multiple pedestrians and some do now not incorporate any pedestrians. Moreover in some of the pix the pedestrians are clearly seen and are large in length(towards the digital camera) whilst in some of the snap shots, the pedestrians are occluded with the aid of items or very small(far faraway from the digital camera). The dataset consists of 11 periods of information amassed from video taken driving around busy streets. Periods 0 to five are assigned to the education set and the final are assigned to the check set. The pics are obtained as .Seq documents which have been preprocessed the use of matlab code received along aspect the database at the Caltech Pedestrian Database web site[3] and python code. The bounding boxes round the pedestrian is likewise Supplied as a set of text documents (again those want to be extracted from a compressed report using matlab code furnished). Each report corresponds to a body/picture inside the database and is empty if no pedestrian is gift or contains the coordinates of the bounding bins if someone/multiple humans are gift.

The dollar et al. Paper cautioned that each 0.33 frame inside the schooling set is taken as a schooling pattern and each 30th image inside the check units are used as take a look at samples. However the sliding technique resulted in the pix being in addition divided into approximately 50 sub images. This made the training and test pattern sizes intractable for this paintings because the schooling times had been becoming extraordinarily long and even trying out a assignment. Consequently the datasets were in addition sampled from. The

schooling dataset changed into sub sampled (randomly) to 2000 snap shots (around one hundred thousand pictures for the CNN) and the check set become also decreased to 1500 pictures through random sampling. The aim is to re- run the answer on larger datasets once basic pipeline is completed validated. The same old evaluation metrics for the accuracy of the detection system is described inside the paintings via greenback et al and additionally in Tome et al. For each set of rules/architecture, the pass over charge (MR) and the variety of false positives in keeping with image (FPPI) are measured. For each bounding container, if the bounding box distinctive by the set of rules and the actual bounding field (reality fee) do now not overlap by greater than 50% of their location, then it's miles considered as miss or a false negative. If the bounding field is particular by the set of rules in a region that does not contain a (fact)bounding container/pedestrian, then it is considered a false fantastic (FP). That is used to compute the quantity of fake positives according to image (FPPI) and averaged. The pass over charge (MR) is the ratio of the range of false Negatives to the variety of effectively diagnosed boxes (Positives). But as defined in the segment under, because the type effects seem unrealistic, the usual CNN metrics of check accuracy are used for the time being. Yet again realistic effects are received by using training/trying out on a larger dataset and making sure that the pipeline itself isn't always fallacious (in its implementation), those metrics could be used/defined.

D. Experiments/ Results/ Discussion

To teach the community, the photos are first handed thru the sliding window detector which generates a fixed of smaller sub snap shots for education. Those are then publish-processed and fed into the CNN for education. The Nesterov momentum method is used for education. Exceptional mastering costs are attempted for each the architectures and the first-class acting values are selected (0.1 for the Resnet and zero.01 for the AlexNet). The momentum value is set at 0.9 and the Weight decay is 1e-4. For both the networks, the training set is run for a couple of epochs (6 for AlexNet, three for ResNet) with a batch size of 32 picsan iteration.

Discern four suggests the evolution of the loss feature in the course of training for each the CNN architectures. Whilst training was performed for more than one epochs, we see that the loss is appreciably decreased inside the first 100 or so iterations after which doesn't alternate drastically. The loss for the ResNet comes down a lot faster than the AlexNet. The education became achieved for 2000 schooling pics that resulted in a complete of about

Fig.3 Samples from the Caltech Pedestrian Database

As hundred thousand photos. The take a look at accuracies for the skilled models had been proven to be extremely high (round five% for both the architectures). This regarded to be an exceedingly constructive measure of performance. A good way to determine the motives, the algorithm and the training and take a look at set changed into checked out in greater element. It turned into determined that the schooling images generated by the sliding window (as proven in figure 5 carries a couple of times of clear human beings (full line character inside the photo) and of sections of humans. Similarly there have been also samples containing just the road, simply the automobile, lampposts and many others (parent 6). The sliding window generator generated only some images throughout education that contained humans a long way away/combined with the background/trees and so on. Consequently the community overfitted for those instances.

Fig.4 Images with/without people that are not classified correctly

Throughout take a look at due to the incredibly small quantity of photographs, maximum of the photos had been dominated no person gift (discern 5) (automobiles, empty avenue) or someone without a doubt gift much like cases proven in figure 5.

The instances that the set of rules had trouble with (shown in figure 6) were smaller in number. Thus the overfitted version done properly on the test set as well. To triumph over this

trouble, using a larger pattern set containing extra check pictures is required. Other reasons are also being investigated.

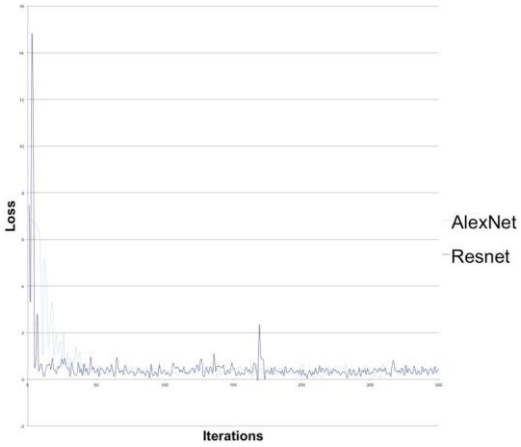

Fig.5 Training results of the CNNs

Fig.6 Images with people clearly defined (easily classified)

Fig.7 Images without people (only road etc) easily classified

It turned into also located that the use of a sliding window method for characteristic detection resulted inside the hassle becoming extremely big (in terms of statistics size) requiring down sampling. Moreover the sliding window carried out become no longer clever sufficient to tug out human beings successfully(with out reducing) especially in cases in which the humans had been a small part of the entire frame (a long way far from the digicam). This likely resulted inside the overfitting and wrong take a look at outcomes. Therefore for future paintings, transferring to an R-CNN primarily based approach in which the CNN acts as each the region inspiration and the feature detection techniques is recommended.

IV. Conclusion and Futurescope

As a part of the take a look at, a pedestrian detection pipeline became installation the use of the Torch7 framework leveraging present implementations [15,16,18,19,20]. A sliding window detector changed into used for area proposal and both the AlexNet and 18 layer ResNet had been used for function detection with the softmax feature serving as a classifier. The hassle turned into formulated as a binary category trouble (individual detected or character now not detected).

Regrettably the effects obtained indicated that the model become possibly overfit and because of the down sampling of the check set, test accuracies had been overoptimistic. The model works fairly nicely for cases wherein people are certainly present inside the frame or completely absent within the frame but doesn't in reality work well for instances of occluded pedestrians or for cases of small pedestrians (far from the digicam).

The subsequent steps to be performed involve schooling the picture on a much larger schooling set and testing the overall performance on a bigger test set, furthermore, which will put off the trouble of too many samples that occurs because of the sliding window technique, transferring to a R-CNN approach, which get rid of the sliding window detector could be attempted.

ACKNOWLEDGMENT

This work is supported by Dr.Sunnetha Manne, Professor and Head, Department of Information Technology from VR Siddhartha. We thank our colleagues who provided insight and expertise that greatly assisted the research.

REFERENCES

[1] Tome, D., Monti, F.,.Baroffio, L., Bondi, L., Tagliasacchi, M., Tubaro, S., “Deep convolutional neural netwoks for pedestrian detection.”, Preprint. Elsevier magazine of sign Processing: photograph communique, 2015.

[2] dollar,. P, Wojek, C., Schiele, B., Perona, P., “Pedestrian Detection: An assessment of the country of the art.”, IEEE Transactions on sample analysis and gadget Intelligence, ISSN:0162-8828, August 2011.

[3] http://www.Vision.Caltech.Edu/Image_Datasets/CaltechPedestrians/

[4] dollar, P., Wojek, C., Schiele, B., Perona, P., “Pedestrain Detection: A Benchmark”, IEEConference on pc vision and pattern popularity, 2009

[5] N. Dalal and B. Triggs, “Histograms of oriented gradients for human detection”, IEEE convention on pc imaginative and prescient and pattern reputation, 2005.

[6] Rowley, A. H., Baluja, S., Kanade.,T, ”Neural network-primarily based face Detection”, IEEE Transactions on sample evaluation and system Intelligence, January 1998.

[7] Viola, P., Jones, M., “strong actual-time item Detection”,2nd global Workshop on Statistical and computational theories of vision, modeling , learning, computing and sampling, 2001.

[8] Sermanet, P., Kavukcuoglu, ok.,Chintala, S., LeCun, Y. “ Pedestrian Detection with unsupervised Multistage characteristic mastering”, global convention on pc imaginative and prescient and pattern recognition, 2013.

[9] Angelova, A., Krizhevsky, A., Vanhoucke, V., Ogale, A., Ferguson, D.,“actual-Time Pedestrian Detection with Deep network Cascades”, White Paper

[10] Fukui, H., Yamashita, T., Yamauchi, Y., Fujiyoshi., H,Murase, H., “Pedestrian Detection primarily based on Deep Convolutional Neural community with ensemble Inference network”, IEEE sensible vehicles Symposium, 2015

[11] Molin,D., “Pedestrain Detection using convolutional neural networks”, Phd Thesis, department of electrical Engineering, LinkopingsUniversitet, Sweden, 2015

[12] Krizhevsky, A, Sutskever, I , Hinton, G.E. “ photo internet classification with deep convolutional neural networks”, Advances in neural information processing structures, 2012

[13] Szegedy, C., Liu, W, Jia, Y., Sermanet, P., Anguelov, D., Erhan, D., Vanhoucke, V., Rabinovich, A., “Going Deeper with Convolutions”,ILSVRC 2014

[14] He, ok., Zhang, X., Ren, S., sun, J., “Deep residual learning for photograph recognition”, ILSVRC 2015

[15] https://github.Com/fb/fb.Resnet.Torch

[16] http://torch.Ch/blog/2016/02/04/resnets.Html

[17] Li, J., Liang, X., Shen, S., Xu, T., Yan, S., ”Scale- aware rapid R-CNN for Pedestrian Detection”, arXiv preprint, arXiv:1510.08160

[18] http://cs231n.Github.Io/linear-classify/

[19] https://github.Com/torch/torch7

[20] https://github.Com/soumith/convnet-benchmarks

Proceedings of the Fourth International Conference on Communication and Electronics Systems (ICCES 2019)
IEEE Conference Record # 45898; IEEE Xplore ISBN: 978-1-7281-1261-9

Fast Error Correction for Header Flit in NoC

V.Taraka Sai Srinatha Reddy, G.Hema Sekhar Reddy, K.Jeshmitha Reddy, M.Vinodhini
Department of Electronics and Communication Engineering
Amrita School of Engineering, Bengaluru
Amrita Vishwa Vidyapeetham
India

***Abstract*—To improve data reliability in NoC, extensively adopted method is the deployment of error correction codes. Errors present in the data flit are corrected by these codes and this is not applicable for correcting errors present in the header flit. So, there is a need for an coding method which will correct errors in data and also the header flit. Further, it is important to have a coding method that will decode the header flit faster compared to data flit, as header flit is used for processing the data flits. Existing single error correction and double error detection code is improved and presented in this paper to support faster error correction in header flit with retaining the same number of redundant bits. This improved code is synthesised and results are compared with existing code. The results show that the header flit are decoded faster compared to data flits as the critical path delay is reduced.**

***Index Terms*—Error correction and detection codes, high-speed networking, Noc, single error correction and double error detection (SEC-DED).**

I. Introduction

In System on Chips (SoC), the reliability issues are increasing gradually when we move towards Deep Sub Micron (DSM) Technology [1]. In SoC's, the information is communicated through an inter communication architecture known as Network on Chip (NoC). Generally, the packets communicated in NoC are more vulnerable to soft errors due to various external and internal noise sources. To improve SoC reliability, Error Correcting Codes (ECCs) are used widely. Error Detection And Correction (EDAC) uses 3D parity check bits to detect and correct multiple errors [2]. This EDAC will correct upto 3 bits of errors. Single Error Correction and Double Error Detection (SEC-DED) code, detect and correct two and one error bits respectively [3]. Horizontal-Vertical Parity and Diagonal Hamming (HVPDH) code, detects 8 bit errors and one bit error is corrected [4]. The extended Hamming code which has similar error correction feature as SEC-DED is also very commonly used [5]. In all the ECC's proposed for Noc and as per the literature survey carried out, detection and correction of error bits are possible only in the corrupted data flit. All these codes are not designed to support error correction in header flit bits.

Various applications of SoC is drastically affected because of the reliability problems present in NoC [6]. In NoC, communication takes place in the form of packets. Packets consists of header and trailer flit each one and body flits between them as shown in Fig. 1. Two or more packets are grouped together to form a message. A packet is further processed in a router based on the information taken from the header flit. If this flit is corrupted, processing of the remaining part of the packet is effected and delayed. Therefore, an ECC which supports error correction in header flit is important. This paper proposes an enhanced SEC-DED Code which can correct and detect errors present in header flit and also in body flit parallelly.

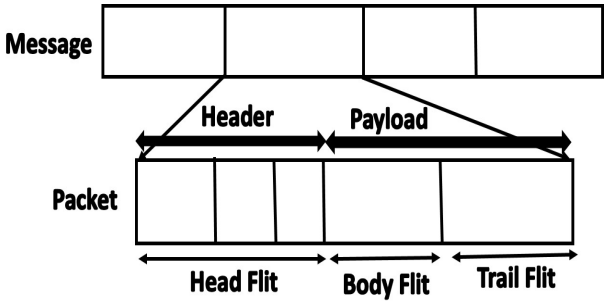

Fig. 1. Packet format of NoC

Further the paper is organised as follows. Survey on all the existing works are presented In Section II. Proposed enhanced SEC-DED code is explained in Section III. Evaluation of proposed work and the conclusion are discussed in Section IV and Section v respectively.

II. RELATED WORKS

There are methods available for constructing the single error correction codes of data bits only with low decoding delay [7].But those methods are not proposed for SEC-DED. In general, there are two methods for detection and correction of errors in the header flit and also in body flit [8]. In first method, two independent ECC's are used for header flit and also body flit, where it requires extra redundant bits. This requires extra storage for the redundant bits. In second method, only one ECC is used for correcting and detecting the errors in both body flit and also the header flit, where same number of redundant bits are used. Therefore, second method is preferred over first method. SEC-DED codes are also widely used in rapid memories [9]. If there are u number of bits in data block, then there will be k number of parity bits to support single error correction which can be specified as given in equation (1).

$$2^k > (u + k) + 1 \tag{1}$$

For example, for a 32 bit data block using equation (1) number of parity bits required is 6. Similarly, for 64 bit data

block, 7 parity bits are required. Further, to extend single error correction feature to single error correction double error detection one extra parity bit is used. So in Hsaio code, here 32 and 64 bit data block requires 7 and 8 parity bits respectively. There are two types of SEC-DED codes they are extended Hamming code and Hsaio code. Hsaio code uses H matrix where every column in this matrix has odd number of ones. Also, the other rules followed in this H matrix are every column should be unique and there should be no all-0 columns. The H matrix for SEC-DED code [10] for data block size of 32 and 64 bits is shown in Fig. 2 and Fig. 3.

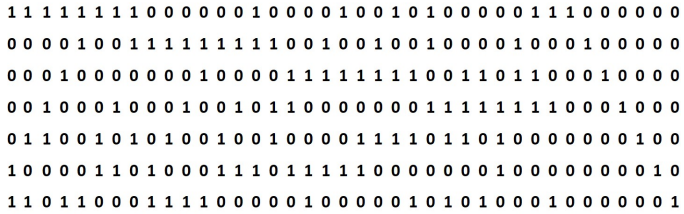

Fig. 2. H matrix for 32 bit data block

Fig. 3. H matrix for 64 bit data block

III. PROPOSED ENHANCED SEC-DED CODE

In this paper, by retaining same number of redundant bits used for SEC-DED code, a extended SEC-DED code is designed. This is designed to protect the entire packet. A fast decoding method is also proposed for header flit bits which reduces the decoding delay of those bits. The same traditional H matrix as shown in Fig. 2 and Fig. 3 are modified to support extended SEC-DED code in our work. To the H matrix of SEC-DED code, which is available for 32 and 64 data block sizes [4], 16 and 32 columns are added to the most significant side to support error correction in header flit bits as shown in Fig.4 and Fig.5.

This extra 16 columns corresponding to the header flit are unique. The bits corresponding to these columns are decoded faster in order to support faster processing of data bits. Faster decoding is performed by considering only fewer redundant bits. In the same way, 32 unique columns are added to facilitate the error correction in the header flit of 64 bit data. In general, the number of bits that can be protected by SEC-DED is always a power of 2. For 32 bit data, 7 parity bits are needed that means $2^7 = 128$ i.e 128 total number of possible bits which are protected by using same 7 parity bits. This is

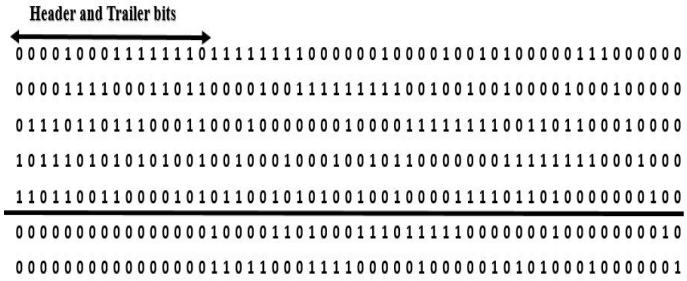

Fig. 4. H matrix for 32+16 bit data block

applicable for 64 bit data also. Therefore, few extra bits can also be protected by the same number of redundant bits.

A. Enhanced SEC-DED encoder

Let h, d, r represents the header flit bits, data bits and redundant bits respectively. In H matrix shown in fig. 4, first 16 columns at the MSB side belongs to headerflit bits (v[0], v[1], v[2],...., v[15]), last 7 columns at the LSB side belong to redundant bits (r[0], r[1], r[2],...., r[6]) and remaining all the 32 bits corresponds to data bits (g[0], g[1], g[2],....., g[31]).

The 48 bit data block (16+32) is given as input to the encoder and the output of the encoder is 55 bits (16+32+7). These 7 redundant bits are calculated by XORing the bits present in the bit position holding 1 in the H matrix [11] without considering the redundant bit columns as shown in equation (2) to equation (8)

$$r[0] = v[4] \oplus v[8] \oplus v[9] \oplus v[10] \oplus v[11] \oplus v[12] \oplus v[14] \oplus v[13] \oplus g[16] \oplus g[17] \oplus g[18] \oplus g[19] \oplus g[20] \oplus g[21] \oplus g[22] \oplus g[23] \oplus g[30] \oplus g[35] \oplus g[38] \oplus g[40] \oplus g[46] \oplus g[47] \tag{2}$$

$$r[1] = v[4] \oplus v[5] \oplus v[6] \oplus v[7] \oplus v[11] \oplus v[12] \oplus v[14] \oplus v[15] \oplus g[20] \oplus g[23] \oplus g[24] \oplus g[25] \oplus g[26] \oplus g[27] \oplus g[28] \oplus g[29] \oplus g[30] \oplus g[31] \oplus g[34] \oplus g[37] \oplus g[40] \oplus g[45] \tag{3}$$

$$r[2] = v[1] \oplus v[2] \oplus v[3] \oplus v[5] \oplus v[6] \oplus v[9] \oplus v[8] \oplus v[10] \oplus v[14] \oplus v[15] \oplus g[42] \oplus g[43] \oplus g[45] \oplus g[19] \oplus g[32] \oplus g[33] \oplus g[34] \oplus g[35] \oplus g[36] \oplus g[37] \oplus g[38] \oplus g[39] \oplus g[46] \oplus g[27] \tag{4}$$

$$r[3] = v[0] \oplus v[2] \oplus v[4] \oplus v[3] \oplus v[8] \oplus v[6] \oplus v[10] \oplus v[12] \oplus v[15] \oplus g[18] \oplus g[22] \oplus g[26] \oplus g[29] \oplus g[31] \oplus g[32] \oplus g[40] \oplus g[41] \oplus g[42] \oplus g[43] \oplus g[44] \oplus g[45] \oplus g[46] \oplus g[47] \tag{5}$$

```
0000000000000000111111111111111 1111111100100110010010011001000000010000000100110001110011100000100000000
0000000111111111000000000111111111 1110000011111111001001100100100110010000000100000001001100011100010000000
0001111000011111000011110000011 1 0001110011100000111111110010011001001001100100000001000000010011001000000
0110011001100111001100110011100 0 0001001100011100111000001111111100100110010010011001000000010000000100000
1010101010101011010101010101101 1 0001000000010011000111001110000011111111001001100100100110010000000010000
1101001100101101100101100110110 1 1001000000010000000100110001110000011100111111110010011001001001000000100
0000000000000000000000000000000 0 0100100110010000000100000001001100011100000111001111111100100110000000010
0000000000000000000000000000000 0 0010011001001001100100000001000000010011000111000001110011111111000000001
```

Fig. 5. H matrix for 64+32 bit data block

$$r[4] = v[0] \oplus v[1] \oplus v[3] \oplus v[8] \oplus v[7] \oplus v[15] \oplus v[13] \oplus v[4] \oplus g[15] \oplus g[17] \oplus g[18] \oplus g[21] \oplus g[23] \oplus g[26] \oplus g[29] \oplus g[34] \oplus g[35] \oplus g[36] \oplus g[37] \oplus g[39] \oplus g[40] \oplus g[42] \oplus g[44] \quad (6)$$

$$r[5] = g[32] \oplus g[33] \oplus g[34] \oplus g[35] \oplus g[36] \oplus g[44] \oplus g[16] \oplus g[21] \oplus g[22] \oplus g[24] \oplus g[28] \oplus g[29] \oplus g[30] \quad (7)$$

$$r[6] = g[16] \oplus g[17] \oplus g[19] \oplus g[20] \oplus g[24] \oplus g[25] \oplus g[26] \oplus g[27] \oplus g[33] \oplus g[39] \oplus g[41] \oplus g[43] \oplus g[47] \quad (8)$$

B. Enhanced SEC-DED decoder

The encoder output is now input to the decoder. For 32+16 data block, the 55 encoded bits are decoded by calculating the syndrome bits. Syndrome bits detect single and double bit errors that are present in the entire packet assuming error free redundant bits. Let nr represents newly calculated redundant bits and r represents the received redundant bits. The syndrome bits (y[0], y[1], y[2]...., y[6]) are calculated by XORing the newly calculated redundant bits and received redundant bits. The calculation of syndrome bits are shown in equation(9) to equation(15). Similarly, for 64+32 data block the 8 syndrome bits are calculated in the same way.

$$y[0] = nr[0] \oplus r[0] \quad (9)$$

$$y[1] = nr[1] \oplus r[1] \quad (10)$$

$$y[2] = nr[2] \oplus r[2] \quad (11)$$

$$y[3] = nr[3] \oplus r[3] \quad (12)$$

$$y[4] = nr[4] \oplus r[4] \quad (13)$$

$$y[5] = nr[5] \oplus r[5] \quad (14)$$

$$y[6] = nr[6] \oplus r[6] \quad (15)$$

For decoding, the syndrome bits corresponding to the ones in the column of H matrix are taken into consideration. In this way the decoding for all the bits are done. In our proposed decoder, bits that are present on the critical time path are to be simplified for low delay. To achieve this, the redundant bits must be divided into two parts. Here, both header flit bits and data bits are shared by the first group and the second group is used only for decoding of data bits. The first group of redundant bits are to be re-computed for header flit bits decoding.

For 32 bit data block with 16 header flit bits, 7 redundant bits are required for protection. As discussed earlier these 7 redundant bits should be divided into two parts. First part is of 5 bits and the second part of 2 bits. First part is used for both header flit bits and data bits and the second part is only for data bits. In this code, for decoding the header flit bits, only the 5 syndrome bits with value ones and zeros are considered. Other 2 syndrome bits are not considered for the decoding of header flit bits. For decoding of data bits, all the 7 syndrome bits with value ones and zeros are considered. For the case of 32+16, in the first part 5 syndrome bits are used. With 5 syndrome bits, 2^5 combinations can be generated. This supports single bit error correction in 32 bits. This way by considering the 5 syndromes bits for evaluating the header flit bits we achieved faster decoding and also we can extend the number of header flit bits from 16 to 32.

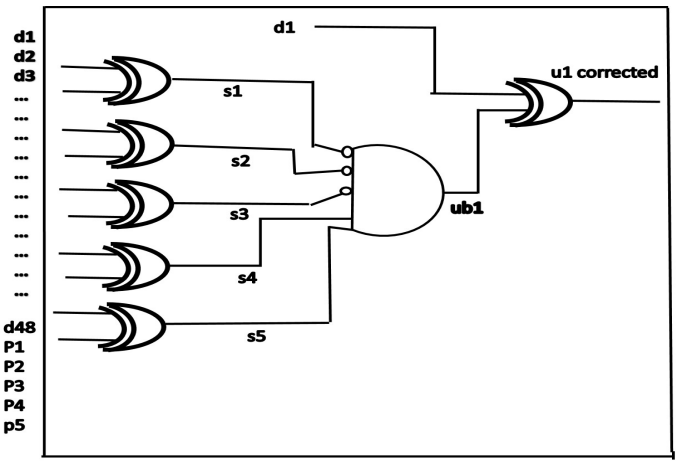

Fig. 6. One bit fast decoding of 32+16 data

Similarly, for 64 bit data block with 32 header flit bits, 8 redundant bits are used for protection. These 8 redundant bits will be divided into two parts. First part is of 6 bits and the second part is of 2 bits as done for 32 bit data block. The

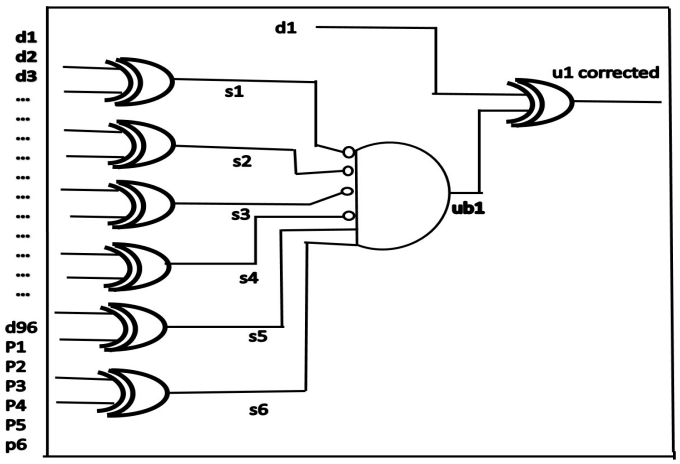

Fig. 7. One bit fast decoding of 64+32 data

first part will protect header flit bits and data bits and second part is only for data bits. In this code for decoding the header flit bits, only 6 syndrome bits with values ones and zeros are considered. Other 2 bits are not considered for the decoding of the header flit bits. For decoding the data bits all the 8 syndrome bits with value ones and zeros are considered. Fig. 6 and Fig. 7 shows Fast decoding hardware architecture for 32+16 and 64+32 data blocks respectively.

IV. EVALUATION

To evaluate the proposed code, this code is implemented for 32, and 64 data block sizes. considering 16 and 64 additional header flit bits respectively. The codec of these codes are compared to the original SEC-DED codes. To evaluate these codes, all these codes are designed in Verilog HDL. The designed codes are synthesized using Cadence RTL compiler for 45nm technology [12]. As per the main design goal, the synthesis for the decoders is to the minimize the delay on the header flit bits with same number of redundant bits. The same synthesis constraints are used for both proposed and original SEC-DED codes. The parameters that are evaluated in this paper are area, power and delay.

The results of the proposed codes are analysed in terms of area, power and delay and are compared to the original SEC-DED code. The encoder results for the case of 32+16 and 64+32 data block size are shown in TABLE I and TABLE II respectively. similarly decoder results for 32+16 data block, header flit bits and 64+32 data block, header flit bits and also the original SEC-DED decoding results are shown in the TABLE III. In this area, power and delay are calculated by separating data and header flit bits. The decoding delay of the header flit bits for 32+16 and original 32 bit is reduced by approximately 3%. In the same way for 64+32 and original 64 the decoding delay of header flit bits is also reduced by 3%. With this delay reduction, it is clear that bits on the critical path are decoded faster. There is a slight increase in circuit area when compared to original SEC-DED codes and there is marginal increase in the delay and power of encoders.

TABLE I
ENCODER RESULTS FOR 32 BIT DATA WITH 7 PARITY CHECK BITS

Number of bits	Area (μm^2)	power(mW)	Delay (pS)
32+16 encoder	410	0.064	1997
original 32 encoder	296	0.038	1295

It is observed that, there is slight impact on the data bits, that is decoding delay is slightly increased for the data bits. However, As discussed earlier,we are concerned only on the fast decoding of header flit bits that are on the critical path. As a result it is observed that AISC circuit area for encoders and decoders have slightest variations when compared to the original SEC-DED codes. Decoding delay of data bits is slower than minimum-weight codes and power consumption increased slightly. However, this proposed code will detect double errors and correct single errors in data and header flit bits with a marginal increase in overall delay and power.

TABLE II
ENCODER RESULTS FOR 64 BIT DATA WITH 8 PARITY CHECK BITS

Number of bits	Area(μm^2)	power(mW)	Delay(pS)
64+32 encoder	830	0.150	2631
original 64 encoder	589	0.090	1567

V. CONCLUSION

This proposed paper presents a code for the construction of SEC-DED code that has a capability to correct and detect the errors in both header flit bits and data bits. These codes are designed for NoC which in turn gives fast decoding of the header flit bits by using minimum number of parity bits that are required for decoding of those header and trailer flit bits. This will eliminate extra memory space that will account for redundant bits. It can also be extended by changing the H matrix which will correct and detect multiple errors. With marginal increase in the overall delay this proposed extended SEC-DED code is able to protect the errors in both header flit bits and data flits and with included advantage of fast decoding of the header flit.

TABLE III
DECODER RESULTS

Number of bits	Area(μm^2)	power(mW)	Delay(pS)
Decoder(32+16, data bits)	722	0.135	3630
Decoder(32+16, header flit bits)	582	0.114	3121
Decoder(original 32+16, data bits)	722	0.135	3630
Decoder(original 32+16, header flit bits)	584	0.104	3227
Decoder(64+32, bits)	1400	0.309	4364
Decoder(64+32, header flit bits)	1131	0.263	4234
Decoder(original 64+32, data bits)	1400	0.309	4364
Decoder(original 64+32, header flit bits)	1150	0.239	4364

REFERENCES

[1] Papanikolaou A., Wang H., Miranda M., Catthoor F., Dehaene W. (2008) Reliability Issues in Deep Deep Submicron Technologies: Time-Dependent Variability and its Impact on Embedded System Design. In: De Micheli G., Mir S., Reis R. (eds) VLSI-SoC: Research Trends in VLSI and Systems on Chip. IFIP International Federation for Information Processing, vol 249. Springer, Boston, MA

[2] Shivani Tambatkar, Siddharth Narayana Menon, Sudarshan.V, M.Vinodhini and N.S.Murty , Error Detection and Correction in Semiconductor Memories using 3D Parity Check Code with Hamming Code , International Conference on Communication and Signal Processing, April 6-8, 2017, India.

[3] E. Fujiwara, Code Design for Dependable Systems: Theory and Practical Application. Hoboken, NJ, USA: Wiley, 2006.

[4] Paromita Raha, M Vinodhini, N. S. Murty, Horizontal-Vertical Parity and Diagonal Hamming Based Soft Error Detection and Correction for Memories, International Conference on Computer Communication and Informatics (ICCCI -2017), Jan. 05 07, 2017, Coimbatore, INDIA.

[5] M. Y. Hsiao, A Class of Optimal Minimum Odd-weight-column SECDED Codes,IBM Journal of Research and Development Vol. 14 , Issue: 4,July 1970.

[6] T Siva Teja, T Sai Kiran, T.V.V Satya Narayana, M.Vinodhini, N. S.Murty , Joint Crosstalk Avoidance with Multiple Bit Error Correction Coding Technique for NoC Interconnect, 2018 International Conference on Advances in Computing, Communications and Informatics (ICACCI), Sep. 2018.

[7] P. Reviriego, S. Pontarelli, J. A. Maestro, and M. Ottavi, A method to construct low delay single error correction (SEC) codes for protecting data bits only, IEEE Trans. Comput.-Aided Design Integr. Circuits Syst., Vol. 32, No. 3, pp. 479483, Mar. 2013.

[8] Pedro Reviriego, Mustafa Demirci, Adrian Evans,and Juan Antonio Maestro"A Method to Design Single Error Correction Codes With Fast Decoding for a Subset of Critical Bits ," IEEE Trans. on circuits and systems-II: Express Briefs, Vol. 63, No. 2, Feb. 2016.

[9] O. Novac, St. Vari-Kakas, F.I. Hathazi, M. Curila and S. Curila , Aspects Regarding the Implementation of HSIAO code to the Cache Level of a memory Hierarchy with FPGA Xilinx circuits , K. Elleithy (ed.), Advanced Techniques in Computing Sciences and Software Engineering,2010.

[10] V. Gherman, S. Evain, N. Seymour, and Y. Bonhomme, Generalized parity-check matrices for SEC-DED codes with xed parity, in Proc. IEEE On-Line Test. Symp., 2011.

[11] Novac Ovidiu, Sztrik Janos, Varikakas Stefan, Kim Che-Soong, Reliability Increasing Method Using a SEC-DED Hsiao Code to Cache Memories, Implemented with FPGA Circuits , Journal of Computer Science and Systems, Vol. 4, No. 2, Oct. 2011.

[12] Sudhakar Alluri, Performance Analysis of VLSI Circuits In 45nm Technology,International Journal of Engineering Science Invention (IJESI), Vol. 07, No. 05, pp.39-51,2018.

Proceedings of the Fourth International Conference on Communication and Electronics Systems (ICCES 2019)
IEEE Conference Record # 45898; IEEE Xplore ISBN: 978-1-7281-1261-9

RCSA scheme with Rayleigh Fading Effect in massive-MIMO system

Umesha G B
Research Scholar
Dept. of ECE
SJCE, Mysore
Karnataka, India
umeshagb@gmail.com

Dr M N Shanmukha Swamy
Research Supervisor
Dept. of ECE
SJCE, Mysore
Karnataka, India
mnsjce@gmail.com

***Abstract*— A multi-user MIMO network system with channel fading effect provide a multiple challenges such as pilot contamination, collision, model complexity, resource allocation and etc. In this paper, we provide minimal collision probability with the less model complexity under consideration of pilot contamination problem and resource allocation using RCSA approach. Here, the uncorrelated Rayleigh fading channels is considered in massive-MIMO network and focused on initial timing variation at urban organizations and proposed a random access process for UEs that want to communicate in the cellular network. In the result analysis, we shown the effectiveness of our proposed model in order to minimize the pilot collision, it also compared with the state-of-art technique to validate the performance of our model.**

Keywords— user equipment's (UEs); massive multiple-input-multiple-output (mMIMO); base station (BS); reactive channel state based allocation (RCSA)

I. INTRODUCTION

A recent enhancement in the field of wireless communication majorly focussed on the MIMO system, which able to provide more spectral efficiency by spatial diversity and multiplexing method at the transmitter side as well as at the receiver end. In paper [1] [2], shows the related research in order to increase the channel capacity with using minimal transmit and receive antennas in MIMO system. In [3], the channel capacity under channels fading effect are analysed using multiple transmission occurrences through emphasizing on the coding structures and multi-path fading equalization of channels. A hyper-geometric matrix is considered in [4] that generates a unique function for the propagation of several scenarios in MIMO correlation fading at receiver and transmitter side. Moreover, an upper bound sum capacity is examined in [5] in order to decentralize the multiple channels, which acknowledge all distributed CSI (channel state information) and receiver CSI.

The method of spectrum sharing is considered in [6] by using new receiver, which enhance the capacity process, minimize collision and decrease problem to obtain efficient optimal power at interference power and transmission scenarios. The power allocation and optimal bandwidth is obtained through frequency-division multiple access protocol in cognitive network [7]. In addition, the security of physical layer in wireless communication network has studied in [8], which compute secure connection probability to provide better secure connection and secrecy capacity process. In [9], effectiveness of several channel capacity and the outage capacity is studied, also it provide probable source distortion for the several outage probabilities under the Rayleigh fading channels. Though the simplified approach to analyse the collision in dual MIMO configuration is considered in [10], which is done by using normalized power distribution in a configured network system.

In [11], studied the spatial correlation through considering two channel models in order to get optimal MIMO capacity at different scenarios, moreover a closed-form appearance for maximizing the efficiency of MIMO channels under at Rayleigh fading is studied in [12] that approximate optimal allocation of antenna, where the transmitter has no acknowledge channel and side CSI. In study [13], the capacity of the several relay channels is investigated under shadowing and fading scenarios with considering constraints of spectrum sharing. Minimum mean square error (MMSE) for multi-cell that based upon the pre-coding method was considered in [14], for each BS the pre-coding matrix was designed to minimalize the sum squared errors of UEs in the cells, but it has some computational complexity because of its huge matrix inversion. In [15], the time-shifted pilot technique is proposed to overcome pilot contamination through distributing the complete system into some smaller groups, then by make use of asynchronous transmission at entire smaller groups. Moreover, the time-shifted method makes definite that the very less pilot contamination among at users in all smaller groups, whenever very large number of the BS antennas is considered this leads towards the communal interference in between transmitted data and the pilot sequences.

A multi-user MIMO network system with the orthogonal block coding was considered that tends to compute both spatial diversity gain and multi user gain under a low complexity of encoding and decoding, in paper [16] a channel fading distribution at several real time scenario is considered, where the behaviour of the channel is subjected to be independent and distributed non-identically such as Nakagami-m fading. Subsequently a relay node may be unable to serve simultaneously multiple source destination pairs, therefore the appropriate design of user scheduling approach is essential. So the drawback of this paper is to not have the opportunistic scheduling and one end-to-end pair under the optimal channel conditions for the transmission in given time period.

In [17], proposed a smart pilot allocation method through minimizing the SINR (signal-to-interference-plus-noise ratio) of users for individual cells in a consecutive manner, but it cannot fulfil the required convergence. Moreover, adaptive pilot allocation based method is proposed in [18] through dividing UEs in a system into the dual group, in according to the present inter-cell interference available number of pilot should be larger than the UEs in individual cell and, if the available number of pilot is limited and considered to be same to UEs in individual cell, then the adaptive pilot allocation based method work same as the random pilot allocation. However, a pilot contamination based elimination pre-coding method is proposed in [19], through exploiting the coefficients property of large-scale fading for channel vector of BSs and users. Figure I.1 shows the MIMO system model.

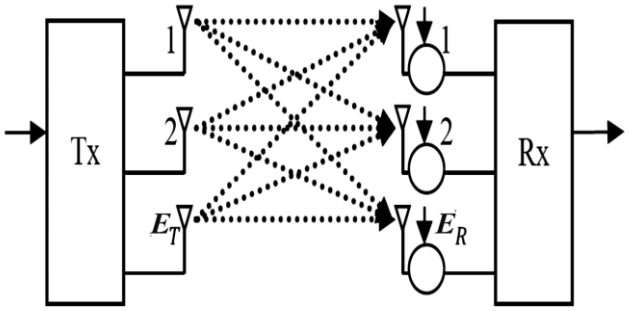

Figure I.1 MIMO system model

In [20], presented a novel approach for intra-cell interference to overcome the problem of pilot contamination in massive MIMO networks, this approach majorly relies on the channel powers stability and the orthogonality at user channels using the graph code method. A random access scheme is proposed in [21] in order to overcome the collision, power and channel estimation through utilizing the huge number of antennas planned in mMIMO network. In this paper, we proposed a RCSA approach with uncorrelated Rayleigh fading channels, the major aim of this is study is to minimize the intra-cell interference in between the UEs. Here we have considered the time-division duplexing (TDD) for the pilot contamination in m-MIMO [22], also we focused on initial timing variation at urban organizations and proposed a random access process for UEs that want to communicate in the cellular network. In addition, UE consigned a pilot sequence before transmitting the data to overcome the pilot collisions at intra-cell. To verify the performance of our proposed model with uncorrelated Rayleigh fading channels effects, in result analysis section we will consider huge number of inactive UEs as compared to active UEs with varying the number of BS antennas.

II. REACTIVE CHANNEL STATE BASED ALLOCATION (RCSA) SCHEME

In this section, we provide a brief of RCSA approach for Massive MIMO that we have proposed in earlier study [23], afterwards in next section we will provide RCSA approach with Rayleigh fading channels. The proposed RCSA approach consist of four major steps as given in fig 1, where the first step stands for queuing and system initialization, the second step provides the response queuing, the third step provides the resource contention and channel state analysis and, at last step stands for the resource allocation. Here, we consider the cellular network, where individual number of BS is having M antennas. The considered network system operates at TDD mode and time-frequency properties are sub-divided to some coherent blocks for the usage of T number of channels. Here, the channel responses at BS and its corresponding UEs are considered to be constant and the frequency remains same with in a same block and vary at different blocks. For this we have considered the OFDM (orthogonal frequency division multiplexing).

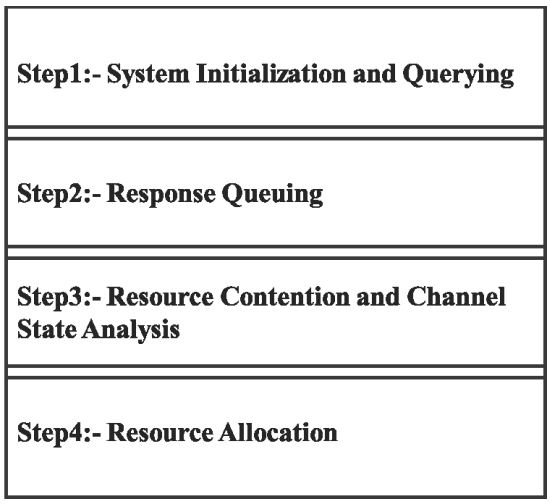

Figure II.1: A proposed RCSA Approach for the Massive MIMO

While assuming huge network of MIMO, the collisions are needed to resolve and recognize as earlier than the UE which is coming into the blocks of payload. Our proposed method can be distributed the approach to resolve a collision at the UEs via using the principle of enormous MIMO. Wherever, the vectors of channel at UE are denoted as $b \in B_0$ and $d_b \in \mathrm{C}^E$ can be denoted as BS, whereas we have though- about the model of generic propagation and also the channels are pre-expected to satisfy these 2 conditions:

$$\frac{\|\mathrm{d}_b\|^2}{E} \xrightarrow{E\to\infty} \beta_b, \forall b, \tag{1}$$

$$\frac{\mathrm{d}_b^{\mathrm{D}}\mathrm{d}_a}{E} \xrightarrow{E\to\infty} 0, \qquad \forall b, a, where\ b \neq a, \tag{2}$$

Here, β_b has much number of strictly values that is well-known to UE b, so that the channels are provided the propagation of asymptotic favorable and the channel hardening [24]. While assuming, the step 1 process for RAP, and the signal is received by the help of BS is known as $\mathbf{F} \in \mathrm{C}^{E\times g_k}$ from the pilot transmission.

$$\mathbf{F} = \sum_{b \in B_0} \sqrt{hb}\, \mathrm{d}_b * \psi_{c(b)}^{\mathrm{T}} + \mathbf{L} + \mathbf{M} \tag{3}$$

Where, $\mathbf{L}$ is represented by the help of inter-cell interference, $\mathbf{M} \in \mathrm{C}^{M \times \tau_p}$ is not dependent the receiver noise and every single distribution of the element is specified as $CZ(0, \sigma^2)$ and it is more complex as Gaussian distribution, where, $\mathrm{C}^{E \times g_k}$ metric represents the interference from various cells. The resources of time-frequency are separated the channel T of coherence block and E denotes the number of antennas. The transmit power is given by the help of h, complex value corresponds to C and the transmitted value is represented by ψ.

During queuing of the response, the BS replies at the side of RAP pilots via transmitting the pre-coded signals of downlink that leads to every single RAP pilots which were being utilized in the uplinks. The reaction towards (ψ_t) can be the sequence of channel $N_t \in \mathrm{C}^{g_k}$ and the sequences of downlink channel can be specified as $N_1, N_2, \ldots, N_{g_k} \in \mathrm{C}^{g_k}$ are the orthogonal to each and everyone and satisfy $\|N_t\|^2 = g_k$. If the BS is considered as the normalized conjugate then $\frac{p_t^*}{\|p_t\|}$ is pre-coded vector at the pilot sequence of N_t in downlink. Then the signal is directed towards MCMR (multi-cast-maximal-ratio) transmission t the UEs in Q_t. Hence, the complete pilot signal of pre- coded downlink $\mathbf{R}$ is specified as;

$$\mathbf{R} = \sqrt{s} \sum_{t=1}^{g_k} \frac{p_t^*}{\|p_t\|} N_t^{\mathrm{T}} \tag{4}$$

Where, down-link sends the power s and it has pre-defined value, the length of pilot channel is mentioned as g_k and it is not dependent from huge number of antennas. The received signal $(\mathbf{U}_b \in \mathrm{C}^{g_k})$ at UE $b \in Q_t$ is defined by;

$$\mathbf{U}_b^{\mathrm{T}} = r_b^{\mathrm{T}} + \eta_b^{\mathrm{T}} + \mathrm{d}_b^{\mathrm{T}} \mathbf{R} \tag{5}$$

Whereas, $\mathrm{h}_k^{\mathrm{T}}$ represented for the channel of reciprocal downlink, and r_b correspond to C^{g_k} which is interference of inter-cell, and η_b can be the receiver noise signal. Though the UE obtain the signal $U_b = \mathbf{U}_b^{\mathrm{T}} \frac{N_t^*}{\|N_t\|}$ by correlating receiver signal $\mathbf{U}_b$ with N_t normalized downlink pilot sequence.

$$U_b = \sqrt{s g_k}\, \mathrm{d}_b^{\mathrm{T}} + \eta_b + r_b^{\mathrm{T}} \frac{N_t^*}{\|N_t\|} \tag{6}$$

In step3, the mechanism of resource contention and analysis of channel state has been proposed to resolve the contention of channel at the distributed manner, so that every single channel can be reiterated only one by the one-UE. The UE $(b \in Q_t)$ can be considered as $h_b \beta_b g_k$ (signal gain) and estimate the signal gain $(\hat{V}_{t,b})$ of the sum of inter-cell interference and contending UEs. The BS (base station) receives the repeated pilot transmission of RAP that followed by the uplink message. The BS can be considered the tth level of pilot signal to estimate the channel UEs which is transmitted ψ_t and decode the corresponded messages. After successfully decoding, the BS can be recognized one-UEs in Q_t and give it to the coherent payload blocks via assigning the sequence of pilot channel. These types of allocation decision can be forwarded through the downlink in the step 4 and equally for step 2. The protocol of RCSA can be reiterated for the fixed number of time, if UEs were not recognized in the step 4, then it is instructed to send via the new RAP channels.

III. RCSA Approach with Rayleigh Fading Channels

Here, we going to consider the uncorrelated Rayleigh fading channels for all UEs, where $b \in B_0$ and d_b can be given as;

$$d_b \sim CZ(0, \beta_b \vartheta_E) \tag{7}$$

Moreover, the model of inter-cell interference can be given as $\mathrm{r}_b \sim CZ(0, \mu_b \vartheta_{g_h})$ which is independent from the other signals, this will allows for relative analysis of traceable performance at any value of E. While considering section II analysis on E for the property of asymptotic favorable propagation and channel hardening, the E value generally will be at larger amount. As per consideration of step 2 (6), the distribution of the random variable under considered uncorrelated Rayleigh fading channels for any UE received signal can be given as;

$$U_b = \mathcal{Y}_b + r_b \tag{8}$$

Where, the $\mathcal{Y}_b$ and r_b parameters are obtained from (9) and (10). The $\mathcal{Y}_b$ consist of scaled chi-distribution with the $2E$ degree of freedom.

$$\mathcal{Y}_b \sim \sqrt{\frac{0.5 h_b s \beta_b^2 g_k^2}{V_t + \sigma^2}}\, m, m \sim \mathfrak{M}_{2E} \tag{9}$$

Where, $\mathfrak{M}$ denotes for the independent chi-distribution and its corresponds lower value denotes the degree of freedom.

$$r_b \sim CZ\left(0, \sigma^2 + \mu_b + s\beta_b g_k - \frac{h_b s \beta_b^2 g_k^2}{V_t + \sigma^2}\right) \tag{10}$$

Through using the statistical property at (8), we will able to calculate the value of expectation and variance related to random variables for received downlink-signal $\frac{U_b}{\sqrt{E}}$, so the mean value can be computed as;

$$\mathbb{M}\left\{\frac{U_b}{\sqrt{E}}\right\} = \sqrt{\frac{h_b s \beta_b^2 g_k^2}{V_t + \sigma^2}} \frac{\mathfrak{D}(0.5 + E)}{\sqrt{E}\, \mathfrak{D}(E)} \tag{11}$$

Similarly, the variance can be computed as;

$$\mathbb{K}\left\{\frac{U_b}{\sqrt{E}}\right\} = \frac{h_b s\beta_b^2 g_k^2}{V_t + \sigma^2}\left(1 - \left(\frac{\mathfrak{D}(0.5+E)}{\sqrt{E}\mathfrak{D}(E)}\right)^2\right) + \frac{1}{E}\left(\sigma^2 + \mu_b + s\beta_b g_k - \frac{h_b s\beta_b^2 g_k^2}{V_t + \sigma^2}\right) \quad (12)$$

While, $\mathfrak{D}(.)$ denotes the gamma function, while considering the E value to infinity, the expected value of received downlink signal can be given as;

$$\mathbb{M}\left\{\frac{z_k}{\sqrt{M}}\right\} = \sqrt{\frac{h_b s\beta_b^2 g_k^2}{V_t + \sigma^2}}, where\ E \to \infty \quad (13)$$

Where, σ denotes the coherence blocks of T channel uses and consecutively, if the E value is tends to infinity, the variance of received downlink signal can be given as;

$$\mathbb{K}\left\{\frac{U_b}{\sqrt{E}}\right\} \to 0, where\ E \to \infty \quad (14)$$

The expected value of received signal with respect to random variables satisfied the considered condition and the variance value tends to zero that confirms the asymptotic satisfactory propagation from the uncorrelated Rayleigh channels fading effect.

IV. Simulation Result and Analysis

In this section, we illustrate the RCSA approach with uncorrelated Rayleigh fading channels (URFC), which is capable to resolve the collision and increase the capacity of network. The simulation of code has done using Matlab 2018a on a Windows operating system. Here, we considered a scenario, where 5000 number of inactive UEs are present in a network, active UEs at the neighboring cells is consider to be 10 and cell radius is 250m. UEs transmit power in the cell is 1 dB, the transmit power of BS is also consider to be 1 dB, the length of the random access pilot sequence is 30 and the noise variance is considered to be 1 dB. The maximum number of BS antennas E is 200, and it varies from 1 to 200, in addition the number of Monte-Carlo realizations is considered to be 1000 in an intra-channel interference module.

In order to make a decision on UE, whether it's a strongest user or not is very difficult, therefore in order to soften the decision we consider the random bias term. As per acknowledgment obtained by b to UEs, the bias term value can made and provide ability to UE to itself appoints the appropriate strongest user under the probability condition. Here, we are going to compared with the existing vertex graph-coloring-based pilot assignment (VGCPA) with URFC [25].

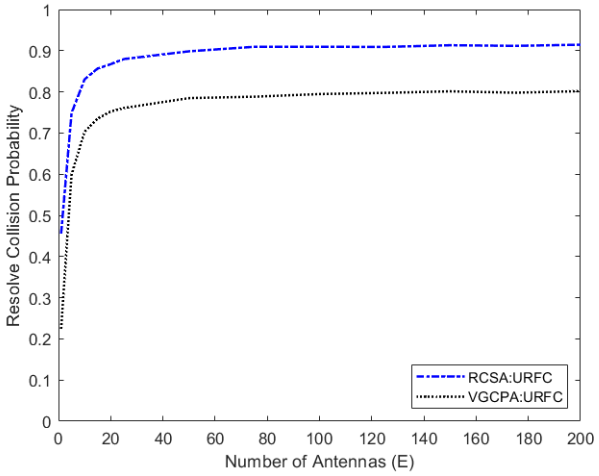

Figure IV.1 Resolved Collision Probability at Zero Bias Term

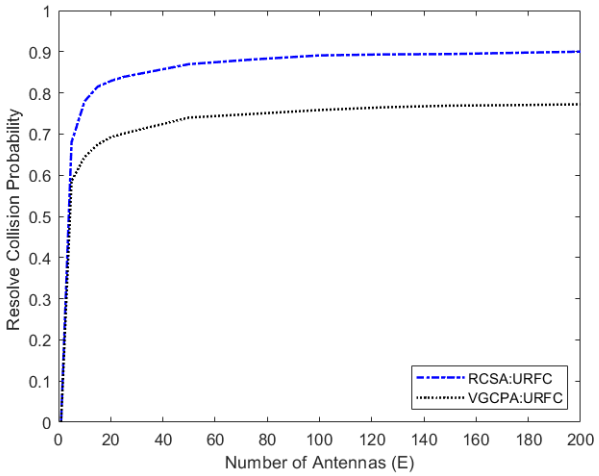

Figure IV.2 Resolved Collision Probability at 0.5 Bias Term

Figure IV.1 shows the resolved collision probability at zero bias term, where the x-axis represents the number of antennas that varies from 1 to 200 and y-axis represents probability at the resolved collision. Here, RCSA-URFC has got minimum and maximum probability score of 0.45 and 0.91, where the average at total number of BSs is 0.84. Whereas, VGCPA-URFC has got minimum and maximum probability score of 0.22 and 0.8, where the average at total number of BSs is 0.7, which is 15.4% less than our proposed approach. Similarly, fig IV.2 shows the resolved collision probability at 0.5 bias term, where our proposed model RCSA-URFC has got maximum probability score of 0.9, where the average at total number of BSs is 0.78. Whereas, VGCPA-URFC has got maximum probability score of 0.77, where the average at total number of BSs is 0.66, which is 15.3% less than our proposed approach.

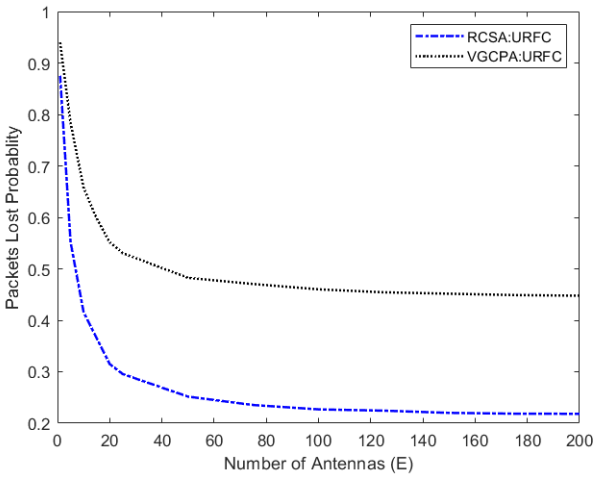

Figure IV.3: Probability at Packets Loss

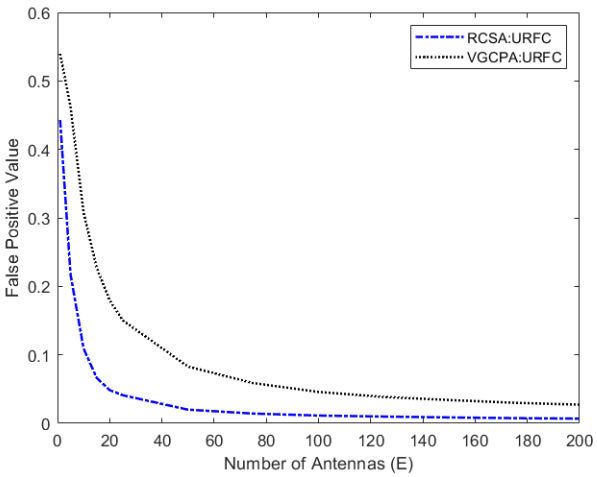

Figure IV.4: False Positive Value at Retransmission

IV.3 shows the probability of packets loss with respect to number of BS antennas, here the x-axis represents the number of antennas that varies from 1 to 200 and y-axis represents probability of packet loss. The minimum and maximum probability of packet loss is 0.44 and 0.94 from VGCPA-URFC approach, and from RCSA-URFC approach the minimum and maximum probability of packet loss is 0.21 and 0.87, in average it is 40% more than our proposed model. Figure IV.4 shows the false positive value with respect to number of BS antennas, where the average false positive value from VGCPA-URFC approach is 0.168 and from RCSA-URFC approach is 0.077, which 54% less than the existing approach.

V. CONCLUSION

The proposed RCSA approach consist of four major steps such as queuing and system initialization, response queuing, resource contention and channel state analysis and, at last resource allocation. The mechanism of resource contention and analysis of channel state has been proposed to resolve the contention of channel at the distributed manner, so that every single channel can be reiterated only one by one UE. From the result section IV, the average resolved collision probability by our proposed model at total number of BSs is 15.4% more than the existing approach. So we can say that the RCSA approach with uncorrelated Rayleigh fading channels is capable to resolve the collision and increase the capacity of network. In future-work, we are going to consider the inter-channel interference along with the intra-channel interference in m-MIMO system.

REFERENCES

[1] G. J. Foschini and M. J. Gans, "On limits of wireless communications in a fading environment when using multiple antennas," Wireless Pers. Commun., Vol. 6, pp. 311-335, 1998.

[2] I. E. Telatar, "Capacity of multi-antenna gaussian channels," European Trans. Telecommun. Rel. Technol., Vol. 10, No. 6, pp. 585-596, Nov. 1999.

[3] Ezio Biglieri, John Proakis, and Shlomo Shamai, "Fading Channels: Information-Theoretic and Communications Aspects," IEEE Transactions on Information Theory, Vol. 44, No. 6, pp. 2619-2692, 1998.

[4] Mario Kiessling, "Unifying analysis of ergodic MIMO capacity in correlated Rayleigh fading environments", European Transactions on Telecommunications, Vol. 16, No. 1, pp. 17-35, 2005.

[5] Nitish Mital, Kamal Singh, and Sibi Raj B Pillai ," On the Ergodic SumCapacity of Decentralized Multiple Access Channels," IEEE Communications Letters, Vol. 20, No. 5, pp. 854-857, 2016.

[6] Neha Singh, and Balaji. Gawalwad," Improving Ergodic and Outage Capacity of Spectrum Sharing Cognitive Radio Networks," International Journal of Advanced Research in Computer Science and Software Engineering, Vol. 5 No. 4, pp. 313-319, 2015.

[7] Xiaowen Gong, Sergiy A. Vorobyov, and Chintha Tellambura, "Optimal Bandwidth and Power Allocation for Sum Ergodic Capacity Under Fading Channels in Cognitive Radio Networks," IEEE Transactions On Signal Processing, Vol. 59, No. 4, pp. 1814-1826, 2011.

[8] Weigang Liu, Zhiguo Ding, Tharmalingam Ratnarajah, and Jiang Xue, "On Ergodic Secrecy Capacity of Random Wireless Networks with Protected Zones," IEEE Transactions on Vehicular Technology, Vol. 65, No. 8, pp. 6146 - 6158, 2016.

[9] Sayantan Choudhury, and Jerry D. Gibson, "Ergodic capacity, outage capacity, and information transmission over Rayleigh fading channels," Journal of Engineering Research and Studies, pp. 1-5, 2011.

[10] Michail Matthaiou, Yannis Kopsinis, David I. Laurenson, and Akbar M. Sayeed," Ergodic Capacity Upper Bound for Dual MIMO Ricean Systems: Simplified Derivation and Asymptotic Tightness," IEEE Transactions On Communications, Vol. 57, Issue 12, pp. 3589-3596, 2009.

[11] Xiaoming Chen," Spatial Correlation and Ergodic Capacity of MIMO Channel in Reverberation Chamber," International Journal of Antennas and Propagation, Article ID 939104, pp. 1-7, 2012.

[12] Mehdi Adibi, and Vahid Tabataba Vakili," An Analytical Closed-form Expression for The Ergodic Capacity of Rayleigh Fading MIMO Channels and Optimal Antenna allocation," 2008 Internatioal Symposium on Telecommunications, IEEE Xplore, doi: 978-1-42442751-2.

[13] Kais Ben Fredj, Sonia Aissa, and Leila Musavian, "Ergodic and Outage Capacities of Relaying Channels in Spectrum-Sharing Constrained Systems" IET Communications, Vol. 7, No. 2, pp. 98 - 109, 2013.

[14] J. Jose, A. Ashikhmin, T. L. Marzetta, and S. Vishwanath, ''Pilot contamination and precoding in multi-cell TDD systems,'' IEEE Trans. Wireless Commun., vol. 10, no. 8, pp. 2640–2651, Aug. 2011.

[15] F. Fernandes, A. Ashikhmin, and T. L. Marzetta, ''Inter-cell interference in noncooperative TDD large scale antenna systems,'' IEEE J. Sel. Areas Commun., vol. 31, no. 2, pp. 192–201, Feb. 2013.

[16] M. Torabi, D. Haccoun, and W. Ajib, "Analysis of the performance of multiuser MIMO systems with user scheduling over Nakagami-m fading channels," Phys. Commun., vol. 3, no. 3, pp. 168–179, Sep. 2010.

[17] X. Zhu, Z. Wang, L. Dai, and C. Qian, ''Smart pilot assignment for massive MIMO,'' IEEE Commun. Lett., vol. 19, no. 9, pp. 1644–1647, Sep. 2015.

[18] M. Alkhaled, E. Alsusa, and K. A. Hamdi, ''Adaptive pilot allocation algorithm for pilot contamination mitigation in TDD massive MIMO systems,'' in Proc. IEEE Wireless Commun. Netw. Conf. (WCNC), Manchester, U.K., Mar. 2017, pp. 1–6.

[19] A. Ashikhmin and T. Marzetta, ''Pilot contamination precoding in multicell large scale antenna systems,'' in Proc. IEEE Int. Symp. Inf. Theory (ISIT), Cambridge, MA, USA, Jul. 2012, pp. 1137–1141.

[20] J. H. Sørensen, E. de Carvalho and P. Popovski, "Massive MIMO for crowd scenarios: A solution based on random access," 2014 IEEE Globecom Workshops (GC Wkshps), Austin, TX, 2014, pp. 352-357.

[21] L. Sanguinetti, A. A. D'Amico, M. Morelli, and M. Debbah, "Random access in uplink massive MIMO systems: How to exploit asynchronicity and excess antennas," in IEEE GLOBECOM, 2016

[22] J. Jose, A. Ashikhmin, T. L. Marzetta and S. Vishwanath, "Pilot Contamination and Precoding in Multi-Cell TDD Systems," in IEEE Transactions on Wireless Communications, vol. 10, no. 8, pp. 2640-2651, August 2011.

[23] Umesha G B "Reactive channel state based allocation scheme in massive MIMO networks", 4th International Conference on Recent Trends on Electronics, Information, Communication & Technology RTEICT-2019

[24] H. Ngo, E. Larsson, and T. Marzetta, "Aspects of favorable propagation in massive MIMO," in Proc. EUSIPCO, 2014.

[25] [H. T. Dao and S. Kim, "Vertex Graph-Coloring-Based Pilot Assignment With Location-Based Channel Estimation for Massive MIMO Systems," in IEEE Access, vol. 6, pp. 4599-4607, 2018.

Proceedings of the Fourth International Conference on Communication and Electronics Systems (ICCES 2019)
IEEE Conference Record # 45898; IEEE Xplore ISBN: 978-1-7281-1261-9

Implementation and Analysis of Adaptive Odd-Even Routing in Booksim 2.0 Simulator

Jaswanth Marri [1], Sunder Manishankar [1], D. Radha [1]
Dept of Computer Science and Engineering
Amrita School of Engineering, Bengaluru
Amrita Vishwa Vidyapeetham, India
jeswanthjashu8@gmail.com

Minal Moharir [2]
Dept of Computer Science and Engineering
RV College of Engineering, Bengaluru, India

Abstract. With the speed in every move in life, the speed of processors is vital for the modern technology. As the single processor has its own limitations, multicore/many-core processor are introduced to compete for the speed. Communication among the cores in a network on Chip(NoC) needs to be expertly handled to avoid needless delay in processing speed. The proposed work presents a deadlock free adaptive odd even routing (OE) to route cache miss packets in the cores with less delay in a 2D mesh topology. The algorithm is implemented and tested in BookSim 2.0 simulator. In a multi-core architecture, as each core processes multiple applications in parallel which results in increase in the chip's overall processing capability. One of the major issue in this NoC is congestion management in the network. As this routing algorithm is adaptive it can change its route accordingly to the traffic present at nodes with help of credits. Simulation result shows the analysis of the routing algorithm in various synthetic traffic patterns such as uniform, tornado, bitrev, shuffle and transpose. It also gives a comparative analysis of performance in terms of latency in various routing algorithms such as XY, adaptive XY, shuffle, transpose.

I. INTRODUCTION

Most of the electronic products, such as mobile phones, smart devices, and so on, consists a lot of software and hardware blocks. Due to usage of several advanced techniques in the products, which results in several number of blocks in a chip. Simultaneously, the system complexity increases with the increase in number of blocks in a chip. With the increase in embedded systems complexity, it is essential to organize the SoCs design and architecture[1].

According to System on Chip (SoC), on a single chip different electronics or computing systems are embedded on to it. As the number of cores increases, which leads to increase in demand for bandwidth for inter core communication to facilitate high core utilization. An essential requirement for scalable interconnection fabrics such as on-chip networks(NoC) is required. The need for better performance is satisfied by increasing the processing cores count on the chip. To address these problems, a new type of interconnect is proposed which is NoC. In NoC context, cores communicate with packet-switching mechanism and all are connected to one another through a network of routers. Routing algorithm is an essential parameter in determining the NoC's performance. For mesh-based NoC, number of routing algorithms have been published and analysed [2].

Routing algorithm is mainly divided into two classes: deterministic and adaptive. In most of the purely deterministic routing algorithms, routing reserves only one path for each communication pair. An example for this type of routing is Dimension Order Routing (DOR) [2]. But this also takes large computational time as they route packets along the same route every time irrespective of the congestion state of the network. Deterministic algorithms are reliable and have low latency in congestion free networks. But the network won't be congestion free always and may need adaptive algorithms for better performance in terms of latency and throughput. On the other side, packets have a choice of multiple paths to reach its destination node in adaptive routing. An example for adaptive routing is Odd-Even (OE) turn model [2]. Network resource utilisation is very high for adaptive routing compared to deterministic routing[3]. The adaptiveness can be in terms of credits, virtual channel etc of the neighbouring cores. There are many simulators in which the algorithms can be analysed in terms of throughput and latency. The topology of the network can like mesh topology, torus topology, spidergon, hypercube etc[4]. In those topologies, variations can be applied for more cores and better connections like 3D connections in mesh topology [5].

The algorithms can be tested on different size of each topology. Performance of NoC can be analysed in terms of throughput, latency, area and power. Apart from these, communication errors are also to be addressed[6].

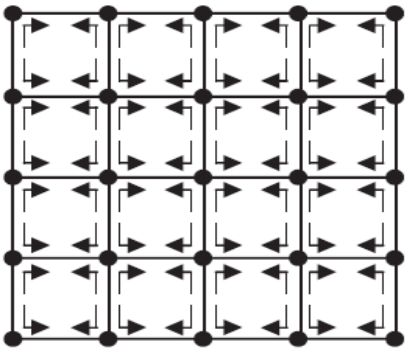

Fig. 1 Restricted turns in XY routing

II. RELATED WORKS

In the literature, most widely studied topic is 2D mesh[7]. In order to avoid deadlock in 2D mesh topology, some 90 degree turns are to be restricted. The system performance is influenced by the number and distribution of the restricted turns. In XY routing, packets are initially routed in X-direction and then in Y-direction. Fig. 1 depicts the restricted turns of XY routing algorithm. In column's perspective same turns are restricted in every column. similarly,same turns are restricted in every row[8].

There were many approaches towards optimizing the routing on different topologies using different routing algorithms and traffics. Some of them are repetitive turn model for adaptive routing [2] their "goal is to exploit the designing space for logic based routing algorithms, and proposed new logic-based routing algorithms that outperformed the state-of-the-art counterparts". The work on "The Odd-Even turn model for adaptive routing"[9] present a model without virtual channels for designing adaptive wormhole routing algorithms for mesh. When Minghua Tang, Chunhui Wu[1] conducted a case study of a adaptive routing algorithm for NoC, known as Odd-Even turn model, Simulation results conclude that in local region there is an high amount of congestion compared to outer regions. It suggests that this issue has to be taken into consideration while designing routing algorithm by researchers.

A model with preemptive approach was applied to odd even routing called PWOE[10].which postpones the saturation traffic rate of NoC by significant percentage compared to odd even under synthetic traffic loads.

Topologies are one of the most essential part of a NoC design, the constraint is performance factor. The parameters which influence the network's performance are latency, throughput, injection rate, hop count etc. Performances are studied and analyzed with the parameters of the topologies in the work "Performance Evaluation of Various Parameters of Network-On-Chip (NoC) for Different Topologies" [11]. Anil Kumar and other authors proposed a machine learning framework[12] that is used on mesh and torus architectures to analyze the performance factors. A comparison was made between the results obtained and the widely used cycle-accurate Booksim-2.0 simulator. Experiments were conducted with various injection rates, virtual channels, and traffic patterns on different topology size ranging from 2×2 to 30×30. The framework showed a prediction error ranging between 5% to 8% and overall minimum speedup ranging between 1500 times to 2000 times. So, considering their analysis, mesh topology is chosen for implementing odd-even routing and run the simulations on 8x8 mesh to analyse and to give out results which can be useful for further research and for development of other routing algorithms.

The proposed work emphasizes on the local region congestion and implemented a fully adaptive non-minimal odd-even routing where the traffic avoidance is the major focus on and the packets may take a longer route in order to avoid the traffic in the mesh.

III. FULLY ADAPTIVE NON-MINIMAL ODD-EVEN ROUTING ALGORITHM

In adaptive routing algorithm there are choices of multiple routing paths between source node and destination node and a single path will be chosen which has the least congestion while routing a packet in the network. According to the dynamic changes in the congestion condition of a network, the paths keep changing. Odd-Even Routing is based upon odd-even turn model [9]. It is classified under the class of distributed adaptive routing algorithm.

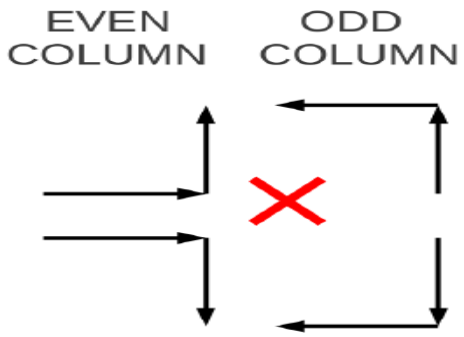

Fig. 2 Restricted turns in odd-even routing

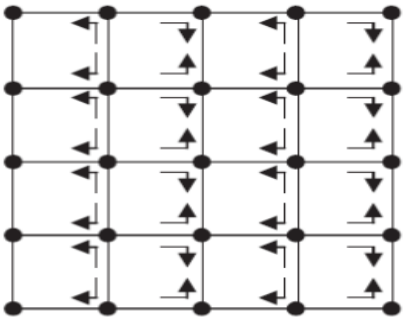

Fig. 3 Restricted turns in Odd-Even Routing at each column is 5x5 mesh.

It introduces various restrictions on taking turns which is depicted in Fig.2. As a result of restrictions in turns, it is deadlock free. Every node in a 2-D mesh has (x, y) co-ordinate. According to the turn model, a column is termed as even or odd based on the x coordinate if it is even then the column is regarded as even column and if it is an odd number then the column is termed as odd column. A turn is regarded as a change in travelling direction in 90- degree. As per these restrictions, there are eight combinations of turns that are possible as shown in the Fig.4. If the packet has 90 degree variation in direction from East to South then it is regarded a ES turn. Likewise if the packet has 90 degree variation in direction from West to South then the turn is termed as WS turn. Similarly, other six types of turns can be described namely EN, WN, SE, SW, NE, and NW turns, where N, S, E and W specify North, South, East and West respectively.

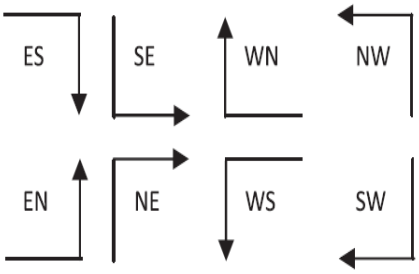

Fig. 4 Combination of turns possible in 90degree angle

The following conditions are necessary to avoid deadlock in OE routing algorithm.

The packets avoid EN and ES turns when present on a even column node. The packets avoid NW and SW turns when present on an odd column node.

ALGORITHM 1

```
//Source nodes are (S1,S2);Destination nodes are (D1,D2);Current nodes are(C1,C2).
Begin
Available_Set ← Ø;
E1 ← D1-C1;
E2 ← D2-C2;
If(E1=0 and E2=0)//current router is the destination router
the packet is delivered to the local node and exits:
If(E1=0)//currently the packet and destination are in same column.
  If (E2>0)
    Append North to Available_Set;
  Else
    Append South to Available_Set;
Else
  If(E1>0)// Eastbound messages
    If(E2=0)
      Append East to Available_Set;
    Else{
      If(C1 is Odd or C1=S1)
        If(E2>0)
          Append North to Available_Set;
        Else
          Append South to Available_Set;
       If (D1 is Odd or E1!=1)//Odd destination column or >= 2 columns to destination
          AppendEast to Available_Set;
          }
 Else{      //Westbound messages
    Append West to Available_Set;
    If(C1 is Even)
      Append North to Available_Set;
    Else
```

```
        Append South to Available_Set;
    }
```

A dimension is selected from the Available_Set for forwarding the packet;

End

****

The above Algorithm 1 is a Fully adaptive minimal OE routing algorithm, available dimensions for forwarding the packet are present in Available_Set.

Available_set is a list of boolean values which contains True or False for the directions North, South, East, West for a packet to route at the current node. This set represents all the available directions excluding the turns in Fig. 2. The congestion detection is implemented through the credit based system present in Booksim 2.0. The detection can be from the delay that is occurred in every core in transferring the packets[13]. The packet is forwarded to the router which has less credits, While routing a packet sometimes non-minimal paths are possible. However, non-minimal paths are not guaranteed to exist.

ALGORITHM 2 - CREDIT BASED

The Available_set in algorithm 1 is used in algorithm 2 to get a a set of available directions of a node and using getusedcredits() function we will save the respective credits for the directions available and find the most feasible or less congested path for the packet.

```
// Initializing the variables.
Counter,ref = 0;
store[2]=null
For  i = 0 to 3 : //  used for finding the no of available directions for a node when Available_set is true.
{
    If(Available_set[i]==true)
   {
      Counter++;//stores the directions
       Store[ref]=j;
       Ref++;
   }
}
If(counter>1)//multiple directions are available
 {  //Cred1 and Cred2 are the respective credits of the available directions.
   Cred1=getusedcredits(store[0]);
   Cred2=getusedcredits(store[1]);
   If(Cred1<Cred2)
   {
     Return store[1];
   Else if(Cred1>Cred2)
   {
     Return store[1];
   }
   Else
   {
     Return store[rand( )%2]
   }
Else  //if only 1 direction is available
  {
   For j =0 to 3
   {
     If(Available_set[j] == True)
     {
        Return  j;
     }
   }
}
**********
```

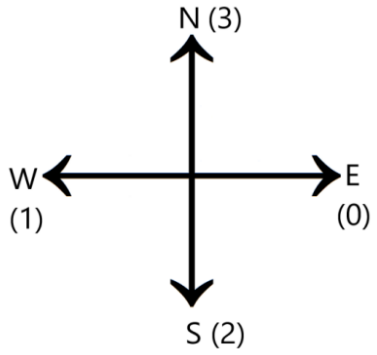

Fig. 5 Encoding of the 4 directions.

In Algorithm 2 we find the number of available directions at a node with help of Available_set and if they are more than 1 direction available then we will find the credits for each direction available and route the packet to that direction in which the credits are less and this will help in congestion avoidance. If both the directions have the same credits then with the help random function we randomly choose one path.

The directions are encoded as depicted in Fig. 5 .When there is only one direction, the algorithm will determine the encoded number for the available path and forwards the packet in that direction. While performing this process the resultant path can be a minimal path or can be non-minimal path depending on the direction.

Existence of non-minimal paths is not guaranteed. If there is only one direction is available, then that is the only direction that can be traversed. A sample selection of routes from source to destination is shown in the Fig. 6.

From Source and Current 49 to Destination 14 : the packet is generated on core 49 which is on odd column. Now using Algorithm 1 it will check the available paths which are East and South. By using Algorithm 2 it will check the credits for both directions and found south direction has less credits and forwards the packet to the router which is in south direction.

From Current 41 to Destination 14: the available directions are east and south from Algorithm 1 and it is still on the odd column. Finds the credits for available directions and chooses the feasible direction which is south and the packet is forwarded to 33, a next router in south direction.

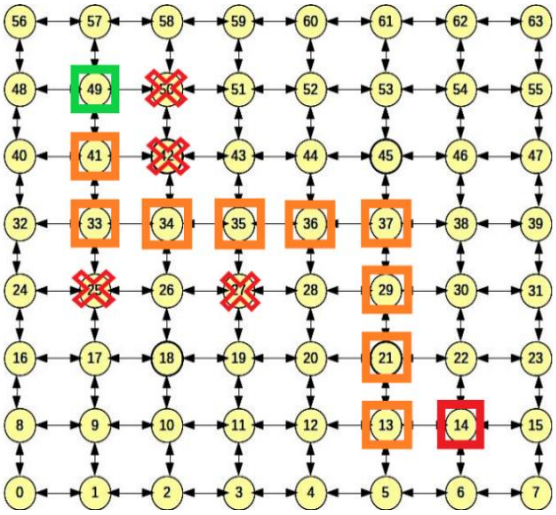

Fig. 6 Route of a packet for source to destination using OE routing and avoiding congested nodes.

From Current 33 to Destination 14 : The available directions are East and South from Algorithm 1.And this time the East direction is preferred over south based on Algorithm 2. So the packet is forwarded to 34.

From Current 34 to Destination 14 : The available direction is only a east direction as it is in even column. ES turn is prohibited and it restricts south direction. So the packet is forwarded to 35.

From Current 35 to Destination 14 : The available directions are east and south using Algorithm 1 . From Algorithm 2 east direction is preferred and is routed to 36.

From Current 36 to Destination 14 : The available directions are only east as the packet is in even column and restricted to take a ES turn. As the packet has only one possibility it is forwarded to the router on east which is 37.

From Current 37 to Destination 14 : The available direction is only south as it is in odd column and the difference between the destination and current is 1,So the east is not added to the Available_set. As the south is the only direction available the packet is forwarded to 29.

Form Current 29 to Destination 14: As its condition is same as the condition at node 37.even at this node it will have only south as the available direction and it will be forwarded to 21.

From Current 21 to Destination 14 : Even this node also has same state as node 37 it also has only south direction in the Available_set .and the packet is forwarded to the node 13.

From Current 13 to Destination 14 : As the vertical distance is zero and only horizontal distance is greater than zero, East direction is added to the Available_set and the packet is forwarded to node 14.

Although the packet had multiple available paths and had to take more turns than a deterministic XY routing algorithm. It avoids the congested routes by using the getusedcredits() function in Booksim 2.0 and routes the packet in the less congested path, thus improving the performance of routing.

V. RESULTS AND ANALYSIS

The simulation is run in Booksim 2.0 for various traffic patterns. The synthetic traffic patterns considered are bitrev, transpose, uniform, and shuffle. In bitrev the node number is converted into binary number and the destination will be the reverse of the source node's binary number. In Fig. 7 the results

show that the odd-even routing has the least packet latency which is till 0.065 injection rate and after 0.065 it saturates. Out of all the traffics the algorithm shows the best results in bitrev traffic when compared with standard deterministic and adaptive algorithms.

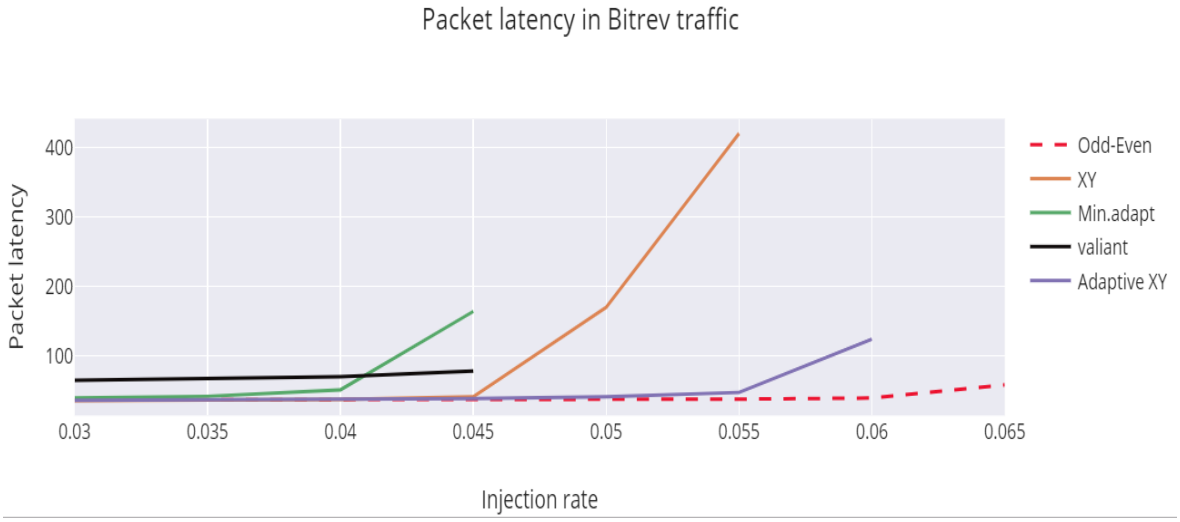

Fig. 7 Packet latency in Bitrev traffic in 8x8 mesh

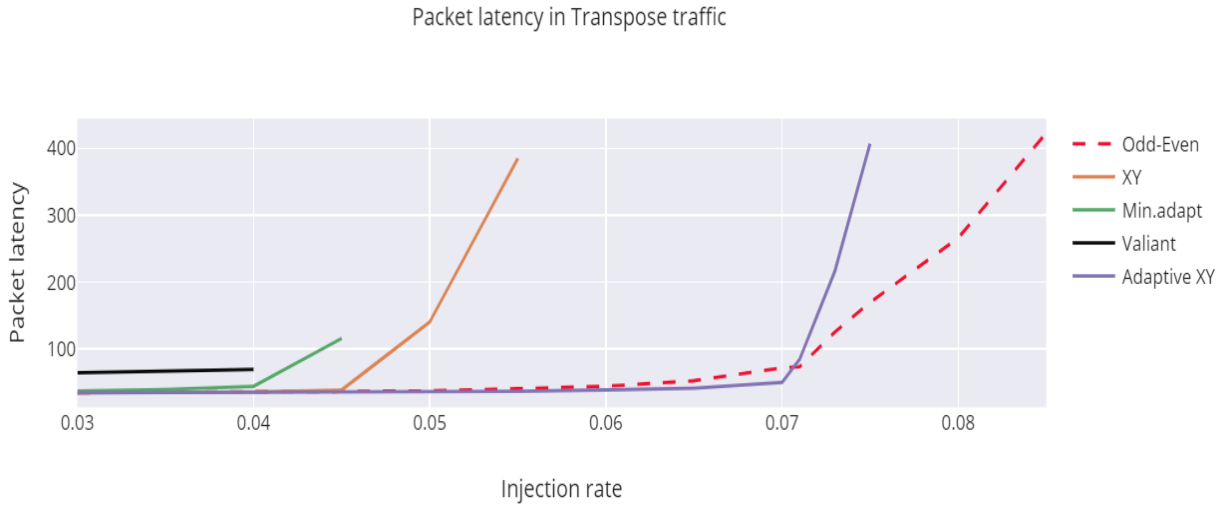

Fig. 8 Packet latency in Transpose traffic in 8x8 mesh

In Transpose traffic, the destination is the transpose of the row, column pair which means for example if the pair (row=1,column=7) is the source which is node 6 will have its destination as node 48 with row=7 and column=1. Fig. 8 shows packet latency for Transpose traffic, the packet latency for Odd-Even algorithm is almost equal to adaptive xy_yx which is the least upto an injection rate of 0.055 and the network latency is least among all other routing algorithms after the injection rate of 0.072. From the Fig. 8 we can conclude that the odd-even routing has the least packet latency or delay which means that it is able to transfer the packet faster than any other algorithms and other algorithms are saturating at low injections whereas saturation point of odd-even is high and saturates after 0.085.

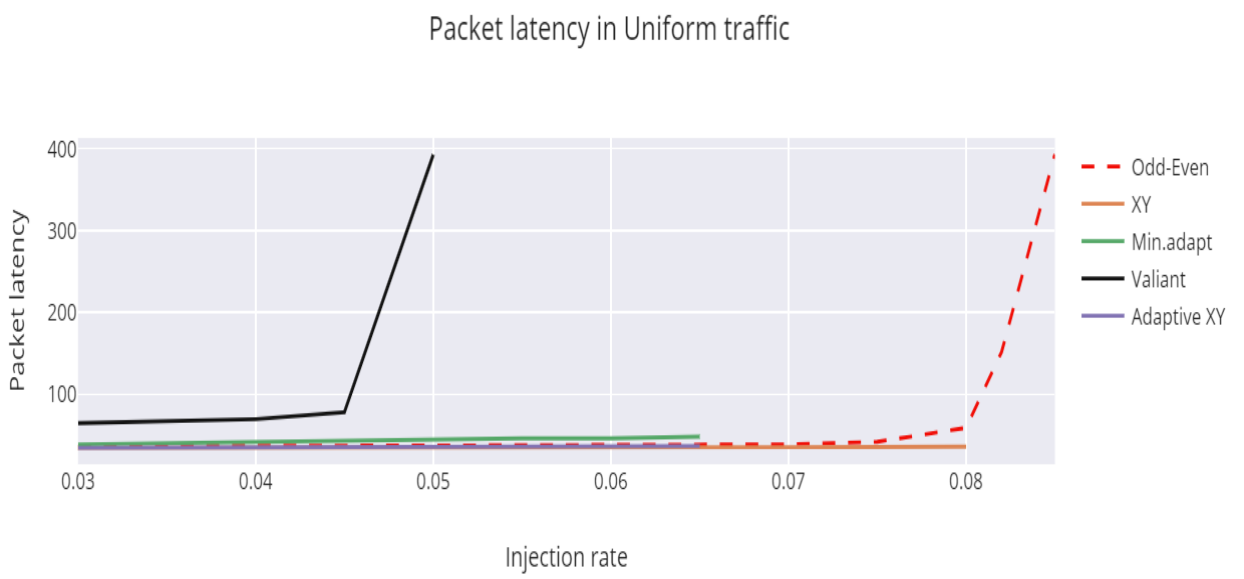

Fig. 9 Packet latency in Uniform traffic in 8x8 mesh

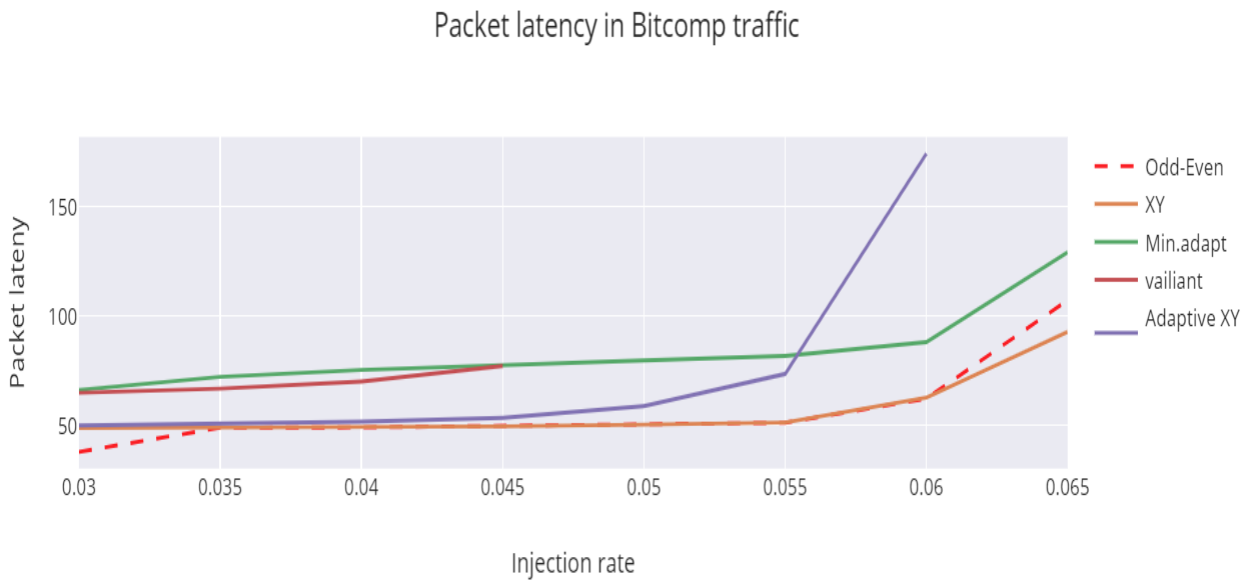

Fig. 10 Packet latency in Bitcomp traffic in 8x8 mesh

In uniform traffic the destination is random to which the packet is sent. From the Fig. 9 we can come to a conclusion that although the odd even routing algorithm's performance is almost same till 0.08 but the XY routing gets saturated at 0.08 and the odd-even still works beyond and saturates at point beyond 0.085 it means although it gives the same performance as the XY routing but it can handle the network with more number of packets than the XY routing.

In bitcomp traffic, the source node number is converted into binary number and negation of the source node number is the destination node. From the Fig. 10, the performance of odd-even routing is almost equal to the XY routing but it shows better performance between 0.03 and 0.035 where the odd even algorithm is able to route packets well by avoiding congestion and as the injection rate increases it is same as XY and at 0.06 it shows a little variation with XY routing. This is because of the vertical and

horizontal distance of the destination is always equal from the source. So, the routing the packets in XY is feasible at higher injection rates.

VI. CONCLUSION

Odd even routing algorithm is a deadlock free algorithm with its own advantages. Addition of adaptiveness results in better performance in routing the cache-miss packets in a dynamic network. Adaptiveness is implemented in terms of credits of each router. The implementation and result analysis are done in Booksim simulator for 8x8 mesh network. The analysis says that it outperforms most of the adaptive algorithms in terms of less latency and extension of saturated injection rates. Latency is better in bitrev type of traffic pattern for the implemented odd even routing compared to all algorithms shown in the graph. It shows better performance in most of the other patterns when compared with other routing algorithms and working of this on larger mesh topology and other topologies is an interesting subject for future work.

VI. REFERENCES

[1] Minghua Tang, Chunhui WuA "Case Study of the Odd-Even Turn Model", Published in 2nd International Conference on Consumer Electronics, Communications and Networks (CECNet) 2012.

[2] Minghua Tang, Xiaola Lin, and Maurizio Palesi "The Repetitive Turn Model for Adaptive Routing",IEEE Transactions on Computers, Vol. 66, No. 1, January 2017

[3] Terrence Mak, Peter Y. K. Cheung, Kai-Pui Lam, and Wayne Luk"Adaptive Routing in Network-on-Chips Using a Dynamic-Programming Network", IEEE Transactions on Industrial Electronics (volume 58, issue:8,August 2011.

[4] Maddula N V Sesha Sai Teja, K Sai Sumanth Reddy, D Radha, Minal Moharir, "Multicore Architecture and Network on Chip: Applications and Challenges", presented at ICIC 2018, Amrita School of Engineering, Bengaluru. India.

[5] Nallasamy Viswanathan, Kuppusamy Paramasivam, and Dr. Somasundaram K., "Vertical Links Minimized 3D NoC Topology and Router-Arbiter Design", International Arab Journal of Information Technology, vol. 15, pp. 469–478, 2018

[6] M. Vinodhini, N.S Murty, "Reliable Low Power NoC Interconnect", Microprocessors and Microsystems, vol. 57, pp.15-22, 2018.

[7]Seema , Pawan Kumar Dahiya"Network-on-Chip: A State-of-the-art Review", IOSR Journal of VLSI and Signal Processing (IOSR-JVSP) Volume 7, Issue-4, Ver. I (Jul. - Aug. 2017), PP 29-35.

[8] Wang Zhang, Ligang Hou, Jinhui Wang, Shuqin Geng, Wuchen Wu,"Comparison Research between XY and Odd-Even Routing Algorithm of a 2-Dimension 3X3 Mesh Topology Network-on-Chip",Published in 2009 WRI Global Congress on Intelligent Systems.

[9]Ge-Ming Chiu, "The Odd-Even Turn Model for Adaptive Routing", Published in IEEE Transactions on Parallel and Distributed Systems(Volume: 11 , Issue: 7 , Jul 2000).

[10] Mohammad Sadrosadati, Ramin Bashizade, Ali Shafie and Hamid Sarbazi "A Method to Improve Adaptivity of Odd-even Routing Algorithm in Mesh NoCs",Published in 24th Euromicro International Conference on Parallel, Distributed, and Network-Based Processing 2016.

[11] Abdul Quaiyum Ansari, Mohammad Rashid Ansari and Mohammad Ayoub Khan"Performance Evaluation of Various Parameters of Network-On-Chip (NoC) for Different Topologies".Published in 2015 Annual IEEE India Conference (INDICON)

[12] A. Kumar and B. Talawar, "Machine Learning Based Framework to Predict Performance Evaluation of On-Chip Networks," 2018 Eleventh International Conference on Contemporary Computing (IC3), Noida, 2018, pp. 1-6.

[13] Nishin Jude C Abraham, D Radha, "Detection and Analysis of Congestion of Nodes in Many-core Processor",presented at First International Conference on Sustainable Technologies for Computational Intelligence (ICTSCI-2019), Amity University Rajasthan, Jaipur, India.

Proceedings of the Fourth International Conference on Communication and Electronics Systems (ICCES 2019)
IEEE Conference Record # 45898; IEEE Xplore ISBN: 978-1-7281-1261-9

Analysis of Load Balancing Algorithms in Software Defined Networking

Himanshi Babbar
Department of Computer Applications,
Chitkara University Institute of Engineering and Technology, Chitkara University, Punjab, India.
Email Id: himanshi.babbar916@gmail.com

Shalli Rani*
Department of Computer Science and Engineering, Chitkara University Institute of Engineering and Technology, Chitkara University, Punjab, India.
Email Id: shallir79@gmail.com

Abstract— With the increasing growth in the network and arising with the latest technologies including cloud and big data, to control and manage the traditional networks is quite tedious. Therefore, it's mandatory to transform conventional network architecture. In order to resolve this issue, Software Defined Networking (SDN) came into existence which makes the management of the network more conformable. To satisfy the fulfilments of Quality of Service (QoS) and with the limited network availability, one of the keynotes that have been taken into consideration is the load balancing issue. It is quite a tedious job to handle the massive amount of load for a single server. Therefore, we can use many servers with the load balancers that behaves as the front end. Although Load balancing is an important aspect in SDN. The basic motive of SDN is to separate the control plane (comprises of intelligent network and this is the area where the controller resides) from the data plane (comprises of routers, switches, and other networking devices that are used in networking). Networks are nowadays more programmable and thus the applications like load balancers don't rely on the dedicated hardware that can be executed with the association of controller and OpenFlow switches in the network can act as a load balancer for this we don't require dedicated hardware for such applications. This paper includes different techniques for SDN that are discussed with their related work and the tool used for load balancing.

Keywords— Software Defined Networking (SDN); Load Balancing; Mininet; OpenFlow; Load Balancing Algorithms.

I. INTRODUCTION

Software Defined Networking (SDN) emerges as one of the noteworthy forms of networking concepts. It helps in lubricating a convenient and efficient flow of network control that facilitates the cost of investment in the meantime which is availing the huge number of users [1]. SDN has transposed the way of managing the network and it is defined by two different tendencies: 1. SDN disassociates the control level (controllers) from the data level (forwarding plane). 2. Decoupling makes the control level programmable by the end users. In conventional networks, it is hardly possible to separate the control level from the data level [2]. Therefore, the end users had to rely on the merchants for the configurations of a software network and its users. In this traditional network data plane, informs your data where it is required to go and control plane, is situated inside a switch or router, in this one device could take the decision of progressing the packet and it also takes into charge of maintaining the routing table information and required to reserve the data and SDN was refined to design, build and manage the networks that decouple the network layer and forwarding layer and becomes directly programmable by the source automation tools [3]. The concept of SDN is explained in Fig. 1. Below:

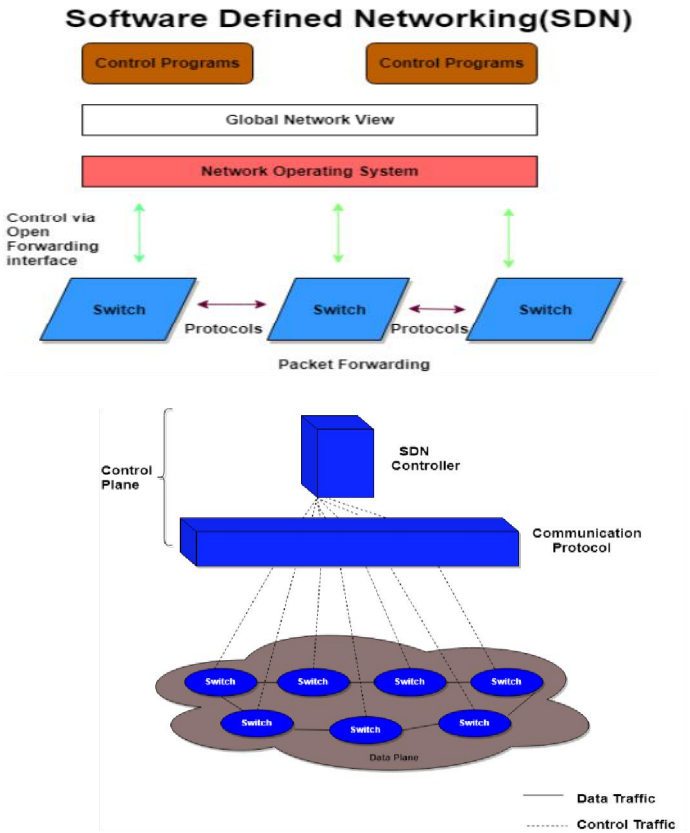

Fig. 1. Software Defined Networking

SDN consolidated the control layer so that the software programmer can have the control over the various data plane elements and SDN interacts the control plane elements with the data plane elements with respect to the defined Application Programming Interface (API).

i. Similarities of Software Defined Networking with Traditional/ Conventional Networking

a. Controllers of SDN has the northbound application programming interface which interacts with the tenders via the API's. It enhances the developers to directly program the network and traditional networks work by using the protocols [4].

b. The main difference between the traditional network and SDN is its virtualization and scalability, the comparison is shown in Table 1 below:

TABLE 1. SDN V/S CONVENTIONAL NETWORKING

Software Defined Networking	Conventional Networking
Forwarding devices and Controller level are disassociated by the API's.	Forwarding devices and Controller level are mingled on the same plane, for every service they require a new protocol.
Facilitates the entire view of the network which leads to consistent and effective policies.	Facilitates the limited information about the networks.

II. MOTIVATION OF RESEARCH

Software Defined Networking is examined to be one of the eminent of the telecom stages. This technology extracts the functions at a lower level of a network on the centralized control level which permits the administers to direct the flow of traffic to the centralized console.

i. The idea of SDN was based on the switch model. The switches process the packets with the system that includes OpenFlow which oppresses the behavior of the switch of the network. This facilitates the control point which coordinates how the switches can handle traffic of the network [5].

ii. The main purpose of choosing load balancing is to keep the network balance the load in SDN. The proposed action is adaptive to the traffic of the network and the flow that is dependent on the integrated path load that relies on the BP Artificial neural network [1]. The primary aim of this proposed action is to optimize the path load and choose the minimal loaded path for the upcoming flow of data.

III. RELATED WORK

Nikhil Handigol et al.,2009, accomplished the coherent technique of optimization algorithm that was developed known as LOBUS (LOad balancing UnStructured networks). We compared this with that of an oblivious or stateful outlook of load balancing.

Chao-Tung Yang et al., 2018, implemented the wildcard mask to execute balancing the load and they even assembled a predicted mechanism that is done in opinion to the traffic of the network.

Ashkan Ghaffarinejad et al., 2014, proposed SDN based load balancing scheme for ASU's Campus Network. In this, approximately 5000 CISCO scattered in unique locations that facilitate the redundant 8 Gbps connectivity to several ten regional 5000 routers.

Sukhveer Kaur et al., 2014, implemented the mininet emulator and compared this emulator with the testbeds which include GENI, VINI, and Emulab. It is accessible to run the real and candid code that are EstiNet, ns-3.

Tariq Emad Ali et al., 2018, proposed the scenario that comprises of fat tree topology SDN Data Center Networks. In this OpenFlow switches are being used. In this, they implemented the OpenDaylight SDN Controller.

Shavan K. Askar, 2016, proposed an adaptive load balancing technique uses the OpenFlow switches that was designed to work using the function it can be a switch, hub or router. OpenFlow switches operate in the charge of the controller that is interconnected to the entire switches and has the overview of the complete network and its corresponding resources.

IV. PROPOSED WORK

i. Data Centre Networks (DCN): The most challenge of SDN is Data Center Networks, which handles the massive number of networks which is not sustained by the changing requirements of the server virtualization. SDN DCN is developed and constructed from a large number of OpenFlow switches which is authoritative for the configuration of switches so to progress the traffic as a layer-2 switch and pertaining the balancing of the load in the DCN [6]. SDN modifies the wide area networks that are required to have the specific API's to provide the changing flow of traffic to degrade the latency and assured the Quality of Service (QoS) for the specific applications.

ii. Load Balancing: Load Balancing is defined as the distribution of load amongst the different servers in order to refinement of the resources, degrade the response time and maximize the throughput. In conventional load balancing networks, it facilitates the support of hardware which is very expensive and suffers from lack of flexibility with this it becomes a single point of failure easily [7]. Availability of Service is predominant in aligning the satisfaction of the end users, which has a higher level of significance on the achievement of balancing the load amongst the process clusters. Connection of most of the people with the internet affects the web traffic which causes the congestion of the network and the loss of packets. With this technique, load balancing refines the efficiency of the network [8].

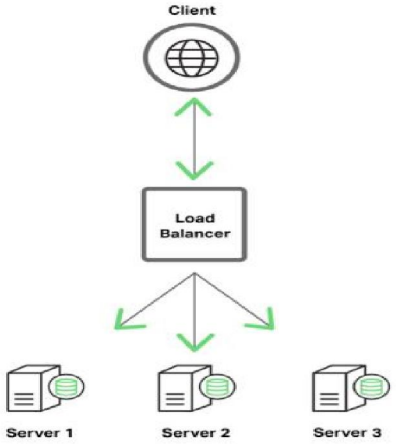

Fig. 2. Load Balancing Architecture

In the process of balancing the load as mentioned in Fig. 2., the traffic is integrated into the multiple servers and it refines the ongoing capacity of the servers [9]. Client's request is forwarded to the backend servers and servers give back the reply and which it then replies to the client. With this client's get directly connected to the backend servers through which the structure of the network is secured, and it inhibits from the attacks on the network.

iii. **Working with Mininet:** In order to work with the SDN, we require many hosts, OpenFlow switches and the wires for creating the connection separating the switches and controller of SDN. Therefore, Mininet is described as the software program that is used to permit the whole network that comprises of controllers, switches, virtual hosts and the links that are to be emulated on a single PC. Mininet has a simple and easy command line API and tools. It is said to be available free i.e. open source software that emulates the OpenFlow devices and the controllers of SDN. Without configuring the physical networks, mininet can generate a topology of the network for the purpose of testing. It reinforces the simplest and adjustable python API for the creation of network and testing.

iv. **Controllers in SDN:** SDN comprises of five topmost controllers that are: POX, Ryu, Floodlight, Open Daylight and Trema. It is considered as the brain of the network and used to facilitate the required information to the switches or routers via Southbound API's [10]. Acts as an intermediator between applications and networking devices. Any interaction between both will be done via the controllers. Controllers are explained briefly in below given Table 2.:

TABLE 2. CONTROLLERS IN SDN

BASICS	POX	RYU	TREMA	OpenDaylight	Floodlight
Language Supported	Python	Python and Message passing reference	Ruby and C	Java	Java and any language that uses REST API
Platform Supported	Linux, Mac OS, Windows	Linux	Linux only	Linux	Linux, Mac OS, Windows
Productivity	Medium	Medium	High	Medium	Medium
Developer	Nicira	NTT, OSRG group	NEC	Multiple Contributors	Big Switch
OpenFlow Version	1.0	1.0, 1.2, 1.3, 1.4		1.0, 1.3	1.0
Used for	Open source platform SDN controller	Used to give logically centralized control and API's of this develops new control	Used to create open flow controllers using C and Ruby programming		It is based on the implementation of Beacon that works with OVSDB.

v. **OpenFlow Protocol:** It is considered as one of the SDN standard protocol which is needed for the building of the solutions of SDN which was established by Stanford University and nowadays is transformed to Open Networking Foundation (ONF) [11]. The most preferable protocol that is required for interaction between the control logic and virtual data plane is OpenFlow. It is orthodox of SDN Southbound Interface Protocol. It is the de-facto interaction between the control plane and the infrastructure plane of the SDN architecture. It is mostly used in wider area networks such as GENI and JGN-X, also useful for ethernet networks.

vi. **SDN based on Load Balancing:** Load Balancing can be administered in either the software or the hardware equipment [12]. The main sole responsibility of load balancer is to distribute the workload requests into multiple servers of a similar type to reduce the burden on the single server. Load Balancer consists of OpenFlow Virtual Switches (OVS) with a controller and various servers that are intermingled to the ports of the OVS [13]. So, in this, each of the servers is assigned its unique IP address and controller has the authority to sustain a list of servers that are interconnected to the OVS. Web service is implemented on every server having a well-known port number as 80.

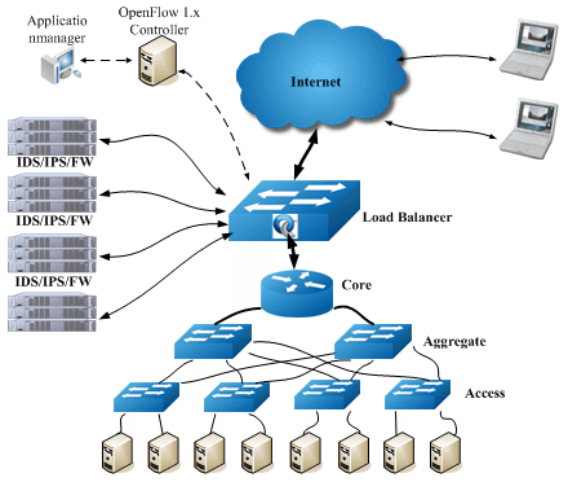

Fig. 3. SDN Based Load Balancer

The controller comprises of the physical location as explained in Fig. 3. All the requests are sent to the physical IP address from the customers [14]. So when the customer is sending the request packet to the physical IP address, then OVS uses the information that is put in the packet header and then later contrast it with the flow entries present in the switch, (1) If the customer's packet header information matches with the flow entry then the switch alters the goal IP address to the location of any one of the servers that are based on strategy of load balancing and forward the bundle of packet to that server. (2) [15] If the packet doesn't match with the flow entry then the switch will advance this packet to the controller. The controller will choose how to deal with the packet, and it embeds new flow entries to the switch by utilizing the OpenFlow [16].

V. Comparative Analysis of Load Balancing Algorithms

Load Balancing divides the workload amongst various links to optimize the efficiency of scheduling and allocation of resources so as to degrade the overloading [17]. We have analyzed the performance of load balancing with time and cost using the cloud analytical tool.

i. Round Robin Algorithm

This algorithm is used to determines the load randomly in the case only when some of the servers are loaded lightly or some of the servers are loaded heavily. This is based on random sampling [18]. The performance analysis is shown in Table 3. and Fig. 4.

Table 3.
Reconfiguration of Time and Cost

Round Robin Algorithm	Time	Cost
R1	40.37	6.09
R10	40.45	10.81
R20	68.9	18.36
R30	48.9	30.7
R40	57.47	39.91
R50	40.73	43.45

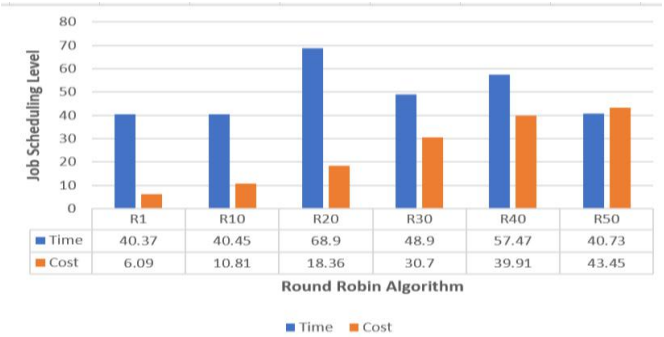

Fig. 4. Performance Analysis of Round Robin Algorithm

ii. Equally Spread Current Execution Algorithm

This algorithm is prepared to deal with priorities. It partitions the load arbitrarily by investigating the size and then later forward the load to only that virtual machine which is said to be loaded delicately and creates the maximum throughput [17]. The performance analysis is shown below in Table 4. And Fig. 5.

Table 4.
Reconfiguration of Time and Cost

ESCE Algorithm	Time	Cost
EC1	40.09	0.89
EC10	40.07	4.5
EC20	40.17	3.03
EC30	40.33	15.03
EC40	40.49	18.12
EC50	40.66	40.67

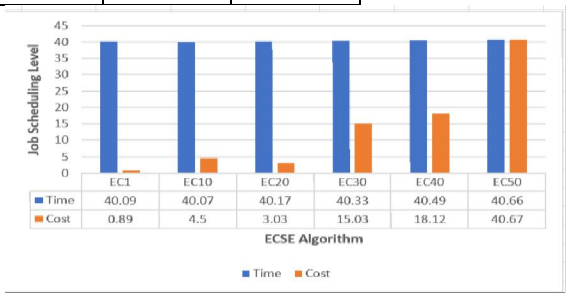

Fig. 5. Performance Analysis of ECSE Algorithm

iii. Throttled Algorithm

This algorithm is done based on the virtual machine and coordinator of cloud couldn't divide this task:

- The request is first sent to the virtual machine.
- The virtual machine has the sole duty to take the choice to move the work as indicated by its size and accessibility.
- Each measure is estimated with its index value.
- The index value is matched with the accessibility. If there is enough space available, then the section sends the response back to the virtual machine.
- After the task is completed the response is stored in the virtual machine allocation table [17].
- The analysis of this algorithm is done in the below Table 5. And Fig. 6.:

TABLE 5.
RECONFIGURATION OF TIME AND COST

Throttled Algorithm	Time	Cost
TH1	40.11	0.89
TH10	40.09	4.5
TH20	40.19	3.03
TH30	40.35	15.03
TH40	40.51	18.12
TH50	40.68	40.67

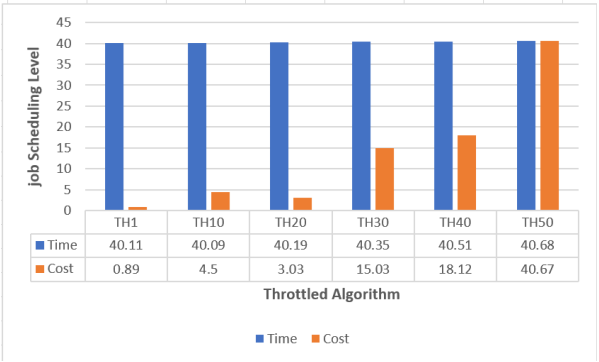

Fig. 6. Performance Analysis of Throttled Algorithm

VI. RESULT ANALYSIS OF LOAD BALANCING ALGORITHMS

We have concluded from the above algorithms that growth of increased strategies using improved jobs and load balancing techniques of allocation of resource. Equally Spread Current Execution (ESEC) algorithm and Throttled algorithm have dynamically allocated the resource to the job in a queue that leads to the cost reduction in the transfer of data and formation of the virtual machine. The result after simulation shows us the result of up to 60% reduction in time and cost.

VII. CONCLUSION

Software Defined Networking is a concept of networking that facilitates the increasing requirements of the network in today's era. As with traditional networks technology redundancy in the path in SDN has efficiently and effectively facilitated the robustness and stability for the whole network. This paper has proposed a domain area to be done in our research work. Load Balancing focusses on how to distribute the massive amount of data into the small portions. Data centers in load balancing handled the huge amount of the data. Load Balancing minimized response time, huge data transfer rate, and how to efficiently and effectively enhance the performance of the whole system are the major key challenges in our research area.

REFERENCES

[1] B. A. A. Nunes, M. Mendonca, X.-N. Nguyen, K. Obraczka, and T. Turletti, "A survey of software-defined networking: Past, present, and future of programmable networks," *IEEE Commun. Surv. Tutorials*, 2014, vol. 16, no. 3, pp. 1617–1634.

[2] M. Mehra, S. Maurya, and N. K. Tiwari, "Network Load balancing in Software Defined Network: A Survey.", *International Journal of Applied Engineering Research,* 2019, pp. 245-253.

[3] A. Jerome, M. Yuksel, S. H. Ahmed, and M. Bassiouni, "SDN-based load balancing for multi-path TCP," *IEEE Conference on Computer Communications Workshops (INFOCOM WKSHPS)*, 2018, pp. 859–864.

[4] C. Chen-Xiao and X. Ya-Bin, "Research on load balance method in SDN," *Int. J. Grid Distrib. Comput.*, 2016, vol. 9, no. 1, pp. 25–36.

[5] K. Govindarajan, K. C. Meng, and H. Ong, "A literature review on software-defined networking (SDN) research topics, challenges and solutions," *Fifth International Conference on Advanced Computing (ICoAC)*, 2013, pp. 293–299.

[6] T. E. Ali, A. H. Morad, and M. A. Abdala, "Load Balance in Data Center SDN Networks," *Int. J. Electr. Comput. Eng.*, 2018, vol. 8, no. 5, pp. 3084-3091.

[7] S. K. Askar, "Adaptive load balancing scheme for data center networks using software defined network," *Sci. J. Univ. Zakho*, 2016, vol. 4, no. 2, pp. 275–286.

[8] C.-T. Yang, S.-T. Chen, J.-C. Liu, Y.-W. Su, D. Puthal, and R. Ranjan, "A predictive load balancing technique for software defined networked cloud services," *Computing*, 2019, pp. 1–25.

[9] A. Ghaffarinejad and V. R. Syrotiuk, "Load balancing in a campus network using software defined networking," *Third GENI Research and Educational Experiment Workshop*, 2014, pp. 75–76.

[10] M. Paliwal, D. Shrimankar, and O. Tembhurne, "Controllers in SDN: A review report," *IEEE Access*, 2018, vol. 6, pp. 36256–36270.

[11] K. Kaur, S. Kaur, and V. Gupta, "Flow statistics based load balancing in OpenFlow," *International Conference on Advances in Computing, Communications and Informatics (ICACCI)*, 2016, pp. 378–381.

[12] V. A. Patrick Von Angelo and W. E. S. Yu, "A Framework for Performance Analysis of Various Load Balancing Techniques in a Software-Defined Networking Environment," *International Conference on Information Science and Applications*, 2018, pp. 67–74.

[13] D. Bhat, K. Rao, and N. Latha, "A survey on software-defined networking concepts and architecture," *Int. J. Sci. Technol. Manag. Vol.*, 2015, vol. 04, pp. 132-141.

[14] S. Kaur, J. Singh, and N. S. Ghumman, "Network programmability using POX controller," *International Conference on Communication, Computing & Systems, IEEE*, 2014, pp. 134-138.

[15] N. Handigol, S. Seetharaman, M. Flajslik, N. McKeown, and R. Johari, "Plug-n-Serve: Load-balancing web traffic using OpenFlow," *ACM Sigcomm Demo*, 2009, vol. 4, no. 5, p. 6.

[16] Y. Hu, W. Wang, X. Gong, X. Que, and S. Cheng, "Balanceflow:

controller load balancing for openflow networks," *IEEE 2nd International Conference on Cloud Computing and Intelligence Systems*, 2012, vol. 2, pp. 780–785.

[17] K. Rishabh, K. Angadi, K. Chegu, D. S. Harikrishna, and S. Ramya, "Analysis of Load Balancing Algorithm in Software Defined Networking," *2nd International Conference on Computational Systems and Information Technology for Sustainable Solution (CSITSS)*, 2017, pp. 1–4.

[18] J. Vashistha and A. K. Jayswal, "Comparative study of load balancing algorithms," *IOSR J. Eng.*, 2013, vol. 3, pp. 45–50.

Proceedings of the Fourth International Conference on Communication and Electronics Systems (ICCES 2019)
IEEE Conference Record # 45898; IEEE Xplore ISBN: 978-1-7281-1261-9

A Multicasting Approach for Path Establishment in Vehicular Ad hoc Networks

Abhander Chaudhary
Department of Computer Science & Engineering
NITTTR, Chandigarh
abhander@gmail.com

Rakesh Kumar
Department of Computer Science & Engineering
NITTTR, Chandigarh
raakeshdhiman@gmail.com

***Abstract*— Vehicular ad hoc network is a decentralized type of network in which vehicles can join or leave the network when they want. Due to such type of the network, path establishment is the major issue of the vehicle ad hoc network. A broadcasting approach is an approach for the path establishment which increases routing over head in the network. In this research work, a multicasting approach is proposed for the path establishment which reduces routing overhead in the network. The proposed approach will be implemented in network simulator version 2. The results will be analyzed in terms of certain parameters.**

***Keywords*— Broadcasting, VANET, Multicasting, NS2**

I. INTRODUCTION

It is very important to ensure the safety, comfort, mobility and quality of huge traffic that is commonly seen within smart cities every day. The Intelligent Transport Systems (ITS) are introduced to provide such facilities within these applications. The Vehicular Ad-Hoc Network (VANET) plays a very important role in developing the ITS for all applications [1]. There are several researchers attracted towards this latest research field from all across the globe. VANETs mainly ensure the safety of vehicles travelling on road along with providing traffic efficiency and level of comfort to the individuals. One of the most important challenges being faced when designing the VANETs is the development of dynamic routing protocol [2]. Lately, in comparison to other traditional approaches, various changes have been made for routing in VANET because of the topology changes arising in highly dynamic and continuous manner. There are several protocols designed for MANETs previously, which are applied and tested within VANET scenarios as well.

The most important challenge here is to reduce the delay related to passing the information from one node to another. If these challenges from MANET protocols are overcome, these protocols can be applied within real time VANET applications. Examining the implications carefully is important [3]. Through the examination of dynamic properties of VANETs, it is possible to control the unpredicted and dynamic nature of vehicular network topologies with the help of routing protocol. The most difficult task to be performed in VANET routing is the identification and maintenance of optimal paths of communication. It is possible to connect the routing protocols of VANET depending upon the topology being used in the network architecture. Further, the performance is also affected whenever the topology of network is changed. With the help of this protocol, it is possible to perform communication amongst the source and destination node with the help of geographical position [4]. It is possible to provide communication amongst the neighboring nodes in such a manner that the beacons are transmitted at regular time interval by using the nodes' geographical positions. The three important components of this protocol are beaconing, location services and forwarding. This protocol also uses the GPS to help in deciding the location of several vehicular nodes. For minimizing the traffic and overhead of VANETs, the Cluster Based Routing (CBR) is applied. The major concern of this routing is generation of network architecture depending upon the clusters that are small groups of vehicles. One of the vehicles present in a cluster is represented as a cluster-head. The size of a cluster completely depends upon the designing of routing algorithm [5]. This design completely relies upon the number of vehicles present within a cluster or geographical positioning of the vehicles. The concept of CBR is also involved previously within ad hoc networks.

The performance of CBR is tested for MANETs that have rigid network conditions. In order to develop the cluster range in most of the routing protocols, a mechanism is generated here. In the next step, the optimal routes are searched to provide communication. Because of the scalability issue, it is not possible to directly apply the cluster formation techniques of MANET in case of VANETs [6]. Broadcast routing is known to be one of the traditional routing approaches of VANETs. The broadcast routing mechanism is applied so that the message that is outside the range of a vehicle can be forwarded. For transmitting the packets, flooding techniques are applied. This routing approach ensures the delivery of information across the network. This approach however, needs to include extensive resources of bandwidth. This approach is applicable in several well established routing protocols particularly within the route discovery process followed towards the destination [7].

Within BROADCOMM, it is possible to simulate the hierarchical structure of highway. The complete region is divided with the help of virtual cells. In case when Cell Reflector (CR) acts like a base station, it is possible to collect the messages from particular call and neighboring calls. CR is used to make judgments when the messages are to be forwarded to individual vehicles. Geocast routing is performed within specific regions that require the need to handle dissemination of information. Due to the increase in use of

VANETS, several geocast routing approaches have been proposed [8]. It is important to perform position based multicasting in several VANET applications in which the vehicles are moving in one similar direction. This routing is also applied for minimizing the search area for next hop to a specific Zone of Relevance (ZOR).

II. LITERATURE REVIEW

Following are the major research work done in the area of VANET:-

Zhiwei Yang et al. (2017) [9] proposed a novel technique for clustering which provides information about the vehicular navigation systems [9]. The author designed a residual route time function which evaluates the overlapping time among the vehicles according to route information. The researchers also designed a method that selects a new cluster head which helps to avoid the exchanging of messages at intersection and maintenance of cluster head is reduced. The comparison is made between the existing algorithms and proposed clustering algorithm, the results shows that the proposed methodology can improve the stability of cluster, in terms of various parameters like lifetime of clusters, number of changed status and so on. Therefore, the researcher draws conclusion from the simulations results that clustering algorithm achieves higher stability and in turn reduces the cost.

Yangyang Xia et al. (2018) [10] presents greedy traffic light and queue aware routing protocol. There are certain benefits provided by applying this approach by performing vehicle clustering at the time of intersection and balance the traffic load among the vehicles. The simulations performed provide results which prove that the designed approach provides better results in comparison to TLRC and GLSR-L. Therefore, the researcher concludes that the simulation performed provides effective results as compared to the other position-based routing protocols.

Abdul Kareem Basil et al. (2017) [11] proposed OSLR routing protocol in which AODV values are evaluated using NS3 simulator [11]. A common geographical topology is used within these applications. There are certain important properties provided within the congestion region. Hence, the researcher concludes that OSLR performs much better than other protocols in terms of the throughput values, PDR values and latency by 17.4%, 7%, and 5% respectively also reduces the density crossroad scenarios.

Wenxiao Dong et al. (2017) [12] proposed a routing protocol called cluster-based recursive broadcast (CRB) which is used to solve the issues and problems faced by other scientists in this field [12]. The re-broadcasting is performed only by the selected vehicles. By taking in consideration the traffic light signal, the CRB is able to achieve the broadcasting along with improvement in efficiency of the forwarded message. The simulations were performed which show that the proposed approach outperform flooding one at a time, in delivery time and delivery ratio. Therefore, the researcher concluded that the proposed approach avoids the storm related issues but outperforms the flooding at the time of high vehicular density and message rate.

Seung-Seok Kang et al. (2017) [13] proposed a simulator called SUMO which is a road traffic simulator and part of NS3 computer based simulator [13]. This proposed simulator is used in monitor the real time traffic of roads and vehicles. The result of this simulation proves that the DSDV routing protocol transfers the information to the network which affects the performance of the packet delivery ratio. Hence, the researcher concludes that the proposed simulator shows better performance and drives at very high speed.

Harinder Kaur et al. (2017) [14] presented two routing protocols called Anchor based street and traffic Aware routing (A-STAR) and Greedy Perimeter Stateless Routing (GPSR) which is used to analyze the real city map [14]. A simulation performed on real map scenario gives accurate results and helps in designing and deployment of VANET in real life. The performance of the proposed approach is evaluated in terms of certain parameters. Simulations were performed by using variable density nodes. Therefore, the simulations of GPSR and A-STAR provide better performance on city map of Bathinda which in turn also shows that A-STAR technique is better. Therefore, the author concludes that the proposed approach is better than the other conventional routing protocols and show effective and satisfactory results.

A. Malathi et al. (2017) [15] presented new multicast routing algorithm for VANET which meets the challenges of multicasting. The proposed approach focuses on the analyzed cluster based routing performance of VANET. The HSSABC optimized algorithm is used to make sure about the effective routing path. The researcher concludes that the proposed algorithm show much better performance in comparison to the already existed routing protocols of ACO, AODV and GA-ACO routing protocols. The experiments were performed which concludes that the proposed approach show effective results in terms of the delivery packet ratio, end-to-end delay, bandwidth and the consumption of energy.

Rajesh Kumar M et al. (2016) [16] proposed quantities like movement of vehicles, vehicular density, and velocity by implementing the Ant Colony Technique. This algorithm responds to the routing protocol having dynamic source routing and improves the working of the MANET. The combined form of algorithm shows much better results at least much better than the end to end delay and packet delivery ratio. In this paper the researcher focuses on the use of ACO technique and provides good routing adaptability at various VANET network. Also, the proposed approach characterizes the dynamic topology, calculation of link quality and so on.

Awos Kh. Ali et al. (2016) [17] proposed routing protocols like AODV, OSLR and GPSR and provides in-depth evaluation of the MANET. This performance is compared in terms of three parameters which are DEL, delay and PDR. The simulations were conducted on NS2 and SUMO and the platforms are configured with the real time situations. Hence, the researcher concluded that the proposed approach OSLR achieves less drop burst length and provides increased PDR results in comparison to the AODV and GPSR load of network. Also, GPSR shows much better results in terms of high node of network and delivers the packets through shortest path.

Arohi Gupta et al. (2016) [18] presented the study of VANET and their routing protocols. The paper also introduces the comparison of AODV, DSR, DYMO and OSLR routing protocols for VANETs along with their advantages and disadvantages [18]. The existing ad hoc routing protocol was also reviewed and elaborated in the respective paper. The paper also shows the comparison between the routing protocols. Every protocol has certain advantages and disadvantages. Therefore, the results of each protocol are compared with one another. Hence, the proposed algorithm is effective and provides much better results.

TABLE I. COMPARISON OF EXISTING ROUTING SCHEME IN VANET

Author's Names	Year	Description	Outcome	Advantages	Disadvantage
Yangyang Xia, Xiaoqi Qin, Baoling Liu, Ping Zhang,	2018	Presents greedy traffic light and queue aware routing protocol. Certain problems are caused due to vehicle clustering at the time of intersection and balance the traffic load among the vehicles.	The proposed approach shows much competitive performance as compared to the other routing algorithms.	It provides better results as compared t other protocols.	Large amount of bandwidth is wasted in this protocol.
Abdul Kareem Basil, Mahamod Ismail, Mohammed A. Altahrawi, Hussain Mahdi and Nordin Ramli,	2017	Presented an OLSR routing protocol and evaluates the value of AODV protocol in various traffic scenarios.	OSLR is effective than the AODV networks in terms of the network metrics.	This protocol is much better than the AODV networks during network blockage scenarios.	Delay in time.
Wenxiao Dong, Fei Lin, Hongling Zhang, Yuping Yin,	2017	Proposed a routing protocol called CRB which is used to solve the issues and problems faced by other scientists in this field	The researcher concluded that the proposed approach avoids the storm related issues but outperforms the flooding at the time of high vehicular density and message rate.	It avoids the storm problems and having high message rate	It increases network congestion.
Harinder Kaur and Meenakshi	2017	Presents two routing protocols called A-STAR and GPSR which are used to analyze the real city map.	The author concludes that the proposed approach is better than the other conventional routing protocols and show effective and satisfactory results.	It is much more effective than previously existed approach.	It shows bad performance for long distance between sources and destination.
A. Malathi , Dr. N. Sreenath,	2017	Presented new multicast routing algorithm for VANET which meets the challenges of multicasting.	The experiments were performed which concludes that the proposed approach show effective results in terms of several parameters.	Shows superior performance in terms of different parameters.	It has no fixed access point.
Rajesh Kumar M and Sudhir K.Routray,	2016	Proposed quantities like movement of vehicles, vehicular density, and velocity by implementing the Ant Colony Technique.	In this paper the researcher focuses on the use of ACO technique and provides good routing adaptability at various VANET network. Also, the proposed approach characterizes the dynamic topology, calculation of link quality and so on.	It provides excellent adaptability to routing protocol at VANET.	The hybrid approaches cannot be used and applied to the VANET environment.

Awos Kh. Ali, lain Phillips and Huanjia Yang	2016	Proposed routing protocols like AODV, OSLR and GPSR and provides in-depth evaluation of the MANET.	The researcher concluded that the proposed approach OSLR achieves less drop burst length and provides increased PDR results in comparison to the AODV and GPSR load of network.	The DEL reduces and PDR increases as per the performance results.	No protocol provides complete information about the path.
Arohi Gupta, Raghuraj Singh, Danish Ather and Ravi Shankar Shukla,	2016	Presents the study of VANET and their routing protocols. The paper also introduces the comparison of various protocols for VANETs along with their advantages and disadvantages.	The proposed algorithm is effective and provides much better results.	It is better and shows satisfactory results.	It requires longer latency for the establishment of the route.
Zhiwei Yang, Weigang Wu, Yishun Chen, Xiaola Lin, Xiang Chen	2016	A novel technique had been proposed for clustering which provides the information about the navigation of vehicles.	The proposed approach shows higher stability and is less expensive.	Higher stability is achieved and becomes less expensive.	The route discovery is floods during the initial phase.

III. INFERENCES DRAWN FROM LITERATURE REVIEW

Following are the various inferences drawn from the literature review:-

1. The vehicular ad hoc network has the self configuring nature and vehicles have high mobility due to which it is difficult to establish stable path. The techniques that are proposed in the previous years have problem of link failure which affect its efficiency.
2. Since the mobility of vehicles is high, road side units plays importance role for the path establishment. The techniques which are already proposed by the authors require extra hardware to deal with the issue of network mobility
3. To establish stable and secure path, clocks of vehicles must be synchronized. An approach needs to be proposed here which can synchronize clocks of the vehicles.

IV. WORK METHODOLOGY

A. Problem Formulation

Most popular amongst all is the reactive routing protocol which establishes the path due to its effective performance. The concept of broadcasting is used in the reactive routing protocol in order to establish the path from source to desired address. Route request packets are flood by the source node when broadcasting the data packets. Route reply packets are sent in response to those requests by the nodes closer to the source node. Hop count and sequence number are the two factors based on which the path for data transmission is chosen.

It had been found that by using broadcasting the nodes which are unable establish a path from source to destination will also receives a request packet which in turn enhances the delay within the network. In this research paper an innovative approach is proposed in which multicasting is used in order to establish a path from source to the desired address.

B. Methodology

In this research work, we will propose scheme for the path establishment using the concept of multicasting. The following are the various steps which are followed for the path establishment:-

1. The VANET is made up of large number of vehicles. In this the road side parameters are employed for the vehicle to vehicle and vehicle to infrastructure interactions.
2. In the second step, the road side units send the control message to each node in the network. The vehicle nodes receive that message and check number of nodes in their direct range.
3. In the third step, each node in the network which presents its number of nodes in their range with the other nodes. The vehicle node which has maximum number of nodes in their range is selected as the zonal head node.
4. The message is transmitted by the source node to its zonal head and verifies that whether it is in its zone or not. When the requesting node is in its zone then path will be directly established from source to the destination and when the requesting node is not in its zone, the zonal head passes the request to the next zonal head. The process is repeated unless the desired path is established.

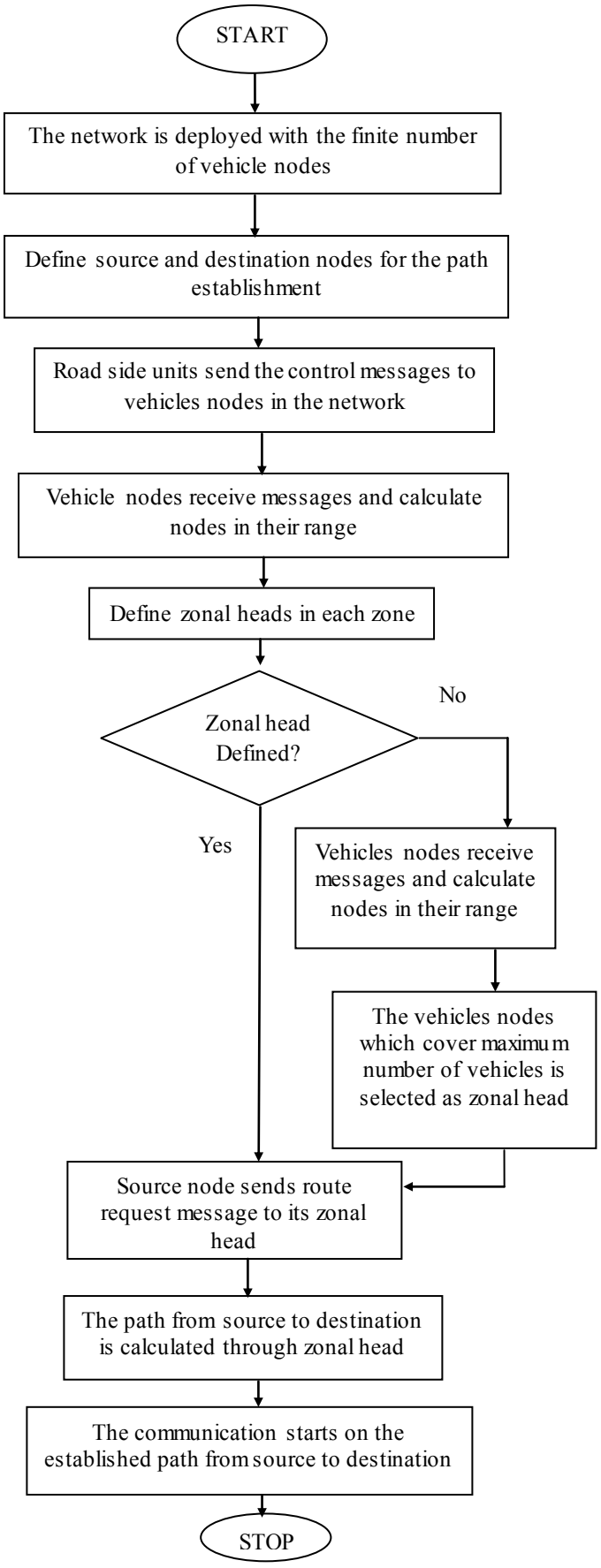

Fig 1: Proposed Flowchart

V. Implementation and Observation

Since VANETs are decentralized in nature, routing is one of the major concerns in these networks. For establishing a path from source to destination, several reactive and proactive types of routing protocols are applied. The reactive and proactive routing protocols are implemented in this research work in network simulator version 2. The table II describes various simulation parameters. The performance of the reactive and proactive routing protocols are compared in terms of throughput and packet loss

Table II. : Simulation Parameters

Parameters	Values
Number of nodes	34
Type of Propagation	Two-Ray Ground
Link layer	LL
Queue type	Priority queue
Queue Length	50
Antenna type	Omni directional

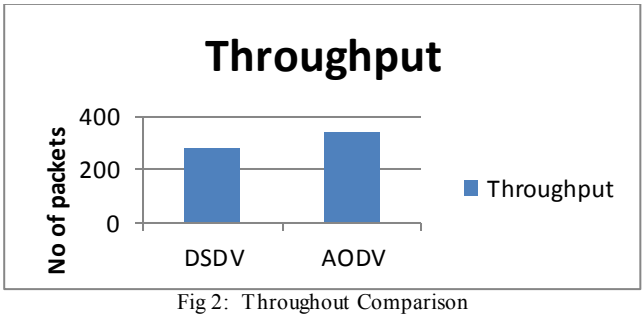

Fig 2: Throughout Comparison

Figure 2 shows a comparative analysis of AODV and DSDV routing protocols in terms of throughput. It is seen that in comparison to DSDV protocol, the throughput achieved when applying AODV protocol is high.

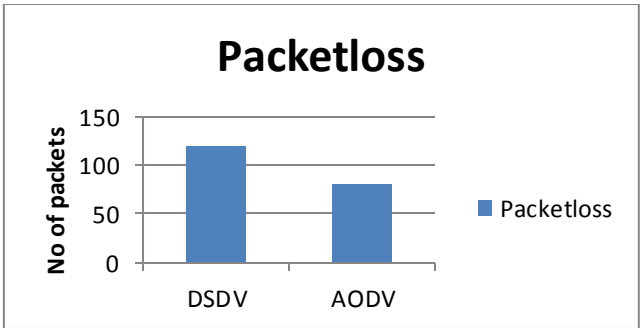

Fig 3: Packetloss Comparison

Figure 3 shows a comparative analysis of DSDV and AODV protocols in terms of packet loss. It is seen that in comparison to DSDV protocol, the packet loss achieved when applying AODV protocol is less.

VI. CONCLUSION AND FUTURE WORK

A decentralized type of network which allows the nodes to enter or leave the network freely is called VANET. VANETs face certain issues while routing is performed due to their dynamic nature. This research work proposes to use multicasting approach to establish paths in these networks. NS2 simulator is used to implement this proposed approach and with respect to certain performance parameters, analysis of outcomes is done at the end.

REFERENCES

[1] S. Dashtinezhad, T. Nadeem, B. Dorohonceanu, C. Borcea, P. Kang, and L. Iftode, "Trafficview: A driver assistant device for traffic monitoring based on car-to-car communication," in Proc. 59th IEEE Semiannual Vehicular Technology Conf., Milan, Italy, May 2004, pp. 2946–2950.

[2] Palak Shandil, Rakesh Kumar: "A novel scheme for isolation of distributed denial of service attack in VANETs," International Journal of Computer Network and Information Security, vol. 11, April 2019, pp.26-34.

[3] O. Riva, T. Nadeem, C. Borcea, and L. Iftode, "Context-aware migratory services in ad hoc networks," IEEE Trans. Mobile Comput., vol. 6, no. 12, Dec. 2007, pp. 1313–1328

[4] A. Nandan, S. Das, G. Pau, and M. Gerla, "Cooperative downloading in vehicular ad hoc wireless networks," in Proc. 2nd Annu. IEEE Conf. WONS, St. Moritz, Switzerland, Jan. 2005, pp. 32–41.

[5] T. Li, S. K. Hazra, and W. Seah, "A position-based routing protocol for metropolitan bus networks," in Proc. 61st IEEE VTC—Spring, Stockholm, Sweden, Jun. 2005, pp. 2315–2319.

[6] J. Tian, L. Han, K. Rothermel, and C. Cseh, "Spatially aware packet routing for mobile ad hoc intervehicle radio networks," in Proc. IEEE Intell. Transp. Syst., Shanghai, China, Oct. 2003, pp. 1546–1551.

[7] M. Jerbi, R. Meraihi, S.-M. Senouci, and Y. Ghamri-Doudane, "Gytar: Improved greedy traffic aware routing protocol for vehicular ad hoc networks in city environments," in Proc. 3rd ACM Int. Workshop VANET, Los Angeles, CA, Sep. 2006, pp. 88–89.

[8] J. Zhao and G. Cao, "VADD: Vehicle-assisted data delivery in vehicular ad hoc networks," IEEE Trans. Veh. Technol., vol. 57, no. 3, May 2008, pp. 1910–1922

[9] Zhiwei Yang, Weigang Wu, Yishun Chen, Xiaola Lin , Xiang Chen, " Navigation Route Based Stable Clustering For Vehicular Ad Hoc Networks", IEEE China Communications, Volume: 15, Issue: 3, March 2016, pp. 2000–2010

[10] Yangyang Xia, Xiaoqi Qin, Baoling Liu, Ping Zhang, "A Greedy Traffic Light And Queue Aware Routing For VANETS", 2018, IEEE China Communications, Volume: 15, Issue: 7, July 2018 , pp. 1920–1926

[11] Abdul Kareem Basil, Mahamod Ismail, Mohammed A. Altahrawi, Hussain Mahdi and Nordin Ramli, "Performance of AODV and OLSR Routing Protocols in VANET under Various Traffic Scenarios", IEEE 13th Malaysia International Conference on Communications (MICC), November 2017, pp. 1819–1828

[12] Wenxiao Dong, Fei Lin, Hongling Zhang, Yuping Yin, "A Cluster-Based Recursive Broadcast Routing Algorithm to Propagate Emergency Messages in City VANETs", IEEE 9th International Conference on Communication Software and Networks (ICCSN), May 2017, pp. 1739–1750

[13] Seung-Seok Kang, and Ye-Eun Chae, Seunguk Yeon, "VANET Routing Algorithm Performance Comparison using ns-3 and SUMO," IEEE 4th International Conference on Computer Applications and Information Processing Technology (CAIPT), August 2017 , pp. 2114–2121

[14] Harinder Kaur and Meenakshi, "Analysis of VANET Geographic Routing Protocols on Real City Map," 2nd IEEE International Conference on Recent Trends in Electronics, Information & Communication Technology (RTEICT), May 2017, pp. 1920–1940

[15] A. Malathi, Dr. N. Sreenath, "Multicast Routing Selection for VANET using Hybrid Scatter Search ABC Algorithm," IEEE International Conference on Power, Control, Signals and Instrumentation Engineering (ICPCSI), September 2017, pp. 1930-1942

[16] Rajesh Kumar M and Sudhir K.Routray, "Ant Colony Based Dynamic Source Routing For VANET," 2nd International Conference on Applied and Theoretical Computing and Communication Technology (iCATccT), July 2016, pp. 1110–1115

[17] Awos Kh. Ali, lain Phillips and Huanjia Yang, "Evaluating VANET Routing in Urban Environments," IEEE 39th International Conference on Telecommunications and Signal Processing (TSP), June 2016 , pp. 1214–1224

[18] Arohi Gupta, Raghuraj Singh, Danish Ather and Ravi Shankar Shukla, "Comparison of Various Routing Algorithms for VANETS," IEEE International Conference System Modeling & Advancement in Research Trends (SMART), November 2016, pp. 1410–1426

Proceedings of the Fourth International Conference on Communication and Electronics Systems (ICCES 2019)
IEEE Conference Record # 45898; IEEE Xplore ISBN: 978-1-7281-1261-9

Developing Augmented Reality Application for All-in-one Interface Card

Rashmi M
Student, M.Tech (IT)
Dept. of Information Science and Engineering
RV College of Engineering
Bengaluru, India
rashmim.sit17@rvce.edu.in

S.G Raghavendra Prasad
Assistant Professor
Dept. of Information Science and Engineering
RV College of Engineering
Bengaluru, India
raghavendrap@rvce.edu.in

***Abstract*— Technologies like Augmented Reality (AR) and Virtual Reality (VR) have been advanced quickly in recent years. Many hardware devices and special techniques have been developed. AR is a technology which integrates the virtual objects with the real time environment. But the critical breakthrough came, when AR spread to the smart phones, this enabled mass spread of AR applications in the field of Education, Manufacturing industries, Military, Medical etc. providing the information about the specified targets to the users. It is also one of the key technologies used in Industry 4.0. AR systems have already reached some level of maturity in educational field and the effectiveness have been widely proven. This paper proposes the development of Marker-based mobile Augmented Reality application, which demonstrates the working of RVCE All-in-one Interface Card.**

Keywords—Augmented Reality, Virtual Reality, Industry 4.0, RVCE All-in-one Interface Card

I. INTRODUCTION

Interaction of Human Computer [1] is a field which is related to Design, Evaluation and implementation of interaction computing systems for use of humans and the study of surrounding phenomena. Augmented reality and Virtual reality are the technologies, which are under Human Computer Interaction. Augmented reality is a technology where virtual reality is combined with real world environments to make it look as if the virtual object is in real world [9]. Augmented Reality can be integrated into daily life and activity, and can be used for various purposes. Augmented Reality (AR) applications provide environment to the users, where they can immerse themselves in to the partially virtual world and interact with the virtual objects and user interface. A lot of Artificial Intelligence (AI) technologies [2] have been used in Augmented Reality. Computer vision is the one area, where AR meets with AI. Computer vision utilizes techniques for computer learning and pattern recognition, that is the reason why it is part of AI.

AR has increased its popularity in both industry and academia, the evolution to Industry 4.0 [3], where during manufacturing , using some of the new technologies in that even AR is also been included.

There are basically two types of Augmented reality,

Marker-Based AR which uses a camera and some type of visual marker from the real-world to produce the result, Virtual objects pop-up only when the marker is sensed by the camera.

Marker-less AR applications [4] have implemented most widely. This is also called as Location-based or GPS, position-based. Uses GPS, Velocity meter, or Accelerometer which is integrated in device to provide the data based on the user's location.

This paper proposes the work of developing a Marker-Based mobile Augmented reality application, which demonstrates RVCE *All-in-one* Interface Card by using AR technology. It gives the information about the Interface card in the form of buttons, videos and other virtual enhancements integrated with real world objects.

A. RVCE ALL-IN-ONE INTERFACE Card

Microprocessors / Microcontrollers is one the core courses studied by under graduate students of computer science, Information Science, Electronics & communication, Instrumentation, Electrical & Electronics Engineering in many universities. R&D Labs of CSE Department, RVCE has taken up the Design & Development of "All In One – Multipurpose Interfacing Card" for PC for X86 Programming and product developments, successfully manufactured and adopted.

RV All-In-One Interface Card can be used to convert PC to PC based product for number of applications and also to create interest and bring innovation among students by using the interface card to conduct different experiments and projects using their computer system.

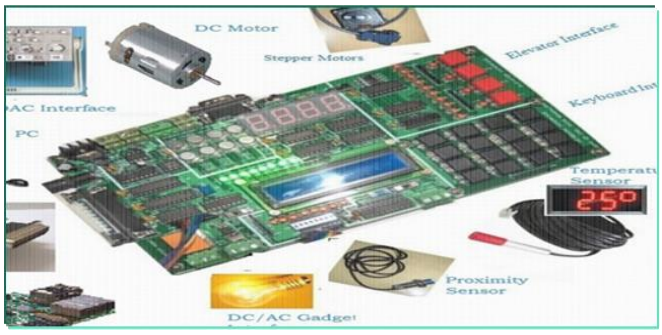

Figure 1: RVCE All-in-one Interface Card

The Different Interfacing Modules Integrated in RV ALL-IN-ONE Interface Board are Logic Controller, Seven Segment Display Module, LCD Interface ,Stepper Motor Interface, DAC Interface, ADC Interface, DC Motor Interface , DC Solenoid , Temperature Sensor Interface , Ac

Gadget Interface, Industrial Sensors Input Interface, Elevator Interface , Keyboard Interface.

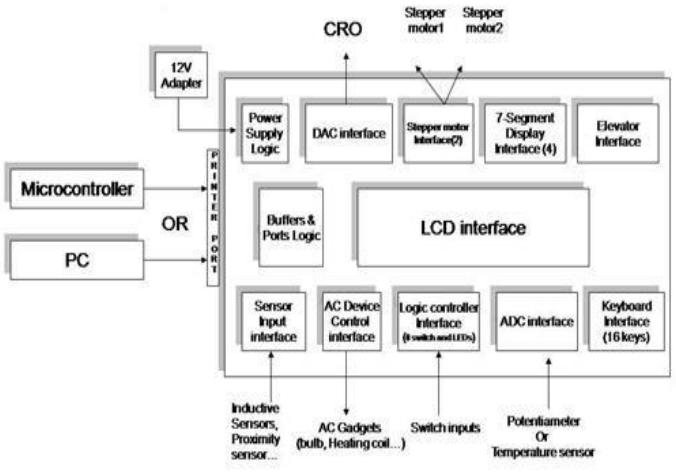

Figure 2 : Block Diagram of RVCE ALL-IN-ONE Interface Card

The application senses the Interface Card and mixes it with virtual objects (like text, graphics and audio) and gives back those information to the users.

II. Objectives and Scope

1. The main purpose of the work is to demonstrate the RVCE *All-in-one* Interface card using Augmented Reality by providing each module's internal working ,functionalities, architecture and code-snippet, and providing all the information at one place and making students understand the concept in easier way.

2. Idea of introducing the technology to the students and make learning as new and creative.

3. This application helps the student to understand about the basic information of Interface card independently.

4. One of the useful technology in the Industry 4.0, which helps engineers while manufacturing by guiding them the procedure.

III. Theory and Concepts

AR uses the device's camera of handheld mobile devices, such as a smart-phones or tablets to capture the video and place virtual objects on top of the real world. To run an AR app on a mobile device, point its camera to the target and application will recognize the target and render computer graphics which is registered for the target position and orientation.

Mobile devices [5] should have the following important features to run AR application

1. Flat panel graphic display touch-screen input. Rear-facing camera.
2. Motion sensors, rotational motion has been recognized by the gyroscope and linear motion has been detected by the accelerometer.
3. GPS and other position sensor for geo-location and wireless.
4. Untethered and battery powered.
5. GPU (Graphics processor), CPU(Main processor) and Memory.

The video frames of the real-world have been captured by the rear-facing camera and displays it in screen. Because the video data is digital, app will modify it and combine virtual graphics in real-time.

AR uses computer vision to recognize targets in the field of view. Whether natural feature tracking (NFT), specific coded markers or other techniques to recognize text or object. The application generates computer graphics that aligns with those real-world transform that overlaps on top of real world imagery when it recognizes the targets and orientation.

The key to the success of mobile AR, also includes sensors which measures orientation, motion and other conditions. A gyroscope for detecting rotational motion around the axes and an accelerometer used for detecting linear motion. The software estimates the device's position and orientation by using three data in real 3D space at any given time. The specific view of the device camera capturing is determined by this data. And uses this 3D transformation to register the computer generated graphics in 3D space as well.

A. Target Based AR

The device camera captures a frame of video [6]. The familiar target is analyzed from the frames by the software, such as a pre-programmed marker, by using the technique called Photogrammetry.

Deformation like size and skew is analyzed as part of target detection, is analyzed to determine its distance, orientation and position relation to the camera in a three-dimensional space. The 3D space is determined from that camera pose that is position and orientation. And these values are used in the computer graphics calculations to reduce virtual objects. Finally, the video frame and rendered graphics are merged and displayed it to the user.

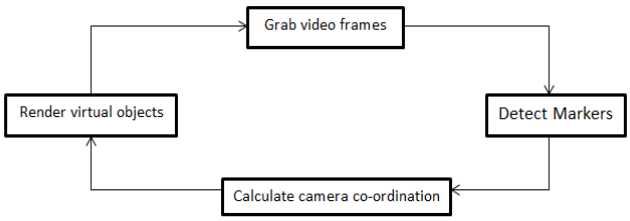

Figure 3: Explains the modules in which AR works

The ability to recognize and track complex 3D objects goes beyond the 2D image recognition [8]. A good marker is detected easily in all the conditions or circumstances. The brightness differences is easily detected than color differences using machine vision techniques. This is because of camera's automatic white balance are poor: it is incorrect color register. The object changes the color depending on the view in the image. The lightening also changes the colors of the objects, that's why color detection becomes challenging. The object detects easily, when there is more contrast in the luminance, that means there should be optimal black and white markers. By using the detected markers, the system also calculates the camera's pose.

B. Marker pose

The object's pose always refers to is location and orientation [6]. Around the three co-ordinate axes, the orientation is expressed with three rotational angles (α, β, γ) and with three translation co-ordinates (x, y, z) location can be expressed. Thus the pose has six degrees of freedom.

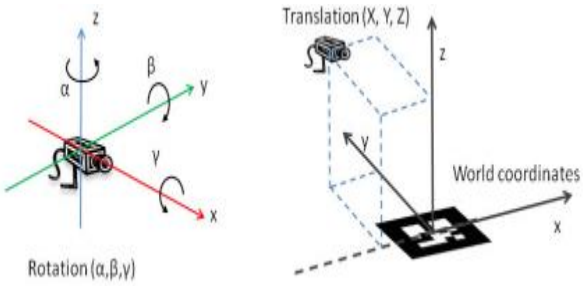

Figure 4: The pose of camera (Orientation and Location in the world co-ordinates)

From a minimum of four coplanar and non-collinear points, the camera's pose can be determined. Thus, calculation of marker's pose in 3D co-ordinate by the system using four corner points of the marker in image co-ordinates.

In digital cameras, co-ordination of elements and image registers on the image sensors differ from ideal co-ordinates. The camera image depends on the camera's physical characteristics such as size and orientation of Image sensor, focal length etc.

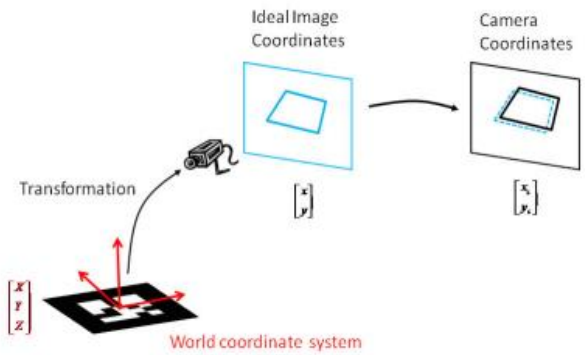

Figure 5: Additional conversion to the camera co-ordinate system is needed as ideal pinhole camera models does not hold for digital camera.

1. Camera transformation

Camera and marker's transformation T

$$x = TX,$$

where X is a point world co-ordinates, x is its projection in ideal image co-ordinates and T is the camera transformation matrix or pose matrix. Transformation T consists 3*3 rotation matrix R and translation vector t and can be expressed in the form of matrix.

x = [R | t] X , which is homogeneous co-ordination is

$$\begin{bmatrix} x \\ y \\ z \end{bmatrix} = \begin{bmatrix} r_1 & r_2 & r_3 & t_x \\ r_4 & r_5 & r_6 & t_y \\ r_7 & r_8 & r_9 & t_z \end{bmatrix} \begin{bmatrix} X \\ Y \\ Z \\ 1 \end{bmatrix}.$$

There are only three parameters in rotation matrix (α, β, γ) which defines its nine elements. There are also three parameters in translation vector and six free parameters in pose matrix. When the marker is detected, the marker tracking system needs to solve this camera for each frame.

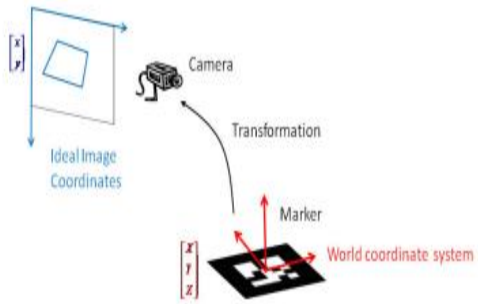

Figure 6: Conversion of worlds co-ordinate to ideal camera co-ordinates by transformation matrix.

2. Detection errors in pose calculation

It is more reliable to detect the x and y translation than z translation. The movement of image plane is smaller It is more reliable to detect the x and y translation than z translation. The movement of image plane is smaller when object moves the same distance in x or y direction than the object moves some distance in z direction.

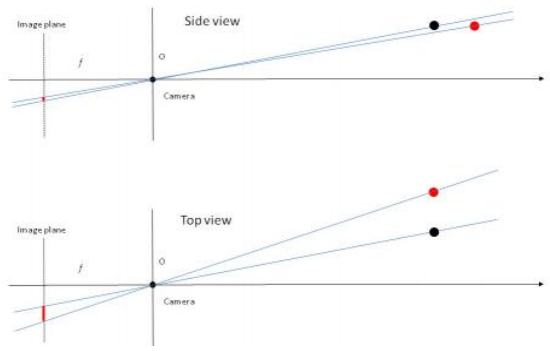

Figure 7: If the black dot (object) moves parallel to the optical axes (on the top) [12], the moment in the image plane is small than the movement of perpendicular to the bottom (optical axes). That's why detection of errors on the image plane have a great detection on the z dimension.

3. Rendering with the pose

The camera is moved to render the virtual object in the right scale and perspective, the camera should be moved to same pose as the real camera and on top of the real image, virtual objects are rendered.

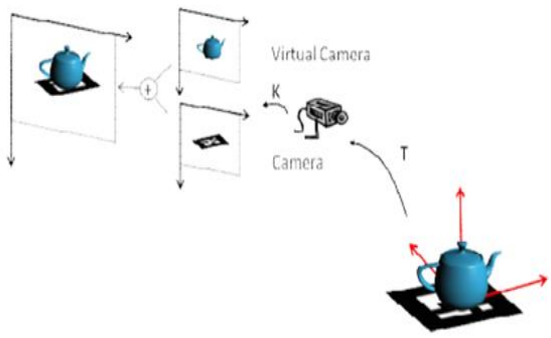

Figure 8: Augmentation in origin

IV. METHODOLOGY

The proposed methodology for the Marker based Augmented reality mobile application has six modules [7]. Below are the names of the following modules.

- Camera
- Capturing Image module
- Processing Image module
- Rendering Image module
- Tracking marker module
- Display the screen

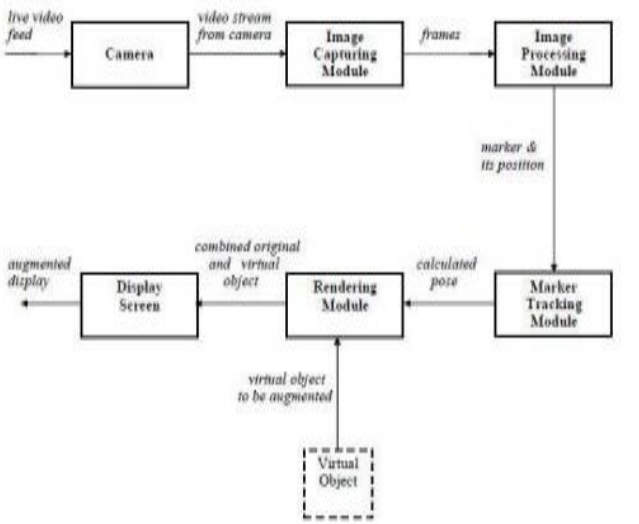

Figure 9: Methodology of the proposed application.

1. Camera module

Camera module takes the live video as an input from the Android smart phone. In Augmented reality displaying this live video is reality

2. Capturing Image module

The live video from the camera module is given as an input for the capturing image module. This module analyses each frames from the live video and generates binary images that has only two values for every pixel. Basically white and black are the only two colors that are used for the binary images.

3. Processing image module

Binary images from capturing module is given as an input to this module. Here binary images are processed by using techniques of image processing to detect the markers for Augmented reality, this is necessary to identify the position to place the virtual objects [10]. Once this is identified, then the location of AR marker is given as an input to the tracking module.

4. Marker Tracking module

The marker tracking module is like heart of AR systems. Calculations of the real-time camera's relative pose is done by this module. 3D orientation and 3D location is the meaning of the term pose, i.e. six degrees of freedom position.

5. Rendering module

Basically the inputs of rendering modules are two. One is tracking module's calculated pose and the

other is virtual objects that needs to be augmented. By using the calculated pose, the rendering module combines the virtual objects with the original image that has been capturing from the camera and displayed on the screen of android smart phone.

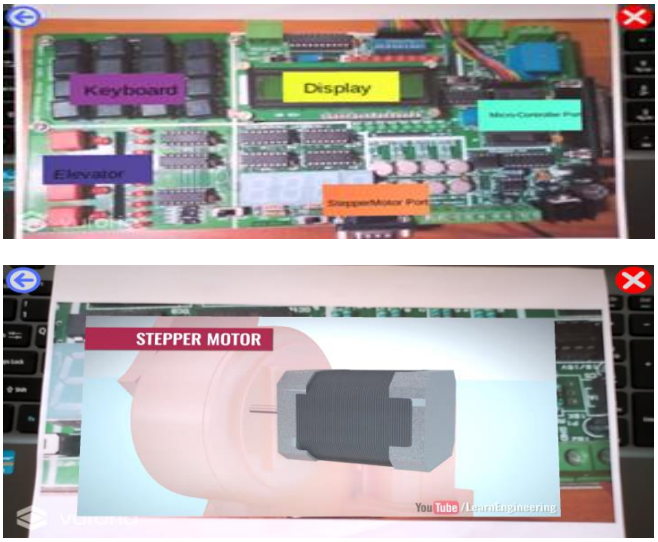

Figure 10: Screenshots of the application which demonstrated the virtual objects of RVCE All-in-one Interface Card.

V. CONCLUSION

This paper proposes the marker based augmented reality using Android, which helps the students to understand the working of RVCE All-in-one Interface card in better way by showing the virtual objects in the form of video (which explains the working of modules like Matrix keyboard, Elevator, Stepper motor) audio and virtual buttons and also provide the program of each module. So that students get all the materials in one place. Further, AR modules can be developed to enhance different electronic devices, machines motors, etc., to enhance the learning [11], in turn enabling the way to adopt and enhance ICT based learning techniques.

REFERENCES

[1] "vuforia sdk," https://deveoper.vuforia.com/, accessed: 2016-02-01. [20] "Unity3d," https://Unity3d.com/, Accessed: 2018-02-01

[2] Ayer, S.K, Messner, J.I, Anumba, C.J Augmenetd Reality gaming in sustainable design education, Journal of Architectural Engineering, 2016, 22(1).

[3] The CDIO INITIATIVE is an innovative educational Framework for producing the next generation for Engineers Available : https :// www. cdio.org/about [Accessed on 2017, 6 March].

[4] Lai, Yoke Chin "Is Augmented Reality a New Paradigm in Design Education when Educational Subsidy Decreases" Published in: Proceeding of The 19th International conference on Engineering Product Design Education.

[5] Assoc. Dr. Oguz Colak, Assist. Prof. Dr. Lokman Yunlu " A Review of Augmented Reality and Virtual Reality in Engineering education".

[6] https://thinkmobiles.com/blog/how-to-make-augmented

[7] Jun He, Peng Han " The research and application of the Augmented reality technology" published in 2017 IEEE 2nd Information Technology, Networking, Electronic and Automation Control Conference

[8] Mikko Kytö, Barrett Ens, Thammathip Piumsomon Pinpointing: Precise Head -and Eye –Based Target Selection for Augmented Reality.

[9] Shaunak Shirish Deshmukh, Chinmay mandar Joshi "3D Object tracking And Manipulation in Augmented Reality. Published in International Research Journal of Engineering and Technology (IRJET) volume: 05 Issue:01|Jan-2018.

[10] Haibin Ling "Augmented Reality in Reality " IEEE Multi Media Honolulu, Hi, USA, Jun.2017,pp.44-50

[11] Siddhart Patil. Chiquitha Prabhu "E-learning system Using Augmented Reality" 17th 2017 , pp. 1-8. IEEE Conference on Emerging Technologies & Factory Automation(ETFA).

[12] Sangeeta Kumari and Nitish Polke "Implementation Issues of Augmented Reality and Virtual Reality: A Survey". International Journal of Engineering Trends And Technology (IJETT)- Volume 32 Number2- February 2017, pp.789-794.

Proceedings of the Fourth International Conference on Communication and Electronics Systems (ICCES 2019)
IEEE Conference Record # 45898; IEEE Xplore ISBN: 978-1-7281-1261-9

Design of low power SR-flip-flop with on/off (ONOFIC) implementation

Masood Ahmad Malik, Vijay Kumar Sharma

School of Electronics and Communication Engineering,
Shri Mata Vaishno Devi University, Kakryal-182320, Katra, (Jammu & Kashmir)

(Email id: malikmasood93@gmail.com ,vijay.sharma@smvdu.ac.in)

Abstract: Metal oxide semiconductor (MOS) devices are the basic building blocks for the logic circuits. Advancement in technology increases the expectation of customer in electronics. Various challenges face by IC designer during the uses of this Nano-scale technology because no one technology is completely satisfied all requirements. Better performance with minimum power dissipation and high stability is become basic need and low power dissipation is possible when power consumption of VLSI device is low. As the need of small electronics components and devices is increased day by day. There is a rapid growth in industry of electronics in few decades. World and technology are growing at the same speed. Day by day as the demand for small devices increases with high efficiency and result in flip-flop came into existence. These flip-flops have number of applications in electronics like used in communication, computers. As the size of the flip-flops decrease there is a problem of leakage current which prevents us to design a low power circuit. To decrease these leakage currents in the SR flip-flops and made it as a low power flip-flop an approach is used in this paper called as ON/OFF (ONOFIC). This ONOFIC implementation of SR flips decreases the leakage current and in this way our SR flip-flop is low power consuming

Keywords—Flip-Flop, ONOFIC, Power Dissipation, VLSI

I INTRODUCTION

World and technology are growing at the same speed. Day by day as the demand for small devices increases with high efficiency and result in flip-flop came into existence. Flip flops have a number of applications in electrons and nowadays these flip-flops are used for optical signal processing and transparent optical fiber processing [1]. Flip-flops is main hardware device that is highly used in synchronous finite state machines [2]. SR flip-flop have number of application one of the application is mechanical bounce and its elimination removal [3]. Flip-flops can be simple or clocked[4], they are positive edge triggered I.e. when clock is raising we are accepting the data from the input and also negative edge triggered which means when clock is falling down at the time data is sampled. There are two types of logic circuits combinational and sequential logic circuits. Combinational logic circuits are the function of current input values but sequential logic circuits are the function of current values of the inputs and also on the preceding input values. Set reset flip-flop is called SR flip-flop and is the simpler one among all the other flip-flops. SR flip-flop has a clock signal and two inputs called as set and reset. When the set input is high output is high and when reset is high output is low. When the set and reset input both are high output is this state is Invalid. NOR and NAND gates are used by simply cross coupling to each other. Due to tremendous use of small devices in electronics field the technology is also scaled down day by day. Scaling has lot of advantages like we are able to make small and small devices like in these days small iPods, tablets, pacemakers and hearing machines but on the other hand we are losing the property of low power. These small devices must be low power dissipation because low power devices are highly demanded in these days. Maximum power consumption of a chip depends on its implementation and technology [5]. Aggressive scaling of MOS devices requires use of ultra-thin gate oxides to maintain a reasonable short channel effect [6].When we are scaling the device parameters we have to scale the supply voltage, threshold voltage and oxide thickness. Supply voltage plays an important factor to reduce the power dissipation in portable devices [7]. Reducing the supply voltage increases the sub-threshold leakage current and decreasing the oxide thickness results in increase of junction tunneling of electrons. When the gate oxide is reduced to a large extent there is exponential increase in gate leakage current and reduction of transistor threshold voltage increases sub-threshold leakage currents [8]. The tunneling of electrons is directly proportional to scaling, new standard CMOS SOCS face major challenges because of leakage current. These leakage currents have a serious effect i.e. the device consumes large quantity of power and this is the main challenge in the VLSI technology.

These leakage currents pose a challenge to the low power devices and lead to the instability of logic circuits. These leakages currents needs to be reduced so that power dissipation of the CMOS devices is low and stability, speed should be improve. This high dissipation power is becoming a serious design concern as we towards the mobile computing world [9]. In this paper CMOS SR flip-flop is designed with ONOFIC implementation which reduces the leakage to a great extent. A comparison is made between the conventional SR flip-flop and our ONOFIC implementation of CMOS SR flip-flop in terms of power dissipation. This paper is divided into four sections. Section 2 explains the related work and ON/OFF (ONOFIC) approach for designing of CMOS SR

flip-flop, section 3 explains the conventional CMOS SR flip-flop and ONOFIC implementation and finally results and conclusion in section 4. All the simulations are done using cadence tool at 45nm.

II RELATED WORK

In [12] a SR flip-flop is designed by using CMOS 90nm technology. Two layout models I.e. semicustom and full-custom design technology are made. A comparison is made between these two in terms of power and fully customized layout is 39%better than semi-custom layout

In [3] SR flip-flop is designed by using 45nm CMOS technology. By using MOS transistors less energy is consumed than by using conventional gates.

ON/OFF (ONOFIC) APPROACH

In the ONOFIC approach design, a logic block consists of one PMOS and one NMOS is inserted between the pull-up and pull-down network. This logic block is known as ON/OFF logic block we usually use PMOS as pull-up and NMOS as pull-down because NMOS will let us go to zero and PMOS will let to go to VDD so we get maximum swing available in this case. If we change the position of the pull-up and pull-down we have to compromise on certain output parameters. This approach is less complex only one logic block is added between the pull-up and pull-down network.

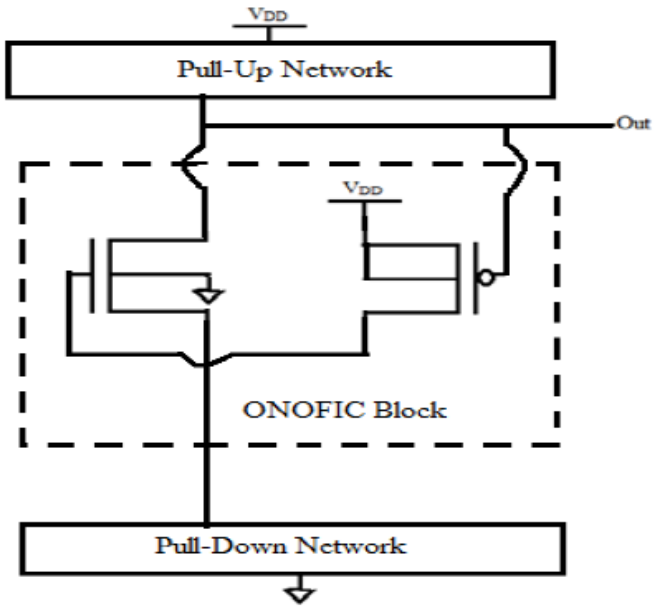

Figure 1.Schematic of ONOFIC approach [10]

This PMOS and NMOS block should work in ON/OFF condition for any logic output. This block works like as force stacking concept providing maximum resistance in OFF condition and minimum resistance in ON condition thus reduces the leakage current. These two transistors should be in cut-off or in linear state depending on the output logic. Figure below shows the schematic of ONOFIC approach. The ONOFIC transistors are connected in this way. The gate of NMOS is connected to the drain of PMOS and source of PMOS is connected to VDD and then the gate of PMOS with the output. The right turning of the ONOFIC transistors helps us in low propagation delay [10].

III CONVENTIONAL AND ONOFIC IMPLEMENTATION OF CMOS SR FLIP-FLOP

The below circuit diagram represents the SR flip-flop with a NOR based design this is the basic design. R and S are inputs and E is clock signal. In this section the SR flip-flop is designed by CMOS technology, designing the SR flip-flop with CMOS technology has number of advantages like low power dissipation, high noise immunity, lower propagation delay and high speed high frequency of operation [11]. The advantage of MOSFET'S is that they draw almost zero control current while idle [12].

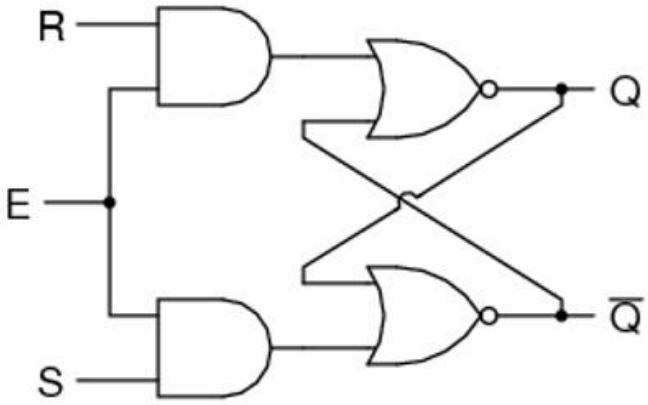

Figure 2 NOR based SR flip-flop

The conventional CMOS SR flip-flop consists of twelve transistors only. The status of the transistors in this design are when clock signal is low in N tree the two series terminals N are and open and also in P tree two parallel transistors are ON by this the state is retaining in the memory cell. When the clock signal is high the circuit is simple a CMOS NOR latch which will answer to inputs S and R.

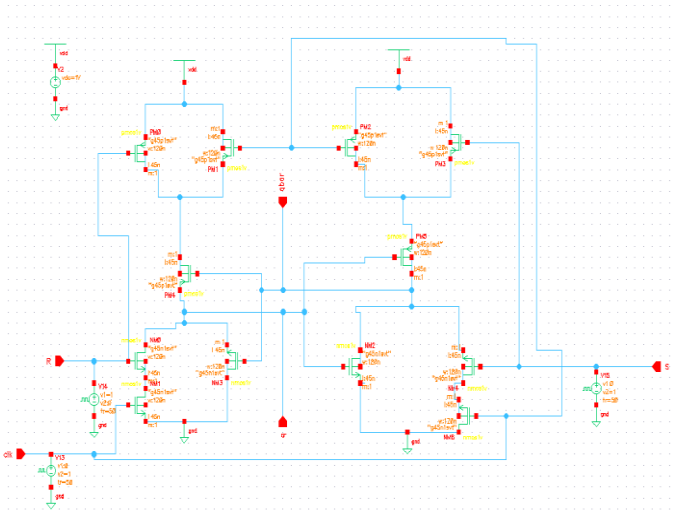

Figure 3.Conventional CMOS SR flip-flop

ONOFIC implementation of CMOS flip-flop

The below circuit represents the ONOFIC implementation of SR flip-flop. It consists of conventional CMOS SR flip-flop and further with addition of ONOFIC logic block. Two logic blocks are added in this implementation between the two pull-ups and pull-down networks. The total number of transistors in this implementation is sixteen. These four extra transistors help us to reduce the leakage current in the network. PMOS transistors control the operation of the NMOS transistors In the OFF state this block provides maximum resistance due to which the leakage currents are reduced because we know these leakage currents arises in OFF state when we go scaling to a to a large extent.

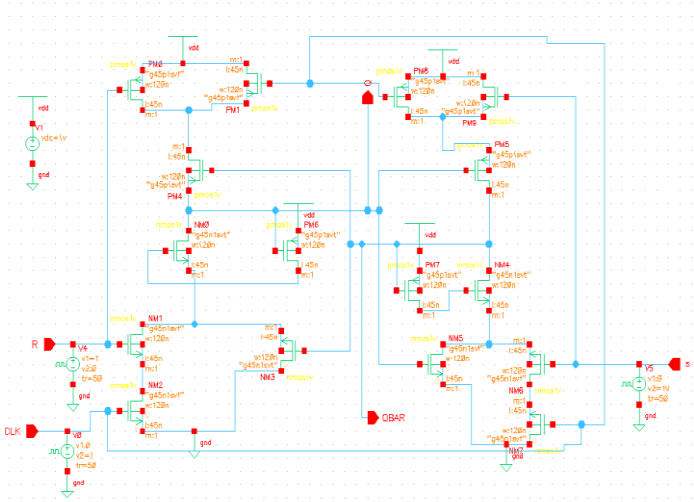

Figure 4.ONOFIC implementation of CMOS SR flip-flop

Static power is consumed even when chip is in quiescent (sleep mode). Static power can also be defined when device is in OFF state still current is flowing from VDD to ground. The main cause of static power consumption is scaling of transistor geometries which cause various leakage currents. Leakage power is about 20-50% today and increasing. The static power can be minimized by using various techniques like in this paper ONOFIC approach is used.

IV RESULT AND CONCLUSION

Table 1 comparison of power dissipation

POWER DISSIPATION OF CONVENTIONAL CMOS SR FLIP-FLOP	POWER DISSIPATION OF ONOFIC IMPLEMENTATION OF CMOS SR FLIP-FLOP
2.8µ	2.1µ

In this section a comparison is made between the conventional CMOS designs of SR with the ONOFIC implementation in terms of power dissipation. The results obtained in ONOFIC implementation are better than the conventional method.

CONCLUSION

In this paper we have discussed various leakage currents and their impact on low power devices. In VLSI technology low power is the main focus of IC designer. The above discussed ON/OFF (ONOFIC) method was used to design a SR flip-flop. ONOFIC technique is easy and only one threshold voltage is used for decreasing the leakage current. The main point of this technique is better ON/OFF property. ONOFIC implementation reduces leakage power and boosts the performance of the digital circuits which is need of the hour. Low power consumption is the outcome of this approach. the future scope of this approach is that if this logic block is turned ON/OFF in a better way it will help in reducing the propagation delay of logic circuits.

References

[1] Tamer A. moniem, “All optical SR flip-flop using 2-D photonic crystal’’ Opt quant electron, PP 2843-2851, 2105
[2] Bhupinder kaur, “ high performance layout design of SR flip-flop using NAND gates,’’ Int. journal of electrical and electronics engineering, vol 2, PP 193-196, 2015.
[3] SV SV Prabhu Deva Kumar, Pagadla venkat, lokesh nayini, “implementation and designing of low power SR flip-flop using 45nm CMOS technology.” International journal of information technology (IJOIT), VOL 1, PP 1-8, 2017
[4] Divya Aggarwal, “ review of flip-flop’’ journal of basic and applied engineering research, vol1, PP 4-19, 2014.
[5] Vijay Kumar Sharma, Manisha Pattanaik, Balwinder Raj, “ONOFIC approach: low power high speed nanoscale VLSI circuits design,’’ International Journal of Electronics, PP 1-13, 2013
[6] Saibal Mukhopadhyay, Cassondra Neau, Rizatamer Cakici, Amit Agarwal, Chris H-kim, kaushik Roy, “ gate leakage reduction for scaled devices using transistor stacking , ’’IEEE transition on very large scale integration (VLSI) sysyem, vol 1, PP-716-730, 2003
[7] K. Haghdad and M. Anis, “Design-specific optimization considering supply and threshold voltage variations”, IEEE Transactions on Computer-Aided Design of Integrated Circuits and Systems, Vol. 27 (10), pp. 1891-1901, 2008
[8] Kaushik Roy, Saibal Mukhopadhyay, Hamid Mahmoodi-Meimand, “Leakage Current Mechanism and Leakage Reduction Techniques in Deep-Submicrometer CMOS Circuits,’’ Proceedings of the IEEE, VOL.91, NO.2,February 2003, PP 305-227
[9] M. Arunlakshman, “ Power and Delay Analysis of Double Edge Triggered D flip- flop based shift Registers in 16nm MOSFET technology ,” International Journal of Advanced Research in Electrical, Electronics and instrumentation Engineering, Vol 3, PP 8560-8568, 2014.
[10] Vijay Kumar Sharma, Manisha Pattanaik, Balwinder Raj,“ leakage reduction ONOFIC approach for deep submicron VLSI circuit design,’’ International journal of electric, computer, energetic, electronics and communication engineering, Vol 7,No 4,2013.
[11] Kaur, Swarnjeet Singh, Sukhdeep Kaur , “Design and Analysis of D flip-flop using different Technologies,” International Journal of Innovative Research in Computer and Communication engineering, Vol. 3. PP 6919-6926, 2015
[12] Anjana S, Rajesh mehra, “ design and implementation of SR flip-flop for efficient power using CMOS 90nm technology ’’ International Journal of scientific research engineering and technology (IJSRET), vol 4, PP 480-483, 2015.

Proceedings of the Fourth International Conference on Communication and Electronics Systems (ICCES 2019)
IEEE Conference Record # 45898; IEEE Xplore ISBN: 978-1-7281-1261-9

Design of 6T FinFET SRAM cell at 7nm

Umayia Mushtaq, Vijay Kumar Sharma

School of Electronics and Communication Engineering,
Shri Mata Vaishno Devi University, Kakryal-182320, Katra, (Jammu & Kashmir)

(Email id: umaiyamushtaq1247@gmail.com , vijay.sharma@smvdu.ac.in)

***Abstract*—Due to the tremendous increase in power dissipation in sub-micrometer region of operation, there arises a need to design low power circuits. The continuous scaling of CMOS logic circuits is not straight forward in the sense that when CMOS devices are scaled below 16nm, short channel effects are observed. These effects increase leakage power dissipation to large extent. The memory occupies about 90% of area in any logic design. The design of memory is of main concern as there occurs parameter variations in CMOS SRAM cells when designed below 16nm. This can be solved by the replacement of CMOS with FinFET in traditional SRAM cells. In this paper, design of 6T FinFET SRAM cell is presented at 7nm technology using ASAP7 PDK and Cadence virtuoso tool. Besides, parameters like power dissipation, delay, power delay products and static noise margins are also analyzed. The simulation results showed that design of SRAM cells using FinFET can be highly efficient in comparison to CMOS SRAM cells.**

Keywords—SRAMt; CMOS; ASAP7 PDK; Power dissipationg;Sub-threshold region; FinFET

I. INTRODUCTION

The parameters like performance, speed, propagation delay and energy per transition improves with continuous scaling. But scaling proves beneficial only upto certain level i.e. below 16nm in complementary metal oxide semi-conductor (CMOS) logic devices. Scaling is not straight forward as it results in degradation of performance. In addition to this, scaling of threshold voltage increases sub-threshold leakage as well [1]

Continuous scaling results in short channel effects. These effects include drain induced barrier lowering, velocity saturation, hot carrier effect, impact ionization, gate induced drain lowering etc. Many methods are devised from time to time to overcome these short channel effects. The methods include channel engineering techniques like retrograde doping, halo doping etc. [2]. Besides, circuit level techniques like INDEP, LECTOR and ON/OFFIC techniques are also suggested [3, 4, 5]. These techniques no doubt reduce leakage power but at the same time increase in propagation delay as well. The best method to reduce leakage in static random access memory cells is to replace CMOS with FinFET logic gates.

FinFETs are best for the design of SRAM cells in the sense that they improve electrostatic behavior of a device. FinFETs are the double gate devices and leakage power dissipation can be controlled by providing two gates instead of one gate which occurs in CMOS logic circuits. Increasing the gate control i.e. by using double gate reduces the leakage power dissipation to huge extent.

FinFETs consist of thin body of silicon and the gate electrodes are wrapped over it as shown in figure 1. There are many types are FinFETs and among them short gate and independent gate FinFET are the common types which are used in digital design [6].

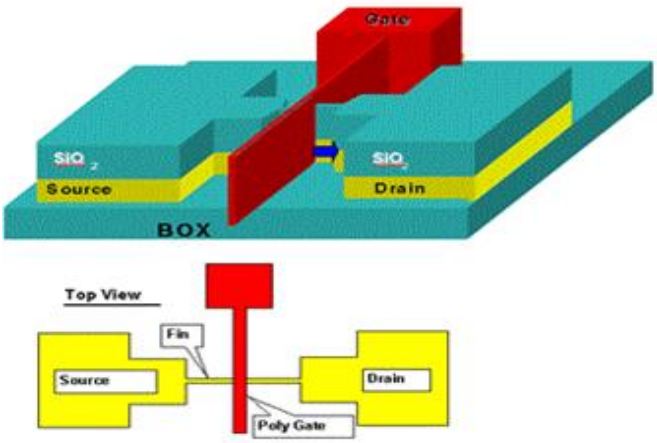

Figure 1: Fin type Field Effect Transistor (courtesy T.J King and C.Hu, UC BERKELEY)

In static random access memory design leakage power dissipation is of primary concern. This can be reduced by the use of FinFET in designing SRAM cells. There occurs increase in area overhead due to the use of FinFET in SRAM cells but this can be compensated by considering the trade-off between

various parameters [7]. The ease and compatibility to design static random access memory (SRAM) cells using FinFET [8] make us to design 6T FinFET SRAM cell.

The design of 6T FinFET static random access memory cell is done using cadence virtuoso tool. Moreover, ASAP7 PDK is used because cadence virtuoso tool does not have any inbuilt library to design FinFET logic circuits. The design of 6T FinFET SRAM cells is performed at 7nm technology.

The development of ASAP 7nm process design kit (PDK) was made at Arizona State university in association with ARM research .This is free PDK used at academic level by various researchers. The PDK has FinFET device models compatible with SPICE for cadence virtuoso tool. The PDK is helpful in designing six transistor (6T) FinFET static random access memory cell at 7nm using Cadence virtuoso tool. The section II describes how FinFET logic circuits are better in comparison to CMOS logic circuits. Section III discussed the modes of operation of FinFET SRAM cells and the section IV consists of simulation results and discussion. Finally the conclusion and future work is provided in the section V.

II. RELATED WORK

To minimize the leakage power many techniques are suggested from time to time for CMOS logic circuits but these techniques have many disadvantages like increase in propagation delay and area. Designing of logic circuits using FinFET is better in the sense because it reduces power dissipation by minimizing short channel effects and at the same time improves subthreshold slope and drive current capability of logic circuits as well. There are certain design challenges which should be taken in consideration i.e. quantized nature of the fin in case of FinFET static random access memory design [9].

The scaling in CMOS logic devices is limited to 16nm only due to scaling obstacles. In case of metal oxide semi-conductor (MOS) devices, high channel doping and moderate thickness of thermal oxide is required at lower dimensions. If these considerations are not satisfied it may lead to degraded performance and reduction in carrier mobility. Better channel control due to dual gate structure, straight process flow and improved on-current capability makes FinFET better in comparison to MOS devices [10, 11].

Due to larger on-current of FinFET devices, FinFET SRAM cells can be operated at higher speed in comparison to conventional CMOS SRAM cells. In addition to this FinFET SRAM cells have low propagation delay for read and write cycles as compared to CMOS SRAM cells [12].

III. PROPOSED SIX TRANSISTOR(6T) FINFET SRAM CELL

Modes of operation in FinFET SRAM cell

FinFET static random access memory (SRAM) cell has three modes of operation i.e. FinFET SRAM hold, FinFET SRAM read and FinFET SRAM write mode. The memory cells are designed at 7nm technology. These cells consist of two cross coupled FinFETs inverters and two access transistors (FinFETS). The access transistors are controlled by word lines. Besides, bit and bit bar voltages are also applied to access transistors.

A. FinFET SRAM HOLD

In hold mode FinFET static random access memory cell has to retain its data and for this word lines are kept at ground or low voltage. Due to this access transistors (FinFETs) are in off state and hence the data present in cross coupled FinFET inverters is retained and the FinFET SRAM cell acts as latch in that case. The circuit diagram for hold operation is given in figure 2. FinFET SRAM cell consists of six FinFETs. The FinFETs used in our design are short gate FinFETs. As shown in figure 2 the word lines are set to “0” or grounded. This suggests that in hold condition 6T SRAM cell acts as latch and latches the value at the output of cross coupled inverters.

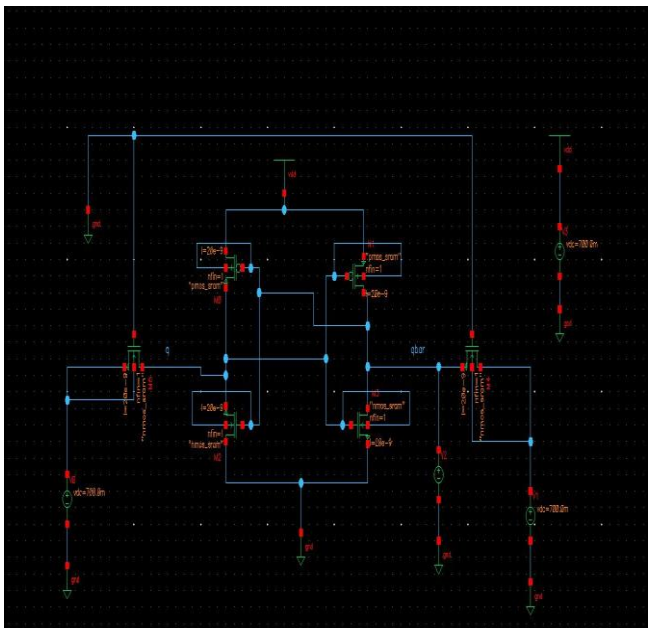

Figure 2: FinFET SRAM hold circuit

B. FinFET SRAM READ

In read mode, which is considered most vulnerable state to parameter variations [13] because both bit and bit bar are set to high voltages (Vdd). The voltage at word lines is also high equal to Vdd (0.7). The node which has "0" value is detected using sense amplifier because this node pulls the respective bit voltages to ground, hence detected by sense amplifier. The circuit diagram for read operation is given in figure 3.

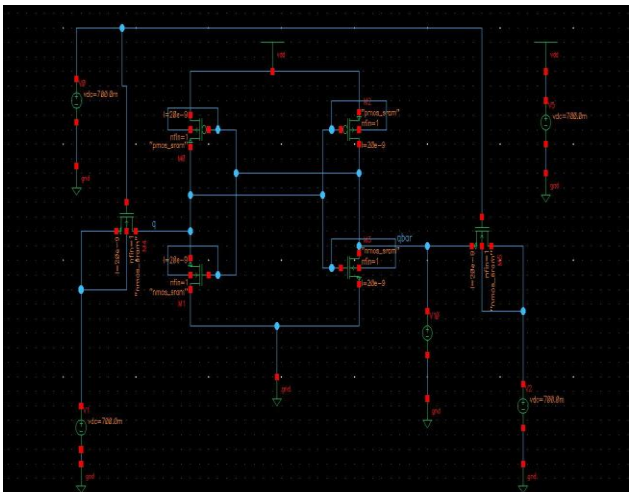

Figure 3: FinFET SRAM read circuit

C. FinFET SRAM WRITE

In write operation also word lines are set to high voltage i.e. equal to Vdd=0.7 in our design of 6T FinFET SRAM cell. For writing "0" at node q , the bit lines are set to "0" and Vdd respectively. To write "0" at qbar, bit and bit bar lines are set to Vdd and "0" respectively.

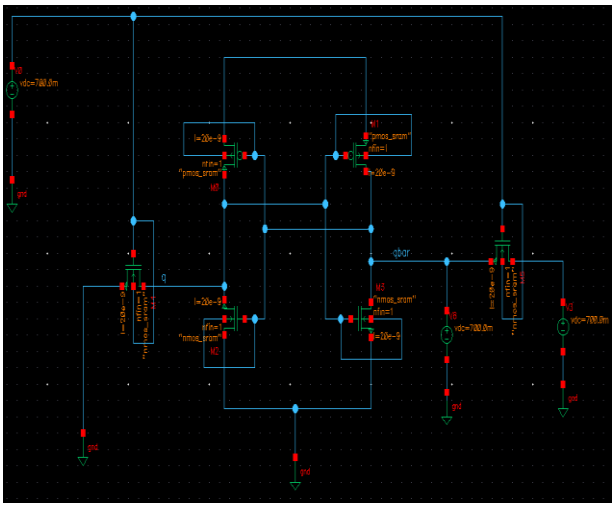

Figure 4: FinFET SRAM write circuit

IV. SIMULATION RESULTS AND DISSCUSSION

As we know power dissipation is one of the major issues which the modern electronic industry is facing these days. The density of chips is increasing day by day and simultaneously increasing power dissipation. Due to this cooling devices are inserted in chips which increase the cost. To overcome this problem FinFET devices can be used which reduce the power dissipation in digital logic circuits.

The parameters like power dissipation, propagation delay and power delay products are obtained for 6T FinFET static random access memory cell in hold, read and write condition.

The power dissipation has gained vital importance now a days due to the reason that as the technology is scaled, there occurs rise in leakage power dissipation to a large extent. The parameters of 6T FinFET SRAM cell at 7nm technology node obtained on cadence virtuoso tool using ASAP 7nm PDK are tabulated in table 1.

Table 1: Parameters of 6T FinFET SRAM cell at 7nm

Parameters of 6T FinFET SRAM cell	**HOLD condition**	**Read condition**	**Write condition**
Power dissipation (µW)	0.10	10.68	31.01
Propagation delay(pS)	11.02	12.8	13.98
Power delay product(aJ)	1.10	136.70	433.52

Besides other important parameter of FinFET SRAM cell i.e. static noise margins are also obtained as shown in figure 5.

The static noise margin curves for read and write are obtained. The static noise parameter is considered as one of the important parameters for FinFET memory design as well.

The static noise margin in 6T FinFET affects both write and read margins of FinFET memory and have a relation with threshold voltage of nfet (n type FinFET) and pfet (p type FinFET) as well, hence determines stability of SRAM cell. The static noise margin curves obtained are given in figure 5 and 6 for read and hold operation respectively.

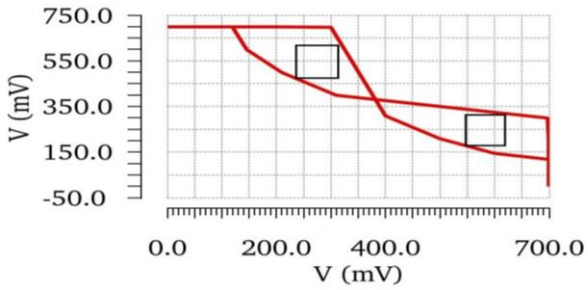

Figure 5: static noise margin for READ operation

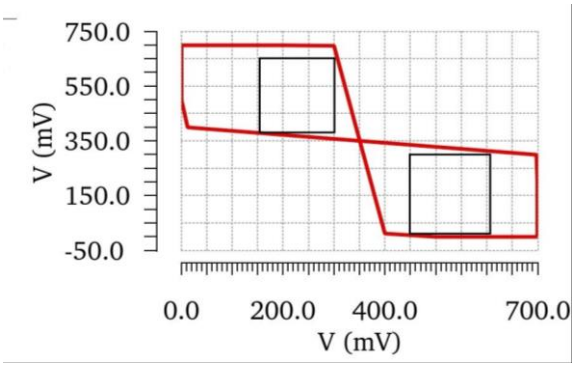

Figure 6: static noise margin for HOLD operation

The static noise margin obtained for hold condition of FinFET memory cell comes is obtained by taking the diagonal length of smallest square obtained from butterfly curves as shown in figure 5 and figure 6. For read and hold operation of 6T FinFET SRAM cell it comes out to be equal to 103mV and 205.06mV respectively.

V CONCLUSION & FUTURE SCOPE

For the minimum possible leakage power and better stability of static random access memory cell, it is preferred to design it with FinFET logic devices. The FinFET logic circuits have lower power dissipation and power delay products compared to complementary metal oxide semi-conductor devices. The various parameters for 6T FinFET SRAM cell are analyzed. In addition to this, stability in terms of static noise margin is analyzed which clearly depict better stability of 6T FinFET SRAM cells. This clearly make us understand that design of 6T FinFET SRAM cell at 7nm has better performance parameters in comparison to CMOS static random access memory cells.

Scaling down of FinFET less than 7nm is the new challenge for design engineers. The Fin height, length and with can be varied which also plays crucial role in determining functionality of logic design. Besides, parameter variation will be carried out to further improve performance of FinFET SRAM cells.

REFERENCES

[1] De, Vivek, and Shekhar Borkar. "Technology and design challenges for low power and high performance [microprocessors]." In *Proceedings. 1999 International Symposium on Low Power Electronics and Design (Cat. No. 99TH8477)*, pp. 163-168. IEEE, 1999.

[2] Roy, Kaushik, Saibal Mukhopadhyay, and Hamid Mahmoodi-Meimand. "Leakage current mechanisms and leakage reduction techniques in deep-submicrometer CMOS circuits." *Proceedings of the IEEE* 91, no. 2 (2003): 305-327.

[3] Sharma, Vijay Kumar, Manisha Pattanaik, and Balwinder Raj. "INDEP approach for leakage reduction in nanoscale CMOS circuits." *International Journal of Electronics* 102, no. 2 (2015): 200-215.

[4] Hanchate, Narender, and Nagarajan Ranganathan. "LECTOR: a technique for leakage reduction in CMOS circuits." *IEEE Transactions on Very Large Scale Integration (VLSI) Systems*12, no. 2 (2004): 196-205.

[5] Sharma, V. K., M. Pattanaik, and Balwinder Raj. "ONOFIC approach: low power high speed nanoscale VLSI circuits design." *International Journal of Electronics* 101, no. 1 (2014): 61-73.

[6] Mishra, Prateek, Anish Muttreja, and Niraj K. Jha. "FinFET circuit design." In *Nanoelectronic Circuit Design*, pp. 23-54. Springer, New York, NY, 2011.

[7] Turi, Michael A., and José G. Delgado-Frias. "Full-VDD and near-threshold performance of 8T FinFET SRAM cells." *Integration* 57 (2017): 169-183.

[8] Manju, I., and A. Senthil Kumar. "A 22 nm FinFET based 6T-SRAM cell design with scaled supply voltage for increased read access time." *Analog Integrated Circuits and Signal Processing* 84, no. 1 (2015): 119-126.

[9] Burnett, David, Sanjay Parihar, Hema Ramamurthy, and Sriram Balasubramanian. "FinFET SRAM design challenges." In *2014 IEEE International Conference on IC Design & Technology*, pp. 1-4. IEEE, 2014.

[10] Rösner, W., E. Landgraf, J. Kretz, L. Dreeskornfeld, H. Schäfer, M. Städele, T. Schulz et al. "Nanoscale FinFETs for low power applications." *solid-state electronics* 48, no. 10-11 (2004): 1819-1823.

[11] Wu, Shien-Yang, Colin Yu Lin, M. C. Chiang, J. J. Liaw, J. Y. Cheng, S. H. Yang, Ming Liang et al. "A 16nm

FinFET CMOS technology for mobile SoC and computing applications." In *2013 IEEE International Electron Devices Meeting*, pp. 9-1. IEEE, 2013.

[12] Farkhani, Hooman, Ali Peiravi, Jens Madsen Kargaard, and Farshad Moradi. "Comparative study of FinFETs versus 22nm bulk CMOS technologies: SRAM design perspective." In *2014 27th IEEE International System-on-Chip Conference (SOCC)*, pp. 449-454. IEEE, 2014.

[13] Bhavnagarwala, Azeez J., Xinghai Tang, and James D. Meindl. "The impact of intrinsic device fluctuations on CMOS SRAM cell stability." *IEEE journal of Solid-state circuits* 36, no. 4 (2001): 658-665.

Proceedings of the Fourth International Conference on Communication and Electronics Systems (ICCES 2019)
IEEE Conference Record # 45898; IEEE Xplore ISBN: 978-1-7281-1261-9

Evaluation of Data Efficacy in Privacy-aware Computing

Geetha P.
Asst Professor, Dept of CSE.
Cambridge Institute of Technology
Bangalore
geetharaghuraj@gmail.com

Dr. Chandrakant Naikodi
Visiting Professor, Dept of CSE
Cambridge Institute of Technology
Bangalore
nadhachandra@gmail.com

Dr. Suresh L.
Principal.&Professor
Cambridge Institute of Technology
Bangalore
suriakls@gmail.com

Abstract
The Digital era marked by the unparalleled growth of Internet and its services with day-to-day technological advancements has paved way for a data driven society. This digital explosion offers huge market value to organizations and business processes who gain valuable information from the collected data to promote futuristic decision making. The aftermath of this large scale analytics is the privacy breach of sensitive information of individuals. The confidential information of people is at a risk of disclosure when it is used for a purpose not intended. Not only should privacy techniques guard classified data, but also ensure that it does not weaken data value when considered for analytical purposes. The proposed work focuses on assessing the expediency of sanitized data for analytics, using a threshold based optimal strategy for improving anonymization with large data. Classification models are trained on the anonymized data using benchmark algorithms and its accuracy is determined. The work is extended to evaluate the performance aspects of the proposed technique on diverse parallel execution environments, Hadoop and Spark.

Keywords: Privacy Preserving, Spark, anonymization, MapReduce

I. INTRODUCTION

Security and Privacy are issues that are a cause of concern in the Digital era. With technological advancement being the norm of the day, data is divulged through many a source and used by organizations for economic benefit. Although regulations regarding privacy are being formulated within an organization's periphery, strict enforcement is a matter of debate, since there is no watchdog policy that ensures the correct use of the data collected. What appears as safe to an end-user may not be the case, in reality. Privacy preservation techniques have been a subject matter in the recent past, in the light of data proliferation from IoT devices and electronic media. These techniques throw light on the challenges that are required to be handled, to sustain quality of data while enforcing privacy. As a matter of fact, utility of data is an important aspect that needs to be considered if analytics should generate meaningful results. Achieving a trade-off between the two is demanding, given the fact that the scale of data is ever-increasing. There is a need for an all-encompassing solution that can handle scale, efficiency and usefulness, while upholding privacy.

The rest of the paper is organized as follows: Section II discusses the privacy scheme used in the paper, discussing the key characteristics of the technique to be considered for privacy enforcement. The section also highlights the processing framework, Spark, used for testing performance aspects of the privacy design in the context of Big Data. Section III defines the overview of the problem stating the objectives of the research. Section IV details the proposed methodology and workflow. Section V details the preparatory data groundwork, categorizing the privacy attributes. Section VI covers the results and discussion, Section VII discusses the related work and Section VIII concludes the paper.

II. BACKGROUND

A. Acronymns

AD	Anonymized Data
NAD	Non-Anonymized Data
AnonyOPT - k	Anonymized Optimal - k
LIL	Local Information Loss
GIL	Global Information Loss
s.t.	Subject to

B. Privacy Scheme

Anonymization is a technique of obscuring published data to prevent sensitive information from disclosure.[1] The parent of all anonymization privacy models, k-anonymity[1][2] is a group anonymization technique that tries to conceal confidential data by creating group of unidentifiable records that avoids the isolation of singular identity by grouping it with k other individuals. The algorithm categorizes the attributes in the dataset into three: sensitive attributes that are not public, but containing personal information of individuals such as salary, disease conditions etc.., quasi-identifying attributes which is a group of attributes that when collectively linked with publicly available data can identify an individual and identifying attributes that are uniquely associated with an individual. Although anonymization literature has shown that the technique fails to handle inference attacks [2] in poorly assorted data belonging to the same equivalence class [2], there are numerous works [2][3] which prove that it can be used as an efficient technique to handle high dimensional data in a context-aware premise.

C. Processing Engine

Spark is a fast in-memory cluster computing framework based on Hadoop MapReduce(MR)[4] capable of handling large workloads. While Spark uses the underlying HDFS[4] for storage, its clusters are utilized for parallel processing of data. Computing is done by creating Resilient Distributed Databases [4] that enables faster MR operations. Due to its in-memory computing it overcomes the slow data transfer associated with Hadoop's MR. The use of Spark data processing has been

XXX-X-XXXX-XXXX-X/XX/$XX.00 ©20XX IEEE

found to be greatly efficient for processing large data streams, text, graph data and high dimensional tabular data. Spark can be integrated with many data querying and processing tools that can be integrated as a stand-alone environment or on a cluster based Hadoop platform.

III. PROBLEM OVERVIEW

A. Objectives

1. To evaluate the efficacy of optimized data anonymization on a data analytic functionality
2. To evaluate the performance improvement of the mining functionality on Apache Spark for Big Data

How does anonymization affect usefulness of data? Can it be used for an effective data analytic functionality in the context of Big Data? A clinical dataset has been used for the purpose. The clinical data is anonymized (AD), the data thus masked is then used for classification. The work evaluates the consequent variation that occurs in the accuracy of classification by comparing it with the classification accuracy on non-anonymized data.(NAD) In addition, the performance of the classification task on Hadoop and Spark is also determined. The parallelization of task on cluster based executing platform brings about significant rapidity in execution. Performance enhancement for large scale data processing is one of the key factors that can be exploited and leveraged in the context of Privacy Preserving Big Data processing. Data worth and performance with scale are challenging issues that have a wide scope of research in the Big Data era while not compromising privacy.

IV. PROPOSED METHODOLOGY

The proposed research goes through two phases of implementation as shown in Fig 1. In the first phase, the data is de-identified by applying the k-anonymity algorithm. This is a preliminary step in the preparation of the data for privacy preserving analytics. Although privacy literature [2] [3] cites a number of variations in the implementation of k-anonymity, the parent algorithm is still known to show convincing results [5] for privacy preservation in the context of Big Data. It is a group based strategy by which the algorithm creates group of anonymous records based on their similarity of certain attributes. The grouping is done by classifying attributes in the dataset into four types [1], sensitive, identifying, quasi-identifying and non-identifying. The identifying attributes are attributes that uniquely identify an individual and are generally removed before the data gets published for analysis. Quasi-attributes are a combination of one or more attributes, which in isolation may not cause privacy breach, but can be linked with publicly available data to identify a data subject. For instance, a voter database may have attributes such as zip code, which can be linked with personal information to zero in on an individual. Information such as disease condition, income etc...are sensitive attributes which are deemed personal and hence should not carry a risk of disclosure. k-anonymity groups data in such a way that the probability of an individual record being identified from the a set of k records is only 1/k. The value of k chosen depends upon the size of the dataset. Here the value of k is chosen optimally based on the general loss information obtained from anonymization. The privacy preserved data is used for classification task implemented using the classic benchmark algorithms such as ID3 and SVM. The results are found to be reasonable and of comparable accuracy with that of the non-anonymized counterpart. In the second phase, the classifiers' performance on Spark is assessed and the result is compared with that of Hadoop execution.

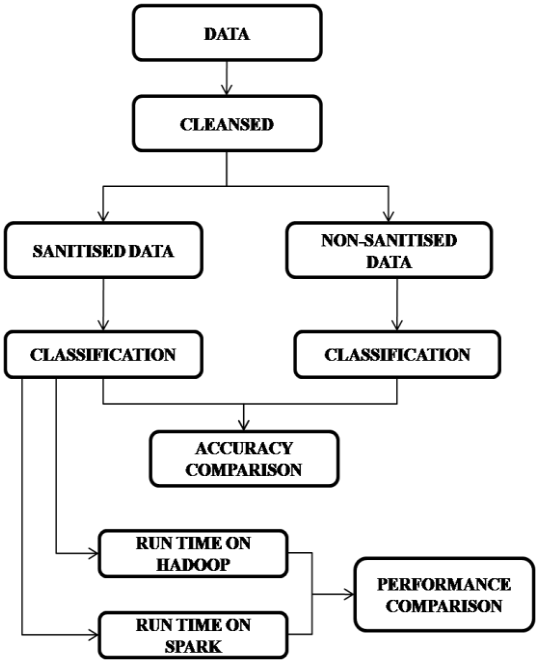

Fig 1 Proposed Workflow

A. Optimal Strategy for anonymity

a) Optimization Formulation

As literature reiterates[1], the choice of k greatly influences the trade-off between privacy and data worthiness. In this work, we propose an optimal algorithm for selecting k value based on the general information loss that occurs when data in a table T is divided into k-anonymous groups. The usefulness of data is prioritized in the formulation of the optimization problem. We call our proposed algorithm as AnonyOPT-k.

b) Definitions

1) Let S represent the total number of data subjects in the input set T, m represent the total number of attributes. The Generic Information Loss [3] is defined as follows:

$$GIL = \frac{1}{S * m} \sum_{i=1}^{S} \sum_{k=1}^{m} \frac{\beta_{ik}^{u} - \beta_{ik}^{l}}{\beta_{k}^{u} - \beta_{k}^{l}} \quad (1)$$

where β_{ik}^{u} and β_{ik}^{l} represent the limiting range of data, β_{k}^{u} and β_{k}^{l} represent the range value of any attribute k.

2) The selection of k is formulated as an optimization problem, considering the following objective function [6]

Maximize 'k' s. t. inequality constraint

$$GIL(T) <= \alpha \quad (2)$$

with range constraint

$$k_l \leq k \leq k_u \quad (3)$$

In Eq. 2, α is the predefined threshold, set for acceptable information loss prioritizing data worth over privacy. The algorithm is repeated for different random seed values of k limited by the range 100-500 as specified in Eq. 3

B. Algorithm AnonyOPT -k

Algorithm AnonyOPT - k (X = { x_1, x_2, x_3….x_n} ϵ T)

// select optimal k

1. k ← Assign a value in the range { k_l, k_u }
2. Repeat until
   a. Generalize the quasi-group and suppress the sensitive attribute using k //Split T into k groups
   b. Calculate LIL for every group
   c. Calculate GIL for T
   d. Increment k

   GIL <= α
3. return k

V. DATA GROUNDWORK

A. Essential Requirements

A clinical dataset has been used for implementation. The data has more than one lakh instances with 24 attributes, containing both categorical as well as numerical attributes. As a preparatory step, data is first checked for missing values and inconsistencies. Numerical data is normalized in order to reduce noise, missing values in categorical data is filled with frequently occurring values. The categorical data are adaptively discretized to facilitate privacy quantification.

B. Privacy Qualifying Attributes

The identifying attribute in the data, patient-id is eliminated, and the disease condition is assumed sensitive. The race, gender, age, occupation, and zipcode attributes are categorized into quasi-group. Generalization is applied to the quasi-group and the data instances are grouped into k-anonymous groups. The disease condition is suppressed to protect sensitivity. Initially, the value of k is chosen randomly, limited by the range constraint of the problem formulation. The upper and lower bounds are assumed for the data under the assumption that the data size and k follow an inverse linear relationship. An optimal value of k is chosen using our proposed AnonyOPT – k, varied at each stage to experiment the change in the level of accuracy of classification task.

VI. RESULTS AND DISCUSSION

The results were considered from two perspectives. Firstly, the usefulness of sanitized data was quantified based on the accuracy of the classifiers on the anonymized data. Results indicate that anonymization technique can be used for privacy preservation, provided an optimal strategy is applied to choose k value. An arbitrary choice of k does not give good results for large data due to the diversity of attribute values. The optimal selection of k using our AnonyOPT – k was found to give reasonable accuracy. Secondly, the execution performance of the technique is evaluated on MapReduce based execution environments, Hadoop and Spark. Results clearly showed that significant performance enhancements are realizable with the in-memory computations of Spark in comparison to Hadoop, both of which are based on MapReduce.

A. Utility of data

The benchmark classification techniques such as Decision Tree and SVM were used to evaluate the usefulness of the transformed data. These results were then compared with the non-anonymized counterpart to assess the variation in the classification accuracies due to the privacy constraints. As shown in the figures [2][3][4][5], anonymization can be used for imposing privacy restrictions, albeit a degree of reduction could be observed in the classification accuracy. The accuracy of the classifiers were checked for differing and increasing sizes of data. The accuracy of classifier was found to reduce as the value of k was increased as shown in figure[6]. A larger value of k minimizes the possibility of an individual record being identified, but reduces the value of data, directly reflected in the reduced accuracy of the classifier. The choice of k is directly proportional to the level of privacy and hence the information loss, and affects data quality that is essential for analytical purposes. In order to bring a balance between the two, AnonyOPT-k followed a threshold based approach so that loss can be kept at check. A threshold of 0.3 for generic information loss was assumed, which helped maintain the usefulness of data. Further increase of k augmented loss. The algorithm was tested with different random seed values for k and experimented for classification accuracy. The data sizes were also gradually increased for testing the effectiveness of the classifiers on AD along with optimal selection for k.

B. Performance

The classification task on anonymized data was tested on Spark to measure speed of execution for increasing data sizes. The results showed that Spark's use of RDD speeded up execution through parallel MapReduce computing in contrast to its equivalent execution on Hadoop. The implementation was optimized using the Dataset API and hence improved the computation speed

of iterative processing required for most of the machine learning tasks. Figure [7] shows the execution time difference between the two environments. For the purpose of testing, initially the experiments were conducted on Hadoop with the cluster environment set in a pseudo-distributed mode. Next, the experiments were carried out on Spark with data on HDFS, and execution on Spark. The task was repeated with Spark set up in stand-alone mode. Stand-alone Spark execution and HDFS based Spark execution did not create much differences in the execution time. The partitioning and splitting of processing into stages was found to vary with expansion in data sizes.

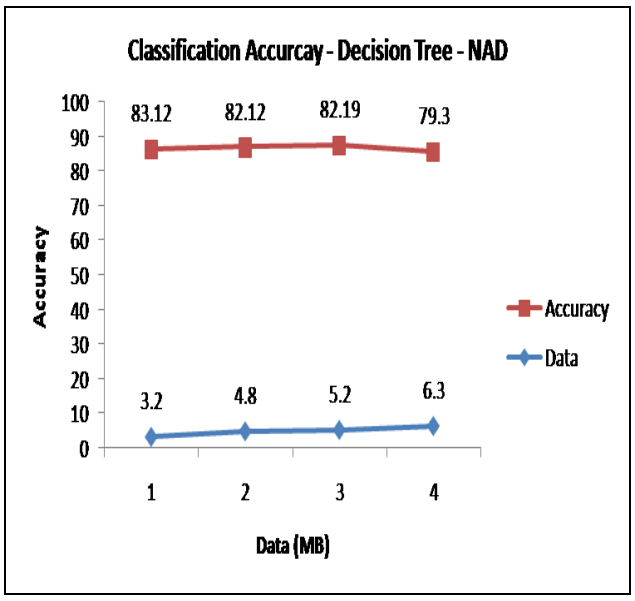

. Fig 2 Classification Accuracy–DecisionTree-NAD

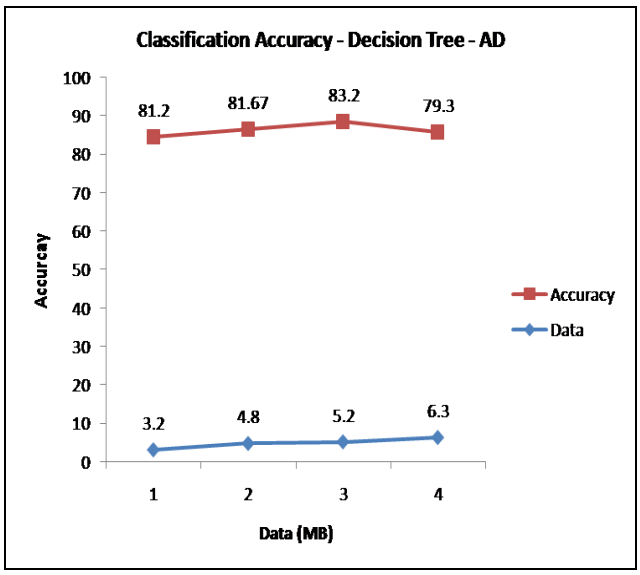

Fig 3 Classification Accuracy–DecisionTree-AD

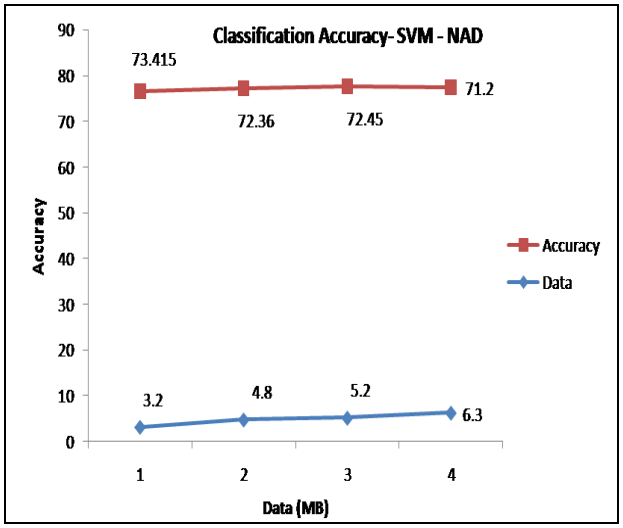

Fig 4 Classification Accuracy – SVM –NAD

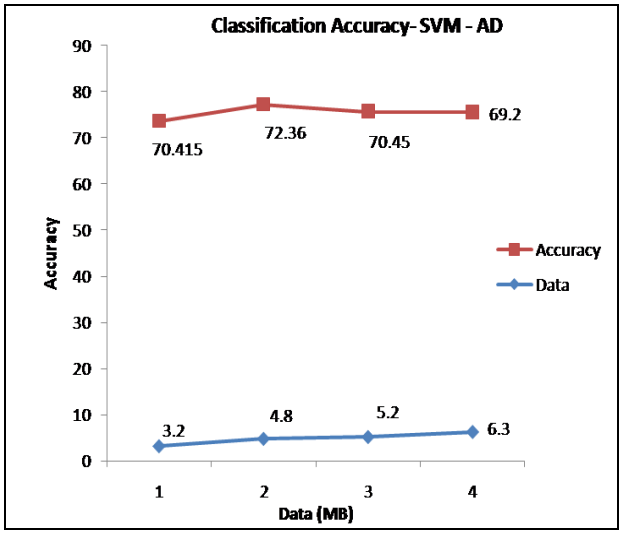

Fig 5 Classification Accuracy – SVM – AD

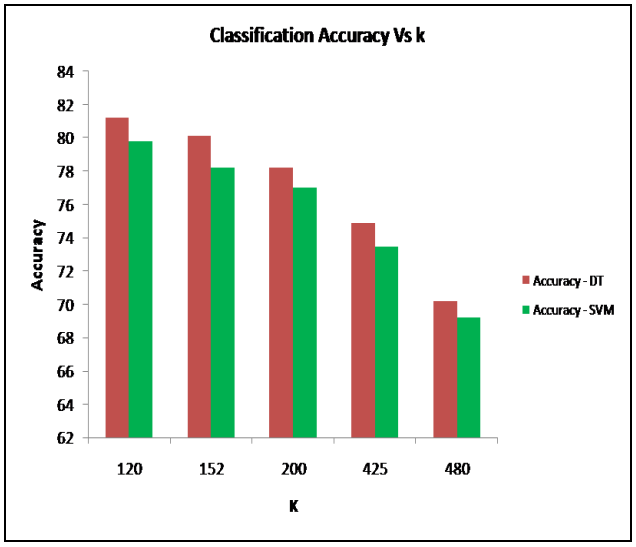

Fig 6 Classification Accuracy Vs K

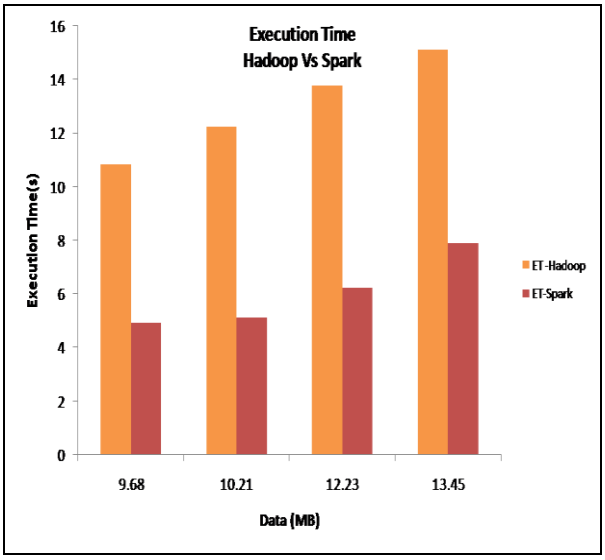

Fig 7 Execution Time Hadoop Vs Spark

VII. RELATED WORK

A vast history of research exists for privacy preserving analytics, primarily classifying work into privacy preserving data publishing [2][3] and privacy preserving data mining [2][3]. A number of privacy techniques have been studied in literature, k-anonymity[1], l-diversity[7], t-closeness[8] and differential privacy[9] being the major ones. Variations of k-anonymity [10] have been discussed, that detail the need to overcome linkage attacks, possible due to linking data with publicly available databases. Although k- anonymity is cited in literature as a poor handler of large data, causing high information loss, the large crowd effect [11] of Big Data is a strong reason to believe that this notion could be proved otherwise. The hindering fact is the optimal choice of k. The value of k chosen largely determines the level of privacy and hence the information loss. The work in [5] uses anonymity to mask large web logs and shows that analytics on such large data can produce acceptable level of correctness. The large crowd effect [11] of Big Data is a fact that can be considered in analyzing the effectiveness of anonymization algorithms for large-scale data. Numerous works has been carried out using k –anonymity as the basic algorithm for privacy preservation, along with MapReduce based computing. The MapReduce based parallel computing platform Hadoop has been used in a number of research innovations for splitting data and working in groups to speed up data execution. The distributed data processing of Big Data using MapReduce gives better performance in terms of scalability as well as speed. The data is uploaded to Cloud, and privacy techniques work on data in the presence of assumptions on the possible attacks on the Cloud Environment. Recent work in anonymization based privacy preservation has focused on improving its effectiveness, by testing heuristic techniques for k value selection. A greedy approach [12] has been used to make an optimized selection, without considering the performance factors. Various techniques of optimization have been tried in order to balance privacy-utility trade-off by using evolutionary [15] algorithms that works on the principle of genetic mutation [15] that works iteratively to arrive at a suitable value of k. Recent work by [16] splits data into homogenous groups, visualizing the data as graphs. It follows a heuristic algorithm [16] that is based on minimum cost flow algorithms. [13] has showed that Spark can be used to improve performance of anonymization due to the use of Resilient Distributed Databases [14]. Anonymization on Spark[13] has been tested on large data of varying sizes and its found that Spark scales well in performance over Hadoop. Algorithms can be fine tuned by using high performance computing techniques that can cater to the Big data technological demands. Spark can also be used with Hive[17] for large scale data querying over millions of instances, and it can be seamlessly integrated with any structured databases.

VIII. CONCLUSION

Large-scale analytics with the onset of Big Data and IoT paradigm is the norm of the day. Useful analytics on data has far-fetched benefits that can be put to advantage in a number of ways for futuristic decision making. But on the downside, lot of personal data is used in the bargain. Hence sensitive information of individuals is disclosed and used for unwarranted reasons. To keep privacy at check and still stride forward with useful analytics in the Big Data era, effective techniques are required that can handle scale and performance. The investigation in this paper firstly uses the classical anonymization algorithm for imposing privacy that is optimized for bounded information loss. Thus the technique prioritizes utility for privacy although reasonably. Secondly, benchmark algorithms are used to train and build classifiers, whose accuracy claim the quality of data. Lastly, the performance of the technique is experimented on parallel execution environments to handle speed of computation. In conclusion, the work suggests that ever growing data sizes require robust algorithms, associated with high performance computations to withstand the growing demands of the digital revolution.

REFERENCES

[1] Latanya Sweeney “Achieving k-anonymity Privacy Protection Using Generalization and Suppression”,May 2002, International Journal on Uncertainty, Fuzziness and Knowledge-based Systems, 10 (5), 2002; 571-588.
[2] Lei Xu, Chunxiao Jiang, Jian Wang, Jian Yuanand Yong Ren, Information Security in Big Data: Privacy and Data Mining, IEEE Transactions , volume 2,2014.
[3] Ricardo Mendes and Jo˜Ao P. Vilela, Privacy-Preserving Data Mining: Methods, Metrics, and Applications, IEEE Transactions, volume 5, 2017.
[4] Apache Spark. Available: http://spark.apache.org/
[5] [5] Jeff Sedayao, Rahul Bhardwaj and Nakul Gorade, “Making Big Data, Privacy, and Anonymization work together in the Enterprise:Experiences and Issues”, IEEE International Congress on Big Data, pp.1-7, 2014.
[6] https://nptel.ac.in/courses/.../IISc.../Optimization

[7] A. Machanavajjhala, D. Kifer, J. Gehrke, and M. Venkitasubramaniam, ‘‘l-diversity:Privacybeyondk-anonymity,’’ACMTrans.Knowl.Discovery Data, vol. 1, no. 1, p. 3, 2007.

[8] Ninghui Li, Tiancheng Li, Suresh Venkatasubramanian, t-Closeness: Privacy Beyond k-Anonymity and ℓ-Diversity, Citiseer 2007.

[9] Shuo Wang, Richard O. Sinnott, Protecting personal trajectories of social media users through differential privacy, Computers & Security (2017)

[10] Mohammed Al-Zobbi, Seyed Shahrestani, Chun Ruan, Implementing A Framework for Big Data Anonymity and Analytics Access Control, 2017 IEEE Trustcom/BigDataSE/ICESS

[11] Xuyun Zhang, Laurence T. Yang, Senior Member, IEEE, Chang Liu, and Jinjun Chen, Member, IEEE", A Scalable Two-Phase Top-Down Specialization Approach for Data Anonymization Using MapReduce on Cloud, IEEE Transactions On Parallel And Distributed Systems, Vol. 25, No. 2, February 2014

[12] Robert Bredereck, André Nichterlein , Rolf Niedermeier, Pattern-Guided k-Anonymity, algorithms ISSN 1999-4893 www.mdpi.com/journal/algorithms

[13] Ugur Sopaoglu, Osman Abul ,"A Top-Down k-Anonymization Implementation for Apache Spark", 2017 IEEE International Conference on Big Data (BIGDATA)

[14] M. Zaharia, M. Chowdhury, T. Das, A. Dave, J. Ma, M. McCauley, M. J. Franklin, S. Shenker, and I. Stoica, "Resilient distributed datasets: A fault-tolerant abstraction for in-memory cluster computing," in Proceedings of the 9th USENIX conference on Networked Systems Design and Implementation. USENIX Association, 2012, pp. 2–2.

[15] S. Mohana ; S. A. Sahaaya Arul Mary",Heuristics for privacy preserving data mining: An evaluation.

[16] "Keisuke Murakami1 Uno2", Optimization algorithm for k-anonymization of datasets with low information loss, Springer-Verlag ,Germany 2017 Takeaki

[17] https://databricks.com/glossary/what-is-spark-sql

Proceedings of the Fourth International Conference on Communication and Electronics Systems (ICCES 2019)
IEEE Conference Record # 45898; IEEE Xplore ISBN: 978-1-7281-1261-9

Saturation Optimization and Extrinsic Timing Analysis for Optically Controlled GFET

S.Chakraborty
Department of Electronics and Communication Engineering
Amrita School of Engineering,Bengaluru
Amrita Vishwa Vidyapeetham, India

K.Bhowmick
Department of Electronics and Communication Engineering
Amrita School of Engineering,Bengaluru
Amrita Vishwa Vidyapeetham, India

N.S. Murty
Department of Electronics and Communication Engineering
Amrita School of Engineering,Bengaluru
Amrita Vishwa Vidyapeetham, India

***Abstract*—In the present work, we propose an optically controlled graphene field effect transistor (OC-GFET) structure where saturation can be attained at lower supply voltage of the order of 1 V. It is compared to present GFET structures using only electrical bias which reaches saturation by using higher supply voltages. The optically induced mobility for the OC-GFET, of the order of 10^5 cm^2/V-s on h-BN substrate allows it to achieve higher current at the aforesaid bias voltage level. An extrinsic timing analysis is carried out and the OC-GFET is found to have a response time of the order of 10 ps and a bandwidth of the order of 60 GHz.**

***Index Terms*—Field effect transistor (FET), mobility, response time, bandwidth**

I. Introduction

The growing need for increased data and process capability has led to the development of advanced electronic systems equipped with complex architectures. The operating frequency designed for the state-of-the-art ICs is in the order of 10^9 Hz. This is devised to cater to the requirement of the on-chip operation bandwidth for high-performance multiprocessor systems [1]. In pursuit of faster ICs a quest for a material with faster response time escalated the interests of researchers towards graphene [2].

Graphene is ideally a one atom thick 2D layer of carbon with a very high mobility, thermal conductivity, optical responsivity and ambipolar transfer characteristics [3]. These properties of graphene can enhance the applications of GFET devices in analog electronics and spintronics [4], [5]. Graphene has extraordinary electronic and optical characteristics and studies have suggested it to be a potential replacement for silicon-based optoelectronic devices [6]–[8].

GFETs are used in electronic sensing applications, non-volatile memory devices and analog RF circuits [9], [10]. Its excellent optical properties provide flexibility in designing highly sensitive photo-detectors [11], electromagnetic wave shields [12] and waveguide polarizers [13]. Graphene has been able to prove its significance in only a handful of digital logic circuit applications, although it has been envisaged for logic circuits for desirable GFET applications [14]. Due to negligible band gap, these devices show low on-off current ratio [15] which does not allow them to achieve saturation region, essential to determine logic '1' in a digital logic circuit [16], [17].

The intrinsic mobility of graphene at room temperature is of the order $2 \times 10^5 \mathrm{cm}^2/V - s$. The effect of scattering due to mismatch in lattice symmetry between graphene and silicon (Si) substrate on electrical biasing limits the mobility of GFET devices thus exhibiting a mobility of the order of $10^3 \mathrm{cm}^2/V - s$ [18]. This decrease in mobility enables GFETs to reach from cut-off region to linear region but fails to attain saturation region even with the industry standard input voltage ranges (1.8-3.3 V) [19], [21]. A perfect cut-off point is also not achieved in GFETs, because graphene has negligible bandgap, but in the present work the attainment of the saturation region is addressed.

In this theoretical work a laser beam of 1550 nm is modelled on the graphene channel of a dual-gated GFET. A comparative analysis is made between the proposed optically controlled GFET (OC-GFET) and conventional electrically biased GFETs (see figure 1(a), (b)) on the performance criteria like saturation velocity attainment voltage, bandwidth and response time. A drain-source voltage (V_{DS}) of around 1 V is required for OC-GFET (see device structure in figure 1(c)) to reach saturation region in contrast to 7 V for an electrically biased GFET [20]. In all the present work endeavours to test the applicability of graphene in FET structure for digital applications. A method of charged impurity scattering into the graphene layer to obtain saturation velocities is reported [22]. However in the present work, we report attainment of saturation around V_{DS} = 1 V by using 1550 nm light incident on intrinsic graphene channel which makes fabrication easy.

II. Device structure

We consider a dual-gated GFET of length (L) and width (W) $1\mu m$, respectively as shown in figure 1(a),1(b) [20]. The top-gate oxide and the back-gate oxide are both made of SiO_2. The thickness of the former (t_{oxt}) is 4 nm whereas that of the latter (t_{oxb}) is 300 nm. The substrate for both the devices as shown in figure 1(a), 1(b) is made of Si. The

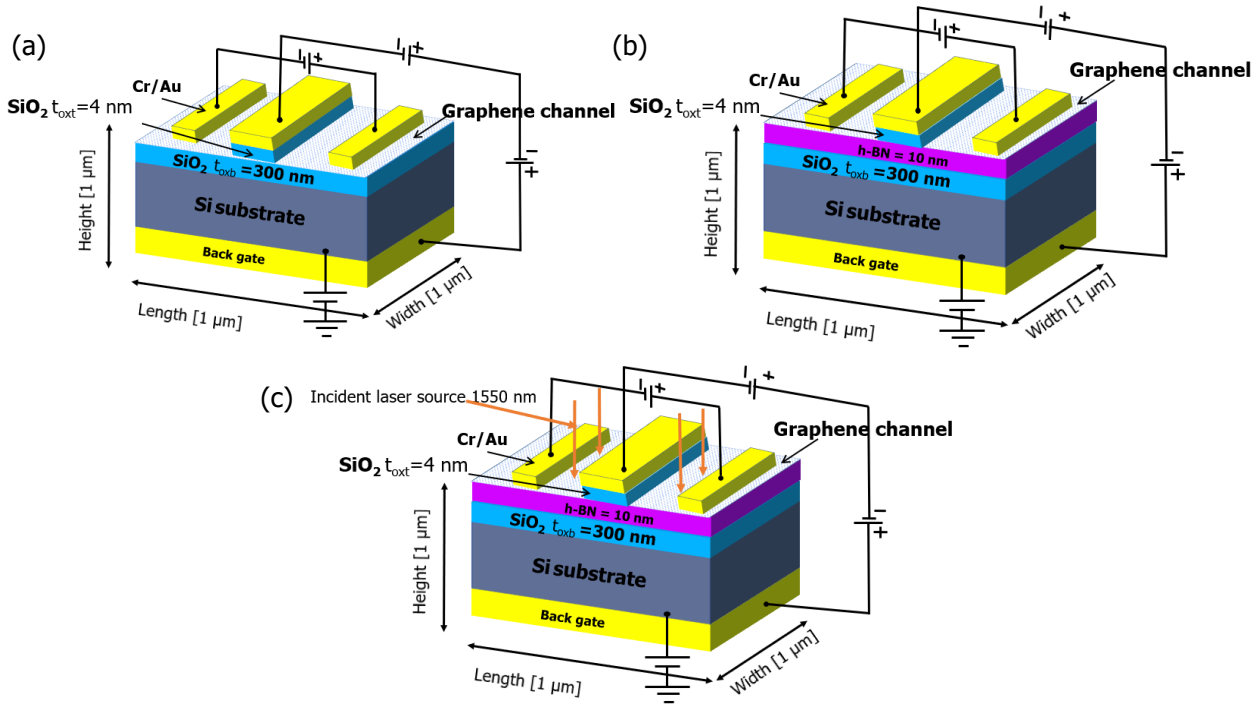

Fig. 1. (a) Schematic of $1\mu m$ electrically biased dual-gated G/SiO_2/Si FET (b) Schematic of $1\mu m$ electrically biased dual-gated G/h-BN/Si FET with graphene on $10nm$ h-BN sheet as channel (c) Schematic of $1\mu m$ dual-gated G/h-BN/Si FET with graphene on 10 nm h-BN sheet as channel and an incident laser source of 1550 nm is modelled on the channel

top-gate, back-gate, and the drain source electrodes are made of Cr/Au. Graphene channel is in direct contact with SiO_2 as shown in figure 1(a) for which it is named as G/SiO_2/Si FET. In figure 1(b) it is shown that graphene channel is in contact with h-BN of thickness 10 nm and is named as G/h-BN/Si FET. Both the FET devices are biased electrically.

1) Electrical characteristics for GFET modeling: A graphene channel has a net mobile sheet charge density (assuming hole conduction) responsible for generation of drain current (I_{DS}) [20] for both G/SiO_2/Si and G/h-BN/Si FETs. The expression for an electrically biased graphene channel potential (V_{ch}) (see equation (1)) is found using Kirchhoffs Laws [18].

$$V_{ch} = \frac{-(V_{GS} - V_{GS0} - V)C_t + (V_{BS} - V_{BS0} - V)C_b}{C_t + C_b + aC_q} \tag{1}$$

where V_{GS} and V_{BS} are top and back-gate source voltages. V_{GS0} and V_{BS0} are the top- and back gate voltages at which I_{DS} reaches minimum. V is the voltage across channel considered as 1 V. C_t and C_b are the top and back gate capacitances. The parameter a is defined as capacitance weighing factor which is 0.5 in this work. The value of quantum capacitance (C_q) is obtained by using V_{ch} value of 0.0034 V (found when V_{GS} and V_{BS} are biased at 0 V) [20] .

2) Drain-Current Model : The effective mobilities (μ_{eff}) at 300 K which is 1125 $cm^2/V-s$ [20] for G/SiO_2/Si/Si and 40000 $cm^2/V-s$ [23] for G/h-BN/Si/Si are substituted in the drain-diffusion model based current equation shown in expression (2) [13], [16] to estimate their respective transfer and output characteristics.

$$I_{DS} = \frac{W\int_0^{V_{DS}} \mu Q_{tot} dV}{L + |\int_0^{V_{DS}} \frac{\mu}{v_{sat_{opt}}}|} \tag{2}$$

where v_{sat} is equated and shown in equation (3) as:

$$v_{sat} = v_F(\frac{e}{1 + fV_{ch}^2} + g) \tag{3}$$

The fitting parameters e, f and g are used from the previously obtained calculations [20].

A. Transfer/Output characteristics for verification

The transfer characteristics (I_{DS} vs V_{GS}) for G/SiO_2/Si FET (refer figure 1(a)) are calculated by varying V_{GS} from -5 V to 5 V for every constant value of drain-source voltage V_{DS} (0.05 - 0.2) V as shown in figure 2(a). The carrier mobility for this device is 1125 $cm^2/V-s$ [20]. The I_{DS} calculated is of the order of $10^{-3}A$.

The output characteristics (I_{DS} vs V_{DS}) shown in figure 2(b) for G/SiO_2/Si FET are calculated by varying V_{DS} from (0-7) V for every V_{GS} (0-4) V. The obtained I_{DS} is of the order of $10^{-3}A$. The device reaches saturation region when V_{DS} applied is 7 V. The obtained I_{DS} is of the order of $10^{-3}A$. A detailed analysis of the I_{DS} vs V_{DS} characteristics for G/SiO_2/Si FET are explained and shown in figure 6(a).

The obtained I_{DS} vs V_{GS} characteristics for G/h-BN/Si FET

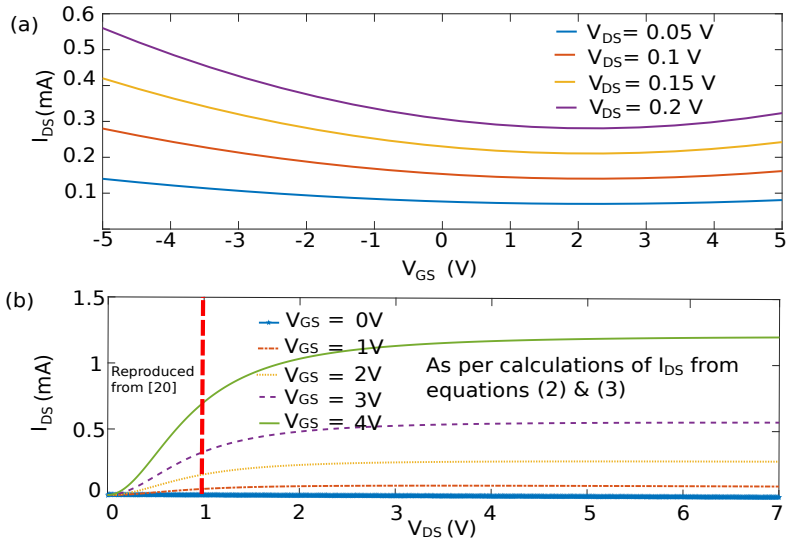

Fig. 2. (a) Transfer characteristics of 1 μm dual gated electrically biased G/SiO_2/Si FET for varying V_{GS} from -5 to 5 V for every V_{DS} ranging from (0.05 - 0.2) V, t_{oxt}= 4 nm, t_{oxb} = 300 nm, T = 300 K, V_{GS0} = 1.1 V, V_{BS0} = 11 V, V_{BS} = 5 V, V_{BS} = 5 V, V = 1 V, m = 0.1 V^2, Δ = 92 meV, μ_{eff} = 1125 cm^2/Vs. (b) Output characteristics of a 1 μm dual gated electrically biased G/SiO_2/Si FET exhibiting the saturation region it attains by applying V_{DS} of 7 V.

are estimated by the same method but the achieved I_{DS} is of the order of 20 mA at V_{GS} -5 V for V_{DS} at 0.2 V and is shown in figure 3(a). The I_{DS} is higher compared to the G/SiO_2/Si FET.

The I_{DS} vs V_{DS} characteristics calculated by the same method as described in sections II(1), II(2) are shown in figure 3(b). It is observed that the G/h-BN/Si FET reaches saturation state on applying V_{DS} of 2 V in contrast to V_{DS} of 7 V used by G/SiO_2/Si to attain saturation. The graphene channel on h-BN has μ_{eff} value 40000 $cm^2/V-s$ [23] which is far higher compared to graphene channel on SiO_2 which has μ_{eff} of 1125 $cm^2/V-s$. On applying V_{DS} of 1.3 V G/h-BN/Si FET can reach saturation region faster than G/SiO_2/Si FET.

III. Effect of Incident Light on Conductivity and Mobility

The optical conductance that occurs as a result of $\pi-\pi^*$ transitions for graphene are mathematically represented by equation(4) [24].

$$\sigma_{\pi-\pi^*} = \sigma_{r1} + i\sigma_{i1} \tag{4}$$

We approximate $\sigma_{\pi-\pi^*} \sim \sigma_0$ (for wavelengths of visible spectrum which doesn't influence the optical conductance [24]) and create universal optical conductance of graphene, identical to conductance of graphene that occurs due to $\pi-\pi^*$ transitions. The intrinsic conduction in graphene is represented by equation(5) [25].

$$\sigma_0 = (\frac{\pi}{2}).(\frac{e^2}{4\hbar}) = \frac{e^2}{4\hbar} \sim 6.08.10^{-5}\Omega^{-1} \tag{5}$$

The term σ_0 (see equation (5)) is the real part of the expression (10) and has minimum conductivity ($6.08.10^{-5}\Omega^{-1}$) at charge neutrality point and is neglected. The imaginary part of the conductivity as shown in equation (4) contributes to the electron transportation in graphene and is expressed in equation (6) [24], [26].

$$\sigma(\omega) = -i\epsilon_r(\omega)\epsilon_0\omega d \tag{6}$$

Here ϵ_0 is the permittivity of free space, ω is frequency of the incident light, d is the thickness of monolayer graphene which has a value of 0.34 nm. The relative permittivity is obtained from the expression (7) [24].

$$n + ik = \sqrt{\epsilon_r(\omega)} \tag{7}$$

The values of refractive indices (r.i.) of a monolayer graphene for the wavelength range (0.2 to 3.5) μm were reported in [24], and are used to calculate $\sigma(\omega)$. The μ_{eff} of a monolayer graphene for corresponding wavelengths $(0.2-3.5)\mu m$ is obtained from expression (8) and is shown in figure 4. The μ_{eff} at 1550 nm is found to be $1.06\times10^5 cm^2/V-s$ (marked by the red dotted line) and the r.i. is found to be 50+50.68i.

$$\mu_{eff} = \frac{\sigma(\omega)}{ne} \tag{8}$$

Here e is the elementary charge and n is the number of charge carriers in the monolayer graphene channel taken as $(6.2\times10^{11} cm^{-2})$.

1) Device structure of OC-GFET: A G/h-BN/Si device of the same device parameters as shown in figure 1(c) is chosen staying consistent with the electrically biased G/SiO_2/Si and G/h-BN/Si FET. It is named OC-GFET, where the graphene channel is on a 10 nm h-BN layer [23]. The choice of interacting layer is considered as h-BN, since it has reported to have achieved a higher μ_{eff} of the order of 60000 $cm^2/V-s$ at 2

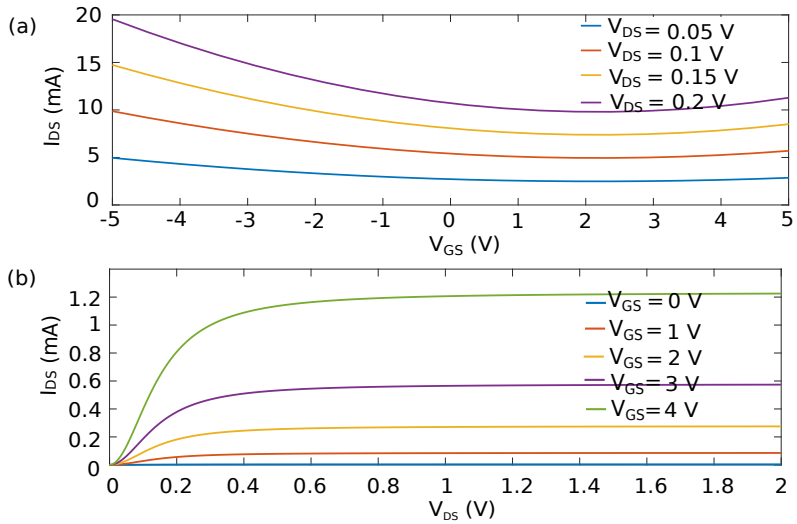

Fig. 3. (a) Transfer characteristics of 1 μm dual gated electrically biased G/h-BN/Si FET for varying V_{GS} from -5 to 5 V for every V_{DS} ranging from (0.05 - 0.2) V, t_{oxt} = 4 nm, t_{oxb} = 300 nm, T = 300 K, V_{GS0} = 1.1 V, V_{BS0} = 11 V, V_{BS} = 5 V, V_{BS} = 5 V, V = 1 V, m = 0.1 V^2, Δ = 92 meV, μ_{eff} = 40000 cm^2/Vs. (b) Output characteristics of a 1 μm dual gated electrically biased G/h-BN/Si FET exhibiting the saturation region it attains by applying V_{DS} of 2V.

K [23]. In this FET a laser source of 1550 nm is modelled on the graphene channel to generate a number of photogenerated carriers as shown in figure 1(c). Due to presence of modulated potential step throughout the graphene channel sheet, the incident laser source does not contribute to generation and transport of photocurrent equally in the channel. However photocurrent due to incident laser beam intensity shows linear dependence due to presence of electrostatic potential steps at the contacts. Such a situation is termed as contact edge effects in OC-GFET which generates a photovoltage of 2 mV [27]. The incident photons on the electrodes will generate less photocurrent compared to graphene channel due to higher resistance of Cr/Au. In this scenario incident photons due to input optical power (P_{opt} result) in a photovoltage (V_{ph}) on the channel as formulated in equation (9) [1].

$$V_{ph} = -0.021 \times ln(P_{opt} - 0.54) \tag{9}$$

As a consequence the μ_{eff} of the graphene channel is found to be $1.06 \times 10^5 cm^2/V - s$ as mentioned in the previous section. A question may arise that the graphene on h-BN interaction may cause scattering in the channel thus reducing the μ_{eff}. However the μ_{eff} is determined from r.i. of monolayer graphene, neglecting the effect of the substrate [24].

A. Channel Potential change due to modelling of Light on the Channel

On the basis of the effect of incident light according to the experimental work [1] on V_{ch} as in literature [27], in the present work it has been assumed that the V_{ph} has an additive effect on the V_{ch}. Hence V_{ph} affects the potential of

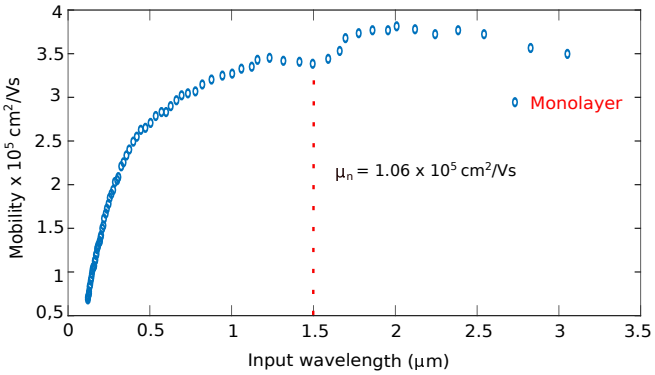

Fig. 4. Input wavelengths ranging from (0.2 to 3.5) μm vs effective carrier mobility μ_{eff} for a monolayer graphene channel.

the electrically biased graphene channel as shown in equation (10). It is a modification to equation (1) with the establishment of V_{ph}.

$$V_{ch_{opt}} = V_{ch} + V_{ph} \tag{10}$$

The effect of $V_{ch_{opt}}$ influences the v_{sat} and is expressed in equation (11):

$$v_{sat_{opt}} = v_F(\frac{e}{1 + fV_{ch_{opt}}^2} + g) \tag{11}$$

which is essential for calculating I_{DS} for OC-GFET.

B. Output characteristics of OC-GFET

The I_{DS} vs V_{DS} characteristics for OC-GFET are obtained by keeping a constant λ at 1550 m anda constant P_{opt} of 10 μW. V_{DS} is varied from (0-1) V for every V_{GS} ranging from (0-4) V. It is evident from figure 5(a) that the device achieves

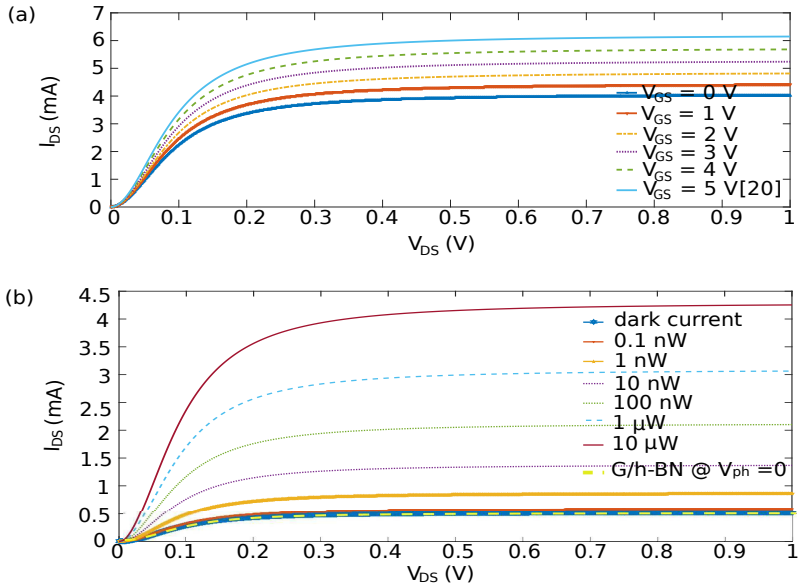

Fig. 5. (a) Output characteristics of 1 μm dual-gated OC-GFET for P_{opt} at 10 μW, t_{oxt} = 4 nm, t_{oxb} = 300 nm, T = 300 K, V_{GS0} = 1.1 V, V_{BS0} = 11 V, V_{BS} = 5 V, V_{BS} = 5 V, V = 1 V, m = 0.1 V^2, Δ = 92 meV, μ_{eff} = 1.06×$10^5 cm^2/V-s$ when light of wavelength λ = 1550 nm is modelled on the channel with V_{DS} varying from (0-1) V for every value of V_{GS} ranging from (0-4) V .(b) Output characteristics of a 1 μm dual-gated OC-GFET for V_{GS} at 0.6 V, t_{oxt} = 4 nm, t_{oxb} = 300 nm, T = 300 K, V_{GS0} = 1.1 V, V_{BS0} = 11 V, V_{BS} = 5 V, V = 1 V, m = 0.1 V^2, Δ = 92 meV, μ_{eff} = 1.06×$10^5 cm^2/V-s$ when light of wavelength λ = 1550 nm is modelled on the channel with P_{opt} as 0.1 nW, 1 nW, 10 nW, 100 nW, 1 μW, 10 μW.

saturation by applying V_{DS} of 1 V. The I_{DS} obtained is of the order of $10^{-3}A$. The achieved I_{DS} for V_{GS} = 5 V (see figure 5(a)) is in close agreement with the results as in [20] for a μ_{eff} value of $1.15 \times 10^5 cm^2/V-s$. Hence the output characteristics of OC-GFET are deemed to be sufficient.

In figure 5(b) the I_{DS} vs V_{DS} characteristics are presented by keeping V_{GS} constant at 0.6 V, λ at 1550 nm and P_{opt} is varied from dark current to 10μW. In this case also the saturation is reached within applied V_{DS} of 1 V. The calculated I_{DS} is of the order of $10^{-3}A$. The reason OC-GFET achieves saturation on applying 1 V is due to its achieved optically induced mobility which is $1.06 \times 10^5 cm^2/V-s$. The I_{DS} vs V_{DS} characteristics were recalculated in terms of G/h-BN/Si FET (see section 2(c)) with V_{GS} as 0.6 V and has been compared with V_{GS} = 0.6 V when V_{ph} = 0 V. Intuitively with no modelled light source on the graphene channel, the OC-GFET should behave like an electrically biased G/h-BN/Si FET. Therefore the output characteristics marked by the yellow dotted lines of G/h-BN/Si FET overlap with the blue line (dark current) of the OC-GFET as shown in figure 5(b).

IV. Comaprison of FETs

This section compares the 3 types of GFETs based on their requirement of V_{DS} values to attain saturation velocity. This also comprises of the comparison based on the response time and bandwidth for each of these devices.

A. Fast attainment of saturation velocity

It is evident from the sections II and III that OC-GFET has the μ_{eff} of 1.06×$10^5 cm^2/V-s$ whereas G/SiO_2/Si and G/h-BN/Si FETs have μ_{eff} values of 1125 $cm^2/V-s$ and 40000 $cm^2/V-s$ respectively. This proves that a FET device with higher μ_{eff} attains saturation velocity, and subsequently the saturation region with less drain-source supply voltage (V_{DS}). The G/SiO_2/Si continues to show a linear behaviour when the applied V_{DS} is 1 V (see figure 6(a)), but it reaches the saturation state on applying a V_{DS} of 7 V as shown in figure 2(b). On the other hand a G/h-BN/Si FET does not attain complete saturation state on applying V_{DS} of 1 V, it attains saturation for the V_{GS} values ranging from (0-3) V, on applying a V_{DS} of 0.73 V, shown by the red dotted lines in figure 6(b). It attains complete saturation on applying V_{DS} of 2 V as shown in figure 3(b). In the case for an optically induced mobility in a monolayer graphene channel, the OC-GFET attains the saturation region with a V_{DS} of 1 V as shown in figure 6(c). For all V_{GS} values ranging from (0-5) V it attains the saturation region on applying a V_{DS} of 0.62 V which is indicated by red dotted lines in figure 6(c). It is inferred from figure 6(c) that saturation has been attained (at V_{DS} = 0.62 V) by using light on pure graphene without any material alteration. However, it can be seen that perfect cut-off is not obtainable. Hence, GFET structures may not be advisable for switching, but for high power applications and RF circuits it shows outstanding performance. Heterostructure variations like graphene/MoS_2/h-BN (G/MoS_2/h-BN) [28] may be tried with light illumination for simultaneous fast saturation attainment and cut-off achievement.

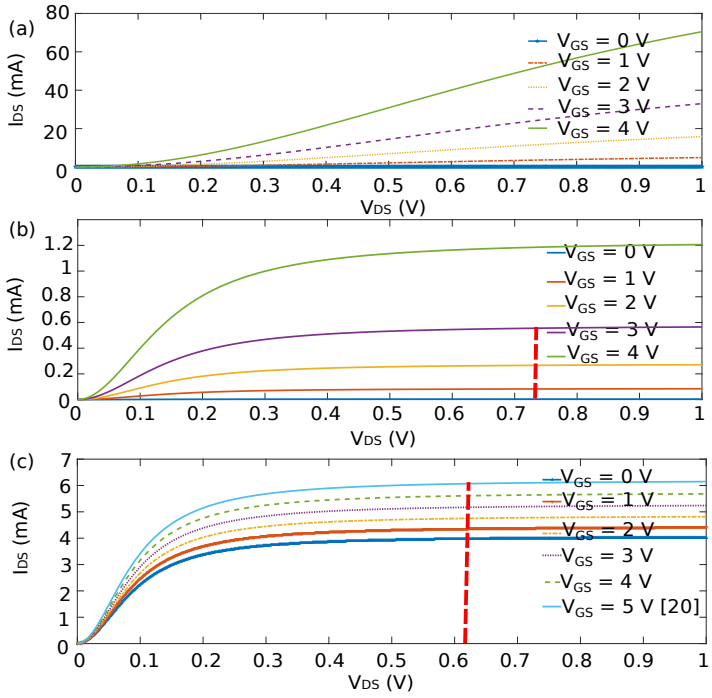

Fig. 6. (a) Output characteristics of a G/SiO_2/Si FET where V_{DS} ranges from (0-1) V for every value of V_{GS} ranging from (0-4) V, the FET exhibits linear behaviour on applying V_{DS} - 1 V (b) Output characteristics of a G/h-BN/Si FET where V_{DS} ranges from (0-1) V for every value of V_{GS} ranging from (0-4) V, the FET reaches saturation region for V_{GS} ranging from (0-3) V correspondingly marked by red dotted lines till V_{GS} of 3 V (c) Output characteristics of a OC-GFET where V_{DS} ranges from (0-1) V for every value of V_{GS} ranging from (0-4) V, the FET reaches saturation region at V_{DS} - 0.62 V marked by red dotted line

B. Extrinsic timing analysis of GFET, OC-GFET and OCFET

The timing analysis is fundamentally characterized by the response time of FET devices. Response time for FETs is measured by rise time (τ_r) and fall time (τ_f) of the output pulse with respect to the given input pulse [29]. It is inversely proportional to the average current (I_{mean}) during the transition of voltage. The power supply (V_{DD}) for all the devices is considered to be 2 V. It is inversely proportional to the average current (I_{mean}) during the transition of voltage. The power supply (V_{DD}) for all the devices is considered to be 2 V. The load capacitance (C_{load}) and load resistance (R_{load}) are connected to the drain electrode from where the output voltage V_{out} is measured. The external load added to all the devices and the output measured from the load at the drain electrode gives the extrinsic timing analysis for the devices. In this work to perform extrinsic timing analysis for the devices R_{load} of 10 $k\Omega$ and C_{load} of 1 pF [29] are chosen. The higher I_{mean} in a device will represent faster rise and fall time compared to a device with lower I_{mean}. It clearly suggests that I_{mean} for OC-GFET in this case has I_{mean} of the order of $10^{-3}A$ in contrast to an optically controlled MOSFET (OCFET) with Ge gate and Si channel [1] which has I_{mean} of the order of $10^{-6}A$. Carrying forward from intrinsic timing analysis of OCFET [1], an extrinsic timing analysis was performed on the same using R_{load} of 10 $k\Omega$ and C_{load} of 1 pF [29]. The τ_r of the OCFET is found to be 4.95 * 10^{-8}s.

While comparing the response time for all the four devices it is found that the OC-GFET has τ_r and τ_f of the order of 10^{-11} s, G/h-BN/Si FET shows τ_r of 1.4*10^{-10} s, G/SiO_2/Si FET bears τ_r of 5.2*10^{-10} s, whereas OCFET delivers τ_r in the order of 10^{-8} s.

When a V_{in} with τ_r and τ_f of 5 ps (see figure 7(a)) is applied to all the FETs, the output voltage V_{out} is observed with respect to time (ps). In figure 7(b), the V_{out} for an ideal inverter is observed at 0.1 ps, where it follows the V_{in} pulse exactly i.e. V_{out} is OFF when V_{in} is ON and vice-versa. In figure 7(c) an OC-GFET observed at 0.1 ps as marked by the red dotted line only shows one V_{out} pulse when already two V_{in} pulses have passed by. It has the τ_r of 6*10^{-11} s which is the fastest among all the other FETs but $\sim$ 10 times slower than input pulse. In figure 7(d,e) the G/h-BN/Si and G/SiO_2/Si FETs observed at the same time 0.1 ps display only the rising half of the V_{out} pulse. However G/h-BN/Si FET (τ_r - 1.4 * 10^{-11} s) is faster than G/SiO_2/Si (τ_r - 5.2 * 10^{-11} s) because of its higher current carrying capability. At 0.5 ps it is clearly demonstrated that G/SiO_2/Si FET is lagging behind the G/h-BN/Si FET (marked by blue dotted line). An OCFET inverter [1] (τ_r - 4.95 * 10^{-8} s) is illustrated in figure 7(f) and it is almost $\sim$ 10^3 times slower than the OC-GFET. At 1 ps the output pulse is very relaxed and only the rising half of the pulse is visible.

Faster response time in photodetectors lead to higher bandwidth (BW) capability which is expressed by the relation (12).

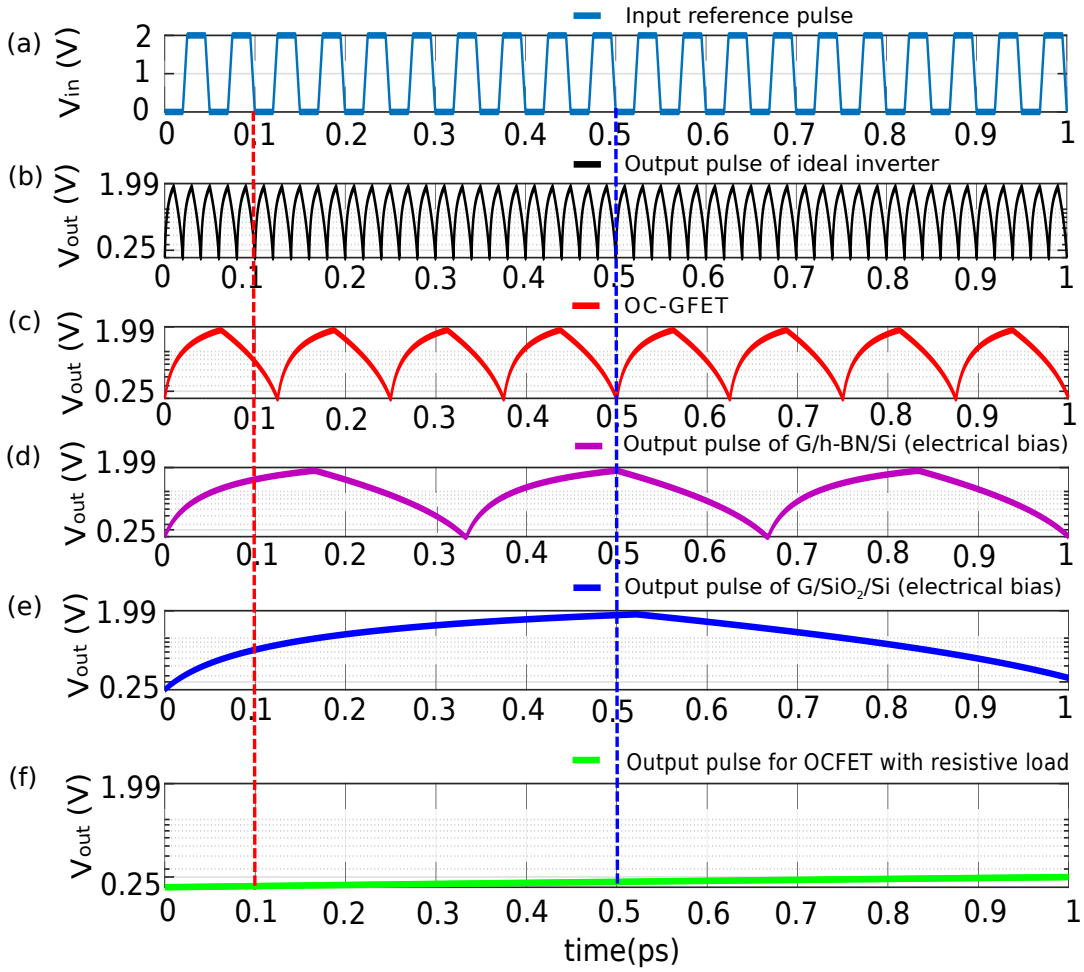

Fig. 7. Timing analysis of FET with devices respect to voltage with resistive load resistance $R_L = 10k\Omega$, load capacitance C_{load} = 1 pF (a) Input reference pulse in $picoseconds(ps)$ (b) Output reference pulse of an ideal inverter (c) Output pulse of OC-GFET with τ_r and τ_f as 60 ps, P_{opt} =10 μW (d) Output pulse of electrically biased G/h-BN/Si FET with τ_r and τ_f as 1.4 * $10^{-10}s$ (e) Output pulse of electrically biased G/SiO_2/Si FET with τ_r and τ_f as 5 * $10^{-10}s$ (f) Output pulse of OCFET [1] with τ_r and τ_f as 4.95 * $10^{-8}s$.

TABLE I
COMPARATIVE RESULTS OF FETS

Device Name(FET)	Supplied V_{DS}(V)	τ_r(s)	BW(Hz)
G/SiO_2	7	5.2*10^{-10}	1.4*10^9
G/h-BN/Si	2	1.4*10^{-10}	5*10^9
OC-GFET	1	6*10^{-11}	1.25*10^{10}
OCFET	-	4.95 * 10^{-8}	5.8*10^7

A high performance FET exhibits an enhanced BW due to its faster response time. A faster τ_r results in higher BW.

$$BW = \frac{0.35}{\tau_r} \tag{12}$$

The performance parameters for all the graphene based FET devices and OCFET are enumerated in table I.

Intuitively it may be argued that OCFET has similar attainment properties in terms of V_{DS} values in order to attain a saturation region faster. However a comparison of τ_r and BW between OC-GFET and OCFET as shown in table I suggests that OC-GFET may outperform an OCFET by an order of 10^3 in performances of both τ_r and BW. It may be noticed that experimental values of I_{DS} for an OCFET are in order of $10^{-6}A$ [1] while graphene based FETs show a possible range of $10^{-3}A$ at similar V_{DS} ranges.

V. CONCLUSION

In this work an OC-GFET with a drain-source supply voltage of 1 V and an incident laser source of 1550 nm reaches saturation in comparison to G/SiO_2/Si and G/h-BN/Si FETs which requires 7 V and 2 V respectively. The extrinsic timing analysis determined in this work establishes that the response time for OC-GFET is of the order of $10^{-11}s$ and bandwidth is in 10^9Hz range. The optically induced mobility is of the order of $10^5cm^2/V-s$ which achieves drain-current in the range of $10^{-3}A$. Light assisted GFET devices have the potential to be used in digital applications.

ACKNOWLEDGMENT

We would like to acknowledge the invaluable insights from Dr. Abhilash Ravikumar, Assistant Professor, Department of Electronics and Communication Engineering, Amrita School of Engineering, Bengaluru.

REFERENCES

[1] L. Colace, V. Sorianello, and S. Rajamani. Investigation of static and dynamic characteristics of optically controlled field effect transistors. Journal of Lightwave Technology , 32(12):22332239, June 2014.

[2] Han Chang, Ultrahigh Responsivity and Detectivity GraphenePerovskite Hybrid Phototransistors by Sequential Vapor Deposition, DOI:10.1038/srep46281, Scientific Reports volume7 2017, Article number: 46281

[3] Geim, A.K. and K.S. Novoselov, The rise of graphene. Nat Mater, 2007. 6(3): p. 183-191.

[4] I. Meric,,Current saturation in zero-bandgap, topgated graphene eld-eect transistors,Nature Nanotech, vol. 3, pp. 654659, Sept 2008.

[5] J.-H. Chen, C. Jang, S. Xiao, M. Ishigami, and M. S. Fuhrer, Intrinsic and extrinsic performance limits of graphene devices on SiO2 , Nature Nanotech,vol. 3, pp. 206209, Jan 2008.

[6] Hariharan.S, Bala Tripura Sundari.B, "Modeling 15nm Graphene FET With Contact Resistance Effects Using Channel Segmentation Technique," International Conference on circuits Power and Computing Technologies [ICCPCT], 2017.

[7] R. Sreenath, B. Bala Tripura Sundari,"Compact model for switching characteristics of graphene field effect transistor,"AIP Conference Proceedings 1724, 020013, 2016

[8] Dimensional Modification Induced Band Gap Tuning in 2D-Photonic Crystal for Advanced Communication and Other Application, Feb 2019. [Online; accessed 11. Feb. 2019].

[9] Y. Q. Wu, K. A. Jenkins, A. Valdes-Garcia, D. B. Farmer, Y. Zhu, A. A. Bol, C. Dimitrakopoulos et al., State-of-the-art gra- phene high-frequency electronics, Nano Letters, vol. 12, no. 6, pp. 30623067, Jun, 2012.

[10] H. Wang, A. Hsu, J. Wu, J. Kong, and T. Palacios, Graphene-based ambipolar RF mixers, IEEE Electron Device Lett., vol. 31, no. 9,pp. 906908, Sep. 2010.

[11] C.-H. Liu, Y.-C. Chang, T. B. Norris, and Z. Zhong, Graphene photodetectors with ultra-broadband and high responsivity at room temperature,Nature Nanotechnol., vol. 9, no. 4, pp. 273278, Mar. 2014.

[12] B. Shen, Y. Li, W. Zhai, and W. Zheng, Compressible Graphene-Coated Polymer Foams with Ultralow Density for Adjustable Electromagnetic Interference (EMI) Shielding, DOI: 10.1021/acsami.5b11715, ACS Appl. Mater. Interfaces 2016, 8, 80508057.

[13] Qiaoliang Bao, Han Zhang, Bing Wang, Zhenhua Ni, Candy Haley Yi Xuan Lim, Yu Wang, Ding Yuan Tang, and Kian Ping Loh. Broadband graphene polarizer. Nat. Photonics , 5(7):411, May 2011.

[14] Dharmendar Reddy Palle. Modeling of graphene-based FETs for low power digital logic and radio frequency applications, Aug 2013. [Online; accessed 18. Apr. 2019].

[15] San-Jose, P.; Prada, E.; McCann, E.; Schomerus, H. Phys. Rev. Lett. 2009, 102, 247204

[16] R. Shishir, F. Chen, J. Xia, N. J. Tao, D. K. Ferry, Room Temperature Carrier Transport in Graphene, J. of Comp. Elec., in press;

[17] D. L Rode,Low Field Electron Transport Semiconductors and Semimetals, vol. 10, Ed. by R. K. Willardson and A. C. Beer (Academic Press, New York, 1975) pp. 1-89.

[18] Dorgan, V. E., Bae, M-H. Pop, E. Mobility and saturation velocity in graphene on SiO2. Appl. Phys. Lett. 97, 082112 (2010).

[19] S. Thompson, P. Packan, and M. Bohr, Intel Technology Journal Q3 1998

[20] Jing Tian, Anestis Katsounaros, Darryl Smith, and Yang Hao. Graphene field-effect transistor model with improved carrier mobility analysis. Electron Devices, IEEE Transactions on , 62:34333440, 10 2015.

[21] G. M. Landauer, D. Jimenez, and J. L. Gonzalez, An accurate and Verilog-A compatible compact model for graphene field-effect transistors, IEEE Trans. Nanotechnol., vol. 13, no. 5, pp. 895904, Sep. 2014

[22] Jyotsna Chauhan and Jing Guo. High-field transport and velocity saturation in graphene. Appl. Phys. Lett. , 95(2):023120, Jul 2009.

[23] C. R. Dean, A. F. Young, I. Meric, C. Lee, L. Wang, S. Sorgenfrei, K. Watanabe, T. Taniguchi, P. Kim, K. L. Shepard, and J. Hone. Boron nitride substrates for high-quality graphene electronics. Nat. Nanotechnol. , 5(10):722726, Oct 2010.

[24] I-Tan Lin,Optical Properties of Graphene from the THz to the Visible Spectral Region, Master of Science in Electrical Engineering, University of California, Los Angeles, United States (2012), - Google Search, Apr 2019. [Online; accessed 5. Apr. 2019].

[25] Stauber, T., N.M.R. Peres, and A.K. Geim, Optical conductivity of graphene in the visible region of the spectrum. Physical Review B, 2008. 78(8): p. 085432.

[26] Helgi Skuli Skulason,Optical Properties of Few and Many Layer Graphene Flakes. McGill University Montreal, Canada (2009). - Google Search, Apr 2019. [Online; accessed 5. Apr. 2019]

[27] Eduardo J H Lee, Kannan Balasubramanian, Thomas Weitz, Marko Burghard, and Klaus Kern. Contact and edge effects in graphene devices. Nature nanotechnology , 3:48690, 09 2008.

[28] Wenyan Zan, Wei Geng, Huanxiang Liu, and Xiaojun Yao. Electric-field and strain-tunable electronic properties of MoS2/h-BN/graphene vertical heterostructures. PCCP , 18(4):3159 3164, Jan 2016.

[29] CMOS Digital Integrated Circuits: Analysis and Design, Feb 2019. [Online; accessed 13. Feb. 2019]

Proceedings of the Fourth International Conference on Communication and Electronics Systems (ICCES 2019)
IEEE Conference Record # 45898; IEEE Xplore ISBN: 978-1-7281-1261-9

Advanced Military Helmet aided with Wireless Live Video Transmission, Sensor Integration and Augmented Reality Headset

Sandeep Jalui [1], Tushar Hait [2], Tulika Hathi [3], Soumes Ghosh [4]

[1,2,3] Bachelor of Engineering in Electronics and Telecommunication, Mumbai University.
MCT's Rajiv Gandhi Institute of Technology, Mumbai, India.

[4] Bachelor of Engineering in Instrumentation, Mumbai University.
MCT's Rajiv Gandhi Institute of Technology, Mumbai, India.

[1] sandeepjalui93@gmail.com ; [2] tusharhait96@gmail.com ; [3] tulika.hathi@gmail.com ; [4] soumes.ghosh@gmail.com .

Abstract - Military and Army need weapons for military activities or operations to safeguard our country and its citizens. They already have exquisite weaponry and ammunition for ensuring our safety. But all these weapons are costly, exclusive and bulkier. Military people face many problems due to the difficult conditions in warfare. Therefore, we came up with an idea of integrating different technologies and implementing augmented reality in helmet to display battlefield information in one screen. This should help improving strategies in war and can get more insights during military operation.

Keywords - Augmented Reality, Wireless Video Transmission, Radar Motion Detection, GPS tracking, Strategic War Improvement.

I. INTRODUCTION

Our military & army are ought to do surveillance in regions of extreme weather and terrain conditions. Military people face problems during their operations like counter insurgency operations, Night operations or surveillance. Bad communication scenarios, surprise attacks by enemy are few of the problems faced. Soldier may be stranded or blinded in desert sand storms or cold winds in snow clad regions, problems such as low visibility might cause hindrance to their operations and might get isolated from their troops.

Indian Army is already provided with advanced machinery and ammunition. They work in extreme weather conditions while securing our nation's borders. They can perform their mission with high awareness if they get information of their surrounding, with enhanced safety, speed and be in close co-ordination with team members, if they get excess to this information by an augmented reality display. Artificial Intelligence, Encrypted Secured Networking, Dedicated Satellite Communication or WiMAX, Night Vision Camera & Radar Technology can be a helping aid to this system.

One of the Successful mission of US military was to catch UN declared Global Terrorist Osama Bin Laden; during this mission they acquainted with technology such that satellite linked camera feeds, wherein the President Barack Obama and several key advisors, saw the real time footage of the operation. High-Tech Drones were also been used with camera with hyper spectral sensor. [1]

It is also expected that in the coming few years, there will be a vast implementation of virtual reality & augmented reality system in military domain. Market of augmented reality is growing worldwide with advancement in technology.[2] If we integrate, all the battlefield parameters, with the augmented reality system, it could result to be a boon for Indian military.

According to 2018 report, use of Artificial neural Networks, Computer Vision, Advanced Computing Autonomous System, Machine Learning and Robotics will keep up with the technological advancements such as warfare platforms, cybersecurity, logistics & transportation, Target recognition, Battlefield healthcare, Combat simulation and Training, Threat Monitoring & situational awareness, thus improving the military intelligence. [3]

Therefore, our project aims to create a best solution by combining all the features into one application that gives output of varied modules on one screen altogether.

II. PROPOSED METHODOLOGY

Our proposed project prototype is attempting to provide a helping aid to the Indian military to strengthen their Defenses and Strategic attack on a whole new level. During the military operation, harsh weather conditions and long-range attacks, our soldiers don't get proper insight, so our main aim here is to provide a modified vision to the soldiers.

The proposed helmet will contain a head mounted display on which we will beam information such as environmental conditions, distance from an enemy/obstacle, motion detection of enshrouded person, to help out with the user's position by displaying GPS co-ordinate to the user if personnel is lost. The helmet will have live wireless encrypted video transmission between the user and the central system. The most important aspect of helmet is built in such a way that it doesn't provide hindrance to the soldier in close combat operations. The Helmet works on a portable power supply.

Here, for visibility problems the solution can be Thermal IR and night vision camera. But it is important to note that undoubtedly, the cost of this accuracy is high enough. There is possibility that the person is separated from his troop & is attacked by the enemy army. In such conditions there is need of personnel's update by location tracking, distance between personal and the attacking troops; so, they could get prepared with their plan of attack. A good communication via audio along with live transmission between his fellowmen can intensify their strategy.

In Military applications, Radar is highly used for its features like stealth, long range coverage, high speed and altitude, maneuvering targets while facing the issues of jamming and fluctuations of radar cross-section with a minute change in the aspect angle of targets. Since, its features are appealing and hence, it is the prime component of helmet. [4]

It is necessary to be equipped with handy devices and be ready for any kind of combat and emergency situations. So

there is a need of provision of real-time information from combat soldiers in battle to their commanders. Hence, we have integrated all sensors onto one headgear, and made a product out of these.

III. PROPOSED SYSTEM

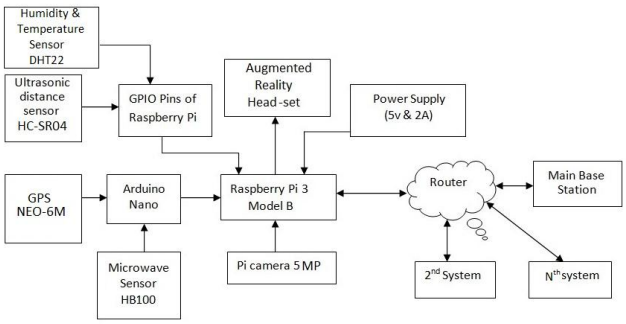

fig. 1 Block Diagram

The above block diagram shows the interconnection of all sensors and flow of data through different devices in a virtual network. The Temperature & Humidity sensor (DHT22) and Ultrasonic distance sensor (HC-SR04) is connected to Raspberry Pi. The GPS (NEO-6M) and Radar module (HB-100) is connected to Arduino. The Arduino is a micro-controller whose function is specific and gives output of sensors accordingly, while Raspberry Pi is microprocessor which integrates all the data coming from sensors and Arduino, combines them in a GUI and send to the display unit of augmented reality headset. Further detailed explanation of individual block is given below.

- **Distance Calculation using Ultrasonic Sensor HC-SR04:**

Ultrasonic sensor works on principle of reflection of sound waves i.e. short high frequency sound pulses which propagates at the velocity of sound. All materials reflect sound, regardless of colour, object shape and size. The time span between the emitting ultrasonic sound wave & receiving echo is termed as Time of flight. It is the measuring factor which determines the distance of the object from the wave source using kinematic formulae.

HC-SR04 Ultrasonic sensor sends 8, 40 KHz signal detecting the echo pulse. The measuring range being up to 400cm with a ranging accuracy of 3mm. High precision sensor can also be used to enhance the range. [5]

- **Motion detection using HB100 Radar module:**

When the Microwave of the Radar sensor are targeted to a particular object, there might be a chance of change in frequency of reflected signal. This change depends upon whether the target is stationary or not. When microwave signal falls on the moving object, the change in the frequency is determined based on that we can identify if there is any motion, this is Doppler effect. The output isn't affected by the presence of factors like temperature, humidity, light, dust or harsh environment.

HB100 uses a frequency of 10.525 GHz, and works up to the range of 20m. The signal detected by Sensor is in range of μV, hence further amplification is required using Operational-Amplifiers. This amplified signal is sent to the Main control unit. Radar systems can be configured in a number of different ways and across many different frequency bands.

- **Temperature and Humidity detection using DHT22:**

Temperature and Humidity are relative parameter when it comes to stating the environmental comfort for any living being. In DHT 22, measurement of temperature and humidity takes place simultaneously by 2 different independent sensors. For the measurement of humidity, capacitance as a principle is used. The moisture present in the atmosphere is adsorbed by the micro fiber material present between the two capacitive plates. The variation of capacitance helps sensor determines the humidity of the environment. A temperature compensation circuit is also taken into consideration for accurate humidity measurement. Also, an independent Thermistor is used for measurement of ambient temperature. Thermistor is a semiconductor device, which has a Negative Temperature Co-efficient (NTC).

Am2302 sensor has a humidity measuring range of 0 %RH to 100 %RH and temperature range of -40°C to 80°C with an accuracy of ± 2 %RH and ± 0.5°C respectively, with an average sensing time of 2 sec.

- **Location detection using GPS NEO-6M:**

GPS uses the method of trilateration to calculate the location. GPS satellites transmit information signal over radio frequency (1.1 to 1.5 GHz) to the receiver. Three GPS satellite revolving around Earth, this GPS module receives information from satellite and calculates the location. This is done by measuring the time required for signal transmission. The satellite transmits the pseudocode; which is received by the GPS receiver. These two signals are compared and the difference between the signals is the travel time.

Neo-6m GPS module has a ceramic antenna with strong satellite search capability. With a default baud rate of 9600 bps and interfaces with RS232 TTL.

- **Live video transmission:**

In this process, Pi-Camera module is connected to the CSI (Camera Serial Interface) port of raspberry pi via 15-pin ribbon cable. Then the camera option is enabled in interfacing options of raspberry pi. The video mp4 format carries huge data and hence for wireless transmission, we needed a device which will provide high speed and bandwidth.

Therefore, Raspberry pi is connected to the router, and transmits video data wirelessly at 15fps. Using python commands, video is uploaded to the virtual network having a specific IP address. Other users can access the data if they are connected to the same network.

Therefore, to access the live video, the end user has to put IP address of the video on the web browser. Also, many users can access this data by making this as one-to-many sharing features. Similarly, many-to-many transmission features is also possible. [6]

- **Virtual Networking:**

In many war zone regions, there is a problem of communication as there is no network available due to bad weather or geographical region constraints. Also there is a high change that the enemy can hack the network if the network is weak and can access our information which can

lead to losing of war. Hence, Military people uses dedicated satellites or transponders for encrypted and effective communication. [7]-[8]

Also in India, ISRO has launched its first military satellite i.e. GSAT-7 which is multi-band military communication satellite, revolves in geosynchronous orbit and connects ocean & land mass covering Indian Navy and Military forces.

In this prototype, we have created virtual network by using Wi-Fi router. As shown in the block diagram, this router is connected to base station i.e. in our case is computer which gets all data. We can connect multiple helmets as shown in fig 1 as nth number of systems. Wi-Fi router works on DHCP principle which connects multiple devices.

• **Augmented Reality:**

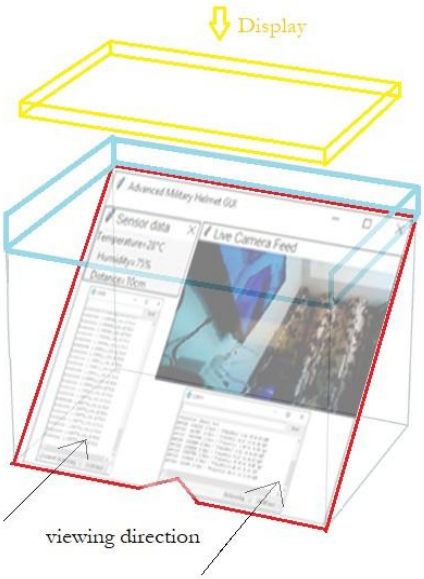

fig. 2 Augmented Reality

The Augmented Reality system is display unit for our Helmet, the data is been collected from the sensors via different modules by Raspberry Pi, is transmitted to a Smartphone with LCD display (6" diagonal length) via Wi-Fi. Augmented reality display is interactive experience with the real world, the normal insights of the ambience can be seen clearly through a transparent glass, also the interactive transparent display will show the LCD Display as shown in fig. 2, the display unit i.e. mobile screen (yellow zone) used as the display and kept on transparent rack (blue zone), the image on the screen from the rack is reflected on the 45° tilted transparent screen (red zone). Since the tilted screen is transparent the ambience can be clearly seen through it. The LCD display reflected on the 45° tilted glass can also be seen superimposed.

Hence, an interactive display could be seen on the transparent glass. This transparent display act as a High-Tech Display system helping the personnel to view the real world as well as the data provided by System. The data helps the personal to analyze the environment in a better way and could be a helping aid in areas with Low visibility. [9]-[10]

VNC server software is already available as android application package file (.apk) format. Hence the UI which we have created using Python Tkinter library is shown on mobile screen for Augmented reality Display. The combination of glass and mirror is structured in such a way that the superimposed image is formed in the glass structure. The augmented reality creates a superficial display of another data to a normal human vision.

IV. IMPLEMENTATION

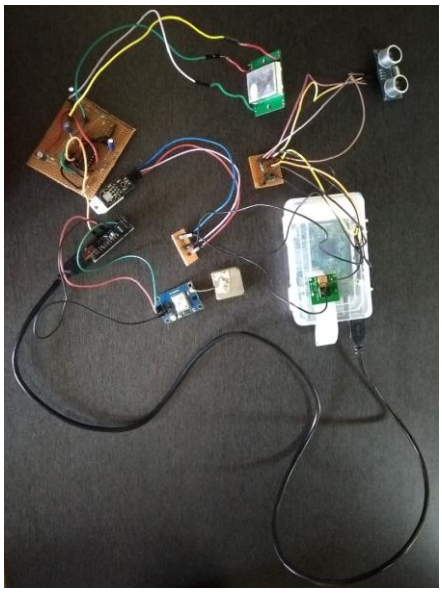

fig. 3 Connection of Components

- The Raspberry Pi is the CPU, the brain of the whole setup. All the modules are connected to it and interfaced via I/O ports and serial communication.
- Since Raspberry Pi is a micro-processor, it needs a screen to access the pi and give commands. We used VNC server software to access the Raspberry Pi User Interface wirelessly via router.
- The Arduino Nano is the microcontroller connected to pi and eases the interfacing of Radar and GPS module via analog and digital pins of Arduino.
- The Radar microwave sensor (HB100) is connected to Arduino Nano which is used for detection of motion of objects which are behind the solid obstacles using doppler principle of radar waves.
- GPS module (Neo-6m) is connected to the Arduino Nano which gives location in terms of longitude and latitude co-ordinates using trilateration methods.
- The DHT22 and Ultrasonic sensor are connected to the GPIO pins of the Raspberry Pi.
- The Temperature and Humidity Sensor DHT22 is connected to the Pi directly, giving the Temperature values in Centigrade and Humidity in percentage.
- The Ultrasonic Sensor HC-SR04 uses SONAR concepts to calculate distance effectively.
- The Raspberry Pi is provided with the power supply of 5 v & 2 amp. The Raspberry Pi Camera of 5 MP is connected the dedicated camera slot of the pi via serial communication. The camera frame rate is 15 fps.

- Raspberry Pi is connected to the router that acts like a satellite/transponder. Here router is an essential component to create a virtual network & imitate a satellite communication for transmission of data.

- The camera is for the live transmission following Master Slave communication protocol and all the 'N' number of systems are connected to the master via router, which had been allotted unique IP address to each device by DHCP.

- All these communications were possible because of the High-speed Router. Router allocates dynamic IP address to Raspberry Pi and other accessing devices as well. This is how we have achieved wireless communication and created a system of virtual network.

- The data of all the modules and video is combined in a GUI using Tkinter Library of python and is projected on mobile screen.

V. RESULT

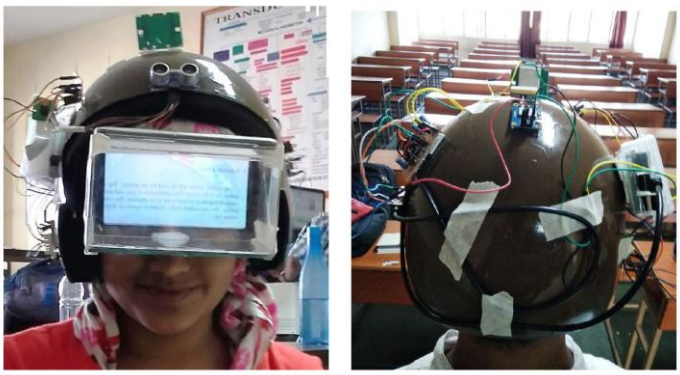

fig. 4 Prototype Model

The fig. 4 shows the prototype hardware model, with all components connected together. The front and rear view is shown on left and right image respectively. The AR is worn separately and then helmet over it. The sensors are kept in front and the processing unit towards sideway.

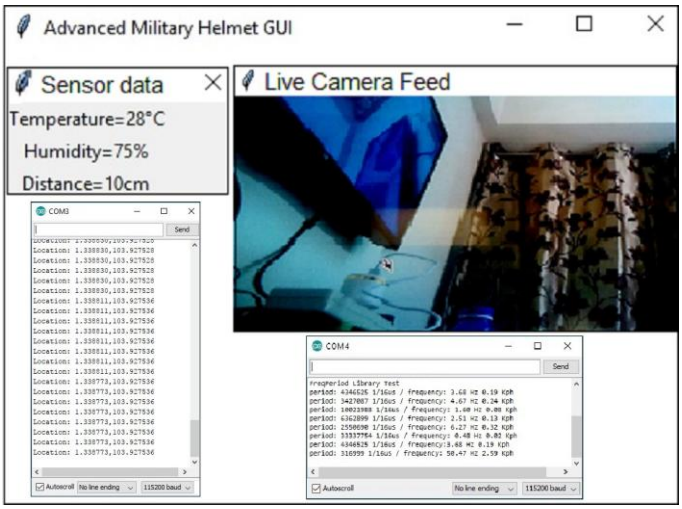

fig. 5 GUI Screen

The fig. 5 shows the GUI Screen. The Ultrasonic sensor shows the accurate distance of 10 cm. The distance shown had accuracy of 3 mm. This distance was also verified with scale. The DHT22 sensor gave us the accurate reading of surrounding temperature and humidity as 28°C and 75% respectively.

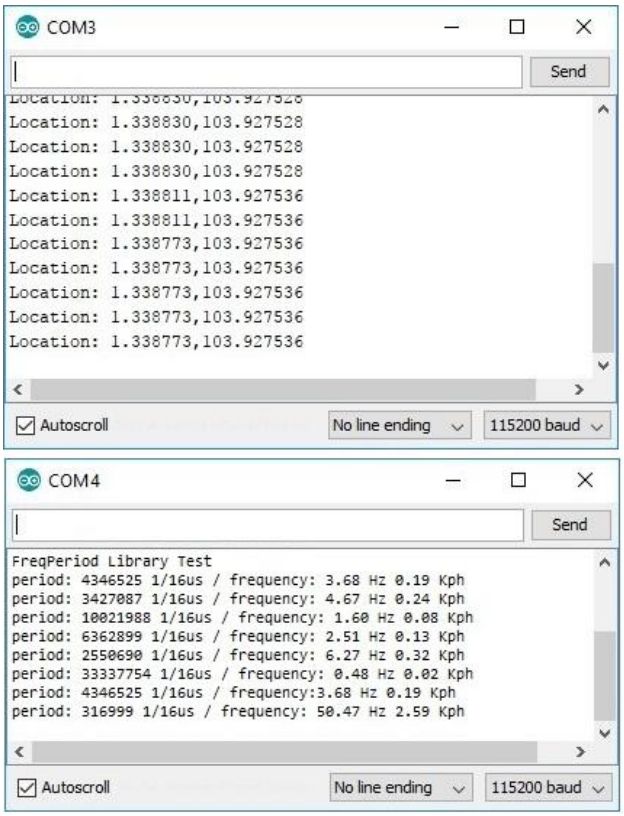

fig. 6 Output of GPS and Radar Module

The fig. 6 shows GPS Co-ordinates and Radar output. The GPS module Neo-6M gave us GPS co-ordinates in terms of latitude and longitude only in open space/ground. The radar module gives us the average frequency value as 3 Hz and velocity reading 0.2 Kph but it shows change in value when it detects the motion of the target. The value of frequency and velocity was 50.47 Hz and 2.59 Kph when we created dummy motion. This module shows motion detection for frequency value above 19.37Hz and velocity 1.0 kph.

In case of wireless transmission, router transmitted sensor and video data properly in a range of 20m radius. This video which was generated by the system was accessible to all the devices by putting the IP address on web browser. We can increase the number of devices if the bandwidth of the network is increased.

VI. CONCLUSION

This prototype project provides solution to all the problems which we discussed. It combines all possible features into one single unit and handles multiple devices simultaneously. The helmet is cost effective and accurate enough to spot the suspect and help making respective combat plans, while being updated about the live data feedback. The implementation of augmented reality in the field of military domain is a new idea and can be developed even more with the upgradation of technologies.

VII. FUTURE SCOPE

- Compact Design can be made using advanced VLSI, mini projector and smaller AR Headset.
- Use of bulletproof material makes it sturdier and more reliable.
- Voice communication between military personnel is an extension of our project. Addition of Voice control system to control all features of helmet with voice commands.
- Implementation of Artificial Intelligence and Advanced Image Computing will make these devices smarter and more reliable by scanning and determining any foreign material.
- Hologram projection of maps.

References

[1] “5 State of the Art Military Technologies That Helped Take Out Bin Laden” an article by FOX News Tech, published on May 05, 2011

[2] Sintia Radu, “The Future of War May Be Virtual-The U.S. is investing billions into virtual reality training for the military by 2022” published on March 20, 2018, on the news article of “US news-Best News”.

[3] Tejaswi Singh, Amit Gulhane, “8 Key Military Applications for Artificial Intelligence in 2018”, an article by market and markets published on October 3, 2018

[4] "Indigenous Radars" published By BULLETIN OF DEFENCE RESEARCH AND DEVELOPMENT ORGANISATION Vol.21 No.2 April 2013

[5] Manpreet Kaur, Jai Pal, “Distance Measurement of Object by Ultrasonic Sensor HC-SR04” issued in IJSRD - International Journal for Scientific Research & Development, Vol. 3; Issue 05, 2015

[6] Omkar Ketkar, Pranay Ninawe, Sagar Panchal, Yash Sonar, "VIDEO TRANSMISSION USING WIRELESS NETWORK" published by International Journal of Technical Research and Applications e-ISSN: 2320-8163, www.ijtra.com Special Issue 40 (KCCEMSR) (March 2016)

[7] Dawson L., "Satellite Technology. In: War in Space". Springer Praxis Books. Springer, Cham, Online ISBN-978-3-319-93052-7, 01 January 2019

[8] David A. Fritz, Bharat T. Doshi, Andrew C. Oak, Steven D. Jones, Jack L. Burbank, Harry L. Miller, John D. Oetting, Ryan M. Collins, Lino A. Gonzalez, and Robert A. Nichols, "Military Satellite Communications: Space-Based Communications for the Global Information Grid", Johns Hopkins APL Technical Digest, Volume 27, Number 1 (2006)

[9] Jun He, Peng Han, Huan Liu, Shiying Men, Lu Ju, Pu Zhen, Ting Wang, “The research and application of the augmented reality technology” published in IEEE 2nd Information Technology, Networking, Electronic and Automation Control Conference (ITNEC), e-ISBN: 978-1-5090-6414-4, 8 February 2018

[10] A. Alhakamy and M. Tuceryan, "AR360: Dynamic Illumination for Augmented Reality with Real-Time Interaction," 2019 IEEE 2nd International Conference on Information and Computer Technologies (ICICT), Kahului, HI, USA, 2019, pp. 170-174., doi: 10.1109/INFOCT.2019.8710982

[11] Brig. Rumel Dahiya, SM (Retd.) is Deputy Director General at the Institute for Defence Studies & Analyses (IDSA), "Indian Army: Internal Challenges in Capability Building and Retention”, October 11, 2012

[12] Richard DeSalvo, Charles Middleton, Elliott Grafer, Alex Cramer, Kevin Anzalone, Elias Soto, Brandon Devenport, "The convergence of microwave photonic and optical wireless systems with military communication and sensor systems", published in IEEE Photonics Conference (IPC) 2016, USA, INSPEC Accession Number: 16637187, 26 January 2017

Proceedings of the Fourth International Conference on Communication and Electronics Systems (ICCES 2019)
IEEE Conference Record # 45898; IEEE Xplore ISBN: 978-1-7281-1261-9

A Comparative Analysis of 8-bit Novel Adder Architecture Design using Traditional CMOS and m-GDI technique

Gautam Nayan
Bachelor of Engineering,
Dept. of ECE,
Sri Siddhartha Institute of Technology,
Tumakuru, Karnataka, India
gautamnayan02@gmail.com

***Abstract*– Addition is a standout amongst the most fundamental operations in VLSI frameworks such as microprocessors and digital signal processing systems. Therefore, the adders must render high speed operation. This paper proposes a novel implementation of 8-bit adder architecture using modified Gate Diffusion Input (m-GDI) approach. The primary blocks of adder are partial full adder, 1-bit full adder, 4-bit ripple carry adder (RCA), 4-bit carry look ahead adder (CLA). The proposed adder architecture devours 70% lesser area, 71% lesser delay and 35% lesser power dissipation w.r.t traditional CMOS design. The proposed adder is implemented utilizing Cadence Virtuoso Tool in 180nm technology.**

***Keywords*– Area, carry look ahead adder (CLA), m-GDI, Power, ripple carry adder (RCA), Speed**

I. INTRODUCTION

LOW-POWER design has turned into a basic concern in VLSI design, exceptionally for portable gadgets and high-density frameworks. As the integration density on the chip increments, fundamental concerns regarding the size and power dispersal of the components emerges. Therefore, the primary point is to lessen the power devoured by the digital circuits.

The design of digital circuits utilizing traditional CMOS technique requires large transistor counts and the circuit consumes larger area. As the technology reduces it results in high leakage power and dynamic power from the CMOS circuits. Digital circuit designed using m-GDI technique outcomes in high speed low power operation and devours lesser area. This approach permits the actualization of large variety of logic functions with a solitary m-GDI cell that's made up of two transistors. Thus, it expends lesser power, area and delay when contrasted with the circuits implemented using traditional CMOS technique [1-3]. Fig. 1 depicts the basic structure of m-GDI cell.

In the first view, the m-GDI cell looks alike to the CMOS NOT gate, but it consists of 3 inputs, one common input to the gate of both NMOS and PMOS, one input to the source/drain of PMOS and another to source/drain of NMOS [1,2].

Table I demonstrates the distinctive logic functions that can be actualized utilizing the single m-GDI cell [1].

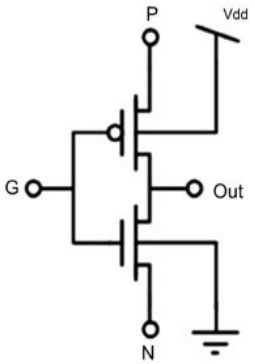

Fig. 1. Basic m-GDI cell

TABLE I. DIFFERENT LOGIC FUNCTIONS REALIZED USING m-GDI CELL

INPUTS			OUTPUT	LOGIC FUNCTION
N	P	G		
V_{SS}	V_{DD}	X	$\bar{X}$	NOT
V_{SS}	Y	X	$\bar{X}.Y$	F1
Y	V_{DD}	X	$\bar{X}+Y$	F2
V_{DD}	Y	X	X+Y	OR
Y	V_{SS}	X	XY	AND
Y	X	S	$\bar{S}X+SY$	MUX

Generally, the realization of basic logic gates utilizing static CMOS technique requires a transistor count varying from 6-12, whereas using a single m-GDI cell different logic functions can be actualized, as the transistor count lessons the circuit becomes compact and devours lesser area and intern offer high speed- low power operation [4].

Adders act as one of the fundamental building blocks of any higher subsystem design such as multiply accumulate units, arithmetic logic units, multipliers, microprocessors and so on [5].

The organization of the present paper is as per the following: Section II discusses the implementation of basic logic gates and full adder circuit. Section III aims at the design and implementation of Ripple Carry Adder and Carry Look Ahead Adder. Section IV aims at the design, implementation and performance analysis of 8-bit novel adder architecture and finally, Section V concludes the paper.

II. DESIGN AND IMPLEMENTATION OF VARIOUS LOGIC GATES AND FULL ADDER ARCHITECTURE.

It ought to be noticed that the producing of all logic gates, in basic m-GDI cell, can't be possible in CMOS process, so twin- well CMOS or Silicon oxide insulator (SOI) technology can be utilized for the cell fabrication [6].

Due to limitation of library in our Cadence simulator, there exists only single-well CMOS in the software, so maximum output voltage swing cannot be achieved. To reduce this disadvantage remarkably, we must use buffer at the output of basic gates to gain maximum output swing. Here, Cadence Schematic Editor was used for the front-end design and the layout was designed using the Cadence Layout XL. In order to carry out the performance analysis of various logic gates and proposed adder architectures Cadence spectre simulator was utilized.

A. AND gate

The realization of AND gate using traditional CMOS technique requires a transistor count of 6. Whereas the using a solitary m-GDI cell the AND operation can be realized. Fig. 2 depicts the traditional CMOS based AND gate. Fig. 3 depicts the m-GDI based AND logic. One input 'A' is applied to the source of NMOS i.e. N input of the m-GDI cell & another input 'B' is applied to the source of PMOS i.e. P input of m-GDI cell. Table II shows the different regions of operation of NMOS and PMOS of the m-GDI cell for the AND operation [3].

TABLE II. Different regions of operation of NMOS & PMOS for logic AND operation

Inputs		PMOS	NMOS	Output
a	b			
'0'	'0'	Linear $V_{in}-V_{tp}<V_{out}<V_{DD}$	Cut off $(V_{in}<V_{tn})$	'0'
'0'	'1'	Cut-off $V_{in}>V_{DD}+V_{tp}$	Linear $0<V_{out}<V_{in}-V_{tn}$	'0'
'1'	'0'	Linear $V_{in}-V_{tp}<V_{out}<V_{DD}$	Cut off $(V_{in}<V_{tn})$	'0'
'1'	'1'	Cut-off $V_{in}>V_{DD}+V_{tp}$	Linear $0<V_{out}<V_{in}-V_{tn}$	'1'

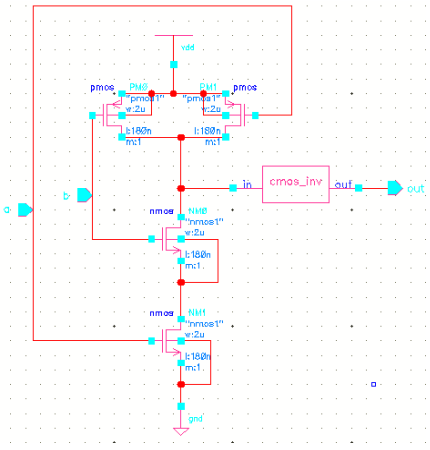

Fig. 2. CMOS AND logic

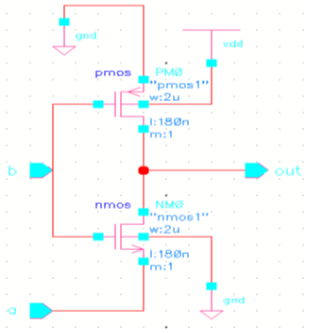

Fig. 3. m-GDI AND logic

Fig. 4 depicts the layout of CMOS based AND gate. In order to achieve full swing output from the m-GDI based AND gate, the output of the logic gate is connected to a buffer. Fig. 5 depicts layout of m-GDI based AND gate with buffer.

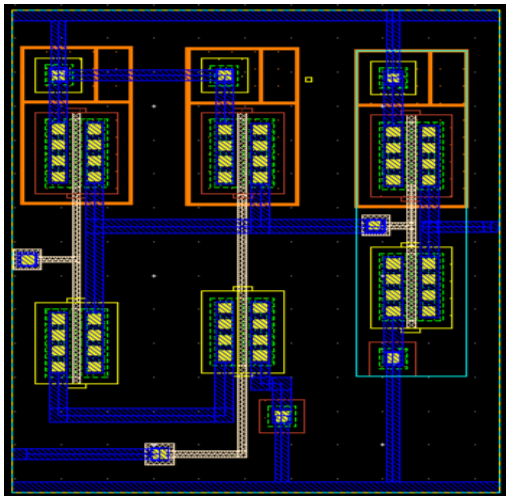

Fig. 4. CMOS AND layout

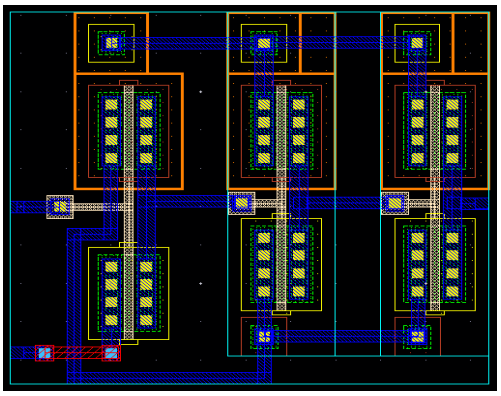

Fig. 5. m-GDI AND layout

B. *OR gate*

In order to actualize OR gate using traditional CMOS technique, it requires a 3 NMOS-PMOS transistor pair that counts to 6 no. of transistors, whereas actualization of basic OR gate using m-GDI technique can be done employing a solitary m-GDI cell.

Fig. 6 depicts the traditional CMOS OR logic and Fig. 7 depicts the m-GDI based OR logic.

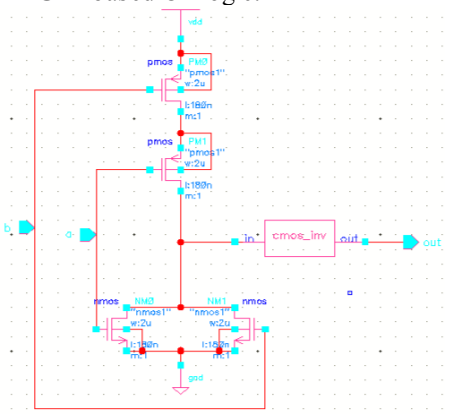

Fig. 6. CMOS based OR logic

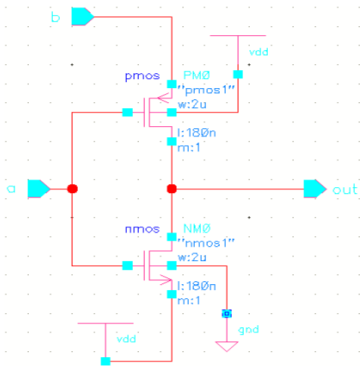

Fig. 7. m-GDI based OR logic

Fig. 8 shows the layout of CMOS based OR gate and Fig. 9 shows the layout of m-GDI based OR gate buffered to achieve full swing output.

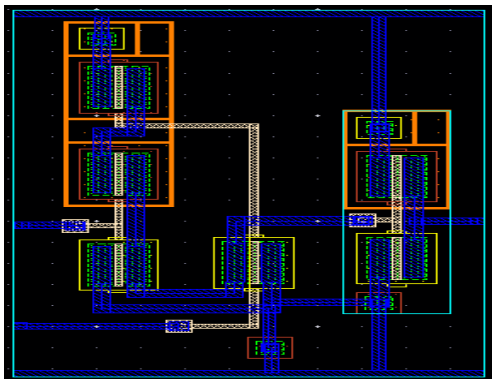

Fig. 8. CMOS OR layout

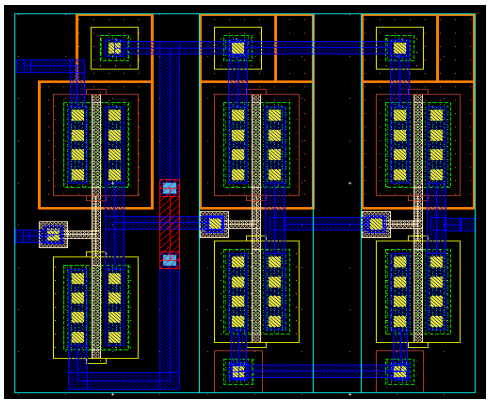

Fig. 9. m-GDI OR layout

C. *EX-OR gate*

The realization of EX-OR gate using traditional CMOS technique requires a transistor count of 12 whereas when realized using m-GDI technique the transistor count reduces to 4 nos.

Fig. 10 depicts the schematic of EX-OR gate realized utilizing traditional CMOS technique and Fig. 11 depicts the m-GDI based EX-OR gate.

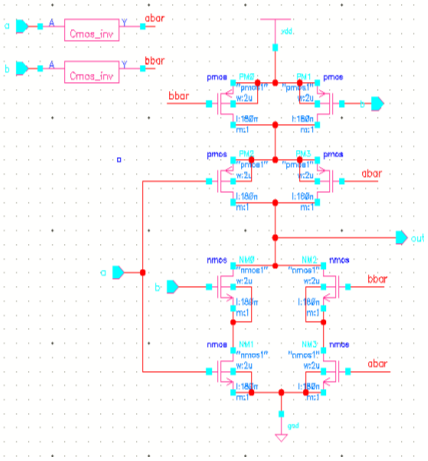

Fig. 10. CMOS based EX-OR logic

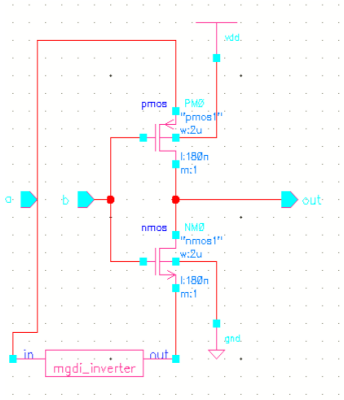

Fig. 11. m-GDI based EX-OR logic

Fig. 12 depicts the layout of the CMOS based EX-OR gate and Fig. 13 depicts the layout of m-GDI based EX-OR gate.

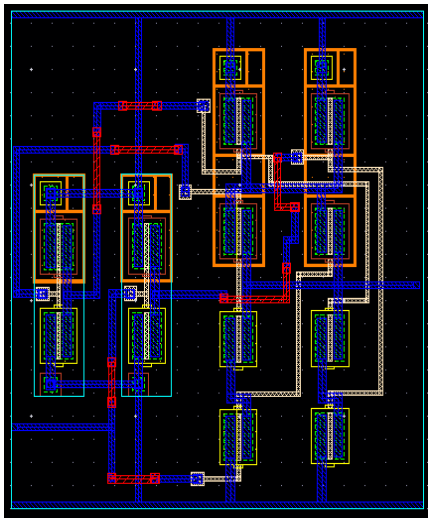

Fig. 12. CMOS EX-OR layout

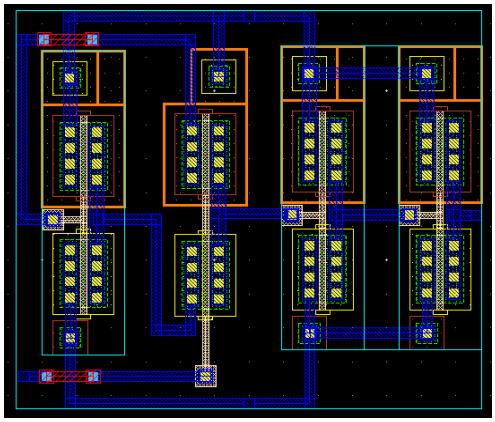

Fig. 13. m-GDI based EX-OR layout

D. Full Adder

A full adder circuits perform the addition of 3 one-bit numbers and often produces a sum and a carry output [5,7]. Table III shows the truth table of 1-bit full adder.

TABLE III. TRUTH TABLE FOR 1-BIT FULL ADDER

A	B	C_{in}	Sum	Carry
0	0	0	0	0
0	0	1	1	0
0	1	0	1	0
0	1	1	0	1
1	0	0	1	0
1	0	1	0	1
1	1	0	0	1
1	1	1	1	1

From the above table, the expressions for Sum can be given as:

$$Sum = A \oplus B \oplus C \quad (1)$$

In order to realize the expression for carry bit, let us examine the table.

When $A \oplus B = 0$;

$$Carry = B$$

Similarly, when $A \oplus B = 1$;

$$Carry = Cin$$

Therefore, this whole carry operation can be realized using a 2:1 MUX circuit. Where, $A \oplus B$ output can be given to the select line S of MUX B can be given to I_0 input and C_{in} can be given to I_1 input of 2:1 MUX.

2:1 MUX can be realized utilizing a single m-GDI cell, where the $A \oplus B$ output can be given to gate input of cell, B can be applied to P input of cell and C_{in} to the N input of the cell. Fig. 14 shows the schematic of m-GDI based Full Adder.

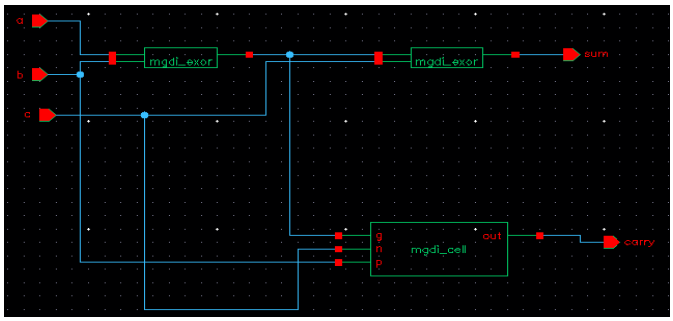

Fig. 14. m-GDI based Full Adder

Therefore, the no. transistors required to implement the full adder circuitry using the above equations employing conventional CMOS technique counts to 42, whereas when implemented using m-GDI the transistor count cut downs to 10 nos. only.

Fig. 15 depicts the layout of 42 transistor CMOS based full adder circuitry and Fig. 16 depicts the layout of m-GDI based Full adder circuitry which is buffered to get the full swing output.

Table IV shows the performance analysis of various logic gates and full adder circuitry. In order to carry out the performance analysis, cadence spectre simulator was utilized. Both the input to the logic gates where varied from 0-1.8V, with one input at 100ns time period and another at 50ns. For the full adder circuitry, the 3 inputs where varied from 0-1.8V and the time period were set to 150ns, 100ns & 50ns respectively.

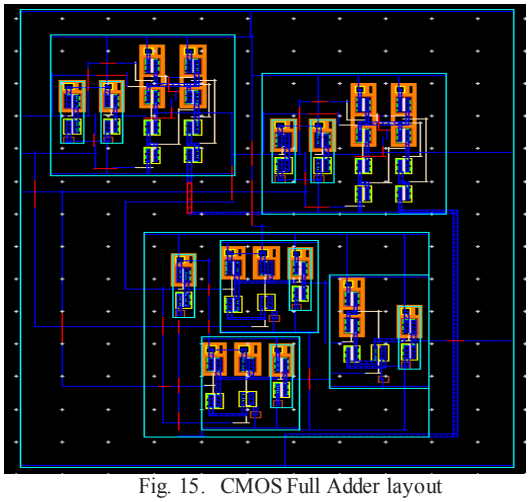

Fig. 15. CMOS Full Adder layout

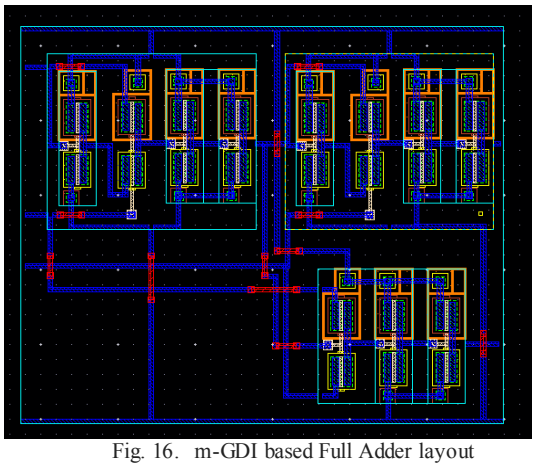

Fig. 16. m-GDI based Full Adder layout

TABLE IV. PERFORMANCE ANALYSIS OF VARIOUS LOGIC GATES AND FULL ADDER CIRCUITRY

Logic		Transistor count	Area (μm^2)	Delay (psec)	Peak power (mW)
NOT		2	21.59	88.46	0.242
Buffer		4	52.219	196.95	0.647
AND	CMOS	6	151.40	146.9	0.638
	mGDI	2	103.36	80.85	0.432
OR	CMOS	6	185.29	187.7	0.547
	mGDI	2	87.19	147.4	0.427
EXOR	CMOS	12	426.92	181.4	0.762
	mGDI	4	158.81	175.1	0.263
Full Adder	CMOS	42	3751.2	154.9	2.180
	mGDI	10	829.23	73.42	1.390

From the above table, it can be seen that the design of basic logic gates using m-GDI technique offers 30% lesser delay, 60% lesser area consumption and 30% lesser power dissipation w.r.t those designed using CMOS technique. Full adder design using m-GDI technique results in 50% lesser delay, 27% lesser power and 80% lesser area in contrast to CMOS based Full adder.

III. DESIGN AND IMPLEMENTATION OF RIPPLE CARRY ADDER AND CARRY LOOK AHEAD ADDER

A. Ripple Carry Adder

Here, a 4-bit Ripple Carry Adder (RCA) is designed by connecting 4 nos. of proposed full adder in cascade. In RCA, the carry bit ripples from each lower stage to the following higher stage and the final sum is only produced when the carry bit reaches the last MSB full adder [8,9].

CMOS based RCA design requires a transistor count of 168 whereas the RCA implementation through m-GDI technique requires a transistor count of 40 only. Fig. 17 depicts the m-GDI based schematic of 4-bit RCA design.

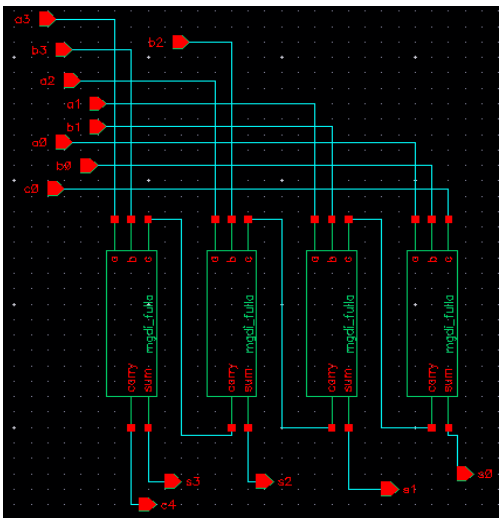

Fig. 17. m-GDI based 4-bit RCA

Fig. 18 depicts the layout of CMOS based 4-bit RCA design and Fig. 19 depicts the m-GDI based 4-bit RCA design employing buffers to obtain full swing outputs.

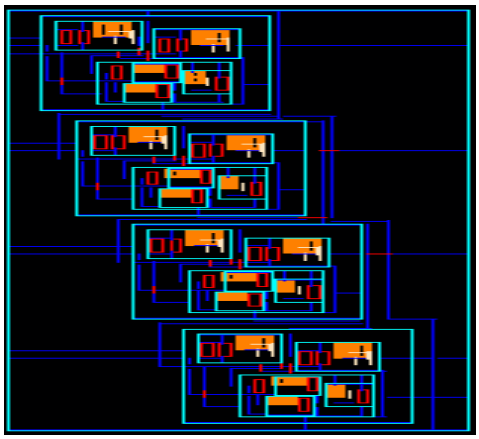

Fig. 18. CMOS based 4-bit RCA layout

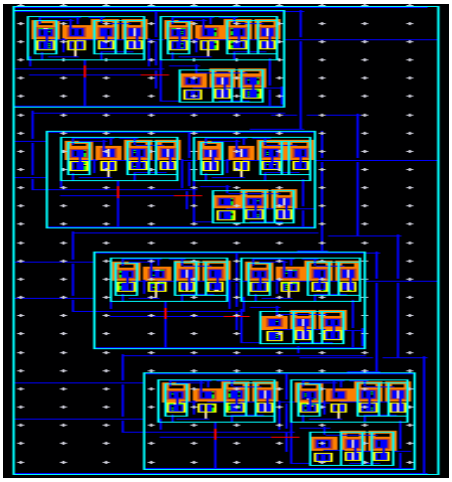

Fig. 19. m-GDI based 4-bit RCA layout

Fig. 20 depicts the simulation results for 4-bit RCA using m-GDI technique for input combination of $B_3B_2B_1B_0$= '1111' and $A_3A_2A_1A_0$ = '1111' & '0000'. Table V illustrates performance analysis of 4-bit Ripple Carry Adder.

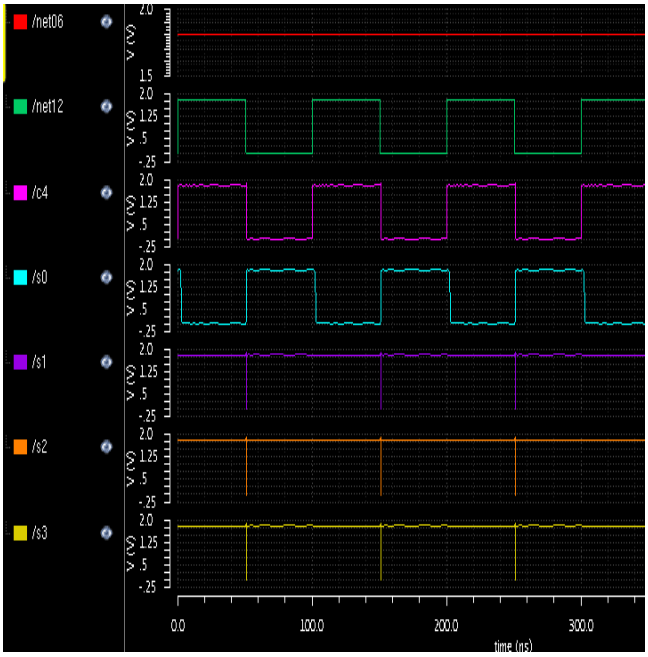

Fig. 20. Simulation result for 4-bit RCA employing m-GDI technique

TABLE V. PERFORMANCE ANALYSIS OF 4-BIT RCA

Design Approach	No. of Transistors	Area (μm^2)	Delay (psec)	Peak Power (μW)
CMOS	168	33767.1	381.50	5.19
m-GDI	40	6292.91	105.08	3.53

B. Carry Look Ahead Adder

This section proposes the implementation of 4-bit Carry Look Ahead Adder. A strategy for accelerating the addition process is by taking out inter stage carry delay. Such an addition operation is termed as look ahead-carry addition. The look ahead approach uses logic gates to look at he lower-order bits of augend and addend to check whether a higher order carry is to be generated. It makes use of two functions carry propagate (P_i) and carry generate (G_i) [10-12].

Where the equations for P_i and G_i can be expressed as:

$$P_i = A_i \oplus Bi \quad (2)$$

$$G_i = A_iB_i \quad (3)$$

For a 4-bit Carry look ahead adder (CLA) the carry output for each stage can be given as:

$$C_1=P_0C_0+G_0 \quad (4)$$

$$C_2=P_1C_1+G_1=P_1.(P_0C_0+G_0)+G_1 \quad (5)$$

$$C_3=P_2C_2+G_2=P_2.(P_1.(P_0C_0+G_0)+G_1)+G_2 \quad (6)$$

$$C_4=P_3C_3+G_3=P_3.(P_2.(P_1.(P_0C_0+G_0)+G_1)+G_2) +G_3 \quad (7)$$

The C_1 stage carry can be realized by using a m-GDI cell, by applying the P_0, the output of 1st partial full adder (PFA1) to the gate input of m-GDI cell, one input to the PFA i.e. C_0 as an input N of m-GDI cell and B_0 input of PFA as input P of m-GDI cell. The carry part of stage 1 i.e. C_1 is used for subsequent stage carry generation C_2, C_3 and C_4.

Fig. 21 stage shows the schematic of 1st partial full adder stage (PFA1) and Fig. 22 shows the schematic for C_1.

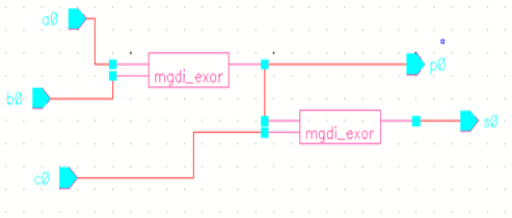

Fig. 21. 1st Partial Full Adder stage

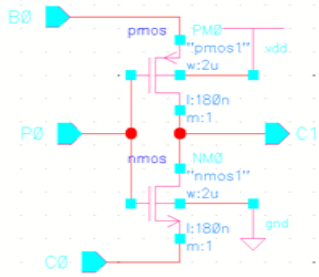

Fig. 22. Schematic of C_1 stage

To realize the sum for subsequent stages the partial full adder shown in the Fig. 23 is utilized.

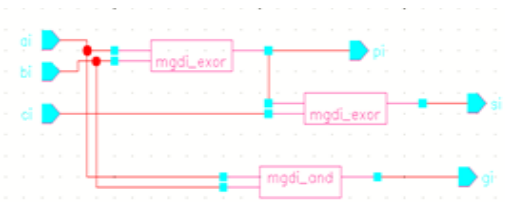

Fig. 23. Partial full adder for the S_1, S_2 & S_3 stage

Fig. 24 shows the schematic of m-GDI based 4-bit Carry Look Ahead Adder. Fig. 25 depicts the layout of 4-bit CMOS based CLA and Fig. 26 depicts the layout of m-GDI based 4-bit CLA. Table VI shows the performance analysis of 4-bit CLA.

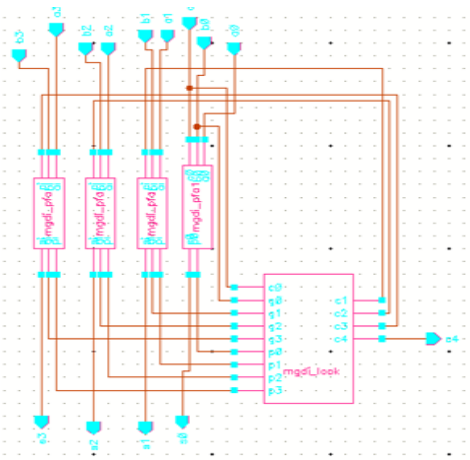

Fig. 24. Schematic of 4-bit m-GDI based CLA

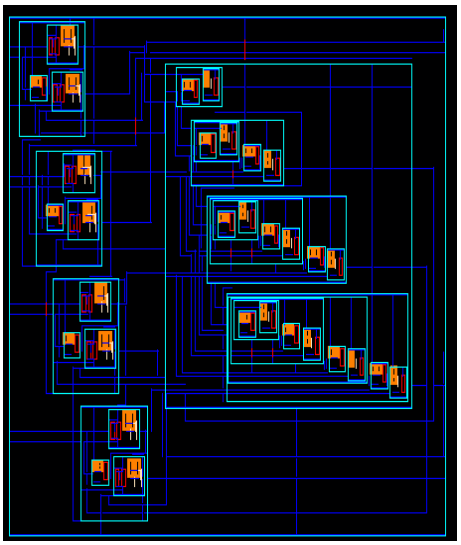

Fig. 25. Layout of CMOS based 4-bit CLA

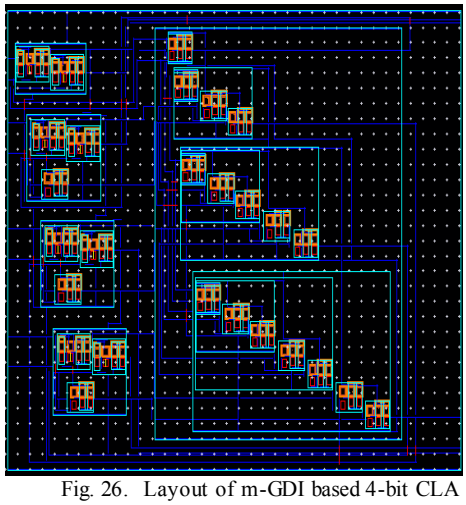

Fig. 26. Layout of m-GDI based 4-bit CLA

TABLE VI. PERFORMANCE ANALYSIS OF 4-BIT CLA

Design Approach	No. of Transistors	Area (μm^2)	Delay (psec)	Peak Power (μW)
CMOS	240	80350.7	261.60	6.38
m-GDI	70	27870.2	22.08	5.58

IV. DESIGN AND IMPLEMENTATION OF 8-BIT NOVEL ADDER ARCHITECTURE

The 8-bit hybrid adder is designed by cascading the two adder modules discussed in section III.

The lower 4-bits of the hybrid adder architecture uses 4-bit Carry Ripple Adder to carry out the summation of 4-LSB inputs to the adder. The carry output C_4 of the 4th stage of the CLA is applied as C_0 input to 1st stage of 4-bit Ripple Carry Adder. The 4-bit RCA calculates the sum of 4-MSB inputs to the adder. The final carry can be obtained at the carry output from the C_4 stage of the RCA.

Thus, the sum of lower 4-bits input $A_3A_2A_1A_0$ and $B_3B_2B_1B_0$ are calculated employing the 4-bit CLA and the higher 4-bits input $A_7A_6A_5A_4$ and $B_7B_6B_5B_4$ are calculated using 4-bit RCA.

Fig. 27 illustrates the schematic of m-GDI based 8-bit Hybrid Adder Architecture and Fig. 28 depicts the layout of proposed 8-bit adder architecture using m-GDI technique.

Fig. 29 depicts the simulation waveforms of 8-bit proposed adder architecture for input combination '11111111' for $A_7A_6A_5A_4A_3A_2A_1A_0$ and '00000000' & '11111111' as input to $B_7B_6B_5B_4B_3B_2B_1B_0$.

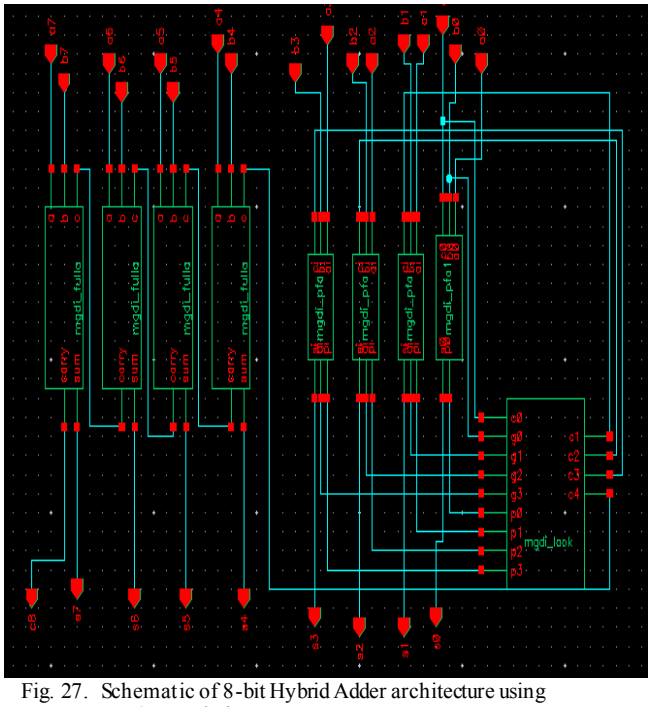

Fig. 27. Schematic of 8-bit Hybrid Adder architecture using m-GDI technique

Fig. 28. m-GDI based 8-bit adder layout

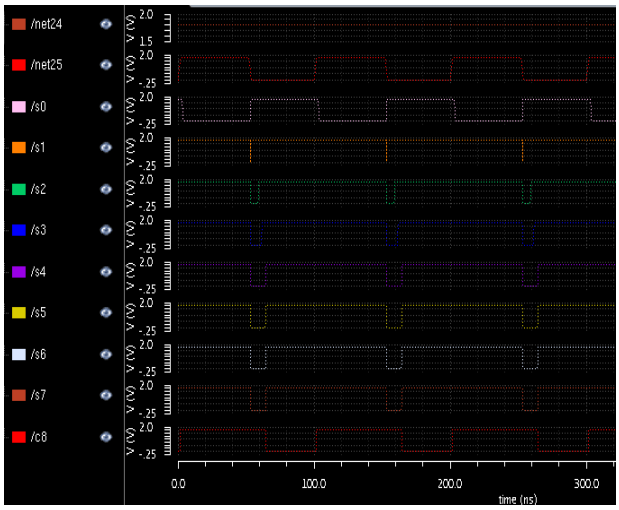

Fig. 29. m-GDI based 8-bit Adder simulation waveform

Table VII gives the performance analysis of 8-bit Hybrid Adder architecture.

TABLE VII. PERFORMANCE ANALYSIS OF 8-BIT NOVEL ADDER ARCHITECTURE.

Design Approach	No. of transistors	Area (μm^2)	Delay (psec)	Power (mW)
CMOS	408	191235.6	286.7	18.50
m-GDI	110	56638.3	82.58	12.05

V. CONCLUSION

This paper proposes a novel design of 4-bit Carry Look Ahead adder and 8-bit novel adder architecture. From the simulation result it was observed that the design of adder architectures using m-GDI technique results in high speed operation and consumes least no. of transistor. For ripple carry adder it was observed that the m-GDI based design consumes 81% lesser area, offers 72% lesser delay and the peak dynamic power reduced by 30% with respect to the traditional CMOS design.

Similarly, for the 4-bit carry look ahead adder it was observed that the m-GDI based design offered 91% lesser delay, a reduction in area by 65%, peak dynamic power reduced by 13% w.r.t the traditional CMOS design.

The proposed 8-bit hybrid adder architecture using m-GDI approach offered reduction in delay by 71%, the number of transistors reduced by a count of 298 when contrasted with the traditional CMOS design. The reduction in peak dynamic power was observed to be 35%. The reduction in area of the proposed adder architecture using m-GDI technique w.r.t the traditional CMOS implementation was found to be 70%.

Thus, from the above results it is clear that the design of 8-bit novel adder architecture using the mGDI technique results in lesser transistor count, dissipates lesser power and results in high speed operation.

REFERENCES

[1] A. Morgenshtein, A. Fish and I. A. Wagner, "Gate-diffusion input (GDI) - a technique for low power design of digital circuits: analysis and characterization", Proc. IEEE International Symposium on Circuits and Systems., Phoenix-Scottsdale, AZ, USA, 2002, pp. I-I.

[2] P. Balasubramanian and J. Joh, "Low power digital design using modified GDI method," International Conference on Design and Test of Integrated Systems in Nanoscale Technology, 2006. DTIS 2006., Tunis, 2006, pp. 190-193.

[3] U. Ramadass and P. Dhavachelvan, "New low power delay element in self resetting logic with modified Gated Diffusion Input technique", 2012 10th IEEE International Conference on Semiconductor Electronics (ICSE), Kuala Lumpur, 2012, pp. 507-511.

[4] S. S. Meti, C. N. Bharath, Y. G. P. Kumar and B. S. Kariyappa, "Design and implementation of 8-bit vedic multiplier using mGDI technique", International Conference on Advances in Computing, Communications and Informatics, Udupi, 2017, pp. 1923-1927.

[5] R.Uma and P. Dhavachelvan, "Modified Gate Diffusion Input Technique: A New Technique for Enhancing Performance in Full Adder Circuits", 2nd International Conference on Communication, Computing & Security, 2012.

[6] E. Abiri, M. R. Salehi and A. Darabi, "Design and evaluation of low power and high-speed logic circuit based on the modified gate diffusion input (m-GDI) technique in 32nm CNTFET technology", 22nd Iranian Conference on Electrical Engineering (ICEE), Tehran, 2014, pp. 67-72.

[7] Khoirom Johnson Singh, Tripurari Sharan, Huirem Tarunkumar. High Speed and Low Power Basic Digital Logic Gates, Half-Adder and Full-Adder Using Modified Gate Diffusion Input Technology. Journal of VLSI Design Tools & Technology. 2018; 8(1): 34–42p.

[8] Kishore, Pinninti & V. Sridevi, P & Babulu, K. "Low Power and Optimized Ripple Carry Adder and Carry Select Adder Using MOD-GDI Technique", Microelectronics, Electromagnetics and Telecommunications: Proceedings of ICMEET, 2016.

[9] Poonam Dhruwe, Chandrahas Sahu, "Low Power 4-Bit Ripple Carry Adder Design in 50nm Technology", International Journal of Advanced Research in Electrical, Electronics and Instrumentation Engineering, Vol. 5, Issue 6, June 2016.

[10] Simran kaur, Balwinder Lakha, & D.K, Jain "Design and Performance Analysis of Various Adders and Multipliers Using GDI Technique", International Journal of VLSI Design & Communication Systems, 2015.

[11] J. Miao and S. Li, "A novel implementation of 4-bit carry look-ahead adder", International Conference on Electron Devices and Solid-State Circuits (EDSSC), Hsinchu, 2017, pp. 1-2.

[12] P. Balasubramanian, C. Dang, D. L. Maskell and K. Prasad, "Approximate ripple carry and carry lookahead adders — A comparative analysis," 2017 IEEE 30th International Conference on Microelectronics (MIEL), Nis, 2017, pp. 299-304.

Proceedings of the Fourth International Conference on Communication and Electronics Systems (ICCES 2019)
IEEE Conference Record # 45898; IEEE Xplore ISBN: 978-1-7281-1261-9

Threshold driven Dual Cluster Head clustering protocol.

Navajyoti Nath, Biswanath Dey
National Institute of Technology Silchar
Silchar, India
navajyoti.cse@gmail.com

***Abstract*—In wireless sensor network, cluster based routing approach is a major step in the direction of energy efficiency. However, research shows that the energy dissipation in cluster based approach predominantly occurs in two cases; first during data transmission to the base station and second during data fusion, which foremost is the job of a Cluster Head (CH). Eventually this leads to sizable energy dissipation ,early death of CHs and lower network lifetime . Thus to address the problem, this paper proposes a new protocol which uses two cluster heads namely Primary CH (PCH) and Secondary CH(SCH).The Primary CH, which is deployed to collect information from sensor nodes and further performs data aggregation, and is elected based on the similar method used in LEACH protocol, but PCH also considers a threshold energy value while election whereas the Secondary Cluster Head (SCH) is selected considering the distance to the Sink and also considers a threshold energy value. Comparisons with LEACH protocol are shown in result area to substantiate the claim of this paper.**

***Index Terms*—LEACH, WSN, DUAL CLUSTER HEAD, Clustering Protocol.**

I. Introduction

Wireless sensor network is a group of huge numbers of sensor nodes which are randomly stationed in harsh conditions or difficult terrains to monitor and gather information of surrounding environment like temperature, humidity, forest fire, automobile movement, etc. Basically, the nodes deployed are limited on battery power and because of the area of deployment, replacing or replenishing of power source becomes very difficult. To overcome this issue, numerous studies [2][12] were brought out to look out for solutions to improve the network lifetime. In clustering based algorithms, the non-CH nodes forward the sensed data to respective CHs where the data aggregation/fusion is carried out and the output data signal is later transmitted to the sink for further processing by the CHs. The CH sends the data to the sink using either a single-hop or a multi-hop communication approach depending upon the distance to the sink [1]. If the distance between the two is greater than the prescribed distance (threshold) multi-hop approach is adopted, else single-hop communication is used. As for the single-hop communication for longer distance would require more energy which will lead to faster death of nodes. Thus, the nodes do not require any more to send data to the sink directly thereby lessening the individual power usage level, however the energy usage level of Cluster Heads (CHs) would increase exponentially, thus a rotation of role of CHs among other nodes is used after a certain interval (rounds) to reduce the burden of the CHs. Therefore, our approach primarily focuses on increasing the network lifetime of a given network. In our approach, we have contemplated the scenario by taking two cluster heads (CHs) in each cluster instead of one CH in LEACH protocol. The fundamental objective behind the election of dual cluster head is to bring down the burden of single cluster head and extent the lifetime. In the proposed approach, two roles of CH are separated and is designated to two different CHs i.e. one CH for data aggregation and other CH for data transmission, thus increasing the lifetime of CHs.

This article is divided into sections: Section II gives brief information about the related protocols, Section III is designed for the network assumptions containing the energy model and network model, in Section IV the proposed protocol is discussed, in Section V the proposed protocol is compared with LEACH protocol, and finally Section VI with a conclusion that concludes the paper.

II. Literature Review

A. Study on Low-Energy Adaptive Clustering Hierarchical Protocol

In LEACH protocol [1], sensor nodes in the WSN claims to be the cluster heads and based on that claim, few of the nodes get elected as CHs and the remaining nodes organize themselves to form clusters. The process of election of CHs, cluster formation and data transmission to the sink, are done in four separate parts: advertisement phase, cluster-setup phase, schedule-creation phase and data-transmission phase. Initially in advertisement phase, the nodes randomly generates any value within 0 to 1 and only if the number is less the value generated by the threshold function generator ($T(i)$), in equation (1) [1], then those nodes are said to be elected as

a CH for that round. The number of CHs in any given round in the network is decided a priori.

$$T(i) = \begin{cases} \frac{p}{1-p*mod(rd,\frac{1}{p})}, & if\ i \in Z \\ 0: & ,otherwise \end{cases} \quad (1)$$

where p = % of nodes being CH assigned a priori, rd = present round and Z = set of nodes that were not elected as cluster heads for the last $1/p^{th}$ rounds and $i = i^{th}$ node. Once the CHs are decided, the non CH nodes decides that to which cluster head it should select based on received signal strength indicator (RSSI)[3-5] to form a cluster. In cluster formation phase, after selecting the cluster heads to join, nodes now inform the cluster heads about the choices made via a control message for cluster formation. In schedule creation phase, the CH, based on the cluster information forms a TDMA schedule, directing the nodes when to send the data to the cluster head. In the final phase i.e. data transmission phase, the sensor nodes send the sensed data in their allotted transmission time to the respective CHs, and after receiving the information from all the non-CH, the CHs performs data aggregation to fuse the data into single data signal. This fused data is then finally forwarded to the sink for further processing.

B. Related Works

Hongjun Wang et al. in [6] proposed an algorithm to improve LEACH using double cluster heads and a mechanism for data fusion. In this algorithm, the clusters are formed on the basis of k-Medoids clustering algorithm, and after the completion of cluster formation the first and the second cluster heads are elected. As the algorithm follows k-medoids, where the value of k is selected based on the ratio of number of CHs required to number of nodes in the network. Election of CHs is same as in the LEACH [2], but with the probability which is based on the ratio between the number of CHs expected to number of nodes in cluster.

Jie Huang in [7], a double CH based algorithm is presented to minimize the effects of untimely death of cluster heads due to hefty energy dissipation. In this algorithm, two cluster heads are used, namely Master-CH, which is selected based on the LEACH protocol and Vice-CH, which is selected among the non-CH nodes in the cluster, based on the distance between other nodes and master node. In [7], the nodes within the cluster sends the data to any of the two cluster heads based on the distance. If the node is in proximity to the master cluster head it transmits the data to the master cluster and if near to the vice cluster head it sends it to the vice cluster head, on receiving the data both the master head as well as vice-CH performs data integration but only master cluster head sends the information to the base station whereas the vice cluster head sends the integrated data to the master-CH from where the data is further forwarded to the base station.

In [8], the clusters numbers are predefined and based on this criterion the network is partitioned into equal sized clusters which are static throughout. Based on the cluster information and the information imparted by the sensor nodes about their location, the sink assigns each node into a cluster. After the nodes are assigned to their clusters, two nodes in each clusters are selected as cluster heads , one being an Aggregating CH (ACH), used for data aggregation and the other being a Transmitting CH (TCH), used for transmitting data to the sink. The ACH is selected among other non-CH nodes in the cluster, based on a fitment factor which includes three weighted criterion residual energy, distance of nodes from sink, and distance of other nodes. The node with highest residual energy and being in the center is given the highest score and is finally selected as the ACH. On the other hand the TCH among other non-CH nodes in the cluster is also selected based on the same fitment factor used by the ACH, but the weightage is mainly focused on the residual energy and the distance between to the sink. Thus a node with highest residual energy and with least proximity to sink is given priority and hence is selected as a TCH. After the selection of cluster heads are completed, the sensor node send their data to the ACH where data aggregation is conducted and then the aggregated data is forwarded to the TCH and the TCH further transmits the data to the sink. This eventually reduces the energy consumption during communication within cluster and outside cluster, and results in overall increase in network lifetime.

III. Network Assumptions

The fundamental objective of this study is to propose a protocol that can improve the network lifetime of nodes with the same initial energy. By increase in network lifetime it is meant that the nodes will have prolonged lifetime or delayed death and to do so the following are the assumptions that are considered for the protocol:

A. Network Model

- Nodes are homogeneous having uniform energy and are energy constrained.
- Location of the sink is fixed and is far off from the nodes.
- Nodes are stationary.
- Every sensor nodes are in communication range with the base station.

B. Energy Model

The energy model for communication and data fusion used in proposed work is fundamentally based on that which was proposed by Heinzelman et al. [2] and are also being used by [1][6-11] . Here two channel models are used, free space channel and the multi-path space model. The option is dependent on the distance to the sink, if the distance is below the threshold distance (D_0), free space is adopted and if the distance is above than threshold distance (D_0), multi-path space model is selected, but in the protocol proposed only free-space communication is implemented. Thus the expression for the energy dissipation in transmitting a n-bit data to a distance d is as follows:

$$E_{tx}(n,d) = E_{tx-elec}(n) + E_{tx-amp}(n,d) = \begin{cases} n(E_{elec} + \varepsilon_{fs} d^2), & d < D_0 \\ n(E_{elec} + \varepsilon_{mp} d^4), & d > D_0 \end{cases} \quad (2)$$

where $E_{tx-elec}(n)$ is the energy required by the transmitter circuit which includes coding, modulation, filtering, and spreading of the signal, to transmit a m-bit message, whereas $E_{tx-amp}(n,d)$ is the amount of energy consumed by the transmitter for transmitting a n-bit message over a distance of d. E_{elec} is the energy consumed by the transmitting circuit to transmit a bit message and the ε_{fs} and ε_{mp} are the constant coefficients for free space and multipath communication respectively. The values of ε_{fs} and ε_{mp} are as per the values used in [2].In addition to the energy consumption on transmission, the expression for the energy consumption on receiving a m-bit message is:

$$E_{rx}(n) = n * E_{elec} \quad (3)$$

Further the expression for threshold value of distance used in our model is as proposed in [7], and is as given as:

$$D_0 = \sqrt{\frac{\varepsilon_{fs}}{\varepsilon_{mp}}} \quad (4)$$

Moreover, as discussed earlier, that for the Cluster Heads, huge amount of energy is dissipated in both the data transmission and data aggregation. Accordingly it becomes utmost importance that we include energy consumption in data aggregation along with the energy dissipation in data transmission. In this paper, therefore we take E_{DA} which represents energy consumption in data aggregation.

IV. Proposed Algorithm

This paper, proposes a new clustering protocol (threshold driven dual cluster head clustering), which surpasses the performance of LEACH protocol. The proposed algorithm is divided into four stages which are shown below:

A. Initialisation Stage:

The objective of this stage is to find the primary cluster heads. This stage follows similar process that is adopted in [2]. But as the LEACH does not consider the residual energy on individual energy, thus there may arise situations where the node elected as cluster head may die without performing its duties. Therefore, in this approach a threshold energy value is computed for primary cluster headE_{PO}, making sure that only that node would be elected as primary cluster head which as residual energy greater than the E_{PO}.

As known that the responsibility of a primary cluster head (PCH) is to collect all the information from all the member nodes and then after performing data fusion on the received data transmit the final data to the secondary cluster head(SCH). The following equation (1) is based on the energy dissipated during reception of m-bit message from the member nodes excluding the PCH ($\frac{1}{p} - 1$) in the cluster and then energy dissipation during data aggregation for all the member nodes and primary cluster head and finally energy consumption while the transmission of fused data to the SCH.

$$E_{P0} = E_{rx}(n) * ((N * p) - 1) + E_{DA}(n)(N * p) + E_{tx}(n,d)$$

$$E_{P0} = n*(E_{elec}*((N*p)-1)+E_{DA}*(N*p)+(E_{elec}+\varepsilon_{fs}*D_0^2)) \quad (5)$$

Where N is the total number of nodes,E_{rx} is the consumption of energy in reception of a $1 - bit$ message , and E_{DA} is the amount of energy that is consumed during aggregation of the nodes and is considered to be a constant and n is the n-bit message.

B. Cluster Formation:

After the election of primary cluster head is over, the primary cluster heads broadcast the information of being the cluster heads with their unique ids. On listening to the broadcast, the remaining nodes chooses to respond cluster heads with the highest signal strength. That is, the nodes selects a cluster head among other cluster heads when the received signal strength is higher than others, which implies that the communication cost with that cluster head would require less energy.

Once all the non cluster nodes selects their cluster heads, they respond with a message indicating their unique ids, residual energy, distance to the base station and the choice it has made. Thereby making the clusters in the network.

C. Secondary Cluster Head Selection:

In this stage, the main intent is to select a node which can act as secondary CH. The role of this very CH is to forward the aggregated data received from primary cluster head. The criterion for the election of SCH is principally based on the residual energy of the node and the distance to the sink. Thus among the member nodes in the cluster, the primary Ch elects a SCH which is at the boundary or near to the cluster boundary (proximity to the base station among other nodes) among the competitors on the information available. The residual energy is considered due the fact that, the node elected as SCH should be able to complete its role without being dead. Here also a threshold energy value for SCH (E_{SO}) is computed, so that only that node which has residual energy higher than the E_{SO} can participate in the election process. As the requirement of SCH is only to collect the aggregated data and later transmission of that data to the BS, therefore only those energy dissipation is considered in the equation (6).

$$E_{S0} = E_{rx}(n) + E_{tx}(n,d)$$

$$E_{S0} = n * (E_{elec} + (E_{elec} + \varepsilon_{fs} * D_0^2)) \quad (6)$$

Where $E_{tx}(n,d)$ is the consumption of energy while transmitting the data to the base station by the secondary CH, and $E_{rx}(n)$ is the energy dissipation while receiving the data from the primary CH.

D. Data Transmission:

After the selection of both the cluster heads and cluster formation, the primary CH broadcasts a TDMA schedule to all the non-CHs within the cluster to inform about when the nodes can transmit data to the primary CH and when to sleep. The primary and secondary cluster heads will always be in the listening mode. Once the schedule is notified, all the non-CH nodes within cluster, as per the schedule passes the data to the primary CH, where the data collection and aggregation is performed and the multiple data signals are transformed in to single signal and as the transmission is within the cluster the energy consumption is way lesser than the original protocol [2]. Further, the data signal is transmitted to the secondary CH for relaying it to the base station. As the secondary cluster head is at the cluster boundary, which enables it to transmit the data with comparatively lesser energy.

Therefore by using the dual CH approach in the proposed algorithm, energy consumption compared to LEACH protocol is reduced. As the role of one cluster head is divided into two and only optimal nodes are used for data transmission which minimizes the energy dissipation in the network, thereby enhancing the network lifetime.

V. Results and Analysis

In this section, the objective is to showcase the performance comparison of LEACH protocol with our proposed algorithm (Threshold driven Dual Cluster Head clustering protocol) in context of network lifetime. The simulation of the algorithm is performed on MATLAB. The network parameters and the network scenarios are given in Table 1 below.

Here for better comparison, two scenarios are implemented, where different combinations of initial energy of nodes(E_0) and the percentage of nodes being CH (p) equals to 10% is considered.

Parameters for Scenario	
Parameters	**Parameter values**
Network-Area	100 m X 100 m
BS position	(100m, 200m)
Total number of nodes	500 & 1000
Initial Energy (E_0)	0.5 J & 1 J
Percentage of clusters p	10%
Ee1ec	50nJ/bit
EDA	5nJ/bit
ε_{fs}	10 pJ/bit/m^2
ε_{mp}	0.0013 pJ/bit/m^4
D_O	87.7m
$E_{PO} - 500nodes$	$5.7 * 10^{-3}$ J
$E_{PO} - 1000nodes$	$1.12 * 10^{-2}$ J
E_{SO}	$3.538 * 10^{-4}$ J
Size of data frames	2000 bit

TABLE I
TABLE CONTAINING THE DETAILS OF PARAMETERS.

Here two network scenarios are being implemented, one of the scenarios consists of 500 nodes and in the another scenario 1000 nodes are deployed, whereas the base station location is same for both the scenarios. Different scenarios are

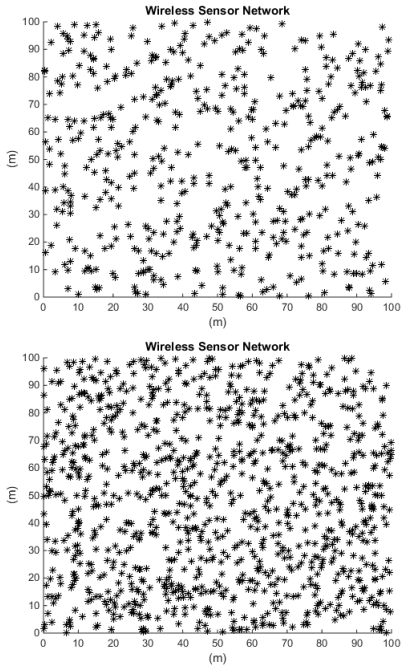

Fig. 1. Network Scenario with 500 and 1000 nodes respectively

As the network scenarios are known, the

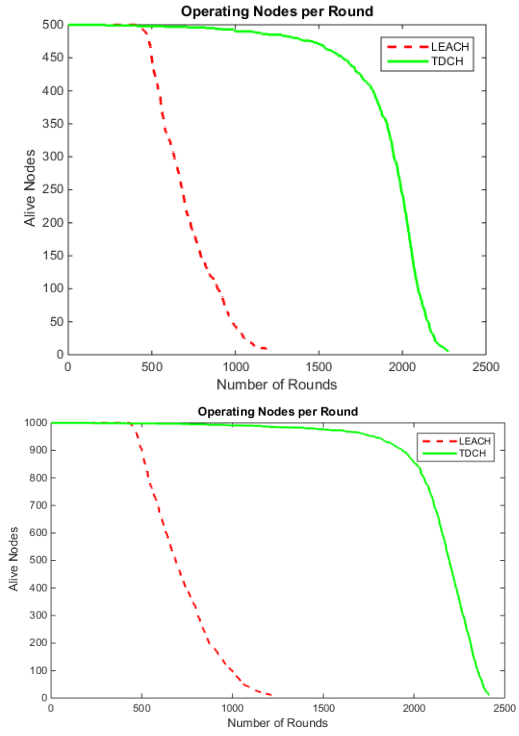

Fig. 2. Simulations comparing LEACH vs TDCH for 500 and 1000 nodes respectively with $E_0 = 0.5J$

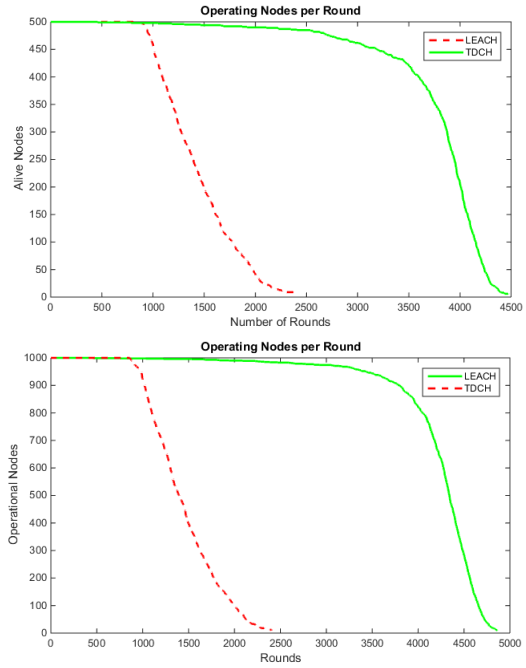

Fig. 3. Simulations comparing LEACH vs TDCH for 500 and 1000 nodes respectively with $E_0 = 1J$

After the comparison it is found that, the proposed algorithm is outperforming the LEACH protocol. In both the scenarios, TDCH is outperforming LEACH protocol by approximately 200%.

VI. Conclusion

The LEACH protocol is considered to be the benchmark of clustering protocols, thus comparison with LEACH protocol substantiate the performance of the proposed protocol. In the above experimental analysis it could be seen that, TDCH protocol has outperformed the LEACH protocol with a whooping difference of 200%. To substantiate the claims of the TDCH further, comparison of TDCH protocol with other well established protocols with few other network scenarios is required. Authors of this paper are working on this and would come with more results to validate the claims further.

References

[1] Heinzelman WB, Chandrakasan AP, Balakrishnan H. An application-specific protocol architecture for wireless microsensor networks. IEEE Transactions Wireless Communication 2002; 1(4):66070.
[2] K. Singh, WSN LEACH based protocols: A structural analysis, 2015 International Conference and Workshop on Computing and Communication (IEMCON), Vancouver, BC, 2015, pp. 1-7.
[3] K. Benkic, M. Malajner, P. Planinsic and Z. Cucej, Using RSSI value for distance estimation in wireless sensor networks based on ZigBee, 2008 15th International Conference on Systems, Signals and Image Processing, Bratislava, 2008, pp. 303-306.
[4] S. Y. Seidel and T. S. Rappaport, 914 MHz path loss prediction models for indoor wireless communications in multifloored buildings, in IEEE Transactions on Antennas and Propagation, vol. 40, no. 2, pp. 207-217, Feb. 1992.
[5] U. Bekcibasi and M. Tenruh, Increasing rssi localization accuracy with distance reference anchor in wireless sensor networks, Acta Polytechnica Hungarica, vol. 11, no. 8, 2014.
[6] Hongjun Wang, Huiqing Chang, Hui Zhao, YoujunYue. Research on LEACH Algorithm Based on Double Cluster Head Cluster Clustering and Data Fusion. In Proceedings of 2017 IEEE International Conference on Mechatronics and Automation August 6 - 9, Takamatsu, Japan.
[7] Jie Huang. A Double Cluster Head Based Wireless Sensor Network Routing Algorithm. In 8th IEEE International Conference on Software Engineering and Service Science (ICSESS); Beijing, China, 2017.
[8] Tripatjot Singh Panaga, J.S. Dhillon. Dual head static clustering algorithm for wireless sensor networks. In International Journal of Electronics and Communications (AEU) 88 (2018) 148156
[9] Xu, D., Zhang, H.: Improved algorithm of LEACH protocol introducing residual energy. Computer Engineering and Applications II 45(28), 115119 (2009)
[10] Thein, M.C.M., Thein, T.: An Energy Efficient Cluster-Head Selection for Wireless Sensor Networks. In: Proceedings of ISMS 201O (2010).
[11] Zahmati AS, Abolhassani B, Shirazi AAB, Bakhtiari AS. An energyefficient protocol with static clustering for wireless sensor networks. International Journal Electronics, Circuits and Systems Volume 1 Number 2, 2007.
[12] S. Misra and R. Kumar, A literature survey on various clustering approaches in wireless sensor network, 2016 2nd International Conference on Communication Control and Intelligent Systems (CCIS), Mathura, 2016, pp. 18-22.

Proceedings of the Fourth International Conference on Communication and Electronics Systems (ICCES 2019)
IEEE Conference Record # 45898; IEEE Xplore ISBN: 978-1-7281-1261-9

Change Detection in Land use-Land cover using Convolutional Neural Network

Sahithi Samudrala
Department of *Information Technology*
V.R Siddhartha Engineering College:
Vijayawada, India
sahithi.rocking25@gmail.com

Mekala Pranvitha nand
Department of *Information Technology*
V.R Siddhartha Engineering College:
Vijayawada, India
mekalapranvithanand@gmail.com

Suhail Mohammad
Department of *Information Technology*
V.R Siddhartha Engineering College:
Vijayawada, India
8125527706ms@gmail.com

Radhesyam Vaddi
Department of *Information Technology*
V.R Siddhartha Engineering College:
Vijayawada, India
syam.radhe@gmail.com

***Abstract*— Change Detection in satellite imagery is a concerning topic for researchers and scientists. Studying changes in satellite images gives enormous amount of knowledge in studying the geography and ecosystem. The dataset used in this work is taken from AVIRIS sensor and normalized in order to reduce time of execution. This paper covers the important aspects of Classification of a satellite imagery using convolutional Neural Networks. Changes are detected basing on the classification maps in multi-temporal imagery. Experimental results show that proposed method got accuracy on par with state of art methods.**

Keywords*— *satellite imagery, Convolutional NN

I. INTRODUCTION

The changes on earth's surface from natural and human causes are rapid. Scientists and researchers are concerned on detecting the changes without knowing the scale of changes which is very hard and need to be addressed. There are many techniques which had been developed for detecting changes on land-cover which are optimal for both satellite imagery and also for digital imagery. Satellite images are different from normal images. They are not to be compared with each other. We can adapt the techniques or algorithms used for normal imagery on satellite imagery. Normal images are three or four channel and are speeded over the Visual Spectrum. Satellite images are multiple channels and are ranged from infrared to ultraviolet in the electromagnetic spectrum with minimal intervals. Digital images represent the intensity of the red-green-blue in the image whereas satellite images are reflection indexes for each interval.

This paper had considered only the push-broom passively scanned images. The spectral images can be collected in multiple ways from satellite to airborne imaging through more complex spectroscopes. Spectroscopes scan land cover in the spatial perspective in all the intervals of the Electromagnetic spectrum collecting the spectral data.

The spectral data collected for each spatial pixel is labeled manually by surveying onsite and respected ground truths of the spectral data are provided. But it is not possible to survey a land in a remote region manually so we are using a deep neural network to learn the patterns of the each spectral data in a remote region from the knowledge of spectral data which was provided with ground truths collected by manual surveys generate the classification maps aka Ground truths.

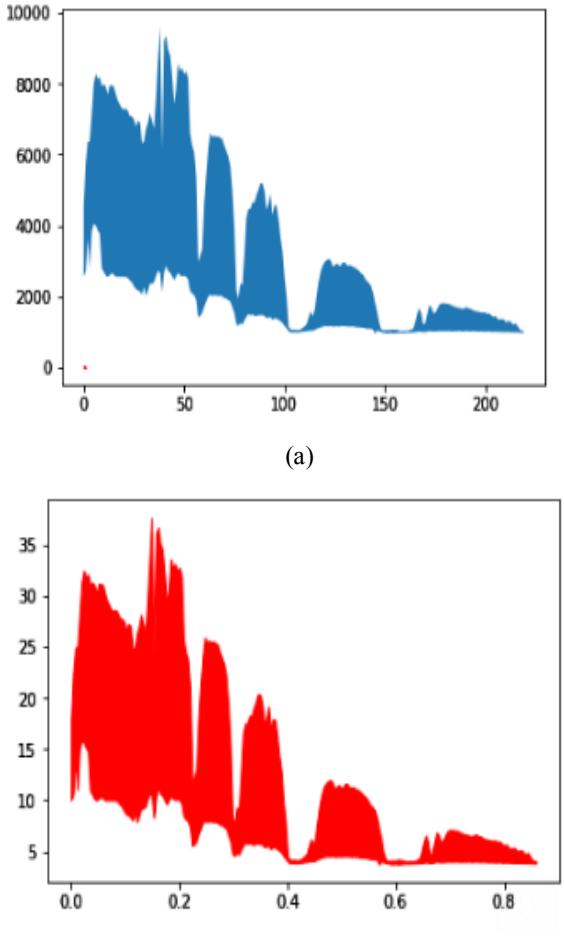

Fig. 1. Scale graph of the data (a) Before normalization (b) After normalization

The paper is organized as follows. This project need a change detection data set, description is shown in section-II. CNN algorithm and methodology is presented in sections III and IV. The complete analysis of results is presented in section V. The last section-VI describes conclusion and future work.

XXX-X-XXXX-XXXX-X/XX/$XX.00 ©20XX IEEE

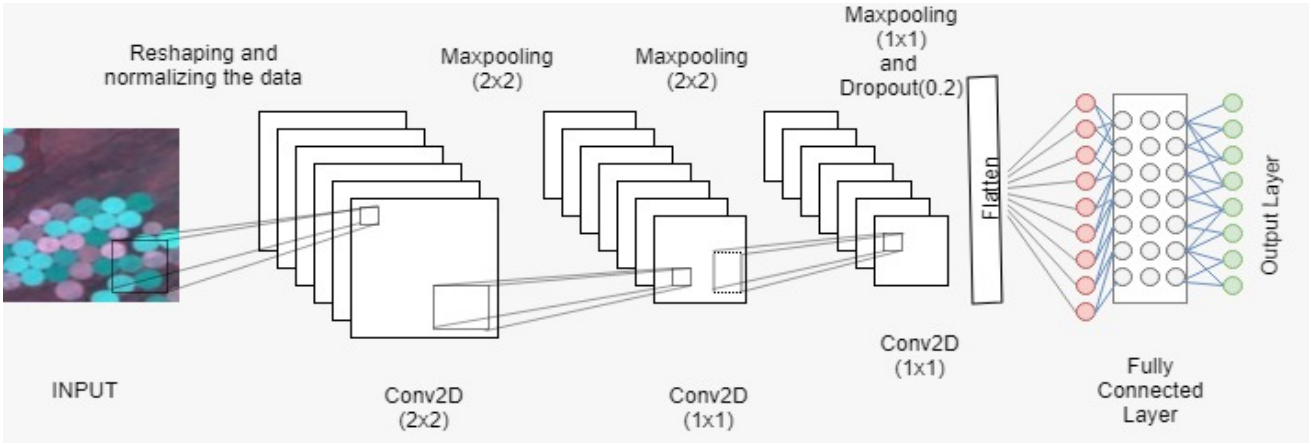

Fig. 2. Different layers of convolutional neural network

II. DATASET DESCRIPTION & NORMALIZATION

The data set used in this work is from AVIRIS sensor [5] with the following features.

- Each class is uniquely represented by an integer in the ground truth.
- They are 16 classes in the dataset
- The spatial resolution of the imagery is 145x145 pixels with spectral resolution of 220 channels for each pixel.

The data consists of a wide range of variables with very high numeric values. Cleaning the outliner values and normalizing the entire data was done for reducing the computation stress. Reducing the scale can fasten the computation and there is no loss in the pattern. The patterns are shown in figure-1.

III. ALGORITHM

There is a wide choice of selection in Deep Neural Networks for supervised learning. Our primary reason of choosing a convolutional neural network and its unique feature to detect new patterns. Recent studies prove that this is one of the best approaches in supervised learning mechanisms.

We used 12 layered CNN(Convolutional Neural Networks). With 3 Convolutional layers, 3 Max pooling layers followed by fully connected neural network layer. The Figure-1 explains the individual layers in detail.

A. Convolutional layer

We had used three Convolutional with relu as activation function and with filters of size (200,100,100). This is using with kernel size of (2,2) for first conv-layer and (1,1) for the next two layers.

B. Pooling layer

We had used Max Pooling layer with kernel size of (2,2). And each layer of pooling uses the Relu as activation function.

C. Fully connected layer

The Fully connected layer has four dense layers the input for the first fully connected layer was flatten and then give to the first layer each layer has RELU as the activation function except the last output layer which we had give activation as softmax, which returns the probability in the range of zero to one.

IV. METHODOLOGY

The change is detected in between two images which are taken from satellite image. Two land-cover images are taken from different time stamps 2013 and 2015. Methodology is represented in figure-3.

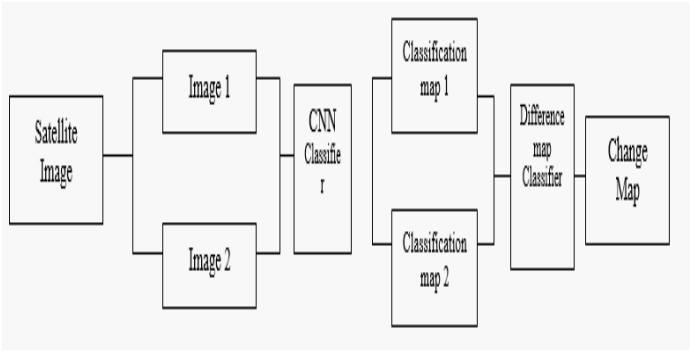

Fig. 3. Architecture diagram of the proposed change detection method

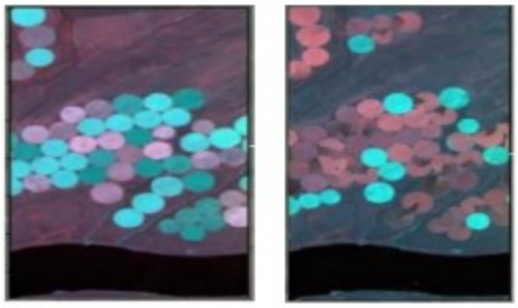

Fig. 4. Sattelite images used for change detection

Using CNN classifier we got two classification maps i.e classification map1 and classification map2.We applied simple difference operation on two classification maps then we got change map with accuracy 97%.

A. Training

Training was done on 8199 samples and test size was 2050. The model was trained for 20 epoches with a learning rate of 0.01. It took 14 seconds to complete the each iteration i.e., an average time of 5 minutes to get a training accuracy of 99% and a test accuracy of 99.66%. The learning curve is shown in figure 5 and the loss curve in figure6.

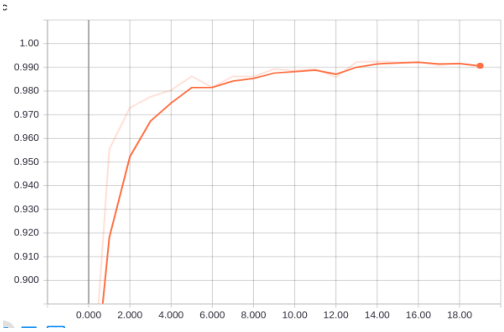

Fig. 5. Learning curve

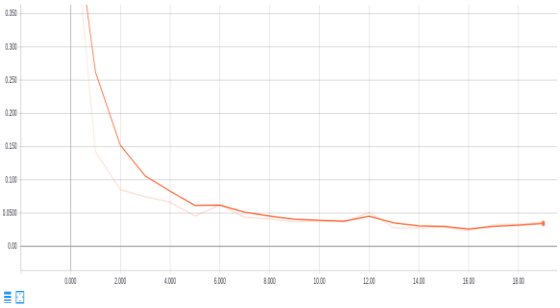

Fig. 6. Loss curve

V. RESULTS

As we can see from the result that is Figure 8 describes about change map from two images that are shown in Figure 7. If we consider these two images they are inputs taken through satellite using AVIRIS (Airborne Visible/Infrared Imaging Spectrometer) sensor data which is temporally varied images that means considered in two different timestamps that are 2013 and 2015 from the area Hermiston located in oregon united states. As we see (390,240,242) these are the width,height and band channel (or) channel colour respectively.

Then both the images are classified using a classifier that is CNN (Convolutional Neural Networks Algorithm) then produces two classification maps by undergoing process of cnn they are conv-layer, batch-normalisation,max-pooling,dropout, flatten, dense. After undergoing cnn process then the two classification maps formed are shown in Figure-7 a and b which are shown below. The height and width of these images will be (390,200) no band channel is considered here.

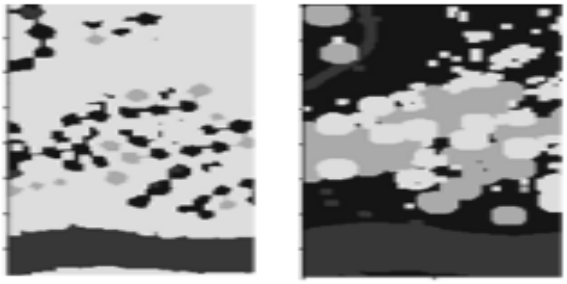

(a) (b)

Fig. 7. Classification Maps (a) 2013 (b) 2015

To get the change map result we find the difference between the two classification maps which the figure is shown below that is Fig 7 change map. This figure shows the difference between two classification maps taken from two different timestamps. In the figure the yellow area indicates the changed area and purple indicates the unchanged area.

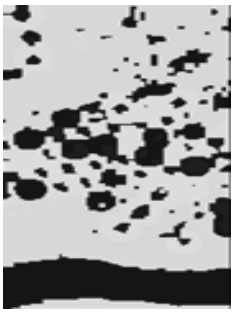

Fig. 8. Change map

The following table 1 illustrates the changes in the classes. The first Column specifies the classes. And remaining columns are the exact count of class labels with Difference in the last column.

TABLE I. CHANGES NOTIFIED WITH NUMBER OF PIXELS TABLE TYPE STYLES

Class	**Year 2013**	**Year 2015**	**Difference**
1	31456	8269	23187
2	14967	11122	3845
7	16239	2236	14003
9	15338	5373	-41035

VI. CONCLUSION AND FUTURE WORK

The technique of using a Deep Convnet model for generating classification maps is optimal for this use case. The generated classification maps for two temporal images are parsed for generating change maps. Using this kind of approach is best, if we need to detect changes in the known

classes. And this approach has wide applications in agriculture, forestry and mineralogy.

The Change Map obtained was well enough to identify the total changes in the complete spatial resolution. We can get the class wise changes from the Convolution Neural networks output layer. Further study can be made in developing a hybrid Convolutional Neural Network, which can classify two satellite imagery and identify the difference in the classification maps by using dual pipelines method.

REFERENCES

[1] D. Lu, P.Mausel, E. Brondizioand E. Moran, "Change detection techniques", International Journal of Remote Sensing, 25, pp.2365–2407, 2004.

[2] A.Singh, "Digital change detection techniques using remotely-sensed data", International Journal of Remote Sensing, 10, pp. 898–1003, 1989.

[3] P.R. Coppin, M.E. Bauer, "Digital change detection in forest ecosystems with remote sensing imagery", Remote Sensing Reviews,13, pp. 207–234, 1996.

[4] T.Blaschke, "Towards a framework for change detection based on image objects",GöttingerGeographischeAbhandlungen, 113.

[5] Baumgardner, M. F., Biehl, L. L., Landgrebe, D. A. (2015). 220 Band AVIRIS Hyperspectral Image Data Set: June 12, 1992 Indian Pine Test Site 3. Purdue University Research Repository. doi:10.4231/R7RX991C.

[6] Superpixel-Based Difference Representation Learning for Change Detection in Multispectral Remote Sensing Images Maoguo Gong, *Tao Zhan, Puzhao Zhang, and Qiguang Miao* IEEE transactions on geoscience and remote sensing 2017.

[7] Feature-Level Change Detection Using Deep Representation and Feature Change Analysis for Multispectral Imagery Hui Zhang, Maoguo Gong, *Puzhao Zhang, Linzhi Su, and Jiao Shi* IEEE geoscience and remote sensing letters,Vol13,No11Nov2016.

[8] *Chang Huang* surface water change detection using change vector analysis IEEE 2016.

[9] E mpirical Relationships for Monitoring Water Quality of Lakes and Reservoirs Through Multispectral Images Carolina Doña IEEE journal of selected topics in applied earth observations and remote sensing, VOL. 7, NO. 5, MAY 2014

Proceedings of the Fourth International Conference on Communication and Electronics Systems (ICCES 2019)
IEEE Conference Record # 45898; IEEE Xplore ISBN: 978-1-7281-1261-9

Efficient Resource Allocation Model For D2D Communication Under Overlapping Area of Multiple Cellular Cell

Professor Ruksar Fatima
Head of the Department Computer science and engineering,
Khaja Bandanawaz college of engineering, gulbarga.
Email- ruksarf@gmail.com

Rohina khanam
PHD scholar,
Khaja Bandanawaz college of engineering, gulbarga
Email-rohina1119@rediffmail.com

Shaik humera tauseef
PHD scholar,
khaja Bandanawaz college of engineering, gulbarga
Email-humera1919@rediffmail.com

***Abstract*— Device-to-Device (D2D) communications was originally projected in cellular networks as an innovative prototype for improving network performance. The rise of new applications such as location aware content distribution introduced new user scenarios for D2D communications in cellular networks. The preliminary studies exhibited that D2D communications has advantages such as reduced communication delay and increased spectral efficiency. However, D2D communication approach introduces problems in terms of interference control overhead and conventions that are still open research problems. Therefore, efficient interference modelling design are required. The existing model has focused on addressing interference considering D2D association operating on same cell and very limited work is carried out in addressing interference issues of D2D user operating on overlapping area of multiple cell. For overcoming research challenges, this work presented Efficient Resource Allocation (ERA) model for D2D under cellular network as a game theory model. Experiment are conducted to evaluate performance of ERA. The outcome shows ERA attained significant performance improvement over state-of-art models in terms of sum rate (utility), successful packet transmission, and revenue.**

Keywords*— *Cellular network, D2D communication, Game theory, Interference management, Overlapping area, Power allocation, Resource allocation.

I. INTRODUCTION

Recently, rapid growth of smart device has been seen resulting in increased traffic and is expected to grow at an annual traffic rate of 53% until 2020 [1]. Therefore, resulting in a requirement of spectrum in cellular network which is expected to go up exponentially in future [2]. However, achieving higher throughput within cellular network owes two challenges. Firstly, it is difficult to increase the physical layer capacity of wireless channel. Since physical layer technologies used in MIMO-OFDM ((Multiple Input Multiple Output-Orthogonal Frequency Division Multiplexing) and 4G/LTE (Long Term Evolution) with interference coordination and capacity-achieving codes, have reached their theoretical limits. Secondly, reducing the size of cell by using femtocell network is a realizable, yet costly, design for improving throughput, as it induces higher cost for offering backhaul connectivity of these small base stations.

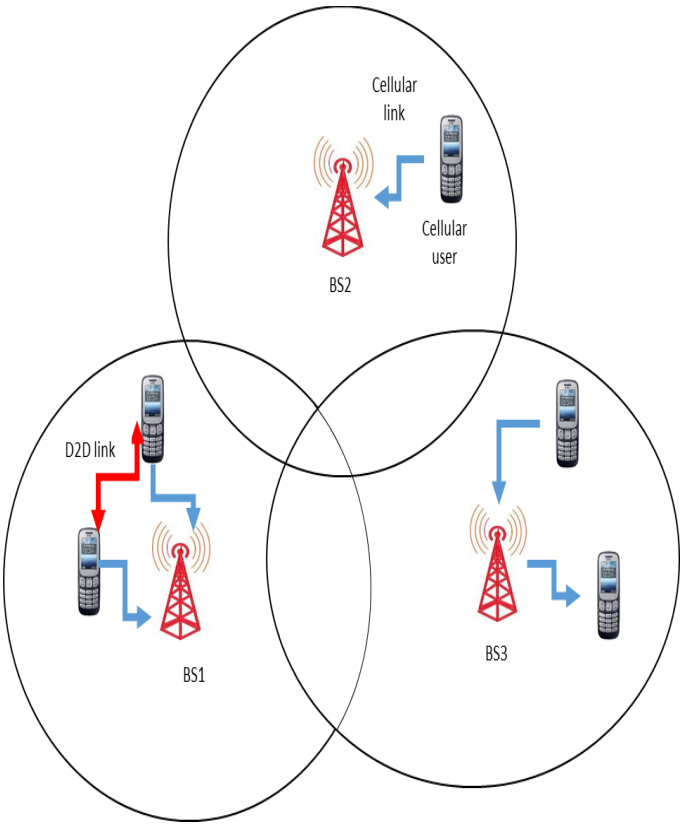

Fig. 1. Architecture of D2D communication under cellular network

Device-to-Device (D2D) communication has emerged has a new paradigm across academic and industries. The architecture of D2D communication is shown in Fig. 1. This is mainly due to unique advantages it offers, the cellular network can offload its traffic, attain higher energy proficiency, better throughput, and robustness to infrastructure failures. Recently, AllJoyn, Qualcomm has aimed at addressing many challenges for

enabling D2D communication. With the new Message Queue Telemetry Transport (MQTT) protocol is specifically designed only for device-to-device communication, the industry is well placed to its real-world deployment. The exiting model on D2D association [3] has still mainly focusing on how device-to-device communication can run proficiently as an underlay to cellular networks. Further, D2D is considered to be one of the promising technique in 5G communications. Here by sharing downlink or uplink resource blocks with cellular subscribers, device-to-device association attains a great potential of increasing network capacity and enhancing spectral efficiency [2]. D2D communication allows direct association among two subscribers which are geographically close to one another without being communicated by based station. This aid in attaining better spectrum utilization, lower delay, and less energy consumption, which can well adapt meet demand of higher transmission rate and larger network capacity [4], [5]. Although enhanced spectral efficiency can be attained by the reutilization of resources in device-device associations. However, it may result in severe cross-tier interference (among cellular subscribers and D2D links) and co-tier interference (among different D2D links transmitting on the same resource blocks) [6], [7].

The existing model [12], [13] has focused on addressing interference considering D2D association operating on same cell with the cellular association. As a result, it incurs interference to the cellular user located in the same cell. For reducing the interference among D2D and cellular subscribers, number of resource management technique adopting game theory [14], [15] approaches has been presented [16], [17], and [18]. However, most of the state-of-art resource allocation model has focused on addressing interference on the intra cell. However, inter cell scenario has be neglected. Therefore, there is need to remodel the game model to provision for inter cell condition. For overcoming the research issues, this work present efficient resource allocation method in intercell D2D association underlying cellular network. Further, this considers base stations as a contender looking for resource allocation of D2D requested load rather than D2D pair as a contender like state-of-art model.

The research contribution as follows

- The novelty of work is this work considers a case where device-to-device link is positioned in the overlapping segment of adjacent cells. Further, the game theory model for resource allocation is presented where base station is considered as contender for contending D2D pairs demand.
- The Efficient resource allocation model attain higher sum rate, successful packet transmission, and revenue.

The rest of the paper is organized as follows. Literature survey is presented in section II. In section III the proposed Efficient Resource Allocation (ERA) model for D2D under cellular network is presented. In penultimate section experimental study is carried out. The conclusion and future work is described in last section.

II. LITTERATURE SURVEY

This section conducted extensive survey on addressing interference issues of D2D association under cellular network for enhancing system performance. Recently, number of approaches is been presented to solve interference issues in device-to-device association underlying cellular networks [8], [9], [10] and, [11]. In [8], presented guard zone based interference modelling for providing QoS requirement of cellular user. For mitigating interference due to presence of D2D association, [9] pairing based interference coordinating model. Further, [10] transmission capacity region which aid in managing interference in D2D environment when both successive interference cancellation and power control were carried out. Limiting co-existence of D2D pairs and cellular user imposed serious interference to the cellular network affecting overall capacity, in [11] considered both uplink and downlink interferences through admission control and power allocation, which intended at maximizing the overall throughput of the D2D associations underlying cellular network. Further, for overcoming (reduce) the interference among D2D and cellular subscribers, number of resource management approaches has been presented [12], [13]. However, most of the state-of-art resource allocation model has focused on addressing interference on the intra cell. However, inter cell scenario has be neglected. In state-of-art D2D resource allocation model, game theory is widely used to obtain characteristics feature of competition between D2D associations. Game theory [14], [15] offers a mathematical solution for effective decision making, which offers a method to predict what may (or would) arise when rational contenders with varying interest. In state-of-art model [16], [17], and [18], D2D pairs is modelled as contender looking for the resources, where the utility of each contender is described as a function of generated interference and realizable data rate. The optimal solution (i.e., equilibrium) for resource allocation can be obtained by using utility function (i.e., contender's best response function). The state-of-art interference model can be used to address inter cell condition by using interference information from adjacent cells. However, it is not efficient when D2D tries to contend with the mutually shared channel of two adjacent cells and it also fails to determine resource configuration. From extensive survey it is clear that a new model is required for addressing interference and enabling D2D association operating in overlapping area of multiple cell in cellular network.

III. EFFICIENT RESOURCE ALLOCATION MODEL FOR D2D COMMUNICATION UNDER OVERLAPPING AREA OF MULTIPLE CELLULAR CELL

This work present efficient resource allocation model for D2D enabled under future high speed and crowded cellular network. Firstly, this work briefly discusses about interference model and architecture considered for resource allocation. Then, this model present a game theory model that maximize the sum rate (utility) of resource allocation considering different assumption. The architecture of interference assumption considered in this work is presented in Fig, 1.

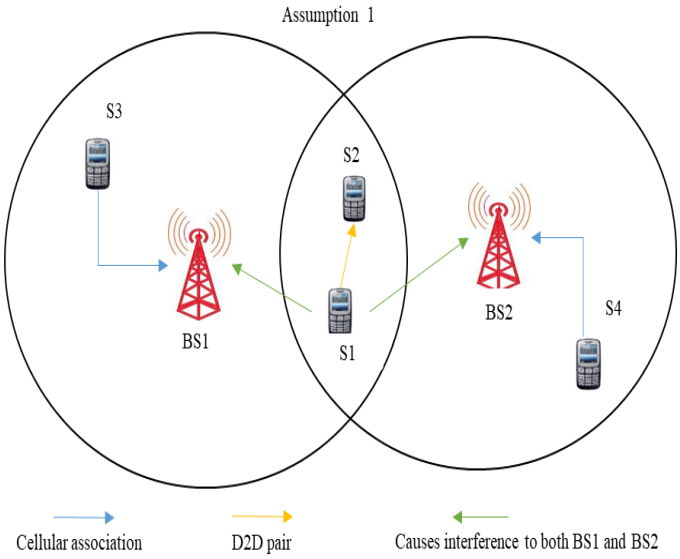

Fig. 1. Architecture of Assumption 1 of D2D communication under cellular network

a) System model for D2D network:

This section describes the D2D system model considered for efficient resource allocation among contending D2D subscribers. This work considers a case where two D2D subscribers are positioned in the overlying region of two adjacent cells using uplink resource for association. In each cell, there exits at least one cellular subscriber that associates with base station. This work further considers that D2D pair reutilize the uplink resources among cellular subscribers while cellular associations use either downlink or uplink resource, thus aid in synchronizing with base stations. The case can be expressed in to following three assumption, where subscriber 1 (source) and subscriber 2 (destination) are the D2D pair, subscriber 3 and subscriber 4 are the cellular subscriber.

Assumption 1: Cellular associations (blue line) in both cells utilize uplink resources. Here, D2D pair (yellow line) induces interference (red line) among base stations as shown in Fig. 1.

Let depict the rate allocation of base station of above assumptions. Let H_{jk} be the channel power gain among source j and destination k over a D2D channel or cellular channel, H_{3B_1} be the gain among subscriber 1 and base station 1, H_{3B_2} be the gain among subscriber 1 and base station 2.The source j power is denoted by q_j, the rate allocation of nth base station in assumption o by S_n^o, the additive white Gaussian noise power at the destination is represented by O_0. Subsequently, for assumption 1, we obtains

$$S_1^1 = C_1 * \log_2\left(1 + \frac{H_{1B_1q_1}}{O_0 + H_{3B_1q_3}}\right), \quad (1)$$

$$S_2^1 = C_2 * \log_2\left(1 + \frac{H_{2B_2q_2}}{O_0 + H_{3B_2q_3}}\right). \quad (2)$$

where S_1 and S_2 are the data rate of base station 1 and base station 2, respectively.

The rate allocation of all base stations aid in obtaining their revenue attained from cellular associations. An important thig to be seen here is that the model to evaluate rate allocation considers interference induced among D2D channel, which aid in impacting revenue of the base station. For example, allocating more bandwidth resource to D2D user will result in reduced interference. As a result, careful planning is required in allocating resource to D2D subscriber in future high speed cellular network. This work present a game theory approach to estimate the amount of bandwidth to be assigned to D2D source subscriber by respective base stations. This work considers that the base station has all information regarding channel state information of each channel in the available cell with respect to base stations. So that overlapping base station can synchronize the radio resource.

b) System Resource allocation using game theory approach for D2D network:

This section describes the resource allocation using game theory approach. Let considers that the each service provider can charge its D2D subscriber. Since D2D channel reutilize the shared channel among two cell. Thus, service providers can maximize their revenue and possess incentive to assign resource to D2D subscriber. The race among service provider can be considered as cooperative game, in which base stations are modelled as contenders. This section present a game theory model where each base station can obtain information of policies and revenue of the base station. Let considers the utility of contender as the regulatory payoffs that composed of two phases. The first phase is obtained from charges obtained from cellular subscribers, and second phase is the charges obtained from D2D association. Therefore, the utility parameter of contenders are expressed as follows

$$V_1^o = \varphi * S_1^o + \omega * C_3^\tau - \mu * C_3^\tau, \quad (3)$$

$$V_2^o = \varphi * S_2^o + \omega * C_3^\rho - \mu * C_3^\rho, \quad (4)$$

where φ and ω are constant depicting the subscription charges of unite bandwidth and resource, respectively. The allocated bandwidth from base station 1 and base station 2 is represented by C_3^τ and C_3^ρ respectively and μ is the cost objective policies of resource. The pricing policies with respect to μ is used similar to [20], [21]. Therefore, it can be formulated as follows

$$\mu = y + z\left(C_3^\tau + C_3^\rho\right)^\alpha, \quad (5)$$

where y, z, and α are constant with non-negative parameter, and $\alpha \geq 1$ assures that the cost objective policies is convex. The Eq. (5), depicts that the cost of all base stations is directly proportional to resource attained by D2D subscriber. Then, the trade-off among data rate and power [22], can be obtained as follows

$$q_3 \propto \frac{1}{C_3^\tau + C_3^\rho}, \quad (6)$$

The proposed resource allocation model attains significant cost reduction and higher sum rate result which is experimentally proved in next section below.

IV. Simulation Result and Annalysis

This section present experiment evaluation of proposed efficient resource allocation (ERA) model for D2D pair under cellular network over state-of-art models. The performance of ERA model is evaluated over existing models in terms of Sum rate, successful packet transmission, and revenue generated to perform data transmission. This work consider a cell scenario, where D2D pairs and cellular users are uniform randomly distributed in a square area of 1000m×1000m with the base station in the center. Further, the D2D pairs and cellular subscribers are mobile in nature with uniform speed. For a fixed number of D2D pairs and cellular subscribers, we repeat the simulation by 2 times and mean of the result is taken. The simulation parameter considered for this work is similar to [17], and [18]. More detail of simulation parameter used for simulation study is described in TABLE I.

TABLE I. Simulation Parameter Considered

Network Parameter	Value
Number of cell	16
Cell width	1000m
Number of cellular and D2D users	200
Modulation scheme	QPSK
Mobility of devices	5 m/s
Maximum distance of D2D	100 m
Sub-carrier bandwidth	1 Hz (15 kHz)
Time slot duration	5 µs
Number of Frequency Channels	10, 20, 30, and 40
Path loss exponent	3.5

a) Sum rate performance evaluation considering varied channel:

This section evaluates sum rate as a utility performance of ERA over existing model [3], [16], [17]. The sum rate performance is evaluated by varying link/channel size and the outcome attained by ERA and exiting model is graphically shown in Fig. 3. The outcome shows that ERA improves sum rate performance by 4.19%, and 34.87%, over exiting model considering varied channel size of 10 and 20, respectively. An average sum rate performance improvement of 19.79% is attained by ERA over existing model.

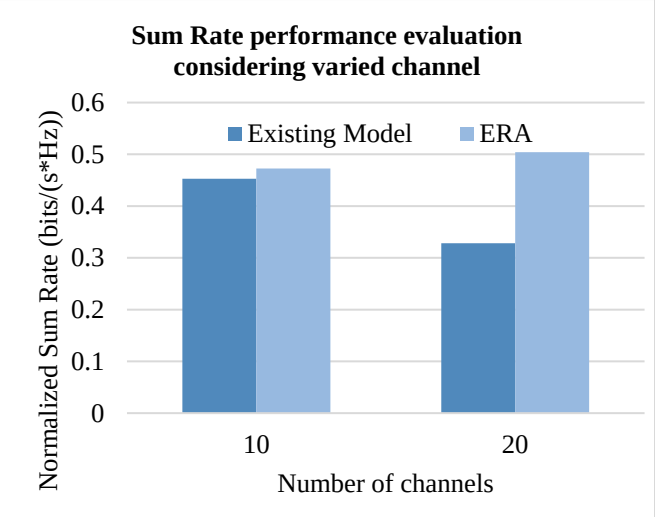

Fig. 3. Sum rate performance evaluation considering varied channel under assumption 1 (Fig. 1).

b) Successful packet transmission performance evaluation considering varied channel:

This section evaluates successful packet transmission performance of ERA over existing model [3], [16], [17]. The successful packet transmission performance is evaluated by varying link/channel size and the outcome attained by ERA and exiting model is graphically shown in Fig. 4. The outcome shows that ERA improves packet transmission performance by 4.87% and 37.18%, over exiting model considering varied channel size of 10 and 20 respectively. An average successful packet transmission performance improvement of 21.02% is attained by ERA over existing model. The overall result attained by ERA is scalable and robust.

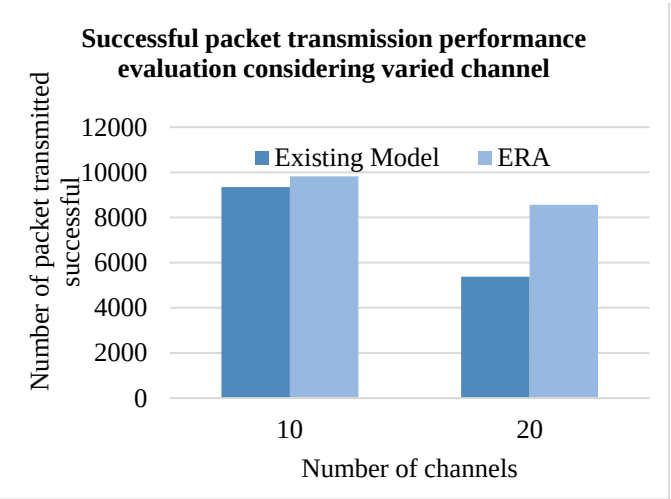

Fig. 4. Successful packet transmission performance evaluation considering varied channel.

c) Revenue performance evaluation considering varied channel:

This section evaluates revenue performance of ERA over existing model [3], [16], [17]. The revenue is computed similar to [13]. The revenue performance is evaluated by varying link/channel size and the outcome attained by ERA and exiting model is graphically shown in Fig. 5. The outcome shows that ERA increase revenue by 30.34% and 4.63%, over exiting model considering varied channel size of 10 and 20 respectively. An average revenue improvement of 17.48% is attained by ERA over existing model. The overall result attained by ERA is scalable and robust.

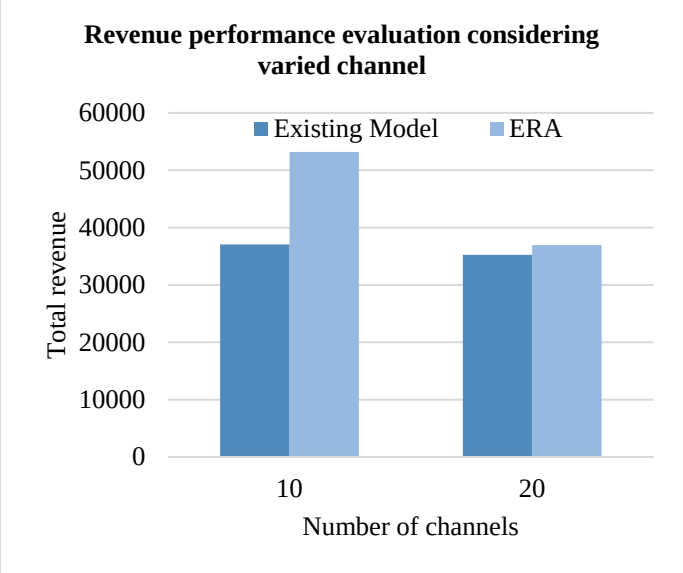

Fig. 5. Revenue performance evaluation considering varied channel.

V. CONCLUSION

For overcoming the interference issues D2D user operating in overlapping area of multiple adjacent cellular network. This work presented an Efficient Resource Allocation model for D2D under cellular network. The resource allocation model is designed as a game theory approach where base station is considered as a contender for meeting resource need of D2D pair presented in overlapping area of adjacent cells. Experiment are conducted to evaluate performance of ERA and outcome shows ERA attain superior performance improvement over state-of-art models in terms of sum rate (utility), successful packet transmission, and revenue. An average sum rate (utility) performance improvement of 19.79% is attained by ERA over existing models considering varied assumption. Further, an average successful packet transmission and revenue performance improvement of 21.02% and 17.48%, respectively is attained by ERA over existing models considering varied assumption. The overall result attained shows scalable and robust performance. In future, this work would consider performance evaluation considering other parameter such as delay and further enhance the resource allocation model.

REFERENCE

[1] Cisco Virtual Networking Index (VNI) Forecast, "Cisco visual networking index: Global mobile data traffic forecast update, 2015–2020," C. V. N. Index, Cisco, Tech. Rep.c11-520862, 2016. [Online]. Available: http://www.cisco.com/c/dam/m/en in/innovation/enterprise/assets/mobilewhite-paper-c11-520862.pdf.

[2] P. Gandotra, R. K. Jha, and S. Jain, "Green communication in next generation cellular networks: A survey," IEEE Access, vol. 5, pp. 11 727–11 758, 2017.

[3] J. Jiang, S. Zhang, B. Li and B. Li, "Maximized Cellular Traffic Offloading via Device-to-Device R. Alkurd, R. M. Shubair, and I. Abualhaol, "Survey on device-todevice communications: Challenges and design issues," in 2014 IEEE 12th International New Circuits and Systems Conference (NEWCAS), Trois-Rivieres, QC, Canada, 2014, pp. 361–364.

[4] P. Mach, Z. Becvar, and T. Vanek, "In-band device-to-device communication in ofdma cellular networks: A survey and challenges," IEEE Communications Surveys Tutorials, vol. 17, no. 4, pp. 1885–1922, 2015.

[5] G. A. Safdar, M. Ur-Rehman, M. Muhammad, M. A. Imran, and R. Tafazolli, "Interference mitigation in d2d communication underlaying lte-a network," IEEE Access, vol. 4, pp. 7967–7987, 2016.

[6] Y. Hassan, F. Hussain, S. Hossen, S. Choudhury, and M. M. Alam, "Interference minimization in d2d communication underlaying cellular networks," IEEE Access, vol. 5, pp. 22 471–22 484, 2017.

[7] S. Lv, C. Xing, Z. Zhang, and K. Long, "Guard zone based interference management for d2d-aided underlaying cellular networks," IEEE Transactions on Vehicular Technology, vol. 66, no. 6, pp. 5467–5472, 2017.

[8] R. Yin, G. Yu, H. Zhang, Z. Zhang, and G. Y. Li, "Pricing-based interference coordination for d2d communications in cellular networks," IEEE Transactions on Wireless Communications, vol. 14, no. 3, pp. 1519–1532, 2015.

[9] M. Shen, J. Liu, X. Wang, Y. Zhang, H. Sun, and J. Li, "On transmission capacity region of d2d integrated cellular networks with interference management," IEEE Transactions on Communications, vol. 63, no. 4, pp. 1383–1399, 2015.

[10] T. Huynh, T. Onuma, K. Kuroda, M. Hasegawa, and W. J. Hwang, "Joint downlink and uplink interference management for device to device communication underlaying cellular networks," IEEE Access, vol. 4, pp. 4420–4430, 2016.

[11] Content Sharing," in IEEE Journal on Selected Areas in Communications, vol. 34, no. 1, pp. 82-91, Jan. 2016. doi: 10.1109/JSAC.2015.2452493.

[12] Z. Zhou, K. Ota, M. Dong and C. Xu, "Energy-Efficient Matching for Resource Allocation in D2D Enabled Cellular Networks," in IEEE Transactions on Vehicular Technology, vol. 66, no. 6, pp. 5256-5268, June 2017.

[13] Y. Liu, R. Wang and Z. Han, "Interference-Constrained Pricing for D2D Networks," in IEEE Transactions on Wireless Communications, vol. 16, no. 1, pp. 475-486, Jan. 2017.

[14] C. Gao, Y. Li, Y. Zhao and S. Chen, "A Two-Level Game Theory Approach for Joint Relay Selection and Resource Allocation in Network Coding Assisted D2D Communications," in IEEE Transactions on Mobile Computing, vol. 16, no. 10, pp. 2697-2711, 1 Oct. 2017.

[15] J. Huang, C. Xing, Y. Qian and Z. J. Haas, "Resource Allocation for Multicell Device-to-Device Communications Underlaying 5G Networks: A Game-Theoretic Mechanism With Incomplete Information," in IEEE Transactions on Vehicular Technology, vol. 67, no. 3, pp. 2557-2570, March 2018.

[16] J. Hu, W. Heng, Y. Zhu, G. Wang, X. Li and J. Wu, "Overlapping Coalition Formation Games for Joint Interference Management and Resource Allocation in D2D Communications," in IEEE Access, vol. 6, pp. 6341-6349, 2018.

[17] Y. Zhao, Y. Li, D. Wu and N. Ge, "Overlapping Coalition Formation Game for Resource Allocation in Network Coding Aided D2D Communications," in IEEE Transactions on Mobile Computing, vol. 16, no. 12, pp. 3459-3472, 1 Dec. 2017.

[18] Y. Chen, B. Ai, Y. Niu, K. Guan and Z. Han, "Resource Allocation for Device-to-Device Communications Underlaying Heterogeneous Cellular Networks Using Coalitional Games," in IEEE Transactions on Wireless Communications, vol. 17, no. 6, pp. 4163-4176, June 2018.

[19] J. Li et al., "On Social-Aware Content Caching for D2D-Enabled Cellular Networks with Matching Theory," in IEEE Internet of Things Journal. doi: 10.1109/JIOT.2017.2749320, 2017.

[20] Manoj C and Amrita Mishra, "Game Theoretic Approaches for Spectrum Sharing in Cognitive Radio Networks: A Survey", Available: http://home.iitk.ac.in/~amritami/index_files/ee670_term_paper.pdf.

[21] Ekram Hossain and Zhu Han, "Game theory for Cognitive Radio Networks", available: http://globecom2009.ieee-globecom.org/Uploads/Public/Docs_Globecom_2009/ekram-zhu-tutorial_14.pdf.

[22] B. P. Lathi and Z. Ding, Modern Digital and Analog Communication Systems. Oxford University Press, 2009.

Proceedings of the Fourth International Conference on Communication and Electronics Systems (ICCES 2019)
IEEE Conference Record # 45898; IEEE Xplore ISBN: 978-1-7281-1261-9

IoT Based Automatic Attendance System

Dharani Devi[1], Devi.A[2], Piriyyadarisani.V[3]

Assistant Professor[1&2], UG Scholars[3], Department of ECE,
IFET College of Engineering, Villupuram.

dharanidevi.ifet@gmail.com[1], deviarumugam02@gmail.com[2], piriyyapinky241197@gmail.com[2]

***Abstract*—Now a days attendance plays a major role in classrooms. The attendance are taken and updated in the lectures logbook manually. Generally the manual work wastes the time for both students and staffs. This problem can be overcomed with the help of the proposed system. The unique characteristics of every human being are their face. In this proposed system, a face recognition technique is used for taking attendance automatically. The proposed system is initially trained with student's database which includes student name, photo and their personal details. The attendance will be taken automatically during every class hours using recognition technique and updated to the student's database. If any student is absent, the message will be automatically sent to their parents or guardian of the absentees using GSM module. The system will also update the everyday attendance database to the Head of department.**

Keywords— Face recognition, Face detection, Open CV, Raspberry pi, web camera

I. INTRODUCTION

IoT makes us to develop a system without human interference. This technology transfers data over the network. It allows objects to be sensed and controlled remotely. Now a day's attendance can be taken manually for every hour by the lectures in an educational institution. The lectures call the students name or their register number. So that, the minimal amount of time can be wasted. And also the lectures manually calculate and overall attendance of the students at the end of the semester. There is a possibility of wrong attendance while calculating overall attendance.

To avoid such problems, the proposed system is implemented on IoT for taking attendance. With the help of IoT, the attendance will be taken automatically which reduces the time and effort of the lecturer. Attendance will be taken for each and every hour in the classroom and it will be automatically updated to the student's database. The absentees are informed to the guardian through SMS. IoT based automatic attendance system will be more secure and efficient technique for taking attendance in the classroom. The login page is created for lecturer using IOT. The attendance database and attendance percentage can also be checked by the lecturer by using the IoT web page.

II. RELATED WORK

In **Face Recognition Attendance System using Raspberry Pi [1],** the attendance are taken using face recognition techniques. The main advantage of face recognition attendance system is to prevent the fake attendance system in the classrooms. The camera module is placed at the center of the classroom. The face recognition method recognizes the face and automatically verifies with the existing database present in Open CV and the attendance is taken.

In **Automatic Attendance system using Face Recognition[2],** the attendance is taken automatically with the help of the face recognition methods. This system is mainly designed to take attendance automatically during class hours. The camera captures the image of the classroom in the beginning of session. The face recognition and detection is performed. Again the image is captured at end of session. Images taken in both the sessions are compared and the attendance is updated in database.

In **Implementation of automated attendance system using face recognition[3],** proposes the attendance system using face recognition. This system can be mainly used in Employee management and Time attendance system. The camera is placed in the entry point of an organization. It can record only the entry time of a student and attendance is updated to the student's database.

In **Smart Attendance system using Face Detection on Raspberry pi[4],** proposes a face recognition attendance system with IOT. Using face recognition and detection algorithm the faces are detected and the attendance is updated to the student's database. The IOT device Raspberry pi use face recognition method for taking attendance automatically and communicates with cloud database.

In **Automated attendance using raspberry pi[5],** the camera is placed at the center of the classroom. Using the face recognition method, the system captures an image of the students in the classroom and compares it with a database already stored. If the image of a student matches it mark it as present otherwise as absent. The attendance will be automatically updated in an attendance database.

III. PROPOSED SYSTEM

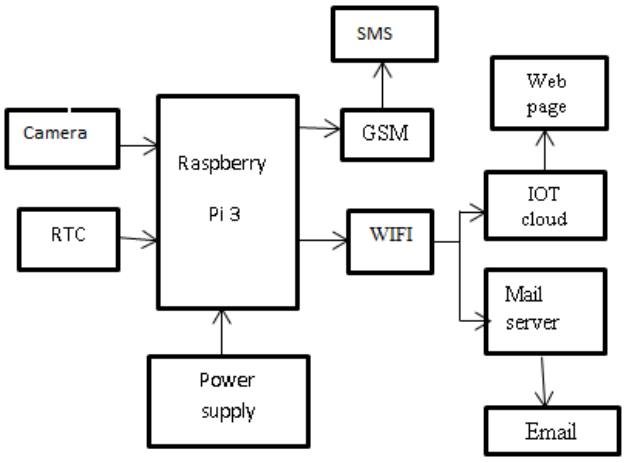

Fig. 1. Automatic Attendance system

The camera is connected with the Raspberry pi. Initially the camera captures images of students present in the classroom and detects the faces as a captured image. The detected faces are compared with the student's database stored in the IOT. When the detected faces matches with the already stored database, then the attendance is marked as present. If not, the absent is marked for the student's those who are not present inside the classroom. After a specified amount of time, the message will be sent to the parents or guardians of the absentees using GSM module. Thus the attendance is automatically updated to student's profile. The web page is created for attendance database using IOT Cloud. The attendance database can also be checked by the faculty advisor by using the web page created with their login id and password. The system will automatically update the attendance database to the Head of the Department. At the end of the semester the faculty advisor can export the student's attendance to calculate overall attendance.

IV. HARDWARE DETAILS

A. *RASBERRY PI 3*

Raspberry pi 3 is ARM based credit card sized single board computer can be used for many applications. Additionally it includes wireless LAN and Bluetooth connectivity for powerful connected designs. The speed of the Raspberry pi 3 is 10 times faster than first generation. Python language is a programming language used in Raspberry pi 3.

Here the Raspberry pi 3 can act major role. It gathers the captured image from the camera. Compare the captured image with the image stored in the database.

Fig. 2. Raspberry pi 3

B. *Camera*

A camera is a hardware device which is used for capturing a photographic images or recording a video which can be stored in a physical medium or photographic film. The image captured can be single image or a sequence of images such as videos or movies. Here the camera is used to capture the images of the students in all the directions. Send the information to the raspberry pi board.

Fig. 3. Camera

C. *RTC*

Real Time Clock (RTC) counts seconds, months, hours, date of the month, month, day of the week and year with leap year compensation up to 2100. RTC is a two wired interface. RTC is the computer clock that keeps tracks of current time.

C. *GSM (Global System for Mobile communication)*

Global System for Mobile communication (GSM) is widely used for mobile communication system. It is a mobile communication modem. GSM is an open and digital cellular technology used for transmitting mobile voice and data services at different frequency levels.

Here the GSM module is used to send the message to the parents or guardians if the student is not available in the class after specified duration of the time.

V. FLOW CHART OF THE PROPOSED SYSTEM

The flow diagram describes the entire operation carried out by the proposed system.

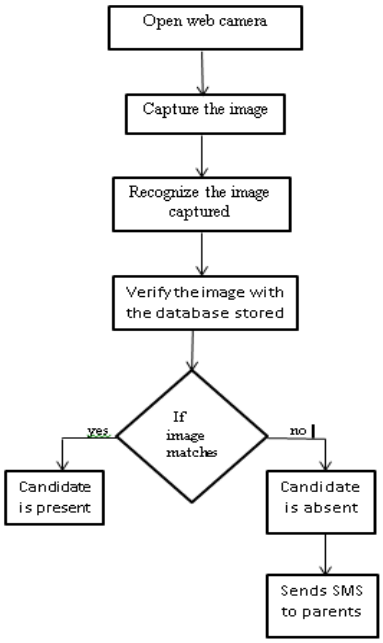

Fig. 4. Flow diagram of the proposed system

VI. EXPRIMENTAL SETUP

Fig. 5. Experimental setup of the proposed system

The different set of images of the students are trained and stored in a student's database. The captured images are compared with trained images and the attendance will be taken automatically using face recognition module.

Fig.6. Trained images

The absentees of the student's will be automatically informed to their's parents through SMS using GSM modem.

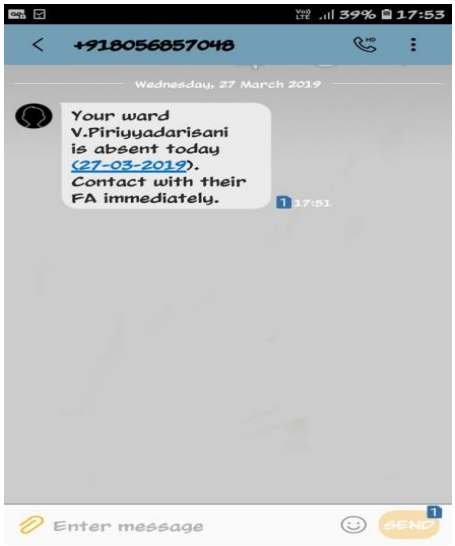

Fig.7. SMS to the parents

The updated attendance can be checked by the faculty advisor using the login page created.

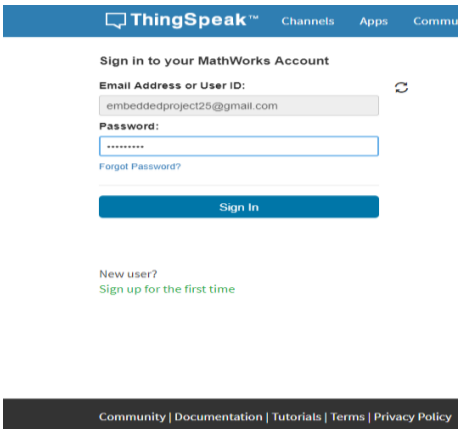

Fig.8. Lecturer login page

The updated attendance of the student's in an excel sheet

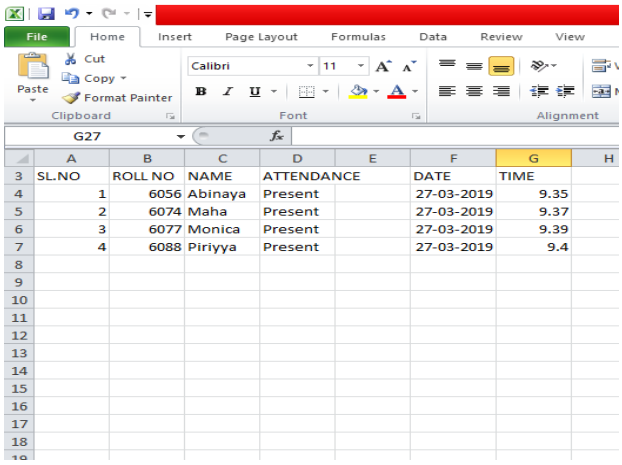

	A	B	C	D	E	F	G	H
3	SL.NO	ROLL NO	NAME	ATTENDANCE		DATE	TIME	
4	1	6056	Abinaya	Present		27-03-2019	9.35	
5	2	6074	Maha	Present		27-03-2019	9.37	
6	3	6077	Monica	Present		27-03-2019	9.39	
7	4	6088	Piriyya	Present		27-03-2019	9.4	

Fig.9. Consolidated attendance at the end of the semester

VII. CONCLUSION

The automatic attendance system using face recognition technique has been developed for replacing a manual attendance system. The propsoed system can capable of working under numerous styles of lighting conditions, different seating arrangements and environments in various classrooms. Most of those conditions are tested on the system and system has shown 95% accuracy for many of the cases. There can also work for exist students depicting numerous facial expressions, varying hair styles, beard, spectacles etc. All of these cases are tested to get a high level of accuracy and efficiency. This proposed system will be enforced for higher results relating to the attendance management. So the proposed system is proved to be more secure, reliable, fast and efficient system. The system can save time, and reduce the quantity of work of the faculty in the administration and can replace the attendance sheets with electronic equipment and reduces the quantity of human resource required for the purpose.

VIII. FUTURE SCOPE

The proposed system can be further developed by improving the recognition rate and by using the Raspberry pi Infra Red camera module. So that the system can be uses as a security surveillance system.

REFERENCES

[1] R.Kiran Kumar, Mekala.S, "Face Recognition attendance system using Raspberry pi", International Journal of Pure and Applied Mathematics, Volume 115,October 2018.
[2] Ashish Choudhary, Abhishek Tripathi, Abhishek bajaj, Mudit Rathi , B.M.Nandini, "Automatic Attendance system using Face Recognition", International Journal of Modern Trends in Engineering and Research, April 2017.
[3] Nirmlaya Kar, Mrinal Kanti Debbarma, Ashim Saha, Dwijen Rudra Pal, "Implementation Automated Attendance System using Face Recognition Technique", International Journal of Computer and Communication Engineering, volume 1, No.2, July 2012.
[4] Aparna Behara, M.V.Ragunadh, "Real time Face Recognition system for time and attendance applications", International Journal of Electrical, Electronics and Data Communication Engineering, volume 1, issue 4, June 2010.

[5] Vishal D. Bikkad, Dr. S.B.Sonkamble, Snehal A.Mane, Surabhi S.Sarada, "Smart Attendance system using face detection on Raspberry pi", International Journal of Computer and Communication Engineering, Volume 6, Issue 5, May 2018.
[6] Rajkumar Soundrapandiyan, J.Prakash, "Automated attendance system using raspberry pi", International Journal of Pharmacy and Technology, September 2016.
[7] Kunal Kishore, Ozwin Neel Lobo, Pranay Saraiwala, Prarthana R, "Design and Development of IOT based Student's Attendance system", International Journal of Innovations and Advanced in Computer Science, Volume 7, Issue4, April 2018.
[8] Kawguchi, Y., Shoji, T., Weijanae, L.I.N., Kakusho, K., Minoh, M.(2005) "Face recognition based lecture attendance system, In the 3rd AEARU workshop on Network Education.
[9] Rohit Chavan, Baburao Phad, Sankalp Sawant, Vinayak Futak, "Attendance Management system using Face recognition", International Journal of Innovative research in Science and Technology, Volume 1, Issue 11, April 2015.
[10] Ofualagba Godswill, Omijie Osas, Orobor Anderson, Ibhadode Oseikhuemen, Odiete Etse, "Automated students attendance management system using Face recognition", International Journal Educational Research and Information Science, Volume 5, September 2018.
[11] Priya Paumarti, P. Purna Sekhar, "Classroom Attendance using Face Detection and Raspberry Pi", International Research Journal of Engineering and Technology, Volume 5, Issue 03, March 2013.
[12] Mathana Gopala Krishnan, Balaji, Shyam Babu, "Implementation of Automated attendance System using Face Recognition", International Journal of Scientific and Engineering Research, Volume 6, Issue 3, March 2015.

Proceedings of the Fourth International Conference on Communication and Electronics Systems (ICCES 2019)
IEEE Conference Record # 45898; IEEE Xplore ISBN: 978-1-7281-1261-9

Gesture and Speech Recognizing Helper Bot

Kailash Gogineni
B.Tech. Student, CSE dept.
Vellore Institute of Technology
Vellore, Tamil Nadu
gkailashnath1998@gmail.com

Akhil Chitreddy
B.Tech. Student, CSE dept.
Vellore Institute of Technology
Vellore,Tamil Nadu
akhilchitreddy@yahoo.com

Anirudh Vattikuti
B.Tech. Student, CSE dept.
Vellore Institute of Technology
Vellore,Tamil Nadu
vattikuti.anirudh97@gmail.com

Dr. Natarajan P
Professor, CSE dept.
Vellore Institute of Technology
Vellore,Tamil Nadu
pnatarajan@vit.ac.in

***Abstract*—** In industries, difficult work is being decreased everywhere scale to expand effectiveness and exactness, and gain benefit by introducing robots that can do repetitive works at lesser expense of preparing. A onetime establishment of such a gadget may cost an enormous sum at first, yet in the more drawn out run, will end up being more beneficial than difficult work. Out of the part, a basic robotic arm is a standout amongst the most generally introduced machines. Robotic arm is one of the significant undertakings in the present computerization industry. Automated arm is a piece of the mechatronic industry which is quickly versatile and developing industry today. Distinctive changes and extra features are being associated with the first kind of straightforward robotic arm to upgrade its ease of use under various conditions. In this project we are building up a robotic arm which will have a free rotation around multiple axes and we are including the technology of Image Processing with it to make it a visual signal based working robotic arm. This project is a pick and place robot, you can take the desired article starting with one place and carry it with its gripper claw using Hand Gestures and, the movement of the whole robot from one place to another place takes place with the wheels attached to the robot using speech recognition. The operations will be constrained by a visual processing framework that read the gestures and will give directions to the Arm for performing various types of movements and tasks.

***Keywords*—** Robotic arm, Image Processing, DC motors, Machine Learning, Gestures, speech recognition.

I. INTRODUCTION

In this project, we will learn diverse parts of Mechatronics, Image Processing, sound processing Mechanics of Machines and their modern execution. We will have a hands-on involvement on working with Python, coding and execution. We will find out about the usage of Artificial Intelligence in the field of Image Processing. The proposed framework comprises of two modules .The first module is Robotic arm control utilizing static hand signals and the second module deals with Maneuverability control utilizing voice commands.

Raspberry Pi acts as a master in perceiving the signals and Arduino will go about as slave by moving the mechanical technology according to the direction issued by raspberry pi. The gestures are prepared utilizing Machine learning procedure utilizing Open CV and SKlearn (essential python libraries utilized for machine learning). At first the motion is distinguished utilizing background subtraction and after that skin segmentation is made and the hand portion is alone segmented and further the features are extracted using Histogram of Oriented gradients and further it is classified using Random Forest. The final model will deployed in the raspberryPi based on the detected gesture it will send command to Arduino to control servo/DC motors of the robotic to perform custom gestures using pulse width modulation.

Further utilizing Google API clients voice inputs are captured and prepared in such an approach to get the string of the specific command given by the client. The strings are further given to Arduino such that the mobility is controlled.

Utilizing Histogram of Oriented Gradients and Random Forests makes the venture increasingly exact in perceiving motions at any rate and parity of exchange off among speed and exactness is kept up.

II. LITERATURE SURVEY

Robots have turned into a substitute for people in unsafe and risky condition. They have turned out to be all the more socially intuitive and this clears path for improvement of algorithms to influence them to perform the tasks productively. Making machines progressively interactive with people and to improve the assignment execution of the robot with less human intervention are the principle goals of HRI. The robot must be equipped for translating, breaking down and understanding a few correspondence components engaged with human to human interaction. The past works in the field of HRI are talked about as for the region of utilization [1].

Sign language is a vital instance of open gestures. Since gesture based communications are exceptionally basic, they are truly reasonable as testbeds for vision calculations [2]. In the meantime, they can likewise be a decent method to assist the crippled with interacting with PCs. Communication via gestures for the deaf is a precedent that has got critical consideration in the gesture literature [3].

The applications like Telepresence and telerobot are regularly arranged inside the area of room investigation and military-based research ventures. The gestures used to connect with and control robots are like completely submerged computer generated experience collaborations, anyway the worlds are regularly genuine, giving the administrator video feed from cameras situated on the robot [4].Gestures can control a robots hand and arm developments to go after and control genuine articles, its development through the world.

Desktop and Tablet PC Applications: In work area figuring applications, gestures can give an elective cooperation to the mouse and console [5]. Numerous gestures for work area registering assignments include controlling illustrations, or clarifying and altering archives utilizing pen-based signals [6].

A player's hand or body position has been followed by Freeman et al. [7] to control development and introduction of intelligent amusement articles, for example, vehicles. Konrad et al. [8] utilized gestures to control the development of symbols in a virtual world, and Play Station 2 has presented a camera named Eye Toy, which tracks hand developments for intelligent amusements [9].

Gestures for virtual and augmented reality applications have encountered one of the best dimensions of take-up in registering. Augmented reality connections utilize signals to empower reasonable controls of virtual items utilizing ones hands, for 3D presentation communications [10] or 2D presentation that mimic 3D associations [11]

Needs for the senior individuals at home are being filled by social-interactive robots. One genuine model is HOBBIT which takes guidelines from the user as motions and facilitates the user with contact screen interface to make a call, stimulation, web, etc. Thus MOBILEROBOTS PeopleBot help the impaired and old individuals in family unit exercises. The association is through Phantom Omni, a haptic interface mounted over robot [12]. Kinect sensor goes about as interface to recognize arm signal for shopping in Mobile Shopping Cart (MSC) which executes the directions inside a large portion of a second time [13].

Recognition of the feelings being a piece of human robot association, where in physiological signals such as tension are registered and sustained through the bio-sensors mounted on human administrator. Moving nearer or casual banter with the user are the extra tasks performed by the robot alongside wall following, obstacle identification dependent on the data sources sustained to the robot. The Robot-based Basketball task (RBB) is an exploratory proving ground where consistent adjustment of its conduct happens as for the human physiological states [14].

Kinder-garten children were made to communicate with robots so as to advance the geometrical thinking while at the same time playing. Thus it improved their geometrical information and appreciated learning. Over the time, the robot is equipped for giving out execution insights of the kids. KindSAR [1], Kinder-garten social assistive robots gives entertainment to youngsters by narrating.

Recognition of the Hand Gesture was executed utilizing the parameters based on the shape [15]. The downside is most extreme parameters adopted in this approached are assumed.

III. *TECHNOLOGY STACK*

The paper deals with identifying the gestures and responding to the speech with the use of Google API and projecting the actions a bot can perform to lift an object. Technology stack includes Machine learning, Image processing and Robotics

- Machine Learning: It is the advanced technology in computer science, which helps the system to behave as human. The base of the Machine learning is pure Mathematics, which helps to perform wonderful tasks. Basically four algorithms such as SVM, logistic regression, Random forest and KNN are used and there accuracy, precision, recall, support are tested and the highest accuracy supported algorithm is used to embed into the Raspberry-pi and further process of loading the data set is done. Now, the machine is trained to recognize some actions. Recognized data is loaded into the program and test against the known and unknown fingers.

- Image Processing: Image processing, helps to do some processing techniques which help to improve the accuracy of recognition of the fingers through the mask. While taking the images of the gestures for dataset collection hog algorithm is used to extract features from the images.

- Robotics: To perform the actions of picking a block or an object a bot is needed which can walk and turn in different direction with respect to the gestures and speech, mostly in the form of a best method called Artificial Intelligence. The bot runs from calculating angles one by one, more likely they are powered by AI blocks that were trained to stand/walk/balance

IV. *ALGORITHMS*

A. Implementation of KNN

1. At the outset, we will generate the data set and send the data
2. Then the value of k is initialized (the nearest neighbor so that, we can make boundaries of each class).
3. Now, for obtaining the class of predicted output, the iteration is to be done from 1 to total number of training data arguments.

- Analyse the test data and each row of the training data and certainly compute the distance between them with the most popular method called Euclidean distance.
- The next step is, we will be using sorting method to the premeditated spaces in ascending order depending on their distance values.
- Now, obtain the top K rows from which the sorting is done.
- Now, just obtain the most recurrent class of the rows.
- Finally, the predicted class is returned and the subsequent output is given.

B. Random forest algorithm Procedure

The procedure consists of two phases which is **creation** and **perform the prediction** from the obtained random forest classifier.

Random forest Pseudocode:

- Arbitrarily pick “k” structures from a whole of “m” structures, only when k << m.
- Amid the different features of “k”, compute the node “d” using best split approach.
- Next, we need to separate the node into offspring nodes using the best split approach.

- Replicate the above 1 to 3 steps until "l" no.of nodes have been occurred and then construct forest by replicating all 1 to 4 steps for "n" no.of times to generate "n" no.of trees.

Prediction technique:
Prediction is performed using the trained random forest algorithm, the steps are:

1. Using the test features and the arbitrarily created decision tree perform the prediction and store it in the form of a target. Then the votes for each predicted target is computed.
2. Finally, the high voted target is the certainly fixed as final prediction.

Voting: Tree one and two would vote that she subsisted, but tree three votes that she expires. If we take a vote, it's 2 to 1 in favor of her existence, so we would classify this commuter as a stayer.

C. SVM: Given a data set containing of features set and tags set, an SVM classifier dimensions a prototype to predict classes for innovative occurrences. It allocates different data arguments to individual classes. If at all, there are only two classifiers means, then the classifier is called Binary SVM classifier.

In SVM algorithm, the plotting of each data element as unique identity in the "n"-dimensional space, where "n" is defined as the no.of features with every feature having a precise coordinate. Then, in the next step the classification is done by recognizing the hyper planes that categorizes the two classes. SVM's are briefly defined as the cutting edge which separates the two classes (hyperplane/ line).

D. Logistic Regression: For logistic regression, we can take any kind of data with wide range. It will run the algorithm on the training set and the model is used to decide the class of the test data.

Pseudocode

- The equation needed to predict the class of the test data is prepared and the data is supplied to the equation to get regression value.
- The regression value is used by the activation function to predict the class of the data. In the project sigma function is used as the activation function.

V. METHODOLOGY

The procedure starts by taking images of hand gestures and creating a dataset. The features from the images taken is extracted by using the HOG (histogram of oriented gradient) algorithm. The dataset is used to train various models such as KNN, SVM, random forest, logistic regression. The best among the algorithms is chosen to create an efficient prediction model using the test data. The model is then fed into raspberry pi module. When the program starts running the camera starts to detect hand gestures using the random forest model, as soon as the gesture has been identified the output is sent in the form binary numbers to the Arduino module. The Arduino module makes use of relays to increase the power voltage from 5 volts to 12 volts and it will be sent to the motors along with the signals from the Arduino board. As per the signals received the robotic arm performs actions in order to pick and place objects. The speech recognizing module includes a chassis which is controlled using the same Arduino module which has Bluetooth module connected to it. The Bluetooth module can be operated by using the google API which is already present in an app, then the signals are sent to Arduino for movement controlling. The movements include forward, reverse, right, left, stop. The power source for the robot is given through plug points and the movement is enabled till two meters.

VI. DESIGN OF THE SYSTEM

The helper bot is designed in such a way that the gesture and speech modules are independently implemented. The gesture recognition system uses machine learning techniques to identify gestures whereas the speech recognition system uses google API to pass the voice commands as signals to the Arduino board.

A. Gesture Recognition

There are two phases in the gesture recognition module. They are the training and the testing phase. From the above diagram, we can see that during the training phase, dataset is collected and then the edge detection algorithms start to act to identify the gestures from our hand. After completing these steps, training of images takes place to classify the gestures. Here we chose random forest algorithm to classify the gestures. Once the model is created we start to take video or an image input to predict the class of the image which will be sent to the raspberry pi for the robotic arm movement.

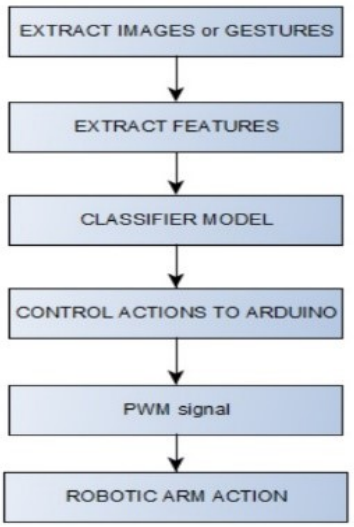

Fig. 1. Gesture Recognition Module flowchart

During the training phase, dataset is collected and then the edge detection algorithms start to act to identify the gestures from the hand. Training of images takes place to classify the gestures. Here we chose random forest algorithm to classify the gestures. Once the model is created we start to take video or an image input to predict the class of the image which will be sent to the raspberry pi for the robotic arm movement

B. Speech Recognition

The speech recognition module works by taking voice input through an android device. The voice commands are converted into signals by making use of a google API. When the Arduino microcontroller receives the signals, it controls the chassis of the robot by making it move front, back, left, right.

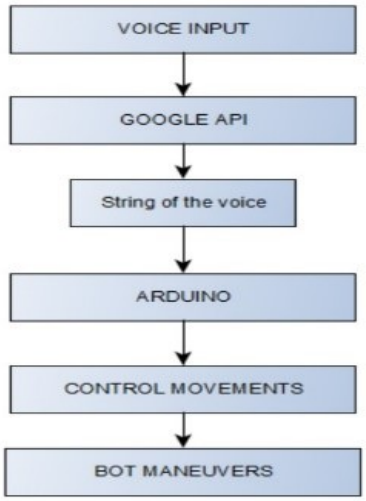

Fig. 2. Speech Recognition module flowchart

The speech recognition module works by taking voice input through an android device. The voice commands are converted into signals by making use of a google API. When the Arduino microcontroller receives the signals, it controls the chassis of the robot by making it move front, back, left, right.

VII. RESULTS

The dataset images of the hand gestures are collected and fed into all the algorithms and then training and tested parts are carried out for calculating the various parameters required to calculate the f1 score which will be helpful for finding accuracy. The results from the various algorithms are as follows:

Algorithms	Precision (avg)	Recall (avg)	F1-score (avg)	Support (avg)
Random Forest	1	1	1	1296
SVM	0.99	0.99	0.99	1296
KNN	0.88	0.88	0.88	1296
Logistic Regression	0.80	0.80	0.80	1296

Table 1. The performance analysis of KNN, LOGISTIC REGRESSION, RANDOM FOREST, SVM Algorithms is done to get the efficient output.

So, from the derived results we can say that, the algorithm of Random Forest and Support vector machine (SVM) gives us the highest values for the parameters precision, recall and f1-score. Among the top two it is obvious that random forest which is an ensemble learning classifier gives the best results. This will now be embedded into the raspberry pi module for recognizing gestures.

Fig. 3

Fig. 4

For the GESTURE 0 the task assingned for the ROBOT is to close its Claw and the Random forest algorithm classifying the gesture on the top left corner as shown in **Fig.3**. When the GESTURE 0 is shown the claw will be closed as shown in **Fig.4**.

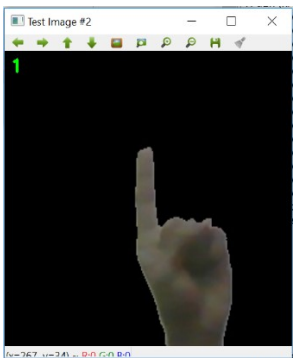

Fig. 5

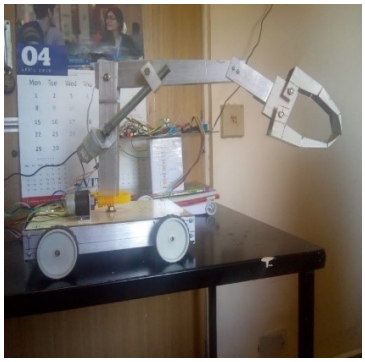

Fig. 6

For the GESTURE 1 the task assingned to the ROBOT is to move its Claw up and the Random forest algorithm classifying the gesture as shown in **Fig.5**. When the GESTURE 1 is shown the claw will move up as shown in **Fig.6**.

Fig. 7

Fig. 8

For the GESTURE 2 the task assingned to the ROBOT is to move its Claw down and the Random forest algorithm classifying the gesture as shown in **Fig.7**. When the GESTURE s is shown the claw will move its Claw down as shown in **Fig.8.**

Fig. 9

Fig. 10

For the GESTURE 3 the task assingned to the ROBOT is to move the Claw to its Left and the Random forest algorithm classifying the gesture as shown in **Fig**.9. When the GESTURE 3 is shown the claw will move to its Left as shown in **Fig.10.**

Fig. 11

Fig. 12

For the GESTURE 4 the task assingned to the ROBOT is to move the Claw to its Right and the Random forest algorithm classifying the gesture as shown in **Fig.11**. When the GESTURE 4 is shown the claw will move to its Right as shown in **Fig.12**.

Fig. 13

Fig. 14

For the GESTURE 5 the task assingned to the ROBOT is to Open its Claw and the Random forest algorithm classifying the gesture as shown in **Fig.13**. When the GESTURE 5 is shown the claw will be Opened as shown in **Fig.14**.

Fig. 15. Robotic arm picking up light objects such as paper balls etc.

After training the model with a dataset of 5000 images, we then test it on some random test data to classify the gesture. The gesture number appears on the top left corner.
The program successfully identifies the gestures when embedded in raspberry pi. The raspberry pi sends the signals to the robot to perform the corresponding action.

VIII. SCOPE

- Robotic devices combined with machine learning is the trending area for developing applications such as automatic plant cutting in a given period of time.
- These can also be used as assistant bots.
- When integrated with large scale equipment, which can send signals in a high range, it will be a great help for the military in detecting the mines.

IX. CONCLUSION

We can imply that the random forest performs better compared to the rest of the algorithms. Therefore, that will be fed into the raspberry pi module for recognizing gestures. When the data set is collected without noise, the gestures can be classified with higher accuracy. The robot picks light objects perfectly with a grip by following the gestures and voice commands.

X. REFERENCES

[1] Balasubramaniyan Chandrasekaran and James M. Conrad, "Human-Robot Collabo- ration: A Survey", *Proceedings of the IEEE SoutheastCon*, pp. 1 - 8, Fort Lauderdale, Florida, USA, 2015

[2] B. Wisenburn, D. J. Higginbotham, "Participant evaluations of rate and communication efficacy of an AAC application using natural language processing", *Augmentative Alternative Commun.*, vol. 25, no. 2, pp. 78-89, 2009.

[3] M. S. Hawley, "A speech-controlled environmental control system for people with severe dysarthria", *Med. Eng. Phys.*, vol. 29, no. 5, pp. 586-593, 2007

[4] J. Todman, N. Alm, J. Higginbotham, P. File, "Whole utterance approaches in AAC", *Augmentative Alternative Commun.*, vol. 24, no. 3, pp. 235-254, 2008.

[5] L. J. Ferrier, H. C. Shane, H. F. Ballard, T. Carpenter, A. Benoit, "Dysarthric speakers' intelligibility and speech characteristics in relation to computer speech recognition", *Augmentative Alternative Commun.*, vol. 11, no. 3, pp. 165-175, 1995

[6] N. Thomas-Stonell, A. L. Kotler, H. A. Leeper, P. C. Doyle, "Computerized speech recognition: Influence of intelligibility and perceptual consistency on recognition accuracy", *Augmentative Alternative Commun.*, vol. 14, no. 1, pp. 51-56, 1998

[7] R. N. Bloor, K. Barrett, C. Geldard, "The clinical application of microcomputers in the treatment of patients with severe speech dysfunction", *IEE Colloquium High-Tech Help Handicapped*, pp. 9/1-9/2, 1990.

[8] U. Sandler, Y. Sonnenblick, "A system for recognition and translation of the speech of handicapped individuals", *9th Mediterranean Electrotech. Conf. (MELECON'98)*, pp. 16-19, 1998.

[9] B. Wisenburn, D. J. Higginbotham, "An AAC application using speaking partner speech recognition to automatically produce contextually relevant utterances: Objective results", *Augmentative Alternative Commun.*, vol. 24, no. 2, pp. 100-109, 2008.

[10] B. O'Keefe, N. Kozak, R. Schuller, "Research priorities in augmentative and alternative communication as identified by people who use AAC and their facilitators", *Augmentative Alternative Commun.*, vol. 23, no. 1, pp. 89-96, 2007

[11] J. Murphy, "I prefer contact this close: Perceptions of AAC by people with motor neurone disease and their communication partners", *Augmentative Alternative Commun.*, vol. 20, pp. 259-271, 2004.

[12] Markus Vincze, Wolfgang Zagler, Lara Lammer, Astrid Weiss, Andreas Huber, David Fischinger, Tobias Koertner, Alexandra Schmid and Christoph Gisinger, "Towards a Robot for Supporting Older People to Stay Longer Independent at Home", *Proceedings of 41st International Symposium on Robotics*, pp. 1 - 7, Munich, Germany, 2014.

[13] Shengnan Gaia, Eui-Jung Jung, Byung-Ju Yi, "Mobile shopping cart application using kinect", *10th International Conference on Ubiquitous Robots and Ambient Intelligence (URAI)*, pp. 289 - 291, Jeju, South Korea, 2013 "Face recognitioin with local binary patterns" by Timo Ahonen, Abdenour Hadid, Matti Pietikainen.

[14] Bekele E., Sarkar N., "Psychophysiological Feedback for Adaptive HumanRobot Interaction (HRI)", *Advances in Physiological Computing, Human Computer Interaction Series*, pp 141-167, Springer, London, 2014.

[15] Meenakshi Panwar, "Hand Gesture Recognition based on Shape Parameters", *Inter- national Conference on Computing,*

Proceedings of the Fourth International Conference on Communication and Electronics Systems (ICCES 2019)
IEEE Conference Record # 45898; IEEE Xplore ISBN: 978-1-7281-1261-9

Cost Efficient Subtractor Designs in QCA

Marshal Raj*, Lakshminarayanan Gopalakrishnan†
*†Department of Electronics and Communication Engineering,
National Institute of Technology- Tiruchirappalli, Tamil Nadu, India
*marshalrgj@gmail.com †laksh@nitt.edu

***Abstract*- The increase in the number of challenges to CMOS technology at extreme Nano meter levels has pushed the research community to find alternative technologies to implement circuits at extremely smaller Nano meter levels. Quantum-dot Cellular Automata is considered to be one of the promising paradigm that can replace CMOS in extreme Nano meter circuit design. It is mainly due to the attractive features it promises to offer such as very high speed, compactness, and extreme low power consumption. Subtractor circuits are widely used in arithmetic and several signal processing applications. In this work, two cost efficient full subtractor designs are proposed using three input and five input majority logic gates. In order to design the circuits with more reliability, the circuits are implemented using clock zone based crossover. Simulation results show that the proposed designs are more cost efficient compared to the existing state-of-the-art designs. The proposed designs can be used to implement any kind of n-bit subtractor design. All the designs are validated and verified using simulation in QCADesigner 2.0.3.**

Keywords- Area, Cell count, Majority Logic, Quantum-dot Cellular Automata (QCA), Subtractor.

I. INTRODUCTION

The challenges in scaling down of CMOS devices to meet the demands of Moore's Law has ignited the research community to find alternatives to CMOS technology for circuit design at very low Nano meter levels. Researchers are trying to find several solutions to keep the CMOS technology relevant to Moore's Law. However, the existing solutions have many limitations and finding an alternative to CMOS has become inevitable [1]. Researchers have come with ideas of several beyond-CMOS technologies. Among the viable beyond-CMOS technologies, Quantum-dot Cellular Automata promises to replace CMOS due to its several promising features such as high speed, small area and low power consumption [2]. Subtractor circuits are used in almost every arithmetic and signal processing application. The existing subtractor designs in QCA have more cells and are vulnerable to fabrication defects due to the type of crossover employed in their implementation. In this paper, in order to reduce the complexity of the subtractor circuits, two cost efficient full subtractor designs are proposed using three input and five input majority logic gates. In addition to that, to increase the reliability of the proposed circuits, the proposed designs are implemented using clock zone based crossover. The proposed cost efficient designs perform better than the existing state-of-the-art designs and it can be used in the implementation of n-bit subtractor of any type. Design verification and validation of the proposed designs are done using QCADesigner 2.0.3 [3].

The authors thank the Visvesvaraya Ph.D. fellowship, Ministry of electronics and Technology (MeitY) for funding this research and DST-FIST, SMDP-C2SD for providing the lab facilities.

The remainder of the paper is organized as follows. Section II provides a crisp and short overview to QCA, Section III discusses the designs and techniques existing in the literature, Section IV presents the proposed subtractor designs and finally, Section V presents the conclusion.

II. QUANTUM-DOT CELLULAR AUTOMATA

A.QCA Cells and wire

QCA cells are the key components of circuit design in QCA. A QCA cell has two electrons and four quantum dots. The quantum dots are interconnected and the electrons can move between the dots but not outside the cell. The repulsion between the two electrons present inside the cell results in occupation of the electrons in one of the two diagonal positions. The cells are considered as binary '1' and '0' depending upon the position of the electrons. A wire is constructed by arranging the cells in an array. Information will be transmitted from one end of the wire and it will be received at the other end. QCA cells are classified into normal cells and rotated cells, based upon the position of quantum dots in the cell. A normal cell logic and a wire formed using normal cells is shown in Fig. 1(a), and Fig. 1(b), respectively. Binary logic transmitted using a normal wire will have the same logic received at the receiver end, irrespective of the number of cells between the transmitter and receiver cell. A rotated cell and rotated wire is shown in Fig. 2(a), Fig. 2 (b), respectively. Compared to a normal wire, the rotated cell wire will have an inverted or non-inverted logic of the transmitted logic, depending upon the even or odd number of cells, respectively, between the input and output cells.

Fig.1. Normal cell. (a) Logic. (b) Wire.

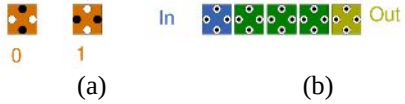

Fig.2. Rotated cell. (a) Logic. (b) Wire.

B. Majority gate and inverter

Majority logic is the key for circuit implementation in QCA. The Boolean logic of the digital circuits is converted to majority logic based expressions and they are implemented using majority gates and inverter. In QCA, three input and five input majority gates are widely used for implementation. The output

of the majority gate depends upon the logic of the inputs. A three input majority gate is shown in Fig. 3(a). To design circuits with optimum number of cells, the majority gate can also be implemented as shown in Fig. 3(b). The Boolean equivalent of a there input majority gate logic with inputs A, B, and C is given by (1).

$$M(A,B,C) = AB + BC + CA \qquad (1)$$

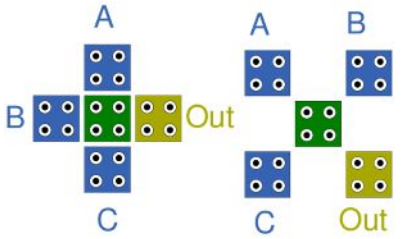

Fig.3. Three input majority gate. (a) Type-I. (b) Type-II.

Several structures of five input majority gates are proposed in the literature. Fig. 4(a) shows the widely used five input majority gate proposed in [4]. Fig. 4(b) shows another version of five input majority gate proposed in [5], which is used in circuits to reduce the complexity.

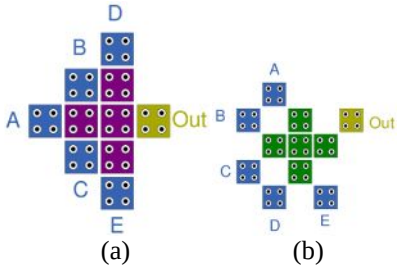

Fig.4. Five input majority gate. (a) Type-I. (b) Type-II.

Inverters are of two kinds in QCA, namely, double path inverter and simple inverter, respectively. Double path inverter is shown in Fig. 5(a) and a simple inverter is shown in Fig. 5(b). Simple inverter is less complex compared to double path inverter. Double path inverter has better fault resistance compared to simple inverter. However, it is achieved at the cost of increased cell count.

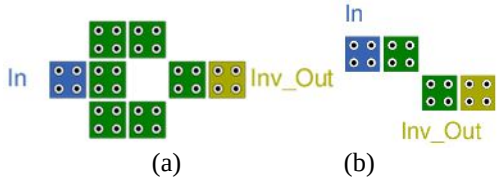

Fig.5. Inverter. (a) Double path. (b) Simple.

C. QCA Clocking

The cells in QCA are not connected to a single clock as done in conventional circuit designs. There are four clock signals (clock 0, 1, 2 or 3) and the cells are connected to any one of the clock. Connection is done in such a way that information flows from one clock zone to another in a pipelined fashion. All the clock signals are in distinct phase and the clock signals will have a 90° phase difference with its neighboring clock signals. Each clock signal follows a sequence of four states in a cyclic order, namely, Relax, Switch, Hold and Release [6]. To differentiate the cells in different clock zones, the cells are represented by different colors as shown in Fig. 6.

Fig.6. Clock zone representation.

D. QCA Crossovers

Wire crossings are the places where two wires cross each other. In QCA, the wire crossings are called as crossovers. QCA crossovers can be broadly categorized as coplanar crossover and multilayer crossover. Coplanar crossovers are the type of crossover where wire crossing is done in the same layer without adding any additional layer. The widely used coplanar crossovers are rotated cell coplanar crossover and clock zone based coplanar crossover. In a rotated cell coplanar crossover, one wire will be a normal wire and another wire will be a rotated cell wire as shown in Fig. 7 (a). In clock zone based crossover, wires which are not connected to the neighboring clock zones can cross each other. Fig. 7(b) shows a clock zone based crossover done between a clock 1 zone wire and clock 3 zone wire. Similarly, Fig. 7 (c) shows a clock zone based crossover done between a wire in clock 0 zone and a wire in clock 2 zone. Rotated cell crossover is more complex compared to clock zone based crossover due to the rotated cells and use of cells with displacement. Placing rotated cells and cells with displacement is very difficult and hence, they are vulnerable to faults that can arise during fabrication. Multilayer crossovers are crossovers where additional layers are introduced in the circuit to aid the wires to cross one another. In general, multilayer crossover is complicated due to the use of multiple layers. In addition to that, the spacing between the layers is also a major factor of concern. Hence, multilayer crossovers are very difficult to fabricate at smaller Nano meter levels. Fig. 7 (d) shows a multilayer crossover done between two clock 0 wires. Additional layers are added over the existing circuit layer and any one of the wire is made to jump the other wire using the additional layers added over the main circuit layer. Multilayer crossover is complex due to the additional layers added to the circuit. Multilayer crossovers are more vulnerable to fabrication faults compared to coplanar crossover.

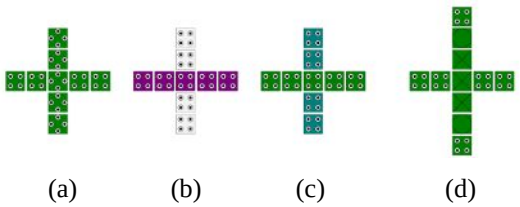

Fig.7. QCA Crossovers. (a) Rotated cell. (b) & (c) clock zone based. (d) Multilayer.

III. EXISTING SUBTRACTOR DESIGNS

In general, subtractor circuits are implemented by combining an adder with an exor gate which functions as a controllable inverter [7, 8]. It reduces the use of a separate hardware for adder and subtractor circuit. However, it is achieved at the cost of increased delay compared to separate implementation of adder and subtractor circuit. In QCA, several subtractor circuits are proposed in the literature. The subtractor circuit comprises of generation of two outputs, namely, Borrow and Difference. The conventional Boolean expression for borrow is given by (2).

$$Borrow = \overline{A}B + \overline{(A \oplus B)}.C \qquad (2)$$

Compared to Boolean logic implementation in CMOS technology, the implementation in QCA is complicated due to the implementation using majority logic. In QCA, only AND and OR gates can be implemented by using majority gates. Hence, implementation of exor operation will require more number of gates compared to CMOS implementation. Although there are dedicated structures proposed to implement exor gates in QCA [9], these structures are vulnerable to faults and it reduces the reliability of the circuit. Hence, to reduce the complexity of circuits, the Boolean expressions are optimized for majority logic based implementations using majority logic. The optimized borrow function using three input majority logic is given by (3). Compared to implementation of conventional Boolean expression using majority gates, (3) requires only one majority gate to implement the borrow function. The Boolean expression for difference given by (4).

$$Borrow = M(\overline{A}, B, C) \qquad (3)$$

$$Difference = A \oplus B \oplus C \qquad (4)$$

Similar to the optimization of Borrow expression, the Boolean expression for difference function is also optimized to reduce the complexity of implementation in QCA using majority logic. Most of the existing designs have used the Three Input ex-or (TIEO) structure proposed in [9], to implement the difference operation [10-12]. Since, the structure is built using the columbic repulsion and not on the conventional logic, the structure is more vulnerable to faults. Hence, it is preferable to implement the circuit using majority logic based expression.

Several subtractor structures are proposed using the optimized majority logic expressions. They have proposed optimized majority logic based expressions for implementation using three input majority gates. Among the proposed equations, the equation used in [13-15] has the least number of inverters and majority gates for its implementation. The optimized three input majority logic expression for difference generation is given by (5). The major advantage of the equation is its ability to generate as a part of its operation. It removes the use of a separate Borrow circuit.

$$Difference = M(M(\overline{A}, B, C), M(A, \overline{B}, C), \overline{C}) \quad (5)$$

Majority logic based expressions are also proposed using 5-input majority logic [16-18]. Among the optimized solutions proposed using 5-input majority logic, the majority logic expression in [17] requires minimum number of inverted inputs and also borrow is generated as a part of difference output generation. Hence, the circuit will be smaller and less complex. The expression used in [17] is given by (6).

$$Difference = M(A, \overline{B}, \overline{C}, Borr, Borr) \qquad (6)$$

IV. PROPOSED SUBTRACTOR

The existing subtractor designs are implemented mainly using rotated cell crossover and multilayer crossover. Hence, the existing designs are complex too implement and are vulnerable to fabrication defects. Hence, in this paper, two simple cost-efficient designs of subtractor are proposed using the three input majority gate and five input majority gate. To reduce the vulnerability to fabrication defects, clock zone based crossover is used for the implementation of the proposed designs. The proposed designs do not require rotated cells and cells with displacement. Hence, the proposed designs are better resistant to faults that can arise due to fabrication defects. The proposed designs are simulated and verified using the default simulation settings used in QCADesigner 2.0.3 as shown in Table I. The cost of QCA circuits is calculated by using (7).

$$Cost = Area * Clock\ phases * Cell\ type * No.of\ Layers \qquad (7)$$

The area used by the circuit depends upon the number of cells used in the design. The speed of the circuit depends upon the number of clock phases needed by the circuit used to generate the output. In other words, the number of clock zones the input has to travel to reach the output. Cell type represents the type of cell used for implementation. For circuits using only normal cells, the value will be 1, for circuits with rotated cells, the value of cell type will be 2, due to its complexity. The number of layers will be 1 for coplanar designs. For multilayer designs, it will be more than 1, depending upon the number of layers used for its implementation.

TABLE.I. SIMULATION SETTINGS

Parameter	Value
Cell dimension	18 nm x 18 nm
Dot diameter	5 nm
Distance between cells	2 nm
Distance between dots	4 nm
Radius of effect	80 nm
Relative permittivity	12.9
Clock High	9.8e-22
Clock Low	3.8e-23
Simulation engine	Coherence vector

A. Proposed Three input Majority Logic design

The first design is implemented using the three input majority logic expression in (5). In order to reduce the complexity of the circuit, the three input majority gate shown in Fig. 3(b) is used for the implementation of the proposed circuit. Fig. 8(a) shows the proposed design-I implemented using three input majority logic and its simulation results are shown in Fig. 8 (b). Table II compares the performance of the proposed design-I with the existing state-of-the-art designs implemented using three input majority logic.

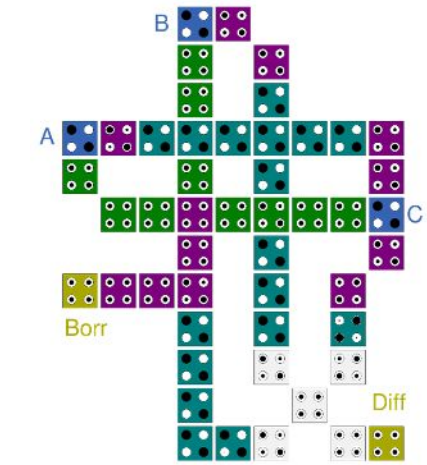

(a)

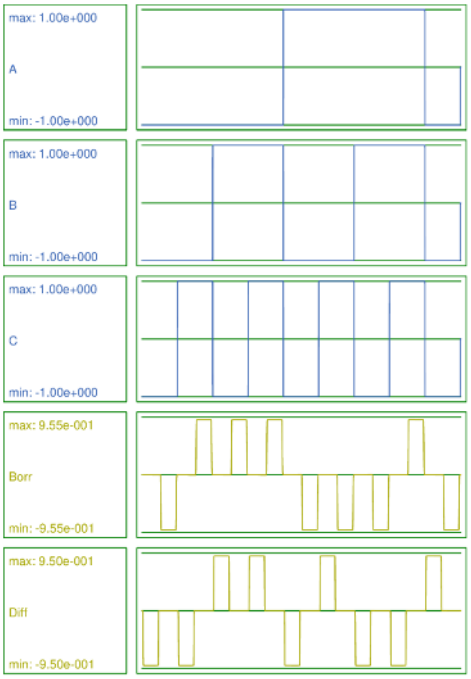

(b)

Fig.8. Proposed Subtractor-I. (a) Circuit. (b) Simulation results.

TABLE II
3-INPUT MAJORITY GATE BASED FULL SUBTRACTOR COMPARISON

Design	Cell count	Area in μm²	Borrow delay	Difference delay	Cost
[13]	233	0.13	2	8	3.12
[14]	272	0.44	5	9	7.92
[15]	90	0.11	4	4	0.88
Proposed-I	49	0.04	2	4	0.16

Table-II clearly shows that the proposed design-I is cost-efficient compared to the existing designs implemented using three input majority logic. The proposed design-I has the least cell count, area, delay, and cost among all the designs. The proposed design-I has the same delay even after implementation using clock zone based crossover.

B. Proposed Five Input Majority Logic design

The second proposed full subtractor is implemented using the five input majority logic expression given in (6). In order to reduce the complexity of the circuit, the five input majority gate shown in Fig. 4(b) is used for the implementation. Fig. 9(a) shows the proposed design-II implemented using five input majority logic and its simulation results are shown in Fig. 9(b). Table III compares the proposed deign-II with the existing designs implemented using five input majority logic expression.

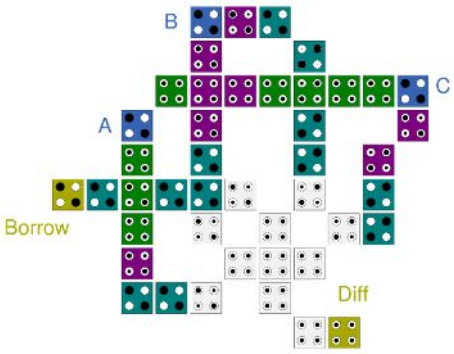

(a)

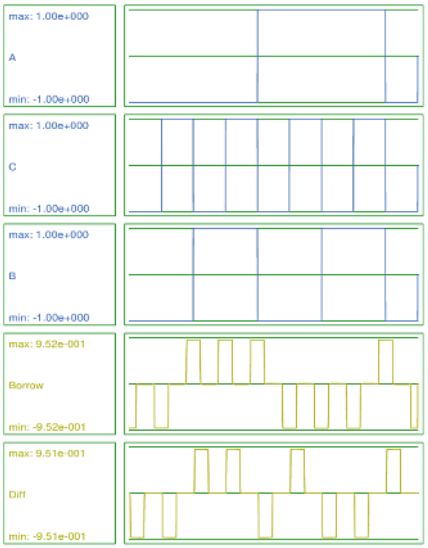

(b)

Fig.9. Proposed Subtractor-II. (a) Circuit. (b) Simulation results.

TABLE III
5-INPUT MAJORITY GATE BASED FULL SUBTRACTOR COMPARISON

Design	Cell count	Area in μm²	Borrow delay	Difference delay	Cost
[17]	63	0.05	3	3	0.30
[18]	53	0.05	3	3	0.30
Proposed-II	44	0.04	3	4	0.16

Table III clearly shows that the proposed deign has the least cell count, area, and cost compared to the existing designs. The delay of the difference circuit is 33% larger than the existing designs due to the clock zone based crossover. However, the

proposed design-II is cost-efficient compared to other designs by more than 45%. In addition to that, both the proposed designs are better resistant to faults that can arise due to fabrication defects. It can be extended to implement any n-bit subtractor designs.

V. CONCLUSION

Quantum-dot cellular automata has the potential to design circuits at extreme Nano meter levels. Subtractor circuits are used predominantly in arithmetic and signal processing blocks. In this paper, two cost-efficient full subtractor designs are proposed using three input and five input majority logic gates. The simulation results show that the proposed designs have fewer cells, area, and cost compared to the existing state-of-the-art-designs. The proposed designs can be implemented in any application that requires a subtractor and also it can be extended to implement any n-nit subtractor design. The proposed designs are simulated and validated in QCADesigner 2.0.3.

REFERENCES

[1] S. S. Binti, M. Sallah, H. Mohamed, M. Mamun, and M. S. Amin, “CMOS Downsizing: Present, Past and Future”, Journal of Applied Sciences Research, vol. 8, no. 8, pp. 4138-4146, 2012

[2] C. S. Lent, P. D. Tougaw, W. Porod, and G. H. Bernstein, “Quantum cellular automata”, Nanotechnology, vol. 4, pp. 49-57, 1993.

[3] K. Walus, T. J. Dysart, G. A. Jullien, and R. A. Budiman, "QCADesigner: a rapid design and Simulation tool for quantum-dot cellular automata," in IEEE Transactions on Nanotechnology, vol. 3, no. 1, pp. 26-31, March 2004.

[4] K. Navi, S. Sayedsalehi, R. Farazkish, and M. R. Azghadi, “Five-input majority gate, a new device for quantum-dot cellular automata”, Journal of Computational Theory and Nanoscience, vol. 7, pp. 1546–1553, 2010.

[5] T. N. Sasamal, A. K. Singh, and A. Mohan, “An efficient design of Quantum-dot Cellular Automata based 5-input majority gate with power analysis”, Microprocessors and Microsystems, vol. 59, pp. 103-117, 2018.

[6] G. L. Snider, A.O. Orlov, I. Amlani, G. H. Bernstein, C. S. Lent, J. L. Merz, and W. Porod, “Quantum-Dot Cellular Automata: Line and Majority Logic Gate”, Japanese Journal of Applied Physics, vol. 38, pp. 7227-7229, 1999.

[7] M. Sangsefidi, M. Karimpour, and M. Sarayloo, "Efficient Design of a Coplanar Adder/Subtractor in Quantum-Dot Cellular Automata," 2015 IEEE European Modelling Symposium (EMS), Madrid, 2015, pp. 456-461.

[8] M. Kianpour, R. Sabbaghi-Nadooshan, and K. Navi, “A novel design of 8-bit adder/subtractor by quantum-dot cellular automata”, Journal of Computer and System Sciences, vol. 80, no. 7, pp. 1404-1414, 2014.

[9] F. Ahmad, G. M. Bhat, H. Khademolhosseini, S. Azimi, S. Angizi, and K. Navi, “Towards single layer quantum-dot cellular automata adders based on explicit interaction of cells”, Journal of Computational Science, vol. 16, pp. 8-15, 2016.

[10] M. Abdullah-Al-Shafi and A. N. Bahar, “An Architecture of 2-Dimensional 4-Dot 2-Electron QCA Full Adder and Subtractor with Energy Dissipation Study,” Active and Passive Electronic Components, vol. 2018, Article ID 5062960, 10 pages, 2018.

[11] J. I. Resht, and M. T. Banday, "Efficient design of nano scale adder and subtractor circuits using quantum dot cellular automata," 3rd International Conference on Electrical, Electronics, Engineering Trends, Communication, Optimization and Sciences (EEECOS 2016), Tadepalligudem, 2016, pp. 1-6.

[12] A. P. Zahoor, Q. M. Khurshid, T. S. Maqbool, W. G. Mohammad, A. Firdous, and B. A. Newaz, “Design of novel QCA-based half/full subtractors”, Nanomaterials and Energy, vol. 6, no. 2, pp. 59-66, 2017

[13] S. Karthigai Lakshmi, G. Athisha, M. Karthikeyan and C. Ganesh, "Design of subtractor using nanotechnology based QCA," 2010 International Conference on Communication Control and Computing Technologies, Ramanathapuram, 2010, pp. 384-388.

[14] E. Ganesh, L. Kishore, and M. Rangachar, “Implementation of quantum cellular automata combinational and sequential circuits using majority logic reduction method,” International Journal of Nanotechnology and Applications, vol. 2, no. 1, pp. 89– 106, 2008.

[15] S. Kim, and E. E. Swartzlander, "Restoring divider design for quantum-dot cellular automata," 2011 11th IEEE International Conference on Nanotechnology, Portland, OR, 2011, pp. 1295-1300.

[16] V. Pudi, and K. Sridharan, "Efficient QCA design of single-bit and multi-bit subtractors," 2013 13th IEEE International Conference on Nanotechnology (IEEE-NANO 2013), Beijing, 2013, pp. 1155-1158.

[17] C. Labrado, and H. Thapliyal, "Design of adder and subtractor circuits in majority logic-based field-coupled QCA nanocomputing," Electronics Letters, vol. 52, no. 6, pp. 464-466, 2016.

[18] R. Jaiswal, and T. N. Sasamal, "Efficient design of full adder and subtractor using 5-input majority gate in QCA," 2017 Tenth International Conference on Contemporary Computing (IC3), Noida, 2017, pp. 1-6.

Proceedings of the Fourth International Conference on Communication and Electronics Systems (ICCES 2019)
IEEE Conference Record # 45898; IEEE Xplore ISBN: 978-1-7281-1261-9

FLOOD FORECASTING BY USING MACHINE LEARNING

Amitkumar Baburao Ranit
Assistant Professor: Department of Civil Engineering
Prof Ram Meghe College of Engineering & Management
Badnera, Amravati, India
amit.ranit@gmail.com

Dr. P. V. Durge
Professor: Department of Civil Engineering
G. H. Raisoni College of Engineering & Management
Pune, India
pvdurge@gmail.com

***Abstract*— Flood is large amount of water passing an overflow on a land. Flood forecast (FF) system issue a warning corresponding to water level or discharges through hydraulic structures. Flood forecast (FF) increase the capability and advancement in hydrology to mitigate the hazards using machine leanings with ANN. Flood forecasting using machine learning algorithm (MLA) method understand to learn and improve system scale to mitigate flood hazards according to the climate change. This research is carrying out for flood forecasting on Upper Wardha project across Wardha river basin. Flood forecasting (FF) using real time estimation gives chances of flood value and by using the forecasted inflow, rate of inflow in reservoir can decide the time of operation i.e. opening and closing of gate in real time with ANN.**

Keywords—Flood; ANN; Machine Learning; Real Time;

Introduction

Flood Forecasting can be defined as a process of estimation of time and duration based on topographical characteristics of any river basin which reduced the hazards to human life and environment also. Flood Forecasting technique challenge to predict occurrence and magnitude with time of flash flood. Flood happened due to continue precipitation with respective time. Ordinary rainfall also contributes to transform with time into deadly flood.

Flood forecasting techniques play a vital and important role to mitigate the hazards for non-structural structures with cost-effective management. Flood forecasting stations cover the network of flood prone area to give flood warning to administration. Forecasting inflow also used for the operation of hydraulic structures such as dam on which opening and closing of gates on spillways.

Flood forecasting techniques and Flood warning system are required different type of architectures of flood. Flood may be reduced by constructing structures such as dams, weirs, dykes but cannot eliminate the risk. Flood forecasting techniques able to mitigate the hazards for population and environment in real time with an early warning [1].

Flood forecasting has been approach through rainfall – runoff and flood routing model. Flood forecast predict inflow at selected location with HFL value at selected locations of river with time depends on watershed or catchment area. Later, downstream side predicts the flood limited with travel time with an assessment of uncertainties to properly support the decision-makers activities [9].

Flood forecasting using machine learning algorithm (MLA) method understand to learn and improve system scale to mitigate flood hazards according to the climate change with the help of AI. Flood forecasting used for creating the machine learning algorithm with past and real records of flood with real time data using rain gauges for different coming back time.

The dataset sources are rainfall-runoff, water levels using automatic rain gauges with satellites technology, infiltration rate etc.

The present study carried out on Wardha River basin .The Upper Wardha project is one of the major irrigation project in Vidharbha region of Maharashtra state. This project is across Wardha River near village Simbhora Taluka Morshi of Amravati district. The Upper Wardha project consists of earthen dam on a both flanks with a centrally located gated spillway and canal on left and right flanks. The Upper Wardha dam has total grass irrigation (GI) of 11690 (ha) with gross capacity of 786 MCM in Godavari River Basin with annual rainfall in the catchment is 840 mm.

Literature Review

Muskingham equation is used for flood forecasting using combination of single and multi inflow model form on Tar River basin [11]. Real time flood forecast is used for Godavari River basin with improved time 12 hr as compared to conventional method with model accuracy improved by computing flood plain inundations [12]. ANN model tool used to forecast flood [13]. Stream flow estimation using multiple linear regression to generate Rainfall – Runoff data [14]. Overview on different methods for Flood Forecast and Early Warning with advanced development in England, Scotland [15]. A comparison between statistical and ANN method for flood forecasting in river Mahanadi, ANN methods are better beyond the calibration and efficient [16].

Different types and classification of floods are as follows.

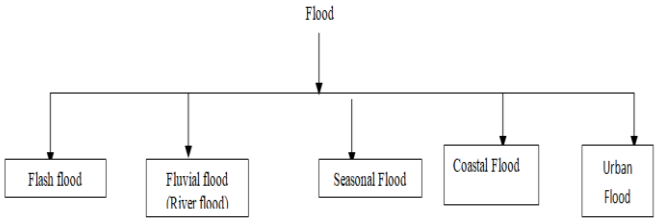

Fig.1:- Types and classification of flood

Methodology

A. Flood Forecasting Models:-

Flood forecasting models depends upon runoff-rainfall duration, intensity of rainfall-runoff, shape with characteristics of catchments and spatial extent. Time series analysis used in hydrology for stochastic model [17]. Flood forecasting is challenge for hydrological models. Different types of Hydrological modeling structure are as follows:

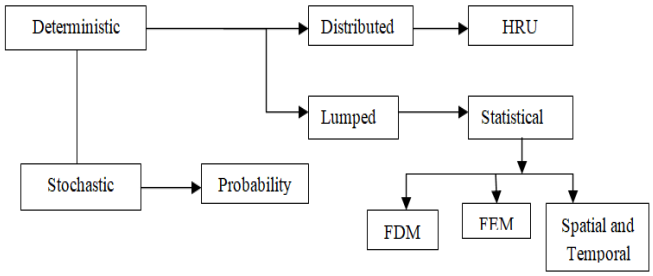

Fig. 2: Hydrological modeling Structures

B. ANN and Machine Learning Approach For Flood Forecasting:-

Neural Networks, which are simplified models of Biological Neuron System. ANN is used to process large data with simple elements [18]. ANN is classified into single layer, multilayer feed forward network and Back Propagation Network.

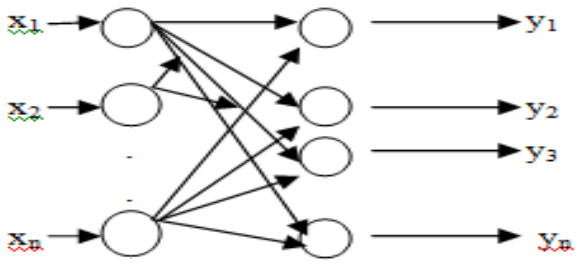

Fig.3. Neural Network Model

C. Machine Learning Method

Real time model is based on actual available and real rainfall and runoff data with time. The following flow chart will give you a concept of real time flood forecasting. Flood forecasting is the process off calculating water levels in reservoir, the storage quantities and outflow rates at particulars inflow hydrograph at various instant. Flood occurrence mainly depends upon various parameters like a rainfall intensity, runoff, evaporation, evapotranspiration, temperature and shape of catchment etc. By interpreting the data for flood routing the technique used i.e. Muskingum Equation which gives the value of inflow and outflow rate. The data obtained from reservoir routing is given to the machine learning, to learn and forecast by the real time data. The Muskingum method of stream flow routing is most frequently used because of its simplicity, as it works with known inflow hydrograph and some fitted parameters without seeking additional information. However, in order to get high degree of accuracy, this method should be for gradually varied flow and not in cases where reach is often affected by back water or unsteady flow condition.

The governing relation between inflow, outflow and change in storage is

Storage=inflow-outflow

$$\vec{I} - \overrightarrow{O} = \Delta S$$

Where,

· = Average outflow during given time period

· = Average outflow during given time period

Δ S= Volume of water stored in the reservoir.

$$\int_{S_j}^{S_{j+1}} S = \int_{j\Delta t}^{(j+1)} I(t)dt - \int_{j\Delta t}^{(j+1)\Delta t} Q\,(t)dt$$

The process of flowing in values at the starting time and end of the jth time interval are I_j and I_{j+1} respectively and corresponding the value of outflow are Q_j and Q_{j+1}.

Machine learning able to learn and improve system in an explicit manner. Machine learning provides computer programs that can approach or obtain or retrieve access data with learning it.

Machine learning able with to calculate large data set. Artificial Intelligent system (AIS) used to train data in such way to improve flood forecasting system with occurring at an early stage development warning system

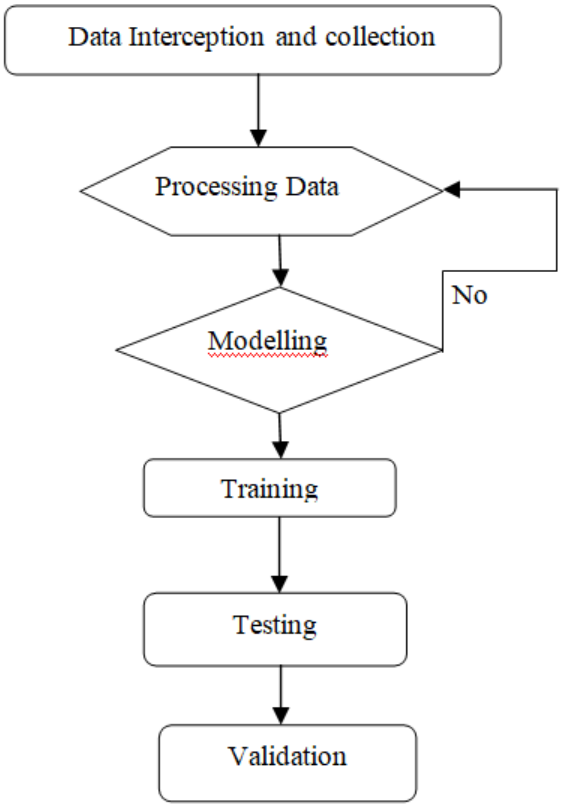

Fig. 4: Flow Chart for Modelling

Results and Conclusion

The Following results are obtained using ANN with machine learning and stochastic Method.

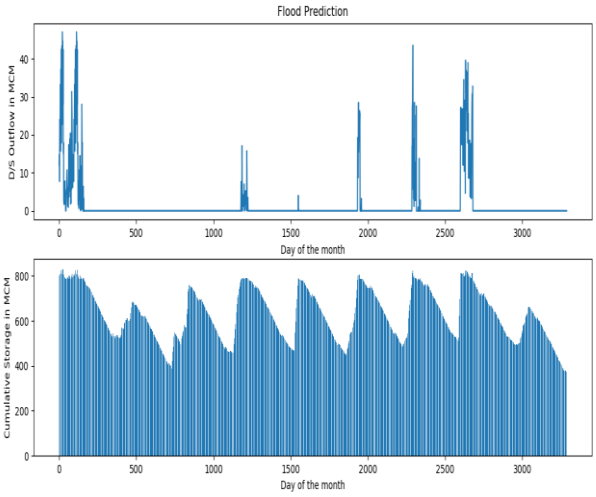

Fig.5: Cumulative Storage and days

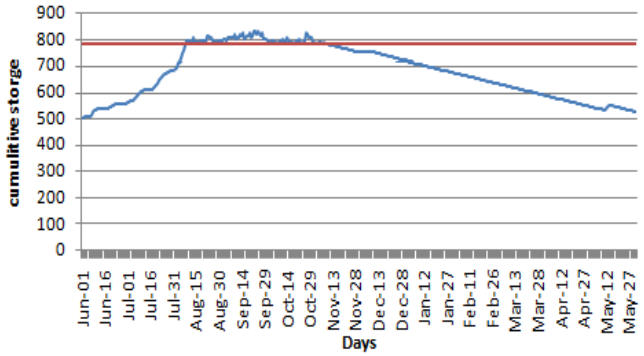

Fig.5: Cumulative Storage and days

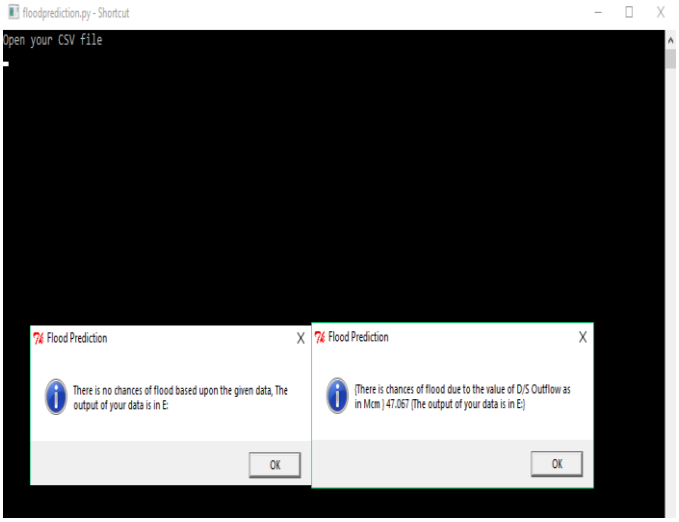

Fig.7:- Flood Forecasted value of outflow for opening of gates

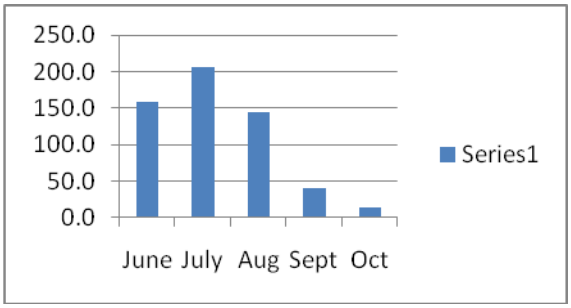

Fig.8:- Hyetograph

Flood forecasting technique organized method suitably based on available data and an appraisal of rating criteria with an inspired performance. Flood forecasting using real time estimation gives chances of flood value in GUI. Flood estimation using Machine Learning in real time can calculate large data instantly. Comparison between flood modelling by machine learning and stochastic method (i.e. Muskinghum method) gives machine learning is accurate, easy and can be applied for numbers of calculation. By using

the forecasted inflow, rate of inflow in reservoir can decide the time of operation i.e. opening and closing of gate.

References:-

[1] Pappenberger, F.; Cloke, H.L.; Parker, D.J.; Wetterhall, F.; Richardson, D.S.; Thielen, J. The monetary benefit of early flood warnings in Europe. Environ. Sci. Policy 2015, 51, 278–291.

[2] Krzysztofowicz, R. Bayesian system for probabilistic river stage forecasting. J. Hydrol. 2002, 268, 16–40.

[3] Todini, E. Role and treatment of uncertainty in real-time flood forecasting. Hydrol. Process. 2004, 18, 2743–2746.

[4] Clark, M.P.; Slater, A.G. Probabilistic quantitative precipitation estimation in complex terrain. J. Hydrometeorol. 2006, 7, 3–22.

[5] Vrugt, J.A.; Robinson, B.A. Treatment of uncertainty using ensemble methods: Comparison of sequential data assimilation and Bayesian model averaging. Water Resources. 2007, 43.

[6] Ebtehaj, M.; Moradkhani, H.; Gupta, H.V. Improving robustness of hydrologic parameter estimation by the use of moving block bootstrap re-sampling. Water Resour. Res. 2010, 46.

[7] He, X.; Refsgaard, J.C.; Sonnenborg, T.O.; Vejen, F.; Jensen, K.H. Statistical analysis of the impact of radar rainfall uncertainties on water resources modeling. Water Resources. 2011, 47.

[8] Legleiter, C.J.; Kyriakidis, P.C.; McDonald, R.R.; Nelson, J.M. Effects of uncertain topographic input data on two dimensional flow modelling in a gravel-bed river. Water Resour. Res. 2011, 47.

[9] Sikorska, A.E.; Scheidegger, A.; Banasik, K.; Rieckermann, J. Bayesian uncertainty assessment of flood predictions in ungauged urban basins for conceptual rainfall-runoff models. Hydrol. Earth Syst. Sci. 2012, 16, 1221–1236.

[10] Montanari, A.; Koutsoyiannis, D. A blueprint for process-based modeling of uncertain hydrological systems. Water Resour. Res. 2012, 48.

[11] Prof.ParthasarathiChoudhary and A. Sankarasubramanian(2009), “River Flood Forecasting Using Complementary Muskingumrating Equations”,Journal of Hydrologic Engineering, Vol. 14, No. 7, July 1, 2009.

[12] KoradaHariVenkataDurga Rao, ValaVenkateshwar Rao, Vinay Kumar Dadhwal, GandarbhaBehera, and Jaswant Raj Sharma, “A Distributed Model for Real-Time Flood Forecasting In The Godavari Basin Using Space Inputs”, International Journal Disaster Risk Sci. 2011, 2 (3): 31–40.

[13] Sulafa Hag Elsafi(2014) “Artificial Neural Networks (Anns) For Flood Forecasting At Dongola Station In The River Nile, Sudan”, Alexandria Engineering Journal (2014) 53, 655–662.

[14] Sharad Patel and Mahesh kumarHardaha(2016),“Multiple Linear Regression Model For Stream Flow Estimation Of Wainganga River”, American Journal of Water Science and Engineering 2016; 2(1): 1-5.

[15] Micha Werner, Michael Cranston,TimHarrison,Doug Whitfield5 and JaapSchellekens, “Recent Developments In Operational Flood Forecasting in England, Wales And Scotland”, 27 February 2009 in Wiley Inter Science.

[16] Wansik Yu, Eiichi Nakakita, Kwansue Jung, “ Flood Forecast And Early Warning With High-Resolution Ensemblerainfall From Numerical Weather Prediction Model”,12th International Conference on Hydroinformatics, HIC 2016.

[17] Hoboken, NJ: John Wiley & Sons “Time series analysis: forecasting and control”, Box, G.E.P, 2016.

[18] Tsoukalas Lefteri, H. and A. Uhrig Robert: John Wiley and Sons; “Fuzzy and Neural Approach in Engineering”, Inc. 1997Krzysztofowicz, R. Bayesian system for probabilistic river stage forecasting. J. Hydrol. 2002, 268, 16–40.

Proceedings of the Fourth International Conference on Communication and Electronics Systems (ICCES 2019)
IEEE Conference Record # 45898; IEEE Xplore ISBN: 978-1-7281-1261-9

Performance analysis of Transformer – Less UPFC

Shaikh Mohammed Tauseef
PG Scholar, Department of Electrical Engineering,
PES College of Engineering, Aurangabad,
Maharashtra, India.
sk.md.tauseef@gmail.com

S. M. Kulkarni
Associate Professor, Department of Electrical Engineering,
PES College of Engineering, Aurangabad,
Maharashtra, India.
smkul_1967@rediffmail.com

Abstract — The paper presents the simulation of an pioneering and unique method of FACTS controller called Unified Power Flow Controller (UPFC) without transformer. Transformer-less Unified Power Flow Controller consist of two cascaded multi-level inverter, which lessen the complication and bulkiness of the circuit. Basically traditional UPFC controller consists of two inverters connected back to back. Conventional methods of UPFC involve complex and bulk circuit resulting in the problem for isolation of the transformers & achieve high power rating with desired output. The proposed Transformer less UPFC controller will be cost effective and acquire low space then the conventional UPFC. A multilevel cascade configuration system will reduce the harmonics of the system hence increases the efficiency of the model and reduce bulkiness.

Keywords — Cascaded Multilevel Inverter (CMI), FACTS, SSSC, STATCOM, UPFC.

I. INTRODUCTION

Power grid is a complicated meshed network which is overcrowded and is subjected to serve congestions. Thus several issues like voltage sag, imbalance of real and reactive power and demand of load supply are introduced. To tackle these issues there is need of introducing control devices which control power flow as per the need. Power electronics based FACTS controller are used for the said issues [1]. UPFC is a mostly used FACTS controller which control selectively or concurrently the parameters of power systems that are line and phase voltages, current, system impedance and etc, which influence power flow of the network. UPFC is a FACTS device which combines the function of SSSC and STATCOM via DC link. The Fig. 1 shows a traditional UPFC. Unified Power Flow Controller is a much flexible & multipurpose controller that can be used for following:

a) Phase Shifting
b) Voltage Regulation
c) Line Impedance Compensation
d) Oscillation Damping
e) Simultaneously control of system parameters.

Thus it provides a flexible controllability to completely control the Real and Reactive power flow over the transmission line. Due to the advantage of FACTS devices and independent control of real and reactive power, many researches is going on in the control, analysis and modeling of it [2].

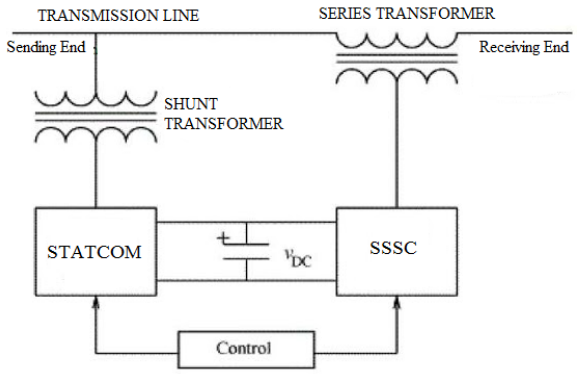

Fig.1. Transformer Unified Power Flow Controller (UPFC).

Though UPFC provides several advantages and controllability in the power system on the transmission line, but it suffers from several disadvantages like bulky size of controller since UPFC requires bulky zig-zag transformers which interface the controller with the high voltage transmission lines. Also these bulky transformers slow down the response of the controller to dynamic load changes. Along with the bulky zig-zag transformer, it also requires 48-pulse high voltage high power inverters to obtain desired high quality waveforms which makes it further complicated. Thus the conventional UPFC has many disadvantages like a) Bulky size, b) expensive and uneconomical (30% – 40% of the cost of the system), c) High Losses and d) Prone to failure [3]. The various disadvantages occurring in the conventional UPFC can be overcome by eliminating the transformer from controller. The innovative transformer-less UPFC provides better performance over existing UPFC due to its advantages such as light in weight, fast dynamic response, better efficiency, cost effective, high reliability and a highly modular structure of two CMIs.

II. SYSTEM MODELLING

The cascade multilevel inverter (CMI) can achieve the high-voltage level independent of using transformers, other semiconductor diodes, or number of coupling condensers. Thus to remove the transformer completely, a new transformer – less Unified Power Flow Controller which is based on an novel design of series and shunt cascaded multilevel inverters has been projected which is represented as shown in Fig. 2.

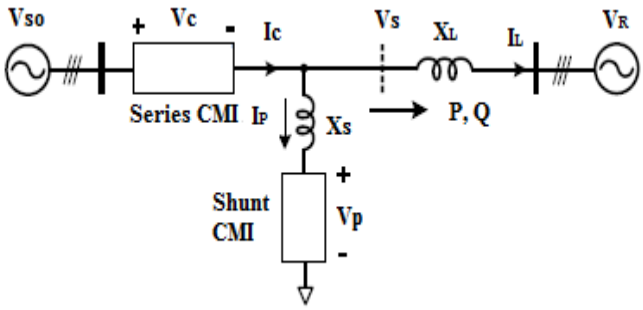

XXX-X-XXXX-XXXX-X/XX/$XX.00 ©2019 IEEE

Fig. 2. Transformerless UPFC using CMI.

The discussed transformer-less UPFC system has two CMIs which are connected in series and shunt. The Series Inverter is in series with transmission line and Shunt Inverter is connected parallel to transmission line just following the series CMI Inverter. Here are some features of the new configuration:

a) In this model there is no need of transformer distinct to the existing UPFC which uses coupling back-to-back dc links, hence, the proposed UPFC can accomplish advantages like economical, light in weight and compact, higher efficiency and reliability, & fast dynamic response to fault;
b) Shunt CMI inverter is connected following series CMI inverter. Also the series and shunt CMI have DC capacitor which supports the necessary dc voltage.
c) The series and shunt CMIs do not share real and reactive power among them and floating dc capacitors have been used;

The proposed UPFC has a modular series and shunt CMI which provides higher flexibility in the system model and high reliability of operation [4].

III. Principle of Operation

Phasor-diagram of the proposed UPFC is represented in the fig. 3. The V_{SO} is sending end voltage and V_R is receiving end voltage. As V_{SO} is along the rael axis thus it makes a phase angle zero. The series CMI can generate a controlled desired voltage to obtain a new sending end voltage V_S, that can control the P and Q of the transmission line. The active power of the system can be made zero by injecting a current through shunt CMI parallel to the voltage of CMIs at the sending end bus. The possibility of both series and shunt CMI using floating capacitors to control reactive power makes the transformer less UPFC a suitable device for the purpose.

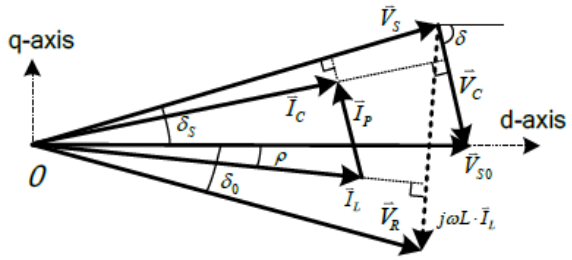

Fig. 3. Phasor diagram of the transformer-less UPFC

The principle of proposed UPFC is structured in detail as shown from Fig. 2 and Fig. 3. The Real Power and Reactive Power flowing on the transmission line can be given as

$$P + jQ = V_R \left(\frac{V_{so} - V_C - V_R}{jX_L}\right)^*$$
$$= \left(-\frac{V_{SO}V_R}{X_L} sin\delta_O + \frac{V_C V_R}{X_L} \sin(\delta_O - \delta)\right) +$$
$$j\left(\frac{V_{SO}V_R cos\delta_O - {V_R}^2}{X_L} - \frac{V_C V_R}{X_L} \cos(\delta_O - \delta)\right)$$

Where asterik (*) indicates complex conjugate of number.

δ_0 = Phase angle of receiving end voltage V_R
δ = Phase angle of series CMIs injected voltage V_C
X_L= Transmission line equivalent impedance.

The uncompensated real and reactive power is given as,

$$P_o = -\frac{V_{SO}V_R}{X_L} sin\delta_O$$
$$Q_O = \frac{V_{SO}V_R cos\delta_O - {V_R}^2}{X_L}$$

The controlled real power (P_C) and reactive power (Q_C) of the Transformer-less UPFC is given by,

$$P_C = \frac{V_C V_R}{X_L} \sin(\delta_O - \delta)$$
$$Q_C = -\frac{V_C V_R}{X_L} \cos(\delta_O - \delta)$$
$$P + jQ = (P_o + P_C) + j(Q_o - Q_C)$$

Since the amplitude and phase angle both of injected voltage V_C of UPFC can be adjusted thus it provide a controlled range of ($-V_C V_R/X_L$) to ($+V_C V_R/X_L$) for real power (P_C) as well as reactive Power (Q_C).

The injected voltage V_C from series CMI is given as,

$$V_C \angle\delta = \frac{X_L}{V_R}\sqrt{{P_C}^2 + {Q_C}^2}\angle\left(\delta_O - \arctan(\frac{P_C}{Q_C})\right)$$
$$V_S = V_S \angle\delta_S = V_{SO} - V_C$$

Where,

$$V_S = \sqrt{(V_{SO} - V_C cos\delta)^2 + (V_C sin\delta)^2}$$
$$\delta_S = \arctan\left(\frac{-V_C sin\delta}{V_{SO} - V_C cos\delta}\right)$$

where

$$I_L = \frac{\sqrt{(V_C sin\delta + V_R sin\delta_0)^2 + (V_{SO} - V_C cos\delta - V_R cos\delta_0)^2}}{X_L}$$
$$\rho = arctan\left(\frac{V_{SO} - V_C cos\delta - V_R cos\delta_0}{V_C sin\delta + V_R sin\delta_0}\right)$$

The new sending end voltage V_S and transmission line current can be controlled as the injected voltage V_C of series CMI is determined. The injected current I_P from the Shunt CMI decouple the Current I_C of series CMI from the line current I_L. Therefore, no real power is exchange between series CMI and shunt CMI which makes possibility to use CMIs with floating capacitors as proposed in the transformer-less UPFC.
Therefore, we have

$$P_{se} = V_c I_c = 0$$
$$P_{sh} = V_s I_p = 0$$

It means series CMI current I_C and Shunt CMI current I_P is to be perpendicular to their voltages V_C and V_S respectively.

$$I_p = I_p \angle \theta_{I_P}$$

Where

$$I_p = I_L \left(\frac{\cos(\rho - \delta_S)}{\tan(\delta - \delta_S)} - sin(\rho - \delta_S) \right)$$

$$\theta_{I_P} = 90 + \delta_S$$

IV. Simulation Model and Results

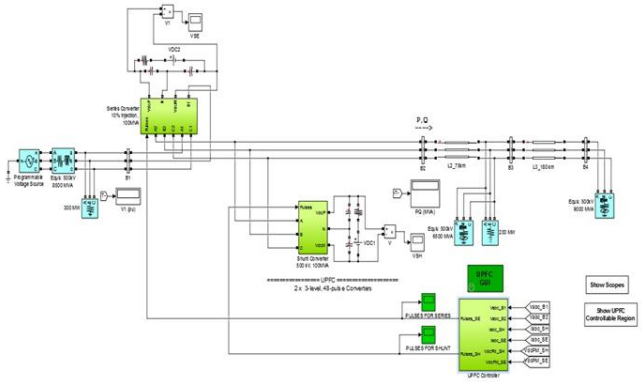

Fig. 4.1 Simulation Model of Transformer-less UPFC

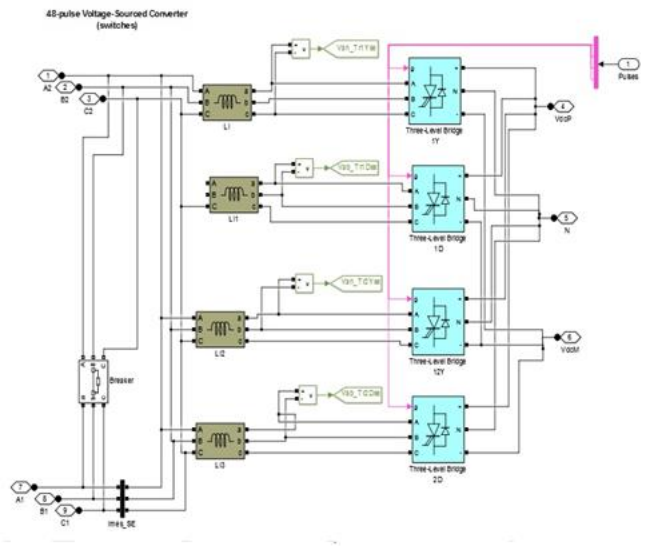

Fig. 4.2 Series Converter

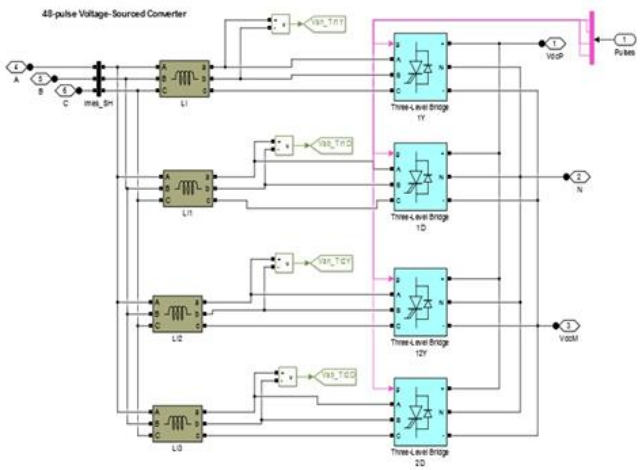

Fig. 4.3 Shunt Converter

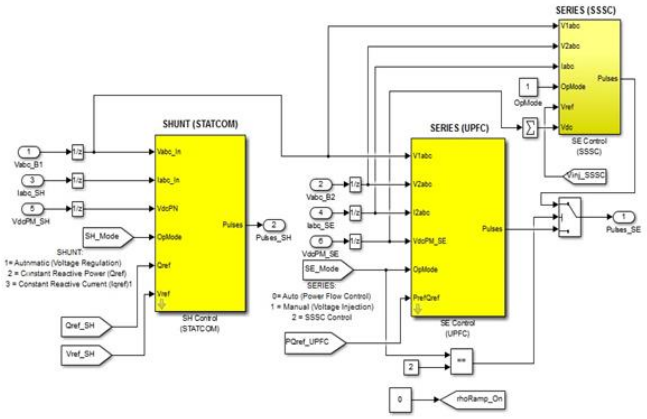

Fig.4.4 UPFC Model

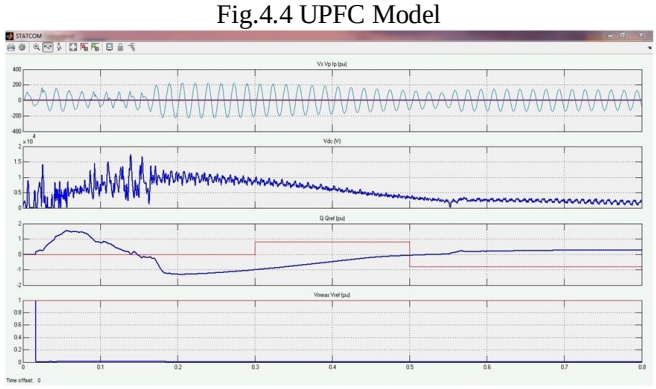

Fig. 4.2 Output waveform of STATCOM

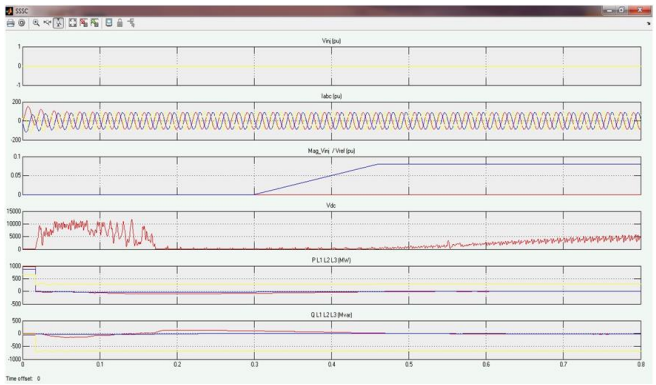

Fig. 4.3 Output Waveform of SSSC

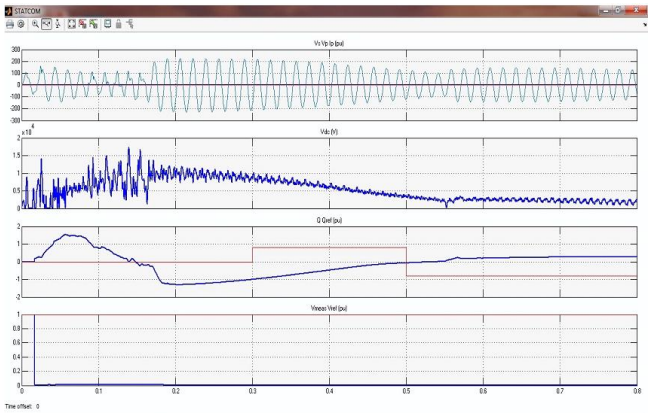

Fig. 4.4 Output Waveform of UPFC

V. Conclusion

The proposed transformer-less UPFC uses a new configuration based on two CMIs. The Proposed UPFC can attain the same controllability as the existing UPFC. The proposed UPFC have two CMIs which offers numerous advantages over the existing UPFC, such as elimination of transformer compact structure & weight, great efficiency, high operation dependability, economical, and fast dynamic response against the fault.

Acknowledgment

I would like to thank Almighty Allah for his blessings and mercy. I would also like to thank my Guide Mr. S. M. Kulkarni for his support throughout and I also thank to all the staff of electrical department for encouraging me.

References

[1] N. Hingrani and L. Guyugyi, “Understandiing FACTS: Concepts and Technology of Flexible AC Transmission Systems”, Wiley, 2000.

[2] R. Nagananthini, K.Ramadas, “Cascaded Multilevel Inverter based Unified Power Flow Controller”, International Journal of Advance Engineering and Research Development, 2017.

[3] K. Sano and M. Takasaki, "A Transformer-less D-STATCOM Based on a Multi voltage Cascade Converter Requiring No DC Sources," Power Electronics, IEEE Transactions on, vol. 27, pp. 2783-2795, 2012.

[4] S. T. Yang, et al “Modulation and control of transformer-less UPFC,” IEEE Trans. Power electron., vol. 31, no. 2, pp. 1050–1063, Feb. 2016.

[5] W. C. Song and A. Q. Huang, “Fault-tolerant design and control strategy for cascaded H-bridge multilevel converter-based STATCOM,” IEEE Trans. Ind. Electron., vol. 57, no. 8, pp. 2700–2708,Aug. 2010.

[6] W. Jin and F. Z. Peng, “Unified power flow controller using the cascade multilevel inverter,” IEEE Trans. Power Electron., vol. 19, no. 4,pp. 1077–1084, Jul. 2004.

[7] B. Gultekin and M. Ermis, “Cascaded multilevel converter-based transmission STATCOM: System design methodology and development of a12 kV 12 MVAr power stage,” IEEE Trans. Power Electron., vol. 28, No. 11, pp. 4930–4950, Nov. 2013.

[8] R.Vishwa Priya and Dr.S.K.Nandha Kumar, “Transformer-less UPFC Using Multilevel Inverter”, International Journal Of Engineering And Computer Science, 2017.

[9] H. Akagi, S. Inoue, and T. Yoshii, “Control and performance of a transformer-less cascaded PWM STATCOM with star configuration”, IEEE Trans. Ind. Appl., 2007.

[10] A. Shukla, A. Ghosh, and A. Joshi, “Hysteresis current control operation of flying capacitor multilevel inverter and its application in shunt compensation of distribution systems”, IEEE Trans. Power Delivery, 2007.

[11] P. Shahanaz Salman, Nandyal, “Implementation of SSSC-Based Cascade H-Bridge Model using Compensation Technique”, International Journal of Advanced Research in Electrical and Electronics and Instrumentation Engineering, 2015.

[12] A. Rajabi - Ghahnavieh, M. Fotuhi - Firuzabad, M. Shahidehpour, and R. Feuillet, "UPFC for enhancing power system reliability," IEEE Trans. Power Del., vol. 25, no. 4, pp. 2881–2890, 2010.

Proceedings of the Fourth International Conference on Communication and Electronics Systems (ICCES 2019)
IEEE Conference Record # 45898; IEEE Xplore ISBN: 978-1-7281-1261-9

The Decomposition methods in Synthetic Aperture Radar Polarimetry

Plasin Francis Dias
Electronics and Communication Engineering
KLS VDIT
HALIYAL,INDIA
plasindias@gmail.com

R. M. Banakar
Electronics and Communication Engineering
BVBCET
HUBLI, INDIA
banakar@bvb.edu

***Abstract*—Synthetic aperture radar is imaging radar to cover the wide range of earth surface with high resolution images. It captures images day and night in all type of weather conditions. The polarization data contains information, on scattering mechanism related to different objects. The objects are land, ocean, ice, snow and forest which are natural distributed targets. Using scattering mechanism different objects are categorized. Scattering mechanism is measured by scattering elements of the matrix. The full polarization of synthetic aperture radar data classifies the obtained image. This paper analyses the two different techniques of decomposition methods related to polarimetry. These are linear decomposition and Pauli decomposition methods. These two methods are helpful for system level design and scattering process considerations.**

Keywords—Synthetic Aperture Radar, Polarimetry, resolution, Decomposition, linear, Pauli

I. INTRODUCTION

To detect targets efficiently advanced airborne and space borne Synthetic Aperture Radars (SAR) are designed. In this radar the two platforms that is sensor and target region both are in relative motion. The SAR processing unit is mounted on a moving system basically aircraft or space craft. The target is covered by single beam by the radar antenna. The target area is continuously illuminated with pulses of radio waves, at wave lengths meters to mm. The obtained synthetic radar image can be classified by the full polarization information of the synthetic aperture radar data. The accessing of full polarization is the basic technique behind the SAR polarimetry. It is a method to obtain the target details which is basically based on amplitude and phase related information. The term full polarization refers to the four main channels used in quad (full) polarimetry. They are polarized in horizontal -horizontal (HH), horizontal -vertical (HV), vertical horizontal (VH) and vertical – vertical (VV) directions.

The scattering mechanism gives the physical details of the target. The physical details of the target are referenced to its dielectric constant and orientation. It is obtained through different scattering mechanisms. The radar SAR sensor transmits continuously the electromagnetic wave towards the target. In response to incident wave the various echo waveforms are received by the receiving antenna. At several different antenna positions, the target is detected with coherency. The received signals which are called as echo signals of polarimetric SAR is mathematically given by equation (1).

$$\begin{bmatrix} E^{r}_{H} \\ E^{r}_{V} \end{bmatrix} = [S] \begin{bmatrix} E^{t}_{H} \\ E^{t}_{V} \end{bmatrix} = \begin{bmatrix} S_{HH} & S_{HV} \\ S_{VH} & S_{VV} \end{bmatrix} \begin{bmatrix} E^{t}H \\ E^{t}V \end{bmatrix} \quad \ldots\ldots(1)$$

Here S is called as scattering matrix representing the four basic elements S_{HH}, S_{HV}, S_{VH}, S_{VV}[1]. The two angles namely ellipticity and orientation angle are the salient features. These parameters illustrate the mechanisms of polarization. The two angles related to field vector are represented in Fig. 1.

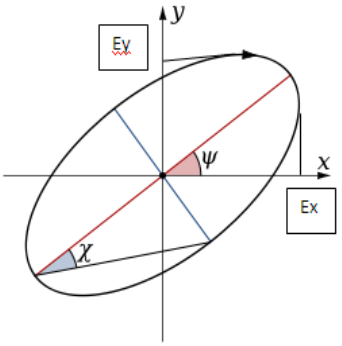

Fig. 1. Relation between ellipticity and orientation

Here ψ^{o} represents the orientation and χ^{o} represents ellipticity for the E vector of an electromagnetic wave. The properties of individual objects of the earth surface are characterized by their scattering nature. This is represented mathematically as the scattering matrix for each pixel of the target image. The received signal obtained by SAR sensor adds for criteria called resolution cell. It is basically the resultant criteria of many distributed targets. These targets are distributed in spatial manner. Every individual or target is represented by each different scattering type of mechanisms. The various scattering mechanisms involved are surface scattering also known as single bounce scattering. The other mechanisms are typically known as double bounce, volume and helix scattering. These are obtained by the natural targets and manmade targets. The physical property surface roughness and its materialistic property namely dielectric constant decide which type of scattering mechanisms occurs. The feature called coherent is basic element criteria of the scattering matrix. It means that the terms in off diagonal element of scattering matrix that is S_{HV} and S_{VH} are equal. Scattering matrix normally gives detail

idea of the working pattern of radar system, in hitting the particular target on the earth surface. It also describes the behavior of the targets on the earth surface for the feature called scatter. This represents the electromagnetic energy returned back towards the radar sensor.

The usual dimension of the S matrix is considered as 2*2. It is considered for every pixel of an image. This concept is illustrated by the authors Fawag Ulaby and Ehsrlon Elactic in contribution toward their paper radar polarimetry for geo science applications [2]. Resolution describes the minimal observable spacing between two same point responses. This is again applied to width of one more response other than previous two. A weaker response among them basically requires larger separation for the detection of the target. Each resolution cell is represented by two pixels. Pixel spacing in SAR imagery is considered for some standard scale. It is normally taken as multiple or division of 100 mts. For ex. ERS -1 data has resolution of 28 mts. In range and azimuth it is delivered with 12.5 mt pixel spacing. In SAR image, the direction of aircraft or space craft is called azimuth direction. The imaging direction is called range direction. SAR processing involves range focusing and azimuth focusing. Range focusing involves de-chirping of received echoes. Azimuth focusing relies on Doppler information produced by target. The difference in dimension of pixel of signal related to SAR image exists to the resolution cell during the data acquisition. It is due to variation of range resolution angle. So pixel resampling is carried out with uniform grid [23], [24].

The various angle related to the target and sensor are categorized as shown in Fig. 2.

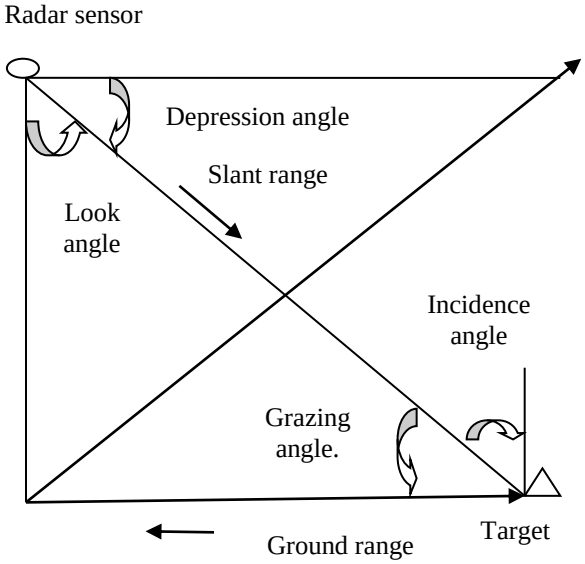

Fig. 2. Synthetic Aperture Radar angles

The slant range is the length representing the line connecting radar sensor and object being observed. The ground range is the range along the ground and target. It is measured from radar nadir track. There exists a line below the sensor base platform is termed as nadir track. The radar beam which hits the target creates a look angle with the orientation normal to ground range. The target also creates an angle with the beam with its normal which is called as incidence angle.

Case 1:

If the surface is smooth

Look angle =incidence angle

Case 2:

If the surface is having curvature

look angle < incidence angle

The depression angle is measured between radar beam by the sensor and horizontal direction of the radar platform. The look is related to depression angle with the difference of 90° minus by each other. The depression angle increases if the look angle decreases. The grazing angle is measured between horizontal surface and incident wave by the sensor [8], [12], [17].

SAR polarimetry provides data about polarization state of received signals for every resolution element or pixel. The behavior of the target is a mathematical representation which is modeled in terms of scattering matrix. This basically gives information of electromagnetic wave by the objects. Current airborne systems have an azimuth resolution of 1m to 0.5m. The resolution of image gives the separation between closest surfaces, which is basically resolved in the final image. The authors in [14], [16] explain with illustrative figures the concept of SAR resolution.

. The recent advances in SAR polarimetry features the fundamentals of processing SAR data using mathematical model in an organized way [13], [7]. Polarimetry is the study of measuring and investigating the polarization pattern of transverse electromagnetic waves. These EM waves are also known as radio or light waves. Polarimetry is carried out on such electromagnetic waves, which are already are reflected or refracted or diffracted waves. These reflection or refraction or diffraction will occur through some material. This change in features will characterize the particular object. Depending on data acquisition method various processing techniques are followed [5], [6]. The processing of SAR data is limited to processing of intensity from target image acquired. The Interferometric processing involves intensity and interferometric phase processing. In interferometry phase and intensity are the main parameters. The target image is processed using various techniques. In interferometry only one image is acquired featuring phase and intensity. In polarimetry the data acquisition is done using different polarization techniques.

Polarimetric processing involves intensity and polarimetric phase processing. In [8], [9], [15] the authors illustrate the fundamental aspects of polarization. The EM wave orientation is discussed in detail. Polarization is method of alignment of electric and magnetic field. These fields are the elementary components of Electromagnetic waves. Although these two fields illustrate the characterization of EM waves, its behavior can be solely done by using the electric field. This is possible because the electric and magnetic field has distinct mathematical relationship. Hence the entire EM wave can be investigated only by knowing the electric field vector. The electric field is represented as a vector. This vector has a length which distinctly represents the amplitude of the electromagnetic wave. The vector rotation rate gives the frequency of the wave. The vector movement can be in different directions namely linear, elliptical and circular. Polarimetric interferometric processing involves intensity, interferometric and polarimetric phase processing which is a new technique.

The radar frequency or wavelength, polarization and incidence angles do affect the scattering mechanisms. If surface is found smooth there is no existence of depolarization. It implies HV or VH back scatter is not present. If the surface is rough there will be some depolarization. Hence HV or VH backscatter exists. For volume scattering such as forest and vegetation high depolarization is found. Thus one can categorize various objects based on the scattering mechanisms. There is peculiar relation exist between scattering mechanisms, scattering matrix and various decomposition techniques involved in the SAR polarimetry [10], [11]. The section II and III highlights the mechanisms related to decomposition techniques.

II. SYNTETIC APERTURE RADAR MATRICES

SAR image is identified with various matrices known as Stokes or Muller matrix or Scattering matrix parameters. The reflected wave from the target has different polarization in relation to incident wave of the radar sensor. The scattering matrix consists of 4 basic elements S_{hh}, S_{hv}, S_{vh} and S_{vv} which are complex numbers. The response of the target is function of incident electromagnetic wave as well as back scattered polarizations. The particular visualization is obtained by polarization signature of the target. The scattering power can be determined by 4 polarization variables HH, HV, VH and VV, the incident angle, elipticity angle, orientation and reflected angles. This variable possibly creates inconvenience in visualization. So backscattered polarizations are considered for two different techniques. The first one has similar polarization that is if the transmitted wave is H then received wave is also H. This is defined as co polarization. The second one has dissimilar polarization that is if transmitted wave is V then received wave is H. This is termed as cross polarization. It is considered for individual incident polarization. This is plotted in two surfaces called co polarization and cross polarization. These plots give proper visualization of proportion related to backscattered wave. The method usually called Back Scattering Alignment (BSA) is used to analyze polarization. When electromagnetic wave energy interacts with objects various scattering mechanism occurs with objects. Polarimetric information of given pixel is combination of scattering mechanisms. To interpret this scattering mechanism and objects properties polarimetric decomposition models are developed [18], [19], [20]. The section III describes the importance of Stokes matrix, along with Muller matrix.

III. SCATTERING AND STOKES MATRIX

A. Sattering matrix

The mechanism involved for the backscattering by the target depends on the wave polarization of incident wave. It may so happen that if the incident wave is horizontal the reflected wave may have either horizontal or vertical polarization. The vertical characterization of beam wave may be reflected by the target in vertical or horizontal directions. S matrix describes the backscattering properties of the target. The two basic component horizontal and vertical component forms the basis in illustrating the electromagnetic wave in terms of electric field. The scattering matrix being complex has both real and imaginary values. It is basically obtained from magnitude and phase measurement by the four channels of the polarimetric radar. To get such values normally a predefined calibration procedure is followed. If the calibration method is not followed then the four scattering matrix are directly measured by the relevant channels of the radar system. The measured scattering properties of the target are dependent on two parameters. These two parameters are nothing but the frequency and radar beam angle. The monostatic radar holds the reciprocity condition true. Here S_{hv} and S_{vh} are equal. Hence scattering matrix is called symmetrical matrix. It has only three independent elements. The two convention method used to describe electromagnetic wave is Forward scatter alignment (FSA) and Backward scatter alignment (BSA). In the FSA for incident and scattered wave the positive Z axis is in the same direction as the traveling of the wave. In BSA the direction of Z axis normally points to the target for two waves called as incident and reflected wave. In both cases the Z axis points in same direction for incident wave and opposite direction for scattered wave. In monostatic radar the coordinate system are same for incident and reflected wave. So in most of the imaging radars the BSA convention is given preference [15]. Therefore naming convention used in BSA for scattering matrix is Sinclair matrix. Similarly in FSA the scattering matrix is termed as Jones matrix.

B. Stokes matrix

The polarization state of electromagnetic wave is illustrated by three parameters. These are orientation, ellipticity and S_o. The parameter S_o is related to intensity of the incident wave. Gabriel Stoke has illustrated the polarization state of the EM wave by vector called Stoke vector. The vector parameters are S_o, Q, U and V

$$\begin{bmatrix} S_0 \\ Q \\ U \\ V \end{bmatrix} = \begin{bmatrix} |E_v|^2 + |E_h|^2 \\ |E_v|^2 - |E_h|^2 \\ 2\,\mathrm{Re}\{E_v E_h *\} \\ 2\,\mathrm{Im}\{E_v E_h *\} \end{bmatrix} = \begin{bmatrix} S_0 \\ S_0 \cos 2\psi \cos 2\chi \\ S_0 \sin 2\psi \cos 2\chi \\ S_0 \sin 2\chi \end{bmatrix} \text{.....(2)}$$

In equation 2 the |.| represents the absolute value. The character * represents the complex conjugate [15]. There are two cases of EM wave. The EM wave may be completely polarized or partially polarized or completely unpolarized. The three stokes parameter are independent in case of completely polarized wave. The total power is given by

$$S_o^{\,2} = Q^2 + U^2 + V^2 \text{.....(3)}$$

For the partially polarized wave, the total power is more than the polarized power.

$$S_o^{\,2} > Q^2 + U^2 + V^2 \text{.....(4)}$$

The polarization of the incident and reflected wave are related to backscattered power of scatterer with the equation (5).

$$P = 0.5(S^S)^T M S^i \text{.....(5)}$$

Here M represents the Stokes matrix. It is another way of transforming incident EM wave into backscattered wave. The Stokes matrix is also symmetric for reciprocity condition. In BSA the other version of Stokes matrix is used. It is called as Kennaugh matrix.

C . Muller matrix.

Muller matrix is mostly used in FSA convention. The various scatterers are distributed on the earth surface. So there is particular measurement to be followed for all N independent values. It is basically asymmetric in nature. The total numbers of pixels are considered as N values. The scattering behavior of the Muller matrix for individual pixel in the obtained image is feature of polarization criteria [21], [22]. All the three different scattering involved are odd, even number of reflections and diffuse scattering. The next section describes the two decomposition methods in scattering matrix called linear and Pauli decomposition methods.

IV. LINEAR AND PAULI DECOMPOSITIONS

The linear decomposition technique is considered as basic decomposition technique. Here information obtained from individual polarization channel is considered. The information obtained corresponds to cross polarized scatter. The three vectors are k_1, k_2, k_3. The k_1 represents the scatter of horizontal oriented target scattering. The second component is by cross polarized scatter. The third component is scatter of vertical oriented target scattering [3], [4]. The target vector for linear decomposition is given as

$$\bar{k}_l = \begin{bmatrix} k_1 \\ k_2 \\ k_3 \end{bmatrix} = \begin{bmatrix} S_{HH} \\ \sqrt{2}S_{HV} \\ S_{VV} \end{bmatrix} .....(6)$$

Pauli decomposition uses Pauli matrices for the extension of scattering matrix. It is basically applied to deterministic targets. It consists of four scattering mechanisms. The first is called single scattering from plane surface. The second and third parameter is called diplane scattering. It is also called as double or even bounce scattering. Such scattering will occur from corners with orientation of 0° and 45°. The fourth element is called anti symmetric component of S matrix. The monostatic radar this term leads to value zero [7]. The Pauli vector is given by

$$\bar{k}_p = \begin{bmatrix} k_1 \\ k_2 \\ k_3 \end{bmatrix} = \frac{1}{\sqrt{2}} \begin{bmatrix} S_{HH} + S_{VV} \\ 2S_{HV} \\ S_{VV} - S_{HH} \end{bmatrix} .....(7)$$

V. DISCUSSIONS

The image characterization is basically obtained by polarization state of the electromagnetic wave. The various scattering mechanisms obtained through natural distributed targets basically depend on wavelength, dielectric constant and polarization of the EM wave. The mathematical modeling of the target identification is carried by different matrices. This basically depends on the scattering alignment technique involved such as BSA or FSA. Why and how different matrices can be used for the target detection is the valid information depicted in this paper. Identifying the target vector and evaluation of the target vector for linear and Pauli decomposition from the SAR image is the contribution of this paper.

The relation between ellipticity and orientation are analyzed using E vector analysis of electromagnetic wave. The component E and H are found to be orthogonal to each other.

Table 1. Comparison of target vectors in linear and Pauli decomposition

Decompositions	**Target Vector Significance**		
	k_1	**k_2**	**k_3**
Linear decomposition	Horizontal orientation	Cross polarized target	Vertical orientation
Pauli decomposition	Single bounce scattering	Double bounce scattering	Volume scattering
	Sphere, plate scatter	Diplane scatter	Dihedral scatter
	Single bounce scattering	Volume scattering	Double bounce scattering

Table 1 depicts the parameters of target vector related to the decomposition technique called as linear and Pauli decompositions. The information in the table reflects the scattering property of the target distributed on the earth surface. The backscattering information helps in identifying the target. SAR image is basically combination of energy present for individual image pixel. It depicts the combination of three images. The interpretation of polarization state change of the backscatter is obtained by target vector of these decomposition techniques.

Fig. 3 represents the overall analysis of decomposition method adopted for scattering matrix of polarimetry data. The two methods are evaluated through image analysis using Python system model.

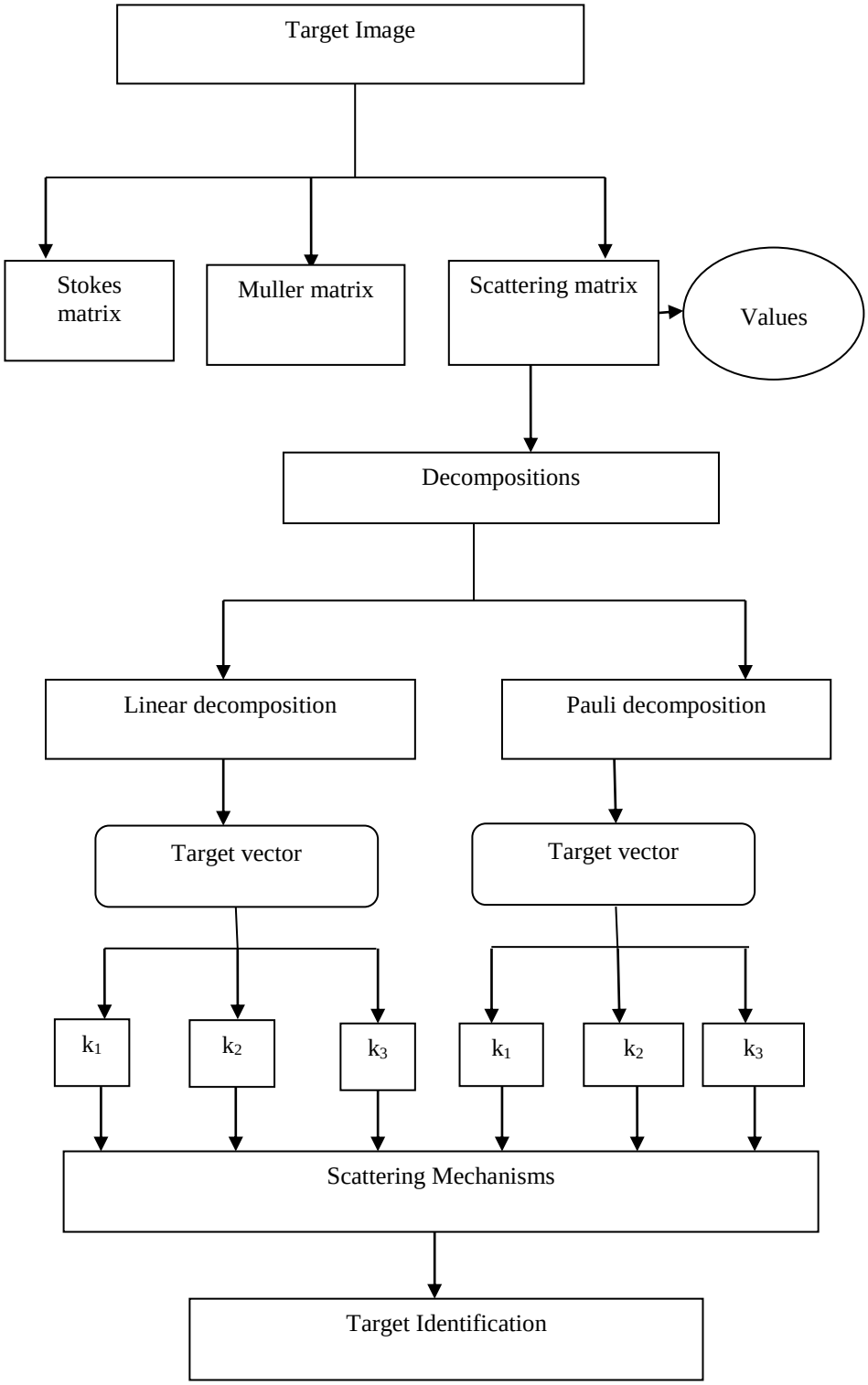

Fig. 3. Decomposition analysis for linear and Pauli decompositions

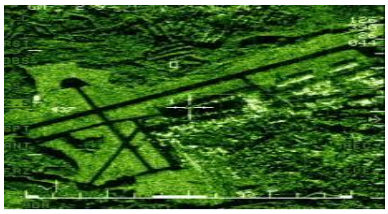

Fig. 4. Original Image

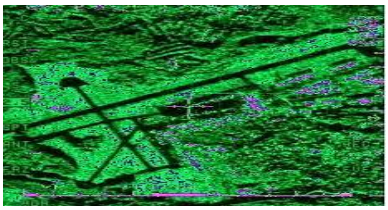

Fig. 5. Linear Decomposition Image

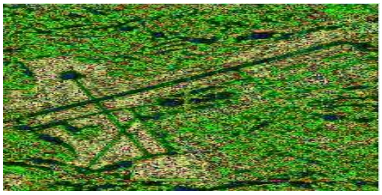

Fig.6. Pauli Decomposition Image

The Fig. 5. and Fig. 6. represents the cross polarization variation.

VI. CONCLUSION

This paper gives basic idea regarding the BSA and FSA conventions. The role of different matrices is highlighted in evaluating the target vector. The effect of polarization of the electromagnetic wave is studied for both conventional methods. System model for each method is developed. The involvement of linear and Pauli decomposition techniques for SAR polarimetry are realized. The target vector depicts the scattering property of the backscattering nature of the distributed targets.

REFERENCES

[1] Kazuo Ouchi, "Recent Trend and Advance of Synthetic Aperture Radar with Selected Topics," Review Remote Sensing ISSN 2072 -4292 , vol., no., pp. 716-765, Feb. 2013.

[2] M.Ouarzeddine, B. Souissi, A. Belhadj-Aissa, "Classification of Polarimetric SAR images based on scattering mechanisms," University of Science and Technology Houri Boumediene, vol., no., pp.1-6, Jan. 2007.

[3] Manuel E. Arrigada, "Performance of scattering matrix decomposition and color space for synthetic aperture radar imagery," Master Thesis for degree of Master of Science, pp. 1–73, Mar. 2010.

[4] Maurizio Sarti, Lucio Mascolo, "An investigation of different polarimetric decomposition techniques for soil moisture estimation," IEEE,vol. 1, no., pp. 209-213, Sept. 2012.

[5] Shenglong GUO, Yang, Wen HONG, Jianfeng Wang and Xiaoyang Guo, "Model based target decomposition with $\pi/4$ mode compact polarimetry data," Science China Information Sciences , vol. 59, no., pp. 1-10, Jun. 2016.

[6] Hongbo Sun,Masanobu Shimada and Feng Xu, "Recent Advances in Syntheic Aperture Radar Remote Sensing-Systems, Data Processing and Applications," IEEE Geoscience Remote Sensing Letter, vol. 14, no. 11, pp. 2013-2016, Nov. 2017.

[7] Shashikumar, "Advances in Polarimetry," SPIE Asia Pacific Remote sensing APRS Symposium tutorial, pp. 1-23, Apr. 2016.

[8] Jacob Van Zyl and Yunjin Kim, "Synthetic Aperture Radar Polarimetry," Jet Propulsion Laboratory, California Information Technology, pp. 88-100, Dec. 2010.

[9] Si-Wei Chen, Yong-Zhen Li, Xue-Song Wang , Shan-Ping Xiao and Motoyuki Sato, "Modelling and interpretation of scattering mechanism in polarimetric synthetic aperture radar," IEEE signal processing magazine, vol., no., pp. 79-89, Jul. 2014.

[10] Sang-Hoon Hong and Shimon Wdowinski, "Revising vegetation scattering theories: Adding a rotated dihedral double bounce scattering to explain cross-polarimetric SAR observations over wetlands," Proceedings, 'Fringe 2011 Workshop', Frascati, Italy, pp. 1-7, Sep. 2011.

[11] Eric Pottier, "Recent advances in the development of the open source toolbox for polarimetric and interferometric polarimetric SAR data processing: The POLSARPRO v4.1.5 software," IEEE, pp. 2527-2530, Aug. 2010.

[12] Jong sen Lee and Thomas L. Ainsworth, "An Overview of Recent Advances In Polarimetric SAR information Extraction: Algorithms and Applications," IEEE International Geoscience and Remote sensing Symposium, pp. 851-854, Jul. 2010.

[13] Alberto Moreira, Pau Prats–Iraola, Marwan Younis, Gerhard Krieger,Iren Hajnsek and Konstantinos P. Papathanassiou,Microwave and Radar institute of the German Aerospace Center (DLR), Germany, "A Tutorial on Synthetic Aperture Radar," IEEE Geoscience and remote sensing magazine, pp. 6-38, Mar. 2013.

[14] C.P. Schwegmann, W. Kleynhans, B. P. Salmon, "The Development of Deep learning in Synthetic Aperture Radar Imagery." International workshop on remote sensing with Intelligent Processing. pp.1-6, May. 2017.

[15] Technical Committee, "Advanced Radar Polarimetry Tutorial-Radar polarimetry," Technical report, Canada centre for remote sensing, pp. 1-24, Nov. 2015.

[16] Yonglei Chang , Jie Yang , Pingxiang Li , Lingli Zhao , Lei Shi , "Sample extraction based on helix scattering for polarimetric sar calibration," The International Archives of the Photogrammetry, Remote Sensing and Spatial Information Sciences, vol. XLII-2/W7, pp. 1-4, Sep. 2017.

[17] Sverre Holm, " Synthetic Aperture Radar and Sonar-SAR and SAS," Lecture notes, Department of informatics, University of OSLO, pp.1-19, May. 2015.

[18] Yoshio Yamaguchi, Toshifumi Moriyama, Motoi Ishido, and Hiroyoshi Yamada, "Four-Component Scattering Model for Polarimetric SAR Image Decomposition," IEEE Transactions on Geoscience and remote sensing, vol. 43, no. 8, Aug. 2005.

[19] Yoshio Yamaguchi, Akinobu Sato, Wolfgang-Martin Boerner, Ryoichi and Hiroyoshi Yamada, " Four-Component Scattering Power Decomposition With Rotation of Coherency Matrix," IEEE Transactions on Geoscience and Remote sensing, vol. 49, no. 6, Jun. 2011.

[20] Shane Robert Cloude and Eric Pottier, "A review of target decomposition theorems in radar polarimetry ," IEEE Transactions on Geoscience and Remote sensing, vol. 34, no. 2, pp. 1-4, Mar. 1996.

[21] Thuy LeToan , "SAR Image classification content scattering physics," ESA most dragon programme Advanced training course in Land Remote sensing , Beijing, pp. 1-4, Oct. 2005

[22] Muhtar Qong, Takeo Tadono, Hiroyuki Wakabayashi and Masanobu Shimada, " Muller Matrix based Classification of Polarimetric SAR Data," Earth Observation Research Center , National Space Development Agency of Japan, IEEE, pp. 375-377, Dec. 2000.

[23] Kohei Arai , " Polarimetric SAR Image Classification with High Frequency Component Derived from Wavelet Multi Resolution Analysis:MRA," International Journal of Advanced Computer Science and Applications (IJACSA), Vol. 2, No. 9, pp. 37-42, Dec. 2011.

[24] Camilla Brekke, Cathleen E. Jones, Stine Skrunes, Benjamin Holt, Martine Espeseth and Torbjorn Eltoft, "Cross correlation between Polarization channels in SAR Imagery over Oceanographic features," IEEE Geoscience and remote sensing letters, pp1-5, jan 2011.

Proceedings of the Fourth International Conference on Communication and Electronics Systems (ICCES 2019)
IEEE Conference Record # 45898; IEEE Xplore ISBN: 978-1-7281-1261-9

Energy Aware Virtual Machine Consolidation for Load Balancing in Virtualized Environment

Bishwabara Panda
School of Computer Engineering
KIIT Deemed to be University
Bhubaneswar, Odisha, India
bishwabarapanda@gmail.com

Suresh Chandra Moharana
School of Computer Engineering
KIIT Deemed to be University
Bhubaneswar, Odisha, India
sureshmoharana@gmail.com

Himansu Das
School of Computer Engineering
KIIT Deemed to be University
Bhubaneswar, Odisha, India
das.himansu2007@gmail.com

Manoj Kumar Mishra
School of Computer Engineering
KIIT Deemed to be University
Bhubaneswar, Odisha, India
manojku.mishra05@gmail.com

***Abstract*— Cloud computing is one of the most prominent technology due to flexibility in distributing the resources. This technology enables the user to pay as per their requirement. In cloud computing virtualization is an essential technology. Reducing the load imbalance level across virtual machines in virtualized environment is of significant interest among researchers. In order to deal with the load balancing problem virtual machine migration is one of the popular technique being applicable. In this paper, we have devised a load balancing mechanism based on virtual machine migration for not only minimizes the load imbalance level but also utilizes the energy efficiently.**

Keywords— virtual machine; load imbalance level; virtual machine consolidation; energy usage

I. INTRODUCTION

Cloud computing is a modern computing model which has achieved the popularity for providing and managing services like software and applications online. Cloud-based services are basically on-demand, scalable, device independent and reliable [1,2]. Virtualization is an essential concept provided by cloud computing. It can control and share the available resources over the datacenters [3]. With the help of virtualization, we can create multiple operating systems like virtual machines and share the resources among these operating system. A virtual machine can be visualized as a software implementation in which an operating system can be installed. In other words a virtual machine work as a complete operating system. In the cloud, multiple numbers of virtual machines can run in a single physical machine by sharing its resources. Virtual machine placement is a process in which a physical machine is selected to host for a virtual machine with fulfilling all the requirements of the virtual machine. Virtual machine migration is an operation in which a virtual machine is a transfer from one host to another host according to its requirements.

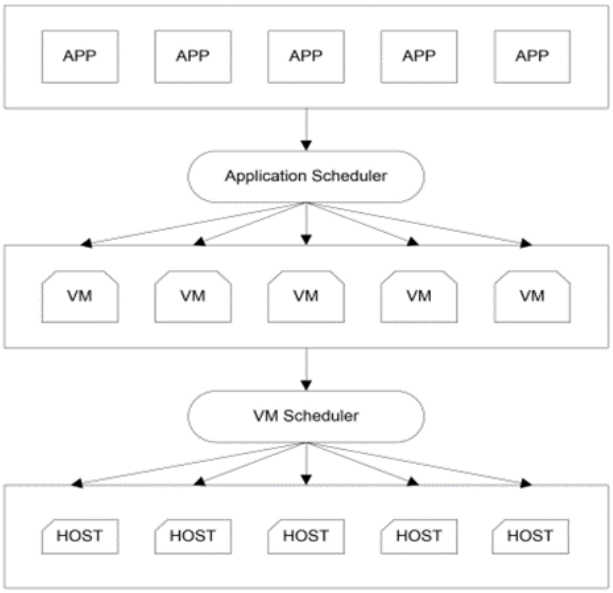

Fig. 1 Cloud System Architecture

In cloud datacenters load imbalance has always been a research subject. The result of load imbalance always leading to performance degradation, SLA violation, etc. To reduce this performance degradation, SLA violation the load balancing needs to be achieved not only across the virtual machines but also within the available host.

The cloud system can be represented as a three-layer architecture as shown in fig.1. According to the above figure the applications exist in the upper layer which is submitted by the user. The multiple numbers of the applications installed onto the virtual machines by the application scheduler. In the next layer, the virtual machines need to be scheduled in the physical machines with the help of virtual machine scheduler. In cloud the load can be possible at application level as well as virtual machine level.

In order achieve the load balancing at the host level there are many scheduling schemes are present. Virtual machine migration one of the popular technique in this direction [4,5,6]. Virtual machine migration is a technique in which a virtual machine is selected to transfer from one host to another host. In this paper, we have proposed a load balancing approach using virtual machine migration technique to achieving energy efficiently.

The next section provides a brief information about the related literature currently present. In Section 3 the proposed load balancing scheme is described. Section 4 highlights the experimental environment and obtained experimental results. Finally, the last section discusses the concluding remarks and future directions respectively.

II. RELATED LITERATURE

In cloud computing environment load imbalance is a well know problem. There are different types of approaches are available to deal with this load balancing problem. Virtual machine migration one of the popular technique in this direction. In this section we are going to discuss some migration based load balancing approaches proposed by different authors.

Zhu et al. [7] provide a heuristic based mechanism using only the CPU load to solve a dynamic virtual machine consolidation problem. For the evaluation, this technique uses historical data. In this technique, the overloaded host has decided by using 85% as an upper threshold value. If the CPU load of the host exceeds the above upper threshold value then that host is selected as overloaded host. Similarly, the lightly loaded host has decided by using 50% as a lower threshold value. If there is a host with the CPU load below the lower threshold value then that host selected as lightly loaded host. This static threshold heuristic doesn't lead to any workload changes as they are not acceptable for the system with the dynamic workload.

Beloglazov et al. [8] provide a consolidation approach which determines two types of threshold values to detect the overloaded and underloaded hosts. Like the previous technique, this technique also uses only the CPU load for the evaluation. The upper threshold value has decided using three types of policies that are MAD (median absolute deviation), local regression(LR) and interquartile range (IQR). If there is host having CPU load exceed the upper threshold value then that host is selected as overloaded host. After the completion of overloaded host detection , this technique selects the virtual machine from the overloaded host for the migration process to balance the load. For the virtual machine selection, this approach used three types of techniques that are MMT(Minimum migration time), Random choice policy(RC) and the maximum correlation(MC) policy. This approach provides a good result for energy consumption and SLA violation. In this approach, the author uses historical data.

Algorithm	**Dominant Characteristics**		
	Resource type	***Citation***	***VM Allocation Dynamicity***
Zhu et al.	Single	147	Dynamic
Beloglazov et al.	Single	1183	Dynamic
Sing et al.	Multiple	440	Dynamic
Wood et al.	Multiple	345	Dynamic

TABLE 1 COMPARATIVE STUDY OF RELATED LITERATURE

Sing et al. [9] proposed a load balancing algorithm to manage the hierarchical and multi-dimensional resource constraint called vector dot. In this approach, the multi-dimensional resource demands are represented by the vectors. Such as the threshold vector of the node u is represented as *PathThresholdVec(u). sItemPathLoadFracVec(u)* captures the resource demand of virtual item on each node along *u*'s flow path. *PathLoadFracVec(u)* represent each node's resource usage fraction along the path. For the virtual machine migration process, this technique evaluates the dot product of *ItemFracLoadVec(u)* and *PathLoadFracVec(u)*. To reduce the highly loaded physical machines, this approach migrates the virtual machine from the overloaded host to the hostwhich has the lowest dot product of *ItemFracLoadVec(u)* and *PathLoadFracVec(u)*.

Wood et al. [10] design a system named sandpiper for hotspot detection and virtual machine migration. This approach also provides new scheduling of virtual machines and physical machines. This technique takes the CPU, network, and memory into the account. This approach predicts the load of the physical machines and compares it with the threshold value. If the load of the physical machine exceeds the threshold value then that host selected as overloaded host. In this approach, a volume is evaluated by multiplying the CPU, memory, and network to capture the multi-dimensional load. This volume represents the degree of a load of each physical

machine. After the overloaded detection, this approach proceeds for the virtual machine migration process. For the virtual machine migration, this approach calculates a VSR(Volume-to-Size Ratio) for each virtual machine, where size is the memory footprint of the virtual machine. The virtual machine with the highest VSR is selected from the physical machine having the highest volume for the migration process.

We have analyzed the surveyed literature in many aspects and provided a comparative study among the considered literature, as illustrated in table 1.

III. PROPOSED WORKING MODEL

The virtualized environment can be thought of virtual machines deployed over physical hosts in order to perform numerous computational tasks provided by various users. The said process of computation may result in uneven distribution of load across virtual machine and hence requires deployment of virtual machine consolidation schemes for achieving load balancing at virtual machine level. In this context, we have proposed a virtual machine consolidation scheme as given in algorithm 1 with an objective of not only minimizing the load imbalance level but also using energy efficiently.

Input: **vmList and hostList**
Output: **Virtual machine consolidation for load balancing**

Algorithm 1: **Energy aware load balancing**

1: Let total_ld = sum of load of all host
2: Let total_host = number of available hosts
3: Let avg_ld = total_ld/total_host
4: Store the host in lower_host_list having total_host_load <= avg_ld
5: Store the host in higher_host_list having total_host_load > avg_ld
6: Let vm_cnt = sum of vms mapped the host in higher_host_list
7: Calculate the curr_thr=100/vm_cnt
8: Let vm_ltt = virtual machine with lowest transfer time within lower_host_list
9: Repeat
10: for each host in higher_host_list
11: if avg_host_load > curr_thr then
12: migrate the current vm_ltt to the considered host
13: for each host in lower_host_list
14: if total_host_load < 10
15: poweroff the considered host
16: until the load among hosts in higher_host_list is balanced

The control flow of the proposed virtual machine consolidation scheme is shown in figure 2. In our proposed model, in the 1st stage we have planned to detect the lower loaded host by determining the average load among the available host. In case, the host having the load lower than the average load then that host will consider as underloaded host. In this situation, we are going to migrate all of the virtual machines from the underloaded host to non-underloaded hosts and keep all the underloaded host in sleep mode. In the next stage, we have selected a virtual machine from that underloaded host for the migration process using LTT (lowest transfer time) method. We have detected the higher-loaded hosts in 3rd stage by applying a current threshold value among the non-lower loaded hosts. Finally, in order to place those migrated virtual machines from the underloaded we have selected the destination host in the last stage.

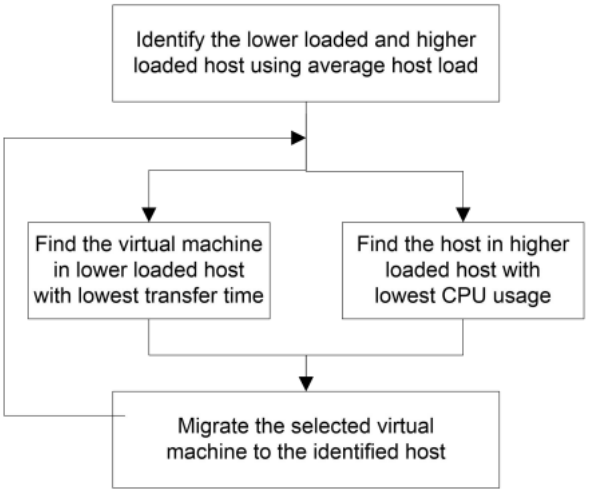

Fig. 2 Proposed Working Model

The proposed load balancing model takes virtual machine consolidation into consideration. Initially, it identifies the hosts with higher loaded as well as lower loaded hosts. Further, it selects appropriate virtual machines from lower loaded hosts and consolidates those virtual machines in the higher loaded ones. This approach looks for achieving load balancing within higher loaded hosts by intelligently consolidating virtual machines among them. The following sections explain the proposed model in detail.

A. Lowerloaded / Higherloaded Host Detection

In this work, we have used an average load to detect the lower loaded and higher loaded host by making use of only the CPU load. The average load can be defined as below,

$$avg\_ld = total\_ld/total\_host \quad (1)$$

where *avg_ld*: average load of the available host.

total_ld: total load of the available host

total_host: the number of available host.

If the CPU load of a host is lower than the average load then that host is considered as lower loaded host and if there is a host having a load greater than this average load value then that host is considered as higher loaded host. In this situation, we are going to migrate all of its virtual machines from lower loaded hosts and keep them in sleep mode.

B. Virtual Machine Selection

Once the lower loaded host has been successfully decided for the migration, we will proceed to identify the virtual machine for the migration process. In order to select the virtual machine we have used the lowest transfer time(LTT) method. In this method, the virtual having that takes the lowest time to migrate will select for the migration process.

C. Destination Host Selection

After identifying the lower and higher loaded host and selecting the virtual machine from the lower loaded host for the migration process, we will move to select the destination hosts to place the migrated virtual machines from the lower loaded hosts. In order to identify the destination host to place the migrated virtual machines we are going to select the host having lowest CPU usage in higher loaded host. We have used a current threshold value to identify the destination host from higher loaded hosts [11,12].

This current threshold value can be determined as,

$$curr\_thr = 100/vm\_cnt \quad (2)$$

where *curr_thr*: current threshold value

vm_cnt: total number of virtual machines available in all the higherloaded hosts.

The host having CPU load lower than the current threshold value will be selected as the destination host to receive the migrated virtual machine from the lowerloaded hosts accordingly.

IV. EXPERIMENTAL EVALUATION

A. Experimental Parameters

For comparing the proposed model, we have taken *Load_Imbalance_Level* and *Energy_Usage_Sum* into consideration. The foremost parameter signifies the level of imbalance in-between the loads assigned to the available virtual machines, whereas the other parameter represents the total energy consumed by the available hosts in the cloud environment.

$$Load\_Imbalance\_Level = \frac{\sum_{i=1}^{k-1} |vmload_i - vmload_{i+1}|}{(k-1)} \quad (3)$$

where $vmload_i$ represents the load present in the *ith* virtual machine.

Further, the *Energy_Usage_Sum* can be defined as,

$$Energy\_Usage\_Sum = \sum_{j=1}^{n} hosteng_j \quad (4)$$

where $hosteng_j$ represents the total energy used by the *jth* physical host.

B. Experimental Environment and Results

We have used Cloudsim simulation environment [12] for implementing and validating the proposed virtual machine placement framework. The simulation environment is realized over Lenovo thinkstation with 4 GHZ processor, 8 GB of RAM and Ubuntu 18.04 operating system. For conducting the experiment, we have varied the number of hosts in the range of 2 to 20 with an interval of 2 over 10 datacenters. Further, we have considered different number of virtual machines over the range of 4 to 40 with a gap of 4 being mapped to the mentioned hosts and these virtual machines executes cloudlets over them. We have assumed that the hosts, virtual machines are homogeneous in nature. In this we have extended the existing VmAllocationPolicy() class of Cloudsim for implementing the proposed scheme. Further, we have computed the *Energy_Usage_Sum* and *Load_Imbalance_Level* upon observing lower level of variations among the loads over the virtual machine. We have used the said parameters to compare the proposed model with existing approaches.

After running the simulation, we have identified that, in terms of the *Load_Imbalance_Level* the proposed scheme outperforms the existing approach in most of the cases as shown in figure 3.

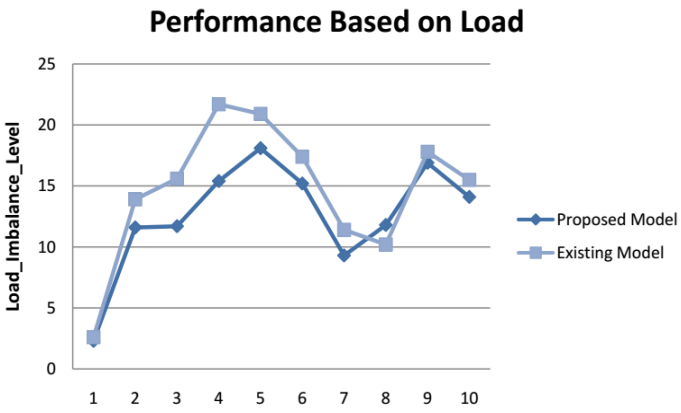

Fig. 3 Comparison based on Load_Imbalance_Level

The graph shown in figure 3 clearly mentions that apart from few iterations, the load_imbalance_level obtained in case of proposed model is less than the existing model. Hence, our proposed model provides a better load balance as compared with the existing model.

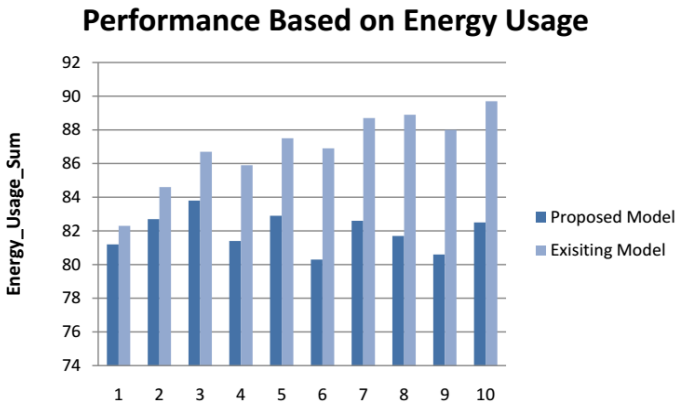

Fig. 4 Comparison based on Energy_Usage_Sum

Further, after comparing the proposed scheme in terms *Energy_Usage_Sum* with the existing model, we have also identified that the proposed consolidation scheme makes use of energy efficiently by suitably powering off the lower loaded physical hosts. It clearly visible in figure 4 that the energy usage in our proposed model is much lower than the existing model. Hence, our proposed model make use of the energy more efficiently as compared with the existing one.

V. CONCLUSION

In virtualized environment load balancing is a significant issue. In order to deal with this problem virtual machine migration is one of the popular technique to achieve load balancing. In our work we have proposed a migration based load balancing approach for the underloaded hosts. We have also compare our proposed approach with the existing technique by using the parameter load imbalance level and energy usage. After the comparison finally we conclude that our proposed approach provide less load imbalance than the existing approach and also the energy consumption of the proposed model is lower than the existing model. In future, our plan is to in-corporate multiple load parameters into the proposed consolidation scheme.

REFERENCES

[1] M. Xu, W. Tian, and R. Buyya, "A survey on load balancing algorithm for virtual machine placement in cloud computing," Concurrency and Computation: Practices and Experience, vol. 29(12), pp. 1-22, Jun. 2016.

[2] EJ. Ghomi, A. M. Rahmani, and N. N. Qader, "Load balancing algorithm in cloud computing: A survey," Journal of Network and Computer application, vol. 80, pp. 50-71, Jun. 2017.

[3] A. Varasteh, and M. Goudarzi, "Server consolidation techniques in virtualized data centers: A survey," IEEE Syst. J, vol. 11(2), pp. 772-783, Jun. 2017.

[4] C. Clark, K. Fraser, S. Hand, J. G. Hansen, E. Jul, C. Limpach, I. Pratt, and A. Warfield, "Live migration of virtual machines," in Proceedings of the 2nd conference on Symposium on Networked Systems Design & Implementation-volume-2, May 2005, USENIX Association, pp. 273-286.

[5] K. Ye, X. Jiang, D. Huang, J. Chen, and B. Wang, "Live migration of multiple virtual machines with resource reservation in cloud computing environments," in Proceedings of 2011 IEEE 4th International Conference on Cloud Computing. July 4-9 2011, Washington, DS, USA, IEEE, pp. 267-274.

[6] S.C. Moharana, and M. SD, "An efficient approach for storage migration of virtual machines using bitmap," in Proceedings of International Conference on Information Processing. August 5-7 2011, Bangalore, India, Springer. pp. 438-447.

[7] T. Wood, P. Shenoy, A. Venkataramani, and M. Yousif, "Sandpiper: Black-box and gray-box resource management for virtual machines," Computer Networks, vol. 53(17), pp. 2923-2938, Dec. 2009.

[8] A. Singh, M. Korupolu, and D. Mohapatra, "Server-storage virtualization: integration and load balancing in data centers," in Proceedings of 2008 ACM/IEEE conference on Supercomputing, November 15-21 2008, Austin, Texas, USA, IEEE Press, p. 53.

[9] A. Beloglazov, and R. Buyya, "Optimal online deterministic algorithms and adaptive heuristics for energy and performance efficient dynamic consolidation of virtual machines in cloud data centers," Concurrency and Computation: Practice and Experience, vol. 24(13), pp. 1397-1420, Sep. 2012.

[10] X. Zhu, D. Young, B. J. Watson, Z. Wang, J. Rolia, S. Singhal, B. McKee, C. Hyser, D. Gmach, R. Gardner, T. Christian, and L. Cherkasova, "1000 islands: Integrated capacity and workload management for the next generation data center," in Proceedings of 2008 International Conference on Autonomic Computing, June 2-6 2008, Chicago, IL, USA, IEEE, pp. 172-181.

[11] S.C. Moharana, S. Samal, A.R. Swain, and G.B. Mund, “Dynamic CPU scheduling for load balancing in virtualized environments,” Turkish Journal of Electrical Engineering & Computer Sciences, vol. 26(5), pp. 2512-2524, Sep. 2018.

[12] M. K. Mishra, Y. S. Patel, Y. Rout, and G. B. Mund, "A survey on scheduling heuristics in grid computing environment," International Journal of Modern Education and Computer Science vol. 6(10), pp. 57-83, Oct. 2014.

[13] R. N. Calheiros, R. Ranjan, A. Beloglazov, C. A. De Rose, and R. Buyya, "CloudSim: a toolkit for modeling and simulation of cloud computing environments and evaluation of resource provisioning algorithms," Software: Practice and experience, vol. 41(1), pp. 23-50, Jan. 2011.

Proceedings of the Fourth International Conference on Communication and Electronics Systems (ICCES 2019)
IEEE Conference Record # 45898; IEEE Xplore ISBN: 978-1-7281-1261-9

Design and Verification of Analog Integrated Circuits Using Free or Open source EDA Tools

Guruprasad
ECE Dept. Manipal Institute of Technology
MAHE, deemed to be University
Manipal, India
guruprasad.mit@protonmail.com

Kumara Shama
ECE Dept. Manipal Institute of Technology
MAHE, deemed to be University
Manipal, India
shama.kumar@manipal.edu

***Abstract*—In this paper, a design methodology for carrying out all the steps involved in a typical analog design flow, using free or open source electronic design automation [EDA] tools is proposed. Implementation of a three stage CMOS operational amplifier is chosen for demonstration. g*EDA-gschem* tool is utilized for schematic capture and SPICE net list generation. *Electric-VLSI* is a state of the art EDA tool which is used for laying out the op-amp, design rule checking [DRC], verifying layout versus schematic [LVS] and generating parasitic extracted SPICE net list. The SPICE net list are simulated with the help of versatile, electronics and electric circuit simulator, *Ngspice.* The scripting language provided by *Ngspice* is used for performing corner analysis and Monte-Carlo simulations. Simulation results reveal that the designed operational amplifier meets the desired specifications. Corner and Monte-Carlo analysis show that the op-amp is robust against process variations and mismatch.**

Keywords—CMOS op-amp; open source or Free EDA tools; Ng-spice; Electric-VLSI; gEDA-gschem.

I. INTRODUCTION

Analog electronics circuit design and verification heavily depend on Electronic Design Automation tools. The accuracy of the circuit simulation relies on how nonidealities and process variations are handled by EDA tools and model files. Unlike the digital circuits, the yield of analog circuits is poor. As technology is shrinking day by day, modeling and simulation are becoming extremely challenging. Cadence, Synopsis and Mentor graphics are the industries which are currently ruling EDA market. They charge millions of dollar for licensing and support which have to be paid periodically. For small scale industries, it is uneconomical and they can not afford. For academic institutions and research organizations, though above mentioned industries provide EDA tools at a concessional rate, still it is considered as costly, especially in developing countries. In this regard, open source and free EDA tools are becoming more and more popular. These tools can do almost all the tasks which are done by proprietary tools but they lack fancy graphic user interface [GUI] and hand-hold approach, hence user must have a fair knowledge in analog design flow to use them. In the present paper, an effort is made to introduce open source/Free EDA tools starting from schematic, layout, post-layout simulations to statistical analysis considering integrated CMOS operational amplifier as an example.

For undergraduate first and second year students, circuit schematic entry, net list creation and simulation tools are enough to understand and appreciate the concepts of basic circuit analysis and design. Instead of purchasing expensive *PSPICE* tool, a combination of schematic capture gEDA-gschem and *Ngspice* can be very effective in teaching and learning process. For higher semesters of undergraduate and post-graduation students can make use of Electric-VLSI along with *Ngspice* for the study and practice of analog circuits. These two tools can eliminate the need of costly softwares like *Cadence Spectre* and *Virtuoso*. One more added advantage is that the students will understand all the intermediate steps of circuit design. Even research scholars pursuing Ph. D program can efficiently use the above mentioned softwares for deeper analysis and design of integrated circuits. *Ngspice* has many builtin functions and scripting language, so that all the complicated analysis like corner analysis, Monte-Carlo statistical analysis can be conducted. Electric-VLSI comes with free MOSIS process design kit [PDK] which is very useful for layout.

Operational amplifiers [Op-amp] are the most common functional blocks found in any analog circuits, so performance metrics of Op-amp are critical. Many typologies like two stage, folded cascode, telescopic cascode, gain-boosted etc.[1-3] are available for implementing an Op-amp, depending on specifications and applications. Two stage Op-amp along with output buffer is the most basic and famous topology which van offer high gain and can drive capacitive loads. In the proposed paper, the design and verification of a two stage Op-amp followed by a source follower is presented. The paper is structured as follows. Section II describes the implementation of CMOS Op-amp. Simulation results and discussion are given in Section III. Conclusion is drawn in last section.

II. IMPLEMENTATION OF OP-AMP USING FREE OR OPEN SOURCE EDA TOOLS

Fig. 1 shows the typical analog design flow. It can be divided into two phases, one is the circuit level deign and other is physical level design [4]. In the first phase, design is validated at transistors level. Schematic capture, net list creation and SPICE simulation tools are required. If design meets the specifications, it will move to second phase else circuit has to be tweaked. In the second phase actual physical aspects of the

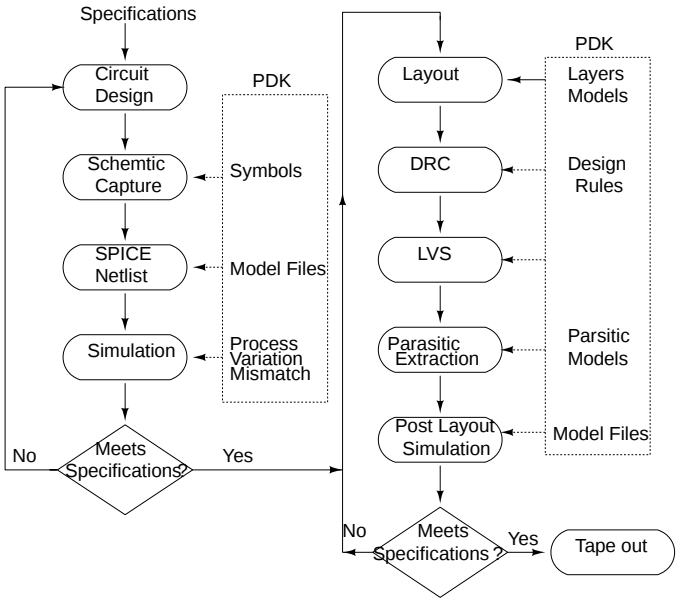

Fig. 1 A typical analog design flow

circuit on the chip is laid out and parasitic capacitance and resistance are extracted. Now again the function of the circuit in the presence of above mentioned parasitic elements is tested. The design flow is repeated till it meets the specifications. When it passes the test, the design is sent to fabrication in a prescribed file format. In this section, how each block can be implemented using open source or free EDA tool is elaborated.

A. Design of op-amp

First stage of op-amp is a differential amplifier which amplifies the only difference between the voltages at its inputs and rejects the common voltage. The second stage is a common source stage which further amplifies the signal received from differential amplifier. Last stage is a source follower which is a class A power amplifier, offers low output resistance. Fig. 2 shows the circuit diagram of op-amp and it is designed for the following specifications [5].

1. Slew rate=0.5 V/µs
2. Open loop gain > 60 dB
3. Phase Margin > 60°
4. Load capacitance=5 pF
5. Common mode rejection ratio [CMRR] > 45 dB
6. Power dissipation > 25 µW

Table I shows the W/L ratio of all the MOSFETs of op-amp.

B. gEDA-gschem

The schematic diagram of the designed op-amp was drawn using gEDA-gschem. gEDA-gschem is a part of General Public Licensed electronic design automation suite. This is used for electrical and electronic circuit schematic capture and producing SPICE net list [6]. It facilitates all SPICE modules, circuit hierarchy and custom symbol creation. Fig. 3 shows the screenshot of gEDA-gschem tool. 'gnetlist' command is used to generate SPICE net list from schematic circuit. The produced SPICE code is ready for the simulation.

TABLE I. TRANSISTORS SIZE

Transistor	W/L
M_1	40
M_2	40
M_3	64
M_4	64
M_5	16
M_6	352
M_7	44
M_8	10
M_9	80
M_{10}	16

C. Ngspice

*Ngspic*e was used for simulating the designed op-amp. *Ngspice* is a mixed signal circuit simulator. It is derived from three open source software packages: Spice3f5, Cider1b1 and Xspice [7]. It handles the following circuit elements: integrated

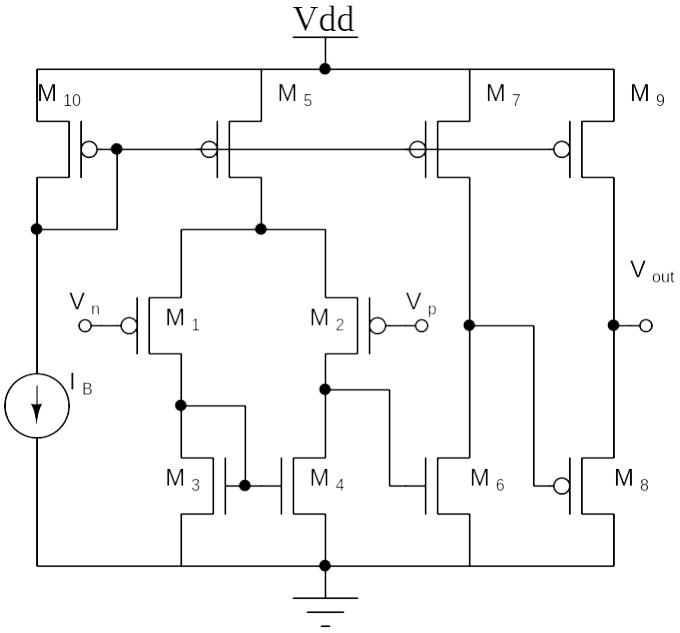

Fig. 2 Schematic diagram of the CMOS op-amp

and discrete resistors, capacitors and inductors, all types of diodes, BJTs, JFETs, MOSFETs, MESFETS, controlled sources, independent sources and many more. All the latest MOSFET device models like level-1 to level-4, Berkeley Short-channel IGFET Model [BSIM] 1 to 4 are supported by *Ngspice*. We can perform all the basic circuit analyses as listed below.

- Operating point analysis
- DC sweep
- Frequency response [phase and gain]
- Pole-zero analysis
- DC or small signal sensitivity analysis
- Transfer function analysis
- Transient analysis
- Noise and distortion analysis

Ngspice comes with *NUTMEG* scripting language which is very useful in plotting and saving the result data and writing the code for complicated circuit analysis like statistical analysis.

D. Electric-VLSI

The layout and parasitic extraction of the op-amp was carried out using *Electric-VLSI* tool. It is a state of the art computer aided design system for VLSI circuit design. Electric can design any type of electronic and electric components and has the capability of facilitating layout, schematics, artwork, and architectural specifications. Along with Ngspice, it can

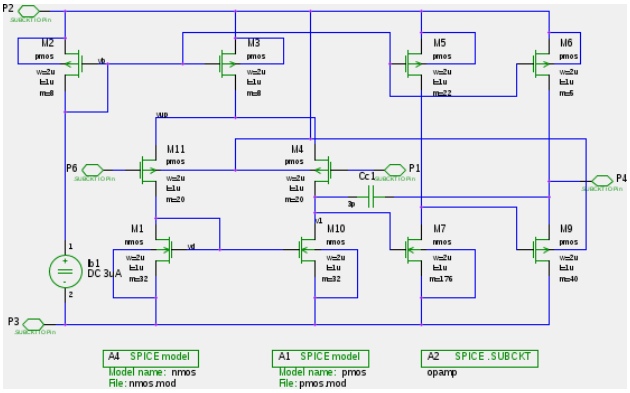

Fig. 3 Snapshot of gEDA-gschem

offer a complete analog design flow from design to fabrication. The salient features of Electric-VLSI are given below [8].

- It has built-in process design kits for different MOSIS technologies.
- Schematic capture
- Custom layout
- Design Rule Check and Electric rule check
- Parasitic extraction
- Layout versus Schematic verification
- It can generate net list for different SPICE engines
- Silicon compiler, placement and routing
- It can export the design to different formats required by the Fabrication units.

III. Results and Discussion

BSIM3v3 model [9] was used for modeling the transistors used in the op-amp circuit. First, stability of the op-amp was investigated by determining loop gain and phase margin [9]. The op-amp exhibited a loop gain of 60 dB with a phase margin of 70^0 as shown in Fig. 4. To determine the slew rate performance of the op-amp, a pulse voltage of 0.65 V with 1 µs rise and fall time was applied to it in voltage follower configuration. The op-amp displayed a slew rate of 0.4 V/µs as shown in Fig. 5. The common mode rejection ratio [CMRR] response of op-amp is shown in Fig. 6. The measured CMRR value was 85 dB.

Ngspice and *NUTMEG* [7,11] have many built-in functions, a few of them are listed in Table II. They are handy in performing statistical analysis and corner analysis. *NUTMEG* scripting language supports conditional statement 'if-else', loop statements 'while' and 'for'. We can run several simulation loops and change device model parameters with the help of 'alter' or 'altermod' commands. Corner analysis is one, which reveals the circuit behavior at different extreme process corners. Using the script, circuit can be analyzed with different process and model parameter values. Fig. 7 shows transient response of the op-amp for different process corners. It shows

that op-amp does not deviate much from nominal for all process corners.

TABLE II. A FEW BUILT-IN FUNCTIONS OF NGSPICE

Function	Notes
Gauss(nom, rvar, sigma)	Gaussian distribution with mean 0 and standard deviation rvar divided by sigma
agauss(nom, avar, sigma)	Gaussian distribution with mean 0 and standard deviation avar (absolute), divided by sigma
unif(nom, rvar)	Relative variation uniformly distributed between +/- rvar

Corner analysis determines the circuit behavior only at extreme process variation values where as local variations and mismatch are not considered. Monte-Carlo simulation is a statistical analysis in which process parameters are varied randomly assuming a distribution model (Gaussian) and also mismatch is considered among the components belong to same category [12]. Ngspice also provides many statistical functions, from which Monte-Carlo simulation can be run on the circuit with the help of scripting language. Table III shows a few statistical functions of Ngspice [6].

TABLE III. STATISTICAL FUNCTIONS OF NGSPICE

Function	Notes
rnd(vector)	A vector with each component a random integer between 0 and the absolute value of the input vector's corresponding integer element value.
sgauss(vector)	Returns a vector of random numbers drawn from a Gaussian distribution (real value, mean = 0,standard) deviation = 1).

The loop gain and phase response of designed op-amp under process variation and mismatch were tested using Monte-Carlo simulation [12]. The loop gain and phase margin of the op-amp for different samples are plotted in Fig. 8 and Fig. 9 respectively. It can be seen that the mean value of loop gain and phase margin matches with the nominal values. This proves the designed op-amp is robust. The layout of op-amp using *Electric-VLSI* is shown in Fig. 10. Op-amp occupies an area of 85 µm × 168 µm on the chip. Table IV shows the comparison between the desired and obtained performance values of the op-amp.

TABLE IV. PERFORMANCE SUMMARY

Parameters	Desired	Achieved
Loop Gain	60dB	60dB
Phase Margin	60^0	70^0
Slew rate	0.5V/µs	0.4V/µs
CMRR	>45dB	85dB

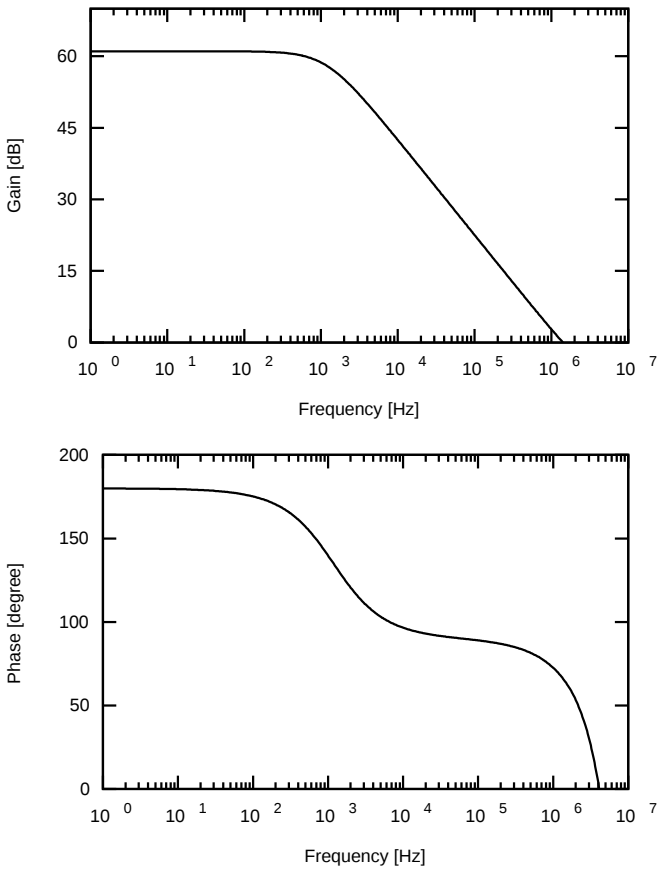

Fig. 4 Loop gain and phase response of the op-amp

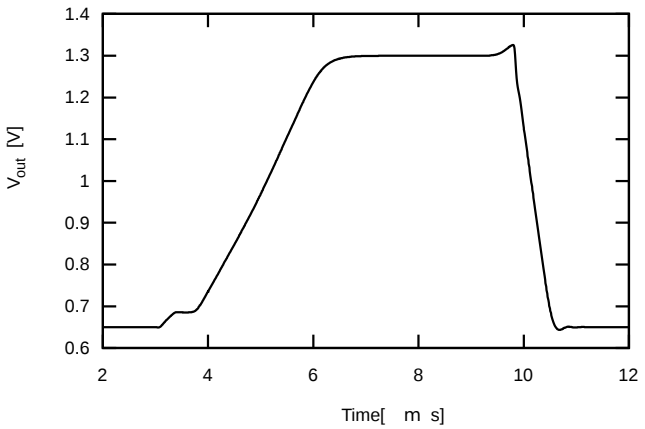

Fig. 5 Transient response of the op-amp

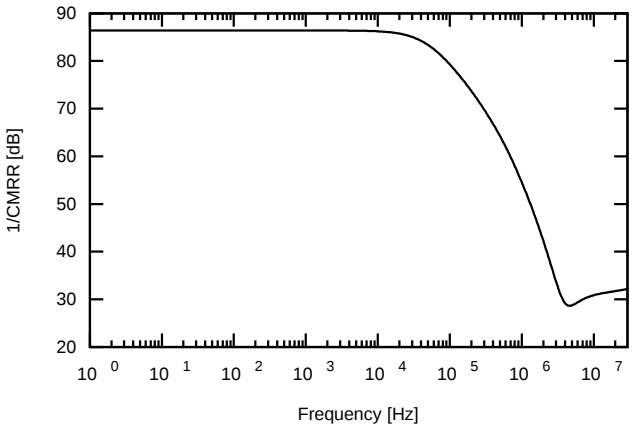

Fig. 6 CMRR Response of the op-amp

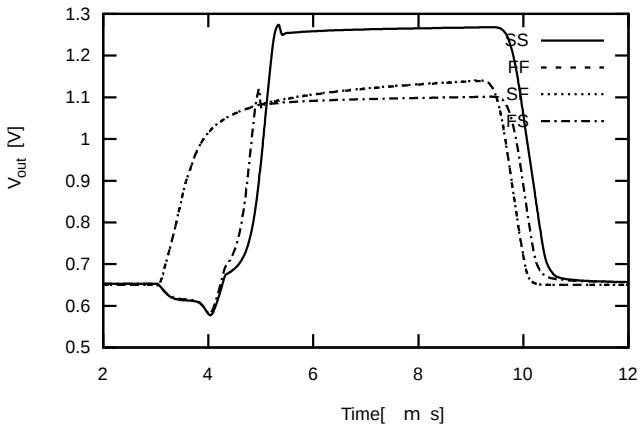

Fig. 7. Corner analysis-Transient response

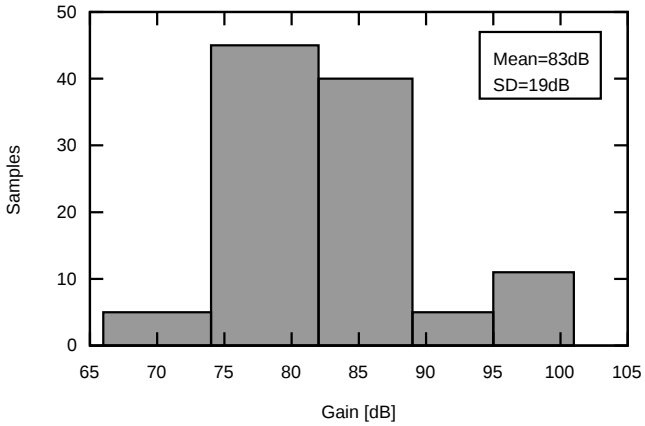

Fig. 8 Monte-Carlo simulation result [loop gain variation]

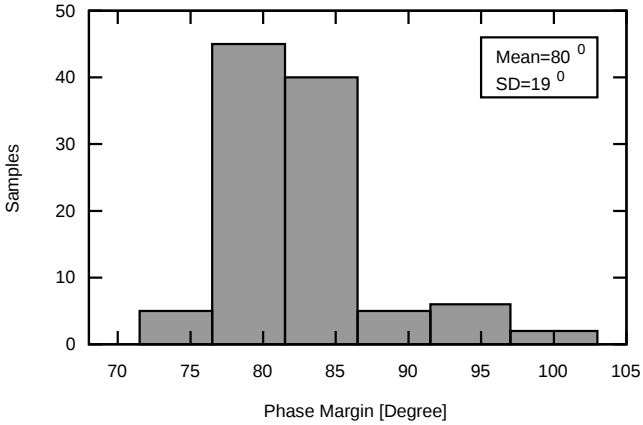

Fig. 9 Monte-Carlo simulation result [loop phase variation]

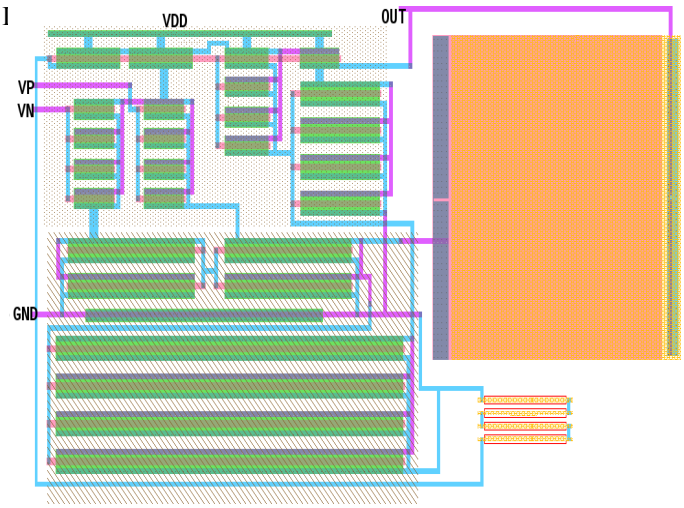

Fig. 10 Layout of the op-amp

CONCLUSION

In the present work the entire analog design flow starting from schematic to post layout simulation and verification have been carried out using free or open source EDA tool considering integrated CMOS op-amp as an example. *Ngspice* and *Electric-VLSI* EDA tools have been used for simulation and laying out op-amp. The op-amp has been designed for a set of specifications and after post layout simulation the results are matched with the desired response. Corner analysis and Monte Carlo simulations have shown the designed op-amp is robust.

REFERENCES

[1] Chen, H., MilovanoviÄĞ, V., Giotta, D.,Zimmermann, H., "Ultra-high bandwidth fully-differential three stage operational amplifiers in 40nm digital CMOS, Design and Diagnostics" of Electronic Circuits and Systems (DDECS), IEEE 16th International Symposium on (pp.76-81).,2013 April.

[2] Adel S. Sedra, Kenneth Carless Smith, "Microelectronic Circuits", 5th Edition,Oxford University press, 2005.

[3] Behzad Razavi, "Design of Analog CMOS Integrated Circuits", Tata McGraw-Hill Education, 2002.

[4] Sutula, S., et al. "Teaching mixed-mode full-custom VLSI design with gaf, SpiceOpus and Glade." 10th European Workshop on Microelectronics Education (EWME). IEEE, 2014.

[5] Allen, P.E. and Holberg, D.R., "CMOS Analog Circuit Design" 2nd Edition, Oxford University Press, 2002

[6] http://wiki.geda-project.org/geda:gaf

[7] Nenzi, P., Vogt, H. “Ngspice Users Manual Version 26”, 2014.

[8] Rubin, S. M. “Computer aids for VLSI design (Vol.21) Reading, Massachusetts”, USA: Addison-Wesley, 1987.

[9] Cheng, Yuhua, et al. "BSIM3v3 manual." University of California 1996 (1995).

[10] http://education.ingenazure.com/ac-stability-analysis-ngspice/

[11] http://bwrcs.eecs.berkeley.edu/Classes/IcBook/SPICE/MANUALS/nutmeg.html

[12] Tuma, Tadej, and Árpád Buermen. “Circuit simulation with SPICE OPUS: theory and practice”. Springer Science & Business Media, 2009.

Proceedings of the Fourth International Conference on Communication and Electronics Systems (ICCES 2019)
IEEE Conference Record # 45898; IEEE Xplore ISBN: 978-1-7281-1261-9

Weighted Pseudorandom Based Deterministic Bist for Fault Testing and Self-Healing

G.Bhavani
Department of ECE
GRIET
Hyderabad, India
bhavani2356@gmail.com

K. Jamal
Department of ECE
GRIET
Hyderabad, India
Kjamal24@gmail.com

B.Veera Reddy
Department of ECE
GRIET
Hyderabad, India
veerareddy57@gmail.com

***Abstract*— The mechanism which involves evaluating design performance is known as Testing. The power dissipation for the circuit in evaluating process is more when compare to standard operation of the circuit. For constricting the power dissipation in testing form delay fault testing method is used in the proposed design. In the proposed design scan architecture with self-healing technique is introduced to enhance the fault coverage. It will be going to sort out number of scan flip flops into uniform group. This paper adds self-healing procedure of scan design that is functioned among two phase clocks for vital scan cell test procedure and faulty scan cell test procedure to pseudorandom pattern generation and deterministic BIST application to increase the fault coverage.**

Keywords— Scan Architecture, Deterministic BIST, LFSR, Pattern Generation, PRPG, CUT.

I.INTRODUCTION

The space at functional power along with test power dissipation is enlarging swiftly. The particulars to impart sufficient explicit power model would be getting within [9] and [17]. Ahead to, explained from Scan based Built in self test (BIST) power consumption is more when differentiated to Deterministic scan testing ascribable to extravagant activating actions originated with random patterns. A weighted pseudorandom test pattern generation and deterministic BIST using reseeding technique to give the low power consumption by disabling the scan chain weight signals while it is executing other application [18].

The procedures introduced in [13], [10], [12] are aimed to reduce functioning between different blocks during scan shift cycles, which has the test generation of allowing directing itself to their parameters. Weighted Pseudorandom testing schemes of [10], [5], [2], and [7] can effectually raise the fault coverage. Yet, which methods are usually resulting in more power consumption with persistent passage at the scan flip-flops in more instances [14].

A DFT method for launch on shift testing[12], [15] ,[16] , It was make sure that combinational circuit logic residues not disturbed among the interleaved capture phases, which was done using computer aided design tools have more search ability for reducing capture switching between scan flip flops. The stipulated operation went by test pattern ordering [20].

As from [13], PRESTO (preselected toggling generator) design which produces binary sequences using preselected toggling activity. The register which is of toggle controlled supervises the hold latches. It has data incorporates zeros and ones; here ones stipulate latches would go to the toggle action, hence recognizable for data attaining from the PRPG. Their portion finds a scan functioning format. Besides that two parameters put in 4-bit Hold along with Toggle registers to encapsulate how will extend whole PRESTO rest each of two in hold mode or toggle mode, respectively. To close either mode, a 1 must yield as T flip flop input. Toggle mode: defines data transferring from PRPG to Phase Shifter. Hold technique: It will encapsulate and reserve measure of clock cycles and equal piece of PRPG giving the phase Shifter with in regards to a eternal value. In absolute operational version of PRESTO , toggle and hold signals are sustain through T_ flip flop which organizes the switching activity, Test data can be done in the design with LBIST(low power built in self test).In which ATPG form of embedded test compression scheme was involved. In this, a pseudorandom pattern generator cascaded with phase shifter which feeds scan chain to form the test pattern. Scan forest design was arranged as individual scan tree it has in deterministic test vector phase. The prototype narrates the scan adopted BIST design for two phase BIST method. Scan forest model will be in active for pseudorandom testing in initial moment. This procedure was heavily diminishing the size of the Phase shifter contrasted with the several scan chain architecture, here individual stage of the Phase shifter directs a scan chain. It leads to area overhead caused by the phase shifter can be diminished significantly. The test response compactor was an included XOR gate network.[8].

As referred from [6], this tells us that test file compression model among hybrid approach and external testing. The designs shows that it has three assessed weights are involved. In reference to the design these signals 0, 1, U are applied to scan element to its represented weight. Here U shows that register takes value of 0 or 1. This Comparision does with three levels, i.e unique part differentiation; each weight set differentiation; and expanded set coalition.

In the extended block diagram of paper Scan Architecture is added to acquire high fault coverage in

pseudorandom pattern generation and Deterministic BIST approach. The Pseudorandom patterns Generation using clock enabling technique is done, Moreover in Deterministic BIST technique will be concealed deterministic patterns are generated. The scan Architecture will be allowing more scan chains to test the pattern generated in PRPG (Pseudorandom Pattern Generation) with respect to CUT (Circuit under Test).

II.BASIC ARCHITECTURE

The basic Architecture for existing design i.e weighted pseudorandom pattern generation and deterministic BIST is shown in Fig.1.The block diagram which is shown in Fig.1.[18]. is architecture for generation of test patterns randomly using weight enable signals and which enables the circuit under test (CUT) to test in Deterministic BIST case. This block diagram validate with scan chain testing. The weights w_0, w_1, w_2..... And w_k are disbursed among the weighted scan enable signals SE_1, SE_2, SE_3.....and SE_k successively. And the values for weight signal w_0, w_1, w_2....., w_k belongs to {0.5, 0.625, 0.75, 0.875}. Persistent values were instantiated by randomizing the output flip flops alongside its position will be explained by dispersing other scan chains. Drained size of sub circuits of discrete scan chain is incited by cutting the entire circuit into sub parts.

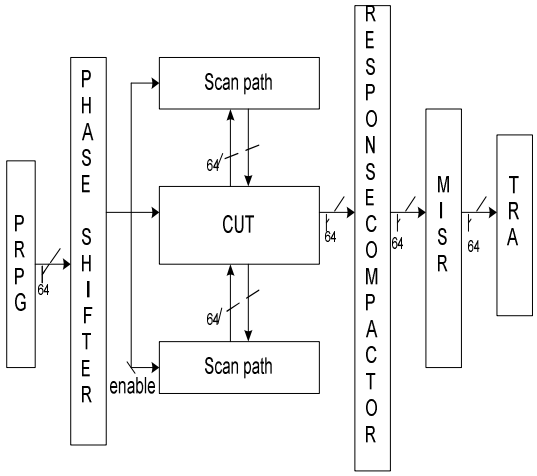

Fig.1. Weighted pseudorandom test pattern generation and deterministic BIST[18].

Where in degraded sub circuit total weight signals were selected. The Testability gain function determines the selection of weight signals. This is shown below:

$$g(f) = \sum_{l/i} \frac{|Co'_1(l) - Co'_0(l)|}{O'(l)}$$

Here, l/i =stuck at i fault at line i. 'f ' represents set of random pattern resistant fault , which accord to segregation of faults which has chance of finding is close to multiple times than thick fault. We aimed to moderate the testability gain function.

A Scan chain has weighted test enable signals which are shown in Fig2.[18]. In the figure test signal is test enable signal, SCin, SCo are Scan in and Scan out signals. Where every D flip flop is selected between Scan chain input and Pseudo primary inputs. Where it is known that each PI have a 0.5 Probability, and the observability calculation of the pseudo primary outputs PO's are declared to l/n. Then the Controllability is.

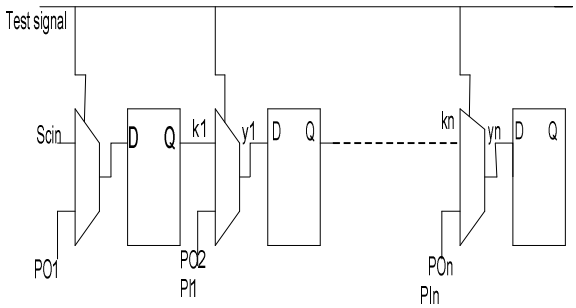

Fig.2. Scan chain with Test enables signals.

$$Co'(PI_i) = P.\ Co1'(x_{i-1}) + (1-P).\ Co1'(PO_i) \quad (1)$$

The Observability of PO_i (PO) can be determined as shown below:

$$O'(PI_i) = (1-P)\ .O'(x_i) \quad (2)$$
$$O'(x_i) = 1-(1-O'(y_i))\ .\ (1-O'(PI_i)) \quad (3)$$
$$O'(y_{i-1}) = P.\ O'(x_i) \quad (4)$$

From equation (1),(2) and(3) p is the chosen weight test enable control, x, y are nodes. Initially the observability coverage of scan out connection will be settled to 1. Yet to test response compactor was intended to course with yield of scan chain by attaching the output chain with XOR gates by perceptive we need to discover zero associating with least system evaluation. The controllability along with Observability measures help to calculate the PI's and PO's. A few iterations are covered to measurement of total nodes present in the benchmark circuits for more coverage.

The PI controllability for i^{th} iteration of scan flip flop is initially set to 0.5 and it has the Observability measurement of the PO is 1/d, where d represents length of the scan chain. It is observed that testing measurement of completely connected nodes become steady after few iterations of testability measure method.

As it is the design of weighted test enable signals separate sets of weights are charge with respect to the test enable control signals. The loads to the design are scan chain set, which are cleaved to sub circuits {SC_0,SC_1,.....SC_{k-1}}, given technique generates k degraded sub circuit formats .To keep down the gain function in the parent method selects the weights respective to initial scan chain. In order to keep down the cost function by specifying next to best among weight

signals, where in second scan chain a weight enable signal port will be chosen. Here in state it states that no weight is initialized for one of the scan chains, through returning the approach was conveyed their test enable control to the similar response as one of the value in standard test per scan BIST scan chains. The evaluation will be continued till the approximate weights should have to be chosen to every test enable signal of scan chains provided. Steps enclosed within existing method.

1. Primitive Polynomial Selection:

The given method includes single LFSR (Linear Feedback Shift Register) consideration to both pseudorandom pattern generation and deterministic states. The procedure gives a modern technique to choose the bits of LFSR and to fix the amount of extra variables to be injected. This will be done to diminish the quantity of deterministic test data. An effectively modeled phase shifter is sufficient for a minimum size of LFSR designed by primitive polynomial. In pseudorandom testing state a combined design of LFSR along with Phase shifter is retained to lend the test patterns. Weighted pseudorandom test patterns are generated from weighted test enable signal.

The amount of care bit length which does not give the maximum size of the LFSR, for every deterministic vector the same LFSR while doing both the phases. For encoding some deterministic test vectors having compute size of care bits, the seed which is kept in the LFSR and inserted control actions were added. It is not needed to provide length of an LFSR which is identical to extreme amount of care bits. At that time, pseudorandom testing state was extended moreover it is needed that effectively intended LFSR was utilized to initiate coded deterministic test vectors. Algorithm 2 referred to[18] , a procedure is explained to choose primitive polynomial that has least degree which is enhanced for the technique of coding of all deterministic test vectors to obtaining hard faults.

Ordinarily, The LFSR which was designed in architecture is shown below Fig.3.

Unlike the method in [8] , it is given that alternative use of an LFSR which has size i.e greater than quantity of care bits. The given procedure selects primitive polynomial with least degree. The commercial tool [5] used the same technique to limit the size of data to be reserved on chip ROM or ATE (Automatic Test Equipment). From Algorithm2 of [1], does choose the polynomial which has the degree should not be less than 20. There will be a rule which is to be provided that LFSR which does not have extra variables is considered first. When the encoding procedure of deterministic vectors cannot done based on LFSR based pseudorandom test generator, we will choose the case where separate extra variable is to be injected to the LFSR. If there is a case of deterministic vectors still cannot be coded in user needed format, the procedure then assessed the situation when two more variables are to be inserted. The process still is continued where given quantity of extra variables considered. If there status where LFSR as crucial portion of test generator cannot encode deterministic test pattern vectors there will be cast of considering second primitive polynomial [18]. The procedure is continued until we get the primitive polynomial which can code in test vector required composition of all deterministic vectors.

The example for LFSR with 64 –bit is presented in the Fig.3.The two extra variables are inserted at the 40 and 19th d flip flop i.e XOR gate is inserted. This gives polynomial i.e to be applied for LFSR.

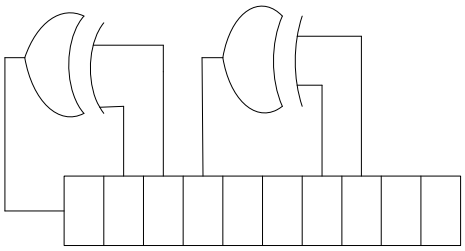

Fig.3. LFSR with variables.

2. Deterministic BIST:

There it is to impart with valuable seed encoding technique in order to cut down storage imperatives inside deterministic test patterns of which random pattern resistant faults. At first, conversion of another code format which gives error free element i.e initial test vector was introduced into LFSR. Every scan in standard in the circuit operates on driving numerical representation with scan trees. Respective scan in input is initialized where it has the equivalent scan tree. After receiving the test data of primary group it is defused and second group is activated then. LFSR prime input i.e seed will be reserved in auxiliary variable i.e shadow register [8]. The scan shift operations iterated till extra variables are placed into the LFSR. This procedure will be continued till scan trees in scan path got test data.. It gives more flexibility for test encoding technique. Minimum No. of clock cycles are basic to convey the entire test vector counter of past test vector, if there should arise an occurrence of scan chain design more clock cycles are assessed for completing the response. All the scan flip flops which were found at earlier level along with the scan chain amass the swearing off condition. i.e singular compound of scan flip flop would have no combinational successor. Process will be continued until the scan trees have been outlined. It has no need that same level scan tree should be kept aside.

The forgoing conditions are necessary to encode format of all deterministic vectors [3],[1].

This can be stated as:

i $L + i.v \geq s_{max}$

ii $\sum_{k=d-1}^{k=d-1-j} b_k \leq (L + V_j$

Where L is the size of LFSR, i represent Figure of sequential cycles to insert extra variables; V_j is the amount of extra variables among j shift cycles, S_{max} is quantity of care bits. b_k gives No. of care bits at scan level k. The previous technique provides reseeding process for LP deterministic BIST. This method partitions all of signals of scan chains to multiple subsets, condition to be remembered that one sub members of scan tree activated at one clock cycle. It will follow the gating logic. The logic was been helped by the shadow register which is of comparable length of LFSR. This register used to store seed values [6].

III. PROPOSED DESIGN

Before going to the proposed architecture, we need to know that what self-healing defines. Self-healing can be characterized that it is designed which has the quality of finding faults or failures and to debug their faults correctly. Essentially all self-healing strategies which were set up on repetition by cumulating spare cells they work same as scan chains in the BIST with executed methodology. The block diagram for proposed architecture is shown below:

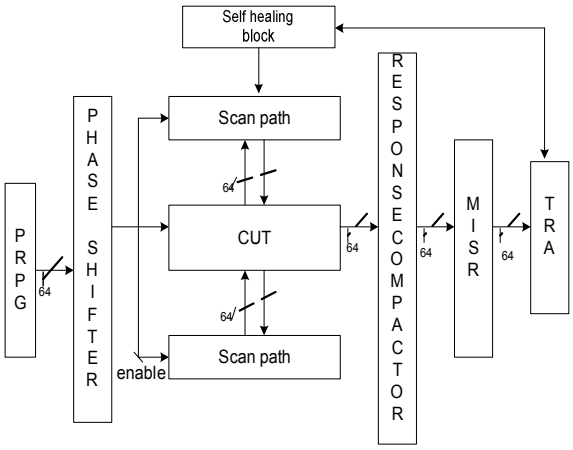

Fig4. Proposed architecture with self healing added block.[19].

As from Fig.4. i.e implementation of executed model, on that instance the defect have been delivered in particular scan cell, alongside the scan cell will condense the control flag which was started will have been assume responsibility for bist controller to bound this fault task was actualized initially. A dual edge triggered cell is introduced to divide the runtime with active scan cell, faulty cells. The primary half of the clock cycle is given switching to active scan cell and second half is given to faulty cell actions to be controlled. The scan cell circuit for self -healing technique is shown below:

In the block diagram, the foremost logic block gives the pattern generation i.e PRPG (pseudo Random pattern generation), these patterns are provided with LFSR and XOR network combination. Succeeding block is Phase shifter which shifts phase of produced patterns. Then other block Scan path will reserve the reference vectors as well as scan chain input is concatenated as input to bist controller. This is given from scan path. CUT shows that the circuit to be tested. Response compactor compresses the data which is under testing. MISR (Multiple Input Signature Register) is grouping of multiple XOR networks. It creates the compacted data to the indication level. This signature is the collection of multiple test data. TRA (Test Response Analyzer) checks the emulation between reference data and test pattern data. While, whether they are contrasted successfully the test will be pass otherwise it is fail. Here, Self-Healing block is joined to enlarge synchronize the clock phasing and test coverage.

The diagram shows the cell structure for DET (dual edge triggered circuit) in Fig.5.[19].There will be added two inputs I_0 and I_1 to the circuit. The control actions are representing that one is debug signal and another one is effective signal. When fault is detected the detection block will get to notice the faulty spot and control block sort the signal to go there location. When the clock rises to positive edge DET will accord normal result and for falling edge of the clock it will drive faulty value [19].

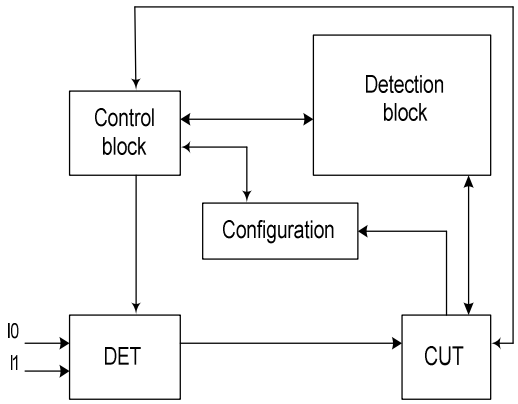

Fig.5. Scan cell structure[19].

IV. EXPERIMENTAL RESULTS

The existing method and propounded method are implemented as well analyzed on synopsys VCS (Verilog language simulation program for chip design) tool. It is quick simulator environment for functional verification. This compilation gives quality in functional verification. In the design truly small scan chain pins were introduced. In order to diminish the area over head a limited size of phase shifter was used. As from the existing design the supplying to the circuit of voltage and frequency are applied to 1.5v and 200MHz, independently. Simulation results from synopsys VCS is

shown in Fig.6. Bist out is the main response from the bist controller, it tells whether the test passing response or fail response.

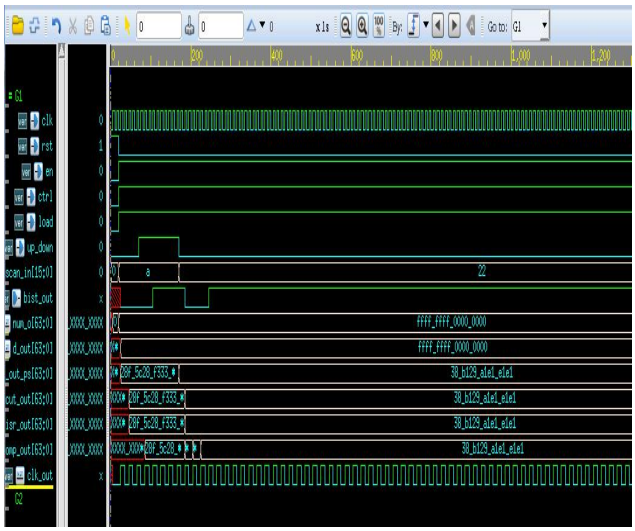

Fig.6. Simulation Results.

The comparison for LP deterministic BIST and low power Pseudorandom pattern generator and extended design is summarized in the below table. What's more, the proceeded is procured to expand the fault coverage. 10% when compared with the existing work. It will also increase fault coverage. For synthesis of both the work will be done by Xilinx vivado tool. Power dissipation calculation was taken from Xilinx vivado environment. This 10 % flip flops are in switching action gives to maximize in rate will give the reason to only switching version of flip flops are assisted in the operation of respective things.

TABLE.I

Comparision of previous work with proposed work(Power reduction)

	Deterministic BIST			**Scan based self healing technique**		
CUT	**Peak (mW)**	**Lppeak (mW)**	**Rate %**	**Peak (W)**	**Lppeak (mW)**	**Rate %**
S38417	6724	643	9.6	6700	620	9.9
b19	41933	5660	13.4	41000	5602	13.7
usb_funct	6261	610	9.7	6108	598	9.86
pci_bridge	8119	984	12.1	8075	978	12.7
74F569	5873	660	10.4	5704	624	10.9

The CUT is the design which is to be test. Contrast checking of deterministic Bist method and self healing technique are evaluated. Peak power and LP peak power are considerable to take the total Power dissipation in the CUT. CUT designs are taken that benchmark environment applications.

V.CONCLUSION

A new technique to raise the fault coverage and to decrease the power dissipation of the circuit is introduced in the proposed design. The proposed technique which has two clocking phases to synchronize error founded data with error corrected data. There it has more signals added, even the signals added it will keep down the power dissipation by using the two edges of clock are involved in the design. LP deterministic BIST is extended to self-healing method to increase power reduction rate.

VI.REFERRENCES

[1] Koenemann, B. "LFSR-Coded Test Patterns for Scan Designs, European Test Conference." (1991): 237-242.
[2] Pomeranz, Irith, and Sudhakar M. Reddy. "3-weight pseudo-random test generation based on a deterministic test set for combinational and sequential circuits." *IEEE Transactions on Computer-Aided Design of Integrated Circuits and Systems*12.7 (1993): 1050-1058.
[3] Hellebrand, Sybille, et al. "Built-in test for circuits with scan based on reseeding of multiple-polynomial linear feedback shift registers." *IEEE Transactions on Computers* 44.2 (1995): 223-233.
[4] Kapur, Rohit, et al. "A weighted random pattern test generation system." *IEEE Transactions on Computer-Aided Design of Integrated Circuits and Systems* 15.8 (1996): 1020-1025.
[5] Rajski, Janusz, et al. "Embedded deterministic test." *IEEE transactions on computer-aided design of integrated circuits and systems* 23.5 (2004): 776-792.
[6] Jas, Abhijit, C. V. Krishna, and Nur A. Touba. "Weighted pseudorandom hybrid BIST." *IEEE Transactions on Very Large Scale Integration (VLSI) Systems* 12.12 (2004): 1277-1283.
[7] Xiang, Dong, Mingjing Chen, and Hideo Fujiwara. "Using weighted scan enable signals to improve test effectiveness of scan-based BIST." *IEEE Transactions on Computers* 56.12 (2007): 1619-1628.
[8] Xiang, Dong, et al. "A reconfigurable scan architecture with weighted scan-enable signals for deterministic BIST." *IEEE Transactions on Computer-Aided Design of Integrated Circuits and Systems* 27.6 (2008): 999-1012.
[9] Yu, Wenjian, Rui Shi, and Chung-Kuan Cheng. "Accurate eye diagram prediction based on step response and its application to low-power equalizer design." *IEICE transactions on electronics* 92.4 (2009): 444-452.
[10] Lin, Xijiang, and Janusz Rajski. "Adaptive low shift power test pattern generator for logic BIST." *2010 19th IEEE Asian Test Symposium*. IEEE, 2010.
[11] Sato, Yasuo, et al. "Low power BIST for scan-shift and capture power." *2012 IEEE 21st Asian Test Symposium*. IEEE, 2012.
[12] Potluri, Seetal, et al. "DFT assisted techniques for peak launch-to-capture power reduction during launch-on-shift at-speed testing." *ACM Transactions on Design Automation of Electronic Systems (TODAES)* 21.1 (2015):
[13] Filipek, Michał, et al. "Low-power programmable PRPG with test compression capabilities." *IEEE Transactions on Very Large Scale Integration (VLSI) Systems* 23.6 (2015): 1063-1076.
[14]. K.Jamal, Dr.P.Srihari "Analysis of Test Sequence Generators for Built-In Self-Test Implementation" 2nd International Conference on Advanced Computing and Communication Systems (*ICACCS* -2015, ISSN: 978-1-4799-6438-3/15/$31.00 ©2015 IEEE)
[15] K.Jamal, Dr.P.Srihari, G Kanakasri "Test Vector Generation using Genetic Algorithm for Fault Tolerant Systems*"International Journal of* Control Theory*and Applications* (IJCTA), 9(12), 2016, pp. 5591-5598. ISSN : 0974-5572.
[16]K.Jamal, Dr.P.Srihari "Low Power TPC using BSLFSR" I*nternational Journal of Engineering and Technology* (IJET), Vol 8 No 2 Apr-May 2016. Page no.759.e-ISSN : 0975-4024
[17] Chitra, A., S. Vijay Murugan, and B. Sathiyabhama. "Detection of Stuck Open and Short Fault in SRAM Based System." *Proceedings of the*

International Conference on Intelligent Computing Systems (ICICS 2017–Dec 15th-16th 2017) organized by Sona College of Technology, Salem, Tamilnadu, India. 2017.

[18] Xiang, Dong, Xiaoqing Wen, and Laung-Terng Wang. "Low-power scan-based built-in self-test based on weighted pseudorandom test pattern generation and reseeding." *IEEE Transactions on Very Large Scale Integration (VLSI) Systems*25.3 (2017): 942-953.

[19] Khalil, Kasem, Omar Eldash, and Magdy Bayoumi. "A cost-effective self-healing approach for reliable hardware systems." *2018 IEEE International Symposium on Circuits and Systems (ISCAS)*. IEEE, 2018.

[20] K. Jamal, P. Srihari, K. Manjunatha Chari, B. Sabitha "Low Power Test Pattern Generation Using Test-Per-Scan Technique for BIST Implementation "ARPN Journal of Engineering and Applied Sciences (ISSN 1819-6608) (VOL.13,NO.8,APRIL2018).

Proceedings of the Fourth International Conference on Communication and Electronics Systems (ICCES 2019)
IEEE Conference Record # 45898; IEEE Xplore ISBN: 978-1-7281-1261-9

Road Crack Detection and Segmentation for Autonomous Driving

Geetika Aggarwal[1] Sarika Jain[2]
[1,2]*Amity Institute of Information Technology*
Amity University Uttar Pradesh
[1]aggarwal.geetika4@gmail.com
[2]ashusarika@gmail.com

Abstract – All things considered, the self-governing vehicle is the vehicles which are fit to detect tits condition and exploring without human contribution under various landscapes especially over pavements. The fact is, limit with regards to auto route for the most part relies upon the vehicle's capacity to screen and exactness so as to translate street surface condition. The improvement of powerful street surface checking instruments is extraordinarily improving the practicality of independent vehicles, while commitment in the decrease of related street mishaps on the planet. The toolbox, in the Mat lab condition, incorporates calculations to pre-process pictures, to identify breaks and describe them into sorts, in light of picture preparing and design acknowledgment procedures, just as modules committed to the execution assessment of irregularity location and portrayal arrangements. An example database of 84 asphalt surface pictures taken amid a conventional street review is furnished with the tool kit, since no asphalt picture databases are freely accessible for peculiarity identification and portrayal assessment purposes. Results accomplished applying the proposed tool kit to the example database are talked about, delineating the capability of the accessible calculations.

Keywords: Image Processing, Pre-processing technique, Image Segmentation, Post-processing technique, Road Surface, Road Anomaly Characterization

I. INTRODUCTION

As there are more improvements in the technology world, cars have become more advanced and thus the evolution of autonomous vehicles.

Self-governing vehicles will be vehicles fit for detecting their condition and exploring without human contribution under various territories, especially over black-top streets. The ability to auto explore to some degree relies upon the vehicle's capacity to screen and precisely decipher street surface conditions the extent that the streets are concerned crocodile part, furthermore called gator breaking and possibly misleadingly shortcoming breaking, is a regular sort of torment in dark top black-top. Cell sizes can fluctuate in size up to 11.80 inches (300 mm) over, yet are normally under 5.90 inches (150 mm) over. Debilitation breaking is commonly a stacking failure, yet various variables can add to it. Usually an indication of sub-base disappointment, poor seepage, or rehashed over-loading. It is vital to avert debilitation splitting, and fix as quickly as time permits, as cutting-edge cases can be all around expensive to fix and can prompt arrangement of potholes or untimely asphalt disappointment. The arbitrariness in increasing speed flags regularly makes street irregularity discovery a troublesome procedure, while rendering portrayal a significantly progressively troublesome and some of the time incomprehensible assignment. For this condition, we hint disclosure as the obvious confirmation of a peculiarity, while delineation is depicted as the certification of the sort of perceived variety from the standard (for this situation on the off chance that it is either a pothole or a pound). From this time forward, giving new frameworks to improving street.

Variety from the standard disclosure and delineation pushed the work revealed in this paper.

We have proposed a a RACA (Road Anomaly Characterization Algorithm) in context on the Wavelet Transformation Scale Space Filtering (SSF) figuring. The SSF figuring shapes the quickening signs by deteriorating them into different scales. It would continue by interfacing the debilitated wavelet coefficients of standard transversely over neighbouring scales and after that separating the loud models through an all around orchestrated spatial channel. The SSF calculation encourages a street irregularity location Algorithm (RADA) to distinguish street abnormalities by means of a fixed limit strategy, while nourishing RACA to describe street peculiarities. RACA accomplishes portrayal utilizing two one of a kind highlights to separate potholes from knocks. On the other end weakness breaking shows itself at first as longitudinal splitting (splits along the bearing of the stream of traffic) in the top layer of the

black-top. These splits are at first light and inadequate dispersed. In the event that further weakening is permitted, these longitudinal splits are associated by transverse breaks to shape sharp sided, kaleidoscopic pieces. This intertwist splitting example looks like the scales on the back of a crocodile or gator, consequently the epithet, crocodile breaking.

II. LITERATURE REVIEW

Yiyang et al. [1] have proposed a break location calculation dependent on computerized picture preparing innovation. By pre-preparing, picture division and highlight extraction [1], they have gotten the data about the break picture. In [4], Threshold strategy for division was utilized after the smoothening of the acknowledged info picture. Adhikari et al. [2] built up a model that numerically speaks to the deformities. Their reconciliation display comprises of split evaluation and recognition, neural system, and 3-D perception demonstrate individually. Alam et al. [3] have suggested an affirmation method at the mix about the pushed picture relationship and sound spread. The past approach permits a distinct estimation of surface re-territories, from now on part openings and break dissipating were settled. Iyer et al. [4] have sorted out a three-advance framework for the split distinctive verification from the high multifaceted nature pictures. The proposed methodology recognizes the split like model in the disorderly condition utilizing shape examination and numerical morphology system. Salman et al. [5] proposed a way to deal with oversee typically see parts in forefront pictures subject to the Gabor confining. Multi-directional break disclosure can be developed by expensive potential Gabor channel. Shan et al. [6] have appeared build part thickness unmistakable verification. In their technique, two cameras were utilized not run of the mill for different suggestion reviewed here. Sinha et al. [7] have researched the breaks by utilizing the two-advance methodology. They have built up a quantifiable channel structure for the break ID. After the limiting, they should the two-advance rationale at which the break incorporate extraction was done locally at the shrouded improvement of the pre-overseeing and some time later they have combined the photos. The second step is to delineate the part among the image zone by the route toward cleaning and accomplice. Talab et al. [8] have shown another system in picture managing for seeing parts in pictures of strong structures. Here the technique wires three phases: First; change the image to a light picture using the edge of the image and after that use Sobel's framework to develop an image using Sobel's channel for seeing parts. Yamaguchi et al. [9] have built up an immersion based break territory strategy. They have gotten their less check time by the modification of the end and avoid consolidate procedure. They have a snappy immersion tally which will utilize the neighboring pixels subject to the circularity of the pixel needs. Yang et al. [10] have proposed a picture examination framework to get slight parts and purpose of constrainment the requirement for pen venturing in invigorated security partner tests. Zou et al. [11] have built up a completely altered strategy to see split the dark top pictures. They utilized geodesic shadow discharge tally to expel the dark top shadows by protecting the break. After shadow clearing, utilizing the tensor tossing a ticket strategies break likelihood map was made. Oliveira et al. [12] have formed a structure for the changed break insistence. Here the break exposure relied on the model perspective. In the model perspective, a subset of the open picture database was usually picked and used for unsupervised getting ready of the structure pictures. Nguyen et al. [13] have proposed a system subject to the edge ID of strong parts from rambunctious 2D pictures of strong surfaces. They have watched the parts as tree-like topology. Lins et al. [14] have developed with the target to mechanize the split estimation process. In their system, they have used only a single camera for the getting ready of the social event of the photos for the split estimation. Li et al. [15] have solidified another structure for seeing the break in the mutilations with the dull shading and the low separation using the enthusiastic discrete curvelet waveform and surface examination.

III. RESULTS AND DISCUSSION

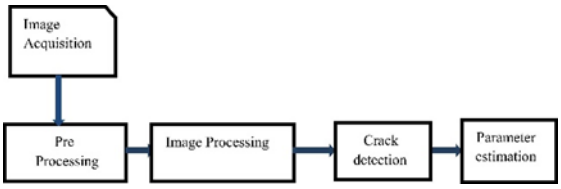

Fig1: The Stages of Image Processing to find road cracks

Picture Acquisition Toolbox gives capacities and squares to associating cameras and lidar sensors to MATLAB and Simulink. It incorporates a MATLAB application that lets you intelligently recognize and design equipment properties. You would then be able to create equal MATLAB code to mechanize your procurement in future sessions. The tool compartment empowers securing modes, for example, preparing tuned in, equipment activating, foundation procurement, and synchronizing obtaining over different gadgets. There are different image acquisition techniques which are used in image processing such as pre-processing technique, image processing technique, crack detection technique, parameter estimation.

I. Pre-processing Technique**:**

Informational indexes can require pre-processing methods to guarantee precise, effective, or significant investigation. Information cleaning alludes to strategies for discovering, expelling, and supplanting awful or missing information. Distinguishing neighbourhood extrema and sudden changes can recognize noteworthy information patterns. Smoothing and detrending are forms for expelling clamour and straight patterns from information, while scaling changes the limits of the information. Gathering and binning strategies are systems that recognize connections among the information factors.

II. Image processing Technique:

Picture examination includes preparing a picture into essential segments so as to extricate factual information. Picture examination can incorporate such undertakings as discovering shapes, recognizing edges, expelling commotion, tallying items, and estimating area and picture properties of an article.

Picture examination is an expansive term that covers a scope of strategies that for the most part fit into these subcategories:

i. Picture improvement to evacuate commotion.
ii. Picture division to seclude areas and objects of intrigue.
iii. Morphological sifting to evacuate more clamour.
iv. Locale investigation to remove measurable information.

III. Crack Detection technique:

Crack detection using computer vision toolbox (sobel edge detection algorithm).

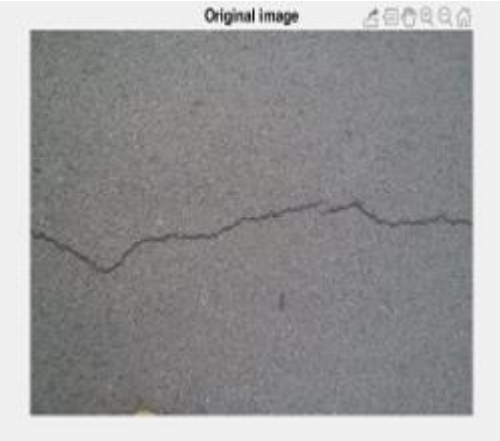

Fig2: Original Image

Fig 3: Contrast Stretched Image

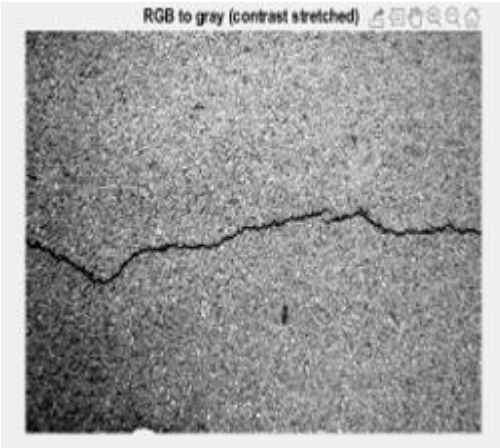

Fig 4: RGB to grey (Contrast Stretched Image)

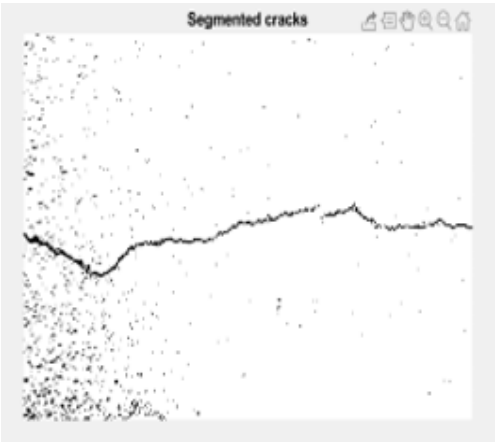

Fig 5: Segmented Cracks

IV. Parameter Estimation Technique

Parameter estimation assumes a basic job in precisely portraying framework conduct through scientific models, for example, likelihood dissemination capacities, parametric powerful models, and information-based Simulink models. Regular assignments for parameter estimation of Simulink models include: bringing in and preparing input-yield test information, for example, the voltage information and rotor speed yield of a DC engine and determining which demonstrate parameters and starting conditions to evaluate, for example, engine opposition and latency. Figure 7 shows genuine (green) and false (yellow) positives. Figure 7 shows in view of the sexually transmitted disease of cco's pixels organizes (level and vertical), indicating choice limits (dashed lines) and highlight space division (strong line).

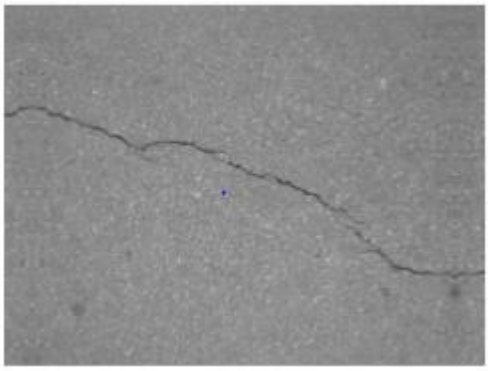

Fig 6: Original Image

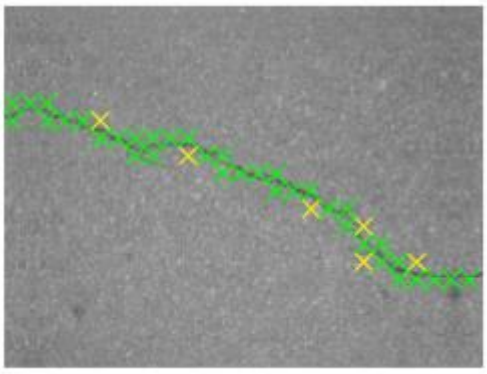

Fig 7: Crack Detected Image

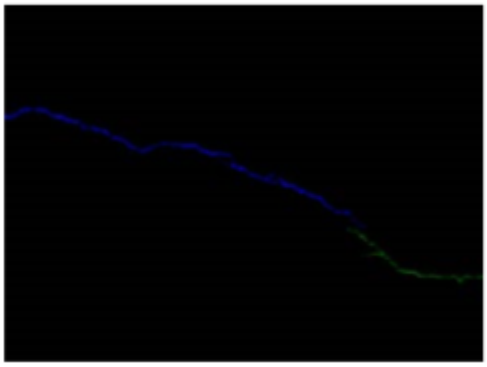

Fig 8: Global Cracks Identified Image

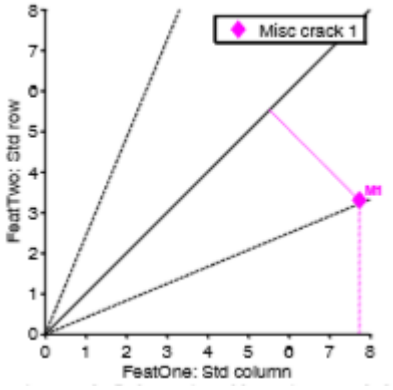

Fig 9: Crack type Assigned Pixels

V. CONCLUSION

The proposed tool compartment permits accomplishing great split location and portrayal results, however managing exceptionally flimsy breaks (of under 2 mm width) can be a troublesome assignment, the same number of false positives may show up, quite because of the trouble of recognize splitting from travelling upsets. There are no accessible conventions or institutionalized techniques for assessing the execution of the created frameworks and to think about the distributed methodologies, driving the creators to think about various conventions, in spite of some current harmonization endeavours. It is normal that this tool kit will be stretched out, for example to incorporate calculations to additionally decrease pixel power difference in non-split squares, or increment strength to picture splendour varieties.

The RACA Algorithm

Here, we depict the progress of our information confirming structure. The system of street surface recognizing is appeared in Fig 10. The three fundamental assignments in this stage combine the street surface information getting process utilizing an Accelerometer, the information parameter introduction, and information show up for visual examination/examination. We note that NI MyRio (1950) Accelerometer was altered utilizing LABVIEW for the information checking action.

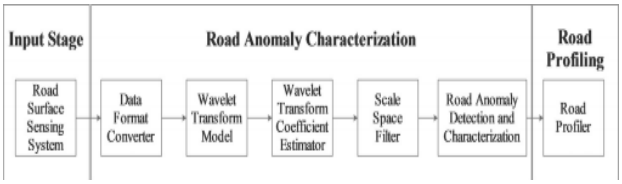

Fig 10: Block Diagram of the street oddity identification, portrayal and profiling framework

We joined a Global Positioning System (GPS) into our arrangement to discover road erraticisms. To do this, we balanced an Arduino microcontroller under the Arduino Integrated Development Environment (IDE). The GPS data getting process is showed up in Fig. 11. On an essential dimension, the system acquaints the GPS module with log the season of data get, and after that records the relating longitude and increase headings of the space where data was gotten. The GPS assessing rate was set at 1 Hz which was found acceptably appealing to give area server ranch in the midst of the drive test.

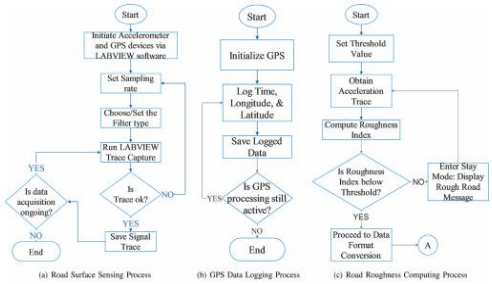

Fig. 10. Components of the Data Acquisition stage

We used the standard deviation of the enlivening flag got over a specific period as a deduced furiousness record to plot road quality. In case the offensiveness list regard is underneath a particular fixed point of confinement regard, RRAA picks that the road surface is smooth (prescribing that the vehicle is on a dull top road), and thusly starts the unusualness assertion and outline computation (delineated in the running with subsections). In any case, if the record regard is over the edge, the estimation enters a stay mode (seeing that the road being used may not be a diminish top road and thusly routinely imperfect). The program demonstrates a "Harsh Road" message in the midst of this stay period. The road abnormality confirmation and depiction check is perhaps established when RRAA measures a severity list underneath the most far off point regard.

REFERENCES

[1] Zhang Yiyang, “The design of glass crack detection system based on image pre-processing technology”, in: Proceedings of Information Technology and Artificial Intelligence Conference, 2014, pp. 39–42.

[2] R.S. Adhikari, O. Moselhi1, A. Bagchi, “Image-based retrieval of concrete crack properties for bridge inspection”, Autom. Constr., 39 (2014), pp. 180-194

[3] S.Y. Alam, A. Loukili, F. Grondin, E. Rozière, “Use of the digital image correlation and acoustic emission technique to study the effect of structural size on cracking of reinforced concrete”, Eng. Fract. Mech., 143 (2015), pp. 17-31

[4] Shivprakash Iyer, Sunil K. Sinha, “A robust approach for automatic detection and segmentation of cracks in underground pipeline images”, Image Vis. Comput., 23 (10) (2005), pp. 931-933

[5] M. Salman, S. Mathavan, K. Kamal, M. Rahman, “Pavement crack detection using the gabor filter”, in: Proceedings of 16th International IEEE Annual Conference on Intelligent Transportation Systems, 2013, pp. 2039–2044.

[6] Baohua Shan, Shijie Zheng, Jinping Ou, “A stereovision-based crack width detection approach for concrete surface assessment”, KSCE J. Civ. Eng., 20 (2) (2016), pp. 803-812

[7] Sunil K. Sinha, Paul W. Fieguth, “Automated detection of cracks in buried concrete pipe images”, Autom. Constr., 15 (1) (2006), pp. 58-72

[8] Ahmed Mahgoub Ahmed Talab, Zhangcan Huang, Fan Xi, Liu Hai Ming, “Detection crack in image using Otsu method and multiple filtering in image processing techniques”, Optik – Int. J. Light Electron Opt., 127 (3) (2016), pp. 1030-1033

[9]Tomoyuki Yamaguchi, Shuji Hashimoto, “Fast crack detection method for large-size concrete surface images using percolation-based image processing”, Mach. Vis. Appl., 21 (5) (2010), pp. 787-809

[10] Yuan-Sen Yang, Chung-Ming Yang, Chang-Wei Huang, “Thin crack observation in a reinforced concrete bridge pier test using image processing and analysis”, Adv. Eng. Softw., 83 (2015), pp. 99-108

[11] Qin Zou, Yu Cao, Qingquan Li, Qingzhou Mao, Song Wang, “CrackTree: automatic crack detection from pavement images”, Pattern Recogn. Lett., 33 (3) (2012), pp. 227-238

[12] Henrique Oliveira, Paulo Lobato Correia, “Automatic road crack detection and characterization”, IEEE Trans. Intell. Transp. Syst., 14 (1) (2012), pp. 155-168

[13] Hoang-Nam Nguyen, Tai-Yan Kam, Pi-Ying Cheng, “An automatic approach for accurate edge detection of concrete crack utilizing 2D geometric features of crack”, J. Signal Process. Syst., 77 (3) (2014), pp. 221-240

[14] Romulo Gonçalves Lins, Sidney N. Givigi, “Automatic crack detection and measurement based on image analysis”, IEEE Trans. Instrum. Meas., 65 (3) (2016), pp. 583-590

[15] Xueqin Li, Honghai Jiang, Guofu Yin, “Detection of surface crack defects on ferrite magnetic tile”, NDT E Int., 62 (2014), pp. 6-13

Proceedings of the Fourth International Conference on Communication and Electronics Systems (ICCES 2019)
IEEE Conference Record # 45898; IEEE Xplore ISBN: 978-1-7281-1261-9

Enhanced Secrecy Capacity under Eavesdropping Attack in Multi-Traffic Industrial WSN

A.Chandra Shaker
Department of Electronics and Telematics Engineering
G.Narayanamma Institute of Technology and Science
Hyderabad, Telangana, India
chandrashakerarrabotu@gmail.com

***Abstract*—Industrial networks are increasingly based on open protocols and platforms that are also employed in the IT industry and internet background. It is essential to secure the important information throughout transmission so highest secrecy capacity is chosen in Wireless Sensor Networks. The employment of sensing element to improve the physical layer security of industrial WSN can counter the eavesdropping attack and optimal sensor scheduling scheme targets to increase the secrecy capacity of wireless transmissions from the sensors to the sink. The system model with one eavesdropper and multiple sources with different data type is used. The scheduling theme satisfies the requirements in multiple traffics and achieves maximal secrecy capacity. Numerical results validate the proposed optimum scheduling theme in Nakagami fading environment. This system model performs better than the traditional Round Robin scheme in terms of the throughput, delay and packet delivery ratio and monitors the packet transmission according to the assigned priorities.**

Keywords—eavesdropping attacks, industrial wireless sensor networks, multi-traffic, secrecy capacity

I. INTRODUCTION

A wireless sensor network is a network which has many sensor devices that are connected with each other wirelessly. The sensor nodes can communicate the collected information from the physical monitored field or environment through the intermediate nodes to the destination. Using like Wireless Ethernet the data is passed to another network through interlinked nodes and gateways. A wireless sensor network are useful in applications where the physical environment like pressure, temperature, sound etc. can be monitored and transmitted to some other device it may be a mobile, laptop, computer or any other electronic device using wireless medium. The monitored information may help to control the application device or to take care of things to be done as per the requirement.

Every industry can have their own network, which is responsible for their own industry and also have a link with the global network. Using Bluetooth, WIFI, router communication one can develop their own personal network in industries by securing the network with passwords and can divide the access availability according to the level of authority in industry. For passing the internal communication the WSNs can be used in between labours and higher authorities.

II. LITERATURE SURVEY

Initial motivation of wireless sensor networks are done by the military [1], and now these are introduced in the industrial applications. These networks are used for line monitoring, automated manufacture of a product to improve the efficiency of factory, to have more productivity and very reliably work in industries [2][3], which can be called as industrial wireless sensor networks [4]-[6].

As the sensor networks are spatially distributed in a region, there is a need of maintaining strict security [7]. If a sensor failed to send exact sensed information to the destination then it is out of production line, or it may cause damage to the machine in factory or sometimes in critical work it may lead to loss of worker. The other aspect in the industrial environment is having machinery obstacles, engine vibrations and the noise generated by the machine.

The wireless sensor network has broadcast nature where the medium access is open to authorized and unauthorized users. So there are more chances of eavesdropper to attack the wireless network than wired networks. The eavesdropper hides within in the industry and the hidden attacker node can steal the information or tap the transmissions if there is no security for the information. Therefore finding the hidden attacker in industrial networks is main concern.

M. Mckay and X. Zhou [15] discussed about the secure transmission with help of generating external noise in the system at the transmitter end. By considering the multiple antennas, the transmitter starts transmitting original signal to the intended receiver and noise signal to the eavesdropper. It acquires systematic secrecy rate and target capacity to optimize the power allocations at the transmitter side for a single eavesdropper.

The specific considerations of industrial WSNs is the fading of channel due to the environmental constraints like machinery affects in the form of frictions and vibrations called as fading signals. Fading affects the signal loss or irrelevant additional signal to the main signal transmission in the channel.

III. PROBLEM FORMULATION

These days many industries are showing interest to implement the wireless networks in their work place for smart work. Sensor network has many advantages that attract industries to take step forward towards implementation of work. The security is the main concern of the industries; any way outside user cannot enter into the network. The intruder may hide within the network. As the technology is improving, intruder is also becoming more intelligent to crack the information. To secure the communication from the eavesdropper, many techniques came up, but still they have some limitations. Few cases how eavesdropper can attack the networks are explained below:

Case 1: Consider the communicational info is hacked by the intruder. In these days of developing technology, labour need not have the knowledge of protocol or algorithm implementation of the machine; it is automatically suggested by the predefined system updating software or new updating instructions may come from the higher technical authority to labour. If the intruder attacks on this information, the wrong updating of protocol installed in the machine damages the

machine functionality with the wrong guidelines of protocol. Sometimes, because of next versions it would not give immediate impact on machine.

Case 2: Consider the interloper has assaulted on the direct information where the human has to communicate with the machine. If a command is given to do an immediate action like switch on or off the machine at different modes according to the situation, that info may be hacked and gives some other mode selection to the machine. Due to this, there will be big loss; sometimes may cause loss of labour at work.

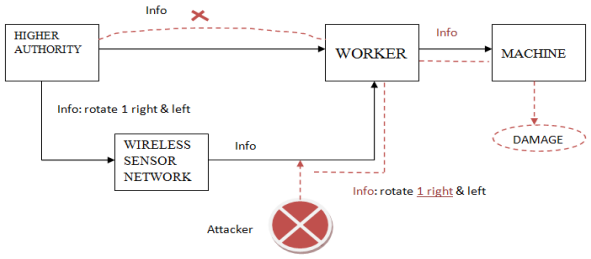

Figure 1: An example for industrial problem

The example in Figure 1 explains the real time problem and how it will damage or loss to the industries considering one higher authority node, worker node and machine with an eavesdropper node. As it is an autonomous network the only chance is having an interloper within the industry. The attack it is not a physical one, but the attacker also uses same nodal device like authority users.

The higher authority thinks to transmit the info 'rotate 1 right and left' to the worker through the wireless main channel link but the eavesdropper attacked on the channel and the info is misguided like 'rotate 1 right & left' to the worker, actual data has changed with the wrong info. If the machines are arranged in synchronous order, this misguided info will affect the machine and it damages the equipment.

Few key parameters are chosen to evaluate the security of the communication technically. By improving the main link channel capacity it shows the improvement of security level at physical layer without any additional power supply or additional relay nodes. As the transmission of data is in the form of packets, the key parameters are to be considered are:

Packet Delivery Ratio: The ratio is calculated in between the number of packets received at the receiver and transmitted from the source. The PDR factor should be at maximum level.

Throughput: The rate of successful packets reception at the receiver end from the transmission end calculates the throughput and this factor is important to see the performance of the introduced algorithm.

Delay: The difference between the estimated time to be reached and to the time when it has reached the destination. For any communication, this is also the main concern for delivering the packet within the time.

Consider the industrial WSN which includes a sink centre point and N sensors with an eavesdropper. Every node device uses a single antenna, the strong lines and dash lines address the main link and wiretap interface, exclusively. The eavesdropper in the Figure 2 could be either absurd user or genuine user who possesses the tapped data. The *N* sensors are indicated by $S = \{Si = 1,2,3 \dots N\}$. As appeared in the Figure 2, the proximity of hardware hindrances, metallic contacts and engine vibrations in mechanical conditions is undermining to the radio spread, which impacts the remote obscuring to change certainly.

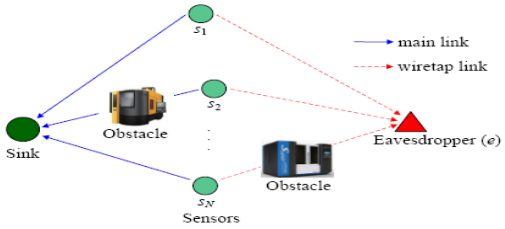

Figure 2: System model

Consider the Nakagami fading model for depicting both essential channel and wiretap channel. It is pointed that Nakagami model is more complex than the other obscuring models like Rayleigh fading model which is most used technique [18][19].

At the point when a sensor is planned to transmit its information to the sink node or destination over a channel, the attacker called eavesdropper attempts to catch the information, which is transmitted from the *Si*. This paper concentrates on the enhancement of wireless physical layer security with the guide of sensor scheduling plan keeping in mind the end goal to successfully shield against the eavesdropper.

IV. Existing Conventional Round Robin Scheme

The existing method conventional Round Robin is used for the reference purpose of this project, where the ***N*** sensors alternate in getting to a given channel and along these lines every sensor has equivalent opportunity to transmit its detected info to the sink without any loss of all inclusive data.

The detected data could be distinctive sorts of information from various sensors. For instance, the sensors might be utilized to identify and screen the distinctive part of the industrial plant conditions, including the movement of a machine, dampness, temperature, pressure and weight of the machine. Despite the fact that the sensors may create diverse sorts of information, their information streams are accepted with the same priority in transmission. The proposed work deals with the multiple data types with the individual priorities.

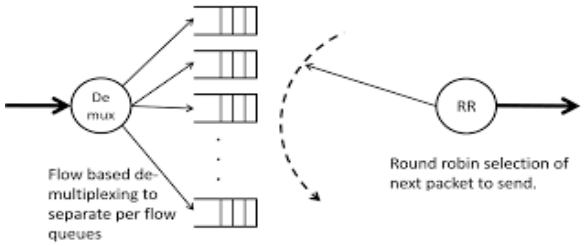

Figure 4: Conventional Round Robin scheme

The Round Robin schedule follows the time slots of a packet which is expressed as $T_{slice=}T_{cycle}/N$, the one circular round of the queue is T_{cycle} and the N defines the number of packets in the queue. The time slice will be changed from one process to other in the system, where the minimum time slice is allotted for the each packet to continue the process with system execution.

The Round Robin algorithm compares the burst time and the time quantum where packet is present in the ready state. If the condition is satisfied then it executes the program for the burst time and complete the process, if not it executes program for the time quantum. If the timer expires then it goes back to the ready state queue.

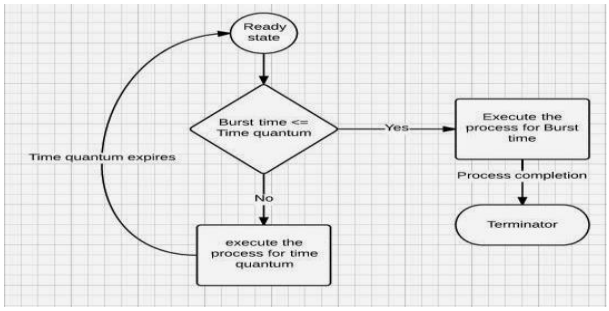

Figure 5: Flow chart for Round Robin method

As in Figure 5, all the packets are stored in the ready state then as per the commands the required program is executed to perform the action. It compares the timer allotted slots to each and every packet prior which packet has to be forwarded for the execution purpose and other packets has to wait till the execution process is done.

A. Secrecy Capacity Calculations for Round Robin Scheme

Considering the *Si* is processed to transmit the scheduled signal $xi(E|xi|^2 = 1)$ along with the power named as *Pi* and rate is termed as *Ri*. The expression for the collecting the signals at receiver, as the received signal is at sink side as:

$$y_s = \sqrt{P_i} h_{is} xi + n_s \quad (1)$$

where fading factor is termed as h_{is} of the original transmission channel or main channel, which transmits the info from *Si* to the intended receiver called sink. The factor n_s will show the additive Gaussian noise with the variances of the signal N_0. As per the Shannon capacity derived formula [9], the capacity of the primary channel can be expressed as:

$$c_s(i) = log_2\left(1 + \frac{|h_{is}|^2 Pi}{N0}\right) \quad (2)$$

where $i \in S$, as per the medium is open in air. The spy may attack on that open space when info is transmitting from the *Si*, as the *xi* is the main signal. In the equation (1), the spy tries to decode the *xi* signal from the transmitting signal.

As per the survey of physical layer [8]-[17], the spy is accepted to have the ideal learning of real transmissions, which includes the details like coding technique, the type of modulation and algorithm used for encryption and the secret key, only the original message signal *xi* is secret to the spy after the many trials also. So from the eavesdropper side *e* the signal is expressed as:

$$y_e = \sqrt{P_i h_{ie} x_i + n_e} \quad (3)$$

where h_{ie} is the factor of fading coefficient at the attacker channel can say wiretap link from *Si* to an eavesdropper and n_e represents the noise at spy link with variance N_0. Considering equation (3), the capacity of the channel at wiretap link is derived in terms of logarithmic expression along with the power *Pi*.

$$C_e(i) = log_2\left(1 + \frac{|h_{ie}|^2 Pi}{N_0}\right) \quad (4)$$

From the [10][11], the difference of channel capacities of the link is considered as the secrecy capacity. In presence of the spy or eavesdropper, we can derive the secrecy capacity as:

$$C_{secrecy}(i) = C_s(i) - C_e(i) \quad (5)$$

where $C_s(i)$ and $C_e(i)$ are expressed in the equations (2) and (4) in terms of capacity their channels respectively.

$$C_{secrecy}(i) = \left(log_2\left(1 + \frac{|h_{is}|^2 Pi}{N_0}\right) - log_2\left(1 + \frac{|h_{ie}|^2 Pi}{N_0}\right)\right) \quad (6)$$

The secrecy capacity is considered with the equation (6) but still the secrecy capacity of the channel is not maximized. So by keeping this as benchmark, an optimal sensor scheduling is proposed.

V. PROPOSED OPTIMAL SENSOR SCHEDULING

The optimal sensor scheduling is the proposed scheme of this paper along with changes in the system model, where the earlier system has only one source and one destination with one type of data traffic. In this proposed system model considering more than one source and one destination along with the different data types which has different priorities.

The optimal sensor scheduling deals with the secrecy capacity of the channel capacity of the spy link and the primary link, where exactly a path has to choose for transmission from source to the intended sink. Among the links it chooses optimally which has the highest secrecy capacity and according to the priority of the queue process it schedules the packets.

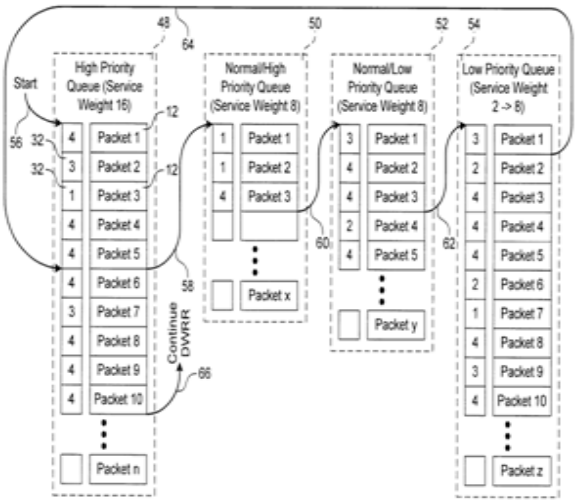

Figure 6: Scheduling queue with priorities

The above example shows the how scheduling process is done according to the priorities of the packets. The priorities levels are divided into four parts. First one is high priority queue with the service weight of 16. Second is normal/high priority of queue with the service weight of 8. Third is normal/low priority queue with the service weight of 8. Fourth is low priority queue with the service weight of 8.

The first queue stores the highest priority packets, remaining will be sent to the next priority queue. Similarly the remaining two priority queues are also filled up. In first queue, packets 1 to packet 10 are stored with their own special priority numbers in left column. It also divides the packets according to the bit size of a packet, compares the

mode of selection with the packet parameters then it sends packet to the schedule queue. It directly executes the packet as First-In-First-Out (FIFO) process.

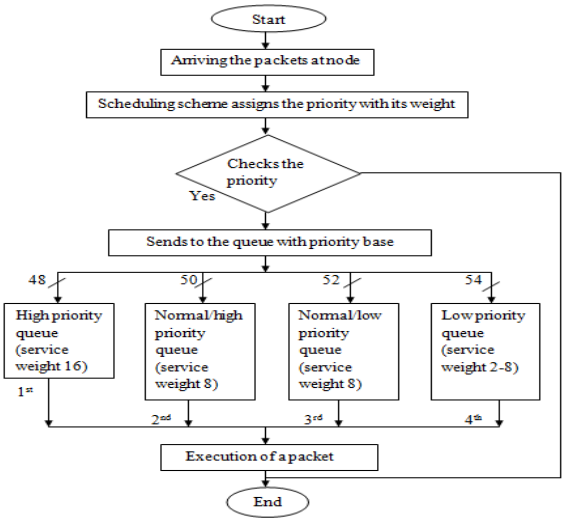

Figure 7: Flow chart for priority checking in queue

The flowchart shows the prioritising of packets according to the queue states. The scheduler divides the four queue states with respect to the prior number and the message weight. The main aim of prioritising the packets is to avoid the latency of emergency packets and to control the long time for low weight packets as the energy saving is the main constraint of WSN.

According to the weights and the priority numbers of packet, scheduler sends that packet into particular queue state then the execution process is started. The next in series of the high priority to the low priority queues will get into the process. The priority of the packets is done to avoid the overhead of the network, which helps to reduce the packet drop rate of the transmission without using any external buffers or memory devices. The flow chart in Figure 8 explains about the calculation of secrecy capacity and selects the optimal highest among the channel capacities by the reference of Round Robin schedule. The node allows transmitting the data by selecting the optimal secrecy capacity.

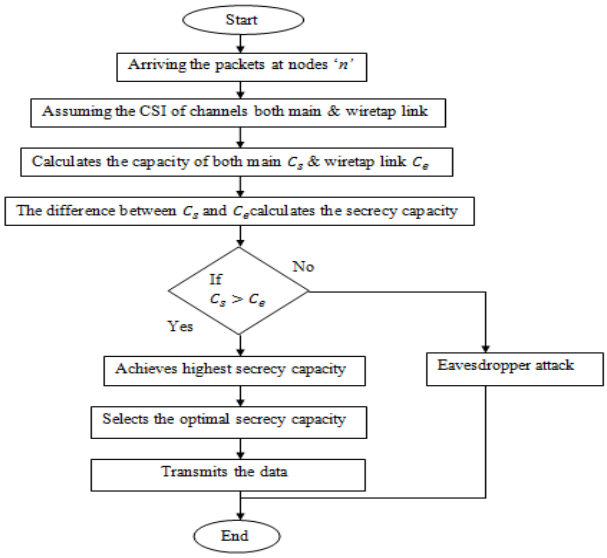

Figure 8: Flow chart for finding secrecy capacity

The system assumes the channel state information of the both main and wiretap link. After arrival of the packet, algorithm calculates the capacity of the channel main and wiretap links as C_s and C_e respectively. The difference of the channel main and wiretap link is called secrecy capacity, $S_c = C_s - C_e$. If $C_s > C_e$, when the channel capacity of the wiretap transmission channel is less than the main channel means a secured connection. S_c will increase with the increase of C_s and decrease of C_e. If $C_s < C_e$, then eavesdropper attacks the network.

Secrecy Capacity Calculations for Optimal Sensor Scheduling

The proposed scheme main objective is to enhance the secrecy capacity factor. Optimal selection of the secrecy capacity is done. Normally, a sensor which acquires the most highest $C_{secrecy}$ is chosen and scheduled in queue for transmitting its data from that sensor node to the destination called sink. Subsequently from the equation (5), the optimal sensor process of scheduling is:

$$\text{Optimal Sensor} = \arg \max_{i \in S} C_{\text{secrecy}} \text{ (i)}$$

$$= \arg \max_{i \in S} \frac{1+\frac{|h_{is}|^2 P_i}{N_0}}{1+\frac{|h_{ie}|^2 P_i}{N_0}} \quad (7)$$

where *S* denotes the arrangement of set of *N* sensor nodes in the scenario. From the above equation (7), the CSI (i.e., $|h_{is}|^2$ and $|h_{ie}|^2$) for every sensor node helps to define or choose the optimal node.

Using channel estimation methods from survey [10], every sensor may evaluate its own CSI with the estimation of a channel and transmits the accessed CSI to the intended receiver. In the wake of gathering all the sensor nodes CSI, the sink can promptly decide the optimal sensor, furthermore the entire network about the CSI of each sensor. When the eavesdropper appeared in the transmission, the secrecy capacity of the proposed system can be derived from (7) as:

$$C_{secrecy}^{Proposed} = \max_{i \in S} log_2 \left(\frac{1+\frac{|h_{is}|^2 P_i}{N_0}}{1+\frac{|h_{ie}|^2 P_i}{N_0}} \right) \quad (8)$$

For the remote connection between any two sensor nodes in system model, the system environment is considered with complex fading coefficients called Nakagami fading channel. The medium is getting very difficult with many signals and interferences that can affect the main signal. Other than eavesdropper effect, there is a need to take interference signals also that lead to the loss of packets or corrupt with interrupt signal.

In this $|h_{is}|$and$|h_{ie}|$ are the random variable coefficients of the channel which represents the fading effects in the transmission medium along with the shaping factors m_i and the k_i, tends to the gamma distributed factors as $|h_{is}|^2$ and the $|h_{ie}|^2$ of the main channel link and the wiretap link respectively.

In terms of the gamma distribution, the source to sink link is $|h_{is}|^2 \sim \gamma \left(m_i, \frac{\sigma_{is}^2}{m_i} \right)$ and for the wiretap to the sink link is $|h_{ie}|^2 \sim \gamma \left(k_i, \frac{\sigma_{ie}^2}{k_i} \right)$, where the expected values of coefficient variables are σ_{is}^2 and σ_{ie}^2 for $|h_{is}|^2$ and $|h_{ie}|^2$

respectively. For the notation convenience, $X_{is} = |h_{is}|^2$, $X_{ie} = |h_{ie}|^2$ for main and wiretap channel respectively.

As the wireless sensor network is the spatial distributed environment, the probability of the density functions of X_{is} and X_{ie} is derived as:

$$fx_{is}(x_{is}) = \frac{1}{\gamma(m_i)}\left(\frac{m_i}{\sigma_{is}^2}\right)^{m_i} x_{is}^{m_i-1} exp\left(-\frac{m_i x_{is}}{\sigma_{is}^2}\right) \quad (9)$$

$$fx_{ie}(x_{ie}) = \frac{1}{\gamma(k_i)}\left(\frac{k_i}{\sigma_{ie}^2}\right)^{k_i} x_{ie}^{k_i-1} exp\left(-\frac{k_i x_{ie}}{\sigma_{ie}^2}\right) \quad (10)$$

The $\gamma(.)$ denotes the gamma function for the density functions of main link X_{is} and the wiretap link X_{ie}. The probability density function of main channel is represented as $fx_{is}(x_{is})$ and for the wiretap channel is $fx_{ie}(x_{ie})$.

VI. Results

The main objective of this proposed system is to achieve the high secrecy capacity than existing scheduled scheme with the system model of one eavesdropper and multiple sources with different types of traffic with different priorities in the scenario. All the results of proposed scheme are simulated and compared with the existing scheme using NS2 software.

A. Secrecy Capacity

The secrecy capacity of a channel is technically measured in terms of the throughput, the speed of the communication in terms of delay factor and the priority rate of the traffic flow. The green portion shows the proposed optimal sensor scheduling scheme and the red portion shows the existing scheme.

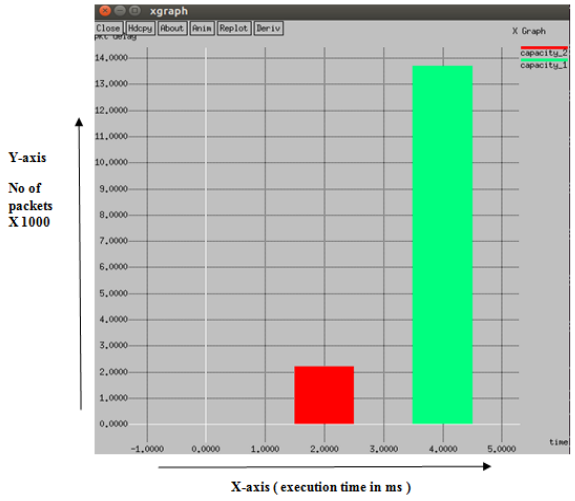

Figure 9: Throughput of existing vs proposed scheme

The optimal sensor scheduling has more throughput level. The secrecy capacity is achieved with the maximised capacity of the main channel. As per the theory it should achieve the more capacity, to have a high security. It is calculated with the successful transmission rate of packets. Hence it has improved the security of the physical layer.

B. Delay

The latency in terms of delay from the Figure 10, the optimal sensor scheduling has less delay compared to the existing model. With less delay it can achieve the fairness of communication without compromising in the speed.

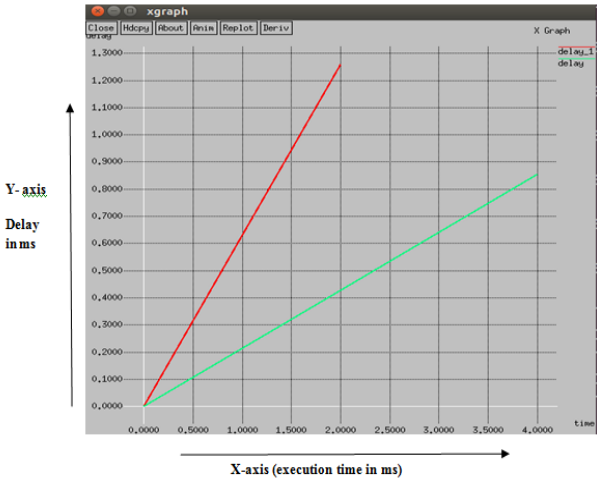

Figure 10: Latency of existing vs proposed scheme

The delay factor is more important in the wireless communication to achieve the QoS requirements. The proposed system has less latency. It also saves the energy of the node.

C. Packet Delivery Ratio

The packet delivery ratio is measured to know the ratio of number of packets received by the number of packets transmitted. The one which achieves maximum rate of PDR will have a secured communication. As per the Figure 11, the proposed optimal sensor scheduling achieved maximum packet delivery ratio than the existing method. This is also a factor which represents the achievement of the maximal secrecy capacity and improved security of physical layer communication.

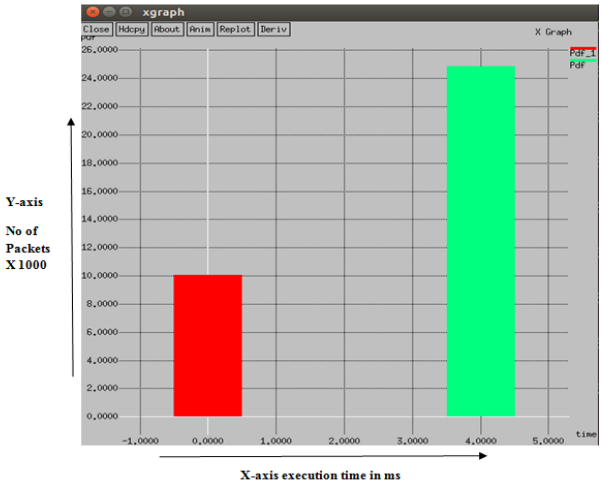

Figure 11: PDR of existing vs proposed scheme

The packet delivery ratio will show the ratio of the number of packets transmitted and the number of packets received. The maximal packet delivery ratio shows the enhancement of the packets that are received successfully at the end. Hence the factor shows the improved delivery ratio.

D. Priorities of Different Data Types

The system model considers the different data types according to their priorities; the graph monitors the priority wise transmission in the network with the same scheduling model. Even though the traffic is increased, the proposed

scheme successfully achieved the requirements of the communication with maximal secrecy capacity.

Considering X-axis as the run time and Y-axis is time taken to complete the transmission, the below graph shows the transmission of different data types with their own priorities, the red colour indicates the high priority traffic with priority0, priority1 is in green colour and priority2 is in blue colour. According to the assigned priority, the data types are forwarding through the nodes.

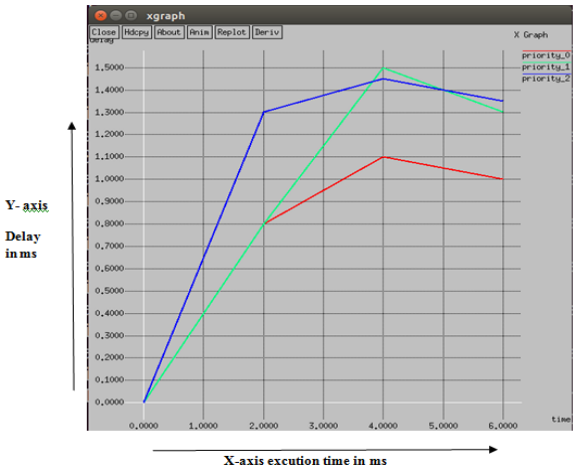

Figure 12: Priorities of different data types

As per the theory, priority0 should take less time to reach the destination which can be observed in the graph with red colour which completed its transmission before the other priority levels.

VII. Conclusion

The employment of sensing element improved the physical layer security of an industrial WSN to counter the eavesdropping attack and the optimal sensor scheduling scheme increased the secrecy capacity of wireless transmissions from the sensors to the sink. The system model with one eavesdropper and multiple sources with different data types in the scenario along with their own priority allocations for successful transmission of emergency data is used.

The scheduling scheme satisfied the requirements of multiple traffics and achieved successfully. The achieved maximal secrecy capacity shows the improved security levels of the physical layer. Numerical results validated the projected optimum scheduling theme in Nakagami fading environment. It performed better than the traditional Round Robin scheme in terms of the throughput, delay and packet delivery ratio and monitored the packets transmission according to the assigned priorities.

The security of the physical layer enhanced with multiple sensor nodes with different data types is only considered. The concept of QoS factor not taken into account and CSI of each sensor is assumed. Also the intercept probability of an eavesdropper in multiple transmissions and multiple eavesdroppers in the scenario for sensor scheduling is not considered. Thus, it is important to investigate the QoS ensured sensor scheduling, endeavouring to enhance the remote security while ensuring every sensor particular QoS necessity. Furthermore, because of the channel estimation mistakes, it is difficult to acquire the ideal CSI for the sensor scheduling. It is of enthusiasm to research the effect of CSI estimation errors with the arrival of intercepts and finding the intercept probability of this sensor scheduling scheme with explained system model. Further idea can be checking the sensor scheduling performance along with the QoS requirement if the multiple eavesdroppers attacked the network.

References

[1] W. Shen T. Zhang F. Barac, and M. Gidlund, “Priority MAC: A priority-enhanced MAC protocol for critical traffic in industrial wireless sensor and actuator networks” *IEEE Trans. Industrial Informatics*, vol. 10, Feb. 2014.

[2] J.-C. Wang C.-H. Lin E. Siahaan B.-W. Chen and H.-L. Chuang, “Mixed sound event verification on wireless sensor network for home automation,” *IEEE Trans. Industrial Informatics*, vol. 10, Feb. 2014.

[3] R.C. Luo and O. Chen “Mobile sensor node deployment and asynchronous power management for wireless sensor networks,” *IEEE Trans. Industrial Electronics*, vol. 59, May 2012.

[4] N. Marchenko T. Andre G. Brandner W. Masood and C. Bettstetter “An experimental study of selective cooperative relaying in industrial wireless sensor networks,” *IEEE Trans. Industrial Informatics*, vol. 10, Aug. 2014.

[5] O. Kreibich J. Neuzil and R. Smid “Quality-based multiple-sensor fusion in an industrial wireless sensor network for MCM,” *IEEE Trans. Industrial Electronics*, vol. 61, Sept. 2014.

[6] T. M. Chiwewe and G. P. Hancke “A distributed topology control technique for low interference and energy efficiency in wireless sensor networks,” *IEEE Trans. Industrial Informatics*, vol. 8, Feb. 2012.

[7] P. T. A. Quang and D.-S. Kim “Enhancing real-time delivery of gradient routing for industrial wireless sensor networks,” *IEEE Trans. Industrial Informatics*, vol. 8 Feb. 2012.

[8] Y. Zou, J. Zhu, X. Wang, and V. Leung, “Improving physical-layer security in wireless communications using diversity techniques,” *IEEE Network*, vol. 29, Jan. 2015.

[9] C. E. Shannon, “Communication theory of secrecy systems,” *Bell System Technical Journal*, vol. 28, 1949

[10] A. D. Wyner, “The wire-tap channel,” *Bell System Technical Journal*, vol. 54, Aug. 1975.

[11] S. K. Leung-Yan-Cheong and M. E. Hellman, “The Gaussian wiretap channel,” *IEEE Trans. Information Theory*, vol. 24, Jul. 1978.

[12] Y. Zou X. Wang and W. Shen, “Optimal relay selection for physical-layer security in cooperative wireless networks,” *IEEE Journal on Selected Areas in Communications*, vol. 31, Oct. 2013.

[13] Y. Zou X. Wang W. Shen, and L. Hanzo, “Security versus reliability analysis of opportunistic relaying,” *IEEE Trans. Vehicular Technology*, vol. 63, Jun. 2014.

[14] S. Goel and R. Negi, “Guaranteeing secrecy using artificial noise,” *IEEE Trans. Wireless Communications*, vol. 7, Jul. 2008.

[15] X. Zhou and M. McKay “Secure transmission with artificial noise over fading channels: Achievable rate and optimal power allocation” *IEEE Trans. Vehicular Technology*, vol. 59, Aug. 2010.

[16] D. Goeckel “Artificial noise generation from cooperative relays for everlasting secrecy in two-hop wireless networks,” *IEEE Journal on Selected Areas in Communications*, vol. 29, Oct. 2011.

[17] Y. Zou X. Wang and W. Shen “Physical-layer security with multiuser scheduling in cognitive radio networks,” *IEEE Trans. Communications*, vol. 61, Dec. 2013.

[18] D. Lee and B. J. Jeong, “Performance analysis of combining space-time block coding and scheduling over arbitrary Nakagami fading channels,” *IEEE Trans. Wireless Communications*, vol. 13, May 2014.

[19] S. Hussain and X. N. Fernando, “Closed-form analysis of relay-based cognitive radio networks over Nakagami-m fading channels,” *IEEE Trans. Vehicular Technology*, vol. 63, Mar. 2014.

[20] J.-C. Chen C.-K. Wen and P. Ting “An efficient pilot design scheme for sparse channel estimation in OFDM systems,” *IEEE Communications Letters*, vol. 17 Jul. 2013.

Proceedings of the Fourth International Conference on Communication and Electronics Systems (ICCES 2019)
IEEE Conference Record # 45898; IEEE Xplore ISBN: 978-1-7281-1261-9

Hybrid Algorithms for Moving Vehicle Plate Recognition System

Shreyas S Bagi[1], Harshith C H[2], Santosh Tuppad[3], Dinu V[4] and Dr. R Srikantaswamy[5]
Department of Electronics and Communication Engineering,
Siddaganga Institute of Technology,
Tumkur, India
[1]shreyas1si15ec097@gmail.com, [2]harshith.1si15ec037@gmail.com, [3]santosh.1si15ec089@gmail.com,
[4]dinu.1si15ec028@gmail.com, [5]rsswamy@rediffmail.com

***Abstract*—The Automatic Number Plate Recognition (ANPR) is a Image Processing innovation that utilizes the vehicle number (permit) plate for vehicle identification. The goal is to utilize the vehicle number plate to plan a productive programmed approved vehicle distinguishing proof framework. The framework is executed in the college entrance for security control.This paper highlights the license plate extraction algorithm where number plate is extracted using Sobel filter, morphological operations and Connected Component Analysis (CCA). Then character segmentation based on CCA and Spectral Analysis, then character recognition based on Support Vector Machine (SVM) technique. In OpenCV-Python, the proposed model is simulated and implemented and its performance is evaluated on the actual image.**

***Index Terms*—Segmentation, Recognition, Sobel filter, Morphological, Connected Component Analysis, Spectral analysis, Support Vector Machine, Python, OpenCV.**

I. INTRODUCTION

ANPR is an technology in image processing that can be used without direct human intervention to peruse vehicle license plate. It is an imperative area of research, because of its numerous applications, for example, traffic observing and law implementation, tracking of automobile, robotizing of vehicle leaving, electronic toll accumulation, Entry and Exit time etc[1]. ANPR framework is still in advancement so as to distinguish and perceive vehicle number plates with different organizations under various natural conditions. Because of variety in the plate models, this undertaking turns out to be extremely troublesome in India. There are various factors that should be considered to increase high precision in the recognition of the number plate, for example, time of day, climate and angles between the cameras and the tags.

The work of ANPR is usually framed in the following steps: Image acquisition, Image pre-processing, Number plate extraction, character segmentation and the last is character recognition[2]. Number plate extraction is most difficult task, mainly because number plate generally occupies a small portion of the entire image and difference in number plate formats.

The proposed ALPR system consists a algorithm for number plate extraction applicable to various standard formats of lic penselate. Figure 1 shows the Block diagram of ALPR system. Character segmentation based on CCA and Spectral analysis and finally, character recognition based on SVM feature extraction that generally applies to different character fonts. . The remaining part of the paper is composed as follows:Section II describes the moving vehicle segmentation , Section IIIdescribes License plate extraction , Section IV explains Character Segmentation,Section V Feature Extraction, Section VI Character Recognition, Experimental results are demonstrated in Section VII. Section VIII concludes the paper.

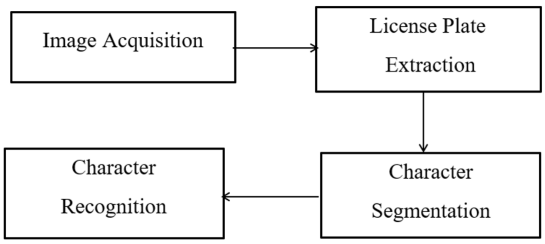

Fig. 1: Process flow diagram of ANPR system.

II. MOVING VEHICLE DETECTION AND SEGMENTATION

The main processing phase of the number plate identification model is the selection of footage frames led by detection and retrieval from a wider scene image of the plate number area to reduce subsequent mathematical calculations and sophistication of the algorithms. A moving object must be recognized & followed by a persistent video arrangement depending on it's essential data, such as visual characteristics, shading, surface, shape and movement characteristics.[3].In video, the car is tracked as it changes its position in each and every frame as it moves from one frame to another. The car throughout the footage is classified as a positive picture and with the Haar Cascade Classifier the entire background is identified as a negative picture. In the proposed model the car region is marked with rectangular box with help of Haar cascade classifier. The car region is extracted based on the

area region for example in the figure 2 the area region of the car is 332 X 332. Based on the x and y values and setting the criteria for the area then we have extracted the car region. Thus, in the overall video, only the car region is extracted as shown in Figure 2.

Fig. 2: Car identified and obtained from video.

A. Extracting the Frames from the video

Depending on the length of the video , the video is divided into six frames. The frames are further processed for plate extraction which recognize the license plate elements. As shown in the figure 3, frames are extracted from the sample video.

Fig. 3: Extracted car images from footage.

III. License Plate Extraction

The extraction of the license plate directly affects the system's accuracy, and is subsequently the most critical stage in the ANPR system. In this phase, a set of possible areas from the input image are produced and a real license plate is selected.

A. Image Acquisition and Preprocessing:

A high- resolution digital camera is utilized in this framework to capture an image. Pictures may be taken in various backgrounds, brightening situations or at different distances between the camera and the vehicle. Pictures are resized to (1000 X 700). Figure 4 demonstrates the preprocessing steps included. Picture will be changed over from RGB to Gray scale.The pre-preprocessing step is utilized for denoising and upgrading picture differentiate. Bilateral filtering is used on the vehicle's gray scale to obtain a smooth, better quality picture with less obscuring effect[4]. With the utilization of histogram leveling on gray scale picture, pictures are upgraded to lessen the issue of low quality and low difference in vehicle images[5]. Figure 5 demonstrates a case of an info picture and Figure 6 demonstrates a case of pre-processed picture with potential number plate region.

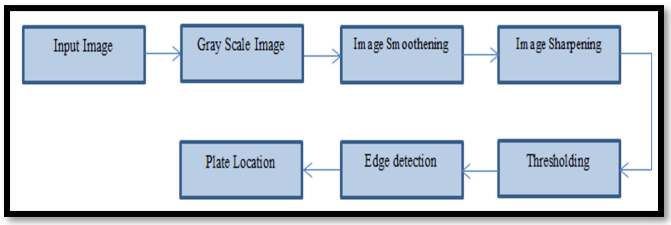

Fig. 4: The Preprocessing flow chart

B. Edge analysis and Morphology

To detect edges, the sobel operation is performed on the threshold image[6]. We mark the pixel as a 1 wherever an edge is presented, otherwise as a 0. Usually the edge pixels are affluent and evenly distributed in the true region of the license plate[7]. In the true license plate region, there are only 2 dominant colors: one for alpha numeric characters and another for the background of license plate. This component is utilized to nd the region of the applicant plate from the picture input. Dilation is connected to fortify the edges extracted by Sobel operation, hole lling is done to ll gaps in the expanded picture, morphological opening is connected to evacuate the undesirable regions in the hole - lled picture, lastly erosion is connected to distinguish hopeful tag districts. Figure 7 indicates consequence of impact of utilizing Sobel operator and Figure 8 shows an example of candidate license plate regions.

C. Candidate Plate Area Detection

Dilation and erosion are used for the entire image to extract candidate plate areas. Figure 9 shows an example of

Fig. 5: Input Image.

Fig. 6: Preprocessed Image.

Fig. 7: Edge analysed Image.

Fig. 8: Morphological analyzed image.

connected component analyzed image with candidate license plate regions[8].Background areas can also be declared as the candidate plate sometimes. This results in plate conrmation using the ratio of width to height, area of region and global image features such as geometrical features, colour and textual features of the number plate to removal of the fake candidates and extract the true license plate region.

D. Spectral Analysis

Characters have the same color and are aligned horizontally. The best way to process such data is to carry out spectral analysis through the Fourier transformation.[9]. In the segmentation of text areas, spectral analysis was normally used. Each row's intensity (gray scale) values are calculated through a periodogram(Equation 1). The periodogram provides a per frequency band energy distribution.

$$\prod_{f}^{Z} F(y) = 1/Z|\sum_{j=0}^{Z-1} f(j)e^{-i2\Pi\eta j}|^2 \quad (1)$$

Fig. 9: Connected Component Analyzed image

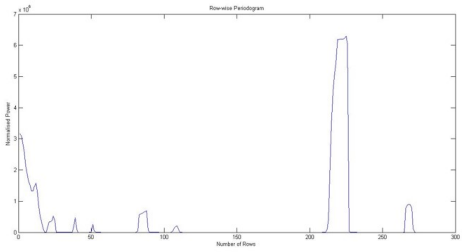

Fig. 10: Effect of spectral analysis on the connected component analyzed image.

1) True Number Plate Extraction: After detecting the area of the potential number plate, the corresponding Column and Row plate area indices will be finally discovered. In the Figure 10 the peak values are corresponding to the license plate rows. So, as soon as the Number Plate indices are known, the number plate is retrieved from the actual gray scale image. The resulting region of the License Plate is as shown in Figure 11.

Fig. 11: Extracted License Number Plate region.

IV. Character Segmentation

The objective of this stage is to segment every one of the characters, without losing character highlights from the given number plate picture.As shown in Figure 12, the segregation of the number plate picture is scaled down to 100 * 100 pixels.Then license plate is morphological opened as shown in Figure 13 and closed as shown in Figure 14 in order to eliminate the background noise on the License Plate. Each labeled 4-connectivity pixel matrix is evaluated based on the area threshold and parts that don't meet predefined zone, height to width ratio and column-row length are required to be non - character areas and are disposed of from the whole picture.The result of connected component analysis is as shown in Figure 15. The connected component are extracted individually which contains the only characters[10] as shown in Figure16

Fig. 12: Segmented License plate Image

Fig. 13: Morphological closing

Fig. 14: Morphological opening

Fig. 15: Connected Component Analysis(CCA)

Fig. 16: Segmented characters

V. Feature Extraction

A feature descriptor is a picture depiction which enhances input image through isolating valuable information and discarding of incidental data.Histogram of Oriented Gradients(HOG) is a feature descriptor.

A. Histogram of Oriented Gradients (HOG)

A technique introduced by Dalal et al[11] is the idea of dense and local gradient-oriented histograms (HOG). The objective of this method is to describe a picture through a set of local histograms. In a local part of the image, these histograms count occurrences of gradient orientation. The model uses the HOG descriptor to obtain character set features (0-9 and A-Z) and incorporate them into a single feature vector. The model is then categorized using the SVM classifier.

Step 1: The image character from the set of characters is resized to 27 X 36.

Step 2: The gradients are calculated horizontally and vertically using the Sobel operator.The sobel operator application on Character M is shown in Figure 17.

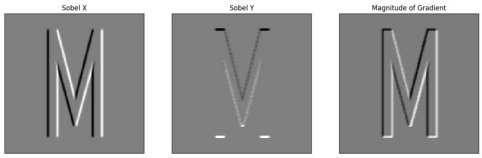

Fig. 17: Character image M

Step 3: Split the Character image into small units, in our case the small unit comprises of 9 rows and 12 columns. In Figure 18(a) The character-0 is of size 27 X 36 and total small units possible are nine units. Then calculate the direction and orientation of the pixels in small unit as the Figure 18(a) shows. The Figure 18(b) provides cell's Magnitude and Angle.

Step 4: Depending on the orientation of the gradient, the

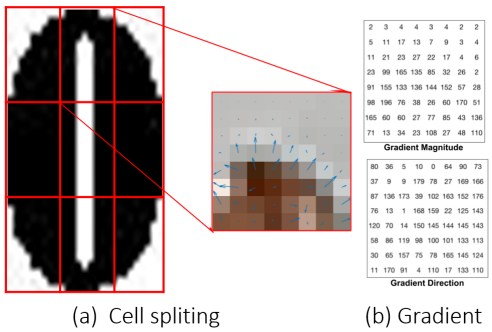

(a) Cell spliting (b) Gradient

Fig. 18: Cell Splitting and Gradient of magnitude and orientation

individual cells will be transformed into symmetrical bins.

Step 5: The adjacent cell grouping is considered to be blocks. The blocks are standardized and represent the histogram of the block.The Figure19 shows how blocks are grouped.

The last step of HOG descriptor is normalization that can

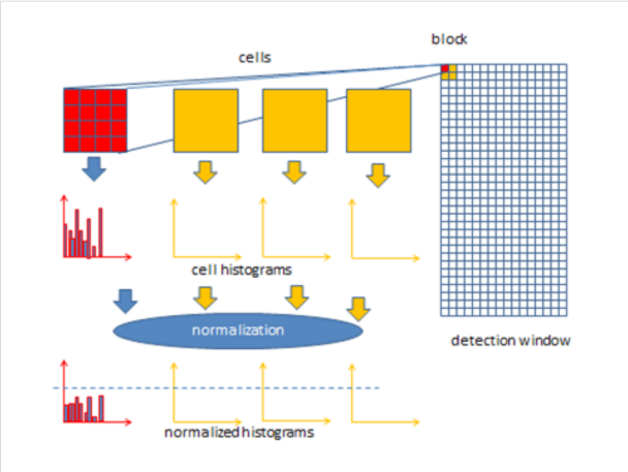

Fig. 19: Histogram computation and normalization

minimize the variability in illumination. By combining all standardized histograms into a single vector, the final feature vector is obtained.

Step 6: Flattening into a feature vector.

Figure 20 (a) is the Dimensional Vector-972(27 X 36 = 972) of character-4 image and Figure 20(b) shows the Dimensional Vector-144 of character-4 image.Their is dimensional reduction from 972 feature to 144 feature.

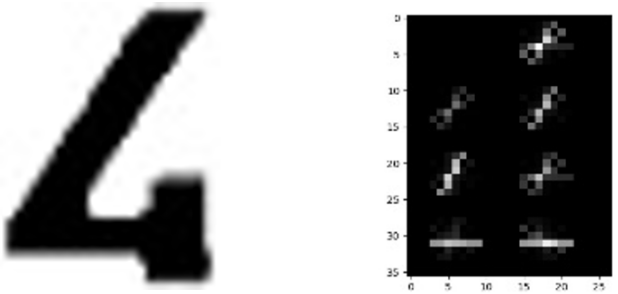

(a) (b)

Fig. 20: (a) input image character-4 (b) HOG image character-4

VI. Character Recognition

After element segmentation, the final interface becomes the phase of recognizing plate numbers and character, i.e. convert segmented Alphanumeric Characters into Text Format readable by machine. Character Recognition model depends on a classifier i.e., Support Vector Machine(SVM)[12].

A. Support Vector Machine (SVM)

SVM belongs to the maximum margin classification hyperplane or binary classifier. Support Vector Machines idea is to map the data input into a high-dimensional feature space. The SVM classifier is utilized to recognize the groups by finding an ideal Hyperplane which are having the most extraordinary partition from the closest dots in the group of preparations called Support Vectors[13]. The preparation set of points $m_j \epsilon R^n$, j=1,2,...,N where each point m_j has a place with the label $n_j \epsilon -1, 1$ as among two classes. The ultimate goal of the SVM classifier is to separate groups by means of a Hyperplane with increasing unification from the support vectors. The formed hyperplane known as Optimal Separating Hyperplane (OSH). The following equation 2 is expression of OSH:

$$f(a) = u \cdot m + z, whereu = \sum_{j=1}^{N} m_i n_i \beta_j \tag{2}$$

Classification is performed on current data point m by calculating sign on the right side of equation 3

$$Q(m) = \frac{u \cdot m + z}{||u||} \tag{3}$$

In Equation 3 the Q sign is used for data point m classification. The $|Q|$ is the perpendicular distance between Q and Hyperplane. The greater Q value the dot is more distant from the decision surface.The result of the classification is therefore more reliable. The system is trained with the number of classes set at 36 with 10 numerals and 26 letters of the English alphabet. The model is programmed with total count of classes set at 36 with 10 Numerals and 26 english characters.

VII. Results

The developed ALPR system automatically extracts the License Plate and segments the elements of the number plate through Connected Component Analysis(CCA). The classification of the Characters through SVM has been implemented. Accuracy of 85% is achieved using One against One SVM classifier. The segmented number plate characters are recognized as shown in Figure 21. A Graphical User Interface (GUI)

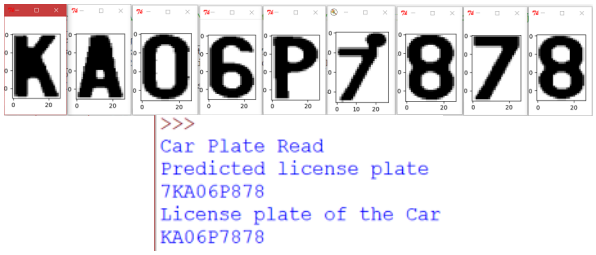

Fig. 21: Segmented Character Image and Recognized license plate number.

is developed. The client can connect with the LPR framework by utilizing the Menu options. Now select the button called Select Image from the GUI then dropdownlist arrives now select the car image and for video analysis select the button called Select Video for video analysis. The execution of the program for still images takes one-second whereas for video it takes around 40 seconds and for HD video it takes around 2-3

minutes.The results of the proposed ALPR system for car, two - wheeler and Taxi, are as illustrated in Figure 22, Figure 23 and Figure 24 correspondingly. The entry time time and exit time of the vehicle is stored in a file as a vehicle log entry to college. The Figure 25 shows the database results stored in file.

Fig. 22: GUI window showing Car image, Segmented license number plate, Segmented characters and Recognized characters of the vehicle license plate.

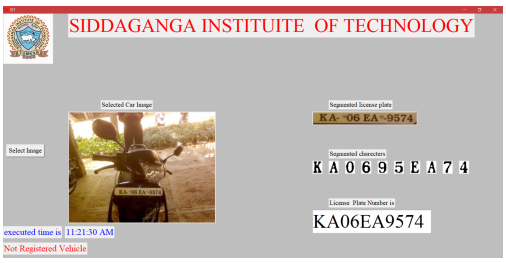

Fig. 23: GUI window showing Scooty image, Segmented license number plate, Segmented characters and Recognized characters of the vehicle license plate.

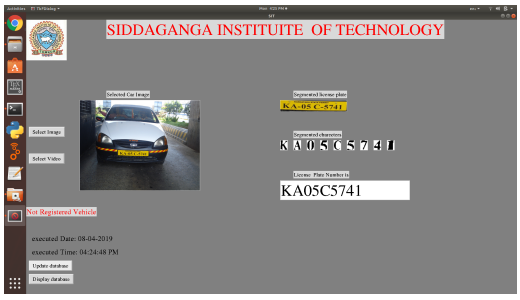

Fig. 24: GUI window showing Taxi image, Segmented license number plate, Segmented characters and Recognized characters of the vehicle license plate.

VIII. Conclusion

License Plate Recognition System has been developed and tested for a video sequence. The selection algorithm for frames is adopted to quickly locate the place of a License Plate and the License Plate is recognized in each frame.Spectral Analysis approach and Connected Component Analysis approach are used for license plate extraction.Connected Component Analysis improves the performance of number plate character segmentation over the technique of projections. The feature extraction based on HOG and followed SVM classifier to recognize the characters gives better recognition accuracy.

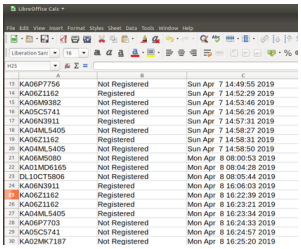

Fig. 25: Database results stored in file

References

[1] A. Yovan Felix, A. Jesudoss and J. Albert Mayan, “Entry and Exit Monitoring using License Plate Recognition”, in 2017 IEEE International Conference on Smart Technologies and Management for Computing, Communication, Controls, Energy and Materials (ICSTM), Veltech,Chennai.

[2] Chengpu Yu, Mei Xie and Jin Qi,“A Novel System Design of License Plate Recognition”,International Symposium on Computational Intelligence and Design in 2008.

[3] Runmin Wang, Nong Sang, Ruolin Wang and Liangwei Jiang “Detection and Tracking strategy for license plate detection in video”, in 2013 ELSEVIER.

[4] Priyanka D. Patil and Dr. Anil D. Kumbhar, “Bilateral Filtering for Image Denoising”,in 2015 International Conference on Green Computing and Internet of Things (ICGCIoT).

[5] Mansour Nejati, Ali Majidi and Morteza Jalalat, “License Plate Recognition Based On Edge Histogram Analysis and Classifier Ensemble”,in SPIS2015, 16-17 Dec. 2015, Amirkabir University of Technology, Tehran, IRAN.

[6] Sheetal Israni and Swapnil Jain, “Edge Detection Of License Plate Using Sobel Operator”,in International Conference on Electrical, Electronics, and Optimization Techniques (ICEEOT) 2016.

[7] Chi-Sung Ahn, Bong-Gyou Lee, Seung-su Yang and Seok-Cheon Park, “Design of car license plate area detection algorithm for enhanced recognition plate”,in 4th International Conference on Computer Applications and Information Processing Technology (CAIPT)- 2017

[8] N.Vishwanath, S.Somasundaram, M.R. Rupesh Ravi, N. Krishnan Nallaperumal, “Connected Component Analysis for Indian License Plate Infra-Red and Color Image Character Segmentation” in 2012 IEEE International Conference on Computational Intelligence and Computing Research.

[9] Jianing Qiu1, Naida Zhu, Yi Wei, and XiaoQing Yu, “An Optimised License Plate Recognition system for complex sistutations”,in 2016 International Conference on Audio, Language and Image Processing(ICALIP).

[10] Tejendra Panchala, Hetal Patel and Ami Panchal, “License Plate Detection using Harris Corner and Character Segmentation by Integrated Approach from an Image”,in 7th International Conference on Communication, Computing and Virtualization 2016.

[11] Navneet Dalal and Bill Triggs.“Histograms of oriented gradients for human detection”,in In Computer Vision and Pattern Recognition, 2005. CVPR 2005. IEEE Computer Society Conference on, volume 1, pages 886893. IEEE, 2005.

[12] M. Bertozzi, A. Broggi, M. Del Rose, M. Felisa, A. Rakotomamonjy and F. Suard “A Pedestrian Detector Using Histograms of Oriented Gradients and a Support Vector Machine Classifier”,in 2007 IEEE Intelligent Transportation Systems Conference.

[13] Shigeharu Miyata and Kenji Oka “Automated License Plate Detection using a Support Vector Machine”,in 2016 14th International Conference on Control, Automation, Robotics and Vision (ICARCV).

Proceedings of the Fourth International Conference on Communication and Electronics Systems (ICCES 2019)
IEEE Conference Record # 45898; IEEE Xplore ISBN: 978-1-7281-1261-9

DIGICERT: A Secured Digital Certificate Application using Blockchain through Smart Contracts

Ms. R.Poorni
Department of Computer Science and Engineering
Easwari Engineering College
Chennai, Tamil Nadu, India.
poorniram21@gmail.com

Mr. M.Lakshmanan
Department of Computer Science and Engineering
Easwari Engineering College
Chennai, Tamil Nadu, India.
lakshmanan1909@gmail.com

Ms. S. Bhuvaneswari
Department of Computer Science and Engineering
Easwari Engineering College
Chennai, Tamil Nadu, India.
rajivanacse@gmail.com

***Abstract*— Deception of Certificates is the major issue that is faced by the educational sector. In order to prevent forgery of certificates and to provide a secure certificate verification environment an authenticated system application is developed using blockchain with smart contracts. The immutability property of blockchain prevents the data stored from being manipulated and helps in implementing a verification system. The system generates a new block for every user in the blockchain. These blockchain are replicated across all the nodes involved in a Peer-to-Peer network and thus it improves the reliability of the system. Whenever a user is validated, their certificates are digitally provided by the system to the user along with a Quick Response code. This helps in sharing of certificates between the employers. The authenticity of certificates is improved by embedding the certificates with imperceptible watermark using the alpha blending process. This helps to avoid various attacks at different phases of certificate distribution.**

Keywords*— *Alpha blending process, Blockchain, Quick Response Code, Smart Contracts.

I. INTRODUCTION

In these modern days a large number of certificates are being duplicated where a large number of these cases go unnoticed. According to a statistical report there have been around 72% of the candidates were pertaining fake credentials. There are various stringent laws and penalties for the forgery of documents yet there are no systems for the prevention on certificate duplication. This system helps to avoid falsification of documents by using blockchain technology. Blockchain is a decentralized technology which utilizes distributed ledger essentially an asset database that can be shared across a network of multiple sites, geographies or institutions. Any changes made in one block can be replicated to all copies of a ledger quickly, ensuring that no participant is left working on outdated information.

The users in the distributed network are non-anonymous that is users need permission to access the blockchain or to get involved in the transactions happening in the blockchain. The applications of a distributed ledger enables information to become almost simultaneous on the blockchain and can be used for keeping records which cannot be manipulated but can be shared among various fields.

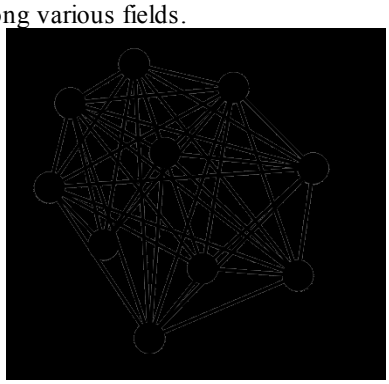

Fig 1.1: Distributed Network

Blockchain is a growing list of records called blocks which are linked through cryptography. Each block contains a cryptographic hash value of the previous block, a timestamp and transaction data generally most often represented as merkle tree root hash. By storing data across its network blockchain eliminates the risk of data getting help up centrally. The blockchain network lacks in a centralized point of contact and hence it avoids the vulnerability of getting hacked.

Smart contracts are protocols enforced to blockchain on which the blocks agree to interact with each other words smart contracts are set of rules which control the nodes in the peer-to-peer based on events taking places in the application. It ensures that the rules are met. Protocols such as Geth are used to develop smart contracts in blockchain. Ethereum is an open source blockchain project that was specifically built to realize the possibility of smart contracts getting executed only when the specific conditions are met.

Smart contracts are capable of implementing compliance

and control on the fly and need information which feed smart contracts with external information. Smart contracts are self verifying, self executing and are tamper resistant. They can turn legal obligations into an automated process and guarantee greater degree of security and reduce reliance on trusted intermediaries.

Fig 1.2: System Structure

The Figure 1.2 shows the structure of the system application. The smart contract establishes all the terms given by the parties included in the system such as the issuing authority i.e., university, the students and the employer. Once the smart contracts are enabled between the parties the events trigger the contract and start the transactions between the users. Based on the contract the execution takes place and the digital certificates will be provided by or to the authorized person.

The system is implemented through a public blockchain ethereum which prevent certificates from being duplicated and helps employers by eliminating the process of physical verification of certificates. It also enables users to have only the digital certificates which can even be shared by holding the security features that avoids certificate duplication.

II. RELATED WORK

EduCTX: A BLOCKCHAIN-BASED HIGHER EDUCATION CREDIT PLATFORM: The need for securely storing digital certificates in blockchain was first determined by Muhamed Turkanovic et al [8]. The idea was to develop distributed application on ARK chain blockchain platform, to securely store digital certificate and transcripts. This helps the user by making their certificates counterfeit proof and lets them carry certificates verified by the issuing authority in a digital wallet. The certificates were successfully stored in a blockchain and therefore protecting the certificates from counterfeiting, accidental damage, etc. Though the idea was broadminded the implementation of the application was narrowminded. The application was developed using ARK blockchain platform which is a private blockchain platform and is an invite only platform. The notion of central authority exists to a certain extent defeating the purpose of the application. The application does not have wide reach to a large audience due these reasons. The non-existence of smart contracts and automation hampers the distributed application from being future proof and also consumes significant amount of resources.

EXPLORING BLOCKCHAIN TECHNOLOGY AND ITS POTENTIAL APPLICATIONS FOR EDUCATION: Guang Chen et al [4] proposed the idea of utilizing a blockchain based application in everyday school activities in order to prevent plagiarism in every day schoolwork such as assignment, homework, project report .The proposed system was developed on the blockchain platform and also suggested to reward students through cryptocurrencies on completion of their work. The idea of incentivizing students on successful completion of their work is not sustainable. The downsides of the proposed idea are teachers need to verify their work only from the blockchain application and it is difficult to perform a perfect assessment through the digital platform. The transaction costs generated will skyrocket due to the amount of transactions taking place due to the a large number of students using the application. They also suggested the use of private blockchain platforms hosted by each school independently in order to reduce transaction cost and make the idea viable for implementation.

EDUCATION-INDUSTRY COOPERATIVE SYSTEM BASED ON BLOCKCHAIN: For any technology or ecosystemto develop it needs the cooperation of the users and the industry providing the technology for the development of tools, one such cooperation was devised by Honming Zhu et al [15]. The proposed idea bought together the education industry and the technology provider IBM to develop frameworks which assist user for developing blockchain applications. The Hyperledger framework and Hyper ledger Peer-Peer network developed by IBM is used to develop distributed application at a faster rate. Though the applications are easy to develop using the framework the applications developed using the framework lack robustness since they have a single point of failure.

UNTWIST BLOCKCHAIN: A DATA HANDLING PROCESS OF BLOCKCHAIN SYSTEMS

Sachin M. Kolekar and et al [10] have discussed the data handling process in blockchain systems. The authors have described how blockchain has grown immensely in the past few years. They eliminate the need for trust among different parties involved in a transaction. They have also eliminated the need for a central authority by using a distributed ledger and hence by doing so the tampering of data is highly difficult. They then present BLOCKBENCH, a criterion skeleton for understanding performance of private block chains and public Blockchain. In this paper they have discussed the circumscriptions of Blockchain. In section 1 they have discussed the workings of blockchain from creation of the genesis node to using clever cryptography in order to hash the nodes present in the network. Section 3 describes the types of blockchains ie private and public blockchains. Section 4 portrays the concepts of blockchain such as the distributed ledger, consensus algorithms and mining. The Intrusion detection systems in detail such as HIDS and NIDS. Their limitations are discussed ranging from updation management to their inability to avoid denial of service attacks. They have conducted comprehensive survey on Blockchain Technology. It is a budding solution for decentralized communication and data management without the need of a trusted third party. It is an open and spread ledger, enabling the recording of contact among various parties in a provable way. Basic clarity and justification of Blockchain is seen and working of the Blockchain in decentralized network has been understood. Also, Combination of Blockchain Technology with Internet of

Things has been studied. Few Advantages and Disadvantages have been seen and various applications of Blockchain Technology are stated. Most Importantly, Future of the Blockchain has been predicted if few of the assumption comes true, then what are the possible technologies which can be created by blockchain technology. Concepts like consensus, distributed ledger, proof of labor, proof of stake, etc. have been explained in short.

LITERATURE SURVEY ON UNTANGLING BLOCKCHAIN: A DATA PROCESSING VIEW OF BLOCKCHAIN SYSTEMS: Tien Tuan Anh Dinh et al [12] discuss about the blockchain systems that are gaining massive momentum in the last few years. The blockchain systems are useful for parties that do not trust each other amidst a transaction. Due to their usage of distributed ledgers parties do not need to depend on a central authority. The authors have focused their discussion on private blockchains and as a result the parties are authenticated. This paper has also discussed about BLOCKBENCH, a benchmarking framework for understanding performance of private blockchains against data processing workloads. They have provided information about the software such as Ethereum, Parity and Hyperledger fabric. The tradeoffs between blockchain and traditional database systems have been discussed in order to evaluate the differences between the former and the latter. They have discussed how a blockchain network is created. The genesis block is initially created whose hash value is stored in the next block and so on until it forms a chain. Consensus algorithms also play a major role in the addition and removal of new nodes in the system which also deals with Byzantine related problems. Blockchain has its advantages over tradition databases in providing robustness and decentralization.

III. PROPOSED SYSTEM

The system proposed is built over a public blockchain based on ethereum platform. The ethereum blockchain platform enables user to develop smart contracts which increases the level of automation and reduces the cost and the number of transactions. Fig 3.1 shows the architecture diagram of Digital Certificate System.

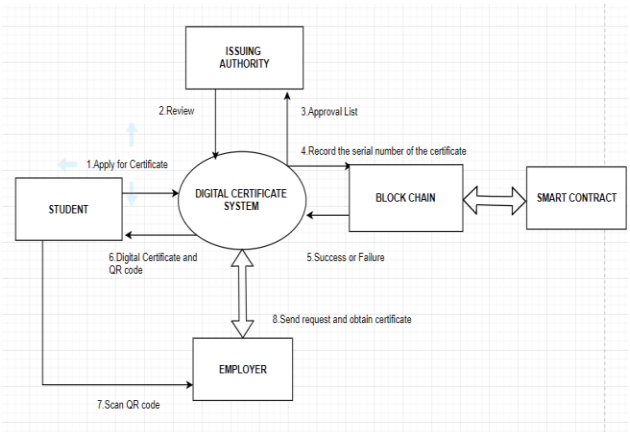

FIG 3.1: Architecture diagram of Digital Certificate System

The students are provided with an application interface through which the students upload their information. The issuing authority provides the authenticated students list to the distributed system which can be verified with the student details that are uploaded through the application interface. The verification list contains the serial number of the certificates that is stored to the blockchain with smart contracts by the Digital Certificate system. When the student request for the digital certificate, only when it is successfully stored in the blockchain they are provided with their digital certificate which is embedded with a data for security and a Quick Response (QR) code for further sharing of certificates. During certificate verification process the QR code is shared by the student to the employer and the certificate is verified.

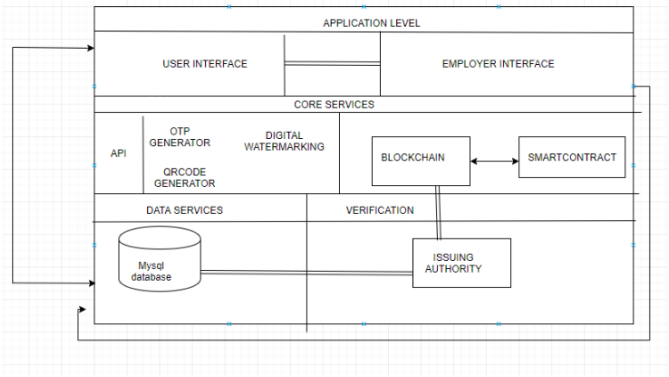

FIG 3.2: Functional Diagram of Digital Certificate System

Fig 3.2 describes the functional architecture of digital certificate system. The application level gives the interface among different users who access the application. The application gets the certificates from the issuing authority which holds the certificates in the database and stores the certificate number in the blockchain through smart contract with the help of hash functions. When the user requests for the certificate the application programming interface embeds the certificate with an imperceptible watermark for authentication and sends an OTP to the user whenever the certificates are shared.

The Digital Certificate System consists of four modules namely

a. Users Validation
b. Hash Generation
c. Securing digital certificates
d. QR code Sharing

The following are the essential components of the system.

a. USERS VALIDATION

Users in the specific module register their details in a form containing various fields in the application. The data collected is stored in a dropbox cloud platform using the dropbox library. Architecture of the dropbox database is of a tree structure which enables easy manipulation of data. Once registered, users are provided with an OTP (one time password) for

authentication. Upon authenticating the users details get uploaded in the concerned issuing authority.

b. HASH GENERATION

The module is the core of the application containing the blockchain system. For every new registered user a new block is created in the blockchain. The data of the user i.e the serial number of the certificate is stored in the block. Hashes are generated using hash function such as SHA-512.

SHA-512 is a cryptographic hash function that is built using Merkle-Damgard structure [3]. It consists of an 80 round module which generates the hashes. The hashes generated use the data stored in the blocks, hence if data changes the hash value will also get change.

The hash of the previous block is stored in the next block and thereby creating a chain of blocks. This is responsible for the property of immutability and any changes can be notified to the user.

c. SECURING DIGITAL CERTIFICATES

Once serial numbers are securely stored in the blockchain they generate a success signal to the system. Upon obtaining the signal and request from the user digital certificates are sent to the user along with a QR code.

The certificates from the digital certification system contain an indistinguishable imprint by using alpha blending process. It is used to display a bitmap which as has transparent and semitransparent pixels. In addition to red, green, blue color channel each channel in alpha bitmap has a transparency component known as alpha channel. An open source API is used for this purpose which imprints the digital certificates through the alpha bending process. This safeguards the digital certificates from being misused after sharing the certificates.

To make the imprint visible the color scale of the digital certificate is changed to a specified value.

The property of the imprint being indistinguishable is that when an unauthorized person tries to duplicate the certificate, they will be unaware of the imprint which can be identified on duplication. This safeguards the digital certificates from being misused after sharing the certificates

d. SHARING QR CODE

In an android interface the users receive the digitally imprinted certificates and are tagged along with a unique QR code. The QR codes are generated through an API (application programming interface). The generated QR codes are shared to the employers on their account. When the QR code is scanned the employer receives the digital certificate of the student after authenticating the user with an OTP.

IV. RESULTS AND DISCUSSION

The results of the above components end up in the system application with login for different users and their specified operation and the sample of user registration is shown below. Similarly the employer will register with their company details so that they can share the documents in a common platform.

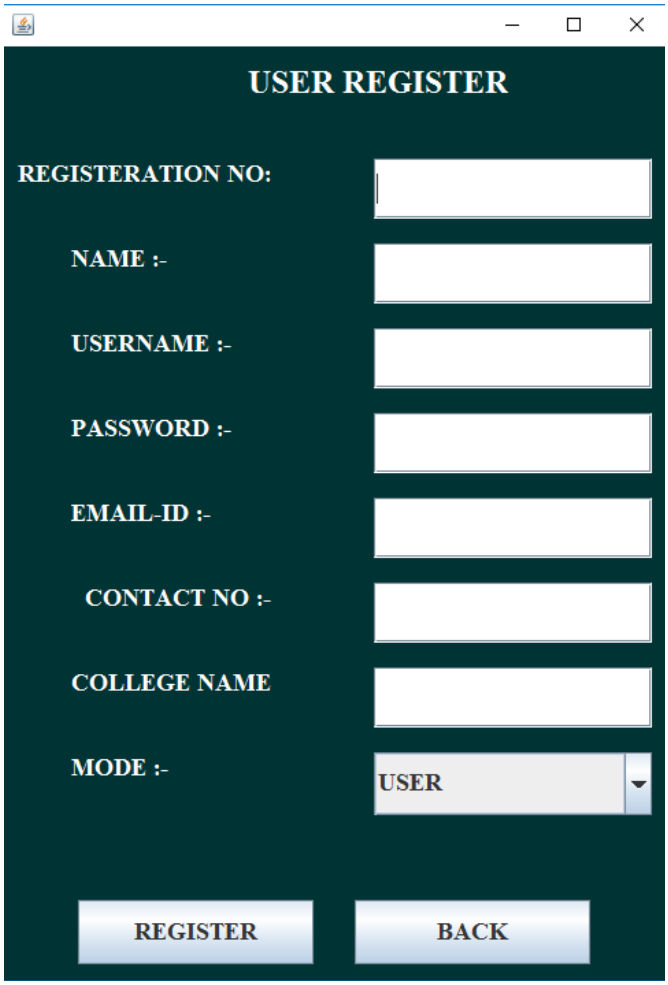

FIG 4.1: Form for Acquiring User Details

The documents are stored in the blockchain. Ethereum is a decentralized platform that runs smart contracts. The Ethereum wallet is installed in the host system and a temporary private test network is executed in order to reduce the cost of development. Genesis block is created and the blockchain is replicated across all the nodes in the Peer-to-Peer network successfully. The ethereum wallet is initialized in the command prompt. The blockchain is implemented on Ethereum blockchain platform. The blockchain is accessed through a command line interface.

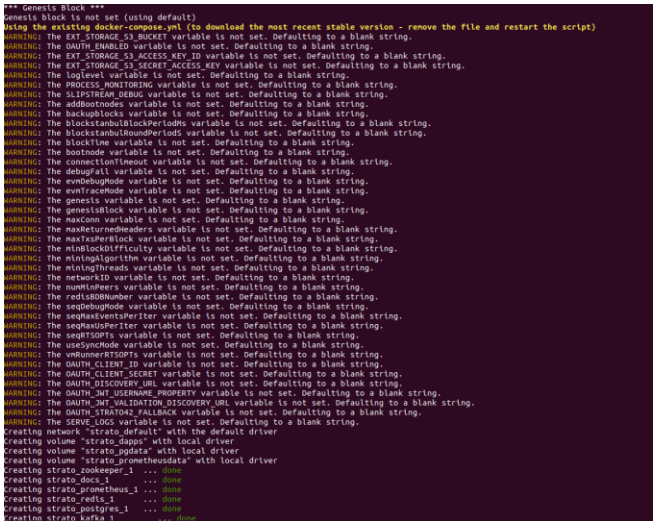

Fig 4.2: Initiating the Genesis block in the blockchain

Once the students register to the application they can request for the mark sheet in the application through blockchain.

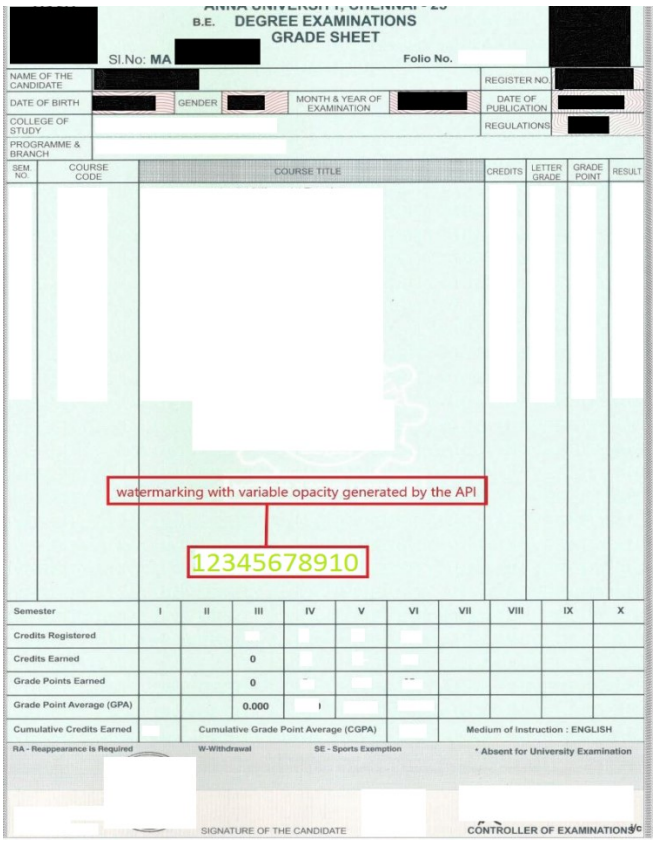

Fig 4.3: Sample watermarked Certificate

The mark sheet is embedded with a watermark for security purpose and can be shared among the employer and the user with the onetime password provided by the application to the user to avoid unauthorized access.

V. CONCLUSION AND FUTURE WORKS

The proposed system demonstrates the effective use of blockchain technology to develop a distributed application and it provides a certified method for preventing duplication of digital certificates. The core of the application is to generate hashes in order to effectively create a blockchain which stores data which cannot be manipulated. As a future work Hyperledger [13] fabric can be used to implement blockchains for effective access. Biometrics of the user can be stored to the application in order to generate highly unique hashes which cannot be decrypted easily.

REFERENCES

[1] Bin Duan ,Ying Zhong,Dayu Liu, "Education Application of BlockChain Technology: Learning Outcome",IEEE Xplore ,2017, Vol 49 ,Issue 14,pg 456-465

[2] Dejan Vujicic ,Dijiana Jagodic,Sinisa Randic, "Blockchain technology,bitcoin,and Ethereum:A briefoverview",2018,IEEE Xplore,Vol 39,Issue 19,pg 723-739

[3] Duo Lei, Feng , Li Feng and Longjiang Qu, "The Design Principle of Hash Function with Merkle-Damgard Construction"

[4] Guang Chen,Bing Xu,manli Lu , Niang - Shing Chen, "Exploring BlockChain technology and its potential application for education", Springer open Journal ,2018.

[5] Jiin-Chiou Cheng ,Narn-Yih Lee, Chien Chi ,Yi-Hua Chen, "Blockchain and smart contracts for digital certificate",2018, IEEE Xplore vol 8 1024-1036.

[6] Massimo Di Pierro, "What is Blockchain",IEEE Xplore, 2018, Vol 19 issue 5 pg 92-95

[7] Mike Sharples, John Domingue, "The Blockchain and Kudos: A Distributed System for Educational record, reputation and Reward",2016,Springer Conference

[8] Muhamed Turkanovic, Marko Holbl, Kristjan Kosic, Marjan Hericko, Aida Kamisalic, "EduCTX: A Blockchain-Based Higher Education Credit Platform", IEEE Access, vol 6, pg. 5112 – 5127, 2018

[9] Nir Kshetri , Jeffrey Voas, "BlockChain in developing countries",2017,Volume 2 Issue 20 ,pg 11-14

[10] Sachin M. Kolekar, Rahul P. More, Smita S. Bachel, Anuradha V. Yenkikar, "Untwist Blockchain: A Data Handling Process of Blockchain Systems", International Conference on Information , Communication, Engineering and Technology, DOI: 10.1109/ICICET.2018.8533868.

[11] Shuai Wang, Yong Yuan ,Xiao Wang, Juanjuan Li, Rui Qin, Fei-Yue Wang, "An overview of smart contract: Architecture , Applications and Future Trends",IEEE Conference ,2018,19310857

[12] Tien Tuan Anh Dinh, Rui Liu, Meihui Zhang∗, Member, IEEE, Gang Chen, Member, IEEE, Beng Chin Ooi, Fellow, IEEE, and Ji Wang, "Untangling Blockchain: A Data Processing View of Blockchain Systems", IEEE, 1041-4347, 2017.

[13] Tomaso Aste , Paolo Tasca , Tiziana Di Matteo, "The Blockchain Technologies: The Foreseeable impact on the society and industry",IEEE Xplore ,2018,Volume 15 issue 9,pg 18-28.

[14] Qin Liu, Qingchen Guan, Xiaowen Yang, Honming Zhu, Gill Green, Shaohan yin, "Education-Industry Cooperative System Based On Blockchain", IEEE International Conference Proceedings 978-1-5386-4870-4/18, 2018.

Proceedings of the Fourth International Conference on Communication and Electronics Systems (ICCES 2019)
IEEE Conference Record # 45898; IEEE Xplore ISBN: 978-1-7281-1261-9

Proceedings of the Fourth International Conference on Communication and Electronics Systems (ICCES 2019)
IEEE Conference Record # 45898; IEEE Xplore ISBN:978[illegible]

Deep Learning Technique for Semantic Segmentation of Satellite Images

Mohammad Yousuf Saifi[1]
School of CSE
Lovely Professional University
Punjab

Dr. Jimmy Singla[2]
Associate Professor
School of CSE
Lovely Professional University
Punjab

Nikita[3]
Former Asst. Prof.
School of CSE
Lovely Professional University
Punjab

Abstract— A sharp increase in the availability of satellite imagery data sets available in the past few years and nowadays made the explanation of all those data a challenging problem. Retrieving useful information and insights from images taken by satellite or any other aerial imagery system requires a good understanding of the information which is present in the images itself. This work searches and studies problem mentioned above by studying, designing and implementation of an automated model to extract semantic maps of waterways, roadways, buildings to track urban cities growth of satellite imagery. As it is a machine learning problem, a deep neural network is implemented and evaluated experimentally. Open source, publicly available frameworks and datasets are used in this work, the result of this work is a pre-processing image model which enables the user to take an input image with different quality and resolution and apply the semantic segmentation on it. U-Net is used as the underlying architecture for this project, because of many advantages and functionalities it provides as an example, we can name less computation time which can help starters in the field of AI and Computer Vision to build their prototype and models fast without the need of too much hardware (GPU, Processor, and RAM). To get a better result and decrease the amount of pressure on machine FCN (Fully Connected Neural Network) is used along with U-Net. As FCN has skip layer function and it also makes the network to learn faster and give more accurate results than CNN due to normalizing the pooling layers which in CNN it makes the network to lose lots of information about the data. The primary purpose of this work is to implement Semantic Segmentation on satellite images taken from Urban areas, SpaceNet dataset provides such a data. The data selected for this project is from Khartoum (Capital of Sudan), it is a developing and deserted city. The result of this work will help in managing resources such as agriculture, natural energy, and water, checking on natural disasters and responding to it, like floods, earthquakes, and tsunamis checking on environmental use such as deforestation and Monitoring Urban Development

Keywords- Satellite, Deep learning, Image, Segmentation

I. INTRODUCTION

Semantic Segmentation is the process of labeling images on pixel level or analyzing all details of an image in pixel level [6]. Segmentation is a process or method of dividing an image into multiple parts and section which can be sets or category of pixels, the main point of segmentation is to make the input image understandable for machines, robots, pc and other purposes. So we can say segmentation helps a computer to analyze and understand images and vides as input and detect boundaries, curves etc. While images given to a segmentation application it subdivides the taken image and classify every pixel available in the mentioned image and label it, after labeling done! There will be certain pixels which can contain same or almost same label, then we can say those pixels share some common characteristic or can be part of same object in the input image.

Fig. 1. Semantic Segmentation

There are 3 types of data sets available: RGB Data sets, RGB Depth and pure volumetric or 3D.

RGB Datasets:

Most of the time and through the years, semantic segmentation focus was on RGB images or data, for the reason RGB or 2D data sets are most widely available and the biggest and can be found easily. In RBB data sets any kind of two-dimensional like as gray measure or RGB images can be contained.

PASCAL Visual Object Classes

There are 5 sub classes available in this data set, which is: Dataset for sorting, appointing, segmentation, action classification and people lareadert. From the mentioned dataset, data for segmentation is interesting since the main objective is to identify objects there above 19 different classes of pictures with objects like: Cow, cat, birds, horse, sheep, person, car, boat, bus, tables…etc.

SBD (Semantic Boundaries Dataset)

This data set is extended version of Pascal Visual Object Classes dataset, the data set (SBD) provide semantic segmentation land fact for the picture which not mentioned in Pascal VOC (Visual Object Classes) which contains annotations for almost 11000 images from Pascal VOC and more than 8000 training images from it is own.

Microsoft COCO (Common Objects in Context)

This is another large scale dataset which is very suitable for image recognition, segmentation and capturing. The part of this data set which is focused on segmentation has more than 80 classes which includes more than 80000 images.

SYNTHetic set of imagery and annotations

It is a big set of photo-realistic renderings of virtual cities, semantically segmented which the main target is context of driving. This data set provides pixel-level annotations for more than 10 classes like river, nature, airplane, highway, house, pole, car…etc. It features more than 13000 training images which is taken from video streams.

Cityscapes

It is a large scale database which is the main focuses of this data set is on semantic understanding of civil road scenes? This dataset supply material in over 30 groups which have flat surfaces, people, cars, buildings, boats, nature and river. This dataset has been captured in over 40 cities during months, during the day when the weather was clear and good.

ReaderTube-Objects

The data available in this dataset mainly prepared from ReaderTube videos which contains objects from ten PASCAL VOC classes: Airplane, animals, different kinds of vehicles and train.

CamVid

It is a driving section, which eventually taken as a film by a camera attached on the dashboard of a car? The dataset covers 32 classes of objects and some of them are

- building
- wall
- tree
- vegetation
- fence
- sidewalk
- parking block

KITTI

It is a famous dataset to be used in mobile robotics and autonomous cars, which is contain couple of hours of traffic conditions filmed with mixture of sensor situations covering high: - Clearness RGB

- grayscale
- 3D scanners

it doesn't contain any data for semantic segmentation but lots of researchers manually marked parts of the database to fit their needs.

II. BACKGROUND WORK

Before deep learning become popular in field of semantic segmentation and computer vision, there were other approaches that we can name TextonForest and Random Forest Based Classifiers and in image classification convolutional neural networks (CNN) were able to be a good answer for most of segmentation problems.

Joao Carreira et.al (2012) In every object recognition or segmentation methods coding, pooling, feature extractions are always included an is basic part of procedure. This paper researched and proposed a method based on pooling, which encodes the second order of local characteristics within a region, to achieve this the multiplicative second order analogue is being introduced and together with good non linearities can give a great result on free form boundry detection and recognition, this can be done without any feature coding.
By researchers of this method it is been found that elevating local descriptors with image information addon can have a huge performance discoveries and gains, even better result can be reached by including the proposed method. In this paper it is been showed that pooling based on second-order technique and free form region has superiority over the other winning systems in Pascal VOC 2011 challenge, sometimes even 20000 time faster. [9]

Alexander Vezhnevets et.al (2012) this paper tried to address problem related to weakly supervised semantic segmentation. In the process the images labeling process only by the classes which is available in them, not regarding their location. On the test input this technique must predict label class for each pixel. The goal of this method is to enable segmentation so make them to use few visual cues in the setting of weakly supervised setting, similar to result which is achieved by full supervised method. Somehow it is difficult to measure the usefulness of different visual cues from data of the purposed method which is Weakly supervised. A group of parametric structured model is defined where each one of the models do the weight process in different way. The maximum expected Agreement is proposed which assesses the quality of model from the group without checking the Supperpixels levels. The process for searching the best and fittest model is a hard process for optimization problem. This problem is looked as Bayesian Optimization and proposed algorithm is based on Gaussian processes to perfectly solve it. The second contribution by this paper is "Extremely Randomized Hashing Forest" which represents varied Supperpixels feature like saparse binary. [10]

Alexander Vezhnevets et.al (2012) the main problem which is addressed by this paper is to solve classifying every pixel in the image related to their semantic class which they belong to for example buildings, water way, cars. Most of methods which exists train from a full supervised image, where every pixel is marked by a group or class label. To reduce the efforts for the process of annotation, recently weakly supervised methods appeared. The weakly supervised method only requires only image labels representing which groups are available or present. While the performance of these methods reaches a acceptable level, there is a huge gap between accuracy of this method and fully supervised method. Which in this paper it is been tried to reduce this gap or even remove it by proposing active learning method with is well suited for this technique. The problem is modeled as a pair-wise CRF along with cast active learning to check for findings it of as most useful node. Which these nodes made the biggest changes in CRF model after revealed the true label of them. After doing test on two different data sets, the proposed methods achieved 97% of accuracy.

Jonathan Long et.al (2015): proposed When in 2010 Deep learning become feasible and made programmers able to integrate it with many widely used software and applications, researchers tried to start their research to find how Deep Learning can contribute more and more in AI field, and one of the areas that Deep learning had a good impact on them is Segmentation. Patch classification is a semantic segmentation using deep

learning that we can name after deep learning invented. What exactly a patch classification does is classifying each pixel into different classes using a method called patch of image around it, the main reason using patches was fully connected layers in classification network and because of this reason the image needed to be of a fixe size. To solve this issue in 2014 Jonathan Long, Evan Shelhamer, Trevor Darrell tried to popularize Convolution Neural Network for dense predictions without any connected layers, and it worked and they named the method FCN Fully Convolution Networks. By using this method in segmentation, users of neural network are able to generate segmentation map of any size image and less time or faster. After this discovery all semantic segmentation start using this paradigm. Beside fully connected layers, we can name pooling layers that semantic segmentation method faced with, what exactly pooling layer is? A pooling layer or pooling tool that CNN using for taking a large image and shrinking them down and preserving important information of image, increase the field of view and ignoring the (where) information, while semantic segmentation needs the alignment of class maps and (where) information as well, different research and work has been done to resolve this issue which semantic segmentation faced with. the encoder and decoder architecture for resolving mentioned problem is introduced, the work process of encoder and decoder is: encoder grade by grade causing the dimension to reduces along with pooling layer after that decoder step recovers grade by grade details of object and spatial elements. One of popular architecture of this method can be named U-Net.

Suarabh Gupta et.al (2016) RGB-D images segmentation sometimes can be tricky; in this paper it is been tried to address that problem and propose a possible solution. The proposed method is "geocentric embedding for depth images" which encodes above the ground, angle with using taking notes on gravity for every and each pixel along with horizontal differences. The geocentric embedding has given better results in most cases than raw depth images for representation of learning features with CNN, which has been demonstrated specifically. The final product achieved average of 37.5% which is almost 56% more precise and accurate than existing methods. Along with other points, the focus on task of segmentation on instance based where the label pixels which belongs to object instances are found by the detector. For mentioned task (instance-based segmentation) the Decision forest technique is proposed which classifies pixels of the input in the detection windows which can be either foreground or background using Unary and Binary tests. Then the output of object detector is taken and given to a Supperpixels classification model for semantic segmentation purpose which had 24% improvement over existing methods that has been studied by this paper. .

Vijay Badrinaryanan et.al (2015) The SegNet which developed and worked on by Cambridge University of United Kingdom is a deep encoder and decoder technique for semantic segmentation. The SegNet architecture is contain structure of non-linear processing layers and set of decoders with pixel wise classifying method, and each encoder has a convolutional layer with batch standardization and ReLU procedure non linearity. One of the main characteristic which makes SegNet special is the use of max pooling indices in the decoders to perform the up sampling process of low resolution functionality maps.

Pedro pinherio et.al (2015) This research has been done by Pedro Pinheiro (and friends) which the main title of the paper is (Learning to Segment Objects), how it works: Given an image, at first outputs a segmentation mask, at the second step outputs the probability that the patch is centred on full object (the mentioned process is being applied on image so it could identify all objects available in the image) and all these process is done in one round or through one CNN. As Deep Mask uses simple feed forward network which is good and successful in creating (coarse object masks) but not for pixel accurate segmentations (or semantic segmentation).

Liang-Chieh Chen et.al (2016) proposed is a method which is using Deep convolutional networks and fully connected CRFs for semantic segmentation, made bellow important contributions in field of semantic segmentation:

- Using of atrous/dilated convolutions
- Propose atrous spatial pyramid pooling
- Use fully connected CRF

It tries to bring together method form DCNNs along with graphical probabilistic framework for solving task of classification on pixel-level, and displaying that responses at the last layer of DCNNs are not Enough local for precise object classification or segmentation, to solve this problem localization characteristic of deep networks by integrating the results at the last DCNN layer with CRF.

III. MATERIAL AND METHODS

Data Set Review

One of few publicly available datasets which provide most complete data for both training and testing purposes is SpaceNet, which contains commercial satellite images. Companies like GosmiQ, NVIDIA along with Radiant Solution partnered to make a possible public release of the data set to make innovation faster in the field of Computer Vision and machine learning and help build algorithms for feature detection from satellite images like buildings, roads, and other man-made structures.

AOI	Satellite	Location	Resolution	Area of Raster	Building Label	Road Labels
1	World View 2	Rio de Janerio	50 cm	2544	4082529	NULL
2	World View 3	Vegas	30 cm	216	151367	3685 km
3	World View 3	Paris	30 cm	1030	23816	425 km
4	World View 3	Shanghai	30 cm	1000	92015	3537 km
5	World View 3	Khartoum	30 cm	765	710960	1030 km

SpaceNet Datset

For a better understanding of the dataset, knowing the main source of the dataset will be helpful. Digital Globe is an American vendor which is main services is providing space imagery and geospatial data, is the main provider of the SpaceNet data as well. The mentioned company has few satellites which some of them can:

- WorldView -1, 2, 3 and 4
- GeoEye 1
- World View
- QuickBird

Each dataset generated from mentioned satellites has different features like geolocational accuracy and resolution.

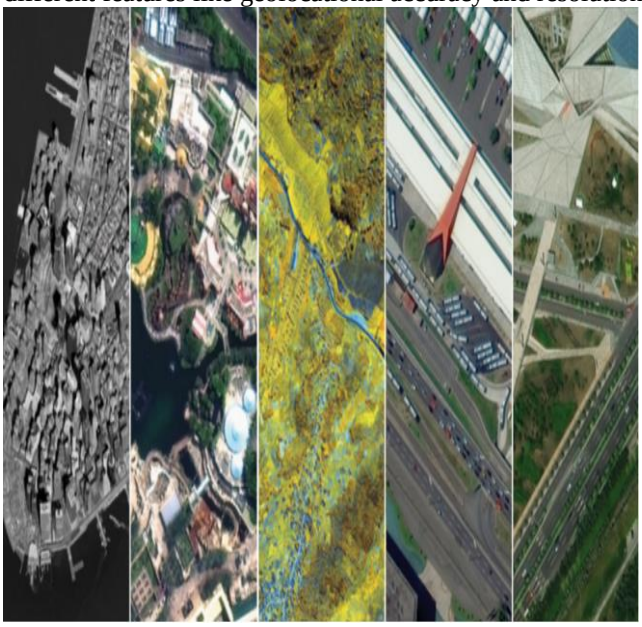

Fig. 2. Data Samples from SpaceNet Data set

Table 1. Different Features of Digital Glove Satellite

Feature	World View 1	World View 2	World View 3	World View 4	Geo Eye Serie
Altitude	495 km	680 km	760 km	615 km	615 km
Characteristics	Pan	Pan + 4 MS	Pan + 8 MS	Pan + 8 MS + 8 SWIR	Pan + 4 MS
Resolution	.50m	0.41m	0.46m	0.31m	0.31m
Multispectral Resolution	NULL	1.64M	1.85M	1.24M	1.24M
40 N Latitude	1.4 Days	< 3 days	1.1 days	1.0 day	1.0 day

Locations covered by SpaceNet Datset

SpaceNet provide satellite data for 5 main areas, which below table is summarizing them

Table 2. SpaceNet AOI (Areas of Interest)

From 2016 SpaceNet organizers started some competitions for the primary purpose of making innovations in the field of computer vision and help to create such algorithm to extract detailed features from satellite images.

The first round of such competition was organized in November 2016, and the target data set was Rio De Janeiro. In the first round, almost 40 developers competed in this challenge which hosted by Top Coder to create such an algorithm to extract building footprints from the input data. The Second competition of SpaceNet main target was from World View 3 satellite which had multiple formats of images like RGB, panchromatic and multispectral.

Raster in SpaceNet

SpaceNet raster is presented in the form of .tiff images. The GeoTiff images are a unique format of images which can be used for georeferencing and pixel in the picture is as real-world distances

Sensor Band of SpaceNet Data Set

Table 3. Sensor Bands of SpaceNet Data Set

Costal	400 – 450 nm	Red	630 – 690 nm
Blue	450 – 510 nm	Red Edge	705 – 745 nm
Green	510 – 580 nm	Near-IR1	770-895 nm
Yellow	585 – 625 nm	Near-IR2	860 – 1040 nm
SWIR-1	1195 – 1225 nm	SWIR-5	2185 – 2225 nm
SWIR-2	1640 – 1680 nm	SWIR-6	2235 – 2285 nm
SWIR-3	1640 – 1680 nm	SWIR-7	2235 – 2285 nm
SWIR-4	1710-1750 nm	SWIR-8	2295 – 2365 nm

Fully Connected Neural Network

Doing Segmentation is far different from classification because the primary purpose of segmentation is required to relate each pixel to a class of the input data, in place of only one class for all the input. To understand what is in the input for each pixel segmentation task is to predict what are contents of the data and to specify the location of the detected object as well.

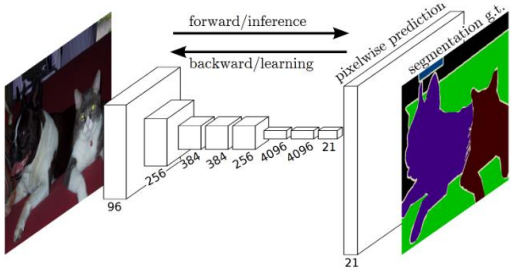

Fig. 3. FCNN

FCN (Fully Convolutional Network)

This model has got its name from the way in which architecture is built which is group of connected layers locally, and the layers are Upsampling, Convolution, and Pooling. This architecture is hugely affecting the number of parameters and computation time. The working method of this model is straightforward where it can work regardless

of the image size, does not require a fixed amount at any of the working stages, because all the layers and connections are local.

To acquire a segmentation result (in our case Map) all segmentation architectures having two main steps:

- Downsampling: which takes contextual information
- Upsampling: which recovers the information

The primary objective of Downsampling is to retrieve the information which is related to WHAT, and the upsampling job is to enable the network to detect exact localization of the detected object WHERE — followed by the recovery phase, to recover the spatial information lost during the pooling or downsampling stage.

Model

There are many FCN architectures available, which the main difference is in their output. the figure shows different types of FCN Architectures like:

FCN 8
FCN 32
FCN 16

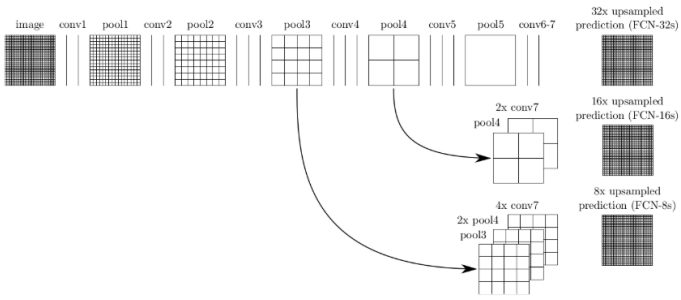

Fig. 4. Different Models

The mentioned FCN models (FCN 8, FCN 16 and FCN 32) differ from each other in the last convolution layer and skip connection. And another main difference between them is that all three mentioned models are using the same downsampling path, but an upsampling path.

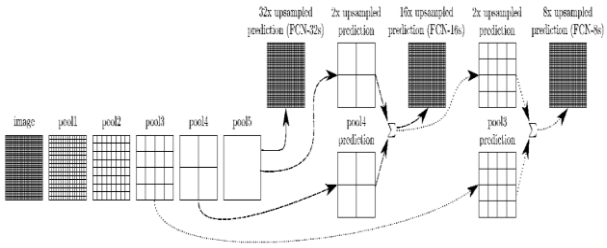

Fig. 5. FCN Models

U-Net Model

This model is built on the base of FCN (Fully Convolutional Network) and then customized which gives better result if used on the medical field and imagining. If we compare this to FCN 8, the main differences between these two models are:

(U-Net is symmetric) and (The skip between upsampling and downsampling uses concatenation instead of a sum operator). The skip connection provides information taken from local to the global during the upsampling stage, and because of it is symmetry characteristics it has a significant number of feature maps in the upsampling stage which enables to transfer information. They named U-Net because of its the symmetric shape which makes it different from other models of FCN Network. The interior architecture of U-Net is separated into three parts.

- Downsampling
- Bottleneck
- Upsampling

Downsampling Section

The downsampling stage is consist of 4 subsections, each section is consisting of

- 3x3 Convolution Layer + activation function
- 3x3 Convolution Layer + Activation Function
- 2x2 Pooling (Max Pooling)

First two layers contain Batch normalization too.

At each pooling block, feature maps double for example if it starts from 64, it will get to 128 at the second and so on. The task of the contracting is to retrieve the context of the input data to do the segmentation job and the result will be transferred to upsampling layer.

Bottleneck Stage

This section locates between the downsampling and upsampling which is built from 2 simple convolutional layers along with batch normalization followed by dropout.

Upsampling Stage

This stage contains the same number of blocks as downsampling, which is 4:

- Deconvolution layer
- Concatenation which contains the cropped feature mask from the downsampling stage
- 3x3 convolution layer + activation function
- 3x3 convolution layer + activation function

Keras

Keras is open source built for neural network library based on Python programming language, which runs by the help of TensorFlow and other technologies like Cognitive Toolkit (Microsoft), Theano. The primary purpose for building the Keras was to enable researchers who work in the field of AI especially Neural Network (Deep Learning) to do very fast experimentation. It helps researchers with the user-friendly environment and modular, the researchers in ONEIROS made some great efforts in building and developing this good platform, Francois Chollet (who is an engineer in Google) is the primary and author of this platform.

This model contains few functionalities which are most commonly used by neural network researchers in the field of deep neural network and can be used for neural network building blocks, optimizers and few useful data toolboxes to make dealing with images and text data a lot easier. The main code used for developing this platform is being hosted in Github and has lots of community support in different forums. Besides supporting the standard neural network, keras support convolutional and RCN (Recurrent Neural Network) as well, along with these it supports other utilities like batch normalization and pooling. The incredible feature of Keras is that let users implement deep models on Smartphones as well (iOS on iPhone and Android), web-based or on JVM.

Basic Approach

The first model which was developed as a single layer consists of 4 layers, with the primary purpose to understand

and implement a neural network model. Then this model firstly used on a small set of data set which mostly included roads and highways and then trained the model on a data set which had over 5000 labelled and ready for training purpose. It is usual to make the number of produced feature map available in each layer as we progress more and more. Our network model is consisting of four convolutional layers with 32 and 64 feature map each, which followed by 0.5 dropouts. The ReLU activation is also used in all function to the wanted probability heat map. All the pooling filter follow a simple 3x3 structure at each layer.

IV. RESULTS

The input data of our model has 712287 pixels in total, from the total number of available pixels about 28.79% are pointed as background and 71.21% segmented as our target points (Buildings, Roads, Water and Corps). Obtained performance parameters are shown in the following table-

Precision	Recall	FPR (False Positive)	TPR (True Positive)	IOU	F1
0.911	0.68	0.16	0.68	0.644	0.778

V. CONCLUSION

Deep Neural Network is studied to find out latest inventions and implodents in the field and possibility to help us out in this work. Segmentation and Semantic Segmentation is studied along with latest literatures to find our improvements in the field. Data sets available for this purpose has been studied and analyzed, and being tried to find the best data set which is suitable for this work and Then by using FCN as main architecture, U Net as pre trained model and python programming language is used to implement the work researched on. At the end in Results, all the output and result of the works have been shown along with training data set.

REFERENCES

[1]https://www.americanscientist.org/article/fifty-years-of-earth-observation-satellites
[2] https://earthdata.nasa.gov/earth-observation-data
[3]https://earthobservatory.nasa.gov/images/87363/bolivias-lake-poopo-disappears
[4] Zhang, Q.J., F. Wang "Neural Network Structures for RF and Microwave Applications" IEEE AP-S 1999
[5] The Swiss AI Lab IDSIA, Istituto Dalle Molle di Studi sull'Intelligenza Artificiale, University of Lugano & SUPSI, Galleria 2, 6928 Manno-Lugano, Switzerland
[6] Yanming GuoYu LiuTheodoros GeorgiouMichael S. Lew "A review of semantic segmentation using deep neural networks", International Journal of Multimedia Information Retrieval, Vol. 7, issue 2, 2018.
[7] Alberto Garcia-Garcia, Sergio Orts-Escolano, Sergiu Oprea, Victor Villena-Martinez, Jose Garcia-Rodriguez "A Review on Deep Learning Techniques Applied to Semantic Segmentation", arXiv, 2017.
[8] Alex Krizhevsky, Ilya Sutskever and Geoffrey E. Hinton "ImageNet Classification with Deep Convolutional Neural Networks", Communications of the ACM, 2012.
[9] Joao Carreira, Rui Caseiro, Jorge Batista, Cristian Sminchisescu "Semantic segmentation with second-order pooling", Proc. Of European conference on computer vision, 2012.
[10] Alexander Vezhnevets , Vittorio Ferrari, Joachim M. Buhmann, "Weakly supervised structured output learning for semantic segmentation, Proc. Of IEEE conference on computer vision and pattern, 2012.
[11] Jonathan Long, Evan Shelhamer and Trevor Darrell "Fully Convolutional Networks for Semantic Segmentation", Proc. Of IEEE conference on computer vision and pattern recognition, 2015.
[12] Saurabh Gupta, Judy Hoffman and Jitendra Malik " RGB-D Image Understanding using Supervision Transfer", SID Symposium digest of technical papers, vol. 47, issue 1, 2016.
[13] S Ren, K He, R Girshick, J Sun "Faster R-CNN: Towards Real-Time Object Detection with Region Proposal Networks", Proc. Of Computer vision and pattern recognition, 2015
[14] Christian Szegedy, Vincent Vanhoucke, Sergey Ioffe, Jonathon Shlens, Zbigniew Wojna "Rethinking the Inception Architecture for Computer Vision", Proc. Of Computer vision and pattern recognition, 2015.
[15] Vijay Badrinarayanan, Alex Kendall, Roberto Cipolla "SegNet: A Deep Convolutional Encoder-Decoder Architecture for Image Segmentation", IEEE Transactions on Pattern Analysis and Machine Intelligence , Vo. 39, issue 12, 2015.
[16] Pedro pinherio et.al "Learning to Segment Objects", NIPS 2015
[17] Abhishek sharma et.al "Recursive Context Propagation Network for Semantic Scene Labeling" NIPS 2014.
[18] Liang-Chieh Chen et.al "Deep convolutional networks and fully connected CRFs for semantic segmentation" Computer Vision and Pattern Recognition , 2016.

Proceedings of the Fourth International Conference on Communication and Electronics Systems (ICCES 2019)
IEEE Conference Record # 45898; IEEE Xplore ISBN: 978-1-7281-1261-9

Real Time Virtual Human Hand Using Leap Motion Controller

R. Satheeshkumar M.E.,(1)
Research Scholar, Department of EEE,
Annamalai University,
Annamalainagar , Tamilnadu ,
India.
satheesh2727@gmail.com

Dr. R. Arivoli M.E., Ph.D.,
Associate Professor, Department of EEE ,
Annamalai University,
Annamalainagar , Tamilnadu,
India.
lnrarivolizc@yahoo.co.in

***Abstract*— The research of robotics needs a good and accurate control. The proposed concept is touch less and non-verbal communication with the use of Leap Motion Controller. The concept has two major parts : first one is "device perceive hand finger moments and send signal", Second one is Robotic hand interfaced with PIC microcontroller which receives signal and controls robotic hand. The paper aims to link virtual environment with real time environment. Here virtual environment consist of leap motion controller and laptop, real time environment consist robotic hand. In real time environment parodist is converts into virtual environment.**

Keywords— ***Leap Motion Controller, Zigbee, Pic16f877a and Robotic Arm.***

I. INTRODUCTION

The development of Advanced Gesture recognition sensors habitually used in robotic hand control. In wide and variety of areas Robotics substitutes human work [1].

Leap motion controller creates virtual screen to visualize hand gesture information and the same information send to robotic hand through wireless device support [2].

For hand gesture recognition many sensors used like MEMS accelerometer, EMG, Gyroscope, flex sensor, pressure sensor…etc [3]

LMC used to achieve hand of human intension by interaction of Robotics. Leap motion controlled good to recognize the intension of human by gesture of human hand and fingers [4].

LMC supports to complete virtual task like virtual game, virtual selection, virtual control, and all virtual environment based applications [5].

Gesture recognition of LMC used to control vehicles, Robotics, drones with the decision of human . at some kind of hazardous situation human brain takes the good decision [7].

LMC creates virtual reality environment for virtual game, virtual pen, virtual instruments performs simulated operations [8]. In this, leap motion controlled can be used like mouse, and joystick. By using LMC gesture recognition, user can interact with virtual reality (VR) environment. This method is a touch less interaction to communicate Robotics [11] [12].

II. RELATED WORK

Leap motion controller finds the touch less Human computer interface. LMC creates virtual environment in computer for various task handling on virtual environment. Interaction of objects By using LMC is an unique way of hand gesture recognition.

It supports various compilers and IDEs such as Visual Studio, Xcode3.0+, Mono version 2.10, Unity Pro and personal version 5.0, java versions 6and 7, python version 2.7.3, and UnrealEngine 4.9. All header files and library files, DLL files provided by leap SDK required to develop leap motion controller enabled application.

Hand gesture recognition is done by LMC on both hands dynamicaly and simultaniously. It can be used in virtual game, virtual air brush, virtual desktop application, virtual mouse and keyboard.

LMC consist of three IR(Infra Red) LEDs and two IR camera which visualize the skeletal point in computer similar to human finger moments. It uses specialized software to visualize skeletal point of finger. Many devices are used for motion capture but leap motion controller has built-in IR sensor to detect human hand and two cameras to capture the gesture of human hand which processed by software.

Distance between the above the Leap Motion Controller and Human hand should be approximately 20 centimeters.

Distance between around the Leap Motion Controller and Human hand should be approximately 45 centimete [6].

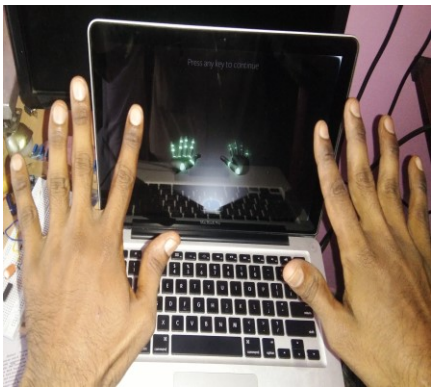

Fig. 1. Leap Motion Controller interface with virtual environment

III. PROPOSED WORK

The main motivation of this paper to is convert virtual hand into real time Robotic hand. LMC generates 3D skeleton image while the information of that virtual image is sent to robotic hand. The following three steps operates Real-Virtual-Robotic hand [9].

1. **Real hand -** Camera of LMC captures the real hand and finger gesture fed into the laptop/PC.
2. **Virtual hand** - Laptop/ PC visualize 3D image(Virtual Hand) and its related information send via wireless.
3. **Robotic hand -** Information of 3D image receive by robotic hand and behave like real and virtual hand.

The proposed design is to convert the HCI (Human Computer Interface) into HCRI (Human Computer Robotic Interface)

A. Schematic of LMC

Fig. 2 shows schematic diagram of leap motion controller. Gesture recognition using leap motion controller provide virtual and robotic hand grip. Each IR Camera is placed between IR LEDs [10].

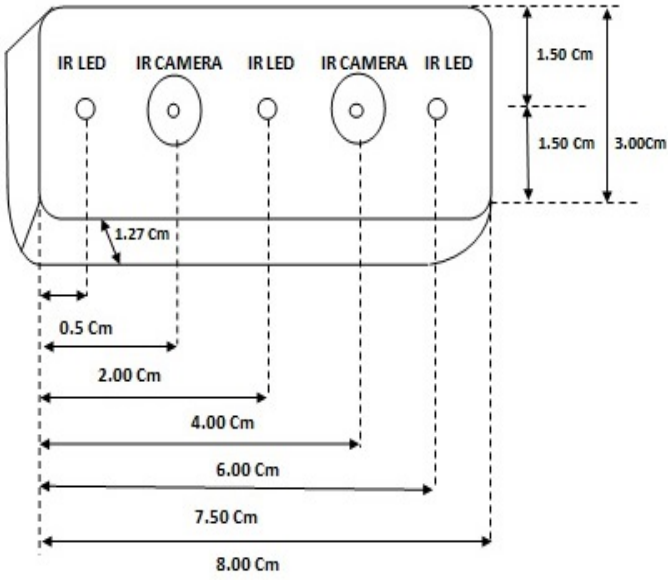

Fig. 2. Schematic of LMC

In Fig. 2 Camera and IR LEDs are placed in unit of Centimeter(Cm). Form the left side of schematic first IR led is placed at a distance of 0.5Cms, first Camera is placed at a distance of 2Cm, second IR led is placed at a distance of 4Cms, second Camera is placed at a distance of 6Cms, third IR led is placed at a distance of 7.50Cms.

Total length, width, and height of Leap Motion Controller is 8Cm, 3Cm and 1.27Cm respectively. The wave length of IR LEDs are 850 nanometers.

B. Software for leap motion controller

Special software program required to use leap motion controller for tracking human hand. Leap motion controller SDK(software development kit) is written in C++, Java, Java Script, Objective C, C#, Python. It support Windows, Linux & MAC operating system. The advantage of this is to make any software program to track human hand. Since for tracking of human hand can make own software.

C. Robotic Hand Design

This Robotic hand has palm and five fingers such as human and it is interfaced with servo motor to control. In this the structure of hand is nearly the same as human hand.

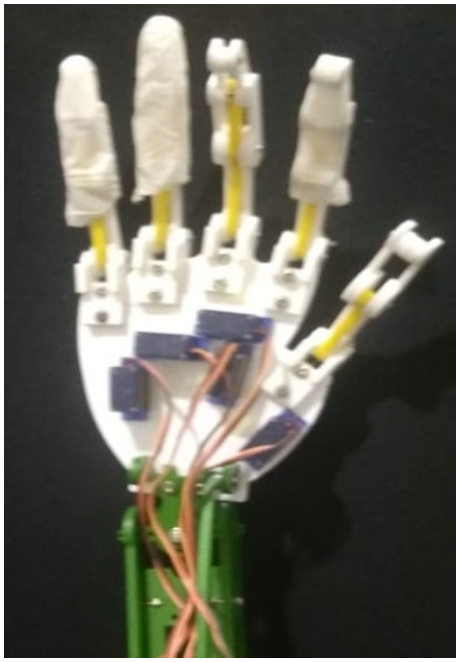

Fig. 3. Robotic Hand Internal View

Fig. 3 shows the internal view of robotic hand with five servo motors to control the five fingers. Each finger has separate control by servo motor [4].

D. Hand Skeletal

Fig. 4 shows the skeletal view of hand fingers. The distal phalanges , intermediate phalanges, proximal phalanges, metacarpals and carpals forms finger of human hand.

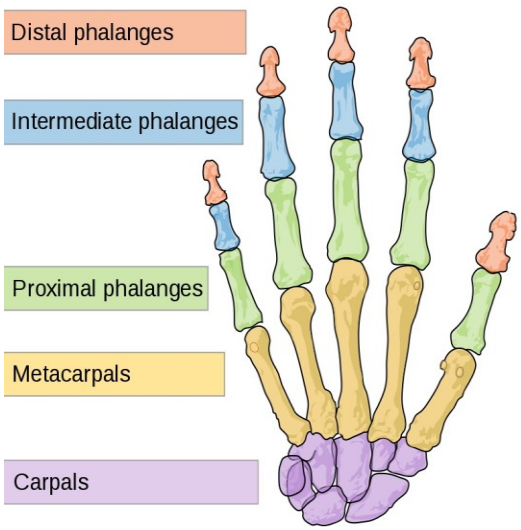

Fig. 4. Skeletal View Of Hand fingers

Fig. 4 Leap motion controller takes standard skeletal model for tracking human hand. Two row of four carpal bones(8 bones) forms wrist of the hand . The area between carpals and distal phalanges called hand. Metacarpals (5 bones), phalanges (14 bones) totally 27 distinct bones forms human hand.

E. Convert Human Hand Gesture into Virtual hand

Gesture of human hand is an input of this leap motion controller. IR sensor built in leap motion controller detects human hand motion and the two cameras built in leap motion controller capture the gesture of hand detected by IR sensors .

Hand gesture of LMC fed to the computer via USB communication port[13]. SDK present on the computer to manipulate the data of hand gesture for virtual simulation by visual C++ language and simulate the hand gesture in virtual environment. This virtual hand information from the computer transfer to robot hand via zigbee wireless device [7].

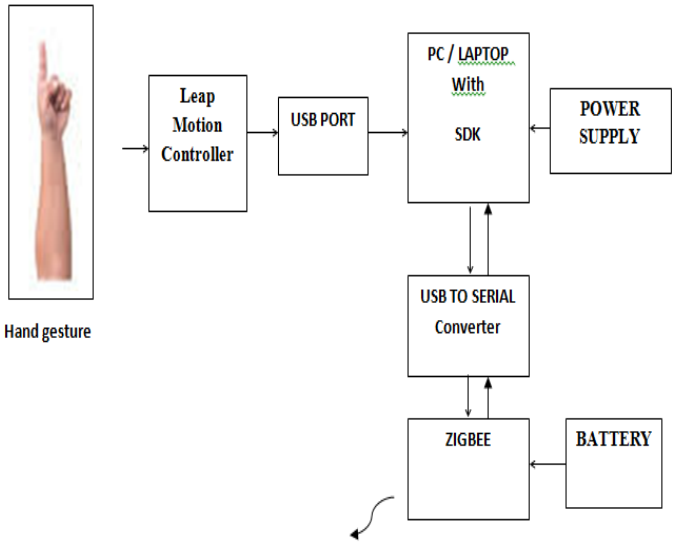

Fig. 5. Hand Tracking Using Leap Motion Controller

Fig. 5 shows the connection of Leap motion controller connected via USB communication port and the wireless device (zigbee) connected via USB communication port with the help of RS232 to USB converter cable which transfers hand gesture information. It operates with a speed of 9600 baud rate.

F. Image acquired by the LMC

Leap motion controller acquires image by camera in the structure of inverted pyramid shape [14]. The frame rate of leap motion controller is 120 frames per second. It has a field view of 135º.

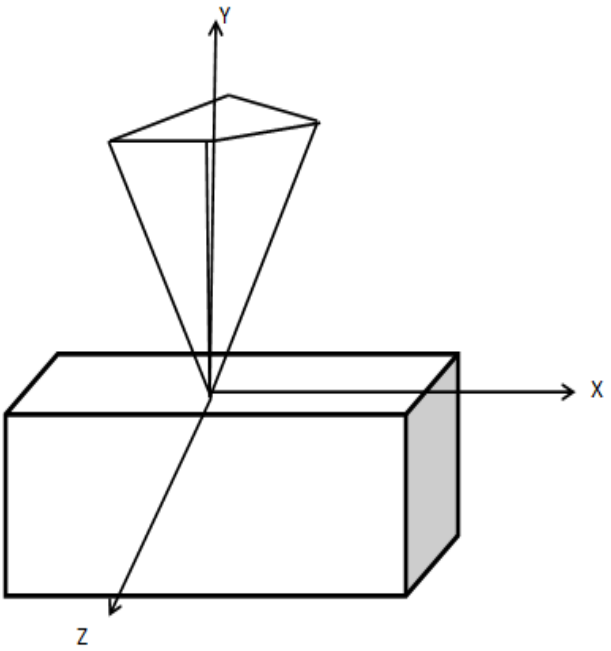

Fig. 6. LMC and Coordinates

Fig. 6 Leap motion controller gets images in inverted pyramid shape and its coordinate value of LMC consist of LMC_X, LMC_Y, LMC_Z in equation is denoted by R.

$$R = \begin{pmatrix} LMC\_X \\ LMC\_Y \\ LMC\_Z \end{pmatrix} \quad \text{----------} (1)$$

$$R' = \begin{pmatrix} 1 & 0 & 0 \\ 0 & 0 & -1 \\ 0 & 1 & 1 \end{pmatrix} \begin{pmatrix} LMC\_X \\ LMC\_Y \\ LMC\_Z \end{pmatrix} + \begin{pmatrix} dx \\ dy \\ dz \end{pmatrix} = \begin{pmatrix} LMC\_X + dx \\ -LMC\_Z + dz \\ LMC\_Y + dy \end{pmatrix} \quad \text{-------} (2)$$

Where dx, dy, and dz are the constants of the distance between origin of the coordinate system of LMC.

G. Convert Virtual hand into Robotic Hand

Virtual hand information is received from remote computer by zigbee transceiver interfaced with pic16f877a microcontroller through UART communication with the speed of 9600 baud rate. It has the same speed as transmitter zigbee connected in computer for real hand tracking.

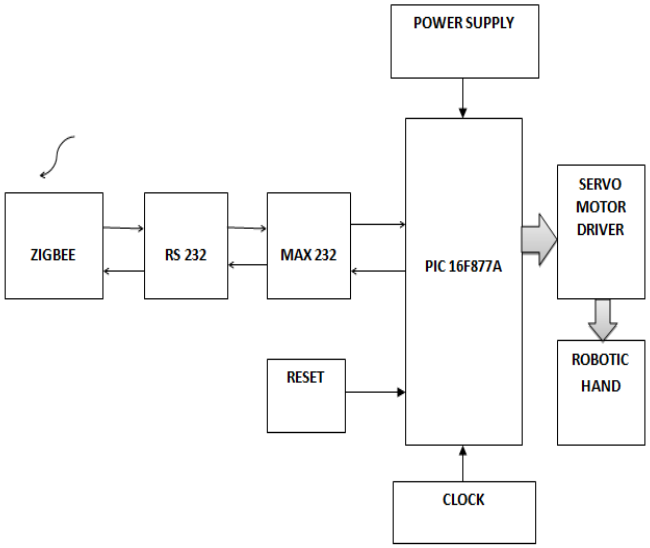

Fig. 7. Robotic Arm Control by LMC

Fig. 7 shows Robotic Arm connected with pic16f877a microcontroller. The robotic Arm receive the commands from real hand via Zigbee wireless communication. This Robotic Arm uses SG 90 servo motor to control fingers of Robotic Arm. Each finger in Robotic Arm has separate SG 90 servo motor our five fingered structure has five SG 90 servo motors.

IV. DATA SET

The Table 1 shows gesture image information analyzed by the Leap Motion SDK. Gesture image information is coded as text for wireless communication to transfer data to the robotic Arm.

Hand Gesture	Code
Swipe	'A'
Grab	'B'
Pinch	'C'
Close	'D'
Release	'E'

Table 1. Gesture Code

Hand gesture recognized by the leap motion controller is coded in Table 1. This text code is sent through zigbee wireless communication.

V. RESULT ANALYSIS

Robotic hand mimics similar to the hand of human controlled from remote area. Fig. 8 shows comparison of Human hand , Virtual hand and Robotic hand.

(a) Real Hand

(b) Virtual Hand

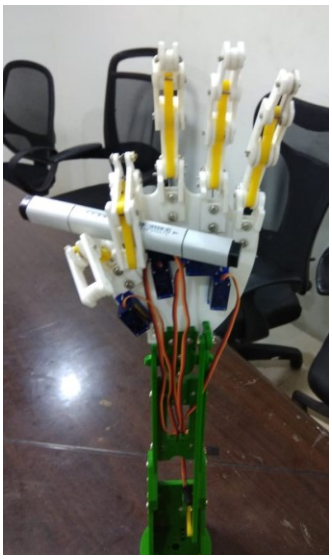

(c) Robotic Hand

Fig. 8. Comparison of hand gesture (a).human hand , (b)Virtual hand and (c) Robotic hand.

Fig. 8(a) shows human hand in front of leap motion controller, Fig. 8(b) shows virtual hand in PC/ Laptop and the Fig. 8(c) shows Robotic hand performs as per human activities. Fig. 9 shows different gesture result of Robotic hand.

The hand gesture method recognized by Leap Motion Controller which transfers the same information to virtual environment of PC/Laptop while same information is transferred to robotic hand through wireless communication [15].

Fig. 9. Gesture Result

Table 2. gives the accuracy of experimental prototype tested under various hand gestures from 4 different person with performance of Swipe, Grab, Pinch, Close, and Release gesture of the hand.

Gesture	Test	Accuracy
Swipe	4 Times	80%
Grab	4 Times	98%
Pinch	4 Times	65%
Close	4 Times	98%
Release	4 Times	98%

Table 2. Gesture Test

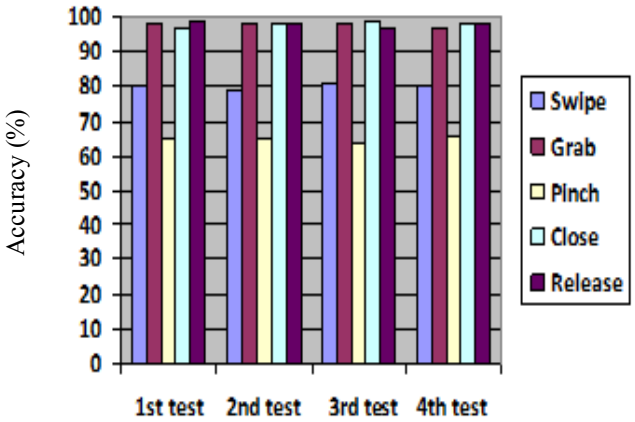

Fig. 10. Gesture Test Under Different Person

Fig. 10. Shows the bar chart of the accuracy obtained under different test conditions.

VI. CONCLUSION

In this research work, hand gesture and its interaction are used to control robotic arm. LMC observes hand and finger gestures. It displays a three dimensional image of hand and mimics Robotic hand like human hand activities. The proposed concept of linked virtual environment with real time environment is found to perform better.

This Robotic hand can perform operations in space research center , satellite, drone control, and places beyond human reach.

VII. FUTURE SCOPE

In future , latency of leap motion controller can be reduced by the new version of SDK.. Speed of wireless communication might be improved by the new types of wireless communication. The proposed concept can be implemented in tele operated Robotic application.

VIII. ACKNOWLEDGEMENT

Author would like to thank SusiRam Educational and Social Service Trust for the financial support and encouragement of this research.

IX. REFERENCES

[1] Saudabayev A, Varol HA. Sensors for robotic hands: A survey of state of the art. IEEE Access. 2015;3:1765-82.

[2] Kofman J, Wu X, Luu TJ, Verma S. Teleoperation of a robot manipulator using a vision-based human-robot interface. IEEE transactions on industrial electronics. 2005 Oct;52(5):1206-19.

[3] Chu NS, Tai CL. Real-time painting with an expressive virtual Chinese brush. IEEE Computer Graphics and applications. 2004 Sep;24(5):76-85.

[4] Kruse D, Wen JT, Radke RJ. A sensor-based dual-arm tele-robotic system. IEEE Transactions on Automation Science and Engineering. 2015 Jan;12(1):4-18.

[5] Jiang H, Duerstock BS, Wachs JP. A machine vision-based gestural interface for people with upper extremity physical impairments. IEEE Transactions on Systems, Man, and Cybernetics: Systems. 2013 Aug 8;44(5):630-41.

[6] Elons AS, Ahmed M, Shedid H, Tolba MF. Arabic sign language recognition using leap motion sensor. In2014 9th International Conference on Computer Engineering & Systems (ICCES) 2014 Dec 22 (pp. 368-373). IEEE.

[7] Hirche S, Buss M. Human-oriented control for haptic teleoperation. Proceedings of the IEEE. 2012 Mar;100(3):623-47.

[8] Vamsikrishna KM, Dogra DP, Desarkar MS. Computer-vision-assisted palm rehabilitation with supervised learning. IEEE Transactions on Biomedical Engineering. 2016 May;63(5):991-1001.

[9] Ponraj G, Ren H. Sensor Fusion of Leap Motion Controller and Flex Sensors Using Kalman Filter for Human Finger Tracking. IEEE Sensors Journal. 2018 Mar 1;18(5):2042-9.

[10] Aditya K, Chacko P, Kumari D, Kumari D, Bilgaiyan S. Recent Trends in HCI: A survey on Data Glove, LEAP Motion and Microsoft Kinect. In2018 IEEE International Conference on System, Computation, Automation and Networking (ICSCA) 2018 Jul 6 (pp. 1-5). IEEE.

[11] Mitra S, Acharya T. Gesture recognition: A survey. IEEE Transactions on Systems, Man, and Cybernetics, Part C (Applications and Reviews). 2007 May;37(3):311-24.

[12] Waldherr S, Romero R, Thrun S. A gesture based interface for human-robot interaction. Autonomous Robots. 2000 Sep 1;9(2):151-73.

[13] Marin G, Dominio F, Zanuttigh P. Hand gesture recognition with leap motion and kinect devices. In2014 IEEE International Conference on Image Processing (ICIP) 2014 Oct 27 (pp. 1565-1569). IEEE.

[14] Sarkar A, Patel KA, Ram RG, Capoor GK. Gesture control of drone using a motion controller. In2016 International Conference on Industrial Informatics and Computer Systems (CIICS) 2016 Mar 13 (pp. 1-5). IEEE.

[15] R.Satheeshkumar and Dr. R. Arivoli , " Real Time Virtual Human Hand For Robotics." *Seventh International Conference On Science and Innovative Engineering and Technology (ICCET)* 2019.

Proceedings of the Fourth International Conference on Communication and Electronics Systems (ICCES 2019)
IEEE Conference Record # 45898; IEEE Xplore ISBN: 978-1-7281-1261-9

Wireless IoT based Solution for Women Safety in Rural Areas

Rahul Paknikar, Shrey Shah, Dr. Prachi Gharpure
Department of Computer Engineering
Sardar Patel Institute of Technology
Mumbai, India
{rahul.paknikar, shrey.shah, prachi_gharpure}@spit.ac.in

***Abstract*—In today's era, women still feel scared to step out of their homes at late nights due to the fear of sexual harassment. This problem is compounded when one shifts the focus from urban to rural sector and interior areas of villages where there is erratic electric supply and poor cellular network connectivity. There are many smartphone based solutions, but the availability of smartphone and cellular network in rural areas is unreliable. This paper proposes a system, by creating a wireless network using IoT technology with a portable device for alerting the concerned authorities to prevent any mishap. Women will be provided with a beacon device consisting of a help button. In case of any emergency, the beacon information will reach the central stations and an alarm will be triggered at the prominent places of the village. One can find out the location of the victim based on her proximity to the nearest access point.**

***Index Terms*—Bluetooth Low Energy, Global Positioning System, Beacon device, Internet of Things, Solar Panels, Access Point, Central Station**

I. Introduction

Even though we live in the 21st century with much technological advancement and social awareness, women face the problem of harassment of any form and get abused physically or mentally. Areas like streets and public spaces have been the territory of such violence. This issue worsens for women living in remote and rural areas, where they might not be aware about these crimes or hesitate to report these crimes to the concerned authorities. There are many existing applications and devices for women security through smartphones. Though the smartphones have increased rapidly, it is not possible that the smartphones and cellular network will be available all the times in rural areas. Also, many people in the village do not have smartphones which can assist them in contacting the concerned authorities, otherwise. Literacy rate of villages is low and parents do not send girls to schools due to the fear of sexual harassment.

The proposed system for women safety is based on BLE (Bluetooth Low Energy) Beacon device due to their low cost, ease of deployment, ease of accessibility to the users and superior interior localization as described in [2], [3]. Kang Eun Jeon, James She, Perm Soonsawad, and Pai Chet Ng [2] specify that BLE has low energy requirements and battery life of BLE Beacon devices can be extended upto 2-3 years on a single coin cell battery if broadcast intervals are set appropriately based on the application. BLE is 60 - 80% cheaper than traditional Bluetooth and is compatible with a wide range of IoT (Internet of Things) boards, mobile phones, tablets and computers. It is ideal for the proposed system which requires small periodic broadcast of data at regular interval of 1 - 1.5 seconds.

The paper has been organized as follows - Section II describes the existing women safety systems and their demerits. An insight into the system that we proposed in Section III includes the overview of system, mathematical model, various components and the working model. The implementation of the system is described in Section IV which consists of a simulation experiment. Section V provides the results of the simulation and its analysis. Lastly, Section VI includes the conclusion and further improvements possible to the system.

II. Related Work

Majority of the approaches for providing women safety concentrate on urban areas where it becomes possible to provide immediate help for women in distress. Additionally, these systems [4], [5], [6] use smartphone and GPS (Global Positioning System) technologies which are difficult to support in undeveloped rural areas.

Implementation of Women Safety based on IoT approach by D. G. Monisha, M. Monisha, G. Pavithra and R. Subhashini [5] involves ARM Controller along with a smartphone, synchronized using Bluetooth to call the preset contacts and record audio for further investigation. It also include components like GPS Module, audio and video recorder in hardware based solution. However, using these components make the device bulky and not feasible to carry it all the time. A reliable GSM network is also required for the smartphone to alert the preset contacts. Noise can be present in the audio recording which can be misinterpreted, making it unreliable.

Another solution by G C Harikiran, Karthik Menasinkai, Suhas Shirol [6] comprises of a wearable Smart Band which continuously communicates with smartphone that has access to the GPS and Internet. The Smart Band sends emergency signal to the smartphone through Bluetooth 4.0 BLE which uses GSM messages and Internet to post on social platform provided by the mobile application. However, many remote areas in the country are difficult to be connected using Internet facilities due to latent requirements and location concerns. Also in distributed housing layout of rural areas, the cost of

providing Internet connectivity is not viable as the subscription fee will exceed the affordability of villagers and it is not feasible to provide reduced subscription rates.

The implementation proposed by Ms. Deepali M. Bhavale, Ms. Priyanka S. Bhawale, Ms. Tejal Sasane, Mr. Atul S. Bhawale [4] provides a unified approach by designing a safety kit for women using Arduino. It consists of a handheld device for alerting and GPS component for tracking the location of victim. But GPS depends heavily on cellular network. Also it is power exhaustive and does not support indoor localization due to its inability to penetrate through the solid rock structures.

III. Proposed System

A. Methodology

Multiple solar powered street light poles are arranged in an optimized formation of triangular geometry such that each pole is within the range of its adjacent poles on either side of it. IoT boards [1] will be positioned on these street poles and will be powered using the solar energy taking into account the unpredictable electricity supply to the rural areas. It will act as an Access Point (AP) of the local wireless network through which the communication between a Beacon device and an AP will occur.

Women will be provided with the Beacon device which will consist of a help button. Based on Beacon device's UUID (Universally Unique Identifier), the user will be identified uniquely and the Transmission (Tx) Power parameter will enable us to estimate the location of the victim. The AP which sense the maximum Tx Power from the Beacon device will give us the accurate location of the victim.

For this, the street poles will be identified by a unique identifier and its pre-defined GPS coordinates in the village area. Beacon communication consists primarily of advertisement broadcast at a regular interval by Beacon device via radio waves. The communication between a Beacon device and an AP, between any two APs and between an AP and a server at central station is governed by BLE Multi-Hop routing protocol [7].

Features of the System:

- Independent of Electricity: Rural areas face the problem of frequent power cuts. To power the APs, our system makes use of solar panels mounted on the street poles. This provides dual benefit by providing power supply to both the AP and street poles. So the system will continue to function even in the absence of electricity.
- Independent of real-time GPS: For accurate tracking of the victim's location, we store pre-defined GPS coordinates of street poles in a database. Also, an offline map of the entire village is stored at the central station to accurately track these GPS coordinates on the map along with the landmark.
- Tracking victim using preset GPS coordinates of APs: Once the victim triggers the help button on the Beacon device, the message is broadcasted and routed to the central station. Based on the information stored in the central station, the concerned authorities can be sure of the victim's location based on the pre-stored latitudinal and longitudinal details of APs.
- Independent of Smartphones and GSM system: The system takes care of Internet issues based on GSM network and smartphones which are not available all the time to make a call or be in range of GSM network.
- Multiple central stations: If multiple help requests are received simultaneously, a single station will not be able to handle and process all the load efficiently. Hence, we introduced multiple stations so that help requests can be routed to the stations and alarm be triggered. This also solves the issue of single point of failure of a station.

B. Mathematical Model

The arrangement of street poles on roads or highway follow 4-in-a-rectangle placement as seen in Fig. 1 indicating that 2 poles face each other in exact opposite direction. To provide adequate visibility for the same area, we optimize the number of poles by placing them in a 3-in-a-triangle placement with each pole placed at the vertex of a triangle as seen in Fig 2. This optimizes the number of APs which need to be mounted on these street poles. Further, we place the poles at some viable distance in the transmission range of APs.

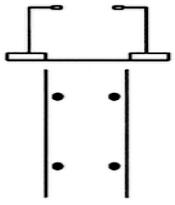

Fig. 1: Rectangular arrangement of poles

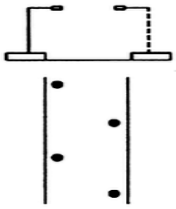

Fig. 2: Triangular arrangement of poles

The maximum transmission range of BLE Protocol is 100 meters. Taking into consideration the attenuation in signals that is caused normally due to interference or fading phenomenon, we restrict the maximum range of transmission to 80 meters. While considering the triangular arrangement, we need to take into account the blind spot, here a centroid, of triangle which is a point outside the normal range of an AP where there is unusually weak signal reception. The centroid is I as seen in Fig 3. To cover it within 3 APs, the distance of the AP to the centroid must be 80 meters which means KI is 80 meters. Based on an equilateral triangle's property, centroid bisects the median KB in the ratio 2:1. So the ratio of segment KI to IB is 2:1 and hence the distance IB is 40 meters. The height $KB = (KI + IB)$ turns out to be 80 + 40 = 120 meters.

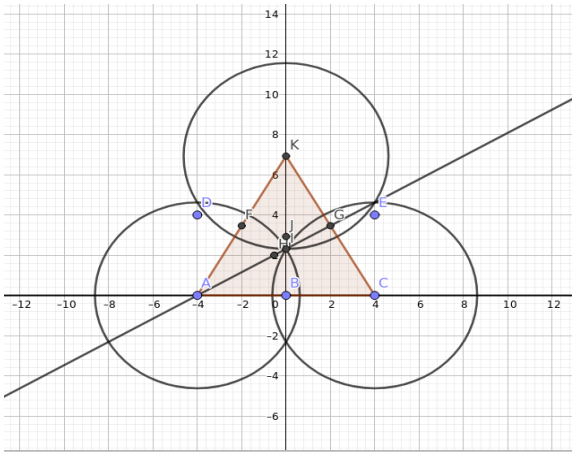

Fig. 3: Calculation of distance between 2 APs

Consider $\triangle KAB$.
Let the distances *AB, BC, CG, KG, FK* and *AF* be *r* meters.
$\implies$ The distance *AK* will be *2r* meters.

Using Pythagoras Theorem,
$(AK)^2 = (KB)^2 + (BA)^2$
$\therefore (2r)^2 = (120)^2 + (r)^2$
$\therefore 4r^2 = 14400 + r^2$
$\therefore r^2 = 4800$
$\therefore r$ = 69.28 meters

Hence, any 2 APs can be placed within a range of 130-140 meters. Thus, an area of 10^6 square meters would require 60 APs to cover the entire region without any blind spot. We can ensure that even if any victim is present at the blind spot and the help button is pressed, the help request will be received by atleast one of the three APs.

C. Hardware Description

Our system consists of five hardware components:

- Beacon device: It is a wearable and portable device [8] which is BLE enabled via radio waves [3], for alerting the concerned authorities in the village and is associated with 4 components - UUID, Major, Minor and Tx Power to uniquely identify the user. It consists of a help button that facilitates the trigger of emergency broadcast.
- AP: We performed a comprehensive review of the IoT boards [1] such as UDOO x86, Intel Galileo, Beagle-BoneBlack, Edison Arduino Kit, Tessel 2 and Raspberry Pi Zero W. All of these boards are BLE enabled, have low energy requirements and can be interfaced with the solar panels. They provide efficient and a reliable platform for development of the IoT boards as an AP.
- Central Station: At each central station, a server is setup by a computer which can be powered by solar panels. It consists of a database that stores the unique mapping of AP identifiers and its corresponding colloquial village region naming. These identifiers and landmarks is plotted on a preset map stored in the server for faster tracking of victim's location.
- Solar Panel: These panels supply power to both street light poles as well as AP. The voltage supply and the electric current drawn from the source are specific to the IoT boards that will be used for APs.
- Buzzer: It is an emergency alarm device interfaced with the server at central station. For effective audibility, the loudness depends on the surrounding environment and the distance from the source. However, the recommended loudness [11] should be 80 - 90 decibels with a region coverage of 60 meters.

D. Working Model

Each woman is provided with a Beacon device. If any woman feels threatened by any perpetrator, she will press the help button on the Beacon device provided. Beacon device will send the information about its unique identifier encapsulated in a broadcast message to APs 1, 2, 3, 4 in its range as shown in Fig 4. Even though AP 4 is down, message will be broadcasted to it, but it will not be able to forward any message to other APs. The APs will route these broadcast messages amongst themselves until they reach the central station. Multiple routes are possible for the message transmission, which will guarantee the delivery of message even in case of losses.

As shown in Fig. 4, the possible paths are as follows:

AP 1 $\rightarrow$ *AP 3* $\rightarrow$ *AP 5* $\rightarrow$ *Central Station*
AP 1 $\rightarrow$ *AP 3* $\rightarrow$ *AP 5* $\rightarrow$ *AP 6* $\rightarrow$ *Central Station*
AP 3 $\rightarrow$ *AP 5* $\rightarrow$ *Central Station*
AP 3 $\rightarrow$ *AP 5* $\rightarrow$ *AP 6* $\rightarrow$ *Central Station*

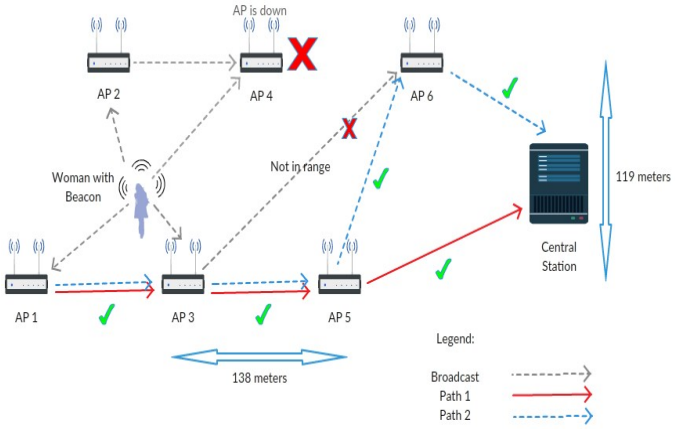

Fig. 4: Working Model of Proposed System

All these paths will route the message to the central station. As soon as the first message reaches the central station, the alarm will be triggered.

IV. Implementation

The proposed system consists of 2 aspects of implementation which are as follows:

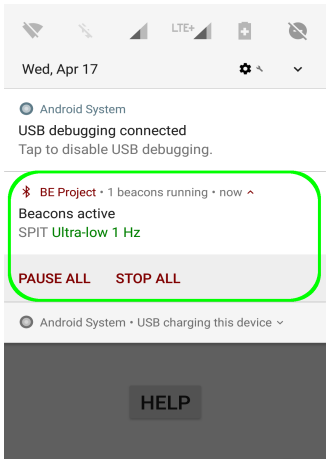

(a) Beacon Configuration

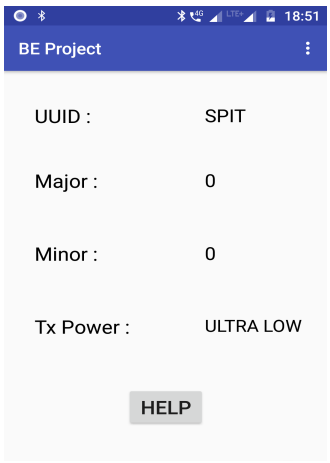

(b) Interface at Beacon device (send regular broadcast)

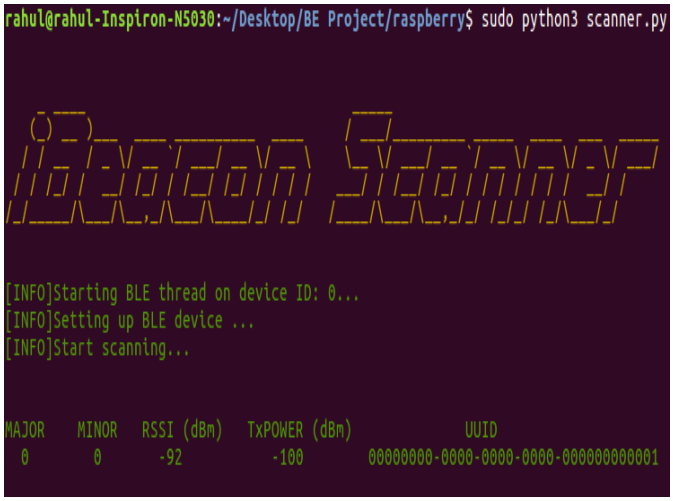

(c) Interface at AP - captured regular broadcast

Fig. 5: Regular Broadcast

(a) Beacon Configuration

(b) Interface at Beacon device (send emergency broadcast)

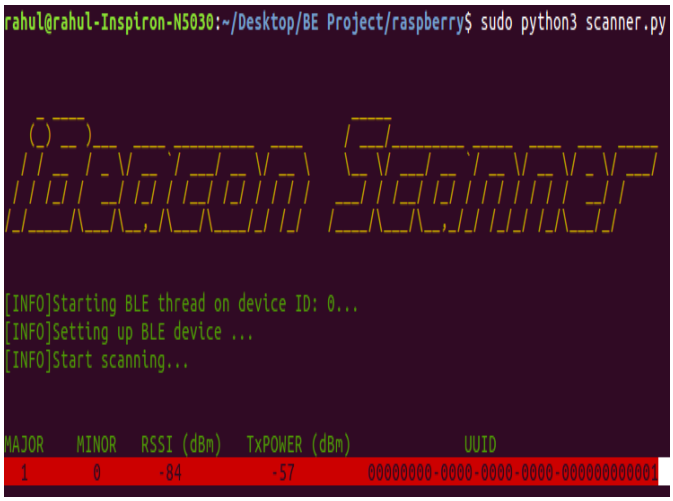

(c) Interface at AP - captured emergency broadcast

Fig. 6: Emergency Broadcast

A. *Beacon Device - AP Communication*

Communication between a Beacon device and an AP was tested by simulating the Beacon device as an Android Application and an AP device with Raspberry Pi Zero W, a single-board computer. The broadcast messages by an AP from the Beacon device is captured with the help of modules specified in [14].

Fig. 5 depicts a simulation of Beacon device, that the user will carry, for a regular use-case. Fig. 5(a) is a screenshot that shows the specification of Beacon device when it is broadcasting BLE packets at Ultra-low frequency as supported by the Android architecture. These packets are regular/normal broadcast packets that contain 4 parameters in its header frame as shown in Fig. 5(b) screenshot. The UUID name ”SPIT” is set at application layer, but at physical layer this parameter will be converted into 16 byte UUID along with Major as 0, Minor as 0 and Tx Power as integer indicating the advertisement mode. Fig. 5(c) is a screenshot that shows the regular broadcast packet captured by an AP device in the range of BLE Beacon device. Since the frequency is Ultra-low, the RSSI (Received Signal Strength Indicator) value and Tx Power are too low for any AP to capture these packets from farther distances and the calculated distance [13] gets restricted to a certain broadcast range. Thus, these packets may not even reach the AP and hence get filtered out. This benefits the system as such packets are regular broadcasts and not emergency broadcast; thus saving energy, increasing lifetime of Beacon devices, reducing load and traffic on APs.

Fig. 6 depicts a scenario for an emergency broadcast by the Beacon device that is triggered by the user. Fig. 6(a) is a screenshot that shows the specification of Beacon device when it is broadcasting an emergency BLE packet at High frequency as supported by the Android architecture. When user clicks

on help button, the Beacon device increases its frequency to transmit the emergency broadcast to a larger distance.

To differentiate between a regular and an emergency broadcast, a flag or some metadata is required in the packet. As shown in Fig. 6(b), the parameter "Major" serves this purpose without increasing the size of the packet. Fig. 6(c) is a screenshot of the extracted information from the packet in a readable format with extra parameter of RSSI sensed by the AP. The broadcast at High frequency facilitates AP to capture the packet with accurate reading of Tx Power and RSSI value, determining the distance with high accuracy [13]. This information from the received packet will then be routed to the central station for further processing.

B. AP - AP Communication and Routing

For testing the efficiency and scalability of our proposed system, we designed a network simulation using ***ns3*** Network Simulator [9], [10] for the scenario described in Working Model.

1) Initial Configuration:

In accordance with the Mathematical model, the horizontal distances between 2 APs is set to 138 meters and vertical distance as 119 meters approximately. As seen in Fig. 7, it depicts the initial state of the system simulating a scenario of 12 APs (red) of which 2 constitute the central stations (black) at prominent places in the region, 3 beacon users (blue) distributed in an approximate area of 261.085×10^3 square meters. Communication between the APs is simulated based on the underlying Multi-Hop routing protocol [7].

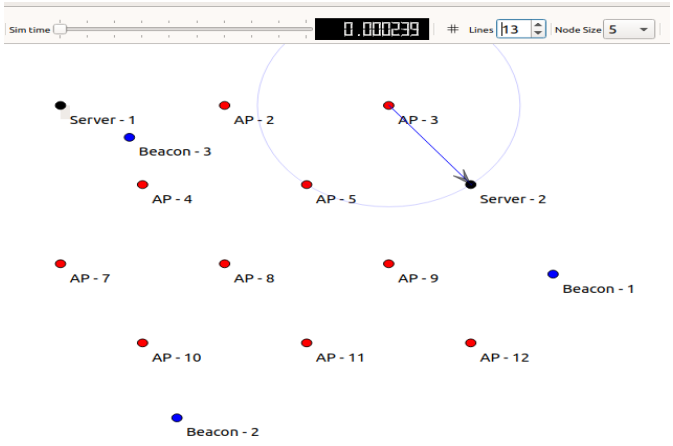

Fig. 7: Initial Configuration of Access Points and Beacons

2) Simulation of Dysfunctional AP:

If certain APs become dysfunctional the system is able to route packets to the central station. To reduce the response time for triggering the alarm, multiple stations have been incorporated so that if packets are unable to reach a particular central station, they are routed to some other central station. As shown in Fig. 8, AP-8 is labelled as 'Down' indicating that it is not in proper working condition. So packets from Beacon devices

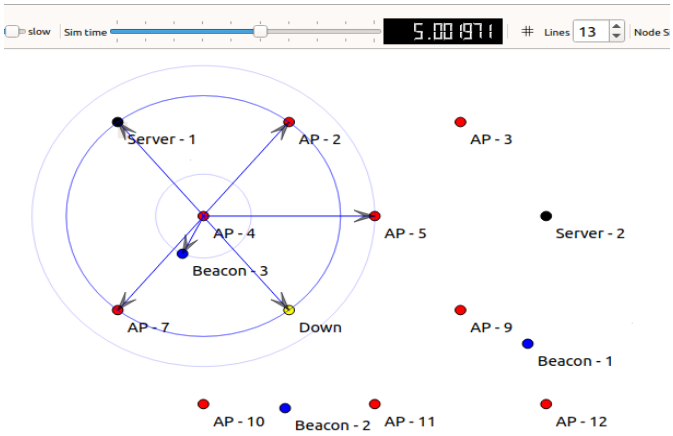

Fig. 8: Considering any random AP as dysfunctional

will be broadcasted to AP-8, but it will not be able to forward any packets.

Tx Power helps to estimate the victim location using RSSI. Fig. 9 shows each distress message packet reaching the central stations and each parameter of BLE header with its value. The message packets from all 3 Beacon devices are received indicating that system efficiently routes the packet even in case of AP failure. It also shows the warning alert - the Beacon device from which it originated and the central station where it is captured along with the time at which the message is received.

```
Trace file generated is BLE_Manet_12Nodes_10SimTime.tr

Starting simulation for 10 s ...

Packet Size (in Bytes): 23
Beacon UUID : 000000000000001
MINOR : 0
MAJOR : 1
SIGNAL POWER : 3
RSSI : 45.0152
Warning! Received Alert Near Access Point 5
Central Server 5 received one packet from Beacon - 1 at 6.50761

Packet Size (in Bytes): 23
Beacon UUID : 000000000000001
MINOR : 0
MAJOR : 1
SIGNAL POWER : 6
RSSI : 64.2705
Warning! Received Alert Near Access Point 4
Central Server 0 received one packet from Beacon - 1 at 6.51536

Packet Size (in Bytes): 23
Beacon UUID : 000000000000002
MINOR : 0
MAJOR : 1
SIGNAL POWER : 1
RSSI : 30.277
Warning! Received Alert Near Access Point 6
Central Server 0 received one packet from Beacon - 2 at 6.70912

Packet Size (in Bytes): 23
Beacon UUID : 000000000000003
MINOR : 0
MAJOR : 1
SIGNAL POWER : 5
RSSI : 64.6725
Warning! Received Alert Near Access Point 0
Central Server 0 received one packet from Beacon - 3 at 6.90857
```

Fig. 9: Distress messages received by the Central Stations

V. Result Analysis

We tested the system for response time to trigger the alarm, scalability and efficiency of the system with the observations as shown in Table I.

Table I: Scalability of the system with increase in the APs, Users and Central Stations

Number of APs	12	50	150	450
Number of Users	3	6	15	30
Number of Central Stations	2	3	7	15
Response Time (in seconds)	0.419	1.019	2.039	4.551

As seen in Fig. 10, we infer that the response time, being a critical parameter, for triggering the alarm varies in an approximate linear fashion with respect to the number of APs, but is within the acceptable range of 0.1 - 15 seconds with the increase in number of APs as described in [12] indicating that first minute during an ongoing violence is most critical and hence the response time should be within 60 seconds. It may be due to the losses and buffer limitations that the time to hear alarm increases due to queuing and processing of packets at central station. Introduction of multiple stations is able to handle the load and packet losses by routing packets to all the stations and alarm be heard. If a station is down, still packets are broadcasted to other stations and alarm is heard. The routing algorithm is able to handle the routing of packets even if multiple Beacon devices are triggered simultaneously.

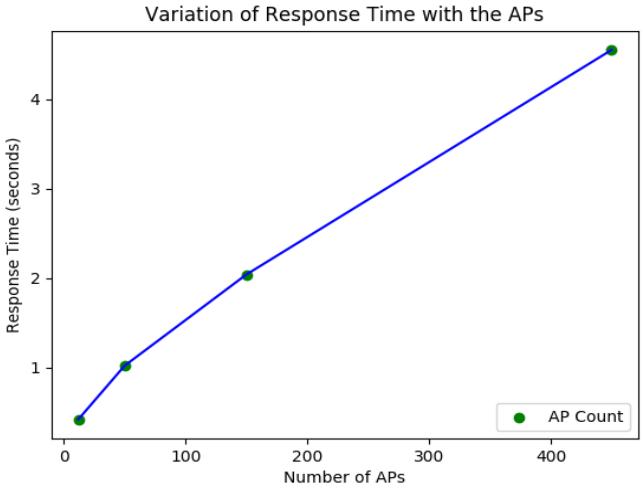

Fig. 10: Variation of Response time (seconds) with APs

VI. Conclusion and Future Scope

In this paper, we have proposed a wireless IoT based solution for women safety in rural areas by taking into account two most critical issues of erratic electricity supply and unreliable cellular network which are common in rural areas. To achieve this, solar panels on the street poles power the APs and an independent local network is created based on BLE routing protocol. Based on the Beacon signal received by an AP, location of the victim is traced out through the RSSI value and supported with a plot on preset map of the village. We introduced multiple central stations so that even if a station fails, the distress message can reach other stations to prevent any mishap.

As for future work to be done, the proposed system can be integrated with Machine Learning to identify most vulnerable and unsafe regions in the village. Thus, security in such regions can be increased by making the local network coverage more stringent. However, such computations need to be done when the system remains idle for long enough, without compromising the safety of women or else it can be done on remote systems. Also, APs can be combined with a surveillance system comprising of audio/video recorder or a camera to record the harassment incident as an evidence and to avoid false accusations. The proposed system can be extended to various emergency situations like fire breakdown, human accident, child abuse, robbery and senior citizen harassment.

References

[1] Ali Raza, Asfand Amin, Ataul Aziz Ikram, Ahmad Jamal Ikram, "A review of low cost and power efficient development boards for IoT applications," in FTC 2016 - Future Technologies Conference 2016 6-7 December 2016 San Francisco, United States.

[2] Kang Eun Jeon, James She, Perm Soonsawad, and Pai Chet Ng, "BLE Beacons for Internet of Things applications: Survey, Challenges, and Opportunities," in IEEE Internet of Things Journal, Vol. 5, No. 2, April 2018

[3] Mahmoud Elkhodr, Seyed Shahrestani and Hon Cheung, "Emerging wireless technologies in the Internet of Things : A comparative study," in International Journal of Wireless Mobile Networks (IJWMN) Vol. 8, No. 5, October 2016.

[4] Ms. Deepali M. Bhavale, Ms. Priyanka S. Bhawale, Ms. Tejal Sasane, Mr. Atul S. Bhawale, "IoT based unified approach for women and children security using wireless and GPS," in International Journal of Advanced Research in Computer Engineering and Technology, Volume 5, Issue 8, August 2016.

[5] D. G. Monisha , M. Monisha, G. Pavithra and R. Subhashini, "Women safety device and application-FEMME," in Indian Journal of Science and Technology, Vol 9(10), March 2016.

[6] G C Harikiran, Karthik Menasinkai, Suhas Shirol, "Smart security solution for women based on Internet Of Things (IoT)," in International Conference on Electrical, Electronics, and Optimization Techniques (ICEEOT) - 2016.

[7] Zonglin Guo, Ian G. Harris , Lih-feng Tsaur and Xianbo Chen, "An On-demand Scatternet formation and Multi-hop Routing Protocol for BLE-based wireless sensor networks," in 2015 IEEE Wireless Communications and Networking Conference (WCNC): - Track 3: Mobile and Wireless Networks

[8] "What is iBeacon? A guide to Beacons." [Online]. Available: http://www.ibeacon.com/what-is-ibeacon-a-guide-to-beacons/

[9] "ns-3 — A discrete-event network simulator for Internet systems." [Online]. Available: https://www.nsnam.org/

[10] "NS-3 Google Groups Support." [Online]. Available: https://groups.google.com/forum/!forums/ns-3-users

[11] "Guide to specifying audible signals." [Online]. Available: http://www.e2s.com/audiblesignals

[12] "Workplace Panic Button." [Online]. Available: https://www.communityresponsesystems.com/blog/workplace-panic-button/

[13] "How to calculate distance from the RSSI value of the BLE Beacon" [Online]. Available: https://iotandelectronics.wordpress.com/2016/10/07/how-to-calculate-distance-from-the-rssi-value-of-the-ble-beacon/

[14] "iBeacon Scanner - Credits: SwitchDoc Labs, LLC June 2014." [Online]. Available: https://github.com/ashokgelal/iBeacon-Scanner

Proceedings of the Fourth International Conference on Communication and Electronics Systems (ICCES 2019)
IEEE Conference Record # 45898; IEEE Xplore ISBN: 978-1-7281-1261-9

Implementation of Power Quality Enhancement using Hybrid Series Active Filter

VANITA NAKADE
Department of Electrical Engineering, G. H. Raisoni Institute of Engineering and Technology, Pune, India,
vanita.nakade@gmail.com

SANGITA PATIL
Department of Electrical Engineering, G. H. Raisoni Institute of Engineering and Technology, Pune, India,
sangita.patil@raisoni.net

***Abstract*- The quality of the power supply is an important concern over the years. The quality of the power can be considered with the factors like current, voltage, and power factor etc. The parameters like the stability and reliability of the power plays an important role in deciding the quality of supply. The end user always faces the economic losses if the quality of the supply is inadequate. The main cause of degradation in power supply is the harmonics. The voltage and current harmonics are the issues to be addresses to enrich the power quality. The active filters are helpful to improve the quality of power by means of mitigating the harmonics. Authors have implemented the hybrid active power filter to improve the quality of the power supply. The sliding mode of the controller is implemented to assure the better performance of the system.**

Keywords- filter, active power filter, power quality, harmonics, hybrid filters, sliding mode controller, etc.

I. INTRODUCTION

The variations in the type of loads connected, moreover the increase in the non-linear loads have caused the power quality degradation. The harmonics are inserted in the grid due to these loads. The protection devices although are smart now a days, experiences the adverse effects of the distorted power. The passive filter provides popular low cost solution over the problem. The problems with the passive filters are mistuning and dependency of impedance on the power supply. [1]

Improving the power quality is on the priority of the researchers since last two decades. The various configurations of filters are presented by the researchers. The reduction of the harmonics is effectively possible with the active power filters. The active filters become more effective with the various configurations. [2-3]

The harmonics present in the source current can be eliminated with the transformer-less hybrid filter. The system can be implemented for the single phase consumers who are really large in numbers. [4]

The harmonics injection at different consumer end or at different non-linear load is going to affect severely at common coupling point. The active filter with proper current selection method can control the impact of harmonics on the power supply. [5]

The inverters (voltage source) are very popular since last few years in micro grids. It provides the reliable conversion of the voltage. It is suitable from the point of view of improving the quality of the power supply as it is capable of handling the power and converting it to the reliable form. It helps in reducing cost also as the complete operations of power control and the conversion is done by the same circuit. [6]

The analysis shows that the power quality issues are increasing in recent years the generation of the electricity is done remotely at different places in small amount. The grid connection of such sources causes the severe effect on the power quality. The smart grid has achieved the performance enhancement to some extent while there is still a huge scope to enhance the grid performance. [7]

Medium distribution systems can work effectively with the unified power control method. The filers are added as per the need in the supply. The circuit is capable of balancing the power. [8]

The reactive power sometimes becomes beyond control of the generalized active filters. The system becomes challenging to control such high distortion in the supply. The selective harmonic reduction becomes an effective strategy to control the power for such situations. The discrete time filtering is another approach to overcome the quality issues. These can be useful in three-phase systems. [9-10]

The non-conventional sources are becoming effective with the enhancement in the technology. When these sources are inter-connected to the grid, there are several issues with the quality of power. It results in low quality of the grid supply and consumers may also be affected. [11]

The closed loop system for the insertion of the current in order to reduce the harmonics is another approach to be used for the micro-grids. It is flexible system to control the harmonic distortion in the power supply. [12]

With enhancement in the technology and number of the energy sources, it becomes more challenging to control the power. The power is generated with different capacities, different strategies and inserted to the grid hence it is very difficult to apply a single solution to control the power. Improving the quality of the supply needs the controlling circuits to be connected at different stages.

II. IMPLEMENTED SYSTEM

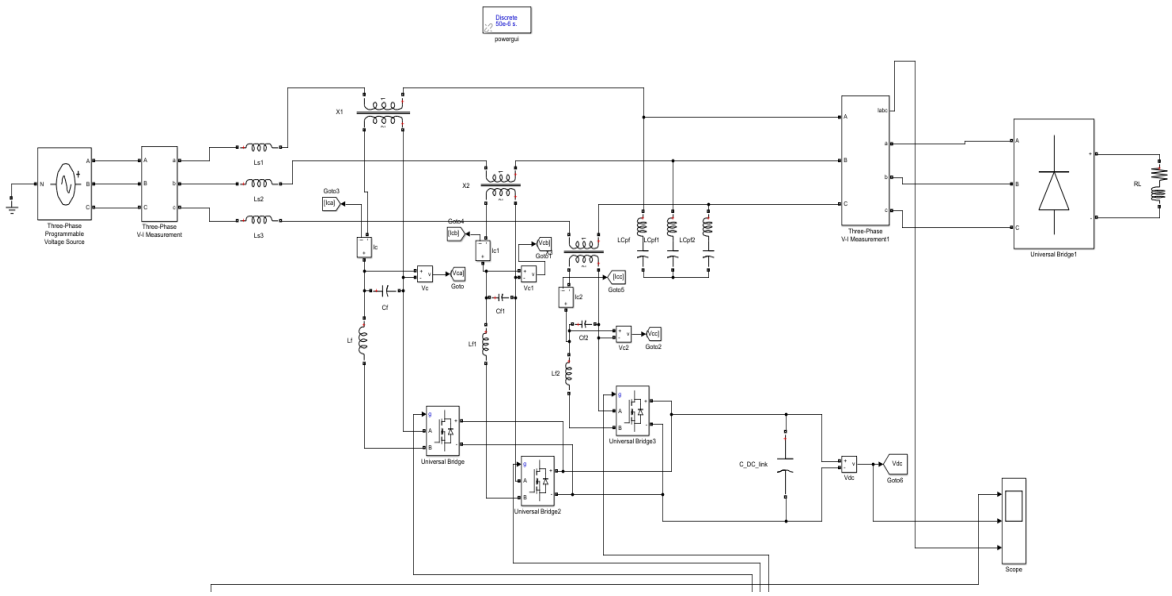

Fig.1. Implemented system for the harmonic control using hybrid active power filter

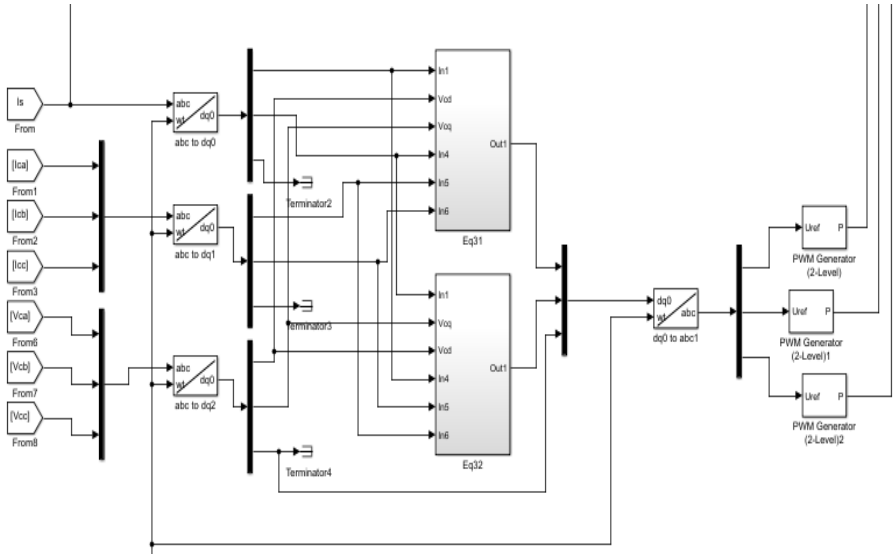

Fig.2. Implemented system –Sliding mode control circuit

Figure 1&2 shows the complete system implemented in MATLAB for controlling quality of power supply. The sliding mode helps in controlling the non-linear power. As it is a closed loop control method, it assures the auto setting of the desire parameters to be set in order to improve the power. The sliding mode control generally operates by comparing the actual quantities with the reference values.

The control scheme for the sliding mode operation is shown in the figure 2 above. The control is developed with the logic diagram controlling the various parameters for the operations. The logic is developed with reference to the following equations:

$$U_d = (\dot{V}^*_{cd} + \alpha \ddot{V}^*_{cd}) + \frac{L_f}{V_{dc}}(C_f\ \omega\ V_{cq} - i_{cd} + i_{sd}) + \frac{\alpha L_f}{V_{dc}}(-C_f\omega^2 V_{cd} - \omega i_{cq} + \omega i_{sq} - \frac{V_{cd}}{L_f} - \omega i_{cq} + i_{sd}) - K_{11}\text{sign}(S_d) - K_{12}\text{sign}(S_d)$$

----------Eq-1

$$U_q = (\dot{V}^*_{cq} + \alpha \ddot{V}^*_{cq}) + \frac{L_f}{V_{dc}}(C_f\ \omega\ V_{cd} - i_{cq} + i_{sq}) + \frac{\alpha L_f}{V_{dc}}(-C_f\omega^2 V_{cq} - \omega i_{cd} + \omega i_{sd} - \frac{V_{cq}}{L_f} - \omega i_{cd} + i_{sq}) - K_{21}\text{sign}(S_q) - K_{22}\text{sign}(S_q)$$

----------Eq-2 [1]

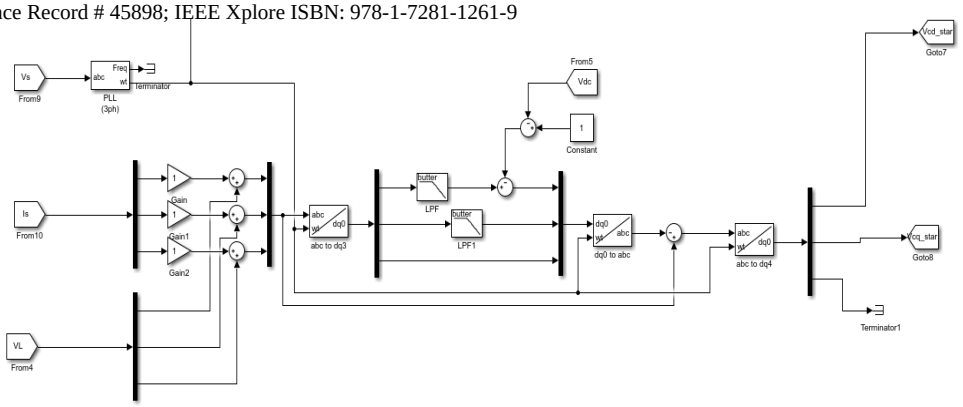

Fig.3. Reference signal generating scheme

Figure 3 shows the reference signal generating scheme. It is very important to have the reference signal in order to compare the real time quantities with the reference values. It helps in identifying the need for the control signal to be generated in order to mitigate the harmonics. The hybrid system detects the source and load parameters at a time.

III. RESULTS AND DISCUSSION

The simulation is implemented and the results are presented in this section. The non-linear load is considered for the experimentation. It leads to the harmonic distortion in supply and load side.

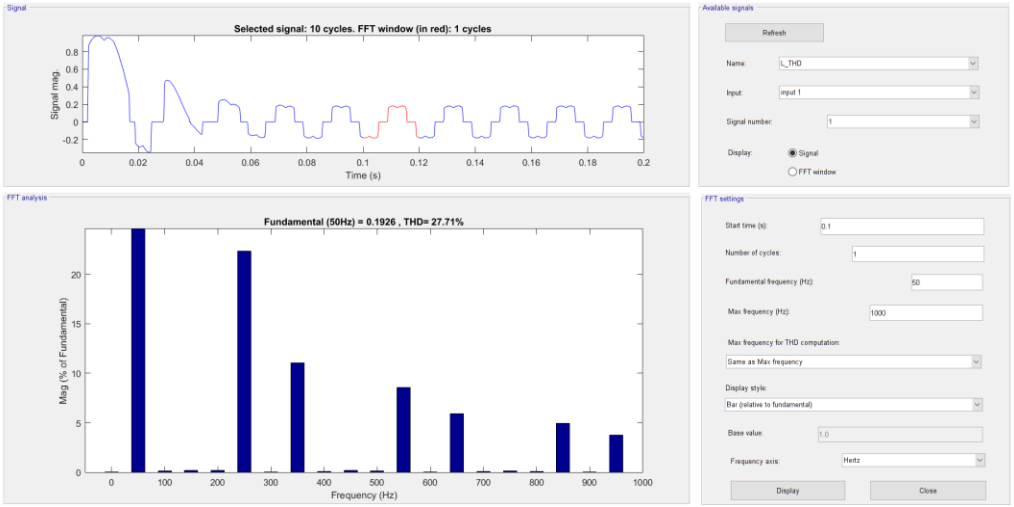

Fig.4 Total harmonic distortion of Supply side

The harmonic distortion of the supply is shown in the diagram 4. The above graph represents the harmonic distortion of the input side. When the input is provided, it is observed that the harmonic distortion of current is 27.71%. This value of the distortion is very high and if the same supply is given to the load, it again creates the problems as the performance of the system deteriorates.

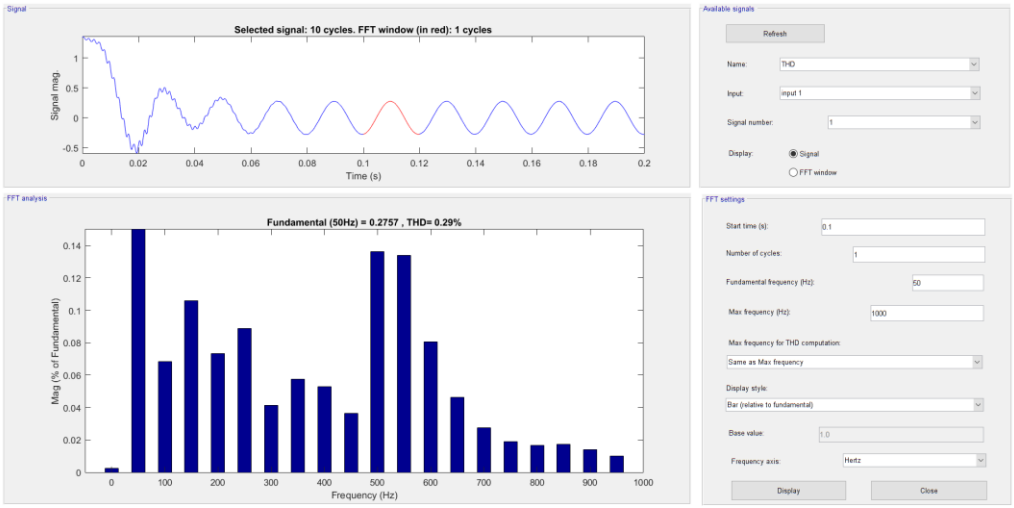

Fig.5 Total harmonic distortion on load side

The harmonic distortion of the load side is represented in the graph above. The hybrid active filter reduces the impact of harmonic distortion satisfactorily. It is observed that the total distortion is 0.29% after implementation of the scheme whereas on load side it was 27.71%. It is observed that distortion is compensated by the implemented hybrid filter scheme.

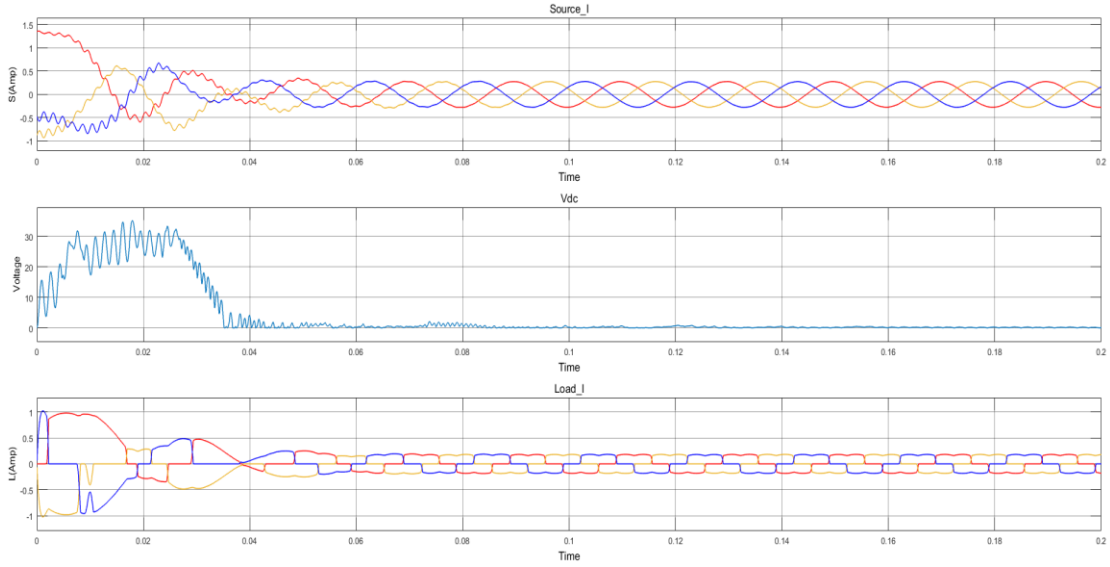

Fig.6. Source current, inverter voltage and load current of the implemented system

The results of the implemented scheme are shown in the waveforms above. It is observed from the above waveforms that, the distortion is reduced in output voltage and current as compared to the input current.

IV. CONCLUSION

The harmonics in the power supply are the severe cause of deterioration of the power quality. As the number of the sources increased and the nature of load is also changed over the years, the harmonic distortion becomes a serious issue to be addressed. Over the wide range of the filters available, it was challenging to select the proper filter to be implemented. The active hybrid filter with sliding mode control is implemented and presented in this paper. Authors have implemented the hybrid active filter scheme for the unbalanced load condition. Authors have achieved the reduction in harmonic distortion from 27.71% to 0.29% from supply to load side. The results achieved in MATLAB are satisfactory. The scheme presented in this paper, is useful for the micro-grid.

REFERENCES:

1. Swain, Sushree Diptimayee, Pravat Kumar Ray, and Kanungo Barada Mohanty. "Improvement of power quality using a robust hybrid series active power filter." *IEEE Transactions on Power Electronics* 32.5 (2017): 3490-3498.
2. Chen, Donghua, and Shaojun Xie. "Review of the control strategies applied to active power filters." *2004 IEEE International Conference on Electric Utility Deregulation, Restructuring and Power Technologies. Proceedings*. Vol. 2. IEEE, 2004.
3. Singh, Bhim, Kamal Al-Haddad, and Ambrish Chandra. "A review of active filters for power quality improvement." *IEEE transactions on industrial electronics* 46.5 (1999): 960-971.
4. Javadi, Alireza, et al. "Experimental investigation on a hybrid series active power compensator to improve power quality of typical households." *IEEE Transactions on Industrial Electronics* 63.8 (2016): 4849-4859.
5. Dey, Papan, and Saad Mekhilef. "Current controllers of active power filter for power quality improvement: A technical analysis." *automatika* 56.1 (2015): 42-54.
6. Miveh, M. Reza, et al. "Power quality improvement in autonomous microgrids using multi-functional voltage source inverters: a comprehensive review." *Journal of Power Electronics* 15.4 (2015): 1054-1065.
7. An, L. U. O., et al. "Overview of power quality analysis and control technology for the smart grid." *Journal of Modern Power Systems and Clean Energy* 4.1 (2016): 1-9.
8. Xu, Qianming, et al. "Analysis and control of M3C-based UPQC for power quality improvement in medium/high-voltage power grid." *IEEE Transactions on Power Electronics* 31.12 (2016): 8182-8194.
9. Wang, Lei, Chi-Seng Lam, and Man-Chung Wong. "Selective compensation of distortion, unbalanced and reactive power of a thyristor-controlled LC-coupling hybrid active power filter (TCLC-HAPF)." *IEEE Transactions on Power Electronics*32.12 (2017): 9065-9077.
10. Badoni, Manoj, Alka Singh, and Bhim Singh. "Comparative performance of wiener filter and adaptive least mean square-based control for power quality improvement." *IEEE Transactions on Industrial Electronics* 63.5 (2016): 3028-3037.
11. Liang, Xiaodong. "Emerging power quality challenges due to integration of renewable energy sources." *IEEE Transactions on Industry Applications* 53.2 (2017): 855-866.
12. Dey, Papan, and Saad Mekhilef. "Current harmonics compensation with three-phase four-wire shunt hybrid active power filter based on modified D–Q theory." *IET Power Electronics* 8.11 (2015): 2265-2280.

Proceedings of the Fourth International Conference on Communication and Electronics Systems (ICCES 2019)
IEEE Conference Record # 45898; IEEE Xplore ISBN: 978-1-7281-1261-9

Neural Differential Equations for Face Recognition

Gadicherla Sameer
Department of Computer Science
PES University
Bengaluru, India
sameergadicherla56@gmail.com

Gogineni Manasa
Department of Computer Science
PES University
Bengaluru, India
manasapriya17@gmail.com

***Abstract*—Recently, Convolutional Neural Networks(CNNs) have been very efficient in many computer vision areas, especially in facial recognition where most CNN models showed near-perfect performance on standard benchmarks.One of the main problems faced by these CNN architectures today is that they need a large amount of processing power and memory to deliver their exceptional performance. This paper aims on comparing and contrasting these CNNs with a new advancement in deep learning called neural differential equations, where the whole architecture is thought of as a differential equation to be solved. This paper aims to show that this method can achieve comparable performance to a residual network with much less parameters. As a part of this project we will show that the models trained over the ODENet, that is neural net using the ordinary differential equations, takes very less memory and time to train when compared to that of CNNs. As to run these models on the benchmark datasets, these models have been run on the standard face datasets named Faces95 and Faces96 respectively.**

Keywords- Face Recognition, Activation Function, Minimum Barrier Detection (MBD), Ordinary Differential Equation network (ODENet), Scaled Exponential Linear Unit (SELU)

I. INTRODUCTION

Face recognition is a task of identifying or recognising a person from an image or a video frame. This involves a lot of training to be undergone for any model to do the prediction. One such methods is the Convolutional neural network(CNN). Recent advances in these networks have made the tasks of tracking[1],recognition[2] and detection[3] pretty much very easy to solve.Deep models have been so influential in this field that almost all the architectures designed have achieved the near perfect results. One of the main challenges faced by CNNs today is that the requirement of heavy processing power hinders the implementation of CNN based solutions on less powerful but ubiquitous devices like embedded systems and mobile phones without diminished performance with wellknown benchmarks[4].

To overcome the existing problem, we have chosen the unique approach from [5] where the whole network being trained is visualised as a differential equation. This neural differential equation is implemented as an ODEBlock in our paper which is a custom keras layer consisting of the differential equation along with weights and the dopri5 method for solving the differnetial equations. This method mainly takes out the very big process of deciding the architecture for training. Any architecture defined with this one block in between will try to learn with shared weights among all the layers which further form the differential equation.

The most interesting part of this network is that it supports supervised learning very effectively. As said in [5], they applied it over the task of classification of written digits by MNIST. The aim in this paper was to show that the ODESolve method written can achieve a comparable performance with the standard residual networks[6]with very less number of parameters. As a result it did perform very well and reduced the parameters from 0.6M in residual network to 0.22M in ODESolve method.Thereby reducing the processing power requirements and the time taken to train the model.

The popularly known datasets Faces95 and Faces96 were used here by pre-processing with Minimum Barrier Detection(MBD) for saliency detection. Upon this we have used the SELU activation function. The motivation behind using this was to avoid overfitting in learning due to less number of parameters being trained using the ODENetwork and the MBD for saliency detection. So as to allow for many levels of abstract representation of the output feeded as input to a neuron, SELU activation function was written, created the Self-Normalizing Neural Networks[7] via inducing the properties for self-normalisation in Feed Forward neural networks(FNNs)[8].

II. RELATED WORK

Neural Ordinary Differential Equations[5] paper introduces a new concept in deep neural network models. It uses a black-box differential equation solver to compute the output. It is a continuous-depth model as it does not use discrete hidden layers. It shows back-propagating through ODE solvers without changing its internal operations. They used this black-box ODE solver for developing new models for time-series modeling, density estimation and supervised learning. These models are evaluated based on computation speed and accuracy. They derived an instantaneous version of the change of variables formula and developed continuous time normalizing flows, which can scale to large layer sizes.

Residual Attention Network[9] is a Convolutional Neural Network with attention mechanism. It incorporates state-of-art feed-forward network architecture. Within each attention module bottom-up top-down structure is used. This architecture is tested on CIFAR-10, CIFAR-100 and ImageNet data sets. It also shows that this network architecture is not affected by noisy channels. This Residual Attention Network outperformed state-of-art image classification methods.

Face Recognition: EigenFace, Elastic Matching and Neural Nets[10] is a relative study between the three face recognition algorithms. EigenFace algorithm works well only when there is very less lighting variations. Elastic Matching algorithm is more adaptable to lighting variations, face positions and expression variations.

Convolutional Neural Networks[11] for Image Classification paper showed image classification using Convolutional Neural Networks. It used traffic signals dataset and classified it.

Face recognition/detection by probabilistic decision-based neural network[12] paper divides face recognition into three parts: Face detection, position of eyes and face recognizer.

Deep Face Recognition[13] paper does face recognition in photos with single face or with multiple faces. It uses very large data sets that are available like LFW, YTF, FaceBook, etc.

III. PROPOSED WORK

A. Overview

Every image from the dataset was pre-processed using two steps. First step was resizing the image into smaller scale, second is "Minimum Barrier Detection (MBD) Transform". MBD Transform is well known for salient object detection. After the MBD Transform is done the image is passed to the neural network with the ODEBlock and trained over the datasets.

B. Minimum Barrier Detection

The aim of salient object detection[14] is to create a prominence map which highlights the face(object) and overcomes the background[15] in the scene. This transform is being widely used in research due to its vast use in computer vision applications. This method is prominently used in mobile devices as they require high quality salient maps using lesser space and is fast in computing it. For this method we used FastMBD Transform Algorithm[16]. Let m be a pixel value in Inverse Raster Scan or Raster Scan. The following distance map can be used to minimize the cost of path m using each n in the neighbourhood of m:

$$DM(m) \leftarrow min\{DM(m), P(I(n).\langle n, m\rangle)\} \quad (1)$$

In this equation,

(1).β_P is used in Image Distance Transform, which is a cost function that is defined as:

$$\beta_P(\pi) = max_{i=0}^{k} P(\pi(i)) - min_{i=0}^{k} P(\pi(i)) \quad (2)$$

where P is the value of a Pixel.

(2).$I(n)$ denotes the assigned path to a pixel n and $\langle n, m\rangle$ is an edge joining pixel m to pixel n. Thus $I(n).\langle n, m\rangle$ is a path for m that appends edge $\langle n, m\rangle$ to $I(n)$ Therefore, the cost function becomes:

$$\beta_P(I_n(m)) = max\{H(n), P(m)\} - min\{L(n), P(m)\} \quad (3)$$

where $H(n)$ and $L(n)$ are the highest and lowest pixel values in $I(n)$ respectively. The value of H and L is updated accordingly when the path assignment changes in each iteration in the algorithm.

To perform the MBD transform following algorithm was used, it is based on [16].

Result: A list DM which is the distance map
Input: Number of Iterations : $iter$ for the Image $Img = (i, V)$;
Algo:$H, L \leftarrow Img, Img$;
set $DM(x)$ to 0 or to inf;
for *m from* 0 *to iter* **do**
  if *m is even* **then**
    InvRasterScan(Img,H,L,DM);
  else
    RasterScan(Img,H,L,DM);
  end
end

Algorithm 1: MBD transform

Result: A list DM which is the distance map
Input: Img, H, L, DM from MBD transform algorithm.; number of rows and columns are set to $rows$ and $cols$ in image Img;
for *m from* $rows - 2$ *to 1* **do**
  for *n from* $cols - 2$ *to 1* **do**
    imx,dist = Img[m][n],DM[m][n];
    high1,high2 = H[m+1][n],H[m][n+1];
    low1,low2 = L[m+1][n],L[m][n+1];
    u1 = max(high1,imx) - min(low1,imx);
    u2 = max(high2,imx) - min(low2,imx);
    if *b1<dist and b1<=b2* **then**
      DM[m][n] = u1;
      H[m][n] = max(high1,imx);
      L[m][n] = min(low1,imx);
    else
      DM[m][n] = u2;
      H[m][n] = max(high2,imx);
      L[m][n] = min(low2,imx);
    end
  end
end

Algorithm 2: Inverse Raster Scan

A sample of how salient object is detected using MBD is shown in Fig 1.

Fig. 1. An example of highlighting salient objects in an image using MBD transform.

C. ODENet

ODENet refers to Ordinary DIfferential Equation Network. In normal neural networks, the previous state vector V_n produces the new state vector V_{n+1} using the formula $V_{n+1} = F(V_n)$. Here function F is $F(x) = \sigma(\sum_i \theta_i x_i)$, where θ is a vector of parameters and σ is an activation function. Whereas in Deep Residual Learning[5], the new state vector is calculated using $V_{n+1} = F(V_n) + V_n$. Using Euler's Method in Residual Networks: Consider a constant $\triangle t \in R$, now the new state in neural network becomes,

$$V_{t+1} = F(V_t) + V_t = \frac{\triangle t}{\triangle t} F(V_t) + V_t = \triangle t G(V_t) + V_t \quad (4)$$

where $G(V_t) = \frac{F(V_t)}{\triangle t}$. If we consider every step of the neural network to be doing Euler's method, then our system can be modeled as

$$\frac{dV(t)}{dt} = G(V(t), t, \theta) \quad (5)$$

Here G is dependent on t and θ. The output of network at some time t_1 is $V(t_1)$. Hence, if we know G, we can use ODE Solvers to evaluate the neural network.

$$V(t_1) = ODE_S(V(t_0), G, t_0, t_1, \theta) \quad (6)$$

If this is substituted in Euler's Method we get something like the residual network state as above.

$$ODE_S(V(t_0), G, t_0, t_1, \theta) = V(t_0) + (t_1 - t_0) G(V(t_0), t_0, \theta) \quad (7)$$

D. Training approach used in ODENet

Train a neural network with ODEBlock as a layer with combination of few other layers, and thereby run as a normal artificial neural network.

The inputs start with preprocessed data, then it is forwarded through the neural network's layers.

In the layers, a function if applied on inputs and weights (inputs and weights are matrices) and then the activation function is applied(SELU). Further in experiment and results section, the exact parameters used will be shown.

The neural network used for ODENet is:

- 1-Conv2D,1-Activation(selu)
- 1-MaxPooling2D
- 1-Conv2D,1-Activation(selu)
- 1-MaxPooling2D
- 1-ODEBlock , 1-Flattening
- 1-DenseLayer , 1-Activation(softmax)

The exact neural network used for CNN for comaparision purpose is

- 1-Conv2D,1-BatchNormalization,1-Activation
- 1-Conv2D,1-MaxPooling2D,1-BatchNormalization,1-Activation
- 1-Conv2D,1-BatchNormalization,1-Activation
- 1-Conv2D,1-MaxPooling2D,1-BatchNormalization,1-Activation
- 1-Flatten,1-XnorDense,1-BatchNormalization,1-Activation
- 1-Dense,1-BatchNormalization

E. Activation Function - SeLU

SeLU is basically useful because it does normalization. Basically there are three types of normalization: input normalization, batch normalization and internal normalization. This function falls in the third category. This activation function needs negative and positive values for y to shift the mean.The gradients are used to adjust the variance. The formula for SeLU is

$$f(x) = \lambda \begin{cases} \alpha(e^x - 1), & for x < 0 \\ x, & for x \geq 0 \end{cases}$$

where λ = 1.05070 and α = 1.67326

This is similar to ReLU for positive values, except the λ. This is the reason for the S(caled). When λ is larger than 1, so is the gradient and the variance can be increased. Normalized outputs are very useful in stabilizing the training process. Additionally, SeLUs learn faster and better on their own compared to other activation functions, even when they are combined with batch normalization. The graph of SeLU looks like Fig. 2.

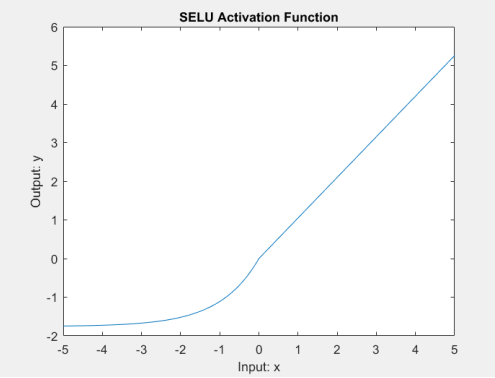

Fig. 2. Graph of SeLU activation function.

IV. EXPERIMENTAL SETUP

For the experimentation, the Faces95 and Faces96 publicly available datasets have been used to compare with current work and do further research.

A. Faces95 Dataset

The Faces95 [17] dataset contains 1440 images, 20 images each of 72 individuals both male and female. The resolution of the images is 180 by 200 pixels taken in portrait format. The subject moves towards the camera as the images are captured introducing head scale substantial variations between the images. Red curtains have been used in the background. Significant head scale variations and background changes were caused by the shadows as the subject moves towards the camera. Major changes in illumination of the face are

seen due to the use of artificial lighting. Minor variations in the facial expressions of the subject and their head tilt, slant and turn were also seen.

Fig. 3. Samples from the Faces95 dataset.

B. Faces96 Dataset

The Faces96 [18] dataset contains 3040 images, 20 images each of 152 individuals. The resolution of the images is 196 by 196 pixels taken in square format. Just like the Face95 dataset, the subject moves towards the camera as the images are captured introducing similar head scale variations in images.Glossy posters have been used for the background increasing the complexity and noise. The hairstyle and age remain same as all images were captured in a single session. Major changes consist illumination of the face are seen due to the use of artificial lighting. Minor variations have the facial expressions of the subject and their head tilt, slant and turn.

Fig. 4. Samples from the Faces96 dataset.

V. EXPERIMENT AND RESULT ANALYSIS

System description in which tests are conducted:

- CPU: Intel core i7 7th generation.
- GPU: NVIDIA GeForce 940MX.

Approach used:

- Images were pre-processed with Minimum Barrier Detection transform and then the processed image was passed as input into the neural network.
- The pre-processed dataset was then split into 80% training and 20% testing images.
- The neural network (training algorithm and architecture described in Subsection 4 of Approach Section) is then used to train upon the training data and tested with the testing data. The network was trained with SeLU for 30 epochs, with 10 as batch size for ODENet and 50 epochs with same batch size for CNN.
- The results are shown as an accuracy table in table I.
- The size consumed by models are described in table II.
- The time consumed for training by models are shown in Fig.10
- The time consumed for loading the models are described in table III.

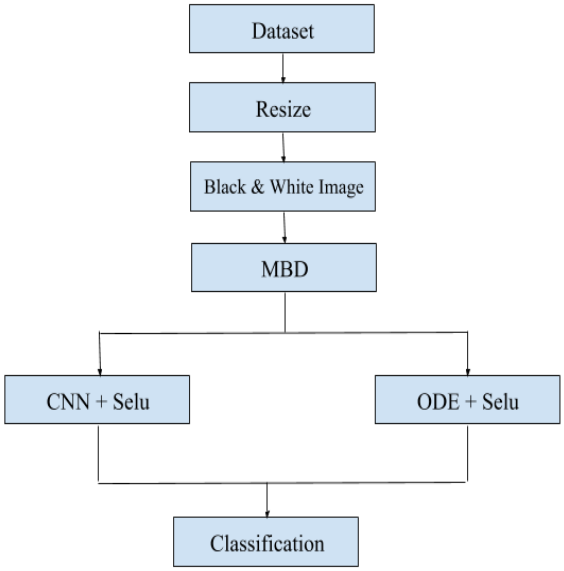

Fig. 5. Block Diagram of the experiment.

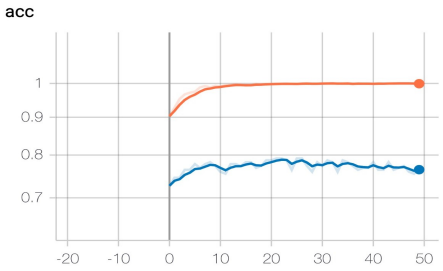

Fig. 6. Accuracy Vs Epochs for CNN over Faces95.

The accuracy for each epoch (50 epochs) for CNN over Faces95 is shown in Fig. 6.

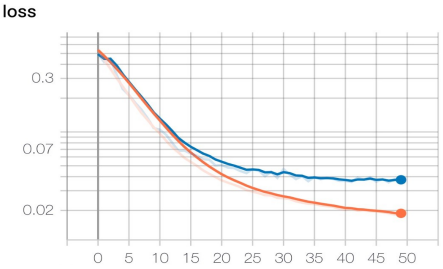

Fig. 7. Loss Vs Epochs for CNN over Faces95.

The loss for each epoch (50 epochs) for CNN over Faces95 is shown in Fig. 7. After training for 50 epochs, the loss of this model in terms or training and testing has reached very much near to zero, which says that the model has avoided overfitting.

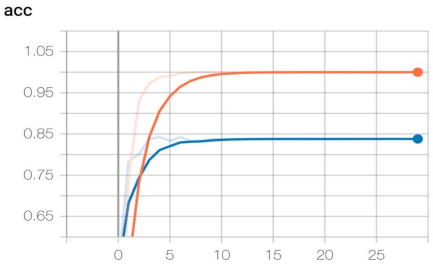

Fig. 8. Accuracy Vs Epochs for ODE over Faces95.

The accuracy for each epoch (30 epochs) for ODENet over Faces95 is shown in Fig. 8.

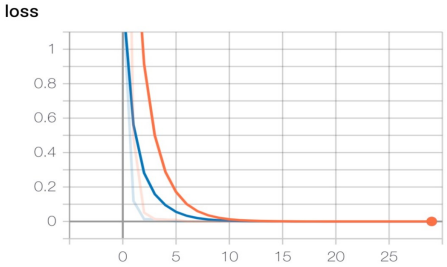

Fig. 9. Loss Vs Epochs for ODE over Faces95.

The loss for each epoch (30 epochs) for ODENet over Faces95 is shown in Fig. 9. Even here the losses have reached near to zero.

* Orange Line - Training Parameters

** Blue Line - Testing Parameters

TABLE I
AVERAGE VALIDATION ACCURACY

	CNN	ODE
Faces95	77.5%	83.46%
Faces96	96.24%	98.79%

From TABLE I, we observe that both the CNN and the ODENet on Faces95 performed poor than that over Faces96 in terms of accuracy. But if we see in Faces96, ODENet performed approximately same as CNN but in Faces95 it performed better than CNN. And all the models have a test loss approximately close to zero.

TABLE II
SIZE OF THE MODEL

	CNN	ODE
Faces95	3.52 GB (3605MB)	29.3 MB
Faces96	3.03 GB (3103MB)	50 MB

In TABLE II, we can see that over Faces95, model on ODENet is 123 times less size of that using CNN. Similarly over Faces96, model on ODENet is 62 times less size of that using CNN.

TABLE III
TIME TAKEN TO LOAD THE MODEL (IN SEC)

	CNN	ODE
Faces95	40	9
Faces96	37	10

TABLE III clearly shows that over Faces95, ODENet loads four times faster and over Faces96 also around four times faster than that over CNN on both the datasets.

Fig. 10. Training Times for each Epoch.

Apart from having less model size, we can also see that ODENet has taken very less time to train as shown in Fig.10. CNN has taken 255 and 235 seconds to train per epoch on the given system specifications. Where are ODENet has taken 45 and 83 seconds for Faces95 and Faces96 respectively. By this we can say that we have reduced the training time per epoch by almost greater than five times.

VI. CONCLUSION AND FUTURE WORK

We can see that the ODENet has outperformed the CNNs in face recognition tasks completely in terms of performance. They have consumed 123 and 62 times lesser the memory on both the datasets Faces95 and Faces96 respectively and also very less training time as shown in results section than the CNNs. Both the architectures performed very well in the recognition tasks,but we know that the ODENet needed less epochs than CNNs to achieve a test loss less than ten percent of 1. The model loading times of the ODENet is one third of CNNs which says that ODENets can be extremely fast to even train and test on devices with lesser computational resources. Thereby we can say that neural differential equations will be a very good advancement in the field of recognition tasks mainly avoiding the task of designing a neural network architecture and giving outperforming results.

Applying these networks over time series is a very good application to be done. We will be using this approach over different tasks like stock prediction and also try to refine the architecture based on the application.Training these networks with different differential equation solvers would be a very good step for doing analysis and getting the most effective one will help us with better training. Training these kinds of networks on small devices like mobiles phones is what our end goal is and will be proceeding with that as the next step.

VII. ACKNOWLEDGMENT

We would like to thank Prof.Shetty Mamatha Gopal for guiding us to carry out this research. Department of Computer Science of PES University has always been very encouraging for us to work on interesting topics like this. Finally our parents and friends have always been motivating and supporting in carrying forward our research, and we are very grateful to them.

REFERENCES

[1] L. Wang, W. Ouyang, X. Wang, and H. Lu. STCT: Sequentially training convolutional networks for visual tracking. In Proceedings of the IEEE Conference on Computer Vision and Pattern Recognition, pages 1373 1381, 2016

[2] Krizhevsky, Alex, Ilya Sutskever, and Geoffrey E. Hinton. "Imagenet classification with deep convolutional neural networks." Advances in neural information processing systems. 2012.

[3] Girshick, R., Donahue, J., Darrell, T., Malik, J.: Rich feature hierarchies for accurate object detection and semantic segmentation. In: Proceedings of the IEEE conference on computer vision and pattern recognition. (2014) 580587

[4] Grm, K., Struc, V., Artiges, A., Caron, M., Ekenel, H.K.: Strengths and weaknesses of deep learning models for face recognition against image degradations. IET Biometrics 7(1) (2018) 8189

[5] Chen, T. Q., Rubanova, Y., Bettencourt, J., Duvenaud, D. K. (2018). Neural ordinary differential equations. In Advances in Neural Information Processing Systems (pp. 6571-6583).

[6] He, Kaiming, et al. "Identity mappings in deep residual networks." European conference on computer vision. Springer, Cham, 2016.

[7] Klambauer, Gnter, et al. "Self-normalizing neural networks." Advances in neural information processing systems. 2017.

[8] Mirjalili, SeyedAli, Siti Zaiton Mohd Hashim, and Hossein Moradian Sardroudi. "Training feedforward neural networks using hybrid particle swarm optimization and gravitational search algorithm." Applied Mathematics and Computation 218.22 (2012): 11125-11137.

[9] Wang, F., Jiang, M., Qian, C., Yang, S., Li, C., Zhang, H., ... Tang, X. (2017). Residual attention network for image classification. In Proceedings of the IEEE Conference on Computer Vision and Pattern Recognition (pp. 3156-3164).

[10] Zhang, J., Yan, Y., Lades, M. (1997). Face recognition: eigenface, elastic matching, and neural nets. Proceedings of the IEEE, 85(9), 1423-1435.

[11] Jmour, N., Zayen, S., Abdelkrim, A. (2018, March). Convolutional neural networks for image classification. In 2018 International Conference on Advanced Systems and Electric Technologies (IC-ASET) (pp. 397-402). IEEE.

[12] Lin, S. H., Kung, S. Y., Lin, L. J. (1997). Face recognition/detection by probabilistic decision-based neural network. IEEE transactions on neural networks, 8(1), 114-132.

[13] Parkhi, O. M., Vedaldi, A., Zisserman, A. (2015, September). Deep face recognition. In bmvc (Vol. 1, No. 3, p. 6).

[14] R. Achanta, S. Hemami, F. Estrada and S. Ssstrunk, Frequency-tuned Salient Region Detection, IEEE International Conference on Computer Vision and Pattern Recognition (CVPR 2009), pp. 1597 - 1604, 2009

[15] Wangjiang Zhu, Shuang Liang, Yichen Wei and Jian Sun, Saliency Optimization from Robust Background Detection, IEEE Conference on Computer Vision and Pattern Recognition (CVPR), 2014.

[16] Jianming Zhang, Stan Sclaroff, Zhe Lin, Xiaohui Shen, Brian Price and Radomr Mch. "Minimum Barrier Salient Object Detection at 80 FPS." http://cs-people.bu.edu/jmzhang/fastmbd/MBS_preprint.pdf

[17] D. L. Spacek, Collection of facial images, http://cswww.essex.ac.uk/mv/allfaces/faces95.html.

[18] D. L. Spacek, Collection of facial images, http://cswww.essex.ac.uk/mv/allfaces/faces96.html.

Proceedings of the Fourth International Conference on Communication and Electronics Systems (ICCES 2019)
IEEE Conference Record # 45898; IEEE Xplore ISBN: 978-1-7281-1261-9

TWO-DIMENSIONAL ECG SIGNAL COMPRESSION BASED ON REGION OF INTEREST USING PCA

ANEESH K N*
Dept. of Electronics and Communication Engineering
SJCE, Mysuru,
India
aneeshkn49@gmail.com

DARSHAN SINGH S*
Dept. of Electronics and Communication Engineering
SJCE, Mysuru,
India
darshans012@gmail.com

M H ABHISHEK*
Dept. of Electronics and Communication Engineering
SJCE, Mysuru,
India
mhabhishek0604@gmail.com

Dr. SHREEKANTH T
Dept. of Electronics and Communication Engineering
SJCE, Mysuru,
India
shreekanth_t@sjce.ac.in

***Abstract*—Several cardiac disorders can be diagnosed by meticulous analysis of ECG signals. The quality of signal determines the accuracy of diagnosis. Usually the size of ECG signals is huge and they are associated with noise. By compressing the ECG signals, they can be stored and transmitted easily. Hence, it is important to pre-process (de-noise) and compress it to a maximum extent. In the recent past many works have been done on ECG compression. Compression techniques have been done using time-domain as well transform domain techniques. In this work an approach through Principal Component Analysis (PCA) has been proposed to compress the pre-processed ECG signal and de-compress it efficiently, such that maximum amount of variance is retained. This algorithm has been tested for 28 ECG signals from the MIT-BIH database. In order to analyze the performance of the algorithm, CR (compression ratio) and PRD (Percent Root Mean Square Difference) have been considered as performance parameters and are calculated. The proposed method achieves a good CR along with small PRD in comparison with algorithms that has been proposed by other researchers.**

Keywords—ECG Signal Compression, Cut align beat, QRS detection, PCA Compression, PRD, CR, Singular Value Decomposition (SVD).

I. INTRODUCTION

Electrocardiography (ECG) is the process in which electrodes are used to record the electrical activity of the heart over a span of time. An ECG signal is used for various diagnostic purposes. They are obtained by placing the electrodes in different parts of body. The ECG signals can be classified as P, Q, R, S, T waveforms. The combination of Q, R, S wave forms the QRS complex wave and represent ventricular depolarization.

The first algorithm for QRS complex detection of ECG signals was developed by Pan and Tompkins (1985) using a band-pass filter of range 5 Hz to 25 Hz which had correctly detected 99.3% of QRS complexes, for the standard 24 h MIT/BIH arrhythmia database [1].

There are various approaches used for compressing the pre-processed ECG signals. Many methods have been proposed [2, 11] to compress the pre-processed ECG signal using jpeg2000 compression technique. Wavelet based approaches to compress ECG signals has also been demonstrated by Suresh Patel et al., and Oliveira et al., [3, 4]. An application of 2-D discrete cosine transforms for coding and compression of ECG signals has been shown by Hanwoo Lee et al., [5].

In this work Principal Component Analysis (PCA) is used to compress and de-compress the ECG signals.

PCA is an approach for obtaining important features from a large set of variables which are of smaller dimensions. PCA has become an important tool in modern data analysis. It is a powerful statistical technique that has found application in fields such as machine learning (such as dimensionality reduction), image compression, and is a common technique for finding patterns in data of high dimension [6]. It is the method of identifying patterns in data, and expressing the data so as to highlight their similarities and differences.

An equivalent 2-D representation (image) of ECG signal is first obtained. This includes various steps like QRS detection and Cut Align and Beat approach to map ECG signal into grayscale. The obtained 2-D representation of ECG signal can be compressed by the PCA image compression algorithm.

II. METHODOLOGY

The proposed methodology is an extension of the previous work done by Shreekanth et al., which uses JPEG2000 compression technique [2]. Since ECG signals are susceptible to various interferences and noises, it is important to de-noise them in the initial stage before compressing, which is done using wavelet de-noising. Two dimensional ECG signal is constructed using Pan-

* = Equal Contribution

Tompkins and Cut-Align-Beat approach. Region of interest is compressed in a way to achieve faithful reconstruction

The following are the sequences of steps which are performed on a raw ECG signal.

A. Baseline drift elimination and wavelet de-noising

The process of removing the noise from a signal is called de-noising and the process of removing baseline drift is called de-trending. The baseline shift is caused by low frequency components and hence such components must be deducted from the signal [9, 13]. A wavelet based approach [2] has been adopted in this work to eliminate baseline drift and noise as shown in Fig 1.

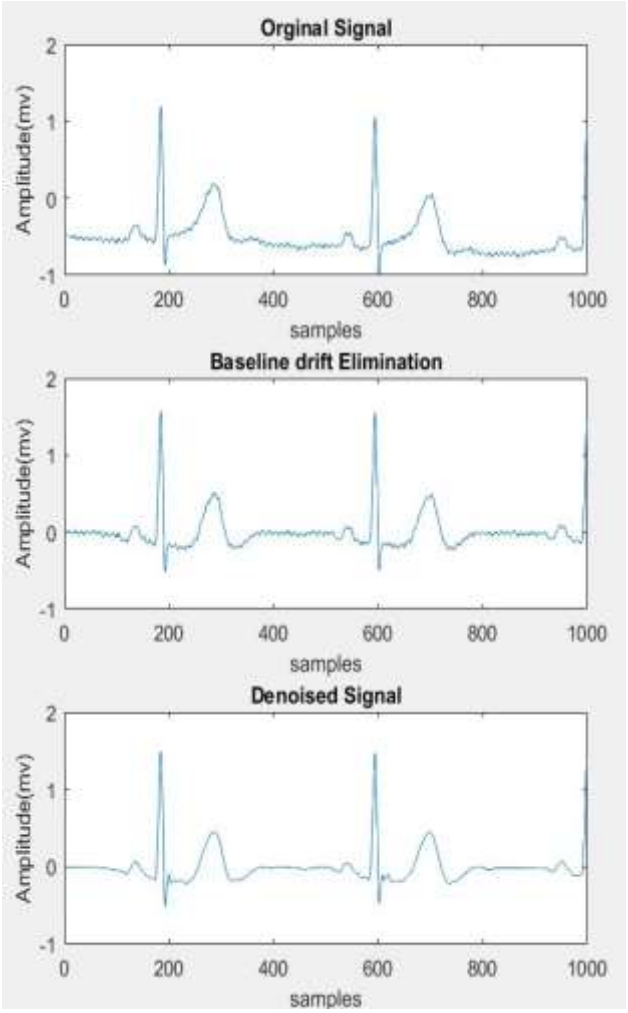

Fig. 1. ECG signal after applying baseline drift elimination and wavelet de-noising.

B. Pan Tompkins QRS detection

This algorithm is used to detect QRS complexes of ECG signal. It recognises QRS complexes based on digital analysis of slope, width and amplitude. Various interferences are removed by a digital bandpass filter which causes false detection of QRS complexes. This algorithm periodically sets parameters and thresholds so as to adapt to the heart rate and QRS morphology [1]. The detection of QRS complexes is as in Fig 2.

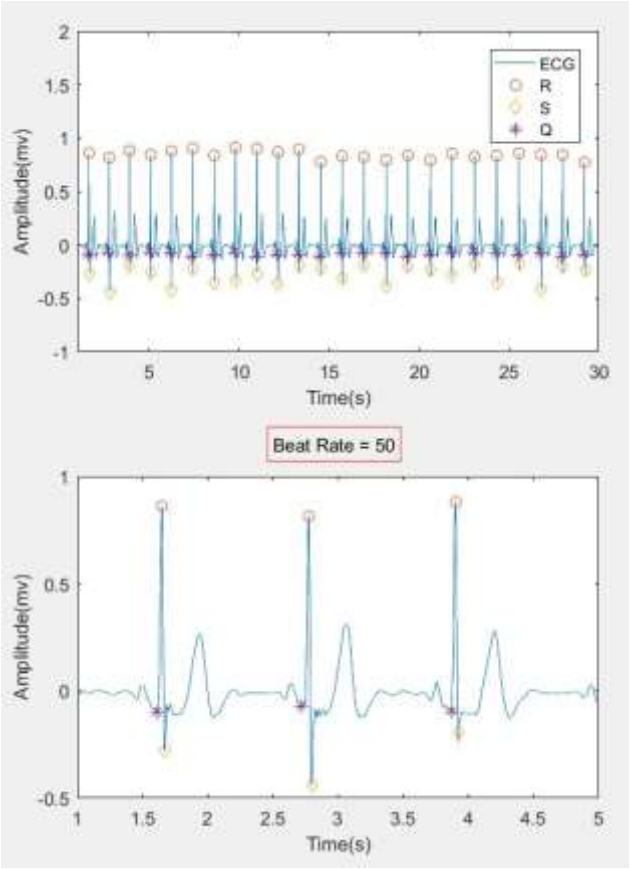

Fig. 2. ECG signal with QRS complexes detected

C. Cut align beat approach

Conversion of 1-D signal to 2-D ECG signal is done by Cut align beat approach. The QRS complexes of the ECG signal detected using Pan-Tompkins method, and the corresponding 2-D data array is obtained by cutting into segments and aligning it with other segments. Since the length of heart beat signal is different, appropriate numbers of zeros are padded [2].

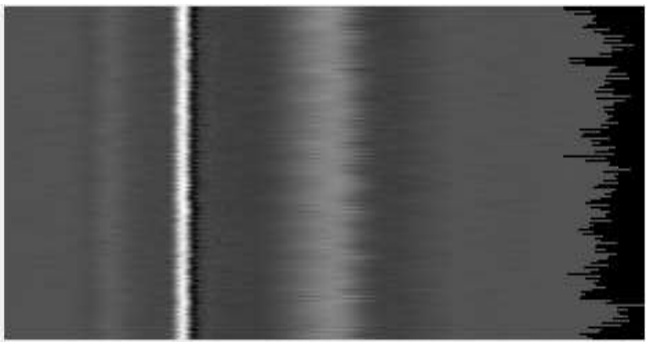

Fig. 3. ECG signal after applying cut and align beat approach

D. Mean extension for equalization of length

An acceptable 2D array can be obtained by the process of equalisation of length of each heartbeat. The period sorting is done first which sorts the beats from longer segments to shorter segments. The mean extension is done by replacing the zeros with the last value of the corresponding segments [2]. Period sorting with

descending order is employed. This improves interbeat correlation and decreases period differences.

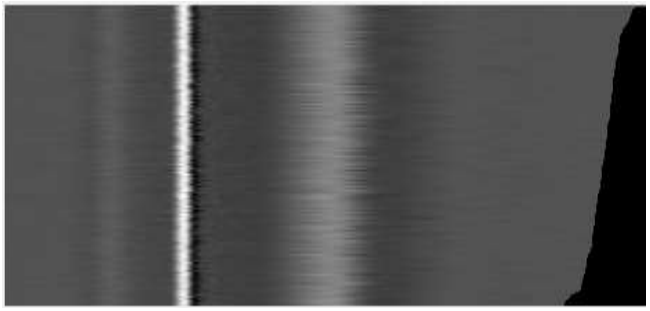

Fig. 4. ECG signal after Period Sorting

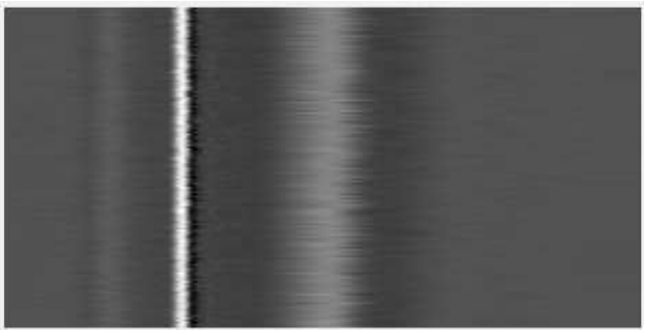

Fig. 5. ECG signal after Period Equalization

E. Period normalization

Each heart-beat has different periods and hence the data points of the 2D array are variable. The data points are normalized in order to ensure that the data occupies fixed number of columns in each row [14]. Within the beat, each sample value is divided with the highest sample value, to achieve amplitude normalization so that each beat will have a maximum amplitude value as unity.

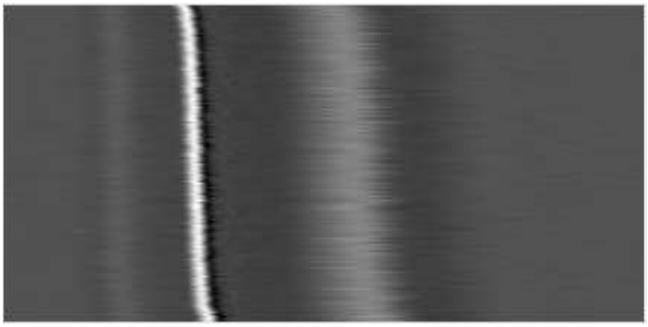

Fig. 6. ECG signal after period normalization

F. Region of Interest (ROI) mapping

Otsu thresholding is applied on the 2D ECG data, and ROI is formed by choosing the data in the QRS region. Then the vertical projection profile of the thresholding image is also found. Vertical projection profile is summation of all the pixel values in vertical direction and its width locates the ROI [2]. The QRS region obtained is compressed at a lower compression rate compared as shown in Fig 7 (a) to that of the Non-QRS region as shown Fig 7 (b). Hence, this results less PRD.

G. Principal Component Analysis (PCA)

In PCA the directions in which the data varies significantly is found. In the covariance matrix, eigenvectors that corresponds to the largest eigenvalues are found and the data is projected onto these directions. This is done because these directions contain most of the second order information.

The following algorithm for PCA is adopted for compression.

Let the data be of n dimensions. The goal is to reduce it to k dimensions where k is less than n.

Step 1: Computing the covariance matrix

For any two variables the degree of linear relationship can be measured by covariance. Positively correlated data is indicated by large positive value. Similarly, negatively correlated data denoted by large negative value. The degree of redundancy is nothing but the absolute magnitude of covariance [6].

$$\Sigma = \frac{1}{m} \sum_{i=`1}^{m} \left(x^{(i)}\right) . (x^{i})^{T} \qquad (1)$$

The resulting matrix Σ will be a $n \times n$ matrix.

Step 2: Computing the Eigen Vectors

The Eigen Vectors of the matrix Σ has to be computed. This can be done using Singular Value Decomposition (SVD).

$$[\, U, S, V \,] = svd\ (\Sigma) \qquad (2)$$

The resulting matrix U will be as follows:

$$U = \begin{pmatrix} | & | & & | \\ u^{(1)} & u^{(2)} & \dots & u^{(n)} \\ | & | & & | \end{pmatrix} \in \mathbb{R}^{n \times n} \quad (3)$$

Step 3: Projecting the data on to the matrix U

Before projecting, a suitable k value has to be chosen. Then only the first k columns of the above matrix U must be selected. Now the matrix U will be of $n \times k$ dimensions. The compressed data is obtained by multiplying the transpose of this new matrix U with the data.

H. Choosing the number of principal components

The number of principal components is chosen such that the average squared projection error should be minimized. It is given as follows:

$$\frac{1}{m} \sum_{i=1}^{m} || \ x^{(i)} - x^{(i)}_{approx} \ ||^2 \qquad (4)$$

Where, $x^{(i)}_{approx}$ is the reconstructed data.
The total variation of the original data is:

$$\frac{1}{m}\ \sum_{i=1}^{m} ||\ x^{(i)}\ ||^2 \qquad (5)$$

Typically, k has to be chosen such that the following value(c) has to be minimized

$$\frac{\frac{1}{m}\ \sum_{i=1}^{m} ||\ x^{(i)} - x^{(i)}_{approx}\ ||^2}{\frac{1}{m}\ \sum_{i=1}^{m} ||\ x^{(i)}\ ||^2} \leq c \qquad (6)$$

The smallest value of k has to be picked such that

‘

$$\frac{\sum_{i=1}^{k} S_{ii}}{\sum_{i=1}^{n} S_{ii}}\ \geq\ 1 - c \qquad (7)$$

Hence, this implies $100 \times (1 - c)\%$ of the variance is retained.

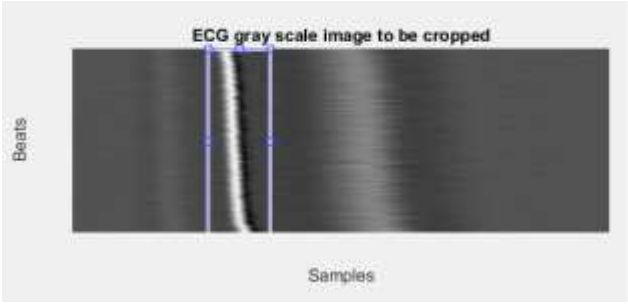

Fig 7. ECG signal with QRS cropped

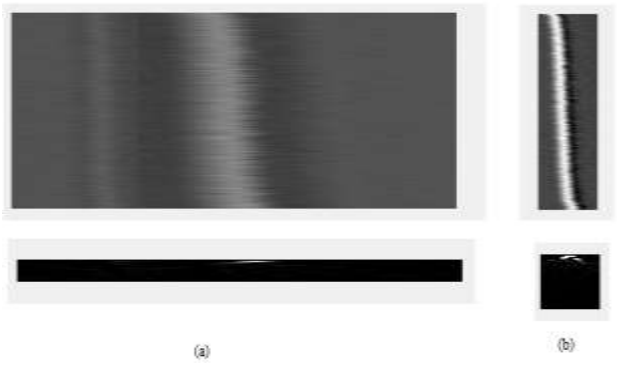

Fig. 8. Image after PCA compression. (a) Non QRS compression. (b) QRS compression.

I. Reconstruction of 1D ECG signal

The decompressed data can be obtained by multiplying the matrix U with the compressed data. The original data is then obtained from decompressed data by applying period denormalization. From the known heart-beat length, a number of samples are picked up. Then they are multiplied to their corresponding mean and amplitude values. Original ECG signal can be obtained by appending all the heart beat’s data to form a sequence [2].

III. RESULTS AND DISCUSSIONS

The algorithm was tested for ECG records obtained of the MIT/BIH dataset. It was sampled at the rate of 360 Hz, 11 bits/s [2]. The ECG signals were considered such that, the patterns were different. The corresponding record the patterns were different. The corresponding record numbers of the considered ECG signals are 102, 111, 114, 124 and 117. These records consisted of ECG signals with different rhythms. The results obtained are compared with other algorithms on the same dataset and are recorded in Table 1. The performance parameters obtained on the proposed algorithm is recorded in Table 2. Figure 8 shows 1000 samples of original signal along with the reconstructed signal and error signal corresponding to the record 117.

The performance of the proposed technique is measured using two parameters namely Compression Ratio (CR) and Percentage Root-mean-square Difference (PRD).

CR is used to quantify the amount of reduction in the size of representation of data due to a data compression algorithm. Compression ratio is defined as follows:

$$CR = \frac{Size\ of\ original\ signal}{Size\ of\ compressed\ data} \qquad (9)$$

Compressed signal quality is evaluated by PRD. It is defined as the square root of the ratio of square of error signal and the square of the original signal.

$$PRD = 100 \times \sqrt{\frac{\sum_{i=1}^{L}(x_{org}(i) - x_{recon}(i))^2}{\sum_{i=1}^{L}(x_{org}(i))^2}} \qquad (10)$$

where x_{org} represents the original signal, x_{recon} represents the reconstructed signal and L is the number of samples in the data.

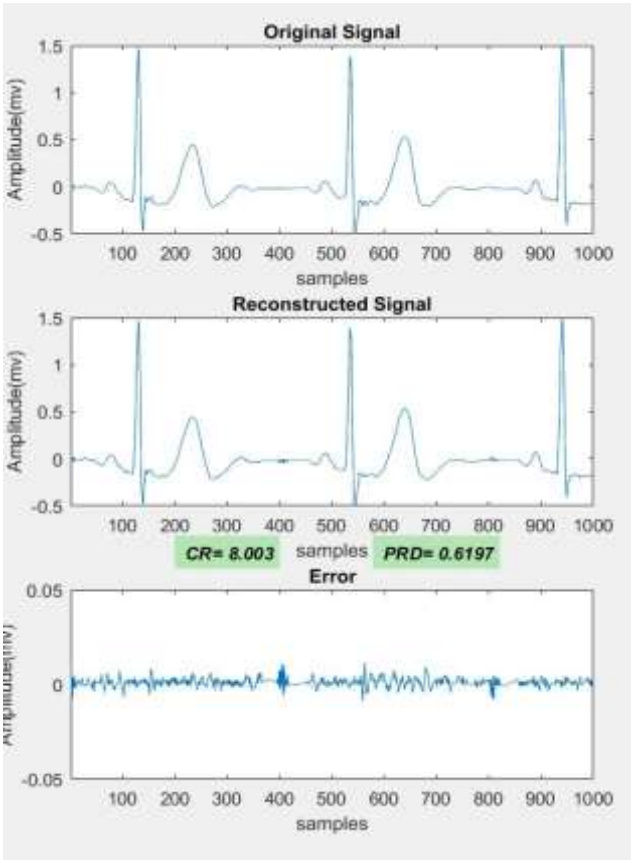

Fig. 8. Reconstructed signal for record 117 and its corresponding error.

Table I. Performance parameters comparison with different algorithm with sampling frequency 360Hz and resolutions 11 bits/sample

Algorithm	Record Number	CR	PRD
Hilton	117	8:1	2.6
Lu et al.	117	8:1	1.18
Djohan	117	8:1	3.9
SPHIT	117	8:1	1.8
Proposed	117	8:1	0.6

Table II. PRD and CR comparison with different data using proposed methodology

Record number	CR	PRD (%)	Sampling Frequency (Hz)	Resolution (bits/sample)
102	8	0.55	360	11
114	10	0.49	360	11
117	8	0.6	360	11
111	8.5	0.9	360	11
124	10	0.5	360	11

IV. CONCLUSION AND FUTURE SCOPE

The compression of ECG signal using PCA based on ROI has been demonstrated. The algorithm has been tested for the ECG signals obtained from MIT/BIH dataset. The performance of the presented algorithm depends on the record which is being used for compression and its signal length. The proposed algorithm outperforms many of the standard algorithms as demonstrated in Table I. The main drawback of this algorithm is the increased computational complexity. The only room for improvement of this work is to reduce error by keeping CR as high as possible. This can be achieved by using superior coding techniques.

REFERENCES

[1] Jiapu Pan and Willis J. Tompkins, "A Real-Time QRS Detection Algorithm", IEEE Transactions on Biomedical Engineering, Vol. BME-32, NO. 3, March 1985.

[2] Shreekanth T, Shashidhar R. (2018) An Application of Image Processing Technique for Compression of ECG Signals Based on Region of Interest Strategy. In: Hemanth D., Smys S. (eds) Computational Vision and Bio Inspired Computing. Lecture Notes in Computational Vision and Biomechanics, vol 28. Springer, Cham.

[3] Suresh Patel, Dr. Ashutosh Datar, "ECG Data Compression using Wavelet Transform", International Journal of Engineering Trends and Technology (IJETT) – Volume 10 Number 3 - Apr 2014.

[4] Oliveira BR, Duarte MAQ, Abreu CCE, Vieira Filho J. A wavelet-based method for power-line interference removal in ECG signals. Res Biomed Eng. 2018; 34(1):73-86. DOI: 10.1590/2446-4740.01817.

[5] Hanwoo Lee and Kevin M. Buckley, "ECG Data Compression Using Cut and Align Beats Approach and 2-D Transforms", IEEE Transactions on Biomedical Engineering, Vol. 46, NO. 5, May 1999.

[6] Jonathon Shlens, "A Tutorial on Principal Component Analysis", arXiv:1404.1100v1 [cs.LG] 3 Apr 2014.

[7] Lu, Z., Kim, D.Y., Pearlman, W.A.: Wavelet compression of ECG signals by the set partitioning in hierarchical trees algorithm. IEEE Trans. Biomed. Eng. **47**, 849–856 (2000).

[8] M. L. Hilton, "Wavelet and wavelet packet compression of electrocardiograms", IEEE Trans. on Biomedical Engineering, vol. 44, pp. 394-402, May 1997.

[9] Jaffery, Zainul and Afroz. (2014). ECG Baseline Drift Elimination Using Wavelet Packets Transform. Australian Journal of Basic and Applied Sciences. 8. 459-466.

[10] Djohan, T., Nguyen, Q., Tompkins, W.J.: ECG compression using discrete symmetric wavelet transform. In: Proceedings of 17th International IEEE Medicine and Biology Conference (1995).

[11] D. S. Taubman and M. W. Marcellin, JPEG2000: Image Compression Fundamentals, Practice and Standards, Kluwer Academic Publishers, Massachusetts, 2002.

[12] Iffat Ara, Md. Najmul Hossain, S. M. Yahea mahbub, "Baseline Drift Removal and De-Noising of the ECG Signal using Wavelet Transform", International Journal of Computer Applications (0975 – 8887) Volume 95– No.16, June 2014.

[13] Tai, S.C., Sun, C.C., Tan, W.C.: 2-D ECG compression method based on wavelet transform and modified SPIHT. IEEE Trans. Biomed. Eng. 52(6), 999–1008 (2005).

[14] Wei, J.-J., Chang, C.-J., Chou, N.-K., Jan, G.-J: "ECG data compression using truncated singular value decomposition. IEEE Trans. Inf. Technol. Biomed. 5, 290-299 (2001).

Proceedings of the Fourth International Conference on Communication and Electronics Systems (ICCES 2019)
IEEE Conference Record # 45898; IEEE Xplore ISBN: 978-1-7281-1261-9

Librany - A Face Recognition and QR Code Technology based Smart Library System

Dhaval Bagal
Dept. of Computer Engineering
Vivekanand Education Society's Institute of Technology
Mumbai, India
dhavalbagal99@gmail.com

Pallavi Saindane
Dept. of Computer Engineering
Vivekanand Education Society's Institute of Technology
Mumbai, India
pallavi.saindane@ves.ac.in

***Abstract*—Libraries play the most important role when it comes to books and reading. Today, libraries have become a great source of information. If we look upon the procedure that most of the conventional libraries in the world follow, we see a great amount of drudgery involved. In this paper, we propose a smart library system, which eliminates most of this drudgery in the conventional library management systems. Using face recognition and QR code based technology, the system automates and eases the tasks of Book Issue, Book Return and Book Search. It resembles 'Just walk out technology' implemented by Amazon in the Amazon Go stores. The proposed system enjoins self-issue and self-return procedures along with the dynamic search feature which provides the real-time location of the books. The proposed system significantly expedites the process of issue, return and search thus avoiding long queues at the reception counter/librarian's desk.**

Keywords—smart libraries; face recognition; QR code technology; dynamic libraries; real time book tracking

I. INTRODUCTION

Traditional library management systems require a great amount of labor, starting from the person at the issue/return counter to the person who puts all the books at their correct locations when they are returned. When the user needs to issue a book, he has to physically visit the library and then carry out the required formalities in order to get the book issued. At peak times, there are long queues at the counter for the issuance of the books. Even for reissuing the book, the user has to physically visit the library and get the formalities done. Apart from all of this, the librarian is largely responsible for the entire library management. He has to properly place the books at the correct location when they are returned. In a conventional library management system, there is no provision to get the real-time location of the books. Also, paperwork is needed to some extent and the library staff must be qualified.

In the proposed system, for issuing a book, the user has to stand in front of a camera and show his face and the book's QR code to the camera to get it issued. This camera is not the usual CCTV camera. It is placed such that only one person can stand in front of it at a time. For returning the book, the user has to drop the book in the drop box such that the book's QR code faces upwards. The camera located at the top of the drop box scans the QR code on the book and updates the database accordingly. Thus, the book is returned. The system also proposes a dynamic search feature. The module for this feature updates the location of the books in the database continuously. Thus if a book is moved from shelf 1 to shelf 2, the location of that book is immediately updated to shelf 2. For this, each shelf has an associated camera which continuously detects the QR codes of the books present on that shelf. If a new book is added to that shelf, the camera for that shelf detects it. It decodes the book's QR code and updates its location to that particular shelf number.

For security purposes, the only labor that needs to be involved includes the person who sits at the exit gate to check whether each user exiting the library doesn't leave the library without issuing the books taken by him.

II. RELATED WORK

A. Smart Library System

Some of the related work in this area includes RFID based smart library systems [2]. They make use of RFID tags. The patron has to scan his ID card and then scan the tags present on the books in order to get them issued. The book drops can be located anywhere in the library and the patron has to simply place the books on the trays available for book drop. The reader reads the tags and notifies the patron of the successful return.

Face recognition based smart library system [1] employs face recognition in combination with RFID technology. The patron needs to stand in the line of sight of the camera until his face is detected and recognized. Once his face is recognized, the patron is logged in to the system after which he can scan the RFID tags of the books in order to get them issued.

The system proposed in [15] uses Near Field Communication based Book Tracking. Each book has an NFC tag attached to it. At the entrance, the user places his/her NFC enabled phone on the NFC reader. If fingerprint and user ID of the user exists in the database, the user is connected to the LAN. For searching a book, the user queries the system through his phone and gets the rack details as a reply from the server. This request is forwarded by the user to the Local Positioning System which further guides him to reach the desired rack. When a new book arrives, it is first registered in a

rack by scanning the book's tag against that particular rack's monitor. For issue procedure, the exit and entrance have NFC scanners. For returning a book, the user drops it in the drop box provided.

The system proposed in [16] focuses on security aspects majorly. When the book is returned by the patron, the librarian scans the book's RFID tag against the RFID reader and retrieves its location. For entering the library, the patron has to verify himself by scanning his tag against the door lock. On successful verification, the door is opened. The book security module checks for outgoing books continuously. If the outgoing book is not issued, then an alarm is activated.

Passive RFID tags at UHF frequencies are used by the system proposed in [17]. The system mainly focuses on smart bookshelves. Antennas are placed on the bookshelves which read RFID tags of the books within the shelf. The system uses microstrip antennas to minimize the spill-over electric field and the radiations emitted by them.

In the approach proposed in [3], the skin area is detected in the image and the facial features are searched in the skin area. The proposed approach considers the nose to be present for a partially occluded face since it does not change much with facial expression. Non-face objects are removed by using morphological operations. The HSV color model is used to avoid illumination variance effect and finally, a bounding box is drawn for the most probable face region.

B. Face Detection

1) Skin Segmentation based face detection: In this approach [3], the skin area is detected in the image and the facial features are searched in the skin area. The proposed approach considers the nose to be present for a partially occluded face since it does not change much with facial expression. Non-face objects are removed by using morphological operations. The HSV color model is used to avoid illumination variance effect and finally, a bounding box is drawn for the most probable face region.

2) Haar cascade combined with other classifiers: In this approach [4], three classifiers are combined with the haar cascade classifier. A face detected by the haar cascade classifier is only accepted when it passes the skin hue histogram test, eye, and mouth detection test.

3) Viola Jones Algorithm: This algorithm [5], [6] involves haar feature selection, creating an integral image, ADA-boost training and cascading classifiers.

C. Face Recognition

1) Support Vector Machines: The approach proposed in [7] uses the eigenfaces algorithm [8] to extract features from the input images. The features are then learned by the SVM. Since SVM is a binary classifier, this approach uses one against one strategy that is it classifies between each pair. A bottom-up binary tree is used for this classification.

2) Radial Basis Networks: In this approach [9], an n-sized input vector is given as input to the hidden unit which gives an m-sized output vector, where m is the number of faces registered. After the training, on feeding the test image we get an output vector. The given face image is recognized as that of a registered person if the maximum value of the output vector is larger than the threshold value. If it is not, the face is rejected as that of an unknown person.

3) EigenFaces Algorithm: This algorithm [8] is based on PCA (Principal Component Analysis). It extracts the variations in the collection of face images and uses this information to encode the face images and compare them individually.

4) LBPH Algorithm: In this approach [11], the central pixels for each window is substituted with a decimal number that is obtained from the binary pattern formed by the surrounding pixels. The LBPH (Local Binary Pattern Histogram) algorithm processes the image and forms binary patterns. It then stores these features into the histogram for later comparison. The histogram to which the test image's histogram is near to is assigned that particular class label.

D. QR Code decoding

Ref. [13] describes the structure of the QR code and its encoding and decoding process.

The approach of [12] uses image processing algorithms for detection of QR code. The grayscale image containing the QR code is binarized based on a threshold value. The alignment patterns and the timing pattern help locate the QR code in the image. The orientation of the QR code and width of one module is a representative of the timing pattern. Once the QR code is detected, a grid is constructed by joining the centers of the three alignment patterns detected. Error correction and decoding are then applied to retrieve the actual message.

The approach in [14] makes use of run length coding for QR code detection. The histogram of the grayscale image is equalized to increase its contrast followed by binarization. Run length coding is then applied to the resultant binary image.

III. Proposed System

A. Book Issue

According to the proposed system, the library can have multiple ATM-like machines for issuing/reissuing the book. The patron has to just stand holding the books in front of one such machine. The camera in it detects the user's face. If the patron is not a registered user, the system does nothing. However, if the patron is a registered member of the library, then upon recognizing his face, the system detects the QR codes present on those books which are held upfront by the patron. On decoding those QR codes, the book ID's of those books are retrieved and the system issues them against the patron whose face was recognized. The patron receives an

email as an acknowledgment for the successful issuance of the books.

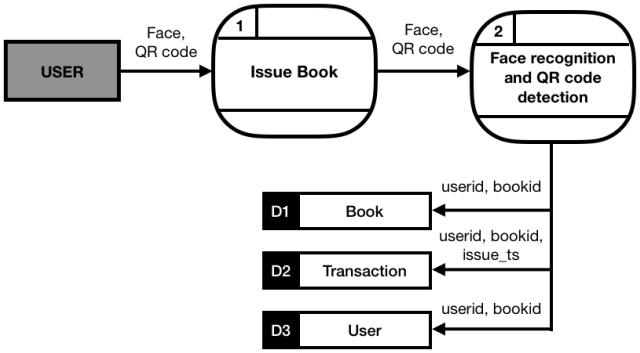

Fig 1. Data Flow Diagram for Book Issue

In Fig. 1, the face and the QR code data are supplied to the issue book module which involves Face recognition and QR code detection and decoding module. In the 'Book' table, the record with ID as 'bookid' is searched and the 'userid' of the patron who has issued that book is added to that book's record. The transaction containing the 'userid', 'bookid' and the 'issue_ts' (timestamp) is added to the 'Transaction table'. The 'User' table is then updated to store the 'bookid' in the details of the patron with ID as 'userid'.

B. Book Return

According to the proposed system, the library can have multiple drop-boxes with each drop-box having a camera situated above it. When the patron drops the books in these drop-boxes, the camera above them detects and decodes the QR code to fetch the book ID of that book. It then updates the database and the book is returned. The patron receives an email as an acknowledgment for the successful return of the book.

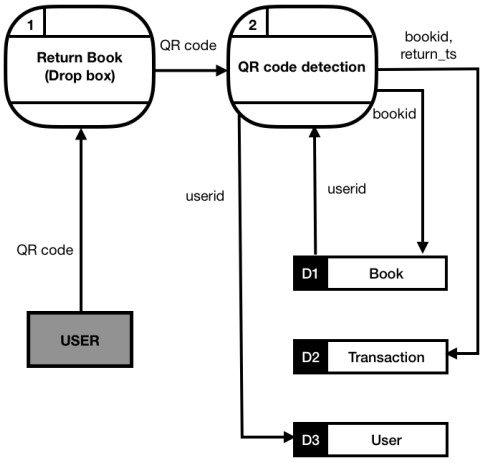

Fig 2. Data Flow Diagram for Book Return

In Fig. 2, the 'bookid' is retrieved from the QR code that is passed to the Return Book module. The 'Book' Table is then queried using 'bookid' to get the 'userid' of the patron who has issued that particular book. The 'return_ts' (return timestamp) which was initially empty is now updated in the 'Transaction' table. The retrieved 'userid' is then used to search for the patron in the 'User' Table and the returned book is removed from the list of his borrowed books.

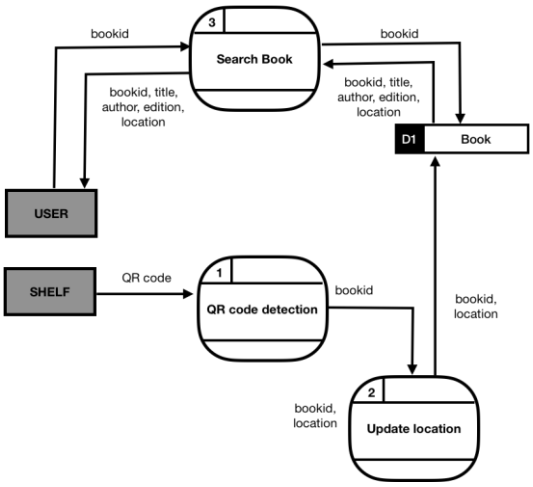

Fig 3. Data Flow Diagram for Dynamic Book Location Updation

C. Dynamic Book Location Updation

The system requires that each shelf has a designated camera which is associated with that particular shelf only. The camera detects all the QR codes found in its associated shelf. It decodes them all to get the book IDs and updates the location of those books to that particular shelf number.

Consider that a book is on shelf 1. The camera associated with shelf 1 will detect this and update the location of that book to Shelf 1. Now if the same book is moved to shelf 2, then the camera associated with shelf 2 will detect this additional QR code and will update the location of the same book to shelf 2. In this manner, the location of the book is updated dynamically in real-time.

The QR codes of the books present on a particular shelf are continuously decoded in real-time and their location is updated in the 'Book' table as shown in Fig. 3.

IV. Technology Used

A. Face Detection

The system uses the Viola-Jones Algorithm (haar cascades) in OpenCV [5], [6] to detect faces in the video frames. Haar cascade classifiers make use of kernels of a given size. Consider the size of the kernel as 3x3. The kernel moves across the image and does matrix multiplication with every 3x3 part of the image, emphasizing some features and smoothing others. Haar-features are good at detecting edges and lines. However, there are certain constraints to the objects that the haar cascade classifier can detect.

The algorithm is so chosen due to its high precision and recall value with respect to the other popular methods of face detection as proved in [6].

B. *Face Recognition*

The system uses the Local Binary Pattern Histogram (LBPH) [11] algorithm for face recognition. Local Binary Patterns are texture descriptors. They compute a local representation of the textures by comparing each pixel value with the surrounding pixel values. If the surrounding pixel value is greater than or equal to the central pixel value, then a zero is assigned at that position, else a one is assigned. The binary matrix (without considering the central pixel) formed is then read in either clockwise or anticlockwise direction and a binary number is generated. This binary number is then converted into a decimal value in the range of 0 to 255. The central pixel value is then replaced by this decimal value.

The above process is repeated for each pixel in the grayscale image and a new image is generated. The histogram for this newly generated image is calculated and is stored. The procedure is repeated for all training images and the histogram values for all the training images are stored. For testing purpose, the test image is processed in the same way and its histogram is calculated. This histogram can be compared with the stored histograms of the training images using distance metrics like Euclidian distance to determine the class label.

C. *QR Code Detection and Decoding*

The system uses the pyzbar library in python along with zbar dependencies to detect and decode QR codes. The advantage of this library is that the QR codes in any decent orientation can be detected and decoded using this library.

V. Experimental Results and Analysis

The system was tested on three datasets for face detection and face recognition viz. Cambridge Olivetti Research Laboratory face dataset, Caltech face dataset and our own manual dataset.

TABLE I. Face Detection Accuracy for Viola Jones Algorithm

Dataset	Total Images	True positives	Accuracy (%)
Cambridge ORL Face Dataset	400	265	66.25
Caltech Face dataset	445	435	97.53
Manual Dataset	200	50	25

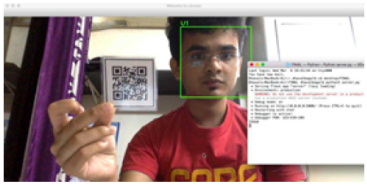

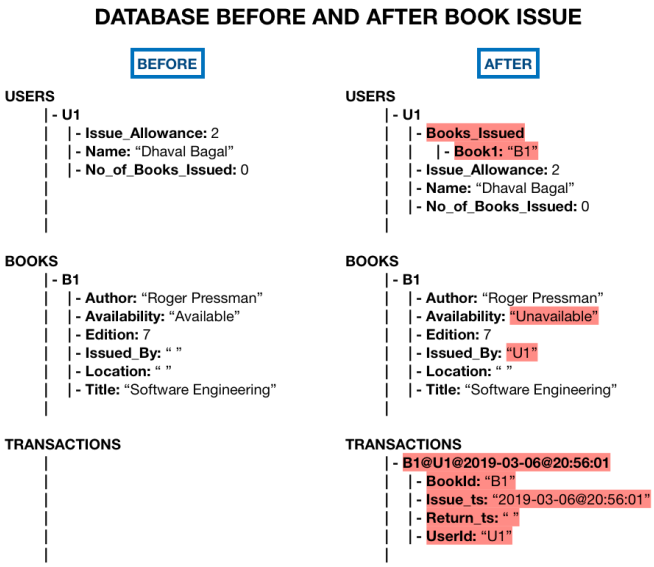

Fig 4. Book Issue

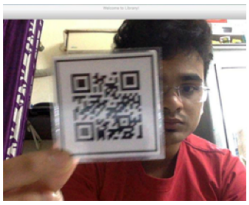

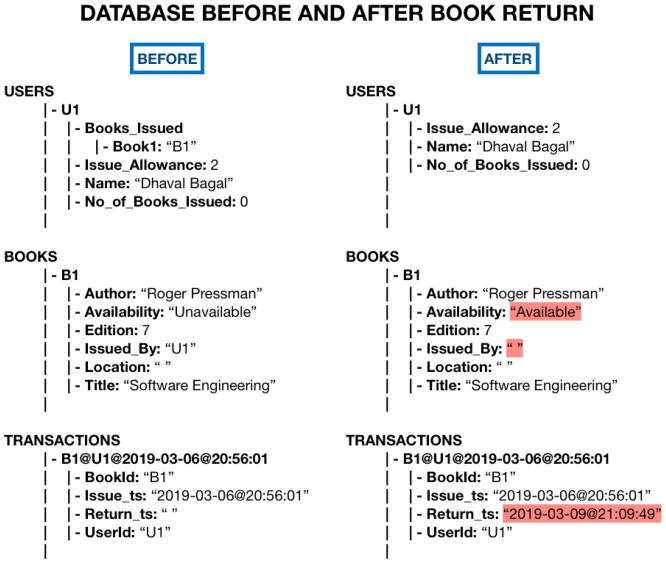

Fig 5. Book Return

TABLE II. RESULTS FOR CAMBRIDGE OLIVETTI RESEARCH LABORATORY FACE DATASET

Algorithm	Accuracy (%)	Avg. Recall	Avg. Precision	F1 Score
Eigenfaces True Pos. = 75 Train size = 181 Test size = 84	89.2857	0.8042	0.8346	0.8191
Fisherfaces True Pos. = 77 Train size = 181 Test size = 84	91.6667	0.8250	0.8317	0.8283
LBPH True Pos. = 77 Train size = 181 Test size = 84	91.6667	0.8292	0.8375	0.8333
LBPH + KNN (n=5) True Pos. = 32 Train size = 198 Test size = 67	47.7612	0.4866	0.3757	0.4241
LBPH + Decision Trees True Pos. = 17 Train size = 198 Test size = 67	25.3731	0.2509	0.1958	0.2200
LBPH + Logistic Regression True Pos. = 29 Train size = 198 Test size = 67	43.2836	0.4662	0.4257	0.4450

TABLE III. RESULTS FOR CALTECH FACE DATASET

Algorithm	Accuracy (%)	Avg. Recall	Avg. Precision	F1 Score
Eigenfaces True Pos. = 85 Train size = 328 Test size = 107	79.4393	0.7269	0.7072	0.7169
Fisherfaces True Pos. = 101 Train size = 328 Test size = 107	94.3925	0.8962	0.9103	0.9032
LBPH True Pos. = 101 Train size = 328 Test size = 107	95.3271	0.9154	0.9615	0.9379
LBPH + KNN (n=5) True Pos. = 34 Train size = 326 Test size = 109	31.1926	0.2629	0.3207	0.2889
LBPH + Decision Trees True Pos. = 25 Train size = 323 Test size = 112	22.3214	0.2022	0.2434	0.2209
LBPH + Logistic Regression True Pos. = 40 Train size = 326 Test size = 109	36.6972	0.3398	0.3123	0.3254

TABLE IV. RESULTS FOR MANUAL FACE DATASET

Algorithm	Accuracy (%)	Avg. Recall	Avg. Precision	F1 Score
Eigenfaces True Pos. = 11 Train size = 25 Test size = 25	44	0.3230	0.3500	0.3359
Fisherfaces True Pos. = 15 Train size = 25 Test size = 25	60	0.5071	0.5300	0.5183
LBPH True Pos. = 15 Train size = 25 Test size = 25	60	0.5849	0.5144	0.5474
LBPH + KNN (n=5) True Pos. = 5 Train size = 37 Test size = 13	38.4615	0.2857	0.3250	0.3041
LBPH + Decision Trees True Pos. = 4 Train size = 37 Test size = 13	30.7692	0.1696	0.3125	0.2199
LBPH + Logistic Regression True Pos. = 9 Train size = 37 Test size = 13	69.2307	0.5357	0.5333	0.5345

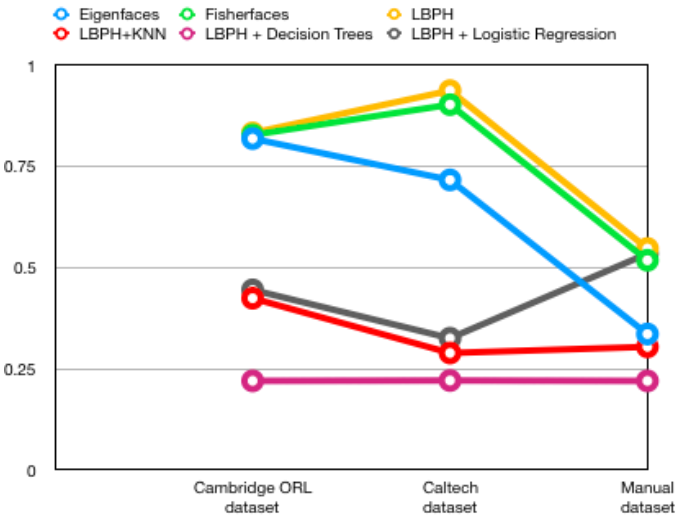

Fig 6. 2D Line plot for F1 scores of algorithms with respect to the three datasets considered

Table I displays the results of the tests performed on the three datasets for Viola-Jones algorithm. It displays the size of each dataset in terms of number of images and the true positives i.e the number of images in which face was detected accurately. The number of true positives divided by the total number of images gives the accuracy of the Viola-Jones algorithm for that particular dataset.

Table II, Table III, Table IV, sum up the results of various algorithms considered for each of the dataset. Since the number of test images for each face in the test dataset was variable, F1 score became significant comparison factor over accuracy. The

recall value is given by the ratio of the number of true positives and the sum of the true positives and false negatives. The precision value is given by the ratio of the number of true positives and the sum of the true and false positives. F1 score is given by the ratio of twice the product of precision and recall values and the sum of the precision and recall values. The empirically obtained F1 scores of LBPH with respect to the ORL, Caltech, and the Manual dataset in Table II, Table III, and Table IV, are 0.83, 0.94 and 0.55 respectively.

Three major algorithms viz. EigenFaces, FisherFaces and LBPH were tested. Other than these, the other three algorithms considered for testing were the combinations with the LBPH. In these algorithms, the histogram of the local binary patterns was extracted for all the training images to create a dataset and then the model was trained on this dataset using KNN, Decision trees, and Logistic Regression.

Fig. 6 justifies the use of LBPH algorithm for face recognition in the proposed system. The 2D line points for the LBPH algorithm in Fig. 6 are maximum with respect to all the three datasets.

VI. Conclusion and Future Work

Owing to the use of software to a great extent in the system, the wear out rate of the system is negligible. If the accuracy of face recognition is improved profusely, then the system would be self-sufficient and can be deployed in the actual libraries which can help reduce the significant amount of load on the librarians. With Librany, all the books in the library can be tracked in real-time. It needs no involvement with the librarian. The system enjoins self-issue and self-return procedures which avoids long queues at the counter.

The system can be extended to detect faces in any orientation. Also, the system can be tuned such that even if multiple faces are detected in the video frame, the book should be only issued to the patron holding it instead of the other detected faces. Buzzers can be deployed at the exit gate which can ensure security and alert the person in charge in case of larceny. Modules which provide business intelligence can be incorporated into the system for knowledge extraction.

Acknowledgement

The authors would like to express their sincere gratitude to the Computer Engineering department of Vivekanand Education Society's Institute of Technology.

References

[1] Vyavahare M.D, Kataria S. S, "Library Management Using Real Time Face Recognition System", Blue Eyes Intelligence Engineering & Sciences Publication Pvt. Ltd., International Journal of Engineering and Advanced Technology (IJEAT), vol. 4, no. 4, pp. 24-27, April 2015.

[2] B.T.Geetha, V.Perumal, S.Hariharan, T.Jayakumar, "A Smart Book Accessing System Using RFID and IR in Library", International Journal of Pure and Applied Mathematics, vol. 118, no. 24, May 2018.

[3] P. Shanmugavadivu and Ashish Kumar, "Rapid face detection and annotation with loosely face geometry", in Proceedings of the 2nd International Conference on Contemporary Computing and Informatics (IC3I), pp. 594-597, 2016.

[4] Li Cuimei, Qi Zhiliang, Jia Nan, Wu Jianhua, "Human face detection algorithm via Haar cascade classifier combined with three additional classifiers", in Proceedings of the IEEE 13th International Conference on Electronic Measurement & Instruments(ICEMI), pp. 483-487, 2017.

[5] Mangayarkarasi Nehru, Padmavathi S., "Illumination Invariant Face Detection Using Viola Jones Algorithm", in Proceedings of the International Conference on Advanced Computing and Communication Systems (ICACCS), 2017.

[6] Kirti Dang, Shanu Sharma, "Review and Comparison of Face Detection Algorithms", in Proceedings of the 7th International Conference on Cloud Computing, Data Science & Engineering – Confluence, pp. 629-633, 2017.

[7] Guodong Guo, Stan Z. Li, and Kapluk Chan, "Face Recognition by Support Vector Machines", in Proceedings of the 4th IEEE International Conference on Automatic Face and Gesture Recognition, 2000.

[8] Matthew A. Turk and Alex P. Pentland, "Face Recognition Using Eigenfaces", in Proceedings of the Conference on Computer Vision and Pattern Recognition, pp. 586-591, 1991.

[9] Kiminori Sato, Shishir Shah and J.K Aggarwal, "Partial Face Recognition using Radial Basis Function Networks", in Proceedings of the 3rd IEEE International Conference on Automatic Face and Gesture Recognition, 1998.

[10] Ghazi Mohammed Zafaruddin, H. S. Fadewar, "Face Recognition: A Holistic Approach Review", in Proceedings of the International Conference on Contemporary Computing and Informatics (IC3I), pp. 175-178, 2014.

[11] Md. Abdur Rahim, Md. Najmul Hossain, Tanzillah Wahid and Md. Shafiul Azam, "Face Recognition using Local Binary Patterns (LBP)", Global Journal of Computer Science and Technology Graphics and Vision, Global Journals Inc., vol. 13, no. 4, 2013.

[12] Yue Liu, Ju Yang, Mingjun Liu, "Recognition of QR Code with Mobile Phones", Chinese Control and Decision Conference (CCDC), pp. 203-206, 2008.

[13] Sumit Tiwari, "An Introduction To QR Code Technology", International Conference on Information Technology (ICIT), pp. 39-44, 2016.

[14] Hou A-Lin, Feng Yuan, Geng Ying, "QR code image detection using run-length coding", International Conference on Computer Science and Network Technology, pp. 2130-2134, 2011.

[15] A. Larsan Aro Brian, L. Arockiam, P. D. Sheba Kezia Malarchelvi, "An IOT based secured smart library system with NFC based book tracking", International Journal of Emerging Technology in Computer Science & Electronics (IJETCSE), vol. 11, no. 5, pp. 18-21, November 2014.

[16] Mohammed I. Younis, "SLMS: a smart library management system based on an RFID technology", International Journal of Reasoning-based Intelligent Systems, vol. 4, no. 4, pp. 186-191, 2012.

[17] I. Markakis, T. Samaras, A. C. Polycarpou, J. N. Sahalos, "An RFID-enabled Library Management System using Low- SAR Smart Bookshelves", International Conference on Electromagnetics in Advanced Applications (ICEAA), pp. 227-230, 2013.

Proceedings of the Fourth International Conference on Communication and Electronics Systems (ICCES 2019)
IEEE Conference Record # 45898; IEEE Xplore ISBN: 978-1-7281-1261-9

Image Representation based on quantum Computation and their Application : Milestone Ontogeny

Sanjay Singh [1], Ashish Mani [2], Rashmi Jain[3]

[1] Department of Computer Science & Engineering, A.S.E.T, Amity University ,Uttar Pradesh, Noida, India , Sanjaysingh.aravali@gmail.com
[2] Department of Electrical & Electronics Engineering, A.S.E.T, Amity University , Uttar Pradesh, Noida, India, amani@amity.edu.in
[3] Department of Electrical & Electronics Engineering , J.C. Bose University of Science and Technology, YMCA, Faridabad, Haryana, India, rashmiagarwal404@gmail.com

Abstract — Image processing is relevant in our day to day life as it is helpful to solve important problems in real world. Recent progress in quantum information and computation led to the birth of a new field called Quantum Image Processing. This new field of image processing in quantum domain focuses on the development of the quantum image processing algorithms, which can run more efficiently on quantum computer. These quantum algorithms are better in terms of Image storage and retrieval with reduced computational complexity. In this article we present recent advancements in quantum image representation with different mathematical models and with their corresponding computational complexity.

Keywords — Quantum computation; Quantum image processing; quantum image depiction; Quantum measurement; Quantum information

I. INTRODUCTION

The field of digital image processing refers to processing of digital images by means of a digital computer. Image processing is well known in our day to day life as the need of extraction of crucial data is also increasing in real world. Computational complexity of an algorithm and visual information are the popular area of research for existing real world problems. Extracting right information from available digital data and removing associated noise in the images are two major problems in this field. Because of the limited architecture of classical computers and the often overwhelming computing complexity of state-of-art algorithms, better ways of storing, processing and retrieving digital images are required. The images of 3D scenes in 2D spaces, visual information and algorithm complexity are all major research areas.

In different fields of computer science, for example information theory, cryptography, emotional depiction and image processing, quantum computation and quantum information have appeared because inefficient tasks on conventional computers can be improved by exploiting the power of quantum computing. The first step in the processing of quantum images involved proposals for capturing and storage of the images on quantum computers. Quantum Computers enables different image illustrations like qubit lattice, Flexible Representation for Quantum Images (FRQI-Model), Multichannel Quantum Image (MCQI Model), Novel enhanced quantum representation model (NEQR), CQIR (Colored Quantum image representation) representation model, Three Channel Representation for quantum color images model (QMCR).

This paper tries to investigate basic of quantum computation, the different quantum image representation, comparison and application of investigated Quantum image representation. Sequence of paper is as follows: In Section 2, the fundamental learning of classical image processing and need of quantum image processing is discussed. In section 3, Basic knowledge of quantum image processing and associated operation used in quantum computation is presented. In section 4, detailed investigation of different quantum image representation, their features and comparison are analyzed. In section 5, Conclusions are drawn and direction for future work is discussed.

II. CLASSICAL IMAGE PROCESSING

Image processing is a technique of enhancement of the raw images received from various sensors or cameras which are placed on the sources like satellites, aircrafts and space probes or the pictures taken during the normal day to day life activities. Different techniques have been developed for improving raw images over the last five to six decades. Image process could be a method where an image is converted into a digital form using some operation to obtain an improved image and to extract a number of useful information. Image processing is used in various applications like: printing industry, film industry, military purpose, graphics arts, forensic studies, material science, medical imaging.

In traditional memory device, memory cells are available in the form of the hardware, i.e., each memory vicinity may be attributed to a truth that is independent of all other reminiscence places. Better ways of storing, processing and retrieving digital images are required because of the limited architecture of classical computers.

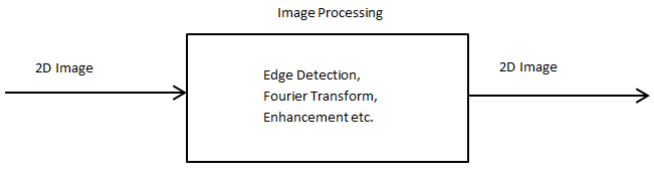

Fig. 1. 2 D Block of Image Processing

III. QUANTUM IMAGE PROCESSING

Image processing is prevalent in our day to day life as it is helpful to extract important information from real world. A new field called quantum image processing emerged after certain major research tasks. Research in this sector has experienced problems owing to its emerging phase. However, efforts continue to identify the diversity of its applicability in different fields of image processing. Most of the work done so far refers to fundamental aspects such as representing and storing an image on quantum computer and the basic processing. The portrayal of 3D scenes in 2D spaces, behaviour of visual information and algorithm complexity are all emerging research area. Quantum image processing is an important and emerging sub-domain in quantum theory.

A. Quantum Image Processing Operation

If we compare the quantum image with the classical image, there is an enormous benefit of the depiction of the quantum image. Let's take X pixel sized quantum image. The general mathematical equation of quantum image is represented as:

$$|\mathrm{QI}\rangle = {}^{1}/_{\sqrt{X}} \sum_{a=0}^{x-1} |\mathrm{Sa}\rangle \otimes |\mathrm{Z}\rangle \qquad (1)$$

Where $|\mathrm{Sa}\rangle$ is color information of quantum image, $|\mathrm{Z}\rangle$ Position of quantum image, $\otimes$ Tensor product.

The bits used to represent information are known as qubits in a quantum computer. These qubits lie in superposition of two basis states in a quantum computing system. As compared to classical bits these quantum bits can store more information because of the quantum-ness like superposition and entanglement. Quantum computer follows the rule of linear superposition principle. A quantum computer can be defined as the computing machine which is used to perform computation based on the laws of quantum mechanics.

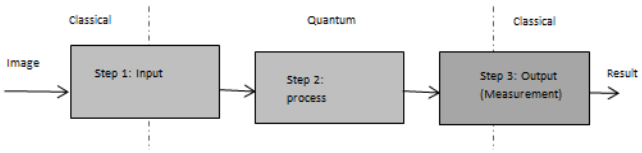

Fig. 2. Basic procedure for Quantum Image Processing

B. Quantum Bits

In the case of Classical Computation, storage and processing of the information used to take place in the form of the bits. As a mathematical structure it involves the processing of the classical bit. It works to represent two 'logical' values, commonly referred to as {0, 1}, and to link these obtained values to two different classical measurement solutions. So, that's why classical bit used to 'live' in the scalar space. Qubit is a real-world entity which is based on Quantum Mechanics law. Simple instances of qubits use two orthonormal polarization of a photon, alignment of a nuclear spin (spin-1/2) in a magnetic area or electron states orbiting an atom. The classical image uses bits that can be either 0 or 1 at a specific location and time.

C. Quantum Gates

Quantum gates are used to perform the manipulation of qubits. A qubit enters a gate of the quantum circuit and exits as another state, so quantum gates represent the time evolution of a state which is required to describe the qubits. The quantum gate satisfies the following criteria:

- Must uphold the norm i.e. norm squared probability amplitudes sum to one after gate application.
- It must be reversible in nature i.e. evolution of every non measured quantum state must be reversible.

The above conditions are equivalent to a restriction that quantum gates must be unitary matrices. In quantum computation most common used quantum gates are Hadamard, NOT and CNOT gates. There are several facts about quantum circuits which can be used in order to express more complex unitary transformations, write circuits more concisely, or adapt circuits to experimental constraints. The gates used to apply on the K qubits are usually represented by 2^k X 2^k unitary matrix; the qubit number in the gate input must be equal to the output end.

D. Quantum Measurement

Quantum physical systems are very susceptible to interference from outside of the scheme compared to conventional physical structures. One sort of external interference mentioned is the quantum measurement that tests a qubit status for the observable state in which it is. A set A_a of non-unitary measurement operators can mathematically describe quantum measurement [19]. Here, a is an index of the base state being evaluated. For instance, if there are two basis states pertaining to $|0\rangle$ and $|1\rangle$, there would be two indices, $a = 0$ and $a = 1$. The probability of the measurement producing the observable state a is given by

$$A(a) = \langle\psi|\, \bar{A}_a A_a\, |\psi\rangle \qquad (2)$$

Where $\bar{A}$ denotes the conjugate transpose of a matrix, $\langle\psi|$ represents the conjugate transpose of $|\psi\rangle$, and the state of the quantum system after measurement is

$$\frac{A_a|\psi\rangle}{\sqrt{\langle\psi|\bar{A}_a A_a|\psi\rangle}} \qquad (3)$$

Applying quantum measurement makes the system "collapse" to one of the basis states [19]. For example, consider the qubit state

$$|\psi\rangle = \alpha\,|0\rangle + \beta\,|1\rangle = \begin{pmatrix}\alpha\\ \beta\end{pmatrix} \qquad (4)$$

So that $\langle\psi| = (\alpha^*, \beta^*)$ (5)

The measurement operator

$$A_0 = \begin{pmatrix}1 & 0\\ 0 & 0\end{pmatrix} \qquad (6)$$

Projects $|\psi\rangle$ onto the observable state $|0\rangle$ with probability

$$\frac{A_0|\psi\rangle}{\sqrt{\langle\psi|\bar{A}_a A_a|\psi\rangle}} = \frac{\begin{pmatrix}1 & 0\\ 0 & 0\end{pmatrix}\begin{pmatrix}\alpha\\ \beta\end{pmatrix}}{\sqrt{\alpha^*\alpha}} = \frac{\alpha|0\rangle}{\sqrt{|\alpha|^2}} = |0\rangle \qquad (7)$$

With the coefficient $\frac{\alpha}{\sqrt{|\alpha|^2}}$ being a phase term, the effect of which on the measurement outcome is negligible and typically ignored. On repeated measurements, one gets a probability distribution over the observable states. The physical, meaningful outcome of quantum measurement can be estimated using quantum state tomography (QuST) [20]—that is, estimation by maximum likelihood. One of the most common tools for this estimation is the Kalman filter approach, as it is the one that is most robust against noise. Therefore, in the field of QuIP, most algorithms created use it to assess the outcomes of quantum measurements

E. Quantum Entanglement

Concept of quantum entanglement occupies the position of primary importance in quantum computing as well as in quantum image processing. Fundamentally entanglement is relationship between two particles. As we know in today's scenario images are being used for communication because they carry information in detail. So by taking advantage of quantum entanglement in images we can improve communication methods.

IV. Representation of an Image in Quantum context

Prof. Salvador E. Venegas-Andraca [2], proposed the quantum image representation, based on qubit lattice. Prof. Jose.I. Labtorre Sentis [4], by using the real ket, proposed the quantum image portrayal. Prof. Kaoru Hirota [3] proposed flexible way of representing the quantum images with a purpose to provide a portrayal of picture at the quantum computers which can be in the shape of a normalized state required to store the information regarding colors and the position associated with them in the given images.

A. Storing and Retrieving an Image in Quantum System using Qubit Lattice

Storing an Image: Let's define ourselves L as a lattice of qubits, that is L= $\{|q\rangle_{i,j}\}$, $I \in \{1,2,...,n_1\}$, $j \in \{1,2,...,n_2\}$ A set of qubit lattices S may be defined as S= $\{L_k\}$, k ∈ {1, 2,...,n_3} Thus, S = $\{\{|q\rangle_{i,j,k}\}$ is a set of n_1 x n_2 x n_3 qubits. Our motive here is to store or accumulate the visual information in S and each lattice, say $L_k \in S$ is used to save the copy of the given image. The process of storing an image using the set of qubit lattices S is described in the algorithm. During the execution of the algorithm, an assumption is made that the lattice L is made up of machine A. On the completion of algorithm, entire set S is initialized; n_3 is used to prepare the same qubit lattices, each of which contains the same image [2].

B. Flexible Representation for Quantum Images(FRQI model)

Le *et al.* [3] proposed the FRQI, which has begun to grow into most widely used quantum image representation (QIR). In this model, the required records i.e. the colors and position of all factors in an image get captured and then integrate with the tensor product to achieve a normalized quantum state. The below equation shows the vector of angles to encode color information in the form:

$$|\mathrm{I}\rangle = \frac{1}{2^n} \sum_{y=0}^{2^{n-1}} |Q_f\rangle \; |i\rangle \qquad (8)$$

$$|Q_f\rangle = \mathrm{Cos}\,\theta\,\mathrm{f}\,|0\rangle + \mathrm{Sin}\,\theta\mathrm{f}|1\rangle \qquad (9)$$

$|0\rangle$ and $|1\rangle$ are 2 Dimension computational basis quantum states, $Q_f \in [0, \pi/2]$ and f = 0, 1, 2.....2^n-1. The equation developed is an integral part of FRQI preparation process and its implementation. By this, the whole preparation of the computational complexity of FRQI image state requires o (2^{4n}). The normalized state of FRQI, i.e., $\| |Q_f\rangle \| = 1$ as follow:

$$\| |Q_f\rangle \| = \frac{1}{2^n}\sqrt{\sum_{f=0}^{2^{2n-1}} (\cos 2\,\theta\mathrm{f} + \sin 2\,\theta\mathrm{f}) = 1} \qquad (10)$$

FRQI illustration and transformation focus on the spatial and geometric data. FRQI has interesting application in quantum watermarking, quantum moves, quantum image data searching and quantum image frameworks and so on [4].

C. Multichannel Quantum Image(MCQI model)

While FRQI can be used in many application of quantum images but still, the concept of "full" color cannot be captured in the images. Sun *et al* [5] proposed the new model of color images processing in quantum computers. The proposed version simultaneously captures the records from R, G, B channels and store the information in quantum state. MCQI model is used to capture and store color information and position at the amplitudes of each image pixel. Thus model supports 2^n x2^n image and can be mathematically expressed as:

$$|QI\rangle = \frac{1}{2^{n+1}} \sum_{f=0}^{2^{2n-1}} |A_{RGB\alpha}^f\rangle \otimes |f\rangle \qquad (11)$$

$$|A_{RGB\alpha}^f\rangle = \mathrm{Cos}\,\theta_R^f|000\rangle + \mathrm{Cos}\,\theta_G^f\,|001\rangle + \mathrm{Cos}\,\theta_B^f|010\rangle + \mathrm{Cos}\,\theta_\alpha^f\,|011\rangle + \mathrm{Sin}\,\theta_R^f|100\rangle + \mathrm{Sin}\,\theta_G^f\,|101\rangle + \mathrm{Sin}\,\theta_B^f|110\rangle + \mathrm{Sin}\,\theta_\alpha^f\,|111\rangle \qquad (12)$$

$|000\rangle, |001\rangle \ldots |111\rangle$ is used to represent the computational premise conditions of the required three qubits. θ_R^f, θ_G^f, θ_B^f, θ_α^f represents the four angles that are used for encoding the data of color channels of the f-th pixel , $|f\rangle$ for f = 0, 1, . . . ,2^{2n}-1 are 2^{2n}-Dimension represents computational premise condition states. The main difference between the FRQI and MCQI is that FRQI require only one qubit to encode an

image color but MCQI uses three qubits to carry multichannel color information. Computational complexity of both MCQI quantum image and FRQI's is same i.e., O (2^{4n}) [5].

D. Novel Enhanced Quantum representation model (NEQR model)

Model representation of NEQR was put forward by Zhang *et al*. [6-7]. Under this model digital image, the basis sate of a qubit collection is used to keep the gray scale cost of each pixel instead of using encoding in a qubit in FRQI. Whereas in NEQR encoded qubit sequences are required to capture the entire image. NEQR requires only pixel's gray-scale and position information. Let us take into account that the value of grey range of the given picture is 2q with given binary collection $c_{ab}^{0} \ldots c_{ab}^{q-2} c_{ab}^{q-1}$ and the required encoding of the gray-scale value *f (a, b) is obtained by:*

$$f\ (a,b) = \ c_{ab}^{0} \ldots c_{ab}^{q-2} c_{ab}^{q-1} \quad (13)$$

Where $c_{ab}^{k} \in [0, 1]$ and *f (a, b)* $\in [1, 2^{q} - 1]$

In NQER quantum image model, first step is quite similar to FRQI. Second step involves the setting of the greyscale value of each pixel. This step is further divided into the 2^{2n} part-operation which is required for the storage of the grayscale information of each and every pixel. Time complexity concerned in preparation of NEQR quantum image shows typically a quadratic decrease, i.e., O($qn.2^{2n}$) whilst in comparison to FRQI. NEQR representation model requires a q +2n qubits for the construction of the quantum image model for the image of size 2^{n} x 2^{n} with gray scale range 2^{q}.

E. CQIR Representation model

CQIR model was proposed by Caraiman and Manta in 2014[8]. CQIR is similar to NEQR. A qubit sequence was used in encoding the colored information required in quantum images. CQIR facilitates histogram equalization of the quantum image. This model requires $m=log_2 L$ qubits to encode all the L grey levels which are available in the picture [8-9]. This model may find potential application in the processing of the images related to medical, radar and astronomy. This may result in enhancement of the contrast of the image for obtaining better details related to the image. The formulation of CQIR illustration is shown:

$$|\mathrm{I}\rangle = \ |C\rangle \mathrm{mx} |P\rangle 2\mathrm{n} \ = \frac{1}{2^{n}} \sum_{i=0}^{2^{2n}-1} \ \sum_{j=0}^{2^{m}-1} \propto i\ j\ |j\rangle\ |i\rangle \quad (14)$$

$$|\mathrm{I}\rangle = \frac{1}{2}(|01\rangle\ \otimes |00\rangle + |10\rangle\ \otimes |01\rangle + |11\rangle \otimes\ |10\rangle + |00\rangle \otimes 11)) \quad (15)$$

$|P\rangle$ is a register in which pixel positions are encoded by using the 2*n* qubits and the information of color pixel is denoted by using $m=log_2 L$ qubits required to encode the L grey level colors. Coefficients $\propto_{i\ j}$ represents the color associated with the pixel whose position is I by using the concept of a superposition of all possible colors with $0 \leq i \leq 2^{2n}$. In this for I, coefficients $\propto_{i\,j}$ holds the value 1 only when the color associated with the pixel is j, otherwise holds 0.

F. Three channel Representation for Quantum Colored images model (QMCR)

RGB three channel representations for quantum colored images model was suggested by Abdolmalekya *et al.* [10]. It is based on the NEQR. The formulation of QMCR representation is shown:

$$|\mathrm{I}\rangle = \frac{1}{2^{n}} \sum_{y=0}^{2^{n-1}} \ \sum_{x=0}^{2^{n-1}} |C_{RGByx}\rangle \otimes\ y\ x\rangle \quad (16)$$

Where the state $|C_{RGByx}\rangle$ is used to encode the information of the R, G and B channels (2^{q} range of each channel) of the pixel. The state $|C_{RGByx}\rangle$ is defined as follows:

$$|C_{RGByx}\rangle = |R_{yx}\rangle||G_{yx}\rangle|B_{yx}\rangle \quad (17)$$

$$|R_{yx}\rangle = \ |\mathrm{r}_{yx}^{q-1}\ \mathrm{r}_{yx}^{q-2} \ldots \mathrm{r}_{yx}^{q-0}\rangle \quad (18)$$

$$|G_{yx}\rangle = |\mathrm{g}_{yx}^{q-1}\ \mathrm{g}_{yx}^{q-2} \ldots \mathrm{g}_{yx}^{q-0}\rangle \quad (19)$$

$$|B_{yx}\rangle = |\mathrm{b}_{yx}^{q-1}\ \mathrm{b}_{yx}^{q-2} \ldots \mathrm{b}_{yx}^{q-0}\rangle \quad (20)$$

Where $\mathrm{r}_{yx}^{k}, \mathrm{g}_{yx}^{k}, \mathrm{b}_{yx}^{k} \in \{0,1\}$ and $R_{yx}, G_{yx}, B_{yx} \in \{0, 1, \ldots 2^{q}-1\}$.

G. Quantum Image representation for log-polar images (QUALPI)

Y. Zhang *et al*. [11-12] proposed the model of QUALPI. For Classical preparing of pictures, idea of log-polar is broadly utilized as an inspecting technique here on account of log-polar picture of size 2^{m} x 2^{n}, examining goals pursuing of the log-range and that of precise introduction are relied upon to be 2^{m} and 2^{n} respectively. This model was investigated for the purpose of processing and storage of the sampled images in log-polar coordinates. Existing quantum computing based image processing models can only present the image sampled in Cartesian coordinates, due to which rotation and scaling operation is not possible to be performed in the existing model. QUALPI utilizes three entangled qubit. In which first one is used for storing the gray scale information, second one is used for log-radius position and the last one is used to retrieve the information for the angular position of all the pixel in case of log-polar image. Estimation of every pixel is to be recorded on the premise condition of a standardized superposition which comprises of qubit groupings, in order to operate on them simultaneously. In the QUALPI model, further geometric transformation can be performed in a simple manner. It also includes the complex one named as symmetric transformation and rotation. The Mathematical formulation of QUALPI representation is shown:

$$|\mathrm{I}\rangle = \frac{1}{\sqrt{2^{m+n}}} \sum_{\rho=0}^{2^{m}-1} \ \sum_{\theta=0}^{2^{n}-1} \sum_{\theta=0}^{2^{n}-1} \ (|g(\rho,\theta)\rangle \otimes |\rho\rangle \otimes |\theta\rangle\ ) \quad (21)$$

Where $g(\rho,\theta)$ used to represent the gray - scale value of each pixels. Gray range of the image is expected to be 2^{q}, so that this can be encoded as:

$$g(\rho,\theta) = \mathrm{C0C1}\ \ldots \mathrm{Cq} - 2\mathrm{Cq} - 1, g(\rho,\theta)\ \in [0, 2\mathrm{q} - 1] \quad (22)$$

It is easy to understand that the pixels lying in different quadrant have different grey scale. *m + n + q qubits are* needed for the storage of information into a QUALPI state for a 2^{m} x 2^{n} log - polar image with gray range 2^{q}. The entire

procedure of arrangement of quantum picture will not cost more than O(q(m+n). 2^{m+n}) for the 2^m x 2^n log-polar quantum image whose grey range value is 2^q . QUALPI is, out of the blue, intended for the pictures tested in log-polar directions.

H. *Simple Quantum (SQR) representation model of infrared images.*

Suzhen *et al*. [13] proposed SQR model. This model was proposed to limit the drawbacks associated with the Qubit lattice and FRQI model. This model depends on qualities of the infrared pictures. SQR model involves the replacement of the color information with the radiation values as the coefficient values. The mathematical formulation of SQR representation is shown:

$$|\mathrm{I}\rangle = |\psi_{ij}\rangle \quad (23)$$

i = 1, 2,…, n_1, *j = 1,2,…,*n_2 *are real numbers. Where* $|\psi_{ij}\rangle$ = = $\cos\theta_{ij}\,|0\rangle + \sin\theta_{ij}|1\rangle$, we can view $|\psi_{ij}\rangle$ in the form of Bloch sphere as a great circle.

SQR model offers the following advantages in comparison to the Quantum Lattice model and latest suggested FRQI model:

1. SQR model requires two n-qubit states so as to keep the extraordinary values. It additionally requires a 2n straightforward quantum gate so as to define the quantum infrared picture in comparison with the Quantum Lattice model. While, n may be neglected because it is a very small number.
2. Simple quantum gate is required to setup the SQR quantum image, which also shows a quadratic decrease compared to the FRQI.
3. It also allows to perform more number of image operations conveniently which are based on SQR in comparison to the original Qubit Lattice representation.

SQR also has the ability to hold more information which includes image information as well as marked information. Here marked information used refers to that kind of information which requires emphasizing, on infrared target or some other vital geographical locations etc.

I. *Quantum states for M Colors and Quantum states for N coordinate (QSMC & QSNC)*

This model requires two sets of quantum states one for *M colors* and the other for *N coordinates*, so that both gray scale and information related to the color of an image can be represented efficiently. This model provides a lossless compression and quantum search enabled image segmentation technique which is universally applicable for both the gray scale and the color images. QSMC & QSNC both require two set of quantum states in order to capture the image, where QSMC is used to represent the M colors while QSNC is required to denote the coordinates of N pixels of an image [14]. Two bijective functions are developed for the purpose of storing the information regarding the coordinate and color of an image with the help of quantum states, *One from M's different colors to M's different angles and the second from N's to N's various angles.* Expression of mathematics associated with QSMC & QSNC Quantum image is shown under:

$$|\mathrm{I}\rangle = \frac{1}{2^n}\sum_{i=0}^{2^{2n}-1} |QSMC_i\rangle \otimes |QSNC_i\rangle \quad (24)$$

Where

$$|QSMC_i\rangle = \cos\phi\,\mathrm{i}\,|0\rangle + \sin\phi\,\mathrm{j}|1\rangle \quad (25)$$

$$|QSNC_i\rangle = \cos\theta\,\mathrm{i}|0\rangle + \sin\theta\,\mathrm{i}\,|1\rangle \quad (26)$$

ϕ_i , $\theta_i \in [0, \pi/2]$, i = 1, 2, ... 2^{2n}-1.

This model is designed in such a way that in a quantum system only 2N + m qubits is stored an image of N pixels and M different colors.

J. *Normal arbitrary Quantum Superposition State (NAQSS)*

This model is designed for multi-dimensional image representation. Li *et al*. [15] proposed this model. Also known as the normal arbitrary quantum superposition state (n+1) qubit. In this model n qubits represents 2n pixel colors and coordinates and the remaining 1 qubit represents information about image segmentation. In this a bijective function is established with the goal that each pixels can locate a relating value for an interval of [0, π/2] by making up a one to one correlation for angle and color. Function is shown as: *g: A→R where A* represents the data regarding the position of the picture in a k- dimensional Euclidean space. The mathematical representation of NAQSS image is shown:

$$|\mathrm{I}\rangle = \sum_{i=0}^{2^n-1} \theta_i\,|v_1\rangle\,|v_2\rangle \ldots |v_k\rangle \otimes |x_i\rangle \quad (27)$$

Where $|x_i\rangle = \cos\propto_0 |0\rangle + \sin\propto_0 |1\rangle$

Represents the information related to the segmentation, where $\propto_0$ is corresponding to the m in order to establish a bijective function. If we divide the image into m sub - images so that it will contains the pixels corresponding to the $|v_1\rangle\,|v_2\rangle \ldots |v_k\rangle$ coordinates.

K. *(2 –D QSNA) Two Dimensional Quantum states and Normalized Amplitude*

Above model for quantum image representation was proposed by *Madhur Srivastava et al. [16]*. The proposed method, two-dimensional quantum state and normalized amplitude, only requires ($[\log_2 \mathrm{N}] + [\log_2 \mathrm{N}]$) qubits. As compared to the previous model like FRQI and NEQR, they are only designed for only square images. Square quantum image needs ($[\log_2 \mathrm{N}] + [\log_2 \mathrm{N}] + l$) qubits. As we see here *l* is the additional qubits representing pixel's amplitude or intensity value, which leads to the increase in storage and reduces the efficiency of representation. For overcoming the above drawbacks Madhur Srivastava *et al. [*16] proposed the 2.D QSNA model, in which square as well as

rectangular images are processed which represent amplitude/intensity without using additional qubits. The formulation of 2-D QSNA representation is shown:

$$Y = \sum_{p=1}^{M} \sum_{q=1}^{N} \propto p,q \; Lp,q \tag{28}$$

Where Y represent the 2-D quantum image,

$$\propto p,q = \sqrt{\frac{A_{p,q}}{\sum_{p=1}^{M} \sum_{q=1}^{N} A_{p,q}}} \tag{29}$$

$$Lp,q = |I\rangle p \otimes \langle J|q \tag{30}$$

By substituting the values of $\propto_{p,q}$ *and* $L_{p,q}$ in equation no. We get,

$$Y = \frac{1}{\sqrt{A_T^{M\,X\,N}}} \sum_{p=1}^{M} \sum_{q=1}^{N} \sqrt{A_{p,q}} \, (|I\rangle \, p \otimes \langle J|_q) \tag{31}$$

L. Quantum representation of Multi Wavelength Images (QRMW)

In Today's scenario, at different wavelength image processing is very important with respect to the hyperspectral imaging, satellite based/airborne remote sending and detection of military target. So according to the application and importance of image processing at different wavelength, we need a model which represent quantum image at different wavelength. QRMW [17] model uses basic states of qubit sequence to store the values at different wavelength of each pixel of the image. This model uses three separate qubit register sequences to hold each pixel's position, wavelength, and color values. The first qubit sequence contains the color value for the pixel wavelength channel in the image, the second qubit sequence encodes the information for the wavelength channel and the last third qubit encodes position information.

The formulation of QRMW representation is shown:

$$|I\rangle = \frac{1}{\sqrt{2^{b+n+m}}} \sum_{\lambda=0}^{2^b-1} \sum_{y=0}^{2^n-1} \sum_{x=0}^{2^m-1} |f(\lambda,y,x)\rangle \otimes |\lambda\rangle \, p \otimes |yx\rangle \tag{32}$$

Where $f(\lambda,y,x) = C_{\lambda_{yx}}^{0} C_{\lambda_{yx}}^{1} \ldots C_{\lambda_{yx}}^{q-2} C_{\lambda_{yx}}^{q-1}$, $C_{\lambda_{yx}}^{0} \in [0,1]$, $f(\lambda,y,x) \in [0, 2^q - 1]$, λ is a channel information and yx is a position information.

QRMW model uses lesser qubits than the QMCR model for all channels.

M. Infra -Red Color Model

Infra-red color model reveals the lucid representation of a quantum infra-red image with respective pixel positions. We use 2x2 dimensional quantum images represented by infra-red model of quantum image. It is given as:

$$|I\rangle = \{|\psi_{ij}\rangle\} \tag{33}$$

Where (I,j) is the pixel position in the image and

$$|\psi_{ij}\rangle = \cos\theta \, ij \, |0\rangle + \sin\theta j|1\rangle \tag{34}$$

Getting quantum image in (2x2) dimensions, we get

$$|I\rangle = \{|\psi_{11}\rangle, \{|\psi_{12}\rangle, \{|\psi_{21}\rangle, \{|\psi_{22}\rangle \tag{35}$$

With,

$$|\psi_{11}\rangle = \cos\theta \, 11|0\rangle + \sin\theta \, 11|1\rangle \tag{36}$$

$$|\psi_{12}\rangle = \cos\theta \, 12|0\rangle + \sin\theta \, 12|1\rangle \tag{37}$$

$$|\psi_{21}\rangle = \cos\theta \, 21|0\rangle + \sin\theta \, 21|1\rangle \tag{38}$$

$$|\psi_{22}\rangle = \cos\theta \, 22|0\rangle + \sin\theta \, 22|1\rangle \tag{39}$$

($|\psi_{ij}\rangle$) these are the pixels represented in the form of qubits. The simplest case without color is assumed here. It is calculated as:

$$P(0) = |\psi_{11}\rangle \otimes |\psi_{12}\rangle \otimes |\psi_{21}\rangle \otimes |\psi_{22}\rangle \tag{40}$$

Simplifying,

$$P(0) = \begin{bmatrix} \cos\theta 11 \\ \sin\theta 11 \end{bmatrix} 2x2 \otimes \begin{bmatrix} \cos\theta 12 \\ \sin\theta 12 \end{bmatrix} 2x2 \otimes \begin{bmatrix} \cos\theta 21 \\ \sin\theta 21 \end{bmatrix} 2x2 \otimes \begin{bmatrix} \cos\theta 22 \\ \sin\theta 22 \end{bmatrix} 2x2 \tag{41}$$

P (0) is the whole initial state of quantum image. Assuming that each pixel faces the de-coherence in the quantum image, we use the following de-coherence channels:

a. Bit Flip Channel
b. Phase Flip
c. Bit Phase Flip

The Kraus operator of Bit Flip channel is given as

$$bo = \begin{bmatrix} \sqrt{p} & 0 \\ 0 & \sqrt{p} \end{bmatrix} \tag{42}$$

and

$$b1 = \begin{bmatrix} \sqrt{p} & 0 \\ 0 & \sqrt{p} \end{bmatrix} \tag{43}$$

Since there are 4 qubits in $[2\,X\,2]$ quantum image, we have to write the Kraus operator for 4 qubits. Let's consider that all qubits are subjected to independent environment. Let's i start with two qubits. On applying the de-coherence channel in the 1st pixel the result will be:

$$P^1(t) = (E_0 \otimes I)\, P(0)\, (E^t_0 \otimes I) + (E_1 \otimes I)\, P(0)\, ((E^t_1 \otimes I) \tag{44}$$

Now with the result obtained above, we evolve the second pixel. So we take p^1 (t) and evolve under the de-coherence noise under the 2nd

$$P(t) = (I \otimes E_0)\, P^1(t)\, (I \otimes E^t_0) + (I \otimes E_1)\, P^1(t)\, (I \otimes E^t_1) \tag{45}$$

$$= (I \otimes E_0)\, [(E_0 \otimes I)\, P(0)\, ((E^t_0 \otimes I) + (E_1 \otimes I)\, P(0)\, ((E^t_1 \otimes I)] \, (I \otimes E^t_0) + (I \otimes E_1)\, [(E_0 \otimes I)\, P(0)\, ((E^t_0 \otimes I) + (E_1 \otimes I)\, P(0)\, ((E^t_1 \otimes I)] \, (I \otimes E^t_1) \tag{46}$$

$$= (I \otimes E_0)\, (E_0 \otimes I)\, P(0)\, ((E^t_0 \otimes I)\, (I \otimes E^t_0) + (I \otimes E_0)\, (E_1 \otimes I)\, P(0)\, ((E^t_1 \otimes I)\, (I \otimes E^t_0) + (I \otimes E_1)\, (E_0 \otimes I)\, P(0)\, ((E^t_0 \otimes I)\, (I \otimes E^t_1) + (I \otimes E_1)\, (E_1 \otimes I)\, P(0)\, ((E^t_1 \otimes I)\, (I \otimes E^t_1) \tag{47}$$

$$= (E_0 \otimes E_0)\, P(0)\, (E^t_0 \otimes E^t_0) + (E_1 \otimes E_0)\, P(0)\, (E^t_1 \otimes E^t_0) + (E_0 \otimes E_1)\, P(0) (E^t_0 \otimes E^t_1) + (E_1 \otimes E_1)\, P(0)\, (E^t_1 \otimes E^t_1) \tag{48}$$

So we get

$$M_1 = (E_0 \otimes E_0) \quad (49)$$

$$M_2 = (E_0 \otimes E_1) \quad (50)$$

$$M_3 = (E_1 \otimes E_0) \quad (51)$$

$$M_4 = (E_1 \otimes E_1) \quad (52)$$

So the two pixels quantum image can be written after passing the quantum image, the Decoherence is as below:

$$P(t) = \sum_{i=1}^{4} Mi\, P(0)\, M_i^t \quad (53)$$

Here it is noted that, for 2 qubits, 2^2=4 kraus operator is needed, so for 4 qubits quantum image, the number of Kraus operator needed will be $2^4 = 16$.

Table: 1 Comparison of Different Image Representation Model

Image	Representation	Qubits Required	Complexity	Color Encoding	Comments
FRQI [3]	$\|I\rangle = \frac{1}{2^n}\sum_{y=0}^{2^{n-1}} \|Q_f\rangle\|i\rangle$	*2m+1*	*O(2^{4n})*	1 angle vector, gray scale	FRQI encodes an image color using one qubit.
MCQI [5]	$\|QI\rangle = \frac{1}{2^{n+1}}\sum_{f=0}^{2^{2n-1}} \|A_{RGB\alpha}^{f}\rangle \otimes \|f\rangle$	*2m+3*	*O(2^{4n})*	3 angle vector, RGB	MCQI uses three qubits to carry color information from multichannel.
NEQR [6,7]	$\|I\rangle = \frac{1}{2^n}\sum_{y=0}^{2^{n-1}}\sum_{x=0}^{2^{n-1}} \otimes_{i-0}^{q-1} \|c_{yx}^{i}\rangle \quad \|y,x\rangle$	*q +2n*	*O(qn.2^{2n})*	Qubit sequence, gray scale	NEQR requires a q +2n qubits for the construction of the quantum image
CQIR [8,9]	$\|I\rangle = \frac{1}{2^n}\sum_{i=0}^{2^{2n-1}}\sum_{j=0}^{2^{2n-1}} \propto_{ij} \|j\rangle \|i\rangle$	*2n, m=log_2L*	*O(log_2L.n. 2^{2n})*	Qubit sequence, gray scale	CQIR image representation is used for better preparing operation for example computing negative, binarization and histograms
QMCR [10]	$I\rangle = \frac{1}{2^n}\sum_{y=0}^{2^{n-1}}\sum_{x=0}^{2^{n-1}} \|C_{RGByx}\rangle \otimes \|y\,x\rangle$	*4q +2n*	*O* (qn x $2^{(2+2n)}$)	RGB	QMCR uses NEQR model to represent RGB-three channel representation
QUALP [11,12]	$I\rangle = \frac{1}{\sqrt{2^{m+n}}}\sum_{\rho=0}^{2^m-1}\sum_{\theta=0}^{2^n-1}$ ($\|g(\rho,\theta)\rangle \otimes \|\rho\rangle \otimes \|\theta\rangle$)	*Gray range 2^q*	*O(q(m+n). 2^{m+n})*	Qubit sequence, gray scale	For the log polar images, QUALPI uses three entangled qubit.
SQR [13]	$\|I\rangle$=Cos $\theta_{ij}\|0\rangle$ + Sin $\theta_{ij}\|1\rangle$	two n-qubit	O(2^{2n})	1 angle vector, infrared	SQR uses to represent the infrared quantum images
NAQSS [14]	$\|I\rangle = \sum_{i=0}^{2^n-1} \theta_i \|v_1\rangle\|v_2\rangle \ldots \|v_k\rangle \otimes \|x_i\rangle$,	(n+1)-qubit	O($\log 2^n.2^{2n}$)	1 angle vector/ gray scale	This model also known as (n+1)-qubit normal arbitrary quantum superposition state. use to store color, coordinate of 2^n pixels and one qubit for picture segmentation information
QSMC & QSNC [15]	$\|I\rangle = \frac{1}{2^n}\sum_{i=0}^{2^{2n}-1} \|QSMC_i\rangle \otimes \|QSNC_i\rangle$	2N + m qubits	O(2^{4n})	I angle vector, gray scale/RGB	QSMC & QSNC both require two set of quantum states in order to capture the image
2-D QSNA [16]	$Y = \frac{1}{\sqrt{A_I^{M\,X\,N}}}\sum_{p=1}^{M}\sum_{q=1}^{N}\sqrt{A_{p,q}}\,(\|I\rangle_p \otimes \langle J\|_q)$	m+n	Pure state	Gray scale/ different color channels	only requires ([Log_2 N] + [Log_2 N]) qubits
QRMW [17]	$\|I\rangle = \frac{1}{\sqrt{2^{b+n+m}}}$ $\sum_{\lambda=0}^{2^b-1}\sum_{y=0}^{2^n-1}\sum_{x=0}^{2^m-1} \|f(\lambda,y,x)\rangle \otimes \|\lambda\rangle_p \otimes \|yx\rangle$	q + 2 + 2n	O(q x $2^{(2+2n)}$)	4 channels and 2^q color scale	QRMW model uses less qubits as compare to MCQI model

V. Conclusion

FRQI illustration utilizes the fundamental quantum gates e.g NOT, CNOT and Toffoli gates. FRQI encodes an image color using one qubit. The representation of CQIR images is used for preparing, negative computing, binarization and histograms. QMCR uses NEQR model to represent RGB-three channel representation. QMCR and MCQI will have more time complexity. Blending operator in MCQI, α is used to mix an image. MCQI uses three qubits to carry color information from multichannel.

It uses quantum image color information R, G, and B. Its color transformation includes the Col operator which is used to shift the gray-scale value to the color channel preselected. CS operator is also used in MCQI which work as swap operator (swap grayscale values between two channels). Numerous mind boggling relative changes, for example, revolution and scaling can't be performed with Qubit Lattice, Entangled Image, Real ket and FRQI models in light of the fact that a great deal of irreversible insertions are required. Only images sampled in Cartesian coordinates can be stored and processed by existing models. For the log polar images, novel quantum representation model QUALPI

Suggested to overcome the disadvantages of current quantum image models. SQR uses infrared quantum images to represent color information from infrared radiation energy that could improve visual capacity in nearly any environment. It uses both qubit Lattice as well as FRQI methods. NAQSS is used to store color, coordinate of 2^n pixels and one qubit for image segmentation information. QSMC and QSNC are used to store image color and coordinate image information by quantum states. QRMW model uses less qubits as compared to MCQI model. QRMW model, 2^n x2^m rectangular images and 2^n x$2^{n \text{ square}}$ images can be represented in other models. In QRMW U_{cc} operator is used. $U_{cc} = x^{\otimes q} \otimes I^{\otimes b+n+m}$. It applies quantum X gate to each qubit of the qubit sequence in the first register. QRMW uses 4 channels 2^q color scale which is more than the earlier discussed image model.

Most of the quantum representation techniques are highly dependent on FRQI. This field's future is to find a way to represent better - performing images than FRQI. In this investigation we have shown some of quantum image representation which is better than FRQI.

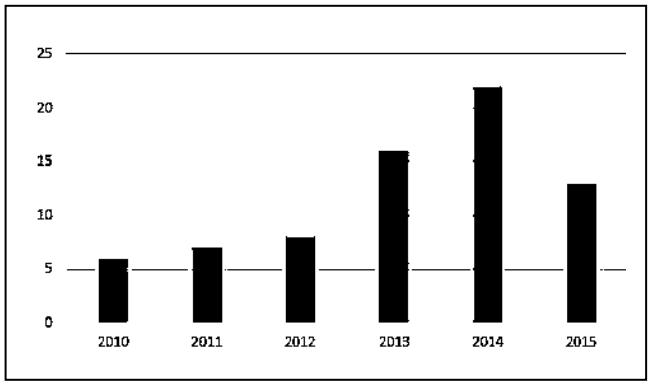

Fig. 3. Bar graph of the number of published works between 2010 and 2015 for Quantum image representation. The number of works has increased, indicating that more attention is being paid to the field of quantum image representation.

It very well may be seen that the consideration around Quantum Image representation has been an expanding pattern, with an especially sharp increment in 2014. In spite of the shortage in 2015 the quantity of concentrates in 2015 has outperformed the number contrasted with years before 2013[18]. Besides, driving diaries have been giving more regard for quantum image representation.

REFERENCES

[1] Kapil K. Sharma. "Milestone developments in quantum information and No-Go theorems", arXiv: 1809.09711

[2] Venegas-Andraca, Salvador E.; Bose, Sougato. "Storing, processing, and retrieving an image using quantum mechanics" ,In: Proceedings of the SPIE Conference of Quantum Information and Computation, Vol. 5105. 134-14(2003)

[3] Le,P.,Dong, F., Hirota, K, "A flexible representation of quantum images for polynomial preparation, image compression, and processing operations", Quantum Inf Process.10(1),63-84 (2011)

[4] Jose I. Latorre. "Image compression and entanglement", arXiv:quant-ph/0510031(2005)

[5] Sun.B.Iliyasu. A., Yan, F., Dong, F., Hirota K. "An RGB multichannel representation for images on quantum computers", J. Adv. Comput. Intell. Intell. Info 17(3), 404-417(2013)

[6] Zhang, Y., Lu, K., Gao, Y.H., Wang, M. "NEQR: a novel enhanced quantum representation of digital images", Quantum Inf. Process. 12(12), 2833-2860 (2013)

[7] Zhang, Yi et al. "NEQR: a novel enhanced quantum representation of digital images", Quantum Information Processing 12 (2013): 2833-2860.

[8] Caraiman, S & Manta, Vasile. "Image processing using quantum computing", 16th International Conference on System Theory, Control and Computing, ICSTCC 2012 - Joint Conference Proceedings. 1-6., (2012)

[9] Caraiman, S & Manta, Vasile "Histogram-based segmentation of quantum images", Theoret. Comput.Sci. 529, 46-20 (2014).

[10] Abdolmalekya M, Naserib M, Batlec J, Faroukd A, Gong L. "Red-green-blue multichannel quantum representation of digital images", Int J for light and Elect Opt 2017; 128:121-132.

[11] Zhang, Y., Lu, K., Gao, Y.H., Xu, K. "A novel quantum representation for log-polar images", Quantum Inf. Process. 12(9), 3103-3126 (2013)

[12] Yi Zhang, Kai Lu, Yinghui Gao, Kai Xu. "A novel quantum representation for log-polar images", Quantum information processing (2013)

[13] Yuan, S., Mao, X., Xue, Y. et al. "Quantum Inf Process", (2014) 13: 1353

[14] Li, H.S., Zhu, Q.X., Zhou, R.G., Lan, S., Yang, X.J. "Multidimensional color image storage and retrieval for a normal arbitrary quantum superposition state", Quantum Inf.Process, 13(4), 991-1011 (2014)

[15] Li, H.S., Zhu, Q.X., Lan, S., Shen, C.Y., Zhou, R.G., Mo, J. "Image storage, retrieval, compression and segmentation in a quantum system", Quantum Inf. Process, 12(6), 2269-2290 (2013)

[16] Madhur Srivastava, Subhayan R. Moulick, Prasanta K. Panigrahi "Quantum Image Representation Through Two-Dimensional Quantum States and Normalized Amplitude", arXiv:1305.2251

[17] Engin Şahin, İhsan Yilmaz. "QRMW:Quantum representation of multi wavelength images", arXiv:1801.10349

[18] Fei Yan , Kehan Chen , Salvador E. Venegas-Andraca , Jianping Zhao, Quantum image rotation by an arbitrary angle, Quantum Information Processing, v.16 n.11, p.1-20, November 2017

[19] Michael A. Nielsen and Isaac L. Chuang. 2000. Quantum Computation and Quantum Information. Cambridge University Press.

[20] Mario Mastriani. 2016. Quantum image processing? arXiv:1512.02942.

Proceedings of the Fourth International Conference on Communication and Electronics Systems (ICCES 2019)
IEEE Conference Record # 45898; IEEE Xplore ISBN: 978-1-7281-1261-9

Translating Artificial Intelligence into Healthcare: Diabetic Retinopathy Detection

Reaya Grewal*, Avleen Malhi*, Palika Chopra*
*Computer Science & Engineering Department, Thapar Institute of Engineering and Technology, India
Email: reaya.grewal@gmail.com, avleen@thapar.edu,palika.chopra@thapar.edu

***Abstract*—Diabetes is a lifelong disease that has the capability to badly hinder the health and damages the retina causing Diabetic Retinopathy. Diabetic retinopathy is majorly identified by exudates.In this paper the coloured fundus images from datasets DIARETDB, MESSIDOR and E-OPTHA are considered.Initially image pre-processing is done for better detection of exudates (bright lesions)in the retina.Gray Level Co-occurrence Matrix (GLCM) is used for extracting the features. Finally, the classification for normal and abnormal retinal images is done by using various machine learning models like decision tree, logistic regression, SVM, kNN, ensemble classifier and analyzing their performances.Ensemble classifier (subspace discriminant), SVM and kNN give better accuracy than the other learners.This automated process will save the manual work and time of the ophthalmologists.Early detection of the exudates in the eyes is crucial for preventing the vision loss in diabetic patients.**

Keywords: **Diabetic retinopathy, exudates, GLCM, Classification**

I. Introduction

Diabetes is a chronic, lifelong condition that affects one's body ability to capitalize the energy found in food. This happens when either the pancreas can't produce enough insulin or the cells in the body become resistant to insulin. Diabetes can cause long term systematic complications that affect heart, nerves, blood vessels, kidneys and eyes.A patient might suffer from serious health problems if diabetes is not treated on time.The people who have suffered diabetes for a long time are affected by Diabetic Retinopathy. It is a micro vascular complication that damages blood vessels supplying the retina.It results in vision loss if care is not taken on medication and treatment. Diabetic Retinopathy is indicated by various features like micro aneurysms, haemorrhages, hard exudates and soft exudates or cotton-wool spots as shown in figure 1.Initially micro aneurysms which are small, dark red spots are the primary abnormality found in the eye and it further results in haemorrhages, that appear alone or in clusters in the compact middle layers of the retina .Micro aneurysms have circular shape and their sizes vary from 10-100 microns.Retinal nerve fibre layer is the location of flame shaped haemorrhages.The most important symptoms of diabetic retinopathy are hard exudates, that have varying sizes and are bright yellow colored lesions.Cotton wool spots which are light yellowish white lesions and also called soft exudates are found in severe stages of diabetic retinopathy.Cotton wool spots are created when the retinal pre-capillary arterioles that supply blood to the nerve fiber layer get blocked and the local nerve fiber axons get swollen.Detection of diabetic retinopathy is very tedious and tough in the initial stages.The earliest visible signs of diabetic retinopathy are exudates. So our focus is early diagnosis of diabetic retinopathy by discovering exudates and protection of the diabetic patients from loss of vision.Drusens are yellow deposits under the retina and made up of lipids (fatty protein) called Bruch's membrane. They shows a sign of dry age-related macular degeneration and can be often confused with exudates.

II. Literature Review

The developing predominance of diabetes overall expands the quantity of cases that should be surveyed by doctors. Furthermore, the cost involving the regular check ups and examination are very high and absence of expert specialists keep many people away from accepting a sufficient and effective medication. It will give the chance to analyze huge datasets of retinal images. Average examination expenses can be lessened as a result of decreasing the workload of prepared classifiers. Clara I. Sánchez et al.[11] focused on the fact that the early symptoms of diabetic retinopathy are hard exudates and used edge detection to differentiate the hard exudates from the other bright lesions. The method was implemented on the dataset of 80 images.Harry Pratta et al. [7] recently approached the problem of detecting the diabetic retinopathy by applying deep learning over a relatively very large dataset of the retinal images. They worked on detection of exudates and drusens with help of colour normalisation and applied CNN attaining accuracy of 75% . Morium Akter et al .[1] performed morphology based exudates detection from colored fundus images.Only morphological operations are used and no machine learning algorithms were used. Enrique V. Carrera et al [2] discovered diabetic retinopathy with the help of SVM and just performed image processing and no features extraction . Vaishali Suryawanshi et al.[4] performed only grayscale preprocessing and only neural network model for classification. Jayant Yadav et al.[5] also worked on fundus images using feed forward neural network. Handayani Tjandrasa et al.[6] did image preprocessing,features extractiona and just used a single model which is SVM for classification of hard exudates.Daniel Welfera et al.[12] worked on detection of exudates using morphological operations only and no machine learning algos were used.Huan Wang et al.[13] worked on detection of exudates using statistical classification and managed to attain accuracy of 70%.Sidra Rashid et al. [14] did detection of exudates by using CLAHE and then applying edge detection algorithm and fuzzy C-means clustering.Dynamic threshold and median filter techniques are used for detecting the hard exudates in [15].

Fig. 1: The images with varying colour and illumination in MESSIDOR dataset (a) Image with red as dominant color, (b) Image having red lesions, (c) A unaffected retinal image, (d) Image of retina with exudates and drusen.

III. Proposed Methodology

An automated method has been put forward for the identification of the bright yellow lesions i.e exudates in

TABLE I: Comparative analysis of the state-of-the-art techniques

Authors	Description	Basic Method
Morium Akter et al [1]	Morphology based exudates detection from colored fundus images	Use of basic morphological operations
Enrique V. Carrera et al [2]	Diabetic retinopathy detection using SVM	Preprocessing of images and use of only SVM
Shuana Yu et al.[3]	Exudate Detection for diabetic retinopathy with CNN	Preprocessing,CNN
Vaishali Suryawanshi et al.[4]	Detection of exudates with help of Neural networks with GLCM features	GrayScale preprocessing ,Neural Network
Jayant Yadav et al.[5]	DiabeticRetinopathy detection using feed forward NN	Features Extraction,Neural Networks
Handayani Tjandrasa et al.[6]	Classification of Diabetic Retinopathy by identifying Hard Exudates	Preprocessing, Feature Extraction ,SVM
Harry Pratta et al.[7]	Detection of exudates and drusens with help of colour normalisation and applied CNN	Image preprocessing,CNN
KH Englmeier et al. [8]	Blood vessels,optic disc and exudates detection	Image processing and features extraction
Osareh et al.[9]	Detection of exudates using simple machine learning alorithms	SVM and neural network application
Rishab Gargeya et al.[10]	Deep Learning for automated identification of Diabetic Retinopathy	Image preprocessing,Deep Learning

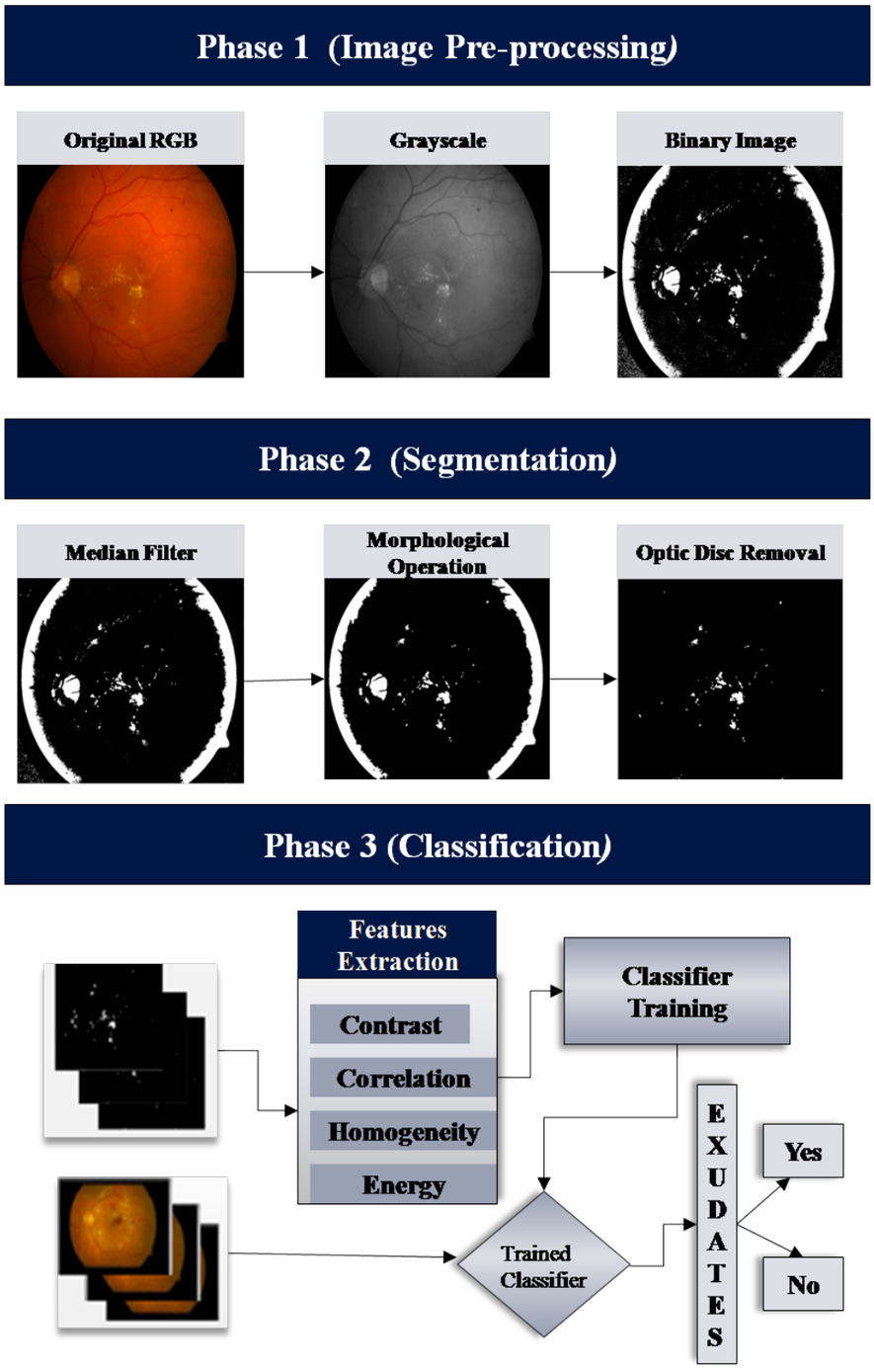

Fig. 2: Proposed methodology for diabetic retinopathy detection

retina which is the major cause of diabetic retinopathy. The figure 2 depicts the methodology used for diabetic retinopathy detection.

A. Image Pre-Processing

Digital image processing is needed for upgrading the visual appearance of an image by extracting important features such as edges , to give more sharpness etc. minor errors can be rectified, image sizes can be increased or decreased , unrecognisable features can be made prominent

etc. thus helping us all to have better vision and adding meaningfulness to the images.The various sub steps used in image processing are :

1) RGB to Grayscale Conversion: The process of converting the RGB image to a grey scale image helps to make the image more uniform as shown in figure 3. The grey scale image uses all the three values of red, green and blue by taking into account only a factor of these three channel values as follows: I = 0.299*R + 0.587*G + 0.114*B; Where I is the resulting grey scale image, R is the pixel colour value of red channel, G is the pixel colour value of green channel and B is the pixel colour value of blue channel.

The major reason to convert the images to grey scale is to reduce the complexities that occur due to colour.

2) Thresholding: Thresholding is an elementary methodology of image segmentation.Thresholding can be used to create binary images with grayscale images as the input. Thresholding segments an image by changing values of all pixels whose intensity values are above a threshold to a foreground value and all the remaining pixels to a background value.A global threshold is used in the conventional thresholding method for all pixels with threshold value T as shown in figure 4a.The gray level values below T are background and those above T are foreground objects.We have used a more sophisticated version of thresholding which is called as adaptive thresholding that varies the threshold dynamically over the image.It assists in the changing lighting conditions in the image, e.g. those occurring due to strong illumination gradient or shadows as shown in figure 4b

3) Median Filtering: It is a highly used nonlinear method for removing noises from images and is very successful at removing noise while maintaining the edges. It is particularly used for removing 'salt and pepper' type noise as displayed in figure 5b .For calculating the median ,all the pixel values are sorted in numerical order from the window and then the pixel being considered is replaced with the middle (median) pixel value as shown in figure 5a .

4) Morphological Operation: These operations depend on the elative ordering of pixel values and are associated with the shape or morphology of features present in an image.An opening operation is composed of an erosion operation which is followed by a dilation operation with the help of the same structuring element that is a disc of radius 3 in our case. The erosion of a binary image f by a structuring element s gives a new binary image g with ones in all locations (x,y) of a structuring element's origin at which that structuring element s fits the input image f, i.e. g(x,y) = 1 is s fits f and 0 otherwise, repeating for all pixel coordinates (x,y) as shown in figure 6a. The dilation of a binary image f by a structuring element s produces a new binary image g with ones in all locations (x,y) of a structuring element's origin at which that structuring element s hits the the input image f, i.e. g(x,y) = 1 if s hits f and 0 otherwise, repeating for all pixel coordinates (x,y) as shown in figure 6b.In erosion the outer boundary of pixels are stripped off whereas in dilation boundary of image is increased .It helps in further removing noise from the image as shown in figure 7.

5) Optic Disc Removal: Optic Disc is extracted using another morphological operation on the binary images using bwareafilt in MATLAB which extracts particular objects from the images . The Optic disc was extracted and subtracted from the images and hence making them free from optic disc which has similar texture to that of exudates.bwareafilt also helps in removal of the boundary of the fundus images of retina as shown in figure 8

B. Features Extraction

Feature Extraction is vital as huge amount of details and information lessens the effectiveness and meaning of data. There can be few data attributes which are collected together for creating and testing a model may not provide meaningful information to the model. Some may actually deviate from the quality and accuracy of the model.In our proposed methodology gray-level co-occurrence matrix (GLCM) is used which is a statistical technique to inspect the texture which takes into consideration the spatial relationship of pixels.The texture of an image is characterized by calculating how often pairs of pixel with specific values and in a specified spatial relationship occur in an image, thus forming a GLCM matrix and then extraction of statistical measures from this matrix are considered which are shown in the table 2.

GLCM is basically second order statistics therefore GLCM collected information regarding pixel of pairs. For creating GLCM, graycomatrix function is used.

C. Classification using machine learning models

The final phase is about application of The Machine Learning Models on the features extracted using GLCM and perform comparative analysis of them .Various models like Decision Trees ,Discriminant Analysis ,Logistic Regression ,Support Vector Machines , Nearest Neighbour and Ensemble Classifiers are trained and tested on the dataset provided with the binary target class as whether exudates are present i.e. class 1 or they are absent i.e class 0.The Models' Accuracy , Confusion matrices and ROC curves are also analyzed.The Ensemble Classifier of subspace discriminant improves the accuracy of discriminant analysis which assumes that different classes generate data based on different Gaussian distributions .Subspace ensemble is better as it makes use of lesser memory as compared to other ensembles with all predictors, and can handle and manage missing values (NaNs).

The basic random subspace algorithm makes use of the following parameters.

1) m, where m is the number of variables or dimensions which have to be sampled in each learner.
2) d, where d is the number of dimensions possessed by the data, that is the number of predictors or columns in the data matrix.
3) n, where n denotes the number of models or learners are present in the ensemble.

The basic random subspace algorithm performs the following steps:

1) A random set of m predictors has to be chosen from the d possible values without replacement.
2) With the help of the m chosen predictors, weak learners are trained.
3) Steps 1 and 2 are repeated until there are n weak learners.
4) Predict by averaging the score prediction of the weak learners, and classify the category with the highest average score.

IV. Results and Discussions

A. Dataset Description

The dataset used for detection of exudates is a combination of three datasets namely MESSIDOR,DIARETDB1 and E-OPTHA .

1) MESSIDOR : This dataset consists of 1200 colored fundus eye images of the rear view of retina which has been acquired by 3 ophthalmologic departments with the assistance of a colored video 3CCD camera on a Topcon TRC NW6 non-mydriatic retinograph with a 45 degree field of view.800 fundus images are obtained by diluting the pupil using a drop of Tropicamide at 0.5% and 400 fundus images are obtained without dilation.
2) DIARETDB1 : This dataset is a collection of 89 colored fundus images.The experts who took part in evaluation of the images confirmed that 84 fundus images display signs of diabetic retinopathy, and 5 images are normal that is they don't show any of the characteristics of diabetic retinopathy. A 50 degree field-of-view digital fundus camera is used for capturing the images which, also has

(a) Original Colored Fundus Image (b) Grayscale Fundus Image

Fig. 3: Conversion of original colored image into grayscale fundus image

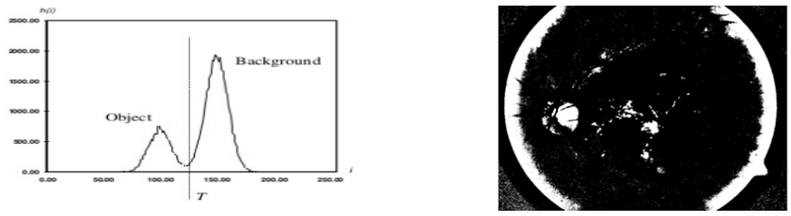

(a) Segmentation on basis of threshold T (b) Binary Image

Fig. 4: Conversion into binary fundus image after thresholding

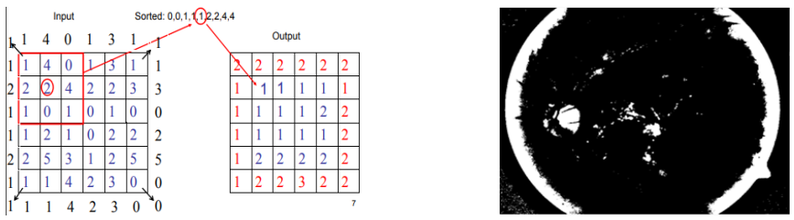

(a) Median Filter method example (b) Filtered fundus image

Fig. 5: Median Filtering to remove ”salt and pepper” noise

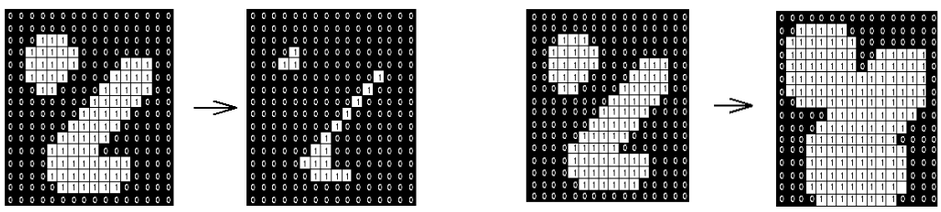

(a) Effect of erosion using a 3*3 square structuring element (b) Effect of dilation using a 3*3 square structuring element

Fig. 6: Morphological Operations Erosion and Dilation

TABLE II: Statistics Of Textural Features Extraction using GLCM

Statistics	Details
Contrast	The local variations in the gray-level co-occurrence matrix are measured
Correlation	The joint probability occurrence of the specified pixel pairs is calculated
Energy	The sum of squared elements in the GLCM is provided.also called as uniformity
Homogeneity	The closeness of the distribution of elements in the GLCM to the GLCM diagonal is measured.

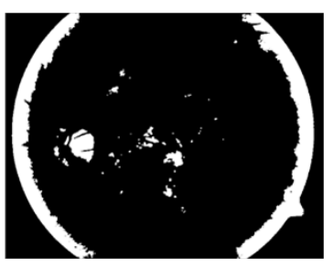

Fig. 7: Fundus image after opening operation to remove objects causing noise.

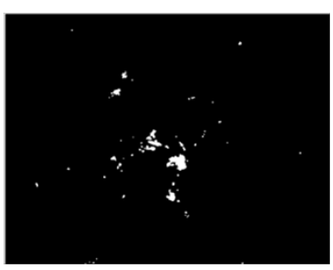

Fig. 8: Removal of optic disc

an advanced imaging settings. This data set is also known as ”calibration level 1 fundus images”.

3) E-OPTHA : This dataset of colored fundus images having 47 images with exudates and 35 images with no signs of exudates or any other lesions is drafted for scientific researches in the field of Diabetic Retinopathy (DR).OPHDIAT© Telemedical network has been used for the generation of the images for screening of DR in a project which has been funded by the French Research Agency (ANR).

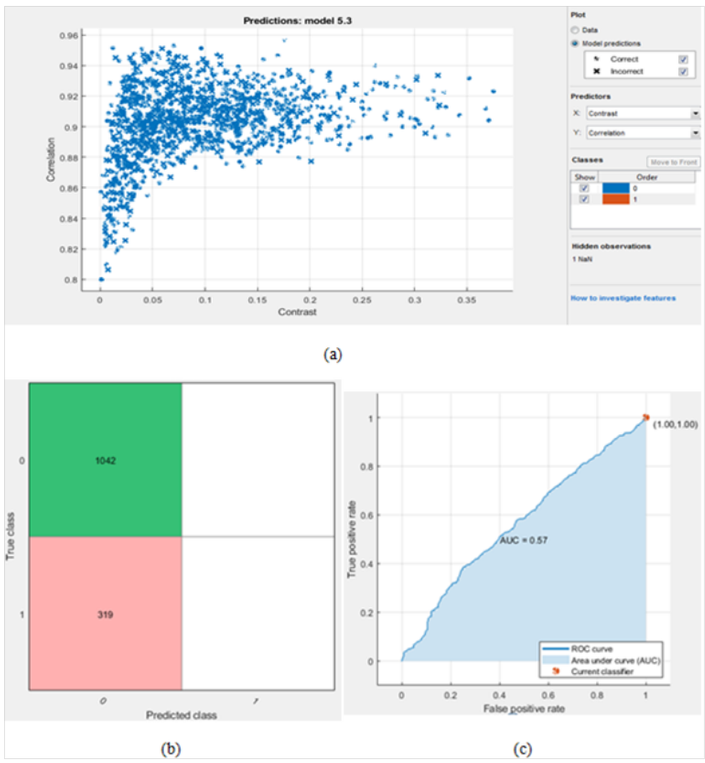

Fig. 9: Scatter plot,Confusion matrix and ROC-AUC curve of Ensemble(Subspace Discriminant) model

TABLE III: Comparison of performance of various models

Model	Accuracy	Sensitivity	Specificity
Proposed ensemble of discriminant analysis	0.760	0.76	0.77
Decision Tree (Fine)	0.700	0.77	0.72
Decision Tree(Medium)	0.750	0.77	0.70
Decision Tree(Coarse)	0.755	0.76	0.66
Logistic Regression	0.765	0.77	1.00
SVM(Linear)	0.746	0.76	0.80
SVM(Quadratic)	0.746	0.76	0.70
SVM(Cubic)	0.633	0.76	0.79
KNN(Fine)	0.659	0.77	0.72
KNN(Medium)	0.757	0.76	0.71
KNN(Coarse)	0.766	0.75	0.70
Ensemble(Bagged Trees)	0.725	0.66	0.78
Ensemble(Sub-space KNN)	0.711	0.78	0.75
Ensemble(RUSBoosted Trees)	0.514	0.77	0.71

B. *Performance Analysis*

The images have a large variation in colour and illumination with in and between the images. Every image can be classified as exudates or not exudates. Hence, the four outcomes of the analysis are two classifications and two misclassifications. The quality measures used in binary classification are sensitivity(SN), specificity(SP) and accuracy(Acc) and these metrics.

The efficiency and authenticity is evaluated by using the formulas and defining necessary terms as follows.

$$Accuracy = \frac{(Correctlyidentifiedimages)}{(TotalNumberOfImages)}\% \qquad (1)$$

or

$$Accuracy = \frac{(T_N + T_P)}{(T_N + F_P + F_N + T_P)}\% \qquad (2)$$

An approach that combines the image processing tools with the machine learning for the discovering diabetic retinopathy by examining the coloured retinal images is followed. It was observed that the detection of the regions that contains the bright lesions(exudates) was achieved effectively by use of normalizing various factors such as conversion of the RGB retinal image into grayscale and binarising them. Morphological operators were used to clarify the candidate regions and remove all unwanted elements. The classification is done with training and testing ratio as 70:30 and also cross validation method of K-Folds is applied with number of folds set as 5 so as to avoid the overfitting problem by dividing the data sets into folds and estimating the accuracy on each fold. Also sensitivity and specificity are measured for various models.Sensitivity, also known as true positive rate, is the ability to correctly measure the proportion of actual positives which have been identified correctly and specificity, also named as true negative rate is the ability to correctly measure the proportion of actual negatives which have been identified correctly.The useful textural features shown in figure **??** are extracted by the GLCM feature extraction technique and further this detailed information is provided to the machine learning models which proved that subspace discriminant ensemble achieved a better accuracy of 76.6% as compared to other models.The overall methodology was effective and robust. The accuracy,sensitivity and specificity of different models are shown in table III and scatterplot, confusion matrix and ROC-AUC curve of ensemble model using subspace discriminant are displayed in figure 9.

V. Conclusion

The prposed approach combines the image processing tools with the machine learning for the recognizing the diabetic retinopathy via exudates in the coloured retinal images. It is achieved effectively by use of normalizing various factors such as conversion of the RGB retinal image into grayscale and binarising them. Morphological operators were used to remove all unwanted elements.The GLCM feature extraction technique is used and the classification of the images proved that ensemble (subspace discriminant), SVM, KNN achieved a better accuracy of 76.6% than the other models. Finally an efficacious automated system for the early detection of diabetic retinopathy based on the identification of exudates can be made based on the methodology carried out.

REFERENCES

[1] M. Akter, M. S. Uddin, and M. H. Khan, "Morphology-based exudates detection from color fundus images in diabetic retinopathy," in *Electrical Engineering and Information & Communication Technology (ICEEICT), 2014 International Conference on*, pp. 1–4, IEEE, 2014.

[2] E. V. Carrera, A. González, and R. Carrera, "Automated detection of diabetic retinopathy using svm," in *Electronics, Electrical Engineering and Computing (INTERCON), 2017 IEEE XXIV International Conference on*, pp. 1–4, IEEE, 2017.

[3] S. Yu, D. Xiao, and Y. Kanagasingam, "Exudate detection for diabetic retinopathy with convolutional neural networks," in *Engineering in Medicine and Biology Society (EMBC), 2017 39th Annual International Conference of the IEEE*, pp. 1744–1747, IEEE, 2017.

[4] V. Suryawanshi and S. Setpal, "Guassian transformed glcm features for classifying diabetic retinopathy," in *2017 International Conference on Energy, Communication, Data Analytics and Soft Computing (ICECDS)*, pp. 1108–1111, IEEE, 2017.

[5] V. Saravanan, B. Venkatalakshmi, and V. Rajendran, "Automated red lesion detection in diabetic retinopathy," in *Information & Communication Technologies (ICT), 2013 IEEE Conference on*, pp. 236–239, IEEE, 2013.

[6] A. Roy, D. Dutta, P. Bhattacharya, and S. Choudhury, "Filter and fuzzy c means based feature extraction and classification of diabetic retinopathy using support vector machines," in *Communication and Signal Processing (ICCSP), 2017 International Conference on*, pp. 1844–1848, IEEE, 2017.

[7] H. Pratt, F. Coenen, D. M. Broadbent, S. P. Harding, and Y. Zheng, "Convolutional neural networks for diabetic retinopathy," *Procedia Computer Science*, vol. 90, pp. 200–205, 2016.

[8] K. Englmeier, K. Schmid, C. Hildebrand, S. Bichler, M. Porta, M. Maurino, and T. Bek, "Early detection of diabetes retinopathy by new algorithms for automatic recognition of vascular changes," *European journal of medical research*, vol. 9, no. 10, pp. 473–478, 2004.

[9] A. Osareh, M. Mirmehdi, B. Thomas, and R. Markham, "Comparative exudate classification using support vector machines and neural networks," in *International Conference on Medical Image Computing and Computer-Assisted Intervention*, pp. 413–420, Springer, 2002.

[10] R. Gargeya and T. Leng, "Automated identification of diabetic retinopathy using deep learning," *Ophthalmology*, vol. 124, no. 7, pp. 962–969, 2017.

[11] C. I. Sánchez, M. García, A. Mayo, M. I. López, and R. Hornero, "Retinal image analysis based on mixture models to detect hard exudates," *Medical Image Analysis*, vol. 13, no. 4, pp. 650–658, 2009.

[12] D. Welfer, J. Scharcanski, and D. R. Marinho, "A coarse-to-fine strategy for automatically detecting exudates in color eye fundus images," *computerized medical imaging and graphics*, vol. 34, no. 3, pp. 228–235, 2010.

[13] H. Wang, W. Hsu, K. G. Goh, and M. L. Lee, "An effective approach to detect lesions in color retinal images," in *Computer Vision and Pattern Recognition, 2000. Proceedings. IEEE Conference on*, vol. 2, pp. 181–186, IEEE, 2000.

[14] S. Rashid *et al.*, "Computerized exudate detection in fundus images using statistical feature based fuzzy c-mean clustering," *International Journal of Computing and digital systems*, vol. 218, no. 1222, pp. 1–11, 2013.

[15] D. Kayal and S. Banerjee, "A new dynamic thresholding based technique for detection of hard exudates in digital retinal fundus image," in *Signal Processing and Integrated Networks (SPIN), 2014 International Conference on*, pp. 141–144, IEEE, 2014.

Proceedings of the Fourth International Conference on Communication and Electronics Systems (ICCES 2019)
IEEE Conference Record # 45898; IEEE Xplore ISBN: 978-1-7281-1261-9

Single Phase AC-DC Cascaded Boost-SEPIC (CBS) Converter for Improved Power Quality at High Duty Cycle

Mohammad Dehan Rahman
Department of Electrical and Electronic Engineering
Islamic University of Technology
Gazipur, Bangladesh
dehanrahman@gmail.com

Md Saif Kabir
Department of Electrical and Electronic Engineering
Islamic University of Technology
Gazipur, Bangladesh
saifkabir@iut-dhaka.edu

Md Nazaf Rabbi
Department of Electrical and Electronic Engineering
Islamic University of Technology
Gazipur, Bangladesh
nazafrabbi@iut-dhaka.edu

Mohammad Abir Hassan Sarker
Department of Electrical and Electronic Engineering
Islamic University of Technology
Gazipur, Bangladesh
abirmctavish@gmail.com

Dr. Golam Sarowar
Department of Electrical and Electronic Engineering
Islamic University of Technology
Gazipur, Bangladesh
sarowarg@gmail.com

Abstract: **Modern day devices often use an AC source as input even though they are operated with DC voltage. In order to have a suitable and flexible DC output, an AC-DC converter is used. However the conventional converters are not suited for high voltage output without sacrificing conversion efficiency. A new topology of Cascaded Boost-SEPIC (CBS) converter is proposed in this paper. This converter is capable of delivering output voltage as high as 1255V at high conversion efficiency. Maximum power factor of 0.97 and minimum THD of 9.94% is ensured by current mode PI controller.**

Keywords—AC-DC converters; High voltage gain; Conversion efficiency; THD; power factor improvement

I. INTRODUCTION

In day to day life electronic devices are used in grid-connected systems, communication systems, power supply systems etc. Devices also operate in variable voltage levels. A converter that facilitates the capability of different level of operating voltage is essential for versatile use. But not all converters are able to make conversion properly without compromising performance. It is almost always the case that a tradeoff has to be made between necessity and performance. High voltage gain will cause for a deterioration of signal shape (high THD). Tradeoff is also visible among performance parameters of the converters. For example, improving power factor tends to decrease the efficiency. [14] These limitations can be addressed introducing cascaded converter topologies. [2 - 7]

The overall efficiency goes down slightly as the duty cycle rises in conventional converter. [1][8] Again increasing duty cycle causes conduction losses and serious reverse-recovery problem in diodes. [9][10] Also Boost converter can operate with lower voltage level of MOSFET. Boost converter also gives output with lower distortion which makes the circuit manage the THD level as low as possible. [11 - 13]

In this paper a new topology is introduced – Cascaded Boost SEPIC (CBS), which is used to avail different voltage level in accordance the duty cycle. Higher voltage conversion can be achieved using cascaded Boost-SEPIC converter. The proposed circuit will provide higher average voltage up to 80% duty cycle. The converter is designed to obtain higher average voltage levels at different duty cycles with appreciable low THD. To further improve the power factor and input current THD, a closed loop implementation is applied using a PI controller.

II. CONVENTIONAL CONVERTERS

A. CONVENTIONAL BOOST CONVERTER

Most commonly used AC-DC converter are boost converters which consisting of a full-wave rectifier and a DC-DC Boost converter following it. The converter is capable of supplying high voltage.

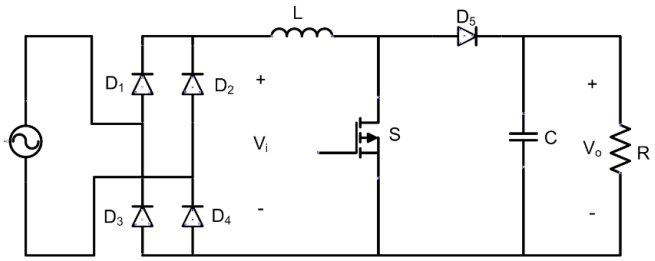

Fig. 1: Conventional Boost converter.

The voltage gain of Boost converter is given as,

$$\frac{V_{o_1}}{V_i} = \frac{1}{1-D}$$

B. CONVENTIONAL SEPIC CONVERTER

A SEPIC converter, followed by a bridge rectifier forms the conventional AC-DC SEPIC converter. DC-DC SEPIC converter is designed as an extension of boost converter by adding a buck-boost converter with it, gives a non-inverting output.

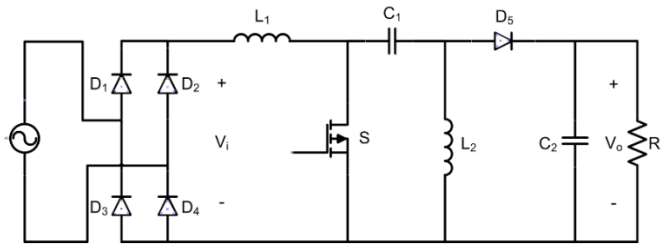

Fig. 2: Conventional SEPIC converter.

The voltage gain of SEPIC converter is mathematically expressed as,

$$\frac{V_{o_2}}{V_i} = \frac{D}{1-D}$$

III. PROPOSED CIRCUIT AND OPERATION

The proposed circuit, CBS converter combines the Boost and SEPIC converter. The proposed CBS converter consists of six diodes (D1-D6), three capacitors (C0-C2), two inductors (L0-L1), a load resistor (RL), and a switch (MOSFET).

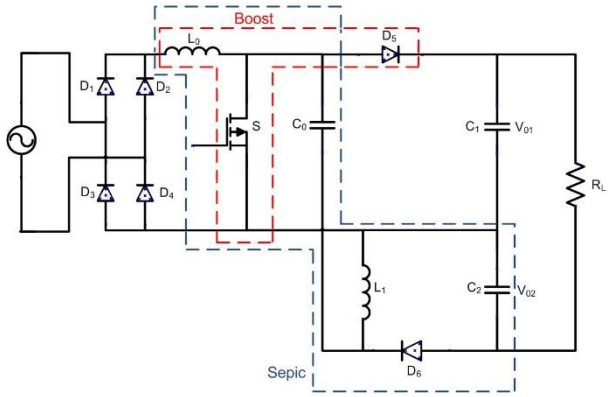

Fig. 3: Proposed CBS converter

Mode 1 of the operation, which is TON of the positive half cycle of line frequency is illustrated in Fig 4(a). Mode 2, TOFF of positive half cycle of line frequency is shown in Fig 4(b). Similarly TON and TOFF of negative half cycle of line frequency is shown in Fig 4(c) and Fig 4(d) respectively.

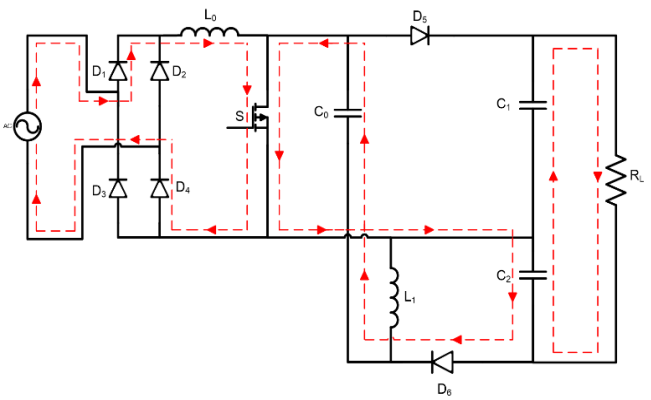

(a)

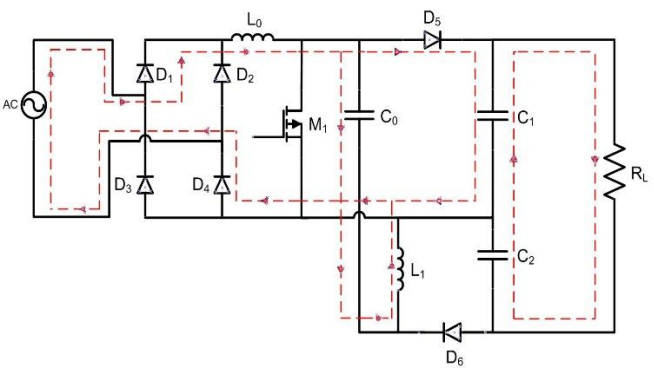

(b)

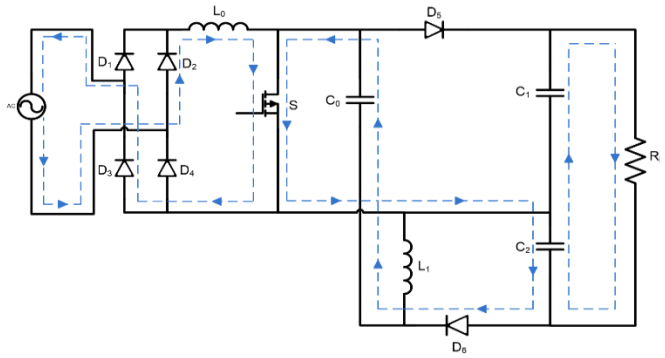

(c)

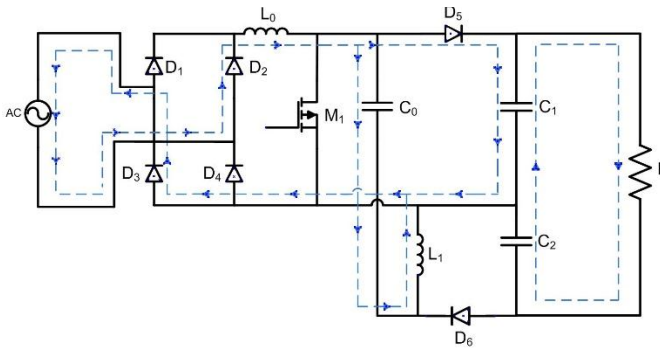

(d)

Fig. 4: Principle of operation of the proposed AC-DC CBS converter (a) Mode 1 (b) Mode 2 (c) Mode 3 (d) Mode 4

Energy is supplied to the load by capacitors C1 and C2. When the switch is off capacitors C0 and C1 are charged by the source, while the load is supplied with energy from capacitor C2. C2 is charged by the capacitor C0 when the switch is on and energy is supplied to the load by C1.

The overall estimated voltage gain of the circuit is given below.

$$V_o = V_{o_1} + V_{o_2}$$

$$V_o = \frac{1}{1-D}V_i + \frac{D}{1-D}V_i$$

$$V_o = (\frac{1}{1-D} + \frac{D}{1-D})V_i$$

$$V_o = \left(\left|\frac{1+D}{1-D}\right|\right)V_i$$

$$V_o = GV_i$$

$$\text{G = Gain} = \left|\frac{1+D}{1-D}\right|$$

IV. CLOSED LOOP TO IMPROVE POWER FACTOR AND THD

In an attempt to improve the input power factor and input current THD, a PI controller is implemented in current mode control. Comparison is made between the actual induction current with the scaled rectified reference current generated from the input voltage. Successive approximation was used to choose the scale factor of the reference current which eventually provided the desired output.

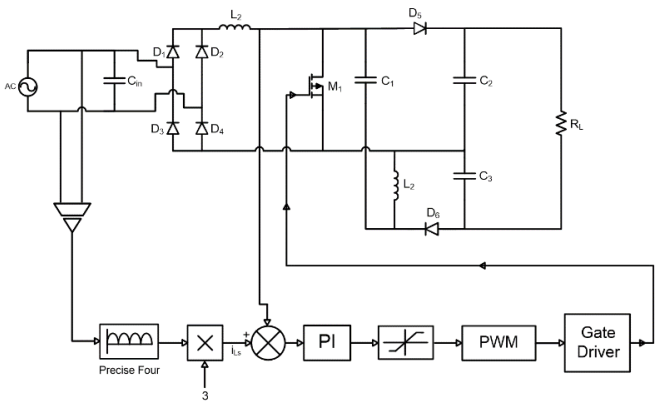

Fig. 5: Close loop implementation of the proposed CBS converter using PI controller

V. SIMULATION RESULTS

For simulation purposes, the following set of data were used in the proposed CBS circuit, as well as the Boost and SEPIC converter.

.TABLE 1 Design parameters

Parameter	Value
Input voltage	325V
Input frequency	50 Hz
Capacitor (C0,C1, C2)	200uF, 500uF, 500uF
Inductor (L0, L1)	5mH, 500mH
Load resistor (RL)	100 ohm

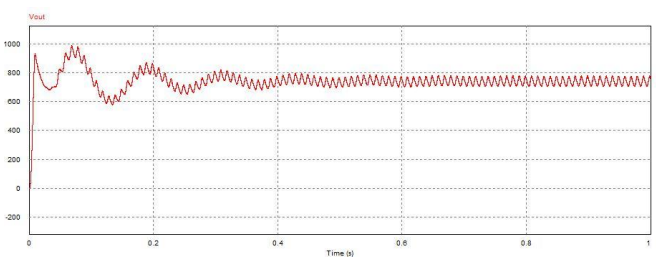

(a)

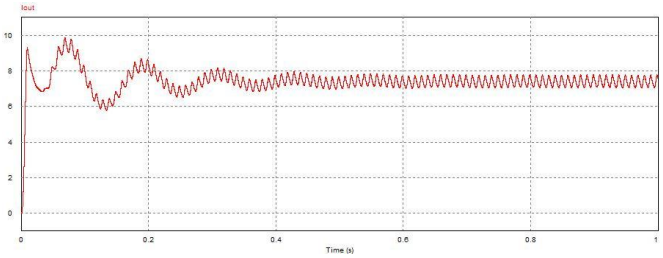

(b)

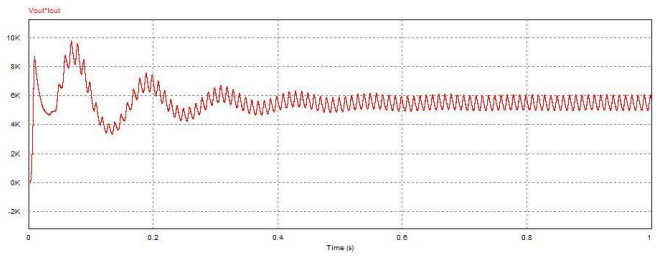

(c)

Fig. 6: (a) Output voltage, (b) current and (c) power of the proposed open loop CBS converter for 50% duty cycle.

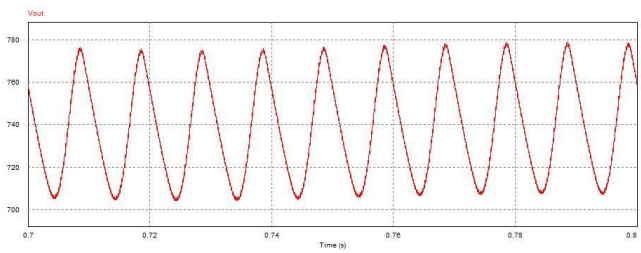

Fig. 7: Output voltage of the proposed open loop CBS converter simulated from 0.4s – 0.5s.

For comparison, the proposed circuit was compared with the conventional Boost and SEPIC converter.

A. Conversion Efficiency

It can be observed from Fig. 8 that the converter proposed here has greater efficiency then conventional SEPIC converter. Initially, the boost converter has slightly higher than the proposed converter but after 0.6 duty cycle, the proposed circuit has higher efficiency. At even higher duty cycles, the proposed circuit has more efficiency than the SEPIC converter.

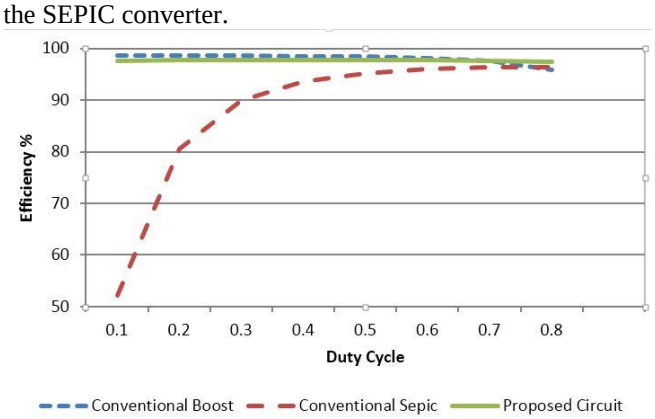

Fig. 8: Conversion Efficiency

B. Input Power Factor

The circuit proposed has a higher input power factor in comparison to the conventional SEPIC converter. Fig. 9 shows that the circuit proposed consistently has a higher input power factor than the SEPIC converter.

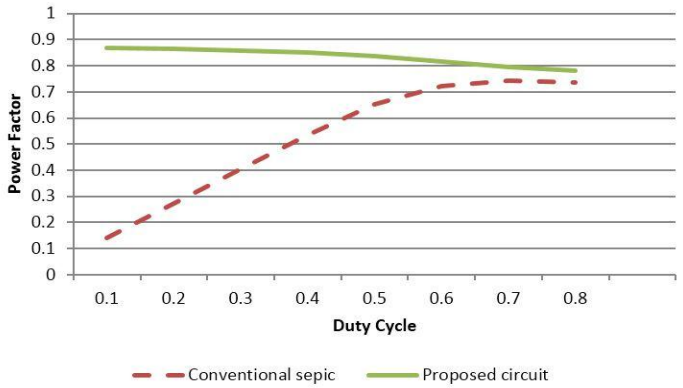

Fig. 9: Input Power Factor

C. Input Current THD

Total Harmonic distortion of the proposed converter is less in comparison to the conventional Boost and SEPIC converter as shown in Fig. 10. However, THD of the proposed converter increases after 0.7 duty cycle.

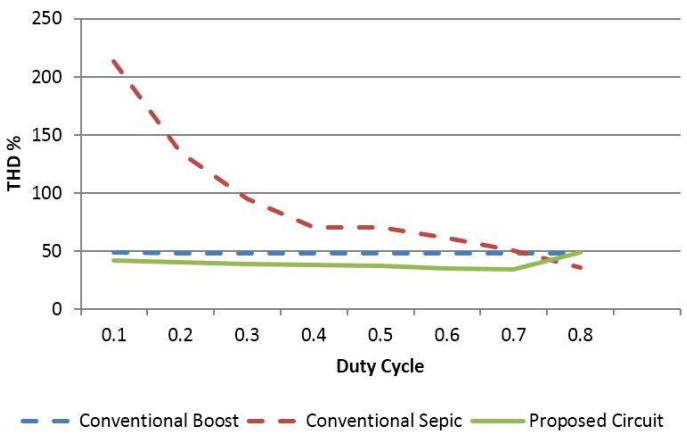

Fig. 10: Input Current THD

D. Average Output Voltage

As illustrated in Fig. 11, the converter proposed has a higher average voltage than the conventional Boost and SEPIC converter. It is also evident that the average voltage of the proposed, as well as the conventional converter increases with increase in duty cycle.

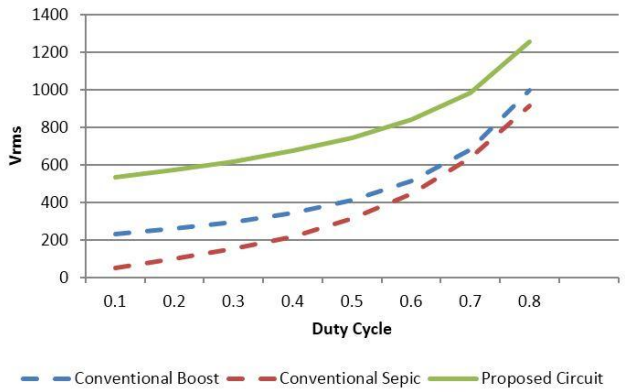

Fig. 11: Average Output Voltage

Implementation of current mode PI controller significantly improved the THD of input current and input power factor with negligible reduction in converter efficiency.

TABLE 2: Open and closed loop comparison

Parameters	Proposed CBS converter (open loop)	Proposed CBS converter (closed loop)
Efficiency (%)	97.8	97.1
THD (%)	39.03	9.94
Power factor	0.86	0.97

The effect of changing the switching frequency on input current THD and conversion efficiency are also observed, keeping 50 duty cycle.

A. Input current THD vs Switching Frequency

From Fig 12, it can be observed minimum THD is achieved around 25Khz of switching frequency.

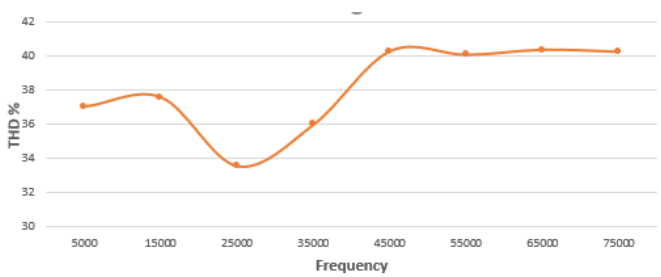

Fig. 12: Input THD comparison with switching

B. Efficiency Comparison with Switching Frequency

As illustrated in Fig 13 conversion efficiency seems to increase at high switching frequency.

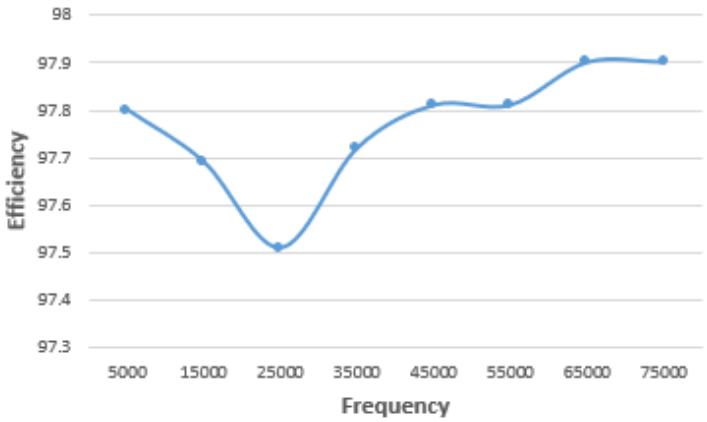

(b)

Fig 13: Efficiency comparison with switching frequency

VI. CONCLUSION

The proposed MBS converter designed by cascading Boost and SEPIC converter to obtain the advantages of both the converters. The maximum efficiency the circuit can produce without any controller is 97.8%. However the THD was quite high which is brought down to 9.94% by using the PI controller. The power factor is also improved with the addition of the PI controller. The proposed MBS converter can be effectively used for high voltage DC application like DC micro grid, heater etc.

REFERENCES

[1] Wilmar Martinez, Camilo A. Cortes, Jun Imaoka, Kazuhiro Umetani, Masayoshi Yamamoto, "Current ripple modeling of an interleaved high step-up converter with coupled inductor", *Future Energy Electronics Conference and ECCE Asia (IFEEC 2017 - ECCE Asia) 2017 IEEE 3rd International*, pp. 1084-1089, 2017.

[2] Y. Liang, "A New Type of Statcom Based on Cascading Voltage Source Inverters with Phase-shitted Unipolar SPWM", *IAS'98*

[3] D.-H. Lee, F. C. Lee, "New Cascade Switch Multilevel PWM Converters", *APEC'99*, pp. 329-324.

[4] L. Huber, M. M. Jovanovic, "A design approach for server power supplies for networking applications", *Proc. 15th Annu. IEEE Appl. Power Electron. Conf. Exp.*, pp. 1163-1169, 2000.

[5] L. Muller, J. W. Kimball, "High gain DC-DC converter based on the cockcroft-walton multiplier", *IEEE Transactions on Power Electronics*, vol. 31, no. 9, September 2016.

[6] J. P. de Souza, DF Oliveira, R. Gules, E. F. R. Romaneli, A. A. Badin, "A high static gain CUK DC-DC converter", *IEEE 13th Brazilian Power Electronics Conference and 1st Southern Power Electronics Conference*, 2015.

[7] A. A. A. Freitas, F. L. Tofoli, E. M. Sa, S. Daher, F. L. M. Antunes, "High-voltage gain DC-DC boost converter with coupled inductors for photovoltaic

systems", *IET Power Electronics*, vol. 8, no. 10, April 2015.

[8] R. W. Erickson, D. Maksimovic, Fundamentals of Power Electronics, Kluwer Academic Publishers, 2001.

[9] . Q. Zhao, F. Tao, F. C. Lee, P. Xu, J. Wei, "A simple and effective to alleviate the rectifier reverse-recovery problem in continuous-current-mode boost converter", *IEEE Trans. Power Electron*, vol. 16, no. 5, pp. 649-658, Sep. 2001.

[10] C. T. Pan, C. M. Lai, M. C. Cheng, L. T. Hsu, "A low switch voltage stress interleaved boost converter for power factor correction", *IEEE Int. Conf. Power Electronics and Drive Systems*, pp. 49-54, 2009.

[11] Mohammad H. Rashid, "Power Electronics: Circuits, Devices and Applications", Prentice-Hall, Inc., Englewood Cliffs, Book, Second Edition, 1993.

[12] Mohan Ned, Undeland Tore M, and Robbins William P, ."Power Electronics ,Converters Applications and Design", John Wiley & Sons, Inc., Book, 1995.

[13] B. W. Williams, " Power Electronics: Devices, Drivers, Applications and Passive Components", Book, Second Edition, Educational Low-Priced Books Scheme; ELBS, 1992.

[14] Bhim Singh, Sanjeev Singh, Ambrish Chandra, Kamal Al-Haddad, "Comprehension Study of Single-Phase AC-DC Power Factor Corrector Converters With High-Frequency Isolation", IEEE TRANSACTIONS ON INDUSTRIAL INFORMATICS, VOL. 7, NO. 4, NOVEMBER 2011

Proceedings of the Fourth International Conference on Communication and Electronics Systems (ICCES 2019)
IEEE Conference Record # 45898; IEEE Xplore ISBN: 978-1-7281-1261-9

Saturable Absorbers for Mode-Locking of Lasers Operating at Ultraviolet Wavelengths

Akshayaa Venkatesh[1,*], Janani MV[1], Arya M Hari[1], R.Kumar[1,*], Dhanalakshmi Samiappan[1,*], Venkatesh Chakravartula[1], Junaid M Laskar[2]

1 Electronics and Communication Engineering, SRM Institute of Science and Technology, Kattankulathur, India.
2 Department of Physics (Research), SRM Institute of Science and Technology, Kattankulathur, India.
∗ akshayaafederer@gmail.com, kumar.r@ktr.srmuniv.ac.in, dhanalakshmi.s@ktr.srmuniv.ac.in

***Abstract*—This paper demonstrates a method to develop a saturable absorber for effective Mode-Locking in the Ultra-violet region. Discovery of graphene's optical property in two dimensional arrangement had led to research of other two dimensional materials. Tungsten Disulphide has been used as a saturable absorber and is fabricated using Liquid Phase Exfoliation Method with N-Methyl,2-Pyrrolidinone as a solvent. The prepared saturable absorber is used for Mode-Locking of laser to produce ultrashort pulses at 355nm. The pulse duration of 12.5ps is achieved with constant amplitude and periodicity. The energy of the of the pulse is 125pJ. The Mode-Locking mechanism is carried on for few hours to ensure its stability. The Mode-Locked laser hence obtained can be used for dentistry and eye treatments.**

***Index Terms*—Transition Metal Dichalcogenides (TMDs), Mode-Locking, Liquid Phase Exfoliation, UV-vis spectroscopy.**

I. Introduction

Using light as medium and transferring information over long distances is termed as optical communication. Light is transferred inside an optical fiber cable by the phenomenon of total internal reflection. In the field of nanotechnology, nano photonics has been evolving rapidly in the last two decades. Studies are taking place with the aim of discovering the interaction of light in nanometer scale. The various devices used in nano photonics include photodetectors, isolators, couplers, waveguides, polarizers, saturable absorbers and electro-optic devices. [1]

Saturable absorption is the ability of a material to decrease its absorption with increase in intensity. The laser comprises of high and low intensities range. When passing through the gain medium of the resonator/cavity, the saturable absorber absorbs the light till a threshold intensity. For any intensity above the threshold, the absorber becomes transparent and transfers the light as it is resulting in locking of modes of the laser.

Graphene and its study of its optical properties led to the discovery of 2D materials and its ability to act as a saturable absorber. The existence of certain drawbacks in graphene such as zero bandgap led to the search of a better 2D material. This led to the discovery of Transition Metal Dichalcogenides (TMDs). [2] TMD monolayers are thin semiconductors of the composition MX_2, in which M is a metal with not wholly filled d-orbital (through group III to XII) and X is a Oxygen family (Chalcogen) atom. TMDs exhibit a idiosyncratic combination of not having high thickness, indirect to direct bandgap and favorable electronic and optical properties along with semiconducting abilities, which give them application in optoelectronics, medical field and spintronics. Fig 1 depicts the arrangement of WS_2 (tungsten atom sandwiched between Sulphur atoms)

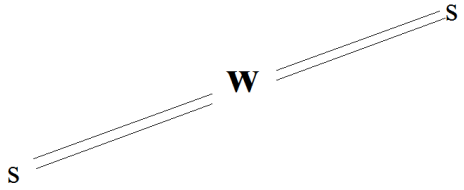

Fig. 1. Arrangement of single layer WS_2

WS_2 is an ideal TMD for its unique optical properties, cost and physical capabilities. WS_2 is a very good lubricant, possesses higher thermal stability, a wider operating temperature range and has absorbance as much as 5-10% of the incident light for thickness of 1nm. WS_2 has high mobility as its effective mass is less. [3] Usually in the insulating regime WS_2 with high mobility at room temperature, shifts to metallic conducting regime at lower temperatures. [4] It can be used in huge temperature and high pressure applications. Liquid phase exfoliation is a process of exfoliation of a TMD in a liquid medium by exploitation of ultrasound to extract 2D layers of the TMD. The nature and properties of the Saturable absorber is characterized by UV-Visible spectroscopy method.

Here, we propose fabricating Saturable absorber using liquid phase exfoliation method which ensures thin film deposition of monolayer or bilayer thickness, also by using this chemical compound Saturable absorber the longitudinal modes in the laser are locked and a gain multiplication inside the cavity is achieved to produce passively mode-locked laser. [5] Passive mode-locking is basically done to modulate the light inside the resonator cavity and to lock the modes of laser light and Q-switching can be obtained when there is a bilayered form of the absorber. Ultra-short pulses hence obtained of UV wavelength can find application in dentistry and eye surgery. In the manufacturing industry, ultra short pulses of laser are used

in laser precision cutting. Its applications range from medicine to manufacturing plants.

II. Methods

A. Fabrication of Saturable absorber

Exfoliation is defined as the addition or removal of the molecule from the layered material structure.The most common materials that undergo the exfoliation method are the Graphites and the Transition Metal Dichalogenides(TMDs). Both the materials comes under two Dimensional materials which has a single or few layers of atoms. Even though the graphite exhibits exotic material properties it has a few drawbacks which leads us to the TMDs a two dimentional material with semiconducting character. Some examples of TMDs are MoS_2 ,$MoSe_2$, and WS_2 etc. Generally exfoliation is done for the layered materials. [6]

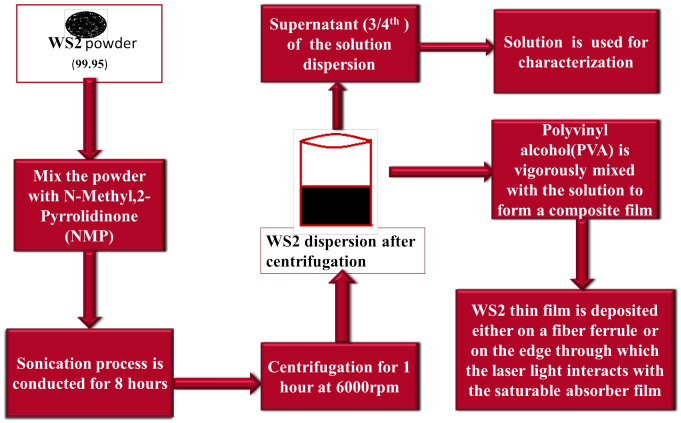

Fig. 2. Liquid phase exfoliation process of tungsten disuphide

Liquid phase exfoliation is very efficient and simple which yields uniform deposition along the substrate. [12] Selection of solvent is very important for the stability of prepared nano flakes. Surface tensions of solute and the solvent should be comparable (solute being WS_2 of 40 mN/m surface tension). As we know surface energies of solid and liquid are almost practically equal, solvent having surface energy near WS_2 is carefully chosen. N-Methyl-2-Pyrrolidone (NMP) has surface tension of 40.79 mN/m, which is closer to WS_2. The lower the difference between the energies the better is the exfoliation process. [7]

The various processes involved in exfoliation process is depicted in Fig 2. WS_2 of 99.9% purity, 2μm particle size is purchased at Sigma-Aldrich, polyvinyl alcohol (PVA) of molecular weight 124000 and NMP is also purchased from Sigma-Aldrich. 5mg/ml WS_2 powder is mixed with the NMP to prepare the solvent mixture. Sonication process is done for eight hours which ensures the breaking down of bonds using ultra sound waves. Centrifugation - The solution is rotated at 6000 rpm for one hour for purification. The upper three forth of the solution is used for characterization. The solution is vigorously mixed with PVA to form a composite film which can be deposited on the fiber ferule for interaction with laser. [11]

B. Mode locking of LASER

The technique of producing ultrashort pulses of very less pulse duration ranging from picoseconds to femtoseconds of the input light is called mode-locking. Mode locking is achieved by inter-locking the different modes oscillating in them that have mildly different wavelengths. [8] Constructive and destructive interference among the modes stimulates the laser to produce pulsating beam. Mode locking is obtained by two methods namely active and passive mode-locking.

Active mode locking is the method of obtaining ultrashort pulses by modulation of the cavity losses. An external modulator is required for actively modulating the resonator losses. An acousto-optic modulator, Pockel's cell can be used for this process. Passive mode locking mechanism is carried out using a non-linear optical device known as saturable absorber. The laser beam oscillates within the resonator through the gain medium and saturable absorber as depicted in Fig 3 and one pulse is sampled after every round trip time.

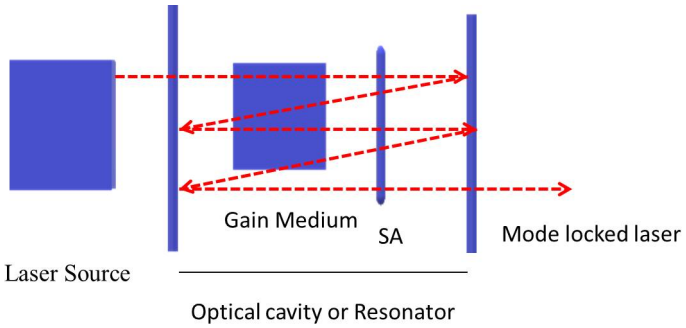

Fig. 3. Mode-locking mechanism

III. Experimental Analysis of Mode Locking

Passive mode-locking is achieved using a saturable absorber. A circuit is designed using VPI photonics software to obtain ultrashort pulses in the ultraviolet wavelength. Simulation is carried out from Table 1.

TABLE I
Simulation Parameters for Mode-Locking Operation

Input Parameters	
Central Frequency (THz)	844.4
Wavelength (nm)	355
Sample Rate (s)	$5120*10^9$
Laser section	Bulk mode, Isotropic
Saturable Absorber	MQW mode, Isotropic
Time delay	1
No. of runs	2
Pulse Duration (ps)	12.5

Fig 4 depicts the circuit designed for mode-locking of laser with saturable absorber and laser section. DC source provides input supply to both saturable absorber and the laser

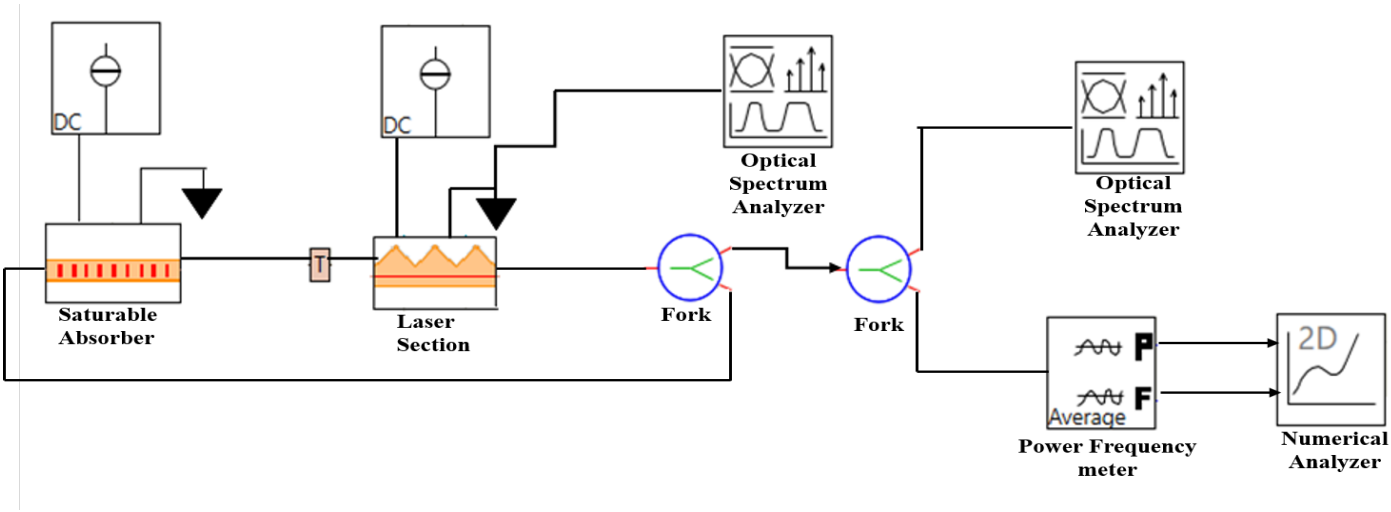

Fig. 4. Experimental set up for mode-locking of lasers

section, Laser section has both bulk and Multiple Quantum Wave (MQW) modes which are respectively used for laser section and saturable absorber. Saturable Absorber is the sample interacting with laser and produce mode-locked pulses. Optical Spectrum Analyzer (OSA) analyses the output signal to produce waveforms. Fork Splits the output from the laser into OSA and back into the circuit for cavity formation. The Optical frequency plot obtained by spliting the signal using a fork is detected using frequency power meter.

IV. Results and Discussion

The simulation of the project was carried out using VPI Photonics design suite (Simulation Software-version 9.9). The LASER section acts as source for the mode-locking using a saturable absorber(Passive modulator). The saturable absorber can be graphene, any 2D materials like Transition Metal Dichalcogenides (TMDs), Metal oxides, Black phosphorous etc. [9] The DC source's output data type was set to samples mode since any passive saturable absorber works only with a sampled input and ultrashort pulses are obtained from sampling the laser light. This output data is collected by the fork, splitting it back to the circuit as feedback as well as to the analyzers. A delay unit of 1 was added between laser section and saturable absorber to avoid deadlocking. Deadlocking has to be avoided since it may lead to ceasing of laser light during the operation. The circuit depicted in Fig 4 is simulated with a input power of 210 mW from where the mode-locking starts. The circuit is run for two cycles since the first cycle has only output through the fork without the feedback whereas the second cycle's output is obtained from feedback signal provided by other arm of the fork back into the circuit hence providing mode-locked regime.

Fig 5 shows the laser signal before Mode-Locking opertion. The waveform depicts many oscillations and irregularities in the laser beam before being locked into modes. This causes uneven power distribution and less energy pulses. Mode-Locking this laser can restricts the power to be delivered

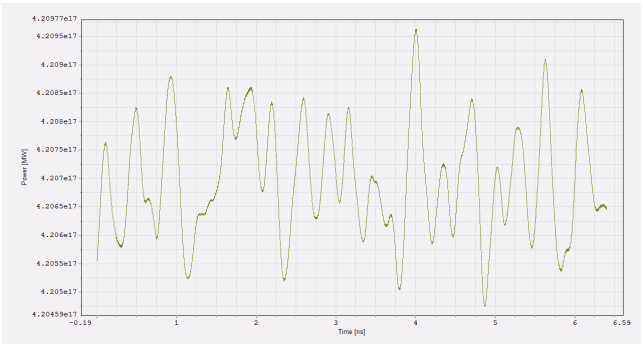

Fig. 5. Laser Pulse before Mode-Locking

at a particular frequency only after every round trip time inside the resonator. The constructive and destructive interference of beams in the resonator

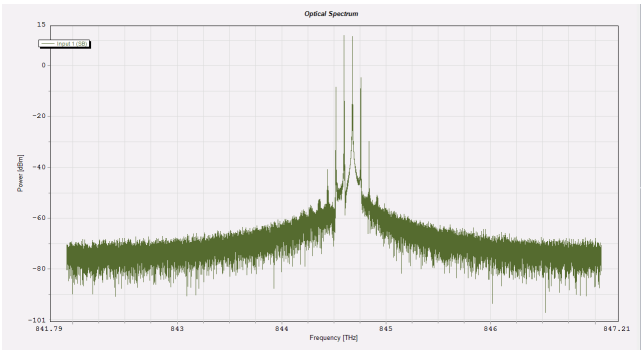

Fig. 6. Mode-locking indicated by Peak at the central frequency of 844.4THz

Fig 6 shows the output simulation of the laser depicting power versus frequency wave which has peak power at the central frequency of 844.4THz. Fig 7 shows optical spectrum of power with respect to the wavelength which indicates high power at 355nm which is in the UV region. Saturable absorber

absorbs the light intensity to a particular threshold and for any intensity above that the saturable absorber acts as a transparent medium giving an output pulse. A peak power of 1mW is obtained at a central frequency of 844.4THz and wavelength of 355nm indicating the mode locked pulse.

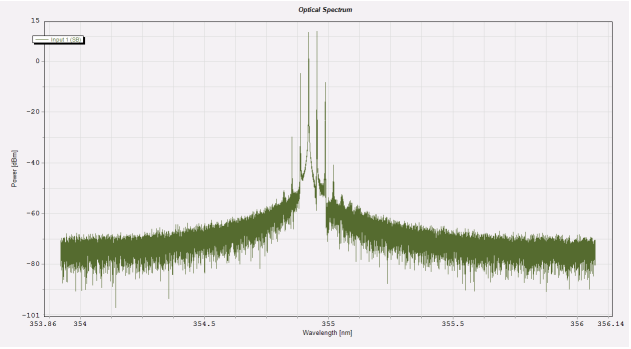

Fig. 7. Mode-locking at a wavelength of 355nm

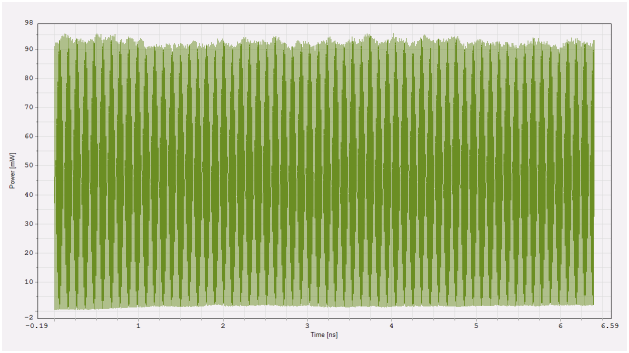

Fig. 8. Mode-locking regime

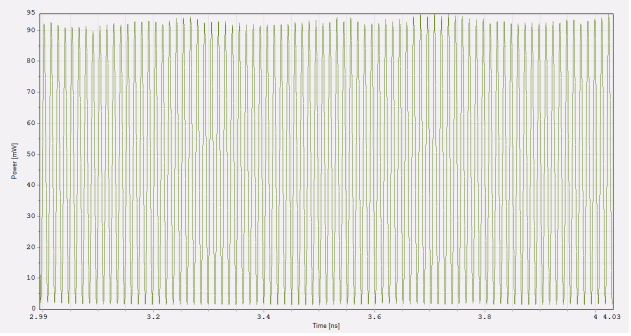

Fig. 9. Mode-Locked pulse over one nanosecond range

The continuous spectrum depicts the periodic mode locking of laser with same amplitude throughout indicating constant mode-locking in Fig 8 after run two. The results indicate the pulses are highly stable. The energy of TE mode locked laser of 125 pJ is achieved. Multiple signal causes high pulse repetition rate in the terahertz range for passive mode locking of the laser pulse, which is caused by the phenomena known as harmonic mode locking.

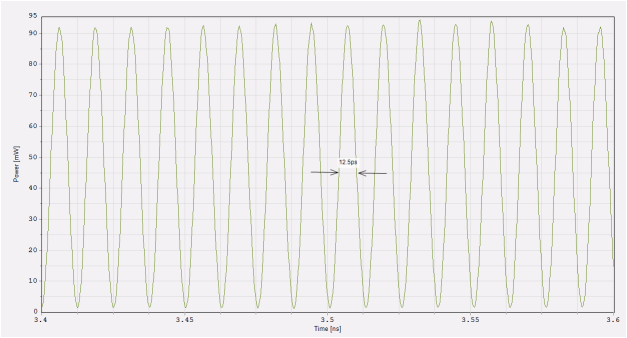

Fig. 10. Pulse duration of 12.5ps

Fig 9 depicts mode-locked laser over one nanosecond range. The waveform shows pulses of equal duration and equally spaced proving it is periodic and stable. Also the pulse duration of each pulse was calculated to be 12.5ps (over 1 ns there was 80 pulses which means 1/80 = 0.0125ns for each mode-locked pulse) is depicted in Fig 10. The pulse duration indicates higher repetition rate. The saturable absorption of the laser depends on the material used as a saturable absorber [10]. WS_2 for saturable absorption with monolayer thickness depends on the rate of transition of electrons from valence band to conduction band due interaction of the laser signal. The optical parameters of the generated pulse is measured using an optical signal analyser. The frequency power ratio is measured using a frequency power meter and a two dimensional numerical analyzer.

The instabilities that can occur during the mode locking operation is caused due to simultaneous Q switching of the laser pulse. Q switched mode locked pulses are not encouraged due to the instabilities it would cause in the pulse train. Q switching is the generation of very high power pulses, which requires higher oscillation in the laser resonator cavity leading to dynamic instabilities. After generating a Q switched pulse the next sequence of pulse would have very low energy, which should be avoided. This instability is avoided by harmonic passive mode locking of the laser and producing ultrashort pulses. [13] If the Mode-Locked and Q-switched condition coexists with no instabilities, a very short pulse of high energy can be obtained which can be useful in providing precision and accuracy.

V. Conclusion

The saturable absorber was developed using tungsten disulphide (WS_2) by Liquid Phase Exfoliation technique, in the range of nano meters. The mode-locking was achieved at the same pump input power of 210mW. The inter-cavity laser was modulated by the Saturable absorber thereby achieving mode-locking at the monolayer thickness areas and Q-switching at bilayer layer areas due to change in modulation depth and absorption coefficient.

Tungsten disulphide is chosen because of its better properties than graphene. Saturable absorption is achieved at ultraviolet frequency of 844.4 THz and wavelength of 355nm.

The pulse duration of the achieved pulse regime was 12.5ps. Hence the energy of TE mode locked laser is 125pJ. The prepared WS_2 is characterized using UV-vis spectroscopy. The measurement of ultrashort pulses could be carried out using auto correlation technique.

VI. Acknowledgements

We thank the support team of VPI photonics Simulation Software and Design Services and Electronics and Communication Department, SRM Institute of Science and Technology, India.

References

[1] Zapata, J. D., David Steinberg, L. A. M. Saito, R. E. P. De Oliveira, A. M. Crdenas, and EA Thoroh De Souza. "Efficient graphene saturable absorbers on D-shaped optical fiber for ultrashort pulse generation." Scientific reports 6 (2016): 20644.

[2] Du, Juan, Qingkai Wang, Guobao Jiang, Changwen Xu, Chujun Zhao, Yuanjiang Xiang, Yu Chen, Shuangchun Wen, and Han Zhang. "Ytterbium-doped fiber laser passively mode locked by few-layer Molybdenum Disulfide (MoS 2) saturable absorber functioned with evanescent field interaction." Scientific reports 4 (2014): 6346.

[3] Yan, Peiguang, Hao Chen, Aijiang Liu, Keyao Li, Shuangchen Ruan, Jinfei Ding, Xuhui Qiu, and Tuan Guo. "Self-starting mode-locking by fiber-integrated WS 2 saturable absorber mirror." IEEE Journal of Selected Topics in Quantum Electronics 23, no. 1 (2017): 33-38.

[4] Ahmad, Harith, N. E. Ruslan, M. A. Ismail, S. A. Reduan, C. S. J. Lee, S. Sathiyan, S. Sivabalan, and Sulaiman Wadi Harun. "Passively Q-switched erbium-doped fiber laser at C-band region based on WS 2 saturable absorber." Applied optics 55, no. 5 (2016): 1001-1005.

[5] Dai, Yu, Lu-Lin Wei, Ming Chen, Jing-Jing Wang, Jie Ren, Qiong Wang, Yan-Ze Wu, Ya-Ping Wang, Xiao-Nong Cheng, and Xue-Hua Yan. "Liquid Exfoliation and Electrochemical Properties of WS2 Nanosheets." Journal of nanoscience and nanotechnology 18, no. 5 (2018): 3165-3170.

[6] Bang, Gyeong Sook, Kwan Woo Nam, Jong Yun Kim, Jongwoo Shin, Jang Wook Choi, and Sung-Yool Choi. "Effective liquid-phase exfoliation and sodium ion battery application of MoS2 nanosheets." ACS applied materials interfaces 6, no. 10 (2014): 7084-7089.

[7] Jha, Ravindra, and Prasanta Kumar Guha. "An effective liquid-phase exfoliation approach to fabricate tungsten disulfide into ultrathin two-dimensional semiconducting nanosheets." Journal of materials science 52, no. 12 (2017): 7256-7268.

[8] Xie, G. Q., J. Ma, P. Lv, W. L. Gao, P. Yuan, L. J. Qian, H. H. Yu, H. J. Zhang, J. Y. Wang, and D. Y. Tang. "Graphene saturable absorber for Q-switching and mode locking at 2 m wavelength." Optical Materials Express 2, no. 6 (2012): 878-883.

[9] Hu, Y., X. Jin, G. Hu, M. Zhang, Q. Wu, Z. Zheng, and T. Hasan. "Hybrid mode-locked erbium-doped fiber laser with black phosphorus saturable absorber." In 2018 Conference on Lasers and Electro-Optics (CLEO), pp. 1-2. IEEE, 2018.

[10] Mao, Dong, Xiaoqi Cui, Xuetao Gan, Mingkun Li, Wending Zhang, Hua Lu, and Jianlin Zhao. "Passively Q-switched and mode-locked fiber laser based on an ReS2 saturable absorber." IEEE Journal of Selected Topics in Quantum Electronics 24, no. 3 (2018): 1-6.

[11] Cao, Liming, Xing Li, Rui Zhang, Duanduan Wu, Shixun Dai, Jian Peng, Jian Weng, and Qiuhua Nie. "Tm-doped fiber laser mode-locking with MoS2-polyvinyl alcohol saturable absorber." Optical Fiber Technology 41 (2018): 187-192.

[12] Xu, Danyun, Pengtao Xu, Yuanzhi Zhu, Wenchao Peng, Yang Li, Guoliang Zhang, Fengbao Zhang, Thomas E. Mallouk, and Xiaobin Fan. "High yield exfoliation of WS2 crystals into 12 layer semiconducting nanosheets and efficient photocatalytic hydrogen evolution from WS2/CdS nanorod composites." ACS applied materials interfaces 10, no. 3 (2018): 2810-2818.

[13] Guo, Bo, Shi Li, Ya-xian Fan, and Pengfei Wang. "Versatile soliton emission from a WS2 mode-locked fiber laser." Optics Communications 406 (2018): 66-71.

Proceedings of the Fourth International Conference on Communication and Electronics Systems (ICCES 2019)
IEEE Conference Record # 45898; IEEE Xplore ISBN: 978-1-7281-1261-9

Level management in connected water reservoirs employing curve fitting based PID control scheme

Mohit kumar
M. Tech: Department of Electrical Engineering
National Institute of Technology, Kurukshetra
Haryana
mohitbcs852@gmail.com

Dr. Sathans
Professor: Department of Electrical Engineering
National Institute of Technology, Kurukshetra
Haryana
sathans@nitkkr.ac.in

***Abstract*— Climate change affects us in almost all daily aspects of life. Specially, disasters like floods. The dam level management system to counter these unpredictable floods has become obsolete. This can been seen in the recent destruction brought upon by floods in the state of Kerala (India). The major reason for the deluge has been reservoir mismanagement. Due to absence of a scientific method to control the outflow from several local dams. Consequently, a first step towards encountering this conundrum in form of a PID controller augmented by a FOPDT (first order plus dead time reinforcement) to manage water levels in a two connected reservoir system is proposed.**

Keywords*— PID controller, FOPDT model, flood control and interacting reservoirs.

I. INTRODUCTION

The interconnected reservoir system regime is common to most of the water management techniques. Some of these include feed-forward control [1, 2], feedback control [2, 3] either without or with feed-forward control and Decentralized and distributed control [4]. Even though these techniques are widely used in normal reservoir level control. Their use in unpredictive situations like floods has been limited. For instance, in Kerala floods, the Idukki dam which is connected to Mullaperiyar dam as shown in figure 1 faced flash floods. The reason for these disastrous floods was the mismanagement of water level and sudden release of water from Mullaperiyar to maintain mandated water level of 139 feet. Hence, to avoid such catastrophes a state of the art system is required. Currently the water level systems are rampant with human biases and myopic constrains.

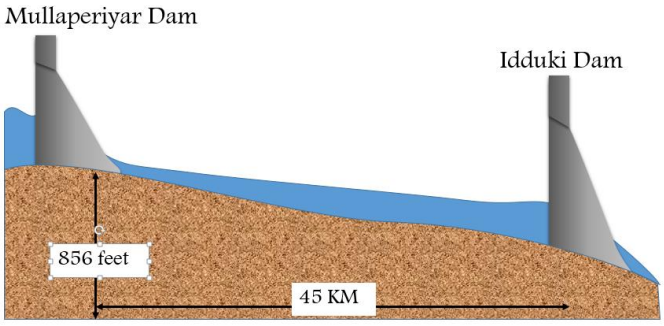

Fig 1: Water flow diagram of two connected reservoir system.

Previously, some amount of work has been done in similar area. In 2009, a paper was published revealing the use of PID and DI (Dynamic Inversion) based nonlinear controller in water management systems [5]. In a different approach fuzzy (logic) supervisor (FZPID) and genetic algorithms (GAPID) have also been utilized [6]. However, a large memory requirement is a prerequisite in these approaches which slows down the response time. Consecutively, in 2010 another research view explored the use of microcontrollers in sensing and controlling water levels [7]. Methods based on this type of techniques helps in creating a robust control scheme. Apart from research papers there are few patents which highlight level sensing systems on small scale [8, 9]. These can further be upsized to larger systems in which level management is required.

Furthermore, in these systems sudden rise of water due to excess rain fall has not been taken into account. Therefore, to avoid such backlashes a system based on PID (Proportional Integral Derivative) controller reinforced by FOPDT (first order plus dead time reinforcement) may serve as a prudent alternative.

II. MATHEMATICAL MODEL FOR TWO RESERVOIR SYSTEM

To understand the governing mathematics behind the operating principles of two interacting reservoir systems, the diagram in figure 1 needs to be expressed in terms of sufficient differential equations. Moreover, these equations must be converted in to a working transfer function. The physical variable such as resistance to water flow should be converted to mathematical entities to handle them in a quantitative manner. The levels of reservoirs which change with time are converted to S-domain. Next, the transfer function is calculated taking q_{in} as the input and h_2 as output. This makes the working relation between these variables easy to counter as they are now mathematical quantities. Finally, this transfer function is incorporated into a Simulink block represented by Tank S-function in figure 3.

A schematic representation demonstrating the mathematical model of figure 1 is depicted in figure 2.

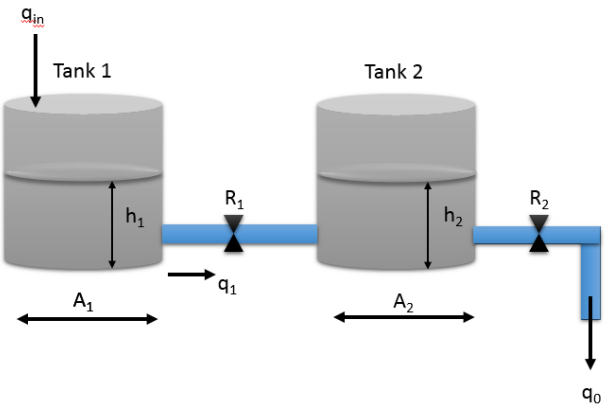

Fig. 2: Mathematical diagram of two connected reservoir system

Wherein,

$q_1(t)=q_{in}(t)$: water flow from external source such as rain in centimeter cube per minute.

$q_2(t)=q_o(t)$:the outflow from tank towards rivers in centimeter cube per minute.

$h_1(t)$: level of water in the first reservoir in meters.

$h_2(t)$:level of water in the second reservoir in meters.

A_s (s=1, 2): area of both the reservoirs in meter square.

and R_s (s=1, 2): the resistances to flow.

In the case of two interacting systems the transfer functions cannot be multiplied directly. Therefore the transfer function of interacting systems can be stated in the form of equation 1 [10].

$$\frac{h_2(s)}{q_{in}(s)} = \frac{R_2}{T_1T_2s^2+s(T_1+T_2+A_1R_2)+1} \qquad (1)$$

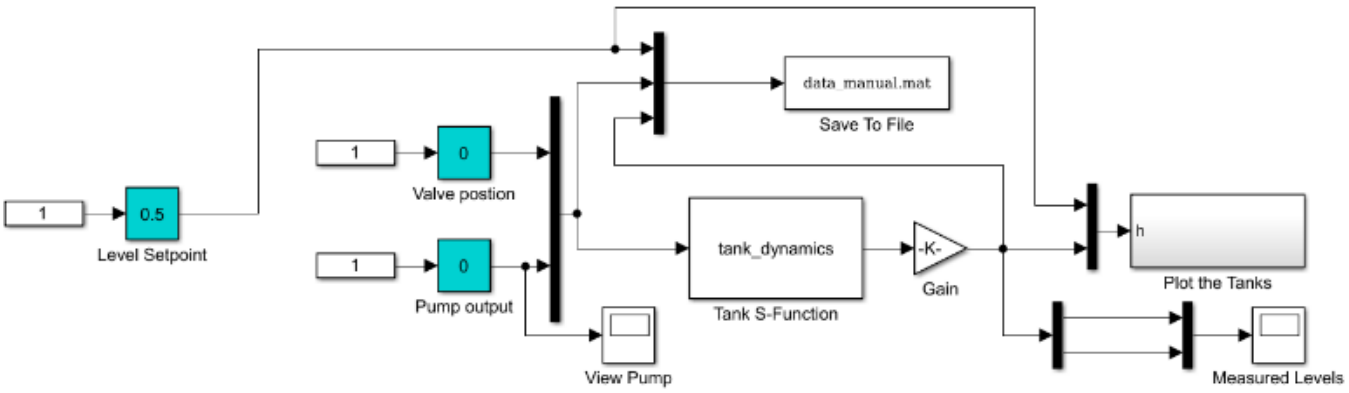

Fig. 3: Simulink model with manual control.

Figure 3 depicts the control strategy used presently modeled in MATLAB [11]. Equation 1 is integrated in this simulation using "Tank S-Function". This scheme is devoid of an automatic controller i.e., the pump output and valve position is controlled manually. To take into account unforeseen circumstances a system backed by a PID controller which will act according to credible information is proposed.

III. PID CONTROLLER

A PID controller is an digitally backed equipment which finds its use in numerous scenarios which need controlling of the control variable to regulate heat level, flow of liquids, pressure in turbines, speed and other process related uncertainties. PID (proportional integral derivative) employs a control loop feedback mechanism to restrain certain conditions in a robust way. They are the most spot on and steady controllers. PID control is a hugely known control regime of goading any system towards a desired outcome or level. PID controller employs closed-loop controlling feedback to guide the actual output regarding a process as proximate to the goal or predefined set point as possible (Figure 4) [12].

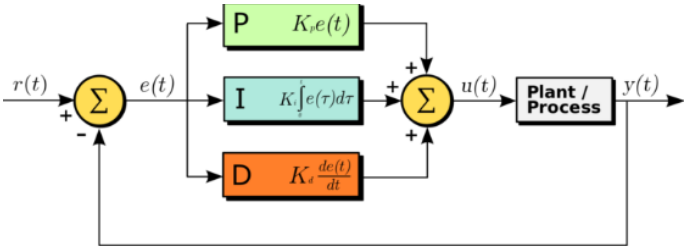

Fig. 4: Block diagram depicting working of a PID controller.

The parameters controlling the working of PID are where Kp, Ki and Kd, all non-negative, denote the coefficients for the proportional, integral, and derivative terms respectively (sometimes denoted P, I, and D). To optimize the stated variables for automatic control of water level in the reservoirs FOPDT (First Order Plus Dead time) technique is employed.

IV. FOPDT MODEL

A FOPDT model is a time tested and sturdy methodology to valuate (give numeric representation to) vital facets of this controller output (CO) to process variable (PV) juxtaposition

for use in determining controller parameter's outline and necessary estimation . In particular, when the CO is a variant quantity: Process gain, Kp, enunciates the distance. Furthermore, how distant the PV can go and remain there. Time constant, Tp, tells us about the pace of the movement for the said control variable.

The reaction graph procedure compels you to perform a step change with respect to the process input, the manipulated variable (MV): From a predefined unchanging state, step and hold the input at a novel value till the reaction variable finally settles to an ultimate steady state. However, disturbances and arbitrary alternate noises stagger the response largely. In continuation, a singular step forces the process far from the needed set point (process response). Furthermore, a single step to the one side of formal will misguide the user away from the nonlinear nature of the process. Therefore, for efficient response graph fitting tests, we usually take into use an up-down-down-up motif, which is a concatenation of step-and-hold leitmotif in the influence. This manufactures four reaction curves. Their average can compensate the influence of noise and perturbations, the pattern takes into account both aspects of the original MV value, makes positive deviations from a nominal response value that are counter affected by negative deviations, and eventually makes the process go back to the mentioned original value. Hence, the controller design is a combination of standard PID controller supported by FOPDT curve fitting technique.

V. CONTROLLER DESIGN

The controller needs to fulfill the prerequisite that the water level mark in concerned reservoirs follows a pattern of predefined set of parameters submitted by the user. Presently, the method used is based upon human intelligence. A dedicated human operator is assigned who is given directions by a bureaucratic committee for controlling the outflow from the concerned reservoir. However, a PID controller can be used pragmatically to avoid any biases. Therefore, dynamic data is needed from the model behavior under set control to feed into the FOPDT model. This will provide the necessary information for robustly approximating the proportional, derivative and integral coefficients of PID controller utilized.

Firstly, without using the PID controller, the pump output was set to 0.5 and the simulation was started.

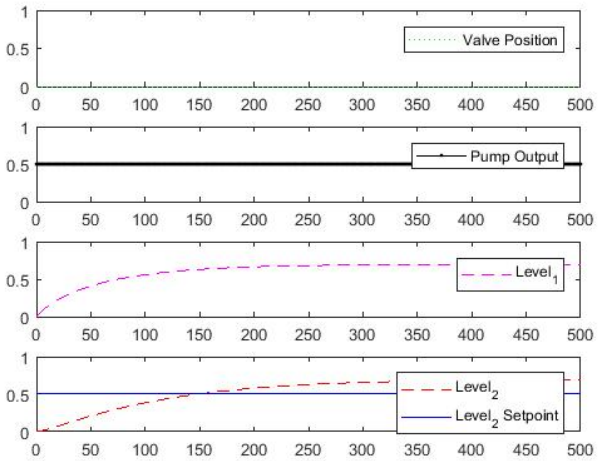

Fig. 5:Level output in reservoirs without using PID controller.

From figure 5 it is observed that the desired set point of 0.5 has been transcended. In real time it means that the water has overflown its set limit.

A data_manual.mat block has been used to extract vital information for the simulation depicted in figure 3. The results stored in the above mentioned block which were then fed into the FOPDT excel calculation sheet.

Model Parameters	
Kp (Gain)	1.388755091
tau (Time Constant)	111.7671239
theta (Time Delay)	8.317417671
Doesn't seem to change with solver	
Minimize Either of These	
Sum of Squared Errors	0.012669935
Sum of Absolute Errors	1.981107474

Fig. 6: Results obtained after curve fitting by FOPDT.

Then curve fitting techniques was used to obtain optimum values of Kp, Ki & Kd (figure 6). After getting the concerned parameters, the pump output block is replaced by a PID controller as demonstrated in figure 7.

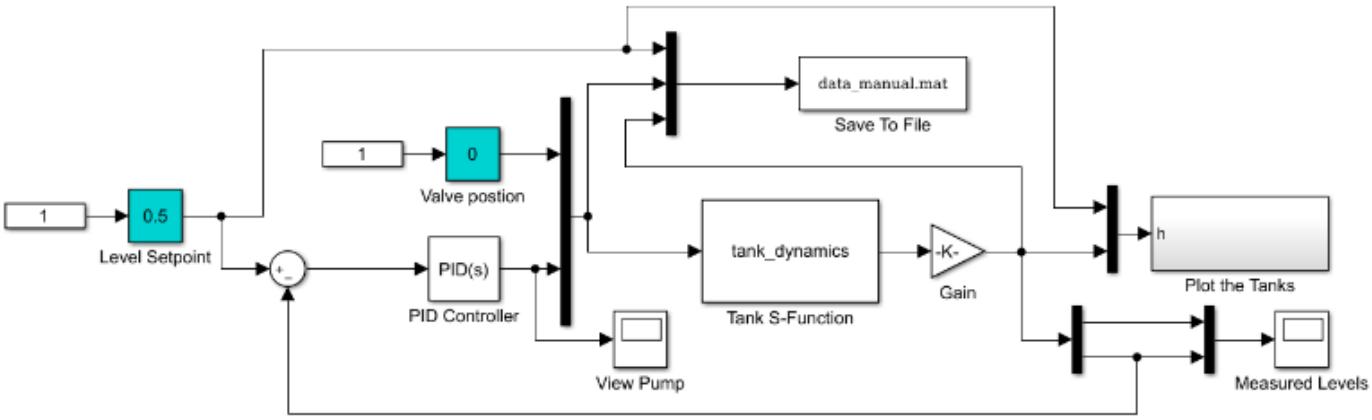

Fig. 7: Results obtained after curve fitting by FOPDT.

Then the simulation was initiated again using the parameters calibrated by curve fitting method.

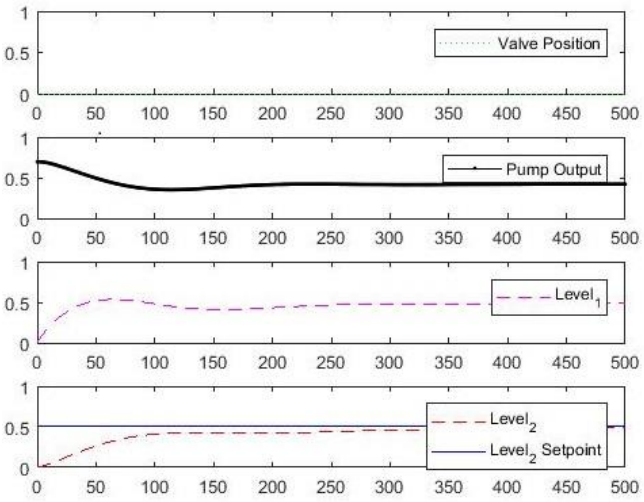

Fig. 8: Level output in reservoirs using PID controller

Now the results have ameliorated which can be observed by the level of water staying below the set limit in figure 8. Notably, the set point given and new output when juxtaposed show negligible diversion from each other. This reduces the chances of a deluge as pump output can be considered as sudden rainfall.

VI. CHALLENGES AND FUTURE PROSPECTS

The main challenge is to practically include a stochastic model which predicts a rainfall pattern. Real time models can be much more efficient and also very complex to develop. Further, the construction aspect of the reservoir also plays a vital role which has not been included in this paper. A large data assimilation is a prerequisite to countering the problem of inaccurate predictions.

Conversely, the future prospects are tremendous. As climate change affects our rain patterns, floods are a real threat. The economical loss of a flood can be saved using scientific methods as proposed.

VII. CONCLUSION

This paper has tried to counter a modern problem of devastating floods with an equally modern solution. The main purpose is to root out the human bias which is currently rampant. The results obtained have exclusively assimilated a method which may prevent future disasters. Finally, this is a step towards a future where such model backed by IOT can usher a new age.

ACKNOWLEDGMENT

Mr. Mohit is grateful to MHRD, India for providing financial support to pursue this research work.

REFERENCES

[1] P. O. Malaterre, “Regulation of irrigation canals”, Irrigation and Drainage Systems, vol. 9, pp. 297-327, November 1995.

[2] P. O. Malaterre and J.-P. Baume, “Modeling and regulation of irrigation canals: Existing applications and ongoing researches”, Proceedings of the 1998 IEEE International Conference on Systems, Man, and Cybernetics (San Diego, California), pp. 3850-3855, October 1998.

[3] J. Schuurmans, “Control of water levels in open channels”, Ph.D. thesis, Delft University of Technology, Delft, The Netherlands, October 1997.

[4] R. R. Negenborn, P.-J. van Overloop, T. Keviczky, and B. De Schutter, “Distributed model predictive control of irrigation canals”, Networks and Heterogeneous Media, vol. 4, no. 2, pp. 359–380, June 2009.

[5] M. P. Kumar and M. S. M. Kumar, “Comparative study of three types of controllers for water distribution networks”, J. Am. Water Works Ass., vol. 101, pp. 74-86, Janusry 2019.

[6] M . P. Kumar and M. S. M. Kumar, “Tuning of PID controllers for water networks - different approaches”, J. Am. Water Works Ass., vol. 101, pp. 95-107, July 2009.

[7] S. M. K. Reza, S. A. Md. Tariq, S. M. M. Reza, “Microcontroller Based Automated Water Level Sensing and Controlling: Design and Implementation Issue”, Proceedings of the World Congress on Engineering and Computer Science (San Francisco, USA), vol. I, pp. 20-22, October 2010.

[8] Liu, Xiangjie; Xi, Chunmiao; Zhao, Liang “Water tank liquid level control method based on generalized prediction control optimization”, CN Patent 104076831, Jun 27, 2014.

[9] M. Z. Farmer and D. B. Farmer, “Automatc level sensing system”, US Patent US4572253A, Feb. 25, 1986.

[10] M. Changela, A. Kumar,“Designing a Controller for Two Tank Interacting System”, International Journal of Science and Research, vol. 4, pp. 589-593, May 2015.

[11] MATLAB and Statistics Toolbox Release 2017a The MathWorks, Inc., Natick, Massachusetts, United States.

[12] ArduProject.es, “Stability control and PID for drones”, 2018. [Online]. Available: http://arduproject.es/control-de-estabilidad-y-pid/.

Proceedings of the Fourth International Conference on Communication and Electronics Systems (ICCES 2019)
IEEE Conference Record # 45898; IEEE Xplore ISBN: 978-1-7281-1261-9

Nonlinear Model Predictive Controller for the Real-Time control of Fast Dynamic System

Mrs. Supriya P. Diwan
Department of Electronics Engineering
Walchand College of Engineering
Sangli, India
supriya.diwan@walchandsangli.ac.in

Dr.(Mrs.)Shraddha S. Deshpande
Department of Electronics Engineering
Walchand College of Engineering
Sangli, India
shraddha.deshpande@walchandsangli.ac.in

***Abstract*—The computational complexity due to the system's non-linearity and non-convexity , restricts the use of nonlinear model predictive control (NMPC) for fast dynamic real time systems. This paper presents the real time development of the NMPC to control the highly nonlinear fast dynamic single rotary inverted pendulum (SRIP) system in inverted position with 20 millisecond sampling period which corresponds to nonlinear non-convex optimization problem. This challenging problem is solved with online successive linearization and optimization on the compact reconfigurable input/output (cRIO) (field programmable gate array (FPGA)) hardware platform from National Instruments. The effectiveness of the control algorithm with the rapid disturbance rejection capability is validated using experimental results.**

***Index Terms*—Rotary inverted pendulum, nonlinear model predictive control, successive linearization, cRIO, FPGA, real-time systems**

I. Introduction

MPC is applicable for complex multiple input and multiple output (MIMO), Linear/Nonlinear LTI or time varying systems. It has inbuilt Constraints handling capability [1], [2].Also the ability to handle the single input and multiple output (SIMO) or multiple input single output (MISO) by restructuring the formulation. However, linear MPC (LMPC) covers limited operating regions or weakly nonlinearity considerations which may not justify for any of the highly nonlinear industrial plants. Therefore the NMPC shows the strong potential to improve the control and operation of the nonlinear systems [3]. But the main disadvantage is a higher Computational Burden as on for nonlinear optimization problems has to be solved at every sampling instant. In addition the problem becomes too large to solve it online. Therefore, it is difficult to apply NMPC in real time for fast dynamic systems [4] -[6]. To reduce the complexity, the successive linearized NMPC which locally linearizes the model at every control interval is still the promising option for real time implementation of it [7] -[9]. But the online fast computation will be the concern for the rapid control action calculation in the fast dynamic processes.

However, due to enhancement in the electronic hardware platforms there is a large possibility to accelerate the computation time of the controllers for the highly nonlinear systems is increased. The vendors provide the flexibility of the hardware and software platforms which can be handled with ease of use by the user. In the current application domain, the FPGA is being used for predictive control applications.In a survey, mentioned the recent progress in FPGA technology and emphasized the key parameters that may considerably contribute to the development of proficient digital systems for industrial applications.FPGA offers cycle-accurate timing guarantee and easily embedded as a system component. Therefore now a days, the researchers are keen to use an FPGA to speed up the on-line computation of NMPC. Computational speed is improved through parallelization and customizability explained [10]. The efforts of MPC implementation on FPGA for the nonlinear systems are appreciable and therefore, a scope for solving optimum solution of the non-convex nonlinear optimization problem with FPGA is increased [11]. But for implementation using, such as platforms a good knowledge of specific languages such as VHDL/Verilog, system C/system Verilog, etc. required. The choice of language is the target dependent. Less expertise in these languages has been often trouble in developing steps for a Real-Time (RT) target which leads towards the more time consumption in development stage. Real time implementation in cRIO using LabVIEW FPGA reported for the LMPC, LQR, etc. [12]-[14].

The main purpose of this paper is to develop and apply the NMPC to the fast dynamic real time system with minimum implementation time. To this aim,the main contribution of this paper covers the successful implementation of NMPC with online optimization with a successive linearized nonlinear model on the cRIO using LabVIEW FPGA (from National Instruments) using Rapid Prototyping Tools (RCP Tool) with millisecond timescale. For experimental validation the SRIP is used due to its nonlinear fast dynamic behavior. It is unstable at the inverted position with non-minimum phase. Its nonlinear state constraints leads to nonlinear optimization problem. Also the controller developed for it may be applied to the similar practical applications like, In missile launch and control, Lifting cranes on shipyards, Self balancing personal transporter, etc. The paper depicted in the following fashion. Section II briefs about the formulation of the NMPC. Section III discusses in details the utilization of NMPC for the balancing SRIP. Section IV mentions the experimental results of the SRIP system with and without applying the disturbance

which is followed by the conclusion and the future scope.

II. PROBLEM FORMULATION OF NMPC

This section briefs about the formulation of the NMPC that controls the nonlinear fast dynamic system using the successive linearized nonlinear model [7].

A. Model Selection

The system to be controlled using NMPC is generalized by the equation(1)

$$\begin{aligned} \dot{x} &= f(x,u), \\ y &= g(x) \end{aligned} \tag{1}$$

The $f(\cdot)$, $g(\cdot)$ are nonlinear functions of the process model. $x \in \Re^m$,$u \in \Re^n$ and, $y(k) \in \Re^r$ are the state, manipulated input and output vectors of dimensions m ,n and r, respectively. The nonlinear functions (1) are linearized around the current trajectory $(x(k), u(k))$ and discretized at the sampling time T_s. After the discetization the model at sampling instant k in the form of nonlinear discrete state space model [4], [5]

$$\begin{aligned} (x(k+1) &= f(x(k),u(k)), k \geq 0 \\ y(k) &= g(x(k)) \end{aligned} \tag{2}$$

B. Problem Formulation and Solution

The objective function $J(k)$ in (3) is based on the output reference and the future predicted output using the measurement at an instant k.

$$V = \sum_{j=1}^{N_P} \parallel \bar{y}(k+j) - y_r(k+j) \parallel_Q^2 + \sum_{j=0}^{N_c-1} \parallel \Delta u(k+j) \parallel_R^2 \tag{3}$$

where, $\Delta u(k+j) = u(k+j) - u(k+j-1) : j = 1, ...N_c - 1$ and $\|x\| \equiv \sqrt{x^T Q x}$ denoted the weighted 2-norm of the vector x. N_p and N_c are the prediction and control horizon based on the desired set-point trajectory $y_r(k+j)$ and the predictive output $\bar{y}(k+j)$ at instant k for $j = 1, 2, 3...N_p$. The prediction and control horizon should satisfy the condition i.e. $N_p \geq N_c$. Q and R are the weights which are used to prioritize the plants output , the rate of change of control action and the change in control action. The optimization problem of NMPC can be defined as

$$\begin{aligned} \min_{U_k} \quad & V(y(k),u(k)) \\ \text{s.t.} \quad & \mathbf{y}_{min} \leq \bar{y}(k+j) \leq \mathbf{y}_{max} j = 1, 2, ...N_p, \\ & \mathbf{u}_{min} \leq u(k+j) \leq \mathbf{u}_{max} j = 0, 1, ...N_c - 1, \\ & \Delta \mathbf{u}_{min} \leq \Delta u(k+j) \leq \Delta \mathbf{u}_{max} j = 0, 2, ...N_c - 1 \end{aligned} \tag{4}$$

The NMPC controller calculates a sequence of optimal solutions of the problem (3)-(4) in which the first optimal control signal is applied to the system, i.e.,$U^* = u_1^*$. The optimization issue is solved at every next interval by using new process parameters by liniarizing the nonlinear problem at sampling instant as shown in Fig. 1.The optimal move calculated by quadratic programming (QP) is sent to the real time plant.

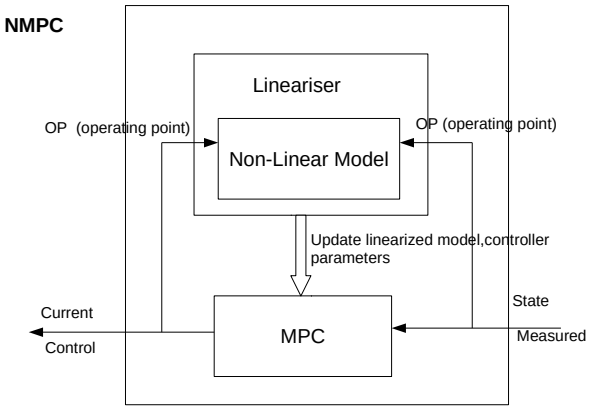

Fig. 1. Successive linearized NMPC

III. NMPC APPLIED TO SRIP

NMPC is implemented using the National Instruments LabView software on the QUARC SRIP Hardware Setup [15]. The highly nonlinear SRIP system is the most popular test platform to assess different control algorithms. The system has a rotational arm and pendulum. The rotation arm is exited by a motor for balancing the pendulum in the inverted position.The SRIP system is represented in Fig.2 which shows that the plan of the rotary arm is orthogonal to pendulum.

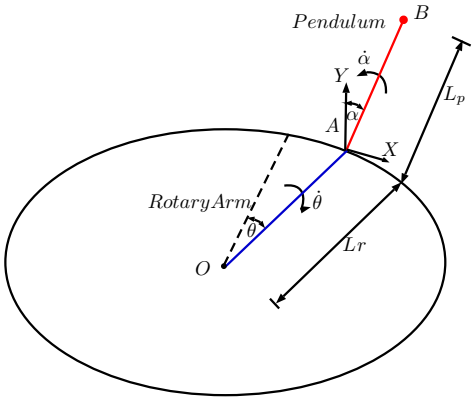

Fig. 2. Typical representation of SRIP system

A. Control relevant model of SRIP

The electrical and torque characteristic equations are formulated by using the values of Inverted Pendulum and Rotary arm parameters for mathematical model derivation. The required hardware system parameters for the state-space model are given in the table 1. There is a state vector x^T=$[\theta, \alpha, \dot{\theta}, \dot{\alpha}]$ and θ represents the rotary arm position, α is the pendulum angle, $\dot{\theta}$ is the rotary arm velocity and $\dot{\alpha}$ is the pendulum angular velocity. The measured outputs are $y^T = [\theta, \alpha]$. The function g maps the rotary arm position and the pendulum position which are the measured outputs. The function f maps the current

state and input to the next state . This model is utilized for prediction of the state trajectory over a prediction horizon N_p and the proper control action taken in order to move the state from an initial condition to the desired position. The nonlinear function of the SRIP based on the states is described by (5) and function for output by (6).

$$\begin{aligned}
f_1 &= \dot{\theta};\\
f_2 &= \dot{\alpha};\\
f_3 &= (d.u + h.cs.cos(\alpha).sin(\alpha) - Br.\dot{\theta}.d\\
&\quad - 2.b.d.sin(\alpha).cos(\alpha).\dot{\theta}.\dot{\alpha}\\
&\quad - d.cs.sin(\alpha).(\dot{\alpha})^2\\
&\quad - cs.cos(\alpha).Bp.\dot{\alpha}\\
&\quad + b.cs.cos(\alpha).cos(\alpha).sin(\alpha).(\dot{\theta})^2)/K_1;\\
f_4 &= (cs.cos(\alpha).u - Br.cs.cos(\alpha).\dot{\theta}\\
&\quad - 2.b.cs.cos(\alpha).cos(\alpha).sin(\alpha).\dot{\theta}.\dot{\alpha} - cs^2.cos(\alpha).\\
&\quad sin(\alpha).\dot{\alpha}^2 - ((a+b) - b.cos(\alpha)^2).Bp.\dot{\alpha}\\
&\quad + ((a+b) - b.cos(\alpha)^2).b.cos(\alpha).sin(\alpha).\dot{\theta}^2\\
&\quad + ((a+b) - b.cos(\alpha)^2).h.sin(\alpha))/K_1; \qquad (5)
\end{aligned}$$

where,$K_1 = (d.(a+b-b.cos(\alpha)^2) - cs^2.cos(\alpha).cos(\alpha))$ and the constants are

$$\begin{aligned}
a &= mpLr^2 + Jr, & b &= 0.25mpLp^2,\\
cs &= 0.5mpLpLr, & d &= Jp + 0.25mpLp^2,\\
d &= Jp + 0.25mpLp^2, & h &= 0.5mpLpg
\end{aligned}$$

The output function $g(\cdot)$ is given by

$$\begin{aligned}
g_1 &= \theta;\\
g_2 &= \alpha; \qquad (6)
\end{aligned}$$

The Jacobian of $f(\cdot)$ and the $g(\cdot)$

$$A = \frac{\partial f}{\partial x} = \begin{bmatrix} 0 & 0 & 1 & 0 \\ 0 & 0 & 0 & 1 \\ 0 & \frac{\partial f_3}{\partial x_2} & \frac{\partial f_3}{\partial x_3} & \frac{\partial f_3}{\partial x_4} \\ 0 & \frac{\partial f_4}{\partial x_2} & \frac{\partial f_4}{\partial x_3} & \frac{\partial f_4}{\partial x_4} \end{bmatrix}, B = \frac{\partial f}{\partial u} = \begin{bmatrix} 0 \\ 0 \\ \frac{\partial f_3}{\partial u} \\ \frac{\partial f_4}{\partial u} \end{bmatrix},$$

$$C = \frac{\partial g}{\partial x} = \begin{bmatrix} 1 & 0 & 0 & 0 \\ 0 & 1 & 0 & 0 \end{bmatrix}, D = \frac{\partial g}{\partial u} = \begin{bmatrix} 0 \\ 0 \end{bmatrix} \qquad (7)$$

by considering the actuator dynamics as

$$\begin{aligned}
A(3,3) &= A(3,3) - Kg^2.kt.km/Rm.B(3);\\
A(4,3) &= A(4,3) - Kg^2.kt.km/Rm.B(4);\\
B &= Kg.kt.B/Rm;
\end{aligned}$$

Therefore, the nonlinear state space equation is given by

$$\begin{aligned}
\dot{x} &= Ax + Bu;\\
y &= Cx; \qquad (8)
\end{aligned}$$

The above described the dynamic model in the continuous time state space form is further descretized with sampling time Ts which is $20ms$. For applying the NMPC, access to the states at the time instant k is required. The output states are mentioned in the (6)directly measured by the by encoders. The other state values (rotary arm velocity $\dot{\theta}(k)$ and pendulum velocity $\dot{\alpha}(k)$ are approximated via a finite difference approximation with respect to the sampling time Ts is mentioned in the (9).

$$\hat{\dot{\theta}}_k = \frac{\theta_k - \theta_{k-1}}{T_s}, \qquad \hat{\dot{\alpha}}_k = \frac{\alpha_k - \alpha_{k-1}}{T_s} \qquad (9)$$

The SRIP is initially at the stable equilibrium position ($\alpha = -180\ \ degree$) and the purpose is the pendulum to be inverted ($\alpha = 0\ \ degree$) and make it stable. Based on the requirement of SRIP controller, the cost function will be formulated as per (3) for stabilizing the inverted pendulum in the upward direction by optimizing the control signal with respective to the constraints defined in (10) position of input (degree) and input voltage (V_m).

$$\begin{aligned}
-10\ degree \leq \alpha \leq +10\ degree \qquad (10)\\
-10\ V_m \leq u \leq +10\ V_m
\end{aligned}$$

TABLE I
DEFINITION OF PARAMETERS IN THE MATHEMATICAL MODEL DEVELOPMENT

Symbols	Parameters	
	Description	***Value***
Rm	Motor armature resistance	2.60 (ohm)
kt	Motor torque constant	0.00767 $(N.m/A)$
km	Motor back-EMF constant	0.00767 $(V.s/rad)$
Kg	Total gear ratio	70
Jr	Motor armature moment of inertia	0.0010 $(kg.m^2)$
g	Gravitational constant	9.81 (m/s^2)
mp	Pendulum Mass with T-fitting	0.127 (kg)
Lp	Full Length of the pendulum (w/ T-fitting)	0.337 (m)
Lr	Distance from pivot to center Of gravity	0.216 (m)
Jp	Pendulum moment of inertia	0.00120 $(kg.m^2)$
Br	Viscous damping coefficient as seen at the rotary arm axis	0.00240 $(N.m.s/rad)$
Bp	Viscous damping coefficient as seen at the pendulum axis	0.00240 $(N.m.s/rad)$

B. Control Mechanism

For the real time control of SRIP, two control actions are required. One is for swing up the pendulum i.e. downward to upward direction and second is to stabilize it in the upward (inverted) position. In this paper two separate controllers i.e. energy based swing up controller [16] and the NMPC for balancing the inverted pendulum are used which are shown in Fig. 3. This paper focused on balance control of the SRIP using NMPC. The switching of two controllers from swing up (switch 1) to NMPC (switch 2) is decided by the pendulum position angle measured by the encoder. The NMPC controller starts working as soon as the pendulum angle is $\pm$ 10 degree. Initially, the values of the different design

parameters were chosen for satisfactory control performance and avoiding excessive computational efforts. The N_p is of 22 samples and N_c is about 3 samples, respectively, with the weight matrices, $R = 0.1$ and $Q = diag([1, 5])$.

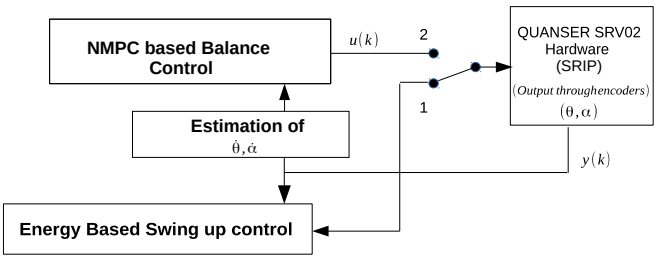

Fig. 3. Block diagram of the control structure for SRIP

C. Real-Time Hardware Implementation on cRIO

The efficacy of an FPGA based implementation of NMPC for the nonlinear real-time system is demonstrated experimentally using the core FPGA hardware. Once the required time and expected accuracy is acquired through the LabVIEW simulation, other interfacing blocks are also embedded to prototype using cRIO platform. This platform is assuring solution for the easy and fast NMPC algorithm verification.

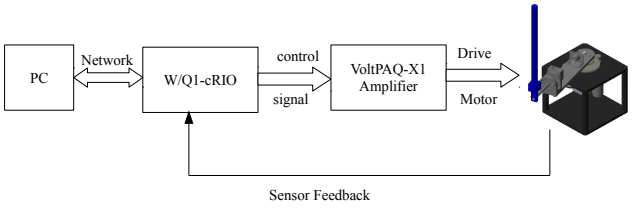

(a)

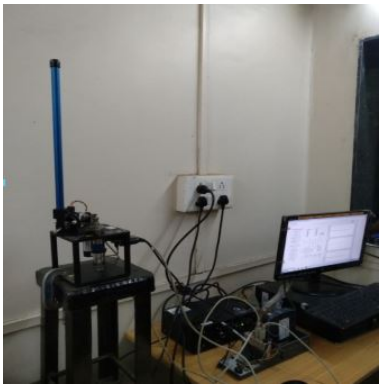

(b)

Fig. 4. (a) Interconnections of devices required for real time implementation(b) Experimental lab set up

The experimental set up has Inverted Pendulum with Q1 data acquisition card, SRV02-ET rotary servo, cRIO FPGA, a PC equipped with RCP toolkit 1.2.903, VoltPAQ-X1 Single Channel Linear Voltage Amplifier and NI MAX Measurement and Automation software provided by National Instruments (as shown in Fig. 4 (a). To realize the implementation of complete NMPC controller on cRIO FPGA, hardware-in-loop (HIL) co-simulation method has been used. The real time implementation of the NMPC, the experimental setup for the SRIP system is as shown in Fig. 4 (b). The dynamic response of the SRIP is observed and monitored through the LabVIEW. On this platform, a LabVIEW project, a HIL included in VI, and a host VI is created. On the development computer, the LABVIEW project file manages the cRIO FPGA and all the VIs. The host VI runs on a cRIO, Real Time target. The TCP/IP protocol is used to link between PC and cRIO. It acquires the signals from the Encoders mounted on the plant via the ADC input modules to calculate the control signal $u(k)$ according to the NMPC algorithm and sends it to the SRIP via analog output modules.

IV. Experimental Results and Discussion

The dynamic response of the Inverted Pendulum is observed and monitored through the LabVIEW. The response of the real-time SRIP system before and after applying the disturbance is shown in Fig. 5 and Fig. 6. In the Fig. 5(a) the real time response of the rotary arm for the stabilizing the pendulum in inverted direction (Fig. 5 (c)) has been shown with swing up control. The control efforts (Voltage) required to the rotary arm for controlling the pendulum in the upright position is shown in Fig. 5(b). Due to energy based oscillatory input the time required to reach at vicinity of the initial condition of the NMPC is somehow more, but the NMPC quickly stabilized the pendulum within a second.

For the testing of the robustness of the controller, manually disturbance is applied at the tip of an inverted pendulum at the 40 second, time instant. The extra efforts required to overcome the disturbance in terms of the rotary arm position and the input voltage shown in Fig. 6(a) and Fig.6(b) respectively. The inverted pendulum stabilized quickly against the disturbance within a second which explored in Fig.6(c).

V. Conclusion

The NMPC is successfully controlled and balanced the inverted position of the pendulum irrespective of the 20 ms fast sampling rate. For checking the disturbance rejection capability, the small disturbance is applied manually at the tip of the inverted pendulum. The control input and the rotary arm position follow their respective limits which is defined as a constraints. The pendulum is swiftly returned to the upright position. Real time challenging problems can handle rapidly on cRIO (FPGA) hardware platform with NMPC. For testing the efficacy of NMPC for the nonlinear plant, rigorous experimentation has performed with different sets of tuning parameters. By selecting an appropriate tuning parameters for NMPC, experimental result shows, the NMPC on FPGA achieve satisfactory performance with robustness.

To avoid the requirement of the two separate controllers, the future work may be focused on the formulation of the NMPC

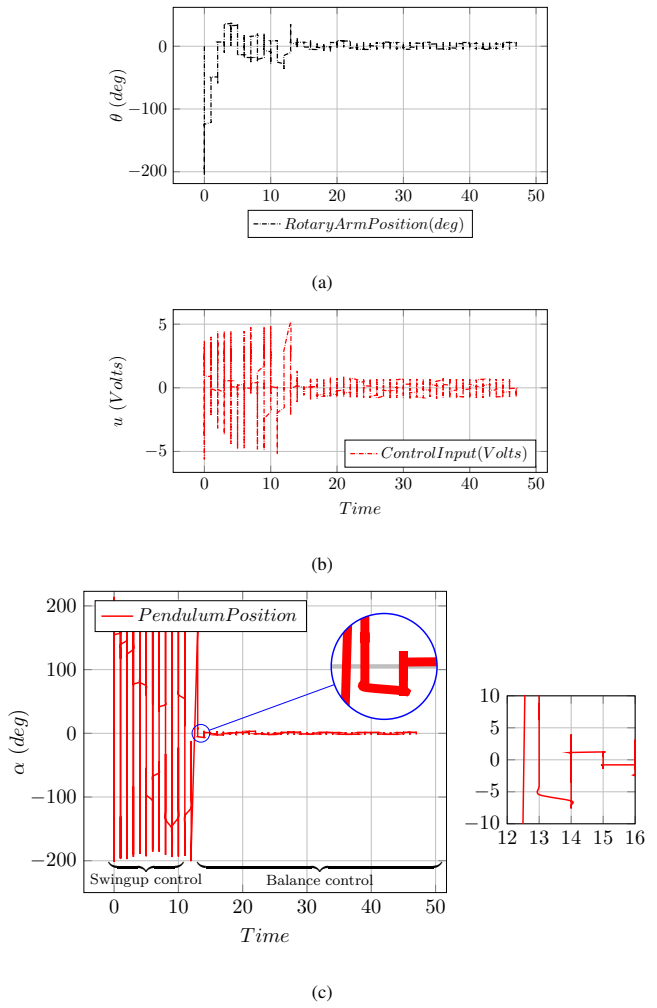

Fig. 5. Qansers SRV02-ET rotary servo systems (SRIP) response of (a) rotary arm (b) control input and (c) pendulum to NMPC algorithm with swing up and balance control without any disturbance

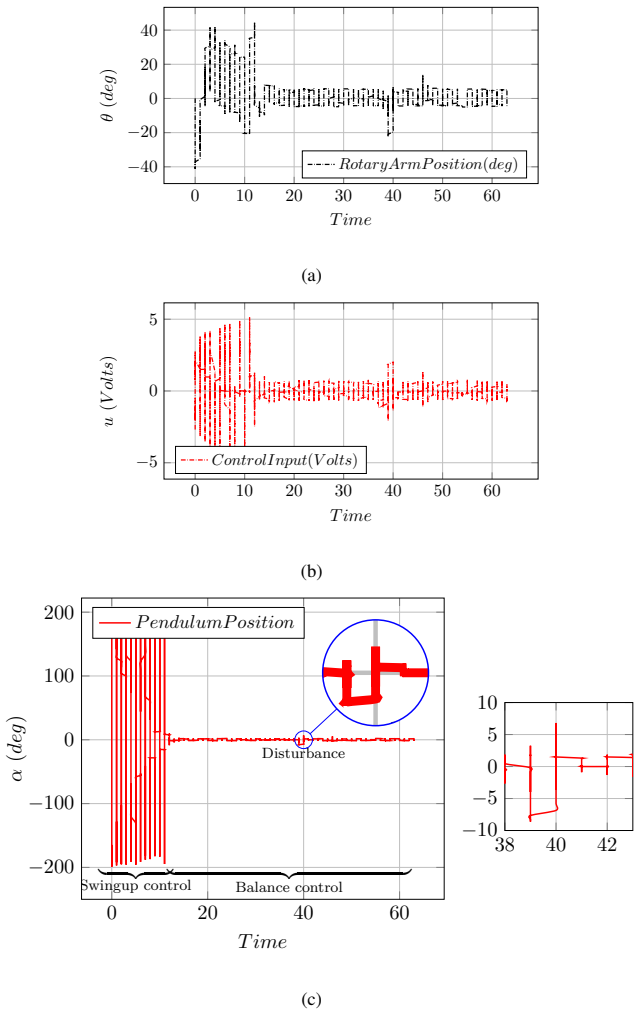

Fig. 6. Qansers SRV02-ET rotary servo systems (SRIP) response of (a) rotary arm (b) control input and (c) pendulum to NMPC algorithm with swing up and balance control with manual disturbance

such that it will be the self sufficient controller for controlling the swing up and the balance control of SRIP efficiently within optimum time.

REFERENCES

[1] J. M. Maciejowski, Predictive control with constraints, UK, Prentice Hall, Harlow, 2000.
[2] E. F. Camacho., C. Bordons, Model Predictive Control, London:Springer-Verlog, 2004.
[3] J. S. Qin, T. A. Badgwell, "A survey of industrial model predictive control technology", Control Engineering Practice, 11(7):733-764, July 2003.
[4] F. Allgower, R Findeisen, L. Biegler, "Assessment and Future Directions of Nonlinear Model Predictive Control",Springer: Berlin, 2007.
[5] H. Han and J. Qiao, "Nonlinear Model-Predictive Control for Industrial Processes: An Application to Wastewater Treatment Process",in IEEE Transactions on Industrial Electronics, vol. 61, no. 4, pp. 1970-1982, April 2014.
[6] H. L. Jay, "Model predictive control: Review of the three decades of development", International Journal of Control,Automation, and Systems, 9: 415, 2011.
[7] S. Hiroya, O. Satoshi, O. Morimasa, "Nonlinear model predictive control using successive linearization: Application to chemical reactors", Transaction of the Society of Instrument and Control Engineers,Vol.E-3,No.1,66/72, 2004.
[8] K. Mina, B. Michael, S. Roland, " Linear vs Nonlinear MPC for Trajectory Tracking Applied to Rotary Wing Micro Aerial Vehicles ", IFAC-Papers On Line,Volume 50, Issue 1, Pages 3463-3469, ISSN 2405-8963, 2017.
[9] A. Bamimore, O. Taiwo and R. King, "Comparison of two nonlinear model predictive control methods and implementation on a laboratory three tank system ", 50th IEEE Conference on Decision and Control and European Control Conference, Orlando, FL, pp. 5242-5247, 2011.
[10] J. J. Rodrguez- Andina, M. D. Valdes-Pena, M. J. Moure, "Advanced features and industrial applications of FPGAs a review", IEEE Transactions on Industrial Informatics, vol. 11, no. 4, pp. 853-864, 2015.
[11] E. N. Hartley, J. L. Jerez, A. Suardi, J. M. Maciejowski, E. C. Kerrigan, G. A. Constantinides , "Predictive control using an FPGA with application to aircraft control", IEEE Transactions on Control Systems Technology, vol. 22, no. 3, pp. 1006-1017, 2014.
[12] H. Kee , S. Mhaske, D. Uliana, A. Arnesen, "Rapid and high-level constraint-driven prototyping using lab VIEW FPGA", IEEE Global Conference on Signal and Information Processing (GlobalSIP), Atlanta, GA, pp. 45-49, 2014.
[13] D. Ricardo ,G Javier , "Graphical MPC for fast dynamic systems", ASME 2008 International Manufacturing Science and Engineering Conference, Volume 1 Evanston, Illinois, USA, pp. 523-532, 2008.
[14] G. Harja, A. Hernandez , R. De Keyser ,I. Nascu , "Embedded real-time MPC implementation using Rapid Prototyping Tools: A thermal process case study", 17th International Conference on System Theory, Control

and Computing (ICSTCC), Sinaia, pp. 250-255, 2013.
[15] Qansers, "SRV02-ET rotary servo and Rotary Pendulum Model" Instructor manual, 2012.
[16] K.J. Astrom, K. Furuta ,"Swinging up a pendulum by energy control", Automatica, 36, pp. 287-295, 2000.

Proceedings of the Fourth International Conference on Communication and Electronics Systems (ICCES 2019)
IEEE Conference Record # 45898; IEEE Xplore ISBN: 978-1-7281-1261-9

PANCHENDRIYA: A Multi-sensing framework through Wireless Sensor Networks for Advanced Border Surveillance and Human Intruder Detection

Arjun D, Indukala P K, K A Unnikrishna Menon
Amrita Center for Wireless Networks & Applications (AmritaWNA)
Amrita School of Engineering, Amritapuri
Amrita Vishwa Vidyapeetham
India
arjund@am.amrita.edu, indukalapk@am.amrita.edu, kaumenon@am.amrita.edu

***Abstract*—Nowadays, almost all countries are facing the problem of internal security from their border areas. Terrorists and intruders are disturbing the tranquillity and consonance of the country. The casualty prompted by the recent Pulwama strike and Uri attack against Indian military force reveals the significance of effective surveillance in the border region and detection of the human intruder in that area to control the terrorist activities on borders. Traditional border patrol systems require a huge number of military persons, and high-cost, high-tech surveillance devices employed in unmanned border patrol systems. Line of sight restrictions and high false alarms are the problems experienced by using any of these techniques. There is a need in developing a multi-sensing system that integrates different technologies to detect the human intrusion with improved system accuracy in flat border areas, border areas with river or pond crossings and border areas covered by dry leaves. The paper proposes a hybrid Wireless Sensor Network system architecture named "PANCHENDRIYA", utilizing the integration of five types of sensors: Geophones, Hydrophones, Microphones, Infrared sensors and Camera sensors for effective surveillance and detection of human intrusion in the above-mentioned border scenarios with early warning capability.**

Keywords—Wireless Sensor Networks, Multi-sensing system, Border surveillance, Intruder detection

I. INTRODUCTION

All governments expressed the necessity of effective surveillance and intrusion detection system to govern the risks of intrusion on borders either for unauthorized goods transportation or for terrorism. India is facing terrorist attacks from Pakistan and violation of truce across the LoC (Line of Control) in Jammu & Kashmir, which presently interrupted the peace and harmony of the nation. Chinese interruptions through the Sino-Indian border also creates problems in that region. Infiltration and violation of truce through LoC is persistent in the last couple of months. These incidents will turn to the need of a multi-sensing system with less human involvement for efficient detection and tracking of human intruders to providing early warning to the Central Monitoring Station after detecting any kind of intrusion by coordinating various technologies.

Wireless Sensor Network (WSN) is an emerging field for connecting the physical and digital world [1]. The WSN framework is used to monitor physical or environmental conditions with the aid of autonomous devices using sensors [2]. WSNs are mainly used in military, health, environmental and home applications [3]. To overcome the challenges faced by the existing surveillance methods, a new multi-sensing system named "PANCHENDRIYA" is proposed to detect the presence and track the human intruder movement through advanced WSNs. PANCHENDRIYA is a new framework with minimum human involvement for solving the problem of unauthorized movement of the human intruders. The paper proposes a new architectural design model for sensing and detection circuits based on the following three scenarios: flat border areas, the border area with river or pond crossings, and the border area covered by dry leaves. The methodology behind the system design is an adaptive platform that could be built later and expanded.

The related works in the border surveillance and intruder detection field is provided in Section II. The system architecture of PANCHENDRIYA is explained in Section III. The block diagram of the system is mentioned in Section IV. WSN model of the system is described in Section V. Section VI explains the overall workflow of the proposed system.

II. RELATED WORKS

The research work of Sun, Zhi, et al., named Border Sense is an architectural proposal consists of three layers namely, Lower layer, Second layer and Higher layer [4]. Underground and ground-based sensors employed in Lower layer improves the quality of monitoring. Multimedia sensors incorporated to the Second layer provides visual information that increases the system accuracy. Unmanned Aerial Vehicles and the lightweight ground robots in the Higher layer provides extra coverage and flexibility to the monitoring system.

Succi et.al., introduced the human intruder detection through footstep signals using kurtosis method under the various style of walking with single and multiple walkers and different test environments [5]. The development of the human

intrusion detection algorithm is based on intrusion detection within the range of the sensors.

Deekshit et.al., work involved a smart geophone sensor network for detecting landslide induced signals by removing different noises that arrive from footstep, rainfall and movement of vehicles [6]. A simple solution using Arduino based data acquisition system with geophone sensor is developed. The resonance frequency is the key factor in a geophone and it has to be kept low for the measurement of the low-frequency signals.

The ground permits the propagation of waves through it. The human footstep signal imposed on the ground is able to detect 100m away from the sensor region under ideal situations. The Rayleigh wave is the main seismic wave considered for human footstep signal detection. It carries 67% of energy from the footsteps and is captured using tri-axial geophones [7].

Passive Infrared sensor (PIR) and MICAz motes are used for human intrusion detection in the border areas [8]. The proposed system captures the direction of the human intruder movement and the speed of walking. The collected information is communicated to the central monitoring station for further analysis. PIR sensor placement follows line topology and a direct line of sight for detection.

Nakadai, Kazuhiro, et al., used a distributed microphone array for human footstep detection. The overall system setup comprises of sound acquisition, event detection and signal conditioning with coarse to the fine procedure for signal peak detection in the time domain [9]. It also uses the Support Vector Machine (SVM) technique for classification of sound signals in a real-life situation and understanding the real event based on the velocity of the sound generated.

Marius Vasile Ghiurcau, Corneliu Rusu, et al., introduced a technique called Time Encoded Signal Processing and Recognition or TESPAR for testing the performance of a monitoring system and concluded that using TESPAR, the classification of sounds generated by human, birds, and vehicles can efficiently be carried out [10]. Complex waveforms can be represented in digital form using TESPAR, which is based on the infinite clipping theory of researchers, Licklidder and Pollack.

Sutin, Alexander, et al., proposed a framework incorporated with Hydrophone sensors named as SPADES (Stevens Passive Acoustic Detection System) for detection, tracing and categorization of dissimilar sounds in surface and submerged outset [11]. The information captured by the Hydrophone sensors is sent to the land-based personal computers for further analysis.

Harish, Palagati, et al., uses video content captured through surveillance camera for intrusion detection and tracking [12]. The proposed method extracts features of the object and semantic contents from the video. The paper also provides information on object movement in the observed area of interest using the semantic content.

III. PANCHENDRIYA - SYSTEM ARCHITECTURE

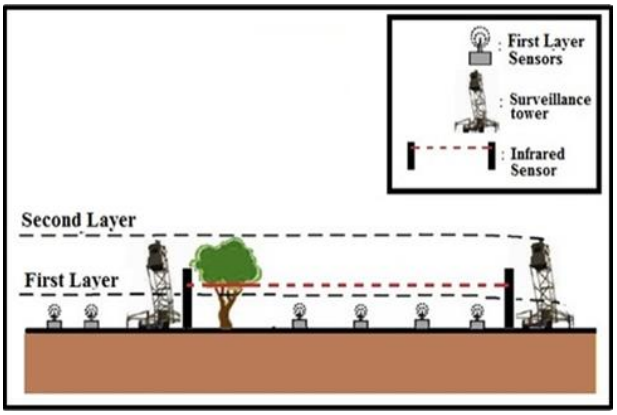

Fig. 1. Different layers of the architecture for a single zone

The proposed system (Fig. 1.) is a multi-sensing system used to monitor and detect any kind of human intrusion in the border area with the aid of low power sensors. The use of low power sensors will improve the efficiency and reliability of the system. A country border is a vast area, which is divided into different zones and the architecture for each zones are designed. The overall architecture of the system contains two layers:

- The First Layer of the architecture contain sensors such as Geophones, Microphones, and Hydrophones that can detect the presence, and track the direction of intruder movements.
- The Second Layer contain surveillance Cameras and Infrared sensors. Cameras provide multimedia information, which enhances the overall system accuracy through visual information and provides better border surveillance. Infrared sensors are used to identify the movement of intruders, whether movement is from Country B (Opposite country) to Country A (Own country) or in reverse direction.

The sensors are deployed based on their coverage range (Fig. 2.), considering the single zone of the overall architecture. The entire deployment region under consideration is covered by the least number of sensors. The proposed system detects the presence and movement of the human intruder by considering three border situations: flat border area, border region with river or pond crossing, and the border region covered by dry leaves. The above-mentioned situations are considered based on the real border region scenarios. When the intruder moves from Country B to Country A, the five sensors involved in the proposed framework performs the following actions. Geophones detect the footstep movement of the human intruder in flat border areas, Hydrophones detects the movement of the intruder crossing the river or pond, and Microphones detects the movement through the dry leaves. The Infrared sensors provide the information of intruder crossing the borderline and finally, the Camera sensors capture the visual information of the intrusion in the border region. The self-excitation capability of Geophone and Hydrophone sensors are helpful to detect the human footstep signals far away from the borderline is helpful to achieve early warning capability.

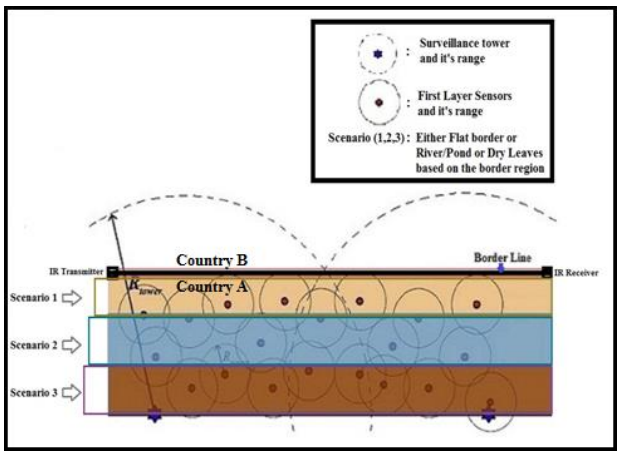

Fig. 2. Deployment of Sensor Nodes for single zone

IV. Block Diagram

The block diagram of PANCHENDRIYA system is shown in Fig. 3. The data acquisition module of the First Layer continuously collect data from each sensors and communicate to the Central Monitoring Station through wireless transmission. The event/signal detection algorithm based on the predefined detection threshold is used for human footstep signal detection in the First Layer. The predefined threshold values of human footstep imposed on each border scenario are fixed based on the various field tests conducted in the testbed. The detected signal is compared with the predefined threshold values. If the detected signal value is greater than the detection threshold value, then there is a human intrusion happening in the border. The Second Layer containing the Infrared sensor with an IR transmitter and receiver section detects the intruder movement between the borderline. The system counts the number of intruders present in the particular sensor region. The Second Layer include Camera sensors that continuously surveillance the border area. Once any kind of intrusion is identified, the Camera sensors rotated immediately to the particular sensor region. The detected signals and the multimedia information captured from the Second Layer through respective data acquisition modules are pre-processed using signal detection algorithm/image processing algorithm in the Central Monitoring Station. Thus, the proposed system achieves in getting a clear picture of the human intrusion occurring in the border area. Once any kind of human intrusion is detected, the Central Monitoring Station sent the warning messages to the border troops for further actions.

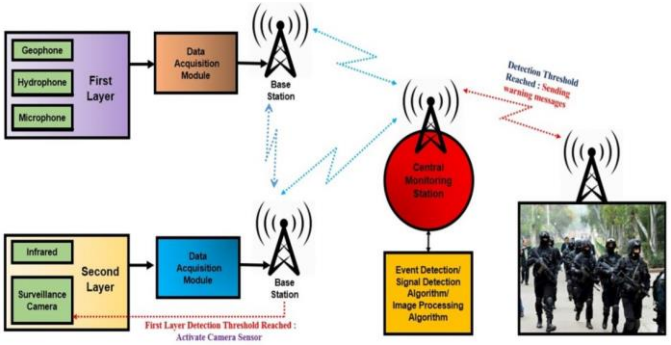

Fig. 3. Block Diagram of PANCHENDRIYA

V. WSN Model

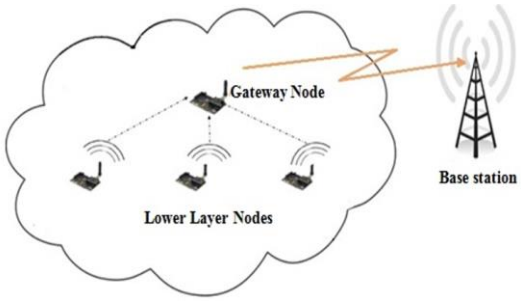

Fig. 4. WSN system architecture

The sensor nodes in the WSN system architecture is shown in Fig. 4. It contains three Lower Layer nodes such as a Geophone, Hydrophone, and Microphone sensors and a Gateway node. The data from Lower Layer nodes are communicate to the Gateway node. Gateway node further forwards the data to the Central Monitoring Station through the base station.

The State diagram of individual Lower Layer sensor nodes in the three particular border scenarios and the state diagram of the Gateway node are shown in Fig. 5. Each individual node is incorporated with different operational states such as:

- OFF: Power null/ energy consumption equals to zero.
- Listen: Radio module is active but no transmission or reception of any packets.
- Sleep: Radio module is inactive and the node is in the sleep mode. It needs some trigger pulse to get back to the listen state.
- Active: Whenever a node is triggered to an active state, it will provide transmission and reception.

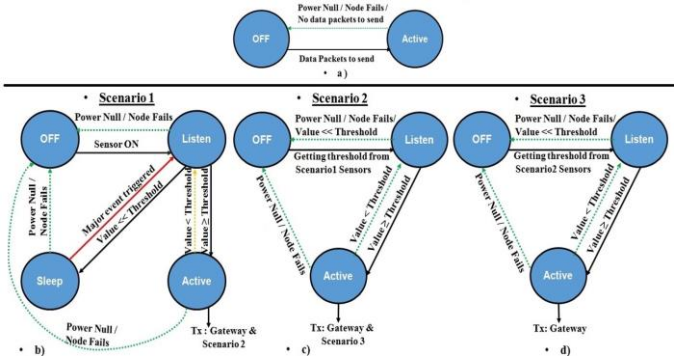

Fig. 5. State diagram of: a) Gateway node, b) Geophone sensor node, c) Hydrophone sensor node and d) Microphone sensor node

VI. Proposed System Flow Chart

The overall work flow of the proposed system is shown in Fig. 6. The test bed is planning to prepare under three border scenarios. The First Level of the testbed include Infrared (IR) and Geophone sensor, the Second Level includes Hydrophone and the Third Level include Microphone and Camera sensor.

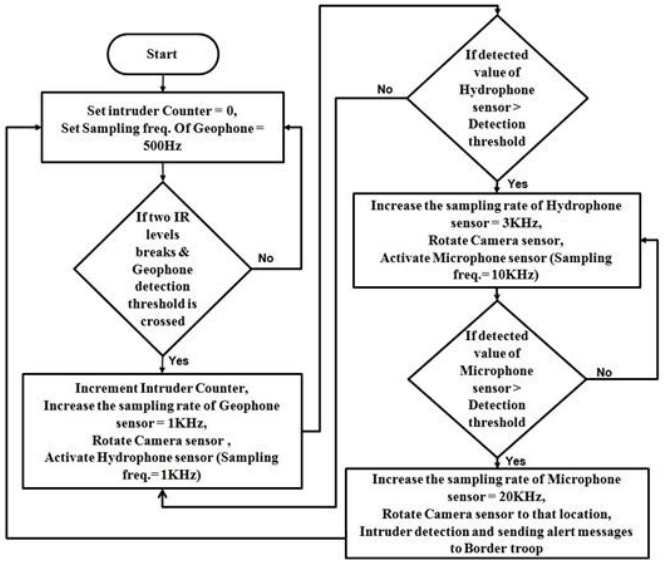

Fig. 6. Overall System Flow Chart

Initially, the bidirectional IR counter circuit is set to zero (no intrusion) and the sampling frequency of Geophone is set to 500Hz. When a human intrusion happens in the border region, the two IR levels are interrupted, showing the sign of intrusion and incrementing the counter value by one. The Geophone continuously monitors the region of interest and self-excited based on the footstep of the intruder. The sampling frequency is increased to 1 KHz, if the predefined detection threshold of the Geophone is crossed. After the First Level intrusion detection, Camera sensor in the surveillance tower immediately rotates into the First Level sensor region, activates the Hydrophone sensor in the Second Level, and collect signals with a sampling frequency of 1 KHz. If the Hydrophone detects signals greater than the predefined detection threshold value, the Camera sensor then rotates into the Second Level sensor region and activates the Microphone sensor in the Third Level. When the detection threshold of the Microphone is crossed, it collects data at a sampling frequency of 3 KHz. If the detection threshold value of the Microphone is greater than the predefined detection threshold due to human intrusion in the Third Level, the Camera sensor immediately rotates into the Third Level sensor region and at the same time, a human intrusion message is sent to the border troop from the Central Monitoring Station. The detection process is iterative. After each detection, the system returns to the initial state and the human intrusion detection process is continued.

VII. Conclusion and Future Scope

The proposed framework "PANCHENDRIYA" delivers a new system architecture, block diagram, overall system flowchart and WSN model for human intruder detection in three different border scenarios such as flat border regions, border region with river or pond crossings, and the border region covered by dry leaves. The proposed multi-sensing approach utilizes Geophones, Microphones, Hydrophones, Infrared and surveillance Camera sensors, and wireless communication capabilities that provide efficient border surveillance and human intruder detection. The future work focuses on building a testbed setup for analyzing the performance of this multi-sensing system and validation of the proposed system based on various test procedures. Thereby the system capability is ensured to detect any kind of human intrusions effectively in the above-said border scenarios, and to provide early warnings.

Acknowledgment

We express our deep gratitude to our chancellor and world-renowned humanitarian leader Sri Mata Amritanandamayi Devi (AMMA), for her inspiration and support towards working on interdisciplinary research that has direct societal benefit.

References

[1] Arjun D; Indukala P K; K A Unnikrishna Menon; "Border Surveillance and Intruder Detection Using Wireless Sensor Networks: A Brief Survey," International Conference on Communication and Signal Processing, 2017, pp. 1125 - 1130.

[2] Ramesh, Maneesha V. "Real-time wireless sensor network for landslide detection." In Sensor Technologies and Applications, 2009. SENSORCOMM'09. Third International Conference on, pp. 405-409. IEEE, 2009.

[3] Ramesh, Maneesha V., and Nirmala Vasudevan. "The deployment of deep-earth sensor probes for landslide detection." Landslides 9, no. 4 (2012): 457-474.

[4] Sun, Zhi, Pu Wang, Mehmet C. Vuran, Mznah A. Al-Rodhaan, Abdullah M. Al-Dhelaan, and Ian F. Akyildiz. "BorderSense: Border patrol through advanced wireless sensor networks." Ad Hoc Networks 9, no. 3 (2011): 468-477.

[5] Succi, George P., Gervasio Prado, Robert Gampert, Torstein K. Pedersen, and Hardave Dhaliwal. "Problems in seismic detection and tracking." In AeroSense 2000, pp. 165-173. International Society for Optics and Photonics, 2000.

[6] Deekshit, V. N., Maneesha Vinodoni Ramesh, P. K. Indukala, and G. Jayachandran Nair. "Smart geophone sensor network for effective detection of landslide induced geophone signals." In 2016 International Conference on Communication and Signal Processing (ICCSP), pp. 1565-1569. IEEE, 2016.

[7] D. Succi, D. Prado, R. Gampert, T. Pedersen, and H. Dhaliwal, "Problems in seismic detection and tracking." Proc. SPIE 4040, Unattended Ground Sensor Technologies and Applications II, July 2000.

[8] Jisha, R. C., Maneesha V. Ramesh, and G. S. Lekshmi. "Intruder tracking using wireless sensor network." In Computational Intelligence and Computing Research (ICCIC), 2010 IEEE International Conference on, pp. 1-5. IEEE, 2010.

[9] Nakadai, Kazuhiro, Yuta Fujii, and Shigeki Sugano. "Footstep detection and classification using distributed microphones." In Image Analysis for Multimedia Interactive Services (WIAMIS), 2013 14th International Workshop on, pp. 1-4. IEEE, 2013.

[10] Ghiurcau, Marius Vasile, Corneliu Rusu, and Radu Ciprian Bilcu. "Wildlife intruder detection using sounds captured by acoustic sensors." In 2010 IEEE International Conference on Acoustics, Speech and Signal Processing, pp. 297-300. IEEE, 2010.

[11] Sutin, Alexander, Barry Bunin, Alexander Sedunov, Nikolay Sedunov, Laurent Fillinger, Mikhail Tsionskiy, and Michael Bruno. "Stevens passive acoustic system for underwater surveillance." In Waterside Security Conference (WSS), 2010 International, pp. 1-6. IEEE, 2010.

[12] Harish, Palagati, R. Subhashini, and K. Priya. "Intruder detection by extracting semantic content from surveillance videos." In Green Computing Communication and Electrical Engineering (ICGCCEE), 2014 International Conference on, pp. 1-5. IEEE, 2014.

Proceedings of the Fourth International Conference on Communication and Electronics Systems (ICCES 2019)
IEEE Conference Record # 45898; IEEE Xplore ISBN: 978-1-7281-1261-9

Disparity Map Estimation Using Combined Cost Measure

Deepa
Department of IS&E
N.M.A.M Institute of Technology, Nitte
Karkala, Karnataka, India
deepashetty17@nitte.edu.in

Jyothi K
Department of IS&E
J.N.N College of Engineering, Shimoga
Karnataka, India
jyothi6575@gmail.com

Abstract— ***Disparity map generation is necessary in many 3D applications. This paper focuses on disparity map estimation using local based stereo matching. Stereo correspondence algorithms are categorized as global method and local method. Global based methods are computationally expensive. This paper proposes an improved stereo matching algorithm by using local method which combines cost computation of gradient information and histogram of oriented gradient. The results obtained shows better quality disparity map.***

Keywords— Disparity; Gradient; Histogram

I. INTRODUCTION

Stereo correspondence between the pair of stereo images results in disparity map. The disparity map finds its use in depth estimation which is used in different applications like robotics, 3D reconstruction of scene, and artificial intelligence. Hence disparity map generation is a crucial and a difficult job in the area of computer vision. Stereo correspondence problem aims at finding matching pixels between stereo pair. The stereo correspondence algorithms are broadly categorized into two methods namely local method and global method [1-9]. Active research is conducted in the recent years to solve stereo correspondence problem to obtain disparity map [10, 11]. Local based methods obtain disparity from local information. Local methods are then classified as area based and feature based. Area based method correlate certain patches of area among the images. This method takes an area on the left image and finds an equal sized area in the right image which is closest match possible. This area is called matching window. The x coordinate difference between the centre of the matching window and the centre of the left window is the disparity value. Usually the small sized window will produce more detail but they are prone to more noise. Large sized window produce a smooth disparity map but with less detail. Hence finding the optimal sized window is the challenging task. Feature based method computes the matching pixel by using certain features extracted from the image. These features include corners, edges. Local based methods are simple and computationally less expensive. The global based method computes the disparity using optimization of the whole image globally. Global stereo matching algorithm focuses on minimizing the global cost function. This method is generally less sensitive to local individualities. These methods gives better result but computationally expensive. The accuracy of the local method depends on appropriate selection of similarity measure function and optimal window size. Generally stereo matching algorithm finds corresponding points based on intensity. But they do not perform well near boundaries and depth discontinuities. To reduce this problem many researches are conducted to determine corresponding points in these regions. Authors in [12, 13, and 14] find the corresponding points based on information such as gradient. These gradient based methods perform well near the boundaries. But the individual gradient information may be prone to noise. Hence the proposed method uses histogram of oriented gradients along with gradient value to reduce noise. The authors in [15] combined the gradient of the image and the intensity to find the matching cost. The combined measurement of the cost produced better result than the individual one. Hence combined cost technique is implemented in this paper.Traditional method computes the disparity by comparing only intensity value or gradient value. This paper proposes a novel technique of generating disparity map based on local method by combining the gradient information and histogram of oriented gradients (HOG) to enhance the reliability of the matches. The disparity map obtained is post processed by applying median filter to generate the refined disparity map. The results produced shows that the method proposed in this paper yields better result than the existing approach which is based on gradient information.

Section II includes details of the methodology described in the paper. The results obtained on various kinds of images are given in section III. Section IV includes concluding remarks

II. PROPOSED ALGORITHM

The various steps of proposed method for disparity map generation are as follows

A. Stereo Matching

Stereo matching using local based method relies on cost function for matching. There are various dissimilarity measures for cost computation such as sum of absolute

difference, sum of squared intensity difference (SSD). Here SSD for matching cost of gradient and histogram of gradients (HOG) is used. Gradient of the image plays a significant role in the area of computer vision. Color intensity is sensitive to distortions and illumination differences.Image gradient has structural details of the image. Hence it is insensitive to differences in illumination. Gradient of images are generated from the initial image by convolving it by a filter. Here Sobel filter is used. Every pixel present in the gradient image computes the variation of intensity of the corresponding point present in the initial image, which is in a particular direction. To get the complete range of the direction, gradient images are calculated in x and y direction.

$$\Delta f = \begin{bmatrix} Gx \\ Gy \end{bmatrix} = \begin{bmatrix} \frac{\partial f}{\partial x} \\ \frac{\partial f}{\partial y} \end{bmatrix} \quad (1)$$

Here $\frac{\partial f}{\partial x}$ gives the image gradient tin the x direction and $\frac{\partial f}{\partial y}$ gives the image gradient in the y direction.

Considering only gradient information may be sensitive to noise, hence HOG descriptor is also used in the proposed method to make it less sensitive to noise. The HOG is a feature descriptor used in computer vision. This counts the number of occurrences of orientation of gradient in a portion of image. HOG descriptor is invariant to photometric transformations. The image is grouped into small connected regions called as cells, and for each connected region we compute a histogram of unsigned gradient orientation. The histograms for all connected regions are then combined to get the HOG descriptor.

The proposed algorithm finds squared differences of gradient value and HOG feature. To compute the squared differences we subtract the gradient value and HOG value of a pixel in the left image with the corresponding gradient value and HOG value in the right image. Then the square of the differences is computed. The sum of squared differences of all the pixels enclosed within the window is then computed. The cost function based on gradient and HOG is calculated as follows

.

$$CG(x,y) = \sum_{(x,y)\epsilon W}^{N} |Gl(x,y) - Gr(x-d,y)|^2 \quad (2)$$

$$CH(x,y) = \sum_{(x,y)\epsilon W}^{N} |Hl(x,y) - Hr(x-d,y)|^2 \quad (3)$$

Here $Gl(x,y)$, $Gr(x-d,y)$ are gradient information of the left reference and the right image. $Hl(x,y)$, $Hr(x-d,y)$ are the HOG values of pixel(x, y) of the left reference image and of the right image, d shows the disparity value. w is the square window of size 8 x 8 that surrounds the pixel (x, y).

The least difference value over the window shows the best matching pixel, and the location of this minimum information gives the optimal disparity of the actual pixel. Here the optimal disparity based on gradient and optimal disparity based on HOG feature is found. This yields two disparity values based on gradient information and HOG value. The disparity map is obtained by combining the weighted sum of two disparities.

$$d = (\propto * d_1) + (\beta * d_2) \quad (4)$$

Here d_1 is the disparity obtained based on gradient, d_2 is the disparity obtained based on HOG and $\propto + \beta = 1$. Here we used $\propto = 0.8$ and $\beta = 0.2$

B. Post Processing

The post processing of initial disparity map is performed using a median filter. Median filter selects the median value of the pixels enclosed in a window and replaces each pixel value in the image by the median value ofl the pixels enclosed in the window. This median value is computed by first sorting the entire pixels contained in the window. Then the pixel under consideration takes the value of the middle pixel.

III. EXPERIMENTAL RESULTS

In the proposed method we used images from Middlebury dataset to assess the performance [16, 17].The images like cones, Teddy, Baby were used. Result is shown in Fig 1.

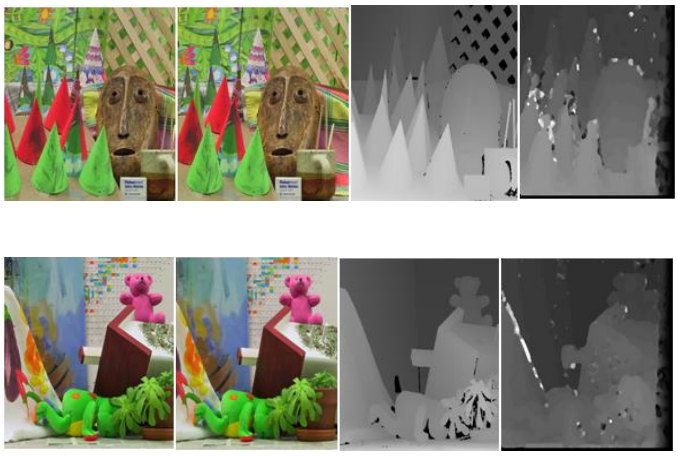

(a) (b) (c) (d)

Fig. 1 Results for images , cones , Teddy, Baby . (a) *Input left* image, (b) Input right image, (c) Ground truth image (d) Disparity Map

Quantitative analysis is done using the metric like percentage of bad matching pixel (PBMP) and root mean square error (RMSE).

PBMP is generally used to analyze the quality of the disparity map.PBP is computed as follows

$$PBMP = \frac{\left[\sum_{x,y} dt(x,y) - dg(x,y) > \delta\right] * 100}{N} \quad (5)$$

Here N is the total count of pixels dt represents the disparity map generated by the proposed method, dgrepresents the disparity map of the ground truth image, and $\delta$is the error threshold. In the proposed method the value of this error threshold is taken as 1. Lower PBMP value gives better quality disparity map.

Table 1 shows the PBMP values calculated using gradient based method and proposed method. We find the bad matching pixel percentage obtained in the proposed method is less than the gradient method.

Table 1: PBMP

	Gradient based	Proposed Method
Cones	2.4246	2.3086
Teddy	1.4160	1.3992
Baby	0.1953	0.1052

RMSE is calculated between the computed disparity map and the ground truth map using the following equation

$$RMSE = \left(\frac{1}{M * N}\sum\sum(dc(x,y) - dt(x,y))^2\right)^{1/2} \quad (6)$$

Here dt is the computed disparity map and dg is the ground truth disparity map. M and N represent the number of rows and columns present in the image. Lower RMSE value gives better quality disparity map.

Table 2 shows RMSE values calculated using gradient based method and proposed method. We find the RMSE of the images obtained in the proposed method is less than the gradient method.

Table 2: RMSE

	Gradient based	Proposed Method
Cones	15.26	14.81
Teddy	15.11	14.87
Baby	8.55	7.27

IV. CONCLUSION

This paper proposes an improved stereo matching method using combination of gradient information and HOG information. The effectiveness of the method proposed is analyzed using different stereo pairs from Middlebury dataset. The results obtained indicate that the proposed method produces high quality disparity map and outperforms the existing method in terms of PBMP and RMSE.

References

[1] Muhlmann K, Maier D, Hesser R, Manner R " Calculating dense disparity maps from color stereo images, an efficient implementation". In: Proceedings of the IEEE workshop on stereo and multi-baseline vision , pp 30–36,2001.

[2] M.Z. Brown, D.Burschka,G.D. Harger "Advances in computational stereo". IEEE Transactions on Pattern Analysis and Machine Intelligence,vol 25,no 8, pp 993-1008, 2003

[3] Hamzah R, Hamid A, Md. Salim S "The solution of stereo correspondence problem using block matching algorithm in stereo vision mobile robot". IICRD, pp 733–737,2010.

[4] D.Scharestein and R.Szeliski "A taxonomy and evaluation of dense two-frame stereo correspondence algorithms".International Journal of Computer Vision, vol 47, no 1-3, pp 7-42, 2002.

[5] K. Zhang, J.Lu,G. Lafruit "Cross-based local stereo matching orthogonal integral images". IEEE Transactions on Circuits and Systems for Video Technology,vol 19, no 7,pp 1073-1079,2009

[6] Prabhakar C.J., Jyothi K. " Adaptive Support Weight-Based Stereo Correspondence Algorithm for Face Images".Emerging Research in Electronics, Computer Science and Technology. Springer, New Delhi ,Vol 248,pp479-485,2014.

[7] Yoon KJ, Kweon IS " Adaptive support-weight approach for correspondence search ". IEEE Trans Pattern Anal Mach Intell 28:650–656,2006.

[8] O. Veksler "Stereo correspondence by dynamic programming on a tree" IEEE CVPR, vol 2,pp 384-390, 2005.

[9] J.Kim, K.M.Lee, B.T.Choi,S.U.Lee "A dense stereo matching using two-pass dynamic programming with generalized ground control points" IEEE CVPR, vol 2, pp 1075-1082, 2005.

[10] G. Calin, V. Roda "Real-time disparity map extraction a dual head stereo vision system" Latin American Applied Research 37, pp 21-24, 2007.

[11] S. Gutierrez, J. Marroquin "Robust approach for disparity estimation in stereo vision" Image and vision computing 22, 2004.

[12] L. De-Maeztu , A. Villanueva , R. Cabeza , "Stereo matching using gradient similarity and locally adaptive support-weight", Pattern Recogniton ,pp1643–1651,2011.

[13] Y. S. Heo and K. M. Lee and S. U. Lee, "Robust stereo matching using adaptive normalized cross-correlation," IEEE Trans. Pattern Anal. Mach.Intell., vol. 33, no. 4, pp. 807-822, Apr. 2011.

[14] I.L.Jung,J.Y.Sim, C.S.Kim, S.U.Lee,"Robust stereo matching under radiometric variations based on cumalative distribution of gradient", IEEE International Conference on Image Processing, pp. 2082–2085,2013.

[15] A. Klaus, M. Sormann, and K. Karner,"Segment-based stereo matching using belief propagation and a self-adapting dissimilarity measure",International Conference ICPR,vol 3, pp. 15-18, 2006.

[16] Middlebury database (2003) http://vision.middlebury.edu/stereo/data/scenes 2003.

[17] Middlebury database (2006) http://vision.middlebury.edu/stereo/data/scenes 2006

Proceedings of the Fourth International Conference on Communication and Electronics Systems (ICCES 2019)
IEEE Conference Record # 45898; IEEE Xplore ISBN: 978-1-7281-1261-9

Object Detection and Gesture Control of Four-Wheel Mobile Robot

M. Jain[1], M. Sehgal[1], Y. Kalra[1], P. Jain[1], N. Aggarwal[1], R.Singh[1*], D. Kumar[1] and T. K. Bera[1]
[1]Mechanical Engineering Department, Thapar Institute of Engineering and Technology, Patiala.

Abstract—In this paper, the development of a four wheel mobile robot with gesture-controlled robot arm manipulator system is presented. The accelerometer and wifi based gesture control model is used to manipulate the motion of its arm with human hand. The glove data is used to control the movement of the robot arm for pick and place operation. The object detection algorithm is also implemented to detect the object autonomously. An ultrasonic sensor is used to detect the upcoming object. Under this work, only single object is considered. The prototype model of four-wheel mobile robot with two movable arms is developed. The proposed object detection algorithm is implemented on the physical model to check the effectiveness of the algorithm. After object detection operation, the gesture control based controller is used for pick and place activity. The novelty of this research is collaborative use of object detection algorithm and gesture control scheme.

Keywords— ***object detection, gesture control, four-wheel mobile robot, ardiuno nano, accelerometer.***

I. INTRODUCTION

Nowadays, robotics is emerging domain in the field of technology. A Robot is an electro-mechanical model, operated by a computer program. It can be autonomous or semi-autonomous. An autonomous robot has no human interfacing. Majority of the industrial robots are autonomous as they require high speed. But, some areas have requirement of semi-autonomous or human controlled robots. Mobile robots are used in home environment in today's scenario [1]. Home robots are now working around us and help us a lot in our daily routine activities. The activities such as cooking, cleaning, watering and pet feeding are done by the home robots [2-5]. There are numbers of methods to interact with these robots, such as voice, gesture, and joystick. The voice command is suitable to control call-and-come service [6]. It has disadvantage that it is not suitable for continuous remote control. In such cases, the gesture control is more appropriate for robot's control. There are several methods to collect a human gesture that a machine would be able to interpret. The camera or data glove is used to capture the gesture information. The gestures data can also be collected via Bluetooth or infrared waves, Tactile, optical or motion technology. The accelerometer/gyroscope is best device to control the minute movement of the arm manipulator [6].

In this paper, an attempt has been made to develop semi-autonomous robot. The four-wheel mobile robot with arm and gripper is considered in this work. Firstly, the robot detects the object from its surrounding environment. The simple and very effective object detection algorithm based on single ultrasonic sensor reading is proposed and its effectiveness is checked on the prototype model and this is the novelty of the research work. Secondly, the gesture based controller is developed to control the motion of the arm. To control the movement of mobile robotic arm, the accelerometer/gyroscope and wireless communication using ardiuno are used. The pick and place operation is considered under this research work. Also, the physical model of the robot is developed and controlled with ardiuno board.

This paper is structured as follow: In Section 2, the object detection algorithm is developed using single ultrasonic sensor. 3-axis accelerometer based gesture controller is developed in Section 3. The pick and place application is considered for validation of the proposed controller. In Section 4, the four-wheel mobile robot is discussed. The prototype model of the four-wheel mobile robot is developed in Section 5. Also, experimental work is considered for pick and place application. The results are discussed in Section 6. Section 7, concludes the paper.

II. OBJECT DETECTION

Many researchers have worked on the subject of obstacle avoidance for robots. The fuzzy controller and vector field histogram (VFH) were implemented to avoid obstacles [7]. The real-time path-planning algorithm for avoiding static obstacle based on two LIDAR sensors reading was proposed in [8] and in this paper, the simulation results were compared with the experimental results. The geometric modelling based obstacle avoidance algorithm was developed in [9] and 2-D geometry shapes were considered to develop the obstacle free path. The on-board monocular camera was used to detect the obstacle for mobile robot [10]. In this paper, the attempt is made to develop very simple object detection algorithm based on an ultrasonic sensor that is mounted on front of the robot.

* Corresponding Author
Rajmeet Singh, Mechanical Engineering Department
Thapar Institute of Engineering and Technology, Patiala.
Email - rajmeetsng@gmail.com

A. Object Detection algorithm

The simple and effective object detection algorithm is developed in this section. Figure 1 shows the flow diagram of the algorithm.

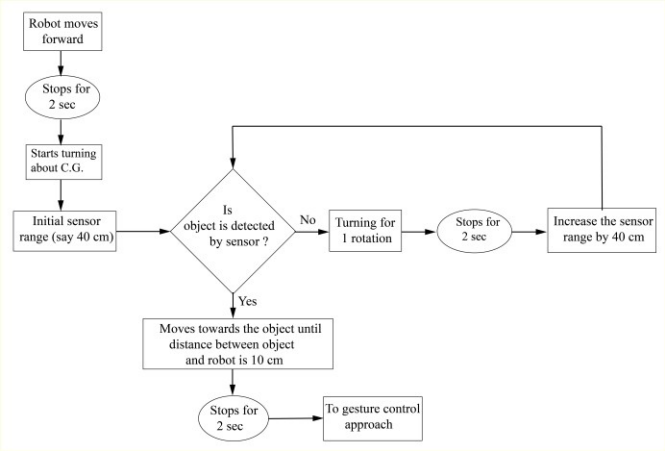

Fig 1. Flow chart of object detection algorithm

Initially, the robot moves in forward direction and then stops for 2 sec. After that, the robot starts turning about its centroid (C.G.). Initially, the ultrasonic sensor range is set to 40 cm. During turning operation, if sensor detects any object within its range, the robot stops in that orientation. If no such object is detected by the robot during first rotation, the robot stops for 2 sec and then, range of the sensor is increased by 40 cm to initial setting i.e. in this case, 40 + 40 = 80 cm. Now, again robot starts turning about its C.G. and searches the object with its range limit of 80 cm. Similarly, same procedure is applied until the object is detected. The proposed algorithm is implemented on the physical model of the robot in later section.

III. GESTURE BASED MANIPULATION

There are many devices available in market to control the gesture manipulation. The full body motion capture device Xsens MVN was used to control the movement of the robot [11]. This device is mostly suitable for animation creation, but could be adapted to other tasks. Myo arm band uses inertia and electromyography (EMG) sensors [12] to control the motion. An image based motion sensing was applied to some situations [13] too. In this paper, 3-axis accelerometer is used to control the 3-DOF (Rotation about vertical and horizontal axis, opening and closing of gripper) of the robotic arm with wifi connectivity.

A. Control approach

A robotic system that allows users to control an industrial robot using arm gestures and postures is proposed. A 3-axis accelerometer is selected to be the input devices of this system and to capture the human gesture-behavior. When compared with other common input devices, especially the joystick/remote interface, this approach using accelerometer/gyroscope is more intuitive and easier to work, besides offering the possibility to control a robot by wireless means. Using this system, a non-expert robot programmer can control a robot quickly and in a natural way. Figure 2 shows the control scheme for controlling the four-wheel mobile robot using blue-tooth, accelerometer and OS module. L298K is used to control the servo motors for wheels.

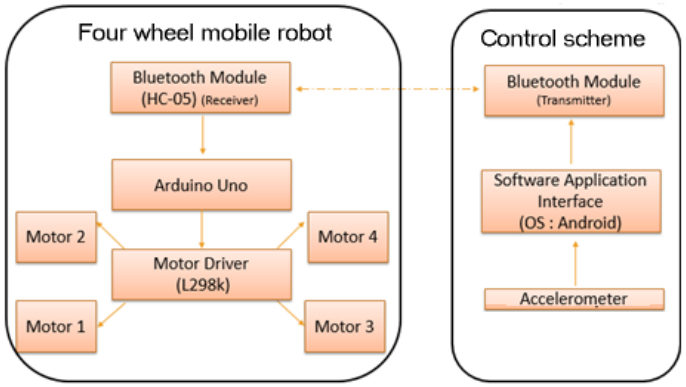

Fig. 2 Control block diagram for four-wheel mobile robot

Figure 3 shows the control scheme for controlling the manipulator action. The manipulator arm is controlled by glove data. The wifi adapter is used to control the arm of the robot. Wifi receiver and transmitter (RC-A-693) are used to control the robotic arm. The accelerometer (MPU6050) is mounted on the glove as shown in Fig. 4 (a).

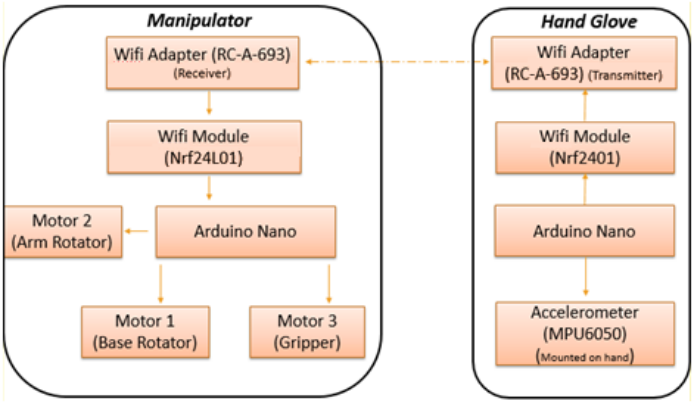

Fig. 3 Control scheme for manipulator

The various actions are assigned to control the movement of the arm. Figure 4 (b-f) illustrates the actions of human hand to control the manipulator. The upward and downward movements of the hand indicate the controlling of the up and down motions of the arm, respectively; left and right movements of the hand indicate opening and closing of the gripper, respectively. After performing numbers of trial runs, the relation between the movement of the hand and arm is developed and is mentioned in Table I.

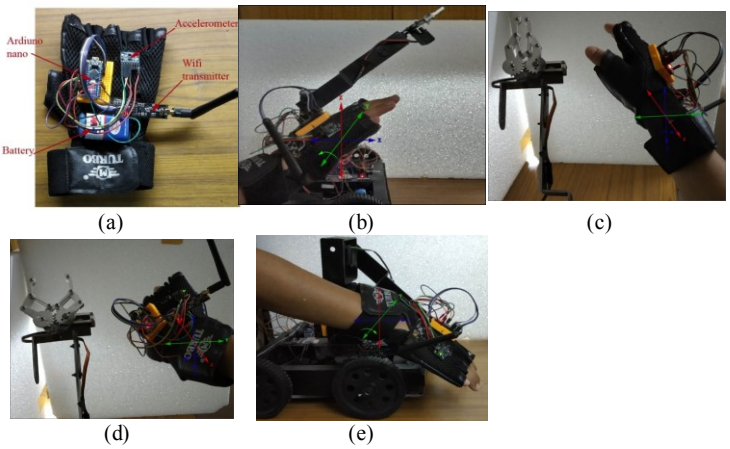

Fig. 4 (a) Glove data, (b) Upward motion, (c) Closing of gripper, (d) Opening of gripper and (e) Downward motion

TABLE I Relations between movement of hand and robotic arm.

Movement of hand (Degree)	**Movement of robotic arm along with gripper**
1^0 CCW/CW pitching motion of hand about y-axis looking from right	1.1^0 CCW/CW pitching motion of robotic arm about y-axis looking from right
45^0 CCW/CW rolling motion about x-axis looking from front	Full closing/opening of gripper

IV. FOUR-WHEEL MOBILE ROBOT

Four-wheel mobile robot without arm is shown in Fig. 5. It is assumed that the robot is symmetrical with respect to its longitudinal axis.

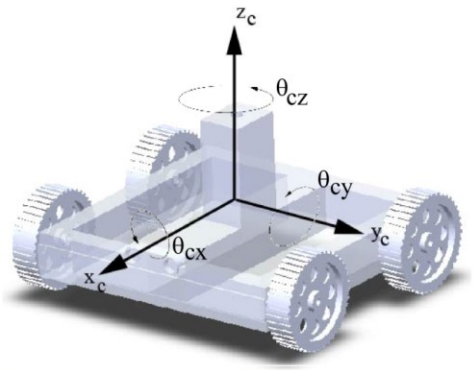

Fig. 5 Four-wheel mobile robot

The robot body motion is described by three linear displacements along three body-fixed axes and the rotational motion is defined by 3 Cardan angles. The robot body is modelled as rigid structure with 6-DOF. The body motion is described by 3 linear displacement along body fixed x, y and z axes and rotation about these axes. The Newton-Euler equations of the robot body are as follows [14]:

$$\sum F_x = m_c\ddot{x}_c + m_c\left(\dot{z}_c\dot{\theta}_{cy} - \dot{y}_c\dot{\theta}_{cz}\right) \quad (1)$$

$$\sum F_y = m_c\ddot{y}_{cb} + m_c\left(\dot{x}_c\dot{\theta}_{cz} - \dot{z}_c\dot{\theta}_{cx}\right) \quad (2)$$

$$\sum F_z = m_c\ddot{z}_c + m_c\left(\dot{y}_c\dot{\theta}_{cx} - \dot{x}_c\dot{\theta}_{cy}\right) \quad (3)$$

$$\sum M_x = J_{cx}\ddot{\theta}_{cx} - \dot{\theta}_{cy}\dot{\theta}_{cz}\left(J_{cy} - J_{cz}\right) \quad (4)$$

$$\sum M_y = J_{cy}\ddot{\theta}_{cy} - \dot{\theta}_{cz}\dot{\theta}_{cx}\left(J_{cz} - J_{cx}\right) \quad (5)$$

$$\sum M_z = J_{cz}\ddot{\theta}_{cz} - \dot{\theta}_{cx}\dot{\theta}_{cy}\left(J_{cx} - J_{cy}\right) \quad (6)$$

First three equations (Eqs. (1)–(3)) are Newton's equations where pseudo-forces appear due to the motions of body about its body-fixed or non-inertial frame. The later three equations (Eqs. (4)–(6)) are Euler's equations which account for gyroscopic moments. The whole set of six equations are referred to as Newton-Euler equations.

V. EXPERIMENTAL WORK

In this section, the physical model of the four-wheel mobile robot with arm is developed using ardiuno module. The proposed object detection algorithm and gesture control approach are implemented on the physical model and are validated for pick and place application. Table II shows the list of electronic equipments used for the development of the physical model of the robot.

TABLE II List of electronic items

Description	**Quality**
Gyroscopic sensor	1
Ultrasonic sensor	1
Servo motor	6
Wireless module	2
Ardiuno (1 uno + 2 nano)	3

A. Development of the physical model

1) CAD model: Initially, the CAD model of the robot is developed using CAD software (*Solidworks*) and the detailed views are shown in Fig. 6 (a-c).

2) Prototype model: In this section, the fabrication of the physical model is done. The chassis of the robot is made of aluminum due to its light weight properties. The ardiuno mega board is used to control the motion of all the wheels of robot and object detection algorithm. Also, the structure of the arms is made of aluminum. The separate ardiuno nano is used to control the motions of the arms. The wifi receiver is used to get command signal from glove data. Figure 6 (d) shows the physical model of the robot.

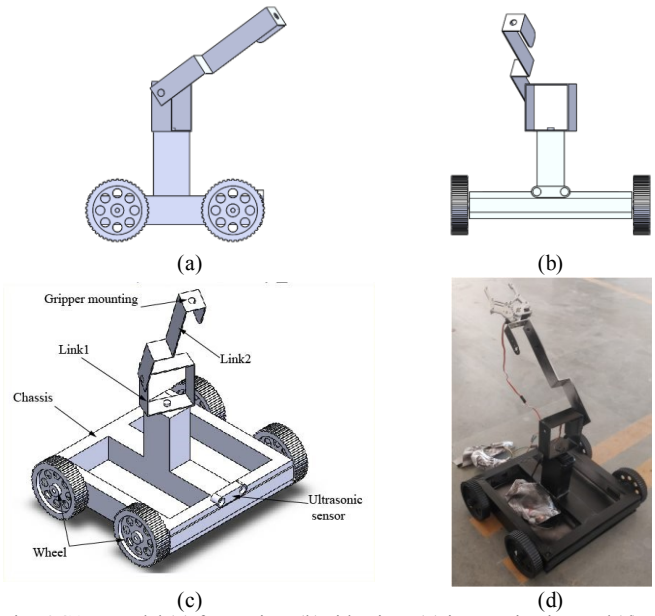

Fig. 6 CAD model (a) front view, (b) side view, (c) isometric view and (d) prototype model

VI. RESULTS

In this section, the experimental results are mentioned and discussed. By performing number of experimental runs, it is estimated that the average maximum linear speed of the robot is 4 cm/s. The experimentation time taken by the robot before pick and place operation is 56s. The linear speed of the robot is shown in Fig. 7 (a). During time 0-36s, the linear speed of the robot is 0 because the robot is turning about its C.G. to find the orientation of the object within its sensor range. After detecting the object, the robot starts to move towards the object. Initially, the speed of the robot is zero and after 2 sec, it reaches to its maximum speed of 4 cm/s. During the period of 38–54s, the robot moves with constant speed of 4 cm/s. Afterwards, when the distance between robot's sensor and object is 10 cm, the robot is stopped. Similarly, the Fig. 7 (b) shows the angular speed (rad/s) of the robot during turning operation. The robot starts turning about its C.G. (first iteration loop) during time span of 0-18s. After 2 sec of stopping, again robot starts turning (second iteration loop) for a time period of 20-33s. The third loop starts from 35s and after 0.34 rad angle, the robot detects the object. Then, the robot starts to move towards the object. Also, the robot's acceleration is shown in Fig. 7 (c). During constant speed of the robot, the acceleration is zero as depicted in Fig. 7(c).

The displacement of the robot is illustrated in the Fig 8. Figure 8 (1-12) shows the overhead pictures of the robot during first iteration loop having ultrasonic sensor range of 40 cm. As depicted from the Fig. 8, the green colored area is 40 cm sensor range zone. During second iteration loop, the range of the sensor is increased by 40 cm to the earlier range value i.e. 40+40=80 cm. Figure 8 (13-26) shows the overhead pictures of the robot while performing second iteration loop. 80cm of sensor range zone is represented by blue colored code. Figure 8 (27-28) shows the result of third iteration loop with sensor range increased by 40 cm to the previous range value i.e. 80+40=120 cm. Once the object is detected by the robot, the robot starts to move towards object until the distance between robot and object is reached by 10 cm as shown in Fig. 8 (29-36). At last, gesture control pick and place operation is done. Figure 8 (37-63) shows the pick and place operation based on gesture controller.

VII. CONCLUSIONS

The purpose of this research-work was to control the movement of the robotic arm with accelerometer/ gyroscope based gesture controller; this was quite effective and easy as compared to other input devices i.e. joystick, keyboard etc. Other important outcome of this research was the implementation of the simple and effective object detection algorithm on physical model of the robot. Also, single ultrasonic sensor was used to detect the object which reduces the cost of the robot. The effectiveness of the proposed algorithm and gesture control scheme were validated on the prototype model of the robot. The pick and place operation was considered under experimental work. The experimental results validate the efficiency of the proposed object detection algorithm and gesture controller. Further, the work will be extended to identify the desired object from the cluster of objects using fusion of ultrasonic sensors and robot mounted camera data.

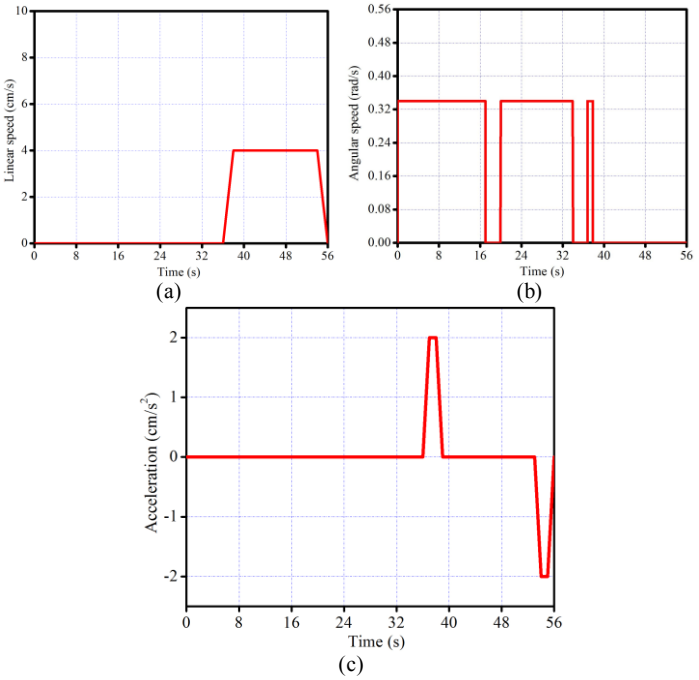

Fig. 7 Experimental results of robot (a) linear speed, (b) angular speed and (c) acceleration.

Fig. 8 (1-12) First iteration with 40 cm sensor range, (13-26) Second iteration with 80 cm sensor range, (27-28) Third iteration with 120 cm sensor range, (29-36) Movement towards object and (37-63) Pick and place operation

Nomenclature

C	robot body
F	Force
J	polar moment of inertia
M	Mass
M	Moment
$x,y,z,$	displacement in three directions
$\dot{x},\dot{y},\dot{z}$	velocities in three directions
$x,\ddot{y},\ddot{z}$	accelerations in three directions
$\dot{\theta},\ddot{\theta}$	angular velocity, acceleration

Acknowledgment

The authors thanks to the mechatronics laboratory at Thapar Institute of Engineering and Technology, Patiala.

References

[1] C. D. Nugent, D. D. Finlay, P. Fiorini, Y. Tsumaki and E. Prassler, "Home automation as a means of independent living ", IEEE Trans. Autom. Sci. Eng., Vol. 5, no. 1, pp. 1–9, 2008.

[2] R. C. Luo, T. Y. Hsu, T. Y. Lin and K. L. Su, "The developement of intelligent home security robot", IEEE Int. Conf. on Mechatronics, Taipei, Taiwan, pp. 422–427, 2005.

[3] G. Song, Y. Zhou, Z. Wei and A. Song, "A smart node architecture for adding mobility to wireless sensors networks", Sens Actuators A Phys. Vol. 147, no. 1, pp. 2016–221, 2008.

[4] G. Song, H. Wang, J. Zhang and T. Meng, "Automatic docking system for recharging home surveillance robots", IEEE Trans Consum Electron, Vol. 57, no. 2, pp. 2034–2039, 2009.

[5] G. Song, H. Wang, J. Zhang and T. Meng, "Automatic docking system for recharging home surveillance robots", IEEE Trans Consum Electron, Vol. 47, no. 2, pp. 428–435, 2011.

[6] Y. Oh, J. Yoon, J. Park, M. Kim and H. Kim, "A name recognition based call-and-come service for home robots", IEEE Trans Consum Electron, Vol. 54, no. 2, pp. 247–253, 2008.

[7] L. Linhui, Z. Mingheng, G. Lie, Z. Yibing, "Stereo vision based obstacle avoidance path-planning for cross-country intelligent vehicle". In: IEEE Int. Conf. on Fuzzy Syst. and Knowledge Discovery, pp. 463–467, 2009.

[8] K. Chu, "Local path planning for off-road autonomous driving with avoidance of static obstacles". IEEE Trans. Intell. Transp. Syst. Vol. 13, pp. 1599–1616, 2012.

[9] S. Ghoshray, K. K. Yen, "A comprehensive robot collision avoidance scheme by two dimensional geometric modeling". In: IEEE Int. Conf. on Robotics and Automation, pp. 1087– 1092, 1996.

[10] J. Jun, W. C. Zhan, J. Juang, "Application of image process and distance computation to WMR obstacle avoidance and parking control". In: IEEE Conf. on Industrial Electronics and Applications, pp. 1264–1269, 2010.

[11] H. Loose and K. Orlowski. " Gait Patterns in Standard Scenarios Using Xsens MTw Inertial Measurement Units". In. 16th conf. on Research and Education in Mechatronics (REM), 2015.

[12] J. Kofman, W. Xianghai, J. Timothy, and S. Verma. "Teleoperation of a Robot Manipulator Using a Vision-Based Human Robot Interface". IEEE Trans. on Industrial Electronics, Vol. 52, pp. 1206–1210, 2005.

[13] H. Mi-Chia, Y. Yu-Hua and S. Tsung-Ying. "Gesture Recognition with Two 3-axis Accelerometers", IEEE Trans. on Industrial Electronics Vol. 978, pp. 4799–4851, 2014.

[14] T. K. Bera, K. Bhattacharya and A. K. Samantary. " Evaluation of antilock braking system with an integrated model of full vehicle system dynamics", Simulation modelling practice and theory Vol. 19, pp. 2131–2150, 2011.

Proceedings of the Fourth International Conference on Communication and Electronics Systems (ICCES 2019)
IEEE Conference Record # 45898; IEEE Xplore ISBN: 978-1-7281-1261-9

Robust Hybrid Image and Audio Watermarking Using Cyclic Codes and Arnold Transform

Bhavneet Sharma
Department of Computer Engineering
National Institute of Technology
Kurukshetra, Haryana (136119)
bhavneetattri@gmail.com

Mayank Dave
Department of Computer Engineering
National Institute of Technology
Kurukshetra, Haryana (136119)
mdave@nitkkr.ac.in

***Abstract*—Hybrid watermarking is a prevailing technique in the latest research and has a significant amount of real-time applications. Digital watermarking is utilized to protect copyright and security to multimedia content. In this paper, an algorithm is an amalgamation of image watermarking and audio watermarking algorithms. In case of image watermarking algorithm discrete cosine transform (DCT) and in case of audio, discrete cosine transforms (DCT) and discrete wavelet transform (DWT) are used to propose this Hybrid watermarking algorithm. Moreover, to refine the performance of the proposed scheme, error correction technique and Arnold transforms are employed. Peak sound to noise ratio and Bit Error Rate (BER) is applied to estimate the performance of this scheme to counter the Time-Scale Modification and numerous attacks possible on images and audio as well.**

Keywords—digital watermarking; DCT; DWT; Arnold transform; cyclic code; signal processing, TSM;

I. INTRODUCTION

Every user, organizations, etc. have a huge amount of data collection and due to ease in availability of technology and internet or communication network, an immense amount of information has forwarded among numerous clients (or users), Twitter, Facebook, WhatsApp and variant social media. In this scenario, attacks probability on data is fairly high because there is a different kind of techniques and tools which can infringe the copyright, copied or modify the information. So, it is mandatory to provide security, duplication control, owner authentication, protection, etc.to digital multimedia (like audio, image, text, video). There are generally three techniques watermarking, steganography and cryptography. Out of these, digital watermarking came out to furnish an effective solution to these problems stated above and turns into a popular technique. Digital Watermarking embeds the original data into another digital data secretly by applying some algorithm [3] and it assures the user's identification, copyright protection, security, etc.

Digital watermarking can be text watermarking, audio watermarking, image watermarking and video watermarking. All these techniques have an overall three processes: Embedding, Detection, and Attack. In the embedding process, user's data (i.e. watermark) is enrooted into another data (data could be image, audio, text, and video) and in the detection process, concealed data is extracted and in the attack process, numerous attacks are possible on watermarked data that tampered the original content and steal the information like copyrights, ownership, and others.

Watermarking is classified based on perceptivity: (1) Visible watermarking, (2) Invisible watermarking, is frequently used one. Visible watermarking is embedding the picture or logo that is noticed easily. Invisible watermarking is piecing the watermark into an unidentified part of the data which cannot be perceived by eyes and watermarking approaches must be invisible. Invisible watermarking has important features which are security, imperceptibility, computational cost, and robustness. For secure watermarking, secret keys must be used and ensure the protection of copyright [15]. Watermarking system should have the potential of survival against processing attacks that is a robust feature of the system. Computational complexity is also a vital and deciding factor in the copyright of the scheme.

Typically, Image watermarking has divided into two based on respective domains: frequency domain and spatial domain. In the spatial domain, the embedding algorithm implant the watermark into the image right away or refurbish the pixel values [3]. Well-known spatial techniques are least-Significant bit technique (LSB) and SSM (spread-Spectrum) Modulation technique. In frequency (or Transform) domain, manipulate the spectral (or frequency) coefficient of the image to embed the watermark. In comparison with the spatial domain, the frequency domain is most preferable for watermarking because of better characterization of human Visual system. This domain is consisting of widely popular techniques DWT, DFT, SVD, and DCT [2, 4, 8, 16].

In audio watermarking, there are two broad domain categories: (1) Time domain (2) Transform domain. In the time domain, imbed the watermark is directly into time domain i.e. mixing the pseudo-noise patterns to the host audio. This technique brings on the deterioration of the sound file due to prompt modification of bits. In Transformation domain, enables implanting of the watermark into a discernible component of host audio and this gives better permanence. It also utilizes the audio masking property of HAS (human auditory system) [5].

The approach in this paper is motivated by aggregation of more than one watermarking techniques, stated above. Here image and audio watermarking are mingled to structure a new

technique of watermarking that will address issues like copyright protection, authentication, security, etc. and to efficiently counter the numerous attacks which can damage either image or audio or secret data. This scheme will persuade others to fuse two or more than two techniques, the resultant scheme will be more effective, strong and efficient and produce better outcomes.

The structure of the paper is as follows: section II will provide about related work and theoretical background useful for this. Section III describes the proposed scheme and algorithm. Section IV demonstrate the analysis and explanation of results. Section V signifies the conclusion and future work, after this there are references.

II. Related work and Preliminaries

Researchers have been trying to design an efficient watermarking approach to resist any kind of attacks and issues associated with it. This section will briefly describe the various schemes that are valuable for designing this scheme.

Soumitra Roy and Arup Pal [1] proposed a multiple image watermarking scheme based on DCT and repetition code. Watermark's bit is loaded into Blue and green component of a color picture, then DCT is employed after decomposing image into blocks and repetition codes are used to update AC coefficients of transformed block. Few larger AC and DC coefficient are kept unspoiled after DCT's block scanning in case of multiple watermark insertion. That makes the scheme stronger and confident.

Ali Al-Haj [2] suggested about aggregated DCT_DWT watermarking procedure for images. First and just next level of DWT Subbands are picked to place the watermark into host picture, in succession DCT is applied on carefully chosen DWT subbands. This enhanced the performance of this scheme in comparison to both individual watermarking approaches.

Palak Garg et al. [4] presented a layout to guard against unauthorized access by integrating DSWT (discrete stationary wavelet transforms), DCT, Arnold transforms and SVD. Colored watermark is inserted into a colored picture. Addition of Arnold transforms into this hybrid algorithm make it more secure. The result shows good indiscernibly.

Weizhen Jiang et al. [6] said, this scheme has designed for audio to counter synchronization attacks. Audio is fragmented into frames. Encrypt the watermark and generate watermark frame sequence number. Then watermarking sequence number is inserted into wavelet coefficients using mean stable property and take advantage of the global characteristic technique to prevent synchronization attacks such as TSM, jittering, pitch shift, etc. This scheme delivered the qualitative result as higher capacity, robustness associated with quantization length.

Rohit M. Thanki and Ashish M. Kothari [7] drafted a technique to provide security and protection of copyrights to image using human speech signals. Hybrid coefficients of speech is evaluated by employing DCT and SVD. Then embedded into coefficients of the image which are obtained by DWT and FDCuT. Its performance is quite better than other techniques for the biometric system. A noise disturbance occurred when there is an increment in the embedding factor.

Subir and Amit M. Joshi [8] intended to deliver an audio watermarking in which watermark is inserted with the aid of DWT and DCT, then error correction codes and arnold transform is used for advancement in the algorithm. Its performance has measured in SNR and BER. It has outstanding results against others scheme.

A. K. Singh, M. Dave and A. Mohan [9] proposed a hybrid dual watermarking technique for images and it will help in telemedicine. DWT and DCT are employed in sequence to embed the watermark and additionally hamming code, BCH code, and Reed-Solomon code are popular error correcting codes. These codes are added to real bits of watermark for enhancement.

M. J. Tsai and H. Y. Hung [10] demonstrate a scheme which is based on DWT, DCT, and sub-sampling. Image is divided into subbands and watermark is embedded by DWT and DCT, subsample the subband's coefficient is also used in insertion. It was robust under different attacks.

Sobha R. V. and Sucharitha M. [12] suggested an audio watermarking scheme for secret transfer of data. It takes audio watermark of lesser length, inserted into the original signal with DCT and DWT-SVD methods, then encrypted with the secure hash method. Its performance evaluation is based on MSE (mean square error) and PSNR (peak signal to noise ratio). On extracting process, watermark has minimum disturbance and quite good performance under synchronization attacks.

A. Preliminaries

Discrete Cosine Transforms is frequency domain-based technique. It is a frequently used and prevailing technique. Itt employed for compression that transforms the signal from spatial to another domain as well as decomposing of signals. It is basically sum of sinusoids with variable frequencies and magnitudes. Any signal can have multiple AC coefficients but only one DC coefficient is there. It displaces the pixel or frame values on the transformation of data. Low-frequency coefficients are used for storage of details about the signal. DC coefficient has all vital details about the signal, but the AC coefficient has only sufficient detailing. Energy compaction property has a crucial role in DCT. The input signal d(m, n) has a sampled value, m as row and n as a column of reshaped signal and N × M size. Its output is transformed signal e(u, v), has DCT coefficients in u, v row and column respectively:

$$e(u,v) = \sqrt{2/M}\sqrt{2/N} \times \alpha(u)\alpha(v) \sum_{u=0}^{M-1}\sum_{v=0}^{N-1} d(m,n) \times \cos\frac{(2m+1)u\pi}{2M}\cos\frac{(2n+1)v\pi}{2N} \quad (1)$$

Where

$$\alpha(u) = 1/\sqrt{2}, u = 0 \text{ and } 1, u \in (1, M-1)$$
$$\alpha(v) = 1/\sqrt{2}, v = 0 \text{ and } 1, v \in (1, N-1)$$

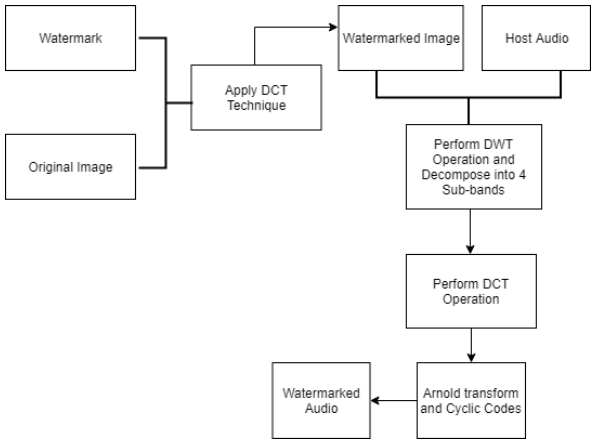

Fig 1. Embedding Procedure

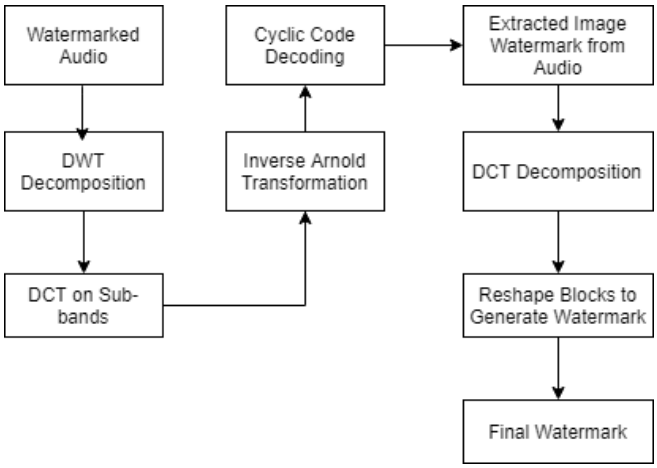

Fig 2. Extraction Procedure

On the extraction process, it is inverse DCT:

$$d(m,n) = \sqrt{2/M}\sqrt{2/N} \times \alpha(u)\alpha(v) \sum_{u=0}^{M-1}\sum_{v=0}^{N-1} e(u,v) \times \cos\frac{(2m+1)u\pi}{2M}\cos\frac{(2n+1)v\pi}{2N} \quad (2)$$

It is well known for the decomposition of a signal into non-overlapping blocks, this is block-based DCT transforms. It has the following output frequency: low, mid, high-frequency subbands. Based on individual's approach, any output frequency band can be picked up for watermark embedding and each band has its own significance.

Discrete wavelet transforms [10,16] is a multipurpose tool and it has its own advantages over DFT and DCT. It compromises with detailed information about the signal (audio/image). It decomposes the signal into several bands which are distributed for watermarked signal and assembled back to get the original signal. When DWT is applied, there are 2-D filters which are used in reshaping and helps in dividing the signal into limited non-overlapping sets that are Lf (lower frequency), Hf (horizontal frequency), Vf (vertical frequency) and Df (diagonal frequency). The first set shows the coarse scale coefficient and other are fine scale. The Level of decomposition is directly proportional to security under attacks.

Error correction code [4, 9]: when there are noise and distortion in the communication channel, it is difficult to recover the data from the channel. The original data is inculcated with extra bits in error correction process. It is used to enhance the recovery process of data. Generally, there are three correcting codes BCH code, Reed-Solomon code, and hamming code. Apart from these three, there is a cyclic code.

Cyclic codes are easy to the device and are linear code over finite fields. Say a block of length n and C is a linear code which is cyclic code. Codes are defined by C only and the next codeword is gained by right shifts operation in between components. C is symbolized into polynomial form,

$$C(x) = c_{0+}\, c_1 X + c_2 x^2 + \cdots \ldots + c_{n-1}\, x^2 \quad (3)$$

This paper uses these cyclic codes.

Arnold transforms [4] is used because it gives supplementary security together with existing watermarking. It does cut and slicing that is aligning the pixel matrix. It worked on the square size matrix of the signal such as M × M. Arnold transform is:

$$\begin{pmatrix} x' \\ y' \end{pmatrix} = \begin{pmatrix} 1 & 1 \\ 1 & 2 \end{pmatrix} \begin{pmatrix} x \\ y \end{pmatrix} \; mod\, M \quad (4)$$

Here, (x, y) belongs to original watermark and (x', y') belongs to displaced watermark. It is also known as a 2-D Arnold transformation. It is employed before embedding. It can be recovered in two ways: inverse transformation by inversing the matrix and periodicity of application. Scrambling key is considered as a secret key. It will be used in decryption of signal.

III. The Proposed Hybrid Watermarking Scheme

In this scheme, there is a sequence of algorithms. The first step is image watermark embedding, it is done with the DCT method, second is audio watermark embedding done with DWT-DCT plus cyclic codes. Then audio and image watermark extraction occur in sequence. Fig 1 and Fig 2 represent the watermark embedding procedure and watermark extraction procedure.

A. Image Embedding

Step 1: Read the image (im) and watermark (wt) with sizes of N × M and n × m respectively. After reading wt convert into binary.

Step 2: divide the image into n × n nonoverlapping blocks by employing DCT (dct()).

Step 3: enroot the watermark into the image's blocks. Each watermark bit will be embedded into the first bit of every block

Step 4: after all embedding, now recombination of every cell to get back the image by changing complete row cells of blocks

Step 5: now change row cells into the particular column to generate a watermarked image by inverse DCT (@dct()), and

finally output is stored. It is treated as watermark in the next algorithm.

Fig 3. Inputs to Image watermarking

B. Audio Embedding

In this algorithms, binary cyclic codes are employed on the image's matrix to encode. The character 'μ' is the constant which is μ × 2 is equal to the size of matrix. The watermark key and Arnold transform is used to figure out transform iterations.

Step 1: Utilize DWT technique on the audio signal and decompose that in subbands {Lf, Hf, Vf, Df}.

Step 2: For embedding and processing, this scheme selects Hf and Vf. Then implement DWT (Haar wavelet) on selected subbands like {Hf1, Hf2, Hf3, Hf4} and {Vf1, Vf 2, Vf 3, Vf 4}.

Step 3: Again, select middle bands {Hf2, Hf3}, {Vf 2, Vf3} from above two for three-level DWT implementation and now further pick four subbands from each subband after three-level DWT {W1, X,2 Y3, Z4}. Uniform sized blocks are created by dividing each block and perform DCT on each. Watermarking key is used to generate random sequence (PN1 and PN2).

Step 4: Reshape the binary watermark of size N × N (output of algorithm 1) U = μ × 2 and apply cyclic codes for encoding the watermark. Then for improving recovery, binary codes are used for encoding.

Step 5: Apply second level of cyclic encoding U1 = U(: , 1:2) and U2 = U(:, 2:3) . Matrix U1 and U2 are reshaped. Now map V1 with U11 and U12, and V2 is mapped with U21 and U22. V is a matrix of V1 and V2. Scrambled the V with watermark key.

Step 6: following rules are employed in watermark embedding:

If V(k) = 0
Then m_coff = m_coff + PN1
If v(k) = 1
Then m_coff = m_coff + PN2

Step 7: To generate watermarked audio, perform inverse DCT and inverse DWT.

Fig 4. Watermarked Image

C. Audio Extraction

Step 1: Implement 3_level DWT and decompose the reshaped watermarked audio as a matrix of H × H.

Step 2: Induce 2 random sequence and they have the same length as DCT's mid_band coefficient. DCT is applied to each block's mid_band coefficient.

Step 3: Extraction rule to find watermark bits:

If correlation (m_coff and PN1)>correlation (m_coff and PN2)
V(k) = 0
If correlation (m_coff and PN2) ≥ correlation (m_coff and PN1)
V(k) = 1, it is mined watermark bit matrix.

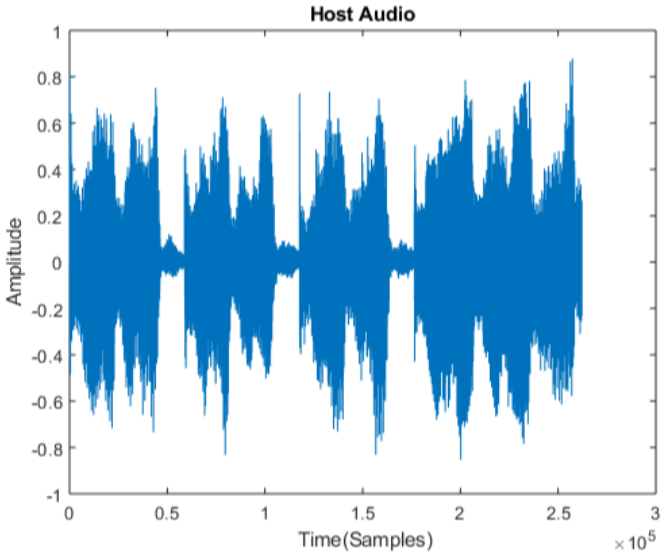

Fig 5. Waveform of Host Audio

Step 4: Apply inverse arnold on V by using watermark key and then reshape it as Ew = μ × 4, create Ew1 and Ew2 from Ew by dividing it horizontally. Then do vertical separation to make Ew11, Ew12, Ew21, and Ew22 of size μ/(2 × 2). Lastly join Ew11 and Ew12 horizontally, as a U1 and same as U2.

Step 5: To create U1' and U2' from U1 and U2 by cyclic decoding. Eliminate the second and first column of U1' and U2' respectively. Then combine these two for finding U.

D. Image Extraction

Step 1: load the extracted watermark picture from the above algorithm and initialize all required parameters and variables.

Step 2: split the picture into nonoverlapping blocks of size n × n.

Step 3: extract the blocks one by one and deploy the DCT method on them. Meantime it store the DCT values in the new block for cross-checking and row_wise formatting in n × n elements.

Step 4: perform the extraction process without using DCT and store its values also.

Step 5: Now compare these values and find the exact watermark by following rules:

If diff ≥ 0
Then ex_bit = 0

If diff < 0

Then ex_bit = 1, extracted bit of watermark is denoted as ex_bit.

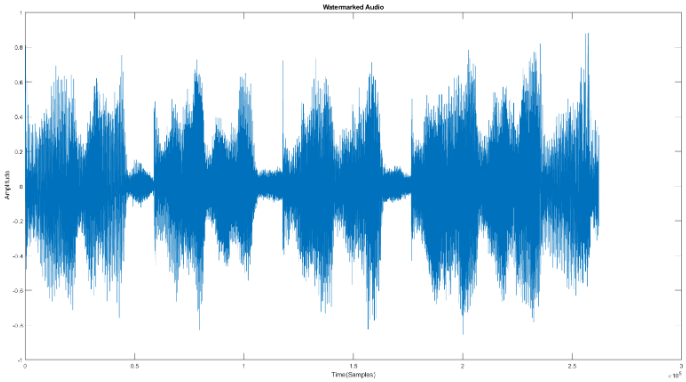

Fig 6. Waveform of Watermarked Audio

IV. Experiment Results and Discussion

In image watermarking procedure, watermark image is taken as 16 × 16 size and other is 32 × 32. Finally, it will generate a watermarked image of 16 × 16 size. In case of an audio procedure, different audio files are taken as original track of 512 × 512 size and all the tracks are of '.wav' format. 7 is the iteration and random sequence length in arnold transform. This paper is implemented on Windows 10 platform, MATLAB v2018Ra and TSM toolbox [11] which will be in action to perform TSM attack.

The proposed scheme is evaluated in terms of the performance parameters like PSNR (peak sound to noise ratio), BER (bit error rate). The Strength of scheme is denoted as BER. Perceptibility property and distortions are recognized by PSNR values. The amount of differentiation between any two signals is calculated as a PSNR value and it also tells about an image's quality (original and extracted picture). It is calculated as:

$$PSNR(dB) = -10log_{10}\frac{MSE}{P^2} \quad (5)$$

Maximum pixel size is P. SNR is calculated for audio signals and is evaluated with respect to noise power. S_{signal} and S_{noise} are the power of audio and noise respectively. SNR is:

$$SNR(dB) = \frac{S_{signal}}{S_{noise}} \quad (6)$$

While communication, the difference between a number of bits in the original image and the extracted image is termed as bit error and the ratio between the number of errored bits to number bit sent is called BER. It is calculated as:

$$BER = \frac{Errored\ Bits}{Sent\ Bits} \times 100 \quad (7)$$

Fig 7. Extracted watermark from Audio

Figures 3 is about initial inputs given to the system, Fig 4 is the output of the image embedding algorithm and it is given as watermark input to audio embedding. Fig 5 and Fig 6 shows the waveform of host and watermarked sounds. Fig 7 is the pulled watermark by the audio extraction process. Fig 8 displays the difference between host and watermarked tracks. Fig 9 is the final watermark which is extracted lastly with image extraction.

This paper also considers the numerous attacks possible on either image and sound. Table I and Table II will show the results of this scheme under two situations when information sharing on safe network and otherwise attacks happen on network. In both scenarios, the scheme is tested and analyzed.

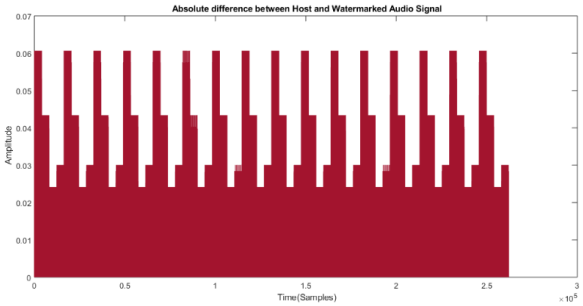

Fig 8. Difference between host and watermarked sounds

In table I, there are five tracks of 5 sec, 7 sec, 1.44 min, 10 sec and 3.34 min same in the order given in the table. For pop audio file BER has value 10 and PSNR value is 62.2154. these values are easily enumerated in MATLAB because it has predefined functions [14]. In the same way, these values are calculated for each example to test the scheme.

Table I scheme analysis under normal scenario.

Sound Tracks	BER	SNR	PSNR
Pop	10	0.201	62.2154
Jazz	3	0.313	52.5294
Classical	4	0.2842	Inf
Bach	0	1.3768	Inf

Looney	3.9	0.198	63.9423

Table II shows the scenario when a scheme is under attacks like signal processing and TSM (time-scale modification). These attacks are either signal processing attacks or synchronization attacks like noise addition, resampling, etc. comes under SP attacks and rest of attacks comes under another type of attacks. In this paper TSM is implemented with variation like TSM – 25%, TSM – 10%, TSM + 10% and TSM + 20%. TSM manipulations are organized with the aid of TSM toolbox [11] which gives TSM implementation. Cropping is done by taking a certain sound length and apply random function. Some minimum and maximum values and attacks happen in-between the range. Resampling is performed by multiplying the original sample rate with an appropriate value.

Table II. The scheme is under attacks scenario

Sound File	**Attacks**	**BER**	**PSNR**
		Proposed Scheme	**Proposed Scheme**
Pop	Random Cropping	18	59.6605
	Requantization	125	51.2441
	Resampling	10	62.2135
	Noise	20	59.2042
	TSM -25%	14	55.2671
	TSM - 10%	21	58.1664
	TSM + 10%	26	60.1893
	TSM + 20%	10	56.1268
Jazz	Random Cropping	19	61.4212
	Requantization	6	Inf
	Resampling	44	55.7781
	Noise	7	Inf
	TSM -25%	13	50.8211
	TSM - 10%	10	54.2545
	TSM + 10%	16	56.2172
	TSM + 20%	9	49.9517
Classical	Random Cropping	22	61.7519
	Requantization	8	Inf
	Resampling	126	52.0104
	Noise	11	72.2169
	TSM -25%	14	62.3642
	TSM - 10%	8	53.9826
	TSM + 10%	13	59.0054
	TSM + 20%	10	56.1833
Bach	Random Cropping	26	62.7523
	Requantization	6	59.3579
	Resampling	95	56.9511
	Noise	0	Inf
	TSM -25%	18	63.1425
	TSM - 10%	12	55.9456
	TSM + 10%	19	64.5297
	TSM + 20%	15	60.3922
Looney	Random Cropping	22	61.9442
	Requantization	6	55.3214
	Resampling	102	57.2584
	Noise	2	Inf
	TSM -25%	20	65.2545
	TSM - 10%	16	62.4006
	TSM + 10%	22	66.2021
	TSM + 20%	18	62.9138

Noises have multiple types like white noise, AWGN noise, etc. In this study, AWGN noise is used to create an attack. Herein audio samples are utilizing for adding AWGN with its specific value. Most of these manipulations are carried out straightly in MATLAB, it has in-built functions which are dynamic according to the requirement.

Fig 9. Finally extracted watermark

V. CONCLUSION AND FORTHCOMING STUDY

This study delivers the new hybrid scheme which is comprised of two contrasting techniques that are Image and Audio Watermarking. This scheme is relying on blind watermarking approach [13]. This hybrid scheme is generally partitioned into two segments. One is embedding, in which the watermark is enrooted into the picture by utilizing DCT method of decomposing into nonoverlapping blocks and then reshaping, rearranging of these blocks after that perform inverse DCT operation to get the image i.e. watermarked. This will be considered as a watermark to audio insertion process which is implemented by three-level DWT decompose, followed by DCT operation on middle-frequency bands. Here cyclic codes (error correction code) are accustomed for encoding of the watermark and arnold transform which will enhance the security and generate a watermarked audio. Another segment is extraction, the output of previous procedure is input to audio watermark pulling and three level DWT after that DCT applies on particular subbands, then cyclic code decoding and inverse arnold transform acted upon it to withdraw the watermark from a sound file. This will be passed to DCT decomposition, reshaping applied to pull the final watermark in image watermark pulling process.

Numerous attacks are carried out to examine the strength, quality, and invisibility of scheme. Experimental results reveal quite effective response in safe or attack scenario in contrast

with existing approaches. The performance of implemented schemes is assessed in BER, SNR, and PSNR.

A forthcoming study on this scheme will be on making it more robust against other serious attacks like pitch shifting, dual attacks, etc. and this idea will be researched by aggregating other techniques to boost the security and protection against manipulations. The performance parameters like PSNR, SNR, and BER can be modified to improve the robustness and security of this approach.

REFERENCES

[1] Soumita Roy and A. Kumar Pal, "A blind DCT based color watermarking algorithm for embedding multiple watermarks" International Journal of Electronics and Communication, vol 72, pp. 149-161, February 2017.

[2] Ali Al-Haj, "Combined DWT-DCT digital image watermarking" journal of computer science, vol 3, pp. 740-746, 2007.

[3] P. Singh and R. S. Chadha "A survey of digital watermarking techniques, Applications and Attacks" International Journal of Engineering and Innovative Technology (IJEIT), vol 2, pp. 165-175, March 2013.

[4] Garg P., Dodeja L., Priyanka, Dave M, "Hybrid Color Image Watermarking Algorithm Based on DSWT-DCT-SVD and Arnold Transform" In Rawat B., Trivedi A., Manhas S., Karwal V. Advances in Signal Processing and Communication. Lecture Notes in Electrical Engineering, vol 526, pp. 327-336, November 2018.

[5] A. M. Chore and Neha Tiwari, "Survey on different methods of digital audio watermarking" International Journal of Engineering Research and Application, vol 7, pp. 113-116, June 2017

[6] Weizhen Jiang, Xionghua Huang, Yujuan Quan, "Audio Watermarking Algorithm against Synchronization Attacks Using Global Characteristics and Adaptive Frame Division" Signal Processing, vol. 162, pp. 153-160, April 2019.

[7] Thanki, R.M. & Kothari, A.M. J, "Hybrid domain watermarking technique for copyright protection of images using speech watermarks" Journal of Ambient Intelligence and Humanized Computing, pp. 1-23, April 2019.

[8] Subir, A. M. Joshi, "DWT-DCT based blind audio watermarking using Arnold scrambling and Cyclic codes", 3rd International Conference on Signal Processing and Integrated Networks (SPIN), pp. 79-84, September 2016.

[9] Singh A.K, B.Kumar, M. Dave, A. Mohan, "Hybrid technique for robust and imperceptible dual watermarking using error correcting codes for application in telemedicine" Int. J. Electronic Security and Digital Forensics, Vol. 6, No. 4, pp.285-305, November 2014.

[10] Tsai Min-Jen, Hsiao-Ying Hung, "DCT and DWT-based image watermarking by using subsampling", Distributed Computing Systems Workshops, pp. 1-6, 2004.

[11] Jonathan Driedger, Meinard Müller, "TSM toolbox: MATLAB implementation of Time-scale modification algorithms" Proc. of the 17th Int. Conference on Digital Audio Effects (DAFx-14), pp. 1-5, September 2014

[12] R. V. Sobha, M. Sucharitha, "Secure transmission of data using audio watermarking with protection on synchronization attack", Global Conference on Communication Technologies, pp. 592-597, December 2015.

[13] X.-L. Liu, C.-C. Lin, S.-M. Yuan, "Blind dual watermarking for color images' authentication and copyright protection", IEEE Trans. Circuits Syst. Video Technol, vol. 8215, no. c, pp. 1-1, December 2016.

[14] Pooya Monshizadeh Naini, "Digital Watermarking Using MATLAB" Engineering Education and Research Using MATLAB, Ali H. Assi., pp. 465-480, October 2011.

[15] Wei Li, "robust digital audio watermarking", Ph.D. dissertation of Fudan University, 2004.

[16] Cai, Yong-mei, Wen Qiang Guo and Hai-yang Ding. "An Audio Blind Watermarking Scheme Based on DWT-SVD." JSW, vol 8, pp.1801-1808, July 2013.

Proceedings of the Fourth International Conference on Communication and Electronics Systems (ICCES 2019)
IEEE Conference Record # 45898; IEEE Xplore ISBN: 978-1-7281-1261-9

ANALYSIS OF BOOST CONVERTERS FOR PV AND WIND IN A HYBRID MICROGRID

RAJALAKSHMI MENON[1], *Mtech Student*, GOMATHY S[2], *Hod EEE Department*, Lakshmipriya K J[3]

Electrical and Electronics Department ASIET, Kalady.

Email ID: rajalakshmimenon94@gmail.com , gomath.eee@adishankara.ac.in , lekshmikj99@gmail.com

ABSTRACT:

This paper presents the analysis of two types of boost converter for PV and Wind in a hybrid Micro-grid. The main aim is to improve the voltage gain capacity of conventional boost converter used in PV and Wind sources for a Hybrid micro-grid. Boost converters are dc to dc converter used to increase the input voltage. Conventional boost converters have low voltage gain capacity with high duty ratio. To eliminate this problem a new three level boost converter which improves the voltage gain capacity with low duty ratio is proposed for PV and a new coupled inductor based boost converter is used for Wind, this also has a high voltage gain capacity. Through this modified converter the voltage gain capacity is increased. The circuit is designed in MATLAB/SIMULINK and results are verified.

Keywords: Renewable Energy, Boost Converters, DC Micro-Grid

INTRODUCTION

There are many isolated locations in the world, which don't have approach to electricity. There are also many places, which are connected to the grid, but, they don't obtain electricity for up to 10-12 hours in the day. Many of such places are rich in renewable energy (RE) sources such as wind, solar and bio-mass.

Contemporary distribution system is experimenting the use of these DERs and thus forming power clusters [1]. This power cluster is called as Micro-grid. Micro-grid is of two types – Alternating Current Micro-grid (ACMG), and Direct Current Micro-grid (DCMG). If the micro-grid has two type of sources, then it is called a hybrid micro-grid. Basically the DERs such as solar PV systems, fuel cell operates at DC. Using power electronics circuits, a DC link capacitor can be formed to feed DC loads. For AC loads we can use an inverter at each section to convert DC power to AC power and this type of grid is AC micro-grid.

In AC micro-grid most of the DERs supply power to AC mains network and require costly and inefficient power inverters, even where the power may ultimately have delivered to a DC device. [3,5]. Whereas in DC micro-grid all the sources will be DC. In current world electrical loads in buildings such as computers, light emitting diodes (LEDs), etc. are supplied by DC power. Also most of the renewable energy sources produce DC power. Apart from decreasing financial costs, a main advantage of DC micro-grid is that the low risk of dangerous electric shocks from low voltage DC makes plug-and-play grids a possibility [8]. This also reduces the cost of installations of micro-grid, and will embolden end users to take responsibility to understand and control their own energy usage. By executing intelligence and internet facility to DC micro-grid controllers it will further enhance consumer involvement with AC devices – through smart metering and in result with dynamic demand management. In association with schedule of high and low power consumption, therefore it will help to reduce costs. [10] The problem with DC micro-grid is that the renewable energy sources produce only a small amount of power therefore we must use a converter to boost this power to integrate to grid only a small amount of power therefore we must use a converter to boost this power to integrate to grid.

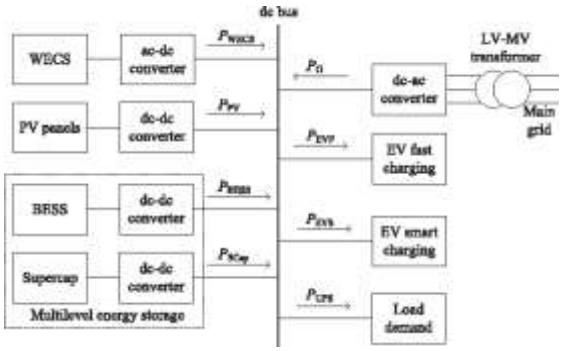

Fig,1. General Micro-grid

Traditionally use of boost converters but these have low voltage gain, hence it should be necessary to increase the number of boost converters. But the efficiency of boost converter is less for high gain i.e. for
very large duty cycle. Therefore, for conventional boost converter we cannot achieve high gain operation. Efficiency will be as poor as 60% for a duty cycle of 0.7[12]. Whereas it will have a highest efficiency for duty cycle of 0.5. To achieve low ripple of ripple free current the use of the Cuk and Sepic converters has been proposed [7]. However, the Cuk and Sepic converters have higher switch voltage and current stresses than the Boost converter, which may result in a low efficiency. Therefore, boost topology may still be preferable.

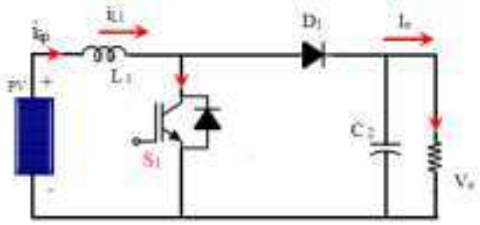

Fig.2. Conventional Converter

Therefore, to overcome these disadvantages of conventional boost converter a modified boost converter is proposed. In this a three level boost converter whose feature includes low devices voltages stress requirement for high voltage application, small inductor size that leads to the reduction of cost and size and can be operated with a wide range input voltage for Wind [13]. And for PV a high gain coupled inductor based interleaved boost converter is used, it has the following features, it improves the transfer characteristics, as well as system efficiency even for high power levels.

PROPOSED SYSTEM

A. Circuit Description

This paper proposes a three level boost converter and a coupled inductor based interleaved boost converter both has high gain. These boost converter has the ability to convert low voltage of PV solar system and wind farm to high voltage without the use of more number of boost converter.

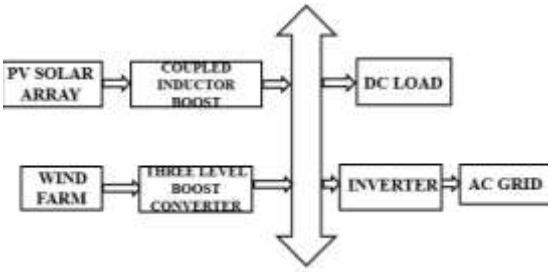

Fig3. Basic Block Diagram

The proposed system consists of a Solar PV array which is designed to give an output of 48V RMS and 67 V Peak. In this each solar cell is designed with 4.75A short circuit current, 1V open circuit voltage, 25deg Celsius system temperature, 1000 W/m2 irradiance. Wind turbine is also designed to have an output of 48V RMS and 67 V peak. The output of solar is boosted using the modified three level boost converter. And the output of wind is boosted using coupled inductor based interleaved boost converter. The output of both these converters are coupled and given to inverter to produce AC voltage for AC applications.

B. Working of Modified converter 1

Fig 4 shows the proposed circuit. It consists of 4 switches S1 to S4, two inductors (L1, L2) and two output capacitors (C4, C5). Output of wind is given to this converter which is AC therefore, first it converted into DC by using diode bridge rectifier boost the voltage to required level of the grid. In this
paper, the output of the converter is coupled with output of coupled inductor boost converter of PV. Then from this coupled output DC loads are directly fed and also an inverter is connected to convert it into AC to feed AC loads.

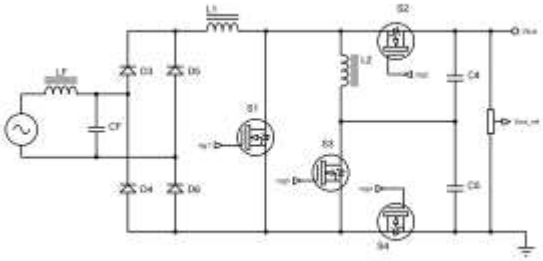

Fig.4. Three Level Boost Converter

Mode 1 : Fig 4 (a) shows mode 1. In this mode the current flows through inductor

L1 , S1, L2 , S3. Therefore, the active switches are S1 and S3. Output is taken across R.

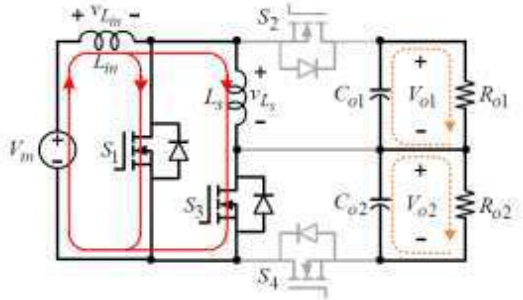

Fig 5. Mode 1

Mode 2 : Fig 4(b) shows mode 2. In this mode there are two current paths. One is through inductor L1 , S1 and Vin. Other one is through L1, L2, S4 and Vin. Therefore switch S1 remains in on state S3 is turned off and S4 is turned on.

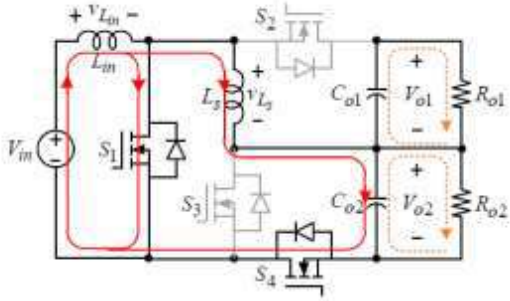

Fig. 6. Mode 2

Mode 3 : In this mode S4 is turned off and S3 is turned on again therefore it is same as that of mode 1.

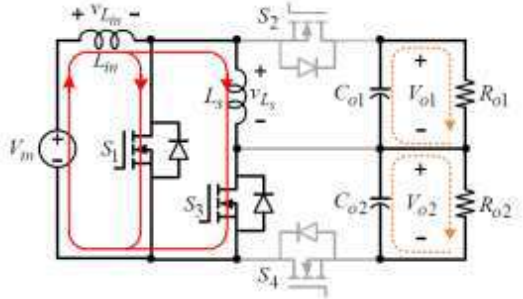

Fig 7. Mode 3

Mode 4 : Fig 4 (d) shows mode 4. In this mode S1 is turned off and S2 is turned on. S3 remains on. Current flows through Vin , L1, L2 and S3. Another path is through Vin L1 , C4 and S3.

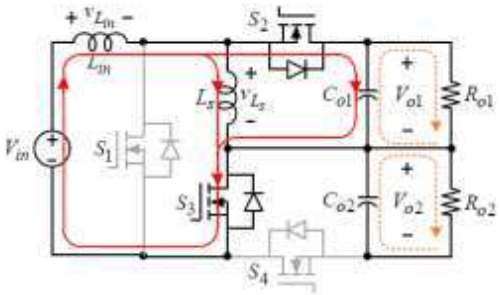

Fig 8 Mode 4

C. Working of Modified converter 2

Fig9. Shows the circuit diagram of coupled inductor based interleaved boost converter. It consists of 2 switches S_1 and S_2, a inductors (L_{in}), coupled inductors(L_1 and L_2) and a output capacitors (C_f) Output of solar is given to this converter which boost the voltage to required level of the grid. The output of the converter is coupled with output of TLB converter of wind.

.

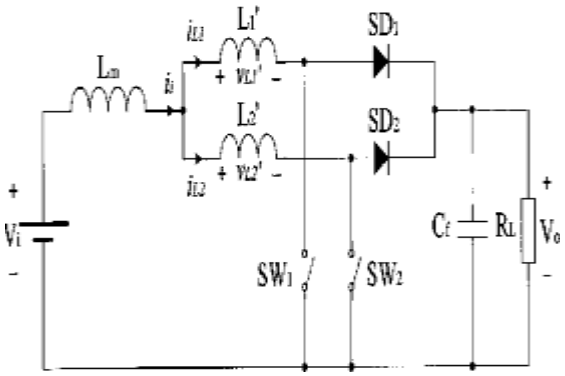

Fig. 9. Coupled Inductor Based Interleaved Boost Converter

Mode 1: Switch S_1 is ON Current flows through inductor L_{in} and L_2 .Both gets charged. Since L_2 is coupled inductor L_1 also get charged due to mutual inductance. Diode SD_1 turns ON and capacitor is charged.

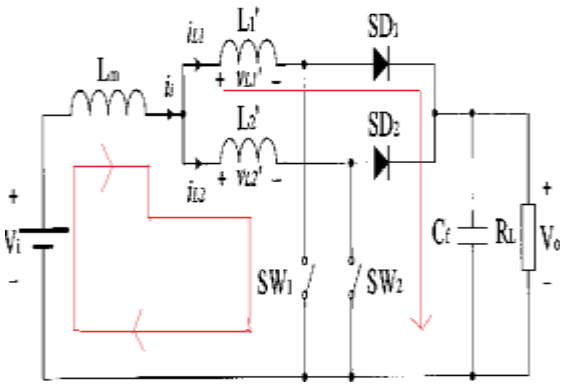

Fig.10 . Mode 1

Mode 2: Switch S_1 and S_2 is ON. All the inductors get charged by the paths of current. Output is supplied from the capacitors.

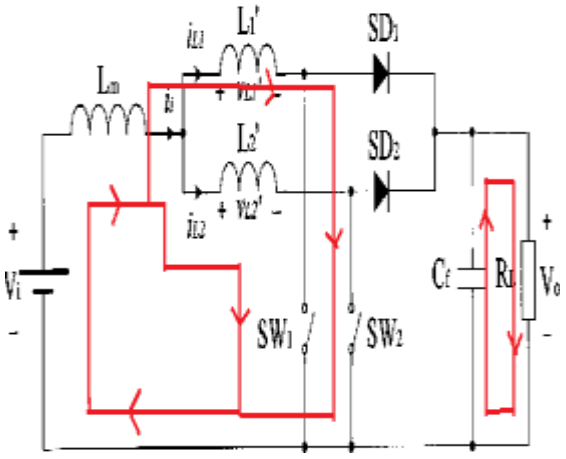

Fig.11. Mode 2

Mode 3: Switch S_2 is turned ON. Current flows through L_{in} and L_1. Since L_1 and L_2 are coupled inductors L_2 also get charged. Diode D_2 is forward biased and capacitor is charged.

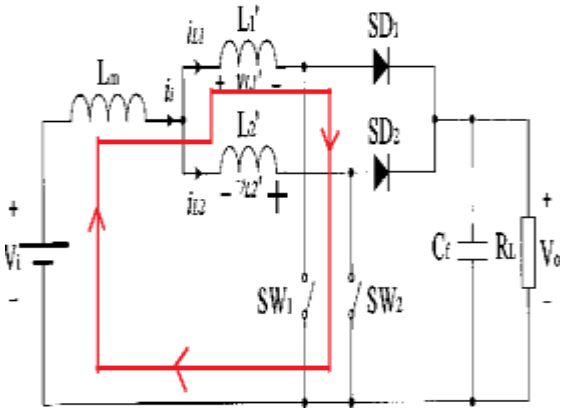

Fig.12. Mode 3

D. DESIGN EQUATION

In the proposed converter the voltage gain is given by

$$V_{in}(1+D)\,T_s/2 = (V_{01}-V_{in})(1-D)\,T_s/2 \quad (1)$$

$$V_{01}(1+D)\,T_s/2 = V_{02}(1-D)\,T_s/2 \quad (2)$$

Where (D) is the duty ratio defined as the time interval when S1 , S3 are both turned on during half switching period (Ts/2).

$$\frac{V_0}{V_{in}} = \frac{2}{1-D} \quad (3)$$

From equation (3) it is clear that the gain is twice than that of conventional boost converter.With minimum input voltage Vin ,maximum current ILin flows through the inductor for a fixed output Po.The inductor value to maintain the ripple is

$$L_{in} \geq \frac{(1-D)DV_0}{4*x\%I_{Lin\,max}} * \frac{1}{2f_s} \quad (4)$$

L_{in}= 280 micro Henry

$$L_s \geq \frac{(1-D)V_0}{z\%*I_{Lin\,max}} * \frac{1}{2f_s} \quad (5)$$

L_s = 960micro henry

In this paper 30% of current ripple of the corresponding average current is given to all the inductors in the circuit.
The current relation between the two inductors is found as

$$I_{Ls} = \frac{R_{01}}{R_{01}+R_{02}} * I_{Lin} \quad (6)$$

Efficiency can be calculated by

$$\frac{Output\ power}{Input\ power} = Efficiency \quad (7)$$

E. CONTROL SYSTEM

Figure 5 shows the control system of the proposed system. During time interval 0 to $DT_s/2$ switches S_1 and S_3 are in on condition. During time interval $DT_s/2$ to $T_s/2$ switch S_1 remain in on condition while S_3 is turned off and S_4 is turned on. In the next interval first situation is repeated. After that upto T_s S_1 and S_4 are off. S_2 and S_3 are in on condition. To obtain this condition it must give same pulse to S_1 and S_3. By giving a delay of half the time period and give it to S_2 and S_4.

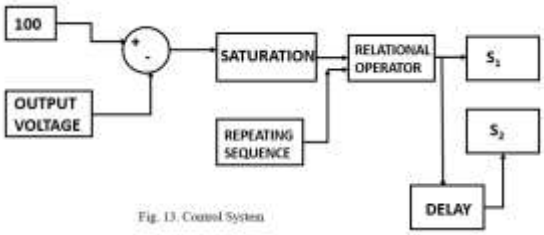

Fig. 13. Control System

SIMULATION RESULTS

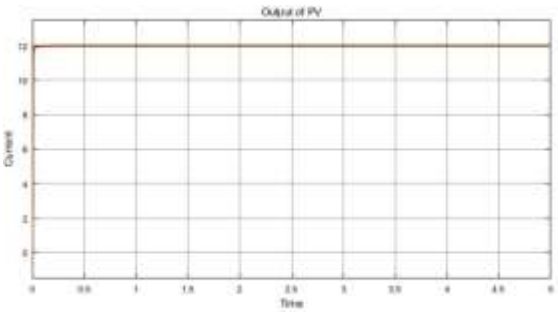

Fig.14. PV Voltage

Fig.14 shows the voltage verses time graph of solar panel. Output voltage is 12V. Voltage increases from zero to 60V. From time 0 to 0.025 voltage is increasing. After that the voltage becomes steady

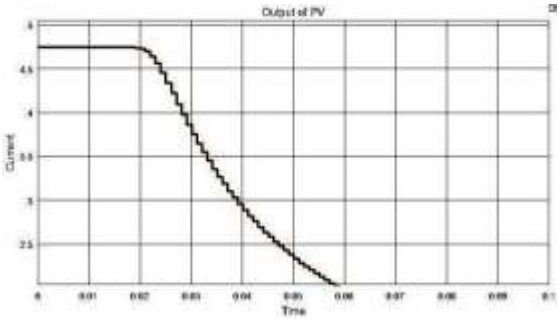

Fig.15. PV Current

Fig.15 shows the current of solar PV. The value of current is 4.7. In these each of these solar cell was designed with 4.75A short circuit current.

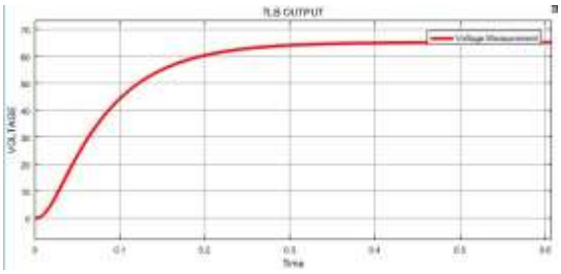

Fig. 16 Output Voltage of Three Level Boost Converter

Figure 16 shows the output voltage of three level boost converter. It is the converter of Wind. It boosts 12V of Wind to 68V after being rectified by the diode bridge rectifier at the front end. It shows a steady increase in voltage. As the PV charges the voltage also increases.

Fig.17. Output Voltage of Coupled Inductor Boost Converter

Figure 17 shows the output voltage of three level boost converter. It is the converter of PV. It boosts 12V of PV to 68V. It shows a steady increase in voltage. As the PV charges the voltage also increases

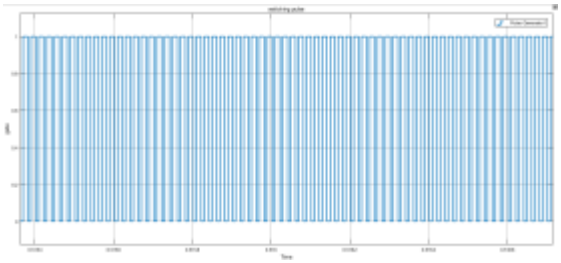

Fig 18. Switching Pulse

Figure 18 shows the switching pulse of the converters. From this it is clear that with this much small duty ration we could boost the voltage 5 times. Therefore, these converters increases the efficiency of the system.

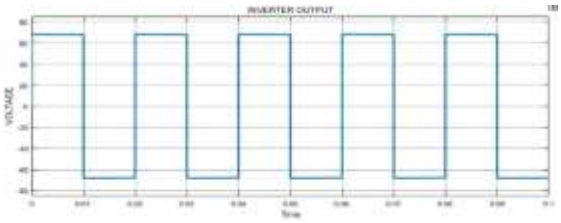

Fig.19. Inverter Output

Figure 19 shows the output voltage of the inverter. The output of both the converters are coupled and given to the inverter. It will produce the AC output for AC applications. It produces 68V AC.

CONCLUSION

This paper proposes two novel high gain boost converter for solar PV system and Wind system in a DC micro-grid. Boost converter is a DC-DC converter used to increase the output voltage. Efficiency of boost converter decreases with increase in duty ratio. This paper showed two high gain boost converter with low duty ratio. Thus we can improve the efficiency of the system. Also the conduction losses are reduced by using three level boost instead of three individual boost converter. Also by using coupled inductor boost the current ripple is reduced. High power. Power sharing. Component rating is reduced and hence cost is reduced. Matlab/simulink based results proved the effectiveness of proposed configuration.

REFERENCES

[1] Octavian Cornea, Member, IEEE, Gheorghe-Daniel Andreescu, Senior

Member, IEEE Nicolae Muntean, Senior Member, IEEE "*Bidirectional Power FlowControl in a DC Microgrid Through a Switched Capacitor Cell Hybrid DC-DC Converter*"DOI10.1109/TIE.2016.263152 IEEE Transactions on Industrial Electronics
[2] Jing Wang William Dunford Konrad Mauch" *A Comparison between Some Proposed Boost Topologies and Conventional Topologies in Discontinuous Inductor Current Mode"*
[3] Simin Sakhavati Department of Electrical Engineering, Shabestar Branch, Islamic Azad University, Shabestar, Iran" *Coupled Inductor Based Boost DC/DC Converter"* 7th Power Electronics, Drive Systems & Technologies Conference (PEDSTC 2016)
16-18 Feb. 2016, Iran University of Science and Technology, Tehran, Iran
[4] Manoj Lonkar,Srinivas Ponnaluri Global R & D Centre, Crompton Greaves Limited Mumbai, India." *An Overview of DC Microgrid Operation and Control"* 2015 6th International Renewable Energy Congress (IREC)
[5] M. Lakshmi and S. Hemamalini, *Member, IEEE," Non-isolated High Gain DC-DC Converter for DC Microgrids*" DOI 10.1109/TIE.2017.2733463, IEEE Transactions on Industrial Electronics.
[6] Shailendra Kr. Tiwari*, *Member, IEEE*, Bhim Singh*, *Fellow, IEEE*, Puneet K. Goel" Design and Control of Micro-Grid fed by Renewable Energy Generating Sources" DOI 10.1109/TIA.2018.2793213 IEEE Transactions on Industry Applications
[7] Mahmood Ul Hassana,b, Muhammad Humayuna, Rizwan Ullahb, Baoquan Liua, Zhuo Fanga"*Control strategy of hybrid energy storage system in diesel generator based isolated AC micro-grids*" Received 5 September 2016; received in revised form 31 October 2016; accepted 7 December 2016
[8] P. C. Sekhar, Member, IEEE, and S. Mishra, Senior Member, IEEE*"Storage Free Smart Energy Management for Frequency Control in a Diesel-PV-Fuel Cell-Based Hybrid AC Microgrid*" This article has been accepted for inclusion in a future issue of this journal. Content is final as presented, with the exception of pagination
[9] A. Elmitwally, Member, IEEE, and Mohamed Rashed, Member, IEEE "*Flexible Operation Strategy for an Isolated PV-Diesel Microgrid Without Energy Storage*" ieee transactions on energy conversion, vol. 26, no. 1, march 2011.

Proceedings of the Fourth International Conference on Communication and Electronics Systems (ICCES 2019)
IEEE Conference Record # 45898; IEEE Xplore ISBN: 978-1-7281-1261-9

VARIOUS DATA DEDUPLICATION TECHNIQUES OF PRIMARY STORAGE

D.Viji
Research Scholar ,Department of Computer Science and Engineering
Sathyabama Institute of Science and Technology
Chennai,India
dviji2k@gmail.com

Dr.S.Revathy
Associate Professor,
Department of Information Technology
Sathyabama Institute of Science and Technology
Chennai,India
ramesh.revathy@gmail.com

***Abstract*— Now a day's rapid amount of data was increased due to new types of data generation device as well as storage devices. So a large amount of repeated data will be generated and stored in cloud service. Repeated data will be drastically reducing the storage space of the cloud environment. So that we need to do the data deduplication that is data block or chunk exactly stored only once in the environment. Data deduplication can be applied in different storage types, archives or backup storage, primary storage, disk drives, and RAM. The contribution of this paper classifies the data deduplication techniques in the primary storage system and identifies the performance and challenges of each technique in primary storage. Finally, ongoing research issues and undefined design points of deduplication techniques in primary storage are recognized and discussed. Primary storage system contains mutable data that means data often changed or removed, but the backup storage system mainly contains immutable data that is which never changed frequently and also some data could not be deleted at any time. In this article, we are analyzed various deduplication techniques of primary storage.**

Keywords*— *Data deduplication, primary storage, cloud service.

I. INTRODUCTION

Data deduplication is the process of scrutinizing a data set or IO files storing and sending distinct data. Additional copies of the same data removed, maintain exactly one copy of the data in the storage system. It is also the process of eliminating repeated copies of blocks of data and reduce storage. Data deduplication methods make sure that only unique contents are present in the storage system like primary, archive, disks, and flash or tape. Repeated data blocks are pointed through the index of unique content.

Deduplication system design change according to the storage environment. Deduplication classified by the following criteria granularity, locality, timing, indexing, technique, distribution scope. Data deduplication classified based on the different types of storage like primary, secondary, RAM, Solid state drive (SSD)[4]. In that primary, RAM, SSD has less attentiveness need to improve throughput, I/O latency and increase space saving. Nitro methodology helps to improve the SSD cache capacity and provide a better trade-off between SSD durability and performance of the primary storage system[8]. For backup system manage scalability, reliability, and security needs further improvements. Primary deduplicating blocks in primary workloads secondary deduplicating in the backup or archival system. Both primary or secondary more or less similar processing operations.[5][6]. Data to be forms of the byte stream and segmented into chunks or blocks. Major two types of chunking algorithm are fixed size chunking and CDC (content defined chunking).

Benefits of deduplication include:

- Reduced an amount of data space in a storage system.
- In primary storage system maximize the flash storage capacity
- Lower bandwidth consumption.
- Higher data holding periods.
- Fast recovery.
- Reduced tape backups

Deduplication methods works based on the data types Fig 1shows the classification of data types. Data deduplication and multimedia deduplication Date deduplication is document or text, multimedia deduplication image video or audio files. Text deduplication again classified as two types of file-level or block level deduplication. File level deduplication entire files are compared with their hash value. In this method does not give high efficiency. Block level deduplication achieve good efficiency compared with file level. Files are divided as blocks are chunks this process also called chunking. That chunks may be a fixed size or variable sizes depend on the deduplication system. Fixed and variable size chunking gives better storage efficiency.

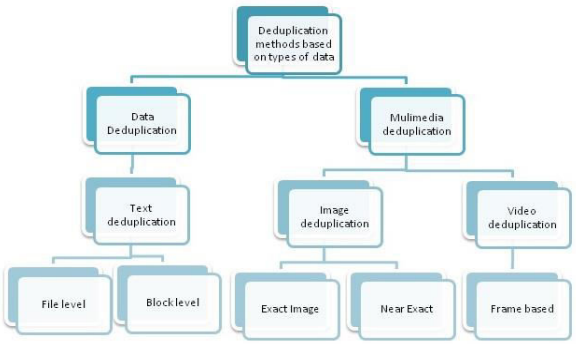

Fig 1. Classification of Deduplication methods

A. *Chunking process*

Each and every chunk have chunk id for unique representation. Chunk id calculated by a cryptographic hash function. Index table maintains the collection of unique chunk information. Chunk information maintained as KV-pair structure, i.e, Key-Value pair. ID denoted as a key and other related information act as a value[7]. Deduplication system searches the newly created chunk id in index table if matches fond new chunk id won't be stored in an index table. Chunking process creates performance issues like time-consuming for chunk id creation and searching process, a large amount of cache memory used for storing index table[7].

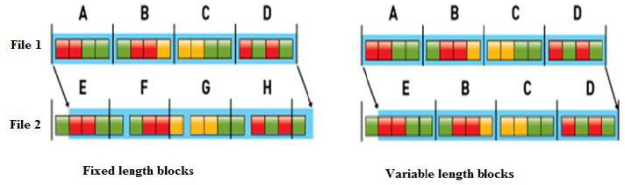

Fig 2. Fixed vs variable size blocks

Figure 2 shows the differences between fixed and variable size blocks for example File 1 sliced as a four fixed block size named A,B,C,D after sometimes file was updated content may be adding or deleting some data from the original file and named as a new file file2, now file2 try to upload in the cloud environment file2 going to be sliced with same fixed size now we get different blocks named as E, F,G, H, all other content of data similar to the file1 except few additional data but even we are getting different block due to fixed size. This what consider as a disadvantage of a fixed length of chunking process small updating will give dramatic changes in the chunking. But processing was easy compared with others. So that variable size chunking reduce the problem of fixed one Fig 2 shows clearly except block E remaining will give the same result So we do not want to save it again simply through indexing we can refer the remaining blocks showed in fig 3. Through this method, we will get effective storage space compared with fixed size block but processing was hard compared with others.

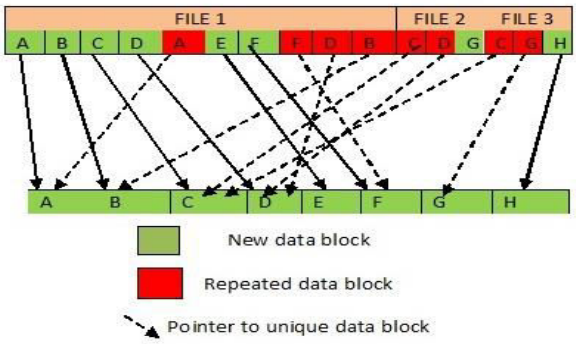

Fig 3.Deduplication reference information

II. Deduplication Methods Primary Deduplication vs Backup Deduplication

For hash deduplication system to find the redundant data whole file break into the block. If data in one chunk similar to data in another chunk, due to changes or updating of any one block even one or two byte of data, two blocks will be generated different hash values and system have to store both the block even major content are similar to each other. Some backup deduplication system used variable size blocks to maximizing the performance of the deduplication system. To find out the block boundaries variable block deduplication needs a lot of computing power. So that primary deduplication system mostly used fixed block size, since primary storage deduplication has to balance write latency against deduplication efficiency.[24]

III. Deduplication Algorithms for Primary Storage

The following two methods are mainly focused on primary storage to decrease storage space and increase the performance of input and output latency.1. Offline deduplication 2. Inline deduplication. Offline deduplication minimizes the additional computational resources and storage area[15]. But it has some following problem of extra reads from the storage, concurrency issues arise. But inline deduplication system overcomes the problem of the offline system as well as reduce the input-output latency.[4]

A Major challenge in primary system tradeoff between space saving and cost. The Smaller size of more number of chunks will give space efficiency but it increases the Larger index structure, so that cost also increased to maintain the index structure. If index too large then partially loaded into the RAM obviously number of disk input and output operations are going to be raised. A Distributed hash table (DST) used to manage the tradeoff between scalability and gain, but it shares the data into distinct client this will arise the problem of privacy and security issues.

Huijun Wu et al., they found the limitations of deduplication techniques in primary storage mainly the following two methods first inline cache, second post-processing deduplication[3]

A. *Inline*

Fingerprint cache mechanism was used to achieve deduplication. Sometimes fingerprint lookup table greater than physical memory size this one considered as a flaw of this method, and also inline cache method does not give a guarantee that all the duplicate blocks are eliminated.

B. *Offline deduplication*

DEDIS one of the offline deduplication method. DEDIS fully decentralized method So it could avoid the single point of failure, It does not depend on storage workload, deduplication achieved on the whole cluster chunks are fixed size of blocks(4KB). most of the techniques do not compare the full content of blocks, in place of checks only chunk signature. DEDIS follows decentralized method so that it maintains an index of unique chunk signature and metadata are distributed. DEDIS overcome the alignment issues of DeDe. Table 1 describes various inline and offline deduplication methods and its performance.

TABLE 1 COMPARISON BETWEEN INLINE AND OFFLINE DEDUPLICATION SYSTEM

Inline deduplication system	Offline deduplication system

• iDedup, Live DFS, DBLK[21] techniques
  • increases the speed of index lookup operation and avoiding disk access.
  • Storage space reduced
  • Centralized deduplication
  • Deduplication target at backup and archival data.
• Opendedup and ZFS
  • reinforce multi-host inline deduplication for dynamic data.
  • Require large RAM capability for indexing chunks.
	• DDE – Duplicate data elimination
	  • For SAN file system
	  • A Centralized metadata server
	  • The Flaw of this method single point of failure.
	• DeDe – Decentralized deduplication
	  • Centralized component avoided
	  • Offline decentralized deduplication for VM volumes
	  • Index structure used that is accessed by all the nodes with the locking mechanism.

C. Post processing

The Drawback of this method before removing the block it was already written into the disk, resource contention was the main problem since a lot of duplicates blocks to be removed.

To improvise the efficiency of caching mechanism they follow a two-phase process, the workload was distributed such a way in the inline phase itself number of duplicates chunks are identified, so that less number of blocks need to be written into the disks. impact of this process input and output performance was increased and the workload of post-processing was reduced.

D. Cache based algorithm

Both LRU and ghost cache carry out poor performance due to memory overhead in the primary storage environment, to accomplish this flaw TLE-LRU (Temporal locality estimation LRU) and hybrid deduplication mechanism arrived. Compared with DIODE SLADE reduce the load of post-processing deduplication process, reduce the cache contention problem for primary storage. In SLADE dynamic locality estimation method was implemented to improve the inline deduplication performance. Table 2 explain about the cache based algorithm and its performance.

In the primary storage environment cache algorithm and ghost cache approach has following drawbacks former cannot manage with fingerprint cache management later it is only for weak locality but it highly affected by memory overhead problem. To overcome these problems the hybrid approach of SLADE with TLE-LRU was implemented. Through this hybrid approach, they achieve high inline cache efficiency, the workload of post-processing deduplication was reduced, improve the inline ration up to 39.70% compared with idedup. Disk capacity also reduced up to 45.08%comparedwith post-processing.[3].

TABLE 2. CACHE BASED ALGORITHM

Algorithm	Performance
1.LRU - least recently used[3]	• Unable to handle a mixed level of temporal locality
2. Ghost cache[3]	• It is For weak locality problem • LIRS(Lower inter-reference recently set) replacement policy and ARC (Adaptive replacement cache). • ARC method better than the LRU
3.SLADE – Stream locality aware deduplication[3]	• Based on the threshold blocks are eliminated whose size greater than the threshold value. • The threshold will be changed dynamically according to the data stream. • It is For primary deduplication.
4. DDFS – Data domain file system [1]	• To improve the fingerprint indexing rate limiting method was used. • It is for backup deduplication
5. DIODE – Dynamic inline off-line deduplication [2]	• It is for primary deduplication. • Deduplication based on file-based file extension, the file type is not enough for deduplication performance

IV. DAC

The single cloud storage server has a number of important issues like vendor lock-in problem, availability, security. Cost increased for user want to migrate from one cloud storage system to another means all the data has to migrate from old service provider to new system this migration cost too higher than the cost of the old service provider this is called vendor lock-in problem. If all the data stored in a single cloud service provider means it can be easily attacked by hackers.

DAC deduplication assisted the primary system in a cloud of cloud it overcomes all the problems in a single cloud server and also avoids the integrity ensure the confidentiality and integrity of outside attacker. DAC removes the unnecessary data and distributes the data among multiple independent clouds. It improves performance and cost efficiency.[16] .DAC used fixed chunking algorithm. Compared to fixed size chunking variable size chunking may be given data redundancy problem in primary storage.[16]. DAC lagging in the reliability analysis and secure data deduplication

A. *Clouds of cloud*

Several systems working under clouds of cloud concept like RACS, HAIL, NC Cloud, Dura cloud, DEPSEY, HYRD, and DAC.RACS used erasure coding to decrease the vendor lock-in problem. HAIL gives the integrity and availability assurance for the stored data. NC Cloud cost-effectiveness, all the above methods used erasure code or network code method for data protection.

In Dura, cloud replication method was used to maintain a copy of user content in different cloud storage provider to give better availability. DEPSEY this method combine the Byzantine quorum system protocol plus cryptographic secret hashing and replication to increase the availability and confidentiality. HYRD integrates both replication and erasure code performance and storage efficient improved but compared to DAC moderate performance only. It also gives a guarantee of availability.

DAC is to address the storage availability issue using replication scheme. Replication method provides better performance and high bandwidth storage overhead, erasure method provides storage efficiency, robustness and high access performance in a cloud of cloud, especially large files.

V. SDM

Once file type was well known then only can apply deduplication manually otherwise not possible for a new type or unknown type[17]. Based on the file type and ratio chunking algorithm will be selected. The ratio for file type less than the predefined threshold means new chunking algorithm will be applied. Problem with this method small size of files because of file size too less than the block size, so a waste of time processing.[19]. SDM overcome the above drawback as well as increase the storage space of the cloud. It automatically detects the deduplication method whether file level or block level based on each file type. For example, mp3 and jpeg are file-level deduplication, pdf, doc and others will perform under block-level deduplication. SDM does not require any configuration process. Its performance level was good in various file type and also improve the speed and accuracy of the system.[18]. The drawback of the SDM method not effective on block-level deduplication scheme compared with others. Processing time increased working under dataset. Sometimes wrong deduplication method selection.

VI. PERFORMANCE ORIENTED AND CAPACITY ORIENTED DEDUPLICATION SCHEME

Performance oriented deduplication scheme (POD) highly improve the performance of the primary storage and reduce the usage of storage space. The following two approaches have achieved these things. Sequence based, idedup and offline deduplication are capacity oriented deduplication. Capacity oriented deduplication scheme mainly focused on storage capacity saving. Table 3 clearly shows the outlook of performance and capacity oriented deduplication scheme.

TABLE 3. OUTLOOK OF PERFORMANCE AND CAPACITY ORIENTED SCHEME

Performance oriented deduplication scheme	**Capacity oriented deduplication scheme**
• Compared with capacity oriented scheme iDedup POD gives better capacity savings.[20] • Small files are a vital role in primary storage of more than 50%. for deduplication, it considers small size files too. • Select –Dedupe • Request-based selective deduplication approach. • Data fragmentation problem minimized. • iCache • Intelligent cache management system.[20] • Read performance and space-saving increased. • It solves the problem of memory contention as well as read amplification	• Capacity oriented concentrate on storage capacity saving. • For deduplication only consider the large request and ignore the small request like less than 4kb, 8kb. • Capacity oriented omitted these small size files this one consider as the most important problem in the performance of primary storage. • idedup • Inline deduplication system [11] • Consider the problem of space allocation between read cache and index cache

VII. TDDFS

Two-Tier storage system implemented to achieve high performance as well as low cost in the primary system. Frequently accessed data stored in the fast tier less active data stored in a low-cost tier. To achieve cost-effectiveness all the file operations are performed in a fast tier and long inactive files are moved from fast to slow tier. Whenever files are migrated from slow to fast tier, if chunks are already available in the fast tier the data migration process could be avoided so that TDDFS gives the best performance in the primary storage system. TDDFS overcome the problem of migration efficiency, deduplication penalty, and isolation between block level management and upper layer application, and also TDDFS solves the deduplication latency and throughput issues. The following four features make TDDFS special and better tradeoff between performance and cost-effectiveness.[7] 1. File migration selection,2. Integration deduplication with file migration,3. Non-Redundant chunk reloading,4.shared chunk management.

SDFS[10] system depends on the situation block size may be fixed or variable size but it cannot manage the two-tier storage system. Lessfs[9] fixed block size for file system it manage the two-tier system but performance less than SDFS and TDDFS. ZFS[13] File-level deduplication compared to other deduplication performance was low. So it does not work under two-tier storage. TDDFS[7] chunking size randomly generated between min(51B) to Max(16KB). TDDFS efficiently manage two-tier storage system and high performance.

VIII. COMPARISON OF DEDUPLICATION METHODS

Table 4 shows a comparison between various deduplication methods with their metrics. In this table, we are compared with the following metrics file system level, performance, efficiency, cost and, its challenges. File system level means whether the file was taken as a whole file or sliced into blocks. The blocks may be sliced as a fixed size or random size.

TABLE 4. COMPARISON OF DEDUPLICATION TECHNIQUES WITH THEIR METRICS

Methods	File system level	Performance	Challenges	Efficiency	Cost
Inline Data Duplication. Idedup [11]	Fixed size	Higher throughput and lower latency. Minimize the extra IOs	Lost the deduplication ratio	H	L
Zettabyte File System ZFS [13]	Fixed size 256 bit block check sums	The most dedup method used the only limited amount of data. ZFS does not have any restrictions. It will be fast while loading dedup tables into the memory	Not optimized for latency.	Mo	L
Duplicate Data Elimination. DDE [22]	Fixed size 32KB	By comparing the hash value of each block, DDE detects duplicate data on the logical block level.	single point of failure system.	Mo	M
Decentralized deduplication DeDe [23]	Fixed size	Decentralized deduplication system. Higher throughput penalty avoided. metadata size was reduced.	In distributed infrastructure needs communication between blocks. Such structure complex and high cost. Alignment issues.	Mo	H
Deduplication of Distrbuted Infrastructure. DEDIS [15]	Fixed size	Fully decentralized avoid the single point of failure.	All distributed service need to maintain both index of unique block signature and metadata	H	H
Stream locality aware deduplication SLADE [3]	Fixed size	Based on the threshold blocks are eliminated whose size greater than the threshold value. The threshold will be changed dynamically according to the data stream.	Designed for primary storage deduplication	H compare with idedup	L
Deduplication-Assisted Cloud-of-Clouds DAC[16]	Fixed size	Overcomes all the problems in a single cloud server and also avoids the integrity ensure the confidentiality and integrity of outside attacker. DAC removes the unnecessary data and distributes the data among multiple independent clouds.	Lagging in the reliability analysis and secure data deduplication	H	L
Tier-Aware Data Deduplication-Based File System TDDFS [7]	Randomly generated between 512B to 16KB	To attain effective capacity utilization of the fast tier TDDFS maintain the deduplicated state of reloaded files.	More intelligent file selection policy needs to improve deduplication ratio.	H	M
Device mapper target for data deduplication Dmdedup [12]	Fixed size	In fast device deduplication structure like fingerprint index. The slower device maintains duplicate data blocks.	Does not have tired storage system concept. Data cannot migrate.	Mo	L
Cache dedup [14]	Fixed size	To increase the space utilization and flash lifespan, cache dedup institute flash-based cache Also, propose cache replacement algorithm (D-LRU, D-ARU) for increase cache performance.	Need distinct data cache for a block in storage and metadata cache for fingerprints	Mo	H
Dynamic inline-offline de duplication DIODE [2]	File level	It is for primary deduplication. Deduplication based on file-based file extension	The file type is not enough for deduplication performance	L	L
Smart deduplication for mobile cloud storage SDM [18]	File level or Block level (fixed size)	Increase the storage space of the cloud. It automatically detects the deduplication method whether file level or block level based on each file type. For example, mp3 and jpeg are file-level deduplication, pdf, doc and others will perform under block-level deduplication.	SDM method not effective on block-level deduplication scheme compared with others. Processing time increased working under dataset. Sometimes wrong deduplication method selection.	L	L
Intelligent cache management system iCache [20]	Fixed size	Improve the read and write performance. Increase the space saving	Lagging in the reliability analysis and secure data deduplication	H	L

CONCLUSION AND FUTURE WORK

The primary deduplication technology has been analyzed in the context of performance, efficiency, challenge, and cost. But still, primary system deduplication techniques have not yet been as successful as backup deduplication technology. Because deduplication achieved in the primary system 68% but in the backup system 83%, and backup deduplication method has drastically increased the efficiency of storing backup data. So that more concentration needs to reduce the deduplication in the backup storage system as well. In future work, we are going to analyze various deduplication techniques in the backup storage system..

REFERENCES

[1] Y. Allu, F. Douglis, M. Kamat, P. Shilane, H. Patterson, and B. Zhu, "Backup to the future: How workload and hardware changes continually redefine data domain file systems," Comput., vol. 50, no. 7, pp. 64–72, 2017.

[2] Y. Tang, J. Yin, S. Deng, and Y. Li, "DIODE: Dynamic inline-offline de duplication providing efficient space-saving and read/write performance for primary storage systems," in Proc. IEEE 24th Int. Symp. Model. Anal. Simul. Comput. Telecommun. Syst., 2016,pp. 481–486.

[3] Huijun Wu , Chen Wang , Yinjin Fu , Member, IEEE, Sherif Sakr, Senior Member, IEEE,Kai Lu, and Liming Zhu, "A Differentiated Caching Mechanism to Enable Primary Storage Deduplication in Clouds" IEEE TRANSACTIONS ON PARALLEL AND DISTRIBUTED SYSTEMS, VOL. 29, NO. 6, JUNE 2018

[4] JO˜ AO PAULO and JOS´E PEREIRA, A Survey and Classification of Storage Deduplication Systems ACM Computing Surveys, Vol. 47, No. 1, Article 11, Publication date: May 2014

[5] Jaehong Min, Daeyoung Yoon, and YoujipWon. 2011. Efficient deduplication techniques for modern backup operation.IEEE Trans. Comput. 60, 6 (2011), 824–840.

[6] Wenji Li, Gregory Jean-Baptise, Juan Riveros, Giri Narasimhan, Tony Zhang, and Ming Zhao. 2016. CacheDedup: In-line deduplication for flash caching. In Proceedings of the 14th USENIX Conference on File and Storage Technologies (FAST'16). 301–314.

[7] ZHICHAO CAO and HAO WEN, JIM DIEHL and DAVID H. C. DU, TDDFS: A Tier-Aware Data Deduplication-Based File System ACM Transactions on Storage, Vol. 15, No. 1, Article 4. Publication date: February 2019.

[8] Cheng Li, Philip Shilane, Fred Douglis, Hyong Shim, Stephen Smaldone, and Grant Wallace. 2014. Nitro: A capacityoptimized SSD cache for primary storage. In Proceedings of the USENIX Annual Technical Conference (USENIX ATC'14). 501–512.

[9] Lessfs. 2012. Retrieved from https://fedoraproject.org/wiki/Features/LessFS.

[10] Opendedup–SDFS. 2012. Retrieved from http://www.opendedup.org.

[11] Kiran Srinivasan, Timothy Bisson, Garth R. Goodson, and Kaladhar Voruganti. 2012. iDedup: Latency-aware, inline data deduplication for primary storage. In Proceedings of the 10th USENIX Conference on File and Storage Technologies (FAST'12). 299–312.

[12] Vasily Tarasov, Deepak Jain, Geoff Kuenning, Sonam Mandal, Karthikeyani Palanisami, Philip Shilane, Sagar Trehan, and Erez Zadok. 2014. Dmdedup: Device mapper target for data deduplication. In Proceedings of the 2014 Ottawa Linux Symposium.

[13] J. Bonwick. ZFS deduplication. 2009. https://blogs.oracle.com/bonwick/entry/zfs_dedup.

[14] Wenji Li, Gregory Jean-Baptise, Juan Riveros, Giri Narasimhan, Tony Zhang, and Ming Zhao. 2016. CacheDedup: In-line deduplication for flash caching. In Proceedings of the 14th USENIX Conference on File and Storage Technologies (FAST'16). 301–314.

[15] JO˜ AO PAULO and JOS´E PEREIRA, Efficient Deduplication in a Distributed Primary Storage Infrastructure ACM Transactions on Storage, Vol. 12, No. 4, Article 20, Publication date: May 2016.

[16] Suzhen Wu, Kuan-Ching Li, Bo Mao,∗, Minghong Liao DAC: Improving storage availability with Deduplication-Assisted Cloud-of-Clouds Future Generation Computer Systems 74 (2017) 190–198

[17] L. Marques, C.J. Costa, Secure deduplication on mobile devices, in: Proc. 2011 Work. Open Source Des. Commun. - OSDOC '11, 2011, p. 19.

[18] Ryan N.S. Widodo, Hyotaek Lim,∗, Mohammed Atiquzzaman SDM: Smart deduplication for mobile cloud storage Future Generation Computer Systems 70 (2017) 64–73

[19] N. Haustein, A. Klein, Troppens, Winarski, Method of and system for adaptive selection of a deduplication chunking technique, U.S. Pat. 2 (12) (2009) 1–7

[20] Bo Mao, Member, Suzhen Wu, Lei Tian, Leveraging Data Deduplication to Improve the Performance of Primary Storage Systems in the Cloud IEEE TRANSACTIONS ON COMPUTERS, VOL. 65, NO. 6, JUNE 2016

[21] Y. Tsuchiya and T. Watanabe. 2011. DBLK: Deduplication for primary block storage. In Proceedings of Conference on Mass Storage Systems (MSST).

[22] Bo Hong and Darrell D. E. Long. 2004. Duplicate data elimination in a san file system. In Proceedings of Conference on Mass Storage Systems (MSST)

[23] Austin T. Clements, Irfan Ahmad, Murali Vilayannur, and Jinyuan Li. 2009. Decentralized deduplication in SAN cluster file systems. In Proceedings of USENIX Annual Technical Conference (ATC).

[24] George Crump APRIL 30, 2013 https://www.networkcomputing.com/data-centers/primary-storage-deduplication-problem

Proceedings of the Fourth International Conference on Communication and Electronics Systems (ICCES 2019)
IEEE Conference Record # 45898; IEEE Xplore ISBN: 978-1-7281-1261-9

LAND COVER CHANGE DETECTION BASED ON SATELLITE IMAGES USING DEEP STACKING NETWORKS

Deepa Palanisamy
Department of Information Technology
MIT Campus, Anna University
Chennai, India
deepapalanisamy25@gmail.com

Radha Senthilkumar
Department of Information Technology
MIT Campus, Anna University
Chennai, India
radhasenthilkumar@gmail.com

***Abstract*—Remote sensing provides timely and reliable information about urban areas and their changing patterns.Detection of urban change is an important factor that affects the supply of food supply, water supply, etc.Detection of land use and land change is essential in order to understand the current situation and plan for the future to avoid scarcity. In this work, we proposed two new framework called Tensor - Deep Stacking Network (TDSN) with back propagation and Deep Stacking Convolution Neural Networks (DS - CNN) for land cover change detection. Changes are detected between the year 2005 and 2015 in the month of September over the Hutong area, Beijing, China. The work has been validated by using Sentinel 2 (4 bands cirrus, water vapor, coastal aerosol, red edge band) and Landsat 8(11 bands) satellite image. All the bands from Landsat -8 image are pan-sharpen to 15m resolution to get more accurate classification result. Bands in the Sentinel -2 satellite image are used to remove cloud present in the raw satellite image. The classification accuracy of proposed work are compared with the traditional classification algorithm Support Vector Machine (SVM). The accuracy of proposed work is 12% is improved in compare to traditional algorithm.**

***Index Terms*—Remote Sensing, Change Detection, Tensor Deep Stacking Network, Back-propagation, Convolution Neural Network.**

I. INTRODUCTION

Remote sensing is the process of obtaining information about the objects or areas from a distance, typically from aircraft or satellites. Remote sensing provides the Earth's periodic image, which is useful in mapping patterns and changes in land use / land coverage over time. Change in land use and land cover has become a central component of natural resource management and environmental monitoring [16]. Growing population was one of the root causes of land cover changes. The effect of changing land cover has resulted in a reduction in fresh water quality. Population growth leads to increased food and fresh water and air demands [1].

Detection of change requires long-term satellite images because scientists are examining an area over a period of time and seeing what changes are being made over that period.Many websites now offer free remote sensing image with high resolution for a day. One of them was USGS [17]. USGS provides free satellite image of Landsat and Sentinel. Landsat-8 is capable of capturing and transmitting 532 Earth images per day. The image is captured using Enhanced Themetic Mapper Plus (ETM+) sensor. This image contains eleven spectral bands. Each bands of 30m resolution except pan-chromatic band which is of 15m resolution. Pan-chromatic band is used for pan-sharpening.

Sentinel - 2 satellite provides 12 bands. Only 4 bands (cirrus, water vapor, coastal aerosol, red edge band) are used in this work. The first three are used to remove the cloud present in the satellite images and the last one helps to detect early signs of food shortages.

The original remote sensing data is severely incomplete and contaminated in the image with artifacts such as cloud, black strip. This increases the difficulty of image analysis.A cloud-free image was formed by cloning the cloud-free satellite image information into their corresponding cloud-contaminated image, assuming that images cover the same coordinates over a short period of time[3]. CNN helps to improve the classification accuracy. CNN is used as a variation of multilayer perceptron designed to reduce preprocessing. In comparison with other image classification algorithms, CNN requires very little pre-processing [15]. This work land cover change are detected for Beijing, china over the period from 2005 to 2015. It is observed that ecological and sustainable changes in agricultural area, water bodies and urban areas.

A. Research Challenges

The (Deep Neural Network) DNN and CNN are proven to be extremely powerful for performing recognition and classification tasks including speech recognition and image classification, training a DNN and CNN are computationally difficult and also extremely difficult to add parallelize across machines [6]. This makes learning at large scale practically impossible. Each satellite image was more than 15 GB in size. It is impossible to train these network with CPU machine. We need a GPU machine to train the network with this huge volume of data. This limitations are overcome by using TDSN but the problem in TDSN was hidden layers are fully

connected layers [14]. Fully connected layer involved more computation and require extra memory to store intermediate results. By replacing the hidden layers with convolution layers reduce computation and also save memory requirement.

II. RELATED WORKS

In Deep learning based predicting missing data for remote sensing analysis [14] use TDSN to predict the missing image in the time series.In predicting remote sensing data using spatial-temporal techniqu. In recent years remote sensing is used in multiple application and it is simple and easy to acquire high-resolution satellite image. By the same time, it creates a challenge for analysis community to interpretation from the images of the huge volume of data. Hence use deep stacking network to predict remote sensing data at the timestamp t. Deep stacking network is stacking of multilayer perceptron with one hidden layer.

In parallel training of deep stacking networks [6] and scalable training of deep stacking network [12] provide parallel and scalable training of deep stacking network. Parallelism reduces the memory and time requirement but arising cost for inter CPU communication. It also demonstrates the full-batch training significantly reduce the error rate by distributing the training dataset over the CPU cluster compare to the mini-batch training using single CPU cluster.Parallelism is achieved by parallelizing the matrix multiplies. The job requires to synchronize all parallel batches distributed over CPU cluster. It must wait for all the dependencies.

In Tensor Deep Stacking Networks (TDSN) [2] the complex functions are calculated from the stacking of multiple simple functions. Each module consists of linear input layer, and output layer, and a two non-linear hidden layer. Non-linear activation function sigmoid is used to map linear input to non-linear output to improve the performance. The input to the first module is corresponding to the first available image in the temporal sequence . For further modules, the output of the previous module along with the new input image is given as input. The final module of the TDSN predicts the actual value. In [11] Forest changes are detected over a period of 29 years (1987 - 2015) using CNN. By using CNN accuracy of image classification was improved around 16%.

III. LAND COVER CHANGE DETECTION

TDSN with back propagation and DS CNN are used to enhance the accuracy of land cover classification. Fig.1 show the overall framework in detail. Our main contribution was adding convolutional and polling layer into Deep Stacking Network. Overall work is divided into three steps. In step one, we applied pre-processing technique on the raw training satellite image, including pan-sharpening, cloud removal. Pan-sharpening helps to get high resolution image and cloud removal helps to remove noise present in the image. In Step 2, land cover classification are done by TDSN with back propagation and DS-CNN. In final step, the performance is measured by comparing the accuracy of two frameworks with the traditional classification algorithms [7].

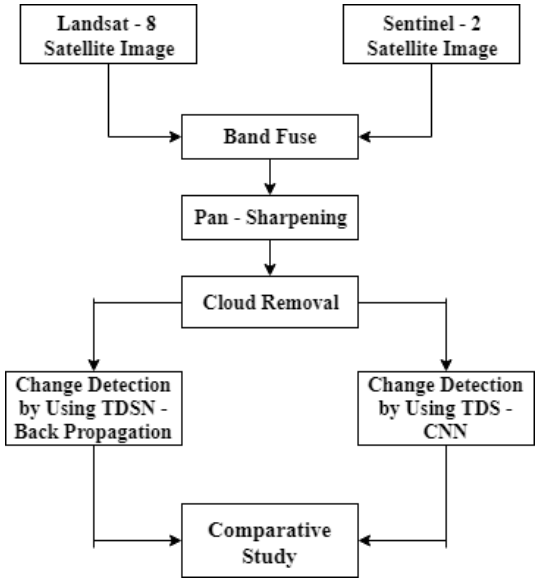

Fig. 1. Overall Flow of Land Cover Change Detection

A. Feature Set Preparation and Pre-Processing

Remote sensing images are collected in the area of Hutong area, Beijing, China, over the year 2005 to 2015. From the year 2005 to 2012 Landsat -7 satellite images are taken. It contain totally eight bands of 30m spatial resolution except panchromatic band which is 15m resolution. For the year 2013 to 2015 Landsat 8 and Sentinel 2 satellite images are taken. Raw satellite image are contaminated with artifacts like cloud, black strips due to fault in sensor used in the satellite. These missing information are formed by clone the information from the cloud-free satellite image into their corresponding clod contaminated image under the assumption that images cover the same coordinates and over a short period of time. Pixel of clod contaminated image are replaced with the pixel from the satellite images. For example, Fig.2 shows how to replace a cloud contaminated pixel from the cloud free image pixel covers the same coordinates as cloud contaminated image.

In the above example 3x3 image are contaminated with cloud and they are replaced with the average of pixel values taken from the cloud free image that covers the same coordinates.

Pan-sharpening was done with the help of pan-chromatic band which is one of the satellite band with high resolution and grayscale bands. For example, consider the Landsat 8 satellite image band 8 (pan-chromatic) have the spatial resolution of 15m, and all other ten bands have 30m spatial resolution. To obtain high resolution multi spectral image, we merge low resolution multi spectral bands of resolution 30 m with high resolution pan chromatic band of resolution 15 m. Bovey pansharpening algorithm shown in Fig.3 was used for pan sharpening. (Red Green Blue)RGB image was converted into (Intensity Hue Saturation)IHS image. After converted into IHS, Intensity part in the image was replaced with pan-chromatic band. Pan-chromatic band (pan) HS was converted

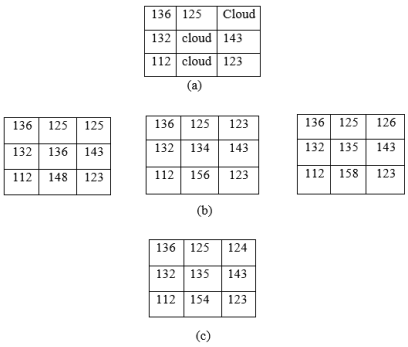

Fig. 2. Cloud Removal. (a). Satellite Image Contaminated With Cloud. (b). Three Cloud Free Satellite Image Covers the Same Coordinates as Cloud Contaminated Image. (c). Cloud Are Replaced With the Average of Cloud Free Image Pixel Values.

back to RGB.

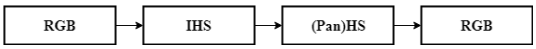

Fig. 3. Pan-sharpening by Bovey Algorithm

Cloud free and pan sharpened satellite image are converted into NDVI image. If NDVI value is negative, it is highly likely that place is covered by water. If the NDVI value is in the range between 0.3 to 1 that area is covered by dense vegetation. Vegetation highly reflects near Infrared and green wavelength. And absorbs blue and red wavelength. If we see more Near InfraRed then it could be a strong vegetation. If the value is nearly by zero that area is it is the highly urbanized area. NDVI image are converted in to pixel and stored in a matrix format. This matrix are converted into dense file format and stored it in .binary extension. The dense format is used to calculate the weight matrix of T-DSN during the training phase. Totally 8 images are used for training from the year 2006 to 2014. The dense file is in the format of N x M matrix. Values are stored in a column-major order. Where N and M are 8 byte signed integer. T-DSN is a supervised learning model. Two images (2005 and 2015) are used for testing purpose, to find the amount changes happened during this 10 years. Target matrix contain three classes -1 represent bare land, 0 represent water area and 1 represent greenery area. Target matrix are stored in the sparse file format. The sparse matrix is in the form of N x M matrix of target labels.

B. Tensor-Deep Stacking Network Model With Back Propagation

The architecture of T-DSN with back propagation for three module is given in the Fig.4. The number of modules in the T-DSN is equal to the number of training images. We designed 8 modules to train 8 images from the year 2006 to 2014. Each module consists of a linear input layer, linear output layer, and two non-linear hidden layers (fully connected layers). The weight matrix W1 and W2 are the maps between the input layer and hidden layers. The weight matrix U map between two hidden layers and the output layer [5].

Each module is basically stacking of simple multi-layer perceptron with two hidden layers [13]. The input to the bottommost layer of T-DSN is raw input image in the first available sequence (2006). The input to the subsequent models are the output of the immediate previous module and the corresponding raw input image in the time series. For example, input to the second module was output of first module and the image vector of time series 2007.The output of each module learns feature for the particular timestamp.

Training vectors are denoted by X= [X1, X2,XN], in which each vector is denoted by Xi=[X1i,.,Xji, .XDi], where D is the dimension of the each input image vector (2947 x 2947), where N is the total number of training samples in the remote sensing time series. L Denote by the number of hidden units and by C the dimension of the output vector.

While training we provide training image as the dense file format and corresponding targets as sparse file format, chunk size (optional), number of blocks, number of iteration network. If chunk size is not provide it automatically get the total available memory of the system and make the chunk size. Once the training gets over it generates weight matrices W1, W2, U for all the blocks of T-DSN. For the first iteration, weights are initialized randomly. For each iteration, weights are modified so as to minimize the root mean square error between actual output and expected output. These weight modifications are made in the backward direction, which is from the last block output layer through each block down to the zeroth block hidden layer. This learning process continues until the weights eventually converge.

Fig.4 shows the block diagram of TDSN- with back propagation. Error at the final block is back propagate in the network. While back propagate make the delta changes in the internal weights to reduce the error in the next iteration. For testing we must provide testing image as a dense file format and path of weight matrices generated during testing and predict flag as command line argument.

We got 90.25% accuracy for first iteration. For the subsequent iteration accuracy was gradually increase. For seventh and eighth iteration there is no change in accuracy (accuracy of seventh iteration = 92.16% and the accuracy of eighth iteration was also 92.16%). So, we stop iterating back the error.

The output at the output layer of the T-DSN is calculated by using the equation 1. The hidden layer output is calculated by using the equation 2 and 3.

$$Y_i = U^T h_i \tag{1}$$

where,

$$h_{1i} = \sigma(W^T X_i) \tag{2}$$

$$h_{2i} = \sigma(W^T X_i) \tag{3}$$

$$h_i = h_{1i} \cdot h_{2i} \tag{4}$$

h1 and h2 are the hidden-layer output vector. U = L x C is an weight matrix at the upper layer of a module. W = D x L

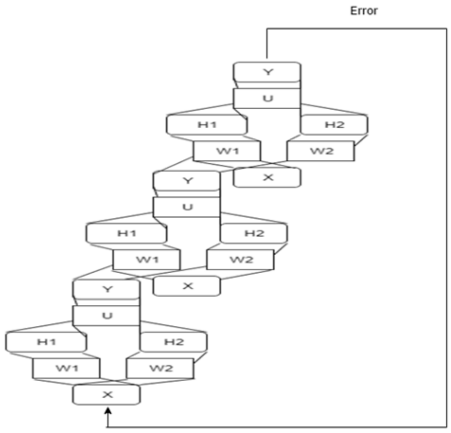

Fig. 4. Block diagram of Deep Stacking Network with Back Propagation with Three Modules.

is a weight matrix at the lower layer of a block, and $\sigma(.)$ is a sigmoid function. Equation 5 gives the formula for sigmoidal activation function.

$$hi = \sigma(W^T X_i) \tag{5}$$

Given target vectors in the full training set with a total of N samples, T = [t1,..,ti,..tN] , where each vector is ti = [t1i,... , tji,..., tCi] T, the parameters and are learned so as to minimize the average of the total square error. At the end of each iteration error is calculated. RMSE is used to calculate the error by using the equation 6. These errors are back propagate in the network and makes the delta changes in the internal weights of TDSN to minimize the error for next iteration. We stop back propagate the error at eighth iteration, there is no change in accuracy of seventh and eighth iteration.

$$RMSE = \sqrt{\frac{1}{n}\sum_{i=0}^{n}(Ve - Va)^2} \tag{6}$$

Where Ve denotes expected output and Va denote actual output. This error is used to alter the internal weight to get expected output.

C. Deep Stacking Convolution Neural Network

Advantage of TDSN are parallel training, scalable, does not required GPU machine for large training data set [6][12]. But it takes more time to get trained. Limitations in the TDSN was overcome by replace hidden layers with the convolution layer, pooling layer and then flatten the output of pooling layer. Similar to the TDSN number of modules in the DS CNN is equal to the number of training images. Each module consist of input layer, convolution layer, pooling layer and output layer. Totally eight modules are designed to train the images from the year 2006 to 2014. One images are chosen for every year in the month of September. Input to the first model is the first image in the temporal sequence. In our case input to the first module was image at the year 2005. The input to the subsequent models are the output of the immediate previous module and corresponding input image. In convolution layer the kernel of dimension 224 x 224 is used. Kernel are initialized randomly. Kernel slide over the complete input image of size 2497 x 2497 and along the way perform dot product between the filter and the input image. The output of the convolution layer is given to the pooling layer. Pooling layers reduce the dimensions of the data by combining the neuron from the convolution layer. It reduce computation work involved in the network. Max pooling layer is used as pooling layer. Kernel size of max-pooling layer was selected as 2 x 2. Hence 4-pixel values are replaced by one pixel value. ReLU is the activation function used for DS CNN. Fig.5 shows the DS CNN with three modules.

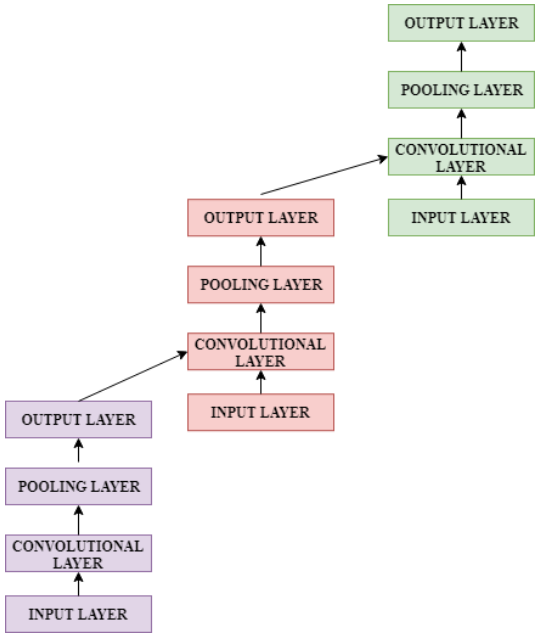

Fig. 5. Block diagram of Deep Stacking Convolution Neural Network

It contains three modules of DS CNN. Each model consists of input layer, two convolution layers, two pooling layers followed by flatten the output of pooling layer and given to the output layer. By adding convolution layer into TDSN, the accuracy of the classification output is improved to 97.37% and also time taken to compute classification was reduced by trimming the image dimension at pooling layer.

IV. RESULT AND ANALYSIS

A. Dataset and Study Area

In order to evaluate the proposed method, the Landsat 5, Landsat 8, and Sentinel 2 satellite images are collected form Land Process Distributed Active Archive Center of the United States Geological Survey (USGS) [17]. These satellite image covers the Hutong area, Beijing, China. It is located at the northern edge of north China. It covers the coordinates of, top-most $39.55°N, 116.23°E$, and bottommost $39.72°, 116.50°E$ around 1370 km^2 study area. The images are collected over the period of 2005 2015 in the month of September. From

the year 2005 to 2012 Landsat 5 image is taken. Landsat 5 satellite uses the Enhanced Thematic Mapper plus (ETM+) sensor to take pictures of the earth. Landsat 5 satellite image contain 8 bands (Band 1 Blue, Band 2 Green, Band 3 Red, Band 4 - Near Infrared, Band 5 - Short-wave Infrared, Band 6 - Thermal Infrared, Band 7 - Short-wave Infrared, and Band 8 Pan-chromatic) except pan-chromatic band all are 30m spatial resolution. The pan-chromatic band has 15m spatial resolution, this band is used for pan-sharpening. Landsat 8 Satellite image, in addition to Landsat- 5 ETM+ satellite bands it also has 3 bands (Cirrus, Thermal Infrared -2, Short-wave Infrared-2). Sentinel 2 satellite we choose only 4 bands (coastal aerosol, cirrus, water vapor and red edge band).

B. Experimental Setup

Pre-processing techniques (band fuse, cloud removal, pan sharpening and NDVI conversion) has been performed using MATLAB (R2018a) in windows 2007 (64-bit OS, 8.00-GB RAM). The framework was designed by using python 2.7 in Linux environment. Keras and TensorFlow are used to build and test the neural network. Keras provides (Application Programm Interface) APIs to design the framework. Keras is build on the top of TensorFlow. Numpy library is used for multi-dimensional matrices multiplication and high level mathematical functions.

C. Performance Metrics

Fig. 6 shows the accuracy of traditional SVM algorithm used in base work [7]and proposed neural network design TDSN back propagation and TDS CNN. Accuracy are calculated by using RMSE given in the equation 7.

$$RMSE = \sqrt{\frac{1}{n}\sum_{i=0}^{n}(Vo - Vp)^2} \tag{7}$$

Where Vo denotes original image and Vp denotes Predicted image. n denotes total number of observations.

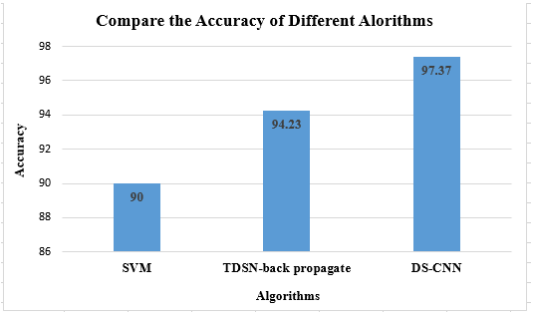

Fig. 6. Accuracy of Land Cover Change Detection.

The accuracy of land cover change detection using DS CNN is improved approximately 7% in comparison to traditional classification algorithm.

Fig.7 shows the accuracy of TDSN output at each iteration. Accuracy had been calculated by using the equation 7.

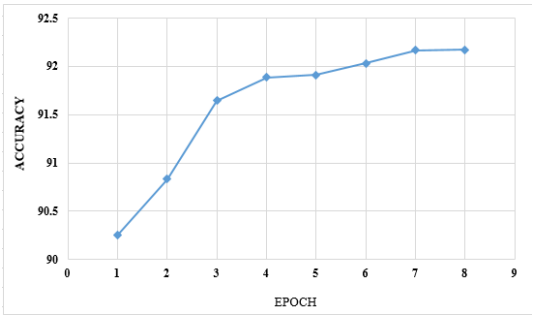

Fig. 7. Accuracy in Each Epoch of Back Propagation.

Accuracy could be improved gradually at each iteration. For each iteration calculate the loss function and make the delta changes in the internal weights of the neural networks to minimize the error and helps to get more accurate output. In the Fig. 7 seventh and eighth iteration was more or less same. So, we can stop propagate the error.

Fig.8 shows the amount of time taken in minutes to find land cover land change detection. From the graph we conclude that DS CNN take less amount of time for classification. Because feature extraction and size reduction was processed by convolution layer and pooling layer respectively, reduce the computation parameters.

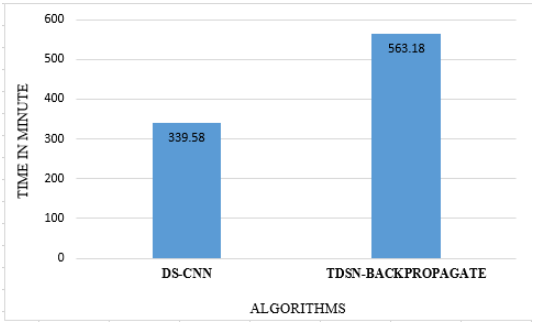

Fig. 8. Time Taken to Complete Classification

V. CONCLUSION AND FUTURE WORK

In this study the accuracy of land cover change detection is improved by adding back propagation into the TDSN it is proven by comparing the classification accuracy to traditional classification algorithm (SVM). But the hidden layers in the TDSN are fully connected so, it takes more time to complete the classification an. Loss function calculation, backpropagate the error to change the internal weights also take time. Limitations in TDSN with backpropagation was overcome by DS CNN. Hidden layers in the TDSN are replaced with the convolutional layer and pooling layer. Convolutional layer helps to extract important feature with the help of kernel and pooling layer helps to reduce the size of the image. The accuracy of DS CNN is also higher in comparison to TDSN with backpropagation. The experiment is carried out during the period of 2005 to 2015 over the area of Hutong,

Beijing, China. Image pansharpening of satellite images into 15m resolution. Raw satellite image contaminates with cloud and artifacts. After land cover changes are detected from the year 2005 to 2015 we collect the 2005 population in Hutong, Beijing, China and population at 2015 and agriculture land, water area and build-ups coverage in 2005 and 2015. Based on this data we calculate the percentage of food shortage arise in the future. This calculator helps to avoid food scarcity in the future. DS-CNN effectively found that the agriculture area was reduced around 12.3%, water bodies are reduced around 9.23% and build-ups are increased to 29.3%.

In future, this work can be extended by changing the filter used in the convolution layer. Edge detection filters like sobel filter can perform well in classification. Replacing the filter used in the convolutional layer with the sobel filter will improve the accuracy of classification result. Which also helps to minimize misclassification error.

REFERENCES

[1] Azzouzi S. A., Vidal-Pantaleoni A. and Bentounes H. A., (2017), Desertification Monitoring in Biskra, Algeria, With Landsat Imagery by Means of Supervised Classification and Change Detection Methods, in IEEE Access, vol. 5, pp. 9065-9072.

[2] Brian Hutchinson, Li Deng and Dong Yu, (2013), Tensor Deep Stacking Networks IEEE Transactions on pattern analysis and machine intelligence, vol. 35, no. 8.

[3] Chao-Hung Lin, Po-Hung Tsai, Kang-Hua Lai, and Jyun-Yuan Chen, (2013), Cloud Removal From Multitemporal Satellite Images Using Information Cloning, IEEE transactions on geoscience and remote sensing, vol. 51, no. 1.

[4] David Palzer, Brian Hutchinson, (2015) The Tensor Deep Stacking Network Toolkit, Neural Networks (IJCNN) International Joint Conference on, pp.- 15.

[5] Deng L. and Yu D., (2014) Deep learning: Methods and applications, Found. Trends Signal Process., vol. 7, nos. 34, pp. 197387.

[6] Deng L., Hutchinson B., and Yu D., (2012) Parallel training for deep stacking networks, in Proc. 13th Annu. Conf. Int. Speech Commun. Assoc., pp. 14.

[7] Haas J. and Ban Y., (Feb. 2018), "Urban Land Cover and Ecosystem Service Changes based on Sentinel-2A MSI and Landsat TM Data," in IEEE Journal of Selected Topics in Applied Earth Observations and Remote Sensing, vol. 11, no. 2, pp. 485-497.

[8] Hu J. and Zhang Y., (Aug. 2013), Seasonal Change of Land-Use/Land-Cover (LULC) Detection Using MODIS Data in Rapid Urbanization Regions: A Case Study of the Pearl River Delta Region (China), in IEEE Journal of Selected Topics in Applied Earth Observations and Remote Sensing, vol. 6, no. 4, pp. 1913-1920.

[9] Jianqiang Z., Xiaolin G. and Xuejun Z., (2018), Deep Convolution Neural Networks for Twitter Sentiment Analysis, in IEEE Access, vol. 6, pp. 23253-23260.

[10] Jyh-Woei Lin , Chun-Tang Chao, And Juing-Shian Chiou, (sept. 2018), Determining Neuronal Number in Each Hidden Layer Using Earthquake Catalogues as Training Data in Training an Embedded Back Propagation Neural Network for Predicting Earthquake Magnitude, Digital object identifier 10.1109/access.2018.2870189.

[11] Khan S. H., He X., Porikli F. and Bennamoun M., (sept. 2017), Forest Change Detection in Incomplete Satellite Images With Deep Neural Networks, in IEEE Transactions on Geoscience and Remote Sensing, vol. 55, no. 9, pp. 5407-5423.

[12] Li Deng , Dong Yu , John Platt, (2012) Scalable stacking and learning for building deep architectures , IEEE International Conference on Acoustics, Speech and Signal Processing (ICASSP), pp. 129-132.

[13] Li Deng, Xiaodong He, Jianfeng Gao,(2013) Deep stacking networks for information retrieval, Acoustics Speech and Signal Processing (ICASSP) IEEE International Conference on, pp. 3153-3157.

[14] Monidipa Das, Soumya K. Ghosh, (2016) Deep-STEP: A Deep Learning Approach for Spatiotemporal Prediction of Remote Sensing Data, IEEE Geoscience and Remote Sensing Letters, vol. 13, pp. 1984 1988.

[15] Nataliia Kussul, Mykola Lavreniuk, Sergii Skakun, and Andrii Shelestov, (2017), Deep Learning Classification of Land Cover and Crop Types Using Remote Sensing Data, IEEE Geoscience and Remote Sensing Letters, vol. 14, no. 5.

[16] Salmon B.P., Wessels K.J., Olivier J.C., van den Bergh F., Kleynhans W. and Steenkamp K.C., (2011), Unsupervised Land Cover Change Detection: Meaningful Sequential Time Series Analysis, in IEEE Journal of Selected Topics in Applied Earth Observations and Remote Sensing, vol. 4, no. 2, pp. 327-335.

[17] USGS Earth Explorer: Land Processes Distributed Active Archive Center, accessed on Aug. 2018. [Online]. Available: https://lpdaac.usgs.gov/usgs earth explorer

Proceedings of the Fourth International Conference on Communication and Electronics Systems (ICCES 2019)
IEEE Conference Record # 45898; IEEE Xplore ISBN: 978-1-7281-1261-9

Influence of trip complexity on optimal driving based Energy Management System of Electric Vehicle

Mousumi Khanra
CSIR-Central Mechanical Engineering Research Institute,
MG Avenue, Durgapur-713209, West Bengal, India
and
Academy of Scientific and Innovative Research (AcSIR),
Ghaziabad-201002, India
Email: mkmit2008@gmail.com

Arup Kr Nandi
CSIR-Central Mechanical Engineering Research Institute,
MG Avenue, Durgapur-713209, West Bengal, India
and
Academy of Scientific and Innovative Research (AcSIR),
Ghaziabad-201002, India
Email: nandi@cmeri.res.in

***Abstract*— Electric vehicles (EVs) have a restricted range due to its inadequate energy storage space, it takes much longer to recharge. Furthermore, charging stations are not as sufficient as fueling stations for diesel or gasoline vehicles. Therefore, the primary motivation in optimal driving based energy management system (DAEM) is to consume the stored energy in a competent way to perform the entire trip. Moreover, due to avoiding accident, quality of road and other reasons, the road speed limits are restricted, and it is observed in both downtown as well as highway. Keeping various speed limits results in increasing the trip complexity which effects in maintaining a same driving strategy throughout a trip. In the present paper, an investigation of the influence of trip complexity on DAEM results was carried out. Two driving cycles (neighborhood and highway) are considered for constructing various trip complexities for this investigation.**

***Keywords*— micro-trip, electric vehicle, optimal driving strategy, trip complexity, energy management, multi-objective optimization, driving cycle**

I. INTRODUCTION

Now a day's EVs are popular in all over the world. Several problems of environment are relevant in recent scenario. To make the EVs as future of personal transportation and to increase the customers' acceptance, these problems should be overcome by developing suitable technology. Limited charging capacity of battery, long charging time and insufficient charging stations are the major hindrances in EV system [1]. Therefore, the primary motivation to overcome such hindrances is the stored energy is to be utilized in an efficient way which leads to the development of energy management system. From previous research studies [2], it was found that driving behavior of a driver play a significant influence of fuel consumption. By realizing such research findings, an optimal driving based Energy Management System to assist drive (so called DAEM) was proposed in [3]. DAEM presents a driving strategy to the driver for optimal driving by solving a multi-objective optimization problem (MOOP) towards minimizing the energy consumption and trip time, and maximizing driving comfort. In [3], the working principle of DAEM was presented in a simple micro trip that consists of a single driving cycle. After analysizing the DAEM results corresponding to various micro-trip lengths, it was revealed that in addition to assist the driver for proper driving, a significant reduction of EV operating cost through minimizing the fuel consumption and increasing the safety factor can be achieved with the used of DAEM.It was found that DAEM system can reduce the energy utilization (above 1.7% per Km) depending on route type of simple micro-trip with low driving cycle. In [4], an extensive study of the influence of initial battery charge and route characteristics on DAEM results was conducted.

Due to avoiding accident, quality of road and other reasons (not overtaking zone, hospital, school, high traffic, narrow road, bridge, etc.) [5][6], it was observed that the road speed limits are restricted, and it is observed in both downtown as well as highway. Keeping various speed limits results in increasing the trip complexity which effects in maintaining a same driving strategy throughout a trip. In the present paper, an investigation of the trip complexity influence on DAEM results was carried out. Different driving cycles are considered for constructing various trip complexities for this investigation. The proposed investigation is carried out based on a comparison of the battery state-of-charge after trip completion (SOC_{Trip_end}) vs. total trip time (T_{Trip}) plots of the optimal solutions obtained in different trips with varying complexities after solving a MOOP towards finding optimal driving strategy (ODS). An ODS comprises of the optimal values of different driving features namely speed, acceleration and deceleration according to the driving mode type.

The rest of the paper is organized as follows: Section II describes the proposed DAEM system for EV trip planning. The related MOOP is formulated in Section III. Description of micro-trip is presented in Section IV. In section V, results and descriptions are presented. Finally, concluding remarks and scope for future research works are highlighted in Section V.

II. PROPOSED DAEM SYSTEM FOR EV TRIP PLANNING

The architecture of DAEM system is presented Fig. 1 [3]. DAEM has two primary modules, such as interface between human and machine (HMI) and optimal trip planning (OTP). The route information (such as road gradient, wind, road surface, weather, etc) is collected by HMI through global positioning system or wireless communication system such as smart phone, etc. HMI also receives the present values of various parameters (namely battery charge, supplementary load, present driving strategy followed, etc.) through various sensors. HMI transfers both the route and vehicle information to OTP module. OTP module solves the related MOOP corresponding to the route chosen for journey and information related to vehicle drive, and provides a set of optimal driving strategy, ODS (solution). DAEM system guides the driver by suggesting

not only the optimal driving strategy (especially, optimal trip speed, acceleration/ deceleration values and durations for changing a speed) but also the predicted range of EV corresponding to the present battery SOC and the suggested ODS, SOC_{Trip_end} and T_{Trip} predictions [7-13].

Driver normally selects a solution (ODS) based on his preference from the set of ODS provided by DAEM for driving the EV. Alternatively, a technique that is used for making decision in a multi-criterion scenario [14] can be adopted to find a preferably best solution. After a certain period, DAEM is allowed to execute again corresponding to the latest data of route characteristics and vehicle drive to find an ODS for subsequent driving. Knowing the range and T_{Trip} in advance provides the driver an adequate flexibility towards efficiently utilizing the energy with ODS, even in urgent situation including shortage of battery charge. In the same manner, DAEM is allowed to execute consecutively according to the collected information that are found after the previous driving until the completion of trip . Such type of driving based on the DAEM suggested ODS assists driver to accurately manage the energy consumption (E).

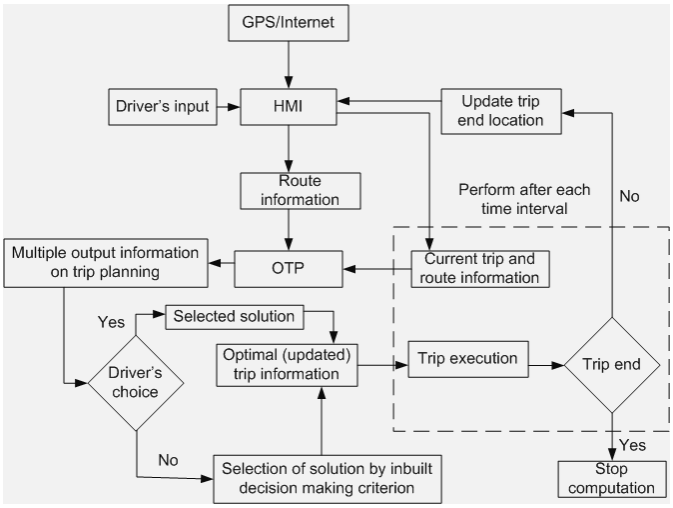

Fig. 1. DAEM system architecture

III. Formulation Of Multi-Objective Optimization Problem

The MOOP for finding an ODS is formulated based on the three objectives, minimizing E, reducing T_{Trip}, and maximizing comfort during driving (i.e., minimization of average jerk experienced), simultaneously [15]. These objectives are depended on various driving features (design variables) and the corresponding relations are expressed as follows:

$$T_{Trip} = f_T\left(v_{ref}, a_{ref}^{1,2,\ldots K}, t_{1,,2,K-1}, k_p, k_i\right) \quad (1)$$

$$E = f_E\left(v_{ref}, a_{ref}^{1,2,\ldots K}, t_{1,,2,K-1}, k_p, k_i\right) \quad (2)$$

$$J_{Avg} = f_{Total}\left(v_{ref}, a_{ref}^{1,2,\ldots K}, t_{1,,2,K-1}, k_p, k_i\right) \quad (3)$$

subject to

$$v_{\min}^{dc} \le v_{ref} \le v_{\max}^{dc} \quad (4)$$

$$a_{\min} \le a_{ref}^{1,2,\ldots,K} \le a_{\max} \quad (5)$$

$$0.3 \ge k_p \ge 0.01 \quad (6)$$

$$3.0 \ge k_i \ge 0.01 \quad (7)$$

During acceleration of speed changing, K number of accelerations ($a_{ref}^{1,2,3,\ldots,K}$) are assumed since in [16] energy consumption is found to be low by utilizing many acceleration rates. $t_{1,2,3\ldots,K-1}$ are the durations of first *K-1* number of accelerations. For simplicity, in this work the deceleration (d_{dec}) was assumed constant depending on v_{diff}_dec (difference between present and desired speeds), as follows:

$$\begin{matrix} a_{dec} = 2.3 \\ a_{dec} = 2.25 \\ a_{dec} = 2.35 \end{matrix} \quad \text{if} \quad \begin{cases} 100 \le v_{diff\_dec} \le 129 \\ 50 \le v_{diff\_dec} \le 100 \\ 0 \le v_{diff\_dec} \le 50 \end{cases}$$

. $v_{\min}^{dc}$ and $v_{\min}^{dc}$ are the allowable EV speed limits that are decided according the type of driving cycle. $a_{\min}$ (=0.1 m/sec^2) and $a_{\max}$ (=3.0 m/sec^2) are the allowable EV acceleration limits., k_p (varying in the range, 0.01, 0.3) and k_i (varying in the range, 0.01, 3.0) are the gains for the PI controller.

IV. Micro-Trip

In real world, the entire travel route of a trip comprises with several micro-trips. A micro trip (MT) is usually described by the portion of two successive stop points (start and end) in the route [17] [18], and the corresponding length is called the micro-trip range. According to safety and road type differentiation, a MT may face four category of road type (driving cycle, DC) based on the speed limits [19] [20] such as (neighborhood (speed range 8 km/h - 40 km/h), urban (40 km/h - 56 km/h), highway (56 km/h - 88.5 km/h), interstate (88.5 km/h - 112.6 km/h). The driving cycle speed limits are required to be followed by a driver as per the traffic rules and regulation.

A MT is considered as a simple type if it follows only one DC throughout its whole length, and such a MT can be demonstrated by the speed vs. distance plot as shown in Figure 2. A simple micro-trip follows three consecutive driving modes in the order, an acceleration mode (a_{ref}) a constant speed mode (v_{ref}), and finally a deceleration model in order to bring the EV to stop.

On the other hand, a complex MT is in general described as a MT consisting of more than one DC. The complexity depends upon the involvement of different driving cycle types, driving cycle lengths, and locations in the micro-trip. Based on such criterions, a micro-trip may be treated as more complex than other. Figure 3 exhibits the speed outline of a typical complex MT that follows first an acceleration mode (a_{ref}) followed by

three different constant speed modes ($v_{ref1\_microtrip}$, $v_{ref2\_microtrip}$ and $v_{ref3\_microtrip}$) and then a deceleration model to stop the vehicle. Unlike to simple micro-trip, the constant speed modes should be associated with at least two different driving cycles in a complex micro-trip. According to micro-trip 1 shown in Figure 3, the first and third constant speed modes correspond to a (high speed) DC and the second (middle) constant speed mode corresponds a low speed driving cycle.

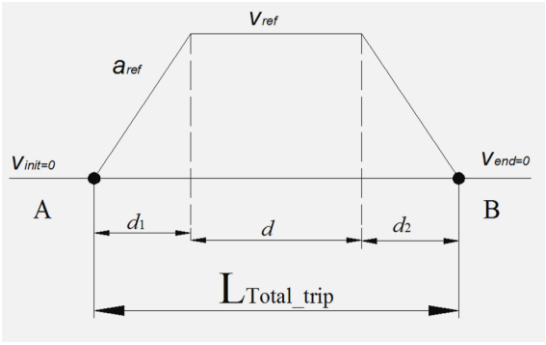

Figure 2. Speed vs. distance of a simple micro-trip

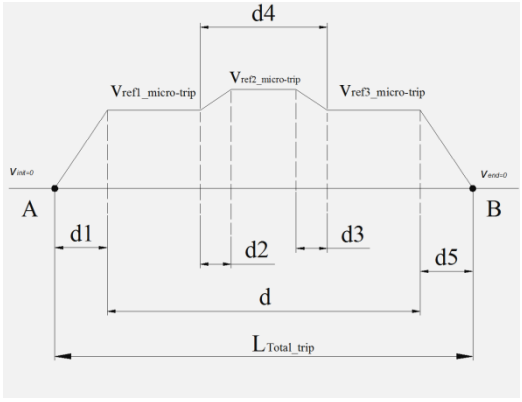

Figure 3. Speed vs. distance of a typical complex micro-trip layout (micro-trip 1)

V. Results and Discussion

For analyzing the MT complexity influence on DAEM results, different case studies are considered, and in each case two micro-trips are assumed, among them one is comparatively more complex than other.

Case I: DAEM results are investigated for a complex MT (microtrip_1) that comprises of two neighborhoods ($v_{ref1\_microtrip}$ and $v_{ref3\_microtrip}$) and one highway ($v_{ref2\_microtrip}$) driving cycles (corresponds to Figure 3) with a simple micro-trip that consists of either a neighborhood or highway DC (corresponds to Figure 2) for the same trip length. Table 1 presents the positions and lengths of the different driving cycles for a 20km trip length. l_h (=d4 in Figure 3) is the length of highway driving cycle in the micro-trip.

TABLE I. ARCHITECTURES OF MICRO-TRIP

Serial No.	Micro-trip distance (km)		Driving cycle
	From	*To*	
1	0	$(L_{Total\_trip} - l_h)/2$	Neighborhood
2	$(L_{Total\_trip} - l_h)/2$	l_h	Highway
3	$(L_{Total\_trip} - l_h)/2$	L_{Total_trip}	Neighborhood

Fig. 4 presents the demonstrative DAEM results (Pareto front) obtained through solving the MOOP presented in Section III using a non-dominated sorting genetic algorithm (NSGA II) [21] for the microtrip_1 of length 20km. Optimization results obtained by varying l_h for the same MT (microtrip_1) are analyzed in order to understand the effect of complexity due to the DC length. . In Fig. 4, highway driving cycle lengths zero and 20 km indicate the corresponding micro-trips are the entirely neighborhood and entirely highway micro-trips, respectively. From Fig. 4, it was found that the Pareto front width in both SOC_{Trip_end} and T_{Trip} is stretched with increasing the highway driving cycle length. With increasing the highway driving cycle length, an opposite phenomenon of the characteristics of SOC_{Trip_end} (increasing) and T_{Trip} (decreasing) is noticed in Fig. 4. The preferred optimal value of SOC_{Trip_end} is determined here using a reference point technique [4] [5] based on ideal point. For different l_h (0, 5, 10, 15, and 20 km), the preferred SOC_{Trip_end} are found as 0.855, 0.856, 0.858, 0.863, and 0.865, respectively. The corresponding values of different parameters of ODS, objectives, etc. are listed in Table 2.

TABLE 2 LIST PREFERRED OPTIMAL SOLUTIONS FOUND IN DIFFERENT HIGHWAY DRIVING CYCLE LENGTH FOR TRIP LENGTH, 20 KM

l_h (km)	SOC	T_{Trip} (sec)	Energy (J)	Jerk (m/sec^3)	V_ref1 (km/h)	V_ref2 (km/h)	V_ref3 (km/h)	1st acc_zone (d1 in Figure 3)			2nd acc_zone (d2 in Figure 3)			k_p	k_i	Actual range (km)
								a_1 (m/sec^2)	a_2 (m/sec^2)	t_1(sec)	a_1 (m/sec^2)	a_2 (m/sec^2)	t_2(sec)			
0	0.855346	1807.38	8397220	11.5067	39.9889	85.9652	39.9235	2.97363	0.387805	2.26759	1.66749	0.408145	24.067	0.155632	1.75886	19986.4
5	0.856298	1611.16	8285350	125.627	39.9996	71.0406	39.9576	2.65058	1.68177	0.850326	1.76513	1.5287	3.17354	0.267 98	2.76021	19986.3
10	0.858101	1388.5	8165130	253.17	39.9941	74.9003	39.9899	2.6917	1.87304	1.08773	1.764	1.52881	5.14697	0.293505	2.87681	19986.3
15	0.863259	1202.53	7894470	57.6981	39.9987	72.8211	39.8996	1.17971	2.00892	0.283359	4.151	1.46134	3.11517	0.277397	0.848691	19986.4
20	0.865426	1008.92	7660530	36.8786	39.9645	74.0497	38.4995	1.29563	0.246616	0.102961	2.64449	2.97196	3.09066	0.274446	1.10591	19987.3

There is a polynomial relationship (presented in Equation (10)) is found among SOC_{Trip_end} and the highway driving cycle length (l_h). According to the nature of trip complexity, the relationship among SOC_{Trip_end} and l_h is varied.

$$SOC_{Trip\_end} = 2x10^{-5} l_h + 2.2x10^{-4} l_h + 0.85508 \quad (10)$$

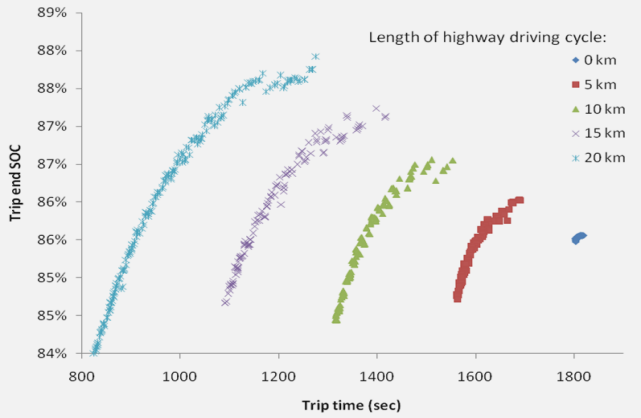

Fig. 4. Variation of SOC_{Trip_end} with T_{Trip} for different complex micro-trips.

Case II: In this case study, two complex micro-trips i.e., micro-trip 1 and micro-trip 2 (as shown in Figure 3 and Figure 5) are considered for investigating the complexity influence on DAEM results. The micro-trip 2 presented in Figure 5 is more complex than micro-trip 1 that presented in Figure 3, in the sense that in Figure 5, there are three highway driving zones with different distributions. In both the micro-trips, the lengths of each driving cycles are kept same for effective comparative analysis.

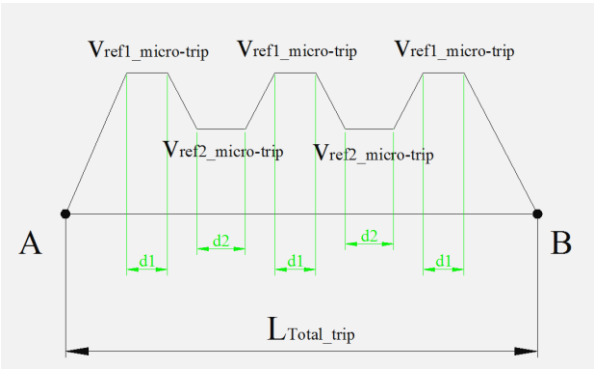

Figure 5. Speed vs. distance of a typical micro-trip layout (micro-trip 2)

The figure 6 shows the Pareto-optimal solutions of SOC_{Trip_end} with T_{Trip} for the two complex micro-trips (as shown in Figure 3 and Figure 5) for different values of highway driving cycle length. The total trip length for both cases was considered as 20 km.

From Figure 6(a), we can see that in complex micro-trip 2, for 15 km highway driving cycle with 20 km trip length, the *SOC* values of the Pareto-optimal range are 0.6754 and 0.7137, respectively. But in complex micro-trip 1, for the same highway driving cycle with 20 km trip length, the SOC values of the Pareto-optimal range are 0.6871 and 0.7168, respectively. For other highway driving cycle say, 10 km and 5 km in complex micro-trip 2 and complex micro-trip 1, the initial and final SOC are 0.6802, 0.7112 and 0.6911, 0.7138 respectively shown in Figure 6(b) and 6(c). On the other hand, the range of T_{Trip} of the Pareto-fronts in both the micro-trips is same. The rate of increase of SOC_{Trip_end} with respect to T_{Trip} was found more or less for both complex trips. But when the highway driving cycle length is low, the micro-trip 2 possess a higher rate of SOC increase with respect to time compare to micro-trip 1, as shown in Figure 6(c). From Figure 6, a low SOC_{Trip_end} in micro-trip 2 compare to micro-trip 1 suggests that the high energy consumption is found when the vehicle runs the same highway cycle distance at a stretch.

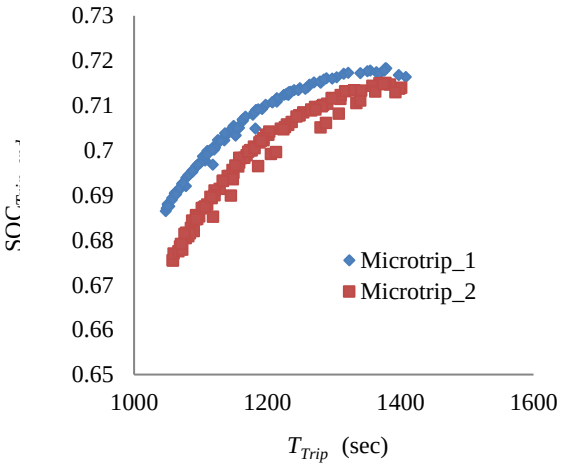

(a)

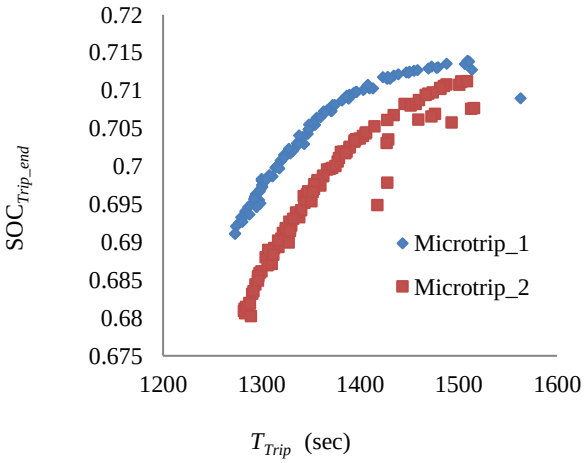

(b)

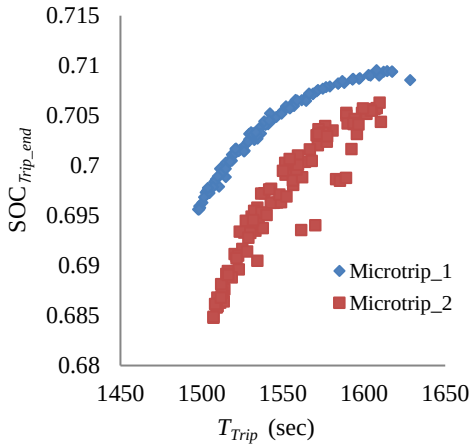

(c)

Figure 6: Comparative results of micro-trips with different highway driving-cycle lengths (a) 15 km (b) 10km (c) 5 km

The above studies of trip complexity effect on SOC_{Trip_end} reveals that it is exceedingly intricate for the inexperienced predictors that use of previous trips to plan or predict current trips in terms of vehicle range or T_{Trip}. Furthermore, inexperienced predictors unable to suggest any appropriate energy-driving parameters. The DAEM system considers for the route features and the driver's preference while suggesting an ODS that yields in an energy-efficient journey with reducing T_{Trip} as well as discomfort.

Figure 7 demonstrate the variations of optimal speeds of different driving cycles in the optimal solutions corresponding to micro-trip presented in Fig. 3 for two highway lengths, 10 km and 15 km. In low driving cycle (neighborhood) the speed of almost all the optimal solutions is found to lie in high side, and such observation is followed in all such low driving cycles in the micro-trip. Whereas, in high driving cycle the speeds of optimal solutions are varied in its entire range. Moreover, the above observations does not depend on the changes of driving cycle lengths in a micro-trip.

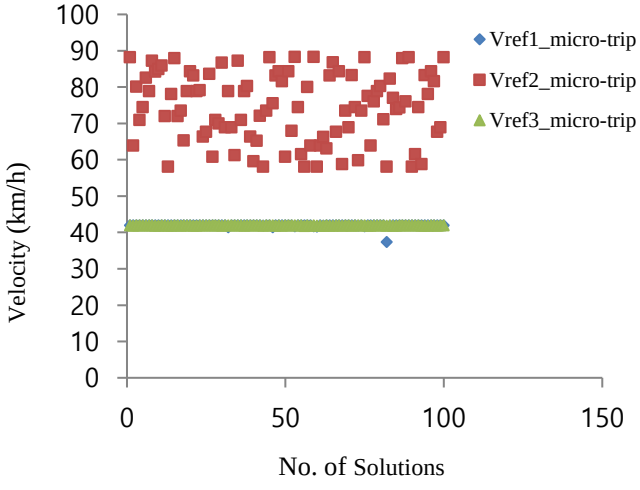

(a)

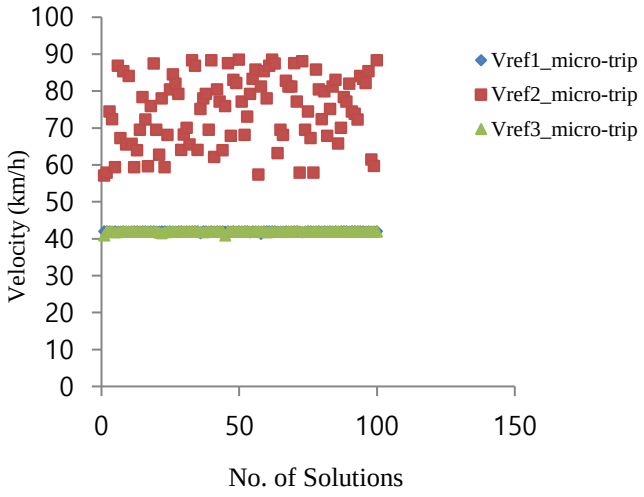

(b)

Figure 7. Variations of optimal speeds of different driving cycles in the optimal solutions corresponding to micro-trip presented in Fig. 3 for highway length (a) 10 km (b) 15 km

VI. CONCLUSIONS

In this paper, the effect of route complexity on the DAEM results is analyzed. Comparisons of two types of route complexity with a simple microtrip draws the following the observations.

- SOC_{Trip_end} varies polynomial with the length of high driving cycle in a fixed length complex micro trip.
- The rate of increment of SOC_{Trip_end} is higher in micro-trip 2 than micro-trip 1 for low highway cycle length.
- With the increase of trip complexity, high Energy consumption is found for same highway cycle length.
- Optimal speed is found as a high values low driving cycle in contrast to a variation in high driving cycle.
- The research findings help to design and develop an EV-oriented highly-intelligent Advanced Driver Assistance System, equipped with other driving assisting systems, suitable monitoring, learning, reasoning, and management capabilities that will implement efficient EV driving and help to increase its range autonomy and decrease energy consumption.

ACKNOWLEDGMENT

First author is thankful to Principal of MIT, Bankura, West Bengal, India to provide the necessary support for her research work at CSIR-CMERI, Durgapur, India. 2nd author acknowledges IUSSTF, New Delhi, India for granting him Indo-US research fellowship, since the present research work is an extension of it.

REFERENCES

[1] Feng, L., Ge, S., Liu, H., Electric Vehicle Charging Station Planning Based on Weighted Voronoi Diagram. Proceedings of Power and Energy Engineering Conference (APPEEC), Asia-Pacific, published by IEEE, pp. 1-5, 2012.

[2] E. Gilman, A. Keskinarkaus, S. Tamminen, S. Pirttikangas, J. Röning, and J. Riekki, "Personalised assistance for fuel-efficient driving," Transportation Research Part C: Emerging Technologies, 58D, pp. 681-705, 2015.

[3] M. Karmakar, A.K. Nandi, "Trip Planning for Electric Vehicle through optimal driving using Genetic Algorithm, International Conference on Power Electronics," Intelligent Control and Energy Systems (IEEE ICPEICES), Delhi, India , 2016.

[4] M. Karmakar, A.K. Nandi, "Driving Assistance for Energy Management in Electric Vehicle, International Conference on Power Electronics," Drives and Energy Systems (IEEE PEDES), Trivandrum, Kerala, India, 2016, .

[5] S. Tsugawa, Super smart vehicle system: Future intelligent driving and the measures for the materialization, in Proceeding of Surface Transportation: Mobility, Technology, and Society. Proceedings of the IVHS AMERICA 1993 Annual Meeting,Washington, D.C., pp. 192–198,1993.

[6] H. Fujii, O. Hayashi, N. Nakagata, Experimental research on intervehicle communication using infrared rays, in Proc. IEEE Intelligent Vehicles Symposium, Tokyo, Japan, pp. 266–271, 1996.

[7] M. Ceraolo, G. Pede, Techniques for estimating the residual range of an electric vehicle. IEEE Transactions on Vehicular Technology 50 (1) 109-115, 2001.

[8] E.J. Yao, M.Y. Wang, Y.Y. Song, T. Zuo, Estimating the cruising range of electric vehicle based on instantaneous speed and acceleration, Applied Mechanics and Materials 361-363, 2104-2108, 2013.

[9] A. Szumanowski, Y. Chang, Battery management system based on battery nonlinear dynamics modeling, IEEE Transactions on Vehicular Technology 57(3), 1425-1432, 2008.

[10] K.A. Smith, C.D. Rahn, C.Y. Wang, Model-based electrochemical estimation and constraint management for pulse operation of lithium ion batteries, IEEE Transactions on Control Systems Technology 18(3), 654-663, 2010.

[11] W.X. Shen, K.T. Chau, C.C, Chan, E.W.C. Lo, Neural network-based residual capacity indicator for nickel-metal hydride batteries in electric vehicles, IEEE Transactions on Vehicular Technology 54(5), 1705-1712, 2005.

[12] F. Baronti, W. Zamboni, N. Femia, R. Saletti, M.Y. Chow, Parameter identification of Li-Po batteries in electric vehicles: A comparative study. IEEE International Symposium on Industrial Electronics, Taipei, Taiwan, doi:10.1109/ISIE.2013.6563887 , pp. 1-7, 2013.

[13] L.L. Du, B. Li, H.D. Zhang, Estimation on state of charge of power battery based on the grey neural network model, Applied Mechanics and Materials 427-429, 1158-1162, 2013.

[14] K. Miettinen, Nonlinear multiobjective optimization. Kluwer, Boston, 1999.

[15] A.K. Nandi, D. Chakraborty, and W. Vaz, "Design of a comfortable optimal driving strategy for electric vehicles using multi-objective optimization," Journal of Power Sources, vol. 283, pp. 1-18, 2015.

[16] W. Vaz, A.K. Nandi, U.O. Koylu, "A multi-objective approach to find optimal electric vehicle acceleration: simultaneous minimization of acceleration duration and energy consumption," IEEE Transactions on Vehicular Technology, (DOI 10.1109/TVT.2015.2497246), 2015.

[17] Haan, M. Keller, Real-world driving cycles for emission measurement: ARTEMIS and Swiss cycles, Final Report, 2001.

[18] M. Andre, Real-world driving cycles for measuring cars pollutant emissions – Part A: The ARTEMIS European driving cycles, Institut National de Recherche sur les Transports et leur Securite (INRETS), Report INRETS-LTE 0411, 2004.

[19] A. G. Ostensen , Effects of Raising and Lowering Speed Limits on Selected Roadway Sections, U.S. Department of Transportation, Federal Highway Administration, Publication No. FHWA-RD-97-084, 1997.

[20] M.I. Berry,The effects of driving style and vehicle performance on the real-world fuel consumption of US light-duty vehicles. Master's Thesis, Massachusetts Institute of Technology, available at http://web.mit.edu/sloan-auto-lab/research/beforeh2/files/IreneBerry_Thesis_February2010.pdf, 2010.

[21] Deb, K., Pratap, A., Agarwal, S. and Meyarivan, T., 2002. A fast elitist non-dominated sorting genetic algorithm for multi-objective optimisation: NSGA-II. IEEE Transactions on Evolutionary Computation 6 (2), 182-197.

Proceedings of the Fourth International Conference on Communication and Electronics Systems (ICCES 2019)
IEEE Conference Record # 45898; IEEE Xplore ISBN: 978-1-7281-1261-9

Load Flow Analysis for Smart Grid With Renewable Energy Resources

Shaikh Mohammad Aamir
Department of Electrical Engineering
Govt. college of Engineering
Karad, India
Shaikhaamer700@gmail.com

Dr. P. M. Joshi
Department of Electrical Engineering
Govt. college of Engineering
Karad, India
dr.pmjoshi@gmail.com

***Abstract*—Smart grid is an electrical network which supply electrical power to consumer in very efficient and economical manner. This paper presents the load flow analysis of smart grid with renewable energy resource and FACTS devices. Newton Raphson method is use for power flow analysis and the objective of this paper is a development of a 14 bus system in PSAT software with FACTS devices, RERs and performs power flow analysis. The main aim of this paper to give initial framework related to load flow in smart grid with the help of RERs.**

Keywords—smart grid, optimal power flow, PSAT, SSSC device, Renewable energy resource

I. INTRODUCTION

Nowadays world population goes on increases continuously, as population increases energy demand increases and to meet the increasing demand renewable energy along with fossil fuel is used. But fossil fuel is not sufficient to meet the increasing demand for long duration that's why it's used is not preferable in the environmental term. The only solution of higher cost and global warming issue of fossil fuel is the use of Renewable energy resources. Power flow analysis is used to find the power transfer from generation side to consumer thorough the grid connected to it is reliable, economical and stable, it is also useful for the calculation of voltage magnitude and phase angle of load bus, active and reactive power flow in transmission line, active and reactive power injected at the buses. There are various methods for power flow analysis but we use Newton Raphson method because it has high convergence speed and it can control inequality constraint easily.

Smart grid is an electrical network that uses information, computer based remote monitoring and control, communication technologies to improve reliability, efficiency, sustainability of the generation and distribution of electricity.

For planning a development of new network or adding a network into an existing system the power flow analysis is required to calculate the voltage magnitude, phase angle, power flow at each bus and line. Also, it is useful to find the optimal capacity of generating station, line and substation.

In this research we create a model of IEEE 14 bus system and connect SSSC (FACT device) to the line of the system and wind turbine generator to slack bus and perform load flow analysis and the effect of such addition is discussed in the result.

II. STATIC SYNCHRONOUS SERIES COMPENSATOR

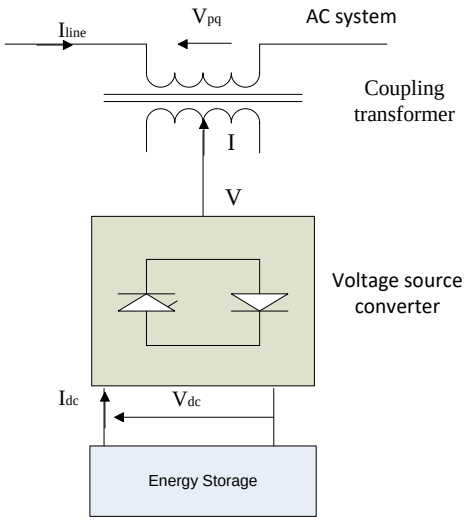

Fig. 1. Functional model of SSSC

SSSC is one of the FACT devices that are used to improve the voltage stability and reduce line losses etc. of existence system. Fig. 1 is functional model of SSSC [4] which consist of voltage source converter which generate a controllable AC voltage at power frequency and connect in series with TL. Output voltage of static synchronous generator is always in quadrature with the line current in order to control the reactive voltage drop and transmitted power. The SSSC work in the two modes, whenever receiving end power is greater than the sending end power or current lags the voltage by 90 degree then it operates on inductive mode. If receiving end power is less than the sending end power or current lead the voltage by 90 degree then it operate on capacitive mode.

III. NEWTON RAPHSON METHOD

Newton Raphson is one of the power flow method and the advantage of this method over the others is convergence occur

very fast, in this research Newton Raphson method is used for power flow and procedure is shown in Fig2.

Steps for load flow analysis by the Newton Raphson method,

Step1: Form nodal admittance matrix.

Step2: Assume initial bus voltage and set nth bus as a ref. bus.

Step3: evaluate P and Q of the system

Step4: form Jacobian matrix

Step5: evaluate power mismatches ΔP, ΔQ.

Step6: set the tolerance value

Step7: if ΔP, ΔQ are less than the tolerance then stop iterations.

Step8: if not then update the value of V and δ and repeat

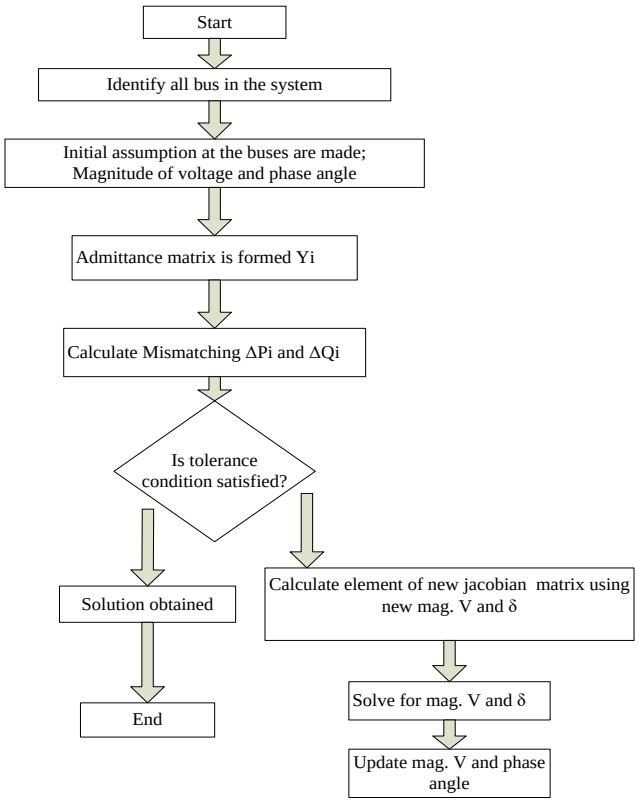

Fig. 2. Flow chart of NR for Load flow

IV. Simulation Model

Creating a simulation model in PSAT software is shown in Fig3. in which IEEE 14 bus system is used which consist of 14 buses, 20 lines, 4 transformer, 11 loads, one generator, two compensator. Input data is taken from the IEEE 14 bus data. Three SSSC are connected to the transmission line between the bus 1 and 5, bus 2 and 3, bus 2 and 4, compensation of SSSC is set to the 25 percent of line and one wind turbine (WTG) generator is connected to the slack bus. Function of wind turbine generator is similar to the other generator but is use is to avoid the the enviromental issue.

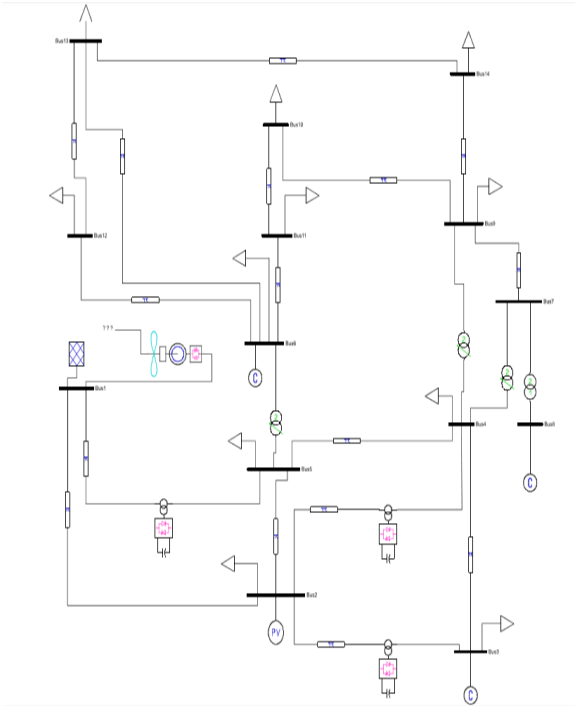

Fig. 3. Simulation model

V. Results

After performing a power flow analysis using Newton Raphson method the result is obtained in the form of voltage magnitude, phase angle, active, reactive power flow etc.

TABLE I. Power Flow Result

Bus	V (P.U)	Phase (P.U)	P gen. (P.U)	Q gen. (P.U)	P load (P.U)	Q load (P.U)
1	1.06	0	2.243	0.063	0	0
2	1.045	-0.078	0.4	0.778	0.217	0.127
3	1.01	-0.181	0	-0.039	0.942	0.19
4	1.0264	-0.148	0	0	0.478	0.04
5	1.031	-0.124	0	0	0.076	0.016
6	1.07	-0.220	0	0.135	0.112	0.075
7	1.055	-0.200	0	0	0	0
8	1.09	-0.200	0	0.211	0	0
9	1.039	-0.228	0	0	0.295	0.166
10	1.037	-0.231	0	0	0.09	0.058
11	1.0498	-0.228	0	0	0.035	0.018
12	1.0539	-0.235	0	0	0.061	0.016
13	1.0479	-0.236	0	0	0.135	0.058
14	1.0247	-0.249	0	0	0.149	0.05

TABLE II. LINE FLOW RESULT

From Bus	To bus	P flow (P.U)	Q flow (P.U)	P loss (P.U)	Q loss (P.U)
1	2	1.4298	-0.1709	0.0356	0.05021
1	5	1.0667	0.3075	0	0.1399
2	3	1.0425	0.404	0	0.1192
2	4	0.9888	0.2938	0	0.0731
4	3	0.21221	0.0002	0.0002	-0.0285
4	7	0.2752	-0.0249	0	0.0146
4	9	0.1578	0.0446	0	0.0133
5	2	-0.2793	-0.0029	0.0041	-0.0238
5	4	0.5674	-0.0658	0.0040	-0.0006
5	6	0.4491	0.1806	0	0.0482
6	12	0.0794	0.0296	0.0007	0.0016
6	13	0.1802	0.0910	0.0023	0.0046
7	9	0.2762	0.1651	0	0.010
8	7	0	0.2113	0	0.0066
9	14	0.0903	0.0133	0.0009	0.0020
10	9	-0.0487	-0.0067	0.00007	0.0001
11	6	-0.0765	-0.0700	0.0009	0.0019
11	10	0.4157	0.0520	0.0003	0.00077
12	13	0.01767	0.0120	0.0009	0.00008
13	14	0.0604	0.0403	0.0008	0.0016

TABLE III. LINE FLOW RESULT

From Bus	To bus	P flow (P.U)	Q flow (P.U)	P loss (P.U)	Q loss (P.U)
2	1	-1.394	0.2211	0.0356	0.0502
2	5	0.283	-0.0208	0.0041	-0.0238
3	2	-1.042	-0.2585	0	0.1192
3	4	-0.2093	-0.2087	0.0028	-0.0285
4	2	-0.9888	-0.2207	0	0.0731
4	5	-0.5634	0.0652	0.0040	-0.0006
5	1	-1.0667	-0.167	0	0.1399
6	5	-0.4491	-0.1323	0	0.0482
6	11	0.0775	0.0720	0.00093	0.0019
7	4	-0.2762	0.0395	0	0.0146
7	8	0	-0.2046	0	0.0066
9	4	-0.1578	-0.0313	0	0.0133
9	7	-0.2762	-0.1549	0	0.0102
9	10	0.0488	0.0068	0.00007	0.0001
10	11	-0.0412	-0.0513	0.0003	0.0007
12	6	-0.0786	-0.0280	0.0007	0.0016
13	6	-0.1778	-0.0864	0.0023	0.0046
13	12	-0.0175	-0.0119	0.00009	0.00008
14	9	-0.0893	-0.0112	0.0009	0.0020
14	13	-0.0596	-0.0387	0.0008	0.0016

VI. CONCLUSION

In this dissertation work initially perform load flow analysis of 14 bus system in PSAT software and compare with the 14 bus standard result, both are approximately equal and then SSSC and wind turbine generator are connected to the system after the connection simulation result shows that active and reactive power flow in that line increase and voltage profile of entire system also increase. In terms of losses active power loss of the system reduces but reactive power loss is increases and this is shown in table IV. Future scope of this project can be extended with other FACTS devices and optimal power flow methodology, also to minimize reactive power losses..

TABLE IV. POWER LOSS COMPARISON

	Without SSSC and WTG		With SSSC and WTG	
	P MW	*Q MW*	*P MW*	*Q MW*
losses	13.58	27.47	5.31	33.52

TABLE V. IMPROVEMENT IN VOLTAGE

Bus	Voltage (P.U) Without SSC and TG	Q load (P.U) with SSSC and TG
1	1.06	1.06
2	1.045	1.045
3	1.01	1.01
4	1.012	1.0264
5	1.016	1.031
6	1.07	1.07
7	1.0493	1.0559
8	1.09	1.09
9	1.0328	1.039
10	1.0318	1.037
11	1.0471	1.0498
12	1.0534	1.0539
13	1.047	1.047
14	1.0207	1.0247

TABLE VI. POWER FLOW COMPARISON

Buses from		Without SSSC and WTG		With SSSC and WTG	
		P (P.U)	*Q (P.U)*	*P (P.U)*	*Q (P.U)*
1	5	0.754	0.054	1.0667	0.3075
2	3	0.735	0.035	1.0425	0.4049
2	4	0.559	0.015	0.9888	0.2938

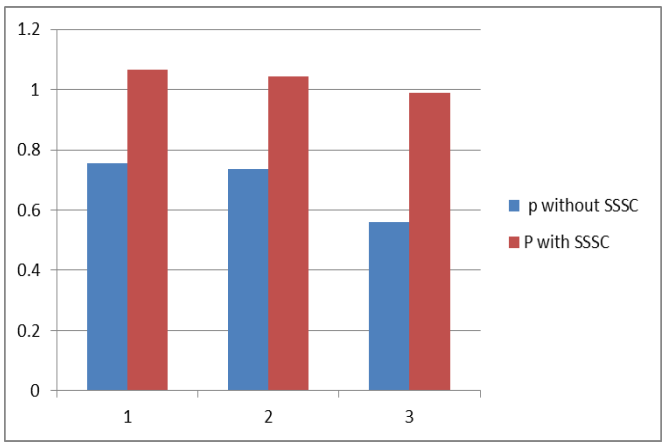

Fig. 4. Active power prifile where SSSC is connected

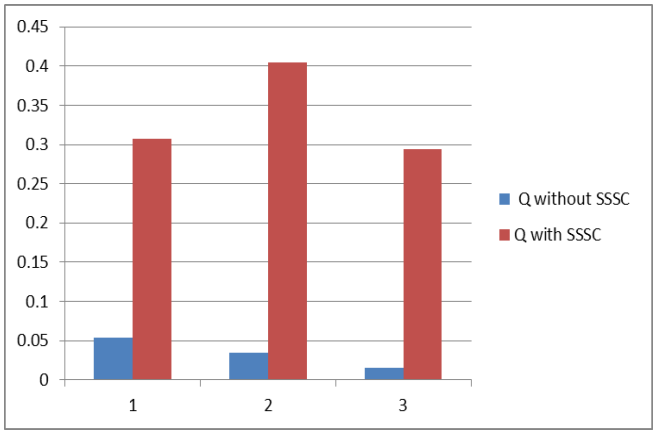

Fig. 5. Reactive power prifile where SSSC is connected

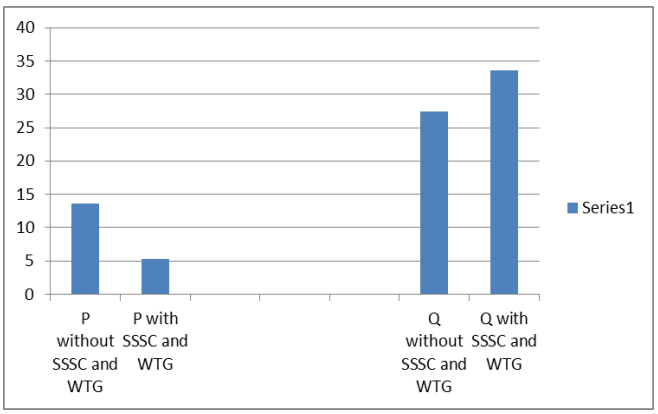

Fig. 6. Power loss comparison

REFERENCES

[1] Pimentel D,Herz M,Glickstein M,Zimmerman M,Allen R,Becker K, Evans J, Hussain B, Sarsfeld R, Grosfeld A, Seidel T. "Renewable Energy: Current and Potential Issues". Bioscience, 2002, 52(12): 1111–1120.

[2] Ummeaiman V. Aleem, CH. Mallareddy , Spruha S. Pitre ,Samarpita S. Bakshi, "Static Synchronous Series Compensator (SSSC) as Stability Booster of a Power System", International Journal of Engineering Trends and Technology (IJETT) – Volume 46 Number 6 April 2017

[3] Koosha Marashi, Sahra Sedigh Sarvestani, and Ali R. Hurson, "Consideration of Cyber-Physical Interdependencies in Reliability Modeling of Smart Grids", IEEE transactions on sustainable computing, vol. #, no. #, #-# 2017

[4] Laszlo Gyugyi, "Dynamic Compensation of AC Transmission Lines By Solid-State Synchronous Voltage Sources",IEEE Transactions on Power Delivery, Vol. 9, No. 2, April 1994.

[5] Aditya Sharma, Manyu Saini and MdIrfan Ahmed, "Power Flow Analysis Using NR Method", international conferrence on innovotive research in science, technology and manegment, 978-93-86171-20-7, 22-23 jan 2017.

[6] Vijay Varma, Prashant Kumar, "Load Flow Analysis in IEEE 14 Bus System Using FACTS Device in MATLAB", IJSART 2395-1052, volume 3, 10 oct. 2017.

[7] P. Srikanth, O. Rajendra, A. Yesuraj, M. Tilak, K.Raja, "Load Flow Analysis Of Ieee14 Bus System Using MATLAB", IJERT ISSN: 2278-0181, Vol. 2 Issue 5, May – 2013.

[8] R.V.Amarnath**, Dr. N. V. Ramana, "State of Art in Optimal Power Flow Solution Methodologies", Journal of Theoretical and Applied Information Technolog, 31st August 2011. Vol. 30 No.2.

[9] S. Surender Reddy, Vuddanti Sandeep, Chan-Mook Jung, "Review of Stochastic Optimization Methods for Smart grid", © Higher Education Press and Springer-Verlag Berlin Heidelberg 2017, 11(2): 197–209.

[10] Deepinder Kaur Mander, GS Virdi, "Result analysis on Load Flow by Using Newton raphson method", IJAREEIE 2278-8875, vol. 6, issue7, july 2017.

[11] "Grid 2030: A national vision for electricity's second 100 years," United States Department of Energy Office of Electric Transmission and Distribution, Tech. Rep., 2003.

[12] "NIST framework and roadmap for smart grid interoperability standards, release 1.0," National Institute of Standards and Technology, Tech. Rep., January 2010.

Proceedings of the Fourth International Conference on Communication and Electronics Systems (ICCES 2019)
IEEE Conference Record # 45898; IEEE Xplore ISBN: 978-1-7281-1261-9

Mathematical analysis of RNN and LSTM for Malicious URL detection

M. Arivukarasi, *Research scholar, Hindustan Institute of Technology and Science*, Chennai
A. Antonidoss, *Associate professor, Hindustan Institute of Technology and Science*, Chennai

***ABSTRACT*-- In the cutting edge age, all data is effectively open through sites and because of this reason individuals depend totally on online assets. On the in opposition to its focal points, protection and security in online media are the primary concern overall as a result of the ascent in phishing assaults propelled on the web. The quantity of phishing sites expands each month focusing on in excess of 450 brands, according to the reports distributed by against phishing working groups. Generally boycotts are utilized to distinguish the URL assaults. In any case, with the exponential increment in the quantity of phishing sites, this strategy has its own restrictions and it additionally neglects to identify recently created phishing URLs which can be unraveled utilizing AI or profound learning strategies. Here we present a near report between established AI procedure - calculated relapse utilizing bigram, profound learning strategies like convolution neural network and Recurrent Neural Network long present moment memory as models used to identify noxious Uniform Resource Locators. On correlation Recurrent neural network and long short term memory gave the best exactness of about 98% for the grouping of phishing Uniform Resources.**

***INDEX TERMS*-- Phishing, Recurrent Neural Network, Long Short Term Memory, Internet Service Provider.**

I. INTRODUCTION

In the course of recent decades physical assaults were normal, in any case, we realized how to tackle the issues brought about by it. Later syntactic assault became possibly the most important factor exploiting the vulnerabilities in the virtual products to bargain the frameworks. These days semantic assaults are normally utilized strategies by assailants to get delicate data of a client. It is still kept on being the most occurring assault in the internet.

Aggressors utilize this method principally in light of the fact that people dependably neglect to confirm the veracity of data that they get through web, and make them a simple prey to the hands of online ruptures. Such assaults are generally helped through spam messages and phishing sites, and trap the client to give the qualifications and other delicate information's of the client. Email is viewed as the main vehicle to convey a wide range of noxious assaults. As per IBMs look into group, the quantity of spam sends are expanding enormously furthermore, aside from that, it is seen that the greater part of the messages created are trick. In first quarter of 2017, the level of spam in email traffic added up to 56.9%. Assailants generally sent messages with phishing sites to counterfeit sites which looks genuine to an ordinary client.

Via the post office they blend true connections and false connections so as to make it look all the more engaging. So as to test the credibility of the email, clients can intently investigate its substance for sentence structure or then again spelling slip-ups or on the off chance that it is requesting individual data like charge card number, telephone number and so forth. Larger part of the web clients who are not taught about the security, neglect to browse the substance of messages and land in pernicious sites. There is no certain flame approach to check in the event that somebody has wound up in phishing sites, however checking the site may help in few cases. Present day internet browsers use additional items and modules to distinguish phishing site. Such instruments use boycotting to distinguish noxious sites. Boycotting approaches are for the most part signature based, where a database is kept up to monitor all the known phishing site. Web creeping, manual revealing, honeypots what's more, different techniques in the vicinity investigation heuristics are the different strategies used to identify the noxious connects to refresh the database. Be that as it may, this technique comes up short when an obscure phishing site is experienced and it requires refreshing the database after following the previously mentioned strategies.

AI is a field of software engineering which is connected in pretty much every zone like science, material science, science, liquid elements, horticulture nowadays. It is conceivable to do so in light of the fact that AI systems gain from the information accessible and after that plan a well-suited model to aid choice making by preparing the future information. Also, the information need not be from a particular field, it very well may be anything. This flexible nature of AI is the explanation behind it to wind up prominent in the current world. In this work, we have utilized strategic relapse utilizing bigram as the model in directed AI to test the exactness acquired to order if a given site is malignant or not. Be that as it may, the disadvantage of AI is that the highlights which alone decides the outcome should be picked physically. Profound learning is a part of unsupervised AI which gain from the information without anyone else and structure a model for future use. It has more prominent probability to identify recently produced phishing sites and furthermore need not require manual element engineering. In this paper we center around RNN and blend of RNN with long present moment memory(LSTM) to acquire the exactness in ordering

the phishing sites. While customary computerized phishing gives 5%-14% precision and physically focused on lance phishing gives 45%. The technique is directly in the center with 30% precision and up to 66% at times with a similar exertion as the robotized one. Security is a worry for any open confronting web application. Great advancement practices can help with shielding against endeavors from clients hoping to uncover information or cut down an application. In any case, in some cases not all assault vectors are taken care of and new endeavors will undoubtedly be found. This is the place security programming can help with checking and anticipating unanticipated assaults. So imagine a scenario where you could utilize the intensity of Google's Tensorflow motor to choose whether a given solicitation is viewed as noxious. Well that was the inquiry I was hoping to reply while taking an interest in Slalom's ongoing AI hackathon. The accompanying post diagrams the specialized subtleties of a PoC for a security observing application which was worked with the assistance of a couple different Slalomites. The goal was to assemble an application that can examine approaching solicitations to an objective API and banner any suspicious movement. The application would likewise have a straightforward UI to show these hailed demands and give the capacity to make preparatory move when vital. The group named the name to this pernicious solicitation identification application 'SecuritAI'.

Similarly as with any Machine Learning issue, the information is the important asset for making a shrewd model. For this situation get to logs from an API is the thing that I required. A fake API must be worked to create a decent dataset of access logs to process. Lumberjacks would should be added to the fake API to aggregate access signs in clusters for preparing reason, just as the capacity to stream logs for constant handling. see in fig 1.

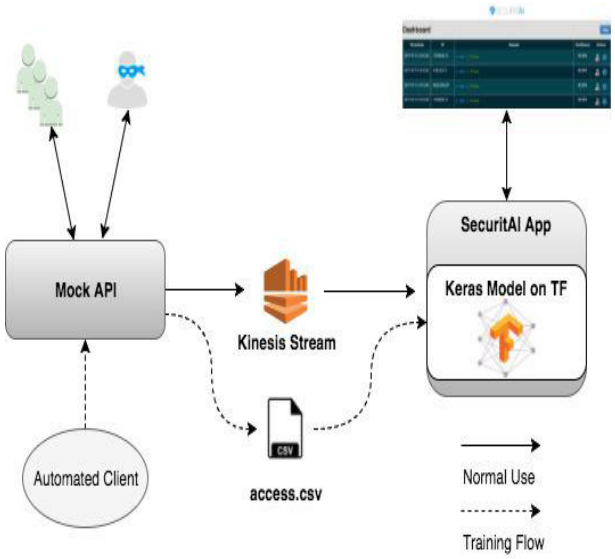

Fig 1. Tensor flow and work model

The paper is composed as pursues. In Section II, we present related work on phishing site recognition. At that point, in Section III, we present the system of Materials and method. In Section IV, we depict result and discussion the point by point procedure of the LSTM and multidimensional highlights. conclusion in Section V. At long last, in Section VI, we finish up the paper what's more, talk about future work

II. RELATED WORK

The Author proposed boycott/whitelist techniques are utilized in numerous examinations and by and by [7], [8], [5], [6], [9], [2]. Be that as it may, these techniques needs to keep up a rundown of phishing sites utilizing a manual/automatically update process as appeared Uniform Resource Locators demands are checked before propelling dependent on a neighborhood database or a database on the cloud. Despite the fact that the boycott/whitelist procedures has fast discovery, overseeing the boycott/whitelist database is wasteful for both the neighborhood database and the cloud database due to the quickly expanding number of phishing destinations. Along these lines, heuristic and Artificial Intelligence approaches have been gotten much consideration in terms of programmed discovery. This can be viewed as a cross breed approach that utilizes boycott/whitelist techniques to ensure clients at the front end while Artificial Intelligence procedures are utilized at the back end (i.e., the server side) to recognize phishing and update on the boycott/whitelist database. A few Artificial Interface systems center around the web structure or web content-based techniques to recognize phishing Uniform Resource Locators [6], [7]. One understood methodology in extricating site page highlights to distinguish phishing destinations is Cantina+ [8]. This methodology depends on 15 highlights web pages, including Uniform Resource Locators highlights and substance highlights, which are costly amid the examination. Another strong work centering on Uniform Resource Locators highlights [2] introduced the adequacy of numerous approaches in the order of phishing Uniform Resource Locators; be that as it may, they didn't solidly think about the blend of numerous highlights to improve the distinguishing proof execution. In view of certain page-positioning highlights, the creators in [5], [7] created web structure-based ways to deal with recognize phishing website pages by utilizing the Google Page Rank esteem. Be that as it may, utilizing just the Page Rank esteem is deficient to distinguish phishing Uniform Resource Locators because of the accompanying reasons. To begin with, numerous phishing sites are made on mainstream sites such as online journals or Google destinations, where the positioning highlights are not helpful for phishing recognizable proof. Second, new Uniform Resource Locators have low positioning qualities that are comparable to phishing Uniform resource Locators. In some particular cases, we can't get Page Rank values from the Application Protocol Interface accurately. Such explicit cases can't be recognized by [8] and [2]. Consequently, consolidating numerous highlights is important to diminish the measure of missed identifications for phishing distinguishing proof .

III. Materials and Methods

With a prepared model the time had come to execute the SecuritAI UI application that would have the model to play out the ongoing expectations. Likewise with the false API, the group stayed with what we knew best, JavaScript. A React UI was worked as a dashboard to screen the movement originating from the flood of solicitation logs. The stream is overseen by AWS Kinesis to connect th e correspondence between the counterfeit API and SecuritAI UI. Now the tech stack is solid, yet one slight issue… Keeras is a python programming library, how is the model assume to make forecasts in JavaScript? Fortunately, there's amp bundle that will help for this need, would be Keras-js p ermits JavaScript applications to run spared Keras models prepared on the Tensorflow motor. Using this python pro gramming library empowered us to run everything from our Node.js application servers.

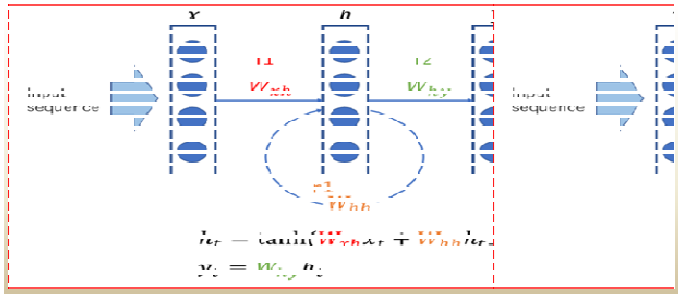

Fig 2. Input and output sequence

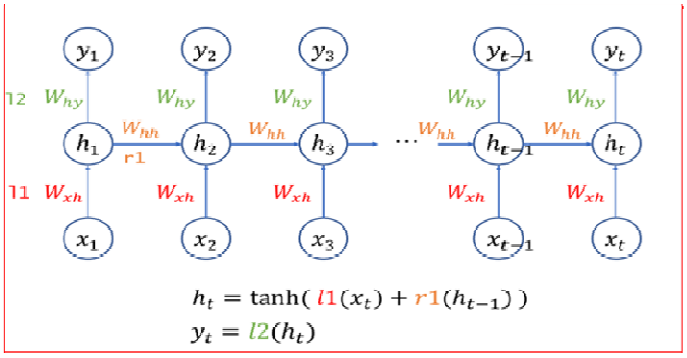

Fig 3. Tanh output

A. Algorithm

Require: Visible layer B={vl1,.....,vlm},Hidden layer H = {hl1,.....,hln}

Ensure : Gradient Approximation Δ θ ← Δwij,Δaj,Δbji
for i in {1.....n}, j in {1.....m}
for (i in {1....n}, j in {1....m} do
Initialize Δwij=Δai=Δbj=0
end for
for each vl in B
vlo ←vl
for time in(0.....k-1)do
for i in {1-n }do
samp hlit ~ p(hli | vlt)
end for
for j in (1.....m)do
samp vltj ~ p (vli | hlt)
end for
end for

B. Algorithm for training process

Require: Period T, Learning Rate η, Momentum ρ,
visible layer Vl, Hidden layer Hl, Number o f visible and hidden layer units nvl, nhl

offset vector a2,b3, Weight Matrix W1
Ensure θ= {W1,a2,b3} Step1:
Initialize W1,a2,b3
Step2: for i ϵ{1...T} do

calling CD-k to generate Δθ= {ΔW1,Δa2,Δb3}
W1←ρW1+ η((1/nvl)ΔW1 a2←ρa2+
η((1/nvl)Δa2)
b3←ρb3+ η((1/nvl)Δb3)
end for

The way to deal with narrowing our attention on paired arrangement with a LSTM RNN i mplies we are performing managed learning with our model. H ence every log passage in the preparation dataset needs a goin g with name to portray if that logged solicitation is typical o r an endeavored infusion assault. Concerning producing inf ormation to prepare the model, the fake API was used to recreate a straightforward web based business application. For example ridiculed out endpoints for a/login,/look,/checkou t. Since the we don't have an authentic progression of clients to the counterfeit API we consolidated a couple runtime alternatives to run the server and execute demands consequently (for example npm run assault infuse). These begin dire ctions went through an average client stream, just as arbitrarily performing endeavored infusion assaults. We tuned these computerized solicitation streams to run ~100 AP I demands every moment to rapidly gather logs for a preparati on dataset.

A custom lumberjack was connec ted to the server system to yield the ideal dataset design. F or this situation, a csv containing columns of solicitation l og JSON and related mark was every one of that was required. So as to separate among ordinary and malignant solicitation s an 'assault' header was added to every malevolent solicit ation performed from the robotized customer. The mark for ea ch solicitation log passage would then be dictated by checkin g for the presence of that header. On the off chance that 'ass ault' header exists at that point mark the log with '1', and expel the 'assault' header before composing the log, genera lly name the log as '0'. Because of certain impediments of utilizing a ridiculed API to deliver a preparation dataset, and furthermore to guarantee we have a progressively summed up c lassifier just fundamental log fields were extricated ami d preprocessing. These properties included: 'technique', 'inquiry', 'statusCode', 'way', 'request Payload'. Counting fluct uating headers presented some arbitrariness which ruined the grouping realizing, so that was let well enough alone for de gree for this stage. Extra information, preprocessing, and per haps a different classifier could be utilized to investigate the header substance.

A robotized customer was left to keep running for a few hours to aggregate an OK sum p reparing information. To prepare the model rapidly an AWS p2.xlarge Deep Learning EC2 example was utilized to play out the calculations. AWS's Deep Learning AMIs are preinstalled with the vast majority of

the mainstream AI libraries and APIs you have to begin performing substantial preparing on GPUs. The 90 pennies for each hour this EC2 occurrence cost isn't just certainly justified regardless of the time spared preparing a model on an extensive dataset, yet in addition worth sparing time on introducing and arranging Tensorflow to legitimately keep running on a GPU. We found the setup and design on another machine demonstrates to be very tedious to get the conditions and GPU arrangement without flaw for the adaptation of Tensorflow wanted.

$$CDk(\theta,v0) = -\sum_{h} p(h|\, v0)\partial E(v0,\, h) \,/\, \partial\theta + \sum_{h} p(h \,/\, vk)\partial E(vk,\, h) \,/\, \partial\theta$$

$$ai = Inp(vi \,/ 1 - p(vi)$$

To decrease predisposition, the dataset created contained ~50/50 typical and vindictive solicitation logs. The dataset was part into 75% preparing and 25% assessment subsets. After a few emphases the model had the capacity to acquire a truly high precision. This was to some degree expected because of the constrained varieties of solicitation blends that were produced, however by and by it was adequate to work within our short time allotment. The precision and misfortune measurements delineated above are likewise caught in logs by means of an appended Tensor board callback inside the Keras preparing content. These logs are an amassing of checkpoints recorded amid preparing which are helpful for envisioning the model's execution amid and subsequent to preparing

$$L\theta = In(L(\theta v)) = In\prod_{i=1}^{n} \rho(vi|\theta) = \sum_{i=1}^{n} In(\rho(vi|\theta))k)\partial E(vk,h)/\partial\theta$$

$$\theta \leftarrow \rho\theta + \eta\partial In(L(\theta)) \,/\, \partial\theta$$

$$\theta \leftarrow \theta + \eta\partial In(L(\theta)) \,/\, \partial\theta$$

IV. Result and Discussion

The initial step on this MVP was to concentrate on picking a forecast model and demonstrate that it was a solid match for our concern. Recognizing whether a given solicitation is proposed to do mischief or uncover delicate data was the issue to illuminate. To begin we chose to limit our attention on deciding whether a solicitation contains content that can be viewed as an infusion endeavor. Infusion assaults can come in different structures: by shrewd addition of SQL, XML, JSON, or source code into solicitations. We were keen on possibly knowing whether given solicitation is an endeavored infusion or not, this is essentially a twofold grouping issue. There are numerous models which can help with this issue: Random forest Naive Bayes Classifier, Support Vector Machines, Neural Networks, and unsupervised models.

Profound Learning/Neural Networks are getting a great deal of consideration with the most recent achievements in the scholarly world and commonsense uses in the field. They have demonstrated to be uncommon at picture acknowledgment and normal language handling (NLP). Imagine a scenario where we could take advantage of the NLP abilities of a neural system for this order issue. This is the thing that we needed to try out. The JSON log passage as is can't be utilized as contribution for a neural system model. Models require

Table 1.Evaluation of LSTM and RNN

Layers	Type	Output shape	Other parameters	Parameters
0-1	Embedding	(None, 2307, 128)	embedding vector	length = 128 18304
1-2	Convolution1D	(None, 2303, 128)	number of filter = 128	filter-length = 5 82048
2-3	Maxpooling1D	(None, 575, 128)	pool-length = 4	0
3-4	LSTM	(None, 50)	memory blocks 50	35800
4-5	Fully connected	(None, 1) 51	5-6 Activation (None, 1)	Sigmoid 0

numeric contributions to work with, in this way message preprocessing is vital. Since substance of a solicitation log contain different character strings, images, and digits we decide to preprocess every passage into a grouping of characters. Handling the log passages as a grouping of characters is performed by mapping the each character of the solicitation log content to numeric qualities inside a populated word lexicon. The related numeric qualities speak to how as often as possible a character is seen. The word reference is at first made and fitted utilizing the preparation information, that way resulting characters can be mapped to recently observed character esteems. E.g In this fragment of the word lexicon, "," character is the seventh most successive character from the preparation dataset.

An incredible decision for learning an arrangement of characters is a Recurrent Neural Network. All the more explicitly a Long Short-Term Memory variation of Recurrent Neural Networks was picked on account of it's wide use and accomplishment in learning arrangements. Long Short Term Memory are somewhat mind boggling and it isn't the focal point of this post, however having an abnormal state understanding helps while tinkering with a model. More on grouping learning and LSTMs practically speaking can be found in this incredible review by Andrej Karpathy — Unreasonable Effectiveness of RNNs. To rapidly build up the neural system model, we picked to utilize the abnormal state Keras API running over Tensorflow, rather than legitimately cooperating with Tensorflow. Keras enables us to rapidly model our model and spare time by giving a standard setup to Tensorflow. Neural system models in Keras are extremely simple to work with, basically instantiate a model article and begin including layers! The underlying implanting layer

indicates the normal elements of the vector inputs, the LSTM concealed layer is characterized with 64 neurons alongside independent dropout layers to decrease fluctuation, lastly a thick yield layer to create the order certainty.

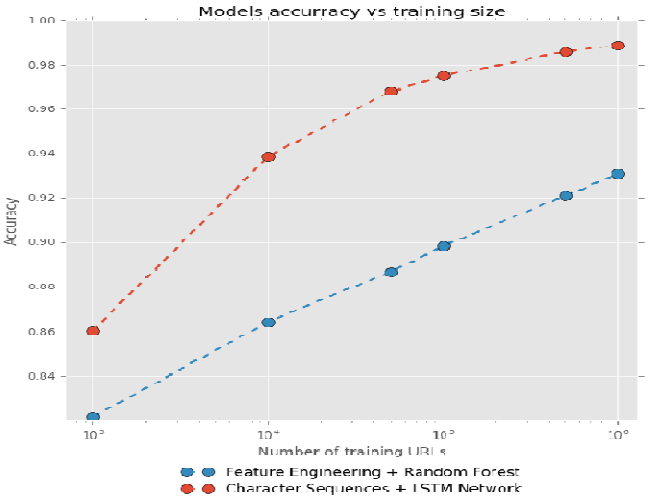

Fig4. Accuracy of LSTM and RF

V. Conclusion

This paper dissected the exhibition of strategic relapse utilizing bigrams, RNN and RNN-LSTM models to distinguish phishing URLs. Profound learning strategies like RNN and RNN-LSTM are ideal over AI techniques as they have the capacity to get ideal component portrayal themselves by accepting the crude URLs as their information. We can guarantee dependent on the outcomes we acquired that, the AI and profound learning based vindictive URL recognition can abandon discovery frameworks assembled utilizing boycotting and customary articulation strategies.

VI. Future Work

A future improvement of our approach will think about applying profound figuring out how to include extraction of website page code and site page content. Furthermore, we plan to actualize our methodology into a module for installing in a Web program

VII. References

[1] R. Dhamija, et.al., “Why Phishing Works,” in Conference on Human Factors in Computing Systems, 2006, pp. 581–590.

[2] J. Vargas, et.al., “Knowing your enemies: Leveraging data analysis to expose phishing patterns against a major US financial institution,” in 2016 APWG Symposium on Electronic Crime Research, 2016, pp. 52–61.

[3] J. Ma, et.al., “Learning to detect malicious urls,” ACM Trans. Intell. Syst. Technol., vol. 2, no. 3, pp.30:1–30:24, May 2012.

[4] S. Marchal, K. Saari, N. Singh, and N. Asokan, “Know Your Phish: Novel Techniques for Detecting Phishing Sites and Their Targets,” in International Conference on Distributed Computing Systems, 2016, pp. 323–333.

[5] T. Thakur and R. Verma, Catching Classical and Hijack-Based Phishing Attacks. Cham: Springer International Publishing, 2014, pp. 318–337.

[6] M. Fernandez-Delgado, E. Cernadas, S. Barro, and D. Amorim, “Do we Need Hundreds of Classifiers to Solve Real World Classification Problems ?” Journal of Machine Learning Research, vol. 15, pp. 3133–3181, 2014.

[7] S. Marchal, R. State, and T. Engel, “PhishScore: Hacking Phishers Minds,” in CNSM, 2014, pp. 46–54.

[8] Z. C. Lipton, “A Critical Review of Recurrent Neural Networks for Sequence Learning,” CoRR, vol. abs/1506.0, pp. 1–38, 2015.

[9] T. Dietterich, “Machine learning for sequential data: A review,” Structural, syntactic, and statistical pattern recognition, pp. 1–15, 2002.

Proceedings of the Fourth International Conference on Communication and Electronics Systems (ICCES 2019)
IEEE Conference Record # 45898; IEEE Xplore ISBN: 978-1-7281-1261-9

Performance Enhancement of OFDM System Using Modified PTS (MOPTS) PAPR Reduction Algorithm

Prabal Gupta
Department of ECE, SCSE
Lovely Professional University
Phagwara, Punjab, India-144411
prabal.gupta9@gmail.com

H. Pal Thethi
Department of ECE, SEEE
Lovely Professional University
Phagwara, Punjab, India-144411
harpalnitr@gmail.com

***Abstract*—This research paper depicts a modified partial transmitted sequence (MOPTS) algorithm by applying the normalized Riemann matrix (C) rows for phase sequences with discrete cosine transform (DCT) in time domain for diminishing of peak to average power ratio (PAPR) of several modulations under many sub-carriers based orthogonal frequency division multiplexing (OFDM) after distributing the information into numerous blocks and optimizing with the assistance of phase sequences. Since, original PTS (ORIPTS) algorithm makes use of phase sequences which are random and designing of those phases are also tedious. Henceforth, in this research manuscript we are suggesting a MOPTS algorithm which has definite phase sequences of normalized Riemann matrix (C) along with DCT. Simulation outcomes clearly indicate the noteworthy PAPR performance of MOPTS in comparison with PAPR of original OFDM (OFDMORIPAPR) and ORIPTS.**

Keywords—Partial Transmitted Sequence (PTS);Orthogonal Frequency Division Multiplexing (OFDM); Discrete Cosine Transform (DCT); Peak to Average Power Ratio (PAPR).

I. INTRODUCTION

In wireless communication system [1], one very promising and efficient multiplexing technique exists which is known as OFDM. It has got significant interest due to very high data rates along with the trusted performance of spatial multiplexing and diversity. Moreover, OFDM system possesses smooth equalization [2], good spectral power efficiency along with the easy implementation on hardware by assistance of Fast fourier transform (FFT). Furthermore, it is better due to significant features like small vulnerable to echoes, well-organized bandwidth utilization, it also has protection against narrow-band-co-channel interferences (NBCCI) hence, it improves the capacity of system by providing reliable transmission of information. OFDM procedure has been adopted by several wireless and wire-line system like wireless local-area network (WLAN) [3] IEEE-802.11 a/b/g/n, Long term Evolution (LTE) [4], European telecommunication standards institute (ETSI)[5], Broadcast radio-access network (BRAN), Digital television broadcasting (DTVB)[6],[7], Digital audio-broadcasting (DAB), Digital video-broadcasting (DVB)[8], worldwide interoperability for microwave access (WiMAX) IEEE-802.16 [9], Asynchronous digital subscriber line (ADSL)[10]-[12], Digital subscriber line (DSL). Since, OFDM has numerous advantages but high PAPR is considered as the key disadvantage of OFDM because of this, it suffers from out of band-radiations (OOB) and in band-distortions (IB) [13] and high PAPR leads to non-linearity in high power amplifier (HPA). Moreover, high PAPR enhance complexity of both analog-to-digital converters (ADC) and digital-to-analog converters (DAC). Henceforth, HPA with huge input back-off- power (IBO) is required along with huge word length so as to follow high PAPR [14].

The several solutions for the lessening of PAPR is to adopt the appropriate method which can reduce PAPR just before sending signals from transmitter side. Many procedures have been presented in literatures to diminish value of PAPR like trellis assisted constellation subset selection (TACSS)[15], clipping[16],non- linear companding transforming [17]-[19], peak windowing [20], clipping and filtering [21],[22], active constellation extension (ACE)[23] the above mentioned procedures be appropriate to group of signals distortion whereas other techniques which belong to the category of scrambling practices of signal like PTS [24],[25], tone-reservation (TR) [26],[27], selective mapping (SLM)[28]-[30], block coding [31], interleaving technique [32], tone injection [33]. This paper is prepared as follows. Section-II provides the comprehensive summary of the works supported for PAPR reduction. In section-III briefly shows OFDM, DCT and original PTS technique. In section IV, we show the proposed modified PTS algorithm. Then simulation results are implemented in section V whereas in section VI conclusions are drawn.

II. RELATED WORKS

In literature, numerous papers have been discussed related to high PAPR in OFDM like, In 2019, Gokceli et al. [34] introduced an effective technique for the diminishing of PAPR where clipping noise can be easily filtered and controlled inside passband of the transmitter which ultimately control signal which going to be transmitted. Several results suggested in 5G new radio (NR) mobile network context which demonstrate the efficiency of presented work. In 2019, Sandoval et al. [35] presented the novel hybrid PAPR diminishing method which uses three techniques like iterative modified companding and filtering, convolutional codes, successive sub-optimal cross antenna-rotations and inversion (SS-CARI). Significant reduction in PAPR is attained with help of hybrid technique.

Tang et al. [36] proposed a clipping noise method of compression in which modification is done in time domain

signal. The reduction in computation complexity has been obtained because it utilizes only one fast fourier transform (FFT). The presented work demonstrated better BER and PAPR reduction performance as compared with traditional ICF method, while Rateb et al. [37] presented a small complexity technique for the diminishing of the PAPR based upon linear scaling of some part of the signals coefficient with the help of a factor. The research work studied many inspections which leads to key choice of factors and finally, achieved large gain. The effective reduction in PAPR is obtained with negligible effects on the bit error rate (BER).

In [38], an effective PAPR lessening method proposed which deals with time domain kernel matrix in order to generate signal with minimum PAPR. It also employed the curve fitting approaches to optimize the scaling factor. The projected method is found to be more efficient as equated with traditional clipping and filtering technique. However, our prior research [39]-[42] have documented several schemes such as, In [39], SLM technique has been proposed which uses DCT matrix based phase sequences. Remarkable gain obtained in comparison with conventional SLM technique. In [40], a combination of PTS and Bose chaudhuri hocquenghem codes (BCH) have been projected to reduce PAPR. Simulation results revealed the significant improvement in the performance with the assistance of proposed work as compared with the conventional PTS and OFDM system. In [41], a highly optimized phases are obtained and applied in SLM algorithm. Simulations results obtained show the extraordinary performance of planned work in contrast with OFDM. In [42], Gupta et al. presented the SLM algorithm along with the usage of Hadamard matrix as a phase sequences which help in diminishing the PAPR. The performance of proposed work is better in contrast with traditional OFDM. In [43], authors projected a different method which is based upon iterative clipping and filtering (ICF) with easy clipping of signals along with filters so that small error vector magnitude and minimum PAPR can be achieved.

In [44], Goel et al., presented a companding method which transform rayleigh distributed-probability-distribution function (PDF) of the magnitude of OFDM signals into a form called as quadrilateral PDF. So, it is called as quadrilateral-companding transform (QCT). This scheme offered a decent tradeoff between PAPR diminishing and BER. Rakshit et al. [45] demonstrated a new small complexity sub-optimal PTS system with its basis in the implementations of differential evolutions (DE) technique in short MBLX-DE, it reduces the PAPR.

Singh et al. [46] proposed a hybrid technique based upon SLM and PTS and this scheme reduced the PAPR from 6 dB to 5 dB. This scheme is compared with other techniques and results are found to be better. Vittal and Naidu et al. [47] planned new small complexity PTS system by using random phase sequences matrix (RPSM) for PAPR decreasing in OFDM. The key aim is to obtain best phase sequence to diminish PAPR and complexity by reducing the number of inverse fast-fourier transform (IFFT).

In this paper, a modified PTS (MOPTS) algorithm has been proposed which uses Riemann matrix (C) rows as the phase sequences along with DCT in time domain for the lessening of PAPR. In this paper firstly, we will propose the algorithm so that smallest PAPR based OFDM signals can be created. The simulation results clearly show the best performance of MOPTS algorithm in comparison with conventional PTS technique and original OFDM system.

III. OFDM, DCT AND ORIGINAL PTS ALGORITHM

A. System Models

In OFDM [36] input information is modulated by phase shift keying (PSK) as sub-carriers in frequency domain. Now, frequency domain OFDM signals consist of N sub-carriers are represented as $X = [X^0, X^1, X^2, \dots X^k, \dots . X^{N-1}]$ where X^k represents block of data for kth sub-carriers.

The discrete signal in time domain of OFDM [2] can be represented as,

$$x(n) = \frac{1}{\sqrt{N}} \sum_{k=0}^{N-1} X^k \, e^{\frac{j2\pi kn}{N}}, n = 0,1,2 \dots . . N-1, \quad (1)$$

where n represents discrete sampling-index, k is index of frequency, N denotes total number of sub-carriers.

Oversampling [8], [36], is generally considered for the better approximation of continuous-time OFDM for PAPR. Now, if the oversampling factor is denoted by L then information can be extended by inserting $(L-1)N$ zeros with LNpoints data block of IFFT. For [2] the enhancement in the accuracy of PAPR, sampling of discrete baseband signal must be under $L \geq 4$.

The time domain conversion [36] of oversampled $X(k)$ is obtained by IFFT module to obtain$x(n)$:

$$x(n) = \frac{1}{\sqrt{NL}} \sum_{k=0}^{NL-1} X^k \, e^{\frac{j2\pi kn}{NL}}, n = 0,1,2 \dots . . NL-1, \quad (2)$$

where X^k represents block of data for the kth subcarriers.

The range of the time domain signal $x(n)$ is evaluated with the assistance of $PAPR$. It is represented as

$$PAPR(x(n)) = 10log_{10} \frac{\max_{0 \leq n \leq NL-1} (|x(n)|^2)}{E[|x(n)|^2]}, \quad (3)$$

where $E[.]$ represents operator of expectation [8], [36]. The $PAPR$ lessening of any technique is calculated by complementary cumulative distribution function $CCDF$ denoted by[39][53]:

$$CCDF = Prob\{PAPR > PAPR^0\}, \quad (4)$$

where $CCDF$ estimates probability of OFDM signal PAPR that exceeds provided threshold $PAPR^0$.

B. DCT Equation

The discrete cosine transform (DCT) is represented [48] as

$$d^n = \sqrt{\frac{2}{N}} \beta^n \sum_{m=0}^{N-1} x^m \cos\left(\frac{\pi n(2m+1)}{2N}\right), \quad (5)$$

Where N different symbols of data.

$$\beta^n = \begin{cases} \frac{1}{\sqrt{2}}, & n = 0 \\ 1, & n = 1, .. N-1 \end{cases} \quad (6)$$

C. Riemann Matrix

The rows of normalized Riemann matrix (C) are preferred as phase sequences for PTS algorithm. Now, Riemann matrix

(M) [49],[50] is attained by eliminating first column and first row of matrix B, where

$$B(i,j) = \begin{cases} i-1 \; if \; i \; divides \; j \\ -1 \; otherwise \end{cases} \quad (7)$$

By using the equation (7), Riemann matrix (M) [51] of the order 4 can be presented as:

$$\text{Riemann matrix } (M) = \begin{pmatrix} 1 & -1 & 1 & -1 \\ -1 & 2 & -1 & -1 \\ -1 & -1 & 3 & -1 \\ -1 & -1 & -1 & 4 \end{pmatrix} \quad (8)$$

If the Riemann matrix (M) with size $D \times D$, then the values of the normalized Riemann matrix (C) will be $\left\{\frac{1}{D}\right\} M$.

D. Traditional PTS Method

In traditional PTS arrangement[24],[52], an oversampled input information symbols X is segregated into numerous sub-blocks $X^v = [X^{v,0}, X^{v,1}, X^{v,2} \ldots\ldots, X^{v,NL-1}]^T$, $0 \le v \le V-1$, with the condition that

$$X = \sum_{v=0}^{V-1} X^v \quad (9)$$

Now, by using $IFFT$ to individual sub-blocks, the vectors of sub-signals $x^v = [x^{v,0}, x^{v,1}, \ldots\ldots x^{v,LN-1}]^T, 0 \le v \le V-1$ are created. The phase rotating factors $b^v = e^{j\emptyset^v}$, where $\emptyset^v \in [0, 2\pi)$ for $v = 1,2, \ldots V-1$. The phase rotating factors are generally the elements of predefined set denoted as $b^v \in \left\{ e^{\frac{j2\pi l}{W}} \middle| \; l = 0,1,2, \ldots . W-1 \right\}$, where W denoted as size of phase rotating factors. The phase factors are $b_u = [b_u^0, b_u^1, \ldots . b_u^{V-1},], u = 0,1 \ldots . U-1$, where U signifies total OFDM signals created. Now, with the uth phase vector, the uth OFDM signal is denoted as

$$x_u = [x_u^0, x_u^1, \ldots\ldots, x_u^{LN-1}]^T \quad (10)$$

$$= \sum_{v=0}^{V-1} b_u^v \, x^v, \;\; u = 01,2 \ldots U-1 \quad (11)$$

Since, all the first factors of phase rotating $b_0^v, 0 \le v \le V-1$ are generally assigned with value 1, $U = W^{V-1}$ signals of the OFDM are created in the traditional PTS method. Lastly, best OFDM signal x_{opt} with smallest PAPR worth among U OFDM signal is chosen for transmission, that is,

$$x_{opt} = \underset{u=0,1,2 \ldots U-1}{argmin} \; PAPR(x_u). \quad (12)$$

Block diagram of above mentioned traditional PTS method is denoted by Fig. 10.

IV. Proposed Modified PTS (MOPTS) Algorithm

The MOPTS algorithm which uses Riemann matrix (C) as phase sequences along with DCT for the diminishing of the PAPR (Fig. 10).

Steps for projected MOPTS algorithm are denoted as:

Step 1: Information Y possesses length N, after passed through digital modulator, is denoted as $G = [G_0, G_1, G_2, \ldots . G_{N-1}]$ where N being total number of the sub-carriers. Oversampling represented by L is performed for the better approximation of the PAPR.

Step 2: The oversampled information symbols is divided into several sub-clocks $G^v = [G^{v,0}, G^{v,1}, G^{v,2} \ldots\ldots, G^{v,NL-1}]^T$ with $0 \le v \le V-1$ as condition given by

$$G = \sum_{v=0}^{V-1} G^v \quad (13)$$

Step 3: Now, after applying IFFT to the separate sub-blocks, time domain OFDM signal is denoted as

$$g(n) = \frac{1}{\sqrt{NL}} \sum_{k=0}^{NL-1} G[k] \, e^{\frac{j2\pi kn}{NL}}, n = 0,1,2 \ldots\ldots NL-1, \quad (14)$$

The vectors for several sub-signals

$$g^v = [g^{v,0}, g^{v,1}, \ldots \ldots . g^{v,LN-1}]^T, 0 \le v \le V-1 \quad (15)$$

Step 4: Taking the DCT of the time domain sequence using equation (5) and represented as

$$s^v = DCT(g^v) \quad (16)$$

The vectors for the numerous sub-signals, $s^v = [s^{v,0}, s^{v,1}, \ldots \ldots . s^{v,LN-1}]^T, 0 \le v \le V-1$

Step 5: The phase rotation vectors are chosen in time domain for the optimization of the data from normalized Riemann matrix (C) obtained by considering $\left\{\frac{1}{4}\right\} M$ from equation (8).

Step 6: The phase factors which are selected from rows of normalized Riemann matrix $(C)$are $p_u = [p_u^0, p_u^1, \ldots . p_u^{V-1},], u = 0,1 \ldots . U-1$, where U denotes total number of OFDM signals is denoted as

$$s_u = [s_u^0, s_u^1, \ldots\ldots, s_u^{LN-1}]^T \quad (17)$$

$$= \sum_{v=0}^{V-1} b_u^v \, s^v, \;\; u = 01,2 \ldots U-1 \quad (18)$$

Step 7: Now, calculate and find out the smallest $PAPR$ which is represented as

$$PAPR\big(s_u(n)\big) = 10log_{10} \frac{\max\limits_{0 \le n \le NL-1} (|s_u(n)|^2)}{E[|s_u(n)|^2]}, \quad (19)$$

$$s_{opt} = \underset{u=0,1,2 \ldots U-1}{argmin} \; PAPR(s_u(n)) \quad (20)$$

*Step 8:*Finally, $CCDF$ for the PAPR is calculated as

$$CCDF(PAPR(s_{opt})) = Prob\{PAPR(s_{opt}) > PAPR^0\} \quad (21)$$

where $CCDF$ denotes the probability of the symbols that exceeds the provided threshold $PAPR^0$.

V. Simulation Results

The significant factors considered for the performance investigation of MOPTS algorithm such as oversampling value (L), sub-blocks partition (V) and rows (U) of normalized Riemann matrix (C) are 4 each whereas sub-carriers (N) are 64,128 and 256. The iterations of 9000 OFDM blocks are also considered. The modulation schemes which are considered for the simulations are 16-PSK,32-PSK and 64-PSK.

From Fig. 1. to Fig. 9. depict CCDF of the PAPR of original OFDM (OFDMORIPAPR), original PTS (ORIPTS), Modified PTS (MOPTS).

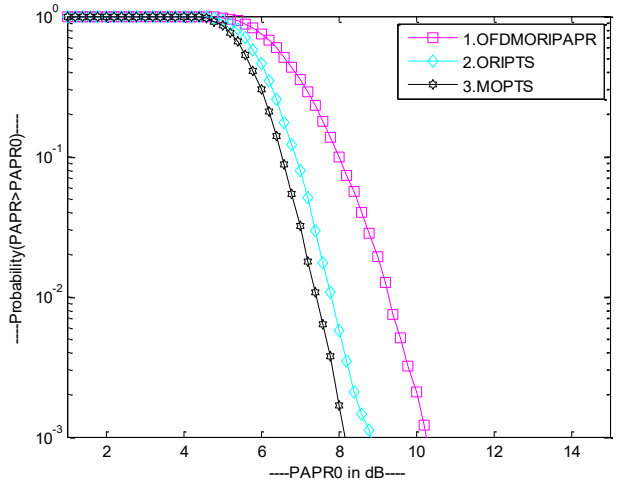

Fig. 1. PAPR diminishing comparison of MOPTS, ORIPTS and OFDMORIPTS under 64 sub-carriers and 16-PSK

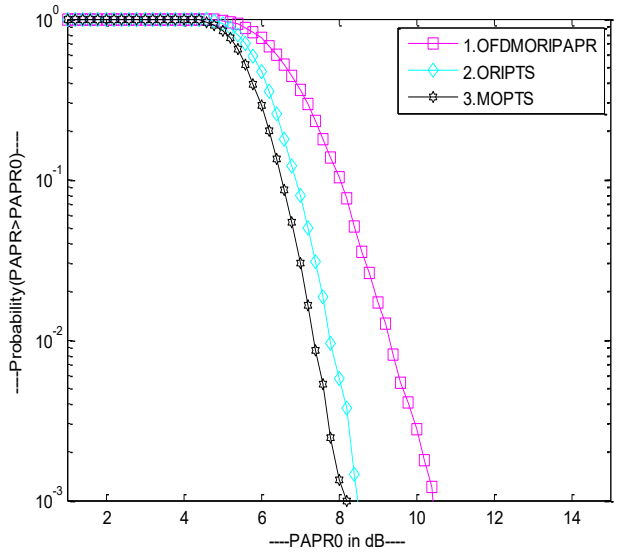

Fig. 2. PAPR diminishing comparison of MOPTS, ORIPTS and OFDMORIPTS under 64 sub-carriers and 32-PSK

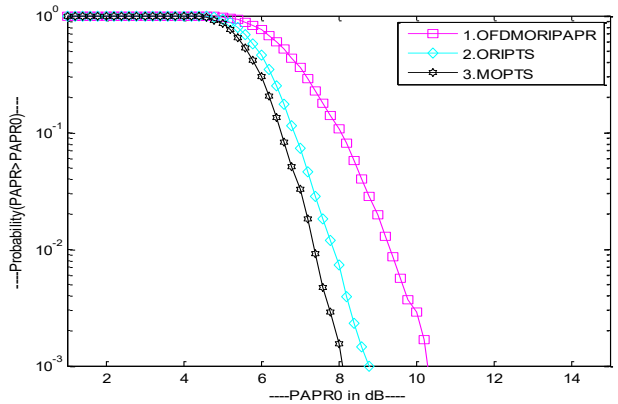

Fig. 3. PAPR diminishing comparison of MOPTS, ORIPTS and OFDMORIPTS under 64 sub-carriers and 64-PSK

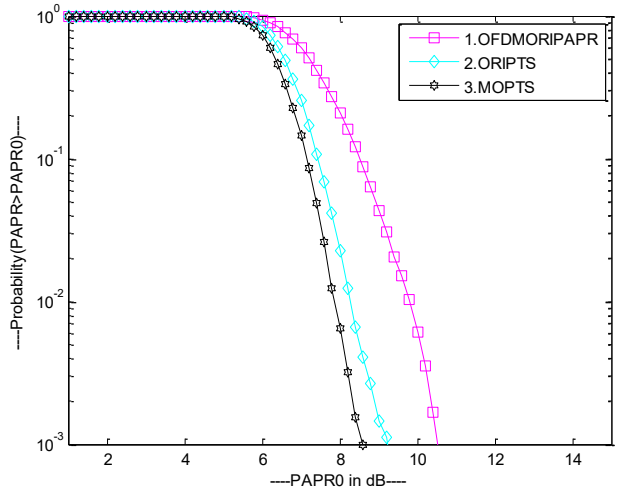

Fig. 4. PAPR diminishing comparison of MOPTS, ORIPTS and OFDMORIPTS under 128 sub-carriers and 16-PSK

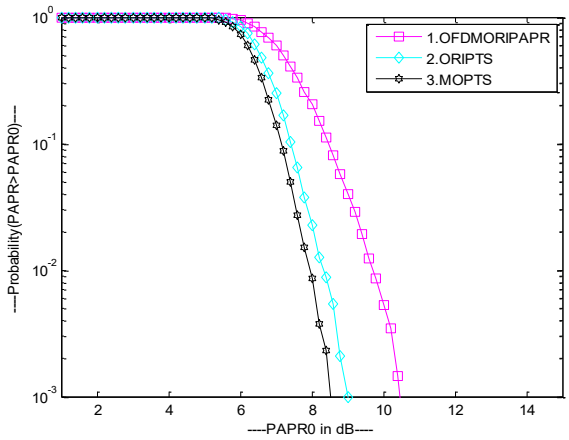

Fig. 5. PAPR diminishing comparison of MOPTS, ORIPTS and OFDMORIPTS under 128 sub-carriers and 32-PSK

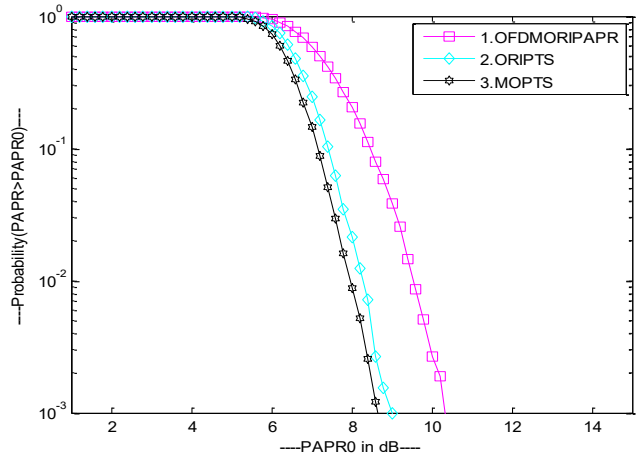

Fig. 6. PAPR diminishing comparison of MOPTS, ORIPTS and OFDMORIPTS under 128 sub-carriers and 64-PSK

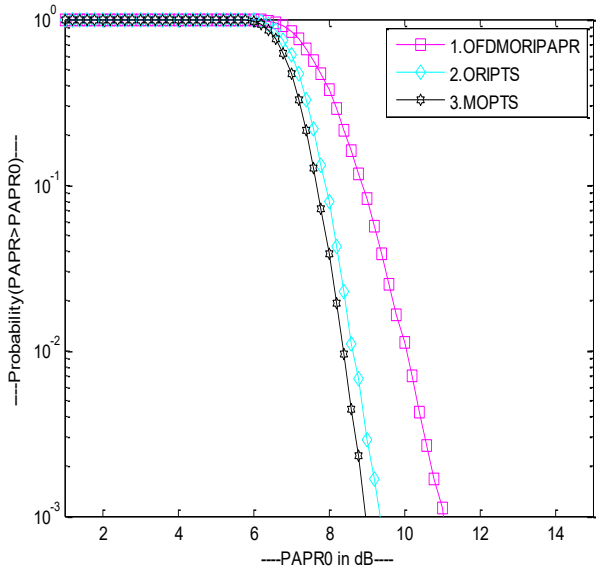

Fig. 7. PAPR diminishing comparison of MOPTS, ORIPTS and OFDMORIPTS under 256 sub-carriers and 16-PSK

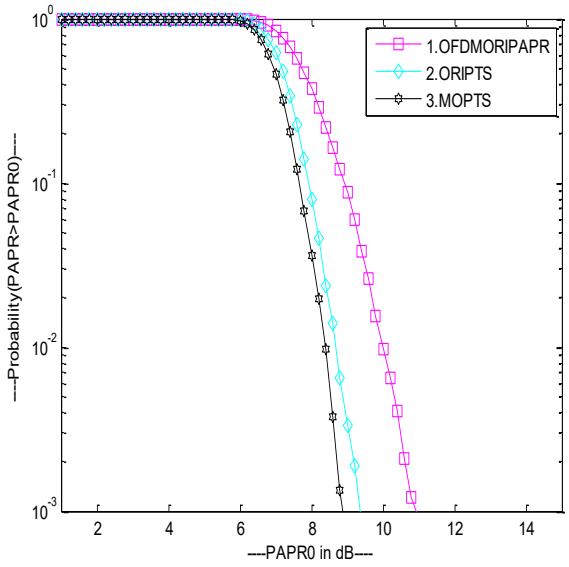

Fig. 8. PAPR diminishing comparison of MOPTS, ORIPTS and OFDMORIPTS under 256 sub-carriers and 32-PSK

In Fig. 1. With 64 sub-carriers and 16-PSK, MOPTS has remarkable PAPR reduction in comparison with ORIPTS and OFDMORIPAPR which is about 0.70 dB and 2.1 dB better than ORIPTS, OFDMORIPAPR respectively similarly it can be easily understood for Fig. 2. and Fig. 3.

In Fig. 4. With 128 sub-carriers and 16-PSK, MOPTS has remarkable PAPR reduction in comparison with ORIPTS and OFDMORIPAPR which is about 0.60 dB and 1.82 dB better than ORIPTS, OFDMORIPAPR respectively similarly it can be easily understood for Fig. 5. and Fig. 6.

In Fig. 7. With 256 sub-carriers and 16-PSK, MOPTS has remarkable PAPR reduction in comparison with ORIPTS and OFDMORIPAPR which is about 0.39 dB and 2.19 dB better than ORIPTS, OFDMORIPAPR respectively similarly it can be easily understood for Fig. 8. and Fig. 9.

It is easily agreed from the Table I. that performance of the MOPTS for N=64 and 64-PSK is best in contrast with 32-PSK and 16-PSK.

As number N depicted in Table I. is increasing from 64,128, and 256 for 16-PSK then the corresponding increase in the PAPR is also observed as 10.21 dB, 10.42 dB and 11.00 dB respectively but remarkable PAPR reduction is achieved by MOPTS algorithm as 8.11 dB,8.60 dB and 8.81 dB respectively.

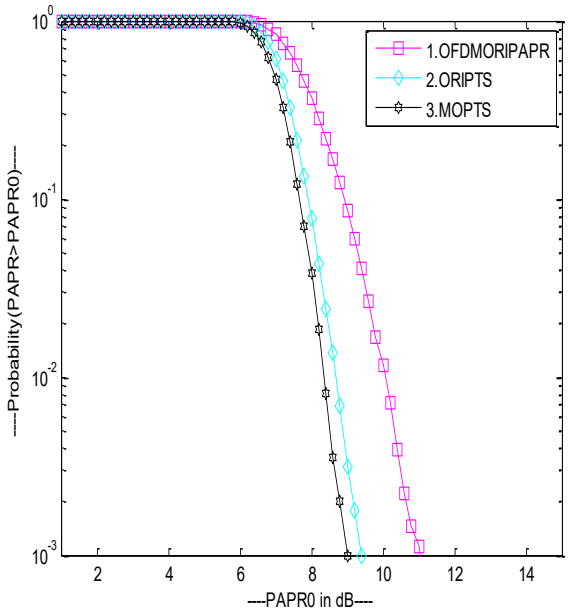

Fig. 9. PAPR diminishing comparison of MOPTS, ORIPTS and OFDMORIPTS under 256 sub-carriers and 64-PSK

TABLE I. CCDF PERFORMANCE ANALYSIS OF MOPTS,ORIPTS AND OFDMORIPAPR FOR N=64,128,256 UNDER 16-PSK, 32-PSK, 64-PSK

PAPR (dB) in order to accomplish $Prob\{PAPR > PAPR^0\} = 10^{-3}$				
Sub-Carriers	**Modulations**	**OFDMORIPAPR**	**ORIPTS**	**MOPTS**
64	16-PSK	10.21	8.81	8.11
	32-PSK	10.40	8.40	8.20
	64-PSK	10.22	8.80	8.05
128	16-PSK	10.42	9.20	8.60
	32-PSK	10.40	9.00	8.41
	64-PSK	10.21	9.00	8.61
256	16-PSK	11.00	9.20	8.81
	32-PSK	10.81	9.21	8.80
	64-PSK	11.00	9.40	9.00

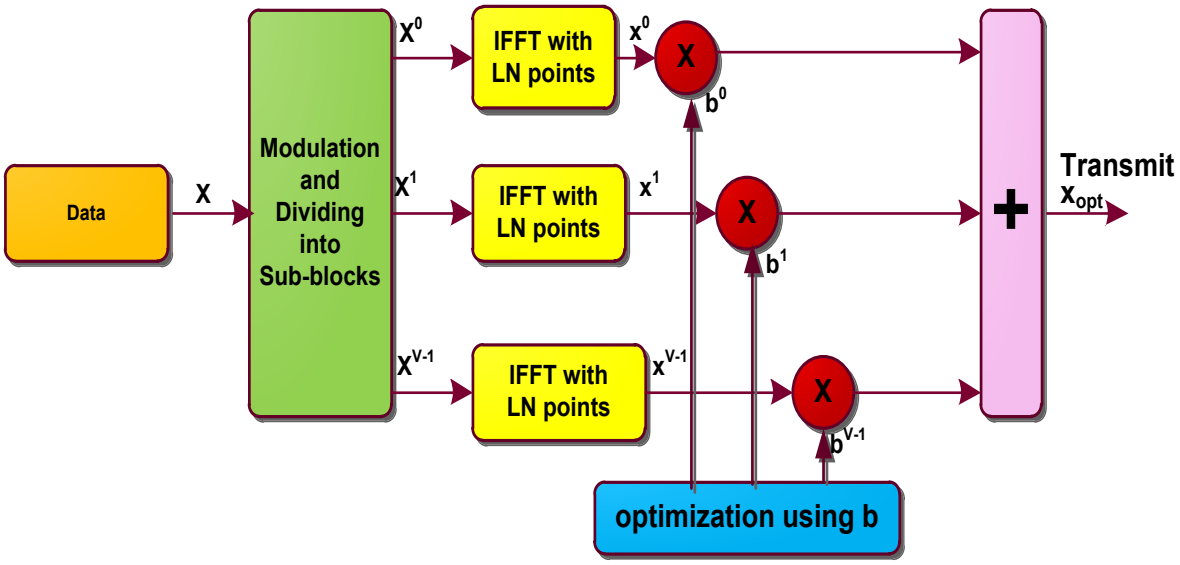

Fig. 10. The block diagram of traditional PTS method [52]

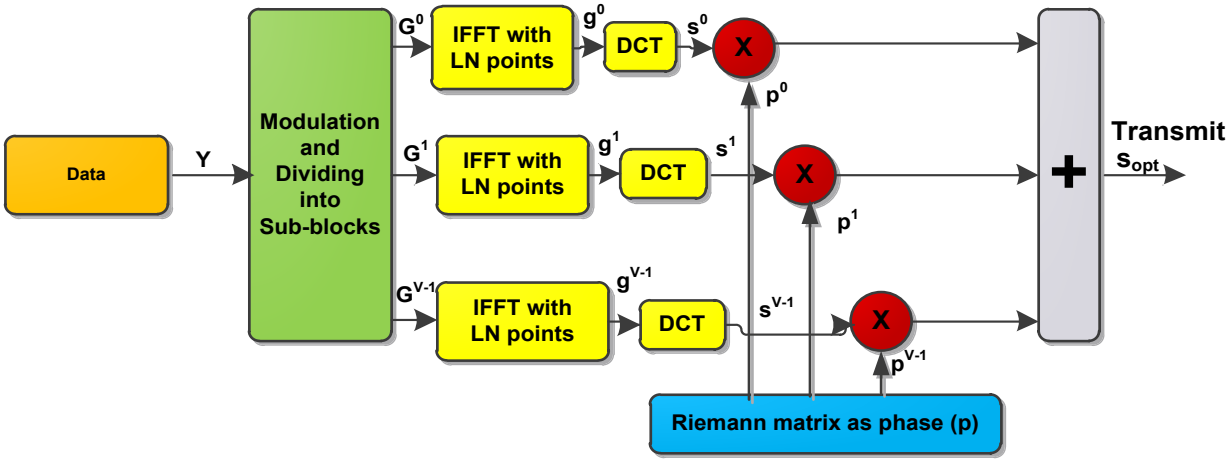

Fig. 11. The block diagram of proposed modified PTS(MOPTS) algorithm

VI. Conclusion

In this paper, PTS scheme has been emphasized to diminish PAPR difficulty of OFDM. Though, PTS scheme undergoes the difficulty of designing and obtaining phase sequences which help in diminishing this problem of PAPR. So, this is the most significant concern which requires the advanced solution. Focusing on this objective, a modified PTS (MOPTS) algorithm has been designed in this paper, which uses normalized Riemann matrix (C) and DCT in time domain whereas the main aim behind using normalized Riemann matrix (C) is the optimization which assists in finding the best phase sequences for the PAPR reduction. Additionally, the proposed MOPTS algorithm can easily generate phase sequences which was difficult in the traditional PTS scheme. Simulation results have been accomplished by comparing MOPTS, ORIPTS and OFDMORIPAPR. The final results, in principle, have depicted that proposed MOPTS algorithm is robust as compared with ORIPTS and OFDMORIPAPR. Furthermore, the futuristic aim of the proposed work is that, it can also be implemented using M-QAM.

References

[1] H. Merah, M. Mesri and L. Talbi, "Complexity reduction of PTS technique to reduce PAPR of OFDM signal used in a wireless communication system," *IET Communications,* vol. 13, no. 7, pp. 939 - 946, 2019.

[2] Y. A. Jawhar, L. Audah, M. A. Taher, K. N. Ramli, N. S. M. Shah, M. Musa and M. S. Ahmed, "A Review of Partial Transmit Sequence for PAPR Reduction in the OFDM Systems," *IEEE Access,* vol. 7, pp. 18021 - 18041, 2019.

[3] Y. A. Jawhar, R. A. Abdulhasan, and K. N. Ramli, "Influencing parameters in peak to average power ratio performance on orthogonal

frequency division multiplexing system," ARPN J. Eng. Appl. Sci., vol. 11, no. 6, pp. 4322-4332, 2016.

[4] S. P. Mohammad and K. Gopal, "Hybrid technique for BER and paper analysis of OFDM systems," Indian J. Sci. Technol., vol. 9, no. 15, pp. 1-5, 2016.

[5] S. H. Han and J. H. Lee," An overview of peak-to-average power ratio reduction techniques for multicarrier transmission," IEEE Wireless Commun., vol. 12, no. 2, pp. 56-65, Apr. 2005.

[6] M. Vidya, M. Vijayalakshmi, and K. Ramalingareddy," Performance enhancement of efficient partitioning technique for PAPR reduction in MIMO-OFDM system using PTS, "in Proc. IEEE Conf. Power, Control, Commun. Comput. Technol. Sustain. Growth (PCCCTSG), Kurnool, India, Dec. 2015, pp. 247-253.

[7] Y. A. Jawhar, R. A. Abdulhasan, and K. N. Ramli," A new hybrid sub-block partition scheme of PTS technique for reduction PAPR performance in OFDM system," ARPN J. Eng. Appl. Sci., vol. 11, pp. 3904-3910, Apr. 2016.

[8] T. Jiang and Y. Wu, "An overview: Peak-to-average power ratio reduction techniques for OFDM signals, "IEEE Trans. Broadcast., vol. 54, no. 2, pp. 257-268, Jun. 2008.

[9] W. Yi and H. Leib," OFDM symbol detection integrated with channel multipath gains estimation for doubly-selective fading channels, "Phys. Commun., vol. 22, pp. 19-31, Mar. 2017.

[10] N. B. Raja and A. Gangatharan," A new low complexity DHT based weighted OFDM transmission for peak power reduction, "Indian J. Sci. Technol., vol. 9, no. 17, pp. 1-4, 2016.

[11] B. H. Alhasson and M. A. Matin, "PAPR distribution analysis of OFDM signals with partial transmit sequence, "J. Commun., vol. 7, no. 11, pp. 784-789, 2012.

[12] J. S. Chow, J. C. Tu, and J. M. Cioffi, "A discrete multitone transceiver system for HDSL applications," IEEE J. Sel. Areas Commun., vol. 9, no. 6, pp. 895-908, Aug. 1991.

[13] E. Costa and S. Pupolin, "M-QAM-OFDM system performance in the presence of a nonlinear amplifier and phase noise,"IEEE Trans. Commun., vol. 50, no. 3, pp. 462-472, Mar. 2002.

[14] G. T. Zhou and J. S. Kenney, "Predicting spectral regrowth of nonlinear power amplifiers," IEEE Trans. Commun., vol. 50, no. 5, pp. 718-722, May 2002.

[15] R. Yoshizawa and H. Ochiai, "Trellis-assisted constellation subset selection for PAPR reduction of OFDM signals, "IEEE Trans. Veh. Technol., vol. 66, no. 3, pp. 2183-2198, Mar. 2017.

[16] P. Miao, P. Chen, and Z. Chen, "Low-complexity PAPR reduction scheme combining multi-band Hadamard precoding and clipping in OFDM based optical communications, "Electronics, vol. 7, no. 2, pp. 1-16, 2018.

[17] H. Bindu and M. Chandrika, "Combined DCT and companding for PAPR reduction in OFDM signals, " Int. J. Innov. Res. Sci. Technol., vol. 2, no. 2, pp. 730-735, 2016.

[18] X. Wu, J. Wang, B. Zhou, Z. Mao, and Z. Gao, " Companding schemes based on transforming signal statistics into trigonal distributions for PAPR reduction in OFDM systems," Int. J. Commun. Syst., vol. 24, no. 6, pp. 776-788, 2011.

[19] C. Kang, Y. Liu, M. Hu, and H. Zhang, "A low complexity PAPR reduction method based on FWFT and PEC for OFDM systems, " IEEE Trans. Broadcast., vol. 63, no. 2, pp. 416-425, Jun. 2017.

[20] S. Cha, M. Park, S. Lee, K.-J. Bang and D. Hong, "A new PAPR reduction technique for OFDM systems using advanced peak windowing method," IEEE Transactions on Consumer Electronics , vol. 54, no. 2, pp. 405 - 410, 2008.

[21] M. Taher, J. Mandeep, M. Ismail, S. Samad, and T. Islam, "Reducing the power envelope fluctuation of OFDM systems using side information supported amplitude clipping approach," Int. J. Circuit Theory Appl., vol. 42, no. 4, pp. 425-435, 2014.

[22] J. Armstrong," Peak-to-average power reduction for OFDM by repeated clipping and frequency domain filtering," Electron. Lett., vol. 38, no. 5, pp. 246-247, 2002.

[23] C. Ni, Y. Ma, and T. Jiang," A novel constellation amplitude modification method for PAPR reduction in OFDM systems," Wireless Commun. Mobile Comput., vol. 16, no. 18, pp. 3307-3315, 2016.

[24] S. H. Müller and J. B. Huber, "OFDM with reduced peak-to-average power ratio by optimum combination of partial transmit sequences," Electron. Lett., vol. 33, no. 5, pp. 368-369, 1997.

[25] Y. Jawhar et al.," New low-complexity segmentation scheme for the partial transmit sequence technique for reducing the high PAPR value in OFDM systems, "Electron. Telecommun. Res. Inst. J., vol. 40, no. 6, pp. 699-713, Jun. 2018.

[26] H. Liang, H.-C. Chu, and C. B. Lin," Peak-to-average power ratio reduction of orthogonal frequency division multiplexing systems using modified tone reservation techniques," Int. J. Commun. Syst., vol. 29, no. 4, pp. 748-759, 2016.

[27] B. Horvath and B. Botlik," Optimization of tone reservation-based PAPR reduction for OFDM systems, " Radio engineering, vol. 26, no. 3, pp. 791-797, 2017.

[28] M. A. Taher, M. J. Singh, M. Ismail, S. A. Samad, and M. T. Islam, " Sliding the SLM-technique to reduce the non-linear distortion in OFDM systems, " Elektron. Elektrotechn., vol. 19, no. 5, pp. 103-111, 2014.

[29] H. Breiling, S. H. Müller-Weinfurtner, and J. B. Huber, "SLM peak power reduction without explicit side information, " IEEE Commun. Lett., vol. 5, no. 6, pp. 239-241, Jun. 2001.

[30] M. M. Rahman, M. N. A. S. Bhuiyan, M. S. Rahim, and S. Ahmed," A computationally efficient selected mapping technique for reducing PAPR of OFDM," Telecommun. Syst., vol. 65, no. 4, pp. 637-647, 2017.

[31] D. D. Falconer, " Linear precoding of OFDMA signals to minimize their instantaneous power variance," IEEE Trans. Commun., vol. 59, no. 4, pp. 1154-1162, Apr. 2011.

[32] A. D. S. Jayalath and C. Tellambura, " Reducing the peak-to-average power ratio of orthogonal frequency division multiplexing signal through bit or symbol interleaving," Electron. Lett., vol. 36, no. 13, pp. 1161-1163, 2000.

[33] S. H. Han, J. M. Cioffi, and J. H. Lee, " Tone injection with hexagonal constellation for peak-to-average power ratio reduction in OFDM, " IEEE Commun. Lett., vol. 10, no. 9, pp. 646-648, Sep. 2006.

[34] S. Gokceli, T. Levanen, T. Riihonen, M. K. Renfors and M. Valkama, "Frequency-Selective PAPR Reduction for OFDM," IEEE Transactions on Vehicular Technology, pp. 1 - 5, 2019.

[35] F. Sandoval, G. Poitau and F. Gagnon, "On Optimizing the PAPR of OFDM Signals With Coding, Companding, and MIMO," IEEE Access, vol. 7, pp. 24132 - 24139, 2019.

[36] B. Tang, K. Qin, X. Zhang and C. Chen, "A Clipping-Noise Compression Method to Reduce PAPR of OFDM Signals," IEEE Communications Letters, pp. 1-4, 2019.

[37] A. M. Rateb and M. Labana, "An Optimal Low Complexity PAPR Reduction Technique for Next Generation OFDM Systems," IEEE Access, vol. 7, pp. 16406 - 16420, 2019.

[38] X. Liu, X. Zhang, J. Xiong, F. Gu and J. Wei, "An Enhanced Iterative Clipping and Filtering Method Using Time-Domain Kernel Matrix for PAPR Reduction in OFDM Systems," IEEE Access, pp. 1-10, 2019.

[39] P. Gupta, R. K. Singh, H. P. Thethi, B. Singh and S. K. Nanda, "Discrete Cosine Transform Matrix Based SLM Algorithm for OFDM with Diminished PAPR for M-PSK over Different Subcarriers," Journal of Computer Networks and Communications, vol. 2893207, pp. 1-10, 2019.

[40] P. Gupta, B. A. Kumar and S. K. Jain, "Peak to average power ratio reduction in OFDM using higher order partitioned PTS sequence and Bose Chaudhuri Hocquenghem Codes," in 2015 IEEE-International Conference on Signal Processing and Communication Engineering Systems, Guntur, India, 2015.

[41] P. Gupta and R. K. Singh, "Highly optimized Selected Mapping based peak to average power ratio reduction OFDM system using different modulation schemes," in 2015 Third International Conference on Image Information Processing (ICIIP), Waknaghat, India, 21-24 Dec. 2015.

[42] P. Gupta, R. Singh, B. Singh and B. A. Kumar, "PAPR Performance Analysis of SLM with Hadamard Matrix Based Phase Sequence under M-PSK Modulation for Diminishing PAPR of OFDM System," in 2018

IEEE-International Conference on Intelligent Circuits and Systems (ICICS), Phagwara, India, 19-20 April 2018.

[43] S.-P. Lin, Y.-F. Chen and S.-M. Tseng, "Iterative smoothing filtering schemes by using clipping noise-assisted signals for PAPR reduction in OFDM-based carrier aggregation systems," IET Communications, vol. 13, no. 6, pp. 802 - 808, 2019.

[44] A. Goela, P. G. Poddarb and M. Agrawal, "A novel quadrilateral companding transform for PAPR reduction in OFDM systems," Digital Signal Processing, vol. 85, pp. 113-123, 2019.

[45] M. Rakshit, S. Bhattacharjee, S. Sil and A. C. Sr., "Modified switching DE algorithm to facilitate reduction of PAPR in OFDM systems," Physical Communication, vol. 29, pp. 245-260, 2018.

[46] A. Singh and H. Singh, "Peak to average power ratio reduction in OFDM system using hybrid technique," Optik, vol. 127, no. 6, pp. 3368-3371, 2016.

[47] M. V. R. Vittal and K.R. Naidu, "A novel reduced complexity optimized PTS technique for PAPR reduction in wireless OFDM systems," Egyptian Informatics Journal, vol. 18, no. 2, pp. 123-131, 2017.

[48] P. Tan and N. C. Beaulieu, "A Comparison of DCT-Based OFDM and DFT-Based OFDM in Frequency Offset and Fading Channels," IEEE Transactions on Communications, vol. 54, no. 11, pp. 2113 - 2125, 2006.

[49] N. Irukulapati, V. Chakka and A. Jain, "SLM based PAPR reduction of OFDM signal using new phase sequence," Electronics Letters, vol. 45, no. 24, pp. 1231 - 1232, 2009.

[50] F. Roesler, Riemann's hypothesis as an eigenvalue problem. Linear Algebra Application, vol. 81, (1986), 153-198.

[51] M. Chandwani, A. Singhal, N. V. I and V. Chakka, "A Low Complexity SLM Technique for PAPR Reduction in OFDM Using Riemann Sequence and Thresholding of Power Amplifier," in Annual IEEE India Conference, Gujarat, India , 2009.

[52] K.-S. Lee, H. Kang and J.-S. No, "New PTS Schemes With Adaptive Selection Methods of Dominant Time-Domain Samples in OFDM Systems," IEEE Transactions on Broadcasting , vol. 64, no. 3, pp. 747 - 761, 2018.

[53] P. Varahram and B. M. Ali, "Partial transmit sequence scheme with new phase sequence for PAPR reduction in OFDM systems," *IEEE Transactions on Consumer Electronics,* vol. 57, no. 2, pp. 366 - 371, 2011.

Proceedings of the Fourth International Conference on Communication and Electronics Systems (ICCES 2019)
IEEE Conference Record # 45898; IEEE Xplore ISBN: 978-1-7281-1261-9

Evaluating Visual Performance of Multi-object Scene Reconstruction using Triangulation from Airborne Geo-spatial Point Clouds

Swati RajeshKumar Maurya
Department of Computer Science
S. K. Somaiya College of ASC, University of Mumbai
Maharashtra, Mumbai, 400077, India
Email: swadrag@gmail.com

Ganesh M. Magar
P. G. Department of Computer Science
S. N. D. T. Women's University,
Maharashtra, Mumbai, 400049, India
Email: drgmmagar@gmail.com

***Abstract*— This paper presents a hybrid framework for reconstructing the scene of objects from a geospatial dataset from point clouds. The method addresses the processing issues of large data points in 3D space and uses spatial clustering to determine the context membership for points. It further uses the min-cut based graph algorithm to segment the resulting polyhedral surface of the object in the scene. Spatial clustering is performed using k-dimension search tree in multidimensional space for segmenting and assigning memberships of point to possible clusters. Size of these clusters controls the background penalties for use during graph cuts for generating multi-object polyhedral objects. The results in this paper are compared to other methods and it is observed that the min-cut graph-based approach outperforms simple Delaunay triangulation and Euclidean estimate based method for surface construction. It can classify objects with better accuracy into separated structures and enabling more efficient visual communication and rendering performance. Geospatial reconstruction problems especially those used for visual communication can use the min-cut based method to construct multi-object scenes for faster rendering performances and reduced data management overheads.**

Keywords*—*min-cut algorithm, point cloud, 3D surface reconstruction, surface triangulation, Visualization

I. INTRODUCTION

Many geospatial applications especially those used for visual communication of a scene of objects often require identifying and processing surface point organized as point clouds. These point clouds contain hundreds and thousands and even millions of points representing 3D spatial occupancy of objects. These points are results of surface returns recorded from sensors like LIDAR devices. This makes computing several geomorphic aspects of the objects and features possible. However, the size of these data sets are very large and results in a lot of computational overheads due to the very discrete nature of the points in the point cloud. Working with point cloud data is actually an informatics problem which relies on processing large data values and involve a higher degree of complexity. Among several interesting application being addressed, reconstruction of the geospatial objects especially from arbitrary point clouds[1] is of greater interest for geospatial computing problems. With these large set of points in the point cloud, computation requirement increases multifold and traditional methods and algorithm perform poorly. Therefore, it becomes a potential candidate for big data processing and management problem.

Reconstruction and visualization are challenging problem especially from an unorganized set of points in point clouds[2]. If surface details are not very important, representing the object surface using the polyhedral structure can lead to a more efficient organization. Triangulation is used for approximating these surfaces and in fact, this itself can lead to improved rendering performances. Various algorithms are available to process these surface data and often combined together for better results. The problem of reconstruction can be broken down into two sub problems. First, it involves identifying separate object structures from an unstructured set of points within the given point cloud data. Second, it requires constructing the triangulated surface from them. Studies suggest that simple clustering algorithms perform poorly for problems involving identifying objects from the scene with multiple objects and experience severe performance issues.

A more robust approach for clustering is needed that is equally applicable to large and big data sets. Representing objects using triangular polygons requires identifying vertices and edges that define the object surface. Simple triangulation from unorganized points often leads to deformed surface approximations. The problem of deformation exacerbates with a scene with multiple objects. Fused objects are often seen while reconstruction and lead to extra and redundant storage requirements. Such results can prove to be a great hindrance for critical geospatial reconstruction based applications and thus must be addressed specifically. Visual communication of the scene under investigation experiences erroneous surface patch and deformed shapes.

This paper addresses the aforementioned challenges and issues in surface reconstruction and proposes a hybrid framework that comprises of spatial clustering of objects in multidimensional space followed by an efficient triangulation using graph cuts. This paper starts with a brief into a literature survey of related work followed by a description of input data and experimental setup. Subsequently, the framework for multi-object scene triangulation is presented followed by experimental results and discussion. Finally, the observation is presented with future pointers for the research in the concluding remarks. The details each of these are described next in discussions to follow.

II. Literature Survey And Related Work

The problem of Identification, segmentation, and triangulation of object surface have been addressed in past research works. As a problem of visual analytics as discussed in [2] and [3], it has been approached in different ways. Segmentation has been one of the fundamental tasks in identifying and thereby reconstruction. Segmentation of object structures from LiDAR point clouds has been discussed by many including work demonstrated in [4], [5], [6] and [7]. The method discussed in [4] is limited to ordered point clouds and uses scan-line-based ground segmentation algorithm. Although it could successfully segment objects its performance on solid surface generation is unknown. Similar work was performed in [5] using the histogram-based methodology to separate the building clusters from other structures. This work is also limited to the geometric description of structures using point data. Other related works of identifying and segmenting objects from point cloud have been addressed. Segmentation of objects from unstructured point cloud has been discussed in [8] and attempts to identify tree crowns from airborne LiDAR point clouds. However, most of them classify the foreground and background objects only and limit object visualization using point description.

Reconstruction of the object's surface using triangulation has proved more efficient for rendering purpose. Variants of surface triangulation include direct triangulation method, ball pivoting method[9], Voronoi-based algorithm[10], Delaunay based method [10] can provide faster ways to generate surfaces. However, most of the experimental attempts have focused on improving the surface quality for a scene with a single object. While these methods largely satisfy expectations for smaller objects, they suffer from performance and deformation issues for large datasets with rapidly varying surface elevations. An optimized method for reconstructing large geospatial structures such as the reconstruction of sand dunes discussed in [13] provides a pathway to generate surfaces from rapidly varying structures. It is noteworthy to see that all these methods treat foreground objects as one object or perform poorly for scenes with multiple objects. The results are deformed structures and often not suited with closely spaced objects.

Multi-object classification and labeling have been addressed at a small level. One way to achieve the objective of multi-object reconstruction and visualization to with optimal performance is to use a graph-based approach for segmenting of objects. This approach can use graph-based concepts especially to cull away weak links between the identified clusters and thus achieving the objective. Correctness and speed is more important in reconstruction based visual communication and therefore unnecessary computations must be avoided. Min-cut based approach discussed in [14] can be used for this purpose. Although this method was limited to the segmentation problem, it can be further extended and used together with some modifications for generating the physical surface of distinct objects in the scene. This forms the basis of our method presented in this paper.

Table 1: Format Of Data For The Experiment

x	y	z
72.250	-18.179	0.850
68.269	-16.610	0.480
71.599	-18.370	0.760
71.940	-18.549	0.820
72.559	-18.879	0.810
72.679	-18.939	0.400
67.789	-16.700	0.390

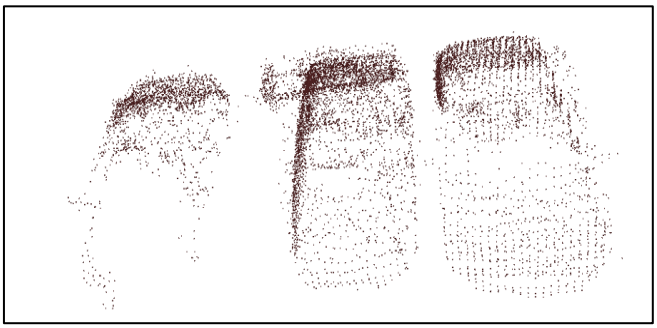

Figure 1: 3D view of the point cloud data sample.

III. Data And Experimental Setup

The experimental validation of the proposed framework for reconstructing polyhedral surfaces of multi-object scene uses geospatial data organized as a point cloud. The point cloud organizes points in 3D space with its spatial coordinates along three dimensions. These points represent the return from the surface obtained during acquisition from LiDAR sensors. The snippet of sample data set presenting a multi-object scene is shown in Table 1. The 3D view of the point data set is shown in figure 1. The data represents the geometrical structure with the center of projection positioned along positive y-axis during data acquisition. Data assumes no point normal information in the originally stored point cloud and hence requires only point processing in raw form. For simplicity of handling, the data is organized in ASCII format. The corresponding height map is shown in Figure 2. Note that, the data represents surface returns and therefore carefully approximates object surface. As it is viewed as a collection of unstructured points, preprocessing is important to prepare and make it suited for experimentation.

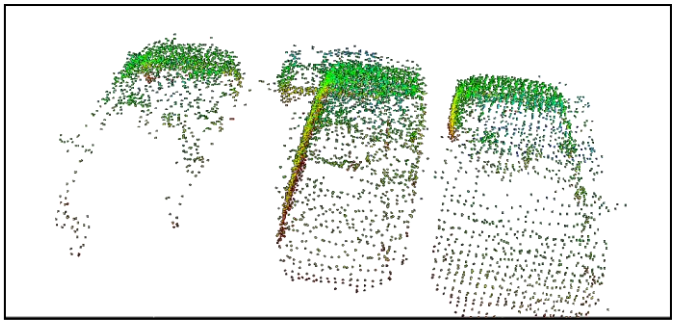

Figure 2: Height map of sample Point cloud

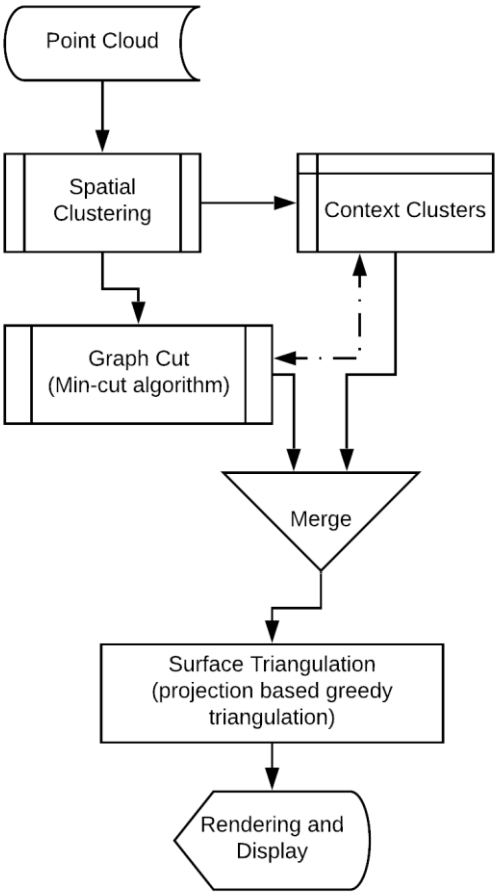

Figure 3: Framework for Multi-object triangulation

The details of the framework and relatedr operations are described next.

IV. Framework For Multi-Object Surface Triangulation

To achieve multi-object segmentation and surface reconstruction, a hybrid framework is proposed comprising of spatial clustering in 3D space and an optimized triangulation controlled by graph based algorithm. The workflow of the proposed framework is shown in Figure 3. The input to the framework is an unstructured set of points stored as a point cloud. The point cloud is subject to initial preprocessing in order to identify isolated outlier points and removed from the data set. The objective function is an odd-ordered filter that culls away point that has no neighbors. These are essentially outlier that is present in the input as the result of acquisition or storage errors. Ground and non-ground sections are identified using the algorithm described in [15] Points classified as non-ground points are taken for further processing. These non-ground points are further processed using the region growing approach as described in [16] for clustering the points into possible objects (see Figure 4a). The simple directed triangulation would result in the poor, fused and deformed surface as shown in Figure 4b. Therefore these clusters are further processed before attempting triangulation of the surface.

Some points especially those at the boundaries of the cluster are sometimes wrongly classified to belong to a different cluster. To overcome these erroneous classifications, a context membership function is used together with graph-based links between the points during the surface reconstruction process. This context membership function assigns the weight to the edges between the neighboring points which are influenced and updated from values of neighbor edges. The weight w_{ij} for the edge between points p_1 and p_j are estimated using the following relation

$$w_{ij} = e^{-\left(\frac{d}{\sigma}\right)^2} \quad \ldots (1)$$

Where d denotes the distance between points and σ defines the common spacing of points. Theoretical approximation of each cluster is computed and distance values are computed for each cluster. A decision criteria together with the distance and weights between points is developed for arriving membership decision for points especially at the boundaries. Intuitively, the farther the points are, the better is the probability for the edge to be culled away.

Edges which have more neighbor edges have more weight and tend to have higher context membership to a specific cluster. Context membership is computed using k-nearest neighbors within the specified radius and thus greater affinity to points relatively closer to each other. This method helps to identify dense clusters inherently comprising of clusters with relative homogeneity of spatial coherence. The result of such coherence is shown in Figure 4c.

Weak edges (longer edges) are identified using distance relationship between points which together with context memberships to respective clusters help in disassociating them. Weak edges have relatively less weight and are links between clusters (potential objects). The links between the points are represented as a graph. The min-cut algorithm discussed in [14] together with context membership is applied to the clusters to segment the objects into distinct objects. Background penalties are computed to control the expected distance d from the center of the cluster. The background penalty is computed as

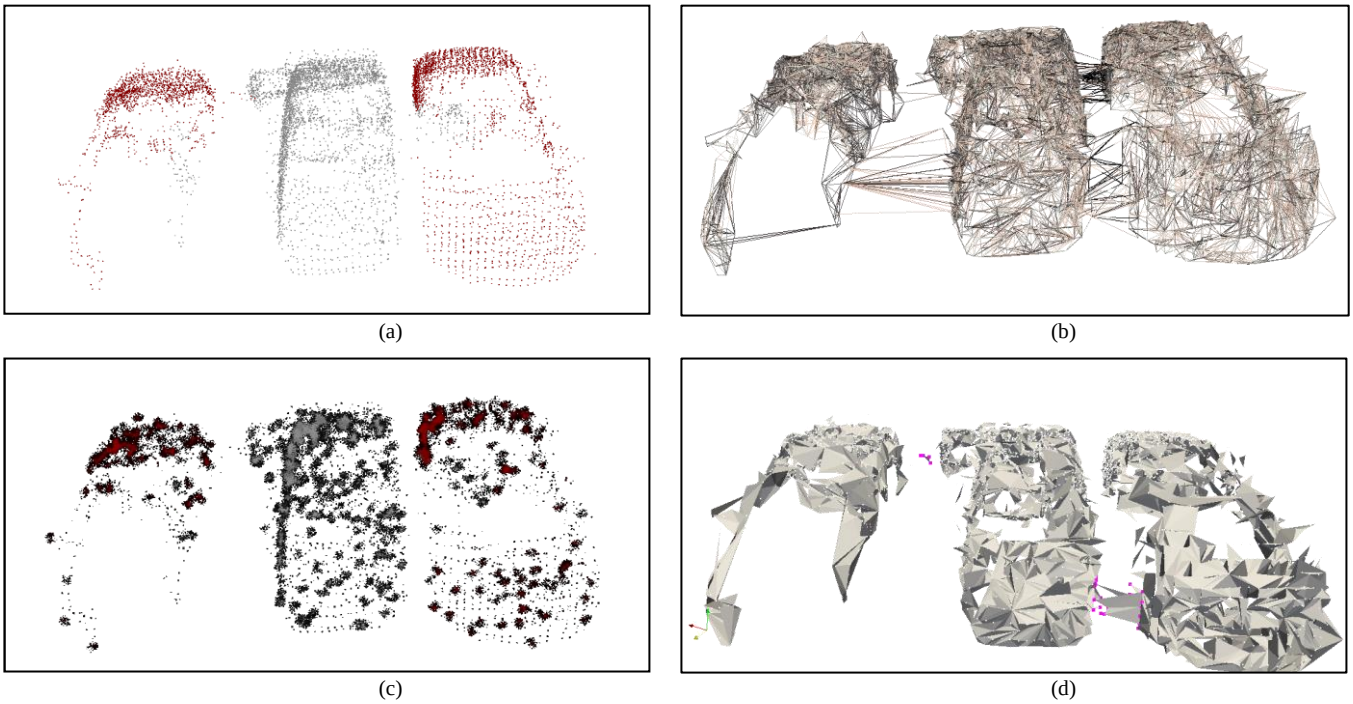

Figure 4: Intermediate stages during surface triangulation: (a) Cluster of objects and point membership (b) Default triangulation using direct triangulation methods (c) Context Clusters and its membership to respective objects (d) Final triangulation of scene using Context Clusters and min-cut algorithm

$$Penalty_{back} = \frac{d_{center}}{radius} \quad \ldots (2)$$

The value of distance to the center is computed as $d_{center} = \sqrt{(x - x_{center})^2 - (y - y_{center})^2}$. The value of radius defines the distance from the center of object beyond which no points are expected.

The optimized triangulation described in [13] is applied to the clustered point cloud for a surface generation as shown in Figure 4d. During triangulation, the membership function is again used to check any cross triangulation arising across clusters. The size of the cluster and thus the resulting object structure is controlled interactively by setting the radius and value of k-nearest neighbors during the triangulation process. The benefit of applying triangulation after the min-cut algorithm is that it reduces false positive links and thus results into improved triangulation and gives better visual results. The algorithm although doesn't offer much flexibility but offer good results for objects that are placed on the planar horizontal surface. The variation on the object surface is handled correctly by the membership function and thus gives better surface approximations.

V. SIMULATIONS AND EXPERIMENTAL RESULTS

The proposed models for generating polyhedral surface has been tested on large dataset encompassing points of the order of several thousand and millions of points on varied geospatial structures. To demonstrate the reconstruction capabilities, the method is applied to a scene comprising of three cars. The scene is stored using point cloud comprising of surface returns represented as points with its elevation values along z-direction. Reconstruction performance is compared for three methods namely direct triangulation, Euclidean estimate based method, and min-cut based method. The result of context cluster which identifies the objects (cars in this case) is shown in Figure 5.

During the process of reconstruction, the non-ground points are first triangulated using the direct triangulation method. For showing the reconstruction capabilities of the proposed method the non-ground points are first triangulated using direct triangulation discussed in [17]. The corresponding mesh model and the solid shaded surface are shown in Figure 5a. Although it performs well on the single object but falls on multiple objects that are lying close to each other. It generated redundant triangular links between possible objects and thus leads to incorrect and deformed surface structures.

The point cloud data is also processed for clustering and identifying possible objects using Euclidean estimator for computing the member points. The result of triangulation is shown in Figure 5b. Results using the proposed framework exhibits significant improvement. The min-cut graph-based method reduces the redundant links and thereby the false

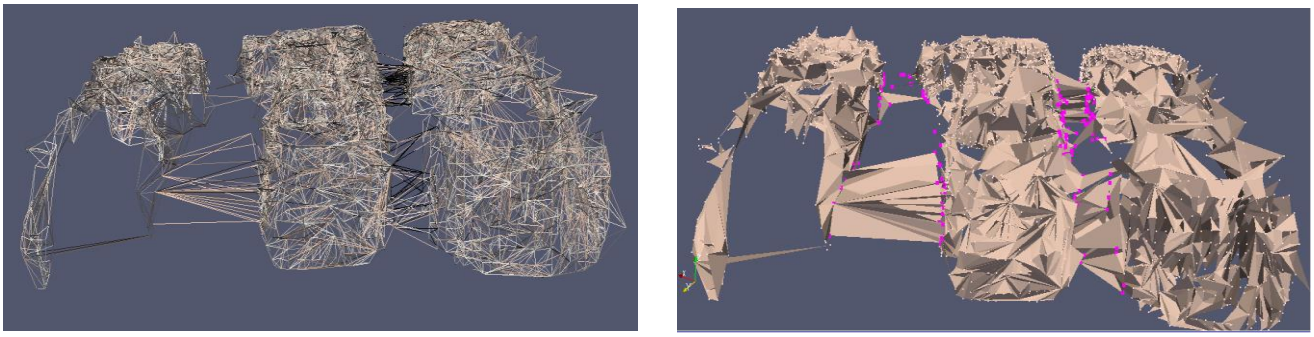

(a) Reconstruction using Direct Triangulation: Mesh Model (left) and Solid Model (right)

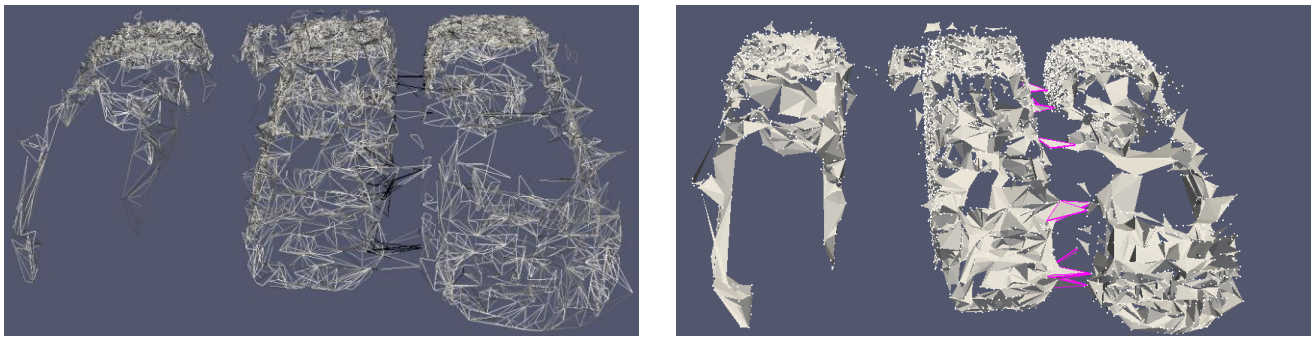

(b) Reconstruction using Euclidean Estimation: Mesh Model (left) and Solid Model (right)

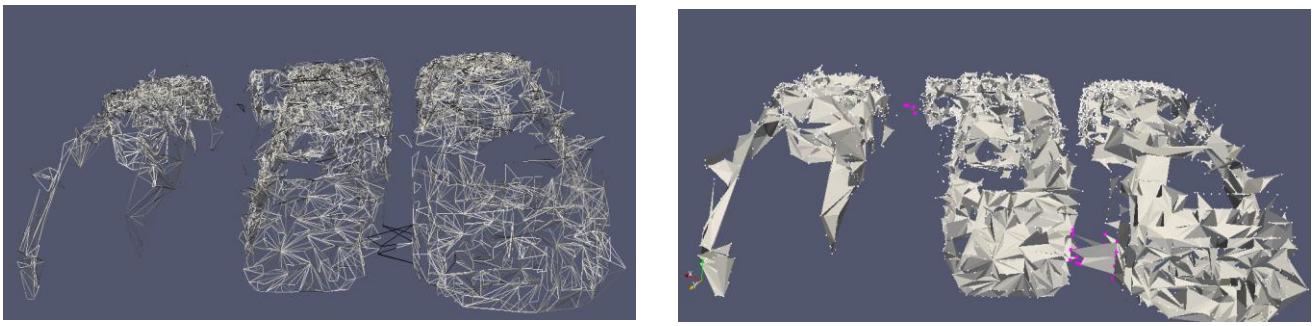

(c) Proposed Method: Context Clusters and Min-Cut based Method

Figure 5: Reconstruction using Various Methods: Surface showing Surface Triangulation (Left) and Solid Surface (Right)

triangulation that fuses the objects together. The segmented point cloud and the corresponding mesh model using the proposed method is shown in Figure 5c.

It is observed that (see Figure 6), the object segmentation and thereby reconstruction performance is significantly improved using the proposed use of min-cut based framework. The accuracy of min-cut based reconstruction is better compared to both direct triangulation and Euclidean estimator based method. The occurrences of false positive are reduced to the considerably both for edge links and for the triangulated cells in the reconstructed scene with multiple objects. Simple triangulation results in maximum false positives and generates deformed and fused structures. Euclidean estimator is good when the cluster of points is distant away from each other. Use of context clustering together with the min-cut algorithm generates good results for close objects in the point cloud.

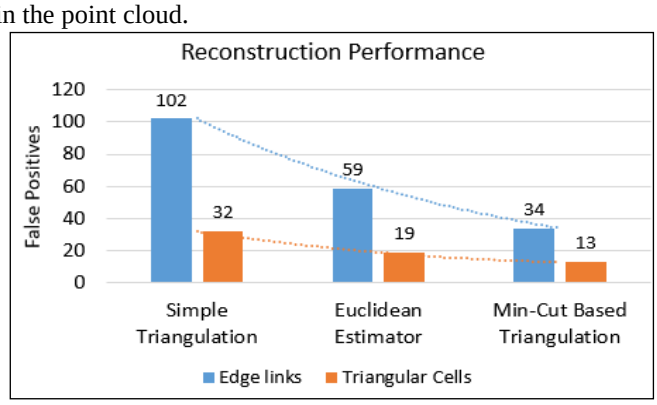

Figure 6: Performance Measure Based on False-Positive Response

VI. Observations and Applications

It is established from the experimental work that min-cut based approach helps to segment object embedded among point cloud and also found useful in surface triangulation as it has influence in determining the weak edges. The use of context membership closely binds the points belonging to the object and prevents surface points from disassociating from its neighbors. The proposed method successfully eliminates loosely connected cluster however cluster of points that are tightly connected with more connected still show some triangulation. This is primarily because of data acquisition error and can be eliminated with more accurate measurements.

Some of the potential applications that are identified where the method discussed above finds its use are listed below.

- Tree crown detection from the sparsely populated forest.
- 3D Building profiling and rooftop detection from airborne surface returns
- Identifying bridges in real 3D space
- Identifying robust microwave coverage in 3D space

Many more related emerging applications can find immense use of the method discussed in this paper for multi-object reconstructions.

VII. Conclusion

This papers demonstrated the successful use of the graph-based min-cut algorithm for identification and reconstruction of the surface for a scene of multi-object spatial structures. Multidimensional clustering of points followed by min-cut based approach gives improved results compared to direct triangulation. The method also established the use of context membership of a point to clusters and its significance in determining the potential links used during min-cut implementation. The accuracy is better than simple triangulation and similar known methods and offers significant performance results. The proposed results set the pointers for fast rendering of multi-object scenes especially reconstructed from unorganized point clouds. Future work can focus on combining triangulated ground surface and multiple objects for interactive visualizations. This work can also be extended for evaluating and studying surface deformations, modeling optimized 3D viewing system for faster rendering requirements.

References

[1] T. Wiemann, I. Mitschke, A. Mock, and J. Hertzberg, "Surface reconstruction from arbitrarily large point clouds," *Proc. - 2nd IEEE Int. Conf. Robot. Comput. IRC 2018*, vol. 2018-Janua, pp. 278–281, 2018.

[2] W. Luo and H. Zhang, "Visual analysis of large-scale LiDAR point clouds," *Proc. - 2015 IEEE Int. Conf. Big Data, IEEE Big Data 2015*, pp. 2487–2492, 2015.

[3] D. A. Keim, F. Mansmann, J. Schneidewind, J. Thomas, and H. Ziegler, "Visual Analytics: Scope and Challenges," in *Visual Data Mining*, Berlin, Heidelberg: Springer Berlin Heidelberg, pp. 76–90.

[4] Ying Zhou *et al.*, "A Fast and Accurate Segmentation Method for Ordered LiDAR Point Cloud of Large-Scale Scenes," *IEEE Geosci. Remote Sens. Lett.*, vol. 11, no. 11, pp. 1981–1985, 2014.

[5] A. M. Ramiya, R. R. Nidamanuri, and R. Krishnan, "Segmentation based building detection approach from LiDAR point cloud," *Egypt. J. Remote Sens. Sp. Sci.*, pp. 1–7, 2016.

[6] Y. Sun *et al.*, "Automated segmentation of LiDAR point clouds for building rooftop extraction," *Int. Geosci. Remote Sens. Symp.*, vol. 2016-Novem, pp. 1472–1475, 2016.

[7] S. Li, L. Su, Y. Liu, Z. He, X. Ave, and W. H. Zone, "Segmentation of Individual Trees Based on a Point Cloud Clustering Method using Airborne Lidar Data, School of Resources and Environment , University of Electronic Science and Technology of China , No . Center for Information Geoscience, University of El," pp. 7524–7527, 2018.

[8] S. R. Maurya and G. M. Magar, "Segmentation and Visualization of Airborne Sparse Forest LiDAR Data using Region Growing Approach," *Int. J. Comput. Appl.*, vol. 156, no. 5, pp. 16–22, 2016.

[9] F. Bernardini, J. Mittleman, H. Rushmeier, C. Silva, and G. Taubin, "The ball-pivoting algorithm for surface reconstruction," *IEEE Trans. Vis. Comput. Graph.*, vol. 5, no. 4, pp. 349–359, Oct. 1999.

[10] N. Amenta, M. Bern, and M. Kamvysselis, "A new Voronoi-based surface reconstruction algorithm," pp. 415–421, 2005.

[11] D. Cohen-Steiner and F. Da, "A greedy Delaunay-based surface reconstruction algorithm," *Vis. Comput.*, vol. 20, no. 1, pp. 4–16, 2004.

[12] W. Gong, Y. J. Liu, K. Tang, and T. Wu, "Approximate Delaunay mesh reconstruction and quality estimation from point samples," *J. Comput. Appl. Math.*, vol. 274, pp. 23–34, 2015.

[13] S. R. Maurya and G. M. Magar, "Performance of Greedy Triangulation Algorithm on Reconstruction of Coastal Dune Surface," in *2018 3rd International Conference for Convergence in Technology (I2CT)*, 2018, pp. 1–6.

[14] A. Golovinskiy and T. Funkhouser, "Min-cut based segmentation of point clouds," *2009 IEEE 12th Int. Conf. Comput. Vis. Work. ICCV Work. 2009*, pp. 39–46, 2009.

[15] K. Zhang, S. C. Chen, D. Whitman, M. L. Shyu, J. Yan, and C. Zhang, "A progressive morphological filter for removing nonground measurements from airborne LIDAR data," *IEEE Trans. Geosci. Remote Sens.*, vol. 41, no. 4 PART I, pp. 872–882, 2003.

[16] M. Li and D. Yin, "A fast segmentation method of sparse point clouds," *Proc. 29th Chinese Control Decis. Conf. CCDC 2017*, pp. 3561–3565, 2017.

[17] X. Zhang, G. Li, J. Zhao, and Z. Hou, "New triangulation method for surface scattered points," *2014 IEEE Int. Conf. Mechatronics Autom. IEEE ICMA 2014*, pp. 541–546, 2014.

Proceedings of the Fourth International Conference on Communication and Electronics Systems (ICCES 2019)
IEEE Conference Record # 45898; IEEE Xplore ISBN: 978-1-7281-1261-9

Network Traffic Optimization in Hadoop MapReduce through Pre-shuffling

D C VINUTHA
Research Scholar, Dept. of CSE
RNS Institute of Technology, Bengaluru
Associate Professor, Dept. of ISE
Vidyavardhaka College of Engineering, Mysuru.
Visvesvaraya Technological University, Belagavi, Karnataka.
E-mail: vinuthadc@vvce.ac.in

G T RAJU
Professor, Dept.of CSE
RNS Institute of Technology, Bengaluru
Visvesvaraya Technological University, Belagavi,
Karnataka.

Abstract*— MapReduce is a popular programming model for handling Big Data in a Distributed computing Environments. Hadoop is popularly used for short jobs and desires low response time. During shuffling phase, large volume of data generated by the map task needs to be accessed to perform shuffling and sorted before being transferred across the network to the reducers. It may generate huge network traffic and consume high bandwidth. Hence a Pre-shuffling scheme is proposed for shuffle intensive applications in this paper to minimize the network traffic because network connects is likely to become limited resource when many applications subscribe the cluster. Here a push model and two stages pipeline being used in shuffling phase of Hadoop MapReduce. Experiments have been conducted on web server log file of NASA and rnsit.ac.in. Experimental result show that proposed Pre-shuffling scheme substantially reduces the network traffic and slightly faster compared to conventional Hadoop. The proposed push model in the pre-shuffling scheme with 2-stage pipeline reduces the run time by an average of 17.3% for click count application.

Keywords — MapReduce, Pipeline, Push Model.

I. INTRODUCTION

Hadoop is an open source implementation of MapReduce framework. It is mainly utilized to process gigantic data in a parallel and distributed environment, the map function is executed on every input data split and emits <key, value> pair as output. Several map tasks may run in parallel either in single/multiple machines. The intermediate data set having the similar key are transferred to same reducer and the reduce task starts after all the map task generates the output, till then reduce task has to wait, because the execution of reduce task will not take place in parallel with the map task. The map output is sent across the network to the reducers, Shuffle is the process of interaction between the map and reduce task of an application. The quantity of map output delivered from mapper to reducer across the network may have an impact on the execution time. Hadoop applications are categorized into Non-shuffle and shuffle intensive application. In shuffle intensive applications, during shuffle phase, huge quantity of intermediate data are generated, which results into network traffic and consumes high bandwidth and large number of I/O operation.

In this paper, a Pre-shuffling scheme is proposed, where in a fraction of intermediate data emitted by map task will be sent immediately through the pipeline to the reducers. Therefore, it is not necessary for the reducer to wait till the map task generates the complete output. It facilitates the overlapping of data computation and data transfer of map tasks, this may result into reduced the network traffic, data transfer time with improved throughput because of data pipelining. The map and reduce task running in the same node are synchronized to provide the overlapping facility, due to which the execution time required for the shuffle intensive applications is reduced.

The rest of this paper is organized section wise and the details of each section are as follows, in Section II related work is described briefly. Detailed description of proposed method Pre-shuffling scheme is given in Section III and its implementation is mentioned in Section IV. Experimental results are presented and discussed in Section V. Section VI presents the conclusion of this paper.

II. RELATED WORK

MapReduce [4] performs the computations on data intensive applications, log analysis etc, using various computing environment like dynamic cloud and multi-core environments [10].Duxbury et al created a scheme to evaluate the performance of network interconnects on MapReduce. During shuffle phase, large amount of data need to be transferred across the network to the reducer causes high network traffic and consume high bandwidth. Shuffle phase consume maximum time, hence in this paper Pre-shuffling model is introduced to decrease the network load. The intermediate data is aggregated at each node to reduce the quantity of intermediate data to be delivered across the network to reducers [8]. Compared to aggregated technique, for shuffle-

intensive applications the partially masking the latencies for reduce tasks is very efficient.

MapReduce is extended to provision database management systems for processing structured files [7]. Parallel data processing policy called pig system is developed to integrate it with Hadoop. Here the compiler generates the Hadoop programs sequentially. Pig latex, a programming language used for pig to execute the data analysis application in parallel and also provides an opportunity to improve the overall performance.

III. PROPOSED PRE-SHUFFLING SCHEME

MapReduce has map, reduce and shuffle phase. During the shuffle phase the map output is partitioned using hashing function and each partition having similar key is transferred to the same reducer, then reduce function is used to process the assigned partitions. To obtain the intermediate data to the shuffle phase, HTTP requests are sent to the five task trackers (default value) by the reduce task. Job tracker has a list and location of all the task trackers and each task tracker transmits the heart beat message periodically to job tracker. If a map or the reduce task is finished then new task is allocated the job tracker. Also, identifies the reduce task start time, the data block to be processed and separate queue is maintained for map and reduce task.

In conventional MapReduce, i.e, in pull model, each reduce task has to fetch the intermediate data and does not provide synchronization between the map and reduce task. Reduce tasks are not started till the complete intermediate data is received. To reduce the shuffling phase time, push model is proposed called as Pre-shuffling scheme. Here, the intermediate data generated from the map tasks are sent immediately to reduce task via shuffle phase, soon after the intermediate data is emitted. The job tracker allocates map/reduce task to the available task tracker. In Pre-shuffling scheme, map tasks are allowed to identify the partitions to be sent to the reducers. The reduce task sorts and keeps the tuples in the node, on which the reduce task is to be launched. After the map tasks are completed, reduce task applies the reduce function to process the allocated <key, value> pairs.

After the submission of the job, if sufficient slots are available for execution, all the tasks are launched. Then the communication channel is established between the map and reduce task, as each map task chooses the reduce task to push the intermediate data, as soon as the small portion of the data is generated. If sufficient slots are not available to execute the reduce task, the output of the map task is stored in the in-memory buffer, the reduce tasks are launched whenever the free slots are available. Then the data is transmitted from the buffer to the reduce task. In conventional MapReduce, the time required to perform the shuffle phase is greater than the map phase. In order to improve the performance, 2-stage pipeline is used in Pre-shuffling scheme. It sends the data through the pipeline to the reduce task soon after the fraction of data is generated from the map task. It overlaps the execution and data transfer during map phase which in turn results in increased throughput.

Two separate threads are created here. The input data is processed and emits the output using the first thread. As soon as the map task output is generated, it will be delivered immediately to reduce task. These threads execute in parallel using pipeline and store the map task output in the buffers, to avoid sending the data directly to the reducers. Buffer sends the map task output to the reduce task as soon as the fraction of data is generated. Suitable threshold value may be used to represent the size of fraction of data (usually 80% of buffer size). Once the size of buffer reaches the predefined threshold, the intermediate results are sorted based on the keys. then the map task output is stored in local disk. Second thread is triggered to verify the availability of sufficient free slot to launch the reduce task. If the node is ready to launch the task, then the communication channel between the mapper and reducer is created. The aggregated data generated using first stage pipeline is delivered to the reducer during the second stage pipeline. If no nodes are not available to launch the task, then the second stage pipeline waits till the map output is received by reduce task. The main objective is to improve the throughput during the shuffle phase using pipeline.

In Pre-shuffling scheme, the amount of data to be sent from map task to reduce task can be controlled dynamically by configuring the buffer size. Large value of threshold represents the huge volume of map output to be delivered to the second stage pipeline. Lesser value of threshold represents each portion to be pushed to the reduce task is large. If the network connects are not overloaded, then the performance of the map task will become bottleneck, to overcome from this, buffer size is increased, so that large amount of data is pushed to the reduce task. It is suggested to have higher threshold value for buffer size with high speed network interconnects.

IV. IMPLEMENTATION

In MapReduce, Map phase has *Map* and *Map-transfer*, the map task processes the input data and then sorts and stores the output into the in-memory buffer. Sort operation will create the partitions consisting of all the tuples having the same key. The map output stored in the buffer is sent to the reducer during map-transfer phase. Reduce task is split into two phases: *shuffle* and *reduce*. Reduce task receives the map output and merge sort is applied on the map task output. The shuffle phase consumes largest time, as it performs merging and sorting operation on the large amount map output. Therefore in the Pre-shuffling scheme, as soon as the data of the map output is generated, aggregate and sort operations are immediately performed. Reduce task applies the merge sort function after receiving the complete map output from all the map tasks during the Pre-shuffling scheme.

Master node observes every task performance and assigns progress score between the range [0, 1]. The value of the progress score for the map task depends on the amount of

input data processed. Pre-shuffling scheme, monitors the progress of reduce task and assigns progress score value, It depends on what amount of data is distributed to the different phases of reduce task, it combines the progress score and the intermediate data, then reduce task receives the partition and the associated partition score. The reduce task progress is estimated by taking the mean progress score of entire corresponding partitions.

In heterogeneous cluster, different nodes execute tasks at different speed. After the considerable progress of reduce task, progress score is stored into a temporary file on HDFS. In this proposed work, the map task output is sent immediately to reduce task using pipeline. This overlaps the transfer time between the mappers and reducers and improves the throughput. During the network congestion in the cluster, Pre-shuffling and the pipeline method shows significant improvement in the performance of the Hadoop MapReduce.

V. Experimental Results and Discussion

For analyzing the performance of Pre-shuffling scheme, Hadoop cluster is created using 10 data nodes and every computing node in the cluster is furnished with two dual-core 2.4GHz processors, 2GB main memory and an operating system Ubuntu 10.4 is used to conduct experiment. The block size is varied to evaluate the performance. Data replication feature is not considered during the evaluation, because the Pre-shuffling scheme with replication substantially improves the performance of the Hadoop. To evaluate the performance Click count application is executed on the Academic and Research Webserver log file such as NASA and rnsit.ac.in with 1 GB data set. Figure 1 display the completion time for both map and reduce task of Click count application on Hadoop with and without Pre-shuffling scheme. Figure 2 shows the execution time for Click count application with 1GB dataset on Hadoop with and without Pre-shuffling scheme. It is found that the proposed scheme decreases the execution time by 17.3% compared to conventional Hadoop. In Figure1, it is also observed that the reduce task begins after the entire map tasks complete their execution. Where as in the proposed scheme, Reduce task starts execution almost soon after the map task has begun. In conventional Hadoop, the map task has completed its execution almost at 50 seconds and at 60 seconds in the proposed work, because some of the operations of the shuffle phase is performed by the map tasks, instead of reduce task in the conventional MapReduce. The Pre-shuffling phase handled by the map task is an effective method to reduce the load on the reduce tasks. Therefore, the proposed work completes the execution much faster than conventional MapReduce.

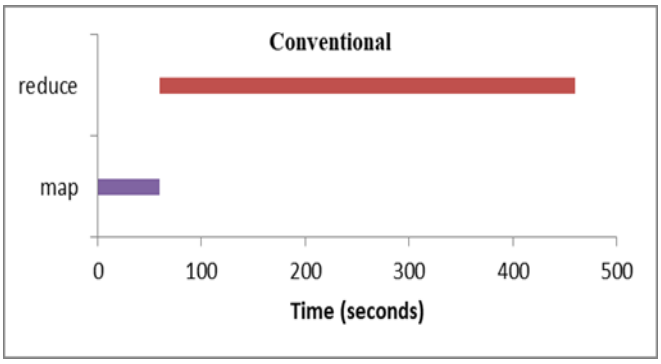

a. Conventional

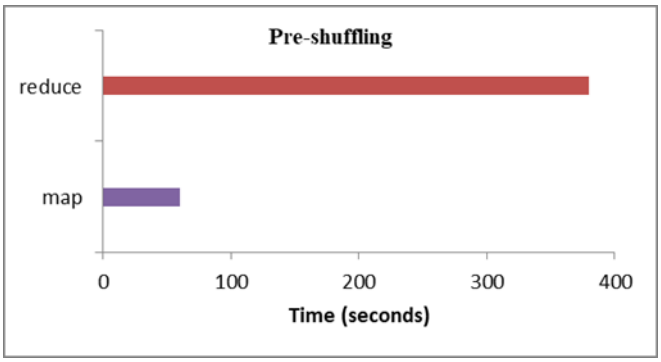

b. Pre-shuffling

Fig 1: Execution Time of both map and reduce task (a) conventional (b) Pre-shuffling Scheme

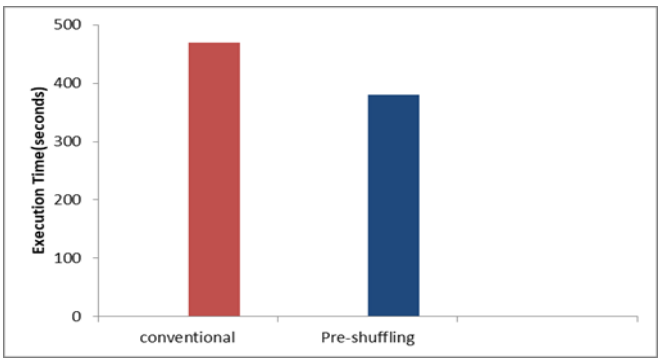

Fig 2: Execution Time of both conventional and Pre-shuffling for click count application with 1GB data set

Experimental results for varied input data blocks

To assess the performance of the Pre-shuffling scheme, Click count application is executed for varied data block size. Figure 3 demonstrates the performance of the Pre-shuffling scheme increases as the block size increases, i.e. from 64MB to 128 MB. Increased block size from 128 MB to 256 MB would results into decrease in the performance by 1.6%.An Experimental results shows the substantial improvement in the

performance of the Hadoop MapReduce using Pre-shuffling method for the block size not greater than 128 MBS.

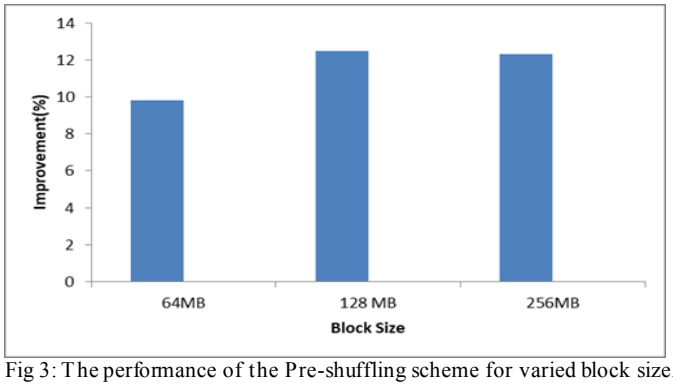

Fig 3: The performance of the Pre-shuffling scheme for varied block size.

VI. CONCLUSION

During shuffle phase, the Shuffle-intensive application generates high network traffic and Disk I/O operations. Hence Pre-shuffling scheme called push model is proposed, here two stage pipelines are used to increase the performance of Hadoop. In Pre-shuffling scheme, map tasks moves the map output across the network to the reducer soon after the data is generated and also reduce task starts execution immediately rather than waiting to receive the complete intermediate data. In first stage pipeline, the aggregated intermediate data of every map tasks are stored temporarily in local buffers. The second stage pipeline identifies the free slots in a node to launch the reduce tasks, and then establishes the communication channel to transfer the intermediate data. Click count application has been used to evaluate the performance. Experimental results revealed that execution time using Pre-shuffling scheme is improved by 17.3% compared to conventional Hadoop. Pre-shuffling scheme *has* improved the execution time by utilizing the resources effectively. In Pre-shuffling scheme, as the size of the input data is unknown, deciding the start time of the reduce task is a challenge. Hence, some adaptive algorithms need to be developed in future.

REFERENCES

[1]. B. He, W. Fang, Q. Luo, N. Govindaraju, and T. Wang. Mars: a MapReduce framework on graphics processors. ACM, 2008.

[2]. Cheng-Tao Chu, Sang Kyun Kim, Yi-An Lin, YuanYuan Yu, Gary R. Bradski, Andrew Y. Ng, and Kunle Olukotun. Map-reduce for machine learning on multicore. In NIPS, pages 281–288, 2006.

[3]. Tyson Condie, Neil Conway, Peter Alvaro, Joseph M. Hellerstein, Khaled Elmeleegy, and Russell Sears. Mapreduce online. In Proceedings of the 7th USENIX conference on Networked systems design and implementation, NSDI'10, pages 21–21, Berkeley, CA, USA, 2010.USENIX Association.

[4]. J. Dean and S. Ghemawat. Mapreduce: Simplified data processing on large clusters. OSDI '04, pages 137–150, 2008.

[5]. Adam Dou, Vana Kalogeraki, Dimitrios Gunopulos, Taneli Mielikainen, and Ville H. Tuulos. Misco: a mapreduce framework for mobile systems. In Proceedings of the 3rd International Conference on PErvasive Technologies Related to Assistive Environments, PETRA '10, pages 32:1–32:8, 2010.

[6]. Apache Software Foundation. The pig project. http://hadoop.apache.org/pig.

[7]. Eric Friedman, Peter Pawlowski, and John Cieslewicz. Sql/mapreduce: a practical approach to self-describing, polymorphic, and parallelizable user-defined functions. Proc. VLDB Endow., 2:1402–1413, August 2009.

[8]. Michael Isard, Mihai Budiu, Yuan Yu, Andrew Birrell, and Dennis Fetterly. Dryad: distributed data-parallel programs from sequential building blocks. SIGOPS Oper. Syst. Rev., 41:59–72, March 2007.

[9]. Heshan Lin, Xiaosong Ma, Jeremy Archuleta, Wu-chun Feng, Mark Gardner, and Zhe Zhang. Moon: Mapreduce on opportunistic environments. In Proceedings of the 19th ACM International Symposium on High Performance Distributed Computing, HPDC '10, pages 95–106,New York, NY, USA, 2010. ACM.

[10]. Fabrizio Marozzo, Domenico Talia, and Paolo Trunfio. A peer-to-peer framework for supporting mapreduce applications in dynamic cloud environments. In Nick Antonopoulos and Lee Gillam, editors, Cloud Computing, volume 0 of Computer Communications and Networks, pages 113–125. Springer London, 2010.

[11]. C. Ranger, R. Raghuraman, A. Penmetsa, G. Bradski, and C. Kozyrakis.Evaluating mapreduce for multi-core and multiprocessor systems. High-Performance Computer Architecture, International Symposium on, 0:13–24, 2007.

[12]. Raplesf. Analyzing network load in map/reduce.http://blog.rapleaf.com/dev/2010/08/24/analyzing-network-lo

[13]. Yuan Yu, Michael Isard, Dennis Fetterly, Mihai Budiu, U´ lfar Erlingsson,Pradeep Kumar Gunda, and Jon Currey. Dryadlinq: a system for generalpurpose distributed data-parallel computing using a high-level language.

[14]. In Proceedings of the 8th USENIX conference on Operating systems design and implementation, OSDI'08, pages 1–14, Berkeley, CA, USA,

Proceedings of the Fourth International Conference on Communication and Electronics Systems (ICCES 2019)
IEEE Conference Record # 45898; IEEE Xplore ISBN: 978-1-7281-1261-9

Intelligent Edge Security with Dynamic Task Offloading in Fog Environment

Albin Mathew
Dept. of Computer Science and Engineering
N. S. S. College of Engineering
Palakkad, Kerala, India
albin.mathew@outlook.com

Namboodiri E I Deepu
Dept. of Computer Science and Engineering
N. S. S. College of Engineering
Palakkad, Kerala, India
eidn.97@gmail.com

Dr. Maya Mohan
Assistant Professor
Dept. of Computer Science and Engineering
N. S. S. College of Engineering
Palakkad, Kerala, India
mayajeevan@gmail.com

***Abstract*— Latency-aware computation is required for prominent technologies like Internet of Things. Things that are connected in IoT environments generate large volumes of real-time data which are generally processed in the cloud. But, the processing of these generated data entirely on the cloud cannot be considered as an efficient solution for time-sensitive IoT applications. To address this issue, a new paradigm, Fog computing, was proposed. Fog computing essentially extends cloud computing and services to the network edges, thus bringing most of the capabilities of the cloud much closer to where the data source is located. Time series analysis is a class of machine learning algorithms that provides deeper insights about the future. The latest trends consist of using deep learning algorithms for performing time series analysis, which have proved to be more efficient than the traditional statistical approaches. This paper aims to replicate a current day Industrial Internet of Things (IIoT) scenario by simulating a secure fog computing environment in which the edge data centers are authenticated by a Certificate Authority, perform time series analysis over pre-collected dataset using Long Short Term Memory (LSTM) neural networks and forecast the required result, along with an intelligent optimization of the network using an efficacious dynamic task offloading mechanism in a secure way.**

Keywords*— *Fog Computing, Internet of Things, Deep Time Series Analysis, Task Offloading, Security, Load Balancing

I. INTRODUCTION

Cloud computing is a method for delivering Information Technology (IT) services in which resources are retrieved from the Internet through web-based tools and applications, instead of a direct connection to a server. Cloud provides three service models: Infrastructure as a Service (IaaS, Platform as a Service (PaaS) and Software as a Structure (SaaS), and enough security features measures. Cloud computing has several advantages and disadvantages as well. But with the change in the networking connectivity and different needs, the cloud computing model has been extensively in use even though it possesses some major potential disadvantages.

Fog computing is extending the cloud computing paradigm network to the edge of the network from the network core. It is an example of highly virtualized platform which provide storage of data, computations, and other networking services between end devices and traditional cloud servers. Fog computing architecture is an arrangement of hardware, and software, and physical and logical elements of the network to implement an IoT network. The major architectural factors include the physical and geographical placements of fog nodes, their hierarchical arrangement, the numbers, types, protocols, topology, and data bandwidth capacities of links between fog nodes, devices, and cloud, the hardware and software design of the individual fog nodes, and how the complete IoT network is established and managed. Fog networks primarily aim at meeting stringent latency requirements, reduced power consumption of end devices, providing real-time data processing, distribution and control of computing resources, and forwarding the network traffic to centralized data centers.

The Fog computing architecture mainly consists of end devices (sensors, mobile devices etc.), edge devices (routers, base stations etc.), Edge Data Centers, which are data centers with limited processing and storage capabilities and Cloud which acts as the central storage having greater processing capabilities. Edge data centers (EDCs) are deployed to reduce the processing and propagation. The nature of EDCs deployment in practice is distributed and they are position between cloud and data sources. Effective load balancing strategies are implemented to reduce the job response time and to improve resource utilization in Fog environment.

Since Fog is a distributed environment, it is susceptible to many security vulnerabilities in the programmability, naming, privacy and scalability such as data tampering, Denial of Service attack, information injection, manipulation, privacy leakage etc. The measures for providing security of data are confidentiality, integrity, availability and privacy requirements. Confidentiality ensures that only the communicating entities have access to the data that is being transmitted. The correct and consistent delivery of data to the authorized users without any undetected modification is achieved by integrity mechanisms. Also, the data should be available to the authorized intended recipients at the required point of time. Authentication and access control is the process of establishing proof of user's identities and providing access to only those users. Finally, privacy requirements ensure the secrecy of all the information and services.

Time series is a continuous or discrete sequence of observations recorded at regular intervals of time. Time Series Analysis is referred to the process of making predictions about the future on the basis of time series data.

In time series analysis, the time period can be measured in any suitable unit of time. The process of using neural networks for forecasting the future values of a time series is known as Deep Time Series Forecasting. There are numerous applications including forecasting and utility studies that employ these methods.

II. RELATED WORKS

In [1] Zhang G.P proposed a hybrid method for time series analysis which combines both Auto-Regressive Moving Average (ARIMA) model and Artificial Neural Network (ANN) model. In [2] Xiaojun C. et al. presents a system that monitors and forecasts air pollution in real-time using IoT. According to the relationship between the pollutants concentration in the last 24 hours and concentration of current pollutants, next 24 hours' network for prediction is established. In [3] Mitra P. et al. proposed a IoT-based approach on a mesh-connected wireless sensor node that uses a simple ANN model for flood forecasting purposes. In [4] Angshuman Ray et al. presented a model that uses ANN for predicting air pressure where the development, training and testing of the model with ground-level air pressure which was collected over a 7-year period. The difficulties that are faced while training artificial neural networks with continuous time-series data were overcame using the model developed in [4].

In [5] Hu P. et al. proposed a framework for face identification and resolution based on fog computing to improve the processing capability and save bandwidth. Security issues includes intrusion detection, data management issues, malicious detection technique, man-in-the-middle attack, data protection, malicious fog node problem. In [6] Alrawais A., et al. provide a scheme and show its usage of fog computing for improving the efficiency of certificate-revocation distribution in connected environments like IoT. In this paper they also give a summary of the major challenges in security and privacy of IoT environments.

In [7] Ningning S., et al. study the architecture of a fog environment and build a graph model of the fog layer and use the vertices to represent the data dependencies between tasks, and edge indicates the link bandwidth. In [8] Verma S, et al. proposed a Load Balancing architecture for the Fog environment. The time required for the clients to access the resources increases with the increase in the distance of servers in Cloud environment. Therefore, the resources are brought as close as possible to the end users in Fog environment to solve this problem.

III. PROPOSED WORK

A. System Design

The technical specifications and requirements were thoroughly analyzed and studied in order to design the system. System design thus had been an approach to solve the issue of creation of the system. Fig 1 describes the design of the proposed system. Initially, a network is created using a no. of Raspberry Pi and a PC which acts as a server. All the Raspberry Pi's except one act as the Edge Data Centers. The one that is not considered as an Edge Data Center is used to send the Air Quality data to the EDCs present in the network. The server device is used to authenticate the EDCs and perform the load balancing. All the EDCs are authenticated at the beginning itself so that the entire system remains secure. The data to be processed from the data sending Pi to the EDCs takes place only after ensuring that the EDC is an authenticated one. Once the data is received at an EDC, it performs the processing. Here, the EDCs perform deep learning using Long Short Term Memory neural networks and perform the pollution forecasting, if any of the EDCs is overloaded, it shares its load to another EDC, only after assuring the authenticity of the destination EDC, and the EDC performs the time series analysis. The load balancing over the Fog environment is done in a dynamic and a secure way.

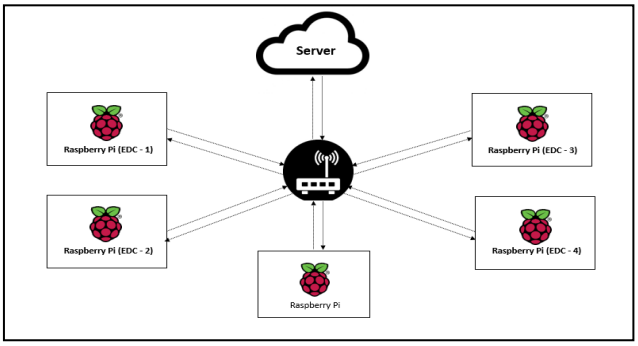

Fig. 1 The Proposed system

B. Secure Authentication

The security of the entire system works on the most fundamental assumption that the server is already secured by some means of hardware installations like the Trusted Platform Module (TPM). Therefore, this server system is considered to be Certificate Authority that performs the authentication of the Edge Data Centers in the network.

A certificate authority (CA) is a credible entity that manages and issues digitally signed documents called digital certificates to the requesting entities. A digital certificate is a kind of document which contains information about the issuer of the certificate and also the information about the requesting entity such as its public key, name, organization, contact information and date of expiration. Whenever an entity needs to be authenticated and if it doesn't have a digital certificate, it requests for one to the CA. The CA verifies the identity of requesting entity and generates a certificate for the applicant, signs it with private key of CA. These certificates can be used at a later time for authentication purposes between entities. Any entity of the system can verify that the certificate is signed by CA using the public key of CA.

In this system, the server, which is the Certificate Authority, issues a self-signed certificate for itself, making it an authenticated entity. The cryptographic algorithm RSA, one of the most efficient algorithms for key management, is used for the public-private key pair generation for the digital certificate. The keys generated using RSA are of 4096 bytes. The digest method used for signing the certificate is SHA-256, and the validity period of each certificate is set to 1 year. Now, the server and the Edge Data Centers generate public-private key pairs of length 4096 bytes, and request the Certificate Authority for getting their certificates signed by the Certificate Authority. The Certificate Authority creates a public key-ring among the Fog nodes by

broadcasting all the public keys to each node. A key-ring is a file that consists of encryption keys. In this case, the public keys are stored, forming a public key-ring. If any EDC wants to send a message to other devices present in the network, it looks up the public key of the corresponding the device to which the message is to be sent, and encrypts the message using this public key. The message can be decrypted by the receiver using its own private key. The certificate generation algorithms are described in Fig 2. The network created in the work consists of five Raspberry Pi's, among which four are chosen to be the Edge Data Centers, and the remaining one is selected as the client device, which has the entire dataset in its storage and sends the data as parts to other EDCs.

The Fog environment is now fully set-up and fundamental security measures are implemented in the system. Next, the data has to be sent to the EDCs present in the network.

Certificate Generation for Certificate Authority

1. If(no self-signed certificate available OR certificate is expired)
2. Create public-private key pairs.
3. Generate certificate signing request .
4. Self-sign the certificate.
5. Add public key to the public key-ring.

Certificate Generation for Edge Data Centers

1. If(no certificate available or certificate is expired)
2. EDC creates public-private key pairs.
3. EDC generates certificate signing request and sends to CA.
4. CA asks for the passphrase.
5. EDC provides the passphrase.
6. If(valid passphrase)
7. CA generates certificate and signs it.
8. Adds EDC to the authenticated list.
9. Sends the certificate to EDC.

Fig. 2 Certificate Generation algorithms

As mentioned before, the one Raspberry Pi, in which the entire dataset is stored, when compared to the industrial implementation, is actually a data generating devices like sensors present at the topmost layer of the Fog computing paradigm. Just like the sensors send the real-time collected data to the EDCs, similarly that single Raspberry Pi sends the data to the EDCs as well. But the difference here is that, the data that is sent to the EDCs is sent in a very secure way.

As per the Fog computing paradigm, only small volume of data that is collected is sent to the EDCs for the necessary processing. Similarly, the client Raspberry Pi, sends only 1000 records from the whole dataset to each EDC. In our system, the client sends the data to any random EDC. Well it has to be noted that data is sent over to only authenticated EDCs.

When the client sends the data to an EDC, the client Raspberry Pi sends its public key to the EDC. The EDC then generates a session key. A session key is a randomly generated key which is used for symmetric encryption and decryption of confidential data that ensures secure communication between two communicating entities. This session key is encrypted using public key of the EDC and sends it to client EDC. The session key can be decrypted only by the intended client EDC using its own private key. Now the communication is made secure and both of them have session keys safely stored with them.

Next the data that is to be sent has to made secure so that no one can use this information that is being sent between them. The data, that is, the 1100 records, are first hashed using SHA-256 (Secure Hash Algorithm 256). SHA-256 is a powerful cryptographic hash function which takes input of any size and produces a 256-bit (32-byte) hash value known as a message digest. This ensures the integrity of the data that is sent. After hashing, the data and the hash value are appended together into one single entity, and encrypted using the AES-256 (Advanced Encryption Standard 256) algorithm. AES is the US government standard for symmetric key block cipher encryption and decryption. It is 128-bit block cipher which can choose key size from 128, 192, 256 bits. The design of AES is based on a substitution permutation network (SPN). The key that is used here for performing the AES operation is the session key that was generated before. Now the data that is to be sent is now secure. This data is sent to the EDC, which performs the decryption operation and stores the data. Once the EDC has the data with it, it runs the LSTM on the data. Once successfully completed, the results are stored into a file. This is how data is sent to all the EDCs in an authenticated manner (described in Fig 3) and once the data reaches the EDC, the LSTM is performed over the data and results from each EDC are appended to the bottom of a single file in the server. After the intermediate results are received, a single variate LSTM is performed over the intermediate results, and the RMSE value is computed.

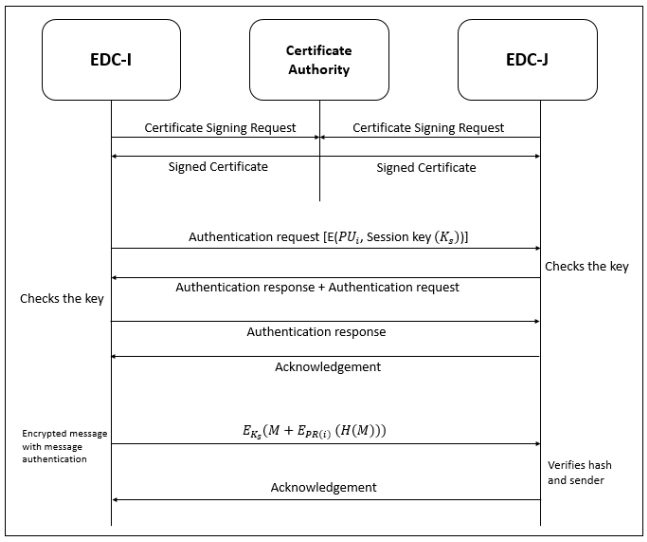

Fig. 3 Secure communication workflow

C. Dynamic Task Offloading

Load balancing is an efficiency improvement strategy in which the workload is distributed among multiple computing resources such as clusters, network links, computer nodes etc. The main aim of load balancing is the optimization of resource usage in minimized response time with maximum throughput. It generally considers multiple factors instead of a single component to increase the reliability and availability. Usually, task offloading involves dedicated software or hardware such as multilayer switch or a DNS server process. In our system, load refers to the CPU load, and along with that, the Memory load, Disk load and the thermal heat is also considered. The task offloading to

other EDCs is based on the values of CPU load of the EDCs.

In the previous section, the secure authentication and communication between the Fog nodes have been explained in detail. The load balancing occurs when the data reaches the EDC. When the data is received by the EDC, it checks its own load, that is the CPU load value. An EDC is considered to be overloaded if the value of the CPU load is greater than or equal to 85%. After checking the load, if it is not overloaded, then the LSTM can be run on the EDC. If the EDC is overloaded, using the Breadth First Search algorithm, it broadcasts requests for the current load information to every EDC in the network. After getting load information from all the EDCs, it sorts all the load information received and selects the EDC with the most minimal load. The data is then sent to the EDC with the most minimum load, and the results are stored in the same file. And if, all the EDCs are overloaded, then the data is sent to the server, and it performs LSTM as a sub-process, the only reason being a PC does not have that processing overhead. This process continues until the entire dataset is sent from the client Raspberry Pi to the EDCs. Note that load balancing is done only after authenticating the EDC to which next data is to be sent, and processed. The load balancing algorithm is described in Fig. 4.

Load Balancing algorithm

```
1.  If(EDC-I is overloaded)
2.    EDC-I broadcasts load request to all EDCs.
3.    Upon receiving the request;
4.      EDC-J determines its current load.
5.      EDC-J sends its load information alongwith its identifier.
6.    Upon receiving load information from all EDCs;
7.      EDC-I checks for EDC with minimum load.
8.      If found
9.        Sends the data to that EDC for processing.
10.     If not found
11.       Sends the data to the upper layer of Fog architecture.
```

Fig. 4 Load Balancing algorithm

D. Long Short Term Memory Neural Network

Unlike the feed-forward neural network, RNNs contain hidden states which are distributed across time, which allows to store a lot of past information efficiently. The core idea is that recurrent connections ensures memory of previous inputs to persist in the internal state of the network, and thereby influence the output of the network. At each time step, the network processes:

1.The input attributes (x_t)
2. Updates its hidden state via activation functions (y_t) and
3. Uses it to make a prediction of its output (z_t).

These steps are similar to the general feed-forward neural networks. However, the value held in the delay unit is fed back to the hidden units as additional input. The delay unit enables the network to have short-term memory. This is because it stores the hidden layer activation values and/or output values of the previous time step. At the subsequent time step, it releases these values back into the network. In other words, the RNN has a "memory" which stores information about those calculated by the hidden units at an earlier time step. Time-series data contain patterns ordered by time. Information about the underlying data generating mechanism is contained in these patterns. Since the delay unit exhibit persistence, RNNs take advantage of this ordering. It is this "short term" memory feature that allows an RNN to learn and generalize across sequences of inputs.

The memory block contains a memory cell and three multiplicative gate units - the input gate, the output gate, and the forget gate. After activation of input gate, the input is multiplied with memory block, output is multiplied with output gate and all the preceding cell values are multiplied with forget gate. The gates control the information flow into and out of the memory cell.

The Role of Gates: Long term dependencies in LSTM are explicitly modeled using gating mechanism. The input, forget, and output gate learn what information to store in the memory, how long to store it, and when to read it out. By acquiring this information from the data, the network learns how its memory should behave. The input gate gradually learns to protect the cell from irrelevant inputs. It controls the flow of input activations into the memory cell. Information enters the cell when the "write" gate is on and those information remains in the cell as long as it's forget gate is "off". The forget gate allows the cell to reset itself to zero when necessary. The output gate controls the output flow of cell activations into the rest of the network. By turning on its output gate, information can be read from the cell. The LSTM learns to turn off a memory block that is generating irrelevant output.

The working of the memory block system can be considered like this: The input gate takes input from the cell at the previous time-step, and the output gate from the current time-step. A memory block can choose to "forget" if necessary or retain their memory over very long periods of time.

IV. RESULT ANALYSIS

The overall system is secured to the maximum limit as much as possible by using most efficient algorithms for the purpose. The basic network security characteristics are assured in the system:

(i) **Confidentiality**: The proposed system uses AES-256 for encryption purposes. For the key management purpose, RSA has been used in the proposed system, since RSA being one of the most secure algorithms used for key-exchange. RSA is better when compared to other key-exchange algorithms as it is not susceptible to attacks like Man-in-the-Middle attack which is present in Diffie-Hellman algorithm. RSA can also be used for signing digital signatures as well.

(ii) **Integrity**: The messages that are being sent between the Fog nodes are properly hashed using one of the best hashing algorithms SHA-256. Any message that is being sent between the Fog nodes cannot be altered by any intruder. Thus ensuring the integrity of messages.

(iii) **Authentication**: Any message that is sent inside the Fog network is sent only to authenticated nodes. The authentication of these nodes is provided by the server which acts as the Certificate Authority and provides certificates to the nodes that request for one. Only nodes having a signed

certificate from the server are sent the information. The system is secured from the masquerading attack by proper authentication of the Fog devices. This is done by storing specific passphrases in the intended Fog devices. Therefore, when EDCs request for getting their certificates signed from the CA, the CA asks the EDCs to provide the passphrase in return. If the EDCs provide the valid passphrase, they get their certificates signed by the CA. Hence if any device somehow enters the network, and requests the CA for getting its certificate signed, the request will be eventually declined by the CA as this malicious device does not know what is the passphrase. Another authentication technique that is introduced in the system is the message authentication between EDCs to ensure that neither of the EDCs can later deny that they haven't sent the message. This is done by hashing the message and encrypting it using the sender EDC's private key which can be decrypted using the sender EDC's public key, which makes the system secure from the repudiation attack.

A. Security Evaluation

The system was subjected to many cryptographic attacks and the results were thoroughly analyzed:

1. Masquerade attack: All of the EDCs have a passphrase stored in them initially. The CA asks for the specific passphrase from the EDC when it requests the CA for getting its digital certificate signed. If the entered passphrase is the valid one, then only the CA signs the certificate coming from the EDC, therefore any other device which tries to pretend as any of the EDCs present in the network cannot even request the CA for signing its request as the device which tries to masquerade an EDC will not have the passphrase with it.
2. Message Modification attack: The proposed system checks for the integrity of the messages that are being sent over the network. The integrity is checked using the hashing algorithm SHA-512 which produces a hash for the message. This hash is validated when the message is received. If the hash value is invalid, then a receiver informs sender to resend the message as the receiver understood that the message has been modified by and intruder.
3. Repudiation attack: In the proposed system, proper message authentication mechanism is incorporated. The message that is being sent is initially hashed by the sender, encrypted using the sender's private key, and then sent to the receiver. The receiver after the getting the message decrypts it using the sender's public key, thus ensuring that the sender cannot refuse later that it ever sent a message.
4. Denial-of-Service attack: The proposed system is invulnerable to masquerade attack as a proper defensive mechanism been taken in the initial stages itself. The DoS attack is very much prevented by keeping a list of authenticated devices in all the EDCs. If in case, a malicious EDC somehow enters the Fog network and starts sending communication requests for performing a DoS attack, the communication with that EDC does not proceed until it is verified that it is an authenticated device by looking in the list of authenticated EDCs. The requests coming from EDCs are multithreaded inside the network, therefore the thread dies if any request from an unauthenticated device is received. The DoS attack is very difficult to handle as it needs very powerful servers to handle the excessive incoming requests coming from different devices based on their time, and block the malicious device for some time. The proposed system does not use powerful EDCs, therefore the DoS attack could be prevented only up to a limit because of the performance constraints of the devices used.
5. Key Brute Force attack: The proposed system uses RSA algorithm for generating the public-private key pairs. The RSA algorithm generates keys of size 4096 bytes. Therefore, it takes centuries to break the keys even if powerful quantum computers are utilized.
6. SSH Brute Force attack: The proposed system is secured from the SSH brute force attack by using passwords that cannot be easily determined for accessing the root. Passwords consisting of special symbols, numbers, upper and lowercase letters and of length 12 characters.
7. Dictionary attack: The proposed system is made invulnerable to dictionary attack by assigning passwords that are not at all present in the dictionary.

B. Load Balancing

The factors that were considered for offloading the tasks are:

1. CPU Load: It is the percentage of the processing workload over CPU. This is the major factor that determines whether the load has to be shared with other Fog nodes or not as processing is what it matters in the Fog architecture.
2. Memory Load: It is the percentage of memory that is currently being used up.
3. Disk Load: It is the percentage of disk that is currently being used up.
4. System Temperature: It is the current temperature of the system. The temperature of the system is another factor as the Fog nodes become more heated up with the increase in temperature, and may get destroyed if more processing load is given to these heated up Fog nodes.

The factors mentioned above for a Fog node decide how the load balancing is performed in the Fog environment. A specific threshold value has been set for each of the factors before-hand. If any of the Fog node has reached the threshold value for any factors, then that node is not considered for sharing the task from other Fog nodes. If all the EDCs are overloaded or heated up, then the PC which acts as the server system is given all of the task based on the assumption that a PC has better system cooling capabilities

and can handle more tasks when compared to the smaller edge devices.

The performance of the load balancing algorithm in the proposed system depends upon the latency in the Fog environment, that is, the time taken for processing the dataset in the Fog environment. It was reported to be 270 seconds on an average with load balancing whereas it was found to be greater without load balancing.

C. Deep Learning

The performance plot of the time series analysis in Cloud environment is shown in the Fig 5. The RMSE value for the analysis in the Cloud environment was found to be 0.031 on normalized values of pollution for the entire test data points. The Fog architecture also brings up an RMSE value very much closer to that observed in the cloud environment and was found to be 0.0386. This is illustrated in Fig 6. The predictions from both environments were found to be similar.

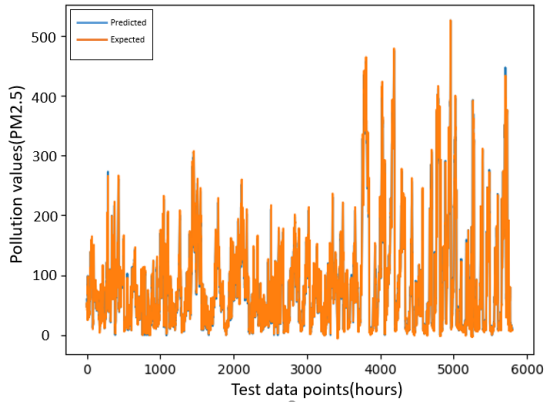

Fig. 5 Line Plot of LSTM Forecast v/s Expected Values in cloud environment

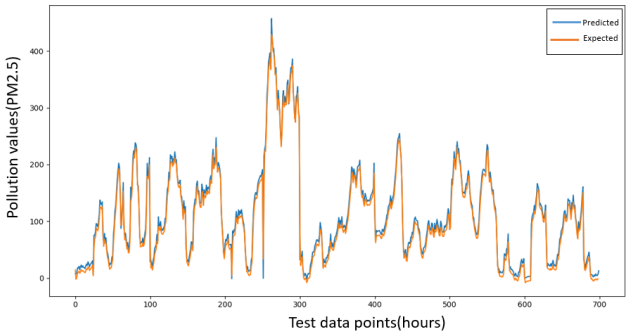

Fig. 6 Line Plot of LSTM Forecast v/s Expected Values in Fog environment

V. CONCLUSION

All the study that has been carried out in this work are by identifying the factors that adversely affect an IoT ecosystem when integrated with a cloud, thus explaining why a new paradigm known as Fog Computing came into existence. Even though the Fog computing environment is a very much optimized IoT network, it still possesses many major issues like security over the network and lack of proper task offloading mechanism since IoT devices are very small and have only limited processing capabilities. Thus overall aim is to create a Fog Computing environment using IoT devices and process a time series data collected before-hand using one of the most efficient deep learning algorithms inside the fog environment and also solve the security and task offloading issues by deploying an intelligent and secure load balancing technique. In future, the work can be extended to wireless, mobile, dynamic and scalable Fog networks, which may have multiple hops in between, with support for multiple applications in different domains.

REFERENCES

[1] Zhang, G.P., 2003. Time series forecasting using a hybrid ARIMA and neural network model. *Neurocomputing*, *50*, pp.159-175.

[2] Xiaojun C., Xianpeng L. and Peng, X., 2015, January. IOT-based air pollution monitoring and forecasting system. In *Computer and Computational Sciences (ICCCS), 2015 International Conference on* (pp. 257-260). IEEE.

[3] Mitra P., Ray, R., Chatterjee, R., Basu R., Saha P., Raha S., Barman R., Patra S., Biswas S.S. and Saha S., 2016, October. Flood forecasting using Internet of things and artificial neural networks In *Information Technology, Electronics and Mobile Communication Conference (IEMCON), 2016 IEEE 7th Annual* (pp. 1-5). IEEE.

[4] Angshuman Ray, Sourav Mukhopadhyay, Bimal Datta, Srimanta Pal, "Prediction of Atmospheric Pressure at Ground Level using Artificial Neural Network". International Journal of Research in Computer Science, 3 (1): pp. 11-18, January 2013.

[5] Hu, P., Ning, H., Qiu, T., Song, H., Wang, Y. and Yao, X., 2017. Security and privacy preservation scheme of face identification and resolution framework using fog computing in internet of things. *IEEE Internet of Things Journal*, *4*(5), pp.1143-1155.

[6] Alrawais, A., Alhothaily, A., Hu, C. and Cheng, X., 2017. Fog computing for the internet of things: Security and privacy issues. IEEE Internet Computing, pp.34-42.

[7] Ningning, S., Chao, G., Xingshuo, A. and Qiang, Z., 2016. Fog computing dynamic load balancing mechanism based on graph repartitioning. China Communications, 13(3), pp.156-164.

[8] Verma, S., Yadav, A.K., Motwani, D., Raw, R.S. and Singh, H.K., 2016, March. An efficient data replication and load balancing technique for fog computing environment. In Computing for Sustainable Global Development (INDIACom), 2016 3rd International Conference on (pp. 2888-2895). IEEE.

[9] J. Zhang, B. Chen, Y. Zhao, X. Cheng and F. Hu, "Data Security and Privacy-Preserving in Edge Computing Paradigm: Survey and Open Issues," in IEEE Access, vol. 6, pp. 18209-18237, 2018.

[10] W. Yu et al., "A Survey on the Edge Computing for the Internet of Things," in IEEE Access, vol. 6, pp. 6900-6919, 2018. doi: 10.1109/ACCESS.2017.2778504

[11] Yi, Shanhe, Zhengrui Qin, and Qun Li. "Security and privacy issues of fog computing: A survey." In International conference on wireless algorithms, systems, and applications, pp. 685-695. Springer, Cham, 2015.

[12] Puthal, D., Obaidat, M.S., Nanda, P., Prasad, M., Mohanty, S.P. and Zomaya, A.Y., 2018. Secure and Sustainable Load Balancing of Edge Data Centers in Fog Computing. *IEEE Communications Magazine*, *56*(5), pp.60-65.

[13] Shi, Weisong & Dustdar, Schahram. (2016). "The Promise of Edge Computing." Computer. 49. 78-81. 10.1109/MC.2016.145.

Proceedings of the Fourth International Conference on Communication and Electronics Systems (ICCES 2019)
IEEE Conference Record # 45898; IEEE Xplore ISBN: 978-1-7281-1261-9

Selection of Optimal Renewable Energy Resources in Uncertain Environment Using ARAS-Z Methodology

Nisha Rathore, M.P.Singh
Department of Computer Science and Engineering,
National Institute of Technology Patna,
Patna-800005, Bihar, India
nisha.rathor271@gmail.com, mps@nitp.ac.in

***Abstract*— In the modern era of globalization, an alarming increment in energy consumption is perceived all over the world which results in the scarcity of primary energy resources in the near future. Due to expeditious economic growth and increasing population, many countries are planning to explore existing Renewable Energy (RE) sources to fulfill increasing energy demand. Selection of suitable alternative RE must be addressed in multi-criteria decision making (MCDM) problem because it involves multiple criteria which are conflicting in nature. This paper proposes an integrated method which is a combination of Additive Ratio Assessment (ARAS) method and Z-numbers. The proposed method namely ARAS-Z, Z-number is used to consider the degree of self-confidence along with the fuzzy number to handle the uncertainty involved in the human judgment used in the evaluation of criteria weights. ARAS is applied for the assessment and prioritization of feasible alternative RE sources based on utility degree. A comparative analysis of the proposed method is done with other MCDM methodologies for checking the effectiveness and capability of the proposed methodology.**

Keywords*— *Renewable Energy Selection, TFNs, MCDM tools, Z-number, Ranking of FNs, ARAS method.

I. INTRODUCTION

In this modern era, Energy becomes an important globally discussed issue. The rising population, rapid economic developments, and technological advancements lead to a huge energy demand for all over the world. The expanding industrialization improves the living standard of people but on the other side, it leads to the rise of global energy demand at a surprising rate. The rising energy demand has been fulfilled by fossil fuels such as petroleum, coal and natural gases. The different countries have different primary energy reservoir and some countries have a limited amount of reservoir that they are unable to fulfill their growing energy demands. The primary resources also have various adverse effects on the environment such as ejection of greenhouse gases and these resources also requires a heavy amount of conservation cost, high maintenance, and pricey in nature. As a result of these issues, developing alternative energy resources is necessary. One remarkable kind of alternative energy sources is non-conventional sources.

In the Paris agreement, India sets an aim to obtain 40% of its total electricity production from non-conventional energy sources by 2030 [1], [2]. A prototype is drafted by the Central Electricity Authority in which 57% of the total electricity capacity will be generated from Renewable Energy (RE) sources by 2027 [3]. So, there is a need to make an effective transition from primary resources to RE sources. Adopting and choosing RE sources is a multi-criteria decision making (MCDM) problem that incorporates both quantitative and qualitative aspects such as technical, environmental, political, economic, and social which are conflicting in nature. MCDM methodologies are efficient methods that are used for the assessment of various RE sources and further used to rank them in order to select the best one.

II. LITERATURE REVIEW

In past research, numerous MCDM approaches have been used widely in the field of RE resource selection. San Cristobal [4] presents the VIKOR method combined with the AHP methodology used to estimate the weights of the criteria and then rank the alternatives resources in order to select the best RE investment project for Spain. Abdolreza et al. [5] present COPRAS methodology integrated with AHP to estimate and evaluate the RE project. Chatzimouratidis and Pilavachi [6] and many other researchers applied an AHP methodology to evaluate the best alternative RE resources considering both quantitative and qualitative criteria.

But the prioritization of suitable alternative RE resources while considering several conflicting criteria becomes more challenging decision process due to the presence of incomplete information and uncertainty in human thought. So, to handle it the concept of fuzzy set theory is used. Turskis and Zavadskas [7] present ARAS method in the fuzzy environment to obtain an appropriate site among several alternatives for the logistics center. Wang, Luo and Hua [8] and Tasri and Susilawati [9] present fuzzy AHP to evaluate the conflicting criteria in an uncertain environment and rank the alternatives in order to select the optimal one. Wang, Huang, Chai and Nguyen [10] propose the TOPSIS method integrated with FAHP for the selection of wind power plants site in Vietnam.

Even though fuzzy numbers have the capability to handle the ambiguity and vagueness, but it is unable to consider the degree of self-confidence of information. To overcome this limitation Zadeh [11], introduced the concept of Z-number. The fuzzy

number along with the certainty degree (reliability) is coined as Z-number which has more expressive power as compared to fuzzy numbers. Chatterjee and Kar [12] present the COPRAS method integrated with Z-number to obtain the optimal RE resource among various feasible alternatives. Z-number concept is practiced successfully in distinct fields to resolve complex MCDM problems, but in the field of RE resource selection, the application of Z-number is little and restricted.

This paper proposes an Additive Ratio Assessment (ARAS) methodology integrated with Z-number and Ranking of generalized fuzzy number concept to choose an appropriate RE alternative. Decision makers (DM) compare the various criteria in a fuzzy environment considering the degree of self-confidence then decision matrix is evaluated to obtain fuzzy weights and to get crisp weights, ranking of generalized fuzzy number is used in which the fuzzy weights are ranked and finally ARAS is applied to rank the feasible RE resources with the help of utility degree. To justify the effectiveness and capability of the proposed method, comparison of the proposed method is done with the several other MCDM methods such as VIKOR, TOPSIS, and COPRAS.

III. PRELIMINARIES

A. Triangular Fuzzy Number (TFN)

Zadeh (1965) [10] gave the fuzzy number concept. DM believes that they are more convenient in expressing their opinion in TFNs as it is a triplet of three values (p1, p2, p3) indicating the lower, the more probable and the higher value (p1 ≤ p2 ≤ p3). Mathematically, the membership value of a TFN $\tilde{E}$ = (p1, p2, p3) can be defined as:

$$\mu_{\tilde{E}}(x) = \begin{cases} 0 & , \quad x < p1 \\ \dfrac{x - p1}{p2 - p1}, & p1 \le x \le p2 \\ \dfrac{p3 - x}{p3 - p2}, & p2 \le x \le p3 \\ 0 & , \quad x \ge p3 \end{cases} \tag{1}$$

B. Z-Number Concept [11]

Zadeh proposed the concept of Z-number [11] to enhance the reliability of the information because it is not enough to consider only fuzziness restriction while dealing with uncertain and imprecise information but also its degree of self-confidence. It is defined as an ordered pair of fuzzy numbers: Z = ($\tilde{A}$, $\hat{R}$) where $\tilde{A}$ determines the restriction of the evaluation and $\hat{R}$ determines the measure of the reliability of fuzzy number $\tilde{A}$.

IV. PROPOSED METHODOLOGY

This section describes the proposed method ARAS-Z, in which both tangible and intangible criteria are evaluated to obtain their weights and then ARAS is applied to rank all the suitable alternatives in order to get the optimal RE resource. The proposed methodology comprises of several steps as described below:

Step 1: Determine the Criteria and Alternatives

This step specifies the various alternative RE resources and the evaluation criteria that are involved in the decision-making process to solve the problem.

Step 2: Construct a pairwise decision matrix Y

A pairwise comparison matrix is formed by the decision maker in which corresponding values are given in linguistic terms expressed in Z-number. The fuzzy restriction values and its certainty degree are described in TFN_S and to obtain the decision matrix, $Y = [Z_{ij}]_{n\times n}$, where Z_{ij} is the evaluation value of criterion i in criterion j and n is the number of criteria, the corresponding value is taken from the codebook by the decision maker. The codebook of fuzzy restriction values [10] and its reliabilities for the criteria are shown in Table I.

Step 3: Conversion of Z-number into TFN_S

Each element of the pairwise decision matrix represented in Z-number is transformed into fuzzy numbers by applying fuzzy expectation [13] to obtain the pairwise fuzzy comparison matrix.

Step 4: Normalization of pairwise fuzzy comparison matrix

The normalization of a comparison matrix is required to scale each criterion value C_i (i=1,2,..n) in the same measurement range as different criteria have different measurement units.

- Summation of each row of pairwise fuzzy comparison matrix is done by applying the fuzzy arithmetic operations [8], $\hat{Y} = \left(\tilde{y}_{ij}\right)_{n\times n}$ where $\tilde{y}_{ij} = \left(p1_{ij}, p2_{ij}, p3_{ij}\right)$, $\tilde{y}_{ij}^{-1} = \left(\frac{1}{p3_{ij}}, \frac{1}{p2_{ij}}, \frac{1}{p1_{ij}}\right)$ for i, j = 1,…, n & i ≠ j.

$$V_i = \sum_{j=1}^{n} \tilde{y}_{ij} = \left(\sum_{j=1}^{n} p1_{ij}, \sum_{j=1}^{n} p2_{ij}, \sum_{j=1}^{n} p3_{ij}\right), \tag{2}$$

$$i = 1, \ldots, n$$

- Fuzzy weights of the evaluation criteria are obtained by normalizing the above rows [8].

$$\hat{W}_i = \frac{V_i}{\sum_{j=1}^{n} V_i} = \left(\begin{array}{c} \dfrac{\sum_{j=1}^{n} p1_{ij}}{\sum_{j=1}^{n} p1_{ij} + \sum_{k=1,k\neq i}^{n} \sum_{j=1}^{n} p3_{kj}}, \\ \dfrac{\sum_{j=1}^{n} p2_{ij}}{\sum_{k=1}^{n} \sum_{j=1}^{n} p2_{kj}}, \\ \dfrac{\sum_{j=1}^{n} p3_{ij}}{\sum_{j=1}^{n} p3_{ij} + \sum_{k=1,k\neq i}^{n} \sum_{j=1}^{n} p1_{kj}} \end{array} \right), \tag{3}$$

$$i = 1,2, \ldots, n$$

Step 5: Determination of the weights of evaluation criteria

After normalization, the fuzzy weights of the criteria are obtained that are represented in TFN_S but in order to get the weights of the criteria in the crisp, ranking of fuzzy numbers are done by using defuzzified value, different heights and different spreads [14].

- Apply the center of area method to defuzzy the fuzzy weights.

TABLE I. LINGUISTIC TERMS OF FUZZY RESTRICTIONS & ITS RELIABILITY AND THEIR TFN VALUES

Fuzzy Restrictions			Fuzzy reliability	
Saaty Scale	**Definition**	**TFN Scale**	**Definition**	**TFN Scale**
1	Equally Important	(1, 1, 1)	Not Very Likely (NL)	(0.1, 0.1, 0.5)
3	Weakly Important	(2, 3, 4)	Likely (L)	(0.1, 0.5, 0.8)
5	Fairly Important	(4, 5, 6)	Very Likely (VL)	(0.5, 0.7, 1)
7	Strongly Important	(6, 7, 8)	Extremely Likely (EL)	(0.7, 1, 1)
9	Absolutely Important	(9, 9, 9)		
2	The intermittent values	(1, 2, 3)		
4	between two adjacent scales	(3, 4, 5)		
6		(5, 6, 7)		
8		(7, 8, 9)		

$$x_{\hat{W}_i} = \frac{(p1_i + p2_i + p3_i)}{3}, \text{i} = 1, \dots, \text{n.} \quad (4)$$

- Calculate the spread $STD_{\hat{W}_i}$ of each fuzzy weight.

$$STD_{\hat{W}_i} = \sqrt{\frac{\sum_{j=1}^{3}(\hat{W}_{ij} - x_{\hat{W}_i})^2}{3-1}}, \quad i = 1, \dots, n. \quad (5)$$

- Then the fuzzy Score of each fuzzy weight is calculated.

$$Score_{\hat{W}_i} = \frac{x_{\hat{W}_i} * 1}{1 + STD_{\hat{W}_i}}, \quad i = 1, \dots, n. \quad (6)$$

- Fuzzy Score gives the final weights of the criteria in crisp. The greater the value of $Score_{\hat{W}_i}$, the higher the weight of $\hat{W}_i$, where i = 1,…,n. The weight vector of the evaluation criteria is $W^T = [w_1, w_2, w_3, \dots\dots, w_n]$.

Step 6: Evaluation of alternative RE resources with ARAS methodology

Evaluation and ranking of feasible alternative resources are done by ARAS method [15]. Utility degree derived from the ARAS method helps to prioritize the alternatives. The utility function value is directly proportional to the evaluated weights of the criteria and the relative effect of values and it is used to determine the complex comparative efficiency of the suitable alternatives. As the RE resources are prioritized based on utility degree, so higher the utility function value better the RE resource.

V. IMPLEMENTATION AND ANALYSIS

Cristobal data [4] is used for the implementation of the proposed method. Cristobal presented the VIKOR method for the evaluation of feasible alternative RE resources for the RE plan started by the Spanish Government in 2005. The proposed methodology is implemented in the following three steps:

Step 1: Two categories of evaluation criteria (C_E) are used in the proposed model namely benefit and cost criteria. Benefit criteria are Power (C_{E1}) in Kilowatt, Operating Hours (C_{E4}) in Hours/year, Useful Life (C_{E5}) in Years and Tons of emissions of CO_2 avoided/year (C_{E7}) in tCO_2/y. Cost criteria are Investment Ratio (C_{E2}) in €/Kilowatt, Implementation Period (C_{E3}) in Years, Operating and Maintaining Costs (C_{E6}) in € $\times 10^{-3}$ / Kilowatt hour.

In this study, thirteen alternatives RE resources are considered namely: Wind power P ≤ 5 MW (R_{E1}), Wind power 5 ≤ P ≤ 10 MW (R_{E2}), Wind power 10 ≤ P ≤ 50 MW (R_{E3}), Hydroelectric P ≤ 10 MW (R_{E4}), Hydroelectric 10 ≤ P ≤ 25 MW (R_{E5}), Hydroelectric 25 ≤ P ≤ 50 MW (R_{E6}), Solar Thermo-electric P ≥ 10 MW (R_{E7}), Biomass (energetic cultivations) P ≤ 5 MW (R_{E8}), Biomass (forest and agricultural wastes) P ≤ 5 MW (R_{E9}), Biomass (farming industrial wastes) P ≤ 5 MW (R_{E10}), Biomass (forest industrial wastes) P ≤ 5 MW (R_{E11}), Biomass (co-combustion in conventional central) P ≤ 5 MW (R_{E12}), Biofuels P ≤ 2MW (R_{E13}). Assessment values of alternatives corresponding to each criterion are shown in Table II.

Step 2: Table III calculates a pairwise comparison matrix using Table I. To determine the evaluation weights of the criteria firstly, Z-numbers are converted into TFN_S using fuzzy expectation then a pairwise fuzzy comparison matrix is normalized using (2), and (3) to obtain fuzzy weights. Further ranking of fuzzy weights represented in TFN_S is done using (4), (5), and (6) to retrieve weights of criteria in crisp. Lastly priority weight vector W = [0.290, 0.109, 0.025, 0.143, 0.154, 0.059, 0.192] is obtained. Based on the opinions of the DM_S, Power (0.290) possess the highest priority and Implementation period (0.025) possess the least priority in the RE selection problem.

Step 3: In this step, the assessment of alternative resources is done by applying the ARAS method on Table II data. The normalized weighted decision matrix, the optimality function value S_i and the utility function value K_i are presented in Table IV. Final ranks of alternative resources are also listed in Table IV. Based on the calculated utility degree value K_i , the optimal alternative RE resource is R_{E12}.

VI. RESULT ANALYSIS

To verify the efficiency and capability of the proposed ARAS-Z method, evaluation of the weights of the criteria and the prioritization of viable thirteen alternative resources are done using utility degree. Spearman's rank correlation coefficient (SCC) [5] is used to compare proposed ARAS-Z methodology with other MCDM methods namely VIKOR, TOPSIS, and COPRAS as shown in Table V. The SCC between the final ranking and the ARAS-Z, VIKOR, TOPSIS, COPRAS methods are 0.99, 0.96, 0.99, 0.99 respectively. Since ARAS-Z method has the highest SCC value (0.99) as TOPSIS and COPRAS, so it justifies the capability and effectiveness of the proposed method.

TABLE II. EVALUATION VALUES OF ALTERNATIVES CORRESPONDING TO EACH CRITERION FOR RE PROJECT.

	C_{E1} (max)	C_{E2} (min)	C_{E3} (min)	C_{E4} (max)	C_{E5} (max)	C_{E6} (min)	C_{E7} (max)
Optimal Value-O	50,000	601	1	7,500	25	600	9,649,680
R_{E1}	5,000	937	1	2,350	20	1,470	1,929,936
R_{E2}	10,000	937	1	2,350	20	1,470	3,216,560
R_{E3}	25,000	937	1	2,350	20	1,510	9,649,680
R_{E4}	5,000	1,500	1.5	3,100	25	1,450	472,812
R_{E5}	20,000	700	2	2,000	25	700	255,490
R_{E6}	35,000	601	2.5	2,000	25	600	255,490
R_{E7}	50,000	5,000	2	2,596	25	4,200	482,856
R_{E8}	5,000	1,803	1	7,500	15	7,106	2,524,643
R_{E9}	5,000	1,803	1	7,500	15	5,425	2,524,643
R_{E10}	5,000	1,803	1	7,500	15	5,425	2,524,643
R_{E11}	5,000	1,803	1	7,500	15	2,813	2,524,643
R_{E12}	56,000	856	1	7,500	20	4,560	4,839,548
R_{E13}	2,000	1,503	1.5	7,000	20	2,512	5,905,270

TABLE III. FORMATION OF PAIRWISE COMPARISON MATRIX IN Z-NUMBER

	C_{E1}	C_{E2}	C_{E3}	C_{E4}	C_{E5}	C_{E6}	C_{E7}
C_{E1}	[1,1,1], EL	[4,5,6], L	[9,9,9], L	[2,3,4], L	[4,5,6], L	[6,7,8], VL	[1,1,1], EL
C_{E2}	[1/6,1/5,1/4], L	[1,1,1], EL	[4,5,6], NL	[1/4,1/3,1/2], NL	[1/4,1/3,1/2], NL	[4,5,6], VL	[1/4,1/3,1/2], NL
C_{E3}	[1/9,1/9,1/9], L	[1/6,1/5,1/4], NL	[1,1,1], EL	[1/6,1/5,1/4], EL	[1/8,1/7,1/6], NL	[1/4,1/3,1/2], VL	[1/6,1/5,1/4], VL
C_{E4}	[1/4,1/3,1/2], L	[2,3,4], NL	[4,5,6], EL	[1,1,1], EL	[1,1,1], EL	[2,3,4], VL	[1/6,1/5,1/4], NL
C_{E5}	[1/6,1/5,1/4], L	[2,3,4], NL	[6,7,8], NL	[1,1,1], EL	[1,1,1], EL	[4,5,6], EL	[1/4,1/3,1/2], VL
C_{E6}	[1/8,1/7,1/6], VL	[1/6,1/5,1/4], VL	[2,3,4], VL	[1/4,1/3,1/2], VL	[1/6,1/5,1/4], EL	[1,1,1], EL	[1/6,1/5,1/4], NL
C_{E7}	[1,1,1], EL	[2,3,4], NL	[4,5,6], VL	[4,5,6], NL	[2,3,4], VL	[4,5,6], NL	[1,1,1], EL

TABLE IV. OUTCOME OF ANALYSIS

	C_{E1}	C_{E2}	C_{E3}	C_{E4}	C_{E5}	C_{E6}	C_{E7}	S	K	Rank
O	0.0572	0.0141	0.0022	0.0156	0.0136	0.0107	0.0397	0.1531	1.0000	-
R_{E1}	0.0051	0.0090	0.0022	0.0049	0.0109	0.0043	0.0079	0.0444	0.2900	12
R_{E2}	0.0102	0.0090	0.0022	0.0049	0.0109	0.0043	0.0132	0.0548	0.3579	7
R_{E3}	0.0255	0.0090	0.0022	0.0049	0.0109	0.0043	0.0397	0.0965	0.6302	2
R_{E4}	0.0051	0.0057	0.0014	0.0065	0.0136	0.0044	0.0019	0.0386	0.2523	13
R_{E5}	0.0204	0.0121	0.0011	0.0042	0.0136	0.0092	0.0011	0.0616	0.4025	5
R_{E6}	0.0357	0.0141	0.0086	0.0042	0.0136	0.0107	0.0011	0.0803	0.5242	3
R_{E7}	0.0511	0.0016	0.0011	0.0054	0.0136	0.0015	0.0019	0.0764	0.4986	4
R_{E8}	0.0051	0.0047	0.0022	0.0156	0.0082	0.0009	0.0104	0.0470	0.3072	11
R_{E9}	0.0051	0.0047	0.0022	0.0156	0.0082	0.0012	0.0104	0.0470	0.3090	9
R_{E10}	0.0051	0.0047	0.0022	0.0156	0.0082	0.0012	0.0104	0.0473	0.3090	9
R_{E11}	0.0051	0.0047	0.0022	0.0156	0.0082	0.0023	0.0104	0.0484	0.3162	8
R_{E12}	0.0572	0.0099	0.0022	0.0156	0.0109	0.0014	0.0199	0.1171	0.7646	1
R_{E13}	0.0020	0.0056	0.0014	0.0146	0.0109	0.0026	0.0243	0.0615	0.4013	6

TABLE V. PERFORMANCE RANKING OBTAINED BY USING DIFFERENT MCDM METHODS

Different MCDM Methodologies									
	TOPSIS		**VIKOR**		**CORPAS**		**ARAS-Z**		
	Score	**Rank**	**Score**	**Rank**	**Score**	**Rank**	**Score**	**Rank**	**Final Rank**
R_{E1}	0.074	12	0.951	13	35.20	12	0.290	12	12.25
R_{E2}	0.147	6	0.798	6	46.14	6	0.358	7	6.25
R_{E3}	0.772	2	0.262	2	91.43	2	0.630	2	2
R_{E4}	0.043	13	0.929	9	27.25	13	0.252	13	12
R_{E5}	0.134	7	0.775	5	42.86	7	0.402	5	6
R_{E6}	0.302	4	0.688	4	56.46	4	0.524	3	3.75
R_{E7}	0.439	3	0.666	3	63.42	3	0.499	4	3.25
R_{E8}	0.086	11	0.946	12	36.32	11	0.307	11	11.25
R_{E9}	0.087	9	0.935	10	36.88	9	0.309	9	9.25
R_{E10}	0.087	9	0.935	10	36.88	9	0.309	9	9.25
R_{E11}	0.090	8	0.917	8	38.08	8	0.316	8	8
R_{E12}	0.841	1	0.000	1	100.0	1	0.765	1	1
R_{E13}	0.272	5	0.823	7	53.40	5	0.401	6	5.75

VII. CONCLUSION

The problem of prioritization of suitable alternative resources becomes complex due to the presence of multiple conflicting criteria and uncertainty in the information. ARAS method integrated with Z-number is proposed for the prioritization of feasible RE sources. In real-world decision problems, uncertainty is pervasive in nature. To handle the uncertainty in this problem, the degree of self-confidence is considered along with fuzzy numbers and a pairwise comparison matrix is formed. Weights are evaluated by ranking the generalized fuzzy numbers which are used further in the ARAS method to prioritize the alternatives using utility degree. Based on the SSC, a comparative analysis is done to validate the capability and effectiveness of the proposed model. Proposed ARAS-Z model has the capability to handle the uncertainty while the other MCDM methods used in the comparison do not consider the uncertainty factor involved in the decision problem which is the main limitation of other MCDM methods.

REFERENCES

[1] Kadian, S. K., Kesari, J. P., & Mishra, R. S. Hydraulic Analysis and Modelling of Small Hydro Power: A Case Study of a Plant at Gogripur, Karnal.

[2] Zhang, W., & Pan, X. (2016). Study on the demand of climate finance for developing countries based on submitted INDC. *Advances in Climate Change Research*, *7*(1-2), 99-104.

[3] Safi, M. (2016). India plans nearly 60% of electricity capacity from non-fossil fuels by 2027. *The Guardian*.

[4] San Cristóbal, J. R. (2011). Multi-criteria decision-making in the selection of a renewable energy project in Spain: The Vikor method. *Renewable energy*, *36*(2), 498-502.

[5] Yazdani-Chamzini, A., Fouladgar, M. M., Zavadskas, E. K., & Moini, S. H. H. (2013). Selecting the optimal renewable energy using multi criteria decision making. *Journal of Business Economics and Management*, *14*(5), 957-978.

[6] Chatzimouratidis, A. I., & Pilavachi, P. A. (2008). Multicriteria evaluation of power plants impact on the living standard using the analytic hierarchy process. *Energy Policy*, *36*(3), 1074-1089.

[7] Turskis, Z., & Zavadskas, E. K. (2010). A new fuzzy additive ratio assessment method (ARAS-F). Case study: The analysis of fuzzy multiple criteria in order to select the logistic center location. *Transport*, *25*(4), 423-432.

[8] Wang, Y. M., Luo, Y., & Hua, Z. (2008). On the extent analysis method for fuzzy AHP and its applications. *European journal of operational research*, *186*(2), 735-747.

[9] Tasri, A., & Susilawati, A. (2014). Selection among renewable energy alternatives based on a fuzzy analytic hierarchy process in Indonesia. *Sustainable Energy Technologies and Assessments*, *7*, 34-44.

[10] Wang, C. N., Huang, Y. F., Chai, Y. C., & Nguyen, V. (2018). A Multi-Criteria Decision Making (MCDM) for Renewable Energy Plants Location Selection in Vietnam under a Fuzzy Environment. *Applied Sciences*, *8*(11), 2069.

[11] Zadeh, L. A. (2011). A note on Z-numbers. *Information Sciences*, *181*(14), 2923-2932.

[12] Chatterjee, K., & Kar, S. (2018). A multi-criteria decision making for renewable energy selection using Z-numbers in an uncertain environment. *Technological and Economic Development of Economy*, *24*(2), 739-764.

[13] Kang, B., Wei, D., Li, Y., & Deng, Y. (2012). A method of converting Z-number to classical fuzzy number. *JOURNAL OF INFORMATION &COMPUTATIONAL SCIENCE*, *9*(3), 703-709.

[14] Chen, S. M., & Chen, J. H. (2009). Fuzzy risk analysis based on ranking generalized fuzzy numbers with different heights and different spreads. *Expert systems with applications*, *36*(3), 6833-6842.

[15] Zavadskas, E. K., & Turskis, Z. (2010). A new additive ratio assessment (ARAS) method in multicriteria decision-making. *Technological and Economic Development of Economy*, *16*(2), 159-172.

Proceedings of the Fourth International Conference on Communication and Electronics Systems (ICCES 2019)
IEEE Conference Record # 45898; IEEE Xplore ISBN: 978-1-7281-1261-9

Secure Defense Mechanism against Data Leakage and Distributed Denial of Service Attacks in Software Defined Networks

P. Mohana Priya
Department of Information Technology
Sastra Deemed University
Thanjavur, India
mohanapriya@it.sastra.edu

***Abstract*—Software Defined Network is an emerging fifth generation network architecture in which data and control planes are decoupled. The programmable network provides standard open interfaces which is vulnerable to data leakage attacks. Existing Open Flow protocol lacks in crypto standard where messages are communicated between data and control planes are in unencrypted form. Open Flow messages are prone to passive attacks such as sniffing and traffic monitoring. Diffie-Hellman Key Exchange algorithm is implemented in Open Flow protocol version 1.3 where random private keys are generated for each incoming network traffic flows. In this research work, secure defense mechanism is proposed where Restricted Boltzmann Machine algorithm is incorporated in controller that detects Distributed Denial of Service attack traffic flows. The performance of Software Defined Network is measured using performance metrics namely bandwidth utilization of controller, delay of request and response messages from switch and controller, encryption and decryption time of Open Flow messages. The proposed secure defense mechanism is an extended work of previous research work on detection of Distributed Denial of Service attack in Software Defined Network controller. The proposed secure defense mechanism out performs existing work with respect to metrics such as bandwidth utilization, delay, encryption and with decryption time.**

Keywords—Software Defined Networks; Data Leakage Attack; Restricted Boltzmann Machine; Man-in-the-Middle Attack; Self-learning; Distributed Denial of Service; Diffie-Hellman Key Exchange Algorithm

I. INTRODUCTION

Data is considered as an important asset in all the sectors like educational institutions, industries etc. Securing data of the intended network is the foremost concern for the network administrator. The most common attacks found in networking environment breach the meaning of data that corresponds to an individual. Man-in-the-Middle attack [1] is the top most category of data leakage attacks which breaks integrity and confidentiality of the stored data. In order to protect the network from data leakage, applying suitable crypto standard for the process of encryption and decryption is needed.

In this research work, data leakage security attack of one of the fifth generation (5G) network named Software Defined Network (SDN) [2] is concentrated. SDN architecture is improvised comparatively from the conventional network. In conventional network [3] setup, data forwarding and data management modules are tightly coupled which lacks in network customization according to the user needs. Researcher communities from Stanford University seek great interest to create an open network that is feasible to integrate customized user applications. Finally SDN is obtained as a product that has Open Flow (OF) [4] protocol that acts as an interface between data forwarding and data management modules.

SDN [5] is an emerging alternate 5G network architecture where data forwarding and data management modules are decoupled each other. SDN is a three layered network architecture where the bottom plane is the data plane whose responsibility is forwarding the incoming network traffic flows. The middle plane is the control plane [6] that is responsible for taking authoritative decisions. In data plane [7], for each and every switch the component named flow table is integrated.

Flow table records the entries of incoming network traffic flows with features such as physical and logical addresses for future analysis. Physical address of incoming traffic flows include source and destination Medium Access Control (SRC MAC) and (DST MAC) address of a machine (or) host where the traffic is originated whereas logical address of network traffic flows include source and IP (SRC IP) and destination IP address (DST IP), Protocol type, Virtual Local Area Network Identifier (VLAN ID). The top most plane is an application plane [8] where user customized applications are incorporated.

The threat vectors of SDN architecture regarding data leakage security attack include vulnerable data plane [3], vulnerable controllers [9], vulnerable data-control plane [10] communication interface, and vulnerable apps in application plane.

The objective of this research work is to incorporate Diffie-Hellman Key Exchange algorithm used for the process of encryption and decryption of messages originated from the data plane to the control plane and vice-versa for providing enhanced security. In control plane, unsupervised Restricted Boltzmann Machine (RBM) algorithm is incorporated that self-

learns network traffic flow features to detect malicious traffic flows.

The major contributions of this research work includes that this is a first paper to use crypto standard to provide additional security in SDN. The messages interacted between data and control planes are in encrypted form so that data leakage (or) man-in-the-middle attack is reduced comparatively than the existing methods. Unsupervised RBM algorithm self-learns network traffic flow features that detect malicious IP addresses that cause data-leakage security attacks. The proposed defense mechanism has higher accuracy in terms of attack detection than the existing methods and it is an extended work of [11] wherein the detection mechanism lacks in OF protocol crypto standard is incorporated to provide security against data leakage attacks.

The paper is organized as follows. Section 2 discusses the related works on data leakage security attacks in SDN. Section 3 discusses the proposed defense mechanism against data leakage security attacks, section 4 details the experimental setup, section 5 reveals the results and discussions and finally section 6 concludes with future research directions.

II. Related Work

Cheng Li et al [12] proposed a prototype system to detect MITM attack with packet modification using Bloom Filters based on SDN by extending the OF protocol. Zhang et al [13] proposed Convincing Mechanism for MITM Detection (CMD) to detect man-in-the-middle attack in OF channel. The topology and connection characteristics of network traffic are fed as inputs to CMD, without analyzing the packet contents. CMD results with good time accuracy and performance.

Sebbar et al [14] proposed a detection mechanism to prevent Man-in-the-Middle attack in Multi-SDN controller environment. The proposed detection mechanism concentrates on the vulnerabilities of Open DayLight (ODL) controller. Effective countermeasure is also proposed to prevent attacks on the league monitor's monitoring service.

Lin et al [15] proposed a defense approach called "Packet forwarding based on BUFfer sharing (PBUF)" that pools the idle switches to mitigate threats in SDN. Buffer management module gleans the statistics of incoming packets and analyzes the table-miss packets. The packet forwarding module is designed to forward table-miss packets to the idle switches to prevent switch (or) controller to be overloaded. Imran et al [16] discussed comprehensive approaches of DDoS attacks in SDN environment. The authors presented various DDoS attack mitigation strategies based on the different classes based on the methodology in handling malicious traffic flows.

Wavelet analysis method was introduced by Julian et al [17] to detect anomalous conditions raised due to man-in-the-middle attack in SDN. Unique characteristics of reported anomalies are used to classify the type of DDoS attack. Mohana Priya & Shalinie [18] proposed a detection system with an unsupervised RBM algorithm in SDN controller. The RBM algorithm self-learns the reliable network metrics to detect DDoS attacks in SDN. Data Leakage Prevention System (DLPS) is proposed by sultan [19] to detect and prevent confidential data in use, transit and at rest.

DLPS use different techniques to analyze the content and context of confidential data. Braga et al [20] discussed a light weight method to differentiate attack traffic flows from normal traffic flows using Self Organizing Map (SOM). Feng et al [21] considered parameters to detect DDoS attack traffic flows include Average Number of Packets in Per Flow (ANPPF), Average of Duration per Flow (ADF), Percentage of Pair-Flows (PPF) and Growth of Single Flows (GSF).

III. Proposed Defense Mechanism

The proposed secure defense mechanism consists of 2 distinct phases namely network traffic flow generation phase and attack detection phase as shown in Figure 1. In phase 1, legitimate and an attack traffic flows are generated using real time network emulator named mininet. SDN controller will monitor the incoming network traffic flows and also analyzes the performance of the network by deeply inspecting the flow structure.

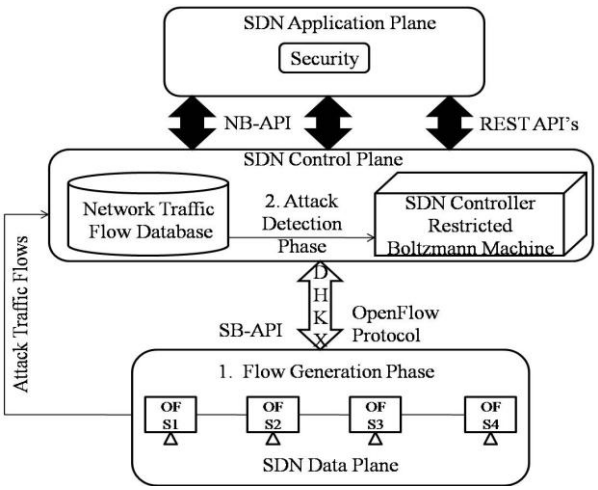

Fig. 1: Block Diagram of Proposed Defense Mechanism

The generated network traffic flows are stored in the database for future analysis. The network traffic flows in the database are pulled through appropriate Structured Query Language (SQL) queries to the SDN controller. It is deployed with RBM algorithm to detect DDoS attack and its variants. In SDN context, for every incoming unknown traffic flows, the data plane switches send PACKET-IN request as a query message to the SDN controller.

The controller in turn reply with the PACKET-OUT response message to the data plane switches through OF protocol. As SDN provides open standard interface as South Bound - Application Programming Interface (SB-API), it is vulnerable to data leakage security attack. In data leakage security attack, the OF messages communicated between SDN

data and control planes are known to attackers. In order to provide enhanced security, all OF messages transferred between data and control planes are encrypted by secretly exchanging the keys between the sender and receiver. Exchanging of secret keys has been done by Diffie-Hellman key exchange algorithm.

In the existing OF protocol version 1.3, if the logic of Diffie-Hellman key exchange algorithm is incorporated, it will generate random prime numbers to generate private and public key pairs to encrypt and decrypt the original message. Finally, key generation process is initiated between the sender and receiver to check whether the secret key exchanged are equal (or) not. Figure 2 shows the Diffie-Hellman key exchange steps as follows:

Algorithm 1 : Diffie Hellman Key Exchange in Open Flow Protocol

Input : OF Request Messages from Data Plane Switches in Encrypted Form.
Output : OF Response Messages from SDN Controllers in Encrypted Form.
1. Assume prime number P.
2. Select α, such that α is less than and primitive root of P.
3. Assume PR_A and PR_A < P.
4. Calculate PU_A :
   $PU_A \rightarrow \alpha^{PRA}$ mod P.
5. Assume PR_B and PR_B < P.
6. Calculate PU_B :
   $PU_B \rightarrow \alpha^{PRB}$ mod P.
7. {Private, Public key pairs} of users are generated
8. Encryption Process of an OF switch Request Message:
   $PU_A = \alpha^{PRA}$ mod P.
9. Decryption Process of a Controller Response Message:
   $PU_B = \alpha^{PRB}$ mod P.
10. Key Generation and Verification at User A, User B:
   10.1 : At OF switch, find the key value K.
   $K = (PU_B)^{PR}{}_A$ mod P.
   10.2 : At SDN Controller, find the key value K.
   $K = (PU_A)^{PR}{}_B$ mod P.

Fig. 2: Diffie Hellman Key Exchange Algorithm in Open Flow Protocol

RBM algorithm is deployed in SDN controller in which for the training phase, the network is trained using contrastive divergence algorithm to update the weight matrix (W_{mn}). The training procedure of CD algorithm has traffic flow features namely source IP address, Destination IP address, Source MAC address, Destination MAC address and protocol type. Visible layer of RBM neural network is trained with the traffic flow features and the hidden layer of RBM processes the input metrics. There exists positive and negative gradient of the network in which the probability of training data is increased by computing the product of visible (v_m) and hidden layers (h_n).

Gibb's sampling procedure is used to update the weights between visible and hidden layers. The network traffic flow features are reconstructed from the available feature vector of traffic flows. The reconstructed network traffic flow features are fed as input to the next level hidden layers. In RBM, two layers exists namely visible and hidden layer. The extracted features of a dataset are fed as inputs to the visible layer where as the reconstructed network traffic flow features are fed as inputs to the higher level hidden layers. Visible layer of RBM has inputs such as source IP address, Destination IP address, Source MAC address, Destination MAC address and protocol type.

RBM is depicted in Figure 3 and its energy configuration [11] of RBM is given as follows:

$$E(V,H) = -\sum_{i=1}^{n}\sum_{j=1}^{m} w_{ij}\, h_i v_j - \sum_{j=1}^{m} b_j v_j - \sum_{i=1}^{n} c_i h_i \quad (1)$$

where,
w_{ij} = Weight matrix connecting hidden and visible layer.
v_j = Visible layer.
h_i = Hidden layer.
b_j & c_i = Bias Units of Visible and Hidden layer.

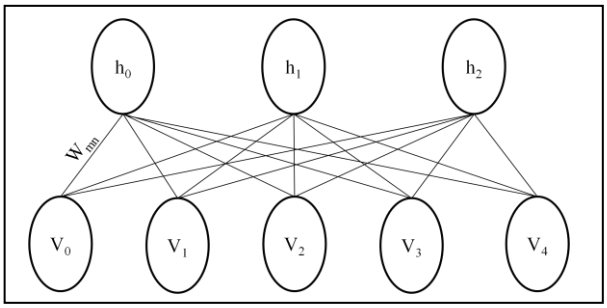

Fig. 3: Structure of RBM

RBM structure is conditionally independent given visible to find the probability of hidden layer and given hidden to find the probability of visible layer.

$$P\left(\frac{h}{v}\right) = \prod_i P\left(\frac{h_i}{v}\right) \quad (2)$$

and

$$P\left(\frac{v}{h}\right) = \prod_i P\left(\frac{v_j}{h}\right) \quad (3)$$

In this research work, the probability of hidden layer is computed given the inputs in visible layer. RBM detects DDoS attack traffic flows and data leakage security attacks with metrics such as hit count of encrypted request packets to the controller from data plane switches, energy consumption of data plane switches (E_{con}(SW)). E_{con}(SW) is measured based on the energy consumption of active switches, energy consumption of active interfaces, number of ports enabled and it is given as follows:

$$E_{con}\ (SW) = E_{con}\ (SW_{active}) + E_{con}\ (Interface_{active}) + \sum_{k=1}^{R} n_{ports\ .r} * E_{con}\ (Ports_{enabled}) \quad (4)$$

where,

$E_{con}\ (SW_{active})$ = Energy consumption of active switches.

$E_{con}\ (Interface_{active})$ = Energy consumption of active interfaces.

$n_{ports\ ,r}$ = Number of ports available in a switch and

$E_{con}\ (Ports_{enabled})$ = Energy consumption of ports enabled.

Figure 4 shows the phases of proposed defense mechanism in a bottom up approach of SDN with all the technical concepts incorporated in each of the component is illustrated. Legitimate and attack traffic flows are generated in data plane, as a follow up modified Diffie Hellman key exchange algorithm is incorporated in OF protocol to enhance its security. The encrypted OF messages from data and control plane is monitored by SDN controller which consists of RBM algorithm that self learns the network metrics, request messages. Based on the knowledge base, SDN controllers identify (or) detect the newly incoming unknown traffic flows.

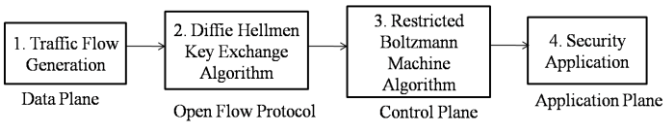

Fig. 4: Phases of Proposed Defense Mechanism

IV. EXPERIMENTAL SETUP

The experimentation has been carried out in Ubuntu Operating system version 15.4 with mininet emulator. In mininet, the data plane of SDN consists of Open Virtual Switch (OVS) that has three hosts namely h1, h2 and h3 interfaced with softwarized POX controller. The procedure of modified Diffie Hellman Key exchange algorithm is incorporated in OF protocol version 1.3 to encrypt the OF request message originated from data plane and decrypt the OF response message from the control plane. RBM algorithm is implemented as a python code named rbm.py in POX SDN controller. RBM algorithm self-learns the OF request messages to detect attack traffic flows. The logic of Diffie Hellman Key Exchange algorithm is implemented using ns-3 [22] tool. POX controller integrated with mininet is bridged with the ns3 simulator tool for interfacing OF protocol with data and control plane.

Wireshark is installed in the target victim to analyze the incoming network traffic flows. nmap tool is used to trace the network performance metrics such as bandwidth utilization of controller, delay of request and response messages from switch and controller, encryption and decryption time of incoming OF messages.

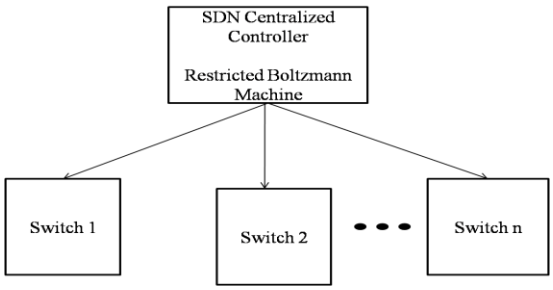

Fig. 5: Experimental Network Setup

V. RESULTS AND DISCUSSIONS

In this section, results are illustrated for various network metrics namely bandwidth utilization of controller and energy consumption of switches. Figure 6 illustrates that bandwidth utilization of controller which can be measured by the generated PACKET-IN request message from the dataplane switch.

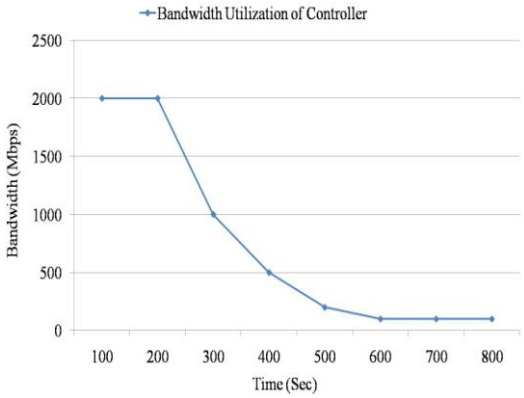

Fig. 6: Bandwidth Utilization of Controller

The inference shows that bandwidth utilization is higher until 299th seconds, when RBM algorithm is deployed in SDN controller at 300th second, bandwidth utilization is reduced gradually and stabilized until analysis with respect to time parameter.

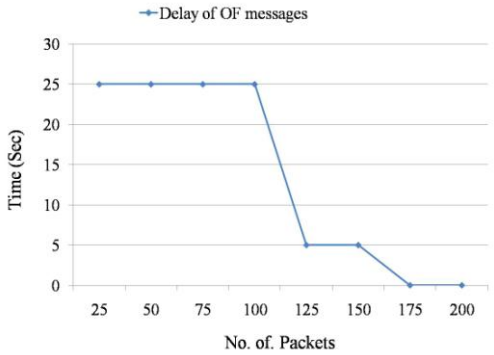

Fig. 7: Delay of SDN Controller

Figure 7 shows the delay of transferring messages from data plane switches and SDN controller. Delay of OF

messages can be calculated based on the Round Trip Time (RTT) originated from data plane switches and SDN controller. When Diffie-Hellman Key Exchange algorithm is deployed at OF protocol, delay parameter is reduced even in case of DDoS attack traffic flows.

VI. Conclusion and Future work

SDN is an emerging fifth generation network architecture subject to active and passive attacks like DDoS attack and traffic monitoring, sniffing etc. The proposed defense mechanism is also deployed with RBM algorithm in SDN controller and Diffie-Hellman key exchange algorithm in Open Flow protocol. The proposed defense mechanism is deployed with RBM algorithm in SDN controller and Diffie-Hellman key exchange algorithm in OF protocol. The proposed defense mechanism outperforms the existing work based on bandwidth utilization, delay of request and response messages from switch and controller, encryption and decryption time of incoming OF messages. The future work is to provide application level security of SDN.

References

[1] K. Zhang and X. Qiu, "CMD: A convincing mechanism for MITM detection in SDN", IEEE International Conference on Consumer Electronics, pp. 1-6, January 2018.

[2] BAA. Nunes, M. Mendonca, XN. Nguyen, K. Obraczka and T. Turletti, "A survey of software-defined networking: Past, present and future of programmable networks", IEEE Communications Surveys and Tutorials, vol. 16, no. 3, pp. 1617-1634, 2014.

[3] HJ. Kim and N. Feamster, "Improving network management with software-defined networking", IEEE Communications Magazine, vol. 51, no. 2, pp. 114-119, 2013.

[4] RM. Kandoi, "Denial-of-service attacks in open flow SDN networks", International Symposium on Integrated Network Management, pp. 1322-1322, 2015.

[5] N. McKeown, T. Anderson, H. Bala Krishnan, G. Parulkar, L. Peterson, J. Rexford, S. Shenker and J. Turner, "Open flow: Enabling innovation in campus networks", ACM SIGCOMM Computer Communication Review, pp. 69-74, 2008.

[6] J. Xie, D. Guo, Z. Hu, T. Qu and P. Lv, "Control plane of software defined networks: A survey", Computer Communications, vol. 67, pp. 1-10, 2015.

[7] M. Kuźniar, P. Perešíni and D. Kostić, "What you need to know about sdn flow tables", International Conference on Passive and Active Network Measurement, pp. 347-359, 2015.

[8] E. Haleplidis, K. Pentikousis, S. Denazis, JH. Salim, D. Meyer and O. Koufopavlou, "Software-defined networking, (SDN): Layers and Architecture Terminology", RFC 7426, 2015.

[9] MA. Karakus, "A survey: Control plane scalability issues and approaches in software defined networks", Computer Networks, Elsevier, Vol. 112, pp.279-293, 2016.

[10] SS. Savas, M. Tornatore, MF. Habib, P. Chowdhury and B. Mukherjee, "Disaster-resilient control plane design and mapping in software-defined networks", International Conference on High Performance Switching and Routing, pp. 1-6, 2015.

[11] P. MohanaPriya and S.M. Shalinie, S.M., "Restricted Boltzmann Machine based Detection System for DDoS attack in Software Defined Networks", IEEE International Conference on Signal Processing, Communication and Networking, pp. 1-6, March 2017.

[12] C. Li, Z. Qin, E. Novak and Q. Li, "Securing SDN infrastructure of IoT–fog networks from MitM attacks", IEEE Internet of Things Journal, Vol. 4, No. 5, pp.1156-1164, 2017.

[13] X. Qiu, K. Zhang and Q. Ren, "Global Flow Table: A convincing mechanism for security operations in SDN", Computer Networks, Vol. 120, pp.56-70, 2017.

[14] A. Sebbar, M. Boulmalf, M.D.E.C. El Kettani and Y. Badd, "Detection MITM Attack in Multi-SDN Controller", 5th IEEE International Congress on Information Science and Technology (CiSt), pp. 583-587, October 2018.

[15] C. Lin, C. Wu, Y. Tian, Z. Wen and S. Ji, "PBUF: Sharing Buffer to Mitigate Flooding Attacks", IEEE 23rd International Conference on Parallel and Distributed Systems (ICPADS), pp. 392-399, 2017.

[16] M. Imran, M.H. Durad, F.A. Khan and A. Derhab,"Toward an Optimal Solution against Denial of Service Attacks in Software Defined Networks", Future Generation Computer Systems, Vol. 92, pp.444-453, 2019.

[17] J. D'Orsaneo, M. Tummala, J. McEachen and B. Martin, "Analysis of Traffic Signals on an SDN for Detection and Classification of a Man-in-the-Middle Attack", IEEE 12th International Conference on Signal Processing and Communication Systems (ICSPCS), pp. 1-9, December 2018.

[18] P. MohanaPriya and S.M. Shalinie, "Restricted Boltzmann Machine based Detection System for DDoS Attack in Software Defined Networks", IEEE Fourth International Conference on Signal Processing, Communication and Networking (ICSCN), pp. 1-6, March 2017.

[19] S. Alneyadi, E. Sithirasenan and V. Muthukkumarasamy, "A Survey on Data Leakage Prevention Systems", *Journal of Network and Computer Applications*, Vol. 62, pp.137-152, 2016.

[20] R. Braga, E. de Souza Mota and A. Passito, "Lightweight DDoS flooding attack detection using NOX/OpenFlow", In LCN, Vol. 10, pp. 408-415, October 2010.

[21] Y. Feng, R. Guo, D. Wang and B. Zhang, "Research on the Active DDoS Filtering Algorithm based on IP Flow", IEEE Fifth International Conference on Natural Computation, Vol. 4, pp. 628-632.

[22] G.F. Riley and T.R. Henderson, "The NS-3 Network Simulator", Modeling and Tools for Network Simulation, Springer Berlin Heidelberg, pp 15–34, 2010.

Proceedings of the Fourth International Conference on Communication and Electronics Systems (ICCES 2019)
IEEE Conference Record # 45898; IEEE Xplore ISBN: 978-1-7281-1261-9

A Machine Learning Approach for URL Based Web Phishing Using Fuzzy Logic as Classifier

Happy Chapla
Research Scholar
Marwadi Education Foundation
Rajkot, India
happypatel2212@gmail.com

Riddhi Kotak
Assistant Professor
Marwadi Education Foundation
Rajkot, India
riddhi.kotak@marwadieducation.edu.in

Mittal Joiser
Assistant Professor
Marwadi Education Foundation
Rajkot, India
mittal.joiser@marwadieducation.edu.in

Abstract- Phishing is the major problem of the internet era. In this era of internet the security of our data in web is must. Phishing is one of the most harmful way to stolen the credential information like username, password or account number from the users. Users are not aware of this type of attack and they become a part of the phishing attacks. It may be losses of financial found, personal information, reputation of brand name or trust of brand. So the detection of phishing site is necessary. In this paper we design a framework of phishing detection using URL.

Keyword – Web mining, data mining, phishing URL, Fuzzy logic, Classifier.

I. INTRODUCTION

Day by day number of phishing URLs have grown rapidly. Phishing sites look same like original sites but the code behind the site is different or the link of the page is followed the incorrect path and collect the information from the users. Every time attackers choose the different options to collect the information. Phishing attempts have grown 65% in the last year according to PhishMe's Enterprise Phishing Resiliency and Defense Report.

According to the research in 3rd quarter of the 2017 the percentage count is[1] 41.99% sites are used to steal the information while using the payment gateways online. 17.7% sites pass the phishing mail via mail address. 15.48% possibilities are there to steal the information from the financial institutions.

II. BASICS OF PHISHING:

Phishing has two types (1) Spear phishing : attack on personal information to increase the probability of the attack. (2) Clone Phishing: Attacker mails the link and previously mail containing the phishing site or web fraud.

Whaling: They target the higher profile and business email on behalf of the high profile manager.

Filter evasion: They were target the users as sending the images and send the hidden text on those images.

Website forgery: They own to fraud

Convert Redirect: They will show the login box on their page or give some popup to the site.

Phone Phishing: They will target the people and send the SMS on the mobile phone as a bank authority and can achieve the credential information from the user via fraud SMS. This techniques borrow ideas from the traditional phishing, phone based social engineering techniques and many more new techniques.

Feature extraction process is also defined in the [3] paper. Authors define the group of features and design some rules for features extraction to check the legitimacy of site. First of all author divide all the features set in to the group of feature set, based on that result they calculate the value of True Positive, True Negative, False Positive and False Negative.

III. FUZZY LOGIC MODEL

A. Fuzzification

The Fuzzification of the fuzzy logic is described by the linguistic variables which is the best advantage of the fuzzy logic system. In this step, linguistic values of the phishing variable are design output such as medium, high and moderator. Fuzzification is also known as the decomposing a system input and / or output into one or more fuzzy sets.

Trapezoidal or Triangular shaped method is most common way to divide your result. Mostly result may be dependent on the rules of fuzzy logic. Hence, rules may be differ from one method to another method although the representation of the result is expressed in simple way.

B. Rule Evaluation

Rule evaluation is used to create the rules for the member functions. Every member functions of the input and output has rules in fuzzy logic. They provide fuzzy rules in form of (If...then) for every member function.

C. Aggregation of the rules

Combine the rules of the membership functions consequents previously scaled into the single fuzzy set. All the rules combine in the same manner and it will combine into a single fuzzy set, this process only occurs once for each output variable. This process works only before the finale defuzzification process.

D. Defuzzification

It is the process of transferring the output of the fuzzy set into the crisp output, in our case we can say that the crisp output in terms of Phishing or Legitimate. Centroid technique is used to defuzzify the data.

VI. PROPOSED METHODOLOGY

Web content mining, web usage mining and web structure mining is also a part of the web mining [7]. We follow the Web URL Mining. The source of phishing attacks are mostly from email, websites and malware. The links (URL) provided in phishing emails draws user into entering phishing website. In website based phishing, website is copy of the original website which looks like same but, the aim is different.

To overcome the problem of phishing we design a framework to detect it using the fuzzy logic as a classifier. We used only URL based features for the extraction process[10]. For that we collect our dataset from the Phish tank site, Open phish site and the URL of the website which can live on the web. We were collecting the 1000 URLs for our dataset purpose.

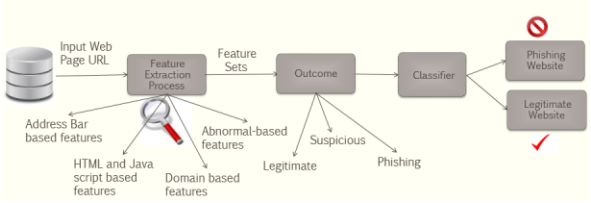

Fig 1. Architecture of the system

Using MatLab tool we code the program which can extract the features from the entered URL. We have different feature sets, out of them we were extract some feature which can based on URL of website. Observed features are conclude in the table 1 [3][4].

TABLE 1
FEATURES OBSERVED IN THE LITERATURE SURVEY

Feature	Legitimate	Suspicious	Phishing
Ip address	Otherwise	-	Exists in URL
Length of URL	-	>=54and <=75	>75
Request URLs in source code	less than 20%	between 20% and 50%	Otherwise
URL of anchor	2	5	Different from anchor
Redirect Page	Correct source <=1	>1and <4	otherwise
On mouse Over	-	-	Use fake URL
Prefix or suffix separated by '_'	Not include	-	Domain part include '-'
Number of '.'	2 dots	3 dots	>3
Number of '%'	2	More than 2	More than 2
Number of '='	2	More than 2	More than 2

URL having '@'	Not present	May be there	Present
Host name	Need hostname	-	-
Popup Window	Not using popup	>2 and<4	More than 4
Age of domain	Otherwise	>1and<2	<1
DNS record	Present	-	Empty
Web page rank 1,00,000	<100000	>100000	Otherwise
Right click	-	Showing an alert	Disable
Status bar	Otherwise	Not change	Change the status bar
Number of '&'	Not present	May be there	Present
Number of '?'	Not present	May be there	Present

V. PROPOSED FEATURES USED FOR IDENTIFICATION OF PHISHING WEBSITE

Long URL

W3 defines the standards and rules for the URL. They were defining maximum54 characters in the URL. Original site not contain more than 54 characters. If length is between 54 to 75 character than it is possible to define the phishing site. It is also known as suspicious site because it may be legitimate also. Maximum numbers of the URL in dataset are defined as phishing due to the long URL.

$$if\{\, URLlength\ < 54\ \rightarrow feature = Legitimate\,\}$$
$$Else\ if\{\, URLlength \geq 54\ and\ \leq 75 \rightarrow feature = Suspicious\,\}$$
$$Else\{\, feature = Phishing\,\}$$

Length of hostname

Hostname has always a fixed length to identify the legitimate URL. When more than 25 characters are present in the URL than it is identifying as phishing site used to make fraud and intentionally collect the credential information from the user.

$$if\{\, Hostname\ length \leq 25\ \rightarrow feature = Legitimate\,\}$$
$$Else\{\, feature = Phishing\,\}$$

Dots:

Number of dotes define the sub domain and multi sub domain in the URL. Top level domain and second level domain is always available in the URL of any website. URL having less than three dots is legitimate sites. If URL having exact 3 dots are known as suspicious site means it may be phishing or may not be; now it is dependent on the other features also.

$$if\{\, Dots\ in\ URL < 3\ \rightarrow feature = Legitimate\,\}$$
$$Else\ if\{\, Dots\ in\ URL = 3 \rightarrow feature = Suspicious\,\}$$
$$Else\{\, feature = Phishing\,\}$$

Slashes

A path with the data is always in a hierarchical form shown as a sequence of a segment separate with the'/'. This feature is also become an important part of the URL when we need to found out the segments of the URL. Less than three slashes are proving the legitimacy of the site. Whereas more than four slashes in the URL is defines as the phishing site.

$$if\{\, Dots\ in\ domain\ < 3\ \rightarrow feature = Legitimate\,\}$$
$$Else\ if\{\, Dots\ in\ domain = 3\ \rightarrow feature = Suspicious\,\}$$
$$Else\{\, feature = Phishing\,\}$$

@ Symbol

'@' symbol leads the browser to ignore everything suffix it and redirect to the link typed after @ symbol. W3 rules says @ symbol rarely used in the real URL. It has low significance because in rare case it is present in the dataset. Only 1% site is phishing out of the total dataset. The probability of this symbol is less according to our research of the dataset.

$$if\{\, URL\ having\ @\ symbol\ \rightarrow feature = Legitimate\,\}$$
$$Else\{\, feature = Phishing\,\}$$

& Symbol

It is one type of the query delimiter to separate the key and value which can be passed through the URL. More than two query variable are passed in the URL cause harm to the website because it shows the value of the key.

$$if\{\, URL\ having\ \&\ symbol\ \rightarrow feature = Phishing\ \}$$
$$Else\{\, feature = Legitimate\ \}$$

 # Symbol

The symbol of '#' is used for the optional fragment. Maximum two optional fragments are used in the legitimate URL. Phishing URL contain more than two '#' symbol. It is optional fragment so rarely present in the URL. It has low significance from all the features. In the dataset of my research are contains only four URLs which has '#' symbol.

$$if\{\, URL\ having\ \#\ symbol \leq 2 \rightarrow feature = Legitimate\ \}$$
$$Else\{\, feature = Phishing\ \}$$

% Symbol

Every URL needs to create in the proper format. But sometimes creator's intentionally put unwanted characters in the URL to confuse the users. Unwanted characters like'%' are present in the URL than it can be a phishing site.

$$if\{\, URL\ having\%symbol\ \rightarrow feature\ Phishing\ \}$$
$$Else\{\, feature = Legitimate\ \}$$

? Symbol

The significance of '?' symbol in URL is more important, however it can be used by attacker to stolen the information from the user. When any developer wants to submit the data of webpage into database at that time question mark symbol is used, but in legitimate sites, this symbol is not used.

$$if\{\, URL\ having\ ?\ symbol\ \rightarrow feature = Phishing\ \}$$
$$Else\{\, feature = Legitimate\ \}$$

DNS Record

Domain Name system stands for DNS. WHOIS database stored the record of the every domain of every URL. We code the program into .net that can provide the connection with WHOIS database and extract the data from the database.

$$if\{\, DNS\ record\ is\ Empty \rightarrow feature = Phishing\ \}$$
$$Else\{\, feature = Legitimate\ \}$$

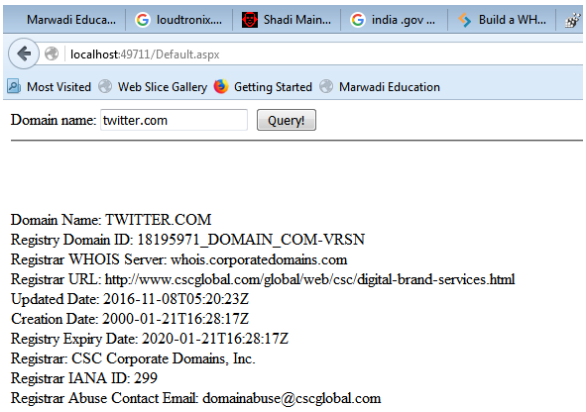

Fig 2. WHOIS Database

For every domain of the URL we check that entered URL is present in the WHOIS record or not. WHOIS database is also known as the third party domain.

Our code connects with the WHOIS database using the port number and extracts the record of entered domain name.

Unicode in URL as PayPal

PayPal is the gateway of the money transferring. PayPal keyword is not used in every URL. Every keyword has its own meaning like 'PayPal' is secured and used when online tractions are done. It follows the proper way to use in URL. Attackers used such type of keyword to confuse the user and to stolen the credential information using the wrong URL.

$$if\{\, URL\ having\ Paypal\ string \rightarrow feature = Phishing\ \}$$
$$Else\{\, feature = Legitimate\ \}$$

We have the three outputs after extracting the features from the URL and that is phishing, suspicious and legitimate. Now, we have the Fuzzy Inference System in the MatLab simulink which can help to decide the output in two forms only named as Phishing and Legitimate.

Now we use the classifier as the next step of our system. We used fuzzy logic for the classifier to classify the suspicious URL into the Phishing and legitimate URL.

For the input and output we have to decide the membership functions and according to those functions rules of the every member are created. According to that rules our final outcome is generated.

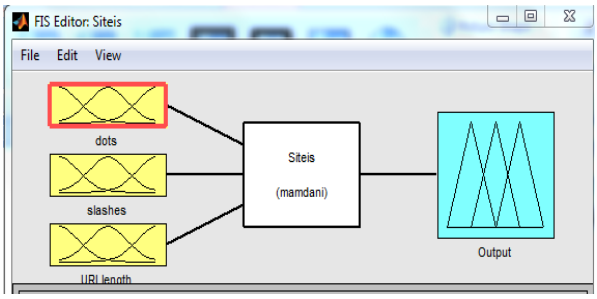

Fig. 3 Fuzzy Inference System design

First of all we design a layer for the features. For the suspicious URL we define the layers to classify it. According to the table1 we can easily examine the significance of the features[12].

Table1: Design a layer for the suspicious site

Criteria	Component	Layer No.
URL & Domain	No. of Dots	**Layer 1**
Weight=0.3		Sub weight=0.5
	No. of Slashes	
Weight=0.2		
Web Address bar		**Layer 2**
	URL Length	Sub weight=0.5
Weight=0.5		

Maher Aburrous et.al [5] designs a layer and a rule for the fuzzy technique. After the design the layer there is next step which is called as the Rule developing. Rules are defined to come with the result which contain either positive or negative in terms of phishing or legitimate[9].

Performance Matrix

There are mainly four possibility exists to find the performance of the system. Four possibility are True Positive, True Negative, False Positive, and False Negative.

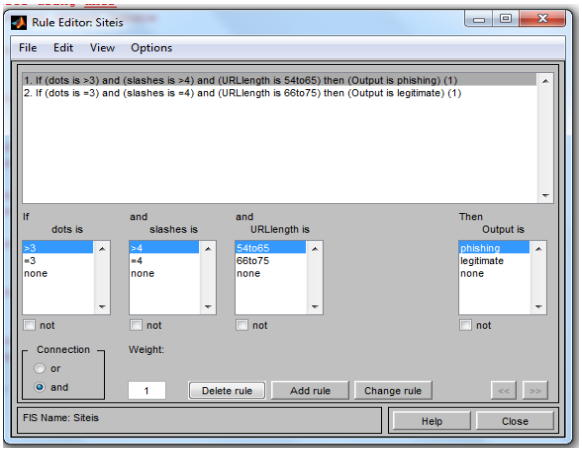

Fig. 4 Rule editor

Assume that Np denotes the total number of original sites Np denotes total number of phishing sites. If $(nh \rightarrow H)$ denotes original URL, then $(np \rightarrow H)$ denotes phishing sites classified as original $(nh \rightarrow P)$ denotes original sites classified as phishing and $(np \rightarrow P)$ denotes phishing sites classified as phishing. The evaluation matrix used in the [6][7].

True Positive Rate: The ratio of the number of phishing sites identify correctly.

$$\text{TP} = \frac{np \rightarrow P}{Np}$$

True Negative Rate: Ratio of original websites identified correctly.

$$\text{TN} = \frac{nh \rightarrow H}{Nh}$$

False Positive: The ratio of number of original websites classified as phishing.

$$\text{FP} = \frac{nh \rightarrow P}{Nh}$$

False Negative: Ratio of number of phishing websites classified as original.

$$\text{FN} = \frac{np \rightarrow H}{Np}$$

Accuracy: Measurement of correctly identifies value. The ratio of true positive rate and true negative rate with the total rate.

$$ACC = \frac{(TP + TN)}{(TP + TN + FP + FN)}$$

VI. CONCLUSION

The group of features is effective in detecting web phishing. Our model constructed using both phishing and legitimate URLs including the features which have been extracted from these models. In this paper fuzzy classifier is implemented using MatLab and the best results are achieved with 91.46% accuracy.

Features of our research are mostly dependent on URL, however using other group of the features user can achieve the best result. Using Different type of data set can be affect to the result of the system. Also the machine learning techniques play the important role as a classifier.

REFERENCES

[1] "Statistic of the website affected by phishing", [Online]. Available: https://www.statista.com/statistics/266161/websites-most-affected-by-phishing/

[2] M. Aydin and N. Baykal, ―Feature extraction and classification phishing websites based on URL, in *IEEE Conference on Communications and Network Security (CNS)*, Florence, 2015, pp. 769-770.

[3] Xin Mei Choo, Kang Leng Chiew, Dayang Hanani Abang Ibrahim, Nadianatra Musa, San Nah Sze, Wei King Tiong, "Feature-based phishing detection Technique", in *Journal of Theoretical and Applied Information Technology,* vol. 91 no. 1, pp. 101-106, 2016

[4] Rami M. Mohammad, Fadi Thabtah, Lee McCluskey, "Intelligent rule-based phishing websites classification", in *IET Information Security*, Vol. 8, no. 3, pp. 153-160, 2014.

[5] Maher Aburrous; M. A. Hossain; Fadi Thabatah; Keshav Dahal, "Intelligent phishing website detection system using fuzzy technique", in *Conference on Information and Communication Technologies: From Theory to Applications",* Damascus, Syria, 2008, pp. 1-6.

[6] B. B. Gupta, Aakanksha Tewari, Ankit Kumar Jain, Dharma P. Agrawal, "Fighting against phishing attacks: state of the art and future challenges", in *Neural Comput & Applic*, vol. 28(12), pp. 3629-3654, Mar 2016.

[7] R. Badlishah Ahmad, Yasmin Yacob, Ammar Yahya Daeef, "Wide Scope and fast websites phishing detection using URLs Lexical features", in *3rd International Conference on Electronic Design (ICED)*, 11-12 Aug. 2016, pp. 410-415, Phuket, Thailand.

[8] R. Cooley, B. Mobasher and J. Srivastava, "Web mining: information and pattern discovery on the World Wide Web", *Proceedings in 9th IEEE International Conference on Tools with Artificial Intelligence*, Newport Beach, CA, 1997, pp. 558-567.

[9] Ying Xue1 Yang Li1, Yuangang Yao, Xianghui Zhao, Jianyi Liu, Ru Zhang, "Phishing sites detection based on urlcorrelation," in *4th International conference on cloud Computing and Intelligence system(CCIS),* Beijing,China, 2016, pp. 244-248.

[10] V. Loia, S. Senatore,"A-Fuzzy oriented sentic analysis to capture the human emotion in Web-based content," in *Knowledge-based system journal of Elsevier Informatica*, Universiy, via Giovanni Paolo II, Fisciano, SA, Italy, vol. 58, pp. 75-85, Oct 2013.

[11] Varsharani Ramdas Hawanna, V. Y. Kulkarni, R. A. Rane, "A novel algorithm to detect phishing URLs," in *International Conference on Automatic Control and Dynamic Optimization Techniques (ICACDOT)*, Pune, 2016, pp. 548-552.

[12] K. N. Manoj Kumar, K. Alekhya, "Detecting Phishing Website using Fuzzy Logic,"in *International Journal of Advanced Research in Computer Engineering & Technology (IJARCET),* vol. 5(10), pp.2413-2417, Oct 2016.

Proceedings of the Fourth International Conference on Communication and Electronics Systems (ICCES 2019)
IEEE Conference Record # 45898; IEEE Xplore ISBN: 978-1-7281-1261-9

Power Analysis of 2-bit Array Multiplier using Adiabatic Logic

Jacob Savio
M.Tech Scholar, Dept. of ECE
N.M.A.M Institute of Technology
Karkala, India
jacb993@gmail.com

Rekha Bhandarkar
Professor and Head, Dept. of ECE
N.M.A.M Institute of Technology
Karkala, India
rekhabhandarkar@nitte.edu.in

Abstract— The importance of digitally integrated circuit is increasing since it has many features such as low power, reliability, propagation delay and noise margin. An energy efficient technique and a new CMOS (Complementary Metal Oxide Semiconductor) logic family called Adiabatic logic, based on reversible switching principle is discussed in this paper. Adiabatic technique is used to increase energy efficiency of logic circuits. The principle is based on energy recovery in which the power supply recovers the charge without heat generation. Minimum power consumption is achieved when the charging and discharging path has a MOS transistor instead of a diode. The simulation is carried out for 2-bit Array Multiplier using 45nm CMOS technology in Cadence Virtuoso environment. Power saving of more than 40% is achieved by Adiabatic logic circuits in comparison with conventional CMOS circuits but with increase in area. The Gate is controlled by power clocks. The method of switching achieves less power dissipation, but complexity of circuit increased. Energy stored in load capacitor is reused in Adiabatic logic whereas energy is discharged to the ground in case of traditional conventional logic.

Keywords— Conventional CMOS; Adiabatic Logic; Half adder; 2-bit array multiplier; PAL; Clocked CMOS logic; CCAL;

I. INTRODUCTION

The power consumption has become a major design parameter for VLSI circuit designers as VLSI technology is improving day by day. Many technologies have been developed to reduce integrated circuit power dissipation. Adiabatic innovation is one of the promising advancements for low power activity of the circuit. The logic of charging recovery or Adiabatic switching techniques is based on slowing down energy transfer and retrieving charge from logic. Dynamic power consumption of the circuit is reduced by Adiabatic logic [26].

In Adiabatic logic, compelling power saving was achieved compared to conventional CMOS circuits. Adiabatic circuits outputs are valid only during a specific phase of the power clock cycle. Therefore, to drive the Adiabatic cascaded Logic chain, multi - phase clocking is required. [20].

In this paper multiplier using Adiabatic Logic is simulated. The method used to multiply two 2-binary numbers is identical to the multiplication of decimal numbers based on partial product calculation, shifting and combining them. A similar approach but that which is simpler than decimal multiplication is to multiply two binary numbers by multiplying the long multiplicand by 0 or 1, as multiplication by 0 or 1 results either in the same number or zero. A representation of a 2-bit array multiplier is as shown in Fig. 1. The maximum product term can be 11 * 11 = 1001, a 4-bit number.

The rest of the paper is organized as follows. Section II provides review of literature. Section III presents description of conventional design. In section IV Adiabatic logic is discussed. Section V presents implementation of 2-bit array Multiplier using Adiabatic Logics. Section VI presents results and their analysis obtaining during the course of the results and Section VII presents conclusion drawn from result obtained from section VI.

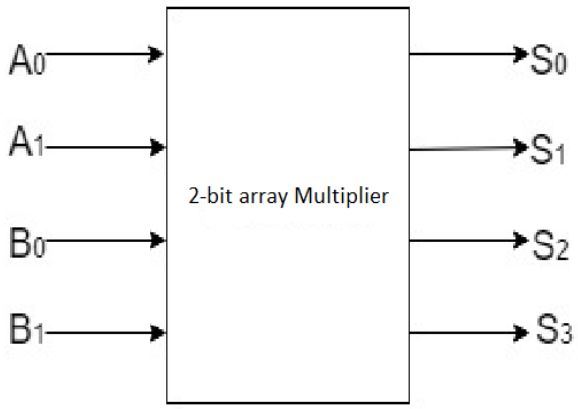

Fig. 1: Block diagram of 2-bit Multiplier

II. LITARATURE REVIEW

A. *Clocked CMOS Adiabatic logic(CCAL)*

He Li et al [15], introduced CCAL technique that is used to reduce consumption of power. Various adiabatic logics such as clocked CMOS, eight level inverter chain CCAL, Quasi Static Energy Recovery Logic (QSERL) are compared with CCAL technique. It has static logic and tristate output which is managed with help of pwr. CCAL has two advantages over QSERL, high operating frequency up to 500MHz and low power dissipation.

B. *Pass transistor Adiabatic Logic(PAL)*

Mahendra Singh Dhaka et al [17], proposed NOR logic Gate using 2PASCL and PAL logics which is simulated on 180nm and 90nm technology to obtain the comparison of significant power saving.

III. Conventional Design

A. Conventional CMOS 2-bit array Multiplier

Multipliers are vital block employed in numerous digital circuits. An overview of the two - bit A_1A_0 and B_1B_0 numbers to produce the four - bit $S_3S_2S_1S_0$ product as shown in Fig. 3. The Multiplication illustrated in Fig. 2 is implemented as shown in Fig. 3. The bits of each partial product are computed by multiplying two bits of the input. Since two-bit multiplication is the same as the logical AND operation, AND Gates can be used to generate the partial products [6]. Half Adders and AND Gates as shown in Fig. 3 are used to implement a 2-bit Multiplier.

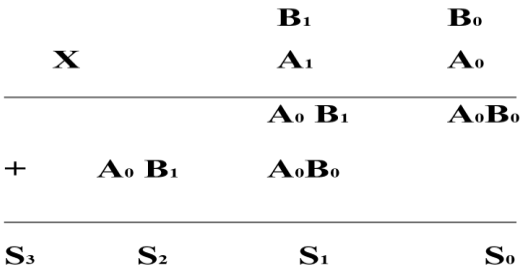

Fig. 2: Illustration of 2-bit Multiplier

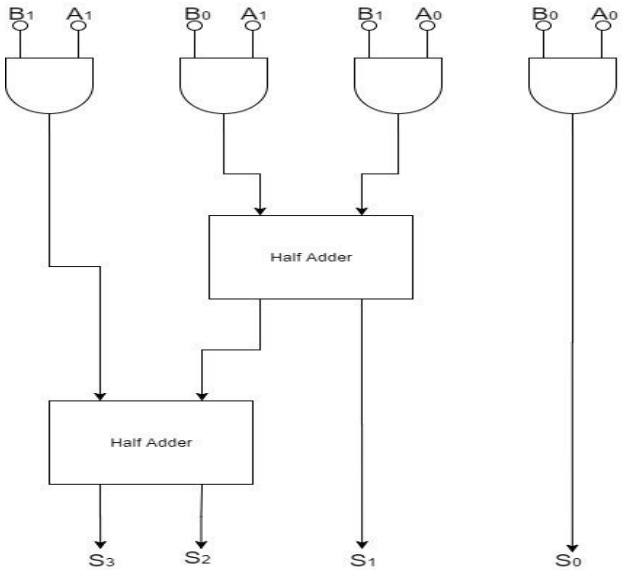

Fig. 3: Block diagram of 2-bit Multiplier

B. Clocked CMOS Logic

Fig. 4 shows the block diagram of a clocked CMOS Gate. It consists of a static logic circuit with clock and /clock controlled tri-state output network. Both P1 and N1 are conducting when clock signal is logic high. Since both the PFET logic block and NFET logic blocks are linked to the output, a standard static logic gate is degenerated by the circuit. When the clock changes from logic one to logic zero, both PMOS P1 and NMOS N1 are in cutoff. Hence the output out is in Hi-Z (high impedance) condition. Both PFETs and NFETs logic blocks are disconnected from the output during this time interval, so there is no effect on the outputs unless the clock reaches the logic one.

IV. Adiabatic Logic Style

Adiabatic word comes from "Thermodynamics" where there is "no exchange of heat with the environment" [22]. But practically this condition cannot be met due to the presence of resistive components in the system or a design. The energy consumption could be minimized in the system by decreasing the switching speed and also obtaining outputs under certain conditions.

In Adiabatic Logic sinusoidal or trapezoidal power source is
in use. As shown in Fig. 5 the output can be analyzed at four phases of the clock namely,

a) Precharge phase

b) Evaluation phase

c) Discharge phase

d) Idle phase

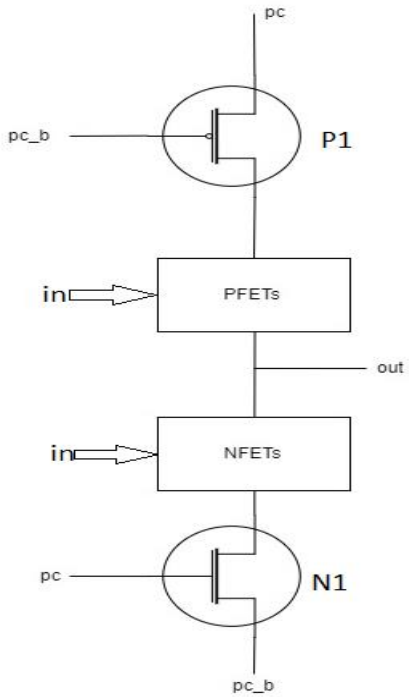

Fig. 4. Block diagram of Clocked CMOS logic

During idle phase/wait phase the circuit is idle. In precharge phase depending upon input the load capacitance (node capacitance) either charge up or does not. In evaluation phase, the output is stable, so that next stage can be analyzed.

Finally, in discharge/ recovery phase the charge is recovered back to power source [23].

Adiabatic Logic is divided into two classes namely,

a) Fully Adiabatic Logic style

All load capacitance charges are recovered in fully Adiabatic circuits and feedback is given to the power supply. Because of which fully Adiabatic circuits are slower and more complex than partial Adiabatic circuits [23].

b) Partial Adiabatic Logic style

In partially Adiabatic circuits a portion of charge stored in the capacitor is transferred to ground, i.e. some heat is dissipated. Therefore, only part of the energy can be recovered, but these circuits can be easily implemented compared to fully Adiabatic Logic circuits [23].

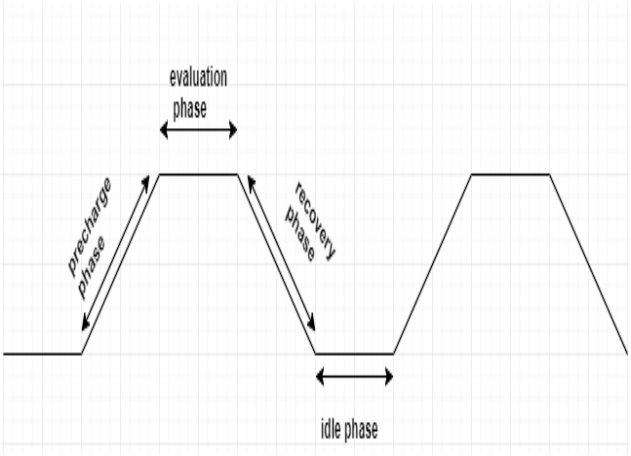

Fig. 5: Four phases of the clock [2]

A. Pass transistor Adiabatic Logic(PAL)

Pass transistor Adiabatic Logic is twin rail Adiabatic Logic with moderately less complex equipment and works through a phase power clock. The basic structure of PAL logic consists of two blocks: memory block and logic block. In pre-charge phase the logic block either charges or discharges based on the input values. In evaluation phase the memory block retains the output values. The inputs make a conduction path from the input to one of the output node when the sinusoidal power clock rises. Output is valid only when sinusoidal power clock at its peak. The supply then tilts down to the zero value from the top, recovering energy stored in the capacitance of the output node. Fig. 6 shows the basic structure of the PAL.

B. Clocked CMOS Adiabatic Logic(CCAL)

Fig. 7 shows the basic structure of Clocked CMOS Adiabatic Logic. Each Clocked CMOS Adiabatic Logic circuit comprises of the CMOS logic component that acts as the logically evaluation component (connected to input) and the clock control component (connected to clock pc) that controls the connection between the logic component and the output node. The CCAL is supplied power by the clock pc and pc_b which are sinusoidal and complimentary.

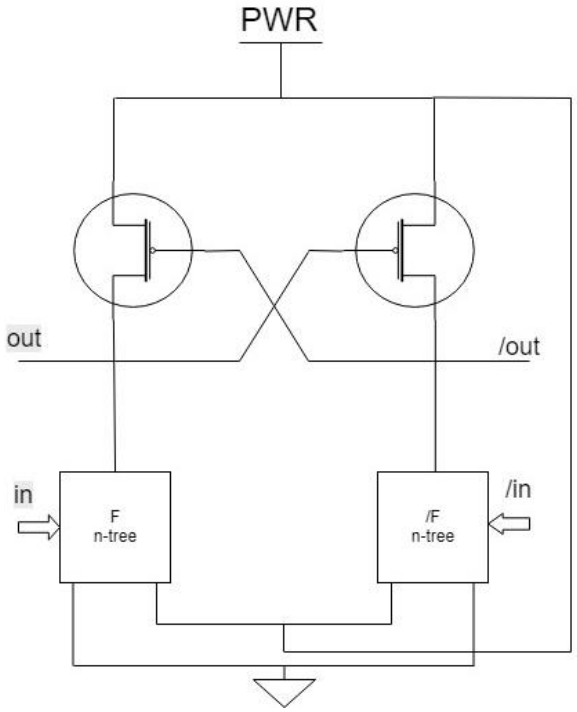

Fig. 6: The basic structure of PAL

V. CIRCUIT IMPLEMENTATION OF 2-BIT ARRAY MULTIPLIER

2-bit array multiplier is designed using conventional CMOS design, Clocked CMOS logic, PAL and CCAL Techniques using Cadence Virtuoso tool 45nm technology with power supply of 1V and 400MHz frequency. For verification of schematic results, the transient analysis is performed by launching ADEL. Graph of the total power is obtained for implemented circuits. 2-bit array multiplier designed using half adders and AND gates are shown in Fig. 3.

A. Conventional CMOS 2-bit multiplier implementation

Fig. 8 shows the schematic implementation of Conventional 2-bit array Multiplier. The 2-bit inputs to the multiplier are a_1a_0 and b_1b_0 and 4-bit output of the Multiplier are $s_3s_2s_1s_0$ bits. Four conventional AND gate and two conventional single bit adders are used to design 2-bit array multiplier. Fig. 9 shows transient response of conventional 2-bit array multiplier.

B. Clocked CMOS 2-bit array Multiplier

Fig. 10 shows the schematic implementation of Clocked CMOS 2-bit array Multiplier. It consists of a static logic circuit that is controlled by clock and clock b with a tri-state output network. Fig. 11 shows transient response of Clocked CMOS 2-bit array Multiplier. From Fig. 11 it is observed that

output is valid only when clock signal is logic high and high impedance when clock is logic low.

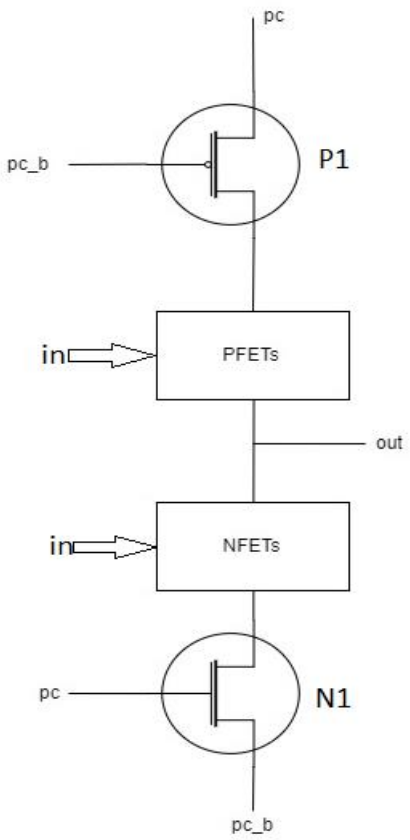

Fig. 7: Block diagram of CCAL

C. PAL 2-bit multiplier implementation

Fig. 12 shows the schematic Implementation of 2-bit array Multiplier using PAL technique. pwr_1, pwr_2 and pwr_3 are power supplies of circuit to drive a cascaded Adiabatic Logic chain [23]. Fig. 13 shows the PAL 2-bit array multiplier's transient response. From Fig. 13 it can be observed that Adiabatic outputs $s_3s_2s_1s_0$ are valid only when the sinusoidal power supply is at its peak value.

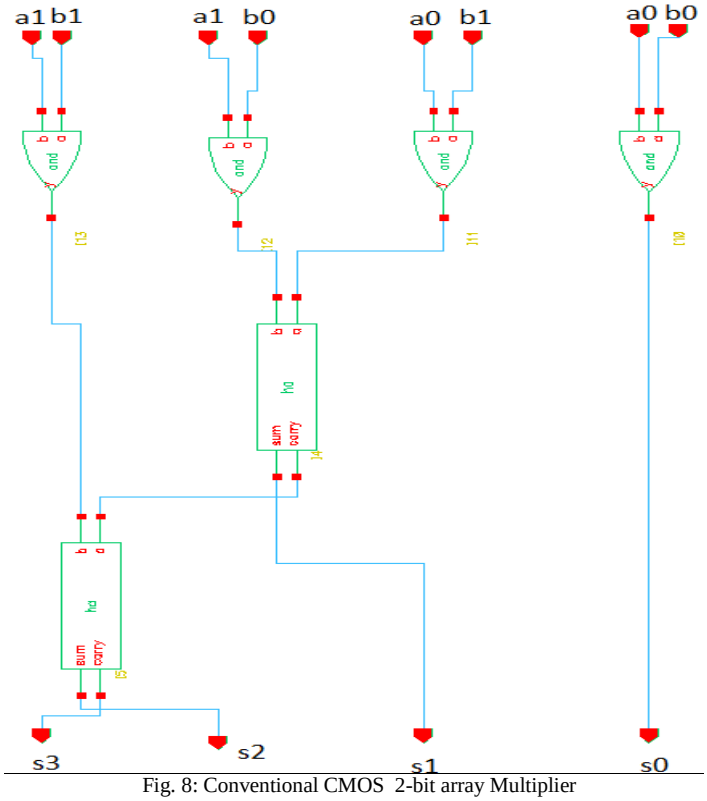

Fig. 8: Conventional CMOS 2-bit array Multiplier

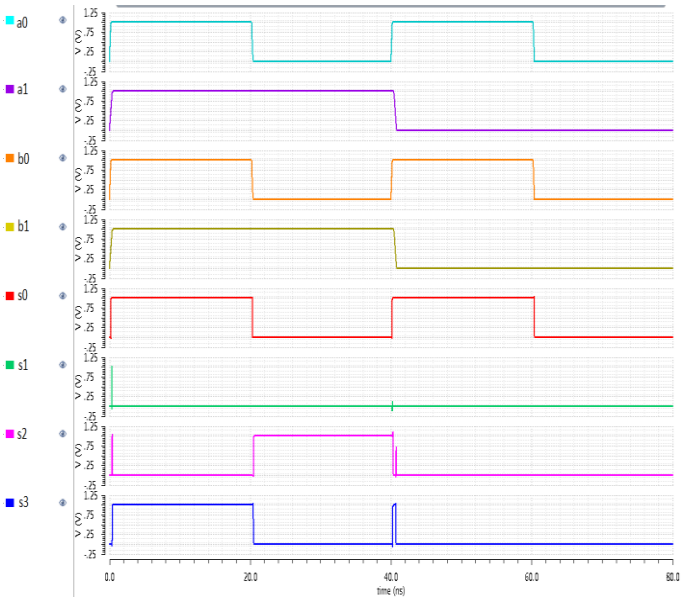

Fig. 9. Transient response of Conventional 2-bit array Multplier

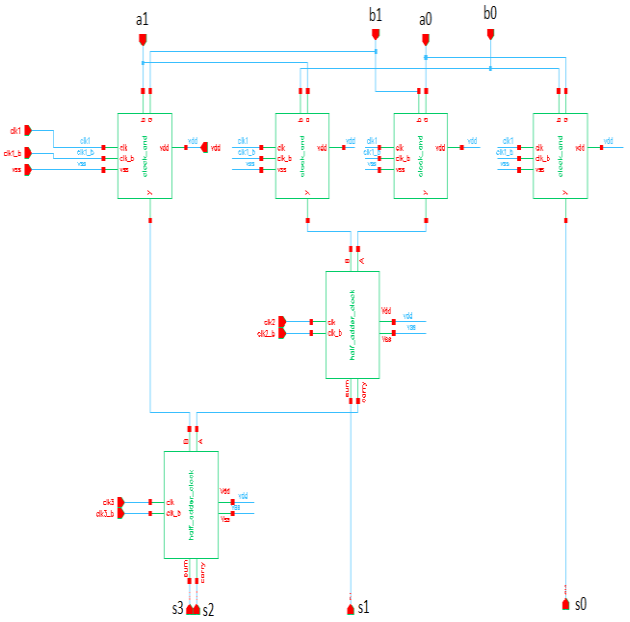

Fig. 10: Clocked CMOS 2-bit array Multiplier

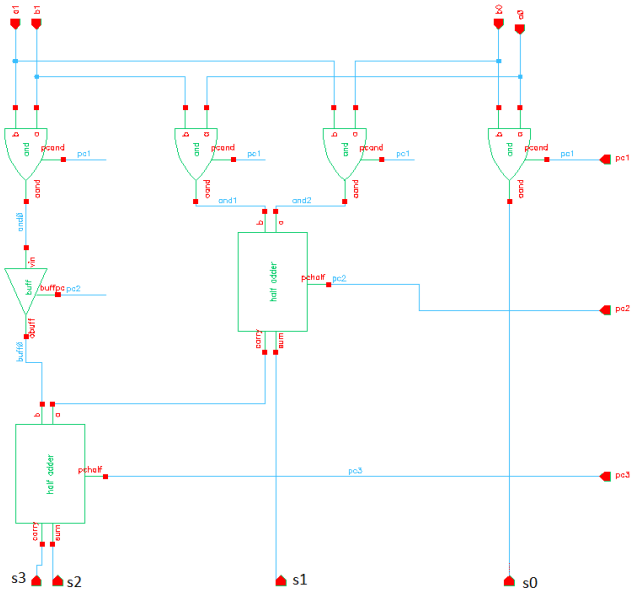

Fig. 12. PAL based 2-bit array Multiplier

D. CCAL 2-bit multiplier implementation

Fig. 14 shows the schematic implementation of 2-bit array Multiplier using CCAL technique. pc_1, pc_2 and pc_3 are power clock of to drive the Adiabatic cascaded logic chain [15]. Fig. 15 shows transient response of CCAL 2-bit array Multiplier. From Fig. 15 it can be observed that Adiabatic outputs $s_3s_2s_1s_0$ are valid only when the sinusoidal power supply is at its peak value.

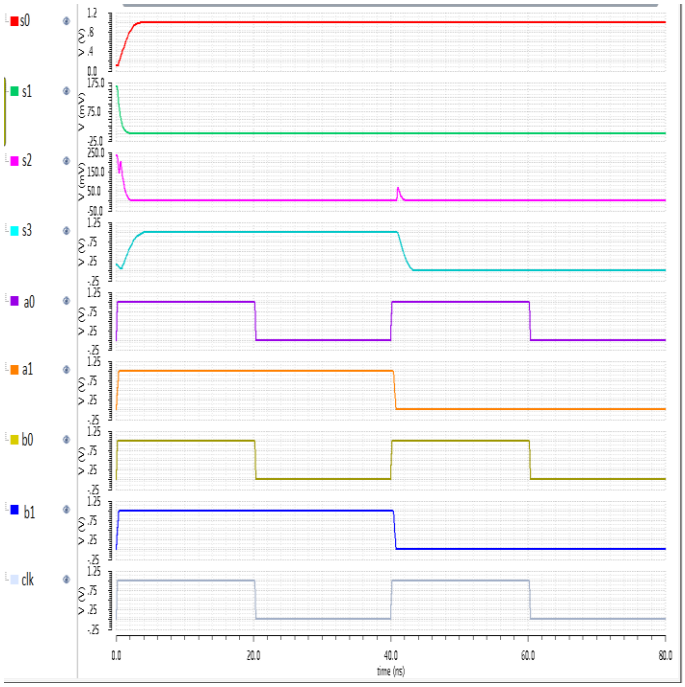

Fig. 11: Transient respond of Clocked CMOS 2-bit array Multiplier

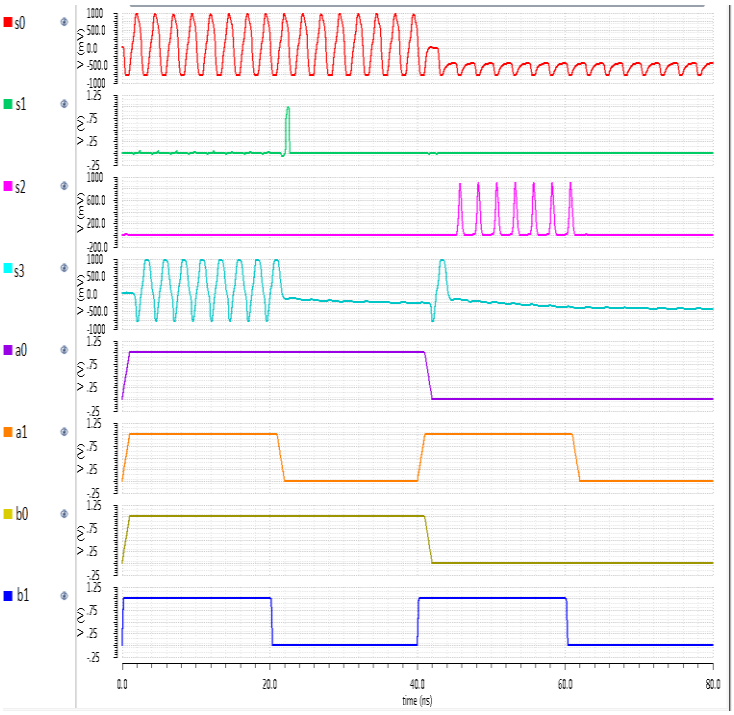

Fig. 13. Transient response of 2-bit array Multplier using PAL

In contradiction to CMOS technique the charge stored in capacitance is recovered by power supply instead of dissipated as heat [23].

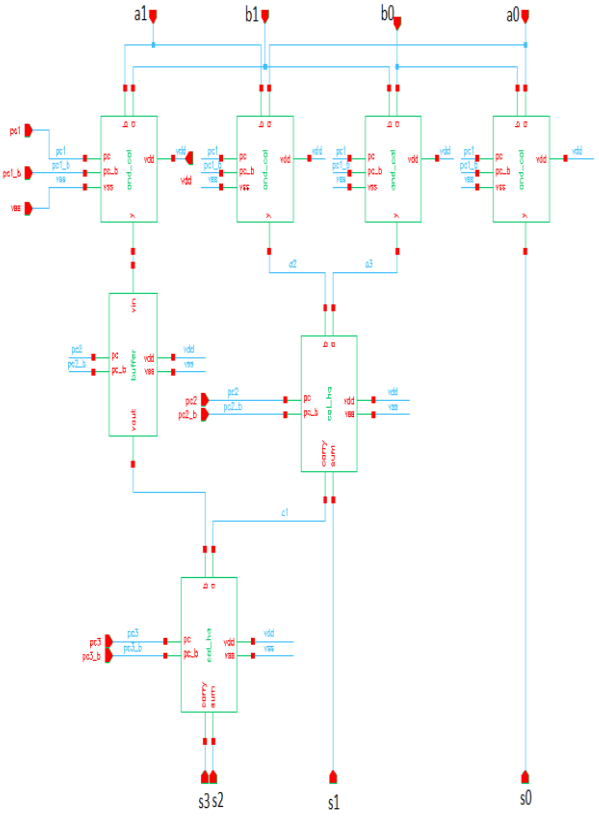

Fig. 12: CCAL based 2-bit array Multiplier

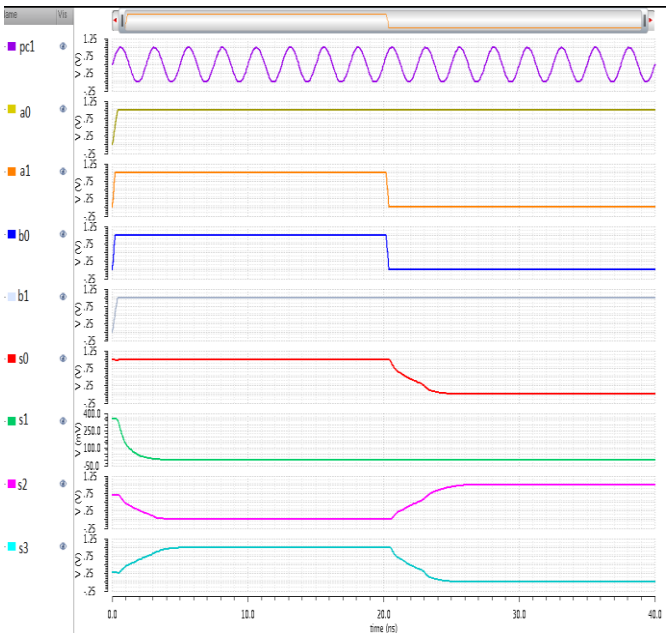

Fig. 13: Transient response of 2-bit array Multiplier using CCAL

E. Power Analysis

Fig. 13, Fig. 14, Fig. 15 and Fig. 16 shows the total power dissipation of 2-bit array Multiplier using Conventional CMOS, Clocked CMOS, PAL and CCAL techniques. Total power dissipation is obtained using Cadence Virtuoso tool.

TABLE I. POWER ANALYSIS OF 2-BIT ARRAY MULTIPLIER

Design Method	Maximum power(μW)
Conventional Design	76.11
Clocked CMOS	94.625
PAL	25.9
CCAL	47.29

Table I. shows the maximum power of 2-bit array Multiplier using conventional CMOS logic, Clocked CMOS logic, PAL and CCAL.

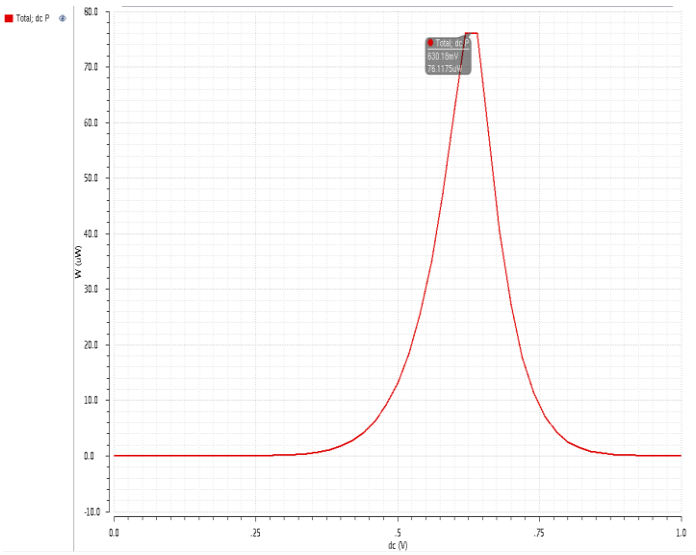

Fig. 14: Total power of Conventional CMOS 2-bit array Multiplier

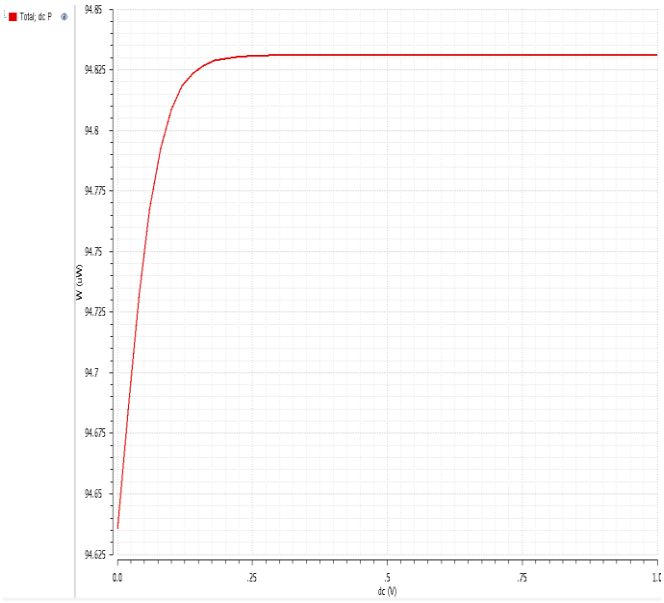

Fig. 15: Total power of Clocked CMOS 2-bit array Multiplier

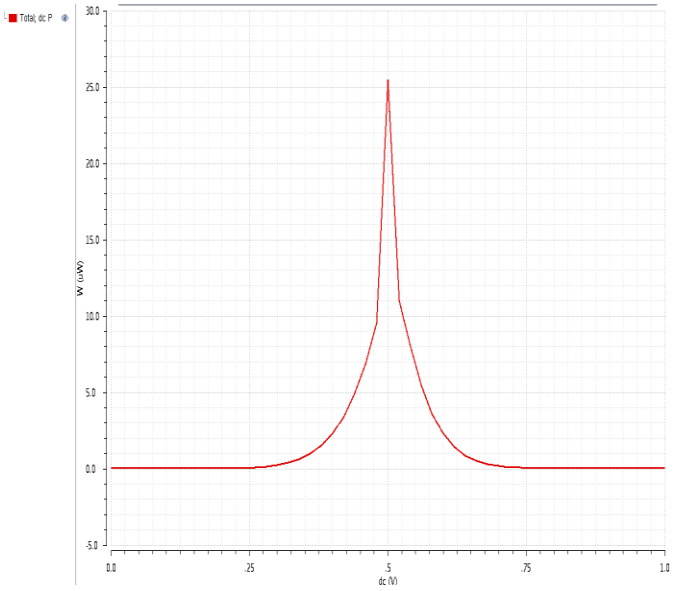

Fig. 16: Total power of PAL 2-bit array Multiplier

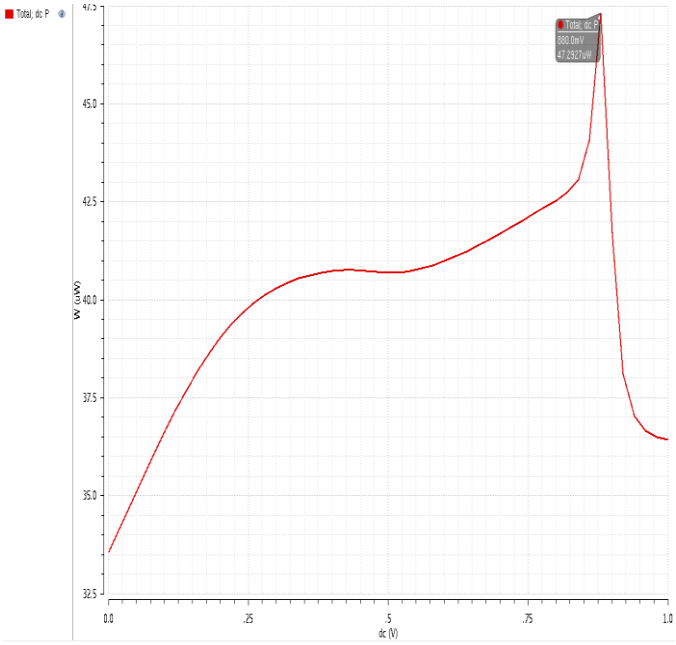

Fig. 17: Total power of CCAL 2-bit array Multiplier

Maximum power consumption of PAL and CCAL logic is less compared to CMOS logic and Clocked CMOS respectively. In CMOS logic and Clocked CMOS logic power is dissipated as heat whereas in PAL and CCAL power is reused. Power reused by turning MOSFETs ON only when they have same potential. When no current flows through MOSFETs they turn off and use a power supply capable of recovering or recycling energy by electric charge. To achieve this, the Adiabatic Logic circuit's power supplies used constant current charging rather than constant voltage charging [18]. From Table I, it is observed that maximum power of PAL is less then maximum power of CCAL.

VI. Conclusion

The 2-bit array Multiplier is simulated and analyzed using GPDK 45nm technology, at 1V, with clock frequency of 400MHz and load capacitance of 0.01 pF for conventional CMOS, Clocked CMOS, PAL and CCAL. From the comparison of the result obtained, the maximum power consumption of the circuit calculated is considerably low in Adiabatic Logic circuits compared to the CMOS circuits. Adiabatic operation promises a significant reduction in power consumption as it reuses the energy stored in the capacitor instead of discharging [17] it to ground and also Adiabatic Logic uses sinusoidal power supply instead of constant voltage supply. It is found that the 2-bit array Multiplier designed using PAL logic consumes less power when compared with CCAL since number of power supply employed in CCAL is more. It is observed that, the circuit area is not increased in CCAL where as there is a 50% area increase in PAL.

Future work includes design and simulation of different multipliers under different Adiabatic techniques. Layout of the Multiplier can be designed in order to find area, delay and other parameters for the same.

References

[1] Arjun Mishra and Neha Singh, “Low Power Circuit Design Using Positive Feedback Adiabatic Logic(PAL-2n)”, International Journal of Science and Research, vol. 3, Issue-6, pp. 46-45, 2018.

[2] Nazrul Anvar, Yasuhiro Takahashi and Toshikazu Sekine, “Two Phase Clocked Adiabatic Static CMOS logic”, Proceedings of the IEEE ICECS, pp.503-506, 2018.

[3] Ruchi Yadav, Amit Bakshi, Joy Chowdhury, J.K.Das, “Adiabatic Approach for Charge Restoration in Low Power Digital Circuits,” 2nd IEEE International Conference on Inventive Systems and Control (ICISC), pp. 473- 477, 2018.

[4] V. Shiva Prasad Nayak, N.Ramchander, R.Sumanth Reddy, T Hemanth Sai Praveen Redy and M. Srisri Reddy, “Analysis and Design of Low-Power Reversible Carry Select Adder Using D-Latch,” IEEE International Conference On Recent Trends In Electronics Information Communication Technology, pp. 1917- 1920, 2016.

[5] V. Shiva Prasad Nayak, N.Ramchander, R.Sumanth Reddy, T Hemanth Sai Praveen Redy and M. Srisri Reddy, “Analysis and Design of Low-Power Reversible Carry Select Adder Using D-Latch,” IEEE International Conference On Recent Trends In Electronics Information Communication Technology, pp. 1917- 1920, 2016.

[6] Ankita Mishra, “Low power cmos cell structures based on Adiabatic switching,” IEEE International Conference on Communication and Electronics Systems(ICCES), 2016.

[7] Preeti Bhati, Navaid Z. Rizvi, “Adiabatic Logic: An alternative approach to low power application circuits”, International Conference on Electrical, Electronics and Optimization Techniques (ICEEOT),2016.

[8] D.Jayanthi, A.Bhavani Shankar, S.Raghavan and G.Rajasekar, “High Speed Multi output Circuits Using Adiabatic Logic,” IEEE International Conference on Emerging Trends in Engineering, Technology and Science(ICETETS), 2016.

[9] Irfan Ahmad Pindoo, Tejinder Singh, Amritpal Singh, Ankit Chaudhary and P. Mohan Kumar, “Power Dissipation Reduction Using Adiabatic Logic Techniques for CMOS Inverter Circuit,” 6th IEEE International Conference on Computing, Communication and Networking Technology(ICCCNT), 2015.

[10] M.L.Keote and Dr.P.T.Karule, "Design and Implementation of Energy Efficient Adiabatic ECRL and Basic Gates," IEEE International Conference on Soft Computing Techniques and Implementations-(ICSCTI), pp. 87-91, 2015.

[11] Arpan Chaudhuri, Mamia Saha, Moumita Bhowmik, Sambhu Nath Pradhan and Subhrajit Das, "Implementation Of Circuitin Different Adiabatic Logic," 2nd IEEE International Conference On Electronics And Communication System(ICECS), pp. 353-359, 2015.

[12] Shiv Pratap Singh Kushawaha, Trailokya Nath Sasamal, "Modified Positive Feedback Adiabatic Logic for Ultra Low Power VLSI," IEEE International Conference on Computer, Communication and Control, 2015.

[13] Sriraj Dheeraj Turaga, E. Arun Jyothi, K. Jaya Datta Sai, "Power Reduction Technique Using Adiabatic Logic," IEEE International Conference on Circuit, Power and Computing Technologies (ICCPCT), pp.1284-1290, 2014.

[14] Deepti Shinghal, Amit Saxena and Arti Noor, "Adiabatic Logic Circuits: A Retrospect," MIT International Journal of Electronics and Communication Engineering, Vol. 3, pp. 108–114, 2013.

[15] He Li, Yimeng Zhang, and Tsutomu Yoshihara, "Clocked CMOS Adiabatic Logic with Low-Power Dissipation," Proceedings of the IEEE, vol 85, no 2, pp.112-126,2013.

[16] M. Bharati, Dilli Kumar, "Design of Energy Efficient Arithmetic Circuits Using Charge Recovery Adiabatic Logic". International journal of Engineering Trends and Technology, vol 4, issue-1, pp.32-40, 2014.

[17] Mahendra Singh haka, Gayatri and Pamendra Singh Dhaka. "Adiabatic Logic Gate for Low Power Application", International Journal of Engineering Research and Applications (IJERA), vol 2, issue-3, pp.24-70, 2012.

[18] Atul Maurya and Gagnesh Kumar, "Adiabatic Logic: Energy Efficient Technique for VLSI application", International Conference on Computer and Communication Technology, Proceedings of the IEEE, pp.234-238, 2011.

[19] Ni Haiyan and Hu Jianping, "Near-Threshold Sequential Circuits Using Improved Clocked Adiabatic Logic in 45nm CMOS Processes", IEEE, pp. 5-8, , 2011.

[20] Nazrul Anvar, Yasuhiro Takahashi and Toshikazu Sekine, "X-OR Evaluation of 4X4 Bit Array Two Phase Clocked Adiabatic Static CMOS logic", Proceedings of the IEEE MWSCAS, vol 3, pp.56-71, 2010.

[21] Cihun Siyong, Muh Tian Shiue, Ci Tong Hong and Kai Wen Yao. "Analysis and Design of an Efficient Irreversible Energy recovery logic in 180 nm CMOS", IEEE Transactions on Circuits and Systems, vol.55.no, pp.2595-2607, 2008.

[22] Kaushik Roy Pandit, Saibal Mukopadhyay and Hamid Mahmoodi Meiand. "Leakage Current Mechanisms and Leakage reduction in Deep Sub-micrometer CMOS Circuits", Proceedings of the IEEE, vol 91, no 2, pp.305-327, 2003.

[23] Yong Bin Kim and Shivakumar Sompur. "An investigation into Adiabatic circuits". IEEE Transactions on Circuits and Systems, vol 1, pp. 294-297, 2001.

[24] H.Mahmoodi-Meimand , A.Afzali-Kusha and M.Nourani, "Adiabatic carry look-ahead adder with efficient power clock generator," IEEE proc. Circuits Devices Sysl, Vol. 148, pp. 229- 234, 2001.

[25] S. G. Younis and T. F. Knight, "Practical implementation of charge recovering asymptotically zero power CMOS," in Proc. 1993 Symp. Integrated Systems, Seattle, WA, Mar. 1993, pp. 234–250.

[26] http://www.techopedia.com

Proceedings of the Fourth International Conference on Communication and Electronics Systems (ICCES 2019)
IEEE Conference Record # 45898; IEEE Xplore ISBN: 978-1-7281-1261-9

Safety and Driver Assistance in VANETs: An Experimental Approach for V2V

C. Suganthi Evangeline
Assistant Professor,
Department of Electronics and communication Engineering
Karunya Institute of Technology and Sciences
Coimbatore, India
evangelineme4@gmail.com

Vinoth Babu Kumaravelu
Associate Professor
School of Electronics Engineering
Vellore Institute of Technology
Vellore, India

Atul Joshi
UG Scholar,
Department of Electronics and communication Engineering
Karunya Institute of Technology and Sciences
Coimbatore, India

Abstract— **In recent years there has been an exponential increase in the number of automobiles available to the consumers. Due to high density of vehicles, the potential threats and road accidents are increasing. The vehicles itself designed in such a way to provide lot of services for users in transit such as toll, infotainment and gaming. The vehicle can able to communicate with other vehicle in order to provide updates about different road situations and dangerous conditions, which results in saving time and lives. This new emerging technology called Vehicular Network (VANET) helps in achieving this communication. The main aim of this work is to develop the prototype for the prevention of chain collisions of vehicles on highways, by sending an indication of collision of the collided vehicle to the preceding vehicles. VANET provides the communication between vehicles and road-side units (RSU) with an aim of providing efficient and safe transportation. The ultrasonic sensor interfaced with the on board unit (OBU) has a controller which detects the collision of the target vehicle and sends the information to the OBU of preceding vehicle. This is accomplished by employing NodeMCUs. Both the NodeMCUs uses user datagram protocol (UDP) to communicate with each other. The RSU provide a hotspot for both NodeMCUs to connect. The present format is a prototype model that can adapted with inputs from different sensors to provide more reliable data to the preceding.**

Keywords— VANET; Collision; User Datagram Protocol; Road Side Unit; On-Board Unit; NodeMCU; Ultrasonic sensor; Target Vehicle; Sensors.

I. INTRODUCTION

Each year many people suffer from different traffic causalities around the world. This leads to the increased investment of financial resources in order to improve the road safety and help the driver by providing assistance. The vehicle internally has its own safety advancements like seat belts, air bags etc. But when during travel the safeness is also being ensured by Intelligent Transportation system (ITS). The major key part of ITS is Vehicular Network (VANET) [1]. VANET is based on the same principle of Mobile Ad hoc Network (MANET) but differs in mobility patterns. The term VANET is first mentioned in 2001 under car-to-car ad hoc mobile communication and networking applications, the networks are formed and relaying of information is done among cars. The architecture of VANET supports vehicle to vehicle (V2V) communication and vehicle to infrastructure (V2I) communication. The communication types are given in Fig.1. This would results in providing applications like road safety, navigation and other internet services.

With the availability of heterogeneous environment, the vehicles in VANET can able to connect with UMTS, Wi-Fi or WiMAX to avail the required services [2]. It is proved that Wi-Fi is the best suitable for vehicles to get access when it moves in high speed. The communication is carried out between vehicles and access points which may be fixed or mobile. The method of dissemination of messages used by the vehicles in VANET environment is broadcasting. This type of message dissemination is done after regular intervals inorder to increase the data rate and resources are get saved. UDP is used to communicate between the two vehicles primarily because establishing low-latency and loss-tolerating connections [1].

There are two vehicular units, the one in the front is termed as target vehicle and the preceding vehicular is termed as host vehicle. Both are connected to the same local network. When the target vehicle is met with a collision, the motor driving the host vehicle is stopped to avoid the collision. This scenario is considered in highways with both the vehicles are assumed to be travelling in the same lane. The collision scenario is depicted in Fig.2.

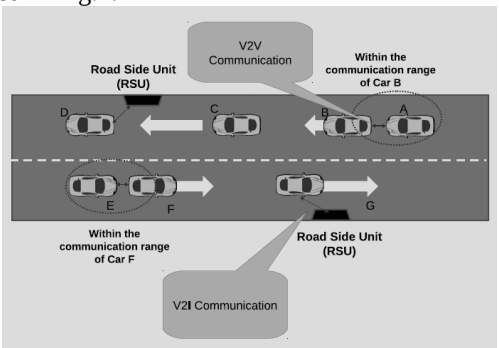

Fig. 1. VANET communication between vehicles and RSU

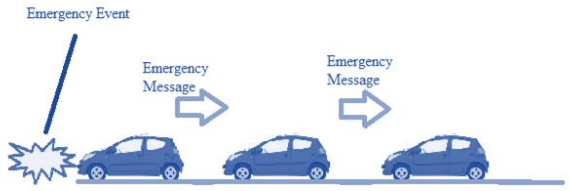

Fig. 2. Application of VANETs in avoiding chain collision

The rest of the paper is organized in the following order:
The recent works on experimental evaluation of VANET is carried out in section II. The methodology adopted is mentioned in section III. The proposed work is presented in section IV. The distance calibration of ultrasonic sensor is given in section V. The experimental setup is presented in section VI The application of VANET is listed in section VII. The future scope of work is given in section VIII and followed by conclusion in section IX.

II. RECENT WORKS

Certain works deals with the implementation of VANET using VNsim, which is a VANET simulator, used to evaluate different VANET technologies. They present novel techniques that substantiate the mobility models of vehicles with good approximation to real-world movement patterns [3]. Previous works deals with the evaluation of performance of V2V and I2V multi-hop communication based on IEEE 802.11b, where the distance and LOS are the factors affecting its performance and have also suggested that the use of ad hoc networks could extend transmission [4]. Others have evaluated the impact of obstructing vehicles on V2V communication using IEEE 802.11p, where the vehicles blocking LOS significantly attenuated the signal [5]. Another also uses IEEE 802.11p standard with 500 byte frame, which obtained the best performance follower by a 50 byte frame which had byte rate decreased by 60% compared to the former. Using a higher byte rate of 1460 was less stable than 500 byte rate transmission [6]. Others have evaluated the IEEE 802.11p standard, which improved safety of vehicles, but have significant downfalls in high dense traffic [7].

III. METHODOLGY

A. Hardware Requirements

- Pic Microcontroller (PIC16F877A) x2
- NodeMCU x2
- Ultrasonic Sensor(HCSR-04)
- L7805 Voltage regulator x3
- L298D Motor Driver x2
- DC motor x2
- Mobile Hotspot

1) PIC16 Series Controller

It is a reduced instruction set computer (RISC) type architecture [8]. It has been made with complementry metal oxide semiconductor (CMOS) type with harvard architecture. The PIC series with this architectcure has separate bus for program and data. The features of the controller is mentioned in Table 1.

The main advantage of CMOS and RISC combination is low power consumption and noise immunity compared to other fabrication techniques. With the use of flash technology the data in the memory is get retained after the power off. It is comfortable to reprogram and erase in PIC16F877A.

TABLE I. GENERAL FEATURES OF PIC16F877A

Parameters	Values
CPU	8-bit PIC
Total number of Pins	40
Voltage needed for operation	2 V > and < 5.5 V
General Purpose Input/ Output Pins	33
Analog to digital Converter (ADC)	Eight Channel and 10 bit
Timer Module	Two 8 bit Timers One 16 bit Timer
Comparators	2
Communication Peripherals	Universal Asynchronous Receiver and Transmitter (UART) , Serial Peripheral Interface (SPI), Inter Integrated Circuit (I2C),

a) Core Features

- High performance RISC CPU.
- It supports instruction in word
- As it is based on RISC architecture the instruction execution takes single clock cycle.
- The clock speed for PIC series is about 200MHz and the time taken for instruction to execute is 200ns
- The stack is about 8 level needed during interrupt servicing.
- The PIC series is capable to support 14 sources of interrupt.
- Power on Reset (POR).
- Power-Up Timer (PWRT) and oscillator start-up timer

2) NodeMCU

It includes an firmware which has Wi-Fi module design for Internet of Things (IoT) applications. NodeMCU is an open source IoT platform. The term "NodeMCU" is actually a firmware works based on Lua scripting language.

a) Steps to program NodeMCU

i) Build the firmware with necessary modules needed.
ii) Perform Flashing the firmware to the chip
iii) Do the uploading part of code to the device.

NodeMCU acts as the communication module between the vehicles in informing about the road situations and further more updates [8].

3) Ultrasonic Ranging Module HC-SR04

The HC-SR04 module provides a non-contact measurement reading from 2cm to 400 cm. The module has four pins which has the function of transmitter and receiver called as trigger and echo pin [10]. The specification of sensor is summarized in Table II.

The basic principle of work:

- It emit short and high frequency sound pulses at regular intervals of time.
- These waves travel with the speed of the sound.
- If it get met with an obstacle it get reflected back as echo which is received by the sensor via echo pin

$$Distance = \frac{Time * Speed\ of\ Sound}{2} \quad (1)$$

TABLE II. SPECIFICATIONS OF ULTRASONIC SENSOR

Parameters	Values
Operating Voltage	+5V
Theoretical Distance measurement	2cm to 450 cm
Practical Distance measurement	2 cm to 80 cm
Accuracy	3mm
Angle Covered	<15 degree

B. Software Requirements

- MPLAB X
- Arduino IDE
- Proteus Professional 7.6

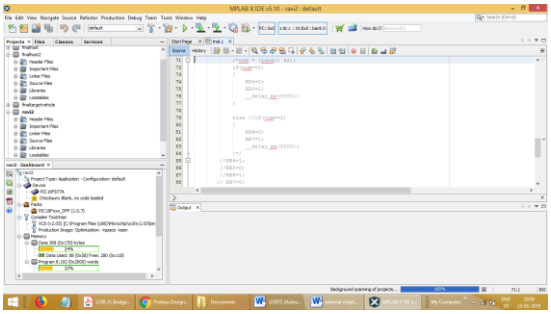

Fig. 3. MPLAB IDE

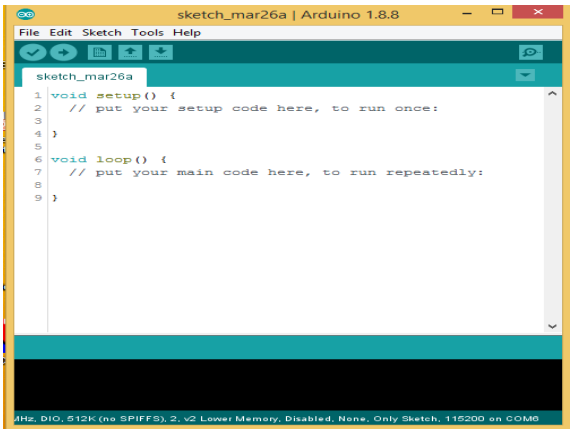

Fig.4. Arduino IDE

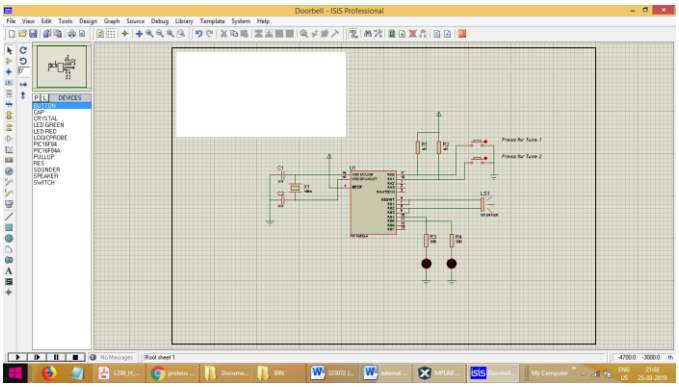

Fig. 5 Proteus Design Suite

The PIC controller is programmed using MPLAB IDE and the environment is shown in Fig. 3. The Wi-Fi module is programmed in Arduino environment and it is shown in Fig.4. The design of the entire prototype is done using proteus software and it is shown in Fig.5.

IV. PROPOSED WORK

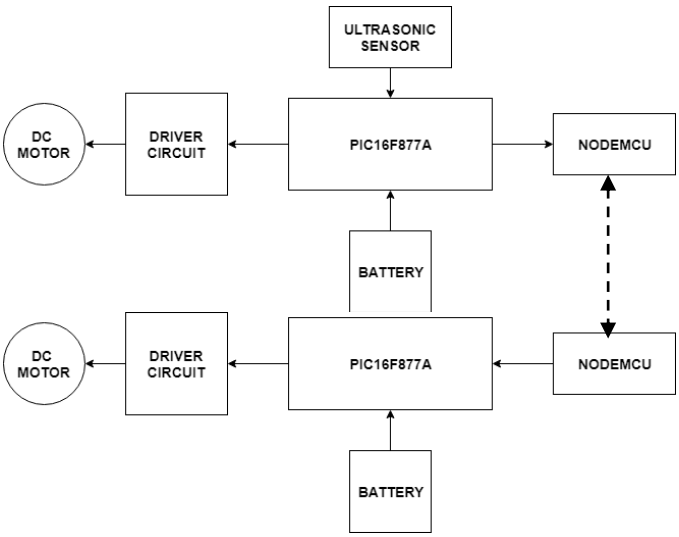

Fig. 6. Block Diagram – a) Target Vehicle b) Host Vehicle

There are two vehicular units, the one in the front is termed as target vehicle and the preceding vehicular is termed as host vehicle. Both units have a Pic microcontroller and a NodeMCU for wireless communication between the two units. The block diagram is given in Fig.6. The ultrasonic sensor is only interfaced with the target vehicle as the distance to collision acts as the real time parameter based on which the two units communicate. When both the host and target vehicle are powered, they connect to the Wi-Fi hotspot which acts as a road-side unit (RSU). After which both the DC motors of the respective vehicular units' starts to rotate depicting the vehicle movement.

When the target vehicle detects an obstacle very close to the ultrasonic sensor, a message indicating collision is passed to the host vehicle and the DC motor of the host vehicle stops rotating. Thus the collision is avoided. This prototype provides the implementation of the VANET using microcontrollers with vehicular to vehicular communication acting as the backbone in this methodology to avoid chain collisions especially in highways.

The circuit diagram is given below.

- The ultrasonic is connected to PORTB with Trigger and Echo of ultrasonic to pins RB1 and RB2 respectively in target vehicle.
- The DC motor is connected to PORTB pins RB4 and RB5 in both the vehicular units.
- PORTB RB7 PIC16F877A is connected to D1 of NodeMCU in target vehicle and D0 of NodeMCU is connected to the PORTB RB2 of PIC16F877A in host vehicle..
- Both driver circuits are powered by 9V batteries separately.

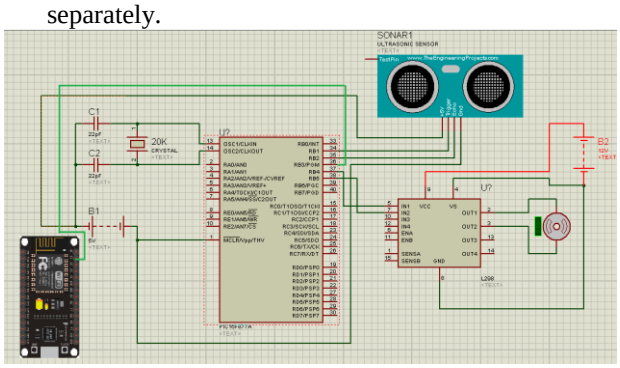

Fig.7. Circuit Diagram – Target Vehicle

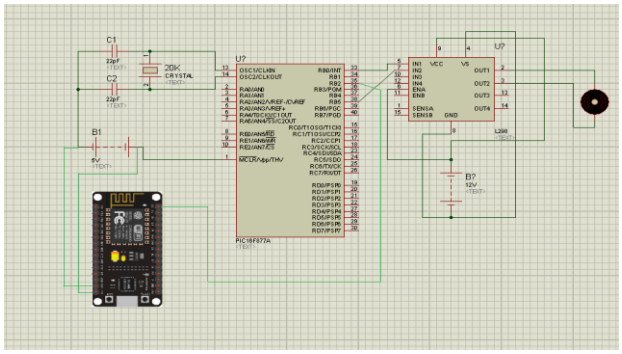

Fig.8. Circuit Diagram – Host Vehicle

The main PIC microcontroller is used to which an ultrasonic sensor and DC motor is interfaced. The NodeMCU is used to take the output from the microcontroller and send the information through the local port to the receiving NodeMCU. The motor driver is connected in between the DC motor and microcontroller. The motor will stop rotating when the distance to collision sensed by the ultrasonic sensor is less than 2cm.

The main PIC microcontroller is used to which the DC motor is interfaced. The NodeMCU receives the message from the other NodeMCU and gives this output to the PIC microcontroller. Upon receiving this the microcontroller stops rotating. The circuit design of target and host vehicle is done and given in Fig 7 and 8 respectively.

The flowchart in Fig.9 gives the flow of the vehicle collision detection using NodeMCU and ultrasonic sensor module.

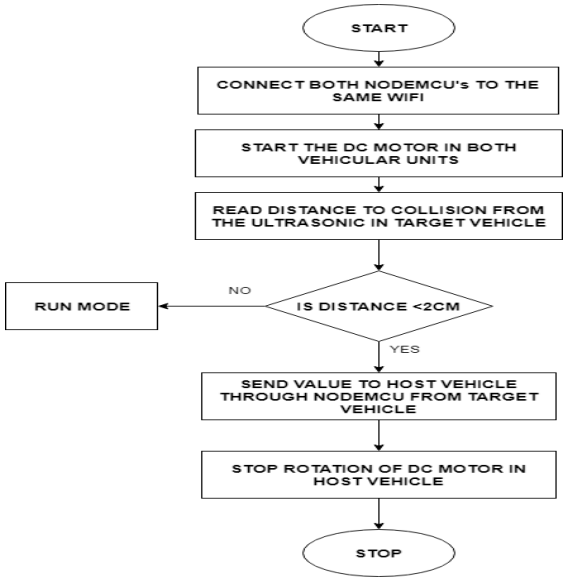

Fig.9. Flowchart of the proposed model

V. DISTANCE CALIBRATION

The pins (1,4,5,7) of PORTB are set as output and pin 2 is set as input. This is done using the keyword TRISB. Timer 2 is used to calculate the distance to collision in ultrasonic sensor use these formulas

$$Time\_Taken = (TMR1L|(TMR1H \ll 8)) \quad (2)$$

$$Distance = \frac{0.0272 * Time\_Taken}{2} \quad (3)$$

When a high pulse is given to trigger pin of ultrasonic sensor the timer 2 is started. It runs until an Echo signal is received from the ultrasonic sensor. By converting this time information to distance and if condition is given which makes pin 7 high when the distance is less than 2cm. This also causes the DC motor to stop rotating. In NodeMCU, it first connects to the Wi-Fi network and configures the UDP protocol

```
udp.beginPacket(ServerIP, 2000);
udp.write(a,1);
udp.endPacket();
```

Once an input signal is given to the pin 1 of NodeMCU it causes it to send information inn a prescribed local port.

The NodeMCU listens to the prescribed local port at all times. When a message is received it causes the pin 0 to go high. This is read by the PIC microcontroller and stops the motor from rotating by setting the pins 0 and 5 low.

```
TRISB5 = 0; //DC motor pin output
TRISB2 = 1; //RB2 is input pin for Wi-Fi module
TRISB0 = 0; // DC motor pin output
```

VI. EXPERIMENTAL SETUP

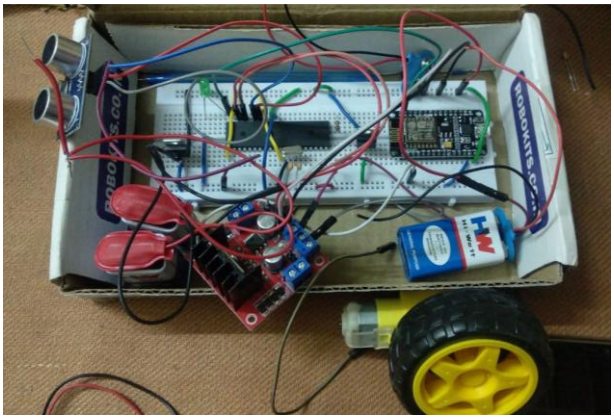

Fig.10. Target Vehicle model

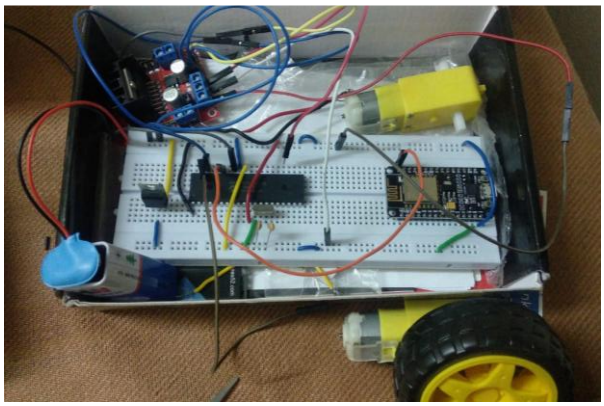

Fig.11. Host Vehicle model

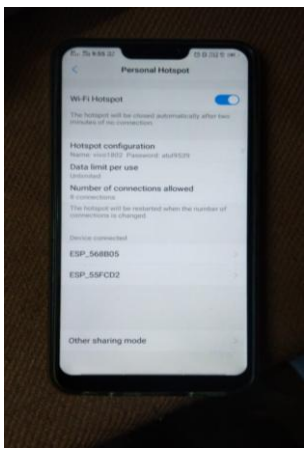

Fig.12. NodeMCU connected to the Wi-Fi Network

The experimental set up of target vehicle and host vehicle is given in Fig 10 and 11 respectively. The mobile is used as hotspot where two Wi-Fi module of host and target vehicles are connected and information got exchanged. The Fig.12 depicts the hotspot for Wi-Fi module.

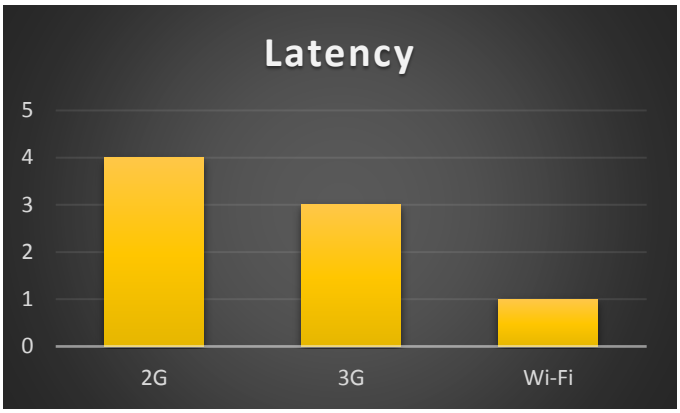

Fig.13 Latency comparison using different network providers

The experiment was conducted using 2G, 3G and Wi-Fi (NodeMCU module). The comparison chart is presented in fig 13. The NodeMCU delivers the messages to neighboring vehicles with less latency which makes the proposed work to provide assistance to driver and to use of safety applications.

VII. APPLICATIONS

THE APPLICATIONS OF VANETS INTO FOLLOWING CLASSES:

A) Safety Applications

- Real-time traffic: The infrastructure unit in VANET is enabled with memory so that all real time information are get stored and it is readily available to the user when they request for it. The real time data can about traffic information, congestion details etc.
- Co-operative Message Transfer: The vehicles in VANET environment are able to cooperate among themselves to exchange messages. Reliability and latency is the major concern but it may automate emergency brakes in case of potential accidents.
- Post-Crash Notification: A vehicle can able to broadcast the warning messages about its position to nearby vehicles.

B) Commercial Applications

- Remote Vehicle Personalization/ Diagnostics: It helps in downloading of personalized vehicle settings or uploading of vehicle diagnostics from/to infrastructure.
- Internet Access: Vehicles can access internet through RSU if RSU is working as a router.

C) Convenience Applications

- Route Diversions: Alternate route can be taken in case of traffic congestion.
- Electronic Toll Collection: Payment in toll can be automated
- Time Utilization: The traveler is able to access net during transit for web browsing and mailing services. The heterogeneous access network provides all requested services for the user.

VIII. FUTURE ENHANCEMENT

The designed prototype can be enhanced by adding more features. The utility of this project can be extended further by increasing the number of sensors to visualize the surrounding environment. This will provide more safety protocols and makes the driving and travelling more safe and enjoyable. Infotainment services can be providing transferring appropriate media through the Wi-Fi network with less latency. The message packet can have more secure protocols so as to stop manipulation of the critical data and to avoid chaos on the roads. With the right equipment it can be implemented on a full scale vehicle and avoid collisions.

IX. CONCLUSION

The designed prototype has all the features to be implemented into a successful commercial model for sales as vehicular equipment. At present there is no cheap technology and haven't been fully deployed on the roads. It has high scope for Indian roads, especially due to persistence of haphazard driver.

REFERENCES

[1] Memon, A., Shaikh, F.K. and Felemban, E., 2015, May. Experimental evaluation of vehicle-to-vehicle based data transfer. In *2015 International Conference on Information and Communication Technology Research (ICTRC)* (pp. 274-277). IEEE.

[2] Evangeline, C.S. and Kumaravelu, V.B., 2017, August. Decision process for vertical handover in vehicular adhoc networks. In *2017 International conference on Microelectronic Devices, Circuits and Systems (ICMDCS)* (pp. 1-5). IEEE.

[3] Ana Gainaru, Ciprian Dobre, Valentin Cristea., 2009, April. A Realistic Mobility Model based on Social Networks for the Simulation of VANET. In 2009, *IEEE 69th Vehicular Technology Conference*

[4] Moez Jerbi, Patrick Marlier, and Sidi Mohammed Senouci., 2007, October. Experimental Assessment of V2V and I2V Communications. In 2007, *International Conference on Mobile Adhoc and Sensor Systems*, *IEEE*

[5] Rui Meireles, Mate Boban, Peter Steenkiste, Ozan Tonguz2 and Jo˜ao Barro.,2010. Experimental Study on the Impact of Vehicular Obstructions in VANETs. In 2010, *IEEE Vehicular Networking Conference.*

[6] FernandoA.Teixeira,ViniciusF.eSilva, JesseL.Leoni, DanielF.Macedo, JoséM. S. Nogueira ., 2014, April Vehicular networks using the IEEE 802.11p standard: An experimental analysis. In *Vehicular Communications Volume 1, Issue 2, pp 91-96*

[7] Renda M Elena, Resta Giovanni, Santi Paolo, Martelli Francesca, Franchini Alessandro., 2016, February. IEEE 802.11p VANets: Experimental evaluation of packet inter-reception time. *In Computer Communications, Volume 75, pp 26-38.*

[8] Di Jasio, L., 2011. *Programming 16-bit PIC Microcontrollers in C: Learning to Fly the PIC 24*. Elsevier.

[9] Barai, S., Biswas, D. and Sau, B., 2017, December. Estimate distance measurement using NodeMCU ESP8266 based on RSSI technique. In *2017 IEEE Conference on Antenna Measurements & Applications (CAMA)* (pp. 170-173). IEEE.

[10] Carullo, A. and Parvis, M., 2001. An ultrasonic sensor for distance measurement in automotive applications. *IEEE Sensors journal*, *1*(2), p.143.

Proceedings of the Fourth International Conference on Communication and Electronics Systems (ICCES 2019)
IEEE Conference Record # 45898; IEEE Xplore ISBN: 978-1-7281-1261-9

Design and Implementation of Automatic Miniature Indoor Plant Cultivator Using Artificial Environment

Akhila S, Shriya Nithyan, Sowmya C, Priya B. K
Department of Electronics & Communication Engineering,
Amrita School of Engineering, Bengaluru
Amrita Vishwa Vidyapeetham,
India
akhiila789@gmail.com, shriya.nithyan@gmail.com, rcksowbhi7896@gmail.com, bk_priya@blr.amrita.edu

***Abstract*— with a lot of people looking forward to greener food and due to declining earth conditions for doing the same, developing a replica of the field from the past century in a small box is a high-time requirement. This is achieved by real-time controlling and monitoring of environmental parameters by designing a space efficient (nullifying the need of balcony farming) and least human interface (in accordance with our busy lifestyle) based system. It is helpful in producing non-toxic vegetables and making the availability of seasonal and exotic crops anywhere anytime. This is achieved by controlling, monitoring and providing environmental parameters like soil moisture, temperature, humidity and light. Real-time monitoring of these parameters and taking necessary control decisions will result in the improvement of yields. Firstly depending on a crop, the required parameters are set and provided by continuous monitoring of the system and when the optimum conditions goes below a threshold value the required action is taken based on the previously stored information. Using microcontroller as a decision maker and Analog-to-Digital Converter along with the sensors to collect the information and to do the needful. This user-friendly application helps in increasing the harvest of organic crops.**

Keywords*— *Indoor Artificial Environment, Real-time monitoring, Arduino UNO

I. INTRODUCTION

There is a constant need for saving agriculture due to the decreasing land space and corresponding climatic conditions. Due to various political and economic reasons the farmers are finding it difficult to survive. Also as the climatic conditions have changed drastically over the past few years, providing the exact required optimum conditions is not possible. Additionally to give more yields out of less available resources, farmers have switched over to chemical methods which over the years proved to be harmful to the human kind. With more people getting awareness about the harmfulness of these chemicals, they are opting towards organic products which are not readily available without any adulteration. So a solution to the problem is to have our own plants and harvest out of it. But this is not possible in an urban household where there is no space. There are places that suffer adverse climatic conditions, where growing what we need is not possible for that environment. So in order to overcome all these problems, a novel design which is completely organic and can fit within the urban kitchen space and which can also provide the liberty to try any exotic plant from any part of the world right in the kitchen has been proposed. It is designed with maximum automation as possible, so there is less human intervention which is in accordance to urban lifestyle. This cultivator uses a microcontroller as the brain to which the required programs are uploaded and the system is controlled [1]. There is a real-time monitoring and corresponding controlling of plant parameters like soil moisture, humidity and temperature. Arduino Uno microcontroller is used. This controller has input/output pins which are easily compatible with most of the sensors in comparison to the other microcontrollers [2]. Arduino is much cost effective and is an open source computer hardware and software company. Any variations in the requirements will trigger the corresponding response. The initial setting of the soil is the only parameter where human hands are required in this proposed work, hence maximizing the automation. Below is the description of the hardware used to build the prototype, followed by system design and experimental results with pictures. The paper is concluded with final observations and its future scope. Finally the paper ends with acknowledgement and the list of references.

II. HARDWARE RESOURCES

Some of the main hardware components used is detailed below:

1. ARDUINO UNO:

It is the brain (micro-controller) of the system. Three Arduino boards have been used in this system. One consists of the LCD screen and the keypad to take the required input from the user, the second one contains all the sensors and their corresponding actuators and the last one is for the grow light. The first two boards work in master-slave fashion, whereas the last one is kept separate to avoid the delay of the system performance. It is open source software and is easily compatible with most of the sensors. Hence, this micro-controller is chosen.

IEEE Conference Record #45982; IEEE Xplore ISBN: 978-1-7281-1261-9

2. DHT 11 SENSOR (TEMPERATURE AND HUMIDITY SENSOR):

Fig.1 DHT11 MODULE

This device has two different sensors incorporated in it as shown in Fig.1. The humidity sensor consists of two electrodes sandwiching a moisture holding substrate. The change in humidity causes respective changes in the conductivity or resistance between the electrodes which is in turn converted to the required value in humidity. The temperature sensor uses a thermistor, which is a variable resistor whose resistance changes with the temperature.

3. SOIL MOISTURE SENSOR:

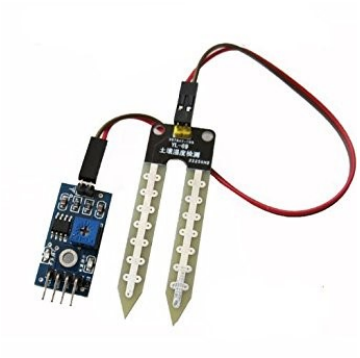

Fig. 2 SOIL MOISTURE SENSOR

This sensor consists of two electrodes which creates a voltage proportional to the permittivity of the dielectric medium between them which in turn gives the water content of the soil as shown in Fig. 2.

4. GROW LIGHT:

Fig. 3 GROW LIGHT

It's an artificial sunlight used for plant growth which provides the exact spectrum required for photosynthesis akin to that of the sun [9]. The Arduino board used for grow light as shown in Fig.3 is programmed to switch the light ON and OFF according to the average photo-period requirement of the plant which is six hours.

5. HUMIDIFIER:

Fig. 4 HUMIDIFIER

This system uses a wick of paper, foam or cloth which draws the water and makes the air absorb the moisture which is then vibrated in ultrasonic range to atomise the water as shown in Fig.4. This is activated in response to the drop in humidity than the optimum required value.

6. LCD (16X2) DISPLAY:

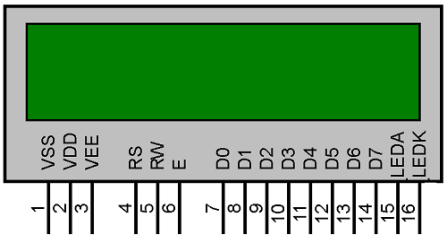

Fig.5 PIN DIAGRAM OF LCD

An LCD display, whose pin diagram is as shown in Fig. 5, is used to give suggestions on the different types of crops available. The data and the optimum parameters are collected for three crops-spinach, coriander and fenugreek. Table 1 shows the parameter requirements of these crops.

Table 1 LIST OF PLANTS AND THEIR PARAMETERS

Sl. No.	Plant	Temperature	Humidity
1.	Coriander	4-24 ^{O}C	30-50%
2.	Spinach	15-35 ^{O}C	60-80%
3.	Fenugreek	8-27 ^{O}C	30-40%

7. HEXADECIMAL KEYPAD (4x4)

Fig. 6 KEYPAD (4x4)

From the different crops displayed on the LCD, a crop is selected to the seed sown, one of the plants is selected using keypad as shown in Fig. 6. Column scanning method is used to program the keypad.

III. SYSTEM DESIGN

The project is designed to create an artificial environment for the optimum growth of the plants where the optimum required conditions are supplied, maintained and controlled as shown in Fig. 7a. In this design three Arduino boards are used to compensate the lack of input/output pins in a single Arduino board required for the design. Here the sensors and their corresponding actuators are connected to the Arduino (Slave) and keypad and LCD is connected to the Arduino (Master) and these two Arduinos are interfaced to each other by master-slave configuration to work according to the required specification.+5V DC power supply is given to the boards through the USB cable.

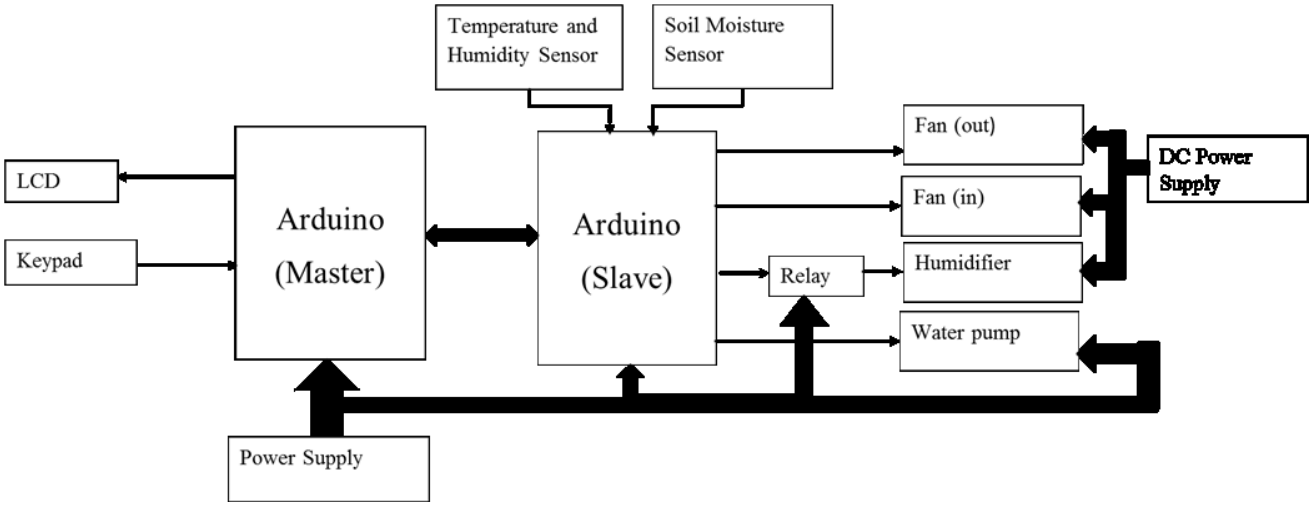

Fig. 7a BLOCK DIAGRAM OF THE PROPOSED SYSTEM

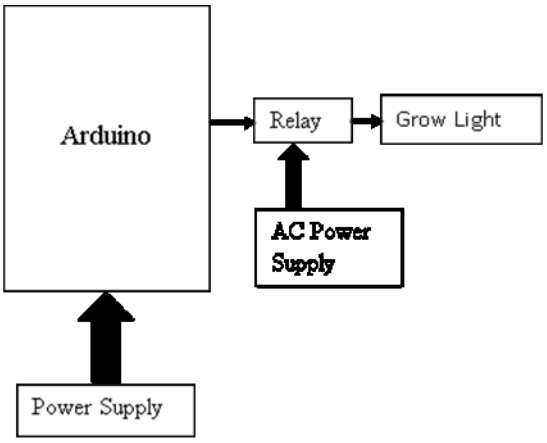

Fig. 7b BLOCK DIAGRAM OF THE PROPOSED SYSTEM

The keypad is used to select a plant out of a list (which contains three kinds of plants: Spinach, coriander and Fenugreek) displayed on the LCD. Threshold parameter values for each plant is stored in the microcontroller so by selecting a particular plant the corresponding plant threshold parameter value is taken and the setting of the microcontroller changes accordingly.

In the design the temperature sensor, humidity sensor, soil moisture sensor are connected to the analog input pins of the controller which receives the analog values from the sensors these values are compared with the defined range of values accordingly fan(OUT), fan(IN), humidifier, water pump correspondingly will be turned ON and OFF. Grow light is connected to the digital output pin via a relay to the third Arduino which is used to control the light as shown in Fig. 7b. , whereas humidifier is connected to the digital output pin of Arduino (Slave) to regulate humidity inside the device. The LCD assures if the plant has got selected or not. Hence the artificial environment is provided to the plants for their optimal growth. The flowchart explains the complete design of the model as shown in Fig. 8.

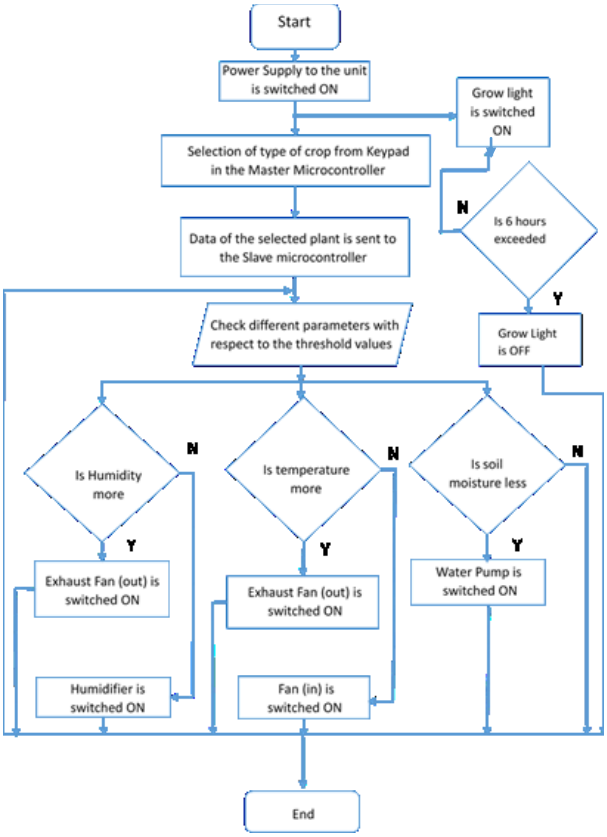

Fig.8 FLOWCHART OF THE PROPOSED SYSTEM

IV. EXPERIMENTAL RESULTS

The prototype of the design is as shown in the Fig 9a. The sensors and actuators are connected to the Arduino boards which respond in accordance to the way it is programmed using Arduino Uno Software. For experimental purpose, a spinach plant was grown inside the device. According to the parameters defined for spinach, the corresponding actuators were observed to be working under the supervision of the sensors.

Fig. 9a Front view of the prototype

1. As soon as the system is switched ON, LCD screen displays the available plants which can be grown in this system, whose parameters are pre-loaded in the Arduino memory.

2. Depending on which crop has to be grown, respective number is chosen through the keypad.

3. Once the number is chosen, the entire set of optimum parameters are sent from the master to the slave and hence the required actuators are activated. The grow light switches ON/OFF according to the plant requirements programmed as shown in Fig. 9b.

4. The soil moisture sensor senses the moisture content of the soil, if it goes below the threshold, then that information is provided to the microcontroller. In turn it switches ON the water pump. Once the requirement is met the water pump is turned OFF.

5. The temperature sensor part of the DHT sensor continuously monitors the temperature of the system. If it is below the threshold Fan (IN) will be switched ON otherwise Fan (OUT) will be switched ON for air circulation as shown in Fig.9c.

6. The humidity sensor part of the DHT sensor monitors the relative humidity of the system. If it is below the threshold humidifier will be switched ON otherwise Fan (OUT) will be switched ON.

Fig. 9b Internal view of the prototype

Fig. 9c Top view of the prototype

V. CONCLUSION

The objective was to design and create an artificial environment for the optimum growth of a plant in an urban kitchen space where the optimum required conditions are supplied, maintained and controlled.

1. When the soil moisture is less than the required quantity the water pump will be switched ON providing sufficient amount of water to the plants.

2. When the humidity is less than the threshold, humidifier will be switched ON else the Fan (OUT) will be switched ON.

3. When the temperature is less than threshold Fan (IN) will be switched ON while Fan (OUT) will be switched ON otherwise.

4. Grow Light will be switched ON and OFF for every 6 hours which compensates the average sunlight requirement for the plants.

The plant cultivator device can make a vegetable plant grow in its artificial environment which is automated in giving necessary conditions for its healthy growth. It can be implemented in urban kitchen spaces and can also be used in restaurants where quality of food is given at most importance. This addresses the problem of rising cost of vegetables and it provides organic vegetables.

It has characteristics of space and cost efficiency and also save time in monitoring the plant. Sensors and its corresponding actuators reduce the effort of the user. It is eco-friendly as well.

VI. FUTURE ENHANCEMENT

This system can be expanded in the following directions:

1. It has only default three plants stored in Arduino's memory. It can be modified in such a way that users can add new plants by using the SD card.

2. It can be used for research purposes of plants in indoor environment by including data logging.

3. Heating Element can be used for increasing heat inside the device so that the device can be used in extreme cold climatic conditions.

4. GSM technology can be used to receive messages regarding plant environment and growth.

5. For more controlled plant growth CO_2 sensor can be used to provide enhanced accuracy of the plant growth.

VII. ACKNOWLEDGEMENT

The advancements in technology that we see today are the perseverance and brain of many engineers. The fact that engineering is creating a significant reform in the way of life of the society for good reasons is what we take pride in as engineers.

We would like to convey our sincere gratitude to Amrita Vishwa Vidyapeetham for providing us with the necessary infrastructure, also to Karnataka State Council for Science and Technology (KSCST), IISC Campus, Bengaluru a wing of Karnataka state government which recognises the projects and provides funding for the projects to carry out the projects based on real time solutions for the problems that is encountered in the society. This work is funded by KSCST under the category 41st Students Project Programme for the academic year 2017-2018 and has been selected for the state level exhibition.

VIII. REFERENCES

[1] T. Saha, M. K. H. Jewel, M. N. Mostakim, N. H. Bhuiyan, M. S. Ali, M. K. Rahman, H. K. Ghosh and Md. Khalid Hossain, "Construction And Development Of An Automated Greenhouse System Using Arduino Uno", I.J. Information Engineering and Electronic Business, 2017, 3, 1-8, 1 March 2017

[2] Sourav Saha, Siddhartha Paul, Sudip Halder and Kanishka Majumder, "Smart Agricultural System: Better Accuracy and Productivity", 2017 Devices for Integrated Circuit (DevIC), 23-24 March, 2017

[3] Dong-Hee Noh, Su-Yong An, Jaeyoung Kim, "Implementation of Optimal Greenhouse Control: Multiple Influences Approach", 9th International Conference on Ubiquitous and Future Networks (ICUFN), 4-7 July 2017

[4] Zhao chan Li1 , Jinlong Wang , Russell Higgs , Li Zhou and Wenbin Yuan, "Design of an Intelligent Management System for Agricultural Greenhouses based on the Internet of Things", 2017 IEEE International Conference on Computational Science and Engineering (CSE) and IEEE International Conference on Embedded and Ubiquitous Computing (EUC), 21-24 July 2017

[5] Jin-Won Song, "Grow Light For Plant Factory Using Quantum Dot Led", Journal of International Council on Electrical Engineering, Volume 6 Issue 1, Pages 13-16, 08 Feb 2016

[6] Supun Athukorala, Irunika Weeraratne, Dumindu Jayathilaka, Asitha Bandaranayake and Roshan Ragel, "Affordable Real-time Environment Monitoring System for Greenhouses", Proceedings of the 1st Manufacturing & Industrial Engineering Symposium, 22 October 2016

[7] Lukas Bajer, Ondrej Krejcar, "Design and Realization of LowCost Control for Greenhouse Environment with Remote Control", 13th IFAC and IEEE Conference on Programmable Devices and Embedded Systems: PDES 2015, 26 September 2015

[8] I. Attar, N. Naili, N. Khalifa, M. Hazami, M. Lazaar, A. Farhat, "Experimental study of an air conditioning system to control a greenhouse microclimate", Energy Conversion and Management 79: Pages 543-553, 25 January 2014

[9] Eva Darko, Parisa Heydarizadeh, Benoıˆt Schoefs and Mohammad R. Sabzalian, "Photosynthesis Under Artificial Light: The Shift In Primary And Secondary Metabolism", Philosophical Transactions of the Royal Society B, Volume 369 Issue 1640, 3 March 2014

[10] Yasunaga Iwasaki, Masaki Aizawa, Chie Yoshida, Masuyuki Takaichi, "Developing a new energy-saving, photosynthesis-promoting, environmental control system for greenhouse production based on a heat pump with a heat storage system", J. Agric. Meteorol. 69(2) Pages 81-92, 2013

[11] V. V. Sajith Variyar, Haridas, N., Aswathy, C., and Soman, K. P., "Pi doctor: A low cost aquaponics plant health monitoring system using infragram technology and raspberry Pi", Advances in Intelligent Systems and Computing, vol. 397, pp. 909-917, 2016.

[12] Giriraja C. V., "Plant Health Analyser", 6th International Conference on Advances in Computing, Communications and Informatics (ICACCI'17), Manipal University, Karnataka, India, 2017.

[13] Ms. A. Susmitha, Ms. T. Alakananda, Ms. M. L. Apoorva, Dr. T. K. Ramesh., "Automated Irrigation System using Weather Prediction for Efficient Usage of Water Resources", at International Conference on Advanced Material Technologies (ICAMT) 2016, at Dadi Institute of Engineering and Technology (DIET), Vishakhapatnam on 27th to 28th December2016.

Proceedings of the Fourth International Conference on Communication and Electronics Systems (ICCES 2019)
IEEE Conference Record # 45898; IEEE Xplore ISBN: 978-1-7281-1261-9

A Network Intrusion Detection Approach Using Variant of Convolution Neural Network

Ashish Kumar Verma
Research Scholar, CSE Department
MANIT Bhopal,India
ashish.verma1194@gmail.com

Dr.Praveen Kaushik
Associate Professor, CSE Department
MANIT Bhopal,India
praveenkaushikmanit@gmail.com

Gourav Shrivastava
Research Scholar, CSE Department
MANIT Bhopal,India
gashr83@gmail.com

***Abstract*—Intrusion detection system(IDS) is a preventing measure against different harmful cyber-attacks. It has a key role in securing our information and communication technology system. As the internet evolved, the dynamic growth of network traffic data generated which become a challenge for traditional machine learning algorithms. Performance of a classifier solely depends on feature selection and classifier. Traditional machine learning algorithms can't perform well with huge network traffic dataset. So ML algorithms are not optimistic. In this paper, we implemented Convolution neural network(CNN-1D) for NIDS(Network Intrusion detection system) on NSL-KDD benchmark dataset. CNN automatically fetch network traffic features from the dataset. in this paper, we trained our model 500 epoch. We also compared performance of different ML(machine learning) algorithms & DL(deep learning) approaches with our CNN-1D approach with metrics of AC (accuracy), DR (detection rate) and FAR (False alarm rate).**

***Index Terms*—IDS, CNN (Convolution neural network), Deep learning, Machine learning, NSL KDD**

I. Introduction

The Internet emerged as a essential way of life for every individual. Rapidly development in computer technology, the Internet transformed the way of living, studying and working environment. Attackers use this development as an opportunity to exploit the Information system. Different type of cyber-threats is increasing day by day which is very harmful to information safety. These attacks are threats for security measures availability, integrity, and confidentiality. Here we have a challenge that how can we identify various network attacks, more especially unforeseen attacks. That why many researchers focused on network security. There are many ways to protect the network from an intrusion i.e. encryption, firewall, authentication,antivirus and IDS. The advantage with IDS is that it can detect abnormal behaviors of security threats before it happens[1]. It provides a better way to identify the attacks than other protection mechanism because it can identify the attack from the network traffic flow. Detection of intrusion is very similar to classification problems such as the problem of binary or multi- class classification, i.e. differentiating the behavior og network traffic is normal or abnormal.So multi-class problem into 5 class classification problem i.e. detect whether this belongs to a normal or any four types to malicious attacks: DOS (Denial of Service), Probe (Probing), U2R (User to Root) and R2L(Root to Local). in fact, our primary objective of IDS is to effectively identify the intrusive behavior. When traffic of network is correctly classifying the malicious attack, then the network administrator would take preventing measure to protect network accordingly.

John Anderson in 1931 introduced a significant work on Intrusion detection in his research paper. Depending of the behavior of network & network types intrusion detection broadly classified into two main categories (1) NIDS:NIDS abbreviated as network intrusion detection & it performs the inspection on the content of the network packet to identify intrusive or harmful behavior in the traffic of network. (2)HIDS:HIDS abbreviated as host intrusion detection and it performs deep investigation on log files, system files, file structure, system log files and other type of logs in every system. In real life application, many organizations implemented the combination of NIDS and HIDS. In this paper, we target the NIDS for intrusion detection.

On the basis of classification and analysis of network traffic,IDS detection methods are divided into 3 main categories: 1)Misuse or signature-based detection. 2)anomaly-based detection and 3)state full protocol detection. Signature-based detection works on the predefined rules and signature. Networks administrator have to write/update a signature to their database for a different attack.They are used to effectively detect the known intrusion or attacks with almost zero FARs. Even though signature-based detection has a high ability to detect known attacks, they are less applicable in real time due to their ineffectiveness to identify the unknown or unforeseen attacks. These unknown attacks can be detected only once they got identified by some other technique or we tagged the signature manually.To identify the unknown attacks,anomaly-based detection works on the heuristic approach. Anomaly-based methods analyze the normal behavior and current behavior of network to detect anomalies as deviations from normal behavior. The main problem with anomaly-based techniques is that they have a high false alarm rate because sometimes they categorized previously unseen system behavior as an anomaly which is actually not an anomaly. To tackle the problem of high false alarm rate, organizations use the hybrid approach of Signature-based and Anomaly-based detection.

Every machine learning technique comes under shallow learning and they mainly focused on feature selection and feature extraction,so they can't efficiently tackle the problem of intrusion data classification of huge networks that comes in

the real-time network environment. With the rapid increment in the size of datasets, many classification problems results in drop in accuracy. Machine learning is not fit for effective analysis and forecasting requirement of high dimensionality with dataset. In shallow learning, features selection process takes long time and need expert knowledge. The effectiveness of most ML algorithms hugely depends on the selected features. On the other side, deep learners extract features automatically from the dataset and help to extract better representation to create better models.

II. Related Works

Professor Hinton [2] introduced the concept of deep learning in 2006, afterward various new models proposed by many researchers. Thus deep learning becomes a subpart of machine learning field. In recent years, many research papers and implementation models developed and generated remarkable development in field of computer vision, image recognition [3] and action recognition [4]- [6]. Although deep learning has been around for decades but due to limited computed resources, it's not implemented. The true potential of deep learning has been recognized widely when Convolution neural network (CNN) has recently established remarkable development in the field of deep learning [7]. There are various papers comes on which ML methods are applied for detection of intrusion. M.N. Mohammed [8] applied SVM to identify intrusion in WLAN (wireless local area network). W. Feng [9] done intrusion detection using combing SVM and ant colony optimization. H. Wang [10] develop a framework which is based on SVM (support vector machine) and in this paper they augmented the features of their dataset. G. Kim [11] uses decision tree for anomaly detection with signature detection. A.S. Eesa [12] uses decision tree for feature selection using cuttlefish optimization algorithm. A. Sharma [13] uses artificial neural network with reduced feature set. Papers [14]- [17] uses Naïve Bayesian approach for intrusion detection. Although for Optimization purpose, Genetic Algorithm used in many papers [18]- [21]. A.A. Aburommman [22] applied an ensembling method using SVM, KNN, and particle swarm optimization techniques for IDS. W. Li [23] applied KNN classifier to wireless sensor network. C. F. Tsai [24] wrote a review paper in which he applied a hybrid approach of various Ml algorithms to classify the harmful traffic.

Performance of a machine learning classifier solely depends on feature we selected during feature engineering. Another limitation of ML classifiers that they are unsuited for huge network where network traffic data is generated at very fast rate. To process this huge traffic data machine learning algorithm are not fit because they not only minimize the accuracy but also increases calculation cost and time. To ensure the security of a network, a good IDS archives a good accuracy in less time. Therefore, we implemented deep learning model to identify the intrusive behavior of the huge network accurately and within time.

E. Hodo [25] briefly discussed the previous work done under shallow and deep learning for the intrusion detection. N. Gao [26] introduced deep belief network (DBN) for the intrusion detection in which training and back propagation performed by Restricted Boltzmann machine (RBN). J. Yang [27] uses the combination of RBN and SVM, in which RBM performed feature engineering and selection while SVM used for training the data comes from RBN to increase training speed.

Due to advancement in technology and processing power, GPU (Graphical process Unit) can perform intensive calculation. They also supported distributed and parallel computing which helps to train the deep learning models easily. Q. Niyaz [28] used auto encoder technique for features selection in unlabeled data and on the second stage for classification purpose they used Random tree or J48 algorithms. J Kim [29] proposed RNN (Recurrent neural network) for intrusion detection, in this paper they used network traffic as a sequence for RNN. H. Sak [30] used LSTM (Long Short Term Machine) that is a variation of RNN for acoustic modeling at large scale. D.Gibert Llaurado [31] applied CNN on the malware classification. In his paper he presented two cases, in first case data converted in gray scale image and features are learned from those images. In the second case, the deciding factor for malware classification was x86 instructions. B. Kolosnjaji [32] used system call sequences for malware classification using CNN. R. Upadhyay [33] used first time CNN for the Intrusion detection system. K. Wu [34] implemented Convolution Neural network using CNN. In his paper, he converted 1*122 dimensional feature vector into 11*11 image data and applied CNN on this image dataset. In this paper he improves the classification accuracy of intrusion detection on NSL- KDD dataset using a variation of CNN model.

This paper is ordered as per section given below sections. Section II comprises proposed methodology and in this step, we discussed every step of our model. Under this section, there are some subsections are presented like A) Dataset description B) Data preprocessing C) Methodology D) Evaluation metrics. Section III contains the experimental result and discussion. And last section IV contains conclusion and future work.

III. Proposed Methodology

Here proposed intrusion detection model using CNN contains the following four phases:

Phase 1: Data Preprocessing – This step involves data unifying process and data normalization. To fit the data to our model categorical data converted to numerical data.

Phase 2: Training – This step involves building the relationship among different features of independent variables and tuning the parameters to improve the accuracy of the model.

Phase 3: Testing - Testing step involves a process in which a subset of original dataset chooses for testing purpose against training. If we are not satisfying with accuracy of model, then model will repeat the training phase again.

Phase 4: Evaluation – This step involves evaluation process of model performance. Evaluation metrics in figure 1 showed above four steps of intrusion detection using CNN and proposed our CNN-1D model for NIDS in this paper.

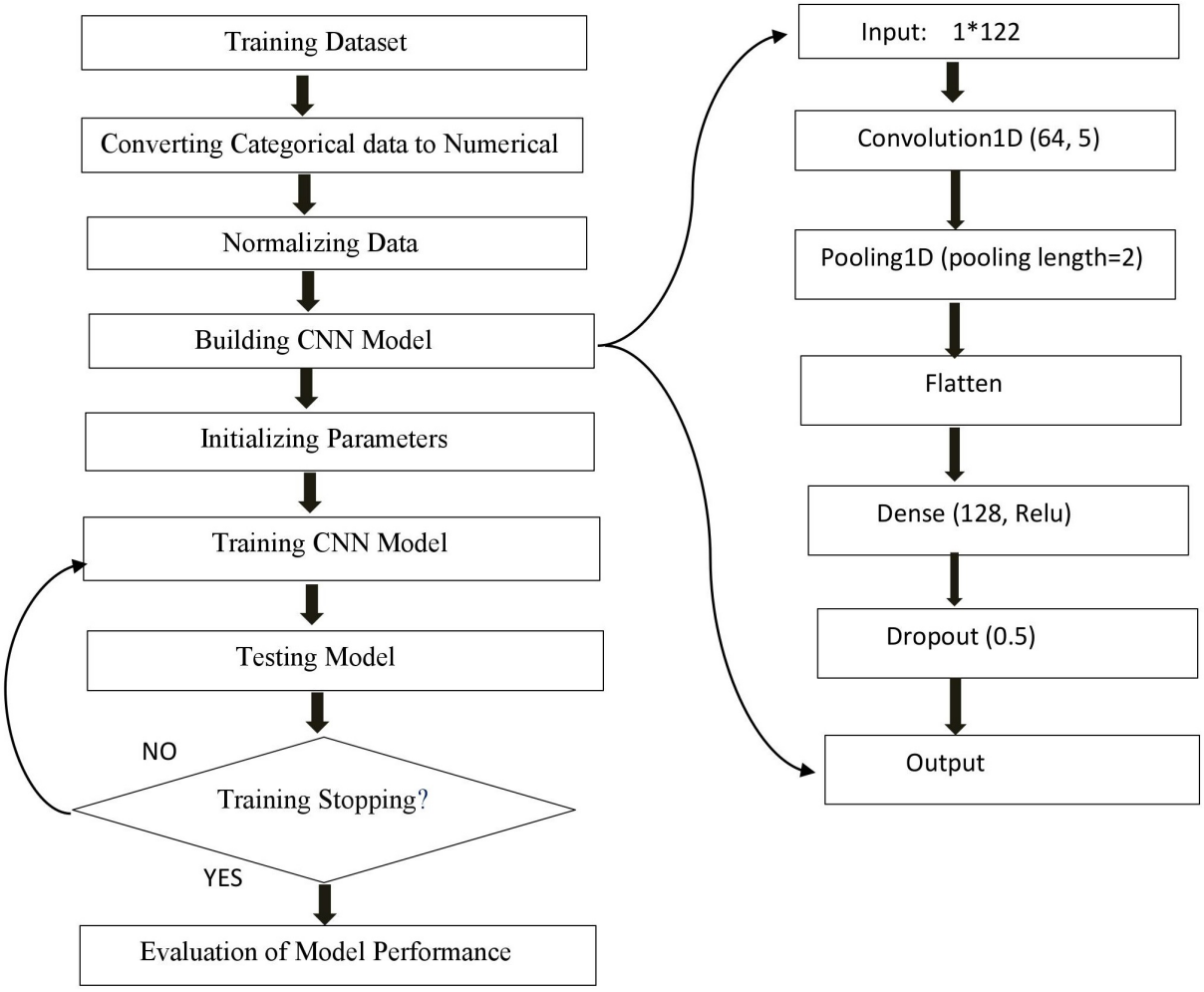

Fig. 1. Flow chart of Intrusion Detection using CNN-1D

A. Dataset Description: NSL KDD Dataset

NSL-KDD dataset is modified version of KDDCUP'99. In 2009 Tavallaee [35] selected NSL-KDD dataset from the most widely used network intrusion detection dataset KDDCUP'99. The number of records in KDDCUP'99 are very redundant that leads a model to be biased towards more frequency of redundant records. Even through NSL-KDD dataset is also old dataset. still, it's used as a benchmark dataset for intrusion detection by many researchers due to lack of public availability of network intrusion detection dataset. The instances of NSL-KDD dataset also reasonable which help to reduce time to run the experiment on whole dataset rather than randomly choosing a portion of the dataset.

NSL –KDD contains one of category named normal which represent normal behavior of traffic and other 22 attacks which are primarily grouped under four categories shown in table 1[35]. Every record of the dataset contains 41 features and one target class label. Out of 41 features attributes, 7 features are symbolic types and others are continuous type.

TABLE I
ATTACK TYPES IN NSL-KDD DATASET[35]

Attack Types	Attacks in NSK-KDD dataset
DOS	Back,land,pod,smurf,teardrop,neptune, MailBomb,Udpstrorm,Processtable,Apache2,Worm
Probe	ipsweep,satan,nmap,portsweep,Mscan, Saint
R2L	imap,warezclient,ftpwrite,named,spy, guesspasswd,multihop,phf,Snmpgetattck, sendmail,Xlook,Httptunnel,Xsnoop,Xlook
U2R	Rootkit,perl,Sqlattck,Ps,Xterm,loadmodule, buffer_overflow

"The NSL-KDD dataset contains four datasets KDDTrain+, KDDTrain+_20Percent as training set and KDDTest+,

KDDTest-21 as testing dataset. KDDTrain+_20Percent contains 20% subset of KDDTrain+ and KDDTest-21 contains subset of KDDTest+ that does not contain some of the records labeled as 21. The instances of four datasets and their attacks are shown in Table II[35]."

TABLE II
INSTANCES OF ATTACK TYPES[35]

	Datasets		
Attack types	**KDDTrain+**	**KDDTest+**	**KDDTest-21**
Normal	67343	9711	2152
Dos	45926	7458	4342
Probe	11655	2421	2402
R2L	995	2754	2754
U2R	52	200	200
Total	12593	22544	11850

B. Data Preprocessing

Before applying our dataset to model, we have to preprocess it because some of fields of our dataset contains categorical data. All of deep learning and machine learning model performs scientific operation on numerical data. So we have to unifying our dataset in numerical data. Our data preprocessing process divided into two subparts: 1) Numericalization 2) Data Normalization.

1) Numercalization: NSL-KDD contains 38 numerical attributes and 4 categorical data. Categorical data fields like 'protocol_type','service','flag' and 'attack label' are converted into numerical values using one hot encoding technique. Categorical field like 'protocol _types' has 3 types of attributes: TCP, UDP and ICMP are encoded into three dimensional vector (1,0,0), (0,1,0) and (0,0,1). Similarly, other feature 'service' has 70 attributes and 'flag' has 11 attributes which are converted into numerical values using one hot encoding. So after numercalization our 41 features converted into 122 features.

2) Normalization: There are some features which are not in same scale. Normalization converts the numerical values of the dataset to bring all feature values within same range.If we are not performing normalization, then our model will bias towards higher values of features. Each feature normalized values within range of [0-1] according to equation (1).

$$S_{normalized} = \frac{S - Min(S)}{Max(S) - Min(S)} \tag{1}$$

Where Max represent maximum value and Min represent minimum value of for every feature.

C. Methodology

The architecture of our CNN model has shown in figure 2[34]. The architecture of CNN model consists of 5 layers which are 1)input Layer, 2)convolution layer, 3)pooling layer, 4)fully connected layer, 5)Output layer. An CNN model has multiple convolution layers and pooling layers. The terminologies and variables of model are described below[34]:

n = n represents the no. of samples
l = l represents no. of convolution layer & pooling layers
$s_p = s_p$ represents the instance p where p = 1,2, 3.....,n
$fm_k = fm_k$ represents the feature map of layers k where k = 1,2,3,.....,l and fm_0 denotes the input sample of s_p.
$w_k = w_k$denotes convolution filter of layer j where k = 1,2,3.....,l
$b_k = b_k$denotes bias of a layer k where k = 1,2,3, ...,l
$o_p = o_p$ denotes output of sample p where p = 1,2, 3.....,n

The network traffic data of TCP/IP packets given to convolution 1D layer in the form of an input vector of dimension $s = (s_1, s_2, s_3....., s_{k-1}), s_{122}, cl)$ where s_k represents features and cl represents class lebel of dataset. Convolution 1D create a feature map fm using convolution operation with filter w_j on input data. The convolution operation can be expressed using following the equation (2).

$$fm_j = f(fm_{(k-1)} \bigotimes w_k + b_k) \tag{2}$$

where $\bigotimes$ =convolution operation
f(x) = Activation function

In this paper, we used a non-linear activation function called Rectified Linear Unit (ReLU). After application of convolution layer, pooling layer applied which minimizes the size of feature map fm_j . The mathematical equation of pooling layer can expressed using following equation (3).

$$fm_k = pool(f(fm_{k-1})) \tag{3}$$

In our paper, we used max-pooling on every feature map which chooses most relevant and significant feature with maximum value . Many features maps collects many features and newly created features provided to fully connected layer. In binary classification we have used sigmoid activation function while in multi-classification we have applied softmax activation function to fully connected layer that gives probability distribution of each class. The mathematical expression of fully connected layer can be given as following equation (4).

$$o_i = softmax(w_{fm0} \bigotimes fm + b_0) \tag{4}$$

After applying various convolution layers and pooling layers, feature map fm transformed into a vector. Then outputo_i obtained from fully connected layer which classify the data into different class labels. After o_i obtained ,the difference between o_i and the expected value calculated using loss function. The goal of our training of our model to decrease the error rate. To calculate the loss function, weight updation of back propagation uses the stochastic gradient descent technique .

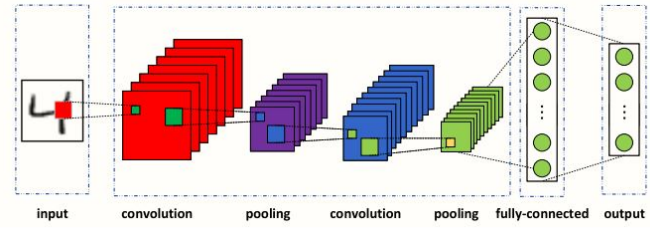

Fig. 2. Architecture of Convolution Neural Network[34]

From table II, we can see KDDTrain+ dataset contains samples unbalanced. For illustration purpose class "normal" having more than 50 percent of records. However other class "U2R" contains only 0.04 percent records. This will create problem in our training, our model will be biased towards higher frequency of records. This whole scenario called class imbalance problem of dataset. To overcome this problem, we used oversampling method called Adaptive synthetic sampling approach (ADASYN).
To tackle the problem of imbalanced problem,there are 3 main approaches which are mostly used:

1) ENSEMBLE-BASED METHOD: This method works on meta-algorithms that uses multiple classification algorithms into one model with the help of boosting and bagging algorithms. This method helps in order to decrease the variance (bagging), bias (boosting) or improves prediction(stacking).

2) COST SENSITIVE BASED METHOD: This method modifies the weights of cost function as per to their distribution of records. The class which contains less frequency of records have larger weights of their cost function and on the other side, the class which has higher frequency of records have small weights of their cost functions.

Lets us suppose we have j classes in our dataset n_1, n_2, n_3..... n_j. Then weights of their cost functions class i will be as:

$$w_j \approx \frac{max}{n_j} \tag{5}$$

Where max represents the maximum number.

3) SAMPLING-BASED METHOD: Sampling based methods either increase or decrease the no. of sample in the total dataset. The oversampling methods increase the frequency of records which are in lower proportion while undersampling decreases the frequency of records which are in higher proportion. And the hybrid approach of oversampling and undersampling not only increment the records having less proportion but also decreases the records of higher proportion. In this paper, we used Oversampling method named ADASYN. Adaptive synthetic sampling approach (ADASYN) is a modified version of Synthetic Minority Oversampling technique(SMOTE). First, it calculates K-nearest neighbors of the minority class of each record in the class. Then draw the line between neighbors and generates random points on lines. After that, it adds some random small values to points thus making it real. Thus these sample points have a little more variance than samples which are taken from their parent samples.

D. EVALUATION METRICS

THere are many criteria to measure the performance of a model. We will choose appropriate metrics according to the problem statement. In our paper we have used AC (accuracy), recall(Detection Rate or DR), FAR (false alarm rate) and confusion matrix as performance measures. There are four parameters which will help to evaluate our model.

TP: TP abbreviated as true positive that are no. of anomaly samples which are classified as anomaly by classifier.

TN: TN abbreviated as true negative that are no. of normal samples which are classified as normal by classifier.

FP: FP abbreviated as false positives that are no. of normal samples which are classified as anomaly by classifier.
FN: FN abbreviated as false negative that are no. of anomaly samples which are classified as normal by classifier.

TABLE III
CONFUSION MATRIX

Actual Class	**Predicted Class**	
	anomaly	***normal***
anomaly	TP	FN
normal	FP	TN

From table III following performance metrics are calculated.

Accuracy(AC): Accuracy is one of the main performance measure of any model. It is the no. of samples correctly classified over total samples.

$$AC = \frac{TP + TN}{TP + TN + FP + FN} \tag{6}$$

DR (Detection Rate): Detection rate also called recall. DR is a measure that tells about percentage of samples correctly classified over the total number of anomaly samples.

$$DR = \frac{TP}{TP + FN} \tag{7}$$

FAR (False Alarm Rate): False alarm rate also called false positive rate. FAR shows the percentage of samples incorrectly rejected by total normal samples.

$$FAR = \frac{FP}{FP + TN} \tag{8}$$

Confusion Matrix: Confusion matrix is a performance measure of a classifier which gives a matrix of predictions over actual samples in classification. Confusion matrix describes how much model is confused among actual class and predicted class as shown in table III.

IV. EXPERIMENTAL AND DISCUSSION

To implement this research paper, we used the most famous deep learning library keras [36] using tensorflow [37] as backend. The experiment performed on the PC that have configuration of Intel(R) Xeon® CPU E5-2650 v3 2.30 GHz, 8 GB memory without GPU acceleration. Our experiment has been performed on both classification binary (normal or anomaly) and multiclass classification (Normal, Dos, Probe, R2L, U2R). There are many algorithms applied to Intrusion detection. Early only ML algorithms used for IDS but now days high end processing power help to use deep learning models for IDS.
In binary classification we compared the performance of machine learning models like J48, Naïve Bayes, NB Tree, Random Forest, Random Tree, Multi-layer Perceptron, SVM, RNN as mentioned in paper [38] with our CNN-1D model. Likewise, we also compared other machine learning algorithms with our model for multiclass(5-category) [34] classification problem.

A. BINARY CLASSIFICATION

In binary classification we have converted 41 dimensional feature set into 122 dimensional feature set. So our model takes 122 input nodes and produces 2 output nodes. In CNN, we can insert as many convolution and Pooling layer. In this paper we called both layers 'multi hidden layer' as combine. We implemented our model for one and two multi hidden layers. Different parameters for multi hidden layer 1 and multi hidden layer 2 are taken as: For One multi-hidden layer, convolution layer 1 filter size & stride are taken as 5 and 1 respectively. And pooling layer 1 filter size & stride taken as 2. In two multi-hidden layer , convolution layer 1 & 2 filter size and stride taken as 5 and 1, and pooling layer 1 & 2 filter size and stride taken as 2.

Accuracy and detection rate for different multi-hidden layers shown in table IV.

TABLE IV
EXPERIMENTAL RESULTS ON DIFFERENT LAYERS

Multi Hidden Layer	**KDDTest+**	
	AC	***DR***
1 Layer	84.29%	74.62%
2 Layer	82.38%	72.18%

From table IV, we can conclude that 1 layer has higher accuracy and detection rate for KDDTest+ dataset. So we have chosen layer 1 for binary classification. The confusion matrix of layer 1 classifier is shown in table V.

TABLE V
CONFUSION MATRIX OF BINARY CLASSIFICATION

Actual Class	**Predicted Class**	
	anomaly	***normal***
anomaly	9576	3257
normal	283	9427

Detection rate and False alarm rate also considered two main measure of performance in classification problem. Table VI compares the detection rate and False alarm rate of given in paper [38] with our CNN-1D model. Here we can clearly see that DR of our model is high with margin 1.72 % and FAR is lower with difference 0.15%.

TABLE VI
DETECTION RATE AND FALSE ALARM RATE OF RNN AND CNN-1D

Metrics	**Models**	
	RNN	***CNN-1D***
Detection Rate (DR)	72.90%	74.62%
False Alarm Rate(FAR)	3.06%	2.91%

Fig.III shows accuracy comparisons between different ML algorithms described in paper [38] with our CNN-1D model. Accuracy of our model is 84.29% in binary classification on NSL-KDD benchmark dataset. Accuracy of our model is higher than all machine learning algorithms and also slightly higher than RNN [38] with margin of 1.01%.

B. MULTICLASS CLASSIFICATION

In multiclass classification (5-category), we performed classification for 5 classes (Normal, Dos, Probe, R2L, U2R). The problem in multiclass classification is that KDDTest+ dataset is highest unbalanced. The number of instances of R2L and U2R are very low in KDDTrain+ dataset. We performed classification algorithm on unbalanced dataset. The accuracy of this experiment is higher than accuracy of balanced dataset. But detection rate and false alarm rate extremely low compared to balanced dataset. So we chose oversampling method (ADASYN) to make the dataset balanced. All results in below section are evaluated on balanced dataset. We trained our model for 500 epochs. The filters used in this experiment 32 & 64 and the filter length was 3 and 5 respectively. The accuracy and detection rate of 64 filter along with 5 filter length was highest. In this subsection we compared accuracy of different ML algorithms & deep learning algorithms with our CNN-1D model as shown in fig.4.

From fig. 4 we can see that accuracy of our CNN-1D model are slightly lower than RNN [38] and CNN [34] model

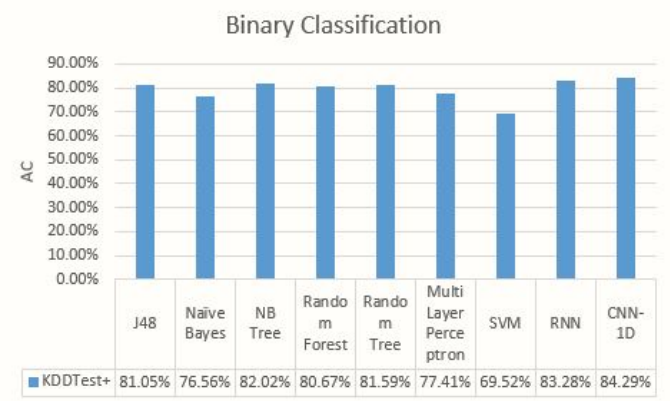

Fig. 3. Performance of CNN-1D and other models in binary classification.

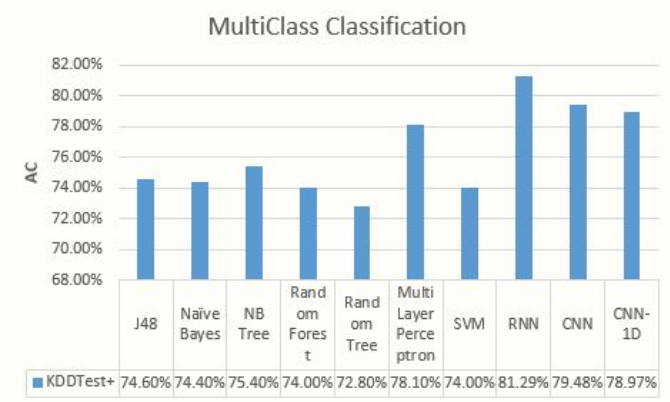

Fig. 4. Performance of CNN-1D and other models in the five category classification.

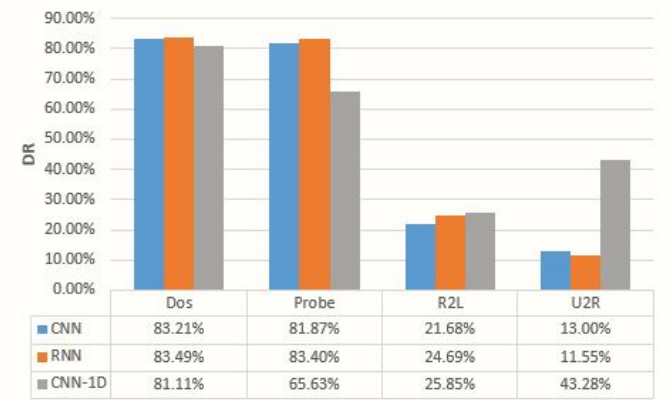

Fig. 5. Detection Rate of Different Models.

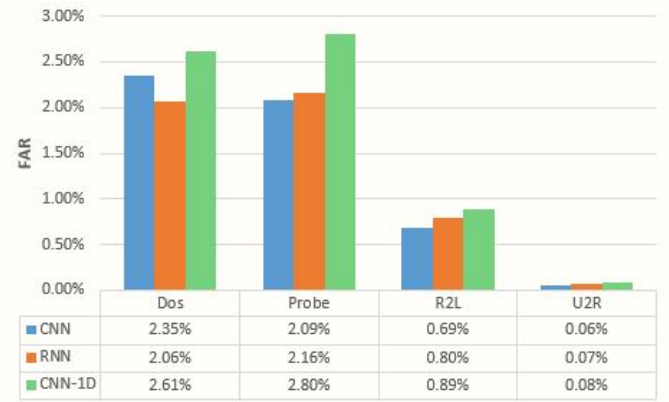

Fig. 6. Detection Rate of Different Models.

with difference of 2.32 percentage and 0.51 percentage. But accuracy of our model is higher than all other machine learning algorithms. Results shows that automatic feature selection of deep learning are better than manually feature selection of traditional ML algorithms. That is the reason deep learning is used in many fields.

TABLE VII
CONFUSION MATRIX OF MULTICLASS CLASSIFICATION ON KDDTEST+ DATASET

Actual	**Predicated Class**				
Class	**Normal**	**Dos**	**Probe**	**R2L**	**U2R**
normal	9389	71	221	20	9
Dos	1245	6051	21	143	0
Probe	512	320	1589	0	0
R2L	2083	3	41	746	12
U2R	24	0	1	13	29

Detection Rate (DR) and False alarm rate (FAR) of our CNN-1D model are computed using confusion matrix shown in table VII. DR's and FAR's of different attacks are compared with CNN [35], RNN [39] and our CNN-1D model in Fig. 5 and Fig.6 respectively. From fig. 5 we can that DR of Dos & Probe are decreased in our model, while DR of R2L and U2R are increased from both models CNN [34] and RNN [38]. FAR's of each attack type shown in fig 6, FAR of our model are slightly lower than CNN [34] and RNN [38] but they are still competitive.

V. CONCLUSION

A deep learning algorithm can automatically extract features from huge dataset. CNN-1D model for NIDS is proposed in this paper to detect anomaly or attack from a huge network IDS. CNN mainly used on image datasets, however we used time series CNN-1D in this paper which shows that CNN can be applied for tabular datasets. To deal with class imbalanced problem in multiclass classification, we used oversampling technique(ADASYN) which improved detection rate and false alarm rate. The evaluation of experimental results we can conclude that our CNN-1D approach for network intrusion detction performs better than all other IDS models. The accuracy & Detection rate of our approach is higher than all existing approaches in binary classification. In multiclass classification our accuracy, DR and FAR are slightly lower but still they are competitive to CNN [34] and RNN [38].

There is still space for improvement in future. We will try to improve the detection rate of Dos and Probe and reduce the

FARs of all four attacks. To achieve the goal, we will modify the structure of our model.

REFERENCES

[1] W. Stalling, Cryptography and Network Security: Principles and Practice, vol. 11, no. 7. Englewood Cliffs, NJ, USA: Printice-Hall, 1999, pp.665-660.
[2] Y. LeCun, Y. Bengio, G. Hinton, "Deep learning", Nature, vol. 521, pp. 436-444, May 2015.
[3] J. Schmidhuber, "Deep learning in neural networks: An overview", Neural Netw., vol. 61, pp. 85-117, Jan. 2015.
[4] L. Liu, L. Shao, X. Li, K. Lu, "Learning spatio-temporal representations for action recognition: A genetic programming approach", IEEE Trans. Cybern., vol. 46, no. 1, pp. 158-170, Jan. 2016.
[5] A.-A. Liu, Y.-T. Su, W.-Z. Nie, M. Kankanhalli, "Hierarchical clustering multi-task learning for joint human action grouping and recognition", IEEE Trans. Pattern Anal. Mach. Intell., vol. 39, no. 1, pp. 102-114, Jan. 2017.
[6] J. Wu, Y. Zhang, W. Lin, "Good practices for learning to recognize actions using FV and VLAD", IEEE Trans. Cybern., vol. 46, no. 12, pp. 2978-2990, Dec. 2016.
[7] A. Karpathy, The unreasonable effectiveness of recurrent neural networks, 2015, [online] Available: http://karpathy.github.io/2015/05/21/rnn-effectiveness
[8] M. N. Mohammed, N. Sulaiman, "Intrusion detection system based on SVM for WLAN", Procedia Technol., vol. 1, no. 10, pp. 313-317, 2012.
[9] W. Feng, Q. Zhang, G. Hu, J. X. Huang, "Mining network data for intrusion detection through combining SVMs with ant colony networks", Future Generat. Comput. Syst., vol. 37, pp. 127-140, Jul. 2014.
[10] H. Wang, J. Gu, S. Wang, "An effective intrusion detection framework based on SVM with feature augmentation", Knowl.-Based Syst., vol. 136, pp. 130-139, Nov. 2017.
[11] G. Kim, S. Lee, S. Kim, "A novel hybrid intrusion detection method integrating anomaly detection with misuse detection", Expert Syst. Appl., vol. 41, no. 4, pp. 1690-1700, 2014.
[12] A. S. Eesa, Z. Orman, A. M. A. Brifcani, "A novel feature-selection approach based on the cuttlefish optimization algorithm for intrusion detection systems", Expert Syst. Appl., vol. 42, no. 5, pp. 2670-2679, 2015.
[13] A. Sharma, I. Manzoor, N. Kumar, "A feature reduced intrusion detection system using ANN classifier", Expert Syst. Appl., vol. 88, pp. 249-257, Dec. 2017.
[14] L. Xiao, Y. Chen, C. K. Chang, "Bayesian model averaging of Bayesian network classifiers for intrusion detection", Proc. Comput. Softw. Appl. Conf. Workshops, pp. 128-133, 2014.
[15] S. Mukherjee, N. Sharma, "Intrusion detection using Naïve Bayes classifier with feature reduction", Procedia Technol., vol. 4, no. 11, pp. 119-128, 2012.
[16] L. Koc, T. A. Mazzuchi, S. Sarkani, "A network intrusion detection system based on a Hidden Naïve Bayes multiclass classifier", Expert Syst. Appl., vol. 39, no. 18, pp. 13492-13500, 2012.
[17] P. Louvieris, N. Clewley, X. Liu, "Effects-based feature identification for network intrusion detection", Neurocomputing, vol. 121, no. 18, pp. 265-273, 2013.
[18] S. Elhag, A. Fernández, A. Bawakid, S. Alshomrani, F. Herrera, "On the combination of genetic fuzzy systems and pairwise learning for improving detection rates on intrusion detection systems", Expert Syst. Appl., vol. 42, no. 1, pp. 193-202, 2015.
[19] P. R. K. Varma, S. S. Kumari, V. V. Kumar, "Feature selection using relative fuzzy entropy and ant colony optimization applied to real-time intrusion detection system", Procedia Comput. Sci., vol. 85, pp. 503-510, Dec. 2016.
[20] A. Chaudhary, V. N. Tiwari, A. Kumar, "Analysis of fuzzy logic based intrusion detection systems in mobile ad hoc networks", Proc. Elect. Perform. Electron. Packag., pp. 690-696, 2014.
[21] A. H. Ali, S. Shamshirband, N. B. Anuar, D. Petković, "DFCL: Dynamic fuzzy logic controller for intrusion detection", Facta Univ., vol. 12, no. 2, pp. 183-193, 2014.
[22] A. A. Aburomman, M. B. I. Reaz, "A novel SVM-kNN-PSO ensemble method for intrusion detection system", Appl. Soft Comput., vol. 38, pp. 360-372, Jan. 2016.
[23] W. Li, P. Yi, Y. Wu, L. Pan, J. Li, "A new intrusion detection system based on KNN classification algorithm in wireless sensor network", J. Elect. Comput. Eng., vol. 2014, no. 5, pp. 1-8, 2014.
[24] C.-F. Tsai, Y.-F. Hsu, C.-Y. Lin, W.-Y. Lin, "Intrusion detection by machine learning: A review", Expert Syst. Appl., vol. 36, no. 10, pp. 11994-12000, 2009.
[25] E. Hodo, X. Bellekens, A. Hamilton, C. Tachtatzis, R. Atkinson, Shallow and deep networks intrusion detection system: A taxonomy and survey, 2017.
[26] N. Gao, L. Gao, Q. Gao, H. Wang, "An intrusion detection model based on deep belief networks", Advanced Cloud and Big Data (CBD) 2014 Second International Conference on. IEEE, pp. 247-252, 2014.
[27] J. Yang, J. Deng, S. Li, Y. Hao, "Improved traffic detection with support vector machine based on restricted boltzmann machine", Soft Computing, vol. 21, no. 11, pp. 3101-3112, 2017.
[28] Q. Niyaz, W. Sun, A. Y. Javaid, M. Alam, "A deep learning approach for network intrusion detection system", Proceedings of the 9th EAI International Conference on Bio-inspired Information and Communications Technologies (Formerly BIONETICS) BICT-15, vol. 15, no. 2015, pp. 21-26.
[29] G. Kim, S. Lee, S. Kim, "A novel hybrid intrusion detection method integrating anomaly detection with misuse detection", Expert Syst. Appl., vol. 41, no. 4, pp. 1690-1700, 2014.
[30] H. Sak, A. Senior, F. Beaufays, "Long short-term memory recurrent neural network architectures for large scale acoustic modeling", Fifteenth Annual Conference of the International Speech Communication Association, 2014.
[31] D. Gibert Llauradó, "Convolutional neural networks for malware classification", 2016.
[32] B. Kolosnjaji, A. Zarras, G. Webster, C. Eckert, "Deep learning for classification of malware system call sequences", Australasian Joint Conference on Artificial Intelligence, pp. 137-149, 2016.
[33] R. Upadhyay, D. Pantiukhin, "Application of convolutional neural network to intrusion type recognition", Ben-Gurion University of the Negev Tech. Rep., 2017.
[34] Kehu Wu,Zuge Chen"A Novel Intrusion Detection Model for a Massive Network Using Convolutional Neural Networks", IEEE Access, vol 6, pp 50850 – 50859, 2018.
[35] M. Tavallaee, E. Bagheri, W. Lu, A. A. Ghorbani, "A detailed analysis of the KDD CUP 99 data set", Proc. IEEE Int. Conf. Comput. Intell. Secur. Defense Appl., pp. 1-6, 2009.
[36] keras documentation "https://keras.io/"
[37] Tensorflow tutorials "https://www.tensorflow.org/tutorials"
[38] C. Yin, Y. Zhu, J. Fei, X. He, "A deep learning approach for intrusion detection using recurrent neural networks", IEEE Access, vol. 5, pp. 21954-21961, 2017.

Proceedings of the Fourth International Conference on Communication and Electronics Systems (ICCES 2019)
IEEE Conference Record # 45898; IEEE Xplore ISBN: 978-1-7281-1261-9

Analysis of Bi-directional DC-DC Buck-Boost Quadratic Converter for Energy Storage Devices

Neeti Dubey
Department of Electrical Engineering
Rajasthan Technical University
Kota, INDIA
neetidebey23@gmail.com

Ashok kumar Sharma
Department of Electrical Engineering
Rajasthan Technical University
Kota, INDIA
aksharma_eck@hotmail.com

Abstract— **The rapid use of renewable and sustainable energy sources in distributed generation system, the importance of energy storage devices forcing the researches to develop new key technologies. For continual power deliver, make greater use of renewable electricity sources, together with solar and wind. Power electronic converters are mostly connected among the different voltage buses and storage systems. Bidirectional dc-dc converter topologies are used for providing charging or discharging. This paper presents the quadratic nature for obtaining higher voltage gain ratios in step-down (buck) and step-up (boost) converter's operating states with reduced charging and discharging ripples. Proposed scheme has been developed and analyzed using MATLAB/ simulink.**

Keywords – Buck converter, Boost Converter, ESD, Quadratic dc-dc converter schemes.

I. INTRODUCTION

Electric power created by sustainable power sources is unsteady in nature, in this way delivering an awful impact on the utility grid [1]. The storage of energy can be possible in two ways, one is magnetically (using inductors) and another one is electrically (using capacitors) [2]. DC-DC converters change the voltage level which might be upper or lower, storing and releasing the energy at distinct voltage. Basically voltage & frequency stability can be realized by the use of such ESDs in sustainable energy sources, for example, sun-based and wind. Because of operational prerequisites of the conveyed age framework, ESDs need such type of DC-DC converters which can permit charging and discharging. The job of Energy storage gadgets in the expanding entrance of inexhaustible and maintainable vitality sources is broadly perceived. Various devices supported electrochemical energy storage systems likewise; ultra capacitor, batteries.

This paper presents traditional buck and boost quadratic converter which comprises of DC-DC boost converter with a coupled inductor for the distributed generation system [3]. Basic step-up converters give higher voltage gain but these converters face the issue--due to limited reverse recovery issue of diode and power losses [4-9]. For obtaining proposed converter for higher voltage gain, two inductors and capacitors have been used [11-14].

In this article buck-boost converter has been simulated which are bidirectional in nature. These converters are very helpful in distribution generation system as conventional converters are less efficient to work in higher frequency regions. This converter is moreover depicted by a fundamental control system since it is only imperative to control one power semiconductor for each movement mode. The additional power semiconductors remain reliably on or continually off. Quadratic converter shows up with DC transformation proportion that offers an essentially more extensive change extend, persistent input and yield current, diminished charging/releasing ripple and moreover direct control hardware.

II. ELECTROCHEMICAL ESD

Electrochemical devices are basic elements of electrochemistry which are highly demanded resources that provide reliability in the solutions of telecommunication applications. These devices are basically eco-friendly in nature.

A. Supercapacitors

Supercapacitor is generally used to store electrical energy in which two parallel plates separated by an insulating medium i.e. dielectric. To achieve a high value of the capacitor, electrochemical double layer capacitance or ultra capacitors used which possessed large surface area carbon electrodes. As compared to conventional capacitor, supercapacitors have greater capacitance and high energy density.

B. Batteries

Batteries are mostly made up of consisting one or more electrochemical cells which obey principle of the electrochemical energy conversion. The Bidirectional nature of the DC-DC converter is responsible to flow

the power from the DC-grid to the battery or vice-versa as shown in fig.1.

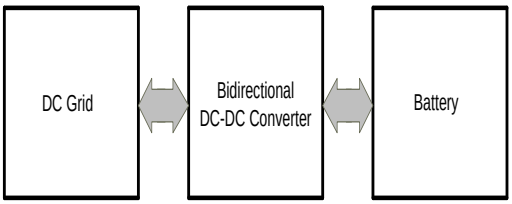

Fig.1.Basic scheme of bidirectional converter

III. QUADRATIC BUCK- BOOST CONVERTER

Figure 2 and 3 show the most known topologies with wide voltage range that is step up and down converter. These topologies are characterized by the use of passive elements.

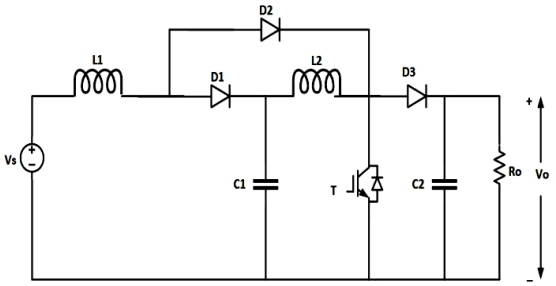

Fig.2. Traditional quadratic boost (Step-up) converter

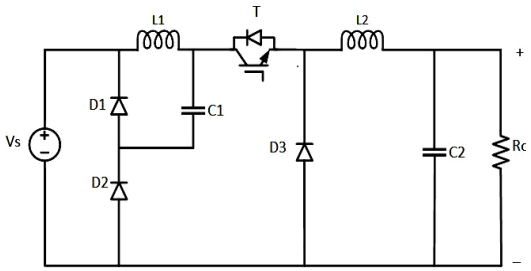

Fig.3. Traditional quadratic buck (Step-down) converter

With the analysis of these previous traditional quadratic buck (step-down) converter and traditional quadratic boost (step-up) converter, it is found that these converters hold the unidirectional power flow using the extra passive elements compared to the normal power circuit, which provide the additional power losses. Individually both the converters possess uncertainty in duty ratio. These limitations are rectified by the new bidirectional quadratic dc-dc converter.

The new bidirectional buck-boost quadratic converter comprises four IGBT switches, capacitors, inductors. Additionally RC filter is connected in the input and output side of the proposed converter which reduces the output voltage spikes and minimizes the charging and discharging ripple. The quality of the proposed converter is, the only one active switch is responsible for each mode of operation.Fig.4. shows the proposed bidirectional quadratic nature buck-boost or step up-down converter.

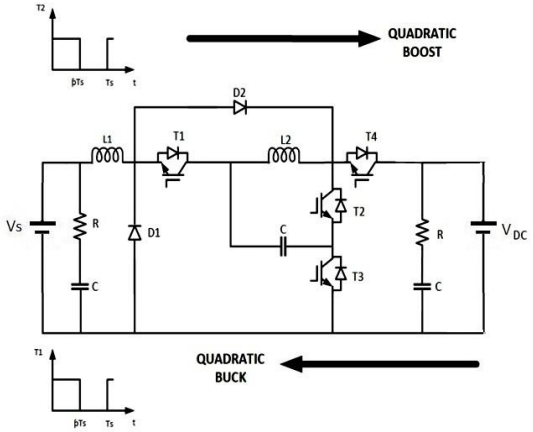

Fig.4. Proposed bidirectional quadratic buck-boost converter

A. *Operation in Boost(step-up)Mode :*

In the discharging mode transistors T_1 and T_4 are turned-off and the transistor T_3 is turned-on. The circuit operation can be split into two different phases over one half cycles as discussed below:

First phase**:** during this time T_2 is turned-on during δTs .during this time period, storage device deliver its energy to the L_1 and capacitor to the L_2, this shows the rising nature of current in both L_1 and L_2. The circuit diagram of the first phase is shown in Fig. 5 (a).

Second phase**:** In the second phase, the transistor T_2 will be turned-off in the duration of (1-δTs). In this stage, both the passive elements (L_1 and L_2) discharge. During this time-interim the inductor L_1 transferred energy to the capacitor and inductor L_2 transferred energy to the load. The circuit diagram of the second phase is shown in Fig. 5 (b).

These phases explained the voltage gain of this converter in Boost mode can be obtained. In this analysis, the average voltages of both the inductors are equal in the first and second phase, the following relationships are received:

$$\delta V_S + (1-\delta)(V_S - V_C) = 0 \quad (1)$$

$$\delta V_C + (1-\delta)(V_C - V_O) = 0 \quad (2)$$

Here, $V_O = V_{DC}$

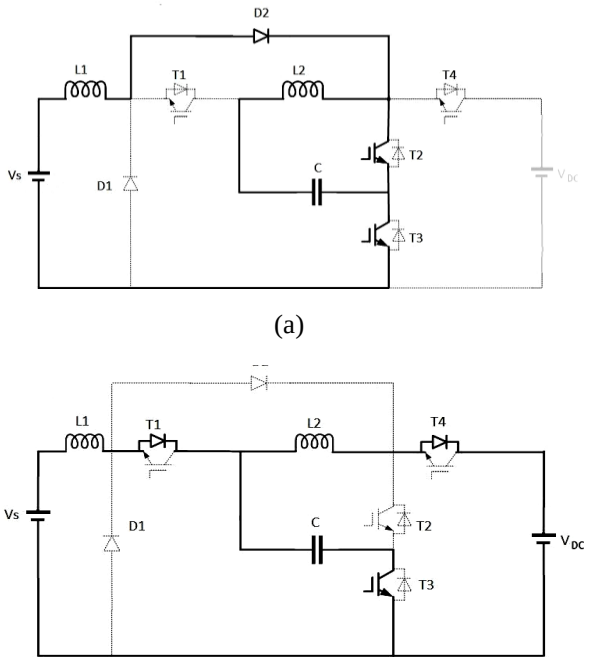

Fig.5. Equivalent circuits during one switching period for the boost mode of the storage system.

By the the preceding equations, the input to output voltage gain in step-up mode can be obtained from equation (3).

$$V_O(1-\delta)^2 = V_I \tag{3}$$

According to the above analysis, these two operating phases present following relationships that are

$$\frac{I_{L1}}{I_{L2}} = 1/(1-\delta) \tag{4}$$

Fig. 6 shows the operational waveform for Boost mode.

B. Operation in Buck (step-down) Mode:

In the charging mode of the buck converter, the energy will be transferred from the load to the storage device i.e. battery. This mode of operation is executed by the transistor T_1. Thus, the transistors T_2 and T_3 are turned-off and transistor T_4 is turned-on. Similarly the two modes of the buck converter as discussed below. First phase**:** In this phase transistor T_1 is turned-on during the time interim of δTs. In this duration of time, the current will be transferred from the load to the inductor L_1 and from the capacitor to the inductor L_2 in Fig. 7 (a).

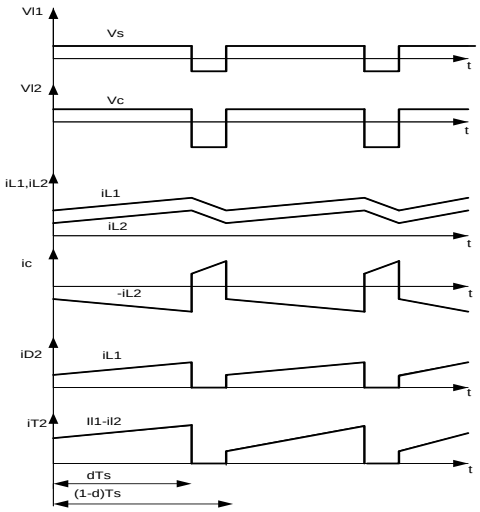

Fig.6. Operational waveforms of boost mode

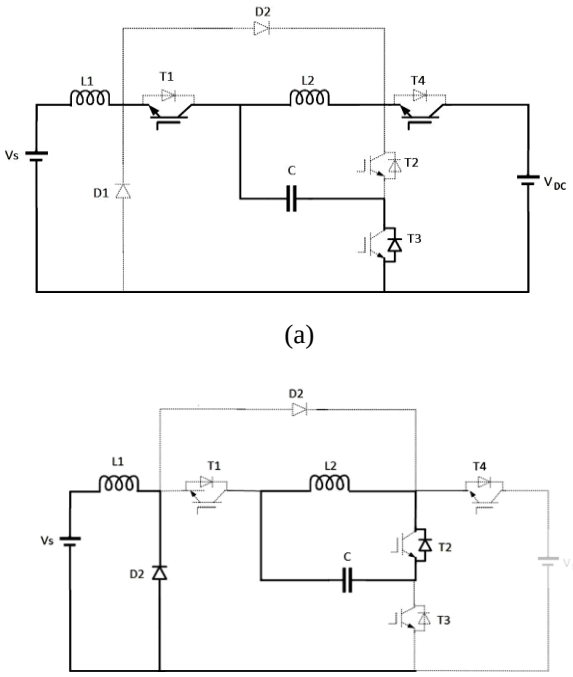

Fig.7. Equivalent circuits during one switching period for the charging mode of the storage system.

Second phase**:** In this phase transistor T_1 is turned-off in the duration of (1-δTs). Energy stored in the inductor L_1 will be delivered to the capacitor C and L_2 will now be transferred to the storage device in Fig.7.b). From the assessment of these two stages is conceivable to accomplish the voltage addition of this converter buck mode. Hence, taking into account that the normal voltages of both the inductors equal to zero, the accompanying connections are acquired.

$$\delta(V_S - V_C) + (1-\delta)V_S = 0 \quad (5)$$

$$\delta(V_C - V_O) + (1-\delta)V_C = 0 \quad (6)$$

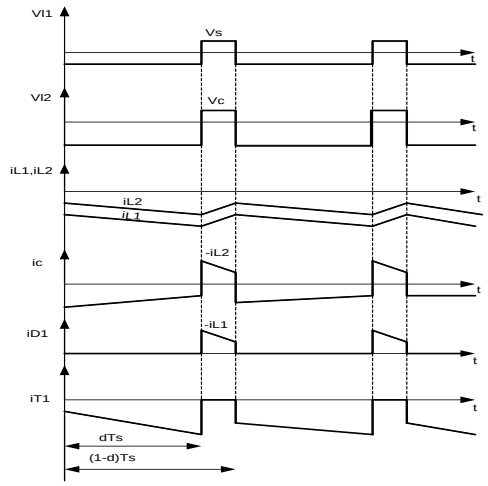

Fig. 8.Operational waveform of the proposed converter during buck mode.

$$\frac{V_o}{V_s} = \frac{1}{\delta^2} \quad (7)$$

The operational waveforms of buck (Step-down) converter during Buck mode are shown in Fig.8.

IV. SIMULATION RESULTS

Boost mode (Forward mode): This mode shows the power stream from the ESD to the load. This simulation has been done using Matlab / Simulink platform. Fig. 9, shows the Matlab model of bidirectional quadratic dc-dc boost converter. The converter operation has been simulated for V_S = 48V (battery voltage), V_O = 180.0 V, L1 = 1.0 mH, L_2 = 2.20mH, C = 150.0 µF ,R_{in}=0.1ohm, C_{in}=47.0µF and with a switching frequency of 15 kHz. The simulated waveforms of the input & output voltage, and ripple in the inductor current as shown in fig. 12.

Buck mode (backward mode): This mode represents the power flow from the load ESD. Operating modes of the proposed bidirectional quadratic converter have been verified through numerical simulations. The simulation depicts the model of bidirectional quadratic dc-dc buck converter.

Similarly, the waveforms of input voltage & current, and ripple current, voltage across transistor T_1,

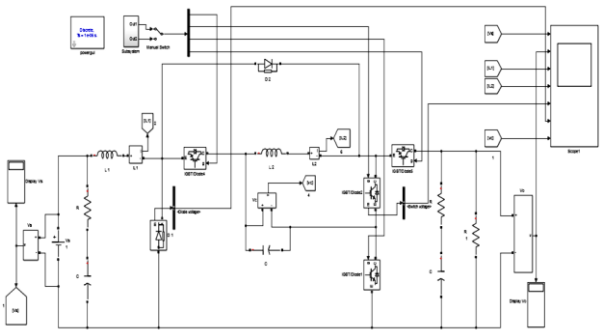

Fig.9.Simulation model of boost converter

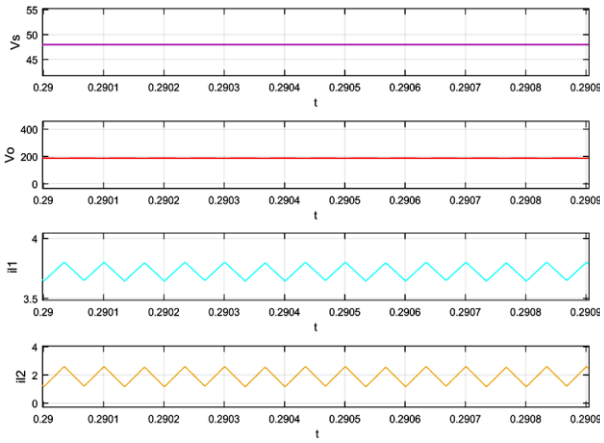

Fig. 10. Simulation waveforms of input voltage V_s, output voltage Vo, inductor current il_1, il_2 in Boost mode.

diode and capacitor as indicated in figure 13 and 14.

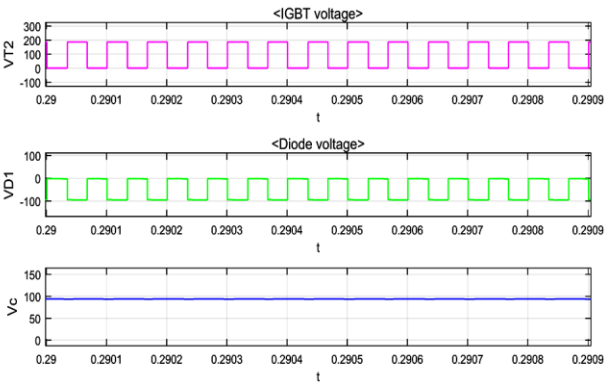

Fig. 11. Simulation waveforms of IGBT voltage V_{T2}, diode voltage V_{D1}, capacitive voltage V_C, in boost mode.

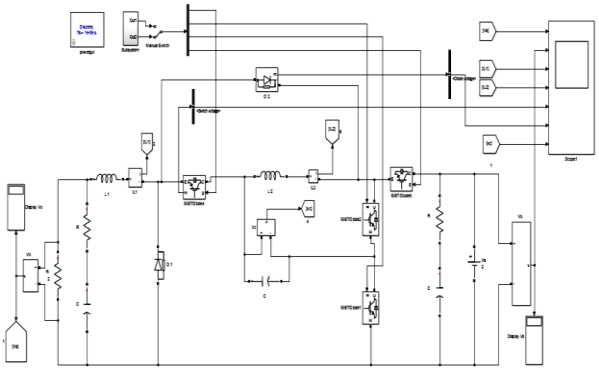

Fig.12.Simulation model of buck converter

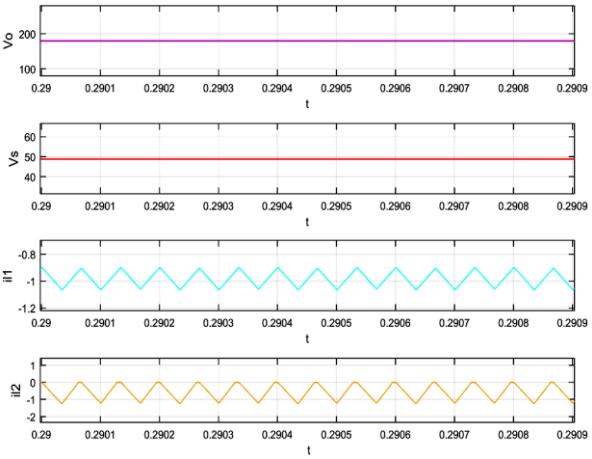

Fig. 13. Simulation results of V_s, V_O, i_{L1}, i_{L2} in buck mode.

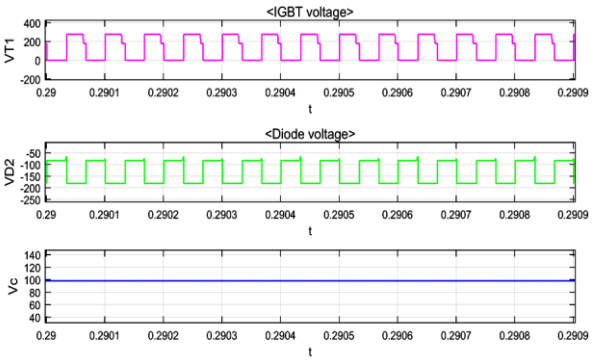

Fig.14. Simulation waveforms of IGBT voltage V_{T1}, diode voltage $V_{D1,}$ capacitive voltage V_C in buck mode.

V. CONCLUSION

The classical quadratic buck and boost converter requires extra passive elements like inductors and capacitors due to which in the case of unidirectional power flow these converters shows the uncertainty in duty cycle and many other drawbacks which make these converters less efficient. In this paper, a bidirectional quadratic buck-boost converter has been analyzed. In this analysis, different modes of charging (buck) and discharging (boost) have been explained. From the analysis, it has been evident that bidirectional DC-DC buck-boost converter provides less ripple with less component count compared to conventional quadratic buck and boost converter which make the system more compatibles for energy storage system. Here, RC filter has been introduced which reduces the spikes in the output voltage and also minimizes the charging or discharging ripple. In charging mode (buck) analysis has been done for 180v (V_{in}) and 48v (V_{out}).Similarly for discharging mode, analysis has been done for 48v (V_{in}) and 180v (V_{out}). MATLAB / Simulink platform has been used to verify the result.

REFERENCES

[1]. J. T. De Carvalho Neto and A. O. Salazar, “One-cycle control applied to a bidirectional buck-boost converter in energy storage applications,” 2015 IEEE 13th Brazilian Power Electron. Conf. 1st South. Power Electron. Conf. COBEP/SPEC 2016, 2015.

[2]. P. S. Tomar, A. K. Sharma, and K. Hada, “Energy storage in DC microgrid system using non-isolated bidirectional soft-switching DC/DC converter,” 2017 6th Int. Conf. Comput. Appl. Electr. Eng. - Recent Adv. CERA 2017, vol. 2018-January, pp. 439–444, 2018.

[3]. S. Inoue and H. Akagi, “A bidirectional DC-DC converter for an energy storage system with galvanic isolation,” IEEE Trans. Power Electron., vol. 22, no. 6, pp. 2299–2306, 2007.

[4]. J. D. Paez, D. Frey, J. Maneiro, S. Bacha, and P. Dworakowski, “Overview of DC-DC converters dedicated to HVDC Grids,” IEEE Trans. Power Deliv., vol. 34, no. 1, pp. 119–128, 2019.

[5]. K. Cui, V. Adrian, B. H. Gwee, and J. S. Chang, “A noise-shaped randomized modulation for switched-mode DC-DC converters,” IEEE Trans. Circuits Syst. I Regul. Pap., vol. 65, no. 1, pp. 394–405, 2018.

[6]. S. M. Lukic et al., “Energy storage for automotives,” vol. 55, no. 6, pp. 2258–2267, 2008.

[7]. Kuldeep jayaswal, Dheeraj kumar palwalia, Gaurav jain, Prakash kumar, “Design-Oriented Analysis of Non-isolated DC-DC Buck Converter”, Ciencia e Tecnica Vitivinicola journal, vol. 30, no. 2, pp. 177-213, February 2015.

[8]. Z. Guo, C. Zheng, L. Zhao, and X. Qi, “Control strategy study of bi-directional energy storage converter,” Proc. 2017 12th IEEE Conf. Ind. Electron. Appl. ICIEA 2017, vol. 2018-February, pp. 567–571, 2018.

[9]. P. Wang, L. Zhou, Y. Zhang, J. Li, and M. Sumner, “Input-parallel output-series DC-DC boost converter with a wide input voltage range, for fuel vell vehicles,” IEEE Trans. Veh. Technol., vol. 66, no. 9, pp. 7771–7781, 2017.

[10]. Kuldeep jayaswal, DK Palwalia, "Performance Analysis of Non-Isolated DC-DC Buck Converter Using Resonant Approach", Engineering, Technology & Applied Science Research, Vol. 8, No. 5, pp. 3350-3354, October 2018.

[11]. J. Zhao, H. H. C. Iu, and T. Fernando, “A design of single-switch two-stage DC-DC converters with PWM and PFM for off-grid solar power system,”

[12]. M. W. Beraki, J. P. F. Trovao, M. S. Perdigao, and M. R. Dubois, “Variable inductor based bi-directional DC-DC converter for electric Vehicles,” IEEE Trans. Veh. Technol., vol. 66, no. 10, pp. 8764–8772, 2017.

[13]. H. Givi, E. Farjah, and T. Ghanbari, “Switch and diode fault diagnosis in non-isolated DC-DC converters using diode voltage signature,” IEEE Trans. Ind. Electron., vol. 65, no. 2, pp. 1605–1615, 2017.

[14]. Y. Ye, K. W. E. Cheng, and S. Chen, “A high step-up PWM DC-DC converter with coupled-inductor and resonant switched-capacitor,” IEEE Trans. Power Electron., vol. 32, no. 10, pp. 7739–7749, 2017.

Proceedings of the Fourth International Conference on Communication and Electronics Systems (ICCES 2019)
IEEE Conference Record # 45898; IEEE Xplore ISBN: 978-1-7281-1261-9

Building a Cloud Solution for Energy Management using Raspberry Pi

Laxmi Khichadi
PG Scholar
Digital Communication Engineering
R V College of Engineering
Bangalore, India
laxmikhichadi9482@gmail.com

Siva Ganesh Kumar
Team Lead
Siemens Technology and Services
Private Limited
Bangalore, India
sivaji.jaya@gmail.com

Dr. Nagamani K.
Professor
Dept. of Telecommunication Engineering
R V College of Engineering
Bangalore, India
nagamanik@rvce.edu.in

***Abstract*— Energy management plays important role in any business. The productivity of an organization will be increased by efficient use of the energy. Energy management reduces system cost and also helps user in analyzing the total energy consumed. In this paper the energy management is carried out efficiently at Siemens by collecting data from the power meters consumed by building and developing a web application in cloud using Raspberry Pi and Modbus Communication protocol. The paper also gives the configuration details of Node RED in Raspberry Pi.**

Keywords— Energy Management, Raspberry Pi, Modbus Communication protocol, Node RED

I. INTRODUCTION

Efficient method of energy management is to use Raspberry Pi for building a web application which gives information about the amount of energy consumed by devices. Raspberry Pi is a small, portable and inexpensive computer which is full-featured on a single board. Keyboard, mouse, monitor, speakers can all be attached to it. In the energy management application Raspberry Pi is used to create documents, web browsing, interface between devices and the cloud. The Raspberry Pi comprises of different interfaces for other external devices. It consists of RAM, graphic chips, processor, Ethernet port, CPU, power source connector UART, memory card etc.

The implementation uses cloud space to store the energy consumed information. Cloud storage provides digital services that enhance the productivity and increase the efficiency of entire business. It is an open platform which allows user to build and run the apps. The data present in cloud can be later analyzed by the user. The cloud has unlimited storage capacity and can be used in any real time application. The project uses serial protocol called Modbus Communication Protocol. It transmits the information from the electronic devices using serial lines. It is used to communicate among the devices which are connected in same network. It is mainly used for industrial applications. Each device communicates with Raspberry Pi with unique address. Based on device address data can be collected from the desired device and analysis of result can be achieved. Displaying and analysis of the data is the last step in the implementation.

The data present in cloud is analysed by different methods like Load monitoring, Load profiling, Load forecasting. Load monitoring is used to analyse the changes in voltage, power and current used by building, home appliances etc. It measures amount of energy consumed at a given instant of time. Using load monitoring sudden rise in the amount of energy consumed can be obtained so that no damage is occurred.

The variations in the electrical load for an instant of time are illustrated by load profiling. It is very useful to plan the amount of power required for future use. In the project bar charts and line charts are used to plot the variations in the power consumptions. Short term, medium term or long-term demand of electrical power required is predicted by load forecasting.

The load forecasting helps the companies in managing electric supply to their customers. Efficiency and revenue of company can be increased by load forecasting. It helps them to plan and act on their capacity and operations.

II. RELATED WORK

When Comparison between microcontroller and Raspberry Pi is carried out, Raspberry Pi is proven to be more useful hardware in IoT projects. Also, the use of Raspberry Pi as a cloud server or as a storage device is given in the paper [1]. Raspberry Pi is used for industrial meter reading to collect data from energy consuming devices [2].

The unnecessary wastage of energy will reduce the efficiency for example in house or industry. Thus to avoid the unnecessary wastage of resource the authors in paper [3] have proposed a method which uses Bluetooth communication present in the user's phone. Raspberry Pi is connected to the Bluetooth which helps in communication. Raspberry Pi usage made the implementation cost effective.

The paper [4] presents self adaptive framework which has steps like planning, monitoring, analyzing, execution etc. The method is based on dynamic power management. It uses control loops. The private cloud infrastructure consists of sensor, virtual machines, hypervisors, host etc. The implementation is carried out in Agile cloud environment. The overall result is that energy consumption is decreased and energy efficiency is increased.

The paper [5] mainly focuses on data logging. The implementation uses communication area network protocol, it

also uses Raspberry Pi and IOT devices. The implementation was carried out to build a data logger system. The system intakes different parameters as input from various sensors like temperature, pressure, coolant temperature sensor, oil sensor, ambient air pressure sensor etc. The calculated sensor data is given to electronic control module and with the interface of the Raspberry Pi controller the data was pushed to cloud and stored data could be viewed in the laptop or PC.

In paper [6] RPiaasa efficient cloud testbed built which uses Raspberry Pi is introduced. The data used to store in the cloud is not secured always. Hence, the paper [7] proposed a method that allowed user to store data securely and also access the data with security from cloud storage. The method prevents the data been leaked to unauthorized users by providing security. It gives access on to the authorized users. The method uses the encryption process; it encrypts the data at client side. The secret key used for encryption is same used for decryption.

The various steps for building IOT platform, creating HTTP connections, Creating assets, sending commands to Raspberry Pi and uploading the information was also mentioned in paper [8]. The collected data from building is represented in smart meters and then forecast tools display it. The data is stored in database and used to plot the variations in data consumed by each building [9].

In the paper [10] ZigBee sensor network is used for energy management. The system proposed consists of three components that is environmental information entity, power monitoring entity and control devices all three are used to monitor and collect environmental information such as humidity and temperature. Each component uses Zigbee interface. The paper [11] gives introduction about Amazon web services, how AWS can be used to compute power and provide various services. The authors in paper [12] explain the importance of energy monitoring, managing and controlling.

III. DESIGN

The design of energy management system comprises of combination of hardware and software implementation. The hardware used here is Raspberry Pi and software part is pushing data to cloud. It has several steps. They can be summarized as follows:

1. The real line data such as voltage or current consumed by the building is read from the power monitoring devices through modbus communication protocol.
2. The interface between the power meters and the cloud is the Raspberry Pi.
3. The Raspberry Pi is configured using Node RED and necessary modbus drivers are installed into the Node RED.
4. Using web tokens, the data is pushed into the cloud.
5. Data visualization in the dashboard consisting of graphs and charts.
6. Analysis of the result.

The complete flow of the system is presented graphical as shown in Fig. 1. And the block diagram is as shown in Fig. 2.

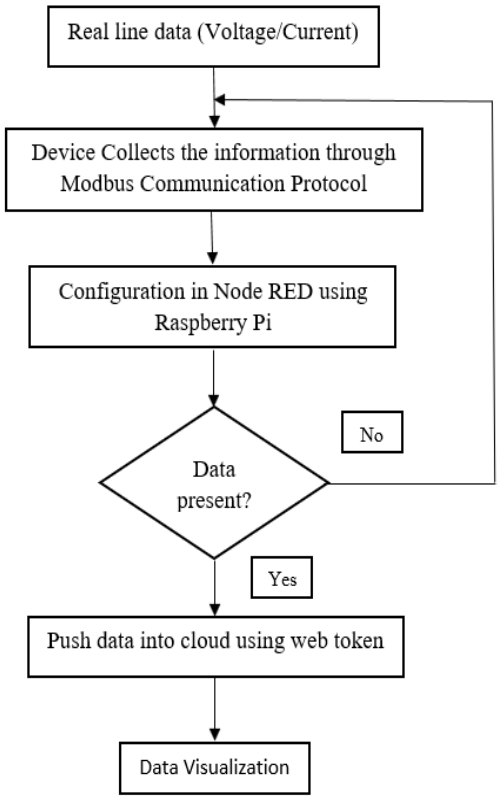

Fig. 1. Flowchart of energy management system

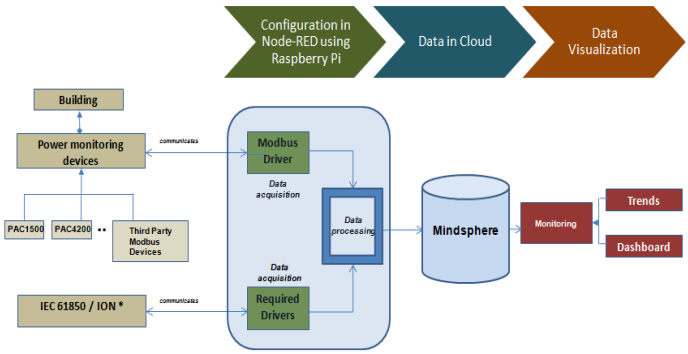

Fig. 2. Block diagram of energy management system

IV. EXPERIMENTAL SETUP

The whole implementation consists of Raspberry Pi 3 B+ as an interfacing tool between power meters and cloud. The main features of Raspberry Pi are:

- Multicore processor which consists of ROM, RAM and Ethernet ports all on single chip.
- Low cost device which is Credit card size.
- Uses Linux operating System.
- Has ability to run multiple programs.
- It is mainly used in IoT-applications.

Various connections that are necessary to configure Raspberry Pi 3 B+ are as shown in Fig. 3.

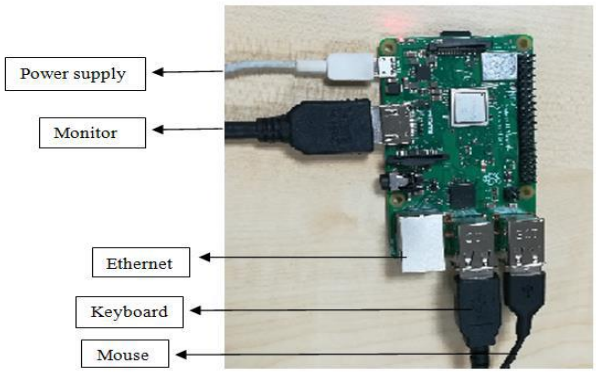

Fig. 3. Raspberry Pi 3 B+ set up

A. *OS Installation*

Steps involved in installing Raspbian OS are as follows:

1. Set up the SD card which acts as an internal storage in Raspberry Pi. Once the card is set up it is ready for Raspbian OS installation.
2. Download the Raspbian OS. To download the Raspbian OS go to raspberrypi.org website and click Download the Raspbian and extract the file.
3. Raspbian OS image file will be installed.
4. Next step is to download Disk Imager to write Raspbian OS in the SD card. To download click on the link installation guide present in raspberrypi.org website. Then download the windows version. Click on source force project page link and download the file. Next extract and install the downloaded file by unchecking the View README.txt and press finish.
5. Win32 Disk Imager-1.0 window will be opened. Select correct drive location according to SD card in Device Selector. Copy the path of Raspbian OS image and paste in Image File. Select the image file once again click on write button and press yes. Success message pops up. Click ok.

B. *Configuring Node RED in Raspberry Pi*

Node RED is a programming tool for creating flow of the hardware devices, APIs, services etc. Node-RED has an internet browser-based editor, which may be used to create JavaScript features. It is communication gateway software which is used to connect modbus drivers and cloud. Node RED has many standard nodes using which flow is created.

Steps to install Node-RED into Raspberry Pi:

1. Insert the configured SD card into the Raspberry Pi.
2. Connect the Raspberry Pi to the monitor in order to have a display of the board.
3. Connect the Pi to the internet.
4. Open command window and install Node-RED using Script command.
5. Open the Node-RED in web browser.
6. If the modbus drivers are not installed then in the root directory of Node-RED install it using the command npm install –g node-red-contrib-mobus.

Fig. 4. shows the Node-RED configured in Raspberry Pi.

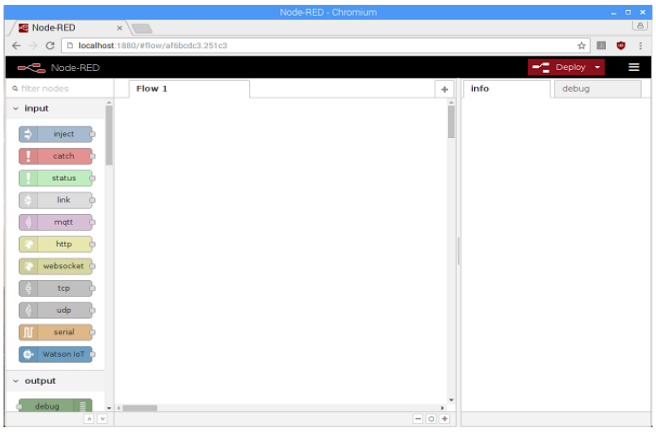

Fig. 4. Node-RED editor

In the device network communication between the devices is carried out by Modbus Communication Protocol hence, modbus drivers are installed in Node RED. Modbus is a serial communications protocol used to connect industrial electronic devices. It is an open source protocol and easily deployed protocol. Three types of Modbus are Modbus RTU, Modbus ASCII and Modbus TCP/IP. Its functions are to read and write the data from and to the devices respectively. Modbus works on master and slave concept. Modbus master is the device which requests the information and Modbus slave is the one which supplies the information. Modbus can have 1 master and 247 slave devices having 247 unique slave addresses for the communication. In this implementation master is the power meters ad slaves are the measuring points like active power, apparent power etc.

V. Results and Analysis

The Node RED flow is created in local browser at http://localhost:1880. Using various nodes like Inject node, Debug node, Function node, Modbus read etc the flow for the project is created. It is as shown in the Fig. 5.

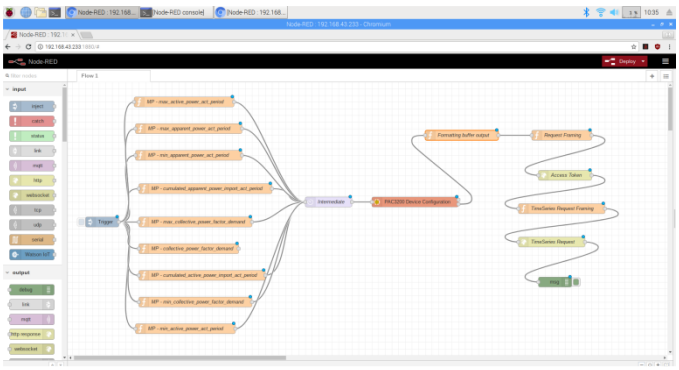

Fig. 5. Json flow in Node RED

The various nodes/steps used to build the above flow are:

1. Inject

The Inject node is used to trigger the flow by clicking the node button. It automatically triggers the flow at regular intervals. The intervals at which the injector can be triggered are at a particular instant, on demand or periodic.

2. Function

Function node passes message though a JavaScript function. Here function node depicts the various measuring points that are supported by power devices. It has function code set to 4 means modbus input register port is set. UnitId is the device ID. Address is the modbus address for each measuring point. dpName is data point name.

3. Intermediate

An intermediate node takes parallel input from every measuring point. If suppose there are 10 data points, each data point should be sent at the output at same time.

4. Modbus Read (Modbus Network)

The IP address is obtained to a device by modbus network; this has to be tagged in the Host address. Default port set is 502.

5. Formatting buffer output

The buffer data is an array. It has to be converted to the float data to give it to the time series. The line msg.result = float [0] is used to convert the buffer output to float.

6. Request framing

It depicts the header in postman software.

7. Access token

It provides security against unauthorized users. It provides authentication by giving user to enter username and password.

8. Time series request framing

Bearer is added to the access token.

9. Time series request

Same asset ID as of device is tagged in the URL.

10. Message

The output status is displayed using deploy node.

The output after creating a flow using above node is as shown in the Fig. 6. The Debug Slider present in the left side of the image gives the information of successful deployment which tells data is pushed into the cloud.

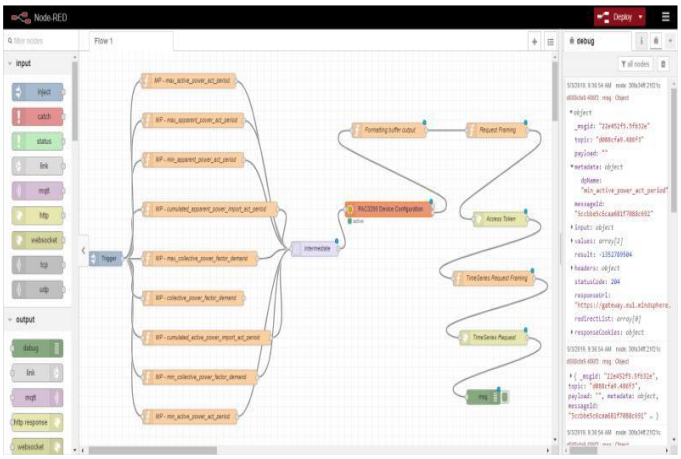

Fig. 6. Node RED output

The next step is displaying data present in the cloud to the dashboard. The data is displayed in the form of gauges, bar chart and line chart. The bar and line chart gives the comparison of data at two different time series. Fig. 7 shows the gauges displaying measuring points such as cumulated active power import, cumulated apparent power import and collective power factor demand.

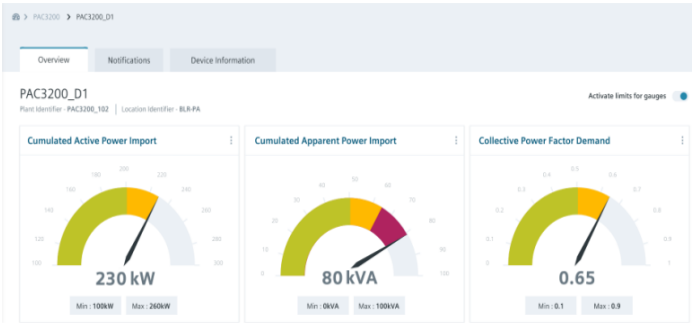

Fig. 7. Energy monitoring dashboard containing gauges

Fig. 8 shows the bar chart, the dashboard has power demand, time of use, usage percentage, minimum value, and maximum value display.

Fig. 8. Energy monitoring dashboard containing bar chart

Fig. 9 shows line chart which displays the cumulated active power import values has date time picker.

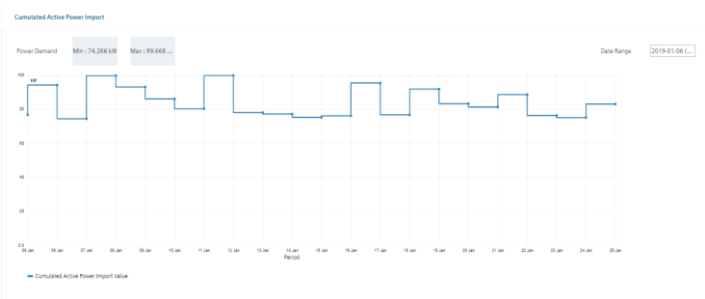

Fig. 9. Energy monitoring dashboard containing bar chart

VI. Conclusions and Future Scope

The energy management system is built efficiently using a cloud application and Raspberry Pi interfacing between power meters and the cloud. As Raspberry Pi is low cost device and consumes less power also Node-RED is open source software. Hence, the system built is cost effective. The data visualization helps user to analyze the power consumed at particular instance and avoid unnecessary wastage of energy.

The future scope of this work is to build a Mobile Application with same features in an optimized way. Also to generate the web application, this would automate the Node-RED flow. The application can be used by industry, homes or any

organizations. Raspberry Pi can also be connected to various sensors to collect data instead of connecting it to network.

ACKNOWLEDGMENT

I acknowledge with immense pleasure the guidance and support extended by Siva Ganesh Kumar and Nithin A, Siemens Technology and Services Private Limited, Bengaluru, India.

I thank Dr. Nagamani K, Professor, Department of Telecommunication Engineering, R. V. College of Engineering, Bengaluru for her timely suggestions and contribution in successful completion of the work.

I thank the company Siemens Technology and Services Private Limited, Bengaluru, India for providing the resources required to carry out the implementation.

REFERENCES

[1] S. E. Princy and K. G. J. Nigel, "Implementation of cloud server for real time data storage using Raspberry Pi," 2015 Online International Conference on Green Engineering and Technologies (IC-GET), Coimbatore, 2015, pp. 1-4

[2] P. H. Kulkarni, P. D. Kute and V. N. More, "IoT based data processing for automated industrial meter reader using Raspberry Pi," 2016 International Conference on Internet of Things and Applications (IOTA), Pune, 2016, pp. 107-111.

[3] Jayanth S, Poorvi MB and Sunil MP, "Raspberry Pi based energy management system," 2016 Online International Conference on Green Engineering and Technologies (IC-GET), Coimbatore, 2016, pp. 1-5.

[4] L. Xu, G. Tan, X. Zhang and J. Zhou, "Energy aware cloud application management in private cloud data center," 2011 International Conference on Cloud and Service Computing, Hong Kong, 2011, pp. 274-279.

[5] T. Tavade and P. Nasikkar, "Raspberry Pi: Data logging IOT device," 2017 International Conference on Power and Embedded Drive Control (ICPEDC), Chennai, 2017, pp. 275-279.

[6] P. Maenhaut, B. Volckaert, V. Ongenae and F. De Turck, "Demo abstract: RPiaaS: A raspberry pi testbed for validation of cloud resource management strategies," 2017 IEEE Conference on Computer Communications Workshops (INFOCOM WKSHPS), Atlanta, GA, 2017, pp. 946-947.

[7] A. Kumar, B. G. Lee, H. Lee and A. Kumari, "Secure storage and access of data in cloud computing," 2012 International Conference on ICT Convergence (ICTC), Jeju Island, 2012, pp. 336-339.

[8] Iot based smart home with real time e-metering using e-controllerr. Bhilare and s. Mali, "iot based smart home with real time e-metering using e-controller," 2015 annual ieee india conference (indicon), new delhi, 2015, pp. 1-6.

[9] CharalamposMarmaras and Omer Rana, “A Cloud-Based Energy Management System for Building Managers”,2014 International Joint Conference

[10] I. Hong, J. Byun and S. Park, "Cloud Computing-Based Building Energy Management System with ZigBee Sensor Network," 2012 Sixth International Conference on Innovative Mobile and Internet Services in Ubiquitous Computing, Palermo, 2012, pp. 547-551

[11] Lingli Fu and Tao Chen, "Building enterprise application based on cloud computing," *2010 International Conference on E-Health Networking Digital Ecosystems and Technologies (EDT)*, Shenzhen, 2010, pp. 534-537.

[12] B. Bitzer and E. S. Gebretsadik, "Cloud computing for monitoring and controlling of distributed energy generations," *2014 49th International Universities Power Engineering Conference (UPEC)*, Cluj-Napoca, 2014, pp. 1-5

Proceedings of the Fourth International Conference on Communication and Electronics Systems (ICCES 2019)
IEEE Conference Record # 45898; IEEE Xplore ISBN: 978-1-7281-1261-9

Test Pattern Generation to Detect Single Stuck-at Faults for Combinational Circuits Using ZBDD.

Antony Thomas, J. P. Anita
Department of Electronics and Communication Engineering
Amrita School of Engineering, Coimbatore
Amrita Vishwa Vidyapeetham, India.
Antony231j@gmail.com, jp_anita@cb.amrita.edu

***Abstract*—In this work generating test pattern using zero suppressed binary decision diagram (ZBDD) to generate test patterns for combinational circuit has been used. The ZBDD for combinational circuits are first obtained then test patterns are generated from it, similar approach is used for fault injected ZBDD and XOR operation is performed of both the set of test patterns to generate test pattern to detect the fault. This approach will reduce the power consumption during test mode of acircuit.**

Keywords— ZBDD, stuck-at-faults, test pattern.

I. INTRODUCTION

The advancement in VLSI technology has enabled us to implement millions of transistors and gates on a single IC. As Moore's law backs up the claim that number of transistors in a circuit doubles every 18 months. The VLSI technology has found its application in many different fields and some situations were performance and robustness are of high demand. Hence testing of these devices becomes an essential part of the development cycle.

As complexity of the circuits increases testing of the circuits become more difficult, challenging and power consuming. Over the last couple of decades or so engineers have constantly tried to develop different approaches to test the ICs, to reduce the effort and power consumption in the test mode. Several algorithms and models have been used to make the process of testing easier. One among these is BDD (Binary Decision Diagram). BDDs have been used studied comprehensively for a theoretical approach. When complexity issue is considered, number of nodes in the BDD are inspected. BDD helps in an easier way to work around and manipulate the Boolean functions [1]. The techniques using BDD is helpful in many applications which uses CAD. Hence the usage of memory becomes a critical factor while using BDD. The order in which variables are present is an important factor which contributes to the size of BDD and hence it also influences the memory consumption. Therefore, there are several approaches which are developed to reduce the size of BDD and thereby reducing the memoryconsumption.

In [2] and [3] different techniques have been introduced to reduce the size of BDDs. In [2] the minimization technique is performed by exchanging the variables in BDD in such a manner that it is optimum. It is performed using and algorithm called Friedman's algorithm. Along with that greedy method is used which is based on exchanging of variables which are adjacent. Mainly performed for 3,4 variables. There are several other methods which are employed in variable reordering. A heuristic method in which the graph is dynamically reorder, that is during the time of BDD construction. It helps the graph to stay more compact [7]. The algorithm that uses bidirectional swapping and oscillates to such that the best possible order of the variable is obtained. This algorithm shows that the number of cycles required for reorder is drastically reduced. One of the main advantages of this is that computation cost is drastically reducing the computation cost. In [4] a different type of approach is used in memory consumption reduction. It is by lessening the number of paths present in BDDs. Also, applications in CAD such as DSOP (disjoint sum of products) minimization and method for integration of SAT and BDD is also described in it. Another approach to make test pattern generation easier is using *Reduced Ordered Binary Decision Diagram* (ROBDD) [5]. In ROBDD based approach redundant paths in the BDD are removed which will reduce the complexity.

Here work proposed is ZBDD based test pattern generation. It further reduces the number of paths present in the BDD. Further explanation of ZBDD and ROBDD is explained in section II. The advantages of using ZBDD are generating a set of relaxed test vectors [6], reducing memory consumption and process of test pattern generation is faster which is evident from the cache hit. ZBDD serves another advantage which is to reduce test power. When circuit the circuit is operated in test mode it tends to consume more power than when operating in functional mode. Hence if ZBDD is used for test patter generation, it will help in reduction of power consumed when the circuit is beingtested.

II. BDD, ROBDD AND ZBDD

BDD is a non-cyclic, graphical and a compact way of representing Boolean functions which are mainly used in CAD based applications. By replacing the nodes in the BDD with multiplexors it can be directly diagramed into circuits [4]. Consider the Boolean function $F(W,X,Y,Z) = \bar{W}X + YZ$. The BDD graph is represented in Fig.1.

From Fig.1 it can be observed that there are two nodes at which the graph terminates. These are called the leaf nodes which can either be '0' or '1'. 'W' is called the parent node or

root node. The leaf not will not have any child nodes. Each intermediate node will have a parent node and child node. The dashed line Represents the case corresponding to which the variable will take a '0' value and solid line represents the case were the variable will take value '1'. From the BDD it can be observed that the areas which are circled are isometric. These isometric subgraphs can be integrated and hence it will further reduce the size of BDD.

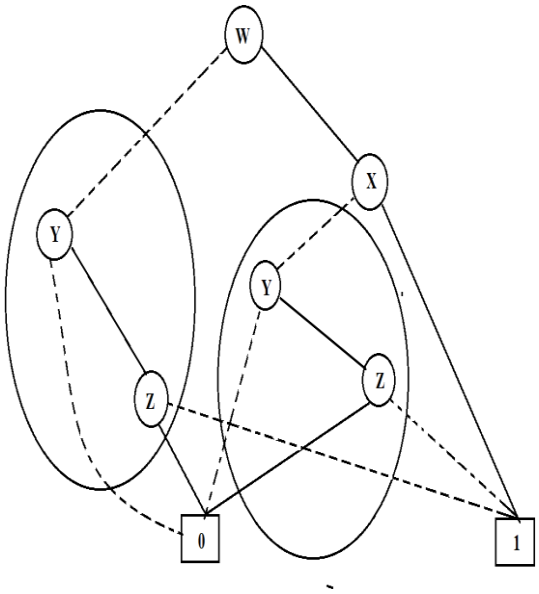

Fig.1: BDD of function $F(W, X, Y, Z)$.

Fig. 2 shows the BDD in which the isometric subgraphs have been removed. It is the ROBDD form of the same function.

ROBDD based implementation can be performed in various manner. One of the ways is to substitute nodes in ROBDD by MUX or INVERT-AND-XOR. The ROBDD based circuits can be further used to test multiple stuck at faults also [6].

Another form of BDD in which the branch which is solid line, that is '1'-branch which will terminate at leaf node '0' is removed. In this situation it helps in removing the redundancy which existed for a better representation. In the work proposed here use of ZBDD is made because of the reasons mentioned above. Analyze the example of the same function, f(W, X,Y,Z), the ZBDD of the function is given in Fig. 3. Here it can be observed that the solid line from Z to leaf node '0' is removed. By the removal of this path the test pattern that is generated will be more relaxed. To extract test vectors, a traversal shall be made from root node of the of the ZBDD to the leaf node. Consider the example, path from root node W through X. The vector generated for that path will be 11XX (assuming order of variables to be W, X, Y, Z).

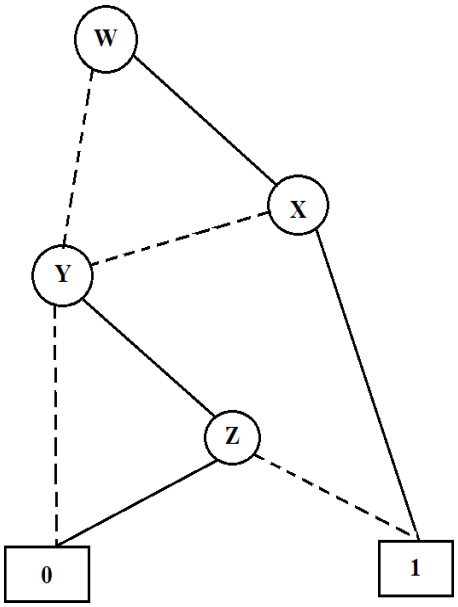

Fig .2: ROBDD of function $F(W, X, Y, Z)$

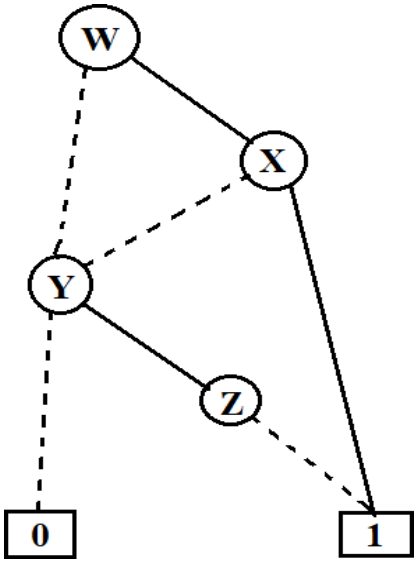

Fig. 3: ZBDD of function $F(W, X, Y, Z)$

III. PROPOSED WORK

Here the method that is employed is manipulation of ZBDDs and generate the test patterns. The approach is to use CUDD (Colorado University Decision Diagram) tool to perform the manipulation on ZBDD. To perform that combinational circuits written in textual form known as BLIF (Berkeley Logic Interchange Format) is used. Using CUDD memory related parameters are also captured. The BLIF format is written in the form as shown. It is described a circuit when viewed as a directed acyclic graph with each node describing combinational logic. Each node will have couple of levels, a single output and a logic function describing it.

Following is an example of a model for a circuit written in BLIF format:

.model<name of the model>

.inputs<input ports>

.outputs<output ports>

<command>

……..

.end.

To generate the ZBDD nanotrav is used. It is a program available with the CUDD package. It takes the input as BLIF file and generates the ZBDDs for the primary outputs. After running the program test vectors are obtained as well. To generate test vectors to detect a stuck at fault, a fault injected circuit is required. Hence, in the BLIF file available for a fault-free circuit a fault is to be injected. The vectors generated by the faulty circuit ZBDD and the vectors generated by the fault free circuit ZBDD, XOR operation is performed among them. The result obtained is the test pattern to detect that stuck atfault.

IV. INJECTING FAULTS

In injecting a fault in a circuit, which can be either stuck-at 0 or stuck-at 1 is done in the BLIF file of the circuit. For stuck- at 0 fault an and gate with one input as '0' and other input the net at which the fault is to be injected is used. Similarly, for stuck-at 1 fault OR gate with one input as '1' and other input as net at which the fault is to be inserted is used. This operation is done in the BLIF file of the circuit which is used to generate the ZBDD. To inject this a C++ program is written. Fig.4 shows the steps that are executed by the program.

Once the faulty BLIF file is generated it is again run using nantotrav. The nanotrav generates the test vectors for the injected fault circuit.

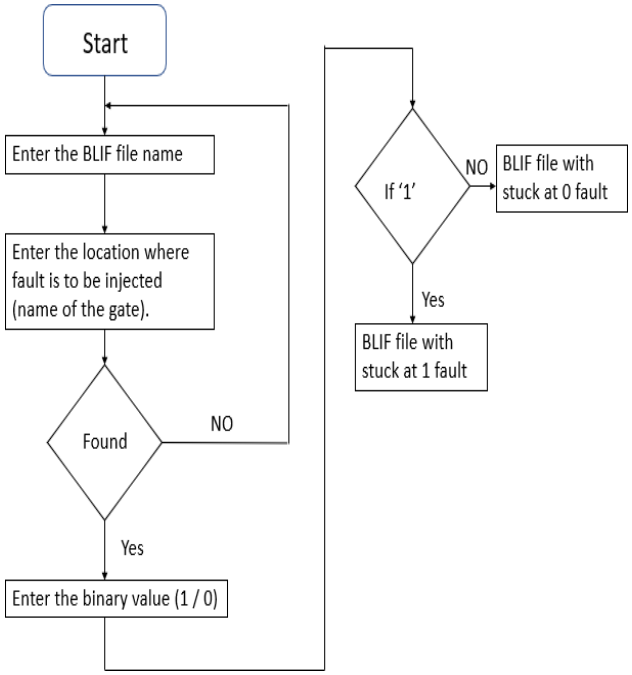

Fig. 4: Steps executed by the C++ program to insert fault.

To obtain the test patterns to detect the fault that is injected, the test vectors from the faulty ZBDD is XORed with the test vectors from the true ZBDD. The vectors which are obtained from ZBDD one which has the greatest number of don't-care conditions are taken because it gives more relaxed set of test patterns.

Along with the test vectors, there are several other parameters which are obtained by running the nanotrav program for both true as well as faulty ZBDDs. Some of them are CUDD modifiable parameters and some of them are non-CUDD modifiable parameters. The description about these parameters are further discusses in section V.

V. RESULTS AND ANALYSIS

After nanotrav program is ran and test vector is obtained for both true and faulty ZBDD, it is XORed to get the test vector to detect that fault. Along with that certain parameters are also considered which are shown in Table I and Table II. Among the CUDD modifiable parameters the following are the parameters that are analyzed.

Maximum number of variables sifted while reordering: It is the number of variables that is removed while the ZBDD is reordered. As discussed in section I, reordering is an important aspect to reduce the size of binary decision diagrams. Sometimes there might be certain variables which can be removed while reordering because those variables act as redundant variables. Variable sifting will help reduce the size of the ZBDD which intern will help in reducing the power consumption required for testing also the computational cost will reduce.

Maximum number of variable swaps per reordering: The number of variables that is are swapped also is a part of reordering which will help in the reduction of size of ZBDD. If the order in which the variables are written, and we can manipulate that ZBDD in such a way that the order in which we write the variables also helps in removing redundant paths and reduces the complexity ofZBDDs.

Cache entries: cache entry is created when a block data from the main memory is written into cache memory it is called cache entry. So, cache entry helps in reducing the time that is required for the computation because the time taken for a program to access data from the main memory is much more than the time required to access from cache memory. The cache mainly holds the data which are frequently used by the program.

Cache hits: when the requested data is present in the cache entry it is called cache hit. More the cache hit faster the execution of the program will take place.

TABLE I.
BDD RELATED PARAMETERS GENERATED BY CUDD

Circuit name	Number of ZBDD variables	Number of ZBDD nodes	Number of variables sifted per reordering	Number of variable swaps per reordering
C17	10	27	1000	2000000
C880	120	7784	1000	2000000
c432	72	2318	1000	2000000
c1335	80	62142	1000	2000000
C1908	66	80194	1000	2000000
C17 with stuck at 0 fault	10	10	1000	2000000
C880 with stuck at 0 fault	120	7718	1000	2000000

TABLE II.
MEMORY PARAMETERS GENERATED BY CUDD PROGRAM

Circuit name	Number of cache entries	Number of cache hits
C17	3276	21
C880	524288	11360425
C432	65536	119531
c1335	484562	10672811
C1908	524288	3079343
C17 with stuck at 0 fault	3276	5
C880 with stuck at 0 fault	524288	113680971

VI. CONCLUSIONS

In the work done, the ZBDDs are used to generate the test vector which helps us to obtain a relaxed set of test vectors. Test vector for testing single stuck at faults for the combinational circuits have been obtained. Apart from these the parameters which are generated by running the CUDD program which includes both memory operation related and ZBDD parameters are also analyzed and it is observed that lesser memory time is consumed for ZBDD to generate test vectors as cache hits is high also a greater number of variable reordering also takes place.

REFERENCES

[1] Bryant, Randal E. Graph-based algorithms for boolean function manipulation. Carnegie-Mellon Univ Pittsburgh Pa School Of Computer Science,2001.

[2] Ishiura, Nagisa, Hiroshi Sawada, and Shuzo Yajima. "Minimazation of Binary Decision Diagrams Based on Exchanges of Variables." ICCAD. Vol. 91.1991.

[3] Fey, Görschwin, and Rolf Drechsler. "Minimizing the number of paths in BDDs: Theory and algorithm." IEEE Transactions onComputer-Aided Design of Integrated circuits and systems25.1 (2006): 4-11

[4] Shah, Toral, et al. "Testing multiple stuck-at faults of robdd based combinational circuit design." 2017 18th IEEE Latin American Test Symposium (LATS). IEEE,2017.

[5] N. Mohan and Anita J. P., “A zero suppressed binary decision diagram-based test set relaxation for single and multiple stuck-at faults”, in the International Journal of Mathematical Modelling and Numerical Optimisation, Vol. 7, No.1, pp 83-96, 2016.

[6] Taher, M., et al. "An oscillating algorithm for variable ordering in binary decision diagram." ICECS 2000. 7th IEEE International Conference on Electronics, Circuits and Systems (Cat. No. 00EX445). Vol. 2. EEE,2000.

[7] Rudell,Richard."Dynamicvariableorderingfororderedbinarydecision diagrams." Proceedings of 1993 International Conference on Computer Aided Design (ICCAD). IEEE,1993.

[8] A. S. Yazhini and Harish Ram D. S., “High level synthesis of data flow graphs using integer linear programming for switching power reduction”, International Conference on Signal Processing, Communication, Computing and Networking Technologies (ICSCCN), pp. 475-479, 2011.

Proceedings of the Fourth International Conference on Communication and Electronics Systems (ICCES 2019)
IEEE Conference Record # 45898; IEEE Xplore ISBN: 978-1-7281-1261-9

Design and performance analysis of WDM optical Communication system with EDFA-DCF and FBG for dispersion compensation using 8x5 Gbps data rate

Nirmala Mahawar
Electronics Engg. Department
Rajasthan Technical University, Kota
mahawarnirmala1993@gmail.com

Ajay Khunteta
Electronics Engg, Department
Rajasthan Technical University, Kota
akhunteta@rtu.ac.in

***Abstract*— The Requirement of system capacity is increasing due to the rise in the number of computer users. This can be achieved by optical communication using WDM technology. Using WDM technology multiply many carrier signals onto a single optical fiber using different wavelength to boost up capacity. Dispersion effects the transmission of the signal along an optical fiber. In the proposed model, three techniques for dispersion compensation (per, post, and mix) has been designed using dispersion compensation fiber (DCF) in 8 channel WDM. According to this topology with the help of 5 Gbps transmission data rate model is compared non-return-to-zero (NRZ), return-to-zero (RZ) pulse in which signal mode fiber (SMF) has been considered using the length of 120 km. The results such as Q-factor and bit error rate (BER) represent pre-compensation scheme using RZ gives better results and also output power at EDFA calculate using optisystem 7.0 software.**

Keywords— WDM, DCF, FBG, SMF, NRZ, RZ, BER, MZM, EDFA.

I. INTRODUCTION

In recent years, glass fiber communication has become one of the most pillars of contemporary telecommunications networks that is because of its fast development and its broad vary of applications. Nowadays, these fashionable telecommunication networks have become additional and additional complicated. In optical network [1], WDM topology is presently widely used in telecommunication infrastructures and is expected to play a key role in upcoming generation networks and the future net. WDM is a strategy for transmitting information from various sources over a similar fiber optic connection in the meantime whereby every datum channel is carried individually exceptional wavelength. WDM innovation can amplify the limit of the current fiber optic system without including extra strands. In WDM [2-4] every correspondence channel is assigned to an alternate recurrence and multiplexed onto a solitary fiber. At the goal, the wavelength is spatially isolated to various collector areas. Henceforth the limit of optical transmission frameworks can be expanded utilizing WDM. When totally different wavelengths of lights pulse propagate in associate glass fiber, it undergoes a development of dispersion which ends up in a very temporal spreading. The most common topology used for compensation of nonlinear effects of dispersion is DCF (negative value of dispersion coefficient minimize the positive value of dispersion coefficient in fiber [5]) and FBG that reflect a particular wavelength [6-8]. Likewise, there are a couple of sorts of enhancers, for instance, SOA, EDFA, and Raman that have been acquainted with experience the lessening impacts. However, EDFA [9-11] still offer higher results. A comparative analysis is done between NRZ and RZ pulse [12]. Difference between NRZ and RZ is the symbol rate use a clock pulse in RZ. Pre, post and symmetric design are generated and describe which give the best result [13].

In this paper, II consists of dispersion compensation techniques, III consists simulation sat up for are applied methods, IV consists of Q-factor, BER result and simulation layout and last discuss the result.

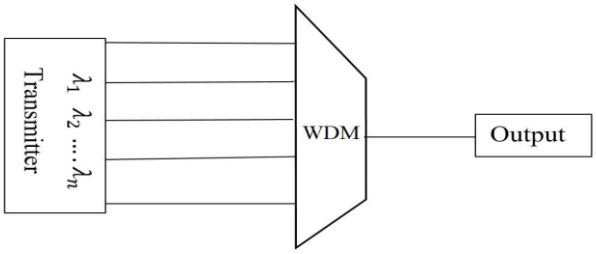

Fig. 1 Simple working block of WDM

II. DISPERSION COMPENSTION TECHNIQUES

In chromatic dispersion, the light totally different wavelengths travel at the side of different velocities in single mode fiber. Beams will arrive at the receiver at different times even beams propagate along with the same path. The result is broadening of the pulse. Pulse spreading in chromatic dispersion applied in the network is calculated using equation (1).

$$\Delta t = DL\Delta\lambda \quad (1)$$

Where D is the dispersion parameter, L is fiber length. DCF, FBG use for compensating dispersion. DCF has negative dispersion between -70 to -90 ps/nm/km. Since the 1980s for compensation of dispersion, the idea of DCF is introduced. DCF has negative dispersion coefficient which reduces/decrease the positive dispersion coefficient when SMF is applied in the WDM model. So that, dispersion is zero.

$$D_{SMF} L_{SMF} + D_{DC\,F} L_{DCF} = 0 \quad (2)$$

D and L represent dispersion and length of fiber respectively. In FBG [14], [15] a particular wavelength is reflected and all rest wavelength is passed. This particular wavelength is reflected by Bragg grating. The wavelength calculates using equation (3).

$$\lambda_{bragg} = 2\, N_{eff}\, \Lambda \qquad (3)$$

λ_{bragg}= Bragg's wavelength, N_{eff} effective refractive index when light propagates in fiber and Λ is the grating period of variation.

III. MODELING OF 8X5 GBPS WDM OPTICAL TRANSMISSION

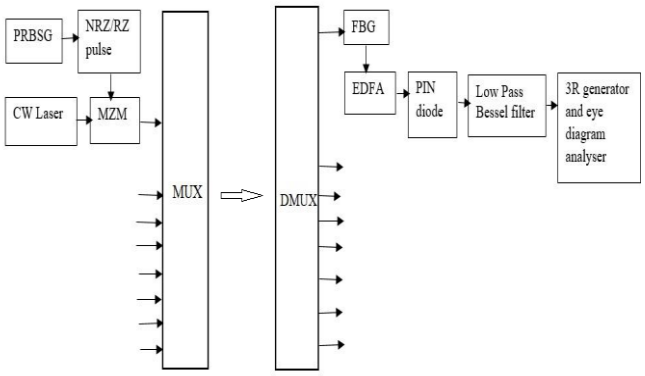

Fig. 2 Principal model of 8 channel WDM for dispersion compensation

Figure 2 shows the principal model of the paper. In this displaying, at transmitter part use CW laser which is nonstop wave laser, NRZ (non-come back to-zero) or RZ (come back to-zero) beat produce, pseudo-arbitrary piece grouping generator (PRBSZ) and Mach Zehnder modulator (MZM). Advanced sign is produced by PRBS generator and heartbeat generator likewise optical sign is created utilizing CW laser which is adjusted with the assistance of MZM show persistent wave laser, NRZ (non-come back to-zero) or RZ (come back to-zero) beat create, pseudo-arbitrary piece succession generator (PRBSG) and Mach Zehnder modulator (MZM). Digital signal is generated at 5 Gbps and optical signal generate using frequency range 193.1 to 193.8 THz (C band) and 0 dB power at the laser. Dense wavelength division multiplexer (DWDM) multiply/set all wavelength at 10 GHz bandwidth. At the end of the demux, an electrical and light signal modulate optical signal generates back in electrical using a pin diode, low pass Bessel filter, 3R generator, and eye diagram analyzer which show the result. The multiple channels using 8 ports DWDM model is introducing, for compensation of scattering in pre, post, and mix or symmetric model. In pre-compensation model DCF placed before SMF and in post-compensation DCF placed after SMF. DCF is used by placing both sides of single mode fiber in the dynamic compensation model.

In the pre-compensation model length of DCF is 25 km. and use 120 km SMF. In modeling gain, EDFA is used which have variable gain between 10 to 30 dB, in first optical amplifier use 10 dB gain and in second use 15dB gain. Different parameters are set in model i.e. dispersion at DCF, attenuation, dispersion slope, dispersion at FBG, Bandwidth of wavelength division multiplexer (WDM). Using 100 GHz spacing frequency range used in the layout is which is start at 193.1THz at every channel. 3R generator performs three types of work like improving the shape of the output pulse, again amplify the data pulse and retiming. Subsystem blocks which connect to WDM are represented transmitter modal at channel 2 to 8. Subsystem 2 and 3 represent receivers at output channels.

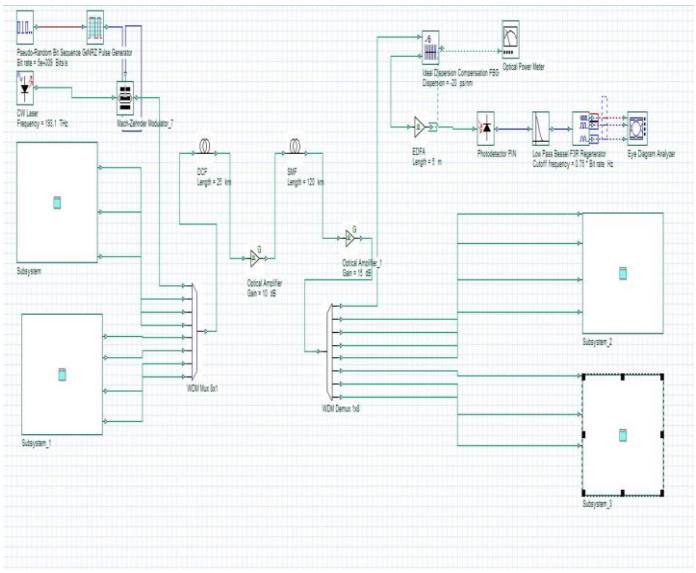

Fig. 3 Simulation layout of pre-compensation using 8 channel

TABLE I. BASIC PARAMETER OF WORK ARE

Parameters	DCF	SMF
Length (km)	25	120
Attenuation (dB/km)	0.2	0.2
Dispersion (ps/nm/km)	-80.4	16.75
Dispersion slop ($ps/nm^2/km$)	-0.3	0.075

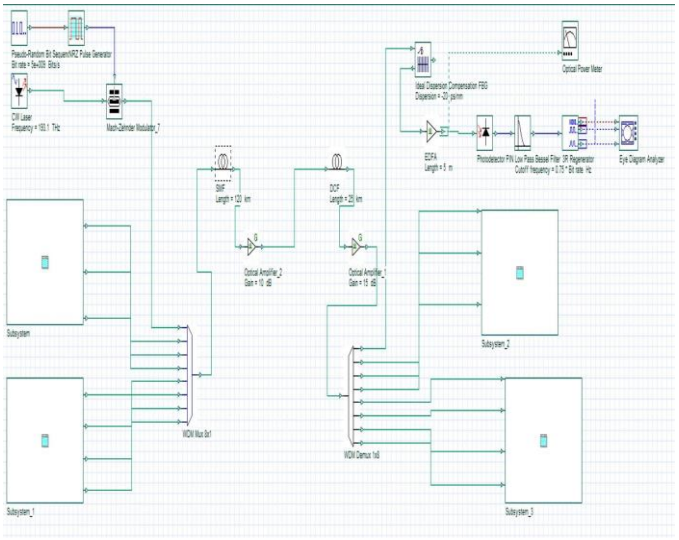

Fig.4 Simulation layout of post-compensation using 8 channel

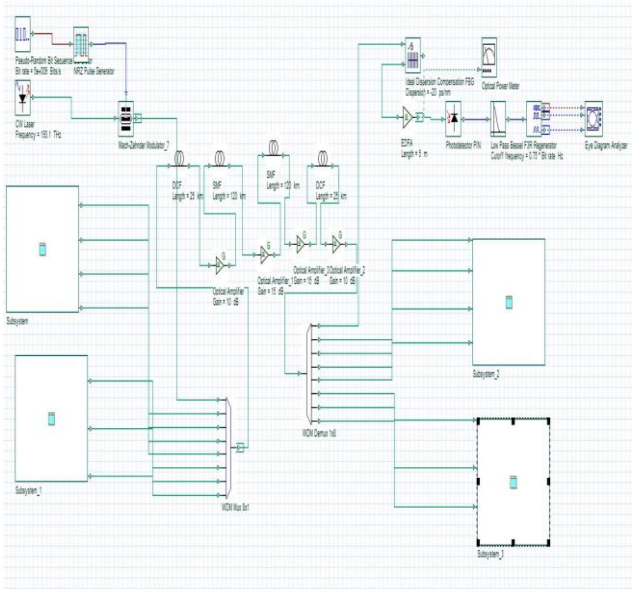

Fig..5 Simulation layout of mix model compensation using 8 channel

IV. RESULT AND COMPARISON

When simulating the model result is generated at eye diagram analyzer, max Q factor and minimum BER of per, post, and mix model at all 8 channel can be seen. The criteria for acceptable value of Q factor is greater than 6 and BER is less than 10^{-12}. Tables are generated using NRZ (table II, III) and RZ (table IV, V) pulse simulation. When seeing RZ pulse performance is better to compare to NRZ pulse. Using NRZ pulse at channel 3 output of Q factor is 8.7355 and BER is $7.51e^{-19}$ which is greater than all output value of post and mix compensation. Like this using RZ max Q factor is 19.3928 and BER is $4.38e^{-84}$ which is better than all pre, post, and mix compensation. NRZ and RZ coded pulse result shown that pre-compensation scheme using RZ pulse gives good performance in table 5. Also, the output power valve of EDFA at the receiver part shown in Table VIII and IX. Eye diagram of NRZ and RZ pulse also shown in figure 6 and 7. Graph plots between Q-factor (NRZ and RZ) and channels are shown in figure 8.

TABLE II. MAXIMUM Q-FACTOR USING NEZ PULSE

Channel	Pre	Post	Mix
1	8.5746	8.3249	7.5027
2	8.0908	8.0528	7.1902
3	8.7355	8.6205	6.7128
4	8.1755	7.4264	7.3812
5	8.5097	8.0749	7.462
6	7.8930	7.5340	7.6535
7	8.1472	7.9531	7.4672
8	8.2699	8.1491	7.6516

TABLE III. MINIMUM BER USING NRZ PULSE

Channel	Pre	Post	Mix
1	$3.64e^{-18}$	$3.18e^{-17}$	$2.27e^{-14}$
2	$1.99e^{-16}$	$2.80e^{-16}$	$2.10e^{-13}$
3	$7.51e^{-19}$	$2.15e^{-18}$	$5.59e^{-12}$
4	$1.03e^{-16}$	$3.93e^{-14}$	$5.47e^{-14}$
5	$5.57e^{-18}$	$2.20e^{-16}$	$2.63e^{-14}$
6	$1.02e^{-15}$	$1.74e^{-14}$	$6.90e^{-15}$
7	$1.27e^{-16}$	$6.40e^{-16}$	$2.76e^{-14}$
8	$4.66e^{-17}$	$1.33e^{-16}$	$6.93e^{-15}$

TABLE IV. MAXIMUM Q-FACTOR USING RZ PULSE

Channel	Pre	Post	Mix
1	17.2737	12.3224	10.0787
2	18.3958	13.588	9.9838
3	16.6783	12.207	10.2937
4	17.4284	13.0928	10.4622
5	18.8222	14.1126	11.7546
6	19.3928	14.8031	11.6204
7	16.4022	12.272	10.2201
8	17.5729	12.9907	10.6545

TABLE V. MINIMUM BER USING RZ PULSE

Channel	Pre	Post	Mix
1	$3.63e^{-67}$	$3.03e^{-35}$	$2.69e^{-24}$
2	$6.96e^{-76}$	$2.13e^{-42}$	$6.55e^{-24}$
3	$8.61e^{-63}$	$1.15e^{-34}$	$2.48e^{-25}$
4	$2.43e^{-68}$	$1.59e^{-39}$	$4.74e^{-26}$
5	$2.38e^{-79}$	$1.37e^{-45}$	$2.52e^{-32}$
6	$4.38e^{-84}$	$6.52e^{-50}$	$1.25e^{-31}$
7	$8.97e^{-61}$	$5.67e^{-35}$	$6.28e^{-25}$
8	$1.91e^{-69}$	$5.93e^{-39}$	$6.08e^{-27}$

TABLE VI. CAMPARE TABLE OF MAX Q-FACTOR USING NRZ, AND RZ PULSE

Pulse	Pre	post	Mix
NRZ	8.7355	8.6205	7.6535
RZ	19.3938	14.8031	11.7546

TABLE VII. COMPARE TABLE OF MIN BER USINGNRZ, AND RZ PULSE

Pulse	Pre	Post	Mix
NRZ	$7.51e^{-19}$	$2.15e^{-18}$	$6.90e^{-15}$
RZ	$4.38e^{-84}$	$6.52e^{-50}$	$2.52e^{-32}$

TABLE VIII. OUTPUT POWER AT EDFA IN PRE,POST,AND MIX COMPENSATION SCHEAM USING NRZ PULSE

Channel	Pre-compensation	Post-compensation	Mix-compensation
1	17.15	17.15	16.72
2	17.12	17.12	16.67
3	17.09	17.09	16.62
4	17.14	17.15	16.72
5	17.11	17.16	16.66
6	17.23	17.22	16.88
7	17.16	17.16	16.77
8	17.16	17.16	16.77

TABLE IX. OUTPUT POWER AT EDFA IN PRE,POST,AND MIX COMPENSATION SCHEME USING RZ PULSE

Channel	Pre-compensation	Post-compensation	Mix-compensation
1	16.65	16.66	15.84
2	16.60	16.61	15.77
3	16.54	16.55	15.69
4	16.65	16.66	15.87
5	16.60	16.60	15.79

6	16.84	16.84	16.18
7	16.70	16.71	15.96
8	16.71	16.72	15.99

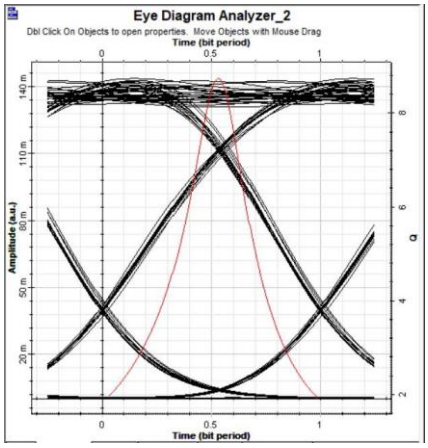

(A)

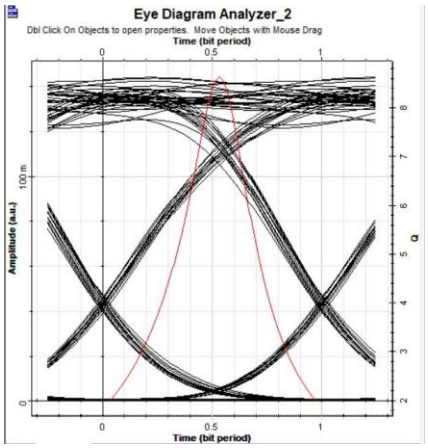

(B)

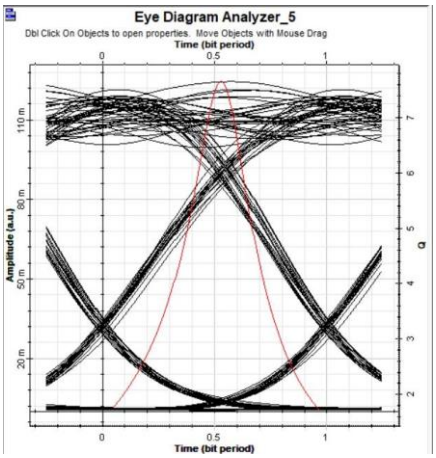

(C)

Fig. 6 Pre (A), Post (B) and Mix (C) dispersion compensation scheme eye diagrams using NRZ pulse

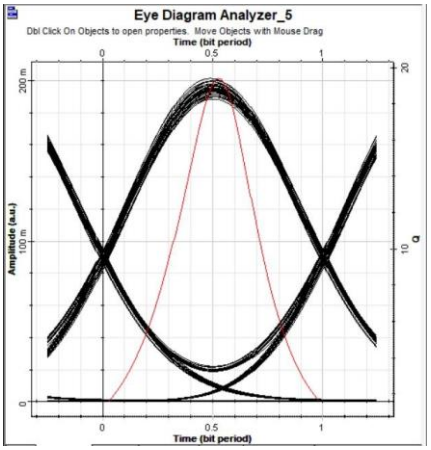

(A)

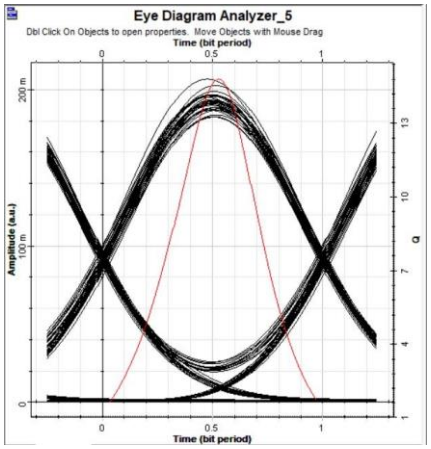

(B)

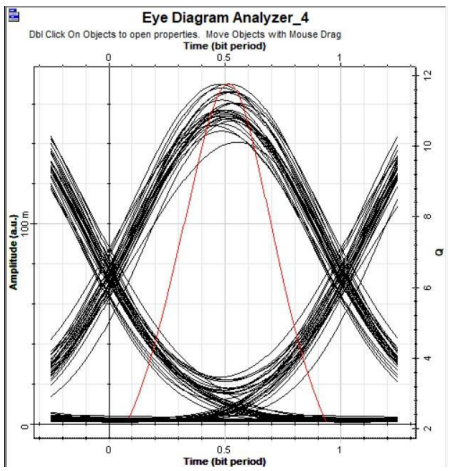

(C)

Fig. 7 Pre (A), Post (B) and Mix (C) dispersion compensation scheme eye diagrams using RZ pulse

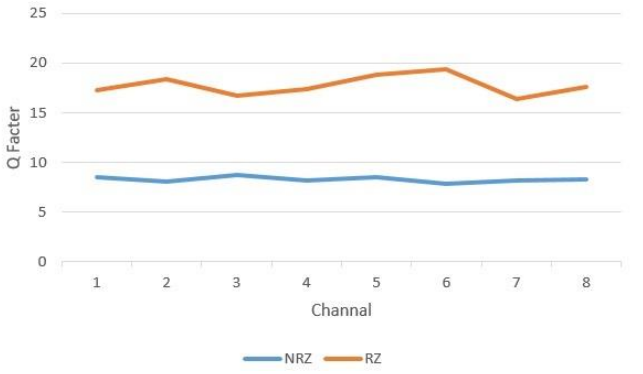

(A)

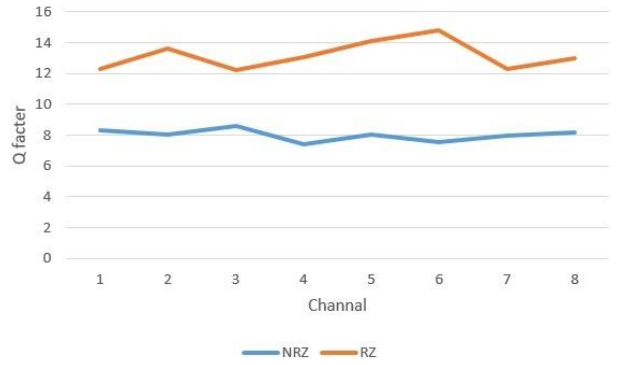

(B)

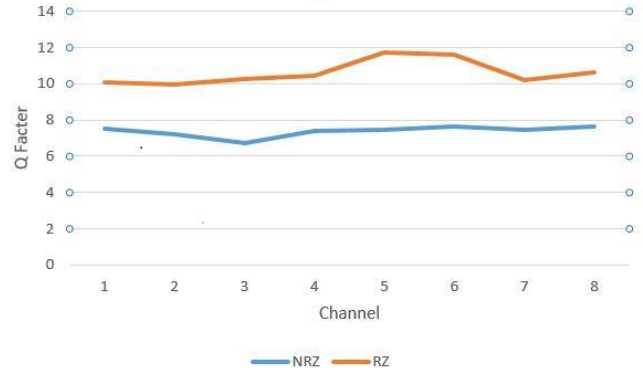

(C)

Fig. 8 Graph plot between channel and Q factor using NRZ, RZ pulse pre-compensation (a) , post-compensation (b), and mix-compensation (c)

CANCLUSION

To minimize the chromatic dispersion a new optical transmission model in introduced using optic system 7.0 software. This design uses 8 channel wavelength division multiplexer (WDM) to test the reliability of the system which increases the use of bandwidth and result remain valid. In this paper use both compensators, DCF, and FBG. DCF use along SMF between MUX and DEMUX and FBG at receiver using -20 ps/nm/km. Pre, post and symmetric (mix) compensator, three scheme are developed to decrease chromatic dispersion using 120 km. SM fiber and 25 km. dispersion compensator fiber. When analyzing the performance of three scheme using Q factor and BER, see that pre model using RZ pulse gives much better result compare to all post and mix model. Using output power meter, the output power is analysis at EDF amplifier. In further, compensation dispersion and nonlinear effect by increasing the number of the channel at multiplexer input point and applied on a complex system.

REFERENCES

[1] I. Journal, O. F. Engineering, P. Analysis, O. F. Dispersion, and C. Using, “1 &*2 ,” vol. 7, no. 2, pp. 513–523, 2018.

[2] M. Chakkour, O. Aghzout, B. Ait Ahmed, F. Chaoui, and M. El Enhancements Using FBG and EDFA-Wavelength Division Multiplexing Optical Transmission System,” *Int. J. Opt.*, vol. 2017, pp. 1–8, 2017Yakhloufi, “Chromatic Dispersion Compensation Effect Performance.

[3] M. M. Ismail *et al.*, “EDFA-WDM optical network design system,” *Procedia Eng.*, vol. 53, pp. 294–302, 2013.

[4] M. I. Hayee and A. E. Willner, “Pre- and post-compensation of dispersion and nonlinearities in 10-Gb/s WDM systems,” *IEEE Photonics Technol. Lett.*, vol. 9, no. 9, pp. 1271–1273, 1997.

[5] M. Kaur and H. Sarangal, “Analysis on Dispersion Compensation with Dispersion Compensation Fiber (DCF),” vol. 2, no. 2, pp. 56–59, 2015.

[6] A. Sharma, I. Singh, S. Bhattcharya, “Performance Analysis of Dispersion Compensation using Ideal Fiber Gratting in a 100 Gbps Single Channal Optical System, ” *IJESRT*, Feb 2018

[7] B. Prasad, K. C. Patra, and N. K. Barpanda, “Performance Analysis of Fiber Optical Communication using Fiber Bragg Grating as Dispersion Compensator,” *Int. J. Adv. Res. Electr. Electron. Instrum. Eng. (An ISO Certif. Organ.*, vol. 3297, no. 4, pp. 2729–2733, 2007.

[8] M. A. Othman, “An Analysis of 10 Gbits/s Optical Transmission System using Fiber Bragg Grating (FBG),” *IOSR J. Eng.*, vol. 02, no. 07, pp. 55–61, 2013.

[9] S. Semmalar and S. Malarkkan, “Output Signal Power Analysis in Erbium-Doped Fiber Amplifier with Pump Power and Length Variation Using Various Pumping Techniques,” *ISRN Electron.*, vol. 2013, pp. 1–6, 2013.

[10] R. Bharti and Y. C. Bhatt, “Dispersion Compensation and Power Optimization using FBG-EDFA in Optical Communication System,” vol. VII, no. 2, pp. 126–130, 2014.

[11] S. Singh, “Analysis of EDFA based 16-Channel C-Band Optical WDM System for Different Pumping,” pp. 4709–4715, 2016.

[12] A. Gupta, “Comparative analysis of NRZ , RZ and Gaussian Pulse generation method in OWC link at different transmitter powers,” vol. 5, no. 6, pp. 3596–3599, 2015.

[13] P. R. Meher, “5 GBPS Data Rate Transmission in a WDM Network using DCF with FBG for Dispersion Compensation,” vol. 4, no. 4, pp. 28–35, 2017.

[14] R. Mishra, “an Analysis of 10 Gbits/S Optical Transmission System Using Fiber Bragg Grating (Fbg) and Double Edfa,” *Int. J. Adv. Res. Comput. Sci.*, vol. 8, no. 8, pp. 349–355, 2017.

[15] K. Kumar, A. K. Jaiswal, M. Kumar, and N. Agrawal, “Performance Analysis of Dispersion Compensation Using Fiber Bragg Grating (FBG) In Optical Communication,” *Int. J. Curr. Eng. Technol.*, vol. 4, no. 3, pp. 1527–1531, 2014

.

Proceedings of the Fourth International Conference on Communication and Electronics Systems (ICCES 2019)
IEEE Conference Record # 45898; IEEE Xplore ISBN: 978-1-7281-1261-9

Collaborative Filtering based Recommender System using Regression and Grey Wolf Optimization Algorithm for Sparse Data

Sneha V.[1], Shrinidhi K.R.[2], Sunitha R. S.[3], Dr.Mydhili K. Nair.[4]
[1,2,3,4] Department of Information Science and Engineering
Ramaiah Institute of Technology, Bangalore, India

***Abstract* - In this epoch of technology, where recommendations are the backbone of E-commerce and Media-services, one of the extensively used approach for implementing recommender systems is Collaborative Filtering. This approach recommends items by identifying users who share similarity in rating the items by observing the user-item ratings matrix. In the real-world, users only rate a limited number of items from the catalogue leading to high sparsity in user-item ratings, which makes it difficult to identify similar users and recommend items accurately. To handle sparsity in user-item matrix, which is one of the major challenges encountered while implementing recommender systems, the paper proposes a technique of Collaborative Filtering using Regression to predict the ratings of unrated items on the basis of the user's history of ratings and similarity to other users, combined with - a nature-inspired algorithm called - Grey Wolf Optimization (GWO) algorithm applied to optimize the loss function. Personalised recommendations can be provided to the users for those highest predicted ratings. The proposed technique is observed to perform well in highly sparse data scenarios in terms of accuracy, user coverage and different variants of hit rate.**

Keywords—Collaborative Filtering; recommender system; sparse matrix; regression; grey wolf optimization; evaluation metrics; hit rate

I. INTRODUCTION

With the striking rise in the number of digital users and it's consequence of rapid increase in the amount of data being generated on the internet, it has become important for industries to filter, map and provide users with the relevant information according to their personalised preferences. Recommender systems have therefore become the backbone in various domains including leading platforms of E-commerce ranging from Amazon, Alibaba and Flipkart, Media-services like Netflix and YouTube, Social-Media Platforms like Facebook and News websites. They help in planning the marketing strategies for these industries in order to increase sales by enhancing user experience and achieving better user satisfaction, as they fulfill the user need by recommending the items of user interest, which in turn leads to establishment of loyalty of users. It also helps in bringing those items into the notice of the user which are not easily seen by the user while browsing through these platforms, until and unless filtered.

One of the extensively used approach in building a Recommender system is Collaborative Filtering (CF), which identifies users who share similar interests in items. The central premise of it being, "if user P shares similar opinions as user Q on topic T_1,T_2,T_3, ... ,T_{n-1} then the user P is likely to have the same opinion as user Q on topic T_n". This technique of collaborative filtering is used when identifying the dominant factors of individual items which are to be recommended are intricate in nature to perform content filtering. Under such circumstances, identifying like-minded users help in recommending a new item to a user which has been rated highly by another user who shares similar choices and preferences. Identifying convergent profiles of users can be done by using the history of identical ratings given by the users to the same set of items.

Most often traditional approaches of CF Recommender System encounters the problem of Data Sparsity since all possible interactions between each user and item are not available in the user-item ratings matrix. This matrix faces the problem of sparsity as users review and rate only limited items when compared to the number of items that are present in the catalogue. [3-4],[11-12] To deal with the missing values in the user-item ratings matrix, the paper proposes the concept of Regression based Collaborative Filtering combined with GWO for a dataset that consists of ratings given by users to items. It searches for similar users on the basis of the user's past record of ratings and predicts the missing ratings. The nature-inspired optimization algorithm GWO[1-2] helps in predicting optimal ratings by optimising the loss function.

The remaining sections of the paper is structured as follows: Section II exhibits the literature review on the challenges faced by recommenders, results of regression techniques applied on sparse datasets and surveys on GWO and its applications. Section III contours the algorithm and equations of GWO proposed by Seyedali Mirjalili et al.[1] Section IV presents the proposed recommender system and Section V examines the results of proposed system and investigations on various evaluation metrics. Finally, Section VI concludes the work.

II. LITERATURE REVIEW

In the recent decade, several works have been conducted in order to build efficient recommender systems. G. Adomavicius et al describe collaborative, content based and hybrid recommender approaches which are the current

generation of methods to implement recommender systems and they provide the overview of implementing these recommenders on a broad scale satisfying high-scaled applications. They also provide insights on the various limitations of these methods including data sparsity and cold start issues.[11] Xiaoyuan Su et al also have investigated on the various research trends and problems faced by the current generation of recommenders. They also talk about data sparsity being one of the major challenges in real world data when collaborative filtering technique is applied to implement recommenders, as finding similar neighbours in a sparse data is difficult, leading to less accurate recommendations being made to the user.[12]

To overcome this major issue of data sparsity, Wang Bailing et al discussed the Three-Tier Network Architecture of a Recommendation System built on the basis of a Regression Model which established that the prediction of preference of the test user for the test item can be calculated using the correlation score between the item and the user. The experimental results presented by them indicated that regression can perform superior when compared to traditional CF algorithm.[5] Similar approach of linear regression using the linear correlation indicated by Pearson Correlation Coefficient discussed by Xinyang Ge et al showed that the approach of regression helps in providing better accuracy in recommending and appealing the users.[8] Slobodan Vuceti et al addresses the problem of data sparsity in CF by using Regression. They also have proposed the approach of predicting the user's preferences for the unrated items on the basis of ratings provided by an active user for the items in the catalogue by combining statistical methods. They provided experimental evidence obtained that their proposed approach is superior to non-personalised predictors even when the rating matrixes are very sparse and also that the regression based recommendations can be applied to data with high sparsity scenarios.[7]

Seyedali Mirjalili et al who proposed the concept of GWO based on inspiration drawn from the nature have discussed on the differences of using conventional gradient optimisation technique vs meta-heuristics optimisation techniques. They proposed GWO stating it had derivation-free mechanism, flexibility, simplicity and avoidance of local optima.[1] Ali Parsian et al used GWO in back-propagation algorithm to find the optimal values for weights and biases. They discussed the drawbacks of gradient based back propagation which usually has slow convergence rate and tends to get trapped in the local minima which is overcome by using GWO. GWO has the feature of global searching where the wolves aim at finding optimal solutions in different directions in order to minimize the risk of being stuck at a local minimum.[1] The GWO algorithm also helps in incrementing the convergence speed by setting the parameter A.[9] S. Hosgurmath et al proposed the technique of using GWO with Linear Collaborative Discriminant Regression Classification for Face Recognition where GWO was again used to find optimal weights that had to be assigned to features. They also show a comparison of their proposed algorithm using GWO working better than Regression Classification without GWO for different image datasets.[10]

III. GREY WOLF OPTIMIZATION ALGORITHM

GWO is a meta-heuristic technique of optimisation which simulates the leadership hierarchy of the grey wolves that are widely known for their hunting strategies in groups. The wolves in the pack are ranked according to their strength and fitness, with Alpha being the chief, followed by the Beta, Delta and Omega. In the pack, generally, Alpha wolves are responsible for taking decision while Beta are subordinate wolves that assist Alpha while taking decisions and ensures that all subordinates obey and give feedback to Alpha. Delta wolves are accountable for watching boundaries and protecting the pack while Omega wolves are the weak ones of the pack that follow the rest.[1-2]

In the GWO algorithm, the objective of the pack is to search the optimal solution for a given problem by implementing the three milestones of hunting as observed in the natural behavior of the wolf packs - exploration (searching for the prey,) exploitation (encircling the prey), and finally launching the attacking on the prey. As multiple iterations of the algorithm are carried out, the wolves try to get as close as possible to their prey by updating their positions. The fittest solution (one with least distance from prey) is considered as Alpha wolf which guides the wolf pack in every iteration along with the help of the second and third fittest solution, called Beta wolf and Delta wolf respectively. The rest solutions are treated as Omega wolves. Algorithm and equations of GWO is briefed in this section.[1]

A. *Parameters Initialisation Phase*

- Initialise the grey wolves in the pack P (pack size)
- Initialise vector 's' which linearly decreases from 2 to 0 as follows -

$$s = 2 - current_{iteration} * (2 / total\ iterations) \quad (1)$$

- In order to initialise vectors U and V two random vectors r_1 and r_2 are initialised in the range [0,1] as follows -

$$U = 2 * s . r_1 - s \quad (2)$$

$$V = 2 * r_2 \quad (3)$$

B. *Population Initialisation Phase*

- Initialise random positions for each wolf in the pack P
- Calculate the fitness of each wolf using -

$$D = |V.X_{prey}(t) - X_{wolf}(t)| \quad (4)$$

where X_{prey} and X_{wolf} is the position of the prey and the wolf at time 't' respectively

$$X_{wolf}(t+1) = X_{prey}(t) - U.D \quad (5)$$

$X_{wolf}(t+1)$ is the positional difference of the wolf with the prey i.e the fitness score for that particular wolf

C. Rank-wise ordering phase

Based on their fitness score for all the wolves in the pack, they are ranked as

- W_{alpha} = Fitness of First best wolf of the pack
- W_{beta} = Fitness of Second best wolf of the pack
- W_{delta} = Fitness of Third best wolf of the pack

D. Updation phase

while $current_{iteration}$ < total iterations or until optimal solution is obtained do

- for each wolf in pack P do

  Update the position of the wolf using the given equations

  $$D_{alpha} = |V_1.W_{alpha} - W(t)| \quad (6)$$

  $$D_{beta} = |V_2.W_{beta} - W(t)| \quad (7)$$

  $$D_{delta} = |V_3.W_{delta} - W(t)| \quad (8)$$

  $$W_1 = W_{alpha} - U_1 . D_{alpha} \quad (9)$$

  $$W_2 = W_{beta} - U_2 . D_{beta} \quad (10)$$

  $$W_3 = W_{delta} - U_3 . D_{delta} \quad (11)$$

  $$W(t+1) = (W_1 + W_2 + W_3) / 3 \quad (12)$$

  end for

- Reinitiate the values of V, U and s
- Update the fitness score for each wolf in the pack
- Update W_{alpha} , W_{beta} , W_{delta} based on their fitness score
- Increment $current_{iteration}$ by one

end while

E. Producing Result

- Return fitness score of the optimal solution (W_{alpha})

The algorithm parodies the search process and hunting strategies of the grey-wolves with an objective of finding the prey. This algorithm is now proposed along with regression for predicting the non-existing values in the user-item rating matrix and optimizing the loss value, thereby addressing the sparse rating matrix in recommender systems.

IV. PROPOSED RECOMMENDER SYSTEM

The process begins with setting arbitrary value for population of the grey wolves (nominee solutions) and assigning ranks to any three wolves as Alpha wolf, Beta wolf and Delta wolf. The parameters initialisation phase of the GWO algorithm is executed. Since the wolves have no idea of where the preys (optimal solutions) lie in the $m * n$ dimensional search space, in order to execute populations initialisation phase each wolf in the pack assigns a set of random values that is used to initialise the weights and bias to be given to identify the user-user similarity. Therefore, each wolf must assign itself a list of $(n * n) + m$ number of random values where m and n indicates the number of items and users in the user-item ratings matrix respectively. The first $(n * n) - n$ values of the wolf can be assigned as the weights to be allotted to each user-user combination (W_u) to check the similarity between them. The remaining $n + m$ values can be assigned as bias for each user (B_u) and each item (B_i). It is to be noted that similarity of a user or item with itself is not allotted a weight.

To prevent users who give high ratings or items that have high ratings from dominating the prediction, we need to tone down all dominating variables by normalising the dataset. This is done by calculating the mean deviation for the all the ratings in the dataset.

$$\sum_{i=0}^{m}\sum_{j=0}^{n} r[i,j] = r[i,j] - \bar{r} \;\; if\; r[i,j] \neq \emptyset \quad (13)$$

$$\sum_{i=0}^{m}\sum_{j=0}^{n} r[i,j] = 0 \; if\; r[i,j] = \emptyset \quad (14)$$

Each wolf now needs to make its prediction of the ratings which is made by using the Regression algorithm. To make predictions based on user similarity, equation (15) which represents the regression line equation is used. Each cell of rating matrix has its regression line equation to check its similarity with other users which are the features to be considered and each of these features are assigned weights chosen by the wolves. The predictions are normalised by calculating their average based on the number of users who have reviewed the item, so that none of the user's ratings dominate the prediction.

For each wolf, $\sum_{i=0}^{m}\sum_{j=0}^{n}\ (p[i,j]\ =$

$$\sum_{k=0}^{n}(Wu[k,j]*(r[i,k]-\ (Bu[k]\ +\ Bit[i]\ )))$$

$$+\ Bu[j]\ +\ Bit[\mathrm{i}]\ +\overline{r}\ )\qquad(15)$$

Root Mean Square Error (RMSE) is the applied loss function for the proposed technique. The loss function is calculated for the predictions made by each wolf based on its prediction on the initial rating matrix which is used to indicate the fitness score of the wolf.

For each wolf,

$$\mathrm{RMSE}=\sum_{i=0}^{m}\sum_{j=0}^{n}(\sqrt{(r[i,j]\ -\ p[i,j])^2})\qquad(16)$$

According to the RMSE obtained by each wolf in each iteration the ranks are re-ordered. Each wolf (nominee solution) updates its list of weights to be assigned to features following the lead of Alpha, Beta and Delta (since they have the least RMSE value), using the GWO algorithm, trying to reach the optimal solution. The central premise being if these wolves have the least fitness scores, it implies that the weights assigned by these wolves are closer to the optimal weights that are needed to be assigned for making accurate predictions while making recommendations. Therefore all other wolves in the pack must update the weights according to the weights of these three wolves using the procedure mentioned in the updation phase.

Over the course of iterations, the wolves estimate the probable ratings, their fitness scores are calculated, their ranks are reordered and weights are updated on the basis of new Alpha, Beta and Delta elected at every iteration. The parameter 's' decreases from 2 to 0 through the iterations with an eye to accentuate exploration and exploitation. The wolves tend to converge towards the prey and diverge from the prey when U < 1 and U > 1 respectively in order to maximise the solution search space as much as possible and also to get closer to the optimal solution. Finally, the termination of the algorithm occurs on satisfying the end criterion i.e., either reaching desired optimal solution or reaching the end of iteration count that was initialised. On running the model, all the sparse values are filled with predictions made by the Alpha wolf (the best solution), hence handling the issue of data sparsity. Based on the prediction matrix retrieved, personalised recommendations are made to each user for those highest predicted ratings since the predicted ratings are obtained on the basis of his earlier ratings of items and the similarity of other users.

V. Experiment Outcomes and Investigation

For the evaluation of the proposed recommender system, the open sourced Movielens dataset is examined. This dataset is highly sparse with sparsity ratio as 0.8630 implying very less interactions between the movies and the users. This dataset was divided into four datasets. Each of the sub dataset was trained using regression and GWO and the testing was carried on 3 folds of the test dataset. Various evaluation metrics for the recommender systems [13] are calculated to investigate the proposed model. To measure the accuracy of the model root mean square error and mean absolute error are calculated. The variants of hit rate like cumulative hit rate and average reciprocal hit rate which are the evaluation metrics to identify how well the recommendations are made using top ' k' recommendations is calculated for the model. Finally the user coverage of the model is measured to identify the spread of the recommender model for the users. The results obtained on implementing the proposed recommender systems are discussed in this section.

A. Root Mean Square Error

Root Mean Square Error (RMSE) is calculated by taking the root of the squared difference between the initial user-item rating and predicted rating denoted in equation (17). It gives a measure of how far the predictions are from the initial ratings using the test sets. If the obtained RMSE is less, it implies that the wolves have reached closer to the actual ratings. The RMSE obtained for the proposed model for the test splits of different datasets is shown in Table I.

$$\mathrm{RMSE}=\sum_{i=0}^{m}\sum_{j=0}^{n}(\sqrt{(r[i,j]\ -\ p[i,j])^2})\qquad(17)$$

TABLE I. RMSE OBTAINED FOR THE DIFFERENT DATASETS

Dataset S.No	Test-Split 1	Test-Split 2	Test-Split 3
1	0.4568	0.4128	0.3081
2	0.5146	0.3890	0.5595
3	0.3053	0.4251	0.3052
4	0.3627	0.2922	0.3110

B. Mean Absolute Error

Mean Absolute Error (MAE) is the absolute difference between the initial user rating and predicted ratings, which has to be ideally less. It gives the average magnitude of the error over the test samples as shown in Table II where all the individual difference of ratings have equal weightages while contributing to the error.

$$\mathrm{MAE}=\sum_{i=0}^{m}\sum_{j=0}^{n}(\ |(r[i,j]\ -\ p[i,j])|\ )\qquad(18)$$

TABLE II. MAE OBTAINED FOR THE DIFFERENT DATASETS

Dataset S.No	Test-Split 1	Test-Split 2	Test-Split 3
1	4.6325	4.3995	3.4678
2	6.9207	4.5682	7.3803
3	3.4179	5.2566	3.0345
4	4.8467	3.6051	4.6019

C. Cumulative Hit Rate

Cumulative Hit Rate (CHR) is the measure to keep the count of hits - a match between the top 'k' recommended items and previously rated items by the user - based on a threshold. The hits are considered if any one among the top 'k' recommendations in the predictions match with the items already rated by the user in the initial ratings test set, given that the rating is above a threshold, say 3.5 as used for results in Table III. This technique of considering a 'hit' based on a threshold ensures that the user actually likes the item that is being recommended to him. Higher CHR is an indication of a good recommendations.

$$CHR = hits \,/\, n \qquad \text{If actual rating} > \text{threshold} \qquad (19)$$

TABLE III. CHR OBTAINED FOR THE DIFFERENT DATASETS

Dataset S.No	Test-Split 1 (%)	Test-Split 2 (%)	Test-Split 3 (%)
1	71.42	63.15	66.67
2	76.92	62.50	79.17
3	88.89	69.23	87.50
4	60.00	68.18	75.00

D. Average Reciprocal Hit Rate

Average Reciprocal Hit Rate (ARHR) is greatly a user-centered metric, which concentrates on considering a hit based on the rank of the prediction in the top 'k' recommended list. Reciprocal of rank of the first hit among top 'k' recommendations is taken for each user in the test set which is further summed up and divided by the total number of users in the set. This metric gives preference to the position of the hit in the recommended list as users tend to concentrate largely at the beginning of the recommendation list. It should preferably be higher. Table IV gives the reading of ARHR for different datasets.

$$ARHR = \left(\sum_{i=1}^{n} 1/rank[i]\right) / n \qquad (20)$$

TABLE IV. ARHR OBTAINED FOR THE DIFFERENT DATASETS

Dataset S.No	ARHR (%)
1	100
2	100
3	100
4	100

E. User Coverage

User Coverage (UC) is the measure of how many users are recommended good recommendations of items from the catalogue. It is calculated by sorting the top 'k' recommendations from the predicted ratings and then checking if the user has been recommended any item with the predicted rating above the set threshold for rating. The higher, the better. For testing the model, the threshold set was 3.5 and the average of the user coverage obtained from the test sets is displayed in Table V.

$$UC = hits \,/\, n \qquad \text{If predicted rating} > \text{threshold} \qquad (21)$$

TABLE V. UC OBTAINED FOR THE DIFFERENT DATASETS

Dataset S.No	UC (%)
1	96.67
2	96.67
3	100
4	100

VI. Conclusion

With the rise of digital content distribution, people now have access to online platforms on an unprecedented scale. Therefore the crucial part of the competition for e-commerce platforms and media services is about how to deliver the right content to the right people at the right time. In the real world, data generated in the platforms is highly sparse which leads to inaccurate recommendations made to the users on implementing CF algorithm. The proposed recommender using regression for prediction and GWO of optimizing loss function is observed to perform well on highly sparse datasets. Observations were made by investigating the proposed model on the prominent evaluation metrics of recommenders like CHR, UC, ARHR and evaluation metrics for accuracy like RMSE and MAE. For future studies, the proposed model can be tested on big data and online A/B tests can be conducted for the proposed model to evaluate the system and the feedback of a user has to be taken into consideration to test the correctness of the model.

References

[1] Seyedali Mirjalili, Seyed Mohammad Mirjalili , Andrew Lewis : Grey Wolf Optimizer https://doi.org/10.1016/j.advengsoft.2013.12.007 (2014)

[2] Mirjalili S, Saremi S, Mirjalili SM, Coelho LDS Multi-objective grey wolf optimizer: a novel algorithm for multi-criterion optimization. Expert Syst Appl 47:106–119 (2016)

[3] Khusro, Shah & Ali, Zafar & Ullah, Irfan. Recommender Systems: Issues, Challenges, and Research Opportunities. 10.1007/978-981-10-0557-2_112. https://www.researchgate.net/publication/294860665 (2016)

[4] Mukta kohar,Chhavi Rana "Survey Paper on Recommendation System", International Journal of Computer Science and Information Technologies, Vol. 3 (2) , 2012,3460-3462. (2012)

[5] Athalye, Shweta, "Recommendation System for News Reader" Master's Projects. 294. http://scholarworks.sjsu.edu/etd_projects/294 (2013)

[6] Wang Bailing, Huang Junheng, Zhu Dongjie, and Hou Xilu A Recommendation System Based on Regression Model of Three-Tier Network Architecture https://doi.org/10.1155/2016/9564293 (2016).

[7] Vucetic, S. & Obradovic, Z. Know. Inf. Sys. 7: 1. https://doi.org/10.1007/s10115-003-0123-8 (2005)

[8] X. Ge, J. Liu, Q. Qi and Z. Chen, "A new prediction approach based on linear regression for collaborative filtering," Eighth International Conference on Fuzzy Systems and Knowledge Discovery (FSKD), Shanghai, 2011, pp. 2586-2590. (2011)

[9] Ali Parsian, Mehdi Ramezani and Noradin Ghadimi, A hybrid neural network-gray wolf optimization algorithm for melanoma detection (2017)

[10] Sangamesh Hosgurmath, Viswanatha Vanjre Mallappa, Grey Wolf Optimizer with Linear Collaborative Discriminant Regression Classification based Face Recognition (2018)

[11] G. Adomavicius and A. Tuzhilin, "Toward the next generation of recommender systems: a survey of the state-of-the-art and possible extensions," in *IEEE Transactions on Knowledge and Data Engineering*, vol. 17, no. 6, pp. 734-749, June 2005. doi: 10.1109/TKDE.2005.99 (2005)

[12] Xiaoyuan Su and Taghi M. Khoshgoftaar, "A Survey of Collaborative Filtering Techniques," Advances in Artificial Intelligence, vol. 2009, Article ID 421425, 19 pages, https://doi.org/10.1155/2009/421425. (2009)

[13] A Survey of Accuracy Evaluation Metrics of Recommendation Tasks, Asela Gunawardana, Guy Shani http://jmlr.csail.mit.edu/papers/volume10/gunawardana09a/gunawardana09a.pdf (2009).

Proceedings of the Fourth International Conference on Communication and Electronics Systems (ICCES 2019)
IEEE Conference Record # 45898; IEEE Xplore ISBN: 978-1-7281-1261-9

Automatic Evaluation of Short Answers Using Deep Neural Networks

Barsha Sharma , Chandni Agarwal , Deep Shikha , Udit Kr. Chakraborty
Department of Computer Science and Engineering
Sikkim Manipal Institute of Technology
Sikkim Manipal University
Sikkim , India
{barsha_201600394 , chandni_201600052 , deep_201600457 , udit.c}@smit.smu.edu.in

***Abstract*—Automatic Short Answer Grading (ASAG) has been an area of active research over the last decade. Researchers and data scientists have tried and proposed various approaches based on classical Natural Language Processing, Information Extraction, Vectorization of text, Frequency Based Techniques etc. However, a single method appropriate for all types of short answers and thereby acceptable to all is yet to be found. This paper presents results of work done on ASAG using a Deep Learning approach. The results show the effectiveness of word embedding, hyperparameter tuning and activation function selection for improved classification.**

***Keywords*—Neural networks ; embeddings ; word2vec ; Doc2vec ; automatic evaluation**

1. Introduction

The increasing reach of the internet has improved the quality of living of individuals in a big way. One of the areas having maximum impact is education. Information and Communication Technology (ICT) has bridged the gap of geography and even time, thereby enabling the successful implementation of anytime anywhere learning. However, for correct evaluation of learning outcome, the assessment methodologies need to be automated. Increased number of enrollments for courses increase the load on human evaluators manifold and it becomes impossible to correctly assess the learners answers. The problem is further compounded if the answers are in free text, where the learner is creating his or her own natural language expressions to present the answer.

While evaluating a large number of free text answers in an unbiased manner becomes difficult for the human evaluator owing to variations in mood, mental fatigue, work load and other influences, automating the process has its own challenges. Natural Language Processing being computationally heavy and a complex domain, extracting semantical sense from the answers and evaluating them with the same finesse and benevolence of a human evaluator is a tough ask. It is for such factors that automated evaluation has shifted towards multiple choice type (MCQ) questions in most high stake examinations.

While the efficacy of MCQ type lies to be debated, text based answers have the propensity to return an evaluation of the learners retention, understanding and application skills. Also, the text based answers enhance the creativity of the learner by restricting the scope of presenting their knowledge to only selection of answers amongst some available choices. However, the aim is to evaluate the knowledge gained and not testing the memorizing capability of a learner,so this scheme of evaluation is not appreciated much. It is for such reasons that Automatic Short Answer Grading (ASAG) has gained importance and is under current study.

In this paper we propose a model that considers the fact that every student has a unique writing pattern and evaluate on the basis of semantics of the answers. In the method proposed in this paper, encoding of answers is done using an available scheme for encoding sentences to paragraph vectors, efficient enough to preserve the semantic relation amongst the constituting words .Then the encoded vectors are fed into another neural network that actually does the grading task.

The next section of this paper shares view on related work, using different methodologies. Section 3 sheds light upon some basics of deep learning and section 4 illustrates its use on the proposed work. Section 5 mentions about the experiments performed, its result and analysis and section 6 shares the conclusion of the mentioned approach.

2. Related Work

Building an automatic evaluator for short answers has been an intriguing task for quite a while. Researchers have adopted various techniques for accomplishing the task, however a common platform is yet to be achieved. The task of evaluation of student answers started long ago with first related work published in 1966 by Ellis B. Page[1] which proposed the idea to grade essays by computer.

This paper focuses on evaluation of short answers. Since the problem of evaluation of short answers has existed for long, concerning many of the researches, many approaches have been suggested to target the problem. One such approach that has always been quite popular is LSA[2](Latent Semantic Analysis). LSA preserves well the semantic relations of text but lacks syntactic relatedness. So, syntactically enhanced models were attempted to be built by [3]Kanejiya, Dharmendra, Arun Kumar, and Surendra Prasad. To enhance the performance of the evaluator, attempts were made to combine it with some other models, [4]Lapata, Mirella, and Regina Barzilay (in 2005) suggested that LSA in combination with some other models can retain entity correlation and semantic relatedness. Also, the idea of LSA being used as corpus based evaluation scheme as proposed by [5]Mohler, Michael, and Rada Mihalcea shows LSA to be a really efficient method but with the restriction of being domain specific and also it being effected significantly by the corpus size. Many other methods may not have the advantages that are possessed by LSA but still have proven to be efficient in their own way.

BLEU[6] (bilingual evaluation understudy) is another method which appeared quite frequently for evaluating short answers automatically. Despite not being able to attain high correlation, the method was suggested to be the sole technique for evaluation of short answers by Pérez, Diana, Enrique Alfonseca, and Pilar Rodríguez[7]. As said, BLEU as a stand alone system performs well while LSA was found to be effective for large corpus. Pérez, Diana, et al.[8] proposed in their work a combined schema of both the techniques. However using both techniques at a time can be computationally inefficient.

A concept that is found to be used along with the said techniques is ontology. Domain ontology in combination with LSA enhances the performance of the evaluator as proposed by Devi, M. Syamala, and Himani Mittal[9].Similarly, a work on collaborative use of BLEU and ontology for grading short answers with considerable result is presented by Selvi, P., and A. K. Bnerjee[10].

Also, many approaches involving NLP methods are administered for evaluation as task involved information extraction and NLP has been doing good in this field[11]. Semantic enhanced NLP performs better than lexical matching[12]. NLP is also used in combination with other techniques or with some alterations,[13]Jana and John used NLP and knowledge representation to develop a scoring model for short content or can be based on particular approach of NLP like parts of speech tagging[14].

Deep Learning being a more recent technique presents itself as a bright option to solve the problem under consideration. However, this has not yet been much employed in the domain of ASAG and hence this work. This paper proposes the idea of using deep learning and neural networks to embed the answers into paragraph vectors and then to evaluate them to assign deserving marks using another network which will be fed with vectors obtained from previous network.

3. Deep learning and neural networks

Deep learning and neural networks with multiple level of abstraction in its processing finds its wide application in the area of text processing and are proven to be considerably efficient. An artificial neuron is designed on the basis of a biological neuron in terms of its functionalities as well as the basic structure[15].An artificial neural network is made up of numerous interconnected artificial neurons organized in multiple layers each performing some computation and conveying the computed output to the next layer.

3.1. Deep Neural Nets

A *deep neural network[16]* is an artificial neural network which has multiple hidden layers, apart from the input and output layers. The essence of a *deep* neural network lies in its *depth.* A deep NN can be a significant tool in representing complex, non-linear relationships.

3.1.1. Biological Neuron

A *biological neuron[17]* is the basic building component of the neural network in the human brain that is responsible for reaction to various stimuli. There are millions of such neurons that collectively form the super complex and powerful network. These neurons communicate with each other through various electrical and chemical signals generated.

Each neuron mainly consists of three components: the *soma*, the *dendrites* and the *axon*. There are numerous dendrites associated with a single neuron which are responsible for collecting signals from other neurons. The signals received are then processed in the soma and then the result,which is also a signal is transmitted to other attached neurons through the axon. The neighboring neurons are not exactly attached to the neuron, and there exists a small gap between them called the synapse.

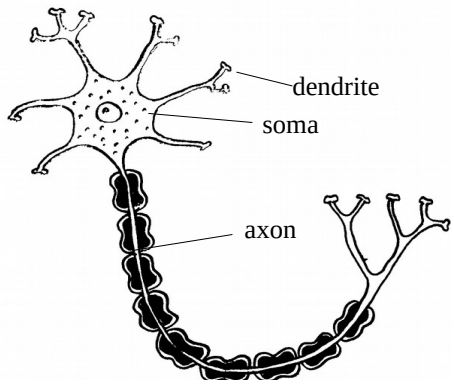

Fig1: Biological neuron

3.1.2.Artificial Neuron

Artificial Neurons were inspired by the concept of biological neurons. Much like a biological neuron, an *artificial* neuron also takes some input values and produces an output. The output value generated decides whether or not the neuron fires. If x_1 , x_2 , x_3 , …. x_n are the inputs provided to the neuron and the respective weights associated with each input are w_1 , w_2 , w_3 , …. w_n then the output is generated in the following manner:

i. Firstly, the sum of the weighted inputs is calculated. Let y_in be the calculated sum. Then y_in is given by,

$$y\_in = x_1w_1 + x_1w_2 + \ldots\ldots + x_nw_n = \sum_{i=1}^{n} xiwi \quad \ldots\ldots\ldots\ldots\ldots\ldots\ldots\ldots\text{eq.(1)}$$

ii. The output associated with the neuron, y_out is given by,

$$y\_out = f(y\_in) \ldots\ldots\ldots\ldots\ldots\ldots\text{eq.(2)}$$

where f is known as the *activation function* since it decides whether the neuron is activated, i.e. it fires, or not.

iii. A few examples of activation functions are identity function, step function, sigmoid function etc.

A simple diagrammatic representation of an artificial neuron is given in Fig2.

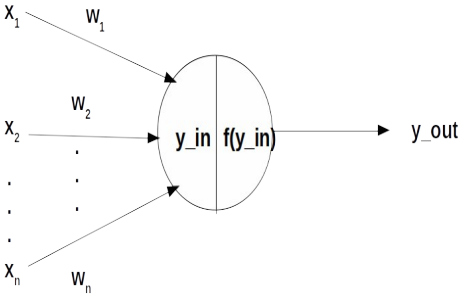

Fig 2: Artificial neuron

3.1.3. Artificial Neural Network

An *Artificial Neural Network* or an ANN is a network of many artificial neurons that interact with each other in an organized way to achieve a certain goal. The neurons in an ANN are structured into three layers, namely the *input layer*, the *hidden layer* and the *output layer.* An ANN consists of exactly one input layer and one output layer, but the number of hidden layers may vary depending upon the developer's choice. However it is always advisable to keep the number of hidden layers at the minimum possible value. No other guidelines are available for the same. The number of nodes per layer is also not fixed, and depends upon the developer to decide. Keeping in mind this flexibility in choice, it is suggested that the developer of a system experiment with small tweaks to the model, as even a slight change may highly affect the accuracy of the system.

In an ANN, each neuron, also known as a "node", is connected to other neuron in the immediate next layer by a connection which has a weight associated with it. These connections may either be unidirectional or bidirectional. An ANN in which each node of a layer is connected to all nodes in the next layer is known as a fully connected network.

A diagrammatic representation of a Feed Forward ANN with one input layer with 'i' nodes,one hidden layer with 'j' nodes and one output layer with two nodes is given in Fig 3.

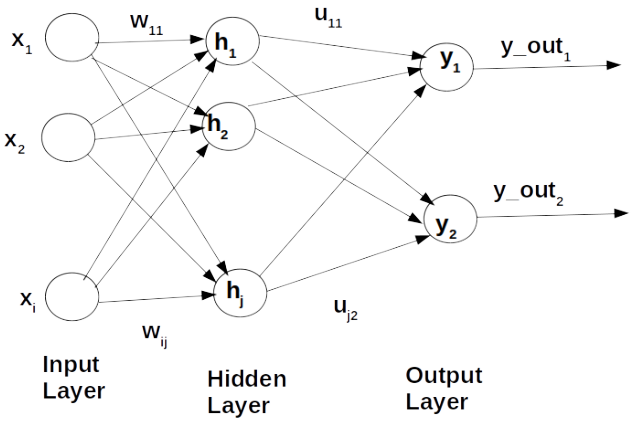

Fig 3: Artificial Neural Network

3.2 Converting Answers to Vectors

It is expected that each student will have a unique way of expressing his/her understanding over the topic. Therefore, it is likely that student answers will be comprising of different words depending on their own preferences. However, neural network computations cannot be directly carried out on words. So, the words must be represented in numeric forms and these numeric representations are expected to be fed into a neural network so that further computations can be carried out.

Initially,an attempt was made to ascertain a function to encode words by using product of three function values, where first function returned the sum of 52 raised to the power of numerical value of the words' compositional alphabets' positional value in english alphabet series, for example, the word "rat" , function f_1(say) would be calculated as,

$$f_1 = 52^{18} + 52^{1} + 52^{20} \quad \ldots\ldots \text{eq.(3)}$$

considering that 1-26 is the positional value of a-z (in lower case) and 27-52 is the positional value of A-Z (in upper case) . The second function returned the part of speech tagged value of the word, i.e., the second function f_2(say) for the same word "rat" would return,

$$f_2 = \text{Part of speech value("rat")} = 10 \quad \ldots\ldots.\text{eq.(4)}$$

considering value for noun (here, "rat") is 10 and similarly for each part of speech a unique value is assigned and the third function returned the positional value of the word in the sentence. If the function is represented by f_3, then for the sentence "rat is a rodent animal", the value returned by this function for the same word "rat" would be,

$$f_3 = \text{position of("rat")} = 1 \quad \ldots\ldots\ldots\ldots...\text{eq.(5)}$$

as the word "rat" appears at position 1 of the sentence and then finally applying summation function to all the values obtained for the constituting words of sentence. However, the function did not result as to what was desired and thus the requirement raised to shift from this customized embedding to some more precise scheme that would provide a representation which could better portray the answers along with preserving the relationships between the words. And thus the idea switched to use already existing schemes for word embeddings.

3.2.1 Word Embeddings

Embeddings in neural networks have proven to be of immense significance to meaningfully represent words in transformed vector space with much reduced dimension. There are various models available implementing word embedding built on some underlying architectures. Some of such schemes are Word2vec[18][19] based on local context window, Glove[20] considering global matrix factorization based on Latent Semantic Analysis and Single Value Decomposition and many more each performing notably in their own way.

3.2.1.1 Word2vec

The model of Word2vec is based on two architectures , namely, Continuous Bag of Words(CBOW) and Skip-gram. The words in the answers are first encoded using one hot encoding and then input to the network. In the former mentioned architecture, the context words are fed into the network and current word is obtained as output and in the later one current word is fed in the network and the context is obtained as output. The network employs one hidden layer which uses usual summation function and the output layer that either uses hierarchical softmax or negative sampling as the activation function. After training the network, when the weights are settled the output layer is tossed off and the weights are retained as vector representations and thus the number of nodes in the hidden layer is equivalent to the vector size thus obtained and therefore is the count of features considered for embedding. The model is said to preserve semantic relations, analogies and linear regularities between the words. Apart from that, the embedding scheme transforms the words into a vector space that is efficient enough to have words to retain the euclidean distance as well as the cosine distance between them.

3.2.1.2 Doc2vec

Based on word2Vec, another model is available known as Doc2Vec[21]. As the name suggests, it is very similar to Word2Vec just that instead of word vectors this model directly converts the answers to paragraph vectors and the input to this type of network is encoded word with a paragraph id. The architectures underlying are Distributed bag of words(DBOW), which is very similar to skip-gram and distributed memory paragraph vector(PV-DM), which is similar to CBOW. The model considered for embedding in this paper is Doc2vec using the distributed memory approach.

For fig.4, pos is the position of target word in its context, n is the size of context window,w(i) is the ith word, w1,w2… w_m are weights of m number of nodes of hidden layer.

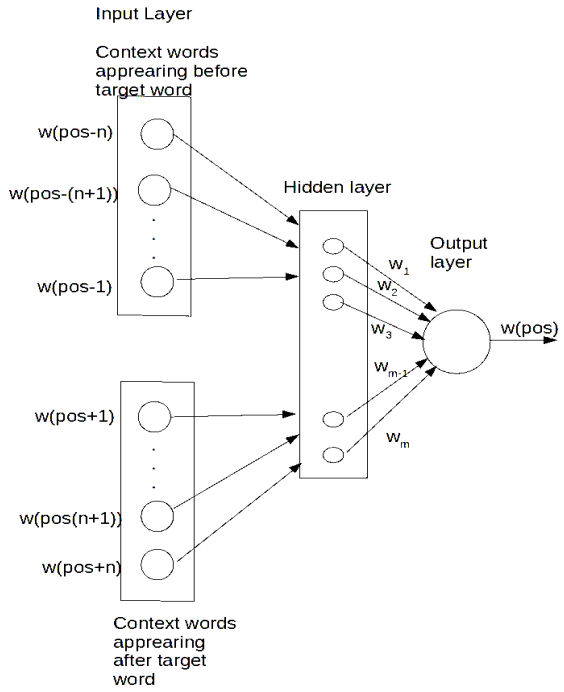

Fig 4: CBOW

4. Proposed Work

The vectors thus obtained from the said network are derived and fed into another neural network which performs the actual evaluation task. Apart from employing another network, grading of answers was also attempted using the cosine similarity between the answers. Although the results obtained were not poor but this approach would be highly rigid to the training set of answers. For instance, if the training set would consist of answers having low marks or very high marks and if an average answer would arrive for testing, then the similarity would be found with either the higher marked or lower marked answer, awarding exact high or low mark respectively. And thus, this is not expected to be a fruitful way of evaluation. So, it is preferred to use another network to do the evaluation.

In this paper, the model uses the dataset consisting of a question , a model answer , sample answers and their respective human evaluator given scores or the actual scores. The question, model answers , sample answers and actual scores were stored in a file and the sample answers and actual scores were read when needed in the program. The sample answers read were stored in (key , value) pairs in the form of dictionary, where the *key* represents the answer and the *value* is the corresponding score of the answer given by the human evaluator. There were a total of 30 answers from which 22 were used for training the model and 8 answers were used for testing the model. The training answers and the testing answers were first converted to vector forms using Doc2Vec as previously said and two models were generated . In another neural model, these vectors of the answers were fed to the neural network and automated scores were generated. The model trained by comparing the automated and the actual score and trying to minimize the difference between them. Hence, the model generated automated scores for the sample answers. The model was then trained on 8 answers of the dataset as mentioned before. Training set consisted of 73.33% of the dataset and testing set consisted of 26.67%.

The model created is Keras sequential model . The sequential[22] model consists of many layers arranged in a linear fashion. In our model , there are four layers and ReLU, that is rectified linear unit is used as an activation function in the first layer, as it cannot be used in the output layer. The Softmax activation function is used in the last layer, that is the output layer and is considered best for multi-classification problems . It gives the output in the form of probabilities whose sum would be equal to one .The activation functions are used to get the sum of the weighted values from the nodes and convert them for the activation of next layer . The ReLu activation used gives same value for the positive weights and zero for weights less than zero . As already said, we cannot use ReLu for output layers as it is considered best to be used as the default activation in the beginning .

The loss function[23] used is ‘sparse_categorical_crossentropy’ .The cross entropy gives the values in between 0 and 1 as the output in the probability form. The loss function is used to calculate the model error . Cross Entropy measures the difference between the two probabilities, that is the estimated and the predicted values. The loss function value is to be minimized to get a better model.

The models used different number of nodes in different layers. The output changes according the the number of nodes . The models need to know the input value , here the vector size is taken in the first layer called the input layer as the input value.

5. Experimentation and Results

In Table 1, observations are noted with different number of nodes in input layer, output layer and hidden layers and it can be seen that how tweaking the number of nodes in each layer will affect the output accuracy of the model. It was further observed that keeping the shape of the model such that number of nodes first increased then decreased gave better results.

Table 1 : Observations noted according to number of nodes in different layers

INPUT LAYER	HIDDEN LAYER 1	HIDDEN LAYER 2	OUTPUT LAYER	OBSERVED ACCURACY (IN %)
35	35	23	11	37.5
35	23	19	11	62.5
50	43	21	11	75
35	29	25	21	25
50	37	29	21	62.5
10	15	17	21	25
10	12	19	21	12.5
10	16	16	21	37.5
9	10	10	11	12.5
9	10	11	11	25
35	42	37	11	50
35	**39**	**23**	**11**	**87.5**
50	62	47	11	75
35	42	30	21	25
50	57	39	21	62.5

With the model tuned with hyper parameters giving the best result (of 87%, mentioned in Table 1) , Table 2 shows the the actual score, that is the human expert awarded score and its corresponding automated score provided by the model proposed in this paper.

Using this score representation the model can be further evaluated for other evaluation metrics such as,

Precision = 0.867/4 = 0.2164

Recall = 2/4 = 0.5

F-score = 0.302

Since, this is a multi class issue these metrics do not give good results, however, some other still give appreciable results,

Mean absolute error = 0.4375

Root Mean Square error = 0.637

Table 2 : score comparison of the best observation value:-

ACTUAL SCORE	AUTOMATED SCORE
4.5	4
4	4
3.5	5
5	5
4.5	4
4.5	4
5	5
4.5	4

6. Conclusion

This paper proposes an idea to evaluate short answers using neural networks. Initially, to embed the free-text answers into appropriate vector representations, Doc2vec is used with underlying architecture of PV-DM. This architecture is highly analogous to the CBOW architecture. Therefore, the vector representations of answers used in this model is quite efficient as Doc2vec not only converts the answers to vectors but also preserves the semantic relationships. The answer vectors thus obtained, when fed into another neural network, with tuning of the hyper parameters would award scores to student answers automatically with appreciable results. Thus, it can be deduced that even without complex algorithms or facing computational overheads, a model can be designed using neural networks which with proper hyperparameter tuning can result in an accuracy of 87.5% . With more exploration and refinements the model can be improved for even better results .

References

[1] Page, Ellis B. "The imminence of... grading essays by computer." *The Phi Delta Kappan* 47.5 (1966): 238-243.

[2] Landauer, Thomas K., Peter W. Foltz, and Darrell Laham. "An introduction to latent semantic analysis." *Discourse processes* 25.2-3 (1998): 259-284.

[3] Kanejiya, Dharmendra, Arun Kumar, and Surendra Prasad. "Automatic evaluation of students' answers using syntactically enhanced LSA." *Proceedings of the HLT-NAACL 03 workshop on Building educational applications using natural language processing-Volume 2*. Association for Computational Linguistics, 2003.

[4] Lapata, Mirella, and Regina Barzilay. "Automatic evaluation of text coherence: Models and representations." *IJCAI*. Vol. 5. 2005.

[5] Mohler, Michael, and Rada Mihalcea. "Text-to-text semantic similarity for automatic short answer grading." *Proceedings of the 12th Conference of the European Chapter of the Association for Computational Linguistics*. Association for Computational Linguistics, 2009.

[6] Papineni, Kishore, et al. "BLEU: a method for automatic evaluation of machine translation." *Proceedings of the 40th annual meeting on association for computational linguistics*. Association for Computational Linguistics, 2002.

[7] Pérez, Diana, Enrique Alfonseca, and Pilar Rodríguez. "Application of the BLEU Method for Evaluating Free-text Answers in an E-learning Environment." *LREC*. 2004.

[8] Pérez, Diana, et al. "Automatic Assessment of Students' Free-Text Answers Underpinned by the Combination of a BLEU-Inspired Algorithm and Latent Semantic Analysis." *FLAIRS conference*. 2005.

[9] Devi, M. Syamala, and Himani Mittal. "Machine learning techniques with ontology for subjective answer evaluation." *arXiv preprint arXiv:1605.02442* (2016).

[10] Selvi, P., and A. K. Bnerjee. "Automatic short-answer grading system (ASAGS)." *arXiv preprint arXiv:1011.1742* (2010).

[11] Smeaton, Alan F. "Progress in the application of natural language processing to information retrieval tasks." *The computer journal* 35.3 (1992): 268-278.

[12] Arun, P., et al. "Automatic answer evaluation: NLP approach." (2016): 1-5.

[13] Sukkarieh, Jana Zuheir, and John Blackmore. "c-rater: Automatic content scoring for short constructed responses." *Twenty-Second International FLAIRS Conference*. 2009.

[14] Patil, Shweta, and Sonal Patil. "Intelligent tutoring system for evaluating student performance in descriptive answers using natural language processing." *International Journal of Science and Research* 3.9 (2014): 779-783.

[15] Roy, S., and U. Chakraborty. "Introduction to soft computing Neuro-Fuzzy and Genetic Algorithm." *Dorling Kindersley (India) Pvt. Ltd, New Delhi, India* (2013).

[16] Karpathy,Andrej “A Beginner's Guide to Neural Networks and Deep Learning.” skymind.ai, Monday April 2019, https://skymind.ai/wiki/neural-network.

[17] Fausett, Laurene V. *Fundamentals of neural networks: architectures, algorithms, and applications*. Vol. 3. Englewood Cliffs: prentice-Hall, 1994.

[18] Mikolov, Tomas, et al. "Efficient estimation of word representations in vector space." arXiv

preprint arXiv:1301.3781 (2013).

[19] Mikolov, Tomas, et al. "Distributed representations of words and phrases and their compositionality." *Advances in neural information processing systems*. 2013.

[20] Pennington, Jeffrey, Richard Socher, and Christopher Manning. "Glove: Global vectors for word representation." *Proceedings of the 2014 conference on empirical methods in natural language processing (EMNLP)*. 2014.

[21] Lau, Jey Han, and Timothy Baldwin. "An empirical evaluation of doc2vec with practical insights into document embedding generation." *arXiv preprint arXiv:1607.05368* (2016).

[22] @misc {chollet2015keras, title={Keras}, author={Chollet, Fran\c{c}ois and others}, year={2015}, howpublished={\url{https://keras.io/getting-started/sequential-modelguide/}}, }

[23] Brownlee,Jason “Loss and Loss Functions for Training Deep Learning Neural Networks.”Machine Learning Mastery, Monday January 2019,https://machinelearningmastery.com/loss-and-loss-functions-for-training-deep-learning-neural-networks/.

Proceedings of the Fourth International Conference on Communication and Electronics Systems (ICCES 2019)
IEEE Conference Record # 45898; IEEE Xplore ISBN: 978-1-7281-1261-9

Comparison of BER and Q-factor in an Is-OWC system using WDM with different modulation techniques

[1]Shubhneet Kaur
M.tech student, Department of Electronics and Communication Engineering
Guru Nanak Dev Engineering College
Ludhiana, Punjab, India
shubhisidhu02@gmail.com

[2]Ameeta Seehra
Associate Professor, Department of Electronics and Communication Engineering
Guru Nanak Dev Engineering College
Ludhiana, Punjab, India
am_ameeta@yahoo.co.in

***Abstract* - Inter-satellite Wireless Communication is the latter day technology in which communication can be done between two satellites. This paper reports the performance of Wavelength Division Multiplexing (WDM) using Chirped modulation technique, CSRZ modulation technique and Alternate chirped NRZ modulation technique. The total number of channels used are 32 with different bit rates of 15 Gbps, 20 Gbps and 42 Gbps with OWC range of 750nm. The main concept of the system is to achieve high Quality factor and minimum Bit error rate. From the observations it has been concluded that Chirped modulation technique shows maximum Quality factor with minimum Bit error rate at 15 Gbps and Alternate chirped NRZ modulation technique shows good results at 20 Gbps and 42 Gbps as compared to CSRZ modulation technique.**

Keywords-Inter-satellite link, WDM, Chirped modulation, ALCNRZ, CSRZ.

I. INTRODUCTION

Inter satellite optical wireless communication links are having momentous role in interchanging of information between satellites. Due to turbulences and pointing errors, FSO systems are less frequently used for the transmission of data and signals. For exchanging of information or data between two satellites Inter satellite link One satellite connect with another satellite through this link as whether the satellite is in same orbit or in the another orbit. Data can send with the speed of light. Is-OWC system also has lot of advantages as there is no license required for such a communication system less cost is involved for designing, small and lightweight components required, less power consumption, can handle huge bandwidth and so on. These links shows a good performance in ultraviolet and infrared bands. Continuous Wave Laser is used as a source of light in inter satellite optical wireless links and due to its high reliability and high speed of operation it can operate at higher transmission bit rates. In order to enhance the system performance latest modulation techniques can be used which also help to increase the system efficiency as well as reduce delays. Wavelength Division Multiplexing is a technology in which number of optical carriers gets multiplex on a single optical fiber by using different wavelengths. Wavelength Division Multiplexing (WDM) technique is used to produce a system with higher data bit rate. WDM multiplexing technique is used to obtain flexibility in Is-OWC system. Is-OWC system is used for earth tracking mission, deep space optical communication is possible, and communication between two satellites is possible through this link. Considering the fact that space being vacuum, chances of distortion of the signal is reduced. Due to misalignments and vibrations, errors such as the pointing error arise in the tracking system of the satellite. In order to reduce the pointing errors and overcome nonlinear effects, a suitable combination of various modulation and multiplexing schemes are used. Important parameters used in Is-OWC system are: Quality factor, Bandwidth, Bit error rate, Power etc. Quality-factor provides a description of an output signal. It is a dimensionless positive value which indicates the quality of signal. Bandwidth plays an important role in Is-OWC system as wider the bandwidth more amounts of data can flow with less number of collisions which produces a high Quality-factor. Bit error rate defines a number of errors received by total number of transmitted bits. As distance increases transmission losses increases. So in order to decrease noise level, the rate of transmission power has to increase.

The paper is organized in five sections. The basic introduction of Is-OWC system is described in section I. The System description of Is-OWC system is provided in section II. Results and discussion is explained in section III. Conclusion is discussed in section IV and finally Future scope is discussed in section V.

II. SYSTEM DESCRIPTION

The design model of the simple Is-OWC system is shown in the fig.II (a). In the system there are two satellites the transmitter being in the first satellite and receiver in the second satellite. In between two satellites the OWC channel can be considered as propagation medium. The electrical and optical signal in the first satellite is modulated and is passed on towards the OWC. Satellite second helps to amplify the low and weak signal so that it can travel to long distance.

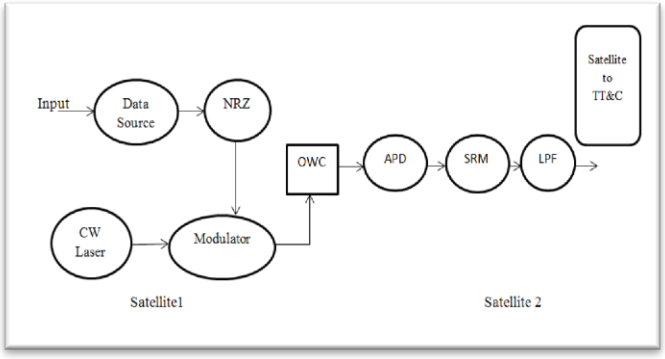

Fig.II (a) Simple Is-OWC system

The system using Wavelength Division Multiplexing technique with different modern modulation schemes namely Chirped, CSRZ and Alternate Chirped NRZ is simulated and analysed in this paper using Optisystem 15 software. 32 channels operating at bit rates of 15 Gbps, 20 Gbps and 42 Gbps are multiplexed together and the signal is passed towards the OWC channel having a distance of 2840 km. Demultiplexer helps to demux the 32 channels and pass the signal to receiver side which will regenerate the signal and amplify it. Fig.II (b) shows the block diagram of the Chirped modulation technique. It is considered as a highly preferred modulation technique in which frequency increases or decreases with time. The chirped rate is defined as a rate at which frequency changes. The chirp with positive rate is defined by one bit period whereas with negative rate it is defined as zero bit periods. Its function is to enhance high immunity to interference, contains high spectral efficiency. The Chirped modulation along with RZ Pulse generator produces high quality factor and shows better performance for long distance transmission in Is-OWC system. It consists of pseudo random bit sequence generator followed by RZ pulse generator that passes its signal through the fork 1*2. The Continuous Wave laser produces an optical input which passes through the LiNb Mach Zehnder Modulator. LiNB MZM controls the amplitude of an optical signal and resulting in an output that can be obtained from the optical spectrum analyser. The frequency taken here is 193.1 THz and the extinction ratio taken is 20 dbm. Fig.II (c) shows output of the chirped transmitter.

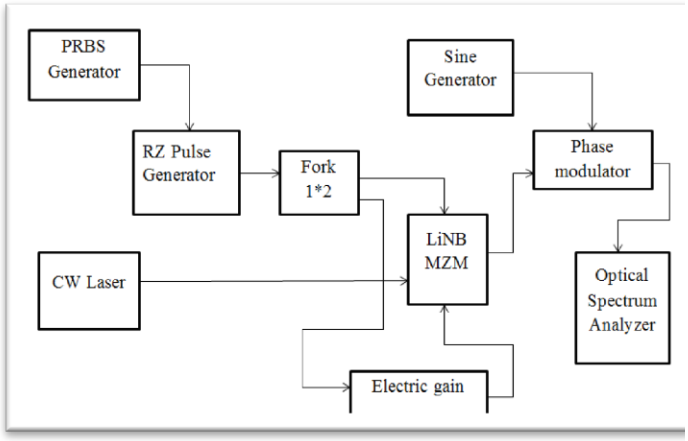

Fig. II (b) Block diagram of Chirped modulation technique

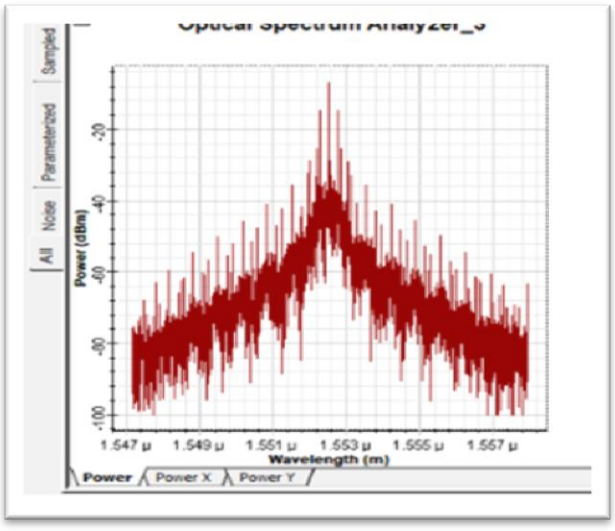

Fig. II (c) Optical spectrum analyser of Chirped modulation technique

Fig.II (d) shows the block diagram of the CSRZ modulation technique block diagram in which modulation takes place in two stages. CSRZ modulation technique has 180^0 phase shift between adjacent bits and also highly immune to cross phase modulation and Self phase modulation. As from the name it indicates that the Carrier signal is suppressed in it. The main motive of using this modulation technique is to reduce nonlinear tolerances in the channels and improvement in the spectral efficiency in high bit rate system. CSRZ modulation technique has no carrier components because during phase alternation, in the optical domain it produces no DC components. In first Mach Zehnder Modulator, intensity modulation is carried out whereas in second Mach Zender Modulator, a sinusoidal signal having frequency equal to half of the bit rate of the original bit sequence and due to this half of the bit rate, the bits 1s have positive sign and rest others have negative sign. Output of CSRZ modulation technique is shown in Fig.II (e).

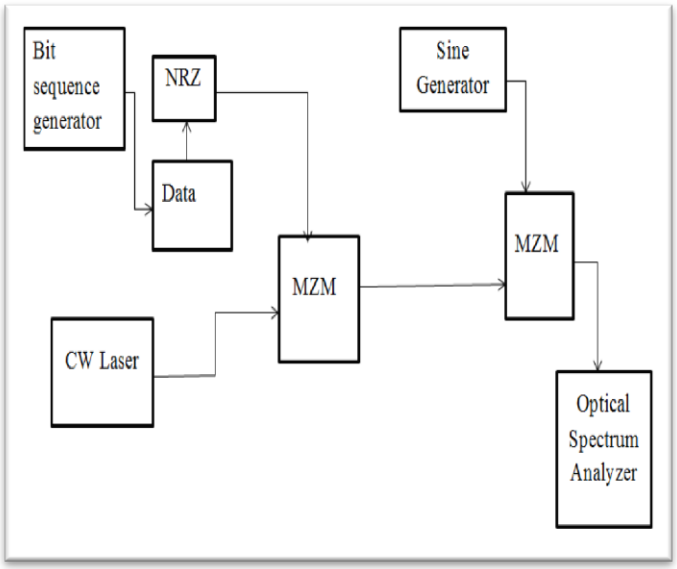

Fig. II (d) Block diagram of CSRZ modulation technique

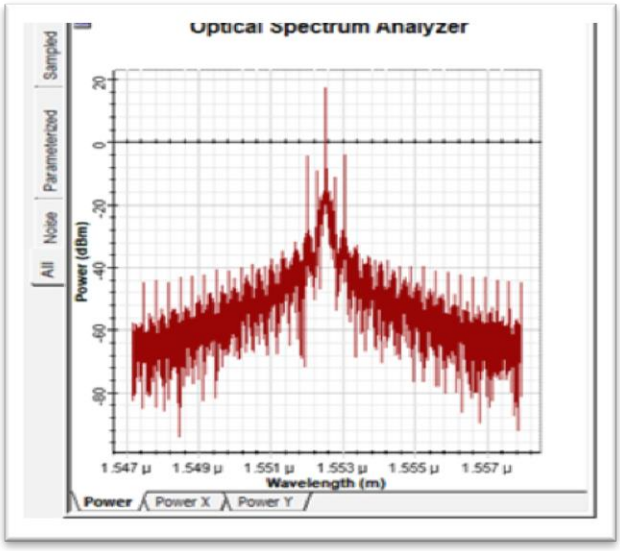

Fig. II (e) Optical spectrum analyser of CSRZ technique

Fig.II (f) shows the block diagram of the Alternate Chirped NRZ modulation technique. The pre-chirping of an optical pulse at the transmitter part makes the better transmission performance of the system but this results in the broadening of the signal spectrum. This implementation of pre-chirping can be realized by using either passive components like optical

fiber, fiber piece or by using active components for example Phase Modulator Or Mach- Zehnder Modulator. Thus this method of pre-chirping has to be chosen very carefully. Alternate Chirped NRZ is considered as an advanced modulation technique as it shows an improvement in the performance of the system as well as helps to increase the efficiency of the system. It also improves nonlinear tolerances due to which error like pointing errors arises which degrades the system performance. Alternate chirped NRZ helps the system to enhance its transmission length and also it is useful because of its simple design. The main target of using Alternate chirped NRZ is to enable a high speed optical transmission over long haul distances. Fig.II (g) shows output of Alternate chirped NRZ modulation technique.

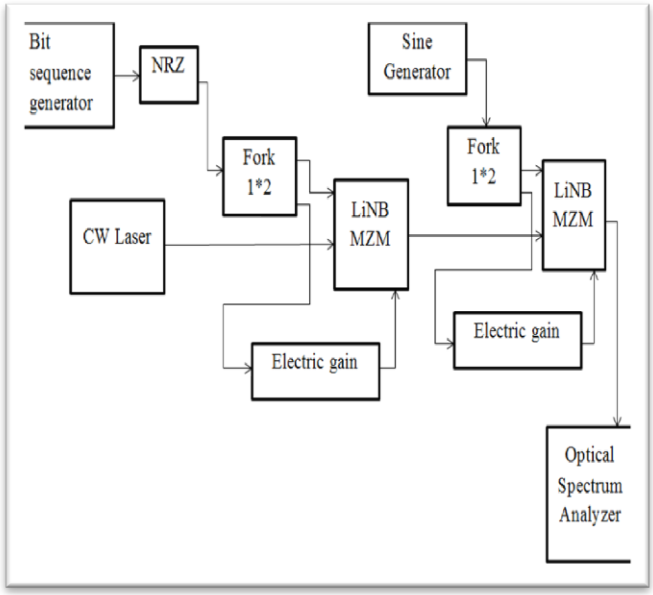

Fig. II (f) Block diagram of Alternate chirped NRZ modulation technique

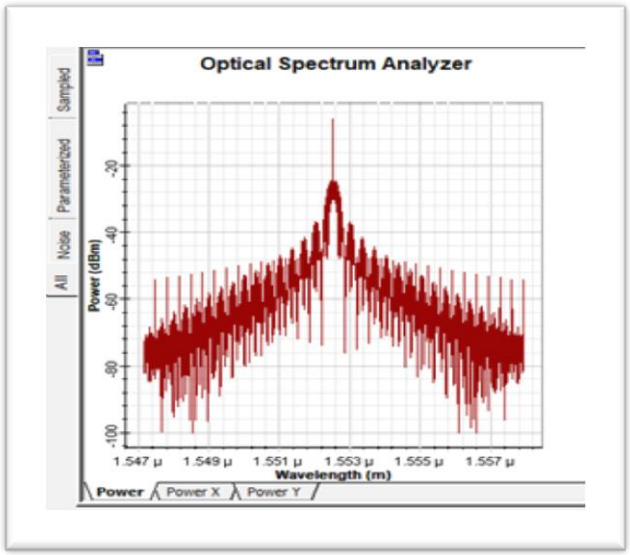

Fig. II (g) Optical spectrum analyser of Alternate chirped NRZ modulation technique

III. RESULTS AND DISCUSSION

The following are the eye diagrams of Chirped, CSRZ and Alternate chirped NRZ modulation techniques at the bit rate of 15Gbps.

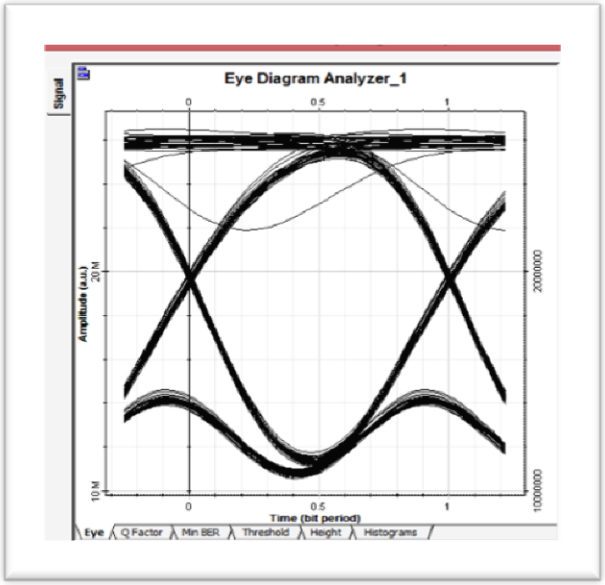

Fig.III (a) Eye diagram of Chirped modulation at 15 Gbps

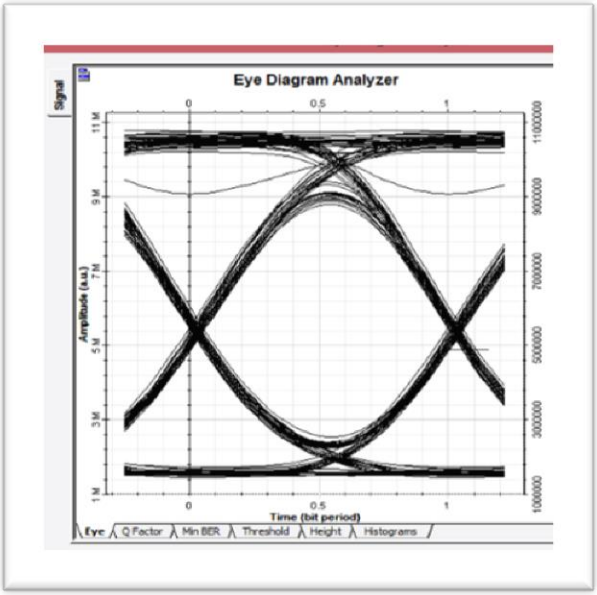

Fig.III (b) Eye diagram of CSRZ modulation at 15 Gbps

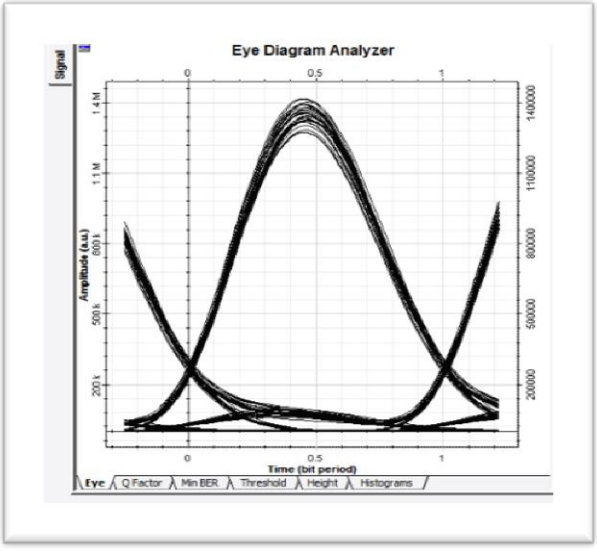

Fig.III (c) Eye diagram of ALCNRZ modulation at 15 Gbps

In this section, the results from simulation of proposed WDM based Is-OWC system are presented and discussed. In Fig.III (a,b,c), from an eye diagrams, it is observed that Chirped modulation technique shows a higher Quality factor , larger eye opening, greater eye height as well as greater eye width which indicates less distortion of the signal.

Fig.III(d,e,f) shows an eye diagrams at bit rate of 20 Gbps and out of the three modulation techniques, Alternate Chirped NRZ modulation technique shows a minimum error with a recorded Quality factor of 13.0075 which indicates a lesser distortion in the signal as compared to the other two modulation techniques.

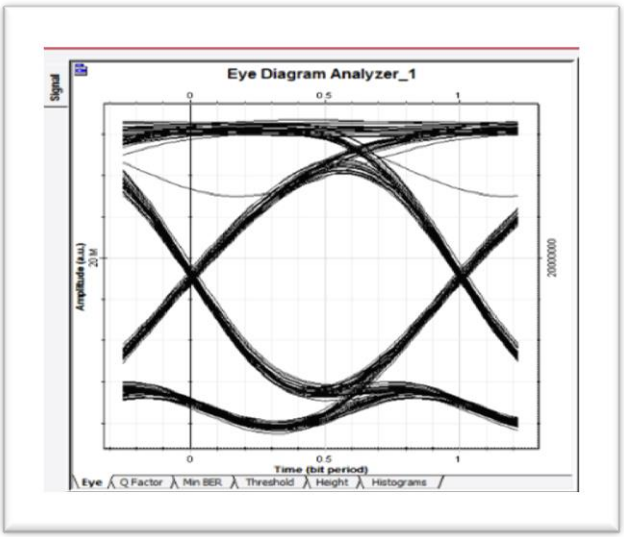

Fig.III (d) Eye diagram of Chirped modulation at 20 Gbps

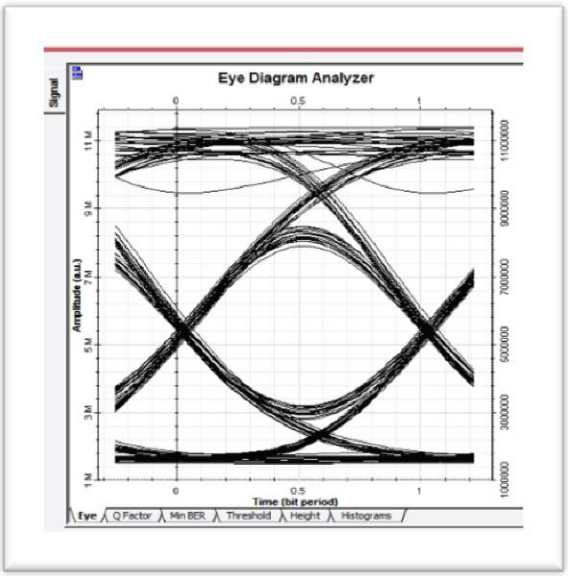

Fig.III (e) Eye diagram of CSRZ modulation at 20 Gbps

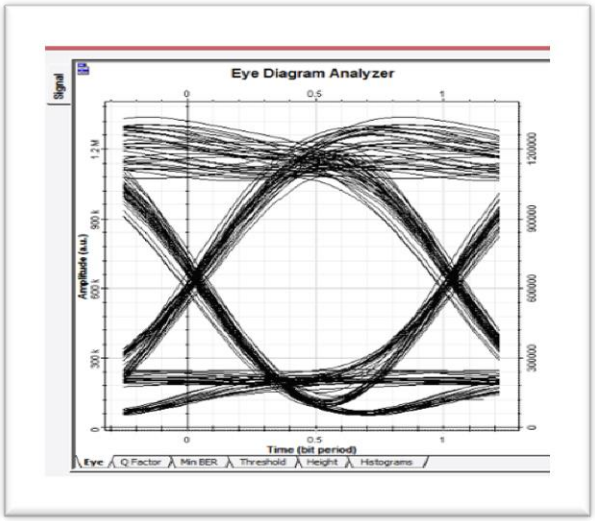

Fig.III (f) Eye diagram of ALCNRZ modulation at 20 Gbps

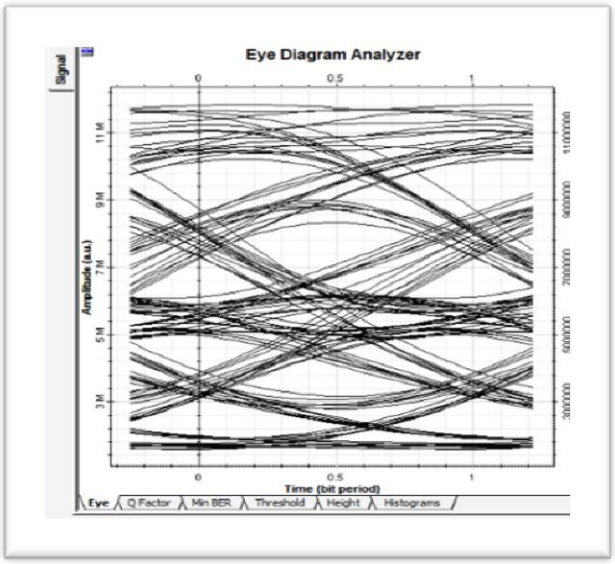

Fig.III (g) Eye diagram of chirped modulation at 42 Gbps

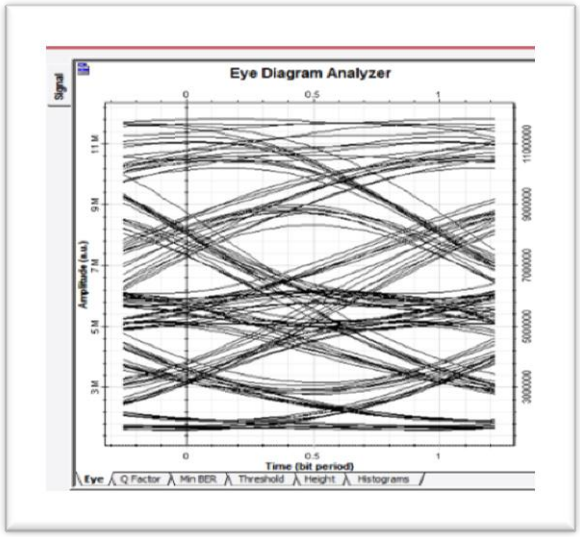

Fig.III (h) Eye diagram of CSRZ modulation at 42 Gbps

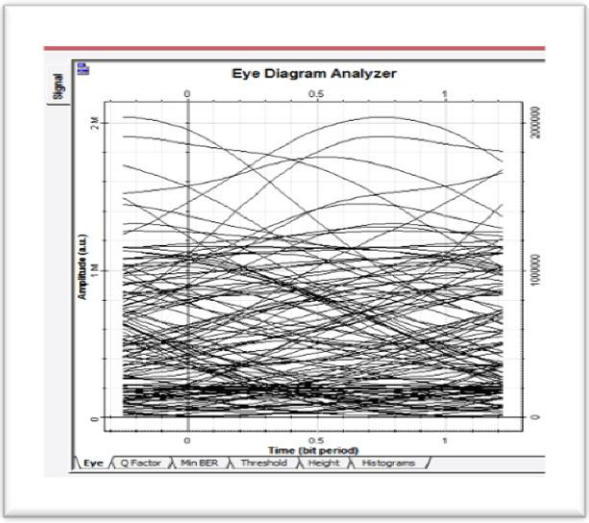

Fig.III (i) Eye diagram of ALCNRZ modulation at 42 Gbps

Fig.III(g,h,i) shows eye diagrams of Chirped, CSRZ and Alternate Chirped NRZ at 42Gbps in which signal Quality degrades as the bit rate goes higher from 20Gbps to 42Gbps.

Table 1 Simulation parameters for the proposed ISOWC system

Parameters used	Values
Bit rates (Gbps)	15, 20, 42
OWC range (nm)	750
No. of samples	4096
Distance (km)	2840
EDFA gain (dbm)	43
Channels used	32
CW laser frequency (THz)	193.1
Extinction ratio (db)	20
Power (dbm)	30

From this section it's clear that out of three modulation techniques namely Chirped, CSRZ and ALCNRZ, Chirped modulation shows maximum Quality factor of 25.9058 with minimum BER of 2.75641e-148 at 15 Gbps .Alternate Chirped NRZ shows best performance at 20 Gbps with Quality factor of 13.0075 and BER of 5.36441e-039 whereas at 42 Gbps again Alternate chirped NRZ shows comparatively better results with Quality factor of 1.62723 and BER of 0.0460834.

Following are the points which help to achieve high Quality factor and minimum Bit error rate

1. EDFA Black box amplifier helps to improve the quality factor of signal.
2. Large WDM bandwidth also improves the signal quality as it reduces the collisions between signals.
3. By increasing CW laser power signal strength increases and it can travel long distance range.

Table 2 shows the comparison of the results for three different modulation techniques used.

Bit rates (Gbps)	Analysed parameters	Chirped modulation	CSRZ modulation	Alternate chirped NRZ modulation
15	Q-factor	25.9058	10.0218	20.3406
	BER	2.75641e-148	5.93527e-024	2.10918e-092
20	Q-factor	9.78423	4.77399	13.0075
	BER	6.44456e-023	8.63686e-007	5.36441e-039
42	Q-factor	1.33877	1.39046	1.62723
	BER	0.0893258	0.0791607	0.0460834

IV. CONCLUSION

From the results and discussion it has been concluded that after comparison between three different modulation techniques having bit rates of 15Gbps, 20Gbps and 42Gbps, Chirped modulation technique shows maximum Q- factor and minimum Bit error rate at 15 Gbps. At 20 Gbps ALCNRZ shows maximum Quality factor with minimum Bit error rate. Whereas at 42 Gbps again ALCNRZ shows better results as compared to other two modulation techniques. From results it has been also concluded that Quality factor decreases as the bit rate and distance increases between two satellites. BER increases with the increase of bit rate and distance between two satellites. Signal with lower bit rate cover long range transmission without much distortion.

V. FUTURE SCOPE

1. Development of Inter-satellite optical network protocol which is used to provide access internet.
2. Transmission of data or information for satellite observation.
3. Communication between satellite clusters.
4. Path prediction model for Is-OWC system.
5. Theoretically advantages of using optical link over RF link have been mentioned in various papers and Books but the performance analysis in terms of QOS has not been done. So it can be considered in future work.

REFERENCES

[1] A. H. Hashim, F. D. Mahad, S. M. Idrus, A. Sahmah, and M. Supa, "Modeling and performance study of inter-satellite optical wireless communication system," Int. Conf. Photonics, pp. 1–4, 2010.

[2] Patnaik and Sahu, "Inter Satellite Optical Wireless Communication System Design and Simulation," IET Communications ,Vol. 6, Issue: 16, November 2012.

[3] S. Tiwari, P. Patel, "A literature review on inter satellite optical wireless link and impact of encoding schemes on performance of 40 gbps system,"IJSRDV4I90283, Volume 4, Issue: 9, Dec. 2012.

[4] N. Kumar, "Enhanced Performance Analysis of Inter Satellite Optical Wireless Communication (ISOWC) System," Optik Volume 125, Issue 8, April 2014.

[5] P. Kaur, A. Gupta, and M. Chaudhary, "Comparative analysis of Inter satellite Optical Wireless Channel for NRZ and RZ modulation formats for different levels of input power," Procedia - Procedia Compute. Sci., vol. 58, pp. 572–577, 2015.

[6] K. Singh, M. Singh, "Performance Improvement of inter-satellite Optical Wireless Communication, International journal of Engineering Research and Technology,vol. 1,no.4, pp. 2278-018, Jun.2015.

[7] S. S. Ganga, R. S. Asha and P. J. Shaija, "Design of a Standardized Inter Satellite Optical Wireless Communication (IsOWC) System with Minimum Input Power," Procedia Technol., vol. 25, no. Raerest, pp. 567–573, 2016.

[8] V. S. Sarath, V. Kumar, A. K. Turuk, and S. K. Das, "Performance Analysis of Inter-Satellite Optical Wireless Communication," no. April, pp. 22–28, 2017.

[9] B. Mallick and B. Patnaik, "Performance Enhancement Of An Inter Satellite Optical Wireless By Employing Various Modulation Techniques," no. January, 2017.

[10] Liu et. al, "Performance Degradation of Typical 1550 nm Optical Inter Satellite Communication Systems in Space Ionizing Radiation Environment", Journal of Lightwave Technology ,vol 35, Issue: 18, Sep. 2017.

[11] R. Kaur and H. Kaur, "Comparative analysis of chirped, AMI and DPSK modulation techniques in IS-OWC system," Optik (Stuttg). vol. 154, pp. 755–762, 2018.

[12] L. Roberto, "Intersatellite link for Earth Observation Satellites constellation," http://www.corista.unina.it/Docs/intersatellite_link.pdf.

Proceedings of the Fourth International Conference on Communication and Electronics Systems (ICCES 2019)
IEEE Conference Record # 45898; IEEE Xplore ISBN: 978-1-7281-1261-9

A Metaheuristic-based Emotional ANN (EmNN) Approach for Rainfall-runoff Modeling

Bishwajit Roy
Computer Science and Engineering
National Institute of Technology Patna
Patna, India
bishwajit.cse15@nitp.ac.in

Maheshwari Prasad Singh
Computer Science and Engineering
National Institute of Technology Patna
Patna, India
mps@nitp.ac.in

***Abstract*— This paper presents a new development in recent machine learning model, a particle swarm optimization (PSO) based Emotional neural network (PSO-EmNN), for daily rainfall-runoff modeling of catchment Seaton at Trebrownbridge, Cornwall, United Kingdom. The EmNN is inspired by neurophysiological information of brain which simulates emotions as additional parameters with conventional weights and biases to improve the networks learning ability. The PSO is used for tuning the parameter set of EmNN to get optimal values of parameters. The performance of the developed model is validated through RR modeling. Further a PSO based artificial neural network (PSO-ANN) is used to compare the efficiency of the proposed approach. The result demonstrates the superiority of the PSO-EmNN over the PSO-ANN in terms of prediction accuracy.**

Keywords*— *Rainfall-runoff modeling; data-driven model; particle swarm optimization

I. INTRODUCTION

Rainfall-runoff (R-R) is a intricate process in the earth's surface. Reliable and accurate assessment of runoff is important for water resources planning to design urban sewer system, flood risk management plan, etc. R-R models are classified as three categories, (i) data-driven model, (ii) conceptual model, (iii) physical law based model [1]. The implementation of physical models and conceptual models requires several environmental parameters and knowledge of the hydrological system. Recently, data-driven models are gaining their popularity because of its ability to handle the non-linear relationship of the generated hydrological data set. These types of models map the input to output data without requiring the knowledge of the hydrological system. When the accurate prediction is much more important rather than the laws of physics, the data-driven models are considered as the best alternative R-R modeling practice. Current studies show that classical models, for example auto-regressive integrated moving average, may not capture significantly the non-linear nature of hydrological processes. Authors of [2] have shown that data-driven models can give similar or better result compare to theory-driven models. The artificial neural networks (ANNs) are the most widely used black box R-R models [3, 4]. But due to gradient based learning ANN may not perform significantly to predict river flow. Currently, hybridization of ANN with metaheuristic algorithm enhances the learning ability of the neural system and overcome from the longer time network training, overfitting and local minima stagnation problem. Several studies show that the antecedent variable for R-R modeling are considered as only rainfall or rainfall and runoff or temperature, evaporation, evapotranspiration in addition to rainfall/runoff [5-7]

This paper considers a new category of ANN called emotional neural network (EmNN) [8]. The EmNN was developed for pattern recognition, clustering, and prediction task. Nourani [9] presented the first hydrological implementation of EmNN in R-R modeling and showed that EmNN has better capability to predict peak flow as compared to ANN. The EmNNs have been successfully used for learning complex systems [10, 11] and in several prediction based applications [12]. They are classified as brain emotional learning (BEL)-based neural networks [13-15] and emotional back propagation (EmBP)-based neural networks [16, 17]. Where the BEL networks closely represent the human emotions and show an efficient learner than the EmBP networks. This paper uses BEL networks for R-R modeling. BEL networks were created from the structural computational model of emotional brain (EB) [8] and applied successfully in various application domains [12, 18, 19]. Authors of this paper use the PSO to learn EmNN and applied in RR modeling. The result of the proposed approach shows the better capability to predict river flow compared to the PSO-ANN.

This paper is organised as follows; Section II presents used data for this study. Section III describes basic framework of EmNN and proposed PSO-EmNN. Results are presented in section IV. Section V presents conclusion of this study.

II. DATA USED

The catchment of the United Kingdom (UK) from one hydrometric area 48 is used to access dataset and downloaded from the national river flow archive (NRFA) website (https://nrfa.ceh.ac.uk/data/search)[20]. Fig. 1 shows the region of the catchment. The daily rainfall and runoff dataset from the Seaton at Trebrownbridge catchment are utilized for river discharge forecast.

Fig. 1: Catchment Seaton at Trebrownbridge

The river Seaton at Trebrownbridge catchment (Fig. 1) increases on the Caradon Hill. The extension of the catchment is linear (no tributaries). It has negligible disturbance with the natural flow regime. The catchment extent is 39.1 km2. The gauge level is at 26.6 m AOD. The highest flow was 13.2 (m^3/s). The catchments data in between 2010 to 2015 is utilized for model run.

The accumulated rainfall rate was taken from the center for ecology and hydrology-gridded estimates of areal rainfall (1km resolution) [21] which is scaled to mm per day.

III. PROPOSED WORK

A. **Emotional Neural Network**

The main findings of EB have been stated in [22-24] by LeDoux. The EB has the shortest path to make a quick response to the input. Such faster response motivated the researchers to design a model of EB and applied the model in several engineering application. The structural model of EB is based on the lymbic system (LS) theory of emotion [25, 26]. Figure 2 shows the anatomical model of emotion. In EB, there are two kinds of responses for amygdala (AMYG) component,

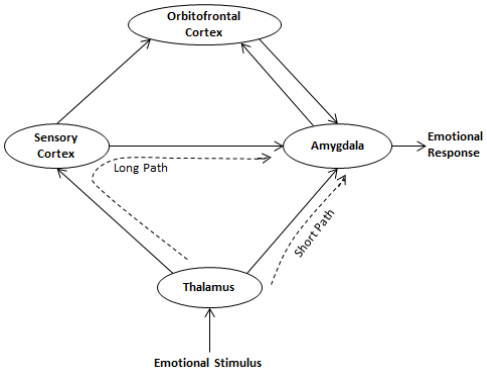

Fig. 2: Anatomical model of EB

one follows the shortest path from thalamus which is faster and imprecise, where the second follows the longest path through sensory cortex (SC) which is slower and precise (Fig. 2). AMYG can provide a quick response based on these paths. The orbitofrontal cortex (OFC) and AMYG interaction control the imprecise information. Where the OFC manages the decision making process under uncertain environment and estimates uncertainty [27, 28]. Overall the utility of EB is to provide a quick imprecise response under the uncertain and unpredictable situation.

B. **A practical EmNN**

The BEL-based EmNN [26] is shown in Fig. 3 which is based on the OFC-AMYG interactions. Where, each of the subsystems related to input dimension. Figure 3 shows the shortest path and the longest path of input flow to the AMYG subsystem. The OFC receives input from AMYG to prevent the final output.

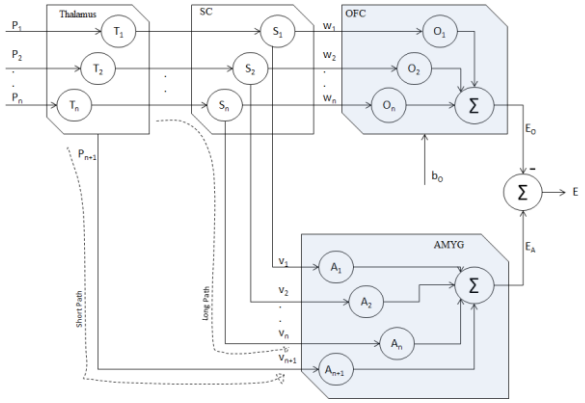

Fig. 3: An EANN based on the OFC-AMYG interconnection

The input pattern is illustrated as {p_1, $p_{2...}$, p_n, p_{n+1}} which are used for feed forward computation. The target value is used for the backward learning process of the model.

The input patterns enter to the thalamus and then forwarded to the SC. The two input patterns are received by AMYG. They are p_1, $p_{2...}$, p_n from SC and an imprecise input p_{n+1} from thalamus. The calculation of input p_{n+1} is formulated by Eq. 1. The related weight of imprecise input is v_{n+1}. The max operator defines the uncertain information.

$$P_{n+1} = \max_{i=1..n}(p_i) \tag{1}$$

The OFC acquires the input pattern from SC. The final output is formulated by Eq. 2.

$$E = E_A - E_O \tag{2}$$

Where, E_A and E_O specify the outputs of AMYG (Eq. 3) and OFC (Eq. 4) respectively.

$$E_A = \sum_{i=1}^{n+1}(v_i \times p_i) \tag{3}$$

$$E_O = \sum_{i=1}^{n+1}(w_i \times p_i) + b_O \tag{4}$$

Where v_i and w_i are the weights of the AMYG and OFC respectively, b_O is the OFC bias and p_i is the input pattern. In the final output (Eq. 2) OFC output inhibits the EMYG output (E_A).

C. **The proposed PSO-based EmNN**

The PSO is used to train the EmNN network by tuning the parameters of EmNN. PSO is a popularly used metaheuristic algorithm for optimization task [29]. PSO minimizes the fitness score (objective function) of particles in order to find

the best solution to the problem domain. Here the particles are represented as follows;

$$Particle_k = [v_1, v_2, .., v_n, v_{n+1}, w_1, w_2, .., w_n, b_O] \quad (5)$$

If the number of inputs is *n* then the number of features in a particle is 2*n*+2. The output of the model is calculated by Eq. 2 with the jth input pattern and assigned weights of kth particle. The fitness function of a particle is calculated as:

$$fitness_{train}(prticle_k) = \frac{1}{m}\left(\sum_{j=1}^{m}\left(O^j - T^j\right)^2\right)^{0.5} \quad (6)$$

Where O^j is the output of the jth input pattern and the related target is T^j. *m* is the total number of samples. The process flowchart of the proposed PSO-based EmNN is shown in Fig. 4.

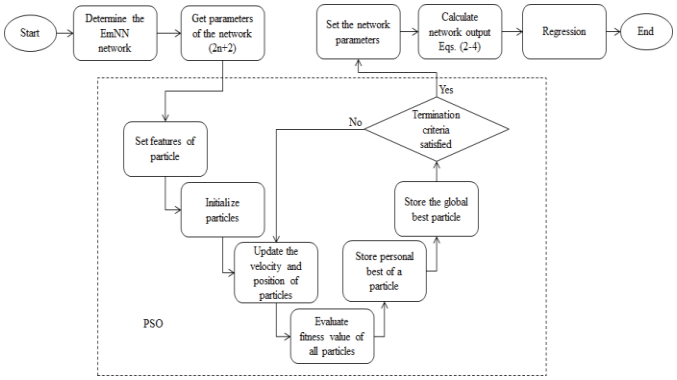

Fig. 4: Process flowchart of PSO-based EmNN

IV. RESULT ANALYSIS

The rainfall and discharge data of the catchment are considered as input to the proposed PSO-based EmNN model to predict next-day discharge. Based on the best performance of models [9], the 2 days lag of runoff value, and current day runoff and rainfall data are considered as the input for the proposed model. The PSO-ANN is used to compare with the proposed model. The catchment's data in between 2010-2015 is bifurcated as 70% training and 30% testing dataset.

To learn PSO-EmNN model, PSO parameters are initialized as: (i) c1=1, (ii) c2=2, (iii) w=0.7, and (iv) wdamp = 0.9. The number of populations is 30. The minimum and maximum values of particle features are considered as -5 and 5 respectively.

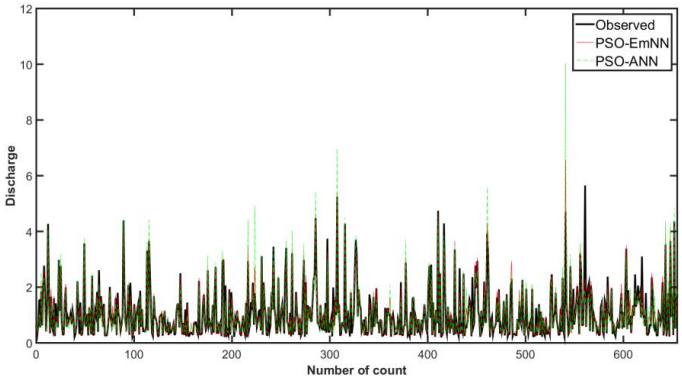

Fig. 5: Predicted vs. observed discharge in test period

The training dataset is used to learn the proposed model. PSO is used to tune 2n+2 number of EmNN model parameters. Where n is the number of inputs. After 50 numbers of run of PSO with EmNN generations, the lowest fitness valued particle is selected to fit the EmNN model. Thereafter, the test data set is used to predict the unknown one-day-ahead discharge.

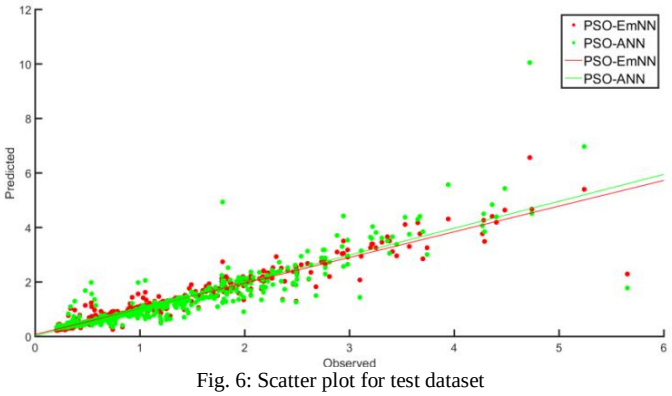

Fig. 6: Scatter plot for test dataset

Figure 5 shows the test case of PSO-ANN and PSO-EmNN. The proposed model shows better prediction capability compare to PSO-ANN. The scatter plot (Fig. 6) shows that the observed vs. predicted points are closer to the regression line of PSO-EmNN compare to observed vs. predicted points of regression line for PSO-ANN. Table 1 described the four performance measure metrics including r, MAE, NSE, and RMSE values of both models. From the Table 1, it is evident that proposed model has better prediction capability compare to PSO-ANN model in R-R modeling. Statistical comparison of training and testing phase with prediction of both models show PSO-EmNN is the most realistic model compare to PSO-ANN (Fig.7).

Table 1: The performance measure matric values of models

Model	R	MAE	NSE	RMSE
PSO-ANN (train)	0.907	0.201	0.819	0.462
PSO-ANN (test)	0.911	0.176	0.8	0.399
PSO-EmNN (train)	**0.936**	**0.132**	**0.876**	**0.383**
PSO-EmNN (test)	**0.964**	**0.106**	**0.929**	**0.238**

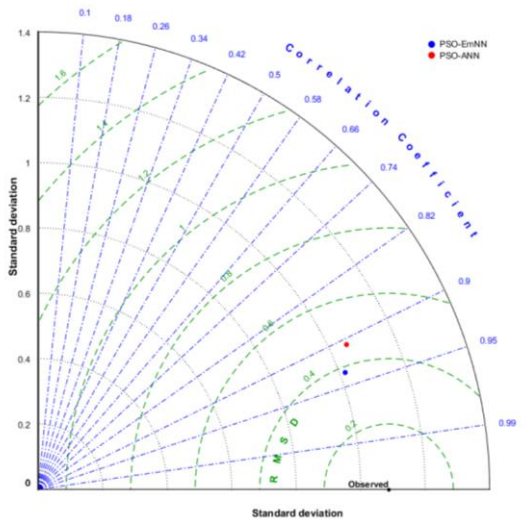

(a)

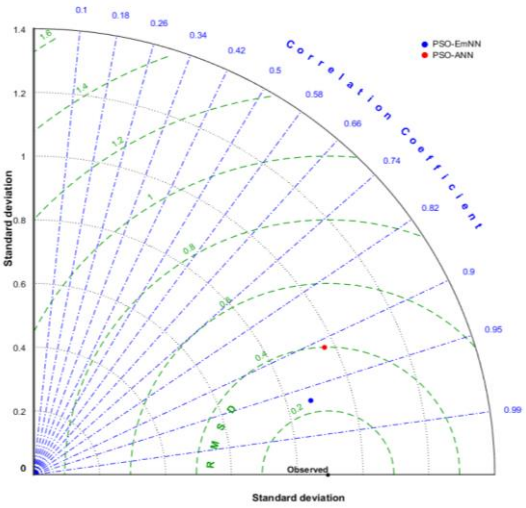

(b)

Fig. 7: The statistical comparison of predictions for both models in (a) training (b) testing phase

V. CONCLUSION

This paper developed a new PSO-based EmNN model and applied in R-R modeling in a catchment. The proposed model is compared with the PSO-based ANN model. The various performance metrics described the superiority of the PSO-EmNN compare to PSO-ANN. Therefore, it is a better alternative data-driven model for hydrological modeling and can be used in other engineering application area. Further, data from the other catchment should be used to validate the performance of the proposed model. Moreover, in future various hydrological models can be considered to compare with the performance of the proposed model in R-R modeling.

ACKNOWLEDGMENT

This research work was made possible by a grant from the Ministry of Electronics & Information Technology (MeitY), Government of India. We gratefully acknowledge the MeitY to provide the financial assistant during research work through "Visvesvaraya PhD Scheme for Electronics & IT".

REFERENCES

[1] Hromadka II, T., Rainfall-runoff models: a review. Environmental Software, 1990. 5(2): p. 82-103.

[2] Chang, W. and X. Chen, Monthly Rainfall-Runoff Modeling at Watershed Scale: A Comparative Study of Data-Driven and Theory-Driven Approaches. Water, 2018. 10(9): p. 1116.

[3] Abrahart, R.J., et al., Two decades of anarchy? Emerging themes and outstanding challenges for neural network river forecasting. Progress in Physical Geography, 2012. 36(4): p. 480-513.

[4] Badrzadeh, H., R. Sarukkalige, and A. Jayawardena, Hourly runoff forecasting for flood risk management: Application of various computational intelligence models. Journal of Hydrology, 2015. 529: p. 1633-1643.

[5] Chua, L.H., T.S. Wong, and L. Sriramula, Comparison between kinematic wave and artificial neural network models in event-based runoff simulation for an overland plane. Journal of hydrology, 2008. 357(3-4): p. 337-348.

[6] Campolo, M., P. Andreussi, and A. Soldati, River flood forecasting with a neural network model. Water resources research, 1999. 35(4): p. 1191-1197.

[7] Tongal, H. and M.J. Booij, Simulation and forecasting of streamflows using machine learning models coupled with base flow separation. Journal of hydrology, 2018. 564: p. 266-282.

[8] Lotfi, E. and M.-R. Akbarzadeh-T, Practical emotional neural networks. Neural Networks, 2014. 59: p. 61-72.

[9] Nourani, V., An emotional ANN (EANN) approach to modeling rainfall-runoff process. Journal of hydrology, 2017. 544: p. 267-277.

[10] Pavlos, G., et al., First and second order non-equilibrium phase transition and evidence for non-extensive Tsallis statistics in Earth's magnetosphere. Physica A: Statistical Mechanics and its Applications, 2011. 390(15): p. 2819-2839.

[11] Babaie, T., R. Karimizandi, and C. Lucas, Learning based brain emotional intelligence as a new aspect for development of an alarm system. Soft Computing, 2008. 12(9): p. 857-873.

[12] 12. Lotfi, E. and M. Akbarzadeh-T. Emotional brain-inspired adaptive fuzzy decayed learning for online prediction problems. in 2013 IEEE International Conference on Fuzzy Systems (FUZZ-IEEE). 2013. IEEE.

[13] Lotfi, E. and M.-R. Akbarzadeh-T. Supervised brain emotional learning. in The 2012 International Joint Conference on Neural Networks (IJCNN). 2012. IEEE.

[14] Lotfi, E. and M.-R. Akbarzadeh-T, Brain emotional learning-based pattern recognizer. Cybernetics and Systems, 2013. 44(5): p. 402-421.

[15] 15. Lotfi, E. and M.-R. Akbarzadeh-T, Adaptive brain emotional decayed learning for online prediction of geomagnetic activity indices. Neurocomputing, 2014. 126: p. 188-196.

[16] Khashman, A., A modified backpropagation learning algorithm with added emotional coefficients. IEEE transactions on neural networks, 2008. 19(11): p. 1896-1909.

[17] Khashman, A., Application of an emotional neural network to facial recognition. Neural Computing and Applications, 2009. 18(4): p. 309-320.

[18] Daryabeigi, E., G.A. Markadeh, and C. Lucas. Emotional controller (BELBIC) for electric drives—A review. in IECON 2010-36th Annual Conference on IEEE Industrial Electronics Society. 2010. IEEE.

[19] Rahman, M.A., et al., Implementation of emotional controller for interior permanent-magnet synchronous motor drive. IEEE Transactions on Industry Applications, 2008. 44(5): p. 1466-1476.

[20] Robinson, E.L., et al., Trends in atmospheric evaporative demand in Great Britain using high-resolution meteorological data. Hydrology and Earth System Sciences, 2017. 21(2): p. 1189-1224.

[21] Keller, V., et al., CEH-GEAR: 1 km resolution daily and monthly areal rainfall estimates for the UK for hydrological and other applications. Earth System Science Data, 2015. 7(1): p. 143-155.

[22] LeDoux, J., Emotion and the limbic system concept. Concepts in neuroscience, 1991. 2: p. 169-199.

[23] LeDoux, J., The emotional brain, fear, and the amygdala. Cellular and molecular neurobiology, 2003. 23(4-5): p. 727-738.

[24] LeDoux, J.E., Emotion circuits in the brain. Annual review of neuroscience, 2000. 23(1): p. 155-184.

[25] Dalgleish, T., The emotional brain. Nature Reviews Neuroscience, 2004. 5(7): p. 583.

[26] Lotfi, E., et al. Wind power forecasting using emotional neural networks. in 2014 IEEE International Conference on Systems, Man, and Cybernetics (SMC). 2014. IEEE.

[27] Herry, C., et al., Processing of temporal unpredictability in human and animal amygdala. Journal of Neuroscience, 2007. 27(22): p. 5958-5966.

[28] Bach, D.R. and R.J. Dolan, Knowing how much you don't know: a neural organization of uncertainty estimates. Nature reviews neuroscience, 2012. 13(8): p. 572.

[29] Eberhart, R. and J. Kennedy. A new optimizer using particle swarm theory. in MHS'95. Proceedings of the Sixth International Symposium on Micro Machine and Human Science. 1995. Ieee.

Proceedings of the Fourth International Conference on Communication and Electronics Systems (ICCES 2019)
IEEE Conference Record # 45898; IEEE Xplore ISBN: 978-1-7281-1261-9

Reconfigurable Warped Digital Filter Architecture for Hearing Aid

Kaustubh Banninthaya K.
Dept. Electronics and Communications
Atria Institute of Technology
(Affiliated to VTU)
Bangalore, India
kaus.bann@gmail.com

Niranjan N.
Dept. Electronics and Communications
Atria Institute of Technology
(Affiliated to VTU)
Bangalore, India
hegdeniranjan97@gmail.com

Risla Fathima P.
Dept. Electronics and Communications
Atria Institute of Technology
(Affiliated to VTU)
Bangalore, India
risla.fathima@gmail.com

Pranav Kumar M. P.
Dept. Electronics and Communications
Atria Institute of Technology
(Affiliated to VTU)
Bangalore, India
mppranavkumar97@gmail.com

Dr. Ipsita Biswas Mahapatra
Dept. Electronics and Communications
Atria Institute of Technology
(Affiliated to VTU)
Bangalore, India
ipsita_bm@atria.edu

***Abstract*—Digital filterbanks in hearing aids employ an array of filters to selectively amplify sound of different frequencies to compensate hearing loss. The use of filterbanks leads to a higher usage of silicon area as there are many filters, each generating a sub-band. Reconfigurable warped digital filter is a Variable Digital Filter (VDF) that can be reconfigured to function as a low-pass, band-pass or high-pass filter with cut-off frequencies that can be varied on-the-go. We propose a system with reconfigurable warped VDF that uses a single prototype filter for generating all the necessary sub-bands. The proposed system automates the generation of the control signals for reconfiguring the filter and pipelines the processing of each sub-band to generate the requisite magnitude response. The proposed architecture is designed to achieve good audiogram matching with minimum matching error.**

Keywords—digital hearing aid, variable digital filter, reconfigurable filter, audiogram matching.

I. INTRODUCTION

A Hearing aid is an electroacoustic device for compensating hearing loss. Hearing loss, as defined by the World Health Organisation (WHO), is the inability to hear 25 dB of sound in, at least one, ear. The WHO categorizes hearing loss as mild (25 to 40dB), moderate (41 to 60dB) and severe (60dB and greater) [1]. The increase in the hearing threshold caused due to hearing loss is not uniform over the range of audible frequencies i.e., there is low hearing sensitivity at certain frequencies. The hearing aid is used to selectively amplify the range of frequencies of sound at which a person experiences low sensitivity. An audiogram is a graph which gives a detailed description of a person's hearing threshold as a function of frequency. Audiograms are unique to the ears of every person; therefore, digital hearing aids are designed in such a way that it should be able to match any audiogram. Digital hearing aids make use of digital filterbanks to adjust the magnitude response for different frequencies of incoming sound signal such that it matches one's audiogram with minimum error.

Digital filterbank is an array filters that split the input signal into multiple sub-bands. Filterbanks used in digital hearing aids have three main components – the analysis block, the processing block and the synthesis block [2]. The analysis block splits the signal into multiple sub-bands. The processing block amplifies each of these sub-bands appropriately and the synthesis block combines all the processed sub-bands to generate the required output signal. A different filter is used to generate each sub-band in the filterbank, which translates to larger silicon area when implemented. A non-uniform filterbank, that generates sub-bands with varying bandwidths and centre frequencies, outperforms uniform filterbanks in terms of matching error and flexibility [3].

The objective of the proposed design is to use a single filter instead of a filterbank, which can be reconfigured without the need to update the structure or the filter coefficients, to generate-process-synthesize audio signals. To achieve the said objective, the reconfigurable warped digital FIR filter designed by Sumit J. Darak et al. in [5] is made use of in the proposed architecture. The filter design proposed in [5] has the capability of being reconfigured to function as low-pass, band-pass and high-pass filter on-the-go, along with fine control over cut-off frequency for low-pass and high-pass, and centre frequency and bandwidth for band-pass modes of operation. In this paper, an architecture is proposed that makes use of the reconfigurable warped digital FIR filter, designed in [5], along with the supporting control system to generate various sub-bands for the application of digital hearing aid. The proposed architecture is capable of generating requisite sub-bands by an automated process that applies minimal changes to the control parameters of the reconfigurable warped filter. The system processes the sub-bands and synthesizes the processed output to match audiograms in digital hearing aids. The proposed architecture inherently saves silicon area because a single filter is used to generate all the required sub-bands at no cost of reduced audiogram matching. The proposed architecture is designed to function like a non-uniform filterbank with comparable audiogram matching capability.

The paper is organized as follows. A survey on the existing filterbanks is presented in Section II. A review on the existing reconfigurable warped filter is given in Section III. The proposed system architecture is presented in Section IV. In Section V, the implementation and the results are presented. Finally, the paper is concluded in Section VI.

II. LITERATURE SURVEY

Various designs of non-uniform filterbanks have been researched recently where Variable Digital Filters (VDFs) are used for sub-band generation. VDFs are filters whose cut-off frequency fc can be changed on-the-fly [4]. Reconfigurable filters are filters whose mode of output responses (lowpass, highpass, band-pass and band-stop) can be changed on-the-fly

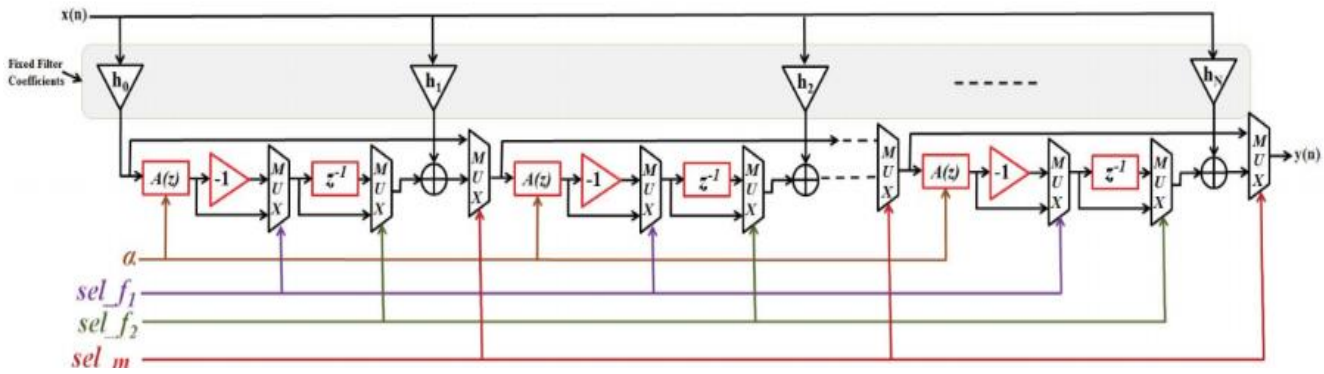

Figure 1. Reconfigurable Warped VDF [5]

[5]. A number of different approaches to VDF design are available. They include transformation approaches [6], Farrow structure-based approaches [7] – [9], and frequency response masking-based approach [10]. It would be beneficial to design a filter structure with a smaller number of bands and which can be reconfigured with minimum change in parameters. In [11], adaptive filters, which are warped filters, are designed using reduced second-order transformation and they provide fixed-bandwidth bandpass responses at an arbitrary centre frequency. However, if the bandwidth needs to be changed, the filter coefficients will need to be updated, which will incur a large number of memory read and write operations. In [12], a coefficient decimation (CDM) technique for realizing low-complexity VDFs with fixed coefficients is proposed. However, filters designed using this technique can only adopt a finite set of cut-off frequencies. In [5], a low-complexity reconfigurable VDF implementation by combining warped filters (using all-pass transform) along with CDM-II technique is proposed to achieve fine control of cut-off frequency over the entire Nyquist band for all 4 modes filter responses.

III. Reconfigurable Warped VDF

The reconfigurable warped VDF is proposed by Sumit J. Darak et al in [5]. The architecture provides variable low-pass and high-pass responses with a fine control over the cut-off frequency and variable bandwidth bandpass or bandstop responses at a tuneable centre frequency on-the-fly without the need to update the filter coefficients. The reconfigurable warped VDF filter architecture is shown in Fig 1 borrowed from [5]. The all pass structure is shown in Fig 2, borrowed from [5]. In this architecture, a low-pass prototype filter with fixed coefficients is used. The fixed-bandwidth bandpass/bandstop responses at an arbitrary centre frequency are obtained using reduced second order all-pass transformation, and the CDM technique is used to change the bandwidth.

When an all-pass structure is used in the place of a unit delay, warping occurs which can be mathematically described as follows,

$$G(z) = H(A(z)) \quad (1)$$

Where,

$$A(z) = \left(\frac{-\alpha + z^{-1}}{1 - \alpha z^{-1}}\right) \quad (2)$$

In this structure the filter coefficients are fixed. Here, α is the warping coefficient which controls the warped frequency response and |α| should be less than 1. The range of values of

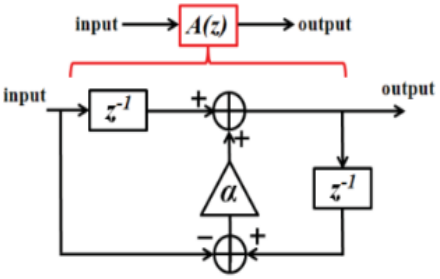

Figure 2. First order all-pass structure [5]

α from -1 to 0 increases the cut-off frequency while the range 0 to +1 decreases the cut-off frequency. At the value 0 of α, the cut-off frequency remains at the same value as that of the prototype filter. Coefficient Decimation (CDM) is implemented using the multiplexers controlled by signal sel_M. The actual multiplexer select line values are stored in lookup tables (LUTs) for each M, where M is the decimation factor, while sel_M provides the address for LUTs. The output of the previous coefficient's adder, which bypasses the present coefficient's operations, is connected to the 0th data-line of the multiplexer and the output of the present coefficient's adder is connected to the 1st data-line. The select signals, sel_f1 and sel_f2, to the two multiplexers after the all-pass structure decide the type of all-pass transform that is applied and thus the output response, i.e., low-pass, high-pass, band-pass, and band-stop responses with values {1,1}, {0,1}, {0,0}, and{1,0} respectively.

IV. Proposed System Architecture

The proposed architecture makes use of the reconfigurable warped filter proposed in [5] by building the necessary control system around the filter. The filter is reconfigured and reused to process the same input multiple times to generate and process each sub-band. This requires memory blocks on either side of the filter to store the input signal and intermediate output signals i.e., sub-bands. Then, the intermediate filter outputs are added together to generate the final output. The reconfigurable filter is operating at a higher rate to process all the required sub-bands, necessitating the use of memory block at the output for rate conversion.

The architecture is composed of 3 basic blocks – input memory block, reconfigurable filter block and synthesis block, shown in Fig 3. The memory block stores the incoming signal. The filter processes a data-block of *l* data elements in one configuration. The same data-block of *l* data elements is

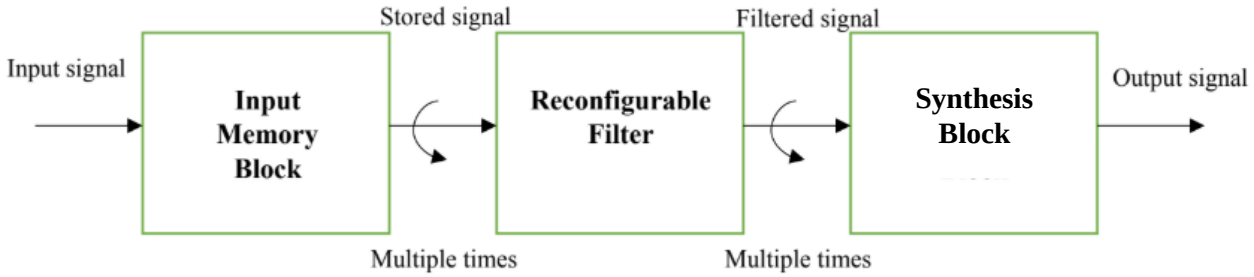

Figure 3. System block diagram

processed again in the next configuration. The output of the filter for each configuration is temporarily stored. At the end of N configurations, all the filter outputs for each configuration are added and the final output is stored. The stored final output is then read at the requisite rate, while at the same time, the filter starts working on the second data-block.

A. Input Memory Block

The incoming signal is stored in a RAM. The write address is generated by a counter counting from 0 to $2l - 1$ at a lower rate. The read address is generated by either of 2 enabled counters, one that counts from 0 to $l - 1$ and the other that counts from l to $2l - 1$, both at a rate of N times higher than the input datarate. Either one of the counters are enabled at any given time. The addresses 0 to $l - 1$ hold the odd indexed data-blocks while the addresses l to $2l - 1$ hold the even indexed data-blocks. Once a data-block is processed, it can be overwritten. Fig 5 shows the input memory block for N = 5 and l = 40000.

B. Reconfigurable Filter Block

The data read from the input memory block enters the reconfigurable filter block. For N configurations, N values of α, sel_f1, sel_f2, sel_M are precomputed and stored in memories. Additionally, the gain values for each of the N configurations are also stored. All the control signal values for each configuration are stored in identical memory locations. Therefore, a single counter counting from 0 to N – 1 incrementing at a rate of (N × Input datarate)/l, can generate the addresses for all the stored control signal values. An increment in the counter changes the control signal values entering the filter which leads to reconfiguration. An edge-detector connected to the same counter generates the reset pulse, such that all the delay elements within the filter are reset at the time of reconfiguration. Each configuration of the filter processes the read data-block of l data elements and generates an intermediate output that has l data elements. Fig 4 shows the reconfigurable filter block for N = 5 and l = 40000.

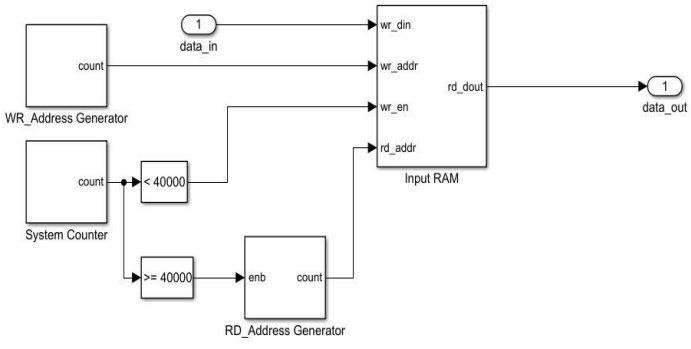

Figure 5. Input Memory Block

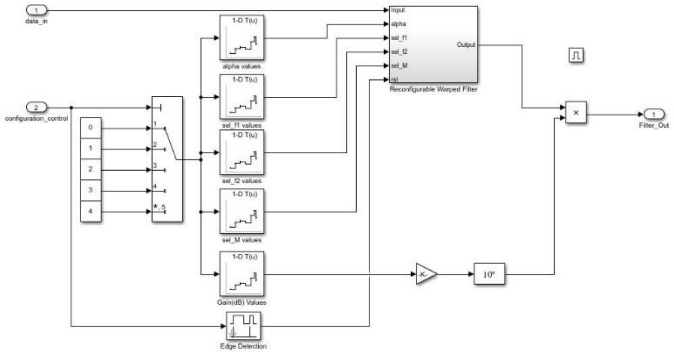

Figure 4. Reconfigurable Filter Block

Table 1 shows the values stored in the LUTs whose address is driven by sel_M and Table 2 shows the filter configurations decided by sel_f1 and sel_f2 values.

TABLE I. LUT STORED VALUES DRIVEN BY SEL_M

Tap No.	sel_M		
	M = 1	***M = 2***	***M = 3***
1	1	1	1
2	1	0	0
3	1	1	0
4	1	0	1
5	1	1	0
6	1	0	0
…	…	…	…

TABLE II. CONFIGURATIONS OF MODES OF OPERATION

Mode of operation	Control Signals	
	sel_f1	***sel_f2***
Low-pass	1	1
Band-pass	0	0
High-pass	0	1

For a given prototype lowpass filter with cut-off frequency β and the required cut-off frequency w_c, both in radians per second, the value for α can be computed by the formula given by [13],

$$\alpha = \frac{\sin(\frac{\beta - w_c}{2})}{\sin(\frac{\beta + w_c}{2})} \qquad (3)$$

For a given prototype lowpass filter with cut-off frequency β radians per second, a bandpass filter configuration of the reconfigurable warped filter has a passband region of β radians

per second. When CDM is applied with a decimation factor M, the passband region is given by [4],

$$Passband\ Bandwidth = M \times \beta \qquad (4)$$

C. Synthesis Block

The intermediate outputs for each of the filter configurations generated must be separately stored. Therefore, there are N registers, each of width l, that are enabled conditionally. A counter counting from 0 to N – 1 incrementing at a rate of $\frac{N \times Input\ datarate}{l}$, is compared to fixed index values to enable the correct registers. At the end of N configurations, all the registers are enabled again to add the outputs of each configuration and at the same time, the first configuration output of the next data-block from the filter is stored in the register. The output of the adder is stored in a RAM, with the write addresses generated by a counter counting from 0 to l – 1 at a rate of $N \times Input\ datarate$, and enabled at the same time as all the registers at the end of N configurations. The stored output in the RAM can be read and sent out as the final processed output at input datarate itself. Therefore, both the input RAM and the output RAM can use the same counters, only, write address generator for input RAM is used as read address for output RAM and read address generator for input RAM can be used as write address for output RAM. Fig 6 shows the synthesis block for N = 5 and l = 40000.

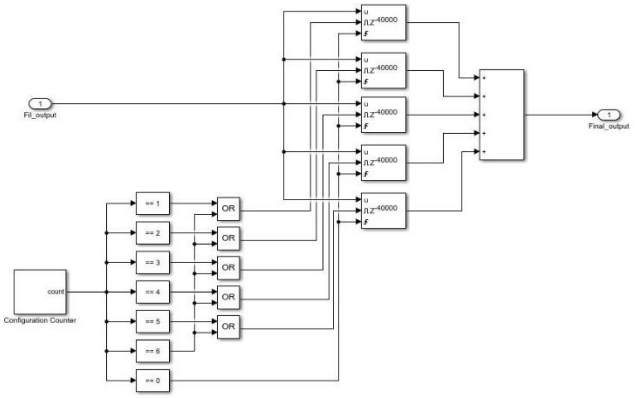

Figure 6. Synthesis Block

V. Implementation and Results

The above mentioned designed is modelled in Simulink using a prototype low-pass filter of the order n = 60, having a cut-off frequency of 500 Hz. The prototype filter has a stop-band attenuation of -60 dB and has 0 dB pass-band gain. The filter architecture is designed for a total number of configurations of N = 9, for a data-block size l = 20.

The audiogram, borrowed from [14], for mild-hearing loss at high frequencies is used for simulating the operation of the filter architecture for verifying audiogram matching operation and computing the matching error. The audiogram used is shown in Fig 7. The hearing sensitivity of the left ear is denoted by circles 'o' and that of the right ear is marked with 'x'. The audiogram for the right ear is used for result analysis here. The reconfigurable filter is reconfigured 9 times to generate 9 sub-bands of varying bandwidths and gains, to best match the audiogram. Equation (3) is used to compute the required α values. The control signals for each configuration is given in Table 3.

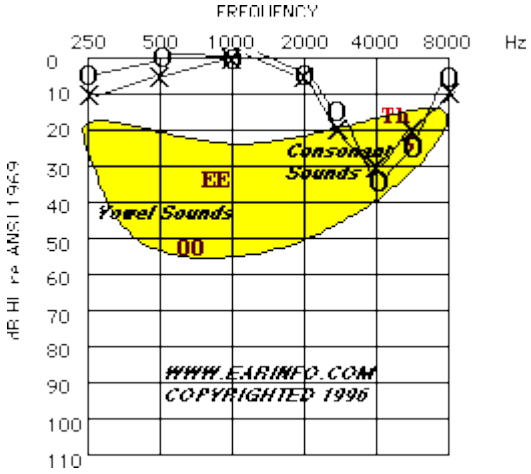

Figure 7. Audiogram for mild hearing loss

TABLE III. Control Signal Values for Simulation

Control Signals	Sub-bands								
	1	*2*	*3*	*4*	*5*	*6*	*7*	*8*	*9*
α	-0.2	0.9	0.75	0.67	0.42	0	-0.3	-0.55	0.6
sel_f1	1	0	0	0	0	0	0	0	0
sel_f2	1	0	0	0	0	0	0	0	1
sel_M	1	2	1	1	2	2	1	2	1
Gain(dB)	4	7	7	13	28	22	18	12	10

The audiogram matching is done by adding the cumulative effect of all the filter responses i.e., sub-bands generated by each configuration of the reconfigurable filter. Fig 8. shows the audiogram matching, where the overall filter response is shown in blue and the audiogram is shown in red. The audiogram matching is done with an error margin of ±6dB. Matching error is shown in Fig 9.

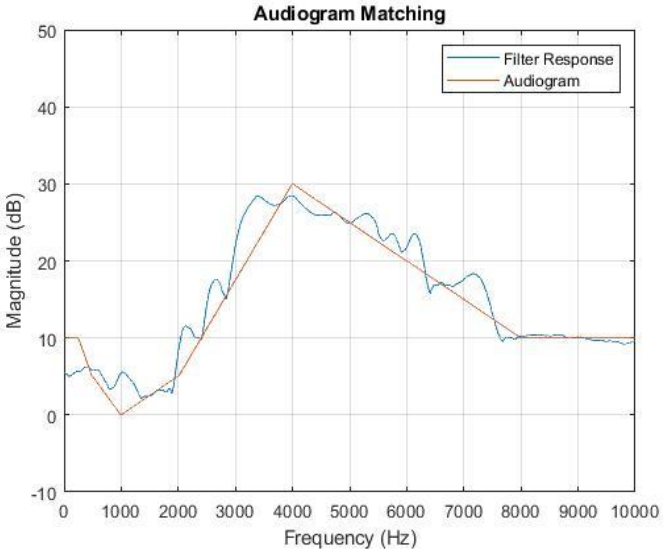

Figure 8. Audiogram Matching

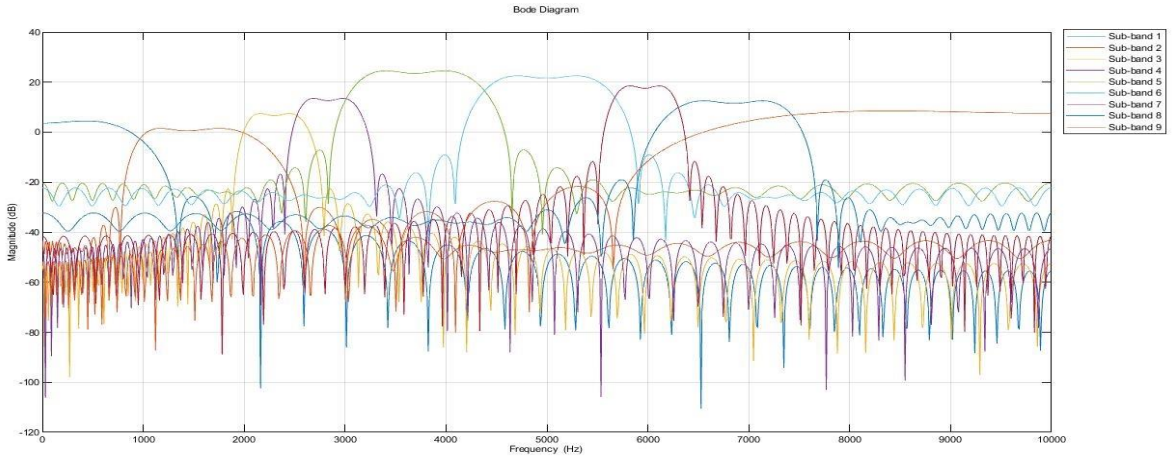

Figure 10. Sub-band Generation

The sub-band generated by each configuration is shown in Fig 10.

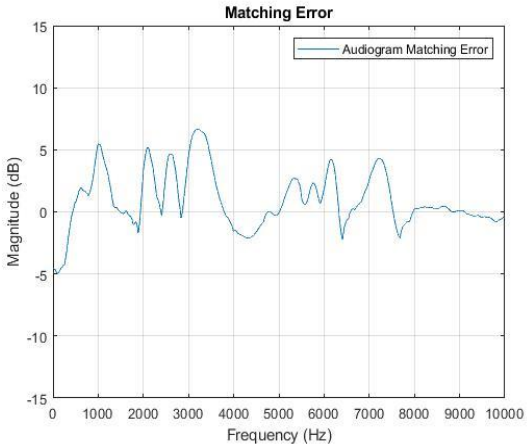

Figure 9. Matching Error

Using the error graph, the matching error is computed as 2.487dB, wherein matching error is the root-mean-squared value of error between the audiogram and the filter response. The matching error of 2.487dB and peak error of 6.1dB is comparable to the matching error in [14] where the same audiogram is used for the analysis of the results.

VI. Conclusion

Reconfigurable warped digital filter is a successfully made use of by the proposed system for the application in digital hearing aids. The proposed system successfully automates the generation of control signals for the reconfiguration of the filter from low-pass to band-pass and high-pass with the required cut-off frequencies. The necessary sub-bands with requisite gains are generated. The proposed system also processes the sub-bands in a pipelined manner to have the magnitude response for optimum audiogram matching. The system achieves good audiogram matching with low matching error comparable to other filterbank designs.

References

[1] G. Eason, B. Noble, and I. N. Sneddon, “On certain integrals of Lipschitz-Hankel type involving products of Bessel functions,” Phil.

[2] S. Raj and A. Shaji, "Design and implementation of reconfigurable digital filter bank for hearing aid," 2016 International Conference on Emerging Technological Trends (ICETT), Kollam, 2016, pp. 1-6.

[3] Ying Wei and Yong Lian, "A computationally efficient non-uniform digital FIR filter bank for hearing aid," IEEE International Workshop on Biomedical Circuits and Systems, 2004., Singapore, 2004, pp. S1/3/INV-S1/17.

[4] Sumedh D., Abhishek A., Smitha K. G., Sumit D. and, A. P. Vinod, "Variable Cutoff Frequency FIR Filters: A Survey," arXiv:1804.02891

[5] S. J. Darak, V. A. Prasad and E. M. -. Lai, "Efficient Implementation of Reconfigurable Warped Digital Filters With Variable Low-Pass, High-Pass, Bandpass, and Bandstop Responses," in IEEE Transactions on Very Large Scale Integration (VLSI) Systems, vol. 21, no. 6, pp. 1165-1169, June 2013.

[6] A. Oppenheim, W. Mecklenbrauker and R. Mersereau, "Variable cutoff linear phase digital filters," in IEEE Transactions on Circuits and Systems, vol. 23, no. 4, pp. 199-203, April 1976.

[7] S. C. Chan, C. K. S. Pun and K. L. Ho, "A new method for designing FIR filters with variable characteristics," in IEEE Signal Processing Letters, vol. 11, no. 2, pp. 274-277, Feb. 2004.

[8] P. Lowenborg and H. Johansson, "Minimax design of linear-phase FIR filters with adjustable bandwidths," 2004 IEEE International Symposium on Circuits and Systems (IEEE Cat. No.04CH37512), Vancouver, BC, 2004, pp. III-657.

[9] S. J. Darak, A. P. Vinod and E. M. Lai, "A new variable digital filter design based on fractional delay," 2011 IEEE International Conference on Acoustics, Speech and Signal Processing (ICASSP), Prague, 2011, pp. 1629-1632.

[10] Ya J. Y., Yong C. L., D. Shi, 2009, "Low -Complexity Design of Variable Bandedge Linear Phase FIR Filters with Sharp Transition Band," IEEE Transactions on Signal Processing, vol. 57, no. 4, pp. 1328-1338.

[11] S. Koshita, Y. Kumamoto, M. Abe and M. Kawamata, "High-order center-frequency adaptive filters using block-diagram-based frequency transformation," 2011 IEEE International Conference on Acoustics, Speech and Signal Processing (ICASSP), Prague, 2011, pp. 4284-4287.

[12] R. Mahesh and A. P. Vinod, "Low complexity flexible filter banks for uniform and non-uniform channelisation in software radios using coefficient decimation," in IET Circuits, Devices & Systems, vol. 5, no. 3, pp. 232-242, May 2011.

[13] A. G. Constantinides, “Spectral transformations for digital filters,” Proc.Inst. Electr. Eng., vol. 117, no. 8, pp. 1585–1590, Aug. 1970.

[14] A. S. Reshma and M. Manuel, "Reconfigurable digital FIR filter bank for hearing aids using minimax algorithm," 2017 International Conference on Trends in Electronics and Informatics (ICEI), Tirunelveli, 2017, pp. 803-808.

Proceedings of the Fourth International Conference on Communication and Electronics Systems (ICCES 2019)
IEEE Conference Record # 45898; IEEE Xplore ISBN: 978-1-7281-1261-9

SUPPRESSION OF CROSS POLARIZATION WITH VARIOUS GEOMETRIES OF DGS IN THE DESIGN OF MICROSTRIP PATCH ANTENNA

B Naveen reddy[1] ,M Hema dharani[2],S Pavithra[3],A Sivapradhayni[4], Mekaladevi V[5]
Department of Electronics and Communication Engineering
Amrita school of Engineering, Coimbatore
Amrita Vishwa Vidyapeetham, India
{pavithrasasi9722@gmail.com, v_mekaladevi@cb.amrita.edu}

***Abstract*— In this paper, microstrip patch antenna is designed with different geometries on the ground plane to achieve low cross polarization level. Linear shaped Defected ground structure (DGS) and fractal defected ground structure (FDGS) have been used to suppress the cross polarization. A microstrip patch antenna with FDGS is designed with lossy substrate FR-4 at 2.2GHz using Ansoft HFSS simulator. Moreover, it is observed that FDGS shows low XP level of -72dB with good return loss and gain.**

Keywords—Square Patch antenna, Cross Polarization(XP), Defected Ground Structure (DGS), Fractal Defected Ground Structure (FDGS).

I. INTRODUCTION

In many applications, antennas should propagate in similar polarization to achieve an optimal performance. A purely polarized antenna will have low cross polarization level. Definitions and applications of XP level are explained in [8]. Formerly, there are number of investigations related with appliance of DGS in reducing the cross-polarization radiation of microstrip patch antennas.Microstrip antenna technology and performance of patch antennas are described in[10][12]. DGS is applied by integrating slots or defects on the ground plane of the microstrip patch antenna. There are various shapes of DGS. Circular patch antenna which has been etched with two circular slots on ground to suppress XP level (5-8dB) has been studied [7] with bandwidth of 160MHz. L shaped asymmetric DGS has been implemented for probe-fed circular microstrip antenna [2] with XP level suppressed up to -15dB. DGS has been used for effective suppression in XP radiation up to -30dB [1] in prob- fed microstrip antenna. In probe fed circular microstrip patch antenna the XP level has been suppressed by (10-12dB) [3]. Circularly polarized patch antenna with arc shaped DGS has suppressed XP level from (18-30dB) [4]. In [6] they have explored circularly polarized microstrip antenna with two different DGS geometries, namely circular ring with suppression (5-7dB) and two arc shaped DGS with suppression (7-12dB). XP suppression level of (7-12dB) has been achieved in [5] with Circular microstrip patch antenna having arc shaped DGS.Since a simple and compact microstrip patch antenna has not yet been designed with low XP level. So, in this paper, a microstrip patch antenna with FDGS has been proposed with low XP level to ensure high isolation between desired and undesired signal.

II. ANTENNA GEOMETRY AND WORKING PRINCIPLE

The proposed antenna is designed to operate at 2.2 GHz. Frequency with FR-4 substrate of dielectric constant 4.4 and thickness 1.6mm. The antenna geometry is chosen as per the equations given below. The ground and patch dimensions are optimized using parametric analysis in HFSS.This antenna is fed using co-axial feed line.

A. Mathematical design

The dimensions of proposed antenna:

- Patch width:

$$W=\frac{c}{2f_r\sqrt{\frac{\epsilon_r+1}{2}}}$$

Where c=speed of light

f_r=resonant frequency

- Patch length(L):

$$L= L_{eff} - 2\Delta L$$

Where $L_{eff} = \frac{c}{2f_r\sqrt{\epsilon_{reff}}}$

$$\Delta L = 0.412h\frac{(\epsilon_{eff}+0.3)\left(\frac{W}{h}+0.264\right)}{(\epsilon_{eff}-0.258)\left(\frac{W}{h}+0.8\right)}$$

- Substrate height(h):

$$\frac{W}{h} >1$$

- Effective dielectric constant (ϵ_{eff}):

$$\epsilon_{eff}=\frac{\epsilon_r+1}{2}+\frac{\epsilon_r-1}{2}\left[1+12\frac{h}{W}\right]^{-0.5}$$

- Ground plane dimension:

$$L_g = L + 6h$$
$$W_g = W + 6h$$

B. *Simple microstrip patch antenna*

A basic microstrip square patch antenna without DGS has been designed for comparative analysis with the proposed antenna with different DGS geometries. Microstrip patch antenna without DGS has been implemented in High-Frequency Structure Simulator (HFSS). It is shown in the Fig. 2.

C. *Microstrip patch antenna with DGS*

The DGS is implemented by placing a slot on the ground plane and adjusted in such a way that it will provide efficient coupling and suppresses the higher order modes. TM_{02} mode is the higher order mode in a rectangular or square microstrip patch antenna. A vertically polarized strong field located near the patch edges ensures the excitation of TM_{02} mode. So, in the design we need to check where the vertically polarized strong fields are located and DGS should be employed on that field ensuring that it should suppress that fields.

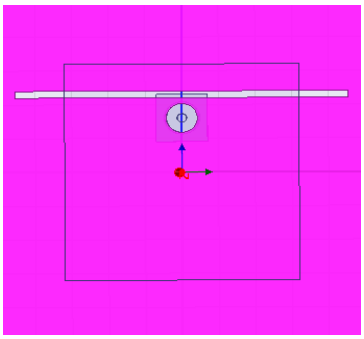

Fig. 1. Square patch antenna with linear shaped DGS

In the design the vertically polarized strong fields appeared at the edges of the patch. So the DGS should be placed on either one of the patch edges. Once the position at which DGS has to be placed is fixed, we need to select the shape of the DGS that we implement. There are different shapes of DGS such as circular, spiral, square, rectangle, L- shaped, Dumbbell, V shaped, U shaped and so on.

D. *Microstrip patch antenna with linear shaped FDGS*

The Linear slot DGS is used as the reference for the FDGS as a self-iterative structure. And as for the positioning it is similar to the design of the DGS.Ansoft High Frequency Structure simulation (HFSS) is used to analyze the performance of antenna. The optimized parameter values of this antenna are:
Ground and patch dimensions:
W_P=32mm, Lp=32mm, Ws=50mm, Ls=50mm
FDGS dimensions:
L_1=10mm, L_2=5mm, W_1=2.5mm, W_2=1.5mm

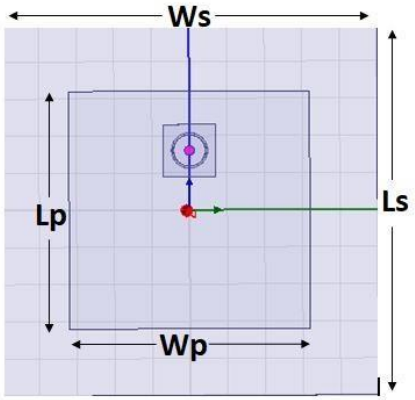

Fig. 2. Microstrip patch antenna

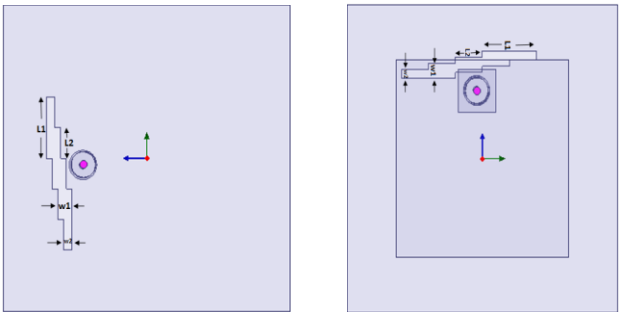

a) b)

Fig. 3 a) FDGS with parameters b) MSP with FDGS

III. SIMULATED RESULTS

XP level plot of the microstrip antenna has been analyzed and the value is 51.2dB. Here XP level has been measured as the distance between the actual polarization and polarization which is 90˚ to that. In the plot two graphs have been plotted with same frequency for $\phi=0^{\circ}$ and $\phi=90^{\circ}$ and the difference between them came to be 51.2dB. For the betterment of XP level suppression, different slot shapes have been attempted.

In this design of microstrip patch antenna with Linear shaped DGS XP level has been suppressed up to -67 dB is shown in Fig. 4.

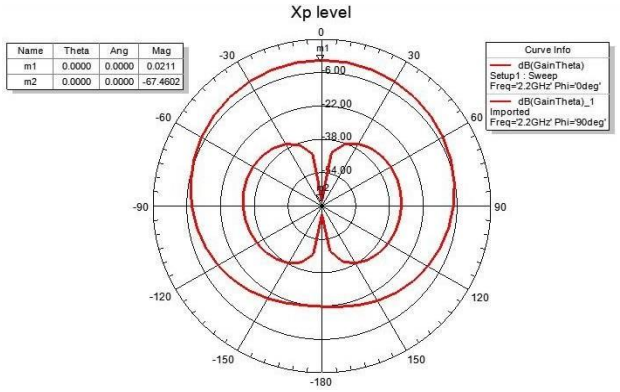

Fig. 4. XP level plot for linear shaped DGS.

E. Microstrip patch antenna with FDGS

In the appliance of linear shaped fractal DGS, the XP level is -72dB.The change in FDGS dimensions will not affect the resonant mode original design. The XP graph with each iterative FDGS geometry is presented for comparison. At the fourth iterative it shows an incremental result obtaining XP level -72dB (Fig. 5.).

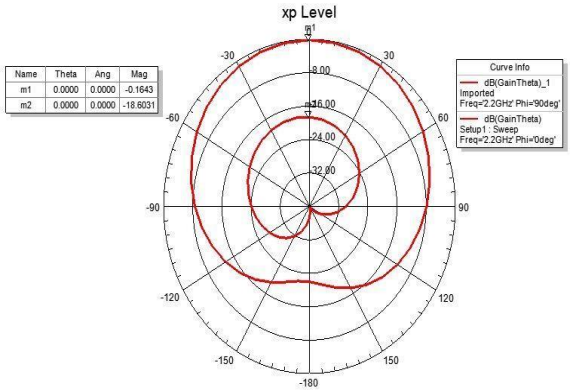

a)

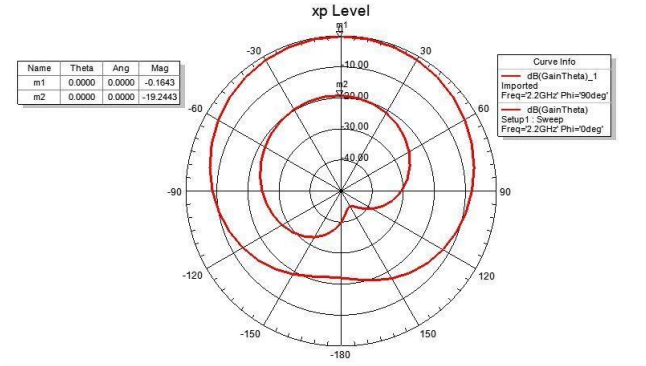

b)

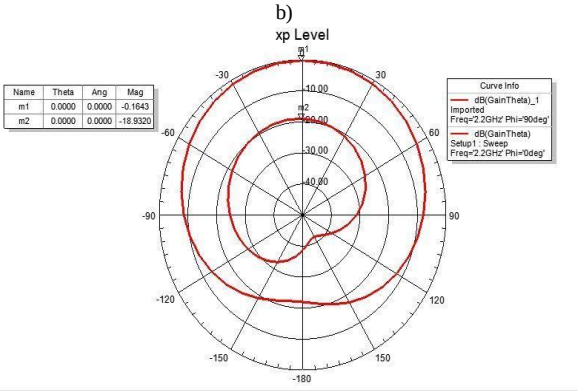

c)

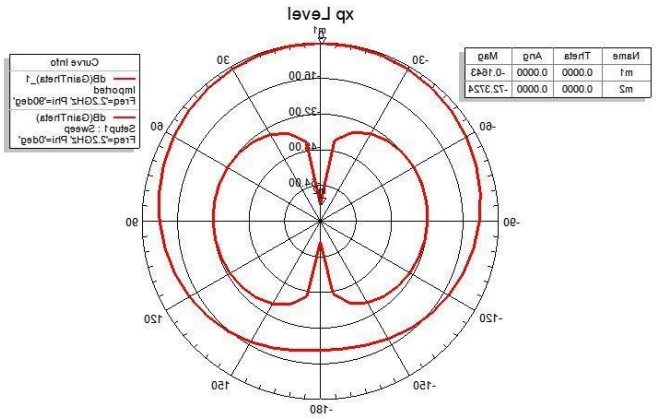

d)

Fig. 5. a) XP plot for 1st iterative. b) XP plot for 2nd iterative c)XP plot for 3rd iterative. d)XP plot for 4th iterative

TABLE 1: XP Suppressions for the different geometries on the ground plane of microstrip patch antenna.

Patch	Design	Geometry	XP suppression
Square	Without DGS	Without DGS	-51dB
Square	With DGS	Linear shaped	-67dB
Square	With FDGS	Linear shaped	-72dB

IV. CONCLUSION

Basic microstrip patch antenna with two different geometrics of DGS have been designed and analysed. With comparative results, it was observed that microstrip path antenna design with FDGS has attained the maximum XP suppression which probably increases the antenna performance. The comparative results are shown in table 1. The proposed design has improved the suppression of XP upto -72dB. Thus, the propounded concept has been implemented to achieve low cross polarization level ensuring the good performance of antenna.

References

[1] C. Kumar and D. Guha, "Asymmetric Geometry of Defected Ground Structure for Rectangular Microstrip: A New Approach to Reduce its Cross-Polarized Fields," *IEEE Trans. Antennas Propag.*, vol. 64, no. 6, pp. 2503–2506, 2016.

[2] C. Kumar, "Nature of Cross-Polarized Radiations from Probe-Fed Circular Microstrip Antennas and Their Suppression Using Different Geometries of Defected Ground Structure (DGS)," *IEEE Trans. Antennas Propag.*, vol. 60, no. 1, pp. 92–101, 2011.

[3] A. Ghosh *et al.*, "Rectangular microstrip antenna with defected patch surface for improved polarization purity," *Proc. 2015 3rd Int. Conf. Comput. Commun. Control Inf. Technol. C3IT 2015*, pp. 1–5, 2015.

[4] C. Kumar and D. Guha, "New Defected Ground Structures (DGSs) to reduce cross-polarized radiation of circular microstrip antennas," *Appl. Electromagn. Conf. AEMC 2009 URSI Comm. B Meet.*, pp. 1–4, 2009.

[5] A. D. Ground and S. Dgs, "Improved Cross-Polarization Characteristics of Circular Microstrip Antenna Employing," *IEEE Antennas Wirel. Propag. Lett.*, vol. 8, pp. 1367–1369, 2010.

[6] G. Singh, R. Rajni, and R. Singh Momi, "Microstrip Patch Antenna with Defected Ground Structure for Bandwidth Enhancement," *Int. J. Comput. Appl.*, vol. 73, no. 9, pp. 14–17, 2013.

[7] A. C. Ludwig, "The definition of cross polarization," *IEEE Trans. Antennas Propag.*, pp. 116–119, 1973.

[8] S. Samanta, P. S. Reddy, and K. Mandal, "Cross-Polarization Suppression in Probe-Fed Circular Patch Antenna Using Two Circular Clusters of Shorting Pins," *IEEE Trans. Antennas Propag.*, vol. 66, no. 6, pp. 3177–3182, 2018.

[9] G. Sudhakaran, B. Kandipati, G. B. Surya, V. K. Shree, M. Sivaprasad and M. Jayakumar, "Evolutionary algorithm based structural optimization for patch antenna design and its performance analysis," 2017 International Conference on *Advances in Computing, Communications and Informatics (ICACCI)*, Udupi, 2017, pp. 2189-2192

[10] Mouna H, Mekaladevi V and Nirmala Devi M, "Design of Microwave Absorbers using Improvised Particle Swarm Optimization Algorithm,"J. Microw. Optoelectron.Electromagn. Appl. vol.17 no.2 São Caetano do Sul Apr./June 2018

[11] Guha, D., Biswas, M., and Antar, Y.M.M., "Microstrip Patch Antenna With Defected Ground Structure for Cross Polarization Suppression", IEEE Antennas and Wireless Propagat. Lett., vol. 4, pp.455-458,2005

[12] K. Carver and J. Mink, "Microstrip antenna technology," *IEEE Trans. Antennas Propag.*, vol. 29, no. 1, pp. 2–24, Jan. 1981.

Proceedings of the Fourth International Conference on Communication and Electronics Systems (ICCES 2019)
IEEE Conference Record # 45880; IEEE Xplore ISBN: 978-1-7281-1261-9

Enhancing Security of AES Using Key Dependent Dynamic Sbox

Yashvir Singh Chauhan
School of VLSI Design and Embedded Systems
National Institute of Technology Kurukshetra
Kurukshetra, India
Chauhanyash23@gmail.com

T.N. Sasamal
Department of Electronics and Communication Engineering
National Institute of Technology Kurukshetra
Kurukshetra, India
tnsasamal.ece@nitkkr.ac.in

***Abstract*— Nowadays most of the data transmission is done through digital communication and hence security and efficient data transmission is always a desirable property for any data communication. At present, Advance encryption standard (AES) is most widely used cryptographic technique. This AES uses static s box for encryption and decryption which remains constant irrespective of the key. Numerous analysts have experimented and revealed that there are some weak points [1] in the static s-box as it is static and known to all. Therefore, in our proposed algorithm we modify AES such that it uses dynamic sbox which is key dependent and compare the avalanche effect of basic AES with our proposed algorithm.**

Keywords—Advance encryption standard(AES),Avalanche effect, Strict avalanche criterion(SAC),Dynamic S-box.

I. INTRODUCTION

Information has been an utmost priority of concern for any country's security. Therefore, there was a strict need for building a highly secure encryption algorithm. In 1997, National institute of standards and technology (NIST)[2] adapted AES as a new cryptographic algorithm to replace age long DES. Vincent Rijmen and Joan Daemen[3] named this algorithm as Rijndael and submitted to NIST where their algorithm was selected among 15 participants.

Since most of the block ciphers uses static s box which is the only non-linear part in AES. So, there was a strict need to make this nonlinear part dynamic that is making it key dependent [4]. Many authors have tried to change s box in the case of-

Krishnamurthy[5]in this paper they created dynamic behavior in sbox by rotating the sbox and this rotation value was key dependent and compared avalanche effect[6] of basic AES with their proposed AES but this scheme has a more complicated decryption algorithm.

Abdullah al mamun[7]in this paper they used random byte to modify s box by performing ex-or on all bytes of s box and hence discussing parameters like time security, avalanche effect and strict avalanche criterion. But this algorithm didn't have key dependent sbox.

Harshali zodpe[8]this paper enhances the security features of AES.in this they have generated a new algorithm for constructing s box and key scheduling algorithm using a PN sequence generator i.e. they have designed PN sequence generator using a 8 bit LFSR and compared avalanche effect of both algorithms and found satisfactory results, but this algorithm violates the basic construction of AES.

Jurumi[9] in this paper they added an extra block in encryption named s-box rotation which uses an offset, generated by performing ex-or on all bytes of round key and the resulting bytes were used to rotate the sbox. Also, they compared avalanche effect on different samples for both schemes and found satisfactory results.

This paper is organized in such a manner that section II consist the explanation of basic AES. In Section III we have described our proposed algorithm which makes sbox key dependent by modifying basic sbox and simulated using Isim simulator from Xilinx ISE. The simulated results are shown in section IV and conclusion in section V.

II. BASIC AES

Advance encryption system is symmetric cipher which uses the same key for encryption as well as decryption. AES is a block cipher which performs operations on blocks of data. AES uses 128-bit plaintext and uses variable keys viz 128,192 and 256. Depending on the size of the key it performs different rounds of operations i.e.10 rounds for 128 bit key, 12 rounds for 192 bit key and 14 rounds for 256 bit key. At present, the most used key size is 128 bit[10].

At internal level of AES, cipher key is expanded to 11, 13 and 15 keys for 10, 12 and 14 rounds respectively. Then the plaintext is copied into an array named state array. State array is 4x4 matrix where each array contains byte of plaintext arranged horizontally [11].

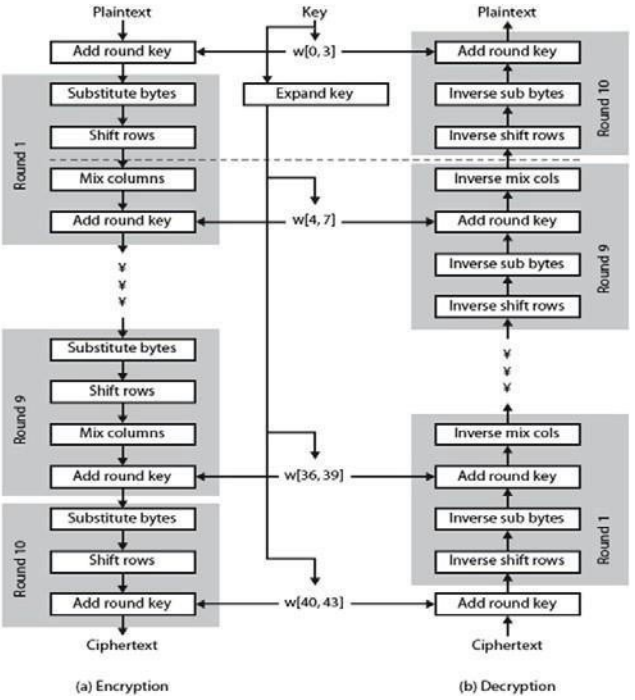

Fig. 1. AES algorithm

A. *Key expansion*

AES involves a key scheduling algorithm which generates a 128 bit unique key for each set of rounds. This algorithm performs operations on words each of word length of 32 bits. Therefore, a key consists of 4 words.

The operations performed in each round to generate a new key are-

- The last word of previous round is rotated 8 bits to the left
- The resulting four bytes are substituted with sbox
- The resulting four bytes are XORed with the first word of the previous round.
- The first byte of result four byte is XORed with round constant (Rcon) that varies for each round.

B. *Add round key*

- It is the initial step of encryption process and also a important step in each round.in this step, 128 bit plaintext array is xor-ed with 128 bit key which is also formed as a state array generating a 128 bit output.

C. *Sub Bytes*

Sub bytes stands for substitution of byte, in this step each byte is substituted with a byte from a 16x16 look up table which contains 256 distinct values. The 16x16 look up table is named as substitution box or S-box.

To substitute a byte from state array, the input left most 4 bits denotes row and right most 4 bits denotes column of s box. Suppose the input byte is a4.so, we inspect rows for a(inhex) and column 4(in hex) and their intersection gives the resultant output.

x \ y	0	1	2	3	4	5	6	7	8	9	a	b	c	d	e	f
0	63	7c	77	7b	f2	6b	6f	c5	30	01	67	2b	fe	d7	ab	76
1	ca	82	c9	7d	fa	59	47	f0	ad	d4	a2	af	9c	a4	72	c0
2	b7	fd	93	26	36	3f	f7	cc	34	a5	e5	f1	71	d8	31	15
3	04	c7	23	c3	18	96	05	9a	07	12	80	e2	eb	27	b2	75
4	09	83	2c	1a	1b	6e	5a	a0	52	3b	d6	b3	29	e3	2f	84
5	53	d1	00	ed	20	fc	b1	5b	6a	cb	be	39	4a	4c	58	cf
6	d0	ef	aa	fb	43	4d	33	85	45	f9	02	7f	50	3c	9f	a8
7	51	a3	40	8f	92	9d	38	f5	bc	b6	da	21	10	ff	f3	d2
8	cd	0c	13	ec	5f	97	44	17	c4	a7	7e	3d	64	5d	19	73
9	60	81	4f	dc	22	2a	90	88	46	ee	b8	14	de	5e	0b	db
a	e0	32	3a	0a	49	06	24	5c	c2	d3	ac	62	91	95	e4	79
b	e7	c8	37	6d	8d	d5	4e	a9	6c	56	f4	ea	65	7a	ae	08
c	ba	78	25	2e	1c	a6	b4	c6	e8	dd	74	1f	4b	bd	8b	8a
d	70	3e	b5	66	48	03	f6	0e	61	35	57	b9	86	c1	1d	9e
e	e1	f8	98	11	69	d9	8e	94	9b	1e	87	e9	ce	55	28	df
f	8c	a1	89	0d	bf	e6	42	68	41	99	2d	0f	b0	54	bb	16

Fig. 2. AES sbox

D. *Shift rows*

This step performs left shift cyclically on different rows. Such as first row of state array is left unchanged, second row is shifted 1 time, third row is shifted 2 times and third row is shifted three times cyclically to the left.

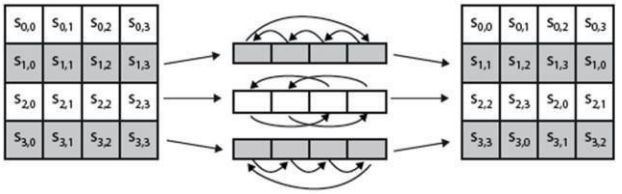

Fig. 3. Shift row operation

E. *Mix column*

This step takes a column from state array and provides matrix multiplication with affixed matrix and produces a output column.

$$\begin{bmatrix} 02 & 03 & 01 & 01 \\ 01 & 02 & 03 & 01 \\ 01 & 01 & 02 & 03 \\ 03 & 01 & 01 & 02 \end{bmatrix} \begin{bmatrix} s_{0,0} & s_{0,1} & s_{0,2} & s_{0,3} \\ s_{1,0} & s_{1,1} & s_{1,2} & s_{1,3} \\ s_{2,0} & s_{2,1} & s_{2,2} & s_{2,3} \\ s_{3,0} & s_{3,1} & s_{3,2} & s_{3,3} \end{bmatrix} = \begin{bmatrix} s'_{0,0} & s'_{0,1} & s'_{0,2} & s'_{0,3} \\ s'_{1,0} & s'_{1,1} & s'_{1,2} & s'_{1,3} \\ s'_{2,0} & s'_{2,1} & s'_{2,2} & s'_{2,3} \\ s'_{3,0} & s'_{3,1} & s'_{3,2} & s'_{3,3} \end{bmatrix}$$

Fig. 4. Mix column operation

III. PROPOSED ALGORITHM

This proposed algorithm consists the same set of rounds as performed on normal AES. Here the key dependent sbox is generated by performing operations on basic sbox and hence we don't violate basic construction of AES and rather enhance the security of basic AES.

We perform following steps to generate key dependent s box-

Encryption

- Select an initial key for encryption.
- Key[z] is selected from lower byte of round key.
- Generate s box, as generated in standard AES as SBOX[i].
- Computing dynamicSBOX[i] =SBOX[i] ⊕ key[z].
- Substitute each byte from dynamicSBOX[i] and continue for each round

Decryption

- Select key[z] from lower byte of round key.
- Generate inverse s box, as generated in standard AES as invSBOX[i].
- Computing invdynamicSBOX[i] =invSBOX[i] ⊕ key[z].
- Retrieving each text by substituting each byte from invdynamicSBOX[i].
- Continue performing above steps for each round.

A. AVALANCHE EFEECT

Avalanche effect is a very important property for a block cipher. It gives the idea that how does output varies by changing one bit in the plaintext. The degree of randomness is calculated through avalanche effect. If the avalanche effect is not of higher degree than cryptanalyst can guess the plaintext by monitoring the cipher text. The avalanche effect is calculated as-

$$\text{Avalanche effect} = \frac{\text{number of times cipher bit changes}}{\text{Total number of bits in plaintext}}$$

Strict avalanche criterion

To measure diffusion and confusion for an algorithm SAC property is used.it was introduced first by Webster and Tavares in 1985[13]. For a function to satisfy SAC it should change the output bits at least by 50% probability when input bits are flipped.

IV. Experimental results

We have simulated AES encryption and proposed AES encryption on Xilinx ISE 14.7. To study avalanche effect, we have considered plaintext 'a56dc6d5230d9529d96c95c019604d10'and key

'31d851641c5044465d8012fa5ce640b6' and generated cipher text for both algorithms.

Then first bit of plaintext is flipped and its variations is compared with the previous cipher text. This is repeated 18 times by flipping various bits of plaintext as shown by bit variance index and at last changing 128th bit of plaintext and compare its cipher text with the cipher text of the original plaintext.

Fig. 3. Simulation of basic AES for bit variance index at 1

Fig 4 Simulation of proposed AES for bit variance index at 1

	0	1	2	3	4	5	6	7	8	9	a	b	c	d	e	f
0	d5	ca	c1	cd	44	dd	d9	73	86	b7	d1	9d	48	61	1d	c0
1	7c	34	7f	cb	4c	ef	f1	46	1b	62	14	19	2a	12	c4	76
2	01	4b	25	90	80	89	41	7a	82	13	53	47	c7	6e	87	a3
3	b2	71	95	75	ae	20	b3	2c	b1	a4	36	54	5d	91	04	c3
4	bf	35	9a	ac	ad	d8	ec	16	e4	8d	60	05	9f	55	99	32
5	e5	67	b6	5b	96	4a	07	ed	dc	7d	08	8f	fc	fa	ee	79
6	66	59	1c	4d	f5	fb	85	33	f3	4f	b4	c9	e6	8a	29	1e
7	e7	15	f6	39	24	2b	8e	43	0a	00	6e	97	a6	49	45	64
8	7b	ba	a5	5a	e9	21	f2	a1	72	11	cd	8b	d2	eb	af	c5
9	b6	37	f9	6a	94	9c	26	3e	f0	58	0e	a2	68	e8	bd	6d
a	56	84	8c	bc	ff	b0	92	ea	74	65	1a	d4	27	23	52	cf
b	51	7e	81	db	3b	63	f8	1f	da	e0	42	5c	d3	cc	18	be
c	0c	ce	93	98	aa	10	02	70	5e	6b	c2	a9	fd	0b	3d	3c
d	c6	88	03	d0	fe	b5	40	b8	d7	83	e1	0f	30	77	ab	28
e	57	4e	2e	a7	df	6f	38	22	2d	a8	31	5f	78	e3	9e	69
f	3a	17	3f	bb	09	50	f4	de	f7	2f	9b	b9	06	e2	0d	a0

Table 1 Dynamic s box of proposed algorithm for round 1

In the above table we have generated dynamic sbox for the first round by using last bytes of round key. Similarly, we can have different s box for different rounds. Therefore, multiple sbox can be generated and hence static behavior of sbox from AES can be avoided hence improving its security. In the below table we have shown avalanche effect variations of basic and proposed AES.

Bit variation index	Plaintext	Cipher text of normal AES	Bit variations
0	a56dc6d5230d9529d96c95c019604d10	4358eda15e52bda915d2768deb9cdb8d	
1	a56dc6d5230d9529d96c95c019604d11	01ba097f1c1d9c095b5b3c397b4fe9e8	55
2	a56dc6d5230d9529d96c95c019604d12	401e3a130088a91fa83d3b78a6eb3d4b	74
8	a56dc6d5230d9529d96c95c019604d90	1438b961ea5f5b54865d0d5a0d8273b0	69
16	a56dc6d5230d9529d96c95c01960cd10	75411c85076732769bfa672f1e83babd	61
24	a56dc6d5230d9529d96c95c019e04d10	e12642ece0e7b0dc999b9404a354100f	63
32	a56dc6d5230d9529d96c95c099604d10	8b07ffff83569f53c63c6bc6bd6008cc	67
40	a56dc6d5230d9529d96c954019604d10	246e14cffcf3ddad7919d7a3ff4abec8	59
48	a56dc6d5230d9529d96c15c019604d10	3132e67ff43162d42269710831cd5675	72
56	a56dc6d5230d9529d9ec95c019604d10	43a6714a0acc64a135218abd33db24ec	65
64	a56dc6d5230d9529596c95c019604d10	537f72876d82ad0831cd1f40d24b34f	60
72	a56dc6d5230d95a9d96c95c019604d10	ba9696956c76dc57db7d1156533b32682	71
80	a56dc6d5230d1529d96c95c019604d10	8a2b0af2210e9af57d98da35a45e1d6f	67
88	a56dc6d5238d9529d96c95c019604d10	ca95a4c2661c1c106e84a9c413739b79	68
96	a56dc6d5a30d9529d96c95c019604d10	3761e1f6bf5efeace7151bf542e55215	60
104	a56dc655230d9529d96c95c019604d10	cc53413a6e877c1ebd7a702803492013	66
112	a56d46d5230d9529d96c95c019604d10	3a585a95e2cd18a6a38206acd220d484	60
120	a5edc6d5230d9529d96c95c019604d10	33dfb26cad3d2e768dd66b81eb67bd15	65
127	e56dc6d5230d9529d96c95c019604d10	2347e42973aa1a352df803aed4d97946	60
128	256dc6d5230d9529d96c95c019604d10	a0628818c21975ad208e09ee1b5533bd	63

Table 2 Avalanche effect on basic AES

Bit variation index	Plaintext	Cipher text of modified AES	Bit variations
0	a56dc6d5230d9529d96c95c019604d10	5632cbfbcf3fe675289d7194d88fd9d9	
1	a56dc6d5230d9529d96c95c019604d11	748110bb0a2e21cecbda4ebob4377fb5	64
2	a56dc6d5230d9529d96c95c019604d12	06e55d4beddca6ac6ae71ed6a9583613	64
8	a56dc6d5230d9529d96c95c019604d90	2715fea975082e3b3b61a8ea605dd501	66
16	a56dc6d5230d9529d96c95c01960cd10	11f22a5de31fc1ad20c872a91c75aefe	57
24	a56dc6d5230d9529d96c95c019e04d10	623e4279b34b2f39fb3a888929613d14	66
32	a56dc6d5230d9529d96c95c099604d10	5a2d73077b2b282dbe7351442efdb063	64
40	a56dc6d5230d9529d96c954019604d10	Fc70d16a46555d62dbec6975b99744c7	60
48	a56dc6d5230d9529d96c15c019604d10	4741c032940634c471756272fbc5ac31	63
56	a56dc6d5230d9529d9ec95c019604d10	6bb21ec7e957935c743a828977f470c2	68
64	a56dc6d5230d9529596c95c019604d10	9ffa23949abf537ee645d4f0959e4c6c	61
72	a56dc6d5230d95a9d96c95c019604d10	9dd5cf86c05b9adc567982da5f9d2fe5	70
80	a56dc6d5230d1529d96c95c019604d10	C37cae28484a1f625e81485c1222b6da	68
88	a56dc6d5238d9529d96c95c019604d10	678e3b0f9678d66e783722bc58322fb8	59
96	a56dc6d5a30d9529d96c95c019604d10	E6da79548c8e79fbc32b077e35988a18	72
104	a56dc655230d9529d96c95c019604d10	7ac947bcc1270cc7a7ab4ac089d24fc8	62
112	a56d46d5230d9529d96c95c019604d10	Cea83bd6205217e5c253d86c73da983f	69
120	a5edc6d5230d9529d96c95c019604d10	238a33617c26be87ce7f3a75b3a4d297	67
127	e56dc6d5230d9529d96c95c019604d10	12bb26dcdbf0e35d90ee74ddf13bd730	56
128	256dc6d5230d9529d96c95c019604d10	B28773ab0946c2ba5381dab9af3fdb4d	64

Table 3 avalanche effect of dynamic AES

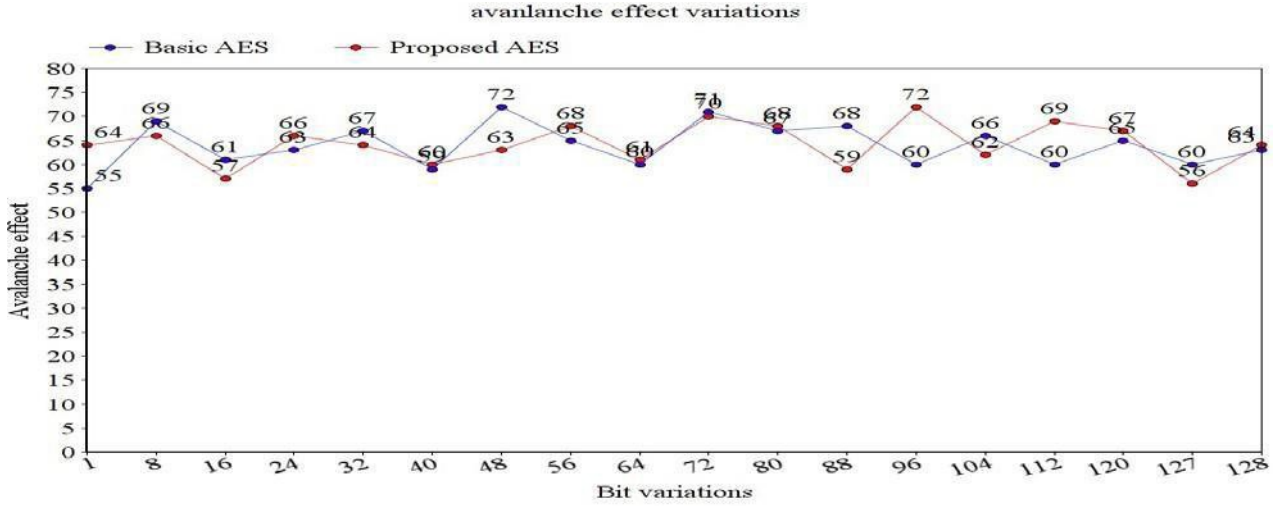

Fig. 5. Variations of basic AES and dynamic AES w.r.t bit variation Index

From the above graph we can infer that proposed algorithm shows better avalanche effect in most cases as compare to the basic AES algorithm and proposed algorithm satisfies strict avalanche criterion greater number of times as compared to basic AES algorithm. In this paper, we don't contradict security of AES rather we take AES as our basic block and doesn't change its mathematical calculations and make SBOX key dependent. Therefore, basic AES algorithm is not violated in this paper.

V. CONCLUSION

In this paper, we have successfully generated key dependent sbox whose avalanche effect is found to be greater than the basic AES.

We have studied that basic AES algorithm uses static sbox which can be attacked in future while in our proposed algorithm it generates multiple sboxes for different rounds that is sbox changes with respect to key and hence increasing the security of cipher. However, it will take extra hardware to ex-or key with sbox as compare to normal AES. So, this algorithm can be used where Security is the utmost priority. Therefore, its application includes military, banking sectors where security is the fore most criteria.

In the future work, this algorithm can be extended to AES-192 and AES-256 implementations and can be verified for larger number of samples.

REFERENCES

[1] Manjula, G., and H. S. Mohan. "Constructing key dependent dynamic S-Box for AES block cipher system." In *2016 2nd International Conference on Applied and Theoretical Computing and Communication Technology (iCATccT)*, pp. 613-617. IEEE, 2016.

[2] NIST, AES. "Advanced encryption standard." *FIPS Publication*197 (2001).

[3] J. Daemen and V. Rijmen, "The Block cipher Rijndael", In the proceedings of *Third International Conference on smart card Research and Applications, CA, Lecture Notes in computer science*, Vol.1820, pp. 227-284, 2000.

[4] Agarwal, Praveen, Amandeep Singh, and Adem Kilicman. "Development of key-dependent dynamic S-Boxes with dynamic irreducible polynomial and affine constant." *Advances in Mechanical Engineering* 10, no. 7 (2018): 1687814018781638.

[5] Krishnamurthy G N and V Ramaswami, "Making AES Stronger: AES wich Key -Dependent S-Box", *International Journal of Computer Science and Network Security,*Vol. 8, No. 9, pp. 388-398, 2008.

[6] Reshma Nadaf and Veena Desai, "Hardware Implementation of Modified AES with Key Dependent Dynamic S-Box", In the proceedings of *International Conference on Advanced Research in Engineering and Technology*, pp. 576-580, 2012.

[7] Abdullah Al- Mamun, Shawon S. M. Rahman, Tanvir Ahmed Shaon and Md Alam Hossain,"Security Analysis Of Aes And Enhancing Its Security By Modifying S-Box With An additional Byte*", International Journal of Computer Networks & Communications (IJCNC) Vol.9, No.2, March 2017.*

[8] Harshali Zodpe, Ashok Sapkal, "An efficient AES implementation using FPGA with enhanced security features", *Journal of King Saud University - Engineering Sciences*,2018,ISSN 1018-3639.

[9] Julia Juremi, Ramlan Mahmod, Salasia Sulaiman and Jazrin Ramli "Enhancing Advanced Encryption Standard S- Box Generation Based on Round Key", *International Journal of Cyber-Security and Digital Forensics*, Vol. 1, No. 3, pp. 183-188, 2012.

[10] Kazys Kazlauskas and Jaunius Kazlauskas" Key - Dependent S-Box Generation in AES Block Cipher System*", INFORMATICA*, Vol.20, No.1, pp. 23-34, 2009.

[11] Yan, Song Y. *Number theory for computing*. Springer Science & Business Media, 2002.

[12] A. Webster and S. Tavares, "On the Design of S-Boxes", In the proceedings of *Advances in Cryptology, Lecture Notes in Computer Science*, Vol. 218, pp.9 523-534, 2000.

Proceedings of the Fourth International Conference on Communication and Electronics Systems (ICCES 2019)
IEEE Conference Record # 45898; IEEE Xplore ISBN: 978-1-7281-1261-9

Performance Analysis of Full Duplex MIMO Fiber-Optical Wireless Communication (OWC) System

Bhumika Narang
Mtech Student:Department of Electronics and Communication
GuruNanak Dev Engineering College
Ludhiana,India
bhumikanarang17@gmail.com

Dr. Baljeet Kaur
Professor: Department of Electronics and Communication
GuruNanak Dev Engineering College
Ludhiana,India
baljeetkaur@gndec.ac.in

Prof.Harminder Kaur
Assistant Professor:Department Of Electronics and Communication
GuruNanak Dev Engineering College
Ludhiana,India
aulakh.harminder@gmail.com

***Abstract*-Full-Duplex Optical wireless system for simultaneous transmission and receiving of MIMO signal in both upstream and downstream. The system representation and simulation is done with higher carrier frequency. The current system is a LOS setup and system also uses 16 QAM modulation techniques. The efficiency of the system is done on the basis of bit-error rate, eye opening, and quality factor and so on.**

Keywords-Wavelength division multiplexing, multiple input/multiple output, optical wireless system, Quadrature amplitude modulation.

I. INTRODUCTION

Next generation communication networks such as 5th Generation or beyond it requires a significant plunge in the data rates. With the increase in capacity, the data rates of the optical downstream system could be alarm by employing digitized transferable method [1].Optical wireless system can be very useful for pliable access networks and resilient for mobile downlink system [2]. Many researchers work on the MIMO OWC system for transmitting the signal efficiently [2]. But in the proposed system, Full duplex is used for sending the signal downstream as well upstream simultaneously. As in the mobile downstream, radio over radio fiber system has been presented for supple, less delay and low data rate transmission. Signal transmitted through MIMO system is 25 GHz of the frequency. MIMO enables to improve the quality of OWC system. Apart from this Full-Duplex fiber optical wireless system is indispensible for the continuous transmission of downstream and upstream of the data without any delay. In addition to it, MIMO [3] signals were transmitted separately in the downstream and upstream direction. Moreover, Quadrature Amplitude Modulation (QAM) is used for lower error rate as the distance is more [4]. OWC caters more coverage area whereas multiple input and multiple outputs provides diversity advantages. The transmission of the optical signal from central station to the base station via optical fiber with the distance of 20 km and further the signal is transmitted to mobile users [5] through OWC. Owing to less error rate providing capacity QAM is generally used. In this, 16-QAM is implemented over a distance of 20 km [6]. As the order of QAM rise the data rates. In 16 QAM 4 bits are used to represent the symbol. The baud rate is ¼.The signal transmitted through local oscillator (LO) from Central station to Base station, it assist to reduce the maintenance cost, complexity and power consumption also[7],[8]. The implementation is done by using LOS conditions by using 16 QAM. As LOS conditions are provided between receiver and transmitter to get high SNR[3], [9], [10]. Even MIMO can give gain under LOS conditions which provides little channel difference. In this paper we proposed the Full- Duplex fiber optical wireless system for MIMO signals at higher carrier frequencies. The current system uses Wavelength division multiplexing (WDM) as intermediate frequency over fiber in the optical link [11]. We

transmit the 16-QAM MIMO OFDM signal over 75 GHz of frequency in bidirectional [12], [13].

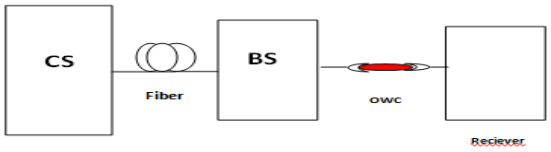

Fig.1. 2 X 2 MIMO system

This paper is organized as follows, the section I is introduction part which explains the literature work of existing paper. Section II demonstrates the experimental setup and III section tells about the results of the work done in the section II and the last IV section is of conclusion.

II. EXPERIMENTAL SETUP

The experimental setup of Performance analysis of Full-Duplex MIMO fiber-OWC system is modeled on Opti-system version 14.0 in Opti-wave. For the analysis of Full Duplex transmission, the OFDM signals send over distinct directions constantly. In downstream, two optical signals transfer from CW laser with a frequency difference of 50 GHz which further modulated by MIMO OFDM. The modulated signals are combined by optical coupler. Circulator is used to separate downstream and upstream signals. The signal transmitted from central station to base station via 20 km bidirectional fiber. Bidirectional fiber are commonly used which has high range of transmission in both the directions. From the base station the signal is further transmitted through optical wireless channel to users. The received signal is amplified by EDFA and filtered by optical Bessel filter. The signal received is optical signal which is converted to electrical signal by suitable photo diode. The desired signal is up converted to 80GHz of the frequency over a distance of 2.5 km. The desired signal amplified and down converted to original signal and outputs captured by an oscilloscope and demodulated and calculated on Eye diagram analyzer. In upstream, the signal is up-converted up to 80 GHz by using mixer. The local oscillator signal for up- conversion could be taken from downlink signals. The signals of up conversions are first amplified and then transmitted through 2.5km of optical wireless channel at remote area unit. The signals amplified before being coupled by photo diode for down converting the original MIMO transmitted signals. The received signals are amplified by low Bessel filter prior to modulating optical signals from CW laser diode using wavelength different from those in downstream. The received signals are transmitted to Central station via 20 km of fiber. Then signals amplified via EDFA and recovered by Bessel filter and photodiodes. The received signal is connected to oscilloscope to receive the output of the signals.

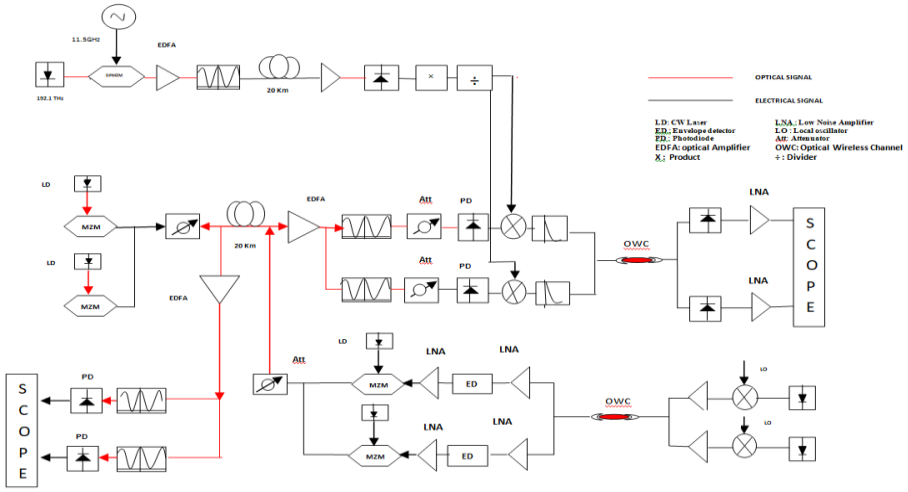

Fig. 2 Experiment Setup of Full Duplex MIMO Fiber-OWC System

III. RESULTS:

The signal is transmitted by CW laser to Dual-Machzender by 16 QAM having 4 bits used to represent the symbol where baud is ¼ of the bit-rate where the signal is up-converted to 11.5GHz of the frequency and the signal is further transmitted to the fiber in single direction and RAU and receiver channel by using following parameters.

Table1.Simulation Parameters used for the proposed Full Duplex MIMO Fiber-OWC System.

Parameters and Components Used	**Values**
CW Laser (Downstream)	193.1THz
CW Laser(Upstream)	192.1THz
Single fiber length	20Km
Bidirectional Fiber	20Km
OFDM Bandwidth	2 GHz
Local oscillator(upstream)	11.5GHz
EDFA length	5 m
OWC distance	2.5km
OWC wavelength	1550nm
Bit rates (Gbps)	40

Simulation Results:

The simulation of 2x2 MIMO 16 QAM OFDM modulations over 20km of the signal through optical fiber as well as bidirectional fiber in both upstream and downstream direction. Fig.3 shows the transmitted signal from central station over the frequency of 80 GHz.

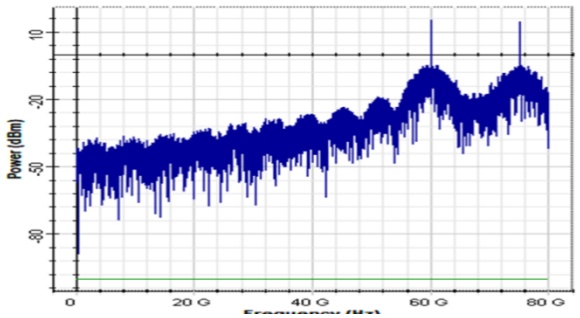

Fig.3 Transmitted Signal of Central Station

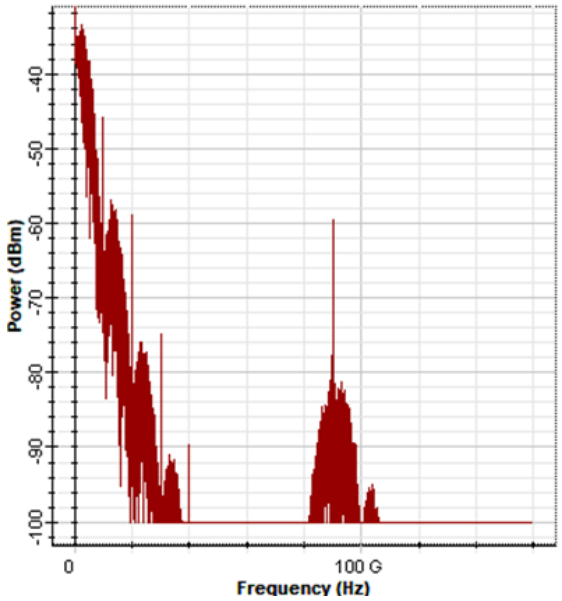

Fig.4 Received signal of MIMO Fiber-OWC System

The received signal of MIMO Fiber-OWC System at the output of the RF spectrum Analyzer_1 is as shown in the Fig.4.The signal analyzed after the transmission of the signal at the output by optical fiber over a distance of 20 km as shown in Fig.5 And signal received and transferred by bidirectional fiber over 20 km is show in fig 6.

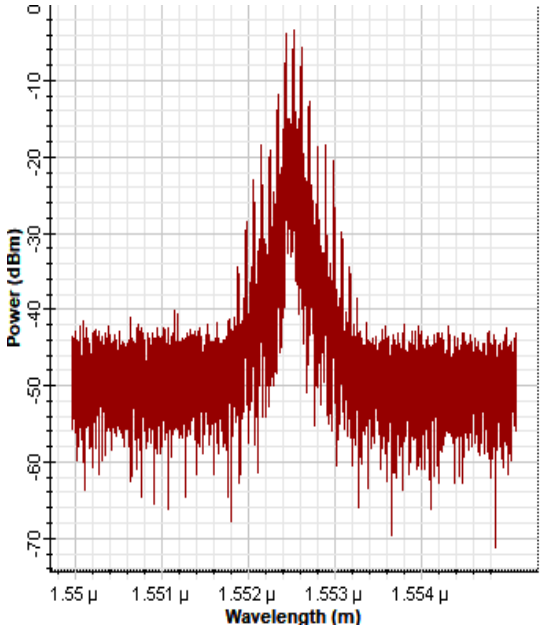

Fig.5 Signal of Fiber

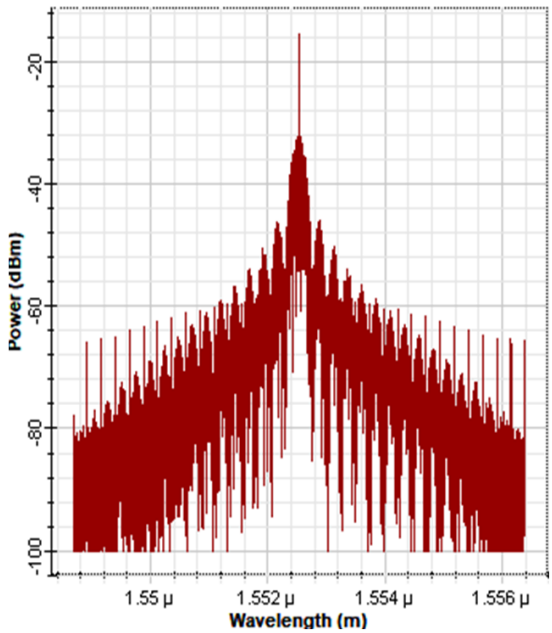

Fig.6 Signal of Bidirectional fiber

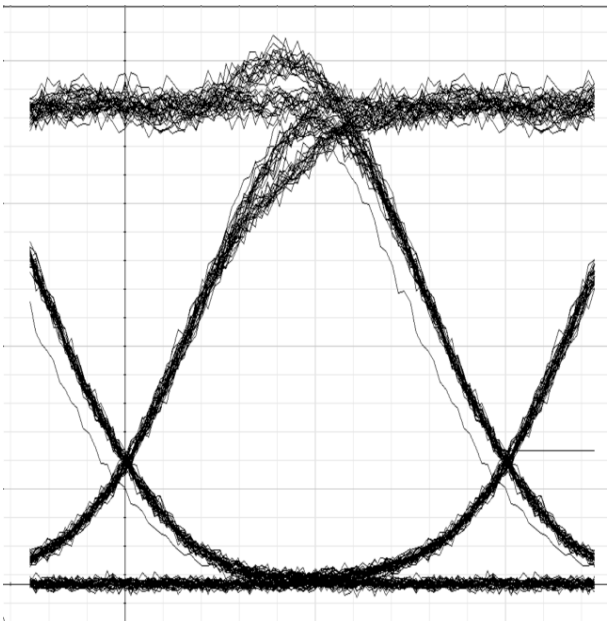

Fig 8. Eye diagram Analyzer

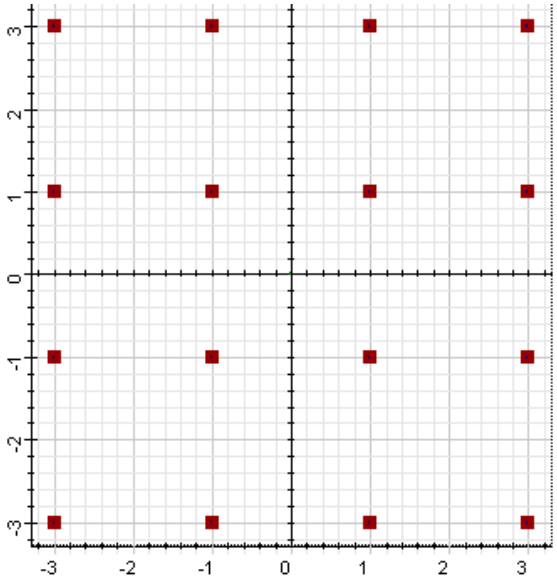

Fig.7 Constellation Diagram of 16 QAM

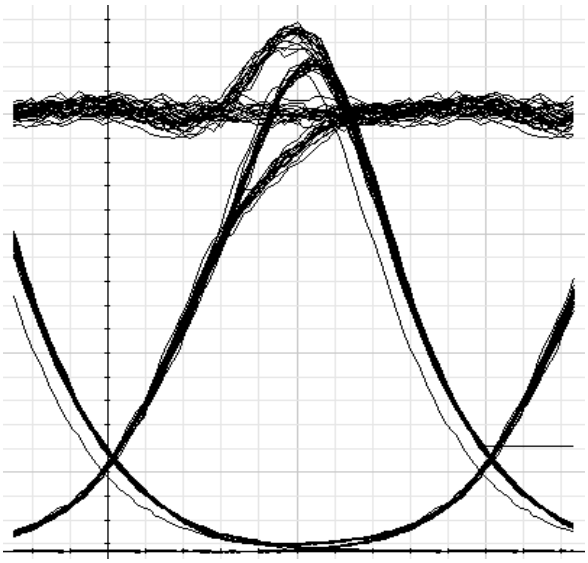

Fig 9. Eye diagram Analyzer_1

The above figure shows the result of 16 QAM at the receiver side. The resulted signal of the Full Duplex 16 QAM OFDM MIMO fiber Optical wireless communication system has been achieved by eye diagram analyzers. The signal of the upstream is shown in Fig.8 and downlink signal in Fig.9and results of the eye –diagrams are written in table 2.

The table below tells about the output received by the eye diagram analyzers and tells the bit error rate, eye height and quality factor of both upstream and downstream of the system.

Table 2. Results of simulation

Parameters	Q-factor	BER	Eye-Height
Eye diagram Analyzer	20.9887	3.72486e-098	1.7488e-005
Eye diagram Analyzer_1	25.1211	1.36735e-139	1.40363e-005

Conclusion:

In this paper, the signal from Full-Duplex MIMO OFDM fiber OWC is send in downstream and upstream by using higher carrier frequencies which lies in W-band. This system is scalable to large-scale MIMO and spectral- efficient owing to the use of WDM system in optical link. The performance of the signal is analyzed by BER and eye diagram. This system is helpful in transmitting large signals for future networking in better way such as tele-medicines, multimedia, telecommuting and many more. The system have full potential to provide the triple play services for upcoming years by increasing its bandwidth so it can be connected to the last miles of network. Apart from this we can increase the efficiency of the system by using Massive MIMO at 64 QAM OFDM to meet the needs of the customers in better way.

REFERENCES

[1] A.kaur and B.kaur " Next Generation Optical Access Networks:A review" ,Proc. ICAET ,pp429-432,2016.
[2] P.W. Berenguer, D. Schulz, J. Hilt, P. Hellwig, G. Kleinpeter, J. K. Fischer and V. Junnickel, " Optical Wireless MIMO in an industrial Environment" ,IEEE J on selected areas in communication vol.36,Issue1,pp.185-193,Nov.16,2017.
[3] P. T. Dat, Kanno and Yamamoto, "Full-Duplex And Scalable MIMO fiber–Wireless Seamless System In W-Band for future mobile networks," IEEE Photonics Tech. Letters, vol. 30, NO. 13, JULY 1, 2018.
[4] H.T. Huang., Wu and Chen L, "High spectral efficient W-band OFDM-RoF system with direct-detection by two cascaded single-drive MZMs," Opt. Exp., vol. 21, no. 14, pp. 16615–16620, 2013.
[5] P.T.Dat, Kanno and Yamamoto,"Bidirectional transmission of LTE-A carrier aggregation signal over a seamless fiber-wireless system in W-band," Proc. OFC, 2015, paper W1F.
[6] J.Zhang, G.K.Chang, Z.Dong and N.Chi,"Multichannel 120-Gb/s data transmission over 2×2 MIMO fiber-wireless link at W-band," IEEE Photon. Technol.Lett., vol. 25, no. 8, pp. 780–783, Apr. 15, 2013.
[7] U. Habib ,C.Wang and N.J Gomes "Radio over fiber transport of mm-Wave 2×2 MIMO for spatial diversity and multiplexing", Proc. IEEE MWP, pp. 39–42, Oct./Nov. 2016.
[8] N. Diamantopoulos., S.Inudo, P. T. Dat, Kanno and Yamamoto,"Mode-division multiplexed W-band RoF transmission for higher-order spatial-multiplexing", Proc. OFC, 2015, paper W4G. 2.
[9] M.Morant and R.Llorente, "Experimental demonstration of LTE-A M×4×4 MIMO radio-over-multicore fiber fronthaul", Proc. OFC, paper Th4E.4, 2017.
[10] X. Pang, J.O. Juan and T.I. Monroy, "Multigigabit W-Band(75–110 GHz) bidirectional hybrid fiber-wireless systems in access networks," J. Lightw. Technol., vol. 32, no. 23, pp. 4585–4592, Dec. 1, 2014.
[11] Naveen H,"2x2 MIMO ROF System At 60 GHz employing 64 QAM Double Sideband Modulation," ICCC, Nov.2015.
[12] R.K.Mungara and A.Lozana "Full-Duplex MIMO in Cellular Networks: System-level Performance" IEEE transactions on wireless communications, vol.5, no.6, pp.3124-3137, 2017.

Proceedings of the Fourth International Conference on Communication and Electronics Systems (ICCES 2019)
IEEE Conference Record # 45898; IEEE Xplore ISBN: 978-1-7281-1261-9

AUTOMATED RAINWATER HARVESTING SYSTEM

Dr. C Kishor Kumar Reddy[1], P R Anisha [2], Rajashekar shastry[3], Dr. B V Ramana Murthy[4], Dr. Vuppu Padmakar[5]
[1,2,3,4]Stanley College of Engineering & Technology for Women, Hyderabad
[5]Methodist College of Engineering & Technology, Hyderabad
e-mail: kishoar23@gmail.com

***Abstract*—With the disturbing rate of utilization of water assets in these days' universal, water deficiency has develop as more noteworthy recognized than any time in recent memory. Collecting water is a territory frequently track upon yet the idea of shrewd water gathering includes handiest come inside the type of thoughts, no longer executions. This proposed framework also is an idea to modernize water collecting anyway the sketches toward its usage is in progress and execution is a genuinely spotless test. The well known setup albeit adaptable, incorporates an expanded floor whereupon a water sensor controlled with the guide of Arduino is fixed. A servo engine also is snared to the water sensor and is fueled through the Arduino. Upon the commonness of water, the water sensor turns on and signals are sent to the Arduino. The code on Arduino is handled following inside the initiation of servo engine with the end goal that a gulf for accumulating water opens up. At the same time, an electronic mail is sent to the individual's cell to tell him/her on each event the gulf endless supply of precipitation and accordingly closes once it's finished. Along these lines, our proposed framework moves in the direction of the advancement of water the board in towns, making it another assignment closer to gathering water the shrewd way.**

Keywords—Arduino, servo motor, water sensor, water management

I. INTRODUCTION

As per the United Nations World Water Development Report, propelled 19 March 2018 all through the eighth World Water Forum, and related to the World Water Day, the overall interest of water has been expanding at a cost of 1% predictable with yr amid the last numerous years as a result of people increment, financial improvement and another in admission design among various components and could keep on developing widely in the predictable fate. It's fundamental to address the world's water requesting circumstances in the meantime as simultaneously giving over additional preferences vital to all components of economical improvement. Supportable improvement has been characterized as "progress that meets the desires of the current without bargaining the limit of things to come ages to satisfy their own needs". In expounding the idea of feasible improvement, the writing has ceaselessly determined that individuals – which incorporate town occupants are people in biological systems, and that they might be at last chargeable for versatility and sustainability of surroundings assets and contributions. Networks in this way need to search for techniques to both remain adaptively inside the stacking capacity offered to them or begin ensuring assets including water. A standout amongst the most not irregular methodologies to moderate water for across the board capacities or for groundwater energize is downpour water gathering [1].

Downpour Water Harvesting is a demonstration of getting and putting away water for later use. As we perceive water is the most perfect state of water, this water can be used for various purposes after significant refinement technique as required. Water lack isn't bizarre in nowadays' enormous urban areas and the regular machine of water reaping is less more then likely for use in the present currently developed houses. Thus despite the fact that water gathering can be incredible in those districts it's presently not renowned adequate because of its technique for usage which has now not prevalent with time [2].

(A) History

The shooting and putting away of water is a way that goes again bunches of years while individuals started to cultivate the terrains and required ways to deal with inundate plants. In warm atmospheres, getting precipitation consistently chosen ways of life or death toll for a couple of networks. While the requirement for keeping water fell away because of urbanization inside a definitive a huge number of years, we by and by need to return to this well established and quintessential piece of greener dwelling.

Human advancements inside the Indus Valley had been far additional unrivaled than we may might suspect lately. In some of the authentic urban areas that still remain, we will in any case find colossal tanks that were sliced into the stone to amass water

while there has been heavy precipitation. These have been utilized to safeguard the masses and neighborhood plants going into more sizzling, dryer times and had been nourished by severa stone ravines that weaved their way through the city. A portion of those stone tanks are as yet utilized these days in segments of India.

Another methodology that has been utilized for many years in India is to develop water reaping frameworks on apex of the tops of homes. It's a basic age that has unfurl the world over, for the most part to nations comprehensive of Brazil and China [3].

The period of water gathering is profoundly established inside the social material of India with an assortment of notable strategies in any case found today. These include:

Talibs: Medium to monstrous measured stores that give water system to plants notwithstanding expending.

Johads: Dams which are utilized to catch and hold water.

Baoris: Wells delved into the ground that are as often as possible regardless utilized for devouring.

Jhalaras: Specially developed tanks which can be utilized for the neighborhood individuals and otherworldly capacities.

Aside from India, for the term of the season of the Roman Empire, water arrangement have moved toward becoming something of a craftsmanship and innovation, with numerous new urban areas fusing kingdom of the fine art time for the time. The Romans had been aces at these new patterns and impressive advancement was made right up till the 6th Century AD and the standard of Emperor Caesar [4]. One of the greatest surprising water gathering structures might be found in Istanbul in the Sunken Palace which ended up used to gather water from the boulevards above. It's large to the point that you can cruise round it in a ship.

(B) Present Day

In China and Brazil, rooftop water reaping is polished for giving water to local use, devouring water, water for animals, water system purposes and reviving ground water. Gansu region in China and semi-dry North East Brazil run considered one of the biggest tasks for water reaping.

In Beijing some lodging gatherings right now are including water in its transcendent water sources after right cure.

In the US, until 2009 in Colorado, water reaping ended up controlled however at this point proprietor of the inhabitant is permitted to put in a housetop downpour accumulation framework as long in light of the fact that it meets the predefined criteria.

In Ireland, Professor Micheal Mcginley of Dublin University College established a dare to structure a downpour water reaping model inside the normal gadget configuration adventure module [5].

(C) Types of Rainwater Harvesting

Water Harvesting is widely isolated into two techniques:

- Surface Runoff Harvesting
- Rooftop Rainwater Harvesting

In this paper, we can be for the most part speakme around housetop water gathering as it's far less exceptionally estimated and more prominent powerful whenever did appropriately can help with enlarging the ground water level of the region.The gadget uniquely comprises of catchments, conveyance and channel out [6].
Catchments: The surface or bay that straightforwardly gets the precipitation is named the catchment of a water reaping framework. It might be the porch, patio, or cleared or unpaved open floor. The porch can be level RCC/stone rooftop or inclining rooftop. The inconveniences that outstanding here are:

i) The tidiness of the rooftop and subsequently the water. A delta that might be evacuated and cleaned off frequently could suggest less cost required for filtration.

ii) Houses in urban areas nowadays aren't worked with open and level housetops. The build of a housetop ordinarily depends upon elements alongside climate, esteem, look and usefulness. Contributed rooftops are regularly utilized atmospheres with heavier downpour and snow fall as they offer quicker and less entangled water dropping and seepage of the rooftop. For example, progressively contributed rooftops might be discovered the northern region of the USA where more snow and downpour gather and a wonderful arrangement all the more level rooftops in the southern region of the USA where considerably less snow and water aggregates.

II. LITERATURE SURVEY

Recent researches have contributed to the improvement in the region of IoT through this paper we can have a short idea of a mission that is to grow a shrewd water gathering process making utilizing IoT. In our writing overview we've alluded and considered uncommon examinations papers in regards to the major idea of IoT. Utilizing IoT in different fields to associate things, administrations

and individuals for reasonable tasks is a pattern now a days in vogue innovation.

The Internet of Things might be utilized for getting the correct amount of water on the correct goal for the best possible time frame and most straightforward when needed. This can be the errand of extraordinary soil sensors and climate sensors as an approach to talk their readings to a particular server. Web of Things age furthermore permits in booking the upkeep just as the shutdown of siphons on a customary establishment. There are streamlining methodologies which could progress of time convey to the inhabitants of a city with respect to the inaccessibility of water for the term of any exact factor in time. This empowers the water guideline government not most straightforward in gathering the alright water needs in a city; rather it additionally helps inside the preservation of benefits and quality [8].

The forces of IoT were utilized significantly by method for a couple of organizations who've taken a stab at keen water control. The accompanying posting obliges of a portion of their endeavors toward the worldwide endeavors of keeping water the utilization of IoT:

- Smart Monitoring-To dissect water cure framework and control it from wherever each time
- Smart Watering Techniques to vegetation-Water the vegetation as steady with their prerequisite
- Smart Water Meters Status-Calculates the use of water and as reliable with the ordinary programming just that tons amount of water is outfitted.
- Potable Water Monitoring-Monitors the top notch of faucet water
- Chemical Leakage Detection in streams Detects the measure of spillages or wastage tossed in waterway
- Swimming pool far away estimation Controls the pool conditions and necessity of water
- Pollution levels in the ocean Controls the seawater to get defiled
- Water Leakages-Detect the spillage and help to find the deficiencies
- River Floods-Monitors water level varieties in water bodies

III. PROPOSED MODEL

The proposed system that we have developed draws inspiration from a combination of various existing smart water management systems that already exist. It is therefore not a direct emulation of said systems but rather a hybrid of the most efficient kind. Firstly, it takes inspiration from the IWCM that has come up with an elaborate water harvesting scheme suitable for both rural and urban areas. The system that it has proposed works in a similar fashion, except that the is collected in different containers that are spread over the entire locality. It also consists of water level indicators fixed to the inside of the containers in addition to vents that open up to catch rainwater. Second inspiration is drawn from Project ph 5.6 that deals with the act of rainwater harvesting but in a smart way [16].

To obtain the most sustainable, economical & efficient water management system, certain architectural requirements are to be fulfilled. Only upon the fulfilment of these requirements can the system produce successful results in the long run, thus enforcing more of its production in the market & enabling various companies & communities to study from it and go on to improvise upon already existing features so as to procure an even better model for smart water management. The body of Integrated Water Resources Management (IWRM) has laid down the following requirements that the architecture of a water management system using IoT devices will need to comprise of:

Requirement no. 1: The following water management functions should be covered by the system:

1) Remote management of physical elements and operation of basic units

2) Identification of resources in the water network

3) Definition of operations and conditions over the network.

Requirement no. 2: It should support interoperability with other applications such as geographic information systems and also databases containing information regarding soils, weather forecast, environment, farming, etc.

Requirement no. 3: It should provide a flexible and extensible architecture for the integration of various systems. To do that, it must define open interfaces among communication and process control layers, and also integrate IoT systems for a direct access to individual water management devices.

Requirement no. 4: It should support integration with legacy systems, controlling current equipment. Water management infrastructures currently deployed in the countryside consist of many interconnected and simple devices that must be managed using legacy systems. They integrate communication functions, data models, and protocols dependent on an specific technology of the

manufacturer. Overriding these systems with new ones is not always a feasible solution [10]. Figure 1 gives the block diagram of the proposed model.

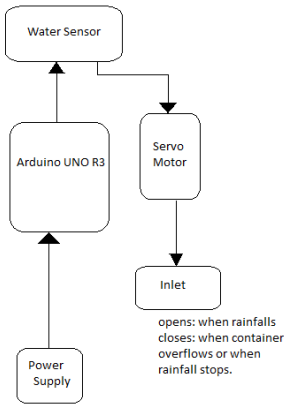

Fig. 1:Block Diagram

The set-up, despite the fact that worked to solid little scale attempts can likewise deal with colossal scale provided the fundamental substance of the gadget is consolidated.Right off the bat, the downpour water falls upon the outside of the water sensor that is fixed onto the surface with the end goal that it faces the skies. After detecting the downpour beads, the water sensor turns on and begins to send alarms to the joined servo engine. A servomotor is a revolving actuator or direct actuator that lets in for explicit oversee of rakish or straight capacity, speed and increasing speed. It comprises of a proper engine coupled to a sensor for capacity remarks. This sensor is in developed to turned out to be associated with the sliding entryway on the floor of the floor that slides open to uncover a social affair compartment for reason of finding approaching precipitation. As the water gathers into this field, alarms are effectively sent to the harnesser to signify water levels. On the exercises of flood of water into the container, the entryway naturally closes in the wake of alarming specialists that the crate has been full to the overflow. This water accumulated is eventually utilized for different human and mechanical games. It can similarly additionally be sent for filtration if in any regard it gets dirtied upon end starting from the earliest stage [14]. Figure 2 depicts the working flow of the proposed model and Figure 3 and 4 shows the result of the model.

Proposed Algorithm

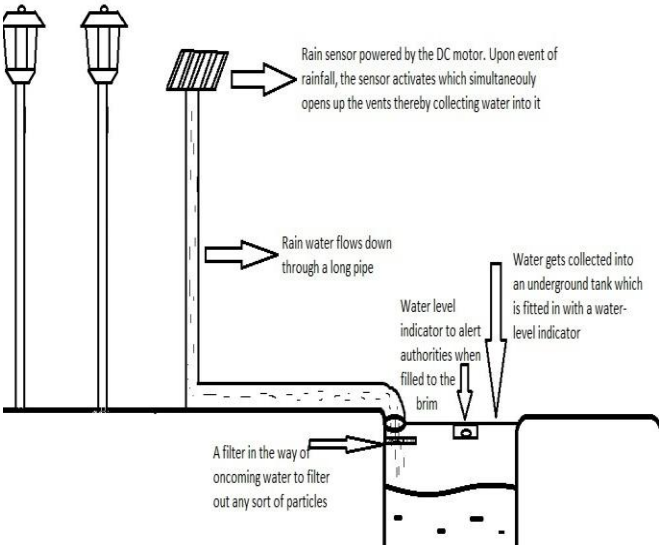

Fig. 2:Proposed model

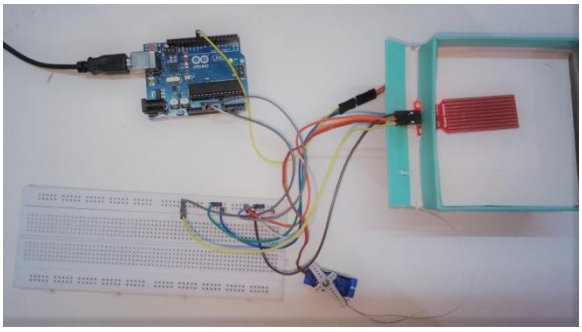

Fig 3: Closed Inlet

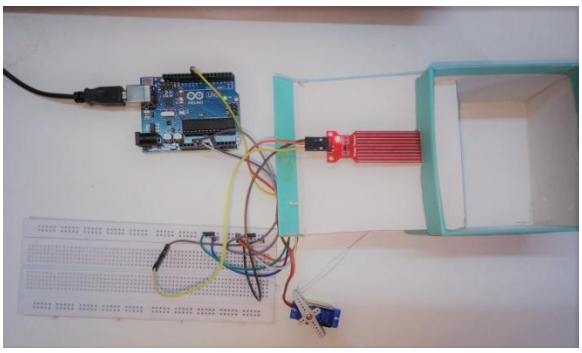

Fig. 4: Opened Inlet

IV. CONCLUSION

The Smart Rainwater Harvesting has to be used in an powerful and possible thing such that it is able to mitigate the effects of depleting groundwater degrees and fluctuating climate conditions. This is extraordinarily a present day research field and it's miles anticipated to grow in future. There is lot of

labor to be achieved in this rising area. Here we get primary expertise on how the water harvesting may be advanced based on the outcomes achieved from this device.

References

[1] G. Santucci, “Internet of Data to Internet of Things”, Paper for the International Conference on Future Trends of the Internet, 2009.

[2] D. Giusto, A. Iera, G. Morabito and L. Atzori, “The Internet of Things”, 2010.

[3] E. Ngai, K. Moon, F. Riggins and C. Yi, “RFID research: An academic literature review (1995-2005) and future research directions”, International Journal of Production Economics, 112:510-520, 2008.

[4] L. Ni, C. Li, L. Qiong, N. Hoilun and Z. Ze, "Status of the CAS/HKUST joint project BLOSSOMS", Proc. Of the 11th IEEE International Conference on Embedded and Real-Time Computing Systems and Applications, pp. 469– 474, August, Hongkong (China), 2005.

[5] L. Atzori, A. Iera and G. Morabito, “The Internet of Things: A survey, Computer Networks”, 2010.

[6] The EPC global Architecture Framework, EPC global Final Version 1.3, Approved 19 March 2009.

[7] K. Sakamura, "Challenges in the age of ubiquitous computing: a case study of T-engine-an open development platform for embedded systems", Proc. Of the 28th International Conference on Software Engineering, pp. 713 – 720, May, Shanghai (China),2006.

[8] Lan Li,” Study of Security Architecture in the Internet of Things,” in Measurement, Information and Control (MIC),2012.

[9] Maciej Kranz, “Internet of Things”, 2016.

[10] M. Yash, “How Internet of Things helps water management”, 2009.

[11] ITU Internet Reports, “The Internet of Things”, November 2005.

[12] International Journal of Computer Applications (0975 8887) Volume 113 - No. 1, March 2015

[13] Jason Pontin,” Bill Joy’s Six Webs,” MIT Technology Review,29 September 2005

[14] Kevin Ashton,” That ’Internet of Things’ Thing”,2009.

[15] H.D. Ma,” Internet of things: Objectives and scientific challenge”, in Journal of Computer Science and Technology,2011.

[16] Debasis Bandyopadhyay, Jaydip Sen,” Internet of Things - Applications and Challenges in Technology and Standardization” in Wireless Personal Communications,2011.

[17] Vaibhav Chakraborty, “Rainwater Harvesting- How it is done and how important is it for future?”,2018

[18] Ashantha Goonetilleke, Godwin A. Ayoko, Prasanna Egodawatta, “Sustainable Urban Water Environment: Climate, Pollution and Adaptation”,2014.

[19] S.Matsuura, H.Ishizuka, H.Ochiai, S.Doui, S.Ishida,”Live E! Project: Establishment of Infrastructure Sharing Environmental Information”, 2007.

[20] MacDonald, L., Pathak, G., Singer, “Water Resource Protection”, 2011

[21] Welle, K. (2010). Strategic review of WaterAid’s waterpoint mapping in East Africa. Based on a review of Ethiopia, Kenya, Tanzania and Uganda. WaterAid

Proceedings of the Fourth International Conference on Communication and Electronics Systems (ICCES 2019)
IEEE Conference Record # 45898; IEEE Xplore ISBN: 978-1-7281-1261-9

File I/O Performance Analysis of ZFS & BTRFS over iSCSI on a Storage Pool of Flash Drives

Devyani Gurjar
Department of Computer Engineering and IT
College of Engineering
Pune, India
devyanig17.is@coep.ac.in

Satish S. Kumbhar
Department of Computer Engineering and IT
College of Engineering
Pune, India
ssk.comp@coep.ac.in

***Abstract*— The demand of highly functioning storage systems has led to the evolution of the filesystems which are capable of successfully and effectively carrying out the data management, configure new storage hardware, have proper backup and recovery it as well. The research paper aims to find out which filesystem can serve better in backup storage (e.g. NAS storage) and compute-intensive systems (e.g. database consolidation in cloud computing). We compare such two most potential opensource filesystem ZFS and BTRFS based on their file I/O performance on a storage pool of flash drives made available over iSCSI (internet) for different record sizes. This paper found that ZFS performed better than BTRFS in this arrangement.**

Keywords—bandwidth, block device, BTRFS, file I/O performance, filesystem, iSCSI, storage pool, subvolume, ZFS

I. INTRODUCTION

Back in 1920s, even storing a byte required expensive magnetic tapes and today just a simple image file shared over internet is in MBs. From magnetic disks to optical ones and from hard disks to flash drives, the hardware evolution for storage has immensely decreased in its physical size and enormously increased in storage capacity, access speed, portability and ease of use. The hard disks have moving mechanical parts to perform operations and the SSDs have none, which makes them less prone to failure due to the physical damage occurring within. Thus, the use of SSDs is a better choice in storage environments. The new NVMe technology is even faster than SSDs but it puts a lot of load on PCI, hence the limited use-cases-- advanced analytical apps, DevOps, etc.

Today storage demand has become so massive that it is a challenge to maintain the data, expensive hardware, its backup & recovery and other infrastructure involved. To address the issues, the industry has evolved to adopt the use of storage controller, storage hypervisors, etc. When the need of more storage strikes, it requires businesses and organizations to expand their storage, mostly to scale it up. To achieve higher, proficient performance and lesser downtimes, the storage has to execute many other CPU intensive tasks such as compression, data deduplication, checksum calculations, snapshots, cloning data, etc. Addition of new hardware and configuring it into the system stresses out the central controlling and processing system. To avoid this, there is a scaling-out storage approach, which adds compute resource along with the storage.

As filesystem are the basis of storage, they need to handle such extreme degree tasks and meet the need. Two such promising and flexible opensource filesystems are ZFS and BTRFS. They are not just filesystems, but include volume managers too, which makes them a faster and complete stack above storage (on the other hand, Ext4, XFS and other filesystems do not have such mechanism built-in). Both ZFS and BTRFS have distinguished features structured into them in their own different ways.

This paper aims to study these two filesystems as per their File I/O performance, when the storage is provided over internet in RAID 6 configuration with default pool settings. We analyzed that ZFS has intelligent ARC cache mechanism which boosts its performance in read operations. We used asynchronous writes that is why its ZIL (ZFS Intent Log) feature was not used (else for synchronous writes this feature makes the writes very reliable) but the approach used to write the data from buffer to disk in form of transaction groups helped. BTRFS on the other was limited by the record size and the absence of cache. Hence, this thesis recommends ZFS as the designated filesystem in the backup storage system (or in NAS storage).

Next section briefs about different work already done to compare these two filesystems. Section III presents the experiment of this paper in detail. Then, performance results are discussed in Section IV. The results are more analyzed in Section V and finally Section VI concludes the outcomes of the experiments conducted.

II. RELATED WORK AND BACKGROUND STUDY

Our previous work [1] presents a detailed literature survey for this experiment. This section includes its brief summary, describes important terminologies necessary to understand the experiments and reasons why the experiments are setup in a certain way.

A. Brief literature survey summary

Most of the experiments previously done were on native computer system, that is, there was no communication between two systems for storage over internet. Several authors have examined the performance of these filesystems over different storage configurations, like for single disk, multiple disk, other RAIDs based on the use of different types of disk accessing protocol, record sizes, file sizes, mount options, hypervisor, microbenchmark and macrobenchmark tests. [2] illustrates the data structure of BTRFS and how checksums are calculated in case of disk failure for data recovery. The paper [3] presented the performance of ZFS and EXT4 on SATA disks over iSCSI and found that ZFS worked better with increasing number of disks. The paper [4] which asserted the effectiveness of the in-built defragmentation tool of BTRFS is a special mention.

XXX-X-XXXX-XXXX-X/XX/$XX.00 ©20XX IEEE

Apart from the performance comparisons, [5] study of end-to-end data integrity about ZFS bought attention to the big security issues of memory corruption for ZFS. Thus, filesystems bring security challenges of access control, encryption & data integrity along with them.

B. Background Study

Filesystem is the data structure that governs how data is written to and fetched from storage media. So, when working for storage, first the disks are to be formatted with a suitable filesystem. Next comes mounting it to the system and one can choose to configure the disks as a storage pool using different RAID combinations instead of using single disks. It is actually faster in performance, proper data management and most important, backup and recovery in case for failure or disaster. Volume managers are required to achieve such configurations. ZFS and BTRFS both have their own volume managers, so they directly communicate with the block devices, which makes them faster than that of using the volume manger provided by the host OS, in our case, by Linux. ZFS has an advantage that when a storage pool is created, it is by default mounted with proper settings as well. Whereas, for BTRFS one has to mount the disks via the native *mount* command provided by Linux. Both of these filesystems provide great features like compression, data deduplication, checksum, creating snapshot, subvolume and clone of data, etc. Checksums prevent the silent data corruption and help in data recovery. When mounted in default mode, the compression and data deduplication are set off for both filesystems and checksum calculations are kept on.

There are different ways to test the working and efficiency of the filesystems. Either to test their functionality one at time or test them under real life working scenarios. The former tests are microbenchmark tests and latter ones termed to be the macrobenchmark tests. This experiment tests the File I/O performance (which majorly focuses on how the filesystem executes its read and write file operations) of the filesystems for various record sizes. The *record size* is the unit of data that will be handled at a time while performing the read and write operations. The operations are to be performed asynchronously, it means, that they are first written to journal of the filesystem and then performed to the actual storage media.

For the experiment setup, Linux OS was the best choice as it is easier for debugging and has compatible options for storage subsystems [5]. iSCSI that is an IP storage protocol for mapping the block-oriented storage data over internet [6], is emerging strong because it can be implemented over larger distances & provides security with IPsec [7]. For iSCSI to work, some target technology is required to configure the LUNS at the target system. The paper [8] studied various Linux iSCSI targets like STGT, LIO, SCST, IET and deduced that SCST has many advantages over others such as it has better support for back-storage handlers in both kernel & user space, has easy session management & target configuration, etc. Flash drives are chosen as the storage which work alike SSDs. The next section covers the detailed approach of the experiment.

III. Approach And Methodology

The approach to this experiment is to create a scenario where an initiator system could use the storage provided by the target system over iSCSI as block device. The target system already would have the storage pool configured with the respective filesystems. The initiator should be able to write and read files to that available storage with the help of open-iSCSI. The tests examined the storage for I/O having variable record sizes of 32 KB to 32 MB and 512 B and results were recorded.

A. Environment Setup

The configuration for this experiment involved three computer systems. Out of which two behave as target, each for ZFS & BTRFS and the third as an initiator. The hardware specification of all these three computer systems are same, the details can be found in Table I and software information in Table II. Table III shows system specific software information.

TABLE I. SYSTEM HARDWARE

System Hardware	Specifications
Processor	Intel(R) Core(TM) i7-3770 CPU @3.40GHz
Memory	3GB
Motherboard	Hewlett-Packard 339A

Each of the target systems creates the RAID 6 storage pool (with default mount and pool settings) out of four 8GB SanDisk Cruzer Blade USB Flash Drives and subvolumes were created to be given as storage block device to hand over the storage over iSCSI to initiator. At a time only one target communicates with the initiator.

TABLE II. SYSTEM SOFTWARE

Software	Specifications
OS	Ubuntu 18.04.1 LTS
Kernel	Ubuntu 4.15.0-44-generic

TABLE III. SYSTEM SPECIFIC SOFTWARE

System	Specifications
ZFS Target	ZFS version 0.7.5-1 ubuntu15
BTRFS Target	btrfs-progs version v4.15.1
Initiator	FIO version 3.1

B. Testing Tool

The Flexible I/O Tester Benchmark is used for the experiments in this thesis (refer Appendix E for installation). Microbenchmark operations such as sequential write, sequential read, random write, and random read help to analyze filesystems better. Each test ran for 600 seconds with a varying record size of 512 B and from 32 KB to 32 MB. After completion of each test, both target and initiator were rebooted. After the completion of all the tests for a particular record size once, the RAID 6 was reconfigured at target system. For more accurate results a set of tests was repeated for a total of five times. The output file has all the metadata of the execution. Here, the output file is of JSON format, hence easy to read and navigate.

C. Capturing IO Statistics

ZFS was benefitted by its built-in *iostat* tool to acquire the I/O. As BTRFS has no such tool of its own, I/O was acquired using the functional Linux utility *sysstat iostat*.

IV. Performance Results

This section presents the final performance results of the experiments organized by the type of experiment. The captured IO results of the five repeated tests were averaged for all of the record sizes.

A. Sequential Write

Fig 1 shows the write performance of ZFS and BTRFS over RAID 6 for sequential write operation. ZFS performs consistently better for increasing record sizes with write bandwidth of 3.3MBps to 4.3 MBps, whereas BTRFS fluctuates more. For record size 512 B and 8 MB there is approximately equal performance difference.

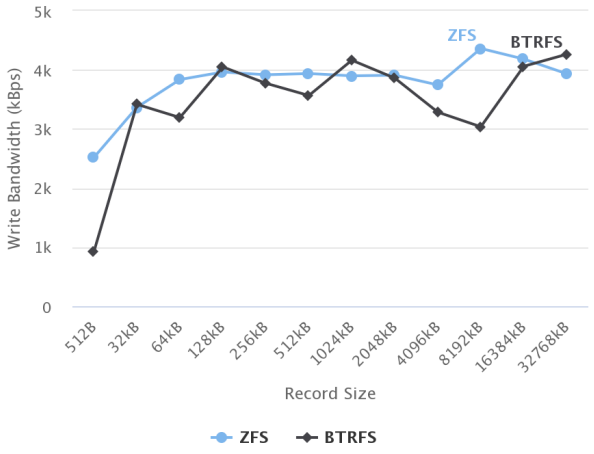

Fig. 1. Write Bandwidth for Sequential Write test.

B. Sequential Read

Fig 2 indicates the read performance of ZFS and BTRFS over RAID 6 for sequential read operation. Clearly, ZFS outperformed BTRFS with read bandwidth of 9.5 MBps to 10.5 MBps. Very vast performance difference can be noticed between these two filesystems.

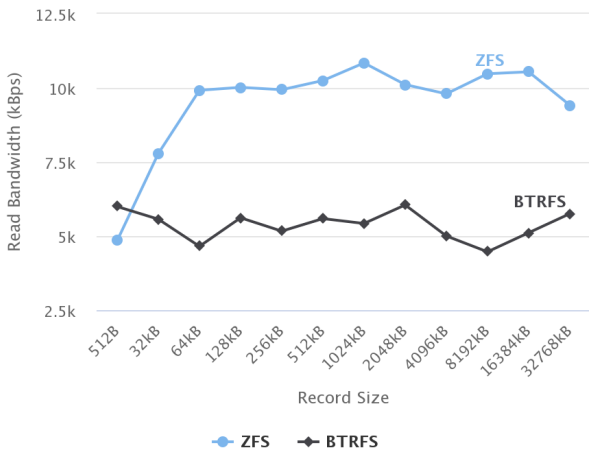

Fig. 2. Read Bandwidth for Sequential Read test.

C. Random Write

Fig 3 depicts the write performance of ZFS and BTRFS over RAID 6 for random write operation. BTRFS performed better than ZFS with write bandwidth of 3MBps to 4.5 MBps. ZFS here again had a consistent run. A big performance difference was seen for 1 MB record size.

D. Random Read

Fig 4 shows the read performance of ZFS and BTRFS over RAID 6 for random read operation. ZFS read better than BTRFS and as record size increased from 256 KB, its read bandwidth hiked. Massive performance difference was observed between these two filesystems.

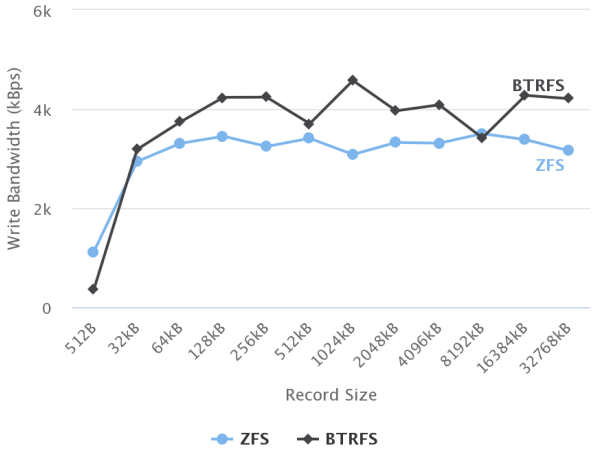

Fig. 3. Write Bandwidth for Random Write test.

V. Analysis

The outstanding difference in ZFS' performance for both sequential and random read operations is the use of primary cache. ZFS by default has the primary cache enabled. This cache is part of RAM and is resizable from 64 MB to 75% of the system's RAM. This cache is governed by the ARC (advanced replacement cache) mechanism which is a combination of MRU (most recently used) and MFU (most frequently used) replacement policies. ZFS keeps data as records and such records are composed of blocks.

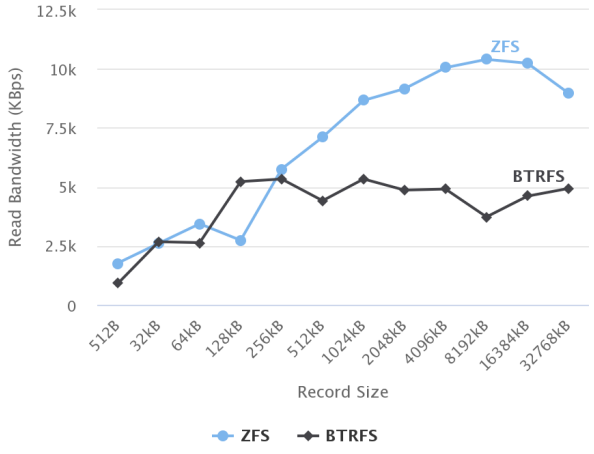

Fig. 4. Read Bandwidth for Random Read test.

For sequential read, as block size increases, the data being transferred increases too. After a certain block size (e.g. 64 KB in) the bandwidth becomes steady due to following reasons: first, as the ARC cache is intelligent to predict the next demand in data, it is pre-fetched, which improves performance. This is helpful in the situation where the block sizes are increasing and there is frequent transfer of data from storage pool to cache. Second, ZFS has to validate data before bringing it into cache which consumes time.

These both factors sort of balance each other and give near to steady performance for varying block sizes.

For random read, similar reasoning is valid. Although, as the data here is accessed randomly, the data pre-fetching does not work as such. But ZFS succeeds in dealing with this by maintaining the ghost MRU and ghost MFU lists in the ARC cache. The data, which is replaced from the cache, gets its metadata linked to these ghost lists, making them faster to access on next demand (also there is no need to validate the data again, thus saving time in checksum validation). Another factor that influenced the performance here is that the random write operation experienced some frequent pool damages (e.g. for block size 128 KB) which led to performance degrade for the next random read operation. Similar dip in performance occurred for block size of 32 MB. There are other block sizes for which the damage occurred, but they were not as frequent as the above-mentioned block sizes. These damages might have taken place due to iSCSI or network connection errors.

Coming to ZFS ability to carry out asynchronous sequential and random write, the ZIL (ZFS Intent Log) feature is not functional by default. ZIL is a logging feature for synchronous writes only. In our case with sync property of pool set as standard, writes are buffered in the cache and after an interval are written to storage disks as transaction groups. So ZIL is not at all functional. But the intelligent mechanism of how blocks are picked up for writing comes into play. The devices in storage pool are divided into metaslabs which contain the blocks. These might blocks vary in size to a maximum of record size. Data blocks are written in localized metaslabs (termed as active metaslab) of the devices and adjacent to same sized blocks. Metaslab has a data structure which keeps track of free space in that particular metaslab. This speed up the process of finding location to save the data. With ZIL enabled, the synchronous write.

Whereas, with ZIL enabled, the synchronous write addresses the data integrity but creates overhead of 2 writes (one to RAM and other to ZIL itself) and another 4 write penalties for the RAIDZ configuration of pool. In such case using a fast device as a SLOG will be beneficial.

BTRFS struggled as its default block size is the page size of the underlying OS, in our case 4 KB. Other limitation was that BTRFS does not use cache which degraded the performance. Also, we know in the case of ZFS that it suffered from some pool damage, but in case of BTRFS we are not sure that no such damage occurred or BTRFS was not able to detect it.

There are several scenarios where ZFS can be included in the storage system solutions. But to avoid monocultures, this paper emphasizes that sequential reads and writes should be considered and that too for backup and data warehouses.

VI. Conclusion

Storage as we know, serves various types of businesses ex. different kinds of servers, computational technologies, data driven support systems, database consolidations, supporting virtualization, backup, etc. The analysis conducted using the filesystem and disk I/O benchmark standard, Flexible I/O Tester on Linux highlighted the behavior of ZFS and BTRFS filesystems for write, read, random write, and random read operations over a storage pool of flash drives in RAID 6 configuration. We recommend ZFS as the designated filesystem in the backup storage system (or in NAS storage). This recommendation is supported by the features of ZFS that amplified its working with variable record sizes. ZFS has intelligent and scalable ARC cache which boosts its performance in read operations. We used asynchronous writes in which the data from buffer to disk was written in form of transaction groups and blocks are picked in a smart manner, which is very functional in random write operation.

Database consolidation and VM snapshot management workload can be designed to test these filesystems further. The setup for such workloads will be heavily intensive on memory, storage and CPU. Although this type of workload should be asynchronous, but if chosen otherwise, use SSDs as storage in RAID 10 configuration and NVMe disk as a SLOG device with ZIL enabled.

References

[1] Devyani Gurjar, Satish S. Kumbhar, “A Review on Performance Analysis of ZFS and BTRFS”, IEEE International Conference on Communication and Signal Processing 2019, April 2019, Chennai, India.

[2] O. Rodeh, J. Bacik, & C. Mason, “BTRFS: The Linux B-tree Filesystem”, ACM Transactions on Storage, Vol. 9, No. 3, Article 9, Publication date: August 2013.

[3] Veerapat Phrornchana, Natawut Nupairoj, and Krerk Pirornsopa, “Performance Evaluation of ZFS and LVM (with ext4) for Scalable Storage System”, 2011 Eighth International Joint Conference on Computer Sci- ence and Software Engineering (JCSSE).

[4] Meaza Taye Kebede, “Performance Comparison of Btrfs and Ext4 Filesys- tems”, Masters thesis, University of Oslo, 2012

[5] Yupu Zhang, Abhishek Rajimwale, Andrea C. Arpaci Dusseau, Remzi H. Arpaci-Dusseau, “End-to-end Data Integrity for File Systems: A ZFS Case Study”, Computer Sciences Department, University of Wisconsin-Madison

[6] Pete Popov, “A SCSI Test Tool for Linux”, ACM

[7] John Huffered, “IP Storage Protocol”, SNIA Education-2011

[8] Jeffrey S. Goldner, “The Emergence of iSCSI”, File Systems and Storage Volume 1, issue 4, ACM Queue July 14, 2008.

[9] Nitin Gode, Rushida Kashalkar, Deepika Kale, Sukhada Bhingarkar, “Feature-Based Comparision of iSCSI Target Implementations”, International Journal of Computer Applications (0975-8887) Volume 85 – No 16, January 2014Virtualization, Wikipedia, Available on internet: https://en.wikipedia.org/wiki/Virtualization

[10] Open-iSCSI Initiator, Available on internet: http://www.open-iscsi.org/

[11] History of Data Storage Technology, Arcserve, Available on internet: https://www.arcserve.com/insights/history-of-data-storage-technology/

[12] What is NVMe?, NetApp, Available on internet: https://www.netapp.com/us/info/what-is-nvme.aspx

[13] Btrfs vs OpenZFS, Linuxhint, Available on internet: https://linuxhint.com/btrfs_vs_openzfs/

[14] Backup Storage, Technopedia, Available on internet: https://www.techopedia.com/definition/13574/backup-storage

[15] BTRFS Wiki, Available on internet: https://btrfs.wiki.kernel.org/index.php/Main_Page

[16] BTRFS Data Structures, Available on internet: https://btrfs.wiki.kernel.org/index.php/Data_Structures

[17] BTRFS Tree Structures, Available on internet: https://btrfs.wiki.kernel.org/index.php/Trees

Proceedings of the Fourth International Conference on Communication and Electronics Systems (ICCES 2019)
IEEE Conference Record # 45898; IEEE Xplore ISBN: 978-1-7281-1261-9

An effective security protocol for GDS (group Data sharing) in Healthcare Cloud Environment

Uma Hombal
Department of CSE
Research Scholar, KSIT Bengaluru
uhombal@gmail.com

Dr. R. B. Dayananda
Department of CSE
KSIT, Bengaluru
rbdayanandakit@gmail.com

Abstract: **The data-sharing in cloud computing will enable many users to share the data. This helps in accessing the information easily and to share the data efficiently. The healthcare data will have to be shared amongst different healthcare centers and the medical practitioners. This involves security issues while sharing the healthcare data within a group. We provide the group model for sharing of data that is based on block based design where the group members will perform the key agreement to get the common group key that helps to shares the data securely. The fault tolerant property is provided by this design which can detect the malicious attackers during the group data sharing. The proposed group data-sharing is compared with the existing data sharing models w.r.t. the time cost of computation for group key generation and sharing of data.**

Keywords— Cloud computing, group data sharing, block based design, key agreement.

I. INTRODUCTION

The Personal health has been brought the great concern in modern residents. The population development and aging, the influence of health-care dictate and demands require for novel and the advanced solutions. At greater integration scale and lower cost, the availability of the computing re-sources has profited healthcare practices. With the help of development and success of the internet that plays an eminent role in maximizing the quality and access so the process is interrelated to the healthcare, which is determine the ICTs (Information of Communication Technologies) [1]. The E-health is defined as the ICTs application to the healthcare, which has come in normal use. While, these ICTs models can be considering many significance in the domain of healthcare, on top of the specific number of ICTs which is based on the emerged paradigm of health-care. There is a widespread use of electronic health record (EHR) [2]. Cloud computing is one of the popular health-IT infrastructures for facilitating EHR sharing. Healthcare providers and all the insurance companies store the electronic medical records in centralized databases .This includes maintaining health records, monitoring of patients etc.

The E-health can be widely defined as the ICTs application to the healthcare that has come in normal use. The co-operation between specialists in terms of the health experts, who can be working together efficiently, and generated their management in sharing and activities their information about the victim easier and in normal manner, and thus they can give cure to the patients. The systems of health are enable for citizen to have control their own health. However, there are security and privacy issues related to the health-care data. The security and privacy protection of cross-institutional electronic patient records is of major importance. The major concern is security in EHR networked systems and for communicating patient data. Here the physical security, network security, application security, internal systems security, secure data-backup strategy, secure internal policies and procedures, third-party certification are considered.

In this paper, our aim is to confirm the security of information sharing within a group in health care cloud security network. Here multiple data owners can freely share the outsourced data with high security. The entity authentication services are provided. The fault detection and fault tolerance is performed to identify the malicious user. We present the block design based key agreement protocol by extending the structure of the symmetric block design to support multiple participants. It enables multiple data owners to freely share the outsourced data. Here the adaptive symmetric block design is constructed as the group data-sharing model to support group data sharing in cloud computing. Here each group member performs the key agreement to derive a common group key to ensure the security of the outsourced group data. The help of group members can produce the normal group key. The semi-trusted and attackers of cloud server has no access to create the key. Cloud Security Service Third Party Verifier takes responsibility for the cloud storage auditing and key updates.

This paper is organized in such a way in section-II Literature survey, section- III described our proposed method, in section- IV, evaluation and medical outcome that is represented and in section- V conclusion.

II. Literature Survey

The research on various security and privacy issues related to health-care data is being addressed and many solutions have been proposed. In [3], the security and privacy issues of HER is given. The paper [4] provides the risk-management methods proposed for health-care environment. It focusses on managing the healthcare by using the fuzzy-logic. In paper [5] [6], it discusses the need in increase of standardized protection levels in the health-care network. In the paper [7], the security of personal-health record is proposed. It addresses the reduction of complexity in key management for the multiple record owners, which is used in the encryption of data being shared by patients to doctors.

In paper [8], it focusses on protected sharing of data in cloud by maintaining the information confidentiality and also the information integrity. The Protected secure data sharing methodology is used which will encrypt the files using only one encryption key. Two key shares technique is used wherein one key is given to user and other key is maintained by the verified third party. This helps in identifying the insider-threat and thereby the stealing of medical files being shared. The response for varying key size is demonstrated in it.

In paper [9], the secure method of resource sharing between more than one people whom from the group, is the main goal. The security and confidentiality is provided which helps in sharing the documents among multiple users of cloud. This paper provides advanced encryption scheme to encrypt the documents to be shared. The documents that are shared can be accessed once the verification of the accessing user is done and is valid. The aim of this paper [10] is provide the dynamic group-data sharing which will is useful for the health-care organizations to share their data that would involve other health organizations. In this paper they use the ternary-based tree approach which can have more health-care organizations and the computation of key used in sharing of messages would increase with the increase in number of member in group.

In [11], introduced the system of E-Healthcare, which is main role in civilization. This type of system aims at storing and collecting the details of patients and also sharing the information, which is related to the health. It has also higher concerns about the privacy of patient's and the security of information. It maximizes the systems of healthcare to isolated and remote locations, that has limited access to the remote healthcare and medical technologies, which can be provided via the telecommunications. They also gather the issues of health and personal information of real-time from the patients and send them to the provider of healthcare for authorized experts to decide on the corresponding cure. They transmit PHI in terms of image and text to Cloud and also personal problem which is interrelated to the medical history. A method for removing the authorized experts to decide on the corresponding cure, and has been broadly utilized in the storage f cloud to minimize the upload bandwidth and storage space.

In [12], MeDshare is addressed which provides a way to share the medical data which can avoid the privacy issues. This system can monitor which entities can access the data for any malicious activities. This can track the data that is being accessed. All activities are recorded and performed in proof way. The model of data sharing is utilized between the cloud-service providers, which is designing by block-chain. This design uses the smart-contracts and certain other mechanisms for accessing the data and to track the nature and behavior of information and have an access to the violated access done by malicious attacks etc. Auditing of data is achieved by this design. In paper [13], proposes the protocol of key exchange protocol that can be based on cipher text –encryption and policy that is attribute based. This establishes secure communication amongst all the participants who exchange messages among them. The attribute based encryption will make to achieve the user level privacy and data access control. Overall it achieves the secure way of communication among the fog-nodes.

III. Proposed Model

A) *System Model*

Fig1 shows the system model of sharing of data among different group according to our Proposed-SM (System Model). The model of system contains 3 entities such as Cloud, CSSTPV (Cloud security service Third party Verifier) and group members.

1) ***Cloud*** **:** the cloud gives the user with unlimited storage services. It gives convenient and efficient storage services for the users. The cloud here semi-trusted party providing data storage and data download services. The users who requires similar information and its related documents or files, will form a group and upload their respective data to cloud. These files can now be shared to other members of group.

2)CCSTPV *:* The client encrypts the information and upload it to cloud using key which is downloaded from the Cloud Security Service Third Party Verifier (CCSTPV) and is responsible for the storage of cloud auditing and give updates to key.

3) Group members: The group participants who wish to share the data to intended user first by identifying the group key, which helps in data sharing. With the fault tolerance capability, the member can identify the changes in the group key if any.

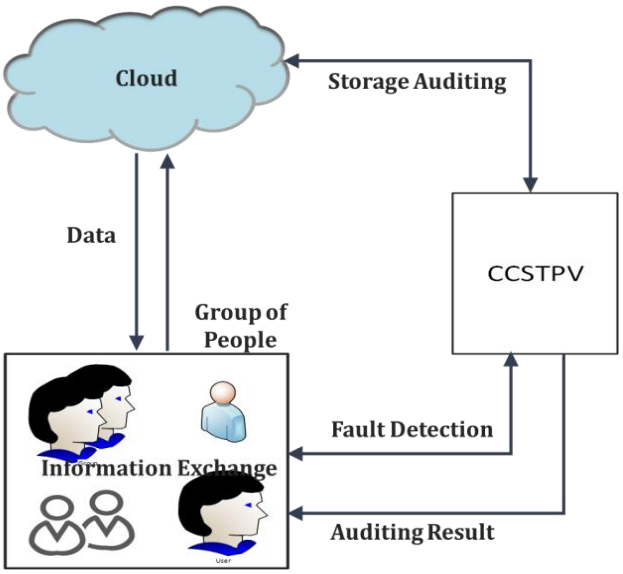

Fig 1: System model of information sharing according to the PSM

B) Construction of the model of Group data-sharing:

The group of information-sharing method applying the symmetric incomplete block based design i.e. (n, i+1, 1) design. It is a decentralized model. By this model, each user can identify the intended sender or receiver of message based on this model. Here n is the total users/participants as well as the number of blocks where blocks decide which user must belong to which block. This is decided by $n= i^2+i+1$. Each block will have i+1participants. Every single 2 participants appears simultaneously in the blocks of n. This in turn will decide to which block and in turn which participant the message must be delivered to. The generation of the (n, i+1, 1) design is explained in flowchart [Fig2].

The flow chart will give step by step details about the block based design. The user pos is the user position which specifies the column number and the block, the user will be belonging to. A sector is said to be group of blocks. For the generation of group key, each $block_i$ must have $user_i$. Therefore similar to above flowchart the steps are followed to generate another structure S which satisfies the block based design technique having property of each block S_i having $user_i$.

The Block diagram [Fig3] shows the block-based technique of group key agreement protocol and it is explained as follows:

There are 3 phases in the method of key agreement.

1. **Initial phase**: In this phase, the CCSPTV generates the parameters of system and distributes the private key to respective user and the public key to all the users. Mapping of private and public keys are done.
2. **Key generation phase:** Involves 2 rounds to generate the common group key. Users will receive the secret messages and then the common group key is generated. This helps in sending the messages to the intended user.
3. **Authentication phase**: This involves identifying the malicious users in the group, verification of authenticity is done.

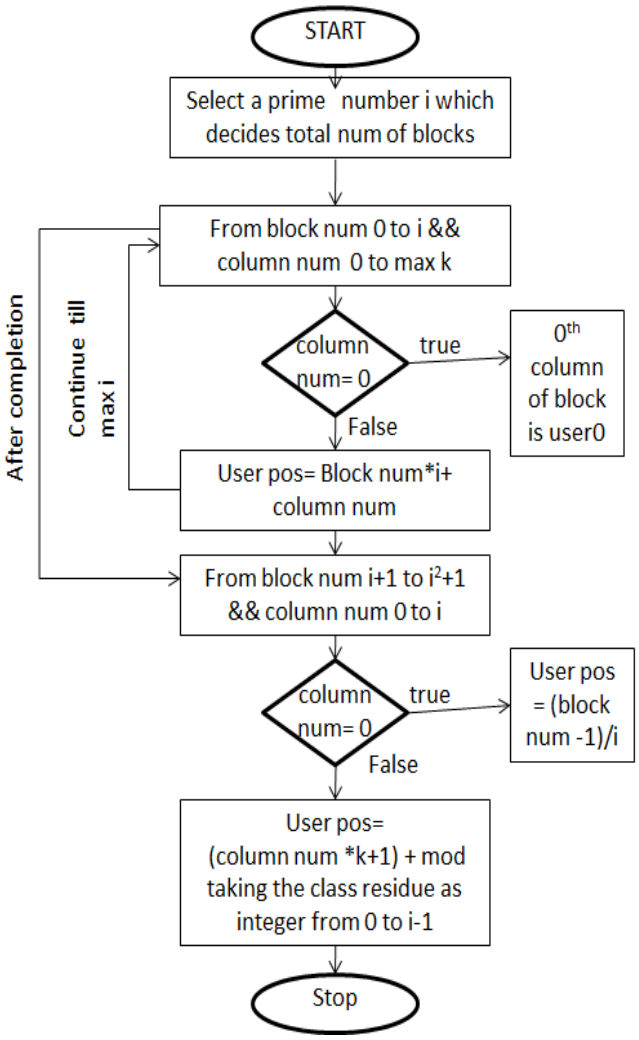

Fig 2: Flow chart of Block based design

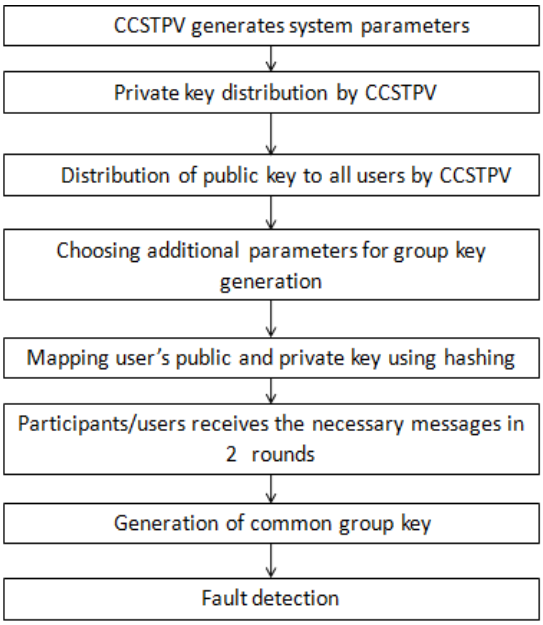

Fig 3: Steps of the key agreement protocol

IV. Simulation Result And Analysis

The experimental evaluation PSM is done using the C programming language. The PSM evaluation uses are the GNU and PBC (Pairing based Cryptography) more than one Precision of Arithmetic Library in VM-ware workstation (12) machine on the Cent-OS (6.7).

Our proposed system PSM is the proposed system model is compared with the IBFTA protocol. IBFTA protocol [14] is an identity based fault tolerant approach which is a key agreement of protocol which is used in exchanging messages among different users. The time cost comparison is done in order to identify which scheme is faster according to the design for exchange of messages, with the increase in the number of participants, both the protocols will have increase in cost for computation. The computation cost for multiple participants and for different phases is found and our protocol efficiency has been compared.

Considering the time cost, the comparison is done first according to the phases of key agreement protocol. Consider initial phase [Fig4], when the number of participants n=7, the time cost for computation in our protocol is 15.7% more efficient than IBFTA protocol [14]. When n=31, our protocol is 65% more efficient. The efficiency of our protocol is more when the number of users increase. When n=993, our protocol is said to be 99% efficient when compared to the IBFTA protocol.

In key agreement phase [Fig5], even when there are less number of users or more the efficiency when compared to IBFTA protocol [14] is high. When there are 7 users, total computation cost is less which is 90% efficient than IBFTA scheme [14]. When n=133 and n=993, the common group key generation is faster and this is 98% efficient to that of IBFTA protocol [14].

In authentication phase [Fig6], time cost when there are less users involved, n=7 our protocol is 8% efficient than IBFTA. In other cases, Yi protocol's time cost is more efficient than our protocol only in this phase. With increasing number of consumers, the time cost of our protocol in this phase increases. IBFTA protocol is 93% efficient than our protocol when n=993.The main reason is that in our case the modular exponentiation is done during this phase which takes more time and this is not the case in IBFTA protocol[14].

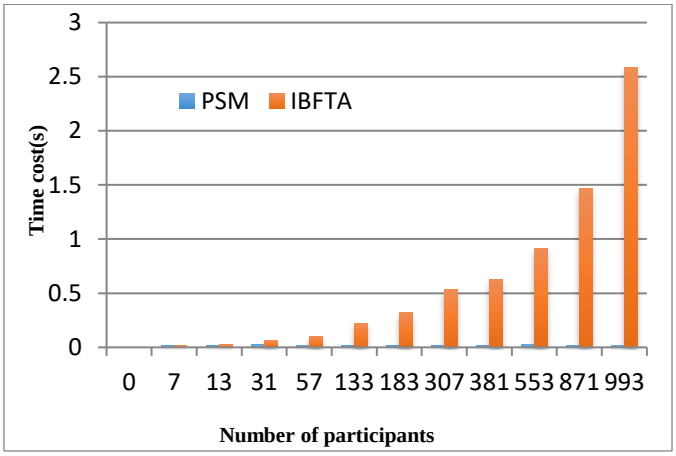

Fig4: Initial Phase

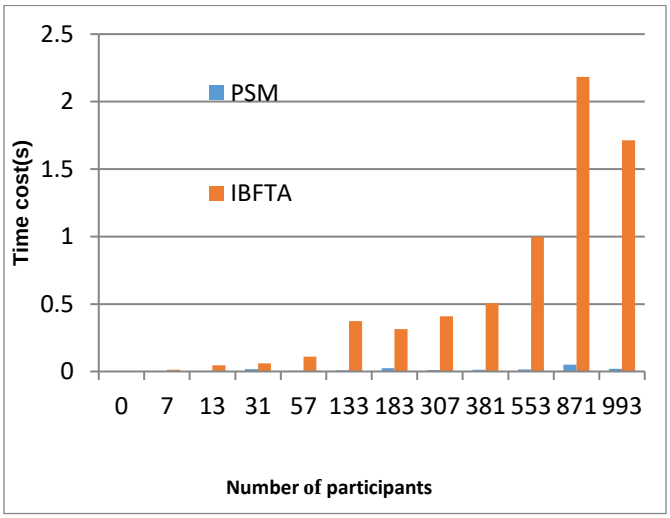

Fig5: Key Agreement Phase

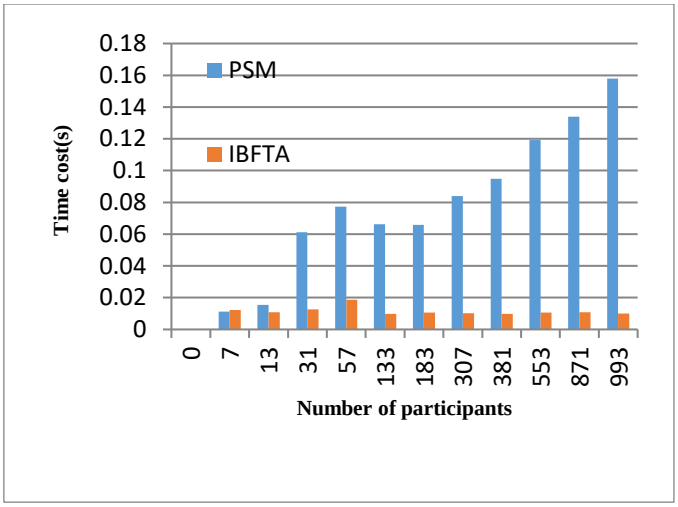

Fig6: Authentication phase

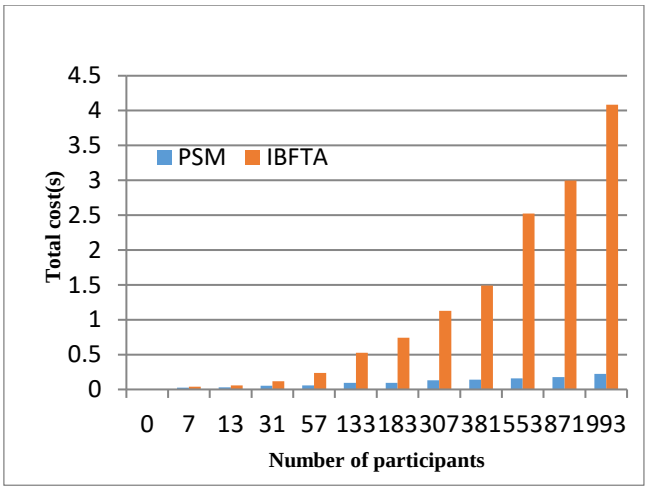

Fig7: Efficiency comparison for multiple participants

Comparing the efficiencies for multiple participants [Fig7], the total computational cost for the participants is considered. The computation cost for IBFTA protocol [14] continuously increases with increase in number of users (n). In our protocol this computation increases based on prime number i, which decides n. For 7 users, our protocol is 34% efficient. For 133 users our protocol is 82% efficient, for 871 and 993 users ours is 94% efficient all in comparison to the IBFTA scheme. Overall, our protocol is supreme compared to IBFTA scheme [14].

V. Conclusion

In this paper, the healthcare of data sharing is achieved by a block based design data-sharing model where, the data can be shared between different groups by generating the common group key. This proposed method involves different phases in group key generation and thereby the data-sharing is obtained. This method is much more efficient when compared with IDFTA w.r.t the computational costs. About 94% efficiency is obtained for the multiple participants for computation cost when compared to the IDFTA protocol. Therefore, our protocol is much more efficient in sharing the data in a faster way.

References

[1] Giuseppe Aceto, Valerio Persico, Antonio Pescap_e, “The role of Information and Communication Technologies in Healthcare: Taxonomies, Perspectives, and Challenges”
[2] Rui Zhang and Ling Liu,” Security Models and Requirements for Healthcare Application Clouds”.
[3] ANSI, ISO/TS 18308 “Health Informatics-Requirements for an Electronic Health Record Architecture”, ISO 2003.
[4] R. Bakker, B. Barber, R. Tervo-Pellikka, A.Treacher, (eds.), “Communicating Health Information in an Insecure World” in: Proceedings of the Helsinki Working Conference. 43:1, 1995. 2.
[5] B. Barber, D. Garwood, P. Skerman, In: Security in Hospital Information Systems, Security and data protection programme presented at the IMIA WH10 Working conference, Durham. 1994.
[6] M. Furnell, P.W. Sanders, “Security management in the health-care environment”, in: R.A. Greenes, H.E. Peterson, D.J. Protti, (eds.), MEDINFO ’95, Proceedings of the eighth World Congress on Medical Informatics. Canada. p. 675–678.
[7] A. Patel, I. Kantzavelou, “Implementing network security guidelines in health-care information systems”. In: MEDINFO ’95. Proceedings of the eighth World Congress on Medical Informatics. Vancouver Trade and Convention Centre, Canada. p. 671–674.
[8] D. Aarthi and N. Indira, "Enabling efficient and protected sharing of data in cloud computing," 2016 International Conference on Information Communication and Embedded Systems (ICICES), Chennai, 2016, pp. 1-5.
[9] S. Mercy and G. U. Srikanth, "An efficient data security system for group data sharing in cloud system environment," International Conference on Information Communication and Embedded Systems (ICICES2014), Chennai, 2014, pp. 1-4.
[10] V. R. Thakare and K. J. Singh, "Ternary tree based TGDH protocol for dynamic secure group data sharing in healthcare cloud," 2016 International Conference on Inventive Computation Technologies (ICICT), Coimbatore, 2016, pp. 1-7.
[11] R. S. Sharon and R. J. Manoj, "E-health care data sharing into the cloud based on deduplication and file hierarchical encryption," 2017 International Conference on Information Communication and Embedded Systems (ICICES), Chennai, 2017, pp. 1-6.
[12] Q. Xia, E. B. Sifah, K. O. Asamoah, J. Gao, X. Du and M. Guizani, "MeDShare: Trust-Less Medical Data Sharing Among Cloud Service Providers via Blockchain," in IEEE Access, vol. 5, pp. 14757-14767, 2017.
[13] A. Alrawais, A. Alhothaily, C. Hu, X. Xing and X. Cheng, "An Attribute-Based Encryption Scheme to Secure Fog Communications," in IEEE Access, vol. 5, pp. 9131-9138, 2017.
[14] X. Yi, “Identity-based fault-tolerant conference key agreement,” IEEE Transactions on Dependable and Secure Computing, vol. 1, no. 3,pp. 170–178, 2004.

Proceedings of the Fourth International Conference on Communication and Electronics Systems (ICCES 2019)
IEEE Conference Record # 45898; IEEE Xplore ISBN: 978-1-7281-1261-9

Obstacle Detection Using Sensor Based System For An Four Wheeled Autonomous Electric Robot

Miss. Shusmita M. Rathod
Student, Department of Electronic Engineering
Sanjay Ghodawat University
Kolhapur, India
shush.rathod19@gmail.com

Mrs. S.K. Apte
Prof., Department of Electronic Engineering
Sanjay Ghodawat University
Kolhapur, India
apte.sk@sginstitute.in

***Abstract*— now day's many industries are using autonomous robot due to their high performance and reliability and which is a great help for human beings. Autonomous cars, one of the most trending topics all over the web a car with no steering wheels, pedal, and with the most advanced technology autopilot. An autonomous vehicle is able to recognize there surrounding and finding the path there itself. Autonomous robot senses their surrounding with the help of different sensors such as Lidar, radar, ultrasonic sensor, infrared sensor; GPS etc. the control system used in autonomous vehicle read the information from the surrounding and find the appropriate path as well as the various obstacles are present on the path. Most of the autonomous vehicles are used for the obstacle detection purpose. In this project, the obstacle detection system is developed and the IR sensor usually used for the distance measurement. The sensor-based four-wheeled autonomous electric robot used to move the vehicle in the predefined path and avoid the obstacle during motion using the data logged from the IR sensor. Suppose during motion the robot doesn't have enough space to pass through the obstacle it must be stopped there itself or otherwise it moves by avoiding the obstacle. The system can be designed in Simulink environment.**

Keywords*— *Autonomous vehicle, Obstacle detection, Arduino mega 2560, Sharp distance IR sensors (Long and Short range IR sensor), Dual shaft DC geared motor, l298n dual h bridge steeper motor controller.

I. INTRODUCTION

The autonomous electric vehicle has received a lot of attention during the past decade and prototype versions of the autonomous vehicle have been developed by different vendors. Now, the research is going on autonomous vehicles all over the world, based on theories of innovation and leading design. According to this research produces various new technologies used in the autonomous vehicle and electric vehicle. Because of this autonomous vehicle there are lots of technology are used for the transportation purpose. Such as where we live, how created a new industry which build our cities and infrastructure. there are various names of Autonomous such as self- driving vehicle , robot or the car without driver etc. Is a vehicle that is able to sense it's surrounding and moves were safe and desirable. There is no human supervision is required for an autonomous electric vehicle, everyone in an autonomous vehicle is a passenger or it can travel with no occupant at all. The primary components of the autonomous electric vehicles are sensors, actuators, and controller unit Autonomous cars consist of multiple combinations of sensors. The real-time data that can be generated from the actuator such as servo motor that must be processed and analyzed to perceive their surroundings. The Autonomous electric vehicles emit less pollutant in the atmosphere rather than the conventional fuel engine-based vehicles.

There are various technologies are required for developing an autonomous vehicle such as radar sensor is used for detection of obstacle and after detecting object it measure the distance and angle of object. Lidar sensor is used for measurement of distance in the form of variable ranges. Ultrasonic sensor is also used for measurement of distance during the object is detected. Video is used for reading the road signals, direction sign, and nearby vehicles. A central computer collects and analyses all this data to help it steer, accelerate, and brake, as needed. The Potential benefits of an autonomous electric vehicle include increased safety, increased mobility, reduced costs, reduced crime, and increased customer satisfaction. And some other advantages are reduces the cost and fuel consumption capacity is also reduces and the size of autonomous vehicle is also reduces because of reducing the size of vehicle the space required for the vehicle of parking purpose is also reduces. The Autonomous electric vehicle has some disadvantages like liability for damage, software reliability, loss of driving-related jobs, loss of privacy; it is very difficult for autonomous vehicle to operate in heavy rain fall and snow and also in heavy disaster. The autonomous electric vehicles must also have the functionality of vehicle collision avoidance systems. In the present vehicles, the vehicle collision occurs due to the distraction of the drivers while driving. In the case of driverless vehicles, the collision of the vehicle will not occur, since the controller unit that controls the vehicle by continuously observing the road conditions.

Most of the Companies are uses autonomous car for developing and testing purpose such as Google, Volkswagen, BMW, etc. In 1920 the experiment of the autonomous vehicle started. In 1980 the first autonomous car is developed. Google has done remarkable work in this field for the past few years. The combination of an autonomous and battery-powered the vehicle has proven to be a breakthrough in the automobile industry. The

autonomous electric vehicle consists of both hardware and software developers such as those involved in sensors, artificial intelligence, mapping, & network connected services for transportation, advanced driver assistance system. The electric car uses battery for storing electric energy and by using this electric energy the car produces the motion in different direction. The electric vehicle does not produce any form of pollution during motion. Because of this the electric vehicle provide pollution free environment as compared to other types of vehicle. The electric vehicle does not uses any form of fuel for driving purpose it uses electric energy instead of fuel. Sometime the battery inside the electric vehicle is discharge so upon charging the vehicle can be moved.

For design automated driving functionality Automotive companies use MATLAB and Simulink software which include computer vision algorithm development, control development, and sensor fusion, etc. Most of the companies' select MATLAB and Simulink software for development purpose because the design of model in Simulink environment is easy as compared to other software and the cost required during design process is very less and size of design is also very compact. Simulink uses block for design the system instead of code used in MATLAB. The Simulink is easy as compared to MATLAB because it provide a simple environment for development of system.

II. LITRATURE REVIEW

Geetinder, Sourabh, Jaspreet and Samreet (2014) give information about the Google driverless car. The car won't have steering wheels the steering can be done while looking out the obstacles, Accelerators or brake pedal can be used for correction of the speed limit and in any traffic condition it can go or stop there itself. All the work of the Google driverless car can be carried out by sensors and software. The Google driverless car consists of three parts such as Google maps that are generally used for navigation. Google maps provide information about the road, traffic signs, etc. the second part is the different types of hardware sensors such as Lidar, video camera, position estimator, distance sensor, aerial and computer these sensors are used for obstacle detection and the third the part is artificial intelligence the data coming from Google maps and hardware sensors are given to artificial intelligence for determining the acceleration. The main part of artificial intelligence to drive the passenger safely and legally to his destination.

Mustapha, Zayegh and Begg (2013) explain about the different sensor used for obstacle detection and distance measurement. There are various sensor used for obstacle detection and distance measurement few of them are IR sensor and ultrasonic sensor. The system uses different type of material for obstacle detection such as paper, plastic, books, plastic etc. The characteristics defined by both the sensors are different the linear characteristics are given by ultrasonic sensor and nonlinear are given by IR sensor. The IR sensor resolution is high as compared to ultrasonic sensor.

Mohammad (2009) gives the information about two distance measurement sensor. The amplitude response of the IR sensor depends on the reflectance properties of the target. The ultrasonic sensor has slightly higher resolution than the IR sensor. The care should be taken while placing the object from the sensor because a slight change in the angle produces a slight difference in the actual distance. The amplitude from the US sensor is dependent on the orientation of the obstacle relative to the sensor and distance, The amplitude of the IR sensor does not have much effect where the small orientation of the reflecting surface. There is no effect of Surface color and smoothness on the output signal of the ultrasonic sensor. The reflectivity of an obstacle is depending on the amplitude of the IR sensor.

Varghese and Boone (2015) explain about the various technologies used to enable autonomous vehicles and advantages, disadvantages associated with each autonomous vehicle sensor. This paper also explained about the internal vehicle systems, external world sensing, sensors, systems, and various factors that play into autonomous vehicle design. Although the single sensor does not provide full information about the autonomous vehicle so that the fusion of sensor is used to drive the autonomous vehicle fully.

Vairavan, Ajith, Shabin and Godwin (2018) they develop one vehicle which is nothing but the robot. This robot is used of obstacle detection and avoidance. The obstacle that are generally detected with help of ultrasonic sensor and avoidance that can be done using arduino microcontroller. In order to detect the obstacle the ultrasonic sensor is placed at the front side of robot. With the help of ultrasonic sensor place on front side of robot the data can be sensed. After data sensing the ultrasonic sensor sense whether the obstacle is present or not if the obstacle is present it detect the obstacle and change the path in which there is no any obstacle are present. After that the data sensed by ultrasonic sensor is given to the controller for the motion of the vehicle and direction of vehicle.

David (2012) explains about the simulation tool used to drive electric vehicle. A simulation is the important tool that provide large amount of benefit for design the model because while designing the cost of the development is reduces. By embedding the entire simulation model during design process can decrease the design time and cost of the design so that most of the companies can complete and test the design with in time. The path changing for an autonomous vehicle is important for the system and to generate a new way to pass the front vehicle without having any collision.

III. METHODOLOGY

The process of measuring the distance to an obstacle can be performed by managing the input and output signals which are coming from the Sharp distance IR sensors. In that input and output signal management there consist of signal processing, conditioning, parameterization, and integration, etc.

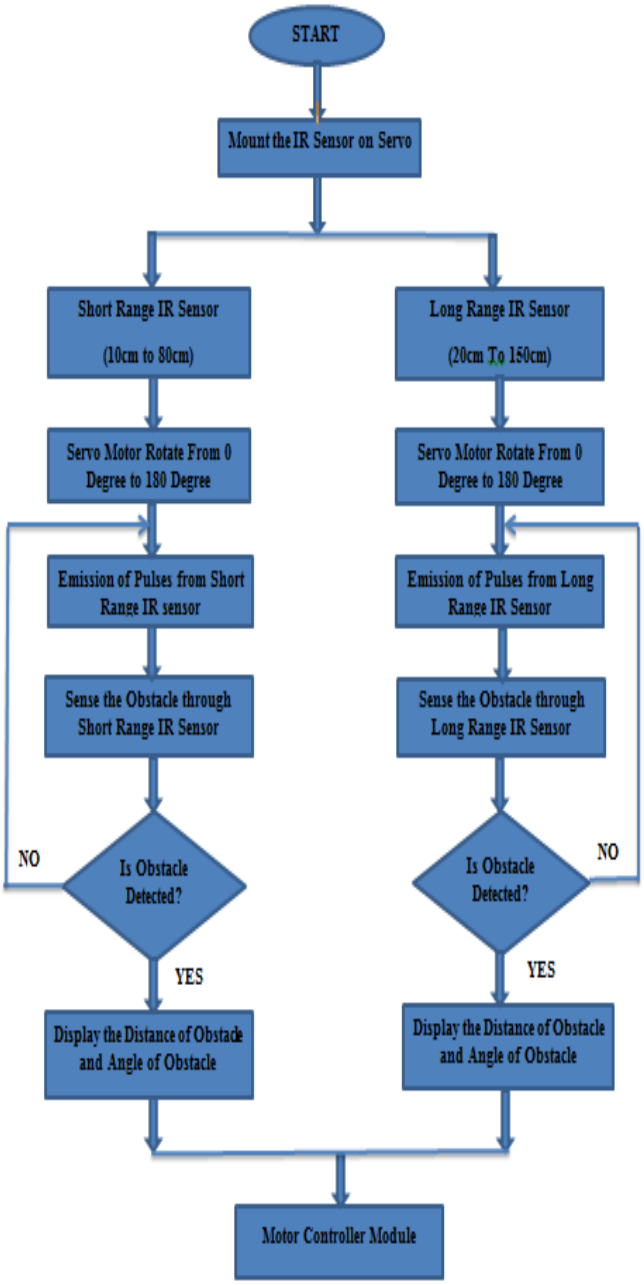

Fig.1. Flow Diagram of Obstacle Detection Using Sharp Distance IR Sensors

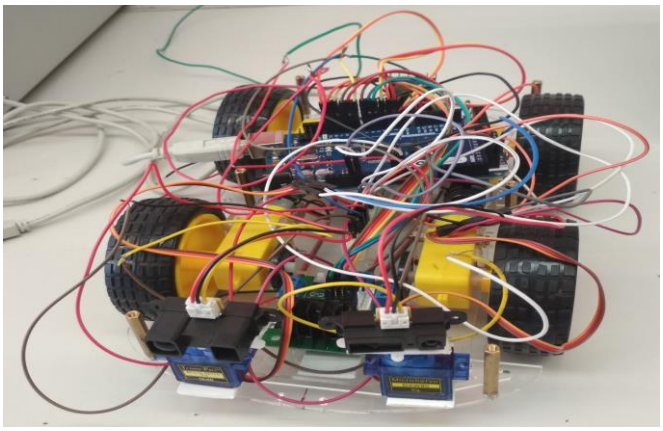

Fig.2. Photograph of Experiment Setup

A. *Signal Processing*

Signal processing is a subfield of information, mathematics, and electrical engineering that is generally used for analysis, synthesis, and modification of the signals. This signal processing that can be done by logging the data coming from both Long range and Short range infrared sensor this logging data are taken from Analog input pin of Arduino i.e. pin A1 for short range IR sensor and A2 for Long Range IR sensor this pin gives the value of ADC count. After using the specific the formula which is based on ADC count i.e. Short-range IR sensor distance can be calculated by using a formula such as

$$\text{Distance (cm)} = 4800/ (\text{Sensor Value} - 20) \quad (1)$$

And another formula used for calculating distance using Long range IR sensor which is nothing but

$$\text{Distance(cm)} = 9462/(\text{sensor Value} - 16.92) \quad (2)$$

B. *Conditioning*

When data is logged from the IR sensor according to logging values the condition is applied in the State flow. There are two State flow are included in single State flow one for servo motor rotation from 0 degrees to 180 degrees. According to condition given in State flow servo motor rotated from 0 degrees to 180 degrees after rotation angle of the servo motor is calculated. And another State flow is used to calculate the obstacle angle from start to end point of the obstacle when the obstacle is detected for both the sensor. This two State flow can be run parallelly because both IR sensors are mounted on the servo motor. According to servo rotate, the IR sensor detects the obstacle.

C. *Parameterization*

Parameterization that is generally used for measurement of a different parameter from the different sensor both the IR sensor detects the obstacle within the specified limit. After detecting the obstacle IR sensor measure the distance of obstacle and this distance can be represented on display. It will also measure voltage, velocity, etc.

D. Integration

Integration of all the components is the final part of my project which is nothing but the process of bringing all the components together with the components such as sub-system into a single system and ensuring that the subsystem works the same as the system and integrating part can be done by embedding all the modules together and tested and assuring their condition to work towards the goal. The integration can be done by combining both the system such as calculate the distance of obstacle using both the IR sensor and the output of IR sensor i.e. distance is given to motor controller model in the form of input according to the distance and speed condition the time can be calculated from that time the condition is given in State flow so that the motor rotates in forward, right, forward and right direction. The benefit of integration is lower development cost, increase reliability and security. Integration is necessary to enable the flow of data through the system as well as provide the necessary data for system functions. If the system that is not integrated results in a significant increase in cost and resource consumption.

IV. RESULTS AND DISCUSSION

The results were discussed by comparing the output of both the IR sensor with respect to distance. Chart 1 shows the distance measurement of both the IR sensor. When the obstacle detected both the IR sensor shows the variations in the distance while when an obstacle is not present it will show the constant distance measurement. By comparing the distance of both long range and short range IR sensor the long range IR sensor gives the accurate result as compared to the short range IR sensor because the range of long-range IR sensor is more as compared to short range IR sensor. The operating voltage for both the IR sensor is kept constant i.e. of (5v).

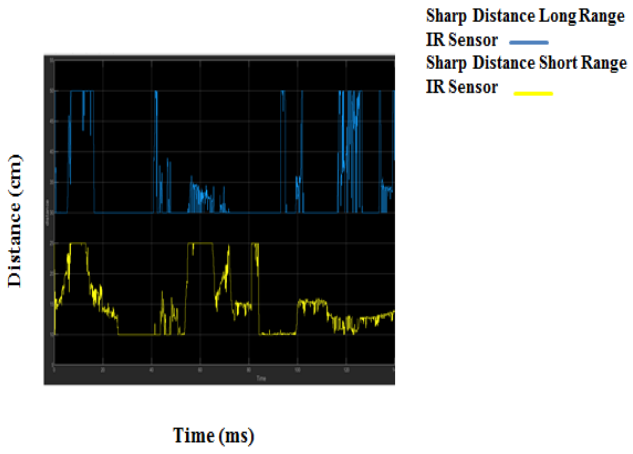

Chart.1. Distance vs time graph

V. CONCLUSION

The goal of my project is to develop a sensor based four-wheeled autonomous robots which detect the obstacle in his path with the help of data logged from the Sharp distance IR sensor and move the robot in the predefined path. During motion if the car doesn't find enough space to pass through the obstacles it must stop there itself otherwise moves in a predefined path by an avoiding obstacle. This project is been designed and implemented with ATmega 2560 Arduino microcontroller in Simulink domain. The work which is performing experimentally has been carried out carefully. Sensor output will be given to the controller. According to signals given to the controller, it will run the wheels in different direction i.e. forward, right, forward, right and speed based on the input signals.

VI. FUTURE SCOPE

The Future scope of my project is to design the same sensor based four-wheeled autonomous electric robot using LIDAR sensor instead of using sharp distance IR sensor because the LIDAR sensor also used for detection of obstacle and measurement of distance but the distance can be easily estimated using LIDAR. The range of LIDAR is very high i.e. 1000feet to 4000 feet. LIDAR provides 360 degrees of resolution. And also develop the GPS system for moving the vehicle from one point to another point.

VII. REFERENCES

[1] G. Kaur, S. Joshi, J. Kaur And S. Kaur, "Going Driverless With Sensors," *International Journal Of Science, Engineering And Technology*, Vol. 2, No. 5, Pp. 298-303, 2014.

[2] B. Mustapha, A. Zayegh and R. K. Begg, "Ultrasonic and Infrared Sensors Performance in a Wireless Obstacle Detection System," *First International Conference on Artificial Intelligence, Modelling & Simulation*, pp. 439-443, 2013.

[3] T. Mohammad, "Using Ultrasonic and Infrared Sensors for Diatance Measurement ," *World Academy of Science, Engineering and Technology*, vol. 3, p. 273, 2009.

[4] J. Z. Varghese and R. G. Boone, "Overview of Autonomous Vehicle Sensors and Systems," *International Conference on Operations Excellence and Service Engineering Orlando, Florida, USA*, , p. 178, 2015.

[5] V. R. A. S. Kumar , . S. L. Ashiff And G. C. Jose , "Obstacle Avoidance Robotic Vehicle Using Ultrasonic Sensor, Arduino Controller," *International Research Journal Of Engineering And Technology (Irjet)*, Vol. 5, No. 2, Pp. 2140-2142, 2018.

[6] D. McDonald, "Electric Vehicle Drive Simulation with MATLAB/Simulink," *Proceedings of the 2012 North-Central Section Conference Copyright © American Society for Engineering Education*.

[7] A. S, M. . S. Kaleemuddin , . D. Bose and . R. . I. K , "Performance comparison of Infrared and Ultrasonic sensors for obstacles of different materials in vehicle/ robot navigation applications," *IOP Conf. Series: Materials Science and Engineering*, pp. 1-7, 2016.

[8] P. B. G, . S. . S. R. Patange, . S. A, R. S and S. . S. J, "Characteristics of different sensors used for Distance Measurement," *International Research Journal of Engineering and Technology (IRJET)* , vol. 4, no. 12, pp. 698-701, 2017.

[9] J. . Z. Varghese and . R. . G. Boone, "Overview of Autonomous Vehicle Sensors and Systems," *International Conference on Operations Excellence and Service Engineering Orlando, Florida, USA,*, p. 178, 2015.

[10] I. R , O. Z and S. S , "Obstacle-avoiding robot with IR and PIR motion sensors," *IOP Conf. Series: Materials Science and Engineering*, pp. 1-6, 2016.

[11] P. A. C and G. . V. Subramanya , "Obstacle Avoidance Robot Using Arduino," *International Journal Of Engineering Research & Technology*, vol. 6, no. 13, pp. 1-4, 2018.

[12] M. Nasucha, "DEVELOPMENT OF AN OBSTACLE AVOIDING ROBOT," *Jurnal Sistem Komputer*, vol. 5, no. 2, pp. 55-60, 2015.

[13] A. Vaghela , . J. Patel and . S. Vaghela , "Obstacle Avoidance Robotic Vehicle Using Ultrasonic Sensor, Android And bluetooth for obstacle detection," *International Research Journal of Engineering and Technology* , vol. 6, no. 2, pp. 339-346, 2016.

Proceedings of the Fourth International Conference on Communication and Electronics Systems (ICCES 2019)
IEEE Conference Record #45983; IEEE Xplore ISBN: 978-1-7281-1261-9

Synchronization of Distributed Photovoltaic Generation with an Active network using Phase Locked Loop technique

Mr. Syed Noorul Faraz[1]
M.E. E. P. S. (PG Student), Electrical Engg.Department,
P.E.S. College of Engineering Aurangabad, Maharashtra, India.
snfaraz121@gmail.com

Prof. S. V. Murkute[2]
Asso. Prof., Electrical Engg. Department,
P.E.S. College of Engineering Aurangabad , Maharashtra, India.
murkutes@rediffmail.com

***Abstract*— The above paper gives the detail design of Solar PV system along with its synchronization with grid connected systems. In this paper detailed design of system along with the design of boost converter, design of inverter system for 180 degree conduction mode along with its SPWM technique and grid synchronization using Phase locked loop technique has been discussed. The PV panel's DC output is amplified by using boost converter up to desired value. which is further converter into A.C. supply by using 3-phase inverter which is working under 180 degree conduction mode which can be controlled by Sinewave pulse width modulation techniques. The reference signal for the system is derived by the grid using phase locked loop so the output of the inverter is in synchronism with grid with respect to phase as well as frequency.**

Keywords—PV panel, Inverter, Boost Converter, SPWM, PLL, Grid Synchronization.

I. INTRODUCTION

In the current scenario of world energy sector, renewable sources are growing their importance every day. This is due to limitation of the conventional resource and adverse environmental impacts of the conventional energy. Among the all Renewable energy sources available, solar energy seems to be a major competitor [1] as it is widely and almost everywhere available in nature and its conversion to electricity through photovoltaic process does not cause harm to environment. The electrical energy which is generated through solar PV system can be used to operate the different types of applications and loads. Solar energy is generated by means of solar photo-voltaic systems, which use arrays of PV panels that convert solar irradiation into electricity. It is reliable and cheap as compared with others.[3]

The Solar generation PV system consist of two types first one is Isolated or standalone system where batteries are used for storing electrical energy and then it is directly fed to load. This system is mostly popular in remote areas, where there is complete absence of grid transmission system or it is impractical to provide power system for light loads. Standalone system is also popular among charging low power appliances. Similar to grid tied system, standalone system also requires similar components for power generation like boost converter, inverter etc. but the addition to that it also requires battery i.e. energy storage system. The size of battery system is directly proportional to the energy requirement of load so it makes system much more costly and bulky for higher power applications. That's why this standalone system is mostly used for low power applications. [12]

The grid tied PV systems also known as ON grid photovoltaic system or grid connected solar photovoltaic system is solar PV system which, instead of storing the energy in the batteries, prefers to transmit the generated energy into the grid, which decreases the cost of battery system but increases the complexity as it need it needs grid synchronization in order to archives stability in the system.[6]

II. LITERATURE SURVEY

A. Photovoltaic System

Photovoltaics is the type of technology and research which directly convert sunlight into electrical energy. The solar cell is the elementary building block of the photovoltaic technology. Solar cells are made of semiconductor materials, such as silicon. [2]

The photovoltaic cells are made up of two or more thin layers of silicon which is common semi-conducting material. When the semiconductor is exposed to light, electrical charges are generated and this can be conducted away by metal contacts as direct current (DC). As the power output from a cell is small inadequate , so more than one cells are combined which forms a 'string'. This increases the output voltage os the system considerably. Classification of Solar pv panels is shown in fig 1.1

Monocrystalline silicon PV panels

Such Monocrystalline panels can be made using cells made up of only one cylindrical crystal of silicon. This system is very effective and has high efficiency as it can transform around 15% of the sun's energy into electrical energy. But the process of production of monocrystalline silicon is very difficult and complicated which increases the cost of them.

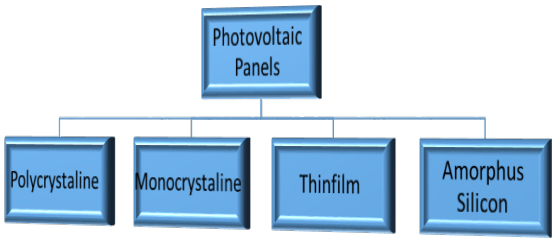

Figure 1: Classification of PV panels

Polycrystalline silicon PV panels

Polycrystalline photovoltaic is also called as multi-crystalline cells. This multi silicon cells are made-up of cells

which are cut from an Ingot of a melted and re-crystallized silicon. They are cut to form thin wafers and again molded into complete cells. This type of panels requires low cost to produce than monocrystalline cells, Though it is low cost and less complicated to manufacture as compare to monocrystalline it has less efficiency i.e. up to 12%.

Thin-film silicon PV panels

Thin film type of panel is a type of multi-crystalline, In this silicon is finely grained .Thin film PV panels are normally enclosed in a transparent and insulating polymer with a tempered glass cover and then fitted into a metal framed module.

Amorphous silicon PV panels

Instead of making rigid crystalline structure, amorphous silicon panels are produced by composing silicon in a thin homogenous layer. These panels can absorbs good amount of solar energy than crystalline type of panels. These panels are very thin that's why it is also called as thin film panels. This type of panels has less efficiency than crystal panels, it can convert only 6% of energy into electrical energy.

B. Off Grid Vs Grid Configuration

As shown in fig. 2 Solar configuration can be of two types i.e. On-Grid & OFF-Grid, depending upon various geographical factor, type of application and availability of resources. On grid system is connected to grid while off grid isolated system.[9]

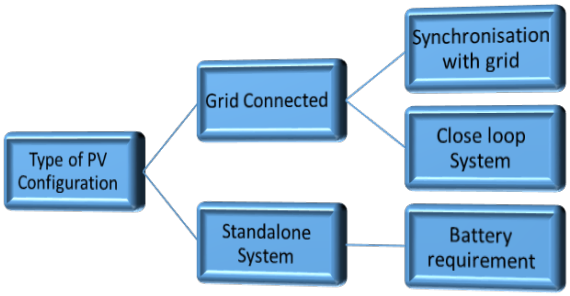

Figure 2:Types of PV panels Configuration

Standalone system requires battery to store the energy, which again increases the cost of the whole system. The drawback of battery requirement will be overcome by grid connected system where instead of storing generated energy it is injected in the grid which omits the energy storage system. Again grid connected system has its own challenges like Synchronization of voltage with the grid, which increases the complexity of the system.[4]

C. Structure of Grid Connected System

The figure no 3 shows the structure of grid tied photovoltaic system. Any energy storage system like battery is absent in grid connected system but feedback control is used from grid to inverter for synchronization. The PV panel generated the D.C. electrical energy in from solar radiation. The generated D.C. Voltage is amplified to desired voltage level by the boost converter. This system is either open loop or close loop system where controller can be used to maintain the output of boost converter. The output power of boost converter is of DC type, which is then fed to inverter to convert it to desired AC voltage which is then either supplied to load or supplied to grid. As discussed earlier there are certain challenges associated which supplying power to grid i.e. synchronization of voltage which is then obtain with help of PLL i.e. Phase Locked Loop system. PLL generated the reference signal which is then fed to the SPWM system of inverter, which generates respective switching signals for inverter and phase & frequency synchronization can be obtain.

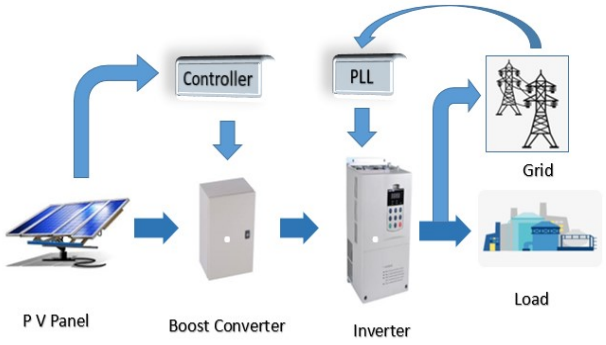

Figure 3: Grid Connected structure of PV System

III. DESIGN & SIMULATION OF SYSTEM

The figure 4 shows the block diagram of MATLAB simulation of the grid connected photo voltaic system. It consists of PV panel block which is the simulation of PV panel, next to it is a boost converter which can be implement to amplify the DC Voltage to desired value. Three phase Inverter circuit is used to convert the DC voltage to three phase AC, SPWM i.e. sine wave pulse width modulation is used to generate switching signal for the three-phase photovoltaic inverter whose output is given to load and Grid. For synchronization of the output voltage PLL i.e. Phase lock loop system is used which measures the frequency along with its phase angle of the grid and according reference is provided to SPWM system.

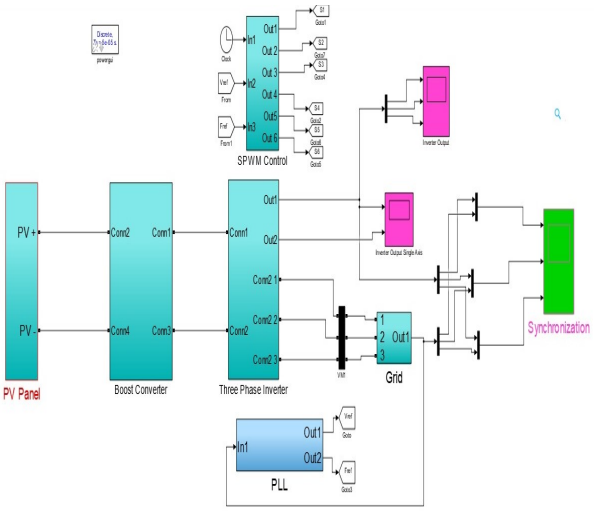

Figure 4: Simulation of Grid Connected PV system

A. PV Panel

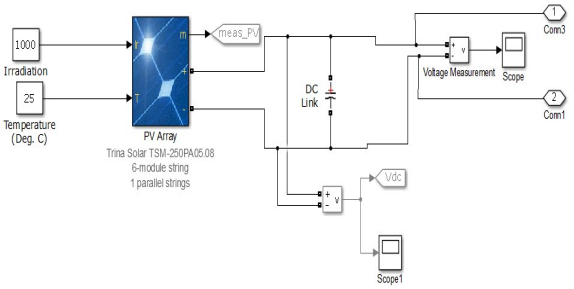

Figure 5: PV panel simulation

The MATLAB simulation of P.V. panel is shown in Fig. 5, input for the panel are temperature & irradiance. DC link capacitor is used to keep the output voltage constant. The VI & PV characteristics of the solar panel is shown in figure 6.

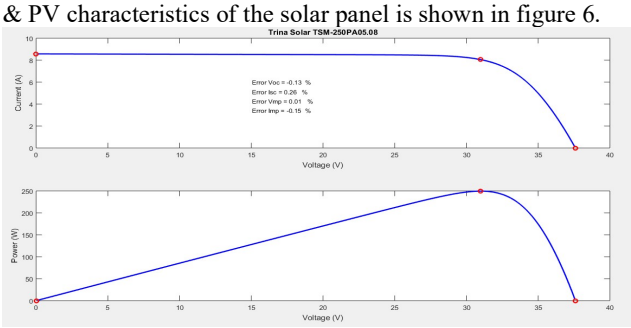

Figure 6: V-I & P-V Characteristics

B. Boost Converter

The function of boost converter is to "step-up" an input voltage to some desired higher voltage level, which is essential for a load. This unique capability is achieved by storing energy in an inductor and releasing it to the load at a higher voltage. This brief note highlights some of the more common pitfalls when using boost regulators. These include maximum achievable output current and voltage, short circuit behaviour and basic layout issues. Figure 7 shows the simulation of Boost converter. Design of boost converter includes design of deciding modulation index along with calculation of switching frequency, inductor & capacitor of the circuit.

i. Selection of Duty Cycle : Duty ratio is the parameter which decides output voltage magnitude. The relation between output voltage is proportional to duty cycle. [8]

$$D = 1 - \frac{V_{in} \times \eta}{V_o} \quad \text{.....(1)}$$

Where η is estimated efficiency of the boost converter.

.

ii. Selection of Inductor : As increases in the inductor value, output current also increases because of the reduction in ripple current. As the inductor value decreases, current limit also decreases. But it is need to take care of the inductor must always have a higher current rating than that of the current.

$$L = \frac{V_{in}(V_o - V_{in})}{\Delta I_L \times f_s \times V_o} \quad \text{.....(2)}$$

V_{in} = input voltage
V_o = required output voltage
f_s = switching frequency (minimum)
ΔI_L = desired ripple current of inductor,
Where ΔI_Lshould be 20% to 40% of output current.

iii. Selection of Capacitor : It is always recommended to implement low ESR capacitors to decrease the voltage ripple. It is recommended to use data sheet while doing the calculation of capacitor and inductor. The following equation is implemented to find the capacitor values of boost converter to attain desired voltage level.

$$C = \frac{I_o \times D}{f_s \times \Delta V_o} \quad \text{.....(3)}$$

Where ΔV_O is the desired o/p voltage ripple.[8]

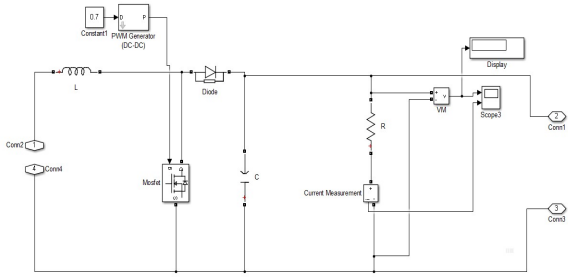

Figure 7: Simulation of Boost Converter

C. Three Phase Inverter

Three single-phase bridge inverters can be connected as shown in Figure 8 to form a configuration of 3-Ø inverter.[10] The individual phase voltages of the 3-Ø bridge circuit are identical to the square voltages output by 1-Ø bridge circuits. The voltages of the 3-Ø inverter are displaced in time by 120^0.

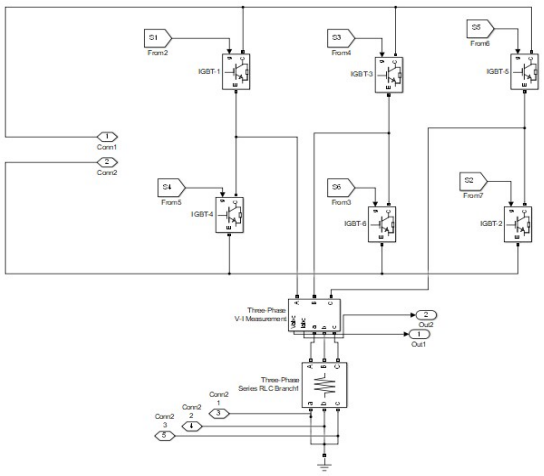

Figure 8: Simulation of Three phase Inverter

D. Sinewave Pulse Width Modullation (SPWM)

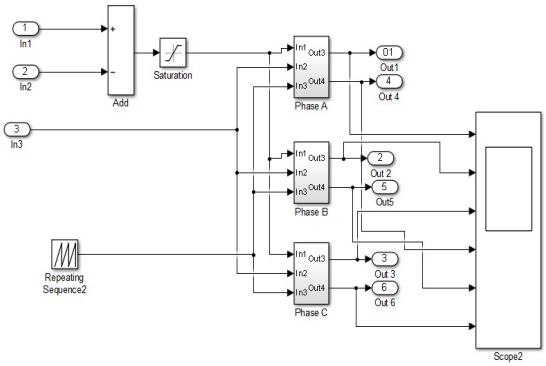

Figure 9: SPWM Simulation

The most common and popular technique for generating sinusoidal wave is SPWM i.e. known as Pulse Width Modulation. Simulation of SPWM is shown in figure 9. This PWM technique includes generating a digital waveform, for which the duty cycle can be modulated in such a way so that the average voltage waveform corresponds to a pure sine wave. The method of producing SPWM signal is comparing sine wave with triangular wave or saw-tooth wave. This Sinewave PWM signal is implemented for controlling power semiconductor switches like IGBT, MOSFET etc. The output produced by inverter is such that it resembles with sine wave. Filter consists of inductor and capacitor which is known as LC-Filter can be implemented to make a smooth sinusoidal waveform out of square wave ac output. With the help of this SPWM method production of much more similar AC waveform than that of others is possible.

E. Phase Locked Loop System (PLL)

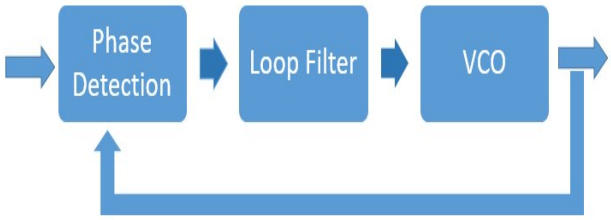

Figure 10: Block Diagram of PLL system

The most important factor of the phase locked loop (PLL), is the phase difference between two given signals. Phase locked loop system also has the ability to detect the phase difference between the two different signals. The difference between reference signals phase and actual signals phase is called as “error signal”. This error signal is used to control phase angle as well as the frequency of two signals. [5]

The basic block diagram of phase locked loop is shown in figure 10 where there are three main elements of the PLL have shown. These elements are respectively phase detector, voltage controlled oscillator i.e. VCO and the filter [13]. At phase detection, the reference signal and the feedback signal which can be generated from VCO are being compared and error signal is generated. This error is then passed to filter for which can be further transmitted to VCO. The Voltage Controlled Oscillator produces an oscillatory signal. This oscillatory signal is again fed to phase detector to get compared with the input reference signal. This identify the phase difference between the two signals, i.e. the error signal. The error signal is then again passing through loop filter. This is the low pass filter which attenuate the high frequency signals and only allows the low frequency signal. Then this error signal is supplied to the control terminal of the VCO.[9] The error of any change in this voltage is considered that it tries to reduce the phase difference and difference in frequency between the given signals. As initial stage the loop is out of lock but as the error reduces the system gets locked and phase angle and frequency gets synchronized with each other .

IV. SIMULATION RESULTS AND ANALYSIS

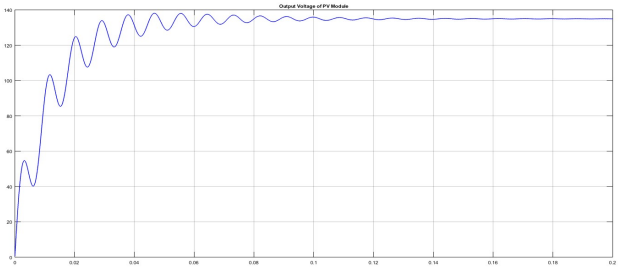

Figure 11: Output of PV panel

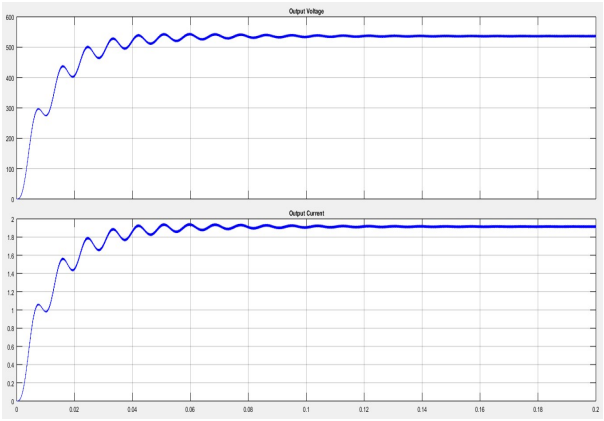

Figure 12 : Voltage & Current of Boost Converter

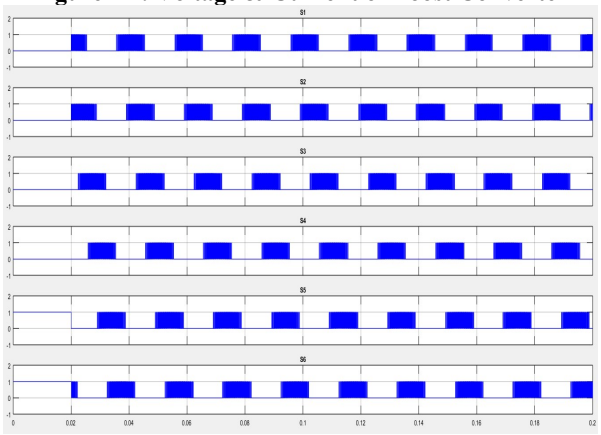

Figure 13: SPWM signal for 3 phase inverter

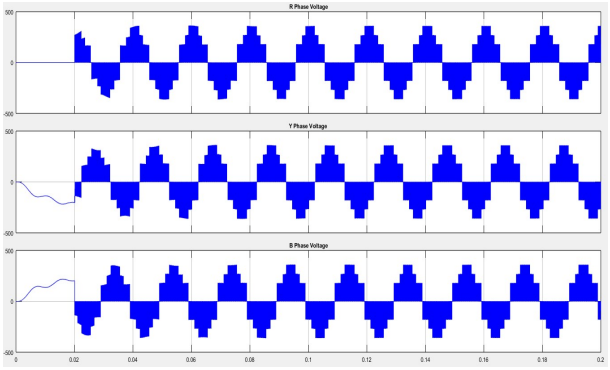

Figure 14: Three Phase Inverter output voltage of three phases

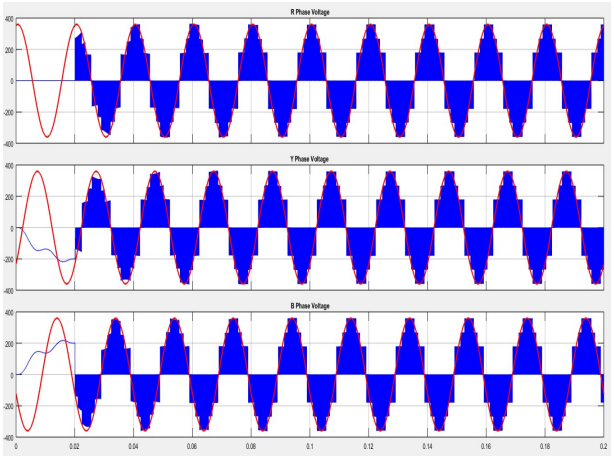

Figure 15: Grid Synchronization

The figure 11 shows the output of the PV panel generated due to solar radiation which is around 132V. This voltage is then fed to Boost converter to amplify the voltage up to 500 V which is shown in figure 12. This DC voltage is applied to 3-Ø inverter which working at 180-degree conduction mode, whose SPWM control signals are shown in figure 13. This inverter converts the DC voltage into 3 phase a.c. voltage which is shown on Figure 14. Inverter gives 440V phase to phase voltage which is same as of grid. This voltage is synchronized with grid voltage which is shown on figure 14. The output of inverter fig no 14 & 15 shows delay of one cycle i.e. delay of 20mlsec, this delay is required PLL loop to measure phase angle of the grid and respectively adjusting & synchronizing output voltage of three phase inverter.

V. CONCLUSION

This paper gives an overview of the grid tied photovoltaic system which includes the selection of PV panels, designing of boost converter depending upon the input and required output, design of three phase voltage source inverter along with Sinewave pulse width modulation system with Phase locked loop system. To synchronize the output of voltage source inverter the reference voltage of grid is fed to phase locked loop system where frequency along with the phase angle of the grid is measured and accordingly reference signal is generated and feed back to SPWM system so that the synchronization can be obtain between inverter output and grid. DGPVs are expected to play important part in future electrical power sector, with consideration of unbalanced grid conditions, islanding and better solutions to power quality issues under high penetration level of DGPV.

ACKNOWLEDGMENT

It is my honor to express acknowledgment to my guide and teachers, who guided me during the preparation of this paper and my project. I would like to present my thanks to my Guide Prof. SV Murkute who motivated me every single time of need, gave his support and valuable time. Last but not least, I am thankful to the almighty. It was his blessing that saw us till the end.

REFERENCES

[1] Sara Freitas, Teresa Santos and Miguel C. Brito, “Impact of large scale PV deployment in the sizing of urban distribution transformers”, Renewable Energy 119 (2018) 767-776.

[2] Lenos Hadjidemetriou, Elias Kyriakides, Yongheng Yang, “A Synchronization Scheme for Single-Phase Grid-Tied Inverters under Harmonic Distortion and Grid Disturbances”, IEEE TRANSACTIONS ON POWER ELECTRONICS

[3] Saeed Golestan, Mohammad Monfared, “Design-Oriented Study of Advanced Synchronous Reference Frame Phase-Locked Loops”, IEEE TRANSACTIONS ON POWER ELECTRONICS, VOL. 28, NO. 2, FEBRUARY 2013

[4] K. N. Dinesh Babu ,R. Ramaprabha ; V. Rajini ; Kamal Bansal, “Auto synchronization of photovoltaic fed grid systems”, 2016 3rd International Conference on Electrical Energy Systems (ICEES).

[5] Sourabh R. Sondawale, Prof. P. P. Jagtap ; Dr. S. G. Tarnekar, “Synchronization of Solar Inverter with Power Grid”, 2018 International Conference on Smart Electric Drives and Power System (ICSEDPS)

[6] Abdalla Y. Mohammed ; Farog I. Mohammed ; Mamoun Y. Ibrahim, “Grid connected Photovoltaic system”, 2017 International Conference on Communication, Control, Computing and Electronics Engineering (ICCCCEE)

[7] Md. Nahid Hossain ; Tushar Kanti Routh ; Abdul Hamid Bin Yousuf, “Design and development of a grid tied solar inverter” , 2012 International Conference on Informatics, Electronics & Vision (ICIEV).

[8] Madhuresh Sontakke “Analysis of Boost Converter and their control strategy”, 2019 JETIR February 2019, Volume 6, Issue 2.

[9] Frede Blaabjerg, Remus Teodorescu, Marco Liserre, Adrian V. Timbus, “Overview of Control and Grid Synchronization for Distributed Power Generation Systems”

[10] K.Arulkumar, K.Palanisamy, D.Vijayakumar, “Recent Advances and Control Techniques in Grid Connected Pv System – A Review”, International Journal Of Renewable Energy Research, Vol.6, No.3, 2016.

[11] Lenos Hadjidemetriou, Markos Asprou, Panayiotis Demetriou, and Elias Kyriakides, “Enhancing Power System Voltage Stability Through a Centralized Control of Renewable Energy Sources”

[12] Lenos Hadjidemetriou, Elias Kyriakides, Yongheng Yang, “A Synchronization Method for Single-Phase Grid-Tied Inverters”, Ieee Transactions On Power Electronics, Vol. 31, No. 3, March 2016

[13] S.N. Faraz, S.V. Murkute, Synchronizing Distributed Photovoltaic Generation with an Active Network (A review on Challenges and Different Schemes), International Journal for Research in Engineering Application & Management (IJREAM) ISSN : 2454-9150 Vol-05, Issue-01, April 2019.

Proceedings of the Fourth International Conference on Communication and Electronics Systems (ICCES 2019)
IEEE Conference Record # 45898; IEEE Xplore ISBN: 978-1-7281-1261-9

Luenberger observer based sensorless speed control of induction motor with Fuzzy tuned PID controller

Vaibhav S. Virkar
Department of Electrical Engg.
Walchand College Of Engineering
Sangli, India
vaibhavvirkar96@gmail.com

Sushil S. Karvekar
Department of Electrical Engg.
Walchand College Of Engineering
Sangli, India
sushil.karvekar@walchandsangli.ac.in

***Abstract*—Induction motors (IM) are utilized in many industries because of their advantages such as high efficiency, high starting torque, low maintenance and economical. Traditional PI controller is sensitive to parametric variations of motor. Additionally, use of PI controller introduces high flux and torque ripples in field oriented control (FOC), this affects performance of motor. This paper discusses use of offline fuzzy tuned PID controller for a space vector pulse width modulation (SVPWM) fed indirect field oriented control (IFOC) of IM drive. The system uses fuzzy Mamdani type I controller to improve transient response. The paper proposes sensorless speed estimation of IM using Luenberger observer. Effectiveness of sensorless speed control of IM is demonstrated in MATLAB/Simulink.**

***Index Terms*—Induction motor, Space vector PWM (SVPWM), IFOC, Fuzzy logic controller (FLC), fuzzy tuned PID, Luenberger observer, Simulink.**

I. Introduction

Nowadays, requirement of controlling of electrical drives is increased. New electronics devices like microprocessors and DSP processors can provide good speed control accuracy. Motors used in an electric vehicle are induction motors, BLDC motors & DC motors. IM is commonly used in the industries because of their special features like, variable speed, rugged operation, self-starting. BLDC motors are utilized in many industrial applications. Induction motors are advantageous over brushed dc motor drives and BLDC. The advantages of IM included ease of operation, high starting torque, high dynamic response [1],[2].

These motors are available for 1 ϕ & 3 ϕ variants. Therefore it is necessary to improve the performance of motor to obtain desired result. Scalar control and vector control are two main types of AC machine control. Due to ease of execution, scalar control is widely used. In scalar control method, direct torque control is utilized to enhance performance of motor. The vector control method is widely used for speed control. Scalar control method has further divided into V/F technique. In V/F technique, the constant Voltage to frequency ratio gives constant motor torque throughout the speed range. The vector control method further divided into two types: direct torque control (DTC) and field oriented control (FOC). DTC is used to control torque of three phase ac motors. DTC further classified as: direct self-control (DSC) & space vector modulation (SVM).

FLC improves the speed response of the system which cannot be improved by the conventional PID controller. Complicated nonlinear systems with uncertainty can be handle by the FLC [4]. The FLC will give a poor response for speed variations and load variation. To reduce this drawback an offline tuning method is introduced with FLC. In this method the PID controller parameters are tuned offline for obtaining better response to load changes. Fuzzy tuned PID controller has all benefits of a FLC and conventional PID controller like simplicity in control [7],[10].

Luenberger observer (LO) gives the best performance under steady state and low speed operation, but dynamic performance is not good. Extended Luenberger observer (ELO) is complicated to design and implement in DSP. Under load condition performance of ELO at low speed is poor [3].

Organization of paper is: Section-II gives introduction about indirect field oriented control system for IM. Section-III describes space vector PWM technique. In Section-IV, Fuzzy tune PID controller is designed. Luenberger observer is designed in section V. Obtained results are shown in section VI. Finally, in section VII conclusion is given.

II. Indirect Field Oriented Control (IFOC) of IM

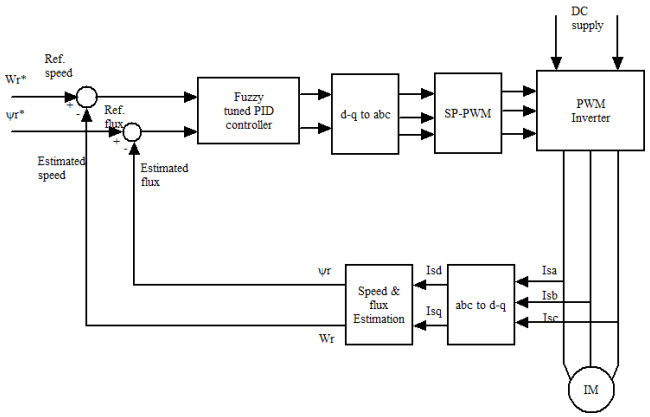

Fig. 1. Schematic of sensorless speed control using FT-PID controller

In FOC, control of IM is complex, because control of decoupled torque & flux generating components of stator currents is complex. To overcome these drawbacks, high performance indirect FOC is used. Proposed work shows high performance of fuzzy tuned PID controller to control speed of AC machine. In this proposed work, performance of PID controller is enhanced by fuzzy logic control and speed estimated by speed estimator. Speed estimators are used instead of speed sensors to reduce the control circuit complexity.

Schematic of proposed work is shown in figure 1, which consist of IM, inverter, FLC with PID tuning, FOC and speed estimator. Here speed is estimated by Luenberger observer and calculated speed is compared with reference speed, error is given to FLC. FLC reduces error and gives signal to space vector PWM and generated SVPWM signals are given to inverter. Feedback signals are taken by sensing the voltage and current.In proposed system speed of IM is controlled through fuzzy tuned PID controller using luenberger observer. For sensor less speed control technique, current senses from motor and converted into d-q format. From that speed is calculated using luenberger observer. An error signal is generated from difference between reference speed & calculated speed. This error given to fuzzy tuned PID controller, from which it gives correct output to achieve reference speed [5],[6].

III. SPACE VECTOR PWM (SVPWM)

PWM technique is employed to inverter to get variable voltage and frequency for variable speed drives. Inverter output in the form of space vectors represents principle of the SVPWM. For execution of SVPWM, reference voltage is calculated using nearest two active vectors & zero vectors. In this control method, simulink model is designed for IFOC. Space vector transformation is as shown in figure 2.

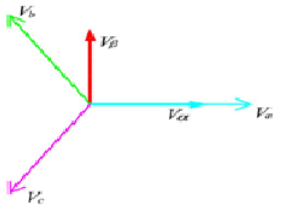

Fig. 2. Space vector transformation

3-phase system $V_a(t), V_b(t) \& V_c(t)$ can be written as;
$V = \frac{2}{3}(V_a(t) + V_b(t)e^{j\frac{2\pi}{3}} + V_c(t)e^{-j\frac{2\pi}{3}})$
The possible space vectors are shown in figure 3,

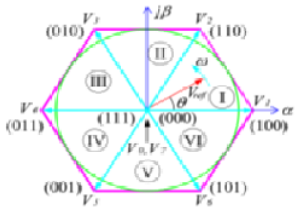

Fig. 3. Eight possible space vectors

TABLE I
SWITCHING STATES AND MAGNITUDE

Space vector	Switching state	Magnitude
V_0	000	0
V_1	100	$\frac{2}{3}V_{dc}e^{j0}$
V_2	110	$\frac{2}{3}V_{dc}e^{j\frac{\pi}{3}}$
V_3	010	$\frac{2}{3}V_{dc}e^{j\frac{2\pi}{3}}$
V_4	011	$\frac{2}{3}V_{dc}e^{j\frac{3\pi}{3}}$
V_5	001	$\frac{2}{3}V_{dc}e^{j\frac{4\pi}{3}}$
V_6	101	$\frac{2}{3}V_{dc}e^{j\frac{5\pi}{3}}$
V_7	111	0

The magnitude of six active vectors is equal to (2/3) V_{dc}. The vectors V_1-V_6 are known as active state vectors and V_7 & V_8 are known as zero state vectors. SVPWM waveforms are shown in fig. 4. SVPWM is a technique utilized in final step of FOC to find PWM signals for inverter switches to generate desired three phase voltages to IM.

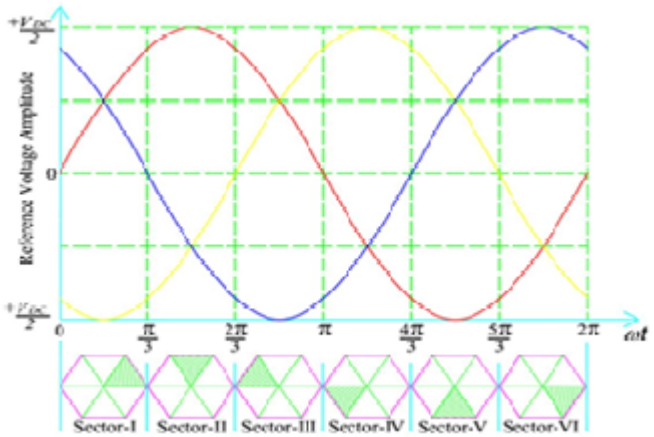

Fig. 4. SVPPWM waveforms

IV. FUZZY TUNED PID CONTROLLER DESIGNING

Fuzzy Logic allows values in between one/zero, high/low true/false, etc. FLC is simple to execute. It consists of fuzzification, fuzzy rules & defuzzification. Fuzzy rules describe relationship between input, output. They are written using IF-THEN statements. Input is taken as error between reference speed & estimated speed [11].

In offline fuzzy tuned PID controller, rules are designed using properties of PID controller & characteristics of IM. Parameters of K_p, K_i, K_d are tuned as load changes. FLC has two inputs: error (e) & change in error (de) and three outputs: K_p, K_i, K_d as shown in figure 6. Equations for offline tuning is acknowledged as below [9],[12].

$$U(t) = K_{pnew}e(t) + K_{inew}(t) + K_{dnew}de(t)/dt \quad (1)$$

$$K_{pnew} = K_{pf}\alpha$$
$$K_{inew} = K_{if}\alpha$$

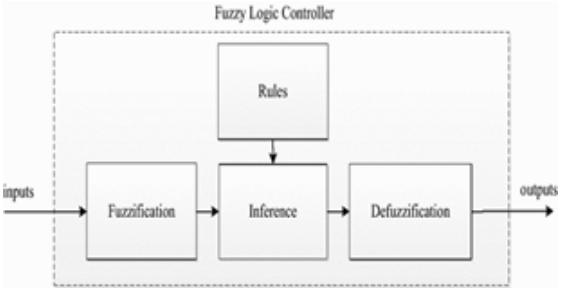

Fig. 5. Schematic of FLC

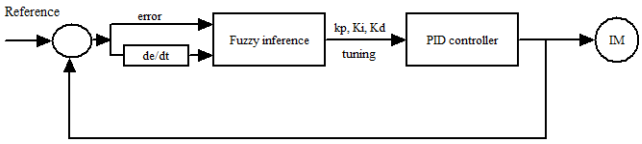

Fig. 6. Block diagram Fuzzy tuned PID controller

$$K_{dnew} = K_{df}\alpha$$

Where,
α = scaling factor, K_p, K_i, K_d are obtained from FLC.

TABLE II
FUZZY RULES FOR KP

e / edt	NL	NM	NS	Z	PS	PM	PL
NL	NL	NL	NL	NL	NM	NS	Z
NM	NL	NL	NL	NM	NS	Z	PS
NS	NL	NL	NM	NS	Z	PS	PM
Z	NL	NM	NS	Z	PS	PM	PL
PS	NM	NS	Z	PS	PM	PL	PL
PM	NS	Z	PS	PM	PL	PL	PL
PL	Z	PS	PM	PL	PL	PL	PL

Fuzzy rules are designed according to error as well as change in error. If value of error is negative large, transient response is high. To reduce high transient response derivative gain of controller is high. Rise time is large. To minimize rise time, proportional gain of controller is increased. To achieve zero steady-state error, value of integral gain is increased. The transient response output from model is improved compared with FLC controller & steady state error is eliminated.

Schematic of FLC is shown in above figure 5. Input variable of fuzzy system is speed error E. Speed error can be represented as:

$$E = \omega_{ref} - \omega_{act}$$

TABLE III
FUZZY RULES FOR K_i&K_d

e / edt	NL	NM	NS	Z	PS	PM	PL
NL	NL	NL	NLM	NM	NMS	NS	Z
NM	NL	NLM	NM	NMS	NS	Z	PS
NS	NLM	NM	NMS	NS	Z	PS	PMS
Z	NM	NMS	NS	Z	PS	PMS	PM
PS	NMS	NS	Z	PS	PMS	PM	PLM
PM	NS	Z	PS	PMS	PM	PLM	PL
PL	Z	PS	PMS	PM	PLM	PL	PL

TABLE IV
FUZZY RULES FOR ALPHA

e / edt	NL	NM	NS	Z	PS	PM	PL
NL	Z	Z	Z	Z	Z	Z	Z
NM	Z	Z	Z	Z	Z	Z	PS
NS	Z	Z	Z	Z	Z	PS	PMS
Z	Z	Z	Z	Z	PS	PMS	PM
PS	Z	Z	Z	PS	PMS	PM	PLM
PM	Z	Z	PS	PMS	PM	PLM	PL
PL	Z	PS	PMS	PM	PLM	PL	PL

The torque reference is controller output variable of IFOC. Controller observes speed error signal and accordingly changes its output. Therefore actual speed w_{act} reaches the reference speed (w_{ref}). Here, for designing FLC, Mamdani method is used. It has fuzzy input and fuzzy output. Choice of fuzzy sets & membership functions are necessary for designing FLC.

Fuzzy sets (linguistic definition) proposed here are defined as follow:
PM = Positive Medium,
PL = Positive Large,
PS = Positive Small,
PLM = Positive Large Medium,
ZE= Zero,
NS = Negative Small,
NM = Negative Medium,
NL = Negative Large,
NLM = Negative Large Medium,
VSE= Very Small Error,
VBE= Very Big Error.

V. DESIGNING LUENBERGER OBSERVER

To determine the Synchronous speed and electrical angle following equations are used to implement flux observer [8]. The simulation diagram is as shown in fig 14
From, indirect vector control,

$$\Theta_e = \int \omega_e = \int (\omega_r + \omega_{sl})dt \tag{2}$$

The rotor circuit equation is given by,

$$R_r i^e_{dr} - (\omega_e - \omega_r)\Psi^e_{dr} + \frac{d\Psi^e_{dr}}{dt} = 0 \tag{3}$$

$$R_r i^e_{qr} + (\omega_e - \omega_r)\Psi^e_{dr} + \frac{d\Psi^e_{qr}}{dt} = 0 \tag{4}$$

Rotor flux linkage is given by,

$$\Psi^e_{dr} = L_r i^e_{dr} + L_m i^e_{ds} \tag{5}$$

$$\Psi^e_{qr} = L_r i^e_{qr} + L_m i^e_{ds} i^e_{qs} \tag{6}$$

From above equations we can write,

$$i^e_{dr} = \frac{1}{L_r}\Psi^e_{dr} - \frac{L_m}{L_r} i^e_{ds} \tag{7}$$

$$i^e_{qr} = \frac{1}{L_r}\Psi^e_{qr} - \frac{L_m}{L_r} i^e_{qs} \tag{8}$$

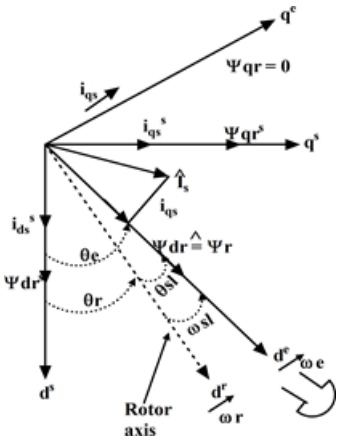

Fig. 7. stator current, Stator flux & Rotor flux vectors on ds-qs plane

If we substitute above values in equations 3 and 4, we obtained,

$$\frac{d\Psi^e_{qr}}{dt} + \frac{R_r}{L_r}\Psi^e_{qr} - \frac{L_m}{L_r} R_r i_{ds} + \omega_{sl}\Psi^e_{dr} = 0 \tag{9}$$

$$\frac{d\Psi^e_{dr}}{dt} + \frac{R_r}{L_r}\Psi^e_{dr} - \frac{L_m}{L_r} R_r i_{ds} - \omega_{sl}\Psi^e_{qr} = 0 \tag{10}$$

For decoupled control,

$$\Psi^e_{qr} = 0 \tag{11}$$

$$\frac{d\Psi^e_{qr}}{dt} = 0 \tag{12}$$

Now, substituting the above values in equation 9 and 10, we obtain,

$$\frac{L_r}{R_r}\frac{d\hat{\Psi}_r}{dt} + \hat{\Psi}_r = L_m i^e_{ds} \tag{13}$$

$$\omega_{sl} = \frac{L_m}{\hat{\Psi}_r}\frac{R_r}{L_r} i^e_{qs} \tag{14}$$

If we consider $\hat{\Psi}_r$ as constant ,then from equation 13 we obtain,

$$\hat{\Psi}_r = L_m i^e_{ds} \tag{15}$$

Therefore, by using equation number (1), (12) and (13) flux observer is designed.

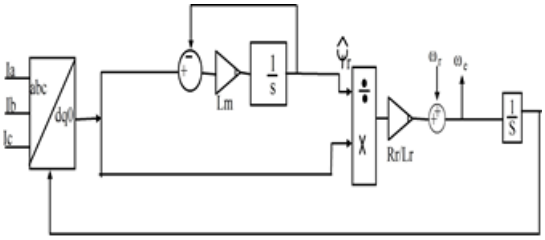

Fig. 8. Block diagram of Luenberger Observer

Where,
ω_e = Estimated speed,
ω_r = Rotor speed,
ω_{sl} = Slip speed,
R_r = Rotor resistance,
L_r = Rotor inductance,
L_m = Magnetizing inductance,
i^e_{qs} = q^e axis stator current,
i^e_{ds} = d^e axis stator current,
i^e_{qr} = q^e axis rotor current,
i^e_{dr} = d^e axis rotor current,
Ψ^e_{qr} = q^e axis rotor flux linkage,
Ψ^e_{dr} = d^e axis rotor flux linkage,

VI. SIMULATION MODEL & RESULTS

The structure of FOC is given in figure 9. Input to speed controller is reference speed & actual speed of motor. Output of speed controller is given to FOC. Actual speed of motor & stator current of motor are also given to FOC. According to the switching pulses, controlled AC voltage produced by the inverter is applied to IM. 3-phase diode rectifier is utilized to convert ac into dc . For sensorless speed control, speed estimator namely Luenberger observer is used. Three stator currents I_a, I_b, I_c, are given to the observer to estimate speed.

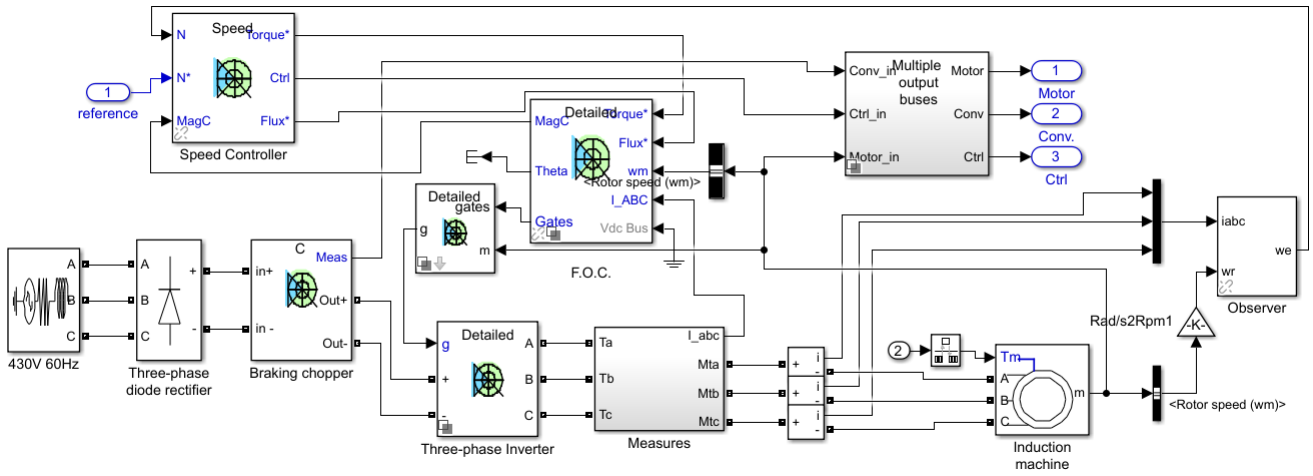

Fig. 9. Simulink diagram of IFOC for speed control of IM

Estimated speed is given to speed controller. In speed controller, 49 rules based on IF-THEN statements as shown in table II, III & IV FLC is implemented to reduce error. For various speed & torque values results are obtained as shown in fig. 10, 11 & 12. Fig. 13 shows output stator current and DC bus voltage for the speed 500 rpm & torque 2 n-m.

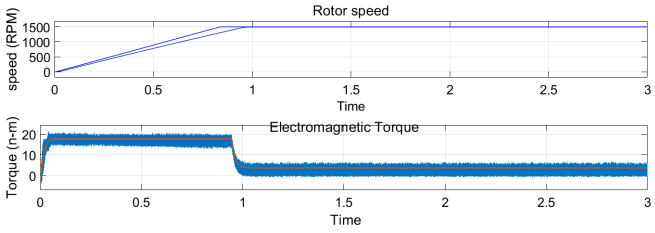

Fig. 10. Output speed at 1500 rpm & torque 2 n-m

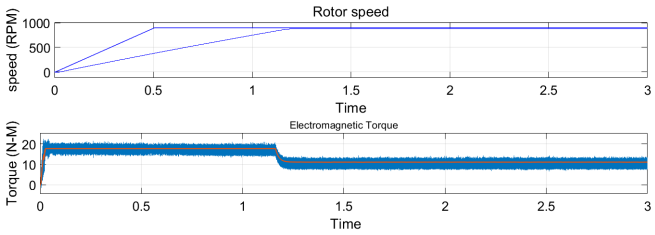

Fig. 11. Output speed at 900 rpm & torque 10 n-m

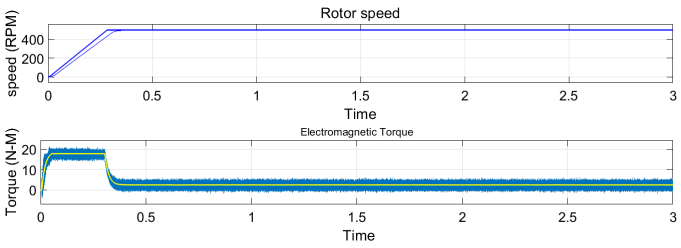

Fig. 12. Output speed at 500 rpm & torque 2 n-m

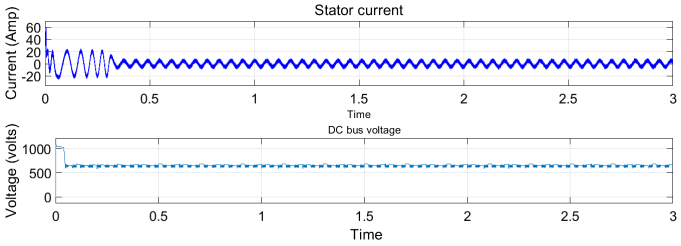

Fig. 13. Output stator current & Dc bus voltage speed at 500 rpm & torque 2 n-m

TABLE V
PARAMETERS OF 3HP IM

Sr. no.	Parameters	3 HP IM
1	Power	2238 W
2	Supply Voltage	430 V
3	Frequency	50 Hz
4	Stator Resistance	0.435 Ω
5	Stator Inductance	0.002 H
6	Rotor Resistance	0.816 Ω
7	Rotor Inductance	0.002 H
8	Mutual Inductance	0.06931 H

VII. Conclusion

The Luenberger Observer based FT-PID (Fuzzy tuned PID) is designed in this paper to estimate rotor speed. FT-PID reduces torque ripples and gives better response. From results, it is seen that FT-PID controller is suitable for all speed ranges with vector control technique. FT-PID has better response as compare to FLC. The actual speed is exactly tracking the reference speed for different speeds as seen in the results. The sensorless speed control using FLC is suitable for applications like electric vehicles, industrial purpose, robotics, etc. Speed controller works accurately with least error between actual speed & reference speed. Moreover, the speed controller improves overall transient response of system.

References

[1] Wei Chen and Changliang,"Sensorless Control of Brushless DC Motor Based on Fuzzy Logi" Xia School of Electrical Engineering & Automation Tianjin University Tianjin 300072, IEEE June 21 - 23, 2006.

[2] Ding Wang Key, "Sensorless fuzzy speed control for single phase induction motor" Laboratory of Automatic Control Heilongjiang University Harbin, China Ying Shi Laboratory of Automatic Control Heilongjiang University Harbin, 2009 China .

[3] Sun Kai, "A Speed Observer for Speed Sensorless Control of Induction Motor" School of Electrical and Electronic Engineering Shandong University of Technology Zibo, China, Zhao Yanlei School of Electrical and Electronic Engineering Shandong University of Technology Zibo, China.

[4] Bahram-Kimiaghalam, Meisam-Rahmani, and Hassan-Halleh,"Speed & Torque Vector Control of Induction Motors with Fuzzy Logic Controller" International Conference on Control, Automation and Systems Oct. 14-17, 2008 in COEX, Seoul, Korea.

[5] M.A. Noroozi, J.S. Moghani and A. Dehnavi, "A Sensorless Direct Speed Control for Brushless DC Motor Drive" Electrical Engineering Dept. Amirkabir University of Technology Tehran, Iran. Feb l3-14, 2013

[6] Tao zhao, Fenghong Xiang, Jianping Wang, Guo Zhang, Jianlin Mao Kunming, "Research on Speed Sensorless Direct Torque Fuzzy Control of Induction Motors", University a/Science and Technology, Kunming, China The Corresponding Author: Jian ping Wang IEEE Feb.13 -14, 2014.

[7] Xiao-Gang Duan, Han-Xiong Li and Hua Deng, "A Simple Tuning Method for Fuzzy PID Control", IEEE November 27, 2007

[8] Bimal k. Bose, "Modern Power Electronics and AC Drives" 1st edition.

[9] Alain Segundo Potts, Basilio Thome de Freitas Jr. and Jose Carlos Amaro, "Fuzzy auto-tuning for a PID controller" Department of Telecommunication and Control. University of Sao Paulo2010 9th IEEE.

[10] Samarth Singh, "Comparative analysis of robustness of optimally offline tuned PID controller and fuzzy supervised PID controller" Electronics and Communication Engineering department IIT Roorkee, R. mitra Electronics and Communication Engineering department IIT Roorkee, India 06 - 08 March, 2014.

[11] P.Thepsatoml , A.Numsomran, V. TipsuwanpoM and T. Teanthong, "DC Motor Speed Control using Fuzzy Logic based on LabVIEW" Department of Electrical Engineering, Faculty of Engineering, Srinakharinwirot University, Nakornnayok, Faculty of Engineering, King Mongkut's Institute of Technology Ladkrabang, Bangkok 10520, Thailand.

[12] Arun Kumar R, Febin Daya J L, "A Novel Self - Tuning Fuzzy Based PID Controller for Speed Control of Induction Motor Drive" School of Electrical Engg., VIT University - Chennai Campus, India, International Conference on Control Communication and Computing (ICCC) 2013.

Proceedings of the Fourth International Conference on Communication and Electronics Systems (ICCES 2019)
IEEE Conference Record # 45898; IEEE Xplore ISBN: 978-1-7281-1261-9

Energy Monitoring of Curing Pumps Using PLC and SCADA

Sahil Desouza
UG Student
ETC Department
Don Bosco College of Engineering
Goa, India
sahildesouza@gmail.com

Roshwyn De Melo
UG Student
ETC Department
Don Bosco College of Engineering
Goa, India
roshwyn17@gmail.com

Shreyas Aigal
UG Student
ETC Department
Don Bosco College of Engineering
Goa, India
aigalshreyas0613@gmail.com

Ketan Dessai
UG Student
ETC Department
Don Bosco College of Engineering
Goa, India
ketandessai16@gmail.com

Duane Dsilva
UG Student
ETC Department
Don Bosco College of Engineering
Goa, India
dsilvaroyed70@gmail.com

Flavia Leitao
Assistant Professor
ETC Department
Don Bosco College of Engineering
Goa, India
flavia.leitao@dbcegoa.ac.in

Mohini Naik
Assistant Professor
ETC Department
Don Bosco College of Engineering
Goa, India
mohini.naik@dbcegoa.ac.in

***Abstract*—The curing section of rubber manufacturing plant requires a lot of manual intervention for checking pump status. The energy of each pump is viewed on the energy meter manually. In case of power failures, pumps in the entire curing section are manually switched on using star-delta configuration. This brings time loss and quality defects. Thus the company incurs huge loss. In order to minimize the manual intervention that is required to check the pump status, the proposed system aims at monitoring the energy consumption of the pump in the curing section of the rubber processing plant. This paper presents a real-time energy monitoring system which has the capability to acquire data from a three-phase supply network connected to the pumps, store the acquired data and display the data on the screen. This data is then used to check the real time status of the pumps and indicate the presence of faults, thus automating the process of monitoring the pumps using PLC and SCADA.**

Keywords— Energy Monitoring; PLC; SCADA; HMI

I. Introduction

Over the past two decades, the electric power industry's involvement in power distribution automation has been principally focused on remote monitoring and control of the distribution systems and their equipments. Advancement in metering and communications have meant that electric power utilities worldwide are increasingly adopting the technology of energy monitoring system to provide better and more efficient services to electric consumers. Development of an online energy monitoring system via PLCs in the industries are accomplished by the use of

- Data Acquisition
- Communication Protocol
- Processing within Energy Meter and host central station [1]

In the Rubber Processing Plant, each of the pumps are controlled by a VFD (Variable Frequency Drive) by comparing the voltage from the header line, transmitted by pressure transmitter, to the set value in the drive [2]. The comparison leads to a change in the frequency of the motor,

thus making an effect on it's pumping. The energy values are tapped from the VFD into an energy meter.

The curing process includes 11 critical stages. Each stage is an important part of the overall curing of tyres. Every stage is a process in itself that must run for a specific time interval to maintain standardised results.

Parameters of concern throughout the curing process are curing time, heating temperature and energy consumed by the pumps. The effect of process parameters on tire vulcanization have been studied [3]. If these parameters are not maintained in all the 11 curing stages, the tyres produced will be scrapped off due to various quality defects. Most importantly, every stage in the curing process is irreversible. This means, if any error occurs due to manual intervention or machine faults, then the output tyre will be scrapped off.

Energy monitoring techniques provides the company with feedback on operating practices, it also provides early warning of unpredicted excess consumption caused by equipment malfunctions, operator error and lack of effective maintenance. Energy monitoring systems helps to envision energy consumption trends (daily, weekly, seasonal, operational) and identify specific areas of wasted energy, observe how it changes to relevant driving factors impact energy efficiency, develop performance targets for EM programs and manage energy consumption, rather than accept it as a permanent cost. The aim is to reduce energy costs through improved energy efficiency and energy management control. Other benefits generally include increased resource efficiency and improved production budgeting [4].

A real-time energy monitoring system is discussed in this paper correctly fetches data from the energy meter of individual pumps through Modbus TCP communication. SCADA systems have been developed which allows the operator to view the logged data in a graphical form. Necessary measures can be undertaken by analysing the data in order to save power and minimize its wastage [5].

The paper is organised as follows: Section II explains the methodology which includes the proposed system. Section III demonstrates the results obtained by using HMI and SCADA which consists of the display of power values of each pump and the set point for the header line pressure. Section IV consists of the conclusion based on the observed results.

II. METHODOLOGY

The proposed system aims at minimizing the efforts of manually checking power consumption of the pump.

The first stage of the project involved using a Human Machine Interface (HMI) panel [6], wherein two pump parameters (power and energy) of a few pumps were displayed in real time. The objective was to temporarily monitor both of these parameters. In order to do so, the following steps were taken:

1. Data of one pump were acquired from its energy meter[7] by using a PLC unit through an Ethernet gateway [8].

2. This data was processed to obtain power and energy values of the pump which were then displayed on the HMI panel.

The second stage of the project involves the following steps:

1. To transfer data from the energy meter into a PLC (Programmable Logic Controller) unit, an Ethernet gateway is used. The gateway device helps in segregating bulk data into single streams.

2. The PLC unit (Micrologix 1400) [9] is used to acquire the power and energy consumed by the pump from the energy meter (EMS network). PLC unit (ControlLogix 5572) [10] is used to fetch the pressure of the header line, which is part of the curing network. Both these networks are then combined into a single network using a network translation device (1783-NATR).

3. The 1783-NATR [11] helps in configuring multiple machines on a single line to have identical network settings. The output of the NATR is connected to the SCADA system. This data comprises of parameters like run-time, power, energy consumed and also displays the mode in which the pump is working.

4. The data on the SCADA screen [12] is analysed depending on the needs of the company.

5. Therefore by using PLC and SCADA we achieve real time energy monitoring of the curing pumps.

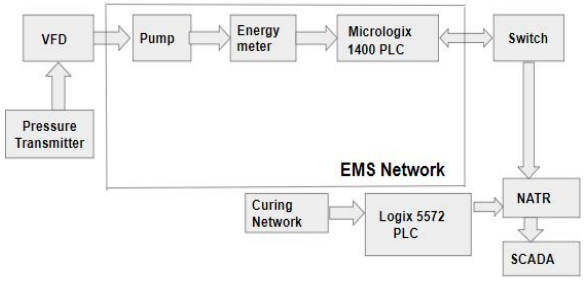

Figure 1. Proposed system block diagram

The inputs to the NATR is given from the EMS network and curing network. The EMS network gives the power consumption of the pumps while curing network gives the pressure from the header line. Fig. 1. shows the block diagram of the proposed system to be implemented. EMS network consists of an Ethernet gateway and PLC. The Ethernet gateway acts as a gateway for data transfer between energy meter and PLC by using Modbus TCP protocol. The energy meter acts as a server and the PLC acts as a client. The input values at the PLC are processed using Micrologix 1400 and then given to the NATR which converts the private port to public port. The second input to NATR is given from the curing network. The Supervisory Control and Data Acquisition (SCADA) system is a communication and control system used for monitoring, operation and maintenance of energy and power.

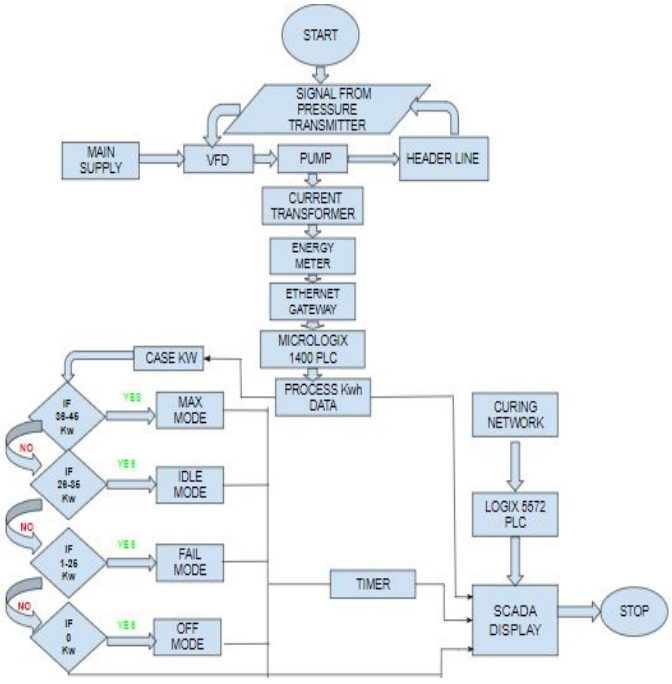

Figure 2. Flowchart

Fig. 2. is the flowchart of the automation process. The flowchart designed can be categorized into three major segments.The first segment shows how the speed of the pump is controlled. A pressure transmitter installed on the header line transmits a signal to the VFD (Variable Frequency Drive). The main supply is also given at the drive. The two voltage levels are processed and accordingly the VFD changes the frequency of the pump thereby varying the speed of the pump. The change in the speed of the pumps results in the change in the pressure in the header line. The next segment identifies the mode in which the pump is working. An energy meter is used to tap values from the current transformer which is present in the VFD panel. The energy meter displays the instantaneous energy, power and operating frequency of the pumps. An ethernet gateway is used to ensure communication between the energy meter and the PLC unit (MicroLogix 1400 PLC). Once the data is received on the PLC unit, with the help of PLC programming the data is processed and thus we determine the mode in which each pump is working. There are four modes in which the pump works depending upon the power consumed by the pump, namely, Max mode, Idle mode, Fail mode and Off mode. The last segment allows a general view of the data monitoring panel on a SCADA software which is displayed on a computer screen. A timer is used to record the time for which the pump is working in a particular mode. A curing network exist which consist of the pressure values of all the pumps in the curing section. These pressure values are processed using a Logix 5572 PLC. The data from this PLC, the timer data, the energy values of the pumps and the data which specifies the mode are all sent onto a SCADA software which is displayed on a computer screen.

III. Results and Discussion

A HMI panel was used to view the pump performance parameters for a certain period. Fig. 3. shows the main screen on the HMI panel. Selecting any one of the first three buttons, we get the screen which displays the pump parameters (ie. power and energy) as shown in Fig. 4.

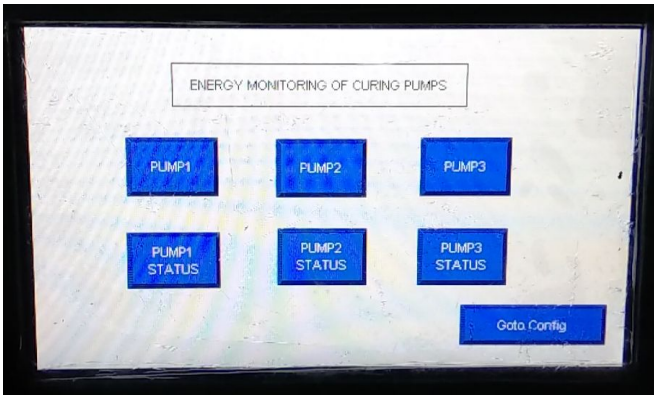

Figure 3. Main Screen of HMI Panel

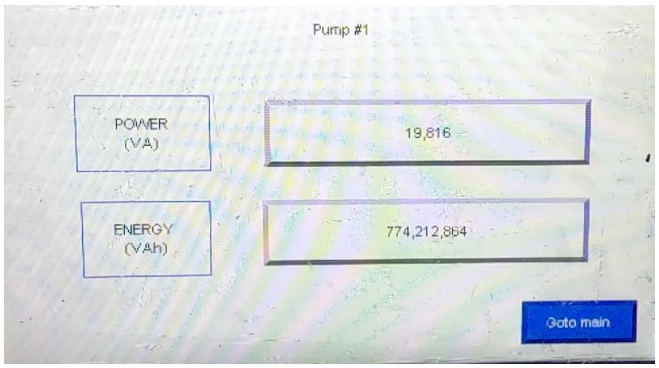

Figure 4. Power and Energy readings of Pump 1 on HMI screen

Figure 5. Pump power status of Pump 1 viewed on HMI Screen

Various pump power status values viewed on the HMI screen (Fig. 5.) include:

- MAX state is used to indicate that the pump is under load and the power is varying between 36-45 kW.
- IDLE state indicates that the pump is in healthy working condition when power drawn is above 20 kW.
- FAIL state is used to indicate that the pump is poorly functioning when the power drawn by the pumps is less than 20 kW.
- OFF state is to indicate that the pump is off.

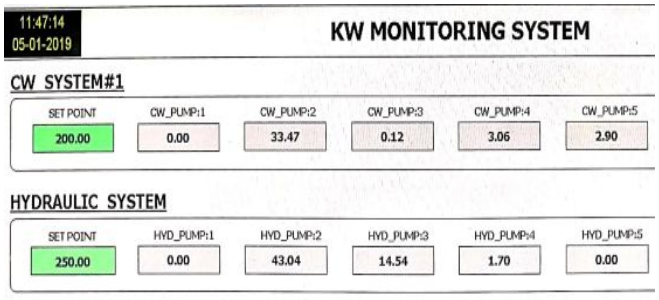

Figure 6. SCADA Screen showing power values of CW SYSTEM#1 and hydraulic pumps

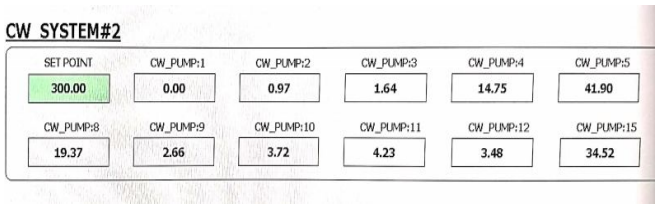

Figure 7. SCADA Screen showing power values of CW SYSTEM#2 pumps

Further on, the monitoring system was implemented on SCADA software to be displayed at the operator's workstation.The general view of the data-monitoring panel is shown in Fig. 6. and Fig. 7. which displays the power values (in kW) for each of the cold water (CW) and hydraulic pumps. The pumps are categorised as CW SYSTEM#1 pumps, hydraulic pumps, and CW SYSTEM#2 pumps. The CW SYSTEM#1 pumps are part of Trenches 1 & 2, whereas the CW SYSTEM#2 pumps are part of Trench 3 up to Trench 9.
The set point value indicates the pressure at the respective header line. This value can be changed by the user as and when required. The kW values are updated each time the pressure at the header line goes below the pressure set point value.

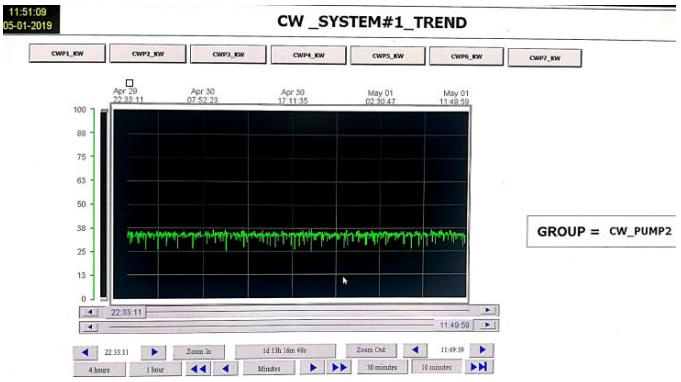

Figure 8. Trend showing power consumed v/s time of CW pump.

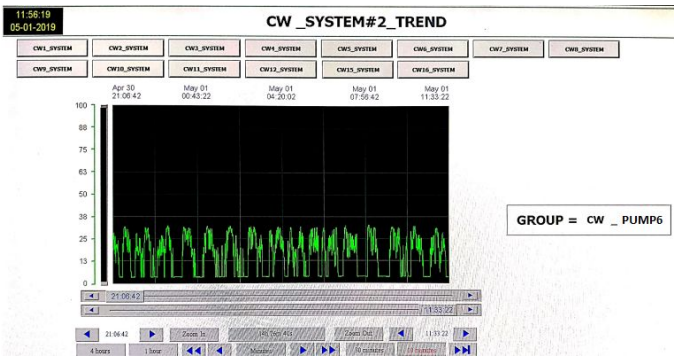

Figure 9. Trend showing power consumed v/s time of CW SYSTEM#2 pump.

Trend determines the gradual change in a process over a certain period of time. Fig. 8., Fig. 9., and Fig. 10. depict the plot of the real time power values. The plotted power values

are continuously updated and displayed depending upon the set time.

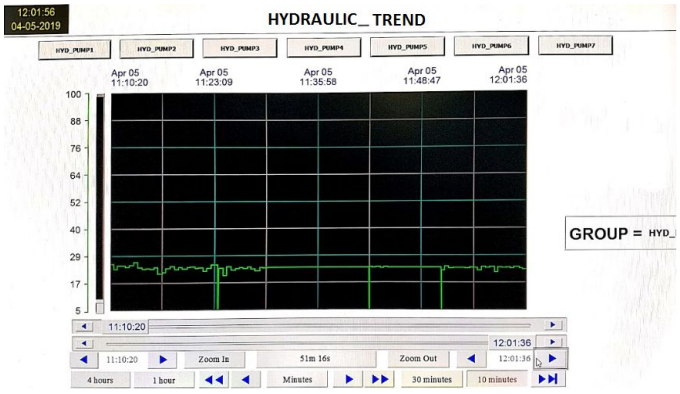

Figure 10. Trend showing power consumed v/s time of hydraulic pump.

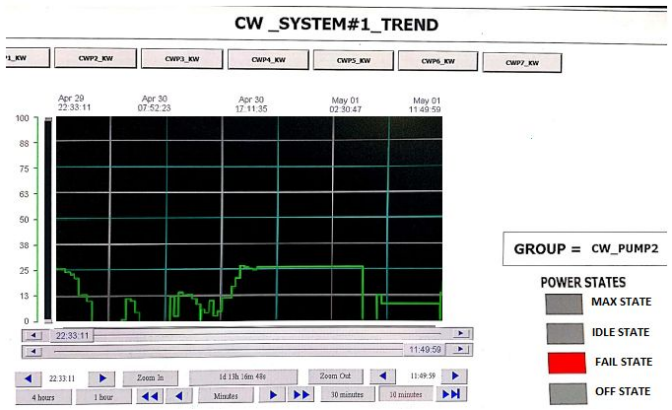

Figure 11. Trend showing power consumed v/s time of CW SYSTEM#1 pump when FAIL state is detected.

In Fig. 11 the onset of failure of the pump inefficiency is detected by the red indication that can be viewed in the power states section. This pump should be frequently monitored. If it remains in the FAIL state for a period of 48 hours, proper troubleshooting procedures should be employed by the operator.

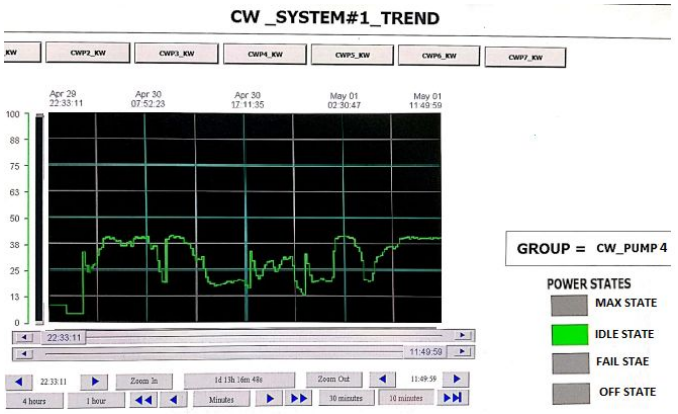

Figure 12. Trend showing power consumed v/s time of CW SYSTEM#1 pump when IDLE state is detected.

Fig. 12. depicts the healthy working condition of a pump (IDLE state). This state indicates that power consumed by the pump is above 20 kW.

IV. Conclusion

The proposed system helps to monitor real-time energy consumption and power values of the cold water pumps and hydraulic pumps used in the curing section of the rubber processing plant. The power values are used to determine the status of each pump. The system logs the measured and calculated electrical data in a database, creating a record of the data for analysis. The data logged can be viewed and analyzed to take measures to save power and minimize its wastage. The implemented trends depicts the power consumed by the respective pump over a period of time. The energy monitoring system therefore minimizes the manual intervention of the operator. Thus human error is minimized resulting in improved reliability.

Acknowledgement

We would like to acknowledge MRF Limited, Goa for providing us the opportunity to implement the energy monitoring system in real time in their factory. We would also like to express our special gratitude and thanks to people from MRF Limited, Goa, for giving us their attention and time.

References

[1] Kamaldeep Kaur, Prof. Ravinder Kaur, “Energy Management System using PLC and SCADA” International Journal of Engineering Research & Technology, Volume 3, Issue 11, November 2014.

[2] Mr.Ankur P. Desai, Mr.Rakesh.J.Motiyani, Dr.Ajitsinh R.Chudasama, “Energy Conservation Using Variable Frequency Drive in Pumping Application” International Journal of Engineering Development and Research, (Two Day National Conference (RTEECE-2014) -17th, 18th January 2014), Energy Conservation Using Variable Frequency Drive in Pumping Application | ISSN: 2321-9939

[3] X Tang et al 2015 IOP Conf. Ser.: Mater. Sci. Eng. 87 012105

[4] Pavan R.Gosavi, Prof. R. S. Khule, “Industrial Energy Monitoring System using PLC and SCADA, International Journal for Research in Applied Science & Engineering Technology, Volume 5, Issue 1, January 2017.

[5] Fatima Mumtaz “Real-Time, PLC Based Energy Monitoring System” IEEE INDICON 2015 1570202521.

[6]https://literature.rockwellautomation.com/idc/groups/literature/documents/um/2711p-um001_-en-p.pdf

[7]https://forum-controlsystems.abb.com/DownloadFile.aspx?file=UserFiles/Answers201712/EM6400_Series_User_M.pdf&filename=EM6400_Series_User_M.pdf

[8]https://www.schneider-electric.com/resources/sites/SCHNEIDER_ELECTRIC/content/live/FAQS/300000/FA300723/en_US/EGX300_User_Guide.pdf

[9]https://literature.rockwellautomation.com/idc/groups/literature/documents/um/1766-um001_-en-p.pdf

[10]https://literature.rockwellautomation.com/idc/groups/literature/documents/um/1756-um001_-en-p.pdf

[11]https://literature.rockwellautomation.com/idc/groups/literature/documents/um/1783-um008_-en-p.pdf

[12] Emami, S. A., & Emami, M. H. (2018). Design and Implementation of an Online Precise Monitoring and Performance Analysis System for Centrifugal Pumps. IEEE Transactions on Industrial Electronics, 65(2), 1636–1644.

Proceedings of the Fourth International Conference on Communication and Electronics Systems (ICCES 2019)
IEEE Conference Record # 45898; IEEE Xplore ISBN: 978-1-7281-1261-9

Security of Cloud Storage based on Extended Hill Cipher and Homomorphic Encryption

Bablu Kumar Das
Computer Engineering Department
National Institute of Technology
Kurukshetra, Haryana, India
bablulaldas21@gmail.com

Ritu Garg
Computer Engineering Department
National Institute of Technology
Kurukshetra, Haryana, India
ritu.59@gmal.com

Abstract*— Cloud computing is one of the emerging area in the business world that help to access resources at low expense with high privacy. Security is a standout amongst the most imperative difficulties in cloud network for cloud providers and their customers. In order to ensure security in cloud, we proposed a framework using different encryption algorithm namely Extended hill cipher and homomorphic encryption. Firstly user data/information is isolated into two parts which is static and dynamic data (critical data). Extended hill cipher encryption is applied over more important dynamic part where we are encrypting the string using matrix multiplication. While homomorphic encryption is applied over static data in which it accepts n number of strings as information, encode each string independently and lastly combine all the strings. The test results clearly manifests that the proposed model provides better information security.

Keywords*— Cloud Computing, Extended Hill Cipher, Homomorphic Encryption, Data Storage, Security.

I. INTRODUCTION

Cloud computing is utilized to get to the assets effectively from the outsider specialist so as to grow the business with low capitalization cost. Due to vast unstructured data over the cloud, information security is the prime concern. Thus, in order to ensure security of the distributed storage, we proposed a framework based on two distinctive encryption algorithms. In this model, user data/information are isolated into two parts such that the secured information is considered as dynamic data while the rest data as static part followed by applying two diverse encryption techniques namely extended hill cipher over the powerful information i.e. dynamic part and homomorphic encryption over static part of the data. The resultant encrypted data is stored in the cloud, thereby making the both common and critical data more secured compared to the previous security techniques that too at the low cost.

Given plaintext x, extended hill cipher converts x into cipher text $y=A\cdot x \pmod n$ where A is the matrix key where $|A| ! =0$ and n represent by 256 [1]. If cryptanalyst knows m pairs (x,y) of successive plaintext and cipher text, he/she can calculate the key matrix A by computing $A=Y\cdot X^{-1} \bmod n$, where X and Y are $m\times m$ matrices of plaintext and cipher text.

In extended hill cipher, strings are divided into group of three and every group is associated with its ASCII values [2]. Extended hill cipher gives better security in comparison to simple hill cipher because hill cipher encrypt only homogenous data and apply modulo 25, while extended hill cipher encrypt heterogeneous data type and apply modulo256.

Further, homomorphic encryption permits executing computations on the scrambled information [3]. It is one of the progressed cryptographic procedures that support arbitrary number of both operations addition as well as multiplication on cipher text. To retrieve user data $x=A^{-1}\cdot y \pmod n$ where A is original inverse matrix, y is encrypted matrix and n represent modulo 256.

The structure of this paper is as follows: Section II describes the related research work. Section III explains the proposed technique in detail. Evaluation of the scheme by different experiments is done in Section IV and finally Section V concludes the paper.

II. RELATED WORK

The significance of security in cloud has pulled the great attention nowadays. Safe cloud storage architectures are of prime concern. Cong Wang et al. [4], have suggested the protection issues related in distributed storage. Whenever a data vulnerability is scrutinize during the storage process, the accuracy identification across the distributed servers are ensured by simultaneous identification of misbehaved nodes through analysis in term of privacy functioning. It is proved that their technique is dominant to handle certain failures, malevolent data modification attack and even server attacks.
J. Shen et al. [5], considered cloud as semi-trusted and proposed a model for urban information sharing by using attribute based cryptography. The procedure they presented is sheltered and can challenge potential assaults. G. Feng et al. [6], point out that when the server load increases the chances of information leakage are there at the time of transmission in cloud servers. They proposed an adequate system encoding in closed cloud environment. Wang et al. [7], proposed a plan that allows clients to review the distributed storage for correctness of the data inside the server. Their plan likewise underpins protected and powerful unique information altering activities. They have accomplished the information uprightness just as information accessibility in distributed storage. J. Hou et al. [8], considered that at peak load, client's

information is put away through CSP (cloud server supplier), regardless of whether CSP is trusty, programmer still gather client information from server in the event that they deal with the distributed storage.

Above mentioned authors attempt to improve the security in cloud service in various terms. Lightly of them used various encryption approaches at different positions, while others attempt to tackle the protection issue with the help of inspecting or building their own security frameworks. Moreover, there is a typical issue in these research works. When the CSP itself is untrusted then these approaches are not effective ones and cannot avoid internal attacks or prevent the CSP from selling user's data to earn illegal profit. Therefore, we introduced a new secure cloud storage technique in this paper. We are dividing file into two parts and applying two cryptographic techniques. We can achieve high degree privacy protection of data. In our scheme encryption helps to protect fine-grained security of the data.

III. PROPOSED FRAMEWORK

The proposed secure cloud storage framework is shown in Fig.1 which consists of seven components namely user, static files, dynamic files over which homomorphic encryption and extended hill cipher encryption algorithms are applied, merged file and cloud server provider. This structure is utilized to store and recover information in a safe way from the cloud server. At server there are numerous customers utilizing the distributed storage services. The cloud server administrator knows the proprietor of the information and deals with the solicitation of the customer. The cloud server director chooses what information ought to be sent by customer's solicitation. Now suppose if CSP itself is untrusted there is a chance of data leakage, thus to avoid this problem, we proposed user level encryption techniques.

In fig.1 initially user data is divided into two separate parts which are static and dynamic. After splitting the data, apply the different encryption techniques on both the data. Static files fall under homomorphic encryption technique while dynamic files representing crucial data fall under more efficient extended hill cipher encryption technique. To retrieve the user data from CSP, user sends the request to the cloud server and CSP grant the user request and sent the user data which is encrypted file. After receiving the file from CSP, both the files fall under reverse decryption technique. Finally merge both files to get original data safely.

A. Extended Hill Cipher Algorithm

Extended hill cipher is a technique based on linear algebra. In extended hill cipher encryption algorithm, each string is grouped into multiple of three and initialized with its ASCII values in matrix form and then multiplied by 3 × 3 matrix whose determinant is not zero. Resultant matrix undergoes modulo 256 and stores the value in another matrix. Then convert resultant valued matrix back to its character form representing the encrypted cipher text. To encrypt the message, each section is multi played by the inverse of the original matrix. In hill cipher we can only encrypt homogeneous data and apply modulo 25. While in extended hill cipher encryption is applied to heterogeneous strings with modulo 256. Thus, the extended hill cipher provides better security to the customer's information.

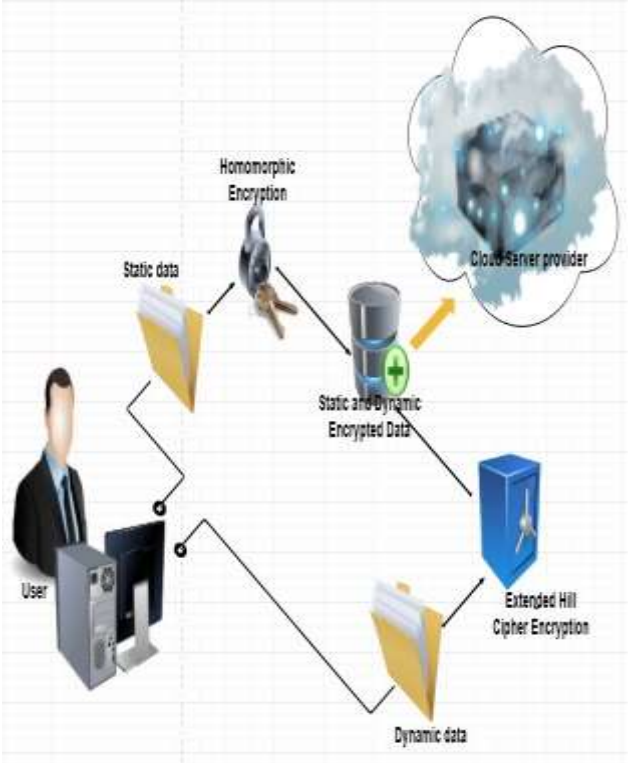

Fig.1 Secure Cloud Storage Framework

- Select invertible matrix A
- Calculate $y=A \cdot x \pmod n$.

  Alice sends (y, A) to Bob.

Where A is key matrix, y represent cipher text and x represent resultant plain text.

a. Encryption Process

- Select a plaintext message to encrypt containing all characters as well as special symbol and digits.

  Let's take an example, Nit_kkr9@gmail.com is our plaintext message and we will convert plaintext to cipher text.

- Initialize a 3x3 square matrix with nonnegative integer each less than 256.

$$A = \begin{bmatrix} 6 & 24 & 1 \\ 13 & 16 & 10 \\ 20 & 17 & 15 \end{bmatrix}$$

- Check its determinant does NOT equal to zero, $|A| \neq 0$

$$\begin{bmatrix} 6 & 24 & 1 \\ 13 & 16 & 10 \\ 20 & 17 & 15 \end{bmatrix}$$ =6(16*15 – 17*10) – 13(24*15 – 17*1) + 20(24*10 – 16*1) = 441

- Group the string into group of three as follows Nit_kkr9@gmail.com

  Example:-[Nit][_kk][r9@][gma][il.][com]

  If the string length does not have mod 3 == 0, repeat the last letter.

- Convert the character into its ASCII value

$N-78$	$\_-95$	$r-114$
$i-105$	$k-107$	$9-57$
$t-116$	$k-107$	$@-64$
$g-103$	$i-105$	$c-99$
$m-109$	$l-108$	$o-111$
$a-97$	$.-46$	$m-109$

- Multiply the converted matrix into given matrix

$$\begin{bmatrix} 6 & 24 & 1 \\ 13 & 16 & 10 \\ 20 & 17 & 15 \end{bmatrix}\begin{bmatrix} 78 \\ 105 \\ 116 \end{bmatrix} = \begin{bmatrix} 3104 \\ 3854 \\ 5085 \end{bmatrix}(\text{mod})256 = \begin{bmatrix} 32 \\ 14 \\ 221 \end{bmatrix}$$

$$\begin{bmatrix} 6 & 24 & 1 \\ 13 & 16 & 10 \\ 20 & 17 & 15 \end{bmatrix}\begin{bmatrix} 95 \\ 107 \\ 107 \end{bmatrix} = \begin{bmatrix} 3245 \\ 4017 \\ 5324 \end{bmatrix}(mod)256 = \begin{bmatrix} 173 \\ 177 \\ 204 \end{bmatrix}$$

$$\begin{bmatrix} 6 & 24 & 1 \\ 13 & 16 & 10 \\ 20 & 17 & 15 \end{bmatrix}\begin{bmatrix} 114 \\ 57 \\ 64 \end{bmatrix} = \begin{bmatrix} 2116 \\ 3034 \\ 4209 \end{bmatrix}(mod)256 = \begin{bmatrix} 68 \\ 218 \\ 113 \end{bmatrix}$$

$$\begin{bmatrix} 6 & 24 & 1 \\ 13 & 16 & 10 \\ 20 & 17 & 15 \end{bmatrix}\begin{bmatrix} 103 \\ 109 \\ 97 \end{bmatrix} = \begin{bmatrix} 3331 \\ 4053 \\ 5368 \end{bmatrix}(mod)256 = \begin{bmatrix} 3 \\ 213 \\ 248 \end{bmatrix}$$

$$\begin{bmatrix} 6 & 24 & 1 \\ 13 & 16 & 10 \\ 20 & 17 & 15 \end{bmatrix}\begin{bmatrix} 105 \\ 108 \\ 46 \end{bmatrix} = \begin{bmatrix} 3268 \\ 3553 \\ 4626 \end{bmatrix}(mod)256 = \begin{bmatrix} 196 \\ 225 \\ 18 \end{bmatrix}$$

$$\begin{bmatrix} 6 & 24 & 1 \\ 13 & 16 & 10 \\ 20 & 17 & 15 \end{bmatrix}\begin{bmatrix} 99 \\ 111 \\ 109 \end{bmatrix} = \begin{bmatrix} 3367 \\ 4153 \\ 5502 \end{bmatrix}(mod)256 = \begin{bmatrix} 39 \\ 57 \\ 126 \end{bmatrix}$$

- Convert each entry in the matrix back to its ASCII string representing the cipher text.

```
Original string is: Nit_kkr9@gmail.com
Encrypted string is: ▯▯¡▒╣D┌q♥F°—β↕'9~
```

Fig.2 Encrypted String (Cipher Text)

b. Decrypting a String

In order to decrypt the cipher test into plain text, you must know the encrypted matrix. Get a cipher message to decode it in plain text or Standard English string.

- Calculate A^{-1}.
- Calculate $x=A^{-1} \cdot y \pmod{n}$.

  Where A^{-1} is invers matrix, y represent cipher text and x represent resultant plain text.

- In the given example decrypt the message

```
Encrypted string is: ▯▯¡▒╣D┌q♥F°—β↕'9~
```

Fig.3 Decoded String

Given extended hill cipher with original matrix

$$A=\begin{bmatrix} 6 & 24 & 1 \\ 13 & 16 & 10 \\ 20 & 17 & 15 \end{bmatrix}$$

- Group all encrypted string into multiple of three and replace each of them into its ASCII values

$$\begin{bmatrix} 32 \\ 14 \\ 221 \end{bmatrix}\begin{bmatrix} 173 \\ 177 \\ 204 \end{bmatrix}\begin{bmatrix} 68 \\ 218 \\ 113 \end{bmatrix}\begin{bmatrix} 3 \\ 213 \\ 248 \end{bmatrix}\begin{bmatrix} 196 \\ 225 \\ 18 \end{bmatrix}$$

- Get the inverse of the original matrix. i.e. Inverse of matrix A^{-1} = Adj (A) / |A|,

$$(Adj)A=\begin{bmatrix} 6 & 24 & 1 \\ 13 & 16 & 10 \\ 20 & 17 & 15 \end{bmatrix}= \begin{bmatrix} \begin{bmatrix} 16 & 10 \\ 17 & 15 \end{bmatrix} & \begin{bmatrix} 13 & 10 \\ 20 & 15 \end{bmatrix} & \begin{bmatrix} 13 & 16 \\ 20 & 17 \end{bmatrix} \\ \begin{bmatrix} 24 & 1 \\ 17 & 15 \end{bmatrix} & \begin{bmatrix} 6 & 1 \\ 20 & 15 \end{bmatrix} & \begin{bmatrix} 6 & 24 \\ 20 & 17 \end{bmatrix} \\ \begin{bmatrix} 24 & 1 \\ 16 & 10 \end{bmatrix} & \begin{bmatrix} 6 & 1 \\ 13 & 10 \end{bmatrix} & \begin{bmatrix} 6 & 24 \\ 13 & 16 \end{bmatrix} \end{bmatrix} =$$

$$\begin{bmatrix} 70 & -343 & 224 \\ 5 & 70 & -47 \\ -99 & 378 & -216 \end{bmatrix}$$

$$A^{-1} = 441 \begin{bmatrix} 70 & -343 & 224 \\ 5 & 70 & -47 \\ -99 & 378 & -216 \end{bmatrix} =$$

$$\begin{bmatrix} 0.158730 & -0.777778 & 0.507937 \\ 0.0113379 & 0.158731 & -0.106575 \\ -0.224491 & 0.857143 & -0.489796 \end{bmatrix}$$

- Multiply the enciphering matrix with inverse matrix and modulo 256.

$$\begin{bmatrix} +0.158730 & -0.777778 & +0.507937 \\ +0.011337 & +0.158731 & -0.106575 \\ -0.224491 & +0.857143 & -0.489796 \end{bmatrix} \begin{bmatrix} 3104 \\ 3854 \\ 5085 \end{bmatrix} =$$

$$(mod)\ 256 = \begin{bmatrix} 78 \\ 105 \\ 116 \end{bmatrix}$$

$$\begin{bmatrix} +0.158730 & -0.777778 & +0.507937 \\ +0.011339 & +0.158731 & -0.106575 \\ -0.224491 & +0.857143 & -0.489796 \end{bmatrix} \begin{bmatrix} 3245 \\ 4017 \\ 5324 \end{bmatrix}$$

$$(mod)\ 256 = \begin{bmatrix} 95 \\ 107 \\ 107 \end{bmatrix}$$

$$\begin{bmatrix} +0.158730 & -0.777778 & +0.507937 \\ +0.011337 & +0.158731 & -0.106575 \\ -0.224491 & +0.857143 & -0.489796 \end{bmatrix} \begin{bmatrix} 2116 \\ 3034 \\ 4209 \end{bmatrix} =$$

$$(mod)\ 256 = \begin{bmatrix} 114 \\ 57 \\ 64 \end{bmatrix}$$

$$\begin{bmatrix} +0.158730 & -0.777778 & +0.507937 \\ +0.011337 & +0.158731 & -0.106575 \\ -0.224491 & +0.857143 & -0.489796 \end{bmatrix} \begin{bmatrix} 3331 \\ 4053 \\ 5368 \end{bmatrix} =$$

$$(mod)\ 256 = \begin{bmatrix} 103 \\ 109 \\ 97 \end{bmatrix}$$

$$\begin{bmatrix} +0.158730 & -0.777778 & +0.507937 \\ +0.011337 & +0.158731 & -0.106575 \\ -0.224491 & +0.857143 & -0.489796 \end{bmatrix} \begin{bmatrix} 3268 \\ 3553 \\ 4626 \end{bmatrix} =$$

$$(mod)256 = \begin{bmatrix} 105 \\ 108 \\ 46 \end{bmatrix}$$

$$\begin{bmatrix} +0.158730 & -0.777778 & +0.507937 \\ +0.011337 & +0.158731 & -0.106575 \\ -0.224491 & +0.857143 & -0.489796 \end{bmatrix} \begin{bmatrix} 3367 \\ 4153 \\ 5502 \end{bmatrix}$$

$$(mod)\ 256 = \begin{bmatrix} 99 \\ 111 \\ 109 \end{bmatrix}$$

- Convert each integer in the plaintext into its corresponding ASCII values.

$$\begin{array}{llll} N-78 & \_-95 & r-114 & g-103 \\ i-105 & k-107 & 9-57 & m-109 \\ t-116 & k-107 & @-64 & a-97 \\ i-105 & c-99 & & \\ l-108 & o-111 & & \\ .-46 & m-109 & & \end{array}$$

- The decrypted string is now as original plain text: Nit_kkr9@gmail.com

B. *Homomorphic Algorithm*

A homomorphic encryption technique allows user to operate on encrypted text directly. Thus, making use of homomorphic encryption assures customer's data secure in all states: storage, transmission and processing. Shi Zhongpan et al. [9], presents a homomorphic calculations focusing on database and fulfill homomorphic expansion and augmentation. Boneh D et al.[10] clarify the homomorphic encryption ideas; this system is connected to the cloud condition to secure the information. The homomorphic encryption procedure permits executing calculations on the encoded information.

Basic concept of homomorphic encryption is shown in figure-2. Suppose a user want to add two numbers 5 and 10, which are stored on cloud data server in encrypted form (assume 5 instead of 10 and 10 instead of 20 respectively). Each digit are multiply by 2 and to reverse divide by 2.

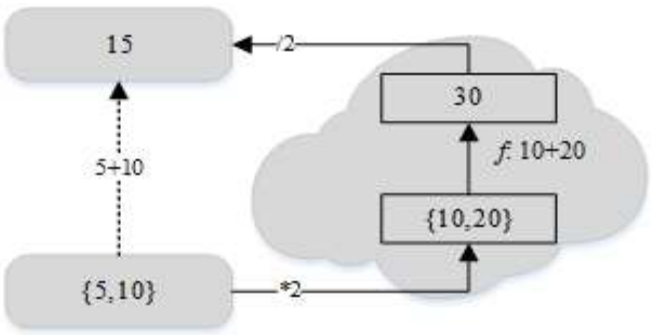

Fig.4 Homomorphic encryption

Homomorphic encryption can be either partial homomorphic or fully homomorphic encryption. Partial homomorphic encryption scheme supports either addition operation (known as additive homomorphic encryption scheme) or multiplication operation (known as multiplicative homomorphic encryption scheme). Such a scheme can perform limited number of operations. On other hand, fully homomorphic encryption (FHE) underpins random number of the two operations.

1. *Encryption Process*

At first we group the message and group length is to be decided as per the user's interest for protection. Now, each group is encoded by the homomorphic calculation.

- Select two random numbers and select two big prime numbers X and Y (more the number of digits are, safer the data is).

- Calculate N=X× Y, and get a random Z;
- Divide the plain text W into sections of length (I) whose count of digits is less than X, W = $w_1,w_2,w_3,\ldots wt$.
- Use the encryption algorithm $C_i = (W_i + I*X) \bmod N$, and compute the cipher text C = $c_1,c_2,c_3\ldots$etc.
- Send the decoded text C to the receiver.

2. *Decryption Process*

- The receiver gets the cipher text C, and groups $C=c_1,c_2,c_3\ldots ct$;
- Use the key X and the decryption algorithm $W_i = C_i \bmod X$ to compute w_i.
- At the last, we can get the plaintext W.

IV. Experimental and Result Analysis

The motivation behind this paper is apply encryption over the cloud data in order to provide information safety and to increment consumer satisfaction by not allowing the third party attack. For evaluating the proposed technique, security attack and time complexity are tested with the other important algorithms.

TABLE I. AVERAGE TIME COMPLEXITY ANALYSIS IN (SEC)

Data size (mb)	001 - 010	011 - 020	021 - 030	031 - 040	041 - 050
Caser cipher	1.0596	2.8152	5.4287	7.5783	8.9846
XOR - Cipher	0.447	1.3581	2.1476	3.0006	3.9989
Vigenere cipher	2.3306	5.7173	8.5286	12.4501	23.5996
Homomorphic	0.4458	2.2071	3.1156	4.5183	6.3086
Hill cipher	860.4412	1806.2217	2440.7313	3086.0851	3832.3503
Extended Hill cipher	1444.3303	2781.1141	4136.5001	5314.4113	6564.2563

A. Security Attacks

Security is the safety of the information that is put away on the distributed storage unit. There are numerous cryptographic techniques for limiting third party attacks. There are many types of attacks on any cryptosystem such as Cipher text Only Attack (COA), Known Plaintext Attack (KPA), Chosen Plaintext Attack (CPA), Dictionary Attack, Brute Force Attack (BFA), and Fault Analysis Attacks (FAA) out of which the extended hill cipher technique is more suitable for data security due to matrix multiplications in comparison to simple hill cipher encryption, caser cipher, xor-cipher, vigenere cipher and homomorphic algorithm [11].

However, mentioned algorithms consume less time but also provide low security. When we transmit 01-10 MB of data, extended hill cipher provides high security at the expense of more time complexity than any other algorithm.

B. Time Complexity

Time complexity of the framework is determined considering the execution time. So when are transmitting (01-10)...(40-50) MB of information, the extended hill cipher encryption takes more time to all others encryption calculations O ($m^{2.373}$) (Table-1). But when we compare security level, extended hill cipher gives more security than all others. Extended hill cipher basically focuses on the high level security.

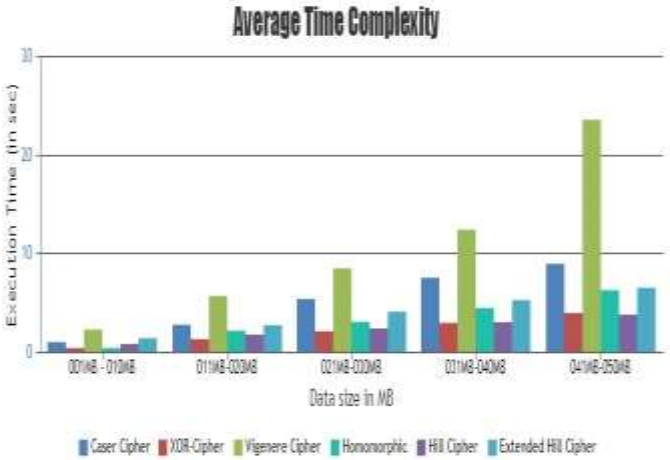

Fig.5 Execution time comparison

When data (in term of megabytes 01MB – 10MB) are encrypted, all the encryption algorithms take approximately same time. However, when we increase the data size, time complexity of all the algorithms increase drastically. In order to represent it in a graph in effective manner, we divided original time (sec) by 1000.

V. Conclusion

Cloud Storage is simply storing data and providing backups of data on virtual cloud server. In cloud storage server, security is a major issue. Encryption is a main technique to solve the data leakage problem. At the point when security level in cloud turns out to be high then integrity and privacy will be high for clients and specialist co-ops. So, we proposed a secure technique to avoid data leakage problem from server side as well as user side. Proposed algorithm which is efficient, secure and unassisted provides security as well as static confidentiality to the data. The technique guarantees the transmission information between the cloud and the customer side safely.

According to [12], the time complexity of matrix multiplication is O ($m^{2.373}$), where m is the degree of the matrix. Also, the time complexity of adding two matrices is O (m^2) , Moreover, the time complexity of XOR two matrices is O(m^2) . Thus, the total time complexity of EHC is O ($m^{2.373}$) + 2 × O (m^2) ~= O ($m^{2.373}$); i.e. the complexity of EHC is O ($m^{2.373}$) which is little bit more then to the complexity of the hill cipher. Time complexity may be improved in future.

VI. REFERENCES

[1] Akgün, Gülbahar. Performance Analysis of Hill Cipher and Its Modifications. Diss. Eastern Mediterranean University (EMU)-Doğu Akdeniz Üniversitesi (DAÜ), 2015.

[2] Muthurajkumar, Sannasy, Muthuswamy Vijayalakshmi, and Arputharaj Kannan. "Secured Data Storage and Retrieval Algorithm Using Map Reduce Techniques and Chaining Encryption in Cloud Databases." Wireless Personal Communications 96.4 (2017): 5621-5633.

[3] Chauhan, Kamal Kumar, Amit KS Sanger, and Ajai Verma. "Homomorphic encryption for data security in cloud computing." 2015 International Conference on Information Technology (ICIT). IEEE, 2015.

[4] Wang, Cong, et al. "Privacy-preserving public auditing for data storage security in cloud computing." *2010 proceedings ieee infocom*. Ieee, 2010.

[5] Shen, Jian, et al. "A secure cloud-assisted urban data sharing framework for ubiquitous-cities." *Pervasive and mobile Computing* 41 (2017): 219-230.

[6] Feng, G. "A data privacy protection scheme of cloud storage." *Software Guide* 14 (2015): 174-176.

[7] Wang, Cong, et al. "Toward secure and dependable storage services in cloud computing." *IEEE transactions on Services Computing* 5.2 (2011): 220-232.

[8] Hou, Jian-zhu, Chun-hui Piao, and Tong-rang Fan. "Privacy preservation cloud storage architecture research." *Journal of the Hebei Academy of Sciences* 30 (2013): 45-48.

[9] SHI, Zhong-pan, Cui-yan CAI, and Xian-feng WANG. "Research of privacy homomorphism algorithm based on encrypted database [J]." *Application Research of Computers* 4 (2009).

[10] Boneh, Dan, and Matt Franklin. "Identity-based encryption from the Weil pairing." *Annual international cryptology conference*. Springer, Berlin, Heidelberg, 2001..

[11] Saeednia, Shahrokh. "How to make the Hill cipher secure." *Cryptologia* 24.4 (2000): 353-360.

[12] Le Gall, François. "Powers of tensors and fast matrix multiplication." *Proceedings of the 39th international symposium on symbolic and algebraic computation*. ACM, 2014.

Proceedings of the Fourth International Conference on Communication and Electronics Systems (ICCES 2019)
IEEE Conference Record # 45898; IEEE Xplore ISBN: 978-1-7281-1261-9

Yaw stability of 4WS with variable steering ratio strategy using inertial delay control based sliding mode control

Tushar Khanke
Department of Instrumentation and Control
College of Engg.,Pune
India
khanketm17.instru@coep.ac.in

Sushant Chaudhari
Department of Instrumentation and Control
College of Engg.,Pune
India
sushantchaudhari2310@gmail.com

Shrivijay Phadke
Department of Instrumentation and Control
College of Engg.,Pune
India
sbp.instru@coep.ac.in

Pramod Shendge
Department of Instrumentation and Control
College of Engg.,Pune
India
pds.instru@coep.ac.in

***Abstract*—In this paper Inertial delay control(IDC) based sliding mode control(SMC) for 4 wheel steering(4WS) vehicle which focuses on the maneuvering flexibility and steering stability of the vehicle. To achieve above a new method for variable steering ratio(VSR) is introduced. A nonlinear vehicle model is considered along with the uncertainties in cornering stiffness, mass and vehicle speed. To compensate the effect of nonlinearities and uncertainties and also controlling lateral dynamics an IDC based SMC is proposed to achieve required side-slip angle and yaw rate of vehicle based on VSR. Further a simulation is executed to analyze the performance of proposed controller for 4WS by tracking the system dynamics to follow the desired model regardless of the nonlinearities and uncertainties. The proposed controller is also validated with Carsim software.**

***Index Terms*—Variable steering ratio, four wheel steering, sliding mode control, inertial delay control, Carsim**

I. Introduction

As automobile industry is developing very fast and most of the people rely on vehicle, stability of vehicle is a big factor. Earlier for yaw stability of vehicle, reseachers used Active front wheel steering(AFS) but it was limited to stability in low to medium speed region of the vehicle due to saturation of lateral forces. As the advancement to get the stability in the high speed region active front steering was combined with braking(DYC), or with ARS i.e 4WS. [1] During turning vehicle performance can be enhanced by actively steering rear wheels as well as front wheels (4WS). The 4WS system can control both yaw rate and lateral velocity of the vehicle. In [2], LPV controller was implemented for velocity varying 4WS vehicle model having uncertainties in mass, cornering stiffness and external disturbances. A second order dynamics decoupling controller was designed in [3] for 4WS vehicle by decoupling the lateral speed and yaw rate. An optimal control theory based controller was designed for model matching in low and high speed of 4WAS is done [4]. An active 4WS non smooth sliding mode controller with finite time convergence was designed for an electric vehicle in [5] to track the desired model. In [6] sliding mode controller having an intergral sliding surface was proposed to eliminate steady state errors. In [7] DOB control strategy for 4WAS was presented, to deal with ignored nonlinear vehicle model and cross wind disturbance.

The steering ratio (SR) is ratio of handwheel and front wheel angle, which has impact on the maneuvering flexibility and vehcile stability [8]. This SR should be varying with vehicle speed because 1) at low speed to get the maneuvering flexibility the SR should be small so that for small handwheel angle it will produce large front wheel angle and 2) at high speed to prevent steering sensitivity a large SR should be given to satisfy the steering stability [9]. Different methods were designed and derived to get the Variable Steering Ratio (VSR) such as constant yaw rate gain , constant lateral acc. gain,combination of both [10] and Fuzzy neural network approach [9]. In summary most of the present researchers focuses on yaw stability, while focus on maneuvering flexibility and steering stability are focused less and very fewer have done the combination of robust yaw stability of 4WS based on VSR strategy.

In this paper the focus is on maneuver flexibility and steering stability and a robust Inertial delay based SMC is applied to achieve yaw stability i.e to follow the desired model of lateral dynamics. The validation is done in Carsim software.

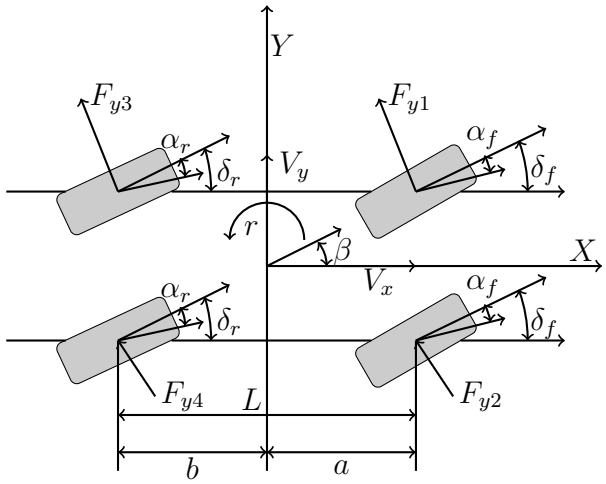

Fig. 1. 4 wheel steering dynamic model

This paper key features are as follow :

- Nonlinear 4WS vehicle model is derived also uncertainties in cornering stiffness, mass, vehicle speed are taken.
- The new function for variable steering ratio is proposed using this strategy the desired model of vehicle lateral dynamics is obtained.
- To track the desired vehicle lateral dynamics regardless of nonlineartities and uncertainties a robust Inertial Delay Control based sliding mode controller is designed.
- Validation of proposed controller in Carsim software.

Organization of this paper is as follow, Section I gives brief introduction of latest work. Section II derives the 4WS nonlinear vehicle model along with desired model of lateral dynamics. An IDC based sliding mode controller is implemented in Section III. Section IV shows the effectiveness of proposed controller and Section V convey robustness through Carsim validation. Section VI is conclusion.

II. Problem Setup

A. Modelling of nonlinear 4WS vehicle

A double track model of 4 wheel steering vehicle is seen in Fig.1 . [11], [12] The 2 DOF vehicle model captures the lateral dynamics obtained as

$$mV_x(\dot{\beta}+r) = F_{y1}cos\delta_f + F_{y2}cos\delta_f + F_{y3}cos\delta_r + F_{y4}cos\delta_r + F_{x1}sin\delta_f + F_{x2}sin\delta_f + F_{x3}sin\delta_r + F_{x4}sin\delta_r \quad (1)$$

$$I_{zz}\dot{r} = a(F_{y1}cos\delta_f + F_{y2}cos\delta_f + F_{x1}sin\delta_f + F_{x2}sin\delta_f) - b(F_{y3}cos\delta_r + F_{y4}cos\delta_r + F_{x3}sin\delta_r + F_{x4}sin\delta_r) + \frac{tw}{2}(F_{y1}sin\delta_f - F_{y2}sin\delta_f + F_{y3}sin\delta_r - F_{y4}sin\delta_r + F_{x2cos\delta f} - F_{x1}cos\delta f + F_{x4}cos\delta r - F_{x3}cos\delta r) \quad (2)$$

where δ_f and δ_r are front and rear wheel angle, $a_y = v_x(\dot{\beta}+r)$ is the lateral acceleration at C.G of vehicle. F_{xi} and F_{yi} are longitudinal and lateral forces simultaneously produced by front and rear tires. i is the sequence of tires .The slip angle of front and rear tires are obtained as

$$\alpha_{1,2} = -\delta_f + \beta + \frac{ar}{v_x}$$
$$\alpha_{3,4} = -\delta_r + \beta - \frac{br}{v_x} \quad (3)$$

we have considered a linear tire model i.e. assuming that slip angles are small thus, the lateral forces are given by

$$F_{y1,2} = -\mu c_{1,2}\alpha_{1,2}$$
$$F_{y3,4} = -\mu c_{3,4}\alpha_{3,4} \quad (4)$$

where μ is co-efficient of friction between road & tyre.$c_{1,2}$ and $c_{3,4}$ are the cornering stiffness of front and rear wheels respectively

The vehicle weight is evenly distributed i.e no logitudinal load transfer occurs.Thus the vertical loads are obtained as

$$F_{z1,2} = \frac{mgb}{2L}$$
$$F_{z3,4} = \frac{mga}{2L} \quad (5)$$

where g is the accceleration due to gravity. Now the longitudinal tire forces are given by

$$F_{xi} = \mu F_{zi} \quad (6)$$

by re-arranging (1–2) equations, vehicle lateral dynamics are derived as

$$\dot{\beta} = \frac{1}{mV_x}(F_{y1}cos\delta_f + F_{y2}cos\delta_f + F_{y3}cos\delta_r + F_{y4}cos\delta_r + F_{x1}sin\delta_f + F_{x2}sin\delta_f + F_{x3}sin\delta_r + F_{x4}sin\delta_r) - r \quad (7)$$

$$\dot{r} = \frac{1}{I_{zz}}[(F_{y1}cos\delta_f + F_{y2}cos\delta_f + F_{x1}sin\delta_f + F_{x2}sin\delta_f)a - b(F_{y3}cos\delta_r + F_{y4}cos\delta_r + F_{x3}sin\delta_r + F_{x4}sin\delta_r)] + \frac{t_w}{2I_{zz}}(F_{y1}sin\delta_f - F_{y2}sin\delta_f + F_{y3}sin\delta_r - F_{y4}sin\delta_r + F_{x2}cos\delta f - F_{x1}cos\delta f + F_{x4}cos\delta r - F_{x3}cos\delta r) \quad (8)$$

As there are uncertainties in cornering stiffness , mass, vehicle speed and lateral and longitudinal forces are multiplied with nonlinear terms all these are lumped together in disturbances and again re-arranging the system equations we get,

$$\dot{\beta} = B_{11}\delta_f + B_{12}\delta_r + d_1 \quad (9)$$

where $B_{11} = \frac{2c_{1,2}}{mV_x}$, $B_{12} = \frac{2c_{3,4}}{mV_x}$ and

$$d_1 = \frac{1}{mV_x}(F_{y1}cos\delta_f + F_{y2}cos\delta_f + F_{y3}cos\delta_r + F_{y4}cos\delta_r + F_{x1}sin\delta_f + F_{x2}sin\delta_f + F_{x3}sin\delta_r + F_{x4}sin\delta_r) - r - B_{11}\delta_f - B_{12}\delta_r$$

$$\dot{r} = B_{21}\delta_f + B_{22}\delta_r + d_2 \tag{10}$$

where $B_{21} = \frac{2ac_{1,2}}{I_{zz}}$, $B_{22} = \frac{-2bc_{3,4}}{I_{zz}}$ and

$$\begin{aligned} d_2 = \frac{1}{I_{zz}}(&F_{y1}cos\delta_f + F_{y2}cos\delta_f + F_{x1}sin\delta_f + F_{x2}sin\delta_f)a \\ &-b(F_{y3}cos\delta_r + F_{y4}cos\delta_r + F_{x3}sin\delta_r + F_{x4}sin\delta_r) \\ &+\frac{tw}{2}(F_{y1}sin\delta_f - F_{y2}sin\delta_f + F_{y3}sin\delta_r - F_{y4}sin\delta_r \\ &+F_{x2}cos\delta f - F_{x1}cos\delta f + F_{x4}cos\delta r - F_{x3}cos\delta r) \\ &-B_{21}\delta_f - B_{22}\delta_r \end{aligned}$$

B. Reference model of lateral dynamics

The desired steering response is obtained from 2 DOF bicycle model of FWS vehicle which requires a desired front wheel angle (δ_{fd}).The VSR strategy is used to get δ_{fd} according to vehicle speed.
By studying conditions for VSR strategy from [8] we have proposed new function of VSR ,

The newly proposed VSR is given by

$$i = i_0 + a(1 - e^{-\alpha V_x^3}) \tag{11}$$

$$\delta_{fd} = \frac{\theta_{hw}}{i} \tag{12}$$

where i is the VSR , θ_{hw} is Handwheel angle, i_0 is initial value ,i_0+a is the final value and α decides rate of exponential term.

The desired lateral dynamics model for 4WS will be same as derived for FWS so that the perception of driver does not change.Thus the desired lateral dynamics are given by

$$\beta_d = \frac{k_\beta}{\tau_\beta s + 1}\delta_{fd} \tag{13}$$

$$r_d = \frac{k_r}{\tau_r s + 1}\delta_{fd} \tag{14}$$

where k_β and k_r are proportional gain : $k_\beta = 0$, $k_r = \frac{V_x}{(L+KV_x^2)}$, K is the understeer gradient $K = \frac{m}{L}(\frac{b}{c_1c_2} - \frac{a}{c_3c_4})$, τ_β and τ_r are time constant for desired side-slip angle and yaw rate respectively,

The state space equation of desired model is obtained as

$$\dot{x}_d = A_d x_d + B_d u_d \tag{15}$$

where , state vector $x_d = \begin{bmatrix}\beta_d \\ r_d\end{bmatrix}$,state matrix $A_d = \begin{bmatrix}-\frac{1}{\tau_\beta} & 0 \\ 0 & -\frac{1}{\tau_r}\end{bmatrix}$, input matrix $B_d = \begin{bmatrix}\frac{k_\beta}{\tau_\beta} \\ \frac{k_r}{\tau_r}\end{bmatrix}$ and desired input $u_d = \delta_{fd}$.

III. Control strategy for yaw stability

Aim of this controller is to enhance maneuvering flexibility and steering stability.
Sliding surfaces used for side-slip angle and yaw rate tracking are stated as follow

$$\sigma_\beta = \beta - \beta_d \tag{16}$$

$$\sigma_r = r - r_d \tag{17}$$

For control strategy the system can be represented in the form of

$$\dot{\beta} = u_\beta + d_\beta \tag{18}$$

where $u_\beta = B_{11}\delta_f + B_{12}\delta_r$

$$\dot{r} = u_r + d_r \tag{19}$$

where $u_r = B_{21}\delta_f + B_{22}\delta_r$
by differentiating both sliding surfaces

$$\dot{\sigma_\beta} = u_\beta + d_\beta - \dot{\beta}_d \tag{20}$$

$$\dot{\sigma_r} = u_r + d_r - \dot{r}_d \tag{21}$$

the required control is obtained as

$$u_\beta = -\hat{d}_\beta + \dot{\beta}_d - K_\beta\sigma_\beta \tag{22}$$

$$u_r = -\hat{d}_r + \dot{r}_d - K_r\sigma_r \tag{23}$$

Estimation of uncertainty using inertial delay control method, the estimation of $d_\beta \& d_r$ are calculated by

$$\hat{d}_{\beta,r} = \frac{1}{\tau_{1,2}}(\int \sigma_{\beta,r}dt + \sigma_{\beta,r}) \tag{24}$$

the dynamics of uncertainties estimator thus becomes [13] [14]

$$\hat{d}_{\beta,r} = \frac{d_{\beta,r}}{\tau_{1,2}s + 1} \tag{25}$$

$$\dot{\hat{d}}_{\beta,r} = \frac{\tilde{d}_{\beta,r}}{\tau_{1,2}} \tag{26}$$

$$\tilde{d}_{\beta,r} = d_{\beta,r} - \hat{d}_{\beta,r} \tag{27}$$

then by differentiating and substituting :

$$\dot{\tilde{d}}_{\beta,r} = \dot{d}_{\beta,r} - \frac{\tilde{d}_{\beta,r}}{\tau_{1,2}} \tag{28}$$

Thus by applying Lyapunov stability, $\tilde{d}_{\beta,r}$ is bounded by $\mid \dot{d}_{\beta,r} \mid \tau_{1,2}$.
Putting u_β and u_r in (20) and (21) we get

$$\dot{\sigma}_{\beta,r} = -K_{\beta,r}\sigma_{\beta,r} + \tilde{d}_{\beta,r} \tag{29}$$

now the sliding condition i.e $\sigma\dot{\sigma}$ becomes

$$\sigma_{\beta,r}\dot{\sigma}_{\beta,r} \leq -\sigma_{\beta,r}(K_{\beta,r} \mid \sigma_{\beta,r} \mid - \mid \tilde{d}_{\beta,r} \mid) \tag{30}$$

This states that $\sigma_{\beta,r}$ will go to zero asymptotically.Thus ensuring side-slip angle and yaw rate will track the desired trajectories.

TABLE I
SPECIFICATIONS OF 4WS VEHICLE

Model specifications	Values
Mass of vehicle (m)	1270 kg
Yaw moment of inertia (I_{zz})	1536 kgm^2
Front axle to C.G distance (a)	1.01 m
Rear axle to C.G distance (b)	1.9 m
Wheel base length (L)	2.91 m
Track width (t_w)	1.55 m
Cornering stiffness of front tires ($c_{1,2}$)	45386 N/rad
Cornering stiffness of rear tires ($c_{3,4}$)	45386 N/rad

IV. SIMULATION RESULTS

To validate, the simulation of the proposed controller is performed on MATLAB/Simulink. In order to verify the robustness of the proposed controller for 4WS we have compared it with passive vehicle and applied same controller to FWS. Observing the limitations of FWS over 4WS by comapring with desired value of yaw rate and sideslip angle.A J-turn maneuver i.e constant handwheel input(θ_{hw}) of 1.74 rad is given by driver and vehicle has been simulated for two logitudinal speed(V_x) i.e for low speed–13.88 m/s (50 $Kmph$) and high speed–33.33 m/s (120 $Kmph$).As all the paramters such cornering stiffness,mass , vehicle speed have uncertainties and are lumped together in disturbances.To compensate this disturbances the IDC is used to make the real time estimate of disturbances.Further controller uses this estimate to attenuate effect of lumped disturbances.Take values of vehicle parameters from Table I and for controller parameters refer Table II for simulation purpose.

The Fig. 2b depicts that yaw rate error for passive is more than AFS and 4WAS.AFS and 4WAS shows almost same response for yaw rate. But the main difference can be seen in Fig. 2a due to the limitation of AFS of controlling only one state the sideslip angle is very poor as compared to 4WAS response.Still it is considerable for low speed region as vehicle stability is mostly depend on yaw rate .Now, for high speed region as sideslip angle increases the vehicle stability not only depends on yaw rate but also sideslip angle.Thus controlling both yaw rate and sideslip angle is important at high speed.The simulation results for high speed from Fig. 3 shows that tracking response of 4WAS for both dynamics are superior than AFS and passive responses.

V. CARSIM VALIDATION

The robustness of the designed controller is observed in simulation section.However ,some assumptions were made at the time of deriving the mathematical model.So,to verify the practicability of IDC based SMC 4WAS Carsim-Matlab co-simulation is performed.Carsim is popular tool used in automobile industry to validate different control strategy.In this Carsim a C-class hatchback car model is considered. In Fig. 4, the CarSim results are obtained for higher speed, from Fig. 4a the side slip angle of passive steering and AFS are not tracking the desired tracjectory but the proposed 4WAS tracks it closely.In Fig. 4b tracking error of yaw rate of passive is not comparable with AFS and 4WAS, the yaw rate tracking error of 4WAS is less than that AFS. For strictly reducing yaw rate error the required steering input by 4WAS is more than that of AFS and passive as shown in Fig. 4c. In Fig. 4d the rear wheel angle is shown which is an additional actuator of 4WAS.

TABLE II
CONTROLLER PARAMETERS

Controller Parameters	Values
K_β, K_r	5
τ_1, τ_2	0.005

VI. CONCLUSION

In this paper an IDC based SMC strategy was implemented on 4WS vehicle.Firstly, a nonlinear vehicle model was derived considering the uncertainties in cornerning stiffness,mass and vehicle speed. Then new VSR strategy was formulated to obatin the desired lateral dynamics.The nonlinearities, uncertainties are estimated by inertial delay control method. To compensate this effect and control the lateral dynamics i.e both yaw rate and sidelip angle to track the desired model of lateral dynamics a robust SMC was designed. The simulation results shows that limitation in FWS was overcome by 4WS. Lastly,the robustness of proposed controller was validated through Carsim for J-turn maneuver. Future scope for this work could be done by reducing the use of additional actuator i.e rear wheel by analysing the $\beta - \dot{\beta}$ phase plane method.

REFERENCES

[1] T. D. Gillespie, "Vehicle dynamics," *Warren dale*, 1997.
[2] M. Li, Y. Jia, and J. Du, "Lpv control with decoupling performance of 4ws vehicles under velocity-varying motion," *IEEE Transactions on Control Systems Technology*, vol. 22, no. 5, pp. 1708–1724, 2014.
[3] R. Marino and F. Cinili, "Input–output decoupling control by measurement feedback in four-wheel-steering vehicles," *IEEE Transactions on Control Systems Technology*, vol. 17, no. 5, pp. 1163–1172, 2009.
[4] M. Ariff, H. Zamzuri, M. Nordin, W. Yahya, S. Mazlan, and M. Rahman, "Optimal control strategy for low speed and high speed four-wheel-active steering vehicle," *Journal of Mechanical Engineering and Sciences*, vol. 8, pp. 1516–1528, 2015.
[5] Q. Meng, Z.-Y. Sun, and Y. Li, "Finite-time controller design for four-wheel-steering of electric vehicle driven by four in-wheel motors," *International Journal of Control, Automation and Systems*, vol. 16, no. 4, pp. 1814–1823, 2018.
[6] L. Tan, S. Yu, Y. Guo, and H. Chen, "Sliding-mode control of four wheel steering systems," in *2017 IEEE International Conference on Mechatronics and Automation (ICMA)*. IEEE, 2017, pp. 1250–1255.
[7] S. Yu, J. Wang, Y. Wang, and H. Chen, "Disturbance observer based control for four wheel steering vehicles with model reference," *IEEE/CAA Journal of Automatica Sinica*, vol. 5, no. 6, pp. 1121–1127, 2018.
[8] Y. Wu, L. Wang, and F. Li, "Research on variable steering ratio control strategy of steer-by-wire system," SAE Technical Paper, Tech. Rep., 2018.
[9] Y. Jiang-Yun, K. Feng, and W. Fang-Yuan, "Control strategy for front wheel angle of steer-by-wire based on variable steering ratio," in *Proceedings of 2011 International Conference on Computer Science and Network Technology*, vol. 2. IEEE, 2011, pp. 852–856.
[10] J. Wei, G. Shi, and Y. Lin, "Design of new variable steering ratio for mechanical active steering system," in *Proceedings of 2013 IEEE International Conference on Vehicular Electronics and Safety*. IEEE, 2013, pp. 27–30.
[11] R. Rajamani, *Vehicle dynamics and control*. Springer Science & Business Media, 2011.

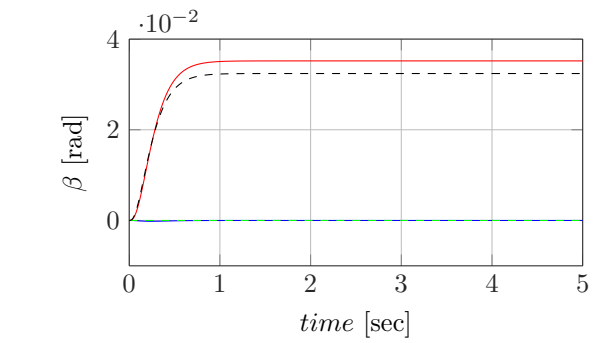

(a)

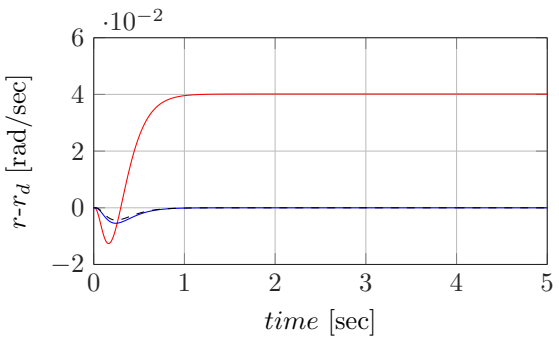

(b)

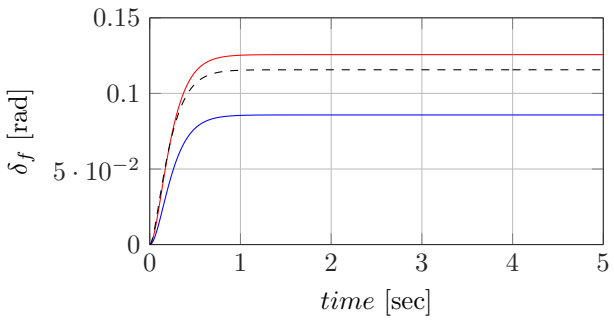

(c)

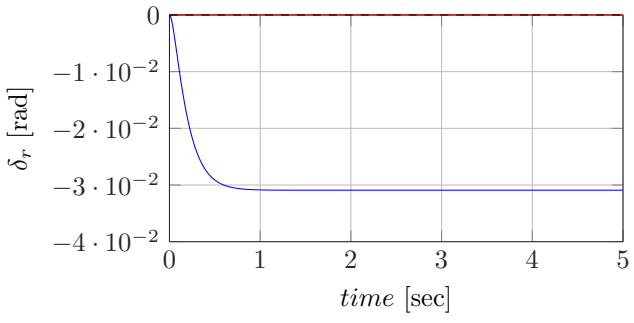

(d)

Fig. 2. Response of the proposed control for 4WS with vehicle speed 50kmph and constant handwheel steering: desired trajectory (dotted green) and passive steering (red) AFS (dotted black) 4WAS(blue) (a) side slip angle (b) yaw rate error (c) controlled front and (d) rear wheels angle

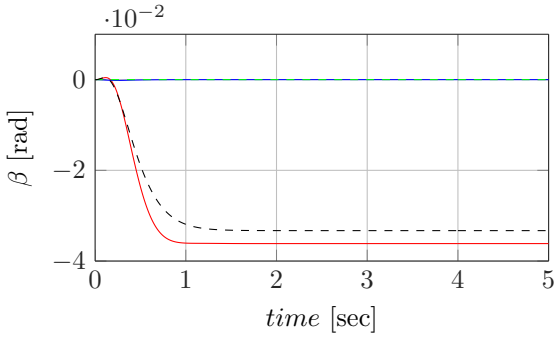

(a)

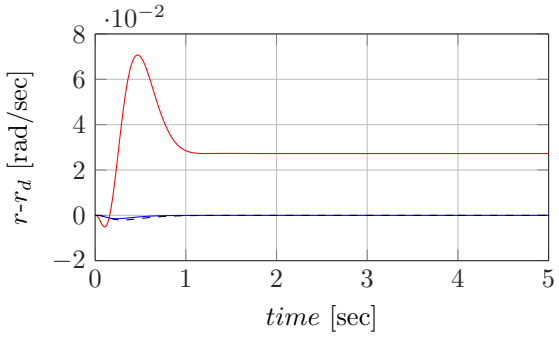

(b)

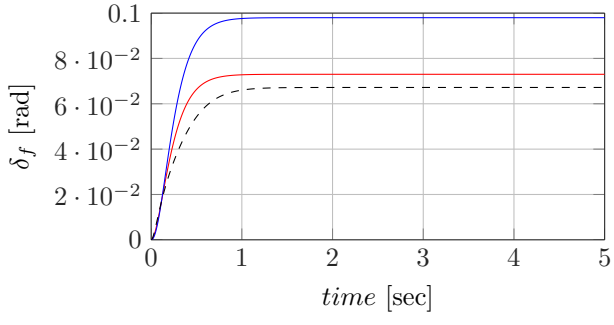

(c)

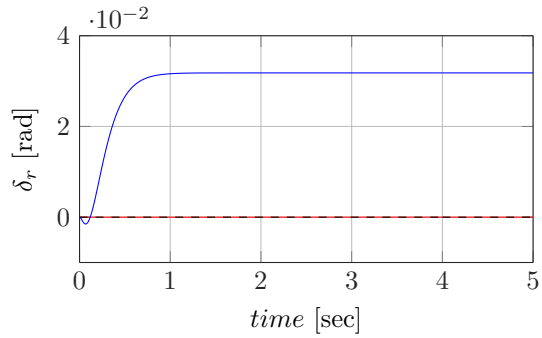

(d)

Fig. 3. Response of the proposed control for 4WS with vehicle speed 120kmph and constant handwheel steering : desired trajectory (dotted green) and passive steering (red) AFS (dotted black) 4WAS(blue) (a) side slip angle (b) yaw rate error (c) controlled front and (d) rear wheels angle

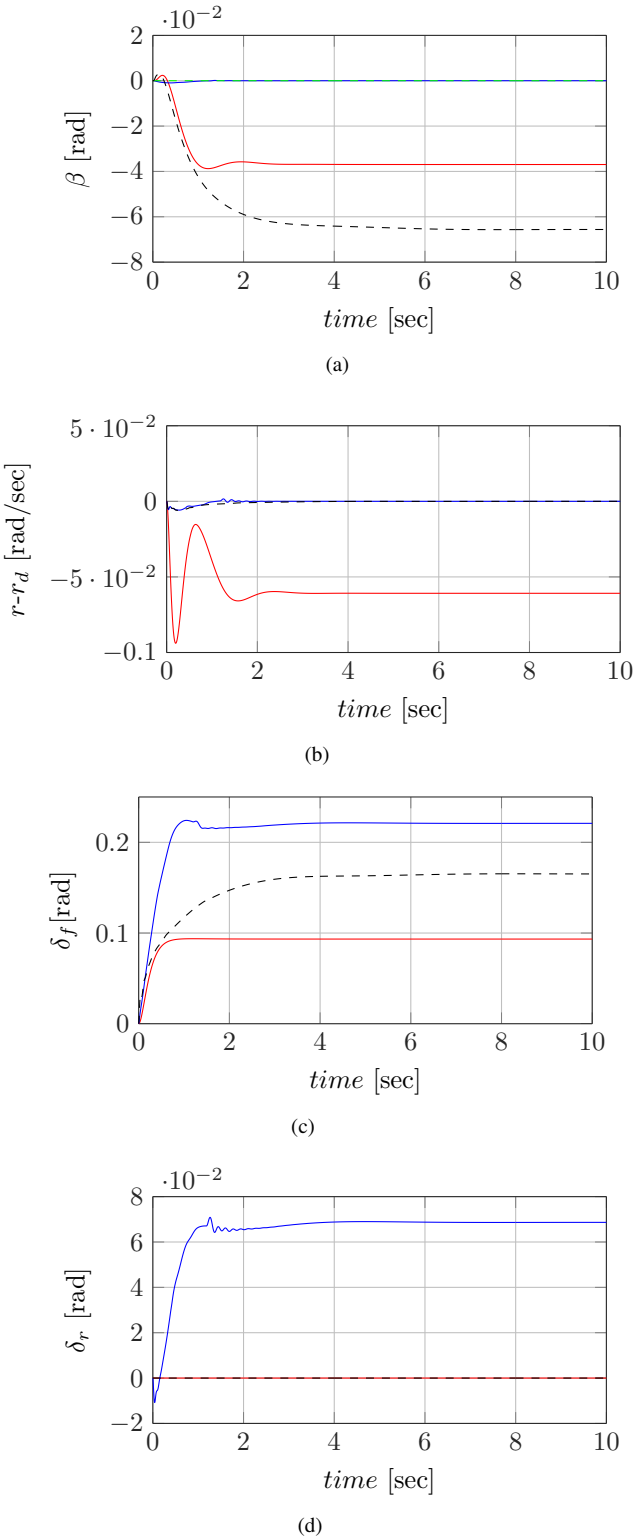

Fig. 4. Validation of proposed control for 4WS with vehicle speed 72kmph and constant handwheel steering : desired trajectory (dotted green) and passive steering (red) AFS (dotted black) 4WAS(blue) (a) side slip angle (b) yaw rate error (c) controlled front and (d) rear wheels angle

[12] A. Marar, D. Ginoya, S. B. Phadke, and P. D. Shendge, "Robust yaw stability control based on disturbance observer using active front steering," in *Industrial Instrumentation and Control (ICIC), 2015 International Conference on*. IEEE, 2015, pp. 1367–1372.

[13] A. Bhowmik, A. Marar, D. Ginoya, S. Singh, and S. B. Phadke, "Inertial delay control based sliding mode control for active suspension with full car model," in *2016 IEEE First International Conference on Control, Measurement and Instrumentation (CMI)*. IEEE, 2016, pp. 376–380.

[14] S. Singh, D. Ginoya, S. B. Phadke, and P. D. Shendge, "Inertial delay control based multiple sliding surface controller for anti-lock braking system with second order actuator," in *2015 International Conference on Industrial Instrumentation and Control (ICIC)*. IEEE, 2015, pp. 1641–1646.

Proceedings of the Fourth International Conference on Communication and Electronics Systems (ICCES 2019)
IEEE Conference Record # 45898; IEEE Xplore ISBN: 978-1-7281-1261-9

Pneumatic Controlled Smart Arecanut Plucking Robot with Raspberry Pi

S Kushal Gowda[1], Prathima K R[2], Yashaswini L[3], Rakesh M D[4] and T R Sateesh Kumar[5]
Department of Electronics and Communication Engineering,
Siddaganga Institute of Technology,
Tumkur, India
[1]skushalgowda1si15ec083@gmail.com, [2]prathima.1si16ec415@gmail.com, [3]yashaswini.1si16ec425@gmail.com,
[4]rakesh.1si16ec417@gmail.com, [5]sateesh_tr@sit.ac.in

***Abstract*—Due to the scarcity of skilled labourers, areca growers are finding it difficult to harvest their crop. Arecanut tree climbing is a risky job which requires skilled labourers. If a person slips while climbing, it will be irreparable damage to him and as well as to his family. In recent years, getting labourers who climb the arecanut tree is a major challenge. Arecanut trees grow to a height of about 60 to 70 feet. It is required to climb the arecanut tree around four to five times in a year for harvesting. Only skilled labourers can carry out these operations. In this paper, a Smart Arecanut Plucking Robot is designed through which some of the above difficulties are addressed. This robot is designed to climb the arecanut trees of varying diameter. Here, the robot can be operated either in manual mode or in automatic mode. Six pneumatic cylinders are used with an air compressor for robot movement. Arduino UNO is used for controlling the pneumatic cylinders. The robot climbs as human climbs the tree and a camera is mounted on the robot to get the live video streaming. Raspberry Pi is used for interfacing camera to get live video streaming of the plucking operation. By watching the live video, the position of the cutter can be adjusted. The android application RaspiCAM Remote installed in users android phone is used to watch the live video stream sent by the Raspberry Pi present in the robotic unit. A robot is successfully tested on an arecanut tree of varying trunk diameter (up to 7 inches) and heights (up to a maximum of 45 feet). The user is successfully able to guide the robot to cut the ripened arecanut bunch.**

***Index Terms*—Pneumatic Cylinder, Solenoid Valve, Air compressor, Camera, Raspberry Pi.**

I. INTRODUCTION

People from the rural part of India mainly depend on agriculture for their livelihood. Arecanut and Coconut are the main crops cultivated in Karnataka and Kerala. Regardless of mass distribution and spread of arecanut trees around these regions, arecanut reaping is still done without safety measures resulting in major issues [1]. Farmers are finding it hard to climb arecanut trees and there is a scarcity of trained arecanut tree climbers. Skilled workers need to climb the tree manually for collecting the arecanuts which is risky and dangerous. To help the farmers in arecanut harvesting, there are numerous machines in the market. They are not successful since they require a lot of muscular power of the labour for its operation. At present, a completely safe device is not available in the market for harvesting the arecanuts. To address both productivity and security, there is a need to invent the machine for arecanut harvesting. In this paper, a robot is designed to climb the arecanut tree and cut the arecanuts. Various models (semi-automatic robots) were created to address the issue but each of them has its own limitation. Here we have examined to beat the above constraint by building up a self-governing robot [2]. Fig. 1. shows the Climber climbing the arecanut tree.

As of now, the shortage of workers has become one of the major challenges in arecanut cultivation. Areca trees grow to a maximum height of around 60-70 feet [3]. It is compulsory to climb the trees around four to five times each year for an effective reap. Only trained workers can do these activities. They need to climb the trees using muscle power. In a hectare of land, around 500 arecanut trees can be grown and a worker needs to climb at least 100 to 150 trees per day to harvest the yield. As this involves real hard physical exertion, youths are losing interest in such risky job resulting in emerging demand for the skilled labourers [4][5].

Fig. 1: Climber climbing the Arecanut tree.

II. Related Works

A. Semi-automatic Robot.

To cut arecanut from trees, Wonder Climber [1] was invented, which is shown in Fig. 2. Skilled workers are required to cut the arecanuts by utilizing this hardware. The greatest advantage of this machine is it can be shifted to anyplace on one's shoulders since it weighs about 6.5 kilograms. This machine can be made to climb the tree and do the hard work related to arecanut tree climbing and cutting. Wonder climber is operated by the assistance of a pulley and rope. With the assistance of two U clamps, the machine can be fitted to any arecanut tree. Once it is fixed, the rope is pulled to climb up. Once it reaches the tree top, by pulling the rope in the correct direction the blade edge can be adjusted to pluck the arecanuts.

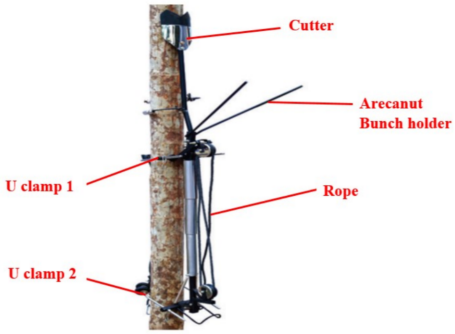

Fig. 2: Wonder climber.

B. Automatic Arecanut Plucking Robot.

The tree climber has two rings, two pulleys, rollers, rope, spring, cutter, collector and the main frame. The power from the motor is transmitted by rope pulley instrument. The machine is placed around the tree and clamped to it by utilizing two rings. Rotation of the motor allows rope to wind and rewind on to the drum. Cutting will happen along the movement of the machine. There is no separate mechanism for cutting operation. Control of the robot is done by a Bluetooth connected via mobile. The upper and lower rings are used to mount the machine onto the arecanut tree. These two rings are fixed to the main frame with the help of pins to arecanut tree. The ring is provided with holes of different diameters so as to climb arecanut trees of different diameter. During the winding operation, the upper ring will be locked to the tree and lower ring will be free to move thus creating an upward movement of the lower ring. After the winding operation, the lower pulley gets locked and upper pulley becomes free. During the unwinding operation the upper pulley displaces and creates a displacement. The cutting operation is carried out by the cutting tool during the unwinding operation. A motor is used for this operation. This operation gives enough power for the cutting tool to produce a cutting action. The remote controlled arecanut plucking machine is shown in Fig. 3.

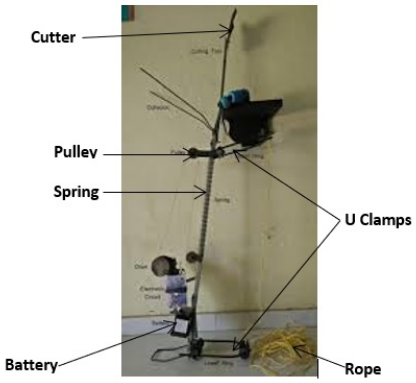

Fig. 3: Remote controlled arecanut plucking robot

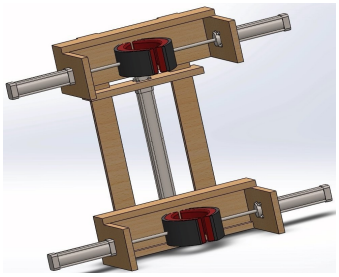

(a) Front view of a Model.

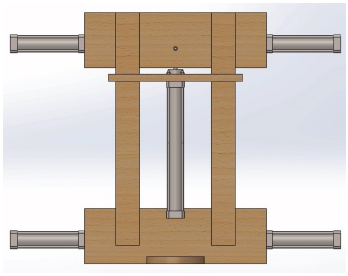

(b) Back view of a Model.

Fig. 4: Design of the Model.

III. Model Design

To address the above issue, the model was designed utilizing the SOLID WORK software as shown in Fig. 4. This design had the capacity to climb up and climb down the tree by considering some mechanisms which will be discussed in the upcoming area. The fundamental material utilized in this robot includes Pneumatic actuators for development of the cylinder bars, to move up and down, Cylinder bars to hold the tree firmly, Grippers to maintain a strategic distance from the scratches on tree and sharper to cut the matured arecanuts, wooden sheets for supporting the cylinders and Pneumatic Poly Urethane (PU) HOSE tube pipe to supply compressed air to pneumatic cylinders [6].

A. Working of Robot(Climbing up)

A Smart Arecanut Plucking Robot is designed and implemented using pneumatic operations. Here, a robot is designed to climb the tree automatically or by manual operation.
The automated robot contains five cylinders in which four cylinders are used for holding the tree and another one cylinder used to climb the tree up and down. There are four stages in climbing the tree.

Subdivision in stages.

1) Stage 1: During the first stage, the cylinder 1 and cylinder 2 holds the tree tightly with the help of piston and gripper by moving the piston forward using compressed air pressure as shown in Fig. 5.

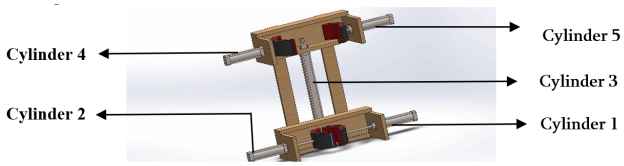

Fig. 5: Movement of the Piston of Cylinder 1 & 2.

2) Stage 2: In the second stage, the third cylinder expands horizontally by the support of cylinder two and three and using compressed air pressure. The cylinder expands almost double in its size by elaborating piston as shown in the above Fig. 6. Hence it is an efficient approach to climb the tree in a short period of time.

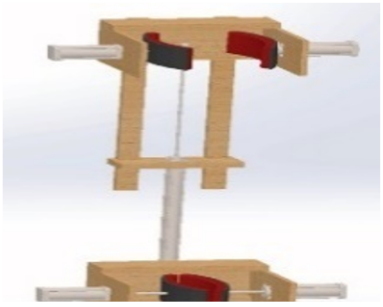

Fig. 6: Movement of the Piston of Cylinder 3 (Climbing Up).

3) Stage 3: In the third stage, cylinder four and five holds the tree with the help of air pressure and third cylinder as shown in the above Fig. 7. The compressed air is passed through the compressor through PU HOSE tube pipe and the cylinders one and two piston gets compressed.

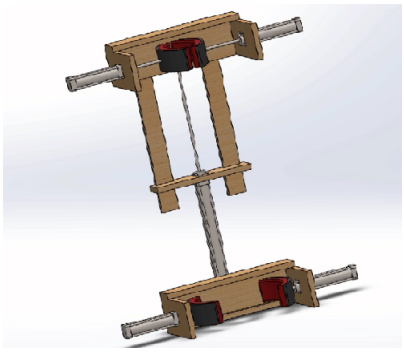

Fig. 7: Compression of the Piston of Cylinder 4 & 5.

4) Stage 4: During the fourth stage, the third cylinder gets compressed hence the robot moves upwards this process continues until the robot reaches the top of the tree were arecanuts are present. Each stage is repeated sequentially with the help of the controlling unit. The fourth stage is shown in Fig. 8.

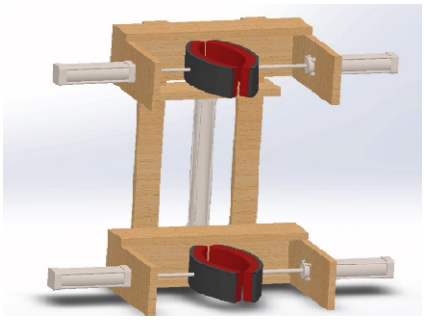

Fig. 8: Piston Movement of Cylinder 3.

B. Climbing Down

When the robot completes cutting of the arecanut bunch it moves down utilizing a similar procedure which is followed during climbing up of the tree but in reverse order.

C. Proposed Arecanut robot

This model is designed to overcome the issue occurred during manual climbing. The robot can be operated by farmers from the ground without manual climbing. This robot is more efficient with different frameworks as far as speed. Farmers can easily operate this robot by understanding the movement of the cylinders.
The designed robot can climb up and climb down the arecanut tree with live video streaming. Depending on the user instructions, the robot cuts the arecanut bunch.

IV. System Description

The block diagram of the robot is shown in Fig. 9. The system comprises of two units in particular Mechanical Unit and User Control Unit. The Automated unit comprises of Pneumatic cylinder, Air compressor, Solenoid valve, Air filter, Control unit and cutter. The user control unit comprise of Raspberry Pi 3, camera, transmitter and receiver.

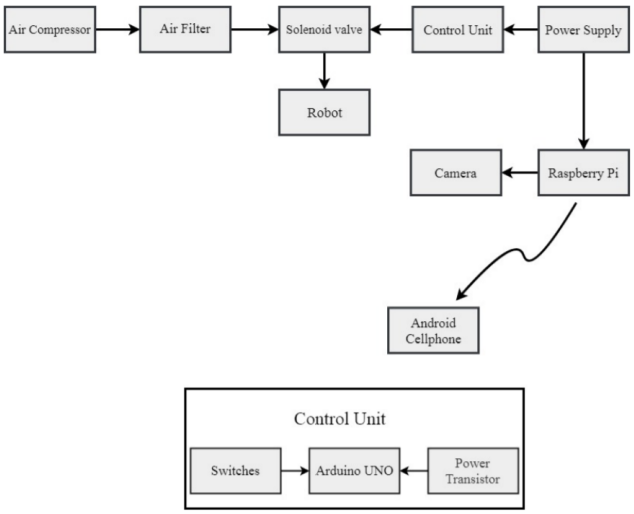

Fig. 9: Block Diagram of Arecanut Plucking Robot.

A compressor can compress air to the required pressure. It can convert mechanical energy from motors into the potential energy in the form of compressed air. At the point when tank weight achieves its built maximum capacity, the air compressor closes off. The packed air is connected to the air channel so as to expel the contaminants from the compacted air [7]. A solenoid valve is a 5/3 solenoid valve series 4-Way solenoid operated valves feature single or double 12v DC, 1Watt solenoids, commonly used to control the stream or heading of air in the framework. The camera associated with the robot will keep track the development of robot and can screen the cutting procedure by giving the guidelines through the control unit to the robot sends the live video streaming through a camera mounted on it. The video can be seen in the Android mobile. The system of the working of the robot is controlled with Pneumatic cylinder. In this task, 5 Pneumatic cylinders are utilized. They will give the appropriate movement to the robot for climbing up or down. Raspberry Pi 3 is the primary useful unit in this undertaking. The cutter which is mounted on the robot cuts the arecanuts dependent on the guidance is given by the user [8].

A. Double acting Pneumatic cylinder

The construction features of a double acting cylinder is shown in Fig 10. The construction of a double acting cylinder is similar to that of a single cylinder. In the double-acting cylinder, a pneumatic force can be connected to either side

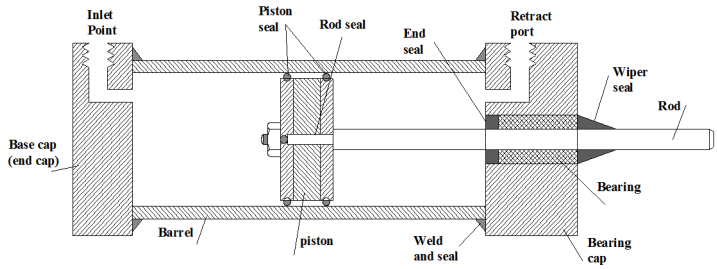

Fig. 10: Double acting Pneumatic Cylinder.

(supply and exhaust) of the cylinder [9]. The double-acting cylinders are normally used in the application where greater stroke length is required.

B. Pneumatic cylinder / Actuator

Pneumatic actuators are the machine used to convert compressed air into the mechanical energy to perform valuable work. In other words, these actuators are used to supply the required power towards the end of the stroke or used to make displacement of the piston [10]. The pressurized air from the compressor is supplied to the pneumatic actuator to move the piston. The pneumatic cylinder is shown in Fig.11.

Fig. 11: Outer View of Pneumatic Cylinder.

C. Flow Chart

The flowchart of the robot operating in automatic mode is shown in Fig. 12. The user needs to press switch SW 1 in order to select the robot to move UP or DOWN. If the user presses the switch SW 1 as ON, the robot starts to climb UP the tree automatically. If the user presses the switch SW 6 as OFF, the robot starts to climbs DOWN the tree automatically. Whenever user press the switch SW 2 (Exit Button) ON, the robot enters in to STOP mode. The cylinder 4, cylinder 5 pistons move forward and holds the areca tree. If user press the switch SW 7 OFF, the robot enters in to IDLE mode.

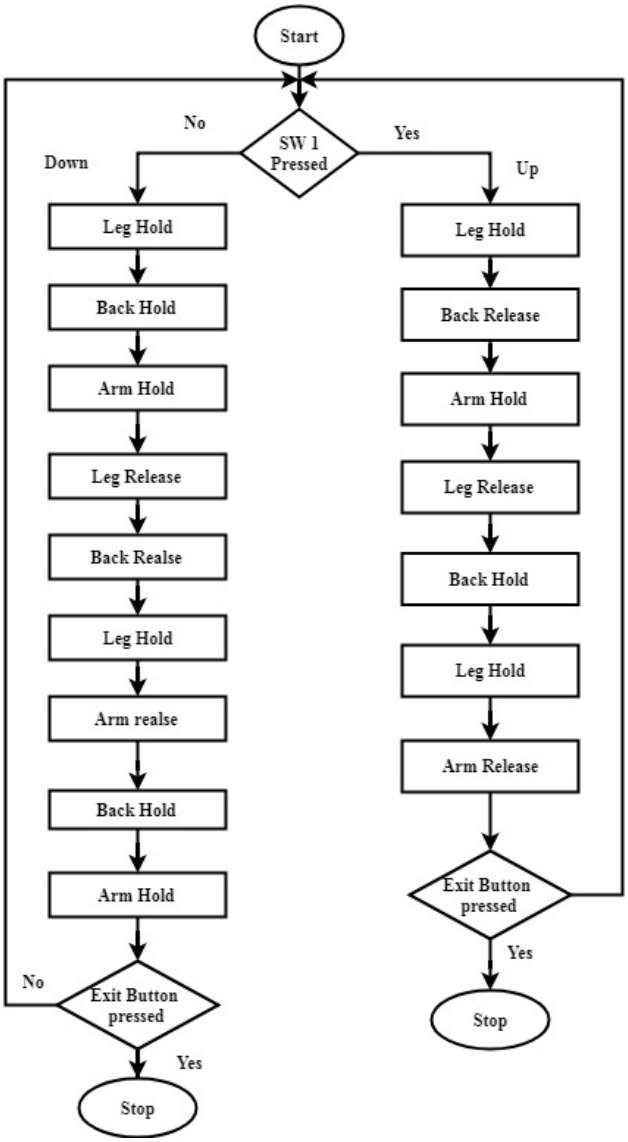

Fig. 12: Flow chart of Automatic Mode.

V. System Software

In this part, programming and working framework utilized for design the robot are discussed. Python is a programming language utilized for controlling the automated unit. For Raspberry Pi 3B, the Raspbian OS is the Linux based working framework which is dependent on Debian streamlined package [11]. Python is the language utilized for coding. Arduino UNO is used for controlling the solenoid valve, Raspberry pi is used for live video streaming of the robot [12].

The Logitech webcam c270 is connected to USB port 1 of Raspberry-Pi through USB cable. The Android mobile is connected to Raspberry-Pi by turning on WiFi. The corresponding IP address of the devices named as Raspberry is entered in RaspiCAM Remote App after that live video streaming of the robot can be observed in the Android mobile.

TABLE I: Control operations or Commands.

Control operations of Robot	
Operations	Digital I/O pins of Arduino
Leg Hold	1 1 0
Back Release	1 0 1
Arm Hold	1 0 0
Leg Release	0 1 1
Back Hold	0 1 0
Arm Release	0 0 1

Table 1 shows different combination of digital inputs from the pins of Arduino to control the robotic actions. When I/O pin is made logic 1 the transistor connected to that I/O pin turns ON and the corresponding valve of the solenoid opens and pressurized air enters the cylinder through this valve moving the piston in one direction. If I/O pin is made logic 0 the transistor connected to that pin turns OFF and closes the valve and stops the movement of piston.

VI. Results Analysis

A Smart Arecanut Plucking Robot is designed and implemented using pneumatic operations. In this paper, a robot is designed to climb the tree automatically or by manual operation.

The robot is constructed using six Pneumatic cylinders.Out of six cylinders, two cylinders are used for the upper arm and 2 cylinders are used for the lower arm to grip the tree. One cylinder is used for the movement of the robot and one more cylinder is used to control the movement of the cutter. The snapshot of the robot with a cutter is shown in Fig. 13. There are six stages in climbing the tree.

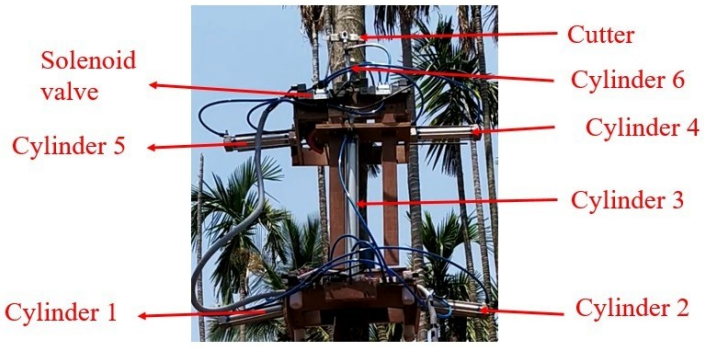

Fig. 13: Snapshot of the Robot with Cutter.

Through these six stages of the operations, the robot moves one step upwards and this process continues until the robot reaches the top of the tree. Each stage is repeated sequentially with the help of the controller. Similarly, to climb down the tree all the stages mentioned in the above section have to be performed in reverse order. The sixth cylinder gets expanded when the user gives the instruction to cut the arecanut. The cutter with piston mounted on the robot is shown in Fig. 14.

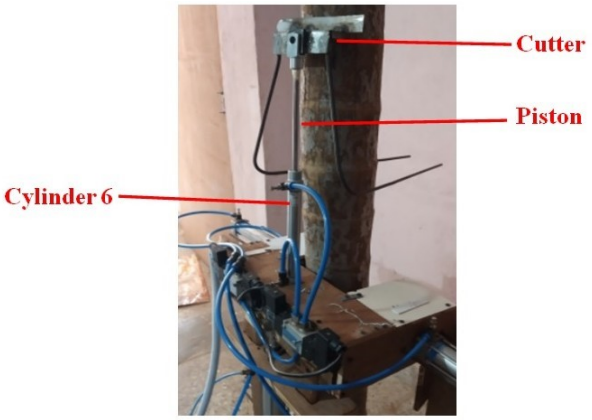

Fig. 14: Movement of the Piston of Cylinder 6 to Cut the Arecanut Bunch.

The robot designed is tested in areca plantation farm. It has successfully climbed up and down the tree and also cut the arecanut bunch. The Fig. 15. shows a picture of the robot while climbing an areca tree.

Fig. 15: Robot Climbing the Tree.

VII. CONCLUSION AND FUTURE WORK

The robot designed in this paper successfully climbed up and climbed down the arecanut tree and cut the arecanuts automatically with minimum manpower. Hence, it reduces the demand for skilled labours. The robot is simple in design and user-friendly. It can climb arecanut trees of varying sizes. The robot is operated in two modes namely Manual mode and Automatic mode. The camera which is interfaced to Raspberry Pi mounted on the robot successfully sent the live video streaming. The video streaming is observed in RaspiCAM Remote App installed in the user's android phone. By watching the video stream, the user can give instruction to the robot to cut the arecanuts. The robot takes around 6 to 8 minutes to climb up, cut the arecanuts and climb down a 45 feet arecanut tree of varying trunk diameter (around 5.5 to 8 inches).

For future work the speed of the robot can be increased by increasing the pressure given to cylinders. The position of the cutter can be made controllable by the user. Image processing can be used for automatic identification of the ripened arecanuts. Wireless connectivity can also be implemented between user and the robot.

REFERENCES

[1] W. Shen, J. Gu, and Y. Shen, , Magnetic system design for the wallclimbing robot, IEEE Signal Processing Lett., vol. 6, pp. 300-303, Dec. 2006.

[2] R. K. Megalingam, T. C. Kattakavam, H. K. Menon, R. V. Madhav, AKinect Based Coconut Tree Climber, International Journal of Applied Engineering Research, Vol. 7, no. 11,pp. 176-282, 2012.

[3] , V. Raghavan and K BaruahArecanut: India's Popular Masticatory - History, Chemistry and Utilization, in Economic Botany - Volume 12, Issue 4,pp 315-345, October 1958.

[4] Fasil TK, Jishnu K Das, Shabeeh AP, Xavier Saji, Prof. Jacob Kuriakose and Prof. Vinod yeldho Baby, Remote Controlled Arecanut Plucking Machine, International Research Journal of Engineering and Technology (IRJET), Volume: 05, Issue: 04, Apr 2018.

[5] Dr.S.Maheswaran, S.Sateesh, G.Saran and Vivek B, Automated Coconut Tree Climber, International Conference on Intelligent Computing and Control (I2C2), 2017.

[6] Lakshmi B, Pooja M, Sahana S, Shwetha K R, Arecanut Plucking Robot, B.E project report, Dept. of Electronics and Communication Engineering, Siddaganga Institute of Technology, Tumkur, 2018.

[7] S. J. Segal, S. Virost, and W. R. Provancher, ROCR: Dynamic vertical wall climb- ing with a pendular two-link mass-shifting robot, IEEE Int. Conf. Robot. Autom., Pasadena, CA, pp. 3040-3045, 2008

[8] R. Aracil, R. J. Saltarn, and O. Reinoso, A climbing parallel robot, IEEE Robot. Autom. Mag., Vol. 50, no. 3, pp. 16-22, 2006.

[9] M. Jawaharlal, S. Chung, P. Jia, L. Park and G. Qi, Coconut Tree Climbing Device Troy High School, Fullerton, IEEE Int. Conf. Canada, pp. 1078-1083, 2009.

[10] B. Lalitha, B. A. Raj, K. S. Parthiabn, Semi-Autonomous Coconut Harvesting Robot, International Journal on Recent Technologies in Mechanical and Electrical Engineering (IJRMEE), pp. 67-71, 2015.

[11] Raspberry Pi,Raspberry Pi Documentation. [Online] Available at https://rasberrypi.org/documentation/ Accessed on 26/04/2018.

[12] Raspbian. [Online] Available at https://raspberrypi.org/documentation/raspbian/ Accessed on 26/04/2018.

Proceedings of the Fourth International Conference on Communication and Electronics Systems (ICCES 2019)
IEEE Conference Record # 45898; IEEE Xplore ISBN: 978-1-7281-1261-9

Implementation of digital lattice filter using Schur Polynomial

Sneha Sivaramakrishnan[1], Swathika Shanmugam[2], B. Bala Tripura Sundari[3]
Department of Electronics and Communication Engineering
Amrita School of Engineering, Coimbatore
Amrita Vishwa Vidyapeetham, India
snehaauh@gmail.com, swathikashanmugam1998@gmail.com, b_bala@cb.amrita.edu

***Abstract*—A lattice filter has multiple applications in adaptive receivers for communication. The design and implementation using high level synthesis has been explored here for trade off between use of conventional computational units and distributed arithmetic. The aim of our work is to implement a digital lattice filter using Schur polynomial. Schur polynomial is an efficient method through which orthonormal polynomials used to compute the lattice coefficients. We have implemented a digital lattice filter in Vivado HLS with regular arithmetic and also with distributed arithmetic, which provides a multiplier-less architecture. By synthesizing the codes in Vivado HLS, The implementation results in the architectures that are compared for resource utilization and latency and delay has been compared for the conventional and distributed arithmetic multiplier less architectures the design based on Schur polynomials.**

Keywords—Lattice filter, High level synthesis, Distributed algorithm, Schur polynomial.

I. INTRODUCTION

Designers have to integrate software processors and application specific hardware that is customized for specific tasks. Describing these features using Hardware Description Language (HDL) allows the designer to adopt tools for Register Transfer Level (RTL) and then use that to burn into target hardware. But the problem faced here is that writing in HDL requires the designer to write in a low level language which is much harder to work with. To overcome this, in recent times, many designers are combining FPGA and HLS. HLS is much easier to work with as the designing can be done using high level languages. Also, the RTL is generated automatically. FPGA is usually reconfigurable and deployment is easier on FPGAs. However, different HLS tools have different specifications. Hence, it isn't easy for all the tools to follow any particular benchmark. High Level Synthesis tools are categorized into Domain Specific language and General Purpose programming language. Despite offering many more functionalities like allowing more input output languages and higher memory bank, it is still more robust than academic HLS tools [1].

In high level synthesis, interconnections are considered to be the key feature that affects performance of the integrated circuit or design. For example, the interconnections account for more than 50 percent of the total dynamic power of an Intel microprocessor. When trying to improve efficiency in terms of area, to minimize area, the complexity of the interconnections has to be minimized as well. In a case where fixed binding of functional units and registers are involved, there will be allocations between both the components through multiplexers. This allocation is called Port Assignment Problem. The main demands of a port assignment algorithm are producing an optimal solution and estimating interconnection complexity as quickly and accurately as possible. To achieve this in a more efficient way, an improvised matrix based algorithm is formulated. Spanning tree and conflict graph methods are used to compute feasible solutions. Elementary tree transformation is used to optimize the obtained feasible solutions. For this, matrix formulation is done using $\oplus$ and $\otimes$ which improves efficiency. Simplex method is used and pivoting is formed. Properties of pivoting are then studied and successive pivoting is proposed. The algorithm is then tested on real benchmarks to evaluate improvements in power, area and delay efficiency [2].

FPGA based digital filters are effective in digital signal processing because of the properties contributed by FPGA like parallelism and logic increases the speed of computation. Distributed arithmetic is based on this concept. FIR filters are widely used because their stability nature and linear response. Usually FIR filters are implemented sequentially incorporating multipliers and accumulators [3] [4].

Lattice filters are versatile architectures are suitable for VLSI design because of their regular and repeated structure. They can be designed for all-pass filter. Usually, filters tend to work only within a certain range of frequencies below or above which the magnitude level reduces. However, with lattice filters, there is no gain reduction and all frequencies can pass through, changing the phase relationship with the multitude of frequencies. Lattice filters scope is explored more in adaptive filter design and hence the applications are signal processing and in future communications of 5G wireless communication.

Distributive arithmetic is one of the most efficient ways to implement a filter. Lattice filter is implemented in High Level Synthesis using Vivado HLS by using Schur Algorithm. The filter is first designed using regular arithmetic and report is obtained through synthesis in Vivado HLS. This report is then compared to the report obtained by designing the filter once again using distributive arithmetic.

This paper has been divided into five parts. The first three parts give brief descriptions about high level synthesis, lattice digital filter and distributed arithmetic respectively. The fourth part gives a detailed explanation of the results obtained. The fifth part gives a conclusion for our findings.

II. HIGH LEVEL SYNTHESIS

RTL level based programming languages demands more work and knowledge on physical level registers and their states at each clock cycle. FPGA requires programming and when they are programmed with RTL level languages, it increases the level of complexity in terms of cost and time. This is because implementation of any function take into account about resources consumed and time taken. There are high possibility of errors occurring during developing and implementing and during testing. Hence it is required to implement at high level of abstraction [5].

Technology like HLS evidently provides the required high level abstraction by incorporating high level programming languages like C or CPP. It has the capability of generating RTL simulations automatically. Test bench are used in verification and validation. These can be written in high level languages in HLS, which can be used validate RTL through co-simulation. Hence it decreases design time and increases productivity [6].

An important application of the high level synthesis is that it allows the designer to write the code easily and use more transformations before the final RTL is generated for design space explorations [13]. Also as mentioned in [14], the methodology used there helps to utilize various design possibilities using timing constraint from the input given.

III. LATTICE DIGITAL FILTER

Digital lattice filter is widely used in digital signal processing. A lattice filter is an example of an all-pass filter. Usually implementation of lattice filters on FPGA involves usage of adders, multipliers, and delayers. The most common implementation technique is array based implementation. To improve the speed and performance lattice structure can be pipelined [7]. The filter coefficients can be found by Schur algorithm [8]. The coefficients can be found by using MATLAB.

Lattice filter has the advantage of frequency insensitivity compared to the other form of digital filters [9]. Lattice filter can be scaled to the required order by iterating the basic structure containing multipliers, adders and delayers. The rounding off of multiplier coefficients can cause error and increase sensitivity. To combat that effect higher word length is chosen for filter realization [10].

IV. DISTRIBUTED ARITHMETIC

Digital lattice filter can be realized by incorporating the concept of distributed arithmetic. Here multiplication can be seen as convolution. The idea is to reduce the number of resources used. This concept takes care of errors caused by rounding off of the multiplication coefficient as well [11].

It follows a mechanism wherein it recognizes values of a multiply then accumulate that occur multiple times and then stores them to a lookup table or a LUT. The values stored in LUTs can be accessed faster from the computer storage than any other external medium. So because of this, the overall cost due to components will reduce by a lot. However this multiplier-less architecture can only follow where there is a multiply and accumulate operation. This makes it perfect for usage in digital lattice filters wherein each module requires a multiplier. With the usage of distributive arithmetic, the architecture becomes multiplier-less which brings down the number of components used, thereby reducing the overall cost as well. The area used by the filter will depend on the number of bits given as input.

Through multiple analysis and experiments conducted, it was found that the implementation using distributive arithmetic, about 86.90% of hardware resources and 67.92% of power consumption was saved [12]. Architectures and design space exploration are implemented for achieving low power implementations[13]. High level synthesis techniques are applicable to be used in determining optimal designs [14].

V. METHODOLOGY AND SYSTEM RESULTS

The code was first written in MATLAB to obtain the lattice coefficients needed while building the filter. For an FIR filter, the Schur Polynomials are derived from the denominator so using that, the required lattice coefficients are obtained.

To implement the filter, the code was written in regular arithmetic at first. In Vivado, the code was written using C++. The same code was written in MATLAB again, and also manual calculation was done to justify the accuracy of the written program and the obtained output.

The filter that we have implemented is of third order. Output has been recorded at the end of every module of the filter, so the final output is the output obtained at the end of the third lattice module. According to the equation being modeled here, the input is split into two, where one is same as the input and the other one is same as input with a delay. Similarly, we have two outputs from the filter, FOUT and GOUT.

After synthesizing the code for a third order filter in Vivado, the utilization estimates were obtained.

LATENCY ESTIMATES OF THIRD ORDER FILTER USING CONVENTIONAL ARITHMETIC

Latency		**Interval**	
Min	Max	Min	Max
21	21	22	22

TABLE I. UTILIZATION ESTIMATES OF THIRD ORDER FILTER USING CONVENTIONAL ARITHMETIC

Name	BRAM_18K	DSP48E	FF	LUT
Expression	-	-	0	12
Instance	-	5	355	727
Memory	0	-	128	6
Multiplexer	-	-	-	53
Register	-	-	121	-
Total	0	5	604	798
Available	650	600	202800	101400
Utilization (%)	0	0.83	0.29	0.78

Similarly, the code is written in Vivado HLS and synthesized for a third order filter using distributive arithmetic to produce the following report.

TABLE II. LATENCY ESTIMATES OF THIRD ORDER FILTER USING DISTRIBUTED ARITHMETIC

Latency		Interval	
Min	Max	Min	Max
118	124	119	125

TABLE III. UTILIZATION ESTIMATES OF THIRD ORDER FILTER USING DISTRIBUTED ARITHMETIC

Name	BRAM_18K	DSP48E	FF	LUT
Expression	-	-	0	324
Instance	-	10	1121	2442
Memory	-	-	-	-
Multiplexer	-	-	-	406
Register	-	-	656	-
Total	0	10	1777	3172
Available	650	600	202800	101400
Utilization (%)	0	1.67	0.87	3.12

VI. CONCLUSION AND FUTURE SCOPE

To summarize the process, we have implemented a digital lattice filter using Schur Polynomial on Vivado HLS using conventional arithmetic and using distributed arithmetic, to synthesize and generate reports accordingly.

The reports that we have obtained display the estimates of resource utilization. From the obtained reports, we can see that the claim about distributed arithmetic needing no memory holds true. However, the implementation using regular arithmetic needs memory resources as well to function. So we can see that using distributive arithmetic requires lesser resources making it more area efficient depending on the number of bits of the input. Also, from the literature survey done on lattice adders, we also know that distributive arithmetic is power efficient and requires lesser power than normal.

Even though distributive arithmetic uses lesser resources, there is a trade off with speed. Since it is bit serial in nature, the latency increases and the total speed reduces. With the addition of more bits, the area used increases and the speed decreases.

Distributive arithmetic is preferred by many especially for filter implementations because the pros weigh out the cons. Power consumption has always been a problem but with this multiplier-less architecture, the efficiency based on area and power has improved. Hence, we can conclude that distributive arithmetic proves better when compared to regular arithmetic, in the ever improving field of technology today.

The filter can be improved in terms of speed by carrying out research to convert bit serial computing to parallel computing. Also further research on multiplier less architectures may help in improving area efficiency as well.

REFERENCES

[1] Nane R, Sima VM, Pilato C, Choi J, Fort B, Canis A, Chen YT, Hsiao H, Brown, S, Ferrandi, F, Anderson, J & Bertels, KA Survey and Evaluation of FPGA High-Level Synthesis Tools, IEEE Transactions on Computer-Aided Design of Integrated Circuits and Systems, vol. 35, no. 10, pp. 1591-1604, 2016.

[2] Cong Hao, Jianmo Ni, Nan Wang, and Takeshi Yoshimura, Interconnection Allocation Between Functional Units and Registers in High-Level Synthesis, IEEE Transactions on Very Large Scale Integration (VLSI) Systems, vol. 25, no. 3, pp. 1140-1153, March 2017.

[3] Ankit Upadhyay , Uday Panwar High Performance VLSI Architecture for Transpose Form FIR Filter using Integrated Module, International Conference on Computer Communication and Informatics (ICCCI) 2018.

[4] M. Sandhya, E. Senthilkumar and J. Manikandan, "Design of distributed arithmetic based reconfigurable filters," IEEE Annual India Conference (INDICON), pp. 1-6, 2016.

[5] F. Montano, T. Ould-Bachir and J. P. David, "An Evaluation of a High-Level Synthesis Approach to the FPGA-Based Submicrosecond Real-Time Simulation of Power Converters," IEEE Transactions on Industrial Electronics, vol. 65, no. 1, pp. 636-644, 2018.

[6] D. Navarro, Ó. Lucı´a, L. A. Barragán, I. Urriza and Ó. Jiménez, High-Level Synthesis for Accelerating the FPGA Implementation of Computationally Demanding Control Algorithms for Power Converters,

IEEE Transactions on Industrial Informatics, vol. 9, no. 3, pp. 1371-1379, 2013.

[7] Yin Liu ; Keshab K. Parhi, Architectures for Recursive Digital Filters Using stochastic Computing, IEEE Transactions on Signal Proceesing vol. 64,no.14, pp. 3705 – 3718, 2016.

[8] DineshBhati, ManishSharma, Ram BilasPachori, Vikram M.Gadre, Time–frequency localized three-band biorthogonal wavelet filter bank using semidefinite relaxation and nonlinear least squares with epileptic seizure EEG signal classification, Digital Signal Processing, vol. 62, pp. 259-273, 2017.

[9] [9] K. Georgopoulos, Grigorios Chrysos, Pavlos Malakonakis, Antonis Nikitakis, Nikos Tampouratzis, Apostolos Dollas, Dionisios Pnevmatikatos, Yannis Papaefstathiou, "An evaluation of vivado HLS for efficient system design," International Symposium ELMAR, Zadar, pp. 195-199, 2016.

[10] Ettore Napoli, Gerardo Castellano, Davide De Caro, Darjn Esposito, Nicola Petra, Single Bit Filtering Circuit Implemented in a System for the Generation of Colored Noise, IEEE Transactions on Circuits and Systems I, vol. 64, no.5, pp.1040 – 1050, 2017.

[11] V. K. Sharma, K. K. Mahapatra and U. C. Pati, An Efficient Distributed Arithmetic Based VLSI Architecture for DCT, International Conference on Devices and Communications (ICDeCom), pp. 1-5, 2011.

[12] S. Venkatachalam and S. Ko, Approximate Sum-of-Products Designs Based on Distributed Arithmetic, IEEE Transactions on Very Large Scale Integration (VLSI) Systems, vol. 26, no. 8, pp. 1604-1608, Aug. 2018.

[13] N. Sowjith, K. Sandeep, S., Sumanth, M., and S. Agrawal, Low power VLSI architecture for combined FMO/Manchester encoder for reusability and FMO/Manchester codecs, 2016 IEEE International Conference on Computational Intelligence and Computing Research, ICCIC, 2017.

[14] Krishnapriya P N, Bala Tripura Sundar B, “High level synthesis for retiming stachastic VLSI Signal Processing Architecures,” Procedia computer science, vol.143, pp.10-19, 2018.

Proceedings of the Fourth International Conference on Communication and Electronics Systems (ICCES 2019)
IEEE Conference Record # 45898; IEEE Xplore ISBN: 978-1-7281-1261-9

Energy Efficient Coverage and Sensor Localization for Scheduling

Miss.Sujata Dhumal
Department of Information Technology
Walchand College of Engineering
Sangli
dhumalsujata123@gmail.com

Prof.B.S.Shetty
Department of Information Technology
Walchand College of Engineering
Sangli
bharathishetty5@gmail.com

***Abstract*—Wireless Sensor Network (WSN) is the collection of already deployed motes which sense the physical phenomena and pass the sensed information to the sink node . Sink node stores information and send that information to users according to the user needs. Wireless Sensor Network (WSN) have self directed, tiny, low powered devices called sensors. Major issue in wireless network is coverage of area . It checks how the sensing area is monitored by motes. Strategy for coverage needs simultaneous activation of multiple sensor nodes as every location get covered by at least n sensors. Therefore scheduling technique alternatively activate the sensor nodes to reduce energy consumption. Due to battery limitation, utilization of energy is an extensive challenge in sensor network .Only few nodes may determine the network-lifetime in existing approach .The main role of sensor is sending and receiving the whole traffic so their "energy efficient coverage " is biggest challenge in sensor network. Sensor localization is used to find the x ,y coordinates of unknown nodes so that scheduling will get easy to cover the area using that particular nodes location. Scheduling is main concept in which sequence of nodes is important which increases the energy efficiency and network lifetime.**

Keywords— Wireless sensor network (WSN), Sensor Localization, Prediction, Scheduling.

I. INTRODUCTION

A. Wireless Sensor Network

Wireless Sensor Network (WSN) is a distributed network of interconnected devices called motes which are connected wirelessly. A mote have multiple sensor modules, for sensing the information of light, information of temperature and report it to the weather forecast. Humidity, pressure and sound each mote have four different components named as processing ,memory, battery modules and communication. Multiple applications like laptop , PC,mobiles are accessing data from internet then sink node access that information from various nodes and send that data to the satellite

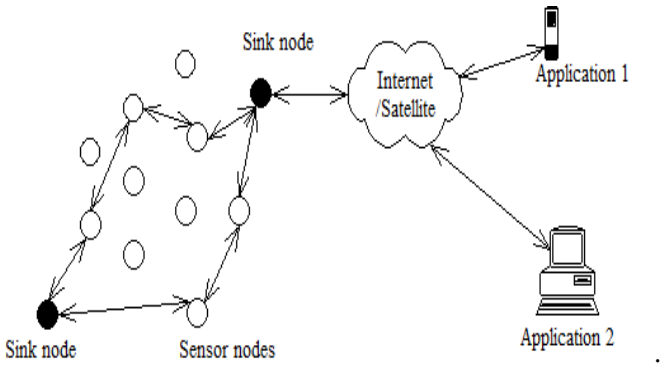

Fig 1. Architecture of wireless sensor network

B. Energy Efficiency

Wireless Sensor Network(WSN) includes many motes with different parameters which have battery power, frequency ,range and accordingly they cover the assigned area. While covering the area they should consider the energy efficiency metric as very important issue as it means that sensor should cover the assigned area in less battery power so that energy ingestion will be less and it will cover the area efficiently. Motes have been used in various fields like engineering, structural health monitoring, health and environment where energy efficiency is very important. There are multiple tasks like data aggregation, receiving and sending data ,data processing which utilizes resources including CPU power ,memory and most important is energy to increase the lifetime of network and productivity.

C. Sensor Localization

Localization is used to find the location of motes which is important to do scheduling of that motes for energy efficient coverage . Distance Orientation method is used to calculate the distance of unknown mote from sink node whose location is already known. This paper is organized such a way that first is discussion on localization literature papers and second covers papers on scheduling concept.

Finding the coordinates of unknown node(x_u,y_u):
Anchor nodes(known) x, y co-ordinates,

(x_1,y_1)=(2,1), (x_2,y_2)=(5,4), (x_3,y_3)=(8,2) with the distance between anchors and node of unknown position $r_1 = \sqrt{10}$, $r_1 = 2$, $r_1 = 3$.

$$2\begin{bmatrix}6 & 1\\ 3 & -2\end{bmatrix}\begin{bmatrix}x_u\\ y_u\end{bmatrix} = \begin{bmatrix}64\\ 22\end{bmatrix} \text{ ……..(1)}$$

Resulting in x_u=5, y_u=2 as the positions of unknown nodes.
The paper is organized as follows:
Section 2 is literature survey and section 3 is proposed work in which some methodologies like localization and formulas are stated. Section 4 presents analysis of simulation results. Finally section 5 concludes the paper.

II. Literature Survey

Sensor Localization: In this following literature, multiple papers on localization are discussed in which sensor localization is important concept which is used to find the location of sensor. Using that location ,sensor can communicate easily in distributed network and increase the accuracy.

R. Jin, Y. Ma, Y. Li, J. Zhao and F. Zhou,(2018), "**High accuracy localization scheme based on time-of-flight (TOF) and directional antenna in WSNs**[1]". In this paper ,they present "high accuracy estimation method" for node localization. Here a sink node contains an antenna having directional information which sends beacons periodically and it has sink nodes position and the location of unknown nodes is find out using antenna orientation . By considering the observations, variations in received signal strength indicates time of flight values and values of beacons , an unknown node calculate the distance relative to the beacon node simultaneously.

I. Strumberger, E. Tuba, N. Bacanin, M. Beko and M. Tuba,(2018), "**Monarch butterfly optimization algorithm for localization in WSNs**[2] ". In this paper they studied about "Optimization Algorithm" which comes in "NP hard " problem. Localization is about finding coordinates which are geograhphically considered for each and every mote which have unidentified position which are deployed accidentally in the observing area. Here the location of anchor node is identified by Global Positioning system(GPS).Distance is calculated using radio signal strength between unknown nodes and neighbour sink nodes .Trilateration method used to get know the (x,y) coordinates of unknown motes which uses the information of motes position.

Lu Dai,Bang Wang, Xianjun Deng ,Laurence T.Yang,(2017)," **An Improved Immune algorithm for Node Relocation to maximize confident information coverage in Hybrid Sensor Network**[3]". This paper studies that the movable mote relocation problem to increase area assured information coverage and reducing the movement cost where it consist the stationary as well as mobile nodes. Stationary nodes can not relocated after initial deployment and mobile nodes minimize the movement cost , maintaining network connectivity and exploit area coverage through moveable node repositioning.

Scheduling: In this following literature papers Scheduling is considered which first uses prediction for classification of sensors according to residual energy, frequency and range which then used by the Scheduling .It is used to give sequence to the motes so that they can activate alternatively and cover the area which they have already assigned .

Manel Chenait, Bahia Zebbane, Chafika Benzaid, Nadjib Badache,(2017),"**Energy-Efficient Coverage Protocol Based on Stable and Predictive Scheduling In WSNs**[4]". Main problem in WSNs is reporting. It says that how well much area is covered by less sensors ,every position must enclosed in at least k motes .Some sensors cover the same,That's why Scheduling alternatively active the sensors so that energy consumption should get reduce hence in this paper SPEC protocol is used. It reduces scheduling energy waste and also prolongs the reporting period.SPEC exactly eliminates unusable switches so that it increases the energy proficiency and network lifetime.

Jia Yufu,Lia Hongjun,(2015**)**,"**Node Scheduling Scheme Based on Coverage Preserving for WSN**[5]". In this paper , Monte Carlo algorithm scheme is used to test whether the nodes deployed are repeated or not. It uses back off mechanism for coverage collision detection. The results shows that the motes covers all concerned zone with minimum motes.

P. Chaturvedi and A. K. Daniel,(2012), "**An Energy Efficient Node Scheduling Protocol for Target Coverage in WSNs**[6]". The major issue faced by WSNs is the energy proficiency and network lifetime. Coverage problem is defines as how well the motes monitor the given area. Scheduling is the most preserving way to remain the motes in active or sleep states. Trust metrics is most important concept for increasing the confidence level that each area is covered by at least one mote. The performance is increased by the aggregation mechanism based on link stability and residual energy of the mote.

III. Proposed Work

Localization is nothing but finding the physical location of sensor nodes as transferring packets to destination will be easier if sensor locations are known. Global positioning system(GPS) is easy method used to find the location of sensor nodes. It is difficult when there is huge number of sensor nodes.

A. Trilateration

Trilateration is nothing but localization of sensor nodes using the distance metric. Node location is estimated through distance calculation from three anchor nodes. Here,

intersection of coverage range of anchor nodes is calculated, which gives a single point as a position of unknown node.
Using the distance calculation equation. If the unknown coordinates are (x, y) and known node coordinates are (x_i, y_i) which are having r_i distance from unknown spot, three equations will be:

$$(x - x1)^2 + (y - y1)^2 = r1^2$$
$$(x - x2)^2 + (y - y2)^2 = r2^2$$
$$(x - x3)^2 + (y - y3)^2 = r3^2$$

Expand out the squares and do minus the second equation from the first and third equation from second, we get

$$2(x2 - x1)x + 2(y2 - y1)y = r1^2 - r2^2 + x2^2 - x1^2 + y2^2 - y1^2$$

$$2(x3 - x2)x + 2(y3 - y2)y = r2^2 - r3^2 + x3^2 - x2^2 + y3^2 - y2^2$$

This is a system of two equations with two unknowns:

$$Ax + By = C$$

$$Dx + Ey = F$$

The values of x and y is obtained from the below equations:

$$x = (CE - FB) / (EA - BD)$$

$$y = (CD - AF) / (BD - AE)$$

B. Distance calculation using Euclidean distance formula

$$\text{Error} = \frac{1}{N_t}\sum_{i=0}^{N_t}\sqrt{(x\hat{}\,i - x)^2 + (y\hat{}\,i - y)^2}$$

where N_t is the network size.
(x,y) is the true location of the unknown node or source. ($x\hat{}_i - y\hat{}_i$) is the estimated location.

C. Ad hoc on-demand distance vector routing protocol (AODV)

AODV is an on-demand distance vector routing protocol which uses routing tables having one entry per target .It is on demand protocol as it creates routes when it is requested by source. while packets are going along the multiple routes from the source to the destination routes will stay active. When the source will not send packets , the routes will get time out and close.

AODV is used as we need routing table to have all information of the nodes instead of having frequent switching to getting information While covering the area routing table should have all the information about sensor nodes as which sensor is available and not while traversing the route for area coverage and accordingly prediction procedure will be applied for the efficient network coverage so it will reduce time consumption and increase energy efficiency and network lifetime.

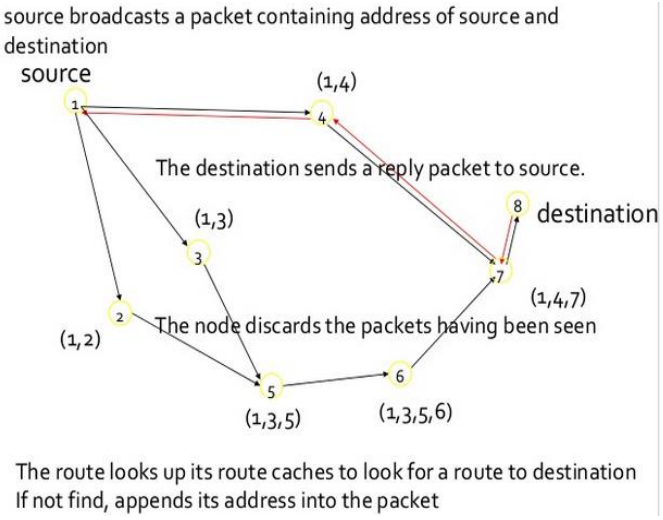

Fig.2 Packet Broadcast Through AODV

D. Network Lifetime

$$\text{Lifetime\_Rate}_{(t)} = \frac{N\_nodes_{(E>0)}}{N\_nodes_{(t=0)}}$$

Network lifetime rate will get changed when no of active sensor value will be changed. Having more no of active sensors will increase the network lifetime as they will cover the maximum area in less energy and increases the energy efficiency.

E. Prediction Procedure

Prediction procedure will check if coverage redundancy algo to apply or not exact after active message.Active Message(AM) have two types of senders.

i)Internal Sender located inside S_i sensing disk.
ii)External ,located between r and $2r^4$, where,r is the redius of s_i sensing disk
iii)Opposite external ,which is an external sender located at the opposite quadrant of another external sender.

F. SPEC (Stable and Predictive Energy-aware Coverage Scheduling)
SPEC is the one way evaluation technique in which routing table have all the information related to sensors using that information sensors get selected to activate. Frequent switching is avoided by SPEC which reduces the energy consumption.

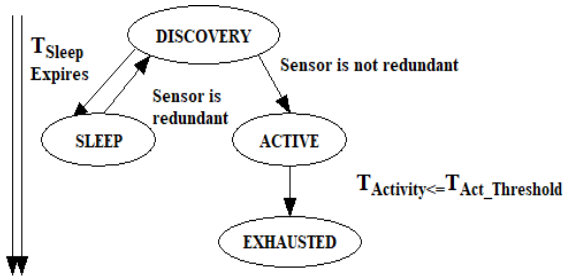

Fig.3 One way evaluation of SPEC protocol.

One way evaluation is used to minimize the frequent switching energy. Here, multiple switches are reduced because of continuous sensor activation.
Wake up method is used to adjust the sleep and active timers considering the energy of motes.
Prediction is to minimize the computation energy loss it reduces the energy required to frequent switches.
Multiple states of SPEC are:

i)Discovery-It will check how many sensors are active right now.
ii)Active-After discovery of sensor node it will get decided to active that particular sensor or not and if that sensor has covered the same area already or not.
iii)Exhausted- sensor will have one threshold value after that limit sensor will go to the exhaust state.
iv)Sleep: sensor will go to the sleep state after its particular timer.

IV. Results and Analysis

Localization is the process of finding the physical or relative location of a sensor node as data and information are useless if the nodes have no idea of their geographical positions. Here, we can give any number to any node and we can make anchor node , any one of them it is not necessary that sequencing is important .

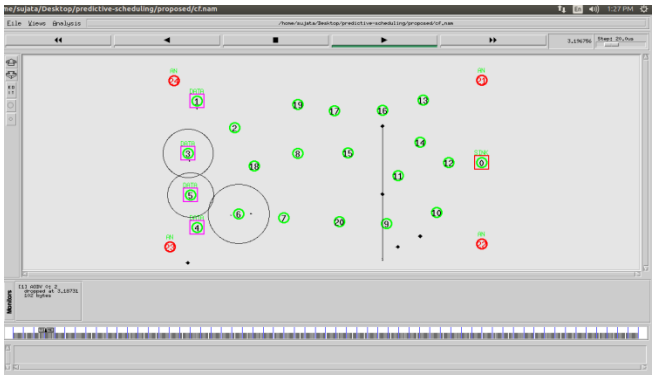

Fig.4 Localization of sensors

Here ,according to the anchor nodes location (x,y) coordinates it will calculate the distance between two nodes and find the location of unknown nodes.

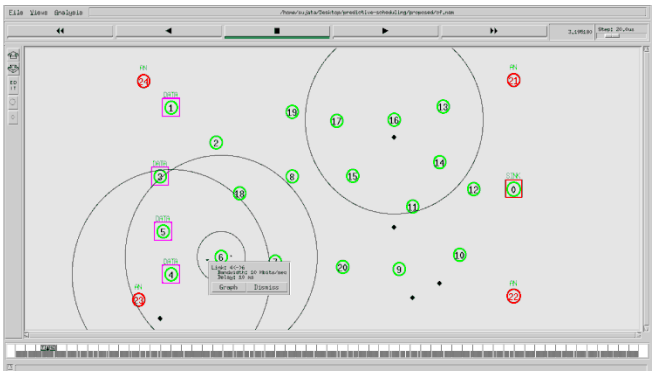

Fig. 5 Communication Links between nodes

While finding the routes,it will select the sensor node having more energy remaining to get active to cover the maximum area.

AODV(Adhoc on Demand Distance Vector Routing protocol)

Here, monitoring of coverage area is done where CBR(Constant Bit Rate),no of bytes transferred per second is calculated.

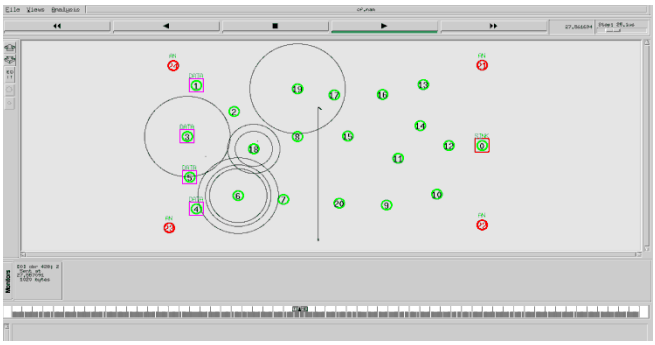

Fig 6 Monitioring of sensors ,CBR(Constant bit rate)

Here, no.of bytes transferred per second is calculated. According to the energy remaining node will demand to pass the packet through it and it will find the route to send the packet to destination.

TABLE I

simulation configuration

Simulation parameters	***Values***
Simulator	NS 2.35
Routing protocol	AODV
Simulation Time	10 Minutes
Transmission Range	100 m
Operating system	Ubuntu 16.04

Energy Consumption in previous systems vs proposed systems.

Energy consumption is nothing but how much more energy is required to cover the assigned area.As there is no frequent switching in proposed systems it reduces the energy consumption.

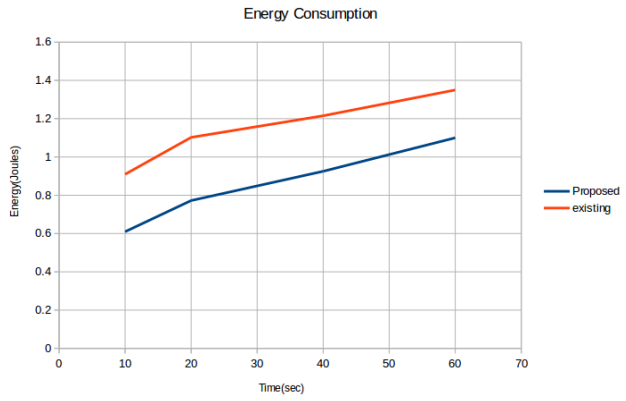

Fig 7 Energy consumption in existing and proposed systems.

In existing systems energy required to cover the area is very much as sensor nodes doesn't have the information if assigned area is overlapped or not .In proposed systems that drawback is overcomed as AODV is having routing table having all the information in the routing table. hence energy consumption is less in proposed system.

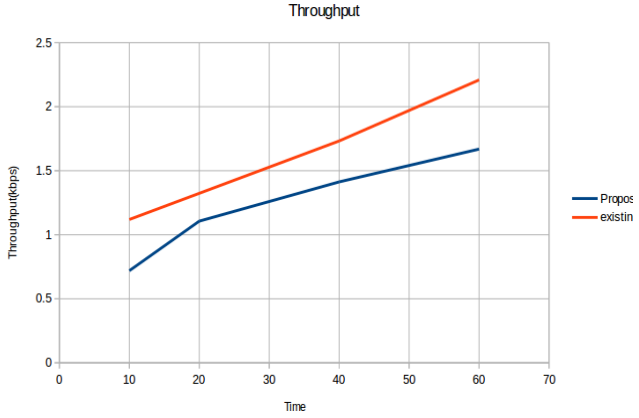

Fig.8 Existing vs Proposed packet throughput

As energy required is less in proposed systems throughput is more.

CONCLUSION

In this paper sensor localization is used to improve the accuracy of sensor location so that activation of motes will be easy for area coverage. Prediction is used for predicting the mote according to its battery power, frequency and range so that more battery powered sensor will activate first and cover the more area proficiently and for activation of motes

Scheduling is used so the sequentially sensor gets activated and cover the area without redundancy of same area coverage and hence it increases the network lifetime and energy proficiency. Future scope is to validate mathematical model for the stability and prediction strategies.

REFERENCES

[1] Rencheng Jin ,Yun Ma,Yingchen Li,Jipeng Zhao,Feng Zhou "High accuracy localization scheme based on time-of-flight and directional antenna in wireless sensor networks" , *Dalian University of technology,Dalian ,Liaoning,*vol 8,pp 136-141,2018.

[2] Ivana Strumberger,E va Tuba,Nebojsa Bacanin ,Marko Beko,Milan tuba,"Monarch Butterfly Optimization Algorithm for Localization in Wireless Sensor Network*",Department of Mathematical Sciences state University of Novi Pazar,*vol 201,pp 42113,2017.

[3] P. Chaturvedi and A. K. Daniel, "An Energy Efficient Node Scheduling Protocol for Target Coverage in Wireless Sensor Networks," *2015 Fifth International Conference on Communication Systems and Network Technologies*, Gwalior, pp. 138-142, 2015.

[4] Lu Dai,Bang Wang,Xianjun Deng ,Laurence T.Yang," An Improved Immune algorithm for Node Relocation to maximize confident information coverage in Hybrid Sensor Network"*The Department of Computer Science,St. Fransics Xavier University,Antigonish,*vol 12 pp-12312,2017.

[5] Manel Chenait ,Bahia Zebbane, Chafika Benzaid, Nadjib Badache, "Sleep Scheduling with stability Predictive Coverage redundancy check in Wireless Sensor Networks", *university of science And Technology Houri Boumedience* , vol.130, pp. 523012, 2015.

[6] Jia Yufu,Lia Hongjun,"Node Scheduling Scheme Based on Coverage Preserving for Wireless Sensor Network",*School of Computer Science and Technology Hubei University of Economics,HBUE Wuhan,China,* vol.225, pp. 432201, 2016

[7] Manel Chenait ,Bahia Zebbane,Chafika Benzaid, Nadjib Badache" Energy-Efficient CoverageProtocol Based on Stable and Predictive Scheduling In Wireless Sensor Networks" *University of Sciences and Technology Houari Boumediene,*vol 6,pp 231-21,2017.

[8]] C. Wang, J. Shih, B. Pan and T. Wu, "A Network Lifetime Enhancement Method for Sink Relocation and Its Analysis in Wireless Sensor Networks," in *IEEE Sensors Journal*, vol. 14, no. 6, pp. 1932-1943, June 2014.

[9] X. Liu,Jiannong C. Shaojie Tang,P. Guo "A Generalised Preserving Scheduling in WSN:a case study in Structural Health Monitoring",IEEE conference on computer Communications, vol.221 , pp. 718-726, 2014

[10] J. Hong ,J. Cao ,Y. Zeng ,S. Lu ,D. Chen ,Z. Li,"A Location Prediction based Sleep Scheduling protocol for Object Tracking in Sensor Networks"State Key Laboratory for NovelSoftware technology ,Nanjing Univ,China, vol.152, pp. 421322, 2009

[11] M. Michel and B. Quoitin, "Impact of a sleep schedule on the AODV convergence time in WSNs," *2013 IEEE Conference on Computer Communications Workshops (INFOCOM WKSHPS)*, Turin, , pp. 69-70, 2013.

[12] So-Tsung Chou, Hann-Tzong Chern and Cheng-Mu Shiao, "AODV protocol with scheduling priority flow in MAC layer (AODV-SPF)," *The 6th International Conference on Networked Computing and Advanced Information Management*, Seoul,, pp. 612-617, 2010

Proceedings of the Fourth International Conference on Communication and Electronics Systems (ICCES 2019)
IEEE Conference Record # 45898; IEEE Xplore ISBN: 978-1-7281-1261-9

An Improvement in Performance and Computational Cost of ANN Based Wind Speed Prediction System

Shashank Sinha, S. Tiwari
Dept. of Instrumentation and Control Engg.
Dr. B. R. Ambedkar National Institute of Technology
Jalandhar, India

***Abstract*-Wind speed prediction is very important as it influences the wind energy and hence wind farm applications. An accurate wind speed prediction will be helpful in scheduling and management of the wind farms. In this work, empirical mode distribution (EMD) and ensemble empirical mode distribution (EEMD) have been used for decomposition of wind speed data into IMFs. An ANN has been proposed to predict the wind speed with IMFS given as the inputs. The accuracy of prediction by the ANN is further increased by using the actual wind speed at the previous instant along with the IMFs as the input to the ANN. This increase in accuracy in prediction was also accompanied by a reduction in the total computational cost.**

***Keywords*- ANN, Wind Speed, Prediction, EMD, EEMD.**

I. INTRODUCTION

The continuously increasing demand of electric power gives rise to the option of use of wind energy s it is abundantly available and clean in nature [1]. But the wind energy comes with a bigger disadvantage of being highly random in nature. To overcome this disadvantage of wind energy, continuous efforts are being made to devise methods for accurate prediction of wind energy [2].

Over past few years many researches have been done to predict the wind speed, Kavasseri [3] has used f-ARIMA model to predict the wind speed, Zhang [4] has used ANN-based and SVM based models for predicting wind speed. Zhou [5] has proposed an improved SVM based model for forecasting short term wind speed. Sun [6] has used Fast EEMD (FEEMD) and regularized extreme learning machine for predicting wind speed. Wang [7] has used a hybrid model of consisting EEMD and Genetic Algorithm and back propagation for the same purpose. Hybrid models for predictions have shown some better results for forecasting wind speed [8]. WD (wavelet decomposition) is also used for decomposing the wind speed data for hybrid model for improving the performance of the system [9] and [10]. Hui Liu [11] has shown and compared various decomposition techniques along with various neural network techniques for prediction of short term wind speed for one to three step ahead.

This work studies the effect of using previous instant wind speed along with IMFs of the wind speed data generated through EMD and EEMD for prediction of wind speed at next instant.

II. WIND SPEED AND ITS EFFECT ON WIND ENERGY

Wind flow is a general phenomenon generally caused by atmospheric air pressure difference. Wind generally flow from high to low atmospheric pressure, and the speed of wind flow is known as wind speed.

The flow of wind contains energy within it which can be further converted into any other form of energy, so the energy of the wind can be defined as[2]:

$$E = \frac{1}{2}mv^2 \quad (1)$$

where m is the mass of wind and v is the wind speed. The mass of the wind (m) can be defined as:

$$m=\rho Av \quad (2)$$

so

$$E = \frac{1}{2}\rho Av^3 \quad (3)$$

where ρ is the air density, A is the cross sectional area of the object on which the wind is falling on.

So because wind speed (v) is variable and random in nature so the wind energy become highly variable and random in nature.

III. DECOMPOSITION OF WIND SPEED DATA

In this paper EMD and EEMD have been used to decompose the wind data. The procedures to do so are as follows.

A. EMD-

The EMD is explained in detail by Huang [12], it is a technique to adaptively decompose a given signal, by means of a process called the sifting algorithm, into a finite set of AM/FM modulated components. These components, called 'intrinsic mode functions' (IMFs), represent the oscillation modes embedded in the data[13]. To find IMF of any time series via EMD steps are as follows[14]-

- Find the local extrema (maxima and minima) of the signal.
- Find the upper envelope $s_+(t)$ and lower envelope $s_-(t)$ by interpolating maxima and minima by cubic spline method.
- Calculate the mean of the envelopes.

$$s(t) = \frac{s_+(t)+s_-(t)}{2} \quad (4)$$

- Subtract the mean from the signal and repeat the process until the resulted signal obtain the criterion of an IMF.

$$c(t) = x(t) - s(t) \quad (5)$$

- Repeat the whole process until the remaining signal is able to decompose i.e. it will have two or more nos. of extremas.
- The remaining signal is called as residue or the trend component.

The IMF should have two properties-

- The no. of zero crossing and no. of extrema should either be equal or at most differ by1.
- The average of the envelope (maxima and minima) should be zero.

But the EMD consist the problem of mode mixing [15] which further was removed by EEMD.

B. EEMD-

To overcome the problem of mode mixing EEMD was proposed in this method different realizations of white noise are added to the signal [14] and [16].

$$S_i(t)=x(t)+w_i(t) \quad (6)$$

where x(t) is the original time series signal and $w_i(t)$ are the different realizations of white noise and i=1,2…..n. Then the IMFs are computed as follows

$$IMF_j = \frac{1}{n}\sum_{i=1}^{n} IMF_j^i \quad (7)$$

So the power of the added noise is consider by the sound to noise ratio of the signal is decided by the formula

$$SNR = 10log_{10}\frac{P_1}{P_2} \quad (8)$$

Where P_1 is the signal power and P_2 is the power of the noise. The SNR should remain in between 50 to 60 dB for successful EEMD [17].

IV. ANN FOR WIND SPEED PREDICTION

Over the past few years artificial neural network have been found to be very much suitable for nonlinear systems and for time series application. In the current work, an ANN with one hidden layer is proposed to predict the wind speed on the basis of the IMFs of the wind speed data. Two different types of activation functions namely *logarithmic sigmoid (logsig)* activation function having a transfer function as-

$$logsig(n) = \frac{1}{1+e^{-n}} \quad (9)$$

and *Tan-sigmoid (tansig)* activation function having transfer function as-

$$tansig(n) = 2/(1+\exp(-2*n))-1 \quad (10)$$

were considered and the best of the two was used. The output layer has a pure linear transfer function.

The ANN use Levenberg-Marquardt back propagation for training. The training algorithm calculates the network parameter as follows [18] to [20]:

$$J = \frac{\partial E(W_k\}}{\partial W_k} \quad (11)$$

$$W_{k+1} = W_k - [J^T J + \mu I]^{-1} J^T E \quad (12)$$

Where J is the jacobian matrix which contains the error with respect to network weights and biases. E is the vector of network error and μ is learning parameter.

The training data set comprised of 100 sec. of wind data. the performance of this ANN is then compared with another ANN using the previous instant actual wind speed as an input in addition to the IMFs.

The comparison of results obtained for predicting wind speed using different methods have been made by using three parameters MAE, MAPE and RMSE by Zhang et al [3]. Therefore, the same parameters have been used to compare results in this work. The computation of these parameter can be done as follows -

$$MAPE = \frac{1}{n}\left(\sum_{i=0}^{n}\frac{|x(t)-x'(t)|}{x(t)}\right) * 100 \quad (13)$$

$$MAE = \sum_{i=1}^{n}|x(t) - X'(t)|/_n \quad (14)$$

$$RMSE = \sqrt{\left(x(t) - x'(t)\right)^2/(n-1)} \quad (15)$$

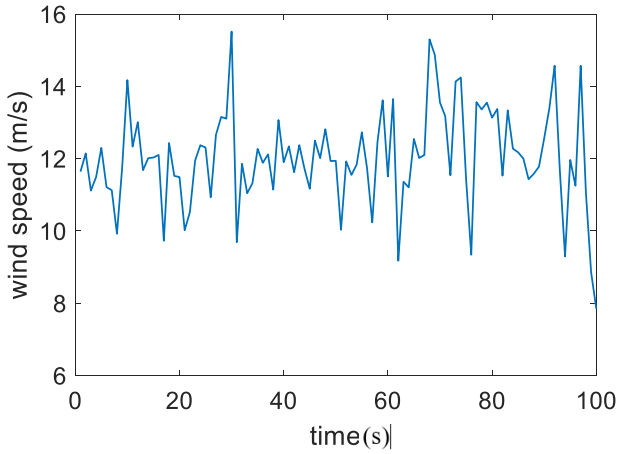

Fig 1 Test Data #1

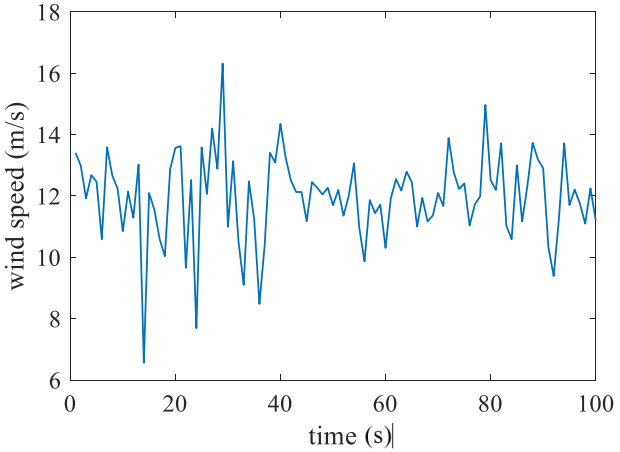

Fig 2 Test Data #2

Where x(t) is the actual value of wind speed, x'(t) is the predicted value.

V. SIMULATION AND RESULTS

The two ANN models were trained using wind speed for 100 sec. The nos. of neurons in the hidden layer was decided using trial and error method. The better of the TANSIG and LOGSIG based on the simulation result was taken as activation function.

These ANNs were then tested using two sets of testing data sets, i.e. Test Data #1 and Test Data #2 (shown in Fig 1 and 2 respectively) each comprise of 100 sec. data.

These data sets were decomposed by EMD and EEMD methods, figure 3 and 4 show the EMD and EEMD of test data #1 and figure 5 and 6 show EMD and EEMD of test data #2.

The architecture of the ANNs and a comparison of their performances are given in Table I and Table II.

Figure 7 and 8 shows a comparison between the wind speed predicted on the basis of IMFs generated using EMD and EEMD without considering the actual wind speed as an input for Test Data #1 and Test Data #2 respectively.

A comparison between the wind speed predicted on the basis of IMFs generated using EMD and EEMD along with the actual wind speed at the previous instant as an additional input for Test Data #1 and Test Data #2 is shown in fig. 9 and 10.

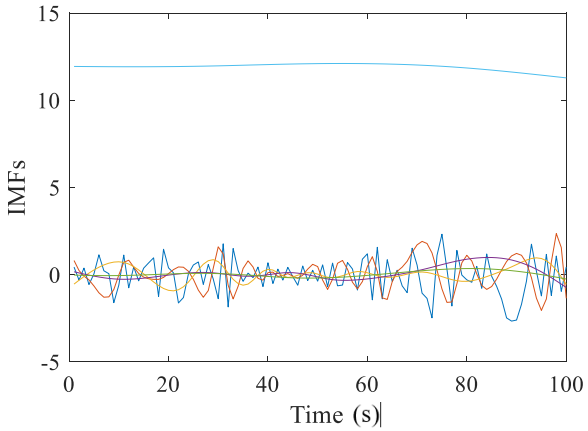

Fig. 3 EMD of Test Data #1

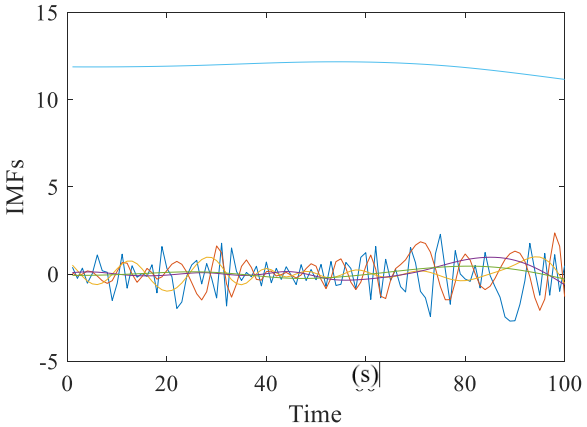

Fig. 4 EEMD of Test Data #1

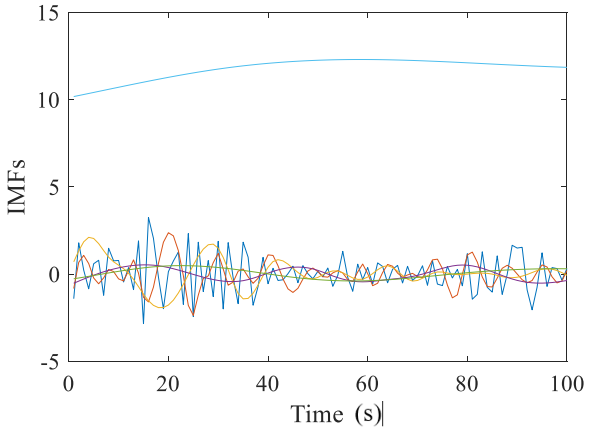

Fig. 5 EMD of Test Data #2

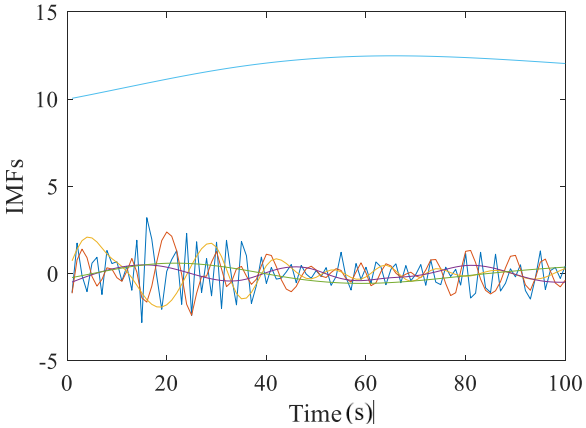

Fig. 6 EEMD of Test Data #2

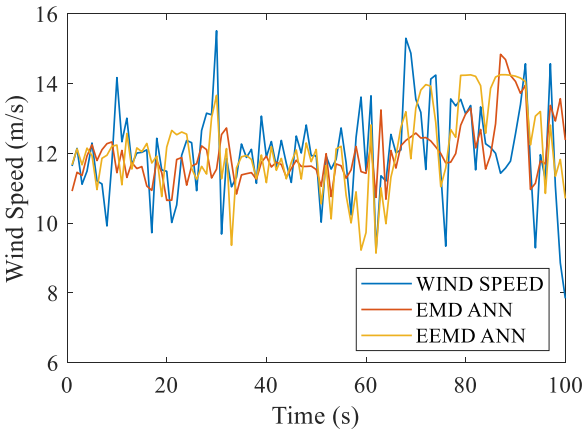

Fig. 7 Results of EMD and EEMD based prediction for Test Data #1

From table I it can be seen that in case of EMD when only IMFs of the wind speed are used for prediction then the error parameters (MAE, MAPE and RMSE) are 1.0408, 8.99 and 1.4216 respectively, but when previous instant wind speed is incorporated along with the IMFs for the prediction then the corresponding error parameters are 1.0236, 8.68 and 1.2971 respectively. So the error parameters are reduced by 1.65%, 3.44% and 8.75% respectively. Similarly, in case

of EEMD when only IMFs of the wind speed are used for prediction the error parameters are 1.0034, 8.65 and 1.3638 but when the wind speed is used along with the IMFs, then the corresponding error parameters are 0.8865, 7.68 and 1.2152 hence the error parameters are reduced by 11.65%, 11.21% and 10.89% respectively.

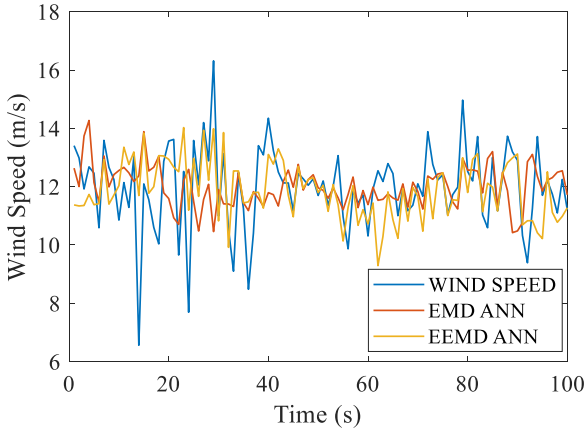

Fig. 8 Results of EMD and EEMD based prediction for Test Data #2

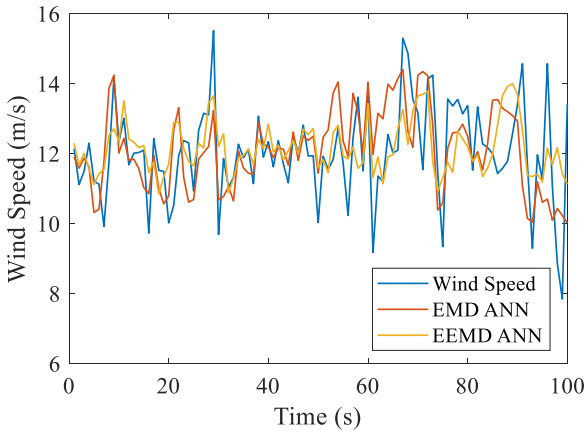

Fig. 9 Results of EMD, EEMD and previous movement wind speed based prediction for Test Data #1

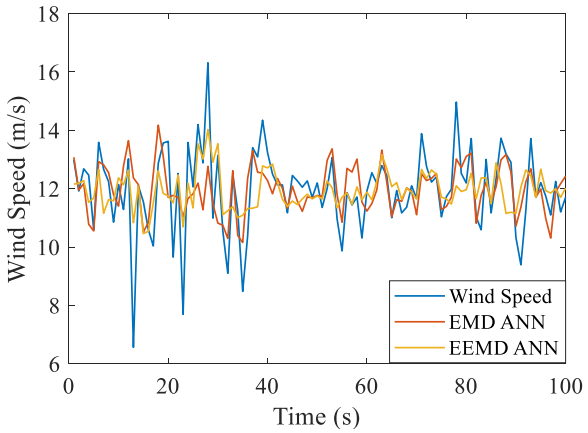

Fig. 10 Results of EMD, EEMD and previous instant wind speed based prediction for Test Data #2

Table I ANALYSIS of TEST DATA #1

Method		ANN Architecture		Performance Analysis		
		No. of hidden layer neuron	Activation Function	MAE	MAPE %	RMSE
EMD	IMF only	14	TANSIG	1.0408	8.99	1.4216
	IMF+ previous instant speed	8	LOGSIG	1.0236	8.68	1.2971
EEMD	IMF only	8	LOGSIG	1.0034	8.65	1.3638
	IMF+ previous instant speed	6	TANSIG	0.8859	7.68	1.2152

Table II ANALYSIS of TEST DATA #2

Method		ANN Architecture		Performance Analysis		
		No. of hidden layer neuron	Activation Function	MAE	MAPE %	RMSE
EMD	IMF only	14	TANSIG	1.1255	10.01	1.5909
	IMF+ previous instant speed	8	LOGSIG	0.8385	7.58	1.2040
EEMD	IMF only	8	LOGSIG	0.9666	8.71	1.3501
	IMF+ previous instant speed	6	TANSIG	0.8551	7.66	1.1631

Table III ANALYSIS of TEST DATA #3

Method		ANN Architecture		Performance Analysis		
		No. of hidden layer neuron	Activation Function	MAE	MAPE %	RMSE
EMD	IMF only	14	TANSIG	1.1753	9.57	1.5484
	IMF+ previous instant speed	8	LOGSIG	1.1108	9.25	1.4024
EEMD	IMF only	8	LOGSIG	1.0007	8.27	1.2998
	IMF+ previous instant speed	6	TANSIG	0.8496	7.15	1.1655

Table IV ANALYSIS of TEST DATA #4

Method		ANN Architecture		Performance Analysis		
		No. of hidden layer neuron	Activation Function	MAE	MAPE %	RMSE
EMD	IMF only	14	TANSIG	1.0092	8.48	1.2704
	IMF+ previous instant speed	8	LOGSIG	0.8389	6.77	1.1122
EEMD	IMF only	8	LOGSIG	0.9373	7.46	1.3423
	IMF+ previous instant speed	6	TANSIG	0.8105	6.76	1.0879

Similarly from Table II it can be seen that in case of EMD when only IMFs of the wind speed are used for prediction, the error parameters are 1.1255, 10.01 and 1.5909 but when the previous instant wind speed is incorporated with the IMFs for the prediction then the corresponding error parameters are 0.8385, 7.58 and 1.2040, so the error parameters are reduced by 25.45%, 24.27% and 24.31% respectively. Similarly for EEMD when only IMFs of the wind speed are used then the error parameters are 0.9666, 8.71 and 1.3505 respectively but when previous instant wind speed is incorporated with the IMFs for the prediction then the corresponding error parameters are 0.8551, 7.66 and 1.1631, so the error parameters are reduced by 11.53%, 12.05% and 10.88% respectively.

Two more data sets, Test Data #3 and Test Data #4, each comprising of 100 sec. data were then used to investigate the prediction accuracy of the ANNs already used for Test Data #1 and Test Data #2. The results obtained are as given in tables III and IV. The results in Table III and IV are in conformity with results reported in Table I and II for Test Data #1 and Test Data #2 respectively.

It is clear from the results in Table I-IV that when previous instant wind speed is incorporated with IMFs (for both EMD and EEMD) the error parameters are reduced (for all Test Data sets). Hence the performance (accuracy) of the prediction is increased when previous instant wind speed is incorporated with IMFs for prediction of wind speed.

From Tables I-IV it can also be seen that the no. of hidden layer neurons are also getting decreased from 14 to 8 in case of EMD and from 8 to 6 in case of EEMD when previous instant wind speed is incorporated with IMFs for wind speed prediction. So because of the reduction in the number of hidden layer neurons the computational cost of the ANN prediction system is also decreasing significantly.

VI. CONCLUSION

The simulation result establish that by incorporating previous instant wind speed along with the decompositions of wind data, not only the accuracy of the prediction improves but the computational cost of the system is also reduced. This reduction in computational cost has a great significance in case of short term wind speed prediction for real time control applications in wind farms.

REFERENCES

[1] World Wind Energy Association, "World wind energy report 2018"

[2] Tawfek K. Mahmoud, Zhao Yang Dong and Jin Ma, "A Developed Integrated Scheme Based Approach for Wind Turbine Intelligent Control" IEEE transactions on sustainable energy, VOL. 8, NO. 3, JULY 2017.

[3] Kavasseri RG and Seetharaman K. "Day-ahead wind speed forecasting using f-ARIMA models." Renew Energy 2009;34(5):1388–93.

[4] Zhang C, Wei H, Zhao J, Liu T, Zhu T and Zhang K. "Short-term wind speed forecasting using empirical mode decomposition and feature selection." Renew Energy 2016;96:727–37.

[5] Zhou J, Shi J and Li G. "Fine tuning support vector machines for short-term wind speed forecasting." Energy Convers Manage 2011;52(4):1990-8.

[6] Sun W and Liu M. "Wind speed forecasting using FEEMD echo state networks with RELM in Hebei", China. Energy Convers Manage 2016;114

[7] Wang S, Zhang N, Wu L and Wang Y. "Wind speed forecasting based on the hybrid ensemble empirical mode decomposition and GA-BP neural network method." Renew Energy 2016;94.

[8] Liu D, Wang J and Wang H. "Short-term wind speed forecasting based on spectral clustering and optimised echo state networks". Renewable Energy 2015;78.

[9] Qin S, Liu F, Wang J and Song Y. "Interval forecasts of a novelty hybrid model for wind speeds". Energy Rep 2015;1.

[10] Kiplangat DC, Asokan K and Kumar KS. "Improved week-ahead predictions of wind speed using simple linear models with wavelet decomposition". Renew Energy 2016;93:38–44.

[11] Hui Liu, Xiwei Mi and Yanfei Li "Comparison of two new intelligent wind speed forecasting approaches based on Wavelet Packet Decomposition, Complete Ensemble Empirical Mode Decomposition with Adaptive Noise and Artificial Neural Networks" Energy Conversion and Management 155 (2018) 188–200.

[12] N.E. Huang, Z. Shen, S.R. Long, M.L. Wu, H.H. Shih and Q. Zheng, "The empirical mode decomposition and the Hilbert spectrum for nonlinear and non-stationary time series analysis", Proc. Roy. Soc. Lond. A 454 (1998) 903e995.

[13] David Looney and Danilo P. Mandic, "Empirical mode decomposition for simultaneous image enhancement and fusion" Imperial College London, UK.

[14] N. Rehman and D. P. Mandic, "Multivariate empirical mode decomposition." *Proc. R. Soc. A* (2010) 466, 1291–1302.

[15] Zhaohua Wu and Norden E. Huang, "Ensemble empirical mode decomposition: A noise-assisted data analysis method", Advances in Adaptive Data Analysis Vol. 1, No. 1(2009) 1-41.

[16] Rais El Hadi Bekka and Yaakoub Berrouche, "Improvement of ensemble empirical mode decomposition by over-sampling", Adavances in Adaptive Data Analysis, Vol. 5, No. 3 (2013) 1350012.

[17] J. Zhang, R. Yan, R. X. Gao, and Z. Feng, "Performance enhancement of ensemble empirical mode decomposition," *Mech. Syst. Signal Process.*, vol. 24, pp. 2104–2123, Oct. 2010.

[18] M. T. Hagan and M. B. Menhaj, "Training feedforward networks with the Marquardt algorithm," IEEE Trans. Neural Network., vol. NN-5, no. 6, pp. 989–993, Nov. 1994.

[19] N. Ampazis and S. J. Perantonis, "Levenberg-Marquardt algorithm with adaptive momentum for the efficient training of feedforward networks," in Proc. IEEE-INNS-ENNS Int. Joint Conf. Neural Netw., 2000, 2000, vol. 1, pp. 126–131.

[20] M. T. Hagan, H. B. Demuth, and M. H. Beale, *Neural Network Design*. Boston, MA, USA: PWS Publ., 1996.

Proceedings of the Fourth International Conference on Communication and Electronics Systems (ICCES 2019)
IEEE Conference Record # 45898; IEEE Xplore ISBN: 978-1-7281-1261-9

An Improved Inverter Control for Grid-Connected PV System

Varun Kumar Mahawar and S. Tiwari
Department of Instrumentation and Control Engineering
Dr. B. R. Ambedkar National Institute of Technology
Jalandhar, India

***Abstract*—The grid-connected solar panel is a distributed power generation device which is connected through an inverter that converts DC power from photovoltaic array to AC power. The voltage regulator to maintain the capacitor voltage at a certain reference level along with a current regulator are required to control the inverter. This paper mainly focuses on control of the inverter with an objective of extracting the maximum power from the solar panel. A fractional order proportional integral controller is proposed to control the inverter in this work. The performance of this controller is compared with the conventionally used PI and PID controllers on the basis of simulation result obtained using MATLAB Simulink.**

Keywords—FOPI, Inverter, PV system, MPPT

I. INTRODUCTION

From the last decades, due to the high increase in the consumption of energy, environment and reserve issues are emerging [1]. It is necessary to find different alternatives for energy consumption. Renewable energy is a good alternative because it is gathered from renewable resources. The most common technologies in renewable energy are Wind power, Hydropower, Solar energy, Geo-thermal energy, Bioenergy, Wave energy. Solar energy is gaining high interest from governments, academia, and industry because it is sustainable and green [2]. Solar energy is an efficient and more feasible alternative option for renewable energy because it is available abundantly. A photovoltaic array is used for generating electricity from the sun. The starting development of solar energy was in space application where cost was not a big issue [3]. Then the photovoltaic (PV) system was started to be used for home application. The multifunctional inverters were proposed in 1998, which have a fuel cell or battery as an auxiliary system [4]. If the storage device such as battery is not connected to the system, the system called as standalone system. PV system was subsequently, connected to the grid and its functionality was monitored in different climate conditions. It has been observed that if the grid is connect to the PV system, the battery size is reduced by 0.5-0.7 factor as compared to standalone system for the same load and solar capacity [5]. In grid-connected PV system, it is important to maintain the capacitor voltage or inverter input voltage at a certain reference level. If it is not set at the reference level, circulating current may flow in the system. Circulating current affects the maximum power of the PV system and it may also damage the system. For increasing the efficiency of the photovoltaic system when PV array is not working, Wu et al suggested a method by using a three-phase rectifier with grid-connected inverter [6]. The maximum power point tracking of PV array is necessary for efficient implementation and operation of the solar system. The quality analysis of the 3.6 KW rooftop solar system in Cairo, Egypt, which is connected to the 220V 50Hz grid is presented in 2011. The system validates the capability of grid-connected photovoltaic in Egypt. The result was analyzed with other studies, which shows the solar system's yearly average production is higher than others [7]. A large scale grid connected photovoltaic plant is installed in Ramagundam, India, where the performance of annual weather variation effect in solar output is observed using SCADA and the actual energy consumption is compared with simulated result in SCADA system [8]. A 91 KW rooftop photovoltaic system was set up on the National Water Research Centre (NWRC), Egypt. A MATLAB Simulink work is proposed mimicking the description of that PV system and Maximum power extract from the solar array has 85% efficiency [9].

The goal of this paper is designing an efficient simulating model, which provides the maximum power from the solar panel while maintaining the capacitor voltage at reference level. The Fractional-Order-Proportional-Integral (FOPI) controller is almost as simple as the conventional PI controller with additional advantage due to the fractional integral. Therefore, the current work envisages to employ FOPI for maintaining the inverter input voltage and compare the performance of the FOPI controller with that of the conventional PI and PID controller on the basis of the simulation results.

II. MODEL DISCRIPTION

The system under consideration is a grid connected solar system consisting of a PV array, DC-DC boost converter, Perturb & Observer Maximum Power Point Tracking (MPPT) controller, 3 phase DC-AC converter, grid and 3 phase resistive load [10]. This system has no storage device such as a battery. The irradiance and temperature values are applied to the solar panel as input. Then DC-DC boost converter is controlled by using Perturb and Observe (P&O) MPPT algorithm and maximum power is extracted from PV panel. Then inverter

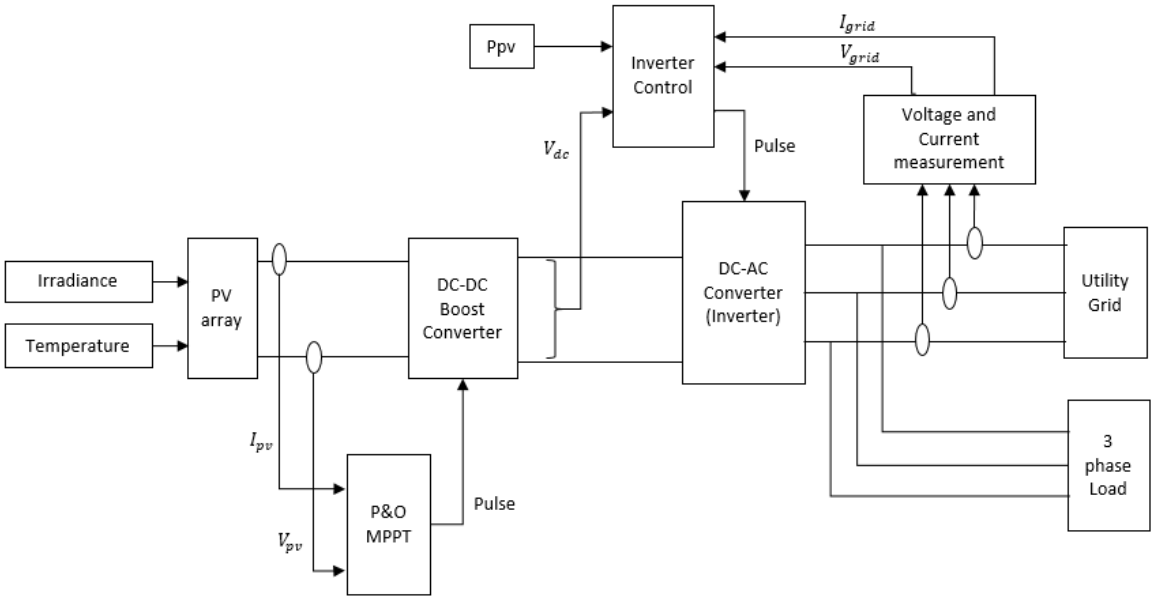

Figure 1 Schematic representation of grid-connected PV system

control scheme is applied to the DC-AC converter (Inverter) for converting DC power to 3-phase AC power. The load is absorbing the power from the inverter and grid both. The simplified configuration is shown in fig (1). This system is modeled and simulated using MATLAB Simulink.

A. PV system

The equivalent circuit for ideal PV cell and practical PV cell are proposed [11] and shown in fig (2) and (3).

The equations (1) and (2) are for ideal PV cell. A series resistance (R_s) and a shunt resistance (R_{sh}) are combined with the ideal equivalent circuit to represent a practical PV cell [11].

$$I = I_{pv} - I_d \quad (1)$$

$$I = I_{pv} - I_0\left[e^{\frac{qv}{aKT}} - 1\right] \quad (2)$$

Where I is current supplied through load (Amp), I_d is current supplied through diode (Amp), I_{pv} is current supplied from PV (Amp), I_0 is reverse saturation current (Amp), q is charge $= 1.602176565 \times 10^{-19}$ Coulomb , v is thermal voltage (Volt), a is diode ideality factor, K is Boltzmann's constant $= 1.3806488 \times 10^{-23}\, JK^{-1}$, T is absolute temperature of p-n junction (Kelvin).

In the PV cell model, the current source is parallel connected with the diode. PV cell act like a diode if there is no irradiance.

$$I = I_{pv} - I_d - I_{sh} \quad (3)$$

$$V_{sh} = V + IR_s \quad (4)$$

$$I_{sh} = \frac{V_{sh}}{R_{sh}} = \frac{V+IR_s}{R_{sh}} \quad (5)$$

$$I_d = I_0[e^{\frac{qV_{sh}}{KT}} - 1] \quad (6)$$

By substituting equation (5) and (6) in equation (3)

$$I = I_{pv} - I_0\left[e^{\frac{q(V+IR_s)}{KT}} - 1\right] - \frac{V+IR_s}{R_{sh}} \quad (7)$$

Where I_{sh} is current supplied through shunt resistor (Amp), R_s is series resistance (Ω), R_{sh} is shunt resistance (Ω), V is load voltage (Volt), V_{sh} is voltage at shunt resistor (Volt) [11].

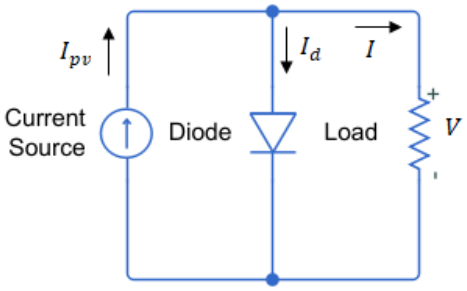

Figure 2 Equivalent circuit of Ideal PV cell

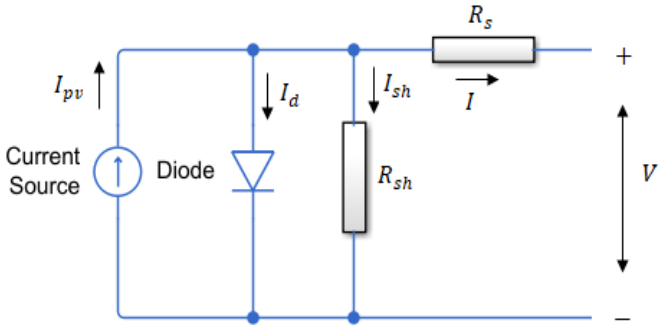

Figure 3 Equivalent circuit of practical PV cell

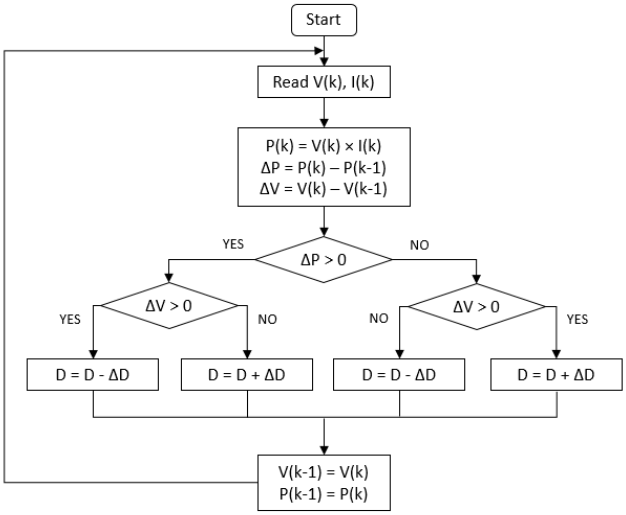

Figure 4 Flowchart of P&O MPPT algorithm

B. Maximum Power Point Tracking (MPPT)

For tracking of maximum power, perturb & observe technique is the most popular because of the low cost and ease to the DC-DC boost converter. In this method, the voltage and current of solar panel are read at time k and the solar power at time instant k is calculated. The voltage and power at time instant k are compared with the sample at time instant (k-1). Voltage from PV array is adjusted by a small amount and the power change is observed. If $\frac{dP}{dV} > 0$, positive sign indicates that the MPP is greater than solar power and the perturbation D is decreased to obtain the MPP. If $\frac{dP}{dV} < 0$, negative sign shows that the MPP is lesser than solar power and the perturbation D is increased to obtain the MPP [14]. If power is increasing continuously with increase in PV voltage, the voltage is increased until $\frac{dP}{dV} = 0$ [14] [15] [16]. The flowchart of the P&O MPPT is shown in Fig. (4), where D is the perturbation step-size.

The MPPT technique requires the knowledge of solar panel parameters. V_{oc} is the open circuit voltage of PV array. Maximum power point voltage (V_{MPP}) and open circuit voltage (V_{oc}) have a linear relationship as shown below

$$V_{MPP} = k \times V_{oc} \tag{8}$$

Where k is constant, and the value of k depends upon the characteristics of the PV cell. The value of k varies between 0.73 to 0.85 [17]. The maximum power at the actual maximum power point (MPP) is calculated by

$$P_{max} = V_{MPP} \times No.of\ series\ modules \times I_{MPP} \times No.of\ parallel\ string \tag{9}$$

Where P_{max} is maximum power at actual MPP, V_{MPP} is the voltage at MPP, I_{MPP} is current at MPP. The efficiency is calculated by the following

$$\eta = \left(\frac{P_{\max tracked}}{P_{max}}\right) \times 100 \tag{10}$$

$$P_{\max tracked} = P_{pv} \tag{11}$$

$$\eta = \left(\frac{P_{pv}}{P_{max}}\right) \times 100 \tag{12}$$

Where η is the efficiency of the MPPT method, $P_{\max tracked}$ is maximum power tracked by the MPPT method [9].

C. Controllers

PI controller is a feedback-based controller. It calculates the output by the received error signal. The function of PI controller is eliminating the steady state error, which are insensitive to system variation [18]. The basic equation of PI controller is given by

$$G_c(s) = K_p + \frac{K_i}{s} \tag{13}$$

PID controller modifies the output based on proportional gain(K_p), integral gain(K_i) and derivative gain(K_d). PID controller make the system stable and more accurate, as it reduces the oscillation present in the system [18]. The equation for PID controller is as follows-

$$G_c(s) = K_p + \frac{K_i}{s} + sK_d \tag{14}$$

FOPI controller is used for improving the performance of the system. As it has three parameters K_p, K_i and λ to tune [19]. The transfer function of FOPI is given by

$$G_c(s) = K_p + \frac{K_i}{s^{\lambda}} \tag{15}$$

The FOPI controller has better control, more flexibility and excellent robustness over PI and PID controller [19]. Ziegler-Nichols method is used for tuning the controller parameters. The

Table I Tuning parameters for controllers

Parameters	PI controller	PID controller	FOPI controller
K_p	112.5	150	112.5
K_i	22500	50000	22500
K_d	-	0.00075	-
λ	-	-	0.6

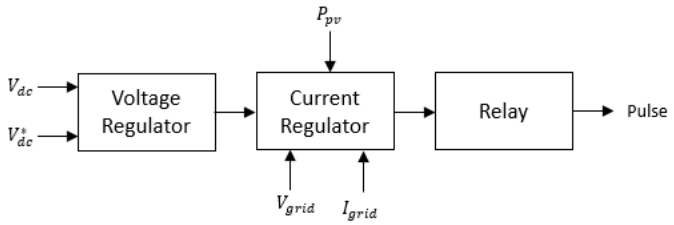

Figure 5 Inverter Pulse Control Scheme

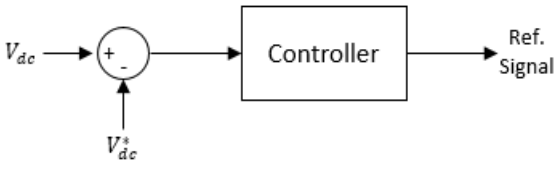

Figure 6 Voltage Regulator

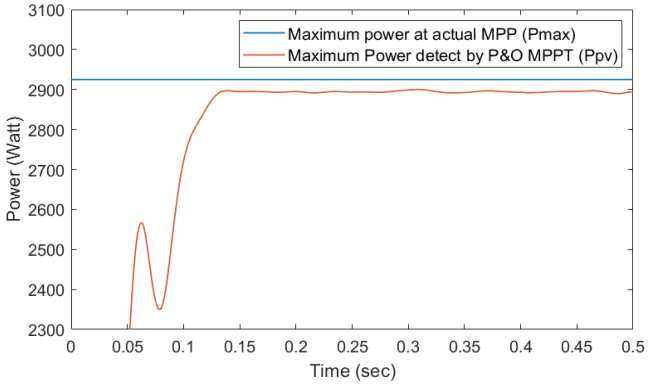

Figure 7 Maximum power extract from Simulink model

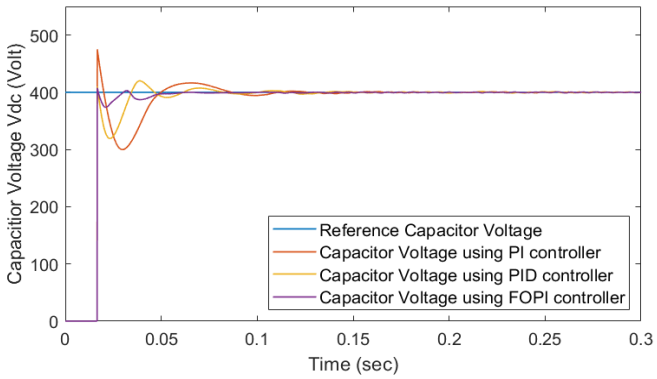

Figure 8 Response of Capacitor Voltage V_{dc}

values of the gains for the different controllers are as given in Table I.

D. Inverter

After extracting the maximum DC power from the solar array, that DC power is converting into 3 phase AC power to supply the demand power to 3 phase load. 3 phase 3 wire inverter is used for converting DC to AC power. 3 phase 3 wire inverter consists of six MOSFET devices. The simplified method for controlling the MOSFET devices is shown in fig (5).

The voltage regulator is designed for maintaining capacitor voltage(V_{dc}) at a certain reference level(V_{dc}^{*}) Fig. The error and signal generated by comparing capacitor voltage(V_{dc}) reference voltage(V_{dc}^{*}). The controller generates a reference signal for the current regulator, which is shown in fig (6). Three controllers PI, PID, and FOPI are used to produce reference signal one by one to control the inerter and their performances are compared. This reference signal is compared with the solar power P_{pv} and a reference power signal is achieved.

Table II Step response parameters for V_{dc}

Parameters	PI controller	PID controller	FOPI controller
Rise Time ($\times 10^{-16}$)	1.5266	1.7347	1.7347
Settling Time (sec)	0.0784	0.0566	0.0440
Peak Overshoot (Watt)	18.7236	4.6681	2.1154
Peak Time (sec)	0.0167	0.0388	0.0167

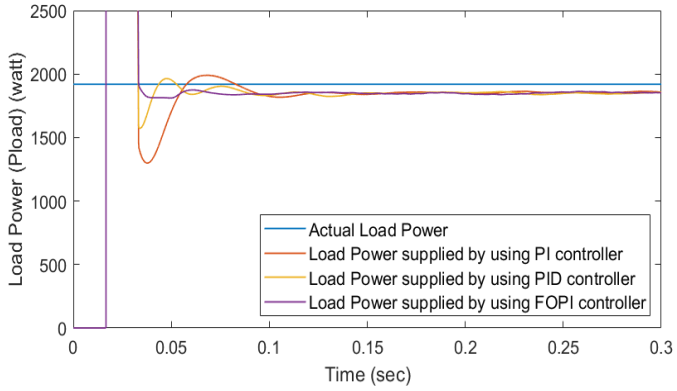

Figure 9 Response of Load Power at 1940W

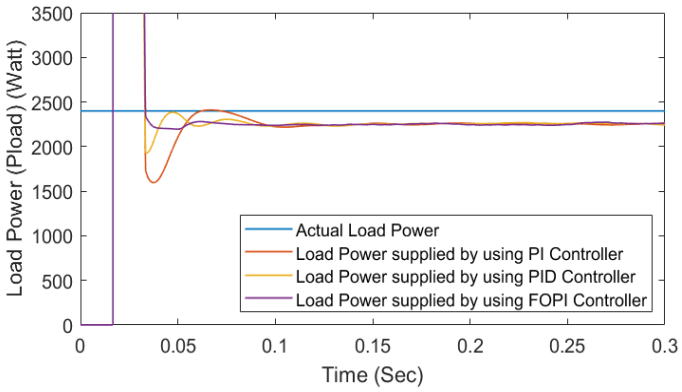

Figure 10 Response of Load Power at 2400W

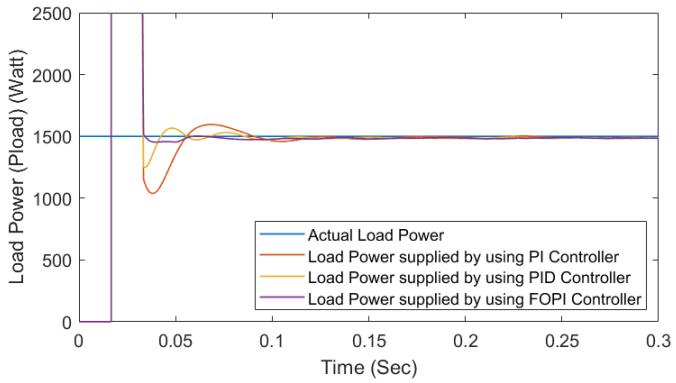

Figure 11 Response of Load Power at 1500W

The phase-locked-loop (PLL) is used to find the phase angle of the grid voltage(V_{grid}). The phase angle is used for park transformation, in which the three-phase grid voltage (abc) reference frame transforms to the grid voltage (dq0) reference frame.

By using the reference power signal and d-axis component of grid voltage, a current reference (I_d^{*}) is generated. An inverse park transformation converts this current reference(I_d^{*}) from the (dq0) reference frame (I_{dq0}) to (abc) reference frame(I_{abc}). Then I_{abc} is compared with the grid current (I_{grid}) and the control pulses for 3 phase 3 wire inverter are generated by using a relay.

III. RESULT

The model is worked in Standard Temperature Conditions (STC). The corresponding values of irradiance and temperature are $1000\ W/m^2$ and 25^0C respectively. The maximum power tracked from the P&O MPPT is compared with the calculated maximum power (2925 W) from (9). The voltage V_{MPP} and current I_{MPP} at calculated maximum power are 37.5 V and 7.8 A respectively.

Fig (7) shows the maximum power tracked by the P&O MPPT. The efficiency of P&O MPPT technique is 98.94% calculated by (12).

The performance of the three controllers in the system are investigated at different levels of 3-phase resistive load. The capacitor voltage is determined by the DC-DC boost converter parameters and hence is kept at 400V and the actual power demand of load in figure (9), (10) and (11) is 1920W, 2400W and 1500W respectively. The capacitor voltage(V_{dc}) and load power for the system equipped with FOPI, PI and PID controllers are shown in figure (8), (9), (10) and (11).

The performance of these controllers in maintaining the capacitor reference voltage in terms of settling time and peak overshoot is given in Table II.

The figure (8), (9), (10) and (11) along with the observations in Table II clearly shows that the PID controller performs better that the PI controller as it takes lesser time to attain the reference target and overshoot value is also very less. However, the least settling time and overshoot are obtain by using for FOPI controller.

IV. CONCLUSION

In this work, a grid-connected PV system is suggested. The P&O tracking method is a precise tracking method and can be used for MPP tracking with an efficiency of 98.94%. A comparative study in to the performances of the FOPI, and the conventional PI and PID controllers for controlling the inverter establishes the superior performance of the proposed FOPI controller in terms of both, the settling time and the peak overshoot that also reduces the distortion in the system. This work can further be expanded by including battery in the grid connected PV system. The future scope includes investigation into hardware implementation of the same.

REFERENCES

[1] Mozaffari Niapour SAKH, Danyali S, Sharifian MBB, Feyzi MR, "Brushless DC motor drives supplied by PV power system based on Z-source inverter and FL-IC MPPT controller," Energy Convers Manage, 2011;52:3043-59.

[2] Pietruszko SM, "Introduction of photovoltaic in Poland, "Proc. Of the 16th European photovoltaic conference and exhibition, Glasgow, London, 01-05.05.2000: James & James; p 2962-6.

[3] Taherbaneh Mohsen, Ghafooifard H, Rezaie AH, Rahimi K., "Evalution end-of-life power generation of a setelite solar array," Energy Manage, 2011; 52; pp. 2518-25.

[4] Kyoungsoo Ro, Saifur Rahman, "Two-loop controller for maximizing performance of a grid-connected photovoltaic-fuel cell hybrid power plant," IEEE Transaction on Energy Conversion, Vol. 13, No. 3, september 1998, pp. 0885-8969.

[5] S. Sopitpan, P. Changmuang, S. Panyakeow, "Monitoring and data analysis of a PV system Connected to a grid for home application," Solar Energy Material & Solar Cell 67, 2001, pp. 481-490.

[6] Wu T.F., Chang C.H., Chen Y.K., "Multi-function photovoltaic power supply system with grid-connection and power factor correction features," IEEE Annual Power Electronics Specialists Conference, vol. 3, 2000, pp. 1185-1190.

[7] Elhodeiby A.S., Metwally H.M.B., Farahat M.A., "Performance analysis of 3.6 kW rooftop grid-connected photovoltaic system in Egypt," International Conference on Energy System and Technologies (ICEST), 2011, Cairo, Egypt.

[8] Shiva Kumar B., Sudhakar K., "Performance evalution of 10 MW grid connected solar photovoltaic power plant in India," Energy Rep. J., 2015, 1, pp.184-192.

[9] Rameen AbdelHady, "Modeling and simulation of a micro grid-connected solar PV system," Water Science, 31, 2017, pp.1-10.

[10] Ahmet Aktas, Koray Erhan, Sule Ozdemir, Engin Ozdemir, "Dynamic energy management for ohotovoltaic power system including hybrid energy storage in smart grid applications," Energy, 162, 2018, pp.72-82.

[11] Chin V.J., Salam Z., Ishaque K., "Cell modelling and model parameters estimation techniques for photovoltaic simulator application: A review," Applied Energy, 2015, 154, pp.500-519.

[12] Aouchiche N., Aitcheikh M.S., Becherif M., Ebrahim M.A., "AI-based global MPPT for partial shaded grid connected PV plant via MFO approach," Solar Energy, 2018, 171, pp.593-603.

[13] Babaa S.E., Armstrong M., Pickert V., "Overview of maximum power point traking control methods for PV systems," Journal of Power and Energy Engineering, 2014, 2(08), p.59.

[14] Muhammad Kamran, Muhammad Mudassar, Muhammad Rayyan Fazal, Muhammad Usman Asghar, Muhammad Bilal, Rohail Asghar, "Implementation of improved Perturb & Observe MPPT technique with confined search space for standalone photovoltaic system," Journal of King Soud University – Engineering Sciences, 2018.

[15] Soualmia A., Chenni R., "A survey of maximum peak power tracking techniques used in photovoltaic power systems," Future Technologies Conference (FTC), 2016, pp.430-443.

[16] Atallah A.M., Abdelaziz A.Y., Jumaah R.S., "Implementation of perturb and observe MPPT of PV system with direct control method using buck and buck-boost converters," Emerging Trends in Electrical, Electronics & Instrumentation Engineering: An International Journal (EEIEJ), 2014, 1(1), pp.31-44.

[17] Schoeman J.J., Wyk J.D., "A simplified maximum power controller for terrestrial photovoltaic panel arrays," IEEE Power Electronics Specialists Conference, June 1982, pp.361-367.

[18] W.J. Praiselin, J Belwin Edward, "Voltage profile improvement of solar PV grid-connected inverter with micro grid operation using PI controller," Energy Procedia, 117, 2017, pp.104-111.

[19] M.A. Ebrahim, Adham Osama, Khaled Mahamed Kotb, Fahony Bendary, "Whale inspired algorithm based MPPT controllers for grid connected photovoltaic system," Energy Procedia, 162, 2019, pp77-86.

Proceedings of the Fourth International Conference on Communication and Electronics Systems (ICCES 2019)
IEEE Conference Record # 45898; IEEE Xplore ISBN: 978-1-7281-1261-9

Design of Low Power FinFET Based Adiabatic Logic Circuits in 18nm Technology

Apoorva Raghunandan
Department of Electronics and Communication Enginerring
RV College of Engineering
Bengaluru, India
apoorva.rsi@gmail.com

Shilpa D R
Department of Electronics and Communication Enginerring RV College of Engineering
Bengaluru, India
shilpadr@rvce.edu.in

***Abstract*—The emergence of Internet of Things (IoT), has increased the demand for design of energy-efficient and secure IoT devices. For example, IoT devices such as Wireless Sensor Nodes (WSN) and Radio Frequency Identification (RFID) tags employ AES cryptographic module which are susceptible to Differential Power Analysis (DPA) attacks. With the scaling of technology, leakage power in the cryptographic device increases, which increases their vulnerability to DPA attack. The FinFET based Adiabatic Logic Circuits are energy efficient and consume low power as compared to normal FinFET circuits. The proposed adiabatic logic is used to design logic gates such as buffers, XOR/XNOR, and AND/NAND circuits. The circuits have been designed using FinFET 18nm technology. The average power of the circuits has been computed and also the output Energy loss of the circuits has been calculated. For the Buffer the Average power consumption was found to be 4.331uW without adiabatic logic and 1.840uW with Adiabatic logic. The reduction of power is 57.51 %. For the AND/NAND circuit Average power consumption was found to be 4.479uW without Adiabatic logic and 2.356uW with Adiabatic logic. The reduction of power is 47.39 %. For the XOR/XNOR circuit Average power consumption was found to be 7.778uW without adiabatic logic and 4.428uW with Adiabatic logic. The reduction of power is 43.07 %.**

Keywords— Adiabatic Logic, FinFET, Low Power VLSI Design

I. INTRODUCTION

Adiabatic logic is a widely used method to design circuits that are energy-efficient and secure. It has been proved that adiabatic logic is one of the most the promising techniques when it comes to dealing with DPA attacks [6],[7],[8],[9]. Techniques such as Symmetric Pass Gate Adiabatic Logic (SPGAL) are used in the design of hardware that is secure and the same time consumes minimum power. These systems are most suitable to be implemented in IoT based devices [1]. When compared to the other widely used DPA resistant families of adiabatic logic, one of the drawbacks of SPGAL is its high leakage power at lower technology nodes. Therefore, with scaling the designer has to deal with the challenges of leakage current. The energy-efficiency of the computing circuits decreases with increase in leakage current. This in turn makes the device more vulnerable to DPA attacks. Low leakage devices such as FinFET can be used for the investigation of crypto circuits. In [1] the design of cryptographic processors, one of the main threats is the DPA attack. To determine the relationship between cipher texts and keys, S-Box is used in cryptographic algorithms like AES and DES [10]. However, due to its high-power consumption, S box is prone to DPA attacks. Due to its resistance against DPA attacks, an 8-bit S-Box circuit has been designed using Symmetric Pass Gate Adiabatic Logic (SPGAL). The verification of results has been performed through SPICE simulations in 180nm technology. As compared to and Secured Quasi-Adiabatic Logic (SQAL) and conventional CMOS, this circuit saves up to 67% and 92% energy. Wireless Sensor Network (WSN) and its sensing applications are of great importance in the present day [2]. With the internet of things, these sensors sense various parameters from the environment and share information across various platforms. Various key technologies and domains that motivate research in IoT have been thoroughly discussed. A cloud centric vision for world-wide implementation of IoT is presented in this paper. A cloud implementation using Aneka has been performed. This is based on the interaction of public and private clouds. There is an emphasis on the need for convergence of WSN, distributed computing and Internet. Paper [3] presents an overview of various radio frequency identification techniques. Traditional ID technologies and RFID techniques have been compared. Various applications of the same have been presented. Each of these applications have their own techniques of which some of them are tag energy supply, frequency range and tag writing capabilities. A circuit contains various components such as transistors and other components. Each of these consume an amount of power which contributes to the overall power consumption of the circuit. Information is leaked through power consumption. Secret keys can be extracted by analysis of side channels. Approaches to prevent DPA attacks and cryptosystems that are secure even when implemented in hardware that leaks have been presented [4]. To reduce power consumption from many charge recovery logic families have been designed. This paper presents a new charge recovery logic style for resistance against side-channel attacks (SDA), especially against DPA attacks. This logic style proves to have better in DPA-resistance level and lower power consumption compared to existing DPA styles proposed this far [5]. Mechanisms such as usage of DC bias instead of ground in the source of NMOS transistors and Pass transistors to discharge the internal parasitic capacitances of function blocks have been proposed to reduce the data dependent power consumption. These methods decrease the dynamic power consumption. This method is more DPA resistant than other proposed styles such as TDPL and SALB. There is also reduced power consumption From the Literature Survey it is observed that most of the Hybrid Full Adder designs employ CMOS Technology. FINFET is known for its high speed of operation. Hence an implementation

of Hybrid Adder using FINFET would further reduce the Delay of circuits [11].

II. Basic of FinFET Based Adiabatic Logic

Adiabatic logic is an efficient method to recycle the charge stored in the load capacitor using power clocks. The main advantage of this method is the reduced dynamic switching energy loss due to charge recycling. The adiabatic charging/discharging of the load capacitors is shown in Fig. 1.

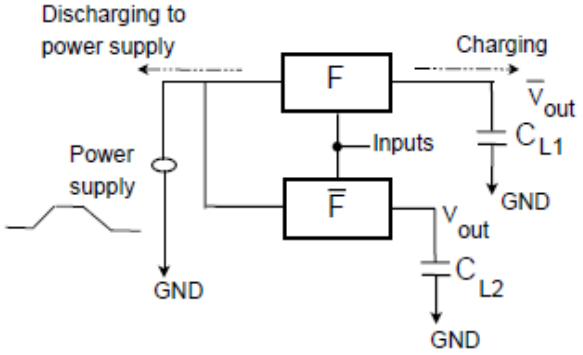

Fig. 1. Adiabatic charging/discharging [1]

Considering that a constant current source is supplying the charge, the energy dissipated in an adiabatic circuit is given by

$$E_{diss} = \frac{RC}{T} CV_{DD}^2 \quad (1)$$

In equation 1, the load capacitor is denoted by C. Vdd is the full swing of the power clock. The charging and discharging time of the capacitor is given by T, Vdd was the full swing of the power clock. Energy dissipation in adiabatic circuits is lesser than, conventional CMOS. As T approaches infinity, energy dissipation tends to zero.

FinFET Device

The FinFET has the gate wrapping the channel in all the three directions. The silicon body is perpendicular to the plane of the wafer. The strudture of the FinFET device is shown in Fig. 2.

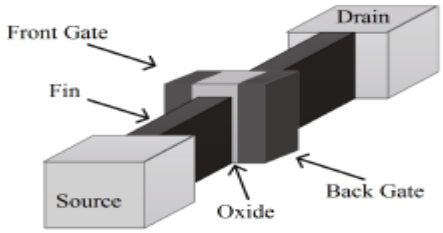

Fig. 2. FinFET Device structure [1]

The main advantage of FinFETs is the effective gate control over the channel. This reduces the threshold current, gate dielectric leakage currents and the short-channel effects than MOSFETs. Higher on state current,lower leakage and faster switching are the advantages obtained from the same. FinFET has different working modes due to its multigate structure. The FinFET has two main working modes. The Independent-Gate (IG) mode and the Shorted-Gate (SG) mode. The two gates are tied together in the Shorted gate mode and the device acts as a three terminal device in SG mode.

III. Implementation of FinFET Based Adiabatic Logic Circuits And Results

The Schematics of FinSAL Buffer, FinSAL AND/NAND gate and FinSAL XOR/XNOR gate were designed using Cadence Virtuoso Tool. The test benches were created, and the working of the Adder was verified through simulations. FINFET 18nm technology was used in the design. The Transient Analysis was performed, and the energy consumption of the circuits was calculated. The Basic Methodology is shown in Fig. 3.

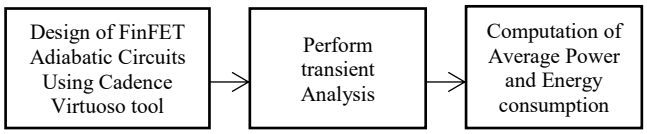

Fig. 3. Basic Overview of Implementation

Table I shows the Basic Overview of Implementation.

TABLE I Different Energy Sources and Their Objectives

Tool Used	**Technology**	**Parameters computed**
Cadence Virtuoso	FinFET 18nm	Energy Average Power

A. Design of Buffer

The Schematic of the buffer with FinFETs in the IG (Independent Gate) mode has been designed as follows. The 18nm technology FINFETs has been used. The n1lvt and p1lvt transistors have been used. The Schematic has been designed in Cadence Virtuoso using FINFETS. Fig. 4 shows the schematic of the buffer. When A is high, capacitor C_L charges and out is pulled up to VDD, while A- bar and out-bar is low.

a. Design of a buffer without Adiabatic Logic

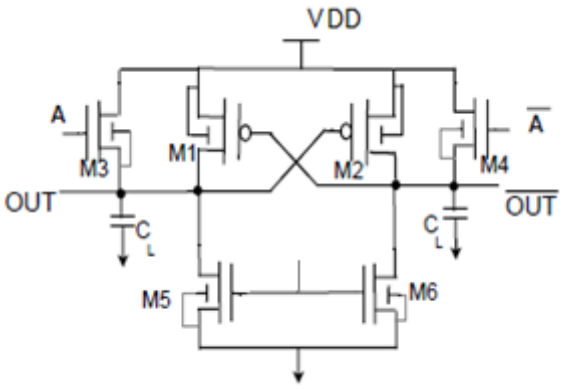

Fig 4. The Schematic of FinFET Buffer

TABLE II SPECIFICATIONS FOR PERFORMING SIMULATION

Library	Model name	Pin Name	Specification
cds_ff_mpt	p1lvt n1lvt	A, Ab	L = 18nm VDD = 1V
analogLib	vdd	Not applicable	1V
	vdc	Not applicable	1V
	gnd	Not applicable	-
	vpulse	Clk	Period = 80ns, Pulse width = 40ns DC Voltage = 1V
	vpulse	A	Period = 80ns, Pulse width = 20ns DC Voltage = 1V

Table II lists the specifications for performing simulation. It contains details about the libraries that are used, the input pins, the model names and the specifications. The average power of the design is computed by performing transient Analysis. The transient analysis waveforms of the buffer is shown in Fig 5.

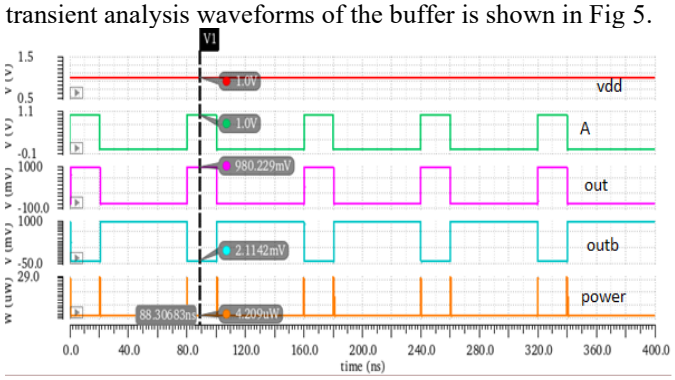

Fig. 5. Waveforms of FinFET Buffer

The maximum output voltage is found to be 980.23mV. The average power consumed by the circuit is 4.331 uW.

b. Design of FinFET Buffer with Adiabatic Logic

The Schematic of the FinFET buffer with Adiabatic logic has been designed as follows. The 18nm technology FINFETs have been used. The n1lvt and p1lvt FINFET transistors have been used. The Schematic has been designed in Cadence Virtuoso using FINFETS. Fig. 6 shows the schematic of the buffer. As compared to the previous design a Vclk pulse is applied as as the supply.

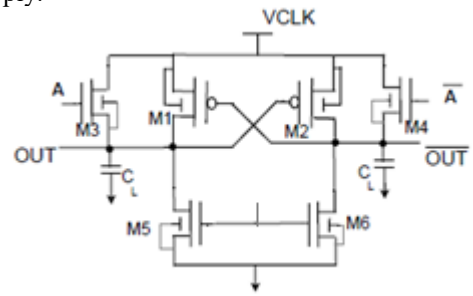

Fig 6. The Schematic of FinFET Buffer with Adiabatic Logic

The specifications for performing synthesis have been shown in Table III.

TABLE III SPECIFICATIONS FOR PERFORMING TRANSIENT ANALYSIS

Analysis	Specification
Transient	Analysis: tran Stop time: 400ns Accuracy defaults: conservative

The transient Analysis was performed, and the working of the Buffer was verified. The stop time was taken to be 400ns. Accuracy defaults were set to conservative.

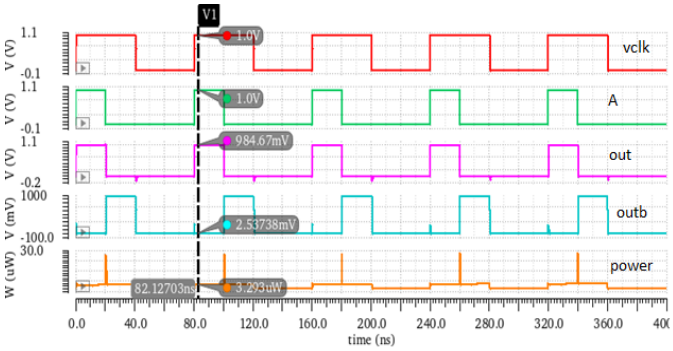

Fig.7. Waveforms of transient Analysis of FinFET Buffer with Adiabatic Logic

Fig. 7 shows the transient analysis waveforms of the FinFET Buffer with Adiabatic logic. The maximum output voltage is found to be 984.66 mV. Average power consumption of the circuit is computed to be 1.84 uW.

B. Design of AND/NAND Gate

The Schematic of the FinSAL AND/NAND gate has been designed as follows. The 18nm technologies FINFETs have been used. The n1lvt and p1lvt FINFET transistors have been used. The Schematic has been designed in Cadence Virtuoso using FINFETS. The specifications remain the same as for the buffer however the period and pulse widths have been changed.

a. Design of FinFET AND/NAND Gate without Adiabatic Logic

Fig 8 shows the schematic of the FinFET AND/NAND

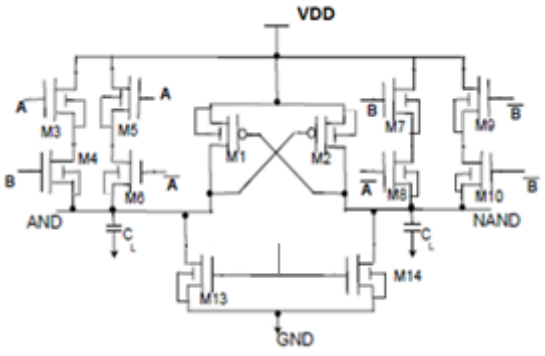

Fig. 8. The Schematic of FinFET AND/NAND Gate

The waveforms of FinFET AND/NAND circuit without Adiabatic Logic is shown in Fig 9. The maximum output voltage is found to be 980.193mV. The Average Power consumption is found to be 4.479uW.

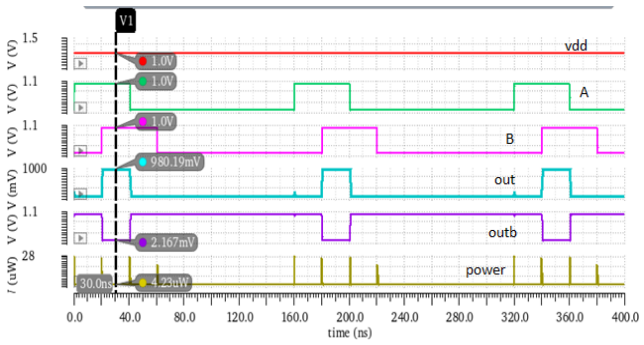

Fig. 9. Waveforms of FinFET AND/NAND circuit without Adiabatic Logic

b. Design of FinFET AND/NAND Gate with Adiabatic Logic

The Schematic of FinFET AND/NAND circuit with Adiabatic Logic is shown in Fig. 10.

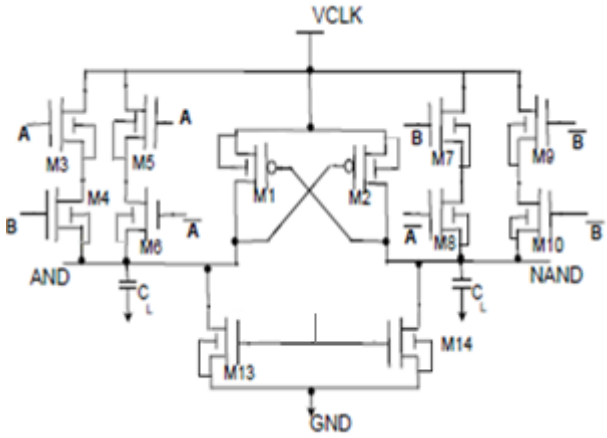

Fig. 10. The Schematic of FinFET AND/NAND Logic

The waveforms of FinFET AND/NAND circuit with Adiabatic Logic is shown in Fig. 11.

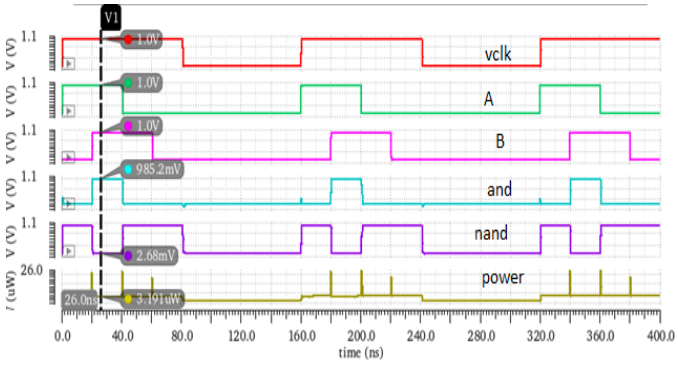

Fig.11. Waveforms of FinFET AND/NAND Logic with Adiabatic Logic

The maximum output voltage is 985.22mV and the Average Power which is computed to be 2.356uW.

C. Design of XOR/XNOR Gate

The Schematic of the FinFET XOR/XNOR gate has been designed as follows. The 18nm technologies FINFETs have been used. The n1lvt and p1lvt FINFET transistors have been used. The Schematic has been designed in Cadence Virtuoso using FINFETS.

a. *Design of FinFET XOR/XNOR Gate without Adiabatic Logic*

Fig. 12 shows the schematic of the XOR/XNOR gate without Adiabatic Logic.

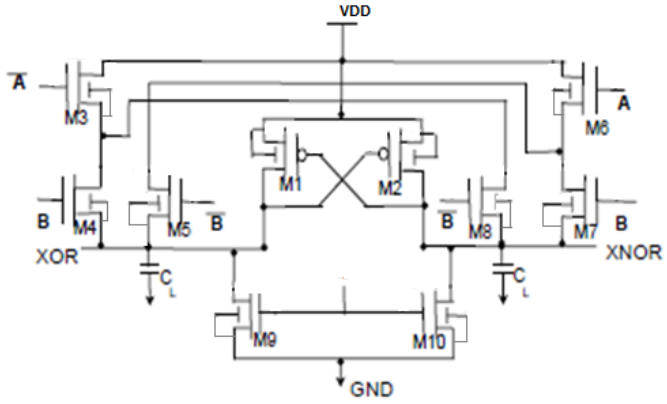

Fig 12. Schematic of FinFET XOR/XNOR Logic without Adiabatic Logic

The Waveforms of FinFET XOR/XNOR Logic without Adiabatic Logic is shown in Fig. 13. The maximum output voltage is 955.36mV. The Average Power consumption is 7.778uW.

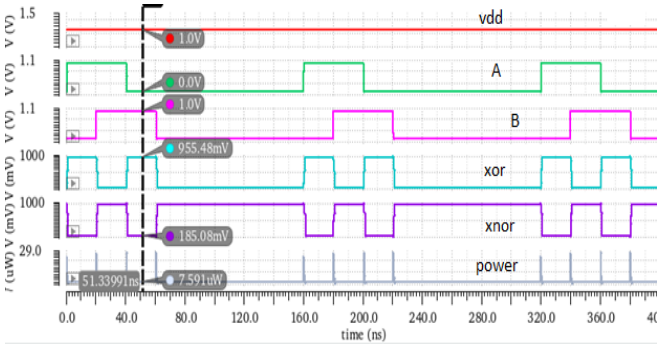

Fig. 13. Waveforms of FinFET XOR/XNOR Logic without Adiabatic Logic

b. *XOR/XNOR Circuit with Adiabatic Logic.*

Fig. 14. shows the schematic of the XOR/XNOR Circuit with Adiabatic Logic.

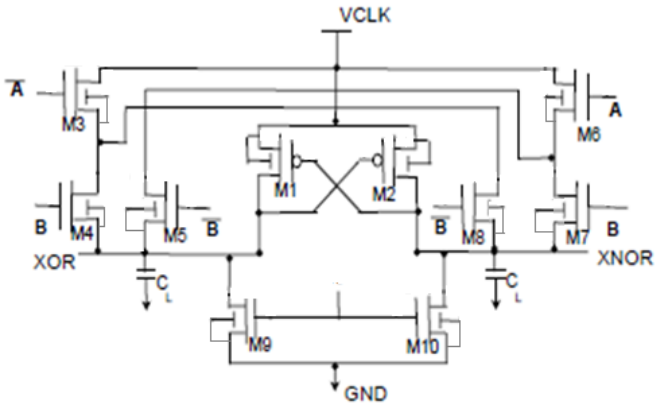

Fig. 14. The Schematic of FinSAL XOR/XNOR with Adiabatic Logic

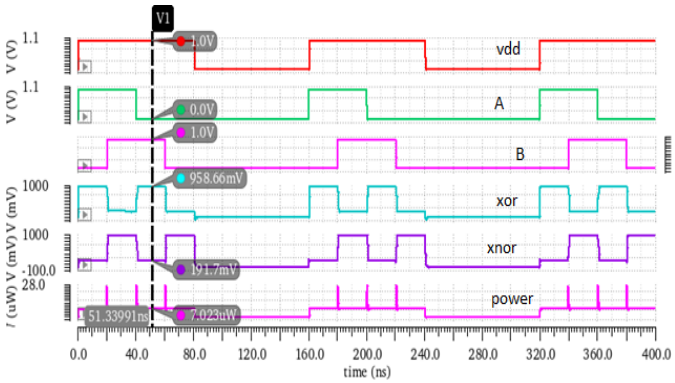

Fig. 15. Waveforms of FinFET XOR/XNOR with Adiabatic Logic

The Waveforms of FinFET XOR/XNOR Logic with Adiabatic Logic is shown in Fig. 15. The maximum output voltage is 958.662mV. The Average Power consumption is 4.428uW.

.

IV. Conclusion

Three circuits were designed using FinFETs – Buffer, AND/NAND circuit and XOR/XNOR circuit. They were designed using FinFET 18nm technology. The Average power and Energy of the three circuits was computed. For the Buffer the Average power consumption was found to be 4.331uW without adiabatic logic and 1.840uW with Adiabatic logic. The reduction of power is 57.51 %. For the AND/NAND circuit Average power consumption was found to be 4.479uW without Adiabatic logic and 2.356uW with Adiabatic logic. The reduction of power is 47.39 %. For the XOR/XNOR circuit Average power consumption was found to be 7.778uW without adiabatic logic and 4.428uW with Adiabatic logic. The reduction of power is 43.07 %.

For the Buffer the Maximum output voltage is 980.23mV without adiabatic logic and 984.66mV with adiabatic logic. The energy of the output signal is is 0.4804 pJ without adiabatic logic and 0.4808 pJ with adiabatic logic. The energy loss is reduced from 3.92 % to 3.84 %. For the AND/NAND circuit the Maximum output voltage is 980.193mV without adiabatic logic and 985.22mV with adiabatic logic. The energy consumption is 0.4803 pJ without adiabatic logic and 0.4853 pJ with adiabatic logic. The energy loss is reduced from 3.94 % to 2.94 %. For the XOR/XNOR circuit, the Maximum output voltage is 955.36mV without adiabatic logic and 958.662mV with adiabatic logic. The energy consumption is 0.4563 pJ without adiabatic logic and 0.4595 pJ with adiabatic logic. The energy loss is reduced from 8.74 % to 8.10 %.

.

References

[1] S. D. Kumar, H. Thapliyal, A. Mohammad, V. Singh, and S. K. Perumalla, “Energy-efficient and secure s-box circuit using symmetric pass gate adiabatic logic,” in Proceedings of the IEEE computer society Annual Symposium on VLSI (ISVLSI). IEEE, 2016.

[2] S. D. Kumar, H. Thapliyal, and A. Mohammad, “Finsal: A novel finfet based secure adiabatic logic for energy-efficient and dpa resistant iot devices,” in IEEE International Conference on Rebooting Computing. IEEE, 2016.

[3] J. Gubbi, R. Buyya, S. Marusic, and M. Palaniswami, “Internet of things (iot): A vision, architectural elements, and future directions,” Future Generation Computer Systems, vol. 29, no. 7, pp. 1645–1660, 2013.

[4] E. Ilie-Zudor, Z. Kem´eny, F. van Blommestein, L. Monostori, and A. van der Meulen, “A survey of applications and requirements of unique identification systems and rfid techniques,” Computers in Industry, vol. 62, no. 3, pp. 227–252, 2011.

[5] S. D. Kumar and H. Thapliyal, “Qualpuf: A novel quasi-adiabatic logic based physical unclonable function,” in Proceedings of the 11th Annual Cyber and Information Security Research Conference. ACM, 2016, p. 24.

[6] W. Cheng, S. Wang, and X. Cheng, “Virtual track: applications and challenges of the rfid system on roads,” IEEE Network, vol. 28, no. 1, pp. 42–47, 2014.

[7] D. Bandyopadhyay and J. Sen, “Internet of things: Applications and challenges in technology and standardization,” Wireless Personal Communications, vol. 58, no. 1, pp. 49–69, 2011.

[8] P. Kocher, J. Jaffe, B. Jun, and P. Rohatgi, “Introduction to differential power analysis,” Journal of Cryptographic Engineering, vol. 1, no. 1, pp. 5–27, 2011.

[9] W. C. Athas, L. J. Svensson, J. G. Koller, N. Tzartzanis and E. Ying-Chin Chou, "Low-power digital systems based on adiabatic-switching principles," in *IEEE Transactions on Very Large Scale Integration (VLSI) Systems*, vol. 2, no. 4, pp. 398-407, Dec. 1994.

[10] M. Alioto, S. Bongiovanni, M. Djukanovic, G. Scotti, A. Trifiletti, "Effectiveness of leakage power analysis attacks on dpa-resistant logic styles under process variations", *Circuits and Systems I: Regular Papers IEEE Transactions on*, vol. 61, no. 2, pp. 429-442, 2014.

[11] D. Hisamoto, W.-C. Lee, J. Kedzierski, H. Takeuchi, K. Asano, C. Kuo, E. Anderson, T.-J. King, J. Bokor, C. Hu, "Finfet-a self-aligned double-gate mosfet scalable to 20 nm", *Electron Devices IEEE Transactions on*, vol. 47, no. 12, pp. 2320-2325, 2000.

[12] L. Joonho, K. Dong-Gyu, C. Soo-Ik, "Reversible energy recovery logic circuits and its 8-phase clocked power generator for ultra-low-power applications", *IEICE transactions on electronics*, vol. 82, no. 4, pp. 646-653, 1999.

Proceedings of the Fourth International Conference on Communication and Electronics Systems (ICCES 2019)
IEEE Conference Record # 45898; IEEE Xplore ISBN: 978-1-7281-1261-9

A Compact Four Port UWB-MIMO Antenna With Notch Band Characteristics And High Isolation

Preeti Pannu, Research Scholar, Devendra Kumar Sharma, Professor & Dean,
Department of Electronics and Communication Engineering,
SRM Institute of Science & Technology, Delhi-NCR Campus, India
Email: preetipannu7@gmail.com, d_k_s1970@yahoo.co.in

***Abstract*—A simple four port antenna with Ultra-wide band (UWB) and multiple- input multiple-output(MIMO) behavior is proposed using two shared radiators. the two shared radiators are making 180^0 angle to each other. The problem of interference in broad-band of UWB from other sources is avoided by forming notch band at 5.5GHz center frequency. The proposed design is of size 48X48mm^2 using FR4 Substrate (dielectric constant 4.4) and fed by micro strip line. The two shared radiator multiple-input multiple-output antenna provides a bandwidth of 2.9 to 11.4 GHz with reflection coefficients S_{11}, S_{22}, S_{33}, S_{44} very less than -10dB and all the mutual coupling coefficients for respective antenna elements are less than or equal to -22 dB. The design also provides triple frequency bands characteristics with wide band behavior. Also, In order to achieve low mutual coupling, the meandered line stub is utilized at the end of the ground plane. The stimulated outcomes of proposed design are shown.**

Keywords—UWB, notch, MIMO

I. INTRODUCTION

UWB antennas has many Characteristics like extremely low transmission energy(less than 1mV), FCC given license of very high bandwidth but with short range, Extremely difficult to intercept, Low cost, use for multiple frequency ranges(3.1GHz to 10.6GHz)- satellite communication, tracking a radar, Mobile devices, sensor, GPS and Bluetooth are narrowband technologies(1.6 and 2.4 GHz respectively). To increase the transmission capacity, we need to reduce the multipath fading. Basically, combination of UWB and MIMO Technology solve the issue of fadedness of signals. In portable MIMO devices, close packing of several antennas degrade diversity performance by introducing mutual coupling between antenna elements. The first major challenge now-a-days is need of small UWB MIMO antenna with minimum coupling for smart and small Electronic devices such as WLAN and UMTS. The UWB MIMO antenna design also affected due to interference from other communication systems radiating at same frequency. The solution for this interference is creation of notch band at that particular frequency. The second major challenge is design of notched compact UWB MIMO antenna. Basically, the main idea from above discussion is to make a small UWB MIMO antenna having stop band behavior as well as low mutual coupling so that channel capacity can be maximize and minimize the cause of interference from other bands.

In Literature, Micro strip antennas accomplished various shapes such as square, rectangular, circular and octagonal proposed for obtaining Ultra-wide band [1-4]. The methods that are study in literature to design UWB MIMO antennas with minimum coupling are defected ground structures, rectangular stubs and tree like structures. T-shaped stub extruded in rectangular ground plane for decoupling in eye shaped UWB MIMO antenna and two antenna elements are orthogonal[3]. In this, concept of orthogonal placement of antenna elements used that provide low coupling between elements. By increasing branches of tree like structure, high isolation is achieved [5]. Fork shaped slot is placed between the antenna elements to enhance isolation and L-shaped slot cut from radiators to create notch band[6]. A shared radiator utilizing meandered line stub with ground plane[7]. T-shaped slot in pentagonal radiator with extending branch of ground plane for improving isolation has been discussed[8]. Method of Double layer slit-patch EBG structure between radiators for low coupling enhance the size of antenna[9]. Dual band MIMO antenna consist of shorted metal strips with ground plane for mutual coupling reduction and "L" slot in radiating patch for dual band[10]. The literature also provide designing methods of UWB antennas with notch band and low mutual coupling like Tapered Micro strip fed compact MIMO UWB antenna consist of two notches using two L shaped slits in patch and T shaped stubs for low coupling[11]. Orthogonally fed slot antennas for UWB systems utilizing uniplanar nature of coplanar waveguide using a diagonal strip on ground plane for maintaining isolation and arc shaped slot resonators in feed structure to reject the desired band[12]. A printed folded monopole UWB antenna uses an open stub to reject the desired WLAN band that interferes with the UWB band[13]. In Literature, two modified coplanar waveguides along with staircase-shaped radiating patches for orthogonal radiation patterns, with a rectangle stub placed at an angle between the feed to get low coupling in entire UWB and by using two split-ring shaped slots over the antenna elements respectively, the stop-band property is achieved[14]. A two CPW-fed floral radiating elements provides ultra wide band along with a decoupling structure to ensure high isolation and the stop-band at the WLAN frequency is obtained through single U-shaped slot on each antenna element [15]. Shared radiator symmetrically shared by two tapered micro strip feed lines placed at an angle of 135° from *X*-axis makes an UWB system and the utilization of meandered line stub with modified ground structure provides maximum amount of isolation between the antenna ports[16]. Many 2x2 port UWB diversity antennas reported in literature[11-16] lack in enhancing the communication channel quality. Therefore, many MIMO UWB antennas are proposed with more than 2-ports recently

[17-22] (consider Table1). Three port antenna design consists of staircase-shaped radiating elements constituting UWB band and also the antennas give stable gain, directional radiation patterns and favorable radiation efficiencies[17]. A four port CPW fed UWB MIMO system with high isolation and stop band behavior[18]. The design of antennas with high radiation efficiencies for UWB signaling and for development of UWB impulse radio communication systems is a most difficult task, especially when these signals and systems exist with previously standardized narrowband services. So, to avoid this problem, an antenna design with quad-element and dual stop-band is communicated in literature[19]. In MIMO UWB Technology, it has been seen that placement of disposed antenna elements orthogonally is the most familiar methodology to maximize isolation of MIMO antenna elements[20]. The orthogonal arrangement of antennas helps to accomplish polarization diversity performance where isolation factor is mainly affected by spacing of individual elements. Also, miniaturization is achieved in UWB MIMO antenna by utilizing the benefit of symmetry property of planar antennas[20]. A design with four circular patches, defected ground structure(DGS) and a mushroom-like electromagnetic band gap structure uses metallic vias method reported in [21]. In this, four ring-shaped slots on the radiators are etched to get stop band behavior[21]. The antenna structure with four triangular monopoles connected symmetrically and orthogonally improves the diversity performance, and by combining a rectangular ring with a straight line further reduces the coupling due to interoperation of the elements[22]. An Koch Fractral geometry is used for UWB performance with C-shaped slot for band rejection and rectangular stub attached to ground plane for mutual coupling reduction [23]. However, many MIMO antennas has been proposed with and without notch bands, and mostly with two ports but they have relatively big size, weak MIMO performance and high coupling in whole band of UWB in comparison with the proposed structure. Many nonconventional shape antenna design that provide compactness are often optimized using different optimization techniques such as genetic algorithm, particle swarm optimization, etc. These antennas offer better impedance matching over wide frequency band. In this communication, a miniaturized MIMO antenna with simple geometry, ultra-wide band and high isolation is proposed. Two shared radiator with two port each designed on 48X48 mm^2. The substrate used for design is FR4_epoxy with 1.6 thickness and relative permittivity of 4.4. The shape of the shared radiator is hexagonal and is fed by perpendicular micro strip line structures of width 1.5mm and height 23.65mm. Each feed line structure consist of two feeds of same width 1.5mm but feed 1 has length 9.9mm and feed 2 has length 13.75mm. feed 1 and feed 2 are orthogonal to each other. The isolation in shared elements is obtained by extending the branch of the ground plane in the symmetry axis of two antenna elements. To get stop band at 5.5GHz, the presented antenna has a slot with inverted L-shaped geometry in Ground plane near feed line of patch. The dimensions of the slot is optimized using Genetic optimization alogorithm in order to achieve sharp notch. This simulated design has ultra-wide impedance bandwidth, the gain is moderate and radiation pattern is omni-directional. The compact size antenna designed due to shared radiator and has stop band at 5GHz to 6.2 GHz. A comparison of other reported UWB MIMO antenna with proposed simulated antenna design is presented in Table 1.

This article is planned as follows: In Section II, Layout for proposed system is discussed with simulation results followed by stop band behavior of MIMO. Experimental results are presented in Section III including isolation, radiation characteristics, and MIMO parameters. Finally, Section IV concludes the Article.

TABLE 1. COMPARISON OF PROPOSED LAYOUT OF UWB MIMO WITH OTHER REPORTED

Reference	Size(WxL geometry) (in mm^2)	Number of Elements	Operating band(in GHz)	Isolation (in dB)	Peak Gain (in dBi)	Notch band (in GHz)
3	18x36	2	2.8-20	≥20	-	-
11	18x34	2	2.9-20	≥20	7	5.1-5.8, 6.7-7.1
12	50x50	2	2.76-10.75	≥15	‹2.8	4.75-6.12
13	55x13.5	2	1.85-11.9	≥17.2	5	5.15-5.85
14	48x48	2	2.5-12	≥15	6	5.1-5.8
15	50x45	2	2.7-10.9	≥15	4	5.1-5.9
16	39x39	2	2.4-12.75	≥15	-	-
17	45x25	3	3.1-11.5	≥19	5.5	-
18	81x87	4	.76-12.75	≥20	4-8.8	3.87-5.94, 7.04-8.7
19	100X100	4	-	≥20	-	3.5, 5.5
20	70x70	4	2.4-14	≥20	-	-
21	60x60	4	3-16.2	≥17.5	-	4-5.2
22	75.19x75.19	4	3.1-17.3	≥20	1-5	-
23	45x45	4	2-10.6	≥17	-	5.1-6
Proposed	48x48	4	2.9-11.4	≥22.5	-	5-6.3

II. ANTENNA LAYOUT

The planned layout is demonstrated in figure 1, has two identical shared patches 180^0 apart with common modified ground structure as represented in figure 2. Two regular

shared Hexagonal radiators are fed by 50Ω Micro strip lines of size (L_F x W_F) where L_F= L_{F1}+L_{F2}. The proposed antenna design has total area of 48x48 mm^2 (i.e. denoted as L_G x W_G) and has printed on low loss FR4 substrate with 4.4 relative permittivity, .02 loss tangent and 1.6mm thickness. The overall MIMO antenna volume is reduced by layout of two shared radiators. One of the major issue in UWB MIMO antenna design is to get resonance at lower cut off frequency i.e. 3.1 GHz and keeping compactness of the layout with it. This can be obtained by increasing current path in radiator so we take hexagonal shared radiator.

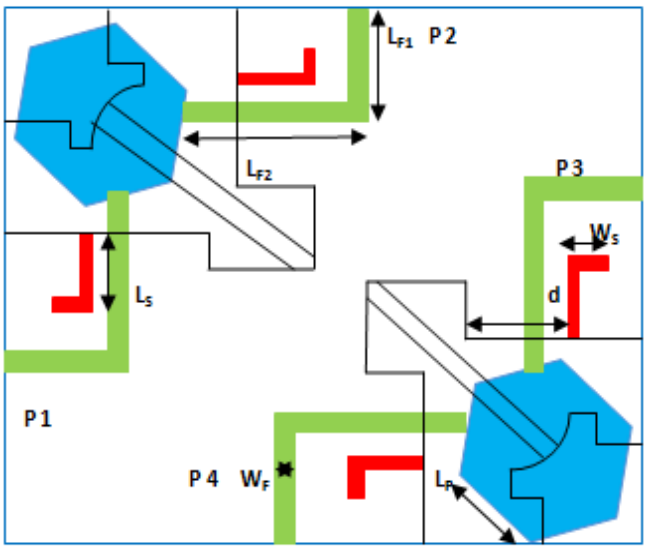

Figure 1: Proposed Geometry

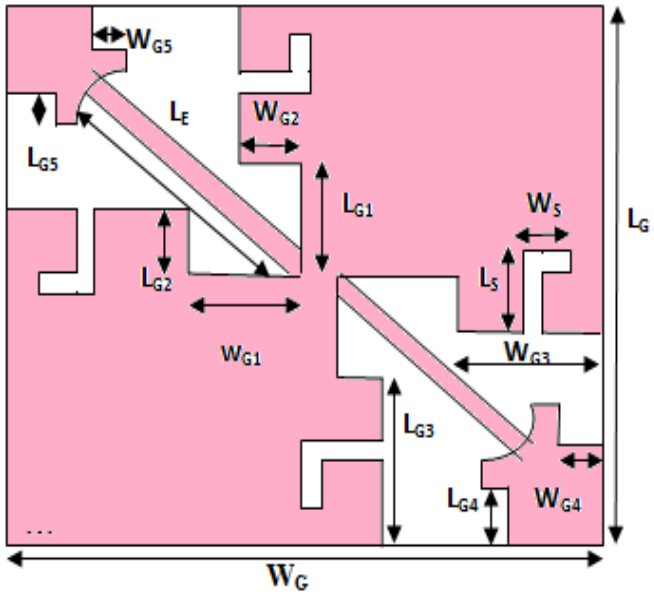

Figure 2: Geometry Of Ground Plane

This design provides wide band of 2.9-11.4 GHz with triple band characteristics and also maintain compactness of the design. In Portable devices, high level of coupling occurs if we utilize multiple radiators that degrades diversity performance. Another major issue is to reduce this coupling between the ports and maintain the compactness of the antenna. In literature, decoupling structure (occupies larger space) is the approach carried out to maximize isolation. The issue of high coupling between ports is minimize by utilizing concept of increasing the distance between respective ports. So, to obtain high isolation between four ports of respective shared radiators , two simple metal branches of length L_E that act as respective reflectors are extended on ground plane on both sides of radiators. These metal branches can also decrease the current on the ground structure flowing between two elements of respective radiators. Further improvement in isolation can be obtained by increasing effective length of the ground. This is accomplished by creating slot in the ground plane. Band stop characteristics in WLAN band also achieve in this design. A inverted L-shaped slot (L_S x W_S) is cut from ground plane near each feed line to create stop band in the region 5.1 - 6 GHz. L-shaped geometry is chosen because of its broad band rejection characteristics. Designing and Optimization process is done by High Frequency Structure Simulator(HFSS). The optimized parameters are given in Table 2.

TABLE 2. PARAMETERS VAUES USED FOR PROPOSED ANTENNA

Parameter	Value(in mm)	Parameter	Value(in mm)
L_G	48	L_{G5}	6.48
W_G	48	W_{G5}	6.7
L_{G1}	9.5	L_S	2.5
W_{G1}	9.5	W_S	5
L_{G2}	5.5	L_E	17.8
W_{G2}	5.5	L_{F1}	9.9
L_{G3}	14	L_{F2}	13.75
W_{G3}	14	W_F	1.5
L_{G4}	6	L_P	8.48
W_{G4}	6	d	7.1

III. OUTCOMES AND DISCUSSION

A. Outcomes

Figure 3 represents the return loss characteristics (S11 and S22 in XY Plot 1, S33 and S44 in XY Plot 2) of the 4-port UWB MIMO proposed design. All reflection coefficients S11, S22, S33 and S44 are < -10dB for entire ultra-wide band (2.9 GHz to 11.4 GHz). These reflection coefficients show triple band characteristics. In XY plot 1, S11 parameter show maximum return loss of -20dB, -25dB and -24dB at 4.1GHz, 7.5GHz and 8.8GHz respectively whereas, S22 has maximum return loss of -27dB, -38dB and -24dB at the respective frequencies. In XY plot 2, return loss(S33) of -28dB, -36dB and -24dB observed at 4.1GHz, 7.5GHz and 8.8GHz respectively whereas, S44 drops to -20dB, -24dB and -23.5dB at these frequencies respectively. It is also shown that, the simulated resonant frequency is given by 7.5 GHz. The existence of L-slot in ground is responsible for notch at frequency of 5.5 GHz. The various mutual coupling parameters S12,S13 and S14 are shown in Figure 4. They all are almost less than -22dB. This shows that the presence of meandered line stub in ground plane avoids the interference between shared patches.

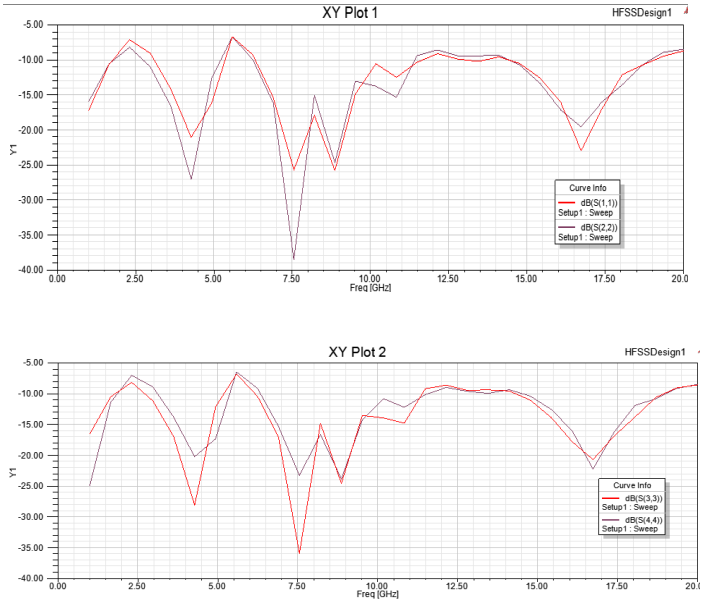

Figure 3: Simulated Results For Return Loss

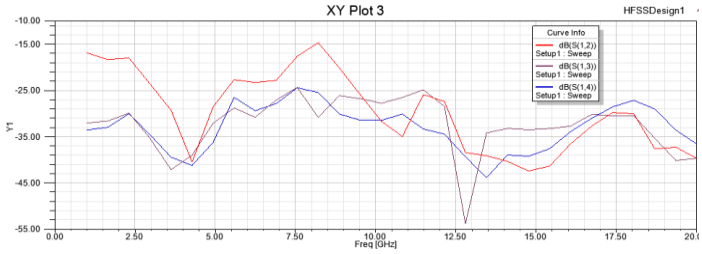

Figure 4: Simulated Results For Isolation Of UWB MIMO Design

B. Stop band behavior

The proposed antenna has simple ground plane represented as Antenna I of Figure 5. This ground plane design show low mutual coupling between shared radiators.

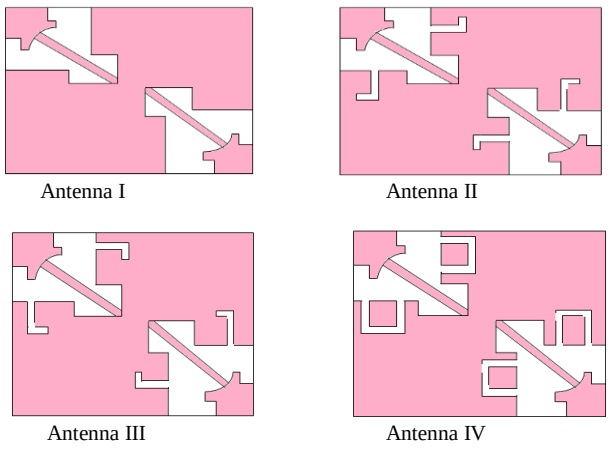

Figure 5. Evolution Of Ground Plane

In order to get rid of interference from other bands, various techniques are displayed in Figure 5 (Antenna II, Antenna III and Antenna IV) to create notch band keeping mutual coupling as low as in Antenna I. Through the comparison in Figure 6, we observed that notch band at 5.5GHz is created using inverted L shaped slot of .7mm thickness with parameter d=7.1mm, using L shaped slots of .7mm thickness at 4.9 GHz(notch center frequency created) keeping distance d= 10.8mm, L_S= 4mm, W_s = 3.1mm and U- shaped slot also create notch at 5.5GHz with distance d=6.2mm, L_S= 4mm, W_s = 3.1mm. The best suitable geometry for notch creation is Antenna II with lower cut off frequency 2.9GHz because in case of Antenna III and Antenna IV, it is difficult to maintain lower cut off frequency that is 3.1GHz as per FCC. The lower cut off frequency in later two cases is 3.2GHz because of different surface current distribution due to different geometry of slots created in ground plane. The upper cut off frequency for Antenna I is 11.4 GHz and in later cases, it is 11.5GHz. So, we concluded that Return loss graph shifted slightly towards right due to either L pattern or U pattern slot in ground.

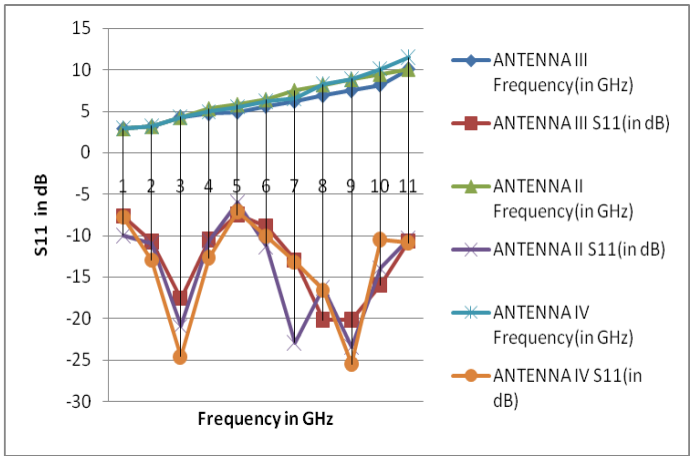

Figure 6. Comparison Of Return Loss For Different Notch Techniques

The comparison of Mutual coupling is shown in Figure4 and it is obtained almost less than -22dB. This shows that the presence of meandered line stub in ground plane avoids the interference between shared patches.

IV. CONCLUSION

A novel micro strip line fed 4X4 UWB-MIMO Layout contain a shared patch and modified ground is communicated. The Layout of antenna has very small size of 48 × 48 mm^2 that makes it best solution for portable devices. By cutting an inverted L-shaped slot in the ground plane, stop band from 5.1 GHz to 6 GHz is created. The meandered line extension in ground plane also has a great impact on the −10 dB bandwidth for entire UWB and on the isolation factor. The simulated results displays consistency where the working bandwidth of the MIMO antenna is from 2.9-11.4 GHz with coupling as low as -22 dB.

References

[1] Preeti Pannu, " A Small Square Monopole Ultra- Wide Band antenna with Band Stop Behavior, " International Journal of Engineering and Technology, vol. 7, no. 3.12, pp. 697-700, 2018.

[2] R. Azim, M. T. Islam and N. Misran, " Compact Tapered shape slot antenna for UWB Applications." IEEE Antenna Wireless Propag. Lett.,vol. 10, pp. 1190-1193.

[3] Richa chandel, Anil kumar“ Design and Packing of an eye-shaped Multiple-Input Multiple-Output antenna with high isolation for wireless UWB applications," IEEE Transaction on Components, packing and Manufacturing Technology, vol. 8, no. 4, April 2018.

[4] A. K Gautam, R. Chandel and B.K. Knaujia," A CPW-fed hexagonal shape monopole like UWB antenna," Microw. Opt. Technol. Lett., vol. 55, no. 11, pp. 2582- 2587, Nov , 2013.

[5] S. Zhang, Z. Ying and S. He, "Ultrawideband MIMO/Diversity antennas with a tree like structure to enhance wideband isolation," IEEE Antenna Wireless Propag. Lett, vol.8, pp. 1279-1282, 2009.

[6] Jun Tao, Quan yuan Feng “Compact isolation-enhanced UWB MIMO antenna with band notch character,” Journal of Electromagnetics waves and Applications., vol. 30, no. 16, pp. 2206-2214, June 2016.

[7] Situ Rani Patre, Surya P. Singh“ Shared radiator MIMO antenna for broadband applications,” IET Microwaves, Antennas & Propagation,vol. 12, no. 7, pp. 1153-1159, Jan 2018.

[8] Chun-Xu Mao, Qing -Xin Chu“ Compact Co-Radiator UWB-MIMO Antenna with Dual Polarization,” IEEE Trans. Antennas Propag., vol. 62, no.9, pp. 4474-4480, September 2014.

[9] Li Q, FeresidisAP, Mavridou M and Hall PS “Miiniturized double layer EBG structures for broadband mutual coupling reduction between UWB Monopoles," IEEE Trans. Antennas Propag., vol. 63, pp. 1168-1171, 2015.

[10] Abdelhaq Boukarkar, Xian Qi Lin“ A miniaturized Extremely Close-Spaced Four-Element Dual-Band MIMO ntenna System with Polarization and Pattern Diversity,"IEEE Antennas and Wireless Propagation Letters, vol. 17, no. 1, January 2018.

[11] Richa chandel, Anil kumar “ Tapered Fed Compact UWB MIMO-Diversity Antenna with Dual Band-Notched Characteristics, ” IEEE Trans. Antennas and Propag, vol. 66, no. 4, pp. 1677-1684, Feb 2018.

[12] Bybi P.C., Augustin G., Tayeb A.D., “Uniplanar polarization diversity antenna for ultrawideband systems, ” IET Microw. Antennas Propag.,vol7,no.10,pp.851-857,2013.

[13] Lee, J.-M., Kim, K.-B., Ryu, H.-K., et al., “A compact ultrawideband MIMO antenna with WLAN band-rejected operation for mobile devices, ”IEEE Antennas Wirel. Propag. Lett., vol. 11, pp. 990–993, 2012.

[14] Gao, P., He, S., Wei, X., et al.: ‘Compact printed UWB diversity slot antenna With 5.5 GHz band-notched characteristics’, IEEE Antennas Wirel. Propag. Lett.,vol 13,pp. 376–379, 2014.

[15] Beegum, S.F., Sanjeev, K.M. ‘Compact WLAN band-notched printed ultrawideband MIMO antenna with polarization diversity’, Prog. Electromagn. Res. C, vol. 61, pp. 149–159, 2016.

[16] Situ Rani Patre, Surya P. Singh, "Shared MIMO antenna for broadband applications, IET Microw., Antennas Propag., vol. 12, no. 7, pp. 1153–1159, 2018.

[17] Thazhe K. Roshna, Unmimadhavan Deepak and Pezholil Mohanan, " Compact UWB MIMO Antenna for tridirectional pattern diversity characteristics, IET Microw. Antennas Propag.,vol 11,no.14,pp.2059-2065, Oct 2017.

[18] Kunal Srivastava, Ashwani Kumar, Binod K. Kanaujia, Santanu Dwari and Sachin Kumar," A CPW-fed UWB MIMO antenna with integrated GSM band and dual band notches, International Journal of RF and Microwave Computer Aided Engineering, pp. 1-10, 2018.

[19] Mohamed Shehata, "Dual Notched Band Quad-Element MIMO Antenna With Multitone Interference Suppression for IR-UWB Wireless Applications, IEEE Transactions on Antennas and Propagation, vol. 66, no. 11, pp. 5737-5746, November 2018.

[20] A.A.R. Saad, "Approach for improving inter-element isolation of orthogonally polarised MIMO slot antenna over ultra-wide bandwidth, Electronics Letters 6th September 2018 Vol. 54 No. 18, pp.1062–1064.

[21] Wenjing Wu, Bo Yuan "A Quad-Element UWB-MIMO Antenna with Band-Notch and Reduced Mutual Coupling Based on EBG Structures, International journal of Antennas and Propagation, pp 1-1, Feb 2018.

[22] Ahmet Kayabasi, Abdurrahim Toktas, "Triangular quad-port multi-polarized UWB MIMO antenna with enhanced isolation using neutralization ring, International Journal Electron Communication Elsevier, pp. 47-53, Feb, 2018.

[23] Shrivishal Tripathi, Akhilesh Mohan and Sandeep Yadav“A Compact Koch Fractral UWB MIMO Antenna with WLAN band rejection, ”IEEE Antennas and Wireless Propagation Letters, vol. 14, pp. 1565-1568,2015.

Proceedings of the Fourth International Conference on Communication and Electronics Systems (ICCES 2019)
IEEE Conference Record # 45898; IEEE Xplore ISBN: 978-1-7281-1261-9

Wireless Power Transfer For Third Harmonics With the Improved Input Power factor

Akhila E. M
Department of Electrical & Electronics Engineering
Government Engineering College Thrissur
Email: akhilahemanth03@gmail.com

Suhara E. M
Department of Electrical & Electronics Engineering
Government Engineering College Thrissur
Email:suharanas@gmail.com

***Abstract*—Power transfer (WPT) without wires in electric vehicle charging is a relevant topic in the present day scenario. From the year of Tesla, the basic method of WPT using magnetic resonance has been developed. The main advantage of WPT is that it does not need any wires and can charge dynamically. So this method is very useful in the case of stationary and dynamic charging of the electric vehicle. WPT can be also used in biomedical types of equipment, electronics appliances charging. This paper proposes a third harmonic WPT system with improved input power factor. The advantage of selecting third harmonics for the power transfer is that it will increase the system frequency up to 3 times without rising the switching frequency. Also, the bigness of the passive components lowered into one by third and thereby the reduction in cost. Reasons for neglecting high order harmonics are also discussed in this paper. The major flaw of ordinary WPT is the poor power factor. So the proposed topology uses a boost PWM rectifier along with hysteresis control, it will increase the input power factor up to 0.9.**

Keywords: Wireless power transfer(WPT), inductive magnetic resonance, Inductive Power Transfer(IPT), Electric vehicle.

I. Introduction

Nowadays the government authorities provide subsidies and reduce taxes to enhance the marketing of the electric vehicle. The shortage of fossil fuels is the major reason for this and also the unlimited emission of pollution from petroleum vehicles. But the charging of the electric vehicle is very difficult. Also, there will be chances for a shock if there are any cracks in the plugged wire. So the concept of WPT for charging will eliminate all these problems[1].

Firstly,Discussing what is the conventional wireless power transfer arrangement done in the electric vehicle. Fig. 1 displays a conventional resonance inductive power transfer arrangement[2] used in EV. There is diode bridge rectifier and high-frequency inverter on the primary part which will draw the power from the grid. The rectifier converts the AC supply into DC. The inverter used is a quasi-square wave inverter having the output of rich in harmonics. The inverter stage transforms DC waveform into a high-frequency square wave. The frequency should be as high as possible in order to boost the efficiency and to limit the losses in transmitting

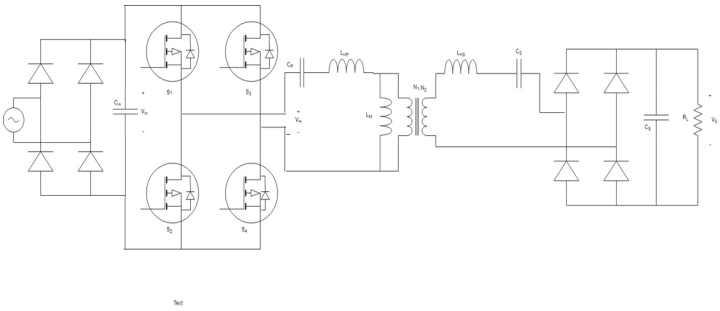

Fig. 1. A Conventional Resonance Inductive Power Transfer system

side. In the primary side transmitter, there is an inductor and a compensating capacitor. These are used to convert a high-frequency square wave into a high-frequency sine wave. Likewise, there is an inductor and a compensating capacitor on the secondary part. So that frequency of the receiver secondary side is made to match with transmitting coil in order to increase the productivity of power transfer. That is the transmitter and receiver are in resonance. The switches used is IGBT for high-power application. Normally, the IGBT carry up to 20 KHz. The power carried from the primary is rectified into dc again in the secondary side, and it is used for charging the battery[3].

Charging of the electric vehicle via WPT is by two types; static and dynamic(in motion)charging. In dynamic charging, the transmitting coil is placed beneath the road, while the receiving coil is placed in the vehicle. So that when the vehicle is passed over the road the battery gets charged[4]. The major parts of the system are a utility grid, a rectifier, a high-frequency H-bridge DC-AC inverter, and two series attached transmitting helices with their series resonant adjusting capacitors, beneath the road. The automobile part of the arrangement contains a receiver helices placed below of the automobile with a resonant adjusting capacitor, a diode bridge rectifier with a DC draining capacitor and the automobile battery. In stationary charging, the primary coil is placed in a particular area, and when the vehicle comes over directly the primary coil, power is transferred through the secondary coil which is placed in the vehicle.
The other advancement in wireless charging is that the

selection of the higher harmonics for the power transfer. The main feature is that the bandpass filter nature of the resonant structure. The resonant network is tuned to pass only one harmonic current to the secondary side. As a result, only the selected resonant component frequency is passed into the secondary side. If the third harmonic frequency of H-bridge inverter is identical to the resonant frequency, then the energy transfer to the second part is the third harmonic frequency. If we change the resonant frequency into fifth, seventh then that component will only transfer to the secondary side. Third harmonic system is introduced by Hulong Zeng. The advantage of this system is that here instead of fundamental frequency 3rd harmonics[5] is selected for the power transfer from primary to secondary. An advantage is that without varying the switching frequency, we can use a large system frequency for the power transfer with the reduced size of the passive components. Also, the cost is reduced due to the dimension cutback of the passive components. Here the output of quasi-square wave inverter contains fundamental, third, fifth harmonics. The receiving side is tuned in such a way that the receiving frequency matches with the third harmonic frequency. As a result the efficiency of third harmonic system is greater than fundamental system.

The major problem of all these systems is that the conventional rectifier on the primary side leads to distorted sinusoidal waveform and a poor power factor. The reduction in power factor affects system performance and efficiency. So the initiated technology is a third harmonic WPT with PWM boost rectifier along with hysteresis control. It will reduces the THD and improve the power factor up to 0.9.

II. Proposed Topology in IPT

Conventional switching power supplies are operated by rectifying the ac line supply and the rectified ac supply is again filtered by large electrolytic capacitors[6]. The main problem behind is that the input current waveform gets largely distorted and input power factor will be very poor(0.35). In order to get best efficiency and the best performance, it is desirable to get a large input power factor and reduction in harmonics. Many of the switching regulator topologies can be used for the power factor advancement and harmonic current deduction[7]. The most used is the boost topology. A high power factor rectifier can be established by using a dc to dc boost rectifier shown in fig 2. The rectifier with a simple circuit is perceived by using an integration of incontinent diode with a boost chopper[8]. This topology has several disadvantages:

- There is a series diode D_S in the power flow path. It will lead to voltage dip, large power damage, poor accuracy.
- At a time, 3 semiconductor losses occur in the power current path.
- There is a particular design required for the inductor on the dc side to bring dc current.
- The essential frequency of the boost switch is very eminent. This will increase the losses in switching and reduce the productivity.

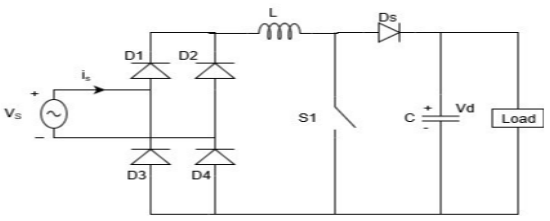

Fig. 2. Boost type rectifier

So by using a simple circuit, which is relevant in the case of ac to dc energy conversion(fig 3). A full bridge pulse width modulated(PWM) boost rectifier using four active switches, that provides controllable dc link voltage, controllable power factor and nearly sinusoidal input current. The overall wireless power transfer with a PWM boost rectifier circuit is shown in figure 3.

In the initiated single-phase power factor correction

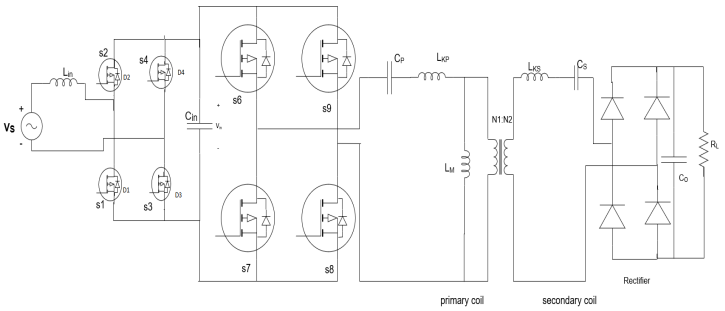

Fig. 3. proposed system

procedure, series diode Ds in the boost topology has been vanished. Another important fact is that instead of the dc-side inductor, an ac-side inductor is used. The merits of the initiated approach are:

- Input current gets sinusoidal and input power factor improved.
- At any time there is two semiconductor drop occurs in the power flow path instead there are 3 semiconductor drop occurs in the power flow path in case of conventional boost topology.
- The ac side boost inductor, L_{in} reduces electromagnetic interference.

A. Working of PWM Boost Rectifier With Power factor improvement

Due to the non-linear characteristics of diode rectifier, there are power quality issues. The THD of the rectifier with filter is having a 10% ripple and THD of 260.46%. In order to

reduce THD and improve power quality, introducing the PWM rectifier fig 3. The PWM converter draws a near sinusoidal input and providing a controlled dc voltage at the output side. It can work both in first and second quadrants of the voltage-current plane. So it will be bidirectional and after the control, the current will be purely sinusoidal.
From the figure, it is clear that the PWM boost rectifier consists of 4 IGBT make a full bridge and input inductance. Its working is discussed here: It has 4 modes
1.Mode 1: When the source voltage is positive and switch S_1 and S_4 are on. During this mode inductor, L is charged through V_S-L-S_1-D_3 or V_S-L-D_2-S_4. The capacitor discharges through the load.

$$V_S = L\frac{di}{dt} \tag{1}$$

2.Mode 2: When the source voltage is positive and S_1 and S_4 are OFF. In this mode, the diode D_2 and D_3 conducts and others remain inactive. Source and inductor feed energy to the capacitor and load.

3.Mode 3: When the source voltage is negative and switch S_2 and S_3 are on. During this mode inductor, L is charged through V_S-L-D_1-S_3 orV_S-L-S_2-D_4. The capacitor discharges through the load.

4.Mode 4: When the source voltage is negative and S_2 and S_3 are off. In this mode the diode D_1 and D_4 conduct, others remain inactive. Source and inductor feed energy to the capacitor and load.

The rectified DC voltage from the PWM rectifier is converted into high-frequency AC by using an inverter. Here the quasi-square wave inverter is used.

The main aim of the paper is that reduce THD and make current in phase with the voltage. So that input power factor can be improved. So we need current control schemes. There are mainly 2 different techniques:

- Hysteresis control
- Sinusoidal PWM [11]

But in this paper, Hysteresis control is used.

III. Control Strategy

By using the proposed boost topology, will get a nearly sinusoidal input current. In order to get a fair sinusoidal input current and improved power factor, a control strategy for PWM rectifier is used. The voltage source rectifier operates by keeping the dc link voltage at a preferred reference value, using a closed loop control[9]. Here the output voltage of the load is compared with a reference value. Then this inaccuracy is given to a PI controller. The output from the PI controller is multiplied with a unity sine. The unity sine will be the ratio of $V_m \sin wt$ to the peak value of the voltageV_m. The resulting output will be reference current. This reference current is compared with the actual current producing switching pulses to the PWM rectifier through a hysteresis controller. The switching signal is used to ON and OFF the four switches of the rectifier[10]. So that the power can come or return to the ac source according to dc link voltage requirements. The control strategy using hysteresis is shown in figure 4.
This control strategy provides almost sinusoidal input current

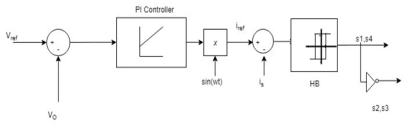

Fig. 4. Block Diagram of Closed Loop Control Strategy

and a high input power factor with THD of 2.59 %.

IV. Power from Harmonics In H-bridge Inverter

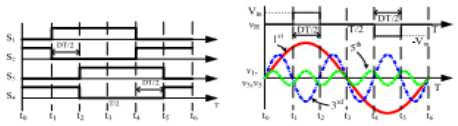

Fig. 5. PWM waveforms, H-bridge output voltage vH , and H-bridge output voltage harmonics.

Now coming into the working of quasi-square wave inverter, each phase leg of the quasi-square-inverter handle under 50 % duty cycle. There is a phase shift among the two legs that manage the outgoing voltage of the inverter V_H. When the switches s_6 and s_8 are on, V_H is the incoming voltage, V_{in}. While if the switches s_7 and s_9 are on then the outgoing voltage V_H equals $-V_{in}$. As there is an energy interchange among the dc source and resonant converter, these states are called active states. There is another condition where both upper switches or lower switches are on state. These states are called zero states as there are energy moves continuously through a closed path within the resonant network. At the same time load continually utilizing the power under zero states. The switching pulses and inverter output is shown in fig.5.

The output of H bridge inverter, V_H is a quasi-square waveform, which contains all the harmonic contents i.e, fundamental,third ,fifth etc. Fourier series representation of quasi-square wave inverter is expressed as[11], Where D is the duty ratio.:

$$v_H = \sum \frac{4V_{in}}{n\pi} \sin(n\pi D) \sin(nt) \tag{2}$$

V. Third Harmonic Selection and Transformer Design

A. Third Harmonic Selection

From the inverter, will get a high-frequency square wave. The power transfer from transmitter to receiver is done by the transformer and the selection of harmonics to transfer power is done by the compensating capacitors and inductors. Third harmonics are selected for the power transfer in this paper. The selection of third harmonics for the power transfer is studied here. It is clear that the switching frequency has a role on the size of the passive components. If the frequency increases three times then the size of the passive components reduced to one by third. Likewise higher harmonic frequency further reduce the size of the passive components. Usually, the electric vehicles are in the kiloWatt range, so that IGBT is used instead of MOSFET. But the maximum frequency that can be carried by IGBT is 20kHz. One way to increase the system frequency is by using the harmonic current to transfer power. The bandpass filter characteristics of inductive power transfer can be used to increase the system frequency by fixing the switching frequency constant. Here a 3rd harmonic frequency is transferred to the secondary side. As a result, the 3rd series resonance compensation(SRC) has merit in volume, weight contrast to the fundamental system. The change from fundamental to the third harmonic system is the frequency of resonance of the resonant network, while the topology used is the same for both. The advantage of High order harmonic system is the small size and low weight. But the dc bus voltage use will be less in higher harmonics and the switches undergoes large current force even if the primary ampere turns is same. The merits of 3rd harmonic discussed below
The power losses in the system mainly are:

- Switching loss P_s. That is the H-bridge inverter loss.
- Capacitor damage P_c.
- Secondary rectifier loss P_d. Diode bridge conduction loss.
- Winding copper loss P_w.
- Transformer Core loss P_t.

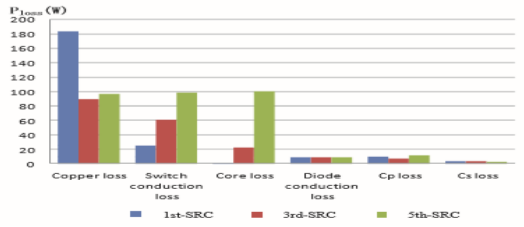

Fig. 6. Loss Comparison of Three IPT Systems

The graph, fig.6 shows a comparison of three IPT systems [12]. P_s is the H-bridge inverter loss. The switching loss, Ps depends upon the switching frequency. As the harmonic order increases, the switching loss increases. Considering the case of copper loss, less number of spins on the windings in higher order harmonic system , as the turns ratio decreases for higher order harmonics. At the same instant, it requires additional winding in analogue to manage the larger primary current. In order to get a good correlation, the three IPT systems current density is calculated to be same. The overall outcome display that copper loss will reduced in higher harmonic system. But from the graph, it is acquit that 5th SRC has over copper loss compared to 3rd SRC. The reason behind is that 5th SRC does not show good performance because it requires a fractional number of turns. As the frequency increases, there is a chance for turns ratio becomes fractional. even with harmonic order more than 5th SRC, this issue will come and effects in a cheaper scheme. The secondary position destruction that are diode loss and secondary side compensation capacitor loss are nearly the same. It means the secondary part only consider resonant component stimulation from the primary part and do not consider which grade of harmonic is selected for the transfer. The copper loss, switching loss, and primary capacitor loss all depends upon primary part current magnitude. As the harmonic order increases, the amplitude of the primary side current increase thereby these losses get increased. In the case of higher order harmonics, there is a chance of a fractional number of turns that affect the overall performance, which leads to an increase in the core loss in higher order harmonics. In WPT application the primary and secondary part are split apart and the form of the core changes a lot. So here window utilization factor expressed in terms of complete winding length(CWL) and winding isolation voltage. CWL is the total of all wires length that is used in the transformer. In case of a higher order, the turns get reduced so that the CWL get reduced. In the case of higher order harmonic system the voltage force on the inductor terminal will be less as the total number of spins get reduced. But the voltage force between the adjacent spins will be higher in the higher order harmonic system. So that 5th SRC having large adjacent voltage stress than 1st and 3rd SRC.
In short, the main reason for selecting the harmonic component is the reduction of copper loss and winding spins.So that it will contract the bigness of the resonant structure. But some limitations are there. There will be higher switching loss and higher insulation voltage between the adjacent spins. There is a need for selecting various core substance for various harmonic order. It limits the higher order harmonic system. Also in the higher order harmonic system, there is a chance for a fractional number of turns in the transformer. It will affect the selection of high grade harmonics.

B. Transformer Design

From the fig 1, it is clear that the ac power is changed into dc power by a PWM rectifier with power factor correction. Then the dc power is changed into high-frequency ac through a high frequency-inverter. A high frequency-inverter is placed between inverter and secondary side with primary

and secondary compensation. The high-frequency current produces an alternating magnetic field in transmitting coil, that induces a voltage on the secondary. By the resonance of secondary compensation, we will get high efficiency. Lastly, the ac is again rectified into dc for charging the battery. The difference from a wired charger is that there is loosely coupled coils in the wireless charger[13].

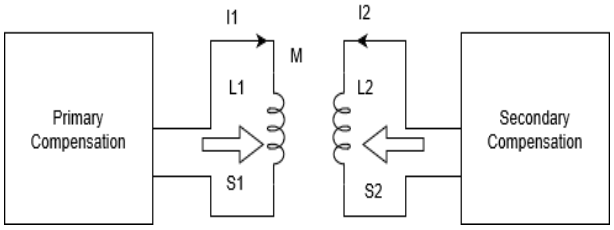

Fig. 7. Two Coil WPT system

To get an idea of WPT principle, the coil and the compensation network is shown in fig 7, where L_1 and L_2 shows the self-inductance of primary side transmitting coil and secondary side receiving coil respectively. I_1 and I_2 are the currents in the primary and secondary side. S_1 and S_2 are the apparent power go into L_1 and L_2 respectively. M is the mutual inductance. For designing we consider only the active power P_{12} transfer from primary to secondary:[3]

$$p_{12} = wMI_1I_2sin\varphi_{12} \tag{3}$$

Taking 400W power transfer from primary to secondary for 230V, 50 Hz supply.we are first calculating the values of passive components for a fundamental frequency. The turns ratio is taken as 15:20 for the fundamental frequency. Assuming 70% efficiency ,can be calculate input power and input current. The secondary current can be calculated by (4)

$$I_1 = I_2k \tag{4}$$

Where k is the ratio of secondary to primary turns. φ_{12} is the phase difference between primary and secondary current, which is taken as 90° for maximum power transfer. From (3), by substituting all values, M will get. The switching frequency is taken as 18kHz. From the M value, primary side inductance can be calculated using(5). From primary side inductance secondary side inductance can be calculated.

$$M = k1\sqrt{L_1L_2} \tag{5}$$

For a WPT, the value of k1 will be very less(0.01) and L_2 is taken as$L_2 = L_1k^2$. From the primary inductance, secondary inductance can be calculated. The compensation capacitor values of primary and secondary can be calculated by 6 & 7 respectively:

$$C_1 = \frac{1}{4\pi^2 f^2 L_1} \tag{6}$$

$$C_2 = \frac{1}{4\pi^2 f^2 L_2} \tag{7}$$

TABLE I
PARAMETERS FOR 1ST AND 3RD SRC

1st SRC	3rd SRC
Turns ratio= 15:20	5:20
L_1=164.5mH	L_1=54.83mH
L_2=291mH	L_2=96.6mH
L_m=2.1884mH	L_m=2.1884mH
C_p=475.2pF	C_p=158.4pF
C_s=269.5pF	C_s=89.83pF
Resonant frequency=18kHz	54kHz

similarly, the values for third harmonics can find out using these equations by changing the turns ratio into 5:20 and the switching frequency becomes three times the fundamental frequency, i.e, 54kHz. The fundamental and third harmonic values are listed in Table1:

VI. SIMULATION RESULTS

The Simulink diagram of the proposed topology is shown in fig.8. In which primary side, there is PWM rectifier along with a hysteresis control is used to enhance the power factor and a high-frequency inverter for converting high-frequency AC. The primary and secondary side inductors and capacitors are for compensation. The secondary side of the transformer is in resonance with the primary side. Again, there is rectification in the secondary side to charge the battery.

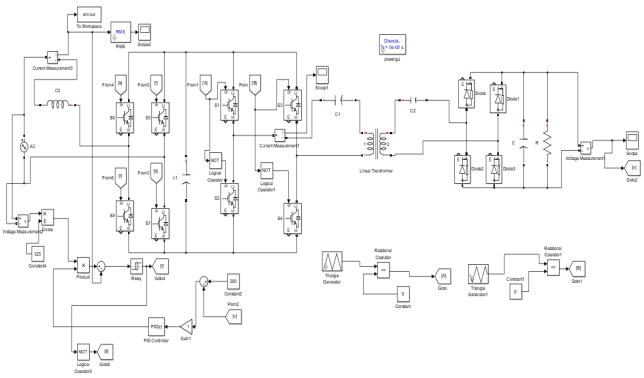

Fig. 8. Simulink Diagram Of the Topology

The parameters used in the simulation are shown in table 2. The switching pulses for the inverter are generated by comparing triangular and a dc value and also there is 90° phase shift between the two legs that is shown clearly in fig.9. The switching pulses and inverter output is shown in the fig.10.

Fig.11 shows the input current waveform and its THD in a conventional rectifier WPT. The THD is 260.46% and pf is 0.35.

Fig.12 shows the inverter output and fundamental current for the selection of fundamental frequency as the resonance frequency. While fig.13 shows the inverter output and third harmonic current for the selection third harmonic frequency

TABLE II
PARAMETERS USED FOR SIMULATION

Components	Values
Input inductor	10.4mH
Input capacitor	266μF
Primary inductor	54.83mH
Secondary inductor	96.6mH
Primary capacitor	158.4pF
Secondary capacitor	89.83pF
Output capacitor	100μF
Load resistor	100Ω
Harmonics	Third

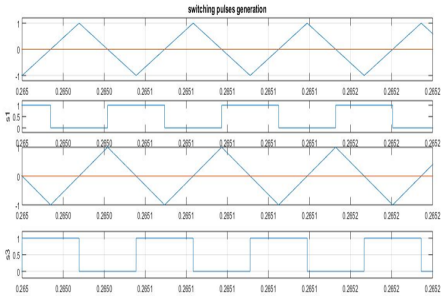

Fig. 9. Switching Pulses For Inverter

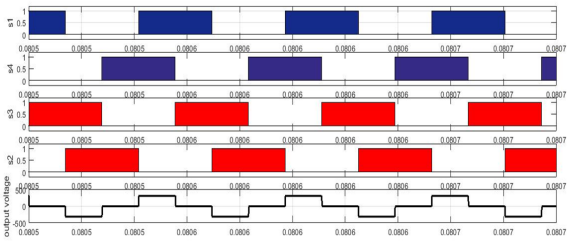

Fig. 10. Switching Pulses And Inverter Output Voltage

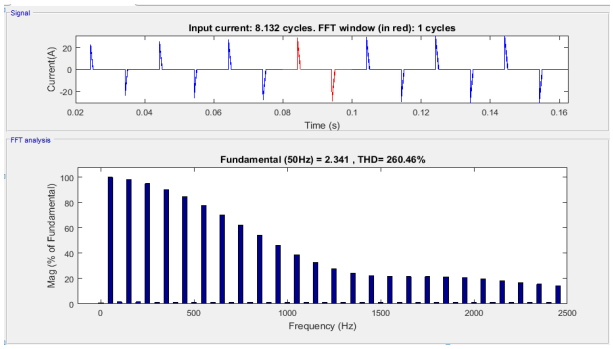

Fig. 11. Input current and its THD in conventional rectifier WPT.

The PWM rectifier control is used to draw a sinusoidal current with improved power factor. From the graph, fig.14 shows the incoming current is sinusoidal which is in phase with incoming voltage having THD 2.59% and a power factor

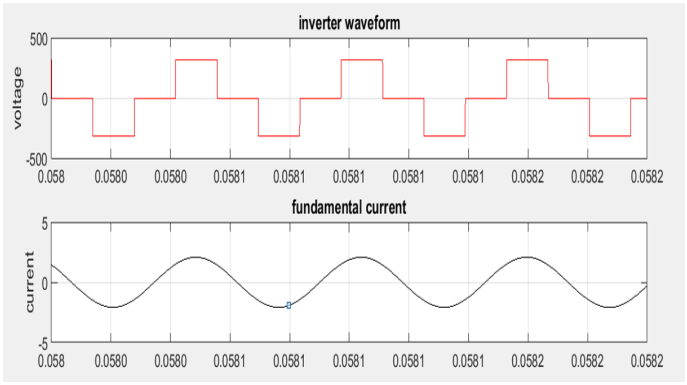

Fig. 12. Inverter Output And Fundamental Current

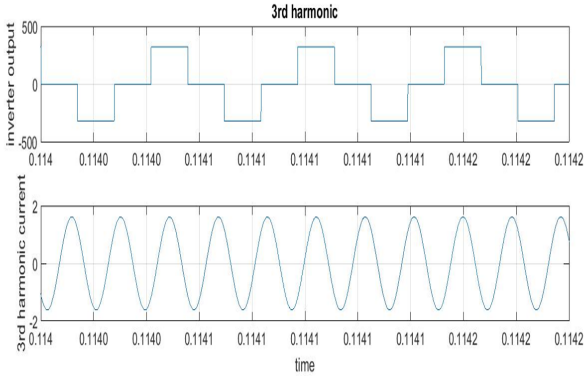

Fig. 13. Inverter Output And Third Harmonic Current

of 0.99.

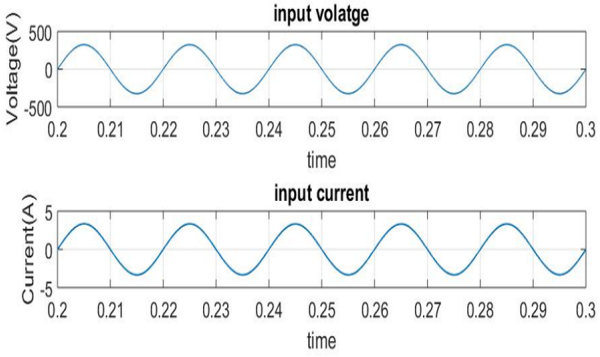

Fig. 14. Input current and Voltage in the Proposed Topology

The FFT analysis of the input current is shown in the fig.15 along with power factor and THD. The power factor is improved greatly.

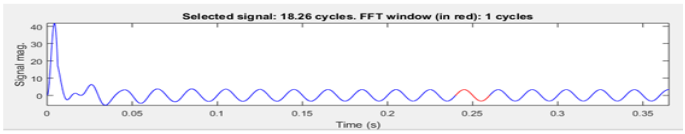

THD	DF	ϕ	COSϕ	PF
0.0259	0.999	0.2	0.999	0.998

Fig. 15. FFT Analysis Of Input Current

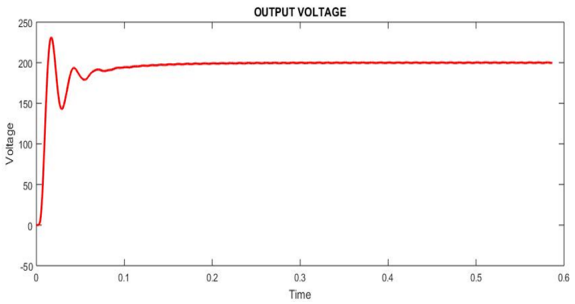

Fig. 16. Output Voltage

The load is regulated by a constant voltage mode. Here making 200V as the output voltage for the battery as shown in fig.16.

VII. Conclusions

In this paper, we are discussed about the wireless power transfer system using third harmonics with input power factor correction. The advantage of using third harmonics for power transfer instead of fundamental is that it decreases the size and volume of the passive components and decreases the overall copper loss. But the input current is not sinusoidal , so that the power factor will be very poor. The PWM rectifier with hysteresis control is used to improve the sinusoidal shape and power factor.

When using a controlled rectifier with 10% ripple filter for rectification, it produces a THD of 260.46% i.e, pf is 0.35. Where as the PWM rectifier with hysteresis control improve the power factor into 0.99 and the THD is 2.59%. Here a 400W, 20cm distance between primary and secondary is introduced with high input power factor and low total harmonic distortion.

References

[1] Mickel Budhia, Student Member, IEEE, John T. Boys, Grant A. Covic, Senior Member, IEEE, and Chang-Yu Huang, Member, IEEE , "Development of a Single-Sided Flux Magnetic Coupler for Electric Vehicle IPT Charging Systems",IEEE Transaction on Industrial Electronics, Vol. 60, No. 1, Januvary 2013.

[2] Honglong Zheng,Zhihui Wang,Yachao Li,Pengqi Deng,College of automation in a Chongqing University,Chongqing,China 400044"Data Transmission through Energy Coil of Wireless Power Transfer System",2017 IEEE

[3] Mustapha DEBBOU, Franois Colet VEDECOM Versailles, France, "Inductive Wireless Power Transfer for Electric Vehicle Dynamic Charging ", 2016, IEEE.

[4] Omer C. Onar, John M. Miller, Steven L. Campbell, Chester Coomer, Cliff. P. White, and Larry E. Seiber Power Electronics and Electric Machinery Group, Energy and Transportation Science Division, National Transportation Research Center, Oak Ridge National Laboratory Oak Ridge, TN 37831 USA ,"A Novel Wireless Power Transfer for In-Motion EV/PHEV Charging ",2013 Twenty-Eighth Annual IEEE Applied Power Electronics Conference and Exposition (APEC) .

[5] Hulong Zeng,student member,IEEE,Shuitao yang,and Fang Z.Peng,Fellow,IEEE,"Design consideration and comparison of wireless power transfer via harmonic current for phev and ev wireless charging",IEEE transaction on power electronics, vol. 32, no. 8, august 2017.

[6] Mahasweta Bhattacharaya" Improvement Of Power Quality Using Pwm Rectifiers", International Journal Of Scientific and Research Publications, Volume 4, Issue 7, July 2014.

[7] Jee-Woo Lim and Bong-Hwan Kwon" A Power factor controller for single-phase Pwm Rectifiers" IEEE Transactions on industrial electronics,Vol 46,No.5,October 1999.

[8] M.A.Ahamed, ass.proffesor,Electrical Engineering Department,Aljouf faculty of Engineering,Aljouf University,Kingdom of Saudi Arabia,"Simulation and Experimental Verification Of Single -Phase PWM Boost-Rectifier With Controlled Power Factor",IRJET,vol.4,issue.3,March 2017.

[9] Roberto Martinez,Member,IEEE and prasad N.Enjeti,senior member,IEEE,"A High -Performance single -Phase Rectier With Input Power Factor Correction",IEEE transactions on power electronics,vol.11,no.2,march 1996.

[10] Vinaya Skanda, Microchip Technology Inc, "Power Factor Correction in Power Conversion Applications Using the dsPIC DSC".

[11] Hulong Zeng, Student Member, IEEE, Nomar S. GonzlezSantini, Student Member, IEEE, Yaodong Yu, Shuitao Yang and Fang Z. Peng, Fellow, IEEE, Dept. of Electrical and Computer Engineering, Michigan State University,East Lancing ,MI 48824,USA,Email:cooloneze@gmail.com,"Harmonic Burst Control Strategy For Full Bridge Series Resonant Converter-Based EV Charging", Citation information: DOI 10.1109/TPEL.2016.2589942, IEEE Transactions on Power Electronics.

[12] Hulong Zeng and Fang Zheng Peng ,Department of Electrical and computer Engineering Michigan State University East Lancing,MI 48824,USA,cooloneze@gmail.com,"Comprehensive design comparison of using different order harmonics as the power carrier in wireless power transfer for phev and ev wireless charging",2016,IEEE .

[13] Siqi Li, Member, IEEE, and Chunting Chris Mi, Fellow, IEEE "Wireless Power Transfer for Electric Vehicle Applications" IEEE journal of emerging and selected topics in power electronics,vol.3,no.1,march 2015.

Proceedings of the Fourth International Conference on Communication and Electronics Systems (ICCES 2019)
IEEE Conference Record # 45898; IEEE Xplore ISBN: 978-1-7281-1261-9

Diagnosing Insomnia Using Single Channel EEG Signal

N Purushotham Raju
Dept of Electrical and Electronics Engineering
Amrita School of Engineering
Amrita Vishwa Vidyapeetham
Bengaluru, India

Purushotham.nb@gmail.com

Venkatesh U
Dept of Electrical and Electronics Engineering
Amrita School of Engineering
Amrita Vishwa Vidyapeetham
Bengaluru, India

Venkateshchowdary005@gmail.com

Sudha Yadhav
Dept of Electrical and Electronics Engineering
Amrita School of Engineering
Amrita Vishwa Vidyapeetham
Bengaluru, India

Sy_sudha@blr.amrita.edu

***Abstract*— The human brain produces different electrical signals in response to the thinking process. These signals are captured using different techniques such as EEG, ECG, EMG, etc. Electroencephalography (EEG) is one of the technique which is being used widely. The data can be detected using EEG Caps, Neurosky Headset. The device used for the project under discussion is Neurosky Headset. The EEG signals Can be used to detect epilepsy, sleep disorders, stroke, head injury, dementia. The EEG signals captured by the headset are transmitted via Bluetooth to the laptop and interfaced with the MATLAB. The obtained signals are deduced to the required parameters which can help us to identify whether a patient is having insomnia or not.**

***Index Terms*—Electroencephalogram(EEG), Non-invasive, Neurosky Mindwave, MATLAB.**

I. INTRODUCTION

No system will continuously work whether it is living or mechanical. Rest plays major role in living organisms to get revitalize. Sleep is the place where every living organism gets rest and the life energy is accumulated. Sleep is the thing which has been harmed in the process of human development. Because of the artificial lights the sleep got troubled and humans started to feel that the sleep is unnecessary thing because of obsession in using gadgets. This the predominant reason for all the disorders and illness in human's life. The international classification of sleep disorders (ICSD, ed 2) lists eight categories of sleep disorders along with appendix A and Appendix B, the four major sleep complaints include excessive daytime sleepiness, insomnia, abnormal movements or behavior during sleep and inability to sleep at the desired time [1].

Insomnia is hassle falling asleep through the night, or arousal too early within the morning. The symptoms of the insomnia include difficulty in starting sleep and maintaining it, early morning awakening and non-restorative sleep at any given time. Among 8 to 40 percent of the general population are suffering from insomnia, 30 to 40 percent are having poor sleep and 8 to 10 percent are suffering from chronic insomnia [2, 3]. Also, about 4% of the population use sleeping pills on a regular basis [4].

Neurons in the human brain produces a voltage of 70 millivolts and the potential difference can be measured using different techniques. Electroencephalogram (EEG) is a technique to measure and record that potential difference in the form of a signal by placing electrodes on the scalp or in the tissue of the brain. There are two methods in EEG, one is invasive and other is non-invasive technique. In invasive method the electrodes are placed inside the brain tissue which will cause problems. The sophisticated non-invasive technique will help to avoid those problems in which the electrodes are placed on the scalp using conventional 10-20 system. Alpha, beta, theta and delta are the four main kinds of the EEG waves which will be used to diagnose diseases like insomnia, epilepsy, Alzheimer's and many other diseases [5]. Similarly, advancements in technology have led to the genesis of many sophisticated devices that can capture the brain waves without wet electrodes. Mind wave headset, Muse, etc. are few of such devices. The mind wave headset is the apparatus used here to serve the purpose. It consists of two dry electrodes namely Fp1 and CAR (according to the 10-20 system). As it consists of only one pair of electrodes it is referred to as a single channel device. The data is wirelessly transmitted via Bluetooth and the signal is mapped at receiver 'send using MATLAB.

II. RELATED WORKS

The literature survey of the work is discussed in this section. The research paper [6] describes about diagnosis of autism based on electroencephalography signal analysis in which discrete wavelet transform is used to obtain major types of EEG waves. Shannon entropy values are calculated for each EEG subband using the feature vector and based on the extracted features artificial neural network classifies the EEG signal into normal or abnormal. In paper [7] Dry electrode is used to get the EEG signal which replaces the conventional 10-20 system and the collected data is sent wirelessly to the cloud from headset where the doctor can examine it in live to interpret the meaning of EEG signal. A single channel EEG signal is used to diagnose insomnia in [8] using PSD approach, the data of insomnia patients and normal patients taken from physiobank and the normalized

power of the EEG subbands is calculated. The working of Neurosky headset is described in [9] [10] [11] and [12].

III. SYSTEM DESIGN

A. *Block Diagram*

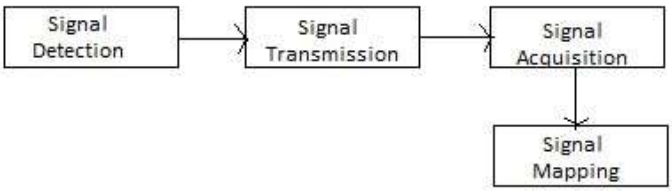

Fig. 1. Block diagram

The block diagram for proposed system is shown in Fig. 1. This system is classified into four stages. These four stages are Signal detection, Signal acquisition, Signal transmission, and Mapping Signal.

1)Signal Detection:

Fig. 2. Headset

In this stage EEG signal is detected through the Neurosky Mindwave headset by placing it on head using a methodology called electroencephalography(EEG). The trifling potential generated by a single neuron is difficult to detect using noninvasive methods. So, the aggregate of electrical potential generated by a cluster of neurons is detected with the single dry electrode which is placed on the forehead. Although, the amplitude of EEG signal varies from 1 micro volts to 100 micro volts in a normal adult, it is amplified and sampled by the headset whose strength is good enough to transmit wirelessly via Bluetooth.

Brainwave Type	Frequency range	Mental states and conditions
Delta	0.1Hz to 3Hz	Deep, dreamless, non-REM sleep, unconscious
Theta	4Hz to 7Hz	Intuitive, recall, fantasy, imaginary, dream
Low Beta	13Hz to 15Hz	Formerly SMR, relaxed yet focused, integrated
Midrange Beta	16Hz to 20Hz	Thinking, aware of self & surroundings
High Beta	21Hz to 30Hz	Alertness, agitation
Gamma	31Hz & above	Cognition, information processing

Table 1. Frequency range for different EEG subbands

2)Signal Transmission:

The detected signal is processed and converted into digital form by the headset. The headset has a thinkgear chip which helps in transferring the aided signal to personal computer or laptop via Bluetooth. 3)Signal Acquisition:

The signal is acquired into laptop where the MATLAB is used as a platform to run code to get the required raw EEG signals.

4)Signal mapping:

The MATLAB uses thinkgear.dll file to access the signal from the headset and the required signal in the form of graph. The raw EEG signal is further classified into delta, theta, alpha and beta from which normalized power is obtained and compared to reference values.

B. *Methodology*

The thinkgear connecter will automatically starts the application when it is installed, unless we stop it. The headset is connected to the laptop via Bluetooth. The thinkgear.dll file should be loaded in MATLAB and the code is executed. The above mentioned steps are basic to run any neurosky applications.

The dry electrode is placed on the forehead of the person through headset to get the raw EEG data. The raw EEG data is filtered using Daubechies wavelet to get delta, theta, alpha and beta. Energy of each segment is calculated using

$$\text{Energy} = \sum\_((j=1)^n)\ CDj \quad (1)$$

where CDj is segment of raw EEG signal. Then Normalized power is calculated and compared with the reference values from [9].

Normalized Power = Energy / number of samples

If the obtained values are falling in the rage of the reference values, we can say that the person might be suffering from insomnia and there is a need to consult doctor.

IV. SYSTEM IMPLEMENTATION AND EXPERIMENTAL RESULT

The Normalized power of each segment of raw EEG data, each of 20 samples is obtained from three persons.

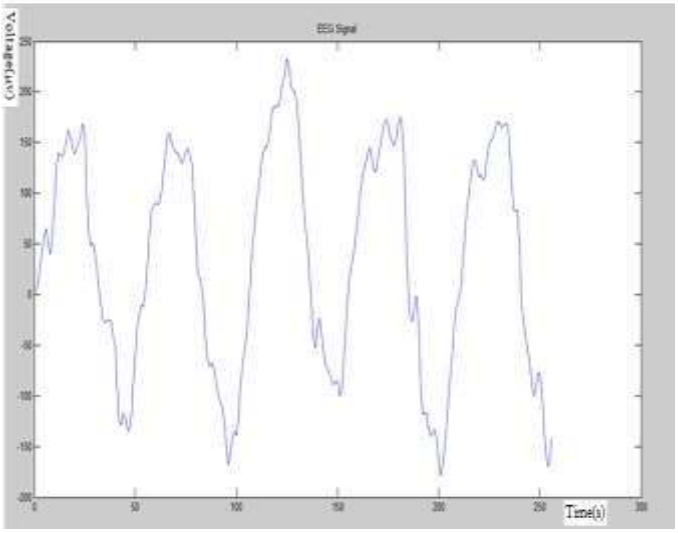

Fig. 4. Raw EEG signal

Fig 4 shows the obtained raw EEG signal from the patient. EEG headset has been used to obtain the signal. The graph was plotted against voltage and time.

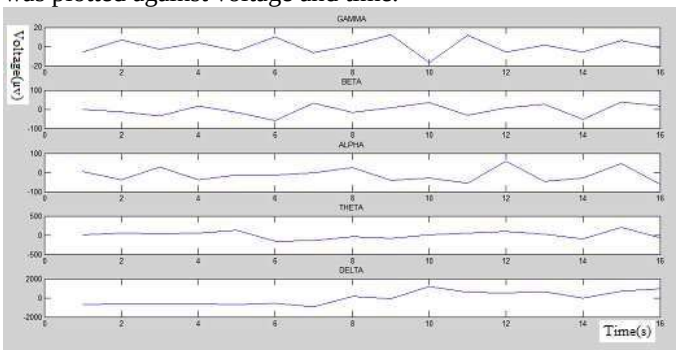

Fig. 5. Different Segments of EEG signal in time domain

The obtained signal (Fig 4) is characterized into four types i.e., Delta, Theta, Alpha, Beta. These signals are plotted in fig 5

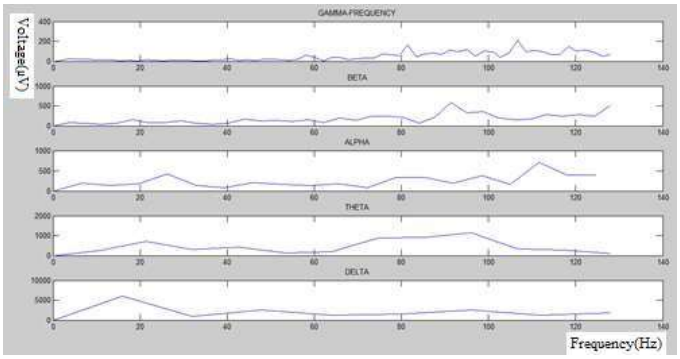

Fig. 6. Segments of EEG signal in frequency domain

Fig 6 shows the signals in frequency domain which are used to calculate the normalized power.

The obtained values are listed in below table

Wave	Person1	Person2	Person3	Reference Value
Delta	0.533	0.086	0.145	0.81-0.89
Theta	0.660	0.080	0.199	0.0078-0.16
Alpha	0.727	0.113	0.1162	0.006-0.02
Beta	0.650	0.122	0.177	0.0005-0.0007

Table 2. Results

From the above results we can say that person2 might be suffering from insomnia.

V. FUTURE SCOPE

This system can be further Developed to diagnose different kinds of illness or disorders and can improved to get the approval for clinical use, which will be useful to doctors and also the people live in remote areas.

VI. CONCLUSION

The proposed system uses the brain signals in the form of raw EEG data to diagnose insomnia.as we are using non-invasive method of electroencephalography, it is easy and harmless to use the headset. MATLAB serves as the platform to obtain the normalized power which helps to diagnose the person.

VII. REFERENCES

[1] S Chokroverty “Overview of Sleep and Sleep Disorders,” The Indian journal of medical research, 131:126-40, February 2010.

[2] EO Bixler, AN Vgontzas, HM Lin, A Vela-Bueno, A Kales,” Insomnia in central Pennsylvania,” Journal of psychosomatic research, pp. 58992, July 2002.

[3] MM Ohayon, “Epidemiology of insomnia: what we know and what we still need to learn”. Sleep medicine reviews, pp. 97–111, 2002.

[4] Y Chong, CD Fryar, Q Gu, “Prescription sleep aid use among adults: United States,” 2005–2010, NCHS data brief, no 127, National Center for Health Statistics, 2013.

[5] Jasjeet Kaur,Amanpreet Kaur, ” A review on eeg signals,” IEEE International Conference on Adavances in Computer Engineering and Applications,2015.

[6] Ridha Djemal, Khalil AlSharabi, Sutrisno Ibrahim, and Abdullah Alsuwailem, “EEG-Based Computer Aided Diagnosis of Autism Spectrum Disorder Using Wavelet, Entropy, ANN,” Bio Med Research International, 2017.

[7] Sonya Dumanis, Patty Osborne Shaffer, “Dry Electrode Headset EEG,” EpilepsyFoundation[Online].Available: https://www.epilepsy.com/learn/diagnosis/eeg/dry-electrode-headset-eeg

[8] Mohd Maroof Siddiqui, Geethika Srivastava, Syed Hasan Saeed, “diagnosis of insomnia sleep disorder using short time frequency analysis of PSD approach applied on EEG signal using channel ROCLOC,” Bio medical research, July 2016.

[9] P P Reddy, P V B. suresh, P T Reddy, P V manitha and K Deepa, “Remote control of an electronic device using EOG,” 2017 International Conference on Smart Technologies for Smart Nation (SmartTechCon), Bangalore, 2017, pp. 780-783.

[10] P P Reddy, P T Reddy, P V B Suresh, Sudha Yadav, "Smart Disease Diagnosing System Using Artificial Neural Network," International Journal of Engineering and Technology (UAE), ISSN: 2227-524X, 2018.

[11] J Katona, T ujbanyi, G sziladi and A Kovari, "Speed Control of Festo Robotino mobile robot using NeuroSky MindWave EEG headset-based brain-computer interface," 7th IEEE International Conference on Cognitive Infocommunications (CogInfoCom), Wroclaw, 2016, pp. 000251-000256.

[12] J Katona, I farkas, T Ujbanyi, P Dukan and A kovari, "Evaluation of the NeuroSky MindFlex EEG Headset Brain Waves Data," 2014, pp. 91-94.

Proceedings of the Fourth International Conference on Communication and Electronics Systems (ICCES 2019)
IEEE Conference Record # 45898; IEEE Xplore ISBN: 978-1-7281-1261-9

Identifying fake user using FRUI, Content and Profile based Algorithm.

Ms. Rohini N Khedkar
M.E Student, Dept. of Computer Engg.
Mumbai, India.
rohinikhedkar10@gmail.com

Prof. Sujata Bhairnallykar
Asst. Prof, Dept. of Computer Engg
Mumbai, India.
bsujata5@rediffmail.com

Prof. Vaishali Jadhav
Assot Prof, Dept. of Information technology
Mumbai, India.
vaishalijadhav_2000@yahoo.com

Saraswati College of Engineering, Mumbai University

***Abstract*—Present time, everybody uses on-line social network for his or her totally different purpose. Mediate dissimilar on-line SMN a few private information is splited any on online SMN. That divided data has abused by fraud person. Fraud person gather the knowledge, use fraudulently it as intimidation to someone, produce sensible relevancy to gain users trust and create some crimes. That occurs gradually. To unravel that drawback cross platform exploration might facilitate in social computing in every theory and real time. Some technique accustomed fraud person targeted on users public profile information, place and temporal property of persons content still as in depth vogue. Existing user identification supported on network structure aren't effective. To discover fraud person, structure projected proposal for FRUI algorithmic program .also use profile and content based identification algorithm. Projected work take a look at 2 on-line social media networks-Facebook and LinkedIn.**

Keywords— SMN, FRUI, Cross Platform, Content and Profile based Algorithm.

I. INTRODUCTION

Currently, large no of on-line social media networking sites are available like Facebook, Twitter, LinkedIn, Instagram, etc. People use this SMN Sites for their different purposes means getting important information, sharing ideas, posting their thoughts, entertainment and always attach with friends. At this time peoples have a no of accounts on on-line SMN same users. Who all are victimization the many accounts on various on-line social media they're victimization those accounts for various purpose. Like obtaining private info of some people, creating fraudulence victimization it and for black mailing reason. In this days fraud peoples toll on-line social media network become greater incessantly.

Facebook is an online social media network. User use the Facebook easily by using internet on computers , laptops mobile phones like smartphones. User first register on Facebook [2]. After doining registration, user can make their account on Facebook by giving personal data like profile picture, birth date, gender etc. Users easily use this account for entertainment, connected with people. User can makes no of friends on Facebook. Users will post their photos, thoughts, and ideas etc on Facebook. People will use varied insert apps, also collect notifications other people's activities. Peoples might part of familiar -interest team. Facebook had over a pair of.3 billion monthly active users as of December 2018 Facebook collect distinguished media coverage, together with several contentious like users account privacy and theoretical impact. Twitter one, the biggest activity service on a social media network. Where people tweets their thoughts [3]. LinkedIn is a professional site. On this site users can post their CV. This site is also used business. LinkedIn allow user to create their profile and connection to connect with each other in on-line SMN [4]. User can make professional relationship using LinkedIn social media network.in planned system used Facebook and LinkedIn social media network. Sina Microblog, the first Chinese microblog social media web site, has over five hundred million accounts and originate run over a hundred million tweets per day [5]

Recently user's interest is increasing on social media network platform on the net, the cross-platform approach has unified utterly completely Different SMN platforms to create richer data and extra and additional complete SMNs for social computing tasks [1]. The cross-platform system finds users on multiple SMN.there are two varieties of SMN connection: single following connections and mutual following connections. If person 1 follows person 2, then person 1 and person 2 have single manner fan during which one is aware of the opposite, however not the other way around. This relationship are common in Twitter and Sina Microblog., mutual manner connections are called friend relationships. The mutual following friend relationship makes as long as a devotee request is shipped only if a friend request is sent by one person and Confirmed by the opposite person. Mutual Friend relationships are terribly tough to pretend by mischievous person[1]. This relationship are common in Facebook, WeChat SMN.

This planned System Projected approach for friend relationship based algorithm. This method is identifying anonymous user in multiple SMN using FRUI algorithm, content and profile based technique .system is applied on two SMN Facebook and LinkedIn. Rest of paper is containing below section: section section II discuss related work, section III introduce proposed work, and section IV introduce result and discussion section VI presenting conclusion and future work.

II. RELATED WORK

Now a days everybody is attracting or using online social media network .between this some social crimes happens by fake user.to identity fake user there are number of methods presented. In this section we discuss some of them.

In [6] M. Motoyama and G Varghese authors present method which is find out a user by using matching and searching account info. This method use three dimension like profile base, connection base and content base to identify users. This presented method check out in two social media network: Facebook and Myspace.

In [7] Author Reza Zafarani presented another method using communities which is connected user identities. This method is called as join analysis algorithm. The connection joining usernames designated by one user in numerous SMN, and on a number of online as regards usernames and communities

In [8] author's. M.A. Kaafar D.Perito, C. Castelluccia, and P. Manils, this methodology traverse the connection users account exclusively by viewing their usernames. The instinct is that the prospect that try of usernames refers to the identical physical person powerfully depends on the entropy of the username string itself.

In [9] Author's presented approach in which users correlation account was used to find the users .authors check out a correlation of users accounts between a five social media networks Facebook ,Flickr, twitter, Google and Myspace.

In [10] Authors Paridhi Jain, et al presented approach was used users account data. Presented system author use users account information like profile photo, date of birth, gender etc .writing style and network structure created by user.

In [11] Authors introduce "Identifying users across social tagging systems". Authours use 2 types of user account info like user id and their tags. This method presented questions and explore either users will determine across social tagging systems.

In [12] in this paper author's Reza Zafarani, et al presented another method which is based on users a behavioral-modeling approach.

III. Proposed work

In this paper System projected a proposal for FRUI (Friend Relationship based User Identification algorithm). During projected model FRUI applied first to detect fake user. On this result of Friend Relationship based User Identification applied two types of technique i.e. content and profile based technique. Lastly this fake person are going to identify.

Below fig1 shows the proposed system architecture.

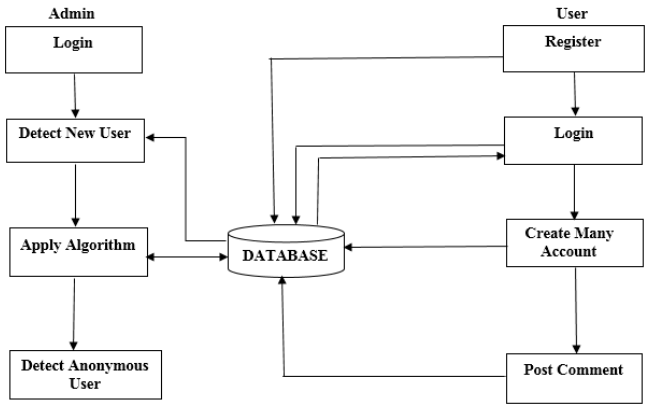

Figure1. Architecture of proposed system

As shown in above Figure (Fig1) there are two roles in the system one is Admin and another is User who have accounts on Social Media. New User can register to Social media network with all details then by using these log in details user can log in into social media. These all details will be saved in database which are entered while registering on social media. One user can create multiple accounts with different name.

After log in into system user can share post, send request, accept request, like and comment the post these all activities of user will be recorded in the database.Admin can log in and see all the details of both social media network Facebook and Linked In.When new account is created admin can see the newly added accounts of user i.e. admin can see registered user. Admin can apply Content based, Profile Based and FRUI algorithms to detect the Anonymous User in system. By using there profile details, Friend list, posts, comments algorithms will find the probable anonymous user of social media and at the end give list of that users.

Content based identification Algorithm-

Content based identification technique detect a fraud user on on-line social media network content based technique used. This planned system used post content which is posted publically by user.

Profile based identification Algorithm-

Profile based identification technique is Identify a fraud user on a SMN involving collection of profile attributes likes profile photo,gender,date of birth, username etc. Profile information is very important in projected system. In this planned system use only two profile attribute birth date and mobile no.

Below algorithm used in this system.

ALGORITHM: FRUI

Input: SMNA, SMNB, Priori UMPs: PUMPs
Output: Identified UMPs: UMPs
1: function FRUI (SMNA, SMNB, PUMP)
2: T= {}, R= dist ( ), S=PUMPs, L= [ ], max=0, FA= [ ], FB= [ ]
3: while Sis not empty **do**
4: Add S to T

5: if max>0 do
6: Remove S from L[max]
7: while L[max] is empty
8: max=max-1
9: if max= =0 **do**
10: return UMPs
11: Remove UMPs with mapped UE from L[max]
12: for each UMPa~B (i, j) in S do
13: for each UEAa in the unmapped neighbors of UEAi **do**
14: FA[i] =FA[i] +1
15: for each UEAb in the unmapped neighbors of UEAj **do**
16: R [UMPA~B (a, b)] +=1, FB[j] =FB[j] +1
17: Add UMPA~B (a, b) to L[R [UMPA~B (a, b)]]
18: if R [UMPA~B (a, b)]>max **do**
19: max=R [UMPA~B (a, b)]
20: m=max, S= {}
21: while s is empty do
22: Remove UMPs with mapped UE from L[max]
23: $C = L[m]$, $m = m - 1$, $n = 0$
24: S = {un-Controversial UMPs in *C}*
25: while *S* is empty do
26: $n = n + 1$, I = {UMPs with top n *Mij* in C using (5)}
27: S = {un-Controversial UMPs in *I}*
28: if $I == C$ do
29: break
30: return T

IV. RESULT AND DISCUSSION

The experimental analysis done using the java programming with set of Facebook and LinkedIn users account .the performance is measured using input user and search time of proposed system.

In this paper an application was developed through which can perform anonymous user identification .To Register this Application, user selects type of social network (Facebook, LinkedIn), gives their user name, password and basic information of user (i.e., mobile no, email, gender and birth date). After the registration process, the user can login their account by giving their user name and password. After login process user can view their profile, add friends and view their friend list, search friends, send friend request etc. The Admin has right to identifies the anonymous user.

Table. 1 and fig. 2 shows the performance analysis of FRUI, Profile and Content based technique with input user and search time (milliseconds).

Technique	Input user	Searching time (milliseconds)
FRUI	600	69868
Profile base	350	4045
content base	50	3067

Table1. Input user and Searching Time.

As shown in above table.1. This system have been tested for 300 users of Facebook and 300 users of LinkedIn accounts (total 600). On this 600 input users, first FRUI algorithm is applied. After that got 350 users as an output of FRUI. Then using this output as an input for profile base, got 50 users as an output of profile base. On this output, content base algorithm is applied and got 3 anonymous users as output.

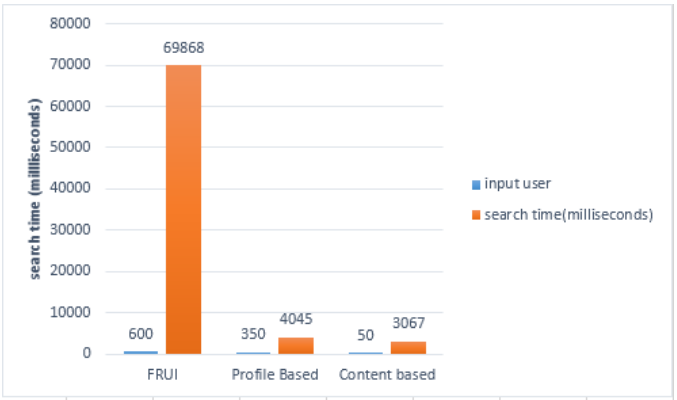

Fig.2 Analysis graph of proposed system.

V. Acknowledgement

After the completion of this work, words aren't enough to specific feelings regarding all people who helped me to achieve my goal. It's an excellent pleasure and moment of huge satisfaction on behalf of me to specific my profound feeling to my guide **Prof. Vaishali Jadhav** and my co-guide academician **Prof. Sujata Bhairnallykar** whose constant encouragement enabled Pine Tree State to figure sky-high. Her perpetual motivation, patience Associate in Nursing glorious experience in discussion throughout progress of the planned work have benefited Pine Tree State, that is on the far side and all members of Computer Engineering department who are giving support to done my work .

VI. CONCLUTION AND FUTURE SCOPE

In this paper finds the difficulty to identify the fraud user's identification in multiple SMN. In SMN network structure is main part. It is help to sort out user identification tasks downside. The planned system for FRUI algorithm. This algorithm finds fraud users by using two another profile based and content based technique (algorithm) to identify fake users. In future work, system have a tendency to aim to assign with that various challenges that system sweet-faced throughout that course of analysis. As an example there are several cases whenever same username doesn't essentially guarantee the identical identity.

REFERENCES

[1]. Xiaoping Zhou, Xun Liang, Senior Member, IEEE,Haiyan Zhang, Yuefeng Ma "Cross-Platform Identification of Anonymous Identical Users in multiple social media network. ". Citation information: DOI 10.1109/TKDE.2016.2485222, IEEE Transactions on Knowledge and Data Engineering.

[2].Wikipedia, "Twitter, "http://en.wikipedia.org/wiki/Twitter. 2014.

[3]Wikipedia,"Facebook"https://en.wikipedia.org/wiki/Facebook.

[4].Wikipedia,"LinkedIn"https://en.wikipedia.org/wiki/LinkedIn.

[5]. Xinhuanet, "Sina Microblog Achieves over 500 Million Users,"http://news.xinhuanet.com/tech/201202/29/c_122769084.htm. 2014.

[6]. M. Motoyama and G. Varghese, "I seek you: searching and matching individuals in social networks," Proc. of the 11th inter-national workshop on Web Information and Data Management (WIDM'09), pp. 67-75, 2009.

[7]. R. Zafarani and H. Liu, "Connecting corresponding identities across communities," Proc. of the 3rd International ICWSM Con-ference, pp. 354-357, 2009.

.[8] D. Perito, C. Castelluccia, M.A. Kaafar, and P. Manils, "How unique and traceable are usernames?" Privacy Enhancing Technol-ogies (PETS'11), pp. 1-17, 2011.

[9]. O. Goga, D. Perito, H. Lei, R. Teixeira, and R. Sommer, "Large-scale Correlation of Accounts across Social Networks," Tech-nical report, 2013

[10]. P. Jain and P. Kumaraguru, "Finding Nemo: searching and re-solving identities of users across online social networks," arXiv preprint arXiv: 1212.6147, 2012.

[11].T. Iofciu, P. Fankhauser, F. Abel, and K. Bischoff, "Identifying users across social tagging systems," Proc. of the 5th International AAAI Conference on Weblogs and Social Media, pp. 522-525, 2011.

[12] R. Zafarani and H. Liu, "Connecting users across social media sites: a behavioral-modeling approach, " Proc. of the 19th ACM SIGKDD International Conference on Knowledge Discovery and Data Mining (KDD'13), pp.41-49, 2013.

[13] J. Liu, F. Zhang, X. Song, Y.I. Song, C.Y. Lin, and H.W. Hon, "What's in a name? An unsupervised approach to link users across communities," Proc. of the 6thACM international conference on Web search and data mining (WDM'13), pp. 495-504, 2013.

Proceedings of the Fourth International Conference on Communication and Electronics Systems (ICCES 2019)
IEEE Conference Record # 45898; IEEE Xplore ISBN: 978-1-7281-1261-9

Fuzzy based Technique for Nodes Coverage with Load Balancing Data collection using Multiple Conflicting Factors

Anjali[1]
Information Technology
Rajkiya Engineering College
Ambedkar Nagar Akbarpur, India
anjalibhandari464@gmail.com

Nidhi[2]
Information Technology
Rajkiya Engineering College
Ambedkar Nagar, Akbarpur, India
nidhi11998@gmail.com

Kumkum Dubey[3]
Information Technology
Rajkiya Engineering College
Ambedkar Nagar, Akbarpur, India
dubeykumkum0607@gmail.com

Prince Rajpoot[4]
Information Technology
Assistant Professor, Rajkiya Engineering College
Ambedkar Nagar, Akbarpur, India
princeraj@recabn.ac.in

Amit Kumar Singh[5]
Assistant Professor (Mathematics)
Rajkiya Engineering College
Ambedkar Nagar, Akbarpur, India
aksingh@recabn.ac.in

Ajeet Kumar[6]
Assistant Professor CSD
Bakhtiyarpur College of Engineering
Patna, India
azit.bce@gmail.com

Ritika Yaduvanshi[7]
Computer Science and Engineering
Mahamaya College of Agricultural Engg and Tech
Ambedkar Nagar, Akbarpur, India
dinkal.ritika@gmail.com

***Abstract*—Due to wide application range in remote areas, Wireless Sensor Network (WSN) is an emerging field of research to prolong the lifetime. Since the battery is not replaceable so there is a need of efficient communication to prolong the lifetime. For this, many techniques are provided by many researchers like: clustering, routing, data aggregation etc. In clustering technique, the whole area is divided into many parts known as clusters. But clustering should be efficient to effect positively. Our aim is to provide load balancing with higher coverage of nodes. So, we have proposed a clustering algorithm based on three conflicting factors using fuzzy. The results positively support the algorithm in order to prolong the network lifetime.**

***Index Terms*—Wireless sensor network (WSN); Clustering; Coverage; Average Lifetime of CHs; Standard Deviation of Lifetime CH; Fuzzy**

I. Introduction

Wireless Sensor Network (WSN) is a collection of tiny sensors [1] having the capability of sensing the surroundings. There may be one or more onboard sensors attached with a node. WSN is having many applications in many areas like: healthcare, military, whether forecasting, agriculture etc. The communication of data may be wired or wireless according to the application of WSN. Sensor can also have chargeable or non-chargeable battery. But most of the applications use wireless communication due to the use in remote areas, so also contains non-rechargeable battery with many other issues like: reliability, security, fault tolerance etc [3] [4] [9]. Due to this there is always a need of efficient utilization of battery to gain data for more time. So our aim is to maximize the lifetime of network. For this many routing [7], clustering [2] [8] etc algorithms have been proposed by many authors. Initially the transmission was direct transmission where the sensor directly transfers the data to the Base Station (BS). After this, data transmission changes to indirect as multi-hop transmission, which reduces the energy consumption by a node and distribute it among all nodes. After it, Clustering algorithm comes into existence that divides the whole network into some clusters and each cluster is having one CH that is responsible for data collection and transmission after processing.

Energy Model We have utilized the same energy model used by [12]. The energy consumption according to this model can be shown as:

$$E_T = \begin{cases} p * E_{electronic} + p * \varepsilon_{fs} D^2_{length}, & \text{if } D_{length} < d_0 \\ p * E_{electronic} + p * \varepsilon_{mp} D^4_{length}, & \text{if } D_{length} \geq d_0 \end{cases} \quad (1)$$

E_T - known as transmission energy utilization in transmission p packets at distance D_{length}. $E_{electronic}$ shows energy in initialization of transmitter.
'd_0'- threshold length
ϵ_{mp}- Transmission with amplification
ϵ_{fs}- Transmission without amplification

Energy utilization in p packet receiving:

$$E_{p_{Rec}}(k) = E_{(Rec-electronic)} * p = p * E_{electronic} \tag{2}$$

We have proposed a clustering algorithm using fuzzy with three conflicting attributes. We have taken heterogeneous WSN where the characteristics of nodes are different to each other. Results verify the superiority of proposed algorithm.
The remaining paper is as follows: Section II explains some previous work done for the lifetime maximization of WSN. Section III explained the proposed algorithm in detail. Section IV shows the comparison of proposed technique with LEACH and base algorithm. Finally the conclusion is given in Section V.

II. Related Work

Clustering is one of the main approaches used for the lifetime maximization by topology controlling and dividing the work among the nodes. The total area is divided into some part and each part is known as cluster. Each cluster is having one CH that is known as the leader of that cluster, whereas, all other nodes work as member nodes. Member nodes sense the data and transmit it to the CH and CH process the data and forward it to the BS either directly or by intermediate CHs. Heinzelman [12] provided LEACH protocol in 2000. LEACH is one of the famous clustering algorithms that work on probabilistic model. It used the probability concept in such a way so that each node would work as a CH after particular number of rounds means it divides the responsibility of CH among the nodes. All remaining nodes join the CHs on the basis of signal distance that shows the corresponding distance. But due to randomness it unbalances the energy consumption. LEACH-C [13] is one of the extended versions of LEACH that specified a restriction that a node is able to be a CH only if its energy is greater than the average of total network energy. Due to this it confirms the division of nodes with higher residual energy. But the energy consumption remains unbalance in this algorithm.
After this H-LEACH [27] came into existence that divides the whole area into some predefine partitions and each LEACH algorithm is applied in each partition to select the CH in each partition. Aaditya et al. [28] provided Hybrid H-LEACH with updating the CH selection process by making it based on distance and residual energy and also using re-clustering phase that validates the minimum distance of member node to the respective CH. Some techniques used centralized control for CHs selection [14] [15]. Yang [19] and Wnag [20] is provided a dynamic approach for clustering and tracking the target. Sharma [21] provided clustering and routing technique using multi-hop path. Many other solutions [5] [6] [10] [11] [23] [24] [25] [26] have been provided for WSN applications to prolong the lifetime.
In our last papers, we have proposed many attributes [30] [31] that can effect to the energy consumption rate and also proposed a multi-attribute based clustering [29] that provided efficient clustering by enhancing the technique given by Elma et al. [27]. As improvement of our previous work, we have proposed fuzzy based clustering using multi-attributes.

III. Proposed Work

The complete proposed algorithm can be described in following steps:
Step 1: First, we find the nodes having remaining energy greater than the total average of network:

$$Energy_{res}(node) > Energy_{res}(Net\_avg) \tag{3}$$

Step 2: Now, we made twenty populations from the node. These populations are generated using k-means clustering and contain only nodes having high residual energy. So here we have used the concept of LEACH-C algorithm to select the CHs from the set of nodes with high amount of energy. It increases the chance that the selected CH will be able to collect data and transmit it to the BS or next CH.
Step 3: Compute Node Coverage: It shows how many normal nodes in the clustered network are within the d0 distance. Its value shows that how many of nodes are within the range where no amplification or regeneration of signal is required. This is calculated for each set of CH or for each population. It is computed as:

$$Node\_Cover = \frac{(Count\_Nodes_k(Distance_{(Node_k - CH)}) \leq d_0)}{n-1} * 100 \tag{4}$$

Step 4: Compute Average Lifetime of CHs: It shows the average of number of rounds till a CH is able to survive or we can say that it shows the time period till the CH is able to collect the data from normal or member nodes and send it to the BS or CH next in the path. It also helps us maintain the same clustering for more time so that there will be no need for frequent clustering. It means we can proceed with the same clusters for next few rounds. It is computed as:

$$Avg\_CHs\_lifetime = \frac{\sum_{c=1}^{CHs_{count}} (Erem\_CH_c / E_{Tran\_Req})}{CHs_{count}} \tag{5}$$

Step 5: Compute Standard Deviation of Lifetime CH: It verifies the load balancing among the CHs. It shows the deviation of lifetime of CHs and lower value helps us to maintain equal energy dissipation and balance lifetime of each CH. Population with lower standard deviation verify the equal energy dissipation in homogeneous WSN and maintain the equal remaining lifetime in both heterogeneous and homogeneous WSN. It plays critical role in where the dead of single node affect the data collection process and we need

whole network to work simultaneously for maximum time. It is computed as:

$$Std\_CH\_life = \sqrt{\frac{\sum_{c=1}^{CHs_{count}} (Lifetime_c - Avg\_CHs\_lifetime)^2}{CHs_{count}}} \quad (6)$$

Step 6: In this step, we use the fuzzy logic to calculate the fitness value for each set of CH or population. All input values are normalized first and then provided as the input. For defuzzification, total 27 rules are generated by us to find the fitness value of a population. The figure explains the fuzzy rules generated by us. We have used triangular membership function for fuzzy calculation.

Fuzzy Description: We have used triangular membership function as shown in Figures 1 and 2 for every input and output.

Fuzzy Rules: We define total twenty one rules as shown in Figures 3 and 4.

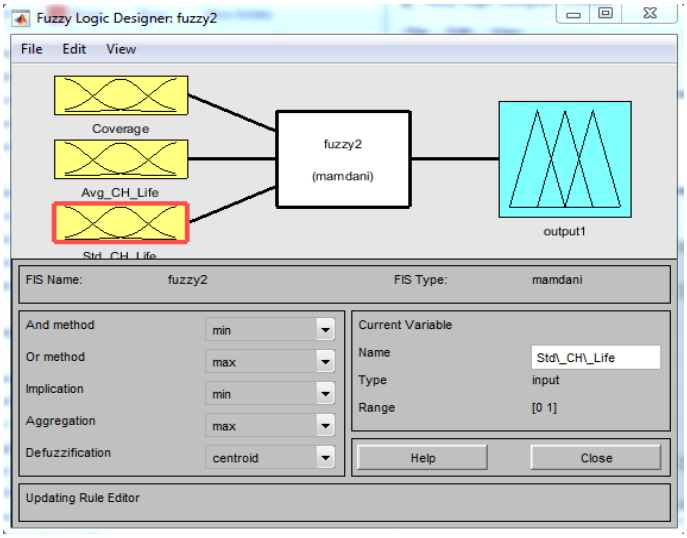

Fig. 1: Fuzzy logic formation

Step 7: Now the population having maximum fitness value selects as the best set of CHs and the nodes in that set select as the final CHs for the data collection.

Step 8: Cluster Formation: All other nodes are known as member nodes and join the nearest CH according to the received signal strength.

IV. Result and Experimental Simulation

We have used MATLAB to simulate all the data collection process with realistic view and better understanding. We have compared with LEACH protocol and our old proposed algorithm. We have processed the whole process in number of rounds and compared all the algorithms. The comparison is done on the basis of number of dead nodes and residual energy and it is shown by Figures 7, 9, 6, and 8.

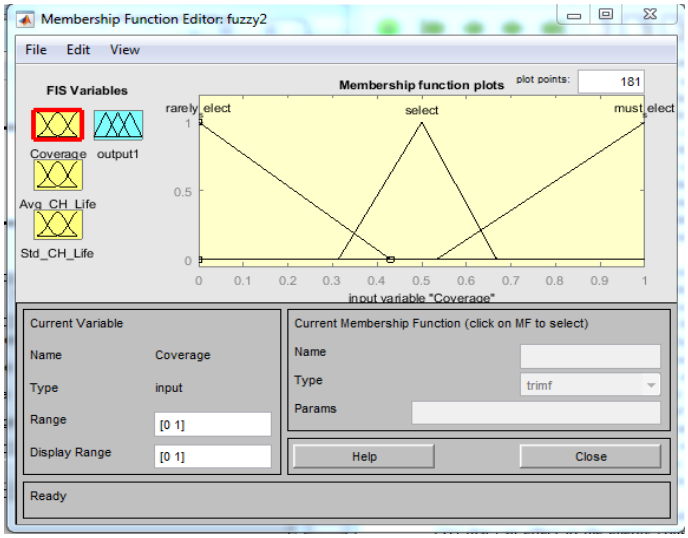

Fig. 2: Membership function for input coverage

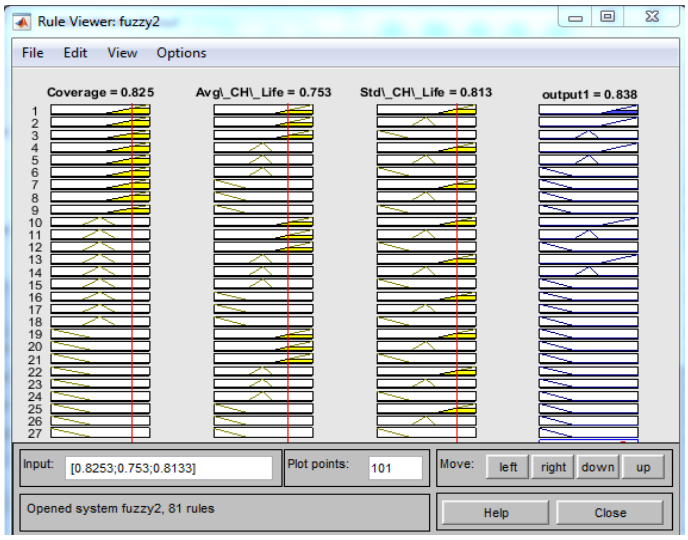

Fig. 3: Fuzzy rules for fitness function

CASE 1: BS position:- (50,50), Sensors Count:- 100, Round Count:- 100

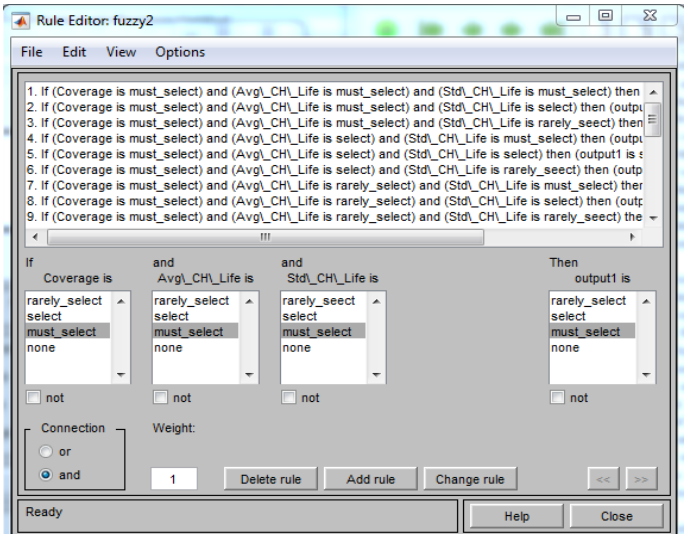

Fig. 4: Fitness example using fuzzy rules

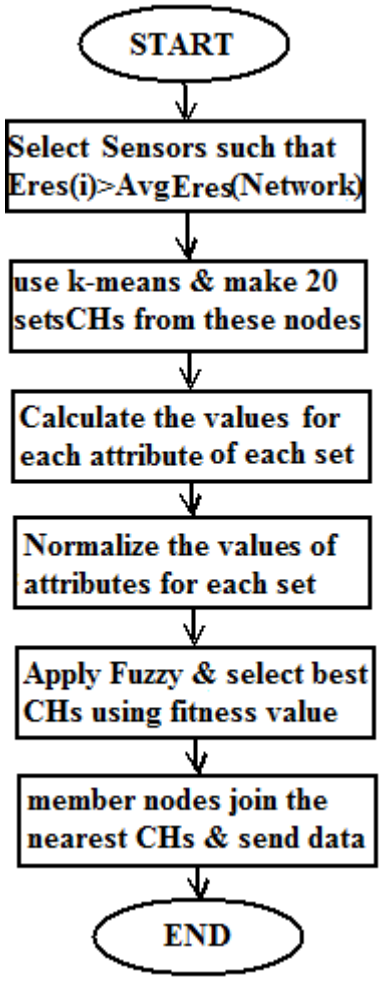

Fig. 5: Proposed clustering technique

Algorithm 1: Fuzzy Based Clustering Technique

Data: $Energy_{prime}$(i), E(Trans.)
Result: Clusters

Begin
for *each sensor s* **do**
  if($Energy_{remain}(s) >$ Avg_Energy_{remain}(Network))
  Mark it as advance node
end
make k sets of node using advance nodes
for *each set k* **do**
  for *each round* **do**
    Quanitfy Node_Cover;
    Quanitfy Avg_CHs_lifetime;
    Quanitfy Std_CH_life;
  end
end
Normalize all the values of each attribute; Use Fuzzy and Calculate the Fitness Value for each Set k;
for *every k_Set* **do**
  Compare with all other Fitness Values of different sets;
end
Declare Best Set of CHs;
CHs in Best Set finally selected as final set of CHs;
for *every Normal Node* **do**
  Find Nearest CH;
  Join that cluster;
end
End

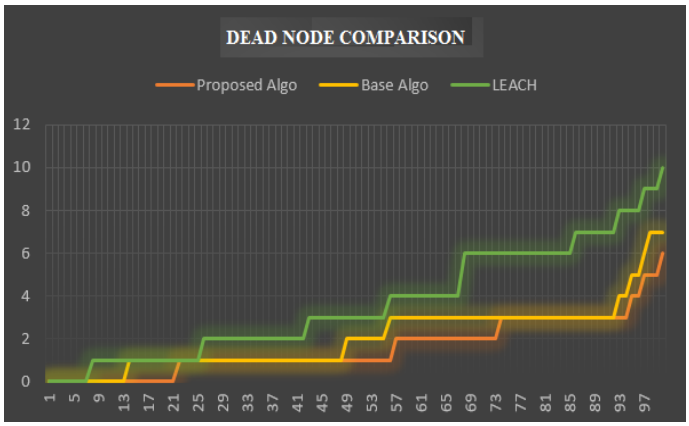

Fig. 6: Dead sensors compare at Rmax=100

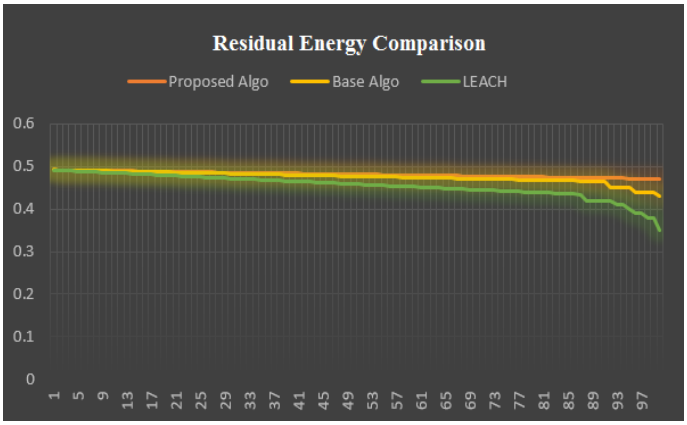

Fig. 7: Residual power compare at Rmax=100

CASE 2: BS position:- (0,0), Sensors Count:- 200 Round Count:- 500

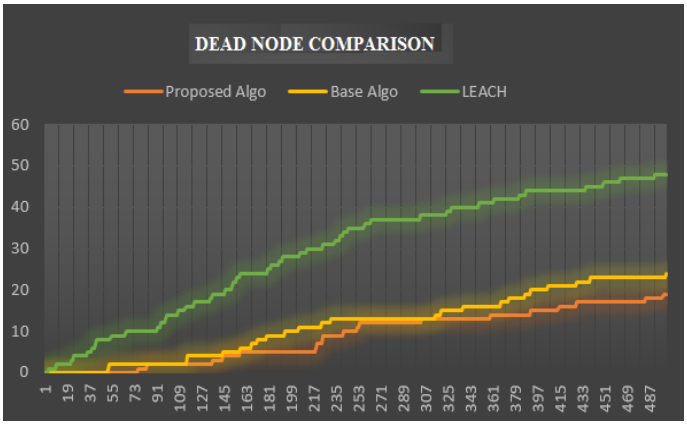

Fig. 8: Dead sensors compare at Rmax=500

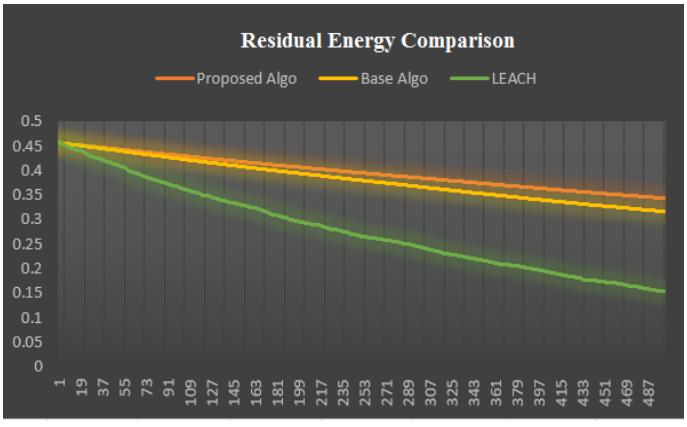

Fig. 9: Residual power compare at Rmax=500

Conclusion

High value of coverage verifies that the member nodes can easily communicate with the chosen CH with out need of amplification of signal. Average lifetime of CHs shows that best nodes are chosen for CHs and they can survive for more period of time. Low standard deviation verifies the load balancing among the CHs. The proposed technique provides us a fuzzy based fitness value generation and selection of set of best CHs among available according to the optimal value of fitness value for the population. This technique removes the manual computation of fitness calculation as was done in our last paper and provides a better approach for the fitness value calculation and selection of CHs based on the fuzzy calculation. Results and simulation part support that our proposed technique provides higher lifetime for network.

Acknowledgment

Special thanks to TEQIPIII REC Ambedkar Nagar for the financial help.

References

[1] H. P. Gupta, S. V. Rao, A. K. Yadav, and T. Dutta, "Geographic routing in clustered wireless sensor networks among obstacles." IEEE Sensors Journal 15, no. 5: 2984-2992, 2015.

[2] J. S. Lee, and W. L. Cheng, "Fuzzy-logic-based clustering approach for wireless sensor networks using energy predication." IEEE Sensors Journal 12, no. 9: 2891-2897, 2012.

[3] Z. Fei, Bin Li, Shaoshi Yang, Chengwen Xing, Hongbin Chen, and Lajos Hanzo. "A survey of multi-objective optimization in wireless sensor networks: Metrics, algorithms, and open problems." IEEE Communications Surveys & Tutorials 19, no. 1: 550-586, 2017.

[4] H. Ma, Shigen Shen, Mei Yu, Zhile Yang, Minrui Fei, and Huiyu Zhou. "Multi-population techniques in nature inspired optimization algorithms: a comprehensive survey." Swarm and Evolutionary Computation 44: 365-387, 2019.

[5] C. Y. Chang, J. P. Sheu, Y. C. Chen, and S. W. Chang, "An obstacle-free and power-efficient deployment algorithm for wireless sensor networks." IEEE transactions on systems, man, and cybernetics-part A: systems and humans 39, no. 4: 795-806, 2009.

[6] F. Marcelloni, and M. Vecchio, "A simple algorithm for data compression in wireless sensor networks." IEEE communications letters 12.6, 2008.

[7] S. Yang, H. Cheng, and F. Wang, "Genetic algorithms with immigrants and memory schemes for dynamic shortest path routing problems in mobile ad hoc networks." IEEE Transactions on Systems, Man, and Cybernetics, Part C (Applications and Reviews) 40.1: 52-63, 2010.

[8] H. Chen, K. T. Chi, and J. Feng, "Impact of topology on performance and energy efficiency in wireless sensor networks for source extraction." IEEE Transactions on Parallel and Distributed Systems 20, no. 6: 886-897, 2009.

[9] F. M. Kiaie, and A. Khanlari, "Coverage problem in heterogeneous wireless sensor network." European Scientific Journal, ESJ 9, no. 27, 2013.

[10] S. Mini, S. K. Udgata, and S. L. Sabat, "Sensor deployment and scheduling for target coverage problem in wireless sensor networks." IEEE sensors journal 14, no. 3: 636-644, 2014.

[11] J. Lee, T. Kwon, and J. Song, "Group connectivity model for industrial wireless sensor networks." IEEE Transactions on Industrial Electronics 57, no. 5: 1835-1844, 2010.

[12] W. R. Heinzelman, A. Chandrakasan, and H. Balakrishnan, "Energy-efficient communication protocol for wireless microsensor networks." In System sciences, 2000. Proceedings of the 33rd annual Hawaii international conference on, pp. 10-pp. IEEE, 2000.

[13] W. B. Heinzelman, A. P. Chandrakasan, and H. Balakrishnan, "An application-specific protocol architecture for wireless microsensor networks." IEEE Transactions on wireless communications 1, no. 4: 660-670, 2002.

[14] D. Kumar, T. C. Aseri, and R. B. Patel, "EEHC: Energy efficient heterogeneous clustered scheme for wireless sensor networks." computer communications 32, no. 4: 662-667, 2009.
[15] F. Bajaber, and I. Awan, "Adaptive decentralized re-clustering protocol for wireless sensor networks." Journal of Computer and System Sciences 77, no. 2: 282-292, 2011.
[16] O. Younis, and S. Fahmy, "HEED: a hybrid, energy-efficient, distributed clustering approach for ad hoc sensor networks." IEEE Transactions on mobile computing 3, no. 4: 366-379, 2004.
[17] Y. Jin, D. Wei, S. Vural, A. Gluhak, and K. Moessner, "A distributed energy-efficient re-clustering solution for wireless sensor networks." In Global Telecommunications Conference (GLOBECOM 2011), 2011 IEEE, pp. 1-6. IEEE, 2011.
[18] I. T. Almalkawi, M. G. Zapata, and J. N. Al-Karaki. "A cross-layer-based clustered multipath routing with QoS-aware scheduling for wireless multimedia sensor networks." International Journal of Distributed Sensor Networks 8, no. 5 (2012): 392515.
[19] W. Yang, Z. Fu, J. Kim, and M. Park, "An adaptive dynamic cluster-based protocol for target tracking in wireless sensor networks." In Advances in Data and Web Management, pp. 157-167. Springer, Berlin, Heidelberg, 2007.
[20] F. Wang, X. Bai, B. Guo, and C. Liu, "Dynamic clustering in wireless sensor network for target tracking based on the fisher information of modified Kalman filter." In Systems and Informatics (ICSAI), 2016 3rd International Conference on, pp. 696-700. IEEE, 2016.
[21] S. Sharma, and S. K. Jena, "Cluster based multipath routing protocol for wireless sensor networks." ACM SIGCOMM Computer Communication Review 45, no. 2: 14-20, 2015.
[22] K. J. Elma, and S. Meenakshi, "Energy Efficient Clustering for Lifetime Maximization and Routing in WSN." International Journal of Applied Engineering Research 13, no. 1: 337-343, 2018.
[23] P. Rajpoot, and P. Dwivedi, "Matrix Method for Non-Dominated Sorting and Population Selection for Next Generation in Multi-Objective Problem Solution." In 2018 8th International Conference on Cloud Computing, Data Science & Engineering (Confluence), pp. 670-676. IEEE, 2018.
[24] N. Verma, N. Pandey, and P. Rajpoot, "Energy Efficient Protocol to Supervise Overground Pipelines using WSN", Proceedings of 2018 3rd IEEE International Conference on Recent Trends in Electronics, Information & Communication Technology (RTEICT-2018), pp 1818-1823, in press.
[25] P. Rajpoot, Data Aggregation and Distance Based Approach to Boost Life Span of WSN. International Journal of Engineering Technology Science and Research, IJETSR, Volume 4, 2017.
[26] S. H. Singh, R. Verma, and P. Rajpoot, "Partition Based Strategic Node Placement and Efficient Communication Method for WSN", Proceedings of 2018 3rd IEEE International Conference on Recent Trends in Electronics, Information & Communication Technology (RTEICT 2018), pp 1807-1812, in press.
[27] V. Gupta, and M. N. Doja, "H-LEACH: Modified and Efficient LEACH Protocol for Hybrid Clustering Scenario in Wireless Sensor Networks." In Next-Generation Networks, pp. 399-408. Springer, Singapore, 2018.
[28] Aaditya, R. Kumar, and P. Rajpoot, "Optimized H-LEACH algorithm for clustering to improve lifetime of WSN", Proceedings of 2018 3rd IEEE International Conference on Recent Trends in Electronics, Information & Communication Technology (RTEICT-2018), pp 2393-2398, in press.
[29] P. Rajpoot, S. H. Singh, R. Verma, K. Dubey, S. K. Pandey, and S. Verma, "Multi-Factor Based Energy Efficient Algorithm for Clustering and Routing in WSN", Soft Computing: Theories and Applications: Proceedings of SoCTA 2018, Springer, (2018), in press.
[30] P. Rajpoot, and P. Dwivedi, "Optimized and load balanced clustering for wireless sensor networks to increase the lifetime of WSN using MADM approaches." Wireless Networks: 1-37, 2018.
[31] P. Rajpoot, and P. Dwivedi, "Multiple parameter based energy balanced and optimized clustering for WSN to enhance the Lifetime using MADM Approaches." Wireless Personal Communications: 1-49, 2019.

Proceedings of the Fourth International Conference on Communication and Electronics Systems (ICCES 2019)
IEEE Conference Record # 45898; IEEE Xplore ISBN: 978-1-7281-1261-9

Power Balanced Efficient Clustering Algorithm for WSN

Prince Rajpoot[1]
Information Technology
Rajkiya Engineering College
Ambedkar Nagar, Akbarpur, India
princeraj2904@gmail.com

Pragya Dwivedi[2]
Computer Science & Engg.
MNNIT Allahabad
Prayagraj, India
pragyadwi86@mnnit.ac.in

Kumkum Dubey[3]
Information Technology
Rajkiya Engineering College
Ambedkar Nagar, Akbarpur, India
dubeykumkum0607@gmail.com

***Abstract*—Wireless Sensor Network is having large number of sensors that sense the surrounding area. Sensing coverage of each nodes are limited that depends on their hardware designing. There is a Base Station (BS) that collects all the packets from sensors and then further processing is done on the collected that are used by the authentic users for taking decision. These information are stored in repository that may be used in future for business models too. Generally these sensors nodes are deployed in remote areas that are not easily reachable so energy is one of the main problem since batteries are not going to be frequently changed once they are deployed. There are lots of proposed work given by many authors and researchers for prolonging the WSNs lifetime. Some of the popular algorithms are LEACH, LEACH-C, HEED etc. Clustering is one of the strategy in which clusters are formed and there is a Cluster Head (CH) in each cluster and the other members nodes transmit data to their respective CHs. In our proposed algorithm we have consider four factors for the selection of CHs.**

***Index Terms*—Wireless sensor network (WSN); Clustering; Delay; Network Lifetime; Maximum power of nodes required; Lifetime of CH; Maximum power of CHs required**

I. Introduction

WSN is a network in which sensors are used in each devices and they all are connected to each other by wireless medium. Each sensor senses the surrounding area. Sensors are used as per our demand that what kind of environment we have to sense. WSN has lots of application in field of medical, agriculture, military and also natural disaster management for the prediction of any tragedy.

In WSN each sensor nodes have their own battery that are treated as non-replaceable since it is not possible to change their batteries frequently once they are deployed. Lifetime of WSN should be as long as possible so we have proposed an approach for prolonging lifetime of whole network. We have used clustering approach in which clusters are formed and in each cluster a CH is selected that receives data from all its member nodes falling under same cluster. After receiving data from all member nodes CHs perform some computation and calculation than further processed data are sent to the sink node i.e. base node that are assumed to having infinite energy since their batteries are easily replaceable because they are easily reachable.

Selection of CHs are our main concern since they have more responsibility with respect to other member nodes. If perfect suitable nodes are chosen as CHs than it may be possible that they dead before time and it will affect our whole network, even whole network may go down. It must be taken care that CHs have to receive data from all nodes after that it must be processed for further processing then it is sent to BS means that more operation that will use more energy so the energy of selected CH must be high. Apart from this the distance of CH to BS will also play a measure role so this distance should be low. We also want to minimize the delay so all the factors that may affect it will be also taken care while selecting CH. We have considered four factors from some previously proposed factors [1] [2] for the selection of CHs. It will select best CHs among all possible nodes that will help us in prolonging lifetime of our network. These factors are:-

1. Delay
2. Maximum power of nodes required
3. Maximum power of CHs required
4. Average lifetime of CH

After considering all these factors a fitness function will be used to calculate fitness value of each nodes. The nodes who has maximum fitness value will be selected as CH and they will work as CHs for some rounds. After some rounds CHs are changed since there fitness value are not perfect to work as CH.

Once CHs are selected they have to collect data from its member's node and forward it to BS. The route followed by CHs to send this data to BS should also be perfect since it may leads to cause delay and more energy consumption too. CH may directly sent data to BS that is called as single hop transmission, no doubt it will take more energy with respect to multi hop transmission. We will select the shortest route for transmission of data from CHs to BS.

Organization of rest of the paper is as: review is described in section 2. Section 3 determines about proposed work whereas the results and comparisons are shown in section 4. Finally, conclusion is explained in section 5.

II. Related Work

Energy is the main concerned in WSN, for this many researches have been done to find its solution [3] [7] [8] [13] [14] - [16]. Topology management [8] - [12] and route analysis [3] - [6] is the main solutions to various issues in

WSN. Low Energy Adaptive Clustering Hierarchy (LEACH) [19] is the main algorithm in field of clustering. It is utilizes probabilistic approach for choosing the CHs in such a way so that every node can become a CH after particular rounds. The selected CHs broadcast a message of selection as a CH so that the normal nodes can find the nearest CH and join that cluster. A TDMA schedule is assign for the data transmission process so that each node can send its available data in its slot. In this way, it distributes the load among the nodes and enhances the lifetime of network. But the selection among the available nodes becomes randomly that creates the unbalance of energy consumption and lead to early dead sometimes.

Centralized control [21], [22] in LEACH can also be given to BS. Here, the BS knows the information about the nodes like: its location and its remaining power and BS selects the CHs for enhancement of lifetime. But this approach is limited to the small WSN.

LEACH-B [23] is an expansion of LEACH algorithm, it optimized number of CHs based on the available remaining energy. Archimedes spiral model is utilized by Halder et al. [24] to optimize the distance between sensors to utilize the energy. LEACH-C [25] applies restriction to LEACH so that no node be able to take a part in CH selection that would have energy less than network's average energy. H-LEACH [26] divides the whole network into many part and LEACH is applied in each part independently. H-LEACH is modified by Aditya et al. [27] by providing dynamic partition that changes after each round of CH selection.

Neetu et al. [29] gave an efficient information collection about abnormal activity in gas pipeline. We have also proposed solution using some factors [30]. Position of nodes may affect the network utility [32] and aggregation of data is also helpful in energy optimization by reducing the redundancy in data packets. Best population selection can be done as the form of next generation [28] and can be applied where many objectives need to fulfill simultaneously. In this paper, we have suggested an algorithm taking a property of LEACH-C that only those nodes take part in CHs selection which will have energy greater than total average energy of WSN. It also utilizes many attributes including some suggested [30] and some new attributes for selecting the CHs.

III. Proposed Work

We designed an algorithm specified as energy optimization using a protocol based on multi parameters of WSNs. The proposed algorithm increases the lifetime of the network by calculating the optimized cluster heads which is the root for lifetime maximization of WSN. The population generated in the network consist of sensor nodes which have the fixed energy and power and cannot be recharged. This energy of sensor nodes gets reduced after certain transmissions of data. So, there is a need to suggest a method or an algorithm which could maximize the lifetime of the sensors. The given algorithm is based on the procedure that, from given nodes, we select certain sets of nodes to be selected as CH. For every set, we generate the fitness function value and the set with the best fitness value is selected. the nodes opted in the set are considered to be final CHs.

Eres represents the total power left in the nodes. more the residual energy less will be the delay as the delay is contrary to Eres. The efficiency of the network depends upon the CHs. selected. CH determination is accomplished by the fitness function explored in the methodology section. Cluster formation is done after the CH determination. The CHs broadcasts the message that they have been selected as final CH and nodes can join them to form the cluster. In return, the nodes send the join message depending upon the signal strength and distance of a node from the CH. A Connection is established among the nodes. CH and base station and the communication starts with the transfer of data. This fitness function proposed is applied to the sets of node periodically so as to maintain the non-uniform distribution of energy nodes considering their residual energy. For the packet delivery to BS from CHs, we require the shortest path which is calculated through Route identification theorem.

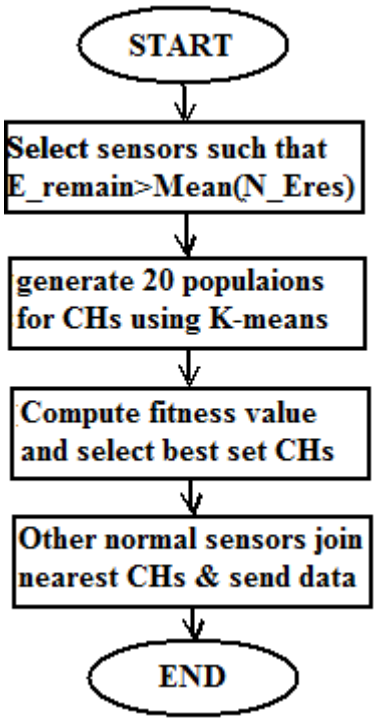

Fig. 1. Proposed Approach for Clustering

A. *An enhanced approach for energy optimization using protocol based on multi factors*

Sensor nodes are distributed in the network in a random manner. The proposed algorithm EOPMF calculates the fitness function value, determines the CHs.

*1) **CH Investigation:**:* As there are n nodes deployed in the network in a random fashion, we take all n nodes and compare their residual energy(remaining energy) with the

total average energy of the network. we select sensors having $E_{res} > E_{avg}$. according to the need of CHs, we choose the sets of nodes to be elected as CHs and apply the fitness function on these sets. The set with the best fitness value is supposed to have the best CHs. The steps involved in the process of CH determination are:

*a) **Step 1**:* **Evaluation of Delay:**
The greater is the residual energy lesser is the delay. Delay evaluation can be given as:

$$Total\_Delay = (\frac{(E_{preliminary} - E_{remaining})}{E_{preliminary}} + random\_num) * RoundTripDelay \quad (1)$$

*b) **Step 2**:* **Evaluation of Maximum power of required by members:**
It determines the max energy dissipation by any one member node. Its evaluation can be given as:

$$P\_Max\_mem = Max(Transmission\_E(Member_j - CH)) \quad (2)$$

*c) **Step 3**:* **Evaluation of Maximum power of CHs required:**

$$CH\_Power\_Max = Maximum(Trans\_E(CH_c - BS)) \quad (3)$$

*d) **Step 4**:* **Evaluation of Average Lifetime of CH:**

$$Avg\_ClustHd\_Life = \frac{\sum_{k=1}^{CHs\_Num}(E_{res} - E_{Trans(CH_k - BS)})}{CHs\_Num} \quad (4)$$

*e) **Step 5**:* **Determination of fitness function:**

$$Fitness = 0.4 * F1 + 0.15 * F2 + 0.2 * F3 + 0.25 * F4 \quad (5)$$

Where factor F1 = Delay, F2 = Maximum power of nodes required, F3 = Maximum power of CH required, and F4 = average lifetime of CH.

*f) **Step 6**:* All the steps described above are rephrased for distinct times and finally, the best CHs are selected based on the optimized fitness value.

*2) **Cluster Formation**:* Once the final set of CH is obtained, all the normal nodes send the join message to the nearest CH depending upon signal strength. These nodes percept the information from their vicinity and transfer information to CH. The CH after receiving information, passes it to the BS through the shortest path algorithm described in the base paper.

Algorithm 1: Proposed CH investigation method

```
Data: Initial Energy E(i), variables values
Result: CHs
Begin
for each sensor n do
    if(E_left(n) > E_left(net))
    add sensor to CH_group
end
originate Q sets in CH_group
for all sets Q in CH_group do
    for all CH Investigation round do
        Enumerate the Delay;
        Enumerate Maximum power of nodes required;
        Enumerate Maximum power of Ch required;
        Enumerate average lifetime of CH for all sets Q;
    end
end
Pick r in (0,1);
Suppose M(Fit_Opt), N(Fit_Opt) are optimization
parameter for two sets M and N;
for each CH set Q do
    if ((M(Fit_Opt) < N(Fit_Opt))
    {
    N is optimal set of CHs
    }
end
End
```

B. Packet Forwarding Process:

Route identification algorithm is required to get the shortest path from CH to BS so that the minimum energy is utilized for the transmission. The Algorithm is discussed in the base paper. The data is transmitted from the CH to base station in a single or multi-hop manner considering the shortest path and minimum energy constraint required.

IV. Result and Experimental Simulation

We have pre-owned the MATLAB software for the simulation of the algorithm and generate the results. the study of different cases visualizes a better picture of base paper and proposed approach comparison. Net Eres and dead nodes are taken as the comparison attributes. The network assumes to be dead when 3/4 of total sensor dies. Dead comparison is is done as 2, 4, and 6 and residual comparison is done as: 3, 5, and 7. The proposed algorithm's results outperforms to the base algorithm by imparting maximized lifetime to the network.

CASE 1: When Node count = 500, sink position (0,0)

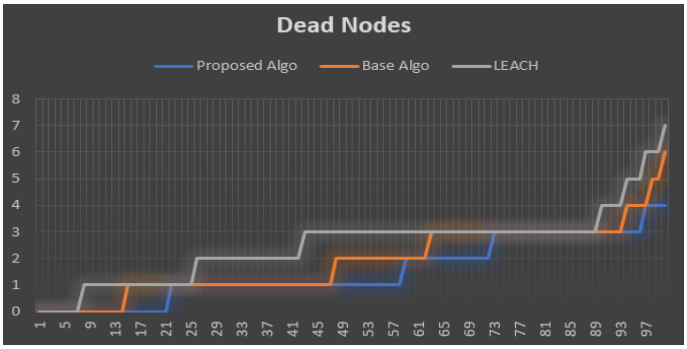

Fig. 2. Dead sensors graph for Rmax=100

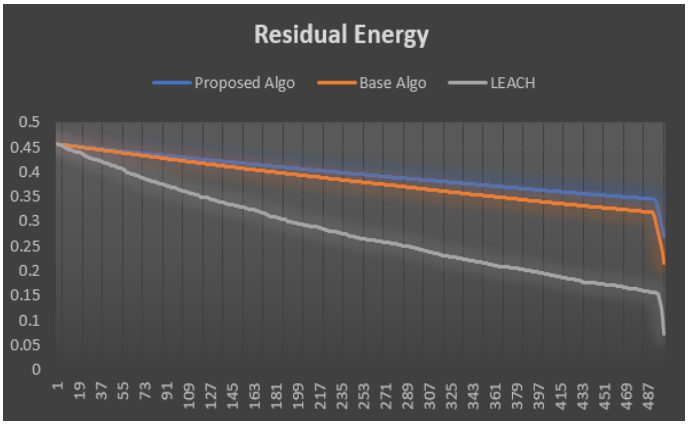

Fig. 5. E_{res} graph for Rmax=100

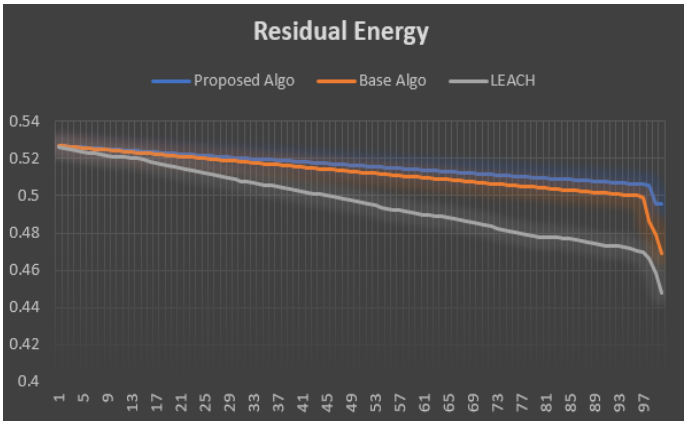

Fig. 3. E_{res} graph for Rmax=100

CASE 3: When Node count = 500, sink position (40,40)

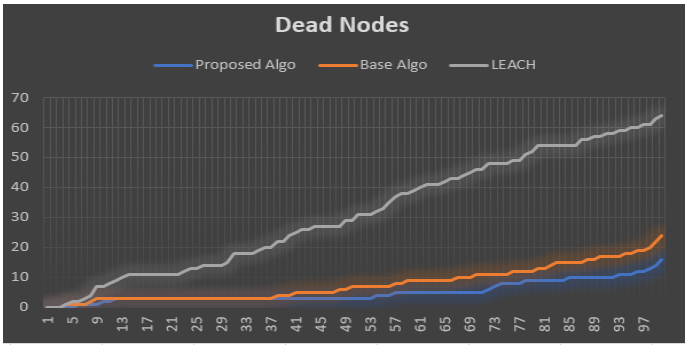

Fig. 6. Dead sensors graph for Rmax=100

CASE 2: When Node count = 100, sink position (20,20)

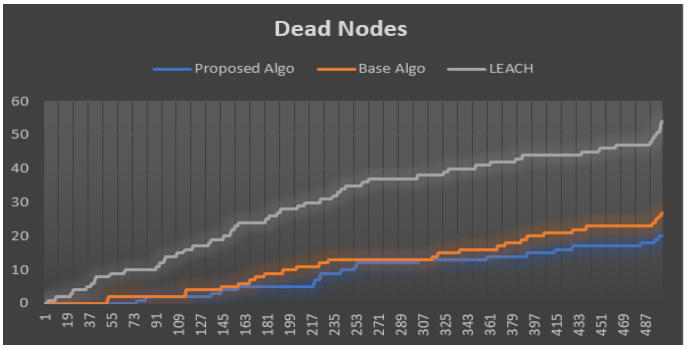

Fig. 4. Dead sensors graph for Rmax=100

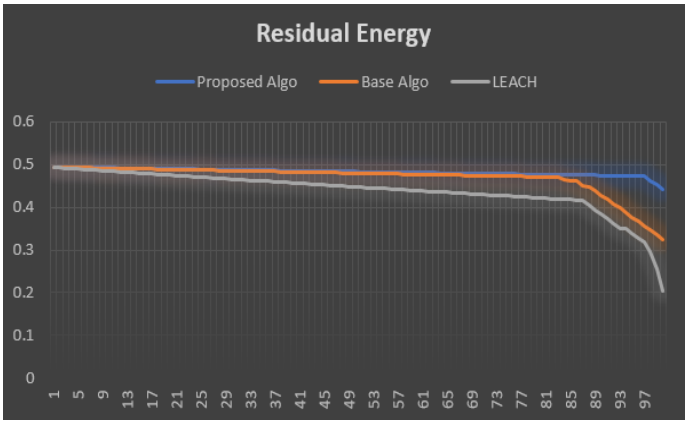

Fig. 7. E_{res} graph for Rmax=100

V. Conclusion

In wireless sensor network our main goal is to collect information from sensor nodes. We have fulfilled our main

motive to prolong lifetime since sensor node batteries are not changed frequently once they are deployed and there is limited power. For our proposed algorithm we have considered the heterogeneous network apart from homogeneous in which sensor nodes are of different configuration with respect to energy and other factors. Proposed method makes information collection process efficient and make higher lifetime. Comparison of the proposed algorithm with the LEACH and base paper assists our concept.

ACKNOWLEDGMENT

We are thanksful to TEQIP-III REC ambedkar Nagar for the financial support.

REFERENCES

[1] P. Rajpoot, and P. Dwivedi, "Optimized and load balanced clustering for wireless sensor networks to increase the lifetime of WSN using MADM approaches." Wireless Networks: 1-37, Springer, 2018.

[2] P. Rajpoot, and P. Dwivedi, "Multiple parameter based energy balanced and optimized clustering for WSN to enhance the Lifetime using MADM Approaches." Wireless Personal Communications: 1-49, 2019.

[3] N. Chilamkurti, S. Zeadally, A. Vasilakos, and V. Sharma, "Cross-layer support for energy efficient routing in wireless sensor networks." Journal of Sensors, 2009.

[4] T. Meng, F. Wu, Z. Yang, G. Chen, and A. V. Vasilakos, "Spatial reusability-aware routing in multi-hop wireless networks." IEEE Transactions on Computers 1: 244-255, 2016.

[5] C. Busch, R. Kannan, and A. V. Vasilakos, "Approximating Congestion+ Dilation in Networks via" Quality of Routing" Games." IEEE Trans. Computers 61, no. 9: 1270-1283, 2012.

[6] A. Dvir and A. V. Vasilakos, "Backpressure-based routing protocol for DTNs". InACM SIGCOMM Computer Communication ACM, Vol. 40, No. 4, 405-406, 2010.

[7] Y. Yao, Q. Cao, and A. V. Vasilakos, "EDAL: An energy-efficient, delay-aware, and lifetime-balancing data collection protocol for wireless sensor networks." In Mobile ad-hoc and sensor systems (MASS), 2013 IEEE 10th international conference on, pp. 182-190. IEEE, 2013.

[8] Y. Zeng, K. Xiang, D. Li, and A. V. Vasilakos, "Directional routing and scheduling for green vehicular delay tolerant networks." Wireless networks 19, no. 2: 161-173, 2013.

[9] X. Luo, Y. Hu, and Y. Zhu, "Topology evolution model for wireless multi-hop network based on socially inspired mechanism." Physica A: Statistical Mechanics and its Applications 416: 639-650, 2014.

[10] M. Li, Z. Li, and A. V. Vasilakos, "A survey on topology control in wireless sensor networks: Taxonomy, comparative study, and open issues." Proceedings of the IEEE 101, no. 12: 2538-2557, 2013.

[11] X. Hu, Y. Li, and H. Xu, "Multi-mode clustering model for hierarchical wireless sensor networks." Physica A: Statistical Mechanics and its Applications 469: 665-675, 2017.

[12] X. M. Zhang, Y. Zhang, F. Yan, and A. V. Vasilakos, "Interference-based topology control algorithm for delay-constrained mobile ad hoc networks." IEEE Transactions on Mobile Computing 14, no. 4: 742-754, 2015.

[13] K. Han, J. Luo, Y. Liu, and A. V. Vasilakos, "Algorithm design for data communications in duty-cycled wireless sensor networks: A survey." IEEE Communications Magazine 51, no. 7: 107-113, 2013.

[14] L. Xiang, J. Luo, and A. Vasilakos, "Compressed data aggregation for energy efficient wireless sensor networks." In Sensor, mesh and ad hoc communications and networks (SECON), 2011 8th annual IEEE communications society conference on, pp. 46-54. IEEE, 2011.

[15] Y. Yao, Q. Cao, and A. V. Vasilakos, "EDAL: An energy-efficient, delay-aware, and lifetime-balancing data collection protocol for heterogeneous wireless sensor networks." IEEE/ACM Transactions on Networking (TON) 23, no. 3: 810-823, 2015.

[16] Y. Xiao, M. Peng, J. Gibson, G. G. Xie, D. Z. Du, and A. V. Vasilakos, "Tight performance bounds of multihop fair access for MAC protocols in wireless sensor networks and underwater sensor networks." IEEE Transactions on Mobile Computing 11, no. 10: 1538-1554, 2012.

[17] F. T. Jaigirdar and M. M. Islam, "A new cost-effective approach for battlefield surveillance in wireless sensor networks". In: IEEE networking systems and security, pp 16, 2016.

[18] K. J. Elma and S. Meenakshi, "Energy Efficient Clustering for Lifetime Maximization and Routing in WSN", International Journal of Applied Engineering Research 13.1: 337-343, 2018.

[19] W. R. Heinzelman, A. Chandrakasan, and H. Balakrishnan, "Energy-efficient communication protocol for wireless microsensor networks." In System sciences, 2000. Proceedings of the 33rd annual Hawaii international conference on, pp. 10-pp. IEEE, 2000.

[20] W. B. Heinzelman, A. P. Chandrakasan, and H. Balakrishnan, "An application-specific protocol architecture for wireless microsensor networks." IEEE Transactions on wireless communications 1, no. 4: 660-670, 2002.

[21] D. Kumar, T. C. Aseri, and R. B. Patel, "EEHC: Energy efficient heterogeneous clustered scheme for wireless sensor networks." computer communications 32, no. 4: 662-667, 2009.

[22] F. Bajaber, and I. Awan, "Adaptive decentralized re-clustering protocol for wireless sensor networks." Journal of Computer and System Sciences 77, no. 2: 282-292, 2011.

[23] M. Tong, and M. Tang, "LEACH-B: an improved LEACH protocol for wireless sensor network." In Wireless Communications Networking and Mobile Computing (WiCOM), 2010 6th International Conference on, pp. 1-4. IEEE, 2010.

[24] S. Halder and A. Ghosal, Lifetime maximizing clustering structure using archimedes spiral based deployment in WSNs. Integrated Network Management (IM), (2015) IFIP/IEEE International Symposium on. IEEE, 2015.

[25] J. Lee, T. Kwon, and J. Song, "Group connectivity model for industrial wireless sensor networks." IEEE Transactions on Industrial Electronics 57, no. 5: 1835-1844, 2010.

[26] V. Gupta, and M. N. Doja, "H-LEACH: Modified and Efficient LEACH Protocol for Hybrid Clustering Scenario in Wireless Sensor Networks." In Next-Generation Networks, pp. 399-408. Springer, Singapore, 2018.

[27] Aaditya, R. Kumar, and P. Rajpoot, "Optimized H-LEACH algorithm for clustering to improve lifetime of WSN", Proceedings of 2018 3rd IEEE International Conference on Recent Trends in Electronics, Information & Communication Technology (RTEICT-2018), pp 2393-2398, in press.

[28] P. Rajpoot, and P. Dwivedi, "Matrix Method for Non-Dominated Sorting and Population Selection for Next Generation in Multi-Objective Problem Solution." In 2018 8th International Conference on Cloud Computing, Data Science & Engineering (Confluence), pp. 670-676. IEEE, 2018.

[29] N. Verma, N. Pandey, and P. Rajpoot, "Energy Efficient Protocol to Supervise Overground Pipelines using WSN", Proceedings of 2018 3rd IEEE International Conference on Recent Trends in Electronics, Information & Communication Technology (RTEICT-2018), pp 1818-1823, in press.

[30] A. K. Yadav, P. Rajpoot, P. Kumar, K. Dubey, S .H Singh and R. Verma, "Multi Parameters Based Heterogeneous Clustering Algorithm for Energy Optimization in WSN" In 2019 9th International Conference on Cloud Computing, Data Science & Engineering (Confluence). IEEE, 2019, in press.

[31] P. Rajpoot,"Data Aggregation and Distance Based Approach to Boost Life Span of WSN". International Journal of Engineering Technology Science and Research, IJETSR, Volume 4, Issue 11, 2017.

[32] S. H. Singh, R. Verma, and P. Rajpoot, "Partition Based Strategic Node Placement and Efficient Communication Method for WSN", Proceedings of 2018 3rd IEEE International Conference on Recent Trends in Electronics, Information & Communication Technology (RTEICT 2018), pp 1807-1812, in press.

[33] P. Rajpoot, S. H. Singh, R. Verma, K. Dubey, S. K. Pandey, and S. Verma, "Multi-Factor Based Energy Efficient Algorithm for Clustering and Routing in WSN", Soft Computing: Theories and Applications: Proceedings of SoCTA 2018, Springer, 2018, in press.

Proceedings of the Fourth International Conference on Communication and Electronics Systems (ICCES 2019)
IEEE Conference Record # 45898; IEEE Xplore ISBN: 978-1-7281-1261-9

Different Input Impedance Matching Circuits for Cascode Common Source LNA with Inductive Degeneration Topology in 45nm CMOS Technology

Malti Bansal , Diksha Singh
Department of Electronics & Communication Engineering,
Delhi Technological University (DTU), Delhi-110042, India
maltibansal@gmail.com

***Abstract*— This paper presents various input impedance matching networks that can be used for cascode common source LNA with inductive degeneration topology in 45 nm CMOS technology. We review the matching networks being used and analyze their performance using simulations. Based on our simulation results, we further conclude that T-Matching network is the best input impedance matching network for cascode common source LNA with inductive degeneration topology in 45 nm CMOS technology.**

Keywords—LNA, IoT, SNR, Inductive Degeneration, Cascode

I. INTRODUCTION

It is an era of amazing developments in technologies. Wireless technologies are improving faster than anything. Alternate options are being explored and efforts are being done to design devices that would save energy. The advancements in technology aim to create sustainable future and are focused on creating devices that are reduced in size and consume less resources. Market for wireless technologies is increasing at a rate faster than one can imagine. Emerging wireless technologies require a receiver system that is compatible with the latest methodologies of wireless systems. Wireless technologies demand a receiver system that provides an optimum performance and consumes low power; which makes it suitable to run for a longer duration of time. Low power receivers are in demand because they also felicitate battery less operation [1]. Recent wireless technologies include ZigBee, Bluetooth, Bluetooth low energy (BLE), etc. which aim at providing a solution for obtaining low energy solutions and also making IoT a future possibility in every aspect of life. With brisk increase in communication technology, additional burden of larger integration also follows up. Better performance delivering integrated circuits are in demand with spectacular improvements in technology. CMOS scaling technologies are also improving day by day which is able to provide better performance at a lower cost and lower chip area. These developments in CMOS process technologies have made realizing a system on chip feasible, for use in almost all domains of life [2]. With scaling of technology integration of circuit is more compact i.e., more no of elements can be placed in a smaller area. This increases the complexity of the circuits. Digital circuits can be easily redesigned according to the changes in the CMOS technology. However redesign of analog circuits to cope up with the advancements in technology has become a challenge for the researchers [3]. This paper is organized in 5 sections. Section I gives a brief review about the recent technologies in wireless communication. Section II of the paper discusses about the Low Noise Amplifier (LNA), its importance in wireless communications and its utility in other domains as well. Further in section III, we discuss the design aspects of the LNA with reference to matching networks and other design parameters as well. Section IV is about the simulation results obtained and further in Section V, we select the preferred matching network based on our analysis.

II. LNA IN WIRELESS COMMUNICATION

A. Low Noise Amplifier(LNA)

At the receiver block, the signal needs to be received and processed further which includes filtering the undesired frequencies, amplification of the signal while maintaining a good value of signal-to-noise ratio (SNR). Signal-to-Noise ratio gives an idea of extent up-to which the signal is affected by noise. A large value of SNR signifies good signal strength and low value of SNR signifies poor signal strength. In most of the receiver architectures, first block in the receiver after the antenna is the Low Noise Amplifier [4]. A low-noise amplifier is an electronic amplifier that amplifies a very low-power signal without significantly degrading its signal-to-noise ratio. It may be preceded by a band select filter in some architectures. LNA is responsible for the overall performance of the receiver to a large extent as it is the first block in the receiver chain and its noise performance dominates the noise performance of the complete receiver. LNA amplifies the signal present at its input and adds a very little noise by the virtue of its components. Hence, it is preferred in many receiver architectures and other domains as well. LNA should provide a high gain, low noise figure, high linearity, low power consumption, etc. LNA's performance is determined by the value of these design parameters [5]. LNA needs to be connected to other components of the receiver system, so input and output impedance should be high enough to prevent loading effect on other components connected. Loading effect tends to decrease the gain of the amplifier as effective load resistance of the amplifier decreases as a consequence of low resistance of the adjacent components. A fully-integrated LNA is the best option. Finally, power consumption is a concern, especially for portable devices. LNA with all parameters perfectly within the limit cannot be designed as trade-off always exists between the different parameters of a LNA. Based on our application area, we need to focus on the parameter to be optimized and accordingly the LNA design procedure is carried out further.

B. LNA in wireless communication

Applications of low noise amplifier involve different frequency ranges but when we want to implement it for

XXX-X-XXXX-XXXX-X/XX/$XX.00 ©20XX IEEE

wireless applications, the frequency that is to be considered is 2.4 GHz or a higher frequency than this as well. Wireless communication is carried out using a narrow band of frequencies or single frequency. Hence we do not need to focus obtaining an optimum performance over a wide range of frequencies. However, there are applications which require wideband LNA's i.e., optimum performance over a wider range of frequency. Darlington amplifier proves to be best for applications for wideband performance [6].

C. Applications of LNA

Applications of LNA also decide the components that can be utilized in the circuit design. If we require a system on chip, we should avoid components which occupy larger chip area, etc. LNAs are used in many applications like industrial scientific and medical band (ISM band), cellular telephones, biomedical applications (at low frequency), satellite communications, etc. For biomedical applications, the low noise amplifier should be designed such that the power consumed by it is within the limit because it may increase the temperature of the tissues; and higher temperature may damage the brain tissues.

III. DESIGN PROCESS

The first step in the design of any circuit or system is creating an outline of expected performance of the circuit or the system. Application for which the circuit is to be designed is the most crucial factor that determines the design process. Unless application is specified, the design process cannot be initiated as the application determines the parameters of concern and we need to proceed with the design following those parameters. The trade-offs like impedance matching, choosing the amplifier technology (such as low-noise component) and selecting the low noise biasing conditions are important parameters for designing a low noise amplifier. Apart from this, low power consumption, small chip area and low cost are also desirable [7]. LNA design process can be categorised into 4 major parts that can be listed as: topology, matching networks, transistor selection and biasing [8].

A. Topology

LNA can be implemented using many topologies such as common-gate, common-source, cascode, etc. Out of all these available topologies, most widely used topology is cascode i.e., common source connected in cascade with common gate transistor [9]. This topology provides an improved performance over others and also improved bandwidth. These topologies can further be enhanced with additional circuitry to provide an improved performance. Common- Gate topology provides a highly linear circuit but noise performance of this topology is relatively low [10]. Inspite of a high noise figure, it can be utilized in wireless communication as it satisfies the standards of the wireless systems. Moreover, with the help of different techniques, desired noise performance can also be achieved by this topology.

B. Matching Networks

LNA is generally placed after the antenna which denotes an impedance of 50Ω. For maximum power transfer between two stages, the output impedance of the first stage should be matched with the input impedance of the second stage. If impedance mismatch occurs between the two stages, maximum power transfer will not take place and reflections are ought to occur. Hence, LNA's input impedance needs to be matched with antenna's output impedance to achieve complete power transfer. This can be achieved by using an input matching network that performs this task of matching the input impedance and it is very crucial for LNA's performance. Matching networks also have different topologies and numerous components are available that can provide matching between two stages. However, choosing a proper matching network that enhances the performance of the circuit is a tedious task that needs to be done properly. A change in matching network affects the circuit performance and hence, a comparison can be done to find which matching network is best for our circuit design.

Similar to the input stage, output matching also needs to be accomplished in order to transfer maximum power to the next stage after the LNA in the receiver block. Different output matching circuits also affect circuit performance.

C. Transistor Selection

Proper selection of transistor is crucial for performance of the circuit. Fabrication process also affects the circuit performance to a large extent. Basically, MOSFET (Metal Oxide Semiconductor Field Effect Transistor) is used to realise LNA, along with additional components.

D. Biasing

After the accumulation of the circuit components as desired, we need to provide biasing to give the device a stable operating point. If the biasing provided to the circuit is not able to provide a stable operating point, it will ruin the circuit performance at the desired frequency, and the circuit will become prone to oscillations and this may destroy the circuit completely. Hence, stability analysis is very crucial for a device's proper operation. Many methods are used to provide biasing to the circuit such as resistive divider biasing, current mirror, etc. Out of these methods, we prefer current mirror biasing as MOSFET current mirror tends to reduce the chip area of the circuit and also provides a good stable operating point to our device. After the design process is complete, we need to convert our design into end-product which can be achieved by fabrication of the circuit. Before fabrication process start,s we need to perform simulations and analyze the stability of the circuit in real time.

IV. SIMULATION RESULTS

We performed the simulations in ADS (Advanced Design System) software and obtained the results required. ADS is a tool which is used by RF designers to simulate circuits and analyze their performance before process of fabrication begins. It helps to reduce the cost of device as its properties can be studied before fabrication, saving unnecessary cost of fabrication. Different from other digital circuits, the value of RLC in RF circuits must be extremely precise due to the sensitivity of the frequency response. A slight change of the value of the circuit components such as inductor, capacitor, etc. within the RF circuit can cause a considerable effect that ruins the expected performance. LNA implemented uses a cascode pair in its basic circuit and a tank circuit is used as a load as it is ought to offer better performance than other

available output loads. We simulate the LNA circuit using 3 different input impedance matching networks and analyze the results obtained, on the basis of LNA parameter specifications. Cascode configuration provides better performance than other configurations and using inductive degeneration enhances the noise performance as well as the gain of the LNA [11]. Input impedance matching is achieved using different input impedance matching circuits and the circuits are simulated.

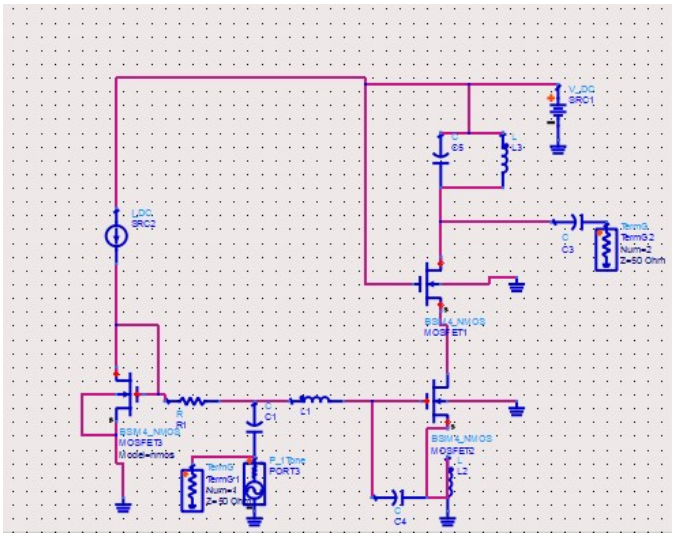

Fig. 1:Implemented LNA

LNA design cannot be perfect in all parameter values a s a trade-off will always exist between the parameters. Input impedance matching circuit can be designed in many configurations such as L matching, T-matching, π-matching, etc. Apart from these configurations, any matching network can be formed using components available that may include inductor, capacitor, transmisson line, stub-matching, etc. For LNA matching, we avoid using matching networks consisting of transmission lines as it may give rise to crosstalk, as the system being designed is going to be fabricated on a chip. Matching networks chosen for analysis are L matching network, T- matching network and third matching network is designed with different configuration than the available matching networks.

A measure of linearity of circuit is obtained by value of its Input Third Order Intercept point (IIP3). A high value of IIP3 implies a high linearity circuit. From the simulation results obtained, we infer that T matching provides a highly linear circuit than the other two combinations.

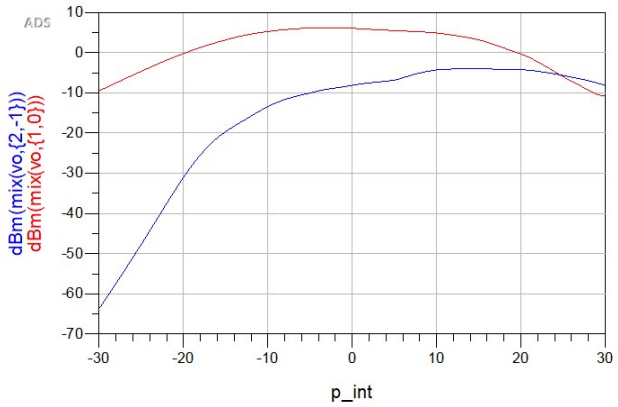

Fig. 2: IIP3 for the LNA circuit with matching network 1

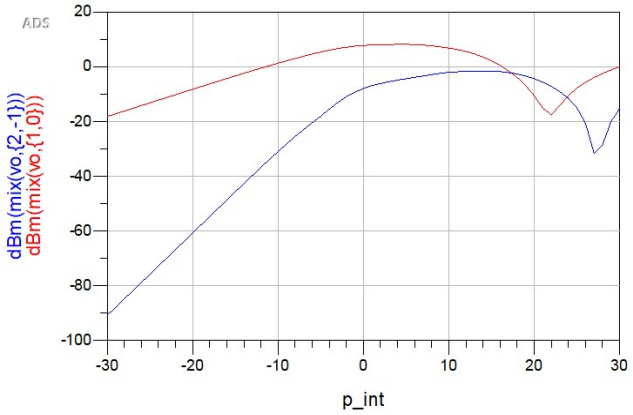

Fig. 3: IIP3 for the LNA circuit with matching network 2

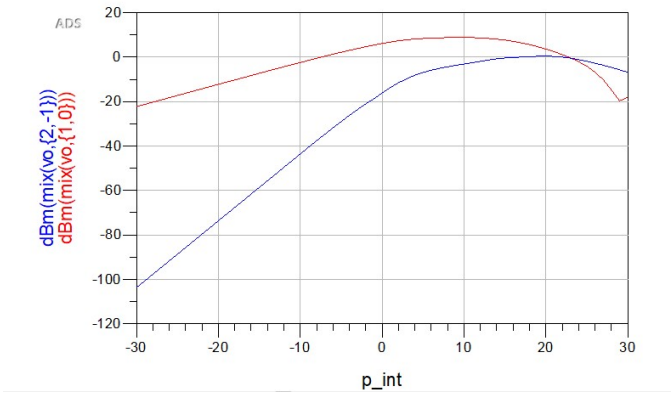

Fig. 4: IIP3 for the LNA circuit with matching network 3

An important parameter in LNA design is the gain offered by the amplifier. In many applications, where the signal to be processed is very weak, gain offered by the circuit is very crucial for the receiver performance. Gain of the system should be sufficiently high so that the effect of noise is suppressed and the SNR maintains a good value. L matching i.e., matching network 1, offers the maximum gain out of the three matching networks. Gain offered by this circuit is sufficiently high with a value of 26.52 dB which is good enough to process signals with very weak amplitudes. Gain offered by matching network 3 was the lowest and hence we conclude that it is not preferable for processing signals which are very weak.

Noise performance of the low noise amplifier is a very critical parameter. As the name implies, the LNA circuit should have a very low noise figure i.e., a good noise performance. It determines the overall noise performance of the receiver system, hence considering this parameter is essential during our design. On the basis of results obtained by simulations, we conclude that the noise figure of the circuit using matching network 2 and 3 is better than using matching network 1.

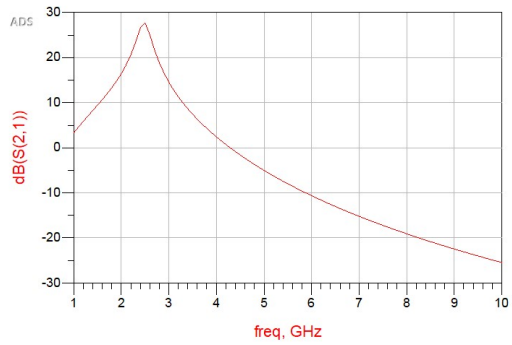

Fig. 5: S_{21} (Gain) of the LNA circuit with matching network 1

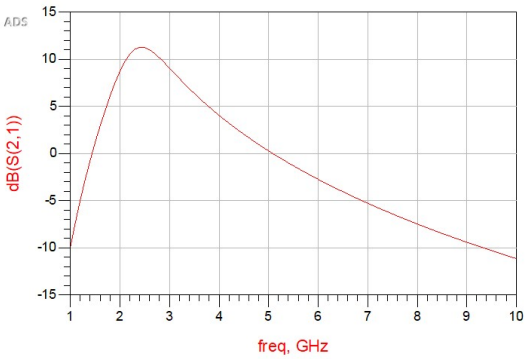

Fig. 6: S_{21} (Gain) of the LNA circuit with matching network 2

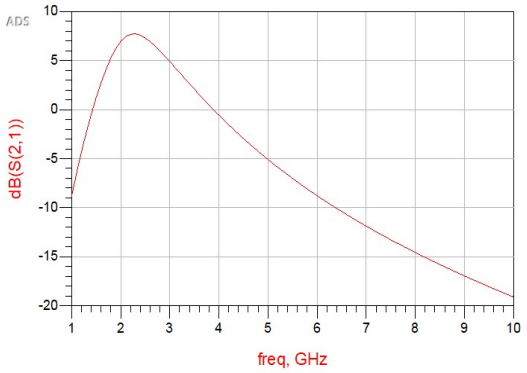

Fig. 7: S_{21} (Gain) of the LNA circuit with matching network 3

.

Either of the two circuits provides a good noise performance. Noise performance of the device is determined by the components being used in the circuit design.

V. CONCLUSION

It is very difficult to design a LNA with all the parameter values perfectly within the limits, which creates a restriction on choosing best circuit among given choices. If we require high gain in our system, while compromising with the noise performance, we can adopt L matching network in our design. On the other hand if we want a circuit with better noise performance, we can adopt T- matching network.

Fig. 8: Noise Figure of the LNA circuit with matching network 1

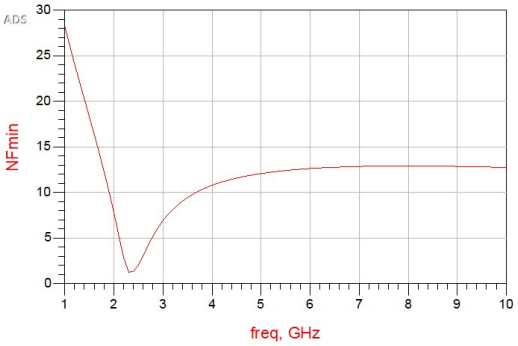

Fig. 9: Noise Figure of the LNA circuit with matching network 2

The results obtained are summarized in tabular form in the table 1.

Table 1: Results obtained for Cascode Common Source LNA with Inductive Degeneration Topology utilizing different input matching circuits

Parameters	Matching network 1 (L matching)	Matching network 2 (T matching)	Matching network 3
Technology	45nm	45nm	45nm
S_{11} (dB)	-12.041	-4.146	-36.5
S_{21}(dB)	26.52	11.281	7.705
S_{22}(dB)	-0.08	-1.202	-1.452
S_{12}(dB)	-51.28	-54.259	-63.25
Noise Figure (dB)	7.464	1.293	1.124
IIP3 (dB)	4.774	9.785	8.765
Power Consumption (mW)	5.45	8.91	9.37

We have simulated and analyzed Cascode Common Source LNA with Inductive Degeneration Topology in 45 nm technology using three different input matching networks and on the basis of the results obtained, we infer that T-matching network provides better overall performance when compared to the other matching networks.

REFERENCES

[1] Sesha Sairam Regulagadda, Nagaveni S, Ashudeb Dutta, “A 550-μW, 2.4-GHz ZigBee/BLE Receiver Front End for IoT applications in 180-nm CMOS”, in proceedings of International New Circuits and Systems Conference(NEWCAS) 2018

[2] Wang Wen-qi, Xu Liang, Zhan Fu-chun, " A Fully Integrated 2.4 GHz 0.25μm CMOS Low Noise Amplifier" in proceedings of Asia-Pacific Microwave Conference 2005
[3] Shaikh K. Alam, "A Novel 2.4 GHz CMOS Variable Gain Low Noise Amplifier Design for Bluetooth and Wireless LAN Applications", in Proceedings of International Conference on Consumer Electronics 2007
[4] Tajinder manku. "Microwave CMOS·devices and circuits" Proceedings of the IEEE 1998 Custom Integrated Circuits Conference. pp. 59-66
[5] Ayari Nadia, Hamdi Belgacem and Fradi Aymen," A Low Power Low Noise CMOS amplifier for Bluetooth applications", in proceedings of International Conference in Applied Electronics 2013
[6] K.W. Kobayashi, "Linearized Darlington cascode amplifier employing gaas PHEMT and GaN HEMT technologies," IEEE J. Solid-State Circuits,vol. 42, no. 10, pp. 2116–2122, Oct. 2007.
[7] G.Gonzalez (1997)," Microwave transistor amplifier: analysis and design", 2nd edition, upper saddle river, NJ:prentics - hall inc. 217, 294-303.
[8 Bhushan R. Vidhale, M.M.Khanapurkar, "Design of Ultra Wideband Low Noise Amplifier with the Negative Feedback using Micro strip Line matching structure for multiple band application and its Simulation based performance analysis", in proceedings of International Conference on Wireless Communications, Signal Processing and Networking(WiSPNET) 2016
[9] B. Razavi, Design of Analog CMOS Integrated Circuits.McGraw-Hill Science/Engineering/Math,2001.\
[10] Lei Liao, Stefan Kaehlert, Yifan Wang, Aytac Atac, Ye Zhang, Martin Schleyer, Ralf Wunderlich, and Stefan Heinen, "A Low Power LNA for Bluetooth Low Energy Application with Consideration of Process and Mismatch", in proceedings of Asia Pacific Microwave Conference 2012
[11] M_ Zamin Khan, Yanjie Wang and R. Raut, "COMPARISON OF DIFFERENT CMOS LOW-NOISE AMPLIFIERS TOPOLOGIES FOR BLUETOOTH APPLICATIONS", in proceedings of IEEE Annual Conference of Wireless and Microwave Technology 2005

Proceedings of the Fourth International Conference on Communication and Electronics Systems (ICCES 2019)
IEEE Conference Record # 45898; IEEE Xplore ISBN: 978-1-7281-1261-9

Cascode Common Source LNA with Inductive Degeneration Topology utilizing Different Output Matching Circuits in 45nm CMOS Technology

Malti Bansal , Diksha Singh
Department of Electronics & Communication Engineering,
Delhi Technological University (DTU), Delhi-110042, India
maltibansal@gmail.com

***Abstract*— One of the most essential component of transceivers is Low Noise Amplifier (LNA). LNA is placed at the initial stage of the receivers and hence, it governs the overall performance of the receiver. This paper compares Cascode Common Source LNA with Inductive Degeneration Topology utilizing different output matching circuits. We list the specific application domains of the different circuits analyzed, on the basis of the results obtained through simulations. We further conclude that RLC circuit is the best one to be used as an output matching network in terms of minimum power consumption and highest linearity.**

Keywords— IoT, Wireless, LNA, Cascode, Inductive Degeneration

I. INTRODUCTION

One of the hottest topics of research nowadays is 'Internet of Things' (IoT) i.e., connecting everything to the Internet to make the dream of smart homes come true. Researchers are working in order to design devices which can be made compatible with the IoT standards. Connecting everything to Internet puts an additional constraint on the components that are being designed. Researchers work to achieve best results using minimum resources in order to make a component that is able to cope up with the rapid growth in technologies day by day. Ability to communicate by the means of wireless medium is the most important feature required in the systems nowadays. For this we require a receiver which should be capable of providing an optimum performance when implemented in real-time systems. LNA is generally the first block in most of the receiver's architectures and hence its performance is crucial for the entire receiver system [1]. Choosing an LNA which is best in terms of performance parameters increases the efficiency of the receiver's system. However with expeditious growth in wireless communication industry, manufacturers aim to design a circuit which is able to deliver best results among the already available hardware at present. In case of LNA performance, target is to achieve a low noise figure, high gain, low loss, high IIP3, etc. [2]. RF circuits have created a tremendous scope of research and this comes due to advancements in semiconductor technologies which makes system level integration more flexible. These have also gained popularity due to their low cost which makes RF more attractive technology to work on. CMOS technology advancements have proved to be beneficial for both analog and digital circuits. However redesign of digital circuits for a newer technology is an uncomplicated process. This is not so in case of redesigning an analog circuit for a newer technology. It is a challenge to redesign analog circuits for newer technologies [3]. The paper is organized into 5 sections. Section I being the introduction followed by Section II that gives a brief about LNA in wireless communication. Further we move to Section III that discusses the topologies prominent for implementing LNA and in Section IV, we discuss the results achieved by us during simulations. In the last section of the paper, we summarize our results and state the application areas depending on the topology being discussed.

II. LNA IN WIRELESS COMMUNICATION

In recent times, focus on technologies consuming low-power has increased and these are being utilized in wireless communications as well. Low power consumption, high gain, low noise figure, etc. are the constraints that are the most important for implementing LNA in wireless communication. Apart from bluetooth communication, low power wireless devices are in demand for other application areas as well. These application areas include neural signal analysis, medical applications, etc. [4]. Since LNA determines the receiver performance, designing a LNA with consideration of all parameters within specified limits presents a demanding situation for all the researchers. Most of the LNA's are generally single band LNA i.e., they are designed to operate at a single frequency. However multiple band LNA's are also being introduced i.e., they are capable of operation at more than one frequency. Operating a single LNA over multiple frequencies increases the complexity of the circuit but it also makes it versatile for multi-standard applications. However LNA's are reported that operate at two frequencies i.e., they are dual band LNA's. Multiple band LNA's are less common as achieving optimum performance at multiple frequencies increases the overheads as well as increases the cost of the LNA. Moreover, it also results in increase in power requirements of the circuit as well as increase in the chip area occupied by the circuit [5]. If we wish to design a broadband LNA, we generally use a single transistor which is being used in common-source configuration [6]. Darlington amplifier is used in case of broadband applications i.e. optimum performance over a larger bandwidth [7]. Wireless communication is generally limited to short distances as compared to other forms of communication. Designing a LNA for short distance communication (up-to 10m) is a smooth process in comparison to designing a LNA for long distance communication (more than 10 m). LNA for long distance communication where the distance between the transmitter and receiver is more than the specified range requires high sensitivity which in turn leads to increase in complex design process. LNA for short distance communication where the distance between the transmitter and receiver module is less than 10 m drives the next block into compression because of the signal at the input being strong in amplitude. This signal leads to an output signal which is distorted. In this scenario we need a LNA that can overcome this problem by

suppressing the input signal to prevent this condition [8]. Bluetooth is also a form of wireless communication which is more prevalent and everybody is more familiar with this form of wireless communication. For Bluetooth communication also, we need a transmitter and receiver and the receiver end utilizes an LNA as the first block of the system. LNA for this particular application will have different characteristics than the LNA for other forms of communication as LNA parameters depend on the application for which they are being designed. More specifically a LNA for Bluetooth applications should provide a higher gain and consume less power than others. Bluetooth Low Energy (BLE) focuses on reducing the power consumption of the circuit and is apt for IoT applications. BLE devices can work for longer hours as they consume less power.

III. LNA TOPOLOGIES

LNA's utilize configurations that were used traditionally to design amplifiers. Other than configuration, additional steps need to be taken to achieve the desired performance. The desired performance can be obtained by introducing a change in the biasing network or it can be through a change in matching networks being used. Most common LNA topologies are common-gate, common-source, cascode, etc. Each of the above topology has its own advantages and disadvantages. In-spite of their own merits and demerits, the cascode configuration is the most common configuration used for implementing LNA. Common source configuration can be used with resistive load as well as inductive load. Resistive load offers less gain and also it does not provide proper matching, which at higher frequency creates a hindrance to the proper functioning of the circuit. Inductive load overcomes the disadvantages offered by resistive load configuration. In the common source configuration, the inductor placed at the output node is responsible for output matching. We also need to provide input matching network to match the input impedance of the amplifier with that of the antenna. In this configuration, a capacitor is also connected across the gate and drain of the transistor which denotes the gate-drain overlap capacitance. The effect of the capacitor is nullified by using an inductor in parallel with the resistance. Since the capacitor is of smaller value, the inductor that should be connected across it should be of a higher value. Using an inductor of large value introduces parasitic capacitances at the ouput node and input node of the circuit and thus degrades the performance of the amplifier. Hence, this topology is rarely used in practical LNA design. Common source stage with resistive feedback is also a possible topology that can be used to implement low noise amplifier. In this topology, a resistor is connected across the output and input nodes i.e., R_F provides a feedback from the output node to the input node. R_F sends a current signal as a feedback to the gate terminal of the transistor depending on the voltage at the output node. This topology does not suffer from the drawbacks as that of common source stage with resistive load. Gain offered by this topology is not restricted by the supply voltage as in case of resistive load. The trade-off between the gain and supply voltage is overcome in this particular topology and hence it is preferable over common source stage with resistive load. Resistive load in case of any transistor configuration i.e., common source or common gate, always creates a trade-off between the supply voltage and the gain of the circuit. Hence, resistive load is not preferred in any practical application, unless required.

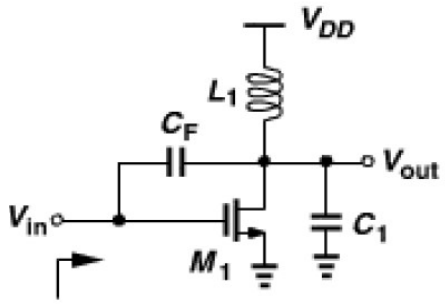

Fig. 1: Common Source Stage in presence of capacitance (reproduced from [9])

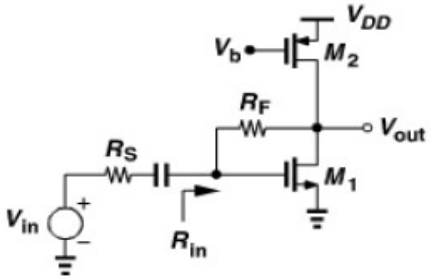

Fig. 2: Common Source Stage with resistive feedback (reproduced from [9])

Apart from common source configuration, common gate configuration can also be used to implement LNA for practical applications. Low input impedance offered by this configuration makes it suitable for practical applications. Inductor is used as a load in this configuration. If the inductor possesses ideal characteristics, it can be connected across the output terminals but if a practical inductor is to be used, a resistor should also be connected across it to model the losses offered by the inductor. Noise performance of this configuration is not optimum as it accounts for a lower gain i.e., better noise efficiency will result in a lower gain. Most widely used configuration is cascode common source stage. This configuration tries to overcome the drawbacks of the topologies discussed so far by introducing certain changes in the circuit. In this configuration, we use active devices to achieve input impedance matching of 50Ω, which limits the noise contribution that was added due to the passive devices in the circuit. One method to achieve this is inductive degeneration that is most widely used in LNA design. The value of the degenerative inductor is crucial in this design process. To achieve an impedance matching of 50Ω, an inductor having a value of about 50 pH, is to be realized. It is difficult to realize an inductor with this value accurately. Hence, in order to realize this inductor, a different method is used. If we wish to achieve impedance matching using degenerative inductor, we need to reduce the f_T of the transistor which can be done by adding an additional

capacitance across the MOSFET terminals. When we start the design process of the cascode LNA, we need to find out the value of the degeneration inductor according to the design specifications.

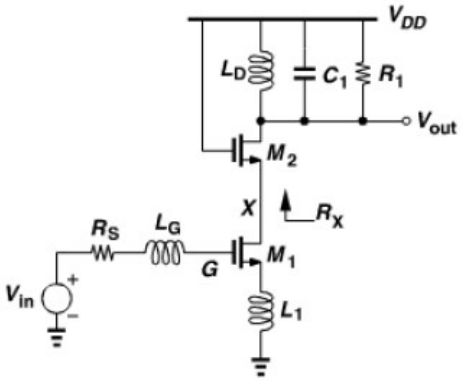

Fig. 3: Cascode Common Source Stage with Inductive Degeneration (reproduced from [9])

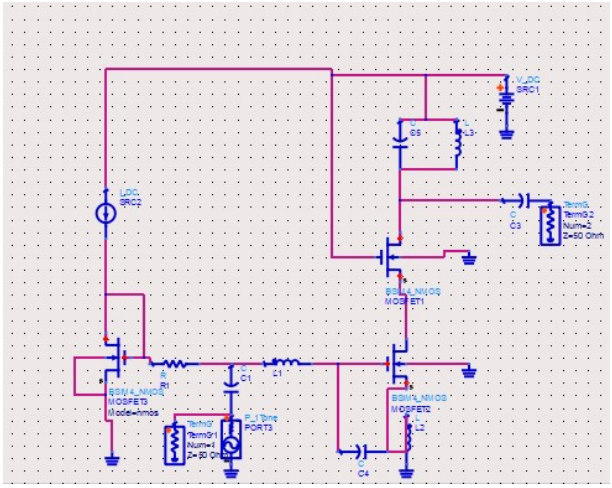

Fig. 4: Implemented LNA

Many other configurations also exist for LNA implementation but they are not widely used in practical applications as their design process is much more complex than these basic configurations. These topologies can be used if we want to design an application specific LNA. Noise cancelling LNA's are available i.e., their design process focuses on improving the noise performance of the LNA, etc.

IV. SIMULATION RESULTS

We can use different circuits as load in our low noise amplifier design and these circuits play a major role in the performance of the low noise amplifier. We have implemented four major output matching networks in our LNA and compared the simulation results obtained to find out the best output matching network for LNA circuits. We observe a trade-off between the various parameters of the LNA. Change in one parameter of the LNA affects the other parameters as well. We observe a trade-off between the gain of the LNA and the linearity of the circuit. We desire a high gain LNA; however a higher gain affects the linearity of the subsequent stages of the receiver. Hence, we need to confine our gain so that the non-linearity of the subsequent stages of the receiver does not become prominent. Generally a pre-select filter is placed before the LNA. This filter is sensitive to the impedance matching at its output terminals [10]. Hence, in our circuit design, we need to focus on impedance matching networks at the input terminal also. Cascode configuration implemented by us incorporates inductors and capacitors to provide this input matching. Inductor placed at the input terminal and the inductor placed at the source end of the MOSFET along-with the capacitance (C_{gs}) creates an input matching network for our configuration. Using a cascode configuration also has a benefit of providing required isolation between the input and output nodes. Isolation is necessary in circuits so that the signals from the output do not leak back to the input terminal. If proper isolation is not provided, signals may leak back and this creates a hindrance in proper operation of the circuit.

Using a resistance as a load is the most common practice but is does not prove to be the best output matching network based on our analysis. When resistance is used as a load, it is observed that it does not provide proper matching and maximum power is not delivered to the output node, which in turn results in more reflected power and losses.

$$|A_V| = g_m.R_D \qquad \text{..... (1)}$$

After substituting the values, we get the gain in terms of voltages as:

$$|A_V| = 2.VRD$$
$$V_{GS}-V_{TH} \qquad \text{.....(2)}$$

Gain obtained in this circuit is lower as it depends on the supply voltage and the voltage drop across the resistance. For new technologies, we work on lower voltages and hence, the gain is further reduced if we use resistance in our circuit. On the basis of results obtained, we conclude that using R as a load in our circuit is not preferable as it ought to increase the noise figure of the circuit as well as it is observed to provide a low value of IIP3. High frequency operation of the circuit is also restricted as the resistance does not provide proper matching at frequency of interest. Thus, this circuit does not provide optimum performance. Using an inductor as a load, overcomes the disadvantages offered by resistive network. Inductor sustains a lower voltage drop than a resistor and hence it can operate at a lower supply voltage as well. Moreover, inductor resonates with the capacitor at the load to offer matching at higher frequency. Value of the inductor is chosen first and then accordingly, the value of the output or load capacitance is chosen such that it will provide matching for desired frequency. Hence, using an inductor in our circuit solves the issue of obtaining matching at our frequency of interest. Using L as a load in our amplifier design overcomes the disadvantages that are observed in circuit with resistance as a load; and it is better to use an inductor in our circuit than using resistance because using a resistance limits the circuit performance and may not deliver the required results.

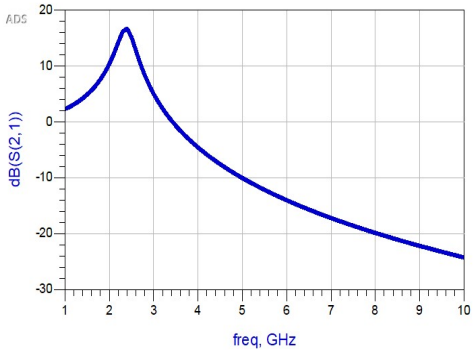

Fig. 5: Gain (S_{21}) obtained when R is used as load

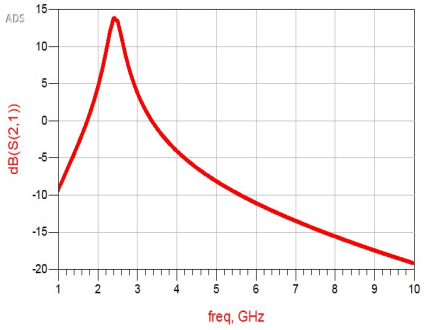

Fig. 6: Gain (S_{21}) obtained when L is used as load

Using LC as a load provides even better results as the inductor being used to realize the circuit is assumed to be a real inductor. Practical inductors suffer from losses which can be modeled by placing a resistor in parallel with the configuration of L and C. It can also be verified from the results obtained during simulation that when a practical inductor is being used in our circuit, the results get downgraded as the inductor being used to achieve output matching is not ideal inductor. Practical inductor properties are also being considered.

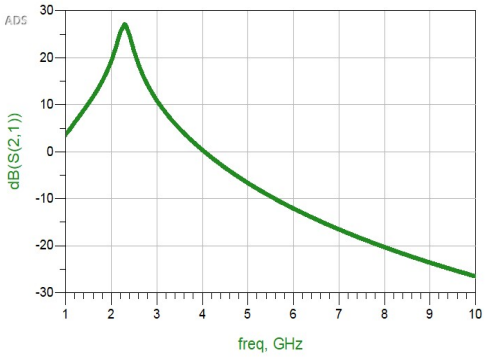

Fig. 7: Gain (S_{21}) obtained when LC is used as load

We know that ideal characteristics never exist. We should prefer the configuration that takes practical aspects into consideration. Using circuit design that is more close to the practical values, is always more realistic to use, as it always provides a better understanding of the real time performance of the circuit. Design process following practical aspects always yields results which are more close to real-time performance of the circuits.

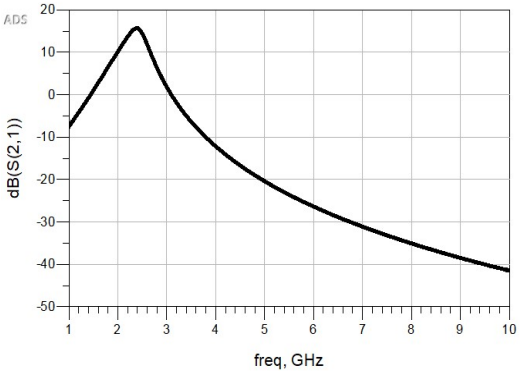

Fig. 8: Gain (S_{21}) obtained when RLC is used as load

We summarize the results obtained in tabular form. However, we compare the performance only on the basis of the gain provided by the circuit. Other parameters can also be used to compare different circuits; and analyze their performance on the basis of parameter values obtained. We need to make a choice of optimizing only one design parameter, keeping others at stake. While implementing these circuits practically, wire bound inductors can be used to realize the given inductance values. Using these inductors reduces the chip area occupied by our circuit design but at the cost of an additional overhead of placing the inductor off-chip rather than integrating on chip [11]. LNA design involves higher level of integration with minimum cost but it also creates a challenge to achieve a better noise performance. MOSFET is being used to implement LNA which possesses a noisy nature; and the noise sources in the MOSET are many. Dominant noise sources are channel noise, gate noise generated due to distributed gate resistance of the MOSFET, etc. These sources degrade the noise efficiency of the LNA. These can be controlled by properly choosing the size of the transistor which provides minimum noise figure. Cascode LNA with inductive degeneration configuration is ought to provide better noise performance and higher gain as compared to other configurations [12].

V. CONCLUSION

We cannot come to a conclusion stating that a particular circuit proves to be the best in terms of all parameters. Every circuit design possesses its own pros and cons making it suitable for one application and not suitable for a different application. This comes forward as a consequence of trade-off between the parameter values of LNA, which makes it a bit difficult to design a circuit with all values perfectly within the limits. On analysis of the results obtained after simulations, we can see the fact come true that there is always a trade-off between the LNA parameters. We observe that one circuit is suitable for application requiring high gain while other circuit is suitable for an application where low noise figure is required. Henceforth, every circuit has its own utility in one application or the other. We need to make a preference in terms of which parameter needs to be optimized and proceed with that aim to design.

Table 1: Results obtained for Cascode Common Source LNA with Inductive Degeneration Topology utilizing different output matching circuits

Parameter	R as load	L as load	LC as Load	RLC as Load
S_{11} (dB)	-13.44	-12.79	-12.041	-14.58
S_{22} (dB)	-11.26	-0.006	-0.08	-19.5
S_{12} (dB)	-47.44	-50.96	-51.28	-50.02
S_{21} (dB)	16.65	13.91	26.52	15.84
Noise Figure (dB)	7.802	8.419	7.464	7.784
IIP3 (dB)	7.023	4.026	5.243	9.783
Power Consumed (mW)	2.95	2.51	5.011	1.98

If we restrict our analysis by considering the gain of the system, LC as a load is observed to be the best design as it offers the maximum gain out of all the above configurations. Even RLC as load offers a sufficient amount of gain. Both these configurations are considered suitable to be utilized in any low noise amplifier design. If we desire a circuit which is highly linear, we need to consider IIP3 value of the circuit. For applications which require a highly linear amplifier, RLC can be utilized as the output matching network as it is observed to provide a higher value of IIP3. Based on our results, we also conclude that if we want to restrict the power consumption of the circuit, we should utilize RLC network in our circuit design, which is observed to consume less power as compared to others. Application specific LNA's are designed by optimizing one parameter and keeping others in the specified limit as trade-off cannot be ignored completely.

References

[1] Tajinder manku. "Microwave CMOS·devices and circuits" Proceedings of the IEEE 1998 Custom Integrated Circuits Conference. pp. 59-66

[2] Ayari Nadia, Hamdi Belgacem and Fradi Aymen," A Low Power Low Noise CMOS amplifier for Bluetooth applications", in proceedings of International Conference in Applied Electronics 2013

[3] Shaikh K. Alam, "A Novel 2.4 GHz CMOS Variable Gain Low Noise Amplifier Design for Bluetooth and Wireless LAN Applications", in Proceedings of International Conference on Consumer Electronics 2007

[4] Lei Liao, Stefan Kaehlert, Yifan Wang, Aytac Atac, Ye Zhang, Martin Schleyer, Ralf Wunderlich, and Stefan Heinen, "A Low Power LNA for Bluetooth Low Energy Application with Consideration of Process and Mismatch", in proceedings of Asia Pacific Microwave Conference 2012

[5] Mou Shouxian, Ma Jianguo, *Yco* Kiat Seng, and Do Manh Anh, "An Integrated SiGe Dual-band Low Noise Amplifier for Bluetooth, HiperLAN and Wireless LAN Applications", in proceedings of European Microwave Conference 2003

[6] Zeenal Aafreen Khan, Amjad Quazi,Mohd Abdulla, "Broad Band Low Noise Amplifier for Wireless Application Using Double Order Gain Flatting Technique" in proceedings of International Conference in Recent Developments in Signal Processing and Embedded Systems(RISE)

[7] K.W. Kobayashi, "Linearized Darlington cascode amplifier employing gaas PHEMT and GaN HEMT technologies," IEEE J. Solid-State Circuits,vol. 42, no. 10, pp. 2116–2122, Oct. 2007.

[8] Florian Kmg, Peter Russer," A switched-LNA in 0.18pm CMOS for Bluetooth applications",in proceedings of Topical meeting on Silicon Monolithic Integrated Circuits in RF systems,2003

[9]B. Razavi, Design of Analog CMOS Integrated Circuits. McGraw-Hill Science/Engineering/Math,2001.

[10] Lin Min , Li Yong-ming , Chen Hong-yi," A 0.18- P m CMOS LNAs with sub-2dB NF and Low Power for Bluetooth Applications" in proceedings of International Conference on ASIC proceedings 2001

[11] Sinyoung Kim, Taejong Kim, and Kuduck Kwon," An Ultra-Low-Power 2.4 GHz Receiver RF Front-End Employing a RF Quadrature *Gm*-Stage for Bluetooth Low Energy Applications" in proceedings of International SoC Design Conference 2017

[12] M_ Zamin Khan, Yanjie Wang and R. Raut, "COMPARISON OF DIFFERENT CMOS LOW-NOISE AMPLIFIERS TOPOLOGIES FOR BLUETOOTH APPLICATIONS", in proceedings of IEEE Annual Conference of Wireless and Microwave Technology 2005

Proceedings of the Fourth International Conference on Communication and Electronics Systems (ICCES 2019)
IEEE Conference Record # 45898; IEEE Xplore ISBN: 978-1-7281-1261-9

An Enhanced Cluster Head Technique for Energy Consumption in DataFusion

E.Brumancia
School of Computing
Sathyabama Institute of Science and Technology
Chennai,India
easpinbrumancia@gmail.com

S.Justin Samuel
School of Computing
Sathyabama Institute of Science and Technology
Chennai,India
drsjustin@gmail.com

A.Sivasangari
School of Computing
Sathyabama Institute of Science and Technology
Chennai, India
sivasangarikavya@gmail.com

Vishwanthi Suvetha.R
School of Computing
Sathyabama Institute of Science and Technology
Chennai,India
vishwanthisuvethar@gmail.com

Sandhiya.M
School of Computing
Sathyabama Institute of Science and Technology
Chennai,India
sandhiyashanaya@gmail.com

Abstract—**Wireless Sensor Network (WSN) could be presently exploitation technology for the data gathering from the hostile surroundings. WSN is consists of an outsized variety of sensing nodes, they are known as sensors. This kind of network is employed to gather the data through base stations (BS). However, it works on restricted batteries consumes lot of loads and power, limited energy is the bottleneck. The data collected from different nodes may give redundant information. To reduce the redundant information data fusion is needed, which will increase the accuracy and robustness of the information. LEACH protocol is one of the typical data fusion algorithms, which will reduce the energy consumption and extend the life cycle of the network. The research results were analyzed and benchmarked with the well-known LEACH and GSTEB protocols. The outcome shows a major improvement within the WSN in terms of energy potency. The results show the overall network energy consumption by scrutiny with existing algorithms.**

Keywords—WSN-Wireless Sensor Networks; LEACH-Low Energy Adaptive Clustering Hierarchy; GSTEB, Data Fusion

I. INTRODUCTION

[1]Wireless is consists of thousands restricted batteries operated nodes. Nodes are unit created of radio transmission and receiving, sensing, storage, processing, mobilize and world positioning system (GPS). These nodes area unit localized in massive geographic region. These nodes area units are localized in massive geographic region. These sensors area unit gift close them then they transform the information into electrical Signals then these signals area unit processed to urge Characteristics remotely gift space wherever sensors unit. The Sensor interconnections have thought-about as promising tool for analysing the physical world, utilize self-organized nodes will sense, method and communicate area unit battery high-powered. In lifetime sensor interconnections node, energy must be a main yet vital resource, wherever exhibits have a restricted characteristic. So that, it is often necessary to optimize specification therefore resources consumed is decreased. Their boundaries kind their style and protocols each stimulating completely different. WSNs are unit shaped by an outsized variety of sensing element.

Depending on the sensors with restricted battery power cannot be superimposed balanced energy exhausting ought be thought-about because the reason for energy-efficient management. The current system has been enforced by the not high Energy adjective bundle Hierarchy (LEACH) theme permits role of collection head evolved among sensing element and makes an attempt distribute energy usage though all buds. It utilizes irregular rotation native base equally distribute energy load among senses within the track though out set-up part, all nodes are unit at instant buds through human action with short messages one lump is chosen as a bunch head per bunch head choice rule. Here we proposed a General Self organized Tree Based Energy Balance routing protocol (GSTEB). We have a tendency to take into account a scenario within which interconnections collects info sporadically from parcel wherever every node regularly senses atmosphere and sends data back to central Station. Commonly parte unit two definitions for lifetime interconnection are time from the beginning of interconnections operation to the death of the primary node within interconnections and also the time from the start of interconnections operation death of last node within interconnections.

The main aim of GSTEB is to do attain extended interconnections a time period various applications. Every spherical, Base station (BS) allots a root hub and communicates its ID and its coordinates to all or any device nodes. Then interconnections computes trail either by transmission of trail data or BS to device nodes or by having identical tree structure being dynamically and singly designed by every node. For each case, GSTEB will amendment foundation reconstruct tree with short delay with low energy exhaustion. Thus, a balanced load is achieved compared with the protocols. The task of GSTEB is part into Initial part, Tree-Constructing part, Self- Organized information aggregation and transmission part, and knowledge Exchanging part.

This paper is organized as following, Section II contains the related works, section III reviews about routing protocol, section IV contains working principles, section V contains results and discussion and section VI concludes the paper.

II. RELATED WORK

In[2] Hongjun Wang, Huiqing Yangtze, Hui Zhao, and YoujunYue projected an formula to balance energy exhaustion of detector nodes in WSN, in order network life additionally gets extended. [3]Zhang Shiyue, Jiande Wu, Xiaodong Wang projected LEACH Cluster

XXX-X-XXXX-XXXX-X/XX/$XX.00 ©20XX IEEE

routing formula for wireless detector Network information Fusion thereby reducing the energy exhaustion and quantity of knowledge communication. In[4] Wei-Qi bird genus ; Bin-Jie Hu projected fusion formula with the gauss distribution characteristic chart therefore the gauss membership operate will improve the information preciseness and measuring stability. In[5] Diksha.J. Ramteke, Amol Boke projected a way supported ICH-LEACH wherever, there'll be hierarchy which is able to encompass Master and slave bunch head thus on enhance life of Master bunch head and lifelong of specific network. In[6] the developing enthusiasm in wireless sensor networks and emerging trend in recent field motivated for measuring the characteristics, operations and communication protocols for a different areas. In[7] proposed the Low Energy Adaptive Clustering Hierarchy to distribute the energy evenly between the sensors in the network. Data fusion is incorporated with routing protocols to reduce the information content that could be transmitted to the base station. Life time also gets extended. In paper [8] redundant data can be eliminated, which will improve the performance. So that energy consumed and network life time also increased. All these done by Improved LEACH algorithm. In[9] Measurement stability and data precision is improved by applying gauss membership function of fuzzy theory and improved leach protocol.

III. HIERARCHICAL ROUTING PROTOCOL

A. Leach

a) LEACH is a simple routing protocol used to reduce energy exhaustion data improve lifetime interconnections nodes. The buds in the LEACH plus cluster buds and bunch head to polling is minimum. Clustering optimization problem in single hop networks: are used to predict lifetime reliability wireless sensor interconnections .Small energy exhaustion data report of distance closer to base clustering in large scale. The distance from the base station far smaller cluster. Every cluster divides into mini clusters and they are organized for each mini cluster define the other mini bunch head. It communicated directly with the bunch head and collects the information about the other nodes to connect and concentrates all nodes for data transmission used resolves some nodes coverage problems.

[10] Each cluster head is having a responsibility to create and manipulate a TDMA schedule during communication process. To transmit the data packets schedule table is used by its cluster member nodes. If any emergency happens in the monitoring environment the sensing elements are triggered to send the information to their own cluster head rather than remote BS by themselves. The data from different nodes are collected by the cluster head and remove the redundant data, then transmits the remaining information to BS. Transmission distance between the nodes will be reduced by the member node with the help of cluster head. Because of this energy consumed.

In [11] To reduce energy consumption in WSN, data fusion is the best solution. Due to sensor failure interruption may occur, by using data fusion techniques we can reduce the redundant data. By doing this entire network energy will be consumed, so that life time of that entire network will be increased.

GSTEB and LEACH is the best suitable algorithm to perform the energy consumption.

The communication process have two different phases such as, Setup phase:

[12]The node which is used to broadcast the message to its surrounding sensing node whose number larger than threshold number will select itself as a bunch head. A node will receive more than one broadcast message from different bunch head, and also judge its distance by the strength of received broadcast message. So, the buds whose number is smaller the threshold will only send request message containing its Broadcast ID to the cluster. Which has the strongest signal strength for saving energy. It records the nodes ID. The CH creates a TDMA schedule slots and broadcast it to all the cluster members and each nodes get their idle slots for transmitting the data, and then the steady state phase starts.

a) *Steady-state phase*

Cluster nodes will form them and send to BS. The formation on the bunch head can reduce the unnecessary bandwidth cost and communication traffic and also a positive reflection to the energy exhaustion where the data transmission distance becomes shorter comparing with transmitting to BS separately which is used to save some energy for the group of nodes.

A. GSTEB

GSTEB protocol is mainly proposed for wireless sensor networks the operation will be divided into phase. They are initial phase, [13]Tree constructing phase, Self-Organized data collecting and transmitting phase and information exchange phase.

a) Initial phase

[14]In the first stage of GSTEB operation data packet to is broadcasted to all the node or few nodes by BS to share the data created time. Every node sends its data to a particular radius. Nearest node's information will be available with the packet. So that packet will be received by its nearest node.It also receives and record the data info in memory. It operates in round, each round generates the data for BS and receives the information of nodes, once all the sensors information is received by the BS then round will be finished.

b) *Tree constructing phase*

Root node will be selected by the BS and broadcast the root id to coordinate with other nodes. Each and every round highest residual energy node will be selected as root node. So the data will be collected by the particular root node and transmits the fused data to the BS. The nodes will choose the parent and its neighbours using vitality. Repeating this process until the tree is constructed. After constructing the tree, sensors will collect the information and transmits the fused data. During the transmission state each child node sends their root id to its parent by choosing them considering their distance.

c) Information exchange phase

Each and every node should generates and transmits a data packet in every round, before its energy goes down. It can persuade the topology. So the node which is about to die need to share their data with other node. This process is

performed based on the time slots, in each time slot random delay will be computed by the node whose energy will certainly be exhausted. This will help to make another broadcasting node in a new time slot. This particular node will broadcast the data packet to the complete network. Mean time remaining nodes will monitor the channel. Root id will be verified based on the data packet received from the node. In order to transfer the information securely the cluster head will be selected based on the degree of energy.

IV. WORKING PRINCIPLE

GSTEB is hierarchical routing algorithm which is most popular for sensor networks. GSTEB sensor nodes are combined in order to form clusters on the basis of received signal strength. The cluster head will act as routers to the sink node. [14]Transmission can be only done by bunch heads instead of all other nodes which will save energy. Existing routing protocol consider balanced energy exhaustion of nodes ignoring elaborative data processing between the sensor nodes. LEACH protocols needs base stations with uneven distribution of bunch heads. Since, the sensor consumes high energy, it should be considered as the issue for energy efficient management. The observation of energy level over sensor network provide as issues in the transmission.

The methodology performs the detector network and selects bunch heads space to the bottom station. The bunch heads are chosen by comparison their crucial values, rather than the crucial values, rather than the standard methodology of choosing bunch heads, during this bunch formula within GSTEB will perform knowledge fusion. The method will acquire higher convergence and price lower message overhead. Clustering in sensing aspect network is economical good topology that encourage planning energy efficient protocols to develop sensing element buds with low price.

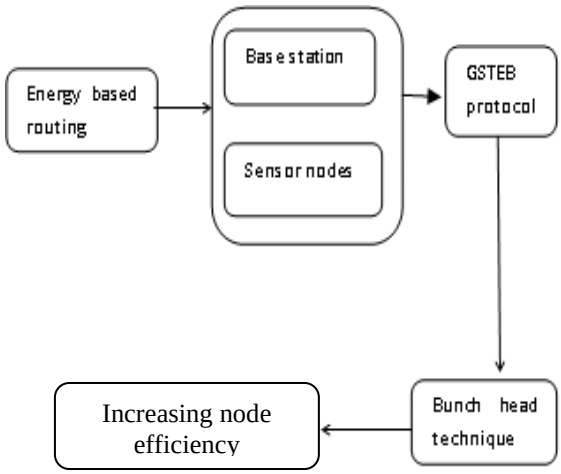

Fig. 1. GSTEB Architecture

A. Low Energy Adaptive Clustering

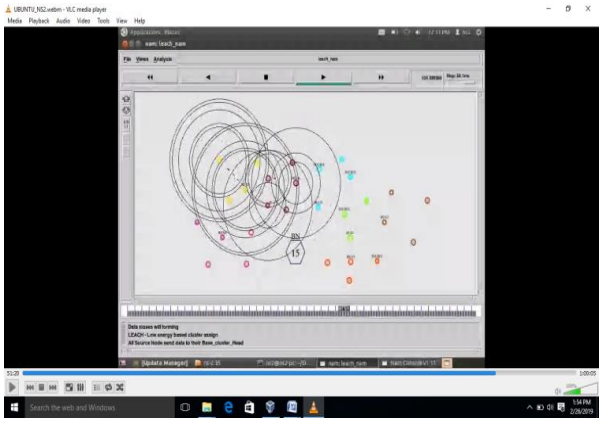

Fig. 2. Source node data to their base head

LEACH is an simple efficiency routing protocol in WSNs. It is integrated with clustering is to lower the energy exhaustion for creating the nodes. It maintains the clusters to improve the lifetime. The performance of LEACH is slightly lower than the proposed method GSTEB.

LEACH will divide the Wireless Sensor network in to number of cluster. Each and every cluster will have a cluster head. The cluster head is responsible to colletct all the data from the other sensing nodes which is shown in fig 2 and fig 3.

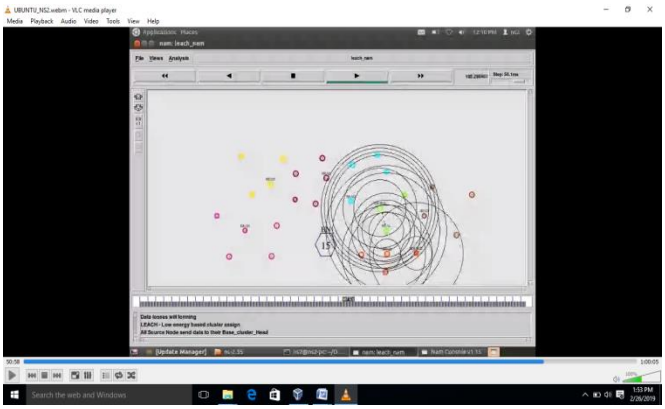

Fig. 3. Implementing LEACH algorithm

B. Tree Based Energy Balance Routing Protocol

G GSTEB is a popular energy balancing routing protocol. For each bunch head process, the base station purposes a node for each bunch head and own its neighbouring ID information which node has highest weight. It is mainly used to balance the energy exhaustion and load.

STEPS OF LEACH ALGORITHM

Step 1: Begin and construct WSS and WSN
Step 2: Send node locations and residual energy information from nodes to base station
Step 3: if Node Energy> Threshold Energy then Wait for cluster
Step 4A: Send join request to CH and wait for TDMA schedule for head announcement

Step 4 B: Node is selected as bunch head.
Step 5: Search for clusters in interconnections
Calculates the modularity (Q) of the clusters
Step 6: if Q>Qmax then
Calculate the centroid of interconnections and its distance from the nodes closest to it
Step 7: Assign highest weights to the nodes close to the centroid having residual energy than others.
Step 8: Compute the estimated (normalized data accuracy) for the sensor nodes in interconnections. Plugin the weights of the nodes in terms of Energy and Precision constraints.
Step 9: In the weights matrix obtain the best set of cluster.

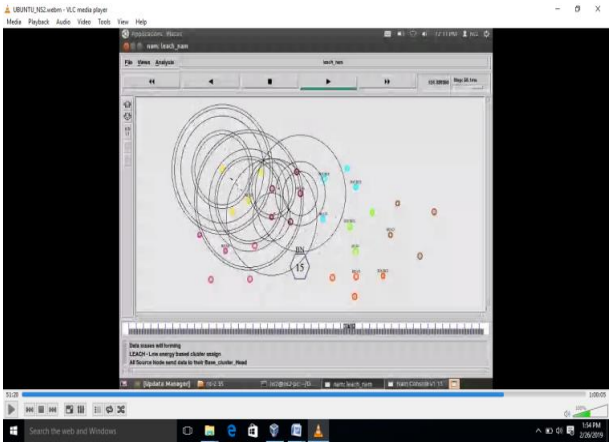

Fig. 4. Group Identification Access

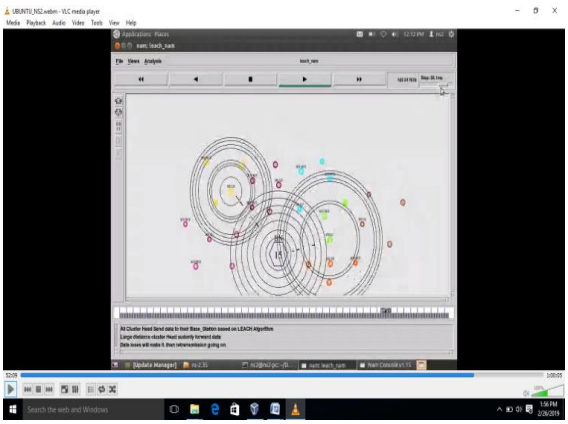

Fig. 5. Bunch head send data to bunch head

STEPS OF GSTEB ALGORITHM

Step 1: Create node
i=nodeid;
Set the routing channel;
Set inienergy, resenergy;
Set rad_range as default;
Step 2: If((node in rad_range) && (next hop!=NULL)
then
Capture data load (node all);
Step3:Create a node and configure
(rreq,rrep,tsend,trev,tdrop, inienergy, resenergy)
Step 4: For i=0 to n
con_energy [i]=inienergy[i]-finalenergy [i]
total_energy[i]=<con_energy [i])
Step 5: if(max_energy[i] <con_energy[i]) then
max_energy = con_energy[i]
nodeid=i;
step 6: If (distance<300 &&max_energy [nodeid]
>energy_neighbor [nodeid]) then
step 7: Max energy node is the cluster head;

V. RESULT AND DISCUSSION

In LEACH, based on the distance the sensor energy consumption was reduced. The nodes will concentrate all the nodes. It only concentrate on specific nodes that transmit the data and information to the other node. It will load the data nodes more and more as shown on figure 4 and figure 5.

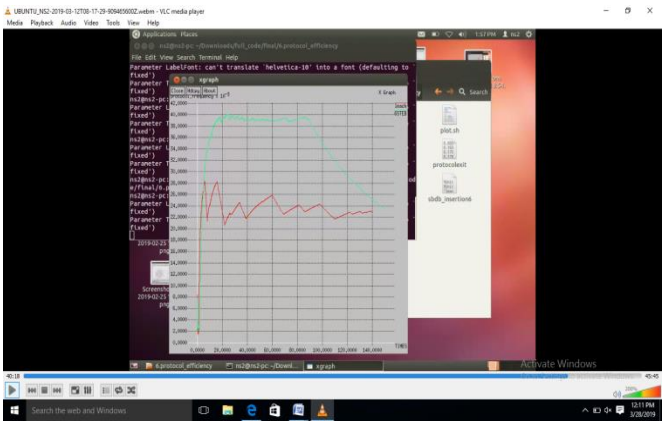

Fig. 6. Delay xgraph loss

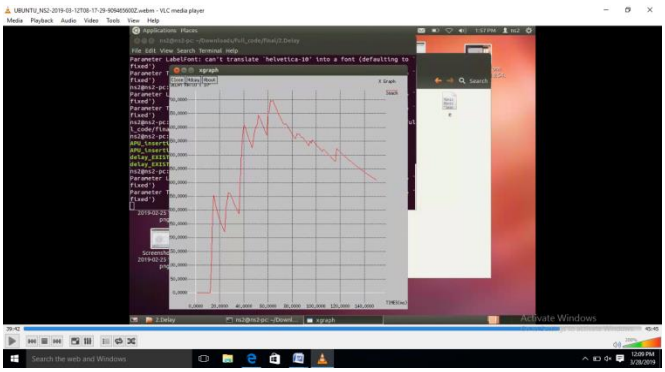

Fig. 7. Delay xgraph loss 1

In GSTEB, the nodes will concentrate all the nodes and do the data processing even though bandwidth is high and minimize energy consumption efficiently compared to LEACH on shown in figure 6 and figure 9. It reduces load. We have used E-GSTEB type of GSTEB for minimizing energy consumption

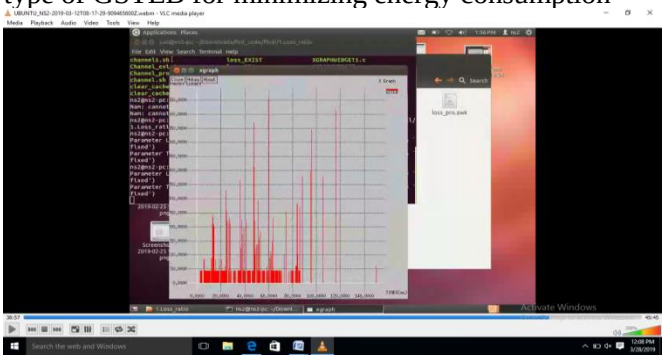

Fig. 8. Parameter xgraph loss

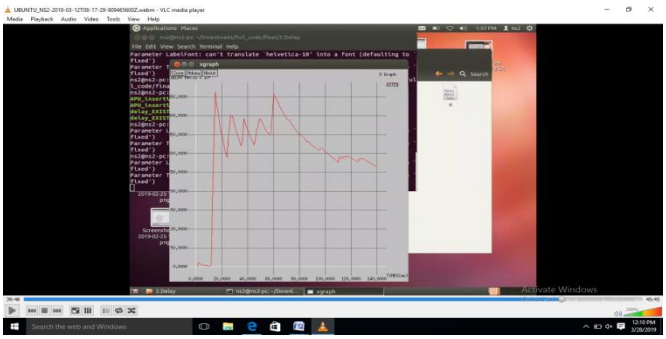

Fig. 9. Parameter xgraph

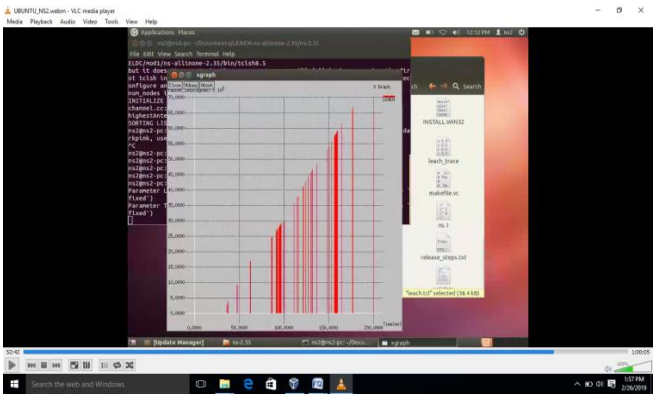

Fig. 10. Xgraph loss 1

The Base station allocates nodes coordinates in each round. Interconnections transmit the data information being dynamically and individually

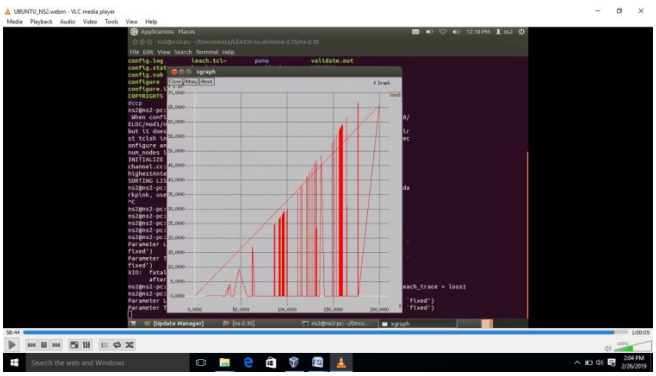

Fig. 11. Xgraph loss 2

The GSTEB chooses the nodes with residual energy to transmission the data information. The allocation of nodes will performed by the Base Station based area unit distance with the radius clusters are shaped. All the nodes will be covered with the other nodes.

VI. CONCLUSION

In this paper, we proposed an enhanced cluster head technique for energy consumption in data fusion. Data from different sensors are grouped and performed cluster heading. The simulation results show the minimized energy with enhanced (E-GSTEB) technique. Because of this energy reduction, network life time will get improve. This clustering techniques gives the more accurate data and data transmission is more efficient. This is done by using a particular data fusion technique.

ACKNOWLEDGMENT

We are thankful to our management Sathyabama Institute of Science and Technology for providing us all the necessary support and facilities required for preparing this manuscript.

REFERENCES

[1] Junguo Zhang, Wenbin Li, Xueliang Zhao, Xiaodong Bai, Chen Chen, “Simulation and Research on Data Fusion Algorithm of the Wireless SensorNetwork Based on NS2”, 2009 World Congress on Computer Science and Information Engineering

[2] Hongjun Wang *1 and Huiqing Chang*1, *2Tianjin Agricultural University,” Research on LEACH Algorithm Based on Double ClusterHead Cluster Clustering and Data Fusion”, Proceedings of 2017 IEEE International Conference on Mechatronics and Automation, August 6-9, Takamatsu, Japan

[3] Zhang Shiyue, Jiande Wu, Xiaodong Wang “A Data Fusion Algorithm Based on Improved LEACH Clustering Routing for Wireless Sensor Network”, icaise.2013.7

[4] Wei-Qi Chen,Bin-Jie Hu, “A Data Fusion Algorithm in Leach Protocol Using Gauss Membership Function”, 2010 6th International Conference on Wireless Communications Networking and Mobile Computing (WiCOM) 23-25 Sept. 2010

[5] Diksha J. Ramteke1 , Amol Boke2, “Modification of LEACH Protocol in Wireless Sensor Network: A Review,” International Research Journal of Engineering and Technology (IRJET), Volume: 05 Issue: 05 | May-2018

[6] K. Akkaya, and M. Younis, “A survey on Routing Protocols for Wireless Sensor Networks,” Elsevier Ad Hoc network Journal, vol.3, pp.325-349, 2005.

[7] W. Heinzelman, A. Chandrakasan, H. Balakrishnan, “Energy efficient communication protocol for wireless microsensor networks,” IEEETransactions on Wireless Communications vol. 1 (4), pp. 660–670, 2002.

[8] Zhang Shiyue, Jiande Wu, Xiaodong Wang, “A Data Fusion Algorithm Based on Improved LEACH Clustering Routing for Wireless Sensor Network”, August 2013

[9] Wei-Qi Chen ; Bin-Jie Hu “A Data Fusion Algorithm in Leach Protocol Using Gauss Membership Function”, 2010 6th International Conference on Wireless Communications Networking and Mobile Computing (WiCOM), 14 October 2010

[10] Fuzhe Zhao, You Xu, and Ru Li,” Improved LEACH Routing Communication Protocol for a Wireless Sensor Network”, International Journal of Distributed Sensor Networks Volume 2012, Article ID 649609, 6 pages

[11] E. Brumancia, S. Justin Samuel, M. Gomathi and Y. Mistica Dhas, “AN EFFECTIVE STUDY ON DATA FUSION MODELS IN WIRELESS SENSOR NETWORKS”, ARPN Journal of Engineering and Applied Sciences, VOL. 13, NO. 2, JANUARY 2018.

[12] SudhanshuTyagia, NeerajKumarb, “ A systematic review on clustering and routing techniques based upon LEACH protocol for wireless sensor networks”, Journal of Network and Computer Applications Volume 36, Issue 2, March 2013, Pages 623-645

[13] M.Sengaliappan1 , Dr.A.Marimuthu2, “Improved General Self-Organized Tree-Based Routing Protocol For Wireless Sensor Network”, Journal Of Theoretical And Applied Information Technology 10th October 2014. Vol. 68 No.1

[14] Manjinder Kaur Dr. Shashi B. Rana*, Performance Comparison of Leach and GSTEB in Wireless Sensor Network, International Journal of Engineering Research & Technology (IJERT), Vol. 4 Issue 04, April-2015

[15] Yan Qiang,1 Bo Pei,1 Wei Wei,2 and Yue Li, “An Efficient Cluster Head Selection Approach for Collaborative Data Processing in Wireless Sensor Networks”, Hindawi Publishing Corporation International Journal of Distributed Sensor Networks Volume 2015, Article ID 794518, 9 pages http://dx.doi.org/10.1155/2015/794518

[16] E. Brumancia, S. Justin Samuel, M. Gomathi and Y. Mistica Dhas, “AN EFFECTIVE STUDY ON DATA FUSION MODELS IN WIRELESS SENSOR NETWORKS”, ARPN Journal of Engineering and Applied Sciences, VOL. 13, NO. 2, JANUARY 2018.

[17] B.Warneke, K.S.J. Pister, "MEMS for Distributed Wireless Sensor Networks," in Proc. of 9th International Conf. on Electronics, Circuits

[18] K. Sohrabi, et al., "Protocols for Self-organization of A Wireless Sensor Network," IEEE Personal Communications, vol. 7, No. 5, pp. 16-27, October, 2000.

[19] I. Akyildiz, W. Su, Y. Sankarasubramaniam, and E. Cayirci, "A Survey On Sensor Networks", IEEE Communications Magazine, vol.40, pp.102-114, 2002.

[20] Sudhanshu Tyagi and Neeraj Kumar, "A systematic review on clustering and routing techniques based upon LEACH protocol for wireless sensor networks," Journal of Network and ComputerApplications vol. 36, pp.623–645, 2013.

[21] Zhao Han, Jie Wu, Jie Zhang, Liefeng Liu, and Kaiyun Tian, "AGeneral Self-Organized Tree-Based Energy Balance Routing Protocol for Wireless Sensor Network," IEEE Transactions On Nuclear Science, vol. 61, No. 2, April 2014.

[22] Dheeraj and Ritu Mishra, "Review Paper on Hierarchal Energy-Efficient Protocols in Wireless Sensor Networks," International Journal of Advanced Research in Computer Science and Software Engineering, vol.4, Issue 6, 2014.

[23] S. Upadhyayula, S.K.S. Gupta, "Spanning tree based algorithms for low latency and energy efficient data aggregation enhanced converge cast (DAC) in wireless sensor networks, Ad Hoc Networks, vol.5, pp.626–648, 2007.

[24] Andrei Gagarin, Sajid Hussain, Laurence T. Yang, "Distributed hierarchical search for balanced energy exhaustion routing spanning trees in wireless sensor networks," J. Parallel Distribution Computer, vol.70, pp.975-982, 2010.

Proceedings of the Fourth International Conference on Communication and Electronics Systems (ICCES 2019)
IEEE Conference Record # 45898; IEEE Xplore ISBN: 978-1-7281-1261-9

Advanced Wheelchair Movement System Using Facial Gestures For Aiding Human With Tetraplegia Condition

Dr.P.V.Ramaraju
Professor & Head of the department
Department of ECE, S.R.K.R
Engineering College
Bhimavaram, India, 534204

K. JaideepSai Narayan
M.Tech Student
Department of ECE, S.R.K.R
Engineering College
Bhimavaram, India, 534204
Mail id:jds14795@gmail.com

G. Naga Raju
Assistant Professor
Department of ECE, S.R.K.R
Engineering College
Bhimavaram, India, 534204

***Abstract*—The major problem faced by the paralyzed people is their mobility. The quadriplegia, one of the serious disabilities affects all the four limbs and such persons need an external help to perform their daily activities. The main objective of this project is to provide an automated system for such people. Abstract discusses the possibility of developing a wheelchair whose motion can be controlled using eye blinks. User's eye gestures are translated to screen position using optical sensing in MATLAB. A camera mounted on the wheel chair recognizes the eye gaze/blinks and if it matches with the gestures in memory, motion control commands are generated by the micro controller depending on the coding. These commands drive the motors of the wheelchair.**

Keywords—Arduino UNO, Hough Transform, MATLAB, Webcam.

1. INTRODUCTION:

Wheel chair is a versatility-based gadget for people with cutting edge/extreme physical disabilities. Different control interfaces have been created for wheelchair control, for example, joystick or head control. These types of interface are not accessible to the general population practically. Now, using eye squint and mouth signal, an alternate type of wheelchair control is conceivable.

This report exhibits the plan, advancement and medicinal effect of a wheelchair with eye control. Individuals with tetraplegia cannot work a wheelchair with joysticks. In any case, a few people truly feel hard to control the bearing of the wheelchair with their hands because of loss of motion, the old, impaired. A wide scope of help gadgets and current hardware have been created to help improve their personal satisfaction. This innovation is a mix of an individual with incapacities in the public eye.

Since all individuals cannot utilize the conventional electric wheelchair, there must be some correspondence between the client and the wheelchair to control it. It is extremely hard for the handicapped client to drive the wheelchair with their arms.Some commonly used methods are mentioned such as: Voice Operated Wheelchair System[1],Head and Finger based Automated Wheelchair System[2], Eye Movement based Electronic Wheelchair System which uses MATLAB[3],Eye Movement based Electronic Wheelchair System which uses Raspberry Pi[5], Hand Gesture based Wheelchair System[4].

- Voice operated Wheelchair System[1] works based on input voice command delivered by the disable person.
- Head and Finger based Automated Wheelchair System[2] works based on head and finger movements.
- Eye Movement based Electronic Wheelchair System which uses MATLAB[3] works based on EOG (Electro-Oculogram).
- Hand Gesture based Wheelchair System[4] works based on EMG (Electromyogram).

In this paper our work mainly emphasizes on the eye blinks with help of mouth gestures. By adding these mouth features number of instructions will be increased as shown in below Table:1. In 'CascadeObjectDetector', to detect eyes we used "Eye Pair Small" and to detect mouth we used "Mouth" in CascadeObjectDetector.

1.1 Model Design algorithm:

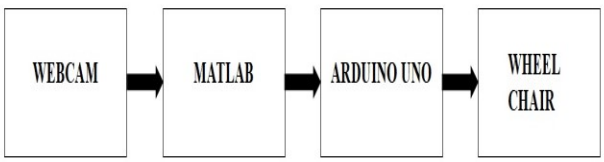

Fig.1- Wheelchair control system block diagram

As shown in Fig.1 Facial features are recorded by the webcam and it is feed to the MATLAB as input. In MATLAB we will use Viola Jones algorithm for detecting facial features and to detect the pupil we will use HOUGH transform. Now to interface the MATLAB with Arduino UNO there presents Arduino packages in the MATLAB toolbox. To run MATLAB code in Arduino, Arduino packages must be installed. Now Arduino is connected to L298N motor diver prototype for wheel moment. This L298N motor diver has

dual full bridge design. An Obstacle detection sensor is used to detect obstacle, when it detects then buzzer sound will be activated.

2. PROPOSED METHODOLOGY :

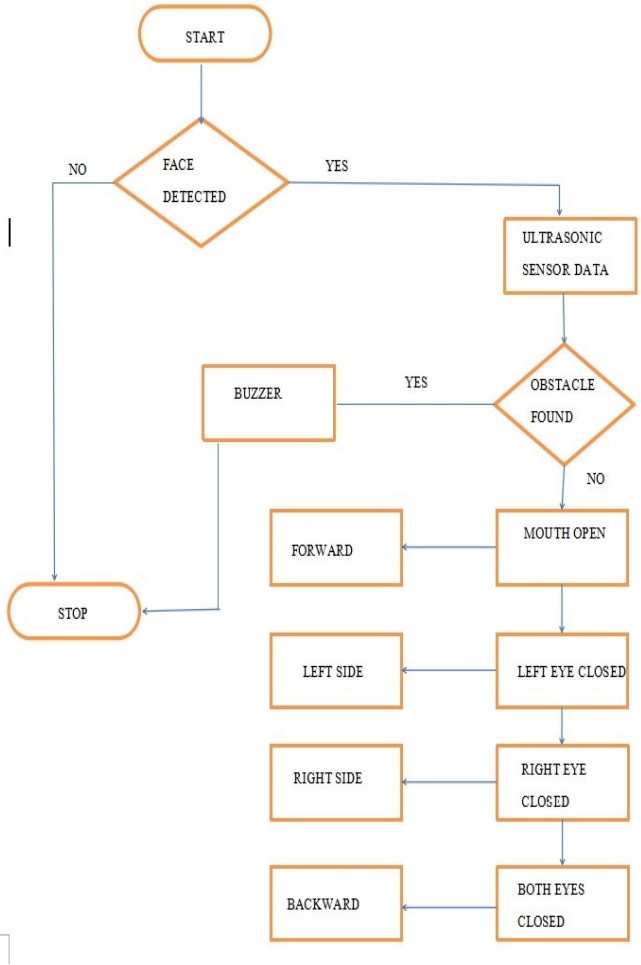

Fig.2-Flow chart

Step by step working :

- Web cam starts recording the facial features. If face is not detected then the program will be stopped, else ultrasonic modulo will be activated.
- If obstacle is found then buzzer will ring otherwise further process will be takes place.
- When mouth is open and 2 eyes are open then wheelchair starts moving forward.
- When left eye is closed, right eye is open and mouth is closed then wheelchair starts moving left.
- When left eye is open, right eye is closed and mouth is closed then wheelchair starts moving right.
- When mouth and 2eyes are closed then wheelchair will move backwards.

2.1 Working:

Working of this project divided into 2 parts:

- Detecting face using Viola Jones algorithm.
- Continuous capturing of eyeball blinks with help of webcam and it is fed to MATLAB and Interfaced with Arduino board.

2.1.1 Detecting face using Viola Jones algorithm :

Using 'CascadeObjectDetector' we will detect eye-shaped objects based on their structure, Viola Jones Algorithm detect similar objects. Continuous snapshots of every 24 frame are taken and feature points are saved.we capture 1 snapshot every second and process it based on the position of the object. Previous snapshot and current snapshot, features are detected and this is communicated to the wheelchair through the serial port.

Viola Jones Algorithm is to scan a sub-window in the detection of a face for the given input. Standard image processing approach will re-scale the input image for different sizes and then run the fixed sized detectors through these images. This approach is taking time instead of being pictures of large sizes. According to the standard perspective, Viola Jones re-measure the detectors rather than the input image and often with different sizes run the detectors with a picture. At first it seems both methods execution will take more time, but Viola Jones has devised a wide-ranging revealing that requires the same number of calculations of any size image. If webcam detects many faces, the program will be stopped because it is difficult to recognize the original input. The above figure is not for example, to detect multiple face or face, it will not come to know the face.

2.1.2 Continuous capturing of eyeball blinks with help of webcam and it is fed to MATLAB and Interfaced with Arduino board:

Continuous snapshots are taken and is given as input to the MATLAB. Using HOUGH transform we will find arbitrary shapes such as circles and ellipses. For detecting eye pupil HOUGH transform is useful. If pupil detected then consider that eye is open, else eye is closed. Where step by step process regarding the moment of wheel chair is discussed in above flow chart. Now the output of MATLAB is given to Arduino through serial communication. Here Arduino UNO board is used to perform moment of wheel chair. It takes around 2 seconds(delay time) of time for each instruction to get executed and display the corresponding output results. Table.1 describes input instructions to the wheelchair.Designed prototype is shown in Fig.3.

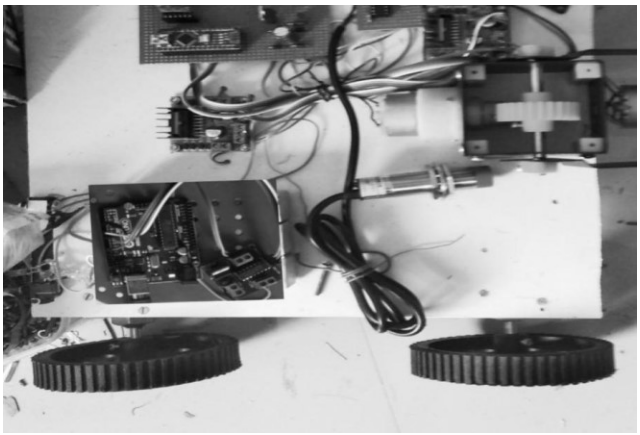

Fig.3-designed prototype

Right eye	Left eye	Mouth	Wheelchair
Open	Open	Open	Forward
Open	Close	Close	Left side
Close	Open	Close	Right side
Close	Close	Close	Backward

Table.1- Input Instruction

3. RESULTS:

The following cases of above table outputs are shown in the below.

- When 2eyes are open and mouth is also open then wheel chair moves forward as shown in Fig.4.
- When left eye is closed, right eye is open and mouth is closed then wheelchair moves left side as shown in Fig.5.
- When left eye is open, right eye is closed and mouth is closed then wheelchair moves right side as shown in Fig.6.
- When 2 eyes are closed and mouth is closed then wheelchair moves backward as shown Fig.7.

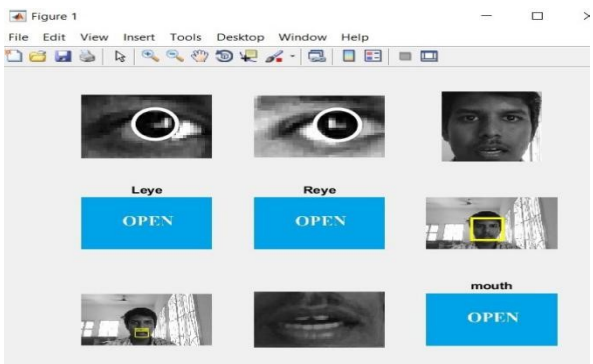

Fig.4- Forward Movement

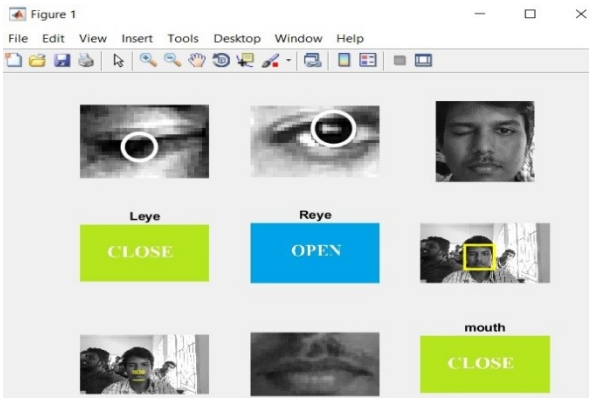

Fig.5- Wheelchair moves left side

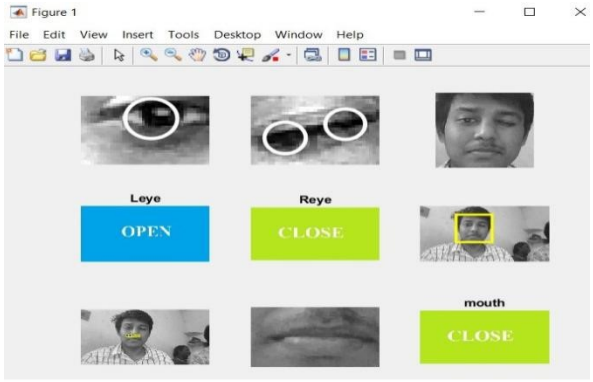

Fig.6-Wheelchair moves right side

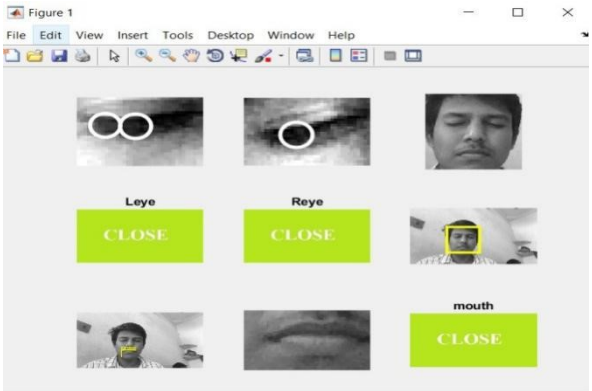

Fig.7-Moves backwards

3.1 Accuracy table:

We conducted different trails on normal and disable people and those results are tabulated in Table.2 and Table.3. The results are quite impressive and percentage of exactness is varied with person to person, but in each case the chances of positive detection are impressive.

Attempts done by normal persons:

Serial no	Total attempts	Favourable outcomes	Percentage of exactness
1	9	8	88.88
2	7	5	71.42
3	9	7	77.77
4	6	6	100
5	5	4	80

Table.2- Percentage of exactness for normal person

Attempts done by disable persons:

Serial no	Total attempts	Favourable outcomes	Percentage of exactness
1	6	4	66.66
2	9	7	77.77
3	4	3	75
4	7	5	71.42

Table.3- Percentage of exactness for disable person

The above data for normal and disabled people are represented in graphical form as show in Graph:1 and Graph:2.
Graph:1 describes number of successful attempts made by the normal people. Graph:2 describes number of successful attempts made by the disable people. X axis describes the person and Y axis describe about the percentage of accuracy

.

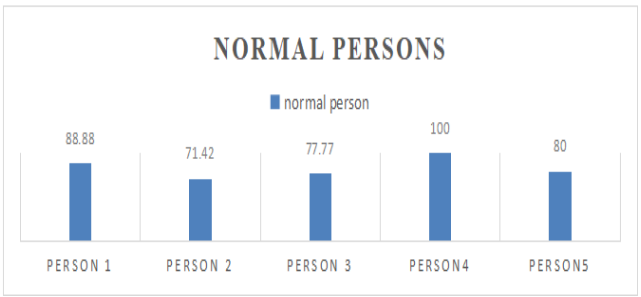

Graph:1

Graph:2

4. Conclusion:

This paper's work has been successful in developing an enhanced wheelchair movement system using facial gestures for the quadriplegia, disabled people. The primary purpose of this work is to develop a prototype that can detect obstacle and make disables self-dependent by increasing their range of mobility through the use of their own facial gestures including both eye and mouth movements. Wheelchair movement system has shown appreciable results with favorable outcomes and the efficiency of this new system is better than the previous developed prototypes for the disables. Future work for this system could be extended by improving speed and power controls of the system for developing a whole optimized systemfor disables.

REFERENCES

[1] M.Senthil Siva Kumar,JayakrishnanMurji, Lightness D Jacob, FrankNyange,M.Banupriya, "Speech Controlled Automatic Wheelchair", PanAfrican International Conference on Information Science, Computingand Telecommunications (2013).

[2] S. Tameemsultana and N. Kali Saranya, "Implementation of Head andFinger MovementBased Automatic Wheel Chair", Bonfring International Journal of Power Systems andIntegrated Circuits, Vol. 1,Special Issue, December 2011.

[3] Ms. HumeraMujawar, Ms. TanayaPatil, Ms. PoojaPatil, Mr. Dinesh O.Shirsath, Mrs. S. S. Sankpal, "Eye Monitored Wheel Chair Control forPhysically Handicapped", International Journal of Innovative Research in Computer Science &Technology (IJIRCST) ISSN: 2347-5552,Volume-3, Issue-3, May 2015.

[4] Jeong-Su Han, Z. Zenn Bien, Dae-Jin Kim, Hyong-Euk Lee, Jong-SungKim, "Human-Machine Interface for wheelchair control with EMG andIts Evaluation", Proceedings of the 25" Annual International Conference of the IEEE EMBS Cancun, Mexico. September 17-21.2003.

[5] DulariSahu, "Automatic Camera Based Eye Controlled WheelchairSystem Using Raspberry Pi", International Journal of Science,Engineering and Technology Research (IJSETR), Volume 5, Issue 1,January 2016.

[6] Hashimoto, M., K. Takahashi, and M. Shimada, "Wheelchair controlusing an EOG- and EMG-based gesture interface," IEEEI ASMEInternational Conference on Advanced Intelligent Mechatronics,AIM.2009.

[7] V Sundara Siva Kumar, G.Ramesh and P Nagesh, ''*MEMSbased Hand Gesture Wheel Chair Movement Control forDisable Persons*'', International Journal of Current Engineering and Technology, Vol.5, No.3 (June 2015).

[8] Deng, L. Y. , Hsu, C. 1. , Lin, T. c. , Tuan, J. S., Chang, S. M. , "EOGbased Human-Computer Interface system development," Journal of Expert Systems with Applications, Vol. 37, pp. 3337-3343, 201

Proceedings of the Fourth International Conference on Communication and Electronics Systems (ICCES 2019)
IEEE Conference Record # 45898; IEEE Xplore ISBN: 978-1-7281-1261-9

An Effective Data Normalization Strategy for Academic Datasets using Log Values

V.Sathya Durga
Research Scholar, Department of CSE
Hindustan Institute of Technology and Science
Padur, Chennai, India
rs.sdv1017@hindustanuniv.ac.in

Thangakumar Jeyaprakash
Associate Professor, Department of CSE
Hindustan Institute of Technology and Science
Padur, Chennai, India
tkumar@hindustanuniv.ac.in

***Abstract* — Data transformation is converting input data from one form to another form. Normalization is a standard data transformation techniques which can be used to transform data. There are many types of normalization techniques, like Min-Max normalization, Cube Root normalization, etc. In this paper, we implement a two-phase normalization process. In the first phase, the data is normalized using Cube Root normalization. Next, the normalized data is still more scaled by applying the logarithmic transformation. Finally, the performance of the transformed values is evaluated against standard metrics.**

Keywords— Data Transformation; Mean Absolute Error; Normalization; ROC Curve;

I. INTRODUCTION

Data Transformation is an integral part of data preprocessing phase in data mining lifecycle. In data transformation, data is converted from the existing form to a form appropriate for mining [1]. Better mining results are yielded if the data in the dataset are appropriately preprocessed and transformed. There are four major categories of transformation techniques. They are smoothing, aggregation, generalization, and normalization [2]. In this paper, we implement a novel normalization strategy by using log values. This normalization strategy can be used by any data mining application of any industry to produce more accurate results.

II. RELATED RESEARCH WORKS

In the research work of Gopal Krishna, a normalization technique named Integer Scaling normalization was introduced. Integer scaling normalization was tested on three datasets. This normalization technique produces values between 0 and 1 effectively [3]. Three normalization technique was compared in the research work of Saranya and Manikandan. Their work normalized the age attribute in the dataset. K-Means clustering was used to test the normalized datasets. This research work reveals that Min Max normalization performed well than other normalization techniques [4]. In the next work of Zuriani and Yuhanis existing normalization techniques was analyzed to predict dengue fever outbreak. Two dengue dataset and one sample dataset for rainfall prediction dataset were used in their work. Maximum accuracy achieved after normalization was 83.4%. In their work, it was found out that decimal scaling normalization performed well than other techniques [5].

III. DESIGN AND IMPLEMENTATION

The required dataset is downloaded from the UCI repository. The dataset used in this work is students academic dataset [6]. This dataset is used to predict the performance of the students. This dataset contains 33 attributes of personal, academic, social, demographic traits of a student. This work mainly focuses on three main attributes in the data set namely grade 1, grade 2 and grade 3. In this work, we implement a two-phase normalization process.

A. Phase 1: Cube Root Normalization

In the first phase, the grade values in grade 1, grade 2 and grade 3 is normalized using cube root normalization. i.e., we take each mark (x) in grade 1, grade 2 and grade 3 find out its cube root value.

Let X be the mark acquired by the students

$$X1 = \sqrt[3]{X}$$

X1 is the output of Phase 1.

B. Phase 2: Log Normalization

In the second stage, we take X1 values and scale it further more by finding log values of X1.

$$X2 = \log (X2)$$

X2 is the output of Phase 2. To the X2 values, we apply decision tree classifier to determine the accuracy and AUC values.

C. Software Implementation

Phase 1 and Phase 2 of this work is carried out in Matlab 2018a. First the dataset is imported. Cube root values (X1) of grade 1, grade 2,grade 3 are found out using the cube root formula, X1 = (sign(x).*abs(x.^(1/3))) [7]. Then we find out log values (X2) of X1 using the log formula (X2=log(X1)). Then we use the classification learner app to determine the effectiveness of the normalized dataset. In the classification learner app, we use Fine Tree classifier to determine the accuracy and AUC values of the normalized datasets.

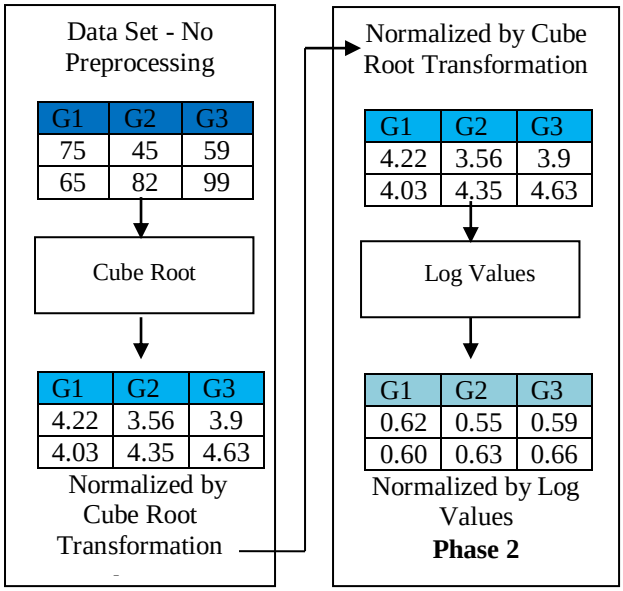

Fig 1: Working Principle

The above figure shows the working principle of this research work. In Phase 1, we perform cube root transformation and Phase 2 perform log normalization.

IV. RESULTS AND DISCUSSIONS

The performance of this proposed work is analyzed in terms three metrics. The metrics are Accuracy, Mean Absolute Error [8] and Roc curve. The experimental values of the metrics are as follows.

A. *Accuracy*

Accuracy of the dataset before preprocessing is 85.6%.
Accuracy after cube root normalization is 85.1 %.
Accuracy after log - cube root normalization is 86.6 %.

B. *ROC Curve*

ROC Curve of the datasets is given below. AUC Value indicated the capability of the model in distinguishing between two groups [9]. The following figures shows the ROC Curve with AUV values of the datasets.

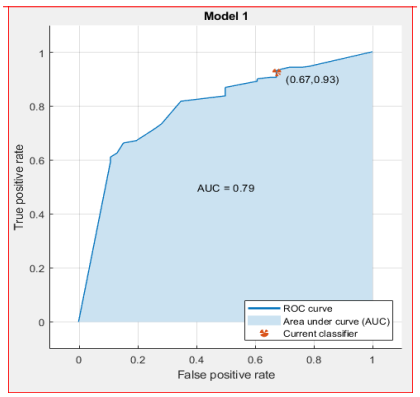

Fig 2: No Preprocessing

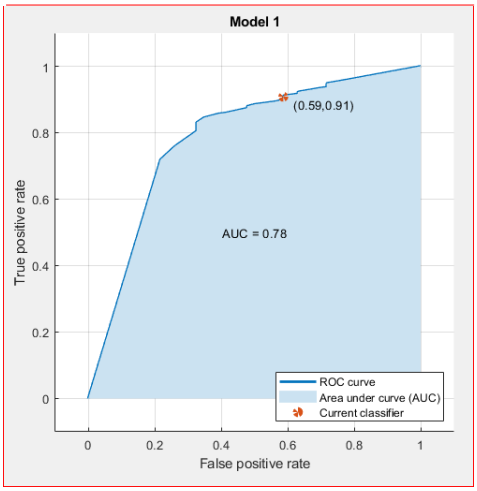

Fig 3: Cube Root Normalization

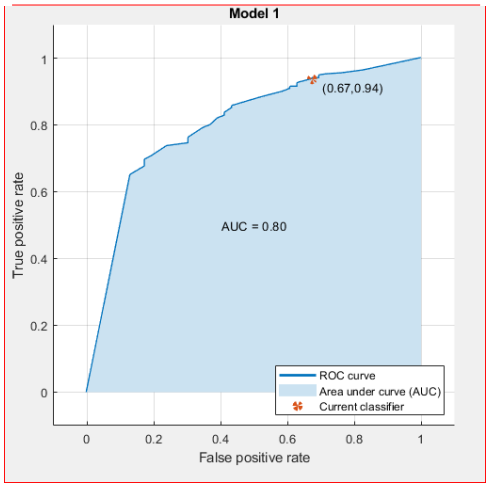

Fig 4: Log - Cube Root Normalization

C. *Mean Absolute Error (MAE)*

MAE before preprocessing is 9.10 %.
MAE after cube root normalization is 0.52 %.
MAE after log - cube root normalization is 0.07 %.

In all the comparisons it is found out that, academic dataset which undergoes two phase normalization performed well than academic dataset with no preprocessing or dataset preprocessed with cube root normalization. Comparing the accuracies, it can be found that high accuracy of 86.6% is achieved by the academic dataset after log cube root normalization. The Mean absolute error is also less (0.07) and AUC value is higher (0.80) for the academic dataset which underwent two-phase normalization. Hence it can be seen, that the proposed normalization strategy decreases the mean absolute error and increases the accuracy and AUC value of academic dataset. It can be taken from here that log - cube root normalization is very effective in improving the performance of mining works related to academic datasets. So, researchers working on academic datasets can use log - cube root normalization to improve the performance of their works.

V. CONCLUSION

In this paper, we introduce a two-phase normalization strategy using the log and cube root values. The academic dataset from the UCI repository is used in this work. From the experimental results of this work, we can conclude that our normalization strategy produces better results in terms of accuracy and mean absolute error. So, for preprocessing academic datasets, it is highly recommended to use log - cube root normalization. As future directions, we can implement log-square root normalization or implement multi phase normalization technique using max min normalization, cube root normalization and square root normalization together.

REFERENCES

[1] Data (Pre) Processing.[PDF] https://www.iitr.ac.in/media/facspace /patelfec/16Bit/slides/Lecture-2-Data-Preprocessing-Part-1.pdf.

[2] Data Preprocessing.[PDF] https://www.cse.wustl.edu/~zhang/teaching /cs514/Spring11/Data-prep.pdf.

[3] Gopal & Kishore," Normalization: A Preprocessing Stage". IARJSET. arXiv:1503.06462.

[4] Saranya & G.Manikandan, "Study on normalization techniques for privacy preserving dm", Int.J.Eng and Tech, vol.5. 2701-2704, 2013.

[5] Z. Mustaffa and Y. Yusof, "A comparison of normalisation techniques in predicting dengue outbreak", Proc. International conference on business and economics research, IACSIT Press, pp. 345-349. 2011.

[6] https://archive.ics.uci.edu/ml/datasets/student+performance (accessed May 23, 2019).

[7] https://www.researchgate.net/post/how_to_find_the_cube_root_on_simu link.

[8] https://www.dataquest.io/blog/understanding-regression-error-metrics/.

[9] https://towardsdatascience.com/understanding-auc-roc-curve-68b2303cc9c5.

Proceedings of the Fourth International Conference on Communication and Electronics Systems (ICCES 2019)
IEEE Conference Record # 45898; IEEE Xplore ISBN: 978-1-7281-1261-9

Saliency Guided Image Super-Resolution using PSO and MLP based Interpolation in Wavelet Domain

Sheetal Shivagunde
Department of Computer Engineering
NIT Kurukshetra
Kurukshetra, India
sheetal_31703103@nitkkr.ac.in

Mantosh Biswas
Department of Computer Engineering
NIT Kurukshetra
Kurukshetra, India
mantoshb@gmail.com

***Abstract*—Super resolution algorithms always used as a trade-off between the cost of the high definition (HD) cameras and the quality and/or clarity of the image obtained. There are various predefined algorithms that obtain Super Resolved images from Low Resolution (LR) images, some (such as, Convolutional Neural Network (CNN), Deep learning, Sparse Representation based algorithms) gives better results for e.g. deburring of zoomed part, removal of noise, color enhancement and so on but are computationally complex or hard to implement in real-time environment whereas some are very simple to use (such as, interpolation based, wavelet based algorithms) but lack quality for e.g. ringing artifacts, edge blurs, poor image quality etc. In this paper, we proposed a method that combines advantages of some of the above mentioned methods. Our proposed method obtains High Resolution (HR) image using saliency model for detection of visually dominant regions, Discrete Wavelet Transform (DWT) for extraction of high frequency details, finally Multi-layer Perceptron (MLP) and Particle Swarm Optimization (PSO) for interpolation. Experimental results visually and quantitatively show that for considered test images our proposed super resolution method appears to be most promising compared to bi-cubic, Chopade *et al.*, Yu *et al.* and Man *et al.* methods.**

Keywords—resolution; saliency; wavelet transform; particle swarm optimization; multi-layer perceptron

I. INTRODUCTION

Nowadays many applications and systems entirely depend upon images for processing, e.g., different biometric systems as, iris recognition system which uses unique patterns of a person's eye veins for recognition, fingerprint scanner that uses physical differences in bridges and valleys or medical imaging systems, radiography, tomography, MRI, ultrasound, elastography, etc. that used for medical diagnosis or surveillance systems and many more. Such applications require very minute details for processing and the outcome relies entirely on the input images therefore quality is the basic necessity for such applications, LR images cannot be used as an input for such applications because these images appear pixelated and contain very less details and we cannot extract required details like, edge information, color information, etc. from such images. High quality images can be obtained using High Definition (HD) cameras but, cost of such cameras is high and cannot be always used as a preferable solution and here come the super resolution (SR) algorithms into the picture. SR algorithms can convert Low Resolution (LR) images into HR images with much less expenses as compared with the cost of HD cameras [1].

Researchers have proposed several solutions for SR problem in both frequency as well as in spatial domain. Frequency domain consists of Complex Wavelet Transform (CWT), Discrete Wavelet Transform (DWT), Stationary Wavelet Transform (SWT), Fast Fourier Transform (FFT), Discrete Fourier Transform (DFT), etc. Eason *et al.* in [2] combined CWT, Wavelet zero padding (WZP) and Cycle Spinning (CS) for obtaining HR image. Gajjar *et al.* [3] used DWT so as to extract high frequency details to reduce edge blurs in combination with learning and maximum a posteriori (MAP) approach, finally gradient descent method is used for minimization of the cost function and the image obtained is the HR image. Anbarjafari *et al.* [4] proposed a method in which high frequency sub bands obtained after DWT and the original LR image are interpolated then Inverse DWT is used in order to obtain the final HR image. Chopade *et al.* [5] proposed SR method that uses SWT in combination with DWT to avoid information loss that occurs due to down sampling in DWT. The extraction of neighbouring information required for the interpolation process is more effective if we are using the decomposed image compared to the use of the original LR image therefore we have used DWT in our proposed method.

Spatial domain methods include interpolation, reconstruction, filtering, sparse representation, learning, optimization etc. Interpolation based techniques are generally categorized as classical interpolations and edge based interpolations [6, 7]. Classical interpolations include linear i.e. nearest neighbour, bi-linear and non-linear i.e. cubic, bi-cubic and spline interpolation methods but mostly these methods are combined with other methods like wavelet based, learning based optimization based methods for obtaining better results because if used alone these methods suffer from reconstruction artifacts like jaggings, saw tooth edges, edge breaks, ringing effects etc. In edge based interpolation techniques recognition of edge region is done and then interpolation is used accordingly therefore such methods provide better results in edge regions. Although edge directed interpolations provide better results than classical interpolations, all these methods use duplication of available information for missing pixel calculation and therefore suffer from jagging, ringing and blurring effects.

To overcome the shortcomings of interpolation based methods several learning based methods have been introduced

[7-10]. CNNs and Deep learning algorithms provide excellent results [7] but are computationally complex to avoid this complexity simple networks like multi-layer perceptron (MLP), Radial Basis Function (RBF), Backpropagation network etc. are widely used [8-10]. San *et al*. [8] have used MLP and RBF in combination with wavelet packet transform for high frequency extraction whereas Man *et al*. [9] have proposed a method that uses registration process for estimation of relative motion between different LR images and then three layer MLP is used for interpolation. Hasan *et al*. [10] have used one of the algorithm from nearest neighbour, bi-linear and bi-cubic interpolation for the upscaling method and then feed forward backpropagation network is used for increasing quality of the interpolation. Instead of duplicating the neighbouring information, learning based methods actually learns to create a new pixel using available neighbouring information this enhances the quality of the resulting HR image therefore in our proposed method we have used learning based interpolation using MLP instead of classical interpolations.

PSO is used to optimize complex and non-convex cost functions obtained after various learning or reconstruction based methods and also for enhancement of the SR results in many algorithms along with classical interpolations or cutting edge learning based methods [11-14]. Gajjar *et al.* [11] have used PSO for final optimization of the cost function obtained after wavelet based learning and Maximum a posteriori markov random field (MAP-MRF). Quraishi *et al.* [12] have evolved a method which uses DWT and linear interpolation for obtaining HR images from input LR images subsequently PSO is used for enhancement of the results whereas Chen *et al*. [13] have used PSO only for the edge region, saliency model is used for the estimation of the edge region, and later, to obtain the HR image Artificial Neural Network-PSO (ANN-PSO) is applied in the estimated edge region and bi-linear interpolation is applied in non-edge region. Yu *et al.* [14] have proposed a mixed PSO algorithm for reconstruction based SR process to avoid shortcomings of basic PSO. Inspired by advantages of PSO, we have used it in our proposed method for visually dominant regions so as to avoid cracked, jagged or blurred edges and indirectly to enhance the interpolation process in that particular region.

Considering above mentioned points, we proposed an approach that integrates benefits of saliency model, DWT and PSO and MLP based interpolation to obtain HR images. The rest of the paper is organized as: In section II proposed method is discussed briefly. In section III experimental results (quantitative as well as visual) are presented for considered test images and section IV concludes the paper.

II. Proposed Method

Saw tooth or cracked edges is the most common problem in classical bi-cubic interpolation however some researchers tried to address this problem, combination of SWT with DWT proved to be better up to certain extent [5, 9], whereas Yu *et al.*'s method uses mixed PSO only for enhancement to overcome problems of all these methods we have proposed saliency guided SR method. In our proposed method Phase Spectrum of Quaternion Fourier Transfer (PQFT) saliency model is used to detect visually dominant regions and to generate the saliency map, DWT is used for extraction of the high frequency details, Missing HR pixel calculation is done with the help of MLP based interpolation in background region and using PSO based interpolation in visually dominant region. In-depth flow of our proposed method is given in the following section and the schematic diagram for obtaining HR image is shown in Fig.1.

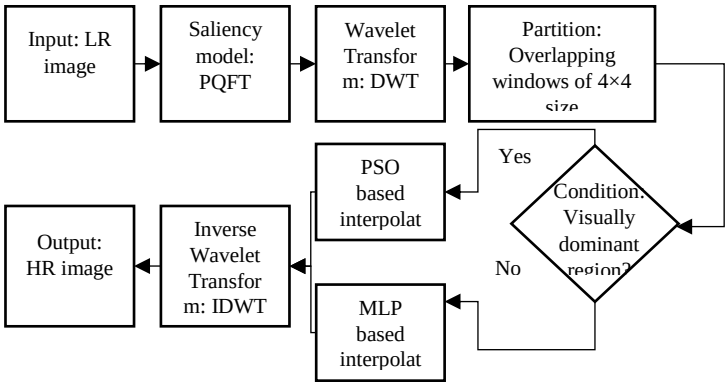

Fig. 1. Schematic diagram of our proposed SR method

A. *Saliency Model: Phase Spectrum of Quaternion Fourier Transform*

Saliency model is used to detect and extract visually dominant regions from an image [15]. Broadly saliency detection methods can be divided as spatial and frequency domain methods. Spatial domain methods are, Classical Itti model, AC algorithm, Region based Contrast (RC) model, Histogram based Contrast (HC) model, Context based CA (Context Aware) model, Graph Theory based algorithm, etc. but shortcomings of these spatial domain based saliency detection methods are these have very high computational complexity and are very sensitive to parameter selections therefore not very useful for real-time systems whereas frequency domain based saliency detection methods have comparatively low computational complexity and feature extraction is easier as compared with spatial domain methods therefore we have chosen frequency domain based saliency detection. Frequency domain based saliency detection methods include, PQFT, Spectral Residual, MSS (Maximum Symmetric Surrounded) and FT (Frequency Tuned) methods.

In our proposed method saliency is used as a sort of image segmentation that segments image into visually important and background part and output of this process is a saliency map. This acquired saliency map is then used for selection of the interpolation process. We have used PQFT algorithm for saliency detection, which uses only the phase spectrum of the input image after application of the Fourier transform but discards the magnitude spectrum and then by applying inverse Fourier transform obtained output is a saliency map of the input image. This saliency map contains only binary values, 1 for visually important regions and 0 for background regions.

Edges play a very vital role in the image. Interpolation process causes smoothing of the edges which degrades the quality of the resultant HR image, therefore to preserve the edge information extraction of high frequency details is essential and

we have used wavelet transform for this. Original LR image is used as an input for DWT and not the saliency map.

B. Wavelet Transform: Discrete Wavelet Transform

Wavelet Transforms decompose signals into both time and frequency domains that means it uses functions localized in both real and Fourier space. There are two main categories of wavelet transform one is a Continues Wavelet Transform (CWT) and other one is a Discrete Wavelet Transform (DWT). When wavelet transform uses discrete set of wavelets it is known as DWT, which fragments image into four mutually orthogonal set of components i.e. one low frequency sub band: LL known as approximation component which can be used for further decomposition and three high frequency sub bands LH, HL and HH represent vertical, horizontal and diagonal details respectively [16]. One – level decomposition using DWT is shown in Fig. 2.

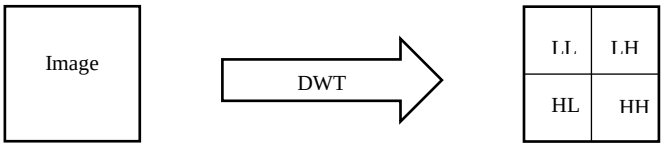

Fig. 2. One - level decomposition of an image using DWT

Haar, Daubechies, Morlets, Symlets, Meyer, Coeiflets and other real wavelets are different kinds of mother wavelets, among these wavelets, Haar wavelet is the simplest and since it is less smooth than other wavelets, it provides better results for the area with sharp edges. Therefore we have chosen Haar wavelet in our proposed method.

Each sub band obtained after DWT is divided into overlapping windows of 4×4 size and compared against the corresponding saliency map to check whether that window falls under the visually dominant region or not. If out of 16 pixels 8 or more pixels are having value 1 in the respective saliency map then that window falls under the visually dominant region and processed using PSO based interpolation otherwise it falls under the background region and processed using MLP based interpolation.

C. Optimization: Particle Swarm Optimization

The particle swarm optimization is a search algorithm motivated by the social behaviour of birds within a swarm and therefore the name is particle swarm. In PSO each particle modifies its position and velocity according to the neighbouring information, which indicates that each particle within the swarm is influenced by other particles [17]. Based on the fitness function, position and velocity updation of each particle is done respectively, by following equations.

$$p_i(t+1) = p_i(t) + v_i(t+1) \tag{1}$$

$$v_i(t+1) = v_i(t) + c \times r_1(t)[b_i(t) - p_i(t)] + s \times r_2(t)\left[\hat{b}(t) - p_i(t)\right] \tag{2}$$

Where $p_i(t)$ and $v_i(t)$ are position and velocity of the particle 'i' at time step 't' respectively, c and s are cognitive and social components respectively, r_1 and r_2 are any random numbers between 0 to 1, $b_i(t)$ is the personal best position which is the best position of the particle from the first iteration/time step till the current time step and $\hat{b}(t)$ is the global best position within the swarm i.e. the best of the personal best.

In our proposed method swarm is a window of size 4×4 and each pixel within the window is a particle. As our proposed method uses PSO only for the visually dominant region, only those particles having value 1 in the corresponding saliency map are considered while modifying position and velocity based on the fitness function. The fitness function is defined as:

$$f = min\left(\left|h_{window} - \frac{p_i \times \hat{b}_{window}}{\sum_{j=0}^{16} p_{j(iff\ p'_j=1)}}\right|\right) \tag{3}$$

Where h_{window} is the actual HR coefficient from the original HR image that is to be calculated, $\hat{y}_{window}$ is the global best for that particular window. Updation of position and velocity using (7) and (8) is done until there is no change in the global bests for continuous five iterations.

D. Learning: Multi-layer Perceptron

MLP is a feed forward neural network that uses supervised type of learning. That means for the learning process target vector is required for each of its input vector, this pair of input and target vector is called as training pair [18]. Number of hidden layers are variable and the values of hidden layer neurons are calculated using following equation.

$$z_j = b_j + \sum_{i=0}^{n} x_i w_i \tag{4}$$

Where, z_j is a hidden layer neuron, b_j is a bias, x_i is an input and w_i is a weight between input layer and hidden layer.

Output of MLP is calculated using

$$y = b + \sum_{j=0}^{m} z_j v_j \tag{5}$$

Where, y is a value of output neuron and v_j is a weight between hidden layer and an output layer.

Learning process of any neural network is associated with the weight updation and in MLP weight updation and bias updation is done using following equations respectively,

$$w_j(new) = w_j(old) + \alpha t x_j \tag{6}$$

$$b_j(new) = b_j(old) + \alpha t \tag{7}$$

Where, α is a learning factor and t is a target pixel value.

In our proposed method we have used two hidden layers for MLP. Input layer consists of 16 pixels which are taken from 4×4 window, first hidden layer also contains 16 pixels which are

calculated using (3), second hidden layer contains 4 pixels which are also calculated using (3), output layer contains only one pixel which is calculated using (4) and this output value is our calculated HR coefficient. This calculated HR value is then compared with the actual HR image's corresponding coefficient and difference is calculated. If this difference is greater than 25 % then weight and bias updation is done using (5) and (6) respectively otherwise no weight updation is required. Fig. 3 shows structure of used MLP in proposed method.

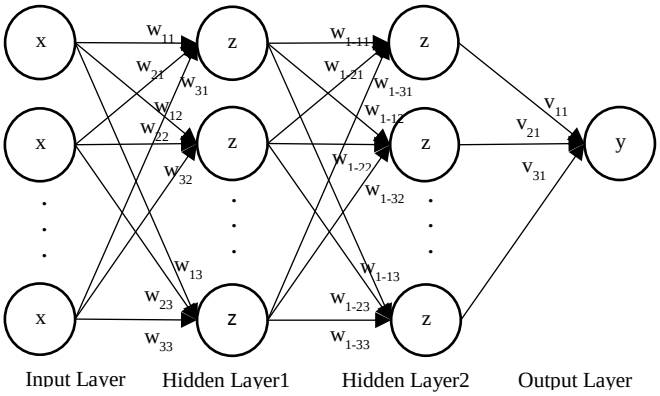

Fig. 3. Structure of the MLP used in proposed method

E. *Interpolation*

Interpolation is a process that uses known neighbouring pixel values for insertion of the new data at unknown points. In a procedure of conversion from LR image to HR image interpolation is used for calculation and insertion of unknown HR pixel with the help of neighbouring known LR pixels [6].

In proposed method interpolation is done using both learning i.e. MLP and optimization i.e. PSO methods, for this bi-cubic interpolation is taken as a base. In bi-cubic interpolation 16 neighbouring pixels of unknown pixel are used for weighted average as shown in Fig. 4.

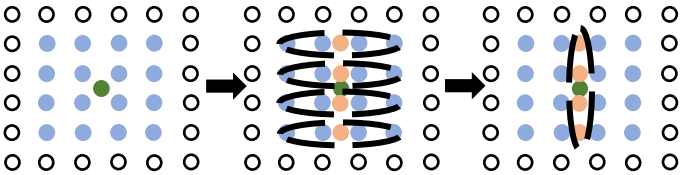

Fig. 4. Process of bi-cubic interpolation

In Fig.4 left most figure represents 16 known LR pixels, middle figure represents intermediate value calculation and final HR pixel calculation is shown in the right most figure. Blue coloured pixels are known LR pixels, as shown in the middle image, using weighted average of these pixels, 4 red coloured pixel values i.e. intermediate values are calculated horizontally, after that as shown in the right most image, vertical weighted average of these 4 intermediate values gives value of HR pixel.

F. *Inverse Discrete Wavelet Transform*

The Inverse of the DWT process is known as IDWT, and it is used to reconstruct the processed sub bands [16]. In our proposed method after PSO and MLP based interpolation, these interpolated high frequency sub bands and the interpolated LR image are combined using IDWT. First-level IDWT is shown in Fig. 5.

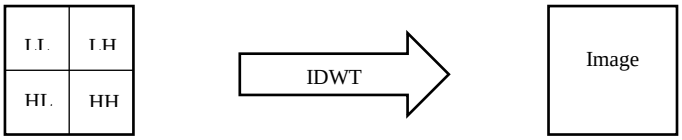

Fig. 5. Inverse Discrete Wavelet Transform of an image

III. Results And Discussions

Here, we have used "Football", "Baboon", "House", "Letters", "Parrot", "Monarch", "Foreman", "Peppers", "Texture 1" and "Texture 2" as test images for experimental purpose, as shown in Fig. 6. Experiments are performed on Intel core 3, 2.3 GHz processor with 4 GB RAM using MATLAB 2016a.

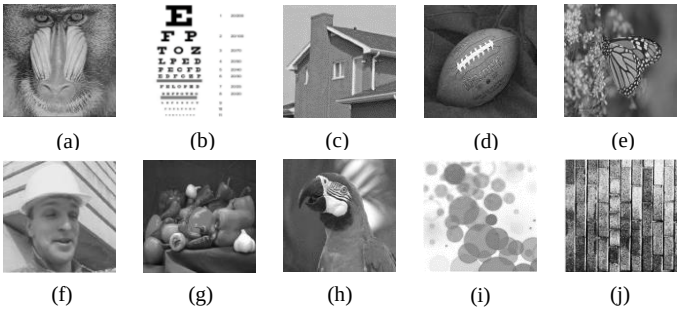

Fig. 6. LR Test images: (a) Baboon, (b) Letters, (c) House, (d) Football, (e) Monarch, (f) Foreman, (g) Peppers, (h) Parrot, (i) Texture1 and (j) Texture2

Performance evaluation of our proposed method with four predefined methods viz., bi-cubic method [6], Chopade *et al.* [5], Yu *et al.* [14], and Man *et al*. [9] using our considered test images is shown visually (as shown in Figs. 7-16) as well as quantitatively. For quantitative performance evaluation, we have used three full reference image quality estimation parameters viz., Peak Signal to Noise Ratio (PSNR), Structural Similarity Index (SSIM) and Normalized Cross Correlation (NCC) [19, 20]. Experimental results of these quality assessment parameters for all the considered methods and for our proposed method are listed in Table I also, Bar charts for each of the quality assessment parameters are shown in Figs. 17 (a-c).

In this paper, we have concentrated our work in the visually dominant region and for that saliency model and DWT are used. Therefore from the cropped part of Figs. 7-16 (e) we can see that our method gives better results in both edge as well as in non-edge region. Also, Results of quality assessment parameters of our proposed method for considered test images are high compared to bi-cubic, Chopade *et al.*, Yu *et al.* and Man *et al.* methods as shown in Table I.

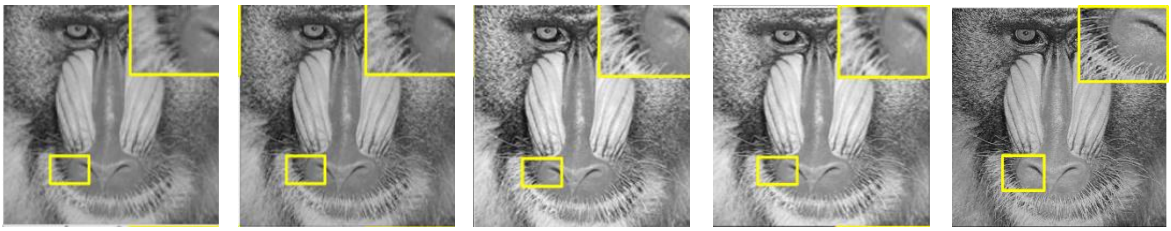

(a) (b) (c) (d) (e)

Fig. 7. Baboon: HR images for methods: (a) Bi-cubic [6], (b) Chopade *et al*. [5], (c) Yu *et al*. [14], (d) Man *et al*. [9] and (e) proposed

(a) (b) (c) (d) (e)

Fig. 8. Letters: HR images for methods: (a) Bi-cubic [6], (b) Chopade *et al*. [5], (c) Yu *et al*. [14], (d) Man *et al*. [9] and (e) proposed

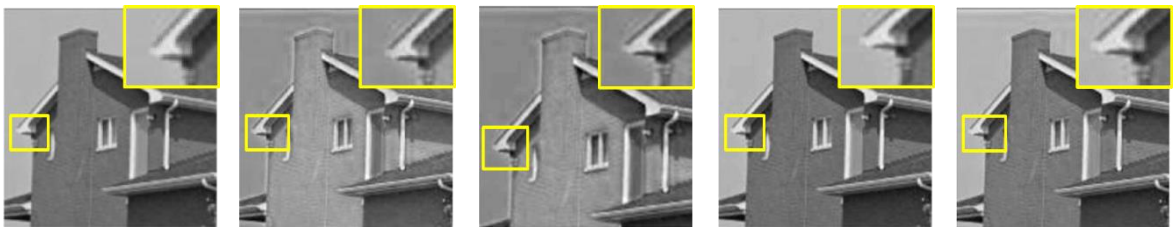

(a) (b) (c) (d) (e)

Fig. 9. House: HR images for methods: (a) Bi-cubic [6], (b) Chopade *et al*. [5], (c) Yu *et al*. [14], (d) Man *et al*. [9] and (e) proposed

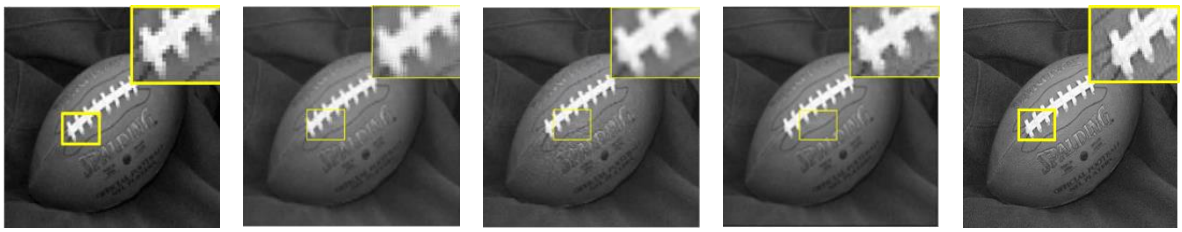

(a) (b) (c) (d) (e)

Fig. 10. Football: HR images for methods: (a) Bi-cubic [6], (b) Chopade *et al*. [5], (c) Yu *et al*. [14], (d) Man *et al*. [9] and (e) proposed

(a) (b) (c) (d) (e)

Fig. 11. Monarch: HR images for methods: (a) Bi-cubic [6], (b) Chopade *et al*. [5], (c) Yu *et al*. [14], (d) Man *et al*. [9] and (e) proposed

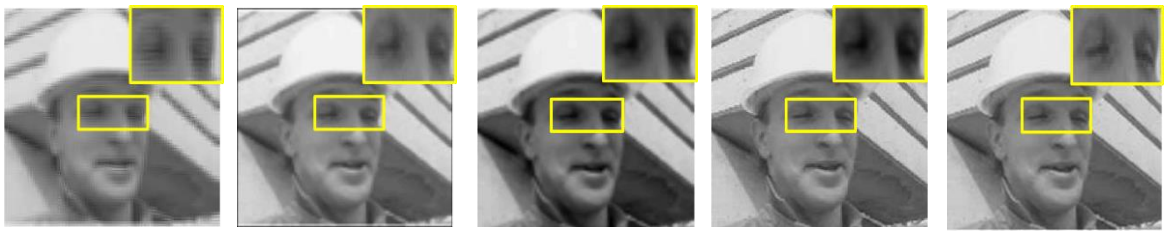

(a) (b) (c) (d) (e)

Fig. 12. Foreman: HR images for methods: (a) Bi-cubic [6], (b) Chopade *et al*. [5], (c) Yu *et al*. [14], (d) Man *et al*. [9] and (e) proposed

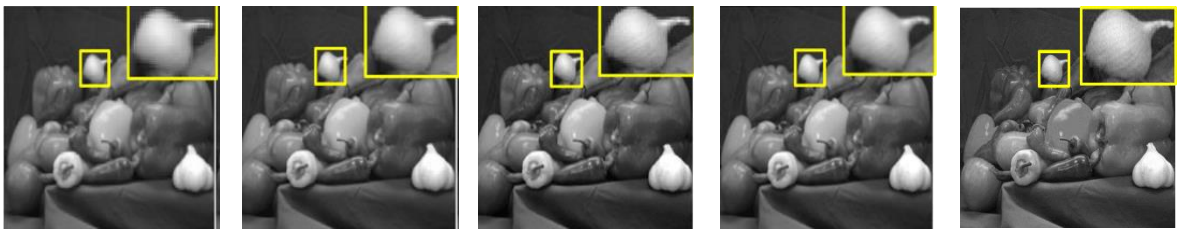

(a) (b) (c) (d) (e)

Fig. 13. Peppers: HR images for methods: (a) Bi-cubic [6], (b) Chopade *et al*. [5], (c) Yu *et al*. [14], (d) Man *et al*. [9] and (e) proposed

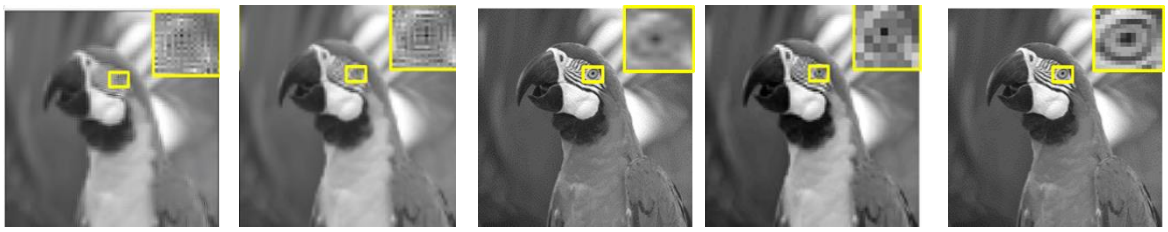

(a) (b) (c) (d) (e)

Fig. 14. Parrot: HR images for methods: (a) Bi-cubic [6], (b) Chopade *et al*. [5], (c) Yu *et al*. [14], (d) Man *et al*. [9] and (e) proposed

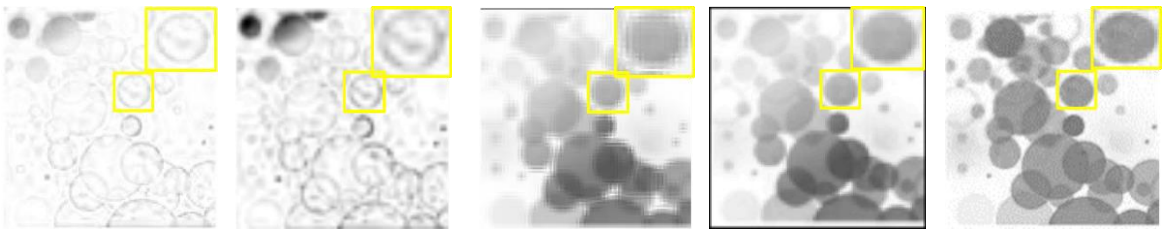

(a) (b) (c) (d) (e)

Fig. 15. Texture1: HR images for methods: (a) Bi-cubic [6], (b) Chopade *et al*. [5], (c) Yu *et al*. [14], (d) Man *et al*. [9] and (e) proposed

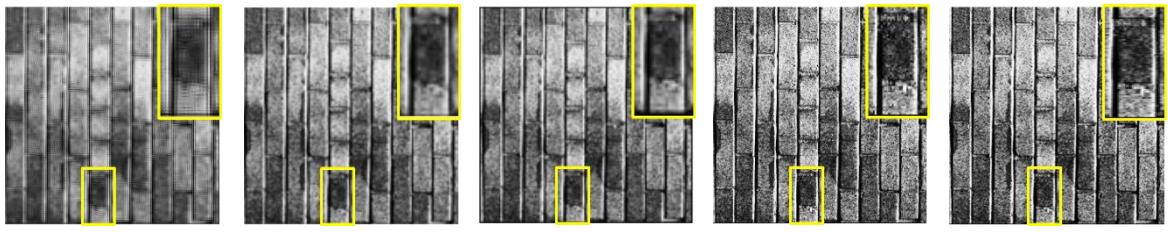

(a) (b) (c) (d) (e)

Fig. 16. Texture2: HR images for methods: (a) Bi-cubic [6], (b) Chopade *et al*. [5], (c) Yu *et al*. [14], (d) Man *et al*. [9] and (e) proposed

TABLE I. RESULTS FOR PSNR, SSIM AND NCC COMPARISON OF OUR PROPOSED SR METHOD WITH BI-CUBIC [6], CHOPADE *ET AL.* [5], YU *ET AL.* [14], AND MAN *ET AL.* [9] METHODS ON CONSIDERED TEST IMAGES

	Baboon	Letters	House	Football	Monarch	Foreman	Peppers	Parrot	Texture1	Texture2
					PSNR					
Bi-cubic	24.973	21.012	22.528	30.075	27.019	19.324	31.096	24.368	17.012	18.637
Chopade et al.	24.608	22.491	26.799	31.015	27.223	24.860	32.631	26.786	22.595	17.113
Yu et al.	24.764	22.745	24.048	28.284	27.138	27.023	32.354	24.677	26.897	18.643
Man et al.	25.368	24.953	31.323	34.414	28.982	27.465	32.352	30.619	35.127	20.373
Proposed	27.834	24.826	31.992	35.347	30.395	27.467	33.989	34.013	38.916	20.994
					SSIM					
Bi-cubic	0.6051	0.7684	0.8269	0.6382	0.6792	0.7399	0.6801	0.6965	0.9131	0.7617
Chopade et al.	0.5360	0.8323	0.9095	0.8761	0.6984	0.9095	0.7263	0.7237	0.8177	0.7566
Yu et al.	0.6297	0.7283	0.9103	0.6120	0.7193	0.7594	0.8823	0.8034	0.9062	0.7509
Man et al.	0.7367	0.9131	0.9446	0.8950	0.8955	0.9210	0.8261	0.9100	0.9723	0.7718
Proposed	0.9453	0.9368	0.9701	0.8992	0.9268	0.9222	0.8792	0.9294	0.9903	0.7959
					NCC					
Bi-cubic	0.5372	0.6073	0.6994	0.8592	0.5970	0.8867	0.6977	0.6828	0.5929	0.4981
Chopade et al.	0.4352	0.5844	0.6798	0.8535	0.5924	0.8801	0.6972	0.6745	0.5382	0.4567
Yu et al.	0.4171	0.5526	0.6640	0.7563	0.5643	0.8521	0.6185	0.6850	0.4378	0.4483
Man et al.	0.4123	0.5487	0.6785	0.8196	0.5673	0.8657	0.6094	0.6456	0.5284	0.4495
Proposed	0.4089	0.5647	0.6473	0.8070	0.5247	0.6670	0.5373	0.6138	0.4937	0.4518

Figs. 17 (a-c) gives bar charts for quantitative performance evaluation of our proposed method with the four considered methods, where, light blue bar represents our proposed method.

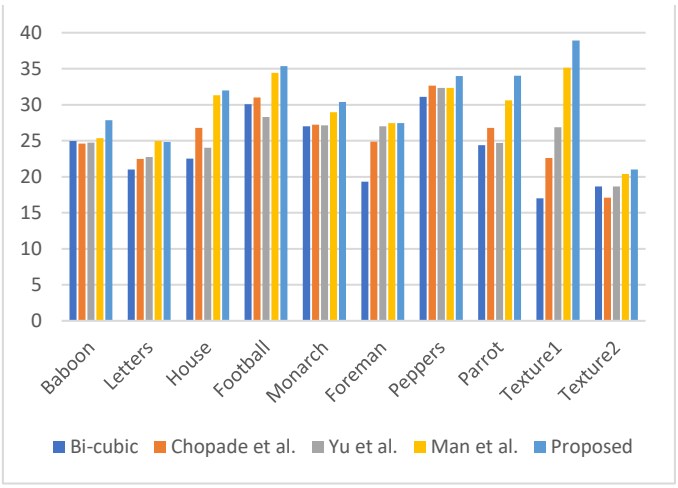

(a)

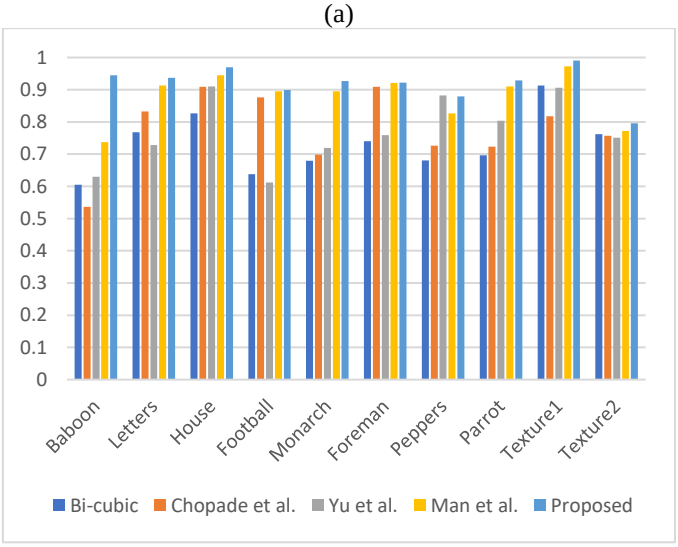

(b)

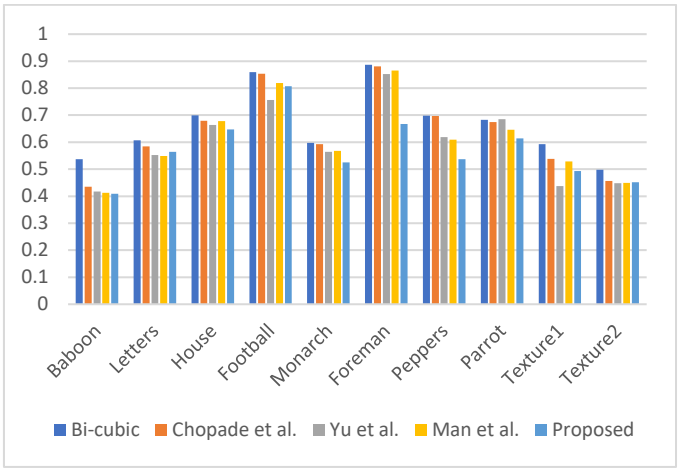

(c)

Fig. 17. Bar charts representing comparison of (a) PSNR, (b) SSIM and (c) NCC of our proposed method with considered SR methods for considered test images

IV. CONCLUSION

In this paper we proposed Saliency guided Image Super resolution using PSO and MLP based interpolation in wavelet domain, and therefore tried to combine advantages of all these methods. Though interpolation based methods produce processing artifacts, combining them with DWT, MLP and PSO avoids this problem also complexity of interpolation based methods is less than other SR methods therefore our proposed method acts as a mid-way between the complexity and the quality. Experimental results for considered test images show that our method gives a promising solution for SR problem and outperforms other considered methods.

However, selection of window for PSO or MLP based interpolation is based on the fixed condition i.e. if window contains 8 or more occurrences of 1 in its corresponding saliency model, then that region is considered as visually dominant region. This condition can be automated, but complexity of the solution will increase subsequently therefore, there is a need to

find a solution that will automate the process but will also not increase the complexity.

REFERENCES

[1] J. Yang, and T. Huang, "Image super-resolution: Historical overview and future challenges", Super Resolution Imaging, pp.4-6, 2010.

[2] G. Eason, B. Noble, and l. N. Sneddon, "On certain integrals of Lipschitz-Hankel type involving products of Bessel functions," Philosophical Transactions of the Royal Society of London., vol.A247, pp.529-551, 1955.

[3] P. P. Gajjar, and M. V. Joshi, "New-Learning Based Superresolution: Use of DWT and IGMRF Prior," IEEE Transactions on Image Processing, vol.19, no.5, pp.1201-1213, 2010, doi: 10.1109/TIP.2010.2041408.

[4] G. Anbarjafari, and H. Demirel, "Image Super Resolution Based on Interpolation of Wavelet Domain High Frequency Sub-bands and the Spatial Domain Input Image," Electronics and Telecommunications Research Institute Journal, vol.32, No.3, pp.390-394, 2010, doi: 10.4218/etrij.10.0109.0303.

[5] P. B. Chopade, and P. M. Patil, "Image super resolution scheme based on wavelet transform and its performance analysis," International Conference on Computing, Communication & Automation, pp.1182-1186, 2015, doi: 10.1109/CCAA.2015.7148555.

[6] R. C. Gonzalez, and R. E.Woods, "Digital Image Processing," pp.64-68, Addison Wesley, 2nd edition, 1992.

[7] G. Pandey, and U. Ghanekar, "A compendious study of super-resolution techniques by single image," Optik, vol.166, pp.147-160, 2018, doi:10.1016/j.ijleo.2018.03.103.

[8] P. E. San, F. Tian, Z. Shi, and M. Deng, "Super-resoloution image reconstruction based on wavelet packet transform and artifcial neural networks," 11th International Computer Conference on Wavelet Actiev Media Technology and Information Processing, pp.124-129, 2014, doi: 10.1109/ICCWAMTIP.2014.7073375.

[9] N. T. Man, and T. Q. Vinh, "Image Super-Resolution Using Image Registration and Neural Network Based Interpolation," International Conference on Advanced Computing and Applications, pp.164-167, 2016, doi: 10.1109/ACOMP.2016.032.

[10] M. S. Hasan, and S. T. Haque, "Single image super-resolution using back-propagation neural networks," 20th International Conference of Computer and Information Technology, pp.1-5, 2017, doi: 10.1109/ICCITECHN.2017.8281778.

[11] P. Gajjar, and M. Joshi, "Zoom Based Super-Resolution: A Fast Approach Using Particle Swarm Optimization," Image and Signal Processing, vol.6134, pp.63-70, 2010, doi:10.1007/978-3-642-13681-8_8.

[12] M. I. Quraishi, K. G. Dhal, J. P. Choudhury, K. Pattanayak and M. De, "A novel hybrid approach to enhance low resolution images using particle swarm optimization," 2nd IEEE International Conference on Parallel, Distributed and Grid Computing, pp.888-893, 2012, doi: 10.1109/PDGC.2012.6449941.

[13] H. Y. Chen, and J. J. Leou, "Saliency-directed color image interpolation using artificial neural network and particle swarm optimization," vol. 23, pp.343-358, 2012, doi: 10.1016/j.jvcir.2011.11.006.

[14] W. Yu, and M. Zhang, "A mixed particle swarm optimization algorithm's application in image/video super-resolution reconstruction," 2nd International Conference on Image, Vision and Computing, pp.526-530, 2017, doi: 10.1109/ICIVC.2017.7984611.

[15] M. Runxin, Y. Yang, and Y. Xiaomin, "Survey on Image Saliency Detection Methods," International Conference on Cyber-Enabled Distributed Computing and Knowledge Discovery, pp.329-338, 2015, doi: 10.1109/CyberC.2015.98.

[16] A. Graps, "An Introduction to Wavelets," IEEE Computational Sciences and Engineering, vol.2, no.2, pp.50-61, 1995.

[17] A. P. Engelbrecht, "Computational Intelligence: An Introduction," pp.289-294, John Wiley and sons, 2nd edition, 2007.

[18] S. N. Sivanandam, and S. N. Deepa, "Principles of Soft Computing," pp.51-56, Wiley, 2nd edition, 2011.

[19] F. Memon, M. A. Unar, and S. Memon, "Image Quality Assessment for Performance Evaluation of Focus Measure Operators," Mehran University Research Journal of Engineering and Technology, vol.34, no.4, pp.379-386, 2015.

[20] M. Gulame, K.R. Joshi, and R.S. Kamthe, "A full reference based objective image quality assessment," International Journal of Advances in Electrical and Electronics Engineering, pp.13-18, 2013.

Proceedings of the Fourth International Conference on Communication and Electronics Systems (ICCES 2019)
IEEE Conference Record # 45898; IEEE Xplore ISBN: 978-1-7281-1261-9

Change Detection in Vegetation Cover Using Deep Learning

Yamini Katta
Department of Information Technology
V.R.Siddhartha Engineering College
Kanuru, Vijayawada-7
yaminikatta07@gmail.com

Nomitha Datla
Department of Information Technology
V.R.Siddhartha Engineering College
Kanuru, Vijayawada-7
nomitha.datla9@gmail.com

Sowmya Sri Kilaru
Department of Information Technology
V.R.Siddhartha Engineering College
Kanuru, Vijayawada-7
sowmyakilaru5@gmail.com

Dr. T. Anuradha
Professor, Department of Information Technology
V.R.Siddhartha Engineering College
Kanuru, Vijayawada-7
atadiparty@gmail.com

***Abstract*— Because of man-made occasions and regular causes, numerous areas on the land are experiencing quick and wide-running changes in vegetation spread. Vegetation is the significant piece of land spread and its progressions have a significant effect on the vitality and mass biochemical cycles. It is also a key marker of territorial natural condition change. Change discovery alludes to the way toward recognizing contrasts in the condition of a state by watching it at various occasions. The Multi Spectral Remote Sensing pictures are proficient for acquiring a superior comprehension of the earth condition and its changes. A Convolution Neural Network (CNN) plays a prominent role in classifying the images more accurately, compared to other Machine Learning algorithms. This paper concentrates on identifying the vegetation change in Bapatla region of Andhra Pradesh state, India between the years 2015 to 2017 using multi spectral Landsat images and deep learning techniques and the experimental results shown a decrease in vegetation land in approximately 240 square kilo meters.**

Keywords*— *Change Detection; Convolution Neural Network; Multi spectral; Vegetation Cover

I. INTRODUCTION

Due to the normal catastrophes and the occasions made by man on nature, fast changes are being seen on the society in numerous countries[1]. To get by on the earth, vegetation is one of the major source and profitable asset accessible on the earth. In order to understand and manage environment at large variety of temporal and spatial scales, up-to-date and reliable information is required all the time.

So as to spare these assets, one way is to gather the satellite pictures of those specific territories amid various timespans and investigate the progressions before they get vanished. Remotely detected information like aerial photos and satellite pictures are the main alternative that permits identifying land spread changes on a vast scale [2].

Satellite pictures have the capability of offering the most exact and most recent data contrasted with measurable, topographic or land use maps.

Manually, the changes cannot be identified from those images. Therefore, advanced techniques and systems are required to find out them. At present the Deep Learning Methods are very commonly used to trace out these changes [3]. In this paper, the vegetation land change in Bapatla region of Andhra Pradesh state, India between the years 2015 to 2017 was identified using Convolution Neural Network (CNN) [4] and to cross-check the acquired outcomes, Natural Difference Vegetation Index (NDVI) [5] concept was used.

The changes obtained through both the concepts were compared and it was observed a decrease of vegetation land in nearly 240 sq. km from both the methods.

II. LITERATURE REVIEW

Kevin and Louis de Jong [6] proposed an effective unsupervised technique for recognizing pertinent changes between two unique images of the equivalent scene. A CNN for semantic division is executed to separate compacted picture highlights, just as to group the identified changes into the right semantic classes. A difference picture is made utilizing the element map data created by the CNN, without unequivocally training on the target contrast pictures.

Kyungsun and Lim [7] proposed a novel change calculation for high goals satellite pictures utilizing CNNs, which does not require any preprocessing, for example, ortho-amendment and classification was proposed. They planned three encoder-decoder-organized CNNs, which yield change maps from an info pair of RGB satellite pictures.

Antonio Mazza [8] proposed a little sans cloud division of the objective picture, a smaller CNN is prepared to play out the ideal estimation. To approve the proposed methodology, they centered around the estimation of the NDVI, utilizing coupled Sentinel-1 and Sentinel-2 time-arrangement obtained over a rural area.

Meera Gandhi. G [9] presented an upgraded Change Detection technique for the examination of Satellite picture dependent on NDVI. NDVI differencing was used as change detection method.

Majed and Ibrahim [10] proposed that Remote Sensing information in blend with the fitting multispectral groups, for example, Landsat OLI/TIR and TM information were utilized to change discovery of vegetation spread utilizing vegetation records for the times of 1990 – 2015 in Ajloun zone, where this investigation zone has the most forest cover in Jordan.

III. THEORETICAL BACKGROUND

Different Algorithms are available in Machine learning and deep Learning for classification. Here CNN was used for accurate classification. And NDVI was used to validate the results obtained from CNN.

A. CNN

Convolutional Neural Networks are complex feed forward neural systems [4]. CNNs are utilized for image classification and recognition in view of its high accuracy. Major steps in classifying the images in the present work are as follows.

Input: Training Data, Output: Classified image
Step-1: Take the image dataset.
Step-2: Pass the data set through the first layer called convolutional layer (Conv2D) with activation function relu and filter of size (1,1).
Step-3: Flatten the output from conv2D layer.
Step-4: Give the flattened image to the Dense layer with 64 neurons and activation function, relu.
Step-5: Repeat Step 4 again with 32, 16 neurons and with same activation function.
Step-6: Give the output from step 5 again to the Dense layer with softmax activation function for 5 classes.
Step-7: Obtain final classified image output.

B. NDVI

The Chlorophyll in the plant observes visible light and transmits the Infrared light. The vegetation rate can be determined dependent on this wonder. NDVI evaluates vegetation by estimating the distinction between near infrared (which vegetation emphatically reflects) and red light (which vegetation assimilates). NDVI dependably extends from - 1 to +1. Negative quantities near -1 represent water bodies, values near +1 represent thick green leaves and NDVI near Zero indicate urban land [5].

NDVI will be calculated using equation 1

$$\text{NDVI} = \frac{\text{NIR}-\text{Red}}{\text{NIR}+\text{Red}} \quad (1)$$

where Red and NIR are the spectral reflectance measurements obtained in the red (visible) and near- infrared regions.

C. Accuracy

Accuracy is the most natural execution measure and it is essentially a proportion of effectively anticipated observation to all observations. The accuracy can be calculated using equation 2 [11].

$$\text{Accuracy} = \frac{\text{TP}+\text{TN}}{\text{TP}+\text{FP}+\text{FN}+\text{TN}} \quad (2)$$

Where, True Positives (TP) and True Negatives (TN) are the effectively predicted positive and negative classes which imply that the predicted positive and negative classes are same as actual positive and negatives. Whereas False Positives (FP) and False Positives (FP) occur when the actual and predicted values are different.

IV. EXPERIMENTAL RESULTS

The essential purpose for this research work is to discover whether the vegetation has expanded or diminished amid various timeframes. Figure 1 indicates the flow involved in this work.

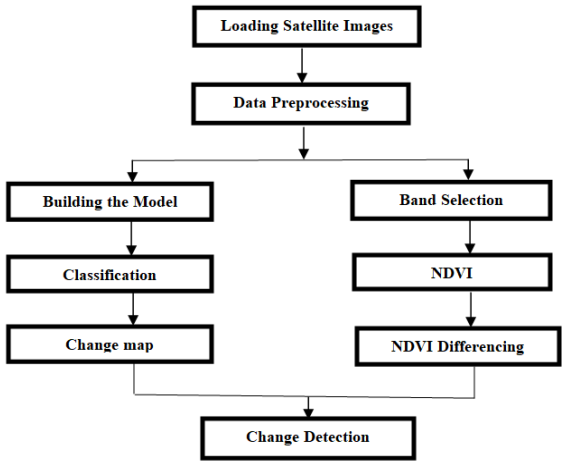

Fig.1. Architecture diagram

A. Dataset and Software used

The Source for the Dataset is US government Earth Explorer website (http://earthexplorer.usgs. gov/) [12]. Here Landsat 7 ETM scenes containing Bapatla, Guntur District, Andhra Pradesh, India Datasets with Latitude 15° 53' 47.8392" N and Longitude 80° 27' 37.5624" E. were considered. These are the multi-spectral images, comprising of 8 bands, for the years 2015 and 2017. To achieve this study, experimentation was done using Anaconda3 Installer version 5.3.0 with Python version 3.7.

B. Data Preprocessing

The aim of Pre-processing is an improvement of the image data that suppresses unwanted distortions or upgrades some image features for further processing. Data preprocessing here involves the Normalization, which evacuate the radiometric errors and effects of atmosphere by 'atmospheric correction' on the satellite images [13]. Next, image cleaning, which involves the removal of noise and Brightness corrections were performed.

C. *Building the Model*

Before building the model, image stacking, combining all bands into a solitary image was done. This was accomplished for both the years independently. There are various CNN architectures/models for image classification [14].

Here a model, which incorporates convolution and dense layers with activation functions 'Rectified Linear Unit (relu)' and 'softmax' were used. Relu [15] is to be used for nonlinear objects and soft max [16] in the case of multi class classification. The convolution layer is the first layer through which the image in the form of matrix of pixel values is passed into it. Then, by passing the channel filter to all positions, a matrix is acquired.

Dense layers perform classification on the features extricated by the convolutional layers. Commonly, a CNN is made out of a heap of modules that include feature extraction. The last module is trailed by at least one dense layer. The last dense layer in a CNN contains one node for each target class in the model, with a softmax function to create a value between 0– 1 for each node.

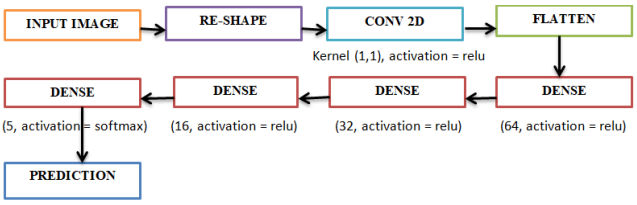

Fig.2. Model for Classification

The Model for classification used in this work is shown in the figure 2. Here the input image is reshaped and given to the Convolutional layer. Then, the software selects a filter with size (1,1) and the activation function used was relu. Next, the image is flattened and given to the dense layers. Initially, 64 neurons were given with relu activation function, followed by 32 and 16 neurons. Here, 5 classes namely Vegetation, Water, Roads, Buildings, Soil were considered. So, 5 neurons were given, one for each target class with soft max activation function in the dense layer. Thus, the image when passed through this model gets classified.

D. *Classification*

Since, a supervised CNN was used, training should be provided for it. The pictures from a similar territory, as shown in the figure 3 and figure 4 were considered as input for training the model. To know how precisely the model is functioning, the entire input was isolated as pixels into 70 percent train data and 30 percent test data. At first, the model was trained with 70 percent of the train data. Next, the test information was given to it. After getting the ideal accuracy, the two satellite pictures of the years 2015, 2017 were given as contribution to the model for classification. In this work, 5 classes, Vegetation, Water, Roads, Buildings, Soil were considered.

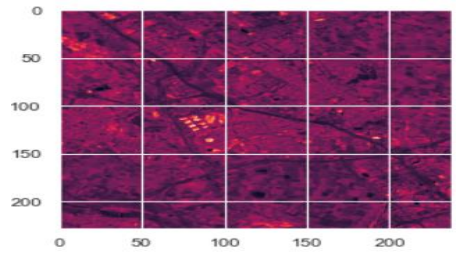

Fig.3. Sample Training Image1

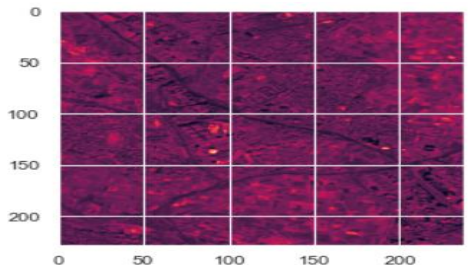

Fig.4. Sample Training Image2

E. *Change Map*

The change map was obtained by differencing the classified images one from the other pixel-by-pixel. The change map contains the changes in all the classes. By isolating each class from the change map, the change can be acquired independently for each class.

F. *Band Selection*

The 8 bands for Landsat 7 ETM are Blue, Green, Red, Near Infrared, Shortwave Infrared 1, Thermal, Shortwave Infrared 2, Panchromatic [17]. For calculating the NDVI, only red and near infrared bands are required [18]. In the Satellite sensor considered here, band 3 represents the red and band 4 represents the infrared. So, these bands were used to calculate the NDVI.

G. *NDVI Differencing*

NDVI Differencing is the process of subtracting one NDVI image from the other NDVI image. The NDVI images were produced by applying the NDVI to 2015, 2017 datasets separately by considering the red and infrared bands using equation 1. Since the Vegetation values of NDVI ranges from 0.3 to 0.8, only those pixel values were considered in the image obtained from NDVI Differencing and the change was calculated [5].

V. Experimental Results

A. *Confusion* Matrix

After training the model, a confusion matrix along with heat map[19], for the pictures used in classification was drawn between the actual and predicted values to know how accurately the model is working. Figure 5 shows the confusion matrix and the heat map for 5 classes. Here 1800, 1000, 3463, 3083, 577 pixels respectively in each class were correctly classified into the corresponding classes.

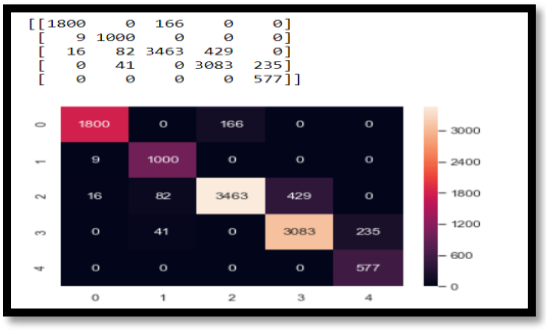

Fig.5. Confusion Matrix and Heat Map

B. *Accuracy of the Model*

By increasing the number of epochs from 1 to 15, the Accuracy of the Model increased from 82% to 92% and the loss decreased from 42% to 17% as shown in the figure 6.

```
Epoch 1/15
 - 20s - loss: 0.4266 - acc: 0.8208
Epoch 2/15
 - 19s - loss: 0.2699 - acc: 0.8888
Epoch 3/15
 - 17s - loss: 0.2476 - acc: 0.9004
Epoch 4/15
 - 14s - loss: 0.2255 - acc: 0.9070
Epoch 5/15
 - 10s - loss: 0.2105 - acc: 0.9149
Epoch 6/15
 - 9s - loss: 0.2085 - acc: 0.9144
Epoch 7/15
 - 10s - loss: 0.2041 - acc: 0.9191
Epoch 8/15
 - 9s - loss: 0.2009 - acc: 0.9215
Epoch 9/15
 - 7s - loss: 0.1923 - acc: 0.9220
Epoch 10/15
 - 7s - loss: 0.1954 - acc: 0.9205
Epoch 11/15
 - 8s - loss: 0.1933 - acc: 0.9232
Epoch 12/15
 - 7s - loss: 0.1796 - acc: 0.9269
Epoch 13/15
 - 8s - loss: 0.1786 - acc: 0.9299
Epoch 14/15
 - 7s - loss: 0.1782 - acc: 0.9296
Epoch 15/15
 - 8s - loss: 0.1720 - acc: 0.9295
```

Fig.6. Accuracy of the Model

C. *Classified Image*

The 8 bands of Landsat 7 ETM Satellite were stacked together into a single image and then processed. The stacked images of 2015 and 2017 were passed to the model for classification. The classified images were shown in the figure 7 and figure 8.

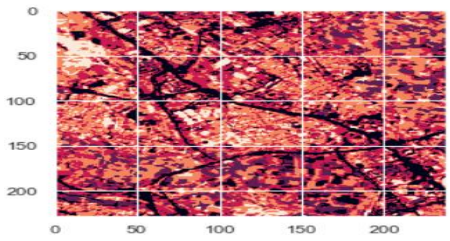

Fig.7. Classified Image of the year 2015

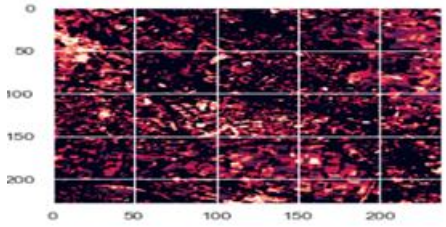

Fig.8. Classified Image of the year 2017

D. *Change in Vegetation*

The Change map was obtained by subtracting the classified images of 2015 and 2017 from one another The 5 classes from the change map were separated and change in each class was found out. Figure 9 shows the change in vegetation.

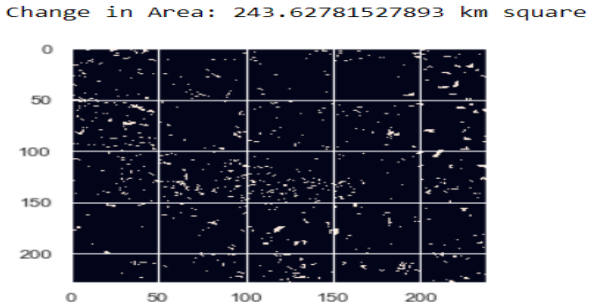

Fig.9. Change in Vegetation

E. *NDVI Images*

The NDVI images of the years 2015 and 2017 images were shown in the figures 10 and 11.

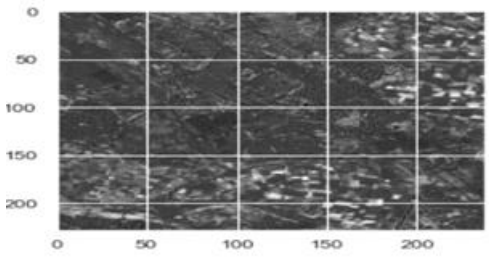

Fig.10. 2015 NDVI Image

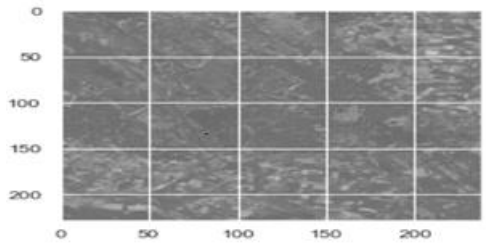

Fig.11. 2017 NDVI Image

F. *NDVI Differencing and Change Detection*

The NDVI Differencing was done through subtracting 2017 NDVI image from 2015 NDVI image. As vegetation index ranges from 0.3 to 0.8, by fixing a threshold as 0.3 to 0.8, the change in Vegetation was calculated and it was observed as 239.35 sq km as shown in the figure 12.

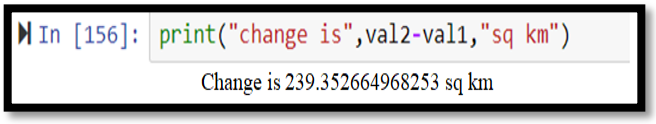

Fig.12. Change obtained through NDVI.

VI. CONCLUSION

The Change discovery is a proficient method to identify the changes in the regular assets and make vital strides before they become evaporated. For recognizing changes over various timespans, Remote Sensing will be extremely useful. This paper identified the change in Vegetation for the years 2015 and 2017 in Bapatla, Guntur District of Andhra Pradesh, India utilizing CNN and NDVI ideas. It has been seen that the Vegetation was diminished from 2015 to 2017. The reduction in vegetation got through CNN with an accuracy of 92 percent was 243.62 square kilometers and through NDVI was 239.35 square kilometers. The change acquired through both the ideas was almost equivalent.

ACKNOWLEDGMENT

This work is supported by Dr. T. Anuradha, Professor, Department of Information Technology from VR Siddhartha. We thank our colleagues who provided insight and expertise that greatly assisted the research.

REFERENCES

[1] Manoj E. Patil, Snehal A. Bhole, “A Comparative Study of Vegetation Change Detection Methods NDVI and LULC with use of Satellite Images”, International Journal of Engineering and Innovative technology (IJEIT), Volume 2, Issue 3, September 2012.

[2] Aly, A. A., Al-Omran, A. M., Sallam, A. S., Al-Wabel, M. I., and Al-Shayaa, M. S, “Vegetation cover change detection and assessment in arid environment using multi-temporal remote sensing images and ecosystem management approach, Solid Earth”, 7, 713-725, https://doi.org/10.5194/se-7-713-2016, 2016.

[3] L. Pearlstein, M. Kim and W. Seto, "Convolutional neural network application to plant detection, based on synthetic imagery," 2016 IEEE Applied Imagery Pattern Recognition Workshop (AIPR), Washington, DC, 2016, pp. 1-4. doi: 10.1109/AIPR.2016.8010596.

[4] Sai V, Bhavya, Narasimha Rao G, Ramya M, Sujana Sree Y, & Anuradha T. "Classification of skin cancer images using TensorFlow and inception v3." *International Journal of Engineering & Technology* [Online], 7.2.7 (2018): 717-721

[5] Berger, Andrés &Ettlin, Guillermo & Quincke, Christopher & Rodríguez-Bocca, Pablo, "Predicting the Normalized Difference Vegetation Index (NDVI) by training a crop growth model with historical data", Computers and Electronics in Agriculture. 10.1016/j.compag.2018.04.028, May 2018.

[6] Louis de Jong, Kevin & Bosman, Anna, "Unsupervised Change Detection in Satellite Images Using Convolutional Neural Networks", ResearchGate, Dec 2018.

[7] Lim, Kyungsun, DongkwonJin and Chang-Su Kim. “Change Detection in High Resolution Satellite Images Using an Ensemble of Convolutional Neural Networks.” 2018 Asia-Pacific Signal and Information Processing Association Annual Summit and Conference (APSIPA ASC) (2018): 509-515.

[8] Scarpa, G.; Gargiulo, M.; Mazza, A.; Gaetano, R. “A CNN-Based Fusion Method for Feature Extraction from Sentinel Data”. Remote Sens. 2018, 10, 236.

[9] Meeragandhi, G & ,bS.Parthiban&Thummalu d Christy. A, cNagaraj, "Ndvi: Vegetation change detection using remote sensing and gis – A case study of Vellore District", ResearchGate, 2015.

[10] Ibrahim, Majed & Al-Mashagbah, Atef, "Change Detection of Vegetation Cover Using Remote Sensing Data as a Case Study: Ajloun Area", Civil and Environmental Research, ResearchGate, 2015.

[11] Renuka Joshi, “ Accuracy, Precision, Recall & F1 Score: Interpretation of Performance Measures”, [online] Accessed on 10th Jan 2019 Available: https://blog.exsilio.com/all/accuracy-precision-recall-f1-score-interpretation-of-performance- measures/

[12] USGS earth explorer home [online] , Available: https://earthexplorer.usgs.gov/

[13] Sowmya D.R, P. Deepa Shenoy, Venugopal K. R, "Remote Sensing Satellite Image Processing Techniques for Image Classification: A Comprehensive Survey", International Journal of Computer Applications (0975 – 8887) Volume 161 – No 11, March 2017

[14] Siddharth Das, CNN Architectures: LeNet, AlexNet, VGG, GoogLeNet, ResNet and more ….,Nov 16,2017 [online] Accessed on 23rd feb 2019, Available: https://medium.com/@sidereal/cnns-architectures-lenet-alexnet-vgg-googlenet-resnet-and-more-666091488df5

[15] Super Data Science Team, Convolution Neural Networks (CNN) Step 1(B): The Rectified Linear Unit (RELU)Description of Relu Function [online] Accessed on 20th Feb 2019, Available: https://www.superdatascience.com/blogs/convolutional-neural-networks-cnn-step-1b-relu-layer/

[16] Softmax Function [online] Accessed on 19th Feb 2019, Available: https://en.wikipedia.org/wiki/Softmax_function

[17] Soares Galvao, Lenio&Vitorello, Icaro& Almeida-Filho, Raimundo. (1999). “Effects of Band Positioning and Bandwidth on NDVI Measurements of Tropical Savannas. Remote Sensing of Environment”. 67. 10.1016/S0034-4257(98)00085-6, 1999.

[18] USGS,Science for changing a world, What are the band designations for the Landsat satellites, [online] Accessed on 2nd March 2019, Available:https://landsat.usgs.gov/what-are-band-designations-landsat-satellites

[19] Daidalos, “How to plot a confusion matrix with matplotlib and seaborn” Jan 18.2019 [online] Accessed on 20th Feb 2019, Available: https://www.science-emergence.com/Codes/How-to-plot-a-confusion-matrix-with-matplotlib-and-seaborn/

Proceedings of the Fourth International Conference on Communication and Electronics Systems (ICCES 2019)
IEEE Conference Record # 45898; IEEE Xplore ISBN: 978-1-7281-1261-9

Design of quadrature error correction loop for communication

Bhagyashri D.Kale

Student of YCCE,Nagpur

Dr.U.S.Ghodeswar

Asso.Prof.YCCE,Nagpur

***Abstract*— The proposed circuit is analog closed loop circuit which corrects quadrature error over high frequency range. The exhibited circuit comprises of stage bolted circle type engineering and it is helpful for quadrature blunder redress. Simple shut circle is utilized to address quadrature mistake for advanced clock. It consumes 1.99mA current from 1v supply over high frequency range. The circuit was design in cadence virtuoso software in 90nm technology file. The circuit works over high frequency range that is 100MHz to 2GHz. In presented method impact of duty cycle distortion due to mismatch in input clocks also discussed. The proposed technique works on high frequency as well as low frequency.**

Keywords— analog closed loop, duty cycle mismatch, quadrature, quadrature correction, quadrature error, phase locked loop,

I INTRODUCTION

Quadrature signal is the pair of periodic signal are said to be in quadrature when they differ in phase by 90 degree. This Quadrature phase separation is critical task, but quadrature separation is very important for wireless and wired communication. Presently a days advance in cmos innovation empower the usage of high recurrence quadrature signal generator, however quadrature partition is in charge of jumble in sign produce quadrature mistake after cautious format dealing with. Imbalance occurs in quadrature clock while separation those are phase imbalance and amplitude imbalance. The sufficiency awkwardness in quadrature clock is effectively cured by utilizing advanced cushion which act as plentifulness modulator and right the adequacy befuddle in clock. If there should arise an occurrence of stage unevenness requires stage change circuit to address it.

Quadrature error leads to different types of errors in different types of communication systems such as poor error vector magnitude performance in wireless transmitter and in wireless receiver it increase bit error rate ratio and wired communication it worsen the jitter which can affect eye parameter.[1] If quadrature error is present it also reduce the image rejection ratio because circuit is depend on the phase separation to achieve good image rejection ratio.

In this paper we present a simple circuit that constantly right the confounds in quadrature signal over the high recurrence extend. This analog circuit is based on phase locked loop type architecture. Low frequency and high frequency challenges are address in this paper. The present circuit is only design for wired and wireless communication. This system is targeted for the application of software define radio(SDR) and cognitive radio(CR).

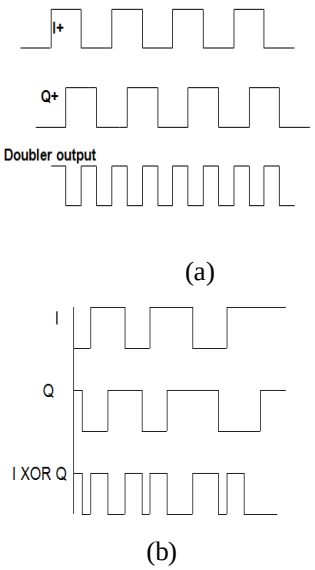

Fig1
(a)xor based doubler output when clocks are in perfect quadrature[1]
(b)xor based doubler output when quadrature error is present[1]

II RELATED WORK

Immual raja, student member ,ieee ,Vishal khatri , Zaira zahir and Gulab Banerjee proposed A 0.1-2GHz Quadrature amendment circle for advanced multiphase check age circuits in 130 nm cmos (2017) this paper shows a simple circuit that can persistently address quadrature mistake over high recurrence run. Here this analog circuit is based on the phase locked loop architecture. Both challenges at high frequency and low frequency are addressed in this paper.[1]

Immanuel Raja ,Gaurab Banerjee, Mohamad A. zeidan, jacob A. Abraham A 0.1-3.5 GHz Duty cycle measurement and correction technique in 130nm CMOS (2016) this paper presents a DCC (duty cycle corrector) technique by using PMC to correct duty cycle of the square wave over the frequency range of 100MHz to 3.5GHz this circuit works over frequency where most of the system fails.[2]

B.Kang Plan and examination of a ultra-wideband programmed self aligning upconverter in 65nm cmos (2012) here ultra-wideband phase interpolator is used to correct quadrature mismatches .ultra-wideband means it use very low energy for short range, high bandwidth

communications over high frequency. Phase interpolator is a circuit in the receiver of the serial link.[3]

Notten, Maxime BeMarc nard, A CMOS quadrature down-conversion mixer with analog i/q correction (2006) in this paper i/q gain and mismatches are corrected for down -conversion mixer with the help of variable resistance over the frequency of 470 MHz to 720MHz.[4]

S.Navid, F.Behbahani, A.Fotowat A Hajimiri Level bolted circle a strategy for broadband quadrature clock age (1997) In this paper mistake right between two quadrature signal a predisposition created by circle to move the dc dimension of info clock over the recurrence scope of 40 to 500 MHz [5]

III BLOCK DIAGRAM DESCRIPTION

A simple shut circle that having negative criticism which is utilized to address quadrature mistake between two clock stage Fig 1(a) describe two clocks that having 50% duty cycle and both are exactly quadrature so after XORing at output we get twice the input frequency and 50% duty cycle. In (b) both clocks are not perfectly quadrature and also not 50% duty cycle so after XORing output will be non 50% duty cycle means quadrature error is present in second case.

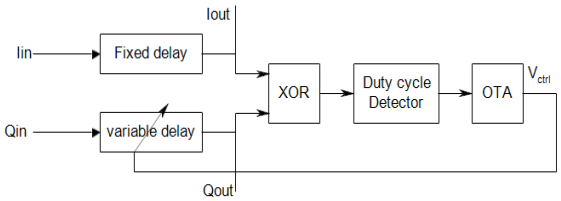

Fig 2 Block diagram of the quadrature correction loop

In Fig2 fixed delay which presented I way and variable delay is presented in Q way here fixed deferral is utilized here in light of the fact that it enables the circle to work over bigger scope of sign. Timekeepers from variable deferral and fixed postpone go to xor and quadrature blunder location is done at the yield of the xor. This yield go to DCD which produce voltage which is corresponding to obligation cycle at the info. Same voltage go to OTA which give addition to circle and create control voltage for variable deferral, as indicated by this control voltage variable postpone will fluctuate and quadrature mistake get remedied. In the event that edge partition between the I and Q tickers is not exactly $\pi/2$, at that point circle will deliver vctrl with the end goal that Q clock will be got more deferral than fixed postponement in I way. What's more, in the event that point partition is more than $\pi/2$, then vctrl produces littler than the fixed postpone way.

IV CIRCUIT LEVEL DISCRIPTION

A.Variable delay:-

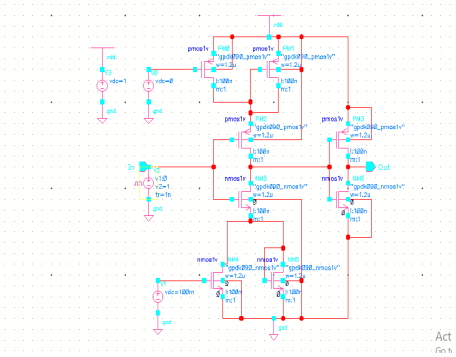

Fig 3 delay used in loop

Delay cell contain two inverter one current starved inverter and is followed by digital inverter. The current kept inverter comprises from a maneatis load for both Nmos and Pmos. Maneatis load gives surety of wide tuning of range, which helps in lessening the quantity of defer cells prompting territory and power saving. between input and output two inverters are present. The charging and discharging current of output capacitance is depends on first inverter i.e current starved inverter. The second stage inverter is for improving the ascent and fall time of circuit. The variety in deferral happen regarding control voltage.

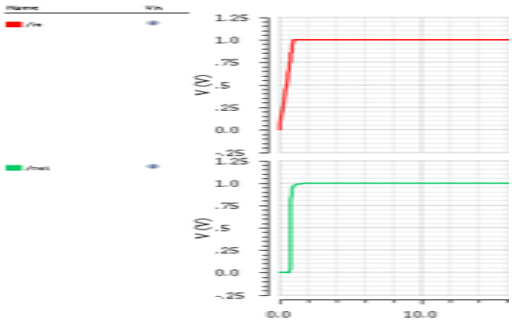

Fig4 output of delay

In presented output, output of delay will be same as input but gives some delay at output. If control voltage will vary then distortion of output will change and get proper output.

B. Current mode logic XOR

The xor rationale is use to change over quadrature blunder to obligation cycle mistake implies at the yield of xor quadrature detecting is performed whether responsibility cycle is half or not. It gives yield as double the information recurrence. For high recurrence input timekeepers it is beyond the realm of imagination to expect to execute with straightforward xor on account of that cml xor is utilized.

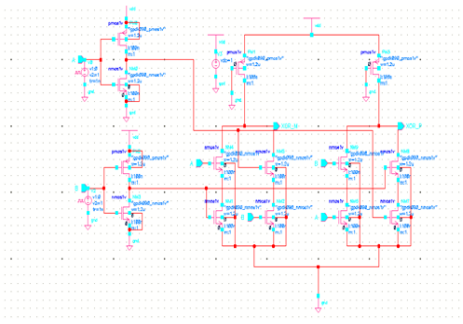

Fig5 schematic of CML-based XOR

In usage Nmos transistors with Pmos load as appeared in the fig. The proportion of the time length for which the sign is more prominent than the regular mode voltage to the all out time is taken as obligation cycle

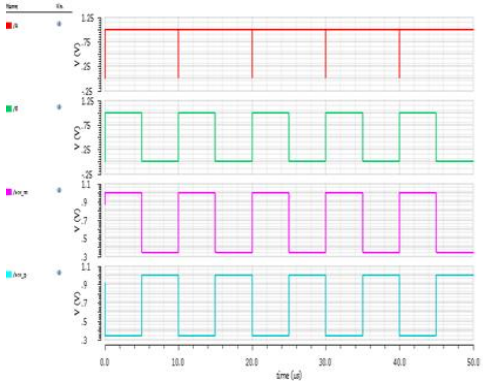

Fig 6.Output of cml xor

Here in output of cml xor will get two output one is xor and another one is xnor output which is totally opposite to the xor output and here useful output is xor.

C. *Duty cycle detector*

DCD is a DA (differential enhancer) based channel ,here current guided through one arm or other by the yield of cml xor . At yield of dcd two capacitors are available on each arm. It is dynamic low pass channel which create differential dc normal voltage yield of xor. This yield is corresponding to the yield of xor. DCD is differential amplifier which produce output difference of two input signal.

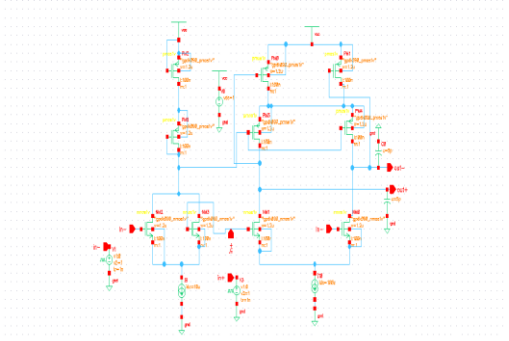

Fig 7. DCD schematics

Output of DCD

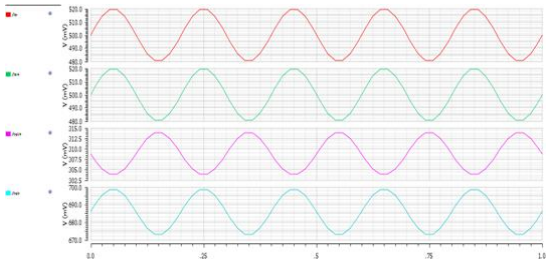

Fig 8 waveform of DCD

The output of DCD is based on differential amplifier, here both input having same phase so at the output we are getting opposite cycles it means difference of both input is zero. If at the output of DCD both the cycle is in same phase that means duty cycle is of 50%

D. *Operational trans- conductance amplifier*

OTA is use to give increase to the circuit and it create control voltage. Ota provide control voltage to variable delay with the help of bias translational circuit. The circuit is biased at 100uA.

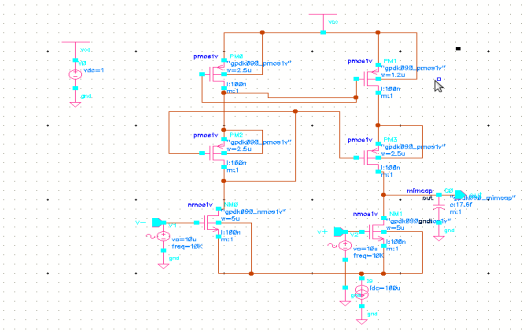

Fig 9. Schematic of OTA

Capacitor is set at the yield of OTA for additionally separating for the control voltage. Here OTA provide gain 21dB. Voltage of OTA transfer to variable delay and according to this voltage variable delay vary and quadrature error will get corrected

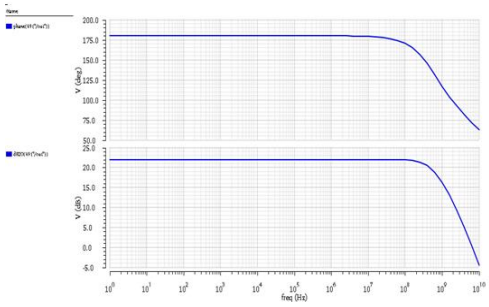

Fig 10 waveform of OTA

From AC analysis we can say that circuit will work 10^9 Hz frequency shows in first waveform and second waveform shows that it gives gain of 21dB.

E. *Bias-translational circuit*

Two voltages for variable delay are send from bias translational circuit. The output voltage of OTA are provided to bias translational circuit. The output voltage is provides for nmos and pmos of control voltage.

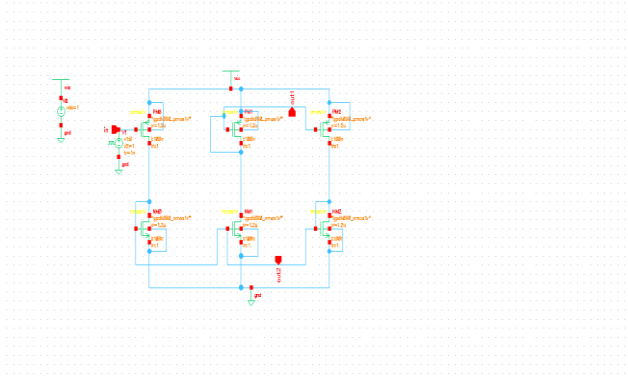

Fig 11 Bias translational circuit schematic

Input to the bias translational circuit is vpulse and at the output we will get two equal voltages. This bias translational circuit gives for 1v at output is 500mv and 500mv of two voltages

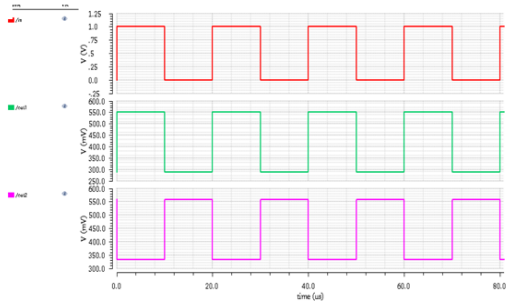

Fig 12 output of bias translational circuit

V MATHEMATICAL ANALYSIS OF THE QUADRATURE LOOP

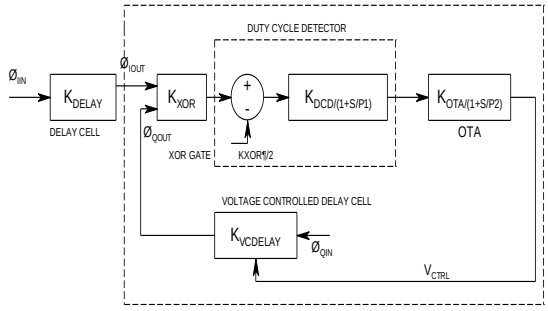

Fig 13. Mathematical representation of quadrature correction loop

Let ΦIin is the period of the information I clock and ΦQin is the period of Q clock. ΦIout is the yield from fixed deferral while ΦQout is yield from variable postponement. The quadrature mistake among ΦIin and ΦQout is limited by second request negative input circle which produce control voltage for the voltage controlled defer cell. Φqe is the quadrature mistake between the ΦIout and ΦQout. The XOR square has gain Kxor and it convert quadrature blunder Φqe into obligation cycle deviation. In the event that obligation cycle is half, at that point at the yield of xor it spoken to by KXOR(π/2).If duty is non 50% then DCD will detect and generate voltage corresponding to duty cycle. DCD is used as low pass filter having pole p1 and gain $K_{DC.}$ This voltage pass to the OTA and it will amplify the voltage. It has dc gain K_{OTA} and pole p2 generate voltage $V_{CTRL.}$ This voltage pass to variable delay introduce some delay in ΦQin and generate ΦQout.
So yield period of quadrature clock ΦQout is given by

$$\phi_{Qout} = K_{xor}.\phi_{Iin} - K_{xor}.\phi_{Qout} - K_{xor.\Pi/2}.\frac{K_{DC}}{(1+s/p1)}.\frac{K_{OTA}}{(1+s/p2)}.K_{VCDELAY}$$

……(1)
Take K_{XOR} common

$$\phi_{Qout} = K_{xor}\left(\phi_{in} - \phi_{Out} - \frac{\Pi}{2}\right).\frac{K_{DC}.K_{OTA}.K_{VCDELAY}}{\left(1+\frac{s}{p1}\right)\left(1+\frac{s}{p2}\right)} \quad \text{……..(2)}$$

Let $K_{xor}.K_{DC}.K_{OTA}.K_{VCDELAY}$ = K
Then closed loop equation for ϕ_{Qout}

$$\phi_{Qout} = \frac{K\left(\phi_{in} - \phi_{Out} - \frac{\Pi}{2}\right)}{\left(1+\frac{s}{p1}\right)\left(1+\frac{s}{p2}\right)} \quad \text{……(3)}$$

After solving equation

$$\phi_{Qout} = \frac{p1p2\left(K\phi_{in} - K\phi_{Out} - K\frac{\Pi}{2}\right)}{p1p2\left(1+\frac{s}{p2}+\frac{s}{p1}+\frac{s^2}{p1p2}\right)} \quad \text{……(4)}$$

Multiply p1p2 to bracket at denominator

$$\phi_{Qout} = \frac{p1p2\left(K\phi_{in} - K\phi_{Out} - K\frac{\Pi}{2}\right)}{p1p2 + p1s + p2s + s^2}$$

$$\phi_{Qout} = \frac{p1p2\left(K\phi_{in} - K\phi_{Out} - K\frac{\Pi}{2}\right)}{s^2 + (p1+p2)s + p1p2} \quad \text{……}$$

..(5)
Multiply denominator with ϕ_{Qout}

$$\phi_{Qout}\left(s^2 + (p1+p2)s + p1p2\right) = p1p2\left(K\phi_{in} - K\phi_{Out} - K\frac{\Pi}{2}\right)$$

$$\phi_{Qout}s^2 + \phi_{Qout}(p1+p2)s + \phi_{Qout}p1p2 + p1p2K\phi_{Out} = p1p2\left(K\phi_{in} - K\frac{\Pi}{2}\right) \ldots$$

……..(6)
Take ϕ_{Qout} common and will get

$$\phi_{Qout} = \frac{K\left(\phi_{in} - \frac{\Pi}{2}\right)p1p2}{s^2 + (p1+p2)s + (p1p2 + p1p2K)}$$

$$\phi_{Qout} = \frac{K\left(\phi_{in} - \frac{\Pi}{2}\right) p1p2}{s^2 + (p1+p2)s + p1p2(1+K)} \quad \text{……..(7)}$$

ω_η is the common recurrence and ξ is the damping coefficient of the framework

$$\omega_\eta = \sqrt{(K+1)\,p1p2}, \quad \xi = \frac{p1+p2}{2\sqrt{(K+1)(p1p2)}}$$

$$\omega_\eta \xi = \frac{p1+p2}{2} \quad [1]$$

The shafts p1 and p2 avoid the middle to limit the settling time. In any case, separate between p1and p2 posts choose the abundancy of the swell on control voltage this presents jitter in the clock. In the event that p1 and p2 are keep nearer to focus, at that point low pass activity is better and control voltage is exceptionally slick. To limit the quadrature mistake a high estimation of K is required.

VI IMPACT OF DUTY CYCLE DETECTOR

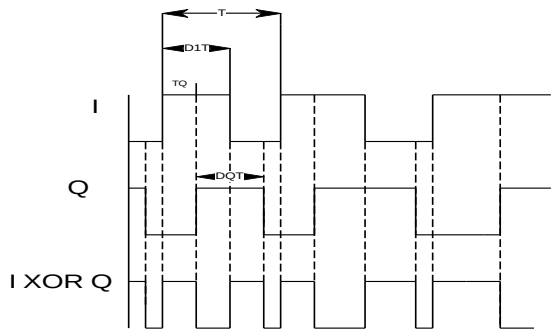

Fig 14. Impact on duty cycle

In above fig I and Q the two tickers having T timeframe and flipping somewhere in the range of 0 and 1. The time slack between two tickers is TQ. At the point when this apply to quadrature circle then non half obligation cycle sway the amendment execution of circle . this system is valuable for location of quadrature mistake. The circles accuracy is rely upon the quadrature finder. Henceforth sway on obligation cycle is broke down.

The output of xor is given to DCD which generate the dc normal of yield of xor

So

$$x(t) = i(t) \oplus q(t) \quad \text{……..(1)}$$

Let d(t) is output of the DCD

$$d(t) = \frac{1}{T}\int_T x(t)dt \quad \text{……..(2)}$$

$$= \frac{1}{T}\left(\int_0^{T_Q} 1dt + \int_{D_I T}^{T_Q + D_Q T} 1dt\right)$$

$$= \frac{1}{T}(T_Q + T_Q + D_Q T - D_I T)$$

$$= \frac{2 \times T_Q}{T} + (D_Q - D_I) \quad \text{……..(3)}$$

To analyze the quadrature error, we can write

$$T_Q = \frac{T}{4} + Q_e \quad \text{……(4)}$$

Here Q_e is quadrature error between I and Q clocks so d(t) can be write

$$d(t) = \frac{1}{2} + \frac{2 \times T_Q}{T} + (D_Q - D_I) \quad \text{….(5)}$$

In above condition demonstrates change of quadrature mistake and obligation cycle blunder in the yield of DCD

On the off chance that the two checks are in ideal quadrature there is no contortion in obligation cycle

$$d(t) = \frac{1}{2}$$

Here is the dc average of a 50% duty cycle .

A nonzero quadrature error (Q_e) result is

$$d(t) = \frac{1}{2} + \frac{2 \times Q_e}{T}.[1] \quad \text{……(6)}$$

VII IMPLEMENTATION CIRCUIT AND RESULTS

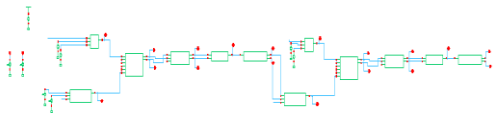

Fig 15.implemented quadrature correction loop

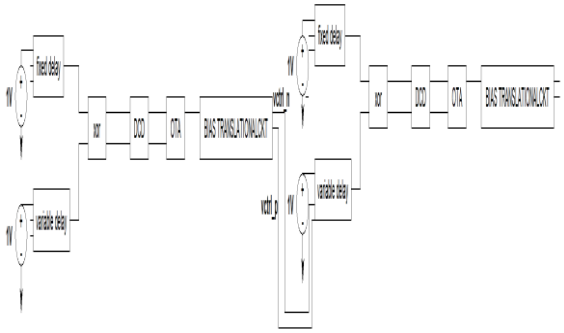

In implemented circuit all modules are combined and voltage provide to the circuit is 1v and the same circuit is built in 90nm technology file. First two block is of delay blocks one is fixed delay and second is of variable delay. Fixed delay inputs are vpulse for main input and other input contains 0v supply and output is given to xor. Variable delay again contain vpulse to main input another input is comes from bias translational circuit. The output of variable delay is given to second input of xor. At the output of xor quadrature sensing is done same output is given to DCD and DCD generate voltage according to input. The same output of DCD is pass to input of OTA and OTA gives amplified voltage to bias translational input and bias translational dive this voltage and pass to variable delay.
The output of this loop is as below

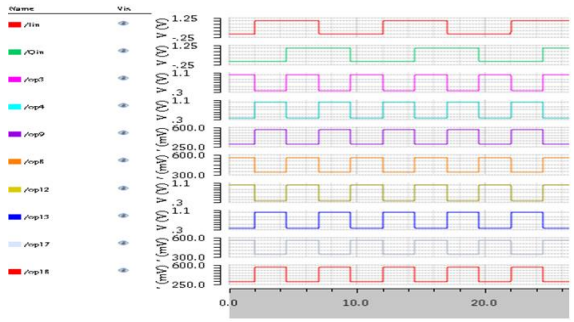

Fig 16. Exact quadrature clock

In fig 16 shows exact quadrature clock here angle between Iin and Qin is 90 degree and therefore at output we are getting 50% of duty cycle it means there is no error present in the clocks.

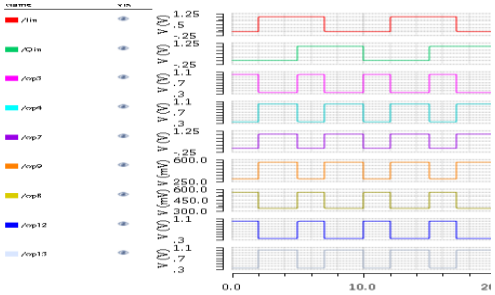

Fig 17. Angle between Iin and Qin is greater than 90 degree.

The above fig 17 shows that angle between Iin and Qin is greater than 90 degree so at the output we are not getting 50% of duty cycle it means here quadrature error is present so after correction the waveform will look like below waveform

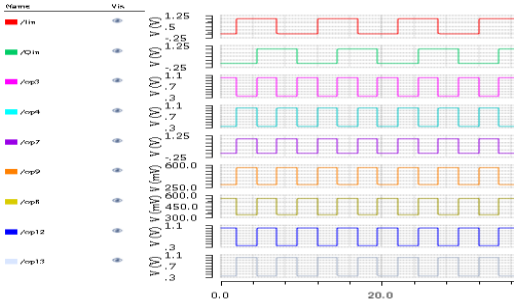

Fig 18 corrected waveform for greater than 90deg.

Now in above fig we can see that duty cycle is of 50% means error is removed in this clocks signal and both clocks in perfect quadrature. Here variable delay get vary it will be less than the fixed delay and before variable delay was greater then it will become less than previous delay

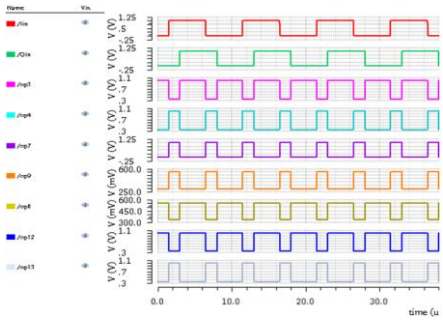

Fig 19. Angle between Iin and Qin is less than 90degree

In above angle between Iin and Qin is less than 90 degree so in output we are getting non 50% duty cycle it means there is quadrature error is present so corrected output waveform is given below

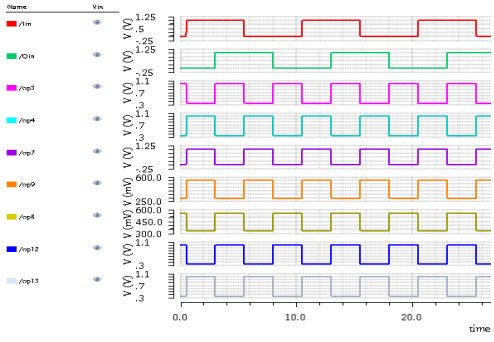

Fig 20. Corrected waveform from less than 90 degree

In above fig quadrature error get corrected because at output we are getting 50% duty cycle. So here variable delay vary and error get corrected. Variable delay is greater than fixed delay means previous variable delay was greater than the after corrected waveform.

Table1 Comparison with previous circuit

Specifications	Previous method	Present method
Technology	130nm	90nm
Power dissipation	4.49 mw	1.19mw
Voltage required	1.2v	1v
Current required	5.4mA	1.99mA

VIII CONCLUSION

In proposed method quadrature error of signal is corrected with the help of analog closed loop circuit the loop is based on the phase loked loop architecture.If angle between two clock signal is greater than 90 deg then variable delay will be less than the fixed delay and when angle between two clock signal is less than 90 deg then variable delay is greater than the fixed delay. power dissipation also minimized as compare to previous technology.

IX FUTURE SCOPE

Through the performancee of the system in terms of quality is satisfactory for the application of quadrature error correction loop that is analog closed loop. But for specific angle measurement and correction is also required for duty cycle correction so this kind of improvement is required
.

REFERENCES

1. Immanuel Raja, *Student Member, IEEE*, Vishal Khatri, Zaira Zahir, *Student* Member, *IEEE*, and Gaurab Banerjee, *Senior Member, IEEE "*A 0.1–2-GHz Quadrature Correction Loop for Digital Multiphase Clock Generation Circuits in 130-nm CMOS," *IEEE Trans. Very Large Scale Integr. (VLSI) Syst.*, vol. 24, no. 3,, March 2017.

2. I. Raja, G. Banerjee, M. A. Zeidan, and J. A. Abraham, "A 0.1–3.5-GHz duty-cycle measurement and correction technique in 130-nm CMOS," *IEEE Trans. Very Large Scale Integr. (VLSI) Syst.*, vol. 24, no. 5, pp. 1975–1983, May 2016.

3. B. Kang *et al.*, "Design and analysis of an ultra-wideband automatic self calibrating upconverter in 65-nm CMOS," *IEEE Trans. Microw. Theory Techn.*, vol. 60, no. 7, pp. 2178–2191, Jul. 2012.

4. M. Notten, M. Bernard, V. Rambeau, and J. van Sinderen, "A CMOS quadrature down-conversion mixer with analog I/Q correction obtaining 55 dB of image rejection for TV on mobile applications," in *Proc. IEEE Radio Freq. Integr. Circuits (RFIC) Symp.*, Jun. 2006, p.

5. S. Navid, F. Behbahani, A. Fotowat, A. Hajimiri, R. Gaethke, and M Delurio, " Level-locked loop: A technique for broadband quadrature signal generation," in *Proc. IEEE Custom Integr. Circuits Conf*, May 1997, pp. 411–414.

6. Elahi, K. Muhammad, and P. T. Balsara, "I/Q mismatch compensation in a 90nm low- CMOS receiver," in *Proc. IEEE Int. Solid-State Circuits Conf., Dig. Tech. Papers, ISSCC.*, vol. 1. Feb. 2005,pp. 542–616.

7. B. Bhukania, S. Ramakrishnan, and Y. Darwhekar, "IQ mismatch compensation using time domain signal processing: A practical approach,"in *Proc. IEEE Int. Symp. Circuits Syst. (ISCAS)*, May/Jun. 2010, pp. 1021–1024.

8. N. Qi, Z. Song, B. Chi, A. Wang, T. Ren, and Z. Wang, "A multi-mode complex bandpass filter with gm-assisted power optimization and I/Q calibration," in *Proc. IEEE Int. Symp. Circuits Syst. (ISCAS)*, May 2013, pp. 1845–1848.

9. M. Notten, M. Bernard, V. Rambeau, and J. van Sinderen, "A CMOS quadrature down-conversion mixer with analog I/Q correction obtaining 55 dB of image rejection for TV on mobile applications," in *Proc. IEEE Radio Freq. Integr. Circuits (RFIC) Symp.*, Jun. 2006, p. 4.

10. J. Carballido *et al.*, "A programmable calibration/BIST engine for RF and analog blocks in So Cs integrated in a 32 nm CMOS WiFi transceiver," *IEEE J. Solid-State Circuits*, vol. 48, no. 7, pp. 1669–1679, Jul. 2013.

11. N. Nguyen *et al.*, "A 16-Gb/s differential I/O cell with 380fs RJ in an emulated 40nm DRAM process," in *Proc. IEEE Symp. VLSI Circuits*, Jun. 2008, pp. 128–129.

12. J. L. Finol and M. Buchholz, "Design of an inphase and quadrature phase and amplitude imbalance compensation in quadrature receivers," in *Proc. 5th IEEE Int. Caracas Conf. Devices, Circuits Syst.*, vol. 1. Nov. 2004, pp. 254–258.

Proceedings of the Fourth International Conference on Communication and Electronics Systems (ICCES 2019)
IEEE Conference Record # 45898; IEEE Xplore ISBN: 978-1-7281-1261-9

Critical Path Delay Improvement in Logic Circuit Operated at Subthreshold Region

Limbasiya Mohit Dhirubhai, Kirti S. Pande,
Department of Electronics and Communication Engineering,
Amrita School of Engineering, Bengaluru
Amrita Vishwa Vidyapeetham, India
mohitlimbasiya42@gmail.com, kirtispande@yahoo.co.in

Abstract **— Lower voltage as well as high-speed subthreshold logic circuits are becoming important factors in modern VLSI technology. At subthreshold region, the effects of the process variations and the diminished ratio of active current to ideal current can introduce timing errors. These timing errors are responsible in the vandalism of the working capacity of the circuits operated at subthreshold region. An increase in propagation delay is observed when the threshold voltage of MOSFET is more than the supply voltage. This paper proposes a circuit to reduce the timing errors keeping the energy consumption to minimum amount. The proposed circuit uses a multiplexer implemented using transmission gates, to be used in the longest delay path of the logic circuit which is operated at subthreshold region. Forward body biasing notion is used to lower the MOSFET's threshold voltage and is incorporated in the proposed circuit, thus, reducing the switching time of the MOSFETs. The proposed circuit is implemented using Cadence Virtuoso at 45 nm technology and compared with the circuit studied from literature survey. The supply voltage for the combinational circuit and the proposed circuit and the D flip-flop was 287 mV. The forward body biasing voltage V_{SB} for NMOS and PMOS MOSFET was equal to 287 mV. The proposed circuit is applied to the longest delay path of the 64-bit ripple carry adder operated at subthreshold region and the switching delay for high going and low going transition are measured and are reduced by 48.14% and 26.60% respectively. Also, the slope of transition of the output signal has been increased by 53.08% & 8.14% for rise and fall respectively. The total propagation delay diminished by 30.12% as compared to existing technique. The energy per cycle and energy-delay product (EDP) turned down by 33.10% and 53.31% respectively, over the existing technique.**

Keywords **— Body biasing, subthreshold logic circuits, critical path delay, transmission gate, multiplexer**

I. INTRODUCTION

In modern VLSI technology, for low-power appliances sub-threshold digital circuits are becoming more important. Dynamic energy used by the digital subthreshold logic circuits can be reduced by decreasing supply voltage. But, whenever supply voltage becomes less than the threshold voltage of MOSFETs, it increases propagation delay. Digital logic circuits endure the process variation effect, whenever they are operated at the subthreshold region.

Furthermore, the subthreshold circuits endure diminished active to idle current ratio. This diminished current ratio and process variations effects encountered at subthreshold circuits can introduce timing errors. These timing errors damages the working ability of the subthreshold circuits.

In this work, a circuit is proposed which is to be used in the longest delay path (critical path) of the logic circuit operated at subthreshold region. The circuit uses multiplexer implemented using transmission gate. As an application, the proposed circuit is used in the critical path of the ripple carry adder with 64 bits to bring down the longest path delay. The MOSFETs using in the transmission gate of the proposed circuits are forward body biased so as to vary the threshold voltage that brings about variation in the switching characteristics of the circuit. Body biasing technique uses the body terminal for changing the threshold voltage of MOSFET. The proposed circuit that is applied to 64-bit ripple carry adder operated at subthreshold region, is implemented in Cadence Virtuoso at 45 nm technology and is compared with the existing circuit.

As an overview of the paper, Section II records the similar work to bring down the delay in critical path of subthreshold logic circuits. Section III, proposes multiplexer based circuit to be used to minimize the critical path delay whereas Section IV explore the implementation of the proposed circuit and its usage in 64-bit ripple carry adder as an application along with the simulation and comparative results with reference to the existing circuit. Section V deals with conclusion and future scope.

II. RELATED WORK

Certain methods to minimize critical path delay and energy for subthreshold circuits that require extremely low power are discussed in this section. Adaptive feedback equalized technique proposed in [1] reduces the critical path delay and provides energy improvement in subthreshold digital circuits. In this, the author used a feedback equalization technique using a variable threshold inverter as shown in Fig. 1(a). The inverter's threshold voltage is also called as mid-point voltage of the voltage transfer characteristics. This technique causes a change in the inverter's threshold voltage based on the output of the logic circuit, so as to introduce faster switching. Changes in the inverter's threshold voltage, in turn, changes the range for logic '0' and logic '1' quickly, based on the variation in the output available in the critical path of the logic circuit operated at subthreshold region of operation. The critical path delay signal is registered in the flip-flop. This feedback equalization circuit improves the switching range at a faster rate, using more number of MOSFETs in the used two feedback paths.

Feedback equalized technique proposed [2] reduces the critical path delay and energy of the circuit operated at

subthreshold. Here, authors have proposed only one feedback path. This technique is not applicable, if previous output and present output of combinational logic block are same. [3] presents the use of feedback equalization technique for the non-subthreshold circuit, using Schmitt-trigger to reduce the switching time. Transistor sizing methodology is proposed in [4] decreases the effect of process-variations. This approach introduces more MOSFET parasitic leading to increase in propagation delay of subthreshold logic circuit.

III. Proposed Model for Critical Path Delay Improvement

The proposed circuit shown in Fig. 1(b), uses a multiplexer implemented using transmission gate to minimize the delay along the critical path. The critical path is the longest path of the logic circuit and is used when operated at subthreshold region to improve the switching characteristics so that the output of the combinational logic circuit is registered in a flip-flop at a faster rate. The shown combinational logic block is operated at subthreshold region, that increases the delay in the generation of the output signal. The suggested circuit is used to improve the working of combinational circuits along the critical path by lowering the delay.

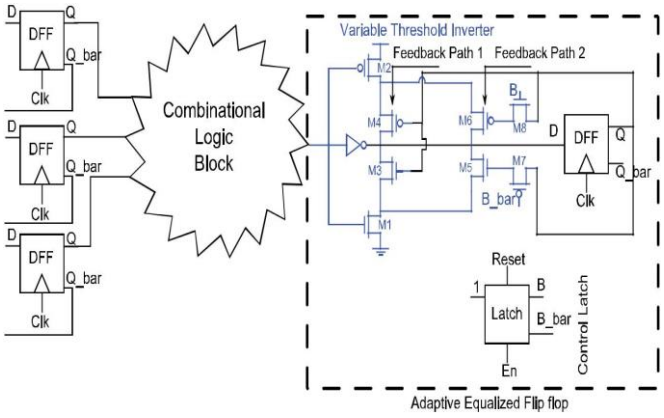

Fig. 1(a). Existing logic design using feedback equalization to improve the critical delay through logic circuit operated at subthreshold region [1].

The multiplexer based circuit uses two transmission gates TG1 and TG2 [5]. A single transmission gate is the parallel connection of PMOSFET and NMOSFET. The input to the NMOSFET of TG1 and TG2 are complement of each other. The MOSFETs used in the transmission gate are body biased. The forward body bias technique is used to reduce the threshold voltage of n-type and p-type MOSFETs. In this circuit, data inputs provided to multiplexer are constant logic '0' and '1'. The select line of the multiplexer is the critical path signal of the logic circuit operated at the subthreshold region. The advantage of transmission gate is that they provide strong '1' and '0' values.

When the TG (transmission gate) is ON, both n-type and p-type MOSFETs are ON and they are in OFF state when the transmission gate is turned OFF.

When the critical path output C_{out} of the logic circuit operated at subthreshold region is equal to zero, TG_1 will be in ON mode (MOSFET M_1 and M_2 are ON as shown in Fig. 1(b).) and at the same time, TG2 will be in OFF mode (MOSFET M_3 and M4 are OFF as shown in Fig. 1(b).), causing the multiplexer output to be strong logic '0'.

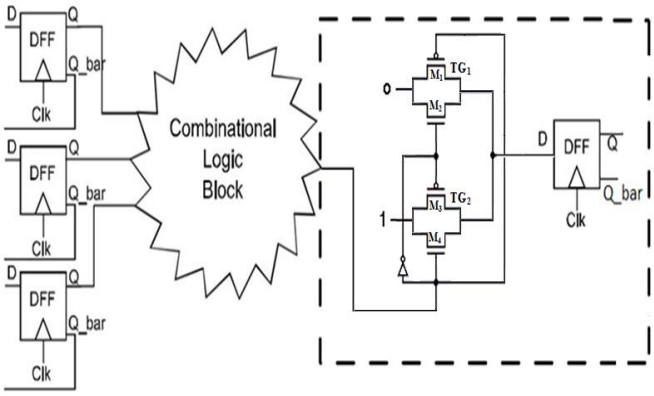

Fig. 1(b). Proposed circuit to improve the working of logic circuit along the critical path.

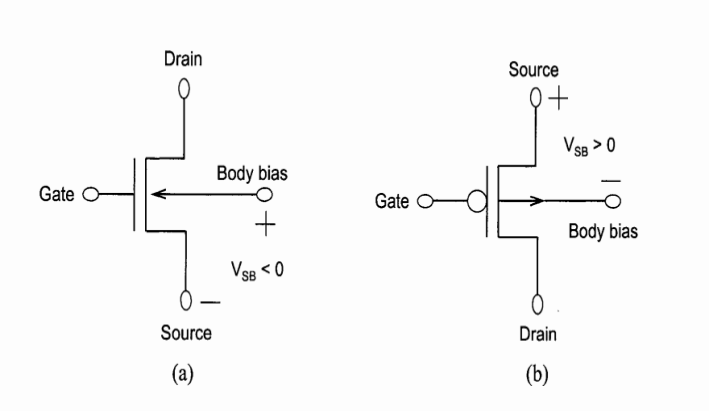

Fig. 1(c). Forward body-biased MOSFETs. (a) NMOS. (b) PMOS [7].

When the critical path output C_{out} of the logic circuit operated at subthreshold region is equal to logic one, TG_1 will be in OFF condition (MOSFET M_1 and M_2 are OFF as observed in Fig. 1(b).) and at the same time the TG2 will be in ON (MOSFET M_1 and M_2 are ON as observed in Fig. 1(b).), producing the multiplexer output as strong logic '1'. The MOSFETs used in the transmission gate are forward body-biased to decrease the threshold voltage of MOSFETs. The idea here is, though the C_{out} switches to the other logic level with higher delay, the MOSFETs used in the transmission gates are made more sensitive to the signal C_{out}, since their threshold voltage is reduced and causes the output of the multiplexer to switch faster. The proposed design can scale-down the transition time of MOSFETs and in turn bringing down the critical path delay of any logic circuit operated at subthreshold region.

The body terminal is used to change the threshold voltage of MOSFETs at the time of circuit operation. The change in threshold voltage of MOSFET using body biasing totally depends on the voltage polarity at source and body terminals (V_{SB}) as shown in Fig. 1(c). Source-substrate p-n junction of MOSFET when reverse or forward biased, increases or decreases the threshold voltage of MOSFET respectively [6]. The width of the depletion region below the gate is reduced by operating MOSFET in the forward-body biasing. Ionic charge in the depletion region will be decreased by reducing the depletion width. To keep up the charge

balance, the mobile charge (number of electrons for an NMOSFET) within the inversion layer increases. After increasing the number of mobile charges within the inversion layer, the gate voltage of the MOSFET required reduces to reach a similar level of the inversion as compared to a zero body biased MOSFET. Therefore, after applying forward body biasing in the MOSFET, the threshold voltage will decrease [7].

Drivability of the MOSFET becomes better with forward body biasing [8-9]. Operating at subthreshold voltage lowers the power consumed [10]. Turning down the supply voltage to near threshold voltage in devices with short channel length, is a constructive solution for ultra-low power applications [11].

IV. Simulation Resuls

The proposed circuit using multiplexer and the existing adaptive feedback equalization circuit are individually applied to 64-bit ripple carry adder operated at subthreshold region, are implemented in Cadence Virtuoso that uses 45 nm technology and results are compared for the two designs for various parameters. Both the designs are operated at 287 mV of supply voltage. 64-bit ripple carry adder has been selected as an application of the proposed delay minimization circuit. The critical path of 64-bit ripple carry adder is found on the final carry output generated at last. Hence, the proposed multiplexer based circuit is used for this carry output signal, C_{out} of the ripple carry adder with 64 bits to decrease the delay along critical path in terms of switching the signal faster so that it can be captured by flip-flop at a faster rate. The supply voltage for the combinational circuit and the proposed circuit and the D flip-flop was 287 mV for both the designs. The forward body biasing voltage, V_{SB} for NMOS and PMOS MOSFET was equal to 287 mV. The threshold voltage of p-type and n-type MOSFETs before body biasing was measured to be 441 mV and 496 mV respectively. The threshold voltage of PMOS and NMOS MOSFET after body biasing was measured to be 387 mV and 455 mV respectively.

A. *Implementation of 64-bit Ripple-carry Adder*

The ripple-carry adder with 64 bits is implemented at 45 nm technology and operated at subthreshold region. Sixty-four full-adder cells are cascaded so that output carry of current stage full-adder is carry forward as an input carry to the consecutive stage full-adder and so on. The block diagram of a ripple-carry adder that can perform operations with 64 bits as input is as shown in Fig. 2. Here, sixty-four inputs A_{63} to A_0 and B_{63} to B_0 are provided to full adder cells 63 to 0. S_{63} to S_0 are the sum outputs of the sixty-four stages of the full-adder. Here, C_{in} acts as initial carry input for the beginning stage full adder and C_{out} is the carry output signal in the final stage of 64-bit ripple carry adder.

B. *Implementation of Proposed Multiplexer-based circuit using forward body-biasing*

The existing circuit of adaptive feedback equalization is implemented and applied to 64-bit ripple carry adder operated at subthreshold region. The entire circuit has been implemented in Cadence Virtuoso at 45 nm technology operating at 287 mV of supply voltage. Fig. 3(a) shows output of this implementation which uses adaptive feedback equalization idea to improve the critical path delay. Here, to bring out more clarity on the analysis, the input applied on A_{63} to A_0 have same input signal and B_{63} to B_0 have same input signal. A_0, B_0 and C_{in} are the input signal of first 1-bit full adder while, C_{out} is the final output carry signal of the combinational logic block. E_Out signal is the output signal of the adaptive feedback equalization technique before reaching the D flip-flop.

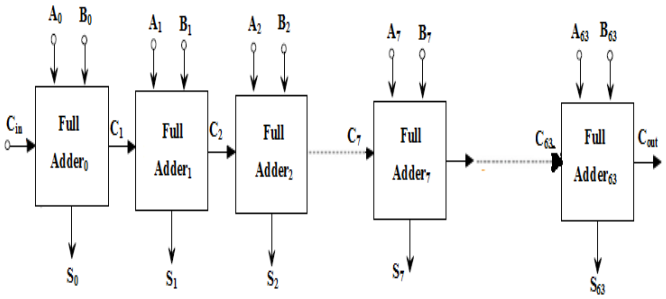

Fig.2. Block diagram of ripple carry adder with 64 bits.

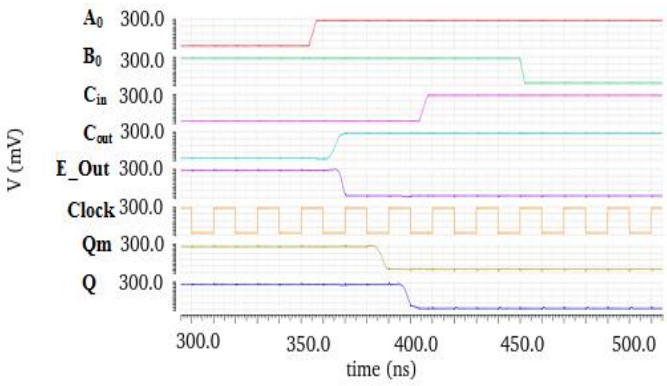

Fig. 3(a) Functionality of existing logic circuit using adaptive feedback equalization technique applied for 64-bit ripple carry adder to improve the critical path delay.

The proposed circuit to decrease the critical path delay uses multiplexer. The multiplexer is implemented using two transmission gates. The select line of the multiplexer is the critical path output signal of the combinational logic block whose delay need to be minimized. The signal that goes to the transmission gates NMOS MOSFETs is complementary of each other, so that when TG1 is ON, TG2 is OFF and vice versa. The MOSFETs used in the transmission gates are forward body biased so as to reduce the threshold voltage of these MOSFETs making them more sensitive to the signal having higher switching delay characteristics. Therefore, this leads to the increase in the slope of the switching characteristics of the signal i. e. rising slope and falling slope of the signal.

The transient analysis showing the functionality of the 64-bit ripple carry adder when used with the proposed circuit to minimize the critical delay is shown in Fig 3(b).

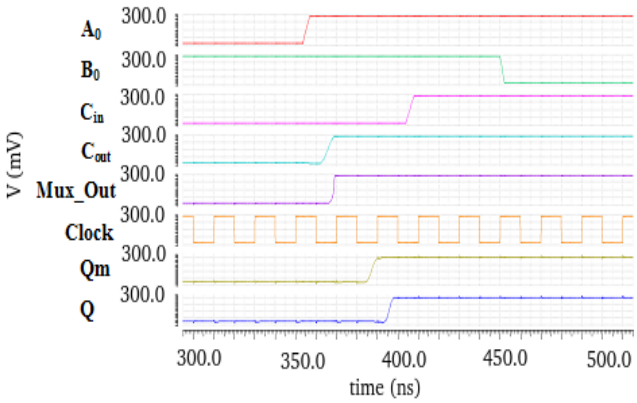

Fig. 3(b). Functionality of proposed logic circuit using multiplexer with forward body biasing technique applied for 64-bit ripple carry adder to improve the critical path delay

Here, to bring out more clarity on the analysis, the input applied on A_{63} to A_0 have same input signal and B_{63} to B_0 have same input signal. A_0, B_0 and C_{in} are the input signal of first 1-bit full adder while, C_{out} is the final output carry signal of the combinational logic block. The Mux-Out signal shown in Fig. 3(b), is the output of multiplexer that gets registered in the followed flip-flop after a clock cycle. The results are measured with respect to the rise time or fall time and the slope associated with the two signals Mux-Out and Q which forms the output of the multiplexer and the output of the flip-flop respectively.

Switching delay of E_Out signal (Fig. 3(a)) is higher than the switching delay of Mux_Out signal (Fig. 3(b)). Reduction in rise or fall time and increase in the slope of these signals indicates the faster switching. The energy per cycle is measured having 33.10 % improvement.

C. Master-slave Positive-edge Trigger D Flip-flop

Fig. 4 shows the used schematic of D flip-flop with positive edge trigger [12] in the design to register the output of multiplexer. The flip-flop uses transmission gates. There is no body biasing technique applied for any of the MOSFET in this circuit of the flip-flop. Master latch becomes active whenever clock goes to lower state and it samples input data signal into Q_m with the slave latch is in hold condition and it retains previous value with the help of feedback. Slave becomes active, when clock goes to higher state and samples the master output (Q_m) into final output (Q).

D. Comparison Between Timing Characteristics of 64-bit ripple carry adder using existing technique and using proposed circuit to lower the delay along the critical path

The supply voltage for the combinational circuit and the proposed circuit and the D flip-flop was 287 mV. The forward body biasing voltage V_{SB} for NMOS and PMOS MOSFET was equal to 287 mV. The threshold voltage of p-channel and n-channel MOSFETs before body biasing was measured as 441 mV and 496 mV respectively. The threshold voltage of p-channel and n-channel MOSFETs after body biasing was measured as 387 mV and 455 mV respectively.

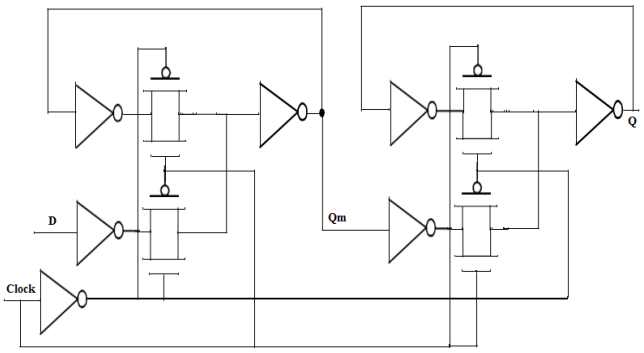

Fig. 4. Schematic view of simple Master-Slave positive edge triggering Flip-Flop [12].

Table I shows the comparison of rise & fall time at the output of the existing technique and the proposed circuit when applied to ripple carry adder with 64 bits. C_{out} is the final output of the critical path of the combinational logic circuit operated at subthreshold region. Table II shows the comparison of rise & fall slopes between the existing technique and the proposed circuit when applied for 64-bit ripple carry adder. Table III shows the comparison of total propagation delay, energy per cycle, energy-delay product (EDP) and corresponding achieved operating frequency of the D flip-flop of the existing technique and the proposed circuit when applied to ripple carry adder with 64 bits.

After providing forward-body biasing in proposed mux-based logic design threshold voltage is lowered-down as compared to zero biased MOSFET. So, MOSFET sensitivity is increased. It has reduced switching delay from logic high to low and low to high (Table I). Therefore, this leads to decrease in total propagation delay of combinational logic block with mux-based logic design. Proposed mux-based logic design gives opportunity to increase clock frequency of the D flip-flop. Total energy per cycle of the proposed mux-based logic design applied for 64-bit ripple carry adder is reduced as compared to existing logic design using adaptive feedback equalization technique applied for 64-bit ripple carry adder. Energy-Delay product has also been lowered down as compared to existing circuit of adaptive feedback equalization when applied to 64-bit ripple carry adder.

V. Conclusion and Future Scope

This paper proposes a circuit to improve the switching characteristic of the longest path (critical path) of the logic circuit operated at subthreshold region of the operation. The proposed circuit comprises of a multiplexer that is implemented using transmission gates and is used in the critical delay path of the logic circuit when operated at subthreshold region. Forward body biasing notion is incorporated in the proposed circuit to lower the threshold voltage of the MOSFETs so as to reduce the switching time of the MOSFETs. The proposed circuit is implemented using Cadence Virtuoso at 45 nm technology and compared with the circuit studied from literature survey at 287 mV. The supply voltage for the combinational circuit and the proposed circuit and the D flip-flop was 287 mV. The forward body biasing voltage V_{SB} for NMOS and PMOS MOSFET was equal to 287 mV.

TABLE I COMPARISONS OF RISE TIME AND FALL TIME AT THE OUTPUT OF THE EXISTING CIRCUIT AND PROPOSED CIRCUIT USING MULTIPLEXER USED TO MINIMIZE THE DELAY ALONG CRITICAL PATH DELAY IN RIPPLE CARRY ADDER WITH 64 BITS

Design Methodology	**Rise time of the flip-flop input signal (ns)**	**Fall time of the flip-flop input signal (ns)**
Existing Adaptive Feedback equalization Circuit applied to 64-bit ripple carry adder [1]	1.99 (at the output of Adaptive feedback equalizer circuit)	1.838 (at output of Adaptive feedback equalizer circuit)
Proposed Circuit Using Multiplexer applied to 64-bit ripple carry adder	1.032 (at the output of the multiplexer)	1.349 (at the output of the multiplexer)

TABLE II COMPARISONS OF RISING SLOPE TIME AND FALLING SLOPE OF THE OUTPUT OF THE EXISTING CIRCUIT AND PROPOSED CIRCUIT USING MULTIPLEXER TO MINIMIZE THE DELAY ALONG THE CRITICAL PATH IN 64 BITS RIPPLE CARRY ADDER

Design Methodology	**Rising Slope of the flip-flop input signal**	**Falling Slope of the flip-flop input signal**
Existing Adaptive Feedback equalization Circuit applied to 64-bit ripple carry adder [1]	61.99	69.96
Proposed Circuit Using Multiplexer applied to 64-bit ripple carry adder	94.90	75.66

TABLE III COMPARISONS OF TOTAL PROPAGATION DELAY, MINIMUM ENERGY POINT, ENERGY DELAY PRODUCT AND CORRESPONDING OPERATING FREQUENCYOF THE OUTPUT OF THE EXISTING CIRCUIT AND PROPOSED CIRCUIT USING MULTIPLEXER TO MINIMIZE THE DELAY ALONG CRITICAL PATH DELAY FOR 64 BITS RIPPLE CARRY ADDER

Parameters	**Existing Adaptive Feedback equalization Circuit applied to 64-bit ripple carry adder [1]**	**Proposed Circuit Using Multiplexer applied to 64-bit ripple carry adder**
Total propagation delay	41.8 ns	29.17 ns
Energy/cycle	1.4048 fJ/cycle	0.9398 fJ/cycle
Energy-Delay product (EDP)	58.72 x 10^{-24} J.s	27.41 x 10^{-24} J.s
Achieved Operating frequency of the D flip-flop	25 MHz	50 MHz

The threshold voltage of p-channel and n-channel MOSFETs before body biasing was measured as 441 mV and 496 mV respectively. The threshold voltage of of p-channel and n-channel MOSFETs after body biasing was measured as 387 mV and 455 mV respectively. The proposed circuit is applied to the critical path of ripple carry adder with 64 bits operated in subthreshold region. The switching delay for high going and low going transition time at the signal given as input to D flip-flop is same as signal produced as output by the proposed circuit using multiplexer and are measured and are reduced by 48.14% and 26.60% respectively. Also, the slope of the transition of the output signal has been increased by 53.08% & 8.14% for rise and fall respectively. The total propagation delay diminished by 30.12%, as compared to existing technique. The energy per cycle and energy-delay product (EDP) turned down by 33.10% and 53.31% respectively, over the existing technique. The operating frequency of the proposed mux-based logic design can increase by 50% as compared to the existing logic design keeping the same supply voltage. The flip-flop used can also be modified to make it more sensitive to detect and capture the critical delay path signal at a faster rate.

REFERENCES

[1] Mahmoud Zangeneh and Ajay Joshi, "Designing Tunable Sub-threshold Logic Circuits Using Adaptive Feedback Equalization," IEEE Transaction Very Large-Scale Integration. (VLSI) System, volume 24, no. 3, March 2016, pp. 884–896.

[2] M. Zangeneh and A. Joshi, "Sub-threshold logic circuit design using feedback equalization," Design, Automation and Test in Europe Conference Exhibition. (DATE), March 2014, pp.1–6.

[3] Z. Takhirov, B. Nazer, and A. Joshi, "Error mitigation in digital logic using a feedback equalization with Schmitt trigger (FEST) circuit," 13th International Symposium Quality Electronic Design.(ISQED), March 2012, pp. 312–319.

[4] J. Kwong, Y. K. Ramadass, N. Verma and A. P. Chandrakasan, "A 65 nm sub-Vt microcontroller with integrated SRAM and switched capacitor DC-DC converter", IEEE Journal of Solid-State Circuits, volume 44, no. 1, pp. 115–126, January 2009.

[5] Sung-Mo Kang, Yusuf Leblebici, "CMOS Digital Integrated Circuits: Analysis and Design": McGraw-Hill, 3rd Edition, 2003.

[6] A. Hokazono, S. Balasubramanian, K. Ishimaru, H. Ishiuchi, Tsu-Jae King Liu, and Chenming Hu, "MOSFET design for forward body biasing scheme," IEEE Electron Device Letters, May 2006, pp. 387–389.

[7] V. Kursun and E. G. Friedman, "Multiple Supply and Threshold Voltage CMOS Cirtuits", New York: John Wiley & Sons, Incorporated.

[8] Rajani Suthar, Kirti S. Pande, and N. S. Murty. "Leakage Reduction in DT8T SRAM Cell Using Body Biasing Technique." IEEE International Symposium on Nanoelectronic and Information Systems (iNIS), December 2017, pp. 215-219.

[9] P. Sreelakshmi, K. S. Pande, N. S. Murty, "SRAM cell with improved stability and reduced leakage current for subthreshold region of operation", IEEE International Conference on Computational Intelligence Computing Research, December 2015, pp. 1-5.

[10] J. Parimala, K. Priyanka, L.S. Kaumudi, K.S. Pande, N.S. Murty, "Subthreshold voltage to supply voltage level shifter using modified revised wilson current mirror", IEEE International Conference and Computing Research (ICCIC), December 2015, pp. 1-5.

[11] Sreyas Mohan, Kirti S. Pande, N. S. Murty, "Stability investigation for 1R-2W and 2R-2W Register File SRAM bit cell using FinFET in subthreshold region", International Conference on VLSI Systems Architecture Technology and Applications, January 2015.

[12] J. M. Rabaey, A. Chandrakasan, and B. Nikolic, "Digital Integrated Circuits: A Design Perspective", Upper Saddle River, NJ, USA: Pearson Education, 2003.

Proceedings of the Fourth International Conference on Communication and Electronics Systems (ICCES 2019)
IEEE Conference Record # 45898; IEEE Xplore ISBN: 978-1-7281-1261-9

SISA : A secret-sharing scheme application for cloud environment

Rohit B. Chilwant
Department of Computer Engineering
Ramrao Adik Institute of Technology
Navi Mumbai,India
Email Id: rohitchilwant1997@gmail.com

Taral S. Sarvagod
Department of Computer Engineering
Ramrao Adik Institute of Technology
Navi Mumbai,India
Email Id: taralsarvagod98@gmail.com

Kunal R. Kumbhar
Department of Computer Engineering
Ramrao Adik Institute of Technology
Navi Mumbai,India
Email Id: kunu6313@gmail.com

Prathmesh N. Gunjgur
Assistant Professor
Department of Computer Engineering
Ramrao Adik Institute of Technology
Navi Mumbai,India
Email Id: gunjgur.prathmesh@gmail.com

Dr. Amarsinh V. Vidhate
Professor
Department of Computer Engineering
Ramrao Adik Institute of Technology
Navi Mumbai,India
Email Id: vidhate.amarsinh@gmail.com

***Abstract*—Security defies one of the galactic barrier when pondering the use of cloud services. Data outsourcing in the cloud (DOC) is conventionally based on data encryption, which imparts impregnable security, but deteriorating the efficiency and rimming the functionalities of cloud. In this proposal we aim to possess them by proposing a secret sharing scheme that depends on partitioning the data and distributed storage over multi-clouds. The scheme used in the proposal uses a combination of symmetric (AES) and asymmetric (RSA) encryption techniques to share the data among the peers in the cloud environment. The proficiency of the suggested scheme has been demonstrated by the empirical results.**

***Index Terms*—multi-clouds, special key, AES, RSA, SISA.**

I. Introduction

The digital revolution has yielded massive amounts of multimedia stats that has become difficult to oversee, thus ultimately induced many organizations to switch to cloud-based solutions. Nevertheless, these cloud-based solutions seem to be economical but there dwells a numerous issue like reliability, accessibility, security & covertness of the content that is being assigned to these Cloud Service Providers (CSPs). Accidental breaches in the cloud services owing to the inadequacy of fault tolerance or server downtime have contributed to formidable forfeit and financial losses in the past.

Multi-clouds have bloomed as a compelling way in offering an eminent cloud service, as it entails outsourcing of data to multiple cloud storage (MCS) servers which are sovereign as a result sealing the data leakage issues. Nevertheless, archiving the data at third-party servers will endanger its security, thus encryption methods are implemented on the information to retain its confidentiality. Encryption methods have been implemented that split the data files into multiple chunks and then archive these shares at distributed cloud server. However, another vital aspect is storage volume at the servers, one such approach is eliminating the data redundancy over the cloud server. Thus, encryption of data will scramble the data so that the hostile will not be able to read it, while removing of redundant data will intend to locate coincident data.

Here in this proposal the data (.pdf, .jpg, .xlsx, .mp3) is converted to its corresponding binary value which further divided into 32-byte blocks. This 32-byte blocks is then encrypted by using a *hybrid encryption* and stored over multi-clouds.

II. Background

Storing data on cloud using a single encryption algorithm became a traditional approach and the system possess various vulnerabilities. Instead of storing data, the trend of uploading files on multiple clouds gathered attention as the data was pretended to be safe as the intruder found it difficult to retrieve data from multiple cloud. Storing the data by splitting it into different chunks and uploading it on cloud was proposed in [1] along with this encrypting the chunks increased integrity authentication of the system to a greater extent also it removed the flaws of encrypting information and uploading it on single cloud.

MCS is a vital service of cloud computing, this grants user to lay in the chunks of encrypted data at distinct cloud drives. Thus, it endorses various CSPs to utilize a single interface in lieu of traditional unique cloud service. Cloud security in the first place aims to the subjects that link to information privacy and protection facets of cloud computing. Such paradigm hubs to the malign insider's ingress to stored information, safeguard from malicious files, elimination of the centralized division of data storage, obsolete files and downloaded files often. The proprietor of the data is less anxious for the future of data stored in such cloud service model. Another aspect is the ingress command on the data, the proposed scheme seeks to ensure the CIA triad which pares malign insider's and file threats with an algorithm that enhances data sharing covertness in MCS services. The proprietor can store and

recover the data in the absence of merging conflicts to procure significant information. The empirical outcomes specify that the suggested model is apt for adopting the MCS services.

III. Related Work

Ken Yang *et al.* [1] found that the use of clouds for storing crucial data in distinct organizations is practiced these days. The data was stored on the server and retrieved at any time and from anywhere. It was made more secure in cloud storage with proper security algorithms and authentication. The analysis increased the availability and security of data at any time at the receiver. For an intruder dealing with the single cloud system is easier than multi-clouds. From this the idea of multi-clouds gathered attention in cloud computing.

Jing Jang Hwang *et al.* [2] introduced the data sharing techniques that were used in the cloud infrastructure were susceptible to various kinds of attacks as many traditional cryptographic techniques fail to provide essential authentication and data integrity for the user. Emphasis was done on using data slicing using AES encryption. The parts of the data were maintained on different clouds servers.

Xiao hua Jiae *et al.* [3] outlined the decline in employing single clouds as the MCS elevated swiftly in CSPs arena. Cloud computing imparts many gains in terms expenditure and uptime. Guaranteeing the security of cloud computing is a prime constituent in the cloud computing environment, as end-user often stores delicate information on CSP which may be untrustworthy. Single cloud became less popular among CSPs as it fails to thrive the CIA triad, thus CSPs moved towards MCS to store important information. It concluded on recent research related to single and multi-cloud security and addressed the use of multi-cloud providers to maintain security. This work motivated to promote the use of multi-clouds due to its ability to reduce security risks that affect the single cloud to the application.

The summary of these papers augmented to storing the data in multi- clouds rather than single cloud. The data should be sliced and each unique chunk is stored in different cloud servers. There was a supreme need of data encryption of data using an optimum and mutually compatible cryptographic algorithms. Finally not acquiescing the available encrypted data to be easily procurable by focusing on encrypting the special symmetric key. The multimedia data used was encrypted using AES algorithm and the special key is being encrypted using an asymmetric public key and all this information is stored in clouds, which strengthens the data integrity of the infrastructure.

IV. Proposed Work

The application built is a secure data sharing application that let us to take advantage of cloud computing using enhanced encryption standards. The application strips away all the redundancies and reduce the complexities of existing systems, acting as a secure endpoint where users can share data securely and in more meticulous way. In this proposal we use *hybrid encryption* which guarantees improved security, confidentiality, integrity of the application. One of the main reason why we use *hybrid encryption* because the public-key cryptosystems often confides to complicated mathematical computations which is generally inefficient in contrast to symmetric-key cryptosystems. A *hybrid cryptosystem* blends the ease of public-key cryptosystem with the efficacy of symmetric-key cryptosystem. The framework of the *SISA* application is shown Fig. 1, here initially the data files (.pdf, .jpg, .xlsx, .mp3) are converted to 32-byte array before performing the AES encryption discussed latter.

TABLE I: Existing vs Proposed

Existing work	Limitations	Proposed work
Data is divided and stored on single cloud	No better encryption	Data is encrypted as well as divided and stored on multiple clouds
Data is encrypted using AES algorithm	Key produced by AES algorithm is not secured	Encryption of Data Using AES algorithm and then splitted.
Data is encrypted using RSA algorithm	RSA is old Algorithm and is not safer for data encryption.	Encryption of AES key using RSA algorithm

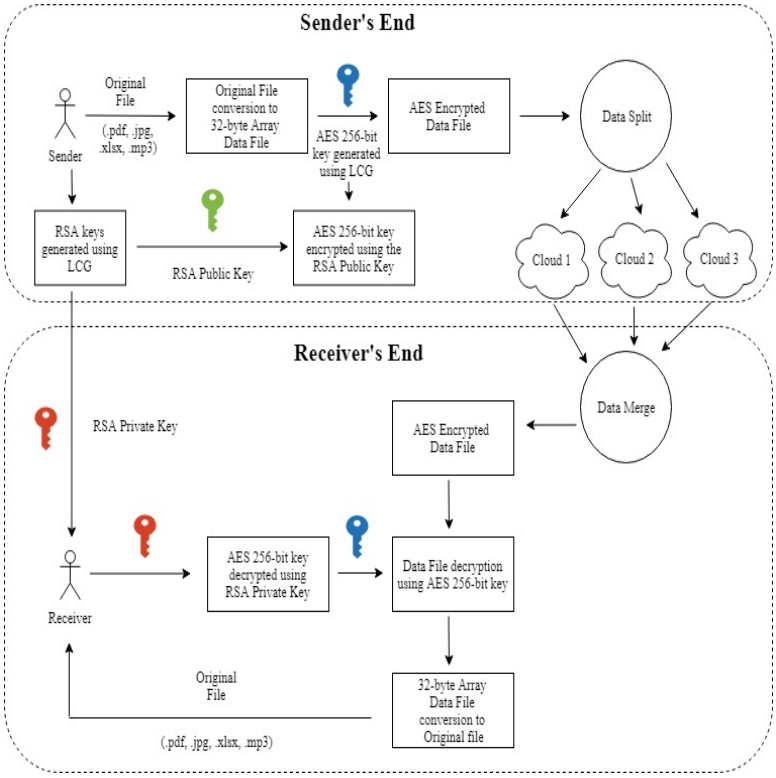

Fig. 1: Framework of SISA

A. Advanced Encryption Standard (AES) Cryptosystem

AES is a symmetric block cipher cryptographic algorithm which is hypothetically impenetrable in a non-trivial time, discussed in algorithm 1. AES allows three variations in key

lengths i.e 128, 192 & 256 bits where the encryption consists of 10, 12 & 14 rounds respectively. All the rounds in each case are identical besides the last round. For encryption, each round consists of four steps : 1) Substitute bytes, 2) Shift rows, 3) Mix columns & Add round key. The last step consists of XORing the output of the previous three steps with four words from the key schedule, the Fig. 2 shows the basic structure of AES cryptosystem. Here we use the AES encryption technique to encrypt the input data file (256 bits), this AES 256-bit encryption key is a *special key* as in our case. In this proposal the AES 256-bit key can be used to encrypt multimedia data (text, audio, pdf, jpg). The integrity of data is ensured by the *special key* which is further encrypted by using an asymmetric key (RSA), thus resulting an *hybrid encryption*. This can be formally realised by the given equations 1 , Let 'P' be the plaintext, K_{AES} be the *special key* which is generated at a real-time using a pseudorandom number generator called Linear Congruential Generator and K_{pri} & K_{pub} be the receiver's private and public RSA keys respectively.

$$\begin{aligned} C_1 &= E_{AES}(P, K_{AES}) \\ C_2 &= E_{RSA}(K_{AES}, K_{pub}) \end{aligned} \tag{1}$$

Then, send both the ciphertexts C_1 & C_2 to the receiver. The receiver can then recover the plaintext as shown in equations 2,

$$\begin{aligned} K_{AES} &= D_{RSA}(C_2, K_{pri}) \\ P &= D_{AES}(C_1, K_{AES}) \end{aligned} \tag{2}$$

B. Linear Congruential Generator (LCG)

Linear congruential generators (LCGs) are class of pseudorandom number (PRNG) algorithms used for generating sequences of random-like numbers. They are prevalent among the other prng's primarily due to their ease of implementation, speed and memory usage. LCGs are defined by the recurrence relation as shown in equation 3 [11]:

$$X_{n+1} = (aX_n + c) \, mod \, m \tag{3}$$

where,
m : the modulus ; a : the multiplier; c : the incrementer; X_0 the starting value, or seed.

Thus, for example if we consider a = 11, c = 37, X_0 = 1 and m = 100 then we can get, X_0 = 1 , X_1 = 48, X_2 = 65, X_3= 52, X_4 = 9 and so on. In this proposal AES 256-bit key is generated in this fashion and stored in 16 $\times$ 16 matrix which is then used in the AES encryption process as discussed above.

C. Rivest–Shamir–Adleman (RSA) Cryptosystem

It is asymmetric cryptographic algorithm popularly used over internet to encrypt data. Generally, RSA algorithm relies on the fact that the factorization of large integer is computationally complex. Here the public-key & private-key both consists of two numbers of which one is the multiplication of the two large prime numbers. So if the private-key is compromised then the encryption fails, thus the encryption strength entirely depends on the key size. Hence, if this key size is doubled or tripled then the encryption strength increases exponentially. Typically, RSA keys are of 1024-bits or 2048-bits so if we used to encrypt large amount of data files (.pdf, .jpg, .xlsx, .mp3) it will consume tremendous amount

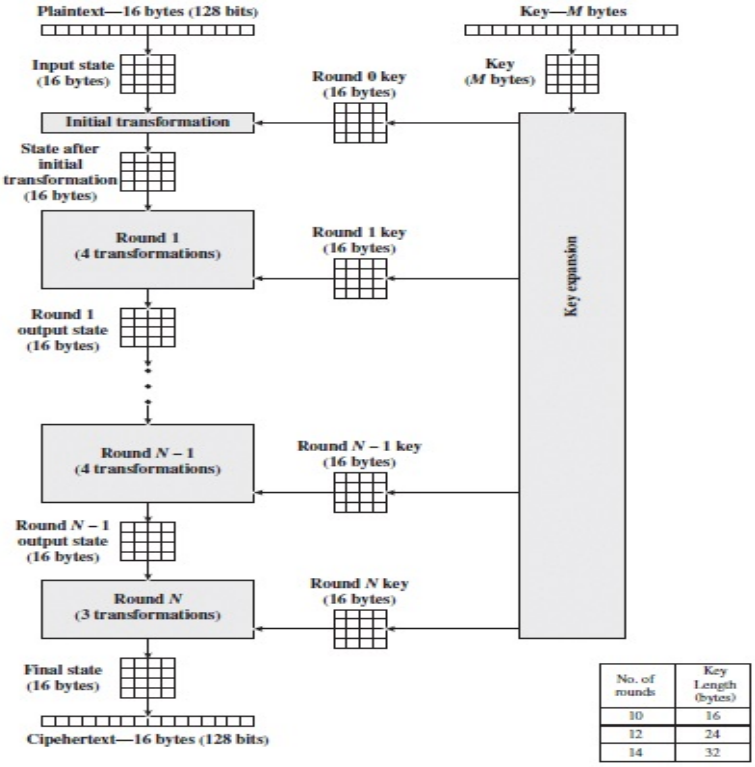

Fig. 2: Basic Structure of AES [7]

Algorithm 1 Data Encryption using AES Algorithm [7].

```
1: procedure MAIN
2:     KeyExpansion (byte key [4 * Nk ], word w[Nb * (Nr + 1)], Nk)
3:     begin
4:     i=0
5:     while(i<Nk)
6:     w[i]s word [key[4*1],key [4t*i +1],key [4*i+2],key [4*i+3]]
7:     end while
8:     while (i <Nb(Nr*1))
9:     word temp= w[i<1]
10:    if (i mod Nk = 0)
11:    temp=SubWord (RotWord (temp)) xor Rcon [i / Nk]
12:    else if (Nk = 8 and i mod Nk = 4)
13:    temp SubWord (temp)
14:    end if
15:    w[i] = w[i - Nk] xor temp
16:    i=i+1
17:    end while
18: end procedure
```

Algorithm 2 Data Splitting Algorithm [10].

procedure MAIN
  Initiate db connection from user to application interface.
  Convert the data to binary
  Generate a Secret key
  Encrypt the data with Secret key.
  Apply Rijndael key Schedule & derive RoundKey
  BitXOR(state of byte, Block(RoundKey))
  Apply Non-linear substitution step
  SubByte: $\frac{oldByte}{newByte}$ (LookUpTable)
  ShiftRow: Transpose(state of Row)
  MixColumn: Mix(state of column)
  Add all the RoundKey
  Check the size of data
  Evaluate remainder = size % cloud no
  Estimate the size of split data (S) = $\frac{Size\,of\,data - remainder}{cloud\,no.}$
  Last data size = S + remainder
  Insert key values to random cloud
end procedure

Algorithm 3 AES key encryption using RSA algorithm [9].

procedure MAIN
  Generate two different primes p and q
  Calculate the modulus$n = p * q$
  Calculate the euler's totient function $\Phi(n) = (p-1) * (q-1)$
  Select for public exponent an integer e such that $1 < e < \Phi(n)$ and $gcd(\Phi(n), e) = 1$
  Calculate for the private exponent a value for d such that $d = e^{-1} mod \Phi(n)$
  Public Key = [e, n]
  Private Key = [d, n]
end procedure

of time. In this proposal, the RSA algorithm provides security to the AES 256-bit key by encrypting it with its public key as shown in equations 1. This encryption of the AES 256-bit key remains anonymous to any intruder, thus provides an one layer additional security. The receiver can decrypt the *special key* using the private-key sent by the admin as shown in equations 2. This enhances the compatibility and efficiency of the *SISA* application and the system guarantees the superior security of the encrypted data stored on the MCS [3].

RSA Key Generation

RSA required two large prime numbers 'p' and 'q' to generate public and private keys. These prime numbers are generated using the Linear Congruential Generator as discussed in subsection IV-B. This LCG algorithm is deterministic and therefore produce sequences of numbers that are not statistically random.

- Generate large random numbers of desired magnitude using LCG.
- Check whether these numbers are prime, otherwise pick successive random numbers.
- Generate the public-key 'e' & the private-key 'd' which are then selected based on the conditions as discussed in the algorithm 3.

Thus, these RSA public-key & private-key of key size 1024-bits is generated and is further used to encrypt-decrypt *special key* as shown in equations 1,2.

D. Working of SISA Application

The application is a client-server based cloud infrastructure where the files can be uploaded, downloaded, shared among the connected server and clients. Initially, the sender / user uploads the data files (.pdf, .jpg, .xlsx, .mp3) to the application which is then converted to 32-byte array. This 32-byte array (i.e. data file) is encrypted by using the AES 256-bit key (i.e. *special key*). Now, before uploading this AES encrypted data file on to the cloud servers the number of blocks are created on to the encrypted data file which are then splitted symmetrically into three parts and are then stored on to the three different cloud servers, discussed in algorithm 2. Thus each cloud server contains the unique part of a file.

The second part of the application is encrypting the *special key* used for data file encryption using the RSA public-key. The system encrypts the *special key* with the RSA public-key and the generated private-key is sent to the receiver by the system. Now, the data as well as the symmetric key is encrypted. This enables hybrid encryption standards which are very difficult to detect and computationally complex to attack easily.

At the receiver's end, the sender first sends the RSA private-key to the receiver only after which he can be able to download the data file. The use of private-key here acts as a obstruction for the decryption of data file using *special key* as it is encrypted using the RSA public-key. Hence, the system first decrypts the special key using RSA private-key and then the data file is decrypted using that *special key*. Finally, 32-byte array is converted back to the original data file (.pdf, .jpg, .xlsx, .mp3) is downloaded at the receiver's end.

Need for Hybrid Cryptosystem

1) Symmetric ciphers are significantly faster than asymmetric in encrypting the files with larger size.
2) Asymmetric ciphers enables key exchange system but at the cost of speed.
3) Asymmetric encryption decelerates the encryption process, but with the concurrent use of symmetric encryption the overall system performance is enhanced.

V. Result Analysis

A. Performance Measurements

The cycle count values for encryption or decryption which depicts the the number of system clock cycles required to en-

crypt or decrypt bytes of data. The amount of time required to execute one of these routines for any system-clock frequency can easily be calculated by using the following formula given in equation 4 [13] :

$$Time = \frac{Cycle\,Count}{System\,Clock\,Frequency} \tag{4}$$

The following are the parameters used for the encryption algorithm performance :

1) **Encryption Time (T_E):** It is the time taken to convert the plaintext (in KB) to ciphertext.
2) **Encryption Throughput (Th_E):** It is defined as the total size of input file (in KB) over the total encryption time (in seconds) as shown in equation 5.

$$Th_E(KB/sec) = \frac{\sum size\,of\,input\,files}{\sum T_E} \tag{5}$$

3) **Decryption Time (T_D):** It is the time taken to convert the ciphertext (in KB) to plaintext.
4) **Decryption Throughput (Th_D):** It is defined as the total size of input file (in KB) over the total decryption time (in seconds) as shown in equation 6 [12].

$$Th_D(KB/sec) = \frac{\sum size\,of\,input\,files}{\sum T_D} \tag{6}$$

5) **Average Time (T_{avg}) :** It is defined as the ratio of total encryption / decryption time over the total number of files as shown in equation 7.

$$T_{avg} = \frac{\sum T_E\ or\ \sum T_D}{\sum number\,of\,input\,files} \tag{7}$$

B. Graphical Analysis

The following Tables II & III shows the comparison of AES & RSA cryptosystem with our proposed system. It is observed that our proposed hybrid encryption is significantly overlapping with the performance of AES algorithm. The graphs 3a & 4a clearly depicts that the *hybrid encryption* is as effective as the AES cryptosystem. On the other hand, in RSA cryptosystem the time take taken for encryption and decryption increases exponentially with the increase of the file size as shown in the graphs 3b & 4b, which is not feasible. Hence, in the proposal the RSA (1024) cryptosystem is used to encrypt the AES 256-bit key which reduces the cost of encrypting the much larger size data files. Thus, the proposal gets the advantage of encrypting the large files using AES which is comparatively faster than RSA and then by encrypting the *special key* with RSA (1024) will computationally complex the decryption process. This will ensure the integrity of the data file.

VI. Conclusion

Despite the benefits of cloud storage of availability, less computation time, etc. in the today's digital world '*data security*' remains the primary focus among the tech giants. This led in the emerging of adapting the cryptographic techniques to the data uploaded over the cloud. In the context, various

TABLE II: Encryption Time (in Milliseconds) [13] [14]

File Size (in KB)	AES	RSA	Proposed System
2	0.761	85	1.854
15	5.705	948	6.799
30	11.410	1949	12.504
55	20.919	3423	22.012
75	28.525	4463	29.619
90	34.231	5545	35.324
150	57.051	10018	58.145
Average Time	22.657	3775.857	23.751
Throughput (KB/msec)	2.629	0.016	2.508

TABLE III: Decryption Time (in Milliseconds) [13] [14]

File Size (in KB)	AES	RSA	Proposed System
2	2.489	400	6.208
15	18.666	3302	22.385
30	37.332	6831	41.050
55	68.441	12426	72.160
75	93.329	16841	97.048
90	111.995	21141	115.714
150	186.659	39381	190.377
Average Time	74.130	14331.714	77.849
Throughput (KB/msec)	0.804	0.004	0.765

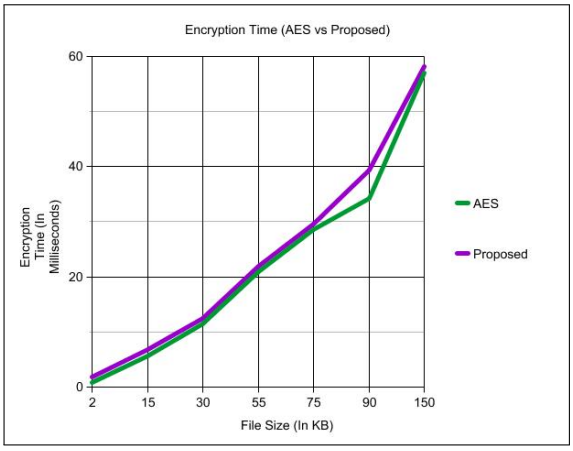

(a) AES vs Proposed

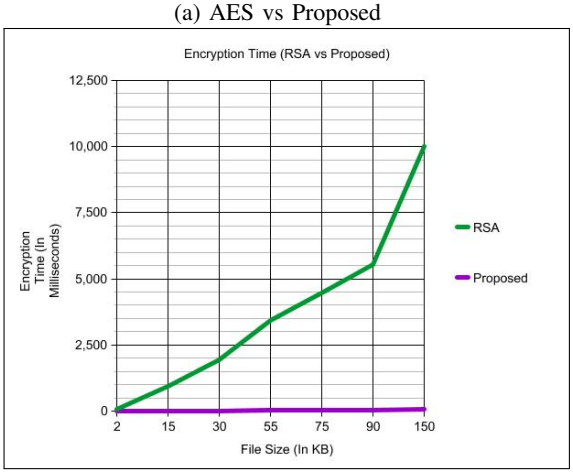

(b) RSA vs Proposed

Fig. 3: Encryption

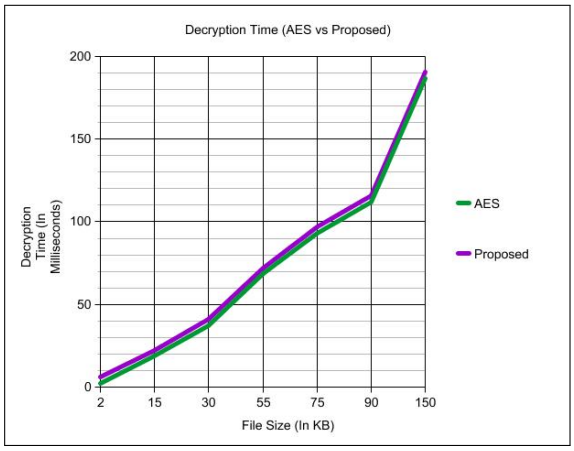

(a) AES vs Proposed

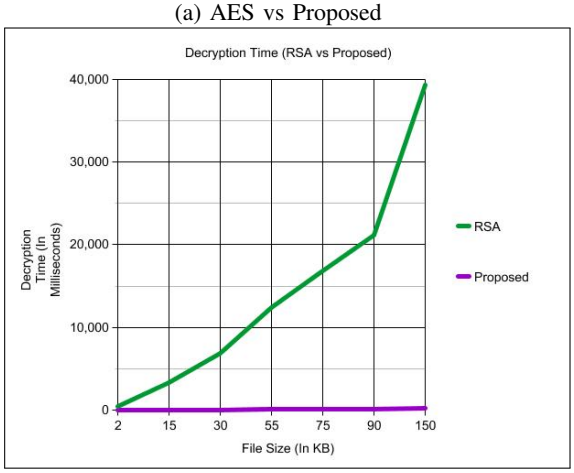

(b) RSA vs Proposed

Fig. 4: Decryption

symmetric and asymmetric key encryption techniques were used to store data on cloud over the period of time. A *hybrid* of symmetric and asymmetric key encryption (i.e. AES and RSA) is proposed which focused on the encryption of data file using symmetric key followed by the encryption of symmetric key with asymmetric key, and storing this crucial data and symmetric key in distributed cloud in encrypted scheme. Encrypting the symmetric key was implemented as the encryption of the key remained anonymous to any intruder and it made the key to be decrypted first before decrypting the data. The asymmetric key was used to further reduce the cost of encrypting symmetric key using another symmetric key algorithm which shows the compatibility of AES and RSA in cryptography is superior.

REFERENCES

[1] J. Bohli, N. Gruschka, M. Jensen, L. L. Iacono and N. Marnau, "Security and Privacy-Enhancing Multicloud Architectures," in IEEE Transactions on Dependable and Secure Computing, vol. 10, no. 4, pp. 212-224, July-Aug. 2013.

[2] J. Hwang, H. Chuang, Y. Hsu and C. Wu, "A Business Model for Cloud Computing Based on a Separate Encryption and Decryption Service," 2011 International Conference on Information Science and Applications, Jeju Island, 2011, pp. 1-7.

[3] K. Yang and X. Jia, "Attributed-Based Access Control for Multi-authority Systems in Cloud Storage," 2012 IEEE 32nd International Conference on Distributed Computing Systems, Macau, 2012, pp. 536-545.

[4] C. Selvakumar, G. J. Rathanam and M. R. Sumalatha, "PDDS - Improving cloud data storage security using data partitioning technique," 2013 3rd IEEE International Advance Computing Conference (IACC), Ghaziabad, 2013, pp. 7-11.

[5] D. Jayalatchumy, P. Ramkumar and D. Kadhirvelu, "Preserving Privacy through Data Control in a Cloud Computing Architecture Using Discretion Algorithm," 2010 3rd International Conference on Emerging Trends in Engineering and Technology, Goa, 2010, pp. 456-461.

[6] B. Lee, E. K. Dewi and M. F. Wajdi, "Data security in cloud computing using AES under HEROKU cloud," 2018 27th Wireless and Optical Communication Conference (WOCC), Hualien, 2018, pp. 1-5.

[7] Abdullah, Ako. (2017). Advanced Encryption Standard (AES) Algorithm to Encrypt and Decrypt Data.

[8] Kartit, Zaid & Azougaghe, Ali & Kamal Idrissi, H & El marraki, Mohamed & Mustapha, Hedabou & Belkasmi, Mostafa & Ali, Kartit. (2016). "Applying Encryption Algorithm for Data Security in Cloud Storage," Advances in Ubiquitous Networking, Springer Singapore, 2016, pp. 141-154.

[9] Xin Zhou and Xiaofei Tang, "Research and implementation of RSA algorithm for encryption and decryption," Proceedings of 2011 6th International Forum on Strategic Technology, Harbin, Heilongjiang, 2011, pp. 1118-1121.

[10] B. Ul Islam Khan, A. M. Baba, R. F. Olanrewaju, S. A. Lone and N. F. Zulkurnain, "SSM: Secure-Split-Merge data distribution in cloud infrastructure," 2015 IEEE Conference on Open Systems (ICOS), Bandar Melaka, 2015, pp. 40-45.

[11] William Stallings,"Cryptography and Network Security Principles and Practices", Prentice Hall Publication, Fourth Edition,2005.

[12] S. Pavithra and E. Ramadevi Pavithra throughput analysis, "Throughput Analysis of Symmetric Algorithms," International Journal Advanced Networking and Applications, 2012,vol. 04, issue. 02, pp. 1574-1577.

[13] Advance encryption standard [Online]. Available: https://www.silabs.com/documents/public/application-notes/AN324.pdf.

[14] S. Y. Bonde and U. S. Bhadade, "Analysis of Encryption Algorithms (RSA, SRNN and 2 Key Pair) for Information Security," 2017 International Conference on Computing, Communication, Control and Automation (ICCUBEA), Pune, 2017, pp. 1-5.

Proceedings of the Fourth International Conference on Communication and Electronics Systems (ICCES 2019)
IEEE Conference Record # 45898; IEEE Xplore ISBN: 978-1-7281-1261-9

Performance Evaluation and Analysis of various Network Security tools

Sinchana K, Sinchana C, Gururaj H L, Vidyavardhaka College of Engineering, Mysore,
Sunil Kumar B R, Adichunchanagiri University, Mandya

***Abstract*— With the developments in the internet and the rise of ecommerce applications and social networks, there is a lot of data generated daily. Thus, the transmission of this data safely through the web is an issue. Also, network security is gaining a greater importance as more and more people are moving towards the age of digital information. As the number of users increase, the cyber-attacks are becoming critical. There are various network security tools which deal with a lot of functions in contributing to the security of network. These network security tools help in finding the vulnerabilities in a website or a web application, to secure wi-fi networks, to crack passwords, to ensure message encryption etc. This paper describes some of such tools, which deal with vulnerability check in a website, wi-fi security, network scanning, network or protocol analyzing.**

***Index Terms*—Network security, Zed Attack Proxy, Aircrack-ng, Wireshark, NMAP**

I. INTRODUCTION

THE fast developments in the internet has attracted a huge number of users, increasing the data production rate. As more and more people are moving towards the digitalized information, this information has to be safely transmitted. The safe transmission of such data is an issue. Along with this, the network security has got a greater importance as there is an increase in the number of users day by day. Due to increase in the number of users, cyber-attacks have become a major threat[1].

Thus, in order to ensure the safe transmission of data and network security, there are various network security tools available. These network security tools perform different functions. There are various types of tools which are used for different purposes[2]. These tools perform variety of operations to contribute to the network security.
Some of them help in sniffing the network or analyzing a protocol, some of them deal in securing a wi-fi network, some of them deal with password security, some check for the website security etc.

In this paper, we describe four such tools which perform certain tasks contributing to the network security[3]. We discuss about Zed Attack Proxy (ZAP) tool which deals in checking for the vulnerabilities in the websites or web application. How the threats in the websites are discovered and solutions are found using ZAP.

Then we discuss about Aircrack-ng tool which deals with password cracking of Wi-fi network. How this helps in discovering the effectiveness in the security of wi-fi network.
Next, we discuss about the NMAP tool that is Network mapper which is a network scanner that helps in finding out the hosts and servers in a computer network. It sends packets and analyses the responses.

The next tool is Wireshark tool, which is a packet analyzer. It is used for network troubleshooting and analyzing the network, development of software and communication protocols.

We discuss how these tools work and their important contributions to ensure network security.

II. ZED ATTACK PROXY

Zed Attack Proxy is an open source web application security scanner which is a free network security tool. It is an OWASP (Open Web Application Security Project) with the flagship status. It is completely free and open source[4]. ZAP is used for penetration testing of your website or a web application. It is ideal for the use of both beginners to the application security as well as professional penetration testers. It is becoming a framework for advanced testing.

A. ZAP PRINCIPLES

- It is free, open source which means anyone can access and use it.
- It's also cross platform that is it works on Linux, Windows and Macs.
- It is easy to use; any user be it beginner or a professional can use it easily.
- It is easy to install; it requires Java Runtime Environment but everything else is included in standard downloads.
- It is fully internationalized, i.e., it's been translated to many other languages.
- It is fully documented, set of useful documents and helpline files are included.
- It works well with other tools, so that we can use other tools in conjunction with zap if we need to.
- It supports the use of well-regarded components.

B. ZAP MAIN FEATURES

- *Intercepting proxy*: we configure the browser to proxy through zap so that zap can see through all the requests and responses.
- *Active and passive scanners*: it provides both the active and passive scanners, so that passive scanners just examine through requests and responses and still recognise the types of problems just on that basis. But the active scanners are different and these can perform wide range of attacks only on applications that you have permission to test.
- *Spider:* it is used to crawl the application, say for example to find the missed-out pages or hidden pages.
- *Report generation*: zap can prepare reports based on the issues found including more advices and links on how to solve that particular problem.
- *Brute force component*: it can also find files even if there are no links to them using brute force component, which is based on owasp dirbuster tool.
- *Fuzzing***:** it can also fuzz parameters and includes fuzzing libraries from the jbrofuzz and fuzz db tools. You can use fuzzing to find more subtle vulnerabilities that the automated scanners cannot find.
- *Extensibility***:** zap can be easily extended

Any web application has to be tested and security testing plays a vital role in it. There are many security threats that a website or a web application may face, like SQL injection, Broken authentication and session management, cross sight scripting, broken access control, security misconfiguration, sensitive data exposure, insufficient data protection, cross site request forgery etc. Zap helps in detecting all such threats and vulnerabilities, and possibly give solutions to the problems[5].

C. WORKING OF ZAP

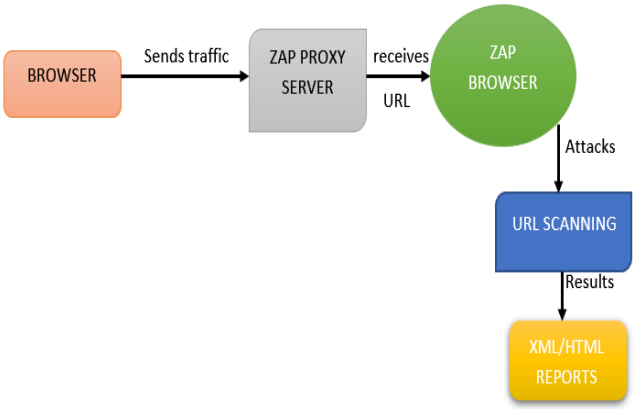

Fig. 1. Block diagram of working of ZAP

Initially, zap creates a proxy server. The browser sends the traffic to pass through the zap proxy server, then the zap browser receives the URL and the attacks on URL with help of auto scanners that helps to find out the vulnerabilities in a website. Finally, a report is generated with the respective problem, its reason and also the solution for it.

E. A SIMPLE PENETRATION TEST

Firstly, configure your browser to proxy through ZAP. Then, explore the application manually. Next, use spider to find 'hidden' content. See what issues the passive scanner has found. Finally, use the active scanner to find vulnerabilities

F. WORKING SCENARIO

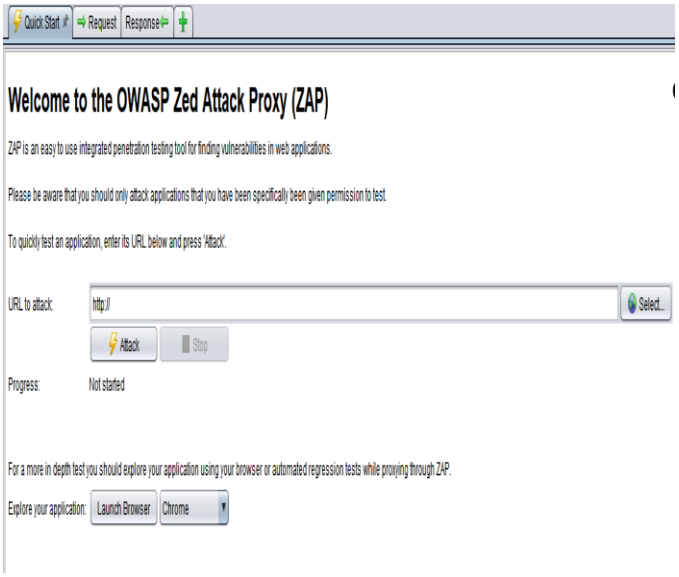

Fig. 2. Initial window of ZAP before entering URL to attack

Initially the zap window looks like this as shown in the above figure.

We give a URL to attack in order to check for the possible vulnerabilities and then the scanning process starts. It is as shown in the below figure.

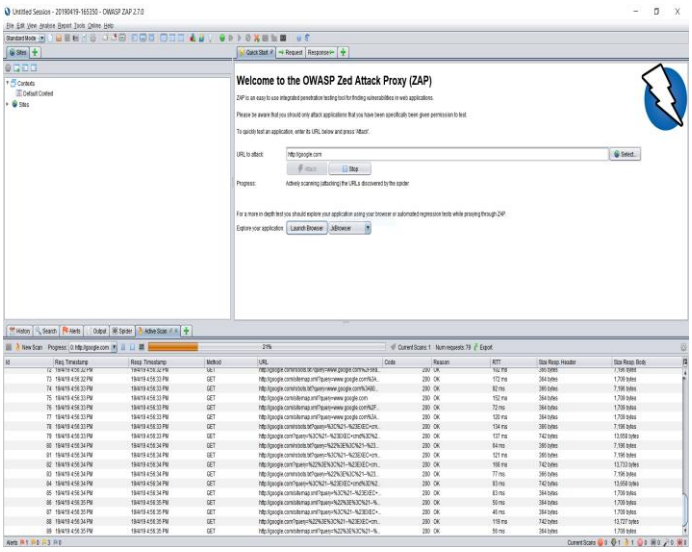

Fig. 3. The scanning process in ZAP.

Once the scanning process is done, the threats or the vulnerabilities discovered through scanning are listed in the alert section.

Fig. 4. The description, type and other details of a threat scanned in scanning process.

The description of the problem and also the possible solution for the threat is also given as shown in figure.

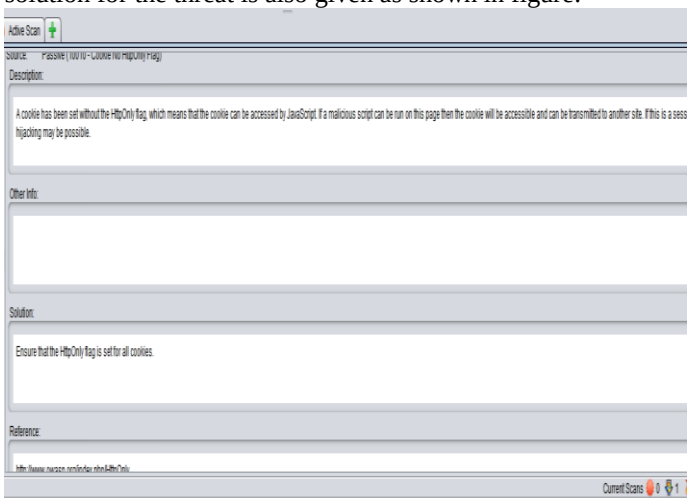

Fig. 5. The solution for the problem given after the description of the vulnerability.

Thus, Zed Attack Proxy is an effective tool to ensure security of the web applications or websites.

III. AIRCRACK-NG

A. FEATURES

It contains a suite of tools for the purpose of checking wireless networks. It is mainly used for:

- *Monitoring:* Packet capturing and exporting of data to text files which is further used for processing by third party tools
- *Attacking:* Replaying attacks, de-authentication, fake access points and others through packet injection
- *Testing:* Checking driver capabilities and Wi-Fi cards (capture and injection)
- *Cracking:* WEP and WPA PSK

It contains four necessary parts [6]:

- *Airodump-ng:* it records the coordinates of the entry or access points and captures the raw 802.11 packets.
- *Aireplay-ng:* it is used for injecting frames into wireless networks.
- *Aircrack-ng:* it is used for recovering keys once enough packets have been captured.
- *Airdecap-ng:* it is used for decrypting the encrypted capture files.

Aircrack-ng is used mainly to test the weaknesses of wireless networks by accessing the network using WEP and WPA-PSK keys by decrypting encrypted packets stored.

B. WORKING OF AIRCRACK-NG

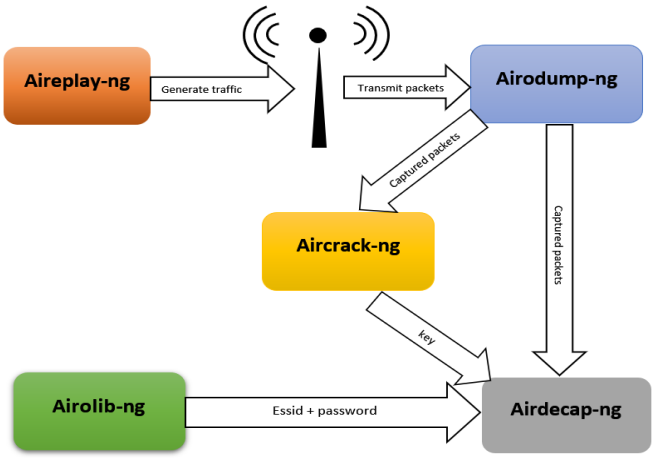

Fig. 6. Block diagram of working of aircrack-ng

Firstly , the aireplay-ng tool generates packets for simulating the traffic. Then the traffic generated, transmits packets and sends it to the airodump-ng tool. The airodump-ng tool captures the packets and then classifies them. Along with this tool, airmon-ng tool changes the adapter to monitor mode to capture all the packets[7]. Once, enough packets are captured, aircrack-ng recovers the key from captured packets. Finally, the airdecap-ng starts decrypting the contents of packets using the recovered key. The airolib-ng tool helps in fastening the password cracking process by precomputing the pairwise master keys[8].

C. WORKING SCENARIO

The password is cracked by checking out all the possibilities in the password list. The output during the cracking process is as shown in fig. 7.

Once the password is cracked, the aircrack-ng tool shows the respective password with the message as “KEY FOUND!”.

The following figures show the output screen while aircracking takes place.

The current passphrase represents the currently parsed password in the password list [9].

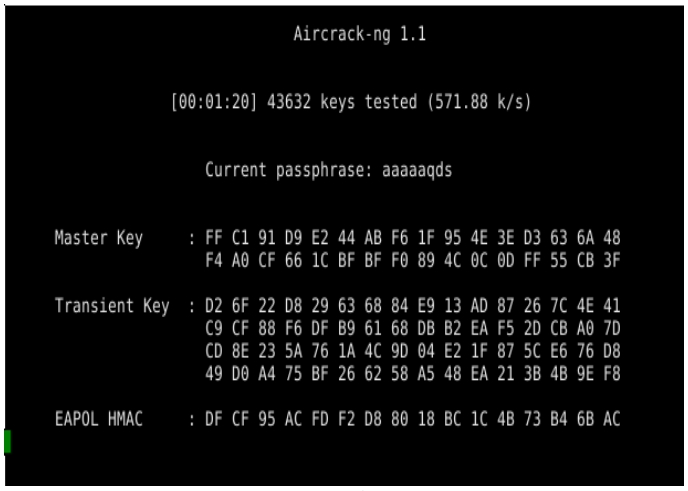

Fig. 7. Output screen while checking for password in the password list.

Once the password is cracked, the output screen is as shown.

Fig. 8. The final output screen when the password is cracked with the message as KEY FOUND and the respective password.

IV. NMAP

Nmap is basically known as foot printing tool or recognisant tool. This is the first step to find information about the target or the IP or the website. Nmap in normally the tool used with Linux, OS and the nmap for windows is known as zenmap.

Nmap is expanded as Network Mapper. It uses innovative raw IP packets to determine which hosts are available on the network, which hosts the services (application name and version), the operating system (and OS versions) that they work on, what packet filters or firewalls are in use and many other characters. It was initially designed to scan large networks quickly. Vulnerability detection, penetration testing, host discovery. The main use is for network exploration and security audits. We will also get to know what the flaws in our network are. It will help us find available ports and services. It will likewise be utilized for finding and abusing vulnerabilities in a system[10]. Nmap supports dozens of advanced techniques to map the network filled with IP filters, firewalls, routers and other hurdles. Many post scanning procedures (both UDP and TCP), OS detection, version detection, ping scraping etc. Nmap is a port scanner and is a tool used by system administrators and attackers (s) to identify vulnerability in operating systems[11]. This takes an IP address or host name and finds the source information associated with it. If an IP address is provided, it then finds the host to which it belongs to[12]. Nmap comes into use when we need to scan huge networks, nearly hundreds of thousands of machines. Nmap is a tool that can be used to find services that operate on Internet connection systems. It could potentially be used for black hat hacking as any other device, as precursor attempts to gain unauthorized access to computer equipment. Nmap is often used by security and systems administration to access the network for impairment.

A. WORKING OF NMAP

Traditional command line and graphical (GUI) versions are available to suit our priorities. Binaries are also available for those who do not want to compile the NMP from the source.Nmap can be used for advanced ethical hacking as well as for scanning a network by using a command line “nmap –v –A target host”.

In the fig 9 the TCP scanning that is done using Nmap. First the command line “nmap –sS 192.168.86.1” is used to syn scan the TCP. This command sends a syn message to the target system (Responder in figure1) using the TCP IP stack, then the responder sends a syn+ack message to the initiator and the initiator sends the ack message which confirms the 3-way hand shake.

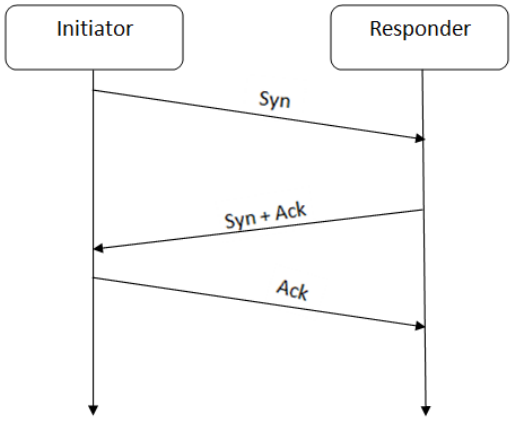

Fig. 9. TCP scanning using nmap.

B. WORKING SCENARIO

Fig 10 shows the initial window of Nmap. Since Nmap is a scanning tool let us take the example of the tcp scanning and show the working scenario of Nmap.

Fig 10 is the initial window of the nmap and this is how it looks when we first open the window. To scan the TCP IP, we need to enter the command line “nmap –v –sn 192.168.0.0” in the command space as shown in fig 11. And once the scanning

of the TCP is done the final window looks like the fig 12 which is the window that shows the entire scanning of TCP.

This is basically just an example to make us understand about the working of nmap. Similarly using the command lines, we can scan any network as shown in the example.

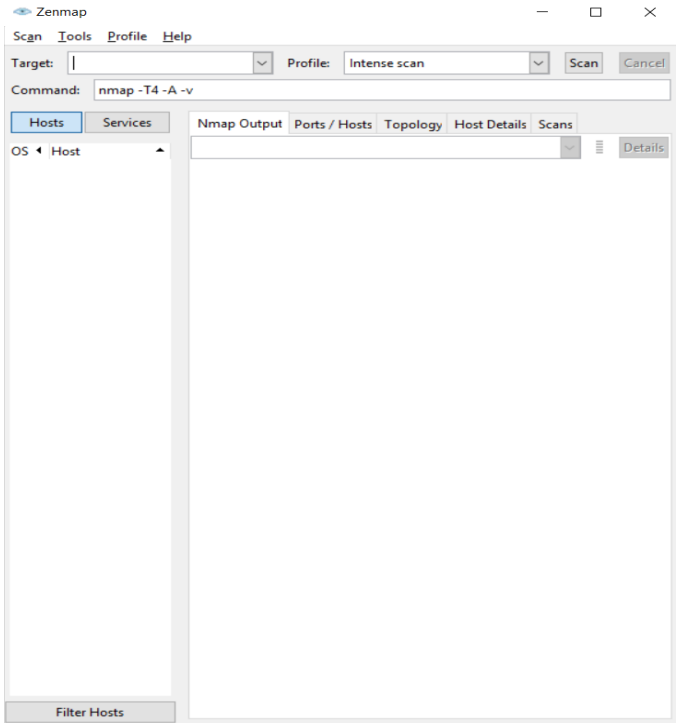

Fig 10. Initial window of nmap.

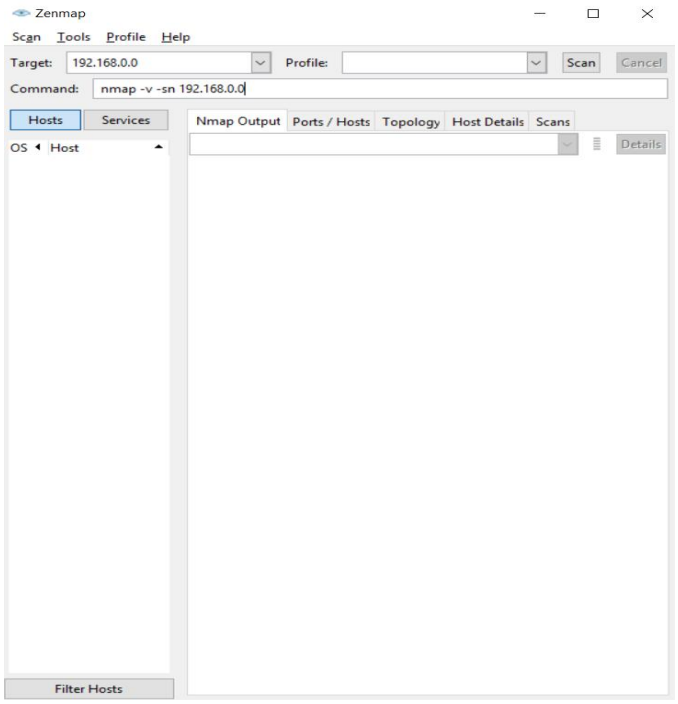

Fig 11: command entering

Command line should be entered to scan the TCP, this is done by using the command line “nmap –v –sn 192.168.0.0”

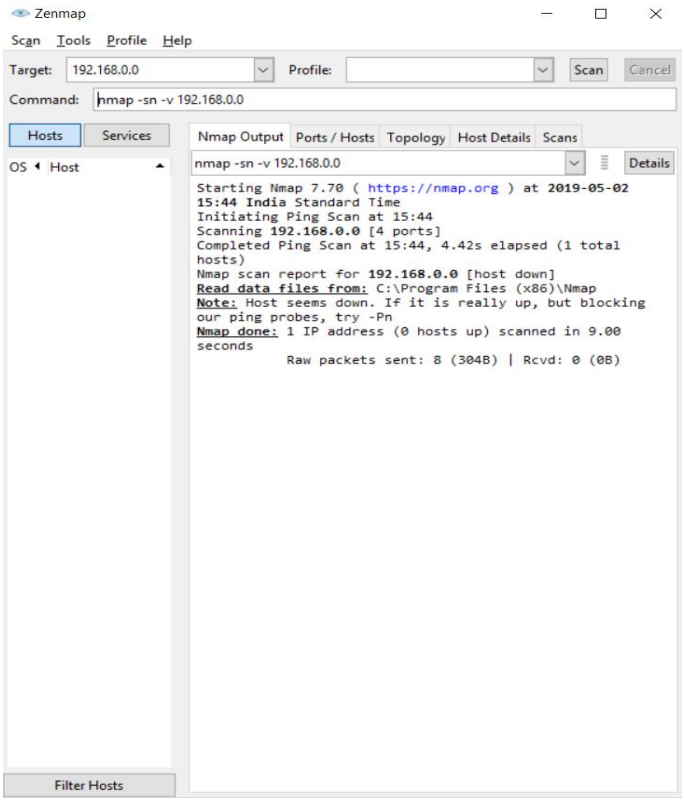

Fig 12:Final window after scanning.

V. WIRESHARK

Wireshark is an open-source and open packet analyzer. It is used for network analysis, software and communications protocol development, troubleshooting and education. It puts the network card into promiscuous mode. This basically means it can intercept packets into the network, it is done by using libraries called as winpcap and libpcap. These winpcap and libpcap provide capture and filter capabilities on different platforms. Wireshark is a free and open-source protocol/ packet tracer[13]. Network attacks are almost identifiable by observing incoming and outgoing traffic, because unusual behavior is caused by the suspicious pattern of packets[14].

A. FEATURES OF WIRESHARK

- The main feature of wireshark is, it has live capture and offline analysis.
- It is a multiplatform i.e., it runs on multiple flatforms like windows, OS, linux etc.
- Captured network data can be browsed through a graphical interface.
- For dissecting new protocols, plug-ins can be created.
- Most importantly it is a data capturing tool and a packet analyzer.

B. WORKING OF WIRESHARK

The first thing we see is the list of all the network interfaces. We have to choose which interface we want

wireshark to capture on. Most of the time it will be the Ethernet or Wi-Fi interface. Once we select the interface the wireshark starts capturing the packets.

Let us take an example of ping packet. Ping packets are a type of internet control message or part of the ICMP protocol. We can ask the wireshark to give us only ICMP packets.

The top part of the screen wireshark shows a list of all the packets seen and gives a brief information about them.
The middle section of the wireshark window shows the lines that corresponds to one of the layers of the internet. Each of the layer is represented by the header that is contained by that packet. So, whenever the wireshark intercepts the packet it looks at all of the header on that packet so that we get complete information about the packet-ed every step of the network stack.

The bottom most part of the wireshark window shows the actual bits of the packets and what their encoding means.

C. WORKING SCENARIO

Fig 13. shows the initial window of wireshark where all the network interfaces are present.

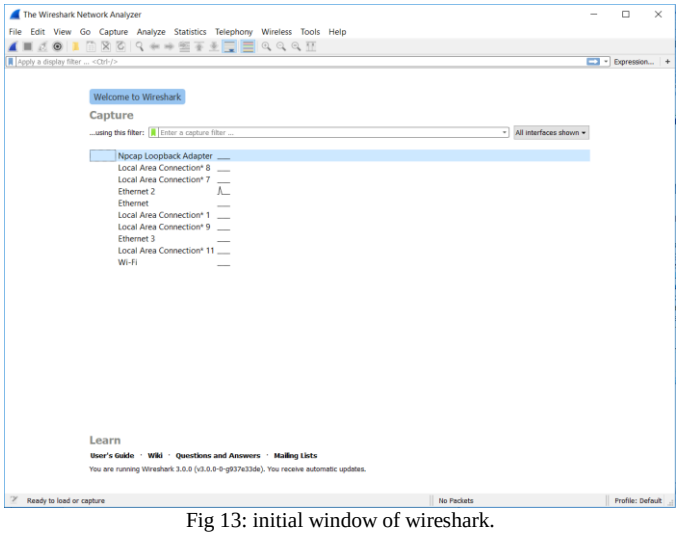

Fig 13: initial window of wireshark.

Fig 14 shows that the packets are being scanned. Here as for the example we have taken i.e., TCP, the packets are being scanned for that.

We can also get the input output graph for this TCP packet analyzer. This option is found in the statistics option and the graph is as shown in fig 15.

Statistics also has many options such as packet length, end points, resolved addresses etc and one such option is capture file properties and this is shown in fig 16.

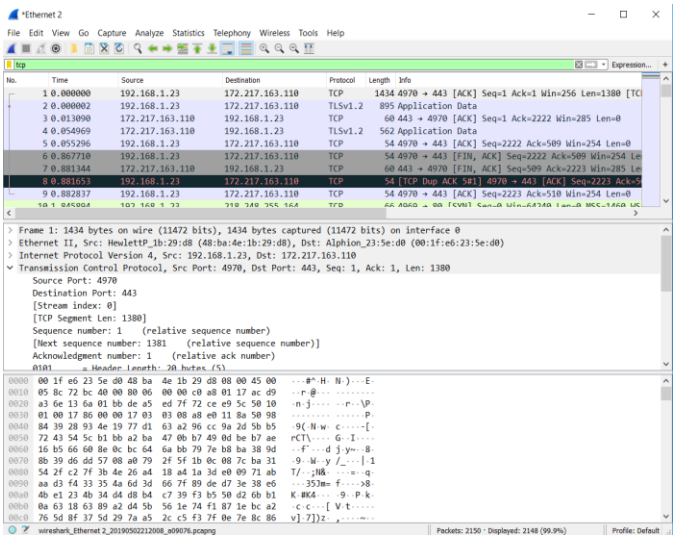

Fig 14: Packet scanning.

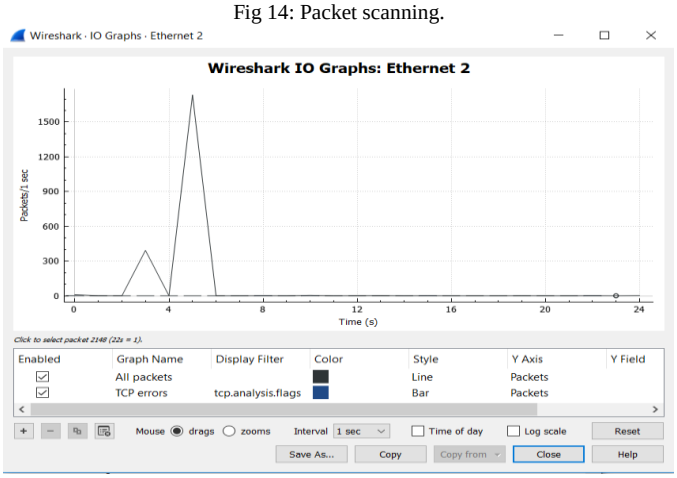

Fig 15: i/o graph.

Under ideal conditions, the graph represents a line develops over time indicating efficient performance the TCP connection [15].

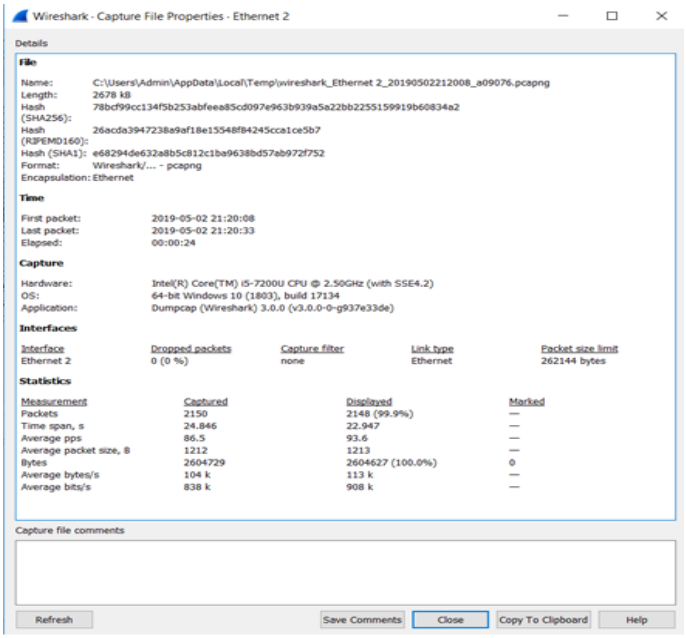

Fig 16: capture file properties.

VI. COMPARISON TABLE OF THE NETWORK SECURITY TOOLS

NO.	TOOL	FUNCTION	USES
1.	Zed Attack Proxy	Web application security scanner	Scans vulnerabilities in a web application, and gives solutions to those problems.
2.	Aircrack-ng	Wi-fi network security checker	used to test the weaknesses of wireless networks by accessing the network.
3.	NMAP	Network mapper	Gives all the information about a network about hosts, operating systems etc.
4.	Wireshark	Packet analyzer	used for network analysis, software and communications protocol development, troubleshooting and education.

VII. CONCLUSION

Here we have exhibited the subject of Network Security and some of the Network Security Tools that will help us in finding the vulnerabilities in a website. In this paper we see the usage, main features, principles and the working scenarios of network security tools like zap, aircrack-ng, Nmap and Wireshark. Thus, all these tools help us in securing the network and preventing it to be vulnerable from any third-party system.

VII. REFERENCES

[1] Importance of Cryptography in network security by T. Rajani Devi

[2] A survey on network security tools for open source by Nabanita Mandal ; Sonali Jadhav

[3] Network security management tool for distribution systems by Zbigniew A. Styczynski ; Chris O. Heyde ; Bernd M. Buchholz ; Olaf Ruhle

[4] Evaluation of vulnerability scanners by Yuma Makino,University of Aizu, Tsuruga, Ikki-Machi, Aizu-Wakamatsu, Fukushima, Japan, 965-8580, Vitaly Klyuev, University of Aizu, Tsuruga, Ikki-Machi, Aizu-Wakamatsu, Fukushima, Japan, 965-8580

[5] Security testing as a service with docker containerization by P. P. W. Pathirathna, V. A. I. Ayesha, W. A. T. Imihira, W. M. J. C. Wasala, Nuwan Kodagoda, E. A. T. D. Edirisinghe, Computing Department, Sri Lanka Institute of Information Technology, Malabe, Sri Lanka

[6] Wi-Fi Protected Access (WPA) –PSK (Phase Shift Keying) Key Cracking Using AIRCRACK-NG by Sheikh Md. Rabiul Islam

[7] Shuaib, K., Boulmalf M., Sallabi F. and Lakas A.," Performance Analysis: Co-existence of IEEE 802.11g with Bluetooth", Second IFIP International Conference on Wireless and Optical communication Networks, WOCN 2005, sponsored by IEEE. Dubai, March 6-9, 2005

[8] Comparison of Wireless Network Penetration Testing Tools on Desktops and Raspberry Pi Platforms Aparicio Carranza, PhD1 , Daniel Mayorga, BTech1 , Casimer DeCusatis, PhD2 and Hossein Rahemi, PhD3 1 New York City College of Technology - CUNY, Brooklyn, NY USA, acarranza@citytech.cuny.edu 2 Marist College, Poughkeepsie, NY USA, casimer.decusatis@marist.edu 3 Vaughn College of Aeronautics & Technology, East Elmhurst, NY USA, hossein.rahemi@vaughn.edu

[9] Z. Trabelsi, K. Hayawi, A. Braiki, and S. Mathew, Network Attacks and Defenses: A Hands-on Approach, Boca Raton, Florida: CRC Press, 2013.

[10] Ms. Gurline Kaur and Navjot Kaur, "Penetration Testing – Reconnaissance with NMAP Tool", International Journal of Advanced Research in Computer Science, Volume 8, No. 3, March – April 2017.

[11] Sandeep Kumar Yadav* Daya Shankar Pandey Shrikant Lade, "A Network Based Approach to Discover Security Vulnerability on Host System", International Journal of Advanced Research in Computer Science and Software Engineering, Volume 4, Issue 12, December 2014.

[12] Sheetal Bairwa, Bhawna Mewara and Jyoti Gajrani, "Vulnerability Scanners: A Proactive Approach to Assess Web Application Security", International Journal on Computational Sciences & Applications (IJCSA) Vol.4, No.1, February 2014.

[13] Jhilam Biswas and Ashutosh, "An Insight in to Network Traffic Analysis using Packet Sniffer", International Journal of Computer Applications (0975 – 8887) Volume 94 – No 11, May 2014.

[14] Vivens Ndatinya, Zhifeng Xiao, Vasudeva Rao Manepalli, Ke Meng and Yang Xiao, "Network forensics analysis using Wireshark", Int. J. Sensor Networks, Vol. 10, No. 2, 2015.

[15] Borja Merino Febrer, Eduardo Carozo and Manuel Belda "Traffic Analysis with Wireshark", The National Communications Technology Institute, February 2011.

Proceedings of the Fourth International Conference on Communication and Electronics Systems (ICCES 2019)
IEEE Conference Record # 45898; IEEE Xplore ISBN: 978-1-7281-1261-9

CONSTRUCTION AND SIMULATION OF VARIOUS STRUCTURES OF UNIMORPH PIEZOELECTRIC CANTILEVER FOR ENERGY HARVEST

Newton Rai
Dept. of Electrical & Electronics Engg
NMIT, Yelahanka, Bengaluru
rainewton444@gmail.com

Nagaraj M J
Dept. of Electrical & Electronics Engg
NMIT, Yelahanka, Bengaluru
rainewton444@gmail.com

Amogh.M.Morey
Dept. of Electrical & Electronics Engg
NMIT, Yelahanka, Bengaluru
rainewton444@gmail.com

V Shantha
Dept. of Mechanical Engineering
SIR MVIT Yelahanka, Bengaluru
shantha_mech@sirmvit.edu

Abstract- Piezoelectric devices are the alternative potential source for energy. The main focus of this paper is to maximize the output voltage in different shapes of piezoelectric cantilever beam with the same dimensions. In this paper we compare the power output between conventional structure and modified structure (E-shape) and conclude that modified structure has more possibilities in generating maximum power. The prototype E-shaped structure shows maximum deflection than the conventional one. This energy harvester is able to remove the battery problem in various fields like wireless, biomedical and so on. The various structure of cantilever beam is designed by using COMSOL multi-physics 5.1. The obtained results are compared using MATLAB simulation.

Keywords- Cantilever, Unimorph Piezoelectric, Energy Harvesting.

1. INTRODUCTION

Advancements in wireless sensors in recent years have had major strides in the piezoelectric domain. When we realize the fundamental properties of piezoelectric effect, we can state that the amount of electric energy produced is directly proportional to the mechanical stress applied. Many researchers have tried to increase the amount of power generated through the use of cantilevers pertaining to the amount of stress and displacement caused by the cantilever beam which has lead to unique design modules like rectangular (cardinal form), step, trapezoidal and much more. Keeping the main focus about structural integrity this paper mainly showcases a new unique form of a cantilever beam design known as the modified E-structure which produces substantial displacement in turn increasing the sensitivity. Here an unimorph cantilever beam is utilized, unimorph has only one piezoelectric layer [4] attached to the substrate. Since energy harvesting is our primary objective, unimorph cantilever is viable choice. Given that the cantilever beam focuses on fundamental modes of frequency [1], the accuracy is tested using MATLAB of different transfer functions pertaining to the E structured cantilever beam [Fig 2]. Basically, there are two model of cantilever that can be used in two different modes-33 mode and 31 mode, where 33 mode (compressive mode) means the voltage is obtained in the 3-direction parallel to the direction of applied force and the 31 mode (Transverse mode) means the voltage is obtained in 1 direction perpendicular to the direction of applied force [5]. The one end of the unimorph cantilever beam is fixed while other end is suspended freely for motion. When the cantilever beam is deflected up and down from the vibrations produced by a mechanical force in the cantilever beam. This mechanical energy of the beam will get converted into electrical energy due to piezoelectric properties [8].

Piezoelectric energy harvesting can be used as the alternative source of energy for the removal of battery problem. PZT materials that can convert the ambient vibration energy surrounding them into electrical energy. This electrical energy can be stored and used to power others devices. Due to advance technology of wireless and MEMS technology the wireless sensor which are in remote area, this piezoelectric electric energy harvesting plays a vital role. In case of biomedical field to power sensors which are implant inside human body, this energy harvesting contributes to supply the power for example the artificial pacemaker.

2. CLASSIFICATION OF CANTILEVERS

This section presents the case study using finite element analysis in COMSOL Multiphysics to compare the traditional rectangular piezoelectric cantilever beam as shown in fig 1 and the derived E shaped as shown in fig 2.

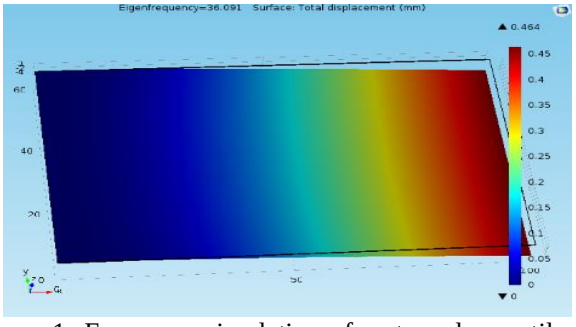

Figure 1: Frequency simulation of rectangular cantilever beam

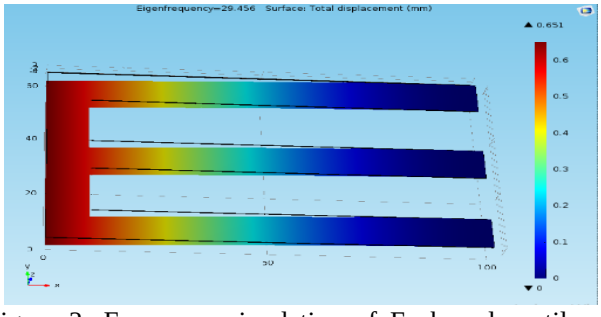

Figure 2: Frequency simulation of E shaped cantilever beam

In order to perform a fair comparison, we need to keep the dimensions of both the beams equivalent as shown in Table 1. The required parameters are compared as shown in Table 2. When the length of piezoelectric and non-piezoelectric are equal the maximum power is generated [11]. The mechanics module of COMSOL Multiphysics is used to simulate the mechanical domains and the piezoelectric devices module to simulate the piezoelectric properties of the PZT5H layer [6].

Table 1: CANTILEVER PARAMETERS

Layer	length (mm)	Width (mm)	Thickness (mm)
Silicon	100	60	0.276
PZT-5H	100	60	0.222

Table 2:MATERIALS PROPERTIES

Material properties	PZT-5H	Silicon
Young's Modulus (GPa)	63	170
Density (kg/m^3)	7500	2329
Poisons Ratio	0.31	0.28

Lead Zirconate Titanate (PZT) is a perovskite ceramic material that shows marked piezoelectric effect[2]. PZT can be prepared in many different forms depending on the application. Here with an approach to create an universal cantilever beam which could be used in multiple ways, we choose PZT based on the conclusions made in the paper[2]. Where temperature change above 20°C does affect the output voltage(PZT-5H). Piezoelectric material works really well under the curie temp (200 °C) and the energy produced increases as the loading increases while the temperature decreases[2].
Table 3 shows comparison of different shapes used for analysis.

Table 3: COMPARISON OF RECTANGULAR AND E-SHAPED BEAMS.

Geometry	Stress, (N/m^2)	Piezoelectric voltage (V)
Rectangular	1.32*10^5	0.278
E-Shaped	1.64*10^5	0.32

3. MESHING

3.1 Meshing

The finite element mesh is used to subdivide the Computer Aided Drawing (CAD) model into smaller domains called *elements*, over which a set of equations are solved. These equations approximately represent the superintended equation of interest via a set of polynomial functions defined over each element. As these elements are fragmented down into figuratively smaller modules, as the mesh is refined, the computed solution will approach the true solution

Meshing is a basic procedure to produce a physical simulation through a grid structure than maps every part of the model to be fabricated. Here the model is meshed with physics control mesh and element size fine. Meshing can be done in many different forms namely tetrahedral [Fig 3] hexahedral and polyhedral. Tetrahedral form is adopted to construct the E cantilever (Fig 4) as it has 4 vertices, 6 edges, and is bounded by 4 triangular faces which provides an immense amount of structural integrity. Tetrahedral meshing is easier to compute than hexahedral, as it simplifies complex geometry. Also another key feature is that tetrahedral can be transitioned into another form of meshing easily when compared hexahedral.

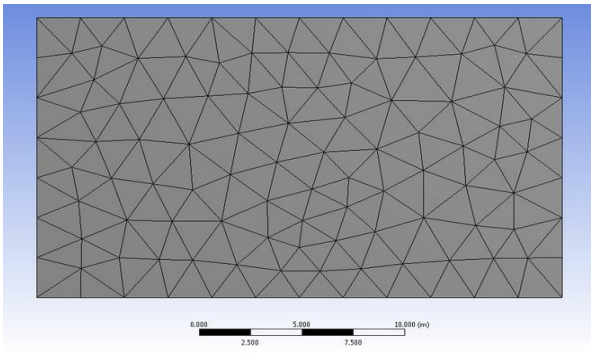

Figure3: Typical Tetrahedral meshing (Comsol)

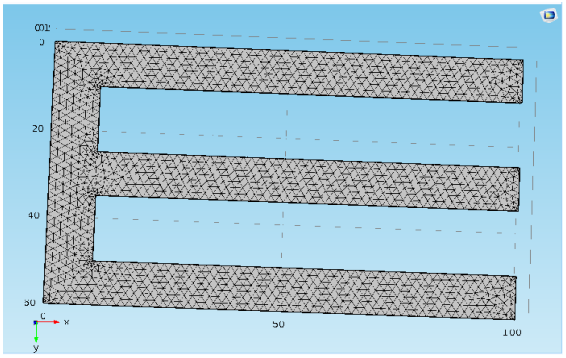

Figure 4: Tetrahedral meshing applied for E cantilever

3.2 Mathematical modelling

A definite system can be represented by different peripherals which may be physical or not depending on its application. A mathematical model as the name states represents this in a mathematical concept. A schematic of converting kinetic energy into electrical energy is represented in figure 5 [1] based on linear elasticity.

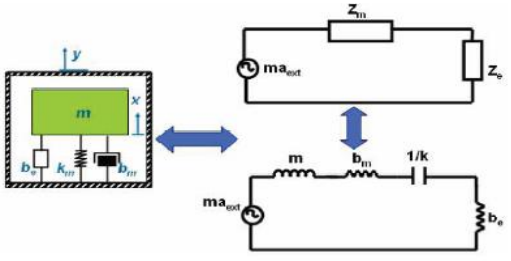

Figure 5: Schematic of a generic vibration energy harvester.

When control system analogy of translating mechanical models to electrical models is applied to the system in

[Fig 5] we get:

$$m\frac{d^2x(t)}{dt^2}+(b_e+b_m)x(t)+kx(t)=f(x)\ldots. (1)$$

$$\frac{X(s)}{F(s)}=TF=\frac{1}{mS^2+k} \ldots\ldots\ldots\ldots\ldots\ldots\ldots\ldots\ldots(2)$$

The above obtained transfer function is used to verify the frequency values using MATLAB.
General equations pertaining to a unimorph cantilever beam are as follows [3]:

$$K=\frac{Ewt^3}{4t^3}\ldots\ldots\ldots\ldots\ldots\ldots\ldots\ldots\ldots\ldots\ldots\ldots\ldots\ldots (3)$$

$$fr=\omega/2\pi=\frac{1}{2\pi}\sqrt{\frac{K}{m_e}} \ldots\ldots\ldots\ldots\ldots\ldots\ldots\ldots\ldots\ldots\ldots\ldots\ldots\

Multiphysics we acquire the following average values:

Table 4: COMPARISON OF RESULTS

Geometry	Eigen frequency (Hz)	Displacement (mm)
Rectangular	36.091	0.464
E shaped	29.456	0.651

4.2 Verification using MATLAB

Taking in consideration of the possible errors caused as the number of iterations are more, the following values were verified in MATLAB using bode plot concept. The frequency obtained from the COMSOL simulation is compared with the frequency obtained from matlab simulation which is shown in figure 7. As the frequency obtained from COMSOL simulation is 29.45 while the frequency obtained from matlab simulation is 32.

Using equation (2) where the following substitutions are made:
m=0.006923 kg
Damping coefficient(B) = 0 (assumption)
Stiffness(K) = 6.8

We get a graph as shown in figure 7, from which we can draw that the eigen frequency value is 29.123Hz.

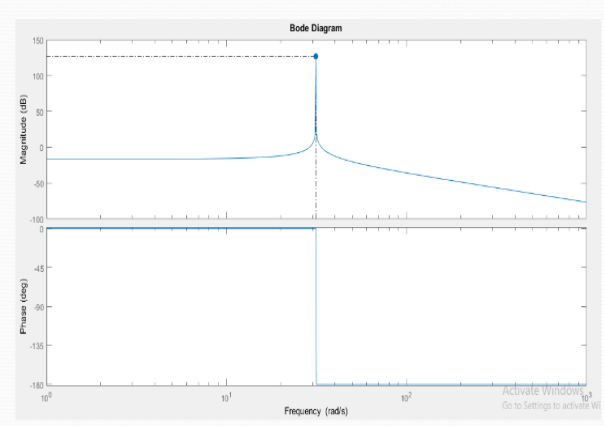

Figure 7: Bode plot obtained from MATLAB simulation

5. CONCLUSION

From the results obtained and verified it is evident that the new formulated E shaped cantilever beam produces more displacement when compared with the traditional Rectangular shaped beam. Since the output power generated is more in this particular prototype as compared to other structures, it can used in bio sensors, wireless sensors, ultrasonic imaging and so on.

5.1 Future scope

The performance of the beams can be estimated by incorporating residual stress of the beams. Mesh less tools can be used to evaluate the performance of the structures. As, it is observed the displacement of the E shaped cantilever beam is considerably more than the conventional structures, different types of structures can be derived to increase the efficiency of this module.

6. REFERENCES

[1] Roundy, S., Wright, P.K and Rabaey, J., "A study of low-level vibrations as a power source for wireless nodes," Computer Communications, Vol.26, pp.1131-1144, 2003.

[2] Butt and R. A. Pasha, "Effect of temperature and loading on output voltage of lead zirconate titanate (PZT-5A) piezoelectric energy harvester". Department of Mechanical Engineering, University of Engineering and Technology, Taxila 47050, Pakistan (2016).

[3] G. Ravi Prakash, K. M. Vinayaka Swamy, S.Huddar and B.G.Sheeparamatti. "Study of Effect on Resonance Frequency of Piezoelectric Unimorph Cantilever for Energy Harvesting". Department of EC Engineering Basaveshwar Engineering College, Bagalkot-587102, Karnataka, India, 2012.

[4] M.Bhanusri and E.varadrajan, "Design and Simulation of Unimorph Piezoelectric Energy Harvesting System". Research and Innovation Centre (RIC), IITM Research Park, Chennai, Tamil Nadu, India and Department of Physics, Indian Institute of Technology (IIT) Madras, Chennai, Tamil Nadu, India, 2013.

[5] Shen, D., Park,J.H., Noh,J.H., Choe,S.Y., Kim S.H., Wikle., H.C. and Kim, D.J., "Micro machined PZT cantilever based on SOI structure for low frequency vibration energy harvesting," Sensors and actuators A:physical,Vol 154, No.1, pp.103-108, 2009.

[6] P. R. Chidambaram, Chris R. Bowen, Sudheer Chakravarthi, Charles Machala and R. Wise "Fundamentals of silicon material properties for successful exploitation of strain engineering in modern CMOS manufacturing." Electron Devices, IEEE Transactions on 53.5 (2006): pp. 944-964.

[7] Priya Chhabra and Anurekha Sharma "Design, Simulation and Fabrication of Piezoelectric Energy Harvester for an Application in Tire Pressure Monitoring System (TPMS)", 1st Winter Workshop on "Engineering at Nanoscale: From Materials to Bio-Sensors" IIT Indore, 10. Dec.2012. [8] Sodano, Henry.

[8] Seema, A., K. R. Dayas, and Justin M. Varghese. "PVDF-PZT-5H composites prepared by hot press and tape casting techniques." Journal of applied polymer science 106.1 (2007): pp.146-151.

[9] V.M Reddy and G.V Sunil, "design and analysis of micro cantilevers with various shapes", International Journal of Emerging and Advance Engineering, Vol 3, 2013.

[10] Priya Chhabra and Anurekha Sharma "Design, Simulation and Fabrication of Piezoelectric Energy Harvester for an Application in Tire Pressure Monitoring System (TPMS)", 1st Winter Workshop on "Engineering at Nanoscale: From Materials to Bio-Sensors" IIT Indore, 10, Dec.2012.

[11] Xiaotong Gao, Wei-Heng Shih, and Wan Y. Shih "Vibration energy harvesting using piezoelectric unimorph cantilevers with unequal piezoelectric and non-piezoelectric lengths Applied physics letters 97 233503, 2010.

[12] Sodano, Henry A., G. Park, and D. J. Inman. "Estimation of electric charge output for piezoelectric energy harvesting." Strain 40.2 (2004): pp.49-58.

ABOUT THE AUTHORS

Newton Rai is a BE student at Nitte Meenakshi Institute of Technology, Bengaluru. His area of interest is in MEMS design and its fabrication, VLSI design, MATLAB simulation.

Nagaraj M J is working as Assistant Professor in Electrical and Electronics Engineering Department of Nitte Meenakshi Institute of Technology, Bengaluru. His research interests are VLSI design, Industrial Automation and Renewable energy of systems.

Amogh M Morey is a BE student at Nitte Meenakshi Institute of Technology, Bengaluru. His area of interest is in MATLAB simulation, MEMS design, VLSI design.

V.Shantha is working as Professor in the Department of Mechanical Engineering,Sir MVIT Bengaluru. Her research area is Materials & Manufacturing

Proceedings of the Fourth International Conference on Communication and Electronics Systems (ICCES 2019)
IEEE Conference Record # 45898; IEEE Xplore ISBN: 978-1-7281-1261-9

Design of laboratory model for demonstration of solid state transformer for smart grid applications

Smita anil sonawale
Deparment Of Electrical Enigineering
Goverment Collage of Engineering
Karad, India
sonawale.smita@yahoo.com

Dr.P.M.Joshi
Deparment Of Electrical Enigineering
Goverment Collage of Engineering
Karad, India
dr.pmjoshi@gmail.com

***Abstract*—Solid state transformer (SST) is an alternative concept of traditional line frequency transformer in the distribution circuits. It has expedience such as small volume, less weight, high power density, controlled power factor etc. It is very beneficial for future power system. This paper encompasses the system design and demonstration of a high voltage SST laboratory prototype model for smart grid applications. The high voltage high frequency 5KVA SST operating at 3 kHz designs are the prime segments of the system, including power stage are highlighted. Transformers magnetic core materials are compare and selected. The high voltage high frequency 5KVA, 3 KHz transformer prototype are designed and integrate with load.**

Keywords – High frequency transformer, dc to dc converter, inverter, rectifier, solid state transformer.

I. INTRODUCTION

Nowadays, power electronics is one of the advance technologies in the power system which has been focused on the improvement of power density and efficiency simultaneously minimising the weight, cost with volume [1]. Varieties of redevelopment technologies are present incorporating high frequency system employed with attachments, such as battery storage system, flexible alternative current transmission system, high voltage dc transmission system, and fuel cell system and power management for computers [2].

We are using SST as an alternative to the traditional line frequency transformer because to overcome the disadvantages of traditional transformer such as bulky size and heavy weight, transformer oil can be harmful when exposed to the environment which are used in traditional transformer cooling as well as insulating purpose, large magnetic inrush current produces harmonics, undesirable results at the input side such as fluctuations effects output waveform with impressions of power deficit at average loads, Voltage regulation is not optimum etc. SST has discriminative characteristics than traditional, as less weight, low volume, high power density, high power factor. Controlled power factor, reactive power compensation, metering or advanced distribution automation, harmonic filtering etc. [9]

Recently, SST is another one high frequency link power conversion system to use in distribution systems with the development of the high voltage power device technology [1].SST exhibits good features such as small weight and volume, controlled power factor, high power density, voltage sag etc. compare to traditional transformer [2]. SST is combination of different materials such as boron, silicon, iron and phosphorus. SST is oil free and dry type insulated high voltage high frequency transformer is mostly preferred due to its safety and environmental consideration; it is one of the advantages of solid state transformer. When line frequency transformer are used in the system then FACTS devices are used to compensating purpose but its alternative SST are used then there will be automatically compensation takes place which is in built in the system.

The remaining part of the paper is drafted as follows. In section II, configuration of SST are explained. In section III, design of high frequency transformer are presented. In section IV, selection of power devices are presented. In section V, summarization of SST function are presented. Finally, conclusion of the paper is given by in section VI.

II. CONFIGURATION OF SST

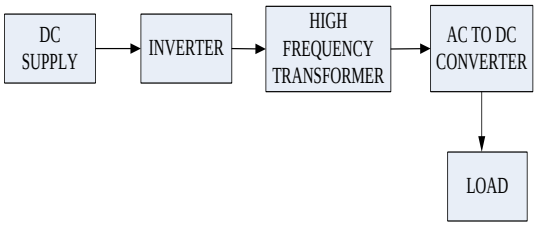

Fig. 1. Configuration of SST

In the recent decade, high power converter is named as power electronics transformer or solid state transformer, has getting more attention and used in the distribution system. Configuration of solid state transformer (SST) are shown in figure 1.

Solid state transformer is one of the best power electronics device which is a coil free, self-regulating, and able to correct the power quality problems, prevents system form load disturbances as well as fault from primary supply side, converts ac to ac, dc to dc, dc to ac with any desired frequency [3].

The basic operation of SST is shown in figure 1. In this operation dc suppy220 volt is given to the system then inverter is the one of the power electronics device used to convert dc to ac and ac supply 230 volt is supply to the high frequency transformer, rating of high frequency transformer is 5KVA and frequency is 3 KHz so size as well as weight will be reduces then output of the high frequency transformer is 48 volt given to rectifier and convert 48 volt ac to 48 volt dc. Output of the rectifier is dc connected to dc load like battery charging, electronic workshop and electrical vehicle charging [1]. If input supply is ac then that time firstly converting 50 Hz ac voltage into dc voltage by using the rectifier. The output of the rectifier is provided to dc to dc dual active bridge converter, in which firstly inverter are used to convert dc voltage into ac voltage at high frequency and supply to high frequency transformer where step up or step down the voltage and output of transformer is provided to rectifier an again convert to dc voltage, finally integrate with dc micro grid as well as ac micro grid [2]. Due to high frequency volume and weight are reduced, so power ratings are required high to reduces weight and volume of transformer effectively.

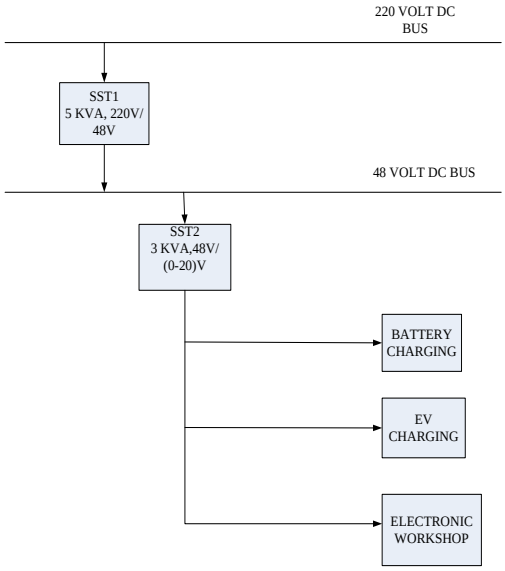

Fig. 2. Innovative architecture of project

Innovative distribution architecture proposed in the project is shown in fig.2.it is proposed to use two solid state transformers. Ratings of these transformers are 5KVA and 3KVA respectively. Input supply is 220V dc and output voltage is variable from 0 to 20V dc. The output is provided to electric vehicle charging, battery charging, and electronic workshop. Also interaction of 48V photovoltaic supply system is proposed for supply to loads through solid state transformer 2, use of this transformer is unidirectional. But when supply is not available then use of main input supply is proposed, which will be provided through solid state transformer 1 as shown in figure 2 and this transformer is bidirectional transformer.

SST is a very beneficial for future distribution power system means in future increases residential load demand and that time required high power rating distribution transformer to improve capacity of the system [2]. If there is a limited space to install transformer, that time SST is a one of the best solution.

The prior work on SST was either components eccentric or had restricted functionality designed for traction systems. Despite of all the distribution system remained destitute from this technique [1].

The concept of solid state transformer is very straight forward and also challenging. High power density power electronic circuit are required, so the operation of SST challenges for both hardware as well as control design. SST contains many components such as high frequency transformer, gate drive, power devices, heat sink, cooling system, control circuit, etc.

The paper can be summarized as follows,

1. Design of solid state transformer
2. Design of high performance system controller for solid state transformer.
3. The demonstration of prototype for loads like as electrical vehicle charging, battery charging, electrical vehicle etc.

III. DESIGN OF HIGH FREQUENCY TRANSFORMER

Table1 shows the specification of 5 KVA solid state transformer. Different parameters are defined like input voltage, output voltage, input current, output current and switching frequency which is the basic parameters required to design the solid state transformer.

A. Specifications of SST :

Table I - Specifications of SST

Power rating	5 KVA	Frequency	3KHz
Input DC voltage	220V	Primary side current	23.92A
Output DC voltage	48V	Secondary side current	104.16A
Primary AC voltage	230V	Secondary AC voltage	48V

B. Selection of Core material :

There are different types of core material are available such as ferrite, amorphous and nanocrystalline and silicon steel. By comparing all materials characteristics, we are selected amorphous core material it has also many advantages as well as disadvantages. Amorphous core material has the highest saturation flux density (1.56T) than

other materials and losses taking place in the core are marginally accepted for a band of several kilohertz. The subjected core is cheaper therefore, it shows the requisite operational cost ratio performance in terms of switching frequency less than 5-10 kHz [5]. Table 2 shows the comparison between different core materials. Core materials are comparing and selected amorphous core material in the c core shape and it has high permeability with 25 micrometre strip thickness.

At the time of transformer design core losses are very important factor to be considered and these are find out by using Steinmetz equation. [1]

$$P_{cv} = K \times f^{\alpha} \times {B_{ac}}^{\beta}$$

Where, P_{cv}= time average power loss per unit volume

B_{ac}= peak flux amplitude

K, α, β = Steinmetz constant

f = frequency of sinusoidal excitation

For different core material has different Steinmetz constant and core losses at 3 KHz frequency which are shown in table 2. Amorphous core material has less core losses than silicon steel.

C. Selection of wire:

Selection of the conducting wire depends on the rating of current. We are selected copper conducting wire for winding purpose at different size for primary and secondary side because primary current is 23.92 A, 10 SWG wire are used and secondary current is 104.16 A, 6×3 fibre glass enamel coating copper foil are used.[4]

D. Calculations :

To find out the different parameters we are using following formulae's [4], [7];

$$\sum VA = \left[\frac{1}{\eta \times \cos\varphi_1} + \frac{1}{\cos\varphi_2}\right] \qquad (1)$$

Equation 1 are used to find out VA rating of a transformer which is 10390.955VA and optimal flux density are calculated by using equation 2. Optimal flux density is less than saturation flux density which is 0.8066T.

$$B_o = \left[\frac{1 \times \sqrt{\Delta T}}{{K_o}^{7/8} \times K_t \times K_f \times K_u}\right] \times \left[\frac{K \times f \times \Delta T}{\sum VA}\right]^{1/6} \times \left[\frac{1}{(\rho_c \times K_c \times f^{\alpha})^{7/12}}\right] \qquad (2)$$

$$A_p = K_o \times \left[\frac{\Sigma VA}{K \times f \times \Delta T}\right]^{4/3} \times [\rho_c K_c f^{\alpha}]^{2/3} \qquad (3)$$

As per [4], all constants and product of area are calculated to selection of core. By using equation (2) product of area 135.1419 cm^4, so we are selected AMCC-160 amorphous c core to high frequency transformer. [5]

$$N_p = \frac{V_p}{k_v \times k_f \times A_c \times B_o \times f} \qquad (4)$$

$$N_s = \frac{V_s}{k_v \times k_f \times A_c \times B_o \times f} \qquad (5)$$

By using equations (4) and (5) we are calculated primary and secondary side number of turns 36 and 8 respectively. Turns ratio are 4.5: 1.

$$\text{MLT} = \frac{\text{Volume of winding}(V_w)}{Window\ area(W_a)} \qquad (6)$$

$$\text{But, } V_w = k_w \times {A_p}^{3/4} \qquad (7)$$

By using equations (6) and (7), calculated mean length of winding are 19 cm. also theoretically core and copper losses are calculated by using (8) and (9). Which are 12.6779 W and 15.1121 W respectively. [4]

$$P_{cu} = \rho_w \times V_w \times k_u \times J^2 \qquad (8)$$

$$P_{fe} = m \times K_c \times f^{\alpha} \times {B_m}^{\beta} \qquad (9)$$

In equations current density J are used which is calculated by equation (10).

$$J = \left[\frac{\beta \times h \times A_t \times \Delta T}{(\beta + 2) \times \rho_w \times k_u \times V_w}\right]^{1/2} = K_t \left[\frac{\Delta T}{{A_p}^{1/4}}\right]^{1/2} \qquad (10)$$

High frequency transformer core AMCC-160 and core with winding are shown in figure 2. [5]

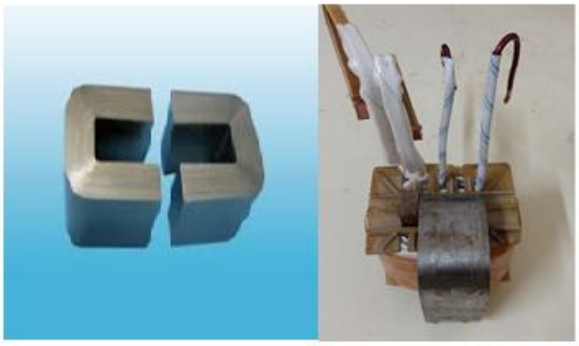

Fig. 3. Core AMCC160 and core type transformer

Material	**Series**	**Saturation Density (T) @ 25°C**	**Strip Thickness (um)**	**Permeability**	**K** (mW/cm^3)	**α**	**β**	**Losses at 3 KHz, 0.3 T** (mW/cm^3)
Silicon Steel	Silicon Steel Arnold Arnon5	1.48	127	High	278.4	1.39	1.80	147
Amorphous	Metglas2605SA1	1.56	25	High	46.7	1.51	1.74	30.2
Ferrite A	Ferroxcube3c96	0.44	N/A	Medium	42.8	1.53	2.98	6.3
Ferrite B	Epcos N97	0.41	N/A	Medium	44.0	1.36	2.72	7.4
Nano crystalline A	Hitachi Finemet FT-3M	1.23	18	High	8.03	1.62	1.98	4.39
Nano crystalline B	VAC Vitroperm500F	1.20	N/A	High	2.48	1.80	2.08	1.47
Nano crystalline C	Magmet Namglas 4	1.23	25	High	3.75	1.71	1.97	2.30

Table 2 – Comparison between different core materials and Steinmetz equation constant

IV. SELECTION OF POWER DEVICES

The input to the transformer should be high voltage and low current means 220-volt dc voltage and 23.92 ampere current. Faster and low loss switching at the high voltage side should be shows satisfactory performance by SiC power devices, however SiC power devices are not commercialized yet and the cost of the devices are higher than Si devices [1].In this project for high voltage side FNB34060T intelligent power module are used for inverting purpose which are shown in fig.4 pin configuration as per datasheet [6]. It is an advance module providing a fully featured, high performance inverter output stage for AC induction, BLDC and PMSM motors. These modules integrate optimized gate drive of the built in IGBT to minimize losses, while also providing multiple protections like under voltage lock out, over current shutdown, thermal monitoring of drive IC and fault reporting. It can support up to 20 KHz. All connections are as per datasheet [6].

For low voltage and high current side means 48-volt 104.166 ampere current side two level H-bridge converter are used to convert 48 ac voltage to 48-volt dc voltage. There are four IRFB3077PbF MOSFEET are used which has rating 75 V/210 A. [1] From the control objective, the phase shift PWM strategy is employed during rectification to cancel harmonics and minimizes size of filter.

Fig. 4. FNB34060T IPM

The switching frequency is selected N times that of rectification stage and boost converter stage. To diminishes the size of passive components higher switching frequency selected. To improve efficiency and thermal design switching losses are big challenge. Between 5 to 20 KHz frequencies are selected for switching the power devices. There are 3 KHz switching frequency are selected which is multiple of 60 Hz.

Zero voltage switching is obtained by dual active bridge converter [11]. In this condition the turn on losses of IGBT and reverse recovery energy losses of parallel connected diode will be very small and turn off losses of the dual active bridge converter remains high due to its inherent operations.

Gate driver design is one of the important parts in the SST design system which are used to high voltage side mosfet into which short circuit protection, active clamping circuit, fault isolation circuit, under voltage protection circuit are integrated. Pulse width modulation technique are used. [9]

V. SUMMARIZATION OF SST FUNCTION

SST are used for different functions such as rejection of load disturbance, rejection of source disturbance, VAR compensation, dc micro-grid integration, ac micro-grid integration etc. All these described characteristics will be evaluated in SST prototype. The advantages over the conventional transformer.

a) SST integrate with both AC and DC micro-grid
b) SST shares both voltage and current
c) Efficiency is good ac as well as dc load condition
d) Source voltage sag means source disturbance rejection capability in SST
e) Load disturbance rejection capabiltity in SST

VI. CONCLUSION

This paper highlights the concept of design and demonstration of 5 KVA SST when input is 220-volt DC and output is 48-volt dc. Also required calculations and selection of material are explained in details. SST has many advantages than conventional line frequency transformer is deeply explained.

REFERENCES

[1] Xu She, Xunwei Yu and Fei Wang, "Design and Demonstration of a 3.6-KV-120-V/10-KVA Solid state transformer for smart grid application,"IEEE transactions on power electronics, vol.29.No.8, August 2014.

[2] Y. Du, S. Baek, S. Bhattacharya, A. Q. Huang, "High-voltage high-frequency transformer design for a 7.2kV to 120V/240V 20kVA solid state transformer," in Proceedings of the 36th Annual Conference on IEEE Industrial Electronics Society, IECON 2010, pp. 493-498, Nov. 2010.

[3] Vijaykrishna Styamsetthi, "A new model Solid State Transformer," Article in International Journal of Research · December 2014.

[4] William Gerard Hurley,Werner Hugo W¨olfle, and John G. Breslin, "Optimized Transformer Design: Inclusive of High-Frequency Effects" IEEE transactions on power electronics, vol. 13, no. 4, July 1998.

[5] www.metaglas.com

[6] www.fairchildsemi.com and FNB34060T Datasheet

[7] A. K. Sawhney "Electrical machine design,"

[8] Haifeng Fan and Hui Li,"High-Frequency Transformer Isolated Bidirectional DC–DC Converter Modules with High Efficiency over Wide Load Range for 20 kVA Solid-State Transformer," IEEE transactions on power electronics, vol. 26, no. 12, December 2011.

[9] Garcia Montoya, Roderick Javier, "High-Frequency Transformer Design for Solid-State Transformers in Electric Power Distribution Systems" (2015).Theses and Dissertations. 1382.

[10] Het Pathak, Mihir Gupte, Ravi Barot and Indrajit Maru," Dual Active Bridge Converter with Solid State Transformer," IJARIIE-ISSN (O)-2395-4396, Vol-3 Issue-3 2017.

[11] www.nptel.com, module3-DC to DC converter, Version 2 EE IIT, Kharagpur.

[12] Sobhi Barg, Kaiyar Ammous, Hanen Mejbri, Abdulrahman Alahdal and Anis Ammous, "Optimum Design Approach of High Frequency Transformer", 978-1-4673-9494-9116/$31.0 © 20161EEE

Proceedings of the Fourth International Conference on Communication and Electronics Systems (ICCES 2019)
IEEE Conference Record # 45898; IEEE Xplore ISBN: 978-1-7281-1261-9

Design and Implementation of Ramp ADC using 45 nm Technology

Sowjanya
Dept. of ECE
NMAM Institute of Technolgy, Nitte
Karkala, India
sowjanyapoojary.1994@gmail.com

Sunitha Lasrado
Dept. of ECE
NMAM Institute of Technology, Nitte
Karkala, India
sunithadsouza@nitte.edu.in

Abstract*---ADC are the important blocks of signal processing systems. Depending on the type of ADC, the blocks involved in the design of an ADC will vary. This paper gives an insight to the design of comparator which will be used in different types of ADC's. This paper also presents design of AND gate, digital counter and DAC used in Ramp ADC. The implementation of 8-bit Ramp ADC is carried out using 45 nm technology in Cadence virtuoso tool and the consumed power is estimated.

Keywords-Analog to Digital Converter (ADC), Digital to Analog Converter (DAC), comparator, digital counter, Operational Amplifier (Op-Amp), Toggle Flip-Flip (TFF), Multi Section Capacitive Digital to Analog Converter (MS-CDAC).

I. INTRODUCTION

Data converters are important building blocks in modern mixed signal processing. The circuit of data converters acts as a link between the analog and digital worlds. Data converters are devices converting analog signals into digital signals and vice versa. It forms the critical components of all the systems. Data converters can be implemented in a number of ways, each taking a different performance parameters in terms of resolution, speed, power consumption, area, etc.

II. REVIEW ON VARIOUS DESIGN TECHNIQUES OF ADC

S. Bashir et al., [1] have proposed different types of ADC's that are used in different application requirements. Different performance parameters like power consumption of different ADC's are compared.

D. Prashanth et al., [2] have designed a dynamic latch based comparator that further provides input and output separation. Thus kickback noise effect is reduced.

P. M. Figueiredo et al., [3] have proposed a different types of comparators out of which latched comparator is one of them. One of the most commonly used comparator is dynamic latched comparator due to its speed.

K. M. Abozeid et al., [4] have designed a dynamic latched comparators, which is power efficient because, in regeneration phase they consume power and absence of static power consumption in reset phase .

Yan Huang et al., [5] have presented the different types of latched comparators like static latched comparator, class AB latched comparator. The fabrication of the comparators are processed using 130 nm technology with power dissipation of 0.75 mW

Raghava Katreepalli et al., [6] have proposed design of synchronous counters which is energy efficient and the power consumption also reduced because clock is applied to different flip-flops simultaneously.

Babita Diana K et al., [7] have designed a SAR ADC using a capacitive array DAC, which works based on charge redistribution principle.

Savitha.M et al., [8] have designed 14 bit SAR ADC. ADC performance is analyzed by using the two split capacitiv e array DAC method to obtain power consumption.

Shinwoong Park et al., [9] have presented a paper that examines the concept of MS-CDAC's, which allows for a broader range of CDAC section segmentation options beyond split - CDAC and C–2C.

Nikhil A. Bobade et al., [10] have presented a modified DAC structure. Hence modification is proposed in modified DAC structure has good power efficiency.

III. Ramp ADC

Ramp ADC is the type of counter ADC. It includes comparator, an AND gate, digital counter, and a DAC. The DAC output is taken as an input to the comparator where it is compared to the analog input signal and produces the comparative output from the designed comparator [2]. If output of the comparator is high then that gives a high input to the digital counter that act as a clock signal. The digital counter makes use of a Toggle Flip-Flop (TFF). Counter starts to count which will be further given as an input to the DAC. Ramp ADC block diagram is shown in Fig. 1. This block is incorporated from [1] and the comparator design is taken from [2]. In this work separate blocks are designed and interconnection between the individual blocks is done.

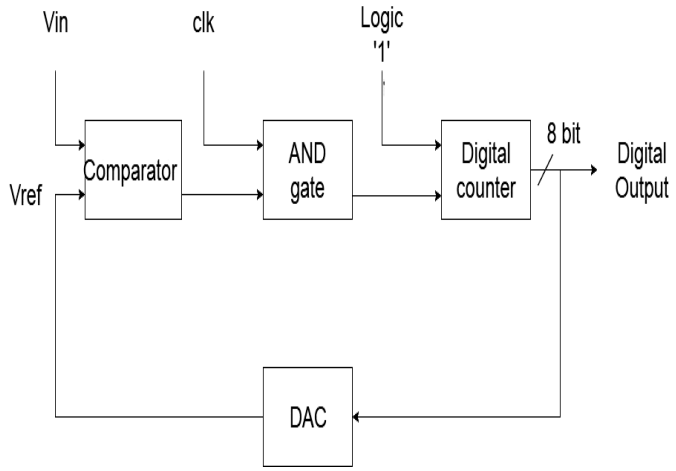

Fig. 1. Ramp ADC block diagram

IV. COMPARATOR

A comparator is a circuit which is used to compare two voltages and it produces the output as either one or a zero, depending on the voltage whether it is at the positive side or at the negative side. The fundamental functionality of the comparator is to find out if an applied input is greater or smaller than the reference signal and, depending on comparison, the binary output is generated.

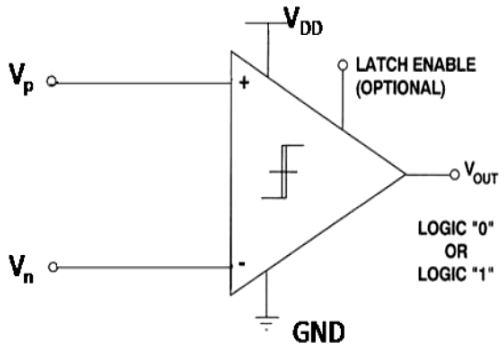

Fig. 2. Symbol of comparator

Fig. 2 displays the comparator symbol. The input voltage is applied to the Vp terminal and Vn is supplied with reference voltage. If Vp terminal input voltage is higher than Vn, then the comparator output is logical '1', where, as if the Vp terminal input voltage is lower than Vn, then the comparator output is none.

ADC's can be implemented using different types of comparators namely Op-Amp based comparator, Static latched comparator, Class-AB latched comparator [11]. Static and Class AB latched comparators are more power efficient, but after regeneration and reset phase there are some supply currents. That problem can be overcome by using Dynamic latched comparator [13]. It allows flow of current only during the regeneration phase [4]. Therefore, due to its high speed and minimized power consumption, Dynamic latched comparator is used in this work.

V. DYNAMIC LATCHED COMPARATOR

The comparator involves two phases of the operation. The output nodes of the comparators are discharged or charged to the source or ground respectively, depending on the architecture in the reset phase. In regeneration phase the digital value is generated at the comparator output. Hence there is power consumption. One of the benefit of Dynamic latched comparator is the absence of static power consumption in the reset phase [4]. Fig. 3 demonstrates the Dynamic latched comparator circuit diagram.

When clk=low, transistors M4 and M3 are in ON state, that precharges the terminal Di+ and Di- to V_{DD} such that transistors M5 and M6 are turned ON. This will discharges the OUT+ and OUT- to ground. When clk=high, M3 and M4 are in OFF state and transistor M15 turned ON, due to which Di node starts to discharge. The difference between voltages Di+ and Di- are applied to transistors M5 and M6. Initially transistors M6 and M5 are in ON state and gradually they becomes OFF. So the output nodes OUT+ and OUT- start regenerating when M5 and M6 are unable to ground the outputs. Power consumed by Dynamic latched comparator is 75.94 pW.

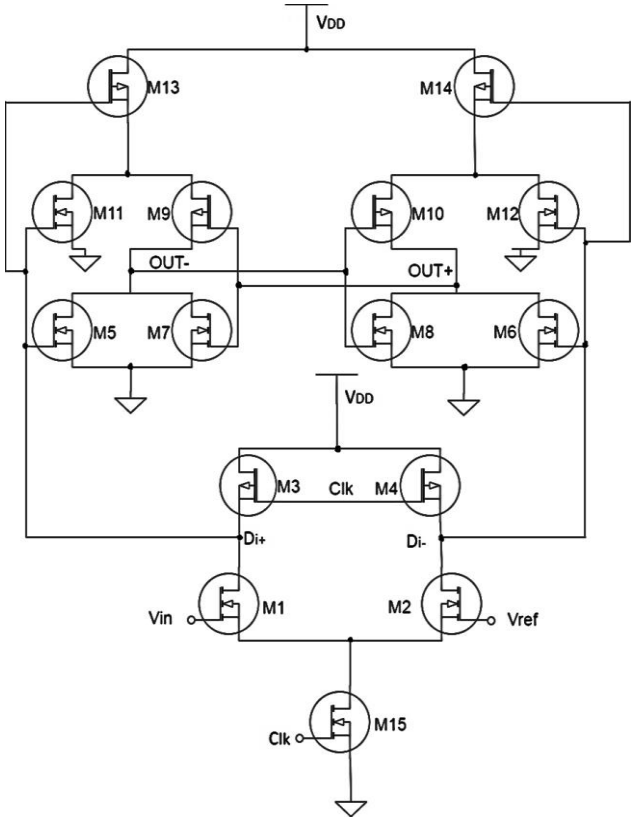

Fig. 3. Circuit Diagram of Dynamic latched comparator

VI. AND GATE

In Ramp ADC, control signal is provided using AND gate. One of AND inputs is the comparator output and another is a clock. The digital counter value increases depending on the AND gate output. Fig. 4 shows the AND Gate schematic.

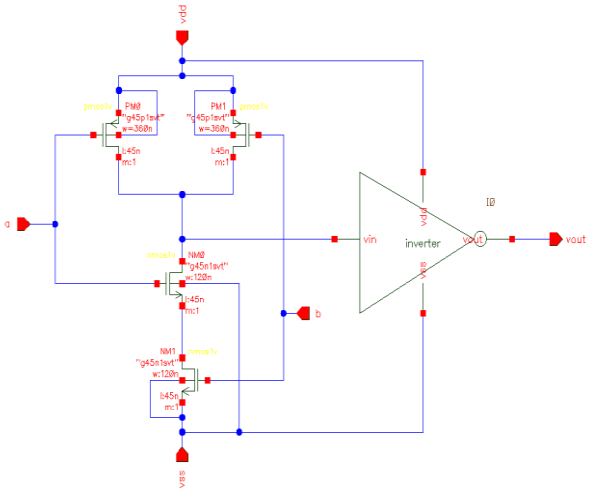

Fig. 4. Schematic of AND gate

VII. Digital Counter

Two types, namely asynchronous counter and synchronous counter, are available. Asynchronous counters are having large propagation. But synchronous counters are more reliable and they can operate at high speed because the same clock is used for all flip-flops, which ensures that every output is changed at the same time. There is therefore more use of synchronous counters. Design of the counters should have high reliability and low power consumption [6]. Hence synchronous counters are used.

Digital counter plays major role in Ramp ADC. When output of the AND gate is applied to digital counter, the digital counter value increases until it becomes equal to sampled input value. The obtained digital output is applied to DAC. The 8-bit digital counter is designed by using TFF [6]. The schematic diagram of digital counter is shown in Fig. 5.

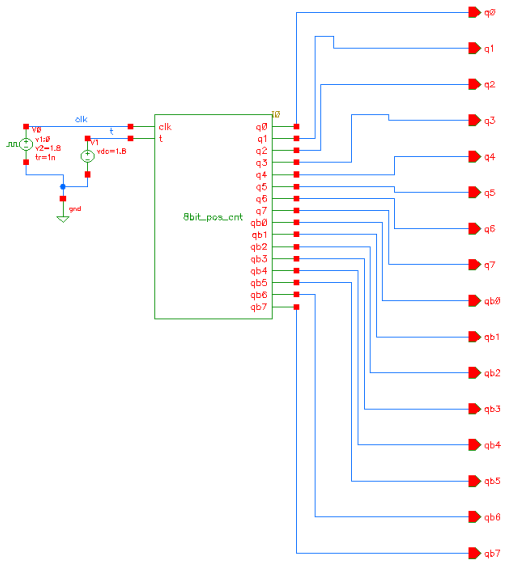

Fig. 5. Schematic of digital counter

VIII. Digital to Analog Converter (DAC)

DAC types are different [8]. Binary weighted and R-2R ladder structure is one of the easiest structures [12]. These structures of the DAC transform digital input into analog output. R-2R ladder type DAC is superior than Binary weighted resistor DAC [12]. Because the resistance changes depending on the binary bit in the Binary weighted resistor DAC. As the number of bits increases, therefore, the resistance will increase causing the effect of loading [11]. Besides that, dissipation of power and non-linearity will also increase. DAC is widely used with capacitor arrays [8]. Compared to conventional R-2R voltage driven techniques, capacitor arrays are easier to manufacture with fewer errors of mismatch [9]. It saves more power based on techniques of charge-redistribution [8]. It is noted that Charge redistribution DAC has a low power consumption of 1.315 µW compared to other DAC types.

Fig 6 shows 8-bit Charge redistribution DAC. It consists of capacitors and switches. The circuit has two modes of operation. One is the reset mode and other is the conversion mode. In reset mode, the bottom plate of the capacitors gets discharge since all the switches are connected to ground. In conversion mode, the switch connection changes from ground to VREF [7], depending on the digital code.

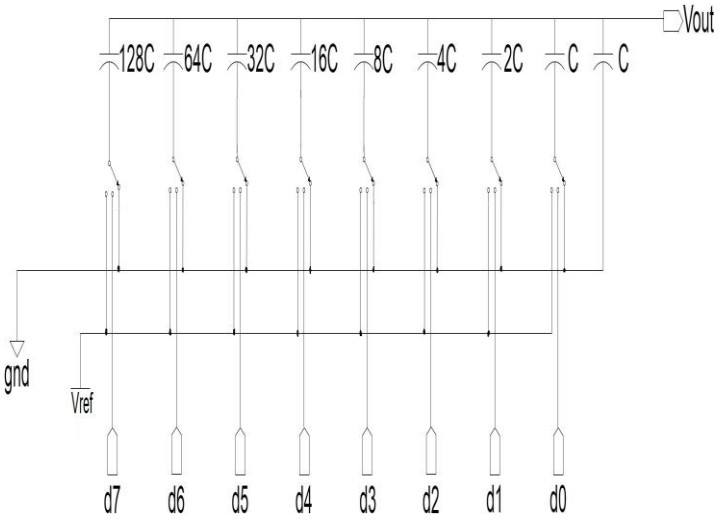

Fig. 6. Schematic of 8-bit charge redistribution DAC

IX. Result

Fig. 7. shows the output of comparator which is simulated in Cadence virtuoso tool with 45 nm technology. Likewise Fig. 8 and Fig. 9 shows the output of AND gate and digital counter respectively.

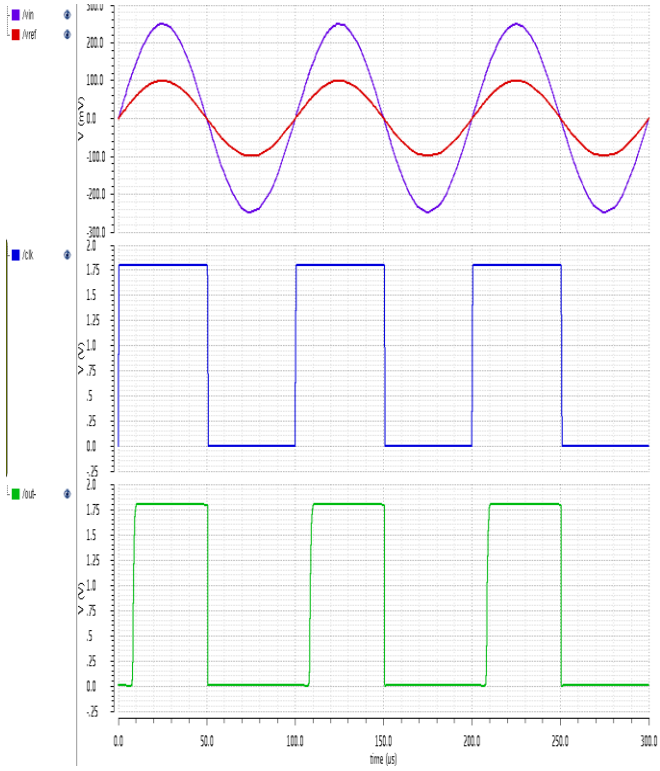

Fig. 7. Output of Dynamic Latched comparator

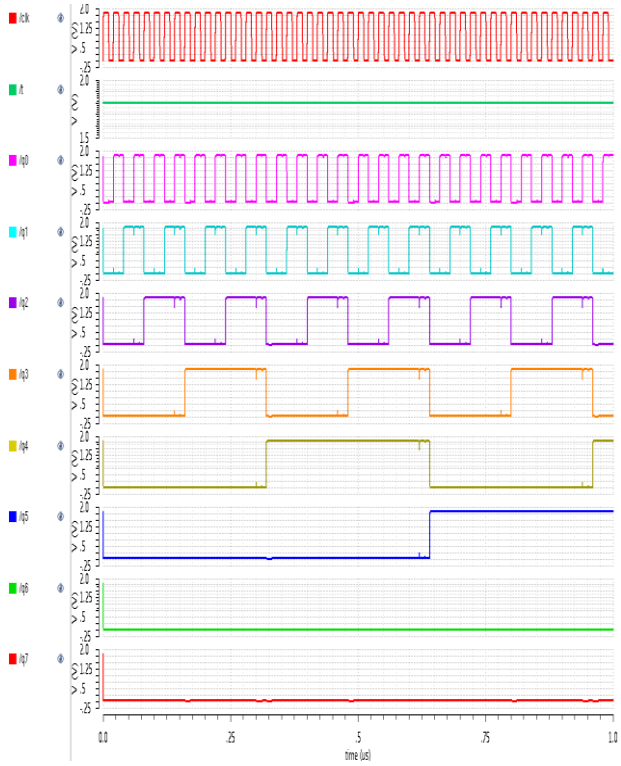

Fig. 9. Output of digital counter

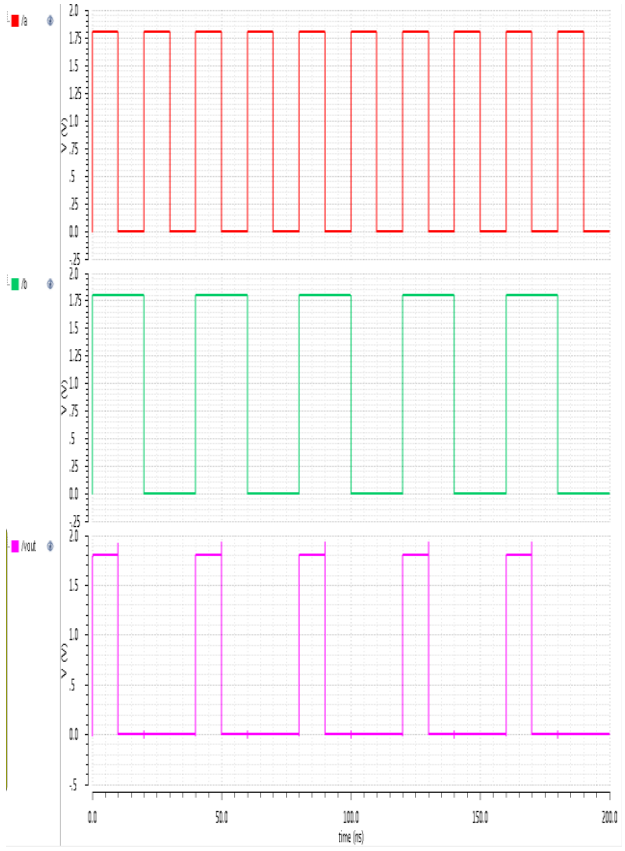

Fig. 8. Output of AND gate

Output of the 8-bit charge redistribution DAC is shown in Fig. 10. It is observed that the digital value ranging from 0 to 255 are converted into analog voltage of 0 to 1.793V.

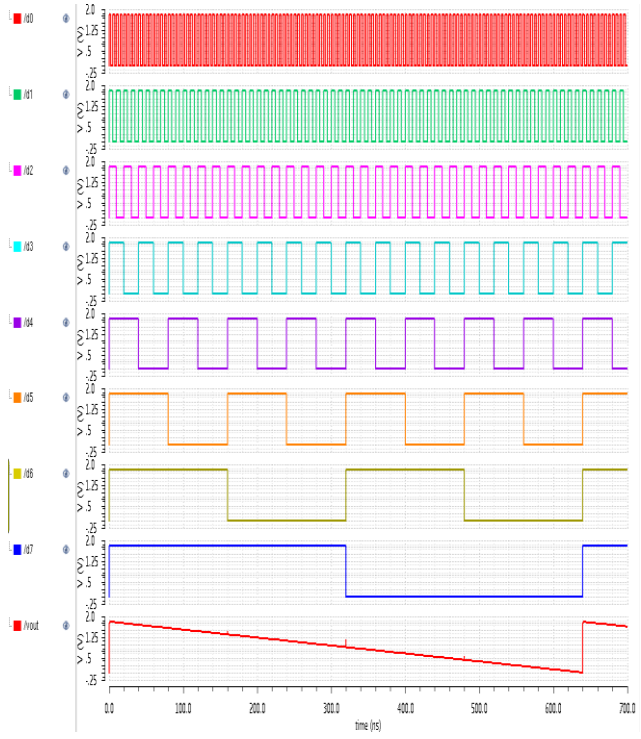

Fig. 10. Output of 8-bit charge redistribution DAC

Transient response of 8-bit Ramp ADC is shown in Fig. 11. Output of the DAC is compared with input voltage. If the comparator output is high, the clock signal to the counter will be provided.Therefore counter value increases, that increased value is again fedback to the DAC. DAC will produce the digital output.

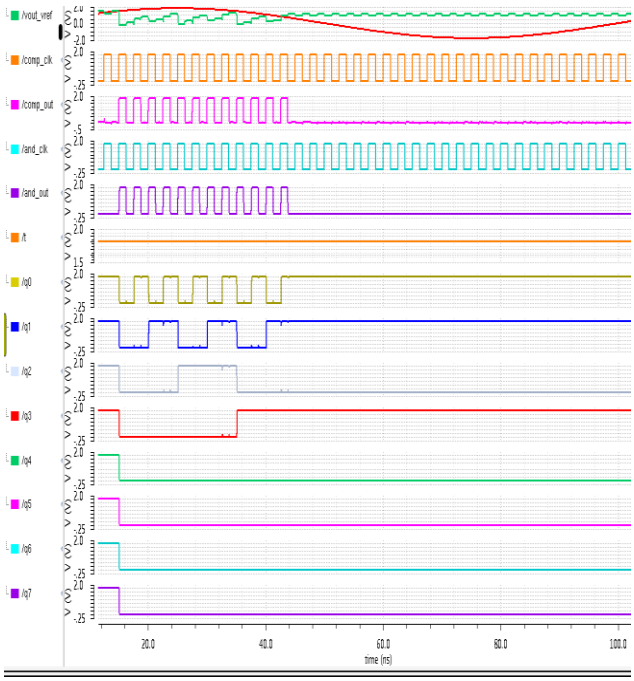

Fig. 11. Output of 8-bit Ramp ADC

The power consumed by 8-bit Ramp ADC is shown in Fig. 12. It is observed that 8-bit Ramp ADC consumes power of 3.247 mW.

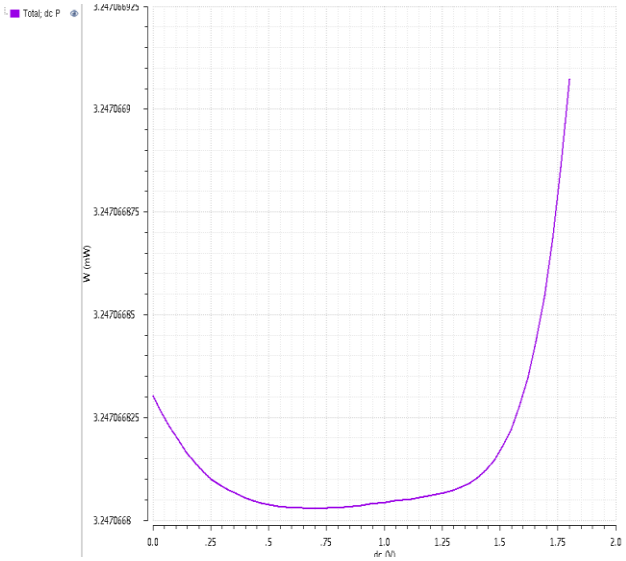

Fig. 12. Power plot of 8-bit Ramp ADC

X. CONCLUSION

The implementation of dynamic latched comparator, AND gate, Digital counter and DAC for Ramp ADC are designed using 45 nm technology and power analysis is made. The power consumed by the 8-bit Ramp ADC is 3.247 mW.

REFERENCES

[1] S. Bashir, S. Ali, S. Ahmed, and V. Kakkar, “Analog-to-digital converters: A comparative study and performance analysis,” Proceeding - IEEE Int. Conf. Comput. Commun. Autom. ICCCA 2016, pp. 999–1004, 2017.

[2] D. Prashanth and H. Lee, “A Sampling Clock Skew Correction Technique for Time-Interleaved SAR ADCs,” Proc. 26th Ed. Gt. Lakes Symp. VLSI - GLSVLSI ’16, pp. 129–132, 2016.

[3] P. M. Figueiredo and J. C. Vital, “Kickback Noise Reduction Techniques for CMOS Latched Comparators,” IEEE Trans. Circuits Syst. II Express Briefs, vol. 53, no. 7, pp. 541–545, 2006.

[4] K. M. Abozeid, M. M. Aboudina, and A. H. Khalil, “Different configurations for dynamic latched comparators used in ultra low power Analog to Digital converters,” ICET 2014 - 2nd Int. Conf. Eng. Technol., 2015.

[5] Yan Huang, Horst Schleifer and Dirk Killat,"Design and Analysis of Novel Dynamic Latched Comparator with Reduced Kickback Noise for High-speed ADCs", Proceeding - Conference on circuit Theory and Design (ECCTD) 2013.

[6] Raghava Katreepalli and Themistoklis Haniotakis,"Energy-Efficient Synchronous Counter Design with Minimum Hardware Overhead", Proceeding - International Conference on Communication and Signal Processing, 2017.

[7] Babita Diana K and D. lackuline Moni, “An Ultra Low Power 8 bit SAR ADC suitable for Wireless Medical Applications”, International Conference on Communication and Signal Processing,978-1-4799-3358-7114/$31.00 ©2014 IEEE, April 3-5, 2014.

[8] Savitha M and R. Venkat Siva Reddy, “14 -bit Low Power Successive Approximation ADC using Two Step Split Capacitive array DAC with multiplexer switching”, Second International Conference on Advances in Electronics, Computers and Communications (ICAECC), IEEE, 2018.

[9] Shinwoong Park and Sanjay Raman, “Analysis and Optimization of Multisection Capacitive DACs for Mixed-Signal Processing”, IEEE Transactions on Very Large Scale Integration (VLSI) systems, 1063-8210 © IEEE, 2018.

[10] Nikhil A. Bobade, Dr. Mahendra A. Gaikwad, Prof. Jayshri D. Dhande, “Design of Successive Approximation Analog to Digital Converter with Modified DAC”,International Journal of Engineering Research & Technology (IJERT), ISSN: 2278-0181, Vol. 3 Issue 7, July - 2014.

[11] Vijay Prathap Singh, Gaurav Kumar Sharma and Aasheesh Shukla, “Power efficient SAR ADC designed in 90nm CMOS technology”, Proceeding - 2nd International Conference on Telecommunication and networks (TEL-NET) 2017.

[12] Sarang Kazeminia, Yashar Hesamiafshar, Khayrollah Hadidi and Abdollah Khoei, “On Matching Properties of R-2R Ladders in High Performance Digital-to-Analog Converters”, Proceedings of ICEE 2010, 978-1-4244-6760-0/10/$26.00 ©2010.

[13] Vaijayanthi, M., Vivek, K., “Analysis of dynamic comparators in ultra-low spply voltages for high speed ADCs”, Proceeding - IEEE Sponsored 2nd international conference on Innovations in information,Embedded and communcation systems (ICIIECS)2015.

Proceedings of the Fourth International Conference on Communication and Electronics Systems (ICCES 2019)
IEEE Conference Record # 45898; IEEE Xplore ISBN: 978-1-7281-1261-9

Intrusion Detection System Based RPL Attack Detection Techniques and Countermeasures in IoT: A Comparison

P.S.Nandhini [1],[2]
Department of Computer Science and Engineering,
Kongu Engineering College [1],
Perundurai, India
nandhinisv1@gmail.com

B.M.Mehtre [2]
Centre of Excellence in Cyber Security (COECS),
IDRBT [2], Established by the RBI,
Hyderabad, India
bmmehtre@idrbt.ac.in

***Abstract*—Routing Protocol for Low power and Lossy Network (RPL) is a light weight routing protocol designed for LLN (Low Power Lossy Networks). It is a source routing protocol. Due to constrained nature of resources in LLN, RPL is exposed to various attacks such as blackhole attack, wormhole attack, rank attack, version attack, etc. IDS (Intrusion Detection System) is one of the countermeasures for detection and prevention of attacks for RPL based IoT. Traditional IDS techniques are not suitable for LLN due to certain characteristics like different protocol stack, standards and constrained resources. In this paper, we have presented various IDS research contribution for RPL based routing attacks. We have also classified the proposed IDS in the literature, according to the detection techniques. Therefore, this comparison will be an eye-opening stuff for future research in mitigating routing attacks for RPL based IoT.**

Key Words - IoT, RPL, IDS, attacks, countermeasures, security, attacks, blackhole, wormhole, knowledge driven approach

I. INTRODUCTION:

IoT is a collection of heterogeneous things or devices that are connected to the Internet. The devices will have a uniquely identity in the network. The devices can be RFID tags, sensors, actuators, smart phones and wide variety of smart devices. The emergence of IoT has led to the connection of people, devices, services and many objects [1]. It is deployed in wide range of applications from smart city to healthcare and intelligent transport systems. There are other domains in which IoT plays a remarkable role to improve the quality of our lives. The IoT has transformed the objects or things from traditional to smart device with the help of Cloud Computing, Big Data, Communication Protocol, WSN and the Embedded Systems.[2]

IoT=Sensing + Communication + Storage + Analysis

The devices in IoT are heterogeneous and so they use various standards. There are many protocols used for communication. 6LoWPAN is one among them. It is a simple low-cost communication protocol. It provides communication in applications where the resources are constrained. The throughput of LLN is not much considered [3]. LoWPAN include devices that work together to connect the physical environment to real time applications. Example of LoWPAN is Wireless Sensors. The main characteristics of LoWPANs are low bandwidth and data rate, star and mesh topology, small sized packets. The architecture of 6LoWPAN is depicted in Fig.1

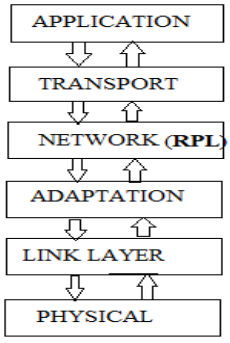

Fig.1. 6LoWPAN Architecture

The major difference in the architecture of 6LoWPAN is the incorporation of a new layer. The new layer is called Adaptation Layer. The main functions of the adaptation layer [4] are: (i) Compression and Decompression of network (IPv6) and transport (UDP) header (ii) fragmentation and reassembly of packets and (iii) routing of packets. The routing can be taken care by Network Layer and Adaptation layer. The routing protocols used in traditional network and WSN are not suitable for IoT. The routing challenges of IoT are: heterogeneous devices, diverse networking, deployment of nodes, intermittent connectivity between nodes, multi-hop communication, fault tolerance, security and context awareness [5]. There

are many standards for IoT. RPL is one of the IoT standards.

The remaining of this paper is organized as follows: Section- II presents the overview of the RPL protocol. Section-III rigorously discusses the classification of recent countermeasures for RPL based routing attacks in IoT. In section-IV, we have provided the concerns, challenges and opportunities related to RPL. The comparison is concluded in section-V.

II. RPL OVERVIEW:

RPLis a routing protocol designed for resource constrained networks. It is a Distance Vector routing protocol. RPL protocol has to find links and select nodes efficiently. It is also a source routing protocol. It allows the sender of a packet to specify the complete or partial route of a packet. The routes of the RPL are enhanced for traffic in both the directions. The root nodes will be a sink node for the topology. Finally, RPL constructs the DAG topology. The DAG consists of one or many DODAGs. There will be one DODAG for every sink node. RPL uses four values for maintaining and identifying a topology. They are RPLInstanceID, DODAGVersionNumber, DODAGID and Rank. RPL protocol and its operation is elaborated in [28].

A. Identifiers of RPL:

- RPLInstanceID: It is used to identify the DODAGs. LLN consists of numerous RPLInstanceIDs. Each of it defines a group of DODAGs that are enhanced for different Objective Functions (OF).
- DODAGID: It uniquely identifies the DODAG in the network. One instance of RPL can have many DODAGs but each have unique ID. (RPLInstanceID, DODAGID) represents a single DODAG uniquely.
- DODAGVersionNumber: A DODAG is rebuild from the root occasionally. The reconstructed DODAG have a version number incremented from the previous one.
- Rank: It determines the location of individual node with respect to the root of DODAG. Fig.2. depicts the DODAG that consists of nodes with various rank.

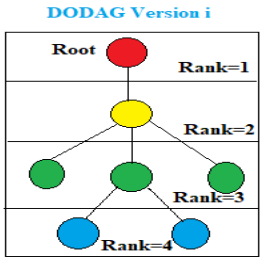

Fig.2. RPL Rank

B. Objective Function (OF):

The objective function [6] defines (i) How the metrics of routing, objectives of optimization and related functions are used in the computation of Rank (ii) Selection of parents during the formation of (iii) Translation of one or more metrics into Rank. The various objective Functions are OF0, MRHOF [7], ETXOF [8], LBOF, TAOF

C. RPL securtiy features:

According to the specification of RPL, the implementation of security features is optional. It provides confidentiality and integrity of messages. RPL can use the link layer security mechanism and in their absences RPL can use its security modes: (i) Unsecured mode: In this mode, RPL message is sent using link layer security to meet the security requirements of applications. (ii)Pre-Installed mode: In this mode, if a node wishes to join an instance of RPL then it should have a pre-installed key. Using that it can generate and process secured message of RPL. (iii)Authenticated mode: As in the pre-installed mode, the nodes will have pre-installed keys in this mode also. Node can use the pre-installed keys to join as leaf in the instance of RPL. If it wishes to join as a router in the RPL instance, it should obtain a key from the authority of authentication. The process of authentication and obtaining keys are based on the implementation. The nodes in the RPL will send CC (Consistency check) message for protecting replay attacks.

III. CLASSIFICATION OF COUNTERMEASURES FOR RPL BASED ROUTING ATTACKS:

The resource constrained nature of nodes and links in the RPL has led to various attacks. IDS is one of the countermeasures for RPL based attacks. Various IDS based countermeasures, knowledge driven technologies approaches are discussed. Fig.3. depicts the classification of IDS. We have reviewed in depth about the detection technique-based IDS for attacks in RPL. The placement strategy of IDS is discussed in [27].

A. NETWORK BASED APPROACH:

The network-based IDS is used for monitoring the traffic in the network. It is also used for analyzing the traffic to protect the system from threats which are based on the networks. NIDS will read all the packets inbound to the network and searches for the pattern that are suspicious. If the threats are detected or discovered, based on the severity, the system can take action such as the IP of the source can be barred from accessing the network, the administrator can be notified, etc.,

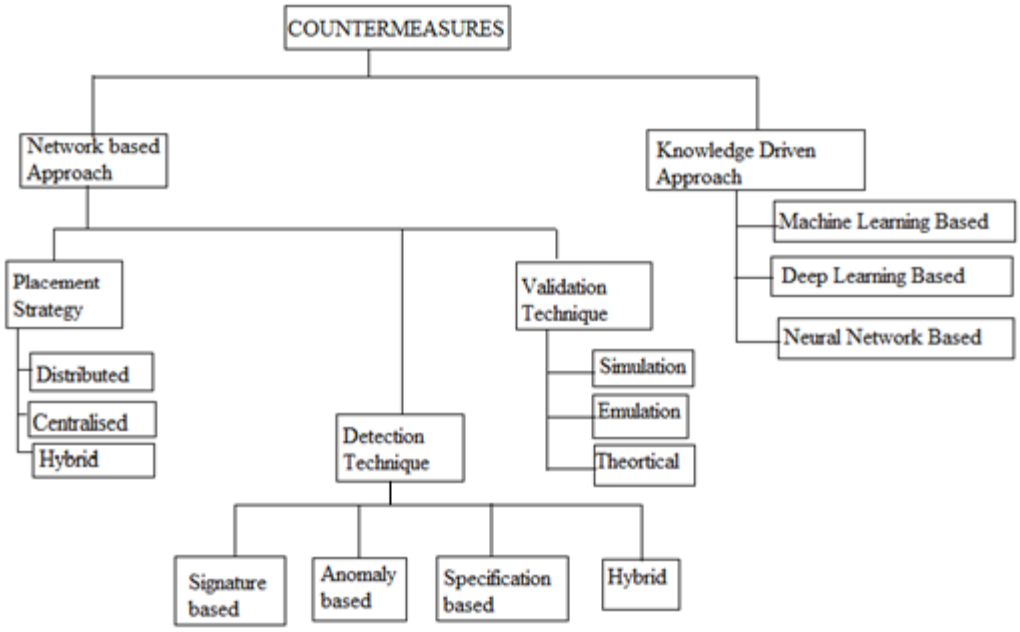

Fig.3. Classification of IDS for RPL Based attacks

1) SIGNATURE BASED DETECTION: In signature-based approach, the signature or pattern of the attack is stored in the IDS internal database. If any network or system activity maps with the stored pattern then the alert will be generated. These IDS are effective in detecting the known threats.

a) Liu [9] et al proposed an IDS based on Immunity Theory. The data in the IoT network is filtered using the immune mechanism. The IoT data is mapped to the elements of the immune environment. The concept of Artificial Immune System (AIS) and the proposed IDS is based on the artificial immunity. The detection element in the proposed IDS evolve dynamically for the purpose of self-learning and self-adaptation.

b) As a large number of devices are connected to the Internet, providing security is a critical challenge. It is difficult to adapt traditional security measures to the nodes since they are constrained in resources, processing power, etc., Oh et al [10] proposed an IDS which operates on the resource constraints. It is a light weight security system which could operate on resource constrained devices. They proposed two techniques: auxiliary shifting and early detection to reduce the number of matchings performed on the constrained systems. The proposed light-weight system also achieved a good performance for a large number of patterns.

c) Pongle [23] et al proposed an Intrusion detection system for real time. It is used for detection of wormhole and the attacker who performs the attack. It uses the location and neighbor information for the detection of worm hole attack. Based on the strength of the received signal, the attacker is identified. This system consumes only fixed number of packets of UDP. So, it is beneficial for resource constrained environment. The centralized module is performing heavy processing and the light weight module will be running on all the sensor nodes. Since it is light weight, it saves energy on the sensor nodes. Based on the placement strategy, it is hybrid placement of IDS. Since the location information of nodes are added, the system is more efficient with less overhead and high detection rate. The memory consumption is also less. The proposed method yields 94% of detection rate.

2) ANAMOLY BASED DETECTION: In anomaly-based IDS, at any instance the activity of a system will be compared with the normal behavior profile. If there is any deviation from the normal behavior i.e., if it exceeds the threshold value then the alert is generated. It is also efficient detect new kinds of attacks. The attacks related to wastage of resources can also be detected using this approach.

a) Gupta et al [12] proposed an IDS based on the computational Intelligence. The malicious activities and intrusion can be detected in less duration. The proposed IDS is a three-tier

architecture. It is Anomaly based IDS. It is suited for both NIDs and HIDS. The majority flaws in the security is also presented in the paper.

b) Cervantes et al [13] proposed Intrusion detection of SiNkhole attacks on 6LoWPAN for InterneT of Things (INTI). It is used for detection of sinkhole attack in the routing services of IoT. The proposed system combines trust, reputation strategies, watch dogs for analyzing the device behavior of the devices. Based on the behavior of the devices the nodes can be classified as attackers or not. The mobility of the node and self-repair mechanism of network are taken into consideration in the proposed INTI intrusion detection system. The effectiveness of the proposed system is measured in terms of detection rate, false positive and false negative rate. The system provided less false positive and negative rate. Since the placement of IDS changes over the time, it consumes more resources. The author in this paper does not discuss the impact of proposed solutions for low power devices.

3) SPECIFICATION BASED APPROACH: In this scheme, specification represents the set of rules or the thresholds which are used to define the behavior of the network components. The network components can be routing tables, protocols and nodes. If there is any deviation from the defined specification, then the alert is generated. This is also similar to anomaly-based approach i.e., identifying the deviation from the normal behavior. But the difference between the two is that in this the specifications are defined manually and there is no need for training phase. Since the specifications are defined manually, it provides lower false positive rate in comparison with the anomaly detection.

a) Le et al [14] proposed a Specification Based IDS for detecting topology attack (local repair and rank attack) in RPL. In the proposed system, the monitoring mechanism is described based on the finite state machine of RPL. The system can detect the threats in the routing operation. The overhead of the system is reasonable. The normal operation of the network is taken as an abstract(specification). This is done manually. If there is any malicious behavior, then that will break the specification. From that it is understood that attack is performed on the routing operation.

b) Surendar et al [15] proposed a detection technique based on the specifications. The specifications are defined considering the constraints of resources. The limitations of INTI and SVELTE are improved. The consumption of energy by the proposed system is also low. It provides quick response against the detected attack. In the proposed system, the nodes in the network will be clustered and a leader will be elected based on the probability. [16] The nodes in the cluster will forward their rank value to the cluster head. Dempster-shaffer theory based on evidence is used to combine evidence from different nodes. The belief degree of the node is derived from it. The cluster head will detect the attack and notify it to the root of DODAG. Once the attacker is detected, the reconstruction of DODAG will be done by the root node without including the attacker node. The proposed system is evaluated by the NS2 simulator.

4) HYBRID APPROACHES: This approach takes the advantage of the scheme and minimize the influence of the drawbacks of the above schemes.

a) The above proposed Intrusion Detection Systems can detect only specific attacks but not the attacks if they are combined. Napiah [17] et al proposed CHA-IDS (Compression Header Analyser) for the detection of combined attacks in 6LoWPAN. The proposed system is a multi-agent system that captures the raw data, manages it and perform analysis based on it. Based on the analysis, the system will take action. The features are selected based on correlation. It also utilizes Best First and Greedy Stepwise to identify the significant features. Only the significant features are identified for detection of attack. Then the features are tested using 6 machine learning algorithms for classifying malicious node and the good ones. The six machine learning algorithms are (i) MLP (ii) J48 (iii)SVM (iv) Navie Bayes (v) Logistic and (vi) Random forest. Among these algorithm J48 shows the better performance in detecting the attacks. So, J48 is used in CHA-IDS which provided 99% of true positive rate. The rule or the signature will be created by the ML algorithm and it is placed at 6BR. It is updated when new signatures are available. It is a hybrid IDS (Anomaly and signature based). The proposed system identifies the following attacks: (i) Flood attack (ii) Sinkhole attack (iii) Wormhole attack when they are combined also.

b) Midi et al [18] proposed Kalis: Knowledge Driven Intrusion Detection System for detecting attacks in real time scenarios of IoT. It is designed for less constrained nodes. The system does not require any changes to the existing IoT system. Based on the IDS detection scheme, the proposed architecture is a hybrid approach (signature and anomaly based) and based on the placement strategy of IDS also it is a hybrid

approach (centralized and distributed). The system is able to detect attacks in various IoT protocols. The evaluation result shows that it is effective in detecting many attacks such as routing attacks, DoS, traditional attacks, etc.,

c) Raza [19] et al proposed an IDS for the detection of various routing attacks (sinkhole, spoofing and selective forwarding attack). The IDS is a hybrid one since it is based on both Anomaly and Signature. It is a light weight effective IDs for constrained nodes. The IDS is also provided with mini firewall. It filters the traffic that are from malicious node before they reach the combined nodes. The IDS is placed in 6BR and all the constrained node. The advantages of the proposed IDS are:(i) The constrains of resources in 6LoWPAN network is taken into consideration. (ii) There is an integrated mini-firewall for the filtering the traffic (iii) It is flexible and it can also be used for the detection of other attacks. The limitation is that the proposed IDS will be affected by Denial of Service (DoS) attack.

B. KNOWLEDGE DRIVEN APPROACH:

a) Geethapriya et al [20] proposed Deep Learning [DL] based IDS for IoT network. The intelligent IDS is tailored into the IoT network. DL is used for detection of malicious traffic. The proposed system provides security as a service. The IDS is implemented in a stand-alone device which is easy to integrate into IoT network. There are three phases in the proposed IDS: (i) Connection phase (ii) Anomaly phase (iii) Mitigation Phase. The DNN (Deep Neural Network) is implemented using Keras. Through this paper, the author has concluded that the usage of DL algorithms for detection of anomaly (blackhole attack, sinkhole attack, DDoS attack, wormhole attack) in IoT environment is feasible and practical. The average precision rate is 95% and the recall rate is 97% for different scenarios of attack.

b) Verma [21] et al proposed NIDS for IoT which are based on RPL. NIDS will be acting as a first line of defense for the networks. There are no reliable datasets for IoT. So, IDS will be suffering in the advancement of accurate performance. RPL-NIDDIS 17 dataset is a synthetic dataset created by NetSim Simulation Platform. The authors have used this dataset for network IDS. They have also discussed 22 attributes that may compromise the IoT network. Correlation analysis is used for the determination of relationship in the future. The dataset developed is evaluated using Machine Learning techniques.

c) Kfoury [22] et al proposed a Self-Organizing Map (SOM) neural network for clustering routing attacks that are inherited from WSN. It is used for notifying the administrator in the early stage itself. It reduces the power consumption of the node and the interruption in the network. SOM is a kind of neural network. It uses unsupervised learning for the conversion of high dimensional space into low dimensional space. This conversion is done for better visualization on a map. In this method, each and every node calculates its distance to the input vector. The Best matching unit holds the node that are closest to the input. Wireshark is used for capturing the traffic and the power tracer module of Contiki is used to get the power consumption of each node during the attacks. Thus, the SOM classified the sample in input training into: sink hole attack, Version attack, Hello Flood attack and clean data. TABLE I represents the summary of the review IDS along with its limitation and challenges.

IV. CONCERNS, CHALLENGES & OPPORTUNITIES:

From the review, it is understood that vast number of researches has been conducted for providing detection and prevention of attacks in RPL. The following issues are discussed below:

- The implementation of security features of RPL remains unexplored.
- There are large numbers of options available in RPL. Most of them remain unused.
- As the number of devices in IoT increases daily, then new security and routing features are also need to be addressed.
- Large number of tools and testbeds should be investigated for evaluation.
- From the review, it is clear that IDS has been serving as one of the countermeasures for the attacks in RPL. The nodes in RPL are resource constrained but IDS need more computation. So, the expandability of IDS for RPL needs to be considered.
- More researches were conducted in simulators especially Cooja. Hence, large number of tools (hardware and software) and testbeds should be investigated for evaluation.

TABLE I. COMPARISON OF IDS DETECTION TECHNIQUES FOR RPL BASED IOT ATTACKS:

References	Intrusion Detection Technique	Threats addressed	Advantages	Limitations	Countermeasure
Cervantes et al [13]	Hybrid (Reputation and trust strategies)	Routing attack	* Node mobility is taken into consideration * The self -repairing mechanism is also taken into account	*More consumption of resources since IDS changes over time	Self repairing mechanism
Lee et al [24]	Anomaly	DoS	*Light weight Intrusion detection system *Detection is accurate	*Only energy of node is considered *Other parameters can be included	-
Wallgren et al [25]	-	Routing attack	*Resource constraints is considered *Less energy consumption in other nodes	*Overhead is high in 6BR *Detection accuracy is less	-
Bhosale et al [26]	Anomaly	Wormhole attack	*Detection rate is high *Different wormhole attacks are considered	*Energy consumption is high *Extended to other attacks also	Real time IDS
Pongle et al [23]	Anomaly	Routing attack	*Packet overhead is low *Resource consumption is low	* Only one type of attack is detected *False positive rate is high	Real time IDS based on Received Signal Strength
Liu et al [9]	Signature	-	*High adaptability *Detection rate is high	*Efficiency decreases with high volume data	Immunity Thoery
Oh et al [10]	Signature	Multiple attacks	* Highly Scalable * Less usage of memory	* Not suitable for real time * Less detection rate	Auxilary shifting & early detection
Gupta et al [12]	Anomaly	-	*Suitable for both NIDS and HIDS *Majority flaws in security is addressed	*Energy consumption is more	Computational Intelligence
Le et al [14]	Specification	None	*Less computation and storage overhead *Energy efficiency is high	*More overhead	Finite State Machine
Surendar et al [15]	Hybrid (Anomaly and signature)	Sinkhole attack	*Constraints of resources are considered *Less drop in the packet *Immediate response against detected attack	*Unknown attacks can't be detected * It is not suitable for real time	InDReS
Napiah et al [17]	Hybrid	Combined attacks	* Detects both individual and combined attack * High detection rate	*Can be extended to detect more attacks	Compression Header analyser
Midi et al [18]	Hybrid (Anomaly and signature)	Routing, DoS attack	*Less usage of CPU and RAM * IDS is Self-adapting * Different IoT protocols are taken into account	* It is not suitable for constrained nodes. * Computational overhead is high	Knowledge driven Technique
Raza [19]	Hybrid	Routing attack	*Constraints of resources are considered * Flexible	*SVELTE can be affected by DoS attack * Less detection rate	Light weight IDS
Geethapriya et al [20]	Deep Learning	Multiple attacks	*Average precision and recall rate are high for different scenarios *Energy efficient	*Large processing power is required *Requires more dataset	Deep Neural Networks
Verma et al [21]	Machine Learning	Modern Routing attack	*False positive rate *Accuracy is high	*More time consumption *Requires more dataset to train	Correlation analysis
Kfoury et al [22]	Neural network	Multiple attacks	*Attacker is detected at the early stage *Power consumption is less *Less interruption of network	*Computationally intensive	Self Organising Map

V. CONCLUSION:

Through this review paper, we have rigorously reviewed recent IDS based countermeasures for the detection and prevention of RPL based attacks. Since, the nodes in LLN are resource constrained, they are easily prone to attacks. The various attacks involved in RPL were discussed. Many investigations should be done to make IDS suitable for resource constrained nodes. The security features that are available in RPL should be explored and implemented for detection of attackers. Thus, this comparison will be an eye-opening stuff for the researches, who conduct further investigation on attacks and countermeasures related to RPL.

REFERENCES:

[1] Conti, Mauro, et al. "Internet of Things security and forensics: Challenges and opportunities." (2018): 544-546.

[2] Al-Fuqaha, Ala, et al. "Internet of things: A survey on enabling technologies, protocols, and applications." IEEE communications surveys & tutorials 17.4 (2015): 2347-2376.

[3] Pongle, Pavan, and Gurunath Chavan. "A survey: Attacks on RPL and 6LoWPAN in IoT." 2015 International Conference on Pervasive Computing (ICPC). IEEE, 2015.

[4] Garg, Ruchi, and Sanjay Sharma. "A study on need of adaptation layer in 6LoWPAN protocol stack." International Journal of Wireless and Microwave Technologies (IJWMT) 7.3 (2017): 49-57.

[5] Dhumane, Amol, and Rajesh Prasad. "Routing challenges in internet of things." CSI Communications (2015): 19-20.

[6] Deshmukh-Bhosale, Snehal, and Santosh S. Sonavane. "A Real-Time Intrusion Detection System for Wormhole Attack in the RPL based Internet of Things." Procedia Manufacturing 32 (2019): 840-847.

[7] Verma, Abhishek, and Virender Ranga. "Evaluation of Network Intrusion Detection Systems for RPL Based 6LoWPAN Networks in IoT." Wireless Personal Communications (2019): 1-24

[8] Kfoury, Elie, et al. "A Self Organizing Map Intrusion Detection System for RPL Protocol Attacks." International Journal of Interdisciplinary Telecommunications and Networking (IJITN) 11.1 (2019): 30-43.

[9] Liu, Caiming, et al. "Research on immunity-based intrusion detection technology for the internet of things." 2011 Seventh International Conference on Natural Computation. Vol. 1. IEEE, 2011.

[10] Oh, Doohwan, Deokho Kim, and Won Ro. "A malicious pattern detection engine for embedded security systems in the Internet of Things." Sensors 14.12 (2014): 24188-24211

[11] Anthi, Eirini, Lowri Williams, and Pete Burnap. "Pulse: An adaptive intrusion detection for the Internet of Things." (2018): 35-4.

[12] Gupta, Abhishek, et al. "Computational intelligence-based intrusion detection systems for wireless communication and pervasive computing networks." 2013 IEEE International Conference on Computational Intelligence and Computing Research. IEEE, 2013.

[13] Cervantes, Christian, et al. "Detection of sinkhole attacks for supporting secure routing on 6LoWPAN for Internet of Things." 2015 IFIP/IEEE International Symposium on Integrated Network Management (IM). IEEE, 2015.

[14] Le, Anhtuan, et al. "Specification-based IDS for securing RPL from topology attacks." 2011 IFIP Wireless Days (WD). IEEE, 2011.

[15] Surendar, M., and A. Umamakeswari. "Indres: An intrusion detection and response system for internet of things with 6lowpan." 2016 International Conference on Wireless Communications, Signal Processing and Networking (WiSPNET). IEEE, 2016.

[16] Surendar, M., and A. Umamakeswari. "InDReS: An intrusion detection and response system for internet of things with 6LoWPAN In: 2016 International

[17] Napiah, Mohamad Nazrin, et al. "Compression header analyzer intrusion detection system (CHA-IDS) for 6LoWPAN communication protocol." IEEE Access 6 (2018): 16623-16638.

[18] Midi, Daniele, et al. "Kalis—A system for knowledge-driven adaptable intrusion detection for the Internet of Things." 2017 IEEE 37th International Conference on Distributed Computing Systems (ICDCS). IEEE, 2017

[19] Raza, Shahid, Linus Wallgren, and Thiemo Voigt. "SVELTE: Real-time intrusion detection in the Internet of Things." Ad hoc networks 11.8 (2013): 2661-2674

[20] Thamilarasu, Geethapriya, and Shiven Chawla. "Towards Deep-Learning-Driven Intrusion Detection for the Internet of Things." Sensors 19.9 (2019): 1977.

[21] Verma, Abhishek, and Virender Ranga. "Evaluation of Network Intrusion Detection Systems for RPL Based 6LoWPAN Networks in IoT." Wireless Personal Communications (2019): 1-24

[22] Kfoury, Elie, et al. "A Self Organizing Map Intrusion Detection System for RPL Protocol Attacks." International Journal of Interdisciplinary Telecommunications and Networking (IJITN) 11.1 (2019): 30-43.

[23] Pongle, Pavan, and Gurunath Chavan. "Real time intrusion and wormhole attack detection in internet of things." International Journal of Computer Applications 121.9 (2015).

[24] Lee, Tsung-Han, et al. "A lightweight intrusion detection scheme based on energy consumption analysis in 6LowPAN." Advanced Technologies, Embedded and Multimedia for Human-centric Computing. Springer, Dordrecht, 2014. 1205-1213.

[25] Wallgren, Linus, Shahid Raza, and Thiemo Voigt. "Routing Attacks and Countermeasures in the RPL-based Internet of Things." International Journal of Distributed Sensor Networks 9.8 (2013): 794326.

[26] Ismail, Nurul Halimatul Asmak, Rosilah Hassan, and Khadijah WM Ghazali. "A study on protocol stack in 6lowpan model." Journal of Theoretical and Applied Information Technology 41.2 (2012): 220-229.

[27] Raoof, Ahmed, Ashraf Matrawy, and Chung-Horng Lung. "Routing Attacks and Mitigation Methods for RPL-Based Internet of Things." IEEE Communications Surveys & Tutorials (2018).

[28] Gaddour, Olfa, and Anis Koubâa. "RPL in a nutshell: A survey." Computer Networks 56.14 (2012): 3163-3178.

Proceedings of the Fourth International Conference on Communication and Electronics Systems (ICCES 2019)
IEEE Conference Record # 45898; IEEE Xplore ISBN: 978-1-7281-1261-9

Integer Wavelet Transform and Arnold Transform based image steganography with cryptanalysis

Rima V G
Department of ECE,
Sree Chitra Thirunal College of Engineering,
Thiruvananthapuram, India
vgrima47@gmail.com

Lakshmi V S
Assistant Professor
Department of ECE,
Sree Chitra Thirunal College of Engineering,
Thiruvananthapuram, India
lakshmivs23@gmail.com

***Abstract*—The rapid development on the field of communication require a secure exchange of information between the sender and the reciepient. Information hiding techniques are widely used in the field of communication such as military applications, scientific research etc. Information hiding is a general process or term which deals with embedding the message for communication in the content.Otherwise we can say that it refers to either producing the data to be hidden making the existence of secret information to be unnoticeable.This process leads to prevent unauthorized access.There are two inputs in the steganography process, one is the cover object and the other is secret object, both these inputs may be image, video, audio e.t.c. Depending upon these cover objects, it can be categorized into image steganography, video steganography, audio steganography e.t.c. In this paper both cover and secret objects are image.**

In this paper image steganography is performed with IWT (Integer Wavelet Transform).Normally the steganography process is performed with DWT (Discrete Wavelet Transform), while applying this transform there exists floating point coefficients,which leads to floating point truncation results in loss of information, to avoid this problem we choose IWT. Arnold transform is an image scrambling technique applied to the secret image to ensure security to it.

***Index Terms*—Integer Wavelet Transform, Arnold Transform, DWT**

I. Introduction

There are some basic criteria to categorize the steganography process. The steganography classification based on the cover objects are image steganography, video steganography, audio steganography and network steganography[14]. The two main process or algorithm in steganography is embedding and extracting. These embedding and extracting processes are performed on certain domains, based on these domains we can classify into six main types. They are spatial domain techniques, transform domain techniques, spread spectrum based domain techniques, masking-filtering technique and cover generation techniques[15].

The steganography processes are generally performed on spatial domain and transform domain. The most frequently used domain is spatial type, where it is easy for implementation (embedding and extracting processes), but security in this domain is less as compared to the transform domain because the unauthorized accessibility will be very high. The transform domain is very difficult for implementation but security will be very high as compared to the spatial domain.

In this paper, two main transforms are used in this steganography process. One is the integer wavelet transform (IWT) and Arnold transform. The IWT is applied to the cover object to transform it for hiding the secret object, where integer to integer or bit to bit mapping takes place. The Arnold transform is implemented to provide secrecy to the secret image , since it is an image scrambling transform.when it is applied to an image, it becomes a diffused form where it is not able to identify the image correctly. The diffused form of secret image is embedded on the sub-bands cH, cV and cD, since the sub-bands are invisible to human eye. This is the entire steganography system. The strength of proposed steganography system is analyzed by security analysis. The security analysis is performed through cryptanalysis.

II. Literature Survey

The techniques for hiding information from an unauthorized access is known as steganography, hence the nature or property of steganography is invisible to human eyes [1]. This paper put forward a secure embedding steganography algorithm that hides the secret object into the least significant bits (LSBs) of integer wavelet transformed cover image in the form of bits or bitstream. This indicates the two level decomposition on LL band, where LL band is similar to the cA band. When decomposition is performed on the image, produces or decomposes to sub-bands are LL, LH, HL and HH sub-bands, in which information on LL sub-band is homogeneous to the original one and is visible to the human eye, because it is the low frequency sub-band and remaining are high frequency sub-bands, not highly visible to the human eye [17].Due to this low frequency, LL sub-band is visible in nature,so the image available from this band appears close to the original image and the sub-bands LH, HL and HH are invisible for human eyes due to its high frequency. These sub-bands are close to cA, cH, cV and cD components or coefficients of the image, where cA is the approximation coefficient of an image and cH, cV and cD are detail coefficients of an image, they are invisible to human eyes. This paper gives idea about choosing IWT instead of DWT.

Based on [2] it was stated that encrypting for hiding an image in another gray image file using Least Significant Bit (LSB) based Steganography and Arnolds transformation algorithm based Cryptography. Here hiding process of secret image into the cover image with minimum distortion made to the cover image.

Steganography methods have many challenges such as high hiding capacity and imperceptibility [3]. Here it proposes integer wavelet transform (IWT) for increasing high hiding capacity and Optimum Pixel value Adjustment algorithm (OPA) for elevating the image quality.The lead of Steganography, over cryptography is that message do not engage attention to themselves.

In [4] steganography is the practice of masking objects like a file, message, image or video within another digital image, simply the purpose of data hiding.Here conceal the secret messages using integer wavelet transform (IWT). IWT is mainly used for signalling tehniques.

According to [5] the main application of DWT (Discrete Wavelet Transform) is image compression. The disadvantage of the DWT is that the wavelet coefficients are real numbers. In this case efficient lossless coding is not possible for linear transforms. Integer Wavelet Transform (IWT) is a fundamental modification of linear transforms, where each filter output is rounded to the nearest integers. IWT can be a unified lossy and lossless codec. The use of IWT is to reduce the memory demands of the compression algorithms as integers are used alternative to real numbers.

In [7] Cryptography and steganography are the two prime fields for information reliability. Cryptography means technique in which the information is unsystematic in a dense rubbish fashion during transference, steganography focuses on masking the existence of the information. Combining both technique gives a higher level of security in which even if the use of covert channel is revealed, the real documentation will not be opened. This paper gives attentiveness on concealing multiple secret images in a single 24-bit cover image using LSB substitution based image steganography. Each secret image is encoded before hiding in the cover image using Arnold Transform. Outputs disclose that the proposed method successfully secures the high capacity data keeping the visual quality of transmitted image satisfactory.

In [8] copyrights protection of plain texts is still a remaining issue that must be improved in order to provide authentication of proprietorship and obtain the desired validity. During the last decade, digital watermarking and steganography techniques have been used as option to block tampering, distortion, and media forgery and also to protect both copyright and authentication. This paper presents a comparative analysis of information hiding techniques, especially on those ones which are focused on modifying the structure and content of digital texts.

In [18] it is a technique, where presence of secret message cannot be detected, so it act as a tool for security purpose to transmit the confidential information in a secure way.There are varity of information hiding approaches exist and they differs from each other depending upon message to be embedded, usage of file types as a carrier or compression method etc. Uncompressed file formats like BMP, GIFF, TIFF e.t.c based on lossless compression provides high data hiding capacity, that means the hiding capacity depends on types of cover images used.

III. PROPOSED TECHNIQUE IN THIS PAPER

The paper proposes steganography based on image with IWT and Arnold transform, here both cover object and secret object are of different images. Both transforms are used namely, IWT and Arnold transform is applied to cover image and the secret image.

A. INTEGER WAVELET TRANSFORM

Widely used wavelet transform in steganography process is DWT (Discrete Wavelet Transform). When it is applied on the image, there exist floating point coefficients, leads to floating point truncation, which may cause loss of information. To avoid this problem, a new transform known as IWT (Integer Wavelet Transform) is utilized in this work. Both the transforms DWT and IWT leads to image compression process. DWT leads to lossy data compression, in which compresses data by discarding some of it. Its aim is to minimize the amount of data that needs to be held. But in IWT it is lossless data compression that allow original data to be perfectly reconstructed from the compressed version.

B. ARNOLD TRANSFORM

Arnold transform is an image scrambling technique, which scrambles the pixels of the image so we can say that it is an image encryption method. When this transform is applied to an image, the pixel location of the image gets changed thus the image appears like a diffused form. We can say that it is an iteration process which leads to change in position of the pixel location, hence this transform depends on the number of iterations and act as a key. The Arnold transform is an image scrambling technique performed on the square image, which shifts the pixel location from (x, y) to (x, y) without changing its size.This transform change the pixel position of the image without removing any information from the image. This transform is area preserving and invertible without loss of information. Let the pixel image be S=(x,y), where [x,y] = [0,1,2,.....N-1] N implies size of the square image [18].

$$\begin{bmatrix} x' \\ y' \end{bmatrix} = A \begin{bmatrix} x \\ y \end{bmatrix} (mod N)$$

$$A = \begin{bmatrix} 1 & p \\ q & pq+1 \end{bmatrix}$$

The values of p and q act as key points in this transform

Generally matrix A is written as

$$A = \begin{bmatrix} 1 & 1 \\ 1 & 2 \end{bmatrix}$$

Another important 'key' used in this transform is 'N', the number of iterations.For the same matrix A, different number of iterations can be performed on an image, which results in diffused form of image. The real image can be obtained by taking contrary of Arnold transform through correct number of iterations, if the number of iterations is incorrect we can't obtain the correct version of the original image.If the number of iterations is very high, the transform takes more time to obtain the output as well as in reverse stage.

Fig. 1. Arnold Transformed image

C. CRYPTANALYSIS

The cryptanalysis is applied to the entire steganography system to analyze its strength for hiding the information. The cryptanalysis is performed by providing certain attacks to the entire steganography system. In this paper there are three keys, p,q and number of iterations. Based on these keys cryptanalysis is performed. The attacks preferred to this steganogrphy system is brute force.

1) Brute Force Attack: Brute force attack is performed by applying trial and error method through all possible keys.In this paper the analysis of this attack should be performed on extracting algorithm.Only the Arnold transformed image is available to the attacker, so to obtain the original secret image by the attacker he/she want to take the inverse of that image.From this it is clear that all possible keys should be applied to the inverse part of the Arnold transform.That is the brute force attack should be performed on inverse Arnold transform of an image by applying all possible keys.

Arnold transform is performed by iteration process on an image to scramble it to obtain the diffused nature however it is not at all clear, where we can perform many number of iterations on the image .An attacker can easily access the original secret image by applying all possible number of iterations on an image, thus the attack can happen easily. To avoid this we introduce new keys rather than the iteration or repetition number. Let p and q are the newly introduced keys along with the iteration or repetition number.By using the values of p, q and iteration number we are performing Arnold transform, thus the combined version of p,q and iteration number act as keys in encryption and decryption. The only source available to the attacker is the stego image, then he/she has to perform extracting process by these three combinations of keys together to obtain the original secret image. The attacker can attack if and only if the combinations of keys should be similar to that used in the embedding process. By this we can say that, Brute force attack is performed by applying trial and error method through all possible combinations of keys. In this paper the analysis of this attack should be performed on extracting algorithm. In extraction algorithm,after extracting the secret image we have to perform inverse Arnold transform by applying the three combinations of keys to extract the original secret image. Only the Arnold transformed image is available to the attacker, so to obtain the exact image by the attacker he/she want to take the inverse of that image.From this it is clear that all possible keys should be applied to the inverse part of the Arnold transform.That is the brute force attack should be performed on inverse Arnold transform of an image by applying all possible keys.As per the experimental analysis, some of the extracted images from different sets of keys results similar images which makes the attacker confused,which is shown in figure 2 and figure 3 . Hence it is the another advantage while analyzing brute force attack.

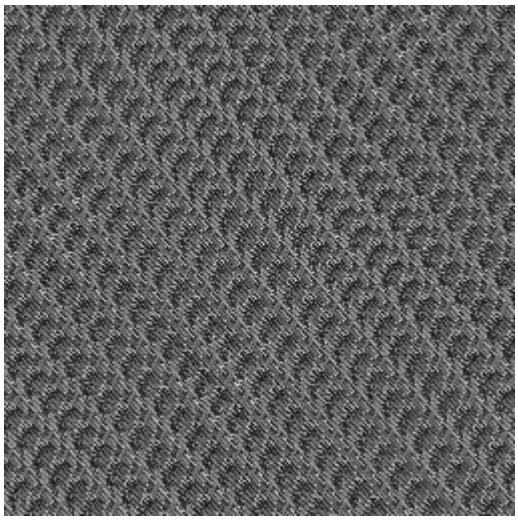

Fig. 2. Extracted image with iteration number=1,p=1 and q=1

IV. ALGORITHMS

There are two phases in image steganography algorithms, the embedding and the extracting phases.

A. Embedding process

There are two inputs in the embedding algorithm or process, one input is cover image and other input is secret image.The cover image is send to the IWT (Integer Wavelet Transform) to obtain the transformed image for embedding the secret image .The secret image is send for the Arnold transform to obtain the scrambled image in diffused nature in order to enhance security or secrecy to the secret image. The output produced in the embedding process is the stego image.The algorithm for embedding process is given below.

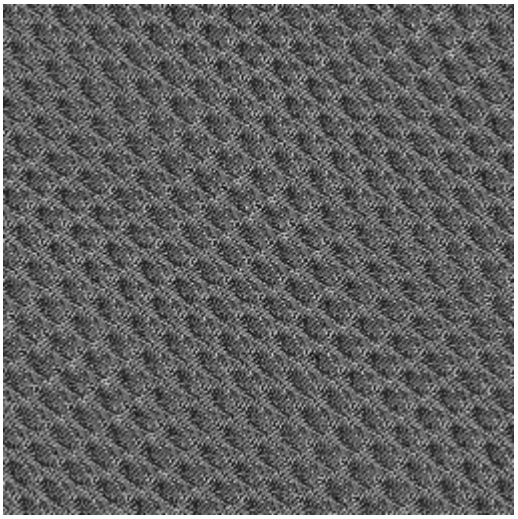

Fig. 3. Extracted image with iteration number=1,p=1 and q=2

- In the embedding phase the IWT (integer wavelet transform) is applied to the cover image (gray scale image)
- Obtained sub-bands of low and high frequencies, LL (low-frequency sub-band), LH, HL and HH (high- frequency sub-bands). These sub-bands can be termed as coefficient bands such as approximation coefficient band (cA) and detail coefficient bands (cV, cH, cD).The three detail coefficients are vertical coefficient (cV), horizontal coefficient (cH) and diagonal coefficient (cD)
- Apply Arnold transform on secret image
- Embed Arnold transformed secret image on the detail coefficient bands of the IWT transformed cover image, since the detail coefficient bands are invisible to the human eye
- After embedding process, perform inverse (IWT) integer wavelet transform to obtain the stego image.

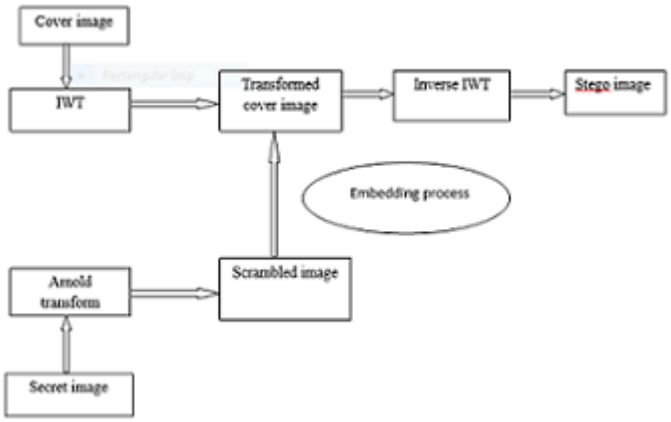

Fig. 4. Embedding Process

B. Extracting Process

The extracting process or algorithm consist of one input as the stego image and two outputs while the cover image and secret image.The stego image is send to IWT to obtain the transformed image from where we have to withdraw the scrambled secret image.The extraction process produces two sets of output as cover image and scrambled image. The scrambled image is send for inverse Arnold transform to obtain the original secret image. The algorithm for extracting process is given below.

- In the extracting phase the IWT (integer wavelet transform) is applied to the stego image
- Extract the secret image from the detail coefficient bands (cV, cH, cD), this secret image is in the form of an Arnold catmap and the transformed cover image
- Apply inverse Arnold transform on extracted image, in order to obtain the real secret image
- Apply inverse IWT to obtain the original cover image

Fig. 5. Extracting Process

V. EXPERIMENTAL ANALYSIS

The proposed steganography algorithm is based on IWT and Arnold Transform. The advantage of this system is analyzed based on its comparison with steganography system based on DWT and Arnold Transform. Mainly the information is available on LL sub band, the figure given below shows the difference in LL sub band applied with IWT and DWT on the same image.

Fig. 6. Difference in LL sub band

From this above figure it is clear that the steganography with IWT is the better one.Comparing IWT and DWT steganography system, clarity on stego image is more in IWT than in DWT. While comparing the performance evaluation PSNR (Peak Signal to Noise Ratio), SNR (Signal to Noise Ratio) of IWT steganography system is higher than DWT steganography system. But in the case of MSE (Mean Squared Error), it is lower in IWT than in DWT. Based on all these criteria we can conclude that the steganography system with IWT and Arnold Transform is the best one. The strength

of entire information hiding system should be analysed by cryptanalysis. The cryptanalysis is performed by taking the possible number of iterations for the iteration matrix A with p and q values. Thus we can say that iteration number, p and q values act as the combination of three keys for encryption and decryption.

VI. PERFORMANCE EVALUATION

A. MSE-Mean Squared Error

It is square of error between original image and stego image image.Mainly used to measure distortion in the image

$$MSE(O,\tilde{S}) = 1/U * V \sum_{i=0}^{U}\sum_{j=0}^{V}(O(i,j) - (\tilde{S}(i,j))^2$$

O(i,j)=Original image
$\tilde{S}(i,j)$=Stego image In this paper a comparison of MSE is made between DWT-Arnold steganography system and IWT-Arnold steganography system. While comparing MSE, it is high in DWT-Arnold steganography system than in IWT-Arnold steganography system.From this it is clear that since MSE is less in the case of IWT, the distortion of the image is less.

B. PSNR-Peak Signal to Noise Ratio

(PSNR) is the ratio between the original cover image and the stego image, in order to compare its quality.

$$PSNR(O,\tilde{S}) = 10log_{10}\frac{(L-1)^2}{MSE(O,\tilde{S})}$$

O=Original image
$\tilde{S}$=Stego image
L=grey-level number On comparing PSNR values of IWT and DWT steganography system,the IWT system have better quality than the DWT-Arnold steganography system.

C. SNR-Signal to Noise Ratio

SNR is calculated as ratio of original image to affected noise. Noise indicates difference between original image and stego image

$$SNR(O,\hat{S}) = 10log\Big(\frac{\sum_{i=1}^{U}\sum_{j=1}^{V}(O_{i,j})^2}{UVMSE}\Big) \quad (1)$$

Transforms	MSE	PSNR	SNR
IWT	6.0900	106.7000	36.1110
DWT	35.5685	89.0519	18.4798

Performance analysis between two transforms

Images	MSE	PSNR	SNR
Cameraman	6.0893	106.7012	36.1122
Lena	6.0900	106.7000	36.1110
Apple	6.0900	106.7000	36.1110
Baboon	6.0900	106.7000	36.1110

Performance analysis on different images

VII. CONCLUSION

The proposed steganography system is based on IWT (Integer Wavelet Transform) and Arnold transform .The developed steganography system is analyzed through cryptanalysis, by introducing simulation attack and brute force attack. Mainly the attack is performed on stego image or cipher text by the attacker. In this work a comparison is made between IWT and DWT steganography system to prove IWT is the best one for hiding the information. Here Arnold transform is used for ensuring security on secret image before hiding. A combination of three keys is used for embedding Arnold transformed secret image to the cover image, to provide high security to the secret image .The combination of three keys are obtained from the Arnold transform in the form of bits .From these keys we can measure the strength of the steganography system in terms of bits by analyzing its computation complexity.The proposed steganography system withstand both simulation and brute force attacks.Simulation attack is performed in extraction section by providing the combination of keys entirely different from the embedding process.The usage of different keys cannot extract the original secret image, thus conclude that the developed steganography system have the ability to withstand the attacks based on simulation.Brute force attack is performed by applying trial and error method through all possible combination of three keys, the steganography medium would be very strong in data hiding.

REFERENCES

[1] Elshazly Emad,Abdelwahab Safey,Abouzaid Refaat,Zahran Osama,Elaraby Sayed and Elkordy Mohamed," A secure image steganography algorithm based on least significant bit and integer wavelet transform",Journal of Systems Engineering and Electronics,Vol.29,No.3,June 2018,pp 639-649
[2] Sadik Ali Al-Taweel, Muhammed Husain Al-Hada, Ahmed Mahmoud Nasser ," Image in image steganography Technique based on Arnold Transform and LSB Algorithms",International Journal of Computer Applications (0975-8887), Vol. 181-No. 10,August 2018
[3] S Jayasudha,"Integer wavelet transform based steganographic method using Opa Algorithm",International Journal Of Engineering and Science,Vol.2,Issue 4(February 2013), pp 31-35
[4] R.Punidha, M.Sivaram,"Integer wavelet transform based approach for high robustness of audio signal transmission", International Journal of Pure and Applied Mathematics,Vol 116 No.23 2017,295-304
[5] Julien Reichel,Gloria Menegaz,Marcus J. Nadenau and Murat Kunt,"Integer wavelet transform for embedded lossy to lossless image compression",IEEE Transactions on Image Processing, Vol 10,No.3, March 2001
[6] Shamim Ahmed Laskar, Kattamanchi Hemachandran,"A Review on Image Steganalysis techniques for attacking Steganography", International Journal of Engineering Research and Technology (IJERT) Vol.3, Issue 1, January 2014
[7] P.Das, S.C.Kushwaha, M. Chakraborty,"Multiple Embedding Secret Key Image Steganography Using Lsb Substitution And Arnold Transform", IEEE Sponsored 2nd International Conference On Electronics And Communication System 2015 (ICECS 2015)
[8] Milad Taleby Ahvanooey, Qianmu Li, Hiuk Jae Shim and Yanyan Huang," A Comparative Analysis of Information Hiding Techniques for Copyright Protection of Text Documents", Security and Communication Networks Volume 2018, Article ID 5325040
[9] Snehal Ghormade, Bhagwat Kakade,"A Survey on Information Hiding Techniques in Digital Media", International Journal of Scientific Engineering Research, Volume 5, Issue 2, February-2014

[10] B.Lavanya, M. Kiran Kumar,"Comparative Analysis of Image Scrambling Sequence Generation Method with Arnold", International Conference on Electronics, Communication and Aerospace Technology ICECA 2017
[11] Kuang Tsan Lin," Image Encryption Using Arnold Transform Technique and Hartley Transform Domain", Ninth International Conference on Intelligent Information Hiding and Multimedia Signal Processing 2013
[12] Gyan VardhanArtist, Dr. Mahesh Kumar Porwal," Dual Layer Image Scrambling Method Using Improved Arnold Transform", American International Journal of Research in Science, Technology, Engineering and Mathematics 2015
[13] Zhiwei Li, Xiyang Yang," A New Measure of Image Scrambling Degree Based on Statistical Hypothesis Testing",3rd International Congress on Image and Signal Processing 2010
[14] Kaur S,Bansal S,Bansal R K,"Steganography and classification of image steganography techniques",Proc.of International Conference on Computing for Sustainable Global Development 2014
[15] Al-Mohammad, Adel(Ghinea, G and Hierons, RM)."Steganography-based secret and reliable communications: Improving steganographic capacity and imperceptibility", Brunel University, School of Information Systems, Computing and Mathematics Theses, 2010.
[16] G. Prabakaran, R. Bhavani, P. S. Rajeswari. "Multi secure and robustness for medical image based steganography scheme", 2013 International Conference on Circuits, Power and Computing Technologies (ICCPCT), 2013
[17] Li, Jian Ping, Simon X Yang, Stephane Jaffard, Bruno Torresani, and John Yen. "Wavelet-Based Initialization for VQ Codebook Generation", Wavelet Active Media Technology and Information Processing, 2006.
[18] Sumeet Kaur, Savina Bansal, R. K. Bansal."Steganography and classification of image steganography techniques", 2014 International Conference on Computing for Sustainable Global Development (INDIACom), 2014

Proceedings of the Fourth International Conference on Communication and Electronics Systems (ICCES 2019)
IEEE Conference Record # 45898; IEEE Xplore ISBN: 978-1-7281-1261-9

Smart Security, Food and Environment Monitoring System for Cows using Microcontroller

Aritro Roy Arko*, Saadat Hasan Khan* and Md Saiful Islam
Department of Computer Science and Engineering
BRAC University
Dhaka, Bangladesh
aritroroyarko@gmail.com, ksaadat09@gmail.com, md.saiful.islam@bracu.ac.bd

***Abstract*—Health and security for cows have been an alarming concern over the South-Asian countries as many people depend on cows for a living. Cows are used for various purposes. For example: It can be used for milk production, crop farming and meat production. It is evident that the health of cows depend on what they eat and where they eat. Many measures can assess the quality of the food. One such way of providing reliable food is by the measurement of pH and temperature of the food. The environment in which the cows stay has significant effects in the wellbeing of the cows. Foot diseases can occur if the cows stay near its own dung for too long. Sadly, no farm takes any measurements during the provision of food. Moreover, farms neither check the environmental conditions nor do they maintain it regularly. Furthermore, the security of cows inside the farm is very tough to maintain, as constant labor need to keep eyes on the cows. Our system looks after the health of cows by measuring pH and temperature of food. It keeps the environment clean by spraying water on the farm at regular intervals of time and security is kept in check by detecting whether the cows have crossed the gate of the farm. The system does all these processes automatically by using pH, temperature, RFID sensors, Arduino micro-controllers, water pump and a 9V battery to power up the pump.**

Keywords—Health, Security, Environment, pH, Temperature, Arduino, RFID, Sensors, Water pump, Cows.

I. INTRODUCTION

Health for cows has always been an important topic for the farmers and is still a difficult issue that needs to be addressed. Our system is the result of a research to help the farmers of any agriculture-based country. The system has undergone thorough revision for quite a number of times after the initial plan. It incorporates three different dimensions which includes the food monitoring system, environment monitoring system and antitheft system of cows. All these components need to be inside the farm. The food monitoring system measures the pH and temperature of the food for the cows and compares the data to a standard chart. If the values are inside the range of the chart, then the food is marked as edible and can be fed to the cows in the farm. The environment monitoring system consists of a water pump which sprays water at frequent intervals of time, generally 4 hours, to drain out all sorts of dirt and wastes produced by cows. If this is not done, it could lead to serious diseases and health hazards for the cows. The anti-theft system consists of RFID tags which is placed on the neck of cows and a RFID sensor placed on the gate of the farm. If any cow escapes the gate or anyone steals a cow, the RFID system will trigger an alarm in the farm, letting all the farmers know that a cow has escaped from the boundaries of the farm. The system is designed to do all the following things mentioned above and we believe that this will not only make the lives of farmers easier but also help farmers to stay away from big losses such as the death of cows, escape of cows or the theft of cows from farms.

II. LITERATURE REVIEW

A lot of work has taken place on the topic of RFID based automatic anti-theft system. Geeth Jayendra, Sisil Kumarawadu and Lasantha Meegahapola have worked rigorously on the topic of RFID based anti-theft auto security system with an immobilizer [1]. Researchers have constantly focused on providing more security that would be efficient. We are now at an era of technology, where RFID systems can track livestock. Nabil Kannouf, Yousef Douzi, Mohammed Benabdellah, Abdelmalek Azizi have written a paper on RFID being used as a security measure on livestock [2]. Rand A. Mahmood has also written about the uses of RFID as a measure of security, starting from security of livestock to library books and personal identification documents [3]. Furthermore, there has also been work and an article on the topic of "CATTLE RFID & TRACKING SYSTEM" [4].

Ensuring food quality is something that is very crucial and many articles provide information on the quality of food provided to cattle. It is very evident that the enzymes can only work most properly in the time of digestion at a suitable pH and temperature range. M.B.de Ondarza added to their website that the enzymes need a pH of 5.7-7.3 and an optimum temperature of 39 degrees to work properly during digestion [5].

Lastly, we can frequently see the use of water pumps where microcontrollers have complete control due to different needs. Madhurima Santra implemented a system to turn on a water pump when the water level of a tank goes beneath a level [6]. Moreover, J. E. Okhaifoh, C. K. Igbinoba, and K. O. Eriaganoma also completed work on the topic of microcontroller based automatic control for water pumping machine with water level indicators using ultrasonic sensor [7]. Furthermore, water wastage from motor pump is a big issue. O Bamigboye, F. Ehiagwina, E. O. Seluwa and K. O. Gbadamosi have also worked together to design a microcontroller based

water pump that works in a way which reduces the water wastage [8].

III. PROPOSED MODEL

The system is designed in such a way that it takes data as input from the sensors according to the environment that the cows are in and then passes the data to the Arduino. The Arduino then computes and converts these electrical readings to scaled values like pH and temperature, which are understandable by humans. The interfaced software compares the computed values with a standard dataset to decide whether the food is appropriate for the cattle. If the pH value lies within the range 5.7-7.3, then it is within the acceptable range. Similarly, if the temperature lies within 38.5-39.5 degrees centigrade, then the temperature is also in the acceptable range. The food can be fed to the cows if and only if both the temperature and pH of the food are within the appropriate range. Lastly, if the temperature and pH are within the standard range, then the system will turn on the green light. Otherwise, it will turn the red light on.

Similarly, the antitheft system detects any RFID card/tag close to the receiver. The cows have RFID tags wrapped around their neck. Any presence of the tag nearby the receiver would indicate that a cow is close to the gate and is about to escape. The RFID receiver would then dump information about the tag to the system, alarming the farmers about the escape.

In addition, the environment monitoring system maintains a clean environment for the cows to live and grow. The motor pump sprays water on the surface of the farm to remove all sorts of wastes and dirt at frequent intervals of time.

A. Flow chart of the system

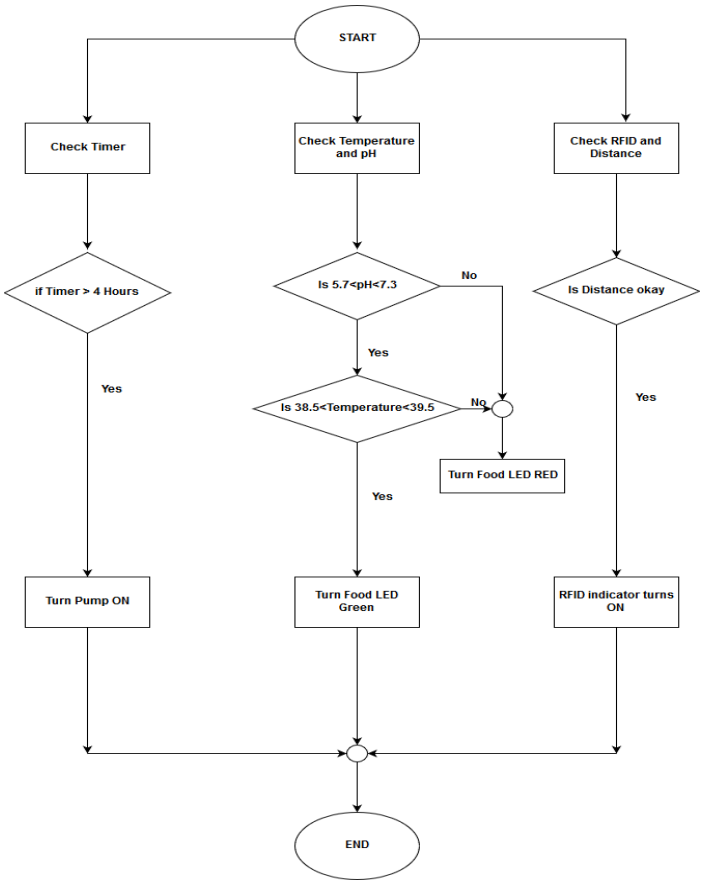

Fig. 1. Flowchart of the system.

The flowchart above represents the overall processes and activities within the system. The system is primarily divided into three parts. Firstly, for the environment management part, there is a timer which checks whether the time that the water pump was last turned on exceeds more than 4 hours. If the condition is true, then the pump automatically turns on to clean the surrounding area. Secondly, the temperature and pH of food is checked regularly. If the pH is within the normal range of 5.7-7.3, then the temperature is checked. The temperature needs to be within 38.5 to 39.5 degree centigrade to be considered normal. If both of them are ok, then the food is good to be fed to the cows and a green light turns on. Otherwise, the red light turns on to warn the farmer that the food is not ok. Lastly, for the antitheft system, if the distance between the tag and receiver is less than the threshold value, it means that the cow is about to escape and the red light or alarm system turns on to warn about the escape.

IV. RELATABLE EQUATIONS

We used the following equation to convert the analog voltage readings taken as input from sensors to digital pH values.

$$pH\ reading = \left(5 - \left(analog\ reading \times \frac{5}{1023}\right)\right) \times \frac{14}{5} \quad (1)$$

V. HARDWARE DETAILS

The overall description of the hardware components are as follows:

A. Arduino Uno R3

In our project, we have used Arduino which is a board to interface between the hardware components, such as the temperature and pH sensors, and the computer. The system uses two Arduino Uno R3 boards in order to serve its needs. One Arduino Uno R3 board controls the pH, temperature, RFID sensors and another one controls the water pump. The latter Arduino also acts as a timer that allows the water pump to spray water on the surface at regular intervals. This is possible by using a delay in our code. The fact that this Arduino deals with only one component, allows the Arduino delay to work exactly like a clock.

B. pH Sensor—SEN0161

The pH sensor's use for our research is to get an analog voltage from the solution that we are using as the food for cattle. The system is designed in the following way. The sensor is placed inside the solution which is the cow food over here. Readings from the sensor pass to the Arduino where it is processed. The sensor produces electric voltages based on the concentration of hydrogen ions in the solution. Furthermore, the pH sensor calculates the pH and gives us the actual reflection about the acidity of the food. The pH reading is obtained by converting the analog voltage using a suitable equation. If the pH lies within the actual range then we can say that the food is okay for the cattle to eat or else it is discarded.

C. Temperature Sensor—DS18B20

For our system, the temperature sensor gives us electric voltages just like the pH sensor. The voltage is directly proportional to the temperature, meaning that the reading is dependent on the temperature of the food. The reading is converted to a suitable temperature value by calling a built in function called getTemp (). Just like the process of collecting temperature, the working methodology is also very much the same. The temperature sensor gives us readings and if the readings are okay i.e. if they lie within the range, the food is accepted. The sensor gives us a reflection of the warmth of the food and whether it is suitable for the cows. However, for the food to be accepted, the temperature and pH should both be within the range. The food will not be accepted if any one of the tests fails.

D. RFID sensor—MFRC522

RFID tag is placed around the cow's neck and RFID receiver is kept on the side of the gate of the farm, which is further connected to the Arduino Uno R3. In general, the RFID receiver module gives a signal to the Arduino board whenever it sees any tag energizing the receiver module at a particular Radio Frequency. This means that whenever a cow passes or escapes through the gate, the RFID receiver module detects the tag and dumps information of the tag to the Arduino. Once information is dumped into the software system, the Red light for the "Cow stolen" signal is turned on in the maintenance room. This would let the farmers know that something is wrong inside indicating either a cow has escaped or someone has entered the farm and is running away with the cow. The RFID system was chosen over many other security systems because it is very cost efficient.

TABLE I. COMPARISON OF RFID SENSORS

Items	Passive RFID	Active RFID	Active RFID new version
Communication. Range	70cm / 3m-7m	Greater than 10m	Approximately 10m
Life of Battery	No battery present	Approximately 1 year	Around 1 year
Security	Weak	N/A , or weak	Strong
Cost	Less than $1	Less than $10	Around $10
Application	Distribution, inventory, tracking of goods	Tracking person (restricted area)	Tracking person

The above table represents how different RFID sensors vary with their applications, cost, battery life and security. This also shows us that the use of RFID sensors for farming purposes is very economic [9].

E. Water pump

Water pump is there to spray water and maintain a clean environment. A 9V potential difference with ample amount of current turns on the water pump. The Arduino controls the water pump via a mosfet which acts as the switch to turn the water pump on and off at regular intervals. The water pump sprays over the surface, cleans off dirt and dung produced cows.

VI. BLOCK DIAGRAM OF THE SYSTEM

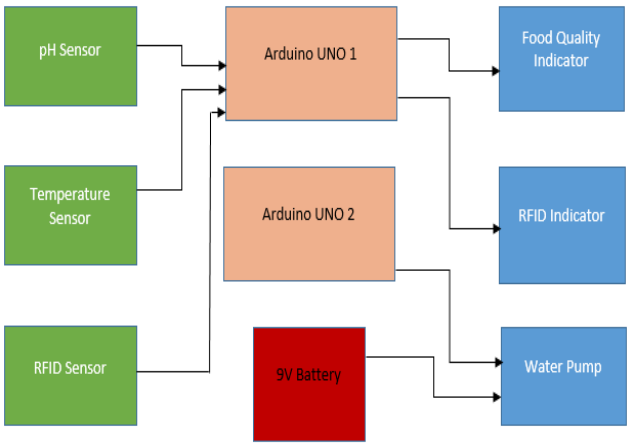

Fig. 2. Block diagram explaining the process

The block diagram above represents the main functions of our system in terms of blocks. There are a total of two Arduinos and a 9V battery. The first arduino has inputs from

pH sensor, temperature sensor and RFID sensor respectively. The arduino mainly processes the inputs. Based on the rules set, it shows appropriate outputs that indicates the food quality and security status of the farm. The second Arduino's output is connected to a water pump which is further driven by a 9V battery. It mainly acts as a switch and is programmed in such a way that when the time that the pump was last turned on becomes greater than 4 hours, the output becomes high and the 9V battery starts driving the water pump for a specific amount of time.

VII. SCHEMATIC DIAGRAM OF THE SYSTEM

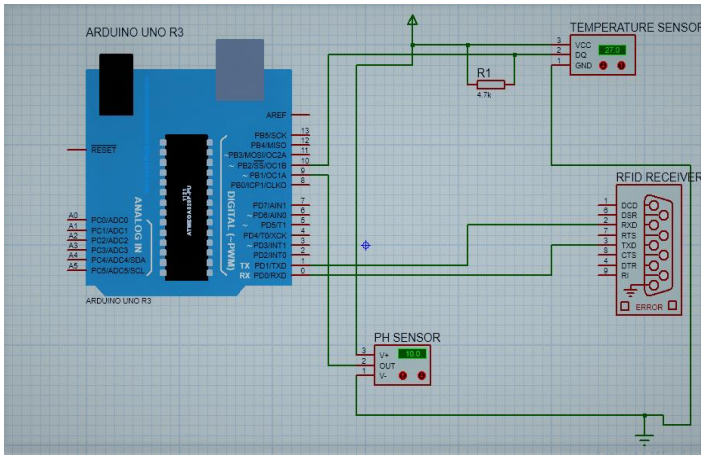

Fig. 3. Schematic diagram of Arduino 1 and corresponding connections

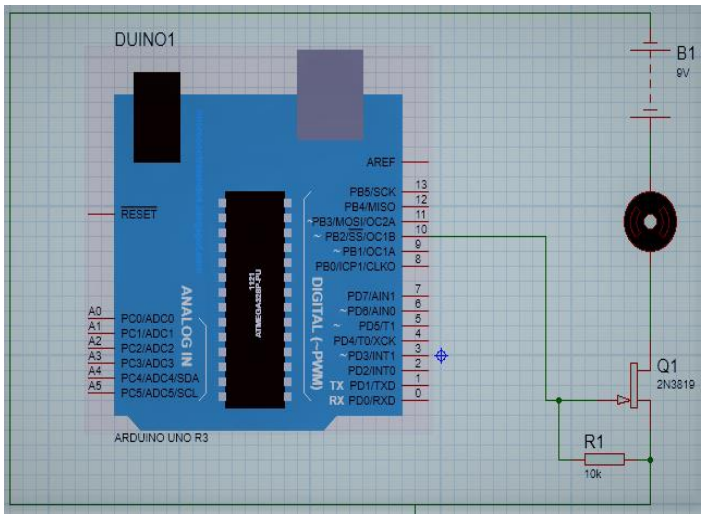

Fig. 4. Schematic diagram of Arduino 2 and corresponding connections

The two schematic diagrams above represent the elements which are connected to the two separate Arduinos in graphical format. Fig. 3 represents the circuit diagram of Arduino 1. This arduino is connected to a pH sensor, temperature sensor and RFID receiver respectively. All the sensors are connected to 5V and ground. There is a 4.7 kilo ohm resistor between the VCC and output of the temperature sensor. Moreover, in Fig. 4, the arduino acts as a switch. The output is connected to the gate of a nmos Q1. The drain is connected to the negative terminal of the pump. The pump is driven by a 9V battery. There is a resistor between the gate and source of Q1. All the components are grounded commonly.

VIII. STATE OF THE SYSTEM

The following table shows the state of the system at different conditions:

TABLE II. STATE OF THE SYSTEM

pH	Temperature range (^{0}C)	RFID range	LED for Food	RFID Indicator
<5.7	<38.5	Not close	Red	X
>7.3	>39.5	Not Close	Red	X
5.7<ph<7.3	38.5<t<39.5	Close	Green	Red

The following figures show the state of the system at different conditions.

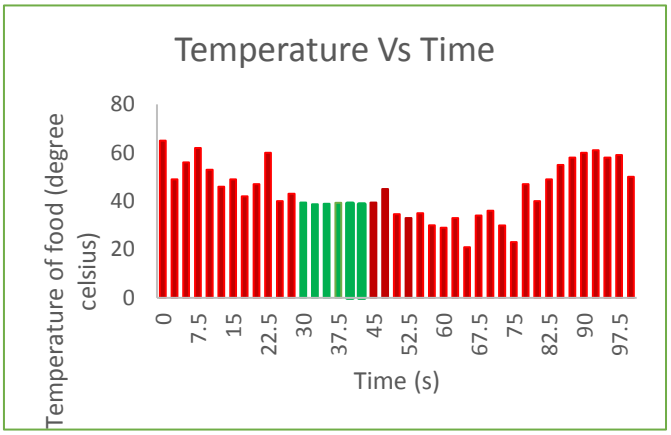

Fig. 5. Temperature vs Time graph

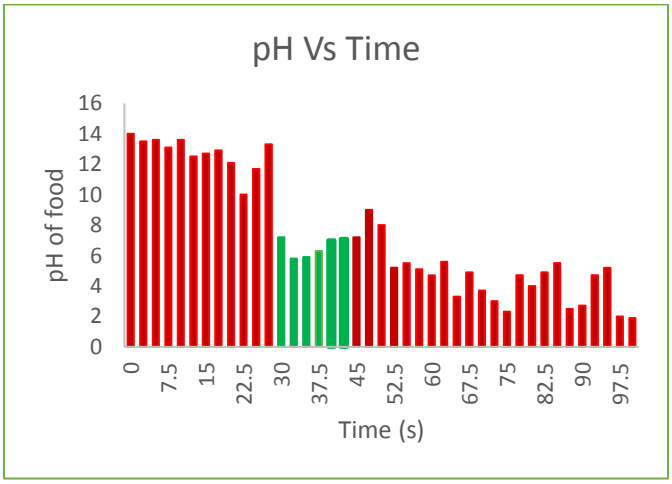

Fig. 6. pH vs Time graph

The green bars in both Figure 5 and 6 show the temperature and ph range of food which is ok to be fed to the cows, whereas the red portion is the range which is unacceptable. If the temperature is within 38.5 to 39.5 degrees celsius, then the food is ok. Moreover, a pH range of 5.7 to 7.3 is acceptable to be fed to the cows.

A. The Overview Of The System

The design and architectural model of our system is as follows. There are two maintenance rooms on either side of the main area, where the cows reside. The room on the left contains a water pump which is powered by a 9V battery. The pump sprays water around the cows at regular period of time to clean any kind of dirt and waste produced by the cows, maintaining a hygienic environment. The room on the right has three main sensors connected to the Arduino inside it. They are: 1) Temperature sensor 2) pH sensor 3) RFID receiver. The temperature and pH sensors are both placed inside the food that will be served to the cow so that the right quality is ensured. The RFID receiver is placed near the exit to notify the owner about the escape of any cow from the farm.

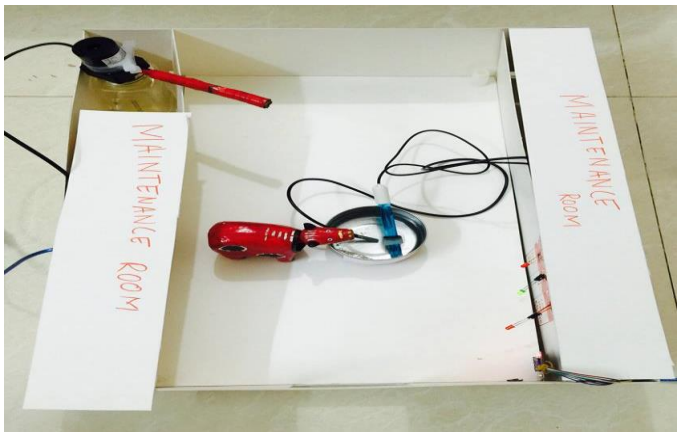

Fig. 7. Overall architecture of the System

B. When The Food Is Okay

When the food that has been provided is within the pH and temperature range, a green light is seen to be turned on. This gives farmers the sign that they can continue to feed the cows.

Fig. 8. Green light turned on , when the food is okay

C. When The Food Is Not okay

If the pH and temperature of the food is outside the standard range, a red light is turned on, meaning that the food cannot be fed to the cows. For example: If the temperature is above 39.5 or below 38.5 or the pH is above 7.3 or below 5.7, then the red light will automatically turn on to tell the farmer that the food provided must be changed.

Fig. 9. Red light turned on, when the food is not okay

D. When Cow Tries to Escape

If the cow tries to escape then a red light would be turned on under the “COW HAS ESCAPED” section, alarming the farmers that the cow has been stolen or escaped and they should look for the cow in the nearby areas.

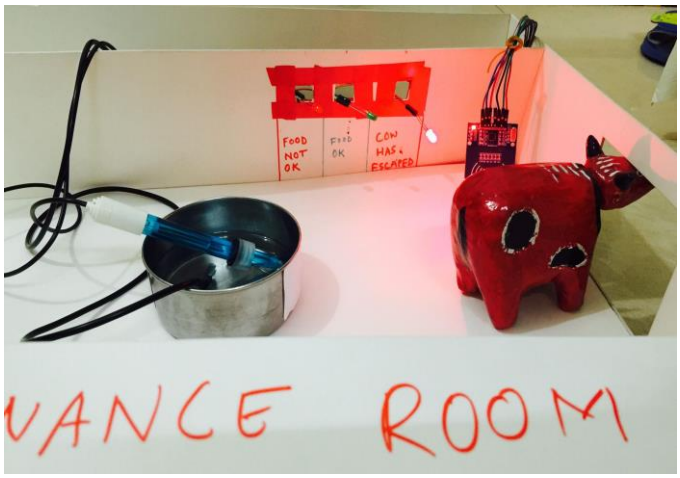

Fig. 10. Red light turned on as cow tries to escape

VI. Conclusion and Future Direction

The design and implementation of smart security, food and environment monitoring system for cows using microcontroller is discussed in this paper. There are some new innovations in our system. For example: Previously, there were very less works on how to check the quality of food which should be provided to cows. In our system, we identified the parameters that can affect the quality of food and then implemented a system that automatically checks whether the food being provided to the cow is healthy, maintains a clean environment around cow's living area and alerts the farmer of any security breach. Another advantage that our system has is that it minimizes big losses for farmers. Although there is an initial installation cost for farmers, the system reduces overall loss through prevention of unhealthy growth and theft of cows. Furthermore, the size of our system is very small, which is a major benefit.

However, there is room for improvement. The system has used less variety of sensors and components in order to measure food quality. Different sensors can be used in order to get measurements that are more accurate and reliable. One such sensor is the turbidity sensor to get a better picture of the quality of the food [10]. It also gives a better understanding of the quality of water [11]. In addition, we are not checking the quality by measuring the vitamin and mineral content of the food. This is something which can be looked after for further research.

A GPS system can also be used in the system to keep track of all the cows and monitor the position of each cow [12]. Hence, it will not only help us to alarm the farmers whether a cow has been escaped or stolen, but also track the exact position of where the cows are.

A heart rate sensor can come in handy to measure the heart rate of all the cows. Records can be kept in the database. This would serve as an indicator to predict any expected disease or attack even beforehand [13].

References

[1] G. Jayendra, S. Kumarawadu and L. Meegahapola, "RFID-based anti-theft auto security system with an immobilizer," Conference Proceedings - 2nd International Conference on Industrial and Information Systems 2007, pp. 441-446, USA: IEEE, 2007.

[2] N. Kannouf, Y. Douzi, M. Benabdellah, and A. Azizi, "Security On RFID," 2015 International Conference on Cloud Technologies and Applications (CloudTech), November 2015.

[3] R. A. Mahmood and W. A. Al-hamdani, "Is RFID Technology Secure And Private?," 10.1145/2047456.2047462, 2011.

[4] Zycom Surveillence (Nig) Ltd, "CATTLE RFID & TRACKING SYSTEM."[Online].Available: http://www.zycomsurvng.com/products/cattle-tracking-system.html

[5] M.B.de Ondarza, "The stomach of the dairy cow." [Online]. Available:http://www.milkproduction.com/Library/Scientific-articles/Animal-health/The-stomach-of-the-dairy-cow/

[6] M. Santra, S. Biswas, S. Bandhapadhyay, K. Palit, "Smart Wireless water level Monitoring & Pump controlling System," *International Journal of Advances in Scientific Research and Engineering*, vol. 03, no. 4, May, 2017.

[7] J. E. Okhaifoh, C. K. Igbinoba and K. O. Eriaganoma, " Microcontroller Based Automatic Control For Water Pumping Machine With Water Level Indicators Using Ultrasonic Sensor," *Nigerian Journal of Technology (NIJOTECH)*, vol. 35, no. 3, pp. 579-583, 2016.

[8] O. Bamigboye, F. O. Ehiagwina, E. O. Seluwa and K. O. Gbadamosi, "Development of Microcontroller Based Water Pump Controller," 8th International Conference Of The School Of Engineering And Environmental, Federal Polytechnic, EDE, July, 2016.

[9] I. Yamada, S. Shiotsu, A. Itasaki, S. Inano, K. Yasaki, and M. Takenaka, "Secure Active RFID Tag System," Ubicomp2005 Workshops, vol no. 5, 2005.

[10] Y. Wang, S. M. S. M Rajib, C. Collins, and A. Azizi, "Low-Cost Turbidity Sensor for Low Power Wireless Monitoring of Fresh Water Course" IEEE Sensors Journal, vol. 18, no. 4, June, 2018.

[11] B. SIgdel, "Water Quality Measuring Station," B. S. thesis, Helsinki Metropolia University of Applied Sciences, Helsinki, Finland, 2017.

[12] J. M. Schieltz, S. Okanga, B. F. Allan & D. Rubenstein, "GPS tracking cattle as a monitoring tool for conservation and management," *African Journal of Range and Forage Science*, vol. 35, no. 3, 2017.

[13] M. Janžekovič, B. Muršec, I. Janžekovič, "Techniques of measuring heart rate in cattle," *Technical Gazette*, vol. 13, no. 1,2, 2016.

Proceedings of the Fourth International Conference on Communication and Electronics Systems (ICCES 2019)
IEEE Conference Record # 45898; IEEE Xplore ISBN: 978-1-7281-1261-9

Coupling Between Automatic Generation Control And Automatic Voltage Regulator While Considering Generation Rate Constraint Of Two Areas

Omer Elmukhtar
Department of computer science and control engineering
North China Electric Power University, Beijing, China
E-mail: omer90mizo@ncepu.edu.cn

Jianhua Zhang
State Key Laboratory of Alternate Electrical Power System with Renewable Energy Sources, North China Electric Power University, Beijing, China
E-mail: zjhncepu@163.com

***Abstract*—This paper describes the implementation of automatic generation control (AGC) and automatic voltage regulator (AVR) under generation rate constraint (GRC) and coupling between automatic generation control and automatic voltage regulator while considering generation rate constrain of two areas for improve and better performance characteristic of load frequency control (LFC) problem. our control aim has to normalize the area control error (ACE), frequency error and tie-line power error in spite of the presences of system uncertainties and external load disturbance, So that the required frequency and power interchange with adjacent structures are maintained in order to reduce the transient deviations and to provide zero steady state error in proper short time, the behavior of the planned is checked by MATLAB SIMULINK software.**

Keywords— Automatic Generation Control (AGC); Automatic Voltage Regulator (AVR); Generation Rate Constraint (GRC); Area Control Error (ACE)

I. INTRODUCTION

Automatic generation control maintains a balance between the whole power generation and load demand, to keep the system frequency (normally 50 or 60 Hz) and regular power interchange with neighboring systems [1].

Load frequency control (LFC) performs a vital role for energy stability between load and era sides. In recent years, several robust design strategies have been delivered for LFC [2]–[4] The dynamic behavior of many industrial plants is heavily influenced by disturbances and, in particular , by change The dynamic conduct of many industrial flowers is closely influenced by disturbances and, in particular, by adjustments in the running point. This is commonly the case for electricity structures [5].

In an electrical grid, many synchronous turbines with different voltage rankings are connected to bus terminals which have the identical frequency and segment sequence as the generators. All generators linked in parallel ought to be run at the suitable capacity to meet the demand. If a generator loses synchrony there'll be changes within the voltage and frequency offer. It's essential to synchronize the bus with the generators for the period of transmission for secure operation. also recognized as synchronous balance refers to the capability of a system to return to synchronism after any disturbance such as a sudden exchange in loading conditions offer frequency and voltage should frequently be among a positive prohibit to confirm safe and reliable operation of electrical instrumentation and equipment every at the client premises and throughout transmission and distribution. So it's crucial to be in an exceedingly position to screen and hold the voltage and frequency among limits. After an annoyance involving a net exchange in power, the System will enter a transient state which is regularly oscillatory and reflected by means of fluctuations in the energy flow over transmission lines. This is referred to as the dynamic system performance. In a tie-line connecting one team of turbines to another, these oscillation can also construct up and be mirrored via excessive fluctuations in power flow in the tie line. This will motive protective equipment to day trip [6].

The goal of this paper is to sketch a controller to perform LFC. At first an evaluation of one of a kind systems from previous research works was performed. The end result obtained. The Matlap/Simulink platform was used for all simulation outcomes obtained. The balance of the systems used to be investigated and the transient and constant country response of the systems have been simulated before any controller used to be designed. The manipulate goal is to minimize overshoot, settling time and steady state error. In LFC, deviation in frequency and tie line strength must return to zero in the minimal time and with minimal overshoot after a load alternate [7]. Controllers had been designed and tested to obtain this. Different kinds of controllers had been simulated in Simulink for the device specifically the PID, Fuzzy, Neuro-Fuzzy and Fuzzy-PID [8]–[11] to enhance its performance. Finally a comparative evaluation of the consequences from the unique

controllers was once achieved and the most appropriate one was once chosen.

II. TWO AREA POWER SYSTEM

Power systems have complex and multi-variable structures. Also, they consist of many one of a kind control blocks. Most of them are nonlinear and/or non-minimum segment systems [12]. Power systems are divided into manipulate areas related by tie lines. All generators are supposed to represent a coherent crew in every manipulate area. From experiments on electricity systems, it can be viewed that every place wants its gadget frequency and tie line strength go with the flow to be managed [3].

In intention of control at this point is to regulate the frequency of each area and at same time to regulate the tie-line power as per inter area power contract. In case of frequency proportional plus integral control is used to get zero steady state error in tie-line power flow as compared to the contracted power, consider that each control area can be represented by an equivalent turbine, generator and governor system. Consider that case of an isolated control area here the incremental power $^{\Delta P_G - \Delta P_D}$ was accounted for the rate of rise of kinetic energy stored, and increase in area load caused due to rise in frequency. A tie-line transmits power in or out an area, so this fact must be taken into the incremental power equation of each individual area.

Power transported out of area-1 is given by

$$P_{tie1} = \frac{|V_1||V2|}{X_{12}} \sin\left(\delta_1^0 - \delta_2^0\right) \tag{1}$$

δ_1^0, δ_2^0 = power angle of equivalent machine of the two area

For incremental change in δ_1^0, δ_2^0 the incremental tie-line power is expressed as follows

$$\Delta P_{tie1}(pu) = T_{12}\left(\Delta\delta_1 - \Delta\delta_2\right)$$

Where

$$T_{12} = \frac{|V_1||V2|}{P_{r1}X_{12}} \cos\left(\delta_1^0 - \delta_2^0\right) = \left[\frac{P_{r1}}{P_{r2}}\right] T_{12} = \partial T_{12} \tag{2}$$

=Synchronizing coefficient

As the incremental power angel are integral of incremental frequencies the equation is written as

$$\Delta P_{tie1} = 2\pi T_{12}\left(\int \Delta f_1 dt - \int \Delta f_2 dt\right) \tag{3}$$

Where Δf_1 and Δf_2 are incremental frequency change in area-1 and area-2 respectively.

In the same way, the incremental tie-line power out of area-2 is given by following equation

$$\Delta P_{tie1} = 2\pi T_{21}\left(\int \Delta f_2 dt - \int \Delta f_1 dt\right) \tag{4}$$

Where

$$T_{12} = \frac{|V_1||V2|}{P_{r1}X_{12}} \cos\left(\delta_1^0 - \delta_2^0\right) = \left[\frac{P_{r1}}{P_{r2}}\right] T_{12} = \partial T_{12} \tag{5}$$

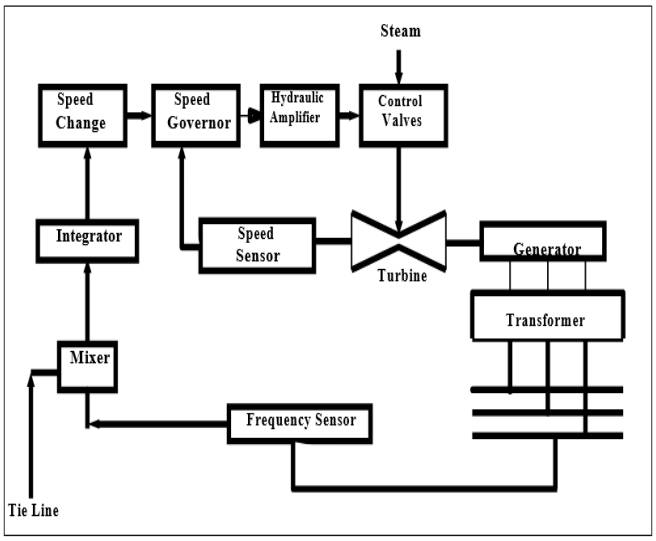

Fig.1. Block diagram of ALFC

Similarly, the incremental power balance equation for area-1 is written as follow

$$\Delta P_{G1} - \Delta P_{D1} = \frac{2H_1}{f_1^0}\frac{d}{dt}\left(\Delta f_1\right) + B_1\Delta f_1 + \Delta P_{tie1} \tag{6}$$

It may be noted that all quantities other than frequency are in per unit in equation, taking Laplace transform of equation and recognizing, the equation is given as

$$\Delta F_1(s) = \left[\Delta P_{G1}(s) - \Delta P_{D1}(s) - \Delta P_{tie1}(s)\right] \times \frac{K_{ps1}}{1 + T_{ps1}S} \tag{7}$$

Where as

$$K_p s1 = \frac{1}{B_1}, T_{ps1} = \frac{2H_1}{B_1 f^0} \tag{8}$$

When compared to the equation of isolated control area case, the only variation in the appearance of the signal $\Delta P_{tie1}(s)$ is shown in fig (1).

Taking Laplace transform of equation (3) the signal $\Delta P_{tie1}(s)$ is obtained as

$$\Delta P_{tie1}(s) = \frac{2\pi T_{12}}{S}\left[\Delta F_1(s) - \Delta F_2(s)\right] \tag{9}$$

From the control area-2, $\Delta P_{tie2}(s)$ is given by taking the Laplace of the equation (9)

$$\Delta P_{tie2}(s) = \frac{-2\pi\partial_{12}T_{12}}{S}\left[\Delta F_1(s) - \Delta F_2(s)\right] \tag{10}$$

III. RESPONSE OF TWO AREA SYSTEM UN CONTROLLED CASE

A. Static Response

The change or deviation result in the frequency.
Tie-line power under steady state conditions flow sudden step changes in load in two area.

Say ΔP_{G1}, ΔP_{G2} are the incremental changes in the generation in area-1 and area-2 owing to the load changes.

Δf Is the static change in frequency, which is same for both the areas, ΔP_{TL} is the static change in the tie-line power that is transmitted from area-1 to area-2 .
For the two areas, the dynamics are described by

$$\left(\Delta P_{G1}-\Delta P_{D1}\right)=\frac{2H_1}{f^0}\frac{d}{dt}\left(\Delta f_1\right)+B_1\,\Delta f_1+\Delta P_{TL1} \tag{11}$$

$$\left(\Delta P_{G2}-\Delta P_{D2}\right)=\frac{2H_2}{f^0}\frac{d}{dt}\left(\Delta f_2\right)+B_2\,\Delta f_2+\Delta P_{TL2} \tag{12}$$

B. Dynamic Response

A power system of two identical control areas is considered for analysis $\tau_{gt}=\tau_t='0'$ for both the areas,

The damping constants of two areas are neglected

$$\mathrm{B}_1=\mathrm{B}_2=0$$

By virtue the second assumption equation (11) and (12) become

$$\left(\Delta P_{G1}-\Delta P_{D1}\right)=\frac{2H_1}{f^0}\frac{d}{dt}\left(\Delta f\right)+P_{TL1} \tag{13}$$

$$\left(\Delta P_{G2}-\Delta P_{D2}\right)=\frac{2H_2}{f^0}\frac{d}{dt}\left(\Delta f_2\right)+P_{TL2} \tag{14}$$

Laplace transformation on both sides of equations (13) and (14)

$$\Delta F_1(s)=\frac{f^0}{2H_1}\left[\left(\Delta P_{G1}(s)-\Delta P_{D1}(s)-P_{TL1}(s)\right)\right]$$

$$\Delta F_2(s)=\frac{f^0}{2H_2}\left[\left(\Delta P_{G2}(s)-\Delta P_{D2}(s)-P_{TL2}(s)\right)\right]$$

From the block diagram, the following equations can be obtained

$$\Delta P_{G1}(s)=\frac{\Delta F_1(s)}{R} \tag{15}$$

$$\Delta P_{G2}(s)=\frac{\Delta F_2(s)}{R} \tag{16}$$

$$\Delta P_{TL1}(s)=\frac{-2\pi\partial_{12}T_{12}}{s}\left[\Delta F_1(s)-\Delta F_2(s)\right]$$

$$\Delta P_{TL2}(s)=-\Delta P_{TL1}(s) \tag{17}$$

From the above equations, the following observations can be made

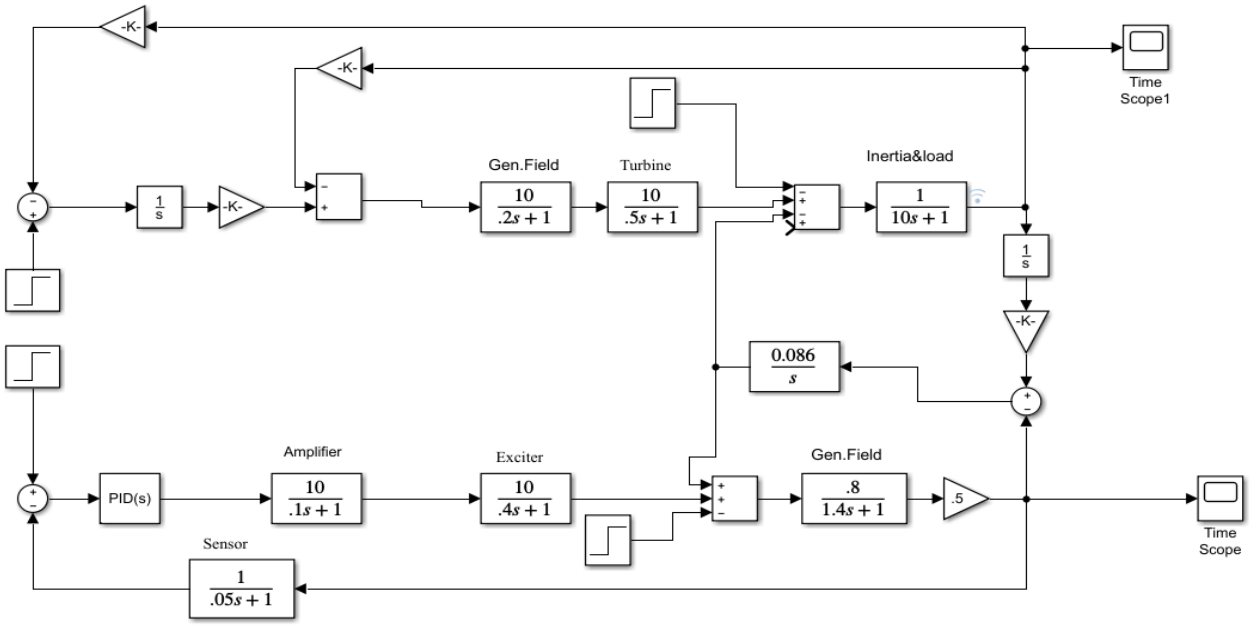

Fig. 2. SIMULINK model of two areas of AGC and AVR considering GRC

IV. SIMULATION STUDY

The AGC and AVR are implementation according to high speed loop of the , since commotion control of generator have little time fixed contributed by field winding, where AGC loop is slow motion loop be forced major time constant take part by turbine and generator determination of inertia. So that the existing transient in excitation control loop mask many fast or does not influence the AGC loop. Practically these two are not non- interacting, the interaction exists but in opposite direction. Since AVR loop influence the magnitude of generated emf this model located in the magnitude of real power and hence AVR loop felt was existed in AGC loop.

In this section develop AGC scheme is employed with AVR and considering generation rate constraint. Here coupling between AGC and AVR scheme is employed. The interaction between frequency domain and voltage cross coupling was exist and can some time disturbing. AVR loop impact the magnitude of generated emf and the internal emf magnitude of the real power. It is complemented that changes in AVR loop is felt in AGC loop. Generation rate constraint is not effect on the terminal voltage because the GRC is applied only from the speed governor system.

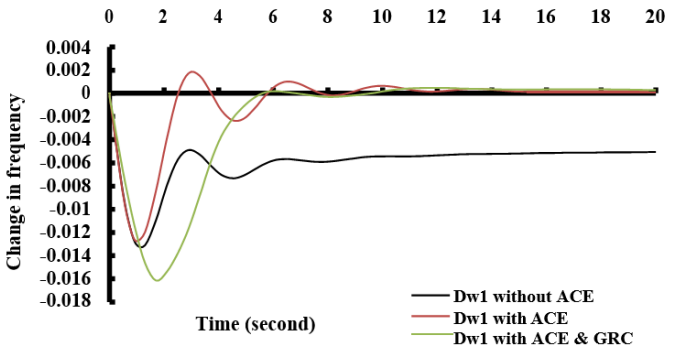

Fig. 3. Comparisons between Dw1 with and without ACE &GRC

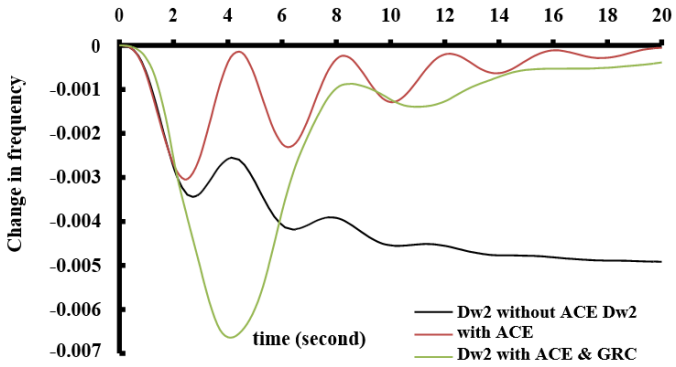

Fig. 4. Comparisons between Dw2 with and without ACE and GRC

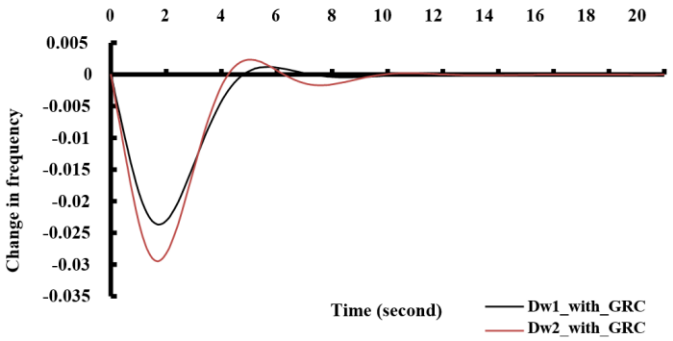

Fig.5. Change frequency of two areas AGC, AVR and GRC

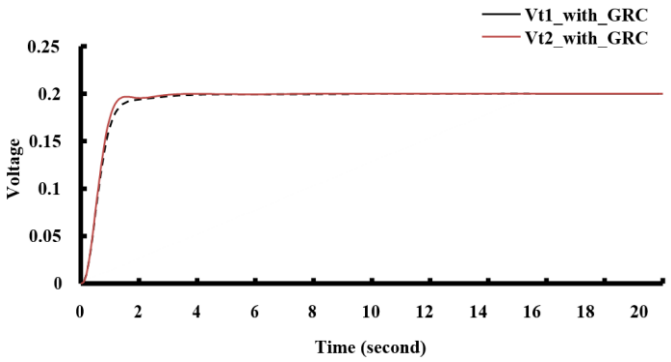

Fig.6. Terminal voltage of two areas AGC, AVR and GRC

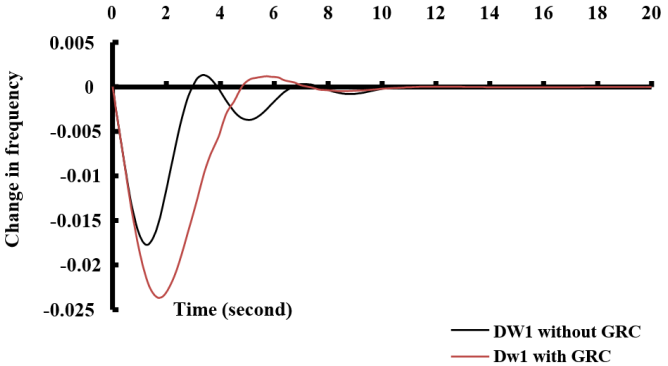

Fig.7. Comparison of change in frequency of area one

In Fig. 5 develop AGC scheme with AVR and considering generation rate constraint of two areas. Here coupling between AGC and AVR scheme is employed. The interaction between frequency and voltage exists and cross coupling does exist and can some time troublesome. AVR loop affect the magnitude of generated emf. The internal emf determines the magnitude of real power. It is concluded that changes in AVR loop is felt in AGC loop.

Fig. 6 represent the change in frequency of area 1 and area 2 the time settling and steady state error is less when coupling, Fig. 7 represent the comparison between frequency of area 1 its clear that the steady state and settling time is less but the over shoot is increase because that the GRC give the real state. Fig. 14 represent the generation rate constraint is not effect on the terminal voltage because the GRC is applied only from the speed governor system.

V. CONCLUSIONS

The two major loops that are AVR loop and ALFC loop has been studied for two areas power system. The frequency of the system is dependent on real power output and is taken care of by ALFC. Terminal voltage of the system is dependent on the reactive power of the system and is taken care of by AVR loop. The cross coupling effects between the two loops are studied that are associated with low-frequency oscillations. It has been observed that even with GRCs the system stays stable and that the response are not much different with and without Generation Rate Constraints.

REFERENCES

[1] Topno, Pretty Neelam, and Saurabh Chanana. "Tilt Integral Derivativecontrol for two-area load frequency control problem." In 2015 2nd International Conference on Recent Advances in Engineering & Computational Sciences (RAECS), pp. 1-6. IEEE, 2015.

[2] H. Bevrani, Robust Power System Frequency Control. Cham, Switzerland: Springer International Publishing, 2014.

[3] S. Saxena and Y. V. Hote, "Load frequency control in power system via internal model control scheme and model-order reduction," IEEE Trans. Power Syst., vol. 28, no. 3, pp. 2749–2757, Aug. 2013.

[4] L. Jiang, W. Yao, Q. H. Wu, J. W. Wen, and S. J. Cheng, "Delay-dependent stability for load frequency control with constant and time-varying delays," IEEE Trans. Power Syst., vol. 27, no. 2, pp. 932–941, May 2012.

[5] G. Eason, B. Noble, and I. N. Sneddon, "On certain integrals of Lipschitz-Hankel type involving products of Bessel functions," Phil.

[6] Unbehauen H, Kocaarslan I. Proceedings of 11th IFAC WoAnderson, P. M. & Fouad, A. A., 1977. Power System Control and Stability. Ames, Lowa: The LOWA State University Press.

[7] El-Saady, G., Mobarak, Y., Wahab, M., Hamada, M.M. and Abdel-Moamen, M., 2013. A new robust technique LFC of multi-area power system using SMES. International Journal of Control, Automation, and Systems, 2(1), pp.56-60.

[8] Chokpanyasuwan, C. Robot Fuzzy logic-PID Controller for Wind-Diesel Power System using Particle Swarm Optimization. In GMSARN International Conference on Sustainable Development: Issues and Prospects for the GMS, 2008.

[9] Mallesham, G., Mishra, S. and Jha, A.N. Automatic generation control of microgrid using artificial intelligence techniques. In 2012 IEEE Power and Energy Society General Meeting ,2012, July, pp. 1-8.

[10] Elmas, C., Deperlioglu, O. and Sayan, H.H. Adaptive fuzzy logic controller for DC–DC converters. Expert Systems with Applications,2009,pp.1540-1548.

[11] Parmar, K.S., Majhi, S. and Kothari, D.P. Load frequency control of a realistic power system with multi-source power generation. International Journal of Electrical Power & Energy Systems, 2012, pp.426-433.

[12] H. Goto, Y. Hasegawa, and M. Tanaka, "Efficient Scheduling Focusing on the Duality of MPL Representatives," Proc. ASME Symp. Computational Intelligence in Scheduling (SCIS 07), ASME Press, Dec. 2007, pp. 57-64, doi:10.1109/SCIS.2007.357670.

Proceedings of the Fourth International Conference on Communication and Electronics Systems (ICCES 2019)
IEEE Conference Record # 45898; IEEE Xplore ISBN: 978-1-7281-1261-9

A Dynamic Coordinator Election Algorithm in Cognitive Radio Networks

Shailendra Kumar
Computer Engineering Department
NIT Kurukshetra
Haryana, India
shailendra2750@gmail.com

Mahendra Kumar Murmu
Computer Engineering Department
NIT Kurukshetra
Haryana, India
mkmurmu9@gmail.com

Abstract*— Cognitive radio network (CRN) is the most emerging technology in wireless communication paradigm. The various components of CRNs include secondary user or cognitive user (CU), primary user or licensed user (LU), and spectrum holes. The CU is an unlicensed user which does not have license to access the spectrum. The license of the spectrum is hold by the LU. The CU nodes exploit the spectrum in an opportunistic manner in the radio environment of LU. The CU node vacates the band if LU appears and starts searching for other available unutilized band. Due to this, the researchers has experienced CRN is a highly dynamic environment. Therefore, one of generic problem coined in CRN is the coordination among the CUs for their resources. It can be viewed as, one, coordination among the CU nodes activities and, other, the channel assignment. To do this, a node may be designated as a special node called coordinator or leader that figure out which bit of the range is accessible, select the best accessible channel, facilitate access to this channel with other node, and clear the channel when another node is identified. Thus, the present contribution proposes a diffusion based coordinator election algorithm, a process to identify a coordinator in CRN. The works also illustrates flow of the algorithm using suitable examples.

Keywords*— cognitive radio network; coordinator; diffusion computation; CU; LU

I. INTRODUCTION

The radio spectrum plays most vital role in the rapid growth of wireless communication technology. In limited availability, various research studies in [1, 2] has observed that the 15% to 85% spectrum are underutilized which imposing credential rip-off in the developments of wireless industries. The cognitive radio networks (CRN) is the emerging technology that ensure the effective utilization of radio spectrum and increases efficiency. The fundamental motivation behind subjective radio system innovation is to move the underutilized authorized range which has a place with the LU which should be possible entrepreneurially. The user(s) in CRNs identifies spectrum range called white space using predefined range task technique for communication. Along these lines, in addition, there is a need of new innovation for better use of range in remote system.

CRNs have two sorts of user; one is primary user or license user (LU) which has the specialist to utilize the specific spectrum. Second is secondary user or cognitive user (CU) which not has the specialist to utilize the specific range band. There ought not to be any obstruction CU within the sight of LU. CU utilizes the spectrum range just without LU interference, artfully. In literature(s), the spectrum of CU is also called as free band or unutilized band of LU. The CRN identifies free band using following fundamental functionalities; spectrum sensing, spectrum detecting, spectrum sharing and spectrum mobility [2, 3]. The CU node keeps up a rundown of edges called local edge set (LES). From LES, few edges are used for control purposes, called public control edges (PCE), which is association set up with neighbors.

A. Problem elucidation

In CRN, a CU node is furnished with an assortment of abilities, for example, learning, proficiency, insight, believability, and working to filter for similarity and enhanced channels. The requirements of a CU node for the spectrum band changes dynamically. This may leads sporadically changes to the radio environment. Usually, the random appearance of LU plays vital impact and adds unique challenges to the CRN. The CU may observe frequent specific spectrum mismatch and hence also adds dynamicity. Therefore, the synchronization of the node(s) activity and channels is examined relative area of research in CRN like other traditional wireless ad hoc networks. The coordinator election process elect a coordinator or leader nodes which may takes care of all synchronization related jobs. In this paper, we present a dynamic coordinator selection protocol for CRN. The coordinator is significant in a CRN in light of the fact that it guarantees better spectrum usage and keeps up the quality of services (QoS). The portrayal of issues present in coordinator choice can be comprehended with the accompanying fig.1. The conduct of the CU node changes quickly to discover the range free from the LU in radio situations. The edges in fig. 1, edge(a, b), edge(a, c, d) , edge(c, d) and edge(c, d) are the free which are detected by CUs nodes 1, 2, 3 and 4 individually. The CU nodes are called neighbors anytime in the event that they have at any rate one public control edge (PCE). Diverse neighborhood look conventions can be utilize to discover a neighbor node in the cognitive radio system [8, 9]. Here, PCE of CU node of 1 and 2 is edge (a) and PCE of nodes 2, 3 and 4 are edge(c, d). The edge list can switch randomly and cause alterations to the topology because the LU can randomly arrive on its license edge at any moment.

For LU interference prediction, on LES, efficient detection method can be used [10]. If CUs have more number of PCE, their links are more stable. For example, links from 2, 3 and 4 are more stable than from 1 to 2. In CRNs CUs can move out of scope or just next to the network. However, PCE may not present because required edge is presently occupies by LU. The monitoring of CU nodes and the allocation of edges in CRNs is therefore highly challenging. We need a suitable network coordinator to ensure stronger cooperation among CUs and assign spectrum holes or edge. Due to significant functional and operational difference with the traditional wireless networks, it is not possible to apply the present coordinator election procedures in CRN. We therefore need to develop a coordinator election technique appropriate for cognitive radio networks.

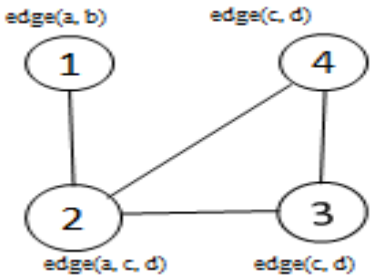

Fig. 1 Example scenario

B. Coordinator election in cognitive radio networks

By and large, coordinator elections are a solitary procedure. Once, the coordinator election computation algorithm is over, there is just a single chief in the networks. The special node act as the coordinator of the allotted task and the rest of the nodes will work ordinarily. The available coordinator can guarantee better coordination among CUs and proficient channel portion as portrayed above.

C. Proposed model

In our proposed framework, we consider a cognitive radio networks which comprises of *m* nodes and *p* edges. The CU is represented using unique *id* for portrayal in the system. Our coordinator decision protocol is based on diffusion computation [11] for extrema finding. Eventually, the proposed algorithm finds the max *id* node as the coordinator. The computation gets started as soon as departure of a leader is observed by any node. The node will be treated as source or initiator *(initial_node)*. As the diffusion method spreads, it creates the spanning tree. In case if multiple nodes start diffusion computation simultaneously, only higher *id* diffusion node survives. If a node receives election message, it is acknowledges using acknowledgement message. On receiving multiple acknowledgements, the initial node selects the highest *id* node as a leader and informs other. If a node *i* observe the presence of LU in the channel, the node removes immediately from the network.

II. RELATED WORK

There are several conventions for ad hoc networks focused on diffusion computation found in literature [12-14]. TORA [18] is a well-known directing convention dependent on diffusion computation. The messages can be tracked among remote system nodes. In CRN, not many coordinator decision conventions have been suggested. Bansal et al. [16] suggested two election coordinator conventions for a single multi-channel jump radio scheme without any identification of effect, one probabilistic and one randomly assigned. The election of the coordinator of this convention takes place at various phases. The measurement of name room is reduced by a factor of 2 in every span of the previous round. The selected node will be proclaimed as the system coordinator at the end of the specific phase. The entire round number depends on the amount of nodes in the scheme. The method used by randomization is probabilistic. In the final phase, only the CU node is dynamic and tuned in. In particular, as a system coordinator, a CU node, involved in the last phase of communication, is declared. In a fully-connected cognitive radio system, Arachchige et al.[17] suggested an unequal strategy to coordinator choice. Furthermore, the designers have used the neighboring revelation coordinator node. Exactly, the scheme coordinator of a CU node participating in the last phase is declared. The neighboring CU node dependably stay associated with one another with at any rate one normal edge. The CU nodes interface in different methods of activity trading control messages so as to play out the decision. Mittal et al.[8] shows a crash-considered cognitive radio system election convention. The assessment suggested in [16] is an extension of the diffusion. The designers anticipate the scheme to be uniform. There might be more than one coordinator in the instinctual systems of size. Two coordinator are 2x times separated.

In the event that two chiefs exist inside the inclusion zone, the determination of a coordinator is performed based on [16]. The work in [18] depicts list strategy for coordinator decision. The creators have figured an articulation for processing sampling components (SF). The parameters include amount of energy (E), CU quantity (Z) and free links (K). The aim is to determine the estimated CU nodes for the sample components (SC). As cognitive radio coordinator a CU node with the highest notable sampling component (SC) value pronounces itself. Author in [15], proposed leader election protocol for CRNs in which diffusion computation technique and message passing is used. A bio-inspired coordination election protocol for CRNs is proposed in [19], the protocol utilizes ant's intelligence to investigate the radio spectrum.

III. SYSTEM MODEL

We assume a cognitive radio networks consists of *m* CUs and *p* correspondence channel. The CU user communicates with each other using communication channel. The communication channels are also termed as links or edges. The edges are bidirectional and not really FIFO.. Every CU has unique identification number(*id*) which is used to

represent by natural number system. We use diffusion computation method and message passing approach to find the maximum identity node in the network. Every node is assumed to maintain some set of data structure during message passing in leader election process. The quantity of all edges acquaints by all CUs is known as the global edge set (GES). We consider various information and message, given in table I. Other assumptions are listed as follows which have been used in our algorithm.

A. Communication edges

The CU nodes are associated intelligently through the correspondence edges.

B. Unique identification number

id is the natural numbers.

C. Diffusion computation

In diffusion computation process, election instance is generated. The election message is spread over the network. This is also called as the expansion of the spanning tree.

D. Highest id node finding

The algorithm finds maximum *id* node as the coordinator in the networks. If we observe more than one initiators, the node with highest *id* will give higher preference.

E. Communication network

CUs are associated in the correspondence organize. We utilize radio range or edges *(channel*) for the system creation in the cognitive radio networks. The communication networks reveal spanning tree while coordination process is in progress.

F. Interference of primary user

When LU appears, the CU needs to disengage itself from that specific edge, immediately, if single PCE present. This situation can be taken care of by *prob_reply ()* function.

IV. PROPOSED ALGRITHM

A. Description of data structure and messages

The following table I and II listed various data structures and message used in the algorithm.

TABLE I.

Abbreviation	***Description***
Buffer	*Stores id of initial node received in Election message*
Count_ (child)	*Signifies number of election message received by ith node.*
Parent_id	*Signifies current parent node for computation.*
Child_id	*Signifies current child node for computation.*
Involve	*Signifies whether node i is participating in election or coordinator.*
Initial_node	*Signifies current node id who started election.*
Ack_buffer	*Stores nodes from where A_ck have to come*
Max_id	*Stores highest downstream node including that particular node*
E_M	*Message to expand the spanning tree*
A_ck	*Message to recognize receipt of an E_M*
Lead_id	*Message to declare the new coordinator*
probe	*Message to decide whether a hub is as yet associated*
Reply	*Message sent because of a Probe message*
Nbl	*Stores neighbor of a node*

TABLE II

Function	***Explanation***
Initiat_prob( )	*If reply from child doesn't come parent remove the child from Ack_buffer* *If probe from parent doesn't come child announce leader*

B. Text of proposed algorithm

The present coordinator election algorithm has been shown in the three procedural steps as following.

Procedure 1: initialization and broadcasting

1. *Node observe departure of leader, initial_node=node_id*
2. *Init(initial_node)*
3. *Involve(initial_node)=1, parent_id=node _id, max_id= node _id, Ack_buffer=Nbl_initial_node*
4. *Broadcast E_M(initial_node,Lead_id ,parent_id) to child*

5. *While parent_id.Lid==child_id.Lid*
    a. *Involve(child_id)=1*
    b. *Max=child_id*
    c. *Initiate_probe(parent_id, child_id)*
    d. *While received E_M*
        i. *Count(child_id)++*
        ii. *Buffer[]=initial_node*
    e. *End While*
    f. *If(count(child_id)>1)*
    g. *Compute_max_initial_node_using_buffer(child_id)*
    h. *Ack_buffer=Nbl_child except parent*
    i. *Parent_node=child_node*
    j. *Broadcast E_M(initial_node, Lid,Parent_node)to child*
6. *End While*
7. *Discard E_M and send N_Ack as node has different leader OR same E_M originator*

Procedure 2: Receiving Acknowledgement

1. *Upon receiving A_ck from node j, Remove j from Ack_buffer compute max_ id*
2. *While ack buffer is empty*
3. *If node is initial node then lead_id=max_id and broadcast lead message(lead_id) to the child*
4. *Else send A_ck(max_id) to parent*
5. *End if*
6. *End while*

Procedure 3: Announcing leader in network

1. *Upon receiving lead message(lead_id)*
2. *While node.involve==1*
3. *Node.lead=lead_id and set Node.Involve=0*
4. *Broadcast leader message to child*
5. *End while*
6. *If node.involve=0*
7. *Then find max leader and broadcast lead message (lead_id)to smaller leader sub network*
8. *End if.*

C. Description of algorithm

The proposed convention is given in content. This convention contains three system procedures: Iinitialization and broadcasting, Receiving Acknowledgment, and Aannouncing leader in the networks. For appraisal of figuring, we use a couple of data structure and messages which are given in the table I. In the midst of the count system every node keeps up that data structure. On amid the computation procedure, every node may reach in any procedure and acts the states of the system, accordingly.

Essentially, we will depict the convention in three cases; in first, there is no interference of LU impedance or node portability and node crashes. In next, it will contain states of disappointment because of LU impedance or node versatility and node crashes. The progress of protocol in first case is appeared in text. Thus, in our proposed convention when any node observe departure of its coordinator, it will begin the computation by instating itself as an initial node, and communicate the election message to its child or neighbor by keeping up the every one of the data structure. The *E_M* message advances data structure, for example, *id* of the initial node for particularly called initiator node. In the event that various elections *E_M* message received by any node *i* from initiator, the message is simply discarded and *N_Ack* send to the parent. The *A_ck* message is utilized to recognize the *E_M* message so as to recoil the spreading over tree. The *A_ck* message answers *Max_id* of node *i*. At the point when the initial node receives acknowledgement *(A_ck)* from all neighbors, the initiator node presently has the most noteworthy *id* put away in *Max_id*. The initiator node declared most extreme node as a coordinator for the associated CU node *i* in cognitive radio networks.

Leader message is used to declare the coordinator. If LU intrude on the channel, the influenced node leaves the channel and this situation can be dealt with by *initial_probe( )*. In this, if reply of child does not come in finite time, the parent will expel child from its *ack_buffer* list. On the off chance that prob from parent does not come in fix measure of time, child node will report the leader in sub network going about as a virtual initiator in light of the fact that in the long run it will have most extreme *id* in its sub network. The partaking CU node *i* have exceptional identifier esteem go from 1….*m*. In the event when node with *involve= 0*, represent it has leader. Otherwise, it is 1 and starts to search for a coordinator. At the point when any node receives *E_M* and on the off chance that its leader and parent leader is same and involve is 0, at that point node involve in the computation. Each time, on receiving *E_M*, every node will augment its *count(child)*. At the point when count of node more noteworthy than 1 node chooses highest *id* CU as initiator node and rest of the nodes are consider as ordinary CU. After getting the *E_M* if node have its leader *(involve=0)* or originator of election message is same node will basically dispose of the message and send *N_Ack*. Otherwise node will take an interest all the while and communicate the election message to neighbor aside from the parent node in the wake of introducing the *Ack_buffer*. Second part of calculation is getting of affirmation. At the point when any node gets the *A_ck* or *N_Ack* from node j it will expel j from the *Ack_buffer* list. Node need to figure the maximum *id* and update *Maxi_id* if *A_ck* got. In the event that *Ack_buffer* is vacant and node isn't starting node it will send the *A_ck* to its parent with most extreme id node of downstream network. Third procedure is receiving the leader message. After accepting leader message there will be two possibilities the node is either have its coordinator or it is hanging tight for the leader. On the off chance that node has its leader, at that point most extreme *leader_id* node will be chosen as leader and new leader will be declared to littler leader sub network otherwise node will store its new leader. The working of algorithm is given in fig. 2, 3, and 4.

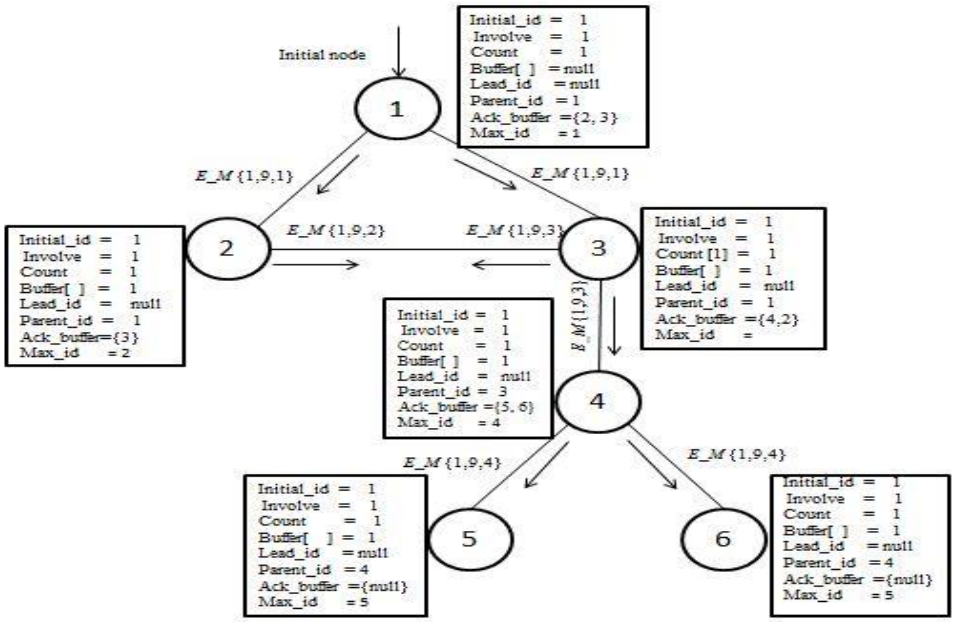

Fig. 2 Initialization and *E_M* broadcasting

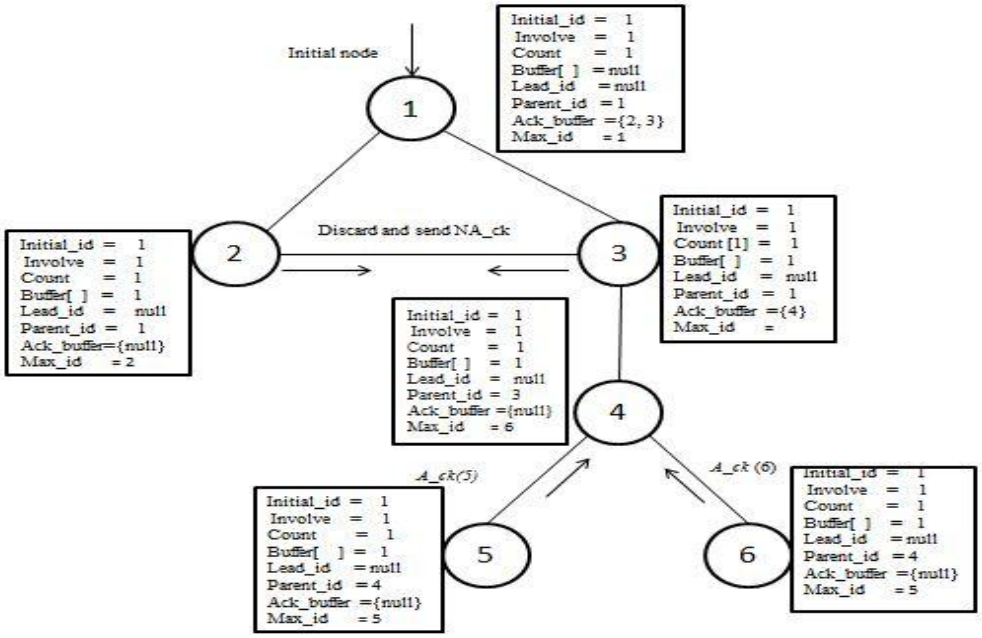

Fig. 3 Acknowledgement delivering

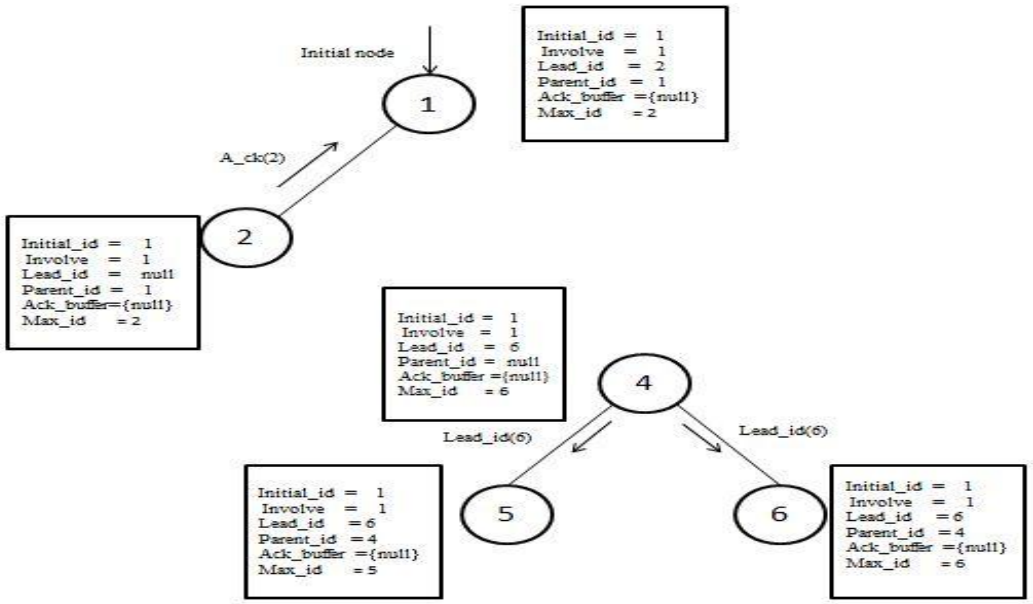

Fig. 4 Handling failure condition and announce leader

V. CONCLUSION

We proposed a coordinator election algorithm to find a maximum *id* node in cognitive radio networks. We have used diffusion computation method to find a coordinator node. The illustration of the algorithm has been included to verify the fairness of the protocol. It is an improved version of the diffusion based leader election protocol in CRN. The example demonstration claims its dynamicity while performing coordination election in cognitive radio networks.

VI. REFERENCES

[1] Fragkiadakis, A., Angelakis, V., & Tragos, E. Z. (2014). Securing cognitive wireless sensor networks: a survey. *International Journal of Distributed Sensor Networks*, *10*(3), 393248.

[2] Akyildiz, I. F., Lee, W. Y., Vuran, M. C., & Mohanty, S. (2006). NeXt generation/dynamic spectrum access/cognitive radio wireless networks: A survey. *Computer networks*, *50*(13), 2127-2159.

[3] Akyildiz, I. F., Lee, W. Y., & Chowdhury, K. R. (2009). CRAHNs: Cognitive radio ad hoc networks. *AD hoc networks*, *7*(5), 810-836.

[4] Kumar, P., & Murmu, M. K. (2015, September). An enhanced leader election for Cognitive Radio Ad-Hoc Networks. In *2015 1st International Conference on Next Generation Computing Technologies (NGCT)* (pp. 192-197). IEEE. *Technologies (NGCT)*, pp. 192-197. IEEE, 2015.

[5] Asterjadhi, A., & Zorzi, M. (2010). JENNA: a jamming evasive network-coding neighbor-discovery algorithm for cognitive radio networks [Dynamic Spectrum management]. *IEEE Wireless Communications*, *17*(4), 24-32.

[6] Kulkarni, S., & Markande, S. (2015, January). Comparative study of routing protocols in cognitive radio networks. In *2015 International Conference on Pervasive Computing (ICPC)* (pp. 1-5). IEEE.

[7] Cheng, Geng, Wei Liu, Yunzhao Li, and Wenqing Cheng. "Spectrum aware on-demand routing in cognitive radio networks." In *2007 2nd IEEE International Symposium on New Frontiers in Dynamic Spectrum Access Networks*, pp. 571-574. IEEE, 2007.

[8] Mittal, Neeraj, Srinivasan Krishnamurthy, R. Chandrasekaran, Subbarayan Venkatesan, and Yanyan Zeng. "On neighbor discovery in cognitive radio networks." *Journal of Parallel and Distributed Computing* 69, no. 7 (2009): 623-637.

[9] Khan, Athar Ali, Mubashir Husain Rehmani, and Yasir Saleem. "Neighbor discovery in traditional wireless networks and cognitive radio networks: Basics, taxonomy, challenges and future research directions." *Journal of Network and Computer Applications* 52 (2015): 173-190.

[10] Guibène, Wael, and Dirk Slock. "Cooperative spectrum sensing and localization in cognitive radio systems using compressed sensing." *Journal of Sensors* 2013 (2013).

[11] Conry, Susan E., Robert A. Meyer, and Victor R. Lesser. "Multistage negotiation in distributed planning." In *Readings in distributed artificial intelligence*, pp. 367-384. Morgan Kaufmann, 1988.

[12] Vasudevan, Sudarshan, Neil Immerman, Jim Kurose, and Don Towsley. "A leader election algorithm for mobile ad hoc networks." *UMass Comp. Sci. Tech. Rep* (2003).

[13] Vasudevan, Sudarshan, Brian DeCleene, Neil Immerman, Jim Kurose, and Don Towsley. "Leader election algorithms for wireless ad hoc networks." In *Proceedings DARPA Information Survivability Conference and Exposition*, vol. 1, pp. 261-272. IEEE, 2003.

[14] Derhab, Abdelouahid, and Nadjib Badache. "A self-stabilizing leader election algorithm in highly dynamic ad hoc mobile networks." *IEEE Transactions on Parallel and Distributed Systems* 19, no. 7 (2008): 926-939.

[15] Murmu, M. K., & Singh, A. K. (2017). A leader election protocol for cognitive radio networks. *Wireless Personal Communications*, *97*(3), 3773-3791.

[16] Bansal, Tarun, Neeraj Mittal, and Subbarayan Venkatesan. "Leader election algorithms for multi-channel wireless networks." In *International Conference on Wireless Algorithms, Systems, and Applications*, pp. 310-321. Springer, Berlin, Heidelberg, 2008.

[17] Arachchige, Chanaka J. Liyana, S. Venkatesan, and Neeraj Mittal. "An asynchronous neighbor discovery algorithm for cognitive radio networks." In *2008 3rd IEEE Symposium on New Frontiers in Dynamic Spectrum Access Networks*, pp. 1-5. IEEE, 2008.

[18] Olabiyi, Oluwatobi, Annamalai Annamalai, and L. Qian. "Leader election algorithm for distributed ad-hoc cognitive radio networks." In *2012 IEEE Consumer Communications and Networking Conference (CCNC)*, pp. 859-863. IEEE, 2012.

[19] Murmu, M. K., & Singh, A. K. (2018). A bio-inspired leader election protocol for cognitive radio networks. *Cluster Computing*, 1-14.

Proceedings of the Fourth International Conference on Communication and Electronics Systems (ICCES 2019)
IEEE Conference Record # 45898; IEEE Xplore ISBN: 978-1-7281-1261-9

A Multi-Hop Low Duty Cycle MAC protocol for Wireless Sensor Networks

Kumar Debasis, M. P. Singh and Rajat Gupta
Computer Science and Engineering Department, National Institute of Technology Patna, Bihar, India
({debasis.cse14, mps, rajat160454}@nitp.ac.in)

***Abstract*— The proposed model, Multi-Hop Low Duty Cycle Medium Access Control (MLDC-MAC) protocol, assumes that the deployment area is composed of equal-sized grids. The sensor nodes that fall within a grid are considered to be the part of the same cluster. The base station appoints the node with the highest residual energy as the cluster head in each grid. The base station also establishes multi-hop paths for communicating with the cluster heads and broadcasts the schedule for inter-cluster communication in the network. After receiving this information, each cluster head broadcasts a schedule for intra-cluster communication within its cluster. When a cluster head receives data from the source nodes in its cluster, it computes the aggregate and sends it to the base station. The simulation results show that MLDC-MAC increases the network lifetime compared with Low Duty Cycle MAC (LDC-MAC) protocol and Bit-Map-Assisted MAC (BMA-MAC) protocol.**

Keywords*— *Data Slot, Control Slot, Energy, Radio, Communication.

I. INTRODUCTION

A Wireless Sensor Network (WSN) is a collection of numerous autonomous devices (sensor nodes) that are deployed in a region to monitor the physical or environmental conditions and report it to a Base Station (BS) [1], [2]. Once deployed, a WSN may be required to provide uninterrupted services for several days or even years. Nonetheless, sensor nodes are powered by small batteries which have low energy storage capacities. Moreover, if the geographic or climatic conditions are not favourable, replacing or recharging the batteries is not a feasible solution. Hence, Medium Access Control (MAC) protocols that are designed for WSNs, inherently include one or more energy saving schemes to meet the network objectives [3], [4].

Usually, the radio/transceiver of a sensor node consumes the maximum amount of energy in its lifetime. It has been found that the radio drains a considerable amount of energy even when it is idle (neither transmitting nor receiving) [5], [6]. To this end, most of the MAC protocols turn OFF the radio when it is not working. In Time Division Multiple Access (TDMA) based MAC protocols, each node is allotted one or more slots in a periodically repeating time frame during which it can send/receive data. At all other times, the node keeps its radio OFF to conserve energy. This helps in minimizing energy consuming factors like overhearing, idle listening and collision.

Clustering is another technique to conserve the energy of sensor nodes in which nodes are grouped into clusters and one node in each cluster is appointed as the cluster-head (CH). The function of the CH is to collect data from all the non-cluster-head (non-CH) nodes and forward it to the BS. Hence, non-CH nodes are involved in short-range communications only.

This paper presents a cluster-based multi-hop routing protocol named Multi-Hop Low Duty Cycle MAC (MLDC-MAC) in which the deployment area is composed of *n* equal-sized grids. Sensor nodes falling within a grid are considered to be the part of the same cluster. The BS appoints the node with the highest residual energy as the CH in each cluster. All the CHs communicate with the BS via multi-hop paths that are established during the setup phase of the protocol. MLDC-MAC adopts a centralized CH election scheme which results in uniform distribution of CHs in the network. An efficient CH rotation scheme (enforced by the rule to appoint the node with the highest residual energy as the CH in each cluster) ensures even distribution of load among the nodes in the network.

This paper is organized as follows. Section II discusses the related work. Section III describes the working of the proposed model. Section IV discusses the results of the simulations and section V concludes the paper.

II. RELATED WORK

In BMA-RR [7], the cluster formation process is same as LEACH [8]. The overall working of BMA-RR is same as BMA-MAC [9]. However, a source node can claim multiple data slots as per its requirement. After receiving control messages from all the source nodes, the CH gets to know how many data slots each source node requires. Based on this information, the CH sets up and broadcasts a TDMA schedule. A one-bit S/R flag informs the node whether it should go into sending mode or receiving mode during the allocated slots. As the name suggests, data slot(s) are allotted on a round-robin basis. A node turns its radio ON during the allocated data slot(s) to perform the assigned task. A one-bit data mode flag informs the CH if the destination is any other node. If the data is for any other node, CH will forward it to that node in the next session. In BMA-RR, nodes with multiple data slots toggle their radios between ON and OFF numerous times within a frame.

BS-MAC [10] follows the same procedure during the set-up phase as discussed above. Towards the end of the set-up phase, each CH broadcasts a Control Slot allocation (CS_ALLOC) message in which it assigns one control slot to each non-CH. This message also contains unique 1-byte short

addresses for the CH and its members to communicate among themselves. A source node sends a control message in its control slot whereas a non-source node keeps its radio OFF to save energy. Each CH uses Shortest Job First (SJF) Algorithm to assign data slots to the source nodes and this information is broadcast through a data slot announcement (ADS_ANN) message. A source node wakes up during the allotted data slot(s) to transmit/receive data to/from its CH. If a node wants to send data to another node, it has to be sent to the CH in the current session. In the next session, the CH will forward the data to the destination node.

BEST-MAC [11] is a modification of BS-MAC in which a Contention Access Period (CAP) is introduced after the control slots. The nodes which could not join the network during the set-up phase send join-request messages during this period. A CH acknowledges the receipt of these messages but does not assign control slots to such nodes. They are allocated control slots in the announcement period when the CH allocates data slots to the source nodes. Data slot allocation is done on the basis of the Knapsack Optimization Algorithm. BEST-MAC also uses shorter time slots which can lead to frequent reservation and scheduling. The CAP may lead to idle listening of CHs after a few sessions. This is so because all the left-out nodes may have joined the network by then.

In LDC-MAC [12], the setup phase is same as LEACH. After the formation of clusters, each CH broadcasts a schedule in its cluster. Every non-CH node is allotted one control slot and one data slot. A source node transmits a control message and a data message in the allocated control slot and data slot respectively. A non-source node keeps its radio OFF for the entire duration of the frame. A CH identifies the source nodes by the control messages received from them and stays awake during the corresponding data slots. However, in this process the CH may have to toggle its radio between ON and OFF multiple times within a frame. Moreover, data slots that are not used by their owners are wasted.

The proposed model is a modification of LDC-MAC in which CHs are appointed by the BS. They communicate with the BS via multi-hop paths that are established during the set-up phase of the protocol. In the next section, the proposed model has been discussed in detail.

III. PROPOSED MODEL

The proposed model assumes that the deployment area is composed of *n* equal-sized grids. Sensor nodes lying in a grid are considered to be the part of the same cluster. All the sensor nodes are homogenous, stationary, and fitted with GPS devices that can be used to know their locations. It is assumed that each node in the deployment area can transmit to the BS directly. It is also assumed that all the nodes are time synchronized. This can be achieved by having the BS broadcast a synchronization pulse at the start of each round. The proposed model divides a round into two phases: Set-up Phase and Steady-state Phase. Fig. 1 shows the working of MLDC-MAC protocol.

A. Set-up Phase

After deployment, each sensor node transmits a HELLO message to the BS. This message contains information which is in the following format – (SN_{id}, SN_{loc}, SN_{re}). Here SN_{id} represents the sensor node ID, SN_{loc} represents its location, and SN_{re} represents its residual energy. After receiving HELLO messages from all the sensor nodes, BS chooses the node which has the highest SN_{re} as the CH in each grid. If two or more nodes fulfil this criterion, then any node can be elected CH randomly. A node whose SN_{re} is below a predefined threshold is not considered in the CH election process.

After CH election, BS broadcasts a duty allocation (DUTY) message that contains information for each node which is in the following format- (SN_{id}, CH_{id}, SN_{loc}). Here, CH_{id} is the ID of the node's CH. If the CH_{id} for a node matches the ID of the node, then the node itself has been elected as a CH for the current round. The DUTY message informs each non-CH node about the allotted CH. It also informs each CH about the non-CH nodes in its cluster.

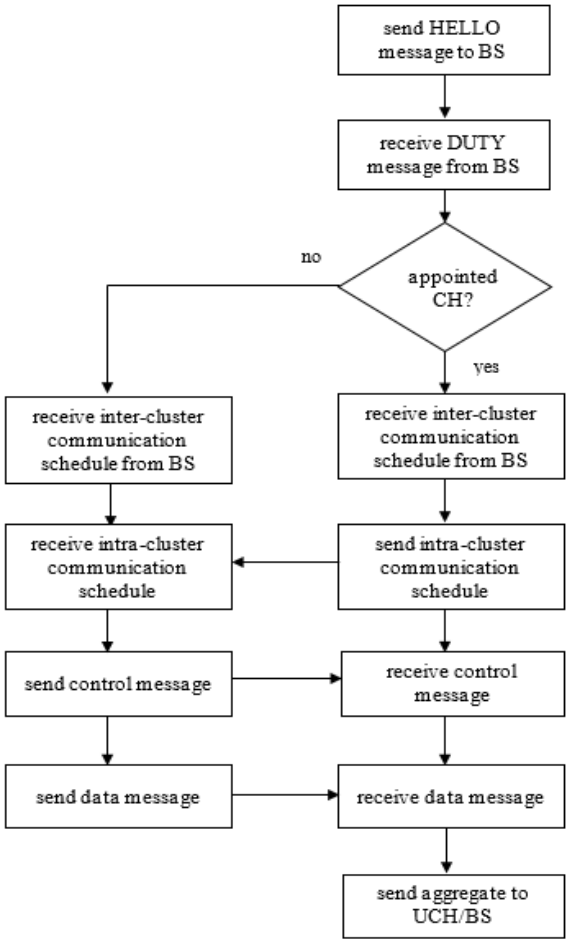

Fig. 1. Working of MLDC-MAC protocol

After a timeout period, BS broadcasts the schedule for inter-cluster communication (SCH_{bs}) in the network. This message contains information about the locations and sizes of control slots and data slots in a frame. The message also contains information for each CH which is in the following format – (SN_{id}, UCH_{id}, DS_{num}, UCH_{loc}). Here, SN_{id} represents the ID of a CH and not a non-CH node. Here, UCH_{id}

represents the ID of the upstream CH, DS_{num} represents the data slot number in which the CH should communicate with its upstream CH, and UCH_{loc} represents the location of the upstream CH. Each CH can identify its upstream CH and the data slot allocated for inter-cluster communication from SCH_{bs} message.

After receiving SCH_{bs} message, each CH broadcasts the schedule for intra-cluster communication (SCH_{ch}) in its cluster. This message contains information for each non-CH node which is in the following format – (SN_{id}, CS_{num}, DS_{num}). Here, SN_{id} represents the ID of a non-CH node, CS_{num} represents the control slot that has been allotted to it, and DS_{num} represents the data slot that has been allotted to it. Each non- CH node identifies the allotted control slot and data slot from SCH_{ch} message. The number of control slots and data slots within the intra-cluster communication period of a frame is fixed. Hence, some data slots and control slots may go unused depending on the size of the cluster.

B. Steady-state Phase

The steady-state phase consists of *k* equal-sized frames. A source node sends a control packet to its CH in the allocated control slot. The control packet informs the CH that the non-CH node will be using its data slot to send a data packet. So, the CH keeps its radio ON during the corresponding data slot. The CH computes the aggregate of all the collected data, and sends it to its upstream CH/BS during the slot allocated in the inter-cluster communication period. A new round begins after k frames in which each sensor node sends a HELLO message and the whole process is repeated again.

IV. Results and Analysis

All the protocols, MLDC-MAC, LDC-MAC, and BMA-MAC are simulated using the Python Programming Language. In all the simulations, the First Order Radio Model [8] is used to calculate the energy consumption in sensor nodes. Table I shows the parameters that are used in the simulations. Here, E_{elec} represents the energy spent in running the transmitter or receiver circuitry, E_{idle} represents the energy spent in idle mode and ϵ_{amp} represents the energy spent in running the transmit amplifier. The BS is assumed to be located outside the deployment area but very close to it. The result shown for a simulation is the average of the results generated in 10 iterations of that simulation.

TABLE I. Simulation Parameters

Parameters	***Values***
Deployment area (A)	50×50 m^2, 100×100 m^2
Initial energy of node	10 Joules
E_{elec}	50 nJ/bit
E_{idle}	40 nJ/bit
ϵ_{amp}	100 pJ/bit/m^2
Threshold energy	0.1 Joules
Data/Schedule message size	500 Bytes
Control message size	20 Bytes
Number of frames in a round	20
Number of CHs (C)	16, 25
Number of nodes (N)	100, 200

Each simulation result is followed by a table that represents the result in terms of RF (round number in which the first node dies) and RL (round number in which the last node dies) for each protocol that is simulated. For each protocol, the RF value is assumed to be the network lifetime in the protocol. Hence, the percentage increase/decrease in the network lifetime can be calculated by comparing the RF value in one protocol with the RF value in another.

For the first simulation, 100 nodes are randomly deployed in a 100×100m^2 area and the number of CHs is 16. Fig. 2 shows the graph that is generated after the first simulation. Table II shows when the first node and the last node of each protocol dies in the first simulation.

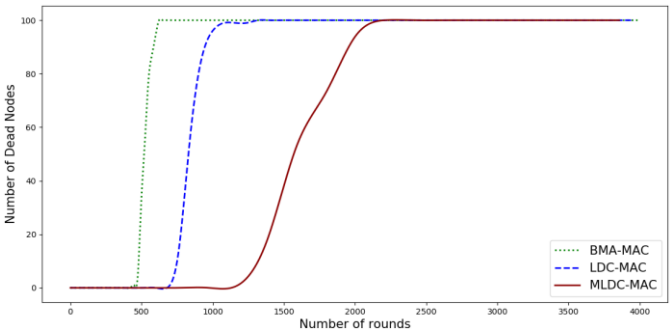

Fig. 2. First Simulation: N=100, A=100×100m^2, C=16.

TABLE II. Results of First Simulation in terms of RF and RL

Protocol	***RF***	***RL***
BMA-MAC	446	600
LDC-MAC	719	1264
MLDC-MAC	1119	2073

For the second simulation, 200 nodes are randomly deployed in a 100×100m^2 area and the number of CHs is 16. Fig. 3 shows the graph that is generated after the second simulation. Table III shows when the first node and the last node of each protocol dies in the second simulation.

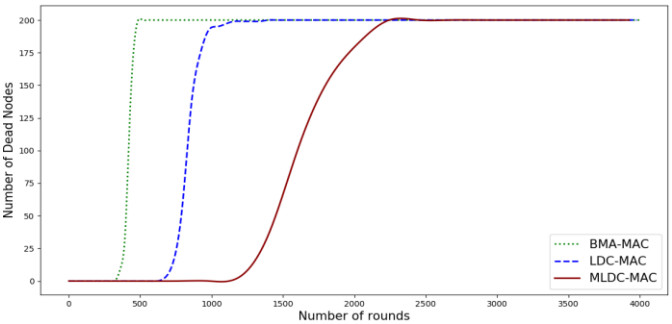

Fig. 3. Second Simulation: N=200, A=100×100m^2, C=16.

TABLE III. Results of Second Simulation in terms of RF and RL

Protocol	***RF***	***RL***
BMA-MAC	312	478
LDC-MAC	636	1350
MLDC-MAC	1126	2106

It is seen that MLDC-MAC saves more energy than BMA-MAC and LDC-MAC in the first and second simulations. Further, the performance of MLDC-MAC is better when 200 nodes are deployed in a 100×100m^2 area than when 100 nodes are deployed in the same area. This is evident from the fact that the RF value in MLDC-MAC is higher in the second simulation than the first simulation.

For the third simulation, 100 nodes are randomly deployed in a 100×100m^2 area and the number of CHs is 25. Fig. 4 shows the graph that is generated after the third simulation. Table IV shows when the first node and the last node of each protocol dies in the third simulation.

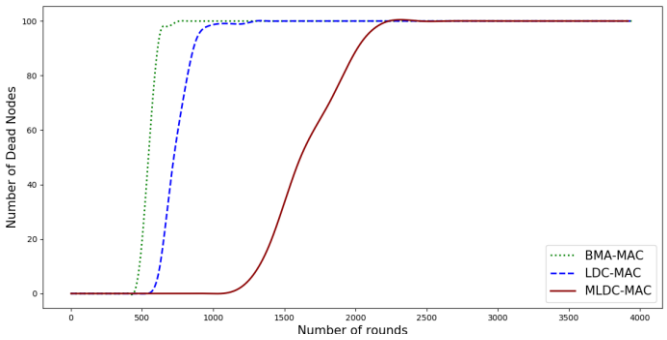

Fig. 4. Third Simulation: N=100, A=100×100m^2, C=25.

TABLE IV. RESULTS OF THIRD SIMULATION IN TERMS OF RF AND RL

Protocol	*RF*	*RL*
BMA-MAC	448	720
LDC-MAC	556	1244
MLDC-MAC	1110	2103

For the fourth simulation, 200 nodes are randomly deployed in a 100×100m^2 area and the number of CHs is 25. Fig. 5 shows the graph that is generated after the fourth simulation. Table V shows when the first node and the last node of each protocol dies in the fourth simulation.

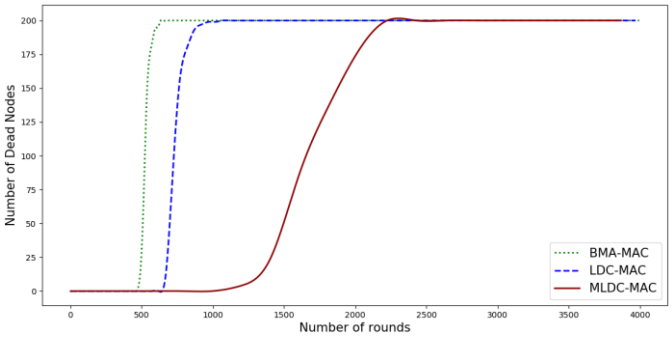

Fig. 5. Fourth Simulation: N=200, A=100×100m^2, C=25.

TABLE V. RESULTS OF FOURTH SIMULATION IN TERMS OF RF AND RL

Protocol	*RF*	*RL*
BMA-MAC	468	618
LDC-MAC	638	1024
MLDC-MAC	1167	2100

It is seen that MLDC-MAC saves more energy than BMA-MAC and LDC-MAC in the third and fourth simulations also. Additionally, the RF value in MLDC-MAC is higher in the fourth simulation than the third simulation. Hence, it can be concluded again that performance of MLDC-MAC is better when 200 nodes are deployed in a 100×100m2 area than when 100 nodes are deployed in the same area.

For the fifth simulation, 100 nodes are randomly deployed in a 50×50m^2 area and the number of CHs is 25. Fig. 6 shows the graph that is generated after the fifth simulation. Table VI shows when the first node and the last node of each protocol dies in the fifth simulation.

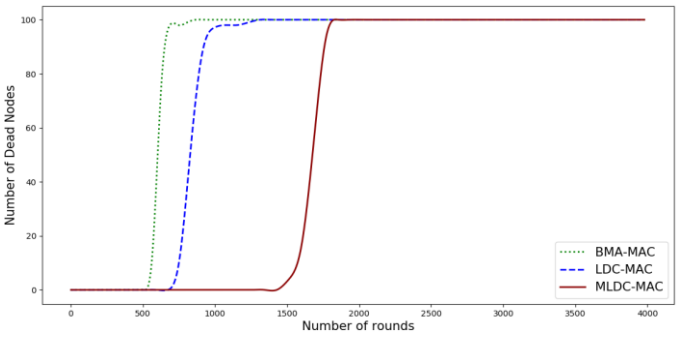

Fig. 6. Fifth Simulation: N=100, A=50×50m^2, C=25.

TABLE VI. RESULTS OF FIFTH SIMULATION IN TERMS OF RF AND RL

Protocol	*RF*	*RL*
BMA-MAC	534	828
LDC-MAC	706	1308
MLDC-MAC	1496	1785

For the sixth simulation, 200 nodes are randomly deployed in a 50×50m^2 area and the number of CHs is 25. Fig. 7 shows the graph that is generated after the sixth simulation. Table VII shows when the first node and the last node of each protocol dies in the sixth simulation.

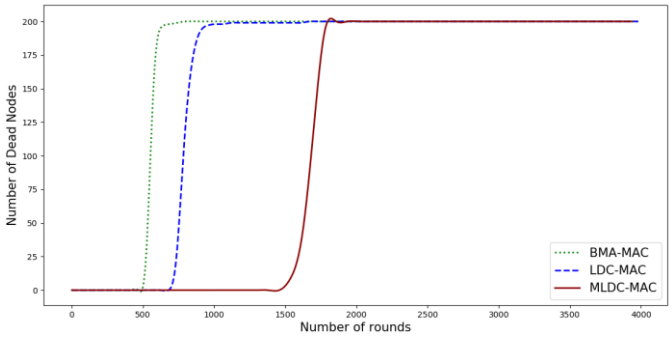

Fig. 7. Sixth Simulation: N=200, A=50×50m^2, C=25.

TABLE VII. RESULTS OF SIXTH SIMULATION IN TERMS OF RF AND RL

Protocol	*RF*	*RL*
BMA-MAC	495	784
LDC-MAC	700	1624
MLDC-MAC	1474	1783

It can be concluded from the results of the fifth and sixth simulations that MLDC-MAC saves more energy than LDC-MAC and BMA-MAC in both the simulations. When the results of the third and fifth simulations are compared, it is found that MLDC-MAC performs better when 100 nodes are deployed in a 50×50 m^2 area than when they are deployed in a 100×100 m^2 area. Similarly, on comparing the results of fourth and sixth simulations, it is found that MLDC-MAC performs better when 200 nodes are deployed in a 50×50 m^2 area than when they are deployed in a 100×100 m^2 area.

V. Conclusion and Future Scope

MLDC-MAC has a centralized approach towards cluster head election unlike LDC-MAC and BMA-MAC. In MLDC-MAC, the BS is responsible for electing cluster heads in the network. This ensures that the cluster heads are evenly distributed throughout the network. MLDC-MAC establishes multi-hop paths between cluster heads and the BS. This eliminates the requirement of long-range communications that are inevitable in LDC-MAC and BMA-MAC. The simulation results show that MLDC-MAC saves more energy than LDC-MAC and BMA-MAC. The performance of the proposed protocol can be further enhanced by dynamically varying the size of grids for even distribution of load.

Acknowledgment

The authors would like to acknowledge the Ministry of Electronics and Information Technology (MeitY), Government of India, for supporting the research work through ‘Visvesvaraya PhD Scheme for Electronics and IT’.

References

[1] Yick, Jennifer, Biswanath Mukherjee, and Dipak Ghosal. "Wireless sensor network survey." Computer networks 52, no. 12 (2008): 2292-2330.

[2] Akyildiz, Ian F., Weilian Su, Yogesh Sankarasubramaniam, and Erdal Cayirci. "A survey on sensor networks." IEEE Communications magazine 40, no. 8 (2002): 102-114.

[3] Demirkol, Ilker, Cem Ersoy, and Fatih Alagoz. "MAC protocols for wireless sensor networks: a survey." IEEE Communications Magazine 44, no. 4 (2006): 115-121.

[4] Akkaya, Kemal, and Mohamed Younis. "A survey on routing protocols for wireless sensor networks." Ad hoc networks 3, no. 3 (2005): 325-349.

[5] Khan, Junaid Ahmed, Hassaan Khaliq Qureshi, and Adnan Iqbal. "Energy management in wireless sensor networks: A survey." Computers & Electrical Engineering 41 (2015): 159-176.

[6] Anastasi, Giuseppe, Marco Conti, Mario Di Francesco, and Andrea Passarella. "Energy conservation in wireless sensor networks: A survey." Ad hoc networks 7, no. 3 (2009): 537-568.

[7] Hsu, T-H., and P-Y. Yen. "Adaptive time division multiple access-based medium access control protocol for energy conserving and data transmission in wireless sensor networks." IET communications 5, no. 18 (2011): 2662-2672.

[8] Heinzelman, Wendi Rabiner, Anantha Chandrakasan, and Hari Balakrishnan. "Energy-efficient communication protocol for wireless microsensor networks." In System sciences, 2000. Proceedings of the 33rd annual Hawaii international conference on, pp. 10-pp. IEEE, 2000.

[9] Li, Jing, and Georgios Y. Lazarou. "A bit-map-assisted energy-efficient MAC scheme for wireless sensor networks." In Proceedings of the 3rd international symposium on Information processing in sensor networks, pp. 55-60. ACM, 2004.

[10] Alvi, Ahmad Naseem, Safdar Hussain Bouk, Syed Hassan Ahmed, Muhammad Azfar Yaqub, Nadeem Javaid, and Dongkyun Kim. "Enhanced TDMA based MAC protocol for adaptive data control in wireless sensor networks." Journal of communications and networks 17, no. 3 (2015): 247-255.

[11] Alvi, Ahmad Naseem, Safdar Hussain Bouk, Syed Hassan Ahmed, Muhammad Azfar Yaqub, Mahasweta Sarkar, and Houbing Song. "BEST-MAC: Bitmap-assisted efficient and scalable TDMA-based WSN MAC protocol for smart cities." IEEE Access 4 (2016): 312-322.

[12] Debasis, K., and Singh, M.P. “A Low Duty Cycle MAC protocol for energy conservation in Wireless Sensor Networks.” International Journal of Control Theory and Applications 9, no. 41 (2016): 991-995.

Proceedings of the Fourth International Conference on Communication and Electronics Systems (ICCES 2019)
IEEE Conference Record # 45898; IEEE Xplore ISBN: 978-1-7281-1261-9

Genetic Algorithm : An Approach on Optimization

Immanuel Savio D[1]
Department of Computer Science and Engineering
Sikkim Manipal Institute of Technology
Sikkim Manipal University, Majitar, Sikkim
Email: immanuelsavio@gmail.com

Udit Kr. Chakraborty[2]
Department of Computer Science and Engineering
Sikkim Manipal Institute of Technology
Sikkim Manipal University, Majitar, Sikkim
Email: udit.c@smit.smu.edu.in

***Abstract*—Solutions for both constrained and unconstrained problems of optimization pose a challenge from the past till date. The genetic algorithm is a technique for solving such optimization problems based on biological laws of evolution particularly natural selection. In simple terms, a genetic algorithm is a successor to the traditional evolutionary algorithm where at each step it will select random solutions from the present population and labels those as parents and uses them to reproduce to the next generation as children with a series of biological operations, namely reproduction, selection, crossover and mutation.**

***Keywords*—Genetic Algorithm, Travelling Salesman, Grammar Induction, Minimal Vertex Cover, Optimization, Evolutionary Algorithms.**

I. Introduction

The use of Genetic Algorithm is not something that started in recently[1]. Genetic Algorithms have been prevalent for more than half a century. Genetic algorithms first came as a result of the research of John Holland in the University of Michigan around 1960, but were unpopular until the 90s. The main purpose is to be used to solve problems in which deterministic algorithms or other traditional algorithms are too costly (time or processing). In simple terms problems which were considered hard or impossible in terms of computation were solved using genetic algorithms in record time and processing capacities. Thanks to the latest advances in research and development of artificial intelligence and soft computing the advancement in genetic algorithm has been enormous. Scientists from using genetic algorithm in their research for optimization have now started to dedicate their total research for the advancement of this very subject.

The Genetic Algorithm (GA) follows the Darwinian theory of Natural Selection[1] which is based upon a bigger class of Evolutionary Algorithms. As mentioned above, Genetic Algorithms are mostly used for optimization of the conventional problems. The genetic algorithm has biologically inspired operations such as mutations, crossover and selection. The "Survival of the fittest" theory of the Darwinian theory is the basis of the Genetic Algorithm[5].

In any genetic algorithm problem, it is started by taking a population of candidate solutions (possible solutions not necessarily the best solution) called individuals or creatures or phenotypes for the problem to be optimized in the given context. Each solution is made up of one or more individual set of properties (called chromosomes or genotype) which undergoes the above operations to be crossed or mutated to arrive at new solutions for the same problem.

This paper is basically divided into three parts. (1)The first part of the paper deals with the introduction of Genetic Algorithm and a brief history of how it all started. (2)The second part will be dealing with the all the operations and the theory which is used in genetic transformations and the (3)final part will include a detailed application of genetic algorithm to three classical problems one an algorithmic problem, one a graph based problem and one finally a Formal language based problem and also we will be looking at how it optimized the solution methodology and also the current and future research applications of GA in some of the most popular machine learning areas.

II. Background

The genetic algorithm is developed from Evolutionary algorithms (EA)[1] which is a 'generic population-based' meta heuristic optimization algorithm. An EA n which the GA is based upon uses biologically inspired mechanisms such as reproduction, mutation, recombination, and selection[7]. The algorithm believes in the theory that the fittest offspring give either the most suitable solution or will produce the fittest set of offspring. This way the EA applies the concept of natural selection.

Like an EA the GA also works similarly[16]. The evolution usually starts with a population of randomly generated solutions or individuals called the initial population. This process is iterative and each iterations population is called a generation.In each of the generations a fitness evaluation is done of all the newly generated population as well as the currently existing chromosomes from the previous generations. The value obtained by an objective function in the optimization problem under consideration is called the fitness. A stochastic selection of the more fit individuals is done from the current population, and modifying the genome of each individual (recombined or mutated randomly) to form a new generation. The newly generated candidate solutions are utilized in the next generation (or iteration) of the genetic algorithm. Commonly, the algorithm comes to a halt if a maximum number(set by the user) of generations specified beforehand has reached, or a fitness level which is considered as optimum or nearly optimum(satisfactory) has been reached for the population[5]. The basic flow of a GA solution will be something as follows:

Algorithm 1: Generic GA

```
Start
Initialize population randomly (say P)
Define fitness function of the problem
Determine the fitness of the population
while !Converging or Optimum not achieved do
    Parent selection from population
    Crossover operation for new population generation
    Perform mutation on the new population
    Calculate fitness of new population
end
If optimum achieved, display the final result
Stop
```

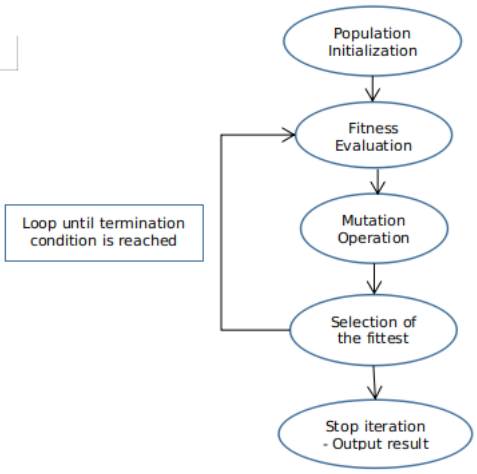

Fig. 1: Flow Chart of a GA

1) A genetically suitable representationx of the solution domain in a format suitable for computation preferably binary representation (0 and 1)[2].
2) A function to evaluate the fitness of the solution or the population generated (fitness function).
3) Data Initialization.

Each candidate solution is usually represented as an array of bits. Arrays or other forms of data structures can be similarly used[16]. The main characteristic of these genetic representations that makes it convenient is the easy alignment of parts, which makes crossover operations simpler. Representations of variable lengths can also be used, but it makes crossover implementations a bit more complex.

III. Initial Population Assignment

The first step in any GA problem is the initialization of population[11] which is a part of the current generation. A generation (say P, P0 is the initial population and Pt is at iteration t) P0 is the initial population which is usually generated randomly. In an iterative process the next generation of population P1, P2... are constituted. When a population for a GA is selected it is made sure that the population diversity (a wide range of possible solutions) is maintained. A failure to maintain population diversity may lead to a condition called Premature Convergence[14].

A. Premature Convergence

Premature Convergence in Genetic Algorithm is analogous to under-fitting in Artificial Neural Networks. The premature convergence in a genetic algorithm is when the algorithm reaches a minimum before it reaches the global optimum solution. Usually, when a genetic algorithm per say any evolutionary algorithm is trapped into a local maxima and doesn't move forward, it's called a condition of premature convergence.

1) Reasons for Premature Convergence

label=

a) Loss of Diversity: Diversity is how many numbers of different solutions are there and how different they are. The loss of diversity refers to how uniform the solutions and thus all solutions are similar to the best one, so the GA is stuck finding the weak and the strong ones.
b) Increased selective pressure to converge to best solution.
c) Over exploitation of the currently existing building blocks from the current generation of population.

2) Prevention of Premature Convergence:

There are certain strategies to prevent the condition of premature convergence

a) Increase the size of the population of the algorithm.
b) Uniform Crossover.
c) Replacing the population's similar individuals
d) Segmentation of chromosomes of similar fitness called fitness sharing

The population size is a crucial parameter to be kept in mind. It shouldn't be too large which might slow down the algorithm and a very small population size might be small for the genetic operations. The optimal size of the population is found by a trial-and-error method.

B. Methods of Initialization

There are two methods of population initialization for a Genetic Algorithm:

Random Initialization: In this method, the initial population is populated with a bunch of totally random solutions.

Heuristic Initialization: This method populates the initial population based on a known heuristic of the problem.

IV. Genetic Operations

Genetic operators are those operators which are applied on the population pool to edit or create new genes from currently existing genes. There are quite a few genetic operators. Their uses, properties and types are discussed below:

Selection: After the initial population initialization then the next step in GA is the selection operation. This is the first genetic operation. There are two types of selections:

a) Selection from the current generation to take part in this generation's reproduction. This is also called the parent selection.

b) Selections from the current generation's parents and offspring to go to the next generation. This is the selection of survivors.

In this step, a single individual chromosome is to be selected as a parent for the next generation of population, based on fitness.

A. Fitness Proportionate Selection

This is a very popular way to select a parent. In this method the parents are chosen on the basis of probability which is proportional to their fitness. This means, higher the fitness of the individuals, the higher chance of being selected to reproduce and propagating the features to the next generation.

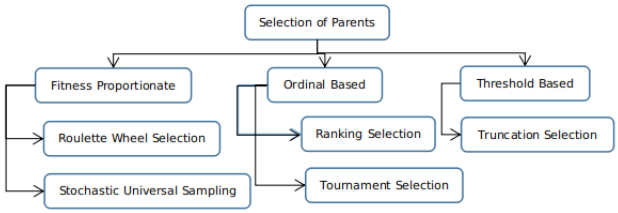

Fig. 2: Different methods to select parents for next generation

There are two ways of implementing the Fitness Proportionate Selection:

1) Routlette Wheel Selection

This selection in this method is based on the proportionality of the fitness of an individual chromosome. The fitter the individual chromosome the higher the chances of the chromosome being selected as a parent. The roulette selection follows a principle of searching linearly through a wheel with slots, where the slots of the wheel weighted proportional to the fitness of the individual chromosomes. Then a chance is taken by throwing a marble in the wheel and selects the chromosome. Chromosome with bigger fitness will be selected more times. A higher the fitness of the individual, greater the size of the area on the pie and so it has a much higher chance of landing in front of the fixed point when the wheel is spun. Therefore, an individual is more probable to be selected if it has a higher fitness value. This implements the " survival of the fittest " law directly. The roulette wheel selection method is show in Fig 3.

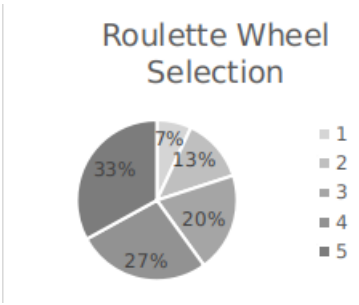

Fig. 3: Roulette Wheel Selection for a sample of 5

There are two main approaches to Roulette Wheel Selection:

a) Approach 1 : Stochastic Sampling with Replacement

This approach selects individual pairs for crossover with probability proportional to their fitness values. Consider a simple fitness and probability of 4 chromosomes. The example as shown in table 1.

TABLE I: Stochastic sampling with 4 Chromosomes

No.	Fitness(f_i)	Probability(P_i)
1	132	0.083
2	521	0.32
3	56	0.035
4	879	0.55
Total	1588	1.0

In this example the probability that an individual is chosen as a parent for crossover is given by:

$$P(i) = \frac{f(i)}{\Sigma f(i)} \tag{1}$$

f(i) : fitness of individual i

P(i) : Probability that individual i is chosen

b) Approcah 2 : This approach has a specific approach which is very similar to the roulette wheel:

It follows a few steps

a) The chromosomes are mapped to a contiguous line such that the length of each individual segment is equal to the size which is proportional to its fitness.

b) A number is generated in random and that chromosome who has a segment falling in the selected random number, is finally selected as parents.

This is done till the number of selected individuals to the required number is obtained.

TABLE II: The table shows the data with some sample population

No.	Rank	Fitness(f_i)	Probability(P_i)
1	9	1.6	0.19
2	8	1.4	0.15
3	7	1.2	0.13
4	6	1.0	0.11
5	5	0.8	0.08
6	4	0.6	0.07
7	3	0.4	0.0.3
8	2	0.2	0.02
9	1	0.0	0.00

Stochastic Universal Sampling : The first step is similar to the approach 2 of the Roulette Wheel Selection. In this the second step there are equally spaced pointers placed over the lines as many individuals are to be selected.

2) Rank-Based Selection

This is an objectively selected selection method[14]. The fitness is dependent on the individual's rank Ranking introduces a sense of uniformity among the individuals and acts as a simple method to control selective pressure. The probability of each chromosome selected is based upon its fitness normalized by the total fitness of the population. There are two types of ranking: Linear and Non-Linear ranking. Linear ranking ranks the individual in population is ranked from 1 to n in the

order of how fit the chromosomes are. Linear ranking assigns a probability proportional to the individuals rank. In the non-linear ranking method, it uses non-linear distribution. Like the linear ranking but the rank is based on but not proportional to the individual's rank.

Tournament Based Selection : This is the simplest of all the selection methods. In this method a K (say =2) is taken and k chromosomes are selected in random and the fittest of the selected k chromosomes is permitted to reproduce.

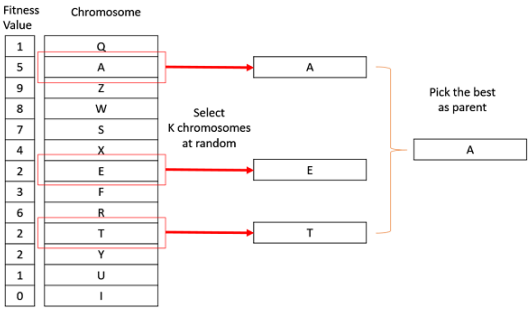

Fig. 4: Tournamen Based Selection

3) Threshold based Selection

a) Truncation Selection

It is an artificial method used to select parents for a large set of chromosomes. A parameter called Trunc is used as a parameter for this method. Trunc indicates what part or fraction of the existing population of chromosomes are to be selected as a parent, The Trunc has a value ranging from 10% - 50%. The chromosomes which are below the limit of the threshold are not allowed to reproduce.

b) Survivor Selection

This selection method is the one which decides which individuals are to be kept for the next generation and which are to be kicked out. This process is known as replacement. This type of selection reduces a population of (N+L) to N where N is the number of parents or population size and L is the number of off springs at the end of a generation. The survivor selection is divided into 2 types as shown below:

c) Age Based Selection

In this method the fitness of the chromosome is not taken into consideration. In this method a certain chromosome is allowed to reproduce for a certain number of generations and then it is kicked out even if it has the highest fitness.

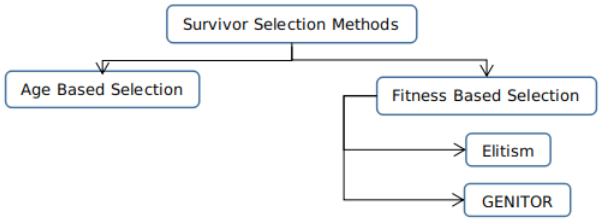

Fig. 5: Survivor selection method and its types

d) Fitness-Based Selection

In this selection, children tend to replace the least fit chromosomes in the population. The selection process followed for the least-fit individuals can be done using one of the above specified methods like tournament selection, fairness proportionate selection etc. In this Elitism is the method which helps preserve the fittest chromosomes during crossover or mutation. In this method there are first copies of the best chromosomes made to the new population. This method increases the performance of the GA drastically.

V. Crossover

Crossover or recombination is an method using in genetic and evolutionary algorithms which is based on the biological process of crossover done during reproduction. This method is one of the few ways to generate new solutions from present population existing by combining the genetic information of parent chromosomes to generate new population or offspring. There are other ways of generating solutions, from a single parent where the parent is cloned as the offspring of the next generation. Mutation of the newly generated off springs are done before being added to the gene pool of the next generation. The different algorithms in evolutionary computing may store the genetic information in different of data structures. It generally uses bit arrays, trees or vectors of real numbers so each genetic representation can be operated with crossover operators of various types.

A. Single-Point Crossover

Both the parents' chromosomes are taken and one point known as the 'crossover point' is randomly assigned. The gene information (bits) to the right of the selected point of one parent chromosome is exchanged with the other parent chromosome shown in fig 6. This results in a child chromosome or offspring which contains genetic material from both the parent chromosomes.

B. Two point and K-point crossover

In this type of crossover, two points are selected from the parent chromosomes randomly. The bits from both the parents between the crossover points are swapped creating new child chromosomes

Fig. 6: Single Point Crossover Method

C. Uniform crossover

The uniform crossover is another type of crossover operation to generate offspring from parent chromosomes. In this, according to a fixed uniform distribution, the child's genetic data is chosen independently from the two parents. In this type of crossover not segments but individual bits are exchanged during the crossover operation unlike the k-point method. Usually the bit chosen from either parent have almost equal probability of being chosen. There are other ways to make the

offspring inherit the genetic information of one parent more than the other by mixing the selection ratios.

VI. Mutation

The Mutation operator is one of the operators used in a genetic algorithm to genetically diversify the genetic population from one generation to the next. This operation of mutation in a genetic algorithm is analogous to biological mutation. In the process of mutation, one or a few values of the genetic information stored in the chromosome are edited or changed. In mutation, there is a probability of the new gene being very similar to the previous configuration or being completely different. So, by the use of mutation, the GA can get a better diversity of population to in turn getting a better solution set in the next generations in comparison to the previous one. This occurs in accordance to the probability of mutation which is set by the user itself. It is recommended that the probability is set low; if set too high the algorithm would work as a primitive random search rather than in an evolutionary manner. There are different types of mutation:

A. Bit Flip Mutation

The mutation of bit strings ensure through bit flips at random positions

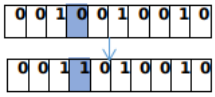

Fig. 7: Bit Flip Mutation

The probability of mutation of a bit is 1/L where L is the length of the binary vector.

B. Flip Bit

This type of mutation takes the selected gene or the chromosome and inverts the bits of the gene. If the bit in a gene is 1 it is inverted to 0 and if it is 0 it is changed to 1

C. Boundary

This type of genetic mutation is useful in integer of float types. In this the operator replaces the chromosome's genetic value with a random value of a lower or an upper bound.

D. Non Uniform

d.The use of non-uniform operators for the mutation operations will increase the probability that the amount of mutation will go to 0 in the next generation. It helps the gene population to grow and evolve rather than staying dormant in the initial stage of the evolutionary timeline. It is also helpful to tune the solution in the later stages but with a price. This operator is limited to integer and float type genes.

E. Uniform

e.This mutation operator inputs an upper and lower bound from the user and replaces value of a selected gene with uniform random values lying between those two bounds. This is also limited to integer and float type gene population

F. Gaussian

f.This operator selects a unit Gaussian Distributed random value and adds it to the selected gene. The obtained gene value is snipped if the added value falls out of the set upper or lower limit specified by the user. This operator is also limited to integer and float genes

VII. Termination

The basic requirement of a genetic algorithm just like any algorithm in computer science has to terminate after a certain amount of time. The rate of progression of a GA is high until it reaches close to the optimum solution and the pace reduces. So the termination condition has to be designed in a way that it stops close to the termination condition as no algorithm can be 100% accurate. Usually, the termination condition is one of the following termination conditions—

a) When there is no improvements in the population for the X iterations
b) We reach an absolute number of iterations.
c) When the objective function value has reached a certain value defined earlier (probable optimum solution)

VIII. Fitness Function

A Fitness function also called as an Evaluation function evaluates how close to the optimum solution or the desires solution has the GA reached[15]. According to the natural selection rule the fittest of the assumed chromosomes are sent to the next level and the rest are killed off. The chromosomes which pass on to the next generation act as parent chromosomes which will be further used for reproduction of new child chromosomes by two methods namely crossover and mutation. But how will the fittest of the chromosomes found. It is done by giving each chromosome a fitness value at the end of each generation. This fitness value will be given by a function known as the fitness function. Each chromosome will award a score and thus indicating how close the chromosome came to the optimum solution. There are a few generic requirements of a fitness function. They are as follows:

a) The fitness function should be clearly defined and the reader should be able to understand clearly how the score for the fitness function is calculated.
b) The optimization of the fitness function is of the prime priority. If the fitness function becomes a bottleneck of the whole algorithm, then the efficiency of the algorithm will be greatly affected.
c) The fitness function should quantitatively measure how fit the given solution is in solving the problem at hand.
d) The fitness functions should give intuitive results. The best and worst chromosomes should be given the best and worst fitness scores.

IX. Applications

The following sections will talk about the different applications of Genetic Algorithm

A. Application 1: Solving the travelling salesman problem with genetic algorithm

The travelling salesman problem always considered as one of the classical problems of computer science optimization theory. It is regarded as an NP-complete problem[3]. This problem serves as an abstract to problems in many engineering fields in the current era. There are two ways of solving this travelling salesman problem in the conventional method which is global and local search. Solving the travelling salesman for a small search space with the traditional methods is easy but the same for a huge search space with the traditional methods is not so efficient. So the genetic algorithms give the problem a biological intelligence simulation and makes it a much more efficient approach to solve the same[4]. The travelling salesman problem will have a GA approach flowchart similar to the one in Fig 1.

As said above the traditional methods are suitable for small number of cities, but when it comes to cities in number of hundreds as it is in the real life scenario the genetic algorithm approach is faster and will take much less time. For the travelling salesman problem we have considered a series of 15 cities and also their latitude and longitudes in table 3

Like any basic GA problem we start by randomly initializing a set of population referred to as a gene pool[11]. This gene pool will be used in the further mutation and crossover to hopefully produce better population for the successive generation. There will be three basic functions followed, namely, reproduction, mutation and crossover.

The first step in this will be reproduction where string from the current generation are copied with the probability based on objective function value. The second operation is crossover where randomly selected pairs of strings are mated which will result in new string.

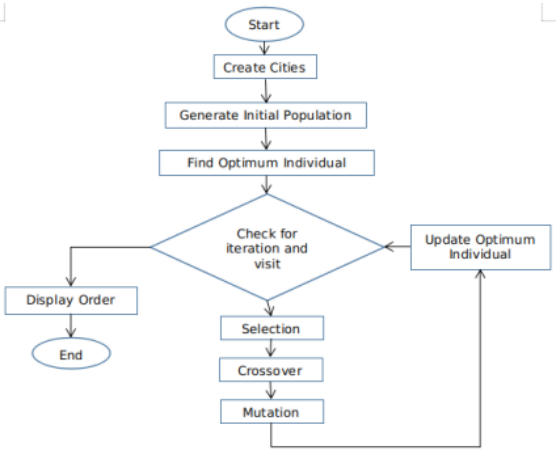

Fig. 8: Solving the Travelling Salesman Problem using GA

The third and final operations in this is mutation Mutation can be done in any one of the methods in the above section but in this we will be following a method of altering the value of a string in random position in some of the population[6]. Mutation is a method by which we can create a diverse population which can protect the genetic material which can probably lost during reproduction or crossover.

TABLE III: Example of cities and their coordinates

Cities	latitude	longitude
City 1	-27.6126	-51.0233
City 2	-26.5716	-52.3229
City 3	-27.4087	-49.822
City 4	-27.2662	-49.708
City 5	-26.9985	-51.5528
City 6	-27.0754	-52.9808
City 7	-26.8794	-52.8568
City 8	-27.6963	-48.8243
City 9	-26.843	-53.5758
City 10	-26.781	-49.3593
City 11	-27.496	-48.6598
City 12	-26.9155	-49.0709
City 13	-27.7455	-49.9423
City 14	-28.3377	-49.6373
City 15	-26.7326	-52.3919

The population which is generated in every generation is checked with the fitness function after the genetic operations to find the fittest of the population for the next generation. In this, we are using a fitness function f(x), where f(x) is defined as:

$$f(x) = \frac{1}{t(x)} \tag{2}$$

Fig. 9: Plot of cities according to Table III

Where t(x) is the objective function. As the travelling salesman problem is a minimization problem t(x) calculates the cost of travelling the cities represented by a chromosomes. This fitness function helps to maintain the darwinian Survival-Of-the-Fittest rule. In our method we also use the Elitism method where the first copies of the best chromosomes are sent to the next generation. This method helps to increase the performance of a GA as it prevents it from losing the best found solution of a particular generation.

The next step of the model is the crossover operation. This method is a very crucial step of the GA. Firstly two chromosomes are randomly selected from the gene pool and then a common crossover length is selected and the both chromosomes are broken at that point and crossed. The crossover operation can be done with a series of steps as follows:

a) Start from the first node c(first node in chromosome C1 and C2)
b) Search both the parent chromosome C1 and C2 and consider the first legit node after the first node in the

parent chromosomes C1 and C2

c) If $C_{px} < C_{py}$ select node X else select node Y
d) If the selected node is node X as the next string in the partially constructed chromosome then copy the remaining genes from the parent C_2 else copy everything from C_1

1) Results

In the example problem we have taken 15 cities. And for the ease of processing we have taken a initial population of 500 chromosomes. Once the program executes the shortest path is represented as in the fig 10. It has to be noted that there is a possibility of the existence of more that one correct answers ,i.e. in this case more than one optimum path for some Travelling Salesman Problems. This depends on the random solutions generated and mutation and the crossover operations.

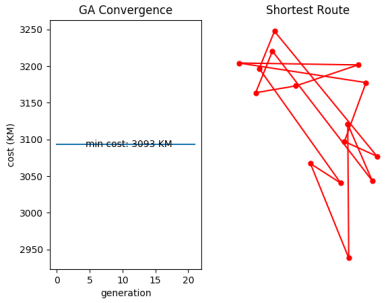

Fig. 10: Final Shortest path calculated using the GA

2) Comparison to other methods

a) Genetic Algorithm

Genetic algorithm is an algorithm with exponential time complexity with a worse case time complexity of O(Kmn). The advantages of using the GA is that the best solution is achieved by the fitness criteria but the disadvantage is that there is no optimum solution,i.e. an approximate solution is reached but an optimum solution is not reached.

b) Greedy Approach

This takes a time of 5 seconds for just a problem with 15 cities. This has a logarithmic time complexity, i.e. the time complexity of the worst case is O(log(n)). This only disadvantage is that there is no best case so no accuracy is reached.

c) Dynamic Programming

3.This is also a slower method of achieving the shortest path. But this takes around 9 seconds for a problem with 15 cities. This has a worst case time complexity of O($n^2 2^n$). The advantage in the method is that this method can achieve a global optimum solution but the biggest disadvantage of this method is that it is inefficient for both memory and time.

B. Application 2 : Grammar Induction

A grammar induction is a method of deciding or finding out a grammar from a set of sample strings collected from the language generated by the grammar[10]. Similar to the travelling salesman problem the grammar induction is also an NP-complete problem for Finite State Grammars. GA has been successfully used for Grammar Induction for Finite State Grammar[13].

Given a set of equivalent and non-equivalent grammars, we use GA to find out a grammar which can successfully parse the given language. Let the initial gene pool be G and next generation be G_{New}. Mutation is performed repeatedly and consists of replacement of an old chromosome by a new one. Steps to use GA for grammar induction[12]:

a) Select one grammar from the initial gene pool G and find the fitness value of the selected grammar
b) Sort the selected grammar in descending order of fitness value
c) Apply the crossover operation between 2 random pairs
d) Sort the resulted new grammar in GNew and find the fitness value of the newly generated grammar
e) If the new grammar successfully finds the positive and negatives, end the iteration
f) Else replace the gene pool G with fitter members from G_{New}. Finally mutate the outputs if repeated
g) Else jump to step (e)

C. Application 3 : Minimal Vertex Cover using GA

Graph-Theory states, " the vertex cover is a term referring to a set of vertices such that every edge of the graph is incident to at least one of the vertices from the set. It can be stated as, G=(V,E), S $\subseteq$ V is a vertex cover if $\forall\{u,v\} \in E : u \in S \vee v \in S$"[9]. Minimum vertex cover for the graph G will be equal to the vertex cover S that minimizes $\|S\|$.

The main issue in finding the minimum vertex cover from a given set of points has been one the most important and classical problems of both graph theory as well as computer science. Unlike both the travelling salesman and the grammar induction problem, the minimal vertex cover problem is said to be an NP-hard problem and this is a very typical example of an NP-hard optimization problem.

Procedure to find the minimum vertex cover using a GA is as follows:

Algorithm 2: Algorithm for finding the Minimum Vertex Cover

```
Input : Graph G
V_c = {}
E^P = E[G]
while E^P !empty do
    Let (x,y) be an arbitraty edge of E^P
    V_c = V_c
    Pop from E^P every edge incident on either x or y
end
Return V_c
```

Using the above methods in combination with the genetic operations we will be able to find out the minimum vertex cover of a set of points in a graph.

X. Conclusion

The research on the field of Genetic and Evolutionary algorithms and also taking into consideration the results obtained in the above experiments and the past work on the same, gives sufficient evidence that the GA has proven to be much more faster and very much efficient in finding solutions to real world problems in comparison to the traditional methods as showing the three applications. The GA also gives rise to new solutions which might not be able to be found by traditional methods.

References

[1] K. F. Man, K.S. Tang, S. Kwong, "Genetic Algorithms: Concepts and Applications", IEEE Transactions on Industrial Electronics, Vol. 43, No. 5, October 1996.
[2] P. K. Yadav, Dr.N. L. Prajapati, "An Overview of Genetic Algorithm and Modelling", International Journal of Scientific and Research Publications, Volume 2, Issue 9, September 2012, ISSN 2250-3153
[3] V Dwivedi, T. Chauhan, S. Saxena, P. Agarwal, " Travelling Salesman Problem using Genetic Algorithm", National Conference on Development of Reliable Information Systems, Techniques and Related Issues
[4] P. Vaishnav, Dr. N. Choudhary, K. Jain, "Travelling Salesman Problem Using Genetic Algorithm: A Survey", International Journal of Scientific Research in Computer Science , Engineering, and Information Technology, Issue 3, Vol 2, ISSN : 2456 - 3307
[5] L. Haldurai, T. Madhubala, R. Rajalakshmi, "A Study on Genetic Algorithm and its Applications", International Journal of Computer Sciences and Engineering, Vol-4, Issue-10, ISSN-2347-2693.
[6] J. Xu, L.Pei, R.Zhu, "Application of a Genetic Algorithm with Random Crossover and Dynamic Mutation on the Travelling Salesman Problem", 8th International Congress of Information and Communication Technology (ICICT-2018)
[7] S. Roy, U. K. Chakraborty, Introduction to Soft Computing – Neuro-Fuzzy and Genetic Algorithms, Pearson Education, 2013.
[8] J. M. Renders, H. Bersini, "Hybridizing genetic algorithms with hill-climbing methods for global optimization: two possible ways", Proceedings of the First IEEE Conference on Evolutionary Computation, vol. 1 (1994), 312,317.
[9] U. K. Chakraborty, D.Konar, C.Chakraborty, "A GA based approach on finding the minimal vertex cover", International Journal of Computer Applications NCWBCB- 2014
[10] U. K. Chakraborty, R. Pradhan, S. Borah, "A Genetic Algorithm Approach for Grammar Induction", International Journal of Emerging Technologies and Applications in Engineering, Technology and Sciences
[11] R. L. Haupt, "Optimum population size and mutation rate for a simple real genetic algorithm that optimizes array factors" IEEE Antennas and Propagation Society International Symposium.
[12] P. Wyard, "Context Free Grammar Induction using Genetic Algorithms", IEE Colloquium on Grammatical Inference: Theory, Applications and Alternatives, April - 1993
[13] N. Choubey, M. Kharat, "Grammar Induction strategy using genetic algorithm : case study of fifteen toy languages", Pacific journal of science and technology, Vol 11, No. 1, May 2010
[14] https://medium.com/the-z/a-gentle-introduction-to-genetic-algorithm-30695a6084c2
[15] https://medium.com/analytics-vidhya/understanding-genetic-algorithms-in-the-artificial-intelligence-spectrum-7021b7cc25e7
[16] https://en.wikipedia.org/wiki/Genetic_algorithm

Proceedings of the Fourth International Conference on Communication and Electronics Systems (ICCES 2019)
IEEE Conference Record # 45898; IEEE Xplore ISBN: 978-1-7281-1261-9

Heterogeneous LEACH protocol with sink node protection in a wireless sensor network

Miss. Bhagyshree Pawde
Department of Information Technology & Engineering
Walchand College of Engineering
Sangli
pawdebhagyshree123@gmail.com

Prof. Bharathi Shetty
Department of Information Technology& Engineering
Walchand College of Engineering
Sangli
bharathishetty5@gmail.com

***Abstract*— wireless sensor network (WSN) is the group of sensing computing and communication components that gives ability to sense a physical phenomenon in a specified environment. The main problem of WSN is energy consumption or battery power, to avoid such problems different type of routing protocols is used. LEACH routing protocol is used to reduce the energy consumption and enhance the battery power and network lifetime. LEACH is a homogeneous WSN protocol and it has some limitations. So there are few version of LEACH homogeneous protocol such as A-LEACH, B-LEACH, T-LEACH and MOD-LEACH. To overcome limitation of homogeneous LEACH protocol heterogeneous LEACH protocol is used. In a heterogeneous LEACH two or more different types of nodes with different battery power and functionality are used. Sink node is a sensor node which has large energy capacity and it collects data from other node. Sometime sink node affected by different type of attack such as sinkhole, black hole attack etc. to avoid these types of attack various technique are used such as intrusion detection, watchdog scenario etc. The sensor has small tiny OS having a capability of sensing physical phenomena and transfer to its base station to convert the sensing information into the human-readable form via internet.**

Keywords— LEACH protocol, Clustering, Heterogeneous WSN, energy Consumption, Network lifetime CH (Cluster Head), BS (Base Station).

I.INTRODUCTION

WSN is the collection of small sensor node also called as a mote. Sensor node (mote) senses the physical phenomena from environment. The battery is an essential part of the sensor. LEACH is standard homogeneous protocol and also it has some version with particular modification. Such as A-LEACH, C-LEACH, M-LEACH, T-LEACH etc.

LEACH protocol has advantages of clustering to reduce energy consumption and enhance the network lifespan. Whereas network lifespan is a time interval or time span from starting of a network to first node death. TDMA scheduling used to reduce the energy consumption because TDMA scheduling allocate some time span to each sensor node then each and every sensor send the data to the CH in particular cluster within allocated time slot. So the data redundancy will be reduced and efficiency will be increased.

LEACH has some drawback such as all sensor nodes have same functionality, parameter, and characteristics. If one of the sensor nodes is destroyed or crashed then the whole network is affected. When we choose the CH if low energy sensor node is chosen then the network lifespan and performance of a particular task will be reduced. Sometimes the distance factor between the sensor nodes in the network will be affected on the performance of the whole sensor network.

The difference between homogeneous and heterogeneous LEACH.

Homogeneous Network	Heterogeneous Network
WSN contain sensor same energy level and almost same parameter such as range, battery power, also all sensor node are identical then such type of network is called as a homogenous WSNs	In heterogeneous WSN, nodes are deployed with different initial energy levels, range, battery power than such type of network is called as a heterogeneous network
It saves energy but does not help in prolonging network lifetime	As compared to homogeneous it saves more energy and helps in prolonging the network lifetime
They are less suitable for real-life applications cause it has some limitation due to homogeneity.	They are more suitable for real-life applications cause its maintain heterogeneity.
Examples-LEACH, PEGASIS	Examples:- DEEC, EDDIEC

Table No.1.comparison of Homo and Hetero LEACH

The work defined in the literature of LEACH Protocol on Homogeneous network which is having sensor nodes with the same parameter which doesn't work efficiently and it has some limitation over a distributed area.

Existing approaches in this area reside big-challenges like the situation where the Sink node affected by a different type of attacks. Due to these limitations, existing approaches are not suitable for sink node security.

In construct, take a LEACH Protocol on Heterogeneous Wireless Sensor Network. Propose the method for Heterogeneous Wireless Sensor Network with Sink Node to improve the security the rest of the paper is organized as follows. Section 2 shows a brief description of the related work performed on the LEACH protocol. Section 3 presents

Methodology. Simulation results discussed in Section 4. Finally, the conclusion introduced in Section 5.

II. Related Work

Salim EL Khedari, Nejah Nasari, Anne Wei, Abedennaceur Kachouri [1] in 2014 described the cluster selection based on different topology because when topology change the whole throughput of sensor network is change. They compare different version of LEACH on homogeneous sensor network and it optimizes performance by using parameter such as mobility, scalability, self-organization, distributed organization, centralized etc.

Reenakamal Kaur Gill, Priya Chawla, Monika Sachdeva [2] in 2014 described that LEACH protocol and its phase's advantages, disadvantages and possible attack on routing protocol. LEACH protocol contains no. of rounds to select the CH of particular cluster. After the formation of cluster no. rounds are divided into two phases one is a set-up phase and another is a steady state phase.

George W. kibirige [3] in 2014 described the total information about sinkhole attack means sinkhole attack is which type attack how it works on LEACH protocol how its affected on sink node and how this attack apply on node by using mint route protocol, challenges in detection of sinkhole attacks communication pattern, prediction or some existing approach such as rule-based, anomaly detection, statistical method anomaly detection method etc. also they detect the attack on sink node by using different detection mechanism.

R.K.Sundararajan, U Arumugam [**4] in 2015** described various threat affection on various layer for physical layer the jamming and tampering for data link layer collision, exhaustion, unfairness for network layer sinkhole black hole, selective forwarding, for transport layer flooding, false messages for application layer data aggregate on distortion etc. this type of threats for different layer and disturb the whole scenario of arranged WSN. Also, they discussed various launching technique to launch a sinkhole attack ex. IDS Architecture and its working or intrusion mechanism also to detect sinkhole attack.

Jitender Grover, Shikha Sharma [5] in 2016 described security requirement such as data confidentiality, data integrity, data authentication, data availability, source localization, self-organization, data freshness etc. to avoid attacks and challenges on the sensor network. They describe the classification of security thread which is based on routing. To avoid different attack some protocol is used such as SPIN, TINYSEC, LEAP, ZIGBEE etc. also they compare the all security protocol performance with all security requirements to verify the effective outcome i.e. they provide security to sink node.

Mohamed Elshrkawey, Samiam, Elsherief, M.Elsayed Wahid [6] in 2017 described that the overview of Homogeneous LEACH protocol i.e. what exact LEACH protocol does, total phase of LEACH protocol such as set up phase, steady-state phase, threshold value calculation formula and TDMA (Time Division Multiple Access) scheduling to improve the network lifespan.

K.Johny Elma, S.Meenakshi [7] in 2018 described that maximize the lifetime of the network by using clustering topology. Clustering is an important factor in the wireless sensor network. Also, they said about energy efficient heterogeneous network by using the sensor node having different functionality and parameter. Route identification technique has minimum time requires sending the packet from source to destination so energy consumption is reduced.

III. Methodology

LEACH protocol is self-adaptive routing protocol which adapts or observes a sudden change in environment. Homogeneous sensor network contain the sensor node which has the same functionality and characteristics. LEACH is fully implemented homogeneous sensor network routing protocol. The cluster has one CH and other is normal sensor node. According to residual energy CH is selected. All sensor nodes can sense the environmental phenomena and store on it then forward that data to CH. Formation of a cluster for LEACH protocol has purpose to reduce energy consumption Improve scalability and network lifespan. Every sensor node selects a random number between 0&1.if this random number is less than a threshold value T(n) that node is chosen as a CH for that current round. An equation of calculating the threshold value T(n) is-

$$\mathrm{t(n)} = \begin{cases} \dfrac{p}{1 - p * rmod\left(\dfrac{1}{p}\right)} & n \epsilon G \\ 0 \end{cases}$$

where:

p: is the percentage of choosing CHs.
r: is the current round.
G: is the set of sensor nodes that have not been CHs in $1/p$ rounds.
n- no. of the sensor node

Set-up phase- it consists cluster formation on randomly deployed sensor node in the sensor network. Each cluster consists one CH depends upon how much energy it contains. In this phase changes the information within sensor node such as node ID, location, energy etc.

Steady-state phase- it consists the data transmission among non CH node i.e. normal node and CH in the particular cluster the data transmission happened according to TDMA (Time Division Multiple Access) fashion. By using TDMA Scheduling CH allocate particular time slot to each and every sensor node in the cluster to transmit their data towards CH. So that all sensors remain inactive till their time slot does not allow to it then energy will less reduce and ultimately network lifespan will be more.

When these two states finish their work then network retreats into the set-up mode and begin an alternate round, starting with a choice of a new CH. In a cluster all sensors sense the physical phenomena in the environment collect it and transmit to the CH accordingly.

Cluster Formation-In LEACH protocol there are different methods w.r.t. attributes and algorithm to form a cluster such k-mean algorithm, fuzzy logic etc. but in LEACH protocol cluster formation in this way.

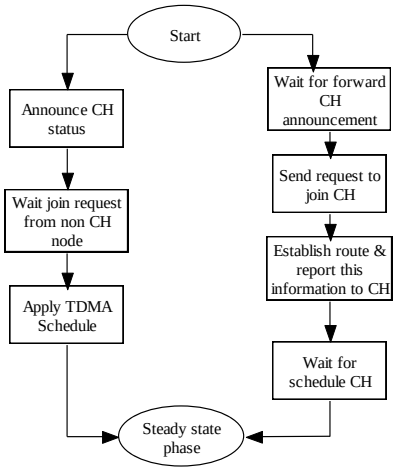

Fig No.1- CH formation.

above flow shows the activity of CH where suppose one node is CH if that node is really CH then he announces his current status i.e I am a CH of current round and he waits to join request from another normal node then he apply TDMA (Time Division Multiple Access) scheduling and send data to the BS.

In each round selected CH broadcast an advertise message to all the nodes in the network informing their new status after receiving this message each sensor node can determine to which cluster they belong to based on received signal strength according to no. of nodes in a given cluster the cluster head generates a TDMA schedule and set a transmission time slot to CH.

If the node is not CH then he waits for forwarding CH announcement from CH of that respective round then he sends the request to join the CH then he establishes the route and reports all information to CH then he waits for scheduling from CH. After doing this task from CH and non CH the whole scenario is going to steady-state phase.

TDMA Scheduling (Time Division Multiple Access)-

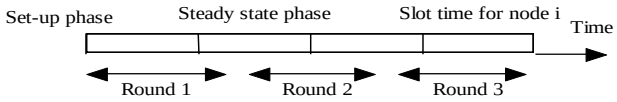

Fig No.2- Time Division Multiple Access.

it is a channel access method network for shared medium i.e. wireless sensor network it allow to share a same transmission medium so that all sensor node use same frequency channel and use it in their particular allotted time slot assigned by CH.by using TDMA scheduling all sensor node sense and transmit data one by one so data should be sent to CH in a uniform manner and it avoids the same data which come from two different node and CH also reduce the redundancy of data.it prevents an intra-cluster collision.

Energy Radio model-

First order radio model is used to calculate the energy consumption when bit data can transmit from sender to receiver. And this data can be transmitting from sensor node to CH and CH to BS.

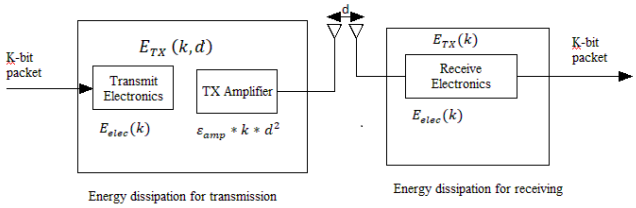

Fig No.3- Energy Radio Model

The radio energy model is shown in fig. 3. Hence to transmit a k- packet at a distance d the radio uses up is given as:

Where,

ETX: required energy utilization for packet transmission.

Eelec: is electronic energy that counts on the filtering, modulation the digital coding and spreading of the signal.

ERX: required energy utilization for packet receiving.

d_0: is equal to the square root of the dividing EDA free space model E_{fd} and multipath fading model Both ${E_{md}}^4$ models are relying on the distance between the receiver and transmitter.

Their value depends on the circuit amplifier model we use a first-order radio model. Whereas it calculates the distance in between two sensor node within a cluster and random function use for sensor distribution within a cluster.

In basic LEACH to find the distance between two hope i.e.

Threshold value distance-

$$d_0 = \sqrt{\frac{E_{fs}}{E_{mp}}}\ , E_{t=0}$$

$$s(i).x_d = rand(1,1) * x_m$$

$$s(i).y_d = rand(1,1) * y_m$$

Transmit amplifier type.

E_{fs} – Amplification coefficient of free space signal

E_{mp} – Multipath fading signal amplification co-efficient

E_{DA} -Data aggregation

Energy dissipation calculation-

Energy dissipation is degradation of energy and irecovareble energy where energy can transform from one phase to another phase. Energy dissipation calculates on the basis of amplifier and the signal transmission, modulation, distance in between transmitter and receiver, filtration bit error rate toleration etc.

$$if\ d > d_0$$

$$s(i).E = s(i).E - (E_{TX} + E_{DA}) * (3000) + E_{mp} * 3000 * (d^4)$$

$$d \leq= d_0$$

$$s(i).E = s(i).E - ((E_{TX} + E_{DA}) * (3000) + E_{mp} * 3000 * (d^2)$$

If adding transmition energy and data aggregation energy with each other w.r.t. no. of rounds then energy dissipated rate is calculated by transmit amplifier for the distance which is greater than threshold value(d_0) then it goes to multipath fading model(d^4)and if the distance which is less than threshold value(d_0) then it goes to free space model(d^2).

Election of associated CH for normal node-

$$\min\_d = \sqrt{s(i).x_d} - (s(n+1).x_d))^2 + s(i).y_d\ (s(n+1).y_d))^2$$

CH can be elected with round by round to sending the data to BS.by using above formula associated CH for the normal node is elected.

This all technique or formulas used in Homo LEACH protocol. In Hetero LEACH there are two types of nodes are used one is a normal node and another one is an advanced node and that is the main difference between Homo and Hetero LEACH.

Random selection of normal node (Hetero LEACH)-

(temp_rand0>=m*n+1)

$E_t = E_t + s(i).E$

S(i).ENERGY=0;

Random election of advanced node (Hetero LEACH)-

(temp_rnd0<m*n+1)

S (i).E=$E_0 * (1 + a)$

$E_t = E_t + s(i).E$

In hetero LEACH protocol a normal and advanced node is elected by using above formulas whereas sensor node has assigned different initial energy and these sensor nodes are randomly elected with their respected energy level.

Sinkhole attack-

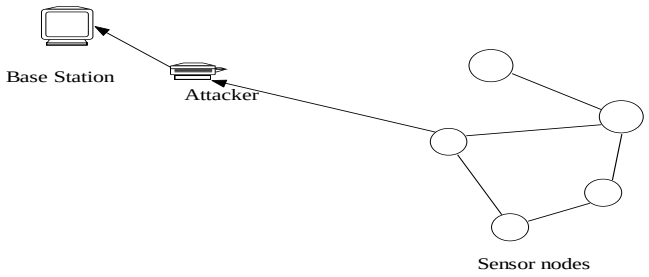

Fig No.4-Sinkhole Attack

Sinkhole attack is one type of active attack it alters information and changes the working of network. It gives the access of network to the unauthorized person and cracks the confidential information. It works on the network layer where one sensor node act as a malicious node which has high energy level and it attracts all remaining sensor node to send their packet towards it and sends fake routing information to all the sensor node and it grabs the packet or information about packet through routing table of any sensor node and also it resides in middle position in any network purposefully. So it works better and fast and it creates an environment in such a way that it attacks easily and fastly on the particular network.

For launching the sinkhole attack there are some method such as mint route protocol and TINY AODV protocol it totally depend upon routing metric so the attacker can make network vulnerable by altering the routing metric this is the most common drawback for routing protocol I.e. the routing metric and that's why all routing protocol can easily affected by the different type of network attack.

LEACH with the attack-

By using below formula attack can be performed on one node which is act as a malicious node whereas it collects data on itself and shows his status to all sensor nodes that is it has large battery power and drop the packet during the epoch.

$$epoch = mod(r, round\left(\frac{1}{p}\right) == 0)$$

The total no. of rounds in which all nodes have become CH once.

$E_{11}(r+1) = 0;$

For i=1:100

E_{11}(r+1)= $S_1(i) =. E + E_{11}(r+1)$

$E_1 =$ Energy left for the round.

After no. of round perform CH check what amount of energy is left to perform more operations.

Ec1(r+1)=Et-El1(r+1)

Et=total energy,

Ec=Energy consumed till previous round

(temp_rand<= (p/(1-p*mod(r,round(1/p)))))

This formula is used to election of CH for next round.

Attack is apply during epoch in different no. of rounds.

4. Simulation Result

Sr. No.	Parameter	Value
1	Simulation Area	100*100(m)
2	Energy model	First order energy radio model, battery
3	Initial node energy	0.5 joule
4	BS position	At center point
5	Node distribution	Random fashion
6	Channel type	Wireless(via signals)
8	Receiving Transmit energy(ERX & ETX)	$50*10^{-9}$

9	EDA data aggregation energy	$1.0*10^{-9}$
10	No.of rounds	3000
11	Network Simulator	MATLAB
12	Routing Protocol	LEACH

Table No.2- Simulation Result

Homogeneous LEACH-

These are the simulation result of Homogeneous LEACH which has the entire sensor node having same capacity and same parameter.

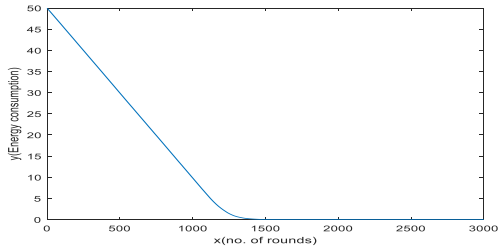

Fig No.5-Energy Consumption

In Homo LEACH this the resulting graph of energy consumption whereas all energy consumed within 50 sensor node then work of the particular cluster is stop because of lack of energy.

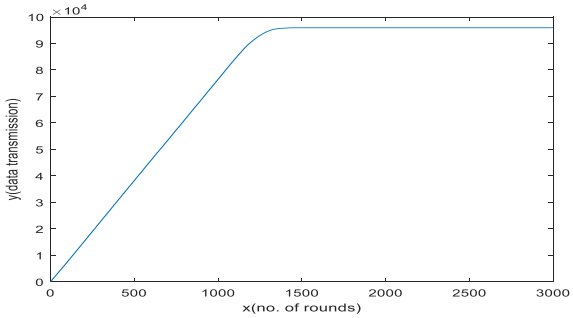

Fig No.6-Data transmission

In Homo LEACH this the resulting graph of Data Transmission whereas all data transmission in between sensor node to Base station can cover the sensing area is around 10*10^4 w.r.t. perticular no. of round.

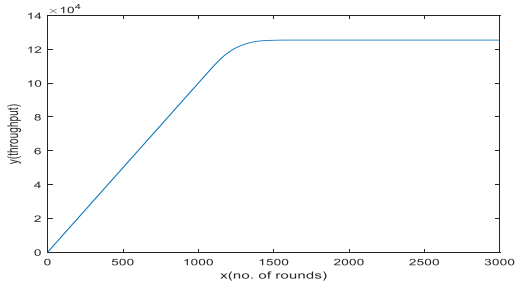

Fig No.7-Throughput

In Homo LEACH this the resulting graph of Throughput nothing but successful performance and packet delivery ratio in between sensor node to Base station can cover the sensing area is around 14*10^4 w.r.t. perticular no. of round

Heterogeneous LEACH-

In Hetero LEACH we use two type of sensor node one is a normal and another one is advanced sensor node having different type of battery power to increase the lifespan of the perticular network.

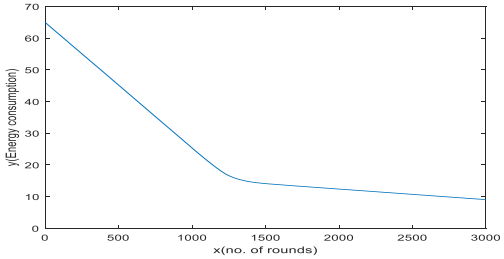

Fig no.8-Energy Consumption

In Hetero LEACH this the resulting graph of energy consumption whereas all energy consumed within 70 sensor node then work of the particular cluster is going to next round as compared to Homo LEACH Hetero LEACH can exceed their work 20 sensor more cause it use advanced node ultimately it gives more throughput.

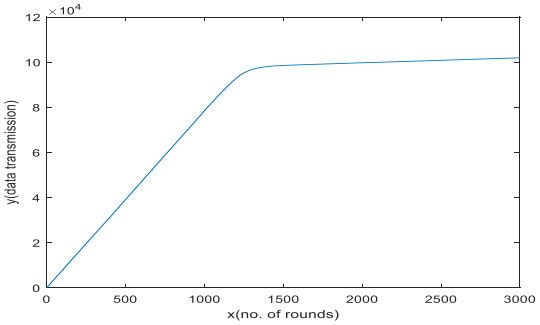

Fig No.9-Data transmission

In Hetero LEACH this the resulting graph of Data Transmission whereas all data transmission in between sensor node to Base station can cover the sensing area is around 12*10^4 w.r.t. particular no. of round.

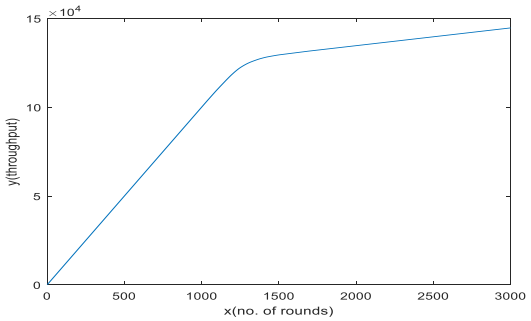

Fig No.10-Throughput

In Hetero LEACH this the resulting graph of Throughput i.e. successful performance and packet delivery ratio in between sensor node to Base station can cover the sensing area is around 15*10^4 w.r.t. perticular no. of round

LEACH with Attack-

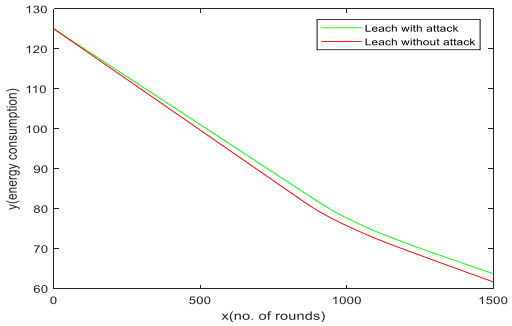

Fig No.11- Energy Consumption of Homo and Hetero LEACH with Attack

This the resulting graph of energy consumption of Homo and Hetero LEACH which is affected by sinkhole attack whereas LEACH with attack have high energy power than the LEACH without attack w.r.t. no. of rounds and energy in joule.

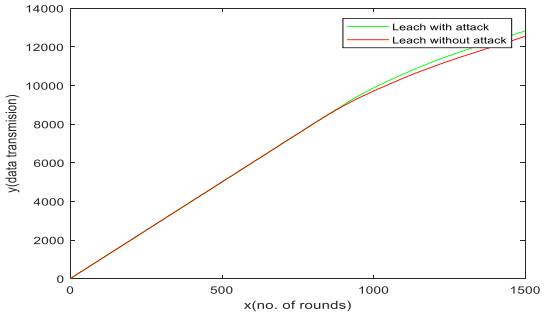

Fig No.12- Data Transmission of Homo and Hetero LEACH with Attack

This the resulting graph of Data transmission of Homo and Hetero LEACH which is affected by sinkhole attack whereas LEACH with attack have more data transmitted to the BS with minimum energy power than the LEACH without attack w.r.t. no. of rounds and energy in joule.
I.e. nothing but LEACH with attack is more data transmitted to the BS with minimum energy as compared to LEACH without attack.

CONCLUSION

This paper present LEACH hierarchical routing protocol and clustering topology on homogeneous WSN used to improve network lifespan and reduce the energy consumption. The basic homogeneous LEACH of WSN has some drawback so to overcome this drawback heterogeneous LEACH of WSN is used. For all parameter such as energy consumption, no. of sensor node (dead and alive node), throughput, data transmission also apply sinkhole attack on LEACH protocol.

REFERENCES

[1] M.Elshrkawey, S.Elsherif M.Wahed "An enhancement approach for Reducing the Energy Consumption in Wireless Sensor Network" *Suez Cana university, Faculty of Computer &Informatics, Information System Department, Ismailia* vol- 6, pp-146-141-2017.

[2] V M.J.Handy, M.Hasse, D.Timmermann "Low Energy Adaptive Clustering Hierarchy With Deterministic Cluster –Head Selection" *Institute of Applied Microelectronics and Computer Science University of Rostock, Richard-Wagner-Str* vol. 32,pp-.31,18119 ,2002.

[3] S.Khediri, Nehaj N.Anne S.Kachoury"A New Approach for Clustering in WSNBased On LEACH" Department of Computer Science Campus University-Sidi Ahmad Zarraouk- vol 24,pp-2112,2014.

[4] Brajesh Mishra, Sarvesh Singh Rai, Navdeep Kaur Saluja "M-LEACH: A modified version of LEACH for WSN", Department of Computer Science & engineering, Infinity Management & Engineering College, Sagar vol-2, Dec2015.

[5] P Batra.P.K ".LEACH-MAC: a new cluster head wireless sensor Network". *Department of Computer Science, Delhi* -D.S vol 35,pp.12-11.-2016.

[6] Sunkara Vinodh Kumar and Ajit Pal "Assisted-LEACH (A-LEACH) Energy Efficient Routing Protocol for Wireless Sensor Networks". *International Journal of Computer and Communication Engineering*, Vol. 2, No. 4, July 2013.

[7] S. K. Singh, P. Kumar, and J. P. Singh, "A Survey on Successors of LEACH Protocol," *in IEEE Access*, vol. 5, pp. 4298-4328, 2017.

[8] Zhenfu Ma, Guangming Li, Qingchao Gong "Improvement on LEACH-C Protocol of Wireless Sensor Network(LEACH-CC)" *school of Communication and InformationSystem, ShandongUniversity, Weihai,264209, China.* Vol-9,2016.

[9] Ioannis Krontiris, Thanassis Giannetsos, Tassos Dimitriou"Launching a Sinkhole Attack in Wireless Sensor Networks the Intruder Side" *Athens Information Technology, 19002 Peania, Athens, Greece* Vol-7,2017.

[10] Lalita Yadav1, Ch. Sunitha"Low Energy Adaptive Clustering Hierarchy in Wireless Sensor Network (LEACH)" *SGT Institute of Engineering & technology,* Gurgaon, Haryana-122505,INDIA, Vol-5,2014.

Proceedings of the Fourth International Conference on Communication and Electronics Systems (ICCES 2019)
IEEE Conference Record # 45898; IEEE Xplore ISBN: 978-1-7281-1261-9

A Review: Parameter Reduction Methods in Soft Set Theory

Priyanka D. Lanjewar
Department of Computer Science and Engineering
Walchand College of Engineering
Sangli, Maharashtra, India
priyanka.lanjewar@walchandsangli.ac.in

B. F. Momin
Department of Computer Science and Engineering
Walchand College of Engineering
Sangli, Maharashtra, India
bashirahmad.momin@walchandsangli.ac

***Abstract*— This paper deals with various parameter reduction methods of soft set theory. It has been found that the problem of uncertainty is too complicated to solve. This paper describes how decision making problem of uncertain and incomplete data solved using soft set theory concept. There are different soft set based parameter reduction methods to solve decision making problems that give optimal solution from big data. The purpose of this article is to explore the soft set theory with its approaches for parameter reduction, classification, clustering and association of rule generations. Comparison of various soft set methods for parameters reduction in terms of computational complexity, computational time and accuracy is provided.**

Keywords*— Soft set theory; uncertaint; parameter reduction; classification; clustering; association rule generation; big data analysis

I. INTRODUCTION

Uncertainty refers to some incomplete or unknown information. In decision making process of big data analysis, this uncertainty increases inaccuracy, which leads to wrong decisions. The problem of uncertainty in the field of engineering, social science and medical science cannot successfully solved by classical models as probability theory, interval mathematics, fuzzy set and rough set theory [1]. Each of this existing theory has their own difficulties as presented below:

A. Probability Theory

This theory is a branch of mathematics and deals with probability which is first investigated in sixteenth centaury by Gerolamo Cardano [1]. Stochastically stable phenomenon is the basis for this theory, where restriction on input is given by equation (1) is:

$$\mu_v = \frac{1}{n} \sum_{i=1}^{n} x_i \qquad (1)$$

If x_i is '1' then event occurs and absent when x_i is '0'. For the existence of limit more number of trials has to do but it is not possible for other field.

B. Interval Mathmatics

In this type of theory, interval is a collection of real numbers having feature that any number lies between '0' and '1'. But there is error while calculating the exact solution to the problem and this theory is unreliable, has partial aim and presents inadequate and defective information [1].

C. Fuzzy Set

In 1965, Lotfi A. Zadeh introduced another kind of set theory. Fuzzy set is a type of set whose elements have the degree of membership. Fuzzy set *F* allows regular assessment of the membership of element which is explained by membership function $\mu_F(x)$ between the interval of [0, 1]. But there is some problem in presenting the membership function for each different case [1].

D. Rough Set

Polish scientist Z. I. Pawlak [2] proposed some new concept over existing set theory with the lower and upper inference of the original set in 1991. But, decision features and conditional features are not directly connected. It means that decision values are not computed with regard to conditional attribute. This is the key difference in rough set and soft set theory.

E. Soft Set Theory

All the existing theories need some pre-specification of few parameter which result in incomplete and imperfect knowledge and leads to many problems. In classical theory there is a need to define mathematical model for exact solution but it is so complicated. The cause of above problem is the insufficiency of the parameterization tool of existing models. Noting such problem in existing theory new mathematical tool is developed by the D. Molodtsov in 1999 [1]. This theory is

free from the above difficulties and has the opposite approach by introducing concept of estimated solution. There is no restriction on estimated explanation in soft set so that this is extremely suitable and uses any parameterization using words, sentence, real numbers, functions and mapping. So difficulties in setting membership function or other difficulty is not available in the soft set theory.

In [2] author P. K. Maji *et al.* has presented how soft set can applied to resolve decision making difficulty for first time by example. Optimal selection can be done by choice value and weighted choice value. Various operations like equality, null, complement of two soft set and soft binary operation as AND, OR, NOT, Union and Intersection are defined in [3]. Soft set is defined in equation (2) is:

$$F: E \rightarrow P(U), \tag{2}$$

Where $P(U)$ is power set of U and pair (F, E) is a soft set if F is mapping of E which is shown in table 1. $\{e_1 \ldots e_5\}$ is set of parameter and $\{h_1 \ldots h_5\}$ be a group of conditional value. In soft set theory conditional value is calculated with respect to decision parameter value so that there is direct relation between these values.

Babitha and Sunil [4] presented definition of some relations and function of soft set such as Cartesian product, equivalence and partition relation and inverse function respectively. Aktas and Cagman [5] showed various characteristic of soft set and compared with rough set and fuzzy set theory and also provided definition of soft group and its soft group properties. U. Acar *et al.* [6] described new thought of soft ring with one more concept of soft ideals of soft ring using some basic algebraic structure of soft set theory.

The rest of this paper organized as follows. Section II presented the literature survey of various soft set based parameter reduction methods for uncertain and incomplete data and soft set based methods for data mining technique. Section III provides research motivation which includes how researcher get motivated because of limited research on soft set based methods for machine learning application is presented in literature survey. Finally Section IV gives conclusion.

II. LITERATURE SURVEY

Parameter reduction methods are described here as soft set algorithms for parameter reduction, soft set approach under incomplete data and soft set approaches for various data mining techniques. Comparative analysis of various methods of reduction of parameter is also given in table 4 and table 5.

A. Soft Set Based Parameter Reduction Methods

There is incorrect calculation in [2]. This is improved by reducing parameters of soft sets as presented by Degang Chen in [7] using parameterization reduction property of soft set. Improved algorithm for reduction of parameter is presented to give optimal solution in which decision value is calculated in accordance to parameters and this is the key difference between soft set theory and rough set theory. As shown in algorithm, Soft set (F, E) given as first input as shown in algorithm and second input is set of parameters P as $\{e_1 \ldots e_5\}$ and as shown in Table 1, it is obvious that h_1 is having highest choice value so h_1 is the optimal selection. But if data is more, then it is difficult to find solution so first find out reduct soft set which is third step of algorithm as by deleting e_1 and e_3 because having same value and it gets reduct soft set as $(F, P) = \{e_2, e_4, e_5\}$. From this reduct soft set optimal choice value h_1 or h_6 will get that has maximum choice value. Accordingly h_2 and h_3 are two suboptimal choices. So here problem of suboptimal choice is not solved by this method. The choice value is defined as follows in equation (3), which is last step of algorithm.

$$c_i = \sum_j h_{ij} \tag{3}$$

Where c_i is the choice value is given by summation of each h_{ij} entries in table and the selection of optimal value is made according to the maximum value of c_i as shown in table 1. The basic algorithmic steps to choose the optimal value is presented in [7] is as follow:

1. Input the soft set (F, E)
2. Input the set P of choice parameters which is a subset of E
3. Identify all reduct-soft-sets of (F, P)
4. Select one reduct-soft-set say (F, Q) of (F, P)
5. Obtain k, for which $Ck = max\ ci$.

Table 1: Binary table of soft set

U	e_1	e_2	e_3	e_4	e_5	Choice value *ci*
h_1	1	1	1	1	1	5
h_2	1	1	1	1	0	4
h_3	1	0	1	1	1	4
h_4	1	0	1	1	0	3
h_5	1	0	1	0	0	2
h_6	1	1	1	1	1	5

Zou and Chen [8] presented various operations for instance union and difference of two soft sets and also provided selection and projection in soft set theory which is based on relational algebra theory. Also it provides the definition of each above operations and applies this relational algebra operation for parameter reduction of soft set. M. I. Ali *et al.* [9] defined new operations because operations presented by [3] are not true generally, so author presented new notion of operations like restricted union, restricted difference, restricted intersection and relative complement in soft set theory for De Morgan's law. K. Gong *et al.* [10] proposed special type of soft set that is Bijective soft set and performed some operation such as relaxed AND, restricted AND, dependency of two Bijective soft set, reduction of soft set and significance of soft set. Z. kong *et al.* [11] presented the normal parameter reduction (NPR) algorithm for soft set in which above problem of suboptimal choice is solved by adding parameter set of soft set. This method computes the parameter importance degree and decision partition to give the optimal

solution for decision making. But this method is not easy to understand and needs more computation. NPR algorithm which is given in [11] is:

1. Input the soft set (*F, E*) along with parameter set *E*
2. Calculate parameter importance degree r_{e_i}, $1 \leq i \leq m$
3. Choose highest subset $A = \{e'_1, e'_2, \ldots, e'_p\}$ from *E* which satisfies total of $r_{e'_i}$ for $1 \leq i \leq p$ afterward place *A* in parameter reduction set.
4. Filter parameter reduction set if $f_A(h_1) = f_A(h_2) = \cdots = f_A(h_n)$ later calculate $E - A$ which is NPR *else A* is removed.
5. Find highest cardinality of *A*
6. Compute $E - A$ which is optimal NPR.

T. Herawan *et al.* [12] shown dimensionality reduction using multi-valued information which is to be transformed into multi-soft sets. AND, OR operations are used to reduct the attribute of soft set. Cagman and Enginoglu [13] explained soft matrices for soft set with its properties and presented soft max-min decision making method for soft decision making model that can be applied to solve uncertainty. So the problem of [11] is solved by X. Ma *et al.* [14] proposed new efficient normal parameter reduction (NENPR) algorithm of soft set without considering parameter important degree and decision partition. The NENPR algorithm proposed in [14] is:

1. Input the soft set (*F, E*) and the parameter set *E*
2. If $e^1{}_j$ and $e^0{}_j$ is occurs then it will becomes reduced parameter called as *C* and new soft set *(F,E')* is created without $e^1{}_j$ and $e^o{}_j$, where $U = \{h_1, h_2, \ldots, h_n\}$, $E = \{e_{1'}, e_{2'}, \ldots, e_{i'}\}$
3. Calculate oriented parameter sum $S(e_{j'})$for soft set *(F,E'), j'*=1',2',…*t'*.
4. Search the subset $A \subset E'$ where, S_A is a several of |U|, next place *A* toward candidate parameter reduction set
5. Examine each *A* in set, if $f_A(h_1) = f_A(h_2) = \cdots = f_A(h_n)$, it will be kept else *A* is obliterated.
6. Find highest cardinality of *A* in set then calculate *E - A- C* which is optimum NPR.

This algorithm takes less computation time as it compute only oriented-parameter sum to give the optimal value. X. Ma *et al.* [15] presented soft set algorithm based on parameterization value reduction that consider least parameter for optimal selection. Z. kong *et al.* [16] stated two cases of normal parameter reduction which is not given by [11] that is altering entries and adding object in soft set with positive and negative changed rates. M. I. Ali [17] has presented other idea on parameter reduction of soft set using classification to resolve the problems of decision making. Soft equivalence relation is introduced for soft set and rough set. Deng and wang [18] initiate idea of parameter significance with the two ideas such as degree of absolute dominance and relative dominance and proposed two algorithms called as pseudo parameter reduction and NPR of soft set. Kumar and Rengasamy [19] also present better decision for soft set theory using parameterization reduction by converting sample data into binary data without any loss of real data.

Han and Li [20] defined a soft set scheme that compile normal parameter reduction with three rules such as Core-Based, Inclusion-Based and Diagonal-Based rules. After combining these three rules one simplification algorithm is proposed. G. Zhang *et al.* [21] proposed algorithm for parameter reduction on soft equivalence relation of soft set. Z. Li *et al.* [22] proposed algorithms for reduction of parameter but using soft covering concept. Z. Liu *et al.* [23] shown the idea of induced soft set and define topology for soft set. T. Bakshi *et al.* [24] proposed several soft set algorithms for automated system of parameterization reduction. And complexity of this algorithm is better than above algorithms that is O (n^3).

Zhang and Wang [25] proposed new method for parameter reduction in soft set theory using the concept of important degrees of parameter that reduce complexity and performed more efficiently than above methods. N. Xie [26] presented attribute reduction in information system and define association among soft set and information system. V. Cetkin *et al.* [27] computed the decision making problems using inverse fuzzy soft set rather than fuzzy soft set so that, decision making process is very fast than existing methods. S. Danjuma *et al.* [28] proposed alternative approach to normal parameter reduction (ANPR) algorithm that overcome difficulty of existing NPR algorithms in terms of computational complexity but last choice not always consider and also give comparisons of NPR, NENPR and ANPR. The ANPR algorithm discussed in [28] is:

1. Input the soft set (*F, E*) and the parameter set *E*
2. If $e_i = e_j$ is present, then select one of them and put it in *Q*, if $e^1{}_j$ and $e^0{}_j$ is exists then it will becomes reduced parameter called as *C* and new soft set *(F,E')* is created without one of the $e_i = e_j$, $e^1{}_j$ and $e^o{}_j$, where $U = \{p_1, p_2, \ldots, p_n\}$, $E' = \{e_1, e_2, \ldots, e_m\}$
3. Calculate oriented parameter sum $S(e_{j'})$ for soft set *(F,E'), j'*=1',2',…*t'*.
4. Ensure each *A* in set, if $f_A(p_1) = f_A(p_2) = \cdots = f_A(p_n)$, also if there exist *B* $f_B(p_1) = f_B(p_2) = \cdots = f_B(p_n)$.
5. Calculate *(A∪B)-(A∩B)* intersection which is represented as *D*
6. Obtain highest cardinality of candidate parameter reduction set next compute *E -C -D -Q* as alternative NPR.

S. Danjuma *et al.* [29] presented analysis on different decision making methods of soft set by reducing parameters. Provide the analysis of different methods for soft set, rough set and for hybrid soft set and also gives real world application of soft set. J. Zhan *et al.* [30] presented survey of various algorithms for NPR, Bijective soft set decision and reduction method built on discernibility matrices in soft set theory. Ma and Qin [31] Distance based parameter reduction of fuzzy soft

set is proposed using distance matrix in which distance of two parameters is computed. And advantage is that low computation and high usability than NPR of fuzzy soft sets. The problem of NPR is overcome by Ma and Qin [32] that proposed new algorithms such as parameter value reduction (PVR), parameterization value reduction (PZVR) , maximal parameter value reduction (MPVR) and maximal parameter value reduction based on NPR (MPVR-NPR).

B. Soft Set Based Approach Under Incomplte Data

Zou and Xiao [33] shown data analysis approach of soft set for incomplete data. If in decision making incomplete data is present then it difficult to give optimal solution. In this, the choice value *ci* of object *hi* calculated as $ci = \sum_{j=1}^{y} hij$ in which *y* is number of parameter and *hij* are the entries in soft set. If there are m possible choice values of object *hi* then decision value *di* is calculated as $di = \sum_{i=1}^{m} kici$ where *ki* is weight of choice value *ci* which is calculated as follows so weighted average for all choice value is computed where, p_e *and* q_e are probability values, *d* is no. of incomplete data given in equation (4),

$$K = \begin{cases} \prod_{e \epsilon E_0^*} q_e \\ \sum_{c_d^x} \left(\left(\prod_{e_i \epsilon E_1^*} p_{e_i} \right) \left(\prod_{e_j \epsilon E_0^*} q_{e_j} \right) \right) \\ \prod_{e \epsilon E_1^*} p_e \end{cases} \quad (4)$$

Z. Kong *et al.* [34] gives the efficient decision making method of soft set for incomplete data which is more simplified than above method.

Table 2: Incomplete Soft Set

U	e_1	e_2	e_3	e_4
h_1	1	1	1	0
h_2	0	1	*	1
h3	0	*	1	1
h_4	*	0	1	*

In Table 2 * represent incomplete information which can be either '1' or '0' which indicates some values are unknown. For Big data analysis it is difficult to give optimal decision of incomplete data. In this method, instead of calculating weight value probability, value of that particular incomplete data is calculated in equation (5) is:

$$p_{e_j} = n_1 / (n_1 + n_0) \quad (5)$$

Where n_1 is the number of value 1 and n_0 is number of value 1. So calculate probability value for each incomplete data. For example for object h_2 in table 2 probability is calculated as $p_{e_j} = 3 / (3+0) = 3$, where n_1 is '3' and n_0 is '0', and then calculate decision value as given in equation (6):

$$d_i = \sum_{j=1}^{m} h_{ij} \quad (6)$$

In this way, optimal decision value will get using incomplete data as shown in table 3 where h_1 and h_2 are optimal selection.

Table 3: Incomplete soft set with decision value

U	e_1	e_2	e_3	e_4	d_i
h_1	1	1	1	0	3
h_2	0	1	3/3	1	3
h_3	0	2/3	1	1	2.67
h_4	1/3	0	1	2/3	2

M. S. Khan *et al.* [35] proposed new method for data filling for incomplete data called as ADFIS which focus on associations of parameters in which missing values are predicted. This method is implemented in Matlab for UCI dataset and overcome the problem of DFIS in terms of accuracy. On Average the performance of this method is improved by 4.44%. Alcantud and Garcia [36] proposed new algorithm to resolve decision making difficulty of incomplete data in Matlab tool. Also provides result in comparison with other methods for critical evaluation. L. Li *et al.* [37] presented the definition of soft incomplete discernibility matrix, soft parameter dominant incomplete discernibility matrix and last for weighted soft set also gives comparison with existing ones.

C. Soft Set Based Approaches for Various Data Mining Techniques

Jothi and Inbarani [38] recommended the soft set approach for unsupervised feature selection using AND operation and cardinality value is computed to give optimal solution. In this method classification is done using feature selection to select most prominent feature. J. Cai *et al.* [39] presented feature selection methods to reduce irrelevant data that result in less computation time and more accuracy. Proposed methods for supervised, unsupervised and semi- supervised which are applicable in machine learning problems such as classification and clustering.

H. Mohamed *et al.* [40] showed Bijective soft set method which include data pre-processing as first step and classification as second step for training and testing data which generate the decision rule using four classifiers to classify student learning pattern and obtain discernibility matrix for every feature. This method of soft set gives better accuracy than other theories. S. Sreedevi *et al.* [41] proposed a fuzzy soft set method that classifies mammogram images between malicious and regular images. Implementation is completed in different steps such as pre-processing, segmentation, feature extraction and selection, and classification. H. Qin *et al.* [42] proposed Novel Soft Set (NSS) method to select clustering attribute that gives faster decision and good scalability than Maximum Dependency Attribute (MDA) approach of rough set theory. This method compute equivalence classes for each attribute and then compute cardinality and degree of dependency to give optimal value. In this paper, cardinality of $a_i(e_j)$ calculated in equation (7) where, *D* is no. of equivalence classes for U/a_l parttions and $F_l(e_j)(X_K) \in \{0,1\}$.

$$|a_i(e_j)| = \sum_{k=D+1}^{D+|U/a_i|} F_1(e_j)(X_k) \times |X_k| \quad (7)$$

R. Mamat *et al.* [43] presented Maximum Attribute Relative (MAR) algorithm of soft set for categorical value to give clustering attribute that gives better performance in terms of execution time and scalability than existing method such as Total Roughness (TR), Min-Min Roughness (MMR), Maximum Dependency Attribute (MDA), Novel Soft Set (NSS). MAR is compared with above four old methods using fourteen datasets of UCI repository. D. Hartama *et al.* [44] proposed the new algorithm to select attribute called as Soft Set Fast Clustering (SSAA) for categorical data to obtain clustering attribute. This algorithm performs better than Maximum Degree of Dominance of Soft Set (MDDS) in terms of execution time using MATLAB software for six different UCI dataset. Herawan and Deris [45] presented soft set approaches for association rule mining from transactional data set. In this, soft regular and soft maximum association rules are defined to compare proposed work. B. Li *et al.* [46] presented association rule mining based on clustering by using Clustering by Fast Search and Find of Density Peaks (CFSFDP) clustering method and soft set to classify transactional database and generate association rule from big database. Results are shown for Adult data set. F. Feng *et al.* [47] defined soft set based association rule mining. Some algorithms are proposed to calculate Parameter taxonomic soft set, M- realization of parameter set and γ -M- reliable maximal association rule. Two case studies presented for Reuters and Web of Science data sets.

Ma and Qin [48] Proposed mixed type of soft set such as fuzzy soft set and interval-valued fuzzy soft set for decision making algorithm based on this hybrid type. F. Xiao [49] Proposed hybrid algorithms for fuzzy soft sets for decision-making by a fuzzy in medical diagnosis. In this algorithm, uncertainty is measured to generate credible value then calculate basic probability using dempster shafer evidence theory to give optimal value. Z. Kong *et al.* [50] proposed the new parameter reduction method based on score decision criteria for fuzzy soft set. At last comparison is given with previous parameter reduction based on choice value decision criteria and some dispensable set analyzes for different case.

Table 4: Comparisons of parameter reduction methods of soft set

Authors	Proposed method	Advantage	Disadvantage
P. K. Maji et al. [2] 2002	Design the algorithm for the selection of house by reducing the parameter with the choice value and the weight value. And give the optimal object selection.	Solve the decision making problems using parameterization property.	Gives incorrect computing in optimal selection of parameter.
H. Aktas [5] 2010	Introduce soft set group concept with its properties.	Overcome the problem of rough set theory.	Here soft ring is not defined which is overcome by [6]
D. Chen et al. [7] 2005	Presented latest method of parameterization reduction of soft set contrast with attribute selection of rough set theory.	Finding optimal decision on Boolean dataset without any influences on the final decision and solve problem in [2].	Problem in selecting sub optimal choice of object.
Y. Zou et al. [8] 2008	Proposed algorithm for parameter reduction using relational algebra and also define various operation like union, difference, selection, projection etc.	The method proves the invariability of optimal solution.	For more parameters, there is explosion of parameter with worst time complexity $O(2^h)$.
Z. Kong et al. [11] 2008	NPR algorithm is proposed to get minimized conclusion and suboptimal decision using added parameter soft set.	More efficient due to decision partitioned and parameter important degree.	Difficult to understand and require more time as computational complexity is $O(n^3)$.
T. Herawan et al. [12] 2009	Presented dimensionality reduction in multi-value information system via AND operation in soft set theory.	Attribute reduction is done for non-Boolean value.	Problems in data cleansing for large dataset and data clustering.
X. Ma et al. [14] 2011	NENPR soft set method that uses the oriented parameter sum exclusive of degree of parameter reduction and decision separation.	Decrease computational complexity by ignoring parameter reduction degree with decision partition and complexity is $O(n^2)$	Require to compute oriented parameter sum.
X. Ma et al. [15] 2011	Algorithm for parameterization value reduction using soft set theory is proposed.	Algorithm holds least parameter value for optimal selection.	Not useful for extended soft set.
Z. Kong et al. [16] 2012	Presents new definition for changing some entries and adding some objects in soft sets.	Problem of [9] varying entries and adding objects are solved.	Difficult for large dataset.

M. I. Ali [17] 2012	Proposed a new soft set for reduction of parameter and introduce the concept soft equivalence.	Reduction of parameter of soft set without distorting its original classification ability.	This method does not provide the algebraic structure.
D. Kumar et al. [19] 2013	Parameterization reduction algorithm converts sample data into Boolean data in information system using soft set theory.	Algorithm gives better decision making over uncertain data.	Difficult for large dataset.
Z. Li et al. [22] 2015	Algorithm for parameter reduction of soft covering is used to obtain lattice structure of soft set.	Attribute reduction for information system is provided.	Not useful for multisource information.
Z. Liu et al. [23] 2015	New definition for induced soft set is presented with topology for parameter reduction.	Soft set mapping is used for induced soft set which may be applicable for science field.	Difficult for large dataset.
S. Danjuma et al. [28] 2017	Propose an (ANPR) alternative normal parameter reduction algorithm for decision making based on soft set theory.	Algorithm reduces the computational complexity which is O (n^2); also execution time is less as existing techniques.	This method does not always consider the last choice.
S. Danjuma et al. [29] 2017	Different soft set based parameter reduction and decision making techniques for soft set is reviewed here with hybrid fuzzy soft sets and rough set.	Give the analysis of previous work and present real world application of soft set.	Problems of multiset on parameter reduction, multi criteria are not solved yet.
X. Ma et al. [32] 2019	PZVR, MPVR and MPVR-NPR algorithms are defined for normal parameter reduction (NPR).	MPVR algorithm gives redundant degree as 93.3% and lower complexity than NPR algorithm.	MPVR-NPR algorithm performance is not good as MPVR.

Table 5: Comparisons of soft set based approaches for incomplete data and data mining techniques

Authors	**Proposed method**	**Advantage**	**Disadvantage**
Y. Zou et al. [33] 2008	Weighted average method is used for optimal choice value of incomplete data for big data analysis purpose.	Problem of decision making using incomplete information is solved.	Not useful for extended soft set.
Z. Kong et al. [34] 2014	Present efficient probability data analysis approach on incomplete data, which is simplified weighted average for decision making.	Computational complexity is less than above method and it is implemented easily.	Not useful for extended soft set.
M. S. Khan et al. [35] 2016	ADFIS method is proposed for incomplete data with better accuracy over DFIS method for various dataset.	ADFIS gives improved performance on average of 4.44% than DIFS method.	Computational complexity is high than DIFS
L. Li et al. [37] 2018	Soft incomplete discernibility matrix and soft parameter dominant incomplete discernibility matrix is introduced.	Decision making problem of incomplete soft set is overcome.	Dost not provide the function mapping form of incomplete soft set.
G. Jothi et al. [38] 2012	For quick reduction of attributes unsupervised feature selection algorithm based on soft set is designed.	Speed and accuracy of the method is good and reduce computational time.	Not useful for extended soft set.
H. Mohamed et al. [40] 2014	To classify student learning fashion Bijective soft set is proposed using standard model.	Method gives good classification accuracy of 97.1%.	Use of more classifier that require more time.
S. Sreedevi et al. [41] 2016	Fuzzy soft set method is developed using fuzzy soft aggregation to classify the images.	Accuracy of algorithm is 94.09% for MIAS dataset.	Not useful for more set of parameters.
H. Qin et al. [42] 2012	NSS technique is proposed to cluster the attributes and compare on UCI dataset for various parameters.	Solved the problem of MDA method of rough set with good scalability.	Not for categorical dataset.
R. Mamat et al. [43] 2013	For the selection of cluster attribute MAR method in multi value information system is developed.	Execution time is less and scalability is good.	Method does not provide for categorical data.

D. Hartama et al. [44] 2016	Proposed the soft set based clustering attribute selection called selecting sub attribute algorithm (SSAA).	Solve the problem of maximum degree of dominance soft set.	Give only 67.56% average percentage of response time.
T. Herawan et al. [45] 2011	Soft set technique for association of rules using co-occurrence of parameters for Boolean dataset is designed.	Capturing of rules is faster than other.	Does not provide approximate reduct in information system.
B. Li et al. [46] 2015	CFSFDP clustering system for soft set is anticipated to reduce big dataset.	Effective technique to produce association rules from big databases	--
F. Feng et al. [47] 2016	Define soft set based association rule mining algorithm and conducted different case study.	Improve problem of transactional dataset	Dose not formalize proposed method in terms of logical formulas

III. RESEARCH MOTIVATION

Now a day's decision making for big data analysis is the most recent issue. Soft set theory is the new theory that solves the problem of previous theories using new property that is parameterization reduction and solve problem of decision making for big data analysis. Explore soft set approach with data mining techniques in machine learning platform is the new concept in artificial intelligence because limited research is done on the practical implementation of soft set method in data mining and machine learning field. Where the decision making problems will be solved by efficient soft set based parameter reduction algorithm for feature selection, classification, clustering and association rule generation to give the optimal selection considering the parameters such as computational complexity, computing time, accuracy, etc. Such algorithms will be implemented in Python platform by proposing the soft set based approach for machine learning with data mining techniques as shown in figure 1.

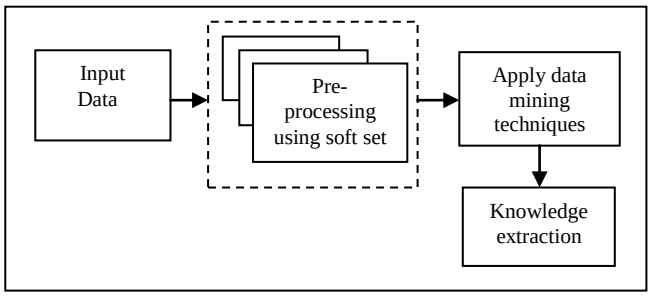

Figure 1: Conceptual framework of research work

Conceptual flow diagram shows the flow of research work in which decision making problem is solved by proposing parameter reduction algorithm using parameterization property of soft set theory, which include dimensionality reduction will be done by considering choice parameter for selecting prominent parameter from original data, then perform classification and clustering attribute selection using soft set concept after that classification based on association rule mining will be done to give the knowledge extraction over uncertain and incomplete data.

IV. CONCLUSION

The latest mathematical theory for parameter reduction is soft set theory that handle uncertainty problem of decision making to give the optimal solution. This theory performs better than existing theory as fuzzy set and rough set theory. Different methods are given in this paper for parameter reduction, few methods for incomplete data and some soft set based methods for various data mining techniques as feature selection, classification, clustering and association rule generation. Performance of these methods is calculated in terms of some parameters such as computational complexity, execution time, accuracy, memory used and scalability etc. Different parameter reductions techniques are relatively compared as shown in table 4 and table 5. As going through literature of soft set, it shown fewer researches on soft set based scheme for data mining techniques applicable for machine learning platform. Few realistic uses of soft set theory seen in literature survey but some of them faces some issues so in future, researcher can give more attention toward such problem. Still there is no such type of soft set method for big data analysis in machine learning platform, so in future researcher will more focus on such new concept.

References

[1] D. Molodtsov, "Soft set theory—First results," *Comput. Math. with Appl.*, vol. 37, no. 4–5, pp. 19–31, 1999.

[2] P. K. Maji, A. R. Roy, and R. Biswas, "An application of soft sets in a decision making problem," *Comput. Math. with Appl.*, vol. 44, no. 8–9, pp. 1077–1083, 2002.

[3] P. K. Maji, R. Biswas, and A. R. Roy, "Soft set theory," *Comput. Math. with Appl.*, vol. 45, no. 4–5, pp. 555–562, 2003.

[4] K. V Babitha and J. J. Sunil, "Soft set relations and functions," *Comput. Math. with Appl.*, vol. 60, no. 7, pp. 1840–1849, 2010.

[5] C. Naim, "Soft sets and soft groups," vol. 177, pp. 2726–2735, 2007.

[6] U. Acar, F. Koyuncu, and B. Tanay, "Soft sets and soft rings," *Comput. Math. with Appl.*, vol. 59, no. 11, pp. 3458–3463, 2010.

[7] C. Dgang, T. E.C.C, Y. D. S., and W. Xizhao, "The Parameterization Reduction of Soft Sets and its Applications," *Int. J. Comput. Math. with Appl.*, vol. 49, pp. 757–763, 2005.

[8] Y. Zou and Y. Chen, "Research on soft set theory and parameters reduction based on relational algebra," *Second Int. Symp. Intell. Inf.*

Technol. Appl., vol. 1, pp. 152–156 2008.

[9] M. I. Ali, F. Feng, X. Liu, W. K. Min, and M. Shabir, "On some new operations in soft set theory," *Comput. Math. with Appl.*, vol. 57, no. 9, pp. 1547–1553, 2009.

[10] K. Gong, Z. Xiao, and X. Zhang, "The bijective soft set with its operations," *Comput. Math. with Appl.*, vol. 60, no. 8, pp. 2270–2278, 2010.

[11] Z. Kong, G. Liqun, W. Lifu, and L. Steven, "The normal parameter reduction of soft sets and its algorithm," *Comput. Math. with Appl.*, vol. 56, pp. 3029–3037, 2008.

[12] T. Herawan, A. Nazari, M. Rose, and M. M. Deris, "Soft Set Theoretic Approach for Dimensionality," pp. 171–178, 2009.

[13] N. Çağman and S. Enginoğlu, "Soft matrix theory and its decision making," *Comput. Math. with Appl.*, vol. 59, no. 10, pp. 3308–3314, 2010.

[14] X. Ma, N. Sulaiman, H. Qin, T. Herawan, and J. M. Zain, "A new efficient normal parameter reduction algorithm of soft sets," *Comput. Math. with Appl.*, vol. 62, no. 2, pp. 588–598, 2011.

[15] X. Ma, N. Sulaiman, and H. Qin, "Parameterization Value Reduction of Soft Sets and its algorithm," *2011 IEEE Colloq. Humanit. Sci. Eng.*, no. Chuser, pp. 261–264, 2011.

[16] Z. Kong, L. Wang, and Z. Wu, "Two cases based on normal parameter reduction in soft sets *," *2012 Int. Conf. Comput. Sci. Electron. Eng.*, vol. 3, pp. 577–581, 2012.

[17] M. I. Ali, "Another view on reduction of parameters in soft set," *Appl. Soft Comput.*, vol. 212, pp. 1814–1821, 2012.

[18] D. Tingquan and W. Xiaofei, "Parameter significance and reductions of soft sets," *Int. J. Comput. Math.*, vol. 89, pp. 1979–1995, 2012.

[19] D. A. Kumar and R. Rengasamy, "Parameterization Reduction Using Soft Set Theory for Better Decision Making," *2013 Int. Conf. Pattern Recognition, Informatics Mob. Eng.*, pp. 365–367, 2013.

[20] B. Han and X. Li, "Propositional Compilation for All Normal Parameter Reduction of a Soft Sets," *springer*, pp. 184–193, 2014.

[21] G. Zhang, N. Xie, and Z. Li, "Parameter reductions of soft equivalence relations," *Int. J. Mach. Learn. Cybern.*, vol. 8, no. 2, pp. 711–720, 2015.

[22] Z. Li, N. Xie, and G. Wen, "Soft coverings and their parameter reductions," *Appl. Soft Comput. J.*, vol. 31, pp. 48–60, 2015.

[23] Z. Liu, K. Qin, Z. Pei, and L. Jin, "On induced soft sets and topology for the parameter set of a soft set," *2015 IEEE Int. Conf. Comput. Inf. Technol. Ubiquitous Comput. Commun. Dependable, Auton. Secur. Comput. Pervasive Intell. Comput.*, pp. 1349–1353, 2015.

[24] T. Bakshi, A. Sinharay, and T. Som, "An introduction towards automated parameterization reduction of soft set," *2016 3rd Int. Conf. Recent Adv. Inf. Technol. RAIT 2016*, pp. 164–171, 2016.

[25] Q. Zhang and X. Wang, "A New Parameter Reduction Method Based on Soft Set Theory," *Int. J. Hybrid Inf. Technol.*, vol. 9, no. 5, pp. 99–108, 2016.

[26] N.-X. Xie, "An Algorithm on the Parameter Reduction of Soft Sets," *Fuzzy Inf. Eng.*, pp. 127–145, 2016.

[27] V. Cetkin, A. Abdukadir, and A. Halis, "A new approach in handling soft decision making problems," *J. Nonlinear Sci. Appl.*, vol. 9, pp. 231–239, 2016.

[28] S. Danjuma, M. A. Ismail, and T. Herawan, "An alternative approach to normal parameter reduction algorithm for soft set theory," *IEEE Access*, vol. 5, pp. 4732–4746, 2017.

[29] S. Danjuma, T. Herawan, M. A. Ismail, H. Chiroma, A. I. Abubakar, and A. M. Zeki, "A Review on Soft Set-Based Parameter Reduction and Decision Making," *IEEE Access*, vol. 5, pp. 4671–4689, 2017.

[30] J. Zhan and J. C. R. Alcantud, "A survey of parameter reduction of soft sets and corresponding algorithms," *Artif. Intell. Rev.*, pp. 1–34, 2017.

[31] X. Ma and H. Qin, "A distance-based parameter reduction algorithm of fuzzy soft sets," *IEEE Access*, vol. 6, pp. 10530–10539, 2018.

[32] X. Ma and H. Qin, "Soft Set Based Parameter Value Reduction for Decision Making Application," *IEEE Access*, vol. PP, no. c, p. 1, 2019.

[33] Y. Zou and Z. Xiao, "Data analysis approaches of soft sets under incomplete information," *Knowledge-Based Syst.*, vol. 21, no. 8, pp. 941–945, 2008.

[34] Z. Kong, G. Zhang, L. Wang, Z. Wu, S. Qi, and H. Wang, "An efficient decision making approach in incomplete soft set," *Appl. Math. Model.*, vol. 38, no. 7–8, pp. 2141–2150, 2014.

[35] M. Sadiq Khan, M. A. Al-Garadi, A. W. A. Wahab, and T. Herawan, "An alternative data filling approach for prediction of missing data in soft sets (ADFIS)," *Springerplus*, vol. 5, no. 1, 2016.

[36] J. C. R. Alcantud and G. Santos-García, "A New Criterion for Soft Set Based Decision Making Problems under Incomplete Information," *Int. J. Comput. Intell. Syst.*, vol. 10, no. 1, p. 394, 2017.

[37] L. Li, Z. Xiao, X. D. Feng, and B. Zhong, "Soft Incomplete Discernibility Matrix for Decision-Making Problems," *IEEE Access*, vol. 6, pp. 32450–32459, 2018.

[38] G. Jothi and H. Hannah Inbarani, "Soft set based quick reduct approach for unsupervised feature selection," *Proc. 2012 IEEE Int. Conf. Adv. Commun. Control Comput. Technol. ICACCCT 2012*, pp. 277–281, 2012.

[39] J. Cai, J. Luo, S. Wang, and S. Yang, "Feature selection in machine learning: A new perspective," *Neurocomputing*, vol. 300, pp. 70–79, 2018.

[40] H. Mohamed, N. B. H. Ahmad, and S. M. H. Shamsuddin, "Bijective soft set classification of student's learning styles," *2014 8th Malaysian Softw. Eng. Conf. MySEC 2014*, pp. 289–294, 2014.

[41] S. S, T. J. Mathew, and E. Sherly, "Computerized Classification of Malignant and Normal Microcalcifications on Mammograms : Using Soft Set Theory," *2016 Int. Conf. Inf. Sci.*, pp. 131–137, 2016.

[42] H. Qin, X. Ma, J. M. Zain, and T. Herawan, "A novel soft set approach in selecting clustering attribute," *Knowledge-Based Syst.*, vol. 36, pp. 139–145, 2012.

[43] R. Mamat, T. Herawan, and M. M. Deris, "MAR: Maximum Attribute Relative of soft set for clustering attribute selection," *Knowledge-Based Syst.*, vol. 52, pp. 11–20, 2013.

[44] D. Hartama, I. T. R. Yanto, and M. Zarlis, "A soft set approach for fast clustering attribute selection," *2016 Int. Conf. Informatics Comput. ICIC 2016*, no. Icic, pp. 12–15, 2016.

[45] T. Herawan and M. M. Deris, "A soft set approach for association rules mining," *Knowledge-Based Syst.*, vol. 24, no. 1, pp. 186–195, 2011.

[46] B. Li, Z. Pei, and K. Qin, "Association rules mining based on clustering analysis and soft sets," *Proc. - 15th IEEE Int. Conf. Comput. Inf. Technol. CIT 2015*, pp. 675–681, 2015.

[47] F. Feng, J. Cho, W. Pedrycz, H. Fujita, and T. Herawan, "Soft set based association rule mining," *Knowledge-Based Syst.*, vol. 111, pp. 268–282, 2016.

[48] X. Ma and H. Qin, "Mixed types of soft set and its extended model based decision making," *2017 4th Int. Conf. Syst. Informatics, ICSAI 2017*, pp. 632–636, 2017.

[49] F. Xiao, "A Hybrid Fuzzy Soft Sets Decision Making Method in Medical Diagnosis," *IEEE Access*, vol. 6, pp. 25300–25312, 2018.

[50] Z. H. I. Kong, J. Ai, L. Wang, P. Li, L. Ma, and F. Lu, "New Normal Parameter Reduction Method in Fuzzy Soft Set Theory," *IEEE Access*, vol. 7, pp. 2986–2998, 2019.

Proceedings of the Fourth International Conference on Communication and Electronics Systems (ICCES 2019)
IEEE Conference Record # 45898; IEEE Xplore ISBN: 978-1-7281-1261-9

INTELLIGENT SYSTEM FOR IDENTIFYING DYSCALCULIA

A. Devi[1], Dr. G. Kavya[2]
Assistant Professor[1], Professor[2]
IFET College of Engineering[1], S.A.Engineering College[2]
Villupuram, Chennai
deviarumugam02@gmail.com[1], kavyavimal@gmail.com[2]

***Abstract*: Specific learning disability is known as learning disorder (neurodevelopmental disorder). Learning disabilities refers to problems in one of three areas (reading called dyslexia, writing called dysgraphia and number related concepts or using the symbols and functions to perform math calculation called dyscalculia). Five to six percentage of school age children are predicted to have dyscalculia. Children are mostly affected by having difficulties in acquiring a basic mathematical skills and they might excellent in other area of interest. The lack of proper detection and assistance in early stages of development of children will affects them being mentally distress and vulnerable. They start to blame themselves for their situation. The proposed system is designed to identify the students whose are at the risk of dyscalculia in an effective manner. So that the students can be identified at their early stage, and by giving proper assistance, they can able to shine in their academics.**

Keywords: Dyscalculia, learning difficulty, detection, mentally distress

I. INTRODUCTION

Mathematics is an universal language which deals with an numbers ,arithmetic's, counting etc. Dyscalculia means having disorder in calculation. It says about the specific difficulty in learning mathematics. It provides difficulty in acquiring mathematical skills and it also involves having difficulty in understanding basic mathematical facts and inability to understand the meaning of number and quantities.

About 6% school going children are having the mathematics difficulties. Generally the basic problem starts at the age of 7. The early screening is an important step in diagnose process. Where the children are tested with the ability to read a number, to understand the number facts, to add and compare the numbers of one-digit and two-digit, ability to acquire basic multiplication skills, basic arithmetic skills, ability to count a number forward or backward, to find a greatest/smallest number, basic geometrical skills. These skill sets are considered for screening test that typically occurred in school children. The screening test is that is used to identify the children having difficulty in acquiring basic mathematical skills and those are need special care and remediation in learning. The diagnostic process of dyscalculia which is based on the test shows a latency between poor numerical ability and good numerical ability. To define a threshold for dyscalculia, there are different criteria has been proposed a difference of 1-2 standard deviation between a skills and mathematical performance. Children who are influenced by dyscalculia regularly feel desolate and they demotivate themselves that they can't do anything like others. This prompts extreme impacts in their grown-up life it might likewise make them drop out their studies. Moreover because of these learning troubles they frequently disregarded by their educators and peers. This cause a person to be frustrated, have the poor self-image. They face trouble in reviewing tables, identifying images, doing fundamental number juggling count, sequencing and so on.

Types of dyscalculia:

Children with developmental dyscalculia finds difficulties to count recognize the mathematical symbol, calculate. Some of the types are,

Acalculia: It is later stage, it occurs due to the injuries in brain. It leads to have difficulty in arithmetic skills like addition, subtraction, multiplication, Division.

Verbal dyscalculia: Children face difficulty in naming verbally, naming the symbol, counting of numbers and items.

Operational dyscalculia: Children find difficulty in applying the rules during the mathematical operations.

Sequential dyscalculia: Facing difficulty in counting according to the sequence.

To overcome the lack of screening tool for identifying dyscalculia and to acquire accurate results, the intelligent embedded system for identifying dyscalculia is proposed. The models consist of the set of test which concerned with basic arithmetic skills, counting numbers, basic geometrical skills.

II. LITERATURE SURVEY

Bane et al. (2012) taken the survey about the people who having learning disabilities on relationships. In this survey, 21 researchers with learning disabilities, 12 supporters and 7 university researchers were considered for the survey. This survey suggested that learning disabilities people have different experiences and views on relationships. This survey concluded that people with learning disabilities need more support from their friends, family, and faculty members to develop new relationships and keep their existing ones[1].

Boyle & Rivera (2012) examined various types of note-taking techniques used by students used during lectures. In this

study, 125 students who having varying disabilities are taken into the survey. This study proved that students those who used note-taking techniques got good score in an effective manner based on the measures of achievement and the quality and quantity of notes recorded[2].

Ho & Siegel (2012) conducted a survey on the identification of students who have reading disabilities, and also reading implications for Chinese Word Recognition and Instructional Methods in Hong Kong Primary Schools. The survey identified that students with dyslexic pattern made more phonological errors, and students with phonological dyslexic pattern made more semantic errors[3].

Kong (2012) conducted qualitative survey on six students with Dyslexia after starting their masters degrees. The students personal accounts were analyzed using thematic analysis. The major themes identified were distress, self-doubt, embarrassment, frustration, relief, confidence and motivation. This survey given better understanding about the consequences of a late diagnosis, and given the special attention for management techniques needed for specific needs of the individuals. The survey revealed that adults diagnosed with Dyslexia can be cathartic or devastating depending on the adults emotional status and personality[4].

Melby & Lervag (2012) given the attention to the students with dyslexia disability and students with non-word repetition. The study concluded that students with dyslexia disability have poorer non word repetition skills when compared to both chronological-age and reading-level controls. And also identified the severity of the non-word repetition problem, where the most important variability is oral language skills[5].

Rose & Rouhani (2012) conducted survey on text oral reading fluency of 64 adolescents who have dyslexia disability, and tested the their verbal working memory on text oral reading fluency. The survey suggested that many shortfalls associated with childhood dyslexia is much important in adolescence, but the nature of the relationships between cognitive and linguistic predictions, and reading fluency were identified to be different for every adolescence[6].

Berninger & May (2011) conducted a survey on evidence-based diagnosis and treatment for people who having learning disability in written and oral language, or both. This survey considered the individual planning differences and evaluation of response to the instruction and modification of the instruction when a student is not responding. And also the survey recognized that teaching alone cannot change heritable changes in gene expression at schooling stage, but not the suited for gene sequences which are vulnerable to complexity and volume in the upper grades[7].

Condition aggregates in variable based math led by Bhattacharya (1988) it was discovered that understudies had more learning inabilities in application than in the information of direct conditions and furthermore it was discovered that the disentangled strategy was more powerful than the technique for transposition in understanding straight condition wholes.

III. PROPOSED SYSTEM

The aim is to build an interactive and easy handling system with high accuracy in detecting the dyscalculia. The proposed system can able to test the children in the age between (8-10yrs), and used to identify the errors made by an individual on the basis of mathematic content prescribed for standard III and IV.

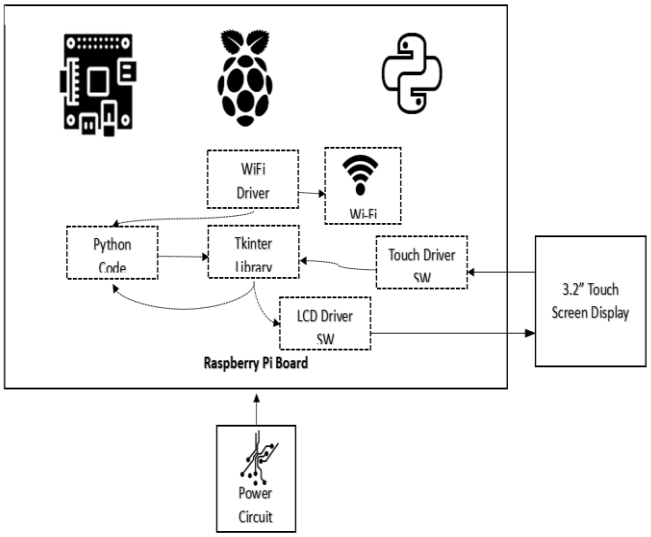

Fig. 1. Schematic diagram of Proposed system

The proposed system consists of raspberry pi board, LCD touch screen, and a power supply. The programming language which used is a python in which it consists of Tkinter and a GUI application for creating the buttons in the test screen. With the usage of Tkinter GUI, the questions will be created. The questions are based on testing the dyscalculia children. The children can able to answer the questions directly by clicking the LCD screen. This can be tested by comparing the latency between a child who suffered with dyscalculia and a normal child. After switching on the raspberry pi board, the result will be displayed on a display. It consist of set of questions for screening test, the children has to take a test for a period of time.

IV. METHODOLOGY

The skills that are checked by this method are given below.

A. Number and comparing:

In this section, the capabilities of the child to count the number in both forward and in reverse direction are checked (for example,1,2,3,4,5,6,7,8,9). And also this section can check whether the child can able to identify which number is odd

number, even number, greater, smaller number in a given questions

B. Basic addition and subtraction

In this section, the addition capability of the child to add the two numbers (example:1+1=2), and addition of doubles like(2+2=4), the subtraction skills (for example 1-2=1) are checked.

C. Basic multiplication skills:

In this section, the multiplication capability of the child (for example:2*3=6) is checked.

D. Missing numbers:

In this section, the missing numbers in given series (for example: 1,2,_,4,5) is checked. And the Identification of the missing number in even place and an odd place are also checked.

E. Place value:

This section involves to check whether the child can able to identify the underlined place value (for example:153=tens).It also involves to identify some of the geometry shapes like triangle, circle etc.

V. FLOW DIAGRAM

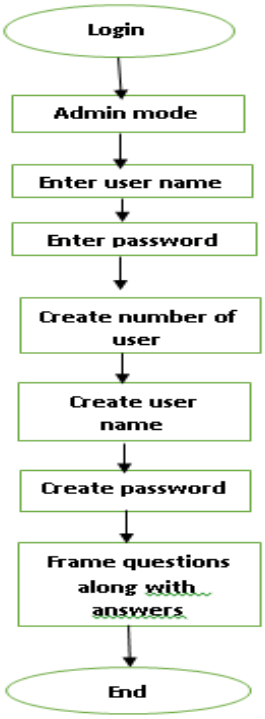

Fig 3. Flow diagram showing admin mode activity

Admin mode: The below flow diagram shows the operation activities carried out by the admin users. In this section, the we can change the type of the questions and we can put an multiple user .The multiple questions can be able to add in the admin section and we can also delete the questions. The number of user also can be created. The total score and the latency is displayed in admin mode. And we can also able to see the progress taken by the children in a parallel manner.

User mode: The below flow diagram shows the actions carried by the user. This section can be used for a children for taking up their test in order to identify whether they are suspected to have dyslexia or not.

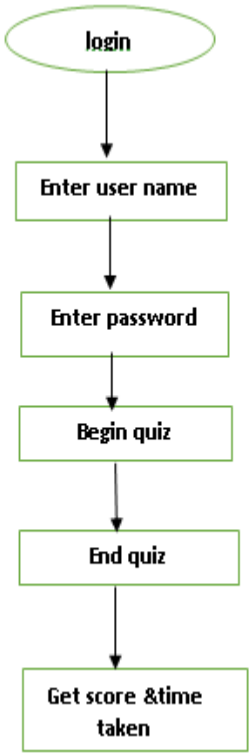

Fig 4. Flow diagram showing user mode activity

VI. EXPRIMENTAL RESULTS

The login page has different modes. They are user mode i.e. login created for normal child and a child suspected to have dyscalculia, and another mode is an admin mode. The user has to login in to the page. Once the child login into the page, they can started to attend the test.

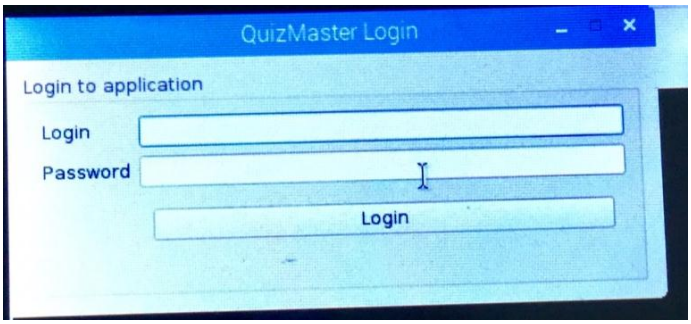

Fig. 5. Login page

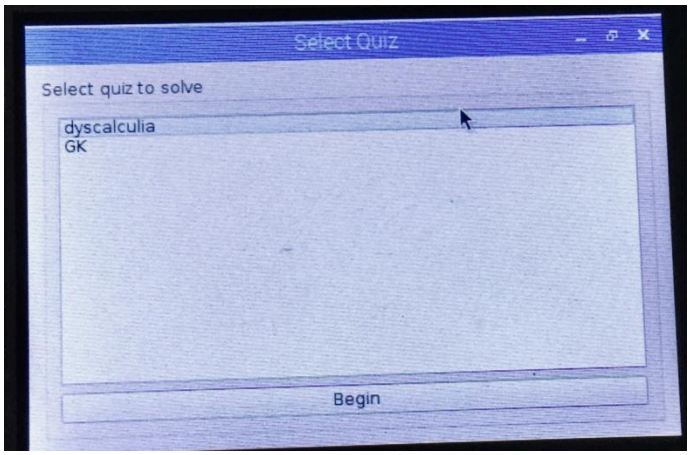

Fig 6. Selection of Quiz

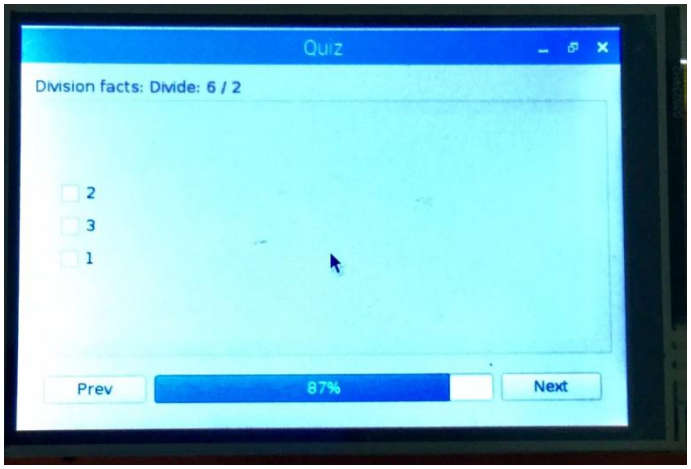

Fig 7a. Questions Set based on division

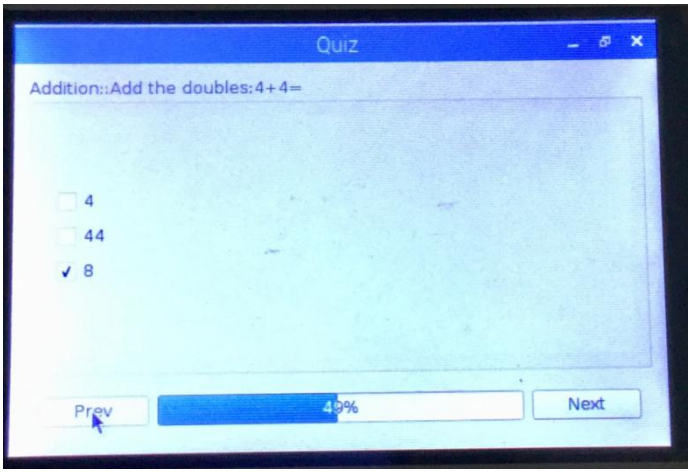

Fig.7b. Questions Set based on addition

Once the students have finished their test, the time taken by them will be displayed in the LCD screen. This is shown below.

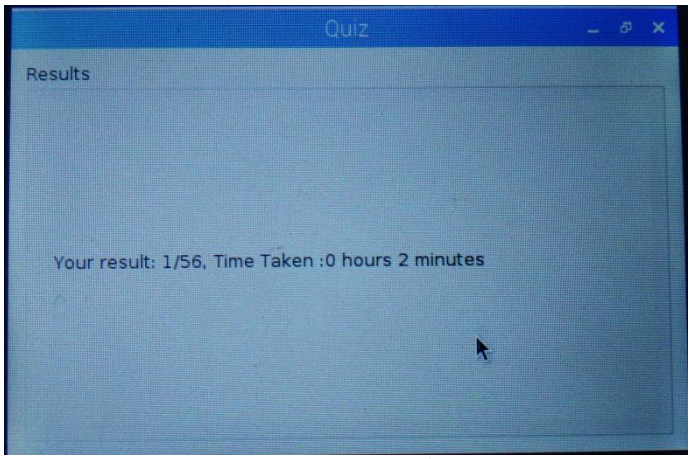

Fig 8. Latency and score of a child

Admin mode: Initially the number of user is created for taking the test. After that, multiple question sets can be added. Some of the question can also be deleted. The time taken for the test has been saved in the admin mode. So the admin can be logged in and the score of each child can be viewed as shown in below figure

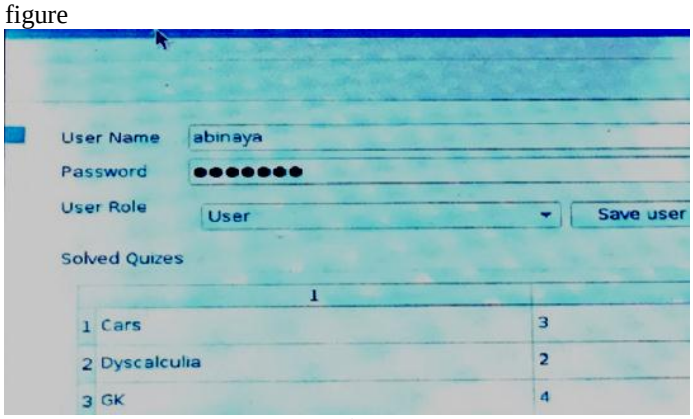

Fig. 9. Score of user statistics

The questions of the test can be updated periodically by using edit mode in the admin side.

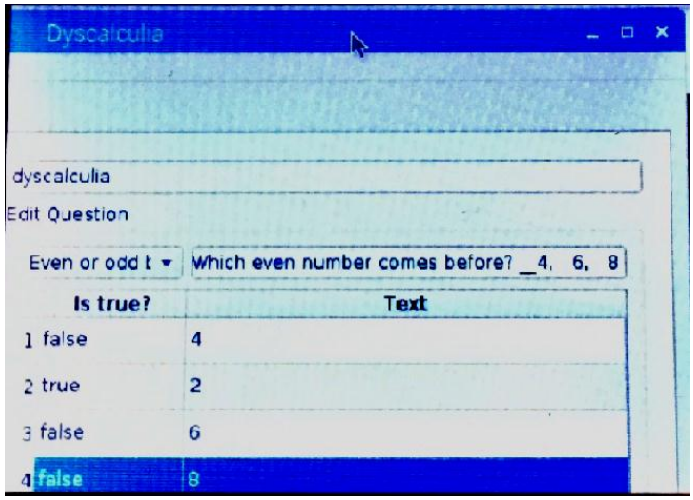

Fig 10. Questions addition page

The given model acts as prototype for the child studying class III. The questions are based on their normal ability. Since there were sixteen kids with two groups. One is normal children (control group) and another one is children (may be learning disabled). Both the groups of the children are allowed to take the test in a intelligent embedded system for identifying dyscalculia. Then the latency and a score of the children has to be calculated. The children are tested on the basis of relevant content.

VII. T- TEST CALCULATION

Sixteen kids of two groups are considered for taking the test. One is normal children (control group) and another one is abnormal children (may be learning disabled). Both groups of children are allowed to take the test in a intelligent system for identifying dyscalculia. Then the latency and a score of the children have to be calculated using T-test calculation. The test analysis of children was given below.

S.NO	Name	Correct answer Attended out of 10
1	Vino S	7
2	Sangeetha M	7
3	Akila K	6
4	vinay P	8
5	Lakshmi R	7
6	Priyanaga K	8
7	Swetha R	9
8	Anjali R	7
Mean		**7.375**

Table. 1 Correct responses of normal child

S.NO	Name	Correct answer Attended out of 10
1	Gayu K	2
2	Durga N	1
3	Gomathi T	4
4	Abinaya D	4
5	Gunaseeli V	5
6	Anusree M	3
7	latha U	2
8	Karthick K	5
Mean		**3.25**

Table. 2 Correct responses of abnormal child

S.NO	Name	Dyscalculia
1	Vino S	3.95
2	Sangeetha M	3.05
3	Akila K	3.07
4	vinay P	2.98
5	Lakshmi R	3.40
6	Priyanaga K	3.02
7	Swetha R	3.50
8	Anjali R	3.95
Mean		**3.365**

Table. 3 Latency of the normal child

S.NO	Name	Dyscalculia
1	Gayu K	7.30
2	Durga N	8.15
3	Gomathi T	7.30
4	Abinaya D	7.06
5	Gunaseeli V	7.13
6	Anusree M	8.02
7	latha U	8.00
8	karthick K	7.95
Mean		**7.613**

Table. 4 Latency of the abnormal children

Formula to calculate mean(μ)

$$\mu = \frac{1}{N}\Sigma x$$

Where,

x = no of correct response or time taken

N= total number of kids

There were two groups of students for identifying learning disabilities. So we found means of both group separately for each SLD.

Formula to calculate standard deviation(σ)

$$\sigma = \sqrt{\frac{\sum|x-\mu|^2}{N}}$$

Formula to calculate T-test

$$T = \frac{\mu_1 - \mu_2}{\sqrt{\left[\frac{\sigma_1^2}{N_1} + \frac{\sigma_2^2}{N_2}\right]}}$$

Where, $\mu_1 > \mu_2$

	Analysis	Dyscalculia
Child with dyscalculia	**Mean**	3.25
	SD	1.391
Normal child	**Mean**	7.375
	SD	0.856
T-Test		2.258

Table. 5 T-test analysis for correct response

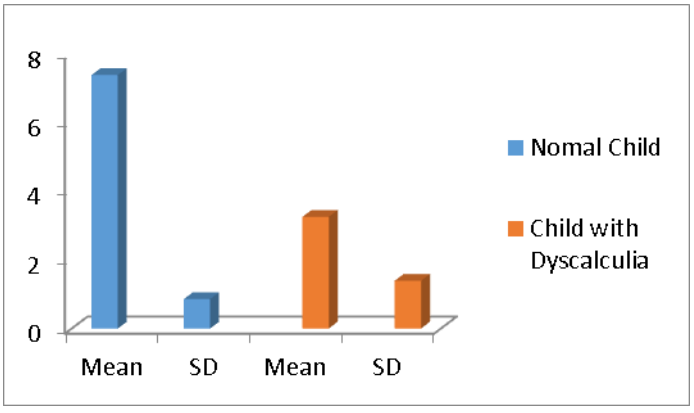

Fig 11. Mean and SD of correct response

	Analysis	dyscalculia
Normal child	**Mean**	3.15
	SD	0.305
Child with dyscalculia	**Mean**	7.52
	SD	0.419
T-test		2.267

Table.6 T-test analysis for time taken

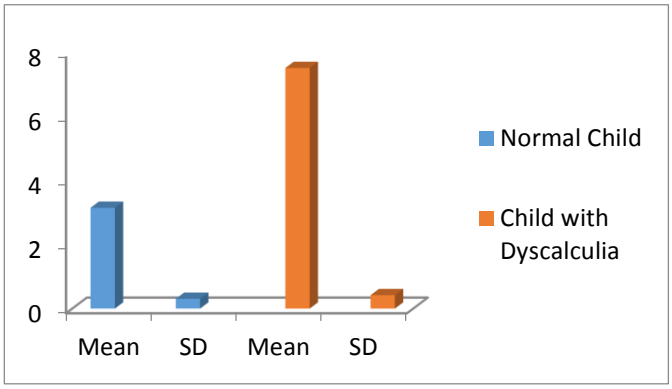

Fig 12. Mean and SD of time taken

VIII. CONCLUSION AND FUTURE SCOPE

The main purpose of this system is to identify the child with dyscalculia who may excel in other area. The main advantage of this system is to handle and use in an easy manner. The proposed is portable, and also it calculate the time taken by the children to answer and calculate the score and compare with the normal children score and latency and says whether the children having dyscalculia or not. The children with learning difficulty have less response for answering the questions. Those children are also taking more time delay when compared with other children's. These types of children should be identified earlier stage itself, and needs special care and guidance. Through practice, the dyscalculia disabilities in the child can be rectified.

The proposed system can be modified to identify the Dyslexia and Dysgraphia disabilities. The calculation of latency can be carried out with a help of screening tool automatically when the students are completing the test and the information can be sent to the parents Emil or mobile phone to aware about the children disability.

REFERENCES

[1]. Bane et al. (2012), "Relationships of people with learning disabilities in Ireland". British Journal of Learning Disabilities. 40. 10.1111/j.1468-3156.2012.00741.x.

[2]. Boyle & Rivera (2012), "Note-taking techniques for students with disabilities: A systematic Review of the Research", in SAGE journals, Volume: 35 issue: 3, page(s): 131-143, https://doi.org/10.1177/0731948711435794v

[3]. Ho & Siegel (2012), " A Study of the Relationships Among Chinese Multicharacter Words, Subtypes of Readers, and Instructional Methods", in Journal of Learning Disabilities, Volume: 49 issue: 1, page(s): 97-110, https://doi.org/10.1177/0022219414529334

[4]. Young Kong, Shelley. (2012), "The emotional impact of being recently diagnosed with dyslexia from the perspective of chiropractic students", Journal of Further and Higher Education. 36. 127-146. 10.1080/0309877X.2011.606898.

[5]. Melby-Lervåg, Monica & Lyster, Solveig-Alma & Hulme, Charles. (2012), " Phonological skills and their role in learning to read: A meta-analytic review", Psychological bulletin. 138. 322-52. 10.1037/a0026744.

[6]. L. Todd Rose, Parisa Rouhani (2012), " Influence of Verbal Working Memory Depends on Vocabulary: Oral Reading Fluency in Adolescents With Dyslexia" in Mind, Brain and Education, Volume 6, Issue 1, https://doi.org/10.1111/j.1751-228X.2011.01135.x

[7]. W Berninger, Virginia & O'Malley May, Maggie. (2011), "Evidence-Based Diagnosis and Treatment for Specific Learning Disabilities Involving Impairments in Written and/or Oral Language", Journal of learning disabilities. 44. 167-83. 10.1177/0022219410391189.

[8]. Devi.A, Sreya prakash.S, Abinaya.D, "Online Rehabilitation Tool for Identifying Learning Disabilities", in the IEEE international Conference on System Computation Automation and Networking, 2019 at Manakula Vinayagar Engineering College, Pondicherry on 29th and 30th March 2019.

[9]. Sakhuja S. Education for all and learning disabilities in India. [Online]. 2004. (Cited 2010); Available from: URL: http://sspeonline.org/article.

[10]. Fergussyn DM, Lynskey MT. Early Reading difficulties and later conduct problems. J Child Psychol Psychiat 1997; 38(8): 899-907.

[11]. Schachter DC, Pless B,Bruck M. The prevalence and correlates of behavioral problems in learning disabled children. Can J Psychiatry 1991 June; 36:323-30.

[12]. John P, George S K, Mampilly A. Handbook on poor school performance. New Delhi: Central Board of Secondary education; 2001.p.7-14.

[13]. Managing learning disability at the post secondary level. [online].(Cited 2010 July 22); Available from: URL: http://www.dyslexia-adults.com/managing.html//

[14]. BrookeU, Wattenberg D, GevaD. [Online]. 2000(Cited 2010); Available from: URL: http://www.pec.journal.com/article.

[15]. Santhanam P.Remedial programs for children with learning disability. [l online]. 2005 (cited 2010); Available from: URL: http://www.ssa.tn.nic.in/research.htm.

[16]. Dr P.M Beulah Devamalar, Dr V.Thulasibai, Dr G.Kavya, T. Jayanandan (2016) , "Design And Implementation Of Wearable Antenna For Biosignal Monitoring" , SENSOR LETTERS, Vol. 13, pp : 1–5, 2015, doi:10.1166/sl.2015.3552.

[17]. Kavya.G, ThulasiBai.V.(2014), "Wearable Advanced Single Chip ECG Telemonitoring System Using SOPC ", IEICE Electronics Express, Japan , Vol.11,No.6, pp: 1-10 . ISSN: 1349-2543

[18]. Dr P.M Beulah Devamalar, Dr V.Thulasibai, Dr G.Kavya (2016) , "Wearable Antenna for Bio Signal Monitoring Applications Using ISM Band" , IEEE sponsored 2nd International Conference on Advances in Electrical& Electronics, Information, Communication & Bio Informatics, AEEICB – 2016 , pp : 32-35.

[19]. V. T. Bai, P. M. B. Devamalar, M. A. Marx and G. Kavya, "An interactive fine motor movements screening e-tool for dyslexia based on kinesthetic perception," *2016 2nd International Conference on Advances in Electrical, Electronics, Information, Communication and Bio-Informatics (AEEICB)*, Chennai, 2016, pp. 296-300.doi: 10.1109/AEEICB.2016.7538294

[20]. Soaner C. Oxford English mini dictionary. 7th Ed. New Delhi: Oxford University Press; 2007. P. 309.

[21]. Joseph R. Boyle, PhD, Tina Z. Rivera, Note-Taking Techniques for Students WithDisabilities *A Systematic Review of the Research* Vol 35, Issue 3, 2012

[22]. J Learn Disabil Evidence-based diagnosis and treatment for specific learning disabilities involving impairments in written and/or oral language 2011 Mar-Apr;44(2):167-83. doi: 10.1177/0022219410391189.

[23]. Psychol Bull Melby-Lervåg M, Lyster SA, Hulme C. Phonological skills and their role in learning to read: a meta-analytic review. 2012 Mar;138(2):322-52. doi: 10.1037/a0026744. Epub 2012 Jan 16.

[24]. Rose LT, Rouhani P. Influence of verbal working memory depends on vocabulary: Oral reading fluency in adolescents with dyslexia. Mind, Brain, and Education. 2012;6:1–9. doi: 10.1111/j.1751-228X.2011.01135.x.

[25]. R Annes Gladia, G Kavya" Design and Development of Non-Invasive Kiosk for Self-Care Health Management" in the Glob. Journal of Pure Applied Mathematics Volume 13, pp: 4787-4794

Proceedings of the Fourth International Conference on Communication and Electronics Systems (ICCES 2019)
IEEE Conference Record # 45898; IEEE Xplore ISBN: 978-1-7281-1261-9

A Detailed survey on Virtual Network Embedding

1st Aqsa Hashmi
Department of Computer Science and Engineering
Rajasthan Technical University
Kota, India
aqsajaved260@gmail.com

2nd C.P Gupta
Department of Computer Science and Engineering
Rajasthan Technical University
Kota, India
cpgupta@rtu.ac.in

***Abstract*—Network virtualization encourages the assured resource management in which particular Virtual Network is allowed to be mapped on common or shared physical infrastructure. This mechanism termed as a problem of Virtual Network Embedding(VNE). It is considered to be NP-hard, and various heuristic, meta-heuristic, and exact solutions are proposed already in the past literature. In this paper study on different categories of VNE is presented. It also discusses multiple different approaches used to solve VNE among various networking environment like wireless networks, optical networks, cloud infrastructure, etc. The paper elaborates taxonomy of VNE optimization methods, considering dynamic or static, centralized or distributed and concise or redundant scenarios. Also focusses on a discussion of crucial algorithmic aspects and possible research directions.**

***Index Terms*—Network virtualization, Virtual network embedding, Embedding algorithms, Virtual networks**

I. Introduction

Network virtualization(NV) is a technique which defines a procedure of merging software as well as hardware network resources. It also performs network functionality into an individual, software-based executive entity, called a Virtual Network (VN). This domain is specific in collecting different virtual networks, that share the hidden resources of multiple substrate networks according to various resource allocation strategies. The physical network supplies network operators along with stretchability, variety, and tractability. Making NV one of the emerging automation in the advance internet architecture. The main advantages of NV are that it can provide more malleability and prevent internet petrification without requiring significant network modification. Network virtualization is made up of some form of network hypervisor, that virtualizes the physical network services to create virtual networks to serve various applications, and ultimately to provide the best possible outcomes, and the most efficient network access possible for the application and workloads. It is already used in business architecture like 4-WARD [1], CABO [2].

Virtualization is used to execute several applications (e.g., Operating System, servers, networking protocol) upon the same shared physical resources. These applications need cloud resources that are standard in the form of a virtual network including many virtual machines(VM) clusters attached by virtual links with undertaking bandwidth. In network tectonics infrastructure as a service (IAAS) [3] is used for defining future internet architecture. NV partition the role of the Internet service provider(ISP) in - 1)Infrastructure Provider (InP), and 2) providers of operation performing in-between the slices of the physical network known as a Service Provider (SP). InP employs and maintains the network appliances, and SP is the in charge of employment of networking protocols and enables end-to-end deployment of the latest networking technologies. There are various business models which are providing separation between InPs and SPs, eg. NetScript, Genesis, X-Bone, AGAVE, etc [4].

The traditional role of management and business of SP divided into three main players [1] (a) Physical Infrastructure Provider(PIP), (b)Virtual Network Operator(VNO)and (c) Virtual Network Provider(VNP). Information about each player is as follows:

1) **Physical Infrastructure Provider(PIP)**: PIP use to locate, command, and maintain the resources of a network such as routers, links, etc. They know the allocation strategy of physical resources assigned to VNP's request by excluding internal protocols. They provide information like prices of resources, the location of the physical network, and the Quality of Service offered. Which in turn, help VNP to build cost-effective decisions for the resources which are used to configure new Virtual networks.
2) **Virtual Network Provider(VNP)**: VNP is an intermediate group amid VNOs and PIPs. They discover practical resources from multiple InPs for granting VNOs requests. It is responsible for slicing and creation of empty containers in which VNOs form the protocol stacks required to configure the VN.
3) **Virtual Network Operator(VNO)**: They Operate the network architecture inside every slice of the virtual network. VNO install, manage, and operate the VN over the topology of VNP to serve the Quality of Service requirements of the client or end user. VNO set up the protocols, and networking infrastructure over the VN, isolated from technologies of the physical network. VNO then make use of VNs to provide services to the client.

A. Virtual Network Embedding

The primary entity in network virtualization comprised of a virtual network which is used to characterize many

network technologies like VPN, Overlay Networks, and Active and Programmable Networks. Virtual Network model defined as the interconnection of nodes and links along with their resource requirements. The requirement of a node is functional resources like Operating System capacity, energy, etc. that will not change with time. A link has a non-functional requirement like bandwidth, propagation delay, etc. that change throughout the time. Hence, this model termed as Virtual Network Request(VNR). Many VNRs with different node and link requirements enable to exist on the shared substrate network. The assignment of embedding VNs on the physical network is the major issue in network virtualization. This issue is known as Virtual Network Embedding problem (VNEP). The goal of VNE is proper utilization of primary resources by accepting many heterogeneous VNs to execute on the same SN. To complete this goal, VN mapped to specified nodes and links of the substrate infrastructure in the most favorable way. The Virtual Network Operator uses different embedding algorithms to determine which virtual resources to invoke from the Virtual Network Provider. Then Virtual Network Provider instantiates Infrastructure Providers substrate resources to handle various Virtual Network Requests. Hence, Virtual Network Embedding becomes an NP-hard problem. VNE is a topic of research in a couple of years because of the demand for network virtualization. In this way, multiple service provider can offer services on the same substrate network. It also can be used for network simulation architecture such as PlanetLab(a research network that supports the global evolution of new network facilities). Presently VNE problem is mainly classified into two subproblems, Virtual Node Mapping (VNoM) and Virtual Link Mapping (VLiM) [5]. The issue is further decomposed to solve the coordination between VNoM and VLiM.

1) VNE Problem Defination: VNE problem is explained as Assume substrate network as an undirected weighted graph G_S=(N, L), where N denotes the number of nodes and L denotes the number of links of the substrate network. Let VNR is represented by another graph $G_V = (N^{'}, L^{'})$, where $N^{'}$ and $L^{'}$ denote set of nodes and links associated to any $VNR^{'}$. Let us consider a function which allocates resources(bandwidth, CPU) to parts of the substrate network represented as equation 1.

$$capacity : [Nodes \bigcup Links \longrightarrow Resourcevectorspace] \tag{1}$$

Then for individual VNR we provide a function as in equation 2.

$$demand^{'} : [Nodes^{'} \bigcup Links^{'} \longrightarrow Resourcevectorspace] \tag{2}$$

This function allocate demand for resources to parts of all VNRs. Then a VNE is consists of two functions 3, 4 and :

$$F_1 : N^{'} \longrightarrow N \tag{3}$$

and

$$F_2 : L^{'} \longrightarrow G_V \subseteq G_s \tag{4}$$

for individual $VNR^{'}$ such that for all the nodes of any VNR and for all the links of any VNR

$$demand(L^{'}) \leq capacity(L) \tag{5}$$

Therefore equation 3 is a node mapping function(VNOM) and equation 4 is represented as link mapping function(VLiM). Model representing multiple VN and a single substrate is shown in figure 1.

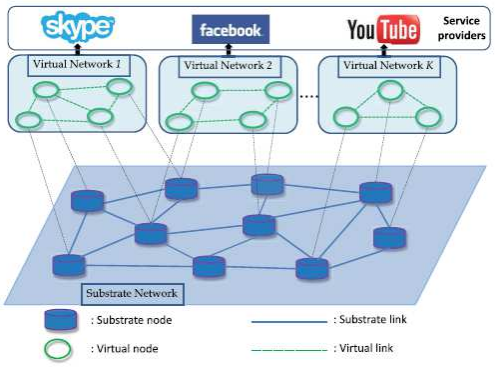

Fig. 1: Network virtualization model [6]

2) VNE problem description: Components of VNE are further described as follows:

1) **Substrate network(SN)**: SN has modeled with the help of a weighted undirected graph in VNE research literature. Substrate topology has formed with routers or switches defined on substrate nodes, and these nodes joined by substrate links such as coaxial cable or optical fiber. Each substrate node has specified by node capacity (CPU capacity) and the location of the node. Substrate links are defined by resources such as bandwidth and propagation delay.
2) **Virtual network(VN)**: The client formulates VN and supervised by the service provider. The task of Service Provider(SP) is to allocate computing resources of the network to a client, and resources hired from InP by using any VNE scheme. A weighted directed graph generally models VN with node and link requirement for computing power and bandwidth. VN termed with virtual network request which arrives from SP to SN in an online or offline manner.
3) **Virtual network mapping(VNE)**: VNEP is split into two subproblems - virtual node mapping (equation 3) and virtual link mapping (equation 4). There must be optimized coordination between these two subproblems. One scheme to achieve better coordination by solving each subproblem separately and output of VNoM termed as input for solving VLiM function. This permutation defined as uncoordinated VNE. Some solutions use coordinated VNE for better performance. Coordinated VNE will work in one stage or two stages. Some VNE approaches embed VNR into multiple adequate InPs by dividing a VNR into sub-requests. This variant termed as InterInP coordination.

978-1-7281-1261-9/19/$31.00 ©2019 IEEE

The rest of this paper is organized as follows. Section II assesses a literature survey. Section III introduces some future research challenges. Section IV concludes the paper.

II. Taxonomy of VNE

VNE can be classified into six categories according to different objectives, as shown in figure 2. A static or dynamic approach used when modification of infrastructure is involved. VNE follow distributed Approach because virtual networks are placed on the physical network composed of multiple InPs. Otherwise, a centralized system is there. When there are no resources saved as a backup, then the Approach is concise otherwise redundant.

1) Scenario-based: Scenario-based approaches are classified as either static or dynamic. When there is a change in the substrate and virtual network with the evolution of the system, then the method is dynamic otherwise static.

Static: In the static category, VNRs arrive following an offline order and stay in the network queue for some time and mapped one by one. There is no reconfiguration of SN and VN involved. Hence it works better for a small-scale network. Limitation of static VNE approach is fragmentation as topologies of both VN and SN cannot be reorganized; due to this, no efficient resource utilization takes place.

Dynamic: Dynamic VNE approach overcomes the limitations of the static Approach by relocating already allocated resources. This Approach involves a change of infrastructure and VNRs arrive following an online manner. Dynamic VNE supports remapping of rejected VNR, which is called virtual network reconfiguration. This algorithm was introduced to improve the rejection rate and load balance. Limitations of dynamic VNE approach is that there is increased complexity of remapping.

2) Modification-based: Modification based approaches can take the form of centralized architecture when only one substrate entity involved for mapping. A Distributed architecture is considered when multiple objects are responsible for mapping the requests.

Centralized: These approaches follow soft programs that run on general computing platforms. The single entity of InP receive VNR and allocate resources to it. This separate entity has information about each resource allocation. In other words, it has global knowledge about the system. But the disadvantage of this Approach is if a single entity failure occurs, the complete process fails. It is tough to maintain scalability on an extensive scale network with this Approach.

Distributed: In this Approach, Virtual Network Requests are distributed over multiple substrate entities. Due to load distribution, every node participates in the embedding process, and it overcomes the limitation of scalability. These approaches provide better robustness compared to the centralized procedure. Deficiency of this Approach is there is communication overhead for maintaining synchronization among multiple InPs.

3) Relocation-based: Relocation based approaches consider the resource requirement. If resources are available only to satisfy the requests, then the method is concise. If resources are saved to handle any substrate failure, then the Approach is redundant.

Concise: In this approach substrate resources are not reserved as a backup when any entity fails. The concise Approach uses algorithms which use as many resources as required for completing the demands. The remaining resources which left after the embedding process they can be used for future VNRs. Failure recovery is not guaranteed in a virtual network. Most algorithms follow the assumption that every time SN is working; hence, most VNE solutions are concise in general.

Redundant: These approaches secure extra resources for virtual network requests in cases of runtime failure. Degree of reliability is directly proportional to the embedding cost. These approaches meant for fault sensitive systems. Substrate entities are monitored if any breakdown happens, so there are fall back resources for them, and switching from primary resource to backup support is performed.

According to the above context the approaches are mutually independent; hence, VNE algorithms are dynamic, distributed, redundant at the same time. Hence notation for identification of the class of the particular algorithm in which it belongs is described with the following syntax:

S—D/C—D/C—R

The first character denotes whether the Approach will work in a Static or Dynamic category. Next character indicates whether the algorithm is Centralized or Distributed. Finally, the third character aims to denote whether the Approach is Concise or Redundant. For instance, a VNE algorithm indicated as S/C/C represents that the algorithm is a static, centralized, and concise algorithm. Class distribution of different embedding approaches can be classified as follows:

A. Centralized/Static/Concise solutions

This section contains a literature survey of VNE algorithms belonging to S/C/C class, as shown in table I. This class is easy to model because virtual network requests arrive offline and processed in batches with a time window. There is only one substrate infrastructure to manage, and it has global knowledge about every component of the network. It works as a base to model the other seven classes described further in the paper. Many types of research have conducted in this class of VNE algorithms.

Limitations of S/C/C category such as:

- S/C/C solutions assume that substrate network remains operational through run time, but in today's substrate network such as MPLS(multi-protocol label switched networks), [13] and real-time system [14] the substrate node or link may fail. Hence, S/C/C solutions will not provide Virtual network survivability, and no extra resources saved for handling substrate failure.

978-1-7281-1261-9/19/$31.00 ©2019 IEEE

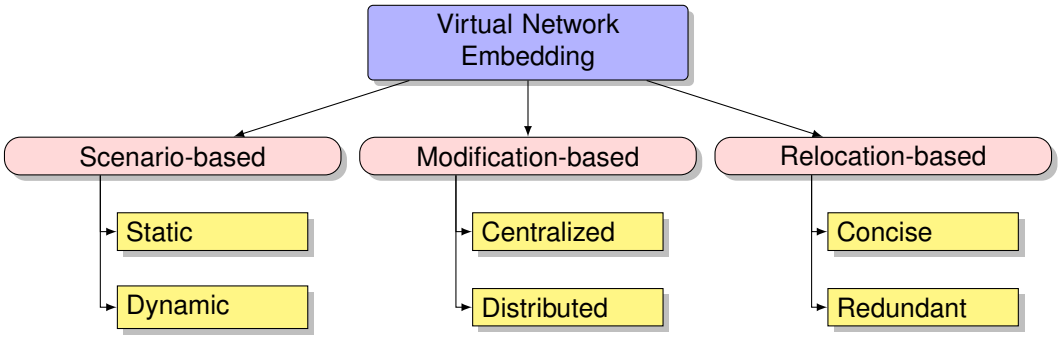

Fig. 2: Taxonomy of VNE

S.No.	References	Contribution	Merits	Limitations
1	Liu *et al.*[7]	virtual network embedding completed by 0-1 programming in one step.	Improved coordination based on nodes proximity	Not feasible for large-scale networks
2	Yu *et al.*[8]	Joint node mapping and link mapping in single stage	Reduced mapping cost and hop length	Not completely optimal
3	Feng*et al.*[9]	Considered multiple attributes of topology for embedding VN	Improved long-term average revenue, acceptance ratio, and revenue to cost ratio.	Does not provide fault tolerance
4	Jarray *et al.*[4]	JNLE column generation with branch and bound technique and auction-based mechanism	Increased infrastructure provider's profit up to 45%	Not able to maintain fairness among clients
5	Mano *et al.*[10]	Investigated trade-off of embedding time and reduced cost of virtual network	This Approach provides faster embedding by reducing dense Virtual Network into sparse.	The feasibility and capacity ratio were not analyzed.
6	Jahani and Khanli[11]	Core decomposition find subnetworks according to a degree of node	More revenue, acceptance ratio, and low embedding cost	It will not provide scalability in handling large complex graphs as memory size was unbounded. Additionally, Approach had more CPU and I/O cost due to inefficient utilization of memory.
7	Moura *et al.*[12]	Proposed A Branch and Price algorithm to solve Virtual network embedding problem of single path.	Fast running time hence memory usage was minimized	Further enhancement is required for performance of the algorithm and no. of nodes can be further reduced

TABLE I: Solution of S/C/C class

- The network scenario under this class of solutions is complicated because of the substantial computational burden on the central unit. Moreover, it is hard to analyze the network in this class.
- As the infrastructure is centralized, there is an issue of scalability arises while implementing S/C/C in large-scale networks. Moreover, static requests also cause fragmentation in the substrate network, which, on the other hand, cause reduced acceptance ratio and long term revenue.

B. Centralized/Dynamic/Concise solutions

C/D/C class includes another variant of S/C/C class by changing one characteristic as shown in table II. Here we are focused on the virtual network embedding with an evolving or dynamic system. The solutions belonging to this class has improved the rejection rate and balances the load of the substrate network efficiently.

D/C/C class provide VNE solutions with the reconfiguration of mapped virtual network requests and reorganize resource allocation. But, there are less number of solutions under this class as compared to S/C/C category. It has some merits as well as limitations.

Limitations are discussed below:

- Fewer VNE solutions are belonging to D/C/C class as compared to S/C/C class, due to the high migration cost of virtual nodes and links resulting in long service disconnection times. Hence, D/C/C solutions are not feasible for critical time applications.
- D/C/C solutions behave in a very complicated manner due to online characteristic; hence, they are more challenging than the static scheme.

C. Distributed/Static/Concise solutions

Above discussed two classes followed the centralized network topology. Where the central substrate entity is handling all VN requests from the clients and is responsible for choosing and assigning virtual nodes to the substrate nodes of the underlying physical network. But the centralized Approach has certain limitations like scalability among vast scaled network, and it is not easy to maintain. Another limitation is productivity and flexibility of VN requirement and management. This becomes challenging research when SN is dynamic with an evolving environment. As shown in table III the section deal with the analysis of distributed network topology which decentralizes the process of making decisions while mapping

978-1-7281-1261-9/19/$31.00 ©2019 IEEE

S.No.	References	Contribution	Merits	Limitations
1	Shuhao *et al.*[15]	Proposed objective functions with both resource and security constraints	Addressed the security requirements of virtual network embedding	Not a traditional pay-as-to-go model.
2	Sun*et al.*[16]	Introduced a MILP model for embedding evolving VN requests	Reduced resource consumption as well as the cost of reconfiguration	Higher link mapping cost
3	Shakya *et al.*[17]	Focused on spectrum consecutiveness, relative loss, and spectrum alignment.	Achieved lower blocking probability for arriving VON requests and enhanced revenue for the Service Providers (SPs)	Alignment and Spectrum consecutiveness will cause excess link load of some region in the network, therefore blocking probability will increase.
4	Han *et al.*[18]	VNE in WiFi network	Increased InP profit and acceptance ratio	The average revenue as well as the average cost declined and RFD increases.
5	Han*et al.*[19]	Green virtual network embedding scheme in virtualized FiWi access network for 5G	Power consumption is reduced with guaranteeing Infrastructure Provider profit	No provisioning of virtual nodes with low flexibility.
6	Hejja and Hesselbach[20]	Embedding focused on peer-to-peer delay as a primary constraint	Reduced the average power consumptions in the physical network by 23.54%.	Non-direct edges are not considered

TABLE II: Solution of D/C/C class

VN on all substrate nodes. This work includes embedding of VN requests on a network which is shared and find optimal mapping with a balanced node on each node and link.

Limitations of S/D/C class of solutions:

- There is a lack in the group of S/D/C solutions in offering resiliency which can be provided by setting up backup resources at provisioning time in a centralized way.
- S/D/C groups algorithms that perform configuration of VNs across multiple substrate networks; hence, there is overhead of exchanging messages; therefore, for vast SNs evaluation is not optimal.

D. Centralized/Static/Redundant solutions

In a network virtualization environment, it is ensured that all virtual links should be unbroken in the presence of failure. As shown in table IV the section focuses on survivability approaches in NV environment. Resources are redundant to provide fault tolerance.

E. Distributed/Dynamic/Concise Solutions

VNE belonged to D/D/C class are grouped in this subsection, as shown in table V. These proposals can perform a dynamic reconfiguration of already mapped Virtual Network Requests when a new VNR arrives. Embedding is concise, and the algorithms run on a primary instance. Dynamic approaches are proactive, hence challenging. It leads to fewer publications in this category, compared to centralized, static methods.

Limitations of D/D/C VNE solutions:

- Distributed solutions for VNE are significantly harder to implement and more difficult to reach near to optimal solutions hence few D/D/C approaches are listed in this section.
- It is hard to find proper convergence direction in multiple Substrate networks.

F. Distributed/Dynamic/Redundant solutions

This subsection defined distributed and dynamic approaches, along with redundant resources to provide fault tolerant behavior. Nguyen *et al.*[6]defined resource allocation and routing in a wireless network environment. The objective of the framework was to prevent disruption caused by traffic for SPs. Provided operation cost for SN was low also it provided promising traffic reduction on link failure. As the formulated model was on a large-scale direct solving of optimization problem was not manageable. Hence, two algorithms were proposed by the application of ADMM (alternating direction method of multipliers) decomposition technique named parallel and distributed algorithm. Limitation of this multi-path addressing is that it also increases the redundant transmission of the target content and the node will exit network when the energy exhausted, and the QoS of the system will deteriorate.

Limitations of D/D/R VNE solutions:

- Most of the algorithms still run on a central instance, and few approaches try to combine redundancy and dynamicity.

G. Distributed/Static/Redundant solutions

This subsection deals with approaches having Decentralized infrastructure and resources are redundant to provide survivability. Order of arrival of VNR is offline

Chowdhury *et al.* [32] proposed PolyVINE allowed mapping of VN in a distributed way and each InP is involved in global competition. They proposed a location dissemination protocol(LAP)and hierarchical addressing system (COST) that allowed InPs to make informed forwarding decisions. Another direction involves modeling this problem as DCOP(distributed constrained optimization problem)[31] and for the solution, there should be minimal information exchange between InPs.

Beck*et al.*[33] proposed a parallel, generic, and distributed technique for mapping virtual networks. Proposed Approach provided minimization in communication than other decentralized VNE solutions. Regardless of its decentralized behavior, mapping costs of DPVNE remain persistent comparable to costs of centralized techniques.

Limitations of S/D/R VNE solutions:

- In S/D/R class of solutions SNs failure of any substrate element is considered thus complexity is higher than usual S/D/C solutins.

978-1-7281-1261-9/19/$31.00 ©2019 IEEE

S.No.	References	Contribution	Merits	Limitations
1	Esposito *et al.*[21]	Distributed auction method for solving slice embedding problem	Quality convergence characteristics and better resource utilization	link is decoupled from node mapping which may result in VNE inefficiency
2	Duan *et al.*[22]	Three virtual machine placement strategies with different features	Saved core switches, Powerfull and flexible also cost saving is achieved	Did not allow link oversubscription
3	Mano *et al.*[23]	Proposed a method which allows optimal VN to built over multiple domains effectively without disclosing private information	Discussed Pareto optimality of VN fragments to reduce search space	A much faster search algorithm can be used for further enhancement
4	Hou *et al.*[24]	Risk assessment framework to recognise unsecure VMs and RVNE framework to accomplish the physical separation among unsecure and safe VMs.	RVNE has undertaken the ODCN protection with an average protection ratio of 0.75	Does not deal with the reply attack hence no optical bandwidth between two risky VMs

TABLE III: Solution of D/S/C class

S.No.	References	Contribution	Merits	Limitations
1	Mashrur Alam khan *et al.*[25](2016)	SiMPLE(Survivability in multi-path link embedding) Highly survivable VN embedding of multiple link failures	Increment in profit, survivability is assured, lower backup bandwidth demand and better acceptance ratio	while implementing under SDN environment, this prototype cannot support path splitting in the substrate network
2	Lee *et al.*[26](2018)	Developed SVNE which was topology aware and it combined those degree and closeness factors	The proposed algorithm may enhance virtual network survivability without lowering the performance and acceptance ratio	Network traffic congestion did not consider for further improvement
3	Xiao*et al.*[27](2014)	Define primary and backup node resources for multiple nodes failures	Achieved rational resource allocation and effectively increased the profit of infrastructure provider	There is no adjustment for dynamic backup quotas to assist the changing Virtual Network and node failure arrival rate.
4	Shahriar *et al.*[28](2017)	Proposed a generalized method to recover from single substrate node failure	Proposed heuristic performed close to the optimal solution and outperforms the state-of-the-art algorithm	Reactive recovery approach take action after failure

TABLE IV: Solution of C/S/R class

S.No.	References	Contribution	Merits	Limitations
1	Houidi *et al.*[29](2010)	Remap VN when a new VN arrives among multiple SNs	Distributed embedding algorithm along with dynamic VN binding for efficient reaction to resource failures	adaptive matching not defined for identification of new candidate resources according to service provider's requirement
2	Esposito *et al.*[30]	Presented a framework for virtual network embedding policy programmability(VINEA).	It is a constrained graph matching problem modeled as network utility maximization. Proposed Approach followed decomposition theory to resolve the VNEP.	Proposed work analyzed the embedding performance with different policies. A secure VN embedding protocol able to function even in the presence of misconfigurations, Byzantine failure, and malicious users is required.
3	R.Gulart *et al.*[31]	First one which was modeled using DCOP(distributed constraint optimization problem) for allocating resources of nodes and link with factor graph	It provided better scalability	features such as geographical location, bandwidth or physical availability not considered

TABLE V: Solution of D/D/C class

III. Future Research Challenges

VNE solutions are still an open field and cover many points. Some future directions in this respective domain are described below:

- **Complexity of VNE**: Static and rigid network systems cannot satisfy an increasingly large amount of mobile traffic. Therefore to leverage, the complexity and scalability of resource allocation in large-scale access networks, various multi-objective or distributed models are already introduced. There are many unresolved issues to resolve complexity in resource distribution.
- **Dynamic VNE**: In studies of static VNE, the assignment of network resources is persistent and excessive in the VNRs lifetime. However, in actual, the user's resource demands evolve with time; therefore, static VN embedding techniques leading to less usage of substrate resources and lowering of revenues. Dynamic methods provide flexibility in virtual and substrate network and provide multiple bandwidth connection in applications like E-health, virtual reality, etc. VNE algorithms with dynamical virtual network mapping for complex computation is an open research issue for future work.
- **VNE Survivability**: Protecting the Virtual Network layer is an uninvestigated spectrum for survivability. Providing survivability at the upper layer (e.g., Internet Protocol

978-1-7281-1261-9/19/$31.00 ©2019 IEEE

(IP)) of a multilayer network is crucial for VNE. Another advantage of giving survivability at the VN layer is that it capitulates more resource effective embedding as compared to providing the same level of survivability at the Substrate Network layer. Survivable VNE with VN level protection saves approximately 33% resources than survivable VNE with SN level protection. Allocation of resources to ensure survivability at the fabric level along with VN level is an essential future challenge to study further.

- **VNE in wireless network**: Operators of the wireless network are observing a considerable rise in data demand because of smart-phones and the abundance of supported Internet applications. Mobility is an important subject that has to be taken into account during the development of the VNE algorithm for wireless networks. Mainly, content caching at the network level is gaining interest as a technique which eases the generated data traffic at the base station and also reduces the access latency and the overall power usage. By caching accessible content along with the network, client requests can be satisfied by closely located mobile clients without the need to recover them from the source, which is assumed to be, in the best case scenario.

IV. CONCLUSION

Network virtualization is an encouraging tool to eliminate the rigidity of modern internet. Virtual Network Embedding is an important matter to resolve resource utilization in network virtualization. Embedding algorithms aimed are essentially exact, heuristic, and meta-heuristic to explain the available virtual network assignment in polynomial time. This paper presented a literature survey of a variety of approaches and also presented a study of many algorithms used to solve different aspects of VNE. A proper explanation and formulation of VNE are given, and a taxonomy is explained in an elaborated manner. As future work issues like InP interactions, reputation management, pricing models, and incentives for InP genuineness. Characteristics such as scalability, stability, and performance require further study

REFERENCES

[1] Jorge Carapinha and Javier Jiménez. Network virtualization: a view from the bottom. In *Proceedings of the 1st ACM workshop on Virtualized infrastructure systems and architectures*, pages 73–80. ACM, 2009.

[2] Nick Feamster, Lixin Gao, and Jennifer Rexford. How to lease the internet in your spare time. *ACM SIGCOMM Computer Communication Review*, 37(1):61–64, 2007.

[3] Sushil Bhardwaj, Leena Jain, and Sandeep Jain. Cloud computing: A study of infrastructure as a service (iaas). *International Journal of engineering and information Technology*, 2(1):60–63, 2010.

[4] Abdallah Jarray and Ahmed Karmouch. Decomposition approaches for virtual network embedding with one-shot node and link mapping. *IEEE/ACM Transactions on Networking (TON)*, 23(3):1012–1025, 2015.

[5] A. Fischer, J. F. Botero, M. T. Beck, H. de Meer, and X. Hesselbach. Virtual network embedding: A survey. *IEEE Communications Surveys Tutorials*, 15(4):1888–1906, Fourth 2013.

[6] H. K. Nguyen, Y. Zhang, Z. Chang, and Z. Han. Parallel and distributed resource allocation with minimum traffic disruption for network virtualization. *IEEE Transactions on Communications*, 65(3):1162–1175, March 2017.

[7] Wenzhi Liu, Yang Xiang, Shaowu Ma, and Xiongyan Tang. Completing virtual network embedding all in one mathematical programming. In *Electronics, Communications and Control (ICECC), 2011 International Conference on*, pages 183–185. IEEE, 2011.

[8] Hongfang Yu, Vishal Anand, Chunming Qiao, Hao Di, and Xuetao Wei. A cost efficient design of virtual infrastructures with joint node and link mapping. *Journal of Network and Systems Management*, 20(1):97–115, 2012.

[9] Min Feng, Jianxin Liao, Jingyu Wang, Sude Qing, and Qi Qi. Topology-aware virtual network embedding based on multiple characteristics. In *Communications (ICC), 2014 IEEE International Conference on*, pages 2956–2962. IEEE, 2014.

[10] Toru Mano, Takeru Inoue, Kimihiro Mizutani, and Osamu Akashi. Reducing dense virtual networks for fast embedding. In *INFOCOM 2016-The 35th Annual IEEE International Conference on Computer Communications, IEEE*, pages 1–9. IEEE, 2016.

[11] Arezoo Jahani and Leyli Mohammad Khanli. Cata-vn: Coordinated and topology-aware virtual network service provisioning in data centers network. In *Computer and Knowledge Engineering (ICCKE), 2017 7th International Conference on*, pages 353–358. IEEE, 2017.

[12] Leonardo FS Moura, Luciano P Gaspary, and Luciana S Buriol. A branch-and-price algorithm for the single-path virtual network embedding problem. *Networks*, 71(3):188–208, 2018.

[13] W. Lau and S. Jha. Failure-oriented path restoration algorithm for survivable networks. In *2004 IEEE/IFIP Network Operations and Management Symposium (IEEE Cat. No.04CH37507)*, volume 1, pages 205–218 Vol.1, April 2004.

[14] Q. Zheng and K. G. Shin. Fault-tolerant real-time communication in distributed computing systems. In *[1992] Digest of Papers. FTCS-22: The Twenty-Second International Symposium on Fault-Tolerant Computing*, pages 86–93, July 1992.

[15] S. Liu, Z. Cai, H. Xu, and M. Xu. Security-aware virtual network embedding. In *2014 IEEE International Conference on Communications (ICC)*, pages 834–840, June 2014.

[16] Gang Sun, Hongfang Yu, Vishal Anand, and Lemin Li. A cost efficient framework and algorithm for embedding dynamic virtual network requests. *Future Generation*

978-1-7281-1261-9/19/$31.00 ©2019 IEEE

Computer Systems, 29(5):1265–1277, 2013.

[17] Sunny Shakya, Nabina Pradhan, Xiaojun Cao, Zilong Ye, and Chunming Qiao. Virtual network embedding and reconfiguration in elastic optical networks. In *Global Communications Conference (GLOBECOM), 2014 IEEE*, pages 2160–2165. IEEE, 2014.

[18] Pengchao Han, Lei Guo, Yejun Liu, Xuetao Wei, Jian Hou, and Xu Han. A new virtual network embedding framework based on qos satisfaction and network reconfiguration for fiber-wireless access network. In *Communications (ICC), 2016 IEEE International Conference on*, pages 1–7. IEEE, 2016.

[19] P. Han and and. Green virtual network embedding framework based on zooming small cells in fiber-wireless access network for 5g. In *2017 19th International Conference on Transparent Optical Networks (ICTON)*, pages 1–4, July 2017.

[20] Khaled Hejja and Xavier Hesselbach. Online power aware coordinated virtual network embedding with 5g delay constraint. *Journal of Network and Computer Applications*, 124:121–136, 2018.

[21] Flavio Esposito, Donato Di Paola, and Ibrahim Matta. A general distributed approach to slice embedding with guarantees. In *IFIP Networking Conference, 2013*, pages 1–9. IEEE, 2013.

[22] Jun Duan, Zhiyang Guo, and Yuanyuan Yang. Cost efficient and performance guaranteed virtual network embedding in multicast fat-tree dcns. In *Computer Communications (INFOCOM), 2015 IEEE Conference on*, pages 136–144. IEEE, 2015.

[23] Toru Mano, Takeru Inoue, Dai Ikarashi, Koki Hamada, Kimihiro Mizutani, and Osamu Akashi. Efficient virtual network optimization across multiple domains without revealing private information. *IEEE Transactions on Network and Service Management*, 13(3):477–488, 2016.

[24] W. Hou, Z. Ning, L. Guo, Z. Chen, and M. S. Obaidat. Novel framework of risk-aware virtual network embedding in optical data center networks. *IEEE Systems Journal*, 12(3):2473–2482, Sep. 2018.

[25] M. M. Alam Khan, N. Shahriar, R. Ahmed, and R. Boutaba. Multi-path link embedding for survivability in virtual networks. *IEEE Transactions on Network and Service Management*, 13(2):253–266, June 2016.

[26] Rongzhen Lee, Qingbo WU, Yusong TAN, and Junyang ZHANG. On the optimal approach of survivable virtual network embedding in virtualized sdn. *IEICE Transactions on Information and Systems*, E101.D:698–708, 03 2018.

[27] A. Xiao, Y. Wang, L. Meng, X. Qiu, and W. Li. Topology-aware virtual network embedding to survive multiple node failures. In *2014 IEEE Global Communications Conference*, pages 1823–1828, Dec 2014.

[28] N. Shahriar, R. Ahmed, S. R. Chowdhury, A. Khan, R. Boutaba, and J. Mitra. Generalized recovery from node failure in virtual network embedding. *IEEE Transactions on Network and Service Management*, 14(2):261–274, June 2017.

[29] Ines Houidi, Wajdi Louati, Djamal Zeghlache, Panagiotis Papadimitriou, and Laurent Mathy. Adaptive virtual network provisioning. 10 2010.

[30] F. Esposito, I. Matta, and Y. Wang. Vinea: An architecture for virtual network embedding policy programmability. *IEEE Transactions on Parallel and Distributed Systems*, 27(11):3381–3396, Nov 2016.

[31] Alexander R. Gulart, Odorico Mendizabal, Raquel Barbosa, and Diana Adamatti. Node and link allocation in network virtualization based on distributed constraint optimization. *Journal of Network and Systems Management*, 1:1–20, 05 2017.

[32] Mosharaf Chowdhury, Fady Samuel, and Raouf Boutaba. Polyvine: policy-based virtual network embedding across multiple domains. In *Proceedings of the second ACM SIGCOMM workshop on Virtualized infrastructure systems and architectures*, pages 49–56. ACM, 2010.

[33] Michael Till Beck, Andreas Fischer, Hermann de Meer, Juan Felipe Botero, and Xavier Hesselbach. A distributed, parallel, and generic virtual network embedding framework. In *ICC*, pages 3471–3475, 2013.

[34] Shun-li Zhang and Xue-song Qiu. A novel virtual network mapping algorithm for cost minimizing. *Journal of Selected Areas in Telecommunications*, 29(1):1–9, 2011.

[35] Aris Leivadeas, Chrysa Papagianni, and Symeon Papavassiliou. Efficient resource mapping framework over networked clouds via iterated local search-based request partitioning. *IEEE Transactions on Parallel and Distributed Systems*, 24(6):1077–1086, 2013.

[36] Hongfang Yu, Chunming Qiao, Vishal Anand, Xin Liu, Hao Di, and Gang Sun. Survivable virtual infrastructure mapping in a federated computing and networking system under single regional failures. In *Global Telecommunications Conference (GLOBECOM 2010), 2010 IEEE*, pages 1–6. IEEE, 2010.

978-1-7281-1261-9/19/$31.00 ©2019 IEEE

Proceedings of the Fourth International Conference on Communication and Electronics Systems (ICCES 2019)
IEEE Conference Record # 45898; IEEE Xplore ISBN: 978-1-7281-1261-9

Modified 802.11b for Co-operative Ad-hoc Networks

Gayathri G
Telecommunication Dept.,
RVCE,
Bangalore, India.
gayathri25th@gmail.com

Usha Padma
Telecommunication Dept.,
RVCE,
Bangalore, India.
kamakshimb@rvce.edu.in

Jhanavi B S
Telecommunication Dept.,
RVCE,
Bangalore, India.
astronaut.janhavi@gmail.com

T Yathin Sai
Telecommunication Dept.,
RVCE,
Bangalore, India.
yathinthammineni@gmail.com

***Abstract*—Cooperative Communication (CC) allows the transmission of information by collaborating different nodes in the network by effective utilization of communication resources. In this paper, a new methodology for relay selection has been proposed where the relay is chosen based on the highest channel capacity of the node with the neighboring nodes as well as destination node. A new frame format ready to forward (RTF) has been proposed to enhance the communication by selecting the relay in a decentralized method. The existing RTS and CTS are modified to support cooperative ad-hoc network.**

Keywords—Cooperative communication, Ready to Forward, Decode-and-Forward.

I. INTRODUCTION

CC for wireless ad-hoc networks have a nature of broadcasting. Remaining nodes or terminals in the communication network behaves like a helping node for the exchange of information on receiving the broadcasted signal for the source node. It is used for improving network connectivity, communication reliability and reduce the signal fading effects.

CC supports both spatial diversity and timing diversity. There are three different types of protocols that are used in CC, namely Amplify and Forward (AF), Decode and Forward (DF) and coded cooperation. We used DF as it decodes the received information and filters the noise, then it encodes the information and broadcasts the information in the network. Whereas, in AF, the relay node will amplify the signal along with the noise which results in fading or loss in signal power and working of Coded cooperation is by transmission of various portions of a user's code-word using two different and independent fading paths.

The primary unit in CC is a three terminal network where the relay cooperates with the source by sharing its resources, to make successful communication between source and destination. Among the resources specified for cooperative communication in [1], relay is one of the important resources to be selected to improve the performance of the network.

CoopMAC was developed for wireless LANs to utilize the multi-datarate capability and reduce the throughput bottleneck that will be caused by the low data rate nodes, such that the throughput can be increased. High data rate stations in CoopMAC, are assisting low data rate stations in their data transmission by forwarding traffic. Each of the low data rate nodes maintained a list in the form of a table and called it CoopTable, of capable helper nodes that is capable of assisting in the transmissions which leads to memory constraints [2]. Relay-enabled DCF *(r*DCF) was developed which enabled packet relaying, in ad-hoc mode of IEEE 802.11 systems, by seeking each station to broadcast the datarate information among the stations explicitly[3].

Every station has to broadcast their rate information, this method consumes more bandwidth. In [4] and [7], authors proposed a new MAC protocol to make a betterment in the lifetime of the Wireless sensor network by considering residual energy information and channel state information of sensor nodes to select the cooperative nodes. A Cooperative Diversity MAC algorithm, which exploited the CC capability in the physical layer for the betterment in robustness of wireless ad hoc networks was investigated in [6].

A good amount of work was done to design cooperative protocols that define the selection of the relay candidate [8], it's coding [9], it's cooperative transmission [10] and it's power allocation schemes. From the recently proposed cooperative protocols, relay selection mechanisms only choose optimal relays among multiple relaying candidates to cooperate with communication links. Most of the research on cooperative communications models the wireless channel as a narrow band Raleigh fading channel with additive white Gaussian noise (AWGN) [11]. Among the relay selection algorithms developed so far, most of the researchers considered centralized relay selection method. Two papers [7] & [12] proposed decentralized relay selections methods, out of which one paper [7] considered location information of the users to

maximize the lifetime of the network by compromising with the reduction of throughput. Since throughput is an important parameter and it depends on the channel strength supported between the users, we propose a decentralized relay selection scheme by considering the location information of the users by modifying the existing IEEE 802.11b MAC protocol.

An effort is made to select the relay in decentralized manner as explained in section II and the proposed mathematical model is explained in III. Modified RTS & CTS frames and newly developed control frame known as Ready To Forward (RTF) for a 802.11b is described in section IV. The proposed model has been compared with wireless ad-hoc networks and an analysis is driven in section V and VI. Conclusion drawn from the proposed work has been explained in section VII along with the Future scope.

II. Relay Selection Model

In a cooperative ad-hoc network there are many nodes which are in range with the source node that may have better channel capacity when compared to the source node while transmitting to the desired destination node. In sequence, to choose the right Relay node, the following algorithm was developed.

Step 1: Source broadcasts RTS. It will be received by all the nodes which are in range (100m) with the source node. Modified RTS will contain the location information of the source.

Step 2: Destination will broadcast CTS, once the RTS is received at the destination The modified CTS frame format will contain the channel capacity supported between the selected source and the destination.

Step 3: The neighbouring nodes will calculate their channel capacity with respect to the destination node.

Step 4: If the channel capacity of the neighbouring node is greater than that supported between the selected source and the destination, a suitable relay with the highest channel capacity will be selected as explained in the mathematical model in section III.

Step 5: The selected relay node will now broadcast the RTF frame in the network to indicate that the other nodes need not be involved in further transmission.

Step 6: The selected relay node will be considered as the helping node to cooperate between the source and the destination.

Fig 1 specifies the methodology at the source node. The first step in the method is to sense the medium to check whether the required channel is free. If it finds the channel is free, then it broadcasts RTS frame i.e. source node broadcast RTS in the network. If the channel is busy then it will wait for the specific back off time.

After broadcasting RTS from the source node, it waits for short inter frame space (SIFS) i.e. the source node will be idle for some amount of time till it gets the response of a CTS frame from desired destination node.

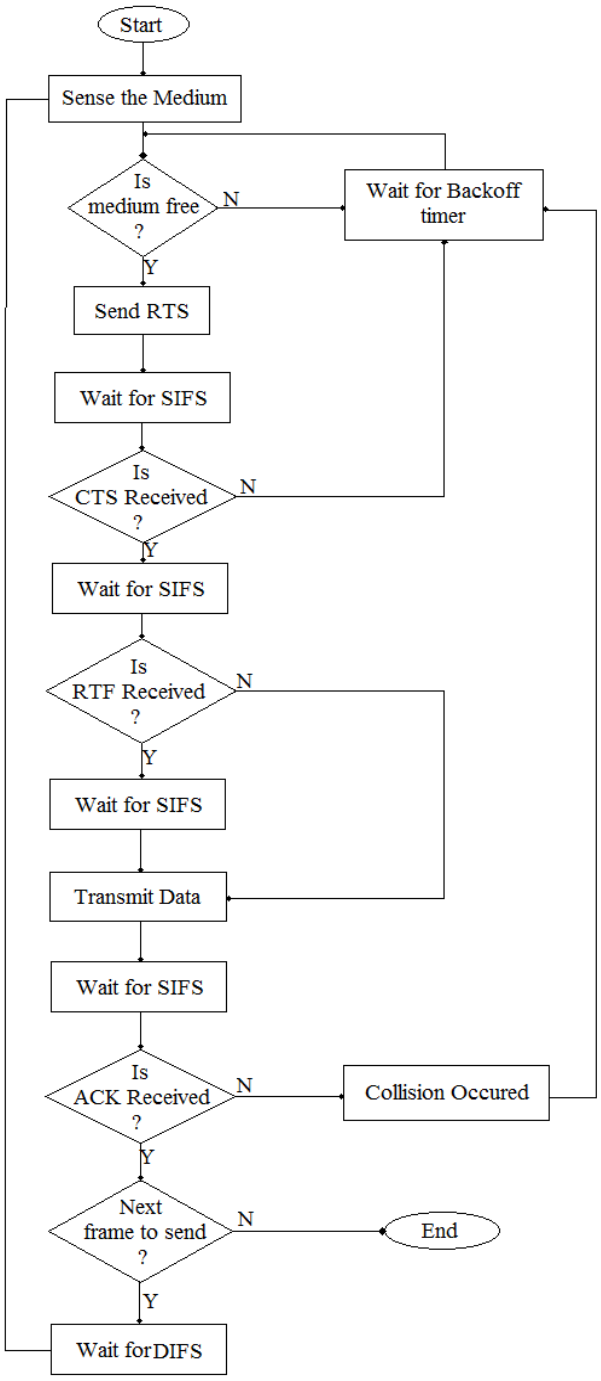

Fig.1: Methodology to be followed at the Source Node

If CTS is received by the source node in response to RTS then it waits for SIFS amount of time and checks for RTF. If RTF is received, then it waits for an SIFS time and transmits data to the destination node. If RTF is not received, it directly broadcasts the data to destination node. If CTS has not been received, then it waits for the specific back off time and makes a new attempt to access the channel.

After the data is transmitted from the source it waits for acknowledgement from the destination node. In the case when acknowledgement is received from the destination node and

there are no further frames to be transmitted then it terminates. If it has some more frames to transmit then it will hold on for a DIFS amount of time. If the acknowledgement has not been received by the source node, then it assumes that the collision has occurred and it waits for back off time and retransmits the data if the channel is free.

Fig 2 specifies the methodology at the relay node. Initially relay nodes are assumed to be in idle state. It receives RTS from the source node and also waits for CTS from the destination node. On receiving the CTS, every relay node computes the channel capacity, in which the relay checks whether the relay node channel capacity is greater than the channel capacity of destination node. If the relay node data rate is greater than that supported between source and destination, Difference between the maximum possible data rate and relay node data rate is assigned to x. The node with smallest value of x will be chosen as the relay node in order to broadcast RTF to remaining nodes.

After broadcasting the RTF it waits for the data transmitted from the source node which is to be transmitted to the destination node. Since the relay node follows the decode and forward mechanism, if first decodes the data and then it

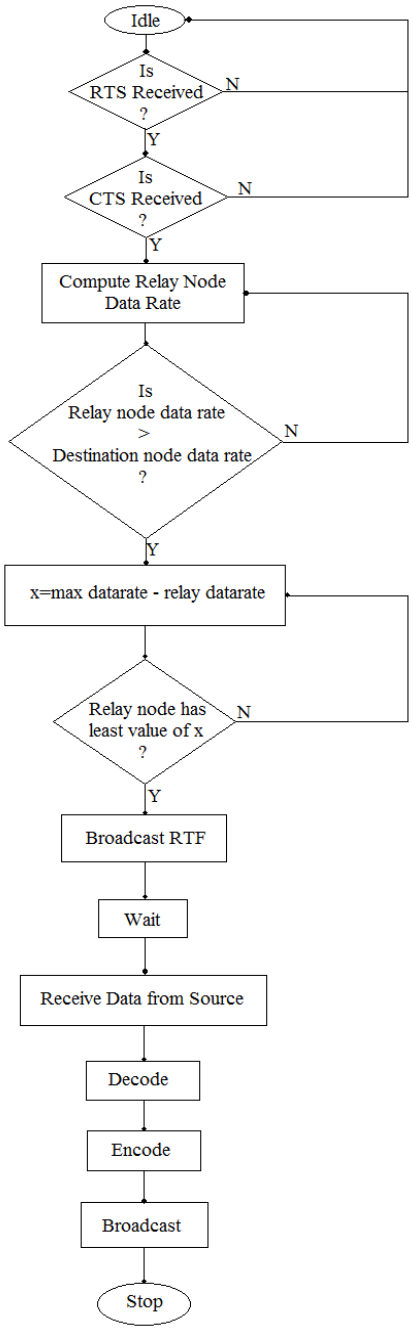

Fig. 2: Methodology at the Relay node.

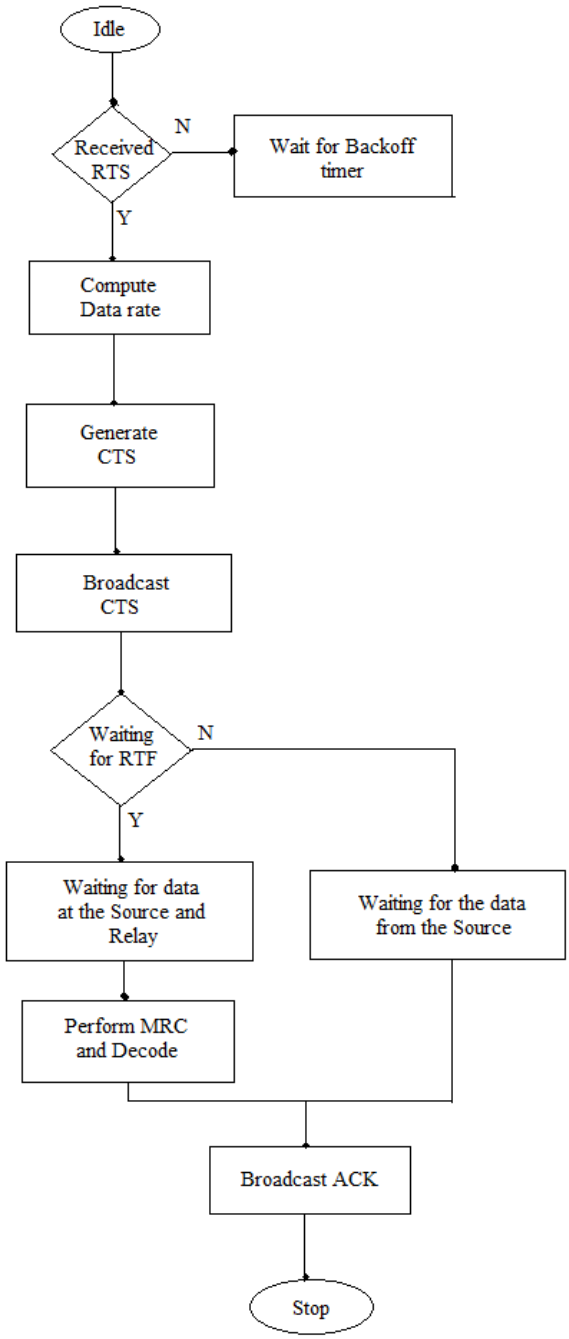

Fig. 3: Methodology to be followed at the Destination node.

encodes and broadcasts the data to the other nodes in the network.

Fig 3 specifies the methodology at the desired destination node. Initially destination node is assumed to be in idle state. If the RTS is obtained at the destination from the source, then it computes the data rate and broadcasts CTS .If it fails to receive RTS then it waits for the amount of time mentioned in the back off timer.

Once the CTS is broadcasted, it waits for the RTF from the relay node. Once the RTF is received it waits for the data from the source node in first time slot and from the relay node in the second time slot. If RTF is not received within a specified time duration, it will hold on until the data is obtained from source node only. On receiving the data, it performs Maximum Ratio Combiner (MRC) and decodes the data .Upon receiving the data the destination node will broadcast the acknowledgement in the network.

III. MATHEMATICAL MODEL

In a cooperative ad-hoc network there are many nodes which are close to the destination node that may have better channel capacity when compared to the source node while transmitting to the destination node. In order to select the right Relay node, the following mathematical model was developed.

Initially, the nodes in range with the destination will receive CTS and every node in that range compares their data rate with that of destination data rate, which is present in the modified CTS frame.

If Relay node data rate > Destination data rate then,

x= Maximum possible data rate - Relay node data rate

where maximum possible data rate supported by 802.11b is 11 Mbps.

If the relay node data rate is greater than destination data rate, then difference between the maximum possible data rate and data rate supported by the relay will be calculated. The relay with the least difference value will broadcast the RTF in the network. The smallest value of x will be set as the back off value in the timer. The relay node that backs off first with minimum back off timer value will be selected as the helper node and this node broadcasts the RTF in the network. Other neighbouring nodes which listen to the RTF will set their backoff value equal to the NAV specified in the RTF.

IV. MODIFICATIONS

A. *Modifications at MAC Layer*

According to the TCP/IP model there are five layers of which CSMA/CA protocol is used at the MAC Layer to facilitate wireless communication. In order to simulate this concept, few modifications were made to RTS and CTS frame formats. A new control frame format known as RTF is also developed to announce the relay that is selected to cooperate with the source in a distributed manner. The modified MAC frame is as shown in the fig 4.

- Subtype defines the values for the control frames such as RTS (1011), CTS(1100), ACK (1101) and RTF (1010).
- Duration of NAV: Network allocation vector is used for virtual carrier sensing and it also specifies the Roundtrip time (RTT) taken to occupy the channel. RTT is computed by considering the processing delay, Transmission delay and propagation delay.

B. *Modified RTS Frame*

It is broadcasted by the sender in the network before the actual data transmission begins. This frame format is as shown in fig 5. Two bytes are added between the destination MAC address and FCS to carry the location information of the source. Location information specifies the X-Y coordinates of the Source in the coordinate plane. The area of the coordinate plane used in this simulation is 250 x 250 m^2.

C. *Modified CTS Frame*

CTS (as shown in fig. 6) is broadcasted by the destination in response to RTS sent by the sender. Four bytes are added between the destination MAC Address and FCS of the CTS to carry the data rate supported between the source and the destination.

D. *Developed RTF Frame*

All the nodes in the network have received a copy of both RTS and CTS. Since RTS contains the location information of the source and every node in the network are also aware of their location information, all the nodes are capable of computing the data rate between themselves and the source. Data rate is computed considering the Euclidean distance from the source and the helping node. Nodes at different locations from the source provide different SNR, which in turn provide different data rates. Since CTS contains the data rate supported between the source and the destination, all nodes other than the destination can compare the data rate with that of the destination data rate. Using the mathematical model explained in section III, a node that is willing to cooperate will be employed as a helper node. The selected helper node will broadcast the RTF in the network. RTF frame format is shown in fig 7. Helping node Address specifies the MAC address of the relay node.

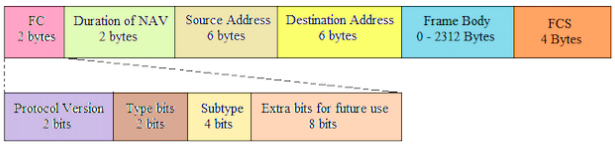

Fig.4: Modified MAC frame format.

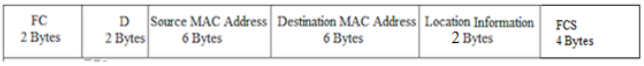

Fig. 5: Modified RTS frame format.

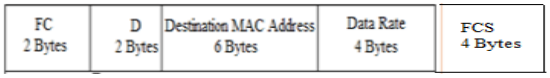

Fig. 6: Modified CTS Frame format.

Fig. 7: RTF Frame format.

V. RESULTS

An ad-hoc network is generated as shown in fig 8 using MATLAB software. These nodes are given fixed positions (or co-ordinates) in the X-Y plane in order to obtain accurate results. Twenty nodes are randomly placed in an area spacing of 250x250 m^2.

After deploying the nodes in the specified network, source node and destination node are selected (here source node is node 13 and destination is node 18) and the desired direction of data transmission is shown in fig 9.

Desired data information which is in random binary format, is generated depending on the number of bits entered that must be used for further transmission. 512 bytes of data bits generated will now be accepted at the application layer. 22 segments, each consisting of 512 bytes of payload are used for the simulation of this work.

Segmentation is performed at transport layer to convert entire stream of information into fixed sized segments and packets. After segmentation, segments are ready to be transmitted in the network. Once the channel is sensed to be free, RTS will be broadcasted from the MAC Layer of the source. CTS will be broadcasted in response to the received RTS from the Destination node. RTF is broadcasted from the selected Relay node as shown in fig 10.

Data information broadcasted by the physical layer of the source node is decoded and encoded again at the selected relay node. Encoded information is broadcasted by the relay node in

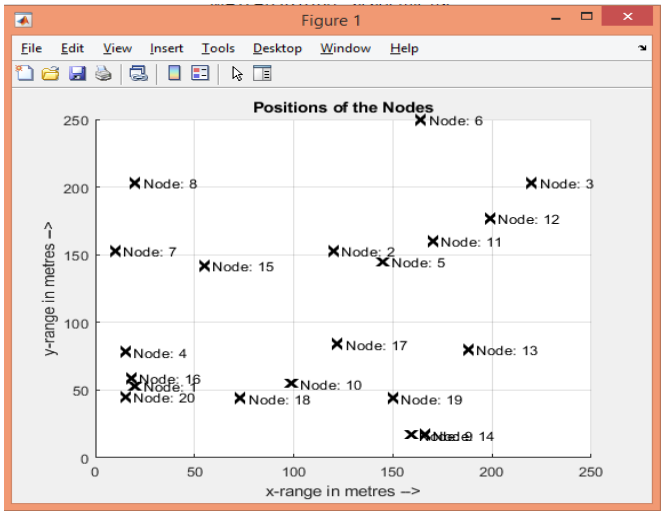

Fig. 8: Positions of nodes in the cooperative ad-hoc environment.

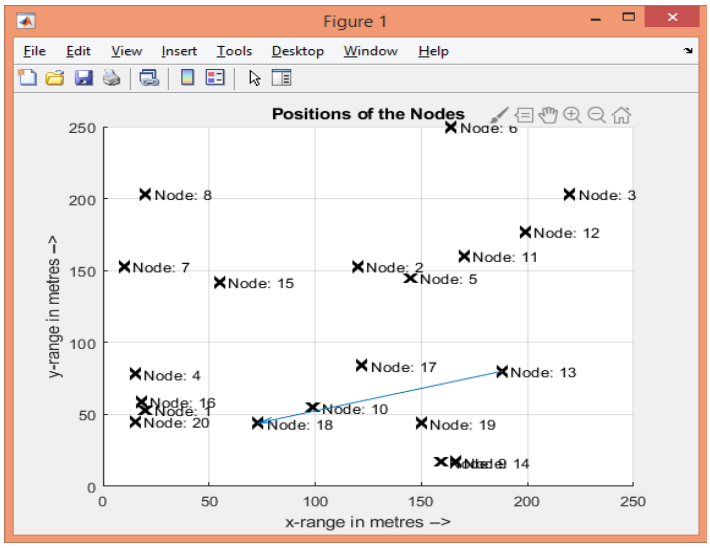

Fig. 9: Plot the direction of the desired transmission.

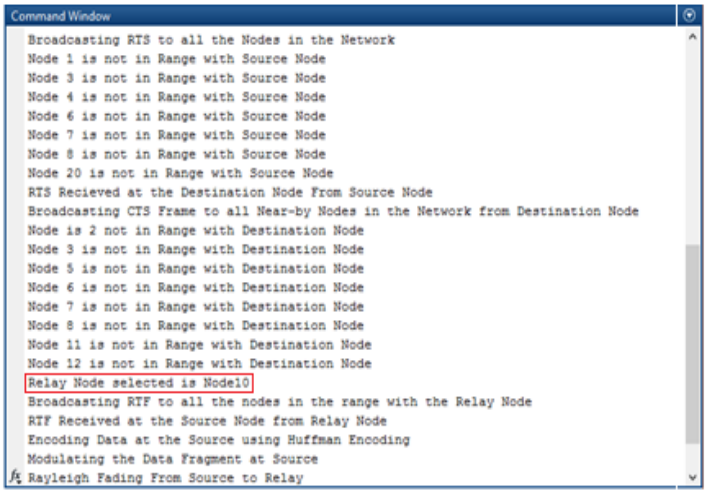

Fig. 10: Relay node selection

the network. This is illustrated in fig 10.

MRC is applied at the destination on the information received from source and the relay, resulting signal is demodulated and error free information bits are delivered to the MAC layer. Performance of the network simulated is evaluated in terms of Packet delivery ratio and Throughput.

VI. PERFORMANCE ANALYSIS

Table 1 shows the performance analysis of Cooperative ad-hoc networks in comparison with normal wireless Ad-hoc networks. The particulars are with respect to number of packets sent using data signal, number of packets dropped due to number of bits in error, packet delivery ratio and throughput in Kbps.

From the results of table 1, it is clear that the throughput and packet delivery ratio are improved in Cooperative Ad-hoc networks in comparison to Wireless Ad-hoc networks for data signals.

TABLE I. PERFORMANCE ANALYSIS OF RESULTS

Type of Network	No. of Packets sent	No. of Packets Lost	Packet Delivery Ratio	Through-put (Kbps)
Wireless Ad-hoc Network	22	13	0.409	$2.8943*10^4$
Cooperative Ad-hoc Network	22	7	0.681	$3.7757*10^4$

VII. CONCLUSION AND FUTURE SCOPE

Wireless Cooperative ad-hoc communication is beneficial in terms of high signal strength, secure network, throughput, packet delivery ratio and high spatial diversity-resistance to fading. The relay selection algorithm for transmission of data over Rayleigh faded channel with AWGN in cooperative ad-hoc network was simulated using MATLAB software. An RTF frame format along with the Distributed relay selection methodology for CC has been proposed for better throughput in the presence of overheads.

Ad-hoc networks are gaining attention amongst recent researches, as the existing mobile computing hardware and wireless networking is capable of supporting today's requirement. As a step towards improvement, an attempt can be made to increase the throughput by using channel coding techniques.

VIII. REFERENCES

[1] Usha Padma, H.V. Kumaraswamy, S. Ravishankar, "Survey of Resource Allocation Techniques in Cooperative Communication", *International Conference on Signal, Image Processing, Communication and Automation (ICSIPCA-2017),* held during 6-7 July 2017.

[2] P. Liu, Z. Tao, S. Narayanan, T. Korakis, and S.S. Panwar, "CoopMAC: A Cooperative MAC for Wireless LANs", *IEEE J.Selected Areas in Comm*., vol. 25, no. 2, pp. 340-354, Feb. 2007.

[3] H. Zhu and G. Cao, "rDCF: A Relay-Enabled Medium Access Control Protocol for Wireless Ad Hoc Networks", *IEEE Trans.MobileComputing*, vol. 5, no. 9, pp. 1201-1214, Sept. 2006.

[4] C. Zhai, J. Liu, L. Zheng, and H. Xu, "Lifetime Maximization via a New Cooperative MAC Protocol in Wireless Sensor Networks", *Proc. IEEE GLOBECOM*, pp. 1-6, Dec. 2009.

[5] M. Gokturk and O. Gurbuz, "Cooperation in Wireless Sensor Networks: Design and Performance Analysis of a MAC Protocol", *Proc. IEEE Int'l Conf. Comm. (ICC '08)*, pp. 4284-4289, May 2008.

[6] Sangman Moh, Chansu Yu, "A Cooperative Diversity-Based Robust MAC Protocol in Wireless Ad Hoc Networks", *IEEE Transactions on Parallel and Distributed Systems*, vol. 22, no. 3, pp.353-363, March 2011.

[7] Xiaoyan Wang, Jie Li, "Improving the Network Lifetime of MANETs Through Cooperative MAC Protocol Design", *Ieee Transactions On Parallel And Distributed Systems*, Vol. 26, NO. 4, 2013.

[8] Xia Chen, Honglin Hu, Shengyao Jin, and Hsiao-Hwa Chen. "Broadcast Reserved Opportunity To Achieve Diversity Relaying And Its Performance Evaluation", *EURASIP Journal On Wireless Communications And Networking*, vol. 7, no. 2, 2008.

[9] Mugen Peng, Jie Zhang, Wenbo Wang and Hsiao-Hwa Chen. Heterogeneous, "Cooperative Relay Selection with Maximal-Ratio Combining for Multi-Radio Access Networks", *International Journal of Communication Systems*, vol. 23, no. 6-7, 732-750, 2010.

[10] Lie-Liang Yang and Hsiao-Hwa Chen, "Error probability of digital communications using relay diversity over Nakagami-m fading channels", *IEEE Transactions on Wireless Communications*, vol. 7, no. 5, 1806-1811, 2008.

[11] Marvin K. Simon and Mohamed-Slim Alouini, "Digital Communication over Fading Channels: A Unified Approach to Performance Analysis" *John Wiley & Sons, Inc*, 2000.

[12] H. Shan, P. Wang, W. Zhuang and Z. Wang, "Cross-Layer Cooperative Triple Busy Tone Multiple Access For Wireless Networks", *Proc.IEEE GLOBECOM*, pp. 1-5, Dec. 2008.

Proceedings of the Fourth International Conference on Communication and Electronics Systems (ICCES 2019)
IEEE Conference Record # 45898; IEEE Xplore ISBN: 978-1-7281-1261-9

A NOVEL FUZZY CONTROLLED INTERLEAVED SEPIC POWER FACTOR PREREGULATOR WITH REDUCED RIPPLES

LAKSHMIPRIYA K J[1] *PG SCHOLAR*, Dr.JENO PAUL [2] *PROFESSOR*, RAJALAKSHMI MENON[3]

ELECTRICAL AND ELECTRONICS DEPARTMENT,ASIET,KALADY

E-mail: lekshmikj99@gmail.com

Abstract - Paper presents a newly modified power quality improved interleaved SEPIC power factor pre regulator with reduced ripples. Main objective is to obtain output voltage with improved efficiency and power factor with inductors directly coupled. Normally, power factor pre regulator with boost converter are used for regulating DC-link voltage for a range of fixed voltages , by using variable DC-link voltage the overall efficiency of the converters can be increased. Single ended primary inductor converter which are interleaved used for power factor pre regulation and PFP stage is the first stage of AC/DC converters .It is used for many applications such as inductive heating , wireless charging , and on board chargers for electric vehicles (PEVs). Here,the presence of coupled inductor reduces magnetic components . Hence new modified power factor pre regulator converter ,provides output voltage with high efficiency and power factor. Presence of coupled inductors decreases the voltage and current ripple. MATLAB simulation based results proved the effectiveness of the proposed system, compared with existing system.

Keywords- Power factor pre regulator (PFP),Single ended primary inductor converter (SEPIC),Coupled inductor, interleaved converter.

I. INTRODUCTION

The first stage of AC/DC converters will be a power factor pre regulator. The converters connected in grid require high power quality, less total harmonic distortion and large power factor. AC/DC converters are consisting of a PFP stage and a DC/DC stage, generally two stage AC/DC converters [1]. Due to soft switching, galvanic isolation, and high efficiency DC/DC converter is chosen as second stage of the converter. Nowadays interleaved SEPIC converters are used as the PFP stage. Power level can be made increased by using interleaved SEPIC converters. The advantage of SEPIC converter is the voltage at the voltage can be made lower or higher than the input voltage [2],[3].

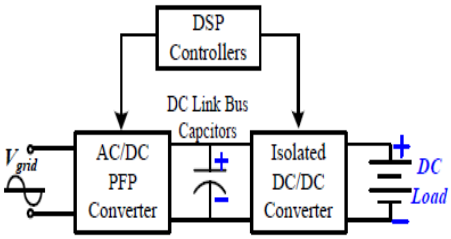

Fig 1. Structure of AC/DC converters

At first Boost type PFP were used. Main aim of PFP is to enhance the power quality also reduces harmonic distortion. This kind of converter is a bridge rectifier followed by Boost converter. But it is having a disadvantage such that by any chance the second converter doesn't get operated near the resonant frequency, then the overall efficiency may get reduced.[5].

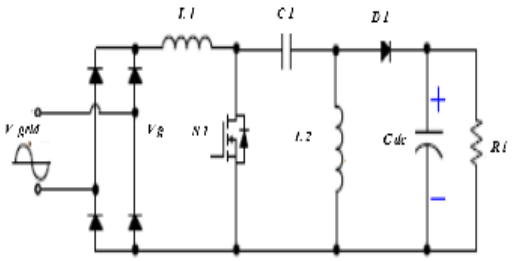

Fig 2. Traditional SEPIC PFP converter

Then a study conducted on the advantages of SEPIC converters as the PFP stage. It is having many advantages such as it reduces voltage ripples, voltage be made high or low than the voltage given to the input [6]. But it is not accepted widely because SEPIC converters cannot be used for high power applications, since the stress of voltage and current on the diodes and switches are higher.

Bridgeless SEPIC and Isolated SEPIC were also their but it is also not contributing much for the reduction of voltage and current stress. By paralleling two SEPIC converters directly, it can be made interleaved [4]. And by interleaving SEPIC converters power level can be increased. This can be designed with coupled inductors for reducing the current stresses and voltage stresses of all the switches and diodes in the circuit.

Here, in this paper an interleaved SEPIC AC toDC converter is designed. The input current is shared among two stages to cut back the present stresses of switches and diodes. Interleaved SEPIC converter having coupled inductors[7]. The presence of coupled inductors, magnetic components will be reduced in the circuit[11]. The new converter will provide output voltage,with improved power quality and high power factor[8][9][10].

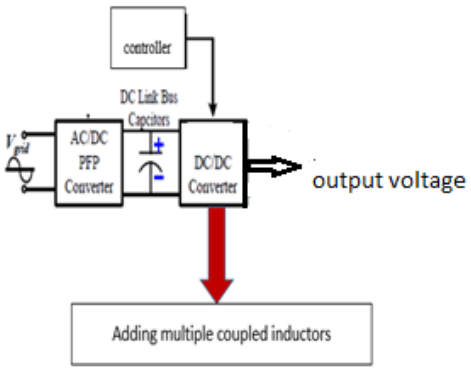

Fig 3. Block diagram of proposed converter

Wide range of DC link output voltage provided by SEPIC AC/DC converter. Large switching losses will be generated by CCM operation, soft switching will be provided by DCM operation. Zero voltage switching can be done for the MOSFET's to reduce the switching losses, and Zero current switching can be done for diodes. In order to reduce the number of magnetic components, the inductors corresponding to the two phases are directly coupled together.[12]

II. PROPOSED SYSTEM

A. CIRCUIT DESCRIPTION

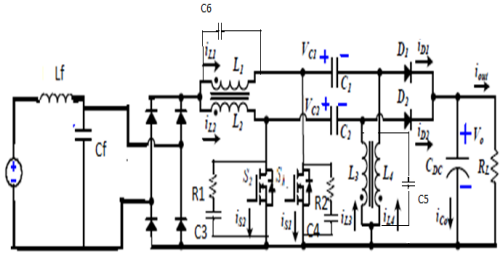

Fig 4. Circuit diagram of proposed converter

This paper proposes a newly interconnected SEPIC AC/DC converter. The input current get shared among two stages. The new interleaved SEPIC converter will provide output voltage, with improved power quality and high power factor and reduced ripples in its output voltage and hence power quality also improved.

ZVS can be realised for reducing switching losses of MOSFET and ZCS for reducing the reverse recovery losses of diodes.Presence of coupled inductors, reduces the number of magnetic components in the circuit and it significantly reduces the voltage ripple. The DC link voltages C_{DC} and the capacitors C_1, C_2, are high and its ripples at the voltage are negligible.[13]

B. MODES OF OPERATION

Mode 1

In this mode switch *S1* is on and switch *S2* is off. The diode D_1 off, and diode *D2* is on. The voltages across both inductors *L1*, *L4* are *Vg* and *L3*, *L2* are - *Vg*. Therefore, the inductor currents *iL1*, *iL4* increases and *Il3*, *Il2* decreases. The inductor current *iL2* decreases all the time and changes the flowing direction in this mode. The current through diode *D2*, *iD2*, keeps on decreasing. The variations of inductor currents, Δ*iL1* and Δ*iL2*, can be expressed as, where, *T* is the switching period, and *D'T* is the time interval between *t0* and *t1*.

$$M = \sqrt{L_{12} - L_{21}} \qquad (1)$$

$$K=\frac{M}{\sqrt{L_1 L_2}} \qquad (2)$$

$$\Delta iL1=\frac{V_g+KV_O}{(1-k^2)L_1} D'T \qquad (3)$$

$$\Delta iL2=\frac{V_O+KV_g}{(1-k^2)L_2} D'T \qquad (4)$$

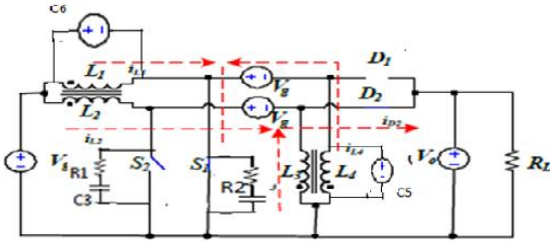

Fig 5. Equivalent circuit of Mode1

Mode 2

At *t1*, current through the diode *D2* is *iD2*..Sum of currents *iL2*,*iL3*, drops to zero. Due to ZCS the diode gets turned off. Currents *iL3* , *iL2* flows through a loop.

Variations of the inductor currents are the same due to the same voltage across the inductors. Average current *iL3* is larger than the average current *iL2*.*The* current of coupled inductor *L2* is constant. when the currents *iL3* and *iL2* drops to minimum, the current *iL3* is very much higher than *iL2* with *iL3* and *iL2* as positive and negative values respectively. Assuming the resistances of inductors and capacitors are small values and can be neglected, the loop current remains constant can be expressed as

$$i_{L3} = -i_{L2} = Constant \qquad (5)$$

Variation of inductor current ΔiL1, can be expressed as,

$$\Delta iL1=\frac{V_g}{L_1}(D - D')T \qquad (6)$$

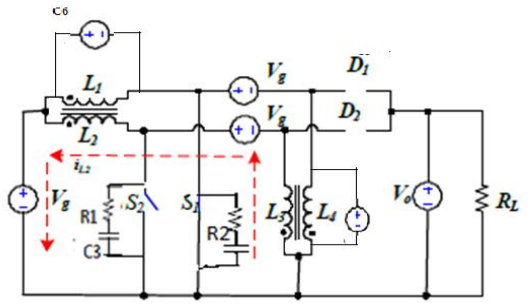

Fig 6. Equivalent circuit of Mode 2

Mode 3

Diodes *D2*, in off condition, while the diode *D1* turned on.Constant current flowing through the loop consisting of *L2* and *L3* inductors.The currents *iL1* and *iL4* decreases from maximum values.The sum of currents through the inductors flows through the diode *D1*. Voltages across inductors *L1* and *L4* are *−Vo*. The current through the inductor *iL1* decreases. It is expressed as,

$$\Delta iL1=\frac{V_O}{L_1}(0.5-D')T \qquad (7)$$

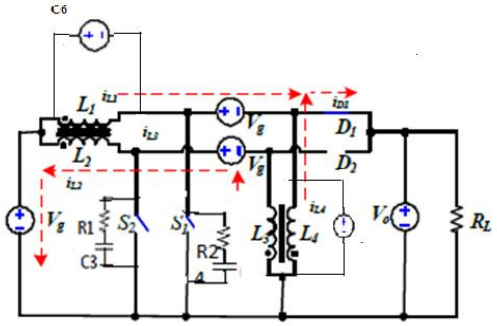

Fig 7. Equivalent circuit of Mode 3

III. DESIGN EQUATIONS

In order to design the proposed converter, certain equations are mandatory .

Equations for snubber design

$$R=\frac{Voltage\ Across\ the\ switch}{Input\ current\ Rating} \qquad (8)$$

$$C=\frac{1}{Voltage\ across\ the\ switch^2\ .\ Switching\ Frequency} \qquad (9)$$

$$P=\frac{V^2}{R} \qquad (10)$$

P is the power output.

$$D=\frac{V_{out}}{V_{out}+V_{in}} \qquad (11)$$

D is the duty cycle it is calculated for the inductor design

$$dt=\frac{1}{F_S\ .\ D} \qquad (12)$$

$$L=V.\ \frac{dt}{di} \qquad (13)$$

Output capacitor design

$$\Delta V_{cs}=\frac{I_{out}D_{max}}{C_sF_{sw}}=I_{out}\sqrt{\frac{V_{out}+V_D}{V_{in\_min}}} \qquad (14)$$

Filter design

$$C_f=\frac{I_m}{\omega V_m}\tan\theta \qquad (15)$$

$$L_f=\frac{1}{4\pi^2 f_c^{\,2} c_f} \qquad (16)$$

IV. CONTROL SYSTEM

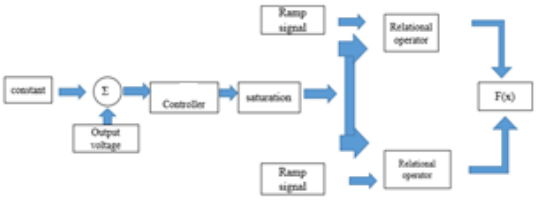

Fig 8. Block diagram of control system

Control system contains three sensors such as voltage and current at the input, and voltage at output. The repeating sequence or saw tooth carrier signals of switches *S1* and *S2* have 180^0 phase shift is used. I controller is implemented here. The error between output voltage and the reference voltage is fed to the voltage-loop. The generated error sum given to the fuzzy controller. In fuzzy controller we need to build fuzzy rules as per our requirement as shown in figure 12.Where as the fuzzy input and output as shown in figure 9,10,11 respectively.

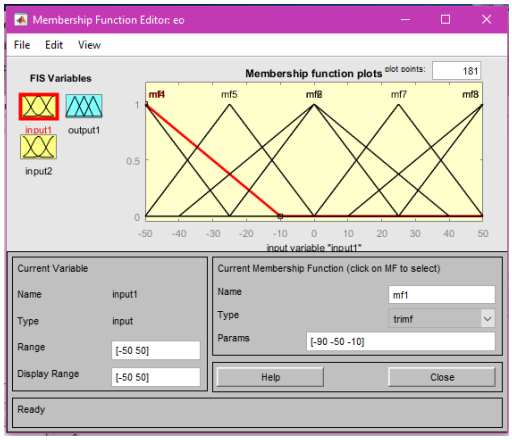

Fig 9.Fuzzy input 1

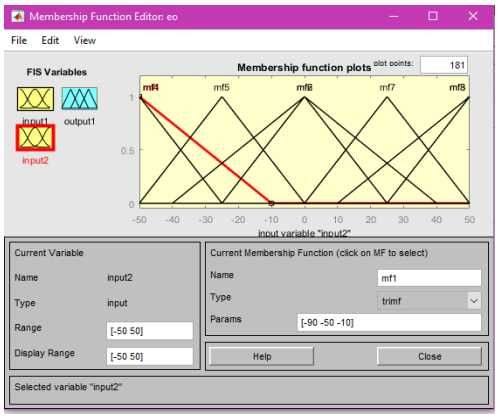

Fig 10. Fuzzy input 2

Fig11. Fuzzy output

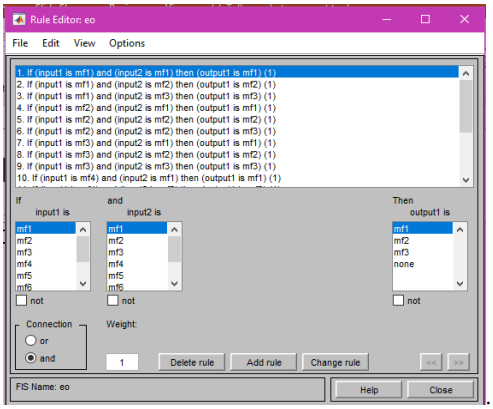

Fig12.Fuzzy rules

V. SIMULATION RESULTS

Simulations were done here for 14V as input voltage and 36 V as the output voltage. Inductance is set as .37mH for all the inductors. Input voltage is in phase with the input current. Power factor is 0.997.

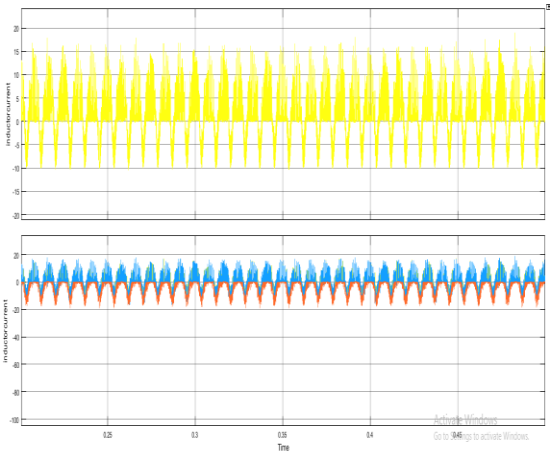

Fig 13. Inductor current

PARAMETER	VALUE
INPUT VOLAGE	14 V
OUTPUT VOLAGE00	36 V
INPUT INDUCTOR	.37mH
OUTPUT INDUCTOR	.37mH
SWITCHING FREQUENCY	30KHz

Table1 . simulation parameters

Figure 13 demonstrate the waveforms of inductor current. Waveforms of input voltage and output voltage are shown in figure 15 .The waveform of switching pulses as shown in figure 14.

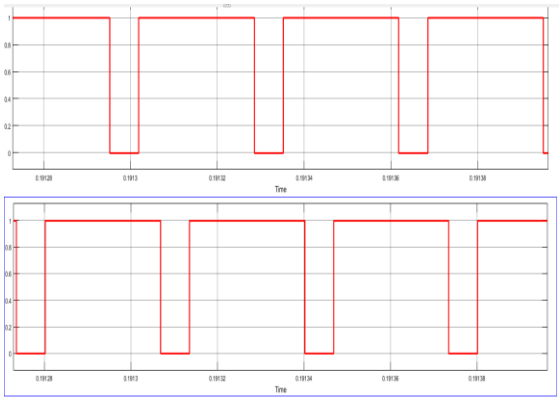

Fig 14. Switching pulses

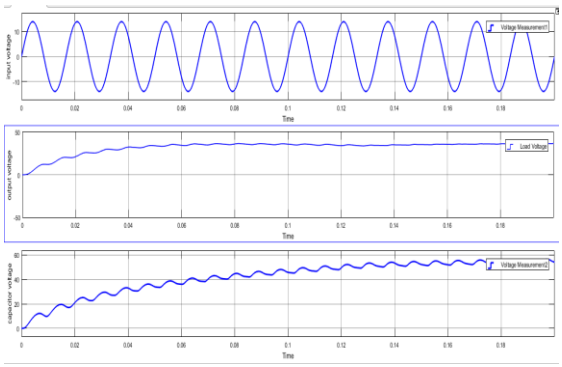

Fig 15. Input output and capacitor voltage

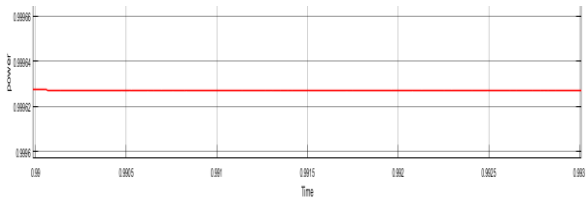

Fig 16. Power output

.

Converter can be used for a large range of input voltages as per our requirement.If the input voltage is 14 V, the output voltage can be boosted to 36V.Limits of output voltage can be varied with input voltage. The output voltage is regulated to 36V, and the output power is 13W with power factor measured as 0.997 and 96% efficiency.

VI. CONCLUSION

This paper proposed a modified power factor pre regulator converter with coupled inductors to provide output voltage with high efficiency and power factor for electric vehicles. Power level can be made increased by interleaving SEPIC converters. The maintenance of high efficiency is achieved . By coupling the inductors reduces the magnetic components can be decreased and decreases the ripples in voltage and current. MATLAB simulation based results proved the effectiveness of the proposed System, compared to the existing system.

VII. REFERENCES

[1] H. Wang, S. Dusmez, and A. Khaligh, "Maximum Efficiency Point Tracking Technique for LLC Based PEV Chargers through Variable DC Link Control," *IEEE Trans. Ind. Electron.*, vol. 61, no. 11, pp. 6041-6049, Nov. 2014.

[2] J. Deng, S. Li, S. Hu, C. C. Mi, and R. Ma, "Design Methodology of LLC Resonant Converters for Electric Vehicle Battery Chargers," *IEEE Trans. Veh. Technol.*, vol. 63, no. 4, pp. 1581–1592, Apr. 2014.

[3] W. Guo, H. K. Bai, G. Szatmari-voicu, A. Taylor, J. Patterson, and J. Kane, "A 10kW 97%-efficiency LLC Resonant DC/DC Converter with Wide Range of Output Voltage for the Battery Chargers in Plug-in Hybrid Electric Vehicles," in *Proc. IEEE ITEC*, 2012, pp.1-4.

[4] H. Wang, S. Dusmez, and A. Khaligh, "Design and analysis of a full-bridge LLC-based PEV charger optimized for wide battery voltage range," *IEEE Trans. Veh. Technol.*, vol. 63, no. 4, pp. 1603-1613, Apr. 2014.

[5] S. Dusmez, and A. Khaligh, "A compact and integrated multifunctional power electronic interface for plug-in electric vehicles," *IEEE Trans. Power Electron.*, vol. 28, no. 12, pp.5690-5701, Dec. 2013.

[6] S. Dusmez, , and A. Khaligh, "A charge-nonlinear-carrier-controlled reduced-part single-stage integrated power electronics interface for automotive applications," *IEEE Trans. Veh. Technol.*, vol. 63, no. 3, pp. 1091-1103, Mar. 2014.

[7] Lyrio Simonetti, Domingos Savio, Javier Sebastian, and Javier Uceda, "The discontinuous conduction mode Sepic and Cuk power factor preregulators: analysis and design," *IEEE Trans. Ind. Electron.*, vol.44, no.5, pp. 630-637, May 1997.

[8] Mahdavi, Mohammad, and Hosein Farzanehfard. "Bridgeless SEPIC PFC rectifier with reduced components and conduction losses," *IEEE Trans. Ind. Electron.*, vol.58, no.9, pp. 4153-4160, Sept.2011.

[9] Jae-Won Yang and Hyun-Lark Do, "Bridgeless SEPIC Converter With a Ripple-Free Input Current", *IEEE Trans. Power Electron.*, vol. 28, no. 7, pp. 3388–3394, Jul. 2013.

[10] Ahmad J. Sabzali, Esam H. Ismail, Mustafa A. Al-Saffar and Abbas A. Fardoun, "New Bridgeless DCM Sepic and Cuk PFC Rectifiers With Low Conduction and Switching Losses," *IEEE Trans. Ind. Appl.*, vol.47, no.2, pp. 873-881, Mar. 2011.
[11] Koh, Hyunsoo, "Z-domain modeling and control design of single-switch bridgeless SEPIC PFC converter with damping circuit," in *Proc. IEEE APEC*, 2013, pp. 2744-2748.
[12] R. Gules, W. Meneghette dos Santos, F. Aparecido dos Reis, E. R. Romaneli, and A. Badin. "A modified SEPIC converter with high static gain for renewable applications," *IEEE Trans. Power Electron.*, vol. 29, no. 11, pp. 5860-5871, May 2014.

Proceedings of the Fourth International Conference on Communication and Electronics Systems (ICCES 2019)
IEEE Conference Record # 45898; IEEE Xplore ISBN: 978-1-7281-1261-9

A Modern Cardiac Monitoring System Based on Wireless Sensing for Human Health Care

Rosmy John
Dept. of Electronics and Communication Engineering
College of Engineering Trivandrum
Kerala Technological University
Kerala, India
rosmy_123@yahoo.com

Dr. Sajith Vijayaraghavan
Dept. of Electronics and Communication Engineering
College of Engineering Trivandrum
Kerala Technological University
Kerala, India
sajithvijayaraghavan@gmail.com

Dr. Pradeep R
Dept. of Electronics and Communication Engineering
College of Engineering Trivandrum
Kerala Technological University
Kerala, India
pradeep@cet.ac.in

***Abstract*— Auscultation is very important to physicians for accurate diagnosis of many heart diseases. Physicians need extensive training and experience in identifying and differentiating the main signs of cardiac diseases based on the heart sound that is being heard. It is essential to continuously monitor the heart activity and transmit the data to a remote centre for analysis. A modern cardiac monitoring system dependent on remote detecting to screen and investigate the cardiovascular condition is presented with the utilization of Internet of Things (IoT) which sends the data to the doctor. The system is low cost, easy and power efficient. The latest MQTT (Message Queuing Telemetry Transport) data protocol is used for data transmission. On the signal analysis part, Empirical Mode Decomposition method in conjunction with Hilbert-Huang Transform is used to realize preprocessing. Heart sound segmentation is done with efficient and accurate combined adaptive threshold method which forms a basis for feature extraction and classification to extract useful physiological parameters from heart sounds.**

Keywords— ***Auscultation, Combined adaptive threshold, Empirical Mode Decomposition, Hilbert-Huang Transform, Internet of Things, MQTT***

I. INTRODUCTION

Early and accurate detection of cardiac illnesses is important to limit deaths caused by cardiovascular diseases. To prevent serious health problems, diseases caused by abnormal heart valves and functions require appropriate detection. Cardiovascular diseases are the number one killer globally and is one of the leading causes of attack in the world. But the death rate depends on where you live. Cardiovascular diseases are the major challenge in worldwide.

Hypertension, high cholesterol and tobacco smoking are some of the risk factors that lead to cardiovascular diseases. The heart diseases can be categorized in to blood vessel diseases, arrhythmias and congenital heart defects [1]. Auscultation is one of the most used techniques for this purpose. Auscultation of the heart can provide clues to the diagnosis of many cardiac abnormalities [2]. It is the action of listening to sounds from the heart, lungs, or other organs typically with a stethoscope as a part of medical diagnosis. It is performed for the purposes of examining the circulatory and respiratory systems, as well as the gastrointestinal system. Auscultation of heart sound is dependent on personal opinion. It relies upon involvement, aptitudes and hearing capacity of the doctor [3].

Cardiovascular diseases (CVD) are the principle causes of death worldwide [4]. Cardiovascular Disease is a class of illnesses that include the heart or veins. Cardiac monitoring is very important and it leads to death if proper monitoring is not there. It is different from hemodynamic monitoring. Most of the cardiac diseases can be predicted by monitoring ECG with the help of electrodes placed on chest or limbs. Therefore, continuous monitoring of ECG is becoming more and more important in both home health care and hospital to prevent diseases related to heart and detect characteristic signs for patients with uncommon events [5].

Normally heart auscultation is done using stethoscope. Electronic stethoscopes are the ones which provide convenient result. The sensors used in electronic stethoscope can be microphone, piezoelectric, capacitive type etc [6]. The most widely used sensor material is piezoelectric. There are many electronic stethoscopes which reduce the ambient noise but the cost is high. Compared to electronic stethoscope digital stethoscopes are more accurate but the cost is very high which is not affordable. However, heart auscultation using stethoscope requires clinical expertise. It is critical to screen and dissect the cardiovascular condition which sends the data to expertise with the utilization of IoT. It is essential for the doctors to diagnose the diseases accurately by analysis of ECG signals. The noise in the ECG signal should be removed otherwise it will interfere the doctor's diagnosis. Many algorithms exist for the signal analysis of heart sound. For signal analysis, mainly three steps are there: preprocessing, feature extraction and classification. Heart sound signals recorded with electronic stethoscope are with external and internal noises. Noises can be due to motion, speech, digestion, respiration etc. Hence preprocessing is essential. Segmentation and classification are the two major challenges in the automated heart sound analysis.

The paper is structured as follows: Section II describes the details of previous works. Section III presents an introduction to functions of Heart and ECG. Section IV presents an overview of system design with the help of block diagrams. Section V describes the details including methodology. Section VI describes the details of experiment and results. Finally, conclusion is described in Section VII.

II. RELATED WORK

Nowadays Internet of Things or IoT is influencing our lifestyle. IoT is a giant network with connected devices. These devices gather and share data. IoT provides a common platform to dump the data. IoT is a combination of hardware and software technologies along with embedded devices which enables to provide facilities and services to anyone, anytime, anywhere using network. Most of the researchers had adopted Bluetooth technology, Zigbee or Radio Frequency Identification for monitoring patient's health and transmitting collected data to distance location. These methods are also meant for short distance communication. There are many cardiac auscultation devices that collect heart sound signals and transmit to a computer for further signal analysis.

XXX-X-XXXX-XXXX-X/XX/$XX.00 ©20XX IEEE

Researchers had adopted many methods for the segmentation of heart sounds as part of signal analysis. Liang et al. recognized S1 and S2 utilizing the Shannon envelope [7]. Wang Xinpei et al. proposed a division technique dependent on Shannon entropy [8]. The segmentation results are not good when noise and interference occur with the above mentioned methods. Ting Li et al. proposed a segmentation method based on cyclostationary envelope [9]. Here segmentation results are more accurate but single threshold method [10] is adopted which had many shortcomings.

This research work presents an advanced heart observing framework dependent on remote detecting for human medicinal services. The system mainly consists of an acquisition module which includes heart sound sensor, a microcontroller board, a microprocessor board and signal analysis part. With the most recent innovation of Internet of Things, clients or specialists can get the prompt response of heart and yield medical intervention. The latest MQTT data protocol is used for transmitting data from one client to another client. This is the most efficient method and the overall system consumes low power and low cost. Signal investigation part incorporates preprocessing, division, highlight extraction and characterization of heart sound sign. EMD method is used to eliminate noises. The EMD method was first proposed by Huang et al. in 1998 [11]. Hilbert Huang Transform (HHT) together with double threshold was implemented for the preprocessing and feature extraction of the signals. This method is explained in detail in H. Ren et al. [12]. Later to improve accuracy, combined adaptive threshold method was adopted [13].

III. FUNCTIONS OF HEART AND ECG

The heart is the engine at the centre of the body's circulation system. The heart is really two pumps in one, working in a continuous cycle. The right side siphons blood to the lungs, while the left side gets blood again from the lungs, then sends it round the rest of the body. The heart pumps out about a cupful of blood about 70 times a minute, speeding up when necessary to meet body cells' increased demand [14]. There are two upper chambers, called the right and left atria, and two lower chambers, called the right and left ventricles. The blood flows in to the atria. The heart muscle is relaxed and blood enters the upper left and right heart chambers. The two atria contract and squeeze blood in to the chambers below them (ventricles). Lastly the ventricles contract and force blood either to the lungs or around the body. There are mainly four locations on the chest wall where these vibrations are more audible. They are Aortic area, Pulmonic area, Tricuspid area and Mitral area.

The heart sound includes four principle sections: the main heart sound (S1), the systolic interim, the second heart sound (S2) and the diastolic interim. At the point when a solid heart pulsates, it produces "lub" "dub" sound. The principal heart sound, "lub", is brought about by the conclusion of the mitral and tricuspid valves toward the start of ventricular systole. The second heart sound, "dub", is brought about by the conclusion of aortic valve and pulmonary valve toward the finish of ventricular systole. Murmurs are typically slosh sound that demonstrate reverse through the valves. S3 and S4 are a "ta" sound that shows ventricles that are either excessively frail or excessively hardened to adequately siphon blood. It can't close or open appropriately. The heart sound segments are shown in in Fig. 1 [15].

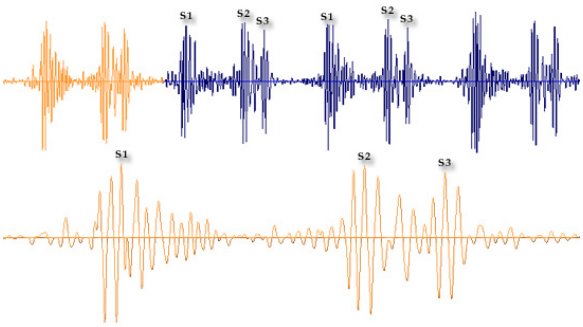

Fig. 1. Heart sound components

An electrocardiogram (ECG) is a tool which is used to visualize the electricity flowing to the heart. The typical electrocardiogram is made out of a P wave, a QRS complex and a T wave. Fig. 2 shows a typical ECG signal.

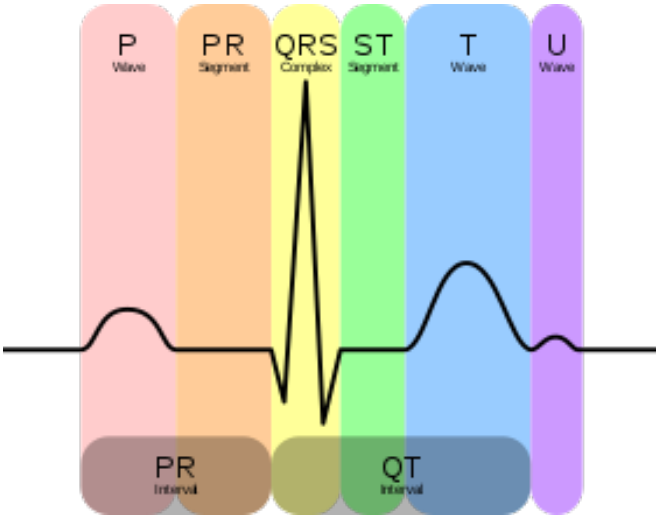

Fig. 2. A typical ECG signal

The P wave is suggestive of the atrial contraction. The first negative deflection is the Q wave, then R and the S wave. The QRS complex denotes the ventricular systole followed by the T wave. The T wave denotes the ventricular diastole. The PR segment is called the iso-electric line of the ECG which is also called the baseline. This is the baseline which compares the ST elevation and ST depression. The PR tell us the AV (Atrioventricular) conduction time. QRS complex is the graphical representation of electrical activity of heart when the ventricles are undergoing the process of depolarization. S1 and S2 corresponds to QRS complex and T wave respectively.

Continuous monitoring of ECG has become an important tool in diagnosing cardiac diseases. Modern ECG machines measure ECG signals in the bandpass of 0.05Hz to 100 or 150Hz. The abnormal sound mainly falls in the region 100-600Hz which can go up to 1000Hz. The heart sound signals together with noise are transmitted wirelessly to remote

centre so that the users or doctors at the other end can diagnose the heart sound signals after signal analysis.

IV. SYSTEM DESIGN

The complete cardiac monitoring system consists of heart sound sensor, the processing element and signal study part. The microcontroller and the microprocessor board together is called the processing unit. The output from the heart sound sensor is given to a microcontroller which digitizes the output value. The microprocessor transmits the information from microcontroller to server. From the server, data is transmitted to the remote client using MQTT data protocol. In the remote centre, signal analysis part is carried out in the PC which includes preprocessing stage (denoising and segmentation), feature extraction and classification of heart sound signals. Fig. 3. indicates the block diagram of complete cardiovascular observing framework.

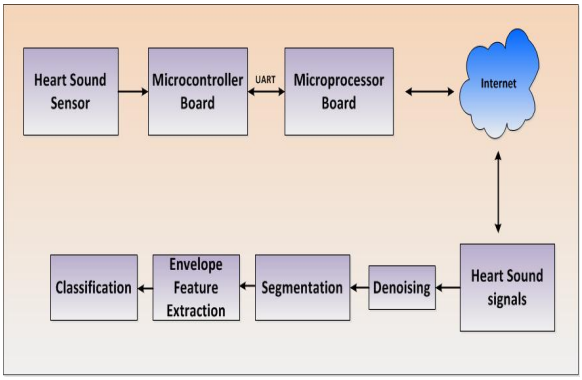

Fig. 3. Complete cardiac monitoring system

The heart rate sensor alongside the securing module measures electrical action of heart through the cathode pads placed on the skin. Here AD8232 is used as the sensor. It will be a little chip which measures the electrical action for heart. Furthermore, it is a single lead heart rate screen front end. If the distance from the AD8232 to the heart is shorter, then there will be less common-mode interference. The output of the board is analog value. The specifications of heart sound sensor are mentioned in Table 1. By connecting this board with Arduino, ECG graph is obtained through transforming IDE window. Heartbeats were recorded at 16-bit accuracy and stored as wav format. The function of Arduino (microcontroller board) is to convert the analog value to digital. Arduino Uno is a general purpose microcontroller board based on the device ATmega328P and has 14 digital input/output pins and 6 analog inputs. Arduino microcontroller have 32KB flash memory. The clock speed is 16MHz and draws less current. The Arduino board is communicated to Raspberry Pi via UART.

Raspberry Pi collects all information from Arduino and finally transmits to the server. Raspberry Pi is used as the microprocessor board. The Raspberry Pi is a credit card sized single board computer which is running a Debian based OS - Raspbian. The Raspberry Pi 3B+ uses a Broadcom BCM2837 SoC with a 1.4 GHz, 64-bit quad- core ARM Cortex-A53 processor, 1GB of SRAM, 2.4GHz and 5GHz integrated Wi-Fi, consuming ultra-low power of 800mA (4.0 W). When the microcontroller is turned on, it will initialize the serial port, for establishing communication with the Raspberry pi computer. It also initializes all necessary digital and analog input and output pins for the proper controlling. The microcontroller listens the serial port for any incoming commands from Raspberry Pi computer, which in turn listens commands from internet.

MQTT data protocol is used for transmitting the heart sound signal. The MQTT protocol is a light weight publish/subscribe informing protocol planned for M2M (machine to machine) telemetry in low bandwidth situations.

Table 1. Specifications of Heart Sound Sensor

Heart Sound Sensor AD8232	
Voltage	2V to 3.5V
Current	230µA
Output	Analog Value

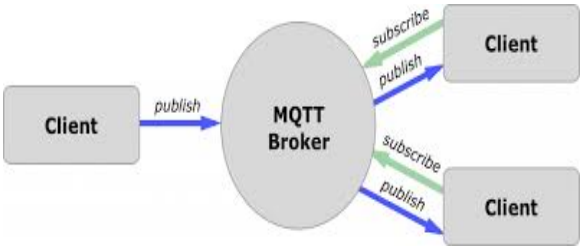

Fig. 4. MQTT protocol

It is useful for connections with remote locations. MQTT may be quick getting to be a standout amongst the fundamental conventions for IoT deployments. Fig. 4. shows how clients in the remote locations uses publish/subscribe messaging model with the application of MQTT server. MQTT is one of the widely used protocol in IoT applications. Its low power usage, less data packet and easy to implement make it ideal for machine to machine or Internet of Things world. It is based on a messaging technique. MQTT is based on clients and server. The server is called a broker and the clients are the connected devices. The MQTT protocol is implemented by using the Mosquitto which is an open source message broker.

The heart sound signals contain external and internal noises which interfere in the final diagnosis. Hence preprocessing is essential. So signal analysis part plays an important role in this. There are many Time-frequency distribution (TFD) methods adopted in signal processing. Some of them are approach based on mathematical model, method based on STFT (Short-time Fourier Transform), Wavelet Transform (WT) based TFD, generalized TFDs in the Cohen class (GTFD). These processing methods have some limitations [16]. So a suitable method should be implemented for heart sound signal analysis.

Hilbert-Huang Transform (HHT) is a time frequency method which is widely used. This is the most effective

method and many researchers have applied in the heart sound signal analysis [17]. There are predominantly two sections in Hilbert Huang Transform: Empirical Mode Decomposition (EMD) and Hilbert Transform. EMD is a time series technique, in which entangled informational indexes can be decayed in to a limited number of Intrinsic Mode Functions (IMFs). transform. For complicate data there should be more than one independent component at any given time. The decomposition should be adaptive in order to study data from nonstationary and nonlinear processes. The adaptive method will represent the characteristics of the signal better. Hilbert Transform offers meaningful Instantaneous Frequency for IMFs.

V. METHODOLOGY

Prior to division, the envelope of the heart sound sign must be separated. Hilbert Transform alone won't be adequate for extricating the envelope of heart sound sign. The Hilbert transformed amplitude oscillates too much. Hence before envelope construction, the signal should be decomposed. The envelope makes sense for each IMF. So Hilbert Huang Transform technique is implemented.

An IMF ought to fulfill the accompanying necessities: The quantity of most extreme and least focuses and the quantity of zero intersections should either be equivalent or their distinction must be one for the full informational collection, and the mean estimation of envelope for the nearby maxima and neighborhood minima ought to be zero.

The signal can be decomposed by applying EMD based on the following assumption [18], which is also depicted in the flowchart shown in Fig. 5.

1. Consider the signal x(t). Identify all the global maximum and global minimum points of x(t). At that point discover neighborhood most extreme and nearby least focuses with the goal that every one of the information are situated between the lower and upper envelope. Obtain the mean curve. Let it be m(t). Then we find the difference between x(t) and m(t) as:

$$x_1(t) - m_1(t) = c_1(t) \qquad (1)$$

where $x_1(t)$ is the original signal and $c_1(t)$ is the first IMF component.

2. $c_1(t)$ becomes the next original signal which is denoted as $x_2(t)$ and find the difference.

$$x_2(t) - m_2(t) = c_2(t) \qquad (2)$$

Here $c_2(t)$ is the next IMF component.

3. The above process is repeated and we define r = $c_k(t)$.

The methodology of extricating one IMF part is filtering. It is represented as

$$x\,(t) = \sum_{k=1}^{n} C_k + r_n \qquad (3)$$

C_k is one of the IMFs changing from C_1 to C_n and r_n is the residual signal.

The sifting procedure stops with a stoppage criteria S and SD. S is defined as the consecutive number of siftings. SD is represented as:

$$SD = \sum_{t=0}^{T} \frac{|h_{k-1}(t) + h_k(t)|^2}{{h_{k-1}}^2(t)} \qquad (4)$$

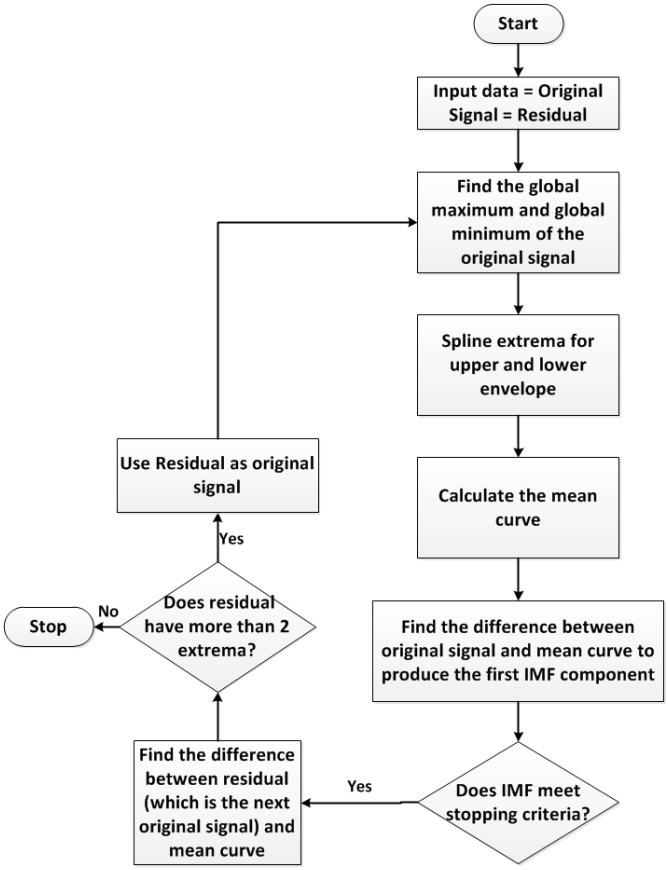

Fig. 5. Flowchart of EMD filtering process

The value of SD ranges from 0.2 to 0.3 [19].
The complex-valued function of heart sound can be expressed as:

$$X_k(t) = \mathrm{c}_k(t) + \mathrm{jH}[c_k(t)] \qquad (5)$$

All IMF enjoy good Hilbert transform:

$$c(t) = a(t)e^{i\theta(t)} \qquad (6)$$

In the Hilbert spectrum analysis, the original signal can be represented as:

$$x(t) = \mathrm{Re}\sum_{k=1}^{n} a_k(t)e^{j2\pi\int f_k(t)dt} \qquad (7)$$

where $a_k(t)$ is the instantaneous amplitude and is represented as:

$$a_k(t) = \sqrt{|c_k(t)|^2 + |H[c_k(t)]|^2} \qquad (8)$$

The most challenging task in the signal analysis part is the heart sound segmentation. The primary operation of segmentation is to detect the boundaries of S1 and S2 discover the begin and end focuses. Selection of threshold value is critical. The threshold may vary for individuals or depending on the cardiac disease. The threshold is mainly dependent on the time interval and the result will be largely influenced by noise peaks. There should a method where accuracy is higher. So we have chosen combined adaptive threshold method. The combined adaptive threshold method is a combination of three independent thresholds.

$$MFR = M + F + R$$

where M indicates versatile soak slant edge, F signifies versatile coordinating edge and R means versatile beat desire edges. The first threshold sets a slew rate value that has an ability to change to suit different conditions, a second one emerges when high recurrence happens and a third one determined to abstain from missing of low sufficiency beats.

VI. Experiment and Results

The information from 10 healthy subjects were gathered utilizing the proposed cardiovascular monitoring framework and this was a non-clinical examination. The test setup of the monitoring system is shown in Fig. 6.

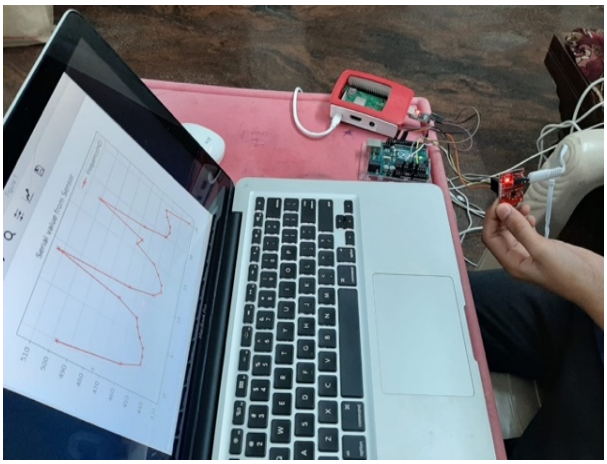

Fig. 6. Real time monitoring System

The data obtained from real time data acquisition is shown in Fig. 7. The data acquired through the processing unit is then transmitted to another client i.e., publish and subscribe of data through MQTT server is implemented here. This is shown in Fig. 8. Aside from this, both typical and irregular heart sound chronicles from the database Physionet/Computing in Cardiology (CinC) Challenge 2016 [20] are utilized to approve the exactness of categorization. The heart sound accounts last from a few seconds to up to more than one hundred seconds. The sum total of what chronicles have been resampled to 2,000 Hz and have been given as .wav group. 50 datasets from normal and 50 from abnormal are selected from the database. Further signal analysis is done in the PC.

The heart sound obtained from 10 healthy subjects was converted to .wav format and transmitted using the MQTT data protocol. These were plotted at the receiving end and found that all were normal beats. The accuracy of the system is 100%.

The decomposition results for the normal and abnormal heart sounds are presented in Fig. 9. The x-axis indicates the samples and y-axis indicates the amplitude in volts. Here the number of IMF shown is 2 with the residual value. All IMF components are the sum of spline functions. Natural cubic spline is used to maintain the smoothness.

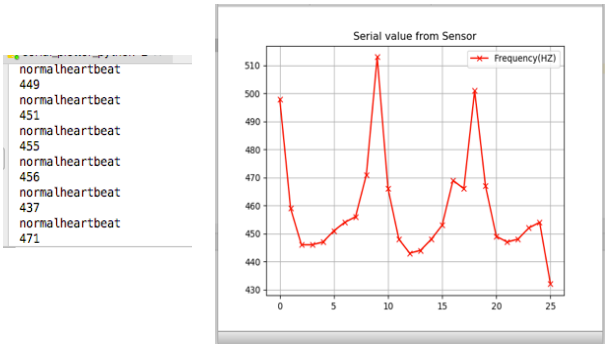

Fig. 7. Data obtained from the real time monitoring system

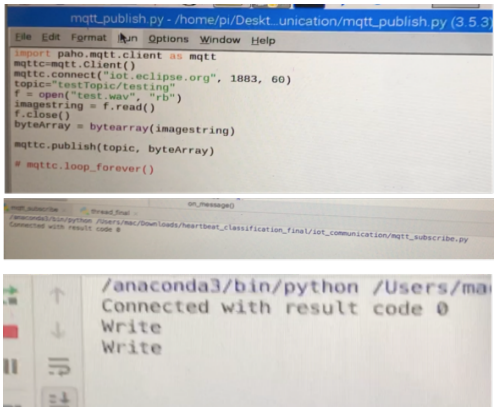

Fig. 8. Data transmission through MQTT server (MQTT publish and subscribe)

Fig. 10 and Fig. 11 shows the Hilbert spectrum for normal and abnormal heart sound respectively. The Hilbert spectrum shows that the normal heart sound frequencies are below 150Hz and that of abnormal are below 1000Hz.

The heart sound segmentation results are shown in Fig. 12. Complete algorithm is developed in Python programming language. The running time of the algorithm is less than 30seconds. The configuration of the computer used is 4 GB RAM, MacBook Pro macos Sierra, 2.5 GHz Intel Core i5.

Feature extraction has a significant role in categorization of heart sound signal. Feature extraction is the method of identifying distinguishing features of the signal. In this research work features are extracted from the time domain. Here Ta is considered as the time gap of first heart sound S1. Tb is considered as the time interval of second heart sound. Ta1 is the time gap from the start of first heart sound of one

cardiac cycle and start of first heart sound of next cardiac cycle. Ta2 is the time gap from the beginning of first heart sound S1 and last part of second heart sound S2 of the same cardiac cycle. These are considered as the highlights for heart sound characterization. So by calculating the appropriate time difference, the heart sounds are classified as normal and abnormal heart sound.

Out of 50 abnormal heart sounds, 48 were correctly identified as pathological. The heart sound sign investigation calculation assessed the typical heart sound exactness to be 100% and anomalous heart sound exactness as 96%.

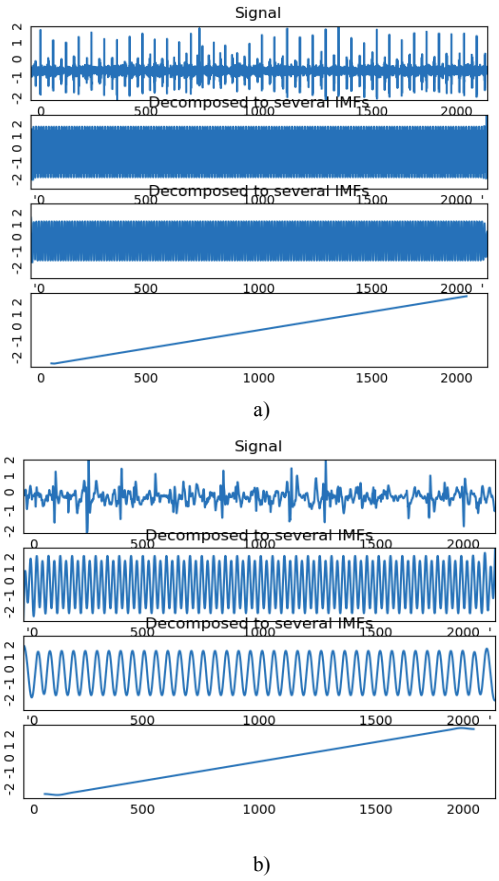

Fig. 9. Decomposition results (a) Normal heart sound (b) Abnormal heart sound

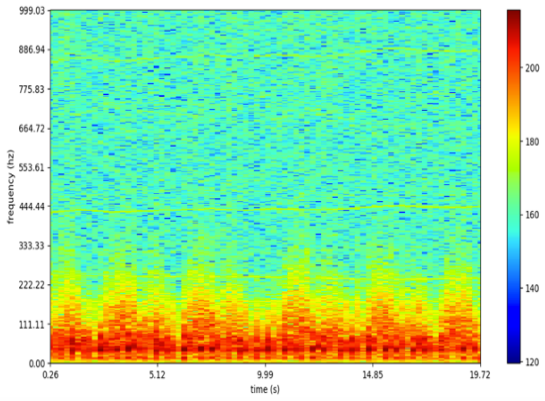

Fig. 10. Hilbert spectrum for normal heart sound

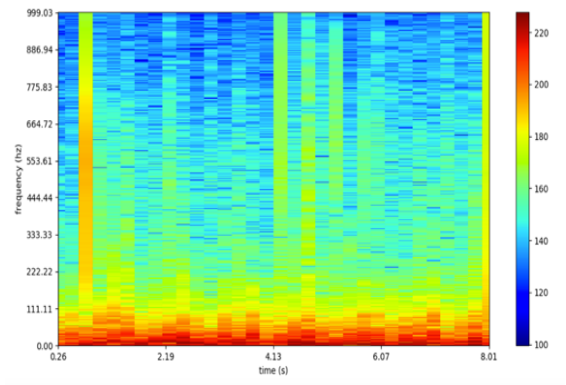

Fig. 11. Hilbert spectrum for abnormal heart sound

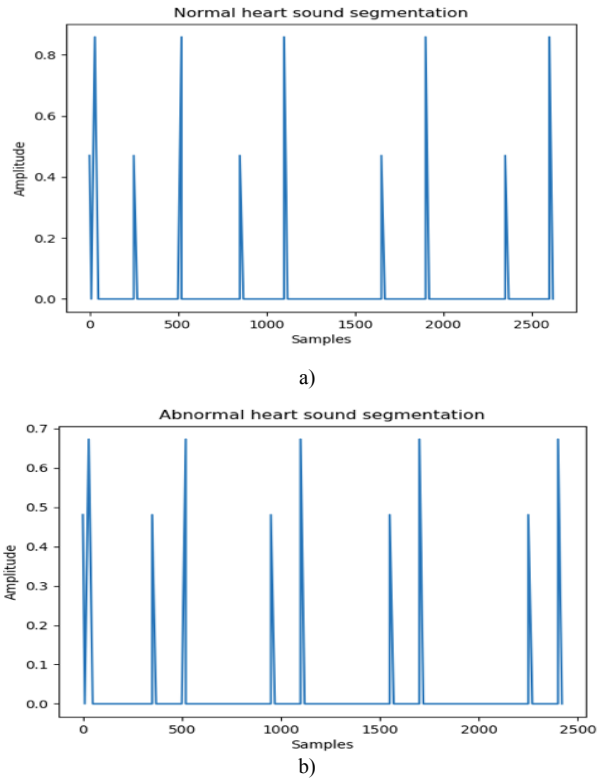

Fig. 12. Segmentation results (a) Normal Heart Sound (b) Abnormal Heart Sound

VII. CONCLUSION

A modern heart observing framework dependent on remote detecting for human medicinal services has been developed. The heart sound is acquired using a simple acquisition module and the processing part is implemented using low cost, low power hardware. The wireless technology is also simple to implement. The MQTT data protocol, which is the latest technology in IoT, is easy to configure and long distance transmission is possible. The signal analysis part was the challenging task. Efficient algorithm for the categorization of normal and abnormal heart sounds is developed using Python programming language, which is faster in execution. Accuracy of 96% is achieved for the abnormal heart sound. The future extent of the framework is to improve the heart sound acquisition module so that it can

be utilized for clinical investigation and furthermore separate the distinctive cardiovascular maladies.

ACKNOWLEDGMENT

The authors would like to thank the Principal and Head of the Department, Electronics and Communication, College of Engineering Trivandrum for providing the facility and support for completing this research work. Also thank the Head of the Department, Cardiology, Medical College, Trivandrum for their guidance.

REFERENCES

[1] *Heart disease - Symptoms and causes - Mayo Clinic*, March 22, 2018. [Online]. Available: https://www.mayoclinic.org/diseases-conditions/heart-disease/symptoms-causes

[2] Sheik Hussain Salleh, Hadrina Sheik Hussain, Tan Tian Swee, Chee-Ming Ting, Alias Mohd Noor, Surasak Pipatsart, Jalil Ali and Preecha P Yupapin, "Acoustic cardiac signals analysis: a Kalman filter-based approach," Published online, International Journal of Nanomedicine, pp. 2873-2881, 2012.

[3] R. E. Perez-Guzman, R. García-Bermudez, F. Rojas-Ruiz, A. Cespedes-Perez and Y. Ojeda-Riquenes, ''Evaluation of algorithms for automatic classification of heart sound signals,'' in *Proc. Int. Conf. Bioinf.Biomed. Eng.* Cham, Switzerland: Springer, pp. 536–545, 2017.

[4] Yuenyong S, Nishihara A and Kongprawechnon W, "A framework for automatic heart sound analysis without segmentation", Biomed Eng Online. 10:13, 2011.

[5] Ritsuko Kohno, Haruhiko Abe and David G. Benditt, "Ambulatory electrocardiogram monitoring devices for evaluating transient loss of consciousness or other related symptoms," Published online, Journal of Arrhythmia; 33(6): pp.583-589, 2017 Dec.

[6] S. Leng, R. S. Tan, K. T. C. Chai, C. Wang, D. Ghista and L. Zhong, ''The electronic stethoscope,'' *Biomed. Eng. Online*, vol. 14, pp. 1-37, Jul. 2015.

[7] Liang H, Lukkarinen S and Hartimo I, "Heart sound segmentation algorithm based on heart sound envelogram," In Computers in Cardiology 1997. Lund: IEEE; pp. 105–108, 7–10 September 1997.

[8] X.-P. Wang, C.-C. Liu, Y.-Y.Li and C.-R. Sun, "Heart sound segmentation algorithm based on high-order Shannon entropy," Research Gate, September 2010.

[9] Ting Li, Tianshuang Qiu and Hong Tang, "A Heart Sound Segmentation Method Based on Cyclostationary Envelope," in Proceedings of the 2nd International Conference on Computer Science and Electronics Engineering (ICCSEE 2013), pp. 2536-2539, 2013.

[10] J. Chen and H. Hou, ''Segmentation of heart sound using doublethreshold,'' in *Proc. 5th Int. Conf. Meas. Technol. Mechatronics Automat.*, pp. 985–988., Jan. 2013.

[11] Norden E. Huang, Zheng Shen, Steven R. Long, Manli C.Wu, Hsing H. Shih, Quanan Zheng, Nai-Chyuan Yen, Chi Chao Tung and Henry H. Liu., "The empirical mode decomposition and the Hilbert spectrum for nonlinear and non-stationary time series analysis," *In Proc. of the Royal Society of London*, vol. 454:903–995, 1998.

[12] Haoran Ren, Hailong Jin, Chen Chen, Hemant Ghayvat and Wei Chen, "A Novel Cardiac Auscultation Monitoring System Based on Wireless Sensing for Health Care," IEEE Journal of Translational Engineering in Health and medicine, Volume 6, 2018.

[13] IvayIo I Christov, "Real time electrocardiogram QRS detection using combined adaptive threshold," BioMedical Engineering Online, 3:28, August 2004.

[14] *The Human Heart-World Invisible.* [Online]. Available: https://www.worldinvisible.com/apologet/humanbody/heart.html

[15] *Basic Heart Sounds*, *2007*. [Online]. Available: www.stethographics.com

[16] Ming Li , Xue-Kang Gu and Shen-Shen Yang, "Hilbert-Huang Transform Based Time-Frequency Distribution and Comparisons with Other Three," INTERNATIONAL JOURNAL OF CIRCUITS, SYSTEMS AND SIGNAL PROCESSING, Issue 2, Vol. 1, pp. 155-160, 2007.

[17] A. Altamirano-Altamirano, A. Vera, L. Leija and D. Wolf, ''Myoelectric signal analysis using Hilbert–Huang Transform to identify muscle activation features,'' in *Proc. Int. Conf. Elect. Eng., Comput. Sci. Autom Control*, pp. 1–4, Sep. 2016.

[18] Lihan Liu, haibin Wang, Yan Wang, Ting Tao and Xiaochen Wu, "Feature Anlysis of Heart Sound Based on the Improved Hilbert-Huang Transform," [Online]. Available: https://citeseerx.ist.psu.edu/

[19] N. E. Huang and Z. Wu, ''A review on Hilbert–Huang transform: Method and its applications to geophysical studies,'' *Rev. Geophys.*, vol. 46, no. 2, 2008.

[20] C. Liu et al., "An open access database for the evaluation of heart sound algorithms," Physiol. Meas., vol. 37, no. 12, pp. 2181-2213, 2016.

Proceedings of the Fourth International Conference on Communication and Electronics Systems (ICCES 2019)
IEEE Conference Record # 45898; IEEE Xplore ISBN: 978-1-7281-1261-9

Mobile Application for Storage and Retrieval of e-learning videos Using Hadoop

Jyoti Parsola
Dept of Computer Applications
Graphic Era University,
Dehradun, India

Durgaprasad Gangodkar
Dept of Computer Science & Engineering
Graphic Era University,
Dehradun, India

Ankush Mittal
Dept of Computer Science & Engineering
Graphic Era University,
Dehradun, India

***Abstract*— With the rapid advancement of mobile phones and low cost, fast internet access students/learners are using smart phones for learning purpose also. Mobile learning (m-learning) has been recognized as a competent method of seeking knowledge. As the quantity of users and lecture video contents is increasing, how to deploy m-learning becomes dubious because of limited memory space in mobile phones. The learning materials like ppt., docs, occupy less space but lecture videos consumes a lot of memory in a mobile device. Therefore there should be some measure where students can store as well as access lecture videos. Hadoop has been evolved as a promising technology to overcome the problems in m-learning. It provides reliable, customized environments for end-users. We present a new mobile application for a mobile learning system integrated with Hadoop, for storage and retrieval of lecture videos from mobile phone to the Hadoop Distributed File System (HDFS). Registered user of the application can perform the functions like upload video, search a video file and download a video file. We have calculated computational time to upload, search and download various size of video file (maximum size is 1.3 GB). The proposed application can be utilized where there is a high demand of exhaustive teaching and learning in higher education.**

Keywords*— Mobile learning, Hadoop, Hadoop Distributed File System (HDFS).

I. INTRODUCTION

With consistent development of internet technology and low cost of mobile phones users have started using it in learning purpose as well. This have increased the size of video data in mobile and due to the low storage power of mobile phones it is not possible to store each and every video in mobile phones. So there is a need of such solution which can provide user to store video data and can easily access or retrieve data when required latter on. One such solution which can resolve such problem is Hadoop, it has achieved remarkable acceptance due to its attributes like, low cost, easy accessibility, fault tolerant, distributed storage and processing , highly scalable [1].

Various researchers have used Hadoop in numerous applications like video Processing [2], query processing [3], video transcoding [4], post event investigation [5], video surveillance [6][7], traffic measurement[8] , event detection[9], face detection[10] and Content Based Image Retrieval [11]. Therefore this gives us motivation to develop a mobile application which can perform the following functions:

- User can send lecture video data from mobile to the Hadoop Distributed File System(HDFS)
- User can retrieve video data when required
- User can download video data easily

Storing video data into HDFS is a challenge as Hadoop was originally designed for text processing [1] so storing video files in HDFS is a challenge for the researchers. Remaining paper is structured as follows: section 2 consists of review of research which is carried out using Hadoop, section 3 discusses the proposed work and section 4 presents experiment and result, finally followed by the conclusion.

II. LITERATURE REVIEW

As data is growing continuously, so to efficiently store and process this consistently increasing data is a challenge. Hadoop which have evolved as a possible solution to this problem, is now been used in various applications which, engender enormous data. A lot of research has been performed by various researchers on how to use Hadoop best for storage and processing, either by changing the architecture of HDFS for increment in processing of mapreduce tasks or by designing efficient algorithms[5] to store data into HDFS, which can be retrieved easily. Apart from this many researchers have used Hadoop for video processing [12] task, video segmentation purpose [2], motion estimation in surveillance videos [13], multi-view object recognition [14].

A video monitoring system that can handle, the users' request of searching video, uploading video, downloading video and trans-coding video is presented in[6]. They also used FFMPEG to trans-code video. A Hadoop based recorder system is proposed in [15] which provides extensible video recording system, data backup, monitoring features and moreover they have used HDFS for storing data. Other video monitoring application proposed where Hadoop is used [16], for extracting metadata (its attributes are vehicle enter time, license plate recognition, type of vehicle) and correction of surveillance videos.

A framework for video playing and storage based on Hadoop is discussed in [17]. It supplies simultaneous access and playing streaming media in mobile phones. A Hadoop-based storage architecture for tremendous MP3 files is proposed in

[18]. Classification algorithm is used in pre-processing component to combine small files into sequence files. They validate that the effective indexing method is excellent quick fix to the issue of small files storage.

Among the huge amount of video data in internet the majority of files are copy of original videos, [19] have attempted to develop a real time video copy detection using Hadoop, they have designed two copy detection algorithms and then they have compared the performance of both the algorithms by implementing on Hadoop platform.

Various researchers have worked in the area of E-learning like reducing data size of e-learning videos [20], generating a time shrunk video by event detection [21], converting e-learning video which consists of power-point presentation into pdf format, enhancing lecture content [22][23] etc. The size on internet data comprising of images and video so [24] uses Hadoop for storage and processing of mass multi-media files for storage. Hadoop has been used for searching lecture videos, it provides list of lecture videos relevant to the user query [25]. But as far as e-learning mobile applications is concerned not many researchers have utilized Hadoop for storing and processing mobile data. So integration of mobile with Hadoop for storing and processing mobile video data is still a challenge.

III. Architecture of Mobile Application

Due to low cost internet and smart phones, students have started using mobile phones for accessing lecture (e-learning) videos, doc files etc for reading purpose, but due to its low memory size it is not possible to store each and every data in it. To resolve this issue we have proposed an android application integrated with Hadoop, where user can store data like e-learning videos. Data Stored can be accessed by other users when required. The components of our proposed application are as shown in fig. 1, it consists of mobile phone in which android application is installed and then the essential learning data i.e. video files is send to the server and third component is the Hadoop HDFS, where data resides and user can access data when required.

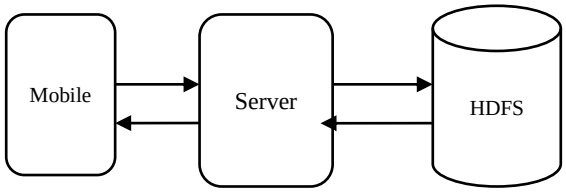

Fig.1 Components of mobile application

A. Mobile Application

We have developed a mobile application which connects with web server and further transfers data to the HDFS. The use case of mobile application user is shown in fig.2, firstly user has to login to perform any operation if user is the registered user then he is directed to the next page where he can perform following functions like upload video file, search a video, download a video. If the user selects an upload video file then again he is directed to the next page where user is asked to select the category like General Awareness, Computer Science, Electrical, Management etc. User selects the category and uploads video. If user selects searching video, then again he is asked to select the category of the video, user selects the category and finally the list of videos related to the category along with the download button is displayed. User clicks on download video option. Video is downloaded into the user mobile device.

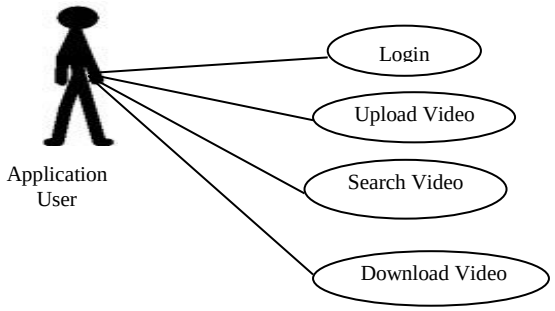

Fig.2 Use cases diagram of mobile application

B. Video Upload & Storage

Multi-media files like images which are usually small in size can be stored in Hadoop, by first converting images into sequential files and Hadoop Archive, CombineFileInputFormat[26], whereas video files are larger in size and some measure have to be done for storing. By default size of a data block is 64MB therefore storing video files becomes challenging as most of the video files are larger than the default size. If file is to saved then it is segmented [2][23] and then stored into various block. Video files is unstructured data so if any encoding scheme is applied to it then it can lead to correlation between video frames. If files are directly stored in HDFS then there is no purpose of using Hadoop for storage and processing. So it is very necessary to store files by first splitting them into various blocks.

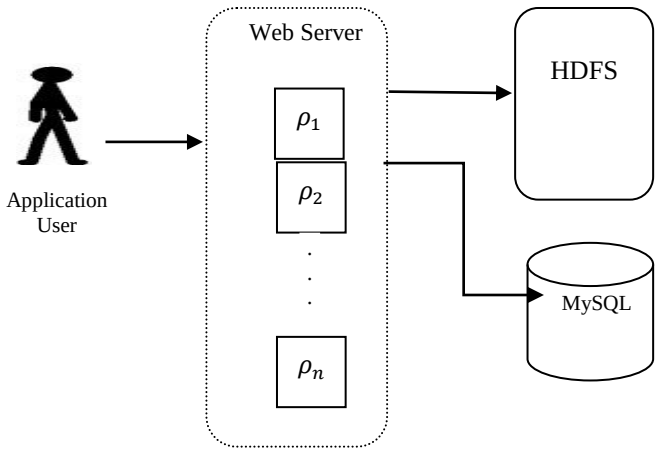

Fig.3 Video Storage Architecture of application

We have used FFMPEG [27] method for splitting video files into ρ segments. We have set size of every segment as ∅, where ∅ = 256MB as lecture videos will be of more than 1 GB, video storage architecture of our application is shown in fig. 3. When user needs to upload a video file, he selects video file, and the category video belongs to, then in the server side FFMPEG converts video file into various segment, and these segments are send to the HDFS, the information about the name of segment, category it belongs to and its HDFS location is stored in a MySQL database.

The segmented video files are stored in such a way that it is easier to access video files. Let's say name of video file is Fundamentals then the segmented video file is named as Fundamental ρ_1. Segmented video files are stored in various DataNode in HDFS, for every segmented file 2 more replica is stored in HDFS so that one of the DataNode fails then data and HDFS can work in spite of the failure. Moreover while uploading video user is asked to select the category of video i.e. which type or which category video file belongs to, this is done for easy accessibility of video files.

C Video Search & Video Retrieval

If the user wants to search any video then he clicks on search button, selects the category, list of videos related to the category along with a download button is displayed. User clicks on download button, with the help of FFMPEG segment video file are merged together and a video file is downloaded into the user mobile device. When user enters for the file name to be searched then *Map* divides the task to various *reducers*, *reducer* then finds the various segment of video files then again FFMPEG merges all the video files and provides the list of video files related to the category selected by the user, MapReduce architecture is shown in figure.4.

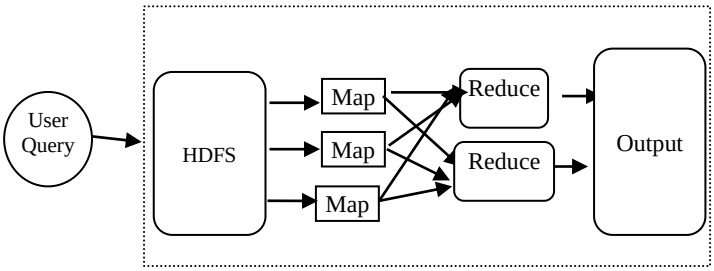

Fig.4 Video Search Architecture of application

IV. IMPLEMENTATION & RESULTS

We have developed our mobile application in android studio version 3.3, the operating system we used for our work is Ubuntu.16.0.4, with 64 bit processor. We have used apache tomcat server which is an open source software implementation of the Java Servlet and JavaServer Pages technologies and eclipse with J2EE for server side programming, and the database used is MySQL. To test our application we have used Genymotion which provides emulator for testing android applications which works very much similar to the real device all the technologies and software used in our application is listed in table. 1. The prerequisite of our application is that both the application user and server should be in the same Wi-Fi range and second is whenever we have to use app, Hadoop have to be started using the shell command.

TABLE.1.TOOLS USED

S. No	Name of Tools	Version
1	Hadoop	2.9
2	Apache Tomcat Server	7.9
3	Eclipse with J2EE	3.7.1,SR1
4	Genymotion	2.10.0
5	MySQL	5.7.22
6	Android version	v8.0 Oreo

A. Video Upload

Working of our video upload module is shown with the screenshot fig.6. Initially when app launches it starts with the login page then user enters the credentials, if user is already registered then he is directed to the next page otherwise user have to register by filling the useful details like username, password, email id etc. Once user logs in, user can perform the following functions clicking on the buttons like upload video, search video, download video. User clicks on Upload Video button then he is asked to select category the particular video belong to, further with the help of browse button user can upload the desired video. A message is displayed that video is uploaded successfully.

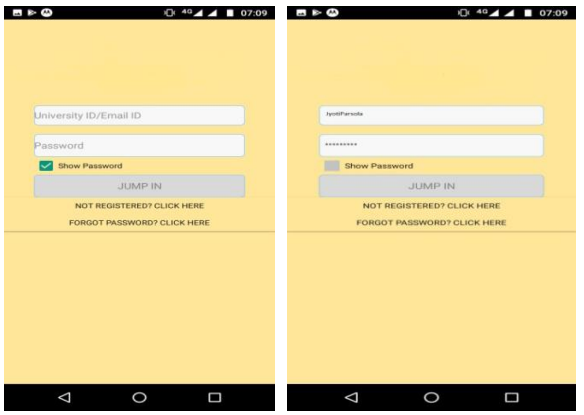

(a) User Login (b) User entered credentials

(c) Task to perform (d) User selected upload button

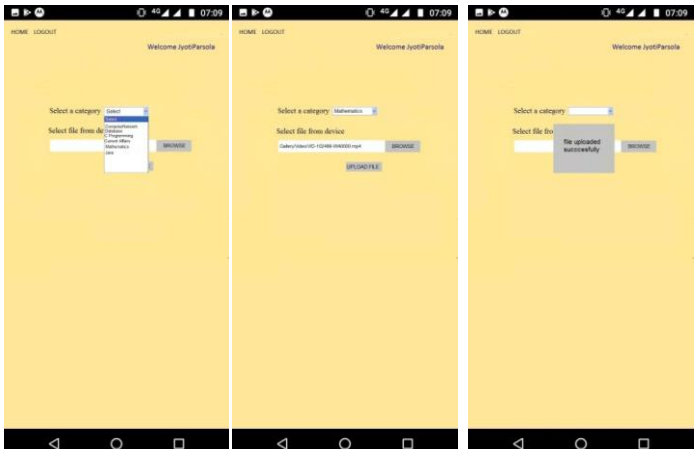

(e)User selected category (f)User has selected category and file from mobile device (g) File is uploaded successfully

Fig.6 Screenshots of our video uploading module of our mobile application

B. Video search and download file

If user wants to search a video in HDFS, user clicks on search video button, user is asked to select the category, once category is selected, the list of video related to the category is displayed along with the Download option and user is informed by message when video downloading is complete shown in fig 7, the same pages appears when user clicks on Download button in home page.

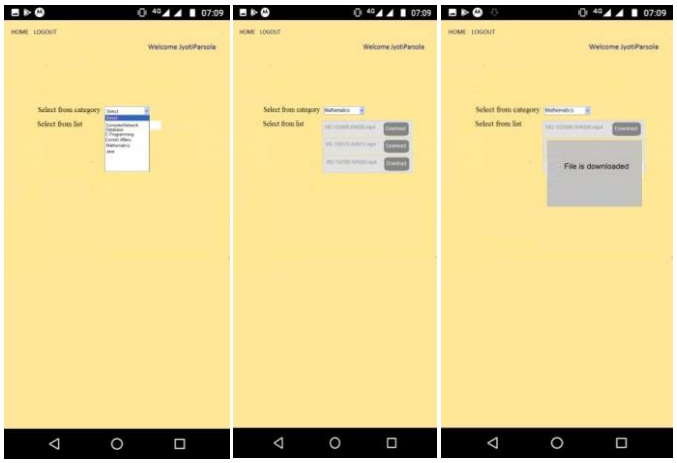

(a) User has to select query to search a video (b) List of video files is displayed (c) User downloaded the video file.

Fig.7 Screenshots of our video search and download module of our mobile application

TABLE. 1 TIME TAKEN FOR UPLOADING VIDEO

Data Size	Upload Time
538 MB	41 s
695 MB	52 s
762 MB	63s
793 MB	69s
853 MB	76s
1.32 GB	87s

Time taken by our application in uploading, searching and downloading video files of various sizes is shown in table.1, table. 2 and table. 3 respectively. Moreover we have reduced the search time of a video file by varying number of reducers. Figure 8 shows how search time changes by varying number of reducers, it is evident from our result that, small data size do not require much reducers but, for large data size in order to reduce search time number of reducers have to be increased. Uploading and downloading time is less as compared to time taken in searching videos. Searching can be reduced further by applying a *combiner* in between *map* and *reduce* task.

TABLE. 2 TIME TAKEN FOR SEARCHING VIDEO

Data Size	Search Time
538 MB	623s
695 MB	722s
762 MB	771s
793 MB	783s
853 MB	815s
1.32 GB	986s

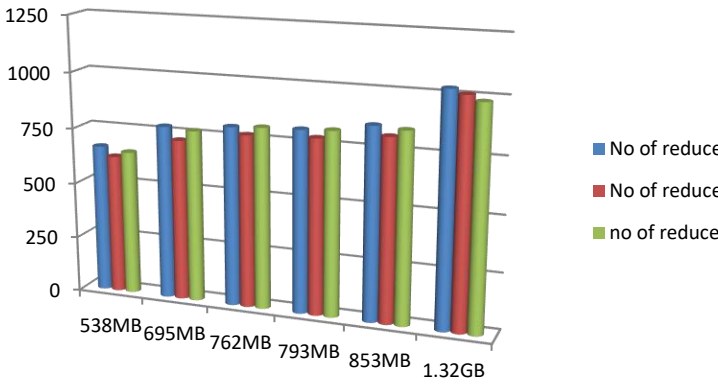

Fig.8 Search time by varying no of reducers

TABLE. 3 TIME TAKEN FOR DOWNLOADING VIDEO

Data Size	Search Time
538 MB	61s
695 MB	73s
762 MB	84s
793 MB	87s
853 MB	91s
1.32GB	128s

V. CONCLUSION & LIMITATION

With the easy access of internet technology and low cost of mobile phones students are using mobile phones for learning purpose by watching lecture videos in their smart phones. Due to less memory space it is not possible for user to store each and every video data in mobile phone, therefore to address this problem we have used Hadoop for storing lecture video. In

this paper we have successfully integrated Hadoop with mobile application, for storage and processing of mobile video data into HDFS. Through this application user can upload a video and store that video into HDFS, search a video and download the required video as well. We have been successfully able to upload and retrieve a maximum of 1.3 GB of video data. The limitation of our work is that the application user and server should be in the same Wi-Fi range, and Hadoop has to be initialized using shell command, with further enhancement in the application user can easily access videos as well as the Hadoop server can be automatically started. Moreover we can further reduce searching time by applying a *combiner* in between *map* and *reduce* task

References

[1] J. Dean, and S. Ghemawat , "Map Reduce: Simplified Data Processing on Large Cluster," ACM Commun., vol.51, no.1, pp. 107–113, 2008.

[2] E. SaatiAlsoruji and S. Majumdar, "A Video Segmentation Strategy for Video Processing Applications on Hadoop Clusters, " in IEEE SmartWorld, Ubiquitous Intelligence & Computing, Advanced & Trusted Computing, Scalable Computing & Communications, Cloud & Big Data Computing, Internet of People and Smart City Innovation (SmartWorld/SCALCOM/UIC/ATC/CBDCom/IOP/SCI) , pp. 1783-1790), Oct, 2018.

[3] H. Wang, X. Qin, X. Zhou, F. Li, Z. Qin, S. Wang, "Efficient query processing framework for big data warehouse: an almost join-free approach, " . Frontiers of Computer Science, vol. 9, no. 12, pp. 224-236, 2015

[4] X. Liu, D. Zhao, L. Xu, W. Zhang, J. Yin, J., & X. Chen, "A Distributed Video Management Cloud Platform Using Hadoop," IEEE Access, vol.3, no. 1, pp. 2637-2643,2015.

[5] J.Parsola, D. Gangodkar, A. Mittal, "Post Event Investigation of Multi-stream Video Data Utilizing Hadoop Cluster", Int. J. of Electrical & Computer Engineering, vol.8, no.6, 2018.

[6] Y. Liu, S. Liang, M. Zhao, and Y. Sun, "Hadoop applications in video monitoring, " in Advanced Materials Research, vols. 1030_1032. Dürnten,Switzerland: Trans Tech Publications, 2014, pp. 1717_1720.

[7] Y.Lee, Y. Lee, "Towards scalable internet traffic measurement and analysis with Hadoop", ACM SIGCOMM Computer Communication Review, vol.43, no.1,2013

[8] K. Shvachko, H. Huang, S. Radia, and R. Chansler, "The hadoop distributed file system, " in: 26th IEEE (MSST201O) Symposium on Massive Storage Systems and Technologies, May, 2010.

[9] J. Hererra, "Detecting Events in Streaming Multimedia with Big Data Techniques," 24th Euromicro International Conference on Parallel, Distributed, and Network-Based Processing, 2016.

[10] Tan, H., & Chen, L. (2014, July), "An approach for fast and parallel video processing on Apache Hadoop clusters," in IEEE International Conference on Multimedia and Expo (ICME), pp. 1-6, Chengdu, China, 14-18 July, 2014,

[11] C.Gu, Y.Gao, "A Content-based Image Retrieval System Based on Hadoop and Lucene", in 2nd International Conference on Cloud and Green Computing, Xiangtan, China, 1-3 Nov 2012.

[12] C. Ryu, D. Lee, M. Jang, C. Kim, "Extensible Video Processing Framework in Apache Hadoop," in IEEE International Conference on Cloud Computing Technology and Science, 2-5 Dec. 2013, Bristol, UK.

[13] J. Parsola, D. Gangodkar, A. Mittal, "Efficient Storage and Processing of Video Data for Moving Object Detection using Hadoop MapReduce, " in Int. Conf. on Signal, Networks, Computing and Systems (ICNCS-2016), JNU, New Delhi, India, 2016

[14] S.Noor and V. Uddin, "MapReduce for multi-view object recognition," in IEEE Int. Conf. on High Performance Computing & Simulation (HPCS), pp. 575-582, Innsbruck, Austria ,18-22 July 2016.

[15] C.-F. Lin, S.-M. Yuan, M.-C. Leu, and C.-T. Tsai, "A framework for scalable cloud video recorder system in surveillance environment, " in Proc. 9th Int. Conf. Ubiquitous Intell. Comput., 9th Int. Conf. Auto. Trusted Comput. (UIC/ATC), pp. 655- 660, Fukuoka, Japan, 4-7 Sept. 2012

[16] X. Zhao, H.Ma, H. Zhang, Y. Tang and G. Fu, "Metadata extraction and correction for large-scale traffic surveillance videos," in IEEE International Conference on Big Data (Big Data) , pp. 412-420, Washington, DC, USA ,27-30 Oct. 2014

[17] C. Liu, K. Fan, Z. Yang, and J. Xiu, "A distributed video share system based on Hadoop, " in Proc. IEEE 3rd Int. Conf. Cloud Comput. Intell. Syst. (CCIS), pp. 587_590, Shenzhen, China, 27-29 Nov, 2014

[18] X.-Y. Zhao, Y. Yang, L.-L. Sun, and Y. Chen, "Hadoop-based storage architecture for mass MP3 files, " J. Comput. Appl., vol. 32, no. 6, pp. 1724_1726, 2012

[19] J. Li, Q.Wu, X. Lian & J. Sun, "Real-time video copy detection based on Hadoop," in IEEE Sixth International Conference on Information Science and Technology (ICIST), pp. 492-497, 6-8 May 2016, Dalian, China

[20] A. Mittal, S. Gupta, S. Jain & A. Jain,"Content-based adaptive compression of educational videos using phase correlation techniques, " Multimedia Syst., vol. 13, no.3, pp.249–259, 2006

[21] T. Yokoi and H. Fujiyoshi, "Generating a time shrunk lecture video by event detection, " in IEEE Int. Conf. on Multimedia and Expo,pp. 641-644, Toronto, Ont., Canada, 9-12 July,2006

[22] P.P. Deolika, "Lecture Video Search Engine Using Hadoop MapReduce, " California State University, Long Beach,2017

[23] F.Wang, C.W. Ngo and T.C Pong, "Lecture video enhancement and editing by integrating posture, gesture and text," IEEE Trans. Multimedia, 9, 397–409, 2007.

[24] J.Lin, K Lin, J. Wang, "Design of mass multi-media files storage architecture based on Hadoop", in 8th Int. Conf. on Computer Science & Education(ICSE2013), April 26-28,Colombo, Sringar, 2013.

[25] Z.Lin, L. Zhen, C.Yingmei, T. Yuqin, "The video monitoring system based on big data processing", in 7th International Conference on Intelligent Computation Technology and Innovation, 25-26 Oct. 2014, Changsha, China

[26] Hadoop official site. http://hadoop.apache.org! .

[27] Bellard F, FFMEPG multimedia system .Http://FFMPEGsourceforge.net.

Proceedings of the Fourth International Conference on Communication and Electronics Systems (ICCES 2019)
IEEE Conference Record # 45898; IEEE Xplore ISBN: 978-1-7281-1261-9

QoS Based Optimal Resource Allocation in Service Composition for Heterogeneous Devices

Y V Dongre, Research Scholar
Department of Computer Engineering
Pune Institute of Computer Technology, Pune
Savitribai Phule Pune University, Pune
yashwant.dongre@gmail.com

R B Ingle, Professor
Department of Computer Engineering
Pune Institute of Computer Technology, Pune
Savitribai Phule Pune University, Pune
rbingle@pict.edu

***Abstract*— Service-Oriented Computing(SOC) rapidly gains importance in the industry to built complex web service applications. The web service plays a very important role in SOC. Service composition is the process of adding services to the existing one using functional attributes of multiple services rapidly and effectively. One of the critical issues in the composition is non-consideration of Quality of service (QoS) parameters which can lead to inaccurate and low performing composite service. Next to selection tasks in the composition process is to allocate resource to selected services in composite service is also crucial. Resource allocation in the composition is the process of allocating component service to selected candidate service for each and every candidate services in composite service. In the cloud environment, component service holds physical computational resource or infrastructural resource. This paper, present mapping of resource allocation problem in composition to 0/1 Multi-dimensional knapsack problem which is NP-hard computational problem. The work in the paper provides the solution to the resource allocation problem with the help of a dynamic programming strategy. The computational simulation was carried out and revealed that the dynamic programming strategy as not suitable for a large number of services considered during the allocation process. Further development of the solutions for such problems should be attempted by applying various heuristics and meta-heuristics approaches. However, after analysis of these approaches, the work suggests to study and apply meta-heuristics to address this type of problems for an optimal solution with the feasibility.**

Keywords— Quality of Service, Service Composition, Resource Allocation, NP-hard Problem, 0/1 Multidimensional Knapsack Problem.

I. INTRODUCTION

In Service-Oriented Computing (SOC), the Quality of Service (QoS) is important for most service-based complex applications. Service composition is the process of adding services using functional attributes of multiple services rapidly and effeectively[1, 2]. In resource allocation for composite web services, a critical problem that must be addressed is to achieve the QoS for composed applications. Overcoming this issue raises two problems. First is resources assignment to every abstract web services(tasks) in the composite web service. The resource allocation problem is critical because it occurred in various research domains out of one is a service-oriented architecture (SOA). An effective way to allocate resources in SOA affects the performance of the web-based system. The resource allocation problem is that a given composite service containing candidate services, each candidate service to be allocated to at least one of the services from a set of component services. Here component service holds a resource. Finding the allocation technique to these resources in order to finish all candidate services is challenging under some set of constraints while satisfying expected QoS. An allocation of very few resources on a cloud computing environment to complete tasks is known resource allocation problem[3].

The resource allocation problem exists in the IoT environment, allocation of tasks to reduce energy consumption devices in it. Due to the use of cloud computing as a platform in IoT applications. Here also the allocation of the resources from the cloud is a challenging issue to address[4]. Cloud computing [5] is an Internet-based computing model where resources and applications are delivered as web services over the Internet are provided on demand as public utilities. This pattern provides a way for the organization to create new composite web services or complex applications.

II. RELATED WORK

Many approaches to solving resource allocation problem have been proposed. Service-oriented computing has attracted huge attention over the past few decades. However, QoS parameters were less addressed as compared to other parameters like duration and storage of computational resources.

In [6] K. Gaia proposed Reinforcement Learning technique using Dynamic Programming to solve the resource allocation problem optimally for IoT content-centric services. They considered Energy, cost and response time parameters in the technique they used. But in this paper authors did not address the feasibility of optimal solution in a large scale environment.

Also, they did not analyses the time complexity of the proposed algorithms.

In [7] C. Tsai presented a solution to the IoT resource allocation problem. The search economics mechanism is used to solve this problem as it is a way to search for the solution of the complex optimization problem. This work considers communication cost whereas other QoS Parameters are missing. The time complexity of the proposed algorithm is $O(n^2.h.iter^{max})$ where n is the number of subsolutions of a complete solution and h the number of regions the solution space is divided.

V. Angelakis et al. [8] focus on IoT devices and network interfaces have heterogeneity in nature which need various services to allocate. Here a resource allocation problem target at getting the best solution. Spiting interface of device and allocation of services to the spat interfaces is called a Service to-interface assignment (SIA) problem. In this paper, they stated this problem is NP-complete problem.

In [9] M. Liu introduced Resource Allocation for non-orthogonal multiple access based Heterogeneous IoT. To solve this problem optimally a deep learning based algorithm is proposed. Energy efficiency was the parameter for the study. Time complexity analysis is not done of proposed algorithms and QoS parameters were missing while optimization of the method.

In [10] A. Singh proposed a resource allocation mechanism using buffering, scheduling and rate limiting. The authors confirms to SLA requirement meeting. The System parameters for study were the capacity and enforcement period where QoS consideration was missing. The work did not focus on the objective to present an optimized algorithm for the best solution to the resource allocation problem.

K. Lee et. al. [11] provided a generic representation of the allocation problem. It is based on the heuristic multi-attribute combinatorial exchange approach which is suitable for large scale environments and greedy optimization methods. The objective of this work is the conceptualization, implementation, and evaluation of proposed mechanism but not to an optimal solution to the allocation problem. The parameters considered for study are energy and cost whereas some important QoS are missing.

Q. Lu et. al. [12] presented quantifying and optimizing the fairness and efficiency of heterogeneous resources as a challenge of resource allocation problem in the cloud platform. A design of Fairness-Efficiency in allocation algorithm is presented. It is an iterative, dynamic-adaptive heuristic for solving the problem. The computation complexity of an algorithm is $O(n^2)$. Along with the solution to the problem the feasibility of solution is not analyzed.

J. Yao et. al. [13] we studied a robust multi-resource allocation problem with uncertainties in resource demands. The cost function is optimized which produces fairness and effiency in a robust manner in the cloud environment.

J. Li et. al. [14] proposed a multiclass resource allocation algorithm for services in IoT. Uplink resource allocation problem is explained. Comparison between different algorithms were presented with respect to delay distribution. Authors claim their algorithms give better performance than fixed allocation algorithms which satisfy the QoS requirements of users.

TABLE I. SUMMARY OF COMPARATIVE ANALYSIS OF THE RESOURCE ALLOCATION ALGORITHMS.

SN	Algorithm	Approach	Technique	Computational Complexity	Author
1	Dynamic Programming	Non-Heuristic	Reinforcement Learning	$O(n)$	K. Gaia et. al. (2018) [6]
2	Demand based	Non-Heuristic	Service-Interface Assignment	$O(n^2\ log(n))$	V. Angelakis et.al.(2016) [8]
3	Gradient method	Non-Heuristic	Dominant Shares	$O(n^2)$	J. Yao et.al. (2017)[13]
4	Multiclass Allocation	Non-Heuristic	Gateway Hierarchy	$O(n^2)$	J. Li et.al. (2016) [14]
5	Gradient method	Non-Heuristic	Deep Learning	$O(n^5)$	M. Liu et. al. (2018) [9]
6	Approximation	Non-Heuristic	Convex Segments	$O(n^2.log(n))$	P. Lai (2015) [15]
7	Greedy	Heuristic	Combinatorial Exchange	$O(2^n)$	K. Lee et. al. (2015) [11]
8	Gradient method	Heuristic	Dynamic Adaptive	$O(n^2)$	Q. Lu et.al. (2016) [12]
9	Dynamic local search	Meta-Heuristic	Search Economics	$O(n^2.h.I^{max})$	C. Tsai (2017) [7]
10	Generalized Ant Colony Optimizer	Meta-Heuristic	Hybrid (ant and global)	$O(m.n.log(n))$	A. Kumar (2018) [16]

A. Comparative analysis of existing approaches

Table I provides a summary of the comparative analysis of existing approaches for solving resource allocation problem. From the table, it has been found that the complexity of the algorithm proposed by K. Gai et. al.[6] is much better than the rest of the existing algorithms. The approaches provided with heuristic led to exponential time on the increasing number of resources. A gradient method with a non-heuristic approach is found computationally heavier than heuristic approaches. However, improvement in complexity was witnessed with metaheuristic approaches[16] with complexity as $O(m.n.log(n))$, where m is the size of initial populations and n is the number of iterations.

The synthesis of the literature revealed that dynamic programming strategy provide the solution in reasonable computational time so, this paper attempts a dynamic programming strategy for solving resource allocation problem. The major challenges can arrive in resources allocation problem are Optimality and Scalability. In case of increase in

scalability of solution space leads to optimality of solution searched in same solution space and vice versa.

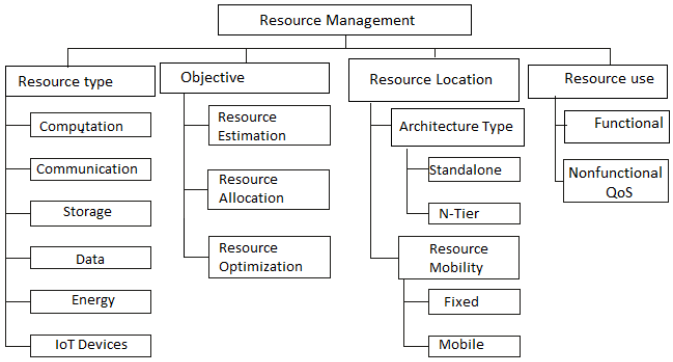

Fig. 1 Taxonomy of resource management

III. RESOURCE ALLOCATION PROBLEM

Fig. 1 illustrates the resource management taxonomy. It gives an overview of research in resource allocation area and presents four dimensions: resource type, an objective of resource management, resource location, and resource use. The first aspect is constructed by reviewing the current type of resources used. Our research focus is on the second aspect which is resource allocation. The resource location plays important role in describing the architecture and the last aspect is used in a survey as allocation criteria of the resource. This paper address resource allocation objective with non-functional QoS as resource use.

There may be many composite services for an activity. Each of the candidate services in a composite service needs to be allocated an instance of the component service. A single instance of a component service may be allocated to more than one candidate service task in the composite service task as long as it used at different time. This is stated as service allocated problem.

To find resource allocation plan which minimizes the aggregated response time of each composite service while satisfying cost constraint is called resource allocation cost constraint problem. The tasks mapping on distributed services is known NP-hard roblem[17,18], which divine computational complexity of resource allocation problem with cost constraint is NP-Hard.

Consider, CS={CS_1, CS_2, CS_3, ... CS_n}, set of composite services, n is total number of services. AS_i ={ $AS_{i,1}$, $AS_{i,2}$, $AS_{i,3}$,..... $AS_{i,m}$ }, set of abstract services, each ith composite service consist of m number of abstract services.

C_i = { $C_{i,1}$, $C_{i,2}$, $C_{i,3}$,..... $C_{i,p}$}, set of p number of candidate service for each abstract service in cloud. $RT_{i,m}$ and $Cost_{i,m}$ response time and cost of candidate service $C_{i,m}$ in the cloud. Now allocation with cost constraint plan P={P_i|i=1,2,3....n}, such that aggregated response time $RT(P)$ is Minimal which is calculated using the following equation.

$$RT(P) = \sum_{i=0}^{m} (RT_i)$$

In above equation total number of candidate services and the constraint which is Cost(P) should not exceed.

A. 0/1 Multidimensional Knapsack Problem

The 0/1multidiamesional knapsack problem consists of an allotment of a specifed capacity items in a knapsack, in which each item has an associated profit and weight[19]. Applications like finance and telecommunication networks can be easily model using this problem[20]. A goal of this problem is to find a subset of items which will lead to the maximum total profit with fulfilling constraints imposed on it. Consider a set of candidate services (s = 1, 2, 3..., n) where n is number of candidate services in composite service and a set of resources (r = 1, 2, 3, ...,m) where m is a number of resources. Each candidate service has a cost associated with it from which maximum capacity is aggregated and resource has cost as well as its associated value of response time of service. Now the problem is an allocation of resources with a minimum response time of component service which holds resource for the given maximum aggregated capacity of candidate service. This can be mapped to 0/1 multidimensional knapsack problem[21].

IV. PROPOSED ALGORITHM

This paper presents an algorithm for resource allocation using a dynamic programming strategy as an *Alogorithm 1*. In this algorithm parameter *CompositeService(CS_n)* is set of candidate services which needs resource/s to execute. *AbstractServices(AS_m)* is set of abstarct services where each service is task in activity of m tasks. *ComponentServices (C_p)* is set of services which holds computational resources and gets allocated to candidate service. *Response Time of C_p (RT) is* response time of component service in other word it is response time of computational resource which is time (in microseconds) required to receive response from component/resource service against request from user/candidate service, *Cost of C_p (Cost)* is monitory cost of component service in terms of price which need to pay to service providers. *Services Allocation Plan (P)* is set of best plans of combination of component services with minimum response time satisfied by cost constraints in user requiremets.

The main idea of the algorithm is to allocate component service to serve the services with the highest resource cost and minimum response time. The algorithm confirms the aggregated response time will be minimized. The algorithm then steps forwards to allocate the services with lower resource shares and so on. The first two lines of the algorithm calculate the aggregated response time and total cost of the composite service. This is done by simple summing of the response time of all services in candidate service and summing of cost as well. Next step calculate aggregated response time of component service using V_n. Plan p with the best response time and cost will get the return.

Algorithm 1	*RESOURCE ALLOCATION ALGORITHM*
INPUT	*Composite Services(CS_n), Abstract Services (AS_m), Component Services (C_p), Response Time of C_p RT), and Cost of C_p (Cost)*
OUTPUT	*Services Allocation Plan (P) while all constratints satisfied*
STEPS	*Calculate aggregated response time of each composite service* *Calculate total cost of each composite service* *if total cost is Maximum then* *$V_n(RT) = Min\ \{V_{n-1}(RT),\ V_n(RT)\}$* *Allocate n^{th} component service with RT to respective Candidate Service in Composite Service.* *Return Plan P*

V. RESULTS AND DISCUSSIONS

The simulations were carried out with machine configuration is Intel Core i3 processor, 4GB RAM, 1TB HDD, Windows 7 64bits OS, and Java Platform(JDK1.7) for implementation. We focus on analyzing dynamic programming as well as a simple iterative method for the implementation of allocation of resources. In our implementation, 3000 component services were use for allocation to candidate services with cost and response time as QoS parameters. The results demonstrate the simulation of dynamic programming for 0/1 multidimensional knapsack version of resource allocation problem. We note down computation time in milliseconds for the number of services by keeping number candidate services constant to 10 in composite service. Fig. 2 shows the performance of dynamic and iterative solutions. From figure 2 it is observed that the brute force algorithm fails to allocate more than 2400 component services. The dynamic programming found to be better than brute force but still get stuck after 3000 services.

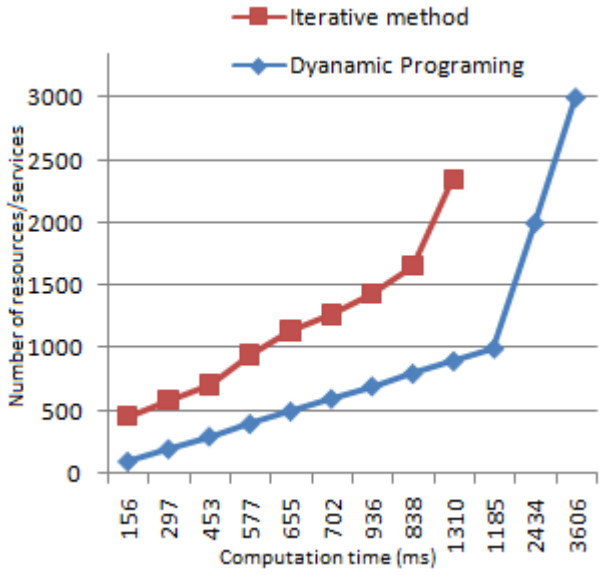

***Fig.**2 Computational time with a number of resources for allocation*

Though dynamic programming is better than brute force but computationally expensive with complexity as $O(n^2)$. From the computational experiments, it can be concluded that dynamic programming strategy fails for a large number of services so attempts for providing the solution with heuristics and metaheuristics technique.

VI. CONCLUSION

This paper presents the resource allocation problem in service composition modeled as 0/1 multidimensional knapsack problem. The stated problem is implemented with brute force and dynamic programing strategy. The computational results revealed that as number of services goes on increasing both the technique failed to allocate the resources. Hence it is concluded that heuristics and metaheuristics based technique should be developed for finding the solutions in reasonable computational time. The analysis results of our simulation show that implementation is good small scale composition. However, all constraints and dependencies are not taken into consideration in current work. The solution accuracy, optimality, and feasibility are not checked in our simulation work.

In future scope we will include the use of meta-heuristics for solving resource allocation problem in service composition with the constraints and dependencies for large scale services along with solution accuracy and feasibility.

REFERENCES

1] L. Zeng and B. Benatallah, "QoS Aware Middle-ware for Web Services Composition," IEEE Transaction on Software Engineering Vol 30 no 5, pp 311-327, (2004).
2] S. Chattopadhay and A. Banerjee, "A Fast and Scalable Mechanism for Web Service Composition," ACM Transaction on the Web, Vol.11 no. 4, Article 26, (2017).
3] B. An, V. Lesser, D. Irwin, and M. Zink, "Automated Negotiation with Decommitment for Dynamic Resource Allocation in Cloud Computing," Proceedings of the International Conference on Autonomous Agents and Multiagent Systems, pp. 981-988, (2010).
4] G. Colistra, V. Pilloni, and L. Atzori, "The problem of task allocation in the Internet of Things and the consensus-based approach," Journal of Computer Networks, vol.73, pp. 98-111, (2014).
5] M. Armbrust, A. Fox, and R. Griffith, "A View of Cloud Computing," Communication of ACM, Vol. 53, No. 4, pp. 50-58, (2010).
6] K. Gaia and M. Qiub, "Optimal resource allocation using reinforcement learning for IoT content-centric services," Elsevier Applied Soft Computing, Vol. 70, pp. 12-21, (2018).
7] C. Tsai, "SEIRA: An Effective Algorithm for IoT Resource Allocation Problem," Elsevier Computer Communication, Vol. 119, pp. 156-166, (2017).
8] V. Angelakis, I. Avgouleas, N. Pappas, E. Fitzgerald, and D. Yuan, "Allocation of Heterogeneous Resources of an

IoT Device to Flexible Services," IEEE Internet of Things Journal, Vol. 3, No. 5, pp. 691-700, (2016).

9] M. Liu and T. Song, L. Zhang and G. Gui, "Resource Allocation for NOMA based Heterogeneous IoT with Imperfect SIC: A Deep Learning Method," IEEE 29th Annual International Symposium on Personal, Indoor, and Mobile Radio Communications, pp.1440-1447, (2018).

10] A. Singh and Y. Viniotis, "Resource Allocation for IoT Applications in Cloud Environments," Workshop on Computing, Networking and Communications, (2017).

11] K. Lee, G. Buss and D. Veit, "A heuristic approach for the allocation of resources in large scale computing infrastructures," Wiley Online Library Concurrency and Computation: Practice and Experience, Vol. 28, pp. 1527-1547, (2015).

12] Q. Lu, J. Yao, Z. Qi, B. He and H. Guan, "Fairness-E_ciency Allocation of CPU-GPU Heterogeneous Resources," IEEE Transactions on Services Computing, pp. 1-14, (2016).

13] J. Yao, Q. Lu, H. Jacobsen, and H. Guan, "Robust Multi-Resource Allocation with Demand Uncertainties in Cloud Scheduler," IEEE 36th Symposium on Reliable Distributed Systems, pp. 34-44, (2017).

14] J. Liu, Q. Sun and G. Fan, "Resource Allocation for Multiclass Service in IoT Uplink Communications," IEEE 3rd International Conference on Systems and Informatics, pp. 777-781, (2016).

15] P. Lai and R. Fan, "Fast Optimal Nonconclave Resource Allocation," IEEE Conference on Computer Communications, pp. 1508-1516, (2015).

16] A. Kumar and S. Bawa, "Generalized Ant Colony Optimizer: swarm-based meta-heuristic algorithm for cloud services execution," Springer Computing, pp. 1-24, (2018).

17] M. Garey and D. Johnson, "Computers and Intractability: A Guide to the Theory of NP-Completeness," Society for Industrial and Applied Mathematics, Vol. 24, No. 1, pp. 90-91, (1982).

18] J. Yu and R. Buyya, "Scheduling scienti_c workow applications with deadline and budget constraints using genetic algorithms," Scienti_c programming, Vol. 14, No. 3, pp. 217-230, (2006).

19] S. Martello and P. Toth, "Algorithm 632: a program for the 0-1 multiple knapsack problem," ACM Transaction on Math Software, Vol. 11 No. 2, pp.135-140, (1985).

20] S. Laabadi, M. Naimi, H. Amri, and B. Achchab, "The 0/1 Multidimensional Knapsack Problem and Its Variants: A Survey of Practical Models and Heuristic Approaches," American Journal of Operations Research, vol. 8, pp. 395-439, (2018).

21] F. Aisopos, K. Tserpes, and T. Varvarigou, "Resource management in software as a service using the knapsack problem model," Int. J. Production Economics, Vol. 141, pp. 465-477, (2013).

Proceedings of the Fourth International Conference on Communication and Electronics Systems (ICCES 2019)
IEEE Conference Record # 45898; IEEE Xplore ISBN: 978-1-7281-1261-9

Faults in CMOS IC's and Their Mitigation Techniques: Review

Sameeksha Munjal
Department of Electronics and Communication
Guru Nanak Dev Engineering College
Ludhiana, India
sameekshamunjal12@gmail.com

Prof. Gurpurneet Kaur
Department of Electronics and Communication
Guru Nanak Dev Engineering College
Ludhiana, India
gurpurneetkaur@gmail.com

Dr. Sandeep Singh Gill
NITTTR,
Chandigarh, India

***Abstract*:** In modern CMOS logic, due to scaling variety of fault occurs which causes reliability issue in circuits. Also in radiation environment, single event upset logic degrades the performance of CMOS IC's. Faults and single event effects becoming a major concern in scaled CMOS devices employed in circuits that have to be used at higher altitudes in space. In this paper, brief history of about the emergence and creation of errors in IC's , types of faults occurring in CMOS logic circuits and their fault tolerance and SEE's mitigation techniques have been discussed.

Keywords: CMOS, SEE, LET, Faults, Radiation effects, Mitigation.

I. INTRODUCTION

CMOS becomes the prevalent technology in past 30 years. CMOS circuits have been utilised at large scale for the construction of IC's which exercised in microprocessor, microcontroller and several other logic circuits. CMOS IC's also used for space application. Moore's Law plays a vital role in the advancement of CMOS circuits which summarised as the transistor density on chip twofold after every 18 months [1]. Speed and complexity of the microelectronic circuit had been boosted to 200-MHz and gate-per-circuit reached beyond million transistors in single chip due to technology scaling. Scaling of CMOS circuits worsen the electronic devices and leads to the establishment of faults in CMOS circuits [2].

Fault is an unsatisfactory behaviour of circuit which needs to be screen out. In CMOS circuits, faults were acknowledged and addressed infrequently in 80's [3]. CMOS being a prevailing technology is certainly focused on shrinking of devices which adds to its design complexity and making it more sensitive to small defects. Leakage current and short channel effects arise due to technology scaling and numerous faults appear in CMOS IC's. In space, radiation effects are principal concern and scaling of CMOS devices further escalate radiation effects in deep submicron dimensions device. Therefore, reliability of CMOS circuit can be enhanced by detecting and correcting the shortcomings and fault masking [4].

Therefore, fault tolerance plays a vital role in analog and digital circuits and it decides the performance of the device. Hence, it is important to work on the fault tolerance capability of the device as it is directly proportional to the reliable performance and it provides assuring successful operation. Fault tolerance system should be well efficient to handle all possible faults occurring in hardware or software components, due to power breakdown or any other possible disaster and still meet expected performance metrics. Owing to increased operating frequencies, the CMOS integrated circuits are more prone to be affected by faults like permanent and transient faults, SEE's and structural faults like interlayer and intra-layer[5].

Vital constituents of fault tolerance are error processing and fault treatment. Error processing features error removal, if there is probability of occurrence of malfunction whereas fault treatment includes elimination of faults before it set in motion. Fault tolerance can be accomplished by combining two fault masking and reconfiguration [6]. Fault tolerant techniques are categorized in static, dynamic and hybrid groups. The static tolerant techniques uses fault masking mechanism which is designed to achieve fault tolerance without requiring any action on the part of the system. The dynamic fault tolerance technique detects, locates and recovers the fault in an attempt to achieve fault tolerance. And hybrid fault tolerance techniques combine both static (passive) and dynamic (active) approaches [7-8].

The paper has been organised as follows: Firstly historical aspects are discussed in part II; In part III different CMOS faults have been discussed including structural faults, SEE's faults and several other faults. Part IV describes SET mitigation techniques and Fault tolerance techniques.

II. Historical Overview

Continuous downsizing of MOSFET technology and upsurge of chip size and area leads to complicated design of integrated circuits and speed and performance had been improved greatly. Operational frequency of MOSFET circuits has been escalated due to which probability of occurrence of faults had been increased. With the advancement and development in IC's design and

structure, faults and SEE's had been observed in MOSFET in late 80's [3].

In 1983, Diehl et al. explained about the digital single event transients and faults occurring in CMOS IC's [9].Faults at transistor level can jeopardize the functionality of CMOS devices and result in erroneous output [10]. Since various circuits were constructed using MOSFET technology, so it was important for analog and digital applications to tolerate various kinds of faults. Faults in CMOS circuits may arise at manufacturing stage. Because of faults occurrence, there has been a probability that transient may latched in a flip flop. Thus, faults and SEE's becoming principal concern in VLSI logic circuits [11].

A report submitted by Intel in 1984describes the dynamic fault imaging technique. This technique describes the voltage transients arising in IC's when it is operating dynamically. This was developed in order to mitigate faults arising due to manufacturing and designing of complex logic circuits[12].

Few years later, Kolasinski performed the experiment under heavy ion radiation and conveyed detailed contribution of SET (single event transients). They emphasis on two extents, LET of SEU particles and cross-section of upsets. It was observed that LET of SEU particles was between 6 and 15 MeV-cm^2/mg and it also witness that dynamic memories has more cross-section than static memories. SETs were observed in memory circuits and microprocessor [13].

New-berry *et al.* examined the transients at the output of devise such as logic drivers and receivers. They scrutinized that minimum LET required for SETs occurrence was 15 MeV-cm^2/mg and pulse width of SETs increases beyond 40ns as LET increase [14].

In 1990,s various papers have been published describing the issue of static and dynamic faults and also it explained that error increases with increase in operational frequencies. The analysis was performed for high speed devices based on Si ECL technologies and this was done at very high frequency i.e. 100Mbps. It concluded that these devices are sensitive for heavy ion interaction and proton irradiation for space applications [15-16]. At low frequencies error were observed in sequential logic circuits whereas at high frequency most of the defect noticed in combinational logic as error rate increases in direct proportion with frequency.

Later in 2000's study was done which describes SET's in digital circuits due to scale down to 150nm technology node. There were significant transients in deep submicron technology due to ion strike in tresstrial environment and the value of LET at which faults were observed in digital circuits was anticipated to be as low as 2 MeV-cm^2/mg [17].

Later it in 2010, it is also showed that reducing the source voltage of digital devices makes it more vulnerable to stuck at faults and SETs and the smaller node capacitances in CMOS circuits unable to protect the nodes from voltage variations. The circuit was designed which can tolerate SETs up to 15GHz of frequency. The amplitude and phase shift due to current and transient pulses injection presented mathematically as:

$$\Delta V = \frac{\Delta q}{C_{tot}} \ldots\ldots (1)$$

$$\emptyset_e = \frac{\Delta q}{q_{max}} \ldots\ldots (2)$$

[18].

Mukherjee *et.al.* Introduced a new defect tolerant technique using transistor redundancy where each transistor is replaced by three transistors. He showed that triple transistor redundancy technique is efficient in terms of area overhead at reasonably good reliability. Triple transistor logic is faster than Quadded transistor technique [19].

Later various error detecting and correcting techniques were proved to be resourceful for CMOS based memory circuit's whereas hardening techniques for combinational logic circuits.

III. Faults in CMOS Circuits

The objective of designing any electronic device using CMOS is to minimize chip area, low power consumption and high Fan-out while maintaining low noise power [20]. Fabrication of CMOS IC's involves various processing steps which may introduce a problem that in turn may introduce a fault. Faults in CMOS devices may occur at transistor level; gate level or system level. But at circuit level, fault can be categorised as follows:

A. Open and Short Faults

Open faults exists a missing link between two interconnects then generally these type of fault occur. They can occur due to missing drains or sources within same transistor or different transistor. On other hand, short faults occur when two or more interconnect lines get shorted. It includes shorting between power supply rails/ lines [21]. These are included in electrical fault models.

B. Stuck at Faults

In such faults, the output of CMOS is trapped at particular logic level; either zero or one. Stuck-at Faults is included at both chip as well as PCB level [19]. Fig 1 represents the stack at faults model, where value of a gate is stuck at 1.

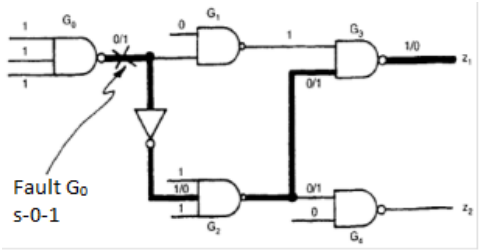

Fig 1 SFs detection [19]

C. Transition Fault

In case of transition fault, CMOS circuit failed to make transition from either 0 to 1 or vice-versa. When a CMOS circuit fails to make transition from 0 to 1 then is known as upward transition fault whereas when it fails to make transition from 1 to 0 then it is called as down transition fault [22]. Figure 2 represents the transition fault.

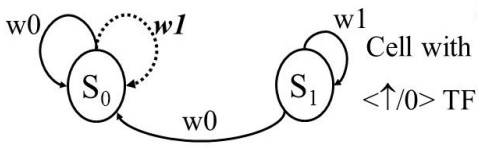

Fig 2 Up- transition faults[22]

D. Bridging Fault

These faults are mainly related to reliability issues of circuit. Bridging faults are the connections formed between two or more wires and performing logical AND/OR between shorting wires. Bridge fault models are shown as follows in fig 3: [23].

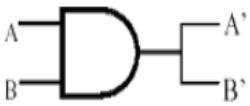

(a) Wired –AND Model

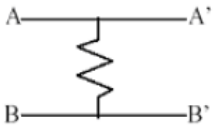

(b) Low Resistance Model

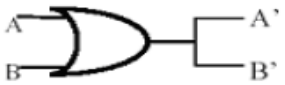

(c) Wired-OR Model

Fig 3: Bridging Faults[23]

E. Single Event Effects

In space, various radiation sources exist that incorporates sun rays, solar winds and cosmic rays. Different particles such as neutrons, protons, electrons and heavy ions are acquainted in radiation environment. These particles when strikes the IC's may introduce error in circuits and these errors are termed as Single Event Effects (SEE). There are different types of single event effects occur in CMOS IC's [24].

In single event upset, when particle hits the IC's it may change the logic level of storage node. Single event transient effect leads to change of voltage in CMOS circuits. Single event transient becomes SEU when it changes the state of storage node. In CMOS, two parasitic BJT are formed which leads to the formation of thyristor like structure and when this thyristor like structure get turned ON due to particle strike then there is direct flow of current from power supply to ground. This triggering of thyristor like structure is termed as Single event Latch up. In Single event gate rupture (SEGR) effect, the gate of CMOS circuit is impaired due to particle strike at gate oxide insulation. Single event burnout happens in power CMOS circuits when drain current increases beyond limit [3],[25]. The energetic particle strike when hits the CMOS circuit, results in formation of charge cloud and it is shown in fig 4.

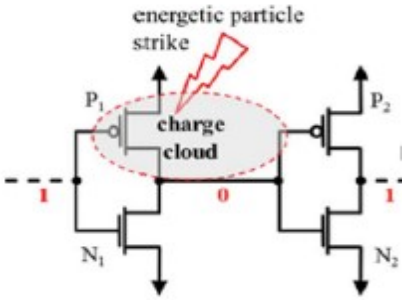

Fig 4 Particle strike CMOS inverter [3]

Therefore in CMOS circuits faults can occur at gate level, transistor level or at switch level. To mitigate the fault occurring in circuits a range of fault detection and correction mechanism are available that has been discussed further.

S.No	Faults	Effects
1.	Open and Short Faults	Produce the floating states at the output of the CMOS logic either at Pull-up network or at pull-down network
2.	Stuck at faults	Single logical connection is permanently stuck at a particular value and does not represents the correct at node
3.	Transition Faults	Spot defects and increases the delay of circuit
4.	Bridging Faults	Two nodes permanently get connect
5.	Single Event Effects	Changes the voltage of circuit because of striking of particle

IV. Fault Tolerance Mechanism and SEE Mitigation

Various fault tolerance and SEE mitigation techniques have been developed in order to prevent

failures in CMOS circuits and these could be implemented in programmable logic [26]. Changing the device structure physically helps to avoids faults and they are termed as fabrication process based techniques. These techniques involve epitaxial CMOS process and silicon-on-insulator process in order to eliminate radiation faults at satisfactory level. The fabrication process- based techniques are quite expensive and therefore, they are not preferred for low level production.

Design based techniques are widely used because they can be applicable to various design level in circuit and also termed as architectural techniques. These techniques include detection, mitigation and recovery techniques. Time redundancy and hardware redundancy techniques generally used for the detection of SEU's in combinational and sequential logic circuits [27]. Fig 5 represents the time redundancy technique.

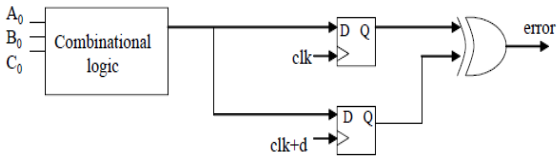

Fig. 5 Time Redundancy duplication scheme to detect SET [27]

Hardware fault tolerance techniques use the concept of duplicity with comparison which could be used for CMOS IC's. The hardware tolerant techniques involve Triple modular Redundancy (TMR), N-Modular Redundancy (NMR), Triple Interwoven Redundancy (TIR), TT (Triple Transistor) Technique and QT (Quad Transistor) Technique [4].

In TMR technique, voter circuit is used which selects one circuit from three different circuit performing same operation but disadvantage associated with this technique is that it assumes voter circuit is fault free [8]. TIR is analogous to TMR technique in which replicated components are arranged randomly. Reliability of TIR technique is main issue [28].

The TT and Quad Technique rectify errors by toggling them from critical to subcritical states.TT technique was categorised as static redundancy technique. In this technique redundancy was added at transistor level and it is highly reliable and occupies less area as compare to other static redundancy techniques. TT is proficient in handling single faults in transistor [18]. QT uses four transistors to function for single transistor due to which error in single transistor can be tolerated. Double faults can also be tolerated using QT technique as long as they are not in parallel. Generally, TT technique is faster than the QT Technique and in addition to TT technique is appropriate because of its efficiency in terms of area and time [29-30]. TT configuration is shown in fig. 6

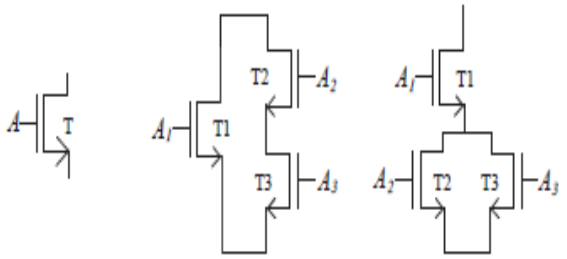

(a) Original Transistor (b) TT version1 of fig. a (c) TT version2 of fig. a

Fig. 6 TT configuration of single transistor [4]

Also, in case of hardware redundancy technique design can be modified logically. In this, we add the redundant bits using error detection and correction techniques which can identify faults and correct upsets.

Reconfiguration, partial reconfiguration and rerouting of bits or information using the programmable matrix in the circuit for detecting and correcting faults. Also detection with codes can be used for sequential or combinational circuits.

Hamming codes can be used for correcting the faults in circuits. It requires changes at circuit level by adding block like decoder blocks, storage cell and encoder. DICE cells can appropriately detect and correct the fault at transistor level [27].

SETs became main issue in CMOS devices in space application when size was reduced below 10μm and critical charge for originating a transient pulse was dropped below 1pC and LET is corresponding to 50 MeV-cm^2/mg. In order to mitigate SETs various techniques have been developed and they are categorised as: Temporal sampling and spatial sampling. Temporal sampling is widely used in deep submicron circuits that have to be employed at high altitudes in space. Generic temporal sampling is widely used form of sampling technique. It is shown in fig. 7:

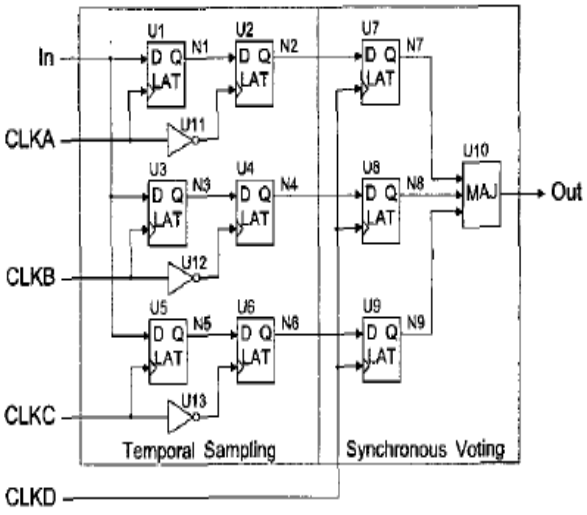

Fig. 7 Generic Temporal Sampling Latch [31]

In this, input data is sampled at different frequencies such that sampling frequency is higher that the single event upset pulse and voting circuitry picks the majority of sampled data [31]. In temporal sampling there exist the trade-off between size and speed.
Table 1 represents the mitigation technique and which fault is diminished by it.

Table 1: Mitigation Technique Summary

Sino.	Mitigation Technique	Fault Diminished
1.	Triple Modular Redundancy technique	Stuck- at fault
2.	Triple Interwoven redundancy technique	Stuck at fault
3.	Triple Transistor redundancy	Stuck at, transition and SET's Fault
4.	Quad Logic Redundancy Technique	Stuck at, Transition faults.

V. Conclusion

This paper discuss about the faults and how they are significant in high speed and complex digital CMOS IC's. Faults being the unsatisfactory behaviour of circuits need to be prevented. Various types of faults have been discussed and their effects on devices have been explained. These faults results in erroneous output and may damage the circuit permanently. Scaling of CMOS technology has increased the number of faults in circuit and also intensified the effects of SEE's. Increase in operational frequency and scale down of capacitance has enhanced the probability of fault and SEE occurrence in CMOS circuits. To mitigate these faults and SEE's various fault tolerance techniques have been discussed at gate level, transistor level and at circuit level. If in future, any kind of fault occur then we can rectify it by using current techniques or by doing advancement.

REFERENCES

[1] S. Shukla, S. S. Gill, H. S. Jatana, V. Nehru, and N. Kaur, "Modelling and mitigation of single-event upset in CMOS voltage-controlled oscillator," Sadhana - Acad. Proc. Eng. Sci., vol. 43, no. 11, pp. 1–10, 2018.

[2] M. H. Bhuyan, "History and Evolution of CMOS Technology and its Application in Semiconductor Industry," SEU J. Sci. Eng., vol. 11, no. 1, pp. 30–42, 2017.

[3] V. Ferlet-Cavrois, L. W. Massengill, and P. Gouker, "Single Event Transients in Digital CMOS-A Review," IEEE Trans. Nucl. Sci., vol. 60, no. 3, pp. 1767–1790, 2013.

[4] S. Salem, H. Zandevakili, A. Mahani, and M. Saneei, "Fault-tolerant delay cell for ring oscillator application in 65 nm CMOS technology," IET Circuits, Devices Syst., vol. 12, no. 3, pp. 233–241, 2018.

[5] C. Bolchini, G. Buonanno, D. Sciuto, and R. Stefanelli, "Innovative Design of CMOS Fault Tolerant Structures," Proc. IEEE Int. Conf. Wafer Scale Integr, San Francisco,USA, pp. 267–276, 1995.

[6] R. D. Adams and P. Drive, High Performance Memory Testing: Design Principles, Fault Modeling and Self-Test. 2005.

[7] J. Zhao, B. Jiang, and P. Shi, "Fault-tolerant Control Design Based on Adaptive Dynamic Sliding Mode Technique for Near Space Vehicles," no. 1, pp. 1618–1623, 2012.

[8] L. Xing, P. Boddu, Y. Sun, and W. Wang, "Reliability analysis of static and dynamic fault-tolerant systems subject to probabilistic common-cause failures," Proc. Inst. Mech. Eng. Part O J. Risk Reliab., vol. 224, no. 1, pp. 43–53, 2010.

[9] B. D. S. E. Diehlt and J. E. Vinson, Shafer and T. M. Mnich, "Considerations for single event immune vlsi logic," IEEE Trans. Nucl. Sci., vol. 30, no. 6, pp. 4501–4507, 1983.

[10] A. Persya and T. Nair, "Fault Tolerant Real Time Systems," Int. Conf. Next Gener. Softw. Appl., pp. 177–180, 2008.

[11] I. Koren and A. D. Singh, "Fault tolerance in VLSI circuits," Computer (Long. Beach. Calif)., vol. 23, no. 7, pp. 73–83, 1990.

[12] T C. May, G. L Scott, E. S Mbieran, P. Winer and V.R. Rao, "Dynamic Fault Imaging of VLSI Random Logic Devices," Proc. Int. Reliab. Phys. Symp., pp. 95–108, 1984.

[13] R. Koga and W. A. Kolasinski, "Effects of heavy ions on microcircuits in space: Recently investigated upset mechanisms," IEEE Trans. Nucl. Sci., vol. 34, no. 1, pp. 46–51, 1987.

[14] D. M. Newberry, D. H. Kaye, and G. A. Soli, "Single Event Induced Transients In I/O Devices: A Characterization," IEEE Trans. Nucl. Sci., vol. 37, no. 6, pp. 1974–1980, 1990.

[15] R. A. Reed et al., "Single Event Upset cross sections at various data rates," IEEE Trans. Nucl. Sci., vol. 43, no. 6, pp. 2862–2867, 1996.

[16] M. P. Baze and S. P. Buchner, "Attenuation of single event induced pulses in CMOS combinational logic," IEEE Trans. Nucl. Sci., vol. 44, no. 6, pp. 2217–2223, 1997.

[17] P. E. Dodd, M. R. Shaneyfelt, J. A. Felix, and J. R. Schwank, "Production and propagation of single-event transients in high-speed digital logic ICs," IEEE Trans. Nucl. Sci., vol. 51, no. 6 II, pp. 3278–3284, 2004.

[18] S. Jagtap, R. Sivaramakrishna, and S. Gupta, "Design of Radiation Hardened Wide Tuning Range CMOS Oscillators," IEEE, 2014.

[19] A. Mukherjee and A. S. Dhar, "New triple-transistor based defect-tolerant systems for reliable digital

architectures," Proc. - IEEE Int. Symp. Circuits Syst., vol. 2015–July, pp. 1917–1920, 2015.

[20] Sung Kang, "A design of CMOS polycell for LSI circuits," IEEE Trans. Circuits Syst., vol. 28, no. 8, pp. 838–843, 2004.

[21] Lang Su, Fault Simulation For Stuck Open Faults In CMOS Combinational Circuits. 1993.

[22] Abhilash kaushal, "Memory fault models and testing | EDN," 2015. [Online]. Available: https://www.edn.com/design/integrated-circuit-design/4439803/Memory-fault-models-and-testing.

[23] D. P. A. S. A. AL-Arian, "Physical Failures and Fault Models of CMOS Circuits," IEEE Trans. Circuits Syst., vol. 34, no. 3, pp. 269–279, 1987.

[24] H. Kim, I. Choi, J. Lim, H. Oh, and S. Kang, "Process variation-Aware bridge fault analysis," ISOCC 2016 - Int. SoC Des. Conf. Smart SoC Intell. Things, pp. 147–148, 2016.

[25] R. Trivedi and U. S. Mehta, "a Survey of Radiation Hardening By Design (Rhbd) Techniques for Electronic Systems for Space," Int. J. Electron. Commun. Eng. Technol., vol. 7, no. 1, pp. 75–86, 2016.

[26] T. S. Nidhin, A. Bhattacharyya, R. P. Behera, T. Jayanthi, and K. Velusamy, "Understanding radiation effects in SRAM-based field programmable gate arrays for implementing instrumentation and control systems of nuclear power plants," Nucl. Eng. Technol., vol. 49, no. 8, pp. 1589–1599, 2017.

[27] F. Kastensmidt, L. Carro, and R. Reis, Fault-tolerance techniques for SRAM-based FPGAs, vol. 32, pp.1-9, 2006.

[28] F. Kastensmidt, L. Carro, and R. Reis, Fault-tolerance techniques for SRAM-based FPGAs, vol. 32,pp. 29-70, 2006.

[29] J. Han, E. Leung, L. Liu, and F. Lombardi, "A Fault-Tolerant Technique Using Quadded Logic and Quadded Transistors," IEEE Trans. Very Large Scale Integr. Syst., vol. 23, no. 8, pp. 1562–1566, 2015.

[30] H. El-Razouk and Z. Abid, "A new transistor-redundant voter for defect-tolerant digital circuits," Can. Conf. Electr. Comput. Eng., no. May, pp. 1078–1081, 2006.

[31] D. G. Mavis and P. H. Eaton, "Soft Error Rate Mitigation Techniques for Modern," Physics (College. Park. Md)., no. I, pp. 216–225, 2002.

Proceedings of the Fourth International Conference on Communication and Electronics Systems (ICCES 2019)
IEEE Conference Record # 45898; IEEE Xplore ISBN: 978-1-7281-1261-9

Full Fledged Automated Fruit Farm

Ganaraj Borkar
Department of Electronics & Telecommunication Engineering
Don Bosco College of Engineering
Fatorda, Goa, India
ganaraj97@gmail.com

Gourav Kanekar
Department of Electronics & Telecommunication Engineering
Don Bosco College of Engineering
Fatorda, Goa, India
gouravkanekar@gmail.com

Parth Ghaware
Department of Electronics & Telecommunication Engineering
Don Bosco College of Engineering
Fatorda, Goa, India
peghaware@gmail.com

Pramesh Budkuley
Department of Electronics & Telecommunication Engineering
Don Bosco College of Engineering
Fatorda, Goa, India
prameshbudkuley@gmail.com

Prannoy Caeiro
Department of Electronics & Telecommunication Engineering
Don Bosco College of Engineering
Fatorda, Goa, India
caeiro.prannoy@gmail.com

Flavia Leitao - Assistant Professor
Department of Electronics & Telecommunication Engineering
Don Bosco College of Engineering
Fatorda, Goa, India
flavia.leitao@dbcegoa.ac.in

Vidhya D.S. – Assistant Professor
Department of Electronics & Telecommunication Engineering
Don Bosco College of Engineering
Fatorda, Goa, India
ds.vidhya@dbcegoa.ac.in

***Abstract*—In our country one of the main challenges facing the farming industry is the paucity of labour. The Farming industry is one of the major employment generators in our country, however the industry employs only seasonal labour resulting in many farm workers moving to cities for other stable occupations such as construction and hospitality. Thus in a country with human resource surplus, finding seasonal labour has become a challenge, and the available labour has become very expensive, resulting in many fields lying barren. Automation of the farming process is a reasonable solution to overcome this problem. An automated farm should be able to pseudo replace tasks which are worker intensive. These include sowing, weeding or disease detection, harvesting and lastly automated inventory. In this project a model is presented for fruit farms. A small farmer bot prototype is also developed. The prototype demonstrates the harvesting step, wherein it detects ripe fruits for plucking.**

Keywords—automated, harvester, apple, YOLO, bot

I. INTRODUCTION

The current farming sector is reliant on the manual based process of plucking and sorting of fruits for making them available for the customers. This is not consistent and is time consuming, thus affecting its efficiency. Nowadays the use of bots in our daily lifestyles such as robotic vacuum which cleans the house and abolishes the age old system of manual sweeping, and the use of chat bots in place of customer care leads to a great profit in the IT sector. A basic farming process includes planting, watering, weeding, harvesting and delivery which are manually done whereas an automated farming process is done with minimum human assistance. Automated farming can be done by using robots for performing the techniques in farming process such as planting the crops with robots, watering using smart drip irrigation system, spraying pesticides and weedicides by identifying the weeds and pests with the help of robots and so on. Taking the positives from this, the project aim at making a bot which will perform the tasks of harvesting and managing the inventory that a labour does on the farm with minimal cost. The proposed system is such that it is capable of automating the process of plucking with no man power and hence making it affordable in comparison to manual system and also maintaining an inventory of the count of the fruits in order to make it available to the customers. Introduction section gives an overview of the objective and the need for Smart Farming. Literature review section gives a brief explanation about the previously conducted research based on different automated techniques used for harvesting apple fruit. Methodology section includes a detailed description of the hardware incorporated in our system. Implementation and result section shows the explanation and analysis of the system. Conclusion section includes capabilities of the project and future work.

II. LITERATURE SURVEY

Different apple harvesting systems were studied to come up with a suitable system design. There are two ways in automated apple harvesting, one being bulk and the other being apple by apple. A mechanical apple harvester [1] is a mass harvester system that is designed for a narrow inclined trellis which requires uniform ripeness. There are two operators on the system which move the harvester towards each apple tree. They adjust the harvester to a tree and cover it with impactors. A shaker attachment then vibrates the tree causing the apples to detach from the tree and the apples fall on the impactors.

Another system engages in robotic bulk harvesting of apples [2]. Its main aim was to check the size and type of catching surface needed, and to use a surface to catch the fruit with no damage. It is a three wheeled harvester. A digital camera captures the images of the apples and the images were processed using a software. The Rapid Displacement Actuator (RDA), a hydraulic cylinder is guided to that position of apple by converting the image pixel coordinates into coordinates in space. Then the actuator is activated for fruit detachment and the apples are collected in the catching surface.

Autonomous Fruit Picking Machine (AFPM) [3] is a robotic apple harvester which uses apple by apple picking system. This system requires a proper fruit gripper. The AFPM is built on an agriculture tractor. The camera inside the fruit gripper will scan for ripe apple and will be then processed under uniform light conditions with the help of high frequency light source. The camera rotates in x and y axis and after the apple is aligned with the image centre and the object centre by using 6 DOF industrial robot then the silicon fruit gripper is in front of the apple. It then uses vacuum suction to detach the apple without damaging it.

A low cost fruit gripper [4] has been used for detachment of apple fruit. It is made of silicon with a camera fitted inside which is looks like a funnel. Its main aim was to detach the apple and enclose the camera. It checks the shape of the apple and encloses it firmly. Then it is activated by vacuum suction and detaches the fruit without damaging.

In this project the object detection approach used is You Only Look Once (YOLO). YOLO [5] is fast and an accurate object detector, thus making it useful for computer vision applications. It is based on regression i.e. instead of selecting parts of an image, it predicts classes and bounding boxes for the whole image in one run for the algorithm.

III. PROPOSED METHODOLOGY

The project aims at developing automated apple harvester bot and maintaining the count of apples in the inventory. "Fig. 1" shows the basic block diagram. The user will give the command from a smartphone to the bot and the bot will initiate its operation. The bot will be controlled by the processor i.e. raspberry pi 3. First the bot will move along the x axis. The camera will take continuous images. The algorithm used for object detection is YOLO and therefore if ripe apple is detected within the frame then the motor is driven by motor driver thereby adjusting the bot in line with the apple. After the bot is aligned in the centre of the apple then the arm in the z plane consisting of a cutter will move towards the apple and will stop until an active signal on the IR sensor is given which will successfully trigger the cutter to cut the apple from the tree. The count of the apple is taken and updated into the inventory mangement site of the user so that the customer can order the apples as per their requirement.

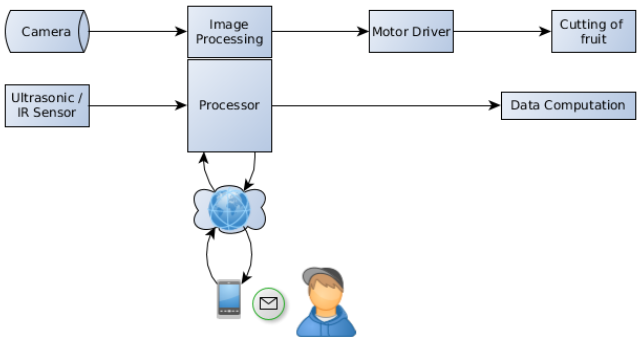

Fig. 1. Block Diagram

IV. HARDWARE USED

1. Motor Driver L293D

Fig. 2. L293D Motor Driver

L293D is a quadruple half H-bridge motor driver IC as shown in "Fig. 2". Motor driver acts as current amplifiers as they take low-current signal and provide a higher-current signal. This current signal is used to drive small DC-geared motors and bipolar stepper motors. It can drive current up to 600mA with a voltage range of 4.5 to 36 volts. The pulsed current per channel driver is 1.2 ampere and has thermal shutdown, back emf and internal ESD protection. L293D can drive two DC motors simultaneously, in both forward and reverse direction. The two motors can be controlled by logic pins 2 & 7 and 10 & 15. Input 00 or 11 stops the motor. Input 01 and 10 rotates the motor in clockwise and anticlockwise direction respectively while enable pins 1 and 9 must be high for motors to operate. When the enable pin goes high, the corresponding driver gets enabled. As a result, the outputs become active and driver drives their associated motors. Similarly, when the enable pin goes low, the associated driver is disabled, and corresponding motor is disabled.

2. DC Geared Motor

A DC geared Motor shown in "Fig. 3", has a gear mechanism connected to the motor. The speed of the motor is calculated in terms of rotations of the shaft per minute (RPM). The dc motor can be operated upto 12v and has 300 RPM. The gear mechanism helps in increasing the torque and therefore causes reduction in speed. The speed of the gear motor can be reduced to any desired speed by using different combination of gears. This hypothesis where gears reduce speed but increase the torque is termed as gear reduction.

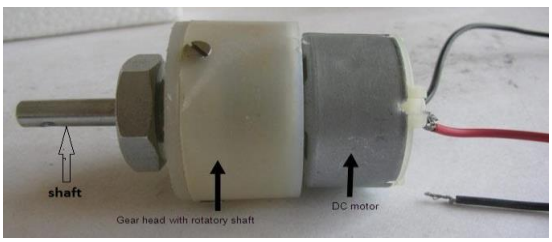

Fig. 3. DC Geared Motor

3. Raspberry Pi 3

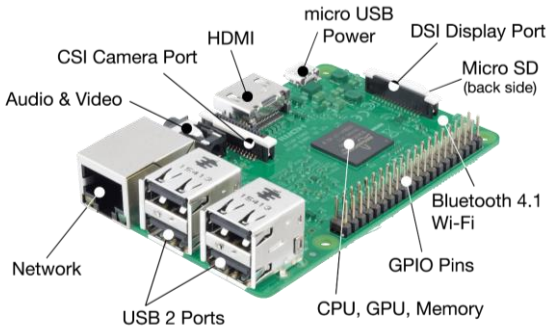

Fig. 4. Raspberry Pi 3

The quad-core Raspberry Pi 3 shown in "Fig. 4" is much more efficient than Raspberry Pi 2. It has a better performance than the other lower version of the pi. Unlike its predecessor, Pi 3 is competent of playing 1080p (Full HD) MP4 video at 60 fps at a rate of about 5400Kbps, and also supports wireless internet, with built-in Wi-Fi and Bluetooth. Raspberry Pi has a separate LCD display and camera port which eliminates the need of monitor and camera so one can connect them directly to the board and has PWM outputs for application use. Raspberry pi 3 uses Broadcom BCM2837 system on chip, ARM Cortex 4 core CPU, Broadcom Video Core 4 GPU, 1GB RAM, 2.4GHz wireless network, 4.1 Bluetooth and has 40-pin GPIO header, and HDMI, Ethernet, 3.5mm audio-video jack, 4 USB 2.0, Camera Serial Interface, Display Serial Interface ports.

4. IR Proximity Sensor

Infrared sensor is used to detect the presence of nearby objects without any physical contact. An IR sensor is shown in "Fig. 5". The IR sensor has builtin IR transmitter and receiver. IR transmitter is a type of LED which radiates infrared radiations. This radiation is invisible to human eye. IR receivers are called infrared sensors as they detect the radiation from an transmitter. IR receivers are typically photodiodes and phototransistors. IR transmitter emits radiation, and when it reaches the object some of the radiation reflects back to the IR receiver. The output of the sensor is shown based on the recepted intensity by the IR receiver. It is operated on 3 to 5 volts. Its detecting range is between 1cm to 30cm and the current consumption is about 23mA to 43mA. When an obstacle is detected its output goes low.

Fig. 5. IR Sensor

V. IMPLEMENTATION

The project uses Yolo V3 technique to implement the proposed idea as shown in "Fig 6". During the time of harvesting, the user will give the command from a smartphone to the bot and a code will be run. The flow chart of the program is shown in "Fig. 7". The bot will be

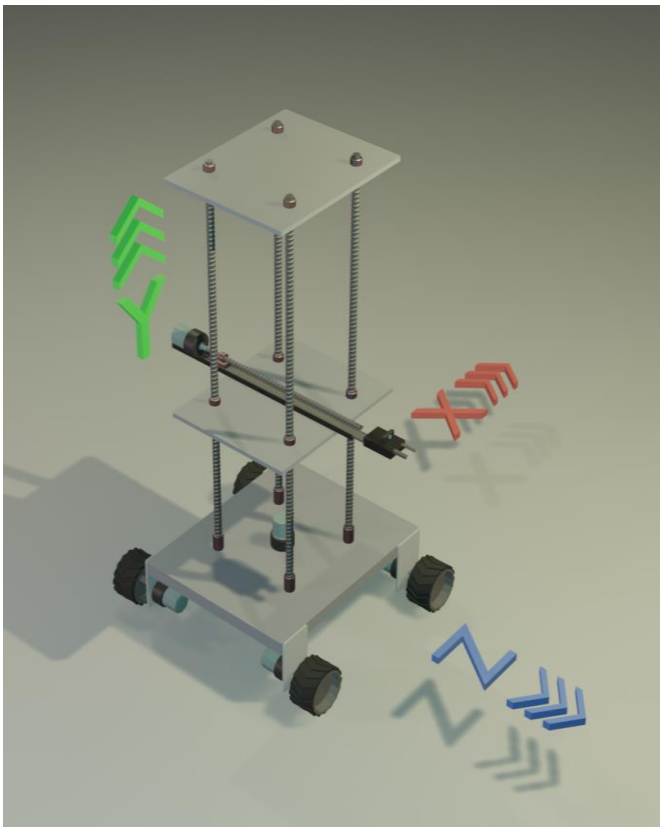

Fig. 6. Basic Model

controlled by the processor i.e. raspberry pi 3. The bot will move along the x axis. The camera will take continous images. The algorithm used for object detection is YOLO. YOLO start its process by dividing the image into SxS grid. For detecting the object, if the centre of an object falls into grid cell, that grid cell is responsible for detecting it. [6] Each grid cell predicts the bounding boxes and also the confidence percentage for those boxes. These confidence scores shows how much confident the model is for an object. It makes prediction across 3 different scales. [7] The detection layer is used to detect 3 different sizes, having strides 32, 16, 8. With an input of 416x416, detection is done on scale of 13x13, 26x26 and 52x52 and each grid cell predicts three bounding boxes. For image of size 416x416, YOLO estimates 10647 bounding boxes. And therefore if ripe apple is detected within the frame it will check if the image center and object center is the same, if not then the motor driver will drive the motors thereby adjusting the bot in x and y direction until the image center and object center is equal.

After the bot is aligned then the arm in the z plane consisting of a cutter will move towards the apple until a high signal on the IR sensor which will successfully trigger the cutter to cut the apple from the tree. Then the arm will move backwards to its initial position and this process will again be repeated. The count of the apple is taken and updated into the inventory of the user so that the customer can order the apples as per their requirement.

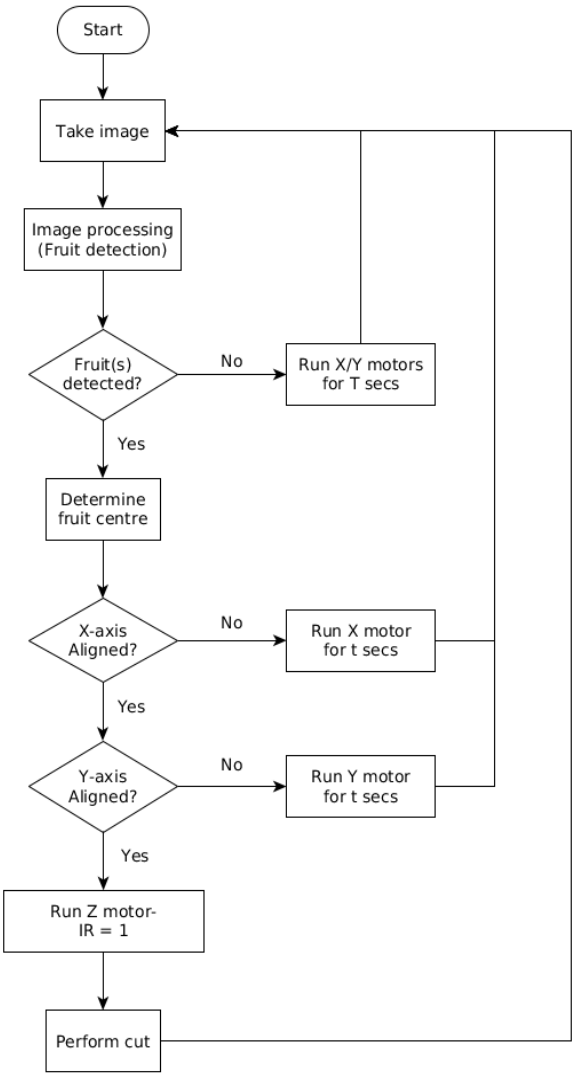

Fig. 7. Flow Chart

VI. RESULTS

The project is divided into three sections, first to detect the apple and move the bot in x axis, second to move to bot in y axis, and third to pluck the apple which is in the z direction and update the inventory. Therefore the results were seen of the project i.e. to detect the apple and aligns itself to the exact coordinates of X and Y. The bot then moved the arm in the z plane consisting of a cutter which on detection of the high signal on the proximity sensor had successfully cut the apple from the tree.

Testing of the program to detect the apple. “Fig. 8.a” and “Fig. 8.b” shows the images taken by the camera and apple has been detected respectively. First, the detection and moving the bot in x direction using only apple was done. Then the detection using two different fruits was tested as shown in “Fig. 9” i.e. for apple and orange to check if the bot will take real time images and classify the objects as apple and orange. The bot was programmed to move towards the apple. So as shown in “Fig. 10”, the bot detects both the fruits but starts moving towards the apple. Therefore after moving and aligning with the object and image centre, the bot stops.

Fig. 8.a

Fig. 8.b

Fig. 9. Detection using two fruits

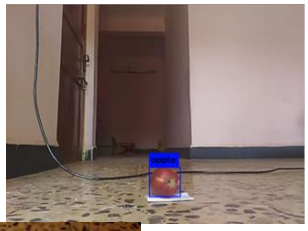

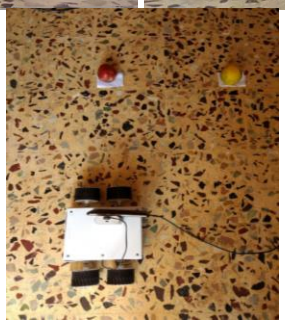

Fig. 10. Bot alinged

Fig. 11. Completed Bot

Fig. 12. Bot alinged in X & Y plane

Fig. 13. Cutting Arm moving in Z plane

Fig. 14. Cutting mechanism

VII. CONCLUSION

The bot was trained to pluck an apple from an artificial tree under normal conditions without the obstruction of leaves and the deam light factor.

VIII. FUTURE SCOPE

The two factors listed in the conclusion that is the obstruction of leaves and the deam light factor can be taken into account for any future research in this domain.

IX. ACKNOWLEDGEMENT

The authors gratefully acknowledge the contributions of our guide Professor Flavia Leitao, co-guide Professor Vidhya D.S. and Sir Joseph Dias for their assistance, suggestions and unconditional support given to us in our project work.

X. REFERENCES

[1] Peterson DL (2005) Harvest mechanization progress and prospects for fresh market quality deciduous tree fruits.

[2] Peterson DL, Bennedsen BS, Anger WC, Wolford SD (1999) A systems approach to robotic bulk harvesting of apples.

[3] Johan Baeten, Kevin Donne, Sven Boedrij, Wim Beckers and Eric Claesen, “Autonomous Fruit Picking Machine: A Robotic Apple Harvester”.

[4] Setiawan AI, Furukawa T, Preston A (2004) A low-cost gripper for an apple picking robot in IEEE Int. Conf. on Robotics and Automation.

[5] Joseph Redmon and Ali Farhadi YOLOv3: An Incremental Improvement, University of Washington,Tech report journal arXiv (2018).

[6] Joseph Redmon, Santosh Divvala, Ross Girshick and Ali Farhadi. You Only Look Once: Unified, Real-Time Object Detection in Conf. on Computer Vision & Pattern Recognition ((2016).

[7] Ayoosh Kathuria, How to implement a YOLO (v3) object detector,16 April 2018 (https://blog.paperspace.com/how-to-implement-a-yolo-object-detector-in-pytorch/)

Proceedings of the Fourth International Conference on Communication and Electronics Systems (ICCES 2019)
IEEE Conference Record # 45898; IEEE Xplore ISBN: 978-1-7281-1261-9

Efficient load Balancing algorithm analysis in Cloud Computing

SONU SAHU
Computer Science and Engineering,
Maulana Azad National Institute of Technology
BHOPAL, INDIA-462003
sahusonu5555@gmail.com

MANISH PANDEY
Assistant Professor,
Computer Science and Engineering,
Maulana Azad National Institute of Technology
BHOPAL, INDIA-462003
manishpandey@yahoo.co.in

Abstract—**Cloud Computing (CC) is a very trendy topic in the research field. Cloud computing has integrated distributing computing, web services, internet, software, and virtualization together. Most of the companies are using cloud computing on large scale. Cloud Computing (CC) services are demanding in the market. Cloud computing has been growing very fast since last few years. Over the past few years, cloud computing has the most powerful technology. A researcher has also shown his interest in cloud computing in past few years. In load balancing, there must be using so many algorithms in one at a time. We have also discussed about response time, turnaround time, and throughput. We have comprehensively analyzed and compared results of the above mentioned LBA. In CC, role of virtual machine is to utilize processor speed, which is discussed in this paper. Cloud Computing models, VM allocation, role of load balancing, simulation, cloudsim have also been explored in this paper.**

Keywords— Cloud computing (CC), Virtual Machine, Load balancing algorithm (LBA), Data Center Controller (DCC).

I. INTRODUCTION

CC could be understood as the delivery service of computing. A cloud must be an environment in which we have around some online services like storage space online compiler, online gaming and so on. Cloud computing provides various resources which can be used online [1]. A cloud can offer some services which should be payable and to be free. Cloud computing is undergoing major changes to allow multifaceted enhancements with each passing day. Nowadays so many companies make use of cloud computing technology like Google, Apple, Amazon, Microsoft, and so on. In a cloud, various data center are located at various locations. A user has been requested to the data center regarding its services [2]. A data center accepts the request of the user and provides its service. A cloud facilitates an online platform like data storage space, online compiler, online video gaming, online music player and so on. This service is provided only on a rented basis. A user can pay for all these services.

Cloud deployment model can be categorized into three types:

a. Public: In a public cloud, service should be public in a public cloud. A public cloud should be a standard Model. In public cloud, Mostly services should be free for a user.

b. *Private*: Private cloud is a service offered to a selected user instead of a public cloud. It provides high-level security and also has some additional feature. All services should be paid in the public cloud.

c. *Hybrid*: A partial mixture of public and private cloud made up of hybrid cloud. It provides more flexibility to enhance IT infrastructure. It provides more data deployed options.

Cloud computing [3] has new emerging technology. Nowadays cloud computing is on the trending list to the company perspective. A cloud computing service can be categorized into four qualities: IAAS, PAAS, and SAAS etc. A service should be offered in the form of layers one by one in cloud computing. It should be performed like a stack. They will accomplish its business goal very easily. There is:

a. Infrastructure as a service (IAAS): It is an infrastructure for instant computing. It should do outsourcing and support to manage an enterprise [1]. It also provides the software. IAAS (Infrastructure as a service) is also known as HAAS (Hardware as a service). It should be a very high-level API.

b. *Platform as a service (PAAS*): It is an architecture of cloud computing and it also just a third party software. It should provide hardware and software as per the user needed. A PAAS provides hardware and software in the platform. A supplier to provides a toolkit and standard parameter has been applying for development and channel for a purchasing purpose.

c. Software as a Service (SAAS): It provides a host a software application over the internet. It is a being third party. The software must always be available for the user in the platform.

CC is a modern technology. Now a days so many companies showing their interest in this emerging technology [4]. A researcher has also showing his interest

in cloud computing. Fig1 shows a cloud computing environment.

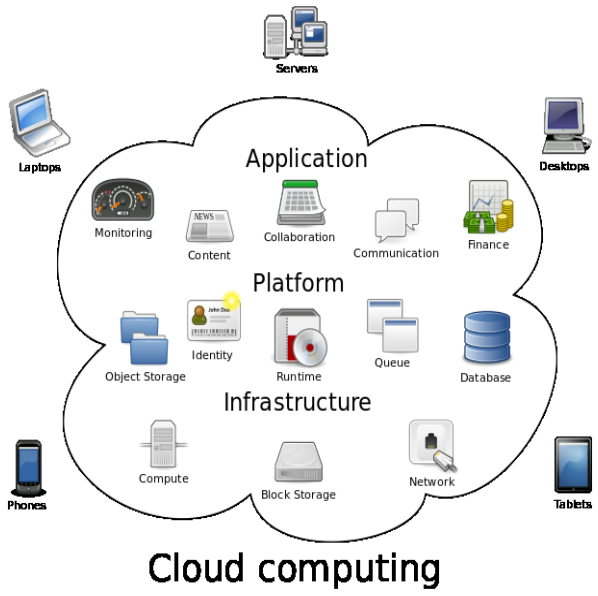

Figure 1: Cloud Computing Environment [Source: Google].

II. LOAD BALANCING

LB could be termed as a process in cloud computing which enhances the accomplishment of CC. It should distribute the load assignment among the nodes in a uniform manner [5]. Load balancing is a model in which we use certain algorithms to fulfill our task. Load balancing works as a part of cloud computing. With the help of load balancer, we are enabled to distribute the load in a uniform manner. In a load balancer, we have to specially take care about load balancing algorithm. An algorithm must have good response time, less turn-around time and good performance [6]. A load balancer is a specific part of CC which enhances the quality of CC. The main motivation for the load balancing algorithm is:

- Good response time.
- Less turn-around time.
- Full utilization of resources.
- No fault tolerance system.
- Improve of efficiency and performance.
- To improve resource utilization.
- Stability maintenance of the system.

Therefore, in a cloud computing environment, we can also try to avoid overloading at a specific node. We have thus categorized the load balance algorithm into two types:

a. *Static*: A static algorithm is basically made for a stable environment like a homogenous system. In the static algorithm, we should have prior knowledge about the system resources, so the load change judgment does not depend on the current system status. That algorithm has a decent mixture in the system that is why it should have low variation in load.

b. *Dynamic*: A dynamic algorithm can be modified effectively in both the homogeneous and heterogeneous environments. Dynamic load balancing may utilize the current state of the system and it ought to be helpful in managing the systemof the load [5].

A static algorithm has been found to be much faster than a dynamic algorithm. But dynamic algorithm has been designed only for the heterogeneous request. If we compare both the algorithms, the static algorithm has less overhead. The main objective in the load balancing algorithm is- to enhance request allocation to VM on the basis of the algorithm. There must be an agreement termed as service level agreement (SLA), existing between the developer and the user. It should generate proper implementation of the algorithm in a successful manner. Fig 2 shows a load balancing process.

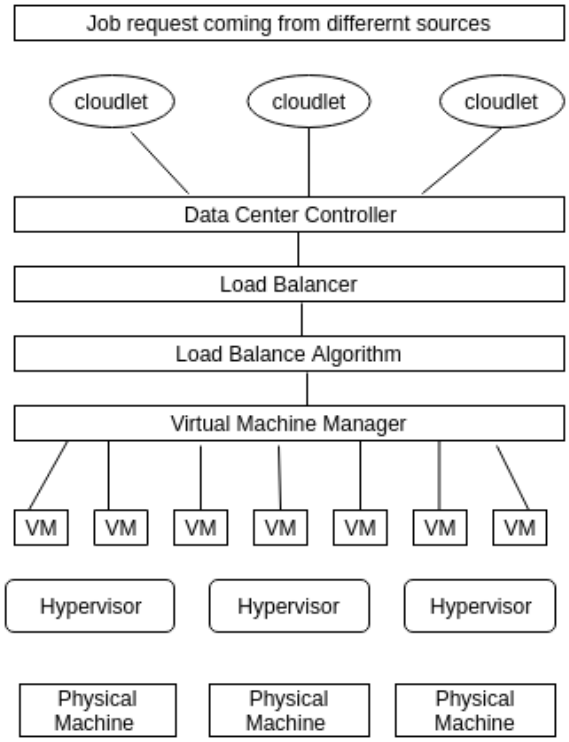

Figure 2: Load Balancing Process.

The algorithm-1 has been shown to balance the load in VM of cloud computing as follows:

```
Algorithm-1
    Begin
      Connect_to_resource()
      L1
      If (resource found)
        Begin
          Calculate connection_string()
          Select fuzzy_connection()
          Return resource to requester
      End
      Else
        Begin
          If (Anymore resource available)
            Choose_next_resource()
```

```
            Go to L1
          Else
            Exit
        End
End
```

Firstly that proposed algorithm has been requested resources for a connection request and then test for obtainable for resources [6]. It measures the connection request and if the resource found. Then choose the connection that is used in the virtual machine to connect the resource as per processor speed and load. Here this graph has been plot energy consumption according to the number of the task and its algorithm. Fig3 shows a graph plotting of various algorithms.

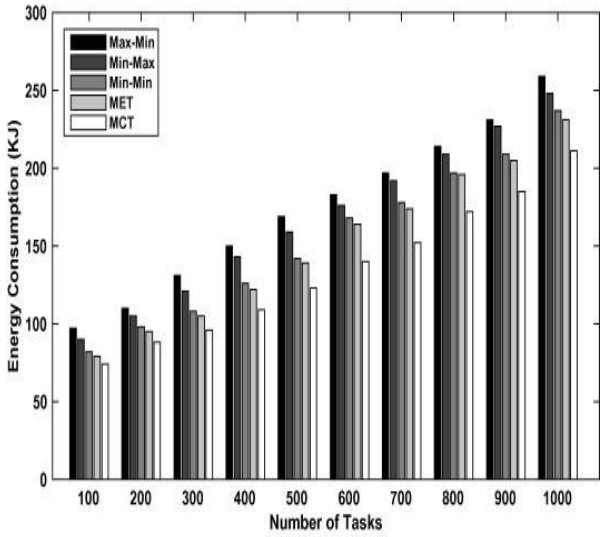

Figure 3: Graph Plotting of various algorithm.

Fig 4 shows plot between before load balancing and after load balancing.

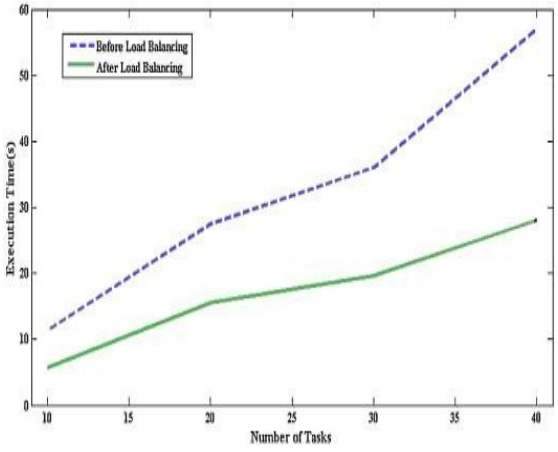

Figure.4 : Before Load Balancing and After Laod Balancing

III. MODELING THE VM ALLOCATION

A virtual machine is an additional layer of an operating system. A virtualization concept in cloud computing is tremendous. It works as an application layer which has only work like hosting, management and execution [7]. Therefore, virtualization has a main key in cloud computing [8]. In order to make proper utilization of available physical resources virtualizations is the best option. In virtualization, various physical machines are integrated assigned to an application dynamically. While using virtualization, several OSs and several applications can run simultaneously on a single server. It rises up the flexibility and utilization of hardware. The basic purpose of virtualization to creates a pragmatic interface. The virtualization environment having some component which we discuss below:

a. *Guest*: It shows as a component in a system. It should communicate with a virtualization layer or even with the host.

b. *Host*: It symbolizes the original environment. This is the palace where guest to be managed.

c. Virtualization: Virtualization allows to us, we will create the same or different environment. Guest operates in virtualization layer. It focuses primarily on computing, storage, and virtualization of the network.

IV. SIMULATION

A simulation is an estimated rendition of a process or system's operation [9]. In the process of simulation, we have required a model which should be developed. That model should be predetermined overview of a subject. It also represents its key features, such as its behavior, functions and abstract or physical properties. Today's simulation tools for CC are: gridsim, simjava, and cloudsim.

V. CLOUDSIM

CloudSim is simulator which helps to create model and simulation of cloud infrastructure [12]. It should create a virtual environment and then we have done some operation in cloudsim. Basically, it was designed for cloud computing and distributing. It should not being a software [10]. It should be a java package. That package we have imported in IDE. Cloudsim was written in java. Cloudsim does not have itself user interface.

VI. CONTEMPORARY VM LOAD BALANCERS

A load balancing algorithms basically allocates the work dynamically. A virtual machine allows the concept of OS and application to run over the hardware. Cloud model make connection request to internal hardware via data center elements. A data center should take care of all service requests and that requests placed in sandbox (processing element) within VM [15]. After that all requests are allocated to the data center host component. A data center object takes care of all the managing activity such as virtual machine creation, virtual machine destruction and routing request of the user request. A virtual machine load balancer controlled by DCC. A DCC creates the table of user's requests which VM allocate for processing. There are various contemporary VM load balancer algorithm which are given below:

a. *Round Robin Load Balancer*: A data center controller contains a list of all VM. A data center controller is being responsible for assigning a request to each VM. If a VM is allocated to a request then it will go the end of the queue. In a Round Robin Load Balancer (RRLB) has a good concept which name is Weighted Round Robin Allocation. In a Weighted Round Robin Allocation, a weight is associated with every VM. If any VM can handle the higher load then its weight is incremented and that VM have treated as more powerful than other VMs [18]. Next time when more than one new request arrives then we will assign that requested to that high weighted VM [19]. It is having a major issue that it doesn't capable of handling the advance load balancing requirements such as execution time for every requests.

b. Throttle Load Balancer (TLB): A Throttle Load Balancer makes a table regarding the state of every individual request of VMs. On this table, TLB keeps the record regarding VMs such that which VM is allocated to a particular request and which one is ideal. If any request has arrived then TLB generate an ID of the ideal VM. That ID send to a data center controller [7]. A data center controller assigns a VM to that request.

c. *Active Monitoring Load Balancer*: The active monitoring load balancer keep the information regards VM and it also keeps that which request assign to a particular VM. When a new request has arrived, it allocated to a new VM arrives. It recognizes the least loaded VM. If there are more than one request comes then it simply follows the FCFS. Active Monitoring Load Balancer sends VM ID to the data center controller. A data center controller recognizes that VM Id and make a request to that VM which is given by active monitoring load balancer. A data center controller will tells about new allocation to Active Monitoring Load Balancer (AMLB). It performs a new allocation and send to the cloudlet.

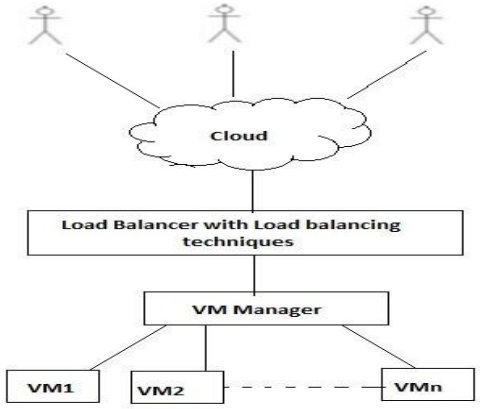

Figure 5: Contemporary VM Load Balancer [Source: Google].

VII. CONCLUSION

L.B [4] is handling a major issue in CC [21]. It allocates the workload dynamically to the server. It also maintains user satisfaction. It makes highly supervised resource utilization [16]. In load balancing, there is two major issues i.e. cost effective and time effective. Cost and time have a major key challenge in the software industry. Both of the parameters enhanced utilization and effectiveness in software industry. In this paper, we have discussed so many algorithms that algorithms are totally dependent on time and cost. Load balancing model and architecture plays an important role in software. Load balancing algorithms make better utilization of processing resources. An ideal load balancing algorithm should have these qualities like maximize throughput and better response time. This is the main aspect of this paper. In load balancing, we can try to use a dynamic algorithm.

REFERENCES

[1] Rodrigo N. Calheiros, Rajiv Ranjan, Anton Beloglazov, César A. F. De Rose, and Rajkumar Buyya, "CloudSim: A Toolkit for Modeling and Simulation of Cloud Computing Environments and Evaluation of Resource Provisioning Algorithms", Software: Practice and Experience, Volume 41, Issue 1, pages 23–50, January 2015.

[2] Rajkumar Buyya, Chee Shin Yeo, Srikumar Venugopal, James Broberg, and Ivona Brandic, Cloud Computing and Emerging IT Platforms: Vision, Hype, and Reality for Delivering Computing as the 5th Utility, Future Generation Computer Systems, Volume 25, Number 6, Pages: 599-616, ISSN: 0167-739X, Elsevier Science, June 2011.

[3] T V R Anandarajan, M A Bhagyaveni, "Co-operative scheduled Energy aware load-balancing technique for an efficient computational cloud", IJCSI, volume 8, issue 2, March 2010.

[4] Menno Dobber, Rob van der Mei, and Ger Koole "Dynamic Load Balancing and Job Replication in a Global-Scale Grid Environment: A Comparison" IEEE TRANSACTIONS ON PARALLEL AND DISTRIBUTED SYSTEMS, vol. 20, no.2, pp 207, Feb 2016.

[5] Kuo-Qin Yan ; Wen-Pin Liao ; Shun-Sheng Wang , "Towards a Load Balancing in a three-level cloud computing network ", 3rd IEEE International Conference on Computer Science and Information Technology (ICCSIT), 2010, Vol-1, pp.-108-113, 2012.

[6] Jeffrey M. Galloway, Karl L. Smith, Susan S. Vrbsky, "Power Aware Load Balancing for Cloud Computing", Proceedings of the World Congress on Engineering and Computer Science 2011 Vol I WCECS 2011, October 19-21, 2011.

[7] Zenon Chaczko Venkatesh Mahadevan, Shahrzad Aslanzadeh and Christopher Mcdermid, "Availability and Load Balancing in Cloud Computing", 2011 International Conference on Computer and Software Modeling IPCSIT vol.14, IACSIT Press, Singapore, 2011

[8] Alexandru Iosup, Member, IEEE, Simon Ostermann, Nezih Yigitbasi, Member, IEEE, Radu Prodan, Member, IEEE, Thomas Fahringer, Member, IEEE, and Dick Epema, Member, IEEE, "Performance Analysis of Cloud Computing Services for Many-Tasks Scientific Computing", IEEE TPDS, MANY-TASK COMPUTING, NOVEMBER 2014.

[9] Martin Randles, David Lamb, A. Taleb-Bendib, " A comparative Study into distributed load balancing algorithm for cloud compuiting,IEEE 24th International Conferece on Advance Inforamation Networking and Application Wrokshops,20-23pp.551-556, April2012.

[10] Meenakshi Sharma, Pankaj Sharma, Sandeep Sharma, "Efficient Load Balancing Algorithm in VM Cloud Environment", IJCST Vol. 3, Issue 1, pp.- 439-441, Jan. - March 2012.

[11] R. Shimonski. "Windows 2000 & Windows Server 2003 Clustering and Load Balancing", Emeryville. McGraw-Hill Professional Publishing, CA, USA (2003), p 2, 2003.

[12] Ali M. Alakeel, "A Guide to Dynamic Load Balancing in Distributed Computer Systems", IJCSNS International Journal of Computer Science and Network Security, VOL.10 No.6, June 2013.

[13] R. Shimonski. "Windows 2000 & Windows Server 2003 Clustering and Load Balancing", Emeryville. McGraw-Hill Professional Publishing, CA, USA (2003), p 2, 2003.

[14] R. X. T. and X. F. Z, "A Load Balancing Strategy Based on the Combination of Static and Dynamic, in Database Technology and Applications (DBTA), 2015 2nd International Workshop 2010, pp. 1-4, 2015.

[15] Patricia E. Figueroa Jesús A. Pérez "Architecture for Interoperability between Instant Messaging and Presence Protocols" International Conference on Networked Digital Technologies (CCIS, volume 88)2010.

[16] Y. F. Wong and W. C. Wong. "A fuzzy-decision-based routing protocol for mobile ad hoc networks" 10th IEEE International Conference on Network, pp. 317–322, 2012.

[17] G. V. S. Raju, G. Hernandez, and Q. Zou, "Quality of service routing in ad hoc networks", IEEE Wireless Communications and Networking Conference, Vol. 1, pp. 263 –265,2015.

[18] W. Pedrycz and F. Gomide, "An introduction to fuzzy sets: analysis and design", complex adaptive systems. MIT Press, 2011.

[19] Yilin Lu," A Hybrid Dynamic Load Balancing Approach for Cloud Storage", 2012 International Conference on Industrial Control and Electronics Engineering 978-0-7695-4792-3/12 © 2012 IEEE.

[20] Ruhi Gupta. "Review on Existing Load Balancing Techniques of Cloud Computing." International Journal of Advanced Research in Computer Science and Software Engineering Volume 4, Issue 2, February 2014.

[21] Martin Randles, David Lamb, A. Taleb-Bendiab . " A Comaprative study into Distributed Load balancing algorithms for cloud computing" , IEEE 24th international conference on Advanced Information Networking and Applications workshops,20-23 pp.551-556,April 2012.

Proceedings of the Fourth International Conference on Communication and Electronics Systems (ICCES 2019)
IEEE Conference Record # 45898; IEEE Xplore ISBN: 978-1-7281-1261-9

Fast and Accurate Traffic Sign Recognition for Self Driving Cars using RetinaNet based Detector

Shehan P Rajendran, Linu Shine, Pradeep R, Sajith Vijayaraghavan
Dept. of Electronics and Communication Engineering
College of Engineering Trivandrum
Trivandrum, India
shehanpr@gmail.com, linu_shine@yahoo.com, pradeep@cet.ac.in, sajithvijayaraghavan@gmail.com

***Abstract*—Increase in the number of vehicles on road necessitates the use of automated systems for driver assistance. These systems form important components of self-driving vehicles also. Traffic Sign Recognition system is such an automated system which provides contextual awareness for the self-driving vehicle. CNN based methods like Faster R-CNN for object detection provide human level accuracy and real time performance and are proven successful in Traffic Sign Recognition systems [1]. Single stage detection systems such as YOLO [2] and SSD [3], despite offering state-of-the-art real-time detection speed, are not preferred for traffic sign detection problem due to its reduced accuracy and small object detection issues. RetinaNet has shown promising results with respect to accuracy and speed required for object detection problems. It uses Focal Loss [4] and Feature Pyramid Network (FPN) [5] for tackling the low accuracy and small object detection problems. In this paper, an approach for traffic sign recognition system for self-driving cars based on RetinaNet is presented with comparative analysis of its performance with Faster R-CNN based sign detector [1] and YOLOv3 [9] based detector. RetinaNet forms the traffic sign detection network and a CNN-based classifier forms the traffic sign class recognizer. The network training and evaluation are done using the German Traffic Sign Detection Benchmark (GTSDB) [6] dataset and the classifier performance is verified using German Traffic Sign Recognition Benchmark (GTSRB) [7] dataset.**

Keywords— Traffic sign detection, CNN, RetinaNet, Faster R-CNN, YOLO

I. INTRODUCTION

Systems for assisting the drivers to avoid accidents are becoming more and more important as the number of vehicles on road is on an exponential increase. Advanced Driver Assistance Systems (ADAS) are being effectively used in automobiles for providing lane keep assistance, forward collision warning, pedestrian warning, driver drowsiness detection, traffic sign assist system etc. These form essential systems in autonomous cars for contextual awareness and road attribute mapping in order to control the vehicle motion trajectory. Traffic Sign Recognition (TSR) is the core component of traffic sign assist system for providing timely instructions and warnings to the drivers regarding traffic restrictions and information. In self driving cars, the inputs from traffic sign recognition system are used to make suitable decisions by the car, for example, to reduce speed or prepare for a detour etc.

Traffic sign recognition involves traffic sign detection and classification. Several studies have been conducted to address the traffic sign recognition problem. Even though some of the existing approaches have demonstrated good results on various benchmark datasets, most do not work very well in adverse conditions like motion blur, poor illumination, rainy or foggy weather, small sized signs etc. Recent studies use deep learning techniques, especially Convolutional Neural Networks (CNNs) for solving the traffic sign detection and classification problems. Majority of such studies use the German Traffic sign Detection Benchmark (GTSDB) [6] and German Traffic Sign Recognition Benchmark (GTSRB) [7] datasets for training and evaluation of their detection and classification networks. Improvements are made in the general CNN based object detection networks for traffic sign detection. A modified version of Faster-RCNN, a two-stage object detection network comprising of Region Proposal Network, bounding box regressor and classifier networks, has shown good accuracy and speed and it is found to be promising for real world problems like self-driving cars. Single stage detectors like YOLO [2] offer real time speed in detection, however these suffer from foreground-background class imbalance problems and does not provide the required detection accuracy. Also, these detectors are not efficient in detecting small objects, which is critical for traffic sign recognition. The recent improvements made as part of YOLOv2 [8] and YOLOv3 [9] have tackled the problems to some extent.

In this paper, RetinaNet object detection network, which is based on feature pyramid network and focal loss, is tuned and used for the traffic sign detection purpose. Very good detection result on the GTSDB database is observed using this approach. The CNN based traffic sign classifier proposed by Li and Wang [1] is used for classification of the traffic signs.

The rest of the paper is organized as follows. Section II covers the related work, Section III describes the technical approach, Section IV details the experiments done, Section V covers the performance evaluation and Section VI draws the conclusion of the work.

II. RELATED WORK

A. Traffic Sign Recognition

Extensive research is being done by the computer vision and machine learning communities to address the problem of automatic traffic sign detection and recognition in the past decade. Issues such as non-uniform scene illumination, blurring due to motion of vehicle-mounted camera with respect to traffic signs, traffic sign occlusion due to other vehicles, trees etc. make the traffic sign recognition task very challenging. Traffic sign detection based on extracting sign proposals and classifying based on a color probability model and Histogram of Oriented Gradients (HOG) is proposed by

XXX-X-XXXX-XXXX-X/XX/$XX.00 ©2019 IEEE

Y Yang et.al [10]. However manual features such as HOG fails due to the challenges mentioned above. Recently, several object detection problems are being better addressed using Convolutional Neural Networks (CNNs). Computer vision research for intelligent transportation systems are also following the trends and many such work are finding practical use in advanced driver assistance applications as well as in autonomous driving vehicles. In line with that, several researchers have attempted to solve the problem of traffic sign recognition using CNN based object detection frameworks.

Y Zhu et al [11] proposed a method based on deep learning components for traffic sign recognition. It consisted of a Fully Convolutional Network (FCN) for proposal generation and a CNN for classifying signs. Later Zhu et al [12] proposed a traffic sign recognition system using an end-to-end multi-class CNN for simultaneous traffic sign detection and classification. They have also created a new dataset called Tsinghua-Tencent 100K dataset for performance analysis. They also proposed a single class detection network for the traffic sign detection and using a separate classifier for classifying the detected traffic signs.

The performance of Fast-RCNN [13] for traffic sign recognition is studied by Zhu et al [12]. Peng et al. [14] analysed Faster R-CNN for traffic sign detection, even though this approach was promising as compared to the previous studies, consistent accuracy and detection speed could not be achieved. Another real time traffic sign recognizer based on Faster R-CNN [15] following the Mobilenet [16] structure proposed recently by Li and Wang [1] could show the real-time performance and accuracy required for applications such as self-driving car, based on their evaluation using GTSDB dataset. In this approach they have also proposed a classifier network using asymmetric kernels for classifying the signs into 43 classes.

B. *Traffic Sign Classification*

CNN based classifiers trained with GTSRB dataset could achieve high classification accuracy in classifying traffic signs. The classifier based on Multi Column Deep Neural Network (MCDNN) proposed by Ciregan et al. [17] and Multi-scale CNN by Sermanet et al [18] could achieve accuracies of 99.17% and 99.65% respectively. These networks however are large and have to learn a huge number of parameters. Another approach by T L Yuan [19] using Spatial Transformer Networks (STN) could achieve an accuracy of 99.59%. Classifier network based on CNN using asymmetric kernels proposed by Li and Wang [1] reported an accuracy of 99.66% when evaluated with GTSRB dataset. Their FRCNN based detector and CNN based classifier combination has proved superior to the state-of-the-art traffic sign recognizers. The CNN based classifier employing asymmetric kernel proposed in [1] is used as the classifier in the proposed traffic sign recognition pipeline.

III. APPROACH

In this section, our approach for traffic sign recognition based on RetinaNet is presented. The traffic sign recognition pipeline, which is illustrated in Figure 1 consists of the RetinaNet based detector, the bounding box pre-processor and the CNN based classifier. The detector trained using GTSDB dataset, detects and localizes the candidate traffic signs. Bounding box pre-processor pre-processes the localized traffic signs for classification. It enlarges the bounding boxes, crops and resizes the boxes containing candidate traffic signs and fed to the classifier. The CNN based classifier classifies the candidate traffic sign as belonging to one of the 43 traffic sign classes.

A. *RetinaNet based Traffic Sign Detection*

RetinaNet is used as the traffic sign detector. RetinaNet is a composite network consisting of the following.

- Feature Pyramid Network (FPN) [5], which forms the backbone network
- A subnetwork for object classification
- A subnetwork for bounding box regression

RetinaNet structure is illustrated in Figure 2.

1) Feature Pyramid Network (FPN): The RetinaNet based traffic sign detector uses FPN as the backbone network and is built on top of ResNet-50 [20] deep feature extractor. FPN is a fully convolutional network, which takes traffic scene image of an arbitrary size and outputs feature maps at multiple scales resulting in a feature pyramid, a semantically strong multi-scale feature representation. This multi-scale feature representation enables the detector to detect candidate traffic signs of varying sizes present in the traffic scene. The feature pyramid network consists of bottom-up and top-down pathways. A feature hierarchy comprises of feature maps of different scales is generated by the bottom-up pathway. The top-down pathway with lateral connections, up-samples the feature map from the higher pyramid level, to generate semantically strong, but spatially coarse feature maps of different spatial sizes. Using lateral connections, the feature maps of same spatial sizes from both pathways are merged, resulting in feature maps of different scales, which are semantically strong with accurately localized activations.

2) Classification Subnet: The object classification subnetwork comprises of fully convolutional networks attached to each feature map level of the feature pyramid. Each subnetwork consists of four convolutional layers of filter size 3×3 with 256 filters with ReLU activations followed by another 3×3 convolutional layer with $C \times A$ filters with sigmoid activation, where C is the number of classes and A is the number of anchor boxes. The output

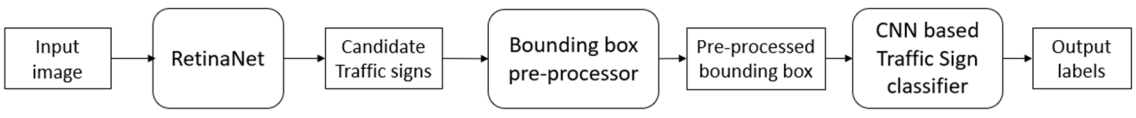

Figure 1. RetinaNet based traffic sign detection pipeline

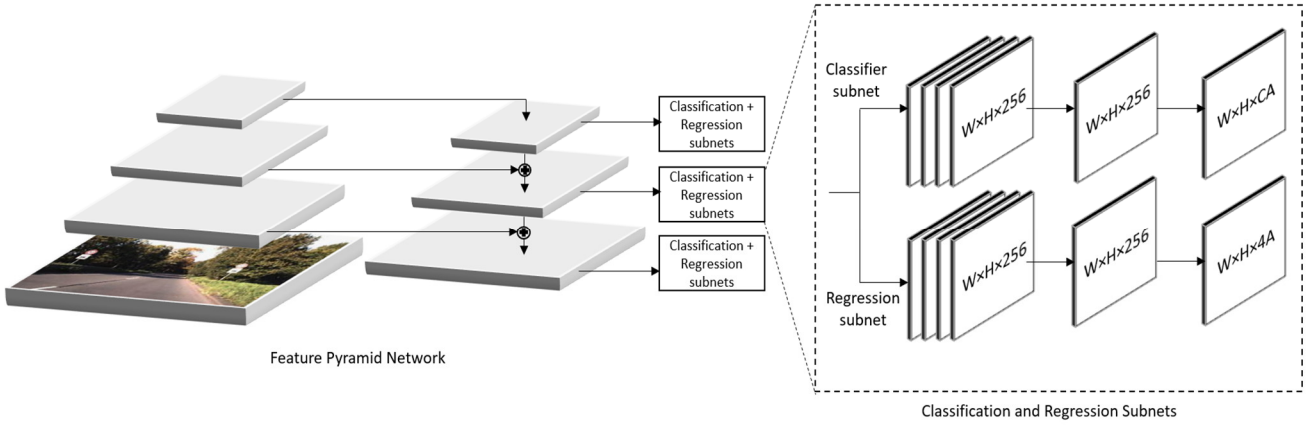

Figure 2. RetinaNet detector architecture

shape would be (*W, H, CA*), where *H* and *W* are proportional to the height and width of the input feature map level respectively.

3) Regression Subnet: The bounding box regression subnet is also attached to each feature map level of the feature pyramid. The subnetwork structure is similar to that of the classification network, the only difference is in the filter count of the last convolutional layer, which is *4A* in this case with 4 bounding box coordinates per anchor box. The output shape would be (*W, H, 4A*) in this case.

4) Loss Functions: RetinaNet uses a multi-task loss that contains two terms – localization loss and classification loss.

$$L = \lambda L_{loc} + L_{cls} \quad (1)$$

Here L_{loc} is the localization loss and L_{cls} is the classification loss. λ is a balancing factor, which balances the two task losses.

In single stage detectors, due to foreground-background class imbalance, the training process is dominated by easily classifiable background examples, which results in less accurate detection performance. RetinaNet resolves the class imbalance problem by using a variant of Focal Loss proposed by Yi Lin et al [4] as the classification loss. For each anchor, the classification loss is defined as:

$$L_{cls} = -\sum_{i=1}^{C} \{\alpha_i y_i (1 - p_i)^{\gamma} \log(p_i) + (1 - \alpha_i)(1 - y_i) p_i^{\gamma} \log(1 - p_i)\} \quad (2)$$

where C denotes the number of classes; $y_i = 1$, if ground trth belongs to i^{th} class and 0 otherwise; p_i is the predicted score for the ith class; γ is the focusing parameter, whose value can range from 0 to +∞; α_i is the weighting factor for the ith class and can range from 0 to 1. Here, the categorical cross entropy loss function is modified by adding the term $(1 - p_i)^{\gamma}$ called the modulating factor which down-weights easy examples and thus focusing training on hard negative examples. For a misclassified example with small p_i value, the modulating factor is close to 1 and hence the loss is not affected, whereas when p_i is close to 1, i.e., for a well-classified example, the modulating factor becomes 0 and the loss is down-weighted. α_i and γ are hyper-parameters, which can be tuned. The effect of the modulating factor is increased with increase in γ. If α_i = 1 and γ = 0, the focal loss becomes equivalent to the categorical cross entropy loss. Smooth L1 loss function [13] is used as the localization loss.

B. Bounding Box Pre-processor

Bounding Box Pre-processor stage extracts and prepares the detected candidate traffic sign boxes for classification. The center of the regressed bounding box is determined and the box is enlarged by 25% to compensate for any regression errors to make sure the traffic sign is completely enclosed in the region. The enlarged boxes are cropped and resized to 48 × 48 size and fed to the classifier network for recognition of the traffic sign class.

C. Traffic Sign Classifier

A fast and accurate traffic sign classifier network architecture proposed in [1] is used here.

In this architecture, an $n \times n$ convolution is replaced by an $n \times 1$ convolution followed by a $1 \times n$ convolution, which reduces both the number of convolution operations and the network parameters. This leads to computational cost reduction and increased speed.

The classifier network structure is in Table I. Batch Normalization and ReLU layers follows all layers other than the final dense layer. The sixth layer forms an inception module where kernels of different sizes are used to extract information from feature map output of the previous layer. The output feature maps from the inception layer are concatenated to combine the feature maps. Dropout layers are also used to regularize the activations of the final stages. To recognize the 43 traffic sign classes, fully-connected layer of an output size of 43 with Softmax activation is used as the last layer.

IV. EXPERIMENTS

The RetinaNet based traffic sign detector and CNN based classifier are implemented using Keras with TensorFlow backend. The detector and classifier are trained and evaluated on the GTSDB and GTSRB datasets respectively. Google Colaboratory environment with Nvidia Tesla T4 GPU having 16GB GPU memory was used for training the detector. The evaluation of the detector, as well as the training and evaluation of the classifier are done on a computer with an Nvidia GTX 1060 GPU having 6GB GPU memory.

Figure 3. Traffic scene image samples from GTSDB dataset [6]. These show different driving scenarios and lighting conditions.

TABLE I. TRAFFIC SIGN CLASSIFIER ARCHITECTURE [1]

Layer	Type		Filter Size/ Parameter	Filters/ Stride	Output shape
1	Conv		3 × 3	32, s1	48 × 48 × 32
2	Conv		7 × 1	48, s1	48 × 48 × 48
3	Conv		1 × 7	48, s1	48 × 48 × 48
4	MaxPool		2 × 2	s2	24 × 24 × 48
5	DropOut		0.2		24 × 24 × 48
6-1	Inception	Conv	3 × 1	64, s1	24 × 24 × 64
7-1	Inception	Conv	1 × 3	64, s1	24 × 24 × 64
6-2	Inception	Conv	1 × 7	64, s1	24 × 24 × 64
7-2	Inception	Conv	7 × 1	64, s1	24 × 24 × 64
8	Inception	Concatenate	-	-	24 × 24 × 128
9	MaxPool		2 × 2	s2	12 × 12 × 128
10	DropOut		0.2	-	12 × 12 × 128
11	Conv		3 × 3	128, s1	12 × 12 × 128
12	Conv		3 × 3	256, s1	12 × 12 × 256
13	MaxPool		2 × 2	s2	6 × 6 × 256
14	Dropout		0.3	-	6 × 6 × 256
15	Dense		256	-	256
16	Dropout		0.4	-	256
17	Dense - Softmax		43	-	43

A. Datasets

The GTSDB and GTSRB datasets are very popular datasets for training and evaluating models for traffic sign detection and recognition respectively.

The GTSDB dataset is generated from video sequences recorded near Bochum, Germany. It consists of images from urban, rural and highway scenarios under different weather and lighting conditions making it pretty representative and challenging. The total dataset consists of 900 images of 1360 × 800 pixels in raw PPM format, which are divided into 600 training images and 300 test images. The training images contain 846 traffic signs and test images contain 360 traffic signs. The traffic sign sizes in the images vary between 16 and 128 pixels.

Representative sample images from GTSDB dataset is shown in Figure 3. It shows traffic scenes from urban, rural and highway driving scenarios in different sizes as well as under different lighting and weather conditions. It can be seen that due to harsh background lighting, traffic sign is barely visible in one of the images. Also, in the highway scene, it can be seen that the traffic sign images are small in size. Being a dataset having images of such diverse conditions, the GTSDB dataset is used to train and evaluate the RetinaNet based detector.

The GTSRB dataset consists of more than 50000 traffic sign images of 43 classes with sizes varying between 15 × 15 pixels and 222 × 193 pixels. Sample images of different traffic sign classes is shown in Figure 4. The classifier is trained using 39209 training images and evaluated on 12630 test images from GTSRB dataset.

B. Evaluation criteria

Intersection over Union (IoU) between the ground truth box and the predicted bounding box > 0.5 is considered as a positive proposal. Mean average precision (mAP) is used for evaluating the detector performance. Speed of detection per image, measured in milliseconds (or number of frames per second) is also used for evaluating the detector. These performance measures are used for comparing the performance of the proposed detector with Faster R-CNN and

YOLOv3 based detectors. Accuracy is used as the measure for evaluating the classifier performance. Confusion matrix-based evaluation for analyzing the accuracy of the classifier across various traffic sign classes is also used.

C. *Detector training*

Detector training was done on GTSDB dataset with 600 training images. Resnet50 model pretrained on COCO dataset was loaded as the backbone model for the RetinaNet. The regression subnets and classifier subnets are trained for 64 epochs with 500 steps/epoch, using minibatch training with a batch size of 4. The Adam algorithm [21] was used as the loss function optimizer with an initial learning rate of 1e-5 with learning rate reduction by a factor of 0.1 if learning plateaus. For focal loss, a weighting factor of $\alpha = 0.25$ and focusing parameter $\gamma = 2$ is used. $\lambda = 1$ is used as the balancing factor for the multi task loss. After 64 epochs of training, the classification loss has reduced to 0.0066 and regression loss to 0.196.

D. *Classifier training*

Classifier was trained on GTSRB dataset with 39209 training images. Minibatch training with batch size of 16 was done. Adam optimizer was used with an initial learning rate of 0.001 and learning rate decay of 1e-6 per mini batch. The classifier was trained for 50 epochs initially without any data augmentation and further for an additional 200 epochs with data augmentation, as proposed in [1], using various image transformations like shifting, shearing, scaling and rotation.

V. EVALUATION

A. *Detector Performance*

The RetinaNet based traffic sign detector was evaluated using the GTSDB test set consisting of 300 images. Mean Average Precision (mAP) is used as the performance measure for the detector. The proposed detector could achieve a state-of-the-art detection performance of 96.7% on the GTSDB test set. mAP of 97.1% is observed when verified with the training

Figure 5. Sample images of 43 traffic sign classes from GTSRB dataset [7]

Figure 5. (a) Traffic sign detection results. (b) Traffic signs labelled with classification results

set images. It took an average of 197ms for processing an image, i.e., an average frame processing rate of approximately 5 frames/sec (fps) could be achieved. Examples of detection results are shown in Figure 5 (a).

The detector performance is compared with traffic sign detector implementations using Faster R-CNN [1] and YOLOv3 [9] evaluated using the GTSDB test set. The proposed RetinaNet based detector outperforms both the detectors in terms of accuracy. However, YOLOv3 could achieve a higher frame rate performance of 9.87 fps with a mAP of 92.2%.

A comparison of the detector performances evaluated on Intel i7 based PC with Nvidia GTX 1060 GPU is in Table II.

TABLE II. TRAFFIC SIGN DETECTOR COMPARISON

Detector	mAP	Time per image	Frame Rate
Faster R-CNN [1]	84.5%	261ms	3.82 fps
YOLOv3 [9]	92.2%	101ms	9.87fps
RetinaNet (proposed)	**96.7%**	197ms	5.07fps

B. *Classifier Performance*

The CNN based custom traffic sign classifier was evaluated using the GTSRB test set consisting of 12630 images. Model trained without data augmentation could achieve an accuracy of 96.46%. With data augmentation, accuracy has improved to 99.6% as reported in [1]. Figure 6 shows the confusion matrix of the classification results from the model trained with data augmentation, where the per class accuracy of the classification results can be seen. It can be seen that most of the classes could be classified with 100% accuracy. A minimum accuracy of 97% is observed for one of the classes.

A complete traffic sign recognition pipeline using RetinaNet based detector, bounding box processor and CNN based classifier has been setup by integrating the components. The final result images with labels generated by the classifier on bounding boxes from the detector are shown in Figure 5(b).

VI. CONCLUSION

In this paper, a traffic sign recognition system based on RetinaNet detector and a custom CNN based classifier is proposed. The detection performance, with traffic-sign being considered as single class, is found to be superior to all previous detectors, based on the detection accuracy, with a reasonably high frame rate. The proposed detector has been proved to be able to detect almost all categories of traffic signs and could regress accurate bounding boxes for the detected signs. The CNN based traffic sign classifier is simple in architecture with very high accuracy. The RetinaNet based detector and CNN based classifier completes the traffic sign recognition pipeline.

The fine-tuning and evaluation of the proposed detection network on other benchmark datasets such as Tsinghua-Tencent 100K can be taken up in future, which could make

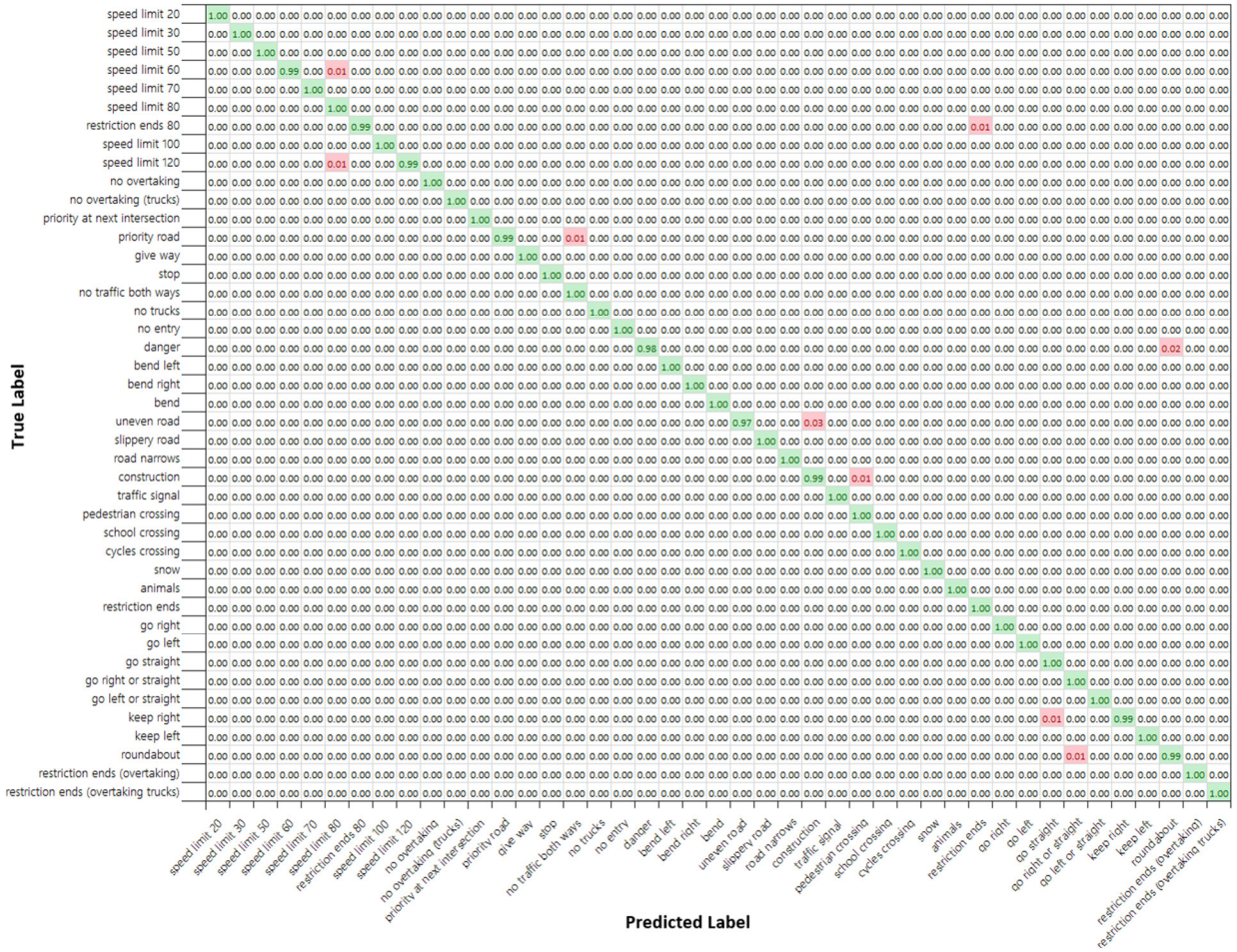

Figure 6. Traffic Sign Classifier Confusion Matrix

the recognition system more robust. Also, there is a possibility of enhancing the datasets with newly added traffic signs, so that the model can be made current with the existing transportation infrastructure in various countries. End-to-end traffic sign recognition pipeline using the proposed detector is another aspect which can be explored further. Based on some of the initial evaluations, it is observed that RetinaNet detector's performance is promising for end-to-end traffic sign recognition. Experiments with fine tuning the network parameters to bring the performance of end-to-end recognition comparable to the detector-classifier combined approach can be taken up in future.

REFERENCES

[1] Jia Li and Zengfu Wang, "Real-Time Traffic Sign Recognition Based on Efficient CNNs in the Wild", *IEEE Trans. Intell. Transp. Syst.*, vol. 20, no. 3, Mar. 2019.

[2] J. Redmon, S. Divvala, R. Girshick, and A. Farhadi, "You only look once: Unified, real-time object detection," in *Proc. IEEE Conf. Comput.Vis. Pattern Recognit.*, pp. 779–788, Jun. 2016

[3] W. Liu *et al.*, "SSD: Single shot multibox detector," in *Proc. Eur. Conf Comput. Vis.* Cham, Switzerland: Springer, 2016.

[4] Tsung-Yi Lin, Priya Goyal, Ross Girshick, Kaiming He, Piotr Dollár, "Focal Loss for Dense Object Detection", [Online] Available: https://arxiv.org/abs/1708.02002, 2017

[5] Tsung-Yi Lin, Piotr Dollár, Ross Girshick, Kaiming He, Bharath Hariharan, Serge Belongie, "Feature Pyramid Networks for Object Detection ", [Online] Available: https://arxiv.org/abs/1612.03144, 2016

[6] S. Houben, J. Stallkamp, J. Salmen, M. Schlipsing, and C. Igel, "Detection of traffic signs in real-world images: The German traffic sign detection benchmark," in *Proc. IEEE Int. Joint Conf. Neural Netw.*, pp. 1–8, Aug. 2013.

[7] J. Stallkamp, M. Schlipsing, J. Salmen, and C. Igel, "The German traffic sign recognition benchmark: A multi-class classification competition," in *Proc. IEEE Int. Joint Conf. Neural Netw.*, pp. 1453–1460, Aug. 2011.

[8] Joseph Redmon, Ali Farhadi, "YOLO9000: Better, Faster, Stronger", [Online] Available: https://arxiv.org/abs/1612.08242, 2016

[9] Joseph Redmon, Ali Farhadi, "YOLOv3: An Incremental Improvement", [Online] Available: https://arxiv.org/abs/1804.02767, 2018

[10] Y. Yang, H. Luo, H. Xu, and F. Wu, "Towards real-time traffic sign detection and classification," *IEEE Trans. Intell. Transp. Syst.*, vol. 17, no. 7, pp. 2022–2031, Jul. 2016.

[11] Y. Zhu, C. Zhang, D. Zhou, X. Wang, X. Bai, and W. Liu, "Traffic sign detection and recognition using fully convolutional network guided proposals," *Neurocomputing*, vol. 214, pp. 758–766, Nov. 2016.

[12] Z. Zhu, D. Liang, S. Zhang, X. Huang, B. Li, and S. Hu, "Traffic-sign detection and classification in the wild," in *Proc. IEEE Conf. Comput.Vis. Pattern Recognit.*, Jun. 2016, pp. 2110–2118.

[13] R. Girshick, "Fast R-CNN," in *Proc. IEEE Int. Conf. Comput. Vis.*, Dec. 2015, pp. 1440–1448.

[14] E. Peng, F. Chen, and X. Song, "Traffic sign detection with convolutional neural networks," in *Proc. Int. Conf. Cogn. Syst. Signal Process.*, Singapore: Springer, pp. 214–224, 2016.

[15] S. Ren, K. He, R. Girshick, and J. Sun, "Faster R-CNN: Towards real-time object detection with region proposal networks," *IEEE Trans. Pattern Anal. Mach. Intell.*, vol. 39, no. 6, pp. 1137–1149, Jun. 2017.

[16] A. G. Howard et al. (2017). "MobileNets: Efficient convolutional neural networks for mobile vision applications." [Online]. Available: https://arxiv.org/abs/1704.04861

[17] D. Ciregan, U. Meier, and J. Schmidhuber, "Multi-column deep neural networks for image classification," in *Proc. IEEE Conf. Comput. Vis. Pattern Recognit.*, Jun. 2012, pp. 3642–3649.

[18] P. Sermanet and Y. LeCun, "Traffic sign recognition with multi-scale convolutional networks," in *Proc. IEEE Int. Joint Conf. Neural Netw.*, Aug. 2011, pp. 2809–2813.

[19] T. L. Yuan. GTSRB_Keras_STN. Accessed: Nov. 1, 2017. [Online] Available: https://github.com/hello2all/GTSRB_Keras_STN

[20] Kaiming He, Xiangyu Zhang, Shaoqing Ren, Jian Sun, "Deep Residual Learning for Image Recognition", [Online] Available: https://arxiv.org/abs/1512.03385

[21] D. Kingma and J. Ba. (2014). "Adam: A method for stochastic optimization." [Online]. Available: https://arxiv.org/abs/1412.6980

Proceedings of the Fourth International Conference on Communication and Electronics Systems (ICCES 2019)
IEEE Conference Record # 45898; IEEE Xplore ISBN: 978-1-7281-1261-9

Asymmetric Multilevel Inverter Induction Motor Drive for Fuel Cell Based Electrical Vehicles

Sumit Kumar
Department of Electrical Engineering
NIT Kurukshetra
National Institute of technology
Kurukshetra,India
sumitsinghnitkkr@gmail.com

Yash Pal
Department of Electrical Engineering
NIT Kurukshetra
National Institute of technology
Kurukshetra,India
yash_pal1971@yahoo.com

***Abstract*— This paper presents direct torque control scheme for an asymmetric multilevel inverter fed induction motor drive for fuel cell based electrical vehicles. The controlling principle is based on Direct torque control (DTC) method. The torque and flux estimator takes input as measured voltage, current and stator resistance. The estimator further calculates the error in flux and torque. The SPWM generates such switching signals which reduce error. The asymmetric multilevel inverter provides almost sinusoidal voltage with less total harmonics distortion (THD) and less switching devices resulting in lesser switching losses. In addition, torque ripple is minimized because of small dv/dt, since each power cell of multilevel inverter operates at switching rate which is very high so we obtain an efficient torque and flux controller. A comparative analysis of two level and multilevel inverter is also done in respect of transient responses and torque ripple. To authenticate the accomplishment of DTC for an asymmetric multilevel induction motor drive for fuel cell electrical vehicles, Simulations are executed in MATLAB/Simulink. The results vindicate advantages of asymmetrical multilevel induction motor drive DTC control for electrical vehicles.**

Keywords—Total harmonic distortion(THD), Direct torque control (DTC), Sinusoidal pulse width modulation (SPWM), Electrical Vehicle (EV) cascaded h-bridge (CHB)

I. INTRODUCTION

Due to extensive use of fossil fuels vehicles, the environmental condition is becoming deteriorating day by day. Co_2 production by these vehicles is increasing at alarming rate, which cause various environmental issues like greenhouse effect and many more. Fossil fuels are limited in nature and if we keep using them at the present rate then the day will be near when we are devoid of them [1]. These all environmental apprehensions have forced to limit the conventional vehicles. Fuel cell based electrical vehicles are one of the most prominent solutions to overcome the challenges caused by conventional vehicles. Due to low weight, small size and low temperature operation, fuel cell is famous in electrical vehicle application. Fuel cell is having high energy density but low dynamic response. Therefore another fast charging storage is required to improve dynamic response of fuel cell. Efficiency and dynamic response of fuel cell can be enhanced by the use of ultra-capacitor [2].

Today induction motors are very famous in variable speed drive. DTC is one of the emerged solutions for better dynamic accomplishment of these machines. DTC method combined with PWM and space vector modulation (SVM) reduces ripple in torque and also maintain the switching frequency of inverter constant [10]. While DTC scheme having no modulator and linear torque controllers which gives significance upswing along with high dynamic performance[3-5]. Additionally, multilevel inverters have emerged as most promising elucidation for high power implementation. Because of output sinusoidal voltage, harmonics spectrum is better and limits the stress on motor insulation windings. It gives the solution over low levels of output voltage and requirement of an expensive and large filter [6].

In this paper, Direct torque control (DTC) enables the natural consolidation of multilevel inverter with induction motor drives. In this model, an asymmetric H-bridge multilevel inverter of seven levels is used [9]. It reduces torque ripple and improve transient responses compared to two level inverter. Simulation results confirm the improvement and advantage of proposed method [7].

This paper has organized in the following sequence. Section II consist a brief discussion about asymmetric CHB inverter. Section III includes DTC scheme for induction motor drive. In section IV results have been discussed for two level and multilevel both. And finally section V concludes the outcomes of the presented work and also discussed about future scope of this work.

II. ASYMMETRIC CHB INVERTER

The asymmetric seven level cascaded h-bridge inverter power circuits exhibited in figure.1. It has three legs each contains two cell fed by independent unequal DC sources. Here DC voltage is obtained by fuel cell.

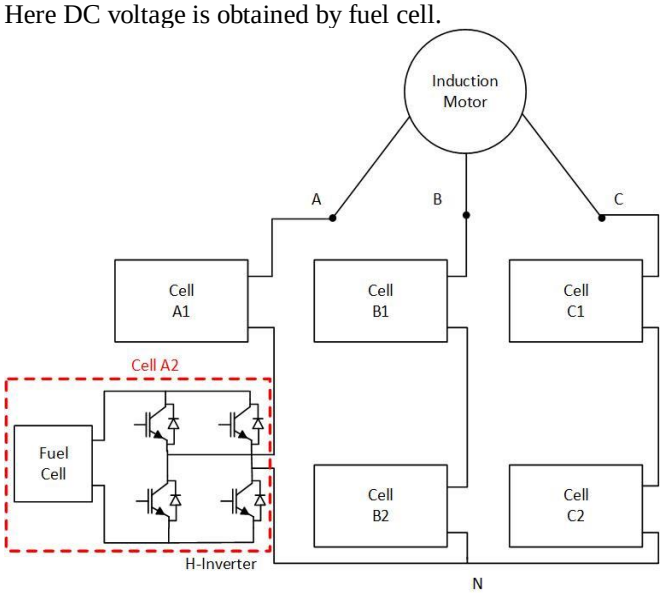

Fig. 1. Presented asymmetrical multilevel inverter

The foremost benefit of an asymmetric multilevel inverter is that with same number of semiconductors switches, it give more number of levels and hence switching losses reduces with a significant factor [8]. If we feed partial voltages of V/(M-1), the all possible redundancies is equal to (3^a -2a -1). If 'a' number of cells are connected to each leg of inverter then the 3^a switching configurations are there [10]. Output voltage of multilevel inverter relies on partial voltage fed to each cell. The feasible switching states can be also minimized if each cell is fed by unequal dc voltage. This result in reduction of cost, volume and switching losses and the conversion efficiency becomes very high.

Particular cell j can give three different voltage levels ($+E_j$, 0, $-E_j$). The asymmetry we can attain from dc voltage is scaled in power of two or three, gives seven or nine distinct levels of output voltage. Seven levels of output can be obtained by two cells, while three cells are required to generate the same seven levels of output with symmetrical multilevel of inverter.

III. INDUCTION MOTOR DTC SCHEME

Direct torque control is an alternate scheme to flux-oriented control(FOC). DTC scheme is generally based on refinement of stator voltage on the basis of torque and flux error. DTC method has advantage that stator flux and current waveforms are almost sinusoidal. The motor parameters won't affect the DTC scheme except the stator resistance. DTC provides superior torque control in transient and also in steady state [12].

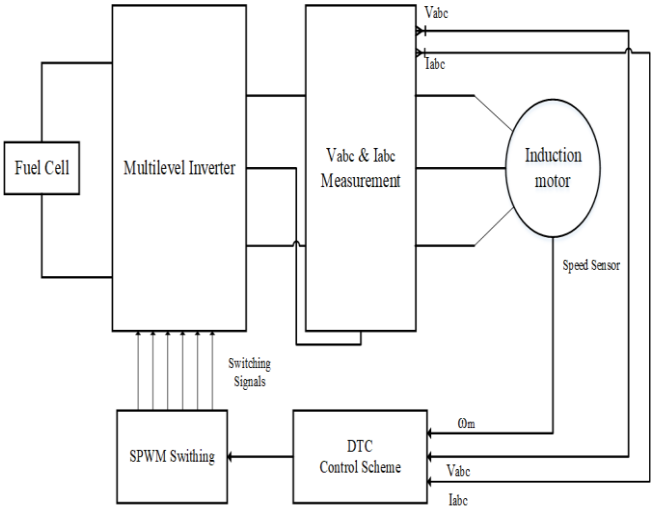

Fig. 2. Block diagram of multilevel DTC induction motor drive

The concerned multilevel drive system is displayed in fig 2 for study point of view. The system consists of multilevel inverter fed by fuel cell (V_{dc}) to drive the induction motor. V_{abc}, I_{abc} and speed are sensed by sensing devices. DTC block used to govern torque and speed of induction motor and with the help of carrier base sinusoidal PWM scheme it generates switching signal for multilevel inverter[11].

A. Modulation strategy

In this paper, the phase shifted multicarrier PWM scheme is accomplished for generating switching signal for multilevel inverter. Usually for P voltage level inverter , (P-1) carriers are needed. In this scheme all carriers have equal frequency and amplitude while two neighbouring carrier signals have some phase shift, given by

$$\Phi = 360/(p-1)$$

The modulating wave is generally a sinusoidal signal having alterable frequency and amplitude. The switching pulse are produced by comparing both modulating and carrier signal. Output wave of each cell is identical except having some phase difference due phase shifted carrier signal.

B. Induction motor modelling

$$\frac{d\Psi_s}{dt} = -\frac{1}{T_s\sigma}\Psi_s + \frac{L_m}{L_r T_s \sigma}\Psi_r + U_s \quad \ldots\ldots. 1$$

$$\frac{d\Psi_r}{dt} = \frac{L_m}{L_r T_s \sigma}\Psi_s - \left(\frac{1}{T_s\sigma} - j\omega_r\right)\Psi_r \ldots\ldots 2$$

Where,

Ψ_s	stator flux
Ψ_r	rotar flux
u_s	stator voltage
L_s	stator total inductances
L_r	rotor total inductances
L_m	magnetizing inductances
R_s	stator resistance of IM
R_r	rotor resistance of IM
ω_r	rotor speed of IM

$\sigma = 1-L_m^2/L_sL_r$, $T = L_s/R_s$, $T_r = L_r/R_r$,

Torque is expressed as

$$T_e = \frac{1.5PL_m}{L_{\sigma_*}^2}\left(\Psi_{s\beta}\Psi_{r\alpha} - \Psi_{s\alpha}\Psi_{r\beta}\right) \quad \ldots\ldots 3$$

Where, P denotes pole pairs and $L_{\sigma_*}^2 = L_sL_r\sigma$

C. Design of Direct torque control scheme

The presented DTC scheme displayed in figure 3, consists three major Parts: torque and flux estimator, PWM gating pulse originator and PI controller.

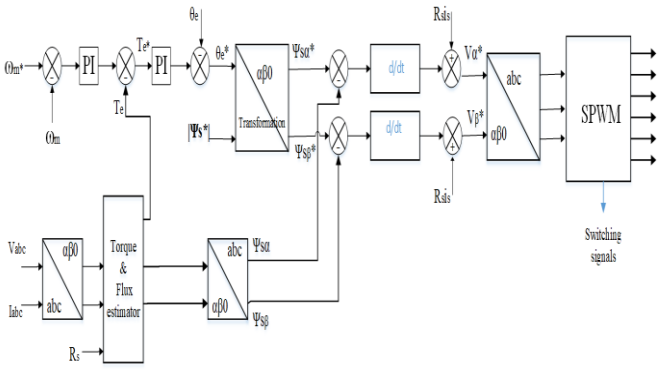

Fig. 3. Presented DTC scheme for multilevel IM drive

The computed voltage, current and stator resistance is given for torque and flux estimation, Evaluated value by torque and flux estimator block are further practiced to determine errors. Speed error is deliberated by comparing

constant speed(ω_{r*}) and computed rotor speed (ω_r) and fed to PI controller which gives reference torque (T_{e*}). PI torque regulator gives reference angle (θ_{e^*}) and after comparing them, we get angle error (θ_{e^*}- θ_e) which further given to transformation block.

The constant stator flux (Ψs^*) is same as rated stator flux ($\Psi s_{\_rated}$) when speed is less the base speed (ω_{br}) and when speed is more than base speed it proportionally reduces. The switching block get three sinusoidal signal which generate the gating pulse for inverter.

$$\Psi_s^* = \Psi_{s\_rated} \; for \; \omega_r < \omega_{br} \; \ldots\ldots\ldots\ldots\ldots 4$$

$$\Psi_s^* = \Psi_{s\_rated} \left(\frac{\omega_{br}}{\omega_r}\right) \text{ for } \omega_r > \omega_{br} \; \ldots\ldots 5$$

The stator flux components are calculated with the help of direct and quadrature axes values of voltage, current and resistance (R_s).

$$\psi_{\alpha s} = \int \left(v_{\alpha ss} - i_{\alpha ss} R_s\right) dt + \psi_{\alpha so} \; \ldots\ldots\ldots\ldots 6$$

$$\psi_{\beta s} = \int \left(v_{\beta ss} - i_{\beta ss} R_s\right) dt + \psi_{\beta so} \; \ldots\ldots\ldots\ldots 7$$

Total stator flux (Ψ_s) is given as

$$\psi_{\alpha s} = \sqrt{\psi_{\alpha s}^{\,2} + \psi_{\beta s}^{\,2}} \; \ldots\ldots\ldots\ldots\ldots\ldots 8$$

The developed torque is enumerated by help of direct and quadrature axis flux and current components.

$$T_e = \left(\frac{3}{2}\right)\left(\frac{P}{2}\right)\left(\psi_{\alpha s} i_{\beta ss} - \psi_{\beta s} i_{\alpha ss}\right) \ldots\ldots 9$$

Where

$v_{\alpha ss}, i_{\alpha ss}, \psi_{\alpha s}$ Direct axis stator voltage, current and flux respectively

$v_{\beta ss}, i_{\beta ss}, \psi_{\beta s}$ Quadrature axis stator voltage, current and flux respectively

V_{abc}, $v_{\alpha ss}$ and $v_{\beta ss}$ is computed using Clarke transformation

$$v_{\alpha ss} = \left(\frac{1}{3}\right)\left(2v_a - v_b - v_c\right) = v_a \; \ldots\ldots 10$$

$$v_{\beta ss} = \left(\frac{1}{3}\right)\left(\sqrt{3}v_b - \sqrt{3}v_c\right) \; \ldots\ldots\ldots 11$$

In Fig.4 scheme for computation of flux and torque is presented. With the help of equation given in 6 and 7 flux can be estimated and by equation 9 torque is estimated.

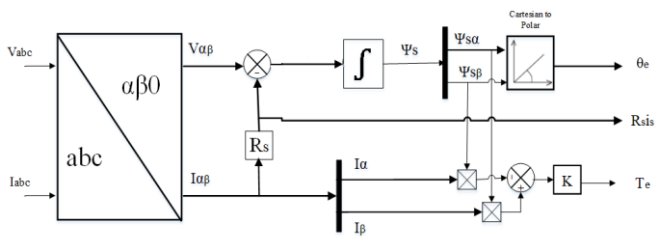

Fig.4. Flux and torque estimation block diagram

IV. SIMULATION RESULTS

For the authentication of presented control scheme for multilevel induction motor drive, simulation of asymmetrical multilevel inverter IM drive and two level inverter fed IM drive are performed using MATLAB. The IM parameters used in MATLAB simulation is presented in TABLE 1.

TABLE 1 : Induction motor parameters

Parameter	Value
Power Rating	4 KW
R_s	1.404 Ω
R_r	1.396 Ω
L_s	0.00598 H
L_s	0.00589 H
L_m	0.1730 H
Inertia(J)	0.0132 Kg.m^2
No of poles	2
Speed (Rated)	1430 rpm
Line voltage	400 V
Rated Frequency	50 Hz

A. *Results of two level Inverter*

Output voltage of two level converter which is fed to IM is displayed in Fig. 5 . The output voltage waveform clearly explains poor dynamic response of induction motor drive as it required notable time to settle at final value.

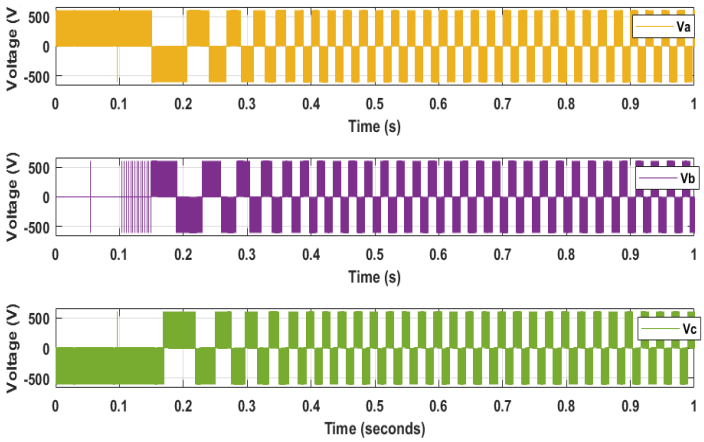

Fig.5 stator voltage in case of two level inverter

In Fig. 6 input current of induction motor is shown. The nature of this current is sinusoidal due to stator winding inductance which acts as filter. The values of current are varying in accordance to the torque.

In Fig.7 stator flux in α and β axis are shown. Both the signals are 90 degree apart from each other sinusoidal in nature. Stator flux is kept invariant in spite of variation in torque and speed.

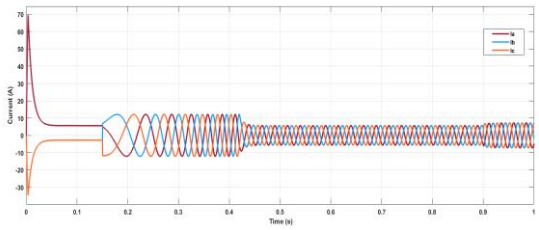

Figure 6 Stator phase current in case of two level inverter

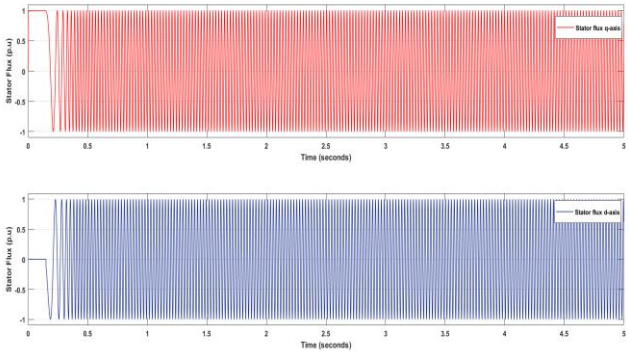

Figure 7 stator flux in α and β axis in case of two level inverter

In Fig. 8 actual and reference speed of induction motor are shown. The reference speed is tracked by actual speed as clearly shown in figure. But the time required by actual speed is 0.4 sec to track the reference speed which indicates poor dynamic response of drive with two level inverter.

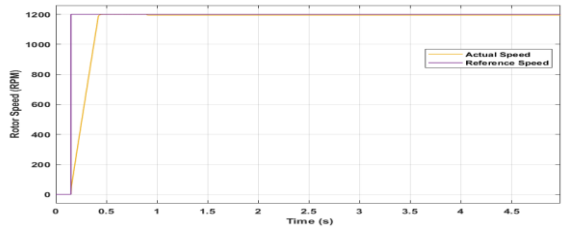

Fig. 8 Reference and actual speed in case of two level inverter

Like speed, actual and reference torque are displayed in figure. 9. Reference torque is tracked by actual torque still dynamic response is worse because actual torque takes approximately 0.8 sec to track the reference torque. In addition to this, transient response also need to be improved as it's value rises to 30 during starting in case of two level inverter.

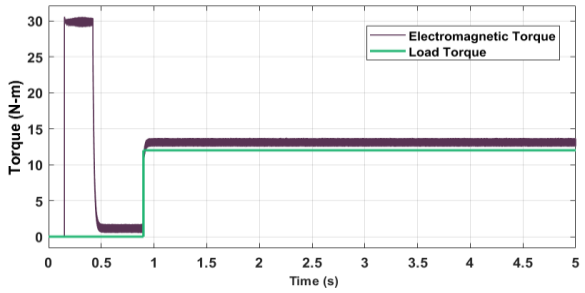

Figure 9 Reference and actual torque in case of two level inverter

B. Results of multilevel inverter

In fig. 10 phase A multilevel inverter voltage signal is shown. Dynamic response compared to two level inverter is much better also total harmonics distortion is less.

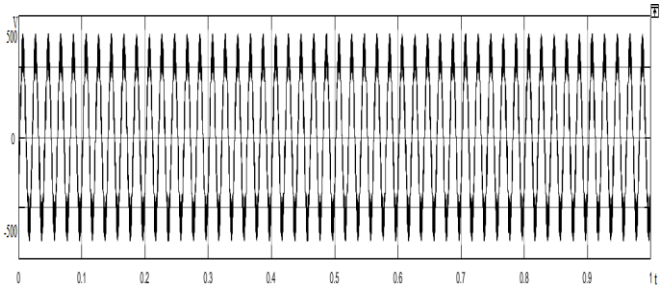

Figure 10 stator phase voltage of multilevel inverter

Likely, stator current is displayed in fig.11 which clearly indicates better dynamic response and current transient as compared to two level inverter . It needs very few time to settle at a final value.

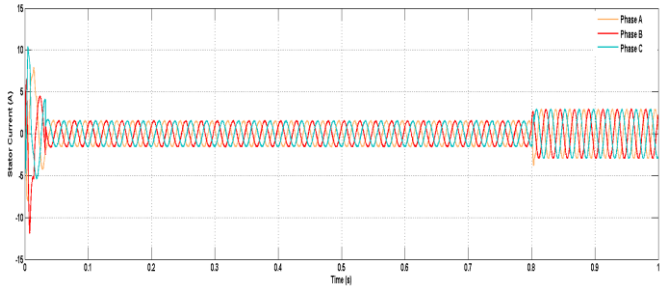

Figure 11 Stator current in case of multilevel inverter

The d and q-axis stator flux are displayed in fig. 12 which is constant everywhere similar to the two level inverter.

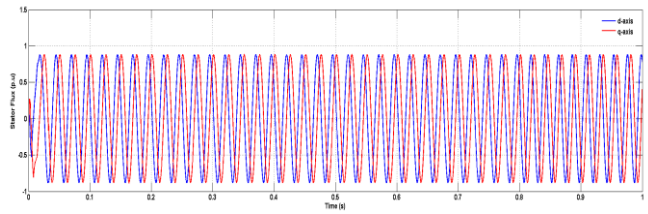

Fig. 12 Stator d and q- axis flux in case of multilevel inverer

In fig.13 actual and reference speeds are shown. We can clearly observe from the figure that it has better dynamic response of IM drive as compared to two level inverter. In case of multilevel inverter actual speed takes 0.2 sec to track the reference speed, While in case of two level inverter, it takes only 0.4 sec.

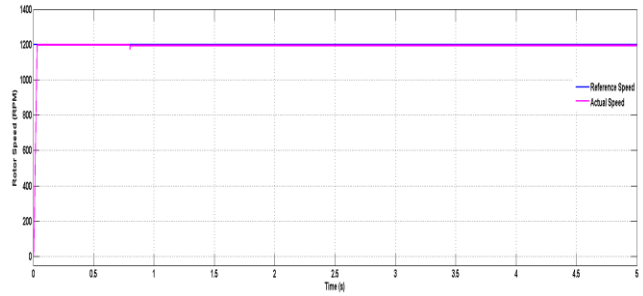

Fig. 13 Reference and actual speed in case of multilevel inverter

Like wise, The reference torque and actual torque is displayed in fig 14. It can be seen from figure that both transient and dynamic resposnse are improved in case of multilevel inverter.

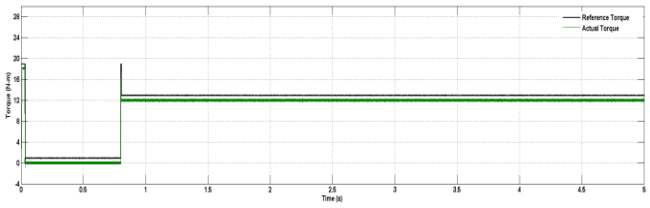

Fig. 14 Actual and reference torque in case of multilevel inverter

VI. CONCLUSION

This paper elucidates performance of asymmetrical multilevel inverter fed induction motor drive with DTC control scheme, which is very popular for electric vehicles. The multilevel inverter drive provides a DTC consolidation for high power application. The major accomplishment of the presented control scheme are minimization in torque ripple, better dynamic response, sinusoidal output voltage having very low THD and lower switching losses in compared of two level inverter. The simulation results validate the better performance of multilevel inverter drive over two level inverter drive. The results also infer that there is yet a chance of further refinement in the presented scheme in terms of new switching techniques and new multilevel topology with reduced number of switches.

REFERENCES

[1] I. Zamora , J.I. SanMartín , F.J. Asensio , V. Aperribay J. García Villalobos, "Plug-in electric vehicles in electric distribution networks: A review of smart charging approaches", Renewable and Sustainable Energy Reviews, vol. 38, pp. 717–731, Oct. 2014.

[2] C. Chan, A. Bouscayrol and K. Chen, "Electric, Hybrid, and Fuel-Cell Vehicles: Architectures and Modeling", IEEE Transactions on Vehicular Technology , vol. 59, pp. 589-598, Oct. 2010.

[3] D. Casadei, F . Profumo, G. Serra, A. Tani, "FOC and DTC: two Viable schemes for induction motors torque control", IEEE Transactions on Power Electronics , vol. 17, Sep 2002

[4] P.Kazmier kowski andB.Kasprowicz"Improved direct torque and flux vector control of PWM-fed induction motor drives," IEEE Trans. Ind. Electron., vol. 42, pp. 344–349, Aug. 1995.

[5] N. M. Nordin, N. R. N. Idris, and N. A. Azli, "Direct Torque Control with 5-level cascaded H-bridge multilevel inverter for induction machines," IECON 2011 - 37th Annual Conference of the IEEE Industrial Electronics Society, pp. 4691–4697, Nov. 2011.

[6] J. Rodriguez, L. G. Franquelo, S. Kouro, J. I. Leon, R. C. Portillo, M. A.M. Prats, and M. A. Perez, "Multilevel converters: An enabling technologyfor high-power applications," *Proc. IEEE*, vol. 97, no. 11, pp. 1786–1817,Nov. 2009.

[7] F. Khoucha, M. S Lagoun, K. Marouani, A. Kheloui, and M. E. H. Benbouzid,"Hybrid cascaded H-bridge multilevel inverter induction motordrive direct torque control for automotive applications,"*IEEE Trans. Ind.Electron.*, vol. 57, no. 3, pp. 892–899, Mar. 2010.

[8] M.Veenstra et *al.*, "Control of a hybrid asymmetric multilevel inverter for competitive medium- voltage industrial drives, *IEEE Trans. Industry Applications*," vol. 41, n°2, pp. 655-664, March-April 2005.

[9] A. M. Trzynadlowski, Control of Induction Motors. Academic Press, Diego, CA, 2001.

[10] C. Lascu, S. Jafarzadeh, "Direct Torque Control With Feedback Linearization for Induction Motor Drives", IEEE Trans. Power Electronics, Vol. 32, Mar. 2017.

[11] M. Manjrekar and T. A. Lipo, "A hybrid multilevel inverter topology for drive application," in *Proc. IEEE APEC1998*, Anaheim, CA, Feb., pp. 523–529.

[12] C. Lascu, S. Jafarzadeh, "Direct Torque Control With Feedback Linearization for Induction Motor Drives", IEEE Trans. Power Electronics, Vol. 32, Mar. 2017.

Proceedings of the Fourth International Conference on Communication and Electronics Systems (ICCES 2019)
IEEE Conference Record # 45898; IEEE Xplore ISBN: 978-1-7281-1261-9

SURVEILLANCE SYSTEM FOR DEAD ZONE

Ayushi Kandoi*, Pradyumna Hegade*, Utkarsh Goel, Venkata Harshavardhan Reddy Allu, Dhanalakshmi Samiappan*, R. Kumar
Department of Electronics and Communication Engineering
SRM Institute of Science and Technology
Chennai, India
ayushikandoi24@gmail.com, pradyumnahegade@gmail.com, dhanalakshmi.s@ktr.srmuniv.ac.in

Abstract:

This paper presents a surveillance system that is capable of transmitting its geo location and the information from real time images to a central unit in no network zone. The system is further configured for using image processing and machine learning algorithms to deduce any suspicious object from the captured image. Thereby, the system is helpful in identifying threats in all kind of weather conditions on land and in oceans. The system is very efficient, cost effective and is simple in design. Once the threat is identified, the system transmits the information to the central unit through the LoRa by using certain communication protocols. Compared to existing devices, this system has the potential to reduce causalities by enhancing navigational and observational features in the surveillance sector.

Keywords:

Image Enhancement; Object Identification; LoRa; LoraWAN; Geolocation; RSSI.

I. INTRODUCTION

Surveillance, a process of monitoring an area, a situation or a person. Borderline areas and restricted territories surveillance are important for any country's safety. In some cases, human forces are deployed to achieve surveillance by constantly monitoring for changes. But the human surveillance is not always a feasible option in cases when the areas to be monitored are risky and inaccessible. There are also the added risks of losing personnel in the event of getting caught by the enemy or any other possible events. With present inventions in modern technology over the years, it is possible to remotely monitor areas of importance by using robots in place of humans. Till date, many remote surveillance robotic systems are available in the market for this purpose. Recently designed robotic systems mostly comprise different types of localization aids such as a GPS system or internal compass, and communication means to exchange information and instructions with a remote-control station.

However, the remote surveillance systems available in recent times highly depend on the availability of communication networks. In case of unavailability of communication network these systems are bound to stop functioning. The communication networks often get affected due to weather conditions or due to destruction of communication channels in war zones. Thus, surveillance becomes difficult in war zones. Hence, a system and method for remote surveillance in no network zones has to be developed. Also, a need to develop a system for remote surveillance that is capable of transmitting geo location and information from real time images to a central unit in no network zone. A system and method of remote surveillance in no network zone could lead to greater advances in surveillance sector by providing: (a) a system to provide a surveillance system that uses image processing and machine learning algorithms to deduce any suspicious object (b) a system that does not rely on Global Positioning System(GPS) but rather relies on the local positing system (c) a system to provide a surveillance system capable of collecting real time images and geo location in no network zones for identifying potential threats (d) a system to provide a remote surveillance system capable of working in all kind of weather conditions on land and in oceans while being more efficient, cost effective and is simple to design.

II. SYSTEM MODEL DESIGN

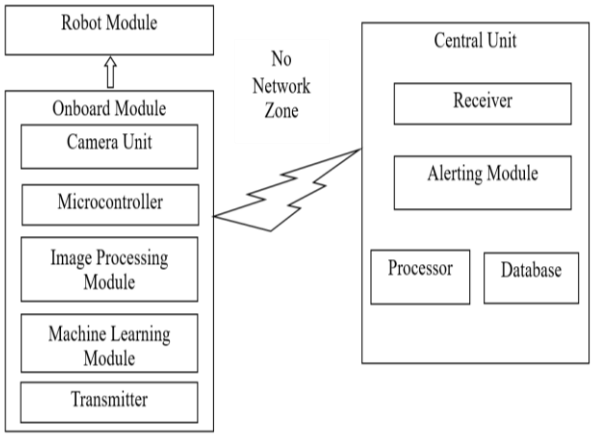

Fig 1: System model

This section briefs on the various components associated with the model. The components were decided mainly focusing the efficiency, the cost effectiveness and power consumption levels. The system has basically two main units as shown in the Fig 1: (a) Robot Module present at the no network zone and (b) the central unit at communicable area.

Robot Module:

The robot module has various onboard components. The robot has been built in a way that it has the dynamic capability to cover any kind of terrain. The chassis is made up of light fiber material, embedded with motor shield for driving the motors, Raspberry Pi as the major microcontroller. Additionally, a camera is deployed for taking the images of the surrounding. The captured image is further processed to extract information using the image processing and machine learning algorithms. The reliable extracted data is then sent over to the central unit via the LoRa module SX1278 (works at a frequency of 433Mhz) which is controlled by the Arduino as a microcontroller.

Central Unit:

The central unit comprises of LoRa module SX1278 which receives the data from the robot module through LORAWAN protocol. Then the received data is further processed with the help of Arduino as a microcontroller. Received information is then processed and classified as the suspicious or non-suspicious object.

III. STATE OF THE ART

The sections followed describes the various state of the art regarding the individual components that are being utilized. Firstly, the image processing algorithms are applied on the captured image for qualitative improvement of the images, that is further processed by implementing machine learning algorithms to identify the elements present in the image. Furthermore, the transmission of information done in no network area with LoRa as a transceiver is discussed. Lastly, the section ends with the integration of individual platforms as a whole.

A. Image Processing:

Due to the limitations of cameras or the presence of non-ideal situation degrade the quality of images. Even different camera devices do not correctly capture the luminance. The contrast, brightness and sharpness of an image are the most important factors which affects its quality. An image which has low contrast and brightness, is associated with dynamic range. The pixels of image can be classified in shadow and highlight. To enhance the images with low brightness, contrast and sharpness we are using conventional algorithms like gamma correction, histogram equalization and unsharp masking to produce the expected results.

Each pixel has some brightness level called luminance [3]. The value of luminance lies between 0 to 1 where 0 means completely dark and 1 means complete bright. So, to correct the luminance we are using gamma correction. Histogram equalization is such a widely used algorithm. Histogram Equalization preserves the brightness and improve the contrast of the image. In our work our main aim is to improve the overall quality of the image so it will easy of the machine to identify the objects in the image.

This section provides a complete description of the proposed method. Figure below shows stepwise flowchart of the proposed method. The proposed method is initiated by calculating the Gamma correction of the image then the conversion of RGB image to YUV image and then the implementation of histogram equalization. In last convert the YUV back to RGB image.[6]

In the gamma correction the gamma is represented by Greek letter which can be described as the relationship between input and output image. The output is proportional to the input raised to the power of gamma.

$$I' = 255 \times \left(\frac{I}{255}\right)^{\frac{1}{y}}$$

Histogram equalization is one the most commonly used contrast enhancement algorithm. It is simple and effective technique. In the equation X = {X(i, j)} denotes an image composed of L discrete gray levels. X(i, j) represents the intensity of the image at (i, j).

$$p(X^k) = \frac{n^k}{n}$$

For k = 0, 1, 2, 3, ……L-1.

Unsharp Masking is most widely used method for image sharpening. This method is simple and work well in many applications also. This algorithm usually decomposes the original image into low frequency component and then process two components [3].

B. Machine Learning:

a) Detection process:

This system comprises of the methodology which is a new approach to the object detection. We are using the YOLO object detection.[8] Previously the object detection required classifiers to perform the detection for them.[12] But this methodology frames the object detection as regression. A single neural network estimates both the probabilities and the bounding boxes from the entire image in one evaluation. Hence improving the performance of the detection. It can process around 45 frames per second. It outperforms various other forms of detection mechanisms present.

The system divides the image into S*S grid. The center of the object which gets in the grid cell is responsible for that object. Each of the grid cell predicts the bounding boxes denoted by B. Also, the scores for these boxes is denoted by the confidence C.

Formally the confidence is defined as

$$\Pr(\text{Object}) * \text{IOU}_{\text{pred}}^{\text{truth}}$$

If no object is present then the confidence is given as zero. Each of the bounding boxes consists a total of 5 predictions: confidence, h, x, y, w. The (x, y) coordinates tell the center of the boxes relative to the grid cell present. The height and width are also then predicted as relative to the entire image.

Confidence prediction shows the IOU between the predicted boxes and any ground truth box present. Here, each grid cell also predicts C conditional class probabilities i.e.

$$\Pr(\text{Classi}|\text{Object})$$

These probabilities are dependent on the grid cell that contains the object. It can only predict one set of class probabilities per grid cell present. It is regardless of the number of boxes B present there. Then multiply the conditional class probabilities and the individual box confidence predictions, which gives the specific confidence scores for each class.[8]

$$\Pr(\text{Classi}|\text{Object}) * \Pr(\text{Object}) * \text{IOU}_{\text{pred}}^{\text{truth}} = \Pr(\text{Classi}) * \text{IOU}_{\text{pred}}^{\text{truth}}$$

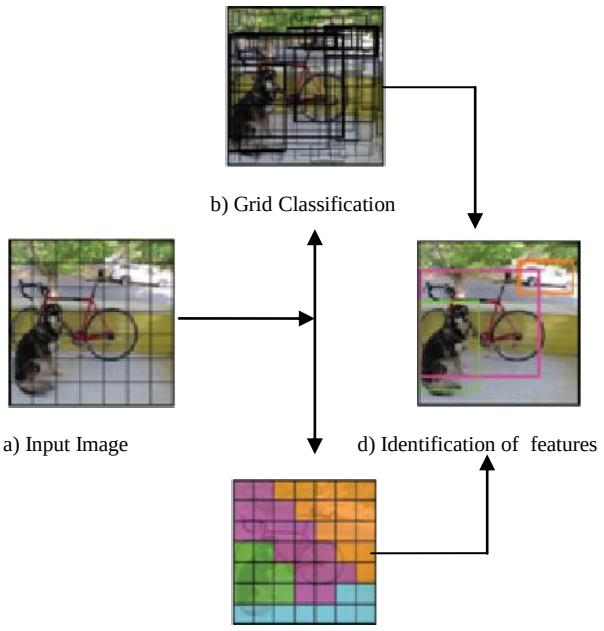

Fig.2. Working structure of Machine Learning

{Image taken from [7]}

Here the problem is taken as a regression. The image is divided into an even grid while simultaneously predicting the various bounding boxes, their confidences and class probabilities. Then these are encoded as a S * S * (B * 5 + C) tensor.

The image has S=7, B=3 and C=20. So, our final prediction is 7*7*35 tensor.

b) Training:

We train our convolutional neural network with the help of the data set of MobileNetSSD [16]. The OpenCV is being used because of its compatibility for multiple platforms and with higher speed and low computational power. We have trained 90 objects for this model.

Once the image is obtained, it is fed to the neural network [7]. But for feeding it to the neural network it has to ben converted into a tensor. A tensor can be described as the pre processed image that serves as the input. The image is converted into 300x300 size for training and the colors are swapped from BGR to RGB. As the OpenCV reads in BGR while RGB is used for training.

Each detection gives us the class probabilities or the confidence (ranges from 0 to 1). The higher confidence objects are selected and the others are discarded. Then based upon the bounding boxes recognized a rectangle is drawn across the objects identified. The class id, confidence and class name are used for drawing the bounding boxes (Figure 2). Further, text is added based upon the image size upon scaling it. So, in this way this method allows us to recognize and get a desired box across our detected objects.

C. LoraWAN for Localization

LoraWAN module SX1278 works at a frequency of 433 MHz band plays a crucial role in this work. This module is considered with the motivation of implementing a system which consumes low power for localization and transmission of data. LoraWAN modules consume 2.8mA of power in steady state and 38.9mA and 14.2mA for transmitting and receiving the data respectively. With these interesting features, the geographical localization becomes a strong application which can be achieved by applying triangulation algorithm with the RSSI values on the gateways from received packages.

a) System Design

The complete system comprises of three blocks: client, 3 gateways, server and a third-party application. The client transmits the packages using LoraWAN protocol and the gateway receives the packages which are

further forwarded to the server using LoraWAN protocol, together with the RSSI signal strength. After the server receives the data, server processes the received data and transmits the messages to the application by using Message Queue Telemetry Transport (MQTT) client. The algorithm for estimating the geographical location is then applied by processing the received information.

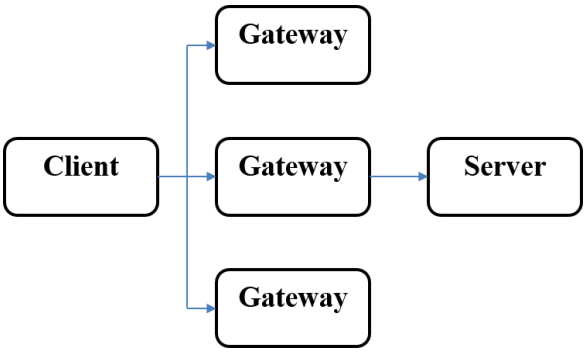

Fig.3. Experimental Setup

- *Client*

The client transmits the data acquired from the machine learning algorithm through a LoraWAN module. The data comprises of the object identification information which is received using the machine learning algorithms and sends it to the server via gateways. The client comprises of a dynamic autonomous robot with the accessories of a camera, 4 motors and a motor driver and a raspberry pi 3B+ module which plays a role of a microcontroller. The camera is used to capture the image which is processed without distortion and keeping the naturalness of the image by using the several image processing algorithms and then the identification of the object is done by using FCNN algorithm, the data is then compressed according to the limitation of the LoraWAN module, which can transmit a limited data. The overall process takes 90 seconds for processing and transmitting the data.

- *Gateways*

The important function of the three gateways is to route the received data from the client to the server via LoraWAN protocol. To estimate the location of the device, the Received Signal Strength Indication (RSSI) value is used to estimate two phases: Distance estimation and Position estimation. The distance is estimated with received RSSI strength value from the client which is considered as an unknown target, the known position of the gateways gives the coordinates of the gateways which receives the signal. By applying the log Normal Shadowing model's algorithm, the estimation of distance (d) is done. The formula for estimation:

$$RSSI(d) = -10n\log(d) - C$$

n= Path loss exponent, C= environmental constant

The estimation of distance d1, d2, d3 from the three gateways respectively is used further to estimate the accurate location of the target.

- *Server*

Server acts as a central unit of the system where the data together with the information of the RSSI value and the estimated distance from each gateway is received via LoraWAN protocol. The estimated distance is used to calculate the accurate position of the target by applying trilateration algorithm.

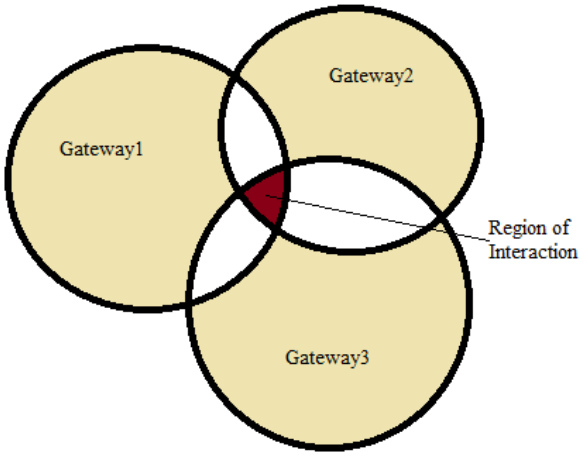

Fig.4. Trilateration Technique

The coordinates of the gateways (x1,y1), (x2,y2), (x3,y3) and the estimated distances d1, d2, d3 from each coordinates of the gateways respectively is used to estimate the unknown coordinates (x,y) by using the least mean square approximation. This is implemented by using the formula:

$$Min\|AX-B\|^2$$

X is a best solution

The circle with the distances d1, d2, d3 as the radius is drawn and the intersection of the three circular boundaries gives the coordinates of the target client.

IV. IMPLEMENTATION AND EVALUATION

This section describes how the entire operation takes place. The system comprises a robot(client) that is deployed in an area. The motion of robot is controlled

by the motor. The onboard module comprises an Arduino board and a raspberry pi board. The image processing [4] and machine learning [8] algorithms are processed in the raspberry pi. Further the raspberry pi is connected with a camera module for taking the input images of the surrounding areas. The Arduino board communicates with the raspberry pi with the help of the serial bridge between them. Also, the LoRa SX1278 module is connected with the Arduino. All the information processed by the raspberry pi is sent to the Arduino board which further sends the only required data with the help of LoRa SX1278 module. Thus, these are the modules present on the client.

The client and the server communicate is achieved using wireless radio frequencies. OpenCV is used to capture the images through the connected WebCam. It is then processed accordingly to feed to the neural network. The neural network is based on the dataset called MobileNetSSD. On detecting the provided set of pre-mentioned targets, the object is detected and its accuracy is sent to Arduino through the Serial interface connected through the USB. The Arduino uses a library called RadioHead which is provided by AirSpayce. It is used to initialize and communicate with the LoRa module. Arduino collects the data sent by Raspberry PI on the serial interface and broadcasts it using LoRa on the specified frequency (433.00 MHz). Then the gateways collect the information being broadcasted and is then combined at the server. The server is designed to show us a real time location of the client along with the detected threats.

When the experiment was conducted under the guidance of the professor the results obtained were cross referenced with the outdoor measurements and locations respectively. The errors noted were minimal. Thus, we were able to locate the object with an error of about 10 meters.

V. EXPERIMENTAL RESULTS

The results at the server side obtained were basically the distance, signal strength and thereby geo locations. Also, the system notified the user if a threat was detected. The following section will show these various components individually.

A. The image enhancement

The image below shows the image prior and after the application of image processing algorithms.

a) Test Image b) Gamma Correction c) After HE & UM

Fig.5. Results for Image Enhancement

Table1. Peak Signal to Noise Ratio

Images	Image 1	GC	HE&UM
PSNR	22.2080	22.2121	21.6612

B. The Threat Identification.

The image shown below was taken while the client was able to recognize the threats in this case humans or persons were present. It describes the various human beings present along with the accuracy of detection.

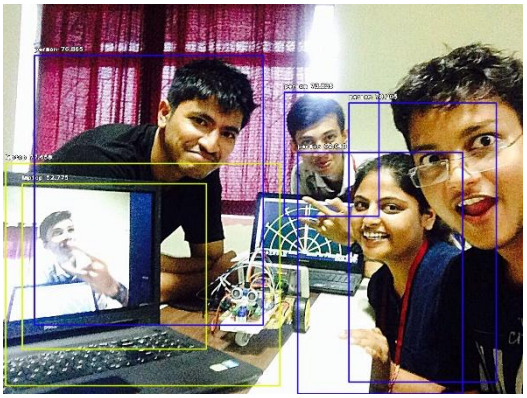

Fig.6. Results for person identification

Table2. Percent Accuracy for Image Identification

Test	Person1	Person2	Person3	Person4	Laptop1	Laptop2
YOLO	78.205	76.865	73.835	62.048	77.658	52.775

This image shows the signal strength received and the distance of the various clients from the fixed positions.

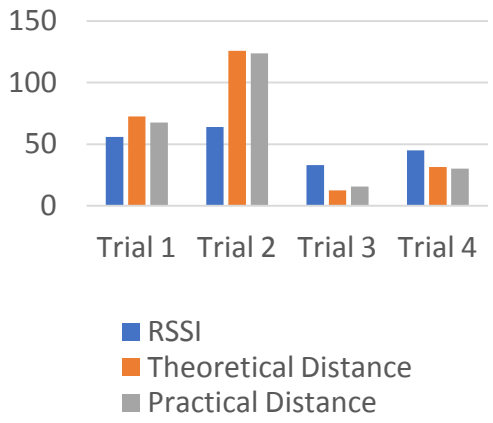

Fig.7. RSSI Strength and Distance Output

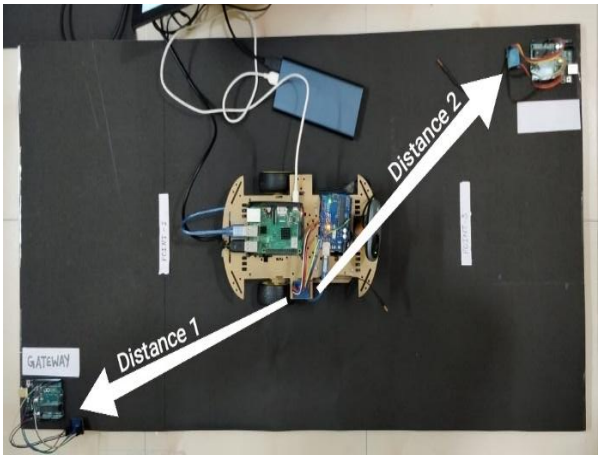

Fig.8. System Setup

VI. CONCLUSION

We here introduce a unified model, for detection of threats in a no network zone. Our model is simple to construct and can be easily used. It also is cost effective and power requirements are minimal. The implementation and evaluation part show that this technology has a lot of applications in the context of surveillance and poor network zones. Furthermore, the system can be improved in future and designed to work in designated areas.

ACKNOWLEDGMENTS

This project has been filed for Indian patent with File No.: 20184101357, with the support of SRMIST.

REFERENCES

1. R. Jin, H. Wang, B. Peng and N. Ge, "Research on RSSI-Based Localization in Wireless Sensor Networks," *2008 4th International Conference on Wireless Communications, Networking and Mobile Computing*, Dalian, 2008, pp. 1-4.
2. C. Fan, Y. Wu and W. Chen, "RSSI-based localization for wireless sensor networks with a mobile beacon," *SENSORS, 2012 IEEE*, Taipei, 2012, pp.1-4.doi: 10.1109/ICSENS.2012.6411544
3. U Goel, B Gupta, M Tiwari, "An Efficient Approach to Restore Naturalness of Non-uniform Illumination Images", Circuit Syst Signal Process (2019) Springer US. https://doi.org/10.1007/s00034-018-01021-w
4. WANG Xianghong, YANG Shi-e, XU Xinsheng, "An Effective Method to Colour Medical Image Enhancement" School of Underwater Acoustical Engineering Harbin Engineering University Harbin, 150001, China
5. Yonghun Shin, Soowoong Jeong, Sangkeun Lee "Efficient naturalness restoration for nonuniform illumination images," IET Image Processing, ISSN 1751-9659
6. Bernat Carbonés Fargas, Martin Nordal Petersen "GPS-free Geolocation using LoRa in Low-Power WANs", IEEE Transaction on Wieless communication
7. You Only Look Once: Unified, Real-Time Object Detection. Joseph Redmon, Santosh Divvala, Ross Girshick, Ali Farhadi, University of Washington, Allen Institute for AI, Facebook AI Research, http://pjreddie.com/yolo/
8. Nico Podevijn , 1 David Plets,1 Jens Trogh,1 Luc Martens,1 Pieter Suanet,2 Kim Hendrikse,1 and Wout Joseph 1 1, "TDoA-Based Outdoor Positioning with Tracking Algorithm in a Public LoRa Network", Department of Information Technology, University of Ghent, IMEC, WAVES, Ghent, Belgium 2 Aucxis CVBA, Stekene, Belgium
9. P.F.Felzenszwalb,R.B.Girshick,D.McAllester,and D.Ramanan., "Object detection with discriminatively trained part based models", IEEE Transactions on Pattern Analysis and Machine Intelligence, 32(9):1627–1645, 2010.
10. M. B. Blaschko and C. H. Lampert, " Learning to localize objects with structured output regression", In Computer Vision– ECCV 2008, pages 2–15. Springer, 2008.
11. L. Bourdev and J. Malik. Poselets, " Body part detectors trained using 3d human pose annotations", In International Conference on Computer Vision (ICCV), 2009.
12. H. Cai, Q. Wu, T. Corradi, and P. Hall, "The crossdepiction problem: Computer vision algorithms for recognising objects in artwork and in photographs.", arXiv preprint arXiv:1505.00110, 2015.
13. https://github.com/opencv/opencv/wiki/TensorFlow-Object-Detection-API

Proceedings of the Fourth International Conference on Communication and Electronics Systems (ICCES 2019)
IEEE Conference Record # 45898; IEEE Xplore ISBN: 978-1-7281-1261-9

A Noval Methodology for Tumor Detection in MRI Images

[1]Ishrat jan / Pg student, 2Giridhar Reddy Bojja
3 Doctoral student, college of business and information systems, dakota state university, madison, south dakota, u.s.a

[3]Er Harish Kumar Dogra / Assistant professor
[1,3] Department of electronics and communication engineering, sri sai college of engineering and technology badhani pathankot

***Abstract*—Brain tumor at beginning period is exceptionally troublesome errand for specialists to distinguish. X-ray images are increasingly inclined to commotion and other ecological impedance. So it winds up hard for specialists to distinguish tumor and their causes. So here we concoct the system, where system will identify brain tumor from images. Here we convert image into gray scale image. We apply channel to image to expel commotion and other ecological obstruction from image. Client needs to choose the image. System will process the image by applying image preparing steps. We connected k-means++ bunching based Division to identify tumor from brain image. Yet, edges of the image are not sharp in beginning period of mind tumor. So we apply image division on image to distinguish edges of the images. In this technique we connected image division to recognize tumor. Here we proposed image division process and many image separating strategies for precision. This system is executed in tangle lab. Tumor is undesirable development of unfortunate cell which increment intracranial weight inside skull. Restorative image preparing is the most testing and imaginative field uniquely X-ray imaging modalities. The system exhibited includes pre-handling, division, highlight extraction, identification of tumor and its grouping from X-ray examined brain images. Attractive Reverberation Imaging (X-ray) is a non-obtrusive imaging modalities which is most appropriate for the location of brain tumor. In this work, Multi Bolster Vector Machines (m-SVMs) has been proposed and connected to brain examined image cuts arrangement utilizing highlights got from slices**.

Keywords—Brain tumor x-ray, k-means++, m-SVMs etc.

1. INTRODUCTION

National Brain Tumor Foundation (NBTF)[1] in the US, around 13 thousand individuals cease to exist of 29 thousand individuals in the U.S. who are determined to have essential mind tumors every year. In light of the estimation of World Wellbeing Association (WHO), mind tumor is viewed as a standout amongst the most well-known cerebrum maladies, so its analysis at beginning time and convenient treatment can help a great many influenced people every year on the planet to expand the odds of survival. In addition, according to review of WHO, numerous instances of death are accounted for overall in light of threatening or destructive tumor.[2-3]

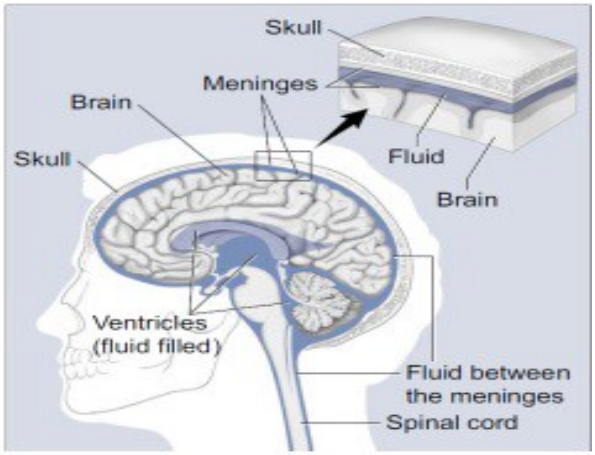

Figure 1: structure of Brain [10]

A. Features of Tumor

In general, the tumor is portrayed as tissue bunch formed as a result of the gathering of unpredictable cells in the body. Routinely, at a fitting time, the old cells are being displaced by new ones. Due to the happening to a destructive tumor(s), this cycle is disturbed. The tumor cells grow exponentially and don't kick the bucket, not under any condition like sound cells. Two sorts of brain tumors are an essential tumor and optional or metastatic tumor [6]. Commonly, the essential brain tumor begins in the brain and will in general stay amid its development residency. While, the auxiliary brain tumor starts elsewhere as disease in the body, later spreads to the brain region.

TABLE I. FEATURES OF TUMOR

Benign Tumor	**Malignant Tumor**
Distinct borders	Invasive borders
Slow Growth	Rapid Growth
Rarely spreads	Often spreads
Less harm	Life- threatening

Generally, Attractive Reverberation Imaging (X-ray) and Registered Tomography (CT) methods are used to dismember the tissues and furthermore tumors appear in the brain. Propelled

picture planning techniques expect a crucial part in the restorative field to look at the medicinal reports. Further, AI Innovation has viably handled different issues in the medicinal history. A part of the systems to recognize and discover the proximity of tumor in the X-ray brain pictures are according to the accompanying: (1) Edge based detection technique, (2) Shape-based detection strategy, (3) Feature-based

Brain tumor recognition is a significant issue in imaging science. By and large, the seriousness of illness is chosen by the size and kind of tumor. A significant advance in examination of mind X-ray check picture is to extricate the limit and locale of tumor. To take care of the issue, the proposed work depicts the system for identification, division and highlight extraction of cerebrum tumor part utilizing MATLAB programming. This product based methodology intends to present a calculation for identifying and fragmenting the cerebrum tumor from ordinary mind utilizing fundamental picture preparing tasks (de-noising picture, sifting), division pursued by highlight extraction.

II. RELATED WORK

Mukambika P. S., Uma Rani K. (2017) Proposed Approach in which Picture is prepared through: Pre-handling, Division, Highlight extraction Order stages. In preprocessing, Morphology procedure utilizing twofold thresholding is connected to expel the skull out of the X-ray cerebrum images.[11]**Astina Minz et.al (2017)** In restorative analytic application, early disfigurement disclosure is a urgent assignment as it gives fundamental comprehension into examination. Medicinal imaging framework is as of now creating field in designing. Attractive Reverberation imaging (X-ray) is one those reliable imaging systems on which restorative symptomatic relies upon. [12]Manual examination of those pictures is a redundant action as the proportion of data and moment focal points are hard to see by the human. **G Rajesh Chandraet al. (2016)** Detection of mind tumor is very normal setback in current circumstance of human services society. Picture division is utilized to isolate the sporadic tumor segment in cerebrum.[13] Mind tumor is an unpredictable mass of tissue in which cells grow besides, copy uncontrollably, clearly unregulated by instruments that control cells.

III. PROPOSED WORK

K-means k-implies grouping is a strategy for vector quantization, initially from sign preparing that is well known for bunch examination in information mining. k-implies bunching plans to segment perceptions into k groups in which every perception has a place with the bunch with the closest mean, filling in as a model of the group. This outcomes in an apportioning of the information space into Voronoi cells. The issue is computationally troublesome (NP-hard); in any case, productive heuristic calculations meet rapidly to a neighborhood ideal. These are normally like the desire amplification calculation for blends of Gaussian appropriations through an iterative refinement approach utilized by both k-implies and Gaussian blend demonstrating.

The two of them use group focuses to demonstrate the information; nonetheless, k-implies bunching will in general discover bunches of tantamount spatial degree, while the desire augmentation system enables bunches to have distinctive shapes the k-implies strategy is a broadly utilized grouping procedure that looks to limit the normal squared separation between focuses in a similar bunch. In spite of the fact that it offers no exactness ensures, its straightforwardness and speed are engaging practically speaking. By expanding k-implies with a basic, randomized seeding system, we acquire a calculation that is O (log k) - aggressive with the ideal bunching. Analyses demonstrate our increase improves both the speed and the precision of k-implies, frequently significantly.

K-Means calculation is an unsupervised bunching calculation that characterizes the information focuses into numerous classes dependent on their characteristic separation from one another. The calculation accept that the information highlights structure a vector space and endeavors to discover normal grouping in them. The focuses are bunched around centroids μI

$$V = \sum_{i=1}^{k} \sum_{x_j \in S_i} (x_j - \mu_i)^2$$

∀I = 1 . . . k which are obtained by minimizing the objective.

The k-implies bunching issue is one of the most established and most significant inquiries in all of computational geometry. Given a number k and a lot of n information focuses in R.

The proposed work performs handling of X-ray cerebrum pictures for location and grouping of tumor and non-tumor pictures by utilizing a classifier. The picture preparing strategies like histogram evening out, picture upgrade, picture division and afterward removing the highlights for discovery of tumor have been utilized. Removed highlights are put away in the learning base. A proper classifier is created to perceive the cerebrum tumors by choosing different highlights.

Attractive Reverberation Imaging (X-ray) is a non-obtrusive imaging modalities which is most appropriate for the discovery of mind tumor. An easy to understand condition has been made by utilizing GUI in MATLAB bringing about a mechanized cerebrum tumor identification framework for X-ray examined pictures. By utilizing the GUI device, the doctor and different specialists are encouraged in recognizing the tumor and its geometrical component extraction. Multi-SVM has used to group the different sorts of tumors like Gliomas, Metastasis, and Astrocytoma and so forth. In this work, Multi Bolster Vector Machines (m-SVMs) has been proposed and connected to cerebrum filtered picture cuts characterization utilizing highlights got from cuts. This work helps in acknowledgment of tumor which thusly spares the valuable time of restorative demonstrative to analyze the tumor naturally in limited capacity to focus time.

K-means++ reliably beaded k-implies, both by accomplishing a lower potential esteem, at times by a few requests of size, and furthermore by finishing quicker. With the manufactured precedents, the k-implies technique does not perform well, in light of the fact that the arbitrary seeding will definitely combine groups, and the calculation will never have the option to part them separated. The cautious seeding technique for k-means++ stays away from this issue by and large, and it quite often achieves the ideal outcomes on the manufactured datasets. The contrast between k-means and k-means++ on this present reality datasets is likewise very generous. On the Cloud dataset, k-means++ ends twice as quick while accomplishing potential capacity esteems about 20% better. The presentation gain is considerably progressively exceptional on the bigger Interruption dataset, where the potential esteem gotten by k-means++ is better by elements of 10 to 1000, and is likewise acquired up to 70%

quicker. The system is designed to be user friendly by using MATLAB GUI tool based on following steps.

Preprocessing: wiener filter
Segmentation: K-means ++ clustering based Segmentation
Feature Extraction: GLCM Based Feature Extract
Classification: Support Vector Machine (SVM)

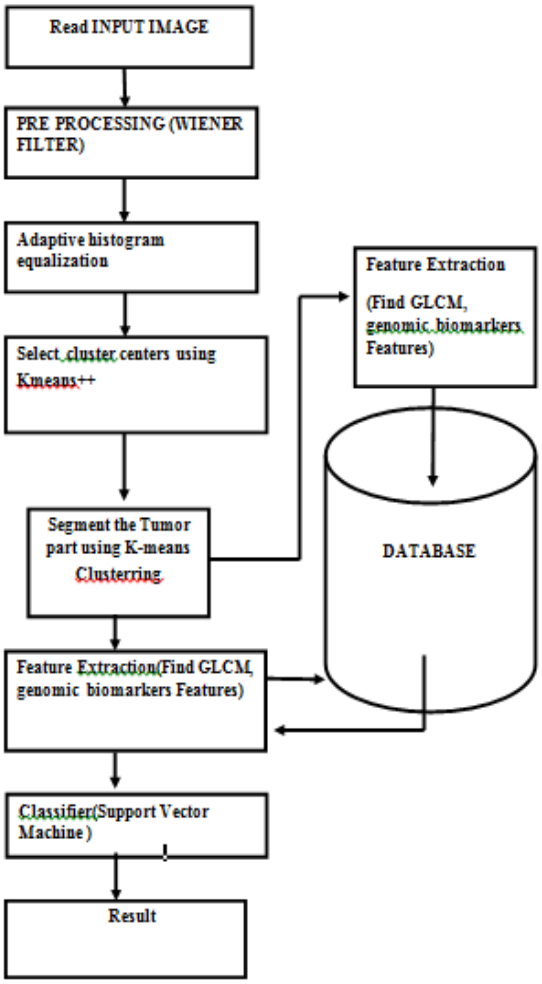

Figure 2: Block diagram

Step 1: Read Input Image
Step 2: Gray Scale conversion
Stage 3: Preprocessing-Evacuate commotions utilizing Wiener channel
Stage 4: Image Upgrade utilizing Versatile Adaptive Histogram Equalization
Stage 5: Pick one focus consistently from among the information focuses.
Stage 6: For every datum point x, figure D(x), the separation among x and the closest focus that has just been picked
Stage 7: Pick one new information point indiscriminately as another inside, utilizing a weighted likelihood dissemination where a point x is picked with likelihood relative to D(x) 2
Stage 8: Rehash Stages 5 and 6 until k focuses have been picked.
Step 9: Now that the underlying focuses have been picked, continue utilizing standard K-mean grouping.
Stage 10: Allot each article to the gathering that has the nearest centroid.
Stage 11: Recalculate the places of the centroids.
Stage 12: If the places of the centroids didn't change go to the following stage, else go to Stage 10.
Stage 13: Concentrate the GLCM highlights and genomic biomarkers from Grouped District.
Stage 14: SVM train
Stage 15: SVM classify

IV. RESULTS

The following samples are taken from the hospital are the tumorous image. So we are applying our proposed work on them in order to test. some statically features of samples are shown graphically also.

SAMPLE 1: This sample had been taken from erode hospital various steps of our proposed work has been compared.

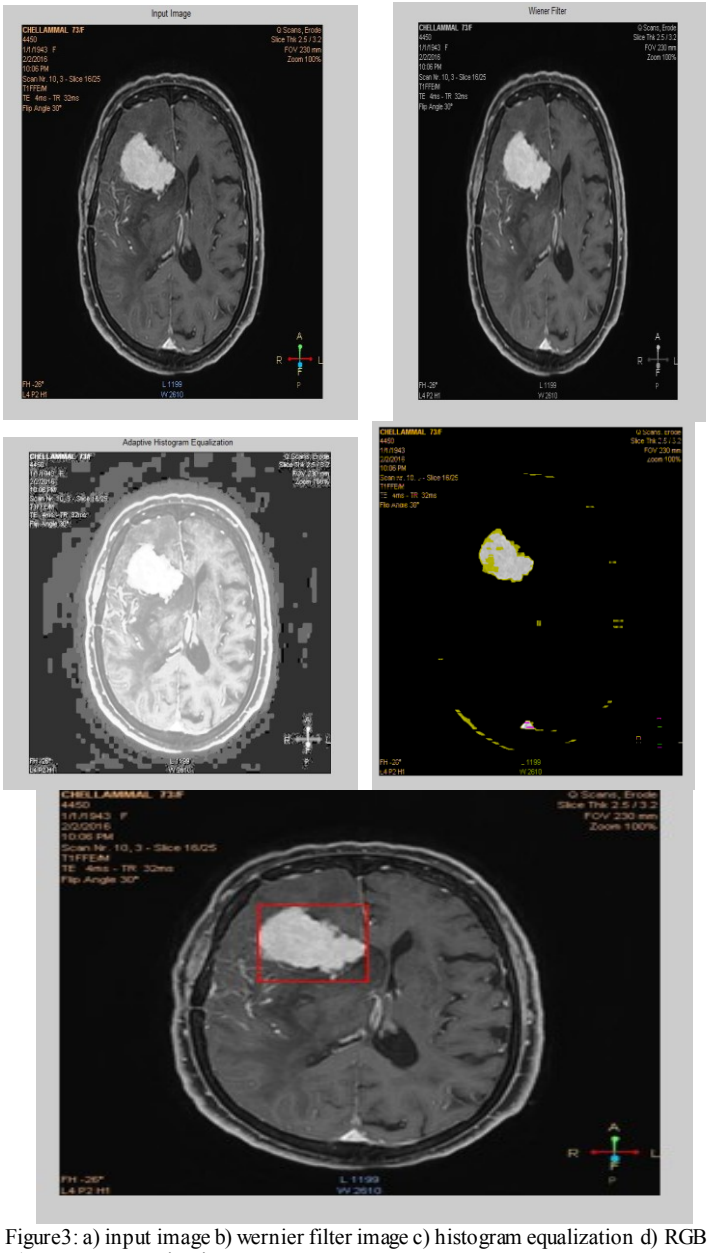

Figure3: a) input image b) wernier filter image c) histogram equalization d) RGB e) Tumor recognization

\

SAMPLE 2

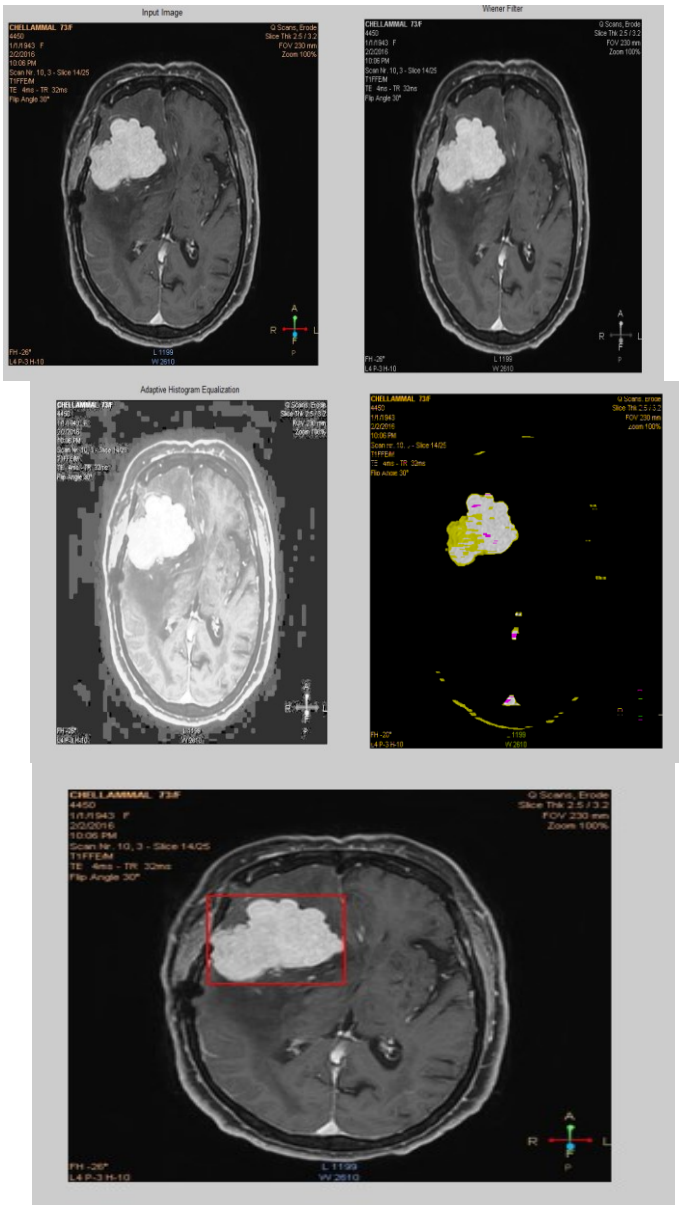

Figure 4: a) input image b) wernier filter image c) histogram equalization d) RGB e) Tumor recognization

SAMPLE 3

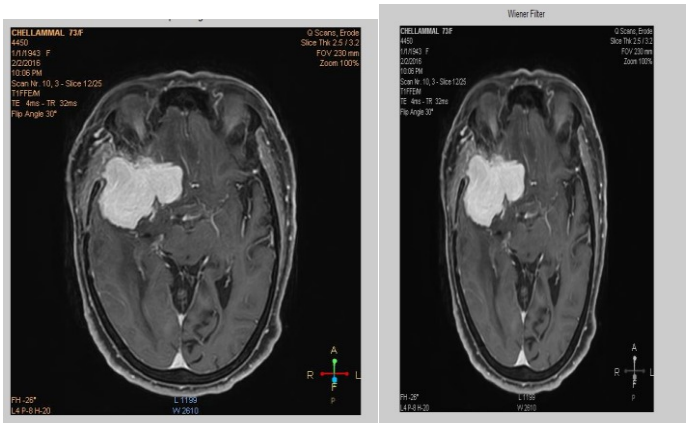

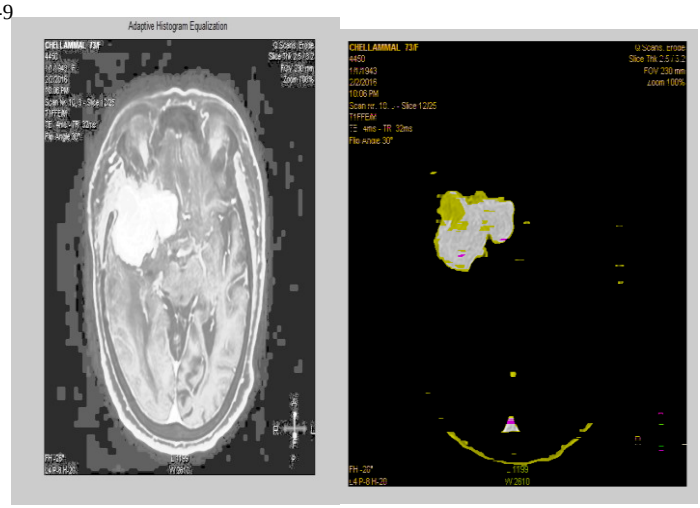

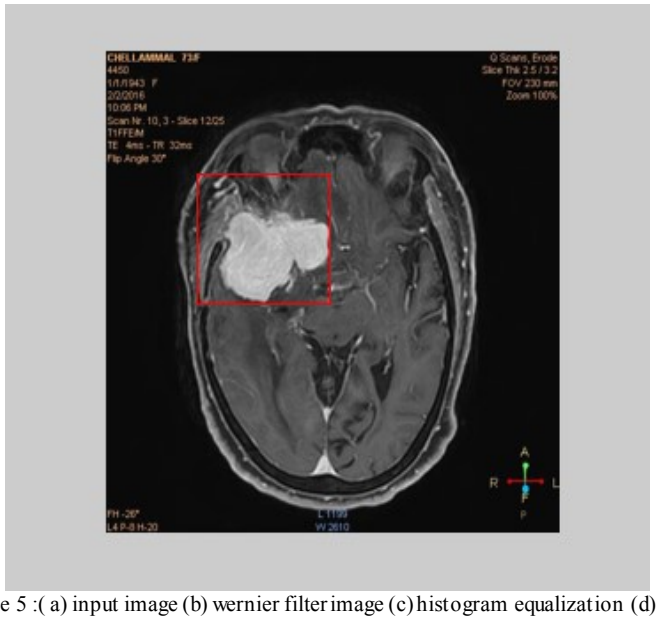

Figure 5 :(a) input image (b) wernier filter image (c) histogram equalization (d) RGB (e) Tumor recognization

SAMPLE 4

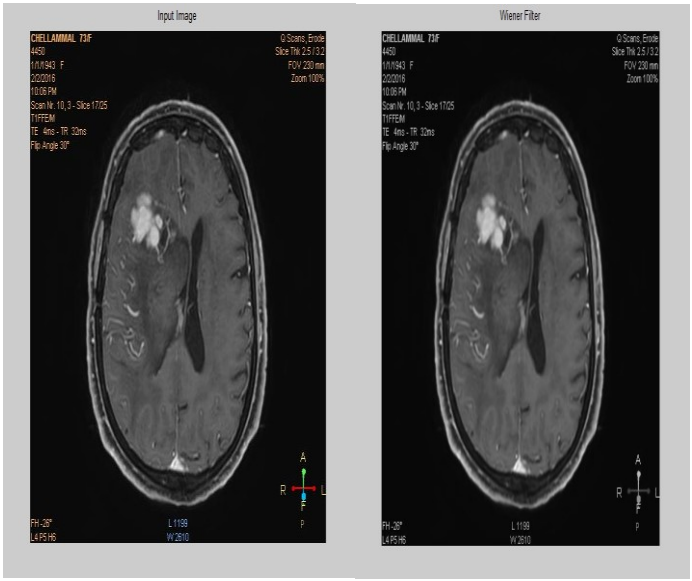

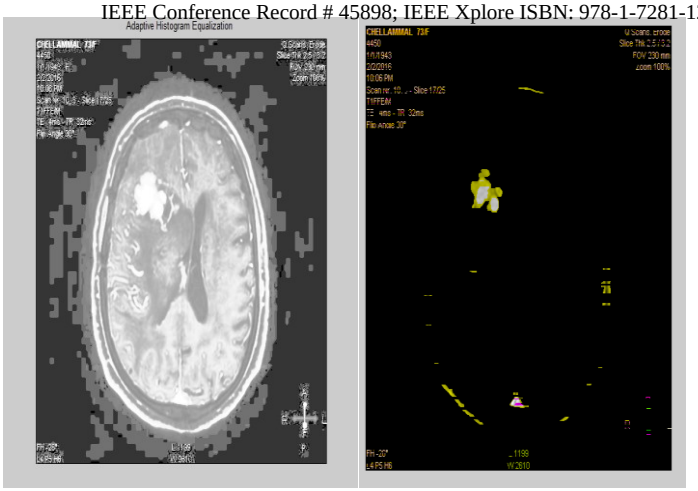

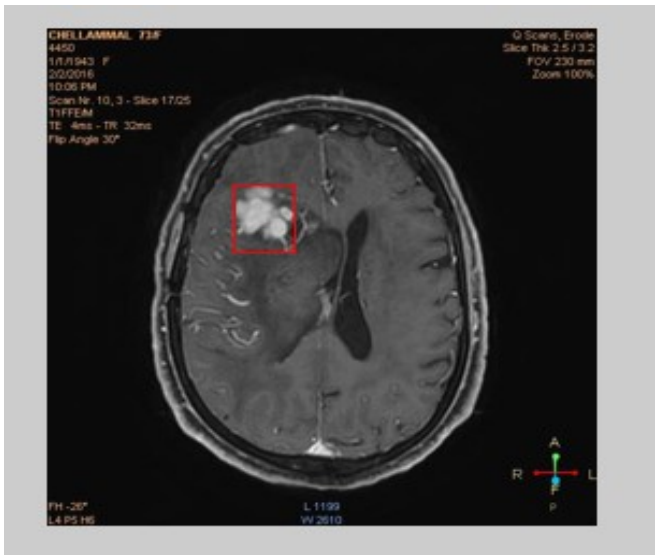

Figure6: : a) input image b) wernier filter image c) histogram equalization d) RGB e) Tumor recognization

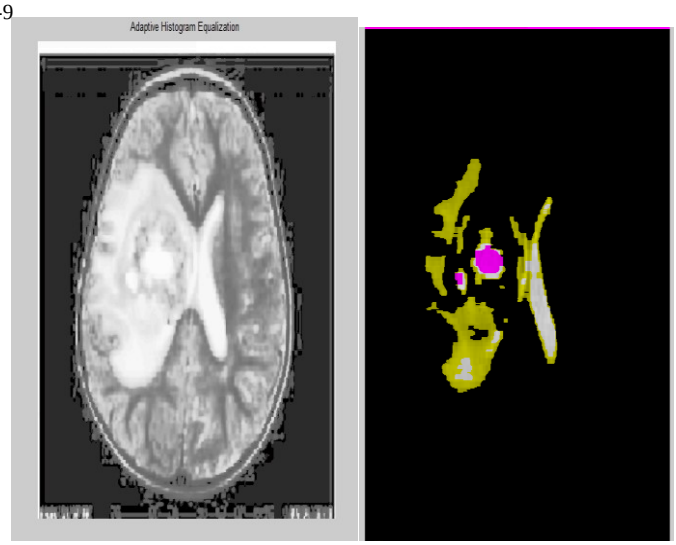

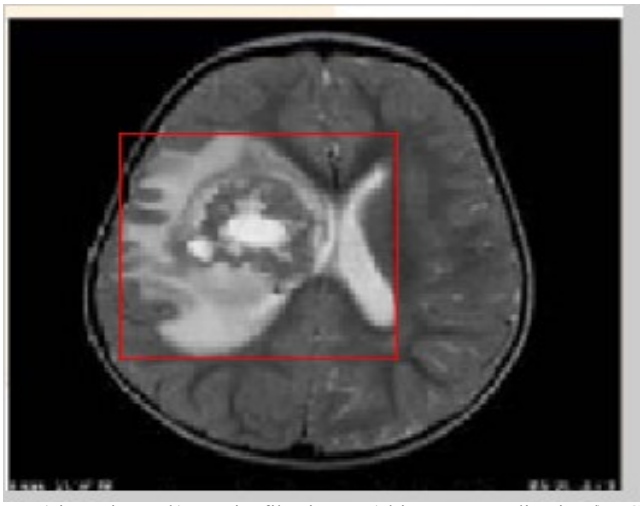

Figure 7: a) input image b) wernier filter image c) histogram equalization d) RGB e) Tumor recognization

SAMPLE 5: PREVIOUS WORK IMAGE [10]

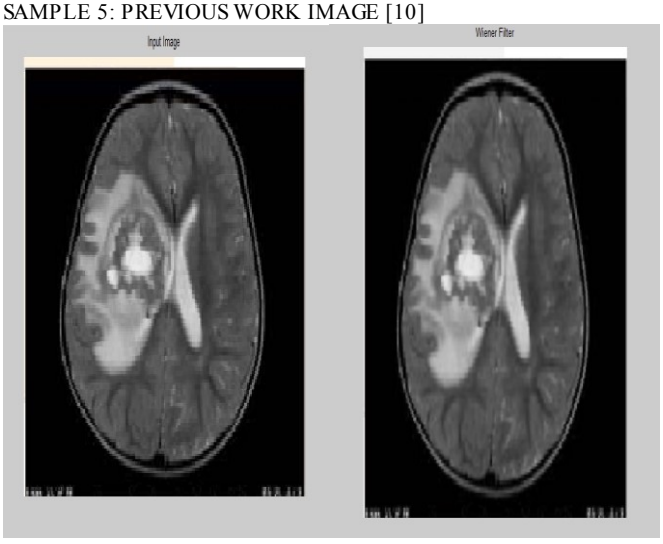

A. Gray level co-occurrence matrices

In statistical texture analysis, surface highlights are figured from the factual conveyance of watched mixes of powers at determined positions in respect to one another in the picture. As indicated by the quantity of force focuses (pixels) in every blend, insights are grouped into first-request, second-request and higher-request measurements. Taken from previous work

Table II: STATISTICAL FEATURES OF GLCM

FEATURES	SAMPLE 1	SAMPLE 2	SAMPLE 3	SAMPLE 4	PREVIOUS WORK IMAGES
CONTRAST	0.887	0.9396	0.8878	0.863	0.398
ENERGY	0.141	0.1215	0.141	0.1233	0.11
ENTROPY	2.5148	2.624	2.51	2.633	2.61

The graphically representation is about the statistical features of various samples taken above and thus compared with the previous work as shown

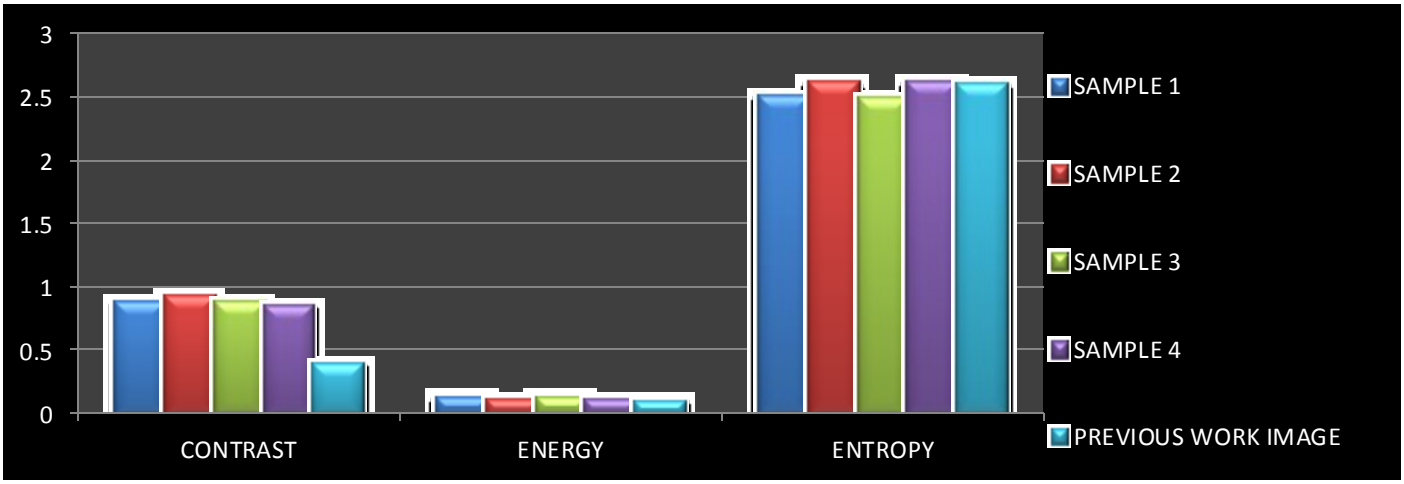

V. CONCLUSION

MR image segmentation is a critical yet unavoidably inconvenient issue in helpful image dealing with. At the point when all is said in done, it can't be fathomed using immediate, standard image dealing with techniques. As a result of the characteristics of MR images, improvement of automated estimations is trying. There is an enormous between patient assortment of sign powers for one same tissue type in light of midway volume sway, regular tumult and wide extent of imaging parameters, which impact the tissue powers. We have proposed a beneficial portrayal structure subject to thickness based batching approach to manage recognize the brain tumor. The MATLAB multiplication is carried on different personality images and tumor is recognized using K-means++ procedure for image division and perfect overall thresholding. The cerebrum tumor acknowledgment is an unprecedented help for the specialists and a guide for the restorative imaging and adventures managing the age of CT Range and X-beam imaging.

In future this program should be possible further developed so tumor can be arranged by its sort. Additionally tumor development can be broke down by plotting chart which can be gotten by examining consecutive images of tumor influenced understanding.

REFRENCES

[1] T. Logeswari and M. Karnan, "An improved implementation of brain tumor detection using segmentation based on soft computing," Journal of Cancer Research and Experimental Oncology, vol. 2, no. 1, pp. 006–014, 2009.
[2] S. Bauer, R. Wiest, L.-P. Nolte, and M. Reyes, "A survey of MRI-based medical image analysis for brain tumor studies," Physics in medicine and biology, vol. 58, no. 13, p. R97, 2013.
[3] P. Kleihues and B. W. Stewart, "World cancer report," 2003.
[4] N. Gordillo, E. Montseny, and P. Sobrevilla, "State of the art survey on MRI brain tumor segmentation," Magnetic resonance imaging, vol. 31, no. 8, pp. 1426–1438, 2013.
[5] J. Mikulka and E. Gescheidtova, "An improved segmentation of brain tumor, edema and necrosis," in PIERS Proceedings, pp. 25–28, 2013.
[6] Parveen, Amritpal Singh "Detection of Brain Tumor in MRI Images, using Combination of Fuzzy c-means and SVM" in 2nd International Conference on Signal Processing and Integrated Networks (SPIN) 2015 IEEE
[7] Mukambika P. S., Uma Rani K. "Segmentation and Classification of MRI Brain Tumor" in International Research Journal of Engineering and Technology (IRJET) Volume: 04 Issue: 07 July -2017
[9] T .Logeswari and M.Karnan "An improved implementation of brain tumor detection using segmentation based on soft computing" Journal of Cancer Research and Experimental Oncology Vol. 2(1) pp. 006-014, March, 2010
[10] Animesh Hazra et.al, "*Brain Tumor Detection Based on Segmentation using MATLAB",* International Conference on Energy, Communication, Data Analytics and Soft Computing (ICECDS-2017) 978-1-5386-1887-5/172017 IEEE
[11] Mukambika P. S., Uma Rani K. "Segmentation and Classification of MRI Brain Tumor" in International Research Journal of Engineering and Technology (IRJET) Volume: 04 Issue: 07 July -2017
[12] Astina Minz, Prof. Chanddrakant Mahobiya "MR Image classification using Adaboost for brain tumor type" in IEEE 7th International Advance Computing Conference (IACC) 2017
[13] G Rajesh Chandra, Dr. Kolasani Ramchand H Rao " TUMOR DETECTION IN BRAIN USING GENETIC ALGORITHM" in 7th International Conference on Communication, Computing and Virtualization 2016

Proceedings of the Fourth International Conference on Communication and Electronics Systems (ICCES 2019)
IEEE Conference Record # 45898; IEEE Xplore ISBN: 978-1-7281-1261-9

Disaster Prediction System using Convolution Neural Network

Purva Mohan Padmawar
Department of Computer Engineering
JSPM's Rajarshi Shahu College of Engineering
Pune, India
purvapadmawar@gmail.com

Ashutosh Sudam Shinde
Department of Computer Engineering
JSPM's Rajarshi Shahu College of Engineering
Pune, India
as.shinde343@gmail.com

Talat Zakirhusen Sayyed
Department of Computer Engineering
JSPM's Rajarshi Shahu College of Engineering
Pune, India
talat.sayyed@gmail.com

Shubham Kalidas Shinde
Department of Computer Engineering
JSPM's Rajarshi Shahu College of Engineering
Pune, India
shubhamkshinde7@gmail.com

Prof.Kavita Moholkar
Department of Computer Engineering
JSPM's Rajarshi Shahu College of Engineering
Pune, India
kavita.moholkar@gmail.com

Abstract—Flood is a cataclysmic event that occurs far and wide causes the extraordinary misfortunes. The floods additionally compromise the human life and the economy of the included nation likewise gets influenced. Neural Networks are generally connected in flood gauging and got great outcomes. The main objective of the project is to predict the flood situation and intimate about it to the people. The importance of predicting the flood is widely increased. The human life can get damaged due to floods; it can prevent loss to economy and human if it is predicted earlier. For prediction there are various methods but the most commonly used method is Neural Networks. This paper develops deep learning approach by combining Convolutional Neural Network (CNN) and Modified Particle Swarm Optimization (MPSO) for the prediction that the area is flooded or not. CNN extracts the attributes cataclysm in all respects productively. CNN is vigorous to shadow. CNN can get the attributes of calamity palatably and it additionally overpowers the misdetection or miscount by administrators, which further influence the handiness of fiasco help. MPSO is applied as optimizer to search for the optimal parameter values for the CNN training process.

Keywords— Convolutional Neural Network; Modified Particle Swarm Optimizer; prediction; disaster; flood; deep learning;

I. INTRODUCTION

Disaster disclosure has been a standout amongst the most unique research zones today since sparing human lives is our earnestness once a catastrophe occurred. It is essential in the administration of fast answer exercises after a hazardous catastrophe, for example, floods. A disaster is an abrupt, disastrous occasion that truly disturbs the working of a network or society and causes human, material, and monetary or natural misfortunes that surpass the network's or society's capacity to adapt utilizing its own assets. [18] Though often caused by nature, disasters can have human origins as well. There can be various types of disaster occur which are categorized as geological disasters, hydrological disasters, meteorological disasters, and wildfires. Among which floods, earthquakes, landslides occur thoroughly.

Predicting flood is the complex process. The flood is predicted at early stage so that the loss to the society can be prevented. Predicting the flood can minimize the risk to human and economical losses. As predicting the flood can intimate the people nearby the flood prone area due which the people are able to relocate to the safer place and prevent the damage [18]. By predicting the flood at earlier stage can cause the preventive and curative measures to be taken by the government.

Flood is a typical cataclysmic event that influencing a quantities of nations around the globe [18]. In spite of it is normal, yet flood can at present be really shocking to a limited extent where it starts to make huge pulverization open offices, private house or even most noticeably awful, passing [1].This influence massively toward to the financial matters structure of the nation that must face this disaster uncommonly for poor people and creating one [1]. To overcome the above issues early prediction systems are

designed using different techniques to provide message to the people before the flood occurs in the area.

Deep Learning is a part of machine learning methods. Machine learning is a technique in computer science which allows data to drive and guide the execution of algorithm [10]. Using a training dataset, the algorithm develops a model which is used to compare against the expected output [10]. An algorithm that uses deep learning goes through much the same process. Each hierarchy applies a transformation on the training input and forms it as a model [10]. This process is repeated until output has reached and an acceptable level of accuracy [10]. Learning can be supervised, unsupervised and semi-supervised. Deep Learning incorporates numerous systems, for example, CNN (Convolutional Neural Network), RNN (Recurrent Neural Network), Recursive Neural Network. These systems are essentially calculations.

Various productions on flood forecast utilizing Artificial Neural Network (ANN) methods have been accounted for [4]. It has been proposed, in light of the fact that it has the incredible ability to display nonlinear and complex frameworks without clear physical clarification [3]. Presently a the very first moment's of the most notable practices in deep learning, CNN is making location showing signs of improvement result in a cataclysm, for example, a flood, earthquake, and landslide. The system is intended to guess the flood on the basis of present image of a specific flood prone area, on the basis of the image the system will guess whether the area is in risk and essential to be relocate or not. The accuracy of the developed model is high due the use of Convolutional Neural Network and Modified Particle swarm optimization. The early prediction leads to save lot of lives and prevent more damage due to flood. The modified particle swarm optimization (MPSO) technique is applied as a parameter searching process for the CNN.

II. RELATED WORK

A. Literature Review

In [13] the writers proposed Bare-Bones multi objective particle swarm optimization (BBMOPSO) algorithm calculation for condition/financial dispatch issues. This paper is having three highlights. The molecule notifying procedure does not require tweaking control parameters. The transmutation administrator is to amplify the pursuit capacity and to maintain a strategic distance from the untimely combination issue. The molecule decent variety is to refresh the all inclusive molecule leaders. From the outcomes, BB-MOPSO calculation is making amazing count of genuine Pareto front and it is reasonable to settle a wide range of multi target advancement issues. BB-MOPSO calculation is giving preferable outcomes over different calculations like multi-objective particle swarm optimization with sigma method (SMOPSO), multi-objective particle swarm optimization method (CMOPSO) and time variant multi-objective particle swarm optimization (TVMOPSO) as far as combination execution. BBMOPSO calculation is superior to CMOPSO and TVMOPSO calculations in the appropriation of arrangements on the acquired Pareto front. BB-MOPSO is accomplishing littlest standard deviation esteem.

In [11] the writers proposed Modified Particle Swarm Optimization algorithm (MPSO) for to take care of building basic streamlining issues. By improving the versatile wellness work we balance the target capacity esteem and imperative infringement particles. The algorithm utilizes the versatile inertial load to adjust abuse. They got outcomes are contrasted and right now accessible advancement calculation which demonstrates that the MPSO calculation is superior to others as far as precision.

III. METHODOLOGY

The Figure 1 shows the proposed system for disaster prediction using deep neural network. Convolutional neural system preparing for stream water flood forecast by utilizing PYTHON.

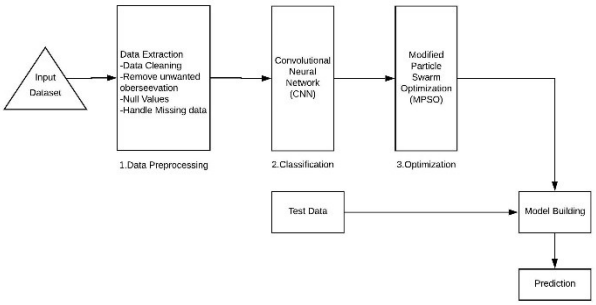

Figure1. Proposed System

B. Data Collection and Used

The prediction done at this paper is to predict the flood in the image. The prediction can be done in three conditions such as flood will occur, flood had been occurred and flood has been occurred. The samples utilized in model improvement were separated into two sets to be specific: training and testing sets. The model was first acquired utilizing training sets. The new testing samples were then nourished to the framework to validate the performance of the system. The data is in the form of images. We obtain images from the Google as input images. Training samples contains 137 images and testing samples contains 500 images.

C. Prediction Model

In this section we are describing our CNN-MPSO model. The model works in three phases such as data preprocessing, MPSO process and CNN training. In first phase the extracted data is pre-processed by performing some operation such as cleaning, removing unwanted observations, removing null values and handling missing values.

In the next phase the particle swarm optimization algorithm is applied to the output of the first phase which optimizes the data so the time taken by the CNN is reduced.

In the last phase the CNN is applied on the optimized data and the output is taken and prediction is performed on the output. The accuracy of the CNN-MPSO model is more than the CNN model.

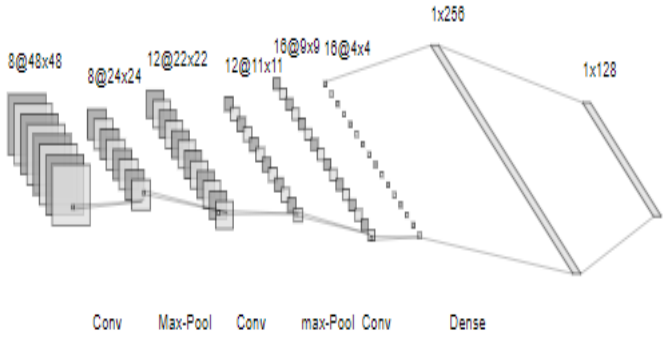

Figure 2. CNN Model

D. Convolutional Neural Network

CNN is a succession of layers, and each layer of CNN changes one volume of actuations to another through differentiable capacity [6]. CNN has concealed layers of 3 essential types, for example, convolution layer, pooling layer, and dense layer which is likewise called as fully-connected layer; the neurons are organized in 3 measurements (width, tallness, profundity).

A Convolution layer is additionally called as conv layer we have utilized keras capacity to execute this model. It is a structure square of a convolution network that does the vast majority of the computational hard work. Convolution layers perform feature extraction on the picture by applying different filters on it. In our model we have utilized 3 convolution layers with 3*3 filters.

It isn't unexpected to occasionally embed a Pooling layer in the middle of progressive conv layers. Pooling Layer capacity is to diminish the spatial size of the portrayal to lessen the measure of parameters and thus to command over fitting. This layer works on each profundity cut utilizing the max operation.

A Dense Layer plays out the characterization on the features which are extricated from the convolution layer and further down inspected by the pooling layer. In this layer every neuron is associated with the previous layer neurons.

In fully connected layer, every neuron is associated with the each neuron of other layer. This layer is like the conv layer just contrast is that the neuron in the conv layer is just associated with the nearby area.

Figure 2 demonstrates the proposed CNN model with the five concealed layers.

E. Modified Particle Swarm Optimization

MPSO algorithm an assessment strategy used to improve the arrangement by advancing the issue. It improves the issue by utilizing particles as an applicant arrangement so these particles fly over a hunt space as per counts to change the area and speed of individual particles, this vacillation of positions is affected by close to home best area and guided toward worldwide best position which is best area in all inquiry space found and affirmed by different particles [8]. The algorithm utilizes the chaotic mapping to produce the underlying population, which guarantees the decent variety of the underlying population and establishes the framework for the worldwide pursuit capacity of the calculation, utilizing instructing component to expand the extent of doable arrangements in the population [11].

The particles of swarm cooperate to accomplish best spot as per the mutual data in the middle of them. Whenever, every particle of swarm can have a local best position (pbest) which is the littlest achieved cost in the cycles [8]. The best position came to in the swarm which known as the global best position (gbest) which is valuable to control the particles toward the global optimum.

The equation (1) is to compute the velocity of the PSO and the equation (2) used to compute the position of the particle.

$$V_{p+1=Vp} + c_1 r_1 (pbest - x_p) + c_2 r_2 (gbest - x_p) \quad (1)$$

$$X_{p+1} = X_p + V_{p+1} \quad (2)$$

Where c1 and c2 are steady qualities and r1 and r2 are arbitrary numbers.

Following are the essential strides of the MPSO calculation:

Step 1.Initialization of fundamental parameters and population. D is the component of capacity, N is the quantity of molecule, T is the most extreme emphasis and set t=0.Initial position xi=(xil,… … ,xiD)is determined by equations (3) and (4).

$$Z_i^{k+1} = \mu Z_i^k (1 - Z_i^k) \quad (3)$$

$$x_{ij} = a_i + (b_i - a_i).z_{ij} \quad (4)$$

Step 2. According to (5) ~ (7), give rise to a new population, that is $(x'_1, x'_2, \ldots x'_N)$. If $f(x'_i) < f(x_i)$, particle x'_i can be replaced with particle x_i. If $f(x'_i) >= f(x_i)$, particle x_i is retained.

$$x'_i(t) = \begin{cases} x_i(t) + r_3\left(gbest - \beta x_{mean}(t)\right), if \ \ r_f < 0.1 \\ x_i(t) + \overline{x_i}(t), \qquad otherwise \end{cases} \quad (5)$$

$$\overline{x_i}(t) = \begin{cases} rand_i\left(x_m(t) - x_i(t)\right), fit(x_m) < fit(x_n) \\ rand_i\left(x_n(t) - x_i(t)\right), fit(x_m) > fit(x_n) \end{cases} \quad (6)$$

$$\beta = round\left(1 + \frac{fit(x_i) - min(fit)}{max(fit) - min(fit)}\right) \quad (7)$$

Step 3. Learning factors c_1, c_2 and inertia weight w is calculated by equations (8) ~ (10).

$$c_1 = (c_{1e} - c_{1s}) \sin(\frac{\pi}{2}\frac{t}{T}) + c_{1s} \quad (8)$$

$$c_2 = (c_{2s} - c_{2e}) \sin(\frac{\pi}{2}\frac{t}{T}) + c_{2e} \quad (9)$$

$$w = w_{max} - (w_{max} - w_{min}) \sin(\frac{\pi}{2}\frac{t}{T}) \quad (10)$$

Step 4. Equations (1) and (2) are used to change the velocity and place of the particle.

Step 5. Change the individual extremum and global extremum of the particle and readjust the particle according to algorithm 1, t=t+1

Step 6. If t > T, algorithm stop. Otherwise, go to Step 2.

MPSO is the advance algorithm of the PSO. MPSO takes the shortest time to process as compare to PSO. The convergence rate of the MPSO is faster than the PSO. Adam is slower than the PSO.

IV. RESULTS AND DISCUSSION

Figure 5 shows the test accuracy of the model at number of epoch. When the epoch is >2 then the accuracy is linear to the epoch. The model takes 137 images at the time of training phase and 500 at the time of testing phase.

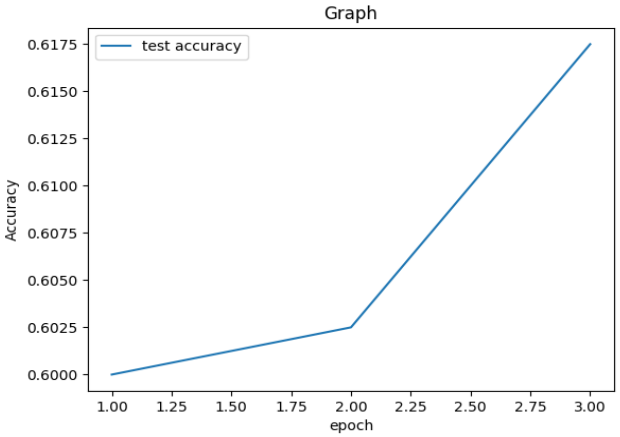

Figure 3. Variation in accuracy with the amount of epoch in the model.

The figure 4 is in view the accuracy at the time of both the phases. The training phase accuracy is 96.88 %. The testing phase accuracy is 64.25 %. The accuracy may vary when the epoch are changed.

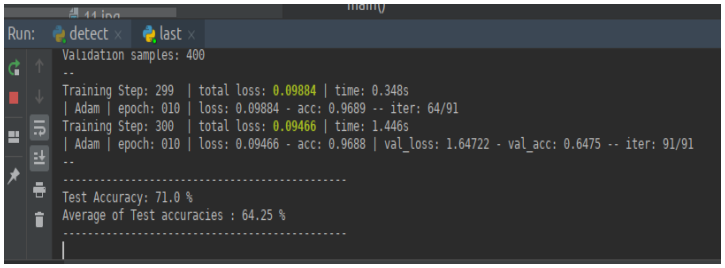

Figure 4. The average accuracy of the prediction model.

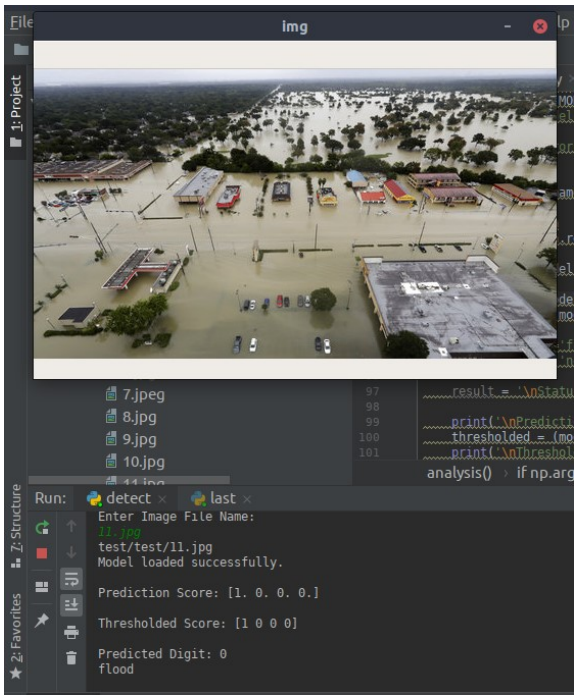

Figure 5. the image is predicted as flood.

The final output is predicted as shown in the figure 5 and figure 6. The images are classified using binary classification i.e. 0 and 1. If the predicted output is 0 means flood and if it is 1 then non-flood.

Change in the number of epoch can affect the accuracy of the model. The image pattern and their types will affect the models accuracy. Different types of pattern and plenty of patches will give a perfect output as compared to bounded ones.

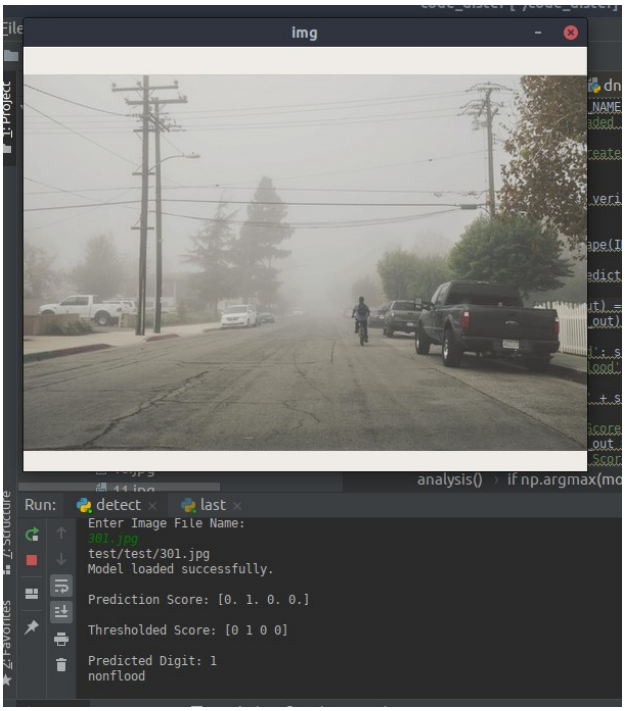

Figure 6. the image is predicted as non flood.

The dataset created by us is tested on Support Vector Machine, K Nearest Neighbors are Traditional Ml algorithm. It is found that results obtained from our proposed system is better than existing system.

Algorithm	Precision	Recall	F1 Score
SVM	0.7317	0.5882	0.6521
KNN	0.5052	0.3773	0.6620
CNN	0.6550	0.7428	0.6552
Proposed System	**0.75**	**0.75**	**0.8**

V. CONCLUSION AND FUTURE WORK

The proposed prediction model using neural network structure is able to predict the flood from the images. In this proposed system, the model applies the CNN on the image and extracts all the features from it. The model also applies MPSO to get the optimized parameters. As per the result we get, it come to know that the proposed model provide relatively high accuracy for flood prediction. The research method which we have suggested in this paper has capability to get executed as a prediction system.

REFERENCES

[1] M. Anuar, R. Rahman, Z. Zulkafi "Early Prediction System Using Neural Network in Kelantan River, Malaysia," IEEE Student Conf.(2017).

[2] P. Panyadee, P.Champrasert, C. Aryupong "Water Level Prediction using Artificial Neural Network with Particle Swarm Optimization Model," IEEE International Conf. ICoICT (2017).

[3] F.Liu, F. Xu, S.Yang "A Flood Forecasting Model based on Deep Learning Algorithm via Integrating Stacked Autoencoders with BP Neural Network," IEEE Conf. on Multimedia Big Data(2017).

[4] K F.Ruslan, A.Samad, M.Tajjudin, R.Adnan "Flood Water Level Prediction Modeling Using NNARX Structure for Sg Pahang Basin",IEEE Internatinal Conf. 27 - 29 November 2015, Penang, Malaysia.

[5] F. Ruslan, A.Samad, R.Adnan "Modelling of Flood Prediction System Using Hybrid NNARXand Extended Kalman Filter" IEEE International (CSPA) 10 - 12 March 2017, Penang, Malaysia.

[6] M. Khalifa, M. Ammar, W. Ouarda, A. Alimi, " Disaster Detection from Aerial Imagery with Convolutional Neural Network." IEEE SCCSIT (2017).

[7] S. Amit, Y.Aoki, " Particle Swarm Optimization for Deep learning of Convolution Neural Network" IEEE (IES-KCIC-2017).

[8] R.Adnan , F.Ruslan" Artificial Neural Network Modelling and Flood Water Level Prediction Using Extended Kalman Filter " IEEE International Conference on Control System, Computing and Engineering (2012).

[9] B. Wang, Y.Sun, B.Xue, M.Zhang " Evolving Deep Convolutional Neural Networks by Variable-length Particle Swarm Optimization for Image Classification",IEEE CEC (2018).

[10] https://searchenterpriseai.techtarget.com/definition/deeplearning-deep-neural-network

[11] R.Yanzi, L.Sanyang" Modified particle swarm optimization algorithm for engineering structural optimization problem"IEEE 13th International Conference on Computational Intelligence and Security(2017).

[12] Geetha T.,Ms.M.Sathya" Modified Particle Swarm Optimization (MPSO) algorithm for Web Service Selection (WSS) problem" 978-1-4673-2149-5/12/$31.00 ©2012 IEEE

[13] Y.Zhang, D.Gong, Z.Ding"A bare-bones multi-objective particle swarm optimization algorithm for environmental/economic dispatch"

[14] H.Li, L.Li" A Novel Hybrid Particle Swarm Optimization Algorithm Combined with Harmony Search for High Dimensional Optimization Problems" 0-7695-3006-0/07 $25.00 © 2007 IEEE.

[15] Pukale.D, Dr.S.Bhirud,Dr.V.D.Katkar" Content-based Image Retrieval using Deep Convolution Neural Network" 978-1-5386-4008-1/17/$31.00 ©2017 IEEE

[16] C.Lee,S.Woo"Decision Boundary Formation of Deep Convolution Networks with ReLu" 978-1-5386-7518-2/18/$31.00 ©2018 IEEE

[17] X.Xu,H.Ge,"An improvement on Recurrent Neural Network by combining Convolutinal Neural Network and a simple initialization of the weights"978-1-4673-7755-3/16/$31.00 ©2016 IEEE

[18] P.Padmawar,A.Shinde,T.Sayyed,S.Shinde"A Survey of Disaster Prediction System"International Conf.(2019)

Proceedings of the Fourth International Conference on Communication and Electronics Systems (ICCES 2019)
IEEE Conference Record # 45898; IEEE Xplore ISBN: 978-1-7281-1261-9

QoS Evaluation of VANET Routing Protocol

B.S. Yelure[1]
Dept.of Computer Science & Engineering
Walchand College of Engineering
Sangli, India
Email: bhushan.yelure@walchandsangli.ac.in

S.P. Sonavane[2]
Dept.of Information Technology
Walchand College of Engineering
Sangli, India
Email: shefali.sonavane@walchandsangli.ac.in

Abstract*— In today's smart revolutionary era, Intelligent Transportation System (ITS) is a buzzword that plays a vital role. Vehicular ad-hoc network (VANET) techniques help ITS for improving efficiency as well as road safety services to vehicles and drivers. The vehicle acts as a node in the special ad-hoc network. Communication in the VANET is accomplished through IEEE802.11p i.e. Dedicated Short Range Communication (DSRC) and Wireless Access Vehicular Environment (WAVE). The ways of communication in the VANET are within vehicles (V2V) and vehicle-to-road (V2R). Routing is a foremost issue in the VANET environment due to the dynamic variation of topology, the restricted movement pattern of the vehicle, unstable links and complex city environments. Implementation of the VANET environment is a difficult task in a real environment. The objective of the paper is to simulate topological routing protocols to evaluate QoS. The simulation uses ManhattanGrid mobility to reflect the realistic vehicular environment. The simulation is conducted in various test environments with the variation in the vehicular density and speed of the vehicle. The influence of both factors on the QoS parameter is evaluated with Packet Delivery Ratio, Throughput, Avg. E2ED and Normalized Routing Overhead. AODV produces better PDR, Throughput and less NRL. OLSR produces less Avg. E2ED with respect to other protocols.

Keywords*— VANET, topological routing protocols, ManhattanGrid, QoS.

I. INTRODUCTION

A. Overview of Vehicular Ad-hoc Network (VANET)

The Indian government started taking initiative towards smart cities recently. An intelligent transportation system is a key component related to the smart city. In addition, a huge investment in the vehicle manufacturers seeks to deploy networks of automotive networks in real time. For example, due to the applicable rules, all new cars in the US will be connected by the end of 2020. The main goal of ITS is to make effective transportation, improve the environmental condition, protection, durability and efficacy of the transport system [3]. It performs information processing, communication, and use of a sensor in vehicles such as cars, trucks, trains and aircraft. In India, tremendous growth is recorded in registered vehicles from about 0.3 million in 1951 to 230 million in 2016 [24]. Urban areas in India are not able to cope up with vehicle growth. Thus, traffic management has a key challenge in many cities that must be paid more attention. According to the survey of World Health Organization (WHO); in India, there is one death every four minutes because of a road accident and in addition to the significant impacts and consequences for the environment [3].

The goal of the VANET is to improve safety of the drivers on the street and provide commercial services. It also disseminates accurate information to vehicle drivers and transport authorities in time [1] [2]. The VANET can help in spontaneous data exchange between various vehicles. Thus, VANET provides a way to connect people on the road. The question is how to achieve this? The solution is to exchange traffic information through the wireless ad-hoc network without infrastructure or through the support of VANET. The vehicular network is the subclass of MANET which achieves communication in vehicular areas by an exchange of messages among vehicles comprising the roadside wireless sensors. This allows information to be communicated to guarantee driver security [4].

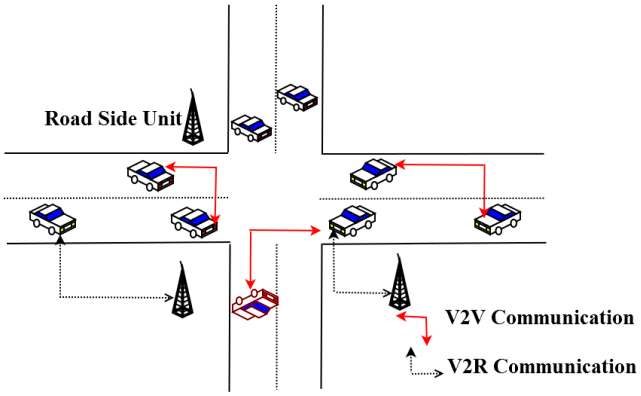

Fig. 1. Vehicular ad-hoc Network Scenario

Communication between the vehicular nodes is very important. Two types of communication that have typically considered in the VANET. One is known as the inter-vehicle communication and the other one is between the vehicle and roadside infrastructure communication. VANET provides communication using hop by hop and multi-hop manner. Components in the VANETs transmit packets in multi-hop mode such as vehicles and road-side units (RSUs). Due to less transmission range, communication is achieved by multi-hop communication amongst intermediate nodes. The vehicle comprises the On-Board Unit (OBUs) that allows short-range wireless V2V communication or V2R communication along with location service like GPS. On the roads, a road-side unit (RSU) is the unit of infrastructure communication. Various OBU and RSU communicate with each other [1] [2]. Fig.1 illustrates the working of VANET.

Thus, VANET is a dynamic network of vehicles without fixed infrastructure like a base station. Vehicles follow the disciplined way for the movement due to its velocity and acceleration. Deployment of VANET is highly expensive as compared to MANET. In terms of mobility; the MANET is having low mobility whereas, VANET is having high mobility being faster vehicles. MANET operates in the 2.4 GHz frequency range whereas, VANET in the 5.9 GHz. The communication range of MANET is up to 250 meters whereas; in VANET it is around 1000 meters. MANET supports infrastructure less operation whereas operations in the VANET supports infrastructure oriented and without infrastructure.

B. Communication Standards in VANET

Vehicles communicate directly with DSRC IEEE 802.11p as well as IEEE 802.16. DSRC is the standard developed by the US and the Federal Communication

XXX-X-XXXX-XXXX-X/XX/$XX.00 ©20XX IEEE

Commission. It allocates a 75MHz spectrum at 5.9GHz for DSRC communication in an approximate range of 1000m. It is used for collision avoidance. Out of seven channels, all channels have a width of 100 MHz. The control channel is dedicated to safe and secure communications. At the end of the spectrum, two channels have reserved for the acute safety of life and high public safety. All other channels are Service Channels (SCHs) [5]. VANET needs rapid bandwidth and interaction because of regular changes in topology and excellent mobility. The American Society for Testing and Materials (ASTM) 2313 working group renamed IEEE 802.11 as a Wireless Access Vehicular Environment (WAVE) [5]. WAVE contains rules for safety, health and the environment.

The Main focus of the paper is:

1. To use ManhattanGrid mobility model to create scenarios for the vehicular density and the speed of the vehicle.
2. To learn and simulate topological routing protocols in VANET.
3. To evaluate the effect of density and speed of the vehicle on the performance measure in terms of quantitative QoS parameters.

It is possible to determine the problems associated with a vehicular node in the simulation environment.

The organization of the paper is as follows: Section II presents related work discussing the basics of routing in the VANET with its protocols. Section III illustrates the QoS evaluation of routing protocols using simulation. Section IV describes an experimental setup for the simulation and section V highlights the conclusion.

II. Related Work

Routing is an intelligent decision process that determines the best appropriate path from the originating node and the target node. Routing in the VANET has various issues like Quality of Service management for several services, network management and road traffic management.

High mobility of the node causes rapid variation in topology, deviation in the velocity and density of the vehicles on the road. The sparse distribution of vehicles in geographical regions degrades network performance. The volatility of the route affects Throughput, with a higher transmission delay and increases in the routing overhead. The VANET area includes buildings, tracks and stringent roads in which vehicles move in a specific direction.

Previously many authors touch the issue of routing protocols evaluation with QoS. These are classified based on the topological routing protocol, transmission strategies and position-oriented routing protocols. The nature of topological routing protocols is proactive and reactive. Table I describes comparative literature of the topological routing with protocol, mobility, nodes, speed, QoS parameters, Time of Simulation (ToS) and tools used.

AODV is a reactive routing protocol. It is always in search of the route in between the source and the sink. It adopts the path discovery procedure with the RREQ, RREP and RERR messages. These messages are exchanged between source and sink. AODV provides unicast multicast and broadcast communication ability. It reduces routing overhead but produces more delay [13] [20].

An enhanced version of AODV routing protocol with the multipath approach is known as AOMDV. In AOMDV, unicast communication is achieved. It is used to compute loop-free and disjoint paths. It produces less routing load while doing the route discovery [14] [21].

OLSR is a pure link state and a proactive routing protocol. The use of Topology Control (TC) and Hello messages determines and disseminates link state information throughout the network. It avoids excessive transmission of Link State Packets (LSP). The main feature of OLSR is the selection of Multi-Point Relay (MPR). One-hop neighbor selects MPR and retransmits all broadcast messages received by it. A multipoint selector is going to select the MPR node, having permission to retransmit the packet. A routing table has preserved in the OLSR [15] [18].

ZRP addresses the routing by acquiring the best properties from both proactive and reactive protocols. Each node has an individual zone. The zone has overlapped with the adjacent nodes. The zone is assigned a radius represented by r. The zone comprises the nodes in its area of radius r. The ZRP consists of peripheral and interior nodes. The node having the minimum distance equal to r with the central node is termed as the peripheral node. The interior nodes are the nodes inside the zone and having distance less than r. It includes a routing component such as IARP and IERP. IARP is a local proactive component comprises routing information related to the nodes within the zone. IERP is a global reactive component that provides services such as improved route discovery and route maintenance. Support for bordercasting is the uniqueness of the ZRP. The bordercasting utilizes the information about the topology provided by the IARP. ZRP also make use of NDP at the MAC layer to locate the new nodes as well as link failures [22] [23].

Table I. Related Work

Reference	Protocol	Mobility	Nodes	Speed (km/h)	QoS Parameters	ToS (s)	Tool used
B. mazarak, and et al. , 2017 [2]	GPSR, AMACAD, MOBIC, DYMO, DSR, OLSR, AODV, DSDV	MOVE	20-100	90-130	PDR, Avg. E2ED, Bandwidth	900	NS-2
Shtaiwi and et al, 2014 [6]	AODV, DSDV, DSR	VANETMOBISIM	20-45	25-55	E2ED, PDR	600	NS-2
A. K. Basil, and et al 2017 [7]	AODV, OLSR	SUMO	18, 72	40	PDR, Delay, Throughput	80	NS-3
M Khairnar, and et al, 2013 [8]	AODV, DSR, GPSR	RWP	30, 50, 150, 300	72	Packet loss ratio, PDR, Avg. E2ED	600	NS-2
L. Rivoirard, and et al, 2017 [9]	AODV, DSR, GRP, OLSR	VANETMOBISIM	30	40	Throughput, Average routing load	300	OPNET

III. Quality Of Service

Quality of Service (QoS) states the network's ability to offer the best service for the specific network traffic by several technologies. It represents the collective outcome of service performance that determines the degree of satisfaction of a user of the service. Each layer in the network is having separate parameters. E.g. delay is used in the

network layer of the OSI model. Working with QoS is one of the most difficult tasks in the VANET because of less accurate QoS, an inappropriate method to estimate QoS and improper selection of route [11].

QoS evaluation plays a major role in various applications of VANET. For instance, an emergency warning application warning is useful only if it hits an appropriate time. If the warning gets delayed then no use of such applications. The VANET uses several quantitative indicators to evaluate QoS.

A. Avg E2ED

Avg E2ED represents the average time for data packets to achieve the goal. It represents the difference between packets arrival time at the destination vehicle and packet transmission time at the source vehicle. It includes MAC layer retransmission time of packets, delay in propagation and the time required for buffering and queuing time.

$$Avg.E2ED = E2ED + \frac{(Et - St)}{count} * 100 \qquad (1)$$

Where, E2ED, St, Et stands for an end to end delay, capture start time on the occurrence of the event and Time at which the packet is completely received.

B. PDR

PDR is the ratio among the number of data packets that arrive at the target vehicle and the number of data packets sent from the source vehicle.

$$PDR = \frac{Tx}{Rx} * 100 \qquad (2)$$

Where PDR stands for Packet Delivery Ratio, Tx represents obtained packets by the target node and Rx indicates generated packets by the source node.

C. NRL

It is the ratio of generated routing packets by delivered data packets.

$$NRL = \frac{Rp}{Dp} \qquad (3)$$

Where, NRL, Rp and Dp represents Normalized Routing Load, sent routing packets and sent data packets respectively.

D. Throughput

It is the total number of successfully received bits by vehicles.

$$Throughput = \frac{Rs}{Et - St} * \left(\frac{8}{1000}\right) \qquad (4)$$

Where Rs, Et and St stands for the size of received packets, end time of the simulation and start time of the simulation.

IV. Experimental Setup

A. Simulation Environment

The simulation is performed on topological routing protocols such as AODV, AOMDV, OLSR and ZRP routing protocols. The objective of the simulation is to analyze quantitative QoS factors such as PDR, NRL, Avg. E2ED and Throughput. It uses network simulator i.e. NS-2.35. The simulation is performed on UBUNTU 14.04 machine comprising a RAM of 8GB with Intel core i-5, 3.2 GHz. processor.

The Manhattangrid mobility model is used for the generation of scenarios. The VANET requires a restricted movement pattern hence the use of the ManhattanGrid model is suitable for such mobility pattern. The ManhattanGrid mobility model is suitable for urban mobility. It uses a grid road topology. It helps the vehicle driver for the selection of a correct path. It works optimally where the roads are in a proper manner. The nodes traverse in the horizontal or vertical direction on the urban map. It hires a probabilistic approach in the selection of node movements. The vehicle selects to keep moving in the same direction at the intersection. The vehicles move straight, left and right with a probability of 0.5 and 0.25 respectively. It is not a good choice for highway scenarios. Even though it offers nodes to change the direction, it levies geographical limitations on node mobility [12] [16] [17].

TABLE II. Simulation Environment

Parameter	Simulation value
Mobility model	Manhattan Grid [19]
Simulation time	600s
Wireless transmission range	250m
Antenna	Omni-directional
Propagation model	Two Ray Ground
MAC protocol	IEEE 802.11p
Simulation area	1100m*1100m
Interface Queue Type	Droptail, priority queue
Number of vehicles	20-70
The speed of the vehicles	Ranging from 8m/s-24m/s
Routing protocols	AODV, AOMDV, OLSR & ZRP
Type of data traffic model	CBR with UDP 10 connections
Data Packet	512 byte
Control Packet	64 byte

Each scenario comprises 50 nodes dispersed in the area having dimension 1100*1100. The 4*4 grid pattern is used in the simulation area. The transmission range used by each node is 250m inside a simulation environment. The node is having 10s pause time. The time of the simulation is 600s. Node density is in the range of 20 -70 by assuming that within 600s approximately 20 to 70 vehicles traveled on the road. The simulation parameters are listed in the Table-II.

The type of traffic used is Constant Bit Rate (CBR) with User Datagram Protocol (UDP). It allows creating traffic at a stable rate by transmitting packets of the same size. It delivers background traffic which matches statistical characteristics of several network applications. In addition, many applications need probable reply times and constant availability of constant bandwidth [10].

B. Observations and discussions

The simulation is conducted to evaluate QoS of the routing protocols in the VANET under various conditions such as according to vehicular density and vehicular speed.

Vehicular Density- The scenarios for the various vehicular densities such as 20, 30, 40, 50, 60 and 70 are used for the simulation. For each density 5 mobility scenarios are generated. The results for the performance measures such as PDR, NRL, Avg.E2ED and Throughput are evaluated. The average of each result is considered and the observation has been made accordingly.

As observed in Fig. 2, PDR is increased across the number of vehicles. For the 20 vehicles, AODV attains 0.49, 1.64 and 1.71 % better PDR as compared to AOMDV, OLSR and ZRP. For the 70 vehicles, AODV attains 3.53, 4.16 and 24.30% better PDR. With the increase in the vehicular nodes, the packet drop ratio decreased.

Related to NRL, AOMDV observed NRL reduction with the increase in the vehicular nodes. In all other protocols, increase in the NRL is witnessed with the increase in the density of the vehicles. Overall AODV produce less NRL as compared to other protocols under study. AODV attains 3.58, 0.96 and 3.89% less NRL for 20 vehicles. In the case of 70 vehicles, AOMDV gets 0.48, 2.38 and 10.68% less NRL compared to the selected protocols.Fig.3 represents NRL performance.

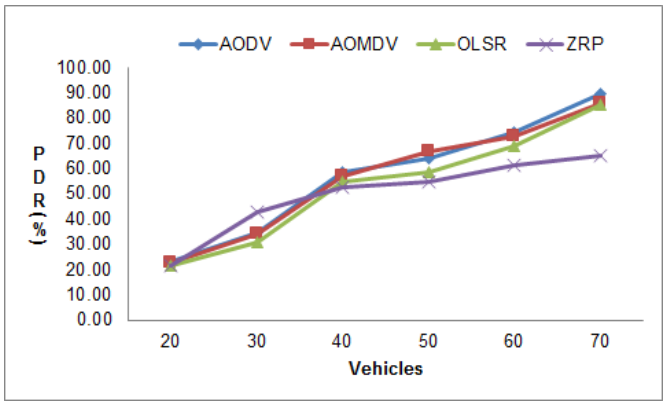

Fig. 2. Measurement of PDR by varying vehicular densities

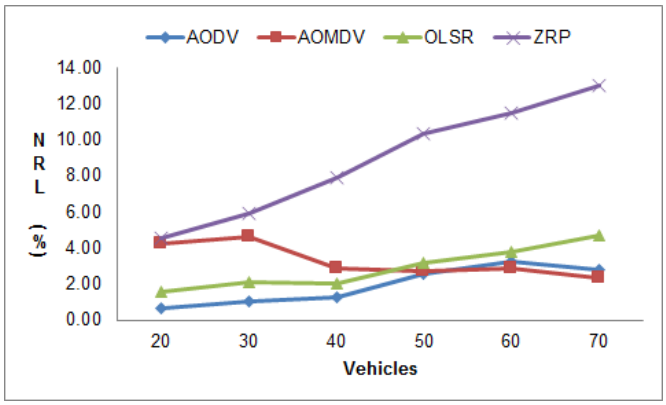

Fig.3. Measurement of NRL by varying vehicular densities

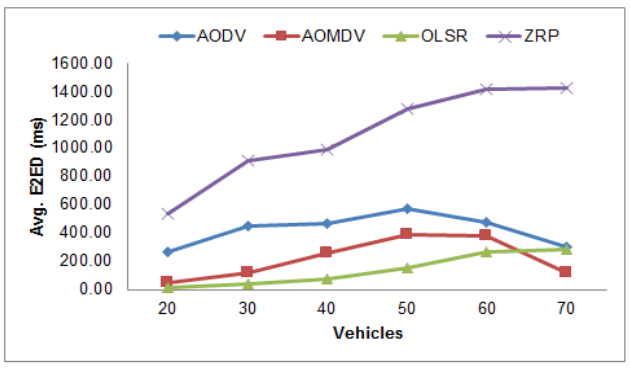

Fig. 4. Measurement of Avg.E2ED by varying vehicular densities

Related to Avg.E2ED, Overall OLSR protocol produces less Avg.E2ED. For the scenario of 20 vehicles, OLSR produces 250.15, 35.48 and 519.31ms less Avg. E2ED as compared to AODV, AOMDV and ZRP. For the case of 60 vehicles, OLSR produces 209.26, 112.34 and 1148.96ms less Avg.E2ED as compared to selected protocols. Fig. 4 shows the behavior of the Avg.E2ED.

AODV produces better Throughput as compared to other protocols. Throughput increases linearly with vehicular nodes for all protocols as shown in Fig.5. In the case of 20 vehicles, AODV produces 0.94, 3.23 and 3.1kbps better throughput with respect to AOMDV, OLSR and ZRP. In the case of 70 vehicles, AODV achieves 7.05, 8.23 and 45.39 kbps better throughput respectively. Table III represents results for the selected protocols of various performance measures.

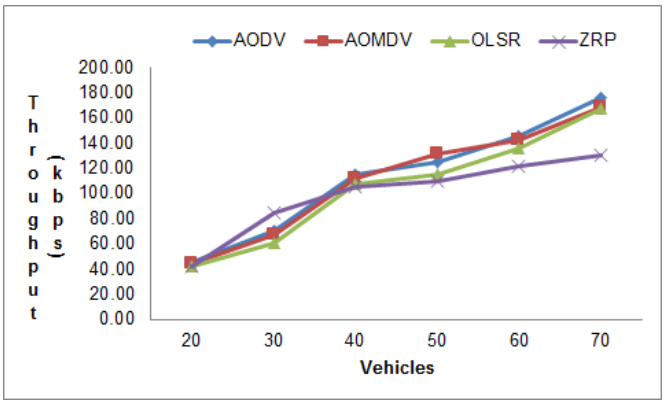

Fig. 5. Measurement of Throughput by varying vehicular densities

Vehicular Speed- The scenarios are generated for the various vehicular speed such as 8, 10, 12,14,16,18,20,22,24 m/s. The results for the various performance measures are evaluated and accordingly, the observation and analysis has been done. Fig. 6. illustrates the behavior of PDR with respect to the varying vehicular speed for the selected protocols. In the case of 8m/s speed, AODV produces 1.04, 4.3 and 6.11% better PDR as compared to the selected protocols. In the case of 24m/s, AODV achieves 4.7, 7.56 and 17.43% better PDR. Thus, PDR for low speed is better but as the speed is increased, a small variation is observed and again when the speed is above 16m/s, an increase in the PDR is observed. The reactive protocols due to their on-demand behavior and quick convergence feature are more appropriate for VANET. Repair of local links in route maintenance provides greater convergence to AODV. Due to the use of route reply, AODV performs better.

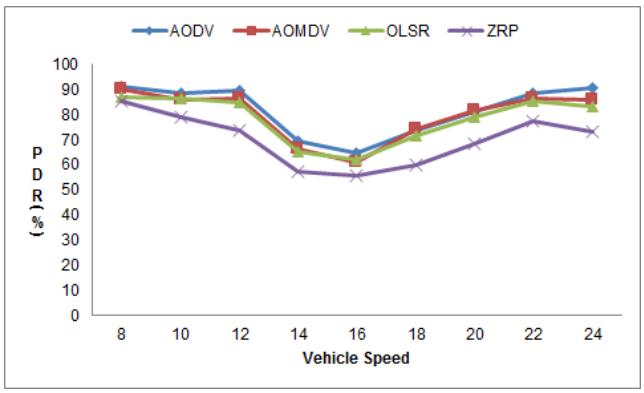

Fig. 6. Measurement of PDR by varying vehicular speeds

Initial development of reactive protocols reduces the routing overheads. AODV generates 0.83, 1.6 and 5.42% as well as 0.4, 0.9 and 6.56% less overhead for the speed of 8m/s and 24m/s vehicles respectively. ZRP generates extra overhead as compared to protocols under study. The RREQ packets control the load of the network in AODV. In ZRP because of mobility, lots of routes are damaged that causes a packet drop. As there is an increase in the vehicles, route search becomes complicated and a large overhead is introduced due to the communication between IARP and IERP. Fig7. illustrates NRL measurements with variation in the vehicular speeds.

TABLE III.SIMULATION RESULTS FOR PERFORMANCE MEASURES FOR VARIOUS VEHICULAR DENSITY (20-70)

Vehicles	PDR (%)				NRL (%)				E2ED(ms)				Throughput (kbps)			
	A	*B*	*C*	*D*	*A*	*B*	*C*	*D*	*A*	*B*	*C*	*D*	*A*	*B*	*C*	*D*
20	23.12	22.63	21.48	21.41	0.63	4.21	1.59	4.52	262.97	48.30	12.82	532.12	45.32	44.38	42.09	42.22
30	34.74	34.06	31.05	42.56	1.04	4.60	2.08	5.94	445.93	117.6	35.73	910.41	70.13	66.78	60.90	84.90
40	58.63	56.95	54.62	52.62	1.30	2.84	2.01	7.86	464.78	258.7	76.60	989.45	114.8	111.2	107.3	105.18
50	63.84	66.94	58.73	54.7	2.57	2.72	3.15	10.33	574.48	389.4	154	1276	125.3	131.3	115.2	109.54
60	74.15	72.62	69.12	61.07	3.25	2.86	3.75	11.50	476.45	379.5	267.2	1416.1	145.4	142.5	135.5	121.99
70	89.55	86.02	85.38	65.25	2.78	2.30	4.68	12.98	297.68	116.8	280.5	1424.3	175.9	168.8	167.6	130.48

Notations- A: AODV, B: AOMDV, C: OLSR and D: ZRP

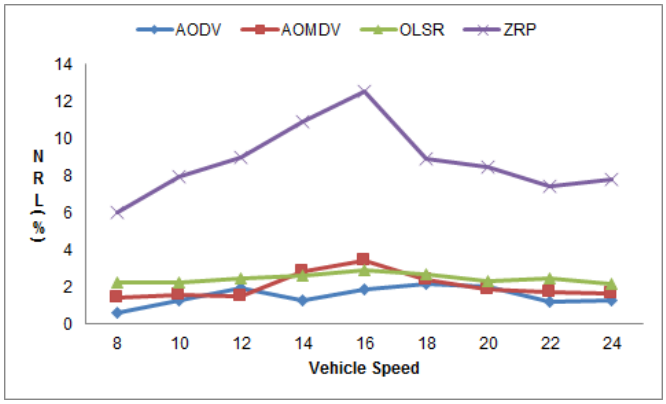

Fig.7. Measurement of NRL by varying vehicular speeds

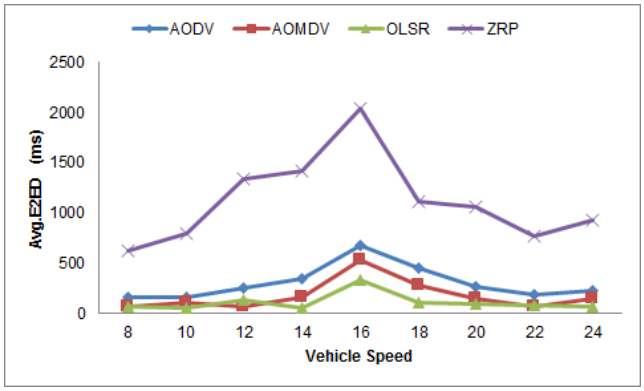

Fig. 8. Measurement of Avg.E2ED by varying vehicular speeds

Precalculating routes reduce the delay in proactive routing protocols. OLSR attains 109.59, 50.88 and 743.15ms as well as 149.25, 75.56 and 852.95ms less Avg. E2ED respectively for the speed of 10 and 16m/s vehicles for the protocols under study. Thus, Avg.E2ED of OLSR is lower in VANET. Repair of local links sometimes increases routing latencies in AODV. In OLSR, it is necessary to look in the routing table while doing a route search. But AODV initializes route search when there is an existence of the valid route. Therefore, a simple search of tables takes less time than flooding a network, which improves the performance of the OLSR protocol in a network sensitive to delay. ZRP produces more Avg.E2ED because the route discovery requires extra time. ZRP produces more control packets since it is composed of protocols i.e. IERP and IARP. IERP initialized by the source vehicle if a destination node is not reachable in the routing zone. Within a local zone, IARP facilitates the maintenance of the routing tables of a node. The interaction between IARP and IERP causes unnecessary traffic on the network that generates a delay in the acquisition of the route. Fig.8. shows Avg.E2ED with variation in the vehicular speeds.

For the smaller speed of the vehicular node, the Throughput generated is more. As the speed of the vehicle increases, the decrease in the Throughput is observed for all protocols. Upto a certain threshold of the speed 16 m/s Throughput decreases in all protocols. Afterward, an increase in Throughput is observed. AODV produces 4.88, 4.69 and 16.03kbps as well as 7.7, 9.31 and 27.41kbps better Throughput for the vehicles with speed of 10m/s and 24m/s compared to the selected protocols. Fig.9. shows Throughput for vehicles with varying vehicular speeds.

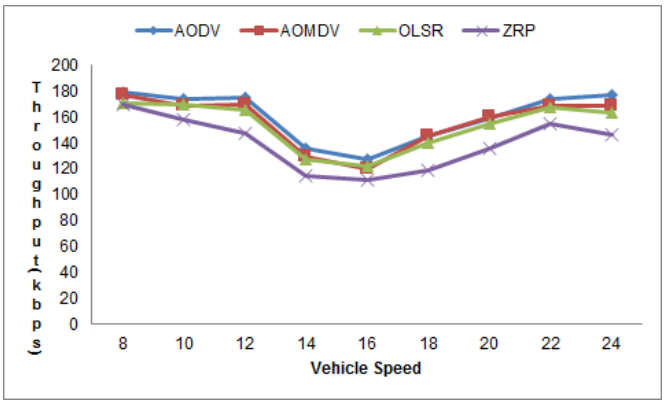

Fig.9. Measurement of Throughput by varying vehicular speed

Table IV represents simulation results for performance measures of various vehicular speeds.

TABLE IV. SIMULATION RESULTS FOR PERFORMANCE MEASURES OF VARIOUS VEHICULAR SPEED

Speed (m/s)	PDR (%)				NRL (%)				E2ED (ms)				Throughput (kbps)			
	A	*B*	*C*	*D*	*A*	*B*	*C*	*D*	*A*	*B*	*C*	*D*	*A*	*B*	*C*	*D*
8	91.47	90.43	87.17	85.36	0.64	1.47	2.24	6.06	163.34	70.29	72.27	629.03	179.57	177.53	171.31	169.58
10	88.65	86.11	86.24	78.99	1.32	1.57	2.25	7.95	166.26	107.55	56.67	799.82	173.95	169.07	169.26	157.92
12	89.46	86.66	84.68	74.01	1.94	1.53	2.5	9.03	255.57	73.98	138.22	1348	175.19	169.88	165.88	147.78
14	69.28	66.16	65.2	57.36	1.28	2.83	2.64	10.94	350.74	163.56	53.57	1414.91	135.91	129.58	127.68	115.16
16	64.88	60.98	62.1	55.55	1.89	3.45	2.95	12.55	676.07	531.99	335.1	2043.28	127.22	119.56	121.99	111.95
18	73.94	74.15	71.4	60.22	2.21	2.43	2.7	8.93	453.13	286.04	106.65	1120.3	145.05	145.29	140.29	119.46
20	81.36	81.52	78.89	68.23	2.01	1.87	2.36	8.5	273.92	144.82	103.42	1063.13	159.63	159.8	155.01	136.32
22	88.66	86.23	85.48	77.43	1.22	1.74	2.47	7.45	185.07	71.01	87.08	770.25	173.5	169.07	167.34	154.84
24	90.64	85.94	83.08	73.21	1.28	1.68	2.18	7.84	223.64	149.95	74.39	927.34	177.58	168.68	163.14	145.96

Notations- A: AODV, B: AOMDV, C: OLSR and D: ZRP

V. CONCLUSION

The vehicular ad-hoc network achieves V2V and V2R communication with the help of IEEE802.11p. Importance of a ManhattanGrid mobility model along with its applicability in the VANET is studied. The simulations are conducted on topological category protocols under various test environments such as density and speed of the vehicle. The QoS affects communication in the VANET. The paper elaborates probable causes towards QoS efficiency along with their parameters with the significance. The influence of density and speed on the QoS parameter is assessed in the VANET environment. The results indicate that AODV, a reactive approach performs better in terms of PDR, Throughput and NRL except some cases in the density environment. AOMDV observed less routing load in case of 60 and 70 vehicles. OLSR produces less Avg.E2ED in all test environments. ZRP achieves moderate results for all parameters except NRL and Avg.E2ED. Overall AODV outperforms all other protocols. Topological routing protocols are less suitable for delay-sensitive networks. In future, a routing protocol will be developed which can cope with the delay sensitive network and intersection oriented environment.

REFERENCES

[1] S. K. Bhoi and P. M. Khilar, "Vehicular communication: a survey," in IET Networks, vol. 3, no.3, pp. 204-217, September 2014.

[2] B. Marzak, H. Toumi, E. Benlahmar, M. Talea, "Performance Analysis of Routing Protocols in Vehicular Ad Hoc Network," In El-(eds) Advances in Ubiquitous Networking 2. Lecture Notes in Electrical Engineering, vol 397. Springer, Singapore 2017.

[3] Rawal, Tejas., "Intelligent Transportation System in India - A Review," Journal of Development Management and Communication. 2015.

[4] F. Li and Y. Wang, "Routing in vehicular ad hoc networks: A survey," IEEE Vehicular Technology Magazine, vol. 2, no. 2, pp. 12-22, June 2007.

[5] J. B. Kenney, "Dedicated Short-Range Communications (DSRC) Standards in the United States," In the Proceedings of the IEEE, vol. 99, no. 7, pp. 1162-1182, July 2011.

[6] Shtaiwi, Abduladhim & Saoud, Abdusadik & Almerhag, Ibrahim.. Performance Evaluation of VANETS Routing Protocols. Computer Science & Information Technology. 4. pp. 305-315, 2014.

[7] A. K. Basil, M. Ismail, M. A. Altahrawi, H. Mahdi and N. Ramli, "Performance of AODV and OLSR routing protocols in VANET under various traffic scenarios," IEEE 13th Malaysia International Conference on Communications (MICC), Johor Bahru, pp. 107-112, 2017.

[8] M Khairnar, D Vaishali, D Kotecha, "Simulation-based performance evaluation of routing protocols in vehicular ad-hoc network", International Journal of Scientific and Research Publications, Volume 3, Issue 10, October 2013.

[9] L. Rivoirard, M. Wahl, P. Sondi, M. Berbineau and D. Gruyer, "Performance evaluation of AODV, DSR, GRP and OLSR for VANET with real-world trajectories," 15th International Conference on ITS Telecommunications (ITST), Warsaw, pp. 1-7,2017.

[10] Y. R. B. Al-Mayouf *et al*., "Real-Time Intersection-Based Segment Aware Routing Algorithm for Urban Vehicular Networks," in IEEE Transactions on Intelligent Transportation Systems, vol. 19, no. 7, pp. 2125-2141, July 2018.

[11] G. Li, L. Boukhatem and J. Wu, "Adaptive Quality-of-Service-Based Routing for Vehicular Ad Hoc Networks With Ant Colony Optimization," IEEE Transactions on Vehicular Technology, vol. 66, no. 4, pp. 3249-3264, April 2017.

[12] F. Martinez,. J., Toh, C. K., Cano, J.-C., Calafate, C. T. and P. Manzoni, "A survey and comparative study of simulators for vehicular ad hoc networks (VANETs)," Wirel. Commun. Mob. Comput., pp. 813 - 828, 2011.

[13] Z. Ismail and R. Hassan, "Effects of Packet Size on AODV Routing Protocol Implementation in Homogeneous and Heterogeneous MANET," 2011 Third International Conference on Computational Intelligence, Modelling & Simulation, Langkawi, pp. 351-356., , 2011

[14] S. G. Kawale and V. Bondre, "Performance evaluation of different density AOMDV routing protocol for VANET," International Conference on Communications and Signal Processing (ICCSP), Melmaruvathur, pp. 1123-1127, 2015.

[15] Joilson Alves Junior and Emilio C. G. Wille, "Routing in Vehicular Ad Hoc Networks: Main Characteristics and Tendencies," Journal of Computer Networks and Communications, vol. 2018.

[16] J. Harri, F. Filali, and C. Bonnet, "Mobility models for vehicular ad hoc networks: a survey and taxonomy," in IEEE Communications Surveys & Tutorials, vol. 11, no. 4, pp. 19-41, Fourth Quarter 2009.

[17] S. A. Ben Mussa, M. Manaf, K. Z. Ghafoor and Z. Doukha, "Simulation tools for vehicular ad hoc networks: A comparison study and future perspectives," 2015 International Conference on Wireless Networks and Mobile Communications (WINCOM), Marrakech, pp. 1-8, 2015.

[18] J. Toutouh, J. Garcia-Nieto and E. Alba, "Intelligent OLSR Routing Protocol Optimization for VANETs," in IEEE Transactions on Vehicular Technology, vol. 61, no. 4, pp. 1884-1894, May 2012.

[19] http://sys.cs.uos.de/bonnmotion/ last accessed in Oct.2018.

[20] https://www.rfc-editor.org/info/rfc3626 last accesed in Oct. 2018.

[21] Mobile Ad-hoc Networking group-https://www.ietf.org/rfc/rfc3561.txt accessed in sept.2018.

[22] Nicklas Beijar, "Zone Routing Protocol (ZRP),"2000.

[23] https://tools.ietf.org/html/draft-ietf-manet-zone-zrp-00 last accessed in Oct.2018.

[24] www.statistica.com/statistics/664729/total-number-of-vehicles-india last accessed on 18 Feb.2019.

Proceedings of the Fourth International Conference on Communication and Electronics Systems (ICCES 2019)
IEEE Conference Record # 45898; IEEE Xplore ISBN: 978-1-7281-1261-9

Things-to-Cloud (T2C): A Protocol Based Nine Layered Architecture

ND Patel*† (ndpatel@idrbt.ac.in),
BM Mehtre* (bmmehtre@idrbt.ac.in), and Rajeev Wankar† (wankarcs@uohyd.ernet.in)
*Centre of Excellence in Cyber Security, Institute for Development & Research in Banking Technology (IDRBT)
†School of Computer & Information Sciences (SCIS), University of Hyderabad (UoH)

***Abstract*—The Internet of Things (IoT) is rapidly becoming a part of our regular activities and environment. According to Cisco by 2030, it is expected that 500 billion devices will be connected on the IoT. Every passing day we see new devices and sensors coming in the market, which use different protocols to connect to the network. With this expected growth of the Internet of Things and the emergence of Fog and Cloud Computing, there is a need for a standard protocol suite to handle different aspects of standardization and cloud protocols in the IoT environment that is not covered by currently existing Three, four, and five layered IoT models.**
We propose a T2C architecture that provides the most prominent standard protocols into nine layers and show why this extension is essential. The proposed T2C architecture fulfills the prescribed activities for smart sensors and fog networking in the backbone. Which brings significant benefits, scalability, and low-power consumption in the IoT architecture. It emphasizes on how IoT device classification can be mapped to our proposed nine layered T2C Architecture.

Keywords: Internet of Things, IoT Protocols, IoT layers, Things-to-Cloud (T2C)

I. Introduction

Things-to-Cloud (T2C) is a bridge between the Internet of Things, Fog Computing, and Cloud Computing. We are putting together IoT and Cloud premises, and calling it as Things-to-Cloud (T2C). Internet of Things (IoT) is a system of interconnected electromagnetic tracking devices, computing devices, and smart digital devices. These devices are capable of transferring the data to the cloud via fog computing. The IEEE has defined an IoT architecture, domains of IoT, the definition of IoT, and identification of public IoT domains. O. Logvinov et al., [1] introduced three-tiered architecture with Sensing layer, Networking & Data Communication layer, and Application layer.

Several attempts were made in the past to provide a layered architecture for IoT based on operations they perform. In the last two-three years, the gap between IoT and Cloud has been bridged due to the introduction of a Fog Computing, which communicates with both these components. IoT-Devices are becoming more powerful and capable of performing various tasks. Due to this advancement, there is a need for re-look-up the five-layered architecture [2]. In this paper, we have proposed nine layered T2C architecture to connect sensor enable IoT-Devices to the Cloud and also explained the required layers for each type of IoT-Devices.

Based on operations performed in each layer, we classified the common standard protocols to handle this operation. The nine layers are IoT-Devices layer, Connectivity layers, Link Protocol layers, Transport & Network layers, Session & Communication layers, Data Aggregation & Processing layers, Data Storage & Retrieval layer, Business Model layer, and Business Application (Apps) layer. At every layer, we have suggested different protocols to be used. Also, we briefly reviewed Things-to-Cloud (T2C) management protocol standards and the current state of security concerns related to specific protocols. We also presented a brief comparison between various IoT protocols and how to choose among these protocols.

The rest of the paper is organized as follows: Section II presents different IoT Architectures available in the literature and present four IoT architecture, in Section III we present the proposed Things-to-Cloud (T2C) which is a protocol based nine layered architecture, in Section IV we discuss IoT Security & Privacy trust framework, and Section V we gave a summary of lessons and future scope of IoT.

II. IoT Architectures

The IoT architecture introduced for smart service domains has to reach the main demands of having Intelligence, Scalability, Interoperability, Think of Security Rights, Challenges in Securing, Managing, and Optimizing. Several IoT architectures are proposed in the literature, but they do not adhere to common architecture design. IoT Basic Model is essentially the architecture which allows us to gather data from various sources, where data has never been traditionally looked at with Three-layer IoT Architecture expressing of the Application Layer, Network Layer, and Perception Layer has been presented in Figure 1 (a) [3] [4]. In the recent survey, another architecture has been considered that add more abstraction to the IoT model [2] [3] [4].

Also, three-layer architecture has been extended to Middle-Ware based architecture and address a different type of communication medium Figure 1 (b). It has been extended to SOA based architecture while having a layer like "Service Composition" to run on resource-constrained devices in Figure 1 (c). The Five-layers architecture is quite similar to the three layers architecture. R. Khan et al., [5] extended the three layers architecture to five layers in Figure 1 (d), that helps to visualize a clear view of IoT architecture with Objects Layer, Object

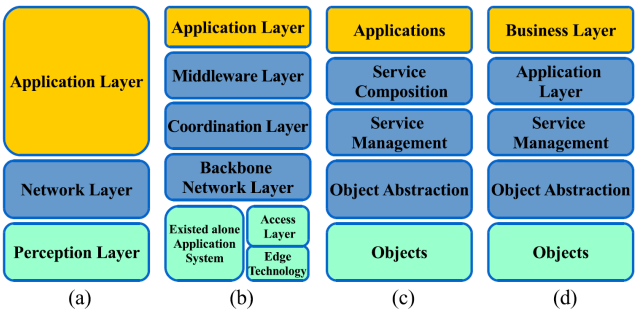

Figure 1: layers Wise IoT Architecture. (a) 3-Layer [4]. (b) Middle-Ware based. (c) SOA based. (d) 5-layer [2].

Abstraction Layer, Service Management Layer, Application Layer, and Business Layer for the easier operation for the IoT ecosystem.

The main limitations for these IoT architectures, the three-layer architecture does not cover all underlying technologies that transfer data to an IoT platform. The SOA-based architecture takes a big fraction of time and energy of the device to communicate with other devices and integrate the required services. The five-layer model is a rather complex model and has very large computational requirements and thus it requires very powerful devices for it's hosting. These models do not cover all standards in the real IoT environment. For example, "Object Abstraction Layer and Service Management Layer" does not cover all Cloud Protocols, neither does it integrate the required services.

III. Protocol Based Nine Layered Architecture for Things-to-Cloud (T2C)

T2C Architecture provides an overview of all the protocols that would be helpful for the performances of the IoT Services. In Figure 2, we present a layered diagram of the important standard protocols and technologies. In the T2C Architecture we extended Object Abstraction Layer to Connectivity Layer, Link Protocol Layer, and Transport & Network Layer. The Service Management Layer has been extended into three different layers; Session & Communication layer, Data Aggregation & Processing layer, and Data Storage & Retrieval layer.

We added Business Model layer to reach Business Application layer with the help of open framework. This extension is brought with intention to reduce the maintenance cost, better services & support, smoother logistics, improved experience, and enhanced security with the low-power. The T2C protocol based architecture defines a protocol based networking architecture to implement protocols in nine layers. Different groups (W3C, IETF, IEEE, EPCglobal, ETSI) are the protocols provided in support of IoT ecosystem. The T2C protocol based nine layered architecture provides the most prominent Standard protocols into nine broad categories.

IoT-Devices Classification and Mapping With T2C Layers: The IoT-Device layer is classified in five parts: Home Automation Based IoT-Devices, Industrial Based IoT-Devices, Health Care Based IoT-Devices, Development Board IoT-Devices, and Virtual Reality & Miscellaneous IoT-Devices. The detailed classification of IoT-Devices can be seen in Figure 3. These devices connect to Link Protocol Layer and receive the data feed over the Transport & Network layer using 2G, 3G, 4G, 5G network technologies. This will not interfere with Transport & Network layer protocols for messages by-passing in the Session & Communication layer. The Session & Communication Layer sends the data feeds to the Aggregation & Retrieval layer to provide low-latency platform for managing real-time, unified, and high-throughput data feeds. For storage purposes, the Aggregation layer sends the data feeds to the Data Storage & Retrieval layer and pop the data feeds with the help of an open framework to the Business Model layer.

However, not all of these nine layers have to be aggregated together to deliver an IoT-Device. Moreover, based on the inherent nature of IoT-Devices, some layers may not be required in them. We provide a mapping for IoT-Devices classification with T2C Layers in Table I.

A. IoT-Device Layer

1) Home Automation Based IoT-Devices: These little devices that consist of the perfect combination of the various sensors to prepare our home intelligent and protected i.e. HD Camera, High Quality Microphone, Smart Temperature, Night-Vision, Motion Detection, Smart Thermostats, Smart Lights, Smart skybell, Intelligently Tracking, Teleportation, 360 degree IR blaster, UV, Humidity, Noise detector, Vibration, Monitor Indoor Air, Outdoor Weather, Energy Consumption, and many more.

These devices intelligently analyze sensor data and send us alerts in case of unusual activity. We empower them to take action when we are traveling.

2) Industrial Based IoT-Devices: Industrial-IoT (IIOT) devices are smart assets providing many benefits, including improvements to Productivity Monitoring, Operational Efficiency Safety, Control Liability Performance, and Diagnostics Regulatory. IIoT eliminates workers from many organizations and industries, allowing IoT-Devices to act autonomously decreasing risks associated with worker injury or human error system failures.

3) Health Care Based IoT-Devices: In the health care industry, it is very difficult to collect samples, patient information, and diagnosing in real-time. The Health Care Based IoT-Devices help in monitoring and keeping track of patients health continuously and are responsible for performing certain actions when the critical condition is triggered. It is expected that by 2025, 80% of all health-care organizations will have implemented IoT technology. Some companies have also designed other health-related IoT products like Thermometers, Fitness Sensors, Baby Monitors, and more.

4) Development Board IoT-Devices: Development Board IoT-Devices have a sensor embedded at the IoT Development Board. In development boards, we realize how a sensible,

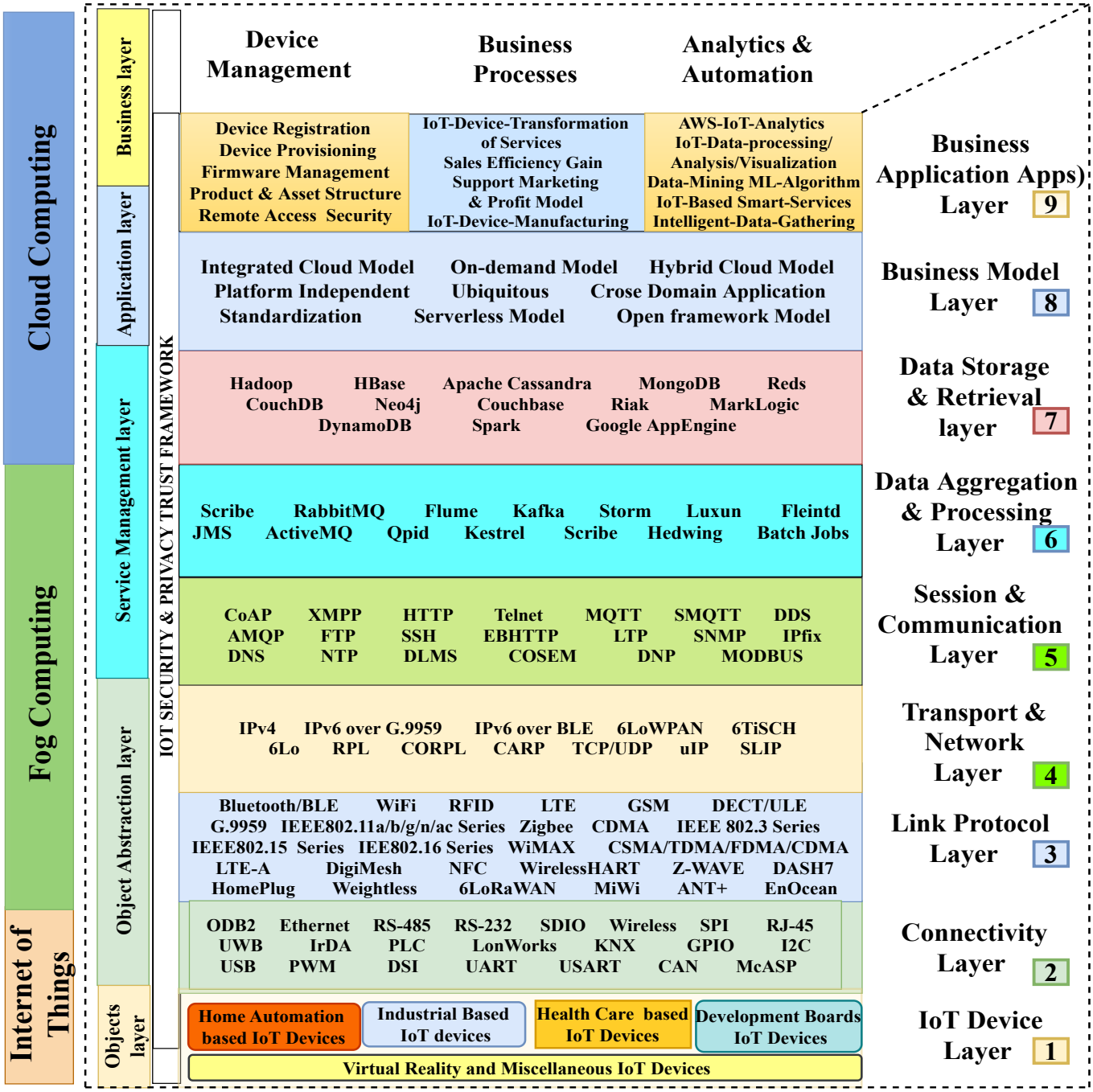

Figure 2: Protocol Based Nine Layered Architecture for Things-to-Cloud (T2C)

IoT-Devices / T2C Layers	Home Automation Based IoT Devices	Industrial based IoT Devcies	Health Care based IoT Devices	Development Boards IoT Devices	Virtual Reality & Miscellaneous IoT Devices
Conectivity Layer		✓		✓	
Link Protocol Layer	✓	✓	✓	✓	✓
Transport & Network Layer	✓	✓	✓	✓	✓
Session & Communication Layer	✓	✓	✓	✓	
Data Aggregation & Processing Layer		✓		✓	
Data Storage & Retrieval Layer				✓	
Business Model Layer	✓	✓		✓	
Bussiness Application Layer	✓	✓	✓	✓	✓

Table I: IoT-Devices and Required Layers

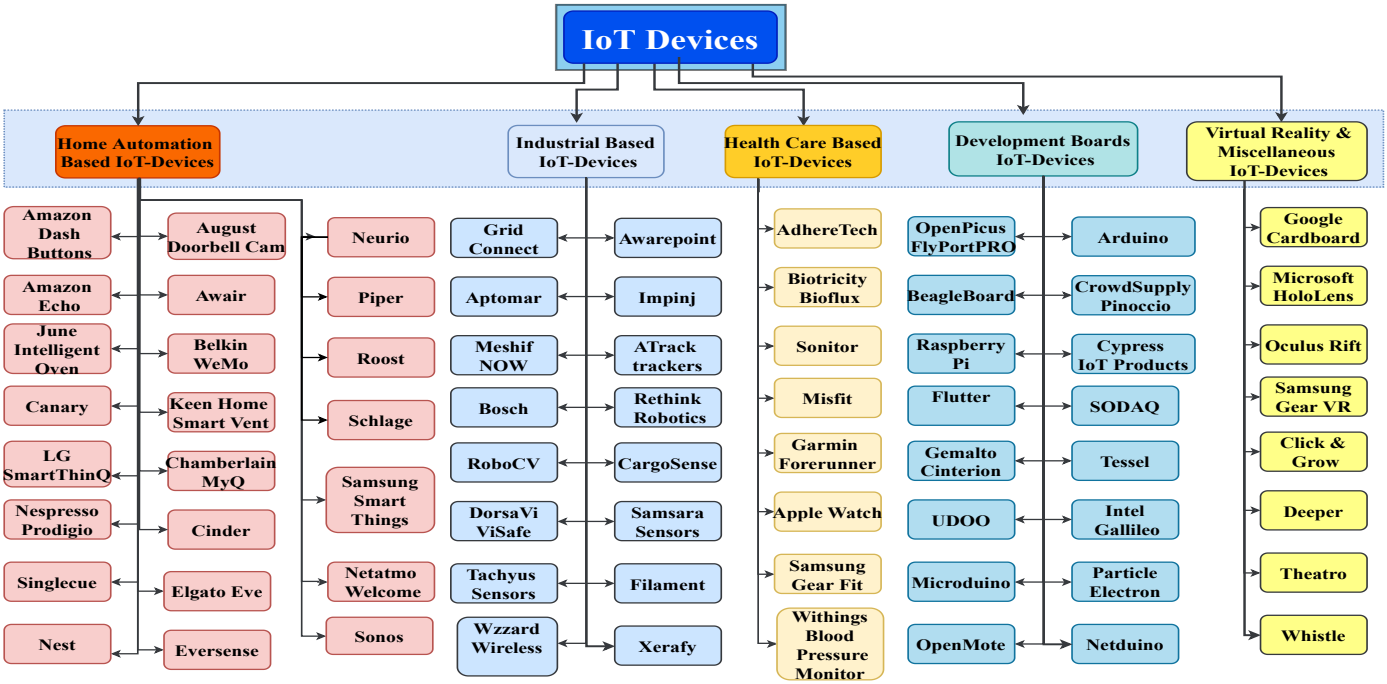

Figure 3: IoT-Devices Classification

smart device acquires, processes, and communicates information to the cloud platform. IoT software and hardware work together to build the IoT Technology stack. In the Development Boards market, there are more than 100+ Single Board Computer (SBC) / Boards available like *Arduino, BeagleBone, Intel, Raspberry Pi families,* etc.

5) Virtual Reality & Miscellaneous IoT-Devices: IoT is also used for the low-Frequency approach to Augmented Reality (AR) / Virtual Reality (VR). There are so many devices designed primarily for enterprise use, *Google Cardboard* for nostalgic toy lovers, *Microsoft HoloLens* augmented reality smart device which can assist with training, design work, communication, and more.

B. Connectivity Layer

While developing any IoT solution big question which arises is how to connect to the above layer? There are so many connectivity protocols available in the literature. We will discuss the most popular connectivity protocols and suggest how to choose the most suitable protocols for an IoT solution. The Connectivity layer protocols provide connectivity to models and interfaces to the set of sensors. We will further continue into detailed features regarding the pros and cons of each of them:

1) OBD-2: Connected Car - The future of automobile, IoT-OBD (On-Board Diagnostics) device is the best car tracking and diagnostic devices for someone who wants to track a car's location, experience travel rates, identify the problem of a check-engine light, and automatically get emergency help after an accident.

2) Ethernet: It is external communication in a local area network. It controls the transmission of the information and avoids simultaneous transmission by various IoT-Devices.

3) RS-485: It is an Industrial protocol. This kit consists of the features of the WiFi connectivity, which establish the real-time overall achievement, authenticity, and accuracy for T2C while transferring information between the application and the fundamental layer.

4) RS-232: It is an Industrial protocol. This kit includes the features of the LoRaWAN connectivity plus the benefits of having an RS-232 connection to be integrated with industrial devices.

5) SDIO: SDIO is an evaluation board. It supports 802.11 series protocols and low-cost IoT USB interface.

6) Wireless: In the IoT, there are a series of factors, all working in tandem to transmit the system records in real time. There are many purposes that fall below the IoT umbrella.

7) SPI: SPI device, gadgets communicate in full duplex mode using a master-slave structure with a single grasp. It's faster than asynchronous serial.

8) RJ-45: RJ-45 is a dual-port connector including with smart sensors, operator terminals, remote input/output, gateways, and transmitters. It supports industrial protocol stacks.

9) UWB: Ultrawideband technology could be an undiscovered option for some IoT applications. A UWB was affiliated to a DCU (data collecting unit), and they send their IoT sensor data to the server, wirelessly [6].

10) IrDA: The Infrared Data Association (IrDA) offers requirement for an entire set of protocols for Wi-Fi infrared communications, and the name "IrDA" also mention that set of protocols.

11) PLC: PLC is a Power Line Communication. For the IoT sensor network SmartGrid, C Chaauvenent et al., [7] proposed G3-PLC (Narrowband Powerline Communication) standard. PLC-IoT Application approves agencies of all sizes to upgrade and enhance their legacy systems for the future.

12) LonWorks: LonWorks is a conversation protocol in the Local operating network (Lon), so it is called LonWorks and open protocol technology. It is a networking platform and individually built address that caters the needs for applications.

13) KNX: KNX is a communication protocol developed for home and building automation. KNX-IoT is state of the art technology. It also supports diverse interactions between KNX and 3rd party equipment driven by relevant use cases from various categories.

14) GPIO: A GPIO (General Purpose Input/Output) port controls both incoming and outgoing signals. It is a standard interface for electronic devices and connects to microcontrollers. It can be used with System-on-Chip (SoC) Modules, Sensors, Displays, and Diodes. It supports Windows and Linux Operating Systems.

15) I2C: Inter-Integrated Circuit (I2C), I2C is a serial and synchronous communication protocol, so they enable apps to speak with Inter-Integrated Circuit devices. In I2C devices EEPROMs, real-time clocks, processors, sensors are used as a control interface. I2C devices have respective data interface (Video Decoders, Digital TV Tuners, Audio processors).

16) USB: USB stands for Universal Serial Bus. Its send and receives a data feed along with clock pules. It is very fast compared with USART and USB. USB have three generations i.e USB1.0, USB2.0, USB 3.0. The USB cable is the only medium that connects Arduino and Computer.

17) PWM: Use Pulse-Width Modulation (PWM) signals for motor control. PWM controls analog circuits with digital outputs. PWM required less heat dissipation, greater efficiency, and higher power output.

18) DSI: Digital Serial Interface (DSI) capabilities allow signals communication (high-speed serial interface) between machines and sensors. Machines to be captured and analyzed the data feeds. DSI could help us to connect machines, devices, things, and sensors in various environment. DSI research & development helps to our Military to reduce the expense of display controllers.

19) UART: Universal Asynchronous Receiver/Transmitter (UART), It's not a communication protocol like I2C, SPI, and more, but it's a stand-alone IC. The main purpose is to transmit, broadcast, and receive serial data.

20) USART: It is a Universal Synchronous & Asynchronous Data Transmitter & Receiver. USART push and pop a block of data with classes pulses. It is a duplex communication. It is fast compared with UART.

21) CAN: Controller Area Network (CAN) is a CSMA-CD/ASM protocol. CAN is an interface for Telit cellular module, as well as a positioning component for the Global Navigation.

22) McASP: Connected McASP is simple to establish a sensor available to work on your existing device, machinery. You need to install the gateway on the devices or machines which we want to track and start monitoring them remotely.

C. Link Protocol Layer

In the IoT ecosystem, connected with millions of devices in the system. We securely transfer the information and data feeds in the Transport & Network layer. Almost all IoT-Devices need some wireless or wired connectivity interface that gives them the ability to collect information from IoT-Devices and transmit the information in The Transport & Network layer with different standard link protocols. These protocols make use of radio waves to transmit the collected information across a network. Link Protocol layer works as a two-way traffic, data or information received from the IoT-Devices will also pass through the IoT Gateway. We shall briefly explain different protocols standards.

1) Bluetooth/BLE: Bluetooth/BLE designed for connecting devices to the internet with low energy consumption. It is an ultra-low power connected devices in short range. Matti et al., [8] investigate Ipv6-based connection over BLE. It is appropriate for future IoT scenarios.

2) Wi-Fi: Any of several standards for short-range wireless data feed transmission. Wi-Fi is a wireless fidelity technology. It is a real-time high-speed less communication protocol [9] for cyber-physical control applications.

3) RFID: RFID tags or smart labels for radio-frequency identification, RFID tags are the small wireless accessory that helps identify people, things, and objects [10]. RFID is a built-in part of our life, which increases convenience and productivity.

4) LTE: LTE is a high-speed wireless communication based on EDGE/GSM and HSPA/UMTS. LTE will pass large packets of data and streamline the IoT Service. It reduces the latency of information delivery.

5) GSM: It is established on eGPRS and construct as a high capacity, long range, low power cellular gadget for IoT applications.

6) DECT/ULE: DECT (Digital Enhanced Cordless Telecommunications) and ULE (Ultra Low Energy) is an ordinary European widespread for cordless phones. They have specific a low-power air interface technological know-how that can be used for IoT applications.

7) G.9959: G.9959 performed at low cost, low bandwidth, and half-duplex reliable wireless communication. It is planned for real-time functions and required the authenticity for low strength consumption [11].

8) IEEE 802.11 series: 802.11 series a/b/g/n/ac/..etc, also known as Wi-Fi for between two wireless clients. It includes a limited range of being connected technology containing wireless LANs (WLANs). IEEE 802.11 wireless communication medium access standard. The basic of 802.11 series MAC layer features include; simultaneous occurrence Frame, Null Data Packet, Short Mac Frame, Efficient Bidirectional Packet Exchange, and Increase Sleep Time.

9) Zigbee: It is high-level intelligence communication protocols based on the IEEE 802.15.4. We can develop personal area networks, helps to a medical device for data collection, and home automation with low-power. ZigBee Pro offers greater aspects such as security the use of the balanced symmetric-key exchange, scalable the usage of random address assignment, and better overall performance the use of environment-friendly many-to-one routing mechanisms.

10) CDMA: C-Code D-Division M-Multiple A-Access P-Protocol (CDMA), It used 2G and 3G wireless communications. The CDMA-based protocol can support IoT traffic in upcoming 5G-MNA (Mobile Network Architecture).

11) Ethernet IEEE 802.3: Ethernet 802.3 is a physical communication in a LAN. Its wired connectivity & networking for computer and data applications.

12) IEEE 802.15 / 802.16: IEEE 802.15 is based on direct sequence spread spectrum, DSSS techniques. IEEE 802.16 is a Wireless Communications Standards (WCS) for metropolitan area networks (MANs).

13) WiMax: Worldwide Interoperability for Microwave Access (WiMax), produce 4G and 5G of wireless Internet. WiMax has average bandwidth in the local LAN connection and offers wireless broadband.

14) CSMA/TDMA/FDMA/CDMA: There are some methods for Signal. Different users share a common channel using F-Frequency D-Division M-Multiple A-Access (FDMA), T-Time D-Division M-Multiple A-Access (TDMA), C-Carrier S-Sense M-Multiple A-Access (CSMA) or C-Code D-Division M-Multiple A-Access (CDMA). These are secure and authentic MAC protocol. They have advance Encryption-Algorithms to encrypt the messages and calculate the coherence and cohesion.

15) LTE-A: L-Long T-Term E-Evolution Advanced (LTE-Advance) is a standard to construct Machine-to-Machine (M2M) communication and IoT-Devices networks. LTE-A is a flexible, scalable, and low-cost protocol related to other cellular protocols [12]. LTE-Advance is a new evolution to help band-aid to increases data speeds, faster, performance, greater stability in the future.

16) DigiMesh: It is the high-latency for information transfer, as the network-dictates in the time-frames for data. They increase network range, and every device performs like a router [13].

17) NFC: Near Field Conversation (NFC) is a set of communication protocols that authorize to electronic devices. It is a flexible system such as a smart-phone and set up authorize communication by bringing them inside four cm of every other [14]. NFC at a receiver apparatus and radio transmitter. The best example is Beacons that come with a built-in NFC tag, and ANT+ provides such strengthens.

18) WirelessHART : It is a wireless sensor networking science primarily based on the H-Highway A-Addressable R-Remote T-Transducer (HART) Protocol. It is advanced developed as an inter-operable wi-fi standard and multi-vendor. WirelessHART was characterized by the necessities of development field system networks. WirelessHART, the first worldwide industrial wi-fi general (IEC 62591), is built on the pinnacle of the IEEE 802.15.4 widespread [15].

19) Z-WAVE: A Z-Wave network consists of IoT units, and a foremost controller additionally acknowledged as a smart domestic hub. Z-Wave is one of the oldest and most commercially profitable IoT protocol, while Thread is one of the most current protocols [16]. Z-Wave protocol used for home appliances to monitoring and control.

20) DASH7: This protocol is a wireless verbal exchange protocol for pushing RFID that operates in universally accessible I-Industrial S-Scientific M-Medical (ISM) smart band, and it is suitable for all T2C requirements [17].

21) HomePlug: It is designed for consistently and especially for Home-Automation and Smart-Grid applications. It is specially constructed to scale down the value and energy utilization of smart HomePlug-AV while maintaining its coverage, interoperability, and reliability.

22) Weightless: Weightless is another Wi-Fi WAN, designed with the aid of the Weightless Special Interest Group (SIG). There are two units of standards, like Weightless-N and Weightless-W. There is the first developed aid with low cost and low energy machine-to-machine conversation with the time division multiple access[18].

23) 6LoRaWAN: It is a recently bobbing up wireless technology constructed for low-power WAN networks with bi-directional communication, low cost, security, and mobility for IoT purposes [19].

24) MiWi: In the MiWi development, there are some different protocols like Miwi protocol, Miwi Mesh, and Miwi P2P. These protocols are used for short range area.

25) ANT+: ANT+ provides such strengthens and features goal for the IoT. It manages the ANT network and defines how to transmit information across the system in a consistent way. ANT+ is an enabled sensor to help health care services.

26) EnOcean: EnOcean is an energy harvesting and energetically exploitation of mechanical motion and other potentials from the IoT Ecosystem, such as temperature difference and indoor lights for building automation and home.

D. Transport and Network:

The Transport & Network layer is responsible for assigning some address and routing of data feeds. At this layer, the data packets are delivered from the Link Protocol layer to the destinations by using the IP address. These layers communicate data to The Session & Communication layer. There are some mechanisms of Network layer encapsulation protocols (IPv4, IPv6 over BLE, IPv6 over G.9959, 6LoWPAN, 6TiSCH, 6Lo, TCIP/UDP, IP, SLIP). IP version 4 (IPv4) is the network layer protocol. IPv4 has five classes, i.e., Class-A IPv4, Class-B IPv4, Class-C IPv4, Class-D IPv4, and Class-E IPv4. Commonly we used Class-A, Class-B, and Class-C. The Class-D and Class-E fixed for multi-casting and some experimental purposes. IPv4 has limited address space (approximately 4.3 billion devices), so we need more address space because there will be more than 50 billion IoT-Devices alone by the year 2025. IPv6 have 128-bit address space (approximately 320

billion devices). In IPv6, there are three types of addresses in standard, i.e., Uni-Cast Address, Multi-Cast Address, Any-Cast Address [20].

6LoWPAN, 6-IPv6 L-Low P-Power W-Wireless P-Personal A-Area N-Network (6LoWPAN) [21] developed for IoT-Devices in a WSN. It is a modified version of IPv6. 6TiSCH, allows IPv6 addresses to pass by T-Time S-Slotted C-Channel H-Hopping (TSCH) mode. Resource-Constrained Nodes (6Lo) is IPv6 protocol for data-links that were left excluded by 6TiSCH and 6LoWPAN. These protocols reduce communication by the following three optimizations, i.e., Header Compression, Fragmentation, and Link Forwarding. The consequence of imparting these protocol standards is to spotlight the main challenge of between particular specific MAC requirements and the variety of protocols. So, the IPv6 and the standard protocol stacks based on the future growths of IoT-Devices. It has sufficient address space for IoT ecosystem while using IPv6.

These are some Routing Protocols (RPL, CORPL, CARPL) presented in IoT. RPL is a measure vector protocol created by IETF in 2012. RPL: IPv6-Routing-Protocol for Lossy Networks and Low-Power. It calculated the de-facto-routing-protocol for IoT. C-Cognitive RPL (CORPL) is an aberrant addition of RPL protocols that are designed for cognitive networks and appropriates the opportunistic sending to deliver packets at each Hop (networking). CA-Channel-Aware R-Routing P-Protocol (CARP) is the only distributed Hop (networking) based routing protocol that is produced for IoT-Devices based network applications. CARP is used for under the water's surface and submarine communication and send the information mostly.

E. Session & Communication Layer

In the Session & Communication layer, we communicate (Request/response, Publisher/subscriber) between Server-2-Server (S2S), Device-2-Device (D2D), Device-2-Server (D2S), and Server-2-Device (S2D). These protocols are very light-weight to publish and receive messages. These protocol designed for constrained IoT-Devices with low-bandwidth.

Things-to-Cloud (T2C) has many standard communication protocols which are briefly highlighted in this section. Those protocols are application structured based and software application specific. For example, if a software application has been constructed with XML, it receives a piece of code in its headers, XMPP may be the considerable option to appoint in the middle of session layer protocols. At the same time, if the application is energy sensitive, then we need to select MQTT. It would be predictable, trustworthy option. However, that appears with the other additional implementation. If the request application needs REST serviceability as it will be HTTP based, then CoAP would be the genuine, authentic alternative if not the single one. The list of alternatives are: CoAP, XMPP, HTTP, Telnet, MQTT, SMQTT, DDS, AMQP, FTP, SSH, EBHTTP, LTP, SNMP, DNS, NTP, IPfix, DLMS, DNP, MODBUS, COSEM, etc.

1) CoAP: The Constrained Application Protocol (CoAP) used with constrained (i.e., lossy, low-power) networks and constrained node. CoAP is the most promising protocol for smart IoT-Devices and M2M applications. CoAP is prescribed in IETF RFC 7252.

2) XMPP: XMPP is a lightweight Publish or Subscribe resource-based constrained IoT-Devices [22]. X-eXtensible M-Messaging & P-Presence P-Protocol (XMPP) reduce interoperability between different networks.

3) HTTP: HTTP is applied for data transfer on the internet, and it is mostly used for IoT-Devices that lack to publish a lot of data feeds.

4) Telnet: Telnet is a Client/Server protocol used in the local area network. It is based on a trust-able connection-oriented transport.

5) MQTT: MQTT is broadly used in T2C Architecture due to the low power consumption. It stands for M-Message, Q-Queuing, T-Telemetry, T-Transport. MQTT is an M2M/IoT connectivity protocol. It is a dial-up connection with home automation, health-care providers, Industrial application, and small device scenarios. It is very small in size, does efficient distribution of information, minimized data packets, and has low power usage to one or many receivers.

6) SMQTT: M Singh et al.,[23] proposed secure SMQTT protocol for IoT. SMQTT is an extension of MQTT and used in lightweight attribute-based encryption.

7) DDS: D-Data, D-Distribution, D-Service (DDS) developed M@M communication by Object Management Group. DDs is low footstep of our devices to cloud.

8) AMQP: A-Advanced M-Message Q-Queuing P-Protocol (AMQP), this is an open source protocol for asynchronous messaging. AMQP gives better performance compared to other protocols [24].

9) FTP: F-File T-Transfer P-Protocol (FTP) is a protocol for exchanging files between a client and a server in the network.

10) SSH: SSH works in the between client and server model. SSH uses public key cryptography.

11) EBHTTP/LTP: E-Embedded B-Binary HTTP (EB-HTTP) and L-Lean T-Transport P-Protocol (LTP) are light-weight protocols. That protocol works on low data rate, low computation complexity, and low energy consumption [25].

12) SNMP: S-Simple N-Network M-Management P-protocol (SNMP) is the most long-range protocol. It supports conventional network equipment like IoT-Devices, scanners, printers, etc.

13) IPfix: I-Internet P-Protocol F-Flow I-Information E-Export (IPFIX), it consists of a unidirectional protocol for export and format the data.

14) DNS: D-Domain N-Name S-Service (DNS), it resolves the host Internet Protocol-Addresses (IP-A) rendering IoT services. There are some Service Discovery protocols, i.e., m-Multicast D-Domain N-Name S-System (mDNS), DNS S-Service D-Discovery (DNS-SD), U-Universal P-Plug n-and P-Play (UPnP), DNS N-Name A-Autoconfiguration (DNSNA),

S-Simple D-Discovery S-Service P-Protocol (SDSP), DNS SEC-Security DNSSEC [26].

15) NTP: N-Network T-Time P-Protocol (NTP), NTP exchange of time-stamped messages in long-range. NTP-client implements a time-request exchange with IoT-Devices and data packet exchange protocol, called Synchronization Protocol for IoT (SPoT) [27].

16) DLMS: D-Device L-Language M-Message S-Specification (DLMS) or D-Distribution L-Line M-Message S-Specification (DLMS) is an advance Utility IoT protocol. DLMS is used for network connectivity that helps smart metering, thermal energy, water, and gas.

17) COSEM: CO-Companion S-Specification for E-Energy M-Metering (COSEM), COSEM is an interface that is used in the communicating of energy-related equipment.

18) DNP: D-Distributed N-Network P-Protocol (DNP). It is a set of communication protocols that communicate with a master station and IEDs of RTUs.

19) MODBUS: Modbus has allowed thousands and thousands of automation units to talk with each other. The embedded operating system start the communication between the stations, and they talk with another device in cyclic repetition in the Modbus Communication Protocol.

F. Data Aggregation & Processing Layer

When IoT-Devices send data feeds, huge data, we require an endpoint to act something with the enormous data. It is a partitioned, distributed, and replicated log service or messaging system. *Storm* help to process in the real-time environment. *Kafka* getting the data feeds and sending at other destination at large scale. Kafka generates IoT data events and gives a continuous stream of data to sources [28]. Other alternate solutions are Scribe, RabbitMQ, Flume, Storm, Luxun, Flint, JMS, ActiveMQ, Qpid, Kestrel, Scribe, Hedwig, Batch Jobs. They help to monitor the traffic of the data in The Data Aggregation & Processing layer.

G. Data Storage & Retrieval Layer

This layer handles the data passes between IoT-Devices and the Business Model layer. In the recent past, a lot of attention has been migrated from computing to data, which can we saw in the form of several data processing software products in the market. From SQL to NoSQL, a normal relational database to Big Data all are used to provide backend solution. Hadoop, HBase, Apache Cassandra, MongoDB, Reds, CouchDB, Neo4j, Couchbase, Riak, MarkLogic, DynamoDB, Spark, Google AppEngine dominate the field. They provide Data-Partitioning, Data-ingest, Data-quality, Data-Governance, Data-Cleansing & Processing, Predictive Capabilities & Normalization in a Distributed Database System (DDS).
This layer is responsible for providing fast services on high-performance distributed databases, highly-scalable, and reconfigurable servers to handle huge amounts of data sets. This allows the user to do reliable, scalable, distributed computing, and cost-effective solutions.

H. Business Model Layer

The basic Business model depends on Cloud Services such as Data as a service, Process as a service, and Product as a service. In a new era industry and people transform their business models and adopt a new business model for social change with the presence of IoT Ecosystem. This business model provides the business value, business purpose, business methods, and business processes by using Integrated Cloud Model, On-demand Model, Hybrid Model, Platform Independent, Ubiquitous, Cross-domain Application, Standardization, Server-less Model, and Open Framework Model, etc.

I. Business Application (Apps) Layer

Business Application (Apps) layer is divided into three parts, i.e., Device Management, Business Processes, and Analytic & Automation. The function of the Device Management Component is device registration, device provisioning, firmware management, product & asset structure with security, and remote access. The Business Processes Component, on the other hand, is responsible for the transformation of services between the IoT-Devices, Marketing for IoT-Devices, and analyzing the impact of IoT-Device-manufacturing on the market. Finally, in the Analytics & Automation Component provide tools for processing data coming from IoT-Devices. It also has a component for data visualization, data mining, and intelligent data gathering services. A Machine learning library can also be incorporated.
With this proposed approach a new nine layered architecture which we call it Things-to-Cloud (T2C) is introduced in which the data can travel from sensor to the cloud and come back to the user with a lot of value added into. It is evident that all layers are not required every time.

IV. IoT Security & Privacy Trust Framework

O-Online T-Trust A-Alliance (OTA) is an Internet Society Initiative [29]. OTA has released two trust framework for IoT i.e "IoT Security & Privacy Trust Framework v2.0 [29]" and "IoT Security & Privacy Trust Framework v2.5 [29]". This framework includes a set of essential principles required to help secure smart IoT-Devices and their data feeds. This framework is divided into four areas, i.e., User Access & Credentials, Security Principles, Notifications & Related Best Practices, and Privacy Disclosures & Transparency. This particular framework can be incorporated in the proposed layer assuming that all the communication between layers are secure in nature.

V. Conclusions

We have proposed a nine layered protocols based T2C architecture. In the protocol environment architecture, we discussed different protocols. These protocols have been developed by W3C, IETF, EPCglobal, ITU, IEEE standards and products are developed by different companies using these standards. An attempt has been made to decentralize the functionality into layers and clearly dividing the role, protocol, and software stacks that can be used to realize a real world scenario.

Any application development of T2C can be designed and implemented using these proposed layers. The purpose of this paper is to provide an insight understanding of this whole ecosystem and the mapping of IoT-Devices with the respective T2C layers. It is a foundation for IoT practitioners and researchers to understand standard protocol classification and to gain an insight into the IoT protocols and standards to understand overall T2C architecture.

REFERENCES

[1] O. Logvinov, B. Kraemer, C. Adams, J. Heiles, G. Stuebing, M. Nielsen and B. Mancuso, 'Standard for an architectural framework for the internet of things (iot) ieee p2413', Tech. Rep. September, Tech. Rep., 2016.

[2] A. Al-Fuqaha, M. Guizani, M. Mohammadi, M. Aledhari and M. Ayyash, 'Internet of things: A survey on enabling technologies, protocols, and applications', *IEEE Communications Surveys & Tutorials*, vol. 17, no. 4, pp. 2347–2376, 2015.

[3] M. Wu, T.-J. Lu, F.-Y. Ling, J. Sun and H.-Y. Du, 'Research on the architecture of internet of things', in *Advanced Computer Theory and Engineering (ICACTE), 2010 3rd International Conference on*, IEEE, vol. 5, 2010, pp. V5–484.

[4] Z. Yang, Y. Yue, Y. Yang, Y. Peng, X. Wang and W. Liu, 'Study and application on the architecture and key technologies for iot', in *2011 International Conference on Multimedia Technology*, IEEE, 2011, pp. 747–751.

[5] R. Khan, S. U. Khan, R. Zaheer and S. Khan, 'Future internet: The internet of things architecture, possible applications and key challenges', in *2012 10th international conference on frontiers of information technology*, IEEE, 2012, pp. 257–260.

[6] Y. Lee, J. Kim, H. Lee and K. Moon, 'Iot-based data transmitting system using a uwb and rfid system in smart warehouse', in *Ubiquitous and Future Networks (ICUFN), 2017 Ninth International Conference on*, IEEE, 2017, pp. 545–547.

[7] C. Chauvenet, G. Etheve and M. Sedjai, 'G3-plc based iot sensor networks for smartgrid', in *Power Line Communications and its Applications*, IEEE, 2017.

[8] F. Martelli, 'Bluetooth low energy', *University of Bologna*, vol. 25, 2014.

[9] Y.-H. Wei and Leng, 'Rt-wifi: Real-time high-speed communication protocol for wireless cyber-physical control applications', in *2013 IEEE 34th Real-Time Systems Symposium*, IEEE, 2013.

[10] A. Juels, 'Rfid security and privacy: A research survey', *IEEE journal on selected areas in communications*, vol. 24, no. 2, pp. 381–394, 2006.

[11] A. Brandt and J. Buron, 'Transmission of ipv6 packets over itu-t g. 9959 networks', Tech. Rep., 2015.

[12] M. Hasan, E. Hossain and D. Niyato, 'Random access for machine-to-machine communication in lte-advanced networks: Issues and approaches', *IEEE communications Magazine*, vol. 51, no. 6, pp. 86–93, 2013.

[13] B. E. Medina and L. T. Manera, 'Retrofit of air conditioning systems through an wireless sensor and actuator network: An iot-based application for smart buildings', in *2017 IEEE 14th International Conference on Networking, Sensing and Control (ICNSC)*.

[14] G. W.-H. Tan, K.-B. Ooi and Chong, 'Nfc mobile credit card: The next frontier of mobile payment?', *Telematics and Informatics*, vol. 31, 2014.

[15] D. Chen, M. Nixon, S. Han, A. K. Mok and X. Zhu, 'Wirelesshart and ieee 802.15. 4e', in *Industrial technology (icit), 2014 ieee international conference on*, IEEE, 2014, pp. 760–765.

[16] S. S. I. Samuel, 'A review of connectivity challenges in iot-smart home', in *Big Data and Smart City (ICBDSC), 2016 3rd MEC International Conference on*, IEEE, 2016, pp. 1–4.

[17] O. Cetinkaya and O. B. Akan, 'A dash7-based power metering system', in *2015 12th Annual IEEE Consumer Communications and Networking Conference (CCNC)*, IEEE, 2015, pp. 406–411.

[18] I. Poole, *Weightless wireless—m2m white space communications-tutorial*, 2014.

[19] L. Alliance, 'Lorawan specification', *LoRa Alliance*, 2015.

[20] M. S. Levine and J. M. Kretchmar, *Correlating nameserver ipv6 and ipv4 addresses*, US Patent App. 15/944,224, Aug. 2018.

[21] P. Thubert, E. Nordmark, S. Chakrabarti and C. Perkins, 'Registration extensions for ipv6 over low-power wireless personal area network (6lowpan) neighbor discovery', Tech. Rep., 2018.

[22] P. Saint-Andre, 'Extensible messaging and presence protocol (xmpp): Core', Tech. Rep., 2011.

[23] M. Singh, M. Rajan, V. Shivraj and P. Balamuralidhar, 'Secure mqtt for internet of things (iot)', in *2015 Fifth International Conference on Communication Systems and Network Technologies*, IEEE, 2015, pp. 746–751.

[24] P. Bhimani and G. Panchal, 'Message delivery guarantee and status update of clients based on iot-amqp', in *Intelligent Communication and Computational Technologies*, Springer, 2018, pp. 15–22.

[25] X. Chen, 'Constrained application protocol for internet of things', *URL: https://www. cse. wustl. edu/~ jain/cse574-14/ftp/coap*, 2014.

[26] S. Lee, J. P. Jeong and J.-S. Park, 'Dnsna: Dns name autoconfiguration for internet of things devices', in *2016 18th International Conference on Advanced Communication Technology (ICACT)*, IEEE, 2016, pp. 410–416.

[27] S. K. Mani, R. Durairajan, P. Barford and J. Sommers, 'A system for clock synchronization in an internet of things', *arXiv preprint arXiv:1806.02474*, 2018.

[28] P. Dobbelaere and K. S. Esmaili, 'Kafka versus rabbitmq: A comparative study of two industry reference publish/subscribe implementations', ACM, 2017.

[29] Online Trust Alliance (OTA), http://otalliance.org.

Proceedings of the Fourth International Conference on Communication and Electronics Systems (ICCES 2019)
IEEE Conference Record # 45898; IEEE Xplore ISBN: 978-1-7281-1261-9

Formulation of Aggregate Key in cloud by Cipher Text storage Reduction for data Outsourcing in healthcare

K.Ketzial Jebaseeli,
Research Scholar, Department of Computer Science,
Sri Ramakrishna college of Arts and science for women,
Coimbatore, Tamil Nadu, India
ketzis88@gmail.com

Dr.V.G.Rani
Associate Professor, Department of Computer Science
Sri Ramakrishna college of Arts and science for women,
Coimbatore, Tamil Nadu, India
ranics@srcw.ac.in

***Abstract*--An extravagant receptiveness to healthcare commercial enterprises is the redistributing of health files to cloud. Howbeit, the exceeding deportments of the cloud system are armament and privacy of sensitive erudition. By the applicability of attribute based encryption dispositions in specification to access control many solutions have been envisaged in order to assuage those challenges. To phase out and also to procure ascendable and decisive secure solution, a distinct key criterion has been milked as multi-signer digital signature paradigms have been made the most of as multi-signer digital signature confrontations. It is entrenched to mollify the measurable attacks. In this paper, a strategic and distinct signature scheme designated as key aggregation scheme which concedes users to decrypt conglomerate classes of file using single key that can be communed betwixt the users in demoniacally fabricated group. The consorted model encompasses aggregate key generation for accessing the files systemized in a pecking order, hashing of key to upturn the security of keys, ring signature has been inculcated to dynamically fabricated group for data admittance using cryptographic proposals. The reserved files will be in the encrypted form which the user can have ingress to capacitate the hoarded files.**

Keywords-- key aggregation, ring signature, Encryption, Health Records, Data preserving, aggregate key.

I. INTRODUCTION:

The up to date onset of cloud Computing has tuned up the confinements of data outsourcing. Cloud-based electronic health records permit medical documents returned and traded amidst medical institutions therefore becoming an imperative model for intensification of productivity and is conventional to contribute improvements in disparate medical services in the offing [1]. Conceivably it springs up with an over-and-above safekeeping threats on incaldenment of millions of users which erects as the foremost impediment surrounded by data owners.

Consequently patients may occurrence disclosure of secretive data that they do not aspire to unveil. For this reason making sure of the security and seclusion on the cloud is a non trifling task. The long-established way to make certain the data is to be dependable on the server to insist on the admission and accession control after substantiation which means any unpredicted dispensation intensification which will supplement depiction on all data [2]. Attribute based encryption has been availed to administer security and ingress control on one and the other attacks to the outsourced data as it became well-liked on harmonization. In Attribute-Based encryption type of impenetrable ingression control where attributes of the users are pre-owned to cobble up access policies and the proprietor of data who ascribes indications are conceded to initiate data in the entity [3].The cryptographic virtuosities are once more deceitful face down to key administration contentions aforesaid key escrow problem, computation power, key denunciation, lampooning, eavesdropping and accelerated attacks. In regulation to chaperon the seclusion of patients, many advents have been contemplated to give accession control to patient documents while providing services related to physical conditions [4]. The extanting data partaking strategy on the cloud is extensible and conducive, if data proprietors can emisorily access rights to their files efficiently to myriad users, who can then access the data unswervingly from the cloud servers. In further cases data owners have a preference to accumulate rift sets of file in cloud and entrust that detachment of file to unusual users with mottled access policies. To accomplish this, data owner has to endow with each user with decryption privileges to unambiguous class of data. This leads to supplementary face ups to and it becomes in competent in large scale appliances. In this paper, the key aggregate format has been sculpted in order to put up a signature for the dynamically establishing group by the data owner and generated signature is again secured using hashing procedure. In adding

together, Constant size aggregate key coalesce the decryption rights of numerous classes of data and uses the public key cryptosystem [5] alongside ring signature to carve up the key to the target deposit of user. Moreover single decryption is conceded out in the midst of the set of user in the intention group in accordance to diminish the multiplication cost, decryption time and memory exploitation through assimilation of substitute attendant to pile up the decrypted data.

II. LITERATURE SURVEY:

Techniques that are relayed on security concerns in cloud have been shared by most of the reviews related to this paper. The recitals which execute pertinent to the projected procedure have been portrayed underneath.

A. Multi Authority Attribute Based Encryption

Control Mechanism with user-centric ingression is a collection of machinery for data admittance to healthiness files accumulate in semi-trusted attendant. To accomplish well-accorded and scalable data admittance have power over files based upon health status, attribute based encryption (ABE) techniques is influenced to encrypt healthiness of apiece patients' file predestined on the insightful attributes [6].The sheltered data outsourcing is paying attention on the manifold data possessor circumstances as to partition the users in the make safe health file coordination into numerous defense domains that significantly lessen the key administration involvedness for owners and users. An elevated degree of unwearied privacy is sure fire concurrently by taking advantage of Attribute based encryption using multi authority.

B. Cipher Text Policy Based Attribute Based Encryption

It tenacities seclusion issue and it makes use of attribute set as confidential key and admittance policies is entrenched into the cipher text for concealed. The key production algorithm takes user's unrestricted as well as secretive attributes to manufacture the undisclosed key for the user. Each cipher text is completed up of access policy. The user can set access policy which consents to set of users to decrypt data. CP-ABE proposals brings into play user's attributes as the reciprocative set for creating new access policy and comparable for creating the private key using a set of user attributes [7]. Nonetheless direct accomplishment of the CP-ABE undergoes two concerns such as access policies are in clear text form and divulge insightful health-related in turn in the encrypted health records (SHRs) and it habitually prop ups small attribute set, which places an detrimental constraints on realistic consumption of CP-ABE because the dimension of its unrestricted parameters grows linearly with the size of the attribute set.

C. Attribute based Encryption by the use of file hierarchy

Cipher text or Key policy Attribute based Encryption has been regarded as to decipher the data allotment disputes in the cloud. It is mulled over as multi layered ingress composition which is incorporated into tree like access structure on lengthening cyclic and acyclic sculpt to engender tree hierarchy of symmetric keys[8]. The admission composition is used to encrypt the hierarchical files with characteristics which exclusively accumulate cipher text production time and data storage time. The cipher text components interrelated to the attributes will be allocated by the files. The massive enlargement in size of the key is the most important negative aspect in this encryption.

III. PROPOSED SYSTEM:

A new theme is being discussed in this section called key aggregate to the secure statuses of data ingression and key distribution among myriad users. The storage bytes have been reduced by the use of this aggregate key scheme.

A. Groundwork

The plot is catalogued into two sections. Hashing model by the data possessor is generated by the use of ring signature scheme and succeeding focuses on production of aggregate key for set of classes in the case. The generated key is at last shared amongst the data users in the set.

B. Data holder

Data proprietor enraptures the file with requirement of class to file detachment and encrypt the partitions for data admission among the data consumers. It is widespread group signature employed to form vibrant contour group towards access of the data files by the holder.

C. Trusted Authority

Trusted Authority is responsible for generating key pairs for data owner and the users.

D. Data User

Data user is consented to access the files of the data possessor which is encrypted with creation of access keys like ring signature and aggregate key. Data owner execute the decryption operation with aggregate key

E. Bilinear Pairing

A coupling is a bilinear map definite over groups. Let's regard as G1 and G2 as subordinate groups of the equivalent prime categorize q. G_T is

passed on as multiplicative group of order q. P and Q are a point which emerges up the G1 and G2.

Bilinear Map is reflected as G1 * G2→ G_T after gratifying the subsequent assets like

Non Degeneracy : If P and Q be the generators for G1 and G2 respectively where neither group only contains the point at infinity

3.1. Threshold model on Aggregate Key generation:

The major beneficiary fact in this proposed system is the lessen in exploitation and increase in its efficiency and decline in storage bytes[9]. The foremost process includes the key generation which is denoted as in figure 3.1. in turn sends it to the data holder as soon as the user‘s schemes are accumulated in the cloud storage. By the formulation of aggregate key through key aggregation, the data holder then passes the data to the encrypted file transmission.

A. Key generation

A data owner disposed to carve up the file registers to obtain her individual public and private key pairs. The data owner is conscientious for classifying each of data file into specific classes. It causes the public key TK and master secret key MSK for data holder.

B. Encrypt

The Classes of file is encrypted by the use of AES encryption procedure and accumulated in the cloud. It attains public key restriction PK, data class d and plain text data T, harvests the cipher text C.

$C= (C0, C1, C2) = (K,(T_m1+K_i), m .e(T_n, K_n)$.

C. Decrypt

When farming out the decryption rights to an unambiguous detachment of message classes, the data owner uses the Extract maneuver to engender an aggregate decryption key that is distinctive to that rift [10]. It acquires Master secret key MSK and data classes’ d. Calculate aggregate key T_K all encrypted messages belonging to this subset of classes.

The cryptographic virtuosities are once more deceitful face down to key administration contentions aforesaid key escrow problem, computation power, key denunciation, and lampooning, eavesdropping and accelerated attacks.

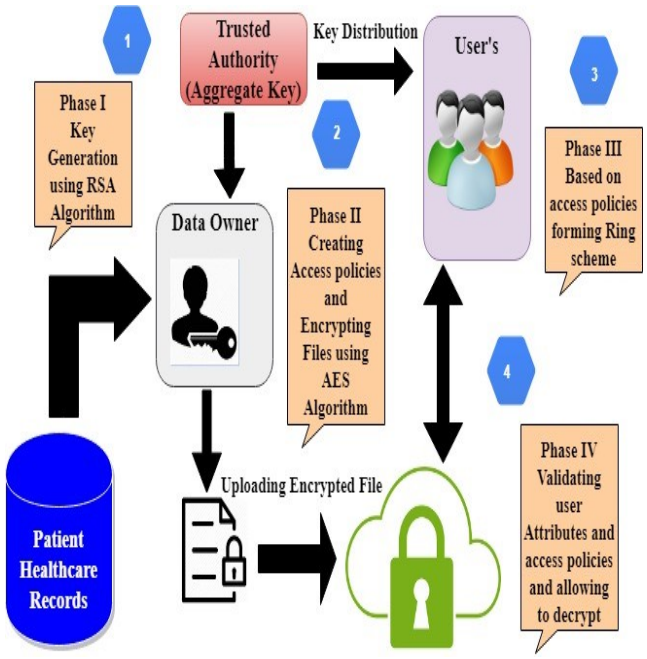

Fig.3.1 Proposed data sharing using Aggregate Key

D. Set Up:

It is used to set up the public parameters param by obtaining the number of data class’s d and security parameter p.

3.2. Aggregate key

Based on bilinear pairing, it is recognized as the most effective one in the cryptographic analysis of aggregation. Especially of Composite order and demonstrated to be sheltered under the postulation that the subgroup pronouncement problem and computational Diffie Hellman predicament are unbreakable [11]. It is carried out on the file surface. Each file fit in to the group is encrypted using the key. AES algorithm is used for the encryption. The key of the dissimilar file utilized for the encryption is combined with tokenize symbol to produce the aggregate key. The aggregate key is produced from encryption of combined key using ring signature [12]. The aggregate key will be mottled on accumulation of file and deletion of files to the group. By the formulation of aggregate key through key aggregation, the data holder then passes the data to the encrypted file transmission

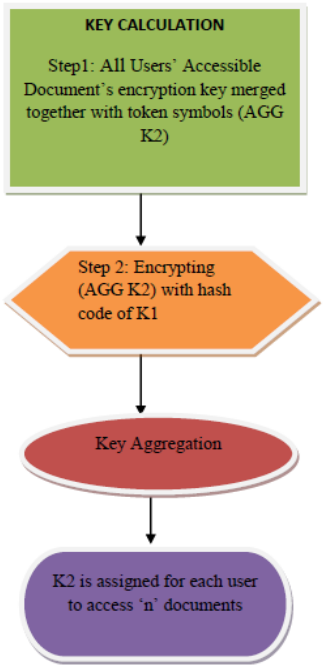

Fig.3.2 Aggregate key calculation

The above figure 3.2. Descripts the accession of users' documents with encryption key concatenated with token symbols (AGGK2). The symbols are ten encrypted with hash code k1 through aggregate key by key aggregation process which is then assigned for each user to access documents.

A. ALGORITHM

Below shows the procedure of Key aggregation using RSA algorithm

STEP I: Generating public key/private key
STEP II: Compute the RSA modulus 'n'
STEP III: Selecting two large primes at random: P, Q
STEP IV: Computing their systemmodulus n=p.q
STEP V: Note ø (n) = (p-1) (q-1)
STEP VI: Consider K secure parameter and outputs the public signing key K_{sig} and Private signing Key V_{sig}

B. Description of Algorithm

The primary process in aggregate method is that the user has to engender either the public key or the private key by choosing the random variables P AND Q followed by the process of enumerating the RSA modulus declared by 'n'. The procedure of termination includes the system computation n=p.q modulus. An authoritative data user can make use of this aggregate key to decrypt any message fitting in to any class. It gets hold of the cipher Text C, data class d and aggregate key AG to generate the decrypted message.

C. Cipher Text Storage Calculation

Step 1: Calculate number of users (Ui).

Step 2: Calculate number of files size decrypted by the user (Fi).

Step 3: Formulate $N = Ui * F_i$

The decryption progression moniterates the ordinary text of the requested file and it will be located in the proxy server in order to set aside the decryption time of further users in the group by abolishing the decryption process for the intact group members. In addition, all process is time embossed for revocation of the group.

IV. EXPERIMENTS

In this segment, we scrutinize the security of the proposed model adjacent to the an assortment of data size is been computed and illustrated in terms of concert charts and tables for cipher text storage Reduction

A. Experimental Set up

The experimental results are obtained with an Intel Core I3 processor with 2620 Processors (2.0 GHz) and 4 GB RAM and 500 GB Hard disk using Dot net programming. The database server and file server has been established in the file system which acts as Cloud infrastructure. The different file sizes are used for computation of the efficiency of the model. Proxy server has been established using virtualization process as Virtual machine.

B. Performance Analysis

The reliability of the system is defined in terms of utilization of proxy server technology in data sharing systems to reduce the storage bytes of the group members. It will greatly facilitate data owner delegating the access rights to other members.

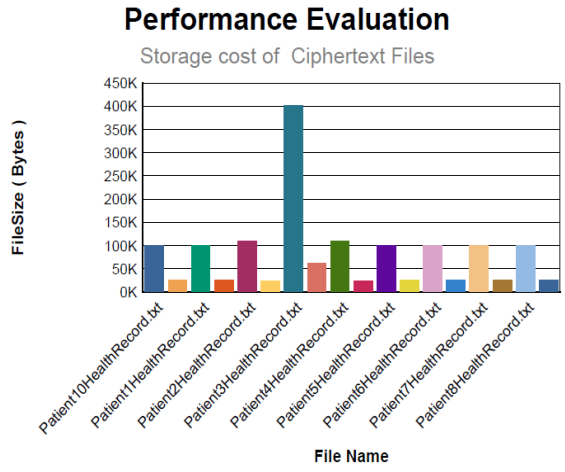

Fig. 4.1. Performance Evaluation of Filesize in storage cost of ciphertext Files.

The statistical figure 4.1 depicts the patients' health records with respect to file sizes in varying storage costs of ciphertext files.

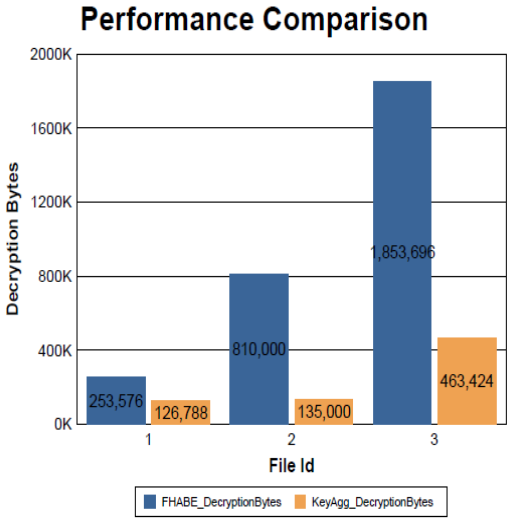

Fig.4.2 Performance comparison of the cipher Text Storage Bytes reduction on the proposed model and existing model to various File sizes

The figure 4.2 and table 1 describes and summarizes the performance of the proposed model and existing models to various files. Arrival of new users and revocation of existing user will lead to changes in key access rights due to expected to change occurs dynamically. User revocation is also achieved without any additional cost. The collusion resistance property ensures that the knowledge of prior aggregate keys does not compromise the knowledge of these new file.

Table 1: Performance Evaluation of the Cipher Text Storage Bytes

Technique	Storage Bytes for File ID 1	Storage Bytes for File ID 2	Storage Bytes for File ID 3
Key Aggregation	126,788	135,000	463,424
File Hierarchy Attribute based Encryption	253,576	810,000	1,853,696

In preference if the data owner desires to adapt an existing document, she could use a dissimilar index for it to make sure that a retracted user cannot ingress it in the outlook.

V. CONCLUSION

In this paper, we have devised and employed the key aggregation application to engender the protected and scalable data allotment model on the multi capability environment. The proposed model explains the effectual of the system on an assortment of phases like key generation, encryption and decryption to an assortment of file sizes and various group member formations. Aggregate key convention has been explained in detail on allocation multi classes of file diverse to set of users. This model has been found to be well-organized among arbitrary number of data classes. The experimental analysis has established Reduction of the storage and decryption time. It has been demonstrated that model is high conspiracy resistant against multiple users. As a future work, competent entree on stipulate data access under emergency circumstances can be enabling under break glass admittance observable fact.

REFERENCES:

[1]. K. Liang, Q. Huang, R. Schlegel, D. S. Wong, C. Tang, “A Conditional Proxy Broadcast Re-Encryption Scheme Supporting Timed-Release,” In Proc. Information Security Practice and Experience, pp. 132146, Springer Berlin Heidelberg, 2013.

[2]. J. Byun, D. Lee, “On a security model of conjunctive keyword search over encrypted relational database,” Journal of Systems and Software, vol. 84, no. 8, pp. 1364-1372, 2011.

[3]. S. S. M. Chow, J. Weng, Y. Yang, and R. H. Deng, “Efficient Unidirectional Proxy Re-Encryption,” in Progress in Cryptology - AFRICACRYPT 2010, ser. LNCS, vol. 6055. Springer, 2010, pp. 316–332.

[4]. C. Hu, P. Liu, “An enhanced searchable public key encryption scheme with a designated tester and its extensions,” Journal of Computers, vol. 7, no. 3, pp. 716-723, 2012.

[5]. Q. Liu, G. Wang, J. Wu, “Time-based proxy re-encryption scheme for secure data sharing in a cloud environment,” Information Sciences, vol. 258, pp.355-370, 2014.

[6]. Scalable and Secure Sharing of Personal Health Records in Ming Li ; Shucheng Yu ; Yao Zheng ; Kui Ren ; Wenjing LouCloud Computing Using Attribute-Based Encryption,IEEE Transactions on Parallel and Distributed Systems (Volume: 24, Issue: 1, Jan. 2013)

[7]. Accountability for Data Sharing in the Cloud" IEEE Transactions on Dependable and Secure Computing (Volume: 9, Issue: 4, July-Aug. 2012)

[8]. Hong Liu ; Huansheng Ning ; Qingxu Xiong ; Laurence T. Yang "Shared Authority Based Privacy Preserving Authentication Protocol in Cloud Computing" IEEE Transactions on Parallel and Distributed Systems (Volume: 26, Issue: 1, Jan. 2015)

[9]. R. Canetti, S. Halevi, and J. Katz, “Chosen-ciphertext security from identity-based encryption,” in EUROCRYPT (Lecture Notes in Computer Science), vol. 3027. New York, NY, USA: Springer-Verlag, 2004, pp. 207–222.

[10]. D. Boneh and J. Katz, “Improved efficiency for CCA-secure cryptosystems built using identity-based encryption,” in CT-RSA (Lecture Notes in Computer Science), vol. 3376. New York, NY, USA: Springer-Verlag, Feb. 2005, pp. 87–103.

[11]. L. Zhou, V. Varadharajan, and M. Hitchens, “Enforcing role-based access control for secure data storage in the cloud,” Comput. J., vol. 54, no. 13, pp. 1675–1687, Oct. 2011

[12]. K.Ketzial Jebaseeli, Dr.V.G.Rani“A Lightweight Data Preserving model using Ensemble Signature Scheme to the outsourced health files in cloud”, Published in Journal of Advanced Research in Dynamical Control Systems, 2019

Proceedings of the Fourth International Conference on Communication and Electronics Systems (ICCES 2019)
IEEE Conference Record # 45898; IEEE Xplore ISBN: 978-1-7281-1261-9

Swarm Optimization techniques using Attribute assortment and Clustering for Machine Learning Classifiers

Vadivu.T, Research Scholar
Department of Computer Science, CMS College of Science and Commerce
Coimbatore, Tamilnadu
vadivuthiyagu19@gmail.com

Sumathi.B, Associate Professor
Department of Computer Science, CMS College of Science and Commerce
Coimbatore, Tamilnadu

Abstract:
Software defined Networking addresses the growth of traffic with static architectures. SDN is a standard which separates the network structures. Quality of Service is used with network traffic to transfer high bandwidth and multimedia information. Fractional Order Darwinian optimization(FODPSO) is used with Particle Swarm Optimization algorithm to enhance the detection accuracy. Comparison with Classification algorithms are used to achieve better performance.

Keywords: SDN, Anomaly detection, Fractional order Darwinian Particle Swarm Optimization.

I. INTRODUCTION

Quality of Service (QoS) is used for allocating the network resources [11] based on the requirements. These services have requirements like throughput, inaccuracy and idleness. Creating a replica by addressing all these requirements is complicated. Intserv and Diffserv are two methods to solve end-to –end connections and scalability. QoS is important for communication network and applications. This is specified in the form of interruption for the navigation of information. Therefore FODPSO [15] is used for accuracy detection. Reinforcement of QoS networking leads to higher cost and effort.

Data plane includes switches to handle network traffic. The information about the networks is gathered by a central organizer. A set of QoS parameters include throughput, end-to end delay [13] and error rates for better performance. The goal of the study is to provide greater QoS performance using Particle Swarm Optimization (PSO) based Delay constrained Least Cost algorithm. PSO is a collective behavior of a system which is used to interact with their location to provide efficient [9] data.

A flock of birds is searching for food without any knowledge of food. So the best criterion is to follow the bird which is near to food. The birds can identify the location using these criteria's: i) birds fly in similar path ii) revisit to path of maximum attention iii) progress through the nearest [10] target. The candidate solution moves towards the target to identify the destination. The confined best, large-scale best and neighborhood solution is calculated. Then the greatest solution is rationalized through entire swarm. This structure of the paper is illustrated as: the prose of the algorithm is explained in sec 2. The illustration of methodologies of PSO based FODPSO is specified in sec 3. Optimization techniques are concluded in sec 4.

II. LITERATURE SURVEY

In 2016, Benuwa.B describes about the swarm behavior and its properties for adapting different environments. An intelligence [1] algorithm is used with an optimization technique.

In 2012, Michael proposed Darwinian algorithm to improve its fitness function. This local optimum has been increased with natural selection.

In 2012, Xu.Y, this approach is used to reduce the interruption constraint direction-finding [12] troubles. Search and relinking optimization method is used scatter search and path.

In 2014, Guck et al proposed an approach for real-time QoS performance. Greedy algorithm [13] and a Mixed Integer Program is used to fix queue allocation. Delay Constrained Least Cost algorithm is used to calculate the minimum cost end-to- end delay.

III. METHODOLOGY

This methodology is used for reducing constant and isolated optimum paths. Particles represent source and location of an element indicates destination. This is swarm intelligence. The communal behavior of the individuals interacting with their surroundings is called as Swarm Intelligence. This optimization technique is used to improve the detection accuracy. This technique is processed with swarm of birds.

A. Particle Swarm Optimization

This is a technique which is called after behavior its birds flocking. A group is started with

random elements. The updation is done by searching optimum solutions. The group of variable gets closer to the member near to the target environment. This algorithm keeps track of three variables such as target value, global value and stop value. The bird has a position and velocity at any time. Position is changed by adjusting the velocity.

Velocity is changed based on the experience and the feedback from the neighbor. Each particle considered with two best values. One is the fitness value called as the pbest. Later one is achieved from any particle with the group called as globbest. The particle gets updated when the best values are established with its velocity and positions. To represent the position of the swarm every element travels through the swarm as:

$$v_{t+1} = \omega v_t + c_1 * \text{rand}(p_i - a_i(t)) + c_2 * \text{rand}(g_i - a_i(t)) + c_3 * \text{rand}(n_i - a_i(t)) \quad (1)$$

$$a_{t+1} = a_i(t) + v(t+1) \quad (2)$$

In above equations, ω denotes the inertia weights and c1, c2, c3 are learning factors denoted as constant values. While determining the velocity p_i denotes the pbest, g_i as global best and n_i as neighborhood best. The parameter rand is random vectors with numbers between 0 and 1.

Initially the element is assigned as null and the position is assigned at random among the borders of its population (Alg 1). Population size is used to optimize the solutions within time limit. Stop criterion is already distinct with the amount of executions.

Alg. Particle Swarm Optimization

Init element (Init a_t^n, v_t^n, $a_t^{\sim n}$, $n_t^{\sim n}$, $g_t^{\sim n}$)
SLoop:
through all elements
find the accuracy of individual element
revise $a_t^{\sim n}$, $n_t^{\sim n}$, $g_t^{\sim n}$
revise v_{t+1}^n, a_{t+1}^n
stop
till stop criterion

The information is called as the individuals decision made for success. Knowledge is termed as the performance of the other neighbor individuals. The virtual value of this factor will differ as of each other decisions. So random weights is applied and its velocity can be considered as

$v_i(t) = v_i(t-1) + \varphi_1.r_1.$ ($s_i^{\sim}$ - $a_i^{\sim}$(t+1)) + $\varphi_2.r_2.$ ($s_g^{\sim}$ - $a_i^{\sim}$(t+1))

where φ_1 and φ_2 are positive numbers and r_1, r_2 are random numbers. The velocity has three components. First, intertia is considered to direct the particle in the same direction. Second, the preeminent location of the element p_i its fitness value is called as pbest, which is scaled by $\varphi_1.r_1$. Third, velocity updation of the best particle g_i found as gbest. This is scaled by $\varphi_2.r_2$. This method can be implemented for this particle swarm optimization technique as:

Step 1: Initially this particle is assigned with arbitrary positions in the group for individual element.

Step 2: Fitness purpose is evaluated for each element.

Step 3: Each individual particle is compared with its fitness value pbest. If it achieves maximum value than pbest then consider this value as present element location a_i as p_i

Step 4: Evaluate the elements maximum fitness value. Fitness function is calculated as globbest and location as g_i.

Step 5: Velocity and position of all the particle is updated by using step 1 & 2.

Step 6: Continue steps 2-5 till stop criterion is acheived.

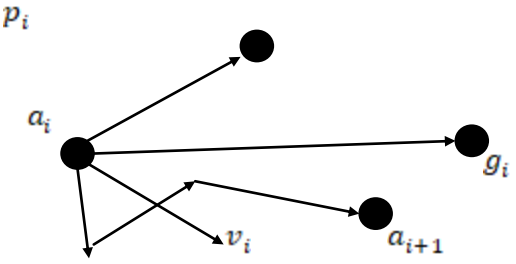

Fig 1. Particle swarm algorithm

Particle swarm algorithm is shown in fig 1. Various criteria's has to consider while implementing the particle swarm algorithm to avoid the sudden increase of the particles. This includes reducing the greatest velocity [6-7], select increase of [8] constants, construction factor or the inertia issue.

Proposed algorithm FODPSO is used to enhance the fitness function. This is composed of particles as a group. This group is managed with a natural selection mechanism. Generally, search to local optima in that area is discarded and new search is started. In order to analyze the state of the group all the particles is executed. So that local position for each group can be rationalized. Finally if it fails, particles are removed. The discarded swarms prematurely move towards non optimal solutions. This algorithm is compared with the clustering algorithms to evaluate detection accuracy. The following procedure can be used for evaluating fractional order Darwinian swarm optimization:

Step 1: Initialize the parameters

Step 2: Update each particles fitness function and best optima
Step 3: Execute all the particles. If swarm obtains best position, extend life of the swarm
Step 4: If Swarm has not improved, delete swarm.
Step 5: End the process

In FODPSO, few attributes has to be considered for efficient best fitness function: population of swarm, min and max of swarm population, initial number of swarms, threshold. Fitness evaluation of best particle is considered.

Feature Subset selection

Subset feature FS={FS| a=1,….,n}
find a subset FS_a, with x < y
max an function F(FS)
$FS_a=\{fn_{a1},fn_{a2},\ldots\ldots fn_{ax}\}$ = arg max= F{ FS| a=1,….,n}

Feature subset selection is described in the above algorithm. FS is initialized with all the particles. Then evaluate the maximum number of swarms in the subset.

B. Experimental Result

Evaluation is done with MATLAB R2017b. The KDDCup99 dataset is used with records. DoS, R2L, U2R are the attacks used for information gathering. Labelled records consist of 25 features as depicted in Table 1. The category name is indicated using target. Decision Tree, Random Forest, Support Vector Machine, AdaBoost classifiers are used for feature selection. Proposed algorithm is compared with feature selection in terms of classification accuracy. This algorithm is compared with Kmeans, MeanShift, Birch. These algorithms are compared in terms of Runtime, Score, Completeness, Degree, Accuracy. Experiments are executed several times under these metrics. FODPSO achieves greater accuracy and runtime compared to other clustering algorithms. Different ranges of clustering algorithms are specified in table 2. This algorithm achieves higher detection accuracy when compared to other cluster algorithms.

TABLE 1. Attributes of KDDCup Dataset

S.No.	Feature Name	Category
1.	Dur_time	C
2.	prot_typ	D
3.	Ser_typ	D
4.	Count	C
5.	Serror-rate	C
6.	Src-byt	C
7.	Dest_byt	C
8.	Num_compr	C
9.	U_attmpt	D
10.	Hot-Log	D
11.	Diff_srv-rate	C
12.	Acc_file	C
13.	Failed_log	C
14.	Flag	D
15.	Dst_srv_cnt	C
16.	Dst_host_srv_cnt	C
17.	Urg	C
18.	Rt_shell	D
19.	Num_shell	C
20.	Wrg_frg	C
21.	Desti_host_serv_rate_typ	C
22.	Desti_host_serv_error_rate_typ	C
23.	Desti_host_reerror_cnt_typ	C
24.	Hot	C
25.	Compr	C

TABLE 2. Comparison using Clustering method

Method	Runtime	Score	Completeness	Degree	Accuracy
KMeans	2.01	1.64	0.691	0.678	75.98
Birch	4.63	1.24	1.697	0.761	85.06
MeanShift	1.65	1.74	0.691	0.823	89.60
FODPSO	1.69	2.10	0.781	0.853	91.24

Through this analysis, FODPSO achieves highest accuracy with all the influential features. Graphical analysis of feature selection algorithms is represented in fig 2.

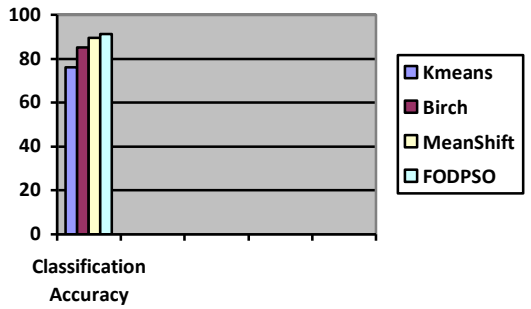

fig 2. Classification accuracy

IV. CONCLUSION

SDN controller estimates the multicast tree based on the network status with delay constraint. This particle algorithm calculates the velocity and position of the element by using fitness function. PSO based FODPSO technique is used to enhance the detection accuracy. Estimation of minimum cost reduces the packet loss. For future work this can be extended for solving multi constrained algorithm for large scale networks.

REFERENCES

[1] Ben-Bright Benuwa, Benjamin Ghansah, Dickson Keddy Wornyo, "A Comprehensive review of Particle Swarm Optimization" , 2016, International journal of Engineering Research, Vol 23, pp 141-161.

[2] C. -J. Ting, K. -C. Wu, and H. Chou, "Particle swarm optimization algorithm for the berth allocation problem, Expert Systems with Applications", vol. 41, pp.1543-1550, (2014).

[3] Y. Shi, "Feature article on particle swarm optimization," IEEE, Neural Network Society, Feature Article, pp. 8–13, Feb. 2004.

[4] M. Salazar-Lechuga and J.E.Rowe, "Particle swarm optimization and auto-fitness sharing to solve multi-objective optimization problems", in Proc. IEEE Swarm Intell. Symp., May 2006, pp. 90–97.

[5] J. Kennedy and R. Mendes, "Population structure and particle swarm performance," in Proc. IEEE Congr. Evol. Comput., May 2002, vol. 2, pp. 1671–1676.

[6] R. Eberhart and Y. Shi, "Particle swarm optimization: Developments, applications and resources", in Proc. IEEE Congr.Evol.Comput. ,May 2001, vol. 1, pp. 81–86.

[7] X. Hu, Y. Shi, and R. Eberhart, "Recent advances in particle swarm," in Proc. IEEE Congr. Evol. Comput., Jun. 2004, vol. 1, pp. 90–97.

[8] R.Eberhart,Y.Shi and J.Kennedy, "Swarm Intelligence", SanMateo, CA: Morgan Kaufmann, 2001.

[9] Del Valle , Y., Venayagamoorthy, G.K., Mohagheghi, S., Hernandez, J.C., Harley, R, " Particle swarm optimization: basic concepts, variants and applications in power systems", IEEE Trans. Evol. Comput. 12(2), 171–195 (2008).

[10] Floreano, D., Mattiussi, C, "Bio-Inspired Artificial Intelligence: Theories, Methods, and Technologies", MIT Press, Cambridge (2008)

[11] Govindarajan, K., Meng, K. C., Ong, H., Tat, W. M., Sivanand, S., & Leong, L. S " Realizing the quality of service (QoS) in software-defined networking (SDN) based cloud infrastructure", in Information and Communication Technology (ICoICT), 2014, 2nd International Conference on (pp. 505-510).

[12] Xu, Y., & Qu, R. (2012), "A hybrid scatter search meta-heuristic for delay-constrained multicast routing problems. Applied Intelligence", 36(1), 229-21.

[13] Guck, J. W., & Kellerer, W. (2014, October), "Achieving end-to-end real-time quality of service with software defined networking", in Cloud Networking (CloudNet), 2014, IEEE 3rd International Conference on (pp. 70-76), IEEE.

[14] Ammar W. Mohemmed,, Mengjie Zhang , and Nirod Chandra Sahoo, "Cooperative Particle Swarm Optimization for the Delay Constrained Least Cost Path Problem", 2008, Springer verlag, pp 25-35.

[15]. Micael S.Couceiro, Rui P.Rocha, " Introducing the Fractional order Darwinian PSO", Springer-verlag, May 2012.

Proceedings of the Fourth International Conference on Communication and Electronics Systems (ICCES 2019)
IEEE Conference Record # 45898; IEEE Xplore ISBN: 978-1-7281-1261-9

Image Segmentation using Convolutional Neural Network for Image Annotation

S. B. Nemade[1]
Department of Computer Science and Engineering
Walchand College of Engineering
Sangli, India
sangita.nemade@walchandsangli.ac.in

S. P. Sonavane[2]
Department of Information Technology
Walchand College of Engineering
Sangli, India
shefali.sonavane@walchandsangli.ac.in

***Abstract* — Due to rapid advancement in the digital display, communication and storage devices with effective techniques are needed to organize, index, retrieve and annotate a large image database. Image segmentation finds application in various areas of image processing and computer vision. Inferring of low level features from the given image is a challenging task in unstructured regions. Most of the annotation and retrieval algorithms fail to consider region semantics. This paper proposes convolutional neural network (CNN) based image segmentation for image annotation application. The proposed CNN includes pixel based prediction of the regions that are applied to obtain low level image features. The algorithm uses image region information based on the precise color distribution within the image. Experimental results demonstrate better results of image segmentation using CNN.**

Keywords — image Segmentation, Convolutional Neural Network(CNN), Automatic Image Annotation.

I. INTRODUCTION

With the advancement of digital capturing technologies, storage devices and communication network, the number of digital images have increased rapidly. Hence, it is necessary to have effective technique for organizing, indexing and searching of these images. Concept-based and content-based image retrieval are two major categories to address problems related to emerging opportunities [1]. However in CBIR system, one of the most significant issues is a semantic gap. Semantic gap is the dissimilarities between the image features extraction interpretation and image features content interpretation by Human Visual System(HVS) . Therefore from last few years, more research is focused on important part of concept-based retrieval i.e. automatic image annotation. The purpose behind the automatic image annotation (AIA) is to allocate textual labels to the image that clearly describes content or objects in the image. Many researchers have developed various methods and frameworks for AIA but more research is carried out on complete image annotation rather than considering the semantics of the regions. Region based image annotation methods have achieved more accurate semantic information than global based image annotation [2]. It focuses on each independent region of an image, making the visual features more accurate in order to present a particular semantic concept. Therefore, image region needs to be analyzed and labeled for attaining accurate image annotation. Image segmentation is used to detect boundaries and objects in images. If the underlying segmentation is inaccurate then image annotation will not provide better results [3]. The good image segmentation aims at segmenting the image correctly and labeling each segment with the respective semantic class. Since image segmentation is a foundation of region annotation, effective image segmentation is needed for an accurate region based image annotation. AIA methods can roughly be classified into five categories[4][5]: (i) Nearest neighbor models, (ii) Generative models, (iii) Discriminative models, (iv) Tag completion-based AIA models and v) Deep learning based models. Nearest neighbor models assume that the images that have similar features may have a high probability of similar labels. Various models used are Joint Equal Contribution (JEC) [6] and Tag Propagation (TagProp) [7]. Generative models emphasis on inferring the correlations between image features and semantic concepts. It finds the probability of a label by computing joint probability of image features and labels from training samples. Some of the generative models are Cross-Media Relevance Model [8], Multiple Bernoulli Relevance Model [9], Latent Dirichlet Allocation [10]. Discriminative models consider AIA as a classification problem where, each label/keyword is treated as a class. Researchers have designed these models for class predictions such as SML [11], SVM [12]. Tag completion-based AIA methods predict and automatically fill the missing labels for any given image ant at the same time correct noisy tags. It consist of various models such as Subspace Clustering and Matrix Completion model [13], TMC model[14]. Deep learning based models enable to solve AIA task using feature representation based on deep learning. For image annotation, CNN is used for robust features generation. Several models are used for this, such as CNN-RNN framework used in the RIA model [15] for image annotation, Deep Multiple Instance Learning (DMIL) model [16]. The AIA framework is basically consisting of steps such as image segmentation, feature extraction and classification. Image segmentation is one of the essential modules in AIA. Images containing natural scenes has unstructured regions that require computationally complex analysis for segmentation. Several segmentation algorithms proposed in the literature use various image elements such as colors, textures, shape and object compositions [17]–[18]. The image segmentation aims at segmenting the image correctly since it is a foundation of the region annotation. Many image segmentation algorithms,

such as JSEG [17] and NCUT [18] have been designed and are commonly used in image annotation. However, it is ineffective in segmenting region bearing similar color distribution. Texture, color and shape are the important features within the image. These features play an important role in the effective segmentation of the objects or regions. Colors are observed by the human eye and are the fundamental feature that differentiates among the objects. Therefore color enhanced segmentation algorithm using CNN is proposed. The algorithm attempts to differentiate objects bearing similar color through separately processing each R, G and B color space effectively assisted by edge detection.

Convolutional based networks are the popular architectures for Image segmentation. Long et al. [19] developed fully convolutional networks that are pre-trained on ImageNet[20] with each pixel classification. For semantic segmentation, contextual hierarchical model is developed by Seyedhosseini et al. [21] for learning contextual information in a hierarchical framework.

The main contribution of this paper is the CNN for image segmentation for the application of image annotation. The algorithm uses image region information based on precise color distribution within the image. The paper is organized as follows. Section II outlines the proposed methodology. Section III demonstrates the experimental result obtained after training and classifications of images. Conclusion and future scope is illustrated in section IV.

II. Colour Enhanced Segmentation Algorithm using CNN

CNN is made up of one or more convolution layers with pooling layer and one or more fully connected layers followed. The CNN architecture is designed in such a way that it takes advantage of two dimensional input image structures. This is achieved through local connections and associated weights followed by pooling (average or max pooling) resulting in translation- invariant features. With the same number of hidden units, a fully connected network needs more parameters than CNN. Therefore, it is easier to train CNN than a fully connected network [20].

The paper proposes a framework for supervised image segmentation based on candidate regions. The framework of the paper consists of two phases of learning and testing. Fig. 1 demonstrates the CNN architecture employed in this algorithm.

A. Convolutional Layer

In the proposed algorithm, each layer of image data is a three-dimensional array of size p x q x r where, p and q are spatial coordinates of the image pixels and r is the feature or channel or color dimension. Predicting each pixel's class independently of its neighbors results in better region / class predictions accuracy. Mostly it is observed that objects have smooth boundaries and well defined shapes, different from the background that tends to be shapeless regions. Convolutional layer initially starts with the smoothing operations to predict a standard pixel with a kernel size of 5x5. The smoothing improves algorithm by forcing each pixel with low probability of being part of an object and improves performance accuracy. The weights of the kernel are initialized to one by twenty five which is updated in the learning / training process so as to predict object through image pixels as given in equation (1). The convolution operation is represented using equation (2) that is applied on each color space (RGB) separately.

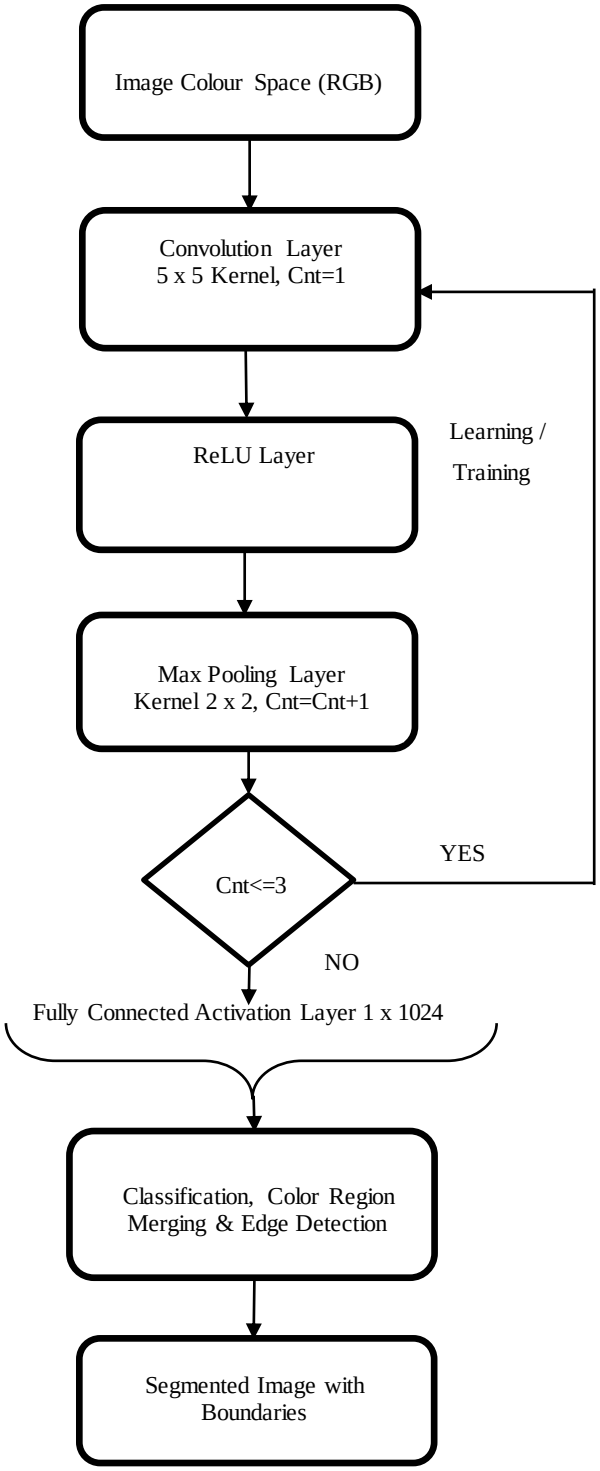

Fig. 1. CNN architecture for image segmentation.

$$w_{ij} = \frac{1}{25}\ for\ i,j = 1\ to\ 5 \quad (1)$$

$$I_c(x,y) = \sum_{x=1}^{p}\sum_{y=1}^{q}\sum_{i=-2}^{2}\sum_{j=-2}^{2} I(x+i,y+j) * w_{ij} \quad (2)$$

Where,

w_{ij} are the initial weights of the kernel that are updated during training process.

$I_c(x,y)$ Output of convolutional layer

B. Rectified Linear Units (ReLU) Layer

There are many activation functions available for neural network models. Deep learning models mostly use ReLU as an activation function due to the reduced probability of vanishing gradient. For every positive value of x, it returns the same value (x), but if it receives a zero or negative value of x, zero is returned[19]. Therefore, mathematically ReLU can be represented using equation (3).

$$f(x) = f(0,x) \quad (3)$$

C. Max Pooling Layer

The accumulation should lead the network towards correct pixel level assignments for each region within the image, so that segmentation task can be performed properly.

An evident accumulation task is to take the average of all pixel positions under consideration. In Max pooling layer, the kernel size is selected at 2 x 2 that provides accumulation of 4 pixels values. It increases the score of the pixels that further helps in classification. The operation performed in max pooling can be represented using equation (4). The advantage of this accumulation is that in the training procedure, pixels with similar scores have a similar weight, while maintaining the goal of predicting similar pixels / regions.

$$I_{mc}(x,y) = \sum_{x=1}^{m}\sum_{y=1}^{n}\sum_{i=1}^{2}\sum_{j=1}^{2} \frac{I_c(x+i,y+j)}{4} \quad (4)$$

D. Implementation Details

The variation image sizes are standardized using image resize at 284x284x3. The three stage convolutional neural networks are illustrated in fig. 1. The input given to network is of the size 284x284x3. Three filters of size 5×5 are used in first convolutional stage. The activations size is 280*280, as no padding is used. These are normalized in the neighboring feature map. With a stride of one, no overlapping spatial pooling is applied in 2x2 local regions

The second and third stages are similar to the first, except that the size of the input data is 140x140 and 68x68 respectively, whereas number of filters remains to 3. The entire network is trained by back propagation using the soft-max function to normalize the logistic regression loss against the predicted scores. The biases are initialized as constant one in the first convolutional layer, as well as the remaining fully connected layers. After each mini-batch of the size 50 images, the network updates all weights. The training starts with a learning rate greater than 0.05 (5%), and reduces it to 0.01 (1%) when the performance of the evaluation set no longer improves. The algorithm separately processes the R, G and B, color spaces through CNN. Thus each object is marked / identified in every color space and effectively backed with edge detection. Finally the result of R, G and B color space are merged that effectively segments the objects.

III. Experimental results

The data set used in this experiment is obtained from the Corel-10k database for segmentation purposes [22]. This dataset contains 10,000 images and 100 categories. The training set contains 10k images. The task is to segment the image into its various regions that include foreground, objects, and background. The images have different sources such as natural scenes, objects such as person, gun, ships, toys, balloon etc. and also images with multiple objects are selected. The images from database are selected randomly to train the proposed CNN. Test image that is excluded in the training is taken from the same dataset in order to validate the algorithm. The experiments are conducted using computer with i7 processor speed 2.8 GHz and 8GB RAM and MATLAB version 9.6 software is employed for implementation of proposed CNN. The step-by-step result obtained after the training and the classification of the balloon image is shown in Fig. 2

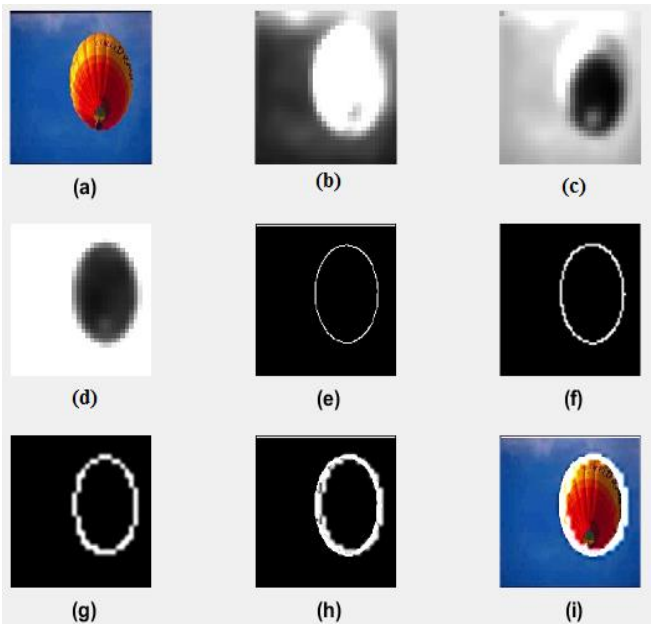

Fig. 2 (a) Original image, (b) The first channel output of CNN, (c) The second channel output of CNN,(d) The third channel output of CNN ,(e)-(g) Result of Edge detection using canny after each layer, (h) Result of color region merging, (i) Segmented image.

Segmented results are illustrated in Fig. 3 after training and classification. In the learning phase, images are applied to the CNN sequentially which updates the weights of the filter in each layer. It is proposed to start with a learning rate greater than 0.05 (5%), and reduces it to 0.01 (1%) when the performance of the evaluation set no longer improves. These updated weights are applied in testing phase that performs segmentation. The results clearly indicate that the proposed image segmentation algorithm using CNN segments regions within the images. It clearly segments foreground, objects and background in the images. The algorithm has been further improved therefore it predicts the map of an image back to its original size without any post-processing. Finally results are obtained in multiple separated region of an image. The metrics commonly used for evaluating image segmentation are variations in pixel accuracy.Let b_{ij} be the number of pixels of class i predicted belonging to class j and let c_i be the total number of pixels of class i. The pixel accuracy (pa) is given by equation (5) and tabulated in table I & II for images containing single and multiple objects respectively.

$$pa = \frac{\sum_i b_{ij}}{\sum_i c_i} * 100 \quad (5)$$

The obtained experimental results are compared with early hierarchical contexts learned by CNN [23] and image segmentation based on CNN and conditional random field [24] depicted in table III & IV respectively. Technique in [23] is applied for single object segmentation whereas technique in [24] is applied for multiple objects.

It is clearly observed that the proposed technique is suitable for multiple and single image segmentation application. Careful observation of the resultant images shows that proposed algorithm effectively segments the objects based color space. Each object consists of some uniform pattern of color which is made from combination of R, G and B color space. Processing each color space separately evaluates each object with uniform distribution followed with edge detection. Finally, merging of each color space with edges enhances the major boundaries of the object whereas suppresses the minor regions within the image.

Fig. 3(c) and 3(d) illustrate some minor boundaries within the object and highlights the major boundaries.

Table I. Pixel accuracy for image containing single object

Sr. No.	Image Type (Single Object)	Pixel Accuracy (%)
1	Balloon	98
2	Gun	90
3	Santa	91

Fig. 3. Segmentation results for images containing single and multiple objects.

Table II. Pixel accuracy for image containing multiple objects

Sr. No.	Image Type (Multiple Objects)	Pixel Accuracy (%)
1	Doll and toy	93
2	Many Balloons	86
3	Many Objects	92

Table III. Comparison of pixel accuracy for single object

Image Type	Pixel Accuracy (%) with Proposed Method	Pixel Accuracy (%) with technique in [23]
Single object	93 (average)	86.83

Table IV. Comparison of pixel accuracy for multiple objects

Image Type	Pixel Accuracy (%) with Proposed Method	Pixel Accuracy (%) with technique in [24]
Multiple objects	90.33 (average)	91.7

IV. CONCLUSION

This paper focuses on CNN based image segmentation for image annotation application. The proposed CNN includes a prediction of the region using image pixels that are applied to obtain low level image features. The algorithm uses image region information based on precise color distribution within the image. Experimental results demonstrate better image segmentation using CNN. Pixel accuracy is calculated to measure the performance of the algorithm to predict and segment foreground, background and objects in the image. Mean filter at the convolution layer and accumulation at the max pooling layer effectively improve the accuracy of the segmentation algorithm. To smoothen the boundaries or ensure consistent segmentation, more sophisticated post processing can be applied. Further, the algorithm can be improved to region based segmentation for semantic segmentation and automatic image annotation applications.

REFERENCES

[1] J. Zhang, Y. Mu, S. Feng, K. Li, Y. Yuan, Chin-Hui Lee, “Image region annotation based on segmentation and semantic correlation analysis,” IET Image Processing, vol.12, no.8, pp.1331-1337, Mar. 2018.

[2] Y. Wang, T. Mei, S.G. Gong, X.S Hua, “Combining global, regional and contextual features for automatic image annotation,” Elsevier Pattern Recognition, vol.42, no.2, pp.259-266, Feb. 2009.

[3] A. Morales-González, E García-Reyes, LE Sucar, “Image Annotation by a Hierarchical and Iterative Combination of Recognition and Segmentation,” World Scientific International Journal of Pattern Recognition and Artificial Int,lligence, vol. 32, no. 01,pp.1860014, Feb. 2018.

[4] X. Jing, F. Wu, Z. Li, R. Hu, D. Zhang, “Multi-Label Dictionary Learning for Image Annotation,” IEEE Trans. Image Processing, vol. 25, no. 6, pp.2712-2725 , June 2016.

[5] Q. Cheng,Q. Zhang, P. Fu, C.Tu, S. Li, “A survey and analysis on automatic image annotation,” Elsevier Pattern Recognition, vol. 79, pp. 242-259, Feb. 2018.

[6] A. Makadia, V. Pavlovic, and S. Kumar, “A new baseline for image annotation,” In Proc. 10th Eur. Conf. Comput. Vis., pp. 316–329, 2008.

[7] M. Guillaumin, T. Mensink, J. Verbeek, and C. Schmid, “TagProp: Discriminative metric learning in nearest neighbor models for image autoannotation,” In Proc. IEEE 12th Int. Conf. Comput. Vis., pp. 309–316, 2009.

[8] J. Jeon, V. Lavrenko, and R. Manmatha, “Automatic image annotation and retrieval using cross-media relevance models,” In Proceedings of the 26th Annual International ACM SIGIR Conference on Research and Development in Informaion Retrieval, SIGIR ’03, pp. 119–126, 2003.

[9] S. L. Feng, R. Manmatha and V. Lavrenko, “Multiple bernoulli relevance models for image and video annotation,” In Proceedings of the 2004 IEEE Computer Society Conference on Computer Vision and Pattern Recognition, CVPR’04, pp. 1002–1009, 2004.

[10] D. Putthividhy, H. Attias and S. Nagarajan, “Topic regressionmulti-modal latent Dirichlet allocation for image annotation,” In Proceedings of the 2004 IEEE Computer Society Conference on Computer Vision and Pattern Recognition, CVPR’10, pp. 3408–3415, 2010.

[11] G. Carneiro, A. B. Chan, P. J. Moreno, and N. Vasconcelos, “ Supervised learning of semantic classes for image annotation and retrieval,” IEEE Trans. Pattern Anal. Mach. Intell., vol. 29, no. 3,pp. 394–410, Mar. 2007.

[12] Y. Verma and C. Jawahar, “Exploring svm for image annotation in presence of confusing labels,” In Proceedings of the 24th British Machine Vision Conference, 2013.

[13] Y. Hou , Z. Lin , “Image tag completion and refinement by subspace clustering and matrix completion,” Vis. Commun. Image Process. (VCIP) ,pp.1–4, 2015.

[14] L. Wu , R. Jin , A.K. Jain, “Tag completion for image retrieval,” IEEE Trans. Pattern Anal. Mach. Intell.,vol. 35,no.3,pp.716, 2013.

[15] Jin , H. Nakayama , “Annotation order matters: recurrent image annotator for arbitrary length image tagging,” International Conference on Pattern Recognition, pp. 2452–2457 ,2017.

[16] J. Wu , Y. Yu , C. Huang , K. Yu , “Deep multiple instance learning for image classification and auto-annotation,” In Proceedings of the IEEE Conference on Computer Vision and Pattern Recognition, pp. 3460–3469,2015.

[17] Deng Y., Manjunath B.S., Shin H, “Color image segmentation”, In Proceedings of the IEEE Conference on Computer Vision and Pattern Recognition, Fort Collins, CO, USA, pp. 446-451, 1999.

[18] C. T. Zahn, "Graph-Theoretical Methods for Detecting and Describing Gestalt Clusters," *in* IEEE Transactions on Computers, vol. C-20, no. 1, pp. 68-86, 1971.

[19] J. Long, E. Shelhamer and T. Darrell, "Fully convolutional networks for semantic segmentation," IEEE Conference on Computer Vision and Pattern Recognition (CVPR), Boston, pp. 3431-3440,2015.

[20] A. Krizhevsky, I. Sutskever, and G. Hinton., "Imagenet classification with deep convolutional neural networks," In Advances in neural information processing systems, pp. 1097-1105, 2012.

[21] Seyedhosseini, Mojtaba, and Tolga Tasdizen, “Semantic Image Segmentation with Contextual Hierarchical Models,” IEEE transactions on pattern analysis and machine intelligence vol. 38,no. 5, pp. 951-64, 2016.

[22] Guang-Hai Liu, Jing-Yu Yang, etc, “Content-based image retrieval using computational visual attention model,” Pattern Recognition, vol. 48,no8 ,pp. 2554-2566,2015.

[23] Zifeng Wu, et. al, “Early Hierarchical Contexts Learned by Convolutional Networks for Image Segmentation,” IEEE 22nd International Conference on Pattern Recognition Stockholm, Sweden, pp. 1538 – 1543, 2014.

[24] Hu Tao, et. al, “Image Semantic Segmentation Based on Convolutional Neural Network and Conditional Random Field,”

IEEE 10th International Conference on Advanced Computational Intelligence (ICACI), China, pp. 568 – 572, 2018.

Proceedings of the Fourth International Conference on Communication and Electronics Systems (ICCES 2019)
IEEE Conference Record # 45898; IEEE Xplore ISBN: 978-1-7281-1261-9

Behaviour of Distance Relay under Faults in presence of Static Synchronous Series Compensator

Priti Sathe
Department of Electrical Engineering,
VPM's Maharshi Parshuram
College of Engineering,
Velneshwar

Pranita Chavan
Department of Electrical Engineering,
Pillai HOC College of
Engineering and Technology,
Rasayani

Dhananjay Borse
R&D Department,
Radium Engineering,
Bavdhan, Pune

***Abstract*—As power flow controllers and voltage compensators, flexible alternating current transmission systems (FACTS) have become popular in transmission systems. The system's power transfer capability increases while the usage of these power electronic devices improves the controllability. The Static Synchronous Series Compensator (SSSC) is a very useful FACTS device that can inject voltage with the line in series. This injected voltage can be described as an inductive or capacitive reaction connected in series to the transmission line that provides control over voltage compensation. This reaction has serious effects on the operation of remote protection systems running along the transmission line as they operate on the line's net impedance basis. Due to the presence of SSSC, this change in system dynamics causes problems of under-reaching or over-reaching and may cause maloperation of the protection scheme. The purpose of this paper is to study the effect of series compensation on distance relaying caused by using SSSC in a fault-condition transmission line. The influence on the distance relay characteristic of mho is studied using MATLAB / Simulink and the results are validated by experiments on a transmission line hardware prototype. A double circuit doubly fed transmission line is considered for this study.**

Keywords: **FACTS, distance relay, SSSC, MATLAB/Simulink, double circuit doubly fed transmission line, fault**

I. Introduction

Introduction of FACTS devices has revolutionized the concept of power flow in transmission lines over last decade. Active and reactive power flow control, control over bus voltages, fast and reliable operation are few of its many advantages [1]. With consumer demand steadily increasing, it was necessary to increase the transmission line's power transfer capacity. FACTS devices made it possible to improve the line's power transfer capability by controlling factors that govern it such as the impedance of the transmission line and the angle of the phase between the voltage sources at both ends of the transmission line. By controlling these factors, transient stability of the line improves such that its power carrying capability improves for same thermal limit.

Of all the FACTS devices, SSSC, which is a series compensating device is very popular and is of particular interest to many researchers owing to its usefulness under any type of loads [2]-[13]. It is a series compensating device used to control the flow of power in transmission lines and improve the damping of power oscillation on power grids. A voltage is injected by SSSC in series with the connecting transmission line and it also acts like a active harmonic filter.

However, a drastic change in current and voltage values is observed due to introduction of SSSC in transmission lines as against their usual values. Distance relay which is most popular method used to protect transmission lines works on the principle of impedance characteristics of the line experiences maloperation in the form of under reaching or over reaching the fault point due to this. Various studies are conducted in this area to investigate influence of SSSC on performance of distance relay [14]-[18].

Hardware demonstration of the concept is not covered in most of the literature presented on this topic. This paper aims to provide experimental results along with simulated results to analyze the effect of SSSC on transmission line protection system and Mho characteristics of the impedance relay on a doubly fed double circuit transmission line. The paper is organized as follows: Section I introduction is immediately followed by Mathematical modelling and operation of SSSC in Section II. Section III discusses the simulated results obtained by simulations using MATLAB/Simulink while Section IV validates the same on a hardware prototype of transmission line. Section V concludes the paper.

II. Mathematical Modelling and Operation of SSSC

SSSC is a series compensated FACTS device and was initially developed in 1989 [3]-[10]. It uses a VSC (Voltage Source Converter) as a VAR compensator that is connected through a transformer in series with the transmission line. It is composed of a VSC, transformer and an energy source. Basic configuration of SSSC connected to the transmission line is shown in Fig. 1.

In capacitive or inductive mode, SSSC can vary the reactance of the transmission line and is thus able to control the active and reactive power flow in the line very effectively. It is capable of maintaining highly effective X / R irrespective of the degree of series compensation. Moreover, a small supply is enough if the operation is only limited for reactive power compensation. With the voltage developed across the line, it

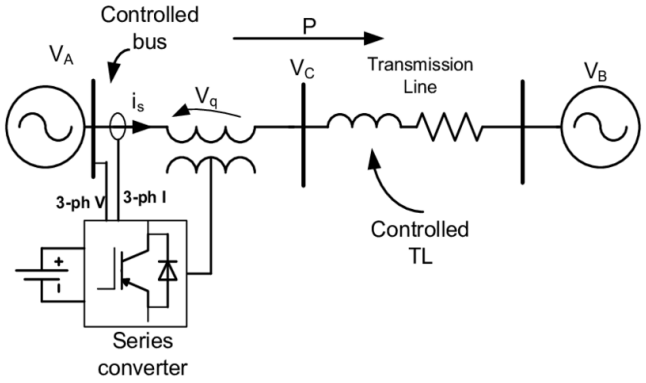

Fig. 1. Basic Configuration of SSSC

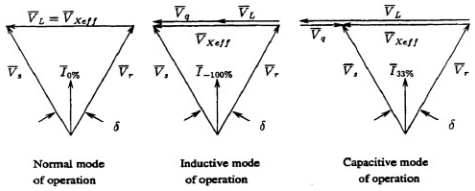

Fig. 2. Phasor diagram showing modes of operation of SSSC

can inject voltage that is of the same magnitude but opposite in phase angle.

Operation of SSSC can be classified into two modes, namely constant mode of reactance and constant mode of quadrature voltage and are represented by phasor diagram as shown in Fig. 2. SSSC voltage is a function of the current flowing through the transmission line in constant reactance mode while it doesnt depend on line current in constant quadrature voltage mode. If an energy storage system is present in the operation of SSSC, an impedance compensation controller acts as a transmission line resistance compensator whereas when energy storage system is absent, it compensates the reactance of the transmission line.

Series capacitor connected in the line counteracts its reactance, thus impedance of the transmission line is reduced. From the phasor diagram, it is seen that the injected voltage acts opposite in polarity to the voltage across series line reactance at a given line current and is given by (1).

$$\mathrm{Vq} = -\mathrm{jkXI} \tag{1}$$

$$\mathrm{k} = \mathrm{X_{SSSC}}/\mathrm{X} \tag{2}$$

Where, V_q is infused voltage, I is line current, X_{SSSC} is SSSC reactance, X is the line reactance and k is the degree of series compensation and j=$\sqrt{-1}$.

Voltage injected by SSSC depends on the flow of power through the line. Active power (P) and reactive power (Q) in the line using sending and receiving end voltages (V_s and V_r) and line reactance (X_L) can be expressed as:

$$\mathrm{P} = \frac{\mathrm{V_s V_r sin}(\delta_\mathrm{s} - \delta_\mathrm{r})}{\mathrm{X_L}} \tag{3}$$

$$= \frac{\mathrm{V^2 sin}(\delta)}{\mathrm{X_L}} \tag{4}$$

$$\mathrm{Q} = \frac{\mathrm{V_s V_r}[1 - \cos(\delta_\mathrm{s} - \delta_\mathrm{r})]}{\mathrm{X_L}} \tag{5}$$

$$= \frac{\mathrm{V^2}(1 - \cos\delta)}{\mathrm{X_L}} \tag{6}$$

$$\delta = (\delta_\mathrm{s} - \delta_\mathrm{r}) \tag{7}$$

$$\mathrm{V_s} = \mathrm{V_r} = \mathrm{V} \tag{8}$$

$$\mathrm{P_q} = \frac{\mathrm{V^2}}{\mathrm{X_{eff}}}\sin\delta \tag{9}$$

$$\mathrm{Q_q} = \frac{\mathrm{V^2}}{\mathrm{X_{eff}}}[1 - \cos\delta] \tag{10}$$

Where,
δ_s is sending end voltage angle,
δ_r is Voltage angle at receiving end,
P_q is Bus 2 active power,
Q_q is Bus 2 rqqeactive power,
X_{eff} is sending and receiving end total effective line reactance.

III. MATLAB Simulation Results and Discussion

A 400 kV, 300km transmission line was used to analyze the performance of the distance relay with and without SSSC connected in series with the transmission line at the mid-point. Fig. 3 represent the model developed using MATLAB/Simulink for calculation of a single phase to ground in double fed transmission line.

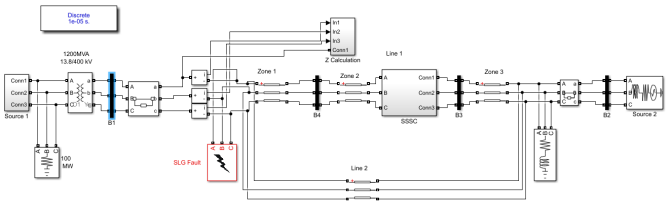

Fig. 3. Modelling Of Double Fed Transmission Line

Figs. 4-6 represent the mho relay characteristics for the fault generated at various locations of the transmission line without SSSC system. Convention uncompensated distance relay was used for this simulation. Typical calculations for finding impedance based on magnitude and phase angle were used.

Figs. 7-9 represent the MHO relay characteristics for the fault generated at various locations of the transmission line with SSSC compensation system.

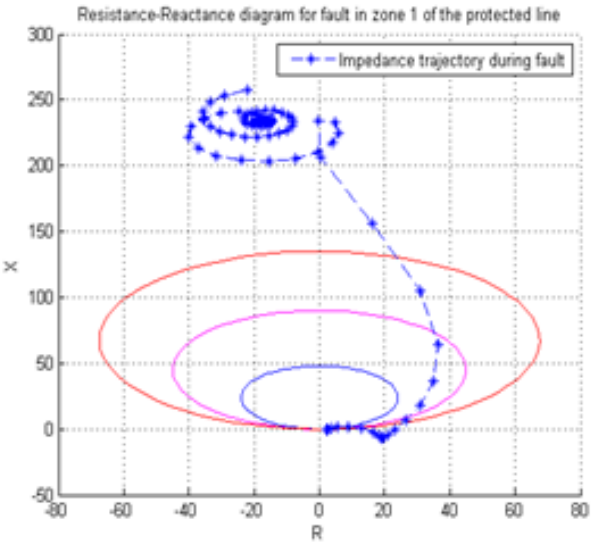

Fig. 4. R-jX plot for the fault in zone 1 without SSSC

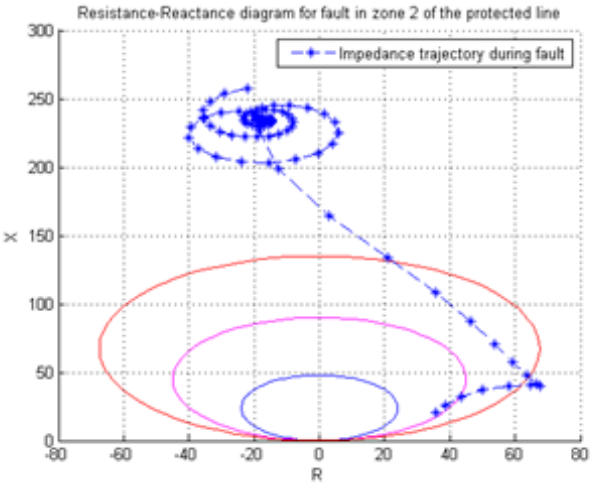

Fig. 5. R-jX plot for the fault in zone 2 without SSSC

An algorithm is used to plot the impedance values of the simulation in a way to represent the impedance characteristics of the line. It can be seen from the figures that mho characteristic under reaches in the presence SSSC connected in zone 2 for fault in zone 3. Similar observations were found for other types of faults as well.

IV. Hardware Experimentation

A hardware prototype of transmission line with distance relaying scheme was designed and constructed with SSSC for validation of the simulation result. A 230V double circuit doubly fed single phase equivalent circuit of transmission line of 300km was design with parameters as shown in Table I. A pair of inductance and resistance is used to represent 100 km section of the line.

Capacitance of the line was neglected as the line was

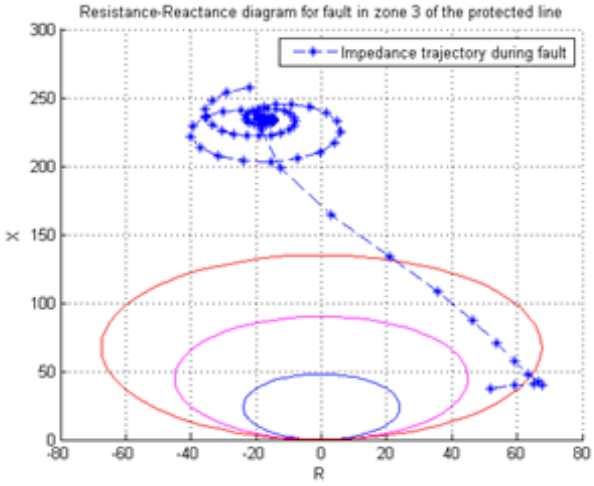

Fig. 6. R-jX plot for the fault in zone 3 without SSSC

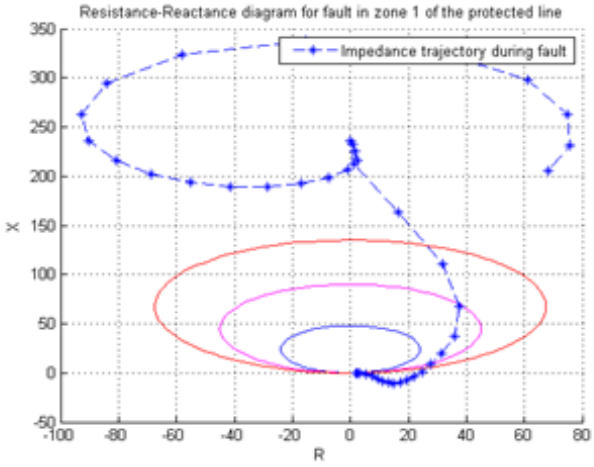

Fig. 7. R-jX plot for the fault in zone 1 with SSSC

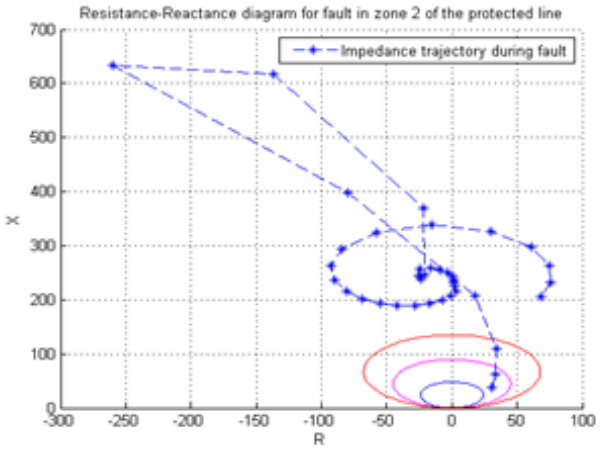

Fig. 8. R-jX plot for the fault in zone 2 with SSSC

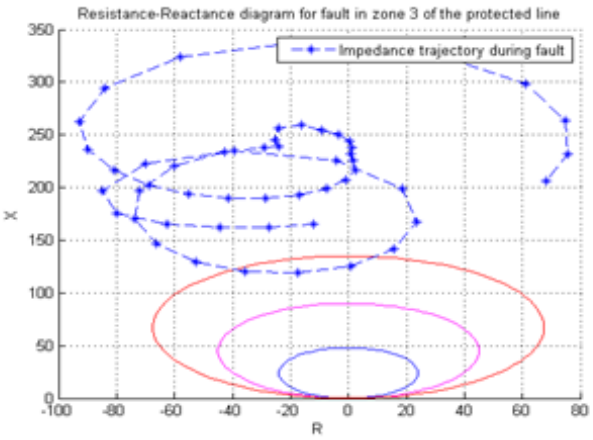

Fig. 9. R-jX plot for the fault in zone 3 with SSSC

TABLE I
PARAMETERS USED FOR HARDWARE PROTOTYPE

Parameter	Value
R1, R2, R3 Line Resistances	4.7 ohms, 10W
L1, L2, L3 Line Inductances	0.1mH, 5A
Voltage	230V, 50 Hz
Line Rating	5A
DC Capacitor for SSSC	1000μF, 63V
Coupling Transformer	230V/24V, 5A

considered to be moderately loads and due to experiments during fault conditions. 100W lamps were used as loads while 200W lamps were used to recreate line to ground fault at various locations of the line. Voltage and current sensors were used for measurement of line parameters. A single phase VSC was connected in series with help of circuit breakers and a step-down coupling transformer. The algorithm for distance relay and for operation of SSSC was implemented using user friendly Arduino Uno platform. Both inductive and capacitive modes of operation were tested on the prototype hardware. The prototype is shown in Fig. 10 and one of its operating modes is shown in Fig. 11.

The distance relays detects the zones of fault location accurately during normal operation. During presence of SSSC, it works effectively to determine fault in zone 1. However, it cannot distinguish between fault in zone 1 and zone 2 as it displays fault in zone 1 for both zones. Thus it under reaches for fault in zone 2. It cannot detect fault in case of fault in zone three as impedance measured is lesser that the relay setting for the same. Phenomenon of over reaching was observed in the case.

V. CONCLUSION

Behaviour of distance protection scheme for transmission under the influence of SSSC during single line to ground fault was discussed in this paper. It was observed that the distance relaying maloperates due to unpredictable change in impedance value in presence of SSSC and thus the distance

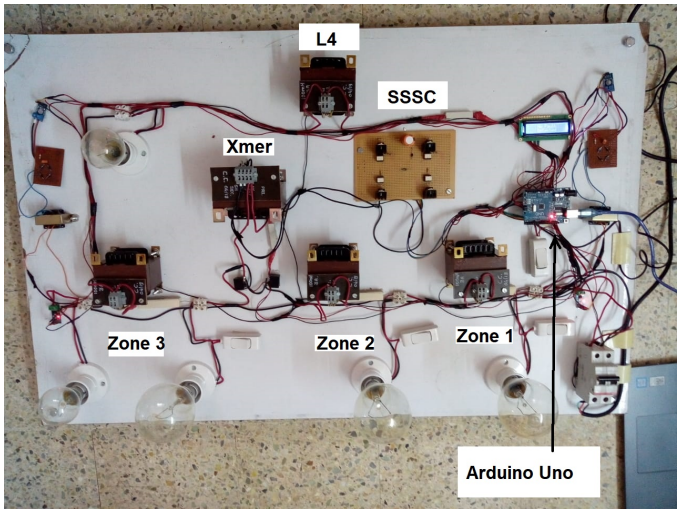

Fig. 10. Hardware Prototype of transmission line with distance relay and SSSC

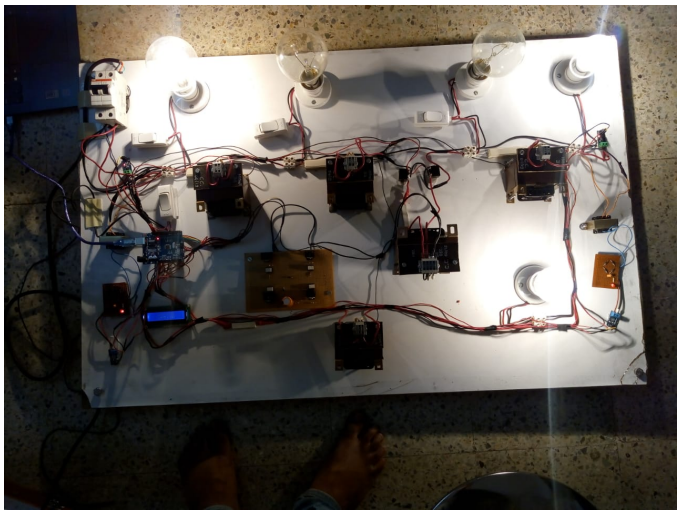

Fig. 11. Hardware Prototype during operation: Fault in zone 1

protection system fails. Both simulated results and experimental results validate these outcomes.

Faults occurring at various locations in the line are studied and its effect is analyzed in this paper. It was found that when SSSC is connected between zone 2 and zone 3 of the transmission line, distance relaying gets affected for these zones while only zone 1 operates ass expected. It can be concluded from the observations that distance relay under reaches for zone 2 if the fault occurs before connection with SSSC while it over reaches for zone 3.

It is very much essential to mitigate the problem of maloperation of distance relay under the presence of SSSC for stable and reliably operation of power system. Various algorithms can be developed for compensation of this error in measurement of distance relay. Recent advancements in Artificial Intelligence, Fuzzy Logic and Artificial neural network can be employed for this task and is a future scope for this research.

REFERENCES

[1] N. G. Hingorani and L. Gyugyi, "Understanding FACTS Concepts and Technology of Flexible AC Transmission Systems" *IEEE Press*, 2000.
[2] M. Faridi, H. Maeiiat, M. Karimi, P. Farhadi and H. Moslesh, "Power System Stability Enhancement Using Static Synchronous Series Compensator (SSSC)", *IEEE Transactions on Power System*, pp. 387-391, 2011.
[3] Dipendra Rai, Sherif O. Faried, G. Ramakrishna and Abdel-AtyEdris, "An SSSC-Based Hybrid Series Compensation Scheme Capable of Damping Subsynchronous Resonance", *JEEE transaction on power delivery*, vol. 127, no.2, 2012.
[4] H. Zenk and A. S. Akpinar, "PI, PID and fuzzy logic controlled SSSC connected to a power transmission line, voltage control performance comparison," 4th International Conference on Power Engineering, Energy and Electrical Drives, pp. 1493-1497, Istanbul, 2013.
[5] A. K. Jadhav and V. A. Kulkarni, "Improvement in Power System Stability Using SSSC Based Damping Controller," 2018 International Conference on Smart Electric Drives and Power System (ICSEDPS), pp. 162-166, Nagpur, 2018.
[6] M. Y. Suliman and S. M. Bashi, "Fast response SSSC based on instantaneous power theory," 2013 International Conference on Electrical Communication, Computer, Power, and Control Engineering (ICECCPCE), pp. 174-178, Mosul, 2013.
[7] M. Rohal and Ravi, "Application of SSSC based power oscillation damping controller for transient stability enhancement of multimachine system for unsymmetrical faults," 2014 6th IEEE Power India International Conference (PIICON), pp. 1-6, Delhi, 2014.
[8] C. Anitha and P. Arul, "Enhancement of voltage stability in transmission system using SSSC," 2014 International Conference on Circuits, Power and Computing Technologies [ICCPCT-2014], pp. 30-33, Nagercoil, 2014.
[9] C. U. Shankar, R. Thottungal and S. Mythili, "Voltage stability improvement and power oscillation damping using Static Synchronous Series Compensator (SSSC)," 2015 IEEE 9th International Conference on Intelligent Systems and Control (ISCO), pp. 1-6, Coimbatore, 2015.
[10] S. Gandhar, J. Ohri and M. Singh, "Application of SSSC for compensation assessment of interconnected Power System," 2014 IEEE 6th India International Conference on Power Electronics (IICPE), pp. 1-5, Kurukshetra, 2014.
[11] S. Arun Kumar, C. Easwarlal and M. Senthil Kumar, "Multi machine power system stability enhancement using Static Synchronous Series Compensator (SSSC)," 2012 International Conference on Computing, Electronics and Electrical Technologies (ICCEET), pp. 212-217, Kumaracoil, 2012.
[12] G. Maheswaran and K. S. Naidu, "Comparison of fuzzy and PI controller based SSSC for damping of sub synchronous resonance," 2014 International Conference on Science Engineering and Management Research (ICSEMR), pp. 1-5, Chennai, 2014.
[13] F. D. Galiana, K. Almeida, M. Toussaint, J. Griffin and D. Atanackovic, "Assessment and Control of the Impact of FACTS Devices on Power System Performance", *IEEE Trans. Power Systems*, Vol11, No 4, Nov. 1996.
[14] A. Kazemi, S. Jamali and H. Shateri, "Effects of SSSC on Distance Relay Tripping Characteristic," 2006 IEEE International Power and Energy Conference, pp. 624-629, Putra Jaya, 2006.
[15] A. Shojaei and S. M. Madani, "Analysis of measured impedance by distance relay in presence of SSSC," 5th IET International Conference on Power Electronics, Machines and Drives (PEMD 2010), pp. 1-6, Brighton, UK, 2010.
[16] Amir Ghorbani, Babak Mozafari and Ali Mohammad Ranjbar, "Digital distance protection of transmission lines in the presence of SSSC" *Elsevier, Electrical Power and Energy Systems*, Vol. 43, pp. 712-719, 2012.
[17] S. Jamali, A. Kazemi and H. Shateri, "Effect of SSSC on measured impedance of distance relay in double-circuit lines," 2007 42nd International Universities Power Engineering Conference, pp. 895-899, Brighton, 2007.
[18] Dhenuvakonda, KR, Singh, A, Thakre, MP, Karasani, RR, Naidoo, R., "Adaptive digital distance relay for SSSC-based double-circuit transmission line using phasor measurement unit", Int Trans Electr Energ Syst., 2019.

Proceedings of the Fourth International Conference on Communication and Electronics Systems (ICCES 2019)
IEEE Conference Record # 45898; IEEE Xplore ISBN: 978-1-7281-1261-9

Modeling of Carbon Nanotube Field-Effect Transistor and Evaluation of an Inverter Circuit

Guru Prasath C, Rakshita Vishali V, Sabarrish S, Khevin Nair, B Bala Tripura Sundari
Department of Electronics and Communication Engineering
Amrita School of Engineering, Coimbatore
Amrita Vishwa Vidyapeetham, India
guruprasath505@gmail.com, rakshitavishali@gmail.com, sabarrish98@gmail.com, khevin.ronaldinho@gmail.com, b_bala@cb.amrita.edu

***Abstract*— The Silicon MOSFET scaling is constrained; because of this CNTFET is observed to be a standout amongst the most encouraging choices. The principle distinction between CNTFETs and MOSFETs is that, the channel in CNTFET is designed by using Carbon Nano Tubes rather than Silicon. This empowers a higher drive current density because of the immense amount of current carrier mobility contrasted with the bulk silicon. Such transistors are being seriously considered for applications in the emerging field of Nanotechnology. A CNTFET can utilize a single CNT or an array of CNTs as the channel material. In this paper, n-type CNTFET and p-type CNTFET will be modeled in Cadence Virtuoso Analog Designing environment and I-V characteristics will be plotted. An inverter will also be designed using the modeled CNTFETs. dc analysis and transient analysis will be done for the designed inverter.**

Keywords*— *CNTFET, device modeling, inverter, circuit designing, dc analysis, transient analysis

I. INTRODUCTION

The gate length of the MOSFETs has been enrolled in the deep sub-micron region because of the 0.35 micrometer node technology. Since 2006, the 65 nm technology has become very common and 45 nm technologies have surfaced in the year 2007. As CMOS enters into nanoscale with respect to size, various device characteristics which are not ideal make the I-V characteristics to extensively differ from that of the MOSFETs, which makes it hard to improve device performance furthermore by downsizing the size of the gate length. In today's technology, one can notice a brilliant advancement and development in electronics which has the device size in the order of nanometers. Few complicated electronic circuits were designed by using leading edge silicon technology. Carbon nanotubes are one of these latest materials because of the rare electronic and mechanical effects. The three logical points why CNTFETs are (1) the theory of operation and the design of the device is very comparable to CMOS devices, (2) the fabrication process of CMOS also can be repeated, (3) CNTFET's current carrying capability has been the best till now.

As CMOS enters into nanoscale with respect to size of the device, various non-ideal characteristics of the device make the I-V characteristics to extensively vary from that of the MOSFETs [1]. The S/D series resistance is a crucial element in the overall device structure. Devices which are fabricated without using silicon such as the CNTFETs work with distinct physics of the device with ballistic conduction in the channel. Also, they work with Schottky barrier contacts at the source terminal and drain terminal. So as to legitimately benchmark future nanoscale Silicon FETs and CNFETs, it is important to build a benchmarking metric that assess the shape of the I-V characteristics with the device that is working in a circuit domain [2]. The major critics are: The absence of a thin equivalent gate oxide, the inclusion of the parasitic capacitance is becoming larger, the growing addition of the S/D resistance to the total resistance of the device [3].

The paper has been divided into five parts. First part gives a detailed explanation about lattice of graphene and computation of circumference and diameter of carbon nanotube. And it also explains how carbon nanotube can be displayed as a sheet of graphene. The second part gives a brief discussion on how carbon nanotubes can be classified based on the chiral number and the operation system. The third part explains the prerequisites for a decent device model and the important parameters that are responsible for deviations and defects brought about by the present CNT manufacturing process. The fourth part gives a detailed explanation about Virtual-Source CNTFET model, user-defined input parameters and hierarchical structure of CNTFET. The fifth part explains the results that are obtained from the model and their interpretations. And it also gives a conclusion of our findings.

II. LITERATURE SURVEY

Carbon atom has an electron configuration of $1s^2 2s^2 2p^2$ in its ground state. sp^2 hybridization develops through covalent bonding. A carbon atom in graphene gathers in a solitary sheet hexagonal lattice. The distance between two adjacent carbon atoms within the hexagonal lattice (d) is 1.44 Å, and the angle between C-C bonds is 120°. The lattice constant (a) is given by $\sqrt{3}\ d$ = 2.49 Å. The inner spacing between the multiple sheets in graphene is approximately 3.35 Å. The frail electrostatic energy between the sheets makes it potential to expect the electrical properties of the graphite sheets are autonomous to each other.

A single-walled carbon nanotube (SWCNT) can be displayed as a sheet of graphite which is folded up and combined along a wrapping vector:

$$C_h = n_1.\bar{a}_1 + n_2.\bar{a}_2 \quad (1)$$

where [$\bar{a}_1$, $\bar{a}_2$] are lattice unit vectors as shown by Figure 1, and the indices (n_1, n_2) are positive integers that determine the chirality of the tube [4]. The length of C_h is therefore the circumference of CNT and it can be computed by the following formula:

$$C_h = a\sqrt{(n_1^2 + n_2^2 + n_1 n_2)} \quad (2)$$

Single-walled CNTs are characterized into three groups depending on the chiral number (n1, n2): (1) armchair, it is in which n1 and n2 are equal, (2) zigzag, it is in which either n1=0 or n2=0, (3) chiral which is said to have different indices.

The CNT diameter is given by the equation $D_{CNT} = C_h/\pi$ [5]. The usual CNT diameters are around a few nanometers. The small diameter of CNTs leads to the wave vector's quantization in the circumferential direction. The electrons in CNT are limited to the atomic plane of graphene. Graphene is an allotrope of carbon which has single layer of carbon atoms organized in lattices which are in the shape of hexagons [6]. The movement of the electrons in the nanotubes is limited due to the quasi 1D structure. Electrons may just move openly along the direction of the tube axis. Therefore, all the wide point scatterings are restricted. Because of electron phonon collaborations only forward and back scattering are feasible for the carriers in nanotubes. The overwhelming transporter transport and conduction trademark makes for nanoelectronics applications CNTs are wanted due to their superior carrier transport and conduction properties for example interconnect and nanoscale devices.

The CNTFET operation principle is similar of conventional Si appliances. In the device that has three terminals, the source and drain contacts are being bridged by the semiconducting nanotubes acting as a conducting channel in the device. Through the gate the appliance is electrostatically switched on or off. Compared to the 3D devices such as bulk Complementary MOS and 2-Dimensional devices, better gate electrostatic control over the channel area is offered by the 1D quasi device structures. CNTFET can be divided as either MOSFET-like FET or Schottky Barrier (SB) controlled FET (SB-CNTFET) depending on the operation system. In consideration of both the usefulness of manufacturing and exceptional working of MOSFET-like CNTFET when contrasted with SB-CNFET, we will concentrate on MOSFET-like CNTFETs.

To assess the appliance execution just along with the work reliance on structure characteristics, the prerequisites for a decent device model include: (1) Decent expandability, (2) At least partially physics based, (3) Large signal and small signal analysis with reasonable accuracy, (4) Tolerable run time. To assess CNTFET device execution with improved precision, a CNTFET device display with an increasingly total circuit-appropriate structure and furthermore fusing the common device non-conceptions is required. A decent harmony among the run-time simulation and precision is wanted. The macro level circuit isn't just constrained by the execution of a single device, yet in addition restricted by the device variation in performance which is vital for nm devices. There are various device conditions deviations and defects brought about by the present CNT manufacturing process: (1) CNT width and chirality control, (2) Adulterating limit control, (3) The likelihood of a CNT to be metallic, (4) Focused-CNT-development. At long last, with the goal for CNTFET to form into a competitive technology, it ought to have great adaptability, for example the advantage in the working of CNTFET over MOSFET is relied upon to enhance (or if nothing else keep up the equivalent) as the technology progresses. And CNTFET is also used to examine the antimicrobial activity of Chitosan-CNT hydrogels [7].

III. Proposed Methodology

The Virtual-Source CNTFET is a semi-empirical model [8] that illustrates the current-voltage (I - V) and capacitance-voltage (C – V) characteristics in a MOSFET having short channel with CNTs as the channel material. The model describes about the dimensional scaling properties and it also includes parasitic resistance (CNT-metal contact resistance and doped extension resistance), parasitic capacitance (metal-to-metal coupling capacitance and metal-CNT fringe capacitance) and tunneling leakage currents (Direct source-to-drain tunneling and gate-to-drain junction band-to-band tunneling). The VS model has only few physical parameters like VS carrier velocity and carrier mobility that can be extracted from experimental I-V/C-V data. In this paper, the equations of the VS model will be used without detailed explanation. Inputs to the VS-CNTFET consist of CNTFET dimensions and CNT diameter. Empirical parameters in this model were extracted from either experimental data or numerical simulations based on the NEGF formalism to ensure the validity. Some equations are empirical but not completely physical. Calibration of the model is performed at room temperature that is 25° C. For temperatures other than 25° C, correctness of the empirical parameter is not guaranteed. This model is only applicable to MOSFET-like CNTFETs but not applicable to Schottky-barrier type CNTFETs. The CNTs are assumed to be all semiconducting [9] [10] [11]. Fig. 1. shows a representation of a CNTFET, whose conduction behavior is similar to a common MOSFET.

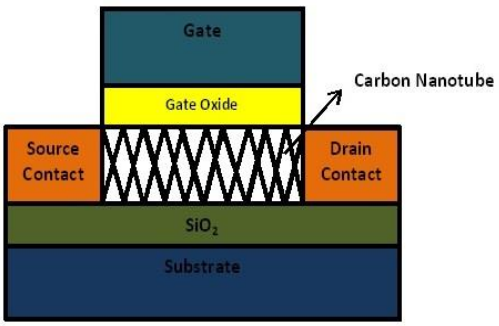

Fig. 1. Representation of CNTFET

Inputs to the VS-CNTFET are design-related parameters such as the gate length (L_g),contact length (L_c), CNT diameters (d), and gate oxide thickness (t_{ox}). The column "suggested scope" shows the range of the input that has been tested. Any

values outside the suggested scope may lead to unexpected results, though the model may still generate outputs as long as the given inputs are valid. The User-defined input parameters are given in Table I.

TABLE I. USER-DEFINED INPUT PARAMETERS

Name	Suggested Scope	Description
Type	-1 or 1	Type of transistor 1: nFET; -1 : pFET
s	[2.5e-9:inf)	Spacing between the CNTs (centre-to-centre) [m]
W	[s:inf)	Transistor width [m]
Lg	[5e-9:100e-9]	Physical gate length [m]
Lc	[1e-9:inf)	Contact length [m]
Lext	(0:inf)	Source/Drain extension length [m]
d	[1e-9:2e-9]	CNT diameter [m]
tox	[1e-9:10e-9]	Gate oxide thickness [m]
kox	[4:25]	Gate oxide dielectric constant
kcnt	1	CNT dielectric constant
ksub	[1:kox]	Substrate dielectric constant
kspa	[1:16)	Source/Drain spacer dielectric constant
Hg	[0:inf)	Gate height [m]
Efsd	[-0.1:0.5]	Fermi level to the band edge [eV] at the source/drain
Vfb	[-1:1]	Flat band voltage [V]
Geomod	1	Device geometry (cylindrical gate-all-around)
Rcmod	0	Contact mode (User-defined value Rs0)
Rs0	[0:inf)	User-defined series resistance (Ω)
SDTmod	1	Source-to-drain tunneling mode (SDT with inter-band tunneling)
BTBTmod	1	Band-to-band tunneling mode (on)
Temp	25	Temperature (°C)

Primarily the given inputs consist of structural and physical parameters. The structural parameters consist of W, L_g, L_{pitch}, L_c, d_{CNT}, N_{CNT} and various other parameters. The physical parameters consist of contact resistance, carrier mean path and various other parameters. By having both the structural and physical parameters as inputs, we will now move on to the next stage, which is called as "First Level" where we are supposed to determine the values of Mobility, Parasitic Resistances and capacitances.

In second level of hierarchical structure, there are two sub-levels where one is derived from the values of first level and the other is derived from the initial conditions (i.e. structural and physical parameters). The second level yields two outputs. One of them is Virtual Source Current and the other on is Tunneling Leakage Current. Tunneling Leakage Current is defined as the sum of Direct Source-to-drain Tunneling Current and band-to-band Tunneling Current [12]. Thus the current at drain terminal can be obtained by:

$$I_D = I_{VS} + I_{TUNNEL} \quad (3)$$

The entire functionality of this structure of CNTFET model is represented in Fig. 2.

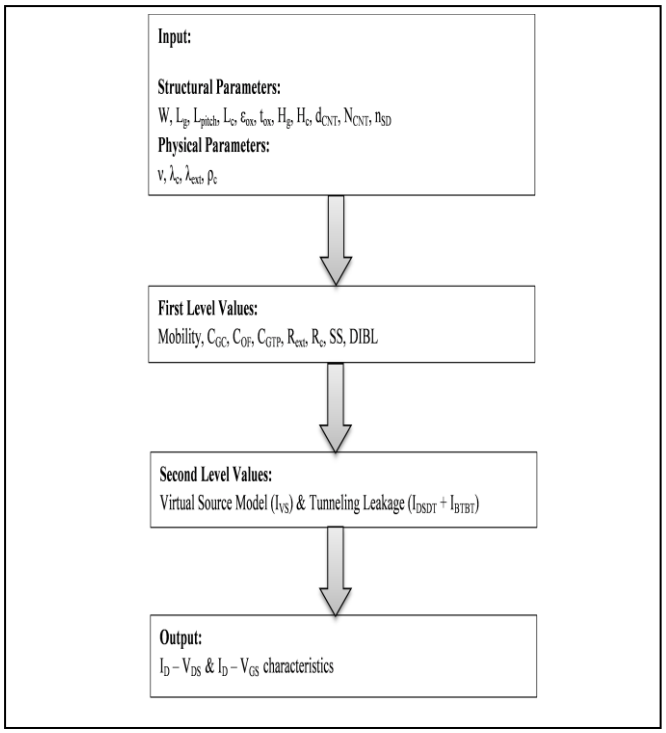

Fig.2. Hierarchical structure of CNTFET model

IV. RESULTS

Fig. 2 displays the graph between drain current and voltage between gate and source for n-type CNTFET. Fig. 3 displays the graph between drain current and voltage between drain and source for n-type CNTFET. Fig. 4 displays the graph between drain current and voltage between gate and source for p-type CNTFET. Fig. 5 displays the graph between drain current and voltage between drain and source for p-type CNTFET. Fig. 2 and Fig. 3 are the graphs obtained from the output of the Virtual-Source n-type CNTFET. Fig. 4 and Fig. 5 are the graphs obtained from the output of the Virtual-Source p-type CNTFET.

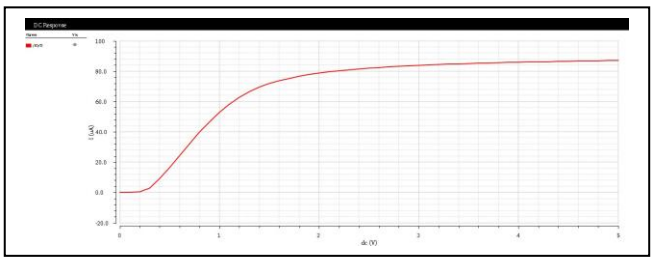

Fig. 2. $I_d - V_{gs}$ graph for n-type CNTFET

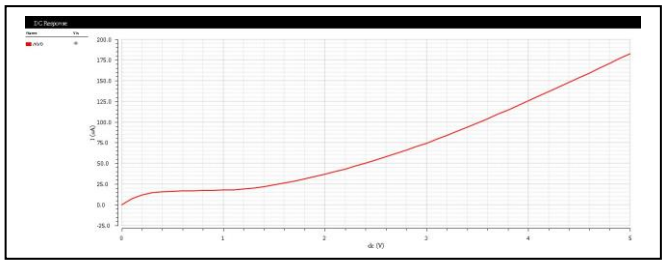

Fig. 3. $I_d - V_{ds}$ graph for n-type CNTFET

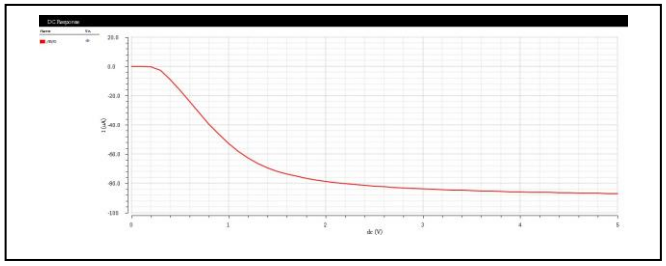

Fig. 4. $I_d - V_{gs}$ graph for p-type CNTFET

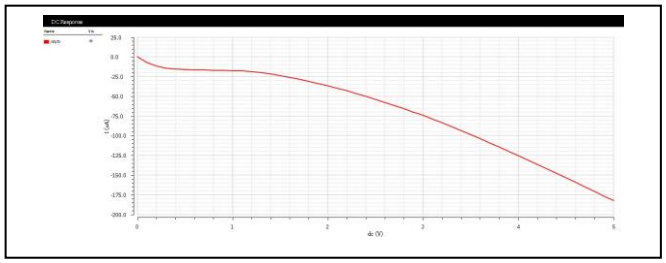

Fig. 5. $I_d - V_{ds}$ graph for p-type CNTFET

Let Vin be the input voltage, Vout be the output voltage and Vdd be the voltage supplied to the inverter. Fig. 6 displays the Voltage Transfer Characteristics (VTC) of an Inverter. When input is low (Vin = 0 V), p-type CNTFET gets switched ON and n-type CNTFET gets switched OFF. Thus, p-type CNTFET pulls Vout to Vdd and hence maximum output voltage occurs. When input is high (Vin = Vdd), p-type CNTFET gets switched OFF and n-type CNTFET gets switched ON. Thus, n-type CNTFET pulls Vout to ground and hence minimum output voltage occurs. The difference between maximum output voltage and minimum output voltage is maximum swing of output signal and this is also known as Logic Swing. Since minimum output voltage is O V and maximum output voltage is Vdd, the logic swing is equal to Vdd. The region between minimum output voltage and maximum output voltage is called Transition Region. Maximum current will flow at Vin = Vout that is at the mid-point of transition region. This is the dc analysis of the designed inverter.

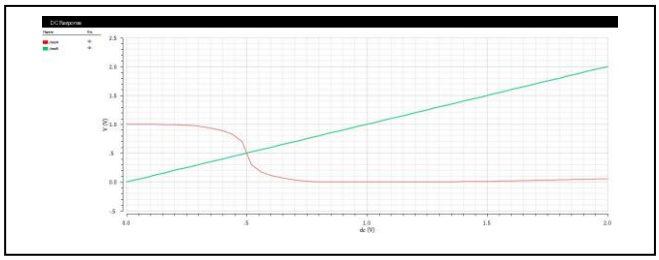

Fig. 6. dc analysis of the inverter circuit

Fig. 7 displays the transient response of an Inverter. When the input voltage is low (Vin = 0 V), output voltage is high (Vout = Vdd). When the input voltage is high (Vin = Vdd), output voltage is low (Vout = 0 V).

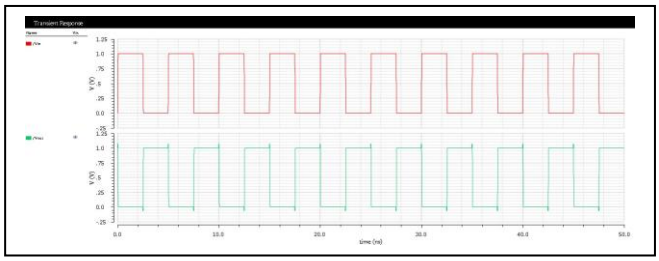

Fig. 7. transient response of the inverter circuit

V. CONCLUSION

In this paper, a semi-empirical model called Virtual-Source CNTFET was proposed that illustrates the current-voltage characteristics in a MOSFET having short channel with CNTs as the channel material. The proposed model describes about the dimensional scaling properties and it also includes parasitic resistance, parasitic capacitance and tunneling leakage currents. In late future, manufacturing a solitary integrated circuit where transistors reaching out in three dimensions is called 3-Dimensional Very large Scale Integration innovation, which will be the prospective of IC manufacturing field rising the stature: from small to miniature. CNTFET could be a fitting device for its miniature size and restrictive ballistic, heat dissemination and low resistive properties. Because of high dielectric material, movement of charges accelerates higher whereas channel measurement diminishes thoroughly. The unique characteristic of channel measurement prompts ballistic transport because of high channel density, showing CNTFET as more reasonable in nanoelectronic devices. What's more, devices that can store the data can be produced by utilizing CNTFET for its high value of current will open another time in nano-computational field. This must be referenced that fabricating the CNTFET is very expensive and it has unwavering quality because of development of misorganised CNTs in development process and expanding leakage power in metallic CNT. Considering all of these, CNTFET is one of the most reliable and assuring competitors and its amazing performance opens a door of new innovations in the field of nanotechnology.

REFERENCES

[1] Md. Alamgir Kabi, Turja Nandy, Mohammad Aminul Haque, Arin Dutta, Zahid Hasan Mahmood, "Performance analysis of CNTFET and MOSFET focusing channel length, carrier mobility and ballistic conduction in high speed switching," International Journal of Advances in Material Sciences and Engineering, Vol.3. No.3/4. pp. 1-11, October 2014.

[2] Sanjeet Kumar Sinha and Saurabh Chaudhury, "Comparative study of leakage power in CNTFET over MOSFET device," Journal of Semiconductors, Vol.35. No.11. pp. 114002, November 2014.

[3] Rasmita Sahoo and R. R. Mishra, "Simulation of Carbon Nanotube Field Effect Transistors," International Journal of Electronic Engineering Research, Vol.1. No.2. pp. 117-125, 2009.

[4] RamBabu.Busi, Swapna.P, Kalyan babu.K, Y.Srinivasa Rao, "Carbon nanotubes Field Effect Transistors: A Review," International Journal of Electronics and Communication Technology, Vol.2. SP-1. pp. 204-208, December 2011.

[5] Sanjeet Kumar Sinha, Saurabh Choudhury, "CNTFET based Logic Circuits: A Brief Review," International Journal of Emerging Technology and Advanced Engineering, Vol.2. Issue 4. pp. 500-504, April 2012.

[6] Sreenath R. and B. Bala Tripura Sundari, "Modelling and Performance comparison of Graphene and Carbon nanotube based FETs," ARPN Journal of Engineering and Applied Sciences, Vol.10. No.9. pp. 4147-4154, May 2015.

[7] J. Venkatesan, Dr. Jayakumar Rangasamy, Mohandas A., Bhatnagar I., and Kim S., "Antimicrobial Activity of Chitosan-carbon nanotube Hydrogels," Materials, Vol.7. Issue 5. pp. 3946-3955, 2014.

[8] M. Claus, M. Haferlach, D. Gross and M. Schroter, "Critical review of CNTFET compact models," Chain for Electron Device and Integrated Circuits (CEDIC), Vol.2. pp. 770-775, 2012.

[9] Chi-Shuen, Eric Pop, Aaron D. Franklin, Wilfried Haensch, H.S. Philip Wong, "A Compact Virtual-Source Model for Carbon Nanotube Field-Effect Transistors in the Sub-10-nm Regime – Part-I: Intrinsic Elements," IEEE Transactions on Electron Devices, Vol.62. No.9. pp. 3061-3069, September 2015.

[10] Chi-Shuen, Eric Pop, Aaron D. Franklin, Wilfried Haensch, H.S. Philip Wong, "A Compact Virtual-Source Model for Carbon Nanotube Field-Effect Transistors in the Sub-10-nm Regime – Part-II: Extrinsic Elements, Performance Assessment, and Design Optimization," IEEE Transactions on Electron Devices, Vol.62. pp. 3070-3078, March 2015.

[11] Jieying Luo, Lan Wei, Chi-Shuen Lee, Aaron D. Franklin, Ximeng Guan, Eric Pop, Dimitri A. Anto niadis, H.S. Philip Wong, "Compact Model for Carbon Nanotube Field-Effect Transistors Including Nonidealities and Caliberated With Experimental Data Down to 9-nm Gate Length," IEEE Transactions on Electron Devices, Vol.60. No.6. pp. 1834-1843, June 2013.

[12] C. Maneux, J. Goguet, S. Fregonese, T. Zimmer, H. Cazin d'Honincthun, S. Galdin-Retailleau, "Analysis of CNTFET physical compact model." International Conference on Design and Test of Integrated Systems in Nanoscale Technology, pp. 40-45, September 2006.

Proceedings of the Fourth International Conference on Communication and Electronics Systems (ICCES 2019)
IEEE Conference Record # 45898; IEEE Xplore ISBN: 978-1-7281-1261-9

Analysis on Machine Learning Algorithms and Neural Networks for Demand Forecasting of Anti-Aircraft Missile Spare Parts

Nikita Pawar
School of Computer Engineering and Technology,
MIT World Peace University, Kothrud, Pune,
Maharashtra, India.
nikitapawar717@gmail.com

Prof. Bhavana Tiple
School of Computer Engineering and Technology,
MIT World Peace University, Kothrud, Pune,
Maharashtra, India
bhavana.tiple@mitpune.edu.in

***Abstract*- Now-a-days demand forecasting is used in many countries for military applications such as spare parts of aircraft and for improving budget efficiency. In supply chain management demand forecasting is a major issue. Currently, time series technique is used to demand forecast but this technique resulted in lack of accuracy and improvement in accuracy is needed .So this paper focused on comparing the features which leads to improvement in the accuracy and propose a system for demand forecasting of spare parts of anti-aircraft missiles, which are based on machine learning and neural networks such that equipment's are properly utilized and alongwith that budget is also maintained. We have compared the existing features with the new features added and applied algorithms and looked upon at the accuracy. Experimental results proves that the new features added gave higher accuracy. Here, we also present an end-to-end boosting system called XGBoost and Multi-layer Perceptron. These new techniques were compared with traditional Machine Learning techniques. This experiment is conducted on the Vietnam War dataset.**

Keywords- Demand Forecasting; Spare Parts; Military; Missiles; Aircraft; MLP;XGBoost..

I. INTRODUCTION

The retail inventory management system has grown significantly over the last two decades with its emergence in the intelligent system for forecasting. Predicting any spare part for its future use itself is a very challenging task.This ultimately affects business reputation and also much loss of time.if a company does not have proper facts and figures regarding the stock required ,time maintenance operation will get affected. This hampers the growth of a company, loss of reputation, may endanger the customer's productivity if there is any sort of delay. Over loading of stock in inventory buffer is a costly job if there are large number of items or if any part is expensive.Effective spare part inventory management is thus a chief but challenging task because it is an issue of time versus availability of the desired service in minimum amount of time. Efficient spare parts management is essential for companies that are increasingly providing services. In most automotive spare parts industry, it is important to conduct sales/demand forecasting and reduce logistics costs due to extras and opportunity costs due to product shortages. To meet these demands, it is necessary to purchase spare parts in order to reduce the cost per inventory, while the demand is being met or an administrative decision is being made.

Machine learning and a data-driven approach are becoming very important in many areas. The scalable learning system uses models and learns models of interest from large data sets. In this paper, we describe MLP AND XGBoost, machine learning technique for the tree boosting. The proposed techniques are supportive of spare parts management in the simplest way that they can be implemented to achieve more accurate results in spare inventory management. The analysis helps to determine how to manage a particular group of parts that represent similar features. The demand for spare originated from maintenance activities and use of this part (known as active installation bases) in combination with component failure behavior and maintenance plans. This forecast is used to manage inventory using the inventory-based policy. The Croston' technique offers precise estimation of the mean level of demand if there is any demand. In this, they compare Croston's and smoothing technique with the bootstrap basis on the uniformity of observed LTD percentiles. This bootstrap technique is more accurate forecasting technique [4].

In this paper, literature review is covered under section II, the proposed approach modules description, Mathematical Modeling, Algorithm and Experimental setup in section III .and at finally concluded in section IV.

II. LITERATURE REVIEW

This chapter focus on the use of machine learning approach in time series forecasting and they consider the three aspects: supervised learning tasks such as validation problems of the single-step predictions, which forecasting approach to use when moving from single step to multi-step prediction and how local learning techniques such as radial basis functions network,k -nearest neighbours method ,etc. deal with data that fluctuates over time.

In this [2], they present the role of supervised machine learning practices in dealing with the forecasting problems. Especially, the role of the local learning approximation is emphasized to cope with important problems in prediction such as error accumulation, nonlinearity, and non-stationary. Constructing an effective predictor is between observations of past and short-term future values, forming historical data, as well as the appropriate strategy for long term vision data. In this [3], they present comparison performance of the different machine learning practices such as NAR, LSTM, ANN and SVM in terms of stepped ahead forecasting error variance and error. The LSTM network gives a slightly worse prediction accuracy with respect to other algorithms. The NAR gives the best accuracy for the short prediction and SVM gives the guaranteed best accuracy. This technique allows performing the forecast processes and training in a parallel manner. They implement efficient training framework and parallel by using power demand traces from the real deployments. Machine learning approach gives less prediction errors in the variance and mean with respect to the ARMA was proved using trial results.In this [4], paper they proposed a bootstrapping system to forecasting delivery of a summation of intermittent demands over the fixed lead time. They combine the values from each of the many inventory items into one and evaluated the accuracy of the overall lead-time demand forecast across all items. The Croston' techniques offer precise estimations of the mean level of demand at moments in case there is a demand. In this, they compare Croston's and smoothing technique with the bootstrap based on the uniformity of observed LTD (Lead Time Demand). This bootstrap technique is more accurate forecasting technique. Hemeimat Raghad, Qatawneh Lina, and Masoud Shadi [5], they proposed a comparison between the five forecasting techniques based on MSE (Mean Squared Error), MAD (Mean Absolute Deviation) and ME (Mean Error) and experimental results showed that the performance for all these techniques. This technique tested on the local paper mill company. Experimental results show that this technique of tracking signal techniques helps companies to better select the ideal forecasting method and minimize forecast errors.

In this paper [6],following types of probabilistic estimation methods are used, threshold-based and percentile-based. The percentile-based rating calculates the frequency of the reference discharge falling below the ensemble percentile. If the combined extent is precise, these frequencies should be consistent with the non-excess percentile probability. The excess probability of great expulsion threshold is overestimated in the prediction, and this overestimation increases with increasing probability level. The contribution to these inaccuracies is similar in the case of spread underestimation but slightly larger in the case of overestimated excess probability.The main objectives of the study are to find out the opportunities and challenges of spare parts management in the durable goods industry through a case-based study conducted by 10 manufacturing companies. Improving capacity helps to better understand current management approaches and methods and its deficiencies, finding the most suitable (though simplistic) improvements, the IT and performance supply chain perspective, and the adoption of integration practices with customers and suppliers, as the last step, will finally come. This visibility also helps to reduce the spare parts management process (each dealer can reduce the stock level of these codes) and the effectiveness (the wait for the end user) [7].Most companies in the automotive spare parts business, it is important to conduct sales/demand forecasting and reduce logistics costs due to surpluses and opportunity costs due to product shortages. To meet these demands, it is necessary to purchase spare parts in order to reduce the cost per inventory, while the demand is being met or an administrative decision is being made. This analysis will be complicated in countries such as Mexico, where fewer companies maintain a good record of their activities, products, and procedures, making it possible at certain moments within the practice. The resulting model of each part is presented first, in order to analyze the results later in the sample and post-sample period[8]. Predicting the demand for spare parts with high accuracy consists of a variety of factors, so a simple predictive model cannot be expected. These include part shipping data, how many products are under operation, and the time since that product was released. In this [9], they proposed a solution on spare parts demand forecasting .It NEC's big data analysis technique called the "Heterogeneous Mixture Learning Analysis Technology".NEC fielding is one of the maintenance businesses based on Know-How and performance of these activities, and appropriate parts management services subcontracted by customers such as manufacturers include endorsements based on demand estimates and cost reduction measures with greater accuracy and high added value. In this paper [10], the demand spare parts are characterized by volatility and fluctuation. It is affected by probabilistic factors, such as the wear behavior, the intensity of the product use, the rate of failure and the type of maintenance. For achieving the competitive advantage of company spare parts strategy aligns with the specific situation of the company. The proposed techniques are supportive for spare parts management is the simplest way that can be implemented to achieve more accurate results in spare inventory management. The analysis helps to determine how to manage a particular group of parts that represent similar features. This decision is how many pieces of stock you have to keep.In this paper [11], they present technology for installed base forecasting of end-of-life spare part demand and formulates research hypotheses on which of four installed base types performs best under which conditions. This technology is illustrated by a case study of

spare parts for six products from appliance manufacturers. The research hypothesis is sustained in the most of cases, and the predictions obtained from the installed base are substantially superior to the simple black-box predictions. The final production decision that supported the past sales stand is a spare part to meet the consumption demand in the future.

III.FORMULATION OF PROPOSED MODEL

A. Proposed System Overview

Spare parts database is considered for forecasting which has features such as unit name, unit NSN, operation date, unit of issue, unit exhausted, consumption number, worker number, worker name, etc. Clusters are formed according to the features extracted. Data mining techniques such as SVM, Random Forest, Linear Regression , MLP and XGBoost are applied on the existing dataset[1] and are compared with the new dataset (Table II) with additional features like unit of issue, unit exhausted ,unit remaining, per unit cost, country budget, total cost of unit, units needed to order. Both these datasets are compared to find out if the additional features give any different prediction in terms of accuracy. When these were compared ,the dataset with additional feature gave higher accuracy .

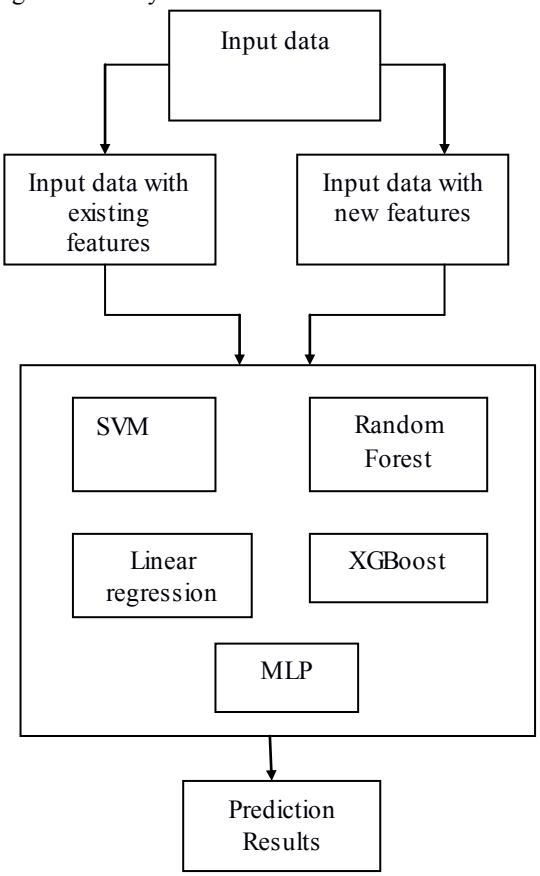

Fig 1 : Proposed System Architecture

- Read input Data:

In this module, it read spare parts data from existing data as well as new data. This data set contains the structured data of anti-aircraft missile.

- Data Mining:

Data mining is the processes which can identify knowledge by modeling, exploring, and analyzing the beneficial information and associations in large-scale data by using classifiers.

- Prediction Results:

Finally, it will predict accurate demand forecast of spare part of aircraft and missiles using XGBoost algorithm.

B. Algorithm

1) XGBoost:

XGBoost is the Extreme Gradient Boosting technique which helps in regularization by avoiding overfitting.It computes optimized results in less amount of time by using less computational resources.

- **Algorithm : XGBoost Model**

i. An initial model F0 is defined to predict the target variable Y. This model will be associated with a residual (Y – F0)

ii. A new model h1 is fit to the residuals from the previous step.

iii. Now, F0 and h1 are combined to give F1, the boosted version of F0. The mean squared error from F1 will be lower than that from F0:

$$F_1(x) < -F_0(x) + h_1(x)$$

iv. To improve the performance of F1, we could model after the residuals of F1 and create a new model F2:

$$F_2(x) < -F_1(x) + h_2(x)$$

v. This can be done for 'm' iterations, until residuals have been minimized as much as possible:

$$F_m(x) < -F_{m-1}(x) + h_m(x)$$

C. Mathematical Model:

S = {I, O, P};
I = Input;
O = Output;
P = Process;

- Process P1

P1 = {I};

- Process 2
  P2 = {P1};
- Process P3
  Perform logistic regression in term of
  $P(T = 1|B) = \Lambda(B^t B)$
  $Where;$
  $T \rightarrow Binary\ random\ variable\ T = m + 1$
  $B \rightarrow Random\ Prediction\ Variable$
  $B = (B_0, B_1, \ldots\ldots\ldots B_m)$
- Process P4
  Perform XGBoost
  $F_m(x) = F_{m-1}(x) + \gamma_m h_m(x)$
  Where,
  $F_m \rightarrow Multiplications\ Factors$
  $h_m \rightarrow Mean\ residual$

- Process P5
  Perform MLP
  $w = w_{old} + \eta\ dx$
  $$O_j = f\left(\sum_i w_{i,j}.x_i\right)$$
  $$y_k = f\left(\sum_i w_{i,j}.O_j\right)$$
  Where;
  $Y_k \rightarrow Output\ layer$
  $O_j \rightarrow hidden\ layer$
  $X_i \rightarrow Input\ layer$

- Process P6
  Perform XGBoost
  $$\frac{\partial\left(y, f^{(m-1)}(x) + f_m(x)\right)}{\partial f_m(x)}$$
  for each x in the dataset.

D. Dataset

We applied various Machine Learning algorithms on Vietnam War Bombing Operations dataset along with some features from [1].In total, we used over 10,000 missiles data. More fields were available ,since these were not relevant for the statistical analysis those were ignored. The features included here are : Aircraft name, aircraft spare parts, aircraft type,unit NSN,Unit series number,Operation date,Spare parts NSN, QPA (Quantity per Assembly Unit),Unit of issue, Unit exhausted, Unit remaining, Country flying mission, Acquisition year, Maintenance year, Procurement Lead Time, Order Shipping Time,etc. This helps to decide when to order,re-order or no order of spare parts.Table 1 describes about the dataset and the features used for forecasting.

IV. RESULTS AND DISCUSSION

A. Experimental Setup

Hardware and software of proposed system given below:

- Software Technology:
  1. Technology: Core Python
  2. Tools: Jet- JetBrains, PyCharm
  3. Operating System: Windows 7
- Hardware Technology
  1. Processor: 1.0 GHz
  2. RAM: 1 GB
  3. Hard Disk: 730 GB

B. Expected Result

Machine learning and Neural Network approach was applied on 10000 observations. The features used in predictive modeling influence the results. The better the features that you prepare and choose, the better the results you will achieve. The main aim of this research is to compare the features which proved to be more useful in predicting the spare parts in minimum amount of time with higher accuracy. In general, Machine learning algorithm learns from its sample data. Feature selection selects only the useful subset of data. This means removing irrelevant data. Experimental results (Table I) show that the added new features such as Unit remaining, Per unit cost of spare part, country budget, total cost of a unit, units needed to order proved to contribute to higher accuracy but it leads to over fitting of data. Here we are trying to improve spare parts utilization rate by maintaining the budget .So including such features obviously helps for better performance. Table I shows the accuracy comparison between existing system and the proposed system. As we can observe from Table I, XGBoost and MLP gives the highest accuracy both in existing system and new proposed model meaning that our model is accurate for most of the times.To evaluate the model we need to understand how good the predictions are[14]. For this we need to understand these basic terminologies:

Accuracy - Accuracy is the most intuitive performance measure and it is simply a ratio of correctly predicted observation to the total observations.[14]

Precision - Precision is the ratio of correctly predicted positive observations to the total predicted positive observations.[14]

Recall (Sensitivity) - Recall is the ratio of correctly predicted positive observations to the all observations in actual class – yes.[14]

F1 score - F1 Score is the weighted average of Precision and Recall. [14]

Table I: Comparison of accuracy for Existing Features and New Features

Algorithms	Accuracy with existing features	Accuracy with new features
SVM	76	93
Random Forest	85	93
Logistic Regression	79	90
Decision Tree	83	90
MLP	93	97
XGBoost	87	98

Table I shows the accuracy comparison between existing system and the proposed sytem with newly added features. Differences in accuracy with existing and new dataset can be contributed to the relevant features and the algorithms applied. SVM, Random Forest, Logistic Regression, Decision Tree have some drawbacks which gives lesser accuracy.For example, a small change in dataset leads to very high changes in model.If the features are correlated it does not reduce variance. Also, Random Forests is not preferred due to its complexity.They are much harder and time-consuming than other algorithms. Gradient boosted decision trees are among the best off-the-shelf supervised learning methods available. Achieving excellent accuracy with only modest memory and runtime requirements to perform prediction, once the model has been trained. Like other decision tree based learning methods, there is no need to apply feature scaling for the algorithm to do well. These are some of the reasons that XGBoost and MLP performed exceptionally well.

The increased accuracy can be contributed to the concept of Economic Order Quantity.Whenever the concept of inventory management comes two factors need to be considered-i) demand to be fullfilled immediately ii) demand to be fullfilled in minimum time in provided budget.So keeping in mind these two factors we contributed this in our novel system.

Table II: Feature Description Table

Aircraft Name	Spare Parts	Unit NSN	Unit Series No	Operation Date	Spare Part NSN	Unit Of Issue	Unit Exhausted	Unit Remaining	Consumption Number
Douglas A-1 Skyraider	Part Shipments	A1111	2000A1	20130228	A12345	69	20	49	1
Douglas A-26 Invader	Golf Parts	B1111	2000B1	20130412	B12345	132	56	76	1
•	•	•	•	•	•	•	•	•	•
•	•	•	•	•	•	•	•	•	•
•	•	•	•	•	•	•	•	•	•
Grumman F-9 Cougar	Water Heater Parts	Z1111	2000Z1	20250412	Z12345	82	17	65	1

Worker Name	Recoverability Code	Organic Code	Representative Code	QPA (Quantity per Assembly Unit)	Unit Standard	Newest Unit	PRO-LT (Procurement Lead Time)	OST (Order Shipping Time)	Acquisition Year	Maintenance Year
Hong Gil Dong	Y	N	Y	1	2000 (Won)	2500 (Won)	250 Days	5 Days	2000	2013
Kim Cheol Soo	Y	N	Y	2	5000 (Won)	6000 (Won)	200 Days	10 Days	2000	2013
•	•	•	•	•	•	•	•	•	•	•
•	•	•	•	•	•	•	•	•	•	•
•	•	•	•	•	•	•	•	•	•	•
Clement Freud	Y	N	Y	26	5000 (Won)	6000 (Won)	1000 Days	130 Days	2000	2013

Per Unit Cost	Country Budget	Total cost of a unit	No of units in the company warehouse	Units Needed to Order
10000	15000	10000	20	1
20000	60000	0	20	0

• • •	• • •	• • •	• • •	• • •
4990000	235666666.7	54890000	14451	11

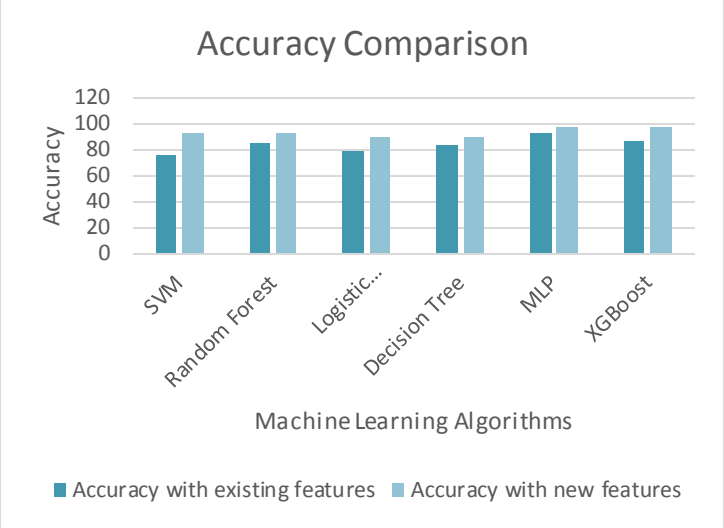

Fig 3: Model accuracy for ML classifiers

IV. CONCLUSION AND FUTURE SCOPE

Developing a precise forecasting model for requesting of spare parts enables the inventory to take necessary actions i.e it can prevent stoppage of spare parts production.Since many decades time series forecasting has been a popular method. But by taking into consideration the drawbacks of each of these methods we continued our research on developing such a model which will improve its accuracy. In this work, we put forward a new prototype for demand forecasting of spare parts of anti-aircraft missiles using Machine Learning approaches and Neural Networks. We compared our new model with that of the existing one which did not take into consideration the country's budget.So we included the concept of Economic Order Quantity (EOQ) which suggested to order optimal number of product units to order.It also helps to re order products in case there is a need to plaace some more orders.The results suggested the dominance of XGBoost and MLP over other classifiers.

Additionally,the analysis on performance results by adding new relevant features improved the accuracy of SVM by 17%,Random Forest by 8%,Logistic Regression by 11%,Decision Tree by 7%,MLP by 4% ,XGBoost by 11%.Thus,it proves that XGBoost proved to be a likely classifer for coorect estimation.

Finally, here we have considered only structured data.Further if unstructured data is considered some new method need to be applied for its prediction. We can also consider geographical conditions in further work.

REFERENCES

[1] Jaedong Kim, Hanjun Lee, Soobin Choi, "Machine Learning Based Approach for Demand Forecasting Anti-aircraft Missiles", 2018.
[2] Gianluca Bontempi, Souhaib Taieb and Yann Borgne, "Machine learning strategies for time series Forecasting"; Chapter in Lecture Notes in Business Information Processing, Springer, [2014].
[3] Bonetto Riccardo and Rossi Michele, "Machine learning approaches to energy consumption forecasting in households"; arxiv: 1706.09648v1 [cs.ne], [2017].
[4] Willemain Thomas, Smart Charles, and Schwarz Henry, "A new approach to forecasting intermittent demand for service part inventories"; International Journal of Forecasting, Elsevier, [2003].
[5] Hemeimat Raghad, Qatawneh Lina, and Masoud Shadi, "Forecasting spare parts demand using statistical analysis"; American journal of operations research, [2016].
[6] Olsson Jonas, and Goran Lindstrom, "evaluation and calibration of operational hydrological ensemble forecasts in sweden"; Journal of Hydrology, Elsevier, [2008].
[7] Bacchetti Andrea, "Challenges and opportunities in managing spare parts for durable goods: an empirical study"; International Annual euroma Conference, [2010].
[8] Vargas Gonzalez, and Cortes Elizondo, "Automobile spare-parts forecasting: a c omparative study of time series methods"; International Journal of Automotive and Mechanical Engineering, Vol.14, [2017].
[9] Noriaki Otsuka, Nishina Mitsuki and Katsunori Higashihara, "Demand forecasting solution contributing to components inventory repair optimization"; Special Issue on Enterprise Solutions to Support a Safe, Secure and Comfortable Life, NEC`s Technical Journal, [2015].
[10] Natalia Kalinowska, "Spare parts categorization in stock management"; Research in Logistic and Production, [2017].
[11] Young Thai, Dekker Rommert, and Heij Christiaan, "Spare part demand forecasting for consumer goods using installed base information"; Erasmus University Rotterdam, [2016].
[12] Thomas R.Willemain, Charles N.Smart,Henry F.Schwarz ,"A new approach to forecasting intermittent demand for service part inventories",Elsevier, 2004.
[13] Zakaria Alameer, Mohamed Abd Elaziz , Ahmed A. Ewees , Haiwang Ye , Zhang Jianhua," Forecasting goldprice fluctuations using improved multilayer perceptron neural network and whale optimization algorithm",Elsevier,2019.
[14] https://blog.exsilio.com/all/accuracy-precision-recall-f1-score-interpretation-of-performance-measures/
[15] Sarah Van der Auweraer, Robert Boute, "Forecasting spare part demand using service maintenance information" , International Journal of Production Economics,2019.
[16] Laura Turrini, Joern Meissner, "Spare parts inventory management: New evidence from distribution fitting",Elsevier,2019
[17] Nikita Pawar,Bhavana Tiple, "Demand Forecasting of Anti-Aircraft Missiles Using Ensemble Techniques.",2019.
[18] A.Regattieria, M.Gamberia , R.Gamberinib , R.Manzinia,"Managing lumpy demand for aircraft spare parts", Elsevier,2004
[19] A.A.Ghobbar, ,C.H Friend ,"Sources of intermittent demand for aircraft spare parts within airline operations", Elsevier, 2002

Proceedings of the Fourth International Conference on Communication and Electronics Systems (ICCES 2019)
IEEE Conference Record # 45898; IEEE Xplore ISBN: 978-1-7281-1261-9

Classification of tumors in brain MRI images with hybrid of global and local DWT features using SVM

Sanjay Kumar C K
Assistant Professor, Department of MCA,
The National Institute of Engineering,
Mysore, India
sanjaykumarck@nie.ac.in

Dr. H. D. Phaneendra
Professor & Head, Department of CS & E,
The National Institute of Engineering,
Mysore, India
hdphanee@nie.ac.in

***Abstract* - Automated brain tumor identification and classification is still an open problem for research in the medical image processing domain. Brain tumor is a bunch of unwanted cells that develop in the brain. This growth of a tumor takes up space within skull and affects the normal functioning of brain. Automated segmentation and detection of brain tumors are important in MRI scan analysis as it provides information about neural architecture of brain and also about abnormal tissues that are extremely necessary to identify appropriate surgical plan. Automating this process is a challenging task as tumor tissues show high diversity in appearance with different patients and also in many cases they tend to appear very similar to the normal tissues. Effective extraction of features that represent the tumor in brain image is the key for better classification. In this paper, we propose a hybrid feature extraction process. In this process, we combine the local and global features of the brain MRI using first by Discrete Wavelet Transformation and then using texture based statistical features by computing Gray Level Co-occurrence Matrix. The extracted combined features are modeled by Support Vector Machine with different kernel functions like Linear, quadratic and RBF for classification of brain tumors in to benign or malignant class.**

Keywords— Brain Tumor, MRI, Segmentation, DWT, GLCM, SVM, RBF

I. INTRODUCTION

Brain tumor is an unwanted collection of cancerous cells that develop in the brain beyond the natural cell cycle. These tumors may be benevolent, usually termed as benign, or malevolent, referred to as malignant. The benign tumors contain non-active cancer cells and many a times have uniform structures where as malignant tumors contain active cancer cells that may stretch to other body parts. Also, the malignant tumors mostly have non-uniform structures. Magnetic Resonance imaging is a non radio-active imaging technique used for study of internal organs to envisage high resolution images of the internal body parts, their structure and functions. With MRI doctors can visualize both surface and deep structures with a high degree of anatomical details and they can detect the occurrence of minute changes in these structures. Early and accurate detection of tumors increases the chances of better planning of treatment and hence better chances of survival of the patient. Automating this process is a challenge as tumors tend to develop in diverse shape, size and position and in some cases they exhibit appearance similar to the normal tissues.

Medical Image Analysis involves processing of image at various stages. First, the **Pre-processing** is done to enhance the image quality where we remove the noise components, boost the image intensity and prepare the image for further processing [2]. In **Segmentation** stage the specific region of interest in the image is identified through one or combination of many intelligent methods [3] to obtain determinant characteristics of tumors from medical images. Following are some of the applications of image segmentation: to locate tumors, to measure tissue volumes, image simplification, classification and recognition of region of interest. **Feature selection** is the general term to represent the methods used for constructing the combination of variables that describe the data effectively [4]. It is the technique of obtaining a subset of highly relevant variables by eliminating irrelevant and redundant variables to build appropriate learning models. Accurate tumor classification is possible with more accurate feature selection techniques. **Classification** is a phase of analysis where we compute the numerical properties of given image features so that the image can be placed into one of the many categories. Classification is achieved by employing two processing phases: first, the training phase and then, the testing phase. In training phase, unique descriptions of each category of classification are obtained using the labeled training samples. In testing phase using an appropriate feature space boundary we classify the unique descriptions of the test image [5].

In this paper we propose an automated method for tumor classification with two class labels namely benign and malignant. We propose a hybrid feature extraction method to get the better representation of image samples by combining local and global wavelet coefficients obtained from DWT and texture based statistical features obtained by computing GLCM. This approach is motivated by the fact that both the local and global features are experimentally found to be uncorrelated and hence upon combining can give enhanced statistical details. This paper is organized into 5 sections. In section II we have summarized related works by various researchers in the field of brain image tumor classification. Section III gives the details of proposed work. The outcomes of the proposed work and evaluation with other benchmarks are discussed in Section IV. Section V has concluding remarks and discusses future enhancement options for this work.

II. Related Work

Many articles have been published by the researchers in the recent years on methods for classification of tumors from MRI images.

Ayush Arora et al [6] suggested a method where the image was segmented using the popular segmentation techniques like thresholding followed by morphological operations. The features ware extracted from the segmented image using DWT. Using principal component analysis the high dimensional features features were reduced to computationally convenient lower dimension without losing much of the classification information. Then, k-NN classification was used to decide if the tumor is benevolent or malevolent.

A scheme for brain tumor identification and further classification from MRI images by probabilistic neural network is suggested by Shree and Kumar [4]. They have used DWT to decompose the images into horizontal, vertical and diagonal components followed by textural image features extraction by computing GLCM. PNN classifier was used for the categorization of tumors.

Another approach for brain tumor classification is suggested by Rathi and Palani [3]. They have extracted shape, intensity and texture features from the normalized images. Prominent features were selected using LDA. SVM was used to classify the tumors.

Adhi Lakshmi et al [7] suggested techniques for tumor analysis. In this method image pre-processing was done with Distribution based Adaptive Mean Filtering and Adaptive Threshold based Edge Detection. Segmentation was achieved by using connected component analysis with Cellular Automata and Multi-angle Cellular Automata. The most representing features were obtained using a method called Dynamic Angle Projection Pattern. Those features optimized with Cockoo Search Optimization and such selected features were passed to SVM with Pointing Kernel Classifier.

A comparative analysis of various feature extraction algorithms is published by El-Gayer et al [8]. They have compared the performances of FAST, SIFT, PCA-SIFT, F-SIFT and SURF algorithms with respect to scaling, rotation, illumination change and other transformations.

Image processing techniques for brain tumor analysis is published by Hemanth and Anitha [2] where they have conducted a survey of many techniques for pre-processing, feature extraction, classification. They have proposed a method where pre-processing was done with connected component analysis. Eight textural features namely Correlation, Contrast, Entropy, Variance, Angular Second Moment (A measure of Uniformity), Skewness (A measure of symmetry), Inverse Difference Moment (A measure of homogeneity) and Kurtosis (A Measure of data distribution) are extracted and these features were used for classification.

Stationary Wavelet Transformation (SWT) which has superior wavelet coefficients as compared to DWT in terms of translation invariant property is proposed by Zhang et al [9]. Those features were reduced with PCA and Fisher Discriminant Analysis (FDA) was used to categorize brain into benevolent or malevolent.

Daljit Singh and Kamaljeet Kaur [5] have observed that GLCM features and classified using SVM with any of the RBF, Linear and Quadratic kernel functions will also yield better classification. They have compared GLCM with PCA for feature extraction.

GLCM features were extracted from the fuzzy clustering based segmented images is proposed by B. Thamaraichelvi and G. Yamuna [10]. Entropy, Correlation, Energy, Contrast, Mean, Standard Deviation and variance features were extracted. SVM with RBF kernel was used to classify brain tumors with an accuracy of 98%.

Using deep learning methods a survey on segmentation of MRI-based brain tumors is published by Işın et al [11]. They have effectively highlighted the challenges in manual, semi-automatic and fully automatic segmentation methods.

III. Proposed Methodology

From the literature Survey we conclude that accurate brain diagnosis can be done by developing more effective and accurate techniques in feature extraction and classification. Literature survey motivated us to look into methods for extracting more meaningful features from the MR Images. In this work, we propose a method for extracting the features as shown in figure 1. First, the image samples are prepared for segmentation. This pre-processing and segmentation stages are described in sections A and B respectively. We extract the local features from the segmented image and global features from the fused images. The details are discussed in sections C, D and E. We were motivated to use a hybrid of local and global features of the image, after closely examining the local and global image features. We found that both the features are not correlated. Hence we hypothesize that use of hybrid features can give better description of the area of interest. These feature vectors obtained from DWT were reduced using PCA and further by computing GLCM, 13 statistical features were computed from them namely, Energy, Contrast, Mean, Correlation, Standard Deviation, Homogeneity, RMS, Entropy, Skewness, Inverse Difference Movement (IDM), Variance, Kurtosis and Smoothness. Using these statistical features the SVM classifier was modeled. The classifier efficiency was tested and compared with Linear, quadratic and RBF kernels functions.

A. Preprocessing

Brain MRI Image data set is obtained from the online repository of IMAGE & DATA ARCHIVE (IDA), University of Southern California [1]. The dataset contains RGB MRI FLAIR image slices with matrix size of 256 x 256, all with axial perspective. Results of various pre-processing stages are shown in figure 2. The images are first converted to gray scale and then enhanced by median filter (Figure 2a).

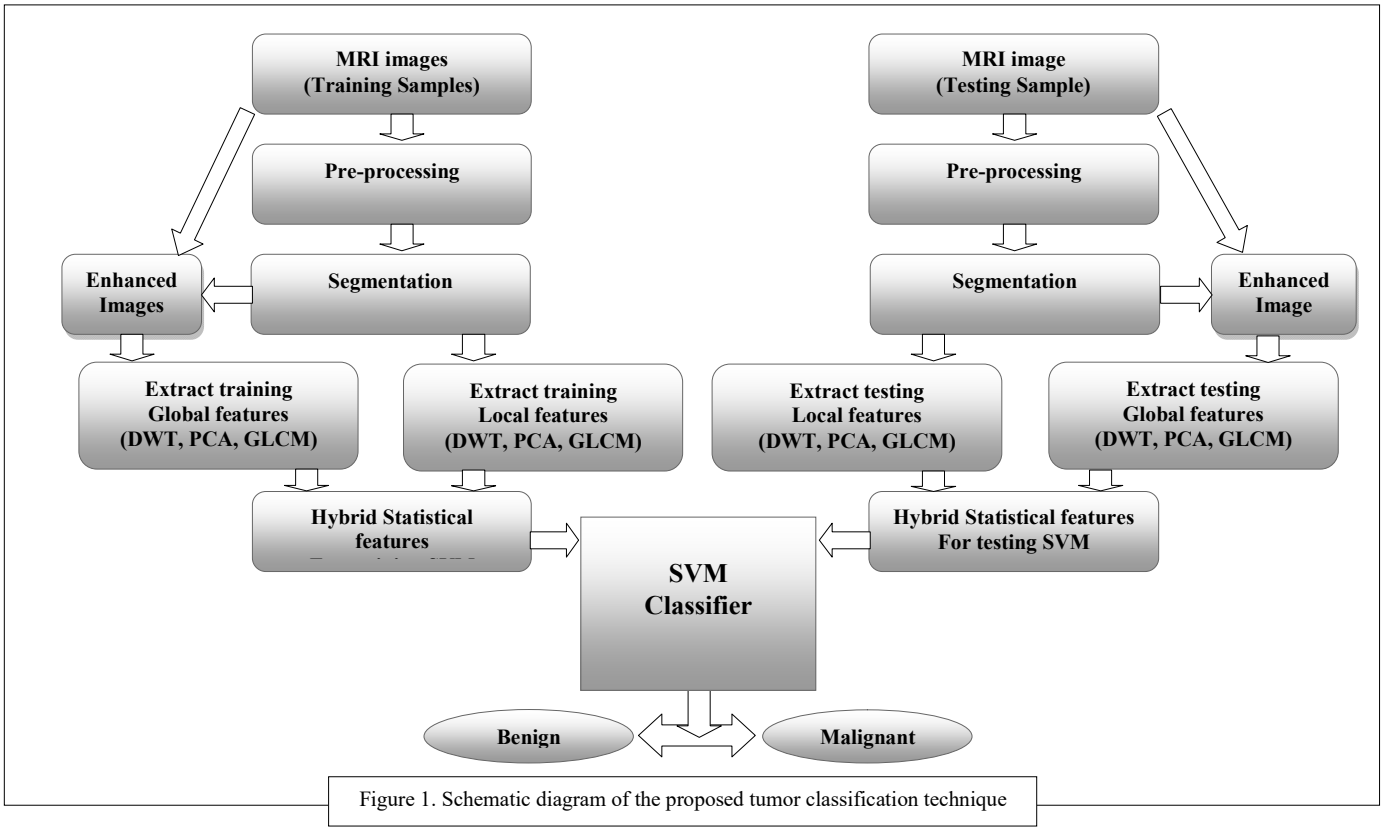

Figure 1. Schematic diagram of the proposed tumor classification technique

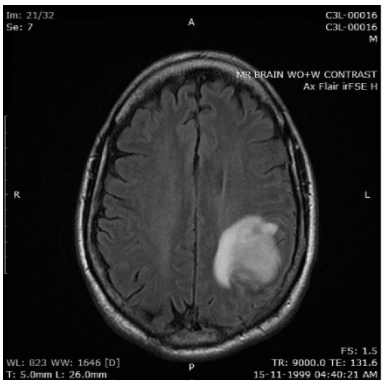

Figure 2 a) Color to Gray Conversion and Enhancement with median filter

2b) Dynamic Thresholding

2c) After flood Fill

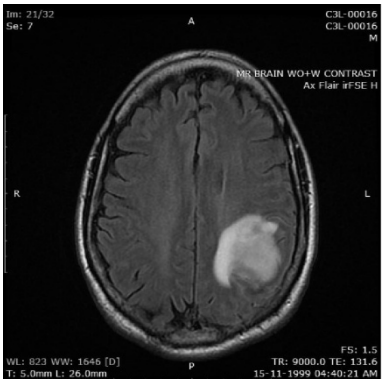

Figure 3a) Original Image

3b) Segmented Image

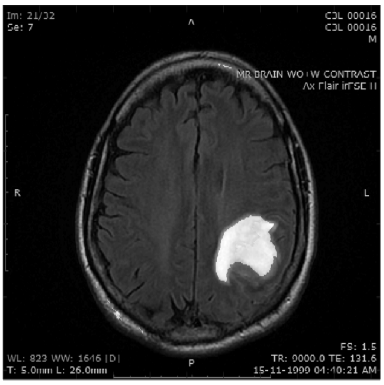

3c) Masked Image

B. Segmentation

The emphasis was on the removal of skull tissues and text in the MRI. Image was segmented using a Dynamic thresholding technique (Figure 2b) along with suitable morphological operations to filter out those undesired pixels (Figure 2c). Filling and Erosion are the two main morphological operations that are performed on binarized image to highlight the area of interest and generate the mask as shown in figure 3b. The original image is fused with the segmented image to get the masked image as shown in Figure 3c.

C. Discrete Wavelet Transformation

MRI image is decomposed using discrete wavelet transform with four sub regions. These regions are called approximate component region and three high-frequency regions, namely horizontal component, vertical component, and diagonal component. Theoretically the approximate component region is obtained by using two successive low-pass filters. The horizontal component is obtained by a pair of high-pass and low-pass filter. The vertical component is filtered using a pair of low-pass and high-pass filter. The diagonal component is created by two successive high-pass filters.

Subsequent levels of decomposition follow the same procedure by decomposing the approximate component sub image of the previous level. 2D discrete wavelet transform was applied with the three-level wavelet decomposition. Here it is important to determine the most suitable decomposition level. With the increase in number of levels more detailed information will emerge. At the same time this will affect the classification model stability and hence reduce the computing efficiency. By trial and error method we have found that at third level all but particularly the diagonal component information is maximized and hence we have taken three levels of Haar wavelet decomposition. 30 MRI images are used to extract the features as training samples with 10 of them belonging to benign class and 20 belonging to malignant class. The masked images (as shown in Figure 3c) are used to compute DWT coefficient vectors of all the four components.

30 MRI images are used to extract the features as training samples with 10 of them belonging to benign class and 20 belonging to malignant class. The masked images (as shown in Figure 3c) are used to compute DWT coefficient vectors of all the four components.

These global features are the input for PCA for further feature reduction. Output of such an image sample is shown in figure 4a. The segmented images (shown in Figure 3b) are used to compute DWT coefficient vectors which are the local features. DWT coefficients of segmented image sample are shown in figure 4b.

D. PCA and GLCM

For feature dimensionality reduction PCA is one of the most commonly used technique. PCA technique preserves the variance of the given input data and finds the linear lower-dimensional closest representation of that data by using orthogonal transformations. It transforms a large set of correlated points into set of principal components.

This reduced feature set of all the components are used to compute GLCM. GLCM is a statistical procedure to tabulate how often different combinations of pixel intensity levels co-occur in an image. Every element in the ith row and j^{th} column of the GLCM is an indicator of how many times a pixel with a specific intensity i occurs in relation with other pixel with

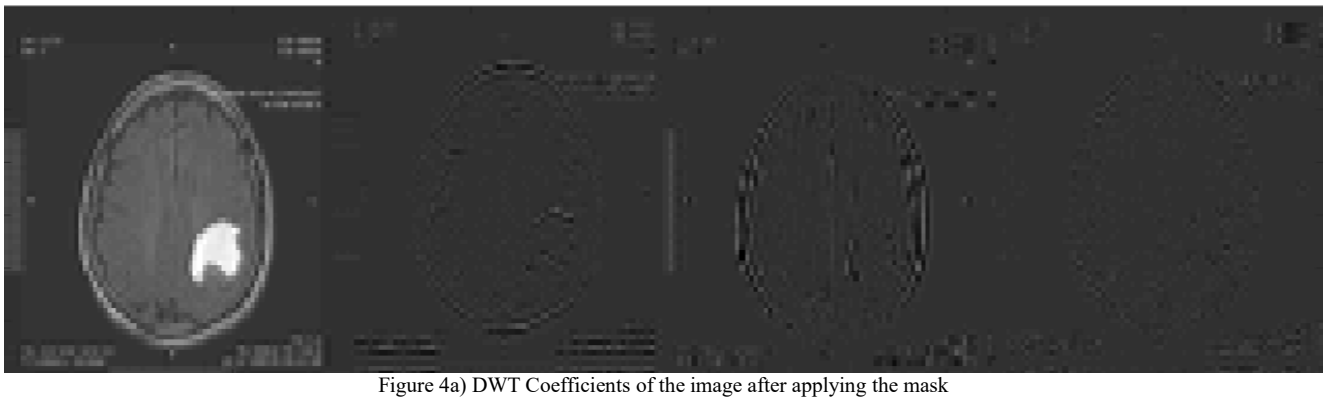

Figure 4a) DWT Coefficients of the image after applying the mask

Figure 4b) DWT Coefficients of the segmented Image

intensity *j*. Two GLCMs are computed, one for local DWT coefficients and the other one for global DWT coefficients.

E. Statistical features

13 statistical features [12] namely Inverse Difference Movement, Skewness, Kurtosis, Smoothness, Variance, RMS, Entropy, Standard Deviation, Mean, Homogeneity, Energy, Correlation and Contrast are computed from both local and global GLCM. A set of 26 features extracted using DWT followed by PCA and GLCM from the sample image is as shown in the following table.

Features	Segmented Image	Fused Image
Contrast	36.54664	98.03584
Correlation	0.84167	0.85767
Energy	0.90735	0.12737
Homogeneity	0.96503	0.60031
Mean	3.87178	31.37863
Standard Deviation	61.48974	108.52944
Entropy	0.39561	2.44954
Root Mean Square level (RMS)	15.74675	62.69145
Variance	3400.14272	6370.37139
Smoothness	0.99998	0.99999
Kurtosis	259.18122	41.06553
Skewness	15.59871	5.03187
Inverse Difference Movement (IDM)	19132.42966	47963.94913

F. Support Vector Machine

SVM is basically a two class linear classifier model built upon numerical learning theory. The idea behind SVM is to build a decision boundary such that the margin of separation between support vectors of both the classes (positive and negative) is maximized. This decision boundary is a hyperplane in high dimensional feature space. This can be represented by $\boldsymbol{w}\ \mathbf{x} + \mathbf{b} = \mathbf{0}$ where w is the weight vector normal to the hyperplane and b is the bias. The training data can be described by

$(\boldsymbol{w_i}\ \mathbf{x} + \mathbf{b}) \geq \mathbf{1}$ for all y_i = Positive Class and

$(\boldsymbol{w_i}\ \mathbf{x} + \mathbf{b}) \leq \mathbf{1}$ for all y_i = Negative Class

Support vectors are basically the planes as shown in figure 5 where: $(\boldsymbol{w_i}\ \mathbf{x} + \mathbf{b}) = +\mathbf{1}$ for hyperplane 1

and $(\boldsymbol{w_i}\ \mathbf{x} + \mathbf{b}) = -\mathbf{1}$ for hyperplane 2

During learning the hyperplane the placement of hyperplane is determined by all training samples with an object of maximizing the distance between hyperplane 1 and hyperplane 2. All samples that are at the distance of the margin are called support vectors. When a new sample is used with unknown class label the value of $(\boldsymbol{w}\ \mathbf{x} + \mathbf{b})$ decides the class of the test sample. Usually along with many other parameters a tuning parameter C is used to define the amount of allowed violation of the margin. Larger the value of C more relaxation is allowed for the model to fit the data.

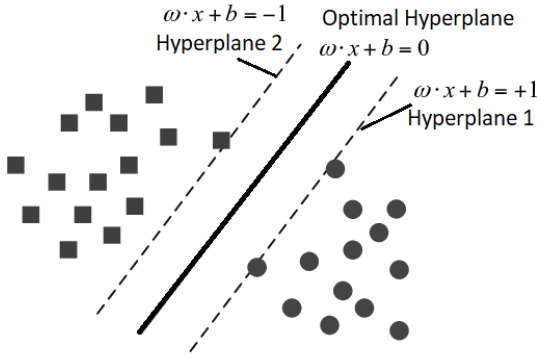

Figure 5. Hyperplanes and Support vectors in SVM

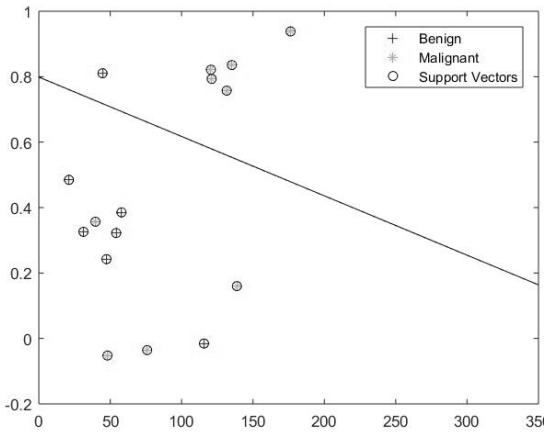

Figure 6a) Trained SVM with Linear Decision Boundary

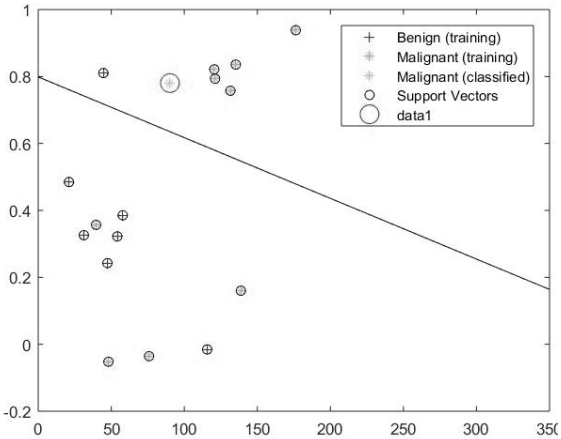

6b) Result of testing new test image where SVM has classified the test sample correctly as Malignant

In this paper we have used linear Support vector where the decision boundary is linear. The SVM training scatter map is shown in Figure 6a with a linear decision boundary. A test sample is being tested in Figure 5b. The test sample as shown in 6b above the linear boundary with bigger circle is classified correctly as malignant.

IV. Result Analysis

Along with the above linear decision boundary model we have also modeled SVM with RBF and Quadratic kernel function to map linear data to nonlinear feature space and the decision boundaries will then be nonlinear. The kernel functions are used to project the data on to the higher dimensional feature space and at this space the data points become linearly separable. The proposed method is yielding acceptable results with linear, RBF and polynomial kernel functions. Polynomial kernel with degrees 2, 3, and 4 are used and best result was found with degree 2 as shown in the below result table.

The performance measure, Accuracy is computed as the probability of correctly classifying the samples. We compute accuracy as:

$$\text{Accurcy} = \frac{TP + TN}{TP + TN + FP + FN}$$

Where TP is True Positive, the number of correctly classified benign tumors; TN is True Negative, the number of correctly classified malignant tumors; FP is False Positive, the number of incorrectly classified benign tumors and FN is False Negative, the number of incorrectly classified malignant tumors. The experimental results are tabulated as follows:

Kernel Function	Feature extraction Method	Accuracy (Rounded)
Linear	GLCM	92%
	DWT	68%
	Proposed Method	**94%**
Quadratic	GLCM	62%
	DWT	73%
	Proposed Method	**89%**
RBF	GLCM	86%
	DWT	93%
	Proposed Method	**95%**
Polinomial	GLCM	92%
	DWT	68%
	Proposed Method	**94%**

V. Conclusion

In this paper we have shown implementation of our proposed method, a hybrid of local and global feature selection with statistical features extracted from the Brain MR Images. They were reduced using PCA and GLCM was computed. Those local and global features were combined to form a set of 26 features are used to train the SVM model. After successful implementation of this model we have tested the model with test image samples and found that this method is having a maximum accuracy of 95% as listed above. There may be many possibilities to improvise this method in future. Different feature selection techniques may also be employed to obtain the hybrid feature set and investigate for even better accuracy over larger datasets. This method can also be employed in analysis of other disease MRI for the purpose of diagnosis.

Acknowledgment

I wish to pay my sincere gratitude to Dr. Narasimha Kaulgod, Professor, Department of E & C, NIE, Mysuru, who has reviewed and suggested modifications. I also thank Dr. A. D. Kulakarni, Professor (Rtd), Department of E & E, NIE, Mysuru, for his continuous motivation.

References

[1] LONI IDA, “LONI Image and Data Archive.” .
[2] D. J. Hemanth and J. Anitha, “Image pre-processing and feature extraction techniques for magnetic resonance brain image analysis,” presented at the International Conference on Future Generation Communication and Networking, 2012, pp. 349–356.
[3] V. P. Gladis Pushpa Rathi, “A Novel Approach for Feature Extraction and Selection on MRI Images for Brain Tumor Classification,” in Computer Science & Information Technology (CS & IT), 2012, pp. 225–234.
[4] N. V. Shree and T. Kumar, “Identification and classification of brain tumor MRI images with feature extraction using DWT and probabilistic neural network,” Brain Inform., vol. 5, no. 1, pp. 23–30, 2018.
[5] D. Singh and K. Kaur, “Classification of abnormalities in brain MRI images using GLCM, PCA and SVM,” Int. J. Eng. Adv. Technol. IJEAT, vol. 1, no. 6, pp. 243–248, 2012.
[6] A. Arora, “k-NN Based Classification of Brain MRI Images using DWT and PCA to Detect Different Types of Brain Tumour,” p. 6, 2017.
[7] A. Lakshmi, T. Arivoli, and M. P. Rajasekaran, “A Novel M-ACA-Based Tumor Segmentation and DAPP Feature Extraction with PPCSO-PKC-Based MRI Classification,” Arab. J. Sci. Eng., vol. 43, no. 12, pp. 7095–7111, 2018.
[8] M. M. El-gayar, H. Soliman, and N. meky, “A comparative study of image low level feature extraction algorithms,” Egypt. Inform. J., vol. 14, no. 2, pp. 175–181, Jul. 2013.
[9] Y. Zhang, S. Wang, Y. Huo, L. Wu, and A. Liu, “Feature extraction of brain MRI by stationary wavelet transform and its applications,” J. Biol. Syst., vol. 18, no. spec01, pp. 115–132, 2010.
[10] B. Thamaraichelvi and G. Yamuna, “GRAY LEVEL CO-OCCURRENCE MATRIX FEATURES BASED CLASSIFICATION OF TUMOR IN MEDICAL IMAGES,” vol. 11, no. 19, p. 12, 2016.
[11] A. Işın, C. Direkoğlu, and M. Şah, “Review of MRI-based brain tumor image segmentation using deep learning methods,” Procedia Comput. Sci., vol. 102, pp. 317–324, 2016.
[12] Namita Aggarwal and R.K. Aggarwal, “First and Second Order Statistics Features for Classification of Magnetic Resonance Brain Images,” J. Signal Inf. Process. 2012 3 146-153.

Proceedings of the Fourth International Conference on Communication and Electronics Systems (ICCES 2019)
IEEE Conference Record # 45898; IEEE Xplore ISBN: 978-1-7281-1261-9

Secure and efficient Session Initiation Protocol authentication scheme for VoIP Communications

Dr. Brij B Gupta,
Dept. of Computer Engineering,
NIT Kurukshetra,
Haryana, India.
gupta.brij@gmail.com

Varun Prajapati,
Dept. of Computer Engineering,
NIT Kurukshetra,
Haryana, India.
prajapativarun570@gmail.com

***Abstract*—Session Initiation Protocol (SIP) is widely used in Voice-over-IP (VoIP) communication to initiate communication between user and server. SIP authentication mechanism was found insecure against various attacks because of its inherent open text architecture. We analyzed different models for SIP authentication and noted their vulnerability against various attacks. Major identified weakness was lack of mutual authentication in various schemes. In this paper, we provide a new authentication model for SIP communication for secure communication establishment. We use AVISPA tool for formal security evaluation of our model. We then prove how our model can resist against various known attacks and provide mutual authentication. Our model is relatively more efficient as we use symmetric key cryptography with ECC instead of asymmetric key cryptography.**

Keywords: VoIP, SIP, AVISPA, mutual authentication, user anonymity, security.

I. INTRODUCTION

We rely mostly on internet and wireless technologies to accomplish various tasks in our daily life. Different architectures, models and applications are developed which are based on these technologies that require a secure user authentication mechanism to validate identity of user and server. As a result multiple authentication schemes were proposed [1], [2], [3], [4], [5], [6], [7] . SIP is a widely used protocol for internet services which is used for authentication [8], [9], [10]. The Internet Engineering Task Force (IETF) designed SIP in 1996. Main role of SIP is to establish, modify and terminate communication between two or more communicating parties. SIP is essential for most of VoIP communications. But SIP was found vulnerable and could easily be hacked [11] .

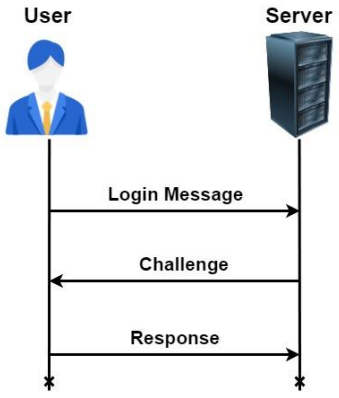

Fig. 1. General Flow of Data in Challenge Response Mechanism in SIP.

In SIP, most commonly used mechanism for login and authentication is challenge response mechanism. In this mechanism, user sends a login message to server which comprises of user specific login data and some dynamically generated parameters. Server verifies user identity on the received login data and generates a server verification token based on dynamic parameters received from user. Server then sends server verification token and some dynamically generated server specific data to user as challenge message. User verifies identity of server through parameters generated at user end. After successful server verification, a user token is generated based on the dynamic data received from server. This token is sent as response message to the server. Server does final verification of user based on user token. A dynamic session key is generated based on the dynamic parameters exchanged in these messages. Figure 1 shows the general flow of data in SIP architecture.

One of the major role of SIP is to provide a secure authentication mechanism. When SIP is implemented, it should ensure to the system that a valid user is accessing its services and to the user that he is connected to a valid system. There are few globally known parameters about the system which varies depending on the implementation. Some knowledge is kept secret by both user and the system. User uses his secret knowledge and public parameters to send a loginrequest to server. Server verifies identity through secret parameters and sends appropriate reply message. Thus client verifies his connection to appropriate server from the received reply message. [12], [13], [14].

Another major aspect in terms of authentication is mutual authentication. Server must ensure that legitimate user is provided access and not an attacker. User must ensure that he is connected to legitimate server and not some malicious spoofed server created by attacker. Multifactor authentication provides advantage over traditional single factor authentication. Amongst Knowledge, Ownership and Inheritance factors of authentication, it is essential to use at least 2 factors for authentication. Knowledge factor can easily be included by including PIN or password for authentication. Ownership factor can be included through devices like smart cards, smart wearable devices or software tokens stored in mobile devices. Inheritance factor is relatively tough to include is system due to nature of biometrics which are used as authenticator. Biometric data is generally tough to replace if leaked from the system. The biometric template of user can

be captured by the attacker if there is vulnerability present in the reader. Biometric data cannot be replaced by user unlike ownership or knowledge factor. Thus it is considered better if only ownership and knowledge factor is used for authentication.

Many SIP schemes used verification table containing user passwords at server for authentication. This made system vulnerable to various attacks like insider attack, password guessing attack, stolen verifier attack, server spoofing attack, etc. Reduced efficiency and lack of scalability is another issue with this approach. To address this problem, new schemes were developed where remote server could authenticate user without verification tables [11], [14] . This new approach also allowed early detection of wrong credentials from user.

Rest of this paper is divided as follows: Section 2 provides literature review for different SIP authentication schemes. In Section 3, proposed model is explained in detail. We evaluate security and functionalities of our proposed model in Section 4. We conclude our paper in Section 5 and provide scope for future work.

II. Literature Review

Several schemes were proposed on SIP to provide secure and reliable authentication [8], [9], [10], [11], [13], [14], [15], [16]. Many of these schemes were vulnerable to many attacks like insider attack, stolen verifier attack, spoofing attacks, etc. Some lacked important functionalities like mutual authentication, secure and dynamic session key generation, or multifactor authentication. Some schemes contained elements like verification tables or global clocks which made them vulnerable.

Yeh et al. [17] proposed an authentication scheme using ECC and smart cards. They provided early wrong password detection by providing offline password verification, Mutual authentication was provided by using a challenge response mechanism. They stated their scheme was resistant to password guessing attacks. However, Farash et al. [18] proved that Yeh et al.'s scheme was vulnerable to offline password guessing attack, user impersonation attack and server impersonation attack.

Farash et al. [18] proposed authentication scheme to overcome weakness in Yeh et al.'s scheme. They stated their scheme could provide security properties like user anonymity, untraceability and offline password changing phase. Alamr et al. [19] proved that Farash et al.'s scheme could not provide user anonymity and confidentiality. Offline password changing phase also made their scheme vulnerable to offline password guessing attack and brute force attack.

Farash et al. [20] stated that their scheme can withstand well known attacks. Kumari et al. [21] showed that Farash et al.'s scheme was vulnerable to user impersonation attack, session specific information leakage attack and password guessing attack. Also there was lack of user anonymity.

Major identified issues in literature review are vulnerability to password guessing attack, user and server impersonation attack, brute force attack and session specific information leak- age attack. Key functionalities which were missing includes mutual authentication and user anonymity.

III. Proposed Model

The proposed model consists of four different phases, i.e. Setup Phase, Registration Phase, Login and Authentication Phase and Password Change Phase. Figure 2 illustrates the workflow of system. We have provided a mechanism for offline password verification to detect invalid password at an early stage. Our proposed model performs multiple checks to verify identity of user and server. A secure session key is dynamically generated based on generated random data. In this section, we see elliptic curve cryptography followed by phases of our system.

A. Elliptic Curve Cryptography (ECC)

Miller [22] and Koblitz [23] were first to explore application of ECC in cryptography. This turned out to be more secure when compared with traditional public key cryptography [24]. Same level of security is provided in ECC but total number of parameters included is reduced. For ECC based cryptography, operations are carried out which completely depends on single equation which is as follows:

$$E_q(i, j): y^2 = (x^3 + ix + j) \bmod q$$

where q is a very large prime number. Size of q is greater than 160 bits and i and j belongs to integers. (x, y) are points that satisfies $94i^3 + 27j^2) \bmod q \neq 0$. Value of integers i and j defines the elliptic curve. Identity element is considered as point at infinity O. Multiplication in ECC is scalar and is considered as repeated addition. So if P is considered as a point over equation $E_q(i,j)$ and v is integer to be multiplied then vP= P + P + P+ P +…P (v times).Computational problems with respect to ECC are as follows:

1. Elliptic Curve Discrete Logarithm Problem (ECDLP)
   ECDLP states that if 2 points R and S are given on an elliptic curve $E_q(i,j)$, then it is computationally hard to find another integer k such that R=kS in polynomial time.

B. Setup Phase

Server generates system parameters in this phase as follows:

- Large prime number: n
- Elliptic curve: $E_p(a, b)$
- Server's private key: $q_s \in Z_n^*$
- Secure one way hash functions: $h_p(.)$, $h_s(.)$ such that $h:\{0,1\}^* \rightarrow \{0,1\}^l$
  where l is the security parameter
- Symmetric encryption/ decryption functions $E_K()/D_K()$ where K is secret key

Server is initialized once all the parameters are set.

C. Registration Phase

Whenever a user wants to register, user and server cooperates to perform following steps via a secure channel. The steps which are performed are as follows:

1) User selects and enters his username as Un and password as Pu. A number M is generate dynamically

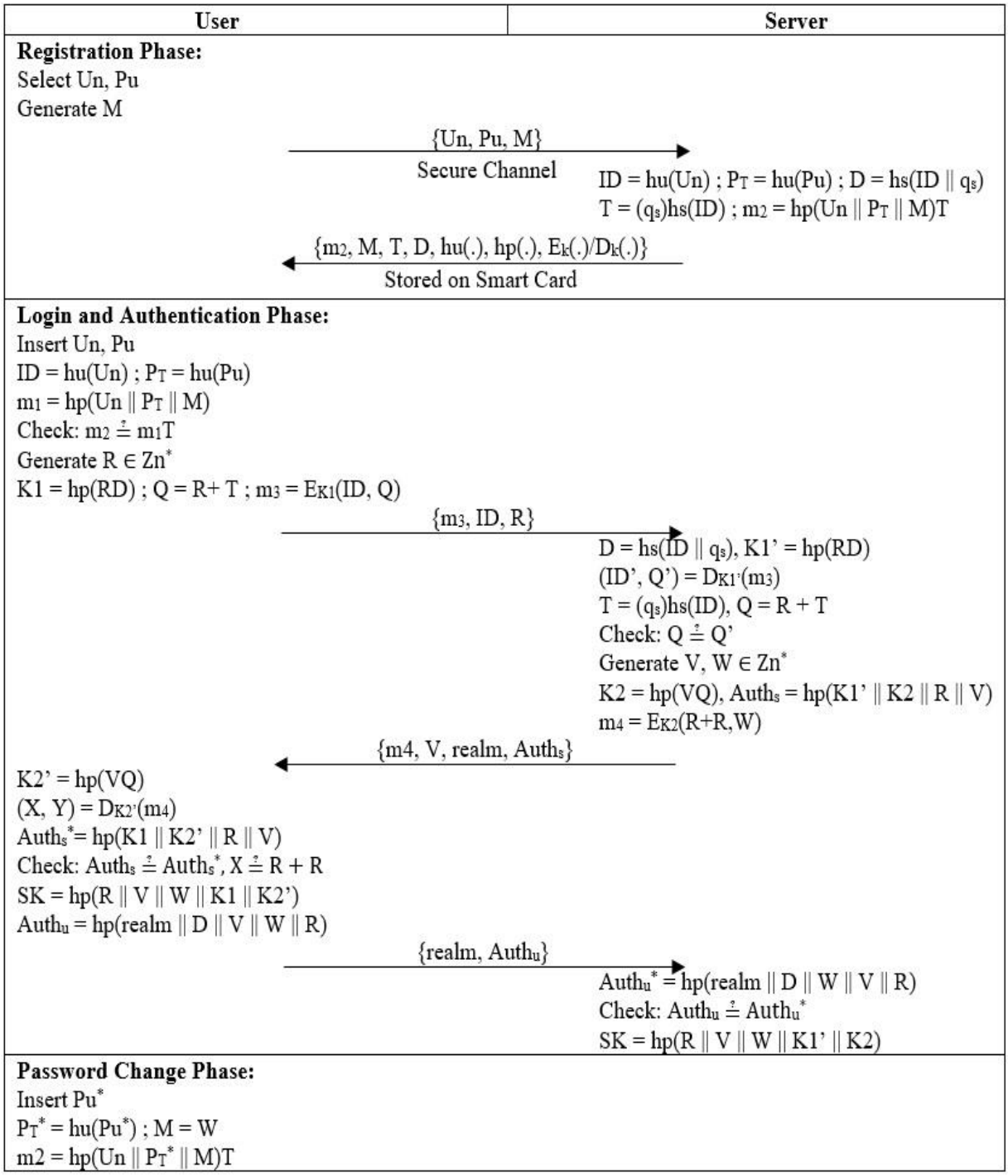

Fig. 2. Data flow in proposed model.

such that $M \in Z_n^*$. All these 3 parameters are then sent to server.

2) Server generates a unique hash function $h_u(.)$ dynamically which is user specific. Then ID is generated as $ID=h_u(Un)$ and P_T as $P_T = h_u(Pu)$. T is generated as $T=q_s(h_s(ID))$ and D as $D=h_s(ID||q_s)$. Secure user authentication parameter (m_2) is generated as $m_2=(h_p(Un||P_T||M))T$.
3) Parameters $\{m_2, M, T, D, h_u(.), h_p(.), E_K(.)/D_K(.)\}$ are stored on smart card. Smart card is sent to the user via a secure channel.

D. Login and Authentication Phase

Whenever user wants to get services of the system, he first passes through this phase to verify identity of system and authenticate himself. Steps followed in this phase are as follows:

1) User enters Un and Pu in the system after entering smart card into the reader.
2) ID is computed as $h_u(Un)$ and P_T as $h_u(Pu)$. Message m_1 is computed as $h_p(Un||P_T||M)$. If value of m_1T equals m2, then user is successfully authenticated, otherwise invalid credentials message is displayed.

3) R is generated dynamically after successful authentication as R Z_n^*. Key K1 is computed as $K1=h_p(RD)$. Q is computed as Q = R+T. Message m_3 is generated by encrypting (ID,Q) with the Key K1. {m_3, ID, R} are sent to the server as login request to the server.
4) After receiving login message, server first computes D as $D=h_s(ID \| q_s)$ followed by key K1' as $K1'=h_p(RD)$. m_3 is decrypted with Key K1' and parameters ID' and Q' are obtained. T is computed as $T=(q_s)h_s(ID)$ and Q as Q=R+T. If Q equals Q', then the identity of user is verified successfully, otherwise the connection is terminated. V and W are generated dynamically after successful authentication as $V, W \in Z_n^*$. K2 is computed as $K2=h_p(VQ)$. Server authentication message $Auth_s$ is computed as $Auth_s=h_p(K1'||K2||R||V)$. m_4 is generated by encrypting (R+R, W) with key K2. {m_4,V,realm,$Auth_s$} is sent as challenge to the user.
5) Key K2' is generated as $h_p(VQ)$. m_4 is decrypted with key K2' to obtain parameters X and Y. $Auth_s^*$ is computed as $Auth_s*=h_p(K1||K2'||R||V)$. Server authentication is successful if $Auth_s$ equals $Auth_s^*$ and X equals R+R. Session key SK is generated as $SK=h_p(R||V||W||K1||K2')$. User authentication message $Auth_u$ is generated as $Auth_u=h_p(realm||D||V||W||R)$.{realm,$Auth_u$} is sent as response to the server.
6) Server generates user authentication message $Auth_u^*$ as $Auth_u^*=h_p(realm||D||W||V||R)$. Final user verification is successful if value of $Auth_u^*$ equals $Auth_u$. After successful authentication, session key is generated as $SK=h_p(R||V||W||K1'||K2)$.

Now server and user communicates securely through the newly generated session key SK.

E. Password Change Phase

This phase is executed when user wants to change his pass- word. In order to change password, entire login and authentication phase is executed first to establish a secure channel with server. Steps performed after generation of SK are as follows:

1) User enters new password P_u^* in the system. P_T^* is computed as $P_T^*=h_u(Pu^*)$. M is modified as M=W.
2) m_2 is then computed as $m_2=h_p(Un||P_T*||M)T$ and the modified value is stored on smart card.

IV. Result Analysis

In this section, we provide security analysis of the proposed model. Then the security of proposed protocol is compared with various proposed schemes. The security provisioning has also been elaborated in this section keeping in contention the aspects that enhance the strength of the system. The key security aspects of the proposed model are mutual authentication ensuring proper identity checks for user and system, user anonymity to prevent access from privileged insider to identify user along with dynamic and secure session key generation for perfect forward secrecy. All these provisions ensure that modularity of the system is maintained to the maximum extent possible. The given system carries forward all the security provisions of symmetric key cryptography as core concepts.

A. Formal Security Evaluation using AVISPA tool

We use Automated Validation of Internet Security Protocols and Applications (AVISPA) tool [25] for formal security evaluation of our proposed scheme. There are different back-ends available to verify security of proposed schemes. We have used On-the-fly Model Checker (OFMC) back-end to evaluate security of our scheme. Figure 3 shows simulation results of our proposed scheme.

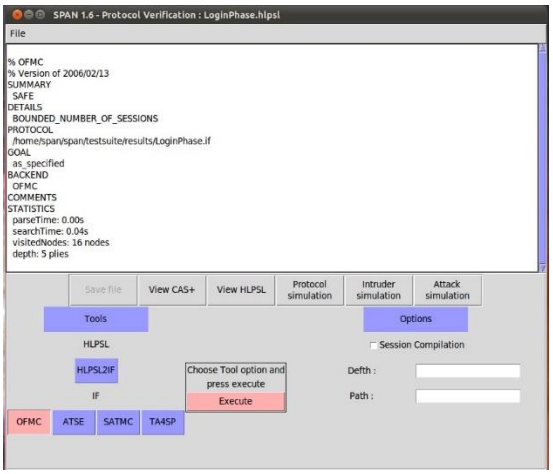

Fig. 3. Simulation result under OFMC model of AVISPA

B. Informal Security Analysis of proposed model

1) Mutual Authentication: In our model, we perform user authentication at server without message freshness in step 3 when we compare Q with Q'. After this preliminary verification, Server is authenticated by user in step 4 when $Auth_s$ is compared with $Auth_s^*$. After successful server authentication, user generates user authentication message as $Auth_u$. Server authenticates user in step 5 when $Auth_u$ is compared with $Auth_u^*$. Thus we provide mutual authentication in our system when we compare $Auth_s$ with $Auth_s^*$ and $Auth_u$ with $Auth_u^*$.

2) Dynamic and Secure Session Key Generation: In our model, we generate session key based on 5 different parameters, (R, V, W, K1 and K2). K1 and K2 are securely generated keys at user and server end respectively, R and V are dynamically generated random values which are transmitted openly between user and server and W is dynamically generated random value at server which is passed securely to user.

Values of W, K1 and K2 is either transferred directly through secure channel or indirectly generated securely by hiding partial information in transferred messages. As a result, it becomes computationally impossible for attacker to guess all 3 secure values correctly. Thus our model supports secure session key generation. Also, as all 5 parameters are random and dynamically generated, our model supports dynamic

session key generation.

3) User Anonymity: In our model, username is accepted from user as Un. This value is then passed from a secure hash function $h_u(.)$ to get a dynamically generated user specific random identity ID. It is impossible to obtain original input value from the hash function. Also, it is impossible for attacker to read contents of message m_3 transferred in step 3 without getting security parameter D. Thus our model supports user anonymity.

4) Resistance against Password Guessing Attack: In our model, we accept 2 different parameters Un and Pu from user to generate user identity ID and password P_T. Neither Pu nor P_T is stored directly on card. ID is transferred through insecure channel to server. But it is impossible to generate Un from ID even if $h_u(.)$ is known to attacker. Thus our model provides resistance against password guessing attack.

5) Resistance against Server Impersonation Attack: In our model, key K1 is generated at user end from a secret parameter D, which was generated by server in registration phase. Q is sent in an encrypted form to server in m_3. Key K2 can only be generated with the knowledge of this Q. Message m4 cannot be sent without K2. As a result, our model provides resistance against server impersonation attack.

6) Resistance against User Impersonation Attack: In our model, user sends message m3 to the server. This message is generated only with the knowledge of security parameter D which is stored on card by server in registration phase. If message is replayed, attacker still cannot generate $Auth_u$ as it contains knowledge of D as well as dynamically generated parameter V and W. Thus our model provides resistance to user impersonation attack.

7) Resistance against Brute Force Attack: In our model, we accept 2 parameters Un and Pu from the user to verify identity of user. None of these parameters are stored directly on the system. It is essential to provide correct Un and Pu in order to login successfully. As it is computationally infeasible to brute force 2 different parameters in polynomial time, our model provides resistance to brute force attack.

8) Resistance against Replay Attack: In our model, values R, V and W are dynamically generated at user and server end. These values are to be included as a reply message to the received message. As attacker cannot modify the messages to add these values, our model provides resistance to replay attack.

9) Resistance against Relay Attack: In our model, session key is generated securely. The parameters which are generated are not transferred directly over insecure channel. Two-factor authentication is also included which gives resistance against relay attacks [26]. Thus our model provides resistance to relay attack.

10) Resistance against Man-in-the-Middle Attack (MITM): In our model, we generate a secure session key in login and authentication phase. This session key is used to transfer data securely through symmetric encryption schemes. Cryptographic techniques are strong security mechanisms to resist MITM attack [26]. Thus by including encryption, we provide resistance against MITM attack.

C. Comparative Security Analysis

We compare security of our proposed model with different schemes from Section 2 to evaluate security of our model relatively in Table 1. Attacks and properties which are considered for security evaluation include password guessing attack, server and user impersonation attacks, brute force attack, relay attack, replay attack, MITM attack and property like user anonymity. Attacks and functionalities which were common for all the schemes are not included in the table.

TABLE I
RELATIVE SECURITY ANALYSIS

Attack Types	Yeh et al. [17]	Farash et al. [18]	Our Model
Password Guessing Attack	Insecure	Insecure	Secure
Server Impersonation Attack	Insecure	Secure	Secure
User Impersonation Attack	Insecure	Secure	Secure
Brute Force Attack	Secure	Insecure	Secure
Relay Attack	Secure	Insecure	Secure
MITM Attack	Insecure	Secure	Secure
User Anonymity	Absent	Absent	Present

V. CONCLUSION AND FUTURE SCOPE

SIP is key component in every VoIP communication. It is responsible for ensuring proper and secure connection establishment between the communicating parties. However there is an inherent vulnerability in authentication phase of SIP due to its open text nature.

In this Paper, a secure authentication model for SIP is proposed. Key functionalities like mutual authentication and user anonymity along with secure and dynamic session key generation mechanism are provided in the proposed model. Lastly informal security analysis is done against various attacks and relative analysis is provided.

Future work can be done to provide security in multiserver environment. Three factor authentication can also be provided for critical applications where smart cards have higher processing power and added functionalities.

ACKNOWLEDGMENT

This publication is an outcome of the R&D works undertaken under the YFRF project under Visvesvaraya Ph.D. Scheme of Ministry of Electronics & Information Technology, Government of India and being implemented by Digital India Corporation.

REFERENCES

[1] D. He, Y. Zhang, and J. Chen, "Cryptanalysis and improvement of an anonymous authentication protocol for wireless access networks," *Wireless Personal Communications*, vol. 74, no. 2, pp. 229–243, 2014.

[2] D. He, N. Kumar, M. K. Khan, and J.-H. Lee, "Anonymous two-factor authentication for consumer roaming service in global mobility networks," *IEEE Transactions on Consumer Electronics*, vol. 59, no. 4, pp. 811–817, 2013.

[3] M. S. Farash and M. A. Attari, "An efficient and provably secure three- party password-based authenticated key exchange protocol based on Chebyshev chaotic maps," *Nonlinear Dynamics*, vol. 77, no. 1-2, pp. 399–411, 2014.

[4] D. He, J. Chen, and J. Hu, "Further improvement of Juang et al.'s password-authenticated key agreement scheme using smart cards,"

Kuwait Journal of Science & Engineering, vol. 38, no. 2A, pp. 55–68, 2011.

[5] D. He, C. Chen, S. Chan, and J. Bu, "Strong roaming authentication technique for wireless and mobile networks," *International Journal of Communication Systems*, vol. 26, no. 8, pp. 1028–1037, 2013.

[6] M. S. Farash and M. Ahmadian-Attari, "A Pairing-free ID-based Key Agreement Protocol with Different PKGs." *IJ Network Security*, vol. 16, no. 2, pp. 143–148, 2014.

[7] M. S. Farash and M. A. Attari, "An efficient client-client password-based authentication scheme with provable security," *The Journal of Supercomputing*, vol. 70, no. 2, pp. 1002–1022, 2014.

[8] M. S. Farash and M. A. Attari, "An anonymous and untraceable password-based authentication scheme for session initiation protocol using smart cards," *International Journal of Communication Systems*, vol. 29, no. 13, pp. 1956–1967, 2016.

[9] W.-E. Chen, Y.-L. Huang, and Y.-B. Lin, "An effective IPv4-IPv6 translation mechanism for SIP applications in next generation networks," International Journal of Communication Systems, vol. 23, no. 8, pp. 919–928, 2010.

[10] S. Wu, Q. Pu, and F. Kang, "Practical authentication scheme for SIP," Peer-to-Peer Networking and Applications, vol. 6, no. 1, pp. 61–74, 2013.

[11] P. K. Dhillon and S. Kalra, "Secure and efficient ECC based SIP authentication scheme for VoIP communications in internet of things," Multimedia Tools and Applications, Apr 2019. [Online]. Available: 10.1007/s11042-019-7466-y

[12] M.-X. Chen and F.-J. Wang, "Session integration service over multiple devices," International Journal of Communication Systems, vol. 23, no. 5, pp. 673–690, 2010.

[13] M. S. Farash, "Security analysis and enhancements of an improved authentication for session initiation protocol with provable security," Peer-to-Peer Networking and Applications, vol. 9, no. 1, pp. 82–91, 2016.

[14] S. Kumari, S. A. Chaudhry, F. Wu, X. Li, M. S. Farash, and M. K. Khan, "An improved smart card based authentication scheme for session initiation protocol," Peer-to-Peer Networking and Applications, vol. 10, no. 1, pp. 92–105, 2017.

[15] L. Zhang, S. Tang, and Z. Cai, "Efficient and flexible password authen- ticated key agreement for voice over internet protocol session initiation protocol using smart card," International Journal of communication systems, vol. 27, no. 11, pp. 2691–2702, 2014.

[16] Q. Jiang, J. Ma, and Y. Tian, "Cryptanalysis of smart-card-based password authenticated key agreement protocol for session initiation protocol of Zhang et al." International Journal of Communication Systems, vol. 28, no. 7, pp. 1340–1351, 2015.

[17] H.-L. Yeh, T.-H. Chen, and W.-K. Shih, "Robust smart card secured au- thentication scheme on SIP using elliptic curve cryptography," Computer Standards & Interfaces, vol. 36, no. 2, pp. 397–402, 2014.

[18] M. S. Farash, S. Kumari, and M. Bakhtiari, "Cryptanalysis and improve- ment of a robust smart card secured authentication scheme on SIP using elliptic curve cryptography," Multimedia Tools and Applications, vol. 75, no. 8, pp. 4485–4504, 2016.

[19] A. A. Alamr, F. Kausar, J. Kim, and C. Seo, "A secure ECC-based RFID mutual authentication protocol for internet of things," The Journal of Supercomputing, vol. 74, no. 9, pp. 4281–4294, 2018.

[20] M. S. Farash, "Security analysis and enhancements of an improved authentication for session initiation protocol with provable security," Peer-to-Peer Networking and Applications, vol. 9, no. 1, pp. 82–91, 2016.

[21] S. Kumari, S. A. Chaudhry, F. Wu, X. Li, M. S. Farash, and M. K. Khan, "An improved smart card based authentication scheme for session initiation protocol," Peer-to-Peer Networking and Applications, vol. 10, no. 1, pp. 92–105, 2017.

[22] Miller, Victor S. "Use of elliptic curves in cryptography." Conference on the theory and application of cryptographic techniques. Springer, Berlin, Heidelberg, 1985.

[23] Koblitz, Neal. "Elliptic curve cryptosystems." Mathematics of computation 48.177 (1987): 203-209.

[24] Johnson, Don, Alfred Menezes, and Scott Vanstone. "The elliptic curve digital signature algorithm (ECDSA)." International journal of information security 1.1 (2001): 36-63.

[25] AVISPA, 2017. http://www.avispa-project.org

[26] B. B. Gupta, M. Quamara, A taxonomy of various attacks on smart card-based applications and countermeasures, Concurrency and Computation: Practice and Experience 0 (0) (2018) e4993.

Proceedings of the Fourth International Conference on Communication and Electronics Systems (ICCES 2019)
IEEE Conference Record # 45898; IEEE Xplore ISBN: 978-1-7281-1261-9

Fully Connected Convolutional Network with Laplacian Filter For Salt Segmentation In Seismic Images

Jasdeep Singh, Tarandeep Singh and Munish Rattan GNDEC, Ludhiana,Punjab,India
jimmy50singh@gmail.com

***Abstract*— Nowadays Convolutional neural networks (CNN) has become very popular, since they are able to surpass human efficiency in image classification task on ImageNet dataset. CNN are able extract features from images. These features has given state of the art accuracy as compare to the hand engineered features. Large deposits of salt normally contain large accumulations of oil and gas. But to pinpoint their accurate location in seismic images require human expertise. As the number of data is increasing now days, it becomes impractical to use human for this task. In this paper, for this task a CNN model based on U-NET architecture, a fully convolutional neural network with Laplacian filter is presented. It has been observed that the preprocessing with Laplacian filter lead to better results.**

***Index Terms*— Convolutional neural network, Salt segmentation, U-NET, Image segmentation, deep neural network, seismic images, Laplacian filter**

I. INTRODUCTION

In sedimentary rocks a dome- shaped structure is formed by evaporation of a large mass of salt. It is known as salt dome. Salt domes have trapped oil and gas reservoirs. Compared with the surrounding strata, salt domes often exhibit chaotic reflections in the form of a distinct texture. Therefore, salt dome interpretation can be formed as a structure segmentation problem. However, the boundaries of salt domes are not easily identified in most geologic scenarios. As the underlying physics with noisy and low-resolution data make it difficult.

Recently Deep neural network methods have been successful in solving problems which require feature extraction[1] .They provide the state of the art results as compare to hand crafted features. In this accuracy can be increased as the amount of the data increases. A subtype of of deep neural network is Convolutional Neural Networks (CNNs). In the field of image analysis it is pushing the state of the art.

LeCun et al. in 1990 [12] and later improved it in 1998 [10] proposed LeNet.It is a Convolutional Neural Network based model. It is used for Handwritten Digit Recognition.It has many applications such as in reading zip codes, digits, etc. But at that time there was a lack of high computing machines which prevented the use of CNN.

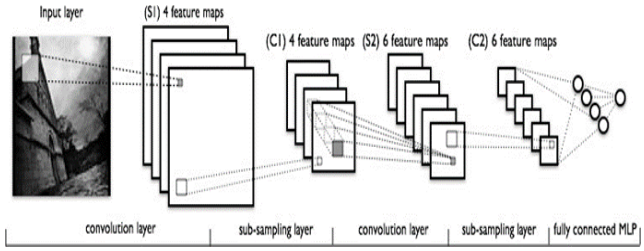

Figure 1: A simple CNN flow diagram [2]

AlexNet architecture was developed by Krizhevsky et al. [3]. It is one of the few works that popularize the Convolutional Neural Networks in the area of image analysis. Its network architecture is similar to LeNet. But AlexNet has larger and deeper architecture with more parameters. In ILSVRC-2012 competition, AlexNet was able to achieve the top-1 and top-5 error rates.

Zeiler M et al. utilize a multilayered Deconvolutional Network (DeConvNet) to see activities within the network[4].It helps in visualizing how the features of the network during the training evolve. They also used it, to troubleshoot the network in case of any issues. They were able to analyze the architecture of AlexNet and did some changing in the network such as decreasing the filter size and stride in the first layer and increase the size of the middle convolutional layers. This new network, which is the improvement of AlexNet,was able to win ILSVRC 2013.

Simonyan et al [11] have done an analysis of network architecture by keeping all the parameters fixed except the depth factor. This could lead to a large number of parameters. But by using small 3x3 convolution filters, they were able to efficiently controll this problem. This result in a development of a new and accurate ConvNet architecture known as VGGNet. It came second in the ILSVRC 2014 contest.

Szegedy et al.[5] introduced a new architecture known as Inception (v1).They were able to win the ILSVRC 2014 competition using it. It utilizes more computing resources than the AlexNet . GoogLeNet is a network, which has a less parameter as compare to AlexNet with twenty-two layers of Inception module. Later, many changes have been done in Inception-v1, which lead to increase in performance. Such as

the introduction of batch normalization by Ioffe et al. [6] which led to Inception-v2. More improvements were done in this version and the architecture was later known as Inception-v3 [7].

Kaiming et. al. proposed a novel CNN architecture known as ResNet. They used residual connection to learn residual function with respect to the input. They propose that it will be easier to learn identity function then compare to unreferenced functions [9].This make it easier to optimize deeper network. It results in increasing the overall performance and accuracy. One of its drawback is that it also increase the number of overall parameters to optimize. Hence make the network much more expansive in terms of resource utilization.But without affecting the performance , overall parameters can be decreased by removing the first Fully-Connected layer .Since this layer contains most of the parameters.

Szegedy et al [8], later in 2015 show that by using residual connection with inception module, model can learn faster. It makes the network more efficient. They were able to win 2015 ILSVRC challenge using this architecture.

Recently, Ross et al [13] review popular facies classification methods based on machine learning algorithms. Huang et al. [14] show that for identifying geologic faults in 3D seismic volumes CNN provides much better results than the methods like support vector machines(SVMs) and logistic regression. Their experiments show much bettrer accuracy in a variety of seismic processing and interpretation tasks. Araya-Polo et al. [15] use pre stack seismic data, without processing the data to seismic image, to identify faults.

Wu et al [16] train a CNN to perform pixel-by-pixel salt body classification. Previous researchers [17][18] discuss salt boundary extraction as a global image segmentation problem. Considering it as an image segmentation problem, it faces problems due to some drawback of deep learning approaches, which only depend on network made for object categorization for pixel wise labelling [19]. It is necessary to have a mechanism such that the deep layer feature are mapped to the same dimension of the input images. Such approaches lead to ad hoc methods to upsample features, e.g. by element replication.

An alternative network architecture, inspired by U-Net [20], that overcomes the problem by mapping the encoder outputs to the final classification labels of image dimension is adopted in this paper. This architecture is include a stack of encoders and their corresponding stack of decoders. Their final output is give to a sigmoid classification layer. Both encoder and decoder are fully convolutional layers. It has dual input channel, one has seismic image as a input and has the Laplacian of the image. The Laplacian operator computes the second derivative of an image and the resultant image highlight regions of rapid intensity changes. Therefore it is often used for edge detection[21][22]. The Laplacian operator for an Image is defined as shown in equations (1), (2) and (3)

$$\Delta^2 f = \frac{\partial^2 f}{\partial x^2} + \frac{\partial^2 f}{\partial y^2} \quad (1)$$

For X-direction,

$$\frac{\partial^2 f}{\partial x^2} = f(x+1,y) + f(x-1,y) - 2f(x,y) \quad (2)$$

For Y-direction,

$$\frac{\partial^2 f}{\partial y^2} = f(x,y+1) + f(x,y-1) - 2f(x,y) \quad (3)$$

Single input channel model which takes only seismic image as an input. The results of both the models are compared. It has been observed that the dual input channel model has outperform the single input channel model.

II. Model Architecture

Firstly, the salt body classification as a semantic image segmentation problem with two classes has been constructed. The algorithm assigns a salt label to each image pixel based on the shape of the seismic image. The frame work of the proposed method is a convolutional encoder decoder network. It is inspired from U-Net[20],an architecture applied to biomedical image segmentation. This encoder-decoder architecture is trained end-to-end such that it jointly optimize all the model parameters of the network. Proposed network architectures for dual input channel is illustrated in figure 2.

First proposed model contain dual input channel with both Laplacian of a seismic image and seismic image as an input where as the second contain only seismic image as input. The rest of the architecture is same in both cases. The Laplacian operator helps in highlighting of the sharp intensity changes in the image which helps in better performance of the model.

The decoder network contains a stack of decoders corresponding to each encoder. It is one of the key components of the proposed network. Each encoder contains a filter bank. By using it for performing a convolutional operation, a set of feature maps is produced.

Element-wise rectified-linear unit ($\sigma(x) = \max\{0,x\}$) is applied as non-linear activation. Following that, max-pooling operation is performed such that the resulting output is sub-sampled by a factor of 2. In the input image dve to max-pooling, over small spatial shifts translation invariance is achieved. The appropriate decoder in the decoder network up samples its input feature maps by resizing-interpolation. This results in a sparse feature maps which are further convolved with a trainable decoder filter bank and produce a dense feature maps. The high dimensional feature representation at the output is fed to a trainable sigmoid function. The output of the classifier is a single channel image of classification probabilities.

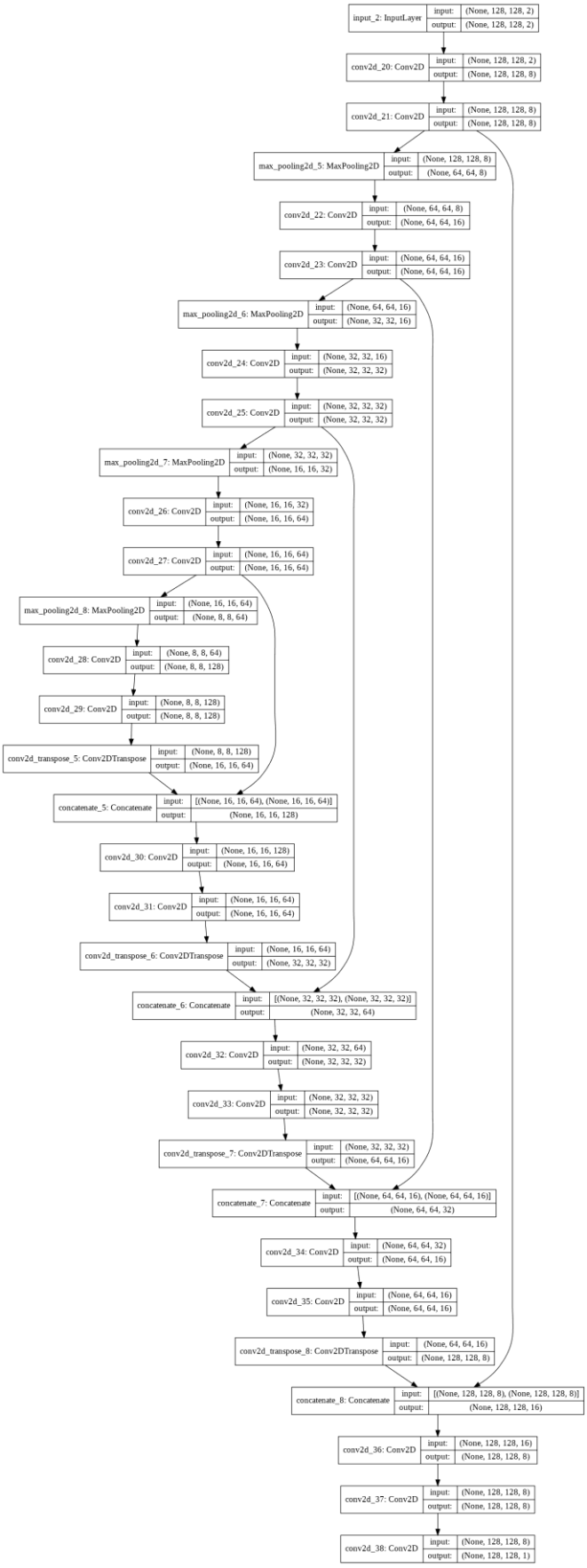

Figure2: Proposed model architecture.Model has dual input channel. Model architecture is inspired from U-net.

III. TRAINING

Dataset is proved by TGS , as they hosted Kaggle Competition of salt segmentation from seismic images [25]. Input seismic images are of 101 × 101 dimension images. They have binary mask of salt deposition. Their is total of 4000 images of train dataset which are divided into training set and validation set. First 3,400 images is used for training and last 600 images is used for validation set.

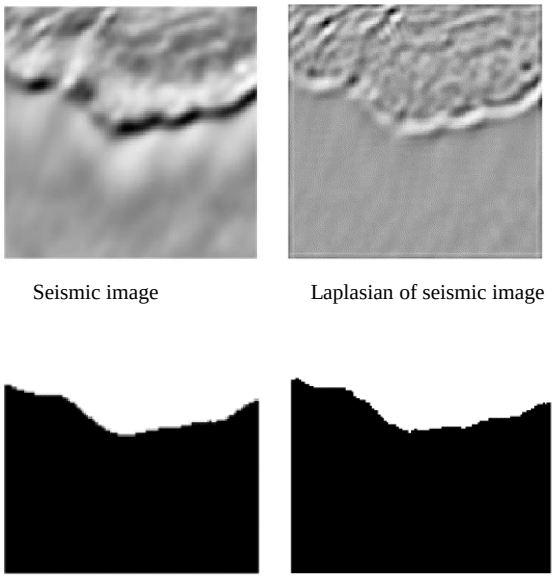

Seismic image | Laplasian of seismic image

Mask | Predicted mask

Figure 3:From left to right first image is a seismic image from validation set and its Laplacian is shown next as the second image. Third image is the output mask of an image which it never seen before while training and its predicted value is shown at last as fourth image.

He et al. [23] propose a technique for weight initializing and it is used for parameters initializing in the proposed network. In this paper binary entropy loss is used as the loss function, and adaptive momentum descent (Adam) as optimization algorithm [24] has been used to iteratively update the model weights. The resolution of input images is increased from 101x101 to 128x128 before giving it to the network. Image pixel are normalized by dividing it by 255.

IV. RESULTS

The model architecture code is written in python using keras library and tensorflow at the backend.Code is available at https://github.com/JASDEEP50SINGH/salt-segmentation-using-laplace-transform.To process the model described above we used a single NVidia GTX 1050 Ti GPU at our disposal. The full training and prediction cycle took about 1 hour for single channel input model and 2 hours for dual input channel input. The value of seed for random variable is set to 125. The results achieved on the validation and training data set during the training process are shown on figure 4.

Model is run for 30 epochs as loss does not decrease further. Whenever validation loss decreases, model weights are saved. From the last saved models weights, it provide 92.28 % accuracy (the percentage of pixels correctly classified in the.

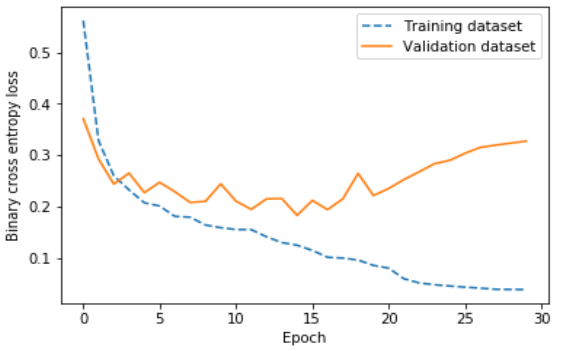

(a)

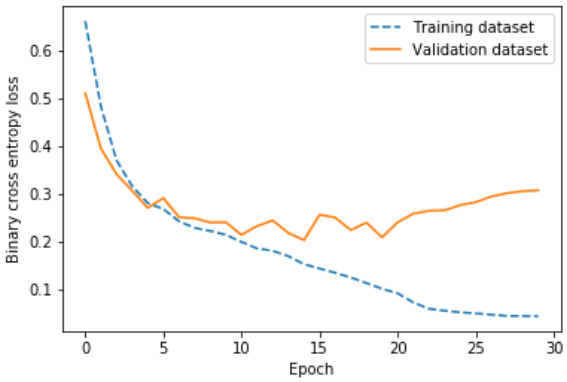

(b)

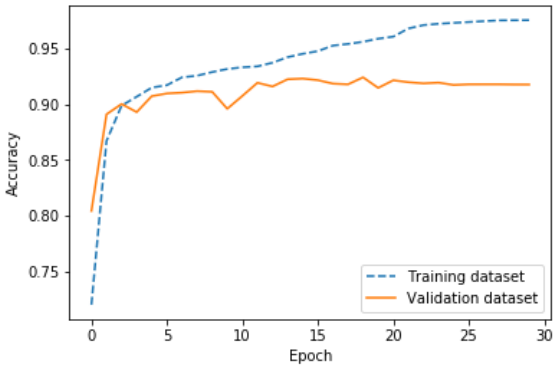

(c)

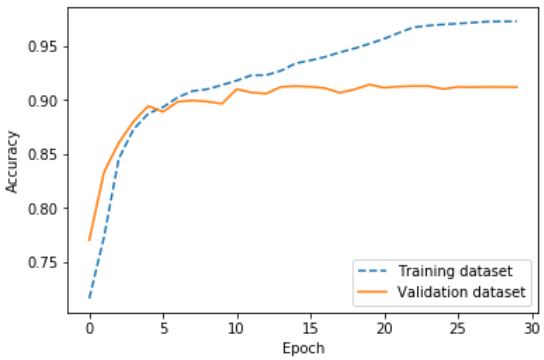

(d)

Figure 4:(a) loss curve of dual input channel model, (b) loss curve of single input channel model, (c) Accuracy curve of dual input channel model, (d) Accuracy curve of single input channel model. As the number of epochs increases accuracy of both models improves and their binary cross entropy losses decreases. Overfitting can be seen as the losses start increasing after they reached their minimum value.

image) and .1825 binary cross entropy loss on validation data by dual input channel model. Single input channel achieves 91.31% accuracy and .2024 binary cross entropy loss on the same data. The Dual input channel outperform the single input channel

V. Conclusions

In this paper a network model with pre-processing of input data is proposed for an end-to-end automatic salt body detection in seismic image based on a convolutional neural networks. The encoder-decoder architecture allows for extracting essential information from training data, and results in high accuracy. The model has been tested on the dataset proved by TGS , as they hosted Kaggle Competition of salt segmentation. With limited amount of manually prepared training samples, the model successfully generalizes to unseen seismic slices produces accurate salt body detection results. The results are further improved by concatenating Laplacian of an image with input image.We believe that with further image pre-processing and data augmentation accuracy can be increased.

References

[1] Waldeland, Anders U., et al. "Convolutional neural networks for automated seismic interpretation." *The Leading Edge* 37.7 (2018): 529-537.

[2] N. Srivastava, G. Hinton, A. Krizhevsky, I. Sutskever, and R. Salakhutdinov, "Dropout: A simple way to prevent neural networks from overfitting," *The Journal of Machine Learning Research*, vol. 15, no. 1, pp. 1929–1958, 2014

[3] Alex Krizhevsky, Sutskever I, and Hinton G.E. "Imagenet classification with deep convolutional neural networks". *In NIPS*, 2012.

[4] Zeiler M., Taylor G., and Fergus R. "Adaptive deconvolutional networks or mid and high level feature learning", *In ICCV*, 2011.

[5] C. Szegedy, W. Liu, Y. Jia, P. Sermanet, S. Reed, "Going deeper with convolutions", *CoRR*, 2014.

[6] S. Ioffe and C. Szegedy." Batch normalization: Accelerating deep network training by reducing internal covariate shift." *In Proceedings of The 32nd International Conference on Machine Learning*, 2015.

[7] C. Szegedy, V. Vanhoucke, S. Ioffe, J. Shlens, and Z. Wojna. "Rethinking the inception architecture for computer vision." arXiv:1512, 2015.

[8] Christian Szegedy, Sergey Ioffe, "Vincent Vanhoucke, Inception-v4, Inception-ResNet and the Impact of Residual Connections on Learning", arXiv:1602.07261, 2016.

[9] K. He, X. Zhang, S. Ren, and J. Sun. "Deep residual learning for image recognition", arXiv:1512.03385, 2015.

[10] B. B. Le Cun, J. S. Denker, D. Henderson, R. E. Howard, W. Hubbard, and L. D. Jackel, "Handwritten digit recognition with a back-propagation network", *in NIPS*, 1990.

[11] Simonyan, Karen, and Andrew Zisserman. "Very deep convolutional networks for large-scale image recognition." arXiv preprint arXiv:1409.1556 (2014).

[12] Y. LeCun, L. Bottou, Y. Bengio, and P. Haffner, "Gradient-based learning applied to document recognition", *Proceedings of the IEEE*, 1998.

[13] Ross, Christopher P., and David M. Cole. "A comparison of popular neural network facies-classification schemes." *The Leading Edge* 36.4 (2017): 340-349.

[14] Huang, L., X. Dong, and T. E. Clee, 2017, "A scalable deep learning platform for identifying geologic features from seismic attributes" *The Leading Edge*, 36, 249–256,

[15] Araya-Polo, M., T. Dahlke, C. Frogner, C. Zhang,T. Poggio, and D. Hohl, 2017, "Automated fault detection without seismic processing" *The Leading Edge*, 36, 208–214

[16] Wu, Xinming, Sergey Fomel, and Michael Hudec. "Fast salt boundary interpretation with optimal path picking." *Geophysics*83.3 (2018): O45-O53.

[17] Lomask, J., R. G. Clapp, and B. Biondi, 2007, "Application of image segmentation to tracking 3D salt boundaries" *Geophysics*, 72, no. 4, P47–P56.

[18] Ramirez, C., G. Larrazabal, and G. Gonzalez, 2016, "Salt body detection

from seismic data via sparse representation" *Geophysical Prospecting*, 64, 335–347.

[19] Grangier, D., L. Bottou, and R. Collobert, 2009, "Deep convolutional networks for scene parsing" *Presented at the ICML 2009 Deep Learning Workshop*.

[20] Ronneberger, O., P. Fischer, and T. Brox, 2015, "U-net. Convolutional networks for biomedical image segmentation" *International Conference on Medical Image Computing and Computer-assisted Intervention*, Springer, 234–241.

[21] Rafael C. Gonzalez & Richard "Digital Image Processing (3rd Edition) Hardcover", (2007).

[22] He, Kaiming, et al. "Delving deep into rectifiers: Surpassing human-level performance on imagenet classification." *Proceedings of the IEEE international conference on computer vision*. 2015.

[23] Kingma, D. P., and J. Ba, 2014, "Adam: A method for stochastic optimization" arXiv, abs/1412.6980.

[24] https://www.kaggle.com/c/tgs-salt-identification-challenge/data

Proceedings of the Fourth International Conference on Communication and Electronics Systems (ICCES 2019)
IEEE Conference Record # 45898; IEEE Xplore ISBN: 978-1-7281-1261-9

A Survey on Effective Data Computation in Inter Cloud Environment

Makrand Samvatsar
Research Scholar
School of Computer Science and Information Technology
Devi Ahilya Vishwavidyalaya, Indore

Priyesh Kanungo
Professor and Head Information Technology, MPSTME,
SVKM's NMIMS, Shirpur

***Abstract*-The need of efficient data computation in the today's world is challenging as the data generated everyday enormously. So in this case the computation resources may be available on demand because of the cloud computing. In this paper an analysis based on the previous study have been discussed and analyzed on the methodological prospects. It includes the attributes like computational parameters, data handling mechanism and data security and authentication. This study also explores the mechanism for the effective data computation in terms of inter cloud environment. It includes the environment variability between public and private clouds.**

Keywords-Cloud Computing, Data Computation, Inter Cloud Environment, Public and private clouds

1. INTRODUCTION

The resource sharing now a days become easier due to the cloud computing [1, 2]. Currently it is an essential platform for the It industry, Business enterprise, University, etc. It is also a mainstay for the Internet of Things (IoT). There are several resources which can be available on demand through the Internet [3, 4]. So cloud computing mainly provides the utility and so it is also called utility computing [5].

For the better utilization of the cloud computing there is the need of efficient handling of the resources and there should be mechanism to provide some sort of ranking and acquiring the mechanism securely [6–10].

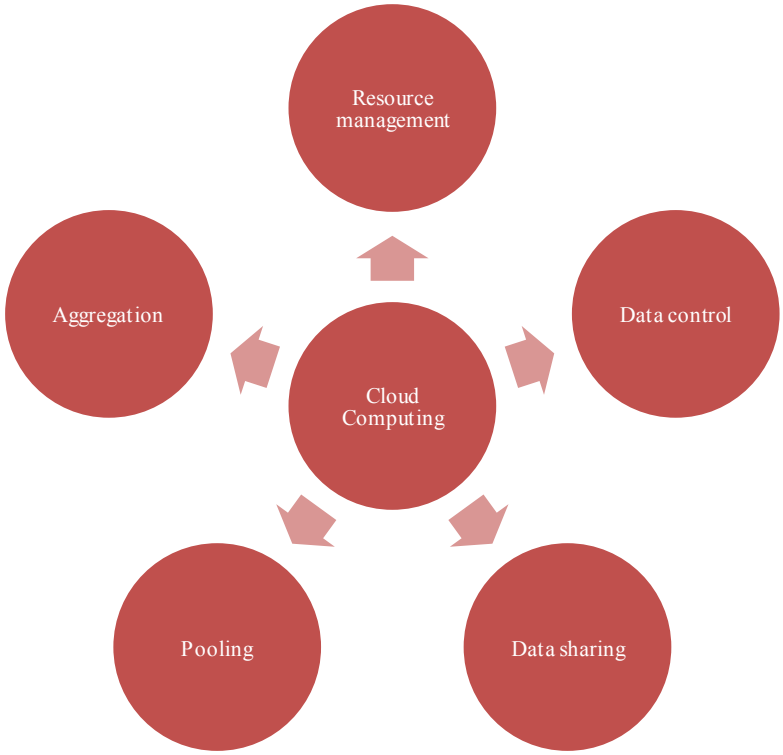

Figure 1 Cloud Computing System

In general cloud computing is categorized in four parts based on the deployment [11–14]. These are public, private, hybrid and community cloud. In terms of resource sharing public cloud is better but it is less secure. Private clod is more secure. In hybrid there is a concrete collaboration of public and private cloud. Community cloud provides the sharing of the resources between organizations [12]. In general based on the services it is categorized in three parts Infrastructure-as-a-Service (IaaS),

Platform-as-a-Service (PaaS) and Software-as-a-Service (SaaS) [12]. IaaS is mainly for the infrastructure like disk and servers (virtual). PaaS is mainly for the platform like database and execution framework. SaaS is mainly for the software resources like mailing services and application services.

The main objectives of this paper are:

1. To explore the methods in the direction of resource utilization and data sharing.
2. To explore the data handling mechanism.
3. To identify the pros and cons and discuss the solution.
4. To explore the security handling mechanism.

2. RELATED WORK

In 2018, Mao [15] discuss the impact of cloud computing environment with the intend of big data. They have suggested the big data transport channel model for improving the channel transmission. For the output features analysis they have used feature extraction and association rule mining. They have auto-correlation beam forming method for the channel equalization design. Their result suggests that their method has better channel equalization.

In 2018, Kim and Chang [16] discussed on privacy preserving techniques in terms of cloud computing. They have proposed a privacy preserving k-means algorithm for solving bit array comparison problem. They have also considered the center point based on the distribution mechanism. They have achieved 300% better performance.

In 2017, Jagli et al. [17] discussed the cloud computing in terms of fully integrated future Internet. They have suggested that the evaluation of best one is needed for efficient service selection and consideration for the development of the new model. They have proposed a model based on fuzzy clustering algorithm.

In 2016, Hong-Qiang et al. [18] discussed about the mobile cloud computing. They have worked on the user demand and their source approvals based on the demand for the fulfillment. For this they have proposed an efficient method based on fuzzy c-means algorithm for the resource scheduling.

In 2017, Lordan and Badia [19] discussed about the computing access in the cloud servers. Their framework that is framework that is COMPSs-Mobile provides the energy-efficient and high-performing applications. The structure gives a framework uninformed programming show that enables engineers to code standard Android applications whose calculation is straightforwardly parallelized and in part offloaded to remote assets. They have provided an outline of the programming demonstrate and depicts the interior parts of the toolbox which underpins it concentrating on the offloading and check pointing systems. It moreover presents the consequences of certain tests directed to assess the conduct of the arrangement and to quantify the potential advantages in android applications.

In 2016, Jing et al. [20] discussed about grey clustering and entropy. They have proposed a grey clustering classification model to evaluate cloud computing credibility. For this entropy is used. It is used for the purpose of weight determination of clustering. Their simulation supports the methods.

In 2016, Jagli et al. [21] discussed about the resource sharing. They have suggested that the SaaS the core of cloud computing. Hereafter interest for programming as a SaaS has been immensely expanded by end clients just as by a specialist organization, yet at the same time, it is a major testing task for cloud specialist coops to assess their administrations, gave to the end client. It is likewise troublesome for end clients to discover the potential programming administrations in the distributed computing condition. At first, depicts the inspiration for assessing SaaS on the distributed computing condition with the issue depiction. Besides, it's portraying the different issues furthermore, challenges for assessing programming administrations on the cloud figuring. Thirdly, it clarifies about the proposed work in assessing Software as a Service. At long last, the answer for the distinguished issue is executed and broke down the outcomes.

In 2017, Awada and Barker [22] discussed about the cloud computing providers. They have suggested a cloud-based management service (CMS) framework. The capability provided by this framework suggested are increased deployment density, scalability and resource efficiency. Their results shows that it is useful in cluster utilization, and reduction in execution time.

In 2017, Dutta and Sengupta [23] discussed about large data sets management. They have implemented k-means for this proposed especially for the enterprise cloud environment.

In 2017, Liu et al. [24] presented a hierarchical multi-cluster big data computing framework. It is based on the Apache Spark. Their system bolsters blend of heterogeneous spark figuring bunches. With a coordinated controller inside the system, it likewise encourages capacity for submitting, observing, executing of Spark work process. Their results shows the effectiveness in group creations.

3. PROBLEM STATEMENTS

The following problem statements have been identified based on the related study analyzed and discussed.

1. Data handling mechanism based on data clustering is missing.
2. Data categorization based on the weight based assignment is also missing.
3. How to handle the data securely in data sharing environment is also a big challenge.
4. Data mining techniques are missing in data sharing and handling.
5. Centralized authentication along with the cloud user control is missing in several research works.

4. ANALYSIS

Gap analysis based on the latest related works has been shown below in Table 1. Comparative analysis based on results is shown in Table 2.

Table 1: Result Analysis

S.no	Authors	Year	Work	Gap
1	Yu et al. [25]	2016	They have used knowledge workloads to predict the workloads of new tasks. For this they have used clustering algorithm. For the characteristic learning they have used neural network. Initial workload is used for the cluster determination. They have used Google dataset.	Other clustering parameters can be added.
2	Tar and Zaw [26]	2017	They have focused on document clustering in the cloud environment. They have proposed a cloud service and an ontology-based technique for identifying cloud service to improve the accuracy of cloud services searching. Their Approach has the capacity to perform cloud administration ideas from cloud administration sources. The fundamental thought behind our technique is cloud administrations utilizing a cosmology based strategy.	The security problem can be discussed.
3	Xiong et al. [27]	2016	They have discussed on resource gathering and data aggregation. They have in the wake of looking at three changed nation's hatchery's administration method, we basically talk about the best approach to structure a cloud-based hatchery stage including its design, principle capacities, and the interface. They expected that the stage can assemble and share a assortment of data and asset, similar to cash, human asset, hardware, office place, etc. So the stage is advantageous for the hatched endeavors, hatcheries, and the administration. For precedent, the stage can give singular administrations through huge information innovation. The stage can investigation the circumstance of hatcheries and caution the organizations in risky condition with the history huge information.	Different methods can be applied on different levels.
4	Yahyaoui and Moalla [28]	2016	They have worked on reducing the storage space. They have used classification for this purpose. For this different clusters have been created and each one represents different entity in the cloud space.	Prioritization should be included for the confliction management.
5	Xu et al. [29]	2016	They have worked in the direction of the predictive power calculation in the cloud environment. They have investigated the status of different machine and validate it.	It can be enhanced with the clustering mechanism.
6	Shangguan and Yue [30]	2018	They have presented MapReduce technique for parallelizing classification. The iterative preparing is changed into iterative Map and Reduce undertakings that can be executed in parallel. The K-Means bunching calculation is tested with the SPARK bunch sent on the OpenStack cloud figuring stage to outline the pertinence and viability of the methodology.	Other clustering parameters can be added.

Table 2: Comparative Analysis based on Results

S.no	Authors	Year	Method used	Results
1	Lee et al. [31]	2019	Trajectory-Aware Edge Node Clustering	The service delay is 2.6 second.
2	Koo et al. [32]	2019	Cloud-based C4I Security Architecture	Security requirements have been analyzed.
3	El-Sofany et al. [33]	2019	Cloud-based Model for Medical Diagnosis	The results shows that it is able to supports the results through fuzzy decisions that is Yes, Maybe, No.
4	Yan et al. [34]	2019	Deep unsupervised learning optimization algorithm based on cloud computing	The error rate is o.16%.
5	Islam et al. [35]	2019	Client Side Encryption in Cloud Computing	They have calculated the execution time for encryption and decryption of different packages like 4000kb, 5000kb, 6000kb and 7000kb.
6	Sharma et al. [36]	2019	Data Privacy in Cloud Computing	They have used AES algorithm with 128, 192, 256 bits length.

5. CONCLUSIONS AND FUTURE DIRECTIONS

This paper provides an explorative way in the direction of studying and analyzing cloud computing with respect to data handling, security and data sharing. This paper explores different related work to find out the problem statements which can be efficiently handle with the future prospects. It also highlights the gaps and the suggested mechanism for the advancement in the performance.

The future suggestions are following:

1. There is the need of working in the direction of data handling and sharing mechanism in efficient way.
2. There is the need of working in the direction of data security and proper virtualization with the ease in data sharing.
3. There is the need of data mining techniques for the pattern discovery in such a way that the load can be reduced or minimized.

References

[1] Mesbahi MR, Hashemi M, Rahmani AM. Performance evaluation and analysis of load balancing algorithms in cloud computing environments. In 2016 Second International Conference on Web Research (ICWR) 2016 Apr 27 (pp. 145-151). IEEE.

[2] Dubey AK, Dubey AK, Namdev M, Shrivastava SS. Cloud-user security based on RSA and MD5 algorithm for resource attestation and sharing in java environment. In 2012 CSI Sixth International Conference on Software Engineering (CONSEG) 2012 Sep 5 (pp. 1-8). IEEE.

[3] Zheng X, Martin P, Brohman K, Da Xu L. Cloudqual: A quality model for cloud services. IEEE Transactions on Industrial Informatics. 2014 May; 10(2):1527-36.

[4] Jagli D, Purohit S, Chandra NS. SaaS CloudQual: A Quality Model for Evaluating Software as a Service on the Cloud Computing Environment. In Innovations in Computer Science and Engineering 2017 (pp. 73-80). Springer, Singapore.

[5] Choi SW, Kim SD. A quality model for evaluating reusability of services in SOA. In2008 10th IEEE Conference on E-Commerce Technology and the Fifth IEEE Conference on Enterprise Computing, E-Commerce and E-Services 2008 Jul 21 (pp. 293-298). IEEE.

[6] Choudhary AR. Baseline requirements and architecture for cloud computing services. International Journal of Advanced Computer Research (IJACR). 2012; 2:1-7.

[7] Luo HY, Lv P, Liu LZ, Yang X. Enterprises trust comprehensive evaluation based on fussy rough AHP in cloud computing. J Shandong Univ (Nat Sci). 2014; 49:111-7.

[8] Alotaibi MB. Antecedents of software-as-a-service (SaaS) adoption: a structural equation model. International Journal of Advanced Computer Research. 2016 Jul 1; 6(25):114.

[9] Bhupendra Kumar, Jayshree Boaddh. A meta-analysis on secure cloud computing. International Journal of Advanced Technology and Engineering Exploration. 2016; 3(15): 15-20.

[10] Zisman A, Spanoudakis G, Dooley J. A framework for dynamic service discovery. In 2008 23rd IEEE/ACM International Conference on Automated Software Engineering 2008 Sep 15 (pp. 158-167). IEEE.

[11] Soni A, Hasan M. Pricing schemes in cloud computing: a review. International Journal of Advanced Computer Research. 2017 Mar 1; 7(29):60.

[12] https://www.globaldots.com/cloud-computing-types-of-cloud/

[13] Shrimali B, Bhadka H, Patel H. A fuzzy-based approach to evaluate multi-objective optimization for resource allocation in cloud. International Journal of Advanced Technology and Engineering Exploration. 2018 Jun 1; 5(43):140-50.

[14] Kalangi RR, Rao MC. A novel multi-user fingerprint minutiae based encryption and integrity verification for cloud data. International Journal of Advanced Computer Research. 2018 Jul 1; 8(37):161-70.

[15] Mao L. Big Data Equilibrium Scheduling Strategy in Cloud Computing Environment. In2018 International Conference on Virtual Reality and Intelligent Systems (ICVRIS) 2018 Aug 10 (pp. 94-98). IEEE.

[16] Kim HJ, Chang JW. A Privacy-Preserving k-Means Clustering Algorithm Using Secure Comparison Protocol and Density-Based Center Point Selection. In2018 IEEE 11th International Conference on Cloud Computing (CLOUD) 2018 Jul 1 (pp. 928-931). IEEE.
[17] Jagli D, Purohit S, Chandra NS. Fuzzy clustering algorithm intended for mining software services on the cloud. In 2017 International Conference on Advances in Computing, Communication and Control (ICAC3) 2017 Dec 1 (pp. 1-4). IEEE.
[18] Hong-Qiang W, Xiao-Yong L, Bin-Xing F, Yi-Ping W. Resource Scheduling Based on Improved FCM Algorithm for Mobile Cloud Computing. In2016 IEEE 22nd International Conference on Parallel and Distributed Systems (ICPADS) 2016 Dec 13 (pp. 128-132). IEEE.
[19] Lordan F, Badia RM. Compss-mobile: Parallel programming for mobile cloud computing. Journal of Grid Computing. 2017 Sep 1; 15(3):357-78.
[20] Jing Z, Rong J, Qiujun L, Jia W, Xiaoyun Y. Cloud computing credibility evaluation based on grey clustering and entropy. In2016 12th International Conference on Natural Computation, Fuzzy Systems and Knowledge Discovery (ICNC-FSKD) 2016 Aug 13 (pp. 772-776). IEEE.
[21] Jagli D, Purohit S, Nalla SC. Implementation of K-means clustering for evaluating SaaS on the cloud computing environment. In2016 International Conference on ICT in Business Industry & Government (ICTBIG) 2016 Nov 18 (pp. 1-5). IEEE.
[22] Awada U, Barker A. Improving resource efficiency of container-instance clusters on clouds. In 2017 IEEE/ACM International Symposium on Cluster, Cloud and Grid Computing (CCGRID) 2017 May 14 (pp. 929-934). IEEE.
[23] Dutta S, Sengupta S. Implementation of K-means clustering in ECB framework of cloud computing environment. In 2017 International Conference on Cloud Computing, Data Science & Engineering-Confluence 2017 Jan 12 (pp. 293-297). IEEE.
[24] Liu Z, Zhang H, Wang L. Hierarchical spark: A multi-cluster big data computing framework. In 2017 IEEE 10th International Conference on Cloud Computing (CLOUD) 2017 Jun 25 (pp. 90-97). IEEE.
[25] Yu Y, Jindal V, Yen IL, Bastani F. Integrating clustering and learning for improved workload prediction in the cloud. In2016 IEEE 9th International Conference on Cloud Computing (CLOUD) 2016 Jun 27 (pp. 876-879). IEEE.
[26] Tar HH, Zaw ZY. Semantic based clustering system with cloud computing. In2017 International Conference on Intelligent Informatics and Biomedical Sciences (ICIIBMS) 2017 Nov 24 (pp. 195-197). IEEE.
[27] Xiong G, Zhang C, Ji T, Guan B, Sun A, Hu Y, Nyberg TR. Cloud computing platform and big data service for incubator cluster. In2016 IEEE International Conference on Service Operations and Logistics, and Informatics (SOLI) 2016 Jul 10 (pp. 60-65). IEEE.
[28] Yahyaoui H, Moalla S. CloudFC: Files Clustering for Storage Space Optimization in Clouds. In 2016 IEEE International Conference on Cloud Computing Technology and Science (CloudCom) 2016 Dec 12 (pp. 193-197). IEEE.
[29] Xu J, Zhou A, Wang S, Sun Q, Li J, Yang F. Machine status prediction for dynamic and heterogenous cloud environment. In 2016 IEEE International Conference on Cluster Computing (CLUSTER) 2016 Sep 12 (pp. 136-137). IEEE.
[30] Shangguan B, Yue P. SPARK Processing of Computing-Intensive Classification of Remote Sensing Images: The Case on K-Means Clustering Algorithm. In 2018 International Conference on Geoinformatics 2018 Jun 28 (pp. 1-4). IEEE.
[31] Lee J, Ko H, Pack S. Trajectory-Aware Edge Node Clustering in Vehicular Edge Clouds. In2019 16th IEEE Annual Consumer Communications & Networking Conference (CCNC) 2019 Jan 11 (pp. 1-4). IEEE.
[32] Koo J, Kim YG, Lee SH. Security Requirements for Cloud-based C4I Security Architecture. In2019 International Conference on Platform Technology and Service (PlatCon) 2019 Jan 28 (pp. 1-4). IEEE.
[33] El-Sofany HF, Taj-Eddin IA. A Cloud-based Model for Medical Diagnosis using Fuzzy Logic Concepts. In2019 International Conference on Innovative Trends in Computer Engineering (ITCE) 2019 Feb 19 (pp. 162-167). IEEE.
[34] Yan H, Yu P, Long D. Study on Deep Unsupervised Learning Optimization Algorithm Based on Cloud Computing. In2019 International Conference on Intelligent Transportation, Big Data & Smart City (ICITBS) 2019 Jan 12 (pp. 679-681). IEEE.
[35] Islam MM, Hasan MZ, Shaon RA. A Novel Approach for Client Side Encryption in Cloud Computing. In2019 International Conference on Electrical, Computer and Communication Engineering (ECCE) 2019 Feb 7 (pp. 1-6). IEEE.
[36] Sharma Y, Gupta H, Khatri SK. A Security Model for the Enhancement of Data Privacy in Cloud Computing. In2019 Amity International Conference on Artificial Intelligence (AICAI) 2019 Apr 29 (pp. 898-902). IEEE.

Proceedings of the Fourth International Conference on Communication and Electronics Systems (ICCES 2019)
IEEE Conference Record # 45898; IEEE Xplore ISBN: 978-1-7281-1261-9

Infrared Vision for Fog Detection System to Improve Road Visibility

Jatin Talwar
ECE Dept, DAV Institute of Engineering & Technology, Jalandhar, Punjab, India
jatintalwar64@gmail.com

Dr. Love Kumar
ECE Dept, DAV Institute of Engineering & Technology, Jalandhar, Punjab, India
Er.lovekumar@gmail.com

Dr. Gurmohan Singh
Electronics & Embedded Computing Division, C-DAC, Mohali, Punjab, India, India
gurmohan@cdac.in

***Abstract*— Fog is a major reason behind road accidents and road side causalities as it reduces visibility, limits contrast and distorts perception. This paper presents some concepts for maturing of a scheme which will be able to increase clearity in winter and foggy conditions using the light rays and heat properties. Various type of foggy environments, their effects on visibility range and remedial measures are discussed. We proposed the Infrared Vision (IV) for fog detection systems to improve object visibility in dense fog.**

***Keywords*— Fog, Fog lights, Infrared Vision (IV), IVFDS, Thermal light**

I. INTRODUCTION

The most dangerous enemy for transportation is dense fog as it reduces the visibility range drastically. Due to dense fog we not only find problem in ground level transportation but even in air as well as in water medium. Therefore, it is necessary to understand the fog formation and the factors related to its formation. In Northern India, during the winter period, a series of low-pressure and high-pressure zones move from Northwest to Northeast along the Himalayas cause dense fog formation while over northern India, ground elevation is the lowest along the Gangetic plains. With the result, cold air drainage from Himalayan higher plateau results in the building up of cold dense air in the trough region. This boosts the relative humidity and the formation of fog takes place. Another type of fog is formed due to the initiation of slightly humid winds from the South-west over the northern region, thus comparatively humid and warm air quash a significantly chilly surface, which forms fog. Further, expanding water and irrigation system are also one of the major reasons today for the formation of fog. The moisture from these bodies contributes to fog formation especially in the rural areas of Northern India.

Fog is a cloud of tiny water particles, ice particles, smoke particles or blend of all these types of particles. This phenomenon is also known as mist/haze if the visibility range is greater than 1000 meters depending upon anonymity caused by mentioned solid particles. The density of fog depends upon the size of particles. The falling velocity of particles abate with smaller size of the water drop. Fog formation can take place in more than one way. Firstly, the air is cooled down to its dew point which results in the occurrence of fog droplets. When the temperature of air is same as compared to the dew point temperature, condensation on tiny water droplets present in the air occurs. The second method for fog formation requires water to evaporate from the ground surface into the air, boosting up the dew point till the time condensation occurs.

Due to dense fog light dispersed down to the earth at a great angle with respect to the line of the sun's light is primarily in the bluish region of the spectrum. The atmosphere changes the evident colour of the sun by scattering of light. This is known as Rayleigh scattering. When violet and blue light undergoes scattering, the mean visible wavelength or colour of the sun shifts towards red. The scattering of light having short wavelength by molecules in the atmosphere is what gives the sky its bluish colour. When viewed across the thicker layer of atmosphere at sunrise and sunset, the sun appears more orange or red. When seen across the thinnest layer of air at midday, the sun shines closest to its real colour, but still it has a hint of yellow colour. The presence of smoke and smog also results in scattering of light and can make the sun appear more orange or red (less blue) in colour [7]. This same phenomenon makes the moon appear more orange or red when it is close to the horizon, but when observed it is slightly more yellow or white when it is high in the sky [7]. The yellow colour has the highest wavelength and does not scatter too easily this is why we prefer using this colour for our headlights so as to make its visibility range higher.

Section II presents earlier types of headlights used in automobile industry. Section III discusses about the proposed solution. Section IV highlights working of Infrared Vision Fog Detection System (IVFDS). Section V presents conclusion and future aspects of proposed solution.

II. TYPES OF HEADLIGHTS

Choosing the right type of headlight plays an important role to meet the requirement of high intensity light, power and long-lasting life. In this section we discussed the different types of headlights and their working principles widely used in the automobile company.

A. Halogen

Halogen lamps functions on halogen gas which elevates brightness. These bulbs are less efficient, as most of the energy is wasted in heat instead of light [4]. Halogen bulbs used in automobiles typically emit a yellow colour light. In terms of units brightness, halogen lamps have a throw of light about 100 metres [4].

B. Xenon headlights

Also referred to as HID (high-intensity discharge), xenon lamps are similar to the universal tube light. There is no filament present that gets heated up, instead, xenon gas is electrically charged [4]. This produces a bluish-white light which is close in colour to natural light [4]. Xenon lamps are more expensive than halogen but they generally last longer and are more efficient. As seen with tube lights, these lamps also have a small delay before lighting up and take some time

to come to full brightness, which is why the high and passing beams get an additional halogen bulb [4]. Another type of xenon headlight is Bi-Xenon. The term bi-xenon headlight 'bi' uses just one xenon lamp for the high beam, which is then either moved or shaded each time a low beam is to be provided [4]. A bi-xenon lamp is cheaper and also takes up less space in the lamp unit [4].

C. LED headlights

LED or light emitting diode discharges light from the movement of electrons and as such, is a simple and highly efficient system [4]. The advantage of LED lights is that they light up instantly, highly efficient and last far longer than other light sources. Thus, they are frequently used in tail-lights and daytime running lights. However, with technology advancing, the problem of lower light intensity is being overcome to the point where LEDs are finding application in headlights [4]. The additional benefit here is that LEDs can emit light that is closer in colour to daylight. These lights consume minimal energy and most people likes them for their designs, style and less cost [4].

D. Laser Lights

These lights trigger a gas with a laser beam, which then glows extremely bright, emitting a powerful and high intensity light [4]. The advantage of laser lights is that they are far smaller than their counterparts. Laser lights have the tendency to throw light for larger distance. This technology is at present available in a few luxury cars worldwide due its high cost.

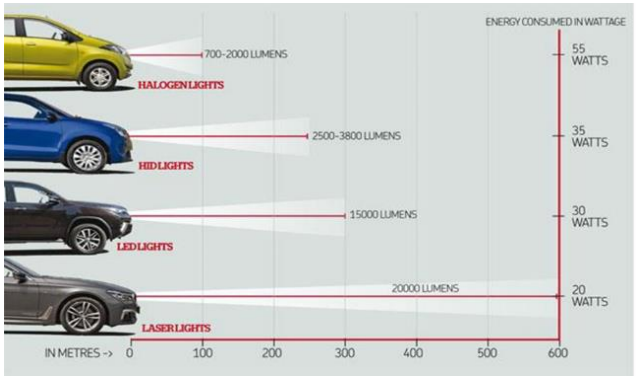

Fig. 1 Graph of headlights with its power range [4]

Fig. 1 show visibility range of various types of headlights. It is clear from Figure 2 that till date laser lights have capability to throw light for more distance as well as with less power consumptions. The less preferred light is halogen light as it has less visibility range as well as it consumes more power approximately 55 Watts [4].

Beside these lights it is necessary to discuss housing and various other components of headlights which play important role to control the emitted light from light source. The body of headlamps acts as a carrier for all the required headlamp components such as cable, reflector etc. Thermoplastics are majorly preferred for the material because of its rigid nature of protecting the body from external factors such as humidity, rain, heat etc. Out of these reflectors play a major role to control the directivity of the emitted light. To increase the efficiency of reflector materials may play a very crucial role. In previous time, most of the reflectors were made of sheet steel, while today, many unaddressed factors like outdated design, quality of material used, production tolerance etc. lead to the solution by using plastics (various thermoplastics) for reflectors. Their manufacturing is done by keeping the high accuracy of mould reproducibility in mind. Thereupon, the reflectors are coated so as to achieve the required surface quality. Aluminum or Magnesium can be used in the case of headlamps with high thermal stress to manufacture reflectors [3]. In the next stage an Aluminium reflection layer and later on a silicon protective layer is vapor-plated onto the reflector surface [3].

Another important parameter of headlight is projection module. Due to their accurate demarcated beam path and high luminous flux the use of projection modules has become quite often in modern headlamps. These modules can be used for wide range of headlamp and individual headlamp concepts because of the availability of different lens diameter, lighting function and easy installation. On the other hand, cover lenses are living up to the expectations by achieving the task of deflecting, scattering, focusing the luminous flux due to cover lenses with dispersion optics. The reflector collects it all in such a way that the desired light distribution, for instance the cut off line is produced [3]. The previous standard concept are now almost out of fashion and been completely replaced with non-patterned systems. Fig. 2 shows a cover lens generally used by headlight manufactures.

(a) (b)

Fig. 2 (a) Mostly used cover lens, (b) Cover lens without dispersion [3]

The improved version of cover lenses is cover lens without dispersion optics. Their main role is to protect the light from harsh weather conditions and rough soiling conditions. They are assigned to different purpose such as DE system used as inner lens, bi-xenon for high and low beam. Within the headlamp system fog lights separate the cover lenses directly in front of the reflector such as Free-form headlamps also known as FF totally without any additional patterning [3]. Glass is preferred mostly to form conventional cover lenses which must be free of errors such as streaks and bubbles. Though, the cover lenses are mostly made of plastic (polycarbonate having various advantages such as impact-resistant, light in weight, smaller production tolerances, more design freedom and special surface coating makes the lens scratchproof in compliance with ECE and SAE regulations [3].

There are four typical headlamp systems, paraboloid, FF-H4, Free-Form (FF) and Super-DE Headlamps (combined with FF headlamps) as shown in Fig. 3.

(a) (b) (c) (d)

Fig. 3 (a) Paraboloid headlamps (b) FF-H4 headlamps (c) Free-Form (FF) headlamps, and (d) Super-DE headlamps with FF headlamps [3]

The shape of reflective surface is parabolic in paraboloid lens. In distribution of headlamp light this is the oldest technology. They are rarely used nowadays. Still they make few appearances occasionally in large H4 headlamps and high-beam headlamps [3]. The reflector upper part is used in low beam from the front view as depicted in Fig. 3(a) [3]. The positioning of light source is carried out in such a way that upwardly radiated light on surface of reflector is downwardly reflected on the optical axis on the roadway as shown in Fig. 3 (b). To meet the standard legal requirements, light is distributed precisely in the cover lens [3]. The distribution of light is carried out by optical elements of two different shapes. The cylindrical vertical profile distributes light in horizontal direction and prismatic structures on a level with the optical axis. This further helps in distributing light in particular a way such that most crucial traffic spots get adequate amount of light as depicted in Fig. 3(c). The cover lens assembly has optical elements in paraboloid headlamp especially for low beam and to provide light distribution as desired as depicted in Fig. 3 (d). In this particular light distribution system, 2 light sources, 1 reflector, 3 bulb shields, and 4 cover lenses are used [3]. The useful light is approx. 27%,

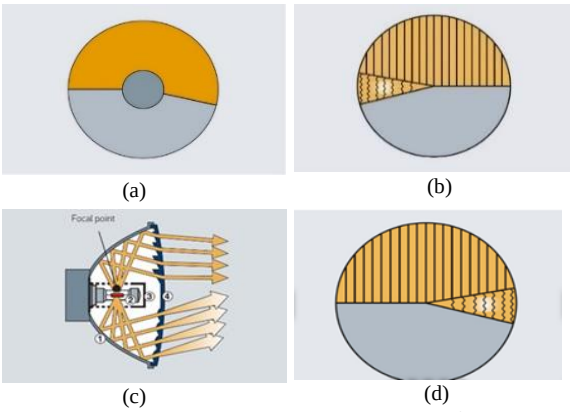

Fig. 4 Light dispersion due to cylindrical optics and deflection by prism in cover lens (seen from above) [3]

The reflective surfaces are freely formed within the space in Free-Form (FF) headlamps. Only computer can compute and optimize them [3]. The various areas of surroundings and road are illuminated by various parts of the reflector. This is specially designed in such ways to use all available reflective surfaces to produce the low beam as depicted in Fig. 4 (a) [3]. The aligning of areas is done in such a way that the light from reflectors is downwardly reflected for having higher visibility on the road as depicted as Fig. 4(b). The reflective surfaces made possible light beams deflection and scattering [3]. The use of clear, non-patterned cover lenses enables to provide the headlamp a brilliant appearance [3]. The horizontally arranged reflector segments generates the illumination and cut-off line of the right-hand edge of the road as shown in Fig. 4(c). The Fig. 4 (d) illustrates distribution of light on the cover lens of an FF headlamp. Nowadays all headlamp reflection systems are furnished with FF reflective surfaces.

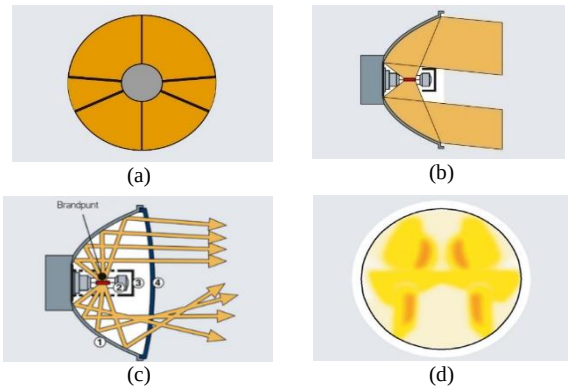

Fig. 5 Dispersion and deflection of light beam caused by reflective surface [3]

In this particular light distribution system, 2 light sources, 1 reflector, 3 bulb shields, and 4 cover lenses are used [3]. The useful light is approx. 27%, [3].

The projector type systems are employed in DE and Super-DE headlamps and they work in same way. The FF technology is used in design of the reflective surfaces [13]. In these headlamps, maximum light is captured by the reflector from the bulb as shown in Fig. 5(a). The light captured from reflector is then guided to fall over the shield and finally directed onto the lens as depicted in Fig. 5(b).

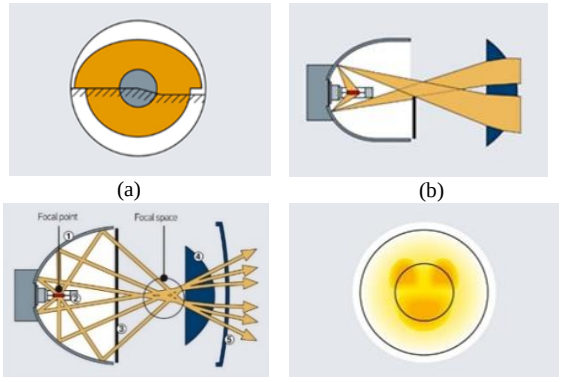

Fig. 6 Intensity of light in focal space and beam path (view from above) [3]

The alignment of light with the reflector in done in such a way that at shield light get distributed which is further projected onto the road with the combination lens as shown in Fig. 5(c). The Fig 5(d) shows a distribution of low beam on cover lens of a Super-DE headlamp.

The use of FF technology facilitates better illumination and wider scatter width on the road edges. To achieve greater visible range and relaxed driving during night time, the light is generally focused near to the cut-off line [3]. The FF reflective surfaces are vital part of all new projector-type systems for low beam. Generally, for greater light output, lenses having diameter between 40 to 80 mm are used. They also result in more weight [3].

As discussed about various types of headlights, the important points and issues related to construction and working of these lamps, there is still a need of improved version of headlamps as existing headlamps are not suitable for dense fog situation due to scattering and reflecting property of the light. The suitable type of headlight which could be the solution to the problems of low visibility due to fog are LED [8]. They have low power consumption, high life

and are eco-friendly. The scattering and reflecting properties of light could cause blindness for the driver in dense foggy conditions [8]. The projected light beam is unable to penetrate deep into the thick fog which makes the vision blurred. The laser-based headlights can be used to improve the vision and visibility for the driver due to high intensity and monochromatic nature of light. Still laser-based head lamps are not in practice due to its high cost and preferred in luxury cars. We require LED with high power and heating effects to achieve the desired result [10]. This approach of breaking down the water droplets by heating effect can be used in smart street lights [11] also they are installed on a specific height so they can also very well help in reduce the low visibility caused by fog.

In this paper, we have introduced a cost-effective solution to visibility problem during dense foggy conditions. We all might have noticed one thing that whenever sunrises the thick fog tends to evaporate. This happens because the fog which is formed due to the condensation effect, when sunlight passes through those tiny water molecules, they get evaporated and results clear sky. Therefore, the concept of evaporation needed to implement by some artificial means to make an effective headlamp. Therefore, some light emitting source which can produce light due to heating effect. Further, heat emitted light needs to be modulated on a carrier which ensures longer propagation distance with high intensity light. Further, high end projection lamps, lenses which can channel the light through them. Coating of Graphene layer must be used as it can withstand high heat temperature so that when the heat rays will pass through it the life line of the bulb in headlight doesn't degrades The light needs to be projected at such an angle and by projecting we need to control the spreading of the light so that the heating property of the light is hot enough to cause evaporation of the tiny water particles, hence the warm air through fog will travel forward causing the same heating effect and making the view much clear for the driver. The angle at which the light is being projected is assumed to follow parabolic profile so that the curvature of light traps the maximum fog under heating effect and clear the path from fog.

III. Proposed Solution

An experiment was conducted to justify the proposed solution to make visibility much more achievable by using thermal light headlight system. An artificial fog like condition was created at home by exhaling warm air on the mirror surface. The mirror surface being cold when it came in contact with the warm air caused condensation. The concept uses to create artificial environment is based on the principal of condensation as when we breathe out, we give out warm air which get freeze when comes in contact with mirror whose temperature is less than air. The moisture begins to come out from the air forming mist of tiny droplets just like fog. After creating artificial conditions just like fog, we noted the time it took to clear off the foggy surface back to clear mirror. So naturally it took around 1minute and 34 seconds.

Then we created an artificial working model just as of the conceptual model of thermal light headlight system. We focused a LED torch on the mirror surface very closely to generate the heating effect as to note what happens and what we noticed that after 1 minute the results were very different. The targeted area under the scope of LED light caused the foggy surface to turn normal into clear screen as the cluster of tiny water droplets the mist on screen broke due to the heating affect and two regions one still with foggy appearance and the other with clear visible appearance was noticed. After the conduction of this small experiment one thing was very much clear that focusing a light with heating properties does break down the condensation to evaporation state which will remove the foggy affect. Based on this small experiment it can be said that if this concept is introduced in headlights with much improved concave lens to converge and then emit light, much improved heating effect could be brought into implementation then it will break down the fog to increase visibility.

IV. Infrared vision Fog detecting system (IVFDS)

After so many discussions about the solution of this problem is not yet achieved. Now the problem has to be addressed not only for the light weight transportation point of view but also as per the requirement of heavy vehicle transportation too. Looking more deeply into the matter fog and its uncontrollable adverse effect on the other modes of transportation like Aeroplanes for air transportation, trains for road transportation, ships for water transportation. Presence of thick fog causes challenging problems for departure of scheduled container as well as passengers boarding their flight or ship which causes inconvenience to the people in form of cancelled flight, delay in importing and exporting of material causing huge bucks as a penalty to the government. So, to make this problem manageable the idea of Infrared vision Fog Detecting System (IVFDS) was proposed which ensures the measurement of the fog thickness for safety and employs thermal cameras to capture a rough idea and image of the any possible obstruction in the path [5]. Depending on the thickness of the fog the system will automatically adjust the intensity of the thermal lights to make sure that safety is not compromised. The preinstalled software will also make sure that it does matches the required conditions in terms to the fog density, the required light intensity and then if the conditions of the surrounding in any way compromises with the safety it will advise not to head start the journey.

For fog detection we will use fog sensors in our IVFDS system. Radar by disparity, operates better not with sound waves, but with electromagnetic waves [6] and this is a vital difference. Like ultrasonic, the waves when travelling collides with an object and as a result they bounce off. They travel at a known speed which is faster comparatively to the ultrasonic waves [6]. Radar is preferred above all because of its nature to not get affected by temperature, an improved consistency and accuracy. Radar also comes very handy and useful in other applications, such as operating in a vacuum, or in high pressure. One of the important reasons is dielectric constant of the target material [6]. Using materials with small dielectric constant does not reflect the electromagnetic wave, so radar passes right through it. To measure such materials having a low dielectric constant is just very gruelling so, to overcome the drawback of low dielectric property of the material which might cause less accuracy for the EM wave when it returns after bouncing back so Guided-Wave Radar (GWR) can also be used. Radar can also help us to detect

vehicles and their position in dense fog if our road visibility is still foggy [9].

A night vision system, based on thermal imaging technology that gives drivers a better view of the road beyond their headlights range. Using infrared technology, it allows driver to see hazards clearly in total darkness and can help in dense fog detecting nearby vehicles, people, and animals [5,12]. It spots the infrared energy (heat) and transforms it into an electronic signal, which is taken care of to generate a thermal image or video because the thermal image camera sees heat not light, it increases the visibility up to four times than headlights and it is not affected by smoke dust or fog. It works in both day and night and is not affected from glare of oncoming headlights.

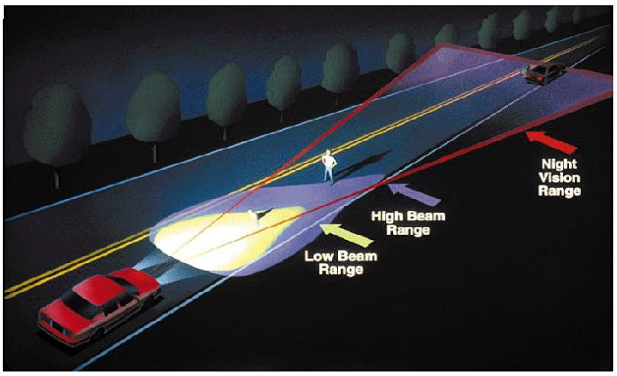

Fig. 7 The schematic illustration range of beam [5]

It will help us to know even if we are not able to see anything as it is not affected due to the fog or darkness. The image can be obtained on our windshield or on the Fog detection system. The sound alerting technology can be used in which if we don't want the image just the presence of any obstacle ahead of us will warn and alert the system and will generate beeping sound. This will also prove to be more economical because we have to make sure the technology should be economical and affordable for all. Fig. 7 illustrates the comparison of different beam ranges that can be used in IVFDS.

V. Conclusions and Future Scope

It is observed that the headlight preferred should be LED as they have low power consumption along with high durability and long-lasting properties. It is proposed that light should be projected in such a way that its heating properties could be used efficiently to reduce the fog. The fog detecting system based on infrared vision will make sure that there is no obstacle in the path of 8 ft to 10 ft. It uses the radio waves from the EM spectrum and does not need any medium to travel. The factors such as fog, hot, humid weather conditions won't affect it. It is also proposed that **IVFDS** will use radar and the magneto-inductive distance sensors for calculating the car speed and distance of impact. It will apply the emergency brakes without the knowledge of driver or it will also give a beeping sound to alert the driver so that when he applies the brake the throttle access is already cut off and it will lessen the impact and the frictional force on the driver.

It is a proposed idea which intends to improve the visibility problems in future faced due to the uncontrolled formation of fog.

References

[1] G. Galati, I. Dalmasso, G. Pavan, G. Brogi, "Fog Detection Using Airport Radar", *2006 International Radar Symposium*, 24-26 May 2006, Krakow, Poland. DOI: 10.1109/IRS.2006.4338037

[2] Xiaojing Wu, Samnei Li "Automatic Fog Detection over Chinese adjacent oceans using Terra/MODIS data," *International Journal of Remote Sensing*, vol 35 (21), pp. 7430-7457, 2014.

[3] "Headlight lens components, types & regulations: HELLA". Available at hyperlink: www.hella.com/techworld/uk/Technical/Automotive-lighting/Headlights-219/

[4] "Types of headlights: AUTOCARINDIA". Available at hyperlink: https://www.autocarindia.com/auto-features/lighting-the-way-headlight-tech-explained-404826

[5] "Infrared vision, thermal detecting:TECHBRIEFS". Available at hyperlink: https://www.techbriefs.com/component/content/article/tb/features/application-briefs/13424

[6] "Fog sensors, radar & challenges:APGSENSORS". Available at hyperlink: https://www.apgsensors.com/about-us/blog/radar-and-ultrasonic-sensors

[7] "Change in color of sun and moon: THOUGHTCO". Available at hyperlink: https://www.thoughtco.com/why-is-the-sun-yellow-603797

[8] Kurniawan B. A., Nakashima Y., Takamatsu M. Analysis of visual perception of light emitting diode brightness in dense fog with various droplet sizes // Optical Review, 2008. – Vol. 15. – No. 3. – P. 166–172.

[9] J. Laneurit, C. Blanc, R. Chapuis and L. Trassoudaine, Multisensorial data fusion for global vehicle and obstacles absolute positioning, IEEE Intelligent Vehicles Symposium, pp. 138-143, June 2003, Columbus, OH.

[10] Christensen A., Ha M. and Graham S., 2007, "Thermal management methods for compact high power LED arrays", 7th International Conference on Solid State Lighting, 14 September 2007 San Diego, 66690Z.1 66690Z.19.

[11] Vitta P., Stanikūnas R., Tuzikas A., Reklaitis I., Stonkus A., Petrulis A., Vaitkevičius H., Žukauskas A. Energy–saving approaches to solid state street lighting // Proceedings of SPIE, 10/2011. – Vol. 8123.

[12] M. Pavlic, H. Belzner, G. Rigoll and S. Ilic, "Image based fog detection in vehicles", Vehicles Symposium (IV), 5 July Alcala de Henares, Spain, 2012

Proceedings of the Fourth International Conference on Communication and Electronics Systems (ICCES 2019)
IEEE Conference Record # 45898; IEEE Xplore ISBN: 978-1-7281-1261-9

2x2 Circular Patch Antenna Array at 2.4 GHz for WSN Applications

Design and Performance Analysis of Circular Antenna Array and Comparison over Rectangular Array

Shravan G. S.
Dept. of Telecommunication Engg.,
BIT, Bangalore, India.
Email: shravansrinivasgs56@gmail.com

L. Sai Suhas
Dept. of Telecommunication Engg.,
BIT, Bangalore, India.
Email: l.saisuhas@gmail.com

Hemanth Kumar N. G.
Dept. of Telecommunication Engg.,
BIT, Bangalore, India.
Email: hemanthng26@gmail.com

Vinay S.
Dept. of Telecommunication Engg.,
BIT, Bangalore, India.
Email: vinayraju84@gmail.com

Girish Kumar N. G.
Assistant Professor,
Dept. of Telecommunication Engg.,
BIT, Bangalore, India.
Email: nggk_bit@live.in

Abstract— **The work is to design a 2x2 circular microstrip patch antenna array resonating at 2.4GHz and it is simulated for Wireless Sensor Network (WSN) applications by using HFSS tool. Circular patch antenna array is designed by depositing circular patches on FR-4 Epoxy substrate and is fed using microstrip feed lines. Fabricated antenna resonates at 2.391GHz. Antenna parameters such as Gain, return loss, Voltage Standing Wave Ratio (VSWR), Directivity, Reflection coefficient and radiation pattern are analyzed. 2x2 circular microstrip patch antenna produces more gain and less return loss compared to 2x2 rectangular microstrip patch antenna. The compact size and higher directivity compared to rectangular array makes it more relatively useful for WSN applications.**

Keywords—Microstrip Antennas; Circular array; Wireless Sensor Networks; Patch Antennas;

I. INTRODUCTION

Antenna basically converts electrons to photons or vice versa. The basic principle involved with the antenna is that the radiation is produced by the accelerated charge, As the separation between the conducting wires reaches the wavelength or more it tends to radiate so that the open end of the transmission line acts as antenna which launches a free space wave. The current on the transmission line flows out as the antenna end there, but the electric field associated will not die out. The radiation of antenna is in the form of circular wavefront at the transmitting antenna whereas at the remote distance the spherical wave transmitted by transmitting antenna arrives at receiving antenna as a plain wave, therefore antenna is a transducer or transition device between guided wave and a free space or vice versa [1]-[3].

On the basis of radiation, Omni-directional antennas are weak directional antennas because they radiate and receive less energy in all directions whereas Directional antenna radiate and receive in a particular direction.

In recent years, Microstrip patch antennas have gained a lot of importance because of their characteristics including light weight, high efficiency, high gain, high directivity and minimum return loss which will help in communication with different range of frequencies and used in applications such as remote sensing, medical fields etc. [4].

Circular antenna shows better results in terms of return loss and VSWR compare to rectangular one. Also, circular antenna shows better result when bandwidth and side lobes are considered. The radiation efficiency is similar in both the antenna which helps in compactable in similar kind of applications [5].

Antennas with more directivity can be used in improving network performance as they increase the alleviating contention and the communication range which can be used primely in Wireless Sensor Networks (WSNs). Along with directivity of the antennas, the compact size of microstrip antenna which are far better than the other enclosed or fabricated types of antenna also helps it in being suitable for WSN application use [6].

In this paper, firstly the related works that have been referred for this paper as a preliminary study have been briefed out in II. Then, we then begin with how the design is done starting from single antenna element in obtaining the array in III, followed by describing the gist of antenna parameters in IV, Further we demonstrate the simulated and testing results in V and compare the set of results for single circular element, simulated and fabricated circular array and the values of that of rectangular array in VI. Finally, we conclude with the future improvements that can be done over the designed antenna array.

II. Related Works

A similar rectangular patch antenna array for LTE applications are studied in [7]. The antenna is designed for 2.1 GHz applications and resonates at 1.86 GHz. Also, another rectangular antenna array is designed in [8] that works in S, C, X- bands. The array arrangements of 1x2 and 1x4 for 2 and 4 antenna elements respectively have been studied in that paper. Roger RT/duroid material with dielectric constant 2.2 and height 1.588 has been used as a substrate material. Microstrip inset line feed has been used for feeding the rectangular patch antenna.

III. Design Procedure

The design procedure can be broken down into two stages viz., Single element design and Array design.

A. Single Element Design

A circular element is characterized by a single parameter i.e., radius of the circle, denoted by a. Given the type of substrate used, desired operating frequency f_r, the radius a can be determined using expression (1) [9].

$$a = \frac{F}{\left\{1+\frac{2h}{\pi\varepsilon rF}\left[ln\frac{\pi F}{2h}+1.7726\right]\right\}^{0.5}} \quad in\ cms \qquad (1)$$

Where,

$$F = \frac{8.791*10^9}{fr\sqrt{\varepsilon_r}} \qquad (2)$$

B. Array design

1) Geometry: The geometrical arrangement of 2x2 is chosen while interelement spacing and the feedline widths are to be determined with the Transmission-line formulae.

2) Inter-Element spacing: Inter-element spacing of λ/2 is chosen in order to obtain the symmetric radiation pattern in both the directions uniformly, i.e., along $\theta = 0^0$ & 180^0 [10].

*3) Coaxial probe dimensions:*The signal from the microwave source is fed to the antenna through coaxial probe, whose dimensions are found using the following expression for characteristic impedance, Z_0 (3).

$$Z_0 = \frac{138*log_{10}\left(\frac{D}{d}\right)}{\sqrt{\varepsilon_r}} \qquad (3)$$

Taking ε_r = 4.4, choosing outer diameter, D=3.4mm, We obtain inner diameter, d=0.7mm. The design is shown in the Fig. 1.

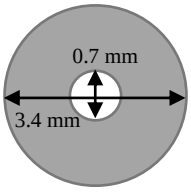

Fig. 1. Dimensions of designed coaxial feed

4) Feed-line widths: The supply from microwave source fed through coaxial feedline are further distributed amongst elements using inset feed lines, whose widths (w) are determined using Transmission line equation [11] shown in (4).

$$Z_0 = \frac{81.0}{(\varepsilon_r+1.41)^{1/2}}\, ln\frac{5.98h}{0.8w+t} \qquad (4)$$

Where, h and t are height of substrate (1.6 mm) and thickness of track (0.035 mm) respectively.

The dimensions of the parameters involved in the antenna design are listed in the Table I.

TABLE I. Values of the Antenna Dimensions

PARAMETER	DIMENSION
Height of the Substrate, h	1.6 mm
Dielectric Constant of substrate (FR4 Epoxy), ε_r	4.4
Radius of the patch, a	17 mm
Inter-Element Spacing	62.5 mm
Thickness of the track, t	0.035mm

The obtained design on HFSS 15.0 is shown in Fig. 2.

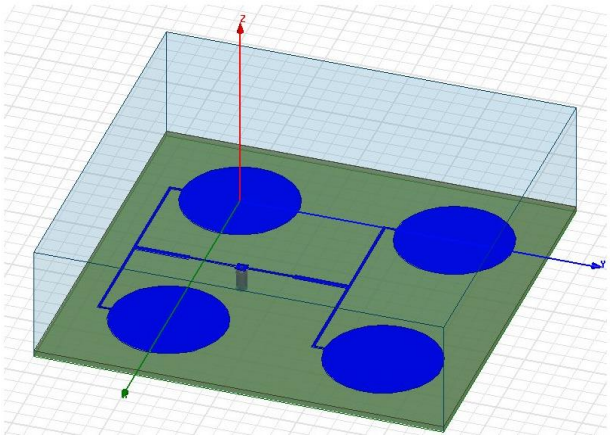

Fig. 2. Antenna design on HFSS 15.0

The fabrication is done and it is depicted in Fig. 3.

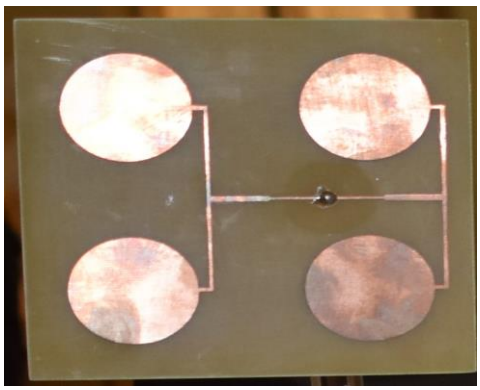

Fig. 3. Fabricated Antenna Design

IV. Parameters of Interest

A. Directivity (D)

Directivity is the pattern used in order to measure how directional an antenna's radiation pattern is. Directivity of a non-isotropic source is determined as the ratios of radiation intensity of the antenna in a reference direction to the radiation intensity of an isotropic source. Isotropic antennas radiate in all directions and hence their directivity will be 1 [12].

$$D = \frac{U}{U_0} = \frac{4\pi U}{P_{rad}} \tag{5}$$

Directivity can also be defined in terms of beam solid angle Ω_A as below

$$D = \frac{4\pi}{\Omega_A} \approx \frac{4\pi}{\theta_E \theta_H} \quad (\theta_E \text{ \& } \theta_H \text{ in radians}) \tag{6}$$

$$D = \frac{32400}{\theta_E \theta_H} \quad (\theta_E \text{ \& } \theta_H \text{ in degrees}) \tag{7}$$

B. VSWR

VSWR gives how efficiently the transmission of power takes place from the source to load. In perfectly matched systems 100% of power is transmitted. Therefore, the VSWR for such systems will be 1. It can be expressed as maximum voltage over minimum voltage of a standing wave.

$$VSWR = \frac{V_{MAX}}{V_{MIN}} = \frac{V_{fwd} + V_{ref}}{V_{fwd} - V_{ref}} = \frac{1 + \sqrt{\frac{P_{ref}}{P_{fwd}}}}{1 - \sqrt{\frac{P_{ref}}{P_{fwd}}}} \tag{8}$$

C. Reflection Coefficient (Γ) and Return Loss (RL)

Reflection coefficient is the one that describes how much of electromagnetic wave is reflected back due to impedance mismatch. It is expressed as the ratio of reflected voltage to forward voltage.

$$\Gamma = \frac{V_{ref}}{V_{fwd}} = \frac{VSWR-1}{VSWR+1} \tag{9}$$

Return Loss (RL) of an antenna can be used as an indication of how effectively the transmitted power of an antenna gets reflected. Since the return loss is the measure of how small the reflection is, more the return loss, less is the reflections and therefore the VSWR.

Return loss in terms of reflection coefficient is

$$RL(dB) = 20log_{10}(\Gamma) \tag{10}$$

D. Gain (G)

Antenna gain indicates how strong an antenna can send or receive a signal in specific direction. The usual description is with respect to the gain of an ideal isotropic lossless antenna. In terms of powers, P_r and P_t, it can be given as below:

$$Gain\ (G) = 10log_{10}\left(\frac{4\pi d}{\lambda}\sqrt{\frac{P_r}{P_t}}\right)\ (dB) \tag{11}$$

E. Antenna Efficiency(ε_r)

The efficiency in regard to an antenna gives the idea about how effective an antenna is in converting frequency power provided at its feedline into radiated power. This can also be defined in terms of gain and directivity as

$$G = \varepsilon_r D \tag{12}$$

V. Simulated Results and Testing

A. Simulated Results

The antenna design is simulated on the simulation tool, HFSS 15.0 and the results are obtained which are found to be almost same as the testing values obtained with the fabricated setup.

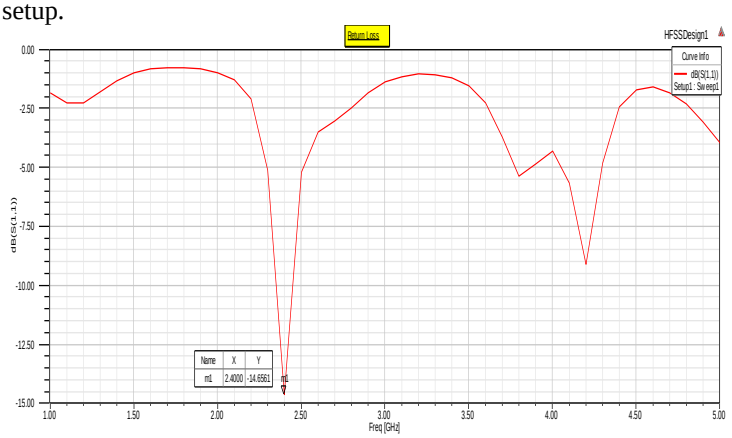

Fig. 4. Simulated value for Return Loss of Circular array

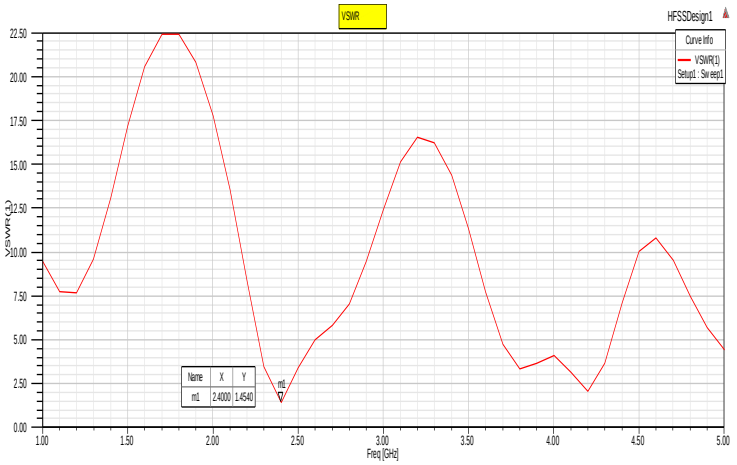

Fig. 5. Simulated value for VSWR of Circular array

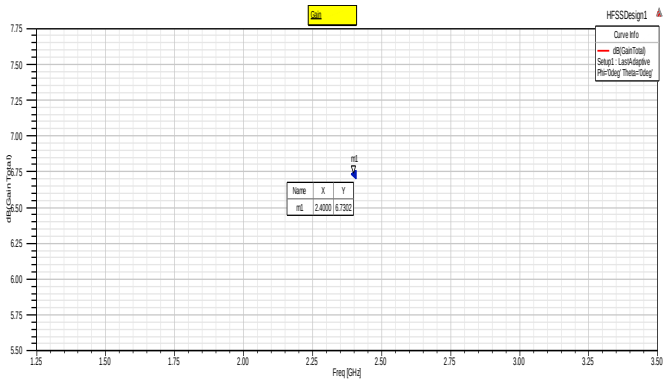

Fig. 6. Simulated value for Gain (in dB) of Circular array

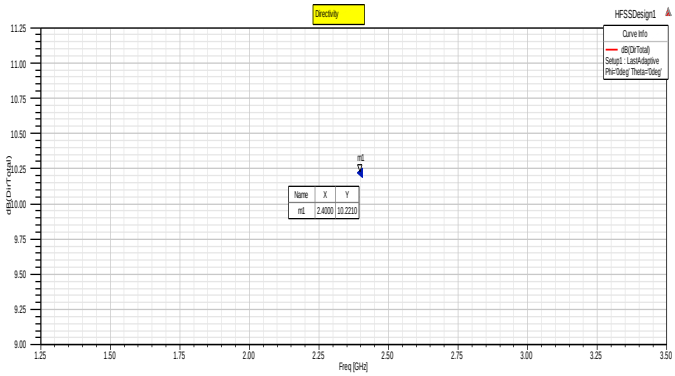

Fig. 7. Simulated value for Directivity (in dB) of Circular array

As shown in the result plots, the antenna array resonates at 2.4GHz as desired. Where, the values of Return loss, VSWR, Gain and Directivity are -14.6561dB, 1.4540, 6.7302dB and 10.2210 dB respectively. Reflection coefficient calculated with its relationship with VSWR is found to be 0.1850.

B. Testing

The minimum distance to be maintained between the Transmitting and receiving antenna are found to be more than 6.6 cm ($2d^2/\lambda$). Here d is diagonal length of the array antenna. Placing the arrays 42 cm away from each other we tested the fabricated antennas for transmission.

Fig. 8. Testing Setup

The transmitted power (P_t) and received power (P_r) are found to be 6.668mW and 50.582µW. From these values gain is calculated and is equal to 5.6dB. The forward power (P_{fwd}) and reflected power (P_{ref}) in an antenna are measured to be 933µW and 1.12µW respectively. Hence, values of VSWR and reflection coefficient are 1.07 and 0.0338. The θ_E and θ_H are found 50^0 and 55^0 hence the directivity is 10.712dB.

The obtained values over testing is tabulated in the Table II.

TABLE II. OBTAINED VALUES ON TESTING

PARAMETER	VALUE
Operating Frequency, f_r	2.391 GHz
Return Loss (dB)	-29.4216
VSWR	1.07
Gain(dB)	5.6
Directivity(dB)	10.712
Reflection Coefficient, Γ	0.0338

VI. PERFORMANCE COMPARISON

The performance comparison between the simulated and fabricated antennas over the rectangular antenna array [8] is tabulated in Table III.

TABLE III. PERFORMANCE COMPARISON

PARAMETER	CIRCULAR ARRAY		RECTANGULAR ARRAY [8]
	SIMULATED VALUE	FABRICATED VALUE	
Operating Frequency (GHz)	2.4	2.391	2.35
Return Loss (dB)	-14.6561	-29.4216	-18.32
VSWR	1.4540	1.07	1.74
Gain(dB)	6.7118	5.6	2.63
Directivity(dB)	10.5220	10.712	6.84
Reflection Coefficient, Γ	0.1850	0.0338	0.27

A circular array of 4 antenna elements was fabricated and tested to obtain parametric values. The obtained parametric values are found to be nearly same as the simulated values. Parameters like return loss, VSWR and Reflection coefficient are found to be better in the fabricated antenna than that of simulated values. In comparison with the rectangular array of 4 elements [8], all the parameters except for that of directivity, where the rectangular array seems to behave more isotropic than that of circular array. Additionally, return loss is found to be much better in the fabricated array with respect to that of rectangular array.

VII. CONCLUSION

A 2x2 circular antenna array that resonates at 2.39GHz frequency is designed using HFSS 15.0 simulation tool and is fabricated and tested to obtain the antenna parametric values. The fabricated antenna values are comparatively similar with respect to the simulated values. It is found to yield better values in terms of Gain, Return loss, Reflection coefficient and VSWR over rectangular array antenna. Wireless Sensor Network applications employ antenna that are highly directional as the data flow from the nodes are unidirectional

towards the control node, which in turn, is directional with the other antennas with other networks. Hence, the designed array can be used in applications of Wireless Sensor Networks due to compact size of microstrip antenna and comparatively high gain in accordance with that of rectangular antenna array at 2.4 GHz frequency. Parameters like the gain and directivity can be further improved by increasing and employing the number of antenna patch elements. It can also be made of lesser patch element size by using a relatively higher dielectric constant material.

ACKNOWLEDGMENT

We thank our Institution, Bangalore Institute of Technology and our Department, Department of Telecommunication Engineering for providing us laboratory facilities for experimenting and testing. Also, we are grateful for Technilab Instruments for helping us in fabrication and fundamental testing of the Antenna.

REFERENCES

[1] Raja, A. H. 2009 Study of Microstrip Feed Line Patch Antenna, Eng. & Tech. Journal, Vol.27, No.2.

[2] Y. F. Cao, S. W. Cheung, Senior Member, IEEE, and T. I. Yuk, Member, IEEE, "A multiband slot antenna for GPS/WiMAX//WLAN systems," IEEE Trans. Antenna Propag. vol. 63, pp. 952-958,Mar. 2015.

[3] Chakraborty, U., Chatterjee, S., Chowdhury,S. K., and Sarkar, P. P.2 011A compact microstrip patch antenna for wireless communication Progress In Electromagnetics Research C, Vol. 18, 211-220.

[4] Minervino, D.R. 20134Arrays of Rectangular Patch Microstrip Antennas for Aerospace Applications 978-1-4799-1397.

[5] P. Saghati, M. Azarmanesh, and R. Zaker, "A novel switchable singleand mulifrequency triple-slot antenna for 2.4-GHz bluetooth, 3.5-GHz WiMAX, and 5.8-GHz WLAN," IEEE Antennas wireless propag. Lett., vol. 9,pp. 534-537,Jun. 2010.

[6] G. Tarter, L. Mottola and G. P. Picco, "Directional Antennas for Convergecast in Wireless Sensor Networks: Are They a Good Idea?," *2016 IEEE 13th International Conference on Mobile Ad Hoc and Sensor Systems (MASS)*, Brasilia, 2016, pp. 172-182.

[7] S. Sudha and N. Sasirekha, "Design of smart antenna array of 2×2 MIMO for 4G-LTE," *2016 International Conference on Wireless Communications, Signal Processing and Networking (WiSPNET)*, Chennai, 2016, pp. 1611-1615.

[8] Design of Rectangular Microstrip Patch Antenna Array for S, C and X-Band; International Journal of Computer Applications (0975 – 8887); International Conference on Advancements in Engineering and Technology (ICAET 2015).

[9] Sanghamitra Dasgupta, Bhaskar Gupta and Hiranmoy Saha, "Development of Circular Microstrip Patch Antenna Array for Rectenna Application", IEEE INDICON 2010, Kolkata, INDIA December 17-19, 2010, pp. 1-6.

[10] Raji A. Abimbola (2017). Effects of Spacing and Number of Elements on the Fields Radiated by Linear Arrays of Equally Spaced Elements. Circulation in Computer Science, 2, 9 (October 2017), 17-22. https://doi.org/10.22632/ccs-2017-252-55.

[11] Andrew J. Burkhardt, Christopher S. Gregg, J. Alan Staniforth, (2000) "Calculation of PCB track impedance", Circuit World, Vol. 26 Issue: 1, pp.6-10, https://doi.org/10.1108/03056120010302133.

[12] Balanis, Constantine A. Antenna Theory: Analysis and Design. 3rd ed. Hoboken, NJ: John Wiley, 2005.

Proceedings of the Fourth International Conference on Communication and Electronics Systems (ICCES 2019)
IEEE Conference Record # 45898; IEEE Xplore ISBN: 978-1-7281-1261-9

A Comparative Analysis of Matrix Based Key Management Schemes For Wireless Sensor Network

Rishabh Kamal
Computer Engineering Department
National Institute Of Technology
Kurukshetra
kamal.rishabh007@gmail.com

Priyanka Ahlawat
Computer Engineering Department
National Institute Of Technology
Kurukshetra
mannpammy@gmail.com

Abstract*—In wireless sensor networks (WSN) key management is a working research subject. As we have large number of key management schemes (KMS) that are designed for sensor network, it is not easy for network designers to know which KMS is perfect fit in a specific WSN operation. This paper presents an exhaustive overview of different schemes along with their advantages and disadvantages. As KMS is the stepping stone of any security mechanism in a sensor network, its effectiveness depends on the underlying scheme. KMS in a WSN guarantees communication between one or two pairs node batch. We have analyzed different schemes based on parameters such as storage cost, communication cost and resilience against node capture.

Keywords— Wireless Sensor Network, Key Management, Computation, Storage.

I. INTRODUCTION

Deploy wireless sensor network (WSN) is a remote, sensitive and sometimes unmanned hostility, environments at a high risk of physical attack. Topology, network size, and sensor density that make it complex to implement the placement of a node before deployment is unknown. Also, wireless communication requires usage of spatial multiplexing. Sensor nodes share media in many other nodes. Thus providing security with wireless sensor network is very difficult. The disparity of the continuity of information in WSN increases all attacks quickly, putting the entire network at risk it is a short time. So in addition to protecting the wireless link we have to limit the range of node capture between sensor nodes Attacks are a very important issue in WSN security.

The main factor is the nature of wireless transmission that leads to WSN vulnerabilities in various situations Malicious networks attack many security mechanisms Proposed against potential attacks In WMN, the non-exhaustive list includes locations technology [3], [4].

Wireless connection, unattended deployment, closedown interaction of nodes makes security a big challenge. In the physical environment. It is helpless against different assaults, for example, getting the knot and transport. Interference also rejection of work also by Information provided by wireless sensor networks Significantly increased. All transmitted information needs to be protected which is exchanged over the network. So one of the first requirements is to distribute encryption key to WSN during setup phase Sensor nodes are used to protect information exchanged with each other each combination or Node set [2].

Every key management scheme (KMS) requires sensor node to store some key information. It is an primary parameter to evaluate its performance. The main storage overhead is the storage capacity required for each sensor node that is used for storing key material. Sensor node with limited storage, so the key management solution should be storage efficient. Most of those already suggested key management scheme based on key pre-allocation of keys. These are schemes are inefficient because each node requires large memory However, several ideas have been proposed recently. The scenario has Reduce these storage requirements

The architecture of WSN is given in Fig. 1. In this architecture given components are shown sink node, user and nodes. All components are connected to the internet and wireless medium. In this source and target are given figure.

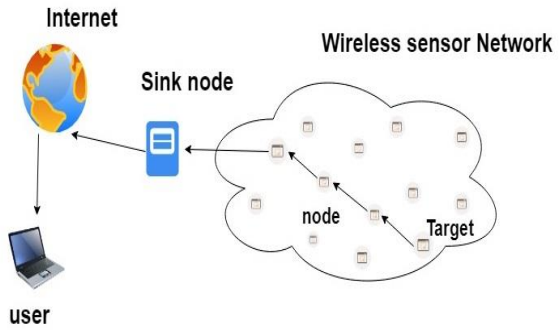

Fig 1: Architecture of Wireless Sensor Network

A. *Key management in WSN*

It is set of process and mechanisms that support effective exchange of keying information among sensor nodes [12]. WSN security requires data confidentiality, authentication, data integrity, availability, durability access Control. Key Management Security solutions in WSN include scalable,

robust and lightweight. Lightweight, effective and efficient management of keys and keys Distribution mechanism and use of the WSN certificate Because the attacker is not secure, one common key Get the key easily. So you can build a WSN Environment to distribute keys in the following manner Scheme:
Data is provided to provide a secure connection Encrypt and authenticate with the key. the key Safety management and distribution planning Applications in such networks should provide scalability. Reliability and confidentiality of integrity and flexibility. From Share one key to communicate with WSN It is not safe because the other party can easily find the key. Thus, the sensor network is used to manage different keys How to ensure communication.

B. Security constrainment

Scalability: The WSN security solution must support in a large network, you must be flexible and work well with tremendous increases.

Authentication: Authentication is a security feature that guarantees messages sent by authentication. There are four main types of resource authentication Technology: One-way, bi-directional or reciprocal authentication , triple authentication, implicit Degree. commonly, input verification allows the recipient to confirm that data is already Posted By requested vendor. If two parties communicate, input verification Achieved in a pure way symmetrical Technique.

Confidentiality: Sensor networks do not leak from Read Sensor the surrounding network. In several appliance, nodes can pass sensitive data a standard way to preserve sensitive data by encrypting data using a private key that is only owned by the beneficiary. In the monitored connection mode, create Secure channel between node and base station, and then route the other secure channels as needed.

Integrity: Data integrity communication that the data received by the recipient does not change in the transfer of the discount. Implement data integrity through authentication. This feature is more powerful.

Lightweight: Because of the power reduction of the sensors Solutions need to use less power by reducing calculations without affecting security services.

Fault-Tolerant: I know wireless media I cannot trust them. The contract can be attacked without notice. Therefore, design your own security solution with these issues in mind and remove problem.

Storage Cost: Capacity costs or storage costs characterized as sensor nodes by exploiting wireless sensor systems heterogeneity. In storage we store the important information of the node.
Computation Cost: It is a parameter to major the performance of key management during key updating, recovery to the key sever. Storage cost and computation cost both are dependent to each other.
Resilience Node capture attack: Node capture attack is define when external adversary can capture Sensor node accesses important information of keys to break the security of linked nodes. This type of attack greatly undermines the security, integrity, and confidentiality of the network. When an attacker captures a series of sensor nodes, these nodes can be modified based on software programming and hardware configuration. You can then use one of the sensor nodes to initiate a further attack on the network.

This paper presents an exhaustive survey of different matrix based KMS. We have evaluated these schemes on different parameters like storage cost , computation cost and resistance against node capture. It aims to provide an insight to different researches about the efficiency and scalability of different schemes for various WSN applications.

This paper organized as follows: Section II describe the introduction of wireless sensor network and key management and second section contribution of this paper. After this existing schemes for key management scheme are explain and make a table I as well as make a table II to define parameter use in table II. After this make a graph between no of nodes and total storage cost for existing scheme given table I and write the conclusion and future work of this paper.

II. EXISTING KEY MANAGEMENT SCHEMES

Du et al presented [1] a predefined random key allocation scheme is utilized to utilize distributing learning, where every node just needs to convey a little piece of the keys required for other pre-master allotment frameworks. [9],[10]. To realize Same level of connected memory minimization. It neither alone reduces the memory requirements of memorization consuming sensor nodes. But more important. It is essentially Network Optimization flexibility for Capture the node.We used our offer to show these improvements analysis and simulations outcomes.
Perrig et al presented a security scheme in wireless sensor system in [2] to explain the networks security services and how to secure a system to various attacks and describe. We need a safe and proficient key distribution mechanism to make keys for large-scale sensor network effectively.
Bahl at el presented [3] Radar a structure RF-based client area and following framework and RADAR works recording and handling signal data to the numerous base stations and present the experimental results of the Location accuracy is high.
Yang et al presented [4] analyse the trilateration limitation and proposed a new novel based scheme inherits the easiness, efficiency of trilateration on time and improve the performance of local nodes also prove correctness and optimal design showing in this paper.
Blom et al introduced the key dissemination based upon[5] the lattice based key administration plot. Blom scheme depends on greatest Distance Separable code utilizing The generator

matrix G of direct code (N, k) on GF (q), N is the length of the secret phrase, k is the elements of the code, i.e. G, are matrices (k × N).Element of GF (P). Where q is the power of prime numbers. MDS The code [6] is characterized by the separation d = N - k + I. Equal to state that any column of k are straight G It's free. Thus, the code can only be specified by: Find out the k element of the line We cannot disclose code information [11].

The program is implemented in two phases. The first is the pre-appointment key and the second is the main stage of incorporation.

Key pre-distribution phase:-

$(\lambda+1)\times$n=public matrix G;

$(\lambda+1)\times(\lambda+1)$ =private symmetric random matrix D.

Key establishment phase:-

K = $(D \times G)^T \times G$, point Kij =Kji figured from open and secret matrix.

the nodes i and j registers the pair astute key as Kij = row x colj = row j x coli=Kji.

Katz et al presented [6] cryptography CRC press in this cryptography algorithm explained also so many algorithm symmetric and asymmetric key cryptography and how to use these algorithm for security and encryption, decryption and shared key cryptography.

Chien et al presented an EPKEM Plan proposed [7] Cheng and Agarwal [8] supports large networks and can Provide a complete network connection, but appears to be vulnerable to Capture the node attacks. They tried to make the network more flexible to catch attacks on the nodes. Unfortunately, this program has not yet provided resistance to Capture the node attacks. The second question that makes this solution What cannot be used is non-scalability. The tertiary question in this solution is that each sensor node compulsory a large storage cells, making it unsuitable for deployment on WSN with many nodes.

Cheng et al exhibited [8] a proficient pairwise key foundation plot for static wireless sensor systems. In this paper, successful designs to build up and oversee two-path changes to accomplish arrange availability and adaptability of fixed wireless sensor systems have proposed. This arrangement underpins enormous networks sizes and has less availability and arithmetic contrasted with current master pre-designation plans.

Eschenauer et al presented [9] a distributed sensor networks Distributed sensor network (DSN) is a mobile network that includes a sensor contract with limited computing and communication capabilities. This paper proposed the main management scheme. Designed to meet the operational and security requirements of the DSN network also show the re-keying concept without computation and communication capabilities.

Chan et al introduced [10] an irregular key redistribution conspire additionally three system for key foundation utilizing the pre-distribution strategies. First is q-composite key, second is multipath reinforcement scheme and finally present a random wise pairwise key scheme. During capture of each node, it completely preserves the confidentiality of other parts of the network and allows for revocation based on authentication and reconciliation between nodes.

Rahman et al introduced [11] a novel for scrabble key administration conventions for remote sensor networks also characterize which conventions are use in key administration thus many think in this novel.

Ankit Gupta et al presented a new plan [12]to overcome this problem deficiencies of two scheme [5] ,[7] and improve the system's Resistance to node catch assaults. In this the solution provides full connectivity and less overhead and more energy efficient. It also provide greater scalability support. In this the third stage of the scheme is the scheme [9]: the pre-allocation of the key, the creation of the double key, and the erasure of the obsolete parameter.

Chaurasia et al presented a [13] mainly focus on weaknesses of Chien [7] and suggest a plan which is placed on Blom's [5] to eeliminate weaknesses from previous plans. Proposal the program offers better protection against attacks captured on node analysed to Chien et al 's scheme. The calculation cost is a bit high, but its memorization requirements are much lower. It is used to store the keys can support more nodes. In this network and using the XOR operation overhead being limited and provides better scalability.

Zhang et al presented a [14] create a key security problem key in wireless technology. technology. Engage Network This paper proposes a new matrix based The pairing key is included by deploying the design in the wireless network. Latest plan is very useful Storehouse sensor node and light correspondence No important accounts provided. In addition, our solutions are scalable, also protected. Opposition attack capture node. The basic design concept This solution This is a heterogeneous wireless network.

Praveena et al presented that [15] they have seen how Modern Encryption Standard version –II algorithm can be used in this document to accomplish safe communication. Compared to any conventional technique, the technique is also very adaptable. Any Java or Matlab can develop a program for encryption or decryption. Even simplified changed vernam cipher is used for the variable block size or variable key, and encryption is achieved in two forms.

Jyothirmai et al presented a [16] Wormhole and black hole attack have been major safety threats that undermine the efficiency of that same Wireless Ad Hoc Network routing protocol. It's tracking and separation is the primary issue for increasing the +quality of a network. In this Major the performance using various parameter Packet shipping ratio, performance, end-end delay, good performance and overhead routing by analysis of the amount of nodes in the network and blackhole nodes.

Priyanka et al presented a [17] vulnerability estimation model that can be used to to strengthen any security mechanism. It exploits various vulnerable factors to build an attack matrix that is later used by network designer to increase the system resistance against node capture attacks

TABLE I. Comparative analysis of existing schemes

S. No	Scheme	Nun	Nus	Storage cost	Computation Cost(C_c)	Resilience node capture attack
1.	Blom's 1985		1	$2(\lambda+1)\|q\| \times N$	$\lambda+1$	yes
2.	W.Du.J.Deng 2004	$P_t(a+b)\tau$	$P_t(1-2a-2b)\tau$	$\tau((\lambda+1)\|q\|+\|q\|) \times N$	$2\lambda-1$	better
3	Chien al's 2008			$(N+3)\times \|Key\|$	$NT_{mul}+T_h+(N+1)T_{add}$	No
4	A.parakh and S.Kak 2011		1	$3N\|q\| \times N$	2N	yes
5	Avinash Chaurasia,Utkarsh Dubey,R.k Ghosh 2012			$(\lceil\sqrt{N}\rceil+2)\|Key\|$	$(N+1)T_{mul}+T_h+T_{pow}+(N-1)T_{add}$	Yes
6	Yuexin $Zhang^1$,Li Xu^{1*},Yang $Xiang^2$, and Xinyi $Huang^1$ 2013	4	7	$\varepsilon_H \times 7$ $\beta \times (\lambda+1)\|q\|+(\|q\|+log_2^N+log_2^\xi H) \times N$	$2\lambda+1$	No
7	Ankit Gupta 2014			Floor($\sqrt{N}$)	Less	No

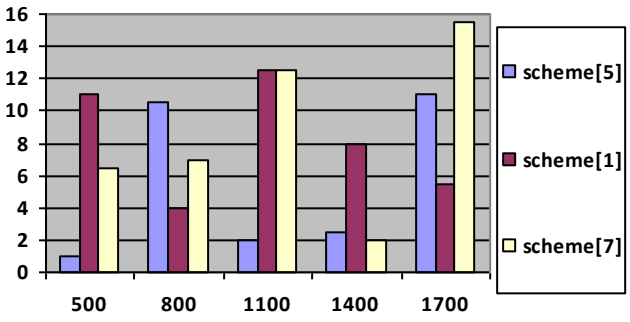

Fig 2. Relationship b/w number of nodes and total storage cost of different schemes

TABLE II. Symbols and their meanings

N	The number of nodes of the sensor
λ	The security parameter of the system
β	Number of sensor nodes per sub-area
ε_H	Number of key locations
P_i	Local Connectivity
N_{un}	Number of key shared spaces between neighbouring nodes
N_{us}	Number of key spaces shared between neighbouring nodes from the same regions
C_c	Computation cost of sensor nodes
τ	Key space
T_{mul}	The cost of beating one
T_h	Calculate the cost of a one-way hash
T_{add}	Single plus cost
T_{pow}	Increase the cost to a certain power
$\|Key\|$	Stored number size

III. Result and Discussion

Table I gives the comparative analysis of different schemes for WSNs. Different parameters such as storage cost, Computation cost and resilience against node capture are used to quantify the performance of different schemes. The performance of any KMS depends upon computation cost and this depend on key length and network size as well as storage cost. Blom's [5] scheme based on matrix and show the node capture attack and node are self-deployed. Zhang [14] scheme was based on deployment and pairwise matrix based in this no node capture attack and computation cost is depend on network size and connectivity between nodes were better. All schemes are analyzed and result are shown in the table I. Fig 2 Show the relationship between total storage cost and number of nodes in this all given scheme in table I.

Each sensor node in Blom's et al scheme [5] is associated with key-spaces, and for each key-space, the node is loaded with the corresponding row of its matrix A. So, the total number of storage cost are $2(\lambda+1)|q| \times N$ and scheme [1] are $\tau((\lambda+1)|q|+|q|) \times N$ and scheme [7] are $(N+3)\times |Key|$.
The cost of light storage at the sensor node is achieved by exploiting the heterogeneity of wireless mesh networks: mesh routers have more storage space than sensor nodes.

In scheme [5], each sensor nodes needs to store $2(\lambda+1)|q| \times N$ bit key material bits for whole networks and similarly the total cost in scheme [1] $\tau((\lambda+1)|q|+|q|) \times N$ Fig. 2 show their relationship when $\lambda = 18$, $\tau = 13$ obviously, the total storage cost of scheme [5] change the values of some points because of depends system security parameter and unique key seed $|q|$ and analysis of all the parameter in Table I. In scheme [7] is also depends on the size of number stored in node.

CONCLUSION AND FUTURE WORK

The Wireless Sensor Network, a set of sensors, performs many of the integrated functions of remote data transfer to remote base stations. Security is the key to strong communication between nodes in WSN. In this paper we describe the classification of the wireless sensor network key management scheme and compare various parameters like, storage cost, computational cost and resilience attack and some scheme focused on local connectivity. Future work improvement is to real time, by considering security, to increase the security and minimize the storage cost of Wireless sensor network as well as computation cost and make a good connectivity between nodes.

References

[1] Du, Wenliang, Jing Deng, Yunghsiang S. Han, Shigang Chen, and Pramod K. Varshney. "A key management scheme for wireless sensor networks using deployment knowledge." In IEEE INFOCOM 2004, vol. 1. IEEE, 2004

[2] Perrig, Adrian, John Stankovic, and David Wagner. "Security in wireless sensor networks." (2004): 53-57.

[3] Bahl, Paramvir, Venkata N. Padmanabhan, Victor Bahl, and Venkat Padmanabhan. "RADAR: An in-building RF-based user location and tracking system." (2000).

[4] Yang, Zheng, Yunhao Liu, and Xiang-Yang Li. "Beyond trilateration: On the localizability of wireless ad hoc networks." IEEE/ACM Transactions on Networking (ToN) 18, no. 6 (2010): 1806-1814.

[5] Blom, Rolf. "An optimal class of symmetric key generation systems." In Workshop on the Theory and Application of of Cryptographic Techniques, pp. 335-338. Springer, Berlin, Heidelberg, 1985.

[6] Katz, Jonathan, Alfred J. Menezes, Paul C. Van Oorschot, and Scott A. Vanstone. Handbook of applied cryptography. CRC press, 1996.

[7] Chien, Hung Yu, Rung-Ching Chen, and Annie Shen. "Efficient key pre-distribution for sensor nodes with strong connectivity and low storage space." In 22nd International Conference on Advanced Information Networking and Applications (aina 2008), pp. 327-333. IEEE, 2008

[8] Cheng, Yi, and Dharma P. Agrawal. "Efficient pairwise key establishment and management in static wireless sensor networks." In IEEE International Conference on Mobile Adhoc and Sensor Systems Conference, 2005., pp. 7-pp. IEEE, 2005.

[9] Eschenauer, Laurent, and Virgil D. Gligor. "A key-management scheme for distributed sensor networks." In Proceedings of the 9th ACM conference on Computer and communications security, pp. 41-47. ACM, 2002.

[10] Chan, Haowen, Adrian Perrig, and Dawn Song. "Random key predistribution schemes for sensor networks." In IEEE symposium on security and privacy, vol. 197. 2003.

[11] Rahman, Musfiq. "A novel scalable key management protocol for wireless sensor networks." (2013).

[12] Gupta, Ankit, and Priyanka Ahlawat. "Improved blom key management scheme for wireless sensor network." In International Conference on Recent Advances and Innovations in Engineering (ICRAIE-2014), pp. 1-5. IEEE, 2014.

[13] Chaurasia, Avinash, Utkarsh Dubey, and R. K. Ghosh. "A robust key management scheme with strong connectivity for wireless sensor network." In 2012 International Conference on Collaboration Technologies and Systems (CTS), pp. 190-194. IEEE, 2012.

[14] Zhang, Yuexin, Li Xu, Yang Xiang, and Xinyi Huang. "A matrix-based pairwise key establishment scheme for wireless mesh networks using pre deployment knowledge." IEEE Transactions on Emerging Topics in Computing 1, no. 2 (2013): 331-340.

[15] Praveena,A., and S. Smys. "Efficient cryptographic approach for data security in wireless sensor networks using MES VU." In 2016 10th International Conference on Intelligent Systems and Control (ISCO), pp. 1-6. IEEE, 2016.

[16] Jyothirmai, Pondi, Jennifer S. Raj, and S. Smys. "Secured self organizing network architecture in wireless personal networks." *Wireless Personal Communications* 96, no. 4 (2017):5603-5620.

[17] Priyanka , Mayank , A Hybrid Approach for Path Vulnerability Matrix on Random Key Predistribution for Wireless Sensor Networks, Wireless personal communications, June 2017, Volume 94, Issue 4, pp 3327–3353

Proceedings of the Fourth International Conference on Communication and Electronics Systems (ICCES 2019)
IEEE Conference Record # 45898; IEEE Xplore ISBN: 978-1-7281-1261-9

Document Management using Artificial Neural Network

Kaustubh Pimparkar
BE-Information Technology
VIIT Pune
kaustubh.pimparkar@viit.ac.in

Rahul Lulla
BE-Information Technology
VIIT Pune
rahul.lulla@viit.ac.in

Pratik Rathod
BE-Information Technology
VIIT Pune
pratik.rathod@viit.ac.in

V Anirudh
BE-Information Technology
VIIT Pune
v.anirudh@viit.ac.in

Suruchi G Dedgaonkar
Professor
Information Technology Engineering
VIIT Pune
suruchi.dedgaonkar@viit.ac.in

***Abstract*- Document Classification is the problem of assigning documents into predefined category making it easier to manage and sort documents. There are several algorithms using which the problem of classification can be solved. We use feed forward neural network with multiple layers (also called multilayer perceptron) trained using backpropagation algorithm for the problem for categorization of resume to make management of these documents easier. Neural networks can learn and model non-linear and complex relationships and model generalize solutions that can predict on unseen data. Applications of neural networks are character recognition, image processing and stock market prediction. Backpropagation algorithm which trains the neural net is a supervised learning approach which learns from errors in order to minimize it, thus, requires a lot of training and storage to produce efficient results.**

Keywords- Multilayer Feed-Forward Neural Network, Backpropagation, K-Nearest Neighbour, Support Vector Machines, Naïve Bayesian, Neural Networks, Artificial Neural Network System.

I. Introduction

With increase in a large amount of information there is always a need to classify documents into a specific category which normally requires manual user intervention. One such problem arises in classification of resumes. Companies receive large number of resumes on a daily basis and have a slight amount of time to have a quick look on every single resume to know for which job specification it belongs. Usually manual intervention is involved for this task. We studied different classification algorithms for solving the problem. The purpose of this paper is to provide a solution using Deep Neural Network for simplifying the task of classifying resumes to predefined category or specification to which it belongs. Using backpropagation algorithm, we trained a neural network model on dataset of resume. We also trained a standard SVM and KNN model on the same dataset and compared their accuracy on testing data and presented the results.

II. Literature Survey

There are many ways in which the problem of document classification can solved. Some of those ways are: K-Nearest Neighbour (KNN), Support Vector Machines (SVM), Naïve Bayesian (NB) and Neural Networks (NN).

A. K-Nearest Neighbour

K-Nearest Neighbour is a non-parametric method for classification. Here, each document is represented as a node or object in euclidean space. K-Nearest Neighbour is an example of classification algorithm in which the objects are categorized into classes considering the smallest distance between the class and the object [3]; The disadvantage of K-Nearest Neighbour is that it takes a large amount of time for classifying objects if the training dataset is large since it has to choose few objects by calculating the distance of each test object using all the data points in the training set.

B. *Naïve Bayesian*

The second method for text categorization is Naive Bayesian. It is different from K-Nearest Neighbour by the fact that it is trained using the training data beforehand to classify the new examples. Naive Bayesian does the classification of documents based by calculating prior probabilities of the predefined categories/classes and probability that a certain attribute value belong to a specific category. Here, we assume that attributes are not dependent on each other; However, this assumption may violate the fact that attributes are not dependent on each other in a text classification application. Also it does not take into account the number of occurence which may be potentially useful [3].

C. *Support Vector Machines*

The next approach is the use of SVM for text categorization. This is a more popular machine-learning algorithm than the other two mentioned above. SVM is based on the idea of classifier which is linear. The idea of SVM is different from that of perceptron model in the sense where if a distribution of training examples are not linearly separable, then the examples need to be mapped into another space where the distribution becomes linearly separable.

D. *Neural Networks*

An Artificial Neural Network (ANN) is an information-processing model inspired by the biological nervous system to process information. Its model replicates the most basic functions of the brain. Artificial Neural Network possess large number interconnected nodes or neurons. They perform computation in parallel way but are configured in a regular architecture. ANNs collective behavior is recognized by their ability to learn, recall and generalize the training patterns to that of a human brain. One of the methods of Artificial Neural Network System (ANS) named Backpropagation can be used to solve text categorization problem. There are good reasons for using it for text categorization. ANS provides a better solution for problems that cannot be solved sequentially or by sequential algorithms. Other applications of artificial neural network include matching of images [5]. They result in better performance. Backpropagation algorithm is widely used among the rest of the algorithms given by ANS. Backpropagation is very useful in recognizing complex patterns and performing nontrivial mapping functions. Neurons are processing elements in the neural network. The lines that connect the neurons are called weights. Every line of processing elements is a layer of a network; Though there can be multiple layers present in ANS in BackPropagation network (BPN) generally there are three.

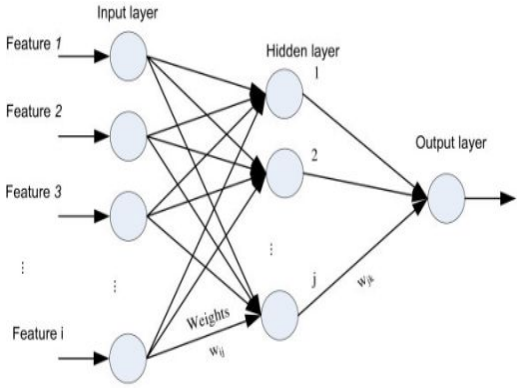

Figure 1 Architecture of neural network

III. IMPLEMENTATION

The general procedure for document classification :

A. *Word Extraction*

In the first step, we are required to convert the document that has many stream of characters into tokens or words for identifying features. In IR, this tokenization process either known as word extraction or word breaking.

B. *Stop Words Removal*

Many words like “a”, “the” are not very helpful in indexing, we need to remove these words from the words that are extracted from previous step. Since these words fall in every English paper they hardly assists in determining the class of that document. We can't differentiate between types of document with these words. The procedure of removing such non influential words from the group of words created by word extraction is called as stop words removal. For this step we create a group of stop words that are to be withdrawn from extracted words.

C. *Word Stemming*

In a document there can be many variations of a word that may be present. One example of this is the word “appear” may also exist as “appearing”, “appeared”. These words basically provide the same meaning but are in different formats. Thus for classification it is desired to combine such variations into one form each. This process of combining joining dissimilar variations of the matching word into a sole form is known as stemming. The module that performs the function of stemming is called a stemmer.

D. *Weights to terms*

We create a vocabulary of terms from document set by measuring the importance of the terms. We assign to each term a weight which indicates the comparative significance of the term in a document. For term frequency(TF), we calculate the total occurence of each term in a document. For inverse document repetition, defined as:

$$IDFi = Log(N/n) \quad (1)$$

Where IDF=inverse document frequency of ith index term, N is nothing but the number of papers in the group and n is an integer number of document ith index terms appear.
For term weighting, which is the multiplication of the term frequency (TF) and the inverse document frequency (IDF):

$$Wji = TFji \times IDFi \quad (2)$$

After calculating the TF-IDF values of each term in a document set, we establish a threshold calculated using mean of all the values and include the terms with higher TF-IDF value than threshold into the vocabulary set. We create bag of words representation of each document using this vocabulary set and pass it on to the neural network.

E. *Neural Network Based Classifier*

For categorization of the documents, vectors representing the documents are handed over to the start level which is input layer of the neural network classifier as input signal. These input signals are then circulate forward along the neural network so that the result which is output of the neural network is calculated in the output layer. We use sigmoid as the activation function in the output units, the result output of the neural network classifier is nothing but the classification vector which contains the values in the scale [0, 1]. This real-valued categorization vector produce a group classification decision, in which the ith vector component represent the likelihood that the input document associate to the ith group [2]. The neural network is trained to reduce errors using backpropagation learning wherein the weights in the layers are adjusted based on output loss function calculated for a particular input. The loss function is absolute difference between the actual and observed values.

Testing:

The dataset collected is randomly separated for training and testing the model. The testing dataset that was held back from training is first preprocessed: words are extracted, stop words are removed and stemming is done. Bags are created of each document using vocabulary set created during training and sent to the now trained neural network for predicting the document. Neural network classifies document to a category based on the certain words appearing in the document.

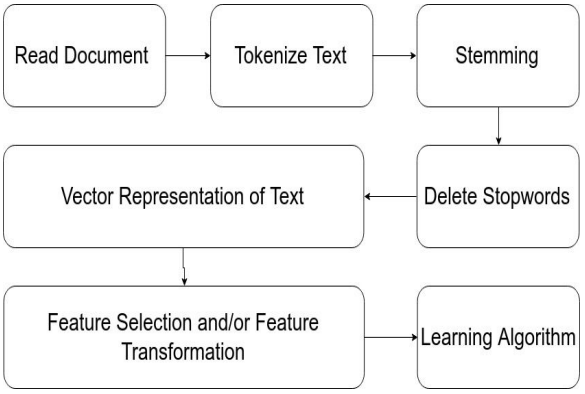

Figure 2:Module division

UI Screenshots:

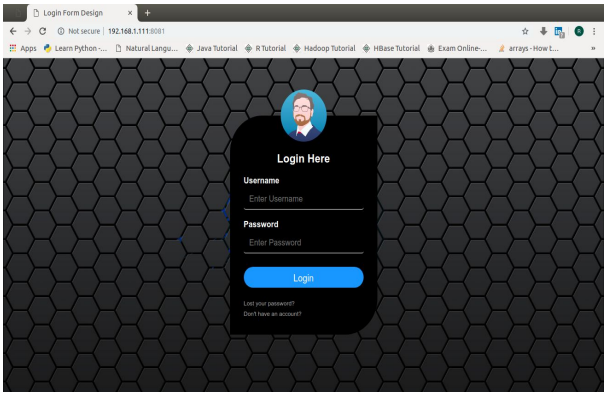

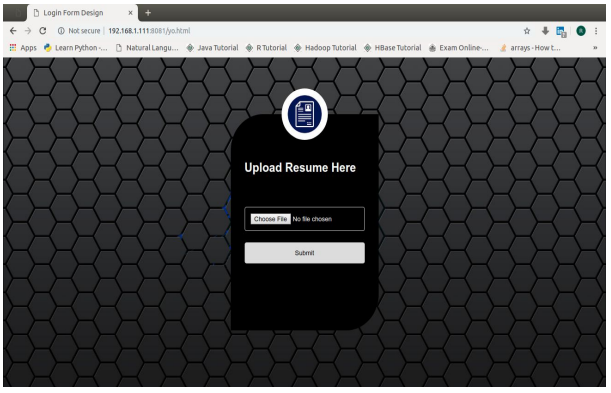

IV. RESULTS

We have implemented three different machine learning models namely K-nearest neighbour, Support vector machine and Neural networks to compare the results.

The training and testing data were common to all three models whose details are as follows

TABLE 1:DATA SAMPLE SIZE

Labels	Training data size	Testing data size	Correct Result	False Result
1.Data Science	150	50	47	3
2.Fashion	75	25	22	3
3.Finance	112	38	35	3
4.HR	81	27	25	2
5.Software	150	50	47	3
	Total=568	Total=190		

The accuracy of each model when trained and tested over the above mentioned data is represented in a tabular format below

TABLE 2:ACCURACY COMPARISON

Model	Accuracy
KNN	61.5%
SVM	82.6%
NN	92.3%

Since the data points are very large in number we have to limit the number of object to which the KNN calculates the distance to find out the similarity factor between the objects, this reduces the accuracy of KNN model largely.

The textual data is an unstructured and correlated data. A particular data point may resemble more than one class. Thus mapping of these data points into another space to achieve a linear separable problem induces an error in classification which affects the accuracy of SVM.

The neural network model is trained using backpropagation algorithm to reduce the error in output by adjusting itself for a particular input, breaking down the problem into smaller parts and ability to handle complicated and unstructured data help it to largely outperforms the other two classifiers into taken into consideration.

IV. Conclusion

In this paper, we have mentioned the need for classification of resume documents and identified different machine learning algorithms used for classification. We have listed the various advantages and disadvantages of each algorithm. While bayesian classification is suitable for low dimension, KNN grows with number of documents. SVM cannot scale well with number of documents. Neural network can be self-adaptive and suitable to complex problem. Classification of resume can ease the task of managing large number of resumes of different types.

For future scope, the neural network model can further be trained to classify more categories of resumes. Much larger dataset is required for accomplishing this task. Documents classified to certain category can be ranked using some machine learning algorithm to find the best applicant for a job.

V. Acknowledgement

We would like to thank our guide Mrs.Suruchi G. Dedgaonkar, for her ideal enlightenment, helpful feedback and persistent motivation from start to end of the project. Her treasured recommendation were of vast help throughout our project phase. Her perspective condemnation kept us working to make this project in an exceptional way. Working under her was a tremendously brilliant training for us.
We would also love to present our heartfelt appreciation to all our friends and colleagues who contribute in the survey, without which this research work would be insufficient.

VI. References

[1] Anubhav Aggarwal, Jasmeet Singh and Dr. Kapil Gupta, “A Review of Different Text Categorization Techniques”, International Journal of Engineering & Technology, 2018.
[2] S.Ramasundaram and S.P.Victor, “Text Categorization by Backpropagation Network”, International Journal of Computer Applications, vol 8– No.6, October 2010.
[3] Vishwanath Bijalwan , Pinki Kumari , Jordan Pascual and Vijay Bhaskar Semwal, “Machine learning approach for text and document mining”, June 2014.
[4] Nidhi and Vishal Gupta, “Recent Trends in Text Classification Techniques”, International Journal of Computer Applications, vol 35– No.6, December 2011.
[5] Chaitanya Naik,Vallari Kothari, “Document Classification using Neural Networks Based on Words”, International Journal of Advanced Research in Computer Science, vol 2, March-April 2015.

Proceedings of the Fourth International Conference on Communication and Electronics Systems (ICCES 2019)
IEEE Conference Record # 45898; IEEE Xplore ISBN: 978-1-7281-1261-9

Memory Optimizing Algorithms for Data Acquisition in Electric Drive of Hybrid Electric Vehicles

Gopika Rajan
Department of Electrical and Electronics Engineering
Federal Institute of Science and Technology
Ernakulam, India
gopikarajan4@gmail.com

Vinoth Ramalingam
Electric and Hybrid Vehicles
Robert Bosch Engineering and Business Solutions Pvt. Ltd
Coimbatore, India
Vinoth.Ramalingam@in.bosch.com

***Abstract*—Data acquisition of electric drive is very much relevant in the context of electric vehicles. Different data like IGBT temperature, diode temperature, coolant temperature, electric machine coolant temperature, motor torque, electric machine speed data etc. have to be acquired and analyzed in electronic control units. Data samples are processed in RAM using various algorithms and relevent information is extracted and transferred to ROM as various maps. These information are useful in life time estimation, failure analysis and optimum design of various electric drive components. Histograms and rainflow counting are conventionally adopted methods in data acquisition. Histograms may include irrelevant information and also require large memory space. Normal offline rainflow counting also demands large memory, which necessitates the need for an optimum memory consuming data acquisition algorithm. An online rainflow counting algorithm based on three point method can minimize the RAM space consumption by significant amount. The data counts remains same as in offline rainflow algorithm. Instead of using histograms for data like electric machine speed, data counts for only the relevant operating range can be stored, which minimizes memory requirement. Also level crossing counting is another algorithm which can be adopted where we are interested only in threshold crossings of the parameter acquired, for example the threshold crossing of inverter phase currents, which can cause serious damage to the system. Memory requirement minimization achieved by the above mentioned algorithms are validated by simulation.**

***Index Terms*—offline rainflow algorithm, online rainflow algorithm, level crossing counting, histograms.**

I. Introduction

Different data acquisition algorithms are used for processing and storing electric drive data. Histograms are conventionally used storage method, which consumes large memory space. Other advanced counting methods are used for filtering and storing input data without losing much granularity. Level crossing counting, as per ASTM standards is implemented, where preset threshold crossing information of acquired data is required[2]. In peak counting the peaks and valleys are counted based on a preset level. Peaks higher than the reference level and valleys lower than the reference level are counted[2]. Simple range counting and maximum edge counting are other conventionally used cycle counting methods[2].Rainflow counting is another widely implemented algorithm in cycle counting and fatigue analysis. Different variants of this algorithm is used. Rainflow algorithm based on pagoda roof analogy proposed by Endo and Matsuishi is the basis for all rainflow varients[3]. One of the most widely implemented rainflow algorithm was proposed by Downing and Socie. This three point algorithm was specified in ASTM E 1049-85[2]. Rainflow cycle counting algorithms provide means for comparing obtained variable amplitude load history with constant amplitude load pattern. Rainflow algorithm identifies closed hysteresis loops in the stress - strain plane and provides a method for treating open loops[4]. Other modern methods like Moshrefifar and Azamfar counting were later proposed, but rarely adopted due to complexity in the procedure[5]. In the above method rainflow counting is widely adopted and efficient method, but consuming lot of memory. An online rainflow counting based on the three point algorithm can considerably reduce the RAM consumption[6]. The input data samples are filtered and processed and relevant data is extracted at the instant when the input samples are obtained and the samples are discarded, reducing RAM memory consumption. The online three point rainflow algorithm can be used in data acquisition of various electric drive parameters like IGBT temperature, diode temperature, coolant temperature, electric machine speed etc. in the electric drive.

II. Offline Rainflow Algorithm

A. Algorithm

For a sample load-time history as in Fig. 1, let 'X' be the current range, 'Y' be previous range adjacent to 'X' and S be the Starting point in the history. The three-point offline algorithm as per ASTM E 1049-85[2] is specified below,

A) Read next valley or peak. If end of data then go to step F.
B) If the number of turning points is less than three then go to step A. Update X and Y with three most recent valleys & peaks that are not eliminated.
C) Check the magnitude of ranges Y & X.
  A) If X<Y, go to step A.
  B) If X>=Y, go to step D.

D) If Y includes S them go to step E, if not count Y as a full cycle and remove the turning points in Y & go to step B.
E) Range Y is counted as a half cycle and remove the initial point in Y and set next point in Y as starting point and go to step B.
F) Count remaining ranges as half cycles.

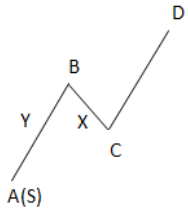

Fig. 1. Sample load history showing ranges and starting point.

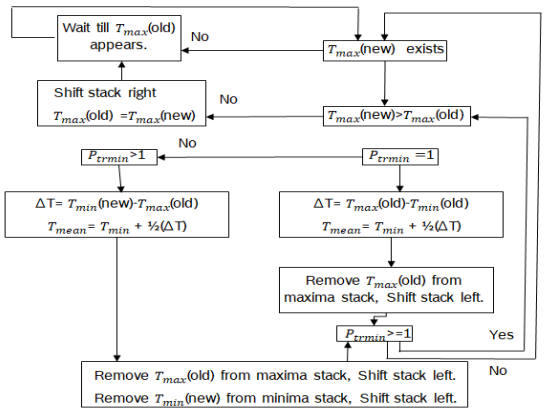

Fig. 2. Online Rain-Flow counting algorithm working on maximal values.

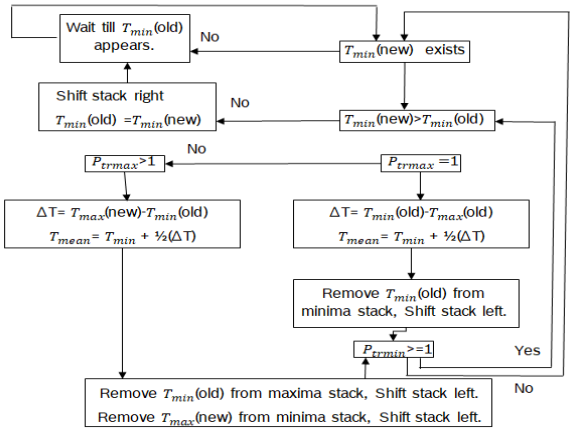

Fig. 3. Online Rain-Flow counting algorithm working on minimal values.

B. Challenges in implementing offline rainflow algorithm

The offline rainflow algorithm is not suitable for real time applications. The load history for significant time should be stored for proper cycle formation from the data. The algorithm cam be applied only on a stored load history. It have a buffer which accommodates the consequent turning points (minima & maxima). The buffer size should be determined before the algorithm is executed. For this the duration between successive usage of the rainflow algorithm, should be predetermined before the algorithm execution. The buffer should have the capacity of holding the entire loading range of the system under consideration. This involves large quantities of data demanding substantial computational resource to process the data during algorithm execution. In real-time applications, coding should be carefully done so that other real-time activities of the ECU are not interrupted.

III. Memory Optimizing Algorithms

A. Online Rainflow Algorithm

The turning points are processed as it occurs. Two buffers are used for this purpose. After processing, the turning points are discarded thus minimizing memory consumption. The load-time history need not be stored. Half and full cycles are extracted in a recursive manner, depending on the buffer contents. The procedure used for obtaining the full and half cycles is similar to the one used in offline rainflow method, and the cycle counts are therefore same for same loading sequences. Pre-ordering of input data points in ascending or decending order as in offline rainflow is not required. The online three point algorithm is depicted in fig. 2 and fig. 3, where, T_{max}-Element of maxima stack, T_{min}-Element of minima stack, P_{trmin}-Element of minima stack elements, P_{trmax}-Element of maxima stack elements. The MATLAB simulation of both online and offline three point rainflow on IGBT temperature input in the range, [20^oC-120^oC] and coolant tempearture input in the range, [20^oC-120^oC] gives similar maps, shown in fig. 4 and fig. 5 respectively, which implies there is no loss of data in the online method.

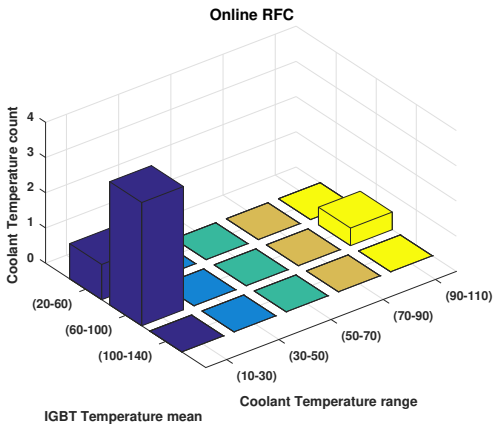

Fig. 4. Online rainflow counting(3D map).

B. Histograms

Histograms are used to represent the distribution of normal data accurately. It is the probability distribution estimate of a continuous variable (quantitative variable). For constructing

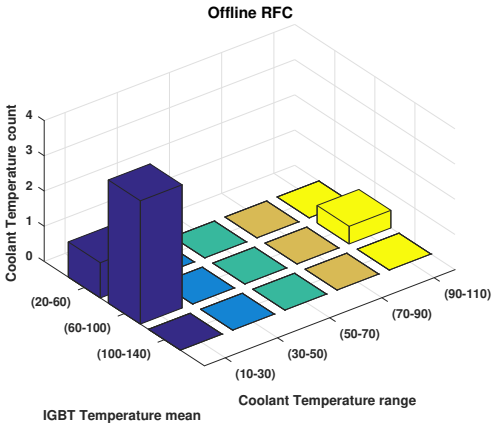

Fig. 5. Offline rainflow counting(3D map).

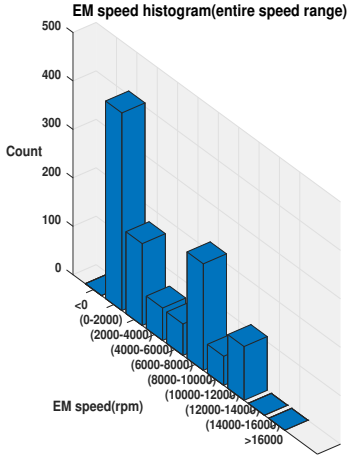

Fig. 7. EM speed histogram for entire speed range(1D).

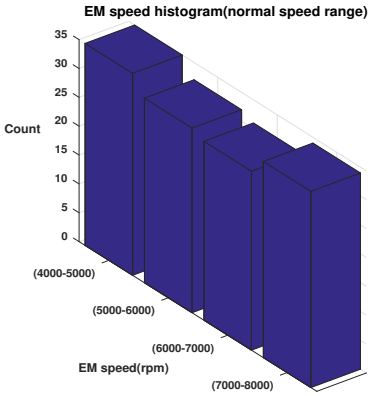

Fig. 8. EM speed histogram for entire speed range(1D).

histograms, the initial step is to make bins of input parameter's value ranges. This means, dividing full operating range of values to series of intervals and then counting how many values is lying in each interval. The bins should be consecutive and non - overlapping. Considering the electric motor speed histogram, the speed may be divided into ten sections as depicted in fig. 6, each section may require a four byte for the count. Thus a total of 40 bytes will be required for the entire histogram in the memory. For the normal driving speeds(40Kmph-160Kmph), the EM speed will be a factor (gear ratio) times the driving speed. This lies between a specific rpm range say, 4000rpm-8000rpm. Histogram for entire EM speed range will be having more sections than this one. Thereby the memory requirement is minimized and also the granularity of the map is now increased as depicted in fig. 6. Only four sections are present in this map. So for each sections of 4 bytes, a total of 16 bytes will only be required, saving 24 bytes of memory. Simulation results for electric motor speed inputs for three minutes are given in fig. 7 and fig. 8.

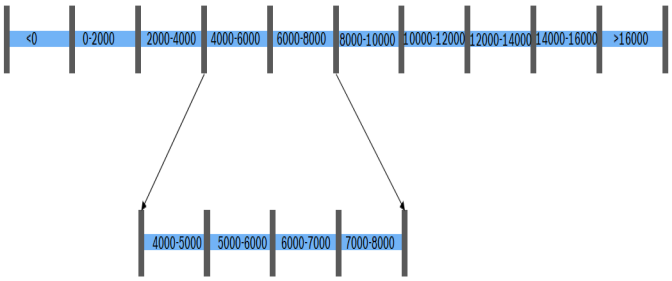

Fig. 6. EM speed histogram sectors for entire speed & normal speed ranges(rpm).

C. Level crossing counting

In level crossing counting, counts are registered when the input data exceeds preset levels. This method can be adopted where we are interested only in threshold crossings of a parameter, which may can have serious effect on the system under consideration. For example, Consider the scenario of a vehicle moving down hill, the electric motor's speed may increase beyond its rated limit which can have adverse effect on the machine. So recording such threshold crossings are of much significance. For such an application the level crossing counting can be used instead of recording a complete histogram. Simulation results of electric motor speed crossing of the rated limit, 16,000rpm for speed inputs for three minutes given in fig. 6 shows that it may require only a byte or two for storing the level crossing counts. Thus the memory requirement can be minimized by a considerable amount than in the case of storing the entire motor speed histogram which may be requring number of sections, having a larger memory requirement say, 4 bytes each.

IV. Conclusion

Different memory optimizing methods were identified for acquiring electric drive parameters. An online rainflow algorithm which minimizes the RAM memory requirement by

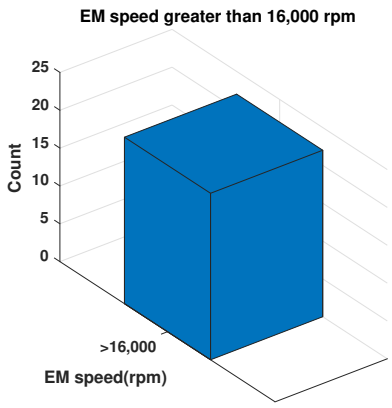

Fig. 9. Offline rainflow counting(3D map).

avoiding the requirement of load history storage can be used in storing parameters like IGBT temperature, diode temperature, coolant temperature etc. Instead of histograms for entire operating ranges , storing only map for normal operating ranges for parameters like electric motor speed memory requirement can be considerably minimized. Level crossing counting can be adopted where only threshold crossings of the acquired parameters are of interest, saving memeory space.

Data acquisition is very much relevant not only in automotive field but also in all areas where a stress cycle analysis is required, as in life time estimation of wind turbine parts, fatigue analysis of mettalic parts of different machines etc. In hybrid electric vehicles the data acquisition functionality will be handled by a particular electronic control unit (ECU) which will be handling other real time electic drive functionalities say, controlling the gate circuit of the electric motors inverter. For such other important real time functions to be performed un - disturbed and efficiently, sufficient memory should be free. So for a functionality like data acquisition, which take up large RAM and EEPROM space, the data acquiring algorithm should be carefully selected. Algorithms should be selected such that the acquired data should maintain maximum possible granularity and consuming minimum memory possible. So techniques with optimum memory usage in data acquisition is of great future scope.

REFERENCES

[1] S. D. Downing and D. F.Socie, " Simple rainflow counting algorithms, " *International Journal of Fatigue*, vol. 4, no. 1, pp. 3140, 1982.
[2] "*Standard Practices for Cycle Counting in Fatigue Analysis, "Annual Book of ASTM Standards*, ASTME 1049-85 (Reapproved 1997), 1999, vol. 03.01, Philadelphia, USA.
[3] M. Matsuishi and T. Endo, Fatigue of metals subjected to varying stress, *Japan Soc. Mech. Engineering*, 1968.
[4] C. H. McInnes and P. A. Meehan, "Equivalence of four-point and three-point rainflow cycle counting algorithms,"*International Journal of Fatigue* 30 (2008) 547-559.
[5] M. Azamfar and M. Moshrefifar, "Moshrefifar and Azamfar method, a new cycle counting method for evaluating fatigue life, " *International Journal of Fatigue* 69 (2014) 2-15.
[6] M. Musallam and C. M. Johnson, "An efficient implementation of the rainflow counting algorithm for life consumption estimation, " *IEEE Transactions on Reliability*, vol. 61, no. 4, December 2012.
[7] M. Musallam and C. M. Johnson, "Real-time compact thermal models for health management of power electronics, " *IEEE Power Electronics Trans.*, vol. 25, no. 6, pp. 14161425, 2010.
[8] M. Musallam, M. Johnson, C. Yin, C. Bailey, and M. Mermet-Guyennet,"Real-time life consumption power modules prognosis using on-line rainflow algorithm in metro applications, " in *IEEE Energy Conversion Congress & ExpoECCE*, Atlanta, Georgia, USA, September 1216, 2010.
[9] I. Rychlik, "A new definition of the rainflow cycle counting method, " *International Journal of Fatigue*, vol. 9, no. 2, pp. 119121, 1987.
[10] M. Meggiolaro and J. Pinho de Castro, "An improved multiaxial rainflow algorithm for non-proportional stress or strain histories, " *International Journal of Fatigue*, vol. 42, pp. 194206, 2011.
[11] "*ASCET V5.2 Reference Guide*, " Document EC010005 R5.2.2 EN, ETAS GmbH, Stuttgart. algorithm for non-proportional stress or strain histories, " *International Journal of Fatigue*, vol. 42, pp. 194206, 2011.
[12] K. L. Singh and V. R. Ranganath, "Cycle counting using rainflow algorithm for fatigue analysis, " in *15th National Conference on Aerospace Structures*, Coimbatore, Tamil Nadu, India, October 1516, 2007.

Proceedings of the Fourth International Conference on Communication and Electronics Systems (ICCES 2019)
IEEE Conference Record # 45898; IEEE Xplore ISBN: 978-1-7281-1261-9

CAPACITOR SWITCHING LOGIC WITH EFFICIENT MAXIMUM POWER POINT TRACKING SCHEME FOR MULTI INPUT SEPIC CONVERTER IN SOLAR POWERED SYSTEMS

Sanoj Kumar Roy S
Power Electronics Research Laboratory
Dept. of Electronics and Communication Engg.
College of Engineering Trivandrum,
Kerala, India
skumarroy.vssc@gmail.com

Shiny G
Power Electronics Research Laboratory
Dept. of Electronics and Communication Engg.
College of Engineering Trivandrum,
Kerala, India
drgshiny@gmail.com

***Abstract* — This paper proposes a capacitor switching logic for a multi input Single Ended Primary Inductance Converter (SEPIC) with efficient Maximum Power Point Tracking (MPPT) scheme for multiple non aligned solar panels. The proposed scheme is an improvement of time division multiplexing control of multi input converters for low power solar energy harvesters. In the proposed design, the capacitor switching logic gives the flexibility of selecting panels on demand providing additional advantage of isolation. For better accuracy an efficient algorithm has been implemented for determining MPPT. The MPPT is practically determined in each cycle when the corresponding capacitor is connected to converter. Using SEPIC converter at the output provides a constant 15V for charging the battery for solar panel voltage range from 8V to 25V. The design improvements will bring increased efficiency for medium power solar systems.**

Keywords— Maximum Power Point Tracking (MPPT), Single Ended Primary Inductance Converter (SEPIC), Perturb and Observe (P&O), Incremental Conductance (InC), Time Division Multiplexing (TDM), Maximum Power Point (MPP).

I. INTRODUCTION

The primary source of energy which helps to retain life on earth is Sun. The importance of extracting energy from renewable sources like solar, wind and tidal gives a solution for the depleting non renewable energy sources. It is considered as green technology as it does not emit any greenhouse gases.

The sun radiates solar energy by electromagnetic waves over a range of wavelengths from 290–2500 nanometers defined as solar spectrum. The solar spectrum consists of three bands namely Ultra-violet (UV) light (290nm–380nm), Visible light (380nm–780nm) and Infra-red light (780nm–2500nm). In the solar spectrum, 51% of the energy is distributed in the infra-red band, 47% in the visible band and 2% in the UV band. A photovoltaic system (Solar panel) is used to generate electricity from solar energy. For the construction of solar cells, monocrystalline and polycrystalline silicon is being used. The mono- crystalline technology creates a homogeneous silicon crystal that achieves a conversion efficiency of 14 to 21% whereas the polycrystalline is a combination of different silicon crystals and achieves a conversion efficiency of 13 to 16.5%. Polycrystalline photovoltaic (PV) cell is cheaper due to the simplest process of fabrication. Compared with silicon solar cells, GaAs solar cells is considered to be ideal for space applications as it possess higher photo electric efficiency, better thermo stability and stronger irradiation resistance [1]. The solar panel efficiency can be improved further by using mirrors and lens to concentrate the solar light to the panel. This concentrated photo voltaic technology (CPV) will provide same power output with lesser solar cell compared with normal panels [2]. The power generated from a solar panel depends on the irradiance which is defined as the amount of power per unit area that is directly exposed to sunlight. At a distance of one astronomical unit (AU) from the sun, the irradiance is approximately 1,368W/m^2 which is defined as Solar constant. The earth atmosphere attenuates the sunlight so that less power arrives at the surface of the earth approx. equal to 1,000W/m^2.

Some applications use multiple PV panels with dissimilar orientations for extracting maximum solar power in a day profile. When aligned configuration of PV panels is used, peak power is obtained at a particular time from both the panels resulting in higher depth of discharge of battery in a daily power profile. Hence the non aligned panels is proposed in [3] provides a smoothened profile by smaller depth of discharge. The method of using non aligned panels will improve the battery life. In [3] time division multiplexing scheme is being implemented for selecting the solar panel. But the above work has got the drawback of sequential switching of solar panels to keep the voltage within the hysteresis window and thereby in Maximum Power Point (MPP) region.

Among the different algorithms used for determining MPP, the P&O and Incremental conductance (InC) method are the most efficient algorithms [4]. Under rapidly changing atmospheric condition InC algorithm is superior compared to P&O, but complexity of implementing InC algorithm in hardware makes P&O method attractive [5][6]. For space applications where accurate tracking is required, P&O or InC method is used. Fractional open circuit voltage or fractional short circuit current method is used for applications where accuracy is not a factor. The reference design uses fractional open circuit voltage (FOV) method whereas the proposed design uses a variant of P&O algorithm to determine MPPT.

This paper proposes an improvement for the scheme presented in [3]. A capacitor switching logic with efficient MPPT scheme has been implemented to obtain improved efficiency. Flexibility of selecting panels on demand provides an additional advantage of isolation. Also the SEPIC converter at the output of the panel provides a constant DC voltage for charging the battery in the entire I-V curve of the panel.

This paper is organized as follows: Section II presents the reference scheme on which improvement has been attempted. Section III describes the proposed architecture. Section IV details about the simulation studies carried out with the mathematical modeling of elements in the design and Section V describes the hardware implementation.

II. REFERENCE SCHEME [3]

A low power, low cost solar energy harvester for non aligned panels using a TDM scheme for selecting multiple panels to a single boost converter with fractional open circuit voltage MPPT scheme is presented in [3]. The scheme is as shown in Fig.1

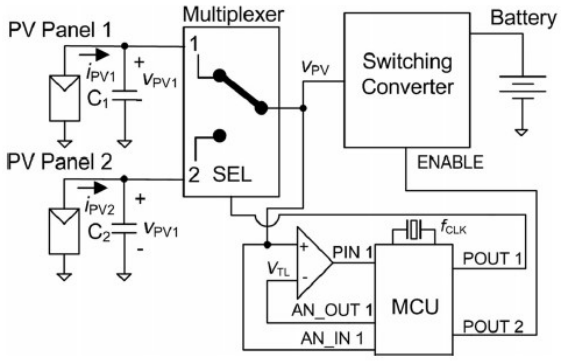

Fig.1 : Reference Scheme [3]

Capacitors (C1 and C2) are permanently connected to the panel and the each panel is selected by a multiplexer. The selected panel is connected to the input of a boost converter and the output of the converter is used to charge a battery [7][10]. The converter is enabled and the logic is selected by a micro controller unit, based on the reference parameters measured. FOV method is being implemented to determine the maximum power point (MPP) of the panel.

Since the panel is hardwired to the capacitor and the capacitor voltage is limited between the hysteresis window during the operation for achieving MPP, the open circuit voltage which is required to determine the MPP voltage can be measured only if the capacitor is allowed to charge to the open circuit voltage. Also the sequential loading of the panel is required to ensure that the capacitor voltage does not cross the upper threshold level of hysteresis window. ie, the switching converter should have a higher current discharge capability than the total current generated by multiple PV panels.

III. PROPOSED SCHEME

In the proposed scheme, pair of switches has been included between the solar panel and the capacitor compared to the reference scheme which provide simple control scheme to make the system in MPP tracking mode even if current discharge capability of the switching converter is less than the sum of currents generated by multiple PV panels. This scheme provide additional feature of isolation between the source and the load and between the sources. A variant of efficient MPP algorithm of perturb and observe is being implemented and calculated in each cycle to give accurate MPP tracking. A SEPIC converter has been used to provide constant DC voltage for charging the battery. The proposed scheme is shown in Fig.2

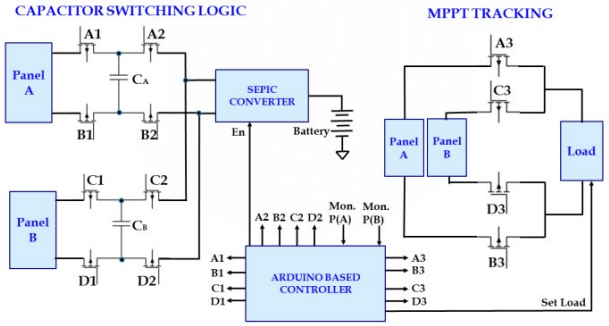

Fig.2 : Proposed Scheme

During initial power on, the open circuit voltage of capacitors is measured and the capacitor with higher voltage is connected to the converter. Assume that voltage across capacitor C_A is greater than voltage across the capacitor VC_B, ($VC_A > VC_B$), then the capacitor C_A is connected to the converter by turning on the switches A2 and B2. During this time, MPP of the solar panel A is determined and the capacitor C_B is charged from solar panel B till upper threshold of hysteresis window (+20% of V_{MP} of panel B). If VC_A falls below the lower threshold of hysteresis window (-20% of V_{MP} of panel A), the capacitor C_B is connected to the converter. During this time, MPP of solar panel B is determined and the capacitor C_A is connected to panel A. In order to determine the MPP of panels, P&O algorithm is used. The solar panel is loaded from no load to short circuit current and the voltage and current is acquired to compute the power. In order to load the solar panel, corresponding switches (A3 and B3 for panel A and C3 and D3 for panel B) are turned on. The load current is varied from 0mA (No load current) to 580mA (Short circuit current) by changing the reference voltage from 0V to 580mV. The maximum power point is practically determined during each cycle accurately. Fig.3 shows the schematic diagram of the capacitor switching logic.

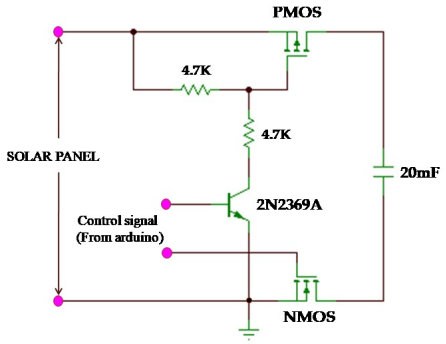

Fig.3 : Electronic load for MPPT Characterization

The control voltage drives the transistor to saturation to make the PMOS turned on till $V_{GS} > 2V_{TH}$ of the PMOS. The NMOS with low $V_{GS(TH)}$ can be driven directly from the arduino controller.

Fig.4 shows the schematic diagram of the electronic load used for MPP characterization.

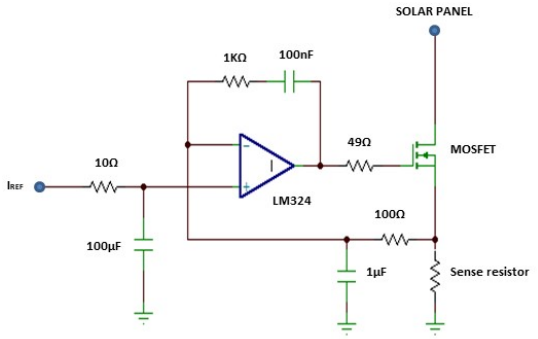

Fig.4 : Electronic load for MPPT Characterization

The current through the sensor resistor will be tracked towards the reference voltage to provide the required loading for the panel. The panel voltage and the load current is measured and characterized from no load to I_{SC} to determine the maximum power point. Sense resistor (1Ω) with temperature coefficient of ±20ppm/ºC is chosen for the application. The RC filter is used to avoid the noise. The panel voltage is scaled down by a factor of 5, buffered and acquired via analog input of Arduino controller. The voltage equivalent of the sense current is buffered and acquired via another analog input of Arduino controller. The voltage and current measurements are multiplied to calculate the instantaneous power of the panel. Fig.5a shows the voltage monitoring scheme and Fig.5b shows the current monitoring scheme.

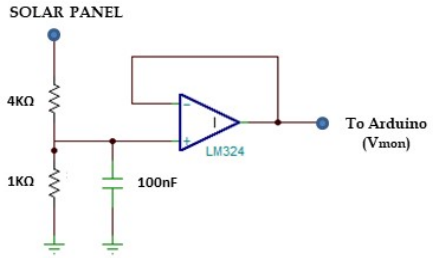

Fig.5a : Voltage monitoring

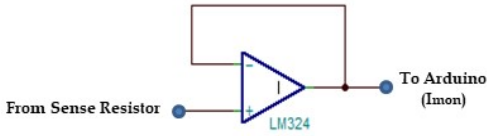

Fig.5b : Current monitoring

Fig.5 : Voltage and Current monitoring

The maximum power point tracking for each panel is determined when the corresponding capacitor is isolated from the panel and the capacitor is connected to converter. A variant of perturb and observe algorithm is being used to determine the MPP of each panel. The panel is loaded from no load to maximum load in steps of 20mA and instantaneous power is calculated from the voltage and current measurements. The voltage (V_{MP}) corresponding to the maximum power output is taken for calculating the hysteresis window (±20% of V_{MP}). Reducing the hysteresis band increases the rate of switching between the panels where as increasing the hysteresis band takes the operating region beyond optimum MPP. So a hysteresis band of ±20% is selected for the proposed design.

The Single Ended Primary Inductance Converter (SEPIC) is used in this design to provide a constant voltage for charging the battery. The SEPIC DC-DC converter provides positive regulated output voltage (+15V) even if the input voltage is above or below the output voltage (8V to 25V). Since the configuration of SEPIC converter requires two inductors, off the shelf coupled inductor is used to reduce the footprint. Coupled inductor will also provide better output ripple performance [8][9]. SEPIC converter is shown in Fig.6

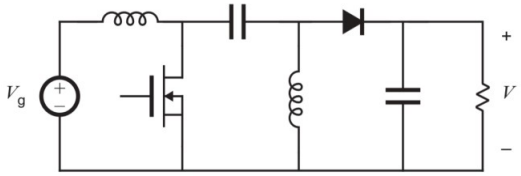

Fig.6 : SEPIC Converter

The input to output voltage relations for a SEPIC converter is given by equation 1.

$$Vo = \frac{D}{1-D} * V_{in} \tag{1}$$

When integrated with the solar panel, the equivalent impedance seen by the solar panel is given by

$$R_{eq} = \frac{V_{in}}{I_{in}} = \left(\frac{1-D}{D}\right)^2 R_{load} \tag{2}$$

For any R_{load}, equation 2 yields

1. As D→0, R_{eq}→α : Open circuit for panel
2. As D→1, R_{eq}→0 : Short circuit for panel

Thus, the SEPIC converter can sweep the entire I-V curve of a solar panel. Also the input ripple current for a SEPIC converter is very low w.r.t the input ripple current of a boost converter.

The battery will be charged at constant voltage continuously if the panels have sufficient irradiance. Multiple panels can be used for continuous voltage output. If the irradiance is not sufficient for continuous operation, then battery will be charged with pulsed current depending on the irradiance. But the panel is ensured to be operated at MPP point at any available irradiance.

IV. SIMULATION

Simulation studies of solar cell, MPPT algorithm and SEPIC converter were carried out using MATLAB and Simulink software prior to finalizing the design for optimum performance.

The mathematical modeling of the solar cell is important for analyzing the power extracted from the solar panel and also to characterize the power-voltage characteristics at different irradiance level and temperature of the panel. Simplest of which is single diode model. Equivalent electrical model of a basic solar cell is given in Fig. 7

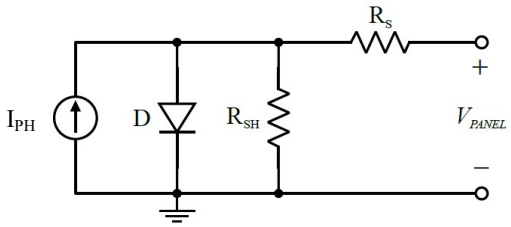

Fig.7 : Electrical model of a PV Cell

The basic mathematical equations governing the current output from the panel is given by equation 3.

$$I_{PH} = I_D + I_{SH} + I_{PANEL} \tag{3}$$

where,

I_{PH} : Generated Photo current
I_D : Diode current
I_{SH} : Shunt Current
I_{PANEL} : Output panel current

The diode current is given by equation 4.

$$I_D = I_{SAT}\left(e^{\frac{V_D}{nVT}} - 1\right) \tag{4}$$

where,

$$I_{sat} = I_s \left(\frac{T}{T_0}\right)^3 e^{qEg/nk} \left(\frac{1}{T_0} - \frac{1}{T}\right)$$

The shunt current is given by equation 5.

$$V_D = V_{PANEL} + Rs * I_{PANEL}$$

$$I_{SH} = \frac{V_{PANEL} + Rs * I_{PANEL}}{R_{SH}} \tag{5}$$

The generated current for a given temperature and irradiance is given by equation 6.

$$I_{PH}(S,T) = I_{PH}(S_0,T_0) + \alpha T(T - T_0)\frac{S}{S_0} \tag{6}$$

The power output from the panel decreases with decreasing irradiance and the power output increases with decreasing temperature of the panel. The P-V and I-V characteristics of the panel at different solar irradiance (1000W/m^2, 800W/m^2, 600W/m^2, 400W/m^2 and 200W/m^2) at constant panel temperature of 25°C [6] is given in Fig.8 and P-V and I-V characteristics of the panel at different panel temperature (30°C, 40°C, 50°C, 60°C and 70°C) at constant solar irradiance of 1000W/m^2 is given in Fig.9

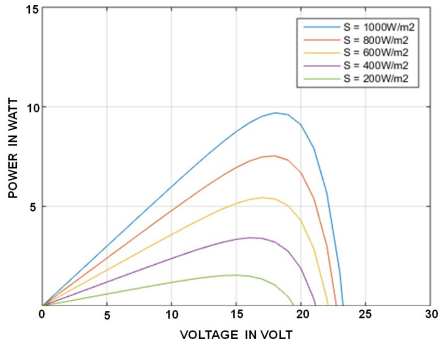

Fig.8a : P-V characteristics for different irradiance at 25°C.

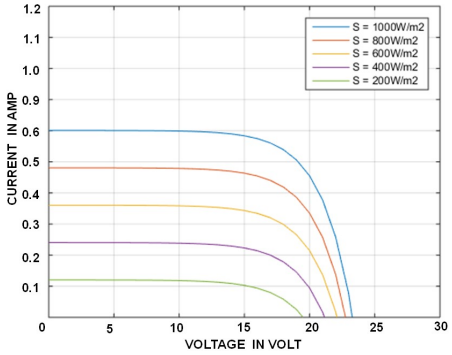

Fig.8b : I-V characteristics for different irradiance at 25°C.

The V_{MP} of the panel is expected to be between 15V and 17V for different irradiance and the short circuit current is expected to be decreasing w.r.t decrease in irradiance level. The I_{MP} determines the charging current for the capacitor and thereby to the load.

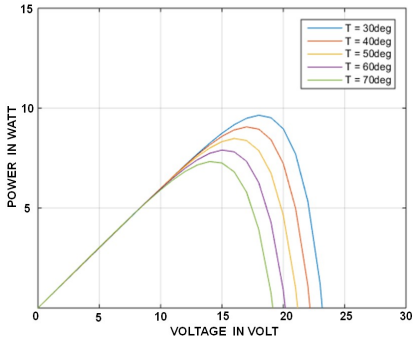

Fig.9a : P-V characteristics for different temperature at 1000W/m^2.

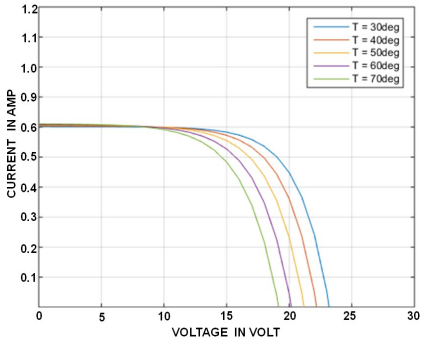

Fig.9b : I-V characteristics for different temperature at 1000W/m^2.

The power output decreases w.r.t the increase in the panel temperature and I_{MP} decreases with increase in panel temperature.

SEPIC converter is simulated using the simulink model as shown in Fig.10. The component values used in the design are L1, L2 : 470µH, C1 : 220µF, C0 : 1000µF and RL : 10Ω. The frequency of the pulse generator is set at 400kHz corresponding to the switching frequency of the converter [9]. Compared to boost converter, the SEPIC has the additional advantage of blocking the input from getting connected to output by the series capacitor, in case of converter disabled for isolating from battery under full charge condition.

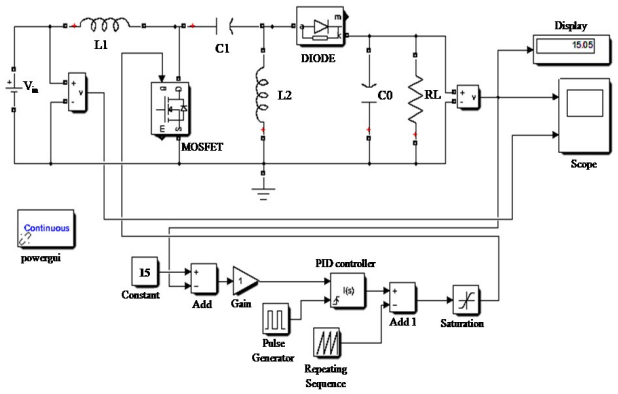

Fig.10 : SEPIC Converter.

The simulation was carried out with input voltage varied from 8V to 25V in steps of 2V and load varied from 20mA to 1.5A and the output voltage is found to be constant at +15V. The inductance and capacitance values are chosen to meet the output voltage ripple within 50mVpp. The simulation result of a SEPIC converter at an input voltage of 24V and load current of 1.5A is shown in Fig.11

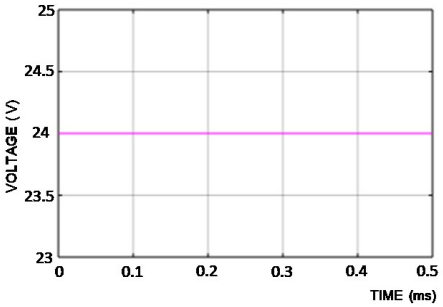

Fig.11a : Input voltage

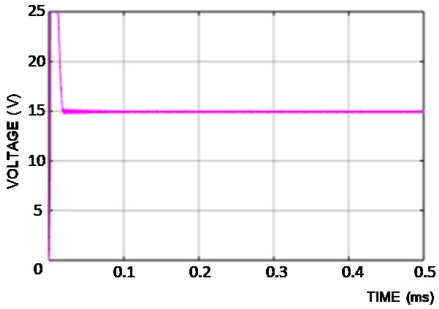

Fig.11b : Output voltage

V. HARDWARE IMPLEMENTATION

The proposed scheme is implemented in hardware to evaluate the performance. The hardware is configured around Arduino Mega 2560 controller, which generates required switching commands based on the upper and lower threshold voltage levels, calculated from the MPP voltage of each solar panel for the capacitor switching logic.

The Arduino Mega 2560 has 15 PWM outputs and 16 analog inputs available out of the 54 digital input/output pins. It also has 4UARTs and operate with a 16 MHz clock frequency. The hardware implementation is shown in Fig.12

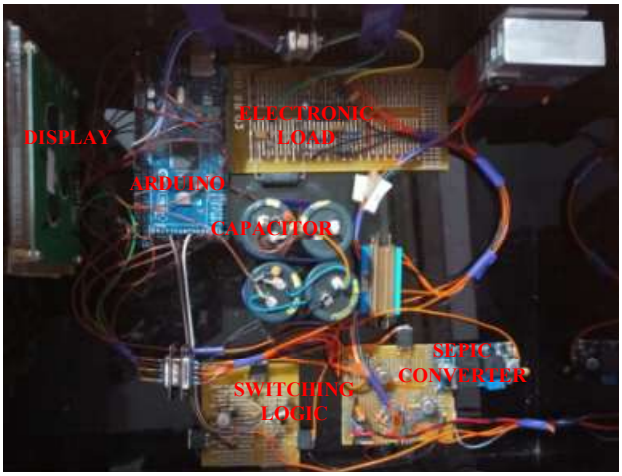

Fig.12 : Hardware model.

Micro Sun make (Model : MS1210) 10W panel is used in the hardware. The open circuit voltage is 22.32V with short circuit current of 0.6A. The maximum power point voltage is 18.1V and the maximum power point current is 0.55A. The MPP voltage of each panel is determined in each cycle by loading each solar panel, when the corresponding capacitor is connected to the converter. The voltage, current of each solar panel during MPPT characterization and voltage across each capacitor is acquired through the analog input of the arduino and digitized by 10 bit ADC in the controller. The maximum power, voltage and current at the maximum power point is displayed in a LCD display.

The XL6009 is a current mode controller used for SEPIC converter and the switching frequency is 400kHz. The converter can be disabled by driving the enable pin of the PWM controller low. The output is scaled down to 1.25V and compared with reference voltage to generate error and thereby adjusting the duty cycle.

The solar panels, the capacitor switching logic circuits implemented using Arduino mega 2560, SEPIC converter and 12V lead acid battery is configured as per Fig.2. The capacitor voltages (VC_A and VC_B) and the output voltages are acquired through Arduino, and is plotted using serial plotter as shown in Fig.13

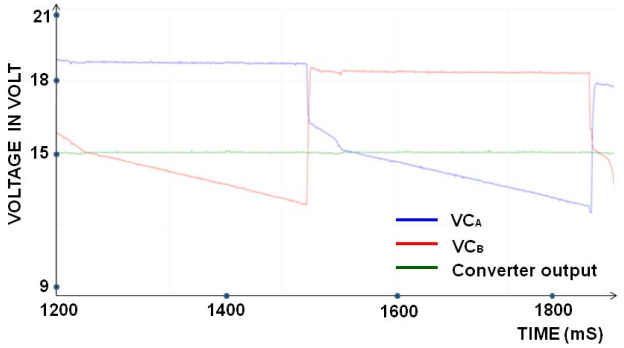

Fig.13 : Voltage waveforms.

P-channel MOSFET is used as switch in the positive supply line and N-channel MOSFET in the return line for simplified drive circuit. The energy, voltage, and capacitance of a capacitor are related by

$$E = \frac{1}{2}(CV^2)$$

The initial energy (E_0) and final energy (E_F) stored in the capacitor is, given by

$$E_0 = \frac{1}{2}(CV_0{}^2)$$

$$E_F = \frac{1}{2}(CV_F{}^2)$$

$$\Delta E = \frac{1}{2}(CV_F{}^2) - \frac{1}{2}(CV_0{}^2)$$

Time required to charge the capacitor is given by eqn.7, where P denotes the power

$$t = \frac{\frac{1}{2}C[V_F{}^2 - V_0{}^2]}{P} \quad (7)$$

During the initial turn on, the initial energy stored in the capacitor is zero and hence the time taken to charge a 20mF capacitor to the V_{MP} voltage of 17V by a 10W panel is 289ms. During the operational cycles the capacitor voltage is charged when connected to panel and discharged when connected to the converter. The capacitor voltage is varied between the 40% hysteresis window and thereby the capacitor charging time from lower threshold voltage to upper threshold voltage is 180ms approx. The output power and the efficiency of the converter determine the input power required to meet the load requirement. This determines the charge discharge cycle duration in the proposed scheme.

Considering the quadratic model of the MOSFET, the drain current equation can be written as equation 8.

$$I_D = \mu C_{ox}\frac{W}{L}\left[(V_{GS} - V_{TH})V_{DS} - \left(\frac{V_{DS}{}^2}{2}\right)\right] \quad (8)$$

$$\text{for } \{V_{DS} < (V_{GS} - V_{TH})\}$$

The gate drive circuit of the MOSFET is designed in such a way that the V_{GS} will provide a drain current which is more than the short circuit current (the maximum expected current from the panel). The resistive divider gate bias ensures the MOSFET turn on till the capacitor voltage greater than $2V_{TH}$ (twice the threshold voltage).

Since the proposed scheme has twelve MOSFET switches, the losses in the MOSFET have been quantified w.r.t to the power converted. The losses can be classified into conduction loss (P_C), switching loss (P_{SW}) and gate charge loss (P_{GC}) [11][12].

$$P_C = (I_D^2\, R_{DS(on)}) \quad (9)$$

$$P_{SW} = \frac{1}{2}(V_{DS}\, I_D\, [t_r + t_f]\, F_{SW}) \quad (10)$$

$$P_{GC} = (Q_g\, V_{GS}^2\, F_{SW}) \quad (11)$$

From equations 9, 10 and11 the conduction loss is calculated be 4mW, switching loss of 1µW and gate charge loss of 1µW. Total MOSFET loss is 0.6% and including the steady state losses in the converter, the total loss is 7.5% of 10W.

CONCLUSION

By implementing capacitor switching logic, option of disconnecting the capacitor from the panel gives the flexibility of selecting panels on demand for characterizing panel for determining MPPT. This feature brings better ground isolation between panels, and between panel and converter thereby better noise performance. The proposed scheme will characterize the panel to determine the MPP point in each cycle and thereby setting the hysteresis window which provides accurate operating condition. Also a variant of perturb and observe algorithm is used to determine the MPP in each cycle compared to fractional open circuit voltage method which is inaccurate. SEPIC converter will provide a regulated output, which makes the system independent of the load, as it cover the entire I-V characteristics of the panel.

As a future scope of work, optimization in the hardware can be attempted considering the actual load requirement. Optimized design w.r.t miniaturization, power and cost can be considered. MEMS capacitor, MEMS switches and switched capacitor converter can be used to implement the scheme for ultra low power application.

REFERENCES

[1] Chen Mingbo Zhang Zhongwei, “Development of the GaAs solar cell for space application”, 25th PVSC; May 13-17, IEEE 1996.

[2] Rizwan Arshad, Salman Tariq, Muhammad Umair Niaz, Mohsin Jamil, “Improvement in Solar Panel Efficiency Using Solar Concentration by Simple Mirrors and by Cooling,” 2014 International Conference on Robotics and Emerging Allied Technologies in Engineering, IEEE 2014.

[3] Oscar Lopez Lapena, “Time Division Multiplexing Control of Multi input Converters for Low Power Solar Energy Harvesters”, IEEE Transactions on Industrial Electronics, vol.65, no.12, Dec. 2018.

[4] Trishan Esram and Patrick L. Chapman :“ Comparison of Photovoltaic Array Maximum Power Point Tracking Techniques” IEEE Trans. Energy Conservation, vol. 22, no. 2, June 2007.

[5] Dalila Beriber and Abdelaziz Talha, “MPPT Techniques for PV Systems” in 4th International Conference on Power Engineering, Energy and Electrical Drives, IEEE May 2013.

[6] A.Durgadevi, S.Arulselvi and S.P.Natarajan, “Study and Implementation of Maximum Power Point Tracking (MPPT) Algorithm for Photovoltaic Systems,” IEEE 2011.

[7] Oscar Lopez-Lapena, Maria Teresa Penella, Manel Gasulla, “A New MPPT Method for Low-Power Solar Energy Harvesting”, IEEE Transactions on Industrial Electronics, Vol. 57, No. 9, September 2010.

[8] Hyun-Lark Do “Soft Switching SEPIC Converter with Ripple-Free Input Current”, IEEE Transactions on Power Electronics, Vol.27, No.6, 2012.

[9] Ebrahim Babaei ; Mir Esmaeel Seyed Mahmoodieh, “Calculation of Output Voltage Ripple and Design Considerations of SEPIC Converter,” IEEE Transactions on Power Electronics, Vol.61,No.3, 2014

[10] Ke Liu and John Makaran “Design of a Solar Powered Battery Charger” IEEE Electrical Power and Energy Conference, 2009

[11] Youthana Kulvitit, “Energy Capapacity of Voltage Dependent Capacitor for the Calculation of MOSFET’s Switching Losses” IEEE conference, 2012.

[12] T.Halder, “Selection of switching skills of the power MOSFET in the Static Converter,” IEEE 2017

Proceedings of the Fourth International Conference on Communication and Electronics Systems (ICCES 2019)
IEEE Conference Record # 45898; IEEE Xplore ISBN: 978-1-7281-1261-9

FOG COMPUTING FOR SMART CITIES

Chintam Muni Kanaka Sri Shalini
Department of CSE
Institute of Aeronautical Engineering
Hyderabad, India

Y. Mohana Roopa
Professor, Department of CSE
Institute of Aeronautical Engineering
Hyderabad, India
ymohanaroopa@iare.ac.in

J. Sirisha Devi
Professor, Department of CSE
Institute of Aeronautical Engineering
Hyderabad, India

***Abstract*— In a world rural area keeps declining and smart cities keep evolving. data is one of the most important resources to maintain as terabytes of data is collected from a single city. data is analyzed using big data analysis and it can be stored by using the fog computing and it also describes how fog computing is effective in IoT when compared to cloud-based computing and how fog-based computing is emerging and how it is leading. it describes cloud and fog architecture and how the data is processed in those architecture and we are going to learn about a new experimental architecture. it is merger of both fog based and cloud-based. Fog computing is technology, which is rapidly in use so, we will discuss some of its applications. The data is used to achieve a proper life where people can live safe and it is also used for analyzing various factors of like economy and employment and to understand its patterns to achieve development. There are many challenges to maintaining the data through fogging these challenges are mentioned along with that the security problems that followed from cloud to fog.**

This paper mainly tells us how fog computing would be the future of IoT and how it would change the world.

Keywords*— *Big data, Data mining and analytics, Smart city, Cloud computing , fog computing.

I. INTRODUCTION

Due to the increase in the urbanization. Cities are rapidly extended their area and along with that population growth has been increased in tremendous amounts. now about fifty-four percentage of the population of world are now living in cities.

It was 30% back in 1950[1]. In 2030 two by third of the population of the world would be live in urban regions and people who are already living in urban areas of countries with developing economies would increase twice in number and the area of these cities could be tripled based on latest UN reports. The proportion of the urban population is expected to increase to 68% by 2050[2].

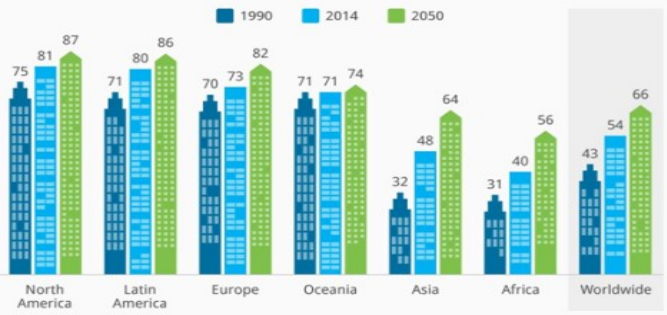

Fig1: Urban population increasing ratio

With the growth of the population of the world will add another 2.5 billion folks to urban areas until 2050. Based on the reports 90% of increase would take place in Asia and Africa.

It is very hard for governments to provide facilities like transportation and water supplies to all the citizens living in that area despite population growth. Big data can be very helpful for the analysis of information in edge computing and in also used in cloud-based computing [3]. Data can be easily analyzed in the fog because of its distributed approached and data can be easily tracked from where it is coming and where it is going to be uploaded. we can provide much security to citizens data

There is much evidence that would suggest that fog computing helps in formatting and sorting data. there are many challenges in these data collection [4]. The challenges may include maintaining sustainable environmental, ideas that would help in developing of both the social and economic conditions of the society and decision making were everyone's opinions are valued. We can create a clever infrastructure and solving these challenges would help achieve to better social life for citizens. Aim of developing this model is provide improved versions of the present smart cities by providing various approaches to collection, integration and analyses of data to help in provide a better life for citizens.

II. BASIC FOG COMPUTING CONCEPT

Smart cities are the traditional cities and as urbanization is at a rapid extent their great need of managing the data that is in these smart cities. Data should be properly managed so that it can be analyzed for various applications. data analytics process of the smart city has quite complexity. Cloud computing is mostly used for maintaining such large data but there are quite disadvantages of using it. There can be many alternatives to cloud computing [6]. When we are talking about the alternatives .one of the best alternative is fog computing .accessing of the data is very easy in fogging when compared to the cloud and the fogging is an extended service of the cloud computing where data is stored nearer to the source and mainly the data can be stored between the cloud and source at a particular point where the data accessing and storage would be easy.fog computing can be called as the edge of the network, this particular name is given because the data is just stored above the ground. accessing data from the cloud becomes more difficult with low internet speed and bandwidth is the most common problem which leads in the difficulty in accessing [7]. Fogging would be the best solution for all the above-

mentioned problems. The following diagram shows the detailed description of fogging.

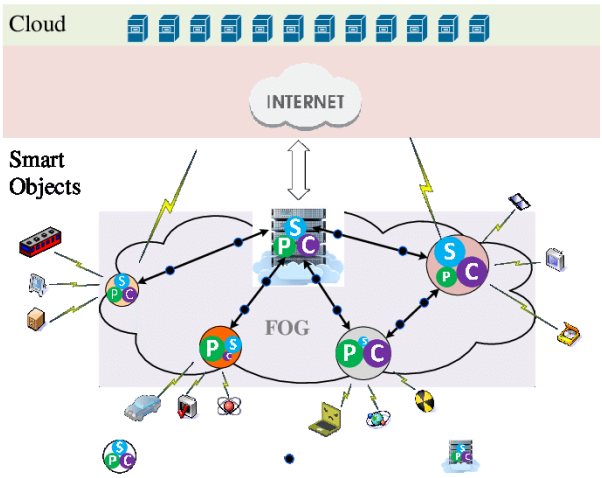

Fig2: Interplay between IoT , Fog and Cloud[4]

III. CLOUD ARCHIETECTURE FOR SMART CITES

Smart cities can provide various solutions which are used to solve real time challenges related to urban regions[8]. there are many challenges and these challenges be providing sustainable environmental, ideas that would help in developing of both the social and economic conditions of the society and decision making were everyone's opinions are valued.

First, we should learn about the cloud architecture for the idea then we can modify that cloud architecture by introducing the fogging into it as the extended form or extended service of the cloud. the architecture of the cloud is given below

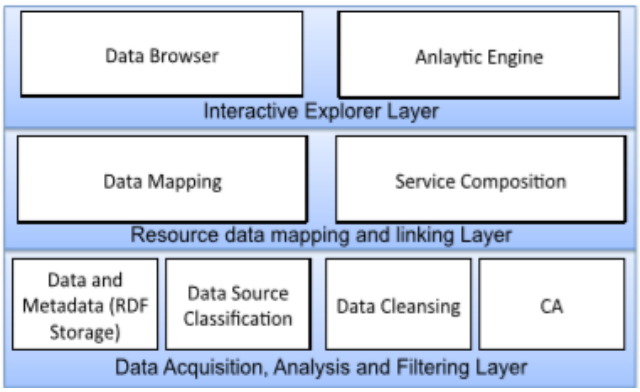

Fig3: Cloud Architecture

It is a three-layered approach and each layered has its own importance.
The bottom layer of this architecture consists of various data warehouses which have data being collected from various data mart and it has a distributed approach and many sensors are connected to this layer and all the data pre-processing steps are performed on the data.

In the middle layer mapping of data based on their Meta characters and linking is performed here this would help in finding new cases and makes the relationship between the attributes stronger. data is collected from various data marts as data collected would have many unique values this would be great help for data linking.

These data browsers present in the upper layer is used to browse the variables and indicators

From the datasets based on the metadata of those variables and indicators and the analytical engine, a great help for the end users use to find the data from the cloud.

difference between cloud computing and for computing. To know about the data storage and data need to understand both the technologies architecture.

IV. FOG ARCHITECTURE OF SMART CITY

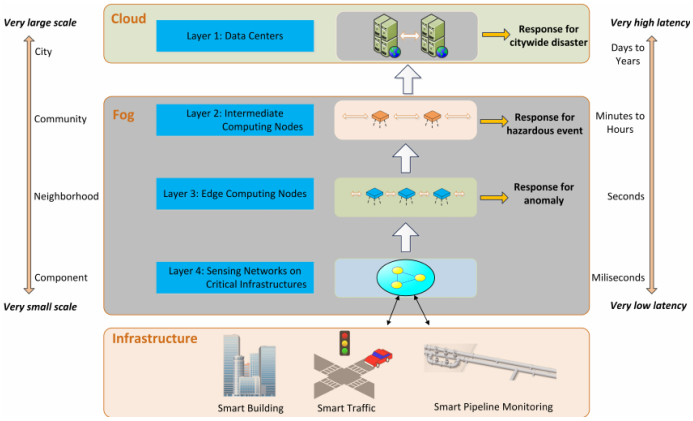

Figure 4: The 4-layer Fog computing architecture in smart cities, in which scale and latency sensitive applications run near the edge.[2]

Layer 4, in this layer sensing action is performed and this can be performed on the data collected from various nodes with consist of many sensors which are of low cost and they are high reliability and they are spread over large public areas so we can monitor different changes and data generated is large from these sensors .data is collected at every node is send to the layer above it..

Layer 3, in this layer nodes are present with power consumption rate would be less than usual and performance of these nodes are also high .local group of sensors and connected to this layer regular analysis should be performed and alerts should be send during the danger and feedback should also be send to respective authorities to improve the local conditions.

Layer 2 may contain nodes which lie between different set of nodes, every intermediate node is connected to a group of edge devices at upper layer and it uses its geospatially collected data to discover the risky events happening.

When any hazardous event is identified it makes fast moves to stop the damage and save the infrastructure and layers 2 and 3 provides feedback which and these feedback act just like the human reflexes that safes us from the dangers. Consider an example, where gas pipeline's certain part has leakage and if the fire starts in that part these intermediate nodes would shut down the whole system [9]. it would reduce the loss to the life and property. Meanwhile, the output of data analysis of these two layers is fed into the to top layer for analysis of behaviour and conditions to be monitored for longer time period and controlling and monitoring of city-wide data can be possible at top layer. long-term data is stored which can be analyzed. It allows spontaneous decision making which makes the municipalities to take better actions across whole city during a natural disaster or large-scale service interruption.

Using this 4-layered approach we can detect the threats easily and we can reduce the damage to the human life's an environment. by using this approach, we can analyze the data many times and problems are rectified immediately we compared to the cloud. Now a day's data is being available for everyone which is termed as open data. which is used for many purposes most of the important purpose is to provide better life for citizens and it helps in visualizing future infrastructure and to improve the present one and all this data is provided by government.

Management of data for each unique domain is used to collect the data from various sources and analysis performed on that data.
By managing such type of data we can get the particular information about the specific thing for suppose we consider the places or areas of a city .we can store the data of all the places in the nodes and we can analyze the crime rate of the area as we already have all the information of the particular area it is also easy to maintain the accident spots of that area. We can analyze many more things about the area by using that data like the real estate and many more because of the tremendous amount of the data present in it and the data trafficking is high whereas in fog-based computing data trafficking would be quite less.
.

IV. FOG-CLOUD-DATA MANAGEMENT

It is a new technique through which data can be more efficiently maintained. Fog-to-Cloud (F2C) Data Management experiments have been conducted on the city of Barcelona.

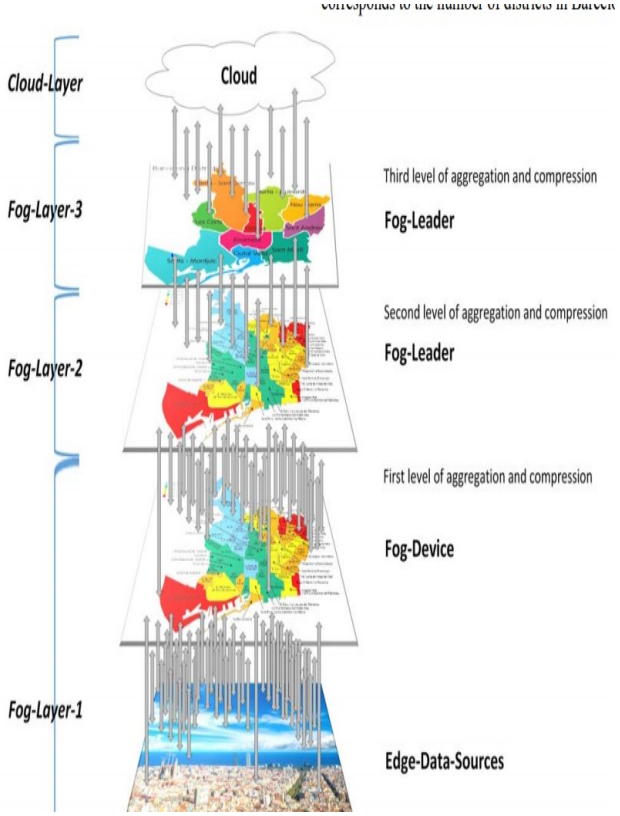

Fig 5: Representation of the F2C data management in Barcelona.[5]

Sensors collect all types of data and this data is classified in data classification phase. Information collected is categorized into five types mostly it is based on energy ,noise, urban, garbage and parking. Where data is again sub divided into types like energy can be divided into solar or wind etc and we can divide noise based on the vehicles or the loudspeakers.

Edge-data-sources collects the data from various sources performs classification in the lowest level. and all classified data is aggregated in fog-layer2 and compression is also done in the same layer. fog-leader is also one of the data classification phases. Sensors are distributed over a large area in Barcelona and layer 1 is spread over 73 respective areas of fog and second layer is spread over one kilometre which has total of ten main areas [5].

V. SECURITY CONCEPTS OF CLOUD COMPUTING THAT FOLLOWED FOG COMPUTING

There are total of 12 critical issues which might act as threats and affect the safety.

A.Advance Persistent Threats (APT)

these would be nothing but the attacks that compromise the security of the companies

B. Access Control Issues (ACI)

This leads in poor management. Unauthorized entries are made and make changes in the software

C.Account Hijacking (AH)
account is being used by unauthorized people who are not allowed to use the account.
D.Denial of Service (DoS)
because of the finite resources even the authorized people cannot use the service sometimes.
E.Data Breaches (DB)
this data breaches cause crisis situation because of the loss of the confidential data.
F.Data Loss (DL)
loss of data can be done by faults in the software or by malicious activates or even by natural resources.
G.Insecure APIs (IA)
The providers of various computing use API's for client use and it is used to provide the security for the applications that we have developed.
*H.System and Application Vulnerabilities (SAV)*Attackers can enter the system by finding loopholes in the system like bugs.
I. Malicious Insider (MI)
A person with authority and he decides to use that power in a wrong way by performing the malicious activity.
J.Insufficient Due Diligence (IDD)
this many occurs when any organization rushes in designing and implementation of the project.
K.Abuse and Nefarious Use (ANU)
If the supply of the resource is for free. it may be used for some malicious activity.
L.Shared Technology Issues (STI)
this is mostly occurring due to shared resources, platforms and infrastructures with more people

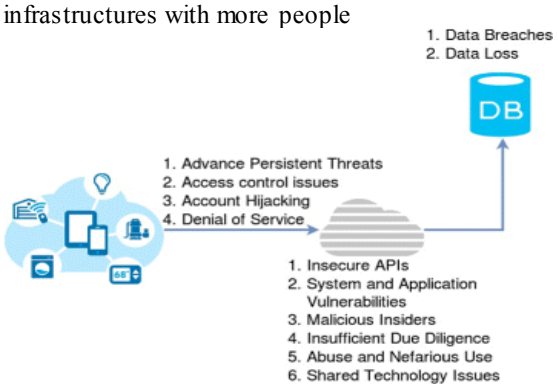

Fig. 6: Potential security issues of Fog Platform inherited from Cloud computing.

Above figure shows how virtualization and other issues of Cloud platform can affect Fog platform as well [10].

VI. APPLICATIONS OF FOG COMPUTING:

A. *Smart Home*

Rapid development of IoT has created many smart devices and sensors are even present at home. there are many home security devices like smart locks and recorders which are can be audio or video or both. Once fog computing platform sets up, every sensor would act as a client[11]. The server-based application is installed in every virtual machine. on this Virtual machine, the advance processing logic is being implemented, which shares the secure.

B. *Smart Grid:*

This is an electricity distributing system where meters are arranged at regular intervals. There is a centralized server with gathers all the information .it also used to analyze that data and inform to the system if any dangers happen. using fog computing, SCADA is added with a decentralized model with micro-grids, which improves scalability and provide security with fog computing, the grid will turn into a hierarchical system which acts as an interface between fog and SCADA. in this kind of systems, fog is in charge of communications with another grid and another fog[12].

C. *Smart Vehicle*

Fog computing can be integrated into automobiles they are 2 ways of integration [14], they are infrastructure-based and autonomous. the formal would be VTube, it basically depends on fog nodes that are placed along the roadside; these nodes are responsible to send/retrieve information to or from the vehicles. The further mentioned in, every fog can communicate to its users within and may be from another fog. There are many applications for fog computing in automobiles. Popular applications would be traffic light scheduling, congestion mitigation, precaution sharing, parking facility management, traffic information sharing, etc.

D. Health Data Management

This have been a delicate topic as the data collected of the patients should be kept confidential because this data is cause harm and disturbs privacy of the patient. By edge computing, the data of the patient will be stored locally so data can be accessed quickly[13]. data collected and stored in those fog nodes like in our Smartphone gadgets. the data is preserved and competed in a more secure manner so there is no way of data leakage. Modification of data can be done easily in patients' fog-node.

E. *Wind Farms*

Wind turbines are a very sensitive piece of equipment. according to the weather you make changes to increase the output. The problem is that most wind farms are located in remote areas. "Edge intelligence" enables us to analyze data locally in real-time without relying on continuous network availability.

F. Trains

As part of the rise in the Internet of Things, trains and tracks are being built with sensors with locomotives acting as the central hub for all the data which has been collected from these sensors. Due to the fast movement of trains, it is difficult

to maintain the connection with "the cloud". it is better to install some fog computing nodes in your locomotive.

G. Pipelines

Gigabytes of data is generated alone from the 100-mile long pipeline [15]. there can be many tetra bytes of data can be collected from a single pipeline. fog computing plays an important role in this case because we can easily detect any leakages if we collect the data at regular intervals cloud only needs to know only important data so it is better to use fog computing.

VII. CHALLENGES IN FOG COMPUTING:

There are several challenges for implementing fog computing and they are

A. Choice of Virtualization Technology

Virtualization can provide a better environment for fog computing. There is a question about which to choose hypervisor or container, we already know that Cloudlet has been utilizing virtualization technique of hypervisor paradrop is choosing the container-based technology because it is lightweight when compared hypervisor and hardware is used for these two technologies[16]. the container cannot host different OS on a single node.

B. Fight with Latency

There are some conditions which lead in having latency at high range in fog computing platforms. Those kinds of latencies would destroy client experience with the fog computing. There are several ways in bringing latency back some of those methods are

- Data aggregation.
- Node mobility.

C. Network Management

Management of the network would be difficult be difficult until you apply techniques like software defined network and network functions virtualization and combination of both can be used to, but it is not easy to combine them to. there can be many difficulties in it. there can be difficulties in design and different directional bounding and genuine design of network can lead to difficulties in design.

D. Security and Privacy

Main priority at every level is to maintain the privacy and security for users and it is also one of the main challenges too. we have use may restrictions on the access and we have to check whether unauthorized people have entered system this makes the model strong.

VIII. CONCLUSIONS

In this paper we have discussed how the population in cities has been increasing and how new technologies should be used for the creation of better cities. How data can be more efficiently accessed and stored in the fog-based computing when compared to the cloud. It also compares the architectures of both cloud and the fog for better data management of the data. it also differentiates between the fog and the cloud computing and it can be done based on the certain characteristics and it highlights some security problems that followed to the fog from cloud. we have also discussed the challenges and the applications of fog computing. In the end we conclude that by adopting fog computing technique we can make better smart cities.

References

[1] Zaheer Khan et.al ," Towards Cloud Based Big Data Analytics For smart future cities", Journal of Cloud Computing Advances, Systems and Applications20154:https://doi.org/10.1186/s13677-015-0026-8, December 2015

[2] Bo tang et. al ," A Hierarchical Distributed Fog Computing Architecture forBig Data Analysis in Smart Cities", DOI:10.1145/2818869.2818898}, October 2015

[3] J. Kane, B. Tang, Z. Chen, J. Yan, T. Wei, H. He, and Q. Yang. Reflex-Tree: A biologically inspired parallel architecture for future smart cities. In International Conference on Parallel Processing (ICPP), 2015.

[4] Jianhau li et.al, "EHOPES: Data-centered Fog Platform for Smart Living", Nov. 2015.

[5] Amir Sinaeepourfard et.al," Fog-to-Cloud (F2C) Data Management for Smart Cities", Future Technologies Conference (FTC) 2017 29-30 November 2017| Vancouver, Canada.

[6] Satyanarayanan M (2015) A brief history of cloud offload: A personal journey from odyssey through cyber foraging to cloudlets. GetMobile : Mob ComputCommun 18(4): 19–23

[7] Alliance CS (2016) The Treacherous 12 Cloud Computing Top Threats in2016 .Online: https://downloads.cloudsecurityalliance.org/assets/research/top-threats/Treacherous-12_Cloud-Computing_Top-Threats.pdf. Accessed 22 Dec 2016

[8] Stojmenovic I, Wen S, Huang X, Luan H (2015)," An overview of fog computing and its security issues: Concurrency and Computation: Practice and Experience ".

[9] Yi S, Qin Z, Li Q, "Security and privacy issues of fog computing: A survey In",International Conference on Wireless Algorithms, Systems, and Applications,2015, 685–695.. Springer

[10] Saad Khan et.al ,"Fog computing security: a review of current applications and security solutions,",Journal of Cloud Computing, December 2017, 6:19

[11] Mohemedfirdhous et.al ,"Fog Computing: Will it be the Future of Cloud Computing?", Conference: Conference: The Third International Conference on Informatics & Applications (ICIA2014), At Universiti Sultan Zainal Abidin (UniSZA), Kuala Terengganu, Malaysia

[12] Shanhe Yi et.al," Fog Computing: Platform and Applications", DOI: 10.1109/HotWeb.2015.22,2015

[13] F. Bonomi, R. Milito, J. Zhu, and S. Addepalli, "Fog computing and its role in the internet of things," in workshop on Mobile cloud computing. ACM, 2012.

[14] C. Wei, Z. M. Fadlullah, N. Kato, and I. Stojmenovic, "On optimally educing power loss in micro-grids with power storage devices," IEEE ournal on Selected Areas in Communications, 2014.

[15] G. Yan, D. Wen, S. Olariu, and M. C. Weigle, "Security challenges in

vehicular cloud computing," IEEE Transactions on Intelligen Transportation Systems, 2013.

[16] T. H. Luan, L. X. Cai, J. Chen, X. Shen, and F. Bai, "Vtube: Towards the media rich city life with autonomous vehicular content distribution," in IEEE Communications Society Conference on Sensor, Mesh and Ad Hoc Communications and Networks

Proceedings of the Fourth International Conference on Communication and Electronics Systems (ICCES 2019)
IEEE Conference Record # 45898; IEEE Xplore ISBN: 978-1-7281-1261-9

Iot Applications in Smart Cities

Sunitha Cheepurishetti
Computer Science And Engineering
Institute Of Aeronautical Engineering
Hyderabad,India

Y. Mohana Roopa
Professor, Computer Science and Engineering
Institute of Aeronautical Engineering
Hyderabad, India
ymohanaroopa@gmail.com

***Abstract*— Here we discuss the integration of sensors with the cloud and their applications which is the highlighting aspect in the future IOT. These concepts are very much important in developing smart cities. These smart cities improve the quality of living. It is estimated that by 2025 there will be atleast 88 smart cities around the world. This idea results in healthy, sustainable and secured environment but, will take lot of investment and time to build. In this paper, we will discuss the areas where the IOT involved to develop a smart city.**

Keywords— sensors; cloud computing.

I. INTRODUCTION

Cloud is the advanced technology of storing and protecting data. Cloud storage is based on the virtualization techniques. In this the uploaded data will store on remote servers and accessed through internet or Cloud. For instance, uploading files to drive that will store on google cloud. The major advantage of cloud, we can access the data that we have uploaded anywhere in the world. Sensors are the devices that sense the physical parameters such as pressure, temperature etc., and gives the signal which can be measured electrically[1][2]. The integration of sensors with cloud can results in many useful applications but this is a bit complex activity. The data in cloud can be pushed to our mobile phones so that the common information can get to know by many people around. In the case of sensor cloud integration, sensors sense the data and transmit it to cloud .This transmission can be done in different ways.

II. HOW THE DATA GO TO CLOUD FROM SENSORS?

A. Sensors to cloud:

The data transmission from sensors to cloud takes place in different ways. At the early stage (1970 to 1980) the transmission process is done by using ethernet which is a wired process but some places do not have wired internet which turns as a disadvantage to this process. This doesn't involve in radio link[5]. This process send information directly from sensor microprocessor to the cloud.

B. sensors to mobile network to cloud:

In this case, the data flows from sensors to mobile phone with the cable(wired). From mobile to mobile tower which involves in radio waves this is a wireless process. After this, the data go to the tower and then to cloud through the cable (wired).This is the cost effective process to the user.

C. sensors to wifi routers to cloud

In this process the data from sensors move to wifi radio through cable (wired) after there to wifi router through radio waves which is wireless process. Wifi routers are connected to cloud by the Ethernet. In another way, from mobile routers the data leave to mobile towers and then to cloud through Ethernet.

D .sensors to mobile to cloud

This is the advanced technology which is in progress. This is used by the mobile phones with the wifi and BT(Bluetooth) radio. Data flows from sensors to BT radio and from there it flows to smart phone to wifi router. From wifi router to cloud.[4]

III. OUTLINE FOR SMART CITIES

Let us assume, Smart cities functions like our body. All the buildings like the muscles in our body, greenery and parks like lungs that provide oxygen and make our life possible. We have roads as veins and arteries which moves the goods and the people (carries the information). Our body has 5sensors which sense the parameters like hot, cold etc., and pass the information to the brain[14]. Similarly, We construct sensor network to the city which senses different parameters, collects the data in the city and transmit it to the cloud. By this sensor layer we can develop many applications that access the data present in the cloud.

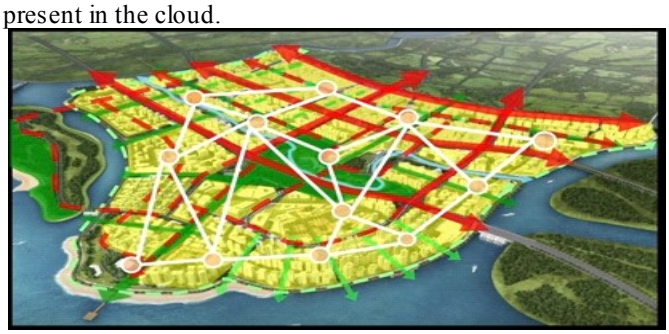

Fig1: Outline for smart cities

A. Smart planning:

Smart planning is to provide a better environment. Firstly, they collect all the information about the city like roads, buildings and parks etc., and also collect data about energy use and waste, save it in database[6]. By this information they can obtain a 3D map of the city. This map gives the status of the city to the developers. The developers continuously observes the changes in the city, update the details to the people in the city through mobile apps or electronic boards.

IV. SOME IOT APPLICATIONS

A. Smart parking:

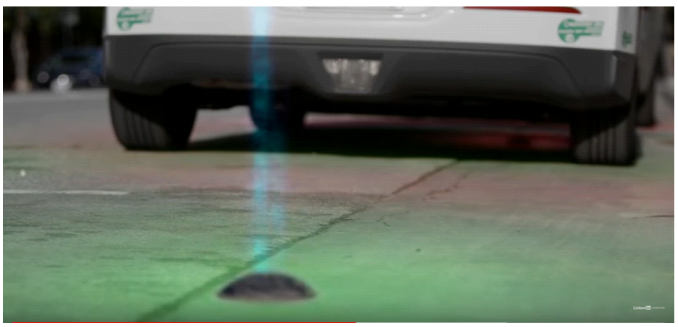

Fig2: Smart parking with sensors

When the city turns out of the traffic cars literally look around for the parking area which ultimately leads to congestion. To overcome this, smart parking came into existence[7]. In smart parking the sensors are affixed into parking slots and these sensors are responsible for giving the information whether the slot is preoccupied or not. This information can be viewed in our mobile phones and the one who drives the vehicle can get to know where the parking place available ,this ultimately saves the time, decreases the traffic and also unexpected damages[8].
To achieve this Nwave wireless parking space sensors are used that track the changes in earth magnetic field caused by presence of iron mass of an object(like vehicles). The status is then transmitted through radio, by a communication network to the cloud.

B. Traffic flow simulation and prediction:

The following are the different applications used in congestion control which is the major headache in the cities

i . In this application, they will push the map filled with traffic conditions (vehicles) of the city ,by seeing that the driver can able to know which way has congestion and can avoid that way .By this we can also know which way is shorter to reach our destination.

ii) Bus passenger count sensor:

Fig 3: Bus passenger count with sensors

From this application we can able to know whether the bus is crowded or not. This can be done by using **bus passenger count sensor.** A single sensor (connected to camera) is fixed at the entry/exit of passengers which is able to increase the count on entry of a passenger and decreases on exit[9]. The passenger movement (exit or entry) can be differentiated by camera which supports the image processing techniques. This complete information is send to cloud. People can access this information via corresponding app by providing the details like bus number.

iii. Fuel level sensor:
When the car is going to be out of fuel the **fuel level sensor** sense it and the software (at the steering) automatically displays alert message along with the data about the gas stations that are nearby.

iv. Connected cars:

Connected car technology is huge and a flexible network of multiple antennas, embedded software, sensors and technologies that provide the communication in order to navigate in this world[10]. The car is given with the internet and the car location and details can be shared by means of internet. It has the responsibility of making decisions with accuracy consistency and speed. These requirements will become more complex when humans lose control over steering wheel and brakes to the autonomous vehicles they can be controlled.

C. Elderly care:

Now-a-days many of the citizens are worried about their parents who will be at home alone when they went to job[11]. To overcome this we will fix sensors in the rooms in which their parents roam, these sensors monitors the movements of

their parents and gives the statistical data to their smart phones.

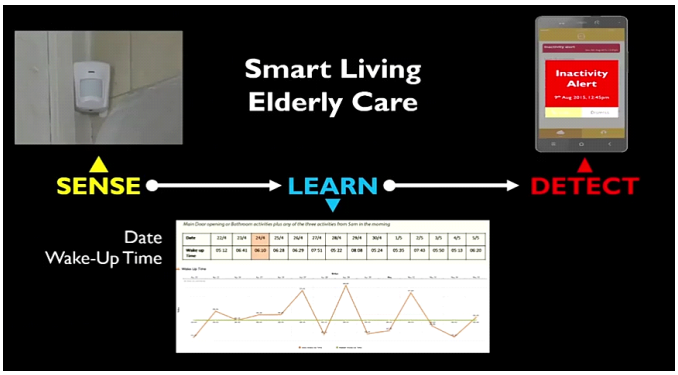

Fig 4: Smart Living Elderly care

D. power consumption:

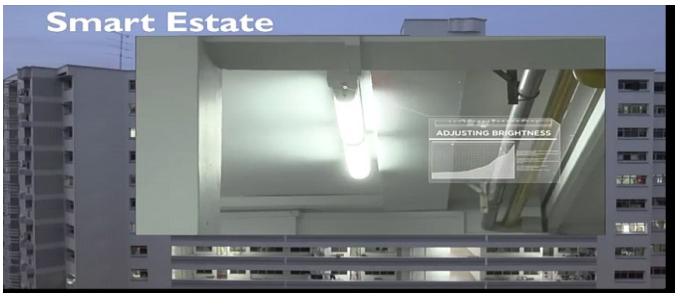

Fig 5: Smart Estate with sensors

In apartments, smart sensors are fixed in the corridor which senses the person movement and brightens the light at that particular place and glooms the remaining lights. Thus less power consumption is achieved.

E. Tele-health:

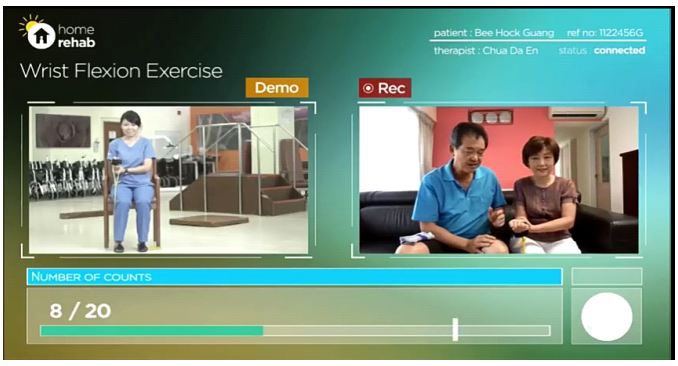

Fig 6: Tele-health is to monitor the patient's heath

The intention behind this tele-health is to monitor the patient's body without moving to the hospital [12]. The doctor can estimate the blood pressure of the patient as the patient catches the sensor. This is also useful for physiotherapy, the doctor can count the number of times the patient is moving his hand for a particular time and if there is any emergency they can suggest the patient to come to hospital.
This approach is used in elderly care where we can use the bed room sensors, call for help push button, toilet sensors etc.,

F. Shadow analysis:

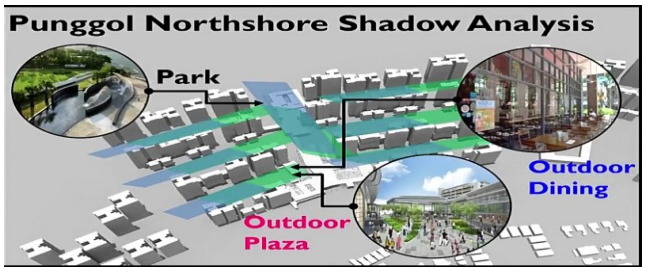

Fig 7: Punggol Northshore shadow analysis

This analysis will make us to know about how much time a particular place will have the shadow [11]. By this we can able to decide where to have which place. For instance, we like to have childcare center in such a place where most of the time it is covered with shadow such that the children can play freely the whole day.

G. Smart estates:

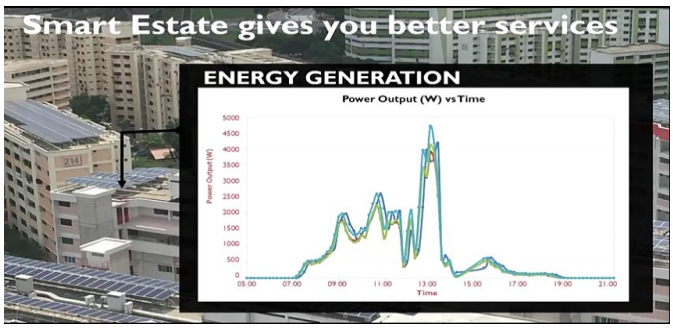

Fig 7: Smart Estate with sensors

In many of the cities we will have the solar panels spread over the buildings, in this case we fix **Uv or solar sensors** to the solar panels sensors to the panels and trace the energy collection by plotting a graph in the computer, by this if there is decreased or poor energy collection by any panel we can able to notice that the panel is not working and be replaced .In another case ,if the panels extending to some extent are collecting the low energy it will be cloudy or rainy in that particular area.

H. logistics:

i. Goods tracking and maintenance :

Good tracking and warehousing is one of the most important parts of the connected logistics. Affixing of small inexpensive sensors will allow companies to easily

track items, monitor their status, condition and construct a smart warehouse system. This idea will also help to check the goods where the human inspection is difficult.

ii. *Location tracking system*:

Location tracking can make the companies to get to know about the driver activities and the location whether he delivered the respective product or not. This can be done using the GPS tracking system this can be largely used in companies like uber, zomato, ola etc.[13].

V. SUSTAINABLE DEVELOPEMENT

Any country in the world, sustainable development will play vital role for its development. In our country about 67.8 percentage of current is produced by using coal which is an indigenous non-renewable resource. Uninterrupted usage of these resources will affect the future generation. If we keep on continuously using them the future generation will get affect in order to reduce that sustainable development should be must in the city.

Solar houses are nothing but construction of houses in which the power that we used to access the electrical appliances inside the house is generated by the solar energy. This can be done by converting solar energy to electrical energy by means of a solar panel and a battery. When the battery is depleted the home appliances will take the energy from the electrical grid.

This ultimately reduces the electrical charges to the common citizen. This is an Environmentally friendly process because it doesn't involve in any pollution raising activity like in thermal power.

VI. CONCLUSION

In this paper we discussed about the different applications used in developing of smart cities through IOT. Smart applications in industry, houses, hospitals, transport are covered which make a person to lead a comfortable life. IOT in transport is very importance because it can prevent many lives to be lost. Applications that are environmental friendly can make the city and the people clean and healthy.

REFERENCES

[1] N. Walravens and P. Ballon, "Platform business models for smart cities: From control and value to governance and public value," IEEE Commun. Mag., vol. 51, no. 6, pp. 72–79, Jun. 2013.

[2] https://readwrite.com/2015/10/13/sensor-data-device-to-cloud/

[3] X. Li, W. Shu, M. Li, H.-Y. Huang, P.-E. Luo, and M.-Y.Wu, "Performance evaluation of vehicle-based mobile sensor networks for traffic monitoring," IEEE Trans. Veh. Technol., vol. 58, no. 4, pp. 1647–1653, May 2009.

[4] https://readwrite.com/2015/10/13/sensor-data-device-to-cloud/

[5] W. Kastner, G. Neugschwandtner, S. Soucek, and H. M. Newmann, "Communication systems for building automation and control," in Proc. IEEE, Jun. 2005, vol. 93, no. 6, pp. 1178–1203.

[6] G. Montenegro, N. Kushalnagar, J. Hui, and D. Culler, Transmission of IPv6 packets over IEEE 802.15.4 networks, RFC4944, s.l.: IETF Sep. 2007. [Online]. Available: http://tools.ietf.org/html/rfc4944.

[7] A. P. Castellani, M. Gheda, N. Bui, M. Rossi, and M. Zorzi, "Web services for the Internet of Things through CoAP and EXI," in Proc. IEEE Int. Conf. Commun. (ICC 2001), Kyoto, Japan, 2011

[8] N. Bui and M. Zorzi, "Health care applications: A solution based on the Internet of Things," in Proc. ISABEL, Barcelona, Spain, Oct. 2011, pp. 1–5.

[9] https://www.youtube.com/watch?v=KEJe-I4ZosU

[10] L. Atzori, A. Iera, and G. Morabito, "The internet of things: A survey," Comput. Netw., vol. 54, no. 15, pp. 2787–2805, 2010.

[11] P. Bellavista, G. Cardone, A. Corradi, and L. Foschini, "Convergence of MANET and WSN in IoT urban scenarios," IEEE Sens. J., vol. 13, no. 10, pp. 3558–3567, Oct. 2013.

[12] A. Laya, V. I. Bratu, and J. Markendahl, "Who is investing in machine-tomachine communications?" in Proc. 24th Eur. Reg. ITS Conf., Florence, Italy, Oct. 2013, pp. 20–23. [4] H. Schaffers, N. Komninos, M. Pallot, B. Trousse, M. Nilsson, and A. Oliveira, "Smart cities and the future internet: Towards cooperation frameworks for open innovation," The Future Internet, Lect. Notes Comput. Sci., vol. 6656, pp. 431–446, 2011.

[13] Y.MohanaRoopa,et.al,"Road and Traffic Enforcement System Using GPSEnabled Mobile Cloud Computing", and Indian Journal of Science Technology, Vol 11(44),November 2018,ISSN:0974. -5645

[14] Y. Mohana Roopa et.al ,"Middleware Architecture for the Internet of Things" Journal of Advanced Research in Dynamical and Control Systems, 2018Vol 10, No 10,pp 1-6.

Proceedings of the Fourth International Conference on Communication and Electronics Systems (ICCES 2019)
IEEE Conference Record # 45898; IEEE Xplore ISBN: 978-1-7281-1261-9

AGRI SUCCOR : Mobile Application for Agriculture

Mrs. J. Jayachitra[1],
Department of IT,
IFET College of Engineering,
Villupuram, Tamilnadu
India
jayachitraifetit@gmail.com

M. Madhu[2] , S.D. Shaik Mohammed Faruk[3]
Deaprtment of IT,
IFET College of Engineering
Villupuram, Tamilnadu
India
Madhumathan155@gmail.com
Faruk140660@gmail.com

***Abstract*—India is an agricultural country with the staple food being rice and wheat. The farmers serve as a backbone to our nation. But, the livelihoods of the agriculturists are at stake. They incur heavy losses due to crop failure and natural calamities. The emerging technology has provided many solutions to upgrade their lifestyle, but still there are challenges. Our main motive is to design a farmer friendly application- Agri Succor to sell their commodities directly to the customers at a reasonable market value without any mediator with the help of volunteers. For the efficient utilization of our mobile application by the farmers, we have incorporated features like information in regional language, crop-disease identification and sell their products directly. This application will emerge out as an essential productivity tool for the farmers if implemented in future**

Keywords—Farmers, Agri Succor, crop disease identification, mobile application

I. INTRODUCTION (*HEADING 1*)

We all are much aware of the fact that India is an agricultural country and tea, cotton and spices are the main exports. Rice and wheat are the most important crops in India because they are the staple food. However, our country, especially Tamil Nadu does not have an accessible agricultural information system for the farmers to gain knowledge on any of the agriculture related problems and solutions. So, there is not much scope in promoting agricultural activities to farmers who serve as a backbone to our nation. But for the past decade or so the lives of the farmers are at stake due to losses incurred during the land cultivation, harvest and natural calamities. The field of information technology has a huge impact on people nowadays and hence, there are many solutions commercially made available for the upliftment of the farmers. Yet, none of them proved to be such helpful in improving their livelihoods. There are also many mobile applications that are specially designed for farmers. Most of these apps mainly focus on only one particular feature like crop management, usage of pesticides, etc. Still, such applications lacked in some aspects as the farmers are unaware about the existence of such applications. Even if they are aware about those applications, the farmer does not know how to access it even though it is in his native language as he might be illiterate.

Our proposed project provides an ultimate solution to all the problems above mentioned. With the assistance of the Tamil Nadu Agritech portal[1], we will handle this situation by establishing a buy-sell platform exclusively for the farmers welfare with almost all kind of facilities.

The main objective of our application is to design a farmer friendly mobile application. So, we have named our app as 'Agri Succor'- Agriculture Helper. The proposed app is interlinked to the TNAU Agritech portal [1] for getting authentic information. Through this application, the farmers can sell their products produced on their farmlands directly to buyers at a reasonable market price. This application bridges the gap between the farmers and consumers through the most crucial role players- the volunteers. There is no intermediate involved in this process. The most astonishing feature of our application is that it is available in the regional language. We also provide another important characteristic – voice to text conversion. As a result, the farmer can enter the details either in text or in speech format. The farmers can get agriculture related information from other fellow farmers or volunteers connected through this application. The solutions for the farm related problems are extracted from the Tamil Nadu Agricultural Agritech application. An additional aspect is employability is created for the volunteers.

First of all, we discuss about the related works about the existing mobile applications on agriculture. Then, we explain about our proposed system which includes the architecture, methodology, as well as the implementation of the Agri Succor application. It is followed by the advantages of the application.

II. RELATED WORKS

A. CCMobile App: CC stands for Connected Crops[2]. User can read the environment metrics like temperature, humidity, etc. Sensor readings are available through SMS or email alerts, graphing and the climate factor historical data. It optimized crop management but it covered only the climate factor

B. Spray Guide: Spray Guide[3] calculates the amount of solute, the amount of solvent, the mixing time and the spraying areas ,etc. Users can share their experience together with data and results to others over their social accounts.by using the this app ,produce quality product but this is not supported crop diseases detection.

C. IFFCO Kisan: It is offered by Indian Farmers Fertiliser Cooperative Limited (IFFCO). IFFCO Kisan[4] seeks advice from the agricultural experts and scientists about crops, agriculture cycle, etc. It is used to provide good Water management but not in the regional language

D. Mandi Trades: Mandi Trades[5] is a buying or selling platform by marketing of farm products. It Uses location intelligence to get a map-based view of both buyer and seller info, along with the geographical proximity. This app eliminates middlemen but it is not ensure the quality check.

E. myRML Farmer: Farm and crop specific precision solutions built with the help of India's top most agriculturists. myRML[6] Works by using specific tools it was designed to analyze or provide information on different aspects of farming habits. It provides high level guidance but there is no provision for weather forecast.

F. AgriSync: AgriSync[7] enables farmers and advisors to connect and resolve support issues using a mobile video customer service platform. It allows the advisor's organization to see open cases, resolution status and farmer feedback in real-time.

G. RainbowAgri Market: RainbowAgri[8] helps in digitizing and branding agriculture. It is a simple mobile and web based tool to profile the farmers, organize and manage farming communities.

III. PROPOSED WORK

The proposed system is designed to provide a friendly interface especially to the farmers. The three main roles of our application are farmers (sellers), volunteers and buyers. The personal details of all the users are highly confidential and secure. In this mobile app, the farmers can provide details about their farmlands and groceries that are being cultivated in their land. The information can be entered either in text or voice format that too in his/her own language. Once the crop has been harvested, the farmer can upload the image of the plant. The plant is checked for the pesticides level and the disease is identified in the app. The recovery solution for the same is provided either in video, audio or text format which are obtained from the Tamil Nadu Agritech application. Once the plant is quality checked, it can be viewed by the buyers who can purchase them at an affordable market price and delivered with the help of the volunteers. Hence all the facilities are available under one roof.

The architecture of the proposed system is shown in Fig.1. The architecture depicted below shows the overall structure of our project. The database plays a major role in gathering and retrieval of data.

a. Collection of Data: The input can be given as text, voice or else as image when the crop is diagnosed for any disease with the help of TNAU application. The interested buyers and sellers can register in this app using the buy- sell platform. The interested volunteers can enroll themselves for uploading the agriculture related news, new government schemes for the betterment of the farmers.

b. Retrieval of Data: The farmers can get the authentic information on crop disorders, recommended pesticides, buyer & seller information, product details and recovery solutions in text, voice and video formats in the corresponding native language. The data which is gathered need to be organized as a report. Using crucial strategies, the data is converted to report before sending them to the farmers, volunteers and consumers. This result can be either in the form of text or voice as per the wish of the user. Data retrieval is the defined as the process of identifying and extracting data from a database, based on a query provided by the user or application. It is achieved through the usage of SQL Processing.

All the features in the architecture are realized through the implementation process

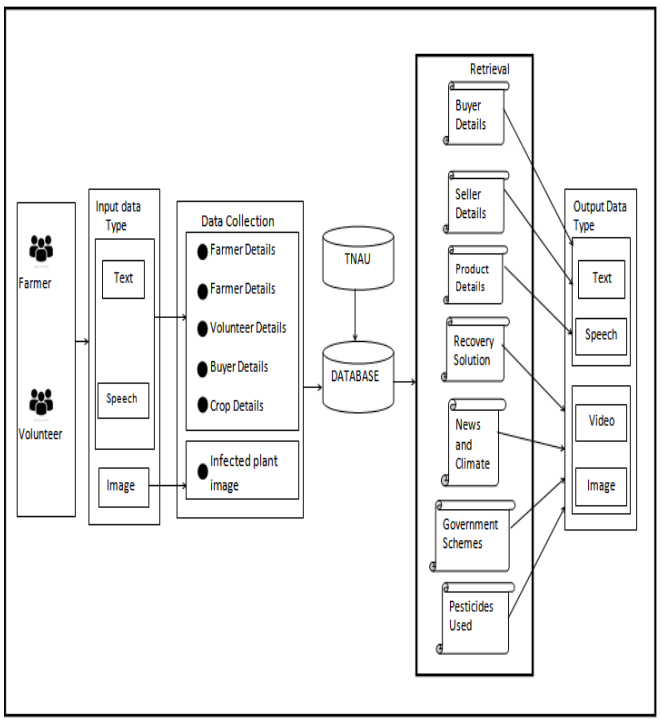

Fig.1. Architecture of the proposed system

A. IMPLEMENTATION

The implementation of the Agri Succor app is divided into three sections:

1. **Interface design:** It consists of three form designs for the use of farmers, volunteers and buyers.

Designing the interface of the application involves three main modules:

a. ***Farmers login***: The farmer login is shown in Fig.2.It consists of the entire details of the farmer including his location, type of crops cultivated in his farmland, price of his farm products, etc. given as text or voice with the option for regional language if required. This information is stored in the database. The farmer can even upload images of his commodities to check the level of pesticides used as well as check for any crop related disorders. He can have access to remedial measures for the crop diseases. In addition to this, he can keep a tab on the agriculture related news and schemes. He can even provide suggestions for the crop diseases to assist other fellow farmers. He can sell his produces to the consumers directly with no intermediary between them.

b. ***Volunteers login:*** The Volunteers login is shown in the Fig.3.The regular updates regarding agricultural schemes, climate and suggestions on crop cultivation are provided by the volunteers. Their main duty is to create awareness among the farmers regarding all kind of agricultural information. The much needed employability is given to these volunteers for their dedicated work. The delivery of farm products to the customers are done with the help of these volunteers

Fig.2. Farmers login

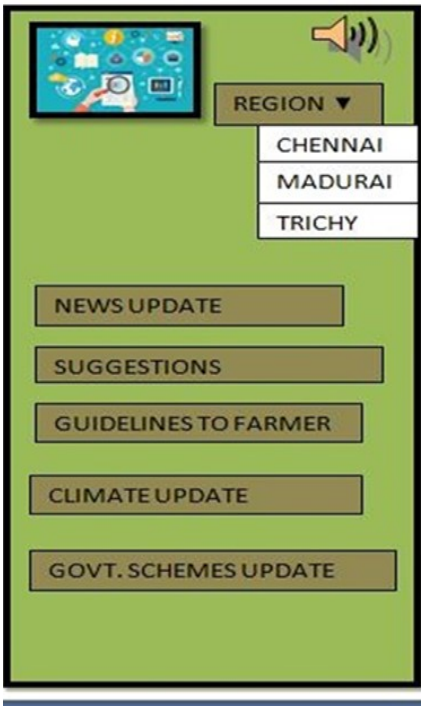

Fig. 3. Volunteers login

c. ***Buyers login***: The Buyers login is shown in Fig.4. The consumers who are willing to buy the farm products directly from the farmers need to enter their information. Once they select the items of a specific farmer, notifications are sent to the respective farmer. The ordered items are safely delivered to the customer.

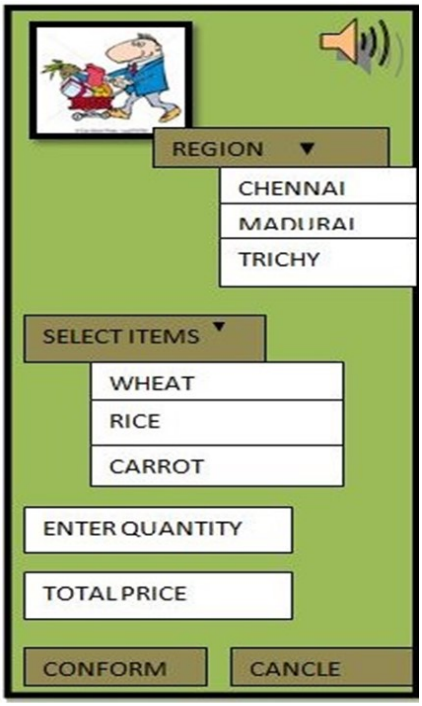

Fig. 4. Buyers login

2. **Voice to text conversion:** For extraction of voice signal, we use Mel-Frequency Cepstral Coefficient algorithm [9] and Minimum Distance Classifier. Support Vector Machine methods are used for speech classification. These techniques are highly efficient in converting the speech to text and vice versa.

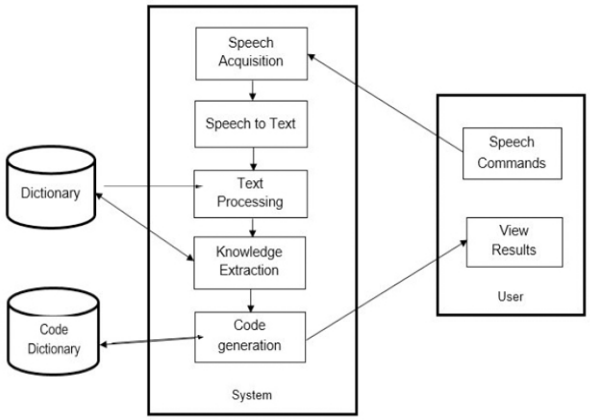

Fig.5.Voice to text conversion

3. **Disease identification:** Crop disease identification is done with the help of suitable image processing techniques. The procedure involves classification, feature extraction, multi-scale signal analysis, pattern recognition and projection

IV. BENEFITS

The Agri Succor will indeed be beneficial in almost all aspects. Some of the most important advantages of the proposed system are listed below:

a. Through the use of the application, both the standards of agriculture and farmers can be raised up.
b. The details can be given as voice or text input.
c. It also increases the job opportunities for the unemployed youth.
d. The commodities are freshly handpicked and delivered to the customers at a reasonable market value.
e. The application can be accessed in the regional language.
f. Instant updates on agricultural schemes, climate, crop diseases and their solutions are provided by the farmers and volunteers.
g. Quality check of the farm products before marketing them ensures that only disinfected items are sold.
h. The remedial measures for the crop diseases are provided in terms of text, voice and video. Considering the above pros of our application, we hope that this project will truly enhance the lifestyle of the farmers.

V. CONCLUSION

Through this mobile application, most of the problems faced by the farmers are provided immediate solutions and guidelines. If this initiative will be implemented in future, unemployability will be reduced to a considerable extent. Moreover, the betterment of the farmers could surely be realized. This application will emerge out as an essential productivity tool for the farmers.

REFERENCES

[1] http://agritech.tnau.ac.in/
[2] https://www.farms.com/agriculture-apps/crops/ccmobile-app
[3] http://www.simplot.com/farmers/products/specialty_products/spray_guide_app
[4] http://www.iffcokisan.com/
[5] http://www.manditrades.com/
[6] http://app.rmlglobal.com/
[7] https://www.agrisync.com/.
[8] http://www.rainbowagri.com/
[9] Zaidi Razak,Noor Jamilah Ibrahim, emran mohd tamil,mohd Yamani Idna Idris, Mohd yaakob Yusoff,Quranic verse recition feature extraction using mel frequency ceostral coefficient (MFCC),Universiti Malaya.

Proceedings of the Fourth International Conference on Communication and Electronics Systems (ICCES 2019)
IEEE Conference Record # 45898; IEEE Xplore ISBN: 978-1-7281-1261-9

Object detection using Adaptive Thresholding, Sobel Operator and Morphological Operations in Underwater Images

Akshita Saini
Department of Computer Engineering
National Institute of Technology, Kurukshetra
Haryana, India
akshitasaini31@gmail.com

Mantosh Biswas
Department of Computer Engineering
National Institute of Technology, Kurukshetra
Haryana, India
mantoshb@gmail.com

***Abstract*— Automation of detecting the shape and boundaries of object in the image is necessary in various object recognition and computer vision tasks but in case of underwater images it poses several challenges because of their degraded quality due to poor lighting conditions, scattering and absorption of light in underwater. A method to detect the object in underwater images is presented in this paper in which degradation of image is dealt by adjusting the image intensity values in order to enhance the contrast of the image. Further, segmentation is done using adaptive thresholding followed by detection of boundaries of object using Sobel operator and then morphological operations are performed to detect the object in underwater image. The results of the proposed method are qualitatively compared with Otsu's thresholding and Fuzzy C-means Clustering (FCM) for segmentation by visual perception and objectively by PSNR and SSIM which gives better and acceptable results on the considered underwater test images.**

Keywords—Object detection; Image enhancement; Image segmentation; Edge Detection; Morphological operations.

I. INTRODUCTION

Within the last few decades, the underwater image processing area has received a considerable attention due to its wide variety of application range from counting of fishes for biological research to the inspections of the structures in underwater for the offshore industries. In order to fulfill the above applications, the detection of objects is necessary in first to make further practice of the task successful. But there are many challenges in the underwater image processing as the physical properties of the water behave differently in water, change of the appearance of a same object with the variations of depth, currents, organic material, temperature and moreover a new set of challenges appear as soon as camera goes into water [1]. The deterioration of materials quickly due to corrosion in water along with waterproofing of cameras and modifications to experimental setups makes them costly, both in resources and time. Underwater images often suffer from low contrast and color-distortion, because of scattering and absorption of light when traveling through water. Color change occurs because of varying degree of attenuation by travelling of light in water with different wavelengths [2]. Due to above reasons the enhancement of the underwater image is a necessary preprocessing task in the underwater image processing. Software methods like histogram equalization, fusion, contrast stretching and polarization have also been used to improve the quality of image [3]. An attempt to enhance the image by modifying contrast-stretching manipulation is done by Yang et al. [4]. Detection of the object from enhanced image is comparatively easier than from raw underwater images. Image segmentation is the easiest way to convert grayscale image to binary image in order to make it easier to analyze and more meaningful and can be done by thresholding methods. Roy et al. made a comparison of different adaptive thresholding techniques in order to choose the most precise method to binarize the image based on texture, contrast, resolution etc. of an image [5]. Segmentation can also be performed using morphological operations [6]. Edge detection techniques gives connected curves indicating object boundaries of the objects which leads to decrement of the amount of information to be processed, filtering out meaningful information. Several attempts to identify object by detecting edges in underwater images is made [7-8]. One of the most important edge detection application in images is the detection of objects present in the image. There are many edge detection techniques used for object detection and image segmentation [9-11]. Edge detection and object detection using morphological operations is also done in [12-13]. Liya et al. has detected object by using morphological operations along with feature extraction [14]. Sudhakar et al. has done foreground extraction from underwater images by using block based enhancement, thresholding and morphological operations [15]. Although, these methods are beneficial but little attempts were made for object detection in underwater image using morphological operations. In our work after the contrast enhancement we have used segmentation followed by edge detection using adaptive thresholding and Sobel operator respectively. Finally, morphological operations i.e. dilation, region filling and erosion is applied to the image in which edges are being detected by Sobel operator. The structure of rest of the paper contains explanation of the proposed work in

detail which is described in section II. Section III consists of the results for considered underwater images. Finally, we have concluded the work in section IV.

II. Proposed Approach

In this paper, a method has been proposed for detection of objects in underwater images consisting of four steps shown in fig. 1. (i) Here, to deal with degradation of image, adjustment of intensity of image is done to enhance contrast of image. (ii) Further, segmentation is done using adaptive thresholding and (iii) Sobel operator used for edge detection. (iv) Finally, morphological operations are performed to detect the foreground object in underwater image.

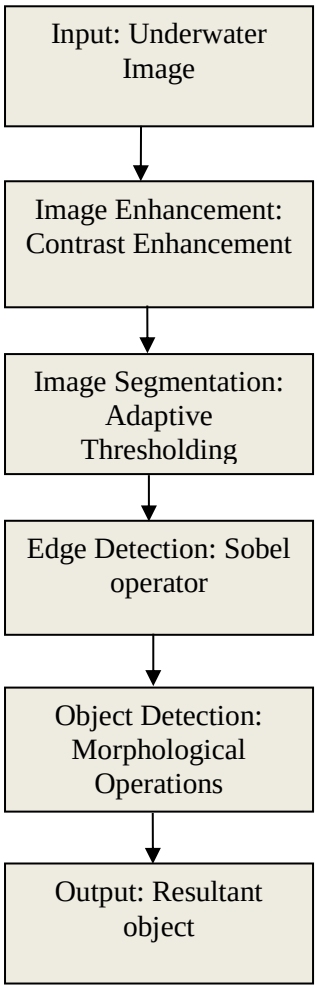

Fig. 1. Flowchart of Proposed Method for Object Detection in Underwater Image.

(i) Image Enhancement:

Underwater images are adversely degraded, hazy in nature and appearance, affected by poor lighting in under water and several atmospheric phenomenon of scattering and absorption of light which affects the quality of image. Due to these factors contrast of the image is heavily affected, therefore, adjustment of intensity of image is done on the grayscale image of the original underwater image by saturating the bottom 1% and the top 1% of all pixel values of the image in order to enhance the contrast of image helping us to distinguish the presence of various objects in the image as shown in fig. 3 (a).

(ii) Image Segmentation:

Image segmentation divides an image into different segments to simplify the image representation and make it more meaningful and easier to analyze. This is typically used to identify the boundaries and objects in images. Here, segmentation of image is done on the enhanced image to convert grayscale image into binary image using adaptive thresholding. In adaptive thresholding, threshold value is changed dynamically over the image and threshold value at each pixel location is dependent on the neighboring pixel intensities. The thresholded image using adaptive thresholding can be seen in fig. 3 (b). Here, the adaptive threshold *Thresh (p, q)* at pixel location *(p, q)* in the image is calculated by first selecting a $a \times a$ region in the image around the pixel location and then calculating the weighted average of the $a \times a$ region by taking the average (mean) of all the pixel location that lie in the $a \times a$ which is represented by *Average (p, q).* Finally, the value of threshold *Thresh (p, q)* is calculated by subtraction of constant parameter *z*, from the weighted average value *Average (p, q),* calculated previously. Therefore, the threshold value *Thresh (p, q),* at pixel location *(p, q)* can be given by:

$$Thresh\ (p, q) = Average\ (p, q) - z \quad (1)$$

(iii) Edge Detection:

Edge detection is an image processing technique used to detect the boundaries of objects in the images. It aims at recognizing the points in an image at which the brightness of image changes sharply and organizing these points into a set of curved line segments termed as edges. Therefore, the image obtained from previous step is further used to detect the boundaries of the object present in underwater images by Sobel operator. The aim of this process is to get clear and more prominent lines of the object as shown in fig. 3 (c). Sobel operator is preferred over others to identify the edges of the object in the underwater image because of its simplicity over others and that it detects edges and their orientations too. A Sobel filter has two 3x3 kernel created for both the X and Y axis of the image shown in fig. 2 in which Y kernel is just a 90 degree rotation of the X kernel. The Sobel filter kernel 2d-convolution is then applied on the image to emphasize lines on the X and Y axis.

-1	0	1
-2	0	2
-1	0	1

(a)

-1	-2	-1
0	0	0
1	2	1

(b)

Fig. 2. Masks used by Sobel operator (a) Horizontal mask G_x and (b) Vertical mask G_y.

The horizontal and vertical kernels are combined together in order find the absolute magnitude, |G|, of the gradients at each point which is given by below function:

$$|G| = \sqrt{G_x^2 + G_y^2} \quad (2)$$

(iv) Morphological Operations:

Morphology has a broad set of operations in digital image processing in which images are processed according to its shape. A structuring element or kernel over the input image is used in these operations and a corresponding output image with same size is produced. A comparison between the pixels of the input image is done along with the neighborhood pixels and corresponding output pixels are obtained. The size and shape of these neighborhoods affects the result of the morphological operations. The following operations are used in our proposed method to remove the noise or the holes present in the background of the image in order to increase the clarity of the object in the image:

Dilation

Dilation is the process of expansion. Dilation operation "grows" or "thickens" the objects in binary image. This lengthening and thickening is controlled by a structuring element. Dilation is useful for filling small holes while preserving the size and shape of the objects in the image and is depicted in fig. 3 (d).

Region Filling

Region filling operation fills the holes in an input intensity image. Hole is an area in which dark pixels are surrounded by lighter pixels. Figure representation is shown in fig. 3 (e).

Erosion

Erosion operation "shrinks" or "thins" the object in the binary image. Structuring element controls the extent and manner of shrinking. Erosion simplifies the structure of an object or their parts and make the structure disappear if width is equal to one. It might also lead the several complicated objects to decompose into simpler ones. Figure representation is shown in fig. 3 (f).

Algorithm: Object Detection in underwater image

Input: Underwater hazy image

Output: Object detected image

i. Take a real underwater image.

ii. Adjusting the pixel intensity of image to enhance contrast of the image.

iii. Obtain a segmented image by applying adaptive thresholding on the enhanced image by using equation (1).

iv. Apply Sobel operator to detect the edges of the segmented image making the edges more prominent.

v. To complete the edges discontinuities apply dilation operation.

vi. For filling the region inside object's boundaries use region filling operation.

vii. To remove small background objects erosion operation is applied.

viii. Detected object can be seen in final image.

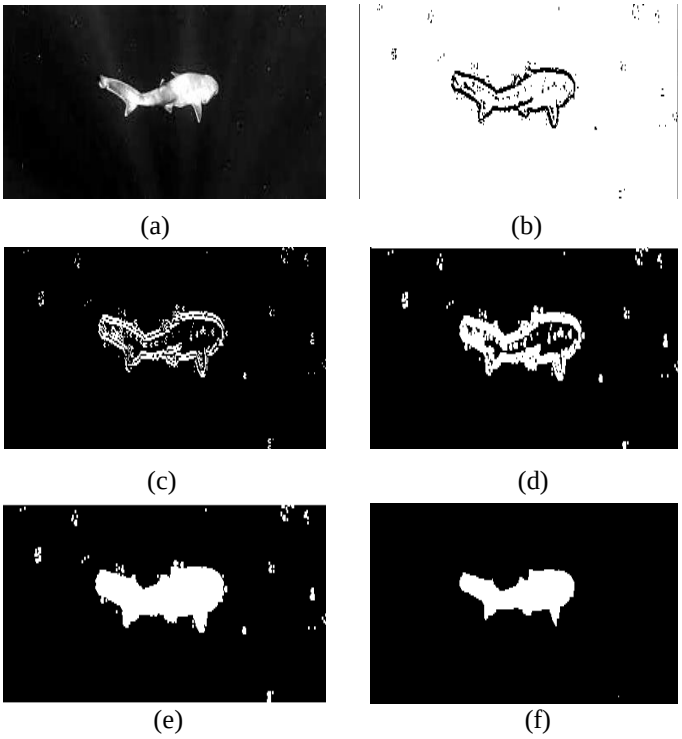

Fig. 3. Visual representation of the steps of the proposed method: (a) Contrast enhancement, (b) Adaptive Thresholding, (c) Sobel operator, (d) Dilation, (e) Region Filling and (f) Erosion .

III. RESULTS AND ANALYSIS

In the experimental results we have evaluated our method on real underwater images as shown in fig. 4-8 (a). The dominant color observed in the images is blue because of its wavelength and therefore, dominance of blue pixels can be clearly observed in images. We have done both objective and subjective comparison of our method with the conventional segmentation techniques i.e. Otsu's thresholding [16] and Fuzzy C-means Clustering (FCM) [17]. We have used Matlab 2016 toolbox running at core 1.70 GHz processor for implementation of all existing and proposed methods which are considered in the paper.

The objective criteria i.e. PSNR and SSIM [18] are considered as significant parameters for the quality of image. Peak Signal-to-Noise Ratio is used to measure compression quality between the original and reconstructed image. The higher PSNR represents the better quality of the reconstructed image. On the other hand, SSIM is defined as structural similarity index which is used for measuring the similarity

between two images. SSIM is a perception- based model in which the degradation of image is a perceived change in structural information, while also including both luminance and contrast masking terms for incorporating important perceptual phenomena. The value of SSIM index is between -1 and 1, and value 1 indicates perfect similarity in images and is reached only in the case of two identical images. Therefore, we can say that an image should possess high PSNR value and high SSIM close to 1 for an image to possess higher quality. Table I and Table II shows the comparison of the performance our method for considered images of underwater with that of Otsu's thresholding and FCM based on evaluation parameters: PSNR and SSIM, respectively and shows that our proposed method gives better results than other methods considered.

The subjective criterion has been fulfilled by considering the restored object in image and comparing it with Otsu's thresholding FCM for segmentation. In fig. 4 and 6 (b-d) we can see that fish boundaries are clearer and the shape of fish is more appropriate in the proposed method. In fig. 5 (b-d) the turtle's shape is complete in comparison to other methods. Similarly, the diver in fig. 7 (b-d) and fishes in fig.8 (b-d) is more fairly detected and visible by our method rather when compared with Otsu thresholding and FCM. Therefore, it is observed that images we get by our proposed method produces better results than other methods considered for object detection.

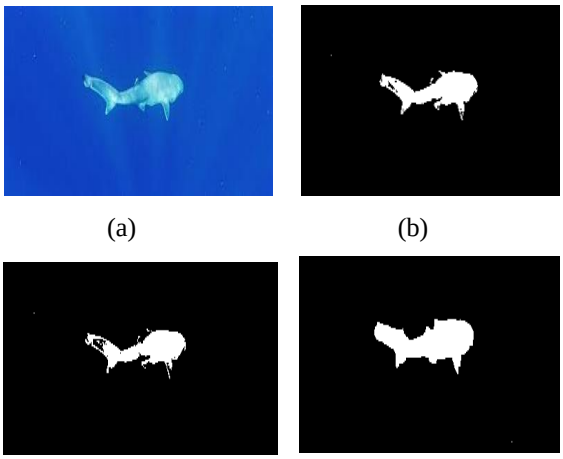

(a) (b)

(c) (d)

Fig. 4. Fish1 (a) Input image; Object Detection methods: (b) Otsu Thresholding (c) FCM and (d) Proposed.

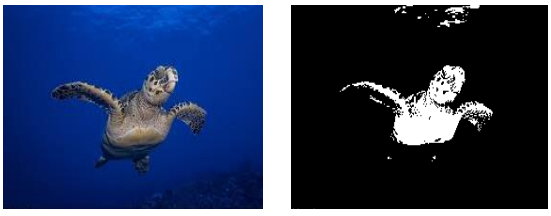

(a) (b)

(c) (d)

Fig. 5. Turtle (a) Input image; Object Detection methods: (b) Otsu Thresholding (c) FCM and (d) Proposed.

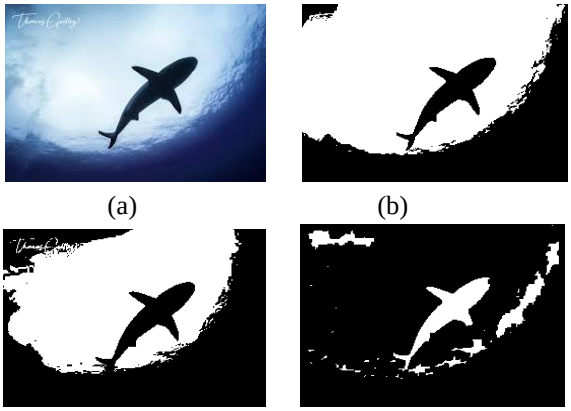

(a) (b)

(c) (d)

Fig. 6. Fish2 (a) Input image; Object Detection methods: (b) Otsu Thresholding (c) FCM and (d) Proposed.

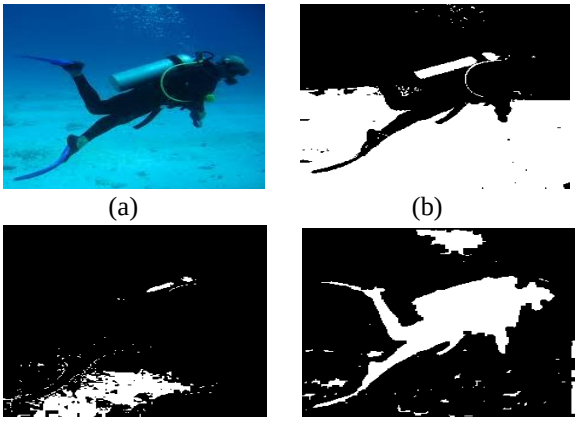

(a) (b)

(c) (d)

Fig. 7. Diver (a) Input image; Object Detection methods: (b) Otsu Thresholding (c) FCM and (d) Proposed.

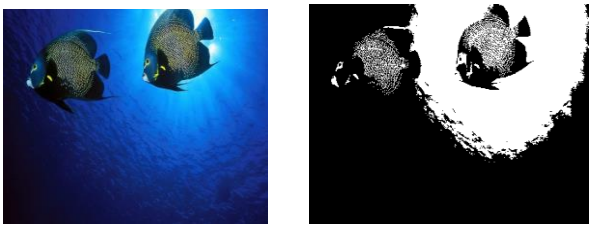

(a) (b)

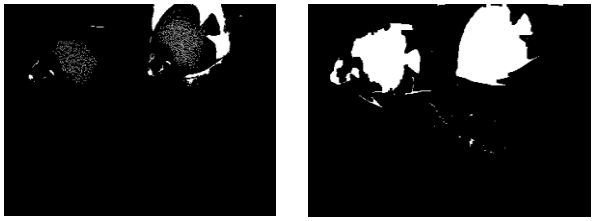

(c) (d)

Fig. 8. Multiple Fishes (a) Input image; Object Detection methods: (b) Otsu Thresholding (c) FCM and (d) Proposed.

TABLE I. RESULTS OF PSNR FOR OBJECT DETECTION METHODS BY OTSU THRESHOLDING, FCM AND PROPOSED FOR CONSIDERED UNDERWATER TEST IMAGES.

PSNR(db)			
Image Name	***Otsu Thresholding***	***FCM***	***Proposed***
Fish1	24.281	24.261	65.332
Turtle	24.522	24.447	58.847
Fish2	28.484	27.036	51.339
Diver	27.030	24.444	51.413
Multiple Fishes	25.945	24.398	55.998

TABLE II. RESULTS OF SSIM FOR OBJECT DETECTION METHODS BY OTSU THRESHOLDING, FCM AND PROPOSED FOR CONSIDERED UNDERWATER TEST IMAGES.

SSIM			
Image Name	***Otsu Thresholding***	***FCM***	***Proposed***
Fish1	0.0303	0.0278	0.9979
Turtle	0.0469	0.0434	0.9893
Fish2	0.5252	0.4279	0.9332
Diver	0.3319	0.0213	0.9358
Multiple Fishes	0.2019	0.0464	0.9782

IV. CONCLUSION

In this paper, we have proposed an object detection method using adaptive thresholding, Sobel operator and morphological operations in underwater images. In our approach the main idea to detect object is that edges or the shape of the object is detected prior to the application of morphological operations in order to detect the object clearly. The proposed method consistently give better results on the considered underwater images when compared with conventional segmentation techniques Otsu's thresholding and Fuzzy C-means Clustering (FCM). The present work can be extended by focusing on the accuracy of the shape of the objects and detection of main object along with the background small objects using soft computing based methods.

REFERENCES

[1] S. Raimondo and S. Corchs, "Underwater image processing: state of the art of restoration and image enhancement methods", EURASIP Journal on Advances in Signal Processing, no. 1, pp.1-14, 2010.

[2] H. Lu, Y. Li, Y. Zhang, M. Chen, S. Serikawa, and H. Kim, "Underwater optical image processing: a comprehensive review" Mobile networks and applications 22, no. 6, pp. 1204-1211, 2017.

[3] A. K. Vishwakarma and A. Mishra, "Color image enhancement techniques: a critical review", Indian Journal of Computer Science and Engineering, vol. 3, no.1, pp. 39-45, 2012.

[4] Ching-Chung Yang, "Image enhancement by modified contrast-stretching manipulation", Optics & Laser Technology, vol. 38, no. 3, pp. 196-201, 2006.

[5] P. Roy, S. Dutta, N. Dey, G. Dey, S. Chakraborty and R. Ray, "Adaptive thresholding: a comparative study", International Conference on Control, Instrumentation, Communication and Computational Technologies, pp. 1182-1186, 2014.

[6] D. Chudasama,T. Patel, S. Joshi, and G. I. Prajapati, "Image segmentation using morphological operations", International Journal of Computer Applications, vol. 117, no. 18,pp. 16-18, 2015.

[7] N. A. Hule, "Underwater Image Processing For Object Detection", International Journal of Innovative and Emerging Research in Engineering, vol. 2, no. 2, pp. 196-201, 2015.

[8] D. Xiaoheng, L. Minghang, M. Jiashu and W. Zhengyu, "Edge Detection Operator for Underwater Target Image", 3rd International Conference on Image, Vision and Computing, pp. 91-95, 2018.

[9] G. M. H. Amer and A. M. Abushaal, "Edge detection methods", 2nd World Symposium on Web Applications and Networking, pp. 1-7, 2015.

[10] A. Ushma, and A.R.M. Shanavas, "Object detection in image processing using edge detection techniques", International organization of Scientific Research IOSR Journal of Engineering, vol. 4, no. 3, pp. 10-13, 2014.

[11] Y. Ramadevi, T. Sridevi, B. Poornima and B. Kalyani, "Segmentation and object recognition using edge detection techniques", International Journal of Computer Science & Information Technology, vol. 2, no. 6, pp. 153-161, 2010.

[12] S. Rani, D. Bansal and B. Kaur, "Detection of Edges Using Mathematical Morphological Operators",Open Transactions On Information Processing, vol.1, no. 1, pp.17-26, 2014.

[13] S. Qian and G. R. Weng, "Research on Object Detection based on Mathematical Morphology",4th International Conference on Information Technology and Management Innovation, pp. 203-208, 2015.

[14] W. Liya, X. Li, and K. Fang, "Object detection based on feature extraction and morphological operation", International Conference on Neural Networks and Brain, vol. 2, pp. 1001-1003, 2005.

[15] M. Sudhakar and M. J. Meena, "A novel method to detect foreground region using morphologicaloperations with block based enhancement for underwater images", International Journal of Engineering & Technology, vol. 7, no. 3, pp. 1751-1756, 2018.

[16] J. Yousefi, "Image Binarization using Otsu Thresholding Algorithm", University of Guelph, Ontario, pp. 1-4, 2011.

[17] M.J. Christ and R. M. S. Parvathi, "Fuzzy c-means algorithm for medical image segmentation", 3rd International Conference on Electronics Computer Technology,vol. 4, pp. 33-36, 2011.

[18] Y. A. Al-Najjar and D. C. Soong, "Comparison of image quality assessment: PSNR, HVS, SSIM, UIQI", International Journal of Scientific and Engineering Research, vol. 3, no. 8, pp. 1-5, 2012.

Proceedings of the Fourth International Conference on Communication and Electronics Systems (ICCES 2019)
IEEE Conference Record # 45898; IEEE Xplore ISBN: 978-1-7281-1261-9

A Study on Label TSH, T3, T4U, TT4, FTI in Hyperthyroidism and Hypothyroidism using Machine Learning Techniques

Afzal Hussain Shahid[1], Maheshwari Prasad Singh[1], Rahul Kumar Raj[2], Rashmi Suman[2], Drakhshan Jawaid[2], Muqtadir Alam[2]

[1]Department of Computer Science and Engineering, National Institute of Technology Patna, Patna, India ({afzal.cse15, mps}@nitp.ac.in)

[2]Department of Computer Science and Engineering, Muzaffarpur Institute of Technology Muzaffarpur, India ({rahulrajab525, sumanrashmi2017, alammit2015, drakhshan933}@gmail.com)

***Abstract*— The thyroid hormone is produced by thyroid gland. This hormone regulates the body's metabolism. Hyperthyroidism and hypothyroidism are the two abnormalities which is caused by the release of too much or too little thyroid hormones respectively. In this study, Random Forest (RF), Support Vector Machine (SVM), and K-Nearest Neighbours (K-NN) classifiers are compared to assess the efficiency of these classifiers in Thyroid disease diagnoses using the thyroid disease dataset that is taken from UCI machine learning repository. The overall classification accuracy of the RF, SVM, and K-NN are 98.50%, 97.02%, and 95.81% respectively. The result shows that the RF classifier performance is better than SVM and K-NN for the diagnosis of thyroid disease using UCI dataset.**

Keywords*— *Thyroid disease diagnosis, Computer-aided diagnosis, Machine learning classifiers.

I. INTRODUCTION

The thyroid gland is one of the endocrine glands that produce thyroid hormone to regulate the body's metabolism [1]. The Levothyroxine (T4) and Triiodothyronine (T3) hormones are produced by thyroid gland. These hormones play a major role in converting nutrients into energy and thereby helps in regulating body temperature, heart rate, and even brain function. Hyperthyroidism occurs when the hormones produced by the gland is more than the requirement of the body. However, hypothyroidism occurs when the hormones produced by the gland is less than the requirement of the body [2]. Severe hyperthyroidism and end-stage hypothyroidism may cause deaths [3] [2]. During pregnancy, it can lead to health problems for the mother and baby [4].

About 70% risk of developing the thyroid disease is found to be associated with genetic background. Also, the contribution of environmental exposures such as perchlorate in rocket fuel, polychlorinated bi-phenols, and radiations (from nuclear fallout and medical radiation) in the disease risk is significant. Most of the environmental exposures reduce thyroid hormone levels [5]. Recently, the thyroid disease risk is found to be linked with systemic lupus erythematosus, an autoimmune disease [6]. There is some evidence of the correlation between thyroid disease and the low level of vitamin D [7].

The amount of T3 and T4 hormone in the blood is controlled by another hormone known as Thyroid Stimulating Hormone (TSH). Low T4 results in more production of TSH that initiates thyroid gland to produce more T4 & vice versa [8].

The different thyroid function tests such as TSH, T3, T4U, Total T4, and Free T4 Index (FTI) are done to assess the various functions related to the thyroid gland. A normal TSH and normal T4 is indicative of normal functioning of the thyroid gland, a low TSH and elevated T4 indicates hyperthyroidism, a low TSH and low T4 indicates secondary hypothyroidism, and a high TSH and low T4 indicates primary hypothyroidism. T3 tests are used for determining the severity of the hyperthyroidism or to diagnose the hyperthyroidism [9].

The classification algorithm is based on supervised learning methodology where the labeled data is used for learning. These algorithms require very large labeled training sets which consist of many features or attributes.

Finding meaningful information from the thyroid datasets of the patients with regard to the thyroid disease diagnosis is important. This paper compares the performance of three classification algorithms, namely, RF, SVM, and K-NN for the diagnosis of thyroid disease by analyzing labels (TSH, TT4, T3, FT4, and T4U) in hyperthyroid, hypothyroid, and normal subjects.

The rest of the paper is organized as follows. Section II briefly describes the related work. Section III presents the methodology that includes the description of the dataset used, a brief introduction about ML classifiers (RF, SVM, K-NN), and the performance metrics used in the analysis. Section IV presents the results and discussions. Section V concludes this

paper.

II. RELATED WORK

Researchers have used various machine learning algorithm for the diagnosis of thyroid diseases. For instance, authors of [10] use Wavelet Support Vector Machine and Generalized Discriminant Analysis to develop an expert system for thyroid disease diagnosis. They achieved the classification accuracy of about 91.86%. Polat et al. [2] hybridize the artificial immune recognition system with fuzzy weighted pre-processing to diagnose the thyroid disease. The classification accuracy of their model was 85%. Feyzullah Temurtas [3] suggests the diagnosis of thyroid disease using Neural Networks. They obtained the accuracy of 93.19%, 94.81%, and 90.05% using multilayer, probabilistic, and learning vector quantization neural networks respectively. Gharehchopogh et al. [11] propose a Multi-layer Perceptron (MLP) which is trained via back propagation learning algorithm for the classification of thyroid disease. The classification accuracy of 96.8% was achieved.

III. METHODOLOGY

A. Dataset description

The dataset for this study is acquired from the UCI machine learning repository. The dataset consists of 7200 instances, 21 attributes of which 15 attributes are categorical and six attributes are numerical. All the instances in the dataset are labelled to one of the three classes: hyperthyroidism, hypothyroidism, and normal subject.

Table 1. Thyroid disease dataset description.

Number of attributes & instances	Values
Total number of attributes	22 including one label set
Attributes with categorical values	15 with two possible values 0/1
Attributes with numerical values	6
Total number of instances	7200
Number of attributes used for analysis	5

The number of instances belongs to hyperthyroidism, hypothyroidism, and normal subject classes are 166, 368, and 6666 respectively. The distribution of instances among three classes shows that the dataset is highly imbalanced. Further for the analysis purpose, the whole dataset was split into a training dataset and test dataset in the ratio of 80/20. Therefore, there are 5760 instances in the training dataset and 1440 instances in the test dataset. Out of the 21 attributes, only 5 attributes are used for the analysis. These attributes represent the various thyroid function tests that indicate the level of thyroid hormones in the blood and are indicative of thyroid disease. These attributes are as follows [12]:

(i) TSH that ranges between 0.4 to 5.0 milli-International Unit per liter.
(ii) Total T4 (TT4) ranges from 4.6 to 12 micrograms per deciliter of blood.
(iii) T3 that ranges between 100 to 200 nanogram per deciliter of blood.
(iv) Free T4 Index (FTI) or FT4 that ranges between 0.7-1.9 nanogram per decilitre of blood.
(v) T4 Uptake (T4U).

B. Support Vector Machine

SVM constructs the hyperplanes in a multidimensional space for the classification task. This space separates classes of different class labels. It is able to deal with non-linear and high-dimensional data. With RBF kernel, the performance is further improved in case of non-linear and high dimensional data. The drawbacks of SVM include: (i) selection of kernel function is difficult as the performance varies with different kernel functions and datasets, and (ii) time-consuming training phase incurs high computational cost [13]. The extreme data points in each class represent the support vectors while the decision boundary between them is the hyperplane which is drawn in such a way that the distance between the support vector and the plane should be maximum.
In this study, the SVM model is trained by using the training samples and the model is tuned by tuning the various parameters to get the optimum result. The parameters used for tuning are Kernel function, C parameter, and gamma coefficients. Kernel function does the mapping of data to different space. The various kernel functions are Linear, rbf, poly, sigmoid, precomputed or a callable. In this study, the SVM model is tuned by using rbf and sigmoid kernel function. The parameter C is the regularization parameter that has the ability to generalize the SVM to perform well on the unseen data. It controls the tradeoff between the achieving a low training error and a low testing error. A large value of C corresponds to a small margin whereas a small value of C corresponds to the large margin between support vectors and hyperplane. In this study the SVM model is tuned at various values of C. Gamma is the kernel coefficient for rbf, poly, sigmoid kernel function which adds complexity in the classification.

C. Random Forest

Random forest (RF) builds multiple decision trees and combine them toger to obtain a more robust, accurate and stable prediction. It adds additional randomness to the model while growing the trees. This algorithm searches for the best feature among a random subset of features for splitting a node.

In RF classification approach, voting strategy is used where each tree votes for a particular class. The rows or instances are then classified into the class for which maximum number of trees have voted. Due to more robustness, the performance of RF it better than AdaBoost, which is also an ensemble learning

technique. The performance of RF is better than DT because, when there is noise in the attribute, trees become deeper and hence overfitting problem occurs. However, RF is less influenced by the noise in the attributes as different sample of the training data is used in the process of averaging the deep decision trees [13]. In this study, the RF model is tuned by varying the n_estimators parameter which represents the number of trees in the forest.

D. K-Nearest Neighbor

K-NN classifies a data point based on how its neighbors are classified. It computes the distance between the new instance and previously known instance to classify the new instance by using the voting strategy. The information about previous instances is given in the training set. It is simplest among all ML classifiers [13]. In this study, the K-NN model is tuned by varying the value of K and compared with each other to get the best classification performance.

E. Performance Metrics

Following performance metrics are used to analyze the performance of different ML classifiers.

Precision: It is used to measures the classifier exactness. It is also known as positive predictive value (PPV).

Recall: It measures the classifier completeness. It is also known as sensitivity or hit rate, or true positive rate (TPR).

Specificity: It measures the proportion of actual negatives that are correctly identified and also called a true negative rate (TNR).

Accuracy: It measures the fraction of predictions our model got right. It can be calculated as the total number of correct predictions divided by the total number of test cases.

F1-Score: It measures the balance between precision and recall.

Class weighted accuracy: It can be calculated as the ratio of the sum of each class size multiplied by its individual accuracy to the total number of test cases.

IV. Results and Discussion

The aim of this paper is to assess the classification efficiency of different ML algorithms on the thyroid disease dataset acquired from UCI. Table 2 shows the classification performance of different ML algorithms in terms of precision, recall, specificity, accuracy, and F1-score for each class. All the models were tuned to enhance the performance. The SVM gives the best result with the *RBF* kernel function and when the values of the parameters C and gamma coefficient are 100 and 1024 respectively. The RF gives the best result when the value of the parameter n_estimators is 32 and K-NN gives the best result when the value of the parameter n_neighbors is set to 1.

It can be observed from Table 2 that for all the classes the RF model gives the best performance in terms of all the performance metrics. It was seen that the performance of the SVM model was improving on increasing the value of the parameter C and best performance is achieved when the value of C is 100 but further increase in the C value results in the performance deterioration. Because the optimal value of C parameters should be large when the feature values in the dataset is small. However, for large value of C, the misclassification rate increases which results in poor performance. Similarly, for RF, the performance increases by increasing the value of the n_estimators as for the higher value of n_estimators, the performance of RF increases. When the value of n_estimators is 32, the best performance is achieved. The further increase in the value of n_estimators results in no change in the performance. However, for the K-NN model, the performance is best at k=1 and starts decreasing by further increasing the value of K. The overall class weighted performance measures for all the classification model is presented in Table 3.

Table 2: Performance of different ML algorithms.

Classes	Performance metrics	Classification models		
		SVM (%)	RF (%)	K-NN (%)
Hyperthyroidism	Precision	91.66	92.68	84.84
	Recall	84.61	97.43	71.79
	Specificity	99.78	99.78	99.62
	Accuracy	99.35	99.71	98.84
	F1-Score	88	95	77.77
Hypothyroidism	Precision	76.8	86.51	69.56
	Recall	75.90	92.77	57.83
	Specificity	98.59	99.11	98.44
	Accuracy	97.27	98.74	63.15
	F1-Score	76.36	89.53	96.08
Normal subjects	Precision	98.18	99.46	97.01
	Recall	98.48	98.86	98.48
	Specificity	80	94.26	65.51
	Accuracy	96.94	98.47	97.74
	F1-Score	96.94	99.16	95.81

Table 3: Overall class weighted performance for the different classification model.

Overall Class Weighted Performance Measures	Classification models		
	SVM (%)	RF (%)	K-NN (%)
Precision	96.77	**98.54**	95.26
Recall	96.80	**98.57**	95.49
Specificity	81.60	**94.69**	70.67
Accuracy	97.02	**98.50**	95.81
F1-Score	96.78	**98.52**	95.35

Figure 1 shows the overall class weighted average performance of SVM, RF, and K-NN with respect to the different performance parameters. For all the performance parameters (precision, recall, specificity, accuracy, and F1-

score), the best performance is achieved by RF followed by SVM and K-NN.

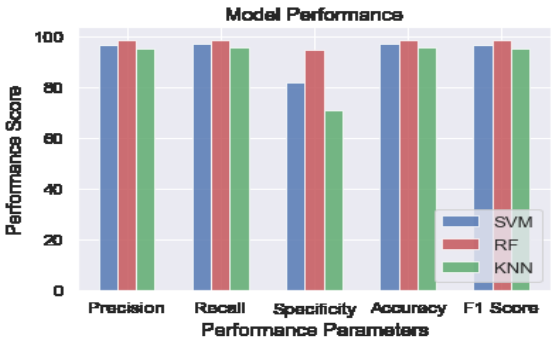

Fig. 1. Overall performance measure comparison for all the classification model

V. CONCLUSION

The paper presented a comparison of three different ML techniques namely, SVM, RF, and K-NN applied for the classification of the thyroid disease into hyperthyroidism, hypothyroidism, and normal subjects. The dataset for this study was acquired from the UCI machine learning repository. To evaluate the performance of different ML algorithms, various performance metrics such as precision, recall, specificity, accuracy, and F1-score were used. Although all the models may be used for the classification, the RF classifier outperformed SVM and K-NN. The maximum weighted average accuracy achieved by RF was 98.50 %. However, the accuracies achieved by SVM, and K-NN are 97.02%, and 95.81% respectively. RF also gives the best performance on all the performance metrics in comparison to SVM and KNN. In future, it would be interesting to assess the classification performance of metaheuristic algorithms on this dataset.

ACKNOWLEDGMENT

The authors would like to acknowledge the Ministry of Electronics & Information Technology (MeitY), Government of India for supporting the financial assistant during research work through “Visvesvaraya Ph. D. Scheme for Electronics & IT”.

REFERENCES

[1] L. Ozyilmaz and T. Yildirim, "Diagnosis of thyroid disease using artificial neural network methods," in *Proceedings of the 9th International Conference on Neural Information Processing, 2002. ICONIP'02.*, 2002, vol. 4, pp. 2033-2036: IEEE.

[2] K. Polat, S. Şahan, and S. Güneş, "A novel hybrid method based on artificial immune recognition system (AIRS) with fuzzy weighted pre-processing for thyroid disease diagnosis," *Expert Systems with Applications,* vol. 32, no. 4, pp. 1141-1147, 2007.

[3] F. Temurtas, "A comparative study on thyroid disease diagnosis using neural networks," *Expert Systems with Applications,* vol. 36, no. 1, pp. 944-949, 2009.

[4] B. M. Casey and K. J. Leveno, "Thyroid disease in pregnancy," *Obstetrics & Gynecology,* vol. 108, no. 5, pp. 1283-1292, 2006.

[5] G. A. Brent, "Environmental exposures and autoimmune thyroid disease," *Thyroid,* vol. 20, no. 7, pp. 755-761, 2010.

[6] J.-S. Yun *et al.*, "Increased risk of thyroid diseases in patients with systemic lupus erythematosus: A nationwide population-based Study in Korea," *PloS one,* vol. 12, no. 6, p. e0179088, 2017.

[7] D. Kim, "The role of vitamin D in thyroid diseases," *International journal of molecular sciences,* vol. 18, no. 9, p. 1949, 2017.

[8] D. A. Fisher, "Physiological variations in thyroid hormones: physiological and pathophysiological considerations," *Clinical Chemistry,* vol. 42, no. 1, pp. 135-139, 1996.

[9] S. P. Fitzgerald and N. G. Bean, "The relationship between population T4/TSH set point data and T4/TSH physiology," *Journal of thyroid research,* vol. 2016, 2016.

[10] E. Dogantekin, A. Dogantekin, and D. Avci, "An expert system based on Generalized Discriminant Analysis and Wavelet Support Vector Machine for diagnosis of thyroid diseases," *Expert Systems with Applications,* vol. 38, no. 1, pp. 146-150, 2011.

[11] F. S. Gharehchopogh, M. Molany, and F. D. Mokri, "Using artificial neural network in diagnosis of thyroid disease: a case study," *International Journal on Computational Sciences & Applications (IJCSA) Vol,* vol. 3, pp. 49-61, 2013.

[12] A. Keleş and A. Keleş, "ESTDD: Expert system for thyroid diseases diagnosis," *Expert Systems with Applications,* vol. 34, no. 1, pp. 242-246, 2008.

[13] A. H. Shahid and M. P. Singh, "Computational intelligence techniques for medical diagnosis and prognosis: Problems and current developments," *Biocybernetics and Biomedical Engineering,* 2019.

Proceedings of the Fourth International Conference on Communication and Electronics Systems (ICCES 2019)
IEEE Conference Record # 45898; IEEE Xplore ISBN: 978-1-7281-1261-9

Fusion of QuickBird Imagery Using Multi-Resolution Analysis Based Algorithms

Vaibhav R. Pandit
Research Scholar, Engineering & Technology,
Sant Gadge Baba Amravati University, Amravati,
Maharashtra, India
vaibhavpandit111@gmail.com

Dr. R. J. Bhiwani
Professor, Dept. of Electronics & Telecomm. Engg.,
Babasaheb Naik College of Engineering, Pusad,
Maharashtra, India
bhiwani_raju@rediffmail.com

***Abstract*—A multispectral image when fused with a panchromatic image acquired on common location to produce another multispectral image with added spatial resolution, the image fusion is known as 'Pansharpening'. Developement of pansharpening algorithms and their quality assessment are the most debated topics of research from the last few decades. In this paper, the authors attempt to compare performances of selective Multi-Resolution Analysis based pansharpening algorithms listed as High-Pass Filtering, Smoothing Filter-based Intensity Modulation, Modulation Transfer Function-Generalized Laplacian Pyramid based algorithms, Indusion and Wavelet Transform based algorithms. These algorithms are applied to two datasets, acquired by QuickBird-2. The performances are evaluated based on popular image quality metrics. This performance analysis will surely help in evaluating the best possible tradeoff between spectral resolution and spatial resolution for fused image produced by the selected algorithms.**

***Index Terms*—Remote sensing, image fusion, pansharpening, panchromatic image, multispectral image, multi-resolution analysis**

I. Introduction

Pansharpening produces an image rich in spatial and spectral resolutions from the fusion of a multispectral (MS) and panchromatic (PAN) imagery; provided both images are acquired on same location [1]. The PAN images are rich in spatial resolution of even lesser than 1 m and MS images are deficient in it, but hold up to eight spectral bands [2]. The physical constraints of the satellite sensors cannot provide rich spatial and spectral resolutions in unique image product. But, the demand for higher resolutions of both types is continuously growing for several remote sensing tasks [3]. These help groundwater prospects mapping, forecast of agricultural output, forest cover mapping, snow & glacier studies, wasteland mapping, visual image analysis, object recognition, change detection, etc. One of the promising attempt to fulfill this demand is seen in terms of 'data fusion' [4]. The pansharpening is a part of this larger research domain 'data fusion' and evolved as a solution with great importance to the problem of physical constraints of satellite sensors. Pansharpening can be regarded as a branch of traditional image fusion.

A. Related Work

Survey of pansharpening algorithms can be found in [5]. The algorithms proposed so far are mostly categorized in two major groups viz. Multi-Resolution Analysis (MRA) [6] and Component Substitution (CS) [7]. The algorithms employing features of both approaches are treated as hybrid [8]. MRA involves an iterative decomposition scheme that constructs an order of 2D-signals holding progressive reduced contents. Here, the content of information is considered as spatial frequency. The decomposition can range from single level to more complex techniques. Thus, MRA is alternatively referred as 'pyramidal approach' [9]. This paper compares the performances of the most recent MRA based pansharpening algorithms listed as High-Pass Filtering (HPF) [10], [11], Smoothing Filter-based Intensity Modulation (SFIM) [11], [12], Modulation Transfer Function-Generalized Laplacian Pyramid based algorithms [11], [13]–[15], Indusion [11], [16] and Wavelet Transform based algorithms [11], [17]–[19].

The outline of the paper is arranged as: Section II briefs the fusion process opting MRA. The selected MRA based image fusion algorithms are presented in Section III. Application of algorithms to image datasets together with a discussion on results is addressed in Section IV. Lastly, the conclusions are noted in Section V.

II. MRA Approach to Image Fusion

The generalized procedure opted by MRA approach involves an iterative decomposition scheme that constructs an order of 2D-signals holding progressive reduced contents, which is obtained by the exploitation of particular analysis operators in repeatable manner.

The result of image fusion exploits computation of subtracting the low-pass filtered PAN image from itself. High-spatial resolution fused product is mathematically defined as:

$$F = M_{up} + g(P - P_L) \tag{1}$$

Where, M_{up} is the MS image now resized to match PAN level, g is the gain factor for spectral bands in MS image, P accounts for the PAN image, P_L is the low-pass form of PAN and F holds the result of image fusion. P_L for (1) is computed as:

$$P_L = \sum_{k=1}^{N} w_k (M_{up})_k \tag{2}$$

Where, w represents optimal weights for spectral bands of MS image denoted as $k = 1, ..., N$.

III. MRA Based Image Fusion Algorithms

This section describes the working procedures of popular MRA approach based image fusion algorithms.

A. High-Pass Filter

In HPF, the PAN image is operated by a small spatial filter of high-pass type. Outcome obtained due to this contains the high-frequency component i.e the information related mostly to spatial details. This spatial filtering removes most of the spectral details. The results of high-pass filtering are added to the MS image rich of spectral resolution in pixel-wise manner. Ultimately, the algorithm combines the spatial details from PAN image to spectral details of MS image [10], [11]. The brief steps of HPF fusion are provided in Algorithm-1.

Algorithm-1: HPF
Input: M_{up}, P **Output:** F
Step-1: Equalize P to match M_{up} scale.
Step-2: Define spatial filter H.
Step-3: P_L = Filter P using H.
Step-4: $F = M_{up} + (P - P_L)$

B. Smoothing Filter-based Intensity Modulation

By using a ratio of PAN image to its low-pass version, spatial information can be modulated. In SFIM algorithm, modulation is performed to a registered MS image deficient in spatial resolution. There are no alterations to spectral properties and contrast of MS. SFIM is actually extended development from the Pixel Block Intensity Modulation (PBIM) technique. The brief steps of SFIM are given in Algorithm-2.

Algorithm-2: SFIM
Input: M_{up}, P **Output:** F
Step-1: Equalize P to match M_{up} scale.
Step-2: Define smoothing filter H.
Step-3: P_L = Filter P using H.
Step-4: $F = \dfrac{M_{up} \cdot P}{P_L}$

Relationship of P to P_L cancels the contrast of spectral, topographical type in the PAN image. It retains the only high-spatial resolution edges. This algorithm is thus considered consistent to the spectral information along with contrast of the input MS image [11], [12].

C. Pyramidal Algorithms

Consideration of Modulation Transfer Function (MTF) with respect to image sensing is important while performing image fusion. These functions for the MS imaging sensors may differ from each other based on decay rate. Also, they differ from MTFs of the PAN image sensor. Typically, the MTF is a bell shaped function. The magnitude value is very much lower than 0.5, when measured at the cutoff Nyquist frequency. It is to avoid aliasing. Generalized Laplacian Pyramid (GLP) is a multi-scale and oversampled structure. For MS sensor, MTF when used to design the GLP reduction filter, it gives 'GLP with MTF matched filter (MTF-GLP)' image fusion [11], [13], [15]. It is briefed in Algorithm-3.

Algorithm-3: MTF-GLP
Input: M_{up}, P **Output:** F
Step-1: Equalize P to match M_{up} scale.
Step-2: Define filter H w.r.t. MTF of QuickBird-2.
Step-3: P_L = Filter P using H.
Step-4: Downsample P_L.
Step-5: Interpolate P_L by 23-coeff. polynomial.
Step-6: $D = P - P_L$
Step-7: $F = M_{up} + D$

Further, a signal-dependent injection scheme 'MTF-GLP with High-Pass Modulation (MTF-GLP-HPM)' is also possible [11], [13]. It is given in Algorithm-4.

Algorithm-4: MTF-GLP-HPM
Input: M_{up}, P **Output:** F
Step-1: Equalize P to match M_{up} scale.
Step-2: Define filter H w.r.t. MTF of QuickBird-2.
Step-3: P_L = Filter P using H.
Step-4: Downsample P_L.
Step-5: Interpolate P_L by 23-coeff. polynomial.
Step-6: $F = \dfrac{M_{up} \cdot P}{P_L}$

Two more versions 'MTF-GLP-HPM followed by Post-Processing (MTF-GLP-HPM-PP)' [11], [14] and 'MTF-GLP using Context-Based Decision (MTF-GLP-CBD)' [11], [13], [15] briefed in Algorithm-5 and Algorithm-6 are also evaluated in experimentation.

Algorithm-5: MTF-GLP-HPM-PP
Input: M_{up}, P **Output:** F
Step-1: Equalize P to match M_{up} scale.
Step-2: Define filter H w.r.t. MTF of QuickBird-2.
Step-3: P_L = Filter P using H.
Step-4: Downsample P_L.
Step-5: Interpolate P_L by 23-coeff. polynomial.
Step-6: $F = \dfrac{M_{up} \cdot P}{P_L}$
Step-7: F = Post-processing F according to [14]

Algorithm-6: MTF-GLP-CBD
Input: M_{up}, P **Output:** F
Step-1: Equalize P to match M_{up} scale.
Step-2: Define filter H w.r.t. MTF of QuickBird-2.
Step-3: P_L = Filter P using H.
Step-4: Downsample P_L.
Step-5: P_L = Interpolate by 23-coefficient polynomial.
Step-6: $g = cov(P_L, M_{up})/var(P_L)$
Step-7: $D = P - P_L$
Step-8: $F = M_{up} + (D \times g)$

D. Indusion

Image fusion algorithms generally interpolate MS image by a bicubic method and finally adds spatial contents of the PAN image to the MS image. Indusion algorithm instead make use of induction scaling technique to get better correlated, sharper and well registered interpolated images. In this algorithm, a pair of Cohen–Daubechies–Fauveau (CDF) 9/7 tap biorthogonal filters is utilized to take out the spatial information of the PAN image, that is further merged to an interpolated MS image [11], [16]. The fusion process is briefed in Algorithm-7, where M represents original MS image.

Algorithm-7: Indusion
Input: M, P **Output:** F
Step-1: Define spatial filter H.
Step-2: $P_L = P$ filtered using H.
Step-3: $P_L = P_L$ decimated by 9 coeff. polynomial.
Step-4: $P_{Leq} = P_L$ equalized to M scale.
Step-5: $P_{up} = P_{Leq}$ upscaled by 7-coeff. polynomial.
Step-6: $M_{up} = M$ upscaled by 7-coeff. polynomial.
Step-7: $P_{Heq} = P$ equalized to match M_{up} scale.
Step-8: $D = P_{Heq} - P_{Leq}$
Step-9: $F = M_{up} + D$

Though the 9/7 filter pair is symmetric, it do not effect in any kind of shift in result image.

E. Wavelet Transform based algorithms

Wavelet transform provides framework for decomposition of input images into a variety of new images. Every new image has a different degree of resolution. Literature shows undecimated discrete wavelet transform called as "à trous" algorithm very effective for pansharpening [18]. Despite nonorthogonality which may affect the spectral excellence of the fused product, the advantageous characteristics like the capability of being easily matched to the MTF of imaging sensor and the shift-invariance property produces accurate pansharpened image. Given an image, it constructs the approximations in a sequence by having consecutive convolutions using filter obtained by scaling function. Here, scaling function refers B_3 cubic spline profile. The differences from two successive approximations are computed in the form of wavelet planes. The foremost wavelet plane from the PAN image possess spatial content that is unavailable in MS image. The image fusion achieved by additive method is referred to as Additive à trous Wavelet Transform (ATWT) [11], [18] and briefed in Algorithm-8.

Algorithm-8: ATWT
Input: M_{up}, P **Output:** F
Step-1: Equalize P to match M_{up} scale.
Step-2: $P_L =$ à trous wavelet transform of P.
Step-3: $P_L =$ Inverse wavelet transform of P_L.
Step-4: $D = P - P_L$.
Step-5: $F = M_{up} + D$.

The alternative implementations viz. à trous Wavelet Transform-Model-2 (ATWT-M2) [11], [17] and à trous Wavelet Transform-Model-3 (ATWT-M3) [11], [17] that are respectively briefed in Algorithm-9 and Algorithm-10 are also evaluated.

Algorithm-9: ATWT-M2
Input: M_{up}, P **Output:** F
Step-1: $W_P =$ à trous wavelet transform of P.
Step-2: $W_M =$ à trous wavelet transform of M_{up}.
Step-3: Equalize W_P to match W_M.
Step-4: $X =$ Injection of W_P in W_M.
Step-5: $F =$ Inverse wavelet transform of X.

Algorithm-10: ATWT-M3
Input: M_{up}, P **Output:** F
Step-1: $W_P =$ à trous wavelet transform of P.
Step-2: $W_M =$ à trous wavelet transform of M_{up}.
Step-3: Covariance based equalization of W_P to W_M.
Step-4: $X =$ Injection of W_P in W_M.
Step-5: $F =$ Inverse wavelet transform of X.

Additive Wavelet Luminance Proportional (AWLP) [11], [19] image fusion is briefed in Algorithm-11 and also tested.

Algorithm-11: AWLP
Input: M_{up}, P **Output:** F
Step-1: Equalize P to match M_{up}.
Step-2: $P_L =$ à trous wavelet transform of P.
Step-3: $P_L =$ Inverse wavelet transform of P_L.
Step-4: $D = P - P_L$.
Step-5: $S =$ Average of M_{up} band images.
Step-6: $IR = M_{up}/S$.
Step-7: $F = M_{up} + (D \times IR)$.

IV. Experimental Results and Analysis

The comparative performance of MRA based image fusion algorithms is obtained and analyzed in this section, where two remotely sensed image datasets acquired by QuickBird-2 satellite are considered. The performance evaluation is done using MATLAB R2019a on the system configuration of core i5 3rd generation processor with 6 GB RAM.

A. Datasets

The details of datsets are shown in Table I and visualized in Fig. 1. The datasets have four bands viz. Blue (B), Green (G), Red (R), and Near-InfraRed (NIR), for MS image covering the visual and near-infrared regions of the spectrum.

B. Experimentation and Performance Measurement

For the two datasets, we perform two experiments applying the MRA based image fusion algorithms discussed in section III. Performance evaluation is carried on a selected region of size 256×256 pixels for MS and 1024×1024 pixels for PAN

TABLE I: Dataset Specifications for QuickBird imagery

Specifications	Dataset-1: Jaipur	Dataset-2: Sundarbans
Satellite Sensor	QuickBird-2	QuickBird-2
Spectral Bands	4-band MS and PAN	4-band MS and PAN
Spatial Resolutions	MS: 2.4 m and PAN: 60 cm	MS: 2.4 m and PAN: 60 cm
Location	Jaipur, India	Sundarbans, India
Data Format	16-bit	11-bit
Dimensions of MS	2955×2970×4	4096×4096×4
Dimensions of PAN	11820×11880	16384×16384
Date of Acquisition	18th September 2013	21st November 2002
Provided by	[20]	[21]

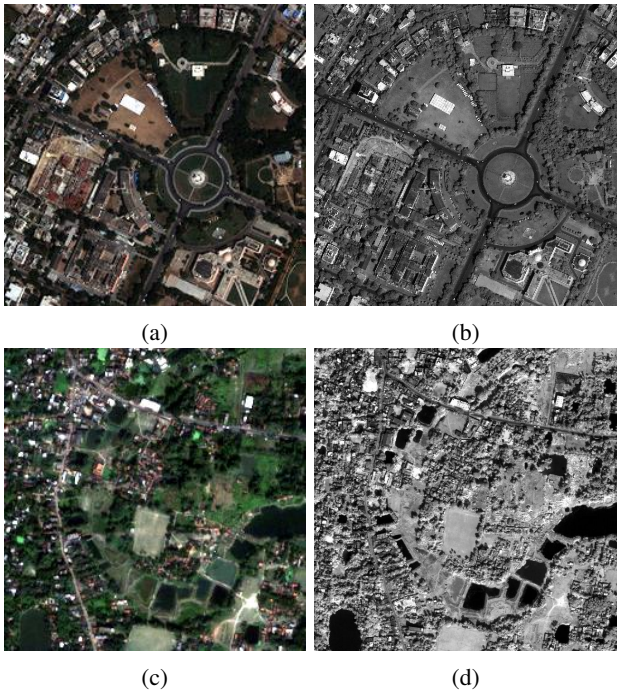

Fig. 1: Dataset-1: Jaipur (a) MS and (b) PAN. Dataset-2: Sundarbans (c) MS and (d) PAN.

image of each dataset. Resultant images after image fusion are displayed in Fig. 2 and Fig. 3 for corresponding datasets. The PAN to MS ratio considering spatial resolutions is 4.

The performances of applied MRA based image fusion algorithms are quantified by measurement of quality metrics. The numerical values for Quality w/ No Reference (QNR) [22], Spectral Distortion (D_λ) [22], Spatial Distortion (D_S) [22] and Spectral Angle Mapper (SAM) [22], [23] are obtained using Full-Resolution assessment [24], whereas Root Mean Square Error (RMSE) [23], *Erreur Relative Global Adimensionnelle De Synthese* (ERGAS) [22], [23], Spatial Correlation Coefficient (SCC) [1] and Quality index Q4 [22], [23] are computed using Reduced-Resolution assessment [24]. Table II shows quality metrics for first experiment, where best result for every parameter is shown in bold, next prominent result is underlined and next to it is shown in italic. Table III correspondingly show quality metrics for second experiment.

C. Objective Analysis

To find the best performance among the selected MRA based image fusion algorithms applied to two different datasets, it is necessary to analyze comparatives of quantitative measurements.

A comparison of QNR values is plotted in Fig. 4. Desired value of QNR is ideally 1. Fig. 5 shows a comparison of D_λ values. D_λ represents spectral distortion and it is a measure of loss. It is totally undesired and ideal value should be 0. To observe both the comparative plots, it is noticed that ATWT-M2 has achieved overall highest results. Next to it, we find Indusion performing at second level. MTF-GLP-HPM-PP remain last to compute desired values of QNR and D_λ.

A comparison of spatial distortion in resultant images can be seen in terms of D_s values in Fig. 6. This metric is achieved at most desired value by Indusion, while ATWT-M3 performs second. More spatial distortion is measured in the result of MTF-GLP-HPM-PP method.

The desired SAM index is also 0. Measurements of SAM are compared in Fig. 7. AWLP computes the most desired value of SAM among other methods. The performance of MTF-GLP-HPM is to be credited next to it, while ATWT-M3 provide highest value of SAM.

Comparatives of RMSE and ERGAS values are plotted in Fig. 8 and Fig. 9 respectively. It is observed that ATWT-M3 has achieved overall most desired results. Next to it, we find ATWT-M2 performing at second level. Indusion remain last to compute desired values of RMSE and ERGAS index.

Fig. 10 shows a comparison of obtained SCC values by all algorithms on all datasets. SCC computes percentage of spatial details injected to final resultant images. On comparison, ATWT-M3 method has achieved highest values, while performance of ATWT-M2 achieves second level. Comparatively Indusion method performs weak in computation of SCC.

A quality content in fused image is derived from computation of Q index. To look at comparison in Fig. 11, ATWT-M2 method maintains highest value. The performance of ATWT-M3 is at second level. Indusion method achieves overall lowest value of Q-index.

Finally, a comparison of time taken by image fusion algorithms to generate high resolution resultant image is plotted in Fig. 12. SFIM results with fused image at lowest computational complexity. HPF also performs very fast to image fusion. ATWT-M3 consumed highest time. Next to it ATWT-M2 also requires considerable time for fusion procedure.

D. Subjective Analysis

After the image fusion by MRA based algorithms is achieved, user is the ultimate judge of results at end use. Hence, visual inspection of resultant images for all the datasets is made.

It is observed for both the datasets, that MTF-GLP-HPM-PP method results in highest spatial distortion in fused images. The results produced by Indusion and MTF-GLP methods are also affected with spatial and spectral distortion. ATWT-M3 and ATWT-M2 are partially successful to reduce these effects,

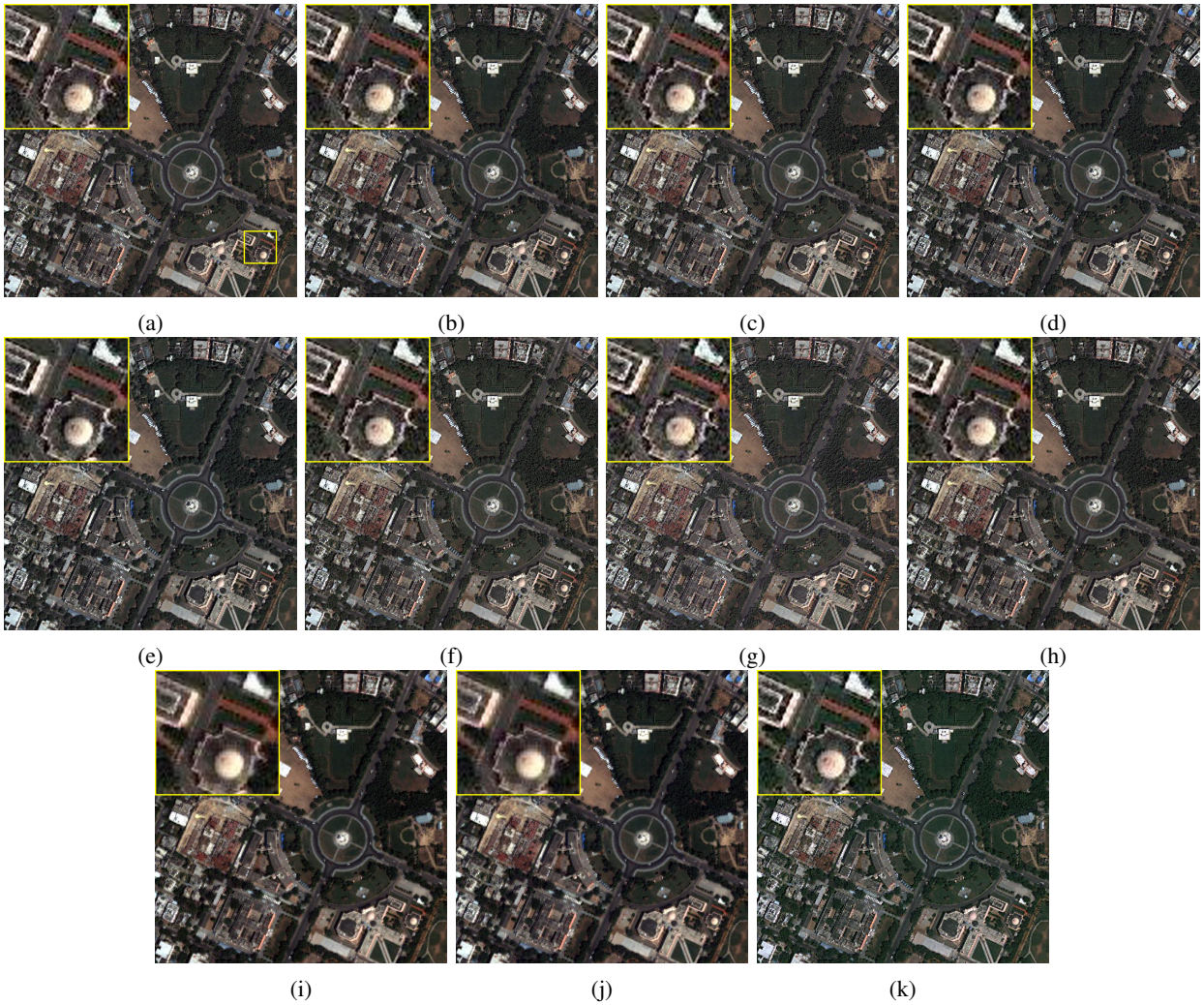

Fig. 2: Experimentation with Dataset-1: Jaipur. Resultant fused images of (c) HPF, (d) SFIM, (e) MTF-GLP, (f) MTF-GLP-HPM, (g) MTF-GLP-HPM-PP, (h) MTF-GLP-CBD, (i) Indusion, (j) ATWT, (k) ATWT-M2, (l) ATWT-M3 and (m) AWLP. The spectral band combinations of only R, G, and B is used for display purpose. The magnification of a region outlined in (a) is represented at top left in every image to help visual distinction.

TABLE II: Measurement of performance metrics: Quality w/ No Reference (QNR), Spectral Distortion (D_λ), Spatial Distortion (D_S), Spectral Angle Mapper (SAM), Root Mean Square Error (RMSE), *Erreur Relative Global Adimensionnelle De Synthese* (ERGAS), Spatial Correlation Coefficient (SCC), Quality index (Q4) and Execution Time Dataset-1: Jaipur.

	Full Resolution Assessment				Reduced Resolution Assessment				
Method	QNR	D_λ	D_S	SAM(°)	RMSE	ERGAS	SCC	Q4	Time(s)
HPF	0.7266	0.1160	0.1780	1.7751	*56.0936*	*3.3502*	0.6335	0.7478	0.3724
SFIM	0.7324	0.1137	0.1736	1.7755	57.2464	3.4934	0.6268	*0.7514*	**0.2446**
MTF-GLP	0.6926	0.1350	0.1994	1.7710	61.3486	3.6641	0.6376	0.7286	1.3620
MTF-GLP-HPM	0.7002	0.1317	0.1935	1.7723	63.1664	3.8559	0.6289	0.7307	1.4900
MTF-GLP-HPM-PP	0.6492	0.1690	0.2187	2.1880	64.8331	3.9531	0.6052	0.7119	2.0650
MTF-GLP-CBD	0.6902	0.1337	0.2034	1.8071	61.8696	3.7844	0.6337	0.7157	1.5420
Indusion	*0.8007*	*0.1016*	0.1088	**1.5068**	70.0831	4.1669	0.5927	0.6538	*0.5506*
ATWT	0.6994	0.1306	0.1956	*1.7693*	59.1852	3.5349	*0.6517*	0.7403	1.7891
ATWT-M2	0.8198	**0.0746**	*0.1141*	2.3250	32.7828	1.8704	0.7210	0.8741	5.5148
ATWT-M3	**0.8350**	0.0778	**0.0945**	2.3634	**29.4886**	**1.7458**	**0.7627**	**0.8764**	5.6637
AWLP	0.7320	0.1153	0.1726	1.7331	63.6851	3.5721	0.6307	0.7503	1.8610

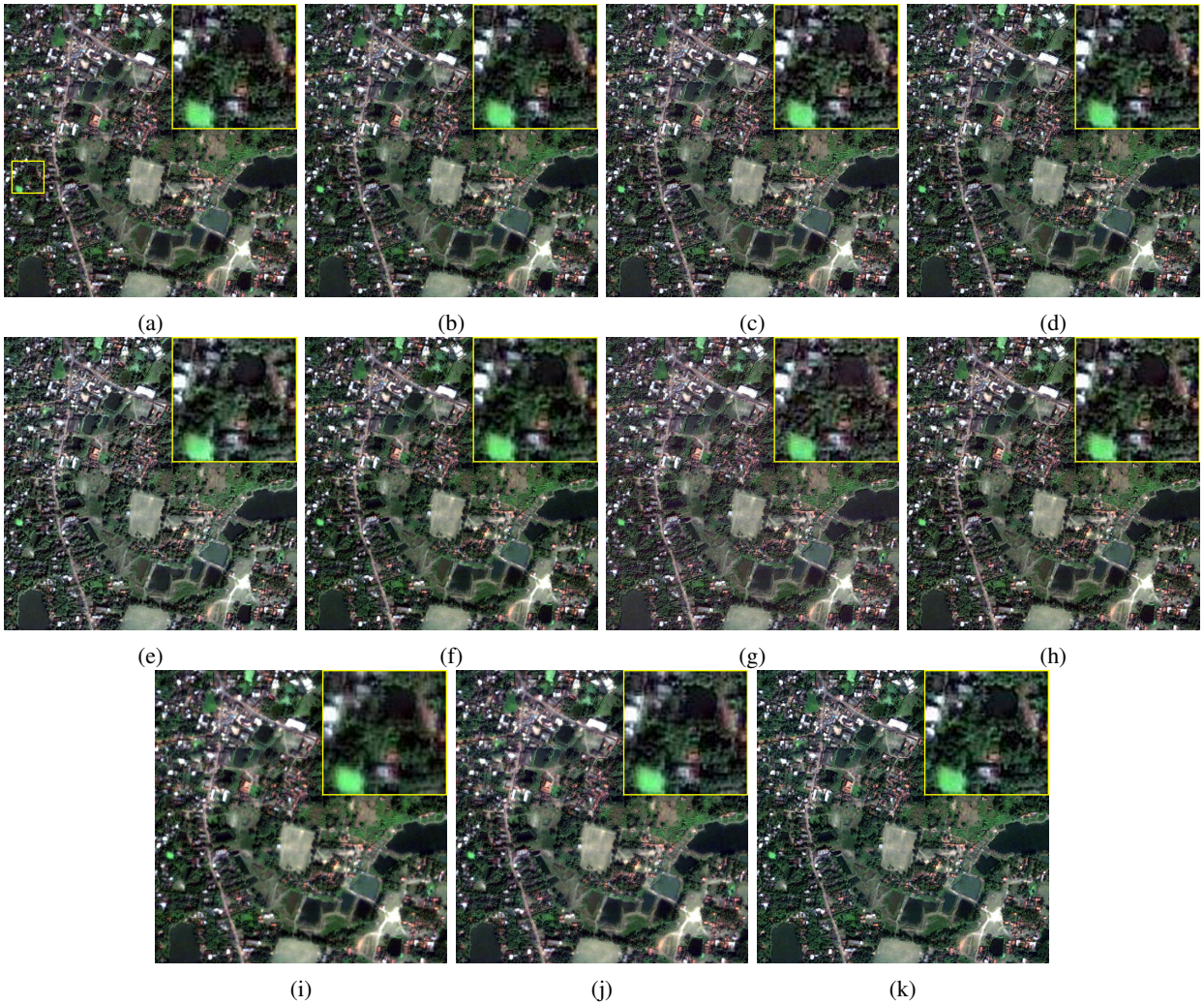

Fig. 3: Experimentation with Dataset-2: Sundarbans. Resultant fused images of (c) HPF, (d) SFIM, (e) MTF-GLP, (f) MTF-GLP-HPM, (g) MTF-GLP-HPM-PP, (h) MTF-GLP-CBD, (i) Indusion, (j) ATWT, (k) ATWT-M2, (l) ATWT-M3 and (m) AWLP. The spectral band combinations of only R, G, and B is used for display purpose. The magnification of a region outlined in (a) is represented at top right in every image to help visual distinction.

TABLE III: Measurement of performance metrics: Quality w/ No Reference (QNR), Spectral Distortion (D_λ), Spatial Distortion (D_S), Spectral Angle Mapper (SAM), Root Mean Square Error (RMSE), *Erreur Relative Global Adimensionnelle De Synthese* (ERGAS), Spatial Correlation Coefficient (SCC), Quality index (Q4) and Execution Time for Dataset-2: Sundarbans.

	Full Resolution Assessment				Reduced Resolution Assessment				
Method	QNR	D_λ	D_S	SAM(°)	RMSE	ERGAS	SCC	Q4	Time(s)
HPF	0.8835	0.0527	0.0673	1.2738	*20.1274*	*1.6500*	0.7330	0.8376	0.3564
SFIM	0.8857	0.0521	0.0656	1.2547	20.1798	1.6640	0.7336	0.8469	**0.2599**
MTF-GLP	0.8444	0.0674	0.0946	1.1970	24.4412	2.0037	0.7231	0.7963	1.3409
MTF-GLP-HPM	0.8482	0.0661	0.0918	*1.1642*	24.5868	2.0292	0.7229	0.8058	1.4131
MTF-GLP-HPM-PP	0.8034	0.0912	0.1159	1.3384	26.5599	2.2131	0.7398	0.7706	1.9179
MTF-GLP-CBD	**0.9230**	**0.0325**	0.0460	1.1542	26.0745	1.9520	0.7062	*0.8674*	1.6279
Indusion	0.9174	0.0454	**0.0389**	1.5763	26.3279	2.1851	0.6517	0.7214	*0.5729*
ATWT	0.8515	0.0637	0.0905	1.1966	23.0492	1.8895	*0.7423*	0.8122	1.8186
ATWT-M2	*0.8990*	0.0407	0.0628	1.7838	10.9650	**0.9258**	0.8571	**0.9207**	5.5662
ATWT-M3	0.8760	0.0703	*0.0577*	1.8718	**10.6671**	0.9764	**0.8629**	0.8678	5.7109
AWLP	0.8978	*0.0438*	0.0610	**1.1126**	31.5079	2.3382	0.6563	0.8236	1.8845

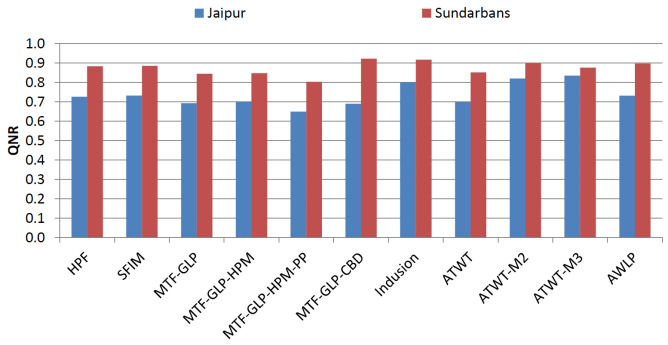

Fig. 4: Performance comparison of MRA based image fusion algorithms considering measurement of QNR.

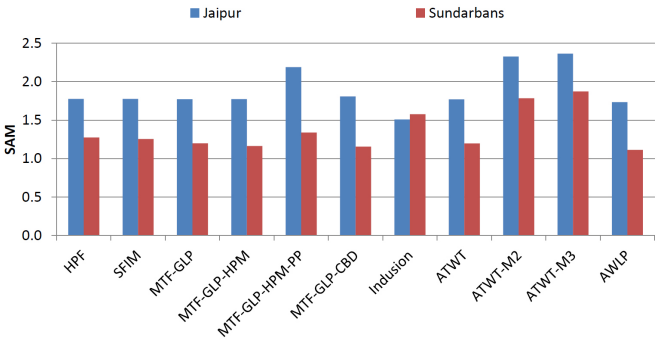

Fig. 7: Performance comparison of MRA based image fusion algorithms considering measurement of SAM.

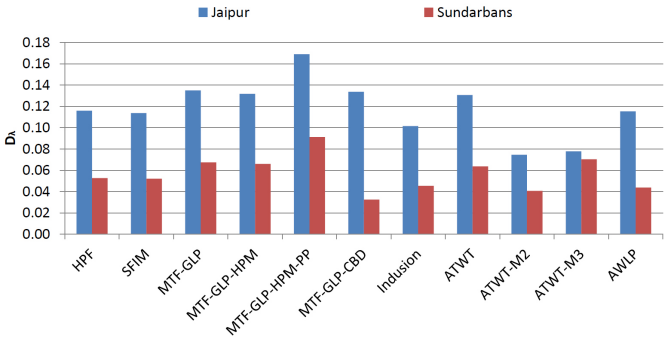

Fig. 5: Performance comparison of MRA based image fusion algorithms considering measurement of D_λ.

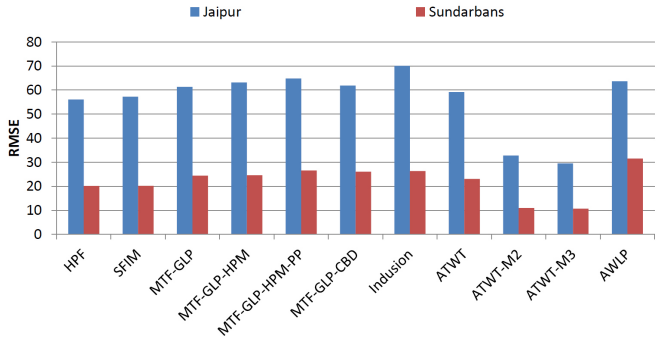

Fig. 8: Performance comparison of MRA based image fusion algorithms considering measurement of RMSE.

but resultant images of these methods are mostly affected with blur. Comparatively, AWLP, ATWT and MTF-GLP-CBD shows better visualization of fused images with respect to input images.

V. Conclusion & Future Scope

The performance evaluation of eleven MRA based algorithms for pansharpening of MS images from two datasets is carried out. The experimental results objectively verify that ATWT-M3 and MTF-GLP-CBD fusion algorithms mostly outperform other state-of-the-art algorithms. But, visual inspection further noticed blur effect in resultant images produced by ATWT-M3 and found comparative better visualizations of objects in resultant images of MTF-GLP-CBD along with AWLP and ATWT. ATWT-M3 and ATWT-M2 have resulted in highest computational complexity, whereas HPF and SFIM performed fast pansharpening. Among the selected algorithms, MTF-GLP-CBD proved its potential achieving quality metrics and computational complexity at optimum.

After analysis of the comparative results based on different quality metrics and visual inspection, a need of more so-

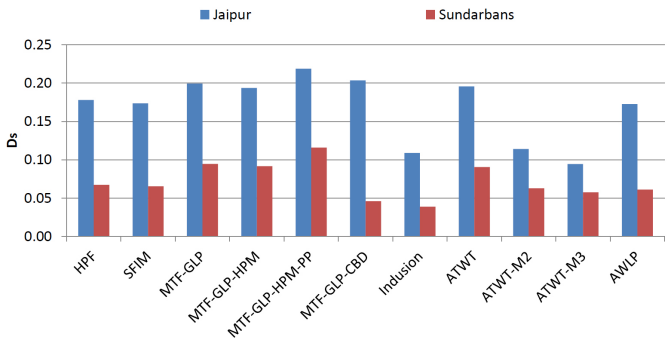

Fig. 6: Performance comparison of MRA based image fusion algorithms considering measurement of D_s.

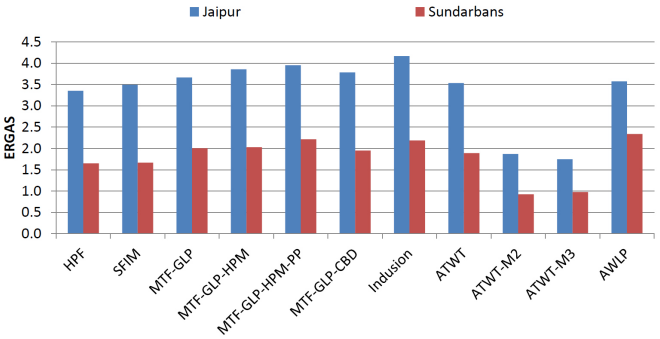

Fig. 9: Performance comparison of MRA based image fusion algorithms considering measurement of ERGAS.

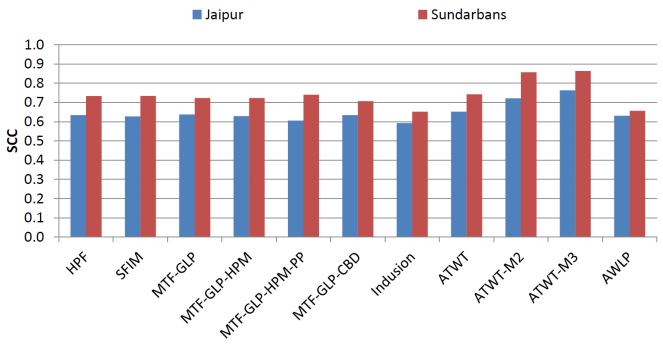

Fig. 10: Performance comparison of MRA based image fusion algorithms considering measurement of SCC.

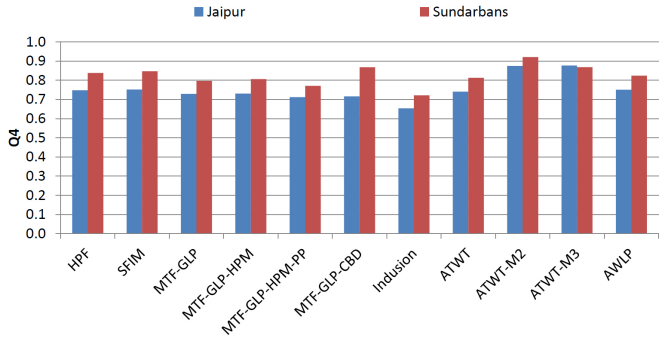

Fig. 11: Performance comparison of MRA based image fusion algorithms considering measurement of Q4 index.

phisticated image fusion algorithm to overcome the observed limitations is underlined. Currently, the selection from available Multi-Resolution Analysis based image fusion algorithms must be specific to application at hand.

REFERENCES

[1] L. He *et al.*, "Pansharpening via detail injection based convolutional neural networks," *IEEE J. Sel. Topics Appl. Earth Observ.*, vol. 12, no. 4, pp. 1188–1204, Apr. 2019.

[2] G. Camps-Valls, D. Tuia, L. Gómez-Chova, S. Jiménez, and J. Malo, *Remote Sensing Image Processing*. Morgan and Claypool, 2012.

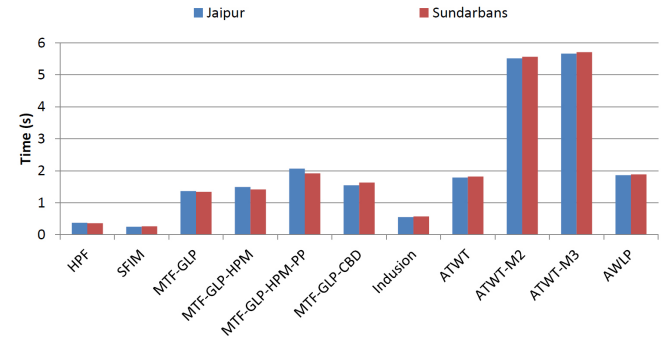

Fig. 12: Performance comparison of MRA based image fusion algorithms considering measurement of Execution Time.

[3] T. Wang, F. Fang, F. Li, and G. Zhang, "High quality bayesian pansharpening," *IEEE Trans. Image Process.*, vol. 28, no. 1, pp. 227–239, Jan. 2019.

[4] H. B. Mitchell, *Data Fusion: Concepts and Ideas*. Berlin, Germany: Springer-Verlag, 2012.

[5] V. R. Pandit and R. J. Bhiwani, "Image fusion in remote sensing applications: A review," *Int. J. Comput. Appl.*, vol. 120, no. 10, pp. 22–32, Jun. 2015.

[6] K. P. Upla, M. V. Joshi, and P. P. Gajjar, "An edge preserving multiresolution fusion: Use of contourlet transform and MRF prior," *IEEE Trans. Geosci. Remote Sens.*, vol. 53, no. 6, pp. 3210–3220, Jun. 2015.

[7] W. Wang, L. Jiao, and S. Yang, "Novel adaptive component-substitution-based pan-sharpening using particle swarm optimization," *IEEE Geosci. Remote Sens. Lett.*, vol. 12, no. 4, pp. 781–785, Apr. 2015.

[8] S. Zhong, Y. Zhang, Y. Chen, and DiWu, "Combining component substitution and multiresolution analysis: A novel generalized BDSD pansharpening algorithm," *IEEE J. Sel. Topics Appl. Earth Observ.*, vol. 10, no. 6, pp. 2867–2875, Jun. 2017.

[9] A. Kallel, "MTF-adjusted pansharpening approach based on coupled multiresolution decompositions," *IEEE Trans. Geosci. Remote Sens.*, vol. 53, no. 6, pp. 3124–3145, Jun. 2015.

[10] J. Pat S. Chavez, S. C. Sides, and J. A. Anderson, "Comparison of three different methods to merge multiresolution and multispectral data: Landsat TM and SPOT panchromatic," *Photogramm. Eng. Remote Sens.*, vol. 57, no. 3, pp. 295–303, Mar. 1991.

[11] G. Vivone *et al.*, "A critical comparison among pansharpening algorithms," *IEEE Trans. Geosci. Remote Sens.*, vol. 53, no. 5, pp. 2565–2586, May 2015.

[12] J. G. Liu, "Smoothing filter-based intensity modulation: A spectral preserve image fusion technique for improving spatial details," *Int. J. Remote Sens.*, vol. 21, no. 18, pp. 3461–3472, Dec. 2000.

[13] B. Aiazzi, L. Alparone, S. Baronti, A. Garzelli, and M. Selva, "MTF-tailored multiscale fusion of high-resolution MS and Pan imagery," *Photogramm. Eng. Remote Sens.*, vol. 72, no. 5, pp. 591–596, May 2006.

[14] J. Lee and C. Lee, "Fast and efficient panchromatic sharpening," *IEEE Trans. Geosci. Remote Sens.*, vol. 48, no. 1, pp. 155–163, Jan. 2010.

[15] B. Aiazzi, L. Alparone, S. Baronti, and A. Garzelli, "Context-driven fusion of high spatial and spectral resolution images based on oversampled multiresolution analysis," *IEEE Trans. Geosci. Remote Sens.*, vol. 40, no. 10, pp. 2300–2312, Oct. 2002.

[16] M. M. Khan, J. Chanussot, L. Condat, and A. Montanvert, "Indusion: Fusion of multispectral and panchromatic images using the induction scaling technique," *IEEE Geosci. Remote Sens. Lett.*, vol. 5, no. 1, pp. 98–102, Jan. 2008.

[17] T. Ranchin and L. Wald, "Fusion of high spatial and spectral resolution images: the arsis concept and its implementation," *Photogramm. Eng. Remote Sens.*, vol. 66, no. 1, pp. 49–61, Jan. 2000.

[18] J. Nu˜nez *et al.*, "Multiresolution-based image fusion with additive wavelet decomposition," *IEEE Trans. Geosci. Remote Sens.*, vol. 37, no. 3, pp. 1204–1211, May 1999.

[19] X. Otazu, M. González-Audícana, O. Fors, and J. Núñez, "Introduction of sensor spectral response into image fusion methods. application to wavelet-based methods," *IEEE Trans. Geosci. Remote Sens.*, vol. 43, no. 10, pp. 2376–2385, Oct. 2005.

[20] (2019, May). [Online]. Available: https://apollomapping.com/download-free-poster

[21] (2016, Mar.). [Online]. Available: http://www.glcf.umd.edu/data

[22] F. Palsson, J. R. Sveinsson, M. O. Ulfarsson, and J. A. Benediktsson, "Quantitative quality evaluation of pansharpened imagery: Consistency versus synthesis," *IEEE Trans. Geosci. Remote Sens.*, vol. 54, no. 3, pp. 1247–1259, Mar. 2016.

[23] S. Li and B. Yang, "A new pan-sharpening method using a compressed sensing technique," *IEEE Trans. Geosci. Remote Sens.*, vol. 49, no. 2, pp. 738–746, Feb. 2011.

[24] J. Liu, Y. Hui, and P. Zan, "Locally linear detail injection for pansharpening," *IEEE Access*, vol. 5, pp. 9728–9738, 2017.

Proceedings of the Fourth International Conference on Communication and Electronics Systems (ICCES 2019)
IEEE Conference Record # 45898; IEEE Xplore ISBN: 978-1-7281-1261-9

A Modified Block Based Biometric Fragile Watermark Technique

Feni Patel
Research Scholar
Electronics and Communication
Sarvajanik College of Engineering and Technology,
Surat, India
patelfeny1810@gmail.com

Chirag Paunwala
Professor
Electronics and Communication
Sarvajanik College of Engineering and Technology,
Surat, India
chirag.paunwala@scet.ac.in

Aarohi Vora
AdHoc Assistant Professor
Electronics and Communication
Sarvajanik College of Engineering and Technology,
Surat, India
vaarohi@gmail.com

***Abstract*— In the era of digital communication data sent through networks has increased. Providing security to data which is in the form of image, text, video, audio has been big challenge. For copyright information and authentication of the data, biometrics authentication is used. At the same time protection of biometrics data is also essential parameter. To increase the security level of biometric data watermarking technique is used. In this, paper we proposed block based biometric fragile watermarking technique which detects slight changes in the watermarked data. Fragile watermark technique generates watermark depending on the embed watermark. In this proposed method authentication data inserted into the least significant bit (LSB) of cover image. The experimental result shows the quality of the image by using conventional LSB technique, with use of key.**

Keywords—Biometric authentication, fragile watermarking, Block based embedding

I. INTRODUCTION

The growth of modern communication, security in network and cloud services is necessary. To provide a security to mitigate the issue of the copyright, unique identification, authentication of that data is very big challenge in network community.

For owner identification and authentication there are types of techniques [1] like passwords, PIN (Personal Identification Number) codes, biometrics etc. But accurate identification can be obtained by using biometrics traits. There are two types of biometrics traits namely physiological and behavioral respectively [1]. Physiological traits consist of fingerprint, hand, iris, face, DNA etc. Similarly, behavioral traits consist of keystroke, signature, voice etc. Security of biometric system is very important. To prevent biometric system from attacks encryption, steganography and watermarking [2] are possible solution. In encryption once the data is decrypted, data is no longer protected so for biometric security encryption is not preferred. Steganography and watermarking used to provide security but steganography is basically used for secret communication not for authentication and ownership protection.

A watermark is defined as the embedded information that is inserted into the cover signal. A watermark can be in form of image, text, biometric etc. In this paper we will concentrate on watermarking based biometric template authentication system.

Watermark technique is divided into three stages: (1) generate watermark and embed that watermark into original media (2) transmit watermark data in the network and (3) detection of embedded watermark [3]. Based on robustness, watermarking technique is classified into two types for authentication like robust watermarking and fragile watermarking [3]. The difference between fragile and robust watermarking is if there is any modification with authenticating data it is not noticeable in robust watermarking. But in fragile watermarking changes are noticeable. So, to identify every possible tampered region in watermarked data fragile watermarking technique has been used [4]. The spatial domain includes Least Significant Bit (LSB) algorithm [5, 6, 7], patch work [8], texture block coding [8] etc. The frequency domain includes Discrete Fourier Transform (DFT) algorithm [6, 9], Discrete Wavelet Transform (DWT) algorithm [6, 10, 11], Discrete Cosine Transform (DCT) algorithm [6, 12, 13].

The rest of the paper is organized as follows. In section II literature review of different watermarking techniques is given. In section III block based technique is explained in detail. The proposed method is describe in Section IV. Experimental results are shows in section V. Section VI conclude the paper.

II. LITERATURE REVIEW

Sabhanayagam et al. [14] presented types of biometric traits and its advantages and disadvantages. Biometric authentication system uses person's biometric data or template and based on comparison of this template with the same person's enrolled data or template. As biometric data of a person is not replicable and it is not secret, numerous attacks are possible in biometric system. Anil et al. [1] shows block diagram of the biometrics system and some attacks like fake biometric, replay old data, override feature extractor, synthesize feature vector, override matcher, modify template, intercept the channel and override decision in the biometrics system.

In [15] Cox et al. present applications of watermarking technique such as, owner identification, authentication, copy protection, broadcast monitoring, medical applications etc. Watermark can be classified as presented in [16]. According to

robustness there are three types namely robust, fragile and semi fragile watermarking. In robust watermarking changes are not noticeable and it can prevent attacks like noisy attack, geometrical attacks etc. In fragile watermarking, changes are noticeable so we can identify that there is any changes with the data. Watermark can be destroyed in this type of technique [3]. Semi fragile is affected from some type of attacks [3] and it is capable to tolerate some limited changes. Based on perceptivity, watermark can be classified into visible which can be observed by human eyes and invisible watermarking which cannot be observed by human eyes [3].

According to data extraction techniques there are three watermarking techniques like blind, semi-blind and non-blind. In blind watermarking original data does not need during extraction process. In non-blind watermarking during extraction process original data is needed.

Watermark can be inserted into the intensity values in spatial domain [16]. LSB is the simplest technique than others and most commonly LSB technique can be used. In this technique watermark is embedded in to the LSB of an image. Verma et al. [17] Proposed watermark image using LSB algorithm in colour for copyright protection. Brindha et al. [3] Proposed Biowatermarking for palm print image using LSB technique. LSB technique divided into two categories: insertion and substitution. Brindha et al. [3] divide palm print image into four quadrants and select fourth quadrant to embed secret data.

He et al. [18] proposed self-recovery fragile watermarking using block neighbourhood tampering characterization to improve the performance of tamper detection and tamper recovery. An image is divided into 8□8 blocks to create an information chain. This technique breaks block-wise dependency and makes technique vulnerable to the counterfeiting attack. Li et al. [19] Proposed multi-block dependency fragile watermarking technique for fingerprint image protection using LSB to prevent fingerprint image from isolated-block tamper. To make watermarking technique not vulnerable to the counterfeiting attack, they are using block wise dependency based watermarking technique. They proposed watermarking technique using LSB for authentication and tamper localization using block division. Security strength and tamper localization can be used for to evaluate the performance of the fragile watermarking.

An image is represented in the form of frequencies in transform domain [16]. Ui et al. [20] proposed a digital image watermarking algorithm based on DWT, DCT and SVD for robust watermarking of digital images in order to protect digital media and copyright efficiently. They used DCT, DWT based blind watermarking for host image and select middle frequency for embedding secret data. Brindha et al. [3] implemented Biowatermarking using DWT, DCT algorithms and for embedding they used palm-print image. For decomposition of an image in DWT haar filter can be used. For embedded an image has been divided into four bands which are HH, LH, LL and HL. They used zigzag scanning to select middle frequency for inserting watermark bits in DCT. Mita et al. [21] Proposed robust biometric based on DCT watermarking algorithm for template protection. They have used finger print feature vector and iris feature vector as watermark. To make system robust against some signal processing and channel attacks they proposed spatial and spectral feature based block discrimination and coefficient estimation strategy.

This research is carried under the minor research project Watermarking based Biometric template authentication System “New era of securing many fold biometrics: research on forensic and cyber security augmentation”, supported by grant from GUJCOST, Government of India. Procured by: Dr. Chirag Paunwala (Grant No. GUJCOST/MRP/2015-16/2640)

III. BLOCK BASED TECHNIQUE

To detect tampering and to authenticate digital image fragile watermarking technique have been proposed. Fragile watermarking technique can be classified into two types namely pixel based fragile watermarking and block based fragile watermarking [22]. In pixel based fragile watermarking technique the authentication data is calculated from the pixels. But this technique is vulnerable to oracle attack [23]. Block based fragile watermarking technique have been proposed to resist this type of attack. In this type of technique cover image is divided into each image blocks and watermark has been embedded into that image blocks. Wong et al. [24] proposed the block wise fragile watermarking technique to detect and localize unauthorized tampered block but that method is vulnerable to vector quantization (VQ) attack [25] and collage attack [26]. These attacks can solve by a self-recovery fragile watermarking for image authentication. This technique also used to improve the performance of tamper detection and tamper recovery [27]. The generalized embedding process of block wise dependency based watermarking is as shown in fig. 2. In this technique blocks are connected in the chain which fails to detect block tamper. For example if Xi0 block suffering from tampering, then watermark is generated from block Xi0 is not same as watermark embedded into the LSB of Xi1 block. Similarly, watermark generated from Xi1 is not equal to watermark embedded into Xi2.

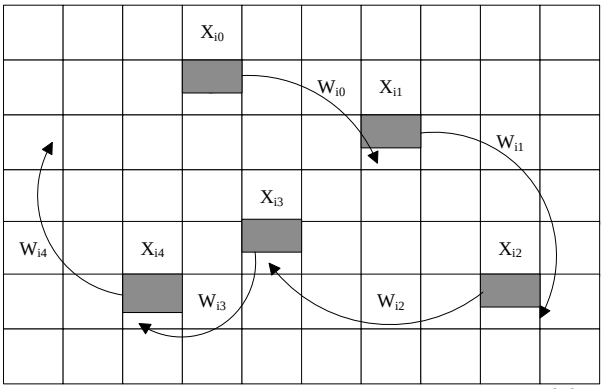

Fig. 1 Block wise dependency based watermarking scheme [19]

IV. PROPOSED WATERMARK EMBEDDING TECHNIQUE

In proposed technique we are using fingerprint as biometric traits.

For security requirement image is divided into 10x10 block. Fig.2. shows multi block dependent structure, 100 bits watermark is generated from each block and it is equally partitioned into ten parts. Each part is embedded into another image block to construct multi block dependent structure as shown in fig. 2.

Block diagram of watermarking generation and embedding process is as shown in fig. 3. LSB of the cover image X is set to zero and noted as X1. An image X1 is divided into its image

blocks $X1_i$, where i=1, 2, ……., N_b with size of 10×10. Where N_b is the number of image blocks.

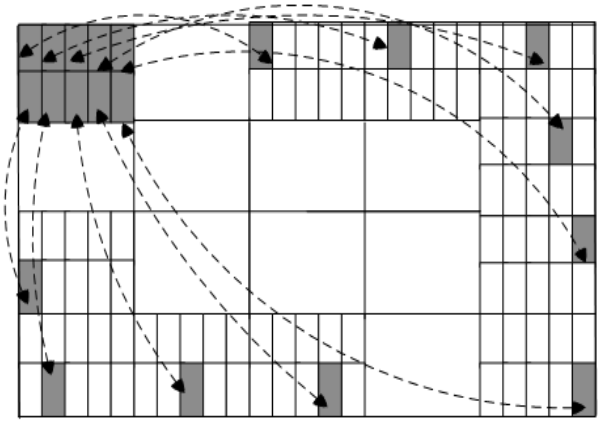

Fig. 2 Multiblock dependent structure [19]

Using jumble watermark bits at random position 100-bit watermark is generated for each image block. In this part, watermark data is embedded into the LSB of the image block at random position.

We have used fixed random numbers to generate key of 100 bits, which is used for encryption to make system secure.

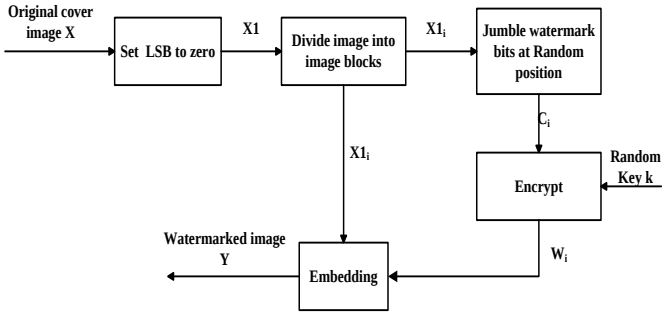

Fig. 3 Block diagram of watermark generation and embedding

To encrypt random position exclusive OR (XOR) operation is used. Using generated key $k = k_1, k_2, \ldots \ldots, k_{100}$ and encrypted random position, watermark bits are generated using eq. 1 $W = W_1, W_2, \ldots \ldots W_{N_b}$ for each block.

$$W_{ij} = C_{ij} \oplus k_{ij} \qquad (1)$$

Where $1 \le i \le N_b, 1 \le j \le 64$

The generated watermark is embedded into the each block of LSB of the original cover image. After embedding, watermark image Y is generated. The process of watermark generation and embedding process is illustrated in below algorithm.

For $i \leftarrow 1$ to N_b
$LSB(X1_i) \leftarrow$ watermark bits
$W_i = C_i \oplus k_i$
$LSB(X1_i) \leftarrow W_i$
$Y \leftarrow X1_i$

Algorithm for watermark generation and embedding

To find the quality of the watermarked image PSNR (Peak Signal to Noise Ratio), MSE (Mean Square Error) and SF (Similarity Factor) are used.

$$MSE = \frac{\sum_{i,j}[f(i,j) - f_w(i,j,a)]^2}{M \times N} \qquad (2)$$

Where $M \times N$ is the size of images. f, f_w are original image and watermarked image respectively.

$$PSNR = 10 log_{10}\left[\frac{b^2}{MSE}\right] \qquad (3)$$

Where *b* is the largest value of the image (typically 255).

Similarity Factor is measure of the similarity of pixel intensities between the original watermark data and watermark data after extraction process.

The formula of similarity factor is given by

$$SF = \frac{\sum_i \sum_j I(i,j) \times I_1(i,j)}{\sum_i \sum_j I_1(i,j)^2} \qquad (4)$$

Where *I (i, j)* is the original watermark data and I_1 *(i, j)* is the watermarked data after extraction process. The value of SF is in between the range [0, 1].

Block diagram of watermark extraction process

The block diagram of watermark extraction process is as shown in fig 4. Let's take test image Y which is received watermarked image. Firstly, do same process as done in process of watermark generated to generate watermark. Divide an image into image blocks $Y1_i$ with size of 10×10. Using XOR operation of key and random position watermark bits are extracted from LSB of the image. And compare with original embedded watermarks.

The process of watermark extraction is illustrated in below algorithm

For $i \leftarrow 1$ to N_b
LSB($Y1^*_i$)←watermark bits
$W_{i1} = C_i \oplus k_i$
Compare W_i and W^*_i

Algorithm for watermark extraction process

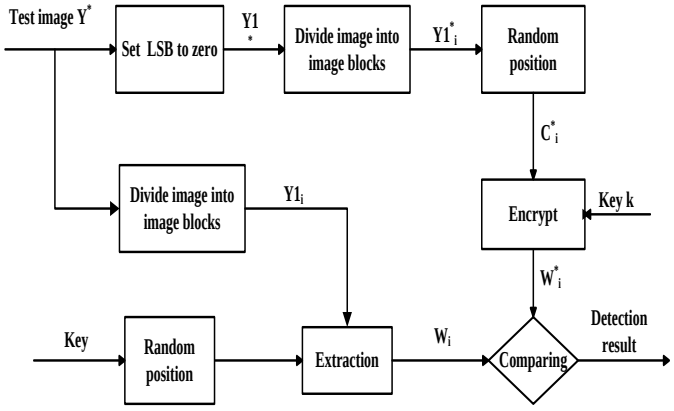

Fig. 4 Block diagram of watermark extraction process

V. EXPERIMENTAL RESULTS

The database for experimentation is created by taking fingerprints of 10 persons from fingerprint scanner named FPCapture_Access_v4.0.2 kit. The fingerprint image is taken as a host image for watermarking. The cover images used for hiding the watermarked bits is taken from standard inbuilt images in MATLAB version 2018. Total 5 different noise attacks are used to prove fragileness of watermarked data. The performance of the proposed watermarking algorithm is evaluated based on SF metrics. The result analysis is detailed in table I. In the result shown in Table I, SF is computed between original watermark data and watermark data after extraction.

TABLE I. COMPARATIVE ANALYSIS OF PERFORMANCE EVALUATION OF WATERMARKING

Sr. No.	Noise	Conventional LSB technique [6]		Proposed method	
		SF %	PSNR	SF %	PSNR
1.	Without noise	100	57.4743	100	51.149
2.	Salt & pepper	93.2692	25.0494	89.968	25.162
3.	Gaussian	3.2446	20.3780	0	20.31
4.	Poisson	1.36	27.3429	0	27.32
5.	Speckle	2.484	18.62	1.13	18.62

Table I shows the comparative analysis of the results of watermark embedding algorithm using conventional LSB technique [6] and proposed algorithm for 5 different noise attacks. As it can be observed form table I, SF is decreasing in proposed algorithm as compared to techniques in [6]. Thus it can be said that tampering is affect much while reconstructing the hidden image from watermarked image. So, we can say that proposed algorithm prove fragileness of the watermarked data. Hence, proposed fragile watermarking algorithm reconstructs not well in case of tampering done due to noise during transmission.

VI. CONCLUSION

The aim of securing biometric traits is being addressed by the proposed watermarking algorithm. This paper addresses novel frame work for biometric fragile watermarking to embed watermark data in block wise manner. Experimental result shows comparative analysis between secret key generation in the presence of noise to find SF. From comparison it is evident that block based technique with jumbling and with key is more suitable for finger print authentication. Experimental result shows that embedded watermarks data are visually insignificant and maintain quality of fingerprint image. The proposed method can detect similarity between embedded watermark data and watermark data after extraction and shows that after attacking SF is decreasing which signifies proposed algorithm is suitable for fragile watermarking. The block based watermarking algorithm provides advantage of enhancing security of the hidden biometric trait.

To make the system robust against various attacks, different techniques of watermarking can be used in future for the Protection of biometric data.

ACKNOWLEDGMENT

This research is carried under the minor research project Watermarking based Biometric template authentication System “New era of securing many fold biometrics: research on forensic and cyber security augmentation”, supported by grant from GUJCOST, Government of India. Procured by: Dr. Chirag Paunwala (Grant No. GUJCOST/MRP/2015-16/2640)

REFERENCES

[1] Anil K. Jain,Umut Uludag, Student Member, IEEE, “Hiding Biometric Data,”IEEE transactions on pattern analysis and machine intelligence, vol. 25, no. 11,pp.1494-1498 November 2003.

[2] Suraj Kumar Dubey, Vivek Chandra, “Steganography, Cryptography and Watermarking: A Review”, International Journal of Innovative Research in Science, Engineering and Technology, vol. 6, no. 2, 2017.

[3] Brindha N V, Meenakshi V S, "Comparison Analysis of Biowatermarking Using DWT, DCT and LSB Algorithms ", Computational Vision and Bio Inspired Computing. Lecture Notes in Computational Vision and Biomechanics, Springer Publication, vol.28, pp.849-863, year-2018.

[4] Jain P and Rajawat A S., “Fragile watermarking schemes for image authentication: a survey”, International Journal of Electronics and Computer Science Engineering, vol. 1, no. 3, pp.1232-1237.

[5] Song, Chunlin, Sud Sudirman, and Madjid Merabti. "Recent advances and classification of watermarking techniques in digital images." In Proceedings of post graduate network symposium, pp. 1-6. 2009.

[6] Preeti Gaur 1, Neeraj Manglani, “Image Watermarking Using LSB Technique”, International Journal of Engineering Research and General Science, Vol. 3, no. 3, pp. 1424-1433, 2015.

[7] A. Bamatraf, R. Ibrahim and M. N. B. M. Salleh, "Digital watermarking algorithm using LSB," *2010 International Conference on Computer Applications and Industrial Electronics*, Kuala Lumpur, 2010, pp. 155-159.

[8] Raghuwanshi, Neetesh, and Anurag Rishishwar. "A Review of Digital Water Marking Techniques and Uses." International Journal of Electrical, Electronics and Computer Engineering, vol. 4, no. 2, pp.66-74, 2015.

[9] Ningombam Jimson and K. Hemachandran, “DFT BASED DIGITAL IMAGE WATERMARKING: A SURVEY”, International Journal of Advanced Research in Computer Science, vol. 9, no. 2, 2018.

[10] Wei-Hung Lin, Yuh-Rau Wang, Shi-Jinn Horng, Tzong-Wann Kao, Yi Pan, “A Blind Watermarking Method Using Maximum Wavelet Coefficient Quantization”, Expert Systems with Applications journal, vol. 36, pp. 11509–11516, Elsevier 2009.

[11] J.E. Fowler, The redundant discrete wavelet transform and additive noise, IEEE Signal Processing Letters Vol.12, pp. 629–632. September 2005.

[12] Yulin Wang, Alan Pearmain, “Blind Image Data Hiding Based on Self Reference”, Pattern Recognition Letters, pp.1681–1689, Elsevier 2004.

[13] Y. Choi and I. Aizawa, “Digital Watermarking using Inter Block Correlation,” in Proceedings of the International Conference on Image Processing, vol. 2, pp. 216–220, October 1999.

[14] Sabhanayagam, T., V. Prasanna Venkatesan, and K. Senthamaraikannan. "A Comprehensive Survey on Various Biometric Systems." International Journal of Applied Engineering Research, vol.13, no. 5,pp. 2276-2297, 2018.

[15] Cox, Ingemar J., Matthew L. Miller, and Jeffrey A. Bloom. "Watermarking applications and their properties." In Proceedings International Conference on Information Technology: Coding and Computing, pp. 6-10, IEEE, 2000.

[16] Hussein, Ensaf, and Mohamed A. Belal. "Digital watermarking techniques, applications and attacks applied to digital media: a survey." International Journal of Engineering Research & Technology, vol.1, no. 7, pp.1-8, September 2012.

[17] Verma, Rajni, and Archana Tiwari. "Copyright protection for watermark image using LSB algorithm in colored image." Advance in Electronic and electric engineering, vol.4, no. 5, pp.499-506, 2014.

[18] He, Hong-Jie, Jia-Shu Zhang, and Heng-Ming Tai. "Self-recovery fragile watermarking using block-neighborhood tampering characterization." In International workshop on information hiding, Springer, Berlin, Heidelberg, pp. 132-145, 2009.

[19] Li C., Wang Y., Ma B., Zhang Z., "Multi-block dependency based fragile watermarking scheme for fingerprint images protection ", Multimedia Tools and Applications, Springer Publication, vol.64, no.3, pp.757-776, year-2012.

[20] Islam, Md Saiful, and Ui Pil Chong. "A Digital Image Watermarking Algorithm Based on DWT DCT and SVD." International Journal of Computer and Communication Engineering, vol.3, no. 5, pp.356-360, September 2014.

[21] Mita Paunwala•, S. Patnaik., "Biometric template protection with DCT-based watermarking", Machine Vision and Applications, Springer, vol.25, no.1, pp. 263–275, 2014.

[22] Dayanand .G Savakar , Shivanand Pujar., "A Survey on Fragile Digital Watermarking", International Journal of Science and Research, vol.5,no.4,pp. 2291-2295, April 2016.

[23] Wu, Jinhai, Bin B. Zhu, Shipeng Li, and Fuzong Lin. "Efficient oracle attacks on Yeung-Mintzer and variant authentication schemes." IEEE International Conference on Multimedia and Expo, vol. 2, pp. 931-934., 2004.

[24] Wong, Ping Wah. "A public key watermark for image verification and authentication." International Conference on Image Processing, vol. 1, pp. 455-459. IEEE, 1998.

[25] Chang, Y-F., and W-L. Tai. "A block-based watermarking scheme for image tamper detection and self-recovery", Opto-Electronics Review, vol. 21, no. 2, pp.182-190, 2013.

[26] Holliman H, Memon N., "Counterfeiting attacks on oblivious block-wise independent invisible watermarking schemes", IEEE Trans Image Process, vol. 9, pp.432–441, 2000.

[27] He, Hong-Jie, Jia-Shu Zhang, and Heng-Ming Tai. "Self-recovery fragile watermarking using block-neighborhood tampering characterization." In International workshop on information hiding, pp. 132-145. Springer, Berlin, Heidelberg, 2009.

Proceedings of the Fourth International Conference on Communication and Electronics Systems (ICCES 2019)
IEEE Conference Record # 45898; IEEE Xplore ISBN: 978-1-7281-1261-9

Data Deduplication with Encrypted Big Data Management in Cloud Computing

Nahlah Aslam K.P.
Department of Computer Science & Engineering
Govt. Engineering College Thrissur
Thrissur, Kerala
Email : nahla057@gmail.com

Dr. Swaraj K.P.
Department of Computer Science & Engineering
Govt. Engineering College Thrissur
Thrissur, Kerala
Email : swaraj.gec@gmail.com

***Abstract*—Cloud storage service is an efficient solution for increasing storage needs of organizations and individuals. In order to ensure security and data privacy, users may encrypt their data before uploading to cloud. In such cases same or different users may up-load same data in encrypted form and it results in the existence of duplicated data. Data deduplication is a technique designed to identify and eliminate redundant data. When users are uploading data in encrypted form, then deduplication is a challenging problem. This project proposes a deduplication system in cloud storage that supports big data deduplication also. The sytem is based on symmetric encryption and re-encryption. The system aims at paragraph-level deduplication of text data files. A token will be generated for each paragraph in a file before uploading to cloud. When a new request for uploading is received, system checks the existence of duplicate files using these tokens. If the file is already exists in the cloud, then system rejects uploading, else system will perform deduplication using re-encryption algorithm.**

Keywords: Cloud Computing, Data De-duplication, Re-encryption.

I. INTRODUCTION

Cloud computing is the on request accessibility of resources, mainly storage of data without direct involvement of user. Cloud storage deliver resources to users over internet. Clouds which are larger in sizes have functions which is distributed over more than one location from central servers. Clouds are of different types. Some are restricted to a single company or organization and it is called enterprise clouds. Some are available to more than one organizations and they are called public clouds and some are combination of both public and private clouds and they are called hybrid clouds. Amazon AWS is the largest among public cloud.

High-capacity networks, economical computers and storage services results in the rapid growth of cloud computing. Cloud computing mainly aims at making the resource sharing economical. By linking together resources over network cloud computing delivers wide collection of information sources to users. Cloud computing provides data processing services to users by offering data storage, computing and so forth. It offers a large collection of data sources by combining resources over a network. It should possess some attributes namely, adaptability, flexibility and fail resistance.

A cloud service provider can retrieve the data contained in the cloud at anytime. Because of this cloud computing has some security problems[9],[13]. The information stored in cloud can get modified or deleted by any other user. In some cases, cloud users may have to share their data with third parties because of some law purposes. In such cases, users will be informed about this in the privacy policy and users can start using cloud services only if they are agreed to it.

Anyway in order to stop unauthorized retrieval of data, users can encrypt their data before storing to cloud[8]. Based on the report of Cloud Security Alliance, main security threats in the cloud are hardware failure, data loss leakage and insecure interfaces [10]. In a cloud storage information belongs to different users are placed on same server. Hackers are ready to spend large amount of time to retrieve all this information. Because a large cloud may contain information of many companies and by attacking this information hackers can get control of these companies and it is termed as hyper jacking[12]. Some examples of such attacks are icloud 2014 leak and Dropbox security breach.

A. Data deduplication in cloud

Presence of duplicated data is a crucial problem in cloud computing. Storage of same data more than once is termed as data duplication. Storing duplicated data results in the wastage of storage space. Even though cloud has large memory, duplicated information results in disuse of large memory and make data processing complex. As a result, deduplication turned out to be vital in cloud data processing. Deduplication aims to lower storage expenditure. This saving will make the cloud more profitable. Governing encoded information with deduplication is a significant issue.

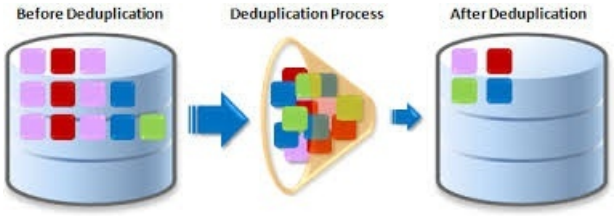

Fig. 1: Data deduplication

Data deduplication is refered as the technique to identify and eliminate redundant data. Many solutions are there for

deduplication of raw data. But in order to ensure security users may save their data in encrypted form in cloud. In such cases deduplication need to be implemented on encrypted data. Deduplication of encrypted data is a challenging issue.

Data deduplication is one of the hottest technologies in storage right now because it enables companies or users to save a lot of money on storage costs to store the data and on the bandwidth costs to move the data. This is great news for cloud providers, because if you store less, you need less hardware. If you can deduplicate what you store, you can better utilize your existing storage space, which can save money by using what you have more efficiently. If you store less, you also back up less, which again means less hardware and backup media. If you store less, you also send less data over the network in case of a disaster, which means you save money in hardware and network costs over time. It is proved that deduplication in cloud results in high cost savings because it can reduce up to 90-95% storage needs for backup applications [6] and up to 68% in standard file systems [7]. These storage savings will benefit cloud users and cloud business.

At a high level, the deduplication process works using software that eliminates redundant data and storing only unique first instances of any data. Any other copies of the same data found by the software are removed, and in their place will be a pointer or reference to the original copy. The deduplication process is transparent both to end users and the applications they use.

Drilling down into the process more, deduplication software typically generates unique identifiers for data using cryptographic hash functions. Deduplication at the file level is inefficient because even if a minuscule part of a file is altered, such as a single bit, a whole new copy of that file will be stored. So this work aims at block-level deduplication on file contents.

The rest of this paper is as follows: Literature survey is discussed in Section 2. Section 3 describes the architecture and different modules of the deduplication system. Section 4 discusses the result. Finally, Section 5 is the conclusion with brief description about the present findings and future direction.

II. RELATED WORKS

Many mechanisms have been developed for deduplication on encrypted data in cloud. Each of them differs in their approaches.

Mihir Bellare, Sriram Keelveedhi and Thomas Ristenpart [1] proposes the primitive method for deduplication on encrypted data, Message Locked Encryption (MLE). As the name implies, in MLE the message is locked under some key. As the key for encryption is derived from message itself, same key is used to encrypt similar messages. So it is easy to recover key used for encryption. This scheme is not resistant to brute-force attack.

Mihir Bellare, Sriram Keelveedhi and Thomas Ristenpart [2] proposes a system architecture that supports secure deduplicated storage which resists brute-force attacks, and realize it in a system called DupLESS. In DupLESS, a group of affiliated clients (e.g., company employees) encrypt their data with the aid of a key server (KS) that is separate from the SS. Clients authenticate themselves to the KS, but do not leak any information about their data to it. As long as the KS remains inaccessible to attackers, system ensure high security. Although DupLESS provides resistance to brute force attacks, it is suitable only for small-sized data.

Xue Yang, Rongxing Lu, Kim Kwang Raymond Choo and Xiaohu Tang [3] proposes another system for deduplication of data. Main aim of this mechanism is to reduce the time taken for search of redundant data. For that this mechanism constructs a decision tree for removal of redundant information and this tree is built based on binary search tree. In this system two companies or organization can have direct agreement with cloud and each client should be afliated with any of those two domain. Each organization or domain will have separate decision tree. After receiving files, cloud will create a decision tree to save these files and this tree is used to check whether newly received file is already existing or not. Result shows that deduplication using decision tree can reduce time complexity of duplicate search significantly.

Xin Tang, Linna Zhou, Yongfeng Huang and Chin-Chen Chang [4] designs a system for removal of redundant data from encrypted information. The working of this system is based on symmetric encryption and Proxy Re-Encryption (PRE). Main merit of this system is that it supports deduplication of big data. This system aims at file-level deduplication. So even a file with small difference with another file will be uploaded as a new file.

From the above methods , it is clear that deduplication on encrypted data is a challenging issue, especially when data size is large. The major problems in existing deduplication systems are listed below:

- To ensure data security and user privacy, data will be stored in an encrypted form to cloud.
- Many of the existing system do not support deduplication on encrypted data especially big data.
- Many of the existing system is not resistant to brute force attack [1],[5].
- Existing system supports only file-level deduplication.
- Secure deduplication in cloud is an arising challenge.

Deduplication on encrypted data is a challenging issue, especially when data size is large[11]. The proposed system aims at a deduplication system which supports block-level deduplication on encrypted files and is resistant to brute force attack.

III. PROPOSED DEDUPLICATION SYSTEM

This project proposes an efficient deduplication system in cloud that supports big data deduplication also. It is resistant to brute force attack and it also manages the storage with deduplication without the direct involvement of data holder. The working of the system is mainly based on paragraph-wise token generation of text data, symmetric encryption and re-encryption to manage encrypted data storage with deduplication.

A. System Architecture

The system contains three entities. They are:

- User: Users transfer and save their data in cloud.
- Authorized Party: The responsibility of authorized party(AP) is to manages deduplication of information.
- Cloud Service Provider (CSP): All uploaded files will be saved in cloud.

The general architecture of the proposed system is shown in figure 1.

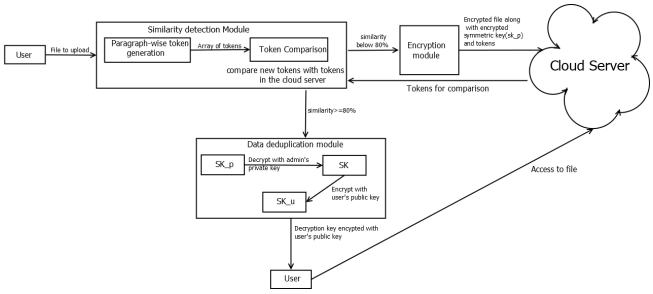

Fig. 2: System Architecture

B. System Modules

The system mainly consists of three modules:

- Similarity detection module - A hash value or token will be generated for each paragraph in a file before uploading to cloud server. These tokens are used for detecting similarity between files.
- Encryption module- If a file shows no similarity to existing files in server, then that file will be encrypted using symmetric encryption method before uploading to cloud server.
- Data deduplication module- When a user is sending duplicate file to cloud server, uploading will be rejected and access to already existing file will be granted to user.

1) Similarity detection: Cloud server will contain some files and corresponding tokens. Tokens are generated for each paragraph in the file using any standard hashing algorithm. When a new file is coming to the system, that file will be split into paragraph using regular expression and tokens will be generated for each paragraph. These newly generated tokens will be compared to tokens corresponding to each file in the cloud server, which has almost similar size of new file.

This comparison is done using retain all() function in java. The retain all() function retains same tokens among newly generated tokens and already existing tokens in the cloud server. If this function returns no to-kens, then it means that there is no similarity and file can be uploaded, so system will go to file encryption module.

If the retain all function returns some tokens, then we take the number of tokens it returned corresponding to each file and the calculate the percentage of similarity the new file shows to that particular file. Similarity percentage can be calculated by:

$$similarity\ percentage = \frac{number\ of\ common\ tokens}{total\ number\ of\ tokens\ in\ new\ file} * 100 \quad (1)$$

The system takes the highest similarity percentage and if it is greater than or equal to 80%, uploading of new file will be rejected and access to the file to which the new file shows highest similarity should granted to new user. To grant access to already existing file, the system will move to data deduplication module.

2) Encryption module: When a user is sending any file to system to get uploaded, the system checks if that file is already existing or not. If the system found that such a file is not existing, then system encrypts that file using symmetric encryption and uploaded to server. The system randomly generates a symmetric key each time a new file is encrypting and this symmetric file will be encrypted with admins public key to get cipher key and this cipher key will be uploaded to server along with the encrypted file and corresponding tokens.

Symmetric Encryption:

- In this encryption technique, a symmetric key which is created by using any standard key generation algorithm and message to be encrypted is given as input. The algorithm encrypts that particular message using the given key and creates cipher message.
- User perform this operation to make their message secure from illegal access.
- This encrypted message can be decrypted using same key which is used for encryption.
- User perform this decryption to decrypt the encrypted data saved in cloud.

3) Data deduplication module: When a client is sending a file which is similar to another file pre-stored by another client, duplication happens. At this time cloud contacts AP to stop uploading of redundant file by granting access to already existing copy of this file to new user. AP allow new user to access duplicate data by providing decryption key of already existing file to new user. AP provide the decryption key to new user using re-encryption algorithm. The overall procedure in this module is explained below.

Deduplication process:

- This process can be described as tuple (E,R,KG,D), in which each element is algorithm.
- Here KG represents standard algorithm for generating keys, E represents algorithm to create encrypted form of input data using the input key and D represents algorithm to create decrypted form of encrypted data which is given as input using the given decryption key.
- Key generation algorithm will produces private key and public key for a particular user.

- The above generated public key and a message will be given as input to encryption algorithm and it creates a ciphertext $C_A = E(pk_A; M)$.
- Then the private key and ciphertext will be given as input to decryption algorithm and it creates the decrypted message $M = D(sk_A; C_A)$.
- R represents re-encryption algorithm. In this algorithm output of E, corresponding decryption key and another public key and private key pair will be given as input.
- Initially the R algorithm will decrypt the cipher key, which is the output of E with its decryption key and this decrypted key will again encrypt using new public key and return.
- The R algorithm will return this re-encrypted key and new private key to D. And the D algorithm will decrypt the re-encrypted key using the given private key and return to user.
- Here, In this system the symmetric key used for file encryption is given as input message to the encryption algorithm and admin's public key is given as key.
- So the output of encryption will be $ck = E(pk; K)$. Where,
  - K is symmetric key for file encryption
  - pk is admin's public key
  - ck is encrypted key or cipher key
- When a new user need to access this symmetric key K, system will go to re-encryption algorithm.
- Here, the R takes as input ck, sk, pk_1 and sk_1. where,
  - sk is admin's private key
  - pk_1 is new user's public key
  - sk_1 is new user's private key
- Initially, R will decrypt ck using sk to produce K. That is, $K = E(pk; ck)$.
- Then this k will be re-encrypted using pk_1 to produce re-encrypted key rk. That is, $rk = E(pk_1; k)$.
- Then this rk will be return to user.
- User can decrypt rk using sk_1 to produce symmetric key. That is, $K = D(sk_1; rk)$.
- Now the user can decrypt the file using symmetric key K.

4) System Procedures:

- Step 1 - System setup: For authorized party(Admin) and each user, a public key and private key pair is generated randomly using any standard keypair generation algorithm. Admin's public key is broadcasted to all users.
- Step 2 - Data token generation: A token will be generated for each paragraph in a file using any standard hashing algorithm.
- Step 3 - Duplication check: User u_1 send a file M to CSP. CSP checks if the duplicated data is stored by finding whether the tokens for M already exists or not. If the check is negative, the file M is encrypted with randomly generated symmetric key DEK_1 and DEK_1 is encrypted with admin's public key (pk_{AP}) to get cipherkey (CK_1). This encrypted file, corresponding tokens and CK_1 will be saved in cloud server. If the check is positive refer to Step 5 for deduplication.
- Step 4 - Duplicated data upload and check: User u_2 later on tries to save the same data M at CSP following the same procedure of Step 2 and 3, Duplication happens and CSP informs it to AP.
- Step 5-Deduplication: CSP decrypts (CK_1) using admin's private key and re-encrypt it using u_2's public key pk_2 and return this re-encrypted key to u_2. Then u2 can get DEK_1 with its private key sk_2.

At this moment, both u_1 and u_2 can access the same data M saved at CSP. User u_1 uses DEK_1 directly, while u_2 gets to know DEK_1 by decrypting it with sk_2.

IV. Results And Discussion

The proposed system was coded and implemented in Java using Eclipse IDE and database is created in MySQL. Text files, word files and pdf files of different size is given as input for result analysis.

A. Similarity detection

Time taken for this phase includes,

- Time for token generation
- Time for token comparison

For token generation SHA-256 hashing algorithm is used here. MD5 and SHA is the prominent method for generating hash values. For unstructured files SHA is better in terms of operation time. Table 1 shows the difference in timetaken for MD5 and SHA-256.

TABLE I: Difference in time taken for hashing using MD5 and SHA-256

Size of file	MD5 Time taken (ms)	SHA-256 Time taken (ms)
12.4KB	843	838
18.2KB	865	861
1MB	987	963
13.6MB	1184	1132
38.6MB	2318	2213
901MB	3459	3129

Table II shows the time taken for similarity detection between text files, word files and pdf files of different sizes.

TABLE II: Time taken for similarity detection

File Size	File Extension	No. of files with similar size	Total No. of Tokens	Execution Time
1 MB	txt	5	3940	4 s
3 MB	txt	5	16021	5 s
5 MB	txt	5	23941	8 s
1 MB	doc	5	9971	6 s
3 MB	docx	5	14760	8 s
1 MB	pdf	5	7719	36 s
3 MB	pdf	5	5161	51 s
5 MB	pdf	5	10381	63 s

B. File Encryption

In this system symmetric encryption is used for file encryption. AES-128 encryption is used here.Table III shows time taken for encryption for different file types.

TABLE III: Time taken for file encryption

SIZE	FILE EXTENSION	TIME
1MB	txt	3s
3MB	txt	3s
5MB	txt	3s
1MB	doc	2s
5MB	doc	3s
10MB	doc	3s
1MB	pdf	3s
3MB	pdf	3s
5MB	pdf	4s

From the above comparison tables, it is clear that AES encryption is not much time consuming. There is not much variation in execution time with increase in the file size. For similarity detection, operation time is increasing with increase in file size. For text files and word documents, there is no considerable increase in time. But for pdf file there is much variation in execution time with increase in file size.

The file uploading process, recovering decryption key and database updation takes only some nanosecond time.

Below figure shows the view of database.

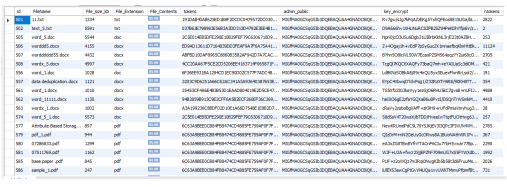

Fig. 3: Database containing files

V. Conclusion

In a secure and well organized cloud storage, removing redundant data has got much importance. Particularly in case of big data storage, removing redundant information will greatly improve utilization of space. Day by day need for cloud services for storing large amount of data is increasing and as a result need for efficient deduplication technique is also arising. Huge data load on storage systems are emphasizing the focus on development of novice techniques to remove duplicate data. With the evolution of data deduplication and its various techniques, cloud computing has potential to remove unnecessary duplicates. Deduplication is an important technique for reducing storage cost, bandwidth and energy consumption.

Many of the existing system aims at file level deduplication and does not support deduplication on encrypted data. So this work aims at block-level deduplication on file contents. The proposed method is capable to find percentage of similarity among files. System perform deduplication on files which shows 80% or above similarity to already existing files. The security of the proposed system is ensured by symmetric key encryption and re-encryption theory.

In Future, this system can be expanded to manage the storage with deduplication when there is any updation or deletion of files and implementing Map Reduce algorithms to reduce execution time. Also the system can be expanded to perform deduplication on other medias such as audio, video and images.

Acknowledgments

I would like to thank Dr, Swaraj K.P. for providing a valuable assistance to complete this research work.

References

[1] M. Bellare, S. Keelveedhi and T. Ristenpart *"Message-locked encryption and secure deduplication"*
In Advances in Cryptology - EUROCRYPT 2013, 32nd Annual International Conference on the Theory and Applications of Cryptographic Techniques, Athens.

[2] S. Keelveedhi, M. Bellare, and T. Ristenpart *"Dupless: Server-aided encryption for deduplicated storage"*
In Proceedings of the 22th USENIX Security Symposium, Washington, DC, USA, August.

[3] Xue Yang, Rongxing Lu, Kim Kwang Raymond Choo and Xiaohu Tang *"Achieving Efficient and Privacy-Preserving Cross-Domain Big Data Deduplication in Cloud"*
IEEE Transactions on Big Data, 2017

[4] Xin Tang, Linna Zhou, Yongfeng Huang and Chin-Chen Chang *"Efficient Cross-User Deduplication of Encrypted Data through Re-Encryption"*
2018 17th IEEE International Conference On Trust, Security And Privacy In Computing And Communications/ 12th IEEE International Conference On Big Data Science And Engineering.

[5] Z. O. Wilcox *"Convergent encryption reconsidered"*
2011 [Online]. Available: http://www.mailarchive.com/cryptography@metzdowd.com/msg08949.html

[6] Opendedup. (2016). [Online]. Available: http://opendedup.org/

[7] D. T. Meyer and W. J Bolosky *"A study of practical deduplication"*
ACM Transaction on Storage, 2012

[8] C. Liu, C. Yang, X. Y. Zhang, and J. J. Chen *"External integrity verification for outsourced big data in cloud and iot: A big picture"*
Future Generation Computer Systems, 2015.

[9] C. W. Tsai, C. F. Lai, H. C. Chao, and A. V. Vasilakos *"Big data analytics: A survey"*
Journal Big Data, 2015.

[10] W.Sharon Inbarani, C.Kumar Charlie Paul, W.Andrew Jerome Jeevakumar *"A Survey on Security Threats and Vulnerabilities In Cloud Computing"*
International Journal of Scientific Engineering Research, 2013.

[11] Zheng Yan, Wenxiu Ding, Xixun Yu, Haiqi Zhu and Robert H. Deng *"Deduplication on Encrypted Big Data in Cloud"*
IEEE TRANSACTIONS ON BIG DATA, VOL. 2, NO. 2, APRIL-JUNE 2016.

[12] Krishna Chaitanya.Y, Bhavani Shankar.Y, Kali Rama Krishna.V, V Srinivasa Rao *"Study of security issues in cloud computing "*
International Journal of Computer science Trends and Technologies, 2011.

[13] M. Ali, S. U. Khan, and A. V. Vasilakos *"Security in cloud computing: Opportunities and challenges"*
Journal of Information Sciences, 2015.

Proceedings of the Fourth International Conference on Communication and Electronics Systems (ICCES 2019)
IEEE Conference Record # 45898; IEEE Xplore ISBN: 978-1-7281-1261-9

Controller Area Network (CAN-Bus) Packet Filtering Firewall – A Survey

Sahana Y P
Digital Electronics and Advanced Communication
Manipal Academy of Higher Education
Karnataka, India
sahanaprakashyarnool@gmail.com

Ajey Gotkhindikar
Subject Matter Expert
Automotive Cybersecurity
KPIT Technologies Ltd, India
ajey.gotkhindikar@kpit.com

Shailendra Kumar Tiwari
Department of ECE
Manipal Academy of Higher Education
Karnataka, India
sk.tiwari@manipal.edu

***Abstract*— The world is moving towards autonomous vehicles and the vehicle is exposed to various types of communication, like Vehicle-to-vehicle (V2V), Vehicle-to-Grid (V2G) and Vehicle-to-Everything (V2X). This communication facilitates telematics, diagnostics and over the air software update features. The vehicle is also connected via various interfaces like Wireless Fidelity (Wi-Fi), Bluetooth (BT), Universal Serial Bus (USB), and On-board Diagnostics (OBD) to the external world for various purposes. This opens possibility for several cyber-attacks through external ports, network interfaces if there are no adequate cyber security mechanisms implemented, and cybersecurity risks are not treated. Controller Area Network (CAN-bus) is a central nervous system of the modern vehicle and most of the in-vehicle communication takes place on it. Unfortunately, the CAN-bus is inherently insecure and lacks basic security features like authentication and encryption. The insecure nature of CAN-bus in a vehicle lead to several security exploits and malicious activities which put driver and passengers at risk. Therefore, security measures need to be implemented in the automotive network.**

This paper addresses CAN vulnerabilities, critical attacks on CAN and security measures to protect CAN bus such as cryptographic measures, firewall and methods to detect and prevent such attacks. Certain approaches have been identified and we are going to discuss these approaches in this paper. However, this paper attempts to bring together essential background knowledge required to work on security for CAN network in automotive embedded systems.

Keywords*— *CAN Vulnerabilities, Attacks on CAN, Security Measures, Packet filtering firewall, Binary Decision Diagram-BDD.

I. INTRODUCTION

In the past two to three decades vehicles are becoming more advanced, more autonomous, more complex in terms of automotive electronics. An embedded system that controls an electrical subsystem is called an Electronic Control Unit (ECU) in a vehicle. There are more than 70 ECUs in a modern car which provides entertainment, navigation, central locking mechanisms, and other safety systems like adaptive cruise control, automated lighting, anti-lock braking system, airbag control, traffic warnings, Collision avoidance etc. There should be quick and reliable communications between these electronic modules for the normal operation of the vehicle. The electronic control modules, the sensors, actuators, and other devices communicate through the in-vehicle networks like Controller Area Network (CAN), FlexRay, Local Inter Network (LIN), and Media Oriented Systems Transport (MOST) as shown in the Fig.1 and Ethernet for higher bandwidth. CAN protocol is considered as a de-facto communication standard for various electronic control units to communicate between sensors, and other devices. As the cars get exposed to the outside world through the internet connectivity, Bluetooth wireless link to connect cell phones to have hands-free calls and Telematics functionalities, this results in increased number of attacking surfaces and entry points for hacking. There is no source identifier or authentication and encryption built into CAN packets. Because of these shortcomings, it is easy to sniff the CAN packets on the network as well as to masquerade as other ECUs and send CAN packets. Therefore, security measures need to be implemented in the automotive network. Firewalls can be considered as the first line of defense and restrict malicious CAN packets entering the in-vehicle network from the external world.

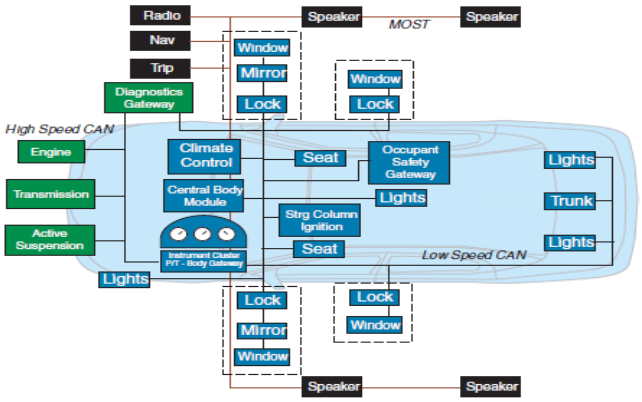

Fig.1. Typical Automotive Network [1]

This paper is divided into different sections as follows. Section I, Introduces the In-vehicle network. Section II is focused on CAN protocol format, CAN vulnerabilities and critical attacks on CAN. Mitigations and security approaches are explained in

Section III and also introduce firewall, its types and the significance of the firewall. The literature survey is focused on firewall technologies which are explained in the Section IV.

II. BACKGROUND

A. *Controller Area Network protocol (CAN-bus)*

In 1985, Robert Bosch developed a serial bus communication protocol for the in-vehicle network called CAN-bus. The protocol was officially released at the Society of Automotive Engineers (SAE) conference in 1986, Detroit, Michigan [2]. There are several versions of the CAN specification were published. There are two parts PART-A and PART-B in the latest standard 2.0 published by the Bosch in 1991. Part-A is for the standard format with an 11-bit identifier CAN 2.0A and Part-B is for the extended format with a 29-bit identifier CAN 2.0B [3]. The CAN standard and extended format are shown in Fig.2.

ISO 11898 standard is released by ISO (International Society of Organization) in 1993 and divided into two parts. The CAN protocol defines the lowest two layers of OSI (open system interconnect) data link layer (ISO 11898-1) and physical layer (ISO 11898-2) for high speed CAN. Later ISO 11898-3 is released, which is for the CAN physical layer for low speed and fault tolerant CAN. In 2012, Bosch released CAN FD 1.0 (CAN with Flexible Data-Rate), which was developed to meet the automakers demands for more accurate and for real-time applications, this is designed for transmitting and record data along with errors between devices and microcontrollers without the help of host computer This specification has different formats which allow different data lengths and for operating with a faster bit rate once the arbitration is decided.

As the CAN-FD is compatible with present CAN 2.0 specification, CAN FD devices can be connected on the same network along with CAN 2.0 devices. There are several CAN-based higher-layer protocols that are standardized. The user choice is according to the application. These are used in a variety of applications including industrial automation, autonomous devices, defense and underwater vehicles and medical equipment. CAN protocol is a message based and it is denoted as a Carrier Sense Multiple Access/Collision Avoidance (CSMA/CA), where the protocol listens to other nodes in the network for avoiding collisions. The CAN also contain error detecting and error handling methods. It can handle bit rate up to 1 Mbps when the physical distance between the nodes is less than 40m within the network. Four different message formats are present in CAN, they are data, remote, error and overload frames.

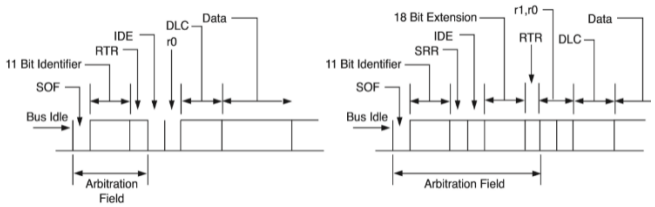

Fig.2. CAN message frames [1].

The CAN data frame is explained in detail and is as shown in the Fig.3.The data frame begins with the Start-of-frame (SOF) bit which is of the single dominant bit, next is arbitration field which consists of eleven-bit Identifier and RTR-bit (Remote transmit request). The RTR-bit must be ‘dominant' in the data frame and ‘recessive' in the remote frame. Followed by the control field which includes data length code (DLC) and two bits for future expansion are reserved. The data length code is four-bit wide which defines how many bytes of data is present in the data field. The data field can be zero to eight bytes of data. The data field is followed by cyclic redundancy checksum (CRC), which enables the receiver that the data received is not corrupted. Acknowledge field (ACK) contains two bits and these will be ‘recessive' at the transmitting station. It is replaced by a dominant bit by the receiver to acknowledge that it received the valid message. Both Data frame and Remote frame ends with EOF (End-of-frame) which contains a flag sequence of seven recessive bits.

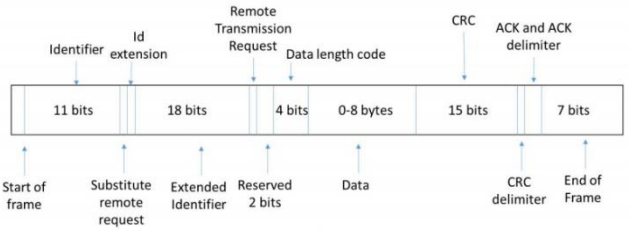

Fig.3. The CAN message format

B. *Arbitration*

As stated earlier, messages are identified by the static identifier (ID). All messages are transmitted over the bus based on the priority. The priority of the messages resolved by the arbitration. The conflict occurs whenever two or more transmitting nodes are sending messages over the same network and at the same time. Arbitration helps to overcome this conflict. Messages with lower Arbitration ID will get the bus and the message transmitted. Arbitration is handled by CAN transmitter. By comparing the value being processed and the value on bus, CAN transceiver checks both the values. If the values are same then it continues transmission else stop transmitting. The transmitted value is AND’ed bit wise with value on the bus. So, the transmitted value is 0 and the bit on the bus is 1, the result zero will be transmitted. Thus, the lower value node wins the arbitration. Due to arbitration DoS type of attack is possible if an attacker send high priority messages for an example sending sequence of dominant bit ‘0’. The bus will not be available for other ECUs to transmit messages and this may affect the normal operation of the vehicle.

C. *CAN Vulnerabilities*

The lack of inherent security mechanism of CAN lead to attacks from physical attack surfaces through OBD port and from wireless attack surfaces such as GPS, GSM module, Bluetooth and Wi-Fi. Various attacking surfaces are shown in

the Fig.4. Table1 gives the summary of vulnerabilities, different possible attacks and security measures for CAN network.

Table 1: Summary of violated security aspects, potential attacks and security measures (to CAN network)

Violated Security aspects	Vulnerabilities of CAN protocol	Possible Attacks	Security Measures
Confidentiality/privacy	Message broadcasting	Eavesdropping	Encryption algorithms
Integrity	Lack of authentication/ addressing	Sniffing/Spoof	Cryptographic hash functions, MAC or Digital signatures
Authenticity	Lack of authentication	Masquerading	MAC or Digital signatures
Availability	Lack of addressing/authentication	Replay, Injection, flooding/DoS attacks	IDS, IPS and Firewalls
Non-Repudiation	Encryption	Sniffing	Forensics support

Weakness of vehicle security arise from the widely used CAN is highlighted in [4], and it is listed below

- Message Broadcasting: Once the message is sent on the CAN bus it is present at every node of the network. Any node or controller has access to it can accept or reject. A passive attacker can read a message by having access from the diagnostic port or by inserting a malicious node on the CAN bus. Eavesdropping can take place which is kind of sniffing on the network.
- Lack of addressing: Nodes in a typical CAN network does not have identification address, all nodes (real or malicious) can send and receive information anytime inside the network without the verification that a source of the information is valid.
- Lack of Authentication: As the source authentication is not present, it is not possible to ensure if message received from valid source. Therefore masquerade attack takes place, in which an attacker acts as an authorized user of the system.
- A common point of entry: Once an attacker gains access to the CAN network, there is no limit that what are the parameters they can obtain within the network. Diagnostics port is the common gateway to the in-vehicle network where all the systems connected. Example OBD-II port provides access to all the systems.
- Limited Bandwidth: Complex authentication or security algorithms requires more bandwidth and processing power for robust communication. But, CAN with 11-bit and 29-bit identifier message structures provides only 64-bit of data in payload and less data for security purposes. The complex authentication algorithms could not be implemented on CAN bus because of the limited bandwidth.
- Lack of Encryption: The robust encryption could not be implemented as there is no higher bandwidth is available in the present CAN bus. For a few sensitive messages and security-related protocol need protection against eavesdroppers. Encryption is necessary for critical data exchange between any two in the CAN network.

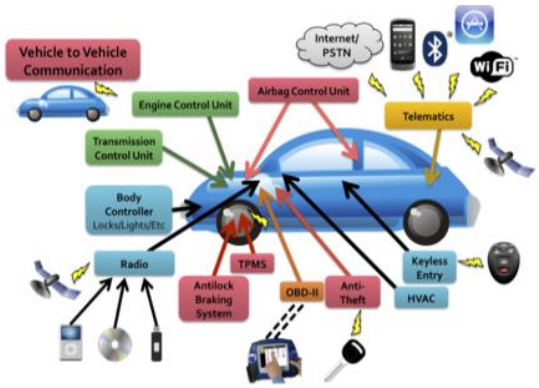

Fig.4. Possible entry points of the modern car [4].

D. Critical attacks on CAN

- Replay attack: The attack in which the transmitted data is delayed or repeated maliciously. Masquerade attack is followed by a replay attack where it needs to pretend to be some other node and retransmits the copy of the message it has received from the CAN bus. The copy of the message may be unaltered or modified. Even though there are tables to match the message id to the sender and determine the identity of the sender at the other nodes but there is no concept to authenticate it. Aruljothi and Priyadarshini [5], have demonstrated a practical wireless attack using a real vehicle in a connected vehicle environment, and they also propose a security protocol for CAN as a countermeasure designed in accordance with current CAN specifications with RKP(random key pre-distribution).
- Injection: In this attack, injecting malicious message on the network appearing to be legitimate. It involves disturbing normal operations of the vehicle. This attack can be done by the node in the trusted network. Any node can send any message in the CAN network.
- Denial of Service (DoS): DoS is a cyber-attack in which the resources are unavailable to intended users temporarily or to damage permanently and weakening the performance of the system. Flooding the network with higher priority messages by sending the sequence of dominant bits continuously. By inducing too many errors to the target node or device where the node on CAN bus goes to so-called bus-off state and removed from the CAN bus so it cannot send or receive further messages. Doing this can disable a device (e.g. critical safety systems) and compromises certain vehicle functionalities. Murvay and Groza [6] have explained about DoS attacks at different layers of

CAN protocol. Concentrated more on DoS attacks of Data link layer as it's very difficult to mitigate with application layer mitigations techniques.

- Man-in-Middle attack: Secretly, an attacker receives and pass the message and alters communication between two nodes for a certain period. Robert Buttigieg et al [7] have explained how the rogue device is inserted in CAN network as a man in middle attack using Proof of Concept (POC) by instrument cluster and vehicle simulator. The main aim of their project was to look into the lack of security in the CAN-Bus protocol, in particular, the lack of authentication of devices and the lack of data encryption. This experiment focused on the possibility that an unauthorized man in the middle device can be connected to the CAN-Bus with the ability to send spoofed messages.

III. SECURITY APPROACHES

A. *Authentication*

There is a possibility of changing the program of an authorized node and spoof the messages on the CAN network and also add a rogue device as there is no authentication. Many researchers have been working to implement effective authentication mechanism for the in-vehicle network. These measures should be implemented at every node of the network. [8] specifies use of Message Authentication Code (CMAC) for authenticating each ECU and CAN messages to prevent spoofing attack. Nicolas Bravo et al [9] proposed Public key/secret key authentication scheme for CAN by using Hash-based Message Authentication Code (HMAC). One pair of public and private keys were given to each node of the network where it shares the signed messages.

B. *Encryption*

Encryption is a cryptographic approach to hide the intelligence of the message from unauthorized users. Complete security of any information is not secured by encryption alone. Authenticity, integrity and confidentiality are ensured by using various cryptographic algorithms. Symmetric and Asymmetric are the two different cryptographic algorithms. Asymmetric algorithms such as RSA (Rivest–Shamir–Adleman), Elliptic curve cryptography (ECC) use different keys and ensures more reliability than symmetric algorithms like Advanced Encryption Standard (AES) which uses a single secret key. To meet the vehicle communication requirements such as computation, capacity, and timing, a combination of symmetric and asymmetric algorithms are used. Asymmetric encryption methods are used for secure key distribution and symmetric encryption for secure communication broadcast inside the vehicle-bus system. Public Key cryptographic techniques are more effective for securing communications with external entities including telematics, service providers and internal communications between safety-critical systems, sensors against cyber-attacks.

Cryptographic algorithms require intense computation to have effective secure communication considering acceptable latencies. Hence, to protect the confidentiality of stored keys, certificates and user credentials requires hardware support. These cryptographic algorithm requirements are beyond the resources available in typical automotive microcontrollers today. A Tiny Encryption Algorithm, Feistel type cipher was used to encrypt the message on CAN bus for a particular microcontroller and proved that this algorithm can be used to hide confidential data on the CAN bus from eavesdropping.
The confidential data like vehicle identification number or other sensitive information. This methodology was designed for a particular processor with the defined parameters by [10]. The mechanism in [11] produces a new field called CAN Message-Authenticator (CMA) which contains both the hash value and timing information which will be used to generate the hash. Authentication of each CAN messages can be done thus it can resist replay attack. Here they have considered CAN Identification Number (CIN) which is unique for each ECU in a particular vehicle. The CMA will be used to verify the legitimacy of the message by a legitimate ECU upon receipt of a frame.

C. *Software & Hardware Approaches*

Gateways in the modern car are used to connect the different networks. In order to have a secure communication between these networks, messages must be checked at the gateways before broadcasting the messages on to the networks. For example, messages from the ECUs connected to the networks like LIN and MOST should be prevented from entering into the critical-safety bus systems such as CAN and FlexRay. Firewalls can control the messages based on certain rules and rules may depends upon the ECU capabilities. Firewalls can be a best option to control the messages and it even checks the incoming network traffic.

Intrusion detection and prevention system (IDPS) can be an alternate for cryptographic techniques to regulate external and internal communications as it needs hardware support which is not beyond what is already there in typical microcontrollers present in ECUs especially to secure CAN bus. IDPS monitors the traffic of vehicle bus and detects if there are an unusual activity and initiate processes to bring back the system to safe-mode and prevent from further damage. By regulating the OBD-II port with creating hardware key or password to access the port where it is physically located can protect against illegal entry of devices into CAN. The security mechanisms are effective until it is upgraded eventually. Security software updates may be over-the-air or dealer distributive, are bound to be an integral part of security and safety of the automotive system.

D. *Significance of Firewall*

Firewalls have been the frontier defense to secure networks against attacks and unauthorized traffic by filtering out

unwanted network traffic coming into or going from the secured network. The filtering decision taken according to a set of ordered filtering rules defined based on predefined security policy requirements [12].The complexity of managing firewall policy limited the effectiveness of firewalls even though it is the main step to secure the network.

Al-Shaer and Hamed [13] have developed an anomaly-free firewall rule editor, which greatly simplifies adding, removing and modifying rules into firewall policy. They used the Java programming language to implement these algorithms in one graphical user-interface tool called the "Firewall Policy Advisor". The rule is set according to one or more different filtering fields.

There are two types of hardware and software firewall as per the user point of view. There two types of firewalls for CAN network as follows [14].

- Packet Filtering Firewalls: Static packet filtering firewalls sequence the packets concerning allow or deny. This is done by considering the field's information on the header such as host/destination address, port number. The depth analysis is not done at this stage. Each packet is examined as a single entity. It is unable to defend the fragment and spoofing attacks.
- Circuit Level Gateway Firewalls: These are deployed at the session layer. To determine the requested session is legitimate or not, Gateway firewalls monitor Transmission Control Protocol (TCP) handshake between the packets. By doing this, the public IP addresses are provided to the outside network and not exposing the internal private IP addresses to the external potential intruders. Circuit-level gateway firewalls do not filter individual packets. An attacker may take advantage of this once the connection is established.
- Application-level Gateway Firewalls: The firewalls decide to allow or drop the packets based on application information which is present in the packet and provide protection for specific application layer protocol. The best example for this kind of firewalls is Proxy server firewalls. Both the client and server are connected to these proxies instead of direct connections so any suspicious data or connections can be dropped by these proxy servers. Application firewalls do deep inspection of each session and decide to drop or allow them to pass through the proxy server by using information present in the application protocol payload or header. Application Gateway firewalls can increase the network performance and makes easier to log traffic.
- Stateful Multilayer Inspection Firewalls: The combination of all the types of firewalls listed till now is called Multilayer Inspection Firewall. These firewalls can filter packet at Network layer using Access Control Lists (ACL), identify the legitimacy of sessions at session layers and evaluates at the Application layer. This firewall can provide a transparent mode in which direct connection is available for the client and server. These can also implement algorithms and complex modules to make connections more secure.

E. Packet filtering firewall in the automotive network

The CAN and its security have become hot-topic for researchers and automakers after a number of high-profile hacking activities in the past couple of years. An attacker can have direct access to the CAN-bus through the OBD port. Charlie Miller demonstrated the vulnerabilities of the onboard computers and networks like CAN-bus by linking these onboard computers in the mid of 2010. Miller and Valasek demonstrated the car attack by altering the CAN message and controlled steering wheel by spoofing park assist [15]. The attackers created software called CarShark to monitor communications between the ECUs and insert fake packets of data to carry out attacks [16].

CAN protocol was designed concerned about reliability but not intended to provide secure communication. The embedded computers present in the cars have strong hardware constraints for computation power and memory left for security mechanisms. Because of which ECUs cannot perform complex cryptographic algorithms to perform strong encryptions. Where an attacker can have limitless hardware to perform cryptanalysis and can break simple algorithms. The security mechanism for a car should be such that its requirements should be within the constraints.

The advantage of packet filtering firewall is, firewall requires fewer resources and computation power. The data exchange with the external world can be restricted by the firewall. Even though an external device is authenticated and starts sending data or signals to the network, it is not wise to accept all those data because those external devices might be compromised. Hence there should be a firewall at the gateway which can control the access to the internal network by external devices and acts as a secondary security mechanism [17].

IV. LITERATURE SURVEY

Wolf et al [18] have given Exposures to Automotive Bus systems, Gateway firewalls and its importance. A secured approach was proposed using modern cryptography which is against manipulation and provides authentication and secrecy. This gives the best way to tackle many of the vehicle security issues.

Alex Oyler and Hossein Saiedian [19] have explained how one can compromise CAN bus and ECU through Telematics and found attacking surfaces. The device can be installed via the cellular network on OBD. Countermeasures for

this is to separate external network from the internal network by combining firewall and Intrusion Detection System (IDS) at Central Gateway System (CGS).

Tharaka et al [20] present a detailed study of firewall technologies and firewall capacity along with other firewall technologies in order to prevent unauthorized accesses. They mentioned that high capacity firewall can provide high performance but it is expensive.

Wei YAN has designed a Bi-directional firewall module which includes vehicle status logger, a CAN message filter and storage module. The storage module is used to store a White-list and a Black-list and the CAN message filter is configured selectively chooses any one of these according to the status of the vehicle [21].

Hamed Salehi et al [22] have mentioned that as soon as detecting higher priority attack by Network Intrusion Detection System (NIDS) send some recommended protection information to the firewall which will set appropriate rule to destroy the connection it. The deep inspection of six layers has been explained in this paper.

Adel El-Atawy and Ehab Al-Shaer [23] explained how rules and policies can be represented as Boolean expressions. Implementation and maintenance of this expression can get complex hence they used Binary Decision Diagram (BDD), where each variable need to be checked only once thus improving packet matching time.

Masud et al [24] have implemented a data-driven firewall. Using a classifier, first finds the packet matching to a class contains a setup of rules. Then finds a matching rule for that respective packet. The results showed that the time required for finding matching rule is six times faster than the conventional methods. In this, they used offline training data for classifier and have considered only the packet header. The last rule is with default empty condition so that any packet could match at least one rule.

Anshu Aneja & Vivek Thapar [25] have explored alternate representations for rule sets which are used to remove the redundant computation using Binary Decision Diagram (BDD) approach and implement the multi-dimensional filtering. This takes less space for storage and less look-up time for accepting or rejecting the incoming packets. They obtained average results of 75.24% and 33.74% for comparison for "Most Reject Packets" and "Most Accept Packets" respectively for about one million incoming packets. Results are shown in the Fig.5.

Dongre and Shikalpure [26] attempted to improve the rule matching time by maintaining two different files. The log file consists of information related to the captured packets recently and this is the sub set of the main file. Another file is Index file, which stores Hash values calculated for each packet. Here each incoming packet is not mapped to the main file instead succeeding packets related to the same flow are compared with the log file.

Gupta and McKeown [27] proposed a method for Packet Classification using Hierarchical Intelligent Cuttings (Hi-Cuts). The HiCut algorithm works by carefully preprocessing the classifier to build a decision tree data structure. Each time a packet arrives, the decision tree is traversed to find a leaf node, which stores a small number of rules. High dimensional (considering many fields) requiring smaller storage and comparable query time when compared with other schemes.

James Joy et al [17] presents an architecture for secure automotive communication both external and internal, by using the Smart Gateway which consists of an external and an in-vehicle gateway and a firewall. The Smart Gateway handles authentication, data integrity and secure key storage and management for both external devices connected to the vehicle as well as for the network communication between ECUs.

Pese et al [28] have shown where internal firewalls can be deployed in the E/E architecture and introduced in automotive. The Hardware (HW) firewall (located at the connectivity gateway) shall handle a large, simple and generic rule set to restrict the traffic between domains whereas the Software (SW) firewall shall focus on a small filter rule set for custom-made rules and Stateful packet inspection. Packets which pass the first layer of security (HW firewall) are shunted to the SW firewall for a deeper analysis.

Wei Si et al [29] proposed a hybrid wired/wireless protocol using Backpressure Collection Protocol (BCP) to mitigate DoS attacks by placing a ZigBee at all critical nodes which monitors link qualities and schedules packet transmission accordingly. Emerge of wireless communication into the intra-vehicular network need to face security issues such as privacy and packet spoofing.

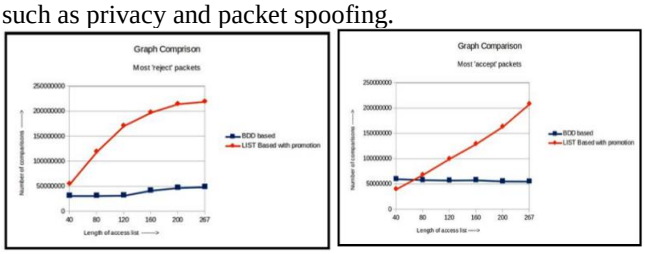

"Most Rejected packets" "Most Accepted packets"

Fig.5. Graph comparison for "Most Rejected packets" and "Most Accepted packets" [25].

V. CONCLUSION

In this paper, we give a brief introduction of in-vehicular networks and explained CAN protocol. We summarize certain vulnerabilities on CAN protocol and possible attacks on it. There are many effective cryptographic techniques to secure any network but when it comes to the automotive systems it has few due to resource constraints. IDPS can track traffic inside the network and detect the anomaly activities and prevent before it affects the system. A firewall prevents unwanted traffic from the outside network and acts as a defender at the entry level. There will be fewer chances of getting hacked if we can control the access before the data or signals enter the trusted boundary.

The effective way of securing CAN bus is to implement Packet filtering firewall at the Central Gateway. It is feasible to

implement a software firewall on the Gateway as the software need not know the developer resources and it is embedded during the ECUs software build process. Software updates can easily be done regularly during the scheduled service visit or by over-the-air updates as the firewall present on the gateway. Algorithms like BDD for packet filtering firewall requires less space for storage and lookup time to accept or reject the incoming packets by comparing the results with the listed order method. One should consider all constraints and develop a security framework for automotive system. Further research is needed to bring out the experimental results to decide which optimizing algorithms are best for the automotive systems. The background knowledge of security measures and its drawbacks depicts that the need for firewall and IDPS systems in the car to reduce attacks on CAN network.

Future work: We are motivated for the development of effective countermeasures to secure CAN bus by focusing on practical CAN based attacks in automotive systems. We are exploring ways to deploy firewall at Central gateway and concentrating on a few ECUs which exchange data between an outside world like telematics, Infotainment, and Diagnostics units. We are working on software firewall for CAN bus with framework considering resource constraints of embedded microcontrollers of ECUs at present.

REFERENCES

[1] J. A. Cook, J. S. Freudenberg, “Controller Area Network (CAN)”, EECS 461. Fall 2008.

[2] https://en.wikipedia.org/wiki/CAN_bus, Date accessed: 5/11/2018

[3] CAN Specification, Version 2.0, Robert Bosch GmbH, 1991.

[4] K. Koscher et al. “Experimental security analysis of modern automobile”, in Security and Privacy (SP), 2010 IEEE Symposium on, Oakland, CA, USA, May 2010, pp. 447–462.

[5] M. Aruljothi and C.S. Priyadarshini, "Security-Based Protocol Design for In-Vehicle Controller Area Network", International Journal of Science and Engineering Research (IJOSER), 2016.

[6] Pal-Stefan Murvay and Bogdan Groza, “DoS Attacks on Controller Area Networks by Fault Injections from the Software Layer”, In Proceedings of ARES’17, Reggio Calabria, Italy,2017.

[7] Robert Buttigieg, Mario Farrugia, and Clyde Meli, "Security Issues in Controller Area Networks in Automobiles", an 18th international conference on Sciences and Techniques of Automatic control & computer engineering - STA'2017.

[8] H. Ueda, R. Kurachi, H. Takada, T. Mizutani, M. Inoue, and S. Horihata, “Security authentication system for in-vehicle network”, SEI technical review, 81, , 2015, pp.5-9.

[9] N. Bravo, S. Koppula and M. Chang, 6.857 Final Project “A Public-Key Authentication Scheme for Controller Area Networks”, 2015, pp. 1-17.

[10] M. Jukl, J. Cupera, “Using of tiny encryption algorithm in CAN-Bus communication”, Research in Agricultural Engineering, 62(2), 2016, pp.50-55.

[11] P. Carsten, T.R. Andel, M. Yampolskiy, J.T. McDonald and S. Russ, “A system to recognize intruders in controller area network (can)”, In Proceedings of the 3rd International Symposium for ICS & SCADA Cyber Security Research. September 2015, pp. 111-114.

[12] U. Thakar, L. Purohit and A. Pahade, “An approach to improve performance of a packet-filtering firewall”, In 2012 Ninth International Conference on Wireless and Optical Communications Networks (WOCN) IEEE, 2012 pp. 1-5.

[13] E.S, Al-Shaer and H.H. Hamed, “Firewall Policy Advisor for Anomaly Detection, Rules Editing and Translation”, Integrated Network Management 2003, pp. 17-30.

[14] I. Kashefi, M. Kassiri and A. Shahidinejad, “A Survey on Security Issues in Firewalls: A New Approach for Classifying Firewall Vulnerabilities”, International Journal of Engineering Research and Applications (IJERA), 3(2), April 2013, pp.585-591.

[15] Charlie Miller, Hackers Remotely Kill A Jeep On The Highway—With Me In It. [Online] Available: https://www.wired.com/2015/07/hackers-remotely-kill-jeep-highway/.

[16] Hack attacks mounted on car control systems, [Online] Available: https://www.bbc.com/news/10119492.

[17] J. Joy, S. Samuel and V.S. Vinu, “Gateway Architecture for Secured Connectivity and in Vehicle Communication”, 16th International Congress Electronics in Vehicles, Oct 2013.

[18] M. Wolf, A. Weimerskirch, and C. Paar, “Secure in-vehicle communication”, In Embedded Security in Cars, Springer, Berlin, Heidelberg, 2006, pp. 95-109.

[19] A. Oyler and H. Saiedian, “Security in automotive telematics: a survey of threats and risk mitigation strategies to counter the existing and emerging attack vectors”, Security and Communication Networks, 9(17), 2016 pp.4330-4340.

[20] S.C. Tharaka, R.L.C. Silva, S. Sharmila, S.U.I. Silva, K.L.D.N. Liyanage, A.A.T.K.K.Amarasinghe, and D.Dhammearatchi, “High-Security Firewall: Prevent Unauthorized access Using Firewall Technologies”, International Journal of Scientific and Research Publications, Volume 6, Issue 4, April 2016, pp. 504-508.

[21] Wei YAN," Vehicle Communication System Based On Controller Area Network Bus Firewall", the United States, Patent Application Publications YAN, October 17th 2017.

[22] H. Salehi, H. Shirazi and R.A. Moghadam, “Increasing overall network security by integrating Signature-Based NIDS with Packet Filtering Firewall”, In 2009 International Joint Conference on Artificial Intelligence, IEEE, April 2009, pp. 357-362.

[23] A. El-Atawy, E. Al-Shaer, T. Tran and R. Boutaba, “Adaptive early packet filtering for defending firewalls against DoS attacks”, IEEE Communications Society subject matter experts for publication in the IEEE INFOCOM 2009, pp. 2437-2445.

[24] M.M. Masud, U. Mustafa and Z. Trabelsi, “A data driven firewall for faster packet filtering”, In Fourth International Conference on Communications and Networking, ComNet-2014 IEEE, pp. 1-5.

[25] A. Aneja and V. Thapar, “Optimizing Packet Filter Firewall using Duple Decision Scheme”, The SIJ Transactions on Computer Networks & Communication Engineering (CNCE), vol.1, issue.2, May-June 20132013, pp.28-33.

[26] S. A. Dongre, S. G. Shikalpure, “Hashing Based Packet Matching Algorithm for Firewall”, International Research Journal of Engineering and Technology (IRJET), vol.2, issue.7, Oct-2015

[27] P. Gupta, and N. McKeown, “Packet Classification using Hierarchical Intelligent Cuttings”, Proc. Hot Interconnects VII Aug. 1999 Stanford, IEEE, vol. 20 no. 1 Jan./Feb. 2000 pp. 34.

[28] M. Pese, K. Schmidt and H. Zweck, "Hardware/Software Co-Design of an Automotive Embedded Firewall", SAE Technical Paper 2017, DOI: 10.4271/2017-01-1659

[29] W. Si, K. Starobinski and M. Laifenfeld, “Protocol-compliant DoS attacks on CAN: demonstration and mitigation”, In 2016 IEEE 84th vehicular technology conference (VTC-Fall), IEEE, 2016, pp. 1-7.

Proceedings of the Fourth International Conference on Communication and Electronics Systems (ICCES 2019)
IEEE Conference Record # 45898; IEEE Xplore ISBN: 978-1-7281-1261-9

Intelligent Storage Device for Commoners

Swarnali Dey
Department of Electronics and Communication Engineering
Future Institute of Engineering and Management
Kolkata, India
dey.swarnali02@gmail.com

Amrita Dutta
Department of Electronics and Communication Engineering
Future Institute of Engineering and Management
Kolkata, India
amrita.sportivo@gmail.com

Madhusmita Mishra
Department of Electronics and Communication Engineering
Future Institute of Engineering and Management
Kolkata, India
riyamishra10@gmail.com

Subhabrata Banerjee
Department of Electronics and Communication Engineering
Future Institute of Engineering and Management
Kolkata, India
subhabrata2010@gmail.com

***Abstract*- An exhaustive investigation has been performed in the field of artificial intelligent since last few decades. Moreover, sophisticated gadgets have also been designed based on those algorithms in an efficient fashion. In this article, an intelligent model is designed to reduce food wastage and hunger problem in a competent fashion. A hardware model of a refrigerator is also made where the needy commoners can come and take food they need to fulfil their hunger. The model only responds if a human stands in front of it. If it finds any other living creature other than human is standing then it shows no response. Furthermore, system exhibits no response if same human being appears twice within next 12 hours.**

***Keywords*-** *Intelligent Storage, Object detection, Object recognition, Text to Speech Conversion Video to image processing.*

I. INTRODUCTION

Food waste is an important global issue the reasons for which are many. Only in the EU, a big amount of food are wasted annually with an associated cost estimated more than hundred billion euro. According to The Guradian, US households waste about thousand tons of food on daily basis. Every year, more than a million tons of food produced for human consumption is lost or wasted.

An intelligent and scalable detection algorithm has been proposed in [1] where "Mean Average Precision" (MAP) has been improved by more than 30% with respect to earlier outcome. Basic viewpoint of this paper combines two features i.e. efficient Convolutional Neural Networks (CNNs) and supervised trained data can be applied for segmentation purpose and application oriented fine-tuning purposes respectively. A wide range of image classification based on objective functions has been introduced in [2]. In this article a comprehensive comparison has been made among several variables like "ovens-rest, multiclass, ranking and weighted average ranking SVMs". In this paper several classification techniques have been chosen to train an independent data. Moreover, binary classifier has also been used to identify the accurate class in an efficient fashion. A detailed comparison of these high-dimensional descriptors was performed in this paper and it has been shown that the Fisher vector representation outperforms the others. Thereafter, an attempt has been made based on "Multi-scale Order-less Pooling" technique in [3]. Moreover, CNN scheme have also been applied to execute the classification of image with higher accuracy. Furthermore MOP-CNN scheme with same power has been adopted to execute the above task.

Moreover, the concept of large-scale visual recognition has been discussed in [4], where an eminent design has been adopted and as a result better performance has been achieved. In this mode Back propagation algorithm triggered CNN along with convolutional filters have been used for training purpose. Moreover, techniques like rectification and pooling have also been adopted. On the other hand an exhaustive investigation has been performed on classifier to recognize the multiple task. In this regard, an "off-the-shelf CNN" as well as "OverFeat" having least complex classifiers has been revealed in [5]. From experiment it has been shown that the structures found from deep learning triggered convolutional nets should be the principal entrant in most chromatic identification errands.

The present item uncovering approaches on these abstract interpretations of substances has been uttered in [6]. Here a comparison has been made among human annotators and numerous standard object detectors on a quantity of Picasso portraits. The Cubist painting has also been bring together as a supplementary features for entity identification. To execute the fact different entities have been reorganized in an efficient which can't be identifiable to the human. Finally real time data has been used for experimental purpose and better outcomes has been observed.

In [7] Akata, Perronnin, Harchaoui, and Schmid proposed an model which has been used for robotic clasp discovery purpose. The model has been triggered by CNN network. By adopting this method clasp

discovery along with entity identification have been performed with higher accuracy level. For this purpose two different approaches entitled as single network based entity identification scheme as well as direct envisage clasp coordinates have been used.

On the other hand "PASCAL Visual Object Class (VOC)" has been suggested in [8] where profligate deformable fragment prototype for entity identification has been considered. The speed tailback of the above mentioned structure has also ben suggested. The projected technique performs four times quicker than the preceding profligate technique on "Pascal VOC". In this article it has also been seen that the proposed scheme performs at frame-rate with higher accuracy level for "pedestrian" and aspect recognition. The limitations of the above article have partially overcome in [9]. In this article "Fast Feature Pyramids (FFP)" for entity identification algorithm with better accuracy has been presented. From result it has been seen that the proposed scheme performs significantly quicker than the earlier methods. The tactic is wide-ranging and is extensively pertinent to vision algorithms demanding Fine-grained Multi-scale" exploration.

Meanwhile, the situational object boundary detection has been described in [10]. In this article initially a wide range of situations and numerous entity boundary detector have been defined and thereafter given test images have been classified within predefined situations based on its context. Then appropriate set of object boundary detectors have been applied and run them for different test condition. This method called situational object boundary detection. Most of the approaches for entity edge discovery are inflexible as single predictor has been used to identify the entity edges without considering their contents.

A novel object detection systems has been proposed in [11] in which "Multi-Region Deep CNN" has been applied. The scheme has been proposed for encoding the semantic segmentation-conscious features. Moreover, an enriched version of CNN has been represented for accurate identification of entity. Furthermore, a thought-provoking scheme named frequently stipulating arrangements connecting with continuous variables has also been introduced. As a result real-time "object-oriented state-based specification language" has easily been pronounced. In this paper an assimilation of Object-Z with explicit symbolization of a streamlined subset of the timed fine-tuning calculus has also been presented.

Research has been continued and novel object classifier based on deep network has been designed in [12]. Usually entity identification has been performed by considering two aspects like feature extractor and an entity classifier. Most commonly usable entity identification method is HOG which is hand engineer component. Multi-layer perceptron module has been used to trigger these systems. Moreover, an exhaustive investigation has also been performed on entity identification scheme based on the perspective of classifiers aside from features.

A new perspective of object detection based on YOLO model has been proposed by Gidaris and Komodakis in [13]. The scheme described as 'You Only Look Once' or YOLO which is the profligate wide-ranging entity identifier used in real-time object detection. Form the analysis it has been seen that performance of YOLO is robust and used for identify any kind of object. Moreover, it has also been observed that better precision has been achieved by adopting YOLO model.

Inspired by above investigation an intelligent storage device has been designed in this paper. For this purpose video file has been taken as input and thereafter unique frames are identified by eliminating redundant frames. Next, adaptive intelligent algorithm has been incorporated for identifying the object and also it has been represented by speech. Then lock of the intelligent storage device has been triggered by this speech signal and lock of this device either in open or close condition.

II.SYSTEM MODEL

The unequal distribution of food has led to the existence of chronic hunger in some parts of the world. In the past decade there has been some success in combating global hunger. The aim of this work is to design an intelligent storage system for retrieval of food. The proposed system will get unlocked only when it recognizes a human being in front of it: otherwise, it remains in the locked state. The functional block diagram of the proposed system entitled is shown in Fig.1.

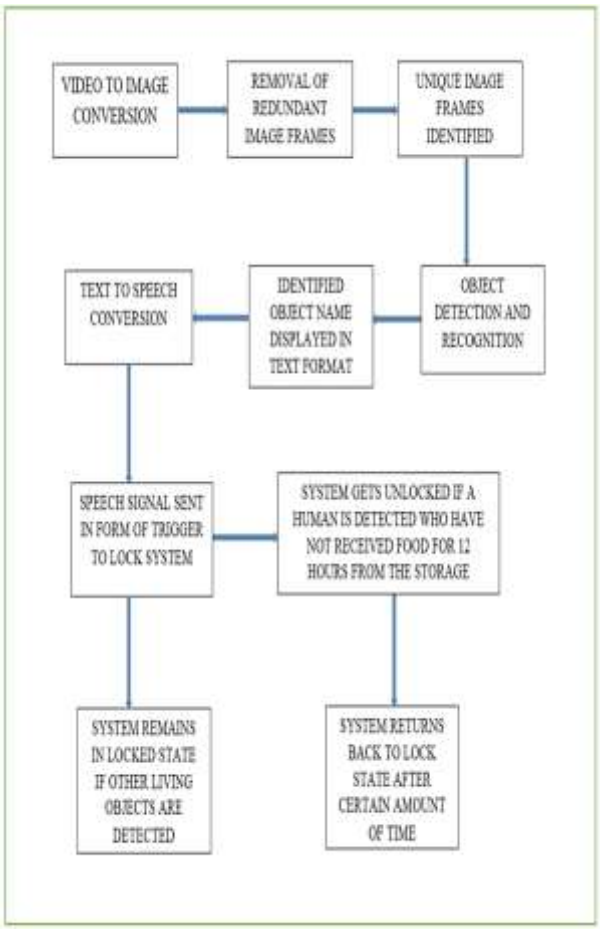

Fig.1 Functional Block Diagram of Intelligent Storage Device

From the above figure it has been seen that unique frames have been identified from the video and thereafter objects has been identified and recognized using Fuzzy K-means algorithm [13]. Next soft computation method has been applied and hence identified object has been described by text and then speech format. Thereafter system becomes lock or unlock based on speech signal which has been treated as a trigger input. After opening the door it becomes close after certain duration (here 10 ms). Moreover, the system can be in locked condition for next 12 hours for the human being who has already taken food.

III.ALGORITHM

The scarcity of food all over the world is not only due to the unequal distribution but also due to the wastage of resources. The flowchart as shown in Fig.2 describes the algorithm of designing the proposed system which will provide food to the commoners and lead to the proper usage of resources.

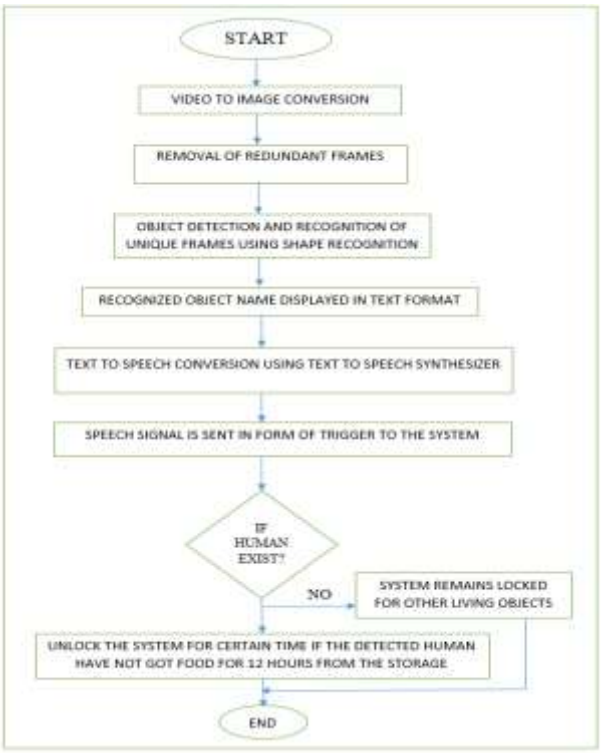

Fig.2. Flowchart of Intelligent Storage Device

From the above figure it has been seen that objects have been detected and identified from the unique frames in an intelligent fashion. Thereafter it has been displayed in text format. From the text, speech signal has been generated and then storage system has been triggered. If human is detected the lock becomes open otherwise closed. The system becomes lock for next 12 hours for the same human being who has already got food from the storage.

IV.RESULTS

The proposed intelligent storage has been implemented both in software and hardware mode. This project consists of a locking system in which the lock is open only and only if the image passes through MATLAB is detected as human. In any other case the lock has been closed. In the simulation part we have taken an image as input to check whether it is a human or not. Depending upon the identification the signal will be sent to the hardware section. Here, The MATLAB 2017b has been used as software and Arduino Uno has been used as hardware. In software section, input and corresponding output have been represented by the following figures:

```
it is a human
Current motor position is 0 degrees
Current motor position is 18 degrees
Current motor position is 36 degrees
Current motor position is 54 degrees
Current motor position is 72 degrees
Current motor position is 90 degrees
Current motor position is 90 degrees
Current motor position is 72 degrees
Current motor position is 54 degrees
Current motor position is 36 degrees
Current motor position is 18 degrees
Current motor position is 0 degrees
```

(a)

```
it is other living object
```

(b)

```
it is other living object
```

(c)

Fig.3 Input images and its corresponding outputs

From the above figures it can be easily conclude that the proposed system easily identified the human being from different types of objects and as human is detected in the image and the text is shown and the speech can also be listened.

Now as the system is able to detect the image as of a human (say Fig. 3a) and the detection will act as the trigger for the hardware system to work. So here the position of servo motor has been changed and start rotating slowly and it has been reached from 0 degree to 90 degree angle and has been stayed in that condition for a predefined time. In that time the door remains open and thus the system allows the user to take the food out from the storage system. After few seconds the motor has been stated for rotating from 90 degree to 0 degree and remains close until and unless next trigger has been sent to the hardware. These facts have been described in Fig.4.

(a)

(b)

(c)

(d)

(e)

(f)

Fig.4 Image of a Human and its corresponding hardware output

On the other hand any species other than human being have been detected door remains close as no triggering input comes in hardware circuit. This fact has been described by the following figures:

(a)

(b)

Fig.5 Image of a Dog and its corresponding hardware output

All the above facts have also been implemented in real time. Some real time captured image and corresponding output have been shown in the following figures:

(a)

(b)

(c)

Fig.6 Real time Human Image and its corresponding hardware output

However, if same person comes more than a time within next 12 hours to the storage it remains close as shown in the following figures:

(a)

(b)

Fig.7 Real time Similar Human Image within 12 Hours and its corresponding hardware output

V.CONCLUSION & FUTURE SCOPE

In this paper an intelligent storage device has been proposed for minimizing the wastage of food as well as distribution of stored food among needy commoners. For this purpose fuzzy K-means classifier has been incorporated within the system for identifying and recognizing the object in an efficient fashion. Moreover, after identifying it has been demonstrated them text as well as speech mode. If human detected door of the intelligent system becomes open due to triggering pulse otherwise it has been closed. Thereafter door becomes open for next 10 ms and then it becomes closed. However door become closed for next 12 hours for the same human being who has already got food from this storage device. The performance of the proposed system can be enhanced in different way. Some intelligent computational algorithms can be incorporated for eliminating the redundant frames. Implementation of model using sophisticated hardware like raspberry pi could be acknowledged as one of the foremost possibilities in future.

REFERENCES

[1] R. Lienhart and J. Maydt. "An extended set of haar-like features for rapid object detection", *in proceedings of International Conference on Image processing*. Sept. 2002.

[2] J. Yan, X. Zhang, Z. Lei, D. Yi, and S. Z. Li. "Structural models for face detection", *in proceedings of 10th IEEE International Conference and Workshops on Automatic Face and Gesture Recognition*. pp.1-6, 2013.

[3] J. Dong, Q. Chen, A. Yuille, "Towards unified object detection and semantic segmentation", *in proceedings of European conference on Computer Vision*, pages 299–314. Springer, 2014.

[4] R. Girshick, J. Donahue, T. Darrell, J. Malik, "Rich feature hierarchies for accurate object detection and semantic segmentation" *in proceedings of IEEE conference on Computer Vision and Pattern Recognition*, pp. 580-587, 2014.

[5] X. Zhu and D. Ramanan, "Face detection, pose estimation, and landmark localization in the wild", *in proceeding of IEEE Conference on Computer Vision and Pattern Recognition*, pp.2879-2886, 2012.

[6] Z. Akata, F. Perronnin, Z. Harchaoui, C. Schmid, "Good practice in large-scale learning for image classification" *in IEEE Transactions on Pattern Analysis and Machine Intelligence*, vol.36, pp.507-520, 2014.

[7] Razavian, H. Azizpour, J. Sullivan, S. Carlsson, "CNN features off-the-shelf: An astounding baseline for recognition", *in proceeding of IEEE Conference on Computer Vision and Pattern Recognition Workshop, pp. 512-519*, 2014.

[8] S. Ginosar, D. Haas, T. Brown, J. Malik, "Detecting people in cubist art" *in proceedings of European conference on Computer Vision*, pp. 101–116. Springer, 2014.

[9] J.Redmonand, A.Angelova, "Real-time grasp detection using convolutional neural networks", *in proceedings of International Conference on Robotics and Automation, pp.1316-1322*,2014.

[10] M. A. Sadeghi, D. Forsyth, "30 Hz object detection with DPM V5", *in proceedings of European conference on Computer Vision*, pp. 65–79, Springer, 2014.

[11] M. Everingham, C. K. I. Williams, J. Winn, and A. Zisserman, "The pascal visual object classes challenge: Aretrospective", International Journal of Computer Vision, 111(1):98–136, Jan. 2015.

[12] S. Gidaris, N. Komodakis, "Object detection via a multiregion & semantic segmentation-aware CNN model", *in Computer Vision and Pattern Recognition*, 2015.

[13] Konar, A. 2005. Computational Intelligence: Principles, Techniques and Applications. Springer. 736 pp.

Proceedings of the Fourth International Conference on Communication and Electronics Systems (ICCES 2019)
IEEE Conference Record # 45898; IEEE Xplore ISBN: 978-1-7281-1261-9

Dynamic Branch Prediction for Embedded System Applications

Subramanya G. Nayak
Dept. of Electronics and Communication Engineering
Manipal Institute of Technology
Manipal Academy of Higher Education, Manipal, INDIA
Email: gs.nayak@manipal.edu

Abstract - As Branch prediction is a performance improving technique adopted in modern processor architectures. Conventional prediction techniques have advantages such as power efficiency and speedy lookup, but with high miss-prediction rate. Neural network based and two level predictions are complex but offer improved accuracy. But disadvantage of these methods are higher power consumption, exponential increase in the complexity and time of execution ranging from 3 – 5 cycles. Optimized branch prediction should have least miss rate, lower power consumption and fewer complexes. It should use minimum resources also. In this paper the algorithm has been implemented for branch prediction which is particularly useful for superscalar or pipelined processors. With current branch prediction algorithms, the success rate of 99% can be achieved but not more than this as some times the prediction fails and whole pipe has to be flushed again. The method that has been currently implemented with increase in the hardware will always predict the branch correctly. The algorithm is very efficient in reducing time and power consumption while implementing code for processor architecture applications used in embedded systems.

Keywords : Branch prediction, hit rate, miss rate.

I. INTRODUCTION

Branches alter the normal flow of control in programs in unforeseen means that changes the normal fetch and operation of instructions. To bring back fetch operation to normal, large number of cycles till branch outcomes are known and target is detected. About 25% instructions are branch in general purpose processors. One of the easy solution to tackle these is to introduce bubbles and stalling the pipeline. Stalling pipeline increase time for execution of entire code. For higher throughput, in high performance microarchitectures, it is essential to have optimization in predicting branch instructions

Static branches are not difficult to forecast and in majority of systems, compilers offer good attention for such branches. Compilers find difficulty with branches whose outcome is found on run-time behavior. The branch outcomes have bimodal distribution and are not random. Dynamic use a prediction mechanism that adapts in runtime and takes the run-time state of the system in order to make the predictions [1]. Dynamic branch prediction techniques have very good accuracy but there exist few limitations.

The drive for advanced performance processors associated with the predictability of branch outcomes propose to use some prediction mechanism to know the outcome well prior the execution of branches. With very good prediction also, there are possibilities of miss prediction which also consume time as it takes for stalling the pipeline. Hence there is a need for smart branch predictors.

Branch prediction is an essential part of highly pipelined and superscalar processors. Its accuracy greatly impacts the efficiency of a processor, as a miss prediction causes fetching and execution of instructions which, in reality, are not needed by the program, and at the end need to be undone. To give a reasonable evaluation of the execution time of a program on a given target MPSoC, modeling branch prediction is required. The main difficulty with simulating branch prediction is to avoid slowing down the simulation, as it uses large tables to maintain per branch confidence state information and guess the branches outcome. Even a simple share [2] with a 16-bit long branch history requires a 216 entries wide counter table. With a memory wise perfectly optimized program, it represents 217 bit if the table contains 2 bit counters. Considering that entries are not accessed sequentially and that the tables are large, naïve modeling of branch predictors will result in an important number of cache misses and decrease simulation performance for any complex predictor. Branch predictors should then be simulated using a method taking memory constraints into account, i.e. the approximate model should be memory efficient while keeping reasonable accuracy.

II RELATED WORK

In a large parallel computing system, branch instructions can cause errors in a natural flow of instruction fetching, decoding and execution. This may cause delay, because the instruction delivering must generally wait until the actual branch outcome is known. The performance loss is great if the pipelining is deeper [2], [3].

To decrease delay, one can try to forecast the way that a branch instruction will take and begin fetching, decoding and delivering instructions before the branch decision is through. However, an incorrect branch prediction may lead to large delay as wrongly fetched instructions lodge useful functional units, like the ALU, registers and memory bus. Hence there is need for precise branch prediction policies.

Branch prediction policies used are static branch prediction which is implemented using software and dynamic branch prediction which uses hardware system

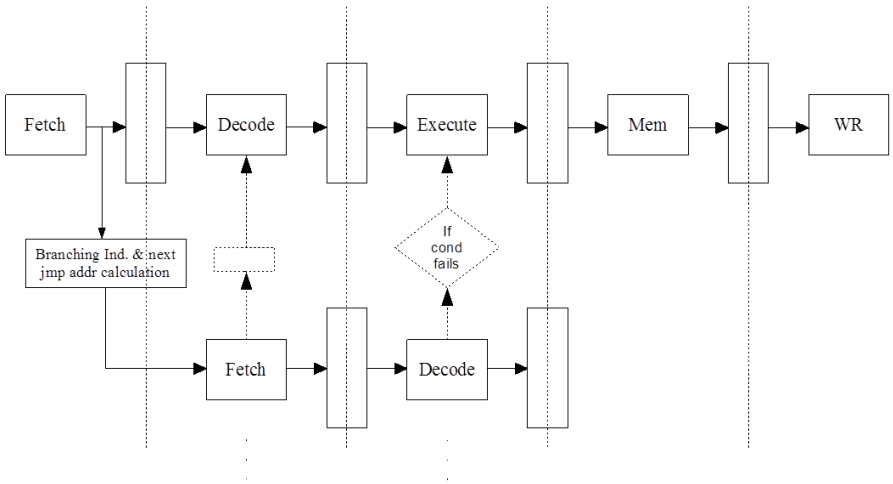

Fig. 1. Hardware for branch prediction in pipelined CPU

III. PROPOSED WORK

The algorithm that has been implemented for branch prediction is particularly useful for superscalar or pipelined processors. The problem is when branching happens, the whole pipe has to be flushed and again filled from the starting of the branched address. Even with current branch prediction algorithms, the success rate of 99% can be achieved but not more than this as some times the prediction fails and whole pipe has to be flushed again. The method that we have currently implemented with increase in the hardware will always predict the branch correctly. This is due to the fact that dedicated hardware is used to check whether the instruction which is fetched is a branching instruction or not [4].

The extra hardware used in our branch prediction is given in figure 1. As we can see from the figure, we will decode the opcode of the instruction for branching in the fetch stage of the pipeline only. This tells the hardware that there is a branch instruction and the address of the branching if the condition is true is also given by the branching instruction itself. For naming purpose, let us call the first pipeline or the original pipeline as pipe 1 and two hardware's for fetch and decode given in the second row of Figure 1 as pipe 2. So, whenever there is a branching instruction, both pipes will be filled by the data, pipe 1 with the consecutive instruction and the pipe 2 with instructions present in the branching address. When this happens, the CPU 1 will check the condition for branching at execution stage, pipe 2 will detect this and if the condition is false, the pipe 2 will flush its contents and the execution will continue regularly [5], [6]. But when the condition for branching turns out to be true, pipe 2 will detect this and pipe 1 will flush its contents. As the pipe 2 is filled with the instructions of the branching address, the contents of pipe 2 will be transferred to
the pipe 1 and the execution of the branching instructions happen. This avoids any stalling in the CPU [7], [8].

This method can be used generally for branching instructions like if-else, for loops etc. But extra and complicated hardware is required in case of 'case' statements and other branching instructions. This can also be used in assembly programming for instructions like BEQ, JMP etc.

IV. METHODOLOGY

The execution and the simulation of the algorithm were done in Linux environment with the help of POSIX Threads and POSIX Message Queues. We used the eclipse environment for the development of the code and the GDB debugger was used for debugging the program. The flow of the program is given in Figure 2.

Algorithm: From the Figure 2, there are two main threads created to simulate the two pipes given in previous section. Then these threads will control the pipeline stages of each pipe. The pipe 2 will have only two stages i.e. Fetch and decode stage. Whenever there is a branching instruction, pipe 2 will detect this and the branching address instructions will be loaded and this also goes through the pipelining along with the actual instructions that goes through the pipe 1[9], [10].

The data that is input this program is a text file which contains the sequence of instructions that needs to be read from the program. Depending on this sequence, the program will execute the instruction. If the sequence is continuous, then it has no branching, but if there are some numbers missing then it indicates that there is a branching instruction [11], [12].

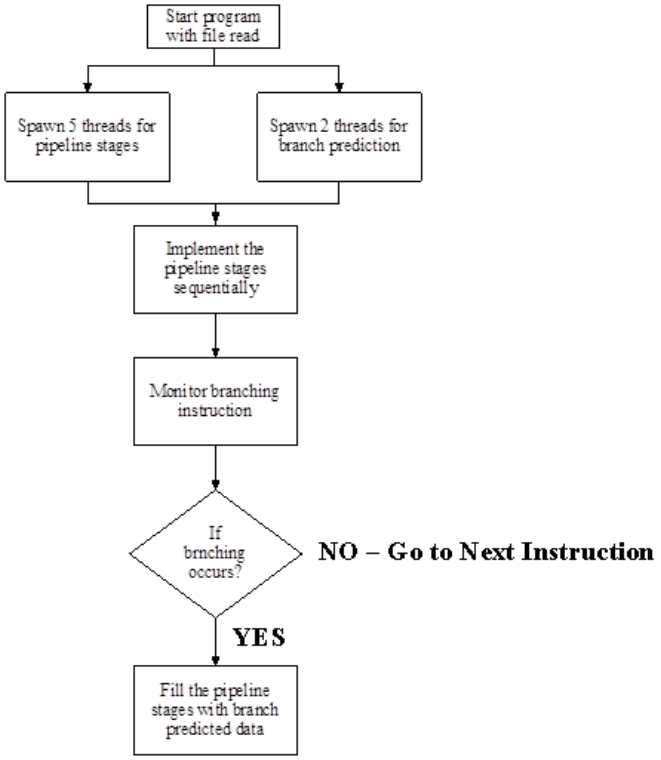

Fig. 2. Flowchart of Simulation

V. RESULTS

When the simulation was done with and without the pipe 2, we can see that there is flushing in pipe 1 if there is any branching instructions, this is not there if we enable the pipe 2 and run the simulation again, this indicates that there is no miss rate and there is 100% hit rate. This is done at the cost of extra hardware. from Figure 3.

In console output of simulation, if there are any branching instructions, the pipe 1 will be flushed and pipe 2 contents will be filled to the pipe 1 and the normal execution happens from then on. This can be used in sophisticated systems where cost of the hardware is not a problem.

```
received in pipe 1 : inst 22
../src/func_util.c:35 : pipe 1, stg: F
../src/func_util.c:49 : pipe 1, stg: D
../src/func_util.c:63 : pipe 1, stg: E
------ flushing pipe 1...
g_curr_inst: 50
 ............. loading pipe 2 ...
received in pipe 1 : inst 23
../src/func_util.c:35 : pipe 1, stg: F
../src/func_util.c:49 : pipe 1, stg: D
received in pipe 2 : inst 30
../src/func_util.c:129 : pipe 2, stg: F
../src/func_util.c:144 : pipe 2, stg: D
received in pipe 2 : inst 46
../src/func_util.c:129 : pipe 2, stg: F
../src/func_util.c:144 : pipe 2, stg: D
received in pipe 2 : inst 48
../src/func_util.c:129 : pipe 2, stg: F
../src/func_util.c:144 : pipe 2, stg: D
../src/func_util.c:63 : pipe 1, stg: E
------ flushing pipe 1...
g_curr_inst: 0
 ............. loading pipe 2 ...
received in pipe 1 : inst 24
../src/func_util.c:35 : pipe 1, stg: F
../src/func_util.c:49 : pipe 1, stg: D
../src/func_util.c:63 : pipe 1, stg: E
../src/func_util.c:94 : pipe 1, stg: M
../src/func_util.c:108 : pipe 1, stg: W
```

Fig. 3. Console output of Simulation

VI. CONCLUSION

There are many aspects which will uphold this method. When the algorithm is implemented we can see that there is no miss prediction of branch, the probability of correct prediction is 1 that is 99%. This method can be employed in high performance systems where the cost of the hardware is manageable. The algorithm is very efficient in reducing time and power consumption while implementing code for signal and image processing applications.

As future scope, the work can be further extended with the detection of branch at decode stage itself and thus latency can be further reduced.

ACKNOWLEDGMENT

I would like to express my sincere gratitude to Dr. Sathish Kumar M, Head of Department, ECE, MIT, Manipal for his continuous and constant guidance. Also, I would like to thank other Professors, lab technicians of ECE department for extending their support and help by providing technical help and ideas for the paper, without which It would not possible to come up with this kind of paper.

REFERENCES

[1] [1] Smith, J.E., 1981, May. A study of branch prediction strategies. In Proceedings of the 8th annual symposium on Computer Architecture (pp. 135-148). IEEE Computer Society Press.

[2] [2]Yeh, T.Y. and Patt, Y.N., 1991, September. Two-level adaptive training branch prediction. In Proceedings of the 24th annual international symposium on Microarchitecture (pp. 51-61). ACM.

[3] [3]Pan, S.T., So, K. and Rahmeh, J.T., 1992, September. Improving the accuracy of dynamic branch prediction using branch correlation. In ACM Sigplan Notices (Vol. 27, No. 9, pp. 76-84). ACM.

[4] [4] Jiménez, D.A. and Lin, C., 2001. Dynamic branch prediction with perceptrons. In High-Performance Computer Architecture, 2001. HPCA. The Seventh International Symposium on (pp. 197-206). IEEE.

[5] [5]Yeh, T.Y., Marr, D.T. and Patt, Y.N., 2014, June. Increasing the instruction fetch rate via multiple branch prediction and a branch address cache. In ACM International Conference on Supercomputing 25th Anniversary Volume(pp. 183-192). ACM.

[6] [6]Jiménez, D.A. and Lin, C., 2001. Dynamic branch prediction with perceptrons. In High-Performance Computer Architecture, 2001. HPCA. The Seventh International Symposium on (pp. 197-206). IEEE.

[7] Nayak, S.G. 2019, Analysis of knowledge accomplishment of an undergraduate engineering course based on attainment of course outcomes, International Journal of Mechanical Engineering and Technology, Volume 10, Issue 1, 248-254

[8] Pavitra D, 2018, Design and Measurement of Performance Parameters of Microstrip Patch Antenna used for Wi - Max and C-Band Applications, *International Journal of Engineering & Technology*, 7 (4.41), 150-153

[9] Nayak, S.G. 2018, Implementation of 32-Bit Arithmetic Logic Unit on Xilinx using VHDL, *Proceedings of the 2nd International Conference on Computing Methodologies and Communication, ICCMC 2018* 8487519, pp. 525-529

[10] Bore Gowda, S.B, 2019, DUCA: An Approach to Elongate the Lifetime of Wireless Sensor Nodes, *Lecture Notes in Electrical Engineering, 478, pp. 329-337.*

[11] Myoung-Keun You, Gi-Yong Song, 2009, SystemVerilog-based verification environment using SystemC custom hierarchical channel,, *8th International Conference on ASIC, IEEE*.

[12] Morris Mano, "Computer System Architecture", PP. 346- 347, 3rd edition, PHI. 1993

Proceedings of the Fourth International Conference on Communication and Electronics Systems (ICCES 2019)
IEEE Conference Record # 45898; IEEE Xplore ISBN: 978-1-7281-1261-9

Performance Analysis of PV & Fuel cell based Grid Integrated Power System

Kuldeep Singh Rathode[1], Santosh Kr Sharma[2], Surbhi Shringi[3]

Department of Electrical Engineering

Rajasthan technical university, Kota, 324010

[1]kuldeepsinghametha@gmail.com,[2] santoshelect@yahoo.co.in,[3] surbhishringi96@gmail.com

***Abstract*- As we all know the crisis of fossil fuels (conventional energy sources) occurs in future, which needs to find an optional choice for them. This makes us to move our attention and attraction to a new and known power generation resources. This new energy generation source become alternate and option for generation, transmission and consumption of conventional energy sources. Renewable energy sources take the place of traditional energy sources. Particularly in recent epoch and speedily developments in recent research work. In this paper we trade photovoltaic cells connected with grid and having solid oxide fuel cell (SOFC) as an alternative for grid interruption or fault condition for uphold the power flow supply. Here we instauration the P&O mppt technique with its specific control strategies along with three phase inverter for controlling DC-AC conversion with respect to grid and connected load. Reference frame theory and PLL methodology will also be provided to system for making it more reliable and advanced. An LC filter will also be used to dispose off distortion and harmonics in the system. This smart grid system will help in continuing the supply even grid is off or isolated for a while with the help of SOFC. This SOFC is used to support the system. All the results and waveforms obtained in this smart system will be explained in the paper. This paper makes the system more flexible and advanced.**

Keywords – PV module, boost converter, LC filter, controlled inverter, d-q reference frame, PLL, grid, circuit breaker, SOFC, smart grid

I. INTRODUCTION

In recent time where the competition between the power generation companies are at its peak. Every company needs to become more advanced and take their interest and attention towards non-conventional energy sources. This makes them seeing and fulfilling customers demand for high quality and clean supply. Every nation and its power generation company are extending their research work to seek new energy generation methodology [1]. This further makes them to switch to micro grid and advanced generation system. This system comprises PV modules connected with grid along with SOFC. Power generated by PV and SOFC are considered as clean energy as per the international law for standard power generation [2].

This advanced system eliminated the fault condition occur when grid is off because of some certain reason [3]. Turn off of grid makes the system and supply unstable which leads to create a system disturbance. So to get rid of such undesired situation we connect a SOFC to overcome this critical condition using specific control strategies [4]. Fig 1 of Extensive block diagram testifies the basic working phenomenon of the system.

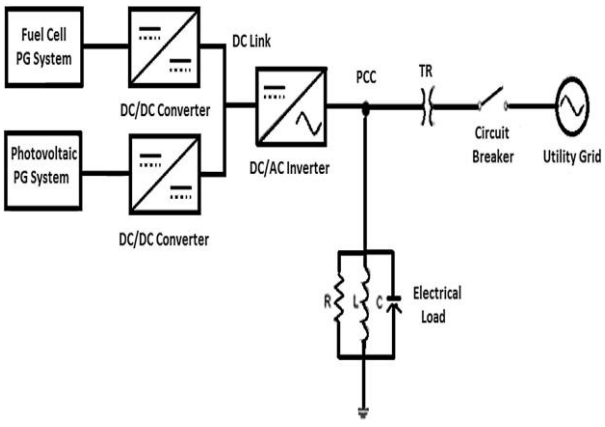

Fig 1 Advanced micro-grid model

For updated and new technology for power generation we believe in micro grids. The main purpose behind this paper is to make a advanced grid connected photovoltaic system which is fed by the SOFC in any fault condition. It works as a backup source of power.

II. GRID CONNECTED PV SYSTEM FOR POWER GENERATION

As we all know the bunch of solar cells called solar array or module. These solar cells basically comprise diode, two resistors and a current source. This PV module generated power is being converted by using a converter.

The introductory PV array model is display in fig.2. this model comprise a diode connected in parallel and two resistors connected in series and parallel combination namely Rs and Rsh with constant current source IL.

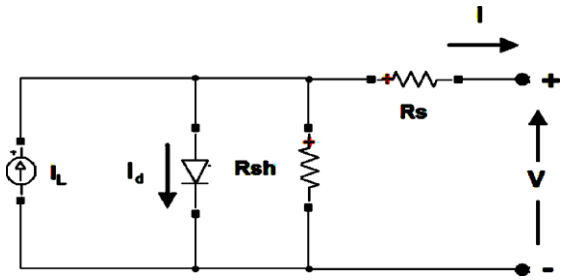

Fig 2 Single diode model of solar PV cell

The characterised equations of PV module and I-V characteristics are explained below.

$$I = I_{pv,CELL}\text{-}I_{Diode}=I_{PVcell}\text{–}I_{0,CELL}\left[exp\left(\frac{q*V}{\propto*K*T}\right)-1\right] \quad \text{- (1)}$$

Where

- $I_{pv,cell}$ the current generated by incident light.
- I_{Diode} is the Shockley diode equation.
- $I_{0,\,CELL}$ is the reverse saturation current or leakage current of the diode.
- [1.60217646 * 10e-19 Coulomb].
- k is the Boltzmann constant [1.3806503 * 10e-23J/K].
- T {K} is the temperature of the PN junction.
- $\propto$ Is the diode ideality constant whose value lies between 1 and 2 for monocrystalline silicon.

An three phase grid associated PV system is specified in fig 3. This model mainly consist a PV module connected with DC link which farther feed the generated supply to the inverter and to a LC filter to reduce harmonics.

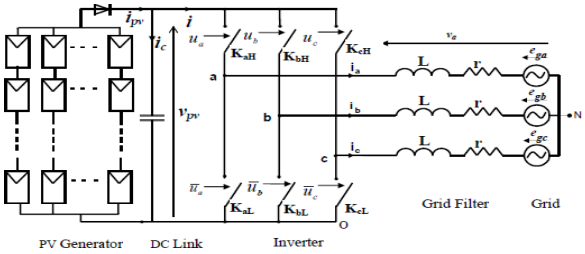

Fig 3 Three phase grid connected PV system.

III. P&O MPPT TECHNIQUE

The perturb & observe technique is broadly used MPPT technique for solar power generation. In this technique we obtain the optimum power output and voltage by comparing the present obtained power with the previously obtained power. When the maximum power is reached we got maximum power point. This technique is basically and practically a "trial and error" analytic approach. P&O algorithm works on sporadically increasing or decreasing the operating current with comparing the previous value. Fig 4 shows the flow chart of P&O technique and Fig 5 shows the P&O mppt algorithm and fig 6 shows the P&O mppt technique used with boost converter.

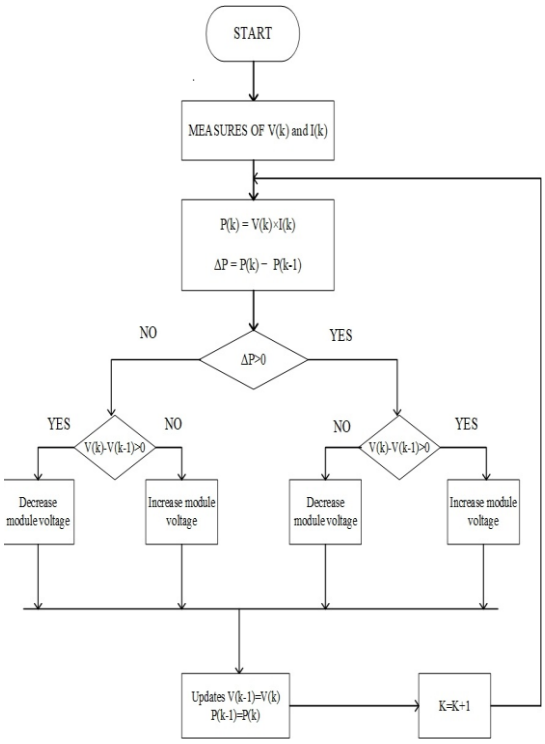

Fig 4 shows the flow chart of P&O technique

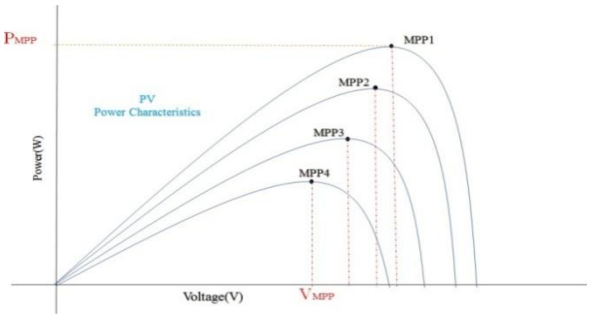

Fig 5 MPP at various Power and voltage

The flow chart of the algorithm is shown in fig 4 reads the value of voltage and current from the module by which the power is calculated. The Kth instant value is saved of current and voltage. The next value is measured again at (Kth+1) instant from which the power is calculated. The difference is calculated by both the instant is taken out. It is observed that on the right hand side voltage is almost constant and slop of the power voltage is negative (dP/dV<0)whereas in left side it is positive (dP/dV>0). The right side curve denotes the lower lower duty cycle near to zero and LHS for higher duty cycle nearly to unity. Depending on the sigh of dP and dV after subtracting dP(P(k+1)-P(k)) and dV(V(k+1)-V(k)) the algorithm decides whether to increase the duty cycle or to reduce it

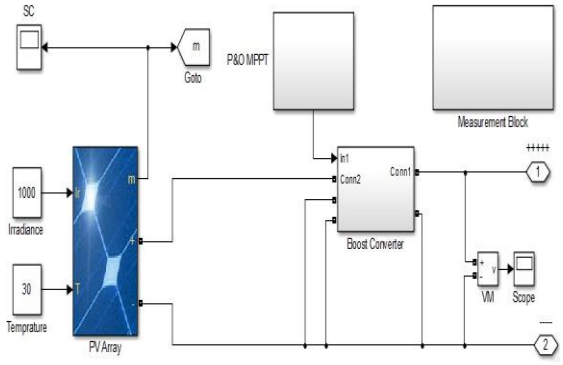

Fig 6 Simulation model of PV array with MPPT and boost converter

IV. Modelling of DC-DC boost converter-

The output voltage obtained by the PV panels is moderately low, so to step up this low level voltage output an DC-DC boost converter is requisite to employ. This converter matches the input voltage magnitude with the desired output voltage. This step up converter comprises a inductor, an diode and high frequency switch. The working phenomenon behind this converter is to manipulate the duty cycle of switch which stimulate the voltage change. Fig 7 shows the basic conventional diagram of DC-DC boost converter.

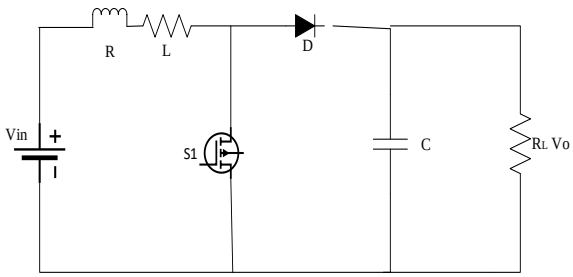

Fig 7 . DC-DC boost converter

Here we have some equations for DC-DC boost converter are specified below

$$D = 1 - \frac{V_{in}}{V_{out}} \quad - \quad (2)$$

$$L_{min} = \frac{(1-D)^2 \times D \times R}{2 \times f} \quad - \quad (3)$$

$$C_{nm} = \frac{D}{R \times F \times Vr} \quad - \quad (4)$$

Where, C_{min} : minimum capacitance ;

L_{NIn} : minimum inductance;

R : boost output resistance;

D : duty ratio;

f : switching frequency;

The continuous conduction mode for converter helps in calculating the inductance value. The inductor current IL flows continuously and never stumble to zero while the desired output voltage ripple is premise by output capacitance.

V. Implementation of Sine Pulse Width Modulation Technique

In all the phases, Pulses are generated by analogized the carrier wave with the reference wave and giving the required output which then provided to the switches

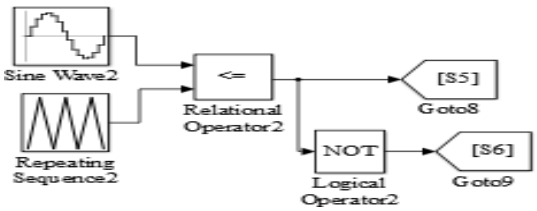

(a)

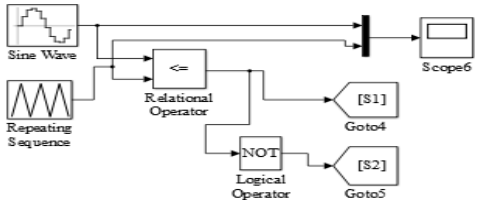

(b)

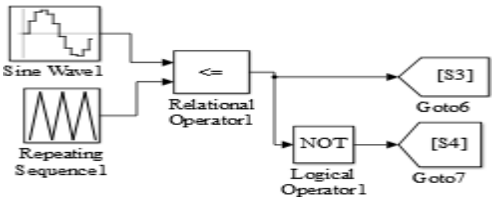

(c)

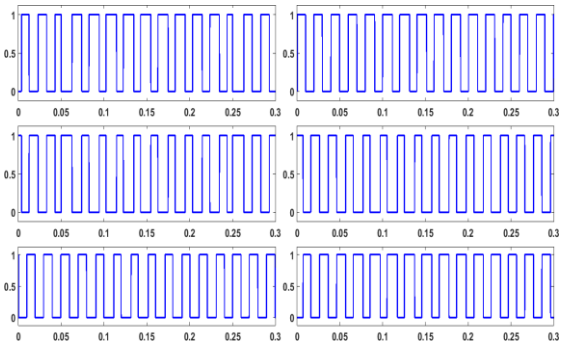

Fig 8. Pulse generated circuit and gate pulses for waveform.

VI. MODELING OF FUEL CELL (SOFC)

SOFC is an electrochemical cell that changes over the chemical energy into electrical energy. The fuel cell is basically differing from traditional batteries as they require a continuous supply of hydrogen and oxygen to corroborate the chemical reaction. This chemical reaction will help in delivering the seriatim DC power supply. Fuel cells have many advantages like better focal point, good and high productivity and better time response without emitting any toxin gases. Following equations will help in foresee the chemical reaction in fuel cell.

$$2H_2+O_2=H_2O \quad \text{- (5)}$$

$$H_2O^{=}=HO+2e^{-} \quad \text{- (6)}$$

$$O_2+4e^{-}=2O^{=} \quad \text{- (7)}$$

The fundamental simulink model for SOFC is shown in fig 9.

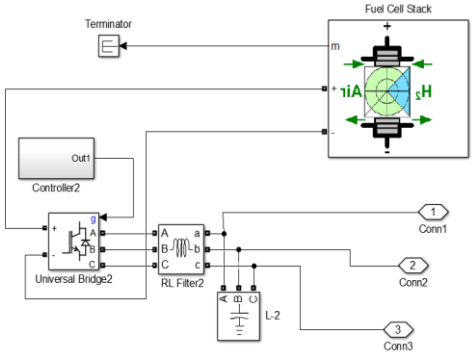

Fig. 9 SOFC subsystem model in matlab

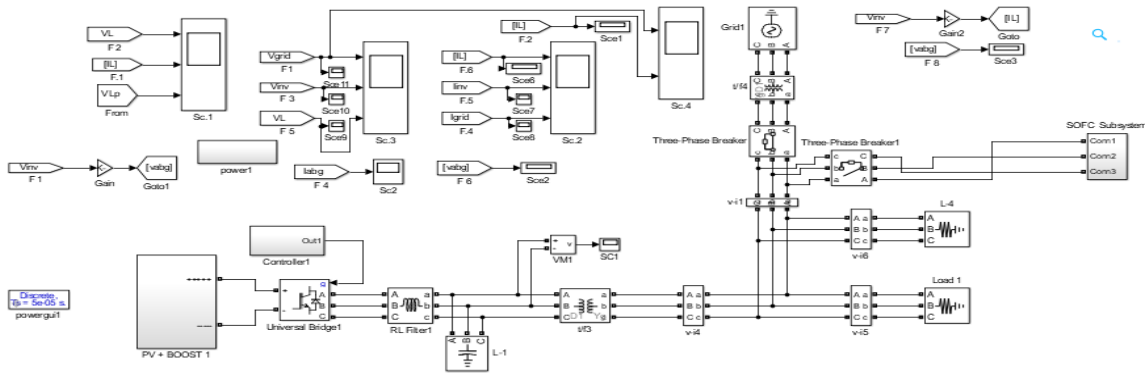

Fig.10 Simulink model of the system in matlab

VII. SIMULATION RESULTS

The simulation result of the above model shows the three phase current and voltage waveform after passing through a LC Filter. The LC filter parameter values are, L= .01 mH and C= 800 µF. Fig 11.1 to 11,3 shows the all possible waveforms.

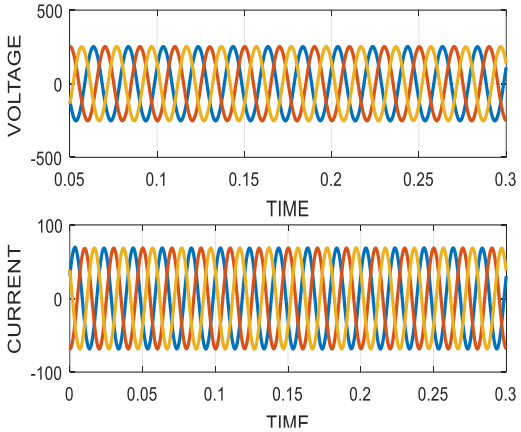

Fig 11.1 Show the three phase voltage waveform of the system when Grid is on.

Grid outage is considered here for specified time duration from 0.05sec., in this condition grid outage voltage, current and power are reduced to zero, so power, voltage and current are disturbed. Due to the condition of grid outage in PV connected system power supplied at loads becomes zero. The Voltage and current waveforms of inverter, grid, loads are shown below when grid is off

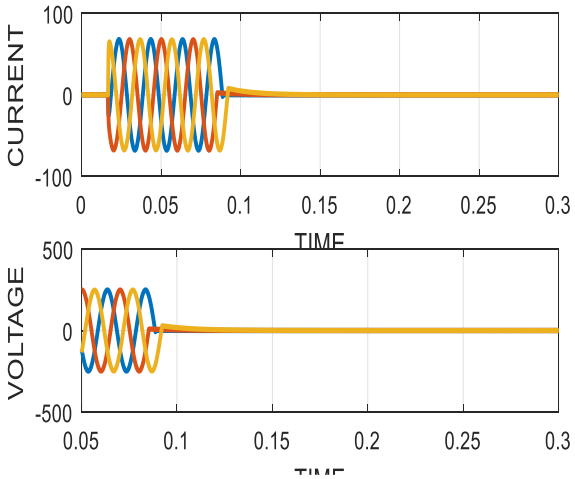

Fig 11.2 show the three phase voltage waveform of the system when Grid is off

Due to the presence of Grid outage all parametric quantities of the system are disturbed, now to resolve this problem we integrated an SOFC in system for specified time duration from 0.05 sec. The voltage and current waveform is shown below

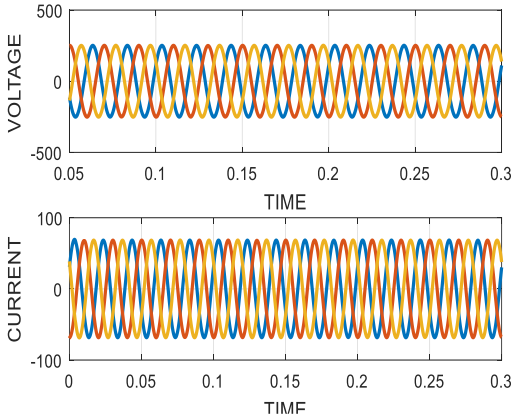

Fig 11.3 Show the three phase voltage waveform of the systemwhen connected with SOFC in it.

Conclusion

The performance of grid connected PV system is analyzed, in which grid connected PV system is compensated by the help of SOFC (solid oxide fuel cell) when grid outage occurs. As soon as there is any fault on the grid side the fuel cell gets switched on to compensate the losses and maintain the three phase output voltage and current. In this hybrid system the fuel cell can be replaced with DG set, wind generator or any other electrical source with the help of PLL technique to maintain the supply output constant. In this hybrid system we can use many energy sources in place of fuel cell like battery, biomass energy generation make this system more advanced . This updation in the sytem makes its usability much easier and reliable in any fault condition and I will place some more energy sources in the system in future.

References

[1] J. Atiq and P. K. Soori, "Modelling of a Grid Connected Solar PV System Using MATLAB/Simulink," International Journal of Simulation--Systems, Science & Technology, vol. 17, 2016.

[2] K. Singh, I. Hussain, and B. Singh, "An improved P&O MPPT algorithm for single stage three-phase grid integrated solar PV system," in Power India International Conference (PIICON), 2016 IEEE 7th, 2016, pp. 1-6.

[3] P. A. Pattanaik, N. K. Pilli, and S. Singh, "Design, Simulation & Performance Evaluation of three phase grid connected PV panel," in Power, Communication and Information Technology Conference (PCITC), 2015 IEEE, 2015, pp. 195-200.

[4] Pacheco, V. M., et al. "Stand-alone photovoltaic energy storage system with maximum power point tracking." Applied Power Electronics Conference and Exposition, 2003. APEC'03. Eighteenth Annual IEEE. Vol. 1. IEEE, 2003.

[5] Mcgowan JG, Manw ell JF. Hybrid/ PV/diesel system experienc es. Revue Renewabl e Energy 1999;1 6:928e33.

[6] H. Bellia, R. Youcef, and M. Fatima, "A detailed modeling of photovoltaic module using MATLAB," NRIAG Journal of Astronomy and Geophysics, vol. 3, pp. 53-61, 2014.

[7] S. S. Mohammed and D. Devaraj, "Simulation and analysis of stand-alone photovoltaic system with boost converter using MATLAB/Simulink," in Circuit, Power and Computing Technologies (ICCPCT), 2014 International Conference on, 2014, pp. 814-821.

[8] M. C. Argyrou, P. Christodoulides, C. C. Marouchos, and S. A. Kalogirou, "A grid-connected photovoltaic system: Mathematical modeling using MATLAB/Simulink," in Universities Power Engineering Conference (UPEC), 2017 52nd International, 2017, pp. 1-6.

[9] F. Mulolani, M. Armstrong, and B. Zahawi, "Modeling and simulation of a grid-connected photovoltaic converter with reactive power compensation," in Communication Systems, Networks & Digital Signal Processing (CSNDSP), 2014 9th International Symposium on, 2014, pp. 888-893.

[10] W. Cao and Y. Xu, "A control strategy of grid-connected photovoltaic inverter under unbalanced voltage conditions," in Harmonics and Quality of Power (ICHQP), 2016 17th International Conference on, 2016, pp. 209-213

[11] S. Verma, H. K. Verma, and M. K. Mohiddin, "Modeling & Analysis of standalone photovoltaic system," International Journal of Research in Engineering and Technology, vol. 2, pp. 259-265, 2013.

[12] B. Xiao, L. Hang, and L. M. Tolbert, "Control of three-phase cascaded voltage source inverter for grid-connected photovoltaic systems," in Applied Power Electronics Conference and Exposition (APEC), 2013 Twenty-Eighth Annual IEEE, 2013, pp. 291-296.

[13] Z. Cen, "Modeling and Simulation for an 8 kW Three-Phase Grid-Connected Photo-Voltaic Power System," Open Physics, vol. 15, pp. 603-612, 2017.

[14] M. A. De Brito, L. P. Sampaio, G. Luigi, G. A. e Melo, and C. A. Canesin, "Comparative analysis of MPPT techniques for PV applications," in Clean Electrical Power (ICCEP), 2011 International Conference on, 2011, pp. 99-104.

[15] L. B. Campanhol, S. A. O. da Silva, L. P. Sampaio, and A. A. Junior, "A grid-connected photovoltaic power system with active power injection, reactive power compensation and harmonic filtering," in Power Electronics Conference (COBEP), 2013 Brazilian, 2013, pp. 642-649.

[16] S.-K. Chung, "Phase-locked loop for grid-connected three-phase power conversion systems," IEE Proceedings-Electric Power Applications, vol. 147, pp. 213-219, 2000.

Proceedings of the Fourth International Conference on Communication and Electronics Systems (ICCES 2019)
IEEE Conference Record # 45898; IEEE Xplore ISBN: 978-1-7281-1261-9

ECG MONITORING SYSTEM USING AD8232 SENSOR

Anitha S Prasad
Assistant Professor, Electronics and Communication,
Sri Jayachamarajendra College of Engineering,
Mysuru, India
anith.sp@sjce.ac.in

Kavanashree N
PG Student, Electronics and Communication,
Sri Jayachamarajendra College of Engineering,
Mysuru, India.
kavanashree5467@gmail.com

Abstract- In this study, we describe the design and successful implementation of the smart healthcare monitoring device. This design helps to view the Electrocardiogram signal and heart beat count can measure at very low cost. The real time ECG signal is viewed on laptops and transmitted to mobile phone through Bluetooth with the help of android software. AD8232 is Electrocardiogram sensor which amplifies the signal extracted with the help of ECG electrode. This design helps in monitoring ECG of patients in remote area.

Keywords- Electrodes; AD8232 Sensor; Arduino controller; Bluetooth module.

I. INTRODUCTION

Medical expert systems are increasing day by day where one part is transferrable and smart healthcare nursing devices which can be used in everyday life. Medical applications have greater importance in this fast moving and competitive world. Any change in heart rate or rhythm, or variation in the morphological ECG signal pattern, is a symptom of an arrhythmia, which could be identified by the analysis of stored data of ECG [1].

ECG monitoring system plays an important role in determining cardiac diseases. There are number researchers working on to archive long term ECG monitoring system. Various types of ECG measuring systems have been introduced. The ECG monitoring system that are used currently in hospitals are big and heavy so it is less portable and also the measuring system have 12 electrodes where 2 on anklet 2 on wrist and other electrodes upon chest of the body. These electrodes are gel electrodes which causes allergy and infection in case of regular use so it is difficult to do long term measurement. These devices are very expensive and home monitoring is not possible so the aged people who need to be tested their heart rate frequently is very difficult in this high population, and it is a main problem in hospitals to check the ECG of all the patients. To provide home monitoring system smart technology place an important role where the result of ECG data collected is analyzed and shared with doctor and the family members.

There are various applications which provide multiple health related data such as ECG, finger photoplethysmography, and blood pressure plethysmography [2]. There are several signal amplification filter methods used in order to get the proper waveform. The delayed signal error is normalized using LMS in order to achieve high speed and low latency and SVM classifier method is used to remove noise [3]. The analysis of signal depends on the P, Q, R and S point in the ECG signal waveform the detection of these point has various algorithm and these points are implemented on IOS based smart phone to serve for remote area people [4]. The doctor is able to axis the data from the cloud and provide the detail analysis of various data collected [5]. The removing of noise is so performed by using FIR and FFT filters [6]. The ECG monitoring system can also be designed as the remoteness as a part of their private home network moderately than being more dependable home control system [7]. There are so many devices which detects the ECG signal and these electrodes are used in textiles, seat belts, wrist watch and mobile case [8]. The signal is controlled by controller and sent to the cloud in this survey they have used MSP430 single chip to control the signal [9]. The original ECG signal is compared with the various filter output and also, they have calculated the power spectral density and signal to noise ratio before and after filtering [10]. There are many sensors available in the market to detect the ECG signal like wireless sensors, MEMS and Nano technology is developing different type of portable wireless sensors for the better life [11]. The command used helps in sending and receiving the data from cloud this process is obtained by HTTP and MQTT protocols [12]. Since the smart phone are limited in power consumption and are very easily portable the heart beat data is transmitted to the smart phone, but it requires great

skills to reach out to provide the mobile application to all OS.

In introduction, The review of ECG system design related work is discussed. In Section II the detailed system architecture was discussed along with its application. Section III introduces steps to read ECG data through electrode for analysis and mobile application design. The last section concludes the project work with future scope.

II. SYSTEM ARCHITECTURE

The ECG monitoring system architecture is exemplified in Figure 1, primarily divided into four parts they are: 1. Sensor module, 2. Controller module, 3. Bluetooth module and 4. Android mobile**.**

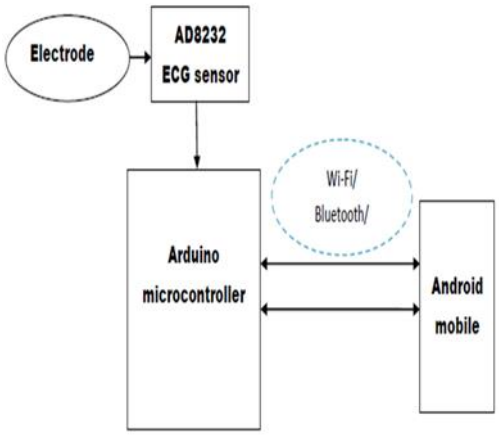

Figure 1: Block diagram of the proposed system

The ECG signal is obtained by placing electrodes on the body part these signals are amplified by using AD8232 sensor which utilize low power and reduce the noise. The output signal of the sensor is given to analog pin of the Arduino Uno board. The threshold level of the heart beat is fixed which will be compared with the obtained signal and thus this data is sent to Android mobile via Bluetooth. Based on the threshold level the real time-tested ECG signal display the result on the mobile with the heartbeat.

A. Sensor module:

The sensor module has two part.

1) Electrodes:

The electrodes used in this project is disposable electrodes which offers fast, easy, and more hygienic which is alternative to reusable electrodes or wet electrodes. These electrodes are pre gelled and these are called dry electrodes which will be good for patient skin. Instead of using 12 lead electrode system and keeping the bulk device its been used 3 lead electrode system devices as shown in Figure 2, where the electrodes are placed on the right-hand wrist (R-Red), left-hand wrist (G-Green) and the right-leg ankle (Y-Yellow).

Figure 2: Dry electrodes with color code pins.

2) AD8232 ECG Sensor:

The heart rate electrical movement is measured by this small chip called AD8232[12]. Figure 3 shows sensor module which is non-harmful and it measure the heart rate and gives the signal which can be directly connected to any controller like MSP430, Arduino, Raspberry-pi. This sensor is designed to extract the signal even when the electrodes are poorly in connection with the body. The extracted signal is then amplified. This design helps to obtain the output signal easily from an embedded controllerdevice or from an analog-to-digital converter (ADC) ultralow power device.

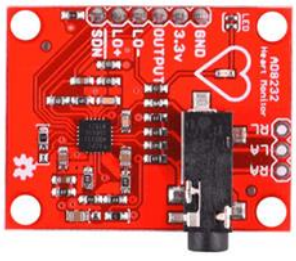

Figure 3: AD8232 Sensor.

The AD8232 is a cohesive front end for signal acclimatizing of heart biopotentials and for heart rate monitoring. It consists of a particular instrumentation amplifier, a right leg drive amplifier, an operational amplifier and a mid-supply reference buffer. In addition, the AD8232 contains leads off recognition circuitry and an

automatic fast reinstate circuit that brings back the signal soon after leads are reconnected. The AD8232 comprises a specialized instrumentation amplifier that amplifies the ECG signal while refusing the electrode half-cell latent on the same stage. This indirect present feedback architecture is possible to achieve by reducing size and power compared with traditional implementations. The below Figure 4 shows pin configuration of AD8232 sensor.

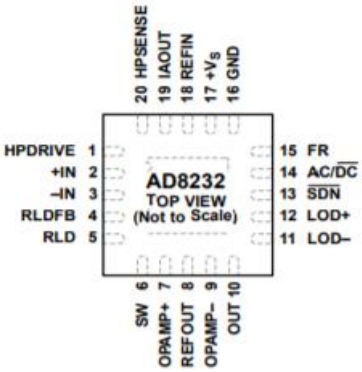

Figure 4: Pin configuration of AD8232 sensor.

B. Controller module:

Based on the Microchip ATmega328P microcontroller Arduino UNO is an open-source microcontroller board which is shown in Figure 5. This board have 14 digital pin and 6 analog pin this controller is programed using Arduino software. This board operates at 5V and its capable of 7V-20V Figure 6 shows the architecture view of arduino uno controller. The Atmel ATmega328 microcontroller is as shown in Figure 7 which is 8bit controller with 32KB program flash memory and it provides 20MHz max clock frequency. The programmable code is written in c.

Figure 5: Arduino Uno controller module.

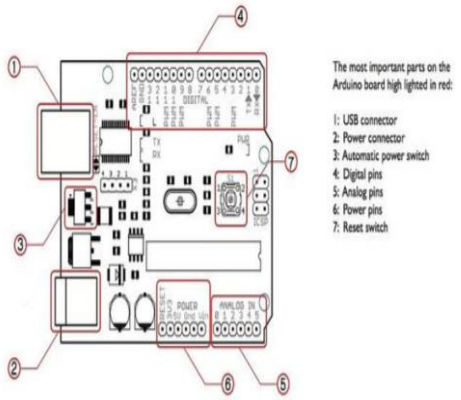

Figure 6: Pin configuration of controller

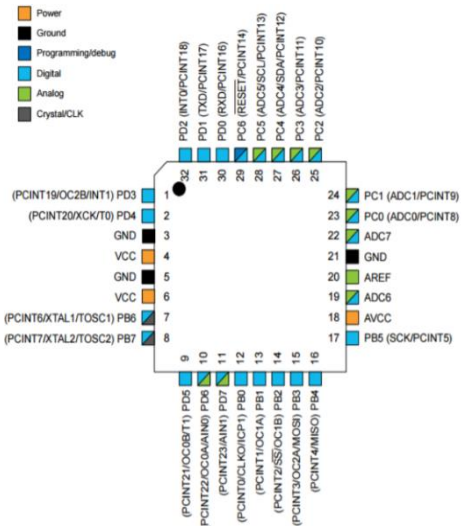

Figure 7: ATmega328 microcontroller coniguration

C. Bluetooth module:

The Transparent serial wireless connection is performed by device HC-05. This module can be used as both master and slave configuration. It has 6 pins and operates at 3.3V. The slave baud rate is fixed to 9600.

D. Android Mobile:

The android code is added to mobile by changing the setting in developers. The run code creates an application. When the Bluetooth of mobile is paired with HC-05 Bluetooth the real time data is sent from controller to mobile during on and display the ECG heart beat and its condition.

III. DESIGN OF MOBILE APPLICATION

This project has two part in software where first part is to control the ECG signal extracted by sensor and second part is sending data to mobile.

Intial the ECG signal obtained from AD8232 sensor is convereted into digital data using Ardunio board. The voltage converted serial data obtained via USB is recived and dispalyed on the monitor. The C program written to filter noise without losing the important data of ECG waveform. The Serial plotter software used to plot the ECG waveform on monitor as shown in Figure 8.

Android application is developed using Java programming language which has built in libraries for Bluetooth connectivity. The filtered signal from Arduino is compared with the threshold value and the condition of the patient is displayed. Figure 9 shows the application before connecting with the Bluetooth . Figure 10 shows the mobile application display window along with the patient result.

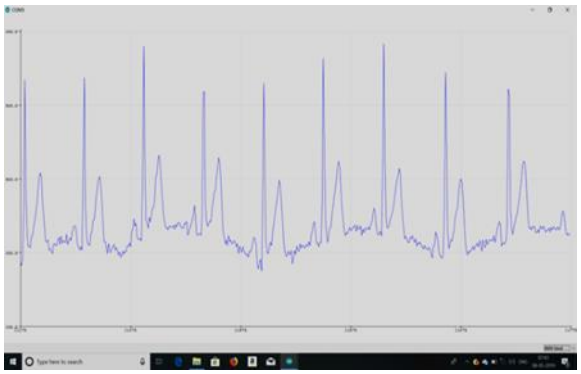

Figure 8: Screenshots of ECG signal

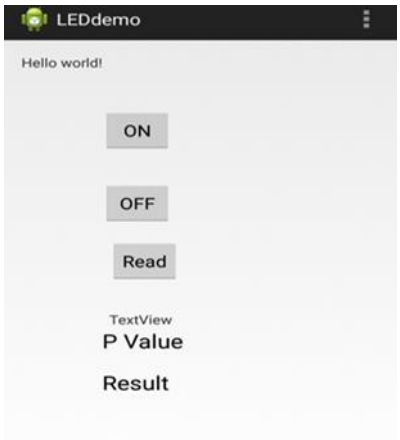

Figure 9: Application developed for android mobile

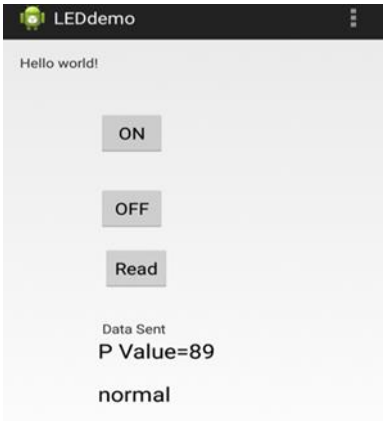

Figure 10: Heartbeat and its condition displayed in android mobile

The working step to monitor ECG signal throgh App is as follow:

Step 1: Placing electrode on the wrist and the anclet based on the color code.

Step 2: Ecg signal acquired throgh electrode is read by sensor and furter processed by controller.

Step 3: Establish connection between the mobile phone and HC-05.

Step 4: Run the code to analyze the signal.

Step 5: ECG signal is displayed with the help of arduino software.

Step 6: Simultaniously the heart rate displayed in mobile application.

IV. CONCLUSION

In this project, we designed and implemented medical related smart technology for remote area and home use which monitors the ECG signal and displays the heart beat in real time use. Three wearable monitoring electrode provides the satisfactory accuracy in real time. These data are filtered and sent to the mobile application. Further studies is on the obtaining the time between R-R interval and also improving the accuracy level of the signal to analyze the various cardiac problems using c code in Arduino software. The future scope of this project is to develop an efficient algorithm for long term analysis and Wifi technology can be used to enhance the data transmission of the signal.

ACKNOWLEDGMENT

I would like to acknowledge the guidance, and opinion given by Mrs. Anitha S Prasad, Assistant professor, Department of E&C, JSS Science and Technology University, Mysuru and Technology for helping as per our need.

REFERENCE

[1] A. Gacek and W. Pedrycz, "ECG Signal Processing, Classification and Interpretation A Comprehensive Framework of Computational Intelligence". London, U.K.: Springer, 2012.

[2] João Martinhoa, Luís Pratesa, João Costaa,b* "Design and Implementation of a Wireless Multiparameter Patient Monitoring System"

[3] C. VENKATESAN1, P. KARTHIGAIKUMAR 2, (Member, IEEE), ANAND PAUL 3, S. SATHEESKUMARAN4, AND R. KUMAR5 "ECG Signal Preprocessing and SVM Classifier-Based Abnormality Detection in Remote Healthcare Applications"

[4] Furkan AVCU*, Adnan KAVAK*, and A. Burak İNNER* *Kocaeli University, Computer Engineering Department, Izmit/Turkey furkanavcu@icloud.com, akavak@kocaeli.edu.tr, binner@kocaeli.edu.tr "QRS Detection on IOS Platform Based on Single Channel Practical ECG Measurement for Remote Patient Monitoring"

[5] Akshatl a, Gauravlb, Zahid1'0, Bhupendrald, Aditi2 e, *Sachin Kumar1'f, Maneesha1'8, Praveen Pandey1,h, 'Department of Electronics, Maharaja Agrasen College, University of Delhi, Delhi, India department of Electronic Science, University of Delhi South Campus, Delhi, India, "A Smart Healthcare Monitoring System Using Smartphone Interface" .

[6] Sudip Deb, Sheikh Md. Rabiul Islam, Jannatul RobaiatMou,Md. Tariqul Islam, "Design and Implementation of Low Cost ECG Monitoring System for the Patient using Smart Device" .

[7] Nilanjan Dey, Amira S. Ashour, Fuqian Shi, Senior Member, IEEE, Simon James Fong and R. Simon Sherratt, Fellow, IEEE, "Developing Residential Wireless Sensor Networks for ECG Healthcare Monitoring".

[8] Md. Shaad Mahmud 1, Honggang Wang1, A.M. Esfar-E-Alam1, Hua Fang1,2, 1, University of Massachusetts, Dartmouth, USA 2, University of Massachusetts Medical School, USA, "A Wireless Health Monitoring System Using Mobile Phone Accessories".

[9] Hongli Yang*, Jihong Chai, "A Portable Wireless ECG Monitor Based on MSP430FG439".

[10] Aneja, Manpreet & Singh, Birmohan &, Seema. (2011). "Comparison of different approaches for removal of Baseline wander from ECG signal". International Conference and Workshop on Emerging Trends in Technology 2011, ICWET 2011 - Conference Proceedings. 5. 1290-1294. 10.1145/1980022.1980307.

[11] Dhruba Jyoti Bora1,2, Neelesh Kumar1, Ritushree Dutta1,3 ISSN 2043-6386 Received on 7th March 2018 Revised 12th June 2018 Accepted on 17th July 2018 E-First on 13th November 2018 doi: 10.1049/iet-wss.2018.5049 www.ietdl.org, "Implementation of wireless MEMS sensor network for detection of gait events".

[12] Zhe Yang1·Qihao Zhou1·Lei Lei2·Kan Zheng1 ·Wei Xiang3, "An IoT-cloud Based Wearable ECG Monitoring System for Smart Healthcare".

Proceedings of the Fourth International Conference on Communication and Electronics Systems (ICCES 2019)
IEEE Conference Record # 45898; IEEE Xplore ISBN: 978-1-7281-1261-9

A Low-Noise Front-End Amplifier with 15 dB Gain Operating at 100-120 GHz in 65 nm CMOS Technique

Rajendra Chikkanagouda,
Research Scholar
Dept. of ECE, M. S. Engineering College,
Bengaluru, India,
e-mail: rajendracg@gmail.com

Cyril Prasanna Raj P.,
Senior Member, IEEE,
Dept. of ECE, M. S. Engineering College,
Bengaluru, India,
e-mail: cyril@msec.ac.in

***Abstract*-This paper illustrates a (100-120) GHz Low Noise Amplifier (LNA) designed for wideband imaging in millimeter (mm) - wave applications. The design has been made in 65 nm CMOS technology. The proposed amplifier model uses Common Source (CS) configuration in cascaded with cascode topology. The optimum transistor geometries are used to obtain large power gain (S_{21}) and minimum Noise Figure (NF_{min}). The inductive peaking technique is utilized to achieve flat gain and bandwidth extension. The designed amplifier provides a 15 dB gain at 100 GHz and 20 GHz 3 dB bandwidth with input and output matching less than -10 dB and -7 dB respectively. The NF of 4.6 dB at 100 GHz and less than 6 dB are inferred across the total band. The amplifier attains a 1 dB compression point (P1dB) at -12 dBm. The designed LNA achieves -5 dBm IIP3 with 10 mW of power consumption from a supply of 1.2 V.**

Index Terms— CMOS: LNA; Wideband-Imaging; Cascode; mm-wave.

I. INTRODUCTION

Traditionally, the millimeter-wave (mm-wave) circuits were implemented using III/V technologies such as InP (Indium Phosphide) and GaAs (Gallium Arsenide). These technologies have superior execution characteristics such as good electron mobility, less threshold voltage and semiconductor material for substrate to implement mm-wave circuits [1-4]. As of late CMOS innovation is favored for its cost viability, and robustness. The transit frequency (f_t) and maximum oscillation frequency (f_{max}) of CMOS is exceeding 200 GHz [5-8]. At mm-wave frequencies there are some disadvantages lower break down voltage, lower available gain and noise performances [6]. The active and passive device modelling is complicated because of conductive substrate used in CMOS which adds parasitic losses. The metal layers of the CMOS are shrink and in close proximity of the conductive substrate [7].The matching elements, resonators and interconnects quality factor are lower than the insulating substrates.

The capacitive coupling increases with substrate density which reduces the passive devices self-resonance frequency. The careful design needs incorporation of losses and parasitic capacitance effects in active devices and passive devices as the transistors are operating in the limited frequency range. Section II discusses the literature review of newly published papers and section III focuses on the design methodology for circuit development. Section IV describes the circuit design and geometries of the LNA. The results and discussions are presented in section V. Section VI contains conclusion.

II. RELATED WORK

The various LNA designs in W-Band have been presented in recent days. Today, LNA front-ends are mainly implemented using InP MMIC [1], InP HEMT [2-4], SiGe [5], FDSOI CMOS [6] and CMOS [7-8] technology.

R. Raja et al. [1] developed a three-stage single-ended LNA in 0.08 µm InP MMIC technology. The width of transistors in each stage is 30 µm. The LNA shows 24 dB of gain and less than 5.5 dB Noise Figure (NF) at 183 GHz. Alexis Zamora et al., [2] presented broad-band 170-280 GHz two-stage single ended LNA based on high frequency InP HEMT technology using coplanar wave guide-MMIC. The gain and NF of LNA are reported to be greater than 10 dB and lower than 7 dB respectively. The NF is reported to less than 6 dB and it covers (190-240) GHz frequency. Pekka Kangaslahti et al., [3] demonstrated a three stage LNA operating at 180 GHz in InP HEMT MMIC technology. The design consists of two-finger HEMT with gate width of 15 µm in each stage, total 30 µm gate periphery per device. The results of the simulated design, a flat gain of 15 dB from 60 GHz to 200 GHz and 2.5 dB of NF is reported in (100-180) GHz frequency range. The S_{11} is less than -5 dB and S_{22} less than -10 dB in (165-183) GHz. Zheng Wang et al., [6] presented a transceiver in 32 nm SOI CMOS process (210 GHz). The design is implemented with OOK modulation. The LNA comprises of seven stage Common Source (CS) differential topology. The amplifier supports a peak gain of 18 dB with 15 GHz of 3-dB bandwidth and S_{11} of -8 dB. S. T Nicolson et al., [8] presented a 140 GHz CMOS receiver with antenna (on-die) in 65 nm. The receiver consumes 100 mW with a supply voltage of 1.2 V. The LNA consists of six stages with CS topology, exhibits 8 dB of gain at 140 GHz with 10 GHz bandwidth and 63 mW of power consumption from a supply of 1.2 V.

The popular topologies used in LNA design are CS and cascode [11]. However, when frequencies near to f_t/f_{MAX}, the coscode device gain decreases almost close to CS and Common

Gate (CG) devices noise contribution is marginally higher side compare to CS device (0.5 dB -1 dB higher). By considering the above discussions, in majority of LNA designs, an inductor (series or shunt) is placed [12] between the CG and the CS stages. This helps for matching and solves performance degradation issues with respect to gain and NF.

III. LNA Design Methodology

The LNA design involves cascade of three distinct blocks such as the matching networks of input side, output side and gain stage as shown in Fig. 1. In this figure, the reflection coefficient is denoted by Γ. The output side of the Input Matching Network (IMN) quantity is denoted by index S and input side of the Output Matching network (OMN) is mentioned by subscript L. The gain stage input and output matching values are denoted by IN and OUT respectively.

The reflection coefficients of the LNA are Γ_a and Γ_b. The 50 Ω characteristic impedance is Z_O. The behavior of the amplification stage is characterized by its scattering parameters [13].

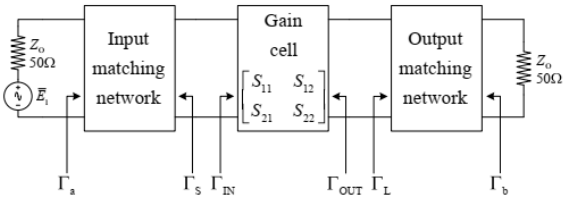

Fig. 1. Basic Amplifier design block

The major trade-offs in designing LNAs are gain, NF and linearity. The matching networks and gain performance are dependent on each other. The two port network theory is used for designing the LNA. To obtain optimum performance of the LNA, the matching networks are the crucial part of the circuit in the design. To improve the available power gain (G_A), the IMN should be modelled.

$$G_A = \frac{1-|\Gamma_S|^2}{|1-S_{11}.\Gamma_S|^2.}.|S_{21}|^2.\frac{1}{1-|\Gamma_{OUT}|^2} \quad (1)$$

and the minimize noise is

$$F = NF_{min} + \frac{4.r_n.|\Gamma_S-\Gamma_{OPT}|^2}{(1-|\Gamma_S|^2).|1+\Gamma_S|^2} \quad (2)$$

In (2), the optimum source reflection coefficient is denoted by Γ_{OPT} and noise resistance is r_n (r_n= R_n/Z_O) and NF_{min} respectively. These three parameters are the noise behavior characteristics of the linear two port network. Since the minimum noise is the main design criteria, Γ_S must be equal to Γ_{OPT}, and to enhance the G_A, Γ_S must be identical to the complex conjugate of the Γ_{IN} (Γ^*_{IN}), where Γ_{IN} is defined by equation (3).

$$\Gamma_{IN} = S_{11} + \frac{S_{12}.S_{21}.\Gamma_L}{1-S_{22}.\Gamma_L} \quad (3)$$

The Γ_{OPT} and Γ^*_{IN} are very distinct in nature, the performance of gain is improved and noise is worsened, and vice-versa. There is a trade-off for designing an IMN between noise and gain performance. The primary objective of the OMN is to boost the operating power gain (G_P)

$$G_P = \frac{1}{1-|\Gamma_{IN}|^2}.|S_{21}|^2.\frac{1-|\Gamma_L|^2}{|1-S_{22}.\Gamma_L|^2} \quad (4)$$

The Γ_L must be equivalent to complex conjugate of the Γ_{OUT} (Γ^*_{OUT}), being Γ_{OUT} given by equation (5).

$$\Gamma_{OUT} = S_{22} + \frac{S_{12}.S_{21}.\Gamma_S}{1-S_{11}.\Gamma_S} \quad (5)$$

The matching networks play an important role to attenuate the noise and enhance the power gain of the LNA which ensure the circuit should be precisely stable. The stability factor (K) is defined in (6)

$$K = \frac{1+|\Delta|^2-|S_{11}|^2-|S_{12}|^2}{2|S_{12}||S_{21}|} > 1 \quad (6)$$

$$\Delta = |S_{11}|.|S_{22}| - |S_{12}|.|S_{21}| < 1 \quad (7)$$

The other two important performance parameters are input and output VSWRs and these parameters are relatively connected to the IMN and OMN. The IMN and OMN are lossless, the conditions to accomplish Γ_a= 0 and Γ_b= 0 are Γ_S= Γ^*_{IN} and Γ_L=Γ^*_{OUT}, respectively. These conditions help to maximize G_A and G_P. The Γ_S=Γ^*_{IN} usually conflicts with the NF_{min} condition at the input side. If the gain stage could be viewed unilateral (S_{12} = 0) the structure of the IMN and OMN is rearranged since the two systems are autonomous of one another. The unilateral condition is practically difficult to accomplish at mm-wave frequencies. The challenging task is to design a matching network for mm-wave frequencies.

The gain stage should be modelled in order to improve the gain and to limit the NF which is satisfying the supply conditions. Inductors are utilized to model IMN and OMN in CMOS process have moderate quality factors (10 to 25), the effect of NF could be exceptionally high. The gain stage should be the most unilateral, possible to achieve the device is unconditionally stable and to minimize the matching networks design complexity.

IV. Circuit Design

Fig. 2 shows the proposed LNA design for wideband support up to (100-120) GHz. The first stage (CS) of the amplifier is designed to minimize the noise level. In this stage, cascode topology will not prefer because of poor noise performance. There are a few choices to defeat this issue such as to minimize the junction capacitance [6], [10] and to use of single transistor design in the early stage to lower the noise produced by the cascade amplifier. The gate resistance (R_G) of the transistor has a large impact on the noise performance. The 100 Ω resistances were used in bias lines. The stability issue at first stage due to poor reverse isolation of a CS transistor is resolved by using a stabilizing resistor (R_C) of 20 Ω between two stages. By placing this resistor the gain diminishes by 2 dB and its impact on overall NF performance is practically immaterial and increases the NF by the value from 0.3 dB to 0.5 dB. The first stage of CS transistor (M_1) m is set to 8 µm. The

cascode circuit is established by the M_2 and M_3 NMOS transistors, both with a length of 65 nm. The widths of M_2 and M_3 are 8 µm respectively. These values were determined using an optimization process based on simulations that use Predictive Technology Models (PTM) [14]. The peaking inductors L_{D1} to L_{D4} are used to enhance the power gain. Both the common source transistors M_1 and M_3 are biased through L_{G1} and L_{G2} respectively with 0.7 V to attain high gain and low NF.

At low frequencies, active devices perform unconditionally stable operation where capacitors acts as an open circuit and at mm-wave frequencies where the substrate losses and parasitic effects are on higher side. The CS transistor offers poor reverse isolation at high frequencies. The first stage of the design suffers stability problem, for avoiding this a resistor is placed between CS and cascode. By adding this resistor, the gain decrease slightly and its impacts on noise is negligible.

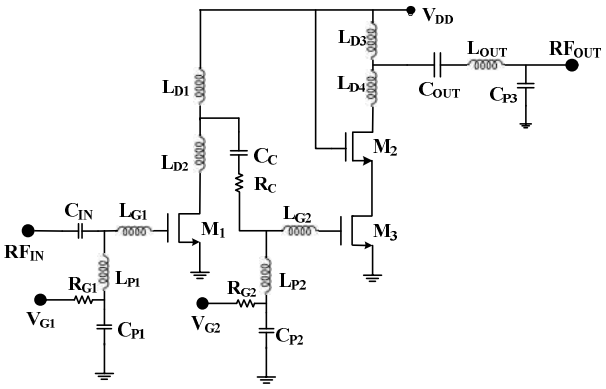

Fig. 2 (100-120) GHz LNA schematic

Cascode is preferred to improve the gain and better reverse isolation in the second stage which is not as crucial for the overall NF. The simultaneous noise and input matching are accomplished by the first stage and the gain performance in a wide bandwidth is obtained by subsequent stages. Table I presents the passive component values of the mm-wave LNA.

TABLE I. PASSIVE COMPONENT DESIGN GEOMETRIES

Inductor	**L_{D1}**	**L_{D2}**	**L_{D3}**	**L_{D4}**	**L_{G1}**
Inductance (pH)	450	150	600	200	59.5
Inductor	**L_{G2}**	**L_{P1}**	**L_{P2}**	--	--
Inductance (pH)	85	85	85	90	--
Capacitor	**C_{IN}**	**C_{OUT}**	**C_{P1}- C_{P2}**	**C_{P3}**	**C_C**
Capacitance	1pF	28 fF	1pF	20 fF	80 fF
Resistor	**R_{G1}**	**R_{G2}**	**R_C**	--	--
Resistance (Ω)	100	100	20	--	--

V. RESULTS AND DISCUSSIONS

The LNA design and its performance evaluation were carried out through Advanced Design System (ADS) simulation using 65 nm CMOS from PTM. This section discusses performances of gain, noise, reflection coefficients, linearity and stability. The biasing voltage of the transistors is set to 0.7 V. The W-band LNA gain and NF performance is represented in Fig. 3 and has a central operation frequency of (100-120) GHz. At this frequency the LNA gain is 15 dB and NF of 4.56 dB. The gain is larger than 14 dB and NF is smaller than 6.3 dB from 92 GHz to 123 GHz.

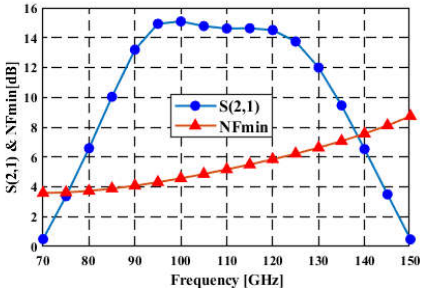

Fig 3. S_{21} and NF of the proposed W-Band LNA

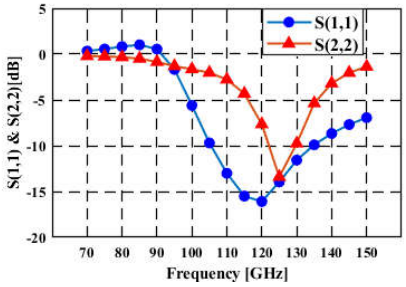

Fig 4. S_{11} and S_{22} simulation results

The proposed LNA matching results are shown in Fig. 4. The input matching S-parameter (S_{11}) is less the -10 dB over the band of interest (106-134) GHz. The minimum S_{11} is reported to -16 dB at 118 GHz. The S_{22} is smaller than -10 dB in the range of frequency (122-130) GHz. The 1dB compression point of the designed LNA is -12 dBm shown in Fig. 5. Fig. 6 depicts the IIP3 and the OIP3 which are-5 dBm and -4 dBm respectively.

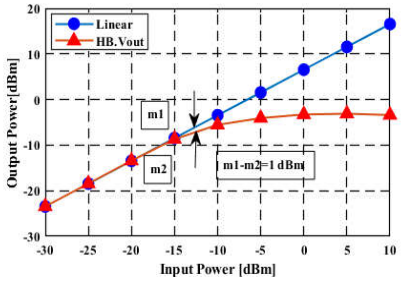

Fig. 5. P1dB simulation result

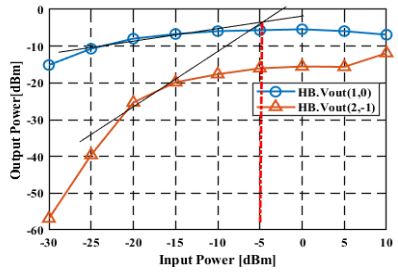

Fig. 6. Simulation result of IIP3 at 100 GHz

The circuit is unconditionally stable in the entire frequency band by taking out the possibility of instability due to noise, might be available in the circuit during power on condition. This is denoted by stability factor (K) and proposed design stability factor is shown in Fig. 7.

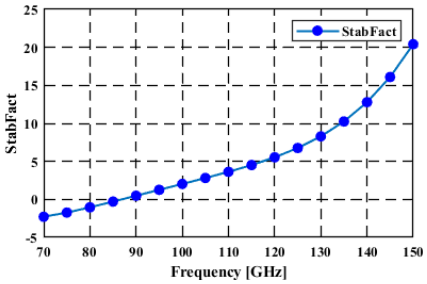

Fig. 7. Stability Factor (K) of the LNA

The performance summary with recently reported cascode mm-wave LNAs is presented in Table II. The presented LNA has good gain, noise and matching performance. The P1dB and IIP3 (linearity) is satisfactory for wireless imaging applications which is achieved with a supply voltage of 1.2 V.

TABLE II. RECENTLY PUBLISHED MM-WAVE CMOS LNAS COMPARISON

Specifications	[7]	[8]	[10]	This work
Year	2016	2008	2015	2019
Technology [nm]	65	65	65	65
Stage	5	6	6	2
Peak Gain	16.7 @104 GHz	9.0 @140 GHz	22.0 (78-92) GHz	15.0 @100GHz
Gain [dB]	>13.7(88.5-110) GHz	8.0@ (135-145) GHz	--	14.0 (92-123) GHz
NF [dB]	7.2-9.0	--	6.8-10.4	6.3
S_{11} [dB]	< -10.0	-15.0@130 GHz	< -10.0	-16.0 @118 GHz
S_{22} [dB]	< -10.0	-10.0 @137GHz	< -10.0	< -13.0 @126 GHz
P1dB [dBm]	--	-12.0	--	-13.0 @126 GHz
IIP3 [dBm]	--	--	--	-5.0
P_{DC}[mW]	48.6	63.0	21.0	10.0

VI. CONCLUSION

A W-Band two stage LNA has been designed and simulated using CS configuration in cascaded with cascode topology. The simultaneous noise and input matching are accomplished by the first stage. The high gain performance in a wide bandwidth is achieved by the subsequent stages. The CMOS LNA achieves a 15 dB of peak gain at 96 GHz along with 3-dB bandwidth of 95-120 GHz. The NF is less than 6 dB reported in the entire W-Band frequency. The IIP3 and P1dB are -5 dBm and -12 dBm respectively. The unconditional stability is achieved from 92 GHz onwards. The proposed design has appreciable gain, NF and good matching performance. Hence the presented LNA is well suitable for 100-120 GHz W-Band imaging applications.

REFERENCES

[1] R. Raja, M. Nishimoto, B. Osgood, M. Barsky, M. Sholley, R. Quon, G. Barber, P. Liu, R. Lai, F. Hinte, G. Haviland, and B. Vacek, "A 183 GHz low noise amplifier module with 5.5 dB noise figure for the conical scanning microwave Imager Sounder (CMIS) program," in *Proc. Int. Microw. Symp. (IMS)*, vol. 3, pp. 1955–1958, 2001.

[2] A. Zamora, K. M. K. H. Leong, T.Reck, G. Chattopadhyay, and W. Deal, "A 170–280 GHz InP HEMT low noise amplifier," in *Proc. Int. Conf. Infr., Millim. Terahertz Waves Electron. (IRMMW-THz)*, pp. 1–2, 2014.

[3] P. Kangaslahti, D. Pukala, T. Gaier, W. Deal, X. Mei, and R. Lai, "Low noise amplifier for 180 GHz frequency band," in *Proc. Int. Microw. Symp. (IMS)*, pp. 451–54, 2008.

[4] G. Moschetti, A. Leuther, H. Mabler, B. Aja, M. Rosch, M. Schlechtweg, O. Ambacher, V. Kangas and M. G. Perichaud, "A 183 GHz Metamorphic HEMT Low-Noise Amplifier with 3.5 dB Noise Figure," *IEEE Microwave and Wireless Component Letters,* vol. 25, no. 9, pp. 618-620, 2015.

[5] J. W. May and G. M. Rebeiz, "A W-Band SiGe 1.5V LNA for Imaging Applications," IEEE Radio Frequency Integrated Circuits Symposium, pp. 241 – 244, 2008.

[6] Z. Wang, P.-Y. Chiang, P. Nazari, C.-C. Wang, Z. Chen, and P. Heydari, "A CMOS 210-Ghz fundamental transceiver with OOK modulation," *IEEE J. Solid-State Circuits*, vol. 49, no. 3, pp. 564–80, 2014.

[7] G. Feng, C. C. Boon, F. Meng, X. Yi, and C. Li, "An 88.5-110 GHz CMOS low-noise amplifier for millimeter-wave imaging applications," *IEEE Microw. Wireless Compon. Lett.*, vol. 26, no. 2, pp. 134–136, 2016.

[8] S. T. Nicolson. A Tomkins, K. W. Tang, A. Cathelin, and S. P. Voinigescu "A 1.2V, 140 GHz receiver with on die antenna in 65 nm CMOS," *IEEE Radio Frequency Integrated Circuits Symposium*, pp. 229-232, 2008.

[9] M. Sato, T. Takahashi and T. Hirose, "68–110-GHz-Band Low-Noise Amplifier Using Current Reuse Topology," *IEEE Trans. Microw. Theory Techn.*, vol 58, no. 7, pp. 1910-1916, 2010.

[10] C. J. Lee, H. J. Lee, J. G. Lee, T. H. Jang, and C. S. Park, "A W-band CMOS low power wideband low noise amplifier with 22 dB gain and 3dB bandwidth of 20 GHz," *Asia-Pacific Microwave Conference (APMC)*, vol. 2, pp.1-3, 2015.

[11] S. Voinigescu, *High Frequency Integrated Circuits*. Cambridge, U.K.: Cambridge Univ., 2013.

[12] P. Heydari, "Design and analysis of a performance-optimized CMOSUWB distributed LNA," *IEEE J. Solid-State Circuits*, vol. 42, no. 9, pp. 1892–1905, 2007.

[13] R. Ribeiro, L. Mendes, J. C Vaz, M. J. Rosario, J. C. Freire, "A 130nm CMOS LNA for 30 GHz applications," IEEE EUROCON- International Conference on Computer as a tool, pp. 1-4, 2011.

[14] Predictive Technology Model, Latest Models [Online]. Available: http://ptm.asu.edu/modelcard/2006/65nm_bulk.pm.

Proceedings of the Fourth International Conference on Communication and Electronics Systems (ICCES 2019)
IEEE Conference Record # 45898; IEEE Xplore ISBN: 978-1-7281-1261-9

Automated Segmentation Technique for Detection of Myocardial Contours in Cardiac MRI.

Sushmitha. R
M.Tech - Computer Science & Engg
Dayananda Sagar College of Engineering
Bengaluru, Karnataka
sushmithagowda325@gmail.com

Dr. Arbind Kumar Gupta
Professor, Dept. of ISE
Dayananda Sagar College of Engineering
Bengaluru, Karnataka
arbind.gupta@gmail.com

Mrs. Chandrakala B M
Assistant Professor, Dept. of ISE
Dayananda Sagar College of Engineering
Bengaluru, Karnataka
chandrakalabm-ise@dayanandasagar.edu

***Abstract* — Segmentation of myocardial contours serves a prerequisite for viability assessment of myocardium which is essential for patient's diagnosis and treatment plan. However, segmenting the myocardial contours more precisely is quite a challenging task. This paper presents an automated segmentation technique for detection of myocardial contours in multiple cardiac MRI frames. Initially, a geometrical template is initialized on each MRI frame using the co-relation technique in order to locate the myocardium region. Later, curved multi-planar reconstruction (curved MPR) image is constructed to detect the epicardial and endocardial edge contours. The detected edges are smoothened using Savitzky Golay filter to obtain final segmentation result. Automated segmentation technique is tested on 12 MRI frames and accuracy is validated on three frames with respect to manually traced endo-epicardial boundaries.**

Keywords – Segmentation, Viability assessment, Cardiac-MRI, Myocardial contours, Curved MPR.

I. INTRODUCTION

Myocardium is a muscular tissue of the heart which consists of striated cardio-muscular fibers that allow heart to contract spontaneously. It is enclosed by two layers with outer layer as epicardium, inner layer as endocardium and the blood is supplied through the coronary circulation. The main function of myocardium is stimulating the heart contractions which are responsible for producing heartbeat. Sample image of myocardium in cardiac MRI is as shown in Figure 1.

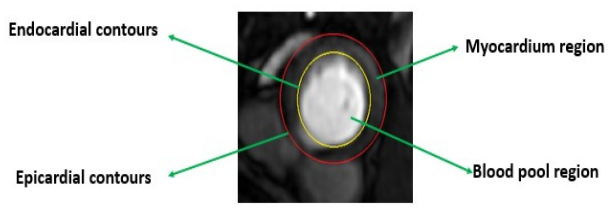

Figure 1: Sample Cardiac MR Image representing myocardium.

In the recent years, there is increase in recognition of cardiac diseases, in particular, myocardial fibrosis. When Myocardial infarction (normally referred as heart attack) occur, there is decrease in blood flow to some portions of the heart that causes the cardiac cells to get damaged. As a result, the damaged cells are replaced by the fibrotic scar or tissue (fibrosis). This remodels the surrounding myocardium and leads to cardiac dysfunctioning. This process is relatively progressive and results in narrowing of ventricular cavities.

Endo-myocardial fibrosis is one such that occurs in inner lining of endocardium where the healthy tissues are replaced by inelastic, thick fibrosis tissues. If the fibrosis is pre-dominant in the left ventricle, then blood flow is reduced from the right portion and causes regurgitation (back-flow) of blood. Also, it may result in left ventricular enlargement, cardiomyopathy, atrial fibrillation etc.

Over various range of imaging modalities, cardio vascular magnetic resonance also referred as Cardiac MR Imaging is popularly used by radiologists for diagnosis rather than CT scans, PETs and ultrasonography imaging. Cardiac MRI provides definite anatomical structure of the heart, detailed information about nature of cardiac disease which helps the doctor to decide about the treatment plan. It's also possible to visualize non-viable, ischemic areas along with the normal tissues with high resolution, by using late-enhanced cardiac MR (LE-CMR) imaging.

Segmentation of myocardium is essential for its viability assessment which is important in patient's diagnosis and treatment planning. This ensures whether revascularization process may benefit the patient. Segmenting myocardium a priory helps to quantify the amount of fibrosis present in it. Proposed segmented result can be used as a template and when superimposed on LE-CMR image, limited search of fibrosis can be done within the template region. Therefore, a prior knowledge of myocardium helps in localization of fibrosis in small region, thereby, improving the accuracy significantly.

In order to locate non-viable tissues in the myocardium, first delineation of endocardial and epicardial contours

should be done. However, segmenting epi-endocardial contours more precisely is quite a challenging task. Manual delineation of contours in the images is intensive procedure and also time-consuming. Therefore, automated or semi-automated algorithms are desired for the purpose. Several related approaches to segment the myocardial contours has been mentioned in the subsequent literature survey.

This paper is organized as follows –
Related work is discussed in section II, automatic myocardium segmentation technique is explained in section III, segmented results are discussed in section IV and concluded in section V.

II. RELATED WORK

In [1], an automated technique is proposed to segment myocardium in LE- CMR images. In every slice of LE-CMR volume, template is deformed such that it fits the myocardial contours. 3D mesh which represents the left ventricle and myocardium thickness is created by using cine MR sequence that provides prior information about the left ventricle. Later it is registered onto the obtained contours to produce the final segmentation.

In [2], an automated technique is proposed to segment left ventricle in 2D LGE-MRI. Circular Hough transforms method is used to detect left ventricle, blood pool region is approximated using morphological active contours method. Later epicardial and endocardial contours are refined using scar and edge information.

In [3], an automated method is proposed to identify microvascular obstruction in LE-CMRI. Initially, the epi-endocardial contours along with scar region is traced manually. Adaptive threshold value is chosen based on normal and scar tissues information and MO regions are identified as the region of pixels with less signal intensity than threshold value. In [4], Fuzzy soft thresholding algorithm is used to identify fibrosis tissues in MR images. First, ROI is defined where the presence of fibrosis is suspected. Image resolution is increased using Interpolation technique. Two classes as (foreground and background) are defined to segment the tissues, where foreground area corresponds to myocardial fibrosis and background represents other tissues.

In [5], fibrosis in left ventricle is detected from delayed gadolinium enhanced images using kernel dictionary learning based clustering. Initially, dictionary is created with two cluster samples i.e. (LGE and non-LGE). Sparse coefficients of input data are used to train K-NN classifier obtained from kernel-based DL approach. Fibrosis is detected in the region between epi-and- endo cardial contours. In [6], myocardial scar is extracted from 3D whole-heart cardiac LE-MRI using max flow-based algorithm. In [7], a 3D visualization tool is developed for detection of left atrial fibrosis from DE-MR images and is compared with EAM.

III. PROPOSED METHODOLOGY

Our proposed automated segmentation technique to detect myocardial contours is described in Figure 2. Initially, Laplacian of Gaussian kernel is modeled as geometrical template and registered on the input MR image using the Co-relation technique. As a result, approximate region of myocardium region is identified with points (x_c, y_c), where (x_c, y_c) are the center points of located myocardium region. Next, the curved multi-planar reconstruction image is constructed using the myocardial center points in order to detect the endo-epicardial boundaries. An edge detector is applied to detect endocardial boundary points initially and later epicardial boundary points are detected. Finally, endo-epi edges are optimized as a smooth curve using "Savitzky Golay Filter" to produce the final segmentation result.

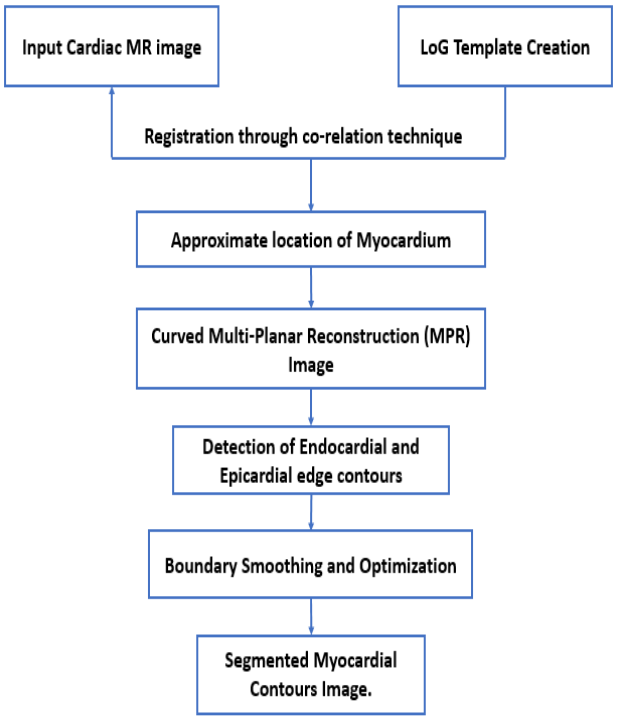

Figure 2: Segmentation Workflow

A. TEMPLATE CREATION

Myocardium is identified robustly as dark, circular annular shape. Hence, a radially symmetric Laplacian of Gaussian kernel with diameter corresponding to the approximate diameter of myocardium is modeled as dark ring. This kernel is correlated with the input MR image.

Kernel's radial profile is defined as follows -

$$f_\rho(r) = \Delta\left(\frac{1}{\sqrt{2\pi\sigma^2}}\, e^{\frac{-(r-\rho)^2}{2\sigma^2}}\right)$$

Depending upon the approximate size and thickness of myocardium, the values of ρ and σ are chosen: where ρ is the radius of the ring whose width corresponds to standard deviation σ and Δ is the Laplacian operator.

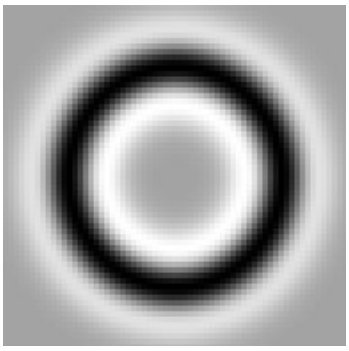

Figure 3a: LoG Template of size $\rho = 20$ and $\sigma = 4$

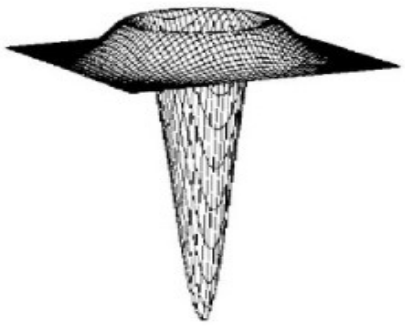

Figure 3b: Three dimensional (3-D) plot of LoG filter.

B. TEMPLATE REGISTRATION

Geometrical template is automatically registered on the input image using the co-relation technique. We compute the co-relation for various values of ρ because size of the myocardium may vary with small value. The value of ρ is chosen as the best response wherever the maximum co-relation match is found. Optimal center co-ordinates (x_c, y_c) of the myocardium is obtained.

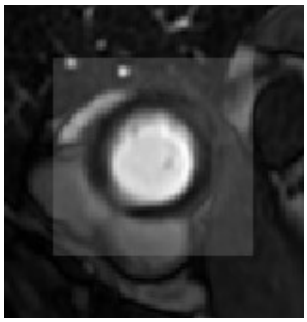

Figure 4: Template superimposed on myocardium region.

C. CURVED MULTI-PLANAR RECONSTRUCTION IMAGE

Myocardium region is constructed as the curved multi-planar reconstruction image with reference of points (x_c, y_c) obtained in the previous step. In the curved MPR image, first the endocardial contour edges are detected and later epicardial contours are obtained. Curved MPR image of myocardium is as shown in figure 5a.

To detect endocardial contours, an edge detector is applied vertically to detect strong edges with maximum intensity change. Average of these edges is considered to obtain the final boundary points. Endocardial contours can be seen as shown in figure 5b.

Since epicardium appears above endocardium, endocardial boundary points and approximate thickness of myocardium is used for detecting the epicardial contours. Edge detector is applied starting from endocardial boundary points up to approximate thickness of myocardium to detect the edge. Epicardial contours can be seen as shown in figure 5c.

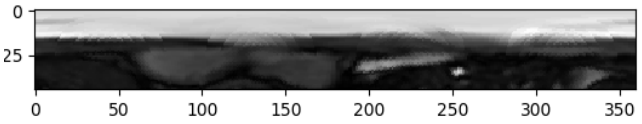

Figure 5a: Curved MPR Image of Myocardium.

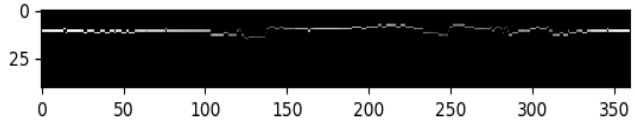

Figure 5b: Endocardial edge contours.

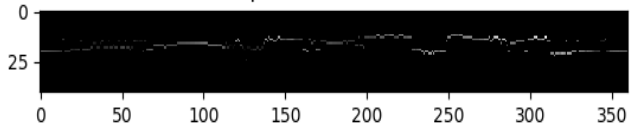

Figure 5c: Epicardial edge contours.

The contours obtained from the above step are drawn on the curved MPR as shown in figure 6a, where blue color

represent endocardial contours and orange color represent epicardial contours. These contours are then optimized as a smooth curve using the Savitzky-Golay filter [12] to produce the final segmentation result.

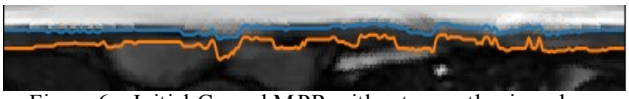

Figure 6a: Initial Curved MPR without smoothening edges.

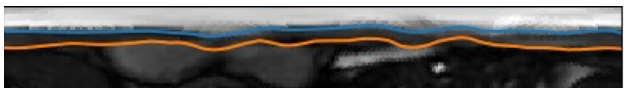

Figure 6b: Smoothened edges using Savitzky-Golay filter.

IV. RESULTS AND ANALYSIS

Figures 7 - 9 illustrates our automated contour detection of myocardium in multiple cardiac MRI frames from different patients. The cardiac images that are used in our project is from the open source Sunnybrook Cardiac Dataset[1].

Sample frames are taken from different patients. For each frame, detected endocardial and epicardial edges images are shown. Curved MPR image with and without smoothening edges is also shown for each image. In order to determine the accuracy of obtained myocardial contours, we have compared with manually traced endo-epi boundaries on the myocardium. Hence, the accuracy of automatic contour detection is validated sufficiently considering manual tracing as gold standard.

Sample MRI Frame 1

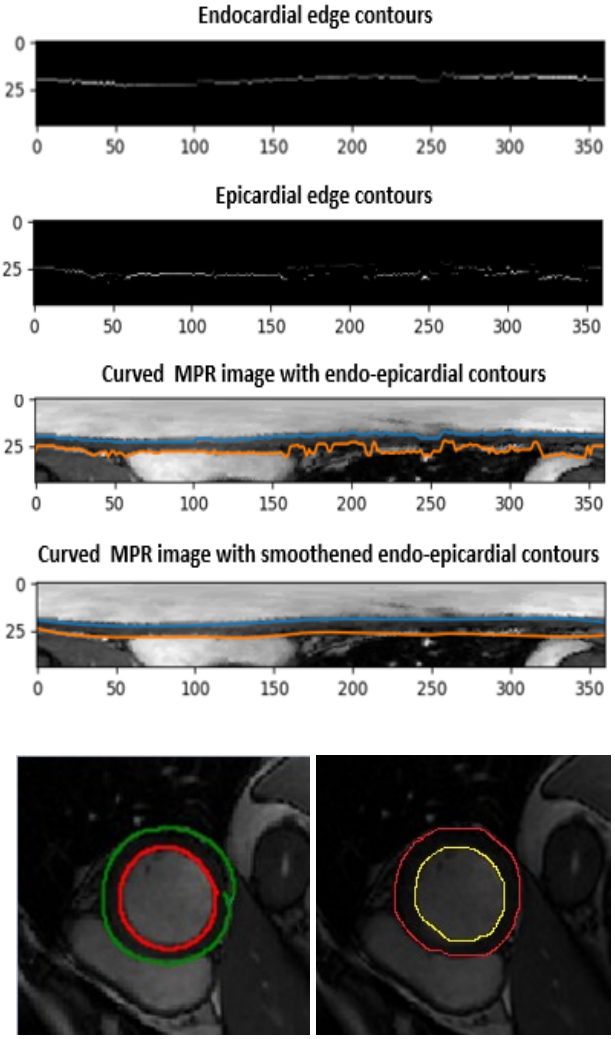

Figure 7: (a) - Segmented Result (b) Manually Traced contours for Frame 1.

Sample MRI Frame 2

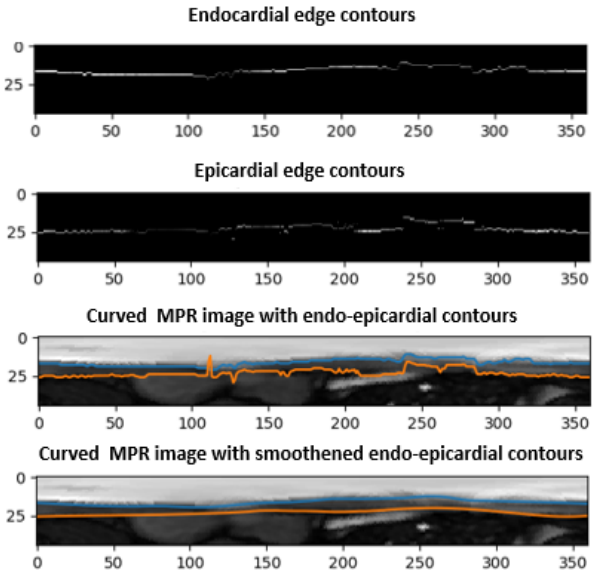

[1] *Sunnybrook Cardiac Data - http://www.cardiacatlas.org/studies/sunnybrook-cardiac-data/*

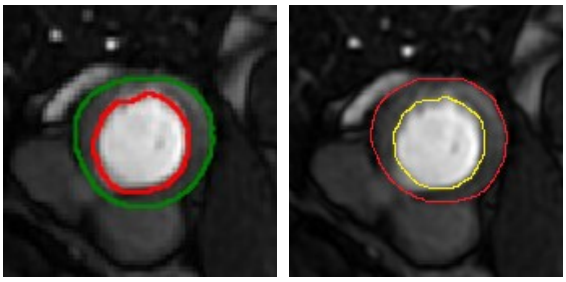

Figure 8: (a) -Segmented Result (b) Manually Traced contours for Frame 2.

Sample MRI Frame 3

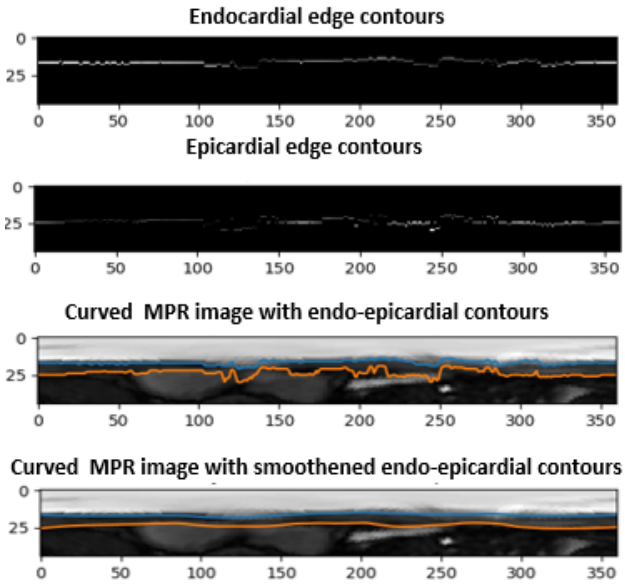

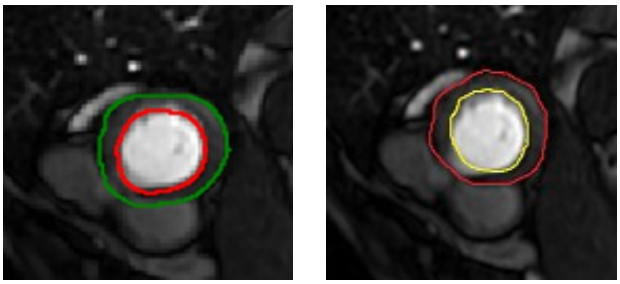

Figure 9: (a) - Segmented Result (b) Manually Traced contours for Frame 3.

V. CONCLUSION

This paper presented an approach for automatic detection of myocardial contours in multiple cardiac MR images. Current work focused on segmenting the myocardial contours in 12 sample MR images from different patients. Future work can be extended to use the proposed work as the template and to superimpose on the LE-CMR image, so that the search of fibrosis can be limited within the template region. This helps to quantify the amount of fibrosis present in the myocardium more accurately.

REFERENCES

[1] C. Ciofolo, M. Fradkin, et.al, "Automatic Myocardium Segmentation in Late-Enhancement MRI", IEEE, pp 225- 228, 2008.

[2] Tanja Kurzendorfer, Alexander Brost, Christoph Forman, Andreas Maier, "Automated left ventricle segmentation in 2-D LGE-MRI", IEEE (ISBI), pp 831-834, 2017.

[3] Trygve Eftestol, Erlend Singsaas, et.al, "Automatic Detection of Microvascular Obstruction in Patients with Myocardial Infarction", computing in Cardiology, pp 757- 760, 2015.

[4] Iveta Bryjova, Jan Kubicek, et.al, "Extraction of Myocardial Fibrosis from MR using Fuzzy Soft Thresholding Algorithm", IEEE (IIAI), pp 1- 6, 2016.

[5] Juan Mantilla, Jose Luis Paredes, et.al, "Detection of Fibrosis in Late Gadolinium Enhancement Cardiac MRI using Kernel Dictionary Learning-based Clustering", computing in Cardiology, pp 357-360, 2015.

[6] Martin Rajchl, Jing Yuan, et.al, "Interactive Hierarchical-Flow Segmentation of Scar Tissue From Late-Enhancement Cardiac MR Images", IEEE Transactions on Medical Imaging, VOL. 33, 2013.

[7] Roberta Leonardi, Federico Veronesi, et.al, "Volumetric identification of left atrial fibrosis from delayed enhancement magnetic resonance imaging in atrial fibrillation: Preliminary results", IEEE Computing in Cardiology, 2014.

[8] Rashed Karim, Aruna Arujuna, et.al, "A Method to Standardize Quantification of Left Atrial Scar from Delayed-Enhancement MR Images", IEEE J Transl Eng Health Med., 2014.

[9] Jeroen J. Bax , Victoria Delgado , "Detection of viable myocardium and scar tissue", European Heart Journal - Cardiovascular Imaging, Volume 16, Issue 10, pp 1062–1064, October 2015.

[10] Marie-Pierre Jolly, "Automatic segmentation of the left ventricle in cardiac MR and CT images," International Journal Computer Vision, Springer vol. 70, no. 2, pp. 151–163, 2006.

[11] G. Hautvast, S. Lobregt, M. Breeuwer, F. Gerritsen, "Automatic contour propagation in cine cardiac magnetic resonance images," IEEE Transactions in Medical Imaging, vol. 25, no. 11, pp. 1472–1482, 2006.

[12] Anupama Bhan , Ayush Goyal, Vinayak Ray, "Fast Fully Automatic Multiframe Segmentation of Left Ventricle in Cardiac MRI Images Using Local Adaptive K-Means Clustering and Connected Component Labeling", IEEE (SPIN), pp 114-119, 2015.

[13] https://docs.scipy.org/doc/scipy0.15.1/reference/generated/scipy.signal.savgol_filter.html (Savitzky-Golay filter).

Proceedings of the Fourth International Conference on Communication and Electronics Systems (ICCES 2019)
IEEE Conference Record # 45898; IEEE Xplore ISBN: 978-1-7281-1261-9

Proposal of smart home resource management for waste reduction and sustainability using AI and ML

Naveen Ananda Kumar J
Institute of management
Christ (Deemed to be University)
Bengaluru, India
jnaveens@icloud.com

Srija Chimmani
Institute of management
Christ (Deemed to be University)
Bengaluru, India
srija.146@gmail.com

Abstract – A research indicated that electricity is obliterating extra non-renewable sources for its production. In that, as per Centre for Policy Research (CPR), about 25% of the total production is diverted to meet the daily consumption in an Indian household. Not only this but also, waste management has become an important issue to deal with. According to Municipal Solid Waste (MSW) of India, waste generation in Indian urban communities extends between 200 - 870 grams per day, contingent on the localities' standard of living and the area of the city. Therefore, in this paper we propose a concept that focuses on a sustainable solution using Artificial Intelligence and Machine Learning algorithms for waste and carbon footprint reduction in a home. This concept explains a solution availed with the help of a proposed model called Home Resource Management (HoReM) that is imbibed in a Smart home.

Key words - Home Resource Management (HoReM), Artificial Intelligence, Machine Learning, Internet of Things, waste management, carbon footprint reduction, Smart home.

I. INTRODUCTION

To divert the load of electricity as a primary source of energy for home appliances, the solution proposed is a smart home that uses renewable source of energy which is Solar. Not just that, the smart home is greatly equipped with waste management quotient. A smart home, also known as domotics, is an advanced automated home system that constitutes of smart lights, smart appliances and smart door locks along with slide and motor sensors for every door and window. This system is heavily relied on Internet of Things that uses Internet in the form of Wi-Fi or Ethernet for connectivity [15]. With the need, waste management has also become the key area of concentration. Beginning of that activity from a home in itself is an achievement. The added features of waste management to a home would constitute solar panels, waste water management system, smart thermostats, smart fridge, smart washing machine, smart AC and air purifier, bio-gas connection, e-dustbin, leak detector.

A green smart home would monitor how and when power is consumed and manage it based on data. Starting from the power to execute all the functions of the home, solar panels can be included for partly distributed power generation along with electricity from other renewable resources such as Hydroelectric plants. Using the sensors and the appliance consumption data, smart power storage system can be charged during the day from the panels and can be consumed at nights by the high-power consumers devices like AC, TV leading to less consumption of electricity generated from non-renewable sources. Also, the system can identify the presence and absence of people which can be further transmitted to disconnect the devices that consume standby power.

Using that power, a typical smart heating/cooling sensor will monitor the external temperature through data from weather websites or from a sensor outside the house and tallies it with the body temperature from the data collected via wearable devices and creates an ideal temperature for the user and their family.

For the regular water consumption in various activities such as washing clothes and utensils, taking a shower - a smart water recirculation system can be built which recycles the used water that will remove calcium and magnesium which are constituents of a hard water [13].

Another safeguarding complimentary solution for decreasing water consumption is leak detection sensors which will be attached to all the pipes at home that will send an alarm to the make motoring system when the tap is not in operation and cuts the supply for that

particular tap. However, integrating a leak detector into smart home network includes actuators that controls water and power sources leading to an alert to the user. And after a certain point of time, if the user fails to react, then it can automatically power off the sources for to control further flow of water [5].

II. LITERATURE REVIEW

According to Bureau of Energy Efficiency (BEE), Indian households accounted represented about 22% of the complete 883 billion units5 of power (whose main source is natural perishable resources) consumption in the year 2014.

As per National Sample Survey Office (NSSO) survey, over 90% of urban family units use power as their key source of lighting. Furthermore, the NSSO's data on families' monthly electricity utilization demonstrates that about 20% of the electrified Indian households expend under 30 units of power for every month while about 80% devour under 100 units for each month. In the urban regions, about 60% of the families expend under 100 units for every month, while 90% of the rural families devour under 100 units depicting in Figure 1.1.

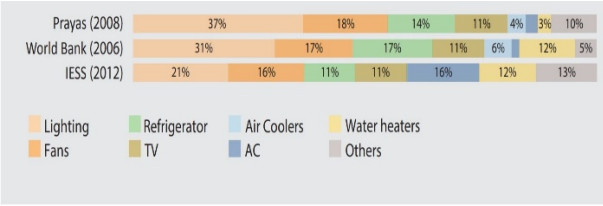

Sources: (Boegle et al., 2010), (NITI Aayog, 2016) and (World Bank, 2008)

Figure 1.1 - 100% stacked column chart demonstrating the electricity consumption of multiple household appliances from different studies

However, electricity is not the only issue that is to be tackled for Indian households. Simultaneously, waste generation has become a major issue. The below mentioned is a waste audit conducted by Press Information Bureau [18], India across 500 households of Hyderabad. Hyderabad is a city with a population of 6.8 million during the 2011 census. The residents were segmented by the income groups as low, middle and high. The incomes were gotten from the property classification they dwelled in. Here, the assumption was that incomes were directly proportional monthly rental costs of the property, real estate value, monthly maintenance costs, and square feet of each flat or villa. Middle (251 households) and High (249 households) income categories were selected as target segments for the waste audit.

Waste was categorized into wet, recyclable and hazardous for variations in food consumption and other factors. Hence, the waste generation was collected across a span of seven days using a digital weighing scale. Each category was again audited in May(summer) and September(autumn) to account for seasonal variations in waste generation.

The results indicated a marginal increase in waste generation amongst High- and Middle-income groups, as shown in Table 1.1. The "middle income" group produced a normal of 0.887 kg of organic waste and 0.235 kg of recyclable waste per house every day. Whereas, the "high income" group produced 0.015 grams higher organic waste and 0.143 grams higher recyclable waste every day.

TABLE 1.1: PRIMARY RESEARCH RESULTS OF THE WASTE AUDIT CONDUCTED ACROSS 500 HOUSEHOLDS

Average Waste Generated per Household per day (in kgs)				
	Wet	**Dry**	**Hazardous**	**Total**
'High income' households	0.902	0.378	0.216	1.496
'Middle income' households	0.887	0.235	0.200	1.322
Final Averages	**0.894**	**0.306**	**0.208**	**1.409**

With rising education and financial gain, the per-capita increment in recyclable waste generated turned as a severe issue for the nation, additional compounded by a population of over two billion. the very fact that nearly 60% of the typical household waste is organic renders options such as RDF and WTE ineffective, due to the low calorific value of organic waste [2].

III. RESEARCH GAP

Even before indulging inside the plans of a Smart home, the key source of entire functioning is possible with the energy in terms of electricity [11]. Also, the highest waste generated would be an e-waste which would contribute majorly in depletion of non-renewable sources of power generation say coal. Therefore, Solar energy will be a dominant electricity source in near future according to Project Drawdown [9]. Currently, the top residential solar panels of 60 individual panels produce an energy between 290 to 360 watts. As per the Tennessee state, a typical 5,000-watt solar electric array that is 80% ideal in terms of output generates about 4,800 kWh per year. Hence, solar energy prevents about 5,760 pounds of CO2 pollution annually.

In the case of Smart lights inside the home, LED lightbulbs set-up cost is initially high however the energy consumption is less than incandescent or compact fluorescent bulbs and lasts longer. An LED bulb consumes up to 25-28 Watts per hour whereas the other mentioned consumes over 40 Watts of energy. Hence, the implementation of alike lighting in smart homes lead to an increase of efficiency by almost 40%.

Installing smart thermostats can also offer major climate benefits. The EPA's Energy Star program confirms that homes with smart thermostats can set aside to $180 every year on warming and cooling.

Recycling, using less water and switching to cleaner cement would all help slow climate change. But the chemicals used in our refrigerators and A/C units trap thousands of times more heat than CO2, so containing them is essential to stopping global warming.

If we prevent refrigerants from leaking and switch to using cleaner chemicals, it would conserve nearly 90 gigatons of C02 out of the atmosphere, according to Project Drawdown's analysis [6]. In fact, the Department of Energy estimates the average household fritters away—and pays for—12,000 unnecessary gallons of water every year. With the implementation of a smart water recirculation system, about two-thirds of water is saved.

IV. COMPONENTS OF PROPOSED MODEL

A. Smart Pay

It is an option enabled via a Smart phone. The Smart Pay will record each and every payment done via credit card, debit card, e-wallets and net-banking. This will keep a track of every transaction performed. These transactions analyzer will help keep a record of money circulation in the system and uploads the data to the cloud.

B. Smart Energy Management

Smart energy management is a combined system of smart grid that react to the local fluctuations. It consists of renewable energy sources. It will help to reduce the monthly expenditure spent on power consumption in the Smart home [4]. This will happen by honing renewable energy source i.e. Solar energy. That will transform the grid system rely less on non-renewable energy leading to reduction of carbon footprint.

C. Smart water recirculation system

The integration of rainwater harvesting system, smart taps, water meters and water flow sensors will help conserve and resend the water into the smart home system for lesser wastage. Additionally, this system will keep a track of the amount of water used, leaked, wasted and future demand as per the consumption pattern [14].

D. Smart appliances

Smart appliances like Smart fridge, Smart lighting, Smart thermostat, Smart washing machine, Smart air conditioner and air purifier will use the smart grid technology to communicates with one another in the system [10]. It helps the user to track as well as work with one tap in the app installed in the smart phone.

E. Smart dustbin(e-bin)

Smart dustbin has a 360-degree camera, LCD interfacing, weight gauge and buzzer that will show the current situation of dustbin to track and segregate the waste. Every motion and regular functionalities are captured via the camera in the form of pictures. This will give the live status of the works being performed inside the smart home. Also, a weight gauge will measure the amount of waste dumped after the camera recognizes the type of waste. Dumping of the waste will intimate the user about the kind of waste being generated on a day-to-day basis for recording and analysis purposes.

Figure 1.2 has two flow charts out of which the first one explains how vegetables/things enter inside the HoReM system. Later, it sends a notification to the user which is tracked from the consumption pattern or about the rotten and unconsumable waste. At last, this data is updated back to the HoReM system.

In the second flow chart, the figure explains how contents inside the fridge is taken out either for cooking followed by consumption or thrown in an e-dustbin. In both ways, the data will get updated in the HoReM system regarding consumption quantity as well as quantity wasted.

Overall, the figure depicts an inter-connection via Smart grid system of Smart pay, Smart refrigerator, Smart dustbin and cloud [16].

V. WORKING PROCESS

In the Smart home system, data is traced at the entry level itself. Figure 1.3 depicts the working model of the smart home. It starts from the minute a product i.e. appliance, groceries, clothes anything is introduced into the Home system. The very first level begins with the Smart Pay option via a Smart phone. The Smart Pay [19]. will record the payment done via credit card, debit card, e-wallets and net-banking which is connected with Home Network of the Smart home [1]. Once that is done, the entire data will perform spend analyzer through it.

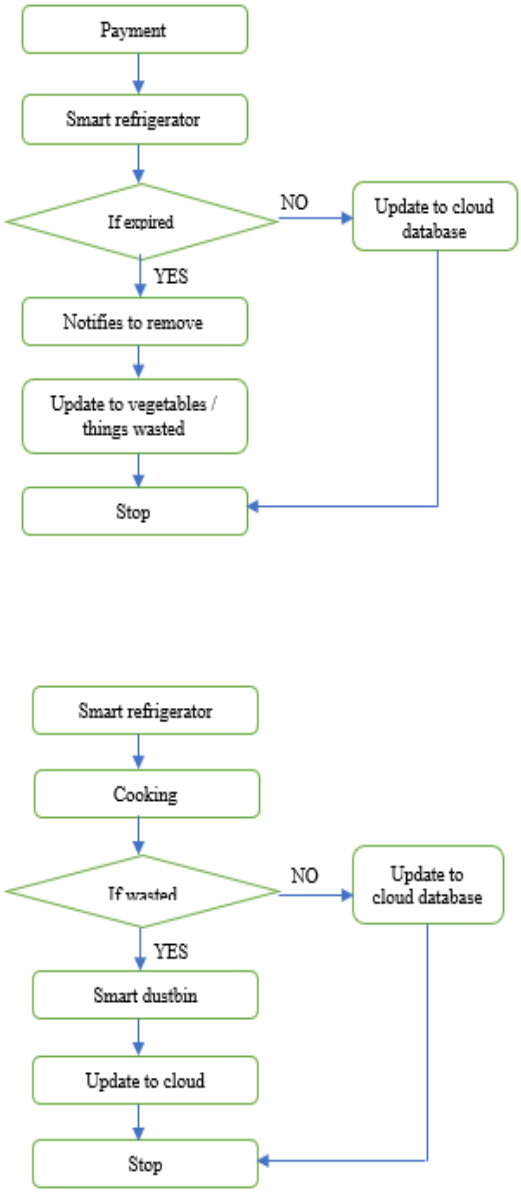

Fig1.2 – Flow chart depicting the process flow of collecting data

Secondly, the data collected will be moved on to the cloud for storage. The cloud here acts as a database for storage and retrieval of the data. Similarly, data is collected from smart lights, programmable thermostats, smart blinds, smart door locks along with slide and motor sensors for every door and window, smart appliances like fridge, washing machine, AC and air purifier. The same would be applicable for a smart Washing machine too. The Washing machine will calculate the amount of detergent stock management and water consumption levels for a particular round of process [12].

As far as the smart water recirculation system, the Water board states that on an average, a low-flow shower head in an Indian household uses about 35 liters of water for a 10-minute shower. Indeterminately, the meter sensors of a smart home shower will measure the amount of water used every single day. The data is run on a probabilistic algorithm say Naive Bayes Classifier and recommends the decrease/increase of flow in tally with the level of water in storage tank as well as on daily usage [8].

When it comes to appliances like Smart fridge, data is collected by sensing the products stored inside it. The bar code scanner would detect the shelf life of the products using the bar codes on the packaging. Later, it will process the time period of product stored inside without regular consumption and notifies about the expiry day that needs to be dumped to the dustbin (which are unfit for consumption). In the same manner, the scanner would measure the products without a packaging like vegetables, fruits and predicts its spoilage period until when it is consumable [17].

Overall all the data is in a process management software called Home Resource Management (HoReM) that allows the smart home to use a system of integrated applications which will manage and automate many background functions related to technology and daily chores.

In this entire process, e-bins would play a key role of detecting what all waste we are dumping out of the system. According to Drawdown's analysis, the food waste accounts for around 8% of the global emissions. Using an ultrasonic sensor, the level of garbage filled in e-dustbin will be analyzed and the LCD interfacing will show the current situation of dustbin. Along with the sensors, the 360-degree camera will identify types of waste using pictures. The detailed analytics measured in kgs/tons will help system to track and segregate the waste based on the image recognition ML algorithm. The waste will be categorized into food wastage – dry and wet, plastic, hazardous and miscellaneous. This will help in order to dump the waste as per the categories. Dumping of the food waste will show the amount of food being wasted on a daily/monthly basis. This data can further reduce waste

generation by intimating the user about the kind of waste being generated on a day-to-day basis.

It is further converted to dashboard using tools and move through Universal Home Gateway. Further, the data collected is sent into the cloud again for analyzing and receiving. After the processing of the data, the information generates a summary using Artificial Intelligence and Machine Learning algorithms. These algorithms will learn from the consumption and waste generation pattern that would result in waste reduction planning. Finally, the summary is shown in the app along with necessary point of changes for efficient saving. It will appear as a recommendation system of what all to consume first and what to dismantle into the garbage.

The summary generated will throw a message to the user saying "The food could have served 200 humans or saved 15 plants" instead of statistical display of numbers. Analogous notification will trigger the user about the waste performed and make them conscious about their decisions. This will lead to a conscious effort of saving and reusing the products in the system without adding it to future waste. Hence, the upliftment will help reduce the wastage, not exactly to zeroth level but to a considerate reduction of wastage. This awareness will bring the waste down leading to a green Smart home which will transform into a sustainable environment.

The app will further assist to generate the upcoming shopping list. It would be rather a recommendation cart that will be created on the basis of consumption pattern of the user. Finally, it will help to manage the money i.e. economy, energy i.e. nature and family i.e. people better – the ultimatum of sustainability.

VI. FUTURE WORK

Overall, sustainability does not reside just in the Smart home as system or few appliances. Rather, the true meaning will be fulfilled with a combination of technology and nature. Currently, the most harmful threat to nature is caused due to lack of regeneration of oxygen and exponential accumulation of Green House gases in the atmosphere. Solution for this threat is planting more trees that will promote the greenery.

In spite of being a grass, bamboo is likewise a genius at putting away carbon and blossoms on a degraded land. It will be equivalent to remove the carbon emissions produced by 50.6 million cars, making it a legitimate environmental change arrangement, according to Project Drawdown's analysis. Hence, bamboo plants will be grown in hydroponic solution as an indoor garden to combat global warming. Also, it would reduce the carbon emissions in the system by circulating more oxygen. Further, the hard water generated out of the Smart water recirculation system can be transferred to hydroponic plants that are used for indoor gardens. The sunlight and soil moisture will be operated via the sensors as well as the actuators.

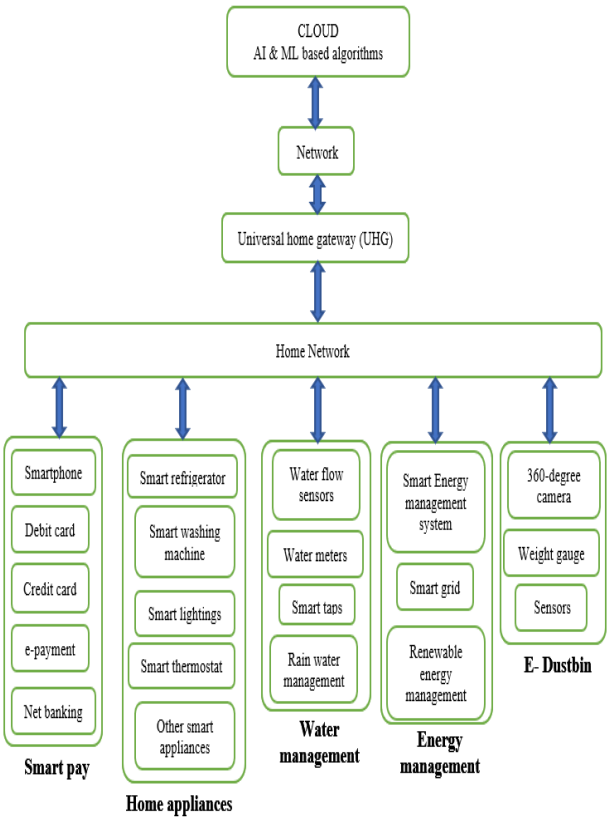

Fig 1.3 – Block diagram of the Smart home integrated with HoReM

VII.CONCLUSION

The proposed Smart home is an apparatus for waste management, reduction of unwanted costs in a household and efficient energy administration. The entire system is built to aid the user for a better way of living. In the quest of an environmental sustainability, the user need not compromise on luxury rather should be mindful of the resources utilized. Hence, the outcome will overall promote sustainability from a very base level. Wherein the base level is home and change begin at home, spreads to the community.

ACKNOWLEDGMENT

We thank our colleagues from the Institute of management, Christ (Deemed to be) University who provided us with insights which were great assistance in shaping our research. We would like to express our gratitude to the faculties and colleagues of Institute of

management, Christ (Deemed to be) University for sharing their pearls of wisdom, reviewing our research and giving us key inputs.

REFERENCES

[1] A Zanella et al, .. (February 2014). Internet of Things for Smart Cities. IEEE INTERNET OF THINGS JOURNAL, VOL. 1, NO. 1.

[2] Annepu, R. K. (2012). Sustainable Solid Waste Management in India. Columbia University, New York city: Central Pollution Control Board and National Environmental Engineering Research Institute.

[3] authors, M. (2014). Prayas Pune organization. Retrieved from Prayas Pune organization: http://www.prayaspune.org/reli/SDI_INFO.htm

[4] B Zhou et al. (March 2016). Smart home energy management systems: Concept, configurations,and scheduling strategies. Elsevier Science Journal Renewable and Sustainable Energy Reviews, 11.

[5] Cara D. Beala et al, .. (2011). A novel mixed method smart metering approach to reconciling differences between perceived and actual residential end use water consumption. Elsevier Science Journal- Journal of Cleaner Production.

[6] D Kann et al. (2019, April 19). CNN. Retrieved from CNN: https://edition.cnn.com/interactive/2019/04/specials/climate-change-solutions-quiz/?fbclid=IwAR1QG1deIbP2Y37sMk7zZIusfn_Vj7i2VDeylHDunTJ1YGs4f-JBD3QwjeI

[7] Debraj Basu et al, .. (2013). Wireless Sensor Network Based Smart Home: Sensor Selection, Deployment and Monitoring. School of Engineering and Advanced Technology, Massey University, New Zealand.

[8] G Hauber-Davidson, E. I. (2006). Smart Water Metering. Demand Management.

[9] Hawken, P. (2019). Project Drawdown. Retrieved from Project Drawdown: https://www.drawdown.org/

[10] J Han et al. (May 2014). Smart Home Energy Management System Including Renewable Energy Based on ZigBee and PLC. IEEE Transactions on Consumer Electronics, Vol. 60, No. 2, 5.

[11] Matt Hamblen, S. (2018, July 17). Las Vegas cleans up with machine learning. Retrieved from www.smartcitiesworld.net: https://www.smartcitiesworld.net/special-reports/special-reports/las-vegas-cleans-up-with-machine-learning-

[12] N Javaid et al, .. (2017). An Intelligent Load Management System With Renewable Energy Integration for Smart Homes. IEEE Access.

[13] Nguyen et al. (2015). Intelligent autonomous system for residential water end use classification: Autoflow. Applied Soft Computing, Griffith University.

[14] R.M. Willis et al, .. (2011). Residential potable and recycled water end uses in a dual reticulated supply system. Elsevier Science Journal on Desalination.

[15] Rita Yi Man Li et al, .. (2016). Sustainable Smart Home and Home Automation: Big Data Analytics Approach. International Journal of Smart Home Vol. 10, No. 8, 177-198.

[16] S Hulyalkar et al, .. (2018). Implementation of Smartbin using Convolutional Neural Networks. International Research Journal of Engineering and Technology (IRJET).

[17] Suhuai Luo et al, .. (2008). Smart Fridges with Multimedia Capability for Better Nutrition and Health. International Symposium on Ubiquitous Multimedia Computing.

[18] Swaminathan, M. (2018, April 21). Engage. Retrieved from Economic and Political Weekly: https://epw.in/engage/article/institutional-framework-implementing-solid-waste-management-india-macro-analysis

[19] Uzialko, A. C. (2019, February 10). Mobile Wallet Guide: Google Pay vs. Apple Pay vs. Samsung Pay. Retrieved from Business.com: https://www.business.com/articles/google-pay-vs-apple-pay-vs-samsung-pay

[20] Zaheer Khan et al,. (2013). Cloud based Big Data Analytics for Smart Future Cities. IEEE/ACM 6th International Conference on Utility and Cloud Computing.

[21] J Chin et al, .. (2012). Understanding and Personalising Smart City Services Using Machine Learning, the Internet-of-Things and Big Data .

[22] A Chandramohan et al, .. (2015). Automated Waste Segregator.

[23] Miao Yun, B. Y. (2010). Research on the architecture and key technology of Internet of Things (IoT) applied on smart grid. 2010 International Conference on Advances in Energy Engineering.

Proceedings of the Fourth International Conference on Communication and Electronics Systems (ICCES 2019)
IEEE Conference Record # 45898; IEEE Xplore ISBN: 978-1-7281-1261-9

Improved IIR tracking by fusion of centroid estimation processing with IMM filter

V S N Murthy A, Chandrakanth V†, P V R R Bhogendra Rao, Ramakalyan Ayyagari*
*Department of Instrumentation and Control, National Institute of Technology, Tiruchirappalli
Defense Research and Development Laboratory, Ministry of Defense, Hyderabad - 500058
Email: †chandrav@drdl.drdo.in

***Abstract*—Imaging Infrared seeker(IIR) is a passive system which works on the reflections from the ambience and tries to deduce intelligible information regarding the targets of interest. Passive systems have complex processing schemes because of the unavailability of active reference signals to synchronize the processing. All the information has to be derived from the raw data obtained using thermal gradients. Manual intervention in these systems is inevitable to provide the initial conditions for the processing to start, unlike active systems where the system automatically configures or maps the surrounding by transmitting a signal. Centroid tracking and image correlation based tracking have been used for IIR tracking extensively in literature. Centroid tracking is highly sensitive to background data and initial tracking window size selected whereas correlation tracking requires a reference template for matching the target parameters which is usually not available up front. Both the techniques have high track loss rate if the background is cluttered. In this work we have proposed a novel infrared tracking technique for IIR seekers by fusing centroid processing with Interacting Multiple Model(IMM) filtering to reduce track loss and improve tracking efficiency.**

Keywords: Centroid Estimation,Correlation tracking, Infrared seeker, IMM filter, Field of view(FOV), Laser range finder(LRF), Readout IC(ROIC), Focal plane array(FPA)

I. Introduction

An infrared system requires specialized optical framework along with integrated ROIC to get the raw image for further processing. Because of complexity and limited expertise, IIR systems tend to be expensive which does not break even for everyday commercial applications which has restricted the technology mostly to military applications. In military applications they are an indispensable tool for territory defence and cross territory enemy intrusion alerts in the border areas especially during dark hours. They form the only source of surveillance available when our optical systems fail. IIR seekers are special class of airborne systems developed for tracking targets of interest, both stationary and mobile, and guide the weapon system towards them culminating in payload delivery for lethal impact. Being mounted on aerial vehicle, the system is tightly constrained by area, processing time and power. Adding to the complexity, IIR systems works on gray scale images which gives very little scope for processing enhancements. Most of the image tracking algorithms proposed in the literature work with colored images [1][2][3][4]. Glasgow and Bell [5] have summarized a brief account of IIR seeker systems available presently and future trends in this field for the interested reader. Traditionally, centroid tracking [4] and correlation based tracking [6][7][11] have been used for tracking the target. While centroid tracking is highly sensitive to background data and initial tracking window size selected, correlation tracking requires a template for matching the target parameters which is usually not available up front. Wanjae Lee et al. [7] proposed a variant of correlation algorithm by estimating the target template every scan with the correlation coefficient between multiple zoomed templates which again requires a reference template for processing. [14][15] propose kalman tracking using single model filters. Single model filters are suitable for no or very little manoeuvring targets. They fail if the target changes direction when passing behind occlusions. In this paper we propose a hybrid approach to fuse data from centroid tracking with IMM filter to handle manoeuvring targets. [8][9][10] present details of IMM filter modelling in detail. We have generated a target model based on background data taken from the field over which we superimposed simulated target data with varying trajectories to closely mimic the real time scenario in the lab. With this approach we improved tracking efficiency and reduced track loss as evident in the simulation results presented. The rest of the paper is organized as follows. Section II briefs on target trajectory modelling. Section III details the proposed methodology. Section IV validates our claim with simulation results followed by conclusions in section V.

II. Target trajectory modelling

The input to the image processor in an IIR seeker is the target image sampled at every 't' seconds. Typically 't' will be in the order of 35ms which should cater for thermal intensity conversion, Non Uniformity correction (NUC), ROIC multiplexing, De-multiplexing and image formation followed by tracking. With this order of sampling rate and pre- processing operations the processing time for tracking is reduced drastically thus, further complicating the problem at hand. There are two methods to generate input video for validating our algorithm.

(a) Generate the trajectory based on the target parameters and map this data to image pixels considering the seeker parameters mentioned in the Table 1.

In this method, at every sampling instant, the range, swath area, pixels occupied by target at that range and range per

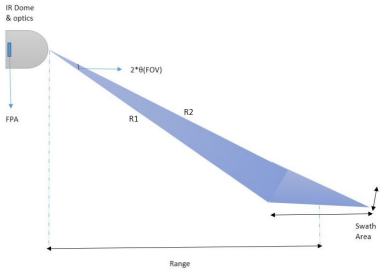

Fig. 1. Seeker Optics

pixel will be calculated. This information is used to generate the target position in the next frame using Equations 1-3 for subsequent processing. This process is continued until the last frame and finally we get a simulated video input to our algorithm.

Table 1	
Parameter	value
Target Parameters	
Range	7000 mtrs
Velocity	70 Kmph
No of Pixel at given range	4 x 4(approx.)
Target Heading	45 deg
IIR seeker Parameters	
Field of view	2 deg $(2 * \theta)$
FPA resolution	256 x 256
Swath area(1D)	2*Range*$tan(\theta/2)$
Range per pixel shift	Swath'area/resolution

$$v(n) = v(n-1) + a * t; \quad (1)$$

$$s(n) = s(n-1) + v(n) * t; \quad (2)$$

$$s(n) = s(n-1) + v(n) * t + 0.5 * a * t^2; \quad (3)$$

where, 's' is the range of the target, 'v' is the target velocity ,'a' is the target acceleration and 't' is the sampling time.

(b) From our previous experience in the field, videos gathered during evaluation trials, discussing with pilots and other colleagues, we narrowed down few trajectory models which we directly simulated at the image level at every frame. From this trajectory, we mapped the target co-ordinates to range and azimuth using parameters from Table 1 and created an input state vector to the IMM filter.

We followed second approach for target generation for our simulations. We considered four phases of target movement. Each phase was coded with a different trajectory model and combined to generate a random trajectory across the image.

III. Proposed Algorithm

A. Centroid processing

$$x = \frac{\sum_{i=1}^{i=m} i \sum_{j=1}^{j=n} I(i,j)}{\sum_{j=1}^{j=m} \sum_{j=1}^{j=n} I(i,j)} \quad (4)$$

$$y = \frac{\sum_{i=1}^{i=m} i \sum_{j=1}^{j=n} I(i,j)}{\sum_{j=1}^{j=m} \sum_{j=1}^{j=n} I(i,j)} \quad (5)$$

where, (x,y) are the centroid co-ordinates, (i,j) are pixel co-ordinates in the received image $I(i,j)$.

Centroid processing is the earliest algorithm used for IIR tracking and still is the most preferred method in ideal conditions. Once the IIR seeker is cooled and ready to view the image, user scans the environment for potential threats and locks on to the target. The initial window enclosing the target and some background is selected and information is passed on to the image processor, We obtain range information using Laser Range Finder(LRF) present in the cockpit. In other scenarios, ground based radar can be used to get initial range information. This information is required to compute the swath area and other parameters in every scan. After locking the target, the feed is handed over to the tracking algorithm which continuously computes the centroid in the given window using equation 4-5 and moves the window keeping the updated centroid in the center. The Problems with this method are

(a) window size is very critical in this method. The window should enclose the target completely with very little background so that background does not dominate centroid calculation.

(b) As the target range decreases the pixels used to represent the target increase i.e, the target template size varies with range. Accordingly, the tracking window has to be adjusted to keep the ratio of "target pixels/background pixels" almost constant.

The main challenge here is to identify the change in target size. Since we are updating the frames at a very high rate, the change from frame to frame is low. The only reference we have to understand this change are the centroid coordinates. They are two possibilities for centroid to be constant in consecutive frames. (a) The target has halted (b) Target size has increased in the frame. Both the cases have to be handled separately so that problem at hand now becomes to identify the condition. The IMM filter precisely does this and solves our problem. It tracks the target even after centroid input is constant and in further frames reacquires the target preventing track loss.

B. IMM tracking

Interacting Multiple model(IMM) filter is primarily developed to use in active radar tracking [9]. It is a combination of multiple state models which are combined according to model probabilities calculated to give a filtered output as shown in figure 5. It consists of state interaction, model probability calculations and combining state estimates for better tracking. We have considered 2 model IMM (CV-CA) for our algorithm. Equations 6-7 represent state and output equation and equations 8-12 represent the equations for state

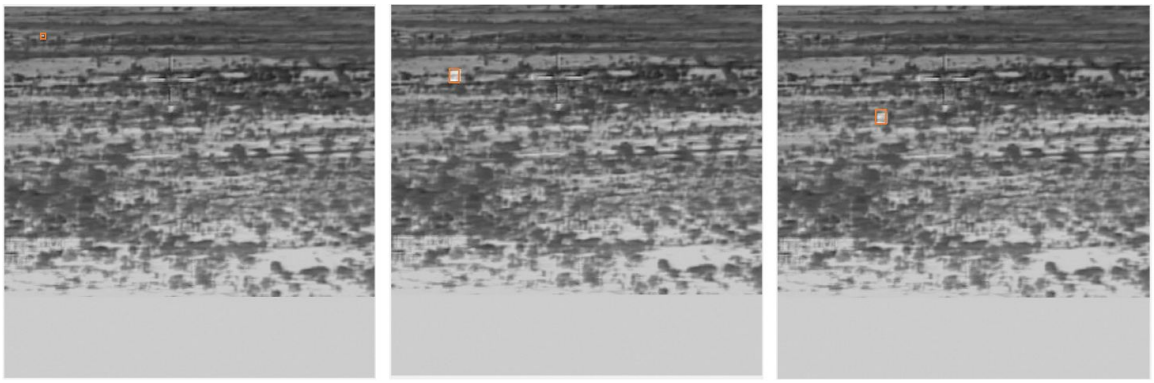

Fig. 2. [a,b,c]Target tracking with centroid processing. It can be observed that the tracking window is following the target correctly in subsequent frames

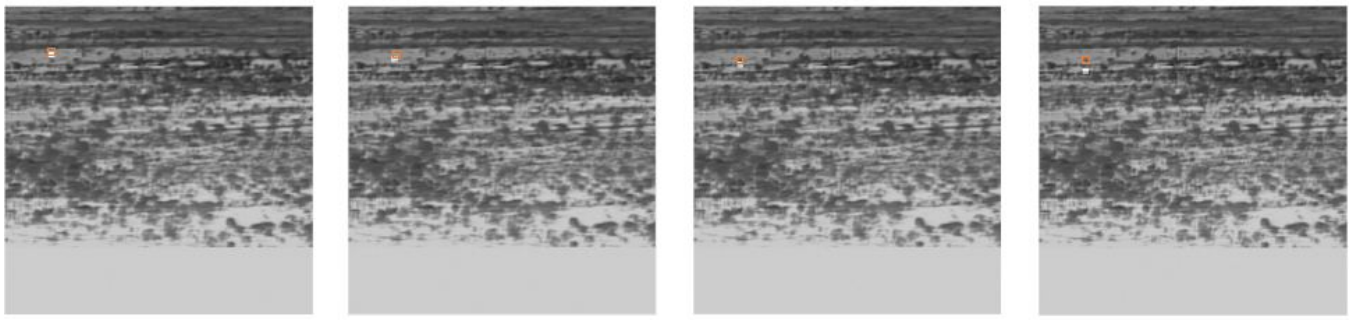

Fig. 3. [a,b,c,d]Target manoeuvre caused centroid jump which led to target window miss as shown in (d).

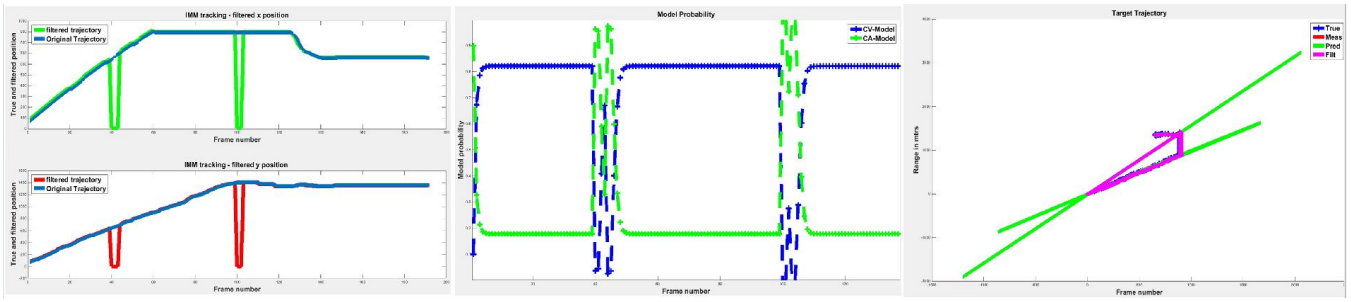

Fig. 4. IMM tracking for missing centroid data (a) Filtered centroid cartesian co-ordinates, (b) Model probability (c) Target trajectory

prediction,state and covariance update equations for kalman filter.

$$X_{k+1} = \phi_k X_k + w_k \tag{6}$$
$$y_k = H_k X_k + v_k \tag{7}$$
$$\widetilde{X} = \phi \hat{X} \tag{8}$$
$$\widetilde{P} = \phi \hat{P} \phi^T + Q \tag{9}$$
$$K = \widetilde{P} H^T (H \widetilde{P} H^T + R)^{-1} \tag{10}$$
$$\hat{X} = \widetilde{X} + K(y_k - H\widetilde{X}) \tag{11}$$
$$\hat{P} = (I - KH)\widetilde{p} \tag{12}$$

where,
X = State estimate
w_k = process noise
v_k = observation noise
P = Covariance matrix
˜ = Predicted values
ˆ = Filtered values
ϕ = State transition matrix
Q = Process noise matrix
K = Kalman gain
R = Measurement covariance matrix
I = identity matrix
y_k = measurement
T = matrix transpose operation

The flow chart of the proposed method is shown in Figure 6. The input to the tracker are the centroid cartesian co-ordinates from the input image which are representative of the target movement across the image surface. Because of the

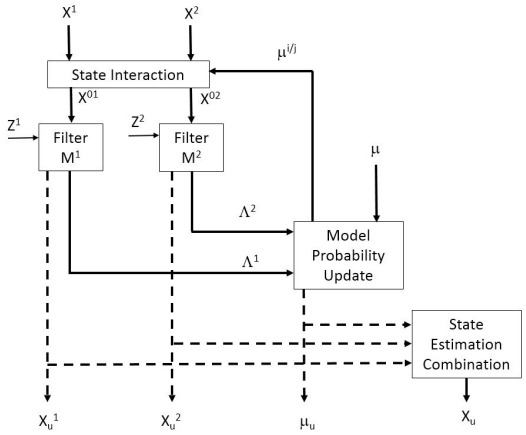

Fig. 5. Block diagram of 2 model IMM processing

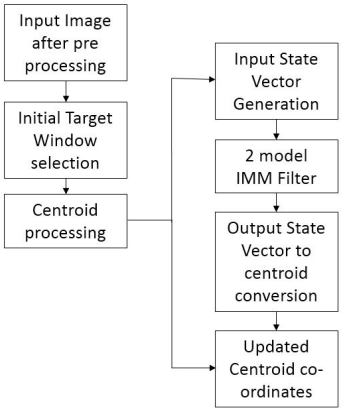

Fig. 6. Flow chart for proposed algorithm

high sampling rate (33 fps) the centroid shift is limited to a few pixels in consecutive frames. This helps in relaxing the input rate to the IMM filter reducing the computations. We have considered every fourth frame for IMM tracking and still obtained good tracking performance. However, when the target moves in and out any obstacle, depending on the area covered by the occlusion we will miss some data frames where the filter will coast or propagates the centroid measurement for few scans. If the obstacle causes a loss in significant number of frames, the target in the visible frame may change in size which may lead to a centroid jump. This jump if in the same direction of previous heading can be handled by single model filter. But if the target changes it course, we need to relock onto the target for tracking. In this case, we can use multiple model IMM filter which can predict different possible positions of the target with varying prediction window sizes to reacquire the target. After acquiring the target from the next measurement, the filter will recalibrate towards the new heading, tracking the target till the hit. Without IMM we cannot acquire targets which have changed heading after the occlusion using only centroid processing. Single model filter is suitable for benign targets where the manoeuvrability of the target is minimum. But this is seldom the case in real time scenario which necessitates the implementation of multi model IMM.

IV. Simulation Results

We have simulated multiple trajectories but due to space constraints presented results for only one trajectory. As mentioned earlier, for our simulations, we have taken background images from the field data and overlaid the simulated target data onto the background image in every frame along with Gaussian noise generating the input video. The video thus generated was fed to the centroid processor with the given initial conditions. The algorithm tracked the target updating the centroid coordinates for the full video without any track loss when there is no manoeuvre as shown in Figure 2. Figure 2 shows the image of the target at different ranges. The target size is divided with range per pixel value at every frame to get the number of pixels to represent the target as seen in the field. Figure 2(a) shows the initial bounding box enclosing the target by the user which is the only input to the tracker. Figure 2(b) and 2(c) show the target with the bounding box tracking the target. Figure 3 shows the case of target miss where the bounding box does not enclose the target due to target manoeuvre. To mitigate this problem, we have used parallel IMM filter channel. After 3 frames of centroid tracking the centroid co-ordinates of the previous 2 frames were input to the 2 model IMM filter in parallel tracking channel as initial conditions. We have simulated the track loss conditions by dropping the centroid co-ordinates in the input vector of IMM filter and observed that tracker was coasting and reacquiring the target in a few frames as seen from the plots in figure 4. It can be observed that when there is loss of data, IMM filter is trying to converge on a suitable model for tracking which is causing the change in model probabilities shown figure 4(b). Figure 4(c) shows the actual trajectory in blue and predicted trajectory in green. As can be observed when there is data loss or change in direction of target motion the predictions go astray but the filter is assigning appropriate weights to the models to get the filtered output(in magenta) which is in line with the true trajectory.

V. Conclusion and Future Scope

In this work we have proposed a novel fusion method of tracking the targets with infrared imaging systems. We have explained the track loss in conventional centroid processing and proposed our method to improve the same. We have implemented parallel channel of target tracking and fused the output to improve tracking efficiency which is apparent from the simulations results. We have considered 2 model IMM which can be further scaled to multiple models to get even better tracking efficiency depending on the complexity of target manoeuvrability and the available resources. We are currently implementing supervised template matching algorithm in third channel to improve resolution in multiple target scenario.

REFERENCES

[1] Stauffer, Chris, and W. Eric L. Grimson.*"Learning patterns of activity using real-time tracking"*. IEEE Transactions on pattern analysis and machine intelligence 22.8 (2000): 747-757.

[2] Wren,christopher R et al. *"Pfinder:Real-Time Tracking of the Human Body."* IEEE Transactions on pattern analysis and machine intelligence 19.7(1997).

[3] Han, Bohyung, and Larry Davis. *"Object tracking by adaptive feature extraction."* Image Processing, 2004. ICIP'04. 2004 International Conference on. Vol. 3. IEEE, 2004.

[4] Comaniciu, Dorin, Visvanathan Ramesh, and Peter Meer. *"Real-time tracking of non-rigid objects using mean shift."* Computer Vision and Pattern Recognition, 2000. Proceedings. IEEE Conference on. Vol. 2. IEEE, 2000.

[5] Glasgow, Bruce, and William Bell. *"The future of anti-aircraft imaging infrared seeker missile threats."* Aerospace Conference, 1999. Proceedings. 1999 IEEE. Vol. 4. IEEE, 1999.

[6] Cui, Ming, Zhiyong Wu, and Yonggang Cao. *"Design of Image Tracking System for Strapdown Seeker based on FPGA+ DSP."* 5th International Conference on Advanced Design and Manufacturing Engineering. Atlantis Press, 2015.

[7] Lee, Wanjae, et al. *"A novel template update method for IR seeker."* Infrared, Millimeter, and Terahertz Waves, 2009. IRMMW-THz 2009. 34th International Conference on. IEEE, 2009.

[8] Ding, Zhen, and Lang Hong. *"An interacting multiple model algorithm with a switching Markov chain."* Mathematical and Computer Modelling 25.1 (1997).

[9] Genovese, Anthony F. *The interacting multiple model algorithm for accurate state estimation of maneuvering targets.* Johns Hopkins APL technical digest 22.4 (2001): 614-623.

[10] Y. Bar-Shalom ve T. E. Fortmann. Tracking and Data Association, New York, Academic Press, 1988.

[11] Teresa L. P. Olson, Carl W. Sanford, *"Real-time multistage IR image-based tracker"*, Proc. SPIE 3692, Acquisition, Tracking, and Pointing XIII, (15 July 1999).

[12] Xu, Liang, *"Information Fusion for Radar/Infrared Compound Seeker based on Federated Filter."* International Journal of Digital Content Technology and its Applications. Volume 5, Number 4, April 2011.

[13] Georgi M. Dimirovski et al. *"A Simulator for Line-of-Sight Missile Control and Guidance Systems: Object-Oriented Design."* Johns Hopkins APL technical digest 22.4 (2001): 614-623.

[14] Mosavi M R, Asadpour M and Farasat M R. *"Design and Implementation of a New Infrared Counter-Countermeasure Algorithm using Kalman Filter."* Proceedings of ICSP 2006.

[15] Aytac, Tayfun and Onur Bekmen. *"Development of a Target Tracking Algorithm for Imaging Infrared Seekers."* Signal processing, communication and application conference, 2008, SIU 2008.

Proceedings of the Fourth International Conference on Communication and Electronics Systems (ICCES 2019)
IEEE Conference Record # 45898; IEEE Xplore ISBN: 978-1-7281-1261-9

A Novel Encryption Algorithm based on DNA Cryptography

A.Vikram*, S.Kalaivani*,G.Gopinath**
*School of Computer Science and Engineering, Bharathidasan University, Tiruchirappalli.
**Professor, School of Computer Science and Engineering, Bharathidasan University, Tiruchirappalli.

Abstract: **The process of information security entails securing the information by transferring it through the networks preventing the data from attacks. This way of securing the information is known as cryptography. The perspective of converting the plain-text into non-understandable format is known as cryptography that could be possible using certain cryptography algorithms. The security could not be offered by the conventional cryptographic algorithms that lacks in their security for the huge amount of growing data, which could be easily broken by the intruders for their malicious activity. This gives rise to the new cryptographic algorithm known as DNA computing that could strengthen the information security, which does not provide any intruders to get authorized to confidential data. The proposed DNA symmetric cryptography enhances information security. The results reveal that encryption process carried out on plain-text is highly secured.**

Keywords: DNA cryptography, Information security, DNA computing.

I. INTRODUCTION

DNA computing was mainly emerged to solve the directed Hamiltonian Path Problem (HPP), which was proposed by Adleman. The concept of HPP is to obtain the shortest path that traverses along each and every node and then return to the last node in the bounded path. A DNA sequence could be formed by fixing the source node second half part to the destination node of the first half path. This DNA computing solved the problem of HPP and gave a new direction in the field of cryptography.

Figure 1: Chromosomal Sequences from a Genetic Database

The most prominent work in DNA cryptography was carried out by Gehani and they proposed an image encryption algorithm with a help of one-time-pads. Substitution method was also bought up that did the pair wise mapping among the plaintext message and ciphertext algorithm. The encryption and decryption were done by the DNA-chip based approach for the 2D images with one-time pads and observed an enhanced version of steganography by reducing the difference among the disorder strands and the plain text. This form of DNA computing was carried out by many researchers in various fields in order to provide a security for the huge amount of data as shown in figure 1. Various cryptographic approaches were also bought to idea known as DNA-BASED cryptographic approaches. Certain attractive properties were also bought in work by DNA computing such as high storage capacity, maximum efficiency in energy, high parallelism that forms high advantage for the concept of data hiding. The application could be a solution for the signal processing, optimization problems, forecasting as well as clustering. One-gram DNA could contain 108 TB of data. This is equal to 1021 DNA-bases.

The objective of this paper is to provide the following:

- To analyze various approached regarding the DNA cryptography.
- To offer a robust ciphertext with the enhanced cryptographic algorithm.
- To offer an advanced data hiding methods with the enhanced approach.

A. DNA

DNA (Deoxyribonucleic Acid) that is formed by the nucleotides is in the form of biological super molecule, which is the source plasma of all living beings. Deoxyribonucleotides is said to be known as the monomer unit of DNA. Four types of nucleotides bases are found in DNA namely,

- Adenine (A),
- Cytosine (C),
- Thymine (T), and
- Guanine (G)

There are two nitrogen bases for the DNA: 1) Purines 2) Pyrimidines. A and G are said to be the double ring molecules and are termed as purines where the single ring molecules are called pyrimidines that has the base C and T. The capability of DNA could be found in the enormous industries that could serve the purpose of image and data encryption, data hiding, steganography, etc. Several parameters such as temperature, pressure, oxygen ratio etc., should be taken care while executing the DNA operations in various laboratories (identical conditions of several parameters should be maintained). Since the DNA is the sensitive module, this could provide several outputs in various environments. Hence, it could be said that the DNA computation totally depends on the environmental conditions as shown in figure 2. Binary form of converting the DNA sequence is known as the binary coding scheme. In this paper the DNA bases such as A, T, C, and G have been used for the binary scheme of 00, 11, 01, and 10. For instance, DNA sequence "AATCGGAT" has the binary sequence of 0000110110100011. RNA (Ribonucleic Acid) also

consist of the main bases as same as the DNA but here the Thymine (T) is replaced by Uracil (U).

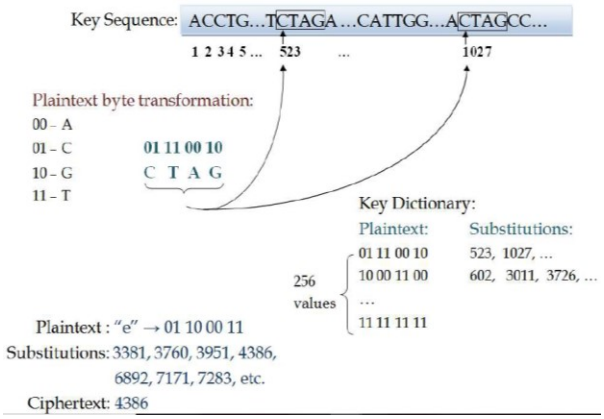

Figure 2: DNA Indexing Algorithm's encryption process

II RESEARCH MOTIVATION AND PROBLEM STATEMENT

The concept behind cryptography is to convert the plaintext into ciphertext (non-understandable format) using several algorithms that falls under cryptography concepts. Cryptography algorithms such as DES, TDES, AES, and RSA that is the multifarious symmetric and asymmetric key algorithms that helps in conversion of plaintext into ciphertext. The security could not be offered by the conventional cryptographic algorithms that lacks in their security over the growing internet usage for the huge amount of growing data, which could be easily broken by the intruders for their malicious activity. DNA could be used in two major roles under the concept of DNA cryptography. DNA acts as a medium for the encryption keys since it has two fundamental properties. The fake DNA and the real DNA sequence have virtually no major sequence. The other point is that there are 163 million DNA sequence available all over the world. Several cryptographic algorithms have been proposed over the last decade. These algorithm ciphertext is more complex than the normal key ciphertext.

III TECHNICAL BACKGROUND AND RELATED WORK

Various algorithms have been created in the concept of DNA computing. Tedious cases such as SAT, DES has been solved with the help of DNA computing in the past two decades. NP complete SAT problem has been solved by Lipton [1] using DNA computing. He also formulated an encoding scheme with the DNA scheme and the author employed a minimum number of variables to solve the SAT problem. In order to crack the Data Encryption Standard (DES), Boneh et al [2] proposed an approach with the DNA computing. Any crypto-system could be cracked with the less key size of about 64-bits with their proposed algorithm. Moreover, their encryption circuit is also small with the cracking mechanism in 916 steps. Each individual step is equal to 32 extractions and it needs at least a day processing for every 10-extraction steps. Altogether, their proposed algorithm could take at least 4 months to crack DES. With the DNA operations hard problem could be solved with the DNA computing techniques that were proposed by Chen et al. [3]. They also solved DES with the DNA technology. Three various functions have been included in the Chen et al.'s anticipated algorithm: 1) Initial function for initialization of the key space with every possibility 2) Encryption process, and 3) Detecting right corresponding key. Enzymes, tubes and short memory strands are all included in the molecular sticker algorithm.

Symmetric-key DNA cryptosystem had been introduced by MingXin et al. [4] that includes the DNA biotechnology imparted into the cryptography technologies. With the DNA probes the encryption and decryption has been formed in this algorithm and the ciphertext has been embedded into the DNA chip (microarray). The advancement of DNA chip leads to the security of the algorithm. For the efficient, reliable and secure transmission of data an algorithm has been proposed by Kar et al. [5]. This algorithm utilizes the DNA keys that utilized 3 keys: 2 keys for the encryption and the remaining one key for sharing the encryption key to the receiver. With the help of string to binary conversion process the plaintext will be converted to binary sequence in this algorithm. Binary coding scheme converts the huge DNA pattern in the form of binary data as the encryption key. The ciphertext could be obtained by applying the XOR and addition operations in the 64-bits plaintext and 64-bits key. Several cryptographic approaches had been proposed by Shiu et al. [6]. The cryptographic approaches with the utilization of DNA approach are as follows: 1) Insertion method 2) Complementary pair method, 3) Substitution method. Finally, they also proved that the substitution method is more efficient than the other two approaches. Data hiding approach has been proposed by Liu et al. [7] with the encryption of ciphertext in a word file with the DNA sequence. Their algorithm utilizes the DNA coding that converts the plaintext into DNA sequence. Chebyshev maps produce two pseudorandom DNA sequence XXOR and YPrimer, and create one time key using preferred DNA sequence key. The output generated includes the YPrimer and the DNA message sequence includes the XXOR. By applying the shift operations in the previously generated output, they could be converted to ciphertext. The word file could be converted to PDF after the encryption of ciphertext into the word file. The receiver will receive the PDF generated. A strong ciphertext algorithm had been proposed by Mandge et al. [8] that include key generation technology with the manipulation of matrix inclusion in the cryptographic algorithm. Initially the plaintext will be converted to a mini-cipher with the several shifting and XOR operations. It is said that if the process is applied to the plaintext each time, we could obtain various mini-

cipher for the similar plaintext since this process includes the secure key generation. After this mini-cipher gets converted to a final ciphertext with several biotechnologies that includes of DNA primers. The substitution method with the single bit complementary rule of Shiu et al. had been enhanced with the table lookup substitution method (TLSM) proposed by Taur et al. [9]. They extended to the two bits complementary rule for the substitution method. The two-bit message is converted to their corresponding letter with the help of TLSM that utilizes the lookup tables [10][11]. On the other hand, Shiu et al. rule could only translate one bit at a time. Moreover, compression of ciphertext is very effective in the TLSM procedure [12].

Complex problem that are difficult to solve in the silicon-based computer could be solved by the DNA computing by the researchers in a polynomial time [13]. The better results could also be generated by the DNA computing that could be used in the field of image processing, clustering and optimization problems. A brief description regarding the problem could be provided by this research work and also helps in analyzing the loopholes from the existing research works[14].DNA operations like Hybridization, Indexing, and PCR have the capacity for a solution of the application in the fields as data hiding, image encryption, and steganography. Several fascinating characteristics have also been present in the DNA that includes vast parallelism, maximum storage capacity as well as maximum efficiency in energy. This forms as an advantage for the data hiding and provides high security for the security purpose for the fast-growing internet data. Hence this could form as a greatest boon to the future for protecting the data [15]. Annealing, Hybridization, Indexing and PCR (Polymerase Chain Reaction) are said to be the DNA operations that has the ability to offer a strong data encryption technique. The powerful cryptography algorithm could be created when the DNA keys and DNA operations are combined together [16]. Cryptographic techniques thus provide greater security for the on-line as well as the off-line private security data. This offers several researchers to find an optimum solution in their research areas. The problem includes the silicon-based computer in polynomial time. Moreover, DNA computing offers greater solution in less amount of time when compared to the silicon computer [17][18].

IV PROPOSED DNA CRYTOGRAPHIC ALGORITHM

The enhanced proposed approaches have been explained in this section that accepts the message in the form of a plaintext and converts it as ciphertext in the form of protein. The receiver receives the protein through the public channel and the decryption process will be applied to receive the plaintext or the message [19]. The binary coding scheme will be shared by the sender and the key will be the codon table of RNA that utilizes the database name, which will be a shared symmetric key with the index number and send through the secure channel to the receiver end in this approach. From the DES algorithm, several substitution and permutation network will be developed through the enhanced algorithm. The functions of the encryption and decryption will be used in the receiver end[20]. Generally, plaintext will be converted into binary value in the encryption algorithm with the utilization of hexadecimal values. A long pattern of DNA sequence will be divided into 32-base pattern such as S1, S2 and S3 respectively. Similarly, k1, k2, k3 will be the 64-bits keys that has the converted 32-base DNA sequence with the binary coding scheme. The encryption block is selected from the 6-bits plaintext. The function of encryption runs from the parameters K1 (64-bits), encryption block, and 64-bits blank cipher block. The output of the encryption will be in the form of cipher block of 64-bits. In the same way, a decryption process will call the parameter k2 for their function with the previous cipher block as input, and 64-bits blank plaintext block. When this process has been executed, the next encryption function will be called with the previous encryption and decryption output with the key k3 as the input. This helps us in receiving 64-bits partial ciphertext block. The fake DNA sequence could be obtained by applying the reverse binary coding scheme inside the partial block. The final ciphertext could be obtained by applying the CDMB technique into the fake DNA sequence. By doing this process, the protein could be obtained which will be send to the receiver end.

The reverse CDMB technique will be applied in the decryption technique, which will be applied to the ciphertext block and it will be first decryption level thereby creating a fake DNA sequence. In order to receive the partial cipher level in the form of bits we tend to use the binary coding technique that tends to produce three 64-bits decryption keys K1, K2 and K3 with the shared information from the sender in the receiving end. Parameter k1 could evoke the decryption function with the selection of 64-bits cipher block as well as the 64-bits plaintext block. Executing this could help in obtaining the plaintext of 64-bits. The encryption function could be evoked with the key k2 with the input of previous output block and 64-bits blank cipher block. Then again, the decryption function should be called after receiving the output of 64-bits block from the previous step that acts as an input in this function with the key k3. This helps in receiving the 64-bits plaintext block. Plaintext P could be obtained by applying the inverse hexadecimal coding.

Algorithm:

I. Procedure for Encrypt (Key K, Plaintext P, Ciphertext C):

Input: Key K, Plaintext P.

Output: Ciphertext C.

Phase 1: Receive K' as 56-bit by applying permutation on K.

Phase 2: Dividing the factor K’ as 28-bits X0 and Y0

Phase 3: Produce Xn and Yn, as 16 blocks such that 1≤n≤16. The set of block Xn and Yn will be formed with the help of the previous block left shift key.
Phase 4: Every concatenated pairs will generate 16 sub-keys, 1≤n≤16.
Phase 5: P that is of 64-bits will be applied with the initial permutation (IP).
Phase 6: IP is divided as P0 and Q0, each consisting of 32-bits.
Phase 7: The pairs of Pn and Qn are obtained for 1≤n≤16, with the help of the two equations:
Pn= Qn-1
Qn = Pn-1 ⊕X (Qn-1, Kn)
Where, X (Qn-1, Kn) = X (Qn-1) ⊕Kn; and X (Qn-1) = Expansion function.
Phase 8: The Q16 P16 blocks of 64 bits is obtained.
Phase 9: The output C is generated by applying final permutation IP-1 to Q16 P16

II Procedure for Decrypt:
Phase 1: Receive K' as 56-bit by applying permutation on K.
Phase 2: Dividing the factor K' as 28-bits X0 and Y0 each.
Phase 3: Produce Xn and Yn, as 16 blocks such that 1≤n≤16. The set of block Xn and Yn will be formed with the help of the previous block left shift key Xn-1 and Yn-1.
Phase 4: Every concatenated pairs Xn and Yn will generate 16 sub-keys, 1≤n≤16.
Phase 5: P that is of 64-bits will be applied with the initial permutation (IP).
Phase 6: IP is divided as P16 and Q16, each consisting of 32-bits.
Phase 7: The pairs of Pn and Qn are obtained for 16≥ n ≥ 1, with the help of the two equations:
Qn-1 = Pn
Pn-1 = Qn ⊕X (Pn, Kn)
Where, X (Pn, Kn) = X (Pn) ⊕ Kn; and Expansion function is X (Pn).
Phase 8: The P0 Q0 blocks of 64 bits is obtained.
Phase 9: The output P is generated by applying final permutation IP-1 to P0 Q0

III Proposed Encryption Algorithm:
Algorithm: Encryption (Plaintext P, Ciphertext C)
Input: Plaintext P, A long DNA sequence > 96 DNA-bases
Output: Ciphertext C
Phase 1: The plaintext or the message is converted in binary form with the help of Hexadecimal value.
Phase 2: S1, S2, and S3 are the 3 DNA sequences chosen from a given 32 bases DNA sequences.
Phase 3: S1, S2, and S3 are converted as K1, K2, and K3 in the form of bits with the binary coding scheme. K1 and K3 are chosen as the encryption key. On the other hand, K2 is made as the decryption. Each key are 64 bits.
Phase 4: Encrypt (K1, P, C')
Phase 5: Decrypt (K2, C', C'')
Phase 6: Encrypt (K3, C'', C''')
Phase 7: C''' is said to be the partial cipher block that is applied with the reverse binary coding scheme and the fake DNA sequence is obtained.
Phase 8: Apply CDMB to obtain the protein sequence from the fake DNA sequence.
Phase 9: PROTEIN sequence is sent to the receiver in the form of encrypted message.

III Proposed Decryption algorithm:
Algorithm: Decryption (Plaintext P, Ciphertext C, Index X and Database D)
Input: Ciphertext C, Key information shared (Index X and Database D)
Output: Plaintext P
Phase 1: Implement reverse CDMB to obtain the fake DNA sequence from the Ciphertext C.
Phase 2: Get the partial ciphertext with the binary coding scheme in the form of bits.
Phase 3: S1, S2, and S3 are the 3 DNA sequences chosen from the shared information by the sender from the DNA databases.
Phase 4: S1, S2, and S3 are converted as K1, K2, and K3 in the form of bits with the binary coding scheme. K1, and K3 are chosen as the decryption key. On the other hand, K2 is made as the encryption key. Each key are 64 bits.
Phase 5: Decrypt (K1, C, P')
Phase 6: Encrypt (K2, P', P'')
Phase 7: Decrypt (K3, C'', M')
Phase 8: Apply the reverse hexadecimal coding to receive the original plaintext P from M.

Conversion of DNA sequence is possible with the proposed scheme that utilizes the DNA encoding table that is shown below. Here the plaintext is been used and each character indicates a DNA pattern with the combination of 3 bases. Several complementary rules has been followed by the proposed algorithm that boost a ciphertext due to perfect complementary rule that follows property like V(W) V(V(W)) V(V(V(W))) V(V(V(V(W)))), where 'W' is any string or alphabet. The complementary rules that have been used in this approach are as follows: (AT) (CA) (GC) (TG), Means V (A) = T.

Table 1: DNA Encoding [6]

A=CGA	H=CGC	O=GGC	V=CCT	2=TAG	…	9=GCG
B=CCA	I=ATG	P=GGA	W=CGG	3=GCA	…	=ATA
C=GTT	J=AGT	Q=AAC	X=CTA	4=GAG	…	,=TCG
D=TTG	K=AAG	R=TCA	Y=AAA	5=AGA	…	.=GAT
E=GGT	L=TGC	S=ACG	Z=AAT	6=GGG	…	:GCT
F=ACT	M=TCC	T=TTC	0=TTA	7=ACA	…	;=ATT
G=TTT	N=TCT	U=CTG	1=ACC	8=AGG	…	_=ATC

Receiver knows DNA encoding table, complementary rules, binary coding scheme and RNA codon table using a secure channel made by the sender. Exploitation of substitution method for the algorithm is obtained from Shiu et al.

V EVALUATION

Complexity analysis for the proposed algorithm was carried out since it exposes the security level of the algorithm for real-time applications.In this work the computational time of the algorithm was analyzed employing complexity theory methods. The input consists of alphabets; special character and alphanumeric.The obtained conclusions were tested to be true through the implementation results.

Table 2: Measurement of Key-Table Computation Run-Time

Nucleotides (key length)	Runtime (ms)
3000	66
4000	300
6000	436
8000	566
9000	636
10000	866

Table 3: Measurement of Encryption Runtime

Size of Plain-Text	Run-time (ns)
86 KB	6
100 KB	13
300KB	36
1000KB	66
13000KB	76

Table 4: Measurement of Decryption Runtime

Cipher-text Size (KB)	Run-time (ns)
86 KB	16
100 KB	33
300KB	46
1000KB	53
13000KB	66

The sum of all the operations represents the execution time of the proposed algorithm. The number of operations contains variable as well as constant based on input parameters. Based on the approximations from complexity theory, the smallest possible class of functions is employed to represent the growing rate of the algorithm's runtime, for instance, the number of operations for 1 + 2n would be O(n) in-terms of complexity; if the number of operations is 4 + n + n3, then the complexity would be O(n3). The experimental results have proved the correctness of the estimated complexity. In order to see the progression of the runtime, the program was executed at different, progressively increasing values of n and m. Figure 3 depicts graphics of the runtime growing rate for the key table computation, encryption and decryption processes. The execution time measurements are presented in Tables 2 - 4.

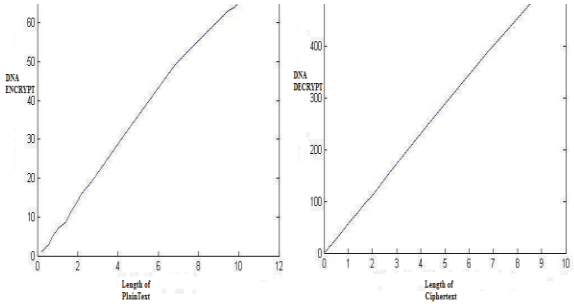

Figure 3: Results of DNA Encryption and DNA Decryption

VI CONCLUSION AND FUTURE WORK

Cryptography based security services could be seen in many sectors that includes several areas that includes digital certificate, banking sectors, image and message encryption etc. Certain algorithms such as DES, TDES, AES, and RSA are multifarious symmetric and asymmetric key cryptography algorithms that exists metamorphosis of plaintext into ciphertext. As the next level of evaluating the efficiency of the proposed algorithms, the following methods will be conferred as future work:

- Statistical measurements
- Key space analysis

REFERENCES

[1] R.J. Lipton, "DNA solution of hard computational problems," Science, New Series, 268(5210), 542-545, 1995.
[2] D. Boneh, C. Dunworth, and R.J. Lipton, "Breaking DES Using a Molecular Computer," DIMACS workshop on DNA computing, 27, 37-51, 1995.
[3] Z. Chen, X. Geng, and J. Xu, "Efficient DNA Sticker Algorithms for DES," IEEE 3rd International Conference on Bio-Inspired Computing (BICTA), 15- 22, 2008.
[4] L. MingXin, L. XueJia, X. GuoZhen, and Q. Lei, "Symmetric-key cryptosystem with DNA technology," Science in China Series F: Information Sciences, 50(3), 324-333, 2007.
[5] N. kar, A. Majumder, A. Saha, A. Jamatia, K. Chakma, and M. C. Pal, "An Improved Data Security using DNA Sequencing," Proceedings of the 3rd ACM MobiHoc workshop on Pervasive wireless healthcare, 13-18, 2013.
[6] H.J. Shiu, K.L. Ng, J.F. Fang, R.C.T. Lee, and C.H. Huang, "Data hiding methods based upon DNA sequences," Information Sciences, 180, 2196-2208, 2010.
[7] H. Liu, D. Lin, A. Kadir, "A novel data hiding method based on deoxyribonucleic acid coding," Computers and Electrical Engineering, 39, 1164-1173, 2013.
[8] T. Mandge and V. Choudhary, "A DNA Encryption Technique Based on Matrix Manipulation and Secure key Generation Scheme," IEEE International conference on Information Communication and Embedded Systems (ICICES), 47-52, 2013.
[9] J.S. Taur, H.Y. Lin, H.L. Lee and C.W. Tao, "Data hiding in DNA sequences based on Table Lookup Substitution," International Journal of Innovative Computing, Information and Control, 8(10), 6585-6598, 2012.
[10] Y.H. Huang, C.C. Chang, C.Y. Wu, "A DNA-based data hiding technique with low modification rates," Multimedia Tools Applications, 1-13, 2012.
[11] M.R. Abbasy, P. Nikfard, A. Ordi, M.R.N. Torkaman, "DNA Base Data Hiding Algorithm," International Journal on New

Computer Architectures and Their Applications (IJNCAA), 2(1), 183-192, 2012.
[12] O. Tornea, M. Antonini, M. Borda, "Multimedia Data Compression and Encryption using DNA Cipher", Communications Department, Technical University of ClujNapoca, winner of 2nd Prize, album SSET 2013.
[13]. W.M. Shih, J.D. Quispe, G.F. Joyce, "1.7-kilobase single-stranded DNA that folds into a nanoscale octahedron", Nature, Vol. 427, pp. 618-621, 2004.
[14] . H. Shiu, K. Ng, J.F. Fang, et al., "Data hiding methods based upon DNA sequences", Elsevier Inc., pp. 2196–2208,2010.
[15] M. Reza Najaf Torkaman et al, "Innovative Approach to Improve Hybrid Cryptography by using DNA Steganography", IJNCAA 2012
[16] Zhihua Chen et el. "Efficient DNA Sticker Algorithms for DES", IEEE 3rd international conference on Bio-inspired computing, 2012
[17] A.P. Thiruthuvadoss, "Comparison and Performance Evaluation of Modern Cryptography and DNA Cryptography," M.S. Thesis, Royal Institute of Technology, 2012.
[18] G. Cui, L. Qin, Y. Wang, X. Zhang, "Information Security Technology Based on DNA Computing," International Workshop on Anti-counterfeiting, Security, Identification, 288-291, 2007
[19] M. Babaei, "A novel text and image encryption method based on chaos theory and DNA computing," Natural computing, 12(1), 101-107, 2013
[20] M.F Vaida, R. Terec, O. Tornea, L. Chiorean, A. Vanea, "DNA Alternative Security", Advances in Intelligent Systems and Technologies Proceedings ECIT2010 – 6th European Conference on Intelligent Systems and Technologies, pp. 1-4, October 2010

Proceedings of the Fourth International Conference on Communication and Electronics Systems (ICCES 2019)
IEEE Conference Record # 45898; IEEE Xplore ISBN: 978-1-7281-1261-9

Design and Analysis of Slotted Ground Rectangular Patch Antenna for Worldwide Interoperability for Microwave Access,Wireless Local Area Network,Ultra Wideband and X-Band Applications

Anjaneyulu Katuru
Assoc. Prof., Dept. of ECE
Tirumala Engineering College
Jonnalagadda, A.P, india
anjikaturu@gmail.com

Mahesh Dronadula
Asst.Prof., Dept. of ECE
Tirumala Engineering College
Jonnalagadda, A.P, India
Maheshdro714@gmail.com

***Abstract*—In the present letter, we are designing a co-planar waveguide rectangular patch antenna with an area of (Lp×Wp) mm^2 .This is exciting by using a feed line having the dimensions of (Lf×Wf) mm^2. An FR-4 substrate occupying the volume of (L×W×H) mm^3 is used. A ground plane having an area of (Lg×Wg) mm^2 is designed on the top of the substrate and an aperture of (Ls×Ws) mm^2 is cut on the ground to improve the bandwidth characteristics. The s designing and simulation was done by using microwave studio computer simulation technology (MS-CST). From the results, it is observed the proposed structure is operating at 3.4 GHz (i.e., IEEE 802.16-WiMAX-worldwide interoperability for microwave access), 5.15 GHz (i.e., IEEE 802.11a-WLAN-wireless local area network), 3.1-10.6 GHz (UWB-ultra-wideband), and 8-12 GHz (X-band) applications. And it is also observed that the proposed antenna exhibits nearly Omni directional radiation patterns, return loss (S11) <-10 dB and VSWR (voltage standing wave ratio) <2 and gain≤5 dB except at the resonant frequency, 6.75 GHz within the UWB range.**

Keywords—rectangular patch; microstrip feed line; WiMAX; WLAN; UWB; return loss; gain

I. INTRODUCTION

Compared to conventional microwave antennas, patch antennas have many merits such as light weight, less cost, linear & circular polarization is possible, dual polarization and dual frequency antennas will be made possible, compatible with MMIC (Microwave Monolithic Integrated Circuits), designs, etc. However the serious disadvantages of microstrip patch antennas (MPAs) are lower bandwidth (BW) and efficiency [1]. These drawbacks can be overcome by introducing ultra wideband (UWB) technology. The Federal communications Commission (FCC) had assigned an unlicensed band of 3.1 to 10.6 GHz for ultra wideband communications in Feb. 2002 [2]. The UWB antennas have several merits compared to conventional patch antennas such as large bandwidth (7.5 GHz), low power consumption (nW), high data rate (> 100Mbps), low complexity, low cost, good time domain resolution etc. [3]. In [4], an elliptical patch with defected ground having step slots was presented to produce UWB characteristics. In [5], an L strip antenna having inverted shape with coplanar waveguide feed and defective ground for UWB applications was proposed. In [6], a triangular patch was designed for providing ultra wideband communication. In [7], a novel antenna having CPW feed for UWB applications was designed. This antenna provides constant return loss and low group delay throughout the frequency band. In [8], a rectangular monopole with truncated ground plane was introduced to operate over a wideband of 3.1 GHz – 11 GHz frequency range. An elliptical patch antenna with co-planar waveguide feed was implemented in [9] to provide UWB characterization. In [10], a monopole elliptical antenna which gives minimum ringing and dispersion of the pulses in time domain were designed. In [11], a UWB octagonal patch with defected ground structure was presented. This antenna produces good impedance matching characteristics by substituting a matching transformer between patch and feed line. In [12], a square patch with parasitic structure and pairs of slots wich are rotated L shape was presented to enhance the bandwidth which includes UWB. In [13], a rectangular antenna which produces triple band like WLAN, WiMAX, and UWB applications were presented. In [14], a patch which has two parallel slots and the antenna became E shaped to produce wideband characteristics for wireless communications. In [15], a U shaped stub is excited by a feed and rectangular slot in the ground was presenting UWB characterization. This paper presents a rectangular slot antenna in which a rectangular patch is excited by CPW feed line to operate at WiMAX, WLAN, UWB and X-band applications. The organization of this paper contains introduction, geometrical structure of

antenna, results and discussion, Far-field gain patterns, surface current distribution and conclusion.

.

II. GEOMETRICAL STRUCTURE OF ANTENNA

The Schematic representation of proposed antenna is depicted in Fig.1. This occupies the volume of (Lp×Wp×Tp) mm^3. A ground plane of size Lg×Wg mm^2 is fabricated on FR-4 material having the dimensions of 50×50×1.6 mm^3.an aperture size of 27.1×40.1 mm^2 is etched on the ground to obtain the wider BW. The parametric values of the proposed structure are represented in table. I. This antenna is operating at various wireless communications that is shown in return loss plot.

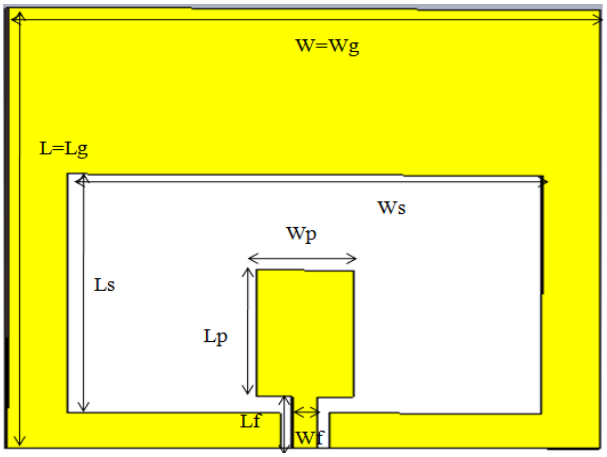

Fig. 1. Desired structure of antenna

TABLE I. ANTENNA PARAMETRIC DIMENSIONS

Parametric symbol	Parametric Value (mm)	Parametric symbol	Parametric Value (mm)
L	50	Wf	2.1
W	50	Tf	0.1
H	1.6	Lg	50
Lp	9.4	Wg	50
Wp	8.2	Tg	0.1
Tp	0.1	Ws	40.1
Lf	4.5	Ls	27.1

III. DISCUSSION OF RESULTS

In our work antenna design software (CST) is used to design and simulating antenna. By optimizing the antenna parameter values, the required return loss (S11<-10 dB) and VSWR (<2) are obtained. Here the S-parameter, S11 represents the square of the ratio of incident wave to reflected wave at the input terminals of antenna. VSWR represents how well the load is impedance matched to the source. The required MPA is operating in the frequency band of 1.48-12.34 GHz, in which it operates at 3.4 GHz (WiMAX), 5.15 GHz (WLAN), 3.1-10.6 GHz (UWB) and 8-12 GHz(X-band) frequencies. These resonating frequencies are shown in S-parameter plot. The antenna provides an absolute bandwidth of 10.86 GHz and fractional bandwidth of 157.16%. The simulated return loss, VSWR and radiation gain pattern at resonant frequency are depicted in Fig. 2.The best value of return loss and VSWR occurred at 1.75 GHz are -27.7 dB and1.08.The far field gain at resonant frequency 6.75 GHz is 6.2 dB.

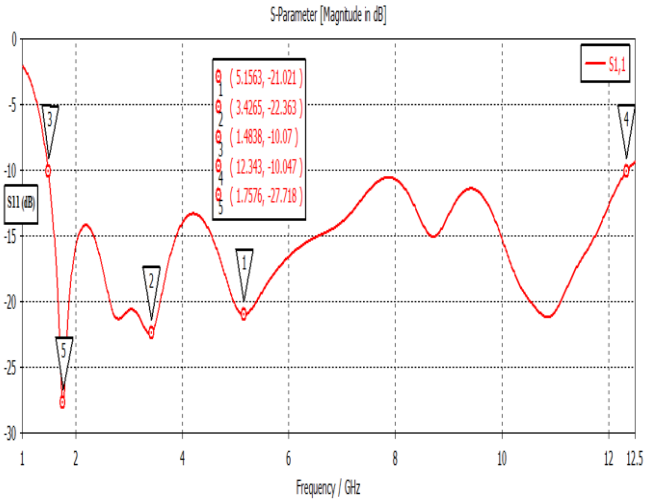

(a)

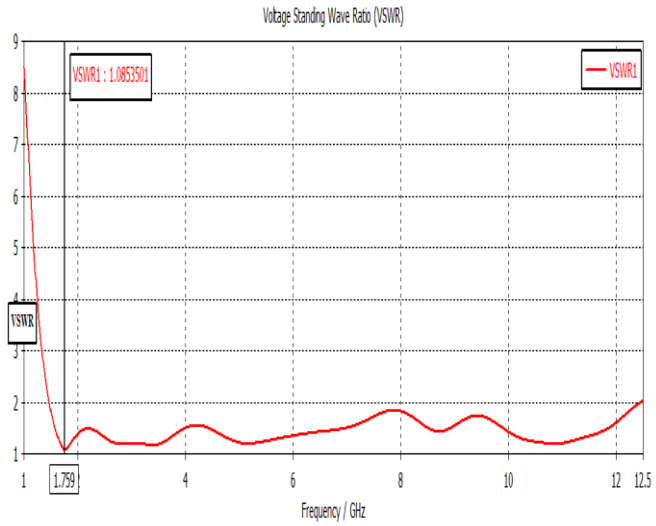

(b)

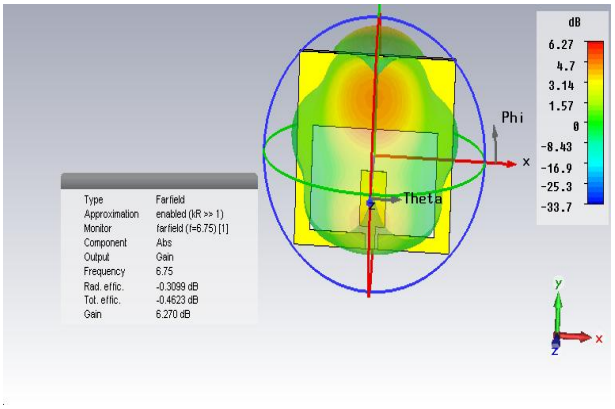

(c)

Fig. 2. (a) Return Loss parameter (b) VSWR parameter (c) Radiation pattern at 6.75GHz

IV. FARFIELD GAIN PATTERNS

The antenna far-field gain patterns in 3-dimensional (3D) and 2-dimensional (2D) H & E plane patterns are represented in below fig. 3 at 3.1, 3.4, 4, 5.7 and 10.6 GHz frequencies from (a) to (o). From these patterns, we concluded that the antenna produces nearly Omni-directional patterns and gain is almost less than or equal to 5 dB except at the resonant frequency, 6.75 GHz. The far field gain values at different frequencies are tabulated in Table II.

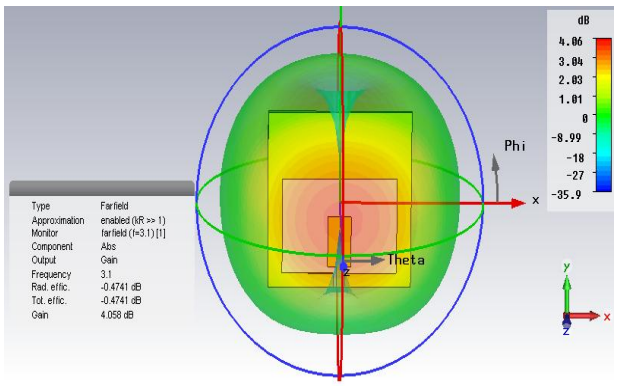

(a)

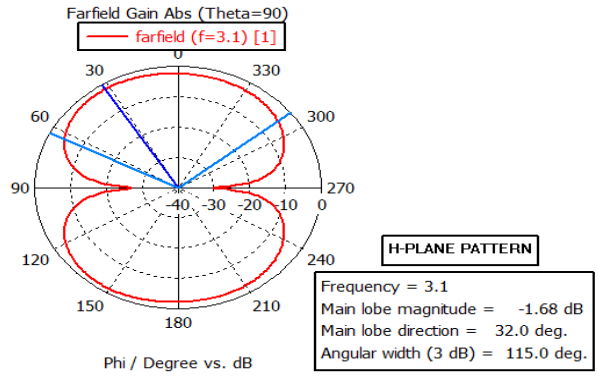

(b)

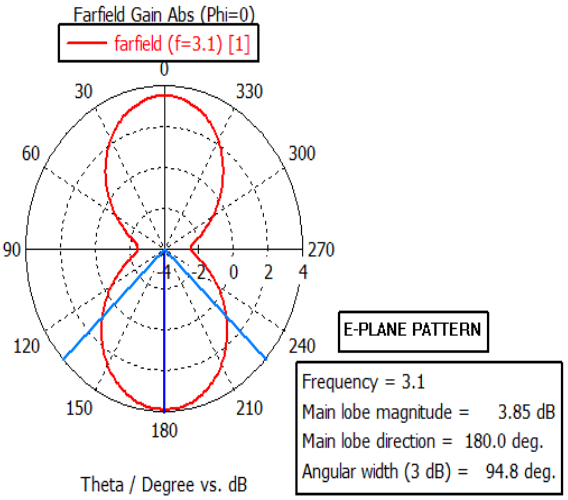

(c) 3.1

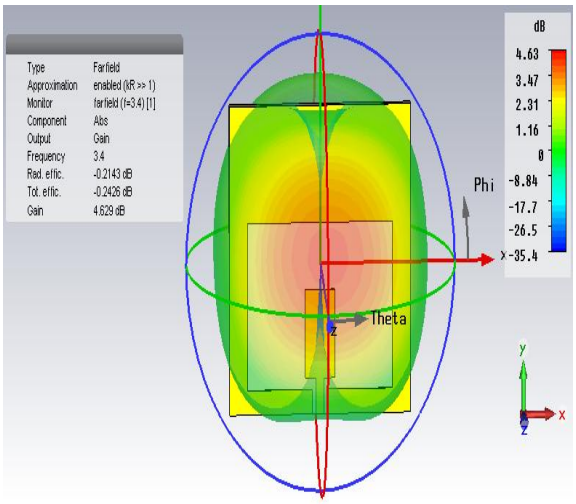

(d)

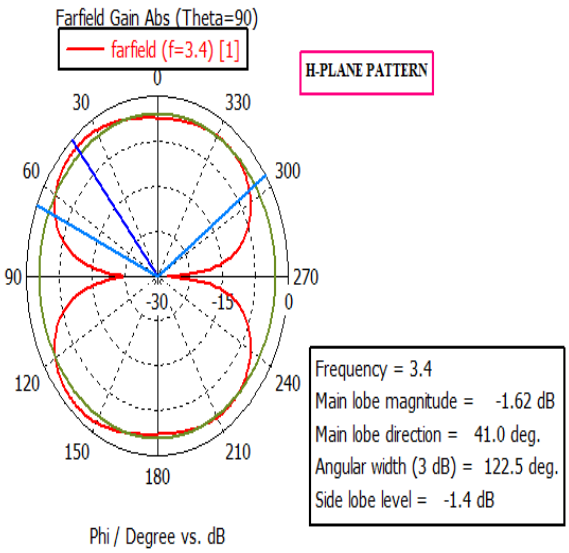

(e)

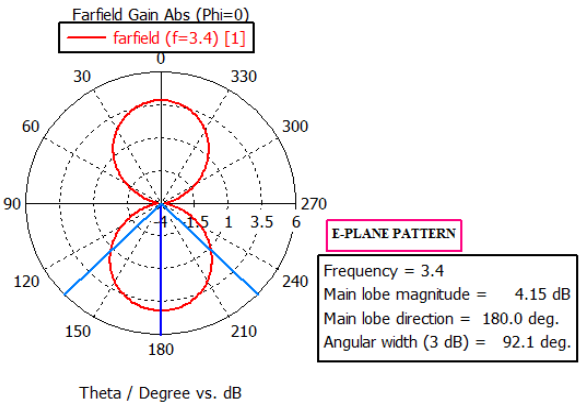

(f) 3.4

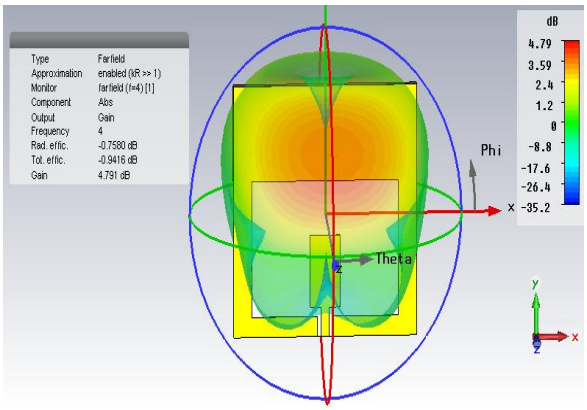

(g)

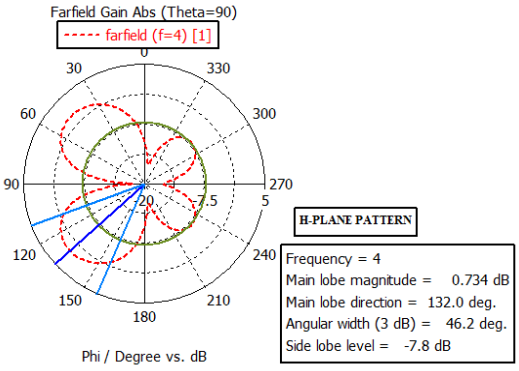

(h)

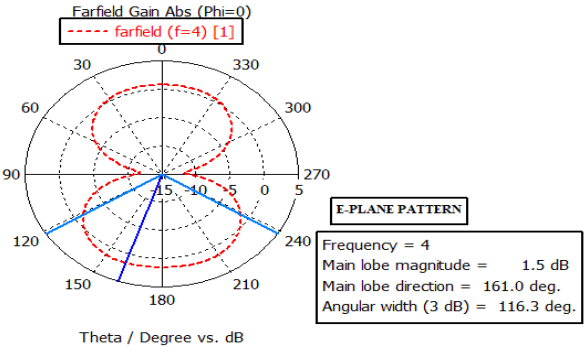

(i) 4

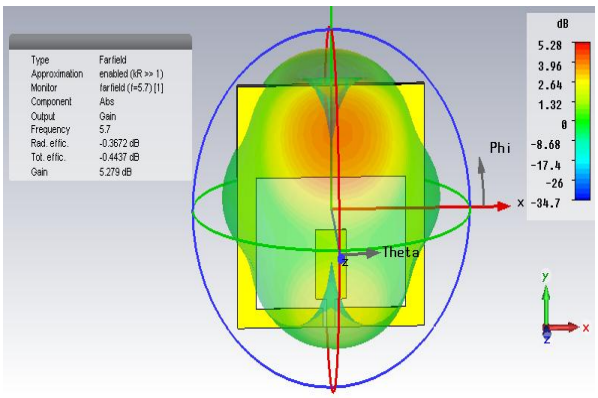

(j)

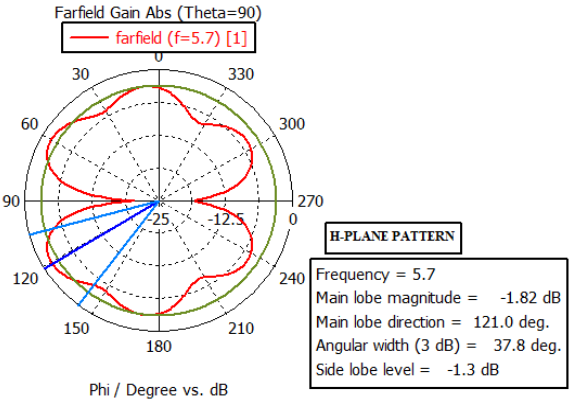

(k)

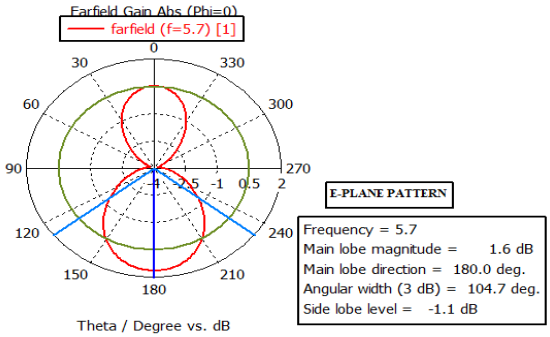

(l) 5.7

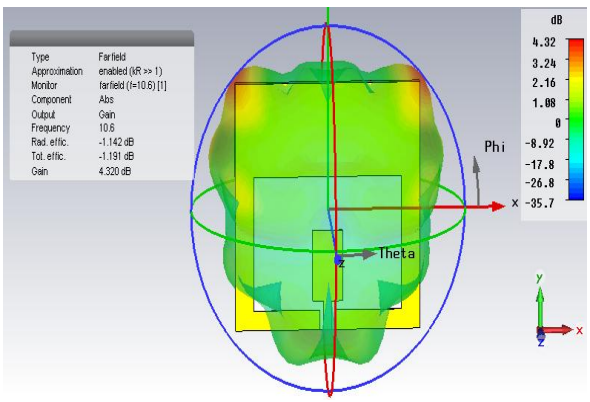

(m)

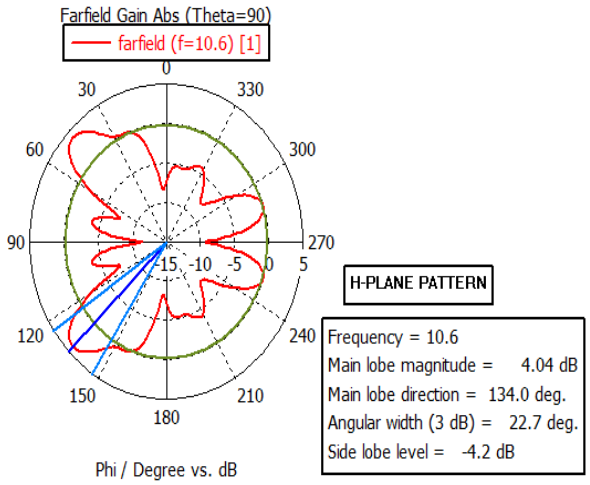

(n)

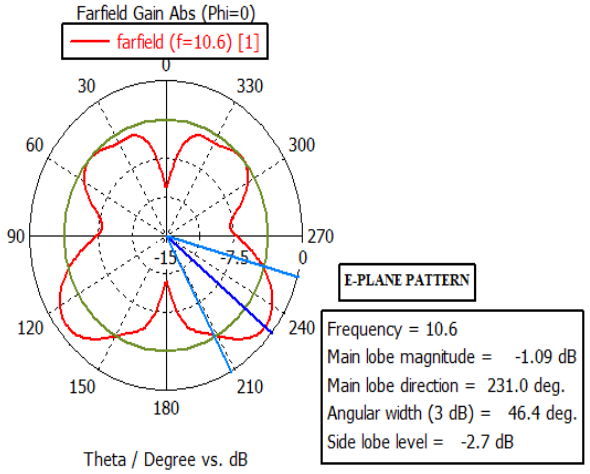

(o) 10.6

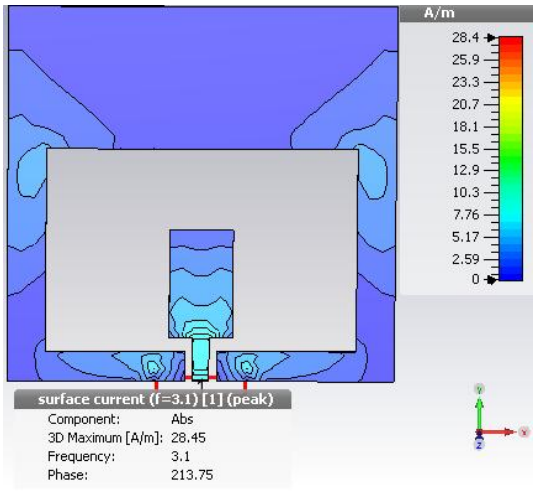

(a)

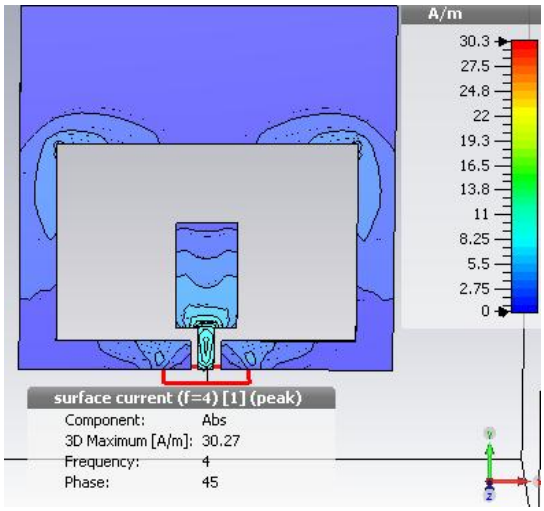

(b)

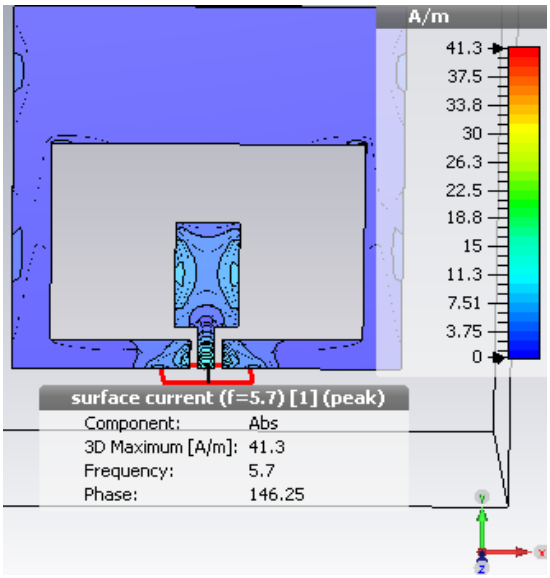

(c)

Fig. 3. 3D, H-plane and E-plane gain patterns at 3.1,3.4,4,5.7,and 10.6 GHz frequencies respectively.

TABLE II. TABLE STYLES

Frequency(GHz)	Gain(dB)
3.1	4.06
3.4	4.63
4	4.79
5.7	5.2
10.6	4.32

V. SURFACE CURRENT DISTRIBUTION

The surface current distribution at 3.1, 4, 5.7 and 10.6 GHz frequencies are shown in Fig. 4. From these figures the distribution of current is maximum at the centre of the patch.

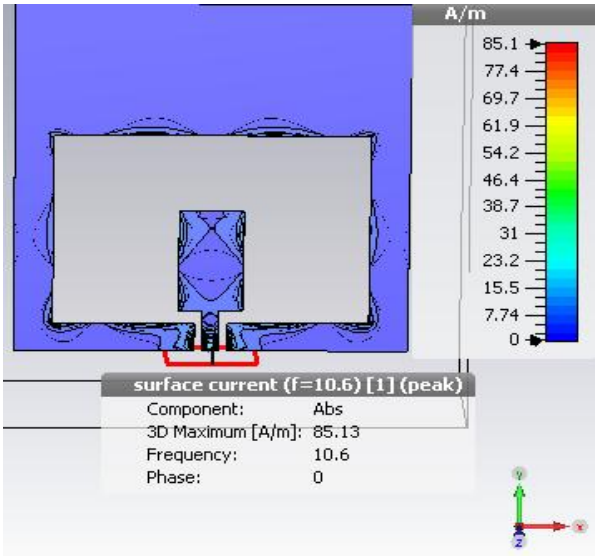

(d)

Fig. 4. Distribution of current at various frequencies (a)3.1 GHz (b)4 GHz (c) 5.7 GHz and (d) 10.6 GHz.

VI. CONCLUSION

A CPW fed ground slotted rectangular patch antenna was designed and simulated by CST. The antenna produces wider bandwidth of 1.48-12.34 GHz, which includes WiMAX, WLAN, UWB and X-band. This antenna also provides S11=-27.7 dB, VSWR=1.08 and almost gain≤5 dB except at the design frequency, 6.75 GHz. The antenna also exhibits nearly omni-directional patterns and also observed the surface current distribution at various frequencies. This antenna is meant for short range and low gain. The transmit power will be increased to increase the range and gain will be increased by antenna array. This antenna is suitable for various wireless communications.

Acknowledgment

My sincere thanks to management, Principal, Dr.Y.V. Narayana and HOD of ECE Dr. Suresh Kumar Pittala of Tirumala Engineering College, Jonnaglagadda, Narasaraopet, and my wife Sravani for their continuous support in completing this work.

References

[1] R. Garg, P. Bhartia, I. Bahl, and A. Ittipiboon, Microstrip Antenna Design Handbook, Artech House, London, 2001.

[2] First Report and Order,Revision of part 15 of the commission's rules regarding Ultra-wideband transmission systems, Federal Communications Commission, FCC,02-48, 2002.

[3] D. Valderas, J. L. Sancho, D. Puente, C. Ling, and X. Chen, Ultra wideband Antennas: Design and Applications, London, Imperial College Press, 2011.

[4] K. M. Hanapi, S. K. A. Rahim, B. M. Saad, M. S. A. Rani and M. Z. A. Aziz, "An elliptically planar UWB monopole antenna with step slots defective ground structure," Microw. Opt. Tech. Lett., vol. 56, no. 9, pp. 2084-2088,September2014.

[5] A. K. Gautam, S. Yadav, and B. Kr. Kanaujia, "A CPW fed compact inverted L-strip UWB microstrip antenna," Microw. Opt. Tech. Lett., vol. 55, no. 7, pp. 1584-1589, July 2013.

[6] C. C. Lin, Y. C. Kan, L. C. Kuo, and H. R. Chuang, "A planar triangularmonopoleantennaforUWBcommunications,"IEEEMicrow. WireL. Compon. Lett., vol. 15, no.10,pp.624626,October2005.

[7] S. H. Lee , J. K. Park, and J. N. Lee, "A novel CPW-fed ultra-wideband antenna design," Microow. Opt. Tech. Lett., vol. 44, no. 5, pp. 393-396, March 2005.

[8] J. Jung, W. Choi, and J. Choi, "A small wideband microstrip-fed monopole antenna," IEEE Microw. WireL. Compon. Lett., vol . 15, no . 10, pp. 703-705, October 2005.

[9] Anjaneyulu. K and A. Sudhakar, "Design and analysis of a compact CPW fed elliptical patch antenna for UWB applications," Int. J. Control Theory and Applications, vol. 10, no. 35, Int. Science press, 2017.

[10] K. P. Ray andY. Ranga, "Ultra wideband printed elliptical monopole antenna," IEEE Transc. Antennas Propag., vol.55, no. 4, pp. 1189-1192, April 2007.

[11] Anjaneyulu. K and A. Sudhakar, "Design and analysis of matched microstrip line feed antenna for ultra wideband applications,"Int. J. Commu. Antennas Propag., vol. 6, pp. 369-374, December 2016.

[12] N. Ojaroundi, "Compact UWB monopole antenna with enhanced bandwidth using rotated L shaped slots and parasitic structures," Microw. Opt. Tech. Lett., vol. 56, no. 1, pp. 175-178, January 2014.

[13] D. Prakash and R. Khanna, "Triple band rectangular shaped monopole antenna for WLAN / WiMAX / UWB applications," Microw. Opt. Tech. Lett., vol. 56, no. 9, pp. 2113-2117, September 2014.

[14] F. Yang, X-X. Zhang, X. Ye, and Y. Rahmat-Samii, "Wideband E shaped patch antenna for wireless communications,"IEEE Transc. Antennas and Propag., vol. 49, no. 7, pp. 1094-1100, July 2001.

[15] R. Chair, A. K. Kishk, and K. F. Lee, "Ultrawidebandcoplanar waveguide fed rectangular patch antenna," IEEE Antennas WireL. Propag. Lett., vol. 3, pp. 227-229, 2004.

Proceedings of the Fourth International Conference on Communication and Electronics Systems (ICCES 2019)
IEEE Conference Record # 45898; IEEE Xplore ISBN: 978-1-7281-1261-9

Fusion Methods & Applications – A Survey

Freceena Francis
PG Scholar
Department of Computer Science &Engineering
NSS College of Engineering
Palakkad, Kerala, India
freceena111@gmail.com

Dr. Maya Mohan
Assistant Professor
Department of Computer Science &Engineering
NSS College of Engineering
Palakkad, Kerala, India
mayajeevan@gmail.com

***Abstract*—Data fusion is the process in which integration of multiple data sources produce more consistent, efficient, and useful information than that provided by any of the individual data source. The fusion methods can be broadly classified with the help of class information. The fusion methods such as serial feature fusion, parallel feature fusion and canonical correlation analysis (CCA) does not contain any class information. That is, they are unsupervised fusion methods. The methods such as cluster CCA, Generalized Multiview Analysis, Linear Discriminant Analysis, Multiview Discriminant Analysis, Discriminative Multiple CCA, Locality Preserving CCA (LPCCA), BGLPCCA, MGLPCCA contain class information. Applications of each fusion methods are also taken into consideration.**

Keywords—Fusion; CCA; Supervised; Locality Preserving; Discriminant Analysis.

I. INTRODUCTION

Real world comprises of huge amount of information. Information can be a text, image, video, audio and so on[1]. This information is obtained from multiple sources and through various acquisition techniques. It is also known as multi modal information. The importance of this type of information is growing expeditiously. Thus, information fusion is becoming significant research topics in pattern recognition, deep learning [2], biometric authentication, real time human action recognition [3][4], behavior recognition [5] etc.

The data obtained from single source can undergo various issues such as noise, unacceptable error rates, occlusions, variations in light conditions and so on. Several attempts were made to improve the performance of systems which capture data from only single source, but they were not so effective due to the problems listed above. Here comes the idea of information fusion, fusing data from different sources and improve the quality of extracted knowledge. The interpretation and integration of two or more information are very important for the effective usage of data in various applications. Information fusion is mainly used in three concepts [6]:

i. Preprocessing: Quality of the raw data is increased before data mining tasks are applied using information fusion in this step. This is referred to as data cleaning.
ii. Model Building: Information fusion is applied to data for building model. It is used in two ways either to define a model or to combine several data models.
iii. Information Extraction: To build summaries or conclusions from the original raw data, to reduce number and dimensionality of records.

Information fusion is considered as the natural integration of multiple sources, features extracted, and the decision thus formed. Information fusion is widely applicable in human action recognition too. Since, it is inefficient or insufficient to characterize various motions of a person. This invariance [7] is due to the variability of same actions by same or different person, and due to the variability of different actions by same or different person. Information fusion thus combines different feature vectors to provide efficient results [8].

In multimodal information fusion we are using data collected from different and variety of sources, these are helpful to improve the classification or recognition accuracy. This multimodal information has the capability to provide complete and effective description of specific pattern with intrinsic characteristics. Fig.1. shows the fusion process.

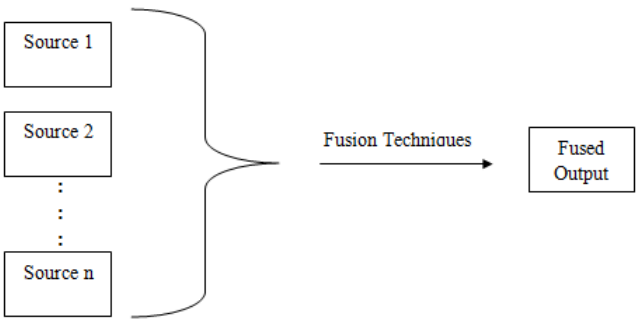

Fig. 1. Fusion Process

The major challenging task in this type of information fusion is the finding of effective method for the task. This method should provide high performance and efficient results. This

survey focuses and discusses on different fusion techniques and their applications in real life.

The rest of this paper is organized as follows. Section 2 briefly provides an overview of the fusion techniques which also explains different supervised and unsupervised fusion techniques. Section 3 compares different fusion techniques. Section 4 concludes the paper with future scopes.

II. FUSION TECHNIQUES

Information fusion is comprised of discriminative feature selection, identification of redundant features and their elimination, preserve information and computational complexity. Information fusion techniques can be broadly classified into supervised and unsupervised fusion techniques. Information collected from multiple sources are then given to the efficient fusion techniques which are capable of making effective use of those information and brings upon more accurate results. A faulty or poorly designed multimodal system could degrade the whole performance of the system and bring upon negative impact.

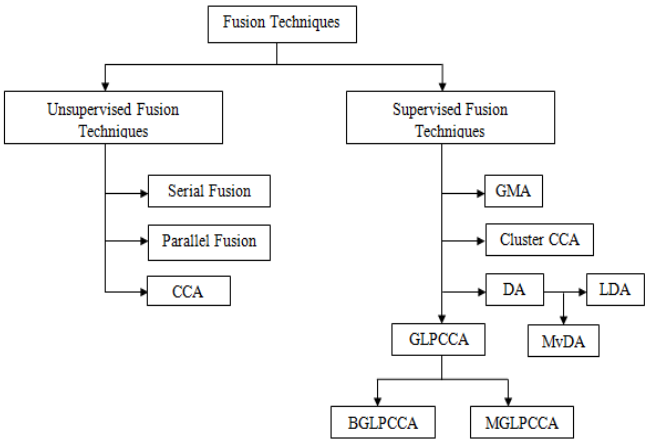

Fig. 2. Overview of Fusion Techniques

Fig. 2. shows how fusion techniques are divided based on their prior knowledge and all. Fusion techniques can be broadly classified into supervised and unsupervised fusion techniques based on the predefined class information. Supervised fusion techniques are those techniques in which predefined class labels are given and training is done on behalf of that. The supervised fusion techniques are then classified into GMA, Cluster CCA, DA, and GLPCCA. While unsupervised techniques are those techniques which do not have any predefined training set and these techniques are classified into Serial fusion, Parallel fusion and CCA.

A. Unsupervised Fusion Techniques

This section discusses about various unsupervised fusion techniques and how it is useful for producing efficient results and their applications in real world. Unsupervised fusion techniques produce results without making use of any training sets.

Serial Fusion [9] is considered as a type of incremental fusion, since it is a method of combining observations from one source to the other sources. In other words, serial fusion can be considered as an information fusion model between two sources. This kind of fusion combines two or more sets of features into a union vector. There exists two feature sets namely, *X* and *Y*. Feature set *X* has *m* dimensions and *Y* has *n* dimensions. Serial fusion will provide a *(m+n)* - dimensional feature vector.

In *Parallel Fusion*, we use a fixed set of sources where all observations from sources are drawn to a central fusion center. It is generally used in reliable information from multiple sources, but their type should be the same or the data should be of equal status. And the solution to this problem is zero padding the lower dimensionality to have same size Parallel fusion model produces better results than the serial fusion model [9]. It produces a complex vector rather than a union vector after combining feature sets.

Canonical Correlation Analysis (CCA) [10], is a type of technique which is used to find a common shared space between two sets. This common shared space maximizes the correlation between the feature samples from two sets. CCA is considered as a version of PCA with multiview. Two views with additive noise related to a hidden class is given, CCA possess a subspace where covariance of noise is directly proportional to the signal covariance. CCA is a multivariate technique which is one of the least frequently used. But is a useful strategy when there are continuous variables for estimating the strength of relationship between two or more dependent and independent variables.

TABLE I. UNSUPERVISED TECHNIQUES

Technique	Application	Description
Serial Fusion	Collaborative Signal Detection	Uses sequential probability ratio test (SPRT)
	Personal identity verification	Fusion between fingerprint and face matchers
	Arrhythmia Classification	Fusion of SVM and logistic regressions
	Iris Recognition	Incremental approach which optimizes the time complexity
	Liver diseases classification	Uses a two-level serial feature fusion procedure
Parallel Fusion	Collaborative Signal Detection	Uses tree-based aggregation scheme
	Channel aware decision fusion in wireless sensor networks	Incorporates fading channel layer
	3D shape-based face recognition	Use combination rules such as consensus voting, rank-sum, nonlinear rank-sum and highest-rank majority rule.
	Membrane Protein Subcellular Localization	Represents the protein sample in complex space.

	Prediction	
	Fusion in distributed sensors	Uses a multiple level parallel decision fusion model
	Kalman Filter	Two-layer fusion structure
CCA	Intelligence and Executive Functioning	Used to found out that the executive functioning measures maintain unique variance with the intelligence.
	Remove Muscle	High performance than a low-pass filter.
	Artifacts from the Electroencephalogram	MANOVA procedure utilized for canonical analysis
	Tourism Industry	n use a steady-state visual evoked potential
	Brain-Computer Interface	(SSVEP) in brain-computer interface (BCI) systems.
	Climate Prediction	By highlighting the spatial patterns of predictor or predictand.
	Fast Active Appearance Model Search	Efficient in modelling the dependency between model parameters and texture residuals.

B. Supervised Fusion Techniques

This section discusses about various supervised fusion techniques and how it is useful for producing efficient results and their applications in real world. Supervised fusion techniques are those techniques which have predefined class information for predicting future labels or for further processing.

Generalized Multiview Analysis (GMA) is a fusion technique which helps in cross modal or cross view classification and retrieval. It can be generalized to further unseen classes and bears an efficient solution which is based on Eigen value. It is also applicable in multiple domains. It is an extension of CCA [11]. Kernel GMA maps to a non-linear space then carries out GMA which helps in obtaining projection directions v_i for the ith view. This is considered as the first step towards multiview feature extraction and a superior alternative for CCA. It leads to a discriminant common subspace. It only considers intra-view discriminant information but not inter-view discriminant information. And also, an extension of Fisher Discriminant Analysis when it is applied to cross-view matching.

Cluster Canonical Correlation Analysis (Cluster CCA) is used in two sets of data points for joint dimensionality reduction [12]. It also helps to find discriminant low dimensional representations that could maximize the correlation between two sets. Meanwhile, it segregates the data sets into different classes. Kernel cluster CCA is an extension of cluster CCA which takes into account the nonlinear relationships between the data sets.

Discriminant Analysis (DA) is used in classifying objects into two or more mutually exclusive and exhaustive categories [13]. Discriminant analysis can be broadly classified into *Linear Discriminant Analysis (LDA)* and *Multiview Discriminant Analysis (MvDA)*. LDA is a supervised data dimensionality reduction fusion technique [14]. It considers the relationships between the various training images and their relationship to the training set as a whole; not plainly use the training set to find the basis vector. The very first stage of the LDA is the labelling of the training data set, which in turn specifies that all images of a single specimen is in the same class and images of different specimen are in the different classes of the training set. The next stage is the cluster separation analysis which uses separation matrix. LDA method makes it easier to distinguish the classes into various clusters by minimizing within-class correlation and maximizing between-class separation.

Discriminative Multiple Canonical Correlation Analysis (DMCCA) is used for information analysis for multimodal and fusion [15]. And is responsible for the extraction of high discriminant characteristics of multimodal information representations. It also finds feature set that could maximize within-class correlation and minimize between-class correlation which in turn can bring upon better utilization of the multimodal information. To bring discriminability, DMCCA uses all features; to bring cross-view correlation, uses all observations from different feature sets; It uses smaller set of parameters. It helps in revealing the complementary representations and the intrinsic structure from different modalities to improvise the recognition task. Different patterns are represented among identified multiple feature subsets by minimizing the Frobenius norm [16].

Globality Locality Preserving CCA (GLPCCA) is a fusion technique which preserves both local and global structures during establishing the correspondences. It improves the discriminative power of the features. Locality Preserving CCA(LPCCA) is used to capture the local structure of given data samples but not the global structure and preserves the local structure in the new found out learned space. GLPCCA is a modifies version of CCA to include both local and global structure details [17]. The GLPCCA technique can be classified into Biset GLPCCA (BGLPCCA) and Multiset GLPCCA (MGLPCCA). BGLPCCA is fusion technique which deals with learning the common feature subspace between two sets. MGLPCCA deals with three or more sets for fusing [18].

TABLE II. SUPERVISED TECHNIQUES

Technique	Application	Description
	Face Recognition	multiple posture images of person are used to

GMA		learn pairs of pose-specific projection directions.
	Text-Image Retrieval	Semantic Correlation Matching (SCM) with a linear kernel is used.
	Facial Expression Recognition	Uses a Discriminative Shared Gaussian Process
Cluster CCA	Cross-Modal retrieval	Brings high correlation between text and image
	Energy Calculation	reproduces high accuracy configuration-interaction correlation energies
DMCCA	Handwritten Digit Recognition	Applicable for postal mail sorting, bank check processing, form data entry etc.
	Audio-based Emotion Recognition	By fusing prosodic features, MFCC features, formant frequency features.
	Visual-based Emotion Recognition	Gabor wavelet features are used to represent visual information
LDA	Analysis of facial images	Allows objective evaluation of the significance of visual information in different parts of the face for identifying the human subject.
MvDA	Face recognition across pose	Performance improvement by employing more discriminant information in both inter-view and intra-view variations.
GLPCCA	Human action recognition	Fuse depth and RGB modalities

III. COMPARISON

TABLE III. COMPARISON TABLE OF FUSION TECHNIQUES

Techniques	Advantages	Disadvantages
Serial Fusion	Fusion model between two sources	Used for fusing from two sources only
Parallel Fusion	Applicable to reliability information from different sources while the type same	Data needed have been obtained or data of equal status
CCA	Multiple dependent and independent variables.	Lacks class information
LDA	Supervised data dimensionality reduction	Homogeneity of variance
GMA	Helpful in cross view application & retrieval	Impossible to compute within-class variations with single sample per class.
cluster CCA	non-linear relationships between two sets	correlation between same classes
MvDA	Even applied to classes not presented in training set	Cannot be used when there is insufficient data to define sample means
DMCCA	Cross-view correlation is obtained from all observations from different feature sets	Can be used only with a much smaller set of parameters
GLPCCA	Improves the discriminative power of features	Difficult to form the projection matrices

Table III is a summary of the performance of fusion techniques discussed so far. The table describes about the advantages and disadvantages of each fusion techniques.

IV. CONCLUSION

In this survey, we have surveyed about different fusion techniques which could bring more efficient results. We have analyzed different fusion techniques and classified them into two dimensions: supervised fusion techniques and unsupervised fusion techniques. The fusion techniques are used to reduce the size of feature set to be given for further processing. Supervised fusion techniques are used nowadays since it increases the chances for better results. The most recent supervised fusion technique is the Biset or Multiset Globality Locality Preserving Canonical Correlation Analysis (BGLPCCA or MGLPCCA) which preserves both the local and global information of the data samples. Even though, they are very much useful for wide sector of fields they have drawback too. they got a complex problem in forming the projection matrices. Future works of fusion techniques could be aimed at optimizing this problem of forming projection matrices.

REFERENCES

[1]. Yongnan Wang, Xihui Mu, Yueting Niu, Fengpo Du and Jianhua Chen, "The application of information fusion in reliability evaluation of complex electromechanical system", In International Conference on Advances in Mechanical Engineering and Industrial Informatics, pp. 1490–1493, 2015.

[2]. Ling Guan, Lei Gao, Nour El Din Elmadany and Chengwu Liang, "Statistical machine learning vs deep learning in information fusion: Competition or collaboration?", In 2018 IEEE Conference

on Multimedia Information Processing and Retrieval (MIPR), pp. 251–256, 2018.

[3]. Chen Chen, Roozbeh Jafari, and Nasser Kehtarnavaz, "A real-time human action recognition system using depth and inertial sensor fusion", IEEE Sensors Journal, vol. 16, pp. 773–781, 2016.

[4]. Qiuxia Wu, Zhiyong Wang, Feiqi Deng, Zheru Chi and David Dagan Feng, "Realistic human action recognition with multimodal feature selection and fusion", IEEE Transactions on Systems, Man, and Cybernetics: Systems, vol. 43, pp. 875–885, 2013.

[5]. Francesco Monti and Carlo S Regazzoni, "Human action recognition using the motion of interest points.", In Image Processing (ICIP), 201017th IEEE International Conference on, pp. 709–712. IEEE, 2010.

[6]. Vicenc Torra, "Trends in information fusion in data mining", In Information fusion in data mining, pp. 1–6. Springer, 2003.

[7]. Nilam Nur Amir Sjarif and Siti Mariyam Shamsuddin, "Human action invarianceness for human action recognition", In Software, Knowledge, Information Management and Applications (SKIMA), 2015 9th International Conference, pp. 1–7, 2015.

[8]. Keyu Li, Zhigang Liu, Liqin Liang, and Yanan Song, "Human action recognition using associated depth and skeleton information.", In Computer and Communications (ICCC), 2016 2nd IEEE International Conference on, pp. 418–422, 2016.

[9]. Jian Yang, Jing-yu Yang, David Zhang, and Jian-feng Lu, "Feature fusion: parallel strategy vs. serial strategy", Pattern recognition, vol. 36, pp. 1369–1381, 2003.

[10]. Nour El Din El Madany, Yifeng He, and Ling Guan, "Human action recognition via multiview discriminative analysis of canonical correlations.", In Image Processing (ICIP), 2016 IEEE International Conference on, pp. 4170–4174, 2016.

[11]. Abhishek Sharma, Abhishek Kumar, Hal Daume, and David W Jacobs, "Generalized multiview analysis: A discriminative latent space.", In Computer Vision and Pattern Recognition (CVPR), 2012 IEEE Conference on, pp. 2160–2167, 2012.

[12]. Nikhil Rasiwasia, Dhruv Mahajan, Vijay Mahadevan, and Gaurav Aggarwal, "Cluster canonical correlation analysis.", In Artificial Intelligence and Statistics, pp. 823–831, 2014.

[13]. Donald G Morrison, "On the interpretation of discriminant analysis" Journal of marketing research, pp. 156–163, 1969.

[14]. PE Robinson and WA Clarke, "Comparison of principal component analysis and linear discriminant analysis for face recognition", In AFRICON 2007, pp. 1–6. IEEE, 2007.

[15]. Lei Gao, Lin Qi, Enqing Chen, and Ling Guan, "Discriminative multiple canonical correlation analysis for information fusion", IEEE Transactions on Image Processing, vol. 27, pp. 1951–1965, 2018.

[16]. Lei Gao, Lin Qi, Enqing Chen, and Ling Guan, "Discriminative multiple canonical correlation analysis for multi-feature information fusion", In Multimedia (ISM), 2012 IEEE International Symposium on, pp. 36–43, 2012.

[17]. Nour El Din El Madany, Yifeng He, and Ling Guan, "Human action recognition by fusing deep features with globality locality preserving canonical correlation analysis", In Image Processing (ICIP), 2017 IEEE International Conference on, pp. 2871– 2875, 2017.

[18]. Nour El Din Elmadany, Yifeng He, and Ling Guan, "Information fusion for human action recognition via biset/multiset globality locality preserving canonical correlation analysis", IEEE Transactions on Image Processing, vol. 27, pp. 5275–5287, 2018.

Proceedings of the Fourth International Conference on Communication and Electronics Systems (ICCES 2019)
IEEE Conference Record # 45898; IEEE Xplore ISBN: 978-1-7281-1261-9

Swheel: Low-Cost Smart Wheelchair with Wireless Control

Tushar Agarwal, Shloka Bhalgat, Chirag Khandhar, Bhumika Khetan

Department of Computer Engineering, Sinhgad College of Engineering, Pune, Maharashtra, India

***Abstract*- The aim of this project is to make a low cost, multi-modal control and an easy to operate a smart wheelchair. To meet the user-specific needs we have implemented a prototype for a smart wheelchair having two major features: (1) Android based application which includes touch-enabled buttons, gesture recognition, voice recognition, and (2) Remote OS installation mechanism. The proposed system is capable of obstacle detection with object detection using Ultrasonic Sensor with real-time object distance, and slope detection using three-axis accelerometer. The accuracy of our system is 91.58% for slope detection as calculated by the 3-axis accelerometer on a variety of slopes and 85.85% for obstacle detection for a variety of obstacles as detected by the ultrasonic sensor. Also, it can send an SOS message which is a notable feature of this project. All these features are controlled wirelessly using Bluetooth on an Android-based application.**

***Keywords*: Smart Wheelchair, Low-cost, Android Application, Wireless controlled, Remote Firmware Update, Slope detection, Obstacle Detection.**

I. INTRODUCTION

According to Census 2011, the disabled population by type of disability in India is found to be significant in the case of movement or locomotive disability. Going by the numbers the movement type disabled population is found to be the highest with 5,436,604 people out of a total 26,810,557 disabled in all, which is approximately around 20.

Although the ongoing improvements in science and technology have changed the way a typical individual carries on with his life, there are a certain group of individuals who have not yet been able to gain an advantage from this advancement. Specifically, impaired individuals that have restricted versatility are not able to do things which a fully functional human (physically) can do. A smart wheelchair aims to help those incapacitated and physically disabled people by empowering them with portability which would incredibly encourage them to do various things and flourish in life. We have aimed to solve this problem based on the Census 2011's report which suggests that the highest number of disabled populations by type is "Locomotive Disabled."

There are no sources in the current document.

Specific mention of the following was made in the definition for Census 2011:

Paralytic persons

- Those who crawl
- Those who can walk with the help of an aid
- Have acute and permanent problems of joints/muscles
- Have difficulty in balancing and coordinating body movement
- Have loss of sensation in the body due to paralysis, Leprosy, etc.

Table I. Disabled Population by Type of Disability in India (2011)

Type of Disability	Persons	Males	Females
Total	26,810,557	14,986,202	11,824,355
In Seeing	5,032,463	2,638,516	2,393,947
In Hearing	5,071,007	2,677,544	2,393,463
In Speech	1,998,535	1,122,896	875,639
In Movement	5,436,604	3,370,374	2,066,230
Mental Retardation	1,505,624	870,708	634,916
Mental Illness	722,826	415,732	307,094
Any Other	4,927,011	2,727,828	2,199,183
Multiple Disability	2,116,487	1,162,604	953,883

Thus, significant research has been carried out so far for the development of a smart wheelchair, which ultimately aimed at packing maximum features on their proposed model, but not many could achieve this and finally restricted their scope. We aim not to eliminate this trade-off but to minimize it in the maximum possible way. This means packing maximum features at a low cost is the aim of this project.

II. SYSTEM OVERVIEW

The smart wheelchair is capable of obstacle detection with the Ultrasonic sensor. Also, slope detection using three-axis accelerometer, along with this facility of sending an SOS message is a notable feature of this project. All these features are controlled wirelessly using Bluetooth on an Android-based app and aim at providing these features at an affordable price. Following Fig. 1 shows the overall system architecture.

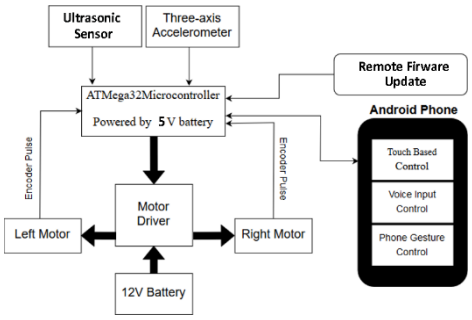

Fig. 1 System Overview Diagram

As per the above diagram, the system is powered by Atmega 32A microcontroller which is controlled through an android application (Swheel). The two important sensors viz. Ultrasonic Sensor for Object Detection and Three-axis Accelerometer for slope detection are also connected to the microcontroller. For the physical locomotion two motors, each of 150rpm is connected through its respective motor driver to the microcontroller. The input power requirement for the motors to operate is 12V which is further stepped down to 5V to power the microcontroller.

There is also a provision to connect a USB programmer which meets the Remote Firmware Installation feature.

III. FUNCTIONAL OVERVIEW

A. Multimodal Input: It refers to the provision of multiple modes to operate the wheelchair through an android application viz. Touch-enabled buttons, Gesture recognition using an accelerometer and, Voice recognition.

B. Obstacle Detection: Obstacle detection is done using the Ultrasonic Sensor where the motion will be suspended for some time until the pathway is clear. This feature has a high priority because it accounts for the user's safety.

C. Slope Detection: Slope detection is done using the 3-axis accelerometer. If any slope detected which is more than the defined threshold then the motion of the wheelchair will be stopped and an SOS message along with the user's location will be sent to the emergency contacts. This feature has a medium-to-high priority because of the threshold calculation.

D. SOS Message Support: SOS message support is provided using the android app. The user can send an emergency message along with the current location to the emergency contacts. This feature has medium priority owing to circumstances which "may" occur. Its usage will be limited.

E. Remote Firmware Update: Firmware updates of the wheelchair will be provided using a web app where the user can download the latest burnable firmware file. This file must be burnt using an executable burner software called "Swheel Burner" to transfer the latest released code to the wheelchair.

IV. OPERATIONAL DETAILS

We have used Atmel Studio for programming of the ATmega32A and Android Studio for the mobile application. The PCB and circuit diagram are designed using EasyEDA and Proteus. The Gerber format specification file created is then used to print the PCB which is mounted atop of the chassis. The circuit diagram given below represents the interconnections between all the circuit components required for the wheelchair. This is the primary circuit of our hardware unit which justifies all the necessary components and connections required.

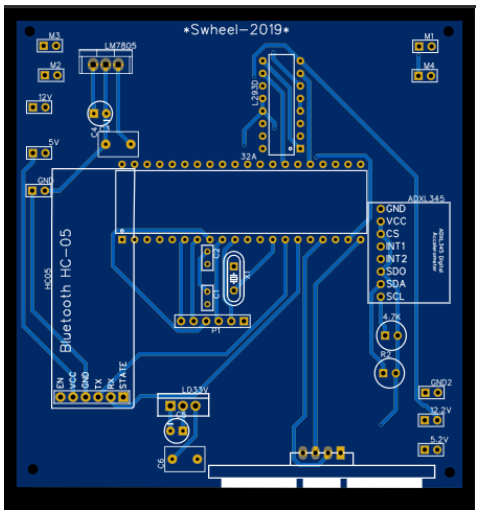

Fig 2. PCB Design

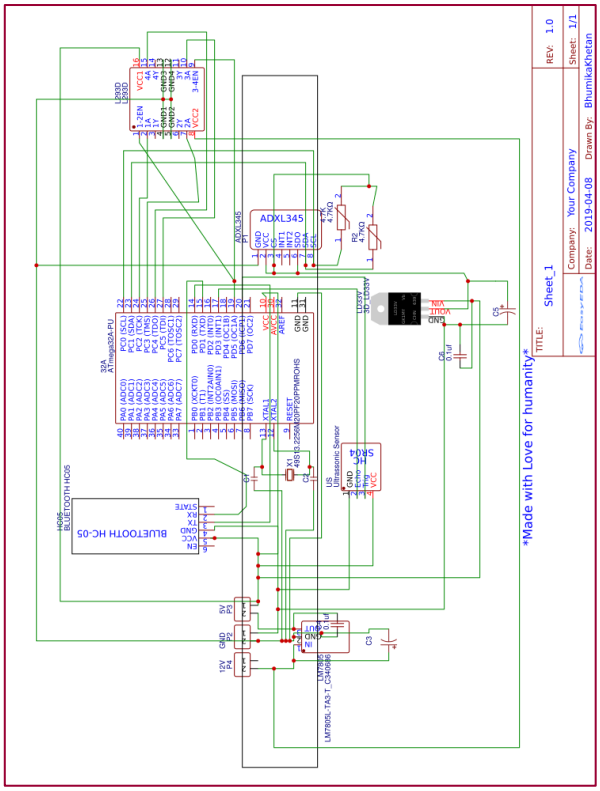

Fig 3. Circuit Diagram

A. Bluetooth Connectivity: The Bluetooth adaptor for the Android phone is checked. If found, the client class makes a socket with the Mac address of the device. the data transfer is done using the send receive class where a buffer is used to store the sent MPC as shown in Table II. We are using the USART module for Bluetooth connectivity. USART is used for communication between ATmega32A and HC-05 which is in turn connected to Android phone. We are enabling receiving and transmitting module in USART. Also, interrupt receiving is enabled.

Table II. Message Passing Codes

Operation	Code	Flow
Forward	F	Mobile to Controller
Backward	B	Mobile to Controller
Left	L	Mobile to Controller
Right	R	Mobile to Controller
Stop	S	Mobile to Controller
Toggle	T	Mobile to Controller
Obstacle Detected	O	Controller to Mobile
Slope- greater than or = 45	a	Controller to Mobile
Slope (Up)- 15 to 45 degrees	b	Controller to Mobile
Slope(Down)- 15 to 45 degrees	c	Controller to Mobile
Slope- less than 15 degrees	d	Controller to Mobile

B. Manual Input: Five buttons are given for manual input as follows- Left, Right, Forward, Backward and Stop. After selecting one button the related MPC as shown in Table II will be sent from Android to HC-05. HC-05 will transfer these codes to microcontroller ATmega32A using use USART module interrupt receiving. At the receiving end, the microcontroller will take those codes and according to the specified functionality, the movement of the chair will be deciphered.

C. Gesture Input: The readings from the inbuilt accelerometer are used to decide the gesture which is given by the user. It depends on the x, y, and z-axis at which the mobile is held. For example, IF (x less than equal to -4 and x less than equal to 4) and (y greater than equal to -9 and y less than equal to -2) and (z

greater than equal to and z less than equal to 10) is satisfied then FORWARD motion is enabled. The related MPC as shown in Table II will be sent from Android to HC-05. HC-05 will transfer these codes to microcontroller ATmega32A using use USART module interrupt receiving. At the receiving end, the microcontroller will take those codes and according to the specified functionality, the movement of the chair will be deciphered.

D. Voice Input: Using the Android TexttoSpeech and RecognizerIntent libraries the voice control module is implemented. The TexttoSpeech object the default language which the user is using on his/her phone. The input will be given in the same language itself. However, we have targeted only the Indian disabled community so English, Hindi, and Marathi will be preferable. After the input is given using the Google text to speech window, the result is displayed on the user's screen. The RecognizerIntent object is used to read out the input command from the screen. The related MPC as shown in Table II will be sent from Android to HC-05. HC-05 will transfer these codes to microcontroller ATmega32A using USART module interrupt receiving. At the receiving end, the microcontroller will take those codes and according to the specified functionality, the movement of the chair will be deciphered.

E. Obstacle Detection: Ultrasonic sensor is being used for obstacle detection. The trigger in the ultrasonic sensor is used for transmitting ultrasonic sound is activated for 15µs. After that, the microcontroller will wait for the Echo of that sound. Based on the time required for receiving the echo we will estimate the distance of the nearest object. If the obstacle is not within a safe distance to the user, then the MPC as shown in Table II for obstacle detection will be sent to the Android phone.

F. Slope Detection: ATmega32A is connected to ADXL345 for slope detection. ADXL345 uses TWO WIRE INTERFACE for communication with ATmega32A. Three-axis values will be determined by the accelerometer module. These values will be used for slope calculation for the wheelchair. If the slope is safe, then the corresponding MPC as shown in Table II will be sent to the Android phone. If not, the motion of the wheelchair will be halted, and the call and SOS message feature will be activated.

G. SOS Message and Call: The telephony library in Android is used for SOS call and message. First, the SMSmanager object is created and then the permission for allowing the application to make call and SMS for allowing the application to make calls and SMS is checked. If allowed, the default SMS is sent to the entered phone number. Similarly, to make a call, action call intent is called.

H. Remote Firmware update: Using this functionality developers can release firmware updates for the wheelchair. Following are the steps to be followed:

Step 1: As shown in Fig. 4 user need to open our web app.

Step 2: Click on Download Update Button.

Step 3: Connect the wheelchair to the PC using a USB cable provided along with the kit.

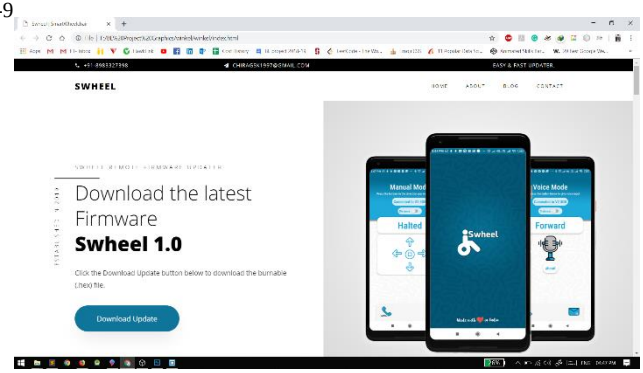

Fig 4. Web app for downloading the latest firmware.

Step 4: As shown in Fig 5. Open the Swheel Burner Application provided along with the kit and select the downloaded file from the file picker.

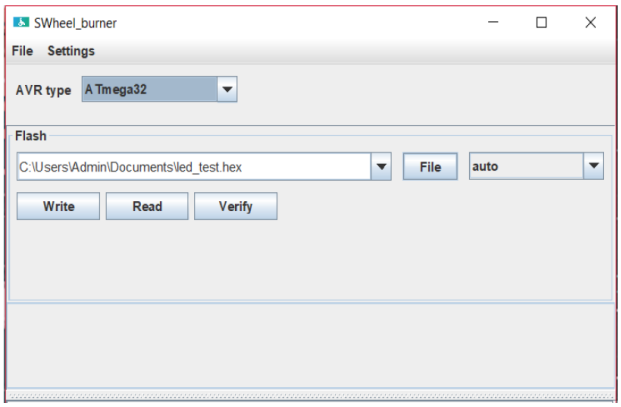

Fig 5. Swheel Burner for burning the firmware.

Step 4: Click Verify and then Burn.
In this way, new firmware can be installed on the wheelchair.

V. COST

It would cost ₹2,500 for developing the system (Kit). In addition to it, wheelchair cost would vary as per the user requirement. Following table describes the cost of the components required in building up this system.

Table III. Cost

No.	Item	Rate(INR)	Quantity	Price(INR)
1	ATMega32 Microcontroller	120	01	120
2	Motor Driver	42	01	42
3	Bluetooth Module (HC-05) 3.3V	300	01	300
4	Battery 12V	380	01	380
5	DC Motor and Wheel Set (100 RPM)	355	01	355
6	Downloader Programmer E-345	200	01	200
7	Resisters	003	010	003
8	Capacitors	005	02	005
9	PCB board 10x10cms	5 Rs./cm^2	01	500
10	Voltage Converter IC	008	02	016
11	Accelerometer	200	01	200
12	Ultrasonic HC-SR04	94	01	094
13	Misc. (Chassis, Wheel, etc.)	-	-	100
	Total			**2357**

VI. RESULTS AND DISCUSSIONS

The following Fig 6 shows the snapshot of our Android application along with the snapshot of the prototype.

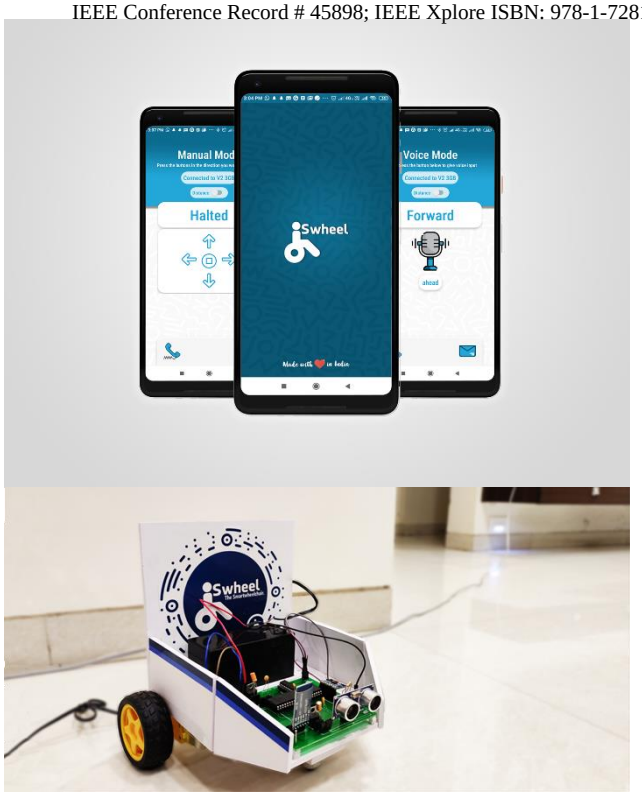

Fig 6. Application and Prototype snapshots

The system was tested for Slope Detection and Obstacle Detection for over 100+ values. The following Table IV illustrates the observed versus the calculated readings obtained by the accelerometer for slope detection.

Table IV. Accelerometer data values

X	Y	Z	Calculated	Observed	Accuracy
684	-64	-700	44.21	49.21	89.84
724	-100	-660	47.32	52.32	90.44
760	-76	-612	50.94	55.94	91.06
808	-64	-596	53.42	58.42	91.44
824	-60	-540	56.6	61.6	91.88
860	-68	-500	59.59	64.59	92.26
876	-76	-480	60.97	65.97	92.42
892	-44	-508	60.24	65.24	92.34
912	-68	-404	65.8	70.8	92.94
944	-36	-400	66.95	71.95	93.05
968	-60	-320	71.41	76.41	93.46
980	-72	-284	73.35	78.35	93.62
996	-80	-256	74.92	79.92	93.74
996	-80	-228	76.36	81.36	93.85
1004	-44	-240	76.34	81.34	93.85
1012	-72	-144	80.96	85.96	94.18
1024	-60	-124	82.33	87.33	94.27
1028	-68	-108	82.92	87.92	94.31
1032	-56	-64	85.28	90.28	94.46
1028	-68	-20	86.05	91.05	94.51
1032	-116	72	82.46	87.46	94.28
1036	-48	44	86.4	91.4	94.53

X	Y	Z	Calculated	Observed	Accuracy
964	-68	-200	77.63	82.63	93.95
892	-60	-484	61.33	66.33	92.46
792	-80	-536	55.61	60.61	91.75
664	92	-872	37.13	42.13	88.13
628	-108	-648	43.7	48.7	89.73
464	-32	-820	29.48	34.48	85.50
392	44	-828	25.3	30.3	83.50
324	-240	-792	21.38	26.38	81.05
436	-344	-780	27.08	32.08	84.41
640	-140	-724	40.95	45.95	89.12
688	-176	-636	46.19	51.19	90.23
748	-192	-620	49.05	54.05	90.75
824	-184	-624	51.7	56.7	91.18
796	-172	-564	53.47	58.47	91.45
860	-124	-520	58.13	63.13	92.08
860	-140	-468	60.4	65.4	92.35
876	-172	-388	64.15	69.15	92.77
872	-96	-412	64.12	69.12	92.77
992	-108	-408	66.95	71.95	93.05
976	-40	-384	68.41	73.41	93.19
Mean Accuracy					91.58

The above Table IV illustrates the value returned by the 3-Axis Accelerometer, which is used to calculate the angle of the chair with the surface on which it is rested i.e. the slope. This is calculated using the following formula:

$$\boldsymbol{\theta = \tan^{-1}\left(\frac{X}{\sqrt{Y^2 + Z^2}}\right)}$$

For example, if the Accelerometer returns the X, Y and Z co-ordinates as say, X = 392, Y = 44, Z = -828 then,

$$\theta = \tan^{-1}\left(\frac{392}{\sqrt{44^2 + (-828)^2}}\right)$$

$$= \tan^{-1}\left(\frac{392}{\sqrt{1936 + 685584}}\right)$$

$$= \tan^{-1}\left(\frac{392}{\sqrt{687520}}\right)$$

$$= \tan^{-1}\left(\frac{392}{829.168}\right)$$

$$= \tan^{-1}(0.4728)$$

$$\theta = 25.30°$$

Thus, the calculated values of the angle are verified with the observed value. The observed values of the slope are calculated using Plum Bob method. Thus, testing the prototype for over more than 50 test cases on a variety of surfaces, we have achieved an accuracy of **91.58 %**.

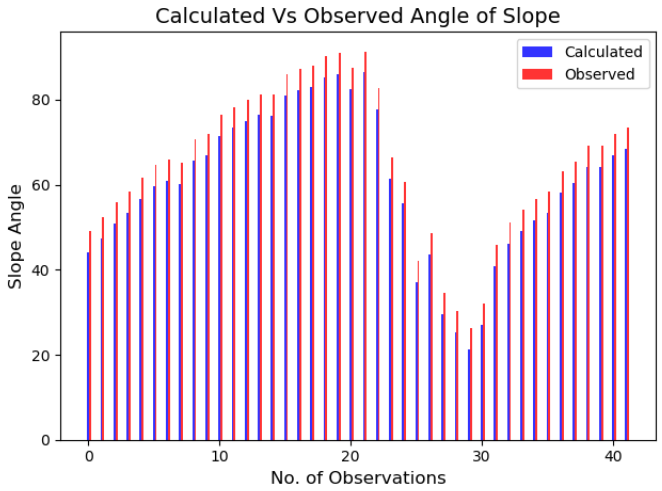

Fig 7. Calculated Values against the Observed value of the angle of Slope

The following Table V illustrates the observed versus the calculated readings obtained by the Ultrasonic Sensor for obstacle detection.

Table V. Ultrasonic sensor data values

Pulse	Calculated	Observed	Accuracy
0	0	0	100
219	3	4	75.00
223	3	4	75.00
225	3	5	60.00
226	3	5	60.00
232	4	6	66.67
274	4	6	66.67
341	5	7	71.43
382	6	8	75.00
397	6	8	75.00
431	7	9	77.78
256	4	6	66.67
514	8	10	80.00
807	13	15	86.67
584	10	12	83.33
599	10	12	83.33
651	11	13	84.62
665	11	13	84.62
678	11	13	84.62
696	12	14	85.71
714	12	14	85.71
735	12	14	85.71
751	12	14	85.71
765	13	15	86.67
790	13	15	86.67
807	13	15	86.67
817	14	16	87.50
822	14	16	87.50
828	14	16	87.50
864	14	16	87.50
855	14	16	87.50
874	15	17	88.24
910	15	17	88.24
922	15	17	88.24
897	15	17	88.24
903	15	17	88.24
934	16	18	88.89
937	16	18	88.89
943	16	18	88.89
925	15	17	88.24
958	16	18	88.89
964	16	18	88.89
945	16	18	88.89
946	16	18	88.89
952	16	18	88.89
1205	20	22	90.91

1204	20	22	90.91
1205	20	22	90.91
1181	20	22	90.91
1205	20	22	90.91
1204	20	22	90.91
1204	20	22	90.91
1205	20	22	90.91
1181	20	22	90.91
1181	20	22	90.91
1205	20	22	90.91
1204	20	22	90.91
1204	20	22	90.91
1205	20	22	90.91
1204	20	22	90.91
1181	20	22	90.91
1204	20	22	90.91
1204	20	22	90.91
1205	20	22	90.91
1204	20	22	90.91
1204	20	22	90.91
1204	20	22	90.91
1205	20	22	90.91
1204	20	22	90.91
1232	21	23	91.30
1208	20	22	90.91
1231	21	23	91.30
1233	21	23	91.30
1290	22	24	91.67
1292	22	24	91.67
1304	22	24	91.67
1352	23	25	92.00
1382	23	25	92.00
1379	23	25	92.00
1400	24	26	92.31
1439	24	26	92.31
1452	25	27	92.59
1488	25	27	92.59
1521	26	28	92.86
1575	27	29	93.10
1580	27	29	93.10
1609	27	29	93.10
1637	28	30	93.33
1657	28	30	93.33
1692	29	31	93.55
1708	29	31	93.55

1723	29	31	93.55
500	8	10	80.00
467	8	10	80.00
460	7	9	77.78
406	7	9	77.78
377	6	8	75.00
358	6	8	75.00
365	6	8	75.00
322	5	7	71.43
310	5	7	71.43
295	5	7	71.43
277	4	6	66.67
271	4	6	66.67
524	9	11	81.82
250	4	6	66.67
316	5	7	71.43
361	6	8	75.00
433	7	9	77.78
582	10	12	83.33
745	12	14	85.71
941	16	18	88.89
1115	19	21	90.48
1308	22	24	91.67
1452	25	27	92.59
1697	29	31	93.55
1906	32	34	94.12
2027	34	36	94.44
Mean Accuracy			85.85

The above Table V illustrates the value returned by the Ultrasonic Sensor, which is used to calculate the distance of an object in front of its line of action. This is calculated as follows:

Speed of sound = 340 m/sec

$$\frac{1}{Speed\ of\ sound} = \frac{29.412\mu s}{cm}$$

$$Distance = \left(\frac{Time\ \times Speed\ of\ sound}{2}\right)$$

… The denominator is 2 because sound travels back and forth.

∴

$$Distance = \left(\frac{Time}{2\ \times 29.412}\right)$$

$$Centimeters = \frac{(microsecond/2)}{29}$$

$$Centimeters = \frac{(microsecond)}{58}$$

Thus, Time is returned by the sensor as output,

$$\boldsymbol{distance = \frac{pulse}{58}}$$

The distance obtained is rounded off to the nearest lowest integer.

For example, if the ultrasonic sensor returns a pulse value say 274 then,

$$distance = \frac{274}{58} = 4.724\ \approx 4cms$$

Thus, the calculated values of the distance are verified with the observed value. The observed values of the distance are calculated manually using a metric scale. Thus, testing the prototype for over more than 50 test cases on a variety of objects, we have achieved an accuracy of **85.85 %.**

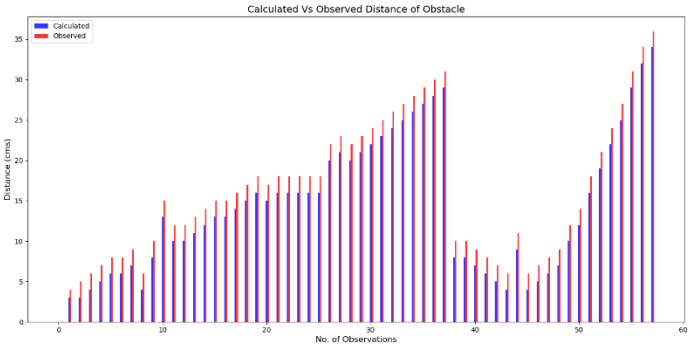

Fig 8. Calculated Values against the Observed value of the distance of the obstacle.

With all these results, the responses on the slope are observed carefully by testing on different slope angles. The Overall accuracy of this system is also compared with the accuracy calculated in the referred base paper titled" Low-cost Smart Electric Wheelchair with Destination Mapping and Intelligent Control Features [1]. The accuracy achieved in this publication is 76% for a 20-degree slope and 96% for the horizontal surface. Whereas our system has achieved an accuracy of 91.58% for a variety of slopes and horizontal surfaces ranging from as low as 20 degrees to as high as 86 degrees.

Table VI. Results

No.	Type of Test	Number of observations	Accuracy
1.	Slope Detection	100	91.58%
2.	Obstacle Detection	120	85.85%

VII. CONCLUSION

In this paper, we have constructed a model of a smart wheelchair which is controlled using an Android phone offering touch, voice control, and gesture-based input modes. Different types of safety measures such as slope detection, real-time distance-based obstacle detection, SOS message, and call are successfully assimilated. Also, a feature for remote OS installation/update is also provided. Everything aforesaid is done in consideration to attain a low cost of the wheelchair.

The accuracy of our system is **91.58%** for slope detection as calculated by the 3-axis accelerometer on a variety of slopes and **85.85%** for obstacle detection for a variety of obstacles as detected by the ultrasonic sensor. The accuracy of slope detection may decrease on a bumpy surface. Overall, the accuracy can be increased by doing 3D surrounding mapping and by GPS outdoor navigation which is a part of the future work.

We have therefore successfully targeted disabled population which accounts for up to 20 percent of the total disabled population in India. Finally, the developed prototype ensures to provide a low-cost, smart and wireless alternative to help the physically challenged, which has a tremendous impact on society.

Greater improvement and feature increments can be made to upgrade client experience and reliability, for instance, by incorporating with EEG signal or EOG signal, finger gesture, 3D surrounding mapping, and so on. GPS module can also be included for tracking and outdoor path navigation. The range for obstacle detection can be improved by incorporating the SONAR sensor.

REFERENCES

[1] Celia Shahnaz, Ahmed Maksud, Shaikh Anowarul Fattah, Sayeed Shafayet Chowdhary "Low-Cost Smart Electric Wheelchair with Destination Mapping and Intelligent Control Features", Institute of Electrical and Electronics Engineer, 978-1-5386-0487--8, 03-2018.

[2] Fitri Utaminingrum, Tri Astoto Kurniawan, M Ali Fauzi, Rizal Maulana; Dahnial Syauqy; Randy Cahya Wihandika Yuita Arum Sari Putra Pandu Adikara, "A Laser-Vision based Obstacle Detection and Distance Estimation for Smart Wheelchair Navigation", Institute of Electrical and Electronics Engineer, 03-2017.

[3] Artee Kunal Dalsaniya, Dhanashri H. Gawali, "Smartphone-based Wheelchair Navigation and Home Automation for Disabled", Institute of Electrical and Electronics Engineer, 978-1-4673-7807-9, 01-2016.

[4] Shraddha Uddhav Khadilkar; Narendra Wagdarikar, "Android phone-controlled voice, gesture, and touchscreen operated smart wheelchair", Institute of Electrical and Electronics Engineer, 04-2015.

[5] Puneet Dobhal, Nishant Singh Bisht, Rajesh Singh, Bhupendra Singh, Shubham Murari, "Smart wheelchair for physically handicapped people using tilt sensor using IEEE 802.15.4 standard protocol", Conference on Advances in Communication and Control Systems 2013 (CAC2S), 01-2013.

[6] The government of India, **http://censusindia.gov.in/**

[7] World Health Organization, **http://www.searo.who.int/india/en/**

Proceedings of the Fourth International Conference on Communication and Electronics Systems (ICCES 2019)
IEEE Conference Record # 45898; IEEE Xplore ISBN: 978-1-7281-1261-9

Internet of Things (IoT) enabled Sustainable Home Automation along with Security using Solar Energy

Swetha Amit[1], Anitha Sarah Koshy[2], Samprita S[3], Shwetali Joshi[4], Ranjitha N[5]
[1]Assistant Professor, Telecommunication Engineering, Ramaiah Institute of Technology, Bangalore, swetha.amit@msrit.edu
[2,3,4,5]UG Student, Telecommunication Engineering, Ramaiah Institute of Technology, Bangalore,
anithaskoshy@gmail.com, sampritaiyer12@gmail.com, shwetalij@outlook.com, ranjithanagendra99@gmail.com

***Abstract*: Home automation is a very important part of "The Internet of Things" popularly called as IoT. IoT provides a solution for seamless control over all the appliances at home. Home automation exists since many decades for controlling basic equipments of home like the lights and simple appliances. Present Technology expects the world to be interconnected with a touch of fingerprints or simple voice commands. The aim of it is to design and construct a home automation system which will switch on or off any household devices that are connected to it, using microcontroller, mobile or Alexa with the help of Wi-Fi. It is socially relevant and its implementation is cost effective. In our project controlling of appliances or equipment is through Alexa or mobile. We have also included an important aspect that is home security by making provisions for door (open and close), movement, fire and gas leak detection. The controllers used here are Node MCU and Arduino mini for automation and security respectively. We are using solar panels as the source of power for the equipments. It has a charging unit and a smart power management unit.**

Keywords: Microcontroller, Alexa, Arduino mini, Node MCU, Solar panels

I. INTRODUCTION

In the 21st Century of Computer age, many tasks are automated. Automation makes every task easier, safer, faster, and cost effective covering a variety of technological capabilities which can be easily installed in our home. It includes controlling the home remotely through a computer or phone by programming the gadgets so that they respond to the variable conditions. All the appliances at home can be centralized too. This new features of home automation not only makes it efficient and easier to operate, but also help in maintaining well. Device can be activity monitored which gives us live updates about the action to be taken. For example, a monitoring furnace reminds us about the cleaning to be done, AC reporting about changing the filters. A lot of countries around the world are using fossil fuels to generate electricity. They are depleting resources and also cause a lot of pollution to the environment. Although it is cheap to use fossil fuels to now, it will eventually cost a lot when the world's fossil fuel starts depleting. That is why more studies and researches have to be done on renewable energy such as solar energy, wind energy, and more as they will be the best source of energy when fossil fuel are depleted.

We in our project are introducing a smart power management system; the solar energy is harvested and used to supply power to carry out the automation and security of the home. We are calling it smart power system because it can switch between solar power and main power based on the availability of the harvested power. The paper demonstrates the complete home automation which is IoT based. Section 2 discusses the overview of the home automation system, section 3 discusses the complete description of the system used to have a home automation system with security. Section 4 and 5 discusses the BLYNK and ALEXA app and their usage in IoT communication and voice controlling respectively. Section 6 discusses the validation of the complete system.

II. OVERVIEW OF THE SYSTEM

In this home automation system, the commands are given through either Alexa or mobile to the Node MCU controller. It is processed in the controller and relayed thus the appliances are controlled. If the person who wants to operate is inside the house then he can use Alexa to give commands, if the person is somewhere else he can control the appliances through mobile phone using the Alexa app.

The home security is taken care with the help of various sensors like door sensor, PIR sensor, gas sensor, fire sensor and glass break sensor (vibration sensor) to detect open/close of the door, movement, gas leak, fire and glass break respectively [1]. The sensed data is given to the Arduino and a signaling message is sent to the mobile through the GSM module. To provide power to all these devices we are implementing a smart power management system. The power from the solar panel is given to the charging unit which consists of a regulator to regulate the voltage level and an indicator which indicates the battery level. The status of the battery level, duration of the battery and the consumption of power will be given to the user. If the battery level that is the stored solar power is getting exhausted then the devices will be powered by the main power. Thus switching between the main power and the solar power will take place.

III. BLOCK DIAGRAM OF THE ENTIRE SYSTEM

The controller receives command from the Alexa or mobile and relays it to the respective device and thus operates it [2,3]. Also the sensors collect data and send it to the controller which is sent to the mobile as an alert

message. The power supply to perform automation and security is given by the harvested solar power. It is a smart power system which switches between solar power and main power based on the availability of the solar power [4].

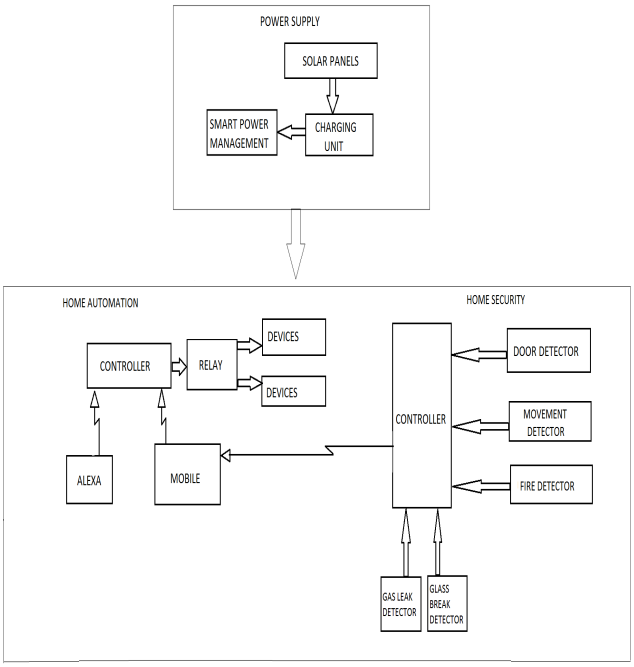

Fig.1: Block diagram of home automation and security system

The solar panel used here gives an output of 21v,30w since the battery used here is of 12v we cannot directly use the 21v output therefore the output is given to the solar charge controller to step down the voltage and making it suitable to use [5].

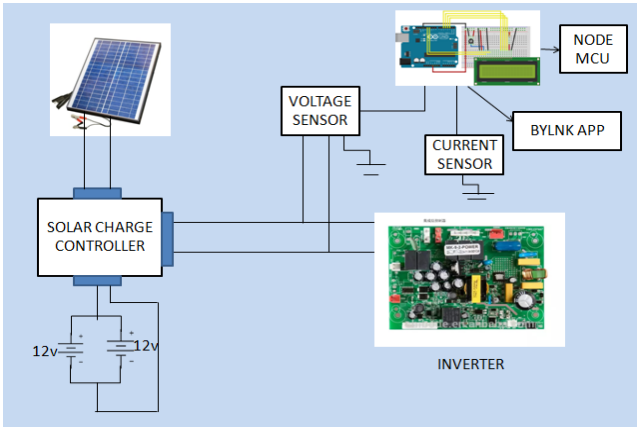

Fig.2: Block diagram of solar power harvesting

The voltage sensor and the battery is parallelly connected to the inverter.The voltage and current are read by the arduino through the voltage sensor and current sensor as they are connected to the respective pins in the arduino. The readings are displayed in the BYLNK app to the user. This solar panel provides a back up power for 6 hours.

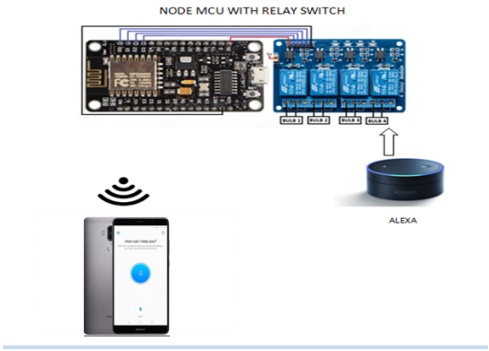

Fig.3: Block diagram of home automation system

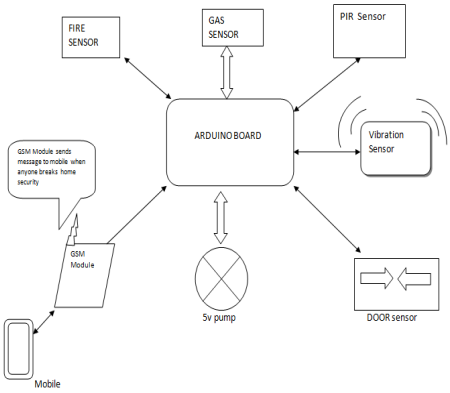

Fig.4: Block diagram of home security system

IV. BYLNK APP

The Blynk app is designed for the IoT. This app can control hardware components remotely, it can also display the sensor data, store it and visualize it. Here the components will communicate with each other to build a fully functional IoT application that can be controlled from anywhere through a preconfigured connectivity type.

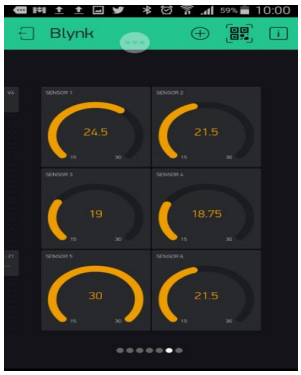

Fig.5: Preview of Blynk App

We can control our hardware from the Blynk app running on our mobile device through the Blynk Cloud or Blynk's personal server. It will work the same in the opposite direction by sending rows of processed data from hardware to your Blynk app. This app has a send on release option, that is, when you move joystick widget, commands are streamed to the hardware, and during a single joystick move you can send dozens of commands. There are use-cases where it's needed, however creating such a load may lead to hardware overload and reset. **Send On Release** is a recommended setting for majority of applications.

There are different types of widgets that control the app. Widgets are interface modules. Each of them performs a specific input/ output function when communicating with the hardware.

The types of Widgets are:

- **Controllers** - used to send commands that control your hardware
- **Displays** - used for data visualization from sensors and other sources
- **Notifications** - send messages and notifications;
- **Interface** - widgets to perform certain GUI functions

V. ALEXA APP

In this proposed work on home automation, ALEXA palys a major role by giving commands through alexa to control the devices when the user is at home. When the user is not at home then with the help of alexa app he can give commands to control the devices. Smart speakers are like gateway devices helping in easy controlling of the smart home.

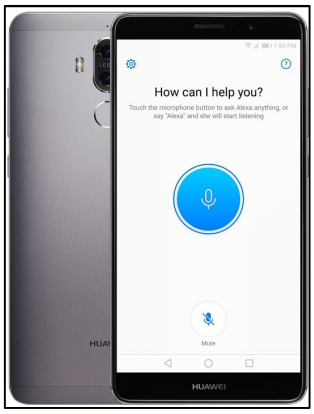

Fig.6: Preview of Alexa App

It gets easier to set up single command groups which can help in controlling multiple lights, plugs and many other devices. Hence, a single command is sufficient to control everything at a time. We can add different devices and rename the devices accordingly.

VI. RESULTS AND DISCUSSIONS

The main aim of the project is to design a system in such a way that by using solar energy we had to control all the devices and we could successfully harvest power from the solar panels which gives us a backup power up to 6 hours as shown in Fig.7 and Fig.8.

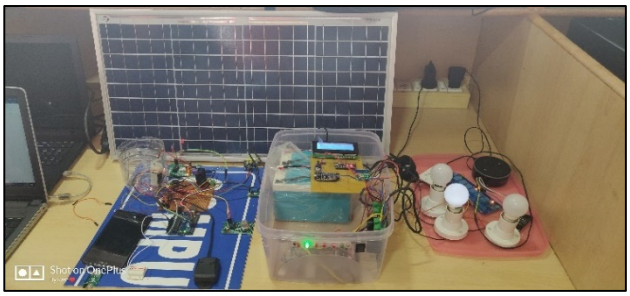

Fig.7: Complete Set-Up of the Project

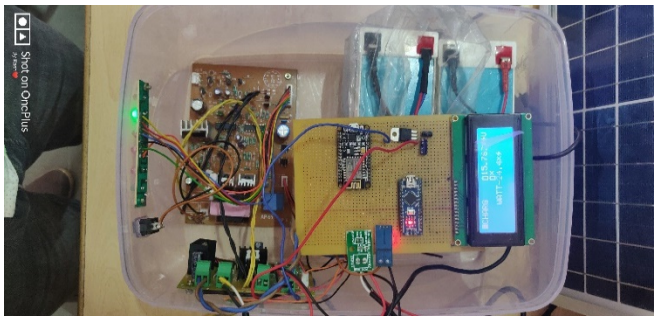

Fig.8: Set-Up of Power Harvesting

We could control the devices at home through alexa and through alexa app and thus we could implement home automation successfully. Refer to Fig.9.

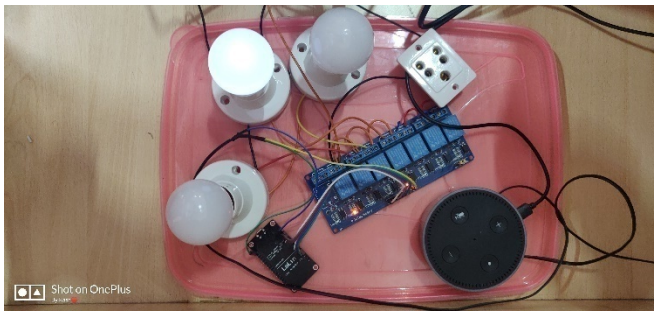

Fig.9: Set-Up of Home Automation

As shown in the Fig.10, the last part of our project is home security where we have deployed all the necessary sensors for various purposes like smoke and flame detection, unusual movement detection, and door and glass break detection. And if there any senses of violation we were successfully able to get messages through GSM module to the mobile phone through an app called BLYNK.

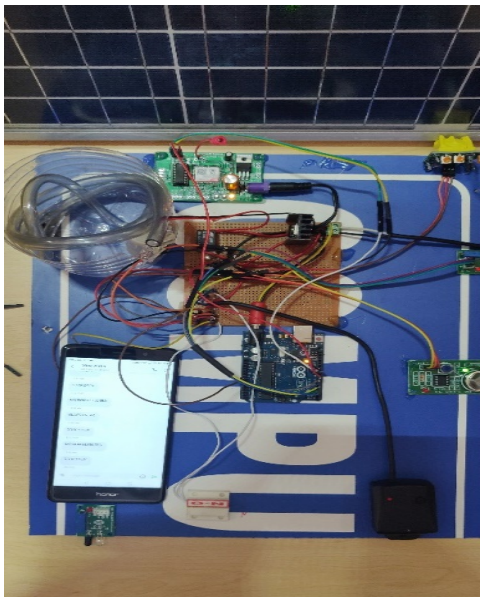

Fig.8: Set-Up of Home Security

VII. CONCLUSION AND FUTURE WORK

Future homes will be capable of offering almost all required services, for example, communication, energy, medical, utility and entertainment. The dream is future in where the data will be communicated between humans and devices without depending on a manual input of individual bytes. Computers can automatically mine data from the database that use the commanded data in changing aspects of home environment.

In future the healthcare service providers will definitely consider automation for effective way to provide remote healthcare services; mainly helping elderly and disabled. As technologies continue to advance, home automation will be a trending technology.

REFERENCES

[1] R. A. Ramlee, M. A. Othman, M. H. Leong, M. M. Ismail, S. S. S. Ranjit, "Smart home system using android application", *Information and Communication Technology (ICoICT) 2013 International Conference of*, pp. 277-280, 2013.

[2] R. S. Ransing, M. Rajput, "Smart home for elderly care based on Wireless Sensor Network", *Nascent Technologies in the Engineering Field (ICNTE) 2015 International Conference on*, pp. 1-5, 2015.

[3] M. Kuzlu, M. Pipattanasomporn and S. Rahman, "Review of communication technologies for smart homes/building applications," *Smart Grid Technologies – Asia (ISGT ASIA), 2015 IEEE Innovative, Bangkok 2015.*

[4] D. Pavithra and R. Balakrishnan, "IoT based monitoring and control system for home automation," *Communication Technologies (GCCT), 2015 Global Conference,Thuckalay, 2015.*

[5] R. Teymourzadeh, Salah Addin Ahmed, KokWai Chan and MokVeeHoong, "Smart GSM based Home Automation System," *Systems Process & Control (ICSPC), 2013 IEEE Conference on, Kaula Lumpur, 2013.*

[6] A A. Pramanik Rishikesh, V. Nagar, S. Dwivedi and B. Choudhury, "GSM based Smart home and digital notice board", *2016 International Conference on Computational Techniques in Information and Communication (ICCTICT), New Delhi, 2016.*

Proceedings of the Fourth International Conference on Communication and Electronics Systems (ICCES 2019)
IEEE Conference Record # 45898; IEEE Xplore ISBN: 978-1-7281-1261-9

Ultra Wide Band Symmetric Slots Antenna for Wearable Applications

Swetha Amit[1], T R Ramya[2], Vandana S[3], Pooja C R[4]
[1]Assistant Professor, Telecommunication Engineering, Ramaiah Institute of Technology, Bangalore
[2,3,4]UG Student, Telecommunication Engineering, Ramaiah Institute of Technology, Bangalore

ABSTRACT: **A low profile antenna for wearable applications is presented. Due to the miniature and low profile compact and flexible property of the antenna, it is well suited for Wearable applications. Moreover, the antenna is completely embedded in a jean material which is used as a substrate. The substrate chosen gives a good robust against external disturbances and also a good flexibility. A circular antenna with symmetrical slots has been built in HFSS and characterized. It is seen that introducing slots in the circular patch antenna enhances the gain. In this paper, the antenna is analyzed for parameters like, bandwidth, VSWR, return loss, gain, impedance matching. The gain of the wearable antenna is 5.8101. The return loss and VSWR are -21dB and 1.1809 respectively.**

Keywords: Symmetric slots, wearable antenna, HFSS, low profile.

I. INTRODUCTION

Microstrip antenna in circular shape are highly recommended antennas for wideband and it is becoming popular with portable devices. It is very easy to manufacture, low cost, low volume. These reasons make the antenna very feasible to be used in wearable applications. Wearable systems are used to monitor the health of people by sensing, processing, actuating and communicating. A wearable antenna acts is the integrated element between cloth and the communication systems, making electronic device less obtrusive.

In this paper, a circular patch antenna is designed at 2.4GHz. The substrate chosen is a textile material; Jeans with a dielectric constant of 1.4 and height of 1.6mm. The antenna is designed on Ansys HFSS v19, which works on the principle of Finite Element Method (FEM). This technique uses a triangular shaped meshes for surface meshing, tetrahedron shape for volumetric meshing. These structures are chosen for two dimensional and three dimensional analyzing structures respectively.

II. DESIGN OF THE SLOTTED CIRCULAR ANTENNA

Since only one parameter of the circular patch antenna is needed ie., the radius of the circular patch, it is very easy to design the antenna. This makes the antenna having only one degree of freedom. The structure of the antenna is as shown in fig 1. The design considerations include knowing the dielectric constant (ε_r) of the antenna, the operating frequency (fr) and the height of the substrate (h). The radius of the antenna can be calculated by the following equation 1 [1];

$$a = \frac{F}{\left\{1+\frac{2h}{\pi\varepsilon_r F}\left[\ln\left(\frac{\pi F}{2h}\right)+1.7726\right]\right\}^{1/2}} \qquad (1)$$

$$\text{Where, } F = \frac{8.791 * 10^9}{f_r\sqrt{\varepsilon_r}}$$

For the wearable application, we have chosen substrate as "Jeans" of dimensions 38mm*25mm with thickness of 1.6mm which satisfies robustness and flexible functionality. The antenna is designed based on frequency which is taken as 3.9GHz. The circular antenna is as shown in fig 1.

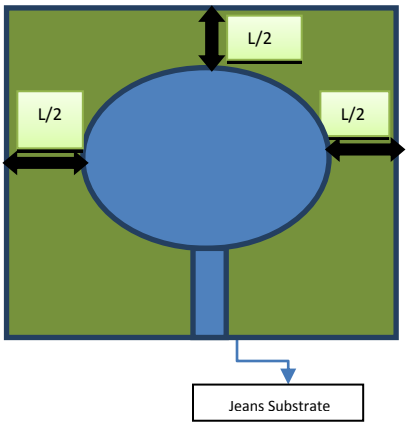

Fig 1: Circular patch antenna

Table 1 shows the dimensions of circular patch antenna with symmetrical slots. The first rectangular slot is chosen to be of dimension 1*19 mm. Further, three iterations are made to the rectangular slot with their dimensions to be 1/3rd the first rectangular slot. Hence the second slot has the dimension of 1*4mm, third rectangular slot has 1*1.3mm and the last slot is of dimension 1*0.4mm. Therefore, for the circular patch antenna, 4 Koch iterations are made so as to enhance the gain of the antenna. Adding slots to the antenna induces capacitance or inductance value which tends to increase the gain of the antenna.

Table 1: Proposed antenna parameters

Parameters	Dimension
Substrate thickness (h)	1
Relative Permittivity (ε_r)	1.4
Ground dimension (mm)	38*25
Patch Radius (mm)	10
First rectangular slot dimension (mm)	1 * 19
Second rectangular slot dimension (mm)	1* 4
Third rectangular slot dimension (mm)	1* 1.3
Fourth rectangular slot dimension (mm)	1*0.4

III. RESULTS AND DISCUSSION

According to the frequency of operation, the designed antenna is calculated at a frequency of 2.9GHz. The antenna was analysed for various parameters like VSWR, S-parameters, Gain, Current distribution. Following figures validates the antenna performance. Fig 2 shows the Symmetric Slotted circular patch antenna with its radiation boundary which tells the near field and far field zone give by the following equation 2.

$$R = \frac{2*a^2}{\lambda} \qquad (2)$$

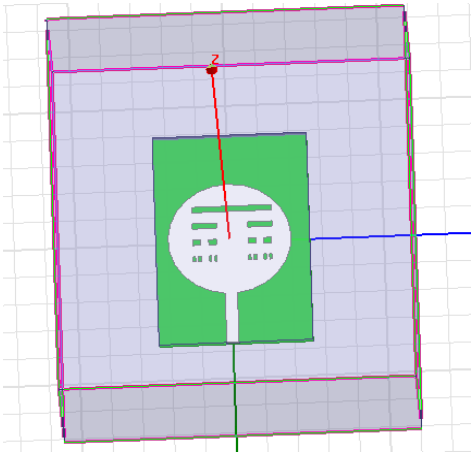

Fig 2: Symmetric Slotted circular patch antenna

Fig 3 shows the lumped port initialized and the patch antenna. The 50 ohm feed line is optimized so as to get a proper impedance matching. The dimensions of the antenna is also chosen such that the design is optimized for the designed frequency.

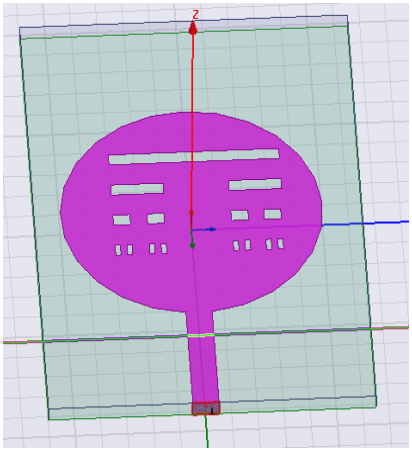

Fig 3: Lumped port initialized and the patch antenna

Fig 4 shows the current distribution in the antenna. Since it is in circular shape, the current distribution tells about the polarization. The antenna is circular polarized which can be used for applications which needs right hand and left hand circular polarized antennas.

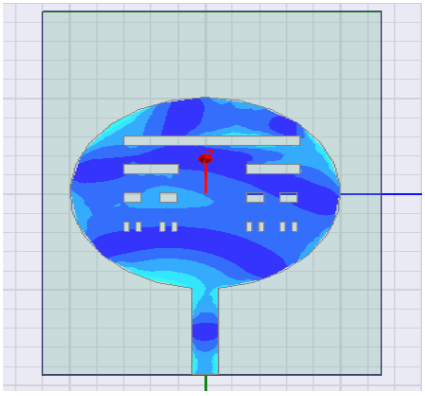

Fig 4: Current distribution in the antenna

The antenna is simulated using the software HFSS and the results were validated. The following fig shows the parameters of interest to be validated the use of antenna. Fig 5 shows return loss of -21dB at 3.9GHz with slots and -15db without slots covering a wideband from 3.5GHz to 5GHz. Fig 6 shows VSWR of antenna with and without slots are less than 2 over a wideband. Though VSWR is same for both with and without slots, we obtain better impedance matching with slots.

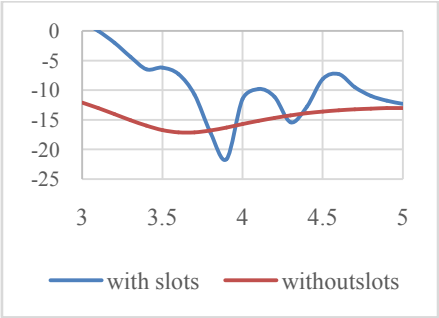

Fig 5: Return loss of -21dB at 3.9GHz with slots and -15dB without slots

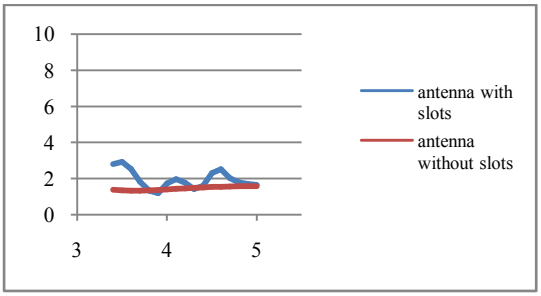

Fig 6: VSWR of antenna with and without slots 1.1809 at 3.9GHz

The bandwidth thus obtained is from 3.5GHz to 5GHz with a centre frequency of 3.9GHz. Thus the percentage bandwidth is given by,

$$Percentage\ Bandwidth = \frac{F_H - F_l}{F_C} \qquad (3)$$

Where, $F_C = Centre\ frequency$

$F_H = Highest\ frequency$

$F_L = Lowest\ Frequency$

On substituting the values, we get the bandwidth of 38.46% which validates the use of antenna as UWB.

Fig 7 shows Smith chart value: 1.080+i0.165. This implies that the antennas is matched perfectly for impedance at 3.9GHz. Fig 8 gives the 3D Radiation pattern of the antenna with a 5dB gain.

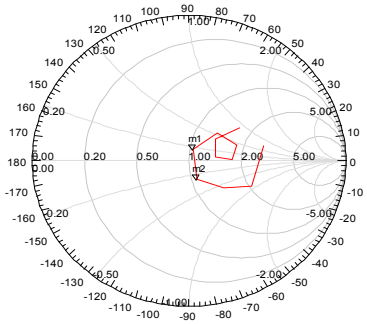

Fig 7: Smith chart value: 1.080+i0.165 at 3.9 GHz

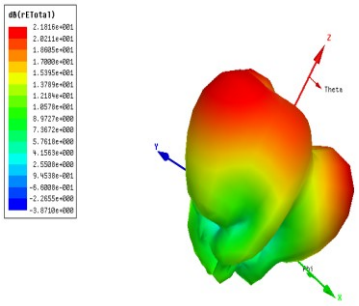

Fig 8: 3D Radiation pattern

Further, few more parameters were checked for the slotted circular patch antenna. Table 2 and 3 shows the parameters and their values at 3.9GHz. The radiation efficiency of the antenna is 86.5%. This implies that the incident power on the antenna is efficiently used since there is a good impedance matching between the feedline and the antenna.

Table 2: Antenna Parameters validated results

Quantity	Value
Max Radiation Intensity	0.201497(W/sr)
Max Directivity	5.56141
Max Gain	5.8101
Radiated Power	0.455307(W)
Accepted Power	2.53215
Incident Power	2.1902
Radiation Efficiency	0.865

Table 3: Radiation parameters

rE Field	Value	(Theta, Phi)
Total	12.3259	(0.872665, 6.10865)
X	8.68542	(0.698132, 3.14159)
Y	9.70529	(0.523599, 1.91986)
Z	9.35585	(1.0472, 6.10865)
Phi	7.63586	(0.523599, 2.26893)
Theta	12.0985	(0.872665, 3.14159)
LHCP	10.896	(0.872665, 5.93412)
RHCP	8.68715	(0.523599, 2.0944)

This circular patch wearable antenna designed on a jean substrate can be used in medical purpose for monitoring, alerting and demanding attention whenever hospital emergency is needed. Also in location based service in supplying the information that is currently needed to the user.

IV. CONCLUSION

The paper presents the design, simulation and validation of circular microstrip antenna at S band. The antenna operates with a good impedance matching. The return loss validates the result for the impedance matching between the antenna and the feeding network. The gain and directivity of the antenna are 5.81dB and 5.56dB respectively. The percentage bandwidth achieved is 38.46%. The radiation efficielcy of the antenna is 38.46% making it use for a wide band application.

In future, the antenna can be integrated with transceivers, microcontroller and sensors for human body monitoring. With the advancement in wearable technology, these devices can be worn on human body and can operate seamlessly.

REFERENCES

[1] Bonfiglio A., De Rossi D. Wearable Monitoring Systems. 1st ed. Springer; New York, NY, USA: 2011. p. 100.

[2] I J Bhal and P Bhartia, “Microstrip antennas”, Artech house, 1980

[3] Arun Singh Kirar, Veerendra Singh Jadaun, Pavan Kumar Sharma, “Design a Circular Microstrip Patch Antenna for Dual Band”, International Journal of Electronics Communication and Computer Technology (IJECCT) Volume 3 Issue 2 March 2013.

[4] Swetha Amit, Oshin S P, “Design, Implementation and Performance analysis of a high gain UWB Slot Wearable Antenna with Human Phantom for Medical Application”, 2017 IEEE International Conference on Antenna Innovations & Modern Technologies for Ground, Aircraft and Satellite Applications (iAIM), 24th to 27th November, 2017,Bangalore

[5] M.Venkata Narayana, Govardhani.Immadi, K.Rajkamal, M.S.R.S Tejaswi, Venkata Raviteja. K, A.K.Chaitanya, B.Bhaskar rao, “Microstrip Patch Antenna for C-band RADAR applications with Coaxial fed” ,International Journal of Engineering Research and Applications (IJERA) ISSN: 2248-9622 , Vol. 2, Issue 3, May-Jun 2012, pp.118-122

Proceedings of the Fourth International Conference on Communication and Electronics Systems (ICCES 2019)
IEEE Conference Record # 45898; IEEE Xplore ISBN: 978-1-7281-1261-9

An AI and ML driven approach for Smart Kitchen to enhance Restaurant like Cooking at Home

Naveen Ananda Kumar J
Institute of management
Christ (Deemed to be University)
Bengaluru, India
jnaveens@icloud.com

Shubashree S
Institute of management
Christ (Deemed to be University)
Bengaluru, India
shreesivakumar96@gmail.com

***Abstract*-With the world moving so fast around us and technology evolving faster than ever, how many of us stop and take a break to cook a healthy meal or even a normal balanced diet meal? We end up going for the easy solution and stop for a burger. Our Smart Kitchen is a way to improvise this situation where the devices in the kitchen, such as, Microwave Oven, Stove, Mixer Grinder and Ingredient Dispenser are all connected by the Smart Refrigerator through a home network which makes the cooking easier as all the devices are communicating to each other controlled by the Smart Refrigerator such as temperature, timing, flavour etc., It also suggests recipes based on the available ingredients. In this paper, we are proposing the concept of Smart Kitchen which is content aware and focuses on personalization for each of its users which in the long term will help in time and waste management, restaurant type cooking and balanced diet. It is an AI driven solution aiming at resolving the problems faced by the current generation and aims at achieving a healthy lifestyle by providing restaurant type cooking in the easiest way possible using AI and ML.**

I. INTRODUCTION

The preparation of food plays a central role in human life. Rapid improvements every day in Artificial Intelligence and Machine Learning powered by Cloud computing has changed the way every household works from a Refrigerator greeting you in the morning to an Induction that reduces the work of every cook, there is a touch of AI and its improvements in every appliance we use at home.[1] The more the people realise the advantages of the integration of technology in their everyday lives, the more the demand for such products. The customers are ready and willing to explore more of it. The consumers are becoming more tech-savvy and want the next big thing in the market at their homes. A Smart Kitchen, where a smart refrigerator is connected to all the other appliances in the kitchen is both personalization and sustainability driven.[2] It has its own unique selling points and is a next-level improvement to today's existing kitchen. The traditional understanding of a refrigerator which was used to store fruits and vegetables or to keep a food cold has changed. These days, smart refrigerator is a device that is connected to the internet and cloud through a network giving it capabilities to develop data and applications focusing on making things easier in the kitchen, optimum and efficient utilization of all the items available and a healthier lifestyle.

In this proposal, we aim at developing a smart kitchen for home where the devices are connected to the Smart Refrigerator where most of the ingredients are stored. The devices are connected and communicating to each other making the routine cooking process easier with minimal supervision. The smart refrigerator also suggests recipes from the cloud database and stores the recipes tried by the user. [3]. The suggestions are personalized based on the customer's taste and requirements for future use. This smart kitchen is restaurant like cooking, personalization and sustainability driven.

Smart Kitchen when achieved will be a revolution to every kitchen making things easier and more comfortable to every user. Using these intelligent devices to bring a range of products and devices reducing the problems faced by homemakers. The smart refrigerator has an idea about all the items stored in it, different ways it can be used in a recipe and its expiration date based on which it suggests recipes to the users. Our smart kitchen proposal takes the smart refrigerator capabilities to the next level where its connected to other appliances. Smart Kitchen, when used to its full extent, will change the eating patterns of every individual leading to a lifestyle change[4].The main reason why people have adopted an unhealthy living is because of lack of time and unawareness about the importance of healthy eating and exercise, laziness and the fast-moving world which disregards the lifestyle of a person. Our smart kitchen will reduce all these problems to a greater extent where cooking

is made easier, the recipes are handed out which is all health oriented and the ability of the devices to communicate with each other about the recipe makes the process easier and the suggested recipe is based on the ingredients available which also avoids the problem of not having an ingredient while cooking. [5]

II. PRESENT SCENARIO

The idea of a smart kitchen environment at homes is not new, there are many ideas which have contributed to the concept of smart kitchen such a user interface robotic arm, sensor enabled kitchen that gives cooking suggestions or instructions through videos and audios, implementing a human behaviour recognition system which stores the actions of humans in the kitchen and suggests new ideas based on the past data etc.,[6] Although these smart kitchen ideas are implemented there are disadvantages to these ideas that are not yet addressed such as:

- The recipes suggested are not linked to the refrigerator which contains the ingredients. Therefore, the recipe suggested might not consider the availability of the ingredients in the kitchen which decreases the convenience of cooking.[7]
- In a smart kitchen, all the appliances such as oven, refrigerator, stove etc are at its best use individually but they are not connected to each other which is again a lot of work for the person cooking and does not make the work easier as much as expected. [8]
- Implementing a healthy lifestyle is an unavoidable component in today's world, these smart kitchens do not consider it as an important feature. They are just focused on making things easier and not healthier. [9]
- There is no automated way to check the progress of the food being prepared like a camera or an alert to notify the progress. Which increases the need of humans to be around all the time when that is the main thing a smart kitchen is trying to avoid to an extent.[10]

A. Problem Statement

To develop a smart kitchen where all the devices such as microwave oven, mixer grinder, stove and ingredient dispenser is controlled by the smart refrigerator through a home network for restaurant like cooking at home which is monitored through a 360-degree camera. This makes the cooking easier and tries to maintain a healthy balanced diet.

B. Objectives

This paper is intended to adapt AI and ML into the devices used in a kitchen connected by the smart refrigerator which assists the other devices in cooking a dish completely.[11] Based on the chosen recipe, the devices adapt and works around the recipe from one device to the other. Even if the user decides to cook their own recipe, the devices are adaptable and stores the information for future cooking of the same recipe. [12]

C. USP of the model

The USP of our model is the network that is developed between the appliances and the refrigerator and its ability to maintain each stage of cooking with minimal human supervision. By integrating AI and ML we are able to better understand the tastes and preferences. This AI features in the smart refrigerator not just understands the items in the refrigerator but how efficiently it can be used in a dish, it also has the ability to control other appliances which renders smooth cooking process. Its ability to adapt and register the new recipes tried by the users is a special feature and keeps the nutrients in check as per the need of the users.

III. PROPOSED MODEL

A. Smart refrigerator

The refrigerator is the centroid which connects all other kitchen appliances through a home network and manages the flow while cooking a recipe. [13] It controls the appliances such as temperature, timing etc. It is also connected to a cloud database of recipes and gives customized suggestions based on the ingredients available and the number of people to be served. [14] It also keeps in check the expiration of the product and makes suggestions based on that. The following devices can be connected to the smart refrigerator network.

1. Microwave oven

The microwave oven is connected to the smart refrigerator. It communicates about the recipe selected and the oven adjusts the temperature and the time as per the requirements.

2. Stove

The stove which is connected to the smart refrigerator also has an automatically controlled valve. Once the recipe is selected, the valve is set as per requirements at different levels and timings are controlled by the refrigerator and the cooking is taken forward from there.

3. Mixer grinder

The mixer grinder is connected to the smart refrigerator. Once the recipe is selected, the

ingredients which needs to be grinded is moved to the mixer and the speed and consistency is selected and controlled based on the recipe or needs of the user through the home network.[15]

4. Ingredient dispenser

The ingredient dispenser is connected to the smart refrigerator. Although this is not a commonly used device is every home, this device when connected to the AI based algorithm in cloud can be very efficient in a smart kitchen. The dispenser has various sections which stores different ingredients such as spices. If the recipe is directly received from the cloud database, the dispenser which has an electronic valve understands the ingredient gives the accurate amount as mentioned in the recipe. The sensors attached to the dispenser is used to check the amount of ingredients to be added.

5. 360 degree - high resolution camera

The smart refrigerator is also connected to a 360-degree high resolution camera which scans and monitors the entire working process in the kitchen. This camera checks the dish at each stage and keeps in check its cooked properly and notifies the user if something goes wrong.

B. Working process

Fig 1.1 explains the working block diagram. The process starts with the smart refrigerator analysing the ingredients in the refrigerator and suggests few recipes based on it and the user can choose one of the recipes as per the interest and feed the quantity needed to serve the number of people in the house. As per the recipe, the ingredients in the refrigerator are taken out and moved to the next step. Based on the recipe, the next needed device is shown by the smart refrigerator according to which the user can move the cooking step by step. [16] The 360-degree camera scans and monitors every step using AI and ML to check the quality, density, colour, mixture and makes sure the dish doesn't get overcooked. It notifies the user to make the necessary changes.

C. Example

In order to comprehend the application of this smart refrigerator, we were given a problem along with how we would tackle this issue.

Problem - Figure 1.2, Martin is a 35-year-old male, he decided to make a brownie for himself for the first time on a Sunday afternoon after absolutely enjoying the brownie he had last night in a restaurant. Initially he tried to bake the brownie just by following the internet recipe and doing it on his own. But he faced various problems like lack of ingredients for which he ran to go out to the store multiple times, the ingredients mix was improper, the cake was burnt due to wrong temperature and the butter and chocolate melt was inconsistent

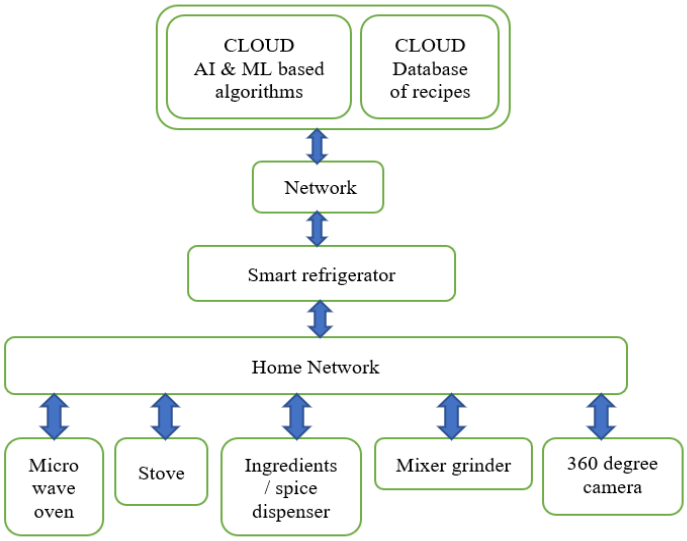

Fig 1.1 Block Diagram

Using the proposed model, he tried to bake the same with the help of a smart kitchen and the process thus went by as follows. First step, he selected the recipe from the cloud database, as per the recommendation by the smart refrigerator. The list of ingredients that was not available was suggested by the refrigerator altogether and the user can buy it in one trip to the store. After the recipe is selected and the ingredients are purchased, the next step is getting the butter and dark chocolate from the refrigerator and melting it. The stove controlled by the smart refrigerator receives the flame level to be maintained and time requirements that these items needs to be melted and adjusts its flame accordingly. Once the mix is ready, the user sets it for cooling. The 360-degree compares the progress of the food with its step-by-step database and alerts if something goes wrong. The next step will be to collect the other ingredients like sugar, flour and cocoa from the ingredient dispenser. The ratio of these items is received from the smart refrigerator and the dispenser dispenses the accurate amount of these items needed. Then the mixer grinder is used to prepare the egg and sugar mix as per the required consistency received from the smart refrigerator. Once all the ingredients are ready with the accurate amount and consistency, it is added to the brownie tin by the user and the tin is placed in the microwave oven. The timing for baking the cake is set up automatically by the smart refrigerator and the cake is ready to be served with no defects as there is a 360-degree camera monitoring the process from step one to the last and notify if something goes wrong. At the end, if the user forgets any step like adding toppings or serving it with ice-cream, the 360-degree camera understands it by comparing it with the database and alerts the user for best results and best tasting food. The use of smart kitchen for baking a

brownie is so much easier and more efficient than baking it manually without the help of the smart kitchen.

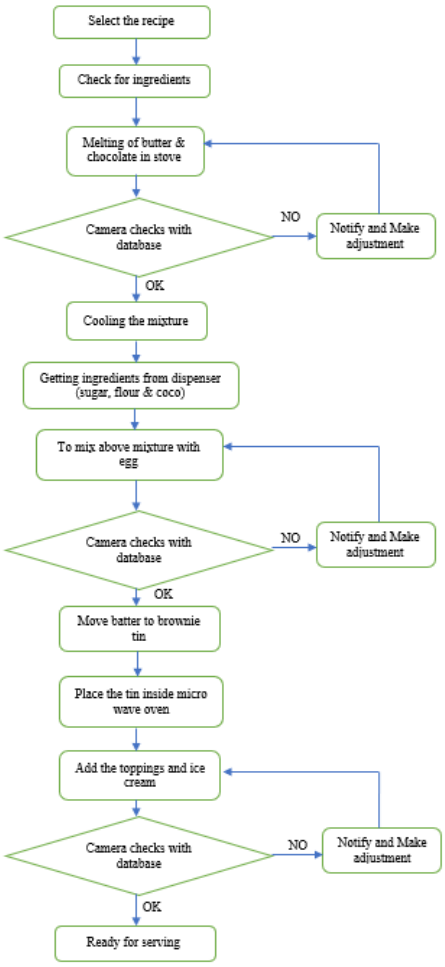

Fig 1.2 Process

D. FUTURE WORK

The future plan for our proposed model is to develop this smart kitchen into a human free kitchen set up where the need for human interaction is minimal to zero. This can be achieved by introducing a robotic arm in the kitchen which is again connected and controlled by the smart refrigerator. Once the recipe that needs to be cooked and the number of people is decided, the smart refrigerator connected to other appliances and the robotic arm takes over from there. And the 360-degree camera keeps in check and notifies if something goes wrong. When this is achieved, cooking becomes very easy and since the kitchen also provides restaurant like cooking, the need to go out and consume unhealthy food is reduced and the complete eating patterns are changed. Since our smart kitchen also provides healthy balanced diet, it is also health focused. However, people might still be interested in cooking their own food, in that case, they can temporarily deactivate the robotic arm and go on with the cooking themselves and use the robotic arm when needed. This smart kitchen makes home-made restaurant like cooking and maintaining a balanced diet very easy which is driven towards making our lives easier.

V. CONCLUSION

This concept of Smart Kitchen which is both AI and ML driven has a great advantage and desirable by the users and is bound to branch out into various other dimensions and appliances that can make the smart kitchen more presentable and automated. The smart kitchen could help the users in making the whole cooking process easy and the benefits of our smart kitchen proposal is double fold. One – Since it cooks restaurant like food, fast food consumption is controlled, packaged food which uses a lot of preservatives is reduced, dependency on the restaurant food is condensed and extra expenses are regulated which in-turn makes their lifestyle better. Two – Smart kitchen is driven towards maintaining healthy balanced diet for its users which is again a feature to attract the users as maintaining good health is a must for everyone. Our smart kitchen idea will open new opportunities and take smart kitchen appliances to a new revolutionary level.

ACKNOWLEDGMENT

We thank our colleagues from Institute of management, Christ (Deemed to be) University who provided us with insights which was a great assistance in shaping our research. We would like to express our gratitude to the faculties and colleagues of Institute of management, Christ (Deemed to be) University.

REFERENCES

[1] Blasco, R., Marco, Á., Casas, R., Cirujano, D., & Picking, R. (2014). A Smart Kitchen for Ambient Assisted Living, (63), 1629–1653. https://doi.org/10.3390/s140101629

[2] Varakian, R. A. (2006). (12) Patent Application Publication (10) Pub. No.: US 2006 / 0043088 A1, 1(19).

[3] Ayes, P. E. O. (1999). United States Patent (19), (19).

[4] Gullà, F., Ceccacci, S., Menghi, R., & Germani, M. (n.d.). An adaptive smart system to foster disabled and elderly people in kitchen-related task.

[5] Kranz, M., Maldonado, A., Rusu, R. B., Benedikt, H., & Rigoll, G. (2007). Context-Aware Kitchen Utilities.

[6] Li, B., Hathaipontaluk, P., & Luo, S. (2009). Intelligent Oven in Smart Home Environment, 247–250. https://doi.org/10.1109/ICRCCS.2009.70

[7] Basu, D., Moretti, G., Gupta, G. Sen, & Marsland, S. (n.d.). Wireless Sensor Network Based Smart Home: Sensor Selection, Deployment and Monitoring.

[8] Schneider, M. (n.d.). THE SEMANTIC COOKBOOK: SHARING COOKING EXPERIENCES IN THE SMART KITCHEN, 416–423.

[9] Cheng, L., & Lu, C. (2010). Design of Interactive e-Care Dining Table for Smart kitchen, 179–182. https://doi.org/10.1109/CASoN.2010.47

[10] Li, Y., Asghar, M. Z., & Pulli, P. (n.d.). 9LVXDOO \ DLGHG VPDUW NLWFKHQ HQYLURQPHQW IRU VHQLRU FLWL] HQV VXIIHULQJ IURP GHPHQWLD, 584–590.

[11] Luo, S., Xia, H., Gao, Y., Jin, J. S., & Athauda, R. (2008). Smart Fridges with Multimedia Capability for Better Nutrition and Health, 39–44. https://doi.org/10.1109/UMC.2008.17

[12] Desai Professor SAL, S. (2016). Understanding IoT Management for Smart Refrigerator, (January), 2–5.

[13] Mahajan, M. P., Nikam, R. R., Patil, V. P., & Dond, R. D. (2017). Smart Refrigerator Using IOT. International Journal of Latest Engineering Research and Applications (IJLERA), 2(3), 86–91.

[14] Singh, D., & Jain, P. (2016). IoT BASED SMART REFRIGERATOR SYSTEM. International Journal of Advanced Research in Electronics and Communication Engineering (IJARECE), 5(7), 2080–2084.

[15] Ghayvat, H., Mukhopadhyay, S., Gui, X., & Suryadevara, N. (2015). WSN- and IOT-based smart homes and their extension to smart buildings. Sensors (Switzerland), 15(5), 10350–10379. http://doi.org/10.3390/s150510350

[16] N. King, Smart Home-What do consumers want?, Intertek Research&Test Centre, 2003

Proceedings of the Fourth International Conference on Communication and Electronics Systems (ICCES 2019)
IEEE Conference Record # 45898; IEEE Xplore ISBN: 978-1-7281-1261-9

An Approach to Secure Data Transmission Through the Use of Cryptography and Steganography

Dr Manjula Shenoy K
Information and Communication Technology Department
Manipal Institute of Technology, MAHE University
Manipal, India
manju.shenoy@manipal.edu

Seema Gulam Shaikh
Information and Communication Technology Department
Manipal Institute of Technology, MAHE University
Manipal, India
seems1995@gmail.com

***Abstract*— In this paper, an approach to transfer data securely is proposed. First, from the sender side, the data is encrypted using Rivest-Shamir-Adleman (RSA) algorithm and then this encrypted data is hidden using Least Significant Bit image steganography concept in a image of the web page and its url is sent to the receiver. Then, at the receiving end, the encrypted data is obtained that is hidden in the image of the web page whose url is sent. This encrypted data is decrypted using the same RSA algorithm . When the sender sends the data to the receiver and incase this data is obtained by the third person or an intruder he will see a URL being sent. Then he will open the URL and he will find a webpage, and he would not find any data being hidden. Then he will try to view the source code of the webpage, and then also he would not find any data being hidden. Thus, the intruder will be assured that no data is been hidden in this and chances are more that he would not go to decode it further. Hence, the chances of doubt an intruder can get that some confidential or private data is hidden in the data being sent is reduced. And hence, the data sent by the sender to the receiver is secured.**

Keywords—RSA, Cryptography, Steganography, LSB

I. INTRODUCTION

Data security is the major issue that people face. Since, we want to make data unreadable by the third person and hide the fact from the third person that data is been sent, we are going to discuss about cryptography and steganography concept. Cryptography consists of the concept of transforming the data into a form that cannot be read by the unwanted users. In cryptography, data is converted to a form that is known only to the sender and the receiver. But it wont hide the fact that some data is being sent. In symmetric key encryption process where same keys are used for encrypting and decrypting the information. In this symmetric system only one key is used to encrypt and decrypt the data. That is, same single key is used for both encryption and decryption and this key will be known to both sender and the receiver and hence it is kept private. Since the key used here is of shorter length, data manipulation is easy here. [16] In asymmetric encryption which is also known as public key cryptography. In asymmetric encryption two keys are used, one for encryption and one for decryption. These two keys are known as the private key and the public key. Data is encrypted using public key of the receiver that can be known to everyone and decrypted using the private key of the receiver that is known only to the receiver. Hence, in this kind of systems security is more. In steganography, the fact that the data is being sent is hidden by hiding the data behind the data. The data that needs to be hidden can be anything like text, video, audio, image, web etc. And also the data that hides the data can be anything like text, video, audio, image, web etc.

The RSA algorithm uses 2 keys one public and the other private. The way in which this algorithm works is as listed in table 1. After following steps we will get public key which is e and n and private key which is d and m. We use this to encrypt and decrypt as follows. If data to be transmitted is called message, then encrypted message we get from Equation 1. And for decryption we use equation 2, LSB steganography concept uses replacement of least significant bits of pixels of the image by the data to be hidden. An example of which is given in table 2.

TABLE 1. RSA STEPS

STEPS	DESCRIPTION
1.	Choose two big prime numbers called p and q which are not equal.
2.	Find their product and call it n=p.q
3.	Let m=Totient(n)=(p-1)(q-1)
4.	Choose a small number e , co-prime to m,with GCD(m,e)=1 where 1<e<Totient(n)
5	Find d such that d mod Totient(n)=1

$$cipher = message^{e} mod\ n \dots\dots\dots\dots\dots (1)$$

$$Message = cipher^{d}\ mod\ n \dots\dots\dots\dots\dots (2)$$

TABLE 2. LSB CONCEPT

STEPS	DATA EMBEDDING USING LSB METHOD
1.	Get the pixels of the image in web page
2.	Get the data to be hidden
3.	Replace LSB of each block by a bit of the data to be hidden
4.	Send the image called stego image
STEPS	DATA EXTRACTION
1.	Extract LSB of each block of pixels and combine it to determine data.

The proceeding sections of paper discusses related work, methodology, results and conclusion respectively.

XXX-X-XXXX-XXXX-X/XX/$XX.00 ©20XX IEEE

II. LITERUTURE REVIEW

A method was proposed [1] using LSB method of Steganography and RSA method of cryptography. Firstly the text that needs to be embedded in the image is converted into binary form. Now, the image in which the text should be embedded is also converted into binary form. Now, binary form of text is embedded in binary form of image using LSB image Steganography method. Now, stego image equivalent to binary form is obtained. Now, this stego image is encrypted into text form using RSA encryption algorithm. However, the chances of doubt an intruder can get that some data is being hidden is not reduced.

An alternate method was proposed [2] using LSB method of Steganography and blowfish method of cryptography. First the image in the suitable format i.e BMP format is used here is encrypted using the blowfish encryption algorithm. Now, this encrypted data is embedded in video by using LSB video Steganography method. The disadvantages of Blowfish algorithm is that it cannot assure authentication and non-repudiation as two people have same key. However, the chances of doubt an intruder can get that some data is being hidden is not reduced.

Another alternate paper[3] introduced a method where data is encrypted using RSA encryption algorithm and then this encrypted data is hidden in an image. The disadvantages of this paper is that it cannot hide large data and itt does assure integrity of the data. However, the chances of doubt an intruder can get that some data is being hidden is not reduced.

Another paper[4] proposed a method using LSB method of Steganography and blowfish method of cryptography. First the text is encrypted using the blowfish encryption algorithm. Now, this encrypted data is embedded in image by using LSB image Steganography method. The disadvantages of Blowfish algorithm is that it cannot assure authentication and non-repudiation as two people have same key. However, the chances of doubt an intruder can get that some data is being hidden is not reduced.

The paper[5] proposed a method using discrete wavelet transforms (DWT) method of Steganography and filter bank cipher method of cryptography. First the text is encrypted using the filter bank cipher encryption algorithm. Now, this encrypted data is embedded in image by using discrete wavelet transforms (DWT) method. The drawbacks of DWT are it becomes it becomes computationaly intensive, it is less efficient and it take some energy to invest in wavelets to become able to choose the proper ones for a specific purpose, and to implement it correcly. However, the chances of doubt an intruder can get that some data is being hidden is not reduced.

The paper [6] proposed a method in which first data is encrypted using RC4 encryption algorithm and this encrypted data is embedded in 3 different images using 3 different Steganography methods. And finally comparison of theses 3 methods is done. The images used here are of BMP format. The disadvantage of this approach is RC4 is not a secure algorithm because keys used here may be weak. However, the chances of doubt an intruder can get that some data is being hidden is not reduced.

The paper [7] proposed a method in which image is encrypted first and then converted into text form. Now, this text data embedded into one more image. Now, the stego image is obtained. However, the chances of doubt an intruder can get that some data is being hidden is not reduced.

The paper [8] proposed a method using cryptography and text steganography. For cryptography, symmetric key algorithm, DES is used. Once the text message is encrypted using DES encryption algorithm, it is hidden behind another text. The text that is used to hide the secret message was created dynamically and it did not reveal the presence of any secret message. Experts have found a weakness in the design of the cipher in DES algorithm. In DES, S box creates same output with two chosen input. In DES the initial and final permutation is not exactly clear and seems confusing. However, the chances of doubt an intruder can get that some data is being hidden is not reduced.

The paper [9] proposed a method in which text is taken as the input data and it is hidden behind the video. The methods used are DCT and DWT, where, frequency domain coefficient of frames were used. The drawbacks of DCT, when the image is compressed there is a chance of data loss. So, if u need the original image for some other purpose the you have to save the original image as a backup before the DCT method is applied. The drawbacks of DWT are it becomes it becomes computationaly intensive, it is less efficient and it take some energy to invest in wavelets to become able to choose the proper ones for a specific purpose, and to implement it correcly. However, the chances of doubt an intruder can get that some data is being hidden is not reduced.

The paper [10] proposed a method where, cipher method is used for cryptography and image steganography method is used for data hiding. First, the text data is encrypted using cipher method and then this encrypted text data is hidden behind an image using LSB steganography method. The disadvantage of this approach is that block ciphers work on large amount of data and hence they need more memory. Stream ciphers do not provide integrity protection or authentication and also it is difficult to implement. However, the chances of doubt an intruder can get that some data is being hidden is not reduced.

The paper [11] proposed a method where, RSA algorithm is used for cryptography and LSB audio steganography method is used for data hiding. First, the message is encrypted using RSA algorithm and then this encrypted message is hidden in an audio using LSB audio steganography method. However, the chances of doubt an intruder can get that some data is being hidden is not reduced.

The paper [12] introduced a method message is compressed using wavelet transform technique and then this compressed data is hidden behind an image using LSB image steganography method. The drawbacks of DWT are it becomes it becomes computationaly intensive, it is less

efficient and it take some energy to invest in wavelets to become able to choose the proper ones for a specific purpose, and to implement it correcly. However, the chances of doubt an intruder can get that some data is being hidden is not reduced.

The paper [13] proposed a method in which first the message is encrypted using AES algorithm of cryptography using a key. Now, this key is hashed using SHA-1 hashing algorithm. Now, the encrypted data can be hidden in image or audio or video using LSB method of Steganography. The drawbacks of this approach is that both AES and SHA1 algorithm are difficult to implement in the approached way. However, the chances of doubt an intruder can get that some data is being hidden is not reduced.

The paper [14] proposed a method in which the original message is encrypted using encryption algorithm using key k. And the encrypted message is converted into ASCII code. After that this ASCII code is converted into binary i.e. in 0's and 1's form. A web page is taken in which data is to be hidden. Then, 4 random methods of hiding data are selected and converted binary data is hidden in a webpage. However, the chances of doubt an intruder can get that some data is being hidden is not reduced.

The paper [15] Proposed a method in which the message is encrypted through Data Encryption Standard algorithm and the message is concealed by applying LSB encoding technique in a spiral manner. Experts have found a weakness in the design of the cipher in DES algorithm. In DES, S box creates same output with two chosen input. In DES the initial and final permutation is not exactly clear and seems confusing. However, the chances of doubt an intruder can get that some data is being hidden is not reduced.

From the research we can conclude that, the cryptography and the steganography concept used above is very useful but the chances of doubt an intruder can get that some confidential or private data is hidden in the data being sent is more. In this project, the main purpose here is to fool the intruder and reduce the chances of doubt an intruder can get that some confidential or private data is hidden in the data being sent, by encrypting the data and hiding this encrypted data in the image that is used in the created webpage. Hence, to secure the data sent by the sender to the receiver. RSA algorithm of cryptography used in this approach is safe and secure for its users through the use of complex mathematics. RSA algorithm is hard to crack since it involves factorization of prime numbers which are difficult to factorize. Moreover, RSA algorithm uses the public key to encrypt data and the key is known to everyone, therefore, it is easy to share the public key. LSB method of steganography used in this approach is known for its simplicity. It embeds the bits of the message directly into the LSB plane of cover-image and many applications use this method.

III. Methodology

The data to be sent is read via GUI (Graphical User Interface) on the sender side. The data is encrypted using RSA technique and encrypted data is hidden behind the image and generates a html page with this image as content and its URL(Uniform Resource Locator) is sent to the receiver. The receiver downloads the image in the web page whose url is sent and decrypts the data hidden behind the image. If an intruder gets url he opens the web page or html source of the web page also he will not be able to guess there is hidden data. Figure 1, shows the sendor side process block diagram.

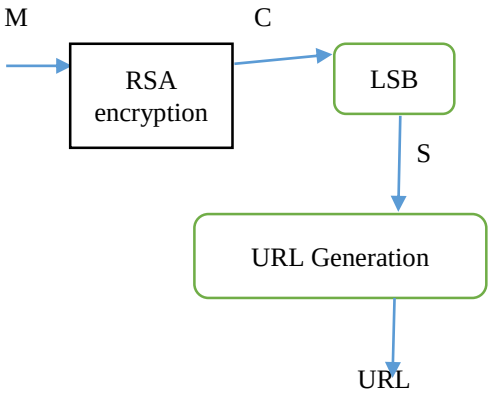

Figure 1. Sendor Side Process

Let M be the message to be sent it is fed to encryption algorithm RSA to result in cipher C. This cipher is then hidden using LSB in a image resulting into S as stego image. The resulting image is put into a web page and its url is sent to the receiver.

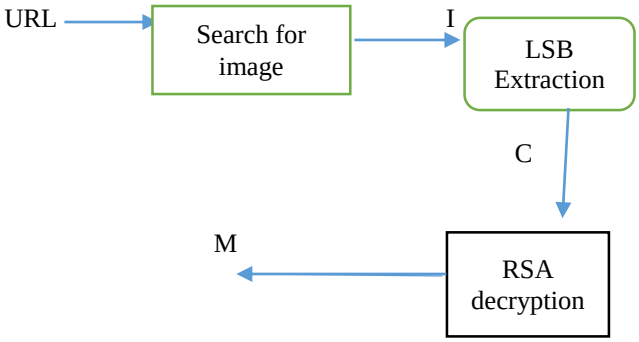

Figure 2. Receiver side process

From web page whose URL is received , the image is extracted and LSB extraction is applied to get encrypted cipher C. Then RSA decryption is applied to get the message which is original.

IV. Results and Discussion

Figure 3. shows the graphical user interface for accepting message to be transmitted.

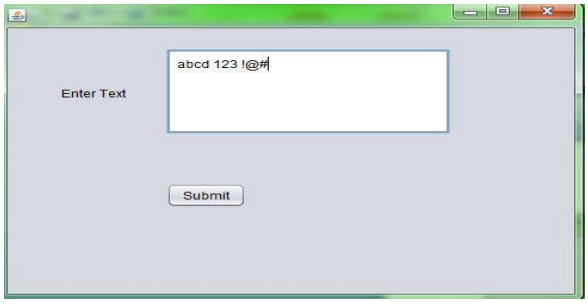

.

Figure 3. GUI to read data to be sent

Figure 4. shows encrypted message output after encryption using RSA.

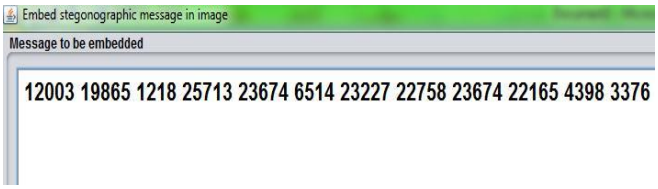

Figure 4. Sender side encrypted data

Figure 5.Shows original and embedded message image.

Figure 5. original and stego image

Figure 6. Decoding Process output

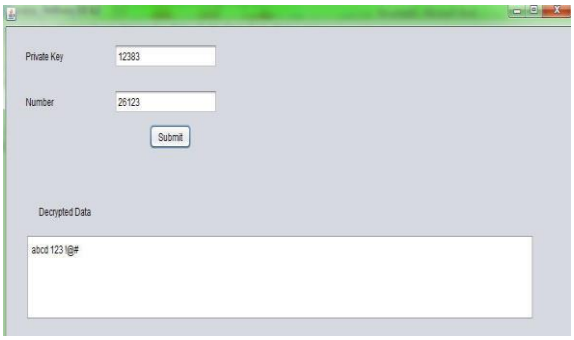

Figure 7. Decryption process output

Figure 6 shows output of decoding process and figure 7 shows decryption step. Figure 8 is the web page containing stego image whose url is sent to the receiver.

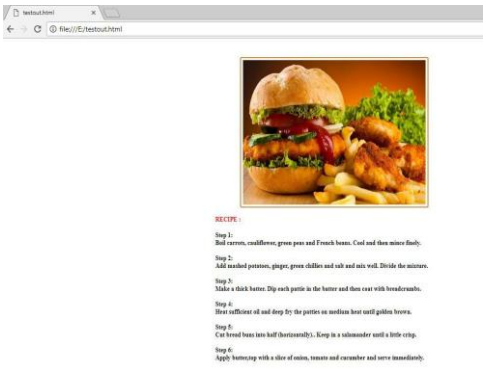

Figure 8. Web page.

When the sender sends the data to the receiver and incase this data is obtained by the third person or an intruder he will see a url being sent as shown in the Fig. 9. Then he will open the url and he will find a webpage as shown in Fig. 8, and he won't find any data being hidden. Then he will try to view the source code of the webpage, then also he won't find any data being hidden. Thus, the intruder will be assured that no data is been hidden in this and chances are more that he won't go to decode it further.

```
run:
Public Key (E,N): 14447,26123
Private Key (D,N): 12383,26123
Please find the the url: E:\testout.html
BUILD SUCCESSFUL (total time: 1 second)
```

Figure 9. Keys and URL.

V. CONCLUSION AND FUTURE SCOPE

This project gives a unique way of hiding the data apart from all other existing methods of data hiding. Hence, the chances of doubt an intruder can get that some confidential or private data is hidden in the data being sent is less when compared to the previous existing methods, since, we have encrypted and hidden the data in the image that is used in the created webpage. When the sender sends the data to the receiver and incase this data is obtained by the third person or an intruder he will see a url being sent. Then he will open the url and he will find a webpage, and he would not find any data being hidden. Then he will try to view the source code of the webpage, and then also he would not find any data being hidden. Thus, the intruder will be assured that no data is been hidden in this and chances are more that he wont go to decode it further. The chances of doubt an intruder can get that some confidential or private data is hidden in the data being sent is reduced. And hence, the data sent by the sender to the receiver is secured.

As an future enhancement some other idea can be proposed using webpage with RSA algorithm and LSB Steganography method to reduce the percentage of doubt an intruder can get that some data is being sent .Also, some work can be done using webpage with RSA algorithm and different Steganography methods and comparing the results. Also, some work can be done using webpage with different

cryptography algorithms and LSB Steganography method and comparing the results.

REFERENCES

[1] Varsha and Dr. Rajender Singh Chhillar, "Data Hiding Using Steganography and Cryptography", International Journal of Computer Science and Mobile Computing, Vol.4 Issue.4, April- 2015, pg. 802-805

[2] Ms. Hemlata Sharma, Ms. MithleshArya and Mr. Dinesh Goyal, "Secure Image Hiding Algorithm using Cryptography and Steganography", IOSR Journal of Computer Engineering (IOSR-JCE), Vol. 13(5), August 2013, pp. 1-6.

[3] M.Juneja, P.S. Sandhu, "Data Hiding with Enhanced LSB Steganography and Cryptography for RGB Color Images", International Journal of Applied Research , ISSN: 2249-555X , Vol. 3(5), May 2013, pp. 118-120.

[4] Ajit Singh, Swati Malik, "Securing Data by using Cryptography with Steganography", International Journal of Advanced Research in Computer Science and Software Engineering, ISSN: 2277 128X, Vol. 3(5), May 2013, pp. 404-409.

[5] Saleh Saraireh, "A SECURE DATA COMMUNICATION SYSTEM USING CRYPTOGRAPHY AND STEGANOGRAPHY", International Journal of Computer Networks & Communications (IJCNC) Vol.5(3).

[6] Wai Wai Zin, "Implementation and Analysis of Three Steganographic Approaches", proceedings of the International Conference on Computer Research and Development, March 2011, pp. 456-460.

[7] N.V Rao and J.TL Philjon, "Metamorphic Crypto- A Paradox between Cryptography and Steganography using Dynamic Encryption", proceedings of the International Conference on Recent Trends in Information Technology, June 2011, pp. 217-222.

[8] Deepali Bhat, Krithi V, Manjunath KN, Srikanth Prabhu and Renuka A., "Information Hiding through Dynamic Text Steganography and Cryptography", Proceedings of the Advances in Computing,Communications and Informatics (ICACCI), India, 04 December 2017, pg. 1826 – 1831.

[9] Vinita V. Korgaonkar and Manisha Naik Gaonkar,"A DWT DCT combined approach for video steganography", Proceedings of the 2nd IEEE International Conference on Recent Trends in Electronics, Information & Communication Technology (RTEICT), India, 15 January 2018, pp. 421 – 424

[10] G.Prashanti, B. V.Jyothirmai and K.Sai Chandana, "Data confidentiality using steganography and cryptographic techniques",Proceedings of the InternationalConference on Circuit ,Power and Computing Technologies (ICCPCT), India, 19 October 2017, pp. 1 – 4.

[11] Ankit Gambhir and Sibaram Khara, "integrating RSA cryptography & audio steganography", Proceedings of the International Conference on Computing, Communication and Automation (ICCCA), India, 16 January 2017, pp. 481 – 484

[12] Humanth Kumar, M.Shareef, R. P. Kumar, "Securing Information Using Steganography", IEEE Xplore International Conference on Circuits, Pwer and Computing Technologies, March 2013, pp. 1197-1200.

[13] Shery Elizabeth Thomas, Sumod Tom Philip, Sumaya Nazar, Ashams Mathew, Niya Joseph, "Advanced Cryptographic Steganography using Multimedia Files", International Conference on Electrical Engineering and Computer Science (ICEECS), May 2012, pp. 239-242.

[14] Lipi Kothari, Rikin Thakkar and Satvik Khara, "Data hiding on web using combination of Steganography and Cryptography", proceedings of the 2017 International Conference on Computer, Communications and Electronics (Comptelix), July 01-02, 2017

[15] B.Karthikeyan, A. Deepak, K.S. Subalakshmi, , Anishin Raj M M, and V.Vaithiyanathan, "A CombinedApproach of Steganography with LSB Encoding technique and DES Algorithm", proceedings of the 3rd International Conference on Advances in Electrical, Electronics, Information, Communication and Bio-Informatics (AEEICB17)

[16] M. Pavani, S. Naganjaneyulu and C. Nagaraju, "A Survey on LSB Based Steganography Methods",International Journal Of Engineering And Computer Science, Volume 2 Issue 8 August, 2013 Page No. 2464-2467

Proceedings of the Fourth International Conference on Communication and Electronics Systems (ICCES 2019)
IEEE Conference Record # 45898; IEEE Xplore ISBN: 978-1-7281-1261-9

Detection and Tracking of Anxiety Related Diseases for Autism Spectrum Disorder Using ECG

Abhirami A , Sudheesh P
Department of Electronics and Communication Engineering
Amrita School of Engineering, Coimbatore
Amrita Vishwa Vidyapeetham, India
Email: *abhisree.4321@gmail.com, p_sudheesh@cb.amrita.edu*

Abstract— Anxiety distress are excessive or continual panic of everyday circumstances causing behavioral and emotional consequences, eventually leading to diseases like heart attack, epilepsy and dyspnea. Anxiety disorders are common for people with developmental disorders like autism spectrum disorder, cerebral palsy, down syndrome. Patients suffering from these diseases have difficulties in communication and emotional recognition eventually leading to narrow interests and repetitive behavior. Sometimes their ways of communicating any symptoms may not be recognizable by the caretakers, hence building up a need of a non-invasive, continuous, real-time detection and tracking of their ECG signals for prediction of these diseases providing possible medications. Here a system framework based on unscented Kalman filter (UKF) is developed to continuously detect and track the R-R interval for anxiety prediction to make these unpredictable diseases predictable and reducing death tolls with timely treatment.

Keywords—Electrocardiography(ECG);Electroencephalogram (EEG); Unscented Kalman filter (UKF); ECG derived respiration (EDR); Hilbert—Huang transform (HHT); Intrinsic Mode functions (IMF); Respiratory Rate(RR); Heart Rate(HR), Autism Spectrum Disorder(ASD).

I. INTRODUCTION

Heart attack is a major medical emergency usually due to blood clot or thrombosis hence blocking blood flow to the heart leading to cell death. Panic attack as a cause of anxiety disorder is a major symptom of heart attack. Chronic anxiety can lead to changes in body's stress response. Anxiety causing an increase in heart rate can easily be diagnosed through electrocardiography (ECG) diagnosis where normal heart rate is 60-100 beats per minutes [20]. Major symptoms includes pain or stiffness in chest, back, arms etc. But in case of ASD the tracking system is very important as they face issues in feeling and communicating their sense of pain [17]. Apart from ECG the methods used for anxiety prediction mechanism are to study the pupil movement of eyes. People tend to have blurred vision with dilated pupil due to severe stress and anxiety since there is high adrenaline level causing pressure on eye [2] . Skin temperature can reveal the stress intensity having a rapid, short-time temperature drop in homeotherms. Stress sweat is released by the apocrine gland of our body due to our stress or anxiety response [1].Epilepsy being a neurological disease, nerve cell activities of brain is disturbed causing seizures, hence disturbing the normal brain cell communication. Seizures are abrupt electrical exertion in brain cells depending on the epileptic discharge location. They are mainly of two types, unilateral and bilateral. The discharge effects the brain cortex without losing consciousness and secondly effecting both hemispheres to lose consciousness respectively. Electroencephalogram (EEG) is the age old technique for detection, But for the early prediction mechanism, the frequency response of the EEG signal can be combined with the R-R interval for better solutions as the epileptic seizures always brings in a change in heart rate(RR).

Respiratory measurements is an important parameter for clinical diagnosis of anxiety. The normal respiratory rate is 12-20 breaths per minute [10][12]. Dyspnea is indicated as short breath or increased breath rate. Increased anxiety lead to increase in breath rate due to panic attack or increase in heart rate. The heart rate variability method is best used for the prediction mechanism to predict changes in the respiratory rate(RR). To have a non-invasive technique to predict dyspnea, an ECG signal and ECG predicted respiratory signal (EDR) analysis is done.

Electrocardiography (ECG) is the technique of recording the hearts electrical activity called heart rhythms over a time period for its functional information and hence diagnosis of complex cardiac diseases. Normal heart rate is 60-100 beats per minute. The wave characterization involves peaks and valleys with R as the main spike as shown in Fig.1. R-R intervals are taken into account to determine arrhythmia's like:1) Tachycardia referring to increase in heart rate, more than 100 beats at rest, hence a decrease in R-R interval, 2) Bradycardia referring to slow heart rate, less than 60 beats at rest hence increasing the R-R interval. Anxiety leads to an increase in heart rate, [6] shorter R-R interval, increase in breath rate hence a predictable method for detection of heart attack and dyspnea[23].The variations in R-R interval can also be used to predict epilepsy as it varies at the onset of the same. 73percentage of seizure can change up to 15 to 20 percentage of heart rate, 55 percentage changes to 20 beats per minute. This ECG is recorded using a non-invasive

external electrodes called skin electrodes. They record the heart muscles electrical activities generated as pulsating electric waves towards the skin surface. These electrodes are wet sensors and they use a conductive gel to increase conductivity between the skin and the wet electrodes.

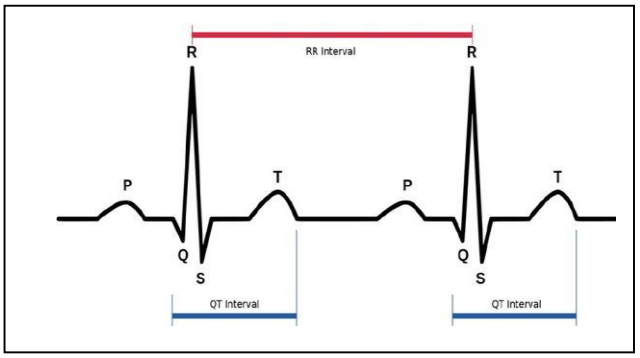

Fig 1. *ECG signal with R-R interval*

Electroencephalogram (EEG) is the test to detect brains abnormal electric activity, for the procedure small metal discs and wires are pasted on the scalp to detect the electrical charges. Mainly used to detect head injuries, brain tumors, epilepsy etc.

A non-invasive technique for tracking of ECG signal using unscented Kalman filter (UKF) technique is developed and predictions from this continual tracking are further used to predict diseases [21]. Extended Kalman filter (EKF) had a very strong disadvantage of linearizing all non-linear models and hence using the linear Kalman filtering equations thus leads to production of highly unstable filter assumption of local linearity [21]. The tracking system is very important as the advantage of a real-time tracking is much more than being subjected to test at the time of seizure or dyspnea. Prediction of such criticality is very important for ASD as they lack communication skills and to sense pain as well.

In Hilbert-Huang transform any non-stationary, non-linear signal is decomposed into intrinsic mode functions (IMF) to obtain instantaneous frequency. This is the algorithm applied to any input signal than being a theoretical tool. They are mainly divided into two parts, one being empirical mode decomposition (EMD) where the main signal is broken into various finite, small and decomposed components and the second being Hilbert spectral analysis (HAS) which examines the instantaneous frequency of above formed IMF as a time function. The section II of the paper contains system overview explaining different techniques, section III having the proposed methodology, section IV with the results and discussions and section V with the conclusions derived.

II. SYSTEM OVERVIEW

A. *Unscented Kalman Filter*

Kalman filter is the basic framework algorithm using a series of measurements with time along with statistical noise with inaccuracies. This algorithm produces estimates of the unknown variable being more accurate than the input signal measurements done by a joint probability distribution of a variable for a given time frame. The major advantages include perfect tracking of linear problem having the disadvantage being no real problems are linear. Any non-linear signals can be divided into smaller linear signals so that the linear algorithm itself can be applicable to the non-linear signal as well, hence giving rise to extended Kalman filter [15]. In this case if the initial estimate is not proper this leads to quick filter divergence hence owing to linearization proving EKF not to be an optimal estimator. The filter tend to have more noise content leading to a reasonable system but not a perfect system. The system is perfect only if the noise content is small. Improvements in EKF leads to unscented Kalman filter for non-linear signal analysis where probability density is approximated by deterministic sampling techniques using unscented transform, setting a set of minimal sample points called sigma points around any given mean. Periodically these points propagate through the non-linear signal function having a new mean and covariance [5]. UKF is the extensively used technique for tracking and evaluation because of its simplicity, robustness, less time and increased accuracy[24].

B. *Hilbert-Huang Transform*

A non-stationary, non-linear input data signal like EEG are divided into various finit, small number of components called intrinsic mode function (IMF) and hence obtain instantaneous frequency of the input signal. Other than Fourier transform, Hilbert-Huang transform algorithm can be applied to a real dataset than a theoretical tool having the advantage of having both frequency and amplitude information with respect to time. The algorithm has mainly two parts empirical mode decomposition (EMD) and Hilbert spectral analysis (HSA). In the EMD part the whole input dataset is divided into extremas i.e. maxima and minima collection over the entire domain range or given domain. There are mainly two conditions to be followed:

1. The zero-crossing must either be equal or different at most by1.
2. Mean value of envelop of local maxima and local minima is equal to 0.

To find the IMF the following procedure is called shifting:

1. Identification of local extrema of the test data
2. Connect all local maxima by interpolation to form upper envelop, repeat the same for lower

The upper and lower envelopes covers all data points between them measuring its mean as m1, having the difference between m_1 and first input component of the range h_1 as in (1).

$$X(t) - m_1 = h_1 \quad \textbf{(1)}$$

This equation must be symmetric with all maxima positive and minima negative having the IMF definition satisfied. In the upcoming shifting h_1 is considered to be the new data hence the shifting equation changes to (2). Then after repeated shifting of k times .$h_1$becomes the IMF and h_{1k} as the first IMF components gives (3).

$$h_1 - m_1 = h_{11} \quad \textbf{(2)}$$

$$h_{1(k-1)} - m_{1k} = h_{1k} \quad \textbf{(3)}$$

□□= sum of $[h_{k-1(t)} - h_{k(t)}]^2 / h^2$ **(4)**

Stoppage criteria of the shifting process: The main type used in this work is standard deviation method (4) and threshold methods. Where the shifting process stops when the deviation is less than an assumed value and in the later method where two values are set with small fluctuations [22]. Once the stoppage criteria are selected, first IMF, c_1 is obtained being the finest scale as the shortest signal component. Follow the above steps finally with residue forming in (5) with residue rn being the monotonic function hence no IMF repetition [22]. To find the instantaneous frequency, Hilbert transform is done on each IMF with u(t) as a real variable with a convolution function of (6). Having the end convolution formulae as(7):

$$X(t) = \text{sum of } (C_j + r_{n\,j}) \quad \textbf{(5)}$$

$$fn(1 \div (\pi \times t)) \quad \textbf{(6)}$$

$$H(u)(t) = 1 \div 2\pi \int_{-\infty} (u(t) \div (T - t))dT \quad \textbf{(7)}$$

C. Cubic-Spline Interpolation

Spline interpolation is one among the type of interpolations, where an interpolate behaves as a type of special piece-wise polynomial called the spline. This has the advantage of having multiple sub-functions at particular period of intervals within the function domain. The errors present are very small even though it gives accurate answer for low degree polynomials of spline. In the prescribed system Cubic-spline interpolation algorithm are used to derive ECG-Derived respiratory signal from the ECG heart rate variability mismatch to obtain a respiratory signal similar to the input ECG. (x_i, y_i):i=0,1,n is the function to interpolate between all the points (xi-1,yi-1)and (xi,yi) with the polynomial equation (8), Where i=1,2,..n.

with curve curvature y=f(x). Spline has the major advantage to minimize the bending of both y' and y" being in the knots above. Hence, only polynomials of degree three or above is the classical approach. Where the ideal case is (9):

$$Y = qi(x) \quad \textbf{(8)}$$

$$1 \le i \le n - 1 \quad \textbf{(9)}$$

$$Q_i(x_i) = q_{i+1}\, x_i \text{ and } q_i(x_i) = q x_{i+1} \quad \textbf{(10)}$$

III. METHODOLOGY

ECG obtained from physionet are filtered and processed to remove artifacts like movement artifacts, baseline wandering, muscle noise etc[19]. A low-pass and high-pass filter is cascaded to get a band pass filtering so that low frequency interference and high frequency artifacts are removed [4] [19]. From these signals R-peak detection and R-R interval detection are done using the conventional Pan Tompkins detection algorithm [4]. Algorithm consists of the following major steps as in Fig.2: low-pass filter, high-pass filter, differentiators, squaring operators, adaptive thresholding, moving window integrator and R-peak detection.

A the low pass and high pass filters are cascaded forming a band pass filter (5Hz-11Hz) having lower or high frequency interference removed for noise rejection function having a sampling rate of 200 samples/sec [11] [20].For determining the slope, derivative or differentiator block is used. In the prescribed system a 5 point derivative is used. Smoothening is done to determine the height of the wave and avoid higher peak distortion. Squaring function is to obtain the positive output and amplifies non-linearity with point-to-point squaring technique. Feature information of peaks is obtained by moving window integrator with its width N approximately equals to widest possible QRS complex [13]. The Pan Tompkins works with altering thresholds to find R-peak and other parameters periodically to adapt to changes hence reduction in false peak detection to get accurate heart rate [3]. They mainly make use of slope, amplitude and width of the ECG waves for R-R interval prediction [16][18].

As shown in the Fig.3 after the R-peak detection the major part of the project is the continuous R-R interval tracking of the system. The early existed system only traced the existence of anxiety but this is the continuous tracking system, using unscented Kalman filter (UKF) framework. These continuous tracking are used for continuous monitoring of the ECG signal for various disease prediction. UKF provides an extended range of accuracy when compared to Kalman filter at the same range of complexity. This technique has unscented transform (UT) as its fundamental component by using a set of assumed weighted points to define the mean and covariance of probability distribution.

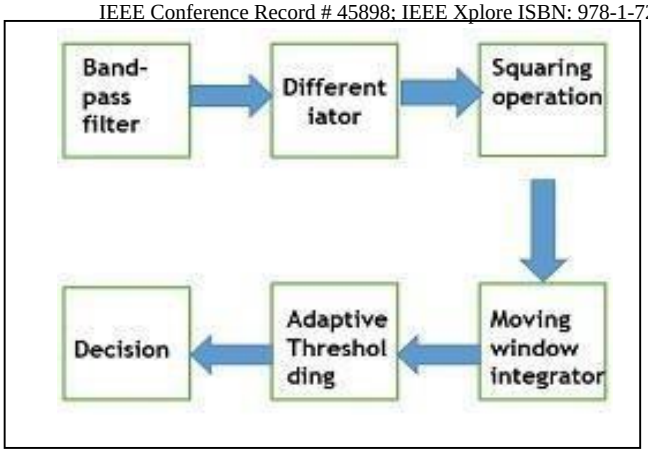

Fig 2. *Pan Tompkins block diagram*

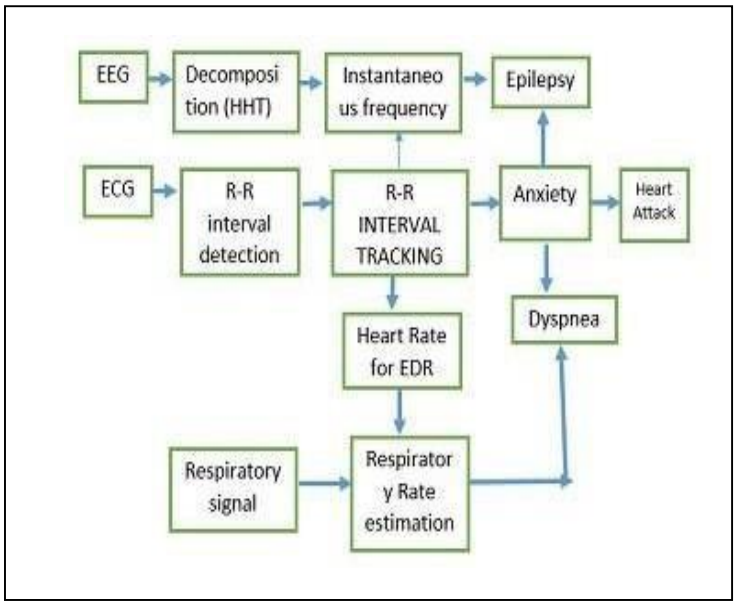

Fig 3.*Block diagram*

The transformation consists of certain steps: Predict new state and the covariance along with noise content [5].

$\hat{x}_{(k+1/k)}$ **(11)**

$P_{(k+1/k)}$ **(12)**

The system contains state-space equation model with (13) (14) governed by prediction step having the estimate of current state variable and uncertainties and updating step being updated by a weighted average having higher weight to higher uncertainties [5]. Mathematically the system equations can be denoted as:

$x_k = x_{k1} + w_k$ **(13)**

$y_k = x_k + v_k$ **(14)**

In equation (13)(14) where Xk is an ideal slow varying R-R wave with time k and wk, vk being the Gaussian noise.

$\hat{x}_{(k+1/k)} = \hat{x}_{(k/k)}$ ***(15)***

$P_{(k+1/k)} = p_{(k/k)} + Q_k$ ***(16)***

$\in_k = y_k \hat{x}_{(k-1/k)}$ ***(17)***

$G_k = P_{(k+1/k)}$ **(18)**

Equations (15) (16) are the prediction and (17) (18) are updating steps respectively. The final outlook of the state space equation is given by (19) (20)

$\hat{x}_{(k+1/k+1)} = \hat{x}_{(k+1/k)} + G_k \in_k$ **(19)**

$P_{(k+1/k+1)} = P_{(k+1/k)}\, G_k\, P_{(k+1/k)}$ **(20)**

The system works in real time as it require only the present state and just past state uncertainty matrix information rather than the past information. UKF has a deterministic sampling technique called unscented transform (UT) towards picking minimum set of points around the mean called the sigma points to propagate through non-linear function with new mean and covariance estimate. To obtain the weight to be applied we use equations having WS0,WC0,WS1 AND WC1 being the weights to be updated as in (21)(22)(23) and α, K being the control sigma points, β – the distribution as in equation (24).

$$ws0 = \frac{\lambda}{\lambda + L} \quad \textbf{(21)}$$

$$wC0 = \frac{\lambda}{\lambda + L} + (1 - \alpha^2 + \beta) \quad \textbf{(22)}$$

$$WS1 = wC1 = \frac{1}{2(\lambda + L)} \quad \textbf{(23)}$$

$$\lambda = \alpha^2 \ (L + K) - L \quad \textbf{(24)}$$

Here 2n+1 sigma points are considered for n dimensions. After R-R interval tracking, anxiety is predicted whenever there is decrease in R-R interval, normal R-R interval being 0.6 to 1.2sec hence increase in heart rate [6]. Further beyond anxiety prediction the system leads to the prediction of three main diseases which is heart attack, epilepsy and dyspnea[25].

From the available ECG, ECG-Derived respiratory signal (EDR) is obtained [7]. Whenever there is a variation in the R-R interval of the ECG there is an amplitude or heart rate variability mismatch in the signal. Hence EDR can be obtained from either of the methods. After R wave detection and RR interval calculation, Heart Rate (HR) can be calculated as (25). cubic spline interpolation and moving average operation over the particular HR value can bring about EDR.

$$HR = 60 \div \text{R-R INTERVAL} \quad \textbf{(25)}$$

To estimate the respiratory rate (RR), EDR is combined with to a reference respiratory signal as (26)

$$RR = (t_{n+1} - t_n) \div 60 \quad \textbf{(26)}$$

Where t_{n+1} is the time of occurrence of $(n+1)^{th}$ R-peak and t_n is the time for the occurrence of nth R-peak. Normal being 12- 20 breath causing any abnormality to dyspnea.

Heart rate can be a bio-marker for seizure prediction as there is a change in the trend of R-R interval of the ECG wave whenever onset of seizures occur [8]. For the prediction purpose we combine the variation in R-R interval along with the instantaneous frequency of the EEG signal of the same patient through Hilbert Huang transform having two major steps for EEG decomposition mainly empirical mode decomposition (EMD) and Hilbert transform for instantaneous frequency [26]. The EEG signal obtained is decomposed into subsequent sub components called intrinsic mode function (IMF). To find IMF the steps are as follows:

1. Identify the local extremas (maxima and minima), mathematically second derivative test. So that all the intermediate data or points are covered within.
2. Connect all maxima's forming upper and all minima's forming lower envelope respectively
3. Find the mean m_1 of this data
4. Difference between the input x(t) and m1 is the first component of the IMF, h_1 i.e.: $x(t)-m_1=h_1$ being it has to be symmetric, maxima positive and minima negative respectively.
5. On next subsequent shifting $h_1-m_{11}=h_{11}$ being the next IMF component. After repeated shifting to K times the equation forms (27):

$$h_{1(k-1)} - m_{1k} = h_{1k} \quad \textbf{(27)}$$

Each IMF contains various input oscillation patterns, 1st IMF having the most and last IMF having the lowest oscillations or residues [14]. This series of IMF are then used to find the frequency using Hilbert transform algorithm [8].Where its amplitude, phase etc. are also obtained. This tool is chosen because of its versatility and its ability to extract a non-linear, non-stationary signal 's frequency component.

IV. RESULTS AND DISCUSSIONS

In the work done Pan-Tompkins algorithm is used for R-peak and R-R interval detection. The Fig.4 depicts the input ECG signal and QRS positions detection. Output are low or high frequency interference removed for noise rejection function using a band pass filter, differentiated, squared and integrated data after complete pre-processing to obtain the slope, feature information and amplitude of the input ECG signal. Threshold-array for filtered data i.e. threshold for each QRS-complex of integrated data are obtained to find the R-peak. The R-R interval obtained from the pan Tompkins algorithm is recorded in the table giving the normal and abnormal variations, where normal R-R interval being 0.6 to 0.8 second heart rate being 60 to100 beats per minute.

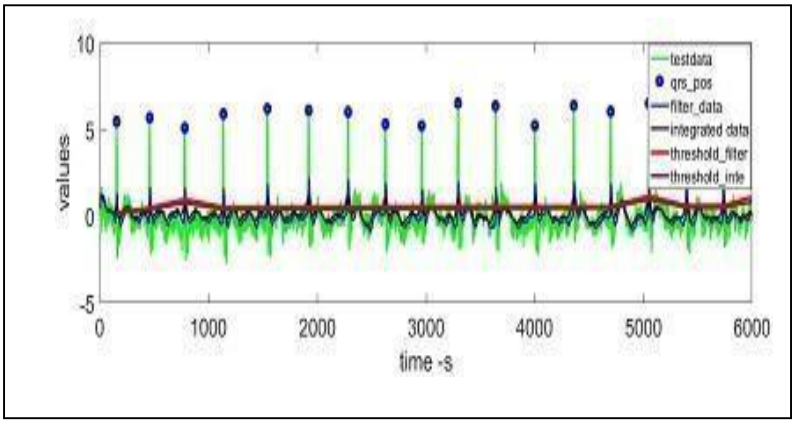

Fig 4. *R-peak detection*

This is the vital sign for a wide spectrum of healthcare strategies. If R-R interval goes beyond this limit it is an evident case of anxiety as shown in Fig.5 and proved by table1. A random signal tracking is done initially giving the results as shown in Fig.6. The figure proves that the algorithm exactly copies the input signal rather than Kalman filter for just linear tracking. The algorithm is suitable for real life tracking of any non- linear signal. For the parallel tracking of ECG-signals an unscented Kalman filter algorithm is used as shown in Fig.7. If variation in R-R interval is evident the system goes for prediction of three diseases. The cases of heart attack like Tachycardia referring to increase in heart rate, more than 100 beats at rest hence a rapid decrease in R-R interval and Bradycardia referring to slow heart rate, less than 60 beats at rest hence increasing the R-R interval. This R-R interval variation can lead to dyspnea prediction, normal being 12-20 breath where any R-R abnormality leads variation since anxiety can be a

major cause of breathlessness. The variations in R-R interval can also be used to predict epilepsy as it varies at the onset of the same. 73 percentage of seizure can change up to 15 to 20 percentage of heart rate, 55 percentage changes to 20 beats per minute.

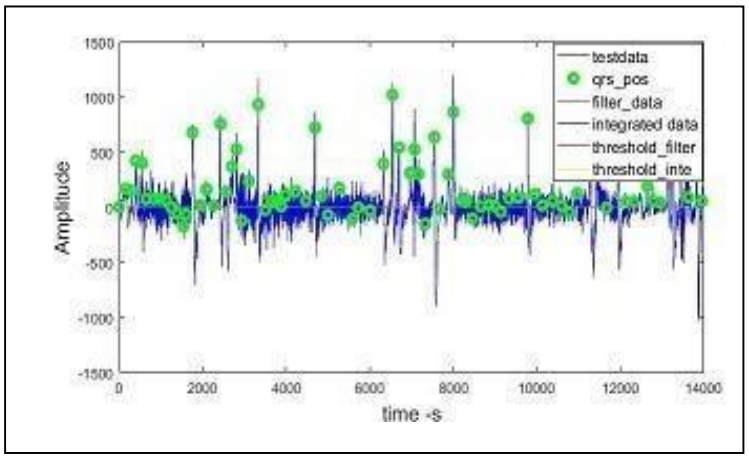

Fig 5 . *R-peak for detection for anxiety*

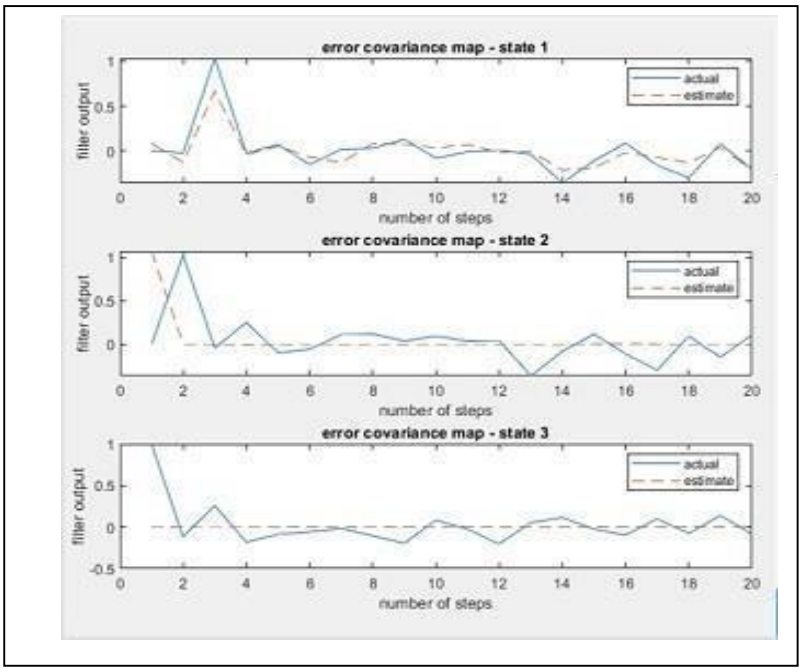

Fig 6. *Tracking of random signal*

UKF is used for tracking of abnormal ECG signals in Fig.7 as this have an advantage of tracking nonlinear signals over Kalman filter. They use deterministic technique using unscented transform setting a set of minimal sample points called sigma points around any given mean of input signal. As indicated the red line indicating sigma points ideally traced the input ECG signal. If an abnormal R-R interval is obtained. there is either heart rate or amplitude miss match as shown in table Heart rate estimation. Heart rate can be calculated from R-R interval as in table2 which is in turn cubic spline interpolated to have EDR in Fig.8. The EDR signal is compared to the respiratory signal for corresponding R-R interval as in table respiratory rate estimation of a subject for respiratory rate estimation hence dyspnea prediction**.**

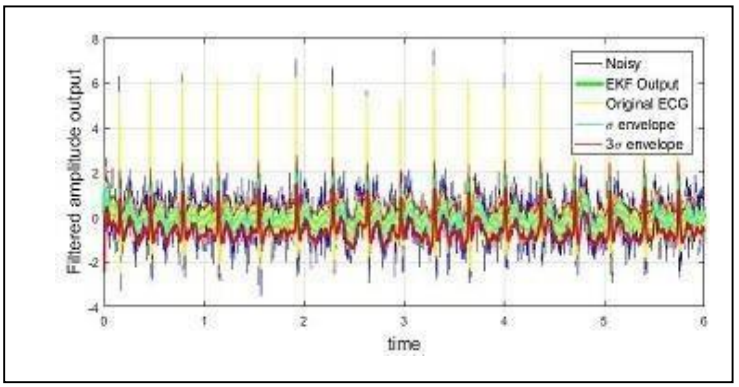

Fig 7. *Tracking of ECG signal*

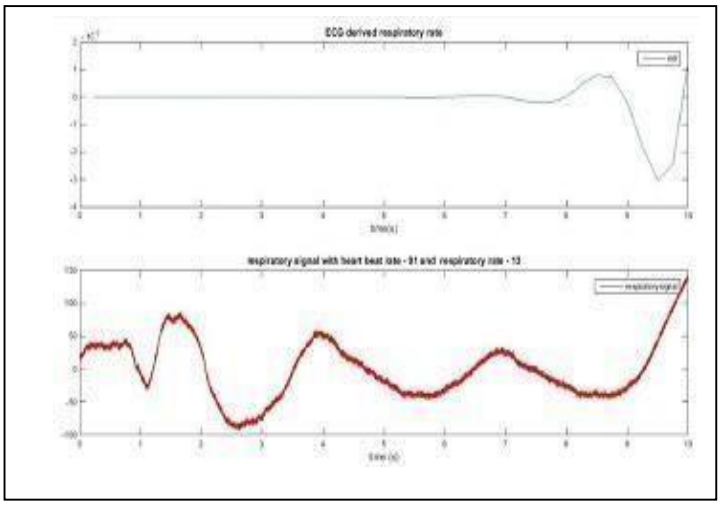

Fig 8. ECG derived respiratory signal

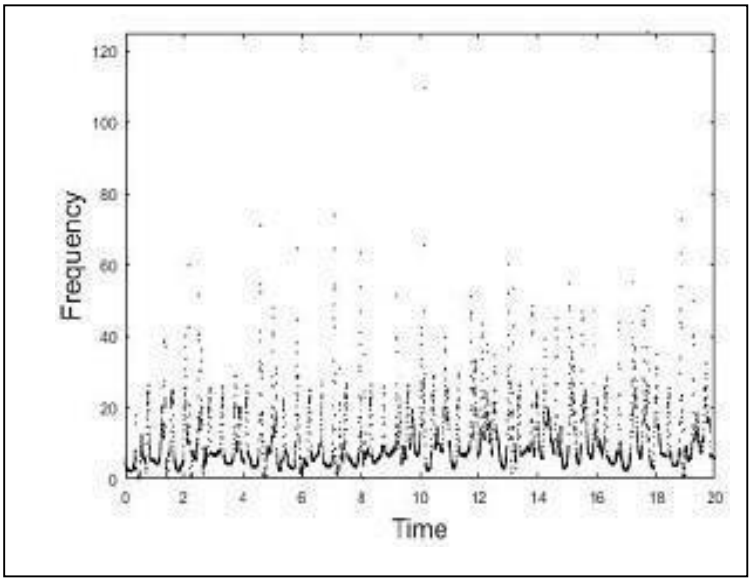

Fig 9. *Hilbert Spectrum analysis- IMF formation*

The table depicts the variation in heart rate and respiratory rate on abnormality For epilepsy prediction along with increase in R-R interval, a decrease in instantaneous frequency of EEG is also considered. In order to obtain the same Hilbert transform as in Fig.10 on input EEG signals are done where the input frequency is divided into smaller IMF and processed for instantaneous frequency by Hilbert spectrum in Fig.9. If the variation is proper this goes intact for epileptic seizure. The variation of instantaneous frequency and R-R interval is evidently plotted in Fig 11

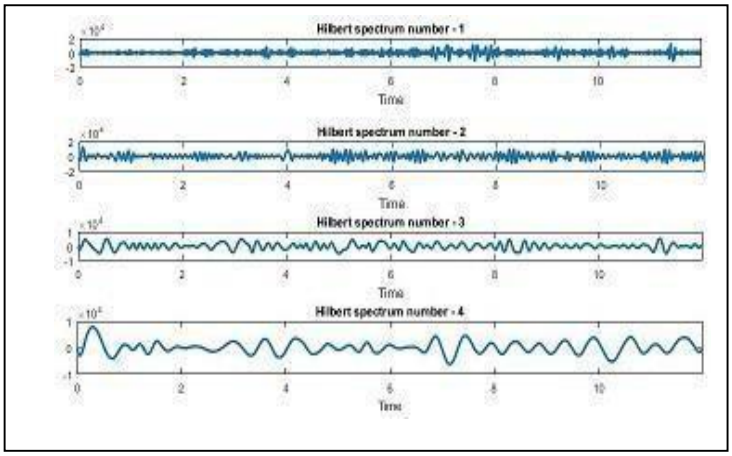

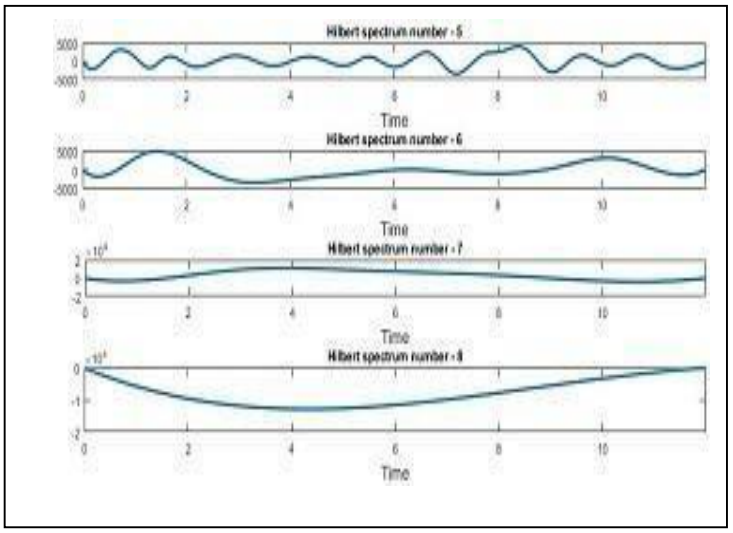

Fig 10 . *Stages of Hilbert spectrum analysis*

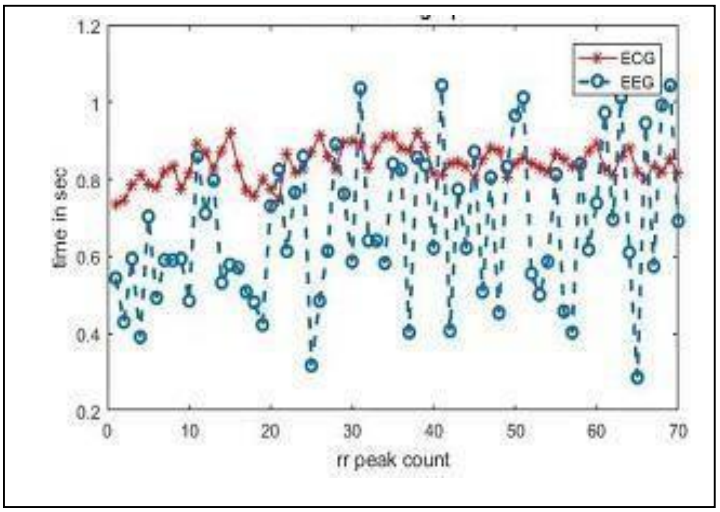

Fig11.*Comparison of R-R interval and Instantaneous frequency*

TABLE 1. R-R INTERVAL VARIATION

S no	Normal ECG			Abnormal ECG		
	First peak (sec)	***Second peak (sec)***	***R-R interval(sec)***	***First peak (sec)***	***Second peak (sec)***	***R-R interval***
1	1,0658	5.9964	0.61	6.04	4.2074	0.845
2	5.09964	5.6968	0.644	4.5488	5.5541	0.8055
3	5.3968	5.9173	0.702	4.207	5.2543	0.8053
4	6.4007	6.347	0.688	5.739	6.1484	0.7855
5	6.1222	6.4007	0.704	6.083	5.5541	0.8055

TABLE2.HEART RATEESTIMATION

Sno:	***R-R interval***	***Heart rate***
1	0.61	98.3
2	0.644	93.16
3	0.702	85.47
4	0.688	87.209
5	0.704	85.22

TABLE3.RESPIRATORY RATE ESTIMATION

Sno:	***R-R interval***	***Respiratoryrate***
1	0.61	1.2438720e+01
2	0.644	2.1238720e+01
3	0.702	2.2838720e+01
4	0.688	1.5638720e+01
5	0.704	1.3238720e+01

V. CONCLUSION

The major proposal of the work is to develop an non-invasive self administered technique for anxiety related disease prediction in children with ASD. These anxiety is especially due to their growth pattern and characteristics. In such a concern, ECG signal was considered due to its bio marking capability in both cardiorespiratory for dyspnea detection and epileptic seizure detection along with heart attack. The variation in ECG during all the three case leads to a new system of parallel tracking the R-R interval and hence the heart rate variability for disease prediction. Already existed system had a Kalman filtering framework to graph the existence of anxiety. It just predicted, if anxiety existed or not, but when it comes to disease prediction the earlier existed system does not find accurate results as continuous, real-time tracking of R-R interval is absent hence there is no continuous tracking of anxiety. The newly proposed system is advancement by using UKF algorithm for real-time tracking. The prescribed system is a true application on Unscented Kalman filter framework for tracking a non-linear system. The system makes use of the deviation in ECG, while tracking to find the R-R interval variations for disease prediction. For epileptic seizure prediction the system combines the instantaneous frequency response of EEG with the variation in the R-R interval and in case of dyspnea prediction EDR is derived from ECG combines with respiratory signal to find breath rate. Hence this system provides an overall noninvasive technique, also proved in terms of its accuracy and stability to get rid of false alarm. Tachycardia referring to increase in heart rate, more than 100 beats at rest, hence a decrease in R-R interval. Bradycardia referring to slow heart rate, less than 60 beats at rest, increasing the R-R interval is noted .In case of epileptic seizure if the instantaneous frequency of EEG signal decreases and RR interval of ECG signals increases it marks its onset. Then R-R interval has a direct impact respiratory rate, as heart rate increases respiratory rate also increases leading to dyspnea. In future the system can be improved incorporating sweat sensors and image processing techniques for eye images and movements for anxiety analysis to increase the sensitivity of the system.

ACKNOWLEDGEMENT

I would like to express my gratitude to my guide, Mr. Sudheesh P for helping me progress in my project with the best possible ideas as well as my friend Miss. Krishnatulasi for the support and suggestions and Our department for giving me the opportunity to do this project on the topic Anxiety detection with all necessary software support, which also helped me in doing a lot of Research.

REFERENCES

[1] ShulamiteA Green and Ayelet Ben-Sasson, "Anxiety Disorders And Sensory Over Responsivity In Children With Autism Spectrum Disorders: Is There A Causal Relationship?,"Journal Of Autism and Developmental Disorders,Springer.Vol10.4,2010.

[2] Richardefrye,"Autism Spectrum Disorder In The Emergency Department: Looking Beyond Behavior,"International Journal of Emergency Mental Health and Human Resilience,Vol.17,No.3,2015.

[3] L.Sathyapriyal,L.Murali And T.Manigandan,"Analysis and Detection Rpeak Detection Using Modied Pan-Tompkins Algorithm,"IEEE International Conference on Advanced Communication Control and Computing Technologies (ICACCT),pp.483-487,2014.

[4] AzadehKushki,AjmalKhan,Jessica Brian and EvdokiaAnagnostou,"A Kalman Filtering Framework For Physiological Detection of Anxietyrelated Arousal in Children with Autism Spectrum Disorder,"IEEE Transactions on Biomedical Engineering, Vol.62,Issue No.3, March2015.

[5] D.A.Dimitriev, E.V.Saperova, A.D.Dimitriev, and Yu.D.Karpenko,"Effect Of Anxiety On The Function Of The Cardiorespiratory System,"Yakovlev Chuvash State Pedagogical Institute, Cheboksary, Russia, Fiziologiya Chelovek Vol.40,Issue No.4,Pp 433-439,July2014.

[6] SuritaSarkar,SaptakBhattacherjee,SaurabhPal,"Extraction of Respiration Signal From ECG For Respiratory Rate Estimation, Michael Faraday IetInternational Summit: Mfiis(2015), Kolkata, India, September2015.

[7] W Orawich Phornsiricharoenphant, Songpol Ongwattanakuf And Y Odchanan W Ongsawae,"The Preliminary Study Of Eeg And Eeg For Epileptic Seizure Prediction Based On Hilbert Huang Transform,The 7th 2014 Biomedical Engineering International Conference (Bmeicon2014 Fukuoka, Japan,22 January2015.

[8] S.Rajasekaran, C. Luteran, H. Qu, Member and C. Riley-Doucet,"A Portable Autonomous Multisensory Intervention Device (Pamid) for Early Detection of Anxiety and Agitation In Patients with Cognitive Impairments, 33rd Annual International Conference Of The IEEEEmbs Boston, Ma, Usa,1st December2011.

[9] P.Calle-Romero,P.Valverde-Galan,Y.Robles-Bykbaev,M.E.Barrosponton,L.Canizares-Jarrn,V.Robles-Bykbaev,P.Ingavelez-Guerra andJ. Orellana-Peralta," Yocasta: A Ludic-Interactive System To Support The Detection Of Anxiety And Lack

[10] Jakub S Gsior,"Heart Rate And Respiratory Rate Inuence On Heart Rate Variability Repeatability: Effects Of The Correction for the Prevailing Heart Rate ,Frontier. Physiology., Vol.7,Article 356,18

August 2016.

[11] Keshava murthy T G ,"Review Paper On Denoising Of Ecg Signal,"2017 Second International Conference On Electrical, Computer And Communication Technologies (Icecct), Coimbatore, Pp. 1-4,2017.

[12] Shephali Gupta And JankiBallabh Sharma," Estimation Of Respiratory Rate From The ECG Using Instantaneous Frequency Tracking Fxlms Algorithm, 2016 International Conferenceon Micro-Electronics And Telecommunication Engineering ,(Icmete), Ghaziabad, Pp.296-300,(2016).

[13] C.Haritha, M. Ganesan And E. P. Sumesh,"A Survey On Modern Trends In ECG Noise Removal Techniques,"2016 Ieee International Conference On Circuit, Power And Computing Technologies, Iccpct,Nagercoil,Pp.1-7, March2016

[14] O. N. Swathi, M. Ganesan And R.Lavanya,"R Peak Detection And Feature Extraction For The Diagnosis Of Heart Diseases, "International Conference OnAdvances inComputing Communications And Informatics (ICACCI) 2017, Pp. 2388-2391, 2017.

[15] P.Sudheesh And M. Jayakumar,"Non Linear Tracking Using Unscented Kalman Filter,": Advances In Signal Processing And Intelligent Recognition Systems,Pp. 38-46,Aisc, Volume 678,27 September2017.

[16] SantanuSahoo ,PrativaBiswalTejaswini Das And SukantSabutb,"Denoising Of Ecg Signal And Qrs Detection Using Hilbert Transform And Adaptive Thresholding,",Global Colloquium In Recent Advancement And Effectual Researches In Engineering, Science And Technology (Raerest 2016),ProcediaTechnology,Vol. 25,Pages68-75,2016.

[17] Richardefrye,"Autism Spectrum Disorder In The Emergency Department: Looking Beyond Behavior,"International Journal Of Emergency Mental Health And Human Resilience,Vol.17,No.3,2015.

[18] L.Sathyapriyal,L.Murali And T.Manigandan,"Analysis And Detection Rpeak Detection Using Modied Pan-Tompkins Algorithm,"Ieee International Conference On Advanced Communication Control And Computing Technologies (Icaccct),Pp.483-487,2014

[19] Azadeh Kushki ,AjmalKhan,Jessica Brian And EvdokiaAnagnostou,"A Kalman Filtering Framework For Physiological Detection Of Anxietyrelated Arousal In Children With Autism Spectrum Disorder,"Ieee Transactions On Biomedical Engineering, Vol.62,Issue No.3, March2015.

[20] D.A.Dimitriev, E.V.Saperova, A.D.Dimitriev,And Yu.D.Karpenko,"Effect Of Anxiety On The Function Of The Cardiorespiratory System,"Yakovlev Chuvash State Pedagogical Institute, Cheboksary,Russia,FiziologiyaChelovek Vol.40,Issue No.4,Pp 433-439,July2014

[21] SuritaSarkar,SaptakBhattacherjee,SaurabhPal,"Extraction Of Respiration Signal From Ecg For Respiratory Rate Estimation,MichaelFaradayIetInternationalSummit:Mfiis(2015),Kolkata, India,September2015

[22] W OrawichPhornsiricharoenphant, SongpolOngwattanakuf And Y Odchanan W Ongsawae,"The Preliminary Study Of Eeg And Eeg For Epileptic Seizure Prediction Based On Hilbert Huang Transform,The 7th 2014 Biomedical Engineering International Conference (Bmeicon2014 Fukuoka, Japan,22 January2015

[23] M Benmaiekl,A. Charej And F.Abdelliche," Preprocessing Of The Ecg Signals Using The His-Purkinje Fractal System,2010 7th International Multiconference On Systems, Signals And Devices,Amman, 2010, Pp.1-5,2010

[24] Jakub S Gsior,"Heart Rate And Respiratory Rate Inuence On Heart Rate Variability Repeatability: Effects Of The Correction forthePrevailing Heart Rate,Frontier. Physiology., Vol.7,Article 356,18 August 2016.

[25] Keshavamurthy T G,"Review Paper On Denoising Of Ecg Signal,"2017 Second International Conference On Electrical, ComputerandCommunication Technologies (ICECCT), Coimbatore,Pp. 1-4,2017.

[26] MaeikeZijlmans, Danny Flanagan and Jean Gotman," Heart Rate Changes And ECG Abnormalities During Epileptic Seizure:Prevalence And Denition of an Objective Clinical Sign , Iecbes28 August2002,2017

Proceedings of the Fourth International Conference on Communication and Electronics Systems (ICCES 2019)
IEEE Conference Record # 45898; IEEE Xplore ISBN: 978-1-7281-1261-9

A proposed model of a Smart Faucet

Naveen Ananda Kumar J
Institute of management,
Christ (Deemed to be University
Bengaluru
jnaveens@icloud.com

Shivani Suresh
Institute of management
Christ (Deemed to be University)
Bengaluru
shivanisuresh109@gmail.com

Abstract- **A low cost, low voltage faucet which is context-aware with a scope of water conservation. The concept propsed is capable of identifying the object in front of it and based on that it will regulate the water flow and is vital for saving water. The faucet uses an in-built sensor like Infra-red camera to identify the object in front of it using machine learning and the micro-controller will recognize the size of the object and on the bases of this it would adjust the position of the nozzle. The pressure of the faucet is determined by this and accordingly, the pressure washer pump would be turned on when the IR sensors recgonises presence of hands under the faucet the water would be sprinkled . This system is useful in large scale kitchens like restaurants, hospitals, households etc. The amount of water conserved would be vast and if implemented in homes then in the long term would be able to make a colossal impact on water conservation.**

Keywords- Micro Controller; Infra-Red camera; Motor Controlled sprinkler; Pressure water pump;Machine Learning.

I.INTRODUCTION

With a population of over 7 billion the resources have become scarce and water is one of the vital sources of survival for all of mankind. Various campaigns have been carried out for bring about awareness regarding water conservation however the impact has been comparatively less with respect to the pace in which the freshwater table is depleting. [1]The proposed faucet is aimed at providing a solution to this problem to an extent by regulating the water flow which if implemented would help to reduce water usage and also make washing and cleaning process more convenient.

The faucet may calculate the water flow required for a shower, bath or for an open faucet activity. This way an entire households water consumption can be reduced immensely and when this is view at from a larger scale i.e. a community the overall water conserved would be sufficient to stabilize the water table.[2] By identifying the content in front of the faucet it would be able to calculate the level of water that should be dispensed and based on the width and density of the object it would adjust the flow of water and would cover more area.[3]

Most of the faucets at present only serve the purpose of dispensing water the flow of water is not regulated and the faucets which have in-built sensors are unable to detect the content present in front of it and as a result, dispense water in at a fixed rate and quantity. [4]The aim of this project is to be able todetect the surface of the object on the bases of which the faucet would change the rate of flow of water and control the volume being dispensed.

Developed countries to an extent have rules and regulations to monitor and regulate water supply to households however most of the developing and third world countries with twice the population of developed countries it is high time that a solution is implemented to cut down on the water wastage. By setting up these faucets in every household would be the perfect market to target in order to tackle this issue.

It is often assumed that software and applications are restricted only to computers and mobile phones. However, the scope for integrating them to daily objects would make smart living a touch away. Implementing software to develop hardware which would help in the day to day functioning of an individual would change the game. [5]

Smart homes are becoming extremely popular and having a smart faucet is an addition to it making the living easy.[6] With the current generation heavily relying on technology, smart faucets would be a gadget that would automatically make its way into their homes.

A combination of an infra-red camera which brings in the advantage of using static overhead camera above the work area, a micro-controller with the ability to interpret the measurements of the object, a pressure pump providing water in the required volume would altogether make the washing process easier.

II.PRESENT SCENARIO AND RESEARCH GAP

The current scenario is taps and faucets are just viewed as a device to dispense water the hidden potential in this is yet to be explored. With motion sensitive and infra-red cameras becoming more common combining these with faucets would help to create smart faucets which can not only control the flow of water but also has the environmental benefit angle as well.[7]

Technology has become extremely affordable when compared to the earlier days. Almost half the world population has a smartphone which was not the case a decade ago. [8]Countries are becoming tech-savvy and the next big thing in the market is smart living. Smart faucets are an untapped market with a lot of scopes.[9]

The faucets available in the market now are mostly the normal faucets which dispense water or are the motion sensitive ones which dispense water on command.[10]

The proposed model in this paper is a novel idea which aims at bringing together different forms of technology to a faucet enabling it to be smart. Bringing home this technology would be a time saver and every homemaker's dream solution to the problem of getting the dishes done on time.[11] It can also be expanded to the bathing segment by using it in showers. Washing our hands and body properly is one of the most effective ways to avoid infection and a faucet which is able to exactly identify the measurements and provide according to it would help to implement this effectively.[12]

Faucets nowadays are equipped with in-built sensors like temperature gauges which help to control the water temperatures. The faucet proposed by us is a combination of hands-free and digital with sensors that would control the flow of water.

III.PROPOSED MODEL

A. Motor controlled sprinkler

The faucet has a 2-way motor controller nozzle which sprinkles the water. A two 2-way motor-controlled sprinkler operates on x and y-axis motion. The nozzle widens and shrinks in accordance with the object in front of it. Once the microcontroller detects the measurements of the object with the help of the infra-red camera the nozzle will adjust accordingly in order to supply water in the required quantity. For instance, if a small plastic cup was brought in front of the nozzle it would detect the width and only open the nozzles center holes for the water to flow. On the other hand, if it was a big bowl all the nozzles would be open in order to cover more area.

B. Infra-Red camera

The infra-red camera is motion sensitive and real time. It would detect motion or hand gesture and turn the faucet on. It is capable of measuring 3D surface and the measurements would then be sent to the microcontroller. This helps the smart faucet to be context-aware giving it the ability to identify what is in front of it and get its dimensions. Once a vessel comes into the washing area it would try to figure out its dimensions. And with the microcontroller, the water flow would be regulated.

The IR camera would be positioned in a manner that it would be still so that it can detect the object properly using ML[13]. Even if the faucet is being moved around the camera would be still near the tail of the faucet so that it can get the measurements easily.[14]

C. Micro Controller

The micro-controller plays a key role in the entire process as it is the deciding body which regulates the flow of the water. Once the measurements are obtained from the infra-red camera the micro-controller determines if the water flow required is high or low. Depending on the width and size of the object the water flow will be decided. If the object is big and requires high pressure then the pressure washer pump will be turned on. This is extremely useful for large scale kitchens which have huge utilizes. It would make the cleaning process a lot easier.

D. Pressure washer pump

The pressure washer pump is meant for heavy cleaning targeting large vessels or while showering or cleaning a car. Mainly when the water requirement is more and the surface area to be covered is large. The pump would get a signal from the microcontroller after which the nozzle would switch to this mode and the water flow would be wider covering the majority of the region in one go rather than having to adjust the object in accordance to the water flow. It's pretty common for people to adjust in the shower in the direction that the water comes in. this faucet would automatically adjust and cover the whole area.

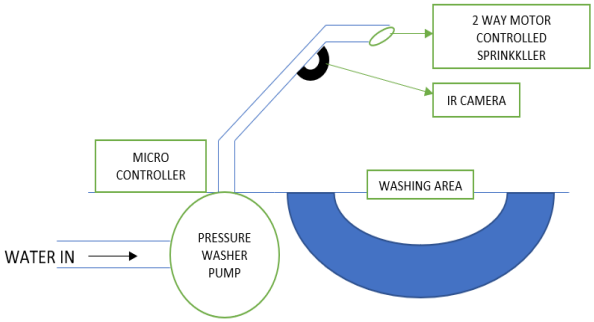

Fig 1.1 Block Diagram

E. Working Process

The models working process starts from the object coming into the washing area. Once it comes in front of the nozzle a hand gesture would indicate that the water should flow out. (Fig 1.1)This would be detected by the infra-red camera which would also check for the measurements and dimensions of the object. These readings would then be sent to the microcontroller which would decide whether to activate the pressure washer pump or not. The pressure washer pump is a high-pressure water dispensing unit which is extremely helpful to wash objects which have a huge surface. The washer would help to pump out water in large quantities so that the object can be washed in one go rather than having to keep the faucet on for a long period of time wasting most of the water. once this decision is made by the microcontroller the next step is for the 2-way motor-controlled sprinkler to adjust the nozzle in either x-axis or y-axis and let the water flow accordingly in order to cover the maximum surface in lowest possible time. This would reduce the amount of time spent on cleaning, the amount spent on electricity bill and most of all the water wastage.

- *Example*

Derek who runs a famous restaurant in the city is experiencing several issues due to the water shortage in the area and is forced to import water. He wants a long-term solution for the problem and wants to contribute to the water conservation front rather than continue wasting water. With the help of the face, he found out that the Infra-red camera sensed the object in front of it and the

Microcontroller uses this image to calculate the area of the object. (Fig 1.2) The 3D measurements obtained helps the micro-controller to combine both this information and decide what position of the nozzle would be able to cover maximum area and what should be the pressure of the water. If pressure calculated is a yes then the water is sprinkled on the object however if it requires more water and the answer is no then pressure washer pump is turned on and the water rushes in.

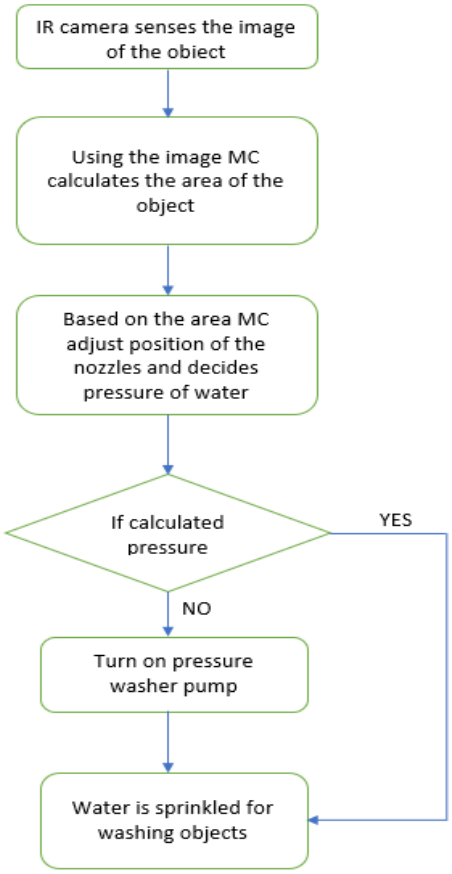

Fig 1.2 Process Flowchart

IV.FUTURE WORK

The future scope of this proposal would be to implement this on a much larger scale and not limit it to just washing utensils. But also in factory's, car washes, hospitals, restaurant and most of all in every household. By widening the scope of this faucet, it would be possible to achieve water conservation and stop having to import water in areas. The long-term aim of this project is to ensure sustainability. By having these faucets in every kitchen, bathroom possible the scope of this idea would increase immensely and the conveince as well.

V.CONCLUSION

It is high time that solutions for tackling water shortage be introduced to the public. Just how change starts at home by targeting the average household to implement this smart faucet the enormous impact it would have on water conservation is more than a first time towards handling global warming. The smart faucet would be user-friendly and the kitchen is a central part of every house starting from there would be more practical.

ACKNOWLEDGMENT

We thank our family and colleagues from the Institute of management, Christ (Deemed to be) University who provided us with insights which were great assistance in shaping our research. We would like to express our gratitude to the faculties and colleagues of Institute of management, Christ (Deemed to be) University for sharing their pearls of wisdom, reviewing our research and giving us key inputs.

REFERENCES

[1] Beal, C. D., Stewart, R. A., & Fielding, K. (2013). A novel mixed method smart metering approach to reconciling differences between perceived and actual residential end use water consumption. Journal of Cleaner Production, 60, 116–128. https://doi.org/10.1016/j.jclepro.2011.09.007
[2] Breuer, P., Eckes, C., & Stefan, M. (2007). Hand Gesture Recognition with a Novel IR Time-of-Flight Range Camera – A Pilot Study, 247–260.
[3] Authors, F. (1983). Eye · in · hand robot vision scores over a fixed camera.
[4] Intelligent autonomous system for residential water end-use classification : Autoflow Author Griffith Research Online. (2015), 0–36.
[5] Bonanni, L., Arroyo, E., Lee, C., & Selker, T. (n.d.). Smart Sinks : Real-World Opportunities for Context-Aware Interaction.
[6] Park, S., Us, M. A., Mark, R., & Us, M. A. (2010). (12) United States Patent, 2(12).
[7] Willis, R. M., Stewart, R. A., Williams, P. R., Hacker, C. H., Emmonds, S. C., & Capati, G. (2011). Residential portable and recycled water end uses in a dual reticulated supply system. DES, 272(1–3), 201–211. https://doi.org/10.1016/j.desal.2011.01.022
[8] Casado, M. (n.d.). Rethinking Packet Forwarding Hardware, 1–132.
[9] Akribopoulos, O., Amaxilatis, D., Georgitzikis, V., Logaras, M., Keramidas, V., Kontodimas, K., … Chatzigiannakis, I. (n.d.). Making P-Space Smart : Integrating IoT technologies in a Multi-office environment.
[10] Cited, R. (2015). (12) United States Patent, *2*(12).
[11] Documents, F. P., & Publications, O. (2016). (12) United States Patent (10) Patent No .: (45) Date of Patent : Primary Examiner — Atif Chaudry water for a period of time regardless of whether an object is, *2*(12).
[12] Sebastian, L., West, G., & Venkatesh, S. (n.d.). Recognition of Emergent Human Behaviour in a Smart Home : A Data Mining Approach, (June 2006).
[13] Lecun, Y., & Huang, F. J. (n.d.). Learning Methods for Generic Object Recognition with Invariance to Pose and Lighting.
[14] Wersing, H., & Edgar, K. (2002). Learning Optimized Features for Hierarchical Models of Invariant Object Recognition, 1–27.

Proceedings of the Fourth International Conference on Communication and Electronics Systems (ICCES 2019)
IEEE Conference Record # 45898; IEEE Xplore ISBN: 978-1-7281-1261-9

SMART AID FOR VISUALLY CHALLENGED PEOPLE

Rohit P
Dept. of Electronics and Communication Engineering
SJCE,Mysuru
rohitp2512@gmail.com

Vinay Prasad M S
Assistant Professor
Dept. of Electronics and Communication Engineering
SJCE,Mysuru
vpms1408@sjce.ac.in

Ranganatha Gowda S J
Dept. of Electronics and Communication Engineering
SJCE,Mysuru
gowdasira26@gmail.com

Krishna Raju D R
Dept. of Electronics and Communication Engineering
SJCE,Mysuru
krishnarajudr95@gmail.com

Imran Quadri
Dept. of Electronics and Communication Engineering
SJCE,Mysuru
imranqad@gmail.com

***Abstract*—This project tries to transform the visual world into the audio world with the potential to inform visually challenged people the spatial locations of the objects in their vicinity. Our paper presents the development of a real-time system based on detection, classification, and position estimation of objects in an outdoor environment to provide the visually impaired individuals with a voice output-based scene perception. The system is low-cost, light weight, simple, and easily wearable. The module is integrated into the stick, and the pi-camera is used to take the picture, and a controller is provided to move the camera in the required direction. The valuable insights gained from the feedback are then used to modify the system to best suit the requirements of the user. The object detection and classification framework exploit a multi-modal fusion-based mask RCNN using motion, sharpening and blurring filters for efficient feature representation. The image recognition classifies the detected objects along with the positions of the objects. Experimental results carried out in the outdoor environment are demonstrated. These data obtained is then converted to voice, and blind people will get the visual of what the environment is around them.**

I. Introduction

Navigation of blind people is an important issue to be considered. They most commonly use sticks for obstacle detection, meanwhile memorizing all locations they are getting familiar. In a new or unfamiliar environment, they depend on individuals passing by to enquire for a certain area. In the world of sophisticated technology along with various sensors, there should be a system with the most basic innovation to make their life a bit easier. Traditional navigation aid methods such as sticks are very limited and are unable to provide a complete scene perception. For example, a stick may just provide information about the presence or absence of an obstacle. However, no information about the kind of obstacle is available. In many cases it may be important to know the obstacle type; specifically, if it is a door needed to be opened or a stair required to be climbed.

Computer vision technologies, especially the deep convolutional neural network [1], have developed rapidly in recent years. It is promising to use the state-of-art computer vision techniques to help people with vision impairment.

The utilization of computer framework advances for navigational purpose is relatively a recent technology. Commonly, the scene is perceived by extracting images/videos using vision sensors and a controller is used to adjust the camera view. The latter is discussed in relation to the recognition of the objects with the help of image processing [2] using mask RCNN [3] [4] multi-modal convolutional neural network and the usage of data that is obtained from the image recognition to identify the position of the object. The processed data is made available to the end-user through voice output and contains information regarding the class and position of the object.

In our project, we have attempted to build a real-time object detection and position estimation pipeline, with a goal to inform the user about the surrounding environment. It is possible to obtain faster results from the mask RCNN image recognition by running the process on the powerful tools. A server can be used to run the process and return the obtained results. For a smaller specifications system, the output will be obtained but the execution time may take long as RCNN requires a higher processing specifications system. So, the end-user system may be designed with low specifications which

can reduce the cost to the end-user. Its main function will be to click the image and send the image data to the server which requires less computational and processing power. The picture in the server will be processed which has a good processing and computational power to handle the RCNN and process the results faster. Once the results are obtained, they are sent back to the end user system in the form of voice output.

II. RELATED WORK

Work has been carried out by various groups in the field of object recognition using image processing techniques that are implemented for an efficient and a quicker way to recognize the object and classify them according to the class.

Mask R-CNN Object Recognition by Kaiming He, Georgia Gkioxari Piotr Dollar [5] have presented a conceptually simple, flexible and a general framework for object instance segmentation which efficiently determines the object in the image by applying the segmentation mask for each instance. They have demonstrated how simple its to train them and how it adds only a small overhead to Faster RCNN running at 5fps.They have demonstrated COCO suite of challenges, including instance segmentation, bounding-box object detection, and person key point detection. Mask R-CNN scores high against all existing, single-model entries on every task. The simple and effective approach will serve as a solid baseline and help ease future research in instance-level recognition.

An Image Matching and Object Recognition System has been developed using Webcam Robot by Sanjana Yadav and Archana Singh [6]. In this work, the image matching and recognition of the image and classification is done by tracking an object and calculating its feature points and classification with the help of trained Data Sets. They have both the manual as well as automated image matching. In the automated system, the picture is taken and uploaded to the database after which the system image matching will be performed. Black and white points of the image is first calculated, then Chamfer Matching Algorithm and 3-4 Distance Transformation with canny edge detector [6] is applied for calculating the pixel values which is used for matching the trained data sets.

pseudo Eye - Mobility Assistance for Visually Impaired Using Image Recognition by A.G.Sareeka, et al., [8] have developed a wearable device which converts the text image to the voice output through a camera click. A SoC (System on Chip) does the processing and tells the user the text thats present in the picture that will guide them through the path.

Visual Assistance for Blind using Image Processing by Deepthi Jain B, Shwetha M Thakur and K V Suresh [9] proposed a wearable model for the blind people which is capable of identifying the objects using image processing techniques and also the distance between the objects is identified using the ultrasonic sensor. Raspberry pi module is used for computation and implementing the algorithm where the modules such as the OpenCV and python language is used for the implementation. Some basic objects and overlapping images were identifiable.

Image Recognition for Visually Impaired People by sound by K.Gopla Krishna, C.M.Porkodi, and K.Kanimozhi[10] have proposed an algorithm to convert the image to the sound format to help blind people understand their surroundings. They have used a canny edge detection package which identifies the object by the edges and by comparing these values with pre- trained dimensions. It has been observed that it is working very good fors simple images but when the images are complicated like overlapping of the images they are obtaining a wrong results and yet to develop the efficient way of image processing.

Voice Assisted Navigation System for the Blind by Ananth Northey , Kishore Kumar M.[11] have designed a cheap and affordable navigators for the blind people where the ultrasonic sensors used will give a voice instruction and guide the route for the person and ground gradient is its improper they have designed an algorithm to guide the correct path for the user. They have incorporated a GPS module which can guide them the route to reach the destination n with the help of the android app which sets the destination and gives the voice output for the user to take the best path.

III. PROPOSED MODEL

The proposed model is used to overcome all the shortcomings of the aid for visually challenged people. There are in the market the sticks that have a sensor which informs whether the object is there or not. Further, there are sticks which use infrared cameras to map the surroundings but are expensive and uses a lot of processing. To address the shortcomings, a model is developed to assist the visually challenged people and read-aloud the names of the objects present in their surroundings and to give them clear estimation of how their surroundings is. To narrow down their range of estimation and to provide precise object position, a controller is given to move the camera to their required view point and then take the photo. The output is read aloud as to what objects are present in that direction.

The photo is taken by the user using joystick switch in the direction he wishes. This photo cant be processed in Raspberry PI as it takes up lot of computation. Hence, this photo is sent to the server dedicated for running the algorithm. The photo is sent through Googles Gmail REST API. Each photo has the unique name in the form of `YYYY_MM_DD_HH_MM_SS` so that there is no replacement of images.

The image is taken up by server from a dedicated Gmail link. This image is then processed using the Mask-RCNN algorithm. The server processes it as it can support multiple clients and can do it fast. The output of the algorithm consists of many parameters which are encoded and sent back to the client from which request has come.

The output from the server is taken up by client and decodes the information. This decoded information is read-Aloud clearly to the user two (2) times. Any flexibility or changes in the read-aloud can be done from provider end.

A. Architecture at the client side

At the client side using the joystick, the user moves the camera in the required position and clicks the pic, the raspberry pi

module takes the picture which is then sent to the mail (pre-coded) using the Gmail API, to make the computations fast in this project and since the raspberry pi module has limited computation al power, its functions are also limited in this project where it performs the main core functions such as uploading the picture and getting the results back and converts them into the voice format which the end user , the blind person is able to hear. The complete working of each section is discussed in detail in the upcoming sections.

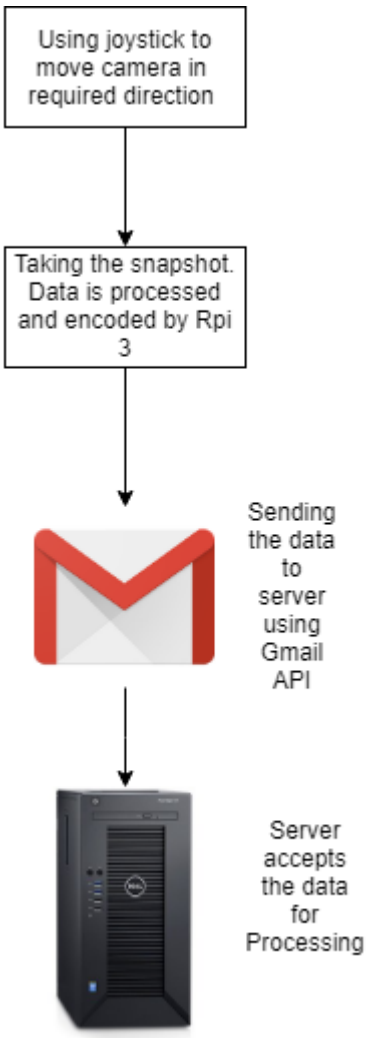

Fig1.Aritecture of the module at the client side

B. Core function of the modules

Each module used has their own core functions and responsibilities, each of the modules functions is explained in detail here.

1) Joystick module: A 2D joystick module is provided along with the push button switch where the user can use this to position the camera in the direction required and push the button. This module is powered and controlled by the Arduino Uno module which is powered by the 9V battery. The joystick provided is able to turn the camera horizontally by an angel of 180 degree and vertically 120 degree.
2) Push button: The push button is provided along with the joystick module where the user once he is done positioning the camera, he can click on the push button (press the joystick vertically) and photo is clicked.
3) Arduino Uno : The joystick along with the push button functions is handled by the Arduino Uno where the values fetched joystick module to the Arduino Uno are in the analog format since the raspberry pi does not have a ADC(Analog to Digital Convertor) Arduino plays a role where it converts the analog data to the digital format and sends the data to the raspberry-pi module which than turns the camera accordingly. Arduino also plays a important role in analyzing the push button push, once the button is pressed it takes that as an interrupt and send the signal to the raspberry pi module which in turn modifies this to take the photo.
4) Raspberry pi: Is the main core at the client side, it is powered by the power bank, it does mainly 3 things, which are.
   a) Receives the signal from the Arduino module to take the picture and once it receives the positive signal then it immediately without much delay clicks a pic and saves it.
   b) The saved picture is than sent to the mail using the Gmail API.
   c) The final results of the image processing is received by the raspberry pi which is also done by using the Gmail API. These final results are than converted into the voice format and through the jack provided the voice output is made available to be heard by the end user.
5) Pi cam: This module is a 5MP (Mega Pixel). Camera which is provided with best interface with the raspberry pi module a 8 line parallel data communication cable is provided for a high speed data transfer of the imaged to the pi module. This module just turns on when the pi send signal to take a pic and a warm up time of 5s is provided to get a clear image and returns the image back to the module

C. Architecture at the server side

The server is pre-installed with python version 3 and required packages for the image processing are also installed. Server is fully automated, and no manual intervention is required for any actions that are required concerned to the project. It is pre trained to object recognition. The Gmail API services are supported by the server. The server does all the required computations and obtains result with the minimum delay possible and max CPU usage. These results are than encoded in the csv file and sent ack to the raspberry pi module using the Gmail API. The flow and the services are explained in detail.

Once server receives the image from the client side, the image processing algorithm is applied to the image for object

recognition. The algorithm that is used is MASK R-CNN which is a robust, efficient algorithm used for object recognition. It even produces accurate results with the complicated images and overlapping images. The results obtained from this algorithm are than converted into the proper csv format which is the best way to send the data with the minimum size over the communication.

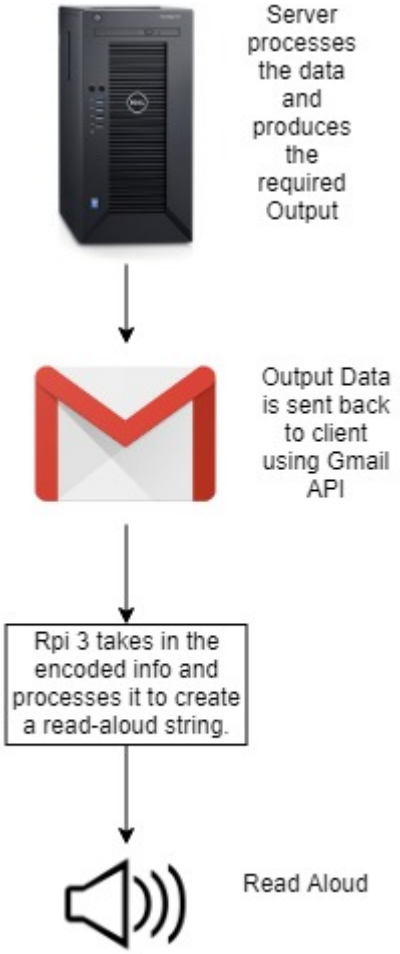

Fig 2. Architecture at the server side

The Server continuously waits for an image to be uploaded by the client. Once the client uploads an image, the authentication is done by google API. If the authentication is successful, the image is fed to object recognition algorithm. The model used by the algorithm might depend on the client's requirement. The default model might be used or the model as per client's requirement might also be used. The algorithm produces the results which are stored as a dictionary which has object as the key and its corresponding position as the value. The data is then converted into a csv format in the form of [object_id, x_left_bottom, y_left_bottom, x_right_top, y_right_top].There might be multiple IDs of this sort based on number of objects being recognized.

The csv file created is renamed the same name as the image processed to produce it to maintain uniqueness among multiple files.The csv is sent back to client through the google API.

D. Mask R-CNN

Mask R-CNN is a conceptually simple, flexible, and a general framework for object instance segmentation efficiently detects objects in an image while simultaneously generating a high-quality segmentation mask for each instance. Mask R-CNN is simple to train and adds only a small overhead to Faster R-CNN, running at 5 fps. Moreover, Mask R-CNN is easy to generalize to other tasks, e.g., allowing us to estimate human poses in the same framework. g instance segmentation, bounding-box object detection, and person key point detection. Without tricks, Mask R-CNN outperforms all existing, single-model entries on every task, including the COCO 2016 challenge winners. The Fig 3. Shows the output of the Mask R-CNN for the images which have overlapped objects, which is using the instance segmentation concept to bring up the result. Mask R-CNN structure is also trained to analyze the human pose estimation also, which means that it can identify the objects even when they are posing in the different position. Fig 4. Shows the insight of what the output would result in.

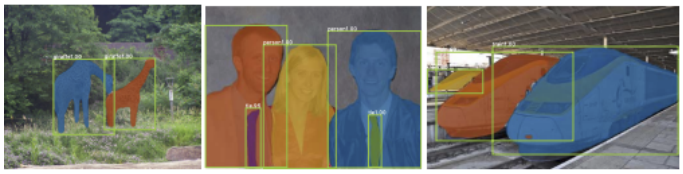

Fig 3. Mask R-CNN output for the overlapping images

E. Gmail-API

The Gmail API is a RESTful API that can be used to access Gmail mailboxes and send mail. For most web applications (including mobile apps), the Gmail API is the best choice for authorized access to a user's Gmail data. The Gmail API, like Gmail itself, is (currently) a free service from Google. The Google Fit REST API enables you to store and access user data in the fitness store from apps on any platform. The REST API provides resources and methods to create, obtain, list, and modify data sources. A data source represents a unique source of sensor data. All requests to the Gmail API must be authorized by an authenticated user. Gmail uses the OAuth 2.0 protocol for authenticating a Google account and authorizing access to user data. You can also use Google+ Sign-in to provide a "sign-in with Google" authentication method for your app. Google has doubled up the Gmail attachment size from 25MB to 50MB for incoming mails, allowing users to receive larger files of size up to 50MB. This means that user can now open file size of maximum of 50MB directly in their inbox mailbox at once.

IV. RESULTS

The fig 5 and fig 7 was sent as input by the Pi cam, the client device sends the image to server which in turn sent back the output in the form the form of fig 6 and fig 8 respectively.

Fig 5. Input Image as taken by camera

Fig 7. Image taken by Picam

2019_04_19_11_38_06.csv

	A	B	C	D	E
1	6	36	0	369	360
2	1	198	411	250	431
3	1	196	146	259	193
4	3	189	442	313	581
5	1	196	427	232	438
6	3	234	0	424	171
7	3	202	358	254	383
8	3	195	364	241	408
9	8	173	367	206	417
10	8	147	441	226	505

Fig 6. Form in which Data is communicated

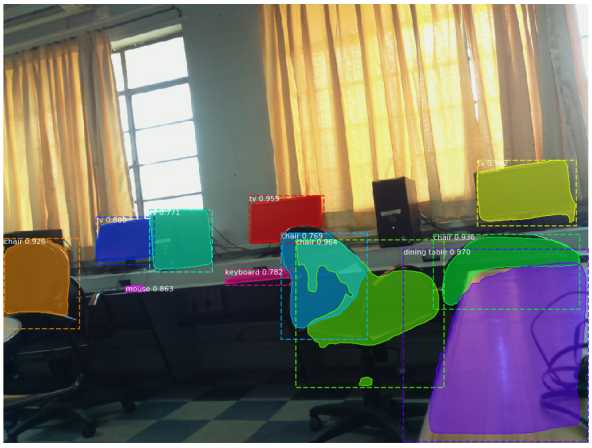

Fig 8. Mask RCNN output

	A	B	C	D	E
1	63	273	829	388	1002
2	57	412	512	671	771
3	63	335	430	418	560
4	57	403	752	534	1009
5	57	410	0	568	132
6	63	373	162	456	264
7	61	429	700	765	1024
8	65	493	213	504	247
9	67	464	387	492	502
10	63	360	255	468	365
11	57	401	486	587	637

Fig 9. The form in which data is communicated

The output has n*5 fields where n is the number of object detected. Each row represents one object. The first element in each row denotes class ID. Each object has a different ID. In the above fig., the ID 6,1,3,8 represents bus, person, car and truck, respectively. The 2nd and 3rd column represents bottom left coordinates of a bounding box i.e. (x1,y1) and 4th and 5th column represents top right coordinate i.e. (x2,y2). It can be inferred that the height of the object is abs(y1-y2) and width of the object is abs(x1-x2) as seen from the camera.

For reading out the object for the visually-challenged, the center line is taken as the reference. Since the images are always 1024 * 768, center line always has x-coordinate 512. The ones having x2 $<$ 512 are in the left of the image, ones having x1 $>$ 512 are in the right of the image and the ones whose x1 $<$ 512 and x2 $>$ 512 pass through the center coordinate.

The voice output for each result would be of format ”The (number of object-name) (object-name) was/were found. One was left/right/straight of the camera, one is .... ” till all the object instances are parsed. The above is repeated for all the objects.

As indicated by Fig 9, first column of eaach row represents the class ID. 57,61,63,65,67 represents chair, table, TV, mouse, keyboard. The read aloud for Fig 9 would be of the form ”There are eleven(11) objects found. ’4 chairs were found; 1 on the left of camera, 2 in line of the camera, 1 on the right

of camera'. '1 table was found; 1 to right of camera'. '4 TV were found; 2 to the left of camera, 1 on line of camera, 1 to the right of the camera'. '1 mouse was found; 1 on the left of camera', '1 keyboard was found; 1 on line of the camera'". This output is repeated to remove ambiguities if any.

The read-aloud is such that, the number of elements in the class are told first followed by position of each. The above result is repeated to get clarity in case of ambiguity the first time.

The Round trip Time takes at max 20 seconds when being tested in the local low power server.

V. CONCLUSION

The paper presents a smart stick which is significantly better than its predecessors with ultrasonic sensors. The sticks with ultrasonic sensors are heavy and expensive. In smart stick, all the operations are done using images which reduces the infrastructure significantly.Therefore it is much cheaper than the ultrasonic ones. The algorithm when hosted on Google servers for testing yielded results in a second. It was observed that the algorithm yielded better results when trained for 30-35 epochs.The accuracy was tested for wide range of objects in various conditions The accuracy was consistently above 90%.Its easy usage combined with powerful detection algorithm makes it an obvious choice in the foreseeable future under wearable tech.

VI. FUTURE ENHANCEMENTS

1) The further goals include creation of micro-controller to perform only the required operation and thus getting rid of Raspberry Pi.
2) As the module is integrated on a stick, the module can be integrated on a cap as it is easily wearable and more portable than a stick.
3) Integrating a night vision and flash cameras for detection in extremely low light.
4) Using depth perception to read-aloud approximate distance of the object which is being recognized.

REFERENCES

[1] https://github.com/matterport/Mask_RCNN
[2] Albawi, S., Mohammed, T. A., Al-Zawi, S. (2017). Understanding of a convolutional neural network. 2017 International Conference on Engineering and Technology (ICET).
[3] King-Sun Fu, Rosenfeld. (1976). Pattern Recognition and Image Processing. IEEE Transactions on Computers
[4] Bappy, J. H., Roy-Chowdhury, A. K. (2016). CNN based region proposals for efficient object detection. 2016 IEEE International Conference on Image Processing (ICIP)
[5] He, K., Gkioxari, G., Dollar, P., Girshick, R. (2017). Mask R-CNN. 2017 IEEE International Conference on Computer Vision (ICCV)
[6] Yadav, S., Singh, A. (2016). An image matching and object recognition system using webcam robot. 2016 Fourth International Conference on Parallel, Distributed and Grid Computing (PDGC).
[7] Wang, B., Fan, S. (2009). An Improved CANNY Edge Detection Algorithm. 2009 Second International Workshop on Computer Science and Engineering.
[8] Takamatsu, M., Nakamura, A., Ishihara, S., Hasegawa, M., Iwata, E. (2018). A study on pseudo stereoscopic vision from a piece of human group picture: Face recognition, segmentation, and depth estimation. 2018 International Workshop on Advanced Image Technology (IWAIT). doi:10.1109/iwait.2018.8369641
[9] Deepthi Jain, B., Thakur, S. M., Suresh, K. V. (2018). Visual Assistance for Blind Using Image Processing. 2018 International Conference on Communication and Signal Processing (ICCSP).
[10] Krishnan, K. G., Porkodi, C. M., Kanimozhi, K. (2013). Image recognition for visually impaired people by sound. 2013 International Conference on Communication and Signal Processing.
[11] Noorithaya, A., Kumar, M. K., Sreedevi, A. (2014). Voice assisted navigation system for the blind. International Conference on Circuits, Communication, Control and Computing.
[12] Kartik Venkataraman Priyam Chatterjee, Robert Mullis Pelican Imaging Corporation, PiCam: An Ultra-Thin High-Performance Monolithic Camera Array 2014.

Proceedings of the Fourth International Conference on Communication and Electronics Systems (ICCES 2019)
IEEE Conference Record # 45898; IEEE Xplore ISBN: 978-1-7281-1261-9

An Examination System Automation Using Natural Language Processing

Indrashis Das
School of Computer Engineering
Kalinga Institute of Industrial Technology Deemed to be University
Bhubaneswar, India
indrashisdas98@gmail.com

Bharat Sharma
School of Computer Engineering
Kalinga Institute of Industrial Technology Deemed to be University
Bhubaneswar, India
yashsharmamgs@gmail.com

Siddharth S. Rautaray
School of Computer Engineering
Kalinga Institute of Industrial Technology Deemed to be University
Bhubaneswar, India
siddharthfcs@kiit.ac.in

Manjusha Pandey
School of Computer Engineering
Kalinga Institute of Industrial Technology Deemed to be University
Bhubaneswar, India
manjushafcs@kiit.ac.in

***Abstract*—This world has seen a lot many examination portals that are deployed over several servers which are used to conduct online examination for various purposes among which some may include conducting a test for entrance examinations, or olympiads at national and international level and while some portals are designed to conduct a test for placement purposes. But what we have seen is that mostly all the portals are designed to conduct tests that contain multiple choice questions. Here our aim is not to work on the technology that is already existing, rather some technology that is very rare. Here we talk of the descriptive online examination system. Multiple choice questions are easy to deal as they have a question, a few options and a field in the same question that stores the correct option in the database. While in the case of descriptive questions it is not so. It brings in or uses the concepts of Natural Language Processing or NLP to assign marks to answers. Answers are nothing but strings and the job of the model is to do some operations on the answer string such that it can assign the correct marks to answers written by the examinee. The data is basically collected from a descriptive online examination system. Further, it is analyzed and the designed model assigns accurate marks to the answers for the question. The back-end is written in Python where the web framework used is Django, the library used for Natural Language Processing includes NLTK and for database purpose, SQLite version 3 is used, while for the front-end HTML version-5, CSS version-3, Bootstrap and Javascript is used.**

Keywords—Exam System; SQLite3; Django; Descriptive System; Natural Language Processing; NLP; Python; NLTK

I. INTRODUCTION

We come to hear news from around the globe that a particular exam was conducted for a job or for a college or examination in schools and the result was published after some time, while this is a good way to conduct an exam but it is inefficient with respect to the current world where automation is the future. The examination system relies on manual work from printing to transporting the paper to the examination hall, then invigilation and the most tedious task of checking the answer sheets which is a huge mess for any examiner which sometimes leads to resource loss. Also, we hear news about paper leaks and answer sheet being lost in the transporting process. The manual checking process will always have that human error based on certain factors like biasing, the mood of the examiner, target completion and much more such factors. Also if we take account of all the paper wastage and the stationary waste which harms our environment leading to do more bad then good as the enormous amount of trees being chopped off across the world for the process. This helps us understand that the offline examination system is not cost effective or time efficient, resources are also wasted in the process and moreover we all know that resources are scarce in nature and we need to utilize it efficiently to get the maximum output of it.

While the offline examination system has a big disadvantage but are not getting replaced at a bigger scale because new online examination system features only multiple choice type of question's while most of the exams contain descriptive question for which multiple choice answers do not work and hence they are not that compatible and efficient to replace it at a larger level. We all know that if we have to remove a universally accepted system, the new system should not be just good, rather it should be able to make a quality difference so that the organizations accept it. While there are some examination system and they are good at evaluating the answers but they have little to no scope for the descriptive ones and the analysis is not well implemented to get meaningful results. Even most famous of them just have a simple system of storing the correct options in the database and just matching the correct option with it to calculate the result.

In the proposed model we are taking the online examination system to a new level by enabling the examinee to write descriptive answers which will get evaluated on their own i.e automating the entire offline examination system with the efficiency of computing having no human error involved, this can be done using NLP or Natural Language Processing. The evaluated answers will be stored in the database and they can be viewed anytime and a particular student profile will be maintained for better evaluation of the student.

This will be a huge boost to the online examination system as this will allow it to overcome its biggest con and it will also help the online examination system to stretch its paw even in the half-yearly or annual examination conducted by schools or college for evaluating the profile of the student. This will have instant benefits like the system will relieve the burden of the teachers and professors of checking copies and in return they can be more productive with their time in teaching things, this will also eliminate biasing in answer script checking and will have leased space for any human error as copies would not be scanned and the entire marks

will be allotted according to the way answers are written by the examinee while he was on and there will be little to no space for acquisition, it will help in resource management as this will cut corners on stationery products, it will also have greater efficiency with respect to time as it will produce instantaneous results and will be more secure and reliable.

Talking about the technology used in order to build such a model for evaluating descriptive answers, NLP or Natural Language Processing is has a great role to play. NLP can do a lot of innovative jobs like predicting if a message or an email is a spam or a ham, the quality search that we can do on shopping websites like www.amazon.in and www.flipkart.com in order to search for different categories of items that include kitchen utensils, electronics gadget, apparels, food items and much more such products that are available online. The basic idea was that did anyone ever think of knowing how these search bars or how these ham-spam classifications work? The answer to this question is that rarest of the rare people have tried getting into this and tried to know what the mechanism or the back-end work in order to give such powerful search results and such predictive classification techniques. For those who are not aware of the mechanism behind this, it's all just about playing with strings of characters, numbers and special characters or what we call as string manipulations to arrive at such results.

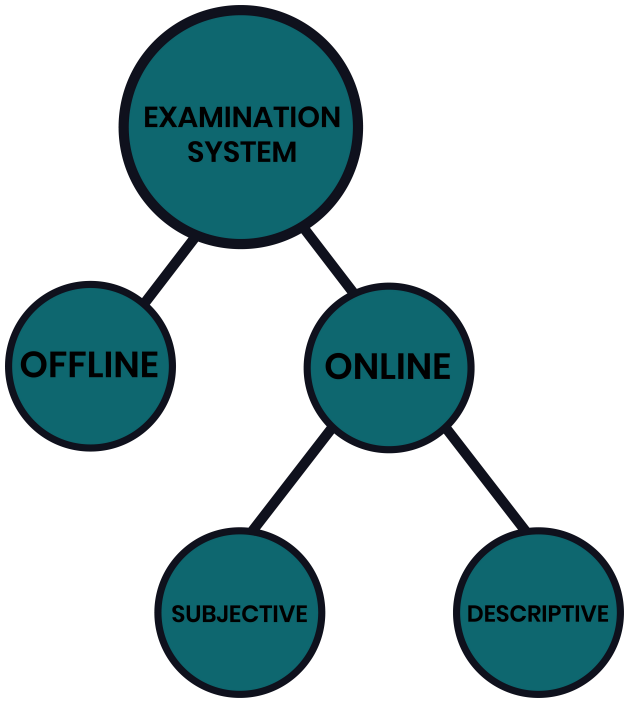

Fig. 1. Types of an examination system

For example when a product is stored in the database of the online shopping website, what happens is that additional keywords are stored for them such that they can be searched using those keywords. The string input by the customer in the search bar contains keywords using which products are searched and displayed on the customer dashboard. Even the back-end for such applications contains quality search algorithms that are out of the scope of this paper's discussion which is on the model of the descriptive online examination system. Similarly, the scenario is quite the same here for evaluating answers for questions that are descriptive in nature. Keywords are stored for every question and on the basis their occurrence in the answer string, the examinee is allotted marks. In order to perform this in Python language, there exists a library that makes it a little easier for the algorithm developers to perform string manipulations. The name of the library used is NLTK which is specifically designed for python to work on NLP. It is discussed in detail in the section where the algorithm is discussed.

In the below section as we can see is critical analysis in the field of Natural Language Processing and online examinations system. Its speaks about the works in the same field by other researchers and what they have done in order to develop such a system. The section below covers all the fields in order to develop and derive such a system out of the demerits of the other systems that are currently in use.

II. State Of The Art

The main aim of such a system is so that human effort can be reduced by introducing proficient computing technologies. Below, there is a discussion by some critical study on the existing technologies and algorithms for Natural Language Processing and examination systems that are already in use. It is by the help of these research papers that we could construct such an algorithm for conducting online descriptive examinations system.

Jayakodi et al.[1] had proposed a concept in the year 2015 to assign weights to questions for a test or basically their end semester question papers. There are multiple educational taxonomies that can be used to assess and assign weights to questions. So they use a taxonomy learning to function the above weight assignment. Here also they are using NLTK which is a library for working with Natural Language Processing along with the Wordnet package using Bloom's taxonomy.

In the year 2010 Ishikawa et al.[2], conceptualized a paper using Natural Language Processing. The idea was to detect users having multiple accounts over a community site. They had to solve this and hence they did some experimental analysis over the messages passed over Yahoo. The users who have multiple user accounts discourage other users in retrieving quality records and hence the credibility of the community site gets decreased.

Kaur et al.[3] in the year 2017 presented and introduced a paper keyword extraction from text. It uses the concepts of data mining along with Natural Language Processing in order to extract keywords. The sub-concepts used to extract keywords from the text include text mining, web mining, graph mining, temporal data mining, sequence mining, spatial data mining, multimedia mining and distributed data mining.

In the year 2009, Futrelle et al.[4] proposed a paper on NLP-NG which a new NLP system for biomedical text analysis. In this system there exist three subsystems depending on which NLP-NG works. The three components include NG-CORE which is used for language processing, NG-DB which is used for the management of the database, and finally NG-SEE that is used for active visualization. Normalization is being used to generate schema which can be used to detect domain-specific text from the main script or the text. The basic advantage of this system is that it can detect domain-specific text from a large variety of text scripts as it uses a 300 million word BioMed Central corpus.

In the year 2017, Revathy et al.[5] introduced a paper for feature extraction from text using NLP. The basic disadvantage of having an LDA system or Latent Dirichlet Allocation process was that it had a very high time complexity. In order to decrease time complexity, they used NLP or Natural Language Processing in order to do the same. LDA uses a generative statistical model that uses an unobserved group of data to explain observations for which time complexity reduces. NLP is faster as compared to LDA because it uses techniques of pattern generation and then ranks documents according to the patterns generated. What exactly happens is that documents related to the existing documents are found and further a cluster of documents are formed. Then an advanced ranking technique is applied to generate an author community so that they can communicate between them.

Nei et al.[6] in the year 2013 gave an emerging concept of simulation training which could improve the response time and could enhance the safety of the system in the real time, which would help to recreate a smart examination system. Also, the interface module works with the communication module which is connected to other modules. The analysis of data can improve the operational steps which will restore those steps and provide a base for further reports.

In the year 2009, Zhang et al.[7] introduced a SQL based online exam system which could show objective questions as well as the SQL questions but this had larger limitations that apart from the SQL questions. There is no way of showing subjective questions and also that time constraints and security could be improved to a greater extent. The system primarily focused on the processing of query statements and process of DML statements which are then compiled and the basic functions of account management and test management could be implemented in the code.

Zhai et al.[8] focussed on the online system with keeping an eye on the security and improving the performance of the system, the system basically which included the addition of the question modules storing the answers in the database, the paper also compared the traditional access methods like the MAC (Mandatory Access Control), DAC and many more such access techniques. The paper is experimenting with the basic concepts and then showing the test results on the access methods, the basic question module interacts with the test module is less reliable.

Luo et al.[9] in the year 2009 differentiated between a normal test and sequenced test and the paper focuses on order and dependency. It goes a step ahead in showing that where the executor can give executing permission or can deny it, it can also set the examinee-set which will lead to the questions module preparation and the exam system is automated as when permission is given to the executor it can start evaluating the sequence test and will generate the result, it combines the traditional model to make an automated system but the lack of security and have no scope for subjective answers is a disadvantage in the system.

Yang et al.[10] in the year 2012 gave an examination system which had a lot of features including the paper generation, to a better mix-up of library system to keep the papers and then arrange them accordingly and another automatic exam generating system which was there for the generation for the exam, the system being good for a hybrid platform for exam system has a little scope for subjective questions, even adding the feature will lead to system being check by an examiner as opposite to the automated system works, though it has new features of difficulty coefficient and also analysis of the paper but this does not use the full potential of automated online exam system.

In the year 2013, Treenantharath et al.[11] also talked about the online examination system with the use of the thin client i.e less connection need in compare to the fat client where we need a centralized server in respect to controlling the online activity also the fat client server typically exist with the client server architecture which is quite heavy to load, using thin client will provide solution to the described problem but it has little to no scope for the descriptive answers to be taken into consideration and thus the scope is only limited to the online multiple choice questions.

As discussed by Atoum et al.[12], the approach taken by the authors was a bit different in this paper as it was supposed to be a monitored online examination system as opposite to the offline center where the invigilator will have a close eye on the examinee there was an online system created to handle that problem by using the webcam and the microphone which will search for any kind of the anomaly and according to that actions will be taken if any kind of malpractice is detected while this system is better but it has loopholes where the above condition will fail, also the system will only have the MCQ based examination which leave us with little to no way for the descriptive answers to be evaluated

III. Algorithm of Online Descriptive Answer Marking System

As discussed earlier it is seen that there exist two types of examination portal or systems that include an offline examination system and an online examination system. Further, the online examination system can be grouped into two examination systems wherein one subjective questions exist while in the other descriptive questions exist. Subjective questions are those in which there exists a question for which a set of multiple choice options are provided such that the examinee has to select one of them. But then it may also happen that there may be multiple answers to a question, then, in that case, multiple check-boxes can be selected. While in the case of the descriptive examination system, a question exists for which the examinee writes an answer that is stored as a string and further marks are assigned to the answer according to the quality and correctness of the answer. Basically, keywords are stored in for the particular question by the teacher who uploads the test and its questions on the portal. The answer's correctness is judged by matching the answer with the keywords i.e basically the words of the answer with the keywords. Further, a sparse matrix is formed and hence it shows the count of each and every keyword in the answer string. Then there occurs some mathematical operation on it so as to count the actual accurate marks for the answer written.

As Python is used in order to code out the algorithm, a module or as we say a library named NLTK is used. This is the library in python that helps out to perform Natural Language Processing. It makes it easier for the algorithm developer to work with NLP. It consists of a list of common words such as prepositions and articles like a, an and the which have no use in the final answer evaluation, so they are removed. These common words are known as "stop-words".

After they are been removed, the keyword existence in the answer is calculated using a sparse matrix. For keyword that exits as a word in the answer string, we put 1 in the cell and go to the next keyword. If the keyword is not present as a word in the list of words in the answer string, then 0 is placed in the cell. This way the sparse matrix is formed. Further with the keyword existence count in the string, marks to be allotted to the answer is calculated.

There are some terms that are important while working on NLP and they are stated below, consider two strings as "Red Pen" and "Blue Pen". Here the keywords that can be obtained are "Red", "Blue", and "Pen". So, the keyword vector can be calculated in the format (Red, Blue, Pen) as,

$$A = (1, 0, 1) \tag{1}$$

$$B = (0, 1, 1) \tag{2}$$

Using this information we can calculate the similarity index between two strings by applying Cosine Similarity on Vectors.

$$sim\ (A, B) = \cos\theta = A\ .\ B\ /\ ||\ A\ ||\ ||\ B\ || \tag{3}$$

The next term is Term Frequency which is nothing but frequency of a term 't' in a document 'd'.

$$TF(d,t) = \#\ of\ occurrence\ of\ term\ 't'\ in\ a\ document\ 'd' \tag{4}$$

where,

$$t = The\ term$$

$$d = The\ document$$

Another term to be introduced is Inverse Document Frequency which is nothing but the importance of the term in the corpus.

$$IDF(t) = \log\ (\ D\ /\ t) \tag{5}$$

where,

$$t = \#\ of\ documents\ with\ the\ term$$

$$D = \#\ of\ total\ documents$$

The final term to be introduced is TF-IDF. It gives the word count along with a notation of how important a word is in a document or a list of documents.

$$W_{x,y} = tf_{x,y}\ \log\ (\ N\ /\ df_x\ ) \tag{6}$$

where,

$$tf_{x,y} = frequency\ of\ term\ x\ in\ document\ y$$

$$df_x = \#\ of\ documents\ containing\ term\ x$$

$$N = \#\ of\ total\ documents$$

Without these terms, NLP is not no possible. Before working on NLP, one should know the meaning of these terms, what they are and how they can be used.

Below we discuss the algorithm used to work the descriptive answer marking system in detail. The merits and demerits of this system are also discussed in detail in the further sections. As we move on through the further sections, we can detect them.

Algorithm for Online Descriptive Answer Marking System

In the below algorithm, variables named KEYWORD and ANSWER are used to store the keywords from the database for the question and answer string input by examinee respectively. While variables NK is used to store number of keywords for the question with which answer string is to be checked, NY is the number of keyword columns for an answer string for which 1 is stored in the cell, MM is the maximum marks assigned to the question and MA is the marks assigned to the student for his answer. Below is the equation used to calculate the marks assigned to the student,

$$MA = (\ NY\ /\ NK\ )\ *\ MM \tag{7}$$

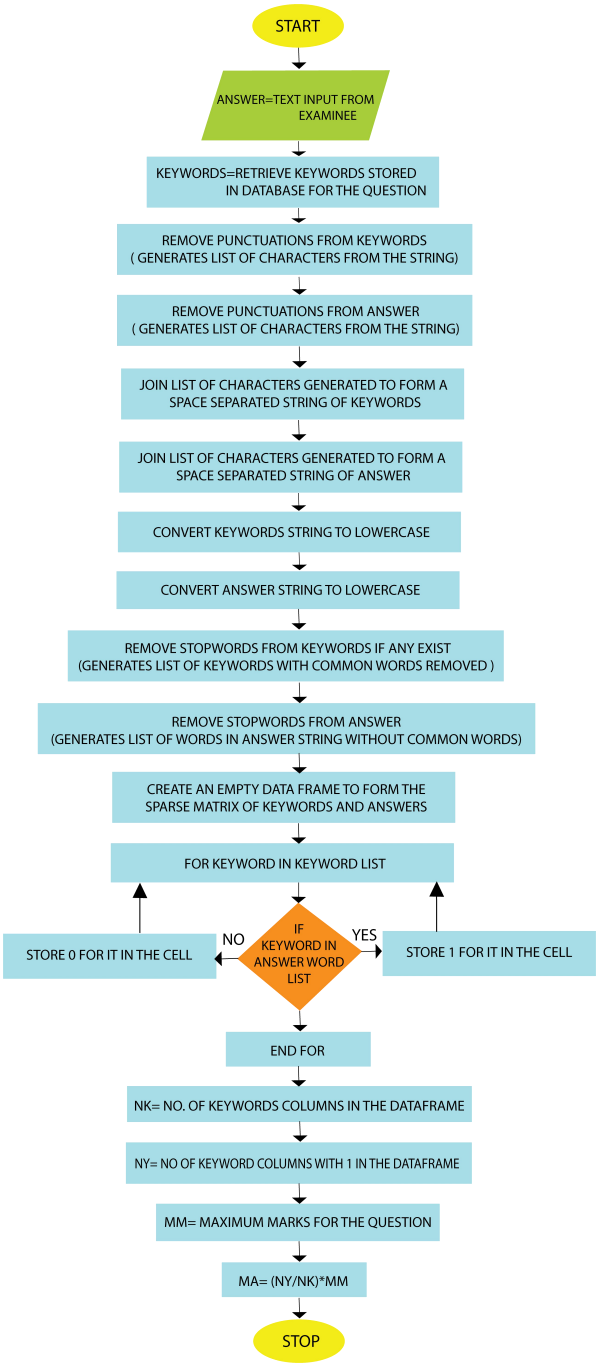

Fig. 3. Algorithm for Online Descriptive Answer Marking System

Now we would take an example of how the algorithm is working. Consider a question as "What is Data Preprocessing ?" for this question the keywords could be

KEYWORD = "data, preprocessing, mining, machine, learning, gathering, range, values, combinations, missing". Now consider the input answer to be ANSWER = "Data preprocessing is an important step in the data mining process. Data gathering methods are often loosely controlled, resulting in out of range values, impossible data combinations, missing values, etc.".

After applying all the string manipulations that include removing punctuation from KEYWORD and ANSWER, then converting the list of characters in KEYWORD and ANSWER into a string and then converting KEYWORD and ANSWER string into lowercase and then on removing stop-words or the common words from KEYWORD and ANSWER and finally after calculating keyword presence in ANSWER, it can be seen that the sparse matrix returned in the form of data-frame looks something like the figure below.

	Answer	data	preprocessing	mining	machine	learning	gathering	range	values	combinations	missing	Marks
0	Data preprocessing is an important step in the...	1	1	1	0	0	1	1	1	1	1	4.0

Fig. 2. Sparse Matrix formed on checking the presence of keywords in the answer string

Further, from here it can be seen that NY = 8, NK = 10, and let MM = 5 marks assigned to the question. Then, marks assigned would be MA = 4.0 using equation (7). Figure (2) shows the algorithm for Online Descriptive Answer Marking System.

IV. Results

The data that we received had the algorithm for online descriptive answer marking system applied to it. Below in figure (4) the sparse matrix for five students who answered the question " What is Data Pre-Processing? " can be seen.

	Name	What is Data Pre-processing?	Answer Words List	data	preprocessing	mining	machine	learning	gathering	range	values	combinations	missing	Marks
0	Lipika	Data pre-processing is gathering of raw materi...	[data, preprocessing, gathering, raw, material...	1.0	1.0	0.0	0.0	0.0	1.0	0.0	0.0	0.0	0.0	1.5
1	Adarsh	Manipulating your data in such way, that it fu...	[manipulating, data, way, fulfils, need, expec...	1.0	0.0	0.0	0.0	0.0	0.0	0.0	0.0	0.0	0.0	0.5
2	Bharat	Removing the irrelevant and redundant value al...	[removing, irrelevant, redundant, value, also,...	1.0	0.0	0.0	1.0	1.0	0.0	0.0	0.0	0.0	1.0	2.0
3	Kashyap	Data Pre-processing is preparing the data acco...	[data, preprocessing, preparing, data, accordi...	1.0	1.0	0.0	0.0	0.0	0.0	0.0	0.0	0.0	0.0	1.0
4	Krishnanshu	Transforming data into a usable format by remo...	[transforming, data, usable, format, removing,...	1.0	0.0	0.0	0.0	0.0	0.0	0.0	0.0	0.0	0.0	0.5

Fig. 4. Applied algorithm of the online descriptive answer marking system on answer generated by five students

In the above figure, it can be clearly seen that there are five rows with students naming Lipika, Adarsh, Bharat, Kashyap and Krishnanshu. Further, there are 14 columns among which the first column contains the Name of the student, answer to the question " What is Data Pre-Processing? ", Answer Word List which contains the keywords generated from the answer generated by the students and then come to the columns which are mandatory keywords that need to exist in the answer and the last column is Marks that consists of the marks obtained by the student.

It can be clearly seen from the algorithm in figure (3) that how the marks are being calculated from the keyword existence in the answer.

Here we have a small data for explaining the instance, while in practical situations when the number of students is huge i.e approximately in the range of 500-1000 or above than that, then quality analytics can be applied to know about the trend of the marks by plotting out some graphs by Python's visualization libraries that include Matplotlib and Seaborn. Below is a histogram showing the frequency of the marks obtained by the number of students.

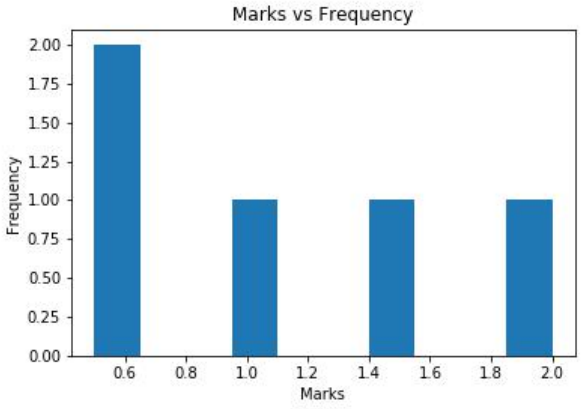

Fig. 5. Histogram for determining frequency of students marks

In the histogram, it can be clearly seen that two students have got the same marks who are Adarsh and Krishnanshu which is 0.5 marks. Further Lipika has got 1.5 marks as three of the keywords match with the answer string input by her. Similarly marks obtained by Bharat is 2.0 and by Kashyap is 1.5. Such histograms are beneficial to know the trend in the marks obtained by students.

V. Conclusion

It can be seen by conducting tests using such an algorithm at regular intervals that one can determine the trend in the marks obtained by different students and we can give them an analyzed report on the different subjects they need to focus on for which they are weak. With the existing data, we can also implement a predictive machine learning model on the data so that it can predict marks that the students will score in the future. It is observed that students mainly study those subjects that are placement oriented or which are required for placement purpose only. While students neglect the subjects of their core domain. Deep knowledge in the domain is required as it is of no use to study if you do not have a core domain knowledge. So it can help students get quality knowledge as everything will be digital and there will be no cumbersome process of conducting a pen-paper test. Also, answers are evaluated at that moment itself and the student can see the solutions and can correct the mistakes or errors committed while appearing for the exam.

The algorithm is also efficient as the faculty conducting the test can himself set the question along with the desired keywords he is expecting in one's answer. With this, there is a generalized model using which such answer marking systems can be developed and all the tests can be conducted over an easy to use dashboard oriented user login portal.

Also, talking about the future works on it, it can be tracked using the system that which student has cheated from any other student. This will again use the concepts of Machine Learning and Data Science to work upon these.

References

[1] K. Jayakodi, M. Bhandara and I. Perera “An automatic classifier for exam questions in Engineering: A process for Bloom's taxonomy”, IEEE International Conference on Teaching, Assessment, and Learning for Engineering (TALE), (2015)

[2] N. Ishikawa, K. Umemoto, Y. Watanabe, Y. Okada, R. Nishimura and M. Murata “Detection of users suspected of using multiple user accounts and manipulating evaluations in a community site”, IEEE Proceedings of the 6th International Conference on Natural Language Processing and Knowledge Engineering, (2010)

[3] B. Kaur, and S. Jain “Keyword extraction using machine learning approaches”, IEEE 3rd International Conference on Advances in Computing,Communication & Automation (ICACCA) (Fall), (2017)

[4] R. P. Futrelle, J. Satterley, and T. McCormack “NLP-NG — A new NLP system for biomedical text analysis”, IEEE International Conference on Bioinformatics and Biomedicine Workshop, (2009)

[5] M. Revathy, and M. L. Madhavu ”Efficient author community generation on Nlp based relevance feature detection”, IEEE International Conference on Circuit ,Power and Computing Technologies (ICCPCT), (2017)

[6] W. Nei, Y. Wu, D. Hu, L. Wang, and Y. Li ”Data Management and Analysis of Intelligent Examination Scoring System of Simulation Training System”, IEEE 5th International Conference on Intelligent Human-Machine Systems and Cybernetics, (2013)

[7] G. Zhang, and H. Ke ”Design of Paperless Examination System for Principles of Database Systems”, IEEE International Conference on Research Challenges in Computer Science, (2009)

[8] L. Zhai, and T. Gong ”The research of examination management system based on network flat”, IEEE 2nd International Conference on Artificial Intelligence, Management Science and Electronic Commerce (AIMSEC), (2011)

[9] S. Luo, J. Hu and Z. Chen ”Task Based Automatic Examination System for Sequenced Test”, IEEE International Conference on Electronic Computer Technology, (2009)

[10] N. Yang, X. Chenguang G. Weiwei and M. Xianmin ”The design of exam system on the basis of .net technology”, IEEE Symposium on Robotics and Applications (ISRA), (2012)

[11] T. Treenantharath and P. Sutheebanjard “Secure Online Exams on Thin Client” , IEEE 11th International Conference on ICT and Knowledge Engineering, (2013)

[12] Y. Atoum, L. Chen, A. X. Liu, S. D. H. Hsu, and X. Liu “Automated Online Exam Proctoring” , IEEE Transactions on Multimedia, (2017)

Proceedings of the Fourth International Conference on Communication and Electronics Systems (ICCES 2019)
IEEE Conference Record # 45898; IEEE Xplore ISBN: 978-1-7281-1261-9

Performance Analysis of Hybrid Transformer-less PFC boost Converter

Prerna Saxena
Department of Electrical Engineering
Rajasthan Technical University, Kota
Rajasthan, India
prernasaxena2@gmail.com

Ashok Kumar Sharma
Department of Electrical Engineering
Rajasthan Technical University, Kota
Rajasthan, India
aksharma@rtu.ac.in

Lata Gidwani
Department of Electrical Engineering
Rajasthan Technical University, Kota
Rajasthan, India
lata_gidwani@rediffmail.com

Mohit Sharma
Department of Renewable Energy Technology
Rajasthan Technical University, Kota
Rajasthan, India
mohitsharma851995@gmail.com

Abstract— **Recently , power electronic devices are widely used in various applications; because of this the shape of input current is greatly affected. Generally, the boost PFC converter provides satisfactory operation for current shaping but for some high voltage application it is not appropriate. In this proposed work a hybrid transformer-less PFC boost converter is introduced. This converter will function in DCM i.e. discontinuous conduction mode to shape current waveform at the input and to obtain a high voltage at output without the need of operating at high duty ratio. The converter uses a minimum number of devices which will enhance the power density and minimizes the cost. Furthermore, power switches voltage stress is decreased leading to low power loss in power switches and therefore making the circuit more cost effective. Finally, simulated results confirm the theoretical analysis and the competence of the presented converter.**

Keywords – PFC converter, Hybrid Boost converter, DCM(Discontinuous conduction mode)

I. INTRODUCTION

With the advancement of technology the use of power electronic devices increased at a rapid rate. Laptops, computers, workstation and power station etc. need of ac- dc power supplies which in turn enhances the use of rectifiers i.e. AC-DC converters inside these power supplies. The problem with conventional rectifier is that being a non-linear device they draw a non-sinusoidal input current which will greatly affect the input current and distort its shape, this on the other hand leads to the deterioration of power factor. In order to accomplish the requirement of high efficiency, many power factor correction technologies have been implemented to shape the current waveform at input. Most of the power factor correction technologies have implemented boost PFC converters owing to its excellent current shaping ability and high performance in terms of efficiency and power factor [1]-[2]. However, the problem with the conventional boost PFC converter displayed Fig .1. is that it is not appropriate for high voltage gain applications required in various biomedical and industrial equipment[3]. Owing, to the limitations of semiconductor devices it is not advisable to use the boost PFC converter at high duty ratio however, to achieve high step up voltage gain the boost PFC converter operates at extremely high duty ratio which leads to deterioration of power factor and increased losses. Also, boost PFC suffers from the problems of low efficiency, high THD at low input voltage and switch voltage stress is relatively high which will lead to increased power loss.

A family of high voltage gain single phase hybrid PFC rectifier suitable for application that require rectification with unity power factor is introduced[4].In [5] a single stage non-isolated switched capacitor AC-DC converter for PFC is proposed that commutes sub harmonics. Unidirectional step up AC-DC converter topologies with voltage multiplier in their output is proposed in [6].In [7] a hybrid switched capacitor voltage double SEPIC power factor correction rectifier to increase the voltage gain is proposed. Other examples of SEPIC PFC converters for universal input applications given in [8],[9],[11].The voltage gain can be improved by using the DC-Dc multilevel boost converter[10],[12].

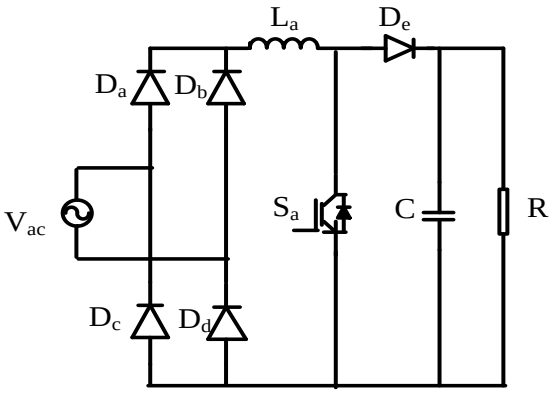

Fig .1. Conventional PFC boost rectifier

This paper presents a boost PFC converter based on hybrid transformer-less boost converter which utilizes a switching topology to replace the inductor of conventional boost converter [13]. This topology helps in reducing the number of switches of the switched inductor PFC boost converter [14] .The proposed converter displayed in Fig.2.has excellent input current shaping ability and reduces the harmonics present in the input current with the help of LC filter present at the input. This converter operates in DCM mode, thereby offering advantage of simple control techniques, soft turn on of switches and low diode reverse recovery loss. The converter uses a minimum number of devices which will enhance the power density and minimizes the cost. Furthermore, the voltage stress of the power switches is decreased so low voltage rating power switches can be used leading to low power loss and therefore making the circuit cost effective.

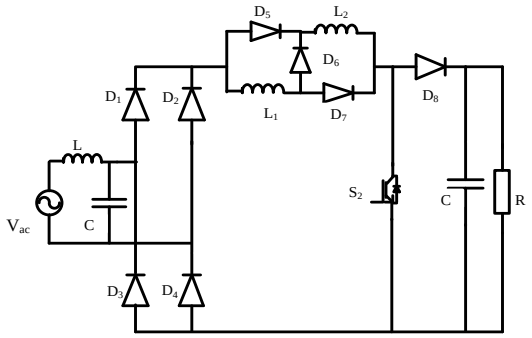

Fig.2. Proposed PFC converter

The section I of this paper includes the introduction of the proposed Hybrid Transformer-less PFC boost converter. The operating principles of the boost converter and its theoretical analysis are presented in section II and III. Finally the simulation result and conclusion is presented in section IV and V.

II. OPERATING PRINCIPLES OF BOOST PFC CONVERTER

The hybrid transformer-less boost PFC converter presented in this paper operates in DCM mode. For the simplification of mathematical calculation of the proposed topology certain assumptions are made as follows:

- Within single switching period the voltage at the input is taken as constant.
- The converter is considered as lossless thereby the power at the input and output can be assumed same.
- The load is taken as resistive.

The different key waveforms of the hybrid boost PFC converter during three distinct states of DCM mode are displayed in Fig.3.

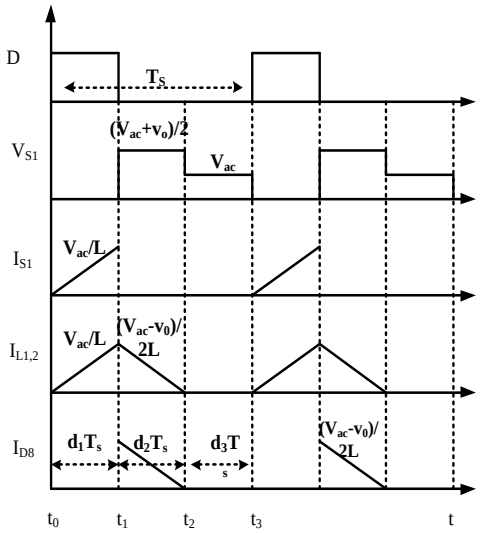

Fig.3. Boost PFC converter key waveforms in DCM mode

Operating in DCM mode, the boost PFC converter has three states during single switching period as represented in Fig.4.

State 1(Fig.4 (a)): During this state the power switch S_1 is turned on and the diode D_8 is off which will charge the two equivalent inductors L_1 and L_2 by the voltage at input which is AC in nature i.e. Vac through the path provided by the diodes D_5 and D_7 respectively. Simultaneously the power is supplied to the load by the bulk capacitor C at the output.

The equation for the current through the inductor and voltage at the output can be derived as:

$$V_{ac} = L_{eq}\frac{d(i_{l1}+i_{l2})}{dt} \quad (1)$$

$$\frac{dv_o}{dt} = \frac{-v_0}{RC} \quad (2)$$

State2(Fig.4 (b)) : During this mode switch S_1 is turned off and diode D_8 is off , the power is supplied to load and the output capacitor from the input AC voltage source following the path made by the inductor L_1, diode D_6 ,inductor L_2 and diode D_8. The inductor current is given by:

$$\frac{V_{ac}-v_o}{2} = L_{eq}\frac{di_{L1}}{dt} \quad (3)$$

State 3 (Fig.4(c)): In the last state the power is supplied to the load by the energy that is stored in the bulk capacitor.

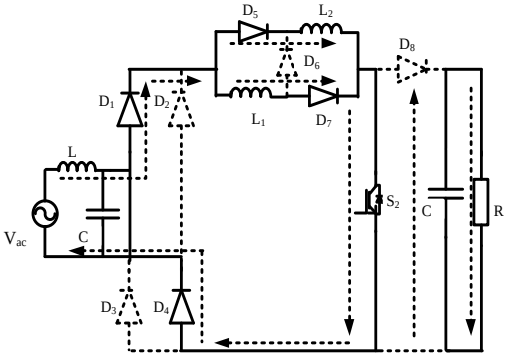

(a)

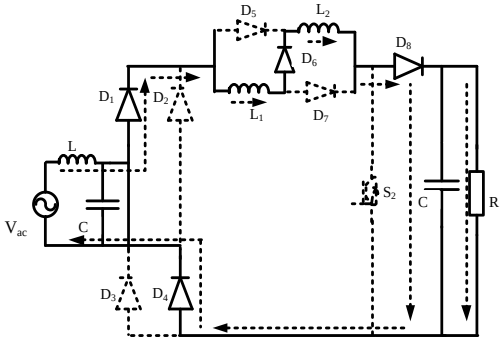

(b)

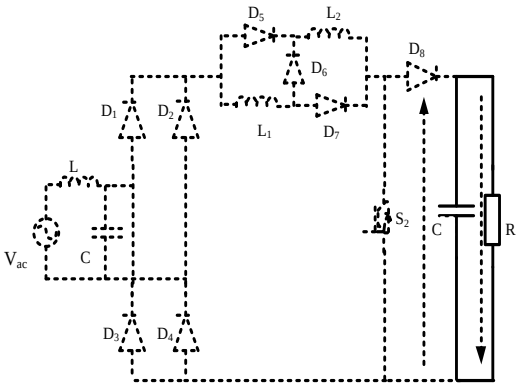

(c)

Fig.4. Different modes of boost PFC converter in DCM mode

III. THEORITICAL ANALYSIS

A. *Hybrid Boost Converter*

The hybrid boost converter is acquired when input inductor of a classical boost converter is replaced by the two inductor of the switching structure represented in Fig.5.

The different switching topologies of basic switching step up structure are represented in Fig.6. The two inductors represented as L_1 and L_2 charged in parallel during topology t_{on} and discharged in series during t_{off}.

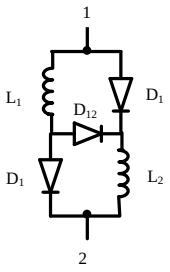

Fig.5. Basic step-up switching structure

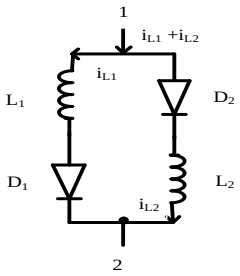

(a) t_{on}

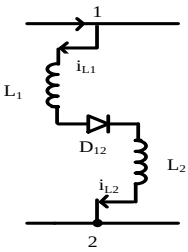

(b) t_{off}

Fig.6. Different switching topologies during t_{on} and t_{off}

B. *Voltage conversion ratio, M*

The voltage conversion ratio of the conventional boost converter is represented as:

$$M = \frac{v_o}{V_{in}} = \frac{1}{1-D} \qquad (4)$$

However, after application of voltage second balance for the inductors L1 and L2 of the hybrid boost converter the voltage conversion ratio can be derived as:

$$v_o = \frac{1+D}{1-D} V_{in} \quad (5)$$

$$M = \frac{v_o}{V_{in}} = \frac{1+D}{1-D} \quad (6)$$

Thus, the voltage conversion ratio is (1+D) times greater than the conventional boost converter.

C. Control technique

The power factor correction converter presented in this paper has excellent input current shaping ability while operating in DCM mode. The control technique for this converter as described in Fig5. Comprises of a simple voltage loop which control the voltage at the output by comparing it with desired reference voltage and the difference between them is overcome with the help of PI controller to acquire the required output voltage.

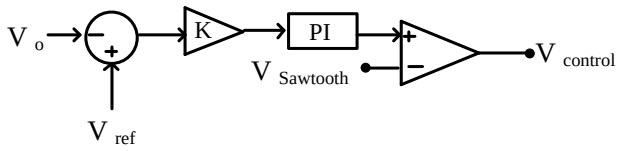

Fig.7. PI Controller

D. Power factor of high gain PFC converters

The PFC converter presented here operates at nearly unity power factor. The power factor can be evaluated by calculating the cosine of the phase difference between the current at the input and voltage at the output.

IV. Simulation and Validation of the PFC Converter

Here MATLAB simulation result is presented. The basic circuit parameters are :

- V_{ac} = 220 V_{rms}
- L_1 & L_2 = 0.4mH
- C = 470 uF
- Switching frequency ,f_s = 20KHz

Fig.8 shows the switching waveform of the switch used in the PFC converters. This switching waveform help to control the on and off timings of the converter. Here, it is noted that the switch duty cycle is very small and therefore, the voltage stress of the switch is minimized.

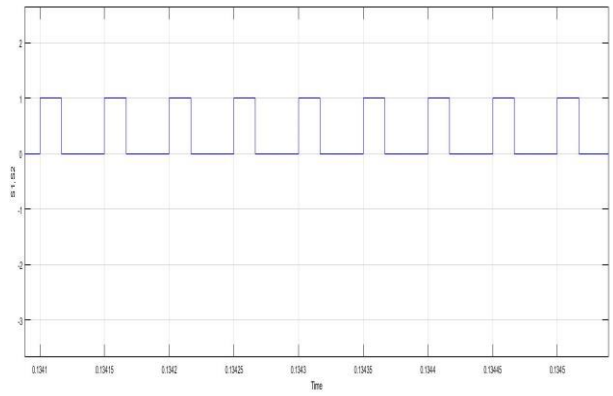

Fig 8. Switching Waveform

Fig.9. Represents the waveforms of voltage and current at the input at V_{rms} = 220V.The figure depicts that the input current waveform approximates to sinusoidal shape showing that the non-linearity and harmonics are reduced. Also, it can be depicted that the waveforms of the voltage and current at the input are approximately in phase showing that the power factor is nearly unity.

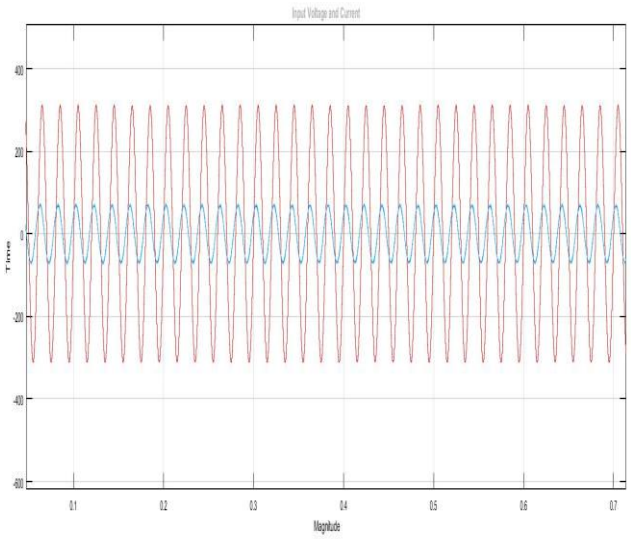

Fig 9. Waveforms of Voltage and Current at the input at V= 220 V_{rms}

The basic simulated key waveforms of the PFC converter presented in this paper are displayed in Fig 10. These waveforms are close to the theoretical waveform and thus prove the effectiveness of converter.

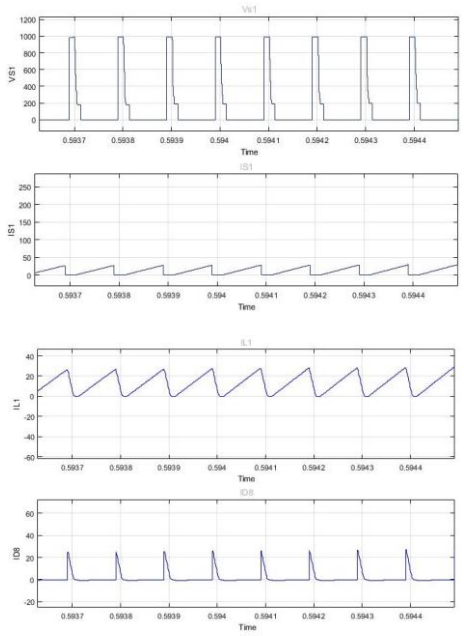

Fig 10. Simulated key waveforms

Fig.11. displays the THD analysis of input current waveform and it clearly depicts that the total harmonic distortion of the proposed converter has reduced to great extent in contrast to the traditional boost PFC converter.

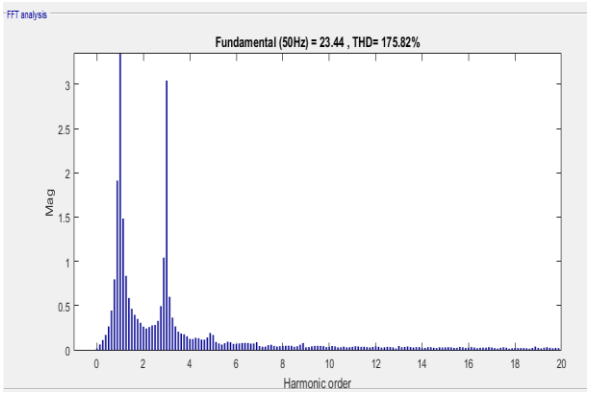

Fig.11 (a) THD analysis of current at input of conventional PFC converter

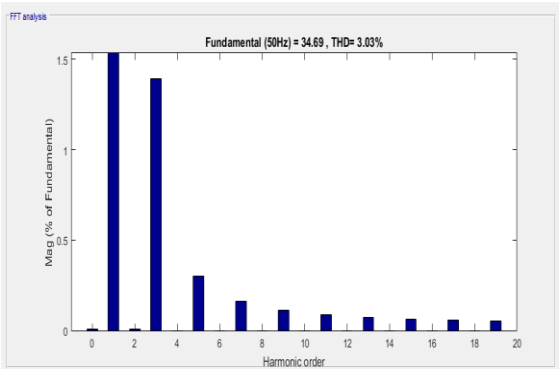

Fig .11 (b) . THD analysis of current at input of proposed PFC converter

Fig.12. represents the voltage at output of the converter which approximates to a constant value of 600 V.

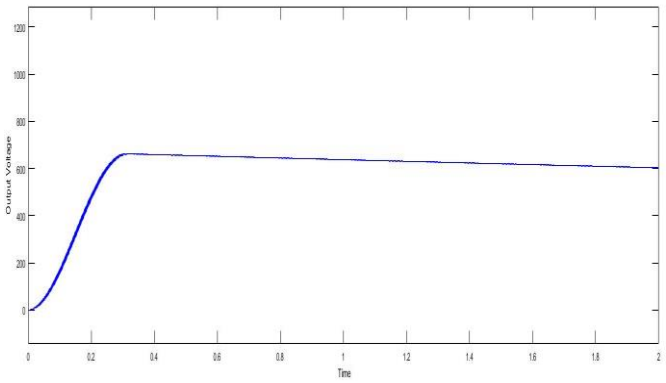

Fig .12. Output voltage

V. CONCLUSION

A hybrid transformer-less PFC boost converter based on the switching topology which replaces the inductor of the standard boost - converter thereby reducing the switching devices is proposed. The converter has input current waveform which follows sine wave i.e. it has excellent current shaping ability .Also, waveforms of voltage and current are approximately in phase i.e. power factor is close to unity. It operates in DCM mode and uses minimal number of devices which has less voltage stresses making the converter cost effective for practical application. The future scope of the proposed converter is it can be analyzed by use of other controller like fuzzy controller in place of PI controller and also it can be analyzed for different load applications.

REFERENCES

[1] Salmon, J. C. (1992). TOPOLOGIES FOR SINGLE-PHASE VOLTAGE-DOUBLER BOOST RECTIFIERS John C. Salmon, 549–556.

[2] Huber, L., Jang, Y., & Jovanović, M. M. (2008). Performance evaluation of bridgeless PFC boost rectifiers. *IEEE Transactions on Power Electronics*,*23*(3),1381–1390. https://doi.org/10.1109/TPEL.2008.921107

[3] Bellar, M. D., Watanabe, E. H., & Mesquita, A. C. (1992). Analysis of the Dynamic and Steady-state Performance of Cockcroft-Walton Cascade Rectifiers. *IEEE Transactions on Power Electronics*, *7*(3), 526–534. https://doi.org/10.1109/63.145140

[4] Rectifiers, S. P. F. C., Cortez, D. F., & Barbi, I. (2015). A Family of High-Voltage Gain Single-Phase Hybrid, *30*(8), 4189–4198.

[5] Kishore, G. I., & Tripathi, R. K. (2018). Single-Phase PFC Converter Using Switched Capacitor for High Voltage DC Applications. *IEEE Transactions on Industry Applications*,*54*(3), 2560–2567. https://doi.org/10.1109/TIA.2018.2807786

[6] Dias, J. C., & Lazzarin, T. B. (2018). A Family of Voltage-Multiplier Unidirectional Single-Phase Hybrid Boost PFC Rectifiers. *IEEE Transactions on Industrial Electronics*, *65*(1), 232–241. https://doi.org/10.1109/TIE.2017.2721919

[7] Costa, P. J. S., Font, C. H. I., & Lazzarin, T. B. (2018). Single-Phase Hybrid Switched-Capacitor Voltage-Doubler SEPIC PFC Rectifiers. *IEEE Transactions on Power Electronics*, *33*(6), 5118–5130. https://doi.org/10.1109/TPEL.2017.2737534

[8] De Melo, P. F., Gules, R., Romaneli, E. F. R., & Annunziato, R. C. (2010). A modified SEPIC converter for high-power-factor rectifier and universal input voltage applications. *IEEE Transactions on Power Electronics*,*25*(2),310–321.

https://doi.org/10.1109/TPEL.2009.2027323

[9] Gabri, A. M. Al, Fardoun, A. A., & Ismail, E. H. (2015). Bridgeless PFC-Modified SEPIC Rectifier With Extended Gain for Universal Input Voltage Applications. *IEEE Transactions on Power Electronics*, *30*(8), 4272–4282. https://doi.org/10.1109/TPEL.2014.2351806

[10] Rosas-Caro, J. C., Ramirez, J. M., Peng, F. Z., & Valderrabano, A. (2009). A DC–DC multilevel boost converter. *IET Power Electronics*, *3*(1), 129. https://doi.org/10.1049/iet-pel.2008.0253

[11] Gules, R., Dos Santos, W. M., Dos Reis, F. A., Romaneli, E. F. R., & Badin, A. A. (2014). A modified SEPIC converter with high static gain for renewable applications. *IEEE Transactions on Power Electronics*, *29*(11), 5860–5871. https://doi.org/10.1109/TPEL.2013.2296053

[12] Yang, L. S., Liang, T. J., & Chen, J. F. (2009). Transformerless DC-DC converters with high step-up voltage gain. *IEEE Transactions on IndustrialElectronics*,*56*(8),3144–3152. https://doi.org/10.1109/TIE.2009.2022512

[13] Axelrod, B., Berkovich, Y., & Ioinovici, A. (2008). Structures for Getting Transformerless Hybrid DC – DC PWM Converters. *IEEE Transactions on Circuits and Systems-I:Regular Papers*, *55*(2), 687–696. https://doi.org/10.1109/TCSI.2008.916403

[14] Lin, X., & Wang, F. (2018). High step-up voltage gain AC-DC rectifier based on transformerless switched-inductor converter for power factor correction.

Proceedings of the Fourth International Conference on Communication and Electronics Systems (ICCES 2019)
IEEE Conference Record # 45898; IEEE Xplore ISBN: 978-1-7281-1261-9

Tree based node verification key management scheme for wireless sensor networks

B Srinivas
SCIS
University of Hyderabad
Hyderabad, India.
b.srinivas@uohyd.ac.in

N Rukma Rekha
SCIS
University of Hyderabad
Hyderabad, India.
rukmarekha@uohyd.ac.in

Subbarao Y.V
SCIS
University of Hyderabad
Hyderabad, India.
yvsrcs@uohyd.ac.in

***Abstract*—** Sensor nodes are geographically placed randomly in the environment. Sensor nodes are limited in capacities like computation power, memory, and processing speed. They collect sensitive information and send to the central base station. A novel TNVS is proposed that identifies certain nodes as authenticator nodes that have relatively high capability in storage, computation and power compared to the regular sensor nodes. These nodes are used for verifying new nodes that are being added into the network, thereby eliminating the entry of malicious nodes into the network. The master key that is shared by all the nodes of the network is renewed periodically to avoid node capture attack. Simulation and results show that in addition to providing authentication TNVS also requires less number of keys when compared to the existing key management schemes there by reducing the burden on memory requirement of the network.

Keywords— ***Authentication, node verification, Key exchange, Key Management, ECDSA, ECDH, Wireless Sensor Networks.***

I. INTRODUCTION

Sensor networks have many applications such as smart home security, military, environment monitoring, healthcare [5]. A wireless sensor network (WSN) consists of sensor nodes that are randomly distributed. Sensor nodes have less battery power, computation power, and storage [8]. They collect the monitor data and communicate with other sensor nodes or base station in the communication range. The proposed approach uses heterogeneous sensor networks (HSNs) that have different capabilities in terms of storage, computation, energy, and communication [9]. Security is a major issue in wireless sensor networks when deployed in an adverse environment. Many key management schemes for WSN were proposed on the security requirements of these environments [7].

It is important to ensure that any new node that enters into a network is properly verified. There is a high chance that it may turn out to be a malicious node if not properly verified. Hence authentication plays a very important role in security of WSN's. Digital signatures are the very best way to authenticate any given node. However, because of the resource constraint environment of WSN's few algorithms like ECDSA [16] are suitable for sensor nodes. The sensor nodes can use an ECDSA algorithm to generate a digital signature for authentication. Tree based node verification key management scheme (TNVS) proposed in this paper will use an ECDSA to authenticate the sensor nodes within the network effectively. The rest of the paper is organized as follows. Section II explains the related work. Section III briefs upon the existing tree-based protocol [12] for key management scheme in wireless sensor networks. Section IV presents the proposed TNVS approach. Section V interprets the results and Section VI is the conclusion of this paper.

II. RELATED WORK

Key management is about generating the keys and updating them in wireless sensor networks. Pre-deployed key management scheme is one of the key management schemes in WSNs [2] where, some keys are stored in the sensor nodes before deploying in the environment. In Adrian Perriz et al. proposed SPINS [1] a pre-deployed key management scheme, which is a master key based key management scheme. It stores the single key in all the nodes. If one node is compromised there is a chance to compromise all the other nodes. It provides good scalability for adding nodes in network but in-efficient security if one node is compromised. Liu et al. proposed a pair-wise key management scheme [3], in this scheme every sensor node stores all pair wise keys with neighbor nodes. It occupies a lot of memory for keys storage but it provides strong security. Sencun Zhu et al. proposed LEAP [14], that establishes four kinds of keys and provides strong security and scalability but requires a huge amount of communication for key establishment and update. Eschenauer & Gligor proposed probabilistic key pre-distribution scheme [10] that is based on the probability of neighbor nodes having common keys. Every node stores only some neighbor nodes pair wise keys from the key pool where some nodes have common keys in their neighbor nodes. Neighbor node selection is based on a chosen probability of common keys. It reduces the energy and storage but if one node is compromised then the probability of the connected nodes being compromised is 0.3. Du et al. proposed a key management scheme using deployment knowledge [4], it uses probabilistic key pre-deployment with the blom's key management scheme to establish the pair wise keys in sensor nodes. It provides node to node authentication but requires a lot of energy for computation. Chan et al. proposed q composite scheme [6], in this scheme any two sensor nodes stores q number of common keys for communication, if one key compromises, they use other keys. It provides strong security but needs a lot of memory and probability of key sharing decreases because pair of nodes has to share q common keys instead of one. Messai M-L et al. proposed a tree-based protocol for key management scheme [12], where every node is pre-

deployed with three keys. One key is the master key stored in all sensor nodes. Other two keys are used for communication between sensor node to base station and vice versa.Also, parent and child nodes compute their pair wise keys for their communication. It is resilient against node capture attack and is energy efficient and also has good scalability but requires storing more number of keys. In a tree-based scheme, new nodes are not verified before adding into the network. If not verfied, it may work as a malicious node in the network and then other nodes may also compromise. So, before adding new nodes into the network, it has to verify its authenticity. In the proposed TNVS approach some sensor nodes are taken as high capable nodes, which are called as authenticator nodes. These authenticator nodes verify the new nodes before adding into the network.

III. TREE-BASED PROTOCOL FOR KEY MANAGEMENT IN WIRELESS SENSOR NETWORKS [12]

Tree-based protocol scheme works as follows.

In tree-based protocol, the base station initiates the tree construction. The base station acts as a root node at level 0 and monitors all the sensor nodes in the network. The base station broadcasts the hello message then sensor nodes that are there in the communication range receive the hello message and respond back. All such sensor nodes are added as children to base station at level 1. Then level 1 nodes broadcast the hello message to next level nodes, and nodes that are there in communication range respond back to received hello message. These nodes will be added in level 2 and so on until the tree formation is completed. Both parent and child calculates their pair wise key and communicates using this key. Nodes send hello messages using the symmetric master key that is there in all the nodes prior deployment.

This tree-based protocol is proposed as a solution for secure node-to-node and node-to-base station communications. Tree based protocol is resistant to node capture attack. Each sensor node's identifier, its level and its parent identifier is calculated to authenticate the sender and the receiver. Hence, a sensor node cannot play a role of other nodes. So, Sybil node creation is not allowed in the network. Hello flood attack is also not allowed in the network until the master key is not known to an attacker.

However, whenever new nodes are added in the network, it has to be verified otherwise it may work as a malicious node in the network leading other nodes to compromise. In tree-based protocol new node verification is not available.

New node verification is implemented in the proposed TNVS approach. Verification is done by some nodes called as authenticator nodes. That has more capability in terms of power, memory, and computation. These authenticator nodes use ECDSA algorithm to verify new nodes.

IV. TREE BASED NODE VERIFICATION KEY MANAGEMENT SCHEME

A novel approach named TNVS is proposed to verify new nodes before adding into the network. The proposed approach is explained in three phases.

1. Key generation.
2. Tree construction.
3. Key renewal.

The following assumptions and notations are used in the proposed approach.

Assumptions

- A root node is a base station that initiates the key management process.
- Authenticator nodes have more capability than the sensor nodes in terms of storage, computation, and power.
- Only authenticator nodes can add the sensor nodes as children.
- In tree organization, internal nodes are authenticator nodes and leaf nodes are called sensor nodes.

Notations:

BS : Base Station id.
BS^{pr} : Base Station private key.
BS^{Pu} : Base Station public key.
$BS_{sign}{}^{Pr}$: Base Station digital signature using its private key.
AN_i : Authenticator node id i.
AN^{Pr} : Authenticator node private key.
AN^{Pu} : Authenticator node public key.
$AN_{i\text{-}sign}{}^{Pr}$: Authenticator node i's digital signature using its private key.
S^{Pr} : Sensor node private key.
S^{Pu} : Sensor node public key.
$S_{sign}{}^{Pr}$: Sensor node digital signature using its private key.
S_n : New sensor node
$S_n{}^{Pr}$: New sensor node private key.
$S_n{}^{Pu}$: New sensor node public key
$S_{n\text{-}Sign}{}^{Pr}$: New Sensor node digital signature using its private key.
K_M : Symmetric master key stored in all sensor nodes.
r_{AN_i} : A random number of AN_i node.
r_{S_n} : A random number of S_n sensor node.
n : n is the total number of nodes in the network.
A : A is the total number of authenticator nodes.

A. Key Generation :

Let $p > 3$ is a prime. The elliptic curve $y^2 = x^3 + ax + b$ over F_p, is the set of solutions $(x,y) \in F_p \times F_p$ to the congruence $y^2 = x^3 + ax + b \pmod p$ where $a,b \in F_p$ are constants such that $4a^3 + 27b^2 \neq 0 \pmod p$, together with a special point O called the point at infinity[13]. A sensor node private Key S^{Pr} is randomly selected from the F_p. B is a generator point on the curve. Sensor node public key $S^{Pu} = S^{Pr}.B$. [15]

B. Tree construction:

The base station is taken as a root node at level 0 and its parent is NULL. Nodes that are there in the communication range of level 0 are called level 1 nodes. In level 1 all nodes are taken as authenticator nodes. First, the base station

broadcast the hello message within the communication range. Authenticator nodes send hello message response to the base station. The base station connects the authenticator nodes as children in level 1.Authenticator nodes are identified by its ID. Level 1 authenticator nodes broadcast the hello message. In level 2, authenticator nodes and sensor nodes that are there in the communication range receive hello message and send hello message response to authenticator nodes of level 1. In this way, sensor nodes and authenticator nodes will form a tree structure until n numbers of sensor nodes in the network are completed.

Sensor nodes in each level collect the monitoring information and send it to their parent. The authenticator nodes collect the same data from the various sensors nodes and send it to the base station. However, the base station communicates with all sensor nodes in the network when key renewal is being performed to avoid communication overhead.

Base Station Node broadcast a Hello Message as follows.

$BS \rightarrow * :$
$\{HELLO\text{-}MSG, BS^{Pu}, BS, 0, NULL, BS_{Sign}^{Pr}(BS, 0, NULL)\}K_M$

Authenticator Nodes decrypt the hello message received from the base station with a symmetric master key and verify the hello message. After verifying, authenticator nodes send hello message response to the base station as follows.

$AN_i \rightarrow BS :$
$\{HELLO\text{-}RESP, AN_i^{Pu} AN_i, 1, BS, AN_{i\text{-}Sign}^{Pr}(AN_i, 1, BS)\}K_M$

BS decrypt the hello message response received from authenticator nodes with a symmetric master key and verifies the hello message response.BS adds authenticator nodes as children at level 1 after verifying hello response.

New node verification:

The next level of nodes broadcast JOIN message in communication range as follows.

$$S_n \rightarrow * :\{ JOIN, S_n, r_{S_n}, S_n^{Pu}, S_{n\text{-}Sign}^{Pr}(S_n, r_{S_n})\}K_M$$

Authenticator Nodes decrypt the JOIN message received from the new sensor nodes with a symmetric master key and verify the hello message. The authenticator nodes verify JOIN message with S_n Signature. After verifying, authenticator nodes send response to the new sensor nodes with received random number and sensor node id as follows.

$$AN_i \rightarrow S_n : \{ r_{AN_i}, AN_i, AN^{Pu}, AN_{i\text{-}Sign}^{Pr}(r_{S_n}, S_n) \}K_M .$$

New sensor nodes decrypt the received message from the authenticator node with a symmetric master key and verify the message. Sensor nodes verify the message with $AN_{i\text{-}Sign}$ signature. After verifying, sensor nodes send a response to the authenticator node with received random number and authenticator node id as follows.

$$S_n \rightarrow AN_i : \{ S_{n\text{-}Sign}^{Pr}(r_{AN_i}, AN_i) \}K_M .$$

Authenticator Nodes decrypt the message received from the new sensor node with a symmetric master key and verify the message. The authenticator nodes verify the message with S_n signature. After verifying, authenticator nodes send a response to the new sensor node with JOIN acknowledgement message as follows.

$AN_i \rightarrow S_n :$
$\{Join\text{-}Ack, AN_i, Level_i, AN_j, AN_{i\text{-}Sign}^{Pr}(AN_i, Level_i, AN_j)\}K_M$

New sensor node decrypts the received message from the authenticator node with a symmetric master key and verifies the message. The sensor nodes verify the message with $AN_{i\text{-}Sign}$ Signature. After verifying, sensor nodes are added to the authenticator nodes

C. Key renewals

It will be necessary to renew the encryption keys because using the same encryption key for extended periods may incur a cryptanalytic risk In order to accomplish the renewal of the sensor keys, the base stations generate the new master key and send the new master key to the authenticator nodes. The master key that is shared by all the nodes of the network is renewed periodically to avoid node capture attack. Authenticator nodes then send the new master key to sensor nodes. This phase first involves calculating a pair wise key between base station and authenticator nodes. Later new master key is shared to authenticator nodes from base station.

Pair wise key calculation between base station and authenticator nodes using ECDH is tabulated as follows:

A base station and Authenticator node shares their public keys.

TABLE I. PAIR WISE KEY CALCULATION BETWEEN BS AND AN_I

BS	**AN_i**
AN_i public key = AN^{Pu}	BS public key = BS^{Pu}
BS Private Key = BS^{Pr}	AN_i Private Key = AN^{Pr}
Public Base Point = B	Public Base Point = B
BS Public key(BS^{Pu}) = BS^{Pr}.B	AN_i Public Key(AN^{Pu}) = AN^{Pr}.B
Pair wise Key ($K_{BS\text{-}AN_i}$) = BS^{Pr}. AN^{Pu} = BS^{Pr}.AN^{Pr}. B $K_{BS\text{-}AN_i}$ = BS^{Pr}.AN^{Pr}. B	Pair wise Key ($K_{AN_i\text{-}BS}$) = AN^{Pr}. BS^{Pu} = AN^{Pr}. BS^{Pr} .B = BS^{Pr}.AN^{Pr}. B $K_{AN_i\text{-}BS}$ = BS^{Pr}.AN^{Pr}. B

After calculating a pair wise key between base station and authenticator node, base station now updates new master key K'_M is updated as follows:

$$K'_{M=} \text{ New-}K_M$$

The base station sends new master key in an update message to authenticator nodes using their pair wise key as below.

$BS \rightarrow AN_i :$
$\{Update, BS, K'_M, NULL, BS_{sign}^{Pr}(BS, K'_M, NULL)\} K_{BS\text{-}An_i}$

Pair wise Key calculation between Authenticator nodes and sensor nodes using ECDH is tabulated as below:

TABLE II. PAIR WISE KEY CALCULATION BETWEEN AN_I AND S_I

AN_i	S_i
S_i public key = S_i^{Pu}	AN_i public key = AN_i^{Pu}
AN_i Private Key = AN_i^{Pr}	S_i Private Key = S_i^{Pr}
Public Base Point = B	Public Base Point = B
AN_i Public key(AN_i^{Pu}) = AN_i^{Pr}.B	S_i Public Key(S_i^{Pu}) = S_i^{Pr}.B
Pair wise Key($K_{AN_i\text{-}S_i}$) = $AN_i^{Pr}.S_i^{Pu}$ = $AN_i^{Pr}.S_i^{Pr}.B$ $K_{AN_i\text{-}S_i}$ = $AN_i^{Pr}.S_i^{Pr}.B$	Pair wise Key($K_{S_i\text{-}AN_i}$) = $S_i^{Pr}.AN_i^{Pu}$ = $S_i^{Pr}.AN_i^{Pr}.B$ = $AN_i^{Pr}.S_i^{Pr}.B$ $K_{S_i\text{-}AN_i}$ = $AN_i^{Pr}.S_i^{Pr}.B$

Authenticator nodes decrypt the update message with pair wise key and verify the update message. After verification, it updates its master key and deletes the old master key. Authenticator nodes then send an updated master key to sensor nodes, after calculating pair wise key between authenticator nodes and sensor nodes.

Authenticator nodes sends new master key in updated message to sensor nodes using their pair wise keys as below:
If parent is BS:

$AN_i \rightarrow S_i$:
$\{Update, AN_i, K'_M, BS, AN_{i\text{-}sign}^{Pr}(AN_i, K'_M, BS)\}K_{AN_i\text{-}S_i}$

If parent is Authenticator node:

$AN_j \rightarrow S_i$:
$\{Update, AN_j, K'_M, AN_i, AN_{j\text{-}sign}^{Pr}(AN_j, K'_M, AN_i)\}K_{AN_j\text{-}S_i}$

Sensor nodes decrypt the message with pair wise key and verify the message. After verification, it updates the master key.

V. SIMULATION AND RESULTS

TNVS is simulated and analyzed in NS2.The NS2 simulation environment set up parameters are as follows.

A. Simulation Environment Setup :

TABLE III. *SIMULATION PARAMETERS*

Parameters	Values
Number of nodes	1020
Area size (m^2)	1200 × 1200
Simulation duration (sec)	300
Agent	UDP
Mobility speed (mb/s)	AN = 10,SN =2
Radio range (m)	AN = 250,SN = 100
Number of AN	25 percent of nodes

In simulation run the experiments for 21 nodes to 69 nodes.

B. Sensor nodes Tree Formation :

Base Station adds the first level of authenticator nodes. Authenticator nodes then verify the sensor nodes and add in each level until tree formation is completed in the network. Tree organization for set of 37 nodes is simulated in the Fig. 1.

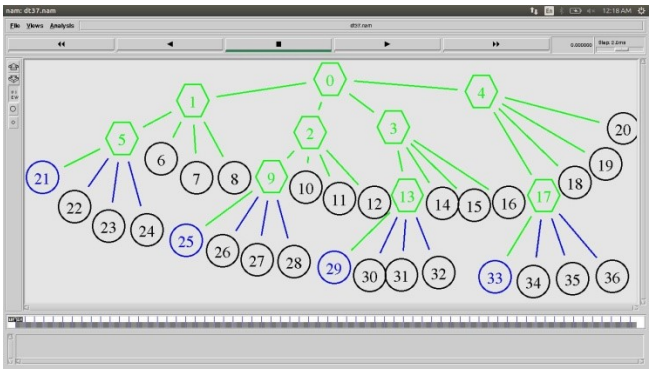

Fig. 1. Tree organization in TNVS.

C. Node verification using ECDSA

Consider n_0 as a root node and n_1 as authenticator node. n_0 node broadcast the hello message. n_1 node verifies the hello message received from base station n_0.In above Fig. 2, it can be seen that n_1 node is verifying the message with ECDSA parameters.

```
bsvs@bsvs-Vostro-1015:~/pw/sefwork$ ns dt1.tcl 37

Decrypted Text at n1=hellomessagen0|0|null


signature:
  r: 0x598b97ba571a37f717e4739504b684d1d1b4ec7d63cdd5ccb0f0c0
6b958d2ea1
  s: 0x4ad9542155db18b44f269f81f708fd1ae41e0005d68493e54621bb
9566b2d0c
valid: true
valid signature
  v: 0x598b97ba571a37f717e4739504b684d1d1b4ec7d63cdd5ccb0f0c0
6b958d2ea1
signature verified
```

Fig. 2. Authenticator node verification.

D. Total number of keys:

In tree based node verification key management scheme approach sensor nodes are pre-deployed with its own private key, public key, and the symmetric master key. Authenticator nodes stores the parent and child nodes pair wise keys, public keys, one symmetric master key, its own private key, and public key. In the proposed approach d is the degree of the node.
In TNVS we have 3 sensor nodes and one authenticator node as children and one parent node resulting in d=5.Total Keys = A*(2d+3) +3*S. Total number of keys required for various existing schemes are analyzed and compared.
In table IV, m is the key pool size, H is the cluster head sensor nodes, C is the number of children assumed for tree

IEEE Conference Record # 45198; IEEE Xplore ISBN Number: 978-1-7281-1261-9

protocol and in TNVS scheme, CC-4 is able to recover the encrypted message without knowing the neighbor nodes pair wise keys. Assume each cluster head is associated with 50 sensor nodes i.e. in 204 nodes 200 nodes are taken as sensor nodes and 4 nodes are taken as cluster heads.

TABLE IV. TOTAL KEYS COMPARISON

Approach	Number of Keys	Sensor Nodes				
		204 S=200 H=4	**408** S=400 H=8	**612** S=600 H=12	**816** S=800 H=16	**1020** S=1000 H=20
Tree Based[12]	S(3+C)	1428	2856	4284	5712	7140
ECC Distributed[17]	(H+2)S+3H	1212	4024	8436	14,448	22,060
EG Scheme[11]	m(H+S)	m=30	m=60	m=90	m=120	m=150
		6120	24,480	55,080	97920	153000
		k=4	k=8	k=12	k=16	k=20
SPINS[1]	S(5+ k)	1836	5304	10404	17136	25500
LEAP[14]	S[(3*k)+2+ k]	3672	13872	30600	53856	83640
TNVS	A*(2d+3)+ 3*S	A=51 S=153	A=102 S=306	A=153 S=459	A=204 S=612	A=255 S=765
		1122	2244	3366	4488	5610

The total numbers of keys required for proposed scheme are compared with the existing schemes for 204,408,612,816 and 1020 sensor nodes. Total number of keys calculated is shown in table IV. A graphical representation of the same depicted in Fig. 3.

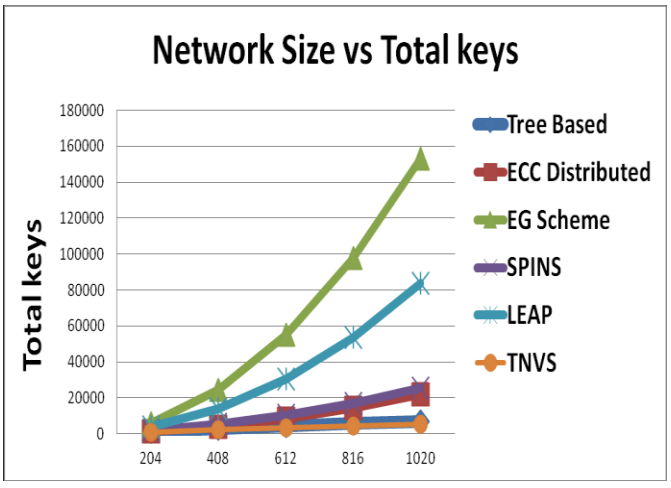

Fig. 3. Network size vs Total keys

The total numbers of keys are less compared to other schemes. In this scheme, new nodes are verified by authenticator nodes using ECDSA algorithm and total numbers of keys are better than existing pre-deployed key management schemes. Proposed scheme reduces the memory required for storing keys and as well provides authentication for new nodes that are being added in the network using ECDSA algorithm.

E. Security Analysis:

In this scheme, assume master key K_M is not known to the attacker then nodes cannot compromise until the pair wise key is calculated in the network. The attacker will not be able to recover the encrypted message without knowing the master key.

Hello Flood Attack: In the TNVS approach, sensor nodes broadcast the hello message that is encrypted using master key for tree construction. An attacker without knowing K_M could not send Hello Flood Attack. Hello message is verified by the authenticator nodes using the ECDSA algorithm.

Node Capture Attack: Every pair of nodes calculate unique pair wise key using ECDH. If one node is compromised attacker can get only one sensor nodes keys. The attacker can't get other sensor nodes keys as base point B is secret and private keys are unique for each sensor node. No matter any number of sensor nodes are compromised other nodes can securely communicate using ECDSA algorithm.

VI. CONCLUSIONS

In this paper a novel tree based node verification key management scheme is proposed for key management scheme in wireless sensor networks. New nodes that are being added in the network are verified by the authenticator nodes using ECDSA. Results shows that TNVS scheme reduces the memory requirement for storing keys and the periodical master key renewal makes the scheme resistant to node capture attack. This approach can be extended for node verification in multi-hop communication.

REFERENCES

[1] A. Perrig, R. Szewczyk, V. Wen, D. Culler, J.D. Tygar, SPINS security protocols for sensor networks, Proceedings of ACM MobiCom'01, Rome, Italy, 2001, pp. 189–199.

[2] DU, W., DENG, J., HAN, Y., AND CHEN, S. 2004. A key management scheme for wireless sensor networks using deployment knowledge. Proceedings of IEEE INFOCOM'04.

[3] Donggang Liu and Peng Ning. Establishing pairwise keys in distributed sensor networks. In 10th ACM Conference on Computer and Communications Security (CCS), October 2003.

[4] Du, W., Deng, J., Han, Y. S., And Varshney, P. 2003. A pairwise key pre-distribution scheme for wireless sensor networks. In Proceedings of 10th ACM Conference on Computer and Communications Security (CCS'03). 42–51.

[5] F. Akyildiz, W. Su, Y. Sankarasubramaniam, and E. Cayirci, "Wireless sensor networks: a survey," Computer Networks, vol.38, no. 4, pp.

[6] H. Chan, A. Perrig, and D. Song. Random key predistribution schemes for sensor networks. In IEEE Symposium on Research in Security and Privacy, 2003.

[7] Ismail Mansour, Gérard Chalhoub and Pascal Lafourcade, "Key Management in Wireless Sensor Networks", *Journal of Sensor and Actuator Networks*, vol. 4, pp. 251-273, 2015.

[8] Jennifer Yick, Biswanath Mukherjee, Dipak Ghosal, Wireless sensor network survey, Computer Networks: The International Journal of Computer and Telecommunications Networking, v.52 n.12, p.2292-2330, August 2008.

[9] L. Girod, T. Stathopoulos, N. Ramanathan, et al., "A System for Simulation, Emulation, and Deployment of Heterogeneous Sensor Networks, "Proc. of ACM SenSys 2004.

[10] L. Girod, T. Stathopoulos, N. Ramanathan, et al., "A System for Simulation, Emulation, and Deployment of Heterogeneous Sensor Networks, "Proc. of ACM SenSys 2004.

[11] L. Eschenauer, V.D. Gligor, "A key management scheme for distributed sensor networks", *Proceedings of (CCS '02.)*, pp. 41-47, 2002.

[12] Messai M-L, Aliouat M, Seba H Tree based protocol for key management in wireless sensor networks. EURASIP Journal on

Wireless Communications and Networking. Springer Publisher,2010;2010 pp. 59:1–59:13, ISSN 1687–1472.
[13] N. Koblitz, "Elliptic curve cryptosystems", Math. Computat., vol. 48, pp. 203-209, 1987.
[14] S. Zhu, S. Setia, and S. Jajodia, "LEAP: Efficient Security Mechanisms for Large-Scale Distributed Sensor Networks," CCS'03: Proc. 10th ACM Conf. Comp. and Commun. Security, New York: ACM Press, 2003, pp. 62–72.
[15] http://andrea.corbellini.name/2015/05/30/elliptic-curve-cryptography-ecdh-and-ecdsa/
[16] X. Du, M. Guizani, Y. Xiao, S. Ci, H.H. Chen, A routing-driven elliptic curve cryptography based key management scheme for heterogeneous sensor networks, in IEEE Transactions on Wireless Communications.
[17] X. Du, S. Ci, X. Yang, M. Guizani, H. Chen, "A Routing-Driven Key Management Scheme for Heterogeneous Sensor Networks", IEEE ICC,2007.

Proceedings of the Fourth International Conference on Communication and Electronics Systems (ICCES 2019)
IEEE Conference Record # 45898; IEEE Xplore ISBN: 978-1-7281-1261-9

Depth Analysis Using Stereo Vision

Mr. Nitin Borhade
Dep. of Electronics and telecommunication
Modern College of Engineering
Pune, India
nitin.mborhade@gmail.com

Mr. Vijay Kunjir
Dep. of Electronics and telecommunication
Modern College of Engineering
Pune, India
vijaykunjir81@gmail.com

Mr. Nandan Andhare
Dep. of Electronics and telecommunication
Modern College of Engineering
Pune, India
nsandhare@gmail.com

Prof. Mrs. Vandana Jirafe
Dep. of Electronics and telecommunication
Modern College of Engineering
Pune, India
vnjpune@gmail.com

Abstract - **Object detection using stereovision is a process to identify a specific object in a sequence of different images. In many years it receives much more attention due to a huge number of applications like navigation, automated inspection, wildlife analysis, etc. The detection of an actual object with different shapes is a difficult task; due to some issues like the external environment, fast movement of an object, shadows, noises, etc., so there is a requirement to choose appropriate methods/algorithms with respect to it. So, this paper specifies depth analysis with stereo vision using an appropriate algorithm.**

Keywords- Deapth,Stereo,Camera,Checkerboard,Calibration.

I. INTRODUCTION

The depth analysis is a predominant tool to investigate various parameters like object detection, distance, size, shape, and many other dimensions. Stereovision is the most versatile and flexible application which used in many applications such as detection, navigation, security, wildlife analysis, etc. Stereo vision systems can be ordinarily used in object detection whereas it generates depth information which detects very small objects with accurate measurement of size and distance. The Stereovision system can be implemented using two cameras that provide a disparity between two objects. Object detection can be achieved by using various traditional methods like Background subtraction, frame differentiation, etc. [1][2][3][4] But due to some limitations, they are not satisfactory for real-time applications. The camera calibration is a primarily important step that uses 3D computer vision to extract metric information for 2D images for object detection, which can be achieved by using various methods. Checkerboard method with black and white square pattern is one of the efficient and accurate methods. It can be used for camera calibration. [8] Firstly the camera initiates too many distortions in the image. Tangential and radial are the major distortions. In a checkerboard image, the lines have appeared as curved due to radial distortion whereas tangential distortion arises due to parallel misalignment of image plane and image. These distortions can be corrected by using appropriate scaling formulas. Another parameter such as intrinsic and extrinsic parameters which include focal length, optical centers, rotational and translational vectors, etc. can be found using sample images of the checkerboard pattern. Distance, size and other dimensions can be estimated using various equations.

The overall idea of this work is, using two cameras the distance between the desired object in frame and the camera is calculated. For this purpose, using camera calibration the distortions are corrected and depth map is generated. After that using regression the depth is calculated.

This paper describes first the related work in that various surveys are considered, after that the detailed explanation about the proposed work is given. In next

II. RELATED WORK

A. Literature survey based on calibration methods

1. Traditional camera calibration method

The traditional camera method is suitable for every type of camera which has high precision calibration which gives high accuracy. The given calibration of the reference object is known in shape and size. The internal and external parameters of the camera are determined by the mathematical transformations. But the algorithm of this method is comparatively complex than other calibration methods.

2. Camera self-calibration method

The camera calibration is done only by comparing the relationship between the images of the surrounding environment during the movement of the camera. Here the 'Kruppa' equations are introduced which determines internal and external parameters. The equations of Kruppa equations are complicated to solve and this method is unstable for the camera calibration. [5]

3. Linear calibration method

The typical calibration method or direct linear transformation method was proposed by 'Abdul-Aziz' & 'Karara' in 1971. Here the parameters are defined while internal and external parameters of the camera should be determined by linear equations without any iterative calculations. The precision in this method is inaccurate. [6]

4. *Tsai two-step calibration method*

This method was proposed in 1987, there was radial distort although directly solving Kruppa equations can get internal and external parameters of the camera. The matrix transform method was used first to determine camera parameters and then achieved as the parameter's initial value, the distortion factor and the use of optimization method improve the calibration and accuracy. Due to high calibration accuracy, it reduces space dimension parameters. This method is not suitable for simplified calibration and it is difficult to obtain noncoplanar 3D points. [10]

5. Zhang calibration method

'Zang' calibration or 'planer pattern method' uses 2D checkerboard to calibrate camera without expensive calibration target. This requires a shoot and calibrate template from more than two images with a different angle. It doesn't need a specific position and displacement information of the planer template movement. The calibration process is complex. [7]

The outcome from all this survey is that the planer pattern method is preferable for the stereo vision than any other method. It gives a better result and accuracy. In this method process of calibration is complex, but still, this method gives a stable result.

B. Literature survey based on camera

1. Logitech C170

The Logitech C170 is a basic camera with a 5 megapixel with a frame rate of 30 fps with resolutions of 1024 X 768 Pixels. It is easy to interface with applications. Passive 3D depth estimation is one of the limitations of this camera. The limitation of the logitechC170 is that, its poor resolution.

2. Logitech C270

The Logitech C270 offers relatively high grade and HD quality image. The maximum resolution 1280 X 720 image capture. The USB 2.0 webcam provides the image. Among this, it yields parameters setting such as white balance, exposure, brightness, gain, and contrast. [8][9]

3. IDS UI-1646 USB

It is a 1.3 MP colored pixel camera with a compact and robust design. The camera can be easily mounted with a various number of applications without any interfacing issue. It is a board level camera that supports the use of M12 S-mount lenses. The maximum resolutions are 1280 by 1024 with the ability of 25 frames/ sec. [12]

4. PB-MV13

PB-MV13 is a 1.3 MP camera, whose frame rate is 500 frames/second. The resolution of the camera is 1280 X 1024micrometer. 12 X 12 micrometer is pixel size. The power consumption of this camera is high and it is also very expensive. [13] [14] [15]

5.HDCS-2020

It is a CMOS structured with very high resolution and less consuming power, which is available in two different types VGA and CIF. Pixel size is 7.4 X7.4 micrometers. Storage is comparatively high around 6 GB. [11]

The LogitechC270 has a high resolution and it fulfills all the featured and technical requirements. It provides high image quality and better accuracy, so it is preferable for a stereo vision system.

III. PROPOSED WORK

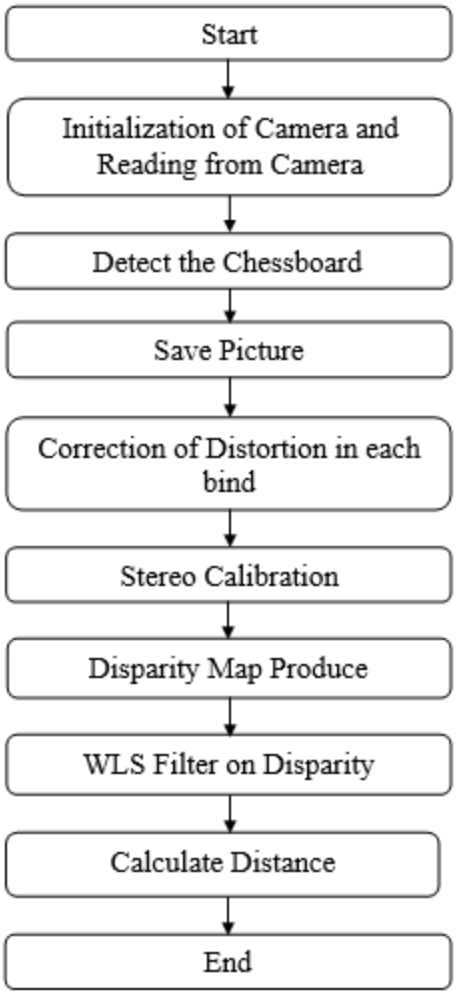

Fig (a). Flow chart of the proposed system

The flow chart consists of several processes. The processes are divided into two parts. The first part determines about images of checkerboard for calibration and the second part describes how the camera calibration is used for depth calculation.

Part I

A.Initialization of camera

Firstly, initiates both cameras which are right and left cameras, after reading the captured video it stores the frames in two variables named frames 'R' & frame 'L'. Convert the captured frames in grey for further operations and computations. [17] [18]

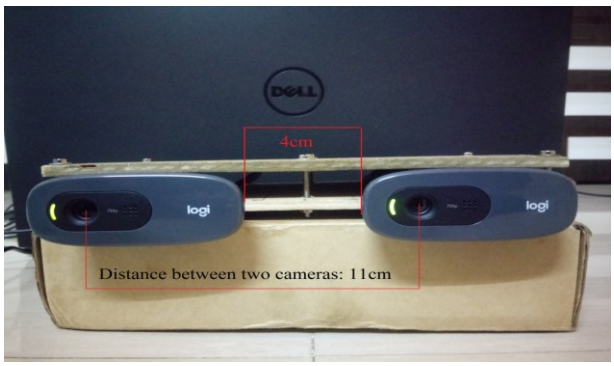

Fig (b). Camera C270 setup and initialization of camera

B. Detect checkerboard

Take Chessboard of either 8x8 blocks (Playing Chessboard) or 10x7 blocks, and find the positions of internal corners of the chessboard. If chessboard corners are detected in both the cameras, 'cv2.cornerSubPix' instruction defines the corner locations. 'cv2.drawChessboardCorners' represents the detected chessboard corners. [17] [18]

Fig (c). Cameras detecting chessboard corners

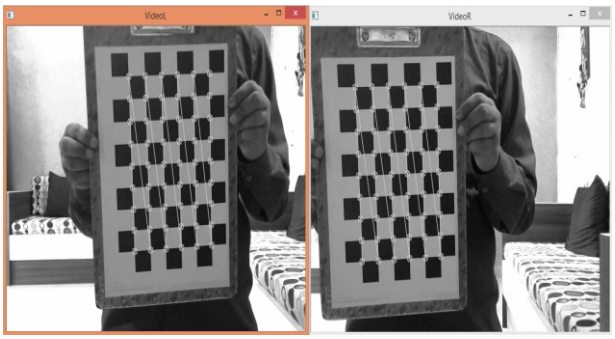

Fig (c). Detection of chessboard pattern

C. Save pictures

The detected images are saved by pressing 's' on the keyboard. Minimum 200 images of the checkerboard are required for calibration (left-100 & right-100). The maximum number of images gives a better result of calibration. [17] [18]

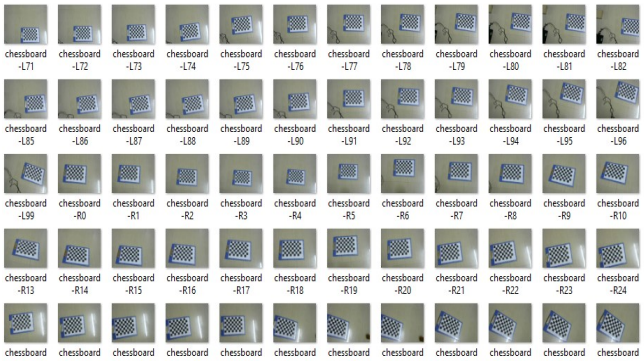

Fig (e). Database of the detected checkerboard

Part II

A. Stereo calibration

With the stored database of Checkerboard images, stereo camera calibration is initiated and the locations of corners are again calculated. The function 'cv.calibrateCamera' determines the camera's intrinsic and extrinsic parameters from several views of a calibration pattern which determines various factors like camera matrices, the distortion coefficient, and translation vector. Calibrate stereo cameras use the function 'cv2.stereoCalibrate', this function estimates transformation between two cameras making a stereo pair. 'cv2.stereoRectify' calculates rectification transforms for each head of a calibrated stereo camera, where this function calculates the rotation matrix for both cameras (right, left), which makes image planes the same (virtually). The function takes the matrices computed by 'cv2.stereoCalibrate' as input and provides 2 rotational and 2 projection matrices as an output with new coordinates. To get horizontal stereo, both the cameras (left and right) shifted to each other along the 'X' axis. In the rectified images, the corresponding 'epipolar' lines in the left and right cameras are horizontal and have the same y-coordinate. 'cv2.initUndistortRectifyMap'corrects the

distortion and rectifies the transformation maps and represents the result in terms of the map. 'StereoSGBM' used to obtain a correlation between the left and right camera. 'cv2.ximgproc.createRightMatcher' (stereo) creates another stereo for right, but the result of this function is difficult to detect the edge of the object because of noise. To remove this WLS filter is used. [18]

B. WLS filters on the disparity

First, set a filter in initialization mode. It consists of a lambda value, which can typically set at 8000, But if it is set at 80,000 it gives a better result. Another stereo object is created with 'cv2.ximgproc.createRightMatcher( )' function. These two cases are used in WLS (Waited least square filter) to generate a disparity map. So, after starting both the cameras, read and store the frames and then applied 'cv2.remap' function to generate a geometric transformation of the images. The result of 'cv2.remap' is then converted into a grey image. Then grey images are converted into a stereo image with the help of WLS filter. The values that come out from the WLS filter are normalized with the help of 'cv2.normalize()' function. In disparity, the value contains too much noise which can be removed by using a morphological filter. The 'cv2.applyColorMap ()' is used to convert a grey scale image into the 'color Image'. To identify the farther and nearer objects, the color map command is used. The nearer object is specified by white ocean color and farther object is specified by dark blue color which shown in fig (f). [18] [19]

Fig (f). Disparity map image using stereo images

C. Calculation of Distance

Once the disparity generated, the distance must be calculated. To determine appropriate distance, there is a need to satisfy the relation between distance and disparity, this can be achieved by 'regression'. In the regression, the disparity values are experimentally measured at several points which finally determine distance.

IV. RESULT ANALYSIS

As discussed in a proposed algorithm, the ocean color shades are used for object representation. The lighter color is used for nearer object and a darker color for the farther objects or background. When a particular object is clicked, then the distance between the 'selected' or 'clicked' object and camera is determined by the algorithm. Fig. (g) shows an ocean colored image, where lighter color is an object and darker part is the background scene. When we click the object in frame, it gives an appropriate distance between camera and object in 'mm' or 'cm'.

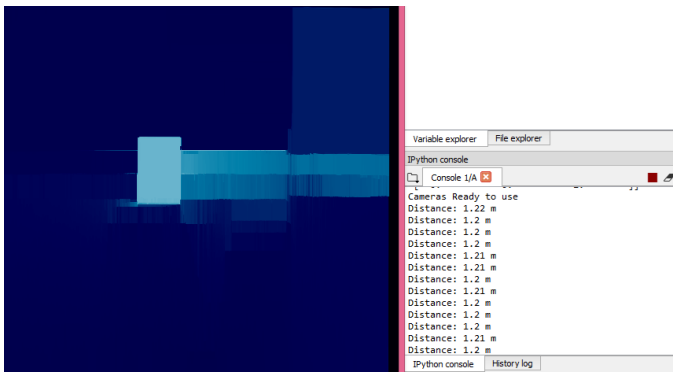

Fig (g). Result: Disparity map and computed distance

After a generation of disparity map, the distance has been calculated. The range of working of this algorithm in our case is around 2 to 3 meters. The min to max values in 10x7 and 8x8 checkerboard is 65 to 200 meters and 68 to 207 meters respectively. The following tables (Fig(h) and Fig(i)) are the result tables that consist of actual distance, computed distance and error for 10x7 and 8x8 checkerboard. Here, the random 10 readings are taken into account. The computed distance is measured with the help of disparity algorithms. According to it, the actual distance is measured manually with the help of scale; where it gives an error range from '+3 to -3'. So here, there is a variation in two different readings with some errors, which will possibly be removed by using a good quality of the camera.

Sr No.	Computed Distance (cm)	Actual Distance (cm)	Error
1	65	68	3
2	70	73	3
3	76	76	0
4	82	84	2
5	90	91	1
6	137	137	0
7	174	173	-1
8	184	182	-1
9	190	192	2
10	200	203	3

Fig (h). Result of a 10x7 checkerboard

Sr No.	Computed Distance (cm)	Actual Distance (cm)	Error
1	68	70	2
2	73	75	3
3	78	80.4	2.4
4	87	84	-3
5	113	113	0
6	142	144	2
7	175	172	-3
8	189	189	0
9	1.94	1.93	-1
10	207	207	0

Fig (i). Result with 8x8 checkerboard pattern

Limitations

- A large number of captured images (database) may lag down the system.
- Less number of captured images may affect accuracy.
- With the use of Logitech C270, its work range is around 2 to 3 meters. With the use of a better quality camera range can be extended.
- The precision of measurement is around +/- 3cm.

V. Conclusion

In this work the various camera calibration methods and various types of cameras are surveyed. Like a human eye, in the proposed system, the stereo vision with calibration algorithm has achieved the depth perception using a two camera, and also achieved calculation of the distance between object and camera without any disturbance. The proposed stereo vision system can detect a selected object and calculates its distance with the precision of +/-3cm in a range of 2 to 3 meters. The performance of this system will be enhanced by using a good quality of the camera and a high-power image processor.

References

1.Jaya S. Kulchandani, Kruti J. Dangarwala," Moving Object Detection: Review of Recent Research Trends ", International Conference on Pervasive Computing (ICPC),2015.

2. S. R. Balaji, Dr. S. Karthikeyan," A Survey on Moving Object Tracking Using Image Processing",11 th International Conference on Intelligent Systems and Control (ISCO),2017.

3. Himani S. Parekh, Darshak G. Thakore,Udesang K. JaJiya, " A Survey on Object Detection and Tracking Methods", International Joulllal of Innovative Research in Computer and Communication Engineering, Vol. 2, Issue 2, February 2014.

4. Massimo Piccardi, "Background subtraction techniques: a review," IEEE International Conference on Systems, Man and Cybernetics, pp. 3099-3104, 2004.

5.Jianfei Li, Research on camera self-calibration method [D], HeFei University of Technology, 2007: 14-16

6. Y. I Abdel-Aziz and H M Karara, "Direct Linear Transformation into object space coordinates in close-rangephotogrammetry," in:Proc. Symp. Close-Range Photogrammetry, Univ. of Illinois at Urbana-Champaign, Urbana, pp.1-18

7. Z. Zhang, "A Flexible New Technique for Camera Calibration," IEEE Transactions on Pattern Analysis and Machine Intelligence, vol. 22, no. 11, pp. 1330-1334, November 2000.

8. Logitech. (n.d.). HD Webcam C270 Specification. Retrieved from http://support.logitech.com/en_us/product/hdwebcam-c270

9. https://www.logitech.com/en-in/product/hd-webcam-c270

10. Tsai R Y, "An efficient and accurate camara calibration technique for 3Dmachine vision" [C], In:Proceedings of IEEE Conference onComputer Vision and Pattern Recognition, 364-374.

11. Henry, P.; Krainin, M.; Herbst, E.; Ren, X.; Fox, D. RGB-D mapping: Using kinect-style depth cameras for dense 3D modeling of indoor environments.Int. J. Robot. Res. 2012, 31, 647–663. [CrossRef].

12. Oleari, F., Rizzini, D. L., & Caselli, S. A Low-Cost Stereo System for 3D Object Recognition.IEEE International Conference on Intellgent Computer Communication and Processing, 127–132, 2013. DOI: 10.1109/ICCP.2013.6646095

13. http://www.cs.carleton.ca/~barbeau/Picosat/CanX_Paper.pdf

14.http://www.datasheetcatalog.org/datasheet2/2/05jj45dcrga6zr0zjg7hrde83cpy.pdf

15. www.datasheetarchive.com/PB-MV40-datasheet.html

16. http://www.cse.iitd.ernet.in/~suban/vision/multiple/node3.htm

17.https://opencv-python-tutroals.readthedocs.io/en/latest/py_tutorials/py_calib3d/py_calibration/py_calibration.html

Proceedings of the Fourth International Conference on Communication and Electronics Systems (ICCES 2019)
IEEE Conference Record #45982; IEEE Xplore ISBN: 978-1-7281-1261-9

Design and Development of Hybrid Powertrain for Motorcycles

Kandi Suyash
Student of B.E, Dept. of Mechanical, Dr. J.J. Magdum College of Engineering
Jaysingpur, India.
suyashkandi@gmail.com

Ghadge Tejraj
Student of B.E, Dept. of Mechanical, Dr. J.J. Magdum College of Engineering
Jaysingpur, India
tejraj.ghadge@gmail.com

Jadhav Vasudev
Student of B.E, Dept. of Mechanical, Dr. J.J. Magdum College of Engineering
Jaysingpur, India
vasudevjadhav2017@gmail.com

Dhaygude Akshay
Student of B.E, Dept. of Mechanical, Dr. J.J Magdum College of Engineering
Jaysingpur, India
iamakshay7777@gmail.com

Mursal Siddique
Student of B.E, Dept. of Mechanical, Dr. J.J. Magdum College of Enigneering,
Jaysingpur, India
siddiquemursal@gmail.com

Kharade Mahesh
Associate Professor, Mechanical Dept, Dr. J.J. Magdum College of Enigneering,
Jaysingpur, India
mahesh.kharade@jjmcoe.ac.in

***Abstract*—Due to rising fuel prices, shortage of fuels and increasing air pollution there is more demand for electric vehicles. But in India the main concern is we do not have enough charging stations to recharge electric vehicles during emergency. So, we cannot use e-bikes for longer range. The hybrid powertrain is used to solve this problem. The primary drive of the powertrain is electric motor and secondary drive uses an IC engine. The power train consists of free wheels and fixed sprocket which allows to operate motorcycle on electric motor as well as IC engine. The use of hybrid powertrain improves overall range of motorcycles.**

Keywords—Hybrid powertrain, freewheels, fixed sprocket, electric vehicles, range, hybrid motorcycle

I. INTRODUCTION

The development in the trends of internal combustion engine vehicles has brought various improvements in automobile sector having great impact on society by satisfying the needs in day to day life, [1]. However, the use large number of automobiles causes large amount of air pollution which has hazardous effects on human life. The combustion products such as nitrogen oxides (NO_x), carbon monoxide (CO) and unburned hydrocarbons (HC) are toxic to human health. Also, carbon dioxide released in atmosphere is responsible for global warming and increasing earth's temperature, [2]-[3]. These are the main reasons for increasing demand of electric and hybrid vehicles. A hybrid vehicle has at least two energy sources, most commonly used energy sources are IC engine and electric motor, [4]. Many researches and studies have been developed in the field of hybrid powertrain to develop the sufficient power to meet the demands of vehicle performance, obtain the sufficient range, improve efficiency and emit few environmental pollutants. The electric vehicles are mainly classified as Plugin electric vehicles (PEV) and Hybrid electric vehicles (HEV), [5]. The various configurations of hybrid vehicle developed are series hybrid, parallel hybrid, series-parallel hybrid, mild hybrid and complex hybrid, [6]-[9].

In India there is demand for electric bikes and cars due to increasing fuel prices, shortage of fossil fuels and rising air pollution. But the electric vehicles have limited mileage per charge, charging of batteries is a time-consuming process. So, it becomes difficult for e-bikes to cover a range of 100-120 kms with limited capacity of battery pack. This paper is aimed to solve the range problem by using hybrid powertrain for bikes. The hybrid motorcycle consists of two power sources. The parallel combination of motor and IC engine is used driving the motorcycle. The hybrid powertrain is designed in such a way that both the power sources are in frontal part of the motorcycle. The motor is used as primary device for driving the bike with a moto of reducing air pollution. The motor used satisfies the performance characteristics of motorcycle i.e. top speed, gradeability, acceleration etc. The engine will be used as a secondary device to drive the bike to improve the range of vehicle. So that even for longer distances 110-130 kms we can use motor for initial 48-50 kms and then use IC engine to cover extra distance. It will also help to reduce air pollution. The throttle of engine and motor is given in right hand only for normal driving experience. The shift from IC engine to electric mode is done by using switch. This design enables us to drive the bike using motor in cities and shift to IC engine for driving on highways.

The paper organization is as follows: In Sect. II the concept of hybrid powertrain is explained along with its CAD model. In Sect. III the working of powertrain is explained. Then in Sect. IV engine selected and its specifications are given. Sect V gives the motor selection and specifications. Sect. VI gives the battery specifications. Sect. VII includes modified frame design for motorcycle. Sect VIII has the powertrain specifications and selected drive ratio. Sect. IX has the observations taken by testing of bike at various speeds. Sect. X consist of graph comparing cost and distance in petrol and hybrid bikes. At last, Sect. XI consists of actual pictures of powertrain developed. Conclusive remarks close the paper.

II. CONCEPT OF HYBRID POWERTRAIN

In two-wheeler segment, the hybridization is usually done by using hub motors as front wheel and engine drives the rear wheel, [10]. But this configuration has very less torque and neglects the driving experience by enabling both wheel drive in two wheelers. To overcome this problem, we have used BLDC motor with gear reduction and by providing drive only to rear wheel. The hybrid powertrain consists of an intermediate shaft present between the power sources and the rear wheel. The direct transmission in bikes is divided in two stages. The length of the intermediate shaft is 300mm. The shaft is supported by the bearings on both the sides such that it has purely rotational motion. One of the freewheels is connected to

engine with chain drive and the other freewheel is connected to motor with chain drive. The fixed sprocket is used for continues power transmission on any of the running mode.

The number of teeth is as follows: -

i. Fixed Chain wheel on motor shaft t_1– 12 teeth
ii. Free wheel (connected to motor) t_2- 18 teeth
iii. Fixed Chain wheel on engine shaft t_3- 14 teeth
iv. Free wheel (connected to engine) t_4 – 22 teeth
v. Rigid chain wheel t_5 – 18 teeth

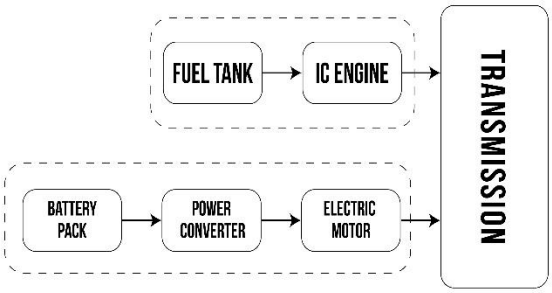

Fig. 1. Concept of Parallel Powertrain

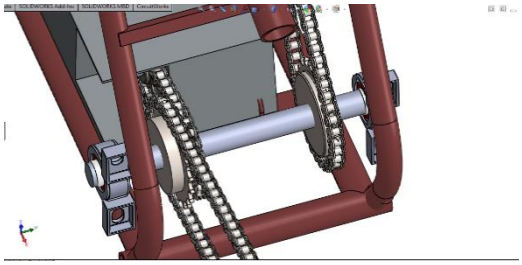

Fig. 2. CAD Model of hybrid powertrain

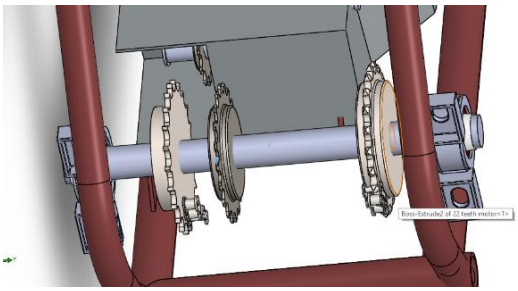

Fig. 3. CAD Model of hybrid powertrain

Fig 1. Shows the basic working of parallel powertrain in which the vehicle can be driven by either electric motor or IC engine or by both. Fig 2. And Fig 3. Shows the design on the powertrain by using counter shaft, 2 freewheels and one rigid sprocket. The freewheel to the extreme right is connected to motor via chain and the centre freewheel is connected to IC engine. And the rigid sprocket to the extreme left is used for providing the final drive continuously. In Fig 3 the centre freewheel is slightly shifted to right for better view of powertrain.

III. WORKING

The hybrid powertrain works on the principle of operation of freewheel. As the freewheel has rachet and pawl mechanism it can transmit power in one direction and not other. This application of freewheel is used to generate hybrid drive.

A. Working on electric mode-

When the electric switch is turned on and the throttle is increased the motor rotates in clockwise direction. The freewheel can transmit power in only one direction, in opposite direction it rotates freely without transmitting power. When the motor freewheel is driven by chain the counter shaft rotates, and the fixed sprocket transmit power to the rear wheel and the vehicle moves. At this condition the engine remains in neutral position or the engine sprocket does not rotate because the freewheel connected to engine does not rotate even though the shaft rotates, it will only rotate when it is driven by chain via engine.

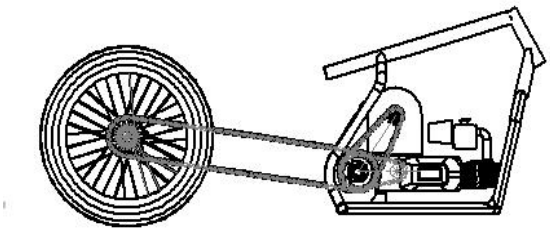

Fig. 4. Working on electric mode

B. Working on engine mode-

While running on engine mode the motor switch is turned off. The operation of freewheel and the sprocket is same. When the engine shaft rotates it transmits power to free wheel via chain drive and the shaft rotates. The fixed sprocket transmits power to the rear wheel and the vehicle moves. At this time the motor freewheel does not rotate and remains in neutral position.

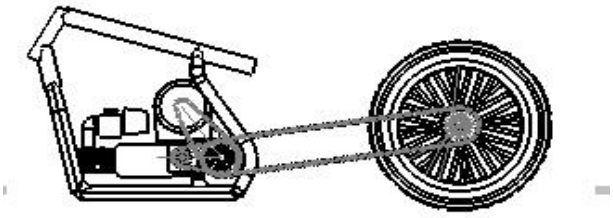

Fig. 5. Working on engine mode

IV. ENGINE SPECIFICATIONS

We have selected Hero splendor's engine which has a horizontal mounting oriented in horizontal plane which enables us more space for mounting of motor and transmission. The engine is used to cover the extra range in hybrid drive mode.

i. Capacity:- 100cc (splendor)

ii. Power:- 8.2 bhp @ 5000 rpm

iii. Torque:- 8Nm @ 5000 rpm

V. MOTOR SPECIFICATIONS: -

We have used BLDC motor as it has higher efficiency and better performance and torque speed characteristics as compared to PMDC motors and HUB motors, [11].

Type- BLDC spindle motor

Nominal Voltage – 48 V

Rated Power – 2000 Watt

Rated torque -9 Nm @3000 rpm

As the motor is primary device and has to satisfy all the performance characteristics of bike the selection of motor is done by calculating power at various driving conditions by using equations. Table 1. gives the theoretical calculated values for various driving conditions.

TABLE 1. TRACTIVE EFFORT AND POWER AT VARIOUS SPEEDS

Case	Vehicle speed (kmph)	Acceleration (m/s^2)	Gradient (Degree)	Tractive effort (N)	Power (KW)
1	40	0	0	39	0.43
2	80	0	0	75	1.66
3	20	0	5	210	1.16
4	15	0	7	281	1.56
5	40	1.2	0	227	2.2
6	20	0.5	5	315	1.75

VI. BATTERY SPECIFICATIONS

Lithium ion Battery pack of capacity 25Ah is required. As the Li on battery pack is smaller in size and lighter in weight compared to lead acid batteries. Lithium ion battery pack has higher charge density than Lead acid batteries, [12].

VII. CHASSIS AND FRAME STRUCTURE

We have used Discover 125 ST for our prototype. There are slight modifications in the frame of the bike. We have designed the frontal part of frame as per requirement which makes it easy for mounting of engine and motor and provides space for mounting shaft. The length of chassis is increased by 4 cm.

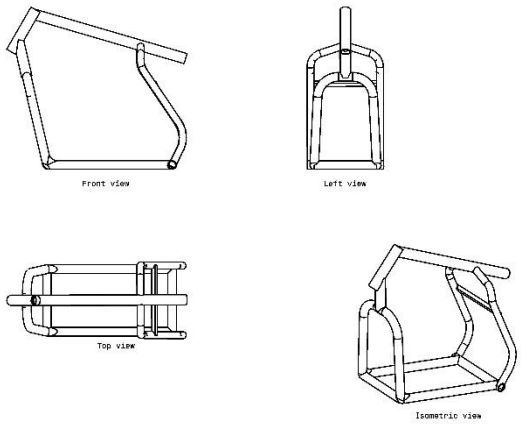

Fig. 6. Views of Frame Modified

VIII. POWERTRAIN SPECIFICATIONS

Fig. 7. Shows the sprocket and drive ratio selection for hybrid powertrain. The powertrain allows the parallel use of IC engine and electric motor for transmission. By using intermediate shaft, the overall drive ratio is obtained in two stages. The selection of drive ratio is done by calculations satisfying maximum torque & maximum speed for the vehicle to satisfy the performance characteristics of the vehicle. Sprockets are selected according to the market availability to maintain overall drive ratio which is 3.165 for electrical drive and 3.31 for IC engine drive. The overall drive ratio for IC engine drive is made constant as per standard vehicle. The first stage reduction for motor is 1.5 and for IC engine is 1.57. The second stage reduction is 2.11.

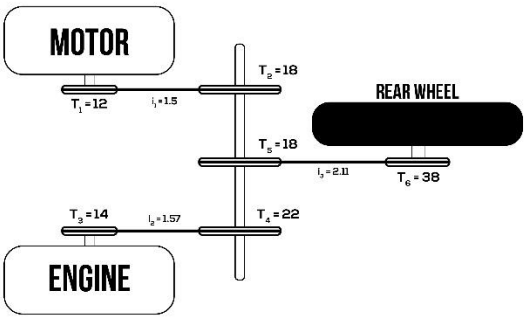

Fig. 7. Sprocket Selection and drive ratio

IX. OBSERVATIONS

A. *Test for current consumption ,mileage covered and cost.*

We have tested the bike for running more than 150 kms using both the power sources with various road conditions. The following are the observations while driving on electric mode. The total load on motor is 210 kg.

TABLE 2. CURRENT CONSUPTION AT VARIOUS SPEEDS

Speed (kph)	Current (A)	Duration For 25Ah capacity (hrs)	Distance (km)
20	10	2.5	50
30	16	1.56	46.8
40	21	1.19	47.6
45	24	1.04	46.8

Following are the observations by keeping the cost parameter constant.

The price of fuel per litre is 78 Rs which is kept constant and range is analysed in case of petrol bikes and hybrid bikes. For petrol bikes the distance covered is 70 kms in one litre of petrol. i.e. 1.11 Rs per km travel. For hybrid motorcycle the average 48 km cost 6 Rs on electric mode. The further distance is covered in engine mode. Thus, range of 112 kms is obtained in 78 Rs. i.e. 0.696 Rs per km travel. If it used for 48-50 kms daily, then motor can be used to cover the whole distance. In this case the cost per km travel is 0.12Rs. This will help to save the money and will benefit common people. For 70 kms of travel using hybrid mode it takes 30.5 Rs. If a bike travels 11000 kms in one year the cost of fuel is 12210 Rs but in case of hybrid bike the cost of travel is 7656 Rs. Thus, we can save fuel of 4554 Rs in one year.

B. *Test for speed and time parameters at normal driving conditions.*

The speed and time parameters are determined while driving bike in petrol mode as well as hybrid mode. The test is conducted as follows: -

i. For petrol mode the bike is accelerated from 0 to 45kmph at normal riding conditions and time is noted down.

ii. For hybrid drive the vehicle is propelled on ICE from 0 kmph to 15-20 kmph approximate to achieve initial momentum and reduce initial high current drain due to high torque required to move the vehicle from stationary position. Although motor provides performance similar to ICE drive but to improve efficiency of overall powertrain by reducing the high current consumption at start the bike initially propelled on ICE then it switched to electrical drive after attaining certain momentum. Time Elapsed in Hybrid mode = ICE engine time (0-15kmph) + Idle time (Switching from ICE to Electrical) + Electrical Drive time (15-45kmph).

Table 3. gives the speed time parameters for both petrol and hybrid mode for the speed up to 45 kmph.

TABLE 3. SPEED TIME PARAMETERS

Test no	ICE Drive (time in seconds)	Hybrid Drive (time in seconds)
1	14.96	26.66
2	18.58	25.28
3	15.04	23.98
4	16.52	23.06
5	16.70	22.24
Mean Time	16.36	24.244

X. GRAPH

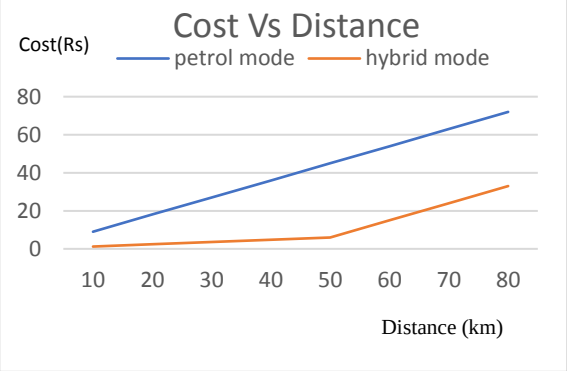

Fig. 8. Graph of Cost VS Distance of a petrol bike and hybrid bike

Fig. 8. shows the comparison of cost and distance travelled in petrol bikes and hybrid bike where the distance covered is 80 km in both cases. In hybrid mode the first 50 kms covered using electric mode.

XI. PROTOTYPE OF HYBRID BIKE WITH PARALLEL CONFIGURATION FOR TRANSMISSION

Fig. 9. Prototype of hybrid powertrain- motor side

Fig. 10. Prototype of hybrid powertrain- engine side

Fig. 9 and Fig. 10 shows the actual hybrid powertrain developed and used in Discover 125 ST.

XII. CONCLUSION

The use of hybrid electric powertrain for motorcycles helps to reduce the fuel crises and reduce the amount of air pollution. The hybrid drive will also reduce the cost of fuel per km travel and will significantly improve the range of bike. It can be used for travelling longer distances and will mainly benefit middle class people. Thus, hybrid drive proves to be more economical, cost effective than conventional petrol bikes. We have designed a powertrain which can be improved in future as the innovation is in its first stage. Researchers can go for automation in the project increasing range and performance of the bike. We can think on manufacturing kits of hybrid vehicle which can turn a petrol bike into hybrid on with small amount of fabrication. The highlighted points for future scope are reduction in weight, regenerative braking, use of solar cell to charge the batteries, ergonomics of hybrid bike, automation, IOT and smart vehicle.

XIII. REFERENCES

[1] Mehrdad Ehsani, Gao, and Ali Emadi, Sebastien Gay Modern Electric, Hybrid Electric, and Fuel Cell Vehicles: Fundamentals, Theory, and Design, 2nd New York, NY, USA: Taylor & Francis, 2009

[2] H. Eren, A. Al-Ghamdi and Jinhua Luo, "Application of zigbee for pollution monitoring caused by automobile exhaust gases," *2009 IEEE Sensors Applications Symposium*, New Orleans, LA, 2009, pp. 164-168.

[3] Barbara. Sokolnicka, Pawel Fuć, Piotr Lijewski, Natalia Szymlet and M. Siedlecki, "Analysis of specific emission of exhaust gases from gasoline direct injection engine in real operation conditions and on dynamic engine dynamometer," *2018 International Interdisciplinary PhD Workshop (IIPhDW)*, Swinoujście, 2018, pp. 231-234.

[4] G. Maggetto, Van Mierlo, Electric, Hybrid and Fuel Cell Vehicles (Ref.No. 2000/050), IEEE Seminar, 2000, pp. 1/1–1/11.

[5] Md Habib Ullah, Teddy Gunawan, M.R. Sharif and R. Muhida, "Design of environmental friendly hybrid electric vehicle," *2012 International Conference on Computer and Communication Engineering (ICCCE)*, Kuala Lumpur, 2012, pp. 544-548

[6] S. Ploumen, Fricke, Miller, and Snyder ," Energy storage devices for future hybrid electric vehicles," *Journal of Power Sources*, volume. 168, no. 1, pp. 2-11, May 2007.

[7] C. Mi, A. Masrur, and Gao, "Hybrid Electric Vehicles: Principles and Applications with Practical Perspectives," Wiley, 2011.

[8] G. Gruosso, "Optimization and management of energy power flow in hybrid electrical vehicles," *5th IET Hybrid and Electric Vehicles Conference (HEVC 2014)*, London, 2014, pp. 1-5

[9] Mattia Morandin, Marco Ferrari and Silverio Bolognani, "Power-Train Design and Performance of a Hybrid Motorcycle Prototype," in *IEEE Transactions on Industry Applications*, vol. 51, no. 3, pp. 2216-2226, May-June 2015.

[10] Sharda Prasad, K. R Natraj, "Design and development of hybrid electric two wheeler suitable for Indian Roads" , *International Journal of Electrical, Electronics and Data Communicatio*n, ISSN: 2320-2084 Volume-2, Issue-9, Sept.-2014

[11] Shahriar Sharifan, Ebrahimi, Ashknaz Oraee and H. Oraee, "Performance comparison between brushless PM and induction motors for hybrid electric vehicle applications," *Intl Aegean Conference on Electrical Machines & Power Electronics, 2015 Intl Conference on Optimization of Electrical & Electronic Equipment & 2015 Intl Symposium on Advanced Electromechanical Motion Systems*, Side, 2015, pp. 719-724

[12] Helmut Weiss, Thomas Winkler and H. Ziegerhofer, "Large lithium-ion battery-powered electric vehicles — From idea to reality," *2018 ELEKTRO*, Mikulov, 2018, pp. 1-5.

Proceedings of the Fourth International Conference on Communication and Electronics Systems (ICCES 2019)
IEEE Conference Record # 45898; IEEE Xplore ISBN: 978-1-7281-1261-9

Performance Evaluation of Power over Ethernet in an Ethernet Switch

Laxmi Khichadi
PG Scholar
Digital Communication Engineering
R V College of Engineering
Bangalore, India
laxmikhichadi9482@gmail.com

Dr. Nagamani K.
Professor
Dept. of Telecommunication Engineering
R V College of Engineering
Bangalore, India
nagamanik@rvce.edu.in

***Abstract*— The trending technology Power over Ethernet (PoE) is a widespread way to send power along with data in a single Ethernet. It uses standard balanced twisted pair cable to send power in an existing Ethernet cable. Devices powered using this technology are Voice-over-Internet (VoIP) telephones, surveillance cameras, wireless access points etc. The technology is more cost effective and can be easily implemented. This paper describes the overview of Power over Ethernet, its methodology, advantages and factors in selecting cable. The paper also gives the factors which influence the performance of PoE system. The PoE using Category 3 or Category 5 cable for power transmission is described.**

Keywords— balanced twisted pair cable, Category 3 cable, Category 5 cable

I. INTRODUCTION

PoE has many industrial applications and is now popularly used everywhere. Because of its compatibility and low cost installation it is the best option for supplying power to existing Internet Protocol (IP) devices .

PoE supplies DC power and supports 10 Mb to 100 Mb Ethernet without installing additional electrical infrastructure. The company named PowerDSine took initiation to standardize the PoE in 1998. The promoting companies were Intel, 3Com, National Semiconductor, Mitel and Novtel Networks. On 12 June 2003 IEEE finally validated PoE standard. PoE provides inline power which reduces the number of power lines to be installed in the network. The two important devices used in a PoE are - the Powered device (PD) and the Power Source Equipment (PSE).Where, the PD accepts the power provided by PSE. The maximum power offered by PoE PSE is 15.4 watts 48vDC. The maximum power offered by PoE+ PSE is 30 watts at 48vDC. The maximum power offered by a Hi-PoE+ PSE is 100 watts. The IEEE standards require 4 pair cable. CAT-5 cable has 4 twisted pairs; in that, two of the pairs out of four are used for data transmission. The specification permits for the spare pairs to send the power. Power over Ethernet (POE) technology carries electrical power through existing network cables.

As an example, a digital surveillance camera generally needs two connections for its installation.

First a network connection, which is used for video recording and display gadget. Second a power connection, which is used to supply the electric power for the camera to function.

In this case, if the digital camera was POE-enabled, only one network cable would be sufficient for transmitting both power and data. This is shown in figure 1.

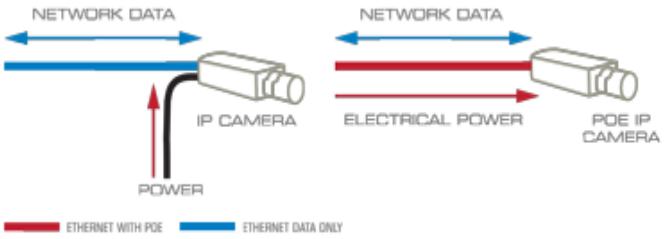

Figure 1: PoE enabled camera

II. RELATED WORKS

The CAT5 cable has four pair; by using all the pairs effectively power delivery to the destination that is power device can be increased [1]. In paper [2] author describes about the architecture present in the power sourcing equipment. The paper [3] and [4] gives specifications for PSE and PD and the power used by the devices. PoE implementation using Endspan insertion and Midspan insertion is given in paper [5]. Different communication protocol used by PoE is mentioned in paper [6] and [7]. The paper [8] and [9] explains the basic principles of a PoE system are explained along with benefits of PoE. Alternative A and Alternative B are the types of implementing PoE which are explained in paper [10].

III.BENEFITS OF POE

1. Time and cost savings

Time and cost is reduced by using PoE. By means of decreasing the time and price of getting electrical cabling established. Network cables can be installed by anyone easily, and can be placed anywhere.

2. Flexibility

PoE allows many devices to connect to it. Without calling to an electrical outlet, gadgets including wireless access points and IP cameras may be placed wherever they are wished most, and repositioned effortlessly if required.

3. Safety

POE delivery is smart, and designed to shield network device from overload, incorrect installation or under powering.

4. Reliability

POE power comes from a significant and universally well matched source, in preference to a set of distributed wall adapters. it could be subsidized-up by an uninterruptible energy deliver, or managed to easily disable or reset gadgets.

5. Scalability

Having electricity available on the network that set up the distribution of network connections straightforward and effective.

6. Enhanced productivity

PoE is capable of collecting data effectively and since it uses same cable for power and data it provides increased productivity to the devices which uses it.

IV.DEVICES SUPPORTED BY POE

PoE has many applications like VoIP phones, IP cameras. Every device can be powered using PoE by estimating how much power the device needs. Any PoE product can be integrated to the design. The figure 2 shows the devices that are PoE enabled.

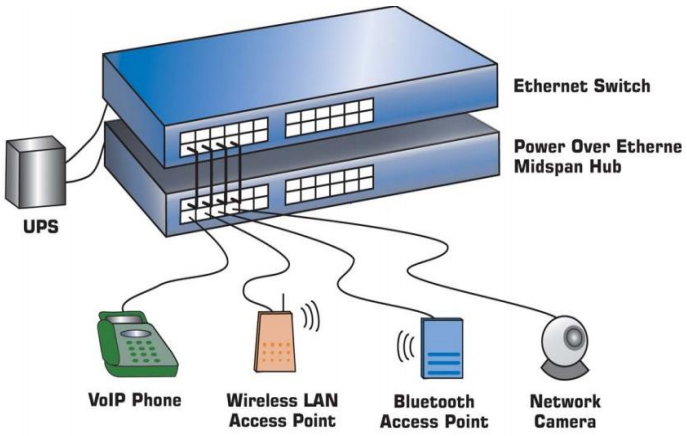

Figure 2: Devices enabled using PoE

Silvertel manufactures a many PoE modules at wattages appropriate for a large number of designs. Table 2 below gives the number of PoE wattages supplied with the aid of Silvertel and examples of a number of the products customer may power with them. Using Silvertel products the selection of PoE enabled devices is less time consuming and less challenging. Different devices require different amount of power to operate is also shown in the table 1.

Table 1: Devices supported by PoE

13W	30W	60W	100W	200W
IP Cameras	IP Telephones	Door Access Systems	Digital Signage Displays	Larger TVs
VoiP Phones	WiMAX Access Points	Video Phones	Point-of-Sale Systems	Larger Displays
Wireless Access Point	PTZ Cameras	Thin Clients	LCD TVs	Larger Monitors
Networked Audio	Remote Computer Terminals		Computer Monitors	Laptops

V. POWER OVER ETHERNET (POE) STANDARDS

The IEEE standards for PoE are 802.3af, 802.3at and 802.3bt.

Type 1 PoE

IEEE 802.3af-2003 was the first PoE standard which IEEE developed. The power given by this type is 15.4 watts at 48vDC with 12.95 watts of power to be assured to devices. Per pair maximum current rating is 350mA. Uses Category 3 cable or higher rate cable.

Type 2 PoE +

IEEE 802.3at-2009 was the second PoE standard developed by IEEE to provide more power. The power given by this type is 30 watts at 48vDC with 25.5 watts of powe.r to be assured to devices. Per pair maximum current rating is 600mA. Uses Category 5e cable or higher rate cable.

Type 3 PoE ++

IEEE 802.3bt-2018 Type 3 provides more power than 802.3at. Provides 90-100 watts at 48 volts DC.

VI. FACTORS IN SELECTING CABLE TYPE AND DIFFERENT CABLE STANDARDS

There are numerous factors that have to be considered while selecting the cable type used to make PoE application. The first one is the quantity of power the PoE device requires for its operation. This power required will dictate which IEEE standard to be selected, and ultimately the minimum class category cabling that can be used .

Other factors have to be taken into consideration for most effective performance of the network. They are heat dissipation, voltage drop and data transmission performance. Voltage drop gives how much of the transmitted power reaches the other end at receiving device. The power that is lost over the length of the cable line transforms to heat and is known as heat dissipation. More heat constructed can add growth in attenuation and also the aging of the cabling jacket.

Another aspect to which is to be considered is the data transmission requirement (e.g., 10GBASE-T, 1000BASE-T) of the device being used. Devices consisting of megapixel IP cameras can also require higher grade cabling if you want to deliver the video signal along with required power. Ethernet uses Modbus/TCP protocol for transmitting and receiving data.

There are 4 standards of twisted pair cabling given by the Telecommunications Industry Association (TIA) which is used mainly for Ethernet application. Those consist of Category 3, Category 5e, Category 6A and Category 6. Based on their power performance characteristics the different cable categories are selected.

As given in the table 1 below, Category 3 cabling makes use of a 24 AWG copper conductor and has a highest bandwidth of 16MHz. Category 3 cabling is permitted for 802.3af devices that require low energy. When compared to other cable Category 6A cable has a maximum bandwidth of 500 MHz and makes use of a 23 AWG copper conductor. The bigger conductor used in Category 6 and 6A cabling is preferred for PoE packages because of its less voltage drop over the cable. Even among all gauge sizes, slight differences in real conductor diameter will have measurable consequences on machine's overall performance. PoE application is also dependent on cable distance.

The table 2 gives the cabling standards, voltage drop and their Approved PoE Applications.

Table 2: Cabling standards and corresponding Approved PoE Applications.

Category	Nominal Conductor Size AWG	TIA Maximum Bandwidth MHz	Common Ethernet Applications	Approved PoE Application(s)	Voltage Drop* volts	Temperature Rise at 500 mA** °C (°F)
Superior Essex Category 3	24	16	10BASE-T	802.3af	1.58	n/a
Superior Essex Marathon LAN® Category 5e	24	100	1000BASE-T	802.3af, 802.3at	1.52	7.2 (12.96)
Superior Essex Cobra Category 5e+	24	100	1000BASE-T	802.3af, 802.3at	1.41	6.95 (12.51)
Superior Essex DataGain® Category 6	23	250	1000BASE-T	802.3af, 802.3at	0.85	6.7 (12.06)
Superior Essex NextGain® Category 6+	23	250	1000BASE-T	802.3af, 802.3at	0.85	6.7 (12.06)
Superior Essex 10Gain® Category 6A	23	500	10GBASE-T	802.3af, 802.3at	0.81	5.1 (9.8)

VII. PRINCIPLE OF POE

An Ethernet cable does not carry power to the devices but Power over Ethernet (PoE) has a only one cable for both data connection and electric power to the devices. The figure 3 explains the principle of PoE. The PoE equipment combines the data and power together into a single cable and is given to the access point.

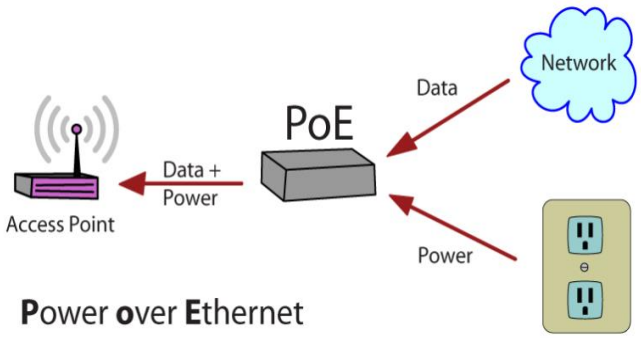

Figure 3: Principle of PoE

Power is "injected" into the cable using "end-span" WAN/LAN switches which include power deliver circuitry. As an alternative, in case user don't need to update existing LAN switches, or simply needs to power a few parts, "mid-span" power injectors may be connected in between the switch and the PD. The end PDs should work with PoE. Power management feature is also supported by many PoE switches so that devices attached to it are power cycled. The PoE power devices turns on telling the endspan or midspan switch that it can receive the power coming through cable.

The figure 4 shows the direct connection using End-Span power source and intermediate source using Mid-Span power injector.

A fully complaint IEEE PoE PD can receive energy over the unused pins or data lines. In this vicinity network administrators should be careful because a few PD's claiming compliancy with the IEEE PoE requirements are constrained to the usage of mid-span power resources using the unused pairs. Mid span injectors does not always verify the end devices hence sometimes it can cause damage to other non PD devices.

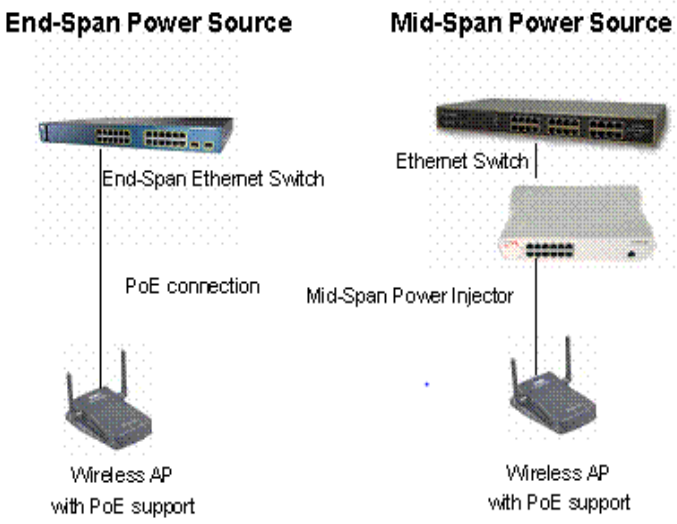

Figure 4: End-Span and Mid-Span Power Injector

To protect the power devices from incoming currents that could occur at some stage in powering up, it is necessary that the PD have inbuilt inrush current safety. The PD having this protection starts with a low current usage stage to prevent the power sourcing equipment (PSE) from getting damaged and then switches to a excessive current level permitting the PD to use its required power of maximum 100 watts.

Fiber extenders are used to extend cable distances up to 100 Miles or 160 km, without the loss of information due to long distance copper cables. LAN extenders increase network distances till 6 miles or 10 km, however if the distance crosses 328 feet cable can have drastically less data speeds. Instead of a 100 Mb/s, the information will decrease lower rate as 2.3 Mb/s. Also, security is provided by fiber cable. Electromagnetic emission is not generated by it so it is very

difficult to detect. Cable is extremely reliable as it is not vulnerable to electrical interferences, or information loss due to temperature, pressure or atmospheric conditions, cable is extremely reliable.

Fiber runs from a present data to a place with power access. A PoE Media Converter is powered by means of either AC or DC electricity. The media converter is hooked up between the power deliver and the fiber cable. In copper cable (STP or UTP) Ethernet can be provided up to 100 meters to the power device. The PoE Media Converter converts the data from fiber to copper, adding power and then transmitting it to the power device.

If Ethernet service has to be extended more than mentioned limits of IEEE 802.3 of 328ft / 100m, Ethernet Extenders are the used. These Ethernet Extenders increase Ethernet connections throughout copper wires. Uses single twisted pair (Category 5/6/7), any copper wiring formerly used in alarm circuits, E1/T1 circuits, RS-232, RS-422, RS-485, CATV and CCTV applications. A PoE Ethernet Extender can operate both as PSE or PD.

VIII. METHODOLOGY [9] [10]

Ethernet is usually transmitted using unshielded twisted pair (UTP) cable which has four pairs. Only two of the pair out of four pairs is used for 10 Mbps and 100 MBps Ethernet. There are two connections used with PoE, namely Alternative A and Alternative B. is In Alternative A, the power is transferred simultaneously along with data over the pairs 1 and 2, 3 and 6. That is the DC+ of 48V is delivered as an industry standard on data pin 1 and pin 2 with DC- data given to pin 3 and pin 6. The figure 5 shows the type 1 Alternative A PoE here spare pairs are used for data transfer and signal pairs are used for power transmission

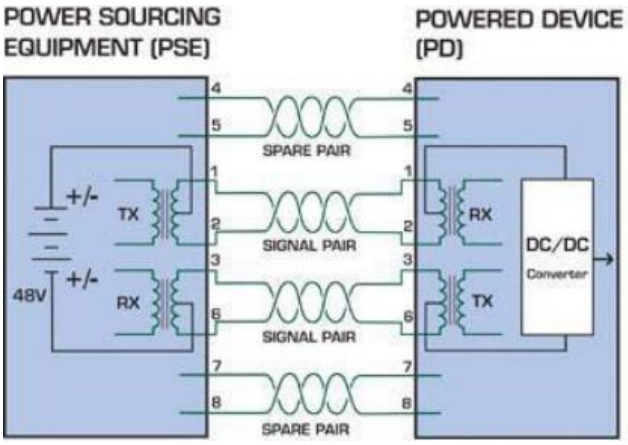

Figure 5: Type 1 Alternative A PoE

In Alternative B, the power is transfered over spare pairs 4 and 5, 7 and 8. That is the DC+ is delivered to unused pin 4 and pin 5 with DC- on pin 7 and pin 8. With PoE data/power interfacing between the two-Ethernet elements is served by LAN cable. The figure 6 shows the type 1 Alternative B PoE it is vice versa of the Alternative A PoE.

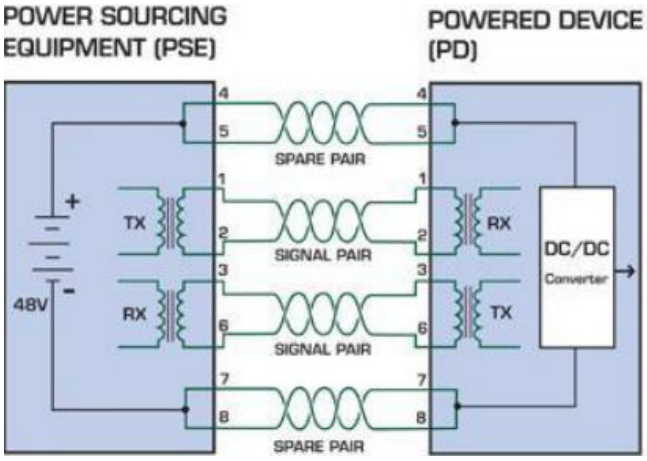

Figure 6: Type 1 Alternative B PoE

Most commonly used is Alternative B by PoE. In Alternative B, the 48V DC power is sent over the cables which are connected to pins 4, 5, 7, and 8 which Base 10/100 networks do not use. The figure 7 shows the Alternative B wiring, there are 8 pins available for the connection.

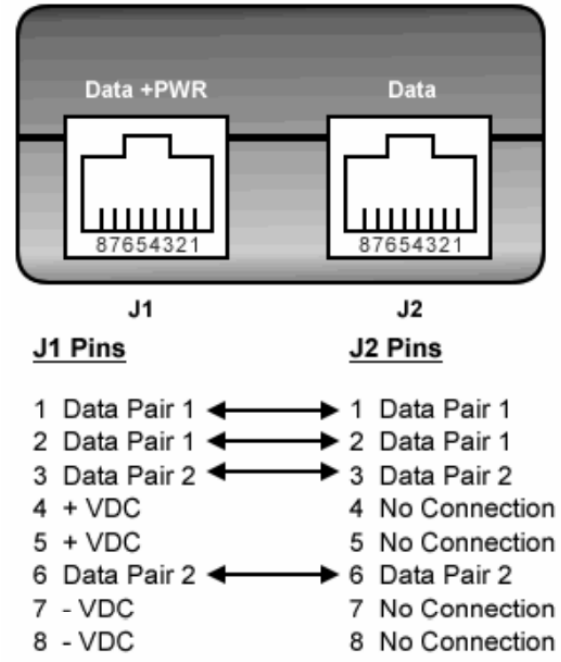

Figure 7: Alternative B wiring

CONCLUSION

Power over Ethernet allows the devices such as VoIP phones, security cameras, Printers; sensors etc transmit data and power on a single Ethernet connection. Deploying PoE technology in the network eliminates the need for installing separate cable for power and data transmission. The PoE deployment is flexible and cost effective while upgrading the Ethernet switch. PoE finds the great scope in almost every field in future as it is cost effective.

ACKNOWLEDGMENT

I acknowledge with immense pleasure the guidance and support extended by Dr. Nagamani K, Professor, Department of Telecommunication Engineering, R. V. College of Engineering, Bengaluru. Her timely suggestions have contributed in successful completion of the paper.

REFERENCES

[1] Z. Xiao, "An Efficient Power Over Ethernet (PoE) Interface With Current-Balancing and Hot-Swapping Control," in *IEEE Transactions on Industrial Electronics*, vol. 65, no. 3, pp. 2496-2506, March 2018.

[2] R. V. White, "Electrical isolation requirements in power-over-Ethernet (PoE) power sourcing equipment (PSE)," *Twenty-First Annual IEEE Applied Power Electronics Conference and Exposition, 2006. APEC '06.*, Dallas, TX, 2006

[3] IEEE Draft Standard for Ethernet - Amendment 2: Power over Ethernet over 4 Pairs," in *IEEE P802.3bt/D3.5, June 2018* , vol., no., pp.1-113, 1 Jan. 2018

[4] IEEE Draft Standard for Ethernet - Amendment 2: Power over Ethernet over 4 Pairs," in *IEEE P802.3bt/D3.6, June 2018* , vol., no., pp.1-36, 1 Jan. 2018

[5] M. S. Alamgir and M. S. Islam, "PoE (Power over Ethernet) switch based remote power control system for the better performance of ISPs in Bangladesh," *2015 18th International Conference on Computer and Information Technology (ICCIT)*, Dhaka, 2015, pp. 23-26.

[6] H. Li, H. Zhang and D. Peng, "Research and design of Industrial Ethernet communication gateway on power station," *Proceedings 2011 International Conference on Transportation, Mechanical, and Electrical Engineering (TMEE)*, Changchun, 2011, pp. 986-989.

[7] L. F. Auler and R. d'Amore, "Power quality monitoring and control using Ethernet networks," *10th International Conference on Harmonics and Quality of Power. Proceedings (Cat. No.02EX630)*, Rio de Janeiro, 2002, pp. 208-213 vol.1.

[8] White Paper | IT and Instrumentation for industry | www.amplicon.com

[9] Technical article on Power over Ethernet by B&B Electronics. www.bb-ele.com

[10] White Paper | Power over Ethernet | Version 0.2 | e | 01.09.2003 | Bouvard White Paper TP061.701_e.doc

Proceedings of the Fourth International Conference on Communication and Electronics Systems (ICCES 2019)
IEEE Conference Record # 45898; IEEE Xplore ISBN: 978-1-7281-1261-9

An Improved Vivaldi Antenna Design for Through-Wall Radar Imaging

Rajashree R Menon[1], Sultana Najeeb[2], Swetha N Prabhu [3], Treesa Angel George[4], Anila Kuriakose[5], Sleebi K Diwakaran[6], Dept. of ECE, Rajagiri School of Engineering & Technology, Kakkanad, India-682039
Email: rmenon05r@gmail.com, sulnajeeb5@gmail.com, swethanprabhu@gmail.com, treesangel15@gmail.com, anilak@rajagiritech.edu.in, sleebi@gmail.com

***Abstract*—This paper presents an improved Vivaldi antenna design for Through Wall Radar Imaging (TWRI). It is one of the most emerging radar technologies that has different applications in real-life situations. Radar uses EM waves to penetrate through the wall, and then detects the objects behind the wall. Antenna plays a very important role in TWRI system. Vivaldi antenna can be used as an ideal candidate for this system. The antenna presented here operates from the frequency 2.5 GHz to 11.3 GHz and shows a constant radiation pattern in the operating bandwidth. The gain obtained is around 6 dBi. The effect of various antenna parameters are also studied in this paper. Furthermore, corrugations and grating elements are added to analyze the effects on gain and bandwidth. With the above enhancements in design, a bandwidth of 8.8 GHz and an improved gain of around 9.6 dBi has been achieved.**

***Index Terms*—Vivaldi, Through Wall Radar Imaging, Grating elements, Corrugations.**

I. INTRODUCTION

The main objective of TWRI is to use electromagnetic (EM) waves to sense and image moving and stationary objects through visually opaque obstacles such as walls[6]. It is a unique application of UWB technology. UWB radio technology has a bandwidth greater than 500 MHz or 20% of the center frequency according to Federal Communications Commission (FCC)[1]. Many existing UWB antennas can be considered for TWRI applications. The choice of the specific antenna depends on the wall material as well. The wall attenuation is comparatively higher at high microwave frequencies. Among the various UWB antenna designs implemented for TWRI application, most of the antennas operate at a higher UWB frequency range (8-12 GHz). Here, we have chosen concrete walls of thickness 19.45 cm for which the optimum range of operating frequency is 2-6 GHz[6]. Hence, designing a UWB antenna for this frequency range (2-6 GHz) remains a challenge.[1-4] represent various UWB antennas that can be used for TWRI application. Among these, Vivaldi and Horn antennas are most suitable antennas which satisfy the TWRI specifications[1,2].

This paper includes the design of UWB Vivaldi antenna for Through Wall applications. Vivaldi antenna is a tapered slot antenna that is based on the principle of travelling wave antenna[5]. Vivaldi antenna was first proposed by P. J. Gibson in 1979[7]. The antenna has an exponentially tapered profile, which provides wide bandwidth and end-fire radiation pattern.

II. DESIRED CHARACTERISTICS OF TWRI ANTENNAS

A. TWRI Antenna Constraints

One of the important characteristics of a TWRI antenna is that, it should be compact and light weight for portability[10]. The antenna should have a gain that is sufficient for the signal to penetrate through the wall and detect the target behind the wall. The return loss should be less than -10 dB so that impedance matching is obtained in the desired frequency range. The antenna must have better transmission and radiation performance with minimum number of side-lobes and back-lobes[6]. The antenna should radiate short transient pulses with minimum distortion[6,10].

B. Antenna in TWRI system

The main elements of the TWRI system are UWB antenna, RF transceiver, duplexer, signal generator and image processing and display unit. Transmission and reception of electromagnetic waves is carried out by the antenna in a TWRI system. In a monostatic radar configuration a duplexer is required to switch between the transmission and reception of signals by the common antenna. The signal generator produces UWB pulses that is transmitted through the wall. The signal after penetrating through the wall is reflected by the target and reaches the antenna in receiver mode. The image of the target is then processed using a focussing algorithm. The main parameters that influence the quality of image produced are cross range and down range resolutions[11]. The Fig 1. shows the configuration of TWRI system components.

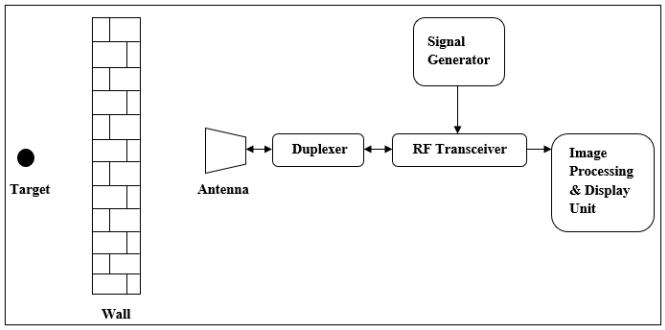

Fig. 1. Monostatic configuration of TWRI system

C. Link Budget Equation

The performance of a communication system depends on the signal-to-noise ratio (SNR) at the receiver. The link budget is generally used to predict the received power in a communication system. For TWRI, the gain required for the receiver antenna is estimated using Link Budget equation[12]:

$$R^4 = \frac{P_t G_t G_r \lambda^2 \sigma}{10(4\pi)^3 K T B L_s L_w^2} \tag{1}$$

where, R is the range, σ is Radar Cross-section(RCS), L_s is system loss, λ is the wavelength of signal transmitted, P_t is the power of the transmitted signal, L_w is the wall attenuation, B is the IF Bandwidth.
Typical values assumed for the above mentioned parameters, in our proposed design are, SNR= 10 dBi, R = 20 m, λ = 0.075 m, σ = 100 cm x 100 cm, P_t = 15 mW, L_s = 10 dBi, B = 10 kHz and concrete wall losses L_w = 15 dBi.
Gain obtained after substituting these values in equation 1 is G=6 dBi. Hence, we need to design a UWB antenna that has a minimum gain of 6 dBi.

D. Vivaldi for TWRI System

Vivaldi antenna is a wide band antenna that has a two-dimensional structure. Being light-weight and planar, the antenna could be mounted on a portable device, thus making it suitable for through wall imaging. Compared to other UWB antennas, Vivaldi antennas show minimum distortion in the shape of the transmitted UWB pulses[6]. The antenna has a constant moderate gain over the wide band of operation. Hence, Vivaldi antenna has been chosen as it satisfies most of the constraints of a TWRI system.

III. DESIGN CONSIDERATIONS

A. Structure Explanation

The designed vivaldi antenna for TWRI is shown in Fig. 2 and Fig. 3. The antenna consists of three layers. The top layer act as the ground plane. The middle layer is composed of substrate. The feeding technique used is microstrip to slotline transition. It forms the bottom layer.

1) Substrate: : The antenna is designed on FR4 material of 0.8 mm thickness that has a permittivity(ϵ_r) of 4.3.

2) Ground plane: : It consist of a uniform rectangular slot that is connected to an exponentially tapered slot. Circular cavity is attached at one end of slot and the other end of the slot is exponentially tapered. The shape of flaring of taper and the cavity determines most of the antenna performance. The slot width affects the highest frequency of operation and the width of antenna affects the lowest frequency[5].

3) Feeding Technique: : The cavity-stub model is used for designing wide band Vivaldi antenna. Micro strip and slot line crosses at right angle to each other to form cross junction. At the cross junction, micro strip line behaves as short circuit, since radial stub is open circuited at the end which is approximately $\lambda/4$ in length[1] and the short circuited slot line behaves as an open circuit. Energy is coupled from microstripline to slotline, which is then radiated from the exponential slot to give an end-fire radiation pattern.

B. Equations

The tapered profile of the antenna is given as,

$$y(x) = \pm ce^{rx} \tag{2}$$

where, constant c is given by,

$$c = \frac{s}{2} \tag{3}$$

$$r = \frac{1}{L}\ln(\frac{W}{s}) \tag{4}$$

where, L, W, r and s are the antenna length, antenna width, opening rate and width of slot at origin[8].

C. Simulated Structure in CST Microwave Studio

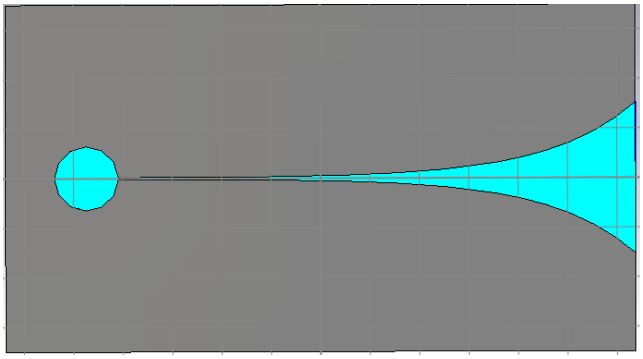

Fig. 2. Vivaldi antenna- top view

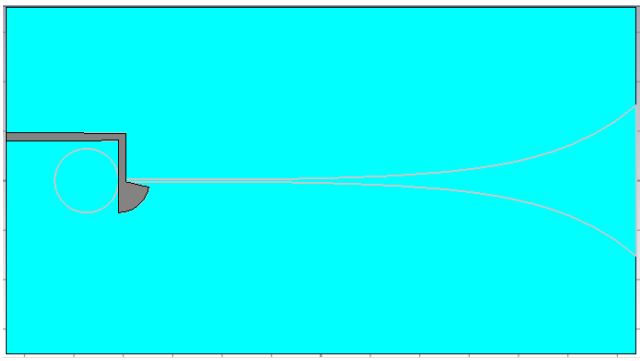

Fig. 3. Vivaldi antenna- bottom view

The values we have chosen for our vivaldi construction are mentioned in Table 1[9].

IV. SIMULATION RESULTS

The proposed vivaldi antenna was simulated in CST simulation tool and results were obtained as follows:-

978-1-7281-1261-9/19/$31.00 ©2019 IEEE

TABLE I
CALCULATED ANTENNA PARAMETERS

Parameters	Dimensions(mm)
Antenna length	128
Antenna Width	70
Taper length	80
Taper width	31
Slot width	0.5
Slot length	25
Taper rate	0.057
Stub angle	80
Substrate thickness	0.8
Circular cavity radius	6.46
Radial stub radius	6.46

A. *Reflection coefficient*

The variations in reflection coefficient with frequency are shown in Fig. 4 for FR4 substrate with ϵ_r=4.3. It is observed that the reflection coefficient is below -10 dB for 2.5-11.3 GHz. The fractional bandwidth for the simulated antenna is 127.5. The antenna has an operating bandwidth of around 8.8 GHz.

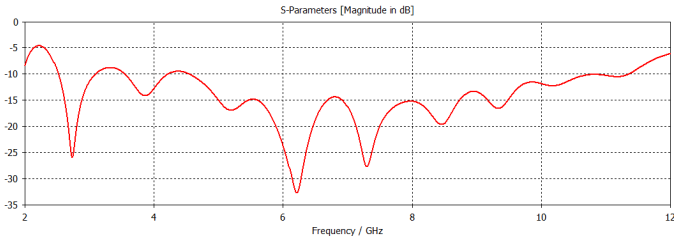

Fig. 4. Variation in reflection coefficient with frequency

B. *VSWR*

The voltage standing wave ratio for the designed antenna is shown in Fig. 5. The value is found to be less than 2 for 2.5-11.3 GHz.

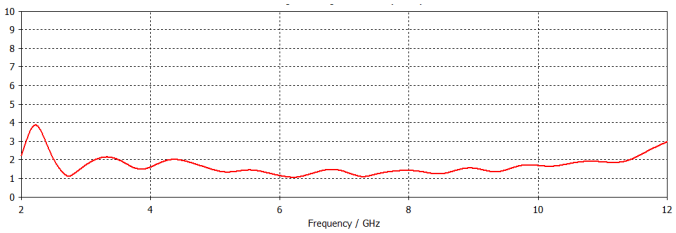

Fig. 5. VSWR Plot

C. *Gain*

It is found that maximum gain of the antenna is always greater than 5 dB in operating frequency range. The far-field directivity of the antenna at 4.5 GHz is shown in Fig. 6. The gain obtained is around 6.6 dBi. The main lobe is directed at 90° and has 3dB angular width of 52°. Further enhancement in gain can be obtained if grating elements and corrugations are added.

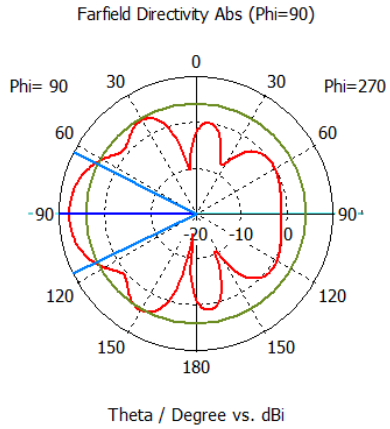

Fig. 6. Far-field Directivity at 4.5 GHz

D. *Effect of adding Grating Elements*

Grating elements were added at the opening end of the exponential slot as shown in Fig. 7. It is observed that as the number of grating elements increased, gain started to increase from a particular point from the radiating region. The side-lobe level also reduced, thus favouring the TWRI application. The length of the grating element was chosen to be 14 mm. Fig. 8 shows the return loss plot of the antenna with grating elements.

When the number of grating elements added was 4, the gain at 4.5 GHz was found to be 7.82 dBi with a reduced amount of side-lobes as shown in Fig. 9. The 3 dB angular width also reduced to 47°, giving a narrow and directive beam suitable for TWRI application.

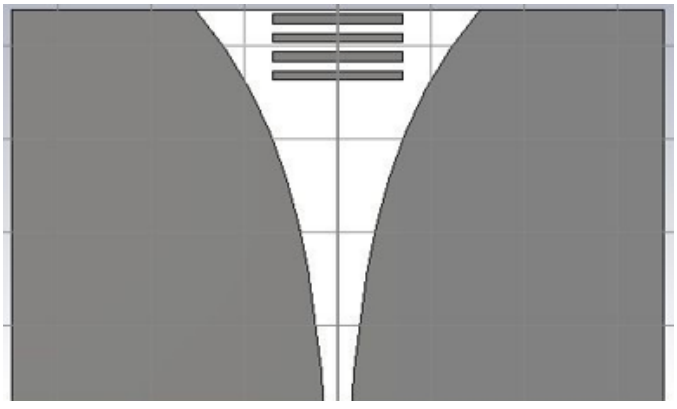

Fig. 7. Vivaldi antenna with Grating elements

978-1-7281-1261-9/19/$31.00 ©2019 IEEE

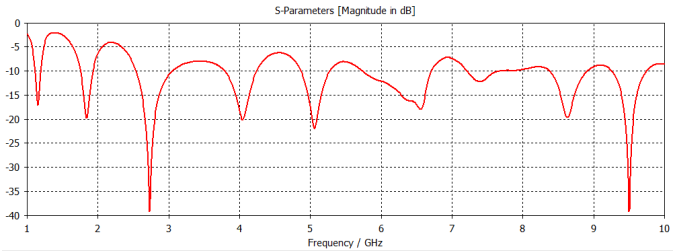

Fig. 8. Return Loss of Vivaldi antenna with Grating

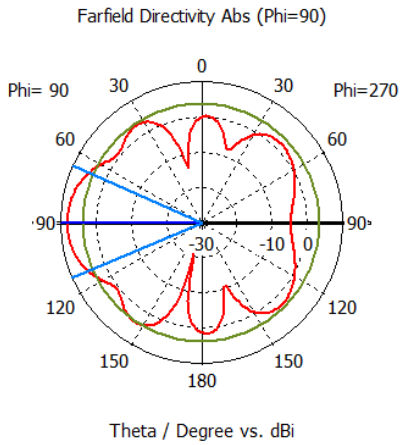

Fig. 9. Directivity of Vivaldi antenna with gratings at 4.5 GHz

E. Effect of adding Corrugations

Corrugations were added along the taper as shown in Fig. 10.As the number of corrugations increased, the gain improved. Eight corrugations each on both sides were added. The width of the corrugation was chosen to be 5mm, maintaining a gap of 1.5 mm between the corrugations. The rate of decrease of corrugation length was fixed to 1.5 mm. Fig. 11 and Fig. 12 show the results of adding 8 corrugations to Vivaldi antenna. The gain obained was 9.6 dBi with a satisfactory side-lobe level. The 3 dB angular width is 63°.

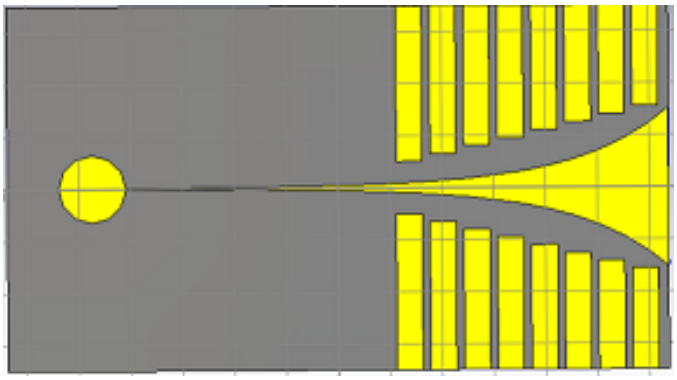

Fig. 10. Vivaldi antenna with 8 corrugations

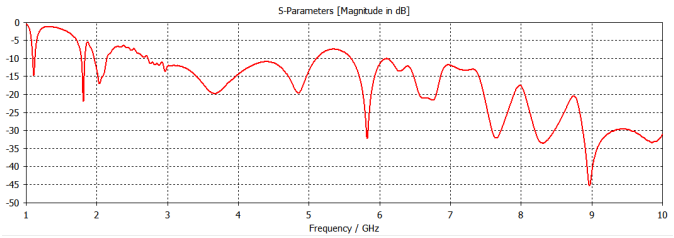

Fig. 11. Return Loss of Vivaldi antenna with corrugations

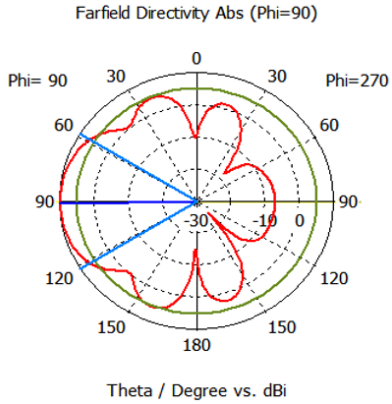

Fig. 12. Directivity of Vivaldi antenna with corrugations at 4.5 GHz

V. Conclusion

This paper presents the design of vivaldi antenna on FR4 substrate suitable for TWRI application.The proposed antenna is developed to operate in the frequency range of 2.5 GHz to 11.3 GHz with a gain greater than 5 dBi. CST microwave suite was used to simulate the antenna. The antenna has return loss less than -10 dB with VSWR value less than 2. Since TWRI system requires a moderate gain, gain enhancement techniques have been introduced in the antenna design. Addition of grating elements and corrugations improved the gain upto 9 dBi with satisfactory return loss for the frequency range 2.5 GHz to 11.3 GHz which can be considered as wide band. The gain obtained is greater than the minimum 6 dBi gain required for the TWRI system.

VI. Future Scope

Array of Vivaldi antenna elements can be implemented to improve the gain. Performance analysis using different feeding techniques like stripline to slotline transition, co-axial to slotline etc could also be considered for vivaldi antenna .

References

[1] B. Kumar, K. A. Vardhan and P. Sharma, ”Design of Slotted Vivaldi Antenna for Through Wall Imaging System” 11th ICIIS, 2016.
[2] B. Ylmaz and C. zdemir,”Design and prototype of a compact, ultra wideband Double Ridged Horn Antenna for behind Obstacle Radar applications”, TUJE, Vol. 1, Issue 2, pages 76-81, 2017
[3] Q. Lu, L. Zhou, C. Tan, G. Lu,”A Novel Wide Beam UWB Antenna Design for Through-the-Wall Radar”, IEEE, 2010

[4] L. Siu, H. Wong, K. Luk,"A Dual Polarized Magneto- Electric Dipole With Dielectric Loading",IEEE Trans. on Antennas and Propag., vol.51, no.3, March 2009.
[5] P.J Gibson,"The Vivaldi aerial.",Proceedings of the 9th European Microwave Conference, pages 101-105, 1979.
[6] M. G. Amin,Through the Wall Radar Imaging, CRC Press, 2010
[7] R. Dhawan, G. Kaur,Vivaldi Antenna Simulation on Defining Parameters, Parametric study and Results", IJCTA, pages 5129-5138, 2016
[8] G. K. Pandey, H.S. Singh, P.K. Bharti and M. K. Meshram,"High Gain Vivaldi Antenna for Radar and Microwave Imaging Applications", IJSPS, 2015
[9] B. Ylmaz and C. zdemir,"Design and prototype of radar sensor with Vivaldi linear array for through-wall radar imaging: an experimental study", Journal of Applied Remote Sensing, 2016
[10] Y. Yang, Y. Wang, A. E. Fathy,"Design of Compact Vivaldi Antenna Arrays for UWB See-Through wall applications", PIER 82, 401418, 2008
[11] C. R. P. Dionisio, S. Tavares, M. Perotoni, S. Kofuji,"Experiments on Through-Wall Imaging using Ultra Wide Band Radar", Microwave and Optical Technology Letters, Vol. 54, No. 2, February 2012
[12] T. Bui, J. Rabig,"Through-the-Wall Imaging Radar", The University of Adelaide, October 2011.

978-1-7281-1261-9/19/$31.00 ©2019 IEEE

Proceedings of the Fourth International Conference on Communication and Electronics Systems (ICCES 2019)
IEEE Conference Record # 45898; IEEE Xplore ISBN: 978-1-7281-1261-9

A Survey on Privacy Preserving Schemes in Cloud Computing

Mr. Sunilkumar, MTech Computer NetworkEngineering
Department of computer Science and Engineering,
Siddaganga Institute of technology Tumkur, India.
sunilhavani@gmail.com

Mr.A.H. Shanthakumara, Asst.Professor,
Department of computer Science and Engineering,
Siddaganga Institute of technology Tumkur, India.
shanthakumara@sit.ac.in

Abstract: Cloud computing furnish services such as storage, database, software and many more and are accessed through cloud service platform via internet. As cloud computing is a most widely used technology there are plenty of user who uses the cloud for their computation and inquire about exercises in the field of information the board. To handle this increased data cloud data storage is the best technology. Keeping data in the cloud more reliable than maintain in the local machine. But providing security for data which is stored in cloud is big issue.it is more important to maintain privacy of the user data if the data is loss it affects the user cloud service. By using some encryption method, we can assure privacy for a certain level in the cloud. There is no complete privacy preservation system is available. This is a survey on different privacy preservation schemes in cloud.

Keywords: Cloud Computing, Two Factor Authentication, RSA, Two-layer encryption.

INTRODUCTION

Cloud computing is most widely used technology and there will be a greater as for number of users because of more user more data will be produced and handling such a huge data in a real world is difficult task so solution for this is cloud. There are different service and deployment models [1] service models are as follows

1. SaaS: it gives feature to use any application through cloud platform. Software as a Service Applications is used by the user from anywhere in the world by internet through web browser. The user need not to have any cloud infrastructure like network, OS, servers, Storage component or even application. it is not applicable for the application that requires real time response such as email and banking related application.

2. PaaS: it gives a user to a platform to run their application for which can't handle the large software and hardware platform. Platform as a Service with help of programming languages, it provides user to put user-developed or acquired applications and tools supported by the provider. PaaS provides application for software development where user will collaborate, deployment and testing services should be automated, PaaS is not suitable if user expecting for portable application and user want to improve performance by some customization.

3. IaaS: it's a delivery model which contains licensed software's based on user needs they

will pay and uses the services. Infrastructure as a Service it is also termed as on-demand services. User will access these services by using browser. Most of the organisation pay for the services for which they need instead buying the software's. Some applications which is provided by SaaS is office software, database software, development software, communication software.

The different deployment models are as follows Public, Private, Community and Hybrid clouds [6]. To store large amount of data storing devises which are high expensive, requires more space and maintenance should be done. Cloud computing provides to store any huge size proportion of information at various limit area and they are dealt with autonomous way. The information stockpiles are taken care of by the CSP. The CSP act as an intermediate which provides different services to the customer such as network, infrastructure and business applications in cloud.

Obligation of the cloud organization is to re-appropriated information with reasonable stage model. The virtual machine official will put the data into any managed Virtual Machine (VM) districts. These virtual machines are made and kept up by the Virtual Machine Manager (VMM). with the assistance of cloud, we can store data in cloud as much we required instead of putting away in local machine yet giving security to the data in cloud is important task. Privacy first important thing to provide privacy for customer data in cloud if the privacy is lost it affects promises to provide good service mainly it affects to the public clouds because data is in unencrypted form present in servers which are handled by cloud service provider. Customer cannot completely trust on CSP for providing privacy for their data for all 3 models priorities of privacy are different.

Privacy Issues in Cloud

Guideline speaking, assurance alludes to the condition or state of concealing the nearness or view. There is a need to achieve this state in the spots where the private things are utilized, for example, information and documents. data of cloud need to be had privacy of client personality and controls leaking of privacy leads to major failure of the framework to keep up information security, it workable for fruitful organization and use of any administration. cloud data storages are disturbed in limited place.it is the responsibility of the CSP to maintain safety of the user data. On the off chance that appropriate security instrument is executed the security is disregarded at the storage service.

Only owner will be able to access data in cloud sometimes CSP can peruse user data for his own benefits' might be sell the user information for some organizations for the sake of money. There might be confidential data which related to the Government records and examination records which might be require for some businessmen's and some organizations can offer personal data of the reputed persons of society such as prime minister, sportsman and actors' personal data can be used for the crime. Using client data is offense some of attackers might change the data of cloud storage.

Dangers malignant programming is acquainted with this stockpiling for getting access and increase knowledge about the information. Privacy manages the availability and accessibility of delicate data to the expected beneficiaries. Re- appropriated information got to and changed just only by clients with suitable access benefits. assume an association has arranged and re-appropriated their information in the cloud. The redistributed information substance is given to the administrator to put in the cloud. It is recommended to guarantee that the administrator can't see or alter the information substance. After record

redistributing, nobody including specialist community can see or alter the substance. If a specialist organization or neighborhood manager is endeavoring to examine the record substance, it must not be done. Protection safeguarding manages the sort of security in redistributed data. This could be guaranteed by utilizing Cryptographic techniques.

Related Works

One of the main solutions for providing privacy in cloud by using different encryption and decryption techniques.

RSA Algorithm RSA [2] algorithm asymmetric block cipher [2], it uses variable size of block. Algorithm is mainly used encrypting and decrypting of data files. The idea of RSA is since it is hard to partition an enormous number open key is a mix of two numbers where one is augmentation of two huge prime numbers.in a similar way private key is gotten from an equivalent two prime numbers. If anyone divides substantial number, the private key is undermined. The encryption depends on key size as key size increases strength of the encryption also increases usually RSA keys are 1024 0r 2048-bit lengths but 1024-bit length key is easy to break than 2048 bit key. But till now it seems to be an infeasible task. An example of asymmetric cryptography

1. A client sends its public key to the server and solicitations for certain information. 2. The server scrambles the information utilizing client's public key and sends the encoded information. 3. Client gets this information and decodes it. There will be two keys public and private where these keys are used respectively to encrypt and decrypt message. The RSA consists of encryption and decryption keys can be calculated by the mathematical operations then it is possible to get cipher text and the plain text by using formula.

$$C = ME \bmod (n)$$
$$P = ME \bmod (n)$$

Q. Xiong and L.T. Yang [3] these authors proposed an authority-based SAPA it is termed as privacy-preserving authentication protocol [4]. this show accomplished shared access master by unapproved access sorting out an instrument with assurance and security thought in this paper principally examined on the following properties 1. Shared access authority is accomplished by anonymous access solicitation coordinating system 2. Attribute-Based Access Control (ABAC) is embraced with the goal that a client can just access to its own information 3. Proxy re-encryption applies to give information to different clients.

In this paper author mainly focused mainly focused on authentication so that user access their data on remotely from cloud model. There will be a different group are there in cloud where each group has its own user which can access data. A supplier makes a request to access information fields, however it isn't ensuring that carrier will permit its access demand. In case the bearer decays its solicitation, the provider's entrance will be uncovered close-by nothing picked up towards the ideal information fields. The supplier may not send the passage solicitation or disadvantage the unaccepted requesting from the get-go if it consistently comprehends that its sales will be denied by the transporter. It is ridiculous to inside and out reveal the provider's private data with no privacy contemplations. A BGKM proposed to overcome the shortcoming of using same key for both encryption and decryption in a public cloud model. It is No longer important that purchaser rely on the public key cryptography. One can select the symmetric keys significantly toward the crowning glory of decryption. A pleasant-primarily based get admission to manage technique used to achieve customer who is having the persona properties can decrypt the substance the creator assuming that a more ultra-modern protection the trouble is seen to perform sharing of prolateness- safeguarding access expert. Through the wrapped traits transmission statistics unsure great is executed. Session

identifiers are utilized for anticipating the session association.

M. H. Au and X. Huang [4] Proposed a model it is based on web-based class computing service [4]. Major problem to provide security for class service is authentication. User received to login to access the class service by using traditional username and password-based system, but it has two problems. Username and password-based system for privacy preserving. Usually computers are shared by different people at that time it is easy for hacker to install spyware to tell details of username and password. To overcome these issue two-factor authentication (2FA) method is used. It is common in most of the web-based services in addition username/password as OTP (one-time password) is received to a service like mobile user needs to enter to complete login process. To provide more security to 2FA a protocol is proposed for web-based service computing service using a lightweight service is having 2 properties It performs some computation also i.e., having exponents. It is tempered i.e.., no one can break to get secrets. With this service protocol proxies 2FA security first the user security key is received.

Services are connected to the computer to authenticate user to access cloud services. User receives both invoked to access security key can't be uses another device belong to other for the access. This design supports a fine-grained attribute-based access control. For the actual abrogation of public keys mediated cryptography was structured. Immediate revocations of public keys are intended for mediated cryptography. A Security Mediator (SEM) model is prepared issue to this cryptography. Regardless, it gives a weight that this SEM dependably continue to be to play out any exchanges. A modified variant of this model planned as protection interceded testament less cryptography. In this framework, the patron has a thriller key, open key, character, and marking calculation. Mystery key & SEM model will be required furthermore required. It takes care of the disavowal issues. Client is mysterious to this model which causes security issue. with short term signature using cryptography added key we can store large haul keys to the protected gadget and unbound gadgets. A Security Mediator (SEM) version is deliberate reliant in this cryptography. It requires a smaller range of prerequisites. Performance analysis and protection evaluation are carried out. It enables a safety framework model to give privateness backing to the data. It normally calls for the gadget to guarantee privacy. Along those lines, it isn't convincing beneath various cloud administrations storage mechanism.

E.Bertino and M. Kantarcioglu [5] has proposed A great grained get admission to manage with first-class grained encryption technique for cloud records [7]. there are many models which are proposed by different authors for outsourcing data which provides encryption. But one problem with these models is that there will be an overhead of computation and communication.so to overcome this issue a Two Layer Encryption (TLE) technique is addressd.in this model at both client side and server-side encryption will be performed that is two-layer encryption and fine-grained encryption respectively. there is a one problem with this model where it can't disintegration Of Access Control Policies (ACPs) at time of TLE.So, in -layer encryption over scrambled information fine grained access control is connected and Various symmetric keys are utilized for correspondence these keys will influences connection between records things. By acting unmarried layer encryption, we will confine the troubles by means of the speak key management plans. customer can access content by using the fine-grained access control using some methodologies this task is done. There are two models in access control push and draw based models. In this way, it is hard to keep up the key mystery in a dynamic information

Sharing framework. Redistribution of the key is struggling besides the assistance of expressive get admission to manage techniques isn't always maintained. Power based totally models required the statistics distributer to live online to furnish get right of entry to. Such works ensures this, using untouchable garage administrations.it is the responsibility of the owner to provide the client privacy and control policies from data publisher. There are six phases are used for Two-layer encryption technique.

TLE perform the encryptions by gathering group key approach to guarantee the security on re-appropriated information It has such overhead on computation on the server facet and inside the get entry to control strategies. Accomplishment of the model is based on the attribute-primarily based keys, access manage strategies.

B.Justus and D.Loehr[7] to provide security for cloud and local administrators authors has designed a model called privacy preservation Mainly provides privacy for data storage provider is needed when we are outsourcing the sensitive data. This data can be leaked this make to build which provides security for both internal and external. In this model, the data is main thing we need to provide security more for that, so all data storage encrypted as backup data should be performed by cloud service. Data backup is automated for encryption proxies. Encryption proxies means which allows third parties to allow cipher text which has been encrypted for one party so that it may be decrypted by another. So, data decryption keys are exchange across secure channel by compressing PCR value we can achieve integrity. If both encryption proxies have same state, then exchange of key matrix take place. For example, when a request is made for data then a new request is designed by developer and sends to an editor, so editor integrates the request and set up access rights for the new request after setting file is signed and sends to next editor and he checks like after that he write sign file. Now encryption proxy access file on condition files is signed by two editors all their signatures are good access if changes rejects the file. The technologies which are used in this model are XML, XML-Encryption, XML Signature and Trusted Platform Module (TPA).

Larry and Ray [8] Propose An algorithm for nameless sharing of private data amongst N parties is evolved [6]. This approach is used to assign nodes ID numbers ranging from 1 to N. The received ID is not known to the other members of the group. If private communication channels used, then collision will not occur. It is likewise tested that there's no collision in personal verbal exchange channels use. This is sent without the use of a relied on crucial authority. The more recent algorithms are developed over a comfortable sum records mining operation the use of Newton ‘s identities and Sturm ‘s theorem. Markov chain technique is used to understand the data on the desired wide variety of iterations.

The pc algebra gives the outcomes towards the finishing touch fees. Author discovered that some cloud primarily based tools used for website control are providing get admission to for a server to saw the traveler moves on a website. For network nodes, such programs are there for requiring dynamic particular ID. This ID is required in sensor community services for administration sports or for protection to the man or woman nodes. It isn't an anonymous community, the contributors acknowledged and identifiable by way of each other’s. Suppose that a set of hospitals with man or woman databases wish to compute and share best the common of a records item, which include the number of clinic acquired infections, without revealing the cost of this facts item for any member of the organization. Thus, N nodes n1. N2, nN have statistics items d1, d2….DN, and desire to compute and share simplest the overall price T=d1+d2+…..+dN A at ease sum algorithm lets in the sum to be amassed with a few guarantees of anonymity T.Secur sum algorithm used for transmitting data securely.

An set of rules for sharing simple integer information on pinnacle of relaxed sum is construct. This is used with the nameless ID

challenge (AIDA) set of rules. It calls for a big range and various iterations. The writer prescribing a evaluate on at ease sum, precise technique of transmitting easy facts with strength sum, sharing complex statistics with an AIDA, and how to discover an AIDA. Comparison of numerous AIDA like Slot selection AIDA, Prime modulus AIDA, Sturm ‘s Theorem AIDA are discussed. Communications Requirements of AIDA methods are defined. Author concluding that the usage of newton identities reduces the communication overhead greatly. So the use of many slots with less number of rounds is needed. The polynomial solution may be avoided by way of making use of strum’s theorem. The non-cryptographic algorithms are simulated. The requirements are based totally best on the secure algorithm chosen.

COMPARIOSN TABLE

Table: Comparison table of different privacy preserving schemes

Comparison Factor / Paper	Q. Xiong and L.T. Yang	M. H. Au and X. Huang	Larry and Ray	E.Bertino and M. Kantarcioglu	B.Justus and D.Loehr
Access Control	Attribute based	Fine grained	No	Fine grained Course grained	Fine grained
Encryption	Proxy re encryption	yes	No	Two layer encryption	XML Encryption
Key management	Broadcast group	yes	No	Group key	No
Policy	No	Two factor authentication	Anonymous ID management	Group key management policy	XACML Policy
proxy	Re encryption	No	No	No	Encryption Proxy
Security person	No	No	No	No	No
Signature	No	yes	No	No	XML signature
Central authority	No	No	No	No	Trusted platform module

Over View of Privacy Preservation

From the relative investigation of existing privacy preservation models, there are different methods and techniques are used different authors but the motive of the all authors is to provide privacy for outsourced data. There some mechanisms which provides access control user and what part of data can be used. These models provide depending on client roles, attribute, policy and group-based access control schemes. to scramble the user data encryption will be performed on a document. different techniques are used to encrypt the data such as single level and multilevel encryption are performed. Some specific parameters are used at the time of access to verify the authenticate user.

providing security for the static files is easier it is difficult for such file where data will be updating and deleting for every time.in such case re-encrypt should be performed on whole file this will be an extra task. For user’s proxy server credentials are given so that user no need to there every time. If the credentials are leaked or meets failure at that time, there is possible of effects of wholeframework. Encryption methods will not support for all the operations of cloud data. homomorphism encryption will not support for analytics operation of data. There is no any scheme is proposed which provides complete security and privacy.

CONCLUSION

Cloud computing more useful for digital data access which provides different services on cloud. There are a greater number of users ofcloud, so it is increasing data storage and retrieval daily.so it is essential to provide security of user data it is priority to provide privacy for client information while storing and retrieving. Different encryption techniques and privacy preserving schemes are used to secure the data. With help of hash functions and signature key privacy is preserved there are some models which provides data recovery techniques. These

models are designed to secure the data of cloud. In destiny with the aid of the result of this audit a consolidated a model of cloud safety framework is planned to guarantee all protection organizations.

REFERENCES

[1]. Dan C. Marinescu, "Cloud Computing Theory and Practice", 1st Edition, Elsevier and Morgan Kaufmann Publication.(p-13)

[2]. https://www.geeksforgeeks.org/rsa-algorithm-cryptography/

[3]. H. Liu, H. Ning, Q. Xiong, L.T. Yang, "Shared Authority Based Privacy-Preserving Authentication Protocol in Cloud Computing," Transactions on Parallel and Distributed Systems, Vol. 26, No. 1,pp-241-251, January, 2015

[4]. J. K. Liu, M. H. Au, X. Huang, R. Lu, J. Li, "Fine-Grained Two-Factor Access Control for Web-Based Cloud Computing Services,", Transactions on Information Forensics and Security, Vol. 11, No. 3, pp.484-497,March, 2016.

[5]. M.Nabeel, E. Bertino, M. Kantarciogluand B.M. Thuraisingham,"Towards Privacy Preserving Access Control in the Cloud," Proc. Seventh Int'l Conf. Collaborative Computing: Networking, Applications and Worksharing (CollaborateCom '11), pp. 172-180, 2011.

[6]. R. G. Gallager, Low Density Parity Check Codes. Cambridge, MA,USA: MIT Press, 1963.

[7]. U. Greveler, B. Justus, D. Loehr, A Privacy Preserving System forCloud Computing, ICCIT, IEEE, pp- 648 - 653, 2011.

[8]. Larry. A. Dunning, Ray. Kresman, "Privacy Preserving Data Sharing With Anonymous ID Assignment", Transaction on Information Forensics and Security, IEEE, Vol. 8, No. 2, pp. 402-413, February, 2013.

Proceedings of the Fourth International Conference on Communication and Electronics Systems (ICCES 2019)
IEEE Conference Record # 45898; IEEE Xplore ISBN: 978-1-7281-1261-9

Optimization Of Vehicle Using Monitoring Systems

Sasvanth Narayan R, Loganathan V, Prateek Lakkar, Suganthan B
Department of Mechanical Engineering
Sri Krishna College of Technology
Coimbatore, India
sasvanth123@gmail.com

***Abstract*— In recent years, vehicle monitoring systems helped riders in gathering real-time information about their vehicles. This paper puts forward, the advancements which can be done using the data's gathered from the monitoring systems and optimize the vehicle. The monitoring system comprises of the following units processing unit, sensors unit, storage unit and a communication unit. The processing unit, communication unit and sensors unit has standard sensors and modules like weight sensor, global positioning module, real-time clock module, speed measuring module, etc. In the storage unit, the data's are stored in the built-in storage module as well as in the cloud. Ishikawa diagram helped to analyze the root causes of the problems faced by the riders. Then by considering those causes, the following solutions current fuel price display, audio communication of the customized details, fingerprint unlocking, mileage indication, automatic maintenance updater and economic travel assistant has been put forward. Towards the end of this paper, a survey related to the research has been described.**

Keywords—vehicle monitoring systems; Ishikawa diagram

I. INTRODUCTION

Road transport is one of the most sophisticated means of carrying around people and things for our day to day life until different problems related to our vehicle maintenance and fuel economy steps in. The present vehicles do not have proper maintenance scheduling or they are integrated with offline data storing methods that are used only for feedback purposes. The development of a unique integrated procedure to find a perfect solution for complete vehicle maintenance including track of fuel usage, tracing of non-economic activities and damage of vehicle parts and performance. Recording and implementing simple technology along with Microcontrollers that can be integrated with numerous cloud and virtual storage devices that are not only secure but also dynamic and provide real-time monitoring. The procedure must be user-friendly and easy to install such that the common man doesn't feel it as a burden but as a pride to have it. "Fig. 1," represents the Ishikawa diagram, also called as fishbone diagram which describes the root cause of the problem. The final problem can be solved by deriving solution for each root causes.

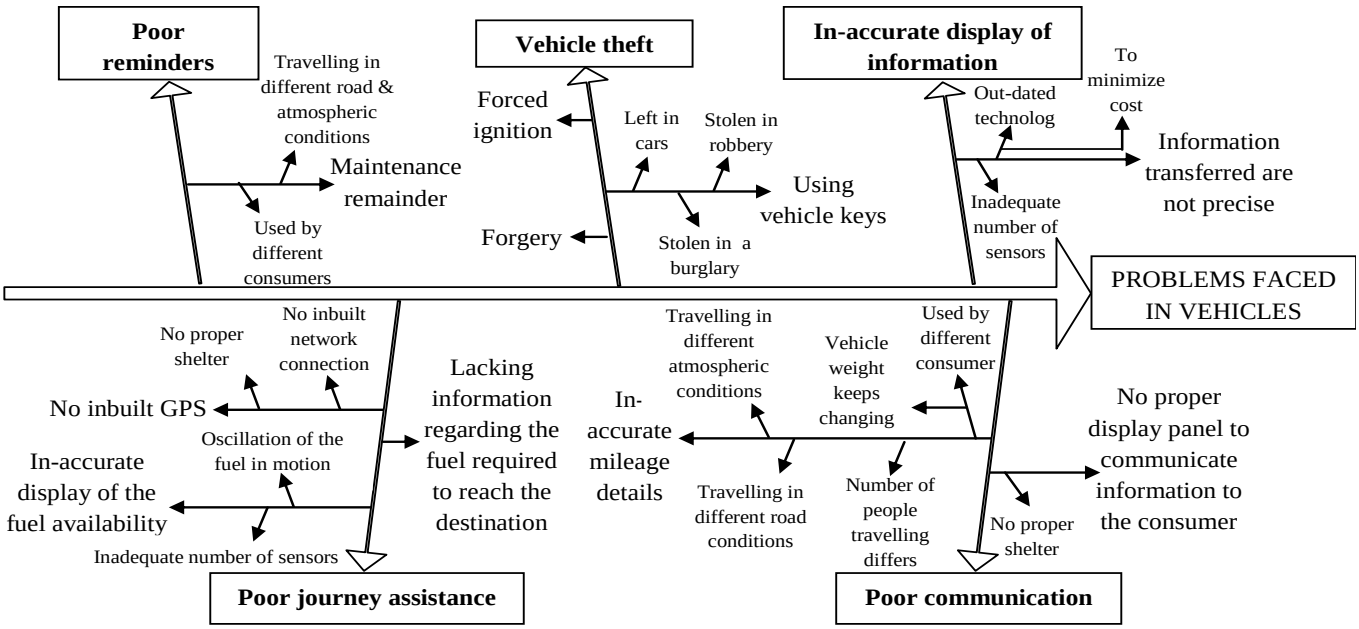

Fig. 1. Ishikawa diagram

II. Proposed Solution For The Causes

A. Maintenance Updater

Vehicles need maintenance at different interval of time, based on the driving conditions, fuel type, etc. So, with maintenance updater, it is possible to time the maintenance according to our daily travel and vehicle conditions, finally alert the consumer that the vehicle needs maintenance. In addition, it suggests the best nearby maintenance station based on the consumer's customization. For predicting the future maintenance schedule we need old maintenance schedule history, along with predetermined calculations. For better communication, we required some of the external parameters like current location, nearby maintenance stations, particular vehicle model details, etc. For updating or calculating maintenance time we need total distance traveled by vehicle between particular intervals as well.

TABLE I. Case Study of Maintenance Updater

Case 1	
From: 02/15/2018	To: 05/15/2018
Initial distance travelled: 0 km	Final distance travelled: 4000 km
Total distance travelled: 15000 km	Total distance travelled: 19000 km
Case 2	
From : 05/16/2018	To: 07/16/2018
Initial distance travelled: 0 km	Final distance travelled: 4000 km
Total distance travelled: 19000 km	Total distance travelled:23000km
Case 3	
From : 07/17/2018	To: 11/17/2018
Initial distance travelled: 0 km	Final distance travelled: 4000 km
Total distance travelled: 23000 km	Total distance travelled: 27000km

[a.] Date format: MM/DD/YYYY

With reference to "TABLE I," if the final distance travel reached a preloaded value say 4000 km, it stores the data using the storage module and sends an alert message to the rider.

B. Fuel Price Diplay

It's difficult for the consumers to keep in trace of the fuel price because of their fluctuating nature. Fuel price display updates the current fuel price on a daily basis with the help of the internet or intranet, respect to location and customized categories, in accordance with the third-party API and electronic device. The customized category indicates selection of fuel type by the customer whether it may be petrol, diesel, bio-fuel, hydrogen fuel, etc. individually or all data can be displayed at the same time if required.

C. Fuel Economy Assistance

Fuel economy assistance helps to make the travel safer, secured and preplanned. It will update the accurate fuel available in the vehicle and analyzes the riding quality based on the past rider's data and suggests the best fuel economic conditions. With the help of this, the future traveling schedule is created by itself. To implement this, we need to access the vehicle speed rate, calculate the distance to be traveled based on the destination location, riders weight and mileage rate based on the previous riding condition. Having these parameters, the fuel economy can be calculated and also suggests the additional fuel to be filled to reach the destination. "TABLE II" implies the case study of fuel economic assistant.

TABLE II. Case Study of Fuel Economic Assistant

Parameters	**Case 1**	**Case 2**	**Case 3**
No. of riders	1	1	2
Riders weight (kg)	60	60	60,60
Avg. speed (km/ liter)	40	60	40
Fuel price (Rs/ liter)	73	73	73
Total distance travelled (km)	10	10	10
Avg. mileage gained (km/ liter)	40	35	30
Fuel economy (Rs/ km)	1.825	2.086	2.433

D. Vehicle Analyzer

Vehicle analyzer gathers information about the vehicle riding route with riding environment and it is integrated with third-party WebPages and APIs for collecting other related information. Once the process is done, it stores all the information in the cloud when the internet is available. If the rider wants to know data between two destinations, the AI matches the current inputs with existing results, finally, it displays the results with its customized predictions. "TABLE III," explains the different parameters necessary for vehicle analyzer.

TABLE III. Case Study of Fuel Vehicle Analyzer

Working condition	**Case 1**	**Case 2**	**Case 3**
No of riders	1	1	2
Weight of the riders (kg)	90	88	120
Model of the vehicle	A001345	A001399	A002005
Mileage of the vehicle (km/ liter)	40	40	35
Speed limit (km/ hr)	60	60	50
Riding method	Continuous	Continuous	Moderate
Environmental conditions	Good	Good	Bad
Result	More efficiency	More efficiency	Less efficiency

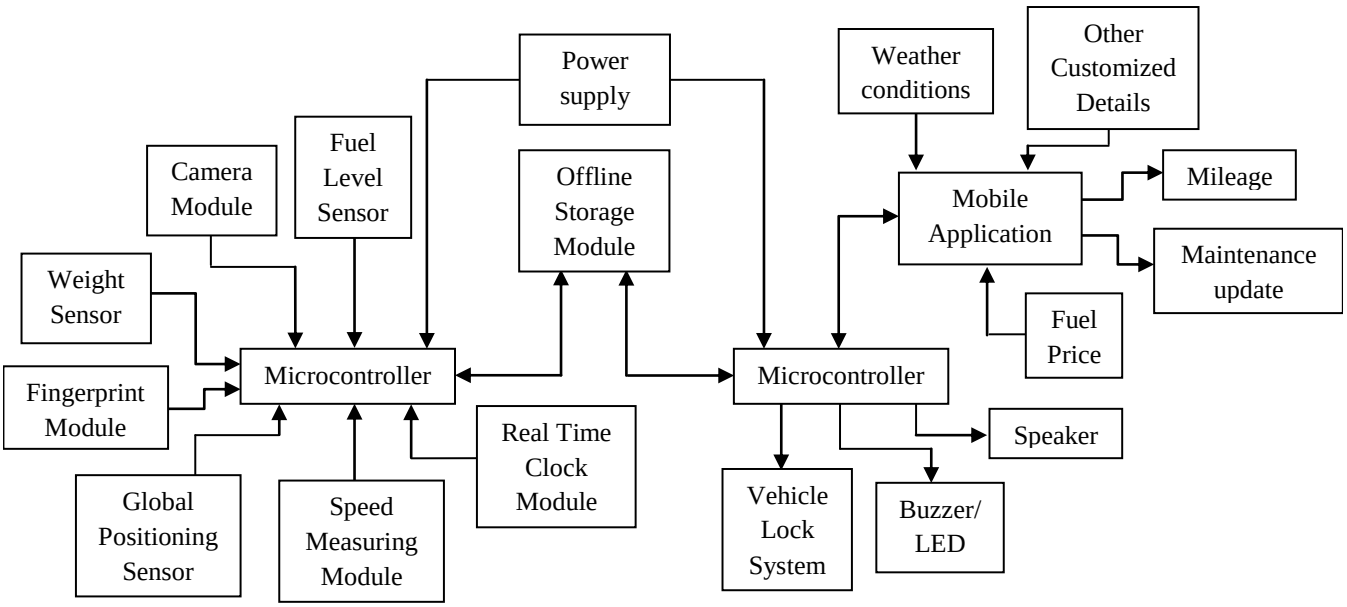

Fig. 2. Block Diagram of the Vehicle Monitoring System.

III. WORKING

With reference to the "Fig. 2," the working of vehicle monitoring system are as follows. Initially, when the rider covers their face and tries to start the vehicle, they get a failed response as the Identification module function was restricted by the rider. Then the rider is authorized by Authentication module by using his/her fingerprint, he/she can switch on the vehicle, and the fuel status will be informed to the customer through Customer communication module by using both audio and visuals after which the rider can start his journey. The Display module projects the economical and fast path using GPS for choosing the best route. The fuel level is displayed and notified regularly by Fuel level indication module so that the driver can refill with the nearest fuel station, fuel price is also projected according to the categories of fuel available in the station with price label by using cloud access module. The rider's weight is found using a weight measuring module, which helps to calculate the mileage of the vehicle preciously. The rider is notified if the vehicle wants maintenance through the maintenance updater in advance by receiving data from the speed measuring module and all the data of the devices which were stored with inbuilt storage system in the form of Offline storage module. With the help of all these modules, we can easily increase the efficiency of customer service.

IV. MOBILE APPLICATION

The first page of the application for the rider is to login to his access for the first level security. Generally, the login details are generated from the riders driving license details and the password is set while installing in the service center. Thus the system is completely secure. "Fig. 3" represents the home page and there are buttons to represent the notification page which displays the warnings and alerts of the vehicle. Separate display page of each button is set in the application. All kinds of notification and warnings based on the location and activities of the vehicle are also displayed for better security in a small map and the vehicle speed and economic speed values are displayed in separate meters. The user can access it by pressing either the notification or the warning button. The application has numerous functions and buttons such that it helps the user to have virtual connect with the vehicle. For example, if the vehicle has changed the route and is not moving towards the destination, notification or warning message will be delivered based on the severity of the problem. If the user finds that his vehicle gets disturbed or being theft or any kind of undesirable change he will get a notification and the warning button is highlighted. If the user finds that his vehicle is being used even after attaining the maintenance period, he will receive a call from the service centers which will help improve vehicle life. The cloud interacts with the customer based on real-time values and provides various facilities. The customer can get timely updates of the location of the vehicle, it can provide the change in the cost of fuel, create maintenance schedules, provide direct contact with the service centers and live navigation.

Fig. 3. Sample mobile application format

V. Survey Report

To evaluate how far our research would be beneficial for the end uses, we took a survey with individuals who are the consumers of the automobile vehicles. The data collection tool which we used is Survey Monkey and the data analysis is done using Microsoft Excel.

From the "Fig. 4," the majority of our survey population are between the age of 20 to 25 years old. Since these age category people are the potential internet users, and survey monkey being an online survey tool, it happened to have a higher proportion of people in this category. This doesn't have any correlation for the number of people who are riding vehicles in that particular age category.

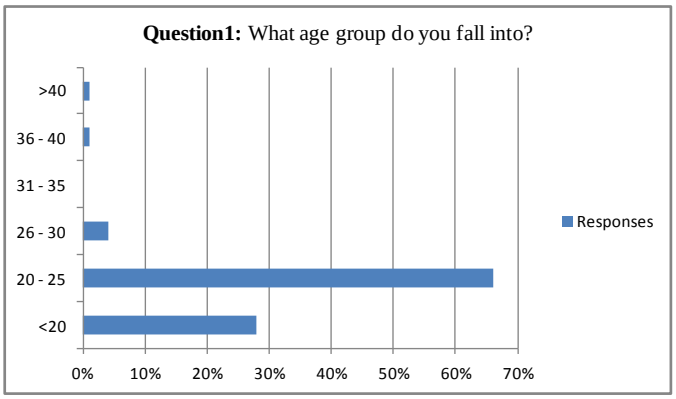

Fig. 4. Survey responders age category

It is a well-known fact that more people use bikes over cars and buses. That replicated in our survey results as well. The population distribution of individuals on their primary mode of transportation is shown in "Fig. 5".

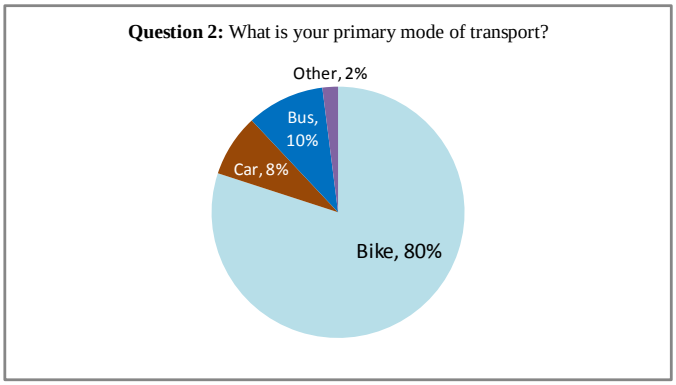

Fig. 5. Survey responders primary mode of transportation

"Fig. 6" shows that, most people in our survey population are the once who ride vehicles every day, this happened to be an advantage for the survey because only the people who use vehicles quite often know the difficulties associated with the vehicle.

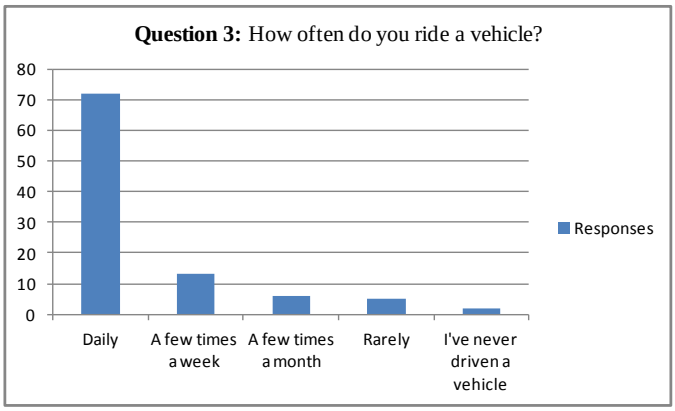

Fig. 6. Survey responders frequency of travel

It has been a mixed response for the advancements which we have proposed in this paper. From "Fig. 7," it is evident that the percentage range between economic travel assistance and current fuel price display (which happened to be the highest and the lowest response) is just 6%. This low variation between each proposed advancements makes it clear that how each advancement contributes value to their vehicle.

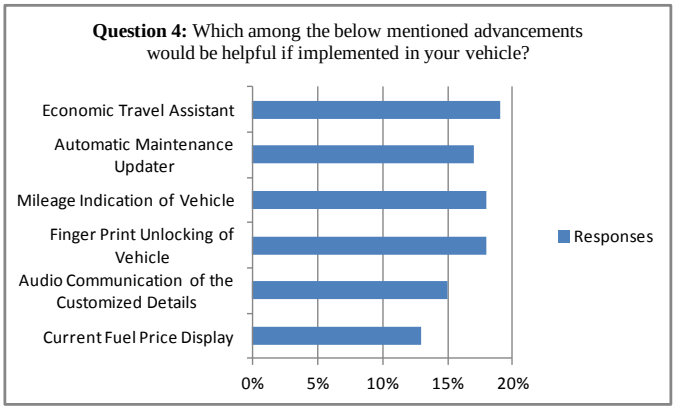

Fig. 7. Survey responders efficaciousness on the proposed advancements

The majority of the survey responders felt that the proposed advancements will be helpful if implemented on the bike. "Fig. 8" gives the evidence for it.

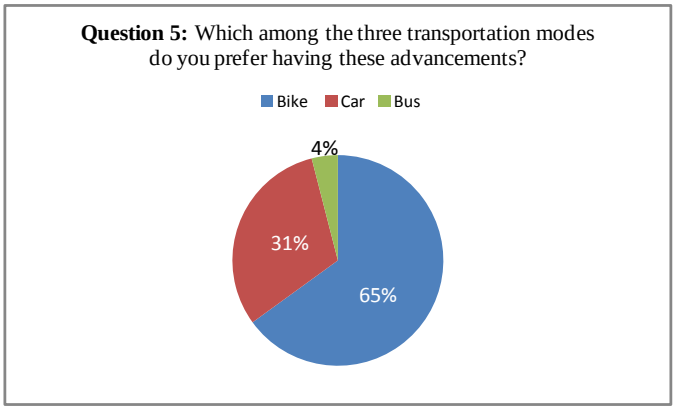

Fig. 8. Survey responders predilection in implementing the advancements

VI. Conclusion

This paper describes solutions for the problems which are being faced by the vehicle riders, using monitoring system technologies. The gathered real-time data's gives the riders the required information to utilize their vehicle optimally which thereby decreases the transportation cost. The proposed solutions also help the manufactures to provide value-added services to their consumers. With the survey results, it's evident that, implementing monitoring system in bikes has far better scope over car. But implementing in bikes leads to other complications, which needs crucial examination.

VII. Future Scope

Apart from the day to day monitoring of the vehicle the people and government organization give higher preference to safety and control. Thus the future scope lies in the fact of implementing various safety methods along with this technology. The suggested methods are alcohol detection, helmet detection, accident detection, and control by sending messages to family, friends and nearby ambulance service.

The future also lies in the concept of Connecting vehicles for better movement on faster platforms without any confusion to cause accidents and to contact nearby workshops and fuel stations for help during the breakdown and guidance. The installation of a GPS based smart route finder to find the best route without traffic and save time and fuel consumption.

If block chain concept is to be implemented successfully in future, we may be able to achieve the secure transfer of data from the vehicles to the OEMs and manufacturing companies along with secure payment methods in fuel station by default setup of encryptions in the vehicle to transfer money without any risk of the breach of our privacy and hacking.

Making all the sensor, microcontrollers and actuators resistant to wear and tear in an open vehicle is a difficult task. Maybe in the future, the shape and design of the vehicle will be modified to provide a secure and resistant atmosphere for the Electronic devices to work effectively.

The manual process of monitoring the vehicle is automated in this project but the vehicle is still to be manually driven by the user and the system provides useful data to the user which is to be analyzed by the user and take necessary actions by himself. In the near future, we can be assured that Artificial Intelligence and Machine learning will be a guiding member and make this also automated. We will be able to develop autonomous driving vehicles that drive on its own and maintains itself on its own.

References

[1] Innovative Global Systems, LLC. (Rock Hill, SC), 'METHOD FOR DATA COMMUNICATION BETWEEN VEHICLE AND FUEL PUMP', US 9633486 B2, 2016.

[2] QUALCOMM Incorporated. (San Diego, CA), 'SMART FUEL INDICATOR', US 9506775 B2, 2016.

[3] Ashwin Srinivasan, "IoT Cloud Based Real Time Automobile Monitoring System", 3rd International Conference on Intelligent Transportation Engineering, 2018.

[4] Linton; Jeb R. (Manassas, VA), Poulin; Christopher M. (Walpole, MA), 'VALIDATING INTERNET OF THINGS DEVICE FIRMWARE', US 20180103023 A1, 2018.

[5] Chaitra B, Raziya Begum M, Aishwarya K and Sachin Patil, "Vehicle Health Monitoring System Using ARDUINO and IOT", International Journal on Recent and Innovation Trends in Computing and Communication, 2017.

[6] Ford Global Technologies, LLC. (Dearborn, MI), 'INFORMATION DISPLAY SYSTEM AND METHOD', US 9499065 B2, 2014.

[7] A. Yasashree and Prateek Lakkar, "Smart Automobile Security System", International Journal of Engineering Research & Technology (IJERT), 2019.

[8] SurveyMonkey Inc. (San Mateo, CA), 'VEHICLE TECHNOLOGY SURVEY',2019.[Online].Avaliable: https://www.surveymonkey.com/results/SM-LZ6KJ235V/ [Accessed:20-June-2019].

Proceedings of the Fourth International Conference on Communication and Electronics Systems (ICCES 2019)
IEEE Conference Record # 45898; IEEE Xplore ISBN: 978-1-7281-1261-9

Design & Development Of AgriculturalRobot Using PLC & IoT

Safin Khan
Dept.of Instrumentation & control
Vishwakarma Institute Of Technology,Pune
safin.khan17@vit.edu

Atul Ingale
Dept.of Instrumentation & control
Vishwakarma Institute Of Technology,Pune
atul.ingale16@vit.edu

Akshara Buchake
Dept.of Instrumentation & control
Vishwakarma Institute Of Technology,Pune
akshara.buchake17@vit.edu

Swaraj Ahire
Dept.of Instrumentation & control
Vishwakarma Institute Of
Technology.,Pune swaraj.ahire16@vit.edu

Prof.Jitendra Gaikwad
Dept.of Instrumentation & control
Vishwakarma Institute Of Technology.,Pune
jitendra.gaikwad@vit.edu

***Abstract*:**
Indian economy mostly depends upon agriculture. More than 60% people of India depends on farming. Farmer has to go through huge losses due to use of historic techniques in agriculture. Most of the activities are done manually by farmers, which consumes time, energy and manpower. So, there is a need to develop an equipment which will reduce efforts of the farmer. Through this project our attempt is to fabricate such a system to automate all the agricultural processes including seeding, ploughing, fertilization and irrigation. As soon as the program is loaded in the PLC, bot starts working.
System has embedded smart technologies like IoT to inform the farmer about the weather conditions. Also the bot is provided with theft security. System has motor-sensor assembly to collect the real field data and according to the data further processes takes place. The dimensions of the field decide the trajectory of the AGROBOT. HMI is used to provide interface between the user and the machine.
***Keywords*-Agricultural robots, Automation, Agriculturalautomation, PLC, HMI, IOT.**

I. INTRODUCTION:

Farming requires a lot of efforts to perform various activities such as seeding, ploughing, irrigation, fertilization. Hence robotics must be implemented to overcome difficulties during farming .But still implementation of robotics in agricultural field is challenging for engineers. Advanced technology helps us to water and fertilize precisely, this results in good quality of food. The idea of applying robotics technology in agriculture is unique.
For this system Programmable Logic Controller is central oriented.

PLC:

PLC is an industrial computer which is rigid, and adapted for the control of processes like assembly lines, robotic devices, etc. It has high reliability control, ease of programming, process fault diagnosis[4]. PLC is an example of hard real time system in which output must be produced in response to input conditions. It consists of input modules, processor, memory, output modules and power supply[4]. PLC receives the information from connected sensors processes the data and produces output based on programming parameters. PLC's are adaptable to almost any application. Various output devices with different voltage ranges can be connected to PLC. Ladder logic is the traditional programming language of PLC[4]. It is usually written on the computer and then downloaded to PLC using serial communication.

HMI:

In order to interact with the PLC users need an HMI. These operator interfaces can be simple displays, keypad, or large touch screen panels .They enable users to review and input information to the PLC in real time. HMI communicates with PLC and sensors to get and display information for users to view [6]. HMI's are used to optimize an industrial process by digitizing data for a viewer. By using HMI operators can see important information like graphs, charts or digital dash board and alarms and can connect with SCADA systems[6].

MOTORS:

- **Stepper Motor**

Stepper motor is used to divide a complete rotation into number of steps. In this project stepper motor is used for seeding and fertilization purpose[8].

- **DC Motor**

This motor coverts electrical energy into mechanical energy. One of the advantage of dc motor is its speed can be controlled over a wide range. In this project DC motor is used in motor sensor and plougher assembly[7].

- **Square Geared Motor**

These motors equipped with gear boxes for providing a great balanced between speed and torque according to requirement. Generally, it provides high torque.In this project, these motors are used to drive the bot on its given trajectory[7].

INVERTER:

Inverters are needed where it is impossible to get AC supply from the mains. An inverter circuit is used to convert DC to AC .here in this project inverter is used to convert 12V DC to 230 V AC, which is given to PLC. Inverter work on the idea to produce oscillations from DC and applying these oscillations to step up transformer to amplify the current.

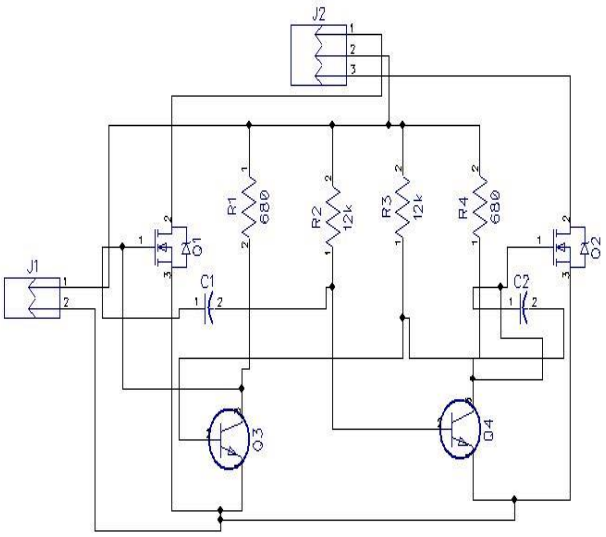

Fig 1.1

II. LITERATURE REVIEW:

Agriculture is the backbone of Indian economy. It supports17% of world population. Nowadays most of us have come across the atomization in various fields which leads great development in industrial products which made our life easier than before. Development of new technologies in agriculture has helped for growing countries. The survival of those people is improved which are totally dependent on agriculture[3]. According to this paper engineers has to make a great efforts for advancement in agriculture complex machinery has to be developed in order to reduce work load of farmers with good quality of food. These equipments are mostly very complex as they are implemented on basics of operation. As these devices are made taking the present scenario in the field of agriculture. The basic objective of developing such a system which detects moisture and PH of field is according the present moisture of soil the irrigation will be carried out in the field which will definitely give a proper way of using water as well as PH will to detect acidity of soil which will turn helpful to fertilize only required nutrients to soil which will help to less damage on soil[1]. The results shows that the robot will successfully work as per physically outlined it will also met the economic and time constraints that it was able to drive up and back along the tracks in the field.

A. Durmus et al.(2015)

In 2015 this team comes with the agrobot term they defined it as a multipurpose robot. They completed their work as per they have divided it was designing team and cloud based service providing team[3]. They built their robot in-house under 2000$ budget using only their available tools, equipment. It was not just a complete mobile robot but also was connected with farmers wirelessly through cloud computing through the farmers mobile devices. But unfortunately implementation of this idea was not completed.

B *Amer et al(2015)*

This team comes up with the prototype of multipurpose robot that is agrobot to perform various agricultural tasks. It has ability to perform various agricultural activities such as harvesting, and weeding. But there was a limitation of this robot was dependency on Wi-Fi.In this work there was impractical to introduce Wi-Fi connections in the open fields, as Wi-Fi routers and cables would be exposed to elements,power and maintenance cost would be high[3].

PROBLEM STAEMENT:

New technologies are introduced in agriculture but question remains the same are they capable to produce good food quality, help farmers, sustain us? According to UN it is needed to gain 3 billion metric tons of food this is very big. Hence for this reason it is necessary to develop a system which will do all work without interference of human to reduce human error. The problem is to make a robot which will be able to do all these work including IoT in it which causes to have all information with farmers. This will reduce the work load of farmers by using smart ways, also will turn helpful for improving food quality by reducing adequate use of fertilizers and maintaining use of water. These will reduce all problems regarding to agriculture and farming will become ease for the farmers as the whole thing will be automated. Thus, the whole process gets automated which isof greater need to the society as well as to the farmers so that they can also enjoy the fruit of life. This technique is definitely going to change the phase of the modern farming in the near future.

OBJECTIVES:

1. Human efforts will be reduced.

2. Just a brief description is more than enough to control the whole system.

3. Efficient use of technology.

4. To design a PLC based more advanced automotive irrigation robot.

5. Efficient use of resources such as water & time.

6. To preserve quality of soil.

III . PROPOSED METHOD:

A complete prototype of agrobot is presented here will first collect weather data to check that all weather conditions are ok that means there is no possibility of raining. The agrobot will start its working as shown in fig 2.

BLOCK DIAGRAM:

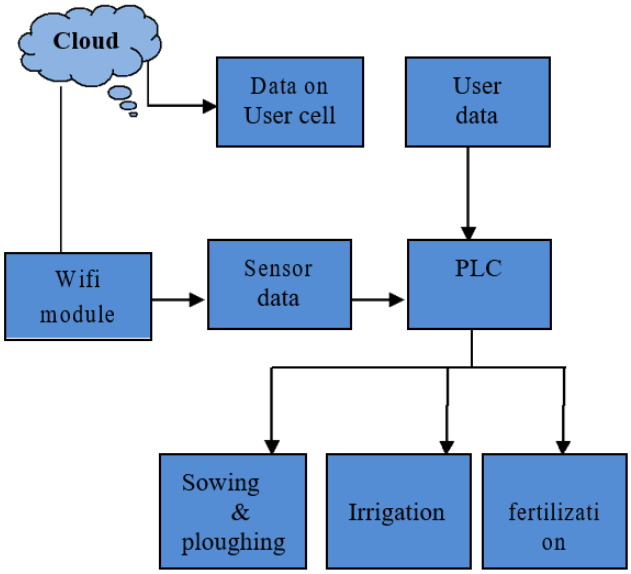

Fig.3.1

Soil fertility testing and weather forecasting:

The land will be suitable for agricultural purpose only if the soil over there is fertile. So the very first task performed by the robot will be testing the fertility of soil as well the weather conditions via IOT as shown in fig 2. Only if the soil is fertile, the further process will be carried on else, message will be given to the farmer about the infertility of the soil.

Sowing and Ploughing:

As shown in fig 2 after checking the fertility of the soil and the weather conditions, and if the soil is fertile, PLC will allow the machine to sow and plough simultaneously. The robot contains a plough, hopper and a container to which a valve is attached. The plough will be connected at the end of the machine and after getting the signal from the PLC, robot moves and thus the ploughing process starts. The only thing that the user has to do is to fill the container with seeds. The level of seeds in the container will be continuously monitored by the robot using a level sensor and thus the PLC, if the level of seeds in the container drops below a specific value, message will be given to the farmer about the shortage of the seeds. As soon as the level of seeds in the container falls below a specific value the PLC will give a signal to the robot to stop so that the container can be filled again with the seeds. The sowing process will again resume by pressing the resume push button on the machine. Thus the ploughing and sowing process will take place. Messagewill be given to the farmer about the completion of the process.

Moisture detection and water supply management:

The robot is at rest after completing both the above Processes. The next task taken into account by the robot is moisture detection. The PLC is being provided with inputs from the moisture sensor. Depending upon the concentration of the moisture present in the soil and after performing the desired calculations in the PLC, the PLC will be able to control the amount of water given to the sprinkler pipes. As the moisture is not even everywhere in the field so the PLC would receive the inputs from the moisture sensors at different stages. Depending upon the data received by the PLC in fig 2 flow rate through the sprinkler is going to vary by actuating a control valve. So the main function of the robot here is to just send the data from different locations to the PLC which will control the flow rate through the pipe. This would save water to a great extent. Again, as per the norms, the message for completion of water supply will provided to the farmer.

Fertilization:

After collecting the data from different locations the robot is at rest. After finishing the above process the next process taken into consideration is the fertilization. Before this if the container contains the seeds the PLC will give an indication to remove the seeds for the farmer by using a bypass valve. The same container will then be filled with the fertilizers. After getting the signal from the farmer to start the fertilization process the PLC will cause the valve to open, thus causing to fertilize the whole field area. As the process gets completed message for the completion of the whole process will be given to the farmer as shown in fig 2.

Overview of the system:

A complete prototype of the agro-bot which will do all the above said processes such as sowing , ploughing , watering, etc. which will be controlled by the heart of the system which in this case is the PLC refer fig 3. The objective of the whole project is to make an automated robot that would be able to do all the work that is done by the farmer. The very first thing done by the agro-bot is to check the fertility of the soil as well as the weather conditions of the field. The weather conditions will be determined by the IOT based technology that would display the real data on the screen of the bot and provide an idea to the farmer that whether the farming is suitable for the present day. If positive signal is given by the farmer the PLC will give the signal to the hopper valve so that it will start sowing seeds within its bounds and plough simultaneously as shown in fig 3. This will tend to reduce the time consumed by the farmer and he will be able to do some productive work during this slot. If level of the seeds in the container drops below a specific value the PLC will cause the agro-bot to stop and at the same instant reduce the time consumed by the farmer and he will be able to do some productive work during this slot. If level of the seeds in the container drops below a specific value the PLC will cause the agro-bot to stop and at thesame instant message

will be given to the farmer about the shortage of seeds.Again after getting the input from the farmer/user the Robot will start the same process further andploughsimultaneously. At last the plough will be lifted up and the hopper valve will close.

FLOW CHART:

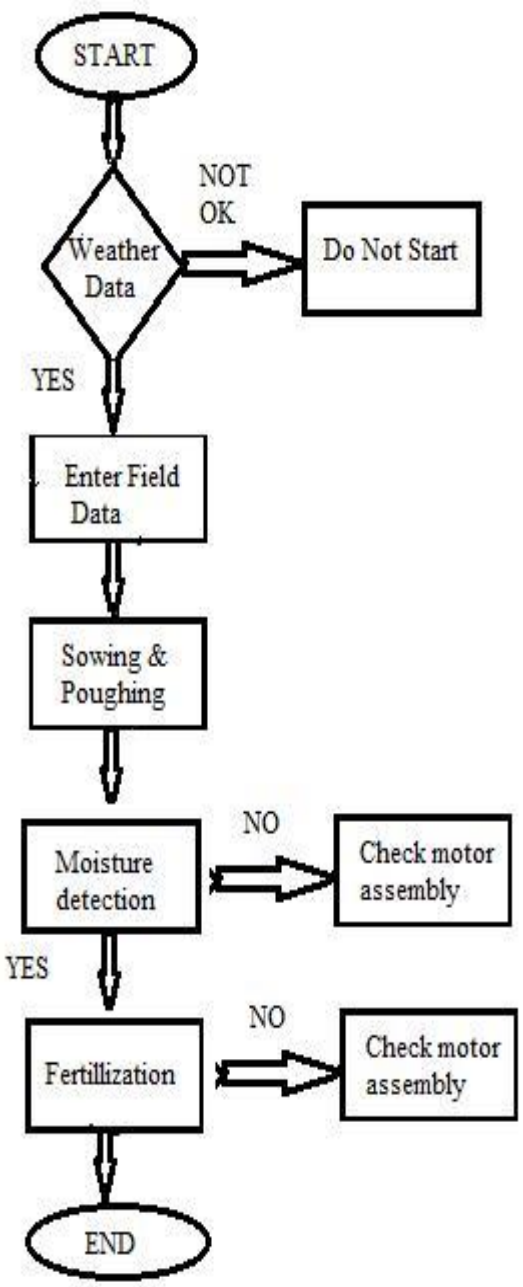

Fig 3.2

System outcomes:

1. Reduced human efforts.
2. Smart use of technology.
3. Visualization of each process is available.
4. Effective time usage.
5. Energy consumption mitigation.

IV. IMPLEMENTATION:

PLC Program:

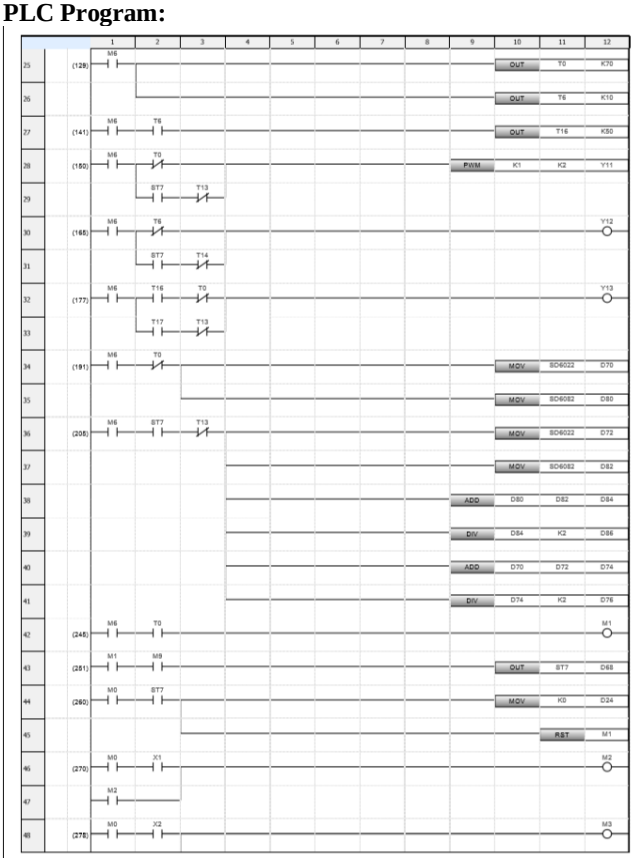

Fig.4.1

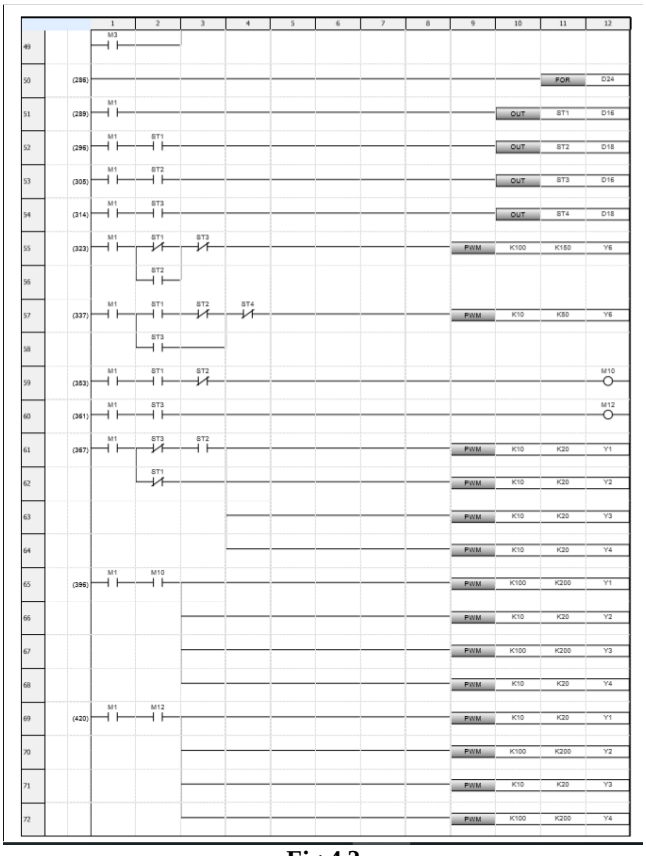

Fig.4.2

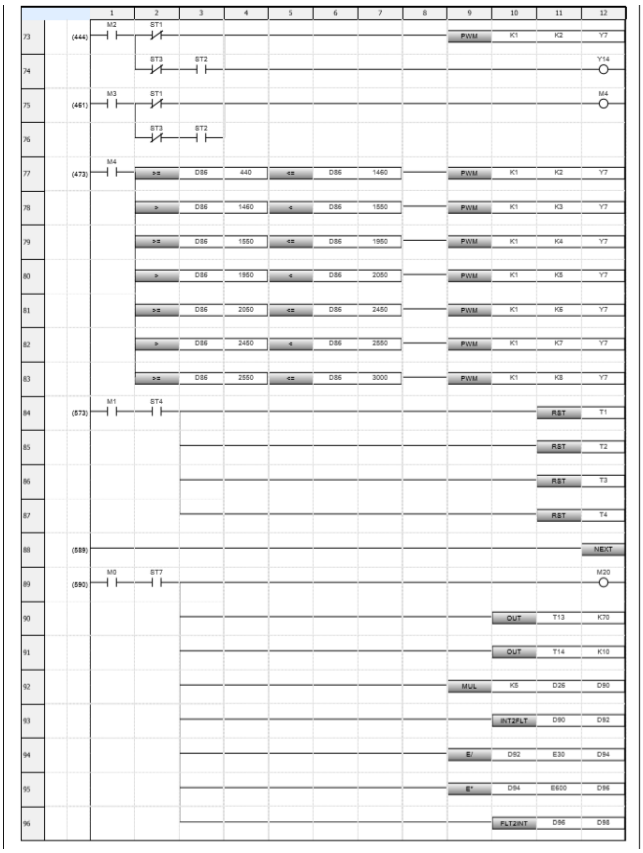

Fig 4.3

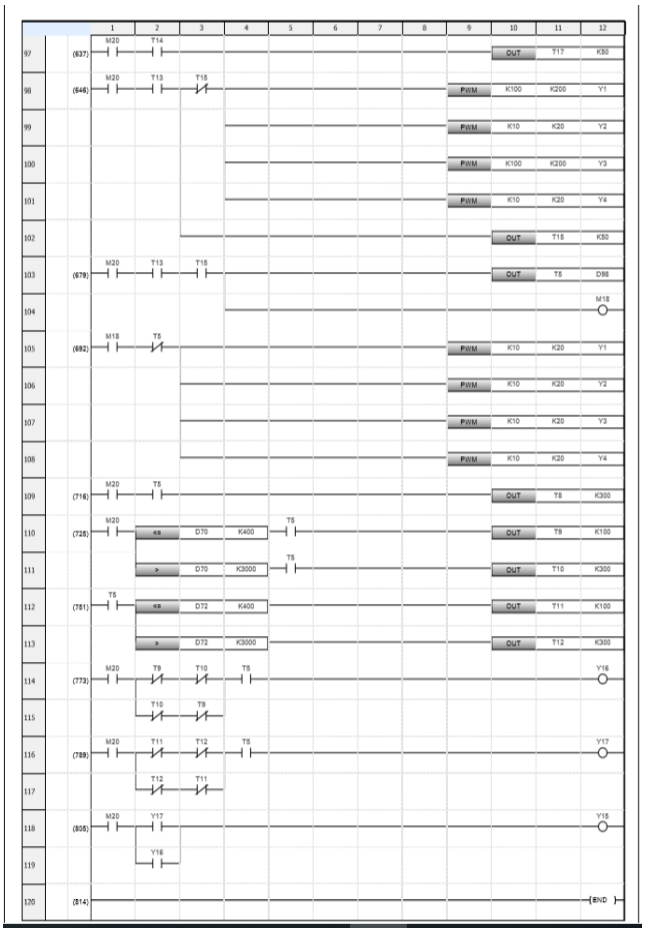

Fig 4.4

HMI Screens:

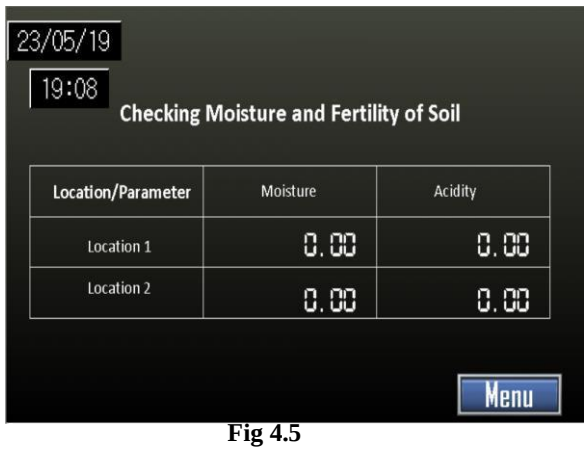

Fig 4.5

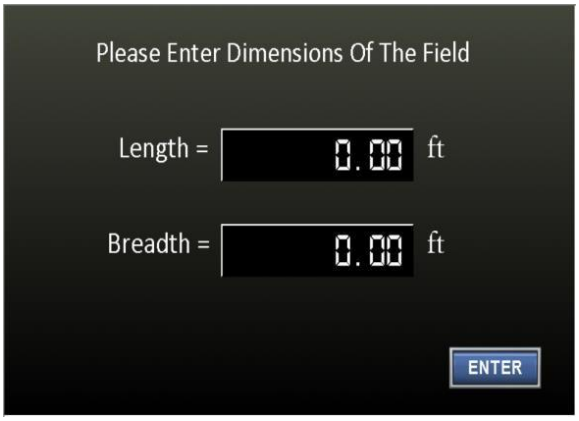

Fig 4.6

Orthogonal view:

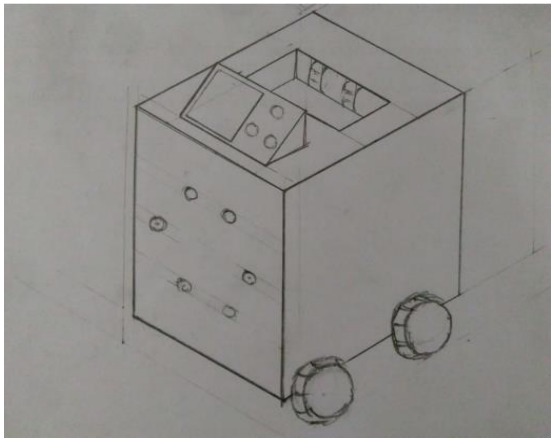

Fig4.7

Fig 11

Result:

1. The bot takes the data from field and the controller and take the respective action depends on the measured values.
2. Speed of bot is fixed so controller can adjust its timing for various dimensions of field given by farmer.
3. Robot will work according to the selection of process user want to do.
4. Fertilizers will be provided in proportion according to acidity of the soil.
5. In irrigation process amount of water provide to field is being control using current moisture data and rain data.

V . CONCLUSION

Through this paper such above mentioned efforts madeto reduce problems in agriculture. The prices of food
grains, fuels, cloths and other things are increasing hencelabors are requesting more wages from owners. This
paper shows that agriculture robots need a supportinfrastructure. This provides wireless connectivity for
the robots in the field.Implementing suchinfrastructure
is challenging the cost of such a robot could be prohibitive. The key to implementing agriculture robots is to find a novel, practical and a reliable approach to implementing the support infrastructure it needs.

REFERENCES:

1. Amrita Sneha, Abirami E, Ankita A :"Agricultural Robot for automatic ploughing andseeding.",IEEE.
2. K Durga Sowjanya, R Sindu,M Parijitham, KShriknt,P Bharghav: "Multipurpose autonomousagricultural robot.",IEEE.
3. Akhila Gollakota, M B Srinivas: "Agribot - Amultipurpose agricultural robot",IEEE
4. https://en.m.wikipedia.org/wiki/Programmable_logic
5. https://unitronicsplc.com/what-is-plc-programmable- logic-controller/
6. https://www.inductiveautomation.com/resources/article/what-is-hmi
7. https://en.m.wikipedia.org/wiki/DC_motor
8. https://en.m.wikipedia.org/wiki/Stepper_motor
9. Neha Naik, Virendra Shete, Shruti Danve**:"**Precision agriculture robot for seeding function."
10. F. Sisteler:"Robotics and intelligent machines in agriculture".

Proceedings of the Fourth International Conference on Communication and Electronics Systems (ICCES 2019)
IEEE Conference Record # 45898; IEEE Xplore ISBN: 978-1-7281-1261-9

An Effective Content Based Image Retrieval Using Dot Diffusion Block Truncation Coding

Admile Nandkumar Sushen

Department of Electronics & Tele-communication Engineering

SVERI's College of Engineering,Pandharpur

nsadmile@coe.sveri.ac.in

Dr.Anup S.Vibhute

Department of Electronics & Telecommunication Engineering

SVERI's College of Engineering,Pandharpur

asvibhute@coe.sveri.ac.in

Abstract -- In the field of image processing application such as medical diagnosis, crime prevention, publishing or advertising, historical research a common image retrieval technique is used. Simple browsing can easily identify images in a small collection of images but for large and different collection of images identification of image becomes critical issue. In this paper for image retrieval four different features are extracted using DDBTC technique. The first two features such as Color Co-occurrence Features (CCF) and Color Histogram Features (CHF) are obtained using color quantizers, Bit Pattern Feature (BPF) and Bit Histogram Feature (BHF) are obtained using Bitmap image. In order to remove the false counter problem and blocking effect different error diffusion kernels are employed. The results shows better accuracy.

Keywords— Average Recall Rate Average Precision Rate, Bit pattern feature, color co-occurrence feature color histogram feature, Dot diffused block truncation coding.

I. INTRODUCTION

Content based Image Retrieval application of computer vision technique to minimize the problem of image retrieval.In annotated based method we have to annote every image based on information of metadata or keywords. In this process the system is not able to capture the exact keywords to represent The images and it becomes time consuming. In CBIR system search of images is based on visual contents rather than metadata. Here "content" is information of texture, shape, or color obtained from images. In 1979 [1] Mitchell and Delp introduces first Block Truncation Coding (BTC). Udpikar and Raina [2] describe the overhead statistical information using source encoding of a block truncation coding. (BTC). Author uses the vector quantization which reduces the bit up to 1.5 bit/ pixel. Yiyan Wu [3] derives Blo for image retrieval. BTC generates the vector quantized bitmap which are then decomposed into a set of vectors. It achieves the compression ratio up to 10:1. G. Qiu [4] uses BTC technique for feature extraction. N. Jhanwara [5] uses motif co-occurrence matrix (MCM) for content based image retrieval. The MCM is similar to the color co-occurrence matrix (CCM), but MCM performs the retrieval task better than the CCM. Experiment shows the MCM improves the retrieval performance as compared to CCM. In [7-10] author uses dot diffusion block truncation coding for image retrieval. To measure the performance of image retrieval various distance metrics are employed.

I.SYSTEM DESIGN

System design flow is mentioned in fig.1

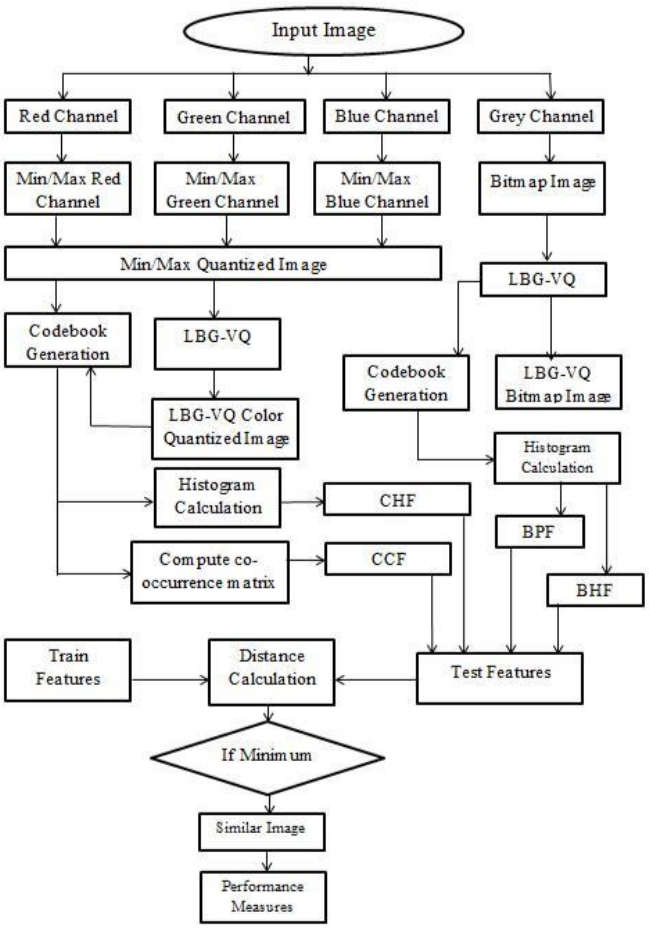

Fig. 1. System Design

A. *Dot Diffused Block Truncation Coding :*

A sample image is used to derive the minimum and maximum quantizers. In this assume at position (i, j) an f (i, j) be the image block. The color images are in RGB color space.

$$Q_{min} = \{\min f_R(x, y), \min f_G(x, y), \min f_B(x, y)\} \quad (1)$$

$$Q_{max} = \{\max f_R(x,y), \max f_G(x,y), \max f_B(x,y)\} \quad (2)$$

In this Red, Green and blue color are represented by R, G and B. The color image is converted into grey image using:

$$f\hat{}(x,y)=1/3[f_R(x,y)+f_G(x,y)+f_B(x,y)] \quad (3)$$

The Bitmap image is also computed using:

$$b_m=1; \text{ if, } f\hat{}(x, y) \ f(i, j) \quad (4)$$

$$0; \text{ if } f\hat{}(x, y) < f(i, j)$$

II.FEATURE EXTRACTION

1.Color Histogram Feature (CHF) :

The Process of CHF is shown in Fig 2.

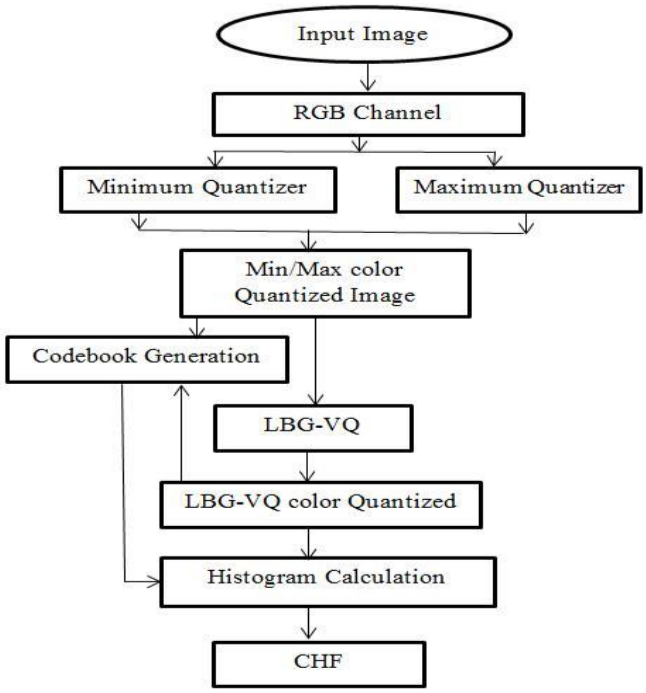

Fig. 2. Design flow of CHF

2. Color Co Occurrence Feature (CCF):

The Process of CCF is shown in Fig 3.

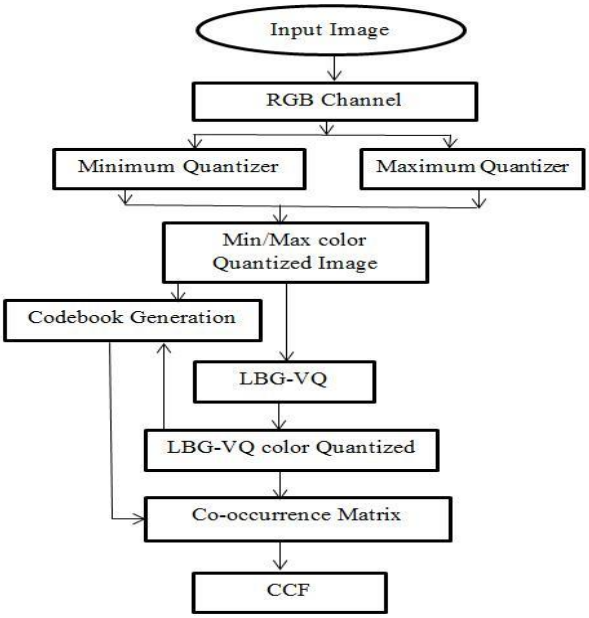

Fig. 3. Design flow of CCF

3. Bitmap Pattern Feature (BPF):

The Process of BPF is shown in Fig 4.

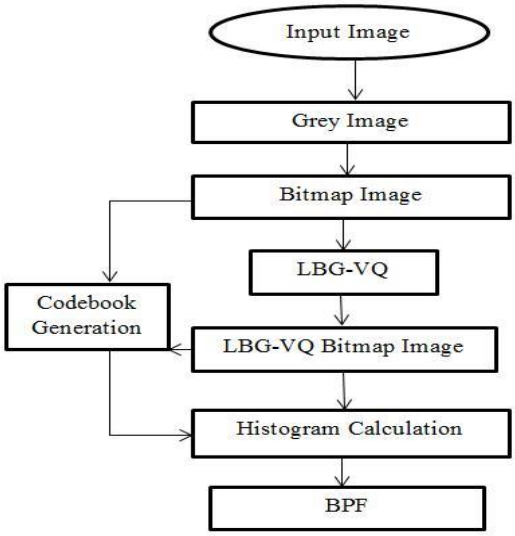

Fig. 4. Design flow of BPF

4. Bit Histogram Feature (BHF):

The Process of BHF is shown in Fig 5.

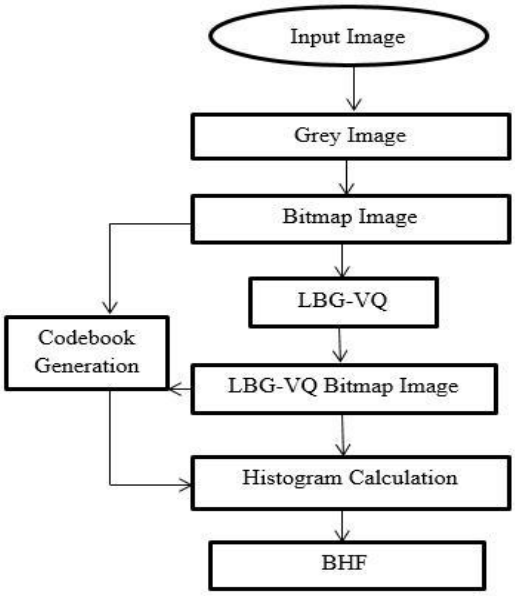

Fig. 5. Design flow of BHF

B. Distance Metrics :

The different distance metrics are given by:

1.L_1 distance

$$\delta(query, target) = a_1 \sum_{k=1}^{Nmin} | CHF_{min}^{query}(k) - CHF_{min}^{target}(k)| + a_2 \sum_{k=1}^{Nmax} | CHF_{min}^{query}(k)\, CHF_{min}^{target}(k)| + a_3 \sum_{k=1}^{Nb} | BPF^{query}(k) - BPF^{target}(k)| \quad (5)$$

2.L_2 distance

$$\delta(query, target) = [\, a_1 \sum_{k=1}^{Nmin} (CHF_{min}^{query}(k) - CHF_{min}^{target}(k))^2 + a_2 \sum_{k=1}^{Nmax} (CHF_{min}^{query}(k) - CHF_{min}^{target}(k))^2 + a_3 \sum_{k=1}^{Nb} (BPF^{query}(k) - BPF^{target}(k))^2]^{1/2} \quad (6)$$

3.x^2 Distance

$$\delta(query, target) = \alpha_1 \sum_{k=1}^{N_{min}} \left(\frac{CHF_{min}^{query}(k) - CHF_{min}^{target}(k)}{CHF_{min}^{query}(k) + CHF_{min}^{target}(k) + \varepsilon} \right)^2 + \alpha_2 \sum_{k=1}^{N_{max}} \left(\frac{CHF_{max}^{query}(k) - CHF_{max}^{target}(k)}{CHF_{max}^{query}(k) + CHF_{max}^{target}(k) + \varepsilon} \right)^2 + \alpha_3 \sum_{k=1}^{N_b} \left(\frac{BPF^{query}(k) - BPF^{target}(k)}{BPF^{query}(k) + BPF^{target}(k) + \varepsilon} \right)^2$$

4. Fu Distance:

$$\delta(query, target) = \frac{L_2 distance}{|CHF_{min}| + |CHF_{max}| + |BPF|}$$

5. Modified Canberra distance

$$\delta(query, target) = a_1 \sum_{k=1}^{Nmin} \frac{|CHF_{min}^{query}(k) - CHF_{min}^{target}(k)|}{CHF_{min}^{query}(k) + CHF_{min}^{target}(k) + \varepsilon} + a_2 \sum_{k=1}^{Nmax} \frac{|CHF_{max}^{query}(k) - CHF_{max}^{target}(k)|}{CHF_{max}^{query}(k) + CHF_{max}^{target}(k) + \varepsilon} + a_3 \sum_{k=1}^{Nb} \frac{|BPF^{query}(k) - BPF^{target}(k)|}{BPF^{query}(k) + BPF^{target}(k) + \varepsilon} \quad (7)$$

C. System Performance:

System performance determined using:

$$APR = \frac{1}{Nt\,L} \sum_{q=1}^{Nt} Nq(L) \quad (8)$$

$$ARR = \frac{1}{Nt\,Nr} \sum_{q=1}^{Nt} Nq(Nr) \quad (9)$$

D. Error Diffusion Kernels:

Here we can mention various Error Diffusion kernels in order to generate the Bitmap images. The advantage of Error diffusion kernels is that it can achieves better image quality as compared to Block Truncation Coding technique. The image compression using BTC and EDBTC and BTC also used in [3, 4, 6]. Here we mention the six different error diffusion kernels.

$$\left(\frac{1}{16}\right)\begin{bmatrix} & * & 7 \\ 3 & 5 & 1 \end{bmatrix} \quad \left(\frac{1}{42}\right)\begin{bmatrix} & & * & 8 & 4 \\ 2 & 4 & 8 & 4 & 2 \\ 1 & 2 & 4 & 2 & 1 \end{bmatrix} \quad \left(\frac{1}{32}\right)\begin{bmatrix} & & * & 5 & 3 \\ 2 & 4 & 5 & 4 & 2 \\ 0 & 2 & 3 & 2 & 0 \end{bmatrix}$$

(a) (b) (c)

$$\left(\frac{1}{32}\right)\begin{bmatrix} & & * & 8 & 4 \\ 2 & 4 & 8 & 4 & 2 \end{bmatrix} \quad \left(\frac{1}{48}\right)\begin{bmatrix} & & * & 7 & 5 \\ 3 & 5 & 7 & 5 & 3 \\ 1 & 3 & 5 & 3 & 1 \end{bmatrix} \quad \left(\frac{1}{200}\right)\begin{bmatrix} & & & * & & 32 & \\ 12 & & 26 & & 30 & & 16 \\ & 12 & & 26 & & 12 & \\ 5 & & 12 & & 12 & & 5 \end{bmatrix}$$

(d) (e) (f)

Error diffusion kernel: (a) Floyd-Steinberg (b) Stucki [62], (c) Sierra (d) Burkers (e) Jarvis and (f) Stevenson filter

Generally while using BTC technique many problems are occurred such as blocking effect and false counter problems. Due to this the image quality can be degraded. In order to overcome such problems various error diffusion kernels are employed

III. EXPERIMENTAL RESULTS

E. Experimental Setup:

Fig.6. Corel Image Dataset

The Fig.6.shows sample images from Corel 1000 Dataset. The Corel 1000 dataset having 10 different Classes. For our image retrieval task we can select 20 images from each class, so that the dataset.

Fig.7. Input color image

Input color image is selected as shown in Fig.7.The Fig.8. is obtained using quantization process From Gray color image Bitmap image obtained as shown in fig.9.

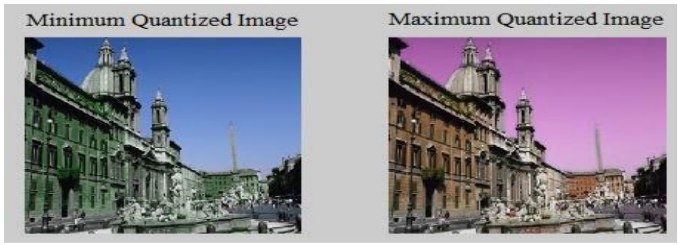

Fig. 8. Min. and Max. Quantized Image

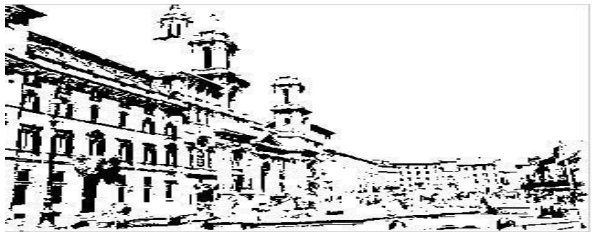

Fig.9. Bitmap Image

The fig.10 and fig. 11 are obtained Using color co-occurrence matrix the image can arrange with vertical, horizontal centered points and diagonally ordered centered points.

Fig.10.Ordered Matrix with centered Points

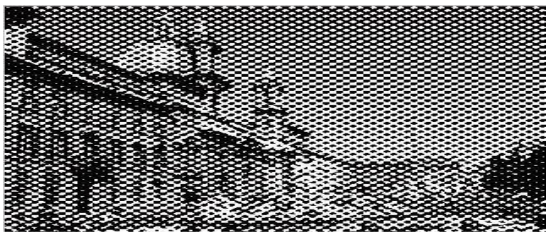

Fig.11.Diagonal Ordered Matrix with Balanced Centered Point

Fig.12.shows the Retrieved images using modified Canberra distance.

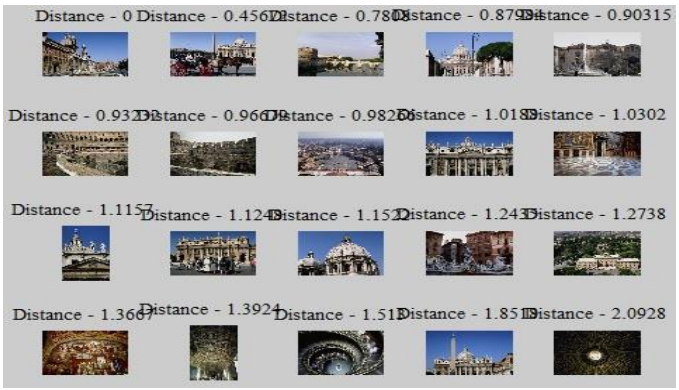

Fig.12. Retrieved Images

The image retrieval task can be performed by using five different distance metrics. The simulated results of L1 and L2 distance listed in Table I and X2 and Fu distance results are listed in Table II.The modified Canberra distance shows the better accuracy listed in Table. III.

Table.I

Class	L_1 distance	L_1 distance	L_2 distance	L_2 distance
	APR	ARR	APR	ARR
African	0.6875	60.19	0.6875	60.19
Beach	0.6875	65.19	0.6875	65.19
Building	0.6875	70.19	0.6875	70.19
Bus	0.8125	80.19	0.8125	80.19
Dinosaur	0.8750	90.19	0.8750	90.19
Elephant	0.5625	60.19	0.5625	60.19
Flower	0.8125	70.19	0.8125	70.19
Food	0.8750	65.19	0.8750	65.19
Horse	0.6875	65.19	0.6875	60.19
Mountain	0.9575	95.19	0.9375	95.19

Table.II

Class	X^2 distance	X^2 distance	Fu distance	Fu distance
	APR	ARR	APR	ARR
African	0.8750	90.19	0.6875	60.19
Beach	0.8750	90.19	0.6875	65.19
Building	0.8750	90.19	0.6875	70.19
Bus	0.9375	95.19	0.8125	80.19
Dinosaur	0.9375	35.19	0.8750	90.19
Elephant	0.9375	90.19	0.5625	60.19
Flower	0.8750	90.19	0.8125	70.19
Food	0.9375	90.19	0.8750	65.19
Horse	0.8750	90.19	0.6875	60.19
Mountain	0.9375	95.19	0.9375	75.19

Table.III

Class	Modified Can. Dist	Modified Can. Dist.
	APR	ARR
African	0.8750	90.19
Beach	0.8750	90.19
Building	0.8750	90.19
Bus	0.9375	95.19
Dinosaur	0.9375	95.19
Elephant	0.9375	90.19
Flower	0.9375	95.19
Food	0.9375	95.19
Horse	0.8750	90.19
Mountain	0.9375	95.19

Performance Image Retrieval is graphicallyshown in Fig.13. And Fig.14.

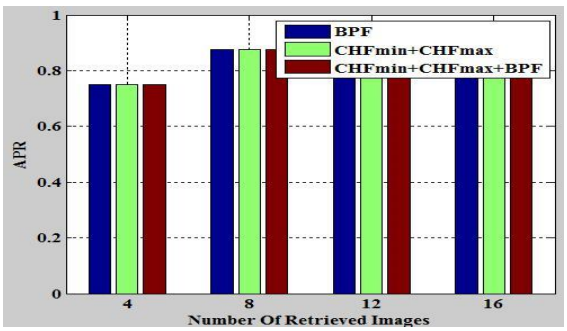

Fig.13. Performance Graph of APR

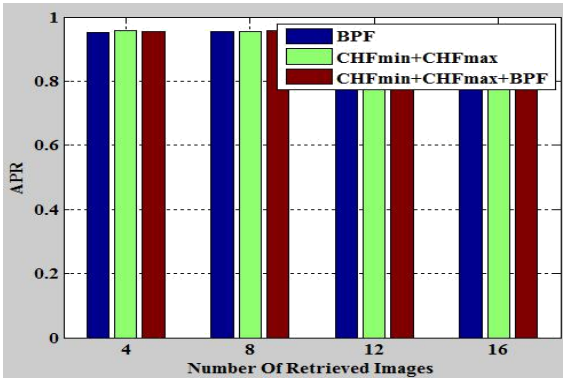

Fig.14.Performance Graph of ARR

COMPARISION OF RESULT WITH OTHER METHODS

In this experiment we measure performance of system and compare with the other retrieval methods.It shows that the proposed system shows the better retrieval accuracy. The Author N.Jhanwar in [4] uses modif co-occurance matrix for image retrieval which achieves 0.5268 accuracy.In our method the average precision rate is 0.9125.Table IV. Shows the comparison of APR with other techniques.

Table IV

Method→ Class ↓	Jhanwar [4]	Qui [5]	Yu [6]	ODBTC [7]	Proposed
People	0.453	0.495	0.849	0.847	0.8750
Beach	0.398	0.423	0.356	0.466	0.8750
Building	0.374	0.405	0.616	0.682	0.8750
Bus	0.741	0.909	0.818	0.885	0.9375
Dinosaur	0.915	0.955	1.000	0.992	0.9375
Elephant	0.304	0.498	0.591	0.733	0.9375
Flower	0.852	0.821	0.931	0.964	0.9375
Horse	0.568	0.689	0.928	0.939	0.9375
Mountain	0.293	0.313	0.404	0.474	0.8750
Food	0.370	0.443	0.682	0.806	0.9375
Average	**0.5268**	**0.5951**	**0.7175**	**0.7788**	**0.9125**

In paper [2] author uses the Error Diffusion Block Truncation Coding and derives the two features which achieves the Precision Rate as 0.797 under Corel 1000.

CONCLUSION

To perform the Experiment DDBTC method and four number of image features are used. The bit pattern feature (BPF) and Bit Histogram Feature (BPH) recognize the contents of image. The color co-occurrence feature (CCF) and color histogram feature (CHF) represents color distribution and image brightness. The simulated results shows better average recall rate and average precision rate. The Error diffusion kernels are employed to minimize the problem of blocking effect and false contour problem. The Modified Canberra distance shows better accuracy as compared to other similarity distance. In the future work, we can increase the size of dataset and computational time for image retrieval can also reduce.

REFERENCES

[1] E. J. Delp and O. R. Mitchell, “Image coding using block truncation Coding,” *IEEE Trans. Comm.*, vol. COM-27, no. 9, pp. 1335–1342, Sep. 1979.

[2] V. Udpikar and J. Raina, \BTC image coding using vector quantization," IEEE Trans.Commun., vol. 35, no. 3, pp. 352{356, Mar. 1987.

[3] Y. Wu and D. C. Coll, \BTC-VQ-DCT hybrid coding of digital images," IEEE Trans. Commun., vol. 39, no. 9, pp. 1283{1287, Sep. 1991.

[4] G. Qiu, “Color image indexing using BTC,” IEEE Trans. Image Process. vol. 12, no. 1, pp. 93–101, Jan. 2003.

[5] N. Jhanwar, S. Chaudhurib, G. Seetharamanc, and B. Zavidovique,\Content based image retrieval using motif co-occurrence matrix," Image Vis. Comput., vol. 22, pp. 1211{1220, Dec. 2004.

[6] Jing-Ming Guo,Heri Prasetyo , " Content-Based Image Retrieval Using Error DiffusionBlock Truncation Coding Features "IEEE Trans.on Image Processing, vol. 25, No. 3, pg.no.466-481 2015

[7] Nandkumar S. Admile and Prof. Rekha Dhawan, “Content Based Image Retrieval Using Feature Extracted from Dot Diffusion Block Truncation coding”, IEEE International conference on communication and Electronics Systems (ICCES-2016) Coimbatore, India,.**DOI:** 10.1109/CESYS.2016.7889864, 21-22 October 2016

[8] Nandkumar S. Admile “Image Retrieval Based on Block Truncation coding”, IEEE International conference on communication and Electronics Systems (ICCES-2018)Coimbatore, India, **DOI:** 10.1109/CESYS.2018.8724097, 15-16 October 2018

[9] Nandkumar S. Admile,Ajit Kanase and Rajesh Khiste ,”User Oriented Image Retrieval Using Feature Extracted by Dot diffusion Block Truncation coding”, IEEE International conference for convergence in Technology (I2CT-2019) Pune, India, 29-31 March 2019.

[10] Nandkumar S. Admile,”Performance Measure of image retrieval using different distance metrics”, IEEE International Conference on Intelligent Computing and Control Systems (ICICCS-2019) Madurai, India, 15-17 May 2019.

[11] Nandkumar S. Admile,”A survey on different image retrieval techniques”, International Research Journal of Engineering and Technology (IRJET-2018), Volume: 05 Issue: 10 | Oct 2018.

[12] Jing Ming Guo and Heri Prasetyo, “Effective Image Retrieval Using Feature Extracted Using Dot Diffused BTC,” IEEE Trans. Vol.24, no.3, pp 1010-1024.

Proceedings of the Fourth International Conference on Communication and Electronics Systems (ICCES 2019)
IEEE Conference Record # 45898; IEEE Xplore ISBN: 978-1-7281-1261-9

Comparative Analysis of DC-DC Converters for Tracking MPP for Roof-Top PV Power Systems with and without Partial Shading Condition

Kamalesh Tripathy
Department of Electrical Engineering
NIT Raipur
Raipur, Chhattisgarh, India
kamaleshtripathy@gmail.com

S. Gupta
Department of Electrical Engineering
NIT Raipur
Raipur, Chhattisgarh, India
sgupta.ele@nitrr,ac,in

***Abstract*—This paper addresses comparative analysis between three basic converters i.e. Buck, Boost and Buck-Boost converter to interface with a rooftop domestic Photo-Voltaic (PV) system to track maximum power point (MPP) effectively in normal conditions and in partial shading conditions. With partial shading, variable atmospheric conditions and variable load, the working value of impedance at MPP (Z_{MPP}) may vary widely. The MPPT algorithm should force the PV system work very near to Z_{MPP} with the help of power electronic interface for varying load and atmospheric conditions in order to make the system work at MPP. The effectiveness of the MPPT algorithm and the power electronic interface can be inferred from this obligation. Although all the three mentioned DC-DC converters can be used as interface between PV source and desired load, the simulation study verifies that the performance of each converter is different. Here the effect of diverse load having different value than Z_{MPP} on tracking MPP for both with and without partial shading condition is analyzed and it is deduced that Buck-Boost converter successfully tracks MPP for varying loading effect and atmospheric condition most efficiently.**

***Keywords*— PV System; Maximum power point tracking; Buck-Boost converter; Boost converter; Buck converter;Partial shading condition**

I. INTRODUCTION

Increase in global warming demands to increase the use of renewable and pollution free energy sources for an environment well suited for human and other living beings. Solar energy can be an ideal energy source which is inexhaustible, having zero carbon emission and completely free. Solar energy is natural source of light and heat. As electricity can be converted into all other form comparatively easily, photovoltaic (PV) technology, which converts solar irradiation (light energy) directly into electricity by photovoltaic effect is more popularly used. Still there are several problems are associated with PV modules such as

a) The electricity generated by PV cell is highly variable with environmental conditions.

b) Efficiency of PV cells to convert energy is very low (12-18%), (although cells over 30% have been fabricated in lab, they are not cost-effective) [1]. Due to low efficiency, it is important to control PV system in such a way to extract maximum power possible.

c) Also practically the V-P curve is highly non-linear, especially due to partial shading there are multiple local maxima on V-P curve, which makes it difficult to track maximum power point.

To get maximum power from PV system for most advantageous utilization, it is utmost important to have a control mechanism to track MPP. However among multiple local maxima, to find the global MPP,frequently usedmaximum power point tracking (MPPT) algorithms like Incremental Conductance (IC) algorithm [2] andPerturb and Observe (P&O) algorithm [3] fail to perform well. So different optimization techniques are used to find the global maximum.

For the variation in solar irradiation, temperature and loading condition, the MPPT algorithm controls the parameters of power electronic interface so that PV system has to work at MPP. Most researchers investigate new methods of MPPT algorithms. Nevertheless performance of DC-DC converters also needed to be scrutinized in different circumstances to build a PV system with an appropriate converter topology.

The presented work includes the modelling of PV system and tracking the MPP using three popular topologies of DC-DC converters i.e. Buck, Boost and Buck-Boost DC-DC converters without partial shading condition and also taking account for partial shading effect. Here Particle Swarm Optimization (PSO) technique is used to get global maximum point for different partial shading condition.

II. PV MODULE MODELLING

Here the relation between output current and voltage (I-V) of a practical PV module is given by equation (1) and the equivalent circuit for an ideal PV cell and practical PV device is given in fig. 1.

$$I = I_{PV} - I_0[\exp(\frac{V+RsI}{V_t\alpha})-1] - \frac{V+RsI}{R_P} \qquad (1)$$

Where I_{pv}= photovoltaic (PV) current, I_0 = reverse saturation current, $V_t = N_s kT/q$ = thermal voltage, k= Boltzman's constant, T= working temperature, q= charge of electron, N_S = no. of series connected cells. If array consists of Np no. of parallel cells, then $I_{pv} = I_{pv,cell}N_p$, $I_0 = I_{0,cell}$ Np. In equation (1), R_s and Rp are intrinsic series and shunt

equivalent resistances respectively. Rp is very large compared to Rs.

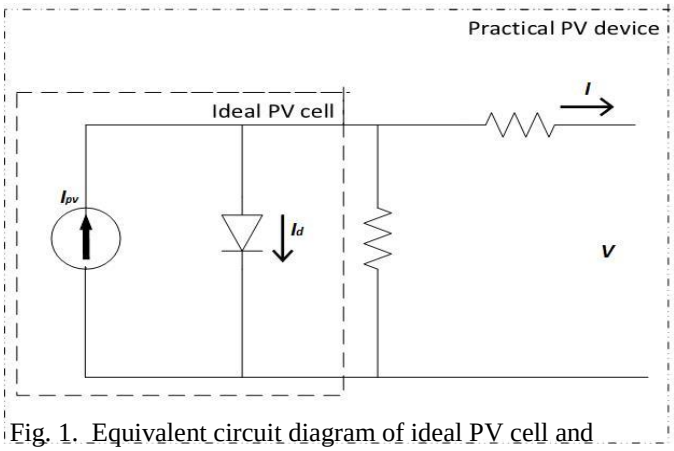

Fig. 1. Equivalent circuit diagram of ideal PV cell and practical PV device

The Bosch Solar Module designation M245 3BB has been successfully modelled from the following mathematical equations. [4]

$$I_0 = \frac{I_{SC,n} + K_I \Delta T}{\exp\left(\frac{V_{OC,n} + K_V \Delta T}{\alpha V_t}\right) - 1} \quad (2)$$

$$I_{PV} = (I_{PV,n} + K_I \Delta T)\frac{G}{G_n} \quad (3)$$

Where,
Vocn = Nominal open-circuit voltage
Imp = Output current at maximum power
Iscn= Nominal short-circuit current
Vmp= Output voltage at maximum power
Pmax_e = Maximum output power = Vmp*Imp
Kv = Temperature coefficient of voltage (%/K)
Ki = Temperature coefficient of current (%/K)
Ns = Number of cells connected in series
G = Solar irradiation
G_n = Nominal solar irradiation
ΔT = (T- 25°C)

List I: Electrical Characteristics of Bosch Solar PV Module c-Si M 60 EU30117 designation M245 3BB

Vocn= 37.7 V
Imp = 8.2 A
Iscn = 8.7 A
Vmp = 30.1 V
Pmax_e = Vmp*Imp = 245 W
Kv= - 0.32 %V/K
Ki = 0.0387 %A/K
Ns = 54
Above list gives the electrical specifications of Bosch Solar Module M2453BB [5] at STC (i.e. irradiation of 1000 W/m^2(=G_n), temperature at 25°C), which is taken as reference in this paper.

III. MAXIMUM POWER POINT TRACKING (MPPT)

(a) Without Partial Shading

Without shading effect the PV panel gets full insolation to generate electricity. Here the P-V curve has only one point where power becomes maximum as shown in fig 2(b). In the simulation here incremental conductance (IC) MPPT algorithm is used [6]. It states that at maximum power, differentiation of power w.r.t. voltage is 0 (zero).

Mathematically,

$$\frac{dP}{dV} = 0 \Rightarrow \frac{dP}{dV} + \frac{I}{V} = 0, \text{ at MPP} \quad (4)$$

$$\frac{dP}{dV} > 0 \Rightarrow \frac{dP}{dV} + \frac{I}{V} > 0, \text{ left of MPP} \quad (5)$$

$$\frac{dP}{dV} < 0 \Rightarrow \frac{dP}{dV} + \frac{I}{V} < 0, \text{ right of MPP} \quad (6)$$

The flow chart of IC algorithm is presented in fig 3. This calculate change in voltage and current and also change in current w.r.t voltage to calculate required duty cycle (D). If equation (6) is satisfied 'D' is increased if (5) is satisfied 'D' is decreased and for equation (4) no change in 'D'. Therefore, by varying duty cycle it will reach at MPP by checking the change in current value w.r.t change in voltage.

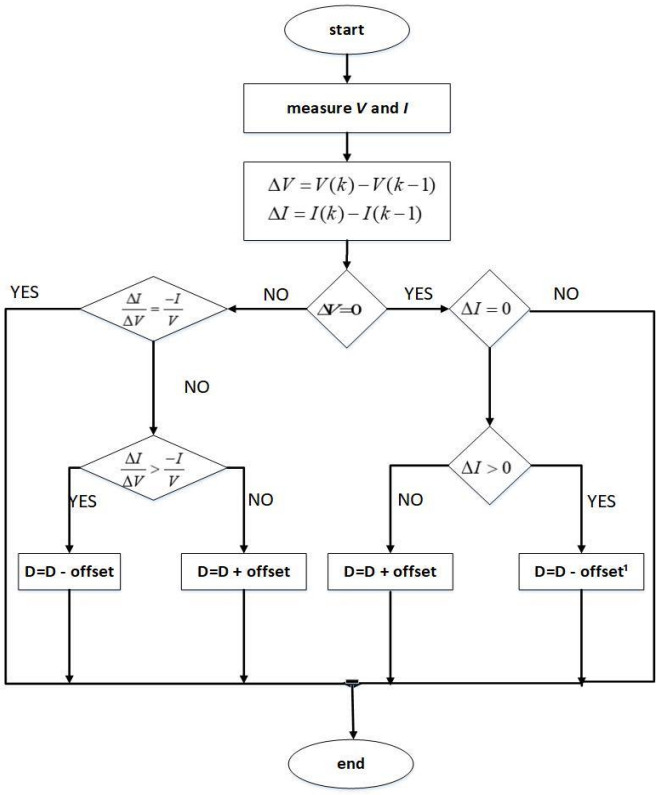

Fig. 3. Flow chart for Incremental conductance MPPT Algorithm

(b) With Partial Shading (effect of shading)

When different parts of a PV panel (shaded cells) get different irradiation than other parts of PV panel (illuminated cells), the generated current by shaded cells is less than that of illuminated cells. Due to this mismatch of current, photodiodes of shaded cells become reverse biased, due to which power loss happens in shaded cells, which in turn leads to hotspot problem.This can damage the PV module permanently[7]. To eliminate this problem, diodes are connected with PV cells in parallel as bypass diodes [8]. These bypass diodes conduct only during shading condition

so that no current can flow through shaded cells. To simulate shading effect in PV module, each group of the PV module is connected to an antiparallel diode and here three groups (connected in series) are used with different insolation given to each group.

Due to bypass diode and mismatch of current P-V characteristics of different PV cells, PV panel has multiple local maxima. Hence MPPT algorithm like IC, P&O may stuck at local MPP and fail to track global MPP. Here to track global MPP particle swarm optimization (PSO) technique [9] is used.

Steps to implement PSO:

1. Create a swarm (i.e. population) of particles (here Duty cycle 'D')uniformly distributed over 0 to 1.
2. Calculatethe objective function(here it is power 'P') for each particle (D).
3. If current position of a particle is betterthan its previous best position, according to the value of corresponding objective function (i.e. $P_{new}>P_{old}$)then update it to new position as its local best.
4. Calculate the best particle position from the total population for global best value.
5. Update the velocity of each particle:

$V_{i+1} = V_i + c_1 * U1 * (pBest - p_i) + c_2 * U2 * (gBest - p_i)$

Where

- P_i: particle's current position
- V_i: current path direction or particle velocity
- c_1: weight of the local bestinfluence
- c_2: weight of the global best influence
- *pBest*: local best position of each particle
- *gBest*: global best position of whole swarm
- *U1 and U2*: random variables

6. Update each particle's new positions:$p = p + V$
7. Go to step 2 until the below criteria is satisfied i.e. $(P_{PV,\,new} - P_{PV,\,old})/\,P_{PV,\,old} < 10^{-4}$

IV. DC-DC CONVERTERS

To maintain the operating point of PV system at MPP, we need a power electronic interface [10] between PV module and load, so that its circuit parameters can be controlled. For PV system DC-DC converters are popularly used for this purpose. The output voltage of DC-DC converter as well as current drawn from the source can be controlled, which in turn controls the input impedance of DC-DC converter by manipulating duty cycle (D). Pulse width modulation (PWM) technique [11] is used here to control duty cycle. Value of 'D' can be obtained by any MPPT algorithm.

For the PV module, both connected load and DC-DC converter (and inverter for ac loads) act as load. Thus by varying input impedance of the converter via duty cycle, slope of load line for the PV source can be manipulated to achieve MPP. Fig. 3 shows operating point of PV module, which is the intersection point between I-V characteristics and the load line (w.r.t PV system the impedance is resistive in nature as the source is dc).

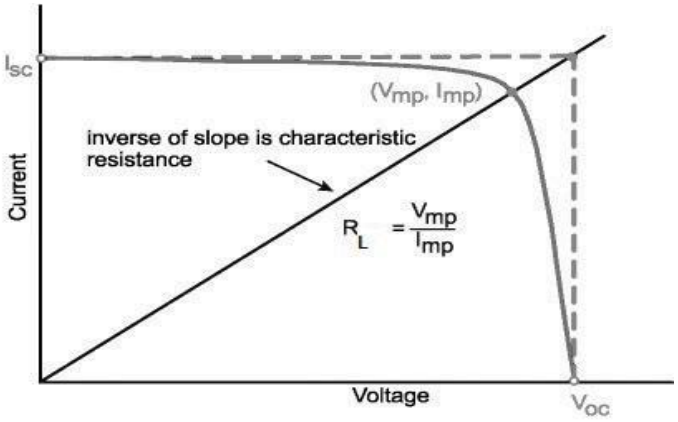

Fig. 3. Operating point for a PV system (V_{MP}, I_{MP})

Fig.4. shows circuit diagram of the Buck, Boost and Buck-Boost converters and the performance characteristics of buck, boost and buck-boost [12] converter are given in table-I

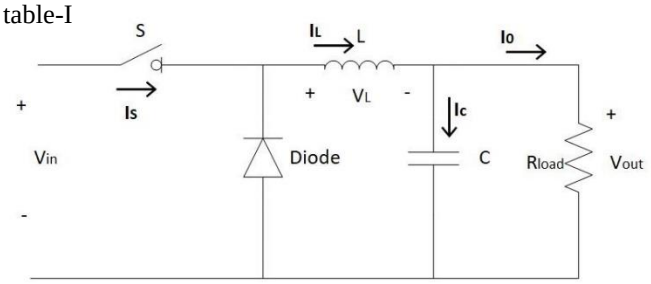

Fig. 4(a). Buck converter circuit diagram

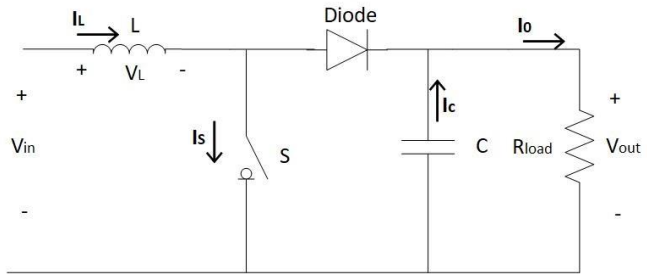

Fig. 4(b). Boost converter circuit diagram

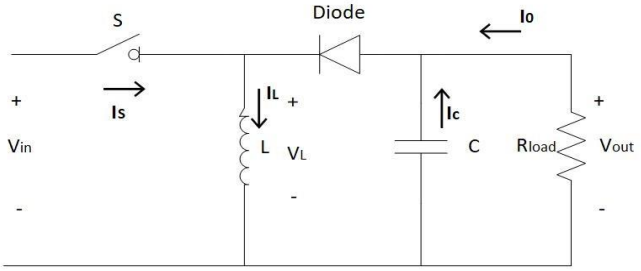

Fig. 4(c). Buck-Boost converter circuit diagram

It can be seen from the table as duty cycle varies from 0 to 1, the impedance reflected by input side of the converter (Z_{in}) also varies differently in each case. This acts as a critical factor which influences tracking ability of MPPT algorithm for any given converter topology for diverse load and atmospheric condition.

Variation of input impedance (Z_{in}) of each converter as D varies from 1 to 0 will be (a) Buck Converter : R_L to ∞ i.e. R_L to open circuit impedance, (b) Boost Converter : 0 to R_L i.e. short circuit impedance to R_L, (c) Buck-Boost

converter : 0 to ∞ i.e. any value of impedance between short circuit and open circuit impedance.

Table- I : Converters performance characteristics

Name of Converters	Gain in voltage	Gain in current	Input impedance (Z_{in})
Buck	D	1/D	$R_L\left(\frac{1}{D}\right)^2$
Boost	$\left(\frac{1}{1-D}\right)$	$(1-D)$	$R_L(1-D)^2$
Buck-Boost	$\left(\frac{D}{1-D}\right)$	$\left(\frac{1-D}{D}\right)$	$R_L\left(\frac{1-D}{D}\right)^2$

If impedance associated with MPP (Z_{MPP}) and Z_{in} have different value due to restrictions of converter topology, then any MPPT algorithm will fail to track global MPP. So for Buck converter if Z_{MPP} is less than R_L, then Z_{in} can never achieve the value of Z_{MPP} and MPPT algorithm will fail to track MPP, for Boost converter if Z_{MPP} is more than R_L, then MPPT algorithm will fail, but for Buck-Boost converter, as Z_{in} can be any value from 0 to ∞, for any load tracking efficiency only depends on MPPT algorithm.

V. Simulation and Results

To show the ability of tracking MPP, here 3.95 KW (~4KW) solar PV array is taken, where 4 modules are connected in parallel and 4 are in series. Each module can provide maximum power 246.82 W at STC. All simulations are done in MATLAB R2016a.

(a) Without Partial Shading

Simulation has been done for three atmospheric condition (i) 500W/m^2 irradiation and 25°C temperature (ii) 800W/m^2 irradiation and 30°C temperature and (iii) 200W/m^2 irradiation and 20°C temperature, for 1st 10 sec, 5 sec, 5 sec respectively i.e. total simulation time is 20 sec.

Table- II : Required operating point parameters for different environmental condition

Sl No.	Atmospheric Condition Irr (W/m^2) T (^{o}C)	P_{max} (KW)	V_{MPP} (V)	I_{MPP} (A)	Z_{MPP} (Ω)= V_{MPP}/ I_{MPP}
1.	Irr=800, T=30	3.119	118.2	26.39	4.478
2.	Irr=500, T=25	2.002	122.7	16.32	7.51
3.	Irr=200, T=20	0.812	122.5	6.583	18.6

Table II shows the impedance value corresponds to MPP from the simulation results with different solar irradiation (I_{rr}) and temperature (T). From simulation it is quite clear that, Z_{MPP} value decrease with increase in irradiation. For domestic load at 220 V ac, heavy load (10.75 KW i.e. 4.5 Ω), medium load (4 KW i.e. 12.1, 1KW i.e. 48.4 Ω) and light load (400W i.e. 121 Ω) are taken for simulation.

The extra power demand of load can be supplied by battery bank. Here it can be observed for variation in irradiation from 200 W/m^2 to 800 W/m^2, Z_{MPP} varies from 4.67 Ω to 18.6 Ω

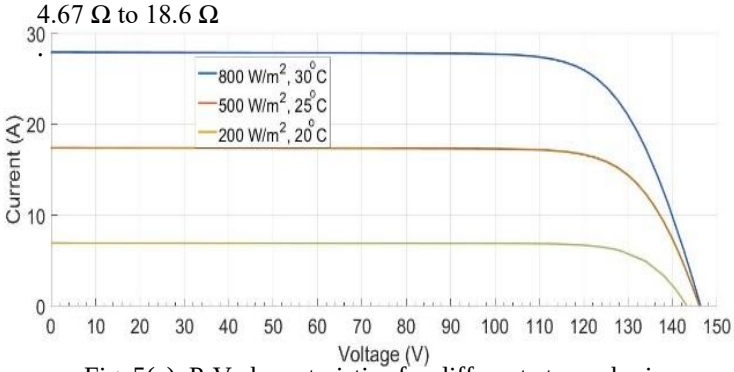

Fig. 5(a). P-V characteristics for different atmospheric condition

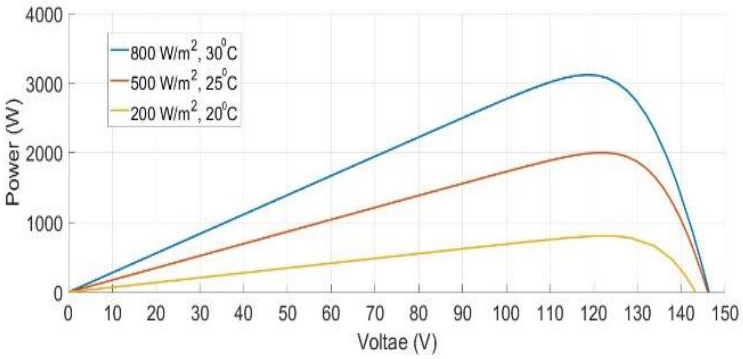

Fig. 5(b). I-V characteristics for different atmospheric condition

As shown in result fig.6, Buck converter tracks properly when load impedance seen by the converter is less than Z_{MPP} i.e. for only very heavy loads (for 4.5 Ω, P=) and for low irradiation level, but for domestic loads it will happen very less time duration in a day. Because generally peak load happens during mid-day when irradiance is very high. So most of the cases it may fail to track MPP.

Boost converter tracks MPP properly when load impedance seen by the converter is more than Z_{MPP} i.e. except for only very heavy loads at low irradiation level. But for high irradiation due to the value of Z_{MPP} is low, at peak load period boost converter may track properly as it happens around mid-day. For medium and light load, it generally can track MPP properly (as sown in fig. 7)

As Z_{in} of Buck-Boost converter can vary from 0 to ∞, so it can track MPP for all values of load impedance and for any irradiation value greater than the threshold value (from fig.8)

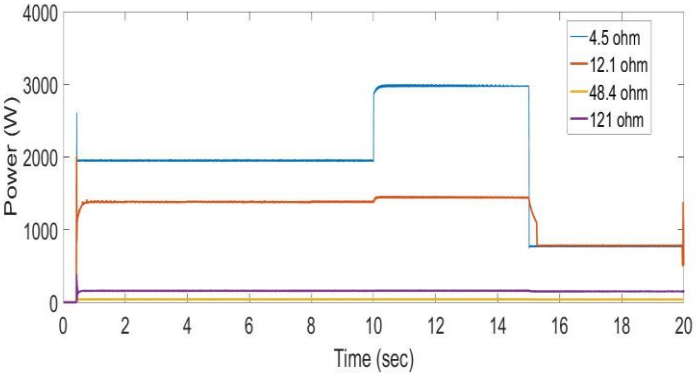

Fig. 6. Tracking of MPP for Buck converter for load resistance 4.5Ω, 12.1Ω, 48.4Ω, 121Ω

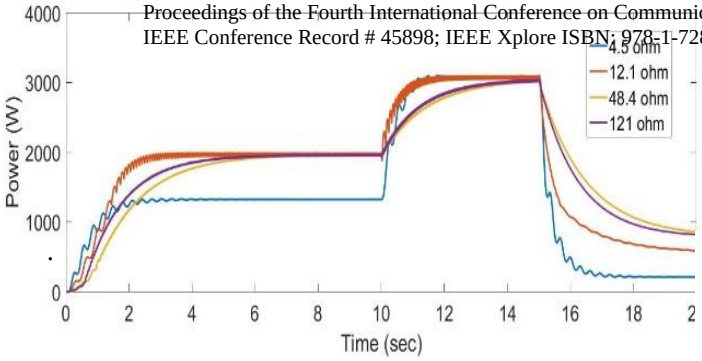

Fig. 7. Tracking of MPP for Boost converter for load resistance 4.5Ω, 12.1Ω, 48.4Ω, 121Ω

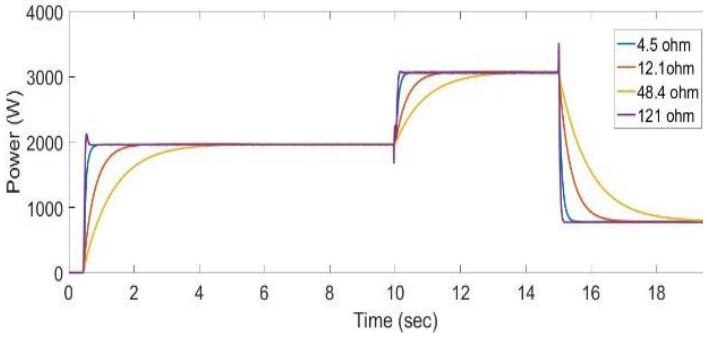

Fig. 8. Tracking of MPP for Buck-Boost converter for load resistance 4.5Ω, 12.1Ω, 48.4Ω, 121Ω

Table III: Output Power produced by different converters without partial shading

Sl. No.	Atmospheric Condition Irr (W/m^2) T (^{o}C)	Load Resistance (in Ω)	Power (KW) produced by PV system (in KW) (for different converters)		
			Buck	Boost	Buck-Boost
1	Irr = 500, T=25	4.5	1.968	1.323	1.97
		12.1	1.393	1.945	1.975
		48.4	0.156	1.973	1.972
		121	0.0404	1.99	1.98
2	Irr = 800, T=30	4.5	3.001	3.044	3.072
		12.1	1.447	3.094	3.078
		48.4	0.157	3.039	3.075
		121	0.041	3.065	3.082
3	Irr = 200, T=20	4.5	793.9	210.7	0.782
		12.1	789.4	589.7	0.797
		48.4	148.5	819.3	0.798
		121	0.038	857.2	0.8

(b) With Partial Shading

Here two partial shading conditions are taken for simulation. All these values are given in below table. After simulation of PV modules also Z_{MPP} values are also given for respective shading condition. Among the four series connected PV modules we provide 3 different irradiation to simulate partial shading condition having the maximum I_{rr} = 800 W/m^2. Here two shading conditions are simulated each for 10 sec.

When partial shading is taken into consideration, for a definite weather condition, Z_{MPP} can vary very widely according to the shading. So even if at the time of peak load sufficient irradiation is available for partial shading, boost converter may not track MPP.

In previous case (without partial shading) for I_{rr}= 800 W/m^2, boost converter tracks MPP properly. But due to different partial shading scenario as presented here Z_{MPP} varies, so boost converter also fails to track MPP for maximum available I_{rr} = 800 W/m^2 and T= 30°C. Similarly for the same reason sometimes buck converter can also track MPP accurately for high irradiation value as Z_{MPP} vary widely for same maximum irradiation available to PV cells.

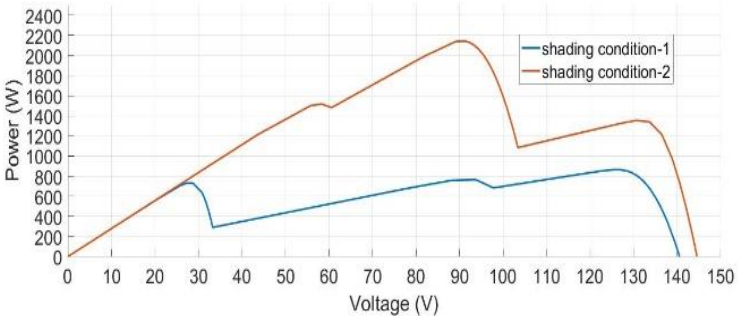

Fig. 8(a). P-V curve for partial shading condition

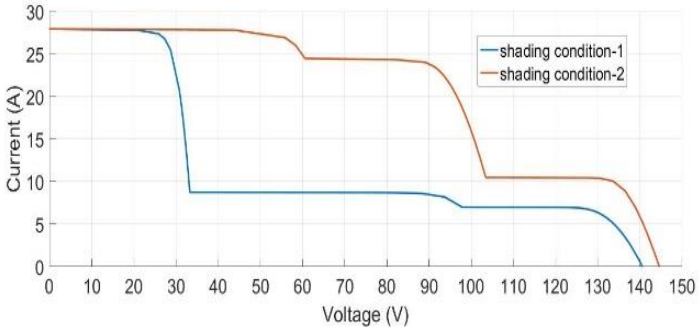

Fig. 8(b). I-V curve for partial shading condition

Table IV: Required operating point parameters for different shading conditions

Sl No.	Series connected Module No.	Irr values (W/m^2)	P_{MPP} (KW)	V_{MPP} (V)	I_{MPP} (A)	Z_{MPP} (Ω)
1. (0 to 10 sec)	Module 1 & 2	250	0.8646	125.6	6.88	18.24
	Module 3	800				
	Module 4	200				
2. (10 to 20 sec)	Module 1 & 2	800	2.143	91.34	23.46	3.893
	Module 3	700				
	Module 4	300				

As from result it is clear that buck converter failed to track MPP in light load condition but successful for high load for first shading condition. For second shading condition it failed to track MPP. Boost converter works

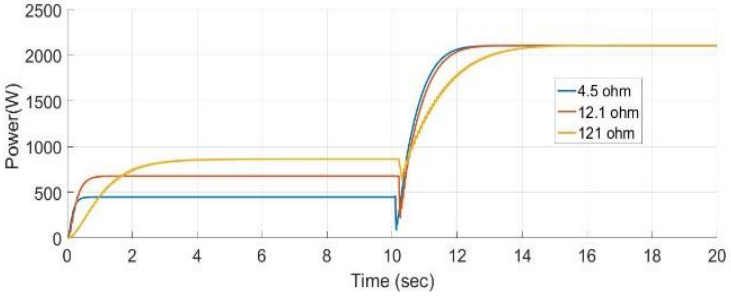

Fig. 8.Tracking of MPP for Buck converter for load resistance 4.5Ω, 12.1Ω, 121Ω with partial shading

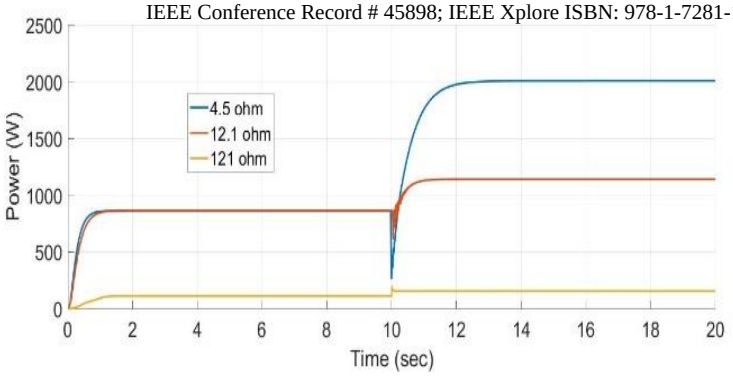

Fig. 9.Tracking of MPP for Boost converter for load resistance 4.5Ω, 12.1Ω, 121Ω with partial shading

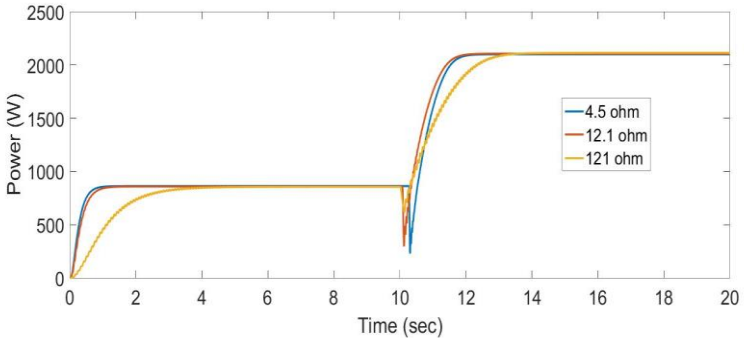

Fig. 10.Tracking of MPP for Buck-Boost converter for loadresistance 4.5Ω, 12.1Ω, 121Ω with partial shading

Table V: Power produced by converters in partial shading

Name of Conver-ters	Power (KW) produced by PV system (for different load)					
	Shading condition-1			Shading condition-2		
	Load Resistance			Load Resistance		
	4.5Ω	12.1Ω	121 Ω	4.5Ω	12.1Ω	121 Ω
Buck	0.854	0.858	0.110	1.97	1.31	0.155
Boost	0.650	0.658	0.861	2.12	2.122	2.123
Buck-Boost	0.860	0.859	0.857	2.12	2.125	2.132

successfully for second shading condition but for first shading condition it failed. But in each case Buck-Boost converter tracks MPP successfully as sown in table-V.

VI. CONCLUSION

If partial shading is ignored, boost converter can track properly for most of the time. But for shading condition as the value of Z_{MPP} is totally unexpected (for a given weather condition), neither Boost nor Buck converter can able to track MPP all the time as each has its own restriction to have required Z_{in} value for all loading conditions. This limitation can be overcome by buck-boost converter. As during lower irradiation and temperature which corresponds to higher value of Z_{MPP}, the converter works in buck mode (for D = 0 to 0.5) and during higher irradiation and temperature which corresponds to lower value of Z_{MPP}, the converter works in boost mode (for D = 0.5 to 1) to adjust the value of Z_{in} of the work near Z_{MPP}. Hence the ability to track MPP gets improved by buck-boost Converter.

Further work in this area may use other converter topologies and also with inverter topologies to show how compatible it is with MPPT algorithm and various loads i.e. industrial loads, medical equipment etc. for less size, cost and reduced ripples in output voltage and current.

REFERENCE

[1] H. Abu-Rub, A. Iqbal, et al., "Adaptive neuro-fuzzy inference-based maximum power point tracking of solar PV modules for fast varying solar radiations", *International Journal of Sustainable Energy. 31(6),383-398(2012)*, 2012.

[2]N. M. Razali and N. A. Rahim, "DSP-based maximum peak power tracker using P&O algorithm", *IEEE First Conf. CleanEnergy and Technol.*, pp. 34-39, 2011.

[3] W. Ping, D. Hui, D. Changyu and Q. Shengbiao, "An improved MPPT algorithm based on traditional incremental conductance method", *4th Int. Conf. Power Electron. Syst. and Appl, PESA2011*, pp. 1-4, 2011.

[4] Marcelo GradellaVillalva, Jonas Rafael Gazoli, and Ernesto Ruppert Filho ,"Comprehensive Approach to Modeling and Simulation of Photovoltaic Arrays",*IEEE Transactions On Power Electronics, Vol. 24, No. 5*, May 2009

[5] Bosch Solar Energy, "Bosch Solar Energy c-Si M 60 EU30117", M245 3BB data sheet, 2012,

[6] A. Loukriz, M. Haddadi, and S. Messalti, "Simulation and experimental design of a new advanced variable step size incremental conductance MPPT algorithm for PV systems," *ISA Transactions, vol. 62, pp. 30–38*, 2016.

[7] S. Motahhir, A. El Ghzizal, S. Sebti, and A. Derouich, "Shading effect to energy withdrawn from the photovoltaic panel and implementation of DMPPT using C language," *International Review of Automatic Control, vol. 9, no. 2*, pp. 88–94, 2016.

[8] Alsayid, Basim A., et al. "Partial shading of PV system simulation with experimental results." *Smart Grid and Renewable Energy* 4.06 (2013): 429.

[9] Duy C. Huynh, TuongM.Nguyen,Matthew, W.Dunnigan,Markus A. Mueller, "Global MPPT of Solar PV Modules using a Dynamic PSO Algorithm under Partial Shading Conditions", *IEEE Conference on Clean Energy and Technology (CEAT)*, 2013.

[10] Chakraborty, Sudipta, Bill Kramer, and Benjamin Kroposki. "A review of power electronics interfaces for distributed energy systems towards achieving low-cost modular design." *Renewable and Sustainable Energy Reviews* 13.9 (2009): 2323-2335.

[11] Tasi-Fu Wu, Yu-Kai Chen, "Modeling PWM DC/DC Converters Out of Basic Converter Units", *IEEE Transactions On Power Electronics, Vol. 13, No. 5*, pp.870-881, September 1998.

[12] Daniel W. Hart,*Power Electronics* ,Tata Mcgraw Hill Edition, 2010

Proceedings of the Fourth International Conference on Communication and Electronics Systems (ICCES 2019)
IEEE Conference Record # 45898; IEEE Xplore ISBN: 978-1-7281-1261-9

Fault Detection and Classification scheme using KNN for AC/HVDC Transmission Lines

Supriya Naik[1] and Dr. Ebha Koley[2]
Department of Electrical Engineering
NIT, Raipur
Chhattisgarh, 492010,INDIA
[1]Supriyanaik775@gmail.com, [2]ekoley.ele@nitrr.ac.in

ABSTRACT— In this paper fault detection and classification scheme using K nearest neighbor (KNN) has been presented for AC/DC transmission line with DFIG (doubly fed induction generator). The power system model consist of 1000 MW synchronous generator, 510 MW wind far, three phase transmission line of 500 kV and 30km length and HVDC line of 1000 MW. The model has been implemented with the corresponding parameters in MATLAB and simulated for different scenario. The raw current and voltage acquired for the sensors have been processed by performing discrete wavelet transform to the derive the discriminatory attributes with maximum disparity between the healthy and faulty cases. Following feature extraction, the required tasks of fault detection and classification scheme in AC and HVDC lines have been achieved using KNN. Further, the efficacy of the proposed KNN based scheme has been validated for varying fault scenarios pertaining to wide variation in fault resistance, inception angle of fault and fault location. For all tested cases, the proposed scheme is able to achieve a fault detection and classification accuracy of 100%.

Keywords- Doubly Fed Induction Generator Windfarm, HVDC, K-nearest neighbor classifier, Discrete Wavelet Transform Fault Detection, Fault Classification

I. INTRODUCTION

In the present era, countries all over the world are trying to enhance their economic conditions by improving industry which demands more energy. It motivates the power system to improve by combining both conventional source of energy and renewable source of Energy. Among renewable sources, wind energy is aggrandized because of its all day wind availability. But most of the wind farms are developed in offshore area. So it is difficult to route wind power to mainland grid efficiently. As HVDC transmission line is more efficient of transferring bulk amount power over long distances due to continuous technical improvement in power electronics [1]. However, the integration of a DFIG Based Windfarm into AC/HVDC system will influence the fault level and network topologies of the power system. These fault levels are intermittent in nature and existing protection schemes may fail to operate because of their pre-set condition. Therefore, the design and selection of a proper protection scheme is essential for reliable control and operation of renewable integrated power systems. Reliability of AC/HVDC system increase by addition of DFIG based windfarm which is possible by improvement of the propensity of its protection scheme. However, the inclusion of windfarm affects the existing protection schemes of AC/HVDC System because of variable speed of wind turbine and its different power rating and others threshold parameters which make the system protection task quite difficult [3]. In AC transmission line two types of fault can occur i.e. shunt fault and series fault. Further, shunt faults are differentiated into asymmetrical fault (LG, LL, LLG) and symmetrical fault (LLL, LLLG). In HVDC line, the DC pole-to-Ground fault and pole-to-pole fault on dc-link can occur. The successful and reliable operation of any transmission network is closely related to the accuracy of the associated fault detection and classification scheme. An accurate scheme minimizes the damage post fault and also helps in attaining the pre-fault condition at the earliest.

Currently, distance relays are used as primary protection for AC lines. In addition, other dominant schemes are based on rate of change of voltage and travelling wave, with under-voltage protection and current differential protection engaged for backup protection schemes. The notable schemes for fault detection/ classification in HVDC lines can be found in [4-9]. A directional pilot protection based on travelling wave has been reported in [4]. Related to fault transient voltage, a non unit dc line protection Approach is published in [5]. In [6], fault detection using power frequency current has been reported. In [7], linear distribution of low frequency voltage signals is utilized to implement distance protection. The unbalance in the current magnitude has been used to incorporate differential protection on the distributed-parameter transmission-line model is presented in [8]. For fault identification and fault pole selection criterion, in this paper the compensated current of the common mode and the differential mode are used. Earlier applications of KNN in power system protection include development of a detection and classification module in [9]. However all the above mentioned protection scheme developed for HVDC line did not consider the impact of integration of a DFIG based wind farm into HVDC system.

The global search capability of heuristic dynamic programming has been exploited for developing an adaptive modulation approach for AC/DC power system in [10]. The

fast power routing capability of HVDC has been analyzed in [11], by interfacing a DFIG wind farm with LCC-HVDC system. Some new protection scheme also developed for multi terminal HVDC connected offshore Windfarm [13]. For microgrid connection extreme learning machine is also developed in [15]

The KNN based scheme for AC/DC network [12, 14] uses the standard deviation of approximate coefficients of current and voltage signals measured at relaying bus (Bus-2). The scheme has been extensive validated for different faults in both the AC and DC line.

II. DFIG WIND FARM BASED AC/HVDC SYSTEM UNDER STUDY

The single line diagram of benchmark power system used in this paper is shown in Fig.1. The model comprises of two sources i.e. a 600 MW wind farm and a 1000 MW synchronous generator, integrated with HVDC transmission line, controlled by two thyristor based converters [10]. A monopolar HVDC transmission line with the earth as a return path which connects two AC systems of different frequencies is considered. The power generated from the sources are transmitted to the grid via a HVDC line of 300 km. Rectifier and inverter are connected on both side of the HVDC link. The raw time domain current and voltage signals acquired from the sensors at the relaying busses are utilized for the development of the fault detection and classification modules.

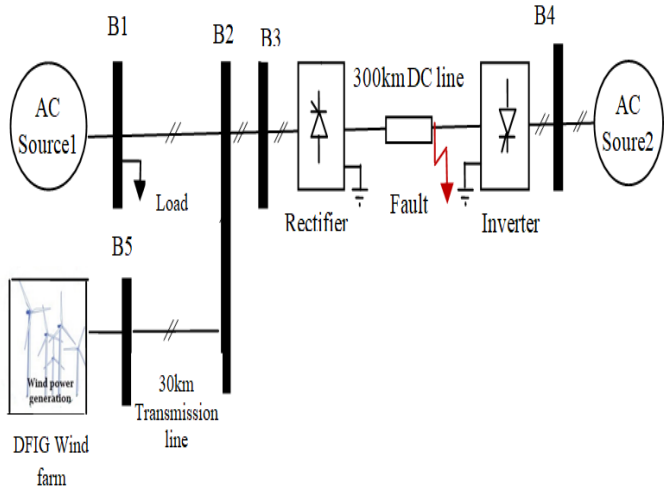

Fig-1 single line diagram of AC/HVDC transmission line with DFIG Windfarm

III. Analysis of Fault

To develop an accurate protection scheme for the HVDC system, fault analysis in terms of variation in the voltage and current profile post-fault has been carried out. In order to depict DC fault, a pole to ground fault has been simulated at 150 km from the relaying point and corresponding voltage and current waveforms are depicted in Fig.2.

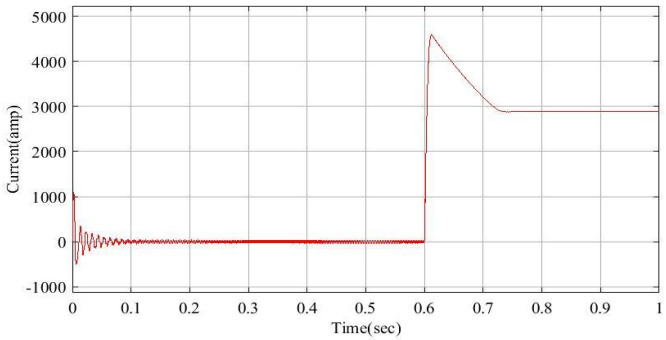

a

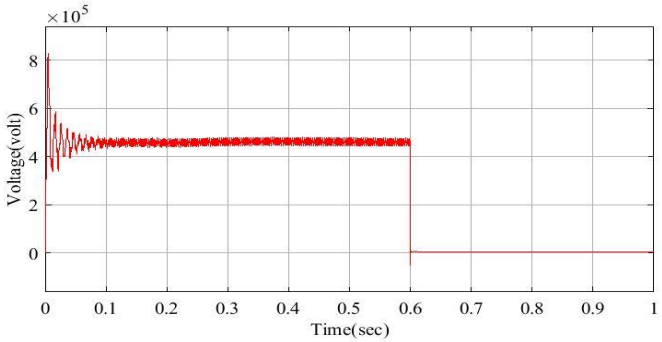

b

Fig-2 (a) Current (b) Voltage in HVDC transmission line during a pole to ground fault at 0.6 sec.

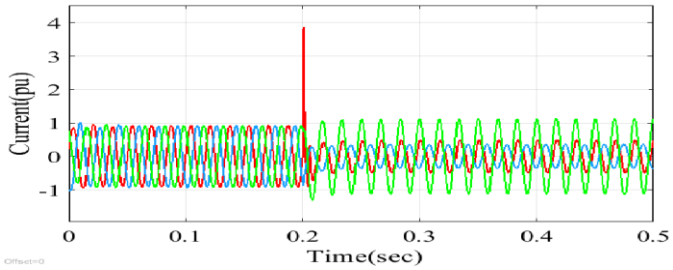

a

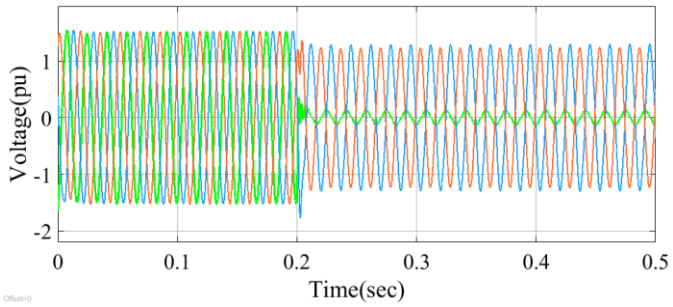

b

Fig-3 (a) Current (b) Voltage of Bus B2 during a AG fault in AC transmission line at 0.2 sec.

Similarly, in the AC a single line to ground fault section between Bus-2 and Bus- 5 has been simulated at 10 km with inception angle of fault(Φ_i) = 0 ° and resistance of fault (R_f)=

20 Ω from relaying point. In fig-3, the corresponding current and voltage waveforms are depicted.

From Fig 2 and Fig. 3, it is confirmed that the magnitude of current signals increases while there is decrement in the voltage signals in both the fault conditions (i.e. fault in HVDC and AC LINES). Thus current and voltage signals are the best indicative of fault conditions.

IV. KNN BASED FAULT DETECTOR AND FAULT CLASSIFIER

A. Pre-processing and Feature Extraction Process

Pre-processing of signals and extraction of discriminatory attributes is useful operation to obtain the suitable feature which can represent the present condition of the line effectively. The time domain instantaneous current and voltage signals are obtained at bus-2 by simulating the power system model under different fault scenarios. Following this, in the proposed scheme, the approximate coefficients are derived from the raw current and voltage signals collected from bus-2 is processed through Discrete wavelet transform (DWT). The attraction of DWT toward protection schemes is due to its both time and frequency domain Delineation. As compared to the more widely used DFT approach, DWT provides a better description since it is not just a single transform, but rather a set of transforms, each with a different set of wavelet basis functions. In this protection scheme, for feature extraction from instantaneous values of voltage and currents and voltages signal DWT technique is utilized. After obtaining the approximate coefficients, the standard deviation of approximate cofficients are then estimated which is fed as inputs to present KNN based fault detector and classifier.

Consider different fault scenarios, six numbers of input features are obtained for the presented KNN based fault protector. Features are

1- Standard deviation of approximate coefficient of voltage signal (σV_a, σV_b, σV_c) of phases a, b and c at Bus -2.
2- Standard deviation of approximate coefficient of current signal (σI_a, σI_b, σI_c) of phases a, b and c at Bus- 2.
3- The detailed description of variation in fault parameters considered in the proposed scheme is deal in Table 1.

Table-I

Fault Simulation Parameter

Simulation Parameters	Parameters Details	Number
Types of feature	Voltage, Current	2
Numbers of Features	Va,Vb,Vc,Ia,Ib,Ic	6
Types of fault	LG,LL,LLG,LLL, DC Pole to ground	12
Fault Resistance (Ω)	0,15,30,50	4
Inception Angles(Degree)	0°,90°	2
Number of Sections	S1,S2,S3	3
Measurement Point	B2	1

3. KNN BASED CLASSIFIER PROTECTION SCHEME

As mentioned in section 1, the inclusion of DFIG windfarm in the HVDC system may affect the conventional protection schemes and demands a new protection strategy which protects both AC and HVDC Transmission Line. For this purpose, KNN based protection method has been developed in the present work. The flowchart detailing the different stages of the algorithm is depicted in Fig. 4.

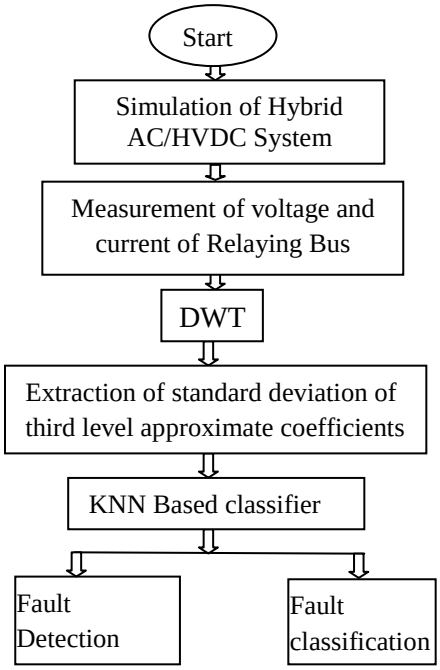

Fig-4 Flowchart of proposed scheme

K-Nearest Neighbour is a supervised learning based classifier, where K is the numbers of classes nearest neighbour to a test case. The value of k varies between 3 to10. The KNN classifier predicts the class of test point. For the protection of the power system model under study, a total of two KNN have been developed. The first KNN will identify the internal fault (fault in HVDC line), external fault (fault in three phase line) and no fault case. Thus for fault detection module has three target values i.e. 1, 2 and 0 representing fault in HVDC line, three phase line and no fault condition. Following detection of fault, KNN-2 classifies the type of faults in AC line. For three phase line the total possible faults are 11 (a-g, b-g, c-g, a-b, b-c, c-a, a-b-g, b-c-g, c-a-g, a-b-c-g). Thus, in case of classification task there are total eleven outputs representing each type of shunt faults in three phase lines. Thus KNN-1 supplies the details idea about the presence of fault and also differentiates between AC and DC faults while KNN-2 classifies shunt faults in AC line.

4. PERFORMANCE EVALUTION OF PROPOSED SCHEME

Following the improvement of the KNN based fault protection technique, testing of proposed KNN is accomplished for a variety of fault conditions to analyze the relay performance. The network was tested using different shunt faults in AC lines and DC faults in DC line with varying fault locations, resistance of fault and inception angles of fault.

A. *Evaluation for varying fault locations*

The appropriateness of the scheme has been evaluated by conducting extensive simulations on both the AC and HVDC line. The exhibition of the suggested scheme for the tested cses are depicted in Table II.

Table II

Test results for different fault detection with varying fault types in AC line

Fault type		Fault Location	Outputs of KNN1 based fault detector/classifier
Fault in AC line	a-g	5 km away from relaying point in AC line	2
	b-g		2
	c-g		2
	a-b-g		2
	b-c-g		2
	a-c-g		2
	a-b		2
	b-c		2
	a-b-c-g		2
Fault in DC line	p-g	150 km away from relay point HVDC line	1
	p-g		1
	p-g		1
	p-g		1
No fault			0

From the test results illustrated in Table II, it is confirmed that the suggested scheme detects AC and DC faults correctly with 100% accuracy.

B. *Evaluation for varying fault locations*

To validate the robustness of the proposed KNN-based detector/classifier, faults of varying types have been simulated at different locations of both the AC and DC lines, with different fault parameters. The different scenarios pertaining to fault resistance of 50 Ω and inception angle of 0°) are detailed in Table III. From the table, it is clear that the proposed network gives accurate results and perfectly identifies the fault. Further, the response of the KNN scheme also tested for fault cases (pole to ground fault) occurring at HVDC line at different locations form the relaying point. The test results detailed in the Table IV confirms that the proposed KNN based detector correctly detects the fault at different locations. Therefore, the proposed KNN based protection strategy is insensitive to the changes in the location of faults.

Table III

Test results for several shunt faults with varying fault locations (L_a) in AC line

Fault location (km)	Fault type	Outputs of KNN2 based fault detector/classifier
1	a-g	1
3	b-g	2
5	c-g	3
10	a-b-g	4
12	b-c-g	5
16	a-c-g	6
22	a-b	7
24	b-c	8
26	a-b-c	9
29	a-b-c-g	10

C. *Evaluation for varying fault resistance*

Any reliable protection scheme needs to validate for different resistance of shunt faults. Achieving robustness against fault variation is a challenge. In this context, the proposed KNN based fault detector and classifier has been gauged for fault resistance varying from 0 Ω to 50 Ω and inception angle of fault varying from 0˚ to 360˚. Results of some test cases are stated in Table III. Fault cases are simulated at fixed fault location (La=15km). From the test clearly that the proposed scheme is immune to fault variation and gives accurate result and perfectly identifies the faulty phases.

Table IV

Test results for DC faults with varying fault locations (L_a) in HVDC line

Fault location (km)	Fault type	Outputs of KNN based fault detector/classifier
1	P_1	1
50	P_1	1
90	P_1	1
150	P_1	1
200	P_1	1

Table V

Test Results for Different Shunt faults with several fault inception angle (Φ=0°) and fault resistance (Ω) at L_a = 15 Km

Fault resistances (Ω)	Inception angle of fault	Type of fault	Outputs of KNN based fault detector/classifier
0.01	0˚	a-g	1
		b-g	2
		c-g	3
50	90˚	a-b-g	4
		b-c-g	5
		a-c-g	6
100	180˚	a-b	7
		b-c	8
		a-b-c	9

.

5. CONCLUSION

In this paper, the feature space to classification output mapping capability of KNN classifier has been utilized to develop a accurate and reliable fault protector (detector and classifier) for AC/DC transmission line. The proposed scheme is able to detect faults of varying types in both the AC and DC sections of the line. Further, the proposed scheme also identify the line (AC or DC) in which fault has occurred. The scheme was extensively validated for faults occurring at various locations with different fault resistance and inception angles .The test results depict that the proposed ANN based protection technique is accurate in detecting and classifying all types of faults in both AC as well as HVDC line.

REFERENCES

1] Mohamed H. OkbaJ, Mohamed H. Saiect, M Z. Mostafa3, and T.M Abdel- Moneim, "High Voltage Direct Current Transmission A Review Part I",. *IEEE Trans HVDC, 2012, 978-1-4673-1835-8/12*

2] Vishnuvardhan Telukunta, Janmejaya Pradhan, Anubha Agrawal, Manohar Singh, and Sankighatta Garudachar Srivani, "Protection Challenges Under Bulk Penetration of Renewable Energy Resources in Power Systems: A Review", *IEEE Trans. CSEE Journal of Power and Energy Systems,2017,3,(4)*

[3] *Sunil K. Shukla, Ebha Koley , Subhojit Ghosh*,"DC offset estimation-based fault detection in transmission line during power swing using ensemble of decision tree" , *IET journal ,2018,doi: 10.1049/iet-smt.2018.5071*

4] Dong Wang, Mengqian Hou, Mengyou Gao, Feng Qiao , "Travelling wave directional pilot protection for hybrid HVDC transmission line", *Electrical Power and Energy Systems, 2019, 107,pp. 615–627*

5] Qiang Huanga, Guibin Zoua, Xiuyan Weia, Chenjun Sunb, Houlei Gaoa, **"**A non-unit line protection scheme for MMC-based multi-terminal HVDC grid*", Electrical Power and Energy Systems,2019, 107, 1–9*

6] D. Wang, H.L. Gao , S.B. Luo, G.B. Zou, "Travelling wave pilot protection for LCC-HVDC transmission lines based on electronic transformers' differential output characteristic", *Electrical Power and Energy Systems,2017, 93, 283–290*

7] Yu Qin, Minghao Wen, Junchao Zheng, Yu Bai, "A novel distance protection scheme for HVDC lines based on R-L model", *International journal of Electrical Power and Energy Systems, 2018,pp. 167–177*

8] Xu Chu, "Unbalanced current analysis and novel differential protection for HVDC transmission lines based on the distributed parameter model", *Electric Power Systems Research,2019, 171 105–115*

9] Jenifer Mariam Johnson, Anamika Yadav, "Fault detection and classification technique for HVDC transmission lines using KNN classifier', *Conference paper 2016*

10] Tang Y., He H., Ni Z., Wen J., Huang T., "Adaptive Modulation for DFIG and STATCOM with High-Voltage Direct Current(HVDC)Transmission", *IEEE Transactions on Neural Networks and Learning Systems,2016, 27(8), pp.1762–1772*

11] Haiping Yin, Lingling Fan, Zhixin Miao, "Fast Power Routing Through HVDC", *IEEE Transaction on Power Delivery, 2012, 27, (3),pp. 1432-1441*

12] Murli Manohar, Ebha Koley,Yuvraj kumar, "Discrete Wavelet Transform and kNN-Based Fault Detector and Classifier for PV Integrated Microgrid", *International Conference on Data and Information Sciences,2017,pp.20-28*

13] Jianwei Li, Qingqing Yang, Hao Mua, Simon Le Blond, Hongwen Hea, "A new fault detection and fault location method for multi-terminal high voltage direct current of offshore wind farm*", Applied Energy journal,2018, 220,pp. 13–20*

14] Omer Faruk Ertugrul,Mehmet Emit Tagluk, "A novel version of k nearest neighbor: Dependent nearest neighbor", *Applied Soft Computing journal, 2016, vol- 55, pp.480-490*

15] Murli Manohar, Ebha Koley, Subhojit Ghosh, " Microgrid protection under wind speed intermittency using extreme learning machine", *Science Direct* journal, *Computers and Electrical Engineering, 2018, vol 72, pp. 369–382*

Proceedings of the Fourth International Conference on Communication and Electronics Systems (ICCES 2019)
IEEE Conference Record # 45898; IEEE Xplore ISBN: 978-1-7281-1261-9

Proceedings of the Fourth International Conference on Communication and Electronics Systems (ICCES 2019)
IEEE Conference Record # 45898; IEEE Xplore ISBN: 978-1-7281-1261-9

Heart Disease Predictions Using Numerous Classification Techniques and Dynamic LSTM Model

Aishwarya Mishra
Information Technology and Computer Applications.
MMM University of Technology,
Gorakhpur (U.P)-273010, India
aishwaryamishra17@yahoo.com

Dayashankar Singh
Information Technology and Computer Applications
MMM University of Technology,
Gorakhpur (U.P)-273010, India
dsscs@mmmut.ac.in

***Abstract*— Now-a-days, a lot of clinical data are used for utilizing the intellectual advancements of clinical basis leadership. In the area of health sector, the need for improving the nature of patient's lives and decreasing the expenses as well as measures the work engaged with their everyday medicinal services condition is very important. An Electronic health record (EHRs) is a data record set which resides patient diagnostic lab records with different parameters, physician/consultants' histories, also in the accounts of different sections of the hospital. Earlier, in the case of heart disease prediction, we have attained a bulk unorganized set of data since the time series of the EHR system. By dividing and taking out these time-sensitive EHRs information, we can distinguish/perceive the aggregate factors among all the obtained set of clinical data for our research purpose. Despite the fact that it is troublesome undertaking to utilize the current EHR information legitimately, on the grounds that they might be repetitive, not in a standardized structure, and some of the data missed/blanked. Consequently, this paper has been proposed a viable and solid design of the Dynamic LSTM model for coronary illness forecast. The main aim of doing this paper has been used to predict heart sickness utilizing an alternate information mining arrangement system. In this paper, we have designed a Dynamic LSTM using classification techniques and generated a training and test model which produce a more accurate result as compare to previously LSTM risk algorithm. One of the advantages of the proposed algorithm is it can work on dynamic dataset records and capable to produce a more efficient classified result for heart disease prediction.**

Keywords—Electronic health record, Deep learning, Dynamic LSTM

I. INTRODUCTION

Heart disease/ Coronary illness is a popular term that implies that the heart isn't used regularly. Children can be brought into the world with heart-related problems. This is called inherent heart disorder [1]. Many of the heart/coronary related diseases can be acquired. Coronary illness, which incorporates ischemic coronary illness, coronary heart disappointment and different sicknesses of the heart, is the main source of all around. It represents the greater part of all s because of cardiovascular illness.

Coronary illness can cause angina (chest torment), heart assaults (myocardial localized necrosis) and unexpected heart failure. A heart assault is typically the principal indication of coronary illness. A Heart disease ordered into three classes:

- Coronary artery disease – This disease occurs when veins are not passing on blood properly in the heart.
- Congestive heart failure – This disease occurs when a heart is not pumping properly.
- Bad heart rhythms – This is a very rare heart disease. This disease defines the electronic pulse like the movement of the heart.

CVDs are the number 1 explanation behind at around the globe. A bigger number of individuals die every year from CVDs than any other reason. A normal 17.9 million people passed on from CVDs in 2016, addressing 31% of each and every overall demise. Of these deaths, 85% is a result of heart strike and stroke. Out of the 17 million startling misfortunes (more youthful than 70) on account of non-transmittable diseases in 2015, 82% are in low-and focus pay countries, and 37% are realized by CVDs. Most cardiovascular ailments can be evaded by keeping an eye on social danger factors, for instance, tobacco use, bothersome eating routine and weight, physical inaction and destructive use of alcohol using people wide philosophies [5][6].

Peoples/Individuals with a cardiovascular ailment or who are at high cardiovascular hazard (because of the nearness of at least one hazard factors, for example, hypertension, diabetes, hyperlipidemia or officially settled malady) need early identification and the board utilizing directing and prescriptions, as fitting. Coronary illness and stroke together added to 28·1% of all-out deaths in India year 2016 — contrasted and 15·2% in 1990. Coronary illness added 17·8% of all-out deaths and stroke contributed 7·1% of complete deaths. The extent of deaths and incapacity from coronary illness was essentially higher in men than in ladies, however, was comparable among people for stroke. Death due to cardiovascular diseases increases from 13 lakh in 1990 to 28 lakhs in the year 2016.

So, diagnoses & prediction of heart disease earlier is compulsory and treatments for individuals/peoples who are probably going to have a coronary illness and help them have a longer life.

A favored technique to determine the issues of precise finding and the conveyance of focused treatments is the continuous execution of complete physical assessments [4]. Be that as it may, total and continuous physical assessments would prompt information over-burden. So, in this paper, we design a novel approach namely Dynamic LSTM model with classification techniques. The main purpose of this algorithm to produce accurate results for finding out heart disease prediction.

A Data mining alludes to extricating or mining information from a lot of information. As it were, Data mining is the science, workmanship, and innovation of finding huge and complex assemblages of information so as to find helpful examples. To accomplish an objective, the proposed calculation deals with information mining characterization strategies. Characterization is an established issue in AI and information mining [1][23]. In other words, the order issue is worried about producing a portrayal or a model for each class from the given informational index. "Characterization" is a standout amongst the most vital information mining strategies. It is utilized to foresee bunch/class enrollment for information cases.

The remainder of the paper is broken down into six sections. Section II gives a review of the previous work in this area and its different aspects. The Background and related work covered in this section. Section III identifies the problems with the existing approach and Section IV presents proposed work. The experimental results define in Section V. This paper concludes with Section VI, which contains a summary and future work for further research.

II. BACKGROUND AND RELATED WORK

Ji.Zhang et.al [1]design a bagging based troupe display is used to anticipate the patient's condition one day ahead of time for creating the last suggestion. A blend of three classifiers artificial neural network, least squares-support vector machine, and naïve Bayes are utilized to develop a group structure. This proposed framework is a promising device for examining time arrangement medicinal information and giving precise and solid suggestions to patients experiencing endless heart infections.

Fen Miao et.al [2] proposed an improved RSF (iRSF) with a novel split standard and a halting basis for distinguishing progressively exact indicators that can isolate survivors and non-survivors and, in this way, improve segregation capacity. Initial, a weighted log-rank test was utilized to part the hub and can be connected to non-relative risk circumstances to improve the test for a scope of elective theories.

Afef Mdhaffar et.al [4] presents a novel wellbeing examination approach for heart failure prediction/ expectation. It depends on the utilization of complex occasion preparing (CEP) innovation, joined with measurable methodologies. A CEP motor procedure approaching wellbeing information by executing edge-based investigation rules. Rather than having to physically set up limits, our novel factual calculation naturally figures and updates edges as indicated by recorded chronicled information.

Chrysa et.al [5] The heart phonocardiogram is breaking down by utilizing Ensemble Empirical Mode Decomposition (EEMD) joined with kurtosis highlights to find the proximity of S1, S2 and concentrate them from the recorded information, framing proposed HSS conspire, to be specific HSS-EEMD/K.

Bo Jin et.al [3] proposes a successful and strong design for heart disease prediction. The primary commitment of paper is to anticipate heart failure(attack) by utilizing a neural network (i.e., to foresee the likelihood of cardiovascular sickness dependent on patient's electronic restorative data). Specifically, they utilized one-hot encoding and word vectors to demonstrate the analysis occasions and anticipated heart disappointment occasions utilizing the fundamental standards of a long short-term memory model.

Assessments dependent on a genuine informational collection show the promising utility and adequacy of the proposed engineering in the expectation of the danger of heart disappointment.

III. PROBLEMS WITH THE EXISTING APPROACH

Coronary illness or CVDs are the number 1 reason for at around the world for death. A bigger number of people die every year from CVDs than from some other reason.

In our proposed approach we have increased the accuracy and efficiency by replacing the static LSTM which was used in the traditional approaches by dynamic LSTM. Our results clearly depict that the dynamic LSTM have higher accuracy than static LSTM. A few investigations/studies in the writing have been led utilizing outfit approaches, with some achievement, in the medicinal area [1][4]. However, none of them drew closer or tackled the issue that we manage in our examination to give exact suggestions to coronary illness persons to take or cure further medical test in for coming days.

IV. PROPOSED ALGORITHM

We contrast to the above-mentioned problems with the existing approach, we develop a classification technique with dynamic LSTM Model framework for heart disease prediction earlier stage. Our proposed model working on the basic LSTM model [3].
To handle Electronic health records data, we proposed a new algorithm namely Dynamic LSTM model (Long Short-

Term Memory Model). In our algorithm we use a training data set and test data set. This algorithm gives better result compare to the above mention algorithms [1]. We are shown details of the algorithm in this section.

We utilize Classification methods of data mining. Classification is the handling of finding a lot of models (or capacities) those define and recognize information classes. A classification technique has two types of data set namely training and test data. First, one is used to implement a model or classifier and the second dataset is used for testing of implemented model. There are some popular classification methods like:

A. CART :

CART represents Classification and Regression Trees. CART is one of the famous techniques for structure choice tree in the AI people group [13][28]. It was created by [Breiman and his team. At 1984] and is portrayed by the way that it develops binary trees, specifically every interior hub/node must be precisely 2 active edges, every one of which presently endeavors to part in a similar way as the root hub/node. The parts are chosen to utilize the Gini index.

B. Bayesian classifier:

A Bayesian classifier is a measurable classifier. This classifier is used for prediction with probabilities.

C. Fuzzy logic:

Fuzzy logic is a set of the rule-based classification system. It improves all the problems of crisp and rule-based classifiers.

D. Association rule mining :

This is an imperative & active field of data mining researcher. One strategy for association rule mining, called associative classification/characterization, comprises of two stages. In the primary advance, affiliation guidelines are produced utilizing an adjusted form of the standard affiliation rule mining calculation known as A prior. The second step builds a classifier dependent on the affiliation rules found.

E. LSTM Model:

Hochreiter and his team design an LSTM model demonstration. It's a unique RNN method. To fulfill a requirement of long-term memory, the RNN capture of condition/situation of the current concealed layer. The result of the calculation comes in the form of an exponential increment and it shows time, cost of a model. That is a reason RNN is not applicable for long term memory calculations.

F. Dynamic LSTM Model:

A collaborative approach is an effective model, which combines all the multiple parent classifiers to solve a problem and increasing performance of every base classifiers. The working principle is taken from LSTM model and deep learning. There are two different datasets namely training data set and test data set. This model is also in working condition if data varies [3].

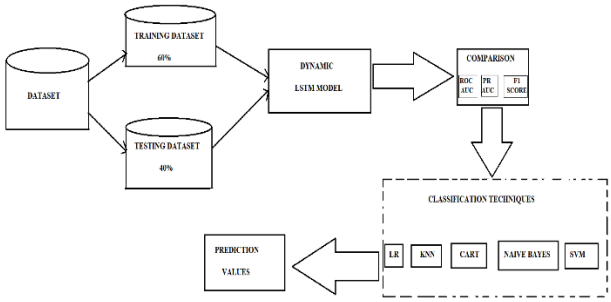

Fig. 1. Framework of proposed dynamic LSTM model.

V. RESULT ANALYSIS

We used a real-life data collection "HEART-DISEASE dataset" occupied from UCI repository. This data composed from four following different locations: Cardiology University Hospital. The characteristics of the multivariate attributes of the dataset are shown in Table 1.

TABLE I. MULTIVARIATE ATTRIBUTES OF DATASET

Attribute name	Attribute type
Age	Numeric
Sex	Binary
Cp	Numeric
Trestbps	Numeric
Chol	Numeric
Fbs	Binary
Restecg	Binary
Thalach	Numeric
Exang	Numeric
Oldpeak	Numeric
Slope	Numeric
Ca	Numeric
Thal	Numeric
Target	Numeric
Bglf	Numeric
Bgl pp	Numeric
Bglr	Numeric

A property of this dataset is that it is a multivariate and generally used for classification purpose. This dataset contains categorical, integer and real attributes. Basically, there are 14 different attributes that were used earlier and 3 more attributes namely Bglf (blood glucose level fasting), Bgl pp (blood glucose level PP) and Bglr (blood glucose level regular) are added to find accurate results.

Table III clearly shows that when dynamic LSTM model is chosen with numerous classification techniques such as LR, KNN, CART, NB and SVM gave the better results. Graphs are plotted in between the Baseline and the prediction values. The corresponding graphs are as given below.

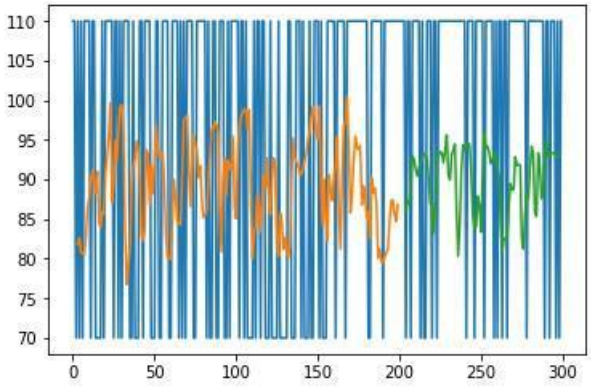

Fig. 2. The layout of Heart disease dataset in histogram format

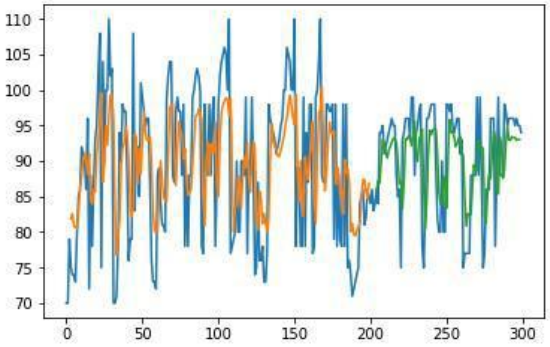

Fig. 3. Dynamic LSTM model Trained on regression Design of Heart Disease Prediction Problem.

Classification techniques with dynamic LSTM model are implemented on Python 3.6 version. This model is tested on different parameters and classification techniques:

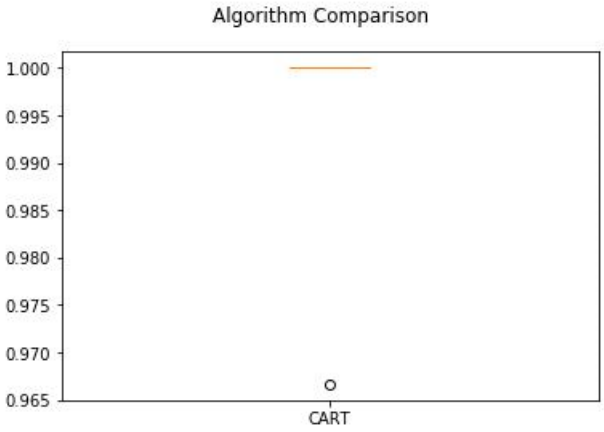

Fig. 4. Classification of Heart disease by CART technique

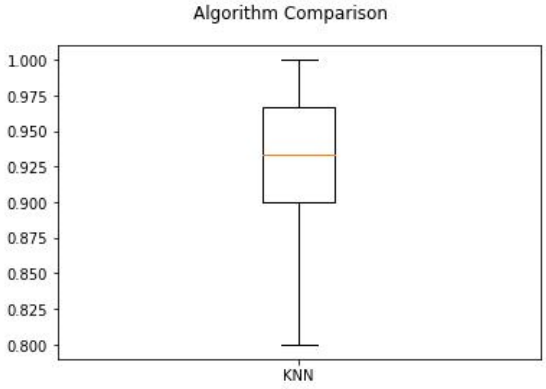

Fig. 5. Classification of Heart disease by KNN technique

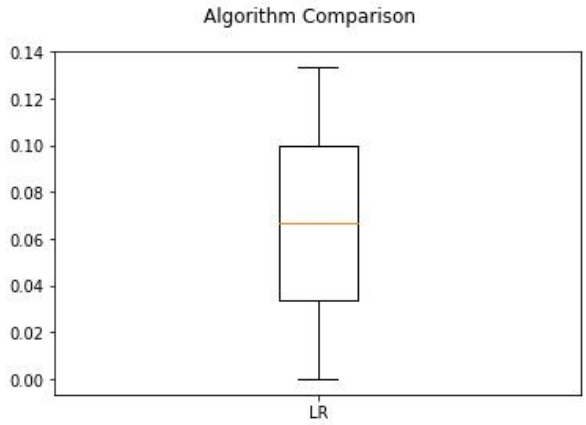

Fig. 6. Classification of Heart disease by LR technique

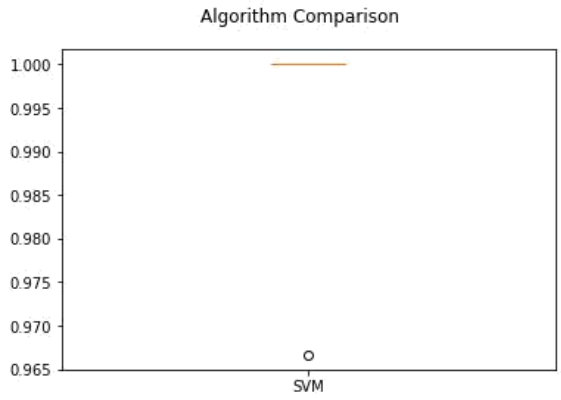

Fig. 7. Classification of Heart disease by Support vector machine

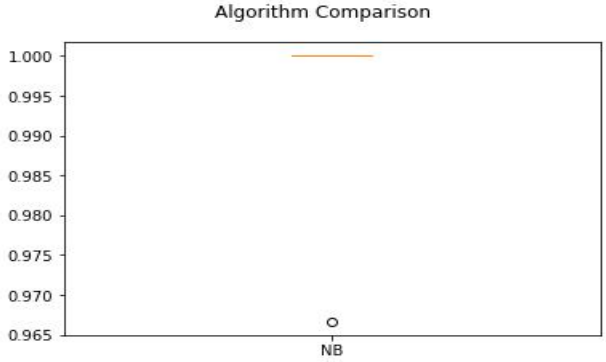

Fig. 8. Classification of Heart disease dataset by Naïve Bayes method

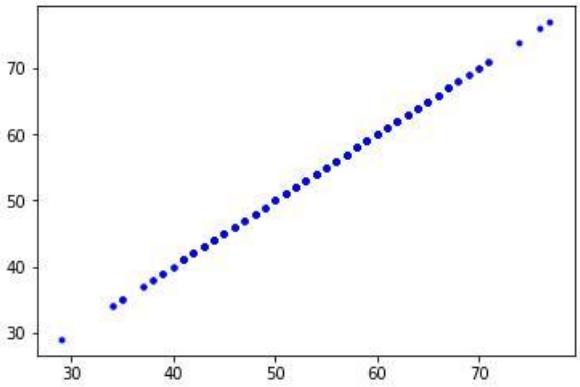

Fig. 9. A line plots of the series creates & shows a clear growing learning.

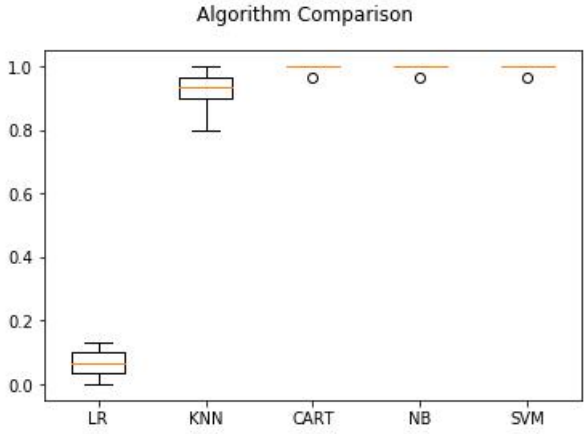

Fig. 10. Collective comparison of classification tehcniques

TABLE II. RESULT OF TEST DATASET

Classification	**Accuracy**
(Test predicts, Train predicts)	(85.97968, 87.23571)

TABLE III. RESULT ANALYSIS BASED ON K-FOLD METHOD

Classification techniques	**Mean Distribution Accuracy**	**Standard Deviation Accuracy**
LR	0.070000	0.043333
KNN	0.926667	0.059255
CART	0.996667	0.010000
NB	0.996667	0.010000
SVM	0.996667	0.010000

TABLE IV. COMPARE LSTM AND DYNAMIC LSTM

LSTM		**DYNAMIC LSTM**	
ROC- AUC	0.6827	LR	0.043333
PR- AUC	0.2678	KNN	0.059255
F1 - SCORE	0.2188	CART	0.010000

VI. Conclusion & Future work

In this section, we conclude the paper with overall findings as well as suggestions for future research work. The paper proposes a design of original methodology for finding accurate result and helps in earlier diagnoses of heart disease predictions. The proposed model gives more efficient and accurate result as compare to previous diagnoses models and algorithms. This classifier varies according to the different data records. One of the advantages of this model is that it can

work on a real, numerical and categorical dataset. In future work, this model can be used in diagnosing of different diseases prediction.

REFERENCES

1. Ji Zhan, R. Lafta, X.Tao, Y. LI," Coupling a Fast Fourier Transformation With a Machine Learning Ensemble Model to Support Recommendations for Heart Disease Patients in a Telehealth Environment", IEEE Access, vol.5,pp.10674-10685,2017
2. Fen Miao, Y.P.Cai, Y.X.Zhan," Predictive Modeling of Hospital Mortality for Patients With Heart Failure by Using an Improved Random Survival Forest" IEEE Access, vol.6,pp.7244-7254,2018 .
3. Bo Jin, C.Che , Z. Liu," Predicting the Risk of Heart Failure With EHR Sequential Data Modeling" IEEE Access, vol.6,pp.9256-9261,2018.
4. A.Mdhaffar, I.B.Rodriguez, K.Charfi," CEP4HFP: Complex Event Processing for Heart Failure Prediction", IEEE Transaction, vol.16,pp.1536-1241,2017
5. C.D.Papadaniil, L.J.Hadjileontiadis, "Efficient Heart Sound Segmentation and Extraction Using Ensemble Empirical Mode Decomposition and Kurtosis Features", IEEE Journal of Biomedical and health Informatic,2013
6. F. M. Bianchi, E. De Santis, A. Rizzi, and A. Sadeghian, "Short-term electric burden estimating utilizing reverberation state systems and PCA decomposition," IEEE Access, vol. 3, pp. 1931_1943, 2015.
7. Pati, B. Kumar, D. Manjhi, and K. K. Shukla, "An examination among ARIMA, BP-NN, and MOGA-NN for programming clone development forecast," IEEE Access, vol. 5, pp. 11841_11851, 2017.
8. Y.- T. Su, Y. Lu, M. Chen, and An.- A. Liu, "Spatiotemporal joint mitosis discovery utilizing CNN-LSTM arrange in time-slip by stage differentiate microscopy pictures," IEEE Access, vol. 5, pp. 18033_18041, 2017.
9. G. Zhu, L. Zhang, P. Shen, and J. Melody, "Multimodal motion acknowledgment utilizing 3-D convolution and convolutional LSTM," IEEE Access, vol. 5, pp. 4517-4524, 2017.
10. G. P. Zhang, "Time arrangement anticipating utilizing a crossover ARIMA and neural system show," Neurocomputing, vol. 50, pp. 159_175, Jan. 2003.
11. G. M. Jenkins and A. S. Alavi, "Some parts of demonstrating and estimating multivariate time arrangement," J. Time Ser. Butt-centric., vol. 2, no. 1, pp. 1_47, 1981.
12. R. G. Dark colored, "Exponential smoothing for anticipating request," Oper. Res., vol. 5, no. 1, pp. 145_145, 1957.
13. G. E. P. Box, G. M. Jenkins, and G. C. Reinsel, Linear Nonstationary Models Time Series Analysis), the fourth ed. Hoboken, NJ, USA: Wiley, 1976, pp. 93_136.
14. S. Hochreiter and J. Schmidhuber, "Long momentary memory," Neural Comput., vol. 9, no. 8, pp. 1735_1780, 1997.
15. F. A. Gers and J. Schmidhuber, "Recurrent nets that time and tally," in Proc. IEEE-INNS-ENNS Int. Joint Conf. Neural Netw. (IJCNN), vol. 3. Jul. 2000, pp. 189_194.
16. Chung, C. Gulcehre, K. Cho, and Y. Bengio. (2014). "Observational assessment of gated intermittent neural systems.
17. G. E. Hinton, "Learning conveyed portrayals of ideas," in Proc. eighth Annu. Conf. Cognit. Sci. Soc., vol. 1. 1986, pp. 47_61.
18. Y. Bengio, R. Ducharme, P. Vincent, and C. Janvin, "A neural probabilistic language show," J. Mach. Learn. Res., vol. 3, pp. 1137_1155, Feb. 2003.
19. C. Buckley and E. M. Voorhees, "Retrieval assessment with deficient data," in Proc. SIGIR, 2004, pp. 25_32.
20. N. Tangri et al., "A prescient model for the movement of endless kidney malady to kidney disappointment," JAMA, vol. 305, no. 15, pp. 1553_1559, 2011.
21. R. Sukkar, E. Katz, Y. Zhang, D. Raunig, and B. T. Wyman, "Disease movement demonstrating utilizing shrouded Markov models," in Proc. Annu. Int. Conf. IEEE Eng. Medications. Biol. Soc., Aug./Sep. 2012, pp. 2845_2848.
22. J. Zhou, J. Liu, V. A. Narayan, and J. Ye, "Modeling illness expert gression through perform various tasks learning," NeuroImage, vol. 78, pp. 233_248, Sep. 2013.
23. Y.- Y. Liu, H. Ishikawa, M. Chen, G. Wollstein, J. S. Schuman, and J. M. Rehg, "Longitudinal displaying of glaucoma movement utilizing 2-dimensional constant time shrouded Markov show," in Proc. Int. Conf. Prescription. Picture Comput. Comput.- Assisted Intervention. (MICCAI), Nagoya, Japan, 2013, pp. 444_451.
24. P. Schulam and S. Saria, "A system for individualizing expectations of malady directions by misusing multi-goals structure," in Proc. Adv. Neural Inf. Procedure. Syst. (NIPS), Montreal, QC, Canada, 2015, pp. 748_756.
25. X. Wang, D. Sontag, and F. Wang, "Unsupervised learning of sickness movement models," in Proc. Knowl. Revelation Data Mining (KDD), New York, NY, USA, 2014, pp. 85_94.
26. E. Choi, N. Du, R. Chen, L. Melody, and J. Sun, "Constructing malady system and fleeting movement show by means of setting touchy Hawkes process," in Proc. Int. Conf. Information Mining (ICDM), Atlantic City, NJ, USA, Nov. 2015, pp. 721_726.
27. N. Hammerla, J. Fisher, P. Andras, L. Rochester, R. Walker, and T. Ploetz," PD sickness state evaluation in naturalistic situations utilizing profound learning," in Proc. AAAI, Austin, TX, USA, 2015, pp. 1742_1748.
28. Z. C. Lipton, D. C. Kale, C. Elkan, and R. Wetzell. (2016). "Learning to determine to have LSTM repetitive neural systems."
29. Karpathy and L. Fei-Fei, "Deep visual-semantic arrangements for creating picture depictions," in Proc. PC. Vis. Example Recognit. (CVPR), Boston, MA, USA, 2015, pp. 3128_3137.
30. Cho et al., "Learning phrase portrayals utilizing RNN encoder-decoder for measurable machine interpretation," in Proc. Observational Methods Natural Lang. Procedure. (EMNLP), Doha, Qatar, 2014, pp. 1724_1734.

Proceedings of the Fourth International Conference on Communication and Electronics Systems (ICCES 2019)
IEEE Conference Record # 45898; IEEE Xplore ISBN: 978-1-7281-1261-9

A Hybrid Approach to Improve Full Coverage in Wireless Sensor Networks

(Full Coverage Improving Hybrid Approach)

Amandeep Kaur Sohal
Department of CSE
GNDEC, Ludhiana
India
amandeepkaursohal@rediffmail.com

Dr. Ajay K. Sharma,
Vice-Chancellor, I K Gujral Punjab Technical University, Jalandhar,
India
vc@ptu.ac.in

Dr. Neetu Sood,
Department of ECE, Dr B R Ambedkar NIT, Jalandhar
India
soodn@nitj.ac.in

***Abstract*— In this paper, we propose a hybrid approach for wireless sensor networks which can reduce the total energy consumption of network operation therefore improving network lifetime along with complete coverage of remote monitoring field. The proposed method named as Hybrid Weight based Coverage Enhancing Protocol (H-WCEP) helps to select appropriate cluster heads and their respective cluster members by using weighted sum method and subsequent routing path by genetic algorithm. The network lifetime and coverage lifetime are computed by implementing this approach to achieve continuously monitoring of remote monitoring areas. The results of H-WCEP outperform as compared to other existing protocols. The network lifetime and full coverage lifetime of H-WCEP increase by 48 percentage and 42 percentage approximately respectively.**

Keywords—wireless sensor networkS; network lifetime; full coverage lifetime.

I. INTRODUCTION

Recently, remote sensing systems have received significant attention in electronic and computer science applications. In wireless Sensor Networks (WSNs), tiny component known as sensors are perform sensing and on-board processing, communication and storage facilities. The WSN provides remarkable benefits for a number of real world problems such as military surveillance, agricultural monitoring and oil pipelining monitoring [1] etc. The WSN has come to stay as one of the highly advanced technologies that can immediately respond against the rapid change in sensed data and send this to data analysis center in areas which could not be connected through cabling. Various applications of WSN are discussed in [2].

In order to tackle design challenges of WSNs, clustering algorithms play a very significant role. The clustering algorithms in WSN can greatly contribute to lifetime, energy efficiency and scalable issues of network [3]. The large number of sensors is deployed in remote monitoring field. In clustering, the sensor nodes are grouped into clusters. Each group/cluster of sensors is managed by a specific sensor called as Cluster Head (CH) and other group/cluster members in cluster are known as Cluster Members (CMs). The CMs monitor or sense the specific environment periodically. The CMs process the

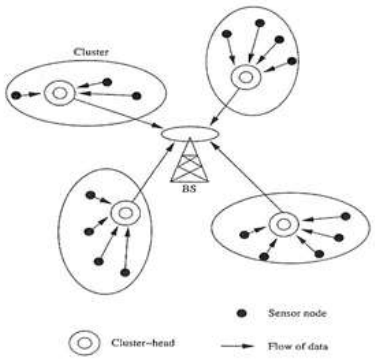

Fig. 1. Cluster based WSN

sensed data and transmit to their respective CH. The CHs aggregate data from their respective CMs and then transmits it to BS. In this way, clustering reduces the energy consumption and numbers of messages communicated to BS decreased. Moreover, data at BS can be encrypted in efficient manner before further transmission to any data centre[4].Thus, clustering achieves prolonged network lifetime [5].The measurements of various performance metrics viz. total energy consumption, network lifetime, number of CHs selected in each round, number of alive nodes in each round, and QoS support like coverage etc. are used to determines the performance of clustered based WSNs.Fig.1 indicates the clustered based network WSN architecture.

The prime objective of this paper is to present an energy efficient clustering protocol which is suitable for remote military area surveillance for achieving prolonged lifetime. Recently, proposed algorithm Weight based Coverage Enhancing Protocol (WCEP)[6] provides the full coverage for longer time as compared to existing clustering protocols. The WCEP works on the basis of weighted sum theory and it increases the lifetime and full coverage by minimizing the energy consumption during cluster formation. But, unable to minimize the energy consumption during inter cluster communication phase.

In this paper, Hybrid-WCEP (H-WCEP) is proposed to decrease energy consumption of the network by using Genetic Algorithm (GA) during data transmission of WCEP. A hybrid approach of weight based method for clusters formation and GA for data transmission is opted to achieve the objective of prolonged full coverage. The cluster head nodes (CHs) and cluster member nodes (CMs) are selected on the basis of coverage governing parameters. The coverage governing parameters taken for this selection procedure are; network remaining total energy, overlapping, node density and degree of sensor node. To conserve the energy consumption, weighted sum method is used. In this method, different weight values are assigned to governing parameters. The optimal set of CHs and alive nodes (as Cluster Member nodes CMs) are selected. Since simple evolutionary optimized algorithm GA has more capability to determine optimal path from CHs to Sink, this GA adopted in inter cluster communication of data transmission in order to conserve the energy consumption.

The rest of the paper is organized as follows. Section II discusses the literature review. Section III discusses the proposed H-WCEP. In Section IV, experimental results are discussed and finally in Section V, the paper is concluded.

II. LITERTURE REVIEW

In literature review, we studied different approaches to optimized energy usage to improve Quality of Service (QoS) in WSNs. The cluster based protocols mimic remote sensing in real time situations. Generally, these protocols are criticized for energy efficiency that involves limited QoS in WSNs. The brief description of related literature is as follows:

[7]proposed distributed cluster based routing protocol namely Low Energy Adaptive Clustering Hierarchy (LEACH) protocol for micro-sensor networks. LEACH improved the network life time, latency and application perceived quality in micro sensor network. However, the study does not investigate good distribution of CHs in the network and sink is assumed only one hop far away from other nodes/ CHs which is not feasible in geographically large network. The work had been extended further based on centralized approach, namely LEACH-C protocol. Still, it cannot solve the limitation of scalability in network. To extend network life time by uniformly CH distribution across the network and load balancing, the amalgamated concept for CH selection, [8] introduced a Hybrid Energy Efficient Distributed Clustering (HEED) protocol. The HEED incorporates two parameters: residual energy of node and node's proximity to its neighbors. However, the rise in iterations involved in cluster formation can lead to overhead cost.

[9] Proposed Distributed Weight-based Energy-efficient Hierarchical Clustering protocol (DWEHC) that designs multi-level structure in intra-cluster communication and limits a number of children of parent node. The author introduced the idea to select CH by calculating weight based on its residual energy and distance to its neighbors. This newly proposed technique improves HEED protocol by developing balanced size clusters and optimizes intra-cluster communication using location

In [10], the authors proposed a protocol incorporating residual energy and other metrics like distance to aggregation point, node reliability, and mobility for CH selection by using evolutionary computing method with purpose of maximizing network life time.

The CHs election techniques called as Coverage Preserving Clustering Protocol (CPCP) was proposed with aim of coverage preservation [11]. The CPCP is based on four coverage aware cost metrics which selects CH, active nodes and routing nodes from densely deployed sensors respectively. The CPCP integrates problem of coverage and energy consumption in network. But these cost metrics cause a large computational burden on sensor nodes. The CPCP is also unable to minimize redundantly covered area in each round.

In [12], the authors described a multi-function based on two factors i.e. choosing optimal CHs locations and minimizing transmission distance. In this protocol, topology of network is designed with three level hierarchical levels. Two CHs at level 2, One CH at level 1and sensor for collecting data placed at level 0. The BS knows the position of all nodes. Thus achieves the minimum distance for transmission.

A GA-based adaptive clustering protocol was proposed by [13] to achieve good performance in network life time in WSNs. Additional information was updates before beginning of first round. In this phase, role of node as sensor or CH, node identifications and geographical position are send to BSs. GA finds an optimal probability of nodes being CHs by minimizing the total energy consumption in one round. The optimal probability was determined by an evolutionary optimization process. This process incorporated non-deterministic rules in probabilistic transitions for prolonging the network life time.

The Distributed Energy Efficient Clustering Algorithm with Improved Coverage (DEECIC) was implemented to increase network lifetime and coverage using average number of clusters in scheme [14]. In this, CH is opted from a crowded area with more remaining energy and more degree of sensor.

Coverage aware Unequal Clustering Algorithm (CUCA) is distributed scheme to prevent hot spot issue and achieves energy efficient coverage preservation in WSNs [15]. The CUCA targets to obtain network load distribution uniformly. The CUCA necessitates overburden of control packets in routing purposes. As a result, unnecessary consumption of energy in each stage takes place that is unacceptable.

The WCEP is an energy efficient full coverage protocol [6]. The WCEP reduces computation burden of sensors and attains pro-longed full coverage with improvement in scalability. The WCEP incorporate the concept of clustering and sleep scheduling efficiently[16]. The WCEP is based on weight values which are assigned to certain governing parameters viz. network remaining total energy, overlapping degree, node density and degree of sensor node. These governing parameters affect the energy and coverage issues magnificently. However, main focus of WCEP is optimal selection of CHs and CMs, whereas energy consumption during data transmission is ignored.

The CPCP [11] and WCEP [6], both primarily focuses on cluster formation process but there is significantly less

importance given to energy consumption during data transmission phase of clustering. Therefore, motivation behind this proposes work is reduction in energy consumption during data transmission phase of WCEP. This has led to more conservation of residual energy and helps in more coverage.

III. PROPOSED WORK

The proposed work presents a hybrid approach using weighted sum method and evolutionary method to achieve coverage of remote and harsh environment for longer period of time. The proposed work is based on Weight based Coverage Enhancing Protocol (WCEP) for clustering and Genetic Algorithm (GA) for transmitting the data to end user controller. In clustering, CHs and CMs are selected in appropriate number for maintaining full coverage in each communication round. The process of clustering considers assigning weight merits to remaining total network energy, overlapping, node density and degree of sensor. The weighted sum method helps in conserving energy using different weight merits to respective governing parameters depending upon situational requirements. Further, GA based optimization procedure performed with each communication round to conserve the energy. The proposed hybrid approach is named as Hybrid -Weight-based Coverage Enhancing protocol using Genetic Algorithm (H-WCEP). The stepwise procedure of H-WCEP is discussed below:

A. *Information Update*

We assume that 'N' sensors are deployed in squared remote monitoring field in uniformly random manner. The deployment of sensors is such that they confirm the 100% coverage at the start of network procedure. The sensors are assumed stationary after deployment and each sensor is awared its own location and BS. The BS is placed at fixed point. The wireless communication channel is symmetric which means monitoring and communicating range is same. The range of sensor and transmission range is modeled as disk sensing model [8]. The transmission range is considered at least double the sensor's range. The network considered for proposed work is homogeneous i.e. all sensors have same computing and communication capacity.

B. *Network Model*

In this step, four coverage observing parameters are incorporated to assign a value to each sensor. These governing parameters are residual/remaining total network energy, overlapping, node density and degree of sensor. At each communication round, sensor dissipates part of their limited energy. As a result, remaining energy is called as residual energy of sensor need to be update periodically. The other governing parameters are node density, degree of sensor and overlapping degree are calculated only once at the start of network procedure. For each sensor, energy dissipation in transmitting and receiving 'L' bit information by each sensor is measured using simple radio model [6], [7], [11]. Equation (1) represents energy consumed by transmitter for performing transmits circuitry operation and Equation (2) indicates receiver's energy consumed due to receiver circuitry when it is receiving data.

$$E_{Tx}(L,d) = L\,E_{elec} + L \in d^{\alpha} \quad \text{where } \alpha=2 \text{ or } 4$$
$$\begin{cases} L\,E_{elec} + L\,\epsilon_{fs}\,d^2 & d < d_0 \\ L\,E_{elec} + L\,\epsilon_{fmp}\,d^4 & d \geq d_0 \end{cases} \quad (1)$$

And Equation [7] indicates formula for energy consumption in receiving L-bit packet.

$$E_{Rx}(L) = L\,E_{elec} \quad (2)$$

In equations (1) and (2),

L=Length of transmitted/ receiving packet,
d=Distance between transmitter and receiver,
d_0=Threshold distance (d_0) calculated from Equation (3):

$$do = \sqrt{\frac{\epsilon_{fs}}{\epsilon_{fmp}}} \quad (3)$$

The electronics energy E_{elec} controlled by digital coding, modulation of signal, filtering of packets, and spreading of the signal.

If $d < d_0$, then free space model is used. It means =2, and amplifier energy becomes $\epsilon_{fs}\,d^2$. Otherwise, $d \geq d_0$ multipath fading channel model is applied which means $\alpha = 4$ and amplifier energy becomes $\epsilon_{fs}\,d^4$.

With each communication round, residual energy is given by Equation (4):

$$E(residual) = E(initial) - E_{Tx} \text{ or } E_{Rx} \quad (4)$$

The other governing parameters such as node density can be calculated by obtaining number of sensors within its cluster range. The degree of sensor is determined by number of covered points in its range. The overlapping degree is number of sensors which produces overlapping area in the monitoring field. Higher the values of these governing parameters (residual energy ($E_{residual}$), overlapping degree ($O_{lapping}$) , node density (ND) and degree of sensor(D_s) for particular sensor make that eligible to become live sensor. The weight w_1, w_2, w_3 and w_4 are assigned to governing parameters using weighted sum method in order to calculate the weight value of each sensor. Equation (5) represents the formulation to compute sensor weight.

For a specific covered point, higher the weight of sensor, higher the chance to become live, otherwise idle or sleep.

$$Sensor.wt = E_{residual}.w_1 + O_{lapping}.w_2 + D_s.w_3 + ND.w_4 \quad (5)$$

Equation (6) is used to obtain CH role for a sensor in terms of CH weight.

$$CH.wt = Sensor.wt + (\text{distance between Sensor and Sink}) \quad (6)$$

C. Clustering Method

In the clustering method, set of sensor nodes are selected as CMs/ CHs which will be active and rest will be in sleep mode for a particular communication round. The proposed clustering algorithm comprises of two phases: cluster formation phase and data transmission phase.

- Cluster Formation Phase:

  The cluster formation phase of proposed algorithm uses a weight based method along with sleep scheduling mechanism to conserve energy while maintaining prolong full coverage of the monitoring field. The total weight of each sensor is calculated on the basis of governing parameters $E_{residual}$, $O_{lapping}$, ND and D_s. The selection of sensor as live sensor is based on maximum value of total weight of sensor for specific covered point. The total weight of sensor and distance from sink determines the CHs. These selected CHs find live sensor as part of cluster and termed as CMs within its cluster radius. These appropriate numbers of specific CMs and CHs are selected repeatedly that maintains the coverage in each communication round.

- Data Transmission Phase:

  In the data transmission phase, intra and inter cluster communication ensures that live sensors communicate to their respective CH directly using single hop method during intra cluster communication. The CHs transmits data to sink via multi hop method. The data transmission phase is optimized using energy and distance parameters using GA. The GA helps to determine path with minimum energy consumption to transfer all data from sensor CHs to sink. To find out an optimum path, the GA generates all possible paths for each of CH. Then, each path is evaluated to determine fitness value using fitness function of GA. The best chromosome is selected among number of generations by means of minimum energy consumption and minimum distance during data transmission. The data transmission phase of WCEGA is further elaborated in Algorithm 1, as follows:

  Algorithm 1: Data Transmission using GA

  D= cumulative distance between sensor and Sink
  w1=weight for residual energy
  w2= weight for distance

Data_transmission (CHs, live sensors, Eresidual, x, y)

```
{
   FOR i=1 to length(Cluster Head)
        FOR generation i=1 to 10
// Create the chromosomes
     FOR i=1 to 20
       Determine the path from each CH to sink
 // Compute the fitness of each chromosome
       Fitness=w1 * Eresidual + w2 * D
      END
// Select best-ranking individuals to reproduce using fitness value
        Min(fitness)  next generation
// Breed new generation using crossover and mutation
  Produce new offspring
  Evaluate the individual finesses of the offspring
  Exchange worst ranked part of population with off-spring
    END //end generation FOR loop
   Obtain the best route from specific cluster head to sink
    END //end Cluster Head FOR loop
    }
```

IV. RESULTS AND ANALYSIS

In this section, the impact of governing parameters on performance metrics for remote WSNs has been investigated. The results of WCEGA protocol is compared with common coverage aware clustering protocol (CPCP) and Weight based Coverage Enhancing Protocol (WCEP). The CPCP discussed four coverage aware cost metrics i.e. energy-aware (Cea), minimum-weight (Cmw), weighted sum (Cws) and coverage redundancy (Ccc). The CPCP (Cmw) focuses longer 100% coverage of monitoring field. Therefore, out of four CPCP cost metrics, CPCP (Cmw) is taken for comparison in these simulations. Generally, coverage related clustering protocols are compared with coverage, lifetime and energy consumption of the network.

In simulations 200 nodes, each with initial energy 1J are taken into monitoring field. The sensors are distributed randomly across 100x100 square units monitoring field. The implementation of WCEGA is iterated based on lifetime of network i.e. energy level of sensors become equal to threshold energy of sensor. The threshold level of energy is assumed zero in this paper. In all communication rounds of network operation, live sensors are selected to collect the sensing data and transmit them to their CHs using single hop communication. Once CH obtained data from its cluster then it transmits the data further to sink using multi-hop communication by GA method. The sink is located at (50,50) co-ordinates. The radius of each sensor is 15m and their communication radius is 30m. The parameters of proposed model are given Table I and parameters for GA approach are listed in Table II.

TABLE I. SIMULATION PARAMETERS

Parameters	***Value***
Initial Energy (E_{int})	1 J
Transmission/Receiving electronics circuitry constant [7]	50 10^{-9}J/bit
Amplifier circuitry constant [7]	10 $^{-12}$J/bit/m^2
Size of Data Packet [7]	240bits
Sensing Range (Rs) [7]	15m
Cluster Radius(Rc) [7]	30m
Transmission Range	40m

TABLE II. SIMULATION PARAMETERS

Parameters	***Value***
Population Size	20
Generation	10
Crossover	0.05
Mutation	0.01
Weight1 for distance factor	0.3
Weight 2 for energy factor	0.7

A. Coverage lifetime Energy Consumption Comparison

The H-WCEP outperforms in comparison to other similar protocols i.e. CPCP and WCEP. By decreasing the consumption of energy during data transmission, it increases the coverage of network. The Fig. 2 depicts comparison of coverage of network in H-WCEP with WCEP and CPCP (Cmw) with time.

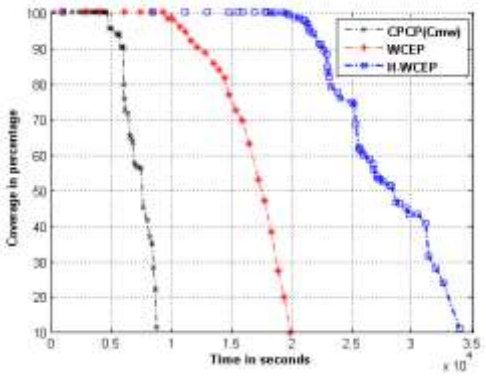

Fig. 2. Comparison of Coverage lifetime with Time for WCEP, CPCP (Cmw) and H-WCEP

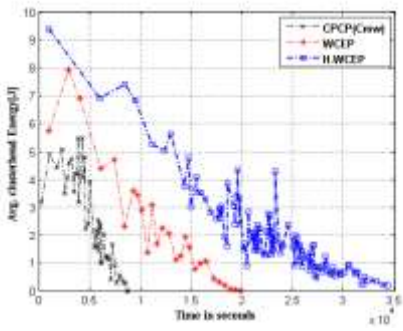

Fig. 3. Average CHs energy with Time for H-WCEP in comparison to CPCP (Cmw) and WCEP

The Fig. 3 indicates higher value of average residual energy of CHs in H-WCEP in comparison to WCEP and CPCP (Cmw) with time.

On the other hand, an important criterion to evaluate energy consumption of WSNs is the average number of CHs with time. If the Number of CHs are high, energy consumption increases. Fig. 4shows that H-WCEP has relatively low number of CHs as compared to CPCP(Cmw) and WCEP.

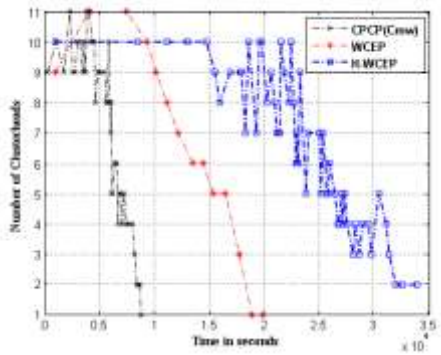

Fig. 4. Comparison of number of Cluster Heads Vs Time for H-WCEP, CPCP (Cmw) and WCEP

B. Lifetime comparison

Network lifetime is defined as start of specific WSNs to death of first sensor. Generally, lifetime of WSN is determined by time taken by First Node Dead (FND), Half Node Dead (HND), Last Node Dead (LND) and these are considered for evaluate performance of cluster based WSNs [11]. Further, FND indicates start of network operation to death of First sensor Node Died. The HND indicates start of network operation to death of Half sensor Node Died. The LND indicates start of network operation to death of Last sensor Node Died. The Fig. 5 represents that H-WCEP exhibits better results than other considered protocols.

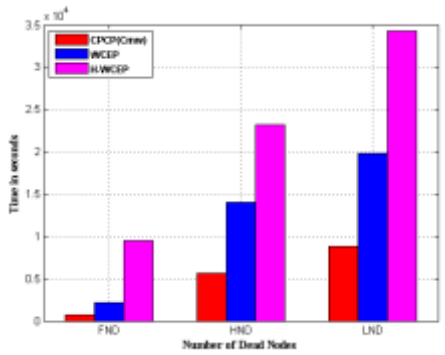

Fig. 5. Lifetime of WCEP, CPCP (Cmw) and H-WCEP in terms of FND, HND and LND

V. CONCULSION

In this paper, an evolutionary based method has proposed to improve longer full coverage in energy efficient clustering protocol. The proposed hybrid method helps in determining efficient optimal path for effective set of CHs and its members. The H-WCEP uses genetic algorithm based routing method that consider distance between cluster head and sink and sensor node's residual energy. Therefore H-WCEP achieves increase in network lifetime and full coverage lifetime. Thus, our hybrid approach uses network energy in effective manner for enhancing the full coverage lifetime in WSNs.

In our future work, we can extend this work by incorporating mobility of sink and pre-determined sensor deployment to enhance the coverage lifetime.

REFERENCES

[1] O. E. Elnaggar, R. A. Ramadan, and M. B. Fayek, "WSN in monitoring oil pipelines using ACO and GA," *Procedia Comput. Sci.*, vol. 52, no. 1, pp. 1198–1205, 2015.

[2] X. Liu, *A survey on clustering routing protocols in wireless sensor networks*, vol. 12, no. 8. 2012.

[3] J. N. Al-Karaki and A. E. Kamal, "Routing Techniques in Wireless Sensor Networks," vol. 2, no. 7, pp. 344–348, 2012.

[4] A. Praveena and S. Smys, "Efficient cryptographic approach for data security in wireless sensor networks using MES V-U," *Proc. 10th Int. Conf. Intell. Syst. Control. ISCO 2016*, 2016.

[5] B. Mamalis, D. Gavalas, C. Konstantopoulos, and G. Pantziou, "Clustering in Wireless Sensor Networks," in *RFID and Sensor Networks: Architectures, Protocols, Security, and Integrations*, Y. Zhang, L. T. Yang, and J. Chen, Eds. New York, USA: CRC Press, Taylor and Francis Group, 2009, pp. 323–354.

[6] A. K. Sohal, A. K. Sharma, and N. Sood, "Enhancing Coverage Using Weight Based Clustering in Wireless Sensor Networks," *Wirel. Pers. Commun.*, vol. 98, no. 4, pp. 3505–3526, 2017.

[7] W. B. Heinzelman, A. P. Chandrakasan, and H. Balakrishnan, "An Application-Specific Protocol Architecture for Wireless Microsensor Networks," *IEEE Trans. Wirel. Commun.*, vol. 1, no. 4, pp. 660–670, 2002.

[8] O. Younis and S. Fahmy, "HEED : A Hybrid , Energy-Efficient , Distributed Clustering Approach for Ad-hoc Sensor Networks," *IEEE Trans. Mob. Comput.*, vol. 3, no. 4, pp. 1–36, 2004.

[9] P. Ding, J. Holliday, and A. Celik, "Distributed Energy-Efficient Hierarchical Clustering for," pp. 322–339, 2005.

[10] G. Ahmed, N. M. Khan, and R. Ramer, "Cluster Head Selection Using Evolutionary Computing in Wireless Sensor Networks." pp. 9–12, 2008.

[11] S. Soro and W. B. Heinzelman, "Cluster head Election Techniques for Coverage Preservation in Wireless Sensor Networks," *Ad Hoc Networks, Elsevier*, vol. 7, no. 5, pp. 955–972, Jul. 2009.

[12] P.-C. Huruială, A. Urzică, and L. Gheorghe, "Hierarchical routing protocol based on evolutionary algorithms for Wireless Sensor Networks," *9th RoEduNet IEEE Int. Conf.*, pp. 387–392, 2010.

[13] J. Liu and C. V Ravishankar, "LEACH-GA : Genetic Algorithm-Based Energy-Efficient Adaptive Clustering Protocol for Wireless Sensor Networks," vol. 1, no. 1, pp. 79–85, 2011.

[14] Z. Liu, Q. Zheng, L. Xue, and X. Guan, "A Distributed Energy-Efficient Clustering Algorithm with Improved Coverage in Wireless Sensor Networks," *Futur. Gener. Comput. Syst. Elsevier*, vol. 28, no. 5, pp. 780–790, May 2012.

[15] N. Mazumdar and H. Om, "Coverage-aware Unequal Clustering Algorithm for Wireless Sensor Networks," *Procedia Comput. Sci.*, vol. 57, pp. 660–669, 2015.

[16] J. J. T. John and S. Ramson, "Energy-Aware Duty Cycle Scheduling for Efficient Data Collection in Wireless Sensor Networks," *Int. J. Adv. Res. Comput. Eng. Technol.*, vol. 2, no. 2, pp. 777–783, 2013.

Proceedings of the Fourth International Conference on Communication and Electronics Systems (ICCES 2019)
IEEE Conference Record # 45898; IEEE Xplore ISBN: 978-1-7281-1261-9

Power Efficient e-Bike with Terrain Adaptive Intelligence

D. S. H. Abhilash , Iqbal Wani, Kiran Joseph, Rashmi Jha, Haneesh K. M.
Electrical and Electronics Engineering
CHRIST (Deemed to be University)
Bangalore, India
h.abhilash@btech.christuniversity.in, haneesh.km@christuniversity.in

***Abstract*— Electric bicycles or e-bikes are gaining momentum in the market as they are offering a smooth, noise less and pollution free option for individual transportation in cities as well as in countryside. E-bikes are usually with a battery powered electric motor drive with an additional option for pedaling. In this work a low cost e-bike was designed and developed with a brushless DC hub motor with controllers. For smart control, smartphone was used a console and the e-bike can be controlled using a mobile application which was connected to the e-bike through Bluetooth. The controller will pick the gradient of the terrain and will control the power of the motor, which results in energy saving. Predicted range of the e-bike, speed, acceleration and total distance covered were displayed in the console along with the geographical position on the map and throttle control options. The bike with the proposed control tested and the results were giving a reduction in current drawn from the battery.**

Keywords*— *Electric bicycle, E-mobility, Range prediction, Intelligent control, Terrain intelligence.

I. INTRODUCTION

Electric bicycles generally known as e-bikes are the bicycles integrated with electric motors for propulsion. These e-bikes are battery powered with either pedal assist provision or with throttle control to ride through different terrains. E-bikes offer more comfort and less noisy operation than usual pedal powered bicycles, so the market for e-bikes is growing all over the world. Increase in fuel prices and polices by various countries to reduce emissions are also driving the market for e-bikes. Riding bicycles is a healthy and eco-friendly practice and e-bikes with pedalling option is adding comfort and efficiency to that. Global opportunity and industrial forecast report by Allied Market research shows that the market of e-bikes expected to grow annually at a rate of 5 % to a total value of 23.83 billion USD in 2025 from the total value of around 20 billion USD in 2018. Market analysis also indicates that countries with higher population density are having higher demand for e-bikes and the Asian countries are leading the trend [1]. Also the development in Lithium-ion battery technologies after the year 2012 and the availability of low cost, efficient and light vehicles are also offer better prospects for the market for e-bikes.

Since e-bikes offer a pollution free and comfortable drive, lot of research and developments are happening in the technological area which offer better solutions in mobility as well as in sports goods category. Multiple fuel options, hybrid vehicle and improved efficiency are the major areas of many of these researches [2]. E-bikes are mainly of two types; a pure electrical powered one with electrical motor which is controlled through a throttle by the user to obtain different power depending on the intention of the user and the second one is a pedal assisted one or a pedelec, in which the power is supplied by both the electric motor as well as pedalling power together. In any e-bike the range of the bike is determined by the battery capacity, motor power, driving terrain, human load and the control mechanism [3]. Pedelecs need pedalling to actuate the motor operation and the comfort level is less compared to a fully battery powered one, but will be having higher range per charge. There were some studies conducted on optimization of power in pedelecs [4].

Fully battery powered e-bikes with BLDC hub motor offer more comfort and can replace conventional fuel based two wheelers in populated cities, especially for short distance commutation. Lower distance per charge and throttle control are the main drawbacks of such vehicles [5]. There were few techniques adopted to improve the efficiency of the vehicle and thus the battery backup, like the regeneration during the slowing down regimes [5]. The regeneration techniques were improved with the help of bi-directional controllers [6] and with EMC compatible controllers [7]. The BLDC motor based e-bikes can additionally save power during when the power demand is less, like in the case of climbing down the hill. Since the controller is feeding the supply to the BLDC motor based on the rotor position, there is an option to save power depending on the road conditions [8, 9].

In this work, we designed and developed a battery powered e-bike with a BLDC hub motor. The rider can control the e-bike using a hand controlled throttle. To improve the efficiency and the range, a gradient senor based controller is provided, which help in suitably giving the throttle based on the gradient of the road in the auto run mode. The rider's mobile phone is used as the console for the e-bike, which will display the predicted range, speed, acceleration as well as the total distance covered. The bike tested in different terrains and the results showed improved power efficiency as well as longer range per charge.

This paper is organised as follows; in section II the design of the e-bike is described, controller details are given in section III. The gradient based control mechanism is described in section IV, integrated e-bike with controllers is presented in section V, results and discussion are given in Section VI and conclusion is given in section VII.

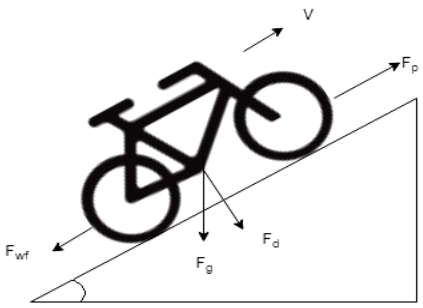

Fig. 1. Forces acting on a bike, while climbing a slope

II. DESIGN OF THE E-BIKE

A single rider bike with some minor additional load carrying capacity which can run for a medium trip length of 50 km is explored. To obtain better comfort and easier mobility, a fully electric powered bike is preferred over pedelecs. If the rider needs to shift to pedalling mode, the motor can be switched off and run as a normal bicycle. The design starts with the propulsion motor, the specification of which depends on the weight of the rider and the other loads on the bike apart from the traction force. There are few options available for the motor type, but a BLDC can provide more torque, stability, higher efficiency as well as lower noise compared to DC motors. Even though the control circuit of the BLDC is complex, lack of commutators and smaller size will give BLDC motors an edge over its competitors.

The following values were selected for the selection of motor power. Mass of bike frame and accessories – 12 kg, battery and controller – 3 kg, cyclist – 80 kg, load – 5 kg. So total weight – 100 kg. As given in Fig. 1, the bike is climbing a slope with an inclination of θ, the traction force F_p has to overcome the normal component of weight F_d and the friction and windage force F_{wf}. If the linear speed of the vehicle V is assumed as 20 km/h. An additional aerodynamic load of 20W is assumed when riding at V km/h [10]. The power is calculated as 260 W and a 36V, 250 W, 250 rpm BLDC hub motor with a maximum torque 32Nm selected to fix on the rear wheel hub.

III. BLDC MOTOR CONTROLLER

BLDC motors offer higher torque over a range of speed with higher efficiency than DC motors. The motor use a set of MOSFET bridge to energize the phase windings according to the position of the rotor with respect to the stator. The position of the rotor is sensed through a set of Hall Effect sensors. In three phase wound motor, three set of Hall Effect sensors are used to precisely locate the position and these signal output from the sensor will be used as the feedback for speed control. For the e-bike speed control, a throttle is connected on the handle, where the rider can adjust it with hand or fingers. Similarly braking and ON-OFF control signals are also fed to the controller through cables. Fig. 2 shows the outline of the controller. In addition to the power control, the controller should be capable of protecting against abnormal voltage and current values. So over voltage and over current protections are also incorporated in the controller.

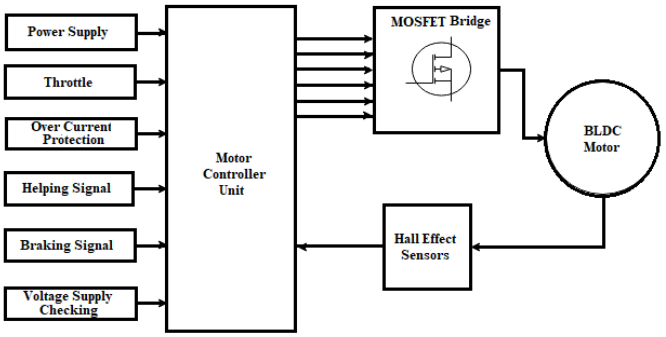

Fig. 2. Block diagram of BLDC motor controller

IV. GRADIENT BASED CONTROL MECHANISM

The gradient of the road is measured by a gradient sensor; the sensor will feed different voltages based on the gradient of the track. If the gradient is negative, the sensor will feed zero and with increasing positive slope, it will give positive voltages. This voltage values are augmented by the throttle output voltage values in the auto run mode. In negative slopes, the motor will be switched off and in positive slopes the motor will be powered based on the voltage values fed by the sensor and processed by the microcontroller.

The rider can opt for normal riding mode or auto run mode. As shown in Fig. 3, the modes are selected based on the relay selection. In auto run mode, the gradient sensor will give voltage values, which the microcontroller will process and categorize into five different levels. For negative slopes it will give zero voltage and for the positive slopes between 10^0 and 50^0 it will a voltage between 3.4V-6.6V and which is calibrated as comparing with the throttle voltage values. While climbing down the slope, the motor will supply with zero power and at higher positive slope motor will be running at highest power. This control scheme is based on the terrain intelligence and which was implemented to improve the power efficiency and thus to improve the range of the bike [11]. The system is compatible with the pedalling mode also, where with the help of a switch; we can totally disconnect the motor from the battery. In case of the battery charge is exhausted the rider can shift to pedalling mode just with toggling the switch.

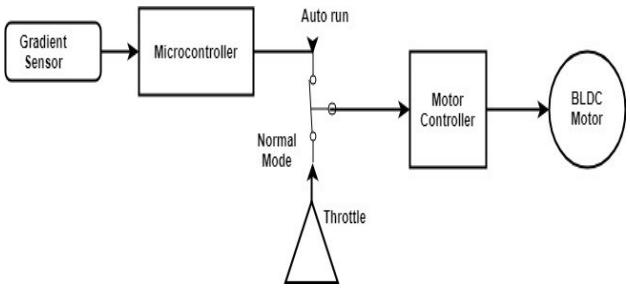

Fig. 3. Gradient sensor based auto run mode

V. E-BIKE INTEGRATED WITH CONTROLLERS

A normal pedal bicycle was converted into the e-bike by fixing a 250W, 36V BLDC hub wheel motor in the hub of rear wheel of the bike. Modifications were done on the wheel holder as well as chassis to accommodate the motor in the hub. The tire size was 66 cm and with a frame size of 45.7 cm. The brake levers are replaced with hybrid brake levers which are capable of controlling mechanically, also capable of producing braking signals for the motor controller [12]. A 5V electric thumb throttle was fixed on the right hand side of the handle to control the acceleration. The throttle was provided with a key to switch ON or OFF the electric motor mode.

The power for the motor is provided with a 37V, 10.4 Ah Li-ion battery packs. It was a custom designed pack with 40 numbers of 3.7V, 2800 mAh batteries connected as 10 in series and 4 such units connected in parallel. The batteries are with 2C rating and suitable for faster charging. A battery pack is provided with charge controllers and protective circuits. Total weight of the battery pack is around 3kgs and a metal holder is provided on the chassis for fixing it comfortably on the bike.

To monitor the State of Charge (SoC) of the battery a voltage sensor and a current sensor were included in the power circuit. The voltage sensor was connected across a high resistance potential divider circuit to reduce power losses and to obtain more reliable readings. The voltage and current sensor output were fed to a Arduino Uno microcontroller and SoC calculations are done there. The current sensor output is used to monitor the current values and to provide protection in case of abnormal operations. These sensor values are also used to calculate the instantaneous power consumption. The Hall Effect sensor outputs were used for speed measurement. Fig. 4 shows the outline of the microcontroller part.

Fig. 5 shows the actual view of the e-bike integrated with the battery pack, motor controller and sensors. The components added to the e-bike were placed carefully to reduce the aerodynamic resistance as well as to improve the comfort of the rider. The controller and the microcontroller circuits were provided with an enclosure to ensure safety and to have a better appearance.

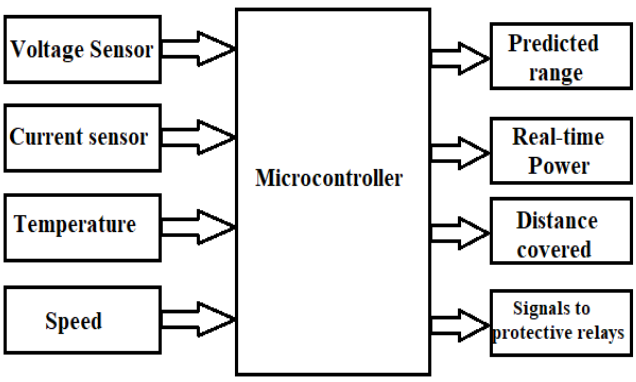

Fig. 4. Outline of the Microcontroller circuit

Fig. 5. The e-bike integrated with controllers and sensors

Terrain intelligence of the e-bike was provided with a set of gradient sensors. These sensors were calibrated to measure the gradient of the road whether it is positive or negative. These sensors will provide voltage signals based on the slope of the road and for better accuracy these sensors were fixed on the horizontal part of the frame. These signals were fed to the microcontroller, which will give a voltage signal output calibrated with the throttle signal values. When the bike is climbing down the hill, the voltage signal output will be zero from the microcontroller and the motor will be disconnected from battery.

Fig. 6 shows the various modes of operation of the e-bike. The rider can select the pedalling mode with the help of the 'kill switch' provided. In normal mode, the rider has to apply the throttle based on the slope of the road. If the rider opts for the 'auto-run' mode, the motor will be driven automatically by providing appropriate power calculated based on the gradient sensors.

Modern e-bikes are provided with consoles to display the measurements like speed, time etc. But such consoles are costly and not suitable for low cost e-bikes. In this project we had developed a mobile phone application which will help the rider to use own smart phone as a console while riding. The mobile application will fetch the predicted range, total distance covered and the instantaneous power consumption of the motor in addition to the current taken from the supply through Bluetooth from the microcontroller unit. Presently the mobile phone application is developed for Android platforms, but can be easily modified to make compatible for other platforms also. A simple holder for the smart phone was provided on the frame of the bike to safely hold the phone.

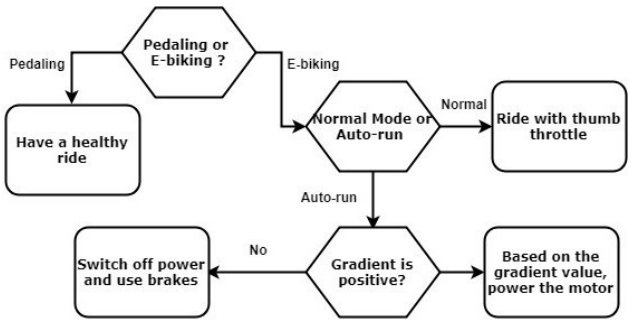

Fig. 6. Flow chart for various modes of operation of the e-bike

VI. RESULTS AND DISCUSSION

The 36V, 250W, BLDC hub motor was tested for the performance using a mechanical loading with spring dials. The motor shown very good speed regulation with a maximum speed of 275 rpm at very light load and with a minimum speed recorded during the test was 224 rpm during the test. The motor was capable of producing a maximum torque of 19.08 Nm. The maximum efficiency of the motor was found to be 81.54% which shows it is much superior to a DC motor. The maximum efficiency recorded at around the half full load and the efficiency at higher loads found to be in close range of maximum efficiency. The load test values are tabulated in Table I. Fig. 7 shows the variation of torque with the output power. Fig. 8 and Fig. 9 show the variation of speed and efficiency with the output power respectively. The vibration of the e-bike with the BLDC was found to be very small even at higher motor speeds.

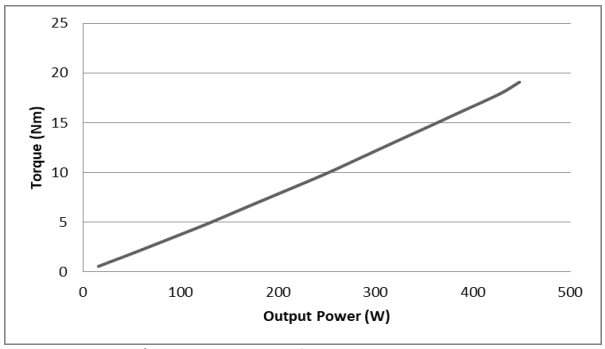

Fig. 7. Torque Vs Output Power curve

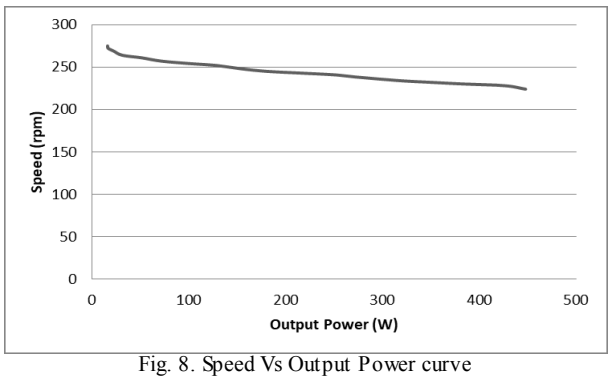

Fig. 8. Speed Vs Output Power curve

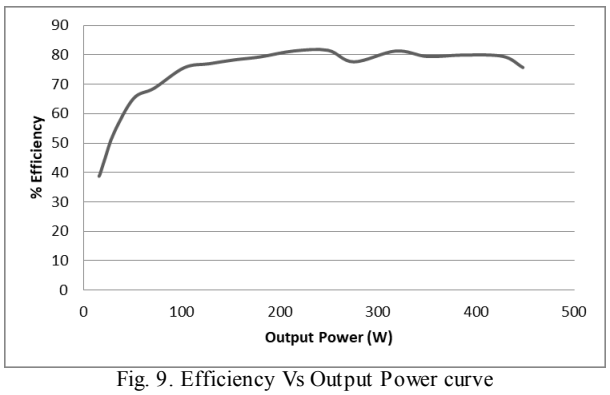

Fig. 9. Efficiency Vs Output Power curve

TABLE I PERFORMANCE OF 250W, 36 V BLDC MOTOR

Sl. No	Voltage (V)	Current (A)	Torque (Nm)	Speed (rpm)	Output power (W)	Effici-ency (%)
1	37.2	1.1	0.55	275	15.85	38.72
2	37.2	1.14	0.584	272	16.64	39.24
3	37.2	1.32	0.78	269	21.98	44.76
4	37.2	1.56	1.12	264	30.98	53.38
5	37.2	2.1	1.86	261	50.86	65.10
6	37.2	2.82	2.675	257	72.02	68.65
7	37.2	3.65	3.86	254	102.71	75.65
8	37.2	4.48	4.86	252	128.30	76.99
9	37.2	5.28	5.92	248	153.81	78.31
10	37.2	6.11	7.024	245	180.28	79.32
11	37.2	7.09	8.426	243	214.50	81.33
12	37.2	8.21	9.864	241	249.04	81.54
13	37.2	9.54	11.048	238	275.46	77.62
14	37.2	10.52	12.98	234	318.20	81.31
15	37.2	11.86	14.42	232	350.47	79.44
16	37.2	12.98	16.02	230	386.01	79.94
17	37.2	14.44	17.88	228	427.08	79.51
18	37.2	15.9	19.08	224	447.74	75.70

The integrated e-bike was tested on different terrains and found to be with easily controllable with thumb throttle. At higher slope the motor takes higher current to supply the higher power requirement. Noise and vibrations were less compared to a normal pedal bicycle. The maximum speed recorded with a rider weighing 80 kg was 25 km/h. The battery pack was capable of providing around 1.5 hours of back up with a single charge. Around 40 km range with a single charge make it a good choice for usual scenarios like urban travel, countryside commutation, in tourism and in sports.

The terrain intelligence system was introduced only in auto-run mode. In auto-run mode no throttle control is required and only braking signal to be applied whenever required. In auto-run mode, the gradient sensor output was used to generate the signal corresponds to throttle signal. In usual throttle control, the throttle voltage signal was varying from 3.4V to 6.6V. In auto-run mode also the voltage signal is calibrated to these levels using the microcontroller

TABLE II PERFORMANCE OF 250W, 36 V BLDC MOTOR

Slope of the terrain (Degrees)	Voltage output from microcontroller (V)
Less than -5	0
-5 to 10	2.4
10-20	2.8
20-30	3.2
30-40	3.5
More than 40	3.66 (max)

program. Only four levels of voltage signals were provided in the terrain intelligent system. In Table II the levels used were consolidated. Presently only a rule based algorithm was used to control the motor power. A more complex intelligent algorithm can be used to control the motor.

The terrain intelligence system was capable of saving power consumed by the motor. In normal thumb throttle controlled mode, the throttle was applied based on the assessment of the rider based on his comfort and the road conditions. Most of the time the perception of the rider will be fuzzy in nature and there will be definitely some scope for optimization in throttle control. To verify the power savings in the terrain intelligent control mode, the currents taken by the motor in throttle control mode and terrain intelligent mode were compared. Since the power consumed by the motor is directly proportional to the current drawn from a constant DC voltage supply, the reduction in current while riding in same terrain with different modes can be seen as the difference in power. The e-bike was tested under some known slopes in different operating modes and the results are tabulated in Table III. The reduction in current is evident in terrain intelligent mode. The percentage power savings can be better if the e-bike run in a complex track with varying slopes.

A mobile phone application was developed for Android platform and the current, predicted range, speed and instantaneous power consumption were displayed on it. The microcontroller fixed on the chassis is acquiring the voltage of battery, current drawn from the power circuit and calculating the above parameters and will send to the mobile application through the Bluetooth module. Fig. 10 shows the display of mobile application. The rider can select the mode and drive accordingly. The predicted range is calibrated to give the minimum distance the bike will run before recharging the battery

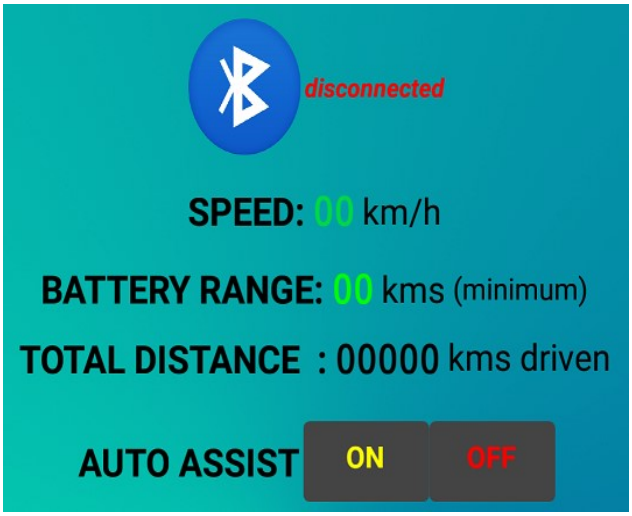

Fig. 10. Display of the mobile application

TABLE III POWER SAVINGS IN TERRAIN INTELLIGENT MODE

Slope of the terrain (Degrees)	Current (A) Thumb throttle mode	Current (A) Auto-run Mode	Power saving (%)
Less than -5	0	0	0.00
-5 to 10	3.4	3.3	3.03
10-20	4.5	4.2	7.14
20-30	5.6	5.2	7.69
30-40	6.4	6.0	6.67
More than 40	6.9 (max)	6.5 (max)	6.35

I. CONCLUSION

E-bikes are gaining popularity especially in populated cities. Riding comfort, long range per charge of battery and capital cost are the major considerations while people selecting e-bikes in present market. In this work a BLDC rear hub motor powered e-bike was developed and tested in various terrains. A gradient sensor based throttle control provided in the auto-run mode was making it terrain intelligent by providing throttle equivalent signals to the motor. The results showed that the terrain intelligent control is capable of saving power consumed by the motor while riding under different slope conditions. A mobile phone application developed and which can display the current, predicted range, instantaneous power of the motor can serve as a console for the e-bike, thus the cost of the e-bike can be reduced. Presently only a rule based terrain intelligent system was employed but a better algorithm can be tried to improve the power savings. Regeneration and charging of battery while pedaling are the future works to be added to the project.

ACKNOWLEDGMENT

The authors acknowledge the facilities provided by the E-mobility Research & Development Facility at Faculty of Engineering, CHRIST (Deemed to be University), Bangalore for the successful completion of this work.

REFERENCES

[1] Salmeron-Manzano, E.; Manzano-Agugliaro, F., "The Electric Bicycle: Worldwide Research Trends", *MDPI Energies,* Vol. 11, pp 1894, 2018.

[2] C. Abagnale, M. Cardone, P. Iodice, R. Marialto, S. Strano, M. Terzo, G. Vorraro, "Design and Development of an Innovative E-Bike*", in Proc. 71st Conference of the Italian Thermal Machines Engineering Association, ATI2016,* 14-16, September 2016, Turin, Italy, 2007, pp. 1–6.

[3] P. Iodice, C. Abagnale, M. Cardone, S. Strano, M. Terzo, G. Vorraro, "Performance Evaluation and Environmental Analysis of an Electrically Assisted Bicycle Under Real Driving Conditions", *in Proc. of the ASME 12th Biennial Conference on Engineering Systems Design and Analysis (ESDA2014), ESDA2014-20438,* Vol. 1, Copenhagen, Denmark, 25–27 June, 2014, pp. 33-40.

[4] M. Cardone, S. Strano, M. Terzo, "Optimal power-assistance system for a new pedelec model", *in Proc. IMechE, Part C: Journal of Mechanical Engineering Science,* vol 3, pp. 332-345, 2015.

[5] *E*. Ceuca, G. Brezeanu and V. Trifa, "Study for developing the energy recovering circuit for modern e-bike controller," *2015 International Semiconductor Conference (CAS)*, Sinaia, 2015, pp. 245-248.

[6] C. Dow, S. Chang, V. Bui and P. Liu, "A Vibration Reduction System for E-bikes," *2018 IEEE 9th Annual Information Technology, Electronics and Mobile Communication Conference (IEMCON)*, Vancouver, BC, 2018, pp. 772-775.

[7] E. Ceuca, I. Pocan and O. Pop, "Electromagnetic compatibility analysis of the assembly e-bike — Power electronic converter with recovery function," *2016 39th International Spring Seminar on Electronics Technology (ISSE)*, Pilsen, 2016, pp. 398-401.

[8] V. N. Kumar, A. Syed, D. Kuruganti, A. Egoor and S. Vemuri, "Measurement of position (angle) information of BLDC motor for commutation used for e-bike," *2013 International Conference on Advanced Electronic Systems (ICAES)*, Pilani, 2013, pp. 316-318.

[9] C. Dow, S. Chang, V. Bui and P. Liu, "A Vibration Reduction System for E-bikes," *2018 IEEE 9th Annual Information Technology, Electronics and Mobile Communication Conference (IEMCON)*, Vancouver, BC, 2018, pp. 772-775.

[10] Roman Nadolski, Krzysztof Ludwinek, Jan Staszak , Marek Jaśkiewicz "Utilization of BLDC motor in electrical vehicles", *in Journal of Przegląd Elektrotechniczny (Electrical Review)*, R. 88, NR 4a/2012

[11] Chris Kiefer, Frauke Behrendt, "Smart e-bike monitoring system: real-time open source and open hardware GPS assistance and sensor data for electrically-assisted bicycles", *in journal of IET Intell. Transp. Syst.*, pp. 1–10,2015.

[12] W. Chlebosz, G. Ombach and J. Junak, "Comparison of permanent magnet brushless motor with outer and inner rotor used in e-bike," *The XIX International Conference on Electrical Machines - ICEM 2010*, Rome, 2010, pp. 1-5.

Proceedings of the Fourth International Conference on Communication and Electronics Systems (ICCES 2019)
IEEE Conference Record # 45898; IEEE Xplore ISBN: 978-1-7281-1261-9

Designing Of Beach Rescue Drone Using GPS And Zigbee Technologies

Sreedevi Nair #1,
Electronics and Telecommunication
Fr. Conceicao Rodrigues Institute of Technology
Sector-9A, Vashi, Navi Mumbai, India
nair.sreedevi@fcrit.ac.in

Gloria Rodrigues #2,
Electronics and Telecommunication
Fr. Conceicao Rodrigues Institute of Technology
Sector-9A, Vashi, Navi Mumbai, India
gloshine26@gmail.com

Cheryl Dsouza #3,
Electronics and Telecommunication
Fr. Conceicao Rodrigues Institute of Technology
Sector-9A, Vashi, Navi Mumbai, India
cheryld0404@gmail.com

Shirin Bellary #4,
Electronics and Telecommunication
Fr. Conceicao Rodrigues Institute of Technology
Sector-9A, Vashi, Navi Mumbai, India
shirin.bellary.sb@gmai.com

Velliza Gonsalves #5,
Electronics and Telecommunication
Fr. Conceicao Rodrigues Institute of Technology
Sector-9A, Vashi, Navi Mumbai, India
vellizagonsalves@gmail.com

Abstract **-- This paper designs a flying lifeguard drone accessory which will deliver an automatic inflating vest to the drowning victim. It is observed that 40% of beach deaths are occurring every year according to statistics due to unavailability of the rescuer on time. There is a need for a system which can increase the victim's survival time. In this project a wrist band is used by the swimmer which has an emergency button. This is suitable for people who go deep into beaches. If a person gets pulled into the sea by the waves, they can press the button on the device, a drone will detect the location of the person using GPS and Zigbee and will go to the victim and drop a life jacket. After which the coast guard can save the drowning victim. There will be many drones present at the beach for the rescue process, but only one drone should be selected for the rescue process for there a GUI is created with the help of Visual C where in the life guard can select the drone for the rescue mission.**

Keywords- global positioning system(GPS), life-ring, Zigbee, Arduino, pixhawk, visual c, servo motor.

I. INTRODUCTION

The drone technology has been used by different organizations and hobbyists. However, the advantages of this technology extends beyond these applications. The use of drone leads to safe, cost-effective solutions ranging from data collection to delivery. In the present scenario where autonomy and collision avoidance technologies improve, so does the drone's ability to perform complex tasks increase [7]. This project presents the design of the ring buoy Delivery Drone System, which delivers ring buoy to the drowning victims before the lifeguard reaches [6]. Once the victim has a ring buoy, he/she can survive until the lifeguard reaches him/her. Lifeguards and rescue crews around the world are now considering drones to be life-saving equipment. These drones can quickly deliver flotation devices to the drowning victims, saving time and reducing panic. Drones could soon become a standard life-saving accessory for lifeguards and rescue teams.

Even just a few seconds in the water can make a difference between life and death, and these drones can fly much faster than people can swim. A drone carries a payload of inflatable ring buoy and can fly to the drowning victim. Upon arrival of the drone above the swimmer, it releases the ring buoy. The whole process is completed within 60 seconds. The swimmer wears a notification device which is like a strap band which fits on the wrist of the swimmer, that can send GPS signals to the drone [1][12].

II. SYSTEM MODEL

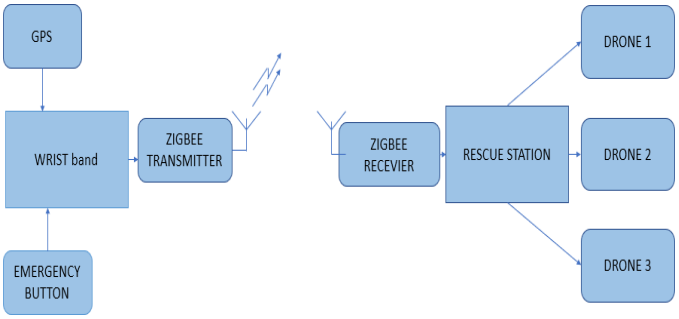

Fig 1. System block diagram

The lifeguard process and the drone system are not dependent on each other, that is if the lifeguard due to some reason is not able to reach the drowning victim in time, the drone will still continue and drop the ring buoy.

The drone process will start and simultaneously the lifeguard has to swim to the drowning victim. This victim is positioned on the rip current and is trying to escape.

As shown in fig(1), with the help of an emergency button on the wrist band the swimmer will be sending GPS signals to the drone with the help of the ZigBee transmitter [1][2].

As shown in fig (5), the rescue station receives the location of the victim with the help of ZigBee receiver and finds the exact spot and coordinates with the victim. The rescue station [5] is where the life guard will select which drone will be selected for the flight. The rescue station will plan the mission for the drone [3]. The rescue station will then command the drone to lift-off. The drone leaves the home point to the given coordinates.

The drone will then detect the exact location of the drowning victim and start hovering towards the drowning victim. When the drone reaches the victim in time, it will drop the ring buoy near the drowning victim. The victim grabs it, and then the drone returns back to its home point [6]. This will increase the victim's survival time. Lifeguard has identified the zone of the victim and is prepared for rescue process.

Working

Let's consider a swimmer named 'X' has gone deep into the sea. Then 'X' is attacked by rip currents in the sea. 'X' has worn the wrist band ,with an emergency button on it. Now when the 'X' feels it can't resist the rip currents it will press the button on the wrist band.

When this button is pressed this sends an SOS signal to the rescue station, fig5 which shows the GUI of rescue station. The rescue station has an option of alarm which turns red whenever the button is pressed. The SOS message consists of the GPS location of 'X'.

This alerts the lifeguard that the swimmer is in in danger. The lifeguard at the rescue station selects the alarm button which has turned red and this creates a notepad.

This updated notepad is uploaded in the mission planner software as shown in fig3. By selecting "do action" in the mission planner software the Pixhawk present on the drone receives the signal and follows the waypoint and drops the ring buoy and saves the swimmer 'X'.

After the drone has dropped the ring buoy the lifeguard will also swim to 'X'.

Hardware used:

1.*Emergency Button* :- It is placed on the wrist band used by the victim. It has a ZigBee module present in the band. This module is used to send GPS co-ordinates to the drone. Whenever the emergency button is triggered the ZigBee module sends GPS co-ordinate to the drone [4].

2.*Zigbee*:- It is used to transmit and receive GPS coordinates. The transmission of the GPS coordinates is done by the wrist band and the reception is done by the rescue station [1][2].

3.*Rescue station* :- It consists of computer hub where the ZigBee receiver will receive the GPS coordinates from the victim and then select the drone which will be sent for the rescue mission[3].

4.*Servo Clamp* :- A servo clamp is used to hold and drop the life ring. The clamp is connected to the pixhawk which instructs when to release the life ring.

5.*Pixhawk:*- This is a flight controller which manages the motion of the drone by setting appropriate speeds for the BLDC motors. It receives commands from on board/off board computer via MAV Link protocol and takes action according to them. [8]

6.*GPS:*- NEO-8m model is used for mapping the GPS co-ordinates.

7.*Arduino Mega:*- The Arduino mega board is used to build the wrist band. On this board is mounted GPS and Zigbee in transmitter mode.

Software Used

1.*Arduino IDE*:- Is the software used to program the GPS module in order to receive the real time coordinates.

As shown in fig 4 are the GPS coordinates that were received from the drowning victim. These coordinates were received via a ZigBee module. The ZigBee module was configured only as a transmitter using the XCTU software. Using this software the ZigBee module was programmed in such a way that when the button was pressed the coordinates were transmitted.

It was also used to handle the interrupts that were generated when the switch was pressed [10].

2.*Visual C*: The GUI for the rescue station is written in visual c.

3.Mission planner: Mission Planner is used as a ground control station for the use of Plane, Copter and Rover. It can be only used with Windows. It can also be used as a configuration utility or as a dynamic control supplement for autonomous vehicles. [11]

II. DESIGN SOLUTION

Design of drone

The drone is designed in such a way that it can carry a payload of 1000g. The rpm of the motors is 980kv. The propellers used are 10inches. It can fly up to a height of 100m. The battery life of the 3s lipo cell is 4000mAH , which can work for15mins. The telemetry used by the drone to communicate with rescue

station has a range of 1000m. Weight of the quadcopter is 2kg.The motors were controlled using ESC of 30mA. The frame used for the drone is S500.

Fig 2. Drone model

Design of Wrist band

The design of the wrist band includes an arduiono mega board, GPS and zigbee. The GPS placed on the arduino board is programmed in such a way that it can take real time GPS coordinates[9]. The zigbee used is configured using XCTU software for transmission. It is also programmed in such a way that it can transmit the GPS coordinates. The arduino board also has a hardware switch which acts as an interrupt. On pressing of the switch the coordinates are transmitted.

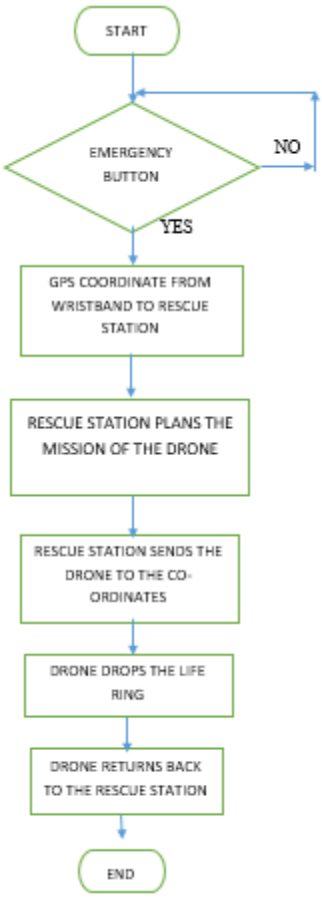

Fig 3. Flowchart of the proposed Solution

The drone rescue process proceeds as follows:

1.The system keeps on checking if the emergency button is pressed.
2.If 'yes', it will send GPS coordinates to rescue station.
3.If 'no' it will keep on checking.
4.Rescue station receives the GPS coordinates and plans the mission for the rescue.
5.Drone then reaches the GPS coordinates and drops the life ring.
6.After the mission is completed it will return back to its home location.

IV. RESULTS AND DISCUSSIONS

An .Autonomous flying of drone

As shown in the fig (4), the mission is planned by the drone to reach the drowning victim. The drone follows the path as shown in the figure. The fig (4) is the snapshot of the screen that can be viewed at the rescue station

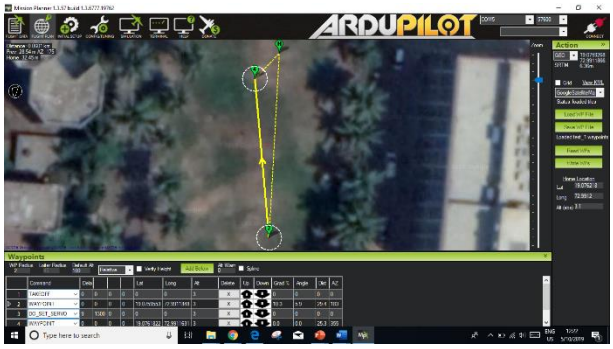

Fig 4. Autonomous settings on mission planner

Transmission of GPS coordinates

As shown in Fig (5) are the coordinates received by rescue station sent by the drowning victim. These are the latitude and longitude values. This is the snapshot seen on the Arduino ide terminal.

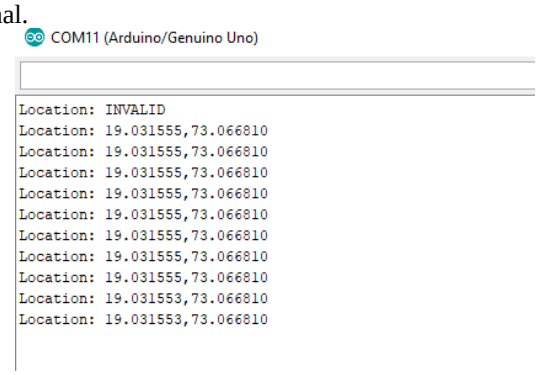

Fig 5. Receiving GPS coordinates

B.GUI of rescue station

As shown in fig. (6), is the GUI of the rescue station. From this window you can select the port from which the data is going to be transmitted to the drone. Also you can read the data that is being received by the Zigbee receiver. The required baud rate can also be selected from the drop down menu. When the send option is clicked the port status will go green when the data is transmitted. The drone selected option will show which drone is being selected.

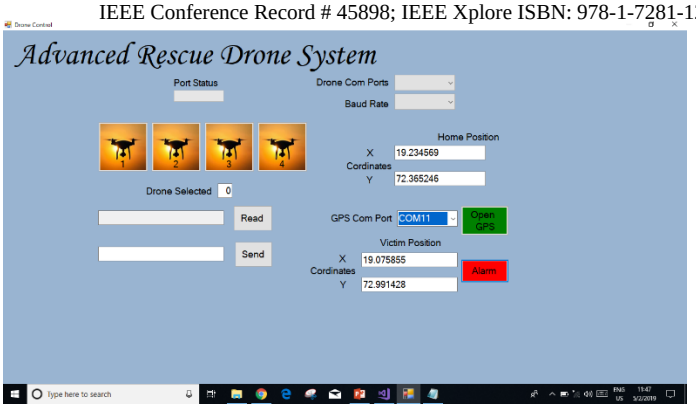

Fig 6. GUI for rescue station

C.Wrist band

As sown in fig (7) is the wrist band that has an emergency button and zigbee transmitter. Whenever the button is pressed the GPS sends the data to the rescue station.

Fig 7. Wrist band

D.Final test of drone using servo motor

As shown in Fig (8),is the drone that was tested using the drop mechanism. It is a holding a ring in the servo clamp. It drops when it reaches the drowning victim.

Fig 8. Drone using drop mechanism

V. CONCLUSION

This concept is developed in order to alert the divers at the beach. So that those drowning in the sea will be sent a life jacket using quadcopter technology before the diver arrives. The drone will reach the site by tracking the location using Global Positioning System (GPS). The proposed model can be used at various levels, for eg: drone companies, healthcare companies, government organizations.

VI. FUTURE SCOPE

1.A camera can be used that allows the lifeguards to view the current situation.
2.In future the drone can send real time video and audio feed to the rescue station for monitoring purposes.
3.Another method is to use artificial intelligence where in it can automatically detect the drowning victim without the need of pressing the hardware switch.
4.Implementing drones in medical field to deliver the medicine and first aid.

ACKNOWLEDGMENT

We express our profound gratitude to our project guide, Ms.Sreedevi Nair, in particular for patience, inspiring guidance, encouragement and freedom given to us during this project, due to which every step was shaped into a stepping stone towards success. We are highly obliged to our college and the management for providing us with best facilities and proper environment to work on our project and for all the moral support and guidance.

REFERENCES

[1]A. Josephin Arockia Dhivya, J. Premkumar ,"Quadcopter based technology for an emergency healthcare",2017 Third International Conference on Biosignals, Images and instrumentation (ICBSII),16-18 March 2017, Chennai, India.
[2]N.Shijith, Prabaharan Poornachandran, V G Sujadevi, Meher Madhu Dharmana, "Spoofing technique to counterfeit the GPS receiver on a drone",2017 International Conference on Technological Advancements in Power and Energy (TAP Energy),21-23 Dec. 2017,Kollam India.
[3]T. K. Venugopalan,Tawfiq Taher, George Barbastathis, "Autonomous landing of an Unmanned Aerial Vehicle on an autonomous marine vehicle",14-19 Oct. 2012, Hampton Roads, VA, USA.
[4]S. Sivakami, K. Janani, K. Janani, R. Ranjana, "Drowning prevention system-at sea level",23-24 Feb. 2017,Chennai, India.
Vineeth Kodire, Sreebha Bhaskaran, Vishwas H.N, "GPS and ZigBee Based Traffic Signal Preemption", 2016 International Conference on Inventive Computation Technologies (ICICT), 26-27 Aug. 2016, Coimbatore, India.
[5]Suriyon Tansuriyong,Motoki Kyan,Kaito Numata,Shuuya Taira,TakashiAnezaki,"Verification experiment for drone charging station using RTK-GPS", 2017 International Conference on Intelligent Informatics and Biomedical Sciences (ICIIBMS), 24-26 Nov. 2017, Okinawa, Japan.
[6]Apurv Saha,Akash Kumar,Aishwarya Kumar Sahu, "FPV drone with GPS used for surveillance in remote areas", 2017 Third International Conference on Research in Computational Intelligence and Communication Networks (ICRCICN), 3-5 Nov. 2017,Kolkata, India.

[7]Gang Xiang,Andrew HardyAndrew Hardy,Mohammed Rajeh, Lahari Venuthurupalli "Design of the life-ring drone delivery system for rip current rescue", 2016 IEEE Systems and Information Engineering Design Symposium (SIEDS), 29-29 April 2016.

[8] Lin Feng,Qi Fangchao "Research on the Hardware Structure Characteristics and EKF Filtering Algorithm of the Autopilot PIXHAWK", 2016 Sixth International Conference on Instrumentation & Measurement, Computer, Communication and Control (IMCCC), 21-23 July 2016, Harbin, China.

[9] S. Chandrasekharan, K. Gomez, A. Al-Hourani, S. Kandeepan, T. Rasheed, L. Goratti, L. Reynaud, D. Grace, I. Bucaille, T. Wirth, S. Allsopp, "Designing and implementing future aerial communication networks", *IEEE Commun. Mag*, vol. 54, no. 5, pp. 26-34, 2016.

[10]Vineeth Kodire,Sreebha Bhaskaran, H. N. Vishwas, "GPS and ZigBee based traffic signal reemption", 2016 International Conference on Inventive Computation Technologies (ICICT), 26-27 Aug. 2016, Coimbatore, India.

[11] Armando Sinisterra, Manhar Dhanak, and Nicholas Kouvaras "A USV Platform for Surface Autonomy", OCEANS 2017 - Anchorage,18-21 Sept 2017 Anchorage, AK, USA .

[12]__Ashok Kumar. R ; Arulselvan. P ; Ashif. A ; Gokul. S ; Kuppusamy. R, "Aero Ambulance Quad copter Based Technology for An Emergency Healthcare", 2019 5th International Conference on Advanced Computing & Communication Systems (ICACCS), 15-16 March 2019, Coimbatore, India.

Proceedings of the Fourth International Conference on Communication and Electronics Systems (ICCES 2019)
IEEE Conference Record # 45898; IEEE Xplore ISBN: 978-1-7281-1261-9

Offline Mobile Application for Train Time Prediction

Ramesh R[1], Divya G[2,] Anaswara Jayan[3], Sonam V Maju[4], and Rosemary Varghese[5]
[1, 2,3,4,5] Assistant Professor, Department of Computer Science and Engineering
Adi Shankara Institute of Engineering and Technology
Kalady, Ernakulam, Kerala, India

Abstract- **Indian Railways is the third largest rail network in the world and provide an efficient service to travelers. Tracks running well over 60,000 KM helps connect about 7500 stations, ferrying nearly 20 million people every day. One of the important problems faced by train travelers in India is to find out whether the destination station has reached or not as the schedule is not always on time. The proposed system consists of 2 sub systems. One is integrated in the train engine for reading RFID tags installed in the entry of the station platforms [1]. Another is the mobile application which works in offline mode for providing useful information regarding the destination arrival time and also offers other features to a train commuter. This system works well during emergency situations where the normal mobile network and other modes of communication fail to provide train station information to travelling commuters.**

Keywords- **Railways, RFID, Information Display Boards;**

I. INTRODUCTION

Passengers travelling in night trains usually wake up early to know which station the train currently passed by. During early morning hours or at night the visibility of outside railway station boards at stations are not clear from travelling trains. Passengers are often frustrated with wanting to know the details regarding the station. The proposed idea is to develop an information system using LED boards in coaches for providing real time information regarding the current station passed by. This cost effective approach enhances user experience by not disturbing the passenger's sleep in night trains as they need to wake up much early to avoid their destination been passed. Currently travelers rely on wakeup call service using 139 services or manually search the place using other map services using GPS. Map services by Google rely completely on availability of Internet services like 3G and above networks which is not a reliable network during train travels and consumes huge battery power and packet data.

There are number of existing online based services which give useful information regarding arrival or departure time, next stop arrival time etc. One such service offered by a private website not connected to Indian Railways is "www.etrain.info" [13]. Another service available to Indian train commuters is Rail Radar [14], a live train tracking service that runs on Google Maps. Available at http://railradar.trainenquiry.com/ the service allows you find out the exact location of a train. One of the oldest IRCTC initiatives for improving customer satisfaction is "Railways on SMS". In this service, train travelers can send an SMS to 139 to avail following services- PNR status enquiry, fare enquiry, train arrival or departure enquiry, accommodation availability, train time table enquiry etc. All of these services rely upon the existing mobile communication networks. If train commuters are travelling through mobile cell networks with low range, internet based services is of little use. Under emergency situations like flooding, earthquakes etc and in the absence of mobile networks, there is not a single service which can offer a reliable train station information details to the customers during their journey in the early morning hours or at night hours.

The proposed system employs broadcasting of station information from a unit at station to the unit in train engine wirelessly upon the entry of that train to a station. The engine unit then updates this information in the LED units at each coach in real time. The proposed system also contains a mobile application. The train code displayed in the display boards can be entered into the mobile application which in turn gives details about estimated arrival time of the destination station. The customer can also set alarms by entering the destination station name or code into the application.

Section II covers working of proposed system using RFID. In section III analysis of various feasibility issues related to integration of proposed system with the existing system is discussed. Cost effectiveness of RFID in our proposed system compared to GPS is evaluated in section IV. In section V brief discussion regarding implementation is provided.

II. PROPOSED INNOVATION

The proposed system employs Radio frequency identification wireless technology [9] and tracking system for updating railway station information from railway platform to the train engine and in turn transfers this information to the LED display boards at each coach in a wired fashion. RFID tags can be used for identifying products and objects uniquely. It contains an integrated chip, an antenna and a memory unit which stores information related to product's electronic product code [EPC]. A Radio frequency identification system consists of 3 parts: - scanning antenna, RFID reader (transceiver) for decoding data and a RFID tag (transponder) [4]. The purpose of scanning antenna part of RFID reader is to radiate RF signals to do two

978-1-7281-1261-9/19/$31.00 ©2019 IEEE

things: One, a means of communicating with the RFID tag and two, it gives the RFID tag the necessary energy for communication.

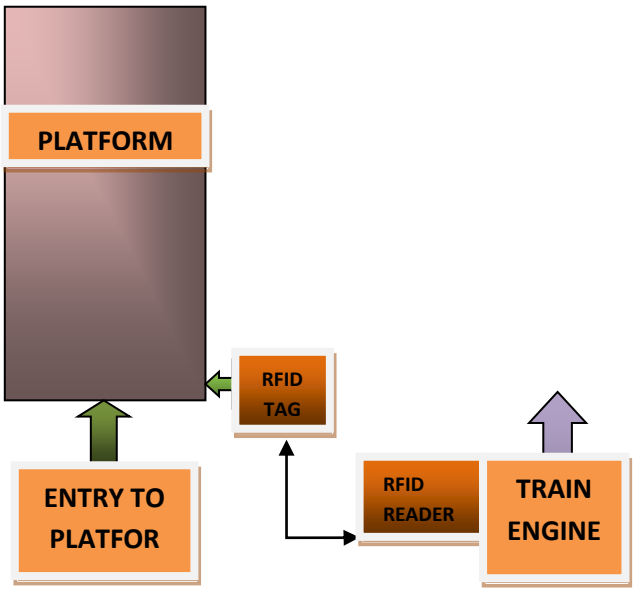

Fig-1: Basic Layout

Figure-1 shows the working our proposed system. The RFID tags installed at entry point of each station stores data related to the corresponding railway station known as "**station tags**". Station tags are the short form notation which uniquely identifies each station name similar to station notations currently used in IRCTC. The train's engine uses an RFID reader to read and track the RFID tags installed in the station. The reader then passes this station tag information to the corresponding coaches in real time. The tag installed at the stations contains details regarding the station name. The basic layout is shown in figure 1. The most optimal location to store RFID tag is at the entry of the platform as shown in figure 2.

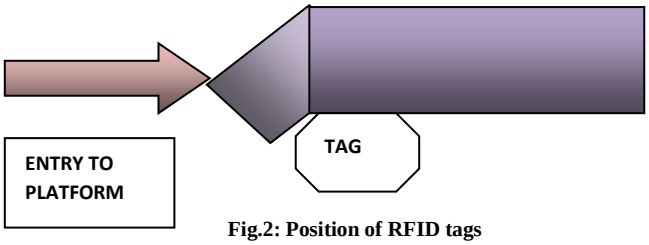

Fig.2: Position of RFID tags

The position of RFID tag (As shown in figure-2) below the entry position of platform is safe enough to protect it from rain water and it gives the optimal shortest distance to the train engine RFID reader. Figure-2 actually depicts the position of RFID tags in the entry point of each station that is below the edge of platform pavement. When the train engine approaches the platform, RFID tag passes through the field of the RFID reader's antenna and activates the RFID tag chip which in turn sends the data in its microchip to the RFID reader. The RFID tags receive their power from the magnetic field generated by the RFID reader in train engine through inductive coupling. Coupling elements of the RFID tag converts the received magnetic field and produces a current which powers the tag. The RFID reader will decode the received signal and send the decoded data to the LED boards in coaches in wired manner.

The main benefit of using RFID systems [11] is its non-contact and non line of sight nature. RFID tags works in various challenging scenarios at remarkable speeds with response time taking less than 100 milliseconds in most cases. It also functions through a variety of substances like fog, snow, paint and could be effective in other visually and environmentally challenging conditions.

WIFI hotspots within the train can provide connectivity with RFID reader so that commuters can obtain the real-time location details [1], [6]. The android application can be equipped with in-built algorithm for calculating the next station details, a machine learning algorithm for finding the expected destination time and other interesting features. Another add-on to the proposed system is using a handheld attachment connected to an android-based mobile device which gives more interesting real time information.

Passengers often wake up early in the morning in night trains due to uncertainty in knowing which railway station the train might have reached. Due to the sudden changes in the railway station it seems harder for a passenger to read a railway station board in a moving station. And passengers can't fully rely on wakeup call service 139 either due to uncertainty of waking up a person in deep sleep and other external noises.

The passenger's experience will get enhanced in trains if they can see which railway station has arrived or which one just passed by. In AC coaches [2 Tier, 3 Tier or Chair car], the visibility of railway station boards is poor in day time and much more difficult during night or early morning hours. The proposed system establishes a simple user friendly display system which gives commuters the necessary railway station details.

One of the enhancement for the proposed system is by creating an android application that can give commuters more information regarding next train information, expected destination time, next stop where food is available in addition to

978-1-7281-1261-9/19/$31.00 ©2019 IEEE

alarm settings. For this enhancement, WIFI technology can be utilized.

III. FEASIBILITY OF IMPLEMENTATION OF THE PROPOSED INNOVATION

Radio frequency identification belongs to a family of Automatic identification and Data capture. RFID tags are simple to use and works very well even during bad weather conditions. It would be impossible to know the station details from AC coaches when it's raining. The RFID tags proposed is used in passive mode which does not require any power source like a battery and hence will remain usable for longer period of time. The power comes from induction method from the RFID reader in the train engine, i.e; the induction from RFID reader is filtered and rectified into DC for powering the tags. Once the RFID tag comes closer to RFID reader, the data in RFID tag's memory will be read by RFID reader. These RFID cards or tags costs about Rupees 50 and the size are analogous to size of a coin.

The RFID reader emits RF waves [5], [7] in ranges varying from few inches to 100 feet or more, depending upon the power output and RF used. The reader's RF waves creates electromagnetic field and if the RFID tag comes within the sphere of this field it gets activated and send the memory data to the RFID reader which in turn decode it and produces useful information.

Currently the railway employs LED display boards in coaches to display whether anyone currently occupied the toilet or not. This same system can be extended to display the current railway station just passed by. The non functional features are fully compatible with the existing system as the same type of contract can be extended to achieve this. The wiring operation can be made simpler by integrating the wiring with the connectivity mechanism already implemented from train engine to each coach for emergency braking system. The power requirement for the LED display is already implemented for toilet occupancy display board. For the start-up cost involves cost for readers, tags, software unit, wiring and display boards.

To integrate with the existing system, the RFID system should be properly tested and implemented. Hence time must be spent as a best practice approach before finalizing the kind of RFID tag to be employed. The hardware should be tested for potential pros and cons. Testing phase should utilize different types of tags after proper type of RFID reader and antenna is selected depending upon the range requirement.

Currently there is no such information system in any public transportation systems which employ RFID tagging methodology for passing station information to the commuter information boards. Presently in public buses the LED boards shows the next stop information.

IV. COST EFFECTIVENESS OF PROPOSED DESIGN

The cost of RDIF reader ranges from 300 to 1000. The setup cost involves cost for packaging the reader unit in engine, wiring to the respective coaches, LED display units per train and the control unit (software unit) which analyses and decodes the railway station information. Also it is expected that with more and more applications switching towards RFID technology both in commercial and industrial in near future the cost will reduce. The cost per unit of RFID tags will be reduced further if orders are in bulk.

GPS: GPS (Global positioning system) reader system [14] offers tracking of objects using a tracking device that obtains signals sent from GPS satellites. And these signals in turn used to view the real-time position of objects like car, busses etc and the digital screen is used for displaying the GPS data. The technology can triangulate the longitude, latitude, speed of the object and direction of movement. Nowadays GPS reading can be tracked using Internet or using mobile applications. The table [1] shows the comparison (relevant to the proposed system) of Passive RFID reading and GPS technology.

Table.1 Comparison of RFID and GPS [12]

KEY FACTORS	PASSIVE RFID TAGGING	GPS METHOD
Range	Limited	100% coverage on the planet
Power Requirement	Not power hungry	Power hungry
Cost	Cheap	Costly
Reliability	Consistency offered within the specified reading range	Accuracy not guaranteed always and may change due to obstacles like trees, buildings and extreme weather conditions
External Battery Source (During power failure)	Not required	Not always possible

The RFID technology offers so many advantages [11] compared to other information transfer systems. RFID technology provides longer operational life as it doesn't require external power source and the power is obtained in wireless mode. The usage of passive tags makes it easy to replace or maintain the tags. The cost of maintenance per passive tag is much lesser compared to active tags. The periodic maintenance can be conducted on the reader device in the train engine by checking the value read from a test RFID passive tag and

978-1-7281-1261-9/19/$31.00 ©2019 IEEE

troubleshooting if any reading error occurs. The tags at the station can also be tested periodically by the same approach.

The main benefit of using RFID systems is its non-contact and non line of sight nature. RFID tags works in various challenging scenarios at remarkable speeds with response time taking less than 100 milliseconds in most cases. It also functions through a variety of substances like fog, snow, paint and could be effective in other visually and environmentally challenging conditions.

Few disadvantages of RFID [8] are discussed in this session. Reader collision occurs when the signals from two or more readers overlap. The tag is unable to respond to simultaneous queries. Systems must be carefully set up to avoid this problem. Few constrains anticipated during set-up phase is that the range should be properly calibrated for the proposed system by the hit and trail method. One of the constrain in using RF waves is the interference effect due to metal bodies. Tag misalignment, the presence of water in the vicinity of RFID reader system and the location selected for installing RFID tags poses some difficulties during reading phase.

V. IMPLEMENTATION

For the implementation purpose we used Raspberry Pi B processor (Fig.3), an RFID reader (based on 125 KHz frequency) and Python programming language. The proposed system can be integrated with mobile application or web based application. Another possible area of improvement is integrating with existing system of arrival or departure time prediction system. The program reads values ("Kottayam" and "Ernakulam") from 2 tags and compares with the stored database to find the station code (Fig.4). The station code can then be sent to the information boards installed in train coaches.

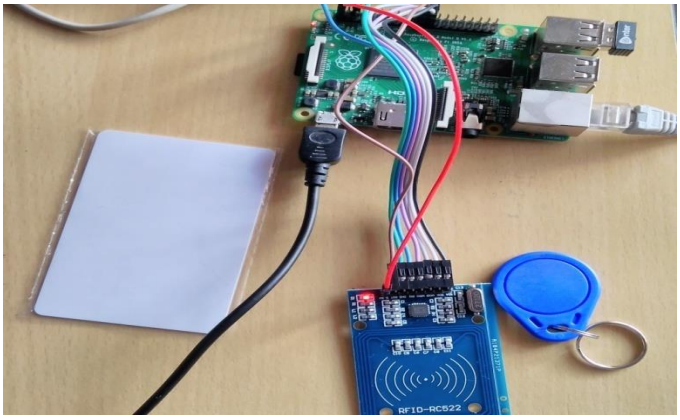

Fig. 3 Prototype: Raspberry Pi B processor with RFID reader

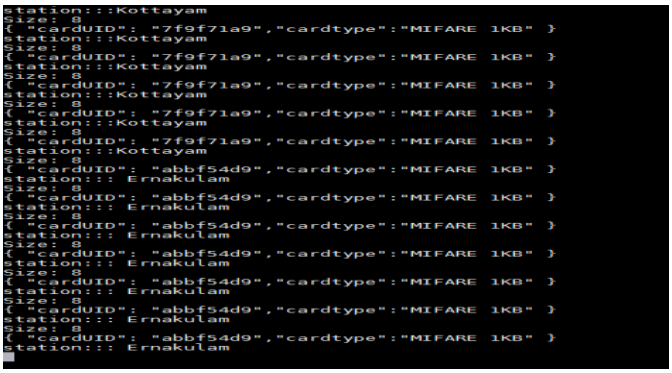

Fig. 4 RFID Reading with Python program

The proposed can be integrated with existing arrival or departure time prediction system like Rail Radar. Indian Railways has launched Rail Radar [13], a live train tracking service that runs on Google Maps. Available at http://railradar.trainenquiry.com/ the service allows you find out the exact location of a train. Trains that are running on time are displayed in blue and those running late are shown in red. Clicking on a train shows the status of the train, and also the route. [15] Active RFID tags give 100% accuracy but in our proposed system we are using Passive tags. The accuracy of Passive tags depends upon environmental factors and metallic interferences at the time of reading. In ideal or optimal reading scenarios the accuracy is 99%.

VI. CONCLUSION

There is immense opportunity for RFID technology yet to be tapped in real world applications like real-time monitoring of logistics, real-time status value extractions of wireless sensors etc. The proposed work gave us in depth insight into the possibilities of RFID technology [10] in solving one of the important problems faced among train commuters in India. The same system can be applied flawlessly in other public modes of transportation especially in tier-1 and tier-2 cities.

VII. FUTURE SCOPE

The proposed system reduces the cost of implementation in public transportation bus's location access systems. The RFID technology along with an offline mobile application can be used in tourism sector. Tourist's locations and national museums can install RFID tags and provide an application so that they will get useful information.

Acknowledgement: We thank Management, Principal and Head of the Department-CSE & IT of Adi Shankara Institute of Engineering and Technology for giving permission to access database of college's vehicle monitoring system. We would like to extend our sincere thanks to all staff coordinators of Data

978-1-7281-1261-9/19/$31.00 ©2019 IEEE

Analytics Research Lab, ASIET, for providing all computing resources and for their whole-hearted efforts put in for the completion of our work.

REFERENCES

[1] Cheng-Ju Kuo; Kuo-Cheng Ting; Jia-Ching Ying; Shyr-Kuen Chen; Yi-Chung Chen, "The RFID-based real-time monitoring system and the management algorithm of RFIDs", 2017 International Conference on Machine Learning and Cybernetics (ICMLC), 2017, Volume: 2.

[2] W. Jeon, J. Melngailis, R.W. Newcomb, "CMOS passive RFID transponder with read-only memory for low cost fabrication", SOC Conference 2005. Proceedings. IEEE International, pp. 181-184, 2005.

[3] Xianwen Ke, Hao Zhou, Nan Jin, Xiaoxia Wan, Jianjun Zhao, "Establishment of Containers Management System Based on RFID Technology", Computer Science and Software Engineering 2008 International Conference on, vol. 6, pp. 329-331,2008.

[4] Stevan Preradovic, Nemai C. Karmakar, Isaac Balbin, "RFID Transponders", Microwave Magazine IEEE, vol. 9, 2008, ISSN 1527-3342.

[5] He Yan, Hu jianyun, Li Qiang, Min Hao, "Design of low-power baseband-processor for RFID tag", Applications and the Internet Workshops 2006. SAINT Workshops 2006. International Symposium on, pp. 4 pp.-63, 2006.

[6] Aislan G. Foina, Silvio E. Barbin, Francisco J. Ramirez, "A new approach for vehicle access control using active RFID tags", Microwave and Optoelectronics Conference 2007. IMOC 2007. SBMO/IEEE MTT-S International, pp. 90-93, 2007.

[7] Yujing Feng, Wei Zhang, Xiaohui Xing, "Digital part in 915MHz UHF RFID tag", Microwave Antenna Propagation and EMC Technologies for Wireless Communications 2009 3rd IEEE International Symposium on, pp. 115-119, 2009.

[8] Daeyoung Kim, M.A. Ingram, W.W. Smith, "Measurements of small-scale fading and path loss for long range RF tags", Antennas and Propagation IEEE Transactions on, vol. 51, pp. 1740-1749, 2003, ISSN 0018-926X.

[9] Wikipedia contributors, "Radio-frequency identification," Wikipedia, The Free Encyclopedia, https://en.wikipedia.org/w/index.php?title=Radio-frequency_identification&oldid=813937183 [Accessed December 6, 2017].

[10] "Types of RFID Systems", Impinj (NASDAQ: PI), 2017.[Online]. Available: https://www.impinj.co
m/ about-rfid/ types-of-rfid-systems/ [Accessed: 06-Dec-2017].

[11] Kundan Pandey, "Advantages and Disadvantages of RFID Technology", Buzzle, 2016, [Online]. Available: https://www.buzzle.com/articles/advantages-and-disadvantages-of-rfid-technology.html [Accessed: 06-Dec-2017].

[12] "Advantages and Disadvantages Global Positioning System", https://www.roseindia.net/services/tracking-system/advantaesanddisadvantagesofgps.shtml

[13] "etrain.info", https://etrain.info/in

[14] "RailRadar GPS", http://railradar.railyatri.in/

[15] https://www.rfidjournal.com/blogs/experts/entry?11454

978-1-7281-1261-9/19/$31.00 ©2019 IEEE

Proceedings of the Fourth International Conference on Communication and Electronics Systems (ICCES 2019)
IEEE Conference Record # 45898; IEEE Xplore ISBN: 978-1-7281-1261-9

AN AMALGAMATION OF FIREFLY ALGORITHM AND WiMAX REFINING BER AND SNR

Garima Behl
Dept. of Electronics and Communication
I.K. Gujral Punjab Technical University
Kapurthala, India
garimabehl12794@gmail.com

Dalveer Kaur
Dept. of Electronics and Communication
I.K. Gujral Punjab Technical University
Kapurthala, India
dn_dogra@rediffmail.com

***Abstract*— The newest favorable technology which supplies to the customer end data amenities at a high speed is the Worldwide Interoperability for Microwaves Access (WiMAX). By witnessing the foundation of the WiMAX physical layer a thought has been excellently attained concerning the system of WiMAX. The foundation improving the BER vs. SNR variation using the Firefly algorithm has been discussed in this paper using MATLAB (R2013b) simulator. The studies and research of the students and scholars are based on the meadow of WiMAX can use this model as a helpful reserve. The reimbursements of using Firefly algorithm in a WiMAX system have been depicted in this paper.**

Keywords— Orthogonal Frequency Division Multiplexing (OFDM), FA(Firefly Algorithm), Wide Area Ntwork(WAN).

I. INTRODUCTION

The showground of telecommunication has a blowup demand of a superior set of amenities, for instance, immediate messaging, video conferencing, or any other kind of communication provision. New technologies are settled for the attainment of high data rates with the hundreds of persons demanding to get entree at an analogous tower. WiMAX (Worldwide Interoperability for Microwave Access) is an encouraging elucidation or a technology conveying digital Broadband Wireless Access (BWA) with augmented rapidity and distance that marks it underneath the Fourth Generation (4G) of expertise [1].

Expansion of the WiMAX was completed by IEEE (Institute of Electrical and Electronics Engineers), a society that mechanisms for the educational and technical origination in innumerable castigations. IEEE 802.16 was the profitable standardization of the WiMAX family for which a group in June 2001 was molded baptized as WiMAX Forum. A wireless auxiliary to cables, DSL, and fiber providing much-advanced bandwidth over the corresponding reportage areas. Another headway in the clan of wireless communication is the forefront version of WiMAX, commonly known as WiMAX 2+ that can exert in amalgamation with LTE (Long Term Evolution) [2]. It is also from time to time termed as MAN (Metropolitan Area Network) interrelating the operators in a geographical section proposing resourceful interconnection to a Wide Area Network (WAN) [3].

Two groups of WiMAX have been volunteered to discourse the supplication of dissimilar types of access. IEEE802.16-2004 is the first version of WiMAX also designated as Fixed WiMAX intended for fixed applications from its base stations. It is centered upon the two standards specifically ETSI HiperMAN (High-Performance Radio Metropolitan Area Network) in addition to IEEE 802.16 agreeing global deployment. It encompasses the usage of 256 carriers Orthogonal Frequency Division Multiplexing (OFDM) and the profiles aimed at compliance testing. This version has its provision expanding to both line-of-sight and non-line-of-sight provinces providing a bit rate ranging from 32 Mbps to 134 Mbps. The second version or the modification i.e. IEEE 802.16e provisions mobile applications [4, 5]. This standard reinforced a lower bit rate of 15 Mbps while providing access in the non-line-of-sight domain. It enabled full nomadic besides mobile users organized with roaming and handoff [6].

In the existence of noise, WiMAX writhes from stark enactment deprivation. In the literature, plentiful approaches have been offered to correct channel noise either in the time domain otherwise in the frequency domain. In previous papers, numerous computational intelligence techniques have been used that does not deliver a better result, here the proposed technique is utilized to deliver an improved result in comparisons to already implemented intelligence technique. For such circumstances, the proposed method in this paper i.e. the firefly algorithm is appropriate wherever performance is very authoritative although the computational cost is less indispensable [7-10].

The result is amended by the application of the firefly algorithm in the MATLAB (R2013b) simulator. The numerous iterations will be evaluated and the finest possible result retains the objective of entire operation i.e. improvement of SNR and BER in CODED-OFDM based WiMAX System by the application of FA [10, 11].

Section II of the paper describes the literature survey and while section III describes problem statement and Section IV provides specifics about the system model. Section V describes the simulation results and Section VI describes the Conclusion.

II. RELATED WORK

In [1] the model construction of the WiMAX physical layer and the enactment valuation for real-time audio data communication in WiMAX using convolution coding has been discussed. BER performance of the signal communicated over the AWGN channel is improved in the WiMAX system by the use of convolution coding. In [5] authors emphases on examining significant QoS parameters in the WiMAX system. Results showed that an optimum WiMAX network should have very a small value of delay and packet plummeted, while high values of throughput. In [6] WiMAX know-how, its simple conceptions, uses, and advantages/disadvantages are studied. Operation of the WiMAX system is corroborated under numerous channels in addition to modulation systems. The graph amongst SNR and BER for performance exploration has been drawn. In [10] discussion is made about various security problems in each version of the WiMAX system. The handling of the security problems and basic evolution of the technology has also been deliberated. The various solutions to tackle such security issues have also been proposed. Basically, a light has been thrown on the security issues and related solutions in the WiMAX system. Under the security's umbrella numerous authentication, access control in addition to encryption technologies fall. After the clearance of all the problems related to security, this broadband technology plays a major role as a future technology of wireless communication. In [29] Non-linear design problems solution by utilizing the newly developed Firefly Algorithm has been shown in this paper. As compared to solutions obtained in the literature previously, FA performs better for an optimization related standard pressure vessel design optimization. Nonlinear design optimization is successfully optimized using the Firefly Algorithm. Some standard test functions were used to validate the algorithms. Unconstrained stochastic functions were solved using the FA after new test functions are designed utilizing the singularity and stochastic components.

III. PROBLEM STATEMENT

WiMAX network lacks quality service because there are hundreds of people trying to get access at the same tower accompanied by various environmental factors like distraction, diffraction, etc. due to this maintaining high SNR and low BER becomes difficult. Hence an efficient technique i.e. Firefly algorithm has been amalgamated with the WiMAX system for the improvement of signal to noise ratio (SNR), bit error rate (BER).

IV. PROPOSED ALGORITHM

The Firefly Algorithm was advanced on the foundation of the idealized behavior of the fireflies and their flashing characteristics.

As per the following three rules, the flashing characteristics are idealized as:

- Regardless of the sex, each firefly is attracted to other fireflies as all fireflies are unisex.
- For any two flashing fireflies, towards the brighter one, the less bright firefly moves since attractiveness and brightness are proportional to each other. Both attractiveness and brightness reduce as their distance upsurges as the attractiveness is proportional to the brightness. A firefly will randomly move in case of non-existence of a brighter firefly.
- The objective function's landscape helps to determine the firefly's brightness or light intensity [11-13].

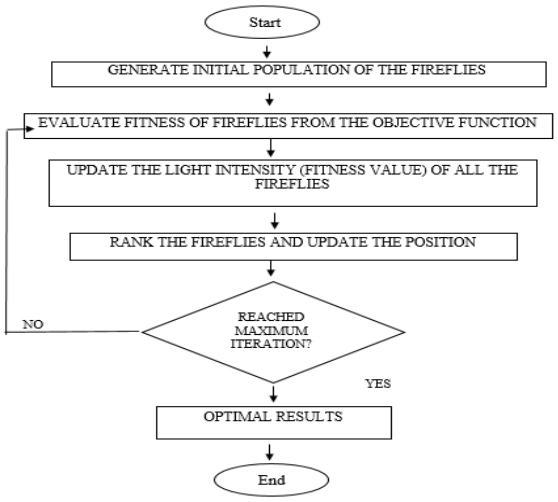

Fig. 1 Flowchart of the Proposed Algorithm

V. SYSTEM MODEL

Following are the steps to be followed in building up the system model in the MATLAB (R2013b) simulator.

A. Assumption and Configuration

Create the input environment with Length of FFT= 256, length of cyclic prefix= 256/8 =32, modulation size =64, 128, and 256, system bandwidth= 20 MHz, null subcarriers (guard and dc) =368, pilot subcarrier= 560, data subcarriers=1120, subchannels = 30, subcarrier spacing =10.93 KHz, guard time=11.4 us, symbol time= 91.4 us, OFDM symbol duration=102.8 us, number of OFDM symbols in 5ms frame=48.

B. Steps followed in model building

1) Signal generation for Transmission

Generate random data that is further passed through various processes such as interleaving, forward error correction, and modulation. Now, implement the subchannelization and frame generation process. Convert the signal to time samples and add the cyclic prefix to it.

2) Signal transmission

Now the message signals are transmitted through the AWGN channel.

3) Improved performance

Convert the signal to frequency samples and remove the cyclic prefix from it. Now the signals are demodulated and decoded. Necessary random data is now obtained. Computational

intelligence technique (i.e. firefly algorithm) is used for the improvement of signal to noise ratio and bit error rate.

4) Necessary computation and comparison

Measure the values of signal to noise ratio and bit error rate after the implementation of the Firefly algorithm using the following formulas.

- Signal to noise ratio= ratio of signal power to the noise power.
- Bit error rate= the number of bit errors divided by the total number of transferred bits throughout a studied time interval.

5) Comparison

Compare the base paper result with proposed results of performance improvement in CODED-OFDM based WiMAX system.

VI. SIMULATION RESULTS

Various results and comparison of proposed results with existing technique result in terms of SNR and BER in MATLAB (R2013b) simulator have been shown in this section.

A. Variation of BER vs. SNR using different modulation techniques

In table 1 and figure 2, it is observed that from the comparison of different modulation techniques and their performance against BER versus SNR results show that 256 QAM performs best (hence also termed as proposed results in next sub-section).

TABLE 1 shows the comparison of BER and SNR for different modulation techniques

	16-QAM		128-QAM		256-QAM	
S.NO	**BER**	**SNR**	**BER**	**SNR**	**BER**	**SNR**
1.	.000299	11.1	.000298	11.3	.000301	11.2
2.	.000296	11.76	.000295	11.8	.000299	13
3.	.000273	13.01	.000289	13.25	.000288	15.1
4.	.000262	13.7	.000278	13.86	.000267	17.2
5.	.0002557	14.0	.000257	14.9	.000250	18.7
6.	.000200	14.9	.000222	16.4	.000216	19.45
7.	.000187	15.01	.000212	16.7	.000200	19.87

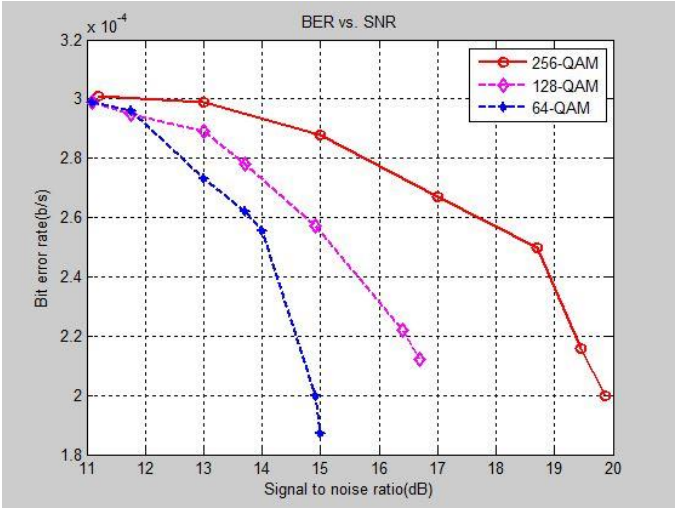

Fig. 2 Variation of BER vs. SNR for 64-QAM, 128-QAM, and 256-QAM

B. Variation of BER vs. SNR for the existing and proposed results

In table 2 and figure 3, it is observed that from the comparison of existing results and proposed results using Firefly algorithm and their performance against BER versus SNR results show that WiMAX system performs best with Firefly algorithm.

TABLE 2 shows the comparison of BER and SNR for existing and proposed results

	EXISTING-RESULTS		PROPOSED-RESULTS	
S.NO	**BER**	**SNR**	**BER**	**SNR**
1.	.000298	11.1	.000301	11.2
2.	.000289	11.76	.000299	13
3.	.000270	13.01	.000288	15.1
4.	.000254	13.7	.000267	17.2
5.	.000244	14.2	.000250	18.7
6.	.00021	14.4	.000216	19.45
7.	.00019	14.7	.000200	19.87

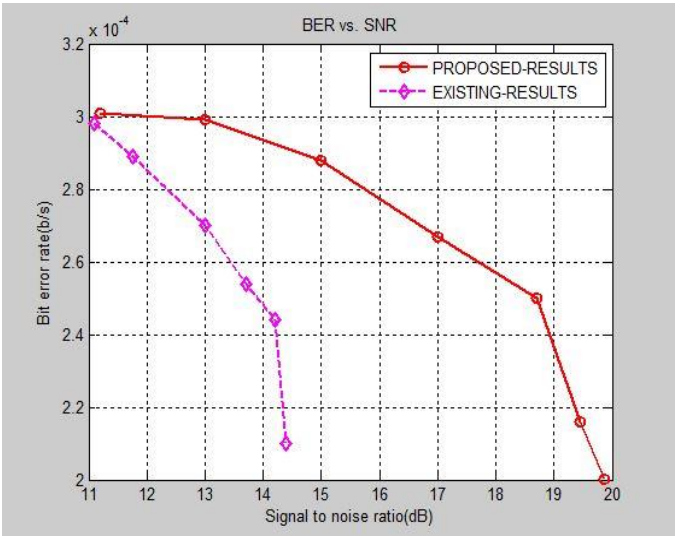

Fig. 3 Variation of BER vs. SNR for existing and proposed results

VII. CONCLUSION

In the noise presence, WiMAX wriggles from stark enactment deprivation. In the collected works, plentiful approaches have been presented to spot-on channel noise either in the time domain or else in the frequency domain. In previous papers, several computational intelligence techniques have been used that does not make available a better result, here the proposed technique is used to provide better upshot in comparisons to previously implemented intelligence technique. For the circumstances, the proposed system is appropriate wherever performance is very authoritative even though the computational cost is less vital.

The result is improved by the application of the firefly algorithm. The numerous iterations are evaluated and the best possible result preserves the objective of the entire operation i.e. improvement of SNR and BER in WiMAX System by the use of FA.

REFERENCES

[1] M. Patidar, Rupesh Dubey, Nitin Dumar Jain, Sarita Kulpariya, “Performance Analysis of WiMAX 802.16e Physical Layer Model,” IEEE, 2012.

[2] Pinola, Jarno, Kostas Pentikousis, "Mobile WiMAX", The Internet Protocol Journal (IPJ), Cisco, 2008.

[3] S. Banerji, R. Singha Chowdhury,“On IEEE 802.11: Wireless LAN Technology”, International Journal of Mobile Network Communications & Telematics (IJMNCT), Vol. 3, Issue. 4, 2013.K. Elissa, “Title of paper if known,” unpublished.

[4] M. Hawawreh, Aymen I. Zreikat, “Performance Analysis of a WiMAX Network in Different Propagation Models,” International Journal of Computer Science and Information Security (IJCSIS), Vol. 15, (pp. 603-609), 2017.

[5] M. Gumaa, Aymen I. Zrekat, “Performance Evaluation of QoS Parameters in WiMAX Network”, International Journal of Science and Research (IJSR), Vol 3, Issue 9, 2014.

[6] S. Ahmed, "Performance analysis of Mobile WiMAX Technology" In Computing for Sustainable Global Development (INDIACom),2014 International Conference on IEEE, (pp. 959-961), 2014.

[7] M. Sing, Komal Arora, Akhil Gupta, “Equalization in WiMAX System”, 2018 International Conference on Intelligent Circuits and Systems, ICICS.2018.IEEE, (pp. 330-333),2018.

[8] V. Kumar, Navpreet Singh, “Analyzing the Performance of CODED-OFDM BASED WiMAX System under Fading Environments with QAM Modulation Technique”, International Journal of Information Research and Review, 2016.

[9] R. Poornima, N.Prabakaran, “Performance Improvement in Mobile WiMAX Using Higher Order Sub Carrier Modulation Techniques”, 2015 International Conference on Circuit, Power and Computing Technologies [ICCPCT], 2015.

[10] R. Yadav, S. Srinivasan, “Evolution of WiMAX Technology, Security Issues and Available Solutions,” International Journal of Computer Applications, Vol. 66, No.2, 2003.

[11] X. Yang, “Firefly Algorithm, Stochastic Test Functions and Design Optimization”, Int. J. Bio-Inspired, Vol. 2, No. 2, pp. 78-84, 2010.

[12] M. Tawhid, A. Ali, “Direct Search Firefly Algorithm for Solving Global Optimization Problems”, Applied Mathematics & Information Sciences, pp. (841-860), 2016.

[13] T. Apostolopoulos, A.Vlachos, “Application of the Firefly Algorithm for Solving the Economic Emissions Load Dispatch Problem”, International Journal of Combinatorics, 2011.

[14] B. Bhushan, S. Pillai, “Particle Swarm Optimization and Firefly Algorithm: Performance Analysis”, IEEE, 2013.

Proceedings of the Fourth International Conference on Communication and Electronics Systems (ICCES 2019)
IEEE Conference Record # 45898; IEEE Xplore ISBN: 978-1-7281-1261-9

A deep learning approach for the classification of diseased plant leaf images

Siddharth Singh Chouhan[1]
(*Student Member, IEEE*)
[1] School of Computer Science and Engineering,
SMVDU, Katra, Jammu and Kashmir, 182320, India
siddharth.lnct@gmail.com

Ajay Kaul[2]
[2]School of Computer Science and Engineering,
Shri Mata Vaishno Devi University, Katra, Jammu
and Kashmir, 182320, India
ajay.kaul@smvdu.ac.in

Uday Pratap Singh[3,*]
[3]School of Mathematics,
SMVDU, Katra, Jammu and Kashmir, 182320, India
*Corresponding author: usinghiitg@gmail.com

***Abstract*—Plant growth monitoring and plant protection are the key elements in the plant production industry. These factors influence the quality and productivity of the plant and its yields. Diseases are the major factor that vitiates the plant health. More often they harm plant parts like fruit, flower, leaf or stem, but quite often the severity of diseases may even result in plant death. In recent years, computer vision techniques, machine learning algorithms, and deep learning models have gained importance due to their capability of dealing with complex data with precision. These techniques are well known for pattern recognition and classification problems. Therefore in this work, a multilayer convolutional neural network is proposed for the classification of diseased plant leaf images. The real-time images of four different plants in healthy and diseased condition are collected for validating the performance of the proposed model. Results, when compared with other methods, shows the higher classification accuracy of the proposed model.**

Keywords—Computer vision, Convolutional neural network, Deep learning, Image classification, Plant pathology.

I. INTRODUCTION

The plant growth monitoring and plant protection are the key concepts for agriculture. The production from a field is completely depended on how healthy is the plant being evolved. This in turns further imitates on the quality and quantity of the plant yields. There are several factors responsible for influencing the plant health, some of them are soil type, moisture level, humidity level, nutrient content, weed, and diseases, etc. Among them, plant disease is the major factor that decreases plant production. These diseases can occur in any part of the plants including stem, flowers, fruits, leaves, stem, etc. More often a severe loss to the plants is observed when a disease is diagnosed in the plant leaves. Since leaves are the main source of producing food for the plants, therefore, entire plant life is depended on them. There is the number of factors responsible for affecting the plant health, but majorly those are categorized among two known as abiotic factors and biotic factors. The abiotic factor is the non-living entities that include temperature, humidity, climate, etc. whereas biotic factors are the living organisms that include fungus, bacteria, or virus. We cannot countermeasure the environmental factors but on the other hand, while espousing suitable mechanisms abiotic factors can be counter-measured [1]-[3].

Generally, the conventional way of diagnosing a disease from the plant is done with the help of an expert. The samples of the plant have been gathered and observations have been made based on both physical and laboratory investigations. The functional part of these systems requires an expert known to be a plant pathologist to make decisions and also physical intervention. Usually, this entire process is time-consuming and often ends up with a high cost [3], [4]. With the increasing demand for food production, it has become essential to adopt some real-time and automated measures to overcome the old-fashioned means of diagnosing plant diseases.

Computer vision methodologies have been used in the number of applications for pattern recognition, classification, object segmentation, etc. Images and image processing techniques are to the core for all the computer vision applications. They play a key role in

storing and analyzing the useful and important information from a scene. Nowadays, it has been observed that a number of methods based on Machine Learning (ML) and Deep Learning (DL) has been used for processing an image. These methods are known for their capability of handling complex images and also for their higher accuracy. Deep learning models are the subpart of machine learning well well-known for their layered structures. These networks simulate the conventional artificial neural networks that map the functional capability to simulate the thinking process of the human brain [5], [6]. These networks are unsupervised in nature generally compromised of the stack of layers over one another. Deep learning is also termed as deep neural networks or convolutional neural network having the capacity of learning from unstructured data [7], [8]. In recent years, deep neural networks have been extensively used for the purpose of classification.

Therefore, in this study, we present a deep neural network for the classification of healthy and diseased leaves images [9]. The real-time images of the leaf have been acquired for this purpose. This dataset compromises of both the healthy and diseased leaf images. The images are then labeled for their classes. Then the entire dataset is divided among training and testing datasets. Three cross fold strategy has been adopted to validate the performance of our proposed multilayer convolutional neural network. The network is first trained with the help of the training database and then the trained model is then validated with the help of testing database for its accuracy. Finally, the results of the proposed model have been compared with other methods for its classification accuracy.

The rest of the article is organized as in section 2 literature related to a disease classification using deep learning has been presented, followed by proposed work in section 3, section 4 presents the details of the multilayer convolutional neural network, followed by results in section 5, finally, section 6 concludes this article followed by references.

II. LITERATURE REVIEW

The various studies related to deep learning have been done and summarized in this part. Edna Chebet Too et al. in [1] have studied the deep learning models named as VGG 16, Inception V4, ResNet, and DenseNets for the plant disease classification. They have broadly presented the fine-tuning and evaluation methodology of these dense layer architectures. The results were validated on the images taken from plantVillage dataset. Shanwen Zhang et al. in [4] have proposed a global pooling dilated convolutional neural network (GPDCNN) for the classification of cucumber plant leaf disease. The presented model also combines the benefits of dilated convolution and global pooling. The model was validated for six different cucumber plant leaf diseases. Among DenseNets has obtained higher classification accuracy. S. Lakshmi and R. Sivakumar in [10] have worked with the artificial neural network and convolutional neural network for the classification of algae disease from the images. In [11] Yuan Yuan et al. have used the concept of transfer learning by utilizing the two-deep networks named as AlexNet and VGGNet for the classification of diseases from the plant images. Eight different kinds of crop diseases were considered for this work. The images were acquired from the plantVillage image dataset. In [12] Artzai Picon et al. have presented an adapted Deep Residual Neural Network-based algorithm for the classification of different diseases. The authors have acquired about 8178 images from the two sites located in Spain and Germany. Konstantinos P. Ferentinos in [13] has used a convolutional neural network for the classification of leaf images among healthy and diseased. For this purpose, the images were selected from the open data repository of about 87848 images with 25 different plants. Focusing on the different diseases of the Grape leave images named as Esca, Black rot and Chlorosis, P. Goncharov et al in [14] have present a deep learning architecture. This research is primarily focused on the classification of diseases and the protection of plant from those diseases.

With the help of the convolutional neural network, K. R. Aravind et al. in [15] have classified three disease form the grape leave images. For this purpose, the authors have used the AlexNet model that is validated with the help of 4063 images taken from the plantVillage dataset. Yang Lu et al. in [16] have presented a deep convolutional neural network for the classification and diagnosis of ten different diseases from the rice leaf images. For this purpose, the 500 images are acquired in the real-time conditions. The proposed work is validated for ten cross strategy for its accuracy. Qiaokang Liang et al. in [18] have proposed a deep network named as Plant Disease Diagnosis and Severity Estimation Network (PD^2SENet) for the classification of diseases from the plant leaf images. This works simultaneously for the diagnosis and

severity of the diseases occurring in the plant. A three-channel convolutional neural network (TCCNN) is proposed by Shanwen Zhang et al. in [19] for the classification of the diseases from the vegetable leaf images. Aravind Krishnaswamy Rangarajan et al. in [20] have used two deep learning models named as AlexNet and VGG16 net for the classification of leaf images among healthy and diseased. The tomato leaf images were taken from the plantVillage leaf image dataset categorized among seven classes. With the capability of learning from the unstructured data, deep learning model has proven to play a significant part in the diagnosis of the diseases from the plant images. So, in this work, we present a study for the classification of plant leaf images among diseased and healthy.

III. PROPOSED WORK

The flowchart for the proposed work is given in Figure 1. At first, our primary focus is on the acquisition of the database. This has been carried out at Shri Mata Vaishno Devi, University, Katra, 182320, India. We have acquired images of 4 different plants containing both healthy and diseased images. Then the collected images are labeled and divided among training dataset and the testing dataset in the ratio 70:30. The proposed multilayer convolutional neural network is the trained with the help of training dataset. After this, the trained MCNN model is then validated for the classification of leaves. Finally, the images are classified among diseased and non-diseased leaf images.

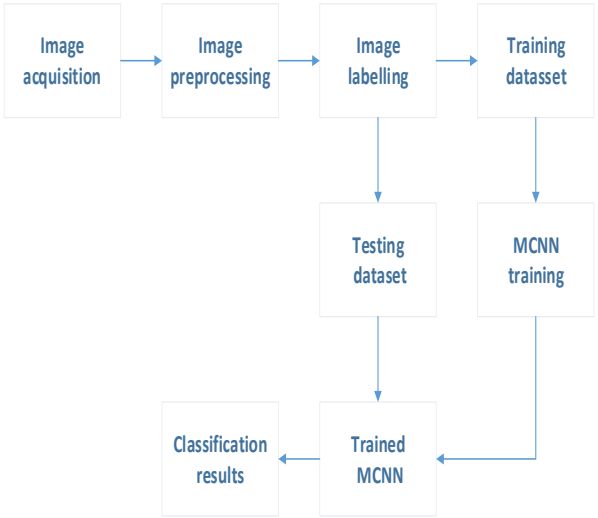

Figure 1. Flowchart for the proposed work

IV. MULTILAYER CONVOLUTIONAL NEURAL NETWORK (MCNN)

Deep learning models are similar in learning capabilities to the conventional artificial neural network. These models are well known for their capability of solving complex problems with higher accuracy. There are a number of deep learning model available like GoogLeNet, AlexNet, ResNet, VggNet etc. These models are varied based on their configuration details like the number of units, their depth, the learning algorithm, etc. These models generally have a layered architecture stacked over one another. More often depending on the complexity of the problems the number of layers namely Convolution layer, Max-pooling layer, Fully-connected layer can be varied to the desired accuracy of the result. This is an important feature of the deep learning model. However, the deeper is structure the more complex is to handle it. This also increases the computational overhead of the network. Deep models are also known for their requirement of a high amount of data to give superior results [9].

For this work, we have proposed a simple convolutional neural network that is inspired by the AlexNet model. The figure 2 shows the architecture of our proposed network. It consists of 6 convolutional layers each followed by ReLU, 3 Max-pooling layers, a flatten, and 2 fully-connected layer, where the last layer acts as an output layer consist of the Softmax activation function. The training of CNN has been performed with the help of BPA or SGD [9]. The various configuration details of the model have been illustrated in Table I.

TABLE I. MCNN CONFIGURATION DETAILS

No. of Convolutional layers	6 with 3×3 filter
No of Max-pooling layers	3 with 2×2 filter
No. of Fully-connected layers	2
Dropout rate	0.2 to 0.5
Learning rate	10^{-2}
Momentum	0.09
Weight decay	1e-6
Activation function	ReLU
Batch size	12
Epochs	100
Training algorithm	BPA / SGD

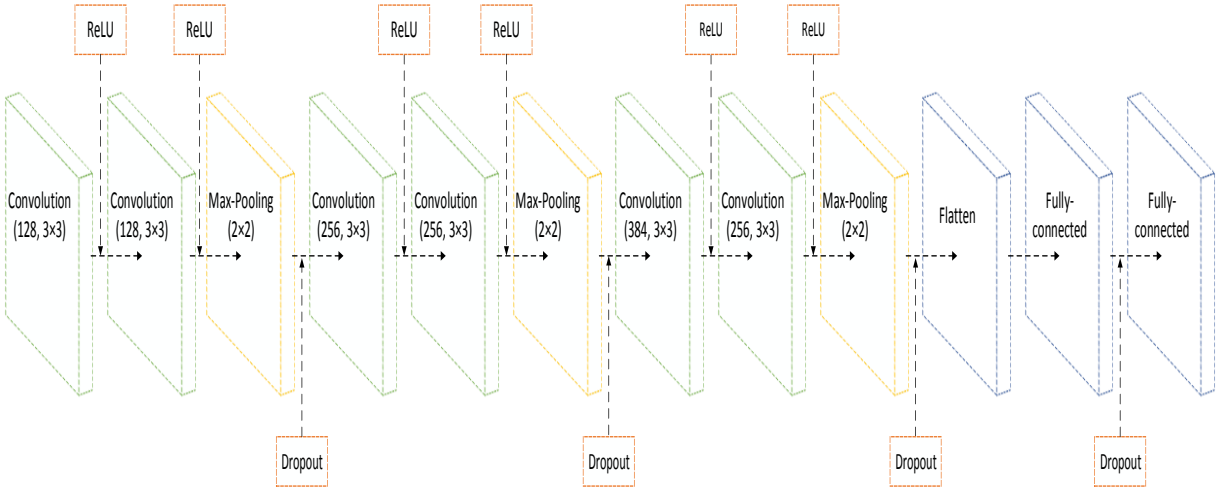

Figure 2. Proposed CNN architecture

V. RESULTS

The training was accomplished on the GPU of an NVIDIA GTX1080 card using the CUDA platform. This process has been completed in about two and a half days. The proposed model has validated on about 1345 images collected for four different plants. Some of the sample images are given in Figure 3. The entire collected images are being first labeled and then divided among two sets in the ratio 70:30. The class labeling for different plant images is given in Table II. The network is trained for three cross-validations i.e. first to classify the given image is of plant leaf or not, second is to classify the given image is the healthy image, and third is to classify the image is the diseased image. The training is accomplished using the 70% images of the database. The result was evaluated using the classification accuracy for the training of the network as well. The average training accuracy of the proposed model is found to be 98.58%. Then the trained network is tested for its accuracy using the testing database. The testing of the network is completed in within six minutes. The classification results of the proposed model are also compared with the other methods. Table III shows the higher classification accuracy of the proposed network.

TABLE II. LABELLING OF IMAGES

Plant name	Healthy class	Diseases class
Arjun	P00	P10
Alstonia	P01	P11
Mango	P02	P12
Sukh chain	P03	P13

Figure 3. Samples images of Arjun, Alstonia, Mango, and Sukh chain plants

TABLE III. RESULTS FOR DIFFERENT METHODS

Algorithms	PSO	SVM	RBFNN	MCNN
Accuracy	87.96	91.57	95.21	98.24
Missing report rate	12.04	8.43	4.79	1.76
False report rate	8.23	5.54	2.36	0

Finally, for the proposed work a number of challenges have been encountered. Most of them are related to the acquisition of the database. The images, when captured in the real environment, are appeared with the number of noises with them. Some of them

include the illumination, temperature, overlapping of leaves, and background details. The proposed CNN performs better under such unavoidable conditions. But, in the future, the model can be more deepen to further overcome the vulnerabilities present in the images.

VI. CONCLUSION AND FUTURE WORK

Plants are important for nature and as well as equally important for the living being. They are the essential part as they provide us with food, shelter, medicine and many more. Plants are also get affected by the diseases and the disorders as the human being does. So in this regard, some appropriate, timely, and accurate methods are to be adopted for suitable plant growth monitoring and plant protection. Therefore in this work, we have proposed a multilayer convolutional neural network for the classification of diseased plant leaf images. The results were validated on the database acquired for four different plant leave images categorized among healthy and diseased. The proposed model with 98.24% achieves higher classification accuracy when compared with the other state of the methods. In the future, the presented model can be further enhanced for the classification of different plant leave and diseases.

TABLE IV. GLOSSARY

Acronyms	
CNN	Convolutional Neural Network
GPU	Graphics Processing Unit
SVM	Support Vector Machine
PSO	Particle Swarm Optimization
RBFNN	Radial Basis Function Neural Network
MCNN	Multilayer Convolutional Neural Network
BPA	Backpropagation Algorithm
SGD	Stochastic Gradient Descent
ML	Machine Learning
DL	Deep Learning
ANN	Artificial Neural Network
ReLU	Rectified Linear Unit

REFERENCES

[1] Edna Chebet Too et al., "A comparative study of fine-tuning deep learning models for plant disease identification," in Computers and Electronics in Agriculture, doi: 10.1016/j.compag.2018.03.032.

[2] Jayme Garcia Arnal Barbedo, "Impact of dataset size and variety on the effectiveness of deep learning and transfer learning for plant disease classification," Computers and Electronics in Agriculture vol. 153, pp. 46–53, 2018, doi: 10.1016/j.compag.2018.08.013.

[3] Siddharth Singh Chouhan, U. P. Singh and S. Jain, "Applications of Computer Vision in Plant Pathology: A Survey," Archives of Computational Methods in Engineering, 2019. doi: 10.1007/s11831-019-09324-0.

[4] Shanwen Zhang et al., "Cucumber leaf disease identification with global pooling dilated convolutional neural network," Computers and Electronics in Agriculture, vol. 162, pp. 422–430, 2019, doi: 10.1016/j.compag.2019.03.012.

[5] Siddharth Singh Chouhan et al., "Image Segmentation Using Computational Intelligence Techniques: Review," Archives of Computational Methods in Engineering, 2018, doi: 10.1007/s11831-018-9257-4.

[6] Siddharth Singh Chouhan et al., "Soft computing approaches for image segmentation: A survey," Multimedia Tools Applications, vol. 77 (21), pp. 28483–28537, 2018, doi: 10.1007/s11042-018-6005-6.

[7] Jayme Garcia Arnal Barbedo, "Plant disease identification from individual lesions and spots using deep learning," Biosystems Engineering, vol. 180, pp. 96-107, 2019, doi: 10.1016/j.biosystemseng.2019.02.002.

[8] Siddharth Singh Chouhan et al., "Bacterial Foraging Optimization Based Radial Basis Function Neural Network (BRBFNN) for Identification and Classification of Plant Leaf Diseases: An Automatic Approach towards Plant Pathology," IEEE ACCESS, 2018, doi: 10.1109/ACCESS.2018.2800685.

[9] U. P. Singh, S. S. Chouhan, S. Jain and S. Jain, "Multilayer Convolution Neural Network for the Classification of Mango Leaves Infected by Anthracnose Disease," IEEE Access. doi: 10.1109/ACCESS.2019.2907383.

[10] S. Lakshmi and R. Sivakumar, "Chlorella Algae Image Analysis Using Artificial Neural Network and Deep Learning," Biologically Rationalized Computing Techniques for Image Processing Applications, Lecture Notes in Computational Vision and Biomechanics, vol. 25, pp. 215-248, 2018, doi: 10.1007/978-3-319-61316-1_10.

[11] Yuan Yuan et al., "Crop Disease Image Classification Based on Transfer Learning with DCNNs," PRCV 2018, LNCS 11257, pp. 457–468, 2018, doi: 10.1007/978-3-030-03335-4_40.

[12] Artzai Picon et al., "Deep convolutional neural networks for mobile capture device-based crop disease classification in the wild," Computers and Electronics in Agriculture, doi: 10.1016/j.compag.2018.04.002.

[13] Konstantinos P. Ferentinos, "Deep learning models for plant disease detection and diagnosis," *Computers and Electronics in Agriculture*, vol. 145, pp. 311–318, 2018. doi: 10.1016/j.compag.2018.01.009.

[14] P. Goncharov et al., "Disease Detection on the Plant Leaves by Deep Learning," Neuroinformatics 2018, SCI 799, pp. 151-159, 2019, doi: 10.1007/978-3-030-01328-8_16.

[15] K. R. Aravind et al., "Grape Crop Disease Classification Using Transfer Learning Approach," Proceedings of the International Conference on ISMAC in Computational Vision and Bio-Engineering 2018 (ISMAC-CVB), Lecture Notes in Computational Vision and Biomechanics 30, pp. 1623-1633, 2018, doi: 10.1007/978-3-030-00665-5_150.

[16] Yang Lu et al., "Identification of rice diseases using deep convolutional neural networks," Neurocomputing, vol. 267, pp. 378–384, 2017, doi: 10.1016/j.neucom.2017.06.02.

[17] Qiaokang Liang et al., "PD^{2}SE-Net: Computer-assisted plant disease diagnosis and severity estimation network," Computers and Electronics in Agriculture, vol. 157, pp. 518-529, 2019, doi: doi.org/10.1016/j.compag.2019.01.034.

[18] Shanwen Zhang et al., "Three-channel convolutional neural networks for vegetable leaf disease recognition," Cognitive Systems Research, vol. 53, pp. 31–41, 2019, doi: 10.1016/j.cogsys.2018.04.006.

[19] Aravind Krishnaswamy Rangarajan et al., "Tomato crop disease classification using pre-trained deep learning algorithm," Procedia Computer Science, vol. 133, pp. 1040–1047, 2018, doi: 10.1016/j.procs.2018.07.070.

Proceedings of the Fourth International Conference on Communication and Electronics Systems (ICCES 2019)
IEEE Conference Record # 45898; IEEE Xplore ISBN: 978-1-7281-1261-9

Cooperative Routing in MANETs Using Trust Inference Framework

Fiza Firdose
MTech, Student ,Dept of E & C
JSS Science and Technological University
Mysuru, Karnataka, India
afsha.firdose76@gmail.com

Dr. Shankaraiah
Professor,Head Of Department of E & C
JSS Science and Technological University
Mysuru, Karnataka, India
shankarsjce@gmail.com

***Abstract*—Cooperative communication in MANETs has grow to be an interesting area, as it perk up system efficiency but still lacks system design. Cooperative routing method includes route discovery, reply, enhancement and data forwarding resulting in mobility conflict and path enhancement. Hosts are typically battery operated, path selection method takes keen on energy utilization, harvesting ability and link break probability to establish suitable path across the network . Using data stored in Cooperative Table and Relay Table we suggest a new Trusted Constructive-Relay-based Cooperative Routing (TCRCPR) protocol with trust inference framework, which provides trust assessment along with results in novel TCRCPR . A new path selection method incorporate route metric value from MAC layer as remaining energy, EH(energy harvest) ability and generally entire network performance is enhanced comparatively and appreciably. Network layer frame unambiguously cover cooperative trusted path discovery, trusted path reply, trusted path improvement and trusted data forwarding. Hence this structure results in efficient throughput lower packet delay ratio, packet control, less energy consumption and secured data transmission and hence can be incorporated by means of existing lower layer mechanisms and can provided great efficiency in performance of MANETs.**

Index Terms—cooperative communication, trust based routing protocol, trust framework, reliability, mobile ad hoc network

I. INTRODUCTION

Mobile ad hoc networks (MANETs) were designed for environment which are co operative and are self-configuring, infrastructure-less network connected wirelessly having features such as frequent change in topology, weak physical protection, no centralized administration, limited bandwidth, limited operating range and high dependence on intrinsic node cooperation which exchange information while there is no central authority and fixed infrastructure. The lack of communications in MANETs makes reliability an issue and data transmission over multi-hop in the occurrence of malicious hosts. Few more issues faced by MANETs are repeated link breaks caused due to mobility along with fast tiredness of energy cause of restricted battery also impacting on the flexibility in MANETs. MANETs are mainly vulnerable to various kinds of routing attack occurred internally [13].It also faces some intrinsic challenge when compared with traditional wireless networks. Earlier proposed routing protocols for ad-hoc networks were ineffective handling attacks.

In paper work, a novel routing protocol called "CRCPR" based on cooperative communication is studied further to support MANETs. By exploring cooperative communication through trust evaluation and available information, energy consumption during transmission is bargained and decreased. Further implementing relay theory based on a Relay Table, [6] TCRCPR introduced offer huge efficiency by providing secure data transmission, trusted path discovered and great robustness adjacent to node mobility by inducing link breaks. Route selecting method selects new route and make use of Route matrix value from Physical/MAC layer as remaining energy [7], EH capability and determine ultimate route by link break probability significantly affect network performance. CRCPR proposes to select new route for assortment mechanism considering energy consumption, energy harvesting, and link break probability that helps determining an appropriate route across a network.

Even after having so many advantages of cooperative communication, there are still some issues in systematically designing in this routing scheme include route discovery, reply, enhancement of path, data forwarding, mobility resistance facilitated, and path selection both effecting energy factors and has less efficiency and performance is also less. TCRCPR remove the mobility concern via self supervision, relay data forwarding and provides secure trusted communicating path between source and destination .There is legacy on association amid participant to attain desired functionalities, with above proposed concept we propose a novel objective that is trust inference structure, which performs assessment plus prediction. The procedure of host trust evaluation based on nodes previous behaviors. To

increase the reliability of data delivery trust establishment scheme which is in Hermes[1], which allow source node to direct data under "trustworthy" with midway nodes. In this design, every host will be assigned"trustworthiness" [3] to its neighbor hosts based over how data is forwarded by analyzing continuous observations. The theory of trust-worthiness runs on conception of "opinion" which hosts in a network have on one other. Then using trusted data sequence info the SCGM (1, 1)-weighted Markov stochastic chain measure predicts trust for upcoming decisions [3]. In this paper we propose a fresh trusted routing protocol with CRCPR to increase the trust, performance, security and efficiency. All simulation result from ns2 tool are shown in the result section. Also a final point, investigational outcome are subjected to convince presented idea via concluding routing valuations.

II.RELATED WORK

A. Energy Efficient Cooperative Routing

Recently, research interest on cooperative communication for efficiency has increased in [11]. Author address orderly approach for evaluating obtainable scheme in cooperative communication. To deal with this concern, the existing routing algorithm for energy efficient cooperative routing algorithm is proposed. Focusing on the transmit set collection strategy, that has huge impact on energy reduction and performance of schemes compared and notional investigation and obtain three theorems to initiate energy efficient cooperative routing.

In paper,[12] a study on cooperative routing for complementary the division of energy amid nodes done. By introduce new method for routing cooperative relay hosts are assigned power for transmission and equilibrium the left over energy amid adjoining nodes to make the most of the lifetime of the set of connections. Targets the systematically cooperative scheme [10] finding the best multiple hop transmission strategy in such a network where we determine hosts implicated in each hop, is a extremely significant trouble to overcome this problem control observation are available at each and every node which describe information organization[11].

In [6] study, the intellect light-weight trust-based routing protocol Intrusion Detection System (IDS) use trust each host posses for other, restricted computational supply needed. In paper,[14] proposed has light weight proactive source routing (PSR) protocol maintaining additional network data compared to distance vector (DV) routes to starting place routing, though it have minor operating cost compared with conventional protocols.

B .Trust Efficiency

In (MANETs), basic start node always depends on supplementary nodes for promoting data packets scheduled multi-hop path to sink. Security with reliability is big issue addressed in ad hoc atmosphere. In this research paper proposed a scheme for trust establishment in MANETs aim provide trustworthiness of data packet forwarded over multiple hop route [1]. Using a Bayesian framework, every node are provided a "trustworthiness" value to neighbor node forming opinion for packet forwarding behavior by direct observation based on trustworthiness value evaluated in network. Opinion metric is implemented to ad hoc routing protocols for getting dependable packet liberation later presented consequences reveal the efficiency of the trust concern design. Many schemes for security are proposed in MANETs to identifying malicious nodes with mean behaviors like packet reducing, alteration, and misrouting on cooperation amongst the host .In paper, [5]proposed defines trust-based detection algorithm factoring in a node's status for MANETs. The algorithm provides less communication overhead with node distributed.

III. TRUST BASED COPERATIVE ROUTING

TCRCPR is a routing protocol which is similar to cooperative protocol that is reactive in nature to built path during transmission and does not maintain any table but proactive routing maintain local table for each data transmission and any modification in network topology updates for betterment.

From a variety of routing scheme for MANETs dynamically routing having been discussed in [2] such as cooperative communication and dynamic routing for energy saving CRCPR[2] is over looked again for betterment of routing with mobility of nodes to decreased energy consumption provide reliability and increase performance.

TCRCPR provides efficient cooperative routing with trust format includes cooperative trusted route discovery, route reply, trusted path enhancement, trusted path selection, and trusted cooperative data forwarding. Further, finds a novel path on basis of energy utilization, EH, and link break probability therefore contributes for cost-effectiveness, energy consumption and **b**etter performance ensuing since mobility-induced frequent link break.

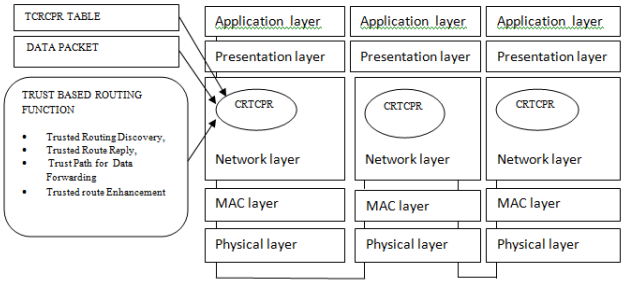

Fig. 1. TCRCPR Structure

Fig. 1 illustrate Cooperative trust frame. It is one tiny sub layer acting without affecting inside the network layer .
It support regular IP traffic, one hop and multi hop ad hoc mobile communication. TCRCPR framework is similar to that of CRCPR frame work its just that trust inference is added to improve efficiency. TCRCPR has three parts:

1) CRCPR tables: the COP Table(cooperative table) with trust, Relay Table, and Cooperative trusted Neighbor Table.
2) Control packets: Trusted Cooperative Hello packet, Trusted Cooperative Route Request Packet, Trusted Cooperative Route Reply Packet, and Trusted Cooperative Confirm Packet.
3) Trust Routing function: Trusted Route Discovery, Trusted Route Reply, Trusted Path Enhancement, and Cooperative Data Forwarding.

A. Neighbor detection

Neighbor discovery is the major role in routing data packet. Many protocols for adhoc networks, includes localization and routing. When neighbor discovery fails, protocols performance decreases. In networks there will be 'N ' no of nodes in which malicious nodes will also be present which can bring down the entire network.

In paper,[2] we present Trust Based Multicast Routing protocol used in network where each node acts as smart agent. Also each agent poses capability of estimate neighbor node trust and select one trusted path for routing of packets.

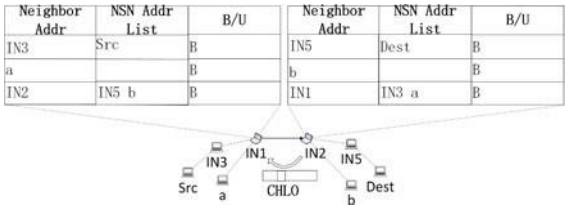

Fig. 2. Cooperative Trusted Neighbor Table Creation.

But once the frame work start working and network established neighbor address tables are created intelligently using algorithm COP possibility detection [2].By using data transformation info as shown in Fig.2 cooperative neighbor table is built with new column added NSN Addr List field and Broadcast/Unicast field[2].

For a topology with more than four nodes Fig.3 it is very difficult for the algorithm to generate and preserve topology but performance will be promising in terms of reduced frequent link break and saving energy but creation and maintenances of algorithm of this kind of topology is very complex. In dynamic MANETs designing and accomplishment of such algorithm is not realistic.

Further, easy results in easy understanding of subordinate layer means for cooperative communication and frame management challenges are studied fully for cooperative communication. Besides, COP topologies know how to coexist with the MANET's .This provide chance to increase performance and save energy, results in forcefulness. Here each node forward data by selecting a trustable entry by broadcasting data packet to there neighbor node and observing time interval of data transmission. The main idea is to detect if any malicious node found in the topology. Ratio of no of packet correctly forwarded to that of number of packets expected in a given time interval[9]defines historical observation .Behavior of node during forwarding of packets are monitored which is required to follow hence consistently data forwarding takes place and the packet are received by the intended node. When a node performs suspiciously value of attributes reduces.

Hence causes packet loss or packet tampering and noted as there was a malicious behavior in the network and mark its entry in COP table.

In detail Host in the network initially receive first data packet is considered as source which has been initialized to value 1 and the intermediary Nodes (INs) will be allotted in table with traveling time from previous node. In the beginning before trusted COP source forwards data, it selects appropriate route by referring to trust attribute value from built COP Table list and packets are placed. Then these packets are sent to all available neighbor routes soon after notifying them to be ready to transmit data via Cooperative (C) nodes. Then, once COP Table is established across the topology data starts forwarding with genuine routes.

Cooperative Network also includes some participants who remain quite are never disturbed until triggered using the COP Table once data is c onfirmed.

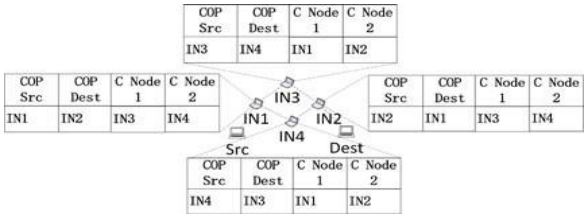

Fig. 3. COP table creation.

Relay Table Creation: As soon as the table Fig.3 is rationalized by the packet, every IN runs the COP algorithm [2] new fill in takes place in COP table and all the reliable entries are obtained and rest entries are deleted as invalid entries. If the neighbor still remains even after the entry in the table is deleted relay table is built. If the entry is deleted but path still stay in the topology then its referred as malicious.

B. Trust-Based Route Discovery and Reply

During data transmission a node is required to route packets to a target, therefore it broadcast demanded packet for search for a path across MANETs. A novel request handling idea of trust based path handling has been implemented and intended to let cooperative topology info to route packets toward destination.This handling is similar to AODV topology. In this COP topology, intermediate node once receives a request packet it immediately finds upstream host of previous hop performs "last hop replacement," where to get closer to COP Des and to decrease the sum hops in the absolute route it replace previous hops IP address through its own IP address within packet IP list. Further with the help of C nodes final route in the topology is selected and this outcome effective point-to-point association of link transversely contained by the COP topology. This not only throw in to saving energy but also improve the robustness cause even if any C host (node) go far from COP topology, a Relay Table is preserved association among

Source and Sink. Additional COP topologies draw, in the ultimate path, then it will lead to huge robustness and increase energy savings. Elaborating more with trusted route discovery and route reply to confirm genuine route:

1.The new fields are added with packets called RPT-Reverse Path Trust RT-Required trust. RPT is calculated using path trust equation [3] .The minimum value of trust flow between the intermediate nodes to reach destination is used and as source does not have any previous node its value is fixed and initialized to one.

2.In Packet Forwarding Strategy ahead getting a data packet from host .The later hop neighbor say 'x' check if it has no route to the previous node then route entry is created stored node ID for backward tracing .

3. Trust value calculated between 'x' and previous node. If obtained RPT value is greater than RT then it's kept in wait state else packet will be discarded. Nodes keep checking if the packets received are same by the receiver if yes understood as lower hop count else goes into wait state in the mean time 'x' node may receive other copies if values as well from other nodes where again step 3 is conceded out . If host 'x' have suitable path to recipient(s) in the table it created and unicast packet to previous nodes else again step 2 carried out. 3. New Fields added here additional fields introduced control package.

1.The Forward Path Trust (FPT) field indicates minimum constant item for consumption of trust data has conceded in the path reply time, also initialized to value 1.

2. The recently added field Required Trust (RT) has the similar denotation.

3. The Reverse Path Trust (RPT) field position to min value obtains from packets and last hop indicated to the multicast receiver.

Once data reached multicast receiver Table Packet Forwarding Strategy is done by intermediate nodes which includes once after packet reaches multicast receiver it calculates trust value previous hop(s). A broadcast packet table created to its neighbors. Intermediate node say '*xm'* receive packet from node 'x*n'*, next node ID is cross checked to see whether its entries matches with its own ID if not from backward learning node recognizes it is malicious.

Now FTP assessment over written to minimum and if this value satisfy the trust condition then host '*xm*' broadcasts its matched entries in the table. If packet forwarding crowd receive numerous packet entries with dissimilar FPT ideals minimum FPT value is selected by the source from packet received. This procedure constructs two-way trusted path starting sources to receivers and vice versa hence trusted packet delivery done.

C. Trusted Path

Path trust represent data will be forwarded from routing path which is used.

$$PathTrust_{sd} = \min_{\substack{s \le m \le d-1 \\ k=m+1}} \{ \bar{TV}_{mk} \}$$

Where *xs* represents a sender, *XD* receiver, *xm* and *xk* are two neighboring nodes on path, and x_m-> x_k indicates that x_k is the next hop of x_m. When control packet are received node tend to, update essential routing records in routing table accordingly.

1. Path Trust Update: Here PTU includes Source Address address of source node, Update Address includes node ID with trust estimation of a given node, Change Address a node with behavior change recorded here and Update Trust Value in control packet. Consider x_k as next node of x_j, then trust of node x_k evaluated by x_j over two succeeding time intervals is bigger or equivalent to the trust revise threshold ζ, host x_j generate PTU. If observed host ought to be no lesser than trust constraint for packet broadcast.

First of all, node x_j looks route set '*X' in* i.e considered as next hop for node there now x_j becomes x_k next node becomes transmitting node where as next node that x_k is not the node needed this info is updated there for trust is node and its path.

Subsequent, PTU data is put on air by x_j for one hop to save energy. Further whichever node getting this data look in favor of the path set 'Y' where later hop x_j, and next hop of x_j is x_k in routing table. Appropriate neighbors update routing info. After execution source node refreshed by node x_j it unicasts a PTU packet using packet table forwarding. Finally route reliance (trust) updated and decided either to employ the novel trail is not.

2. Path Hand-off Procedure is a way to find alternate route when trust value of an exacting node becomes inferior to needed trust constraint for packet broadcast. Initially, host x_m following confirm that host x_k is a unfriendly host , its takes care of path hand-off procedure and informs the downstream node x_j should stop forwarding packets to node x_k then routing entries are also deleted from routing table. Routing entries of x_k is deleted by x_m and again re-transmission takes place for next neighbor node.

Once after receiving packet, again each neighbor will build and unicasts packet to its next. If no route is known packets simple broad casting and specify there is no next hop available and malicious. This is entered in table and flag set done. Until a new efficient trusted path is recognize this redundancy is enough to set up alternate trusted route.

D. Route Enhancement

In this section we discuss about those routing path which do exist in routing table but not in neighbor table this kind of route are deleted. C nodes created between the source and destination nodes will enhance the routing of packets where neighbor association among C host in COP Table along with the Relay Table is enhanced by the unicast scheme when some unwanted routes not present in neighbor table are removed. Therefore both broadcast and unicast are considered valid. Both this casting confirms subsequently hop legitimacy. And hence increase chance of finding valid reliable route. This unicast design flows as follows when a host receive a data from its C hosts it unicasts this to further C host or spread to neighbor. To make use of improved neighbor connections in communication of packets increases overall path robustness.

E. Data Forwarding

Once after final path for data transmission refer Fig.5 is confirmed before data is about to send there are three ways contributing in trust based constructive data forwarding normal manner is executed only when next hop address matches of its own, cooperative manner C nodes starts sending data cooperatively with trust to destination which is alike the "Usual form for Cooperative Communication"[10].

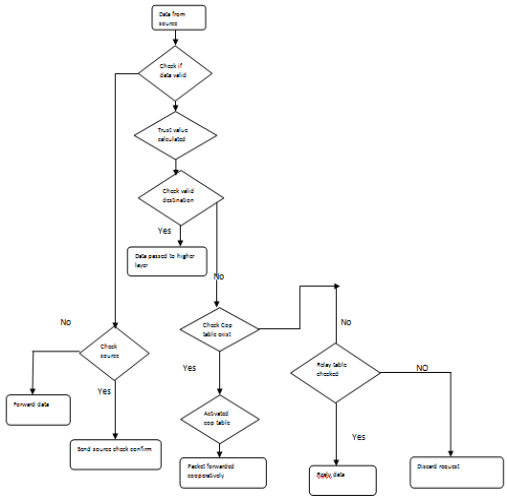

Fig. 4. Flowchart of data forwarding in TCRCPR.

F. Route Selection Criteria

In TCRCPR, to obtain the ultimate path with maximum performance coefficient *Q*, we require info distinct in [2].

1) Energy Harvest Degree*:*

$$H_i = C_e\left(-e^{\frac{-K_1}{n}}+1\right). \qquad (1)$$

From (1), Node *i* has energy harvest degree with stable values of '*n'* associated to energy translation effectiveness C_e and energy harvest involvement K_i, where K_i is determined by battery capability C_{ai}.

Generally it's fixed for all devices. R_i as energy accumulation rate is different.

$$K_i = \frac{R_i}{C_{a_i}}. \qquad (2)$$

2) Real-Time Residual Energy Degree

$$E_i = \left(-e^{-E_i^r(1+H_i)/n_1}+1\right)^{n_2}. \qquad (3)$$

$E_{r\,real}$- time remaining energy of node *i* and $E_r \geq 0$.

H_i Energy harvests degree. n_1 and n_2 are the stable ideals.

Equation (3) guarantee Ei is contained by the range [0, 1].

3) Energy Drain Rate Coefficient

Reveal the power consuming rate of each host. Even if single host has outstanding energy, its life span will be extended even if it has more energy intense rate.

$$a_i = \begin{cases} 1, & \frac{R_i}{E_i} < R_{\text{thr}} \\ 0.1, & \frac{R_i}{E_i} \geq R_{\text{thr}} \end{cases} \qquad (4)$$

$$R_i = \frac{1}{N-1}\sum_{k=i-N+1}^{l} R_k(t). \qquad (5)$$

Therefore, a_i (energy drain rate coefficient) used in ultimate path selection scheme eliminate node with high energy drain rate.

4) Link Break Degree Li make use of reflected stability of each connection, which is evaluated using.

$$L_i = \frac{1}{\left(1+e^{-10(p_i-p_0)}\right)} \qquad (6)$$

where p_i is the diverse link probabilities in TCRCPR, selected factors makes our ultimate chosen path more secure.

5) Link Break Probability for TCRCPR, p_i has of three diverse link break probabilities a normal link p_n two host converse with every one other directly, COP link p_c (i.e., a link between IN1 and IN2) an separate COP link p_{nc} (i.e., a link do not survive among IN1 and IN2). Where *pn=p (7)*

$$P(L_{dotted}) = 1-(1-pn)\,2 = 2p-p2 \qquad (8)$$
$$P(L_{solid}) = pn = p \qquad (9)$$
$$P(L_{dashed}) = 1-(1-pn)\,2 = 2p-p2 \qquad (10)$$

Here the dotted "link" for unconnected COP link L_{dotted}, solid "link" L_{solid} and also dashed "link" L_{dashed}.

IV. SIMULATION RESULTS WITH COMPARISION

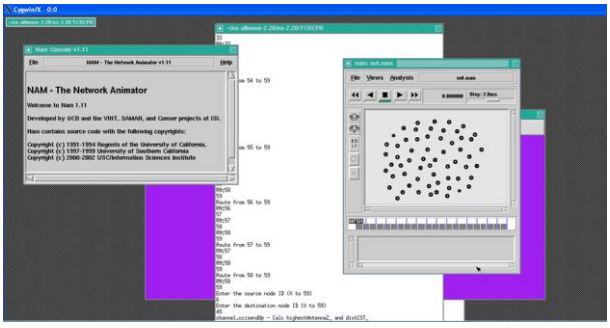

Fig. 5. Topology of MANET nodes

According to the experiment, several advantages of the design have been proved in this result. First, with Trusted Cooperative Neighbor Table, COP Table, and Relay Table stored in the help of topological data structure has helped to improve the performance of the CRCPR greatly. Second, security issue also has solve to great extend with the help of building trust among the neighbor which has reduced control overhead by detecting malicious node with the trust value and excluding them without affecting overall network performance while routing the packets and packet loss also reduced with genuine node transformation and resulted in higher through

put comparatively . Third, the liveliness factor (EH and ER) when choosing the finishing path, the network duration is extended actually.

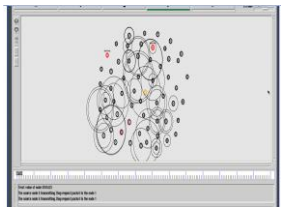

Fig.6. Connection Establishment

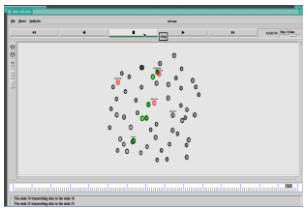

Fig.7. Detection of Trusted path

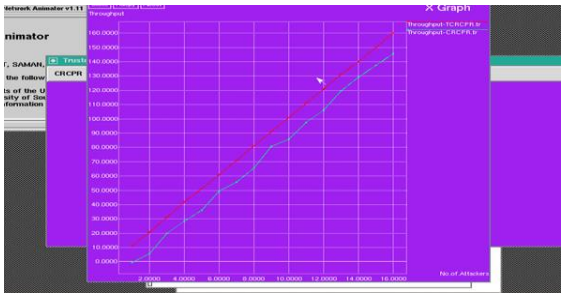

Fig.8. Xgraph Indicating Throughput between TCRCPR and CRCPR

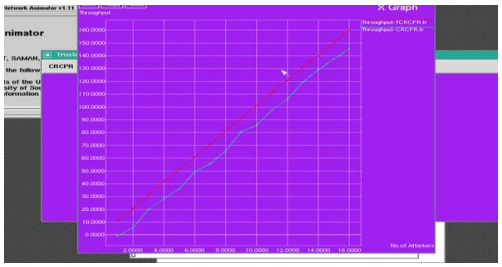

Fig.9. Xgraph to show Control packet between TCRCPR and CRCPR

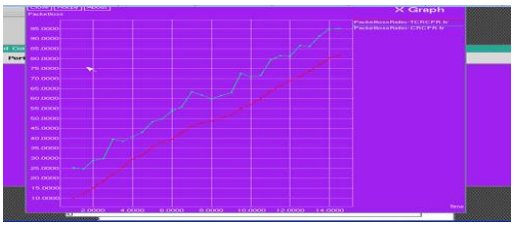

Fig. 10. Xgraph to show Packet loss ratio between TCRCPR and CRCPR

V. Conclusion and Future Work

In this work, we focus on a routing protocol called "CRCPR" based on cooperative communication to supports MANETs which are dynamically reconfigurable. By exploring this communication more adoptable by using information structure, energy utilization during transmissions can be radically decreased. Further introduced CRCPR [07] deals with node mobility issue robustness is providing flexibility from induced link breaks by using relay principle but still lacks in efficiency. This paper presents Trust based Routing Protocol in MANETs which takes trust idea to provide trusted routing protocol. The concept CRCPR incorporates with Trust to increase the efficiency of energy consumption providing effectiveness by allowing nodes to act as smart agent. Where agent has the ability to estimate the trust of neighbor and selects a trusted route for data transmission with trust assessment and hence achieving reliability, robustness and increase in performance and lower energy consumption with TCRCPR. In future work, deep study on trusted strategy can be done majorly focusing on security levels that can be provided to make the topology more secure and in turn enhance performance.

References

[1] C. Zouridaki, B.L. Mark, M. Hejmo, and R.K. Thomas, "A quantitative trust establishment framework for reliable data packet delivery in MANETS," Proc. 3rd ACM Workshop on Security of AdHoc and Sensor Networks (SASN '05), pp. 1-10, 2005.

[2] Jingwen Bai ,Yan Sun ,Chris Phillips and Yue Cao, "Toward Constructive Relay-Based Cooperative Routing in MANETs", IEEE Systems Journal (Volume: 12 , Issue: 2 , June 2018),INSPEC : 17750488,IEEE,11 July 2017.

[3] X Hui Xia ,Zhetao Li ,Yuhui Zheng ,Anfeng Liu , Young-June Choi and Hiroo Sekiya, "A Novel Light-weight Subjective Trust Inference Framework in MANETs",IEEE Transactions on Sustainable Computing (Early Access),IEEE,19 March 2018.

[4] A. Pirzada and C. McDonald, Establishing trust in pure ad-hoc networks, in: Proc. 27th Australasian Computer Science Conference (ACSC04), 2004, pp. 47–54.

[5] W. Li, J. Parker, A. Joshi, "Security through Collaboration and Trust in MANETs," Mobile Networks & Applications, vol. 17, no. 3, pp. 342-352, 2012.

[6] N. Marchang and R. Datta, "Light-weight trust-based routing protocol for mobile ad hoc networks," IET-Information Security, vol. 6, no. 2, pp. 77-83, 2012.

[7] H. Xia, Z. Jia, X. Li, L. Ju and E. Sha, "Trust prediction and trust-based source routing in mobile ad hoc networks," Ad Hoc Networks, vol. 11, no. 7, pp. 2096-2114, 2013.

[8] Lei Gong , Yuebin Bai , Ming Chen and Depei Qian,"Link Availability Prediction in Ad Hoc Networks" ,14th IEEE International Conference on Parallel and Distributed Systems 1521-9097, Melbourne, VIC, Australia ,2008.

[9] H. Xia, J. Yu, C. Tian, Z. Pan and E. Sha, "Light-weight trust enhancedon-demand multi-path routing in MANETs," Journal of Network and Computer Applications, 62, pp. 112-127, 2016.

[10] B. Wang, X. Chen and W. Chang, "A light-weight trust-based QoS routing algorithm for ad hoc networks, " Pervasive and Mobile Computing, 13, pp. 164-180, 2014..

[11] Y. Wang et al., "Towards energy-efficient cooperative routing algorithms in wireless networks," in Proc. IEEE Consumer Commun. Netw. Conf.,Jan. 2013, pp. 79–84.

[12] S. Chen, M. Huang, Y. Li, Y. Zhu, and Y. Wang, "Energy-balanced cooperative routing in multihop wireless ad hoc networks," in Proc. IEEE Int.Conf. Commun., Jun. 2012, pp. 307–311 .

[13] M. Mahmoud and X. Shen. A cloud-based scheme for protecting source location privacy against hotspot-locating attack in wireless sensor networks. IEEE Transactions on Parallel and Distributed Systems, 23(10):1805–1818, 2012.

[14] Zehua Wang ,Yuanzhu Chen and Cheng Li ,"A Lightweight Proactive Source Routing Protocol For Mobile Ad Hoc Networks " IEEE Transactions on Vehicular Technology (Volume: 63 , Issue: 2 , Feb. 2014) pp 859 - 868 ,2013-2014.

[15] D. Balfanz, D.K. Smetters, P. Stewart and H.C.Wong, Talking to strangers: Authentication in ad-hoc wireless networks, in: Proc. Symposium on Network and Distributed Systems Security (NDSS'02), 2002.

Proceedings of the Fourth International Conference on Communication and Electronics Systems (ICCES 2019)
IEEE Conference Record # 45898; IEEE Xplore ISBN: 978-1-7281-1261-9

Performance analysis of three phase integrated generation of SOFC (solid oxide fuel cell), PV (photovoltaic), with IC MPPT (maximum power point tracking) Controller

Kritika Sharma*[1]
Department of Renewable Energy & Tech., RTU,
[1]kritikas289@gmail.com

Dr. Seema Agrawal*[2]
Department of Electrical Engineering, RTU, Kota
[2]seema10dec@gmail.com

Dr. R.K. Somani[3]
Department of computer science BKIT, RTU, Kota
[3]rksomani1@gmail.com

Pankaj Kumar
Department of Electrical Engineering, RTU, Kota
[4]rudrraa777@gmail.com

Abstract— following research paper presents hybrid photovoltaic array (PVA), Solid oxide fuel cell (SOFC) and generation network having some related to MPPT, Availability of Sun irradiance, PV String failure & Shadow effect on PV Panel. Solid Oxide Fuel Cell [SOFC] generates electricity directly by electro chemical process. Here SOFC model will generate electricity whenever Solar power fails to generate electricity according to grid code due to switching harmonics. This proposed system increases the Reliability of local distribution system. This proposed hybrid Solar plus SOFC model will sure help in Smart grid implementation. In this paper we have implemented complete three -phase PV with IC MPPT Controller SOFC hybrid generating power system in MATLAB Software.

Keywords— Maximum power point tracking (MPPT), PV, Solid oxide fuel cell (SOFC), Power quality (PQ), Total voltage harmonic distortion (THD).

I. INTRODUCTION

Recent research and development towards finding alternate generation sources has encouraged exploration of non-conventional energy sources in order to meet growing load demand, decentralised generation has remarkable advantages duo to locally available non-conventional sources of energy[1,4]. Electricity can be obtained explicitly by PV system. Aside these energy sources like PV and wind are stochastic in back up unit to assure uninterrupted power supply. Current harmonics, unbalanced liner loads, reactive power and excessive neutral current are among the sole factors responsible for power quality at distribution end [6].

PV cell is one unit of PV array. Several PV cells can be connected in series or parallel combination to develop PV module as shown in Fig.1. They may be assembled to make panels[2,13]. BP MSX 60 PV Module having two parallel string with 18 cells in one string is used as basic unit of model. PV panel modelling describe in section II with Boost converter and Incremental conductance MPPT [3].

It is feasible to employ PV in coordination with fuel cell to meet variable load demands for either utility or stand-alone application [10, 14]. Non-linear power electronic (PE) loads insert high harmonic components in figure of non-sinusoidal current/voltage and need to be forced to improve supply quality at user end actively.

Together as a hybrid power supply system as solar ia intermittent in nature, SOFC and battery will provide back up when solar generation is reduced. In this way combined operation of sources will improve the reliability of supply to consumers. These sources provide DC power output, which may be converted in to AC supply for AC loads. This conversion is done by PWM inverters at particular frequency power System.

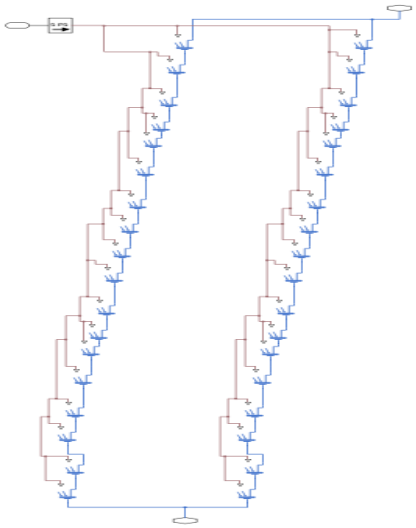

Fig. 1. Photovoltaic panels

Further Solid oxide fuel cell mathematical modelling [9,11,12], MATLAB Simulink model is described in section-III. In the section-IV Hybrid PV & SOFC Simulink Model is proposed, whose schematic is depicted in Fig.2. The Simulink output load voltage waveform with time reference shows the reliability of proposed system. Three phase filter, pulse width modulation (PWM) based voltage source inverter (VSI) [8, 15], SOFC and incremental conductance (IC) MPPT based Controller are the main highlights of the proposed system.

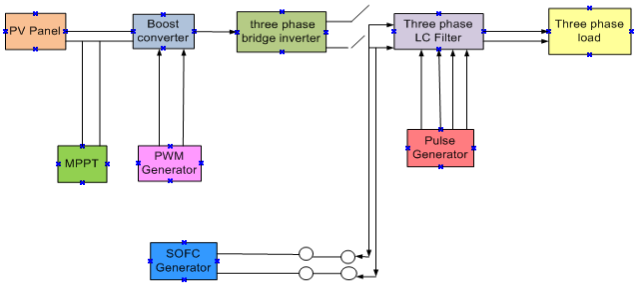

Fig. 2. Block diagram of three phase isolated (PV+SOFC) hybrid generating power system.

II. SOLID OXIDE FUEL CELL MODELLING

PV panel output depends upon the irradiations received on its surface. Sun light is not available equally and moreover different environmental condition may break the

process of PV panel, hence voltage output is not fully guaranteed. This makes the system unreliable in terms of output voltage available at boost converter end. Thus, to enhance the reliability of the system SOFC is added here. Assumptions in SOFC modelling are all gases having deal state, temperature invariant so that Nernst's equation applies. Simulink architecture is shown in Fig. 3.

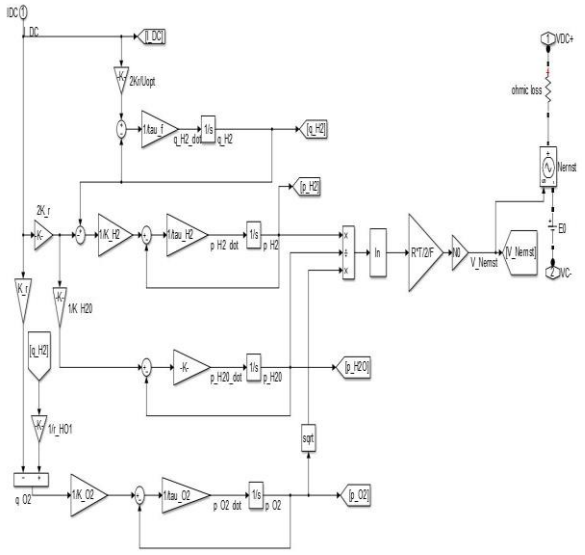

Fig. 3. Simulink model of solid oxide fuel cell (SOFC)

SOFC is based on electro-chemical properties and Nernst Equation (9) which is described from equation (4) to (6).

$$E = N_o\left\{E_o + \frac{RT}{2F}\ln\left(\frac{P_{H_2}\sqrt{po_2}}{p_{H_2o}}\right)\right\} \quad (1)$$

$$P_{H_2}(s) = \frac{1/K_{H_2}}{1+\tau_{H_2}s}\left(q_{H_2}^{in} - 2K_r I_{fc}\right) \quad (2)$$

$$P_{H_2}(s) = \frac{1/K_{H_2o}}{1+\tau_{H_2o}s}\left(2K_r I_{fc}\right) \quad (3)$$

$$P_{o_2}(s) = \frac{1/K_{H_2o}}{1+\tau_{o_2}s}\left(q_{o_2}^{in} - 2K_r I_{fc}\right) \quad (4)$$

$$sq_{H_2}(s) = \left(q_{H_2}^{out} - q_{H_2}^{in}\right)\frac{1}{\tau f} \quad (5)$$

$$q_{H_2}^{in} = \frac{q^r H_2}{uf} = \frac{2K_r Ifc}{uf} \quad (6)$$

Where :-

U_f =fuel uutilization factor

q_r = Molar flow rate

Kr = No/4F is constant

$r_{OH} = \frac{q_{H_2}^{in}}{q_{O_2}^{in}}$ = Hhydrogen to oxygen flow rate

I_{fc} = Fuel cell stack current

$p_{H_2}, p_{H_2O}, p_{O_2}$ = Hydrogen, Water & Oxygen pressure

The SOFC mathematical model parameters values used in MATLAB is illustrated in Table 1.

TABLE 1 SOFC parameters details

Parameter	Detail	Value
T	Absolute Temperature	1273 K
I_FC_0	Primary Current	100 A
F	Faraday Constant	96.487e-6
R	Universal Gas Constant	8314
Eo	Standard Potential	1.18 V
No	Series Cells	525
Umax	Maximum Utilization Factor	0.9
Umin	Minimum Utilization Factor	0.8
Uf	Utilization Factor	0.85
K_{H2}	Hydrogen valve Molar Constant	8.43 e-4
K_{H2O}	Water Valve Molar Constant	2.81 e-4
K_{O2}	Oxygen Valve Molar Constant	2.52 e-3
τ_{H2}	Hydrogen Response Time	26.1 sec
τ_{H2O}	Water Response Time	78.3 sec
τ_{O2}	Oxygen Response Time	2.91 sec
R_{ohm}	Ohmic Loss Per Cell	3.2813e-4
τ_e	Electrical Response Time	5 sec
r_{HO}	Hydrogen to Oxygen Ratio	1.145

III. SOLAR INVERTER MODELLING

Equivalent circuit of the PV cell contains a current source, diode, shunt resistance and a series resistance. Solar cell equivalent circuit is shown in Fig. 4.

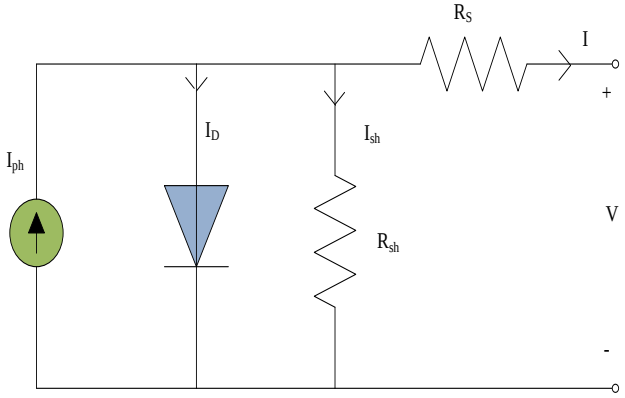

Fig. 4. PV cell network.

$$I = I_{pv,cell} - I_{0,cell}[\exp\left(\frac{qv}{\alpha kT}\right) - 1] \quad (7)$$

Where,

$I_{pv,\,cell}$ = Iincident light current

I_d = Shockley diode equation

$I_{o,\,cell}$ = Reverse saturation current

q = Electron charge

k = Boltzmann constant

T = Temperature

R_p = P-N junction resistance due to leakage current

R_s = Contact resistance of semi-conductor layers

In Two stage Solar inverter, PV power produced by PV Panel here is optimized by IC MPPT with boost controller which work on basis of switch duty cycle, boost converter amplifies applied input PV array voltage. To obtain maximum power, duty cycle of switch is controlled by MPPT in proposed work. Calculations for inductor and capacitor value are calculated as follows:

$$L = \frac{Edc\alpha}{Fs\nabla I} \quad (8)$$

$$C \geq \frac{Eo\alpha}{Fs\nabla V} \quad (9)$$

$$\alpha = \frac{Eo - Edc}{Eo} \quad (10)$$

IV. THREE-PHASE INVERTER

The three-phase VSI square wave inverter as described can be applied to create balanced three-phase AC voltages with fundamental supply frequency.

However 5th, 7th and other odd multiples fundamental frequency voltages distort the output voltage not desirable at all. VSI based on MOSFETs switch is explained in Fig.5.

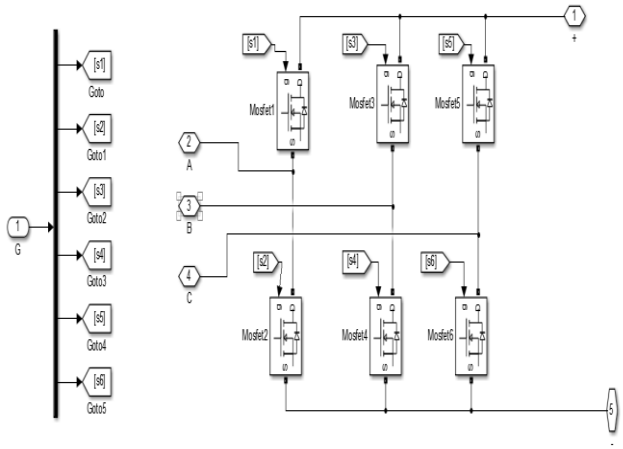

Fig. 5. Basic diagram of three phase VSI invertrer.

Distributed generation is now utilized more and more in world with aim to integrate renewable electrical energy sources into traditional electrical energy power system.

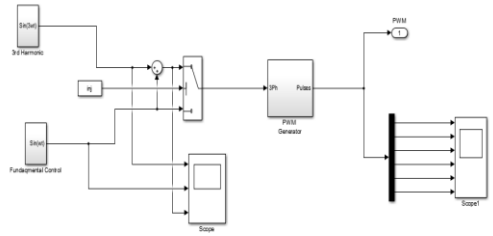

Fig. 6. Three phase PWM inverter module.

Normally, energy sources utilized in DG are linked to a DC-bus, while utility grids work with alternating current (AC). Therefore to merge such energy into grid it is needed to use power electronic converters (PEC), it is applied to step-up the alternative energies voltage, convert DC to AC and for synchronization with utility grid. So, VSI is mostly applied to convert DC-AC signal.

Passive filter system is applied to manage priority of power quality improvement using L_C filter. This system is given away in Fig.7.

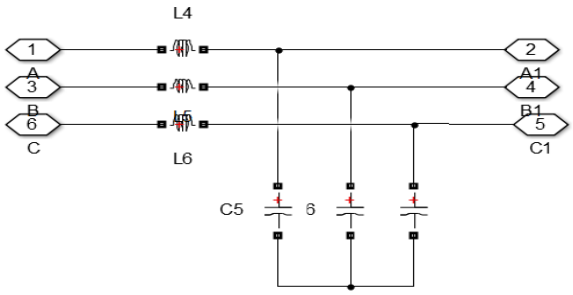

Fig. 7. Performance of three phase filter.

V. PROPOSED THREE PHASE HYBRID MODEL

Here our main aim is reliable power system for smart grid implementation which is realized by means of high speed DC circuit breaker. Operation of these circuit breaker is based on time signal. Through above methodology we connect solar inverter and SOFC in hybrid mode to overcome deficiencies of solar power. Generally, to get connection with grid it requires filter. Thus most common exercised passive filters are inductor (L), capacitor(C) and pi (π) LCL filter.

Active power filter(APF) is also a solution for harmonics. It detects electric current/voltage of nonlinear load and injects a compensation of electrical signal to compensate components that feds to grid.

The filter voltage, current, frequency and overall power handling are affected by designing of particular device or circuitry. The variable DC signal output of a photovoltaic (PV) panel is converted into a fundamental frequency alternating current (AC) using solar inverter.

The proposed hybrid Simulink model of single phase isolated (PV+SOFC) generating power system is examined in Fig.8.

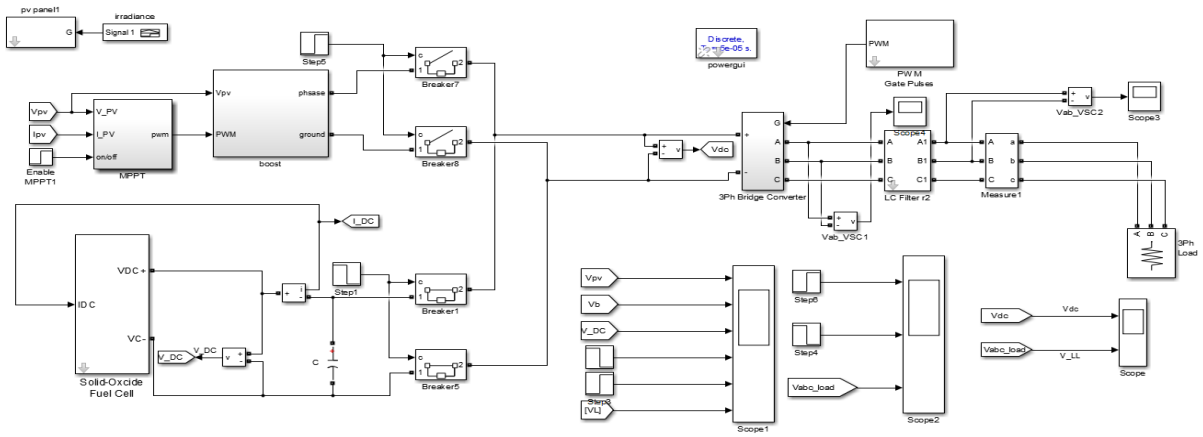

Fig. 8. Matlab Schematic 1 of Proposed 3-Phase Isolated (PV+SOFC) Hybrid Generating Power System.

VI. SIMULINK RESULTS

As per parameters describe in Table 1 results are obtained with Simulink model PV+SOFC for supply quality in distribution system energy sources. These are illustrated Fig. 9 to Fig.14.

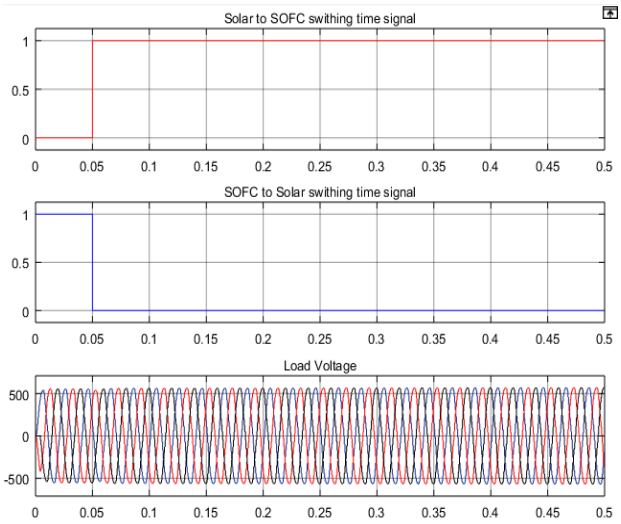

Fig. 9. System load voltage waveform with time signal of three phase isolated (PV+SOFC) hybrid generating power.

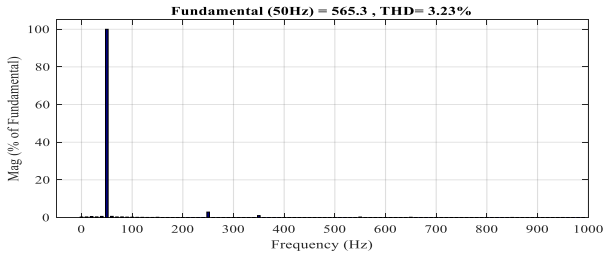

Fig. 10. THD_v (Total voltage harmonic distortion) with LC filter

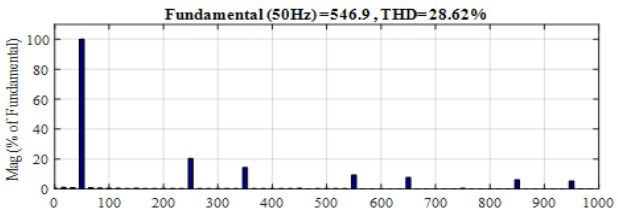

Fig. 11. THD (Total voltage harmonic distortion) without LC filter.

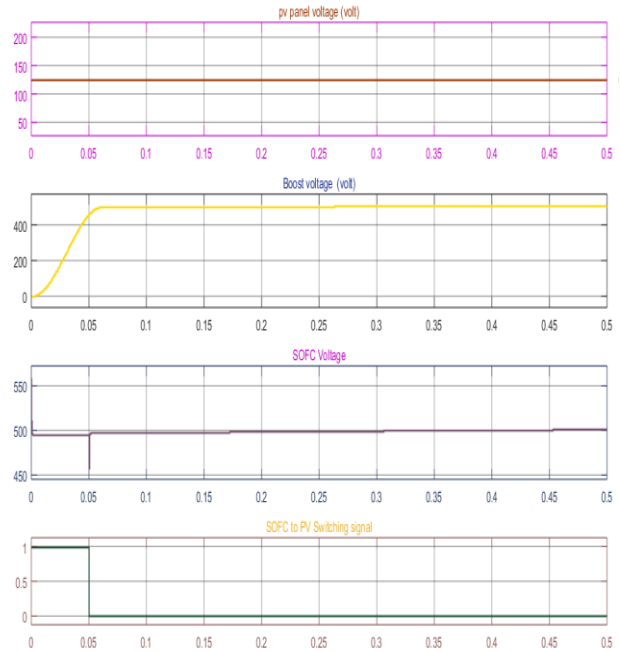

Fig. 12. Voltages at different stages of model and switching signal.

Load voltage waveform and time signals having simulation time period 0.2 second above model is shown in Fig.4. From simulated waveforms it is clear that we has achieved a reliable three-phase hybrid PV+ SOFC generating power system.

VII. CONCLUSION

Hybrid PV+SOFC (photo voltaic + solid oxide fuel cell) three phase isolated power system model is implemented in MATLAB 2015 Simulink software. Complete load waveform shows improved reliability of distribution system. The implemented hybrid model practically suitable for local distribution system, agriculture, multi buildings societies etc. Total voltage harmonic distortion with LC filter at fundamental frequency (50Hz) with level of voltage 565.3V is 3.23% and without LC filter is 28.62%. Pulse width modulation is including and filtering is also include performance analysis three phase PV (photovoltaic) and MPPT (maximum power point tracking) Controller.

VIII. REFERENCES

[1] Seema Agrawal, Seemant Chorsiya, D.K Palwalia, "Hybrid Energy Management System design with Renewable Energy Sources (Fuel Cells, PV Cells and Wind Energy): A Review", IJSET, vol. 6, no. 3,. pp.174-177, 2018 DOI : 10.5958/2277 1581.2017.00104.8 .

[2] S. Jiang, D. Cao, Y. Li and F. Z. Peng, "Grid-Connected Boost-Half-Bridge Photovoltaic Microinverter System Usingm Repetitive Current Control and Maximum Power Point Tracking", IEEE Trans on Power Electr), vol. 27, no. 11, pp. 4711 – 4722, 2012.

[3] K. H. Hussein, I. Muta, T. Hoshino and M. Osakada, "Maximum photovoltaic power tracking: an algorithm for rapidly changing atmospheric conditions," IEE Proc. Gen. Trans and Distri, vol. 142, no. 1, pp. 59 – 64, 1995.

[4] Navadol Laosiripojanaa, Wisitsree Wiyaratnb,Worapon Kiatkittipongc, rnornchai Arpornwichanopd, Apinan Soottitantawat, Suttichai Assabumrungrat; Reviews on Solid Oxide Fuel Cell Tech; Engineering Journal, vol. 13, no. 1, 2009.

[5] M.G. Villalva, J.R. Gazoli and E.R. Filho, "Comprehensive approach to modeling and simulation of photovoltaic arrays," IEEE Trans Power Electr., vol. 24, no. 5, pp. 1198 – 1208, 2009.

[6] L.P. Sampaio, M.A.G.D. Brito, G. De, and C.A. Canesin, "Grid-tie three-phase inverter with active power injection and reactive power compensation," Renew. Energy, vol. 85, pp. 854 – 864, 2016.

[7] S. Agrawal, D. K. Palwalia and M. Kumar, "Performance analysis of ann based three-phase four-wire shunt active power filter for harmonic mitigation under distorted supply voltage conditions", IETE Journal of Research, 2019.
DOI.10.1080/03772063.2019.1617198.

[8] M. Ciobotaru, T. Kerekes ,R. Teodorescu and A. Bouscayrol ,"PV inverter simulation using MATLAB/Simulink graphical environment and PLECS blockset," IEEE Annual Conf on Industrial Electr. , pp. 5313 – 5318, 2006.

[9] R. Yadav and G. Shankar, "Modelling and Simulation of Solid Oxide Fuel Cell", Int Conference on Computation of Power, Energy, Information and Comm., 2014.

[10] Seema Agarwal, Seemant Chourasiya, Rakesh Kumar Kumawat, D.K. Palwalia, "Performance Analysis of Standalone Hybrid PV-SOFC- BATTERY Generation System'' Int Adv Research Journal in Science, Engg. and Tech. (IARJSET), vol 2, no. 1, pp. 49-53, 2015.

[11] X. Xue, J. Tang, N. Sammes and Y. Du, "Dynamic modeling of single tubular SOFC combining heat/mass transfer and electrochemical reaction effects," J. Power Sources, vol. 142, no. 1/2, pp. 211 – 222, 2005.

[12] T V V S Lakshmi, P Geethanjali and K. Prasad S, "Mathematical modelling of solid oxide fuel cell using Matlab/Simulink" Int Conf on Microelectronics, Comm and Renew Energy, 2013.

[13] M. Bouzguenda, A. Gastli, A. H. Al. Badi and T. Salmi, "Solar photovoltaic inverter requirements for smart grid applications", IEEE PES Conf. on Innovative Smart Grid Technologies - Middle East, pp. 17-20, 2011.

[14] Seema Agrawal, D.K. Palwalia, "Analysis of Standalone Hybrid PV-SOFC-Battery Generation System Based on Shunt Hybrid Active Power Filter for Harmonics Mitigation," IEEE 7th Power India International Conference, pp. 1-6, 2016.
DOI: 10.1109/POWERI.2016.8077229.

[15] R. K. Kumawat, S. Agrawal, S. Chourasiya, D. K. Palwalia, "A Comparative Study of Power Inverter Topology and Control Structures for Renewable Energy Recourses", Int Adv. Research Journal in Science, Engineering and Technology, , vol 2, no. 1, pp. 350 – 354, 2015.

Proceedings of the Fourth International Conference on Communication and Electronics Systems (ICCES 2019)
IEEE Conference Record # 45898; IEEE Xplore ISBN: 978-1-7281-1261-9

Emotion Recognition Using Feature-level Fusion of Facial Expressions and Body Gestures

Tanya Keshari
Dept of Computer Science & Engineering
Amrita School of Engineering, Bengaluru
Amrita Vishwa Vidyapeetham, India
tanya251108@gmail.com

Suja Palaniswamy*
Dept of Computer Science & Engineering
Amrita School of Engineering,Bengaluru
Amrita Vishwa Vidyapeetham, India
p_suja@blr.amrita.edu

***Abstract*—Automatic emotion recognition using computer vision is significant for many real-world applications like photo-journalism, virtual reality, sign language recognition, and Human Robot Interaction (HRI) etc., Psychological research findings advocate that humans depend on the collective visual conduits of face and body to comprehend human emotional behaviour. Plethora of studies have been done to analyse human emotions using facial expressions, EEG signals and speech etc., Most of the work done was based on single modality. Our objective is to efficiently integrate emotions recognized from facial expressions and upper body pose of humans using images. Our work on bimodal emotion recognition provides the benefits of the accuracy of both the modalities.**

Keywords—facial emotion recognition, body gestures,bimodal emotion recognition,feature-level, hog feature, SVM.

I. INTRODUCTION

The world of computing has changed over last 40 years. In the recent years technology has developed where 3D gestures are used in television, smartphones and PC for Human Computer Interaction (HCI). Universal gesture recognition market size is increasing at a fast pace and global annual rate is predicted to expand at 22.2% by 2025 [1].

In the present-day context of interactive and intelligent computing, an efficient HCI is of utmost importance. Emotion and gesture recognition can be coined as an approach in this direction.

Emotions are conscious expressions categorized by powerful cerebral activity and a firm intensity of pleasure or displeasure. Humans direct their emotional state through several conduits: facial expression, speech, and body gesticulations etc., The process of identifying emotions from facial expressions is called Facial Emotion Recognition (FER). There are 7 basic emotions: disgust, anger, fear, neutral, surprise, sad, and happy.

Gestures can be described as any non-verbal communication that is expressed to communicate a particular message. In the epoch of gesture recognition, a gesture is well-described as any corporal body movement, that can be understood by a motion sensor. Recognizing gesture is the capability of a computer to comprehend gestures and accomplish commands based on those gestures. Gesture recognition systems finds applications in several interesting areas: Lie detection, Distance learning, photojournalism, tutoring system and biometrics etc.,

In this work, a feature-level fused bimodal emotion recognition model is proposed based on two different modalities: facial expressions and upper body gestures.

The remaining sections of the paper are systematized as follows: Section 2 brief the literature surveyed for this work. In Section 3 dataset description is specified. Phases in emotion recognition are detailed in Section 4. In Section 5, experiment and results are discussed. Finally, the last section includes conclusion and future works.

II. LITERATURE REVIEW

For human behavior understanding and HCI, facial emotion recognition has gained interest of several researchers. Emotion recognition has attracted researchers in computer vision from mid 1970s. Several methods for emotion recognition from images and videos have been proposed by researchers since 1990. Recognition of emotion from facial expression is researched thoroughly in past few decades but emotion recognition from body gesture is a challenging task. An emotion recognition system has 3 main components: face/body detection, feature extraction and classification. The literature survey focuses on the several methods that have been developed for the aforementioned modules.

According to [2] the admixture of facial expression and body gesture overpower all other channels in making judgements about human expressive behavior. This work reflects the combination of the two channels at feature and output level to achieve better recognition rate. For extracting facial features, skin segmentation and histogram equalization are applied followed by feature extraction for body using segmentation and bounding box methods. 94.02 % accuracy was achieved by using BayesNet classification algorithm for feature-level fusion.
Some of the works support the fusion of more than one channel and better results are obtained as compared to single channel. In [3], speech, gestures, and facial expressions are used and overall performance of 78.3% was achieved at feature-level fusion. For feature extraction from facial expression, and body gesture, MPEG 4 FAPs and EyeWeb platform are used respectively. Intensity, pitch, silence length, and MFCC are the features extracted from speech.

Other modalities are facial expressions and physiological signals. For facial expressions, features are extracted using Lucas-Kanade algorithm and 5 physiological signals are extracted using PROCOMP Infiniti system [4]. SVM classifier has been used. A novel fusion of depth and inertial sensor data for hand gesture recognition has been proposed in [5]. The authors have used Kinect SDK and wireless inertial sensor for data collection and Hidden Markov Model (HMM) for classification. Overall recognition of 93% was achieved.

There are various existing technologies for gesture recognition like radar, and image-based gesture recognition etc., [6]. The authors in [7] presented a detailed survey on techniques used in image based emotional body gesture recognition. A survey of gesture recognition illustrating numerous methods and tools for gesture recognition like HMM, FSM, soft computing and connectionist approach are discussed in [8].

Hand gestures can be recognized using accelerometer and IMU [9]. A real-time emotion recognition using Raspberry Pi is illustrated in [10] where emotions are recognized using active appearance model and Adaboost classifier for embedded system applications. The authors in [11] proposed real-time FER using images with pose, age variations, and illumination using CMU-MultiPIE database and an in-house developed Amrita Emotion Database (AED). Apart from images, emotions can be recognized from videos using several techniques and

Fig. 1 shows some of the images from Amrita Emotion Dataset-2

authors [12] proposed method for the same using curves and surface normal.

In all the above previous works, it is shown that the fusing two modalities or data from two modalities results in improved accuracy. Combination of upper half of body and facial expressions in emotion recognition is an emerging area of research and we have proposed a method for the same. The two modalities will complement each other and are expected to provide efficient recognition of emotions in case of ambiguity or if the subject is not expressive in one of the modalities.

III. DATASET

Several databases are available for emotion recognition from facial expressions like CMU-MultiPIE, BU3DFE, BU4DFE, and CK+ [13-15]. Databases for emotion recognition using both body gestures and facial expressions are not openly available. So, we developed an in-house "Amrita Emotion Database-2" (AED-2). The age group of the subjects are 20-25. There are 3 females and 6 males posed for 7 basic emotions (disgust, anger,

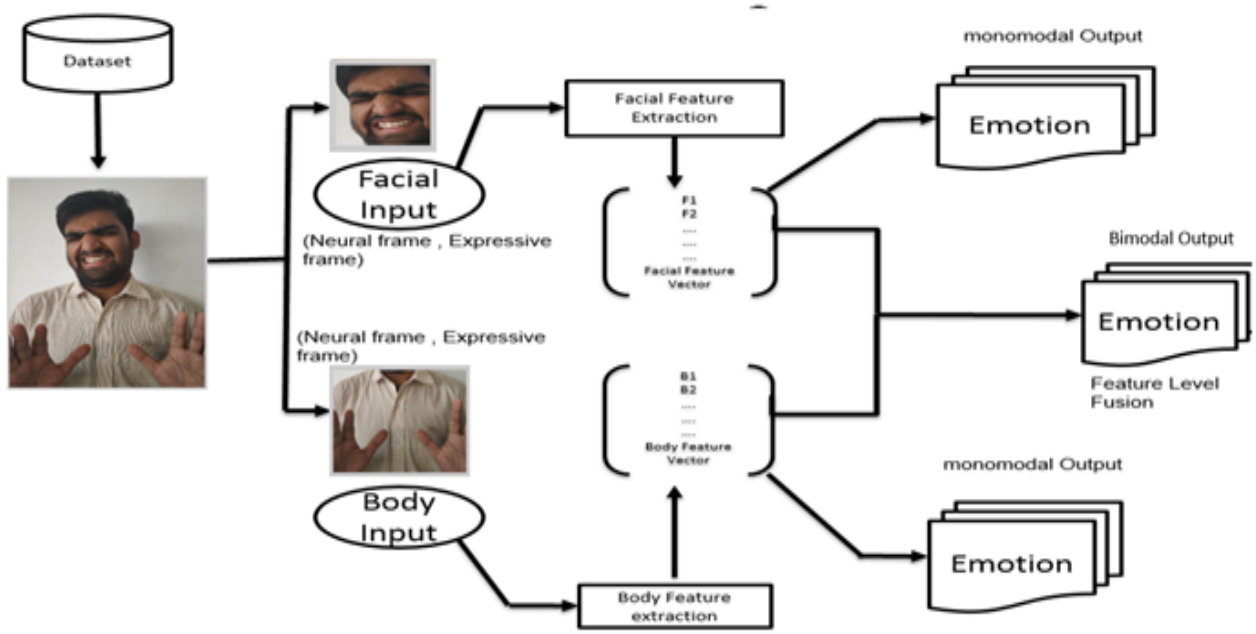

Fig.2 Overview of the proposed method.

happy, fear, sad, neutral and surprise). Fig.1. shows sample of images from AED-2. The dataset contains a total of 100 images.

IV. Implementation

A. Proposed Method

In this work, we have proposed 2 approaches for emotion recognition. An overview of the proposed method is shown in fig.2. In the first approach, emotions are recognized from facial expressions and upper body gesticulations independently. In the second approach the extracted features from facial part and upper body part are combined together to recognize emotion.

The rationale in proposing two approaches is to evaluate and analyse the accuracies of both the approaches and to choose the optimal emotion recognized in case of ambiguities in the expressions in any of the modalities. The ambiguity may arise when the subject express different emotions using facial expression and upper body part. For example, facial expression may give happy and body parts may express surprise. In this case, the combined feature extraction approach will recognize correct emotion. In other cases, the emotion recognized will be the same using first approach.

The basic steps in emotion recognition are image pre-processing, feature extraction & selection and classification. All these phases are discussed in detail in this section.

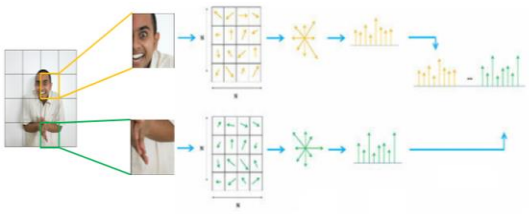

Fig. 4: Process of HOG features extraction: image is divide in cells of siz N x N pixels. The orientation of all pixels is computed and accumulated an M-bins histogram of orientations. Finally, all cell histograms a concatenated in order to construct the final features vector. The examp reports a cell size of 4 pixels and 8 orientation bins for the cell histograms

1) Image Preprocessing

The images in AED-2 are of size3456 X 3456. So, we pre-processed the image by cropping it to 512 X 512 to include only the key region (face and body) in the image.

2) Face and Body Detection

Detecting face and body in an image is a vital step in emotion recognition system. For an optimal detection of face and body separately, the image is segregated into two parts: face image and body image as shown in fig.3(a). Detection of face is done by Voila-Jones face detector [16]. Detection of torso, hands and shoulder are done by using K-means segmentation. Using K-means clustering we segmented the image into two regions,

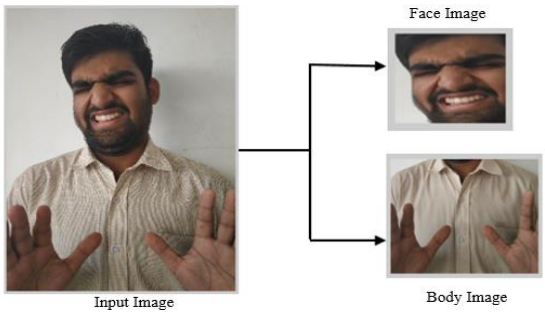

Fig.3(a)Detecting face and body in the image

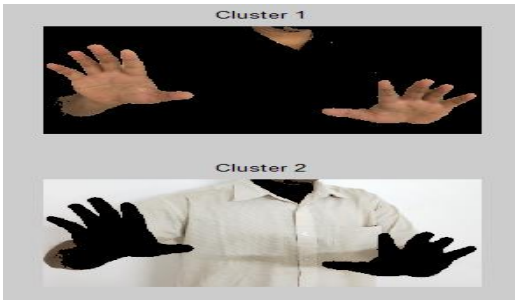

Fig.3(b) K-means segmentation

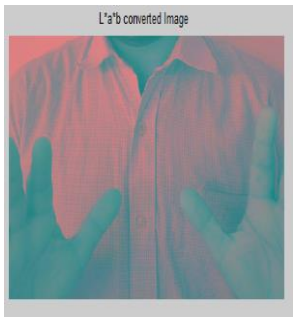

Fig.3(c) CIELAB (L*a*b) converted

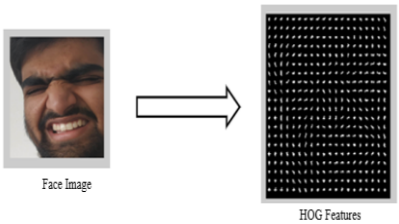

Fig.3(d) HOG features for face

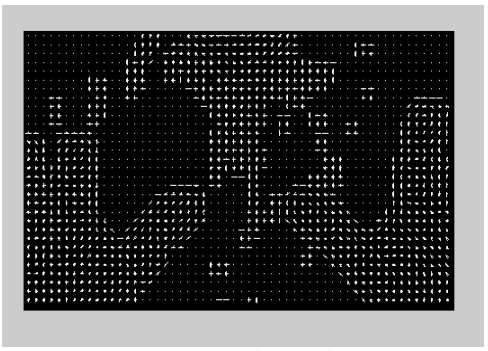

Fig.3(e) HOG features for Body

differentiating the body part from background as given in fig.3(b). The goal of K-means clustering is to classify set of patterns, points or objects into given number of clusters. Each pixel of image (with rgb values) is treated as a feature point taking a position in space. The standard K-means algorithm then randomly pinpoints, the various cluster midpoints in multidimensional space. Each point is then allocated to the group or cluster having closest random mean vector. The process is repeated until there is no noteworthy modification in the position of cluster mean vectors between two consecutive repetitions. K-means clustering [17] is an unsupervised approach and is used in several areas like data mining, image analysis, pattern recognition, face detection, and image segmentation etc.,

3) Feature Extraction

Detecting face/body in the image is the first step of extracting feature in emotion recognition system. The subsequent step is to ensure normalized color and so cropped body images are converted in CIELAB color space, as shown in fig.3(c).

In this work, Histogram of Oriented Gradients (HOG) method is applied which is illustrated in fig.3(d) and 3(e). The HOG has been discovered as an effective technique for detecting face as well as for FER [18, 19]. The elementary notion of HOG features is to map the local object shape and appearance by scattering of edge directions or local intensity gradients. This orientation study is robust to illumination variations. The very initial step behind building the histogram is evaluation of gradient values. Generally, this technique filters the intensity data or color of the picture using filter kernels given below:

$$[-1, 0, 1] \; and \; [-1, 0, 1]^T.$$

The next step is to form histograms. The image is divided into number of cells and each cell covers group of pixels. Based on the gradient values calculated, each and every pixel in the cell have power to casts a vote for an orientation-based histogram mode. Extraction process using HOG method is illustrated in fig.4.

4) Feature Fusion

Feature-level fusion is a critical phase in the approach 2. There are plenty of feature-level fusion procedures such as concatenation, mutual information results, and Principal Component Analysis (PCA) etc., A description of feature-level fusion methods is discussed in [4]. The corpus used in this work is locally created and is small in size and so concatenating the features from two different modalities is the best approach to achieve improved accuracy.

5) Classification

Most of the surveyed literature have used Artificial Neural Network, Support Vector Machine (SVM), and HMM as a classifier [3], [4], [7], [8], [20]. SVM is extensively cast-off in many fields like image classification, text & hypertext categorization, face detection, protein fold and remote homology detection, bioinformatics, and handwriting recognition etc., MATLAB software is used for evaluation and *svmtrain* & *svmclassify* are the inbuilt functions in MATLAB.

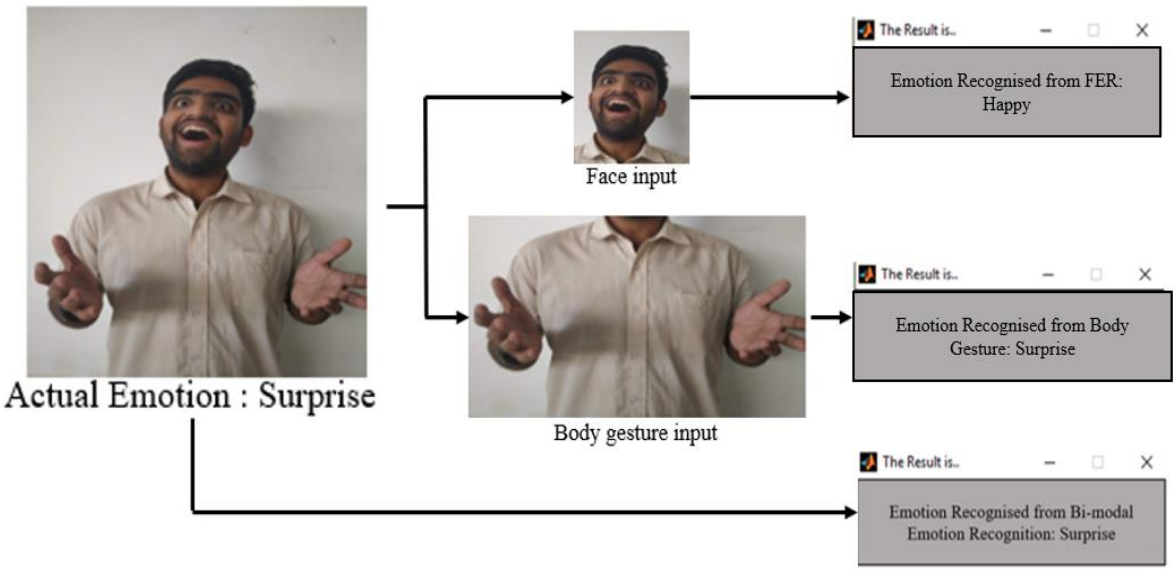

Fig.5 Emotion recognized using two modalities for the same input image

TABLE 2 Emotion-wise accuracy (%) for approach 1 and 2 for 7 emotions

Approach	Modality	Anger	Fear	Happy	Disgust	Neutral	Sad	Surprise
Approach 1	Facial Expression	92	85	85	95	85	85	75
	Body Gesture	80	90	90	80	75	90	80
Approach 2	Bimodal (facial expression and body gesture)	95	91	95	96	95	94	93

We have developed an algorithm *multiSVM* classifier for classification of seven emotions. *MutliSVM* is described as follows:

- Initially SVM is trained for dataset AED-2 for 7 different emotions using *svmtrain*. It will generate train data containing classes with their feature set.
- For each class *i*, where *i*<=*n* (where *n* =number of emotions, i.e. 7)
- Execute *svmclassify*.
  The extracted features are classified using the procedure described and results

V. EXPERIMENT AND RESULTS

Out of 100 images, 70% and 30 % of the images are taken for training and testing respectively. Table 1 represents the overall average accuracy using both approaches for 7 emotions. It shows that fusion of two modalities at feature–level results in better recognition rate as compared to any of the single modality. Inclusively, we have identified that fusion at feature-level of two channels delivers noteworthy enhancements in emotion recognition. Proposed method proves that when we combine two modalities it can achieve better accuracy.

Emotion wise accuracy for approach 1 and 2 are discussed in Table 2. It illustrates that 'disgust' and 'anger ‘are well expressed by facial expressions whereas 'happy' and 'surprise' are recognized better by body gesture. Expressions like 'happy' and 'surprise' are confusing and are often misinterpreted as one another. In fig.5 the input image expressing 'surprise' emotion, is recognized as 'happy' by facial expression because the facial features for 'happy' and 'surprise' emotion are quite similar (eye wide open or wrinkle around the corner of the eyes mouth open). Fusion of features from two modality brings out the best of two different modalities and helps to overcome the drawback of any of the modality. For example, in fig.5 when the feature from both modalities is combined then correct emotion is recognized. Merging different modalities are beneficial in case of missing and unreliable feature due to noisy environmental conditions and corruption of signals during transmission. Approach 2 delivers better result for 'anger', 'happy', 'disgust', 'neutral' and 'sad’. It proves that merging two modalities significantly improve the recognition rate for emotions like happiness, surprise, fear, sad and neutral as shown in Table 2.

TABLE 1 Overall average accuracy for approach 1 and 2 for 7 emotions

Modality	Accuracy (%)
Facial Expression	86
Body Gesture	83.57
Bimodal (facial expression and body gesture)	94

VI. CONCLUSION

In this paper, we have presented a bimodal emotion recognition system constructed on face expressions and upper body gestures. We have proposed two approaches: In the first approach, emotions are recognized from upper body gesticulations and facial expressions independently. In the second approach the extracted features from facial part and upper body parts are combined together to recognize emotion.

We have found that approach 2 achieves higher recognition rate than approach 1. This shows that combination of two modalities will provide the benefit of achieving better accuracy than uni-modal approach.

In future, this work can be extended using deep learning and for images with pose & illumination variations. More number of subjects will be added to the database.

REFERENCES

[1] https://www.grandviewresearch.com/industry-analysis/gesture-recognition-market

[2] H. Gunes, M. Piccardi, “Bi-modal emotion recognition from expressive face and body gestures”, Computer Vision Research Group:Jounal of Networkd and Computer applications, vol. 30 Issue4, pp 1334-1345,Nov 2007.

[3] Loic Kessous, Ginevra Castellano, George Caridakis, “Multimodal emotion recognition in speech-based interaction using facial expression, body gesture and acoustic analysis”, Journal on Multimodal User Interfaces, vol. 3, Number 1-2, pp 33, 2010.

[4] F. Abdat, C. Maaoui and A. Pruski, “Bimodal system for emotion recognition from facial expressions and physiological signals using feature-level fusion,” 5th European Symposium on Computer Modeling and Simulation, 2011.

[5] Kui Liu, Chen Chen, Roozbeh Jafari, Nasser Kehtarnavaz, “Fusion of Inertial and Depth Sensor Data for Robust Hand Gesture Recognition”, IEEE SENSORS JOURNAL, vol. 14, no. 6, June 2014

[6] A. Asokan, A. J. Pothen and R. K. Vijayaraj, "ARMatron — A wearable gesture recognition glove: For control of robotic devices in disaster management and human Rehabilitation," *2016 International Conference on Robotics and Automation for Humanitarian Applications (RAHA)*, Kollam, pp. 1-5, 2016.

[7] Fatemeh Noroozi, Ciprian Adrian Corneanu, Dorota Kamińska, Tomasz Sapiński, Sergio Escalera, Gholamreza Anbarjafari, "Survey on Emotional Body Gesture Recognition," JOURNAL OF IEEE TRANSACTIONS ON AFFECTIVE COMPUTING, Jan 2018.

[8] S. Mitra and T. Acharya, "Gesture Recognition: A Survey," in IEEE Transactions on Systems, Man, and Cybernetics, Part C (Applications and Reviews), vol. 37, no. 3, pp. 311-324, May 2007.

[9] Amritha Purushothaman, Suja Palaniswamy, " Development of smart home using gesture recognition for disabled and elderly", accepted for publication in Journal of Computational and Theoretical Nanoscience.

[10] Suchitra, Suja, S.Tripathi, "Real-Time Emotion Recognition From Facial Images using Raspberry Pi," Proc. of 3rd International Conference on Signal Processing and Integrated Networks, (SPIN), IEEE, Noida, India, pp 666-670, Feb 2016.

[11] Suja P., Shikha Tripathi, "Emotion Recognition from Facial Expressions using Images with Pose, Illumination and Age Variations for Human-Computer/Robot Interaction," Journal of ICT Research and Applications, Institut Teknologi Bandung (ITB), Indonesia, vol.12,no.1, pp.14-34, 2018.

[12] Prathyusha, Suja P., S.Tripathi, R. Louis, "Emotion Recognition from Facial Expressions of 4D Videos Using Curves and Surface Normals", International Conference on Human Computer Interaction, LNCS, Springer, pp.51-64, 2016.

[13] 14 J. F. Cohn, and Y. Tian, "Comprehensive Database for Facial Expression Analysis," *Proc. 4thIEEE Int'l Conf. Automatic Face and Gesture Recognition*, pp. 46-53, 26-30, March 2000.

[14] 15.R.Gross, I. Matthews, J. Cohn, T.Kanade and S. Baker, "Guide to the CMU Multi-PIE Database," *Technical Report*, The Robotics Institute, Carnegie Mellon University, 2007.

[15] L. Yin, X. Wei, Y. Sun, J. Wang, M. J. Rosato, "A 3D Facial Expression Database For Facial Behavior Research," *Proc. 7th Int'l Conf. Automatic Face and Gesture Recognition*, pp. 211 – 216, 10-12 April 2006.

[16] V. Paul and M. J Robust, "Real-time Face Detection", *Int'l J. Computer Vision*, vol.57, no.2, pp. 137-154, 2004.

[17] Yousef Farhang, "Face Extraction from Image based on K-MeansClustering Algorithms" (IJACSA) *International Journal of Advanced Computer Science and Applications*, vol. 8, No.9, 2017.

[18] Deniz O., Bueno G., Salido J., De La Torre F. ," Face recognition using Histograms of Oriented Gradients," *Pattern Recognition Letters*, pp. 1598-1603, 2011.

[19] Meena, Hemant & Joshi, S.D. & Sharma, Kamalesh,"Facial Expression Recognition Using Graph Signal Processing on HOG." IETE Journal, 2019.

[20] A. Sarrafzadeh, S. Alexander, F. Dadgostar, C. Fan and A. Bigdeli, "See Me, Teach Me: Facial Expression and Gesture Recognition for Intelligent Tutoring Systems," 2006 Innovations in Information Technology, Dubai, pp. 1-5of Research. 1-7, 2006.

Proceedings of the Fourth International Conference on Communication and Electronics Systems (ICCES 2019)
IEEE Conference Record # 45898; IEEE Xplore ISBN: 978-1-7281-1261-9

A Hybrid Cloud Approach for Efficient Data Storage and Security

Sandeep HR [1], Dr. Thangam S. [2]
Dept. of Computer Science & Engineering
Amrita School of Engineering, Bengaluru
Amrita Vishwa Vidyapeetham, India
E-mail: sandeephr68@gmail.com [1], s_thangam@blr.amrita.edu [2]

***Abstract*— Cloud computing these days, may be an elementary amendment happening within the space of data technology. It plays a vital role in terms of information storing and reducing the value to entrepreneurs. However, knowledge security continues to be one in all the highest issues for cloud computing. To produce the secure knowledge storage and retrieval, several techniques are projected however the bulk of them face some drawbacks that diminish the practicality of Cloud Computing. This work scrutinizes a hybrid cloud approach for efficient data storage and security. The aim is to propose a model to identify duplication and prevent it thereby using the cloud storage efficiently.**

***Keywords*—Hybrid cloud, security, deduplication, authentication, tokenization**

I. INTRODUCTION

Moving ahead with time, we are all becoming smart and thus making the things we use smarter too. We are developing more and more devices and complicating the device by giving it various tasks to perform and making our own lives simpler because all the tasks that we are to do is done by the devices that we invented over time. For example, a coffee maker, its only supposed to make coffee upon putting the ingredients to make coffee in it. But now we have made it a smart coffee maker. So, it not only makes the coffee but also before leaving home intimates the user that his coffee is ready. Another example is of a smart home. Earlier one should have to remember to turn off all the lights and fans before leaving home. Else they would be running till they get back home in the evening. But now, since we have a smart home, we don't need to remember and turn off all the lights and fans before leaving home. After 20 minutes the fans and lights are automatically turned off if no one is in the house because it's a smart home. One more such example is a smart watch. Earlier the watch was just a device to give information about what time of the day it is. But now since it's a smart watch, the watch gives many more details such as 'xyz' number of steps have been walked by the user, 'abc' number of calories have been burned, what is the rate at which the heart is beating or the user hasn't moved from his place for more than an hour. So, what is the understanding is that, by making devices smart we are not only saving energy in doing the tasks that have to be done but also do much more work in the same time. There are many advantages in devices being smart and helping mankind do their daily routine much faster and in a much more efficient manner. Hence the more and more the devices becomes smart, the more and more time is available to do various other tasks but at the same time important and sensitive data is being shared over the internet which is some food for thought. After all, with every boon comes a bane!

Another example is of the photo gallery in a smartphone. What's new in the market these days is an app called the 'Google Photos' instead of the traditional 'Photo Gallery' which used a fixed storage space in the smartphone. Whereas the 'Google Photos' is a cloud where the photos are uploaded when taken. The cloud is linked with a Gmail account and since it's a big cloud there is no need to worry about how many photographs are there in our phones. And there is absolutely no need to worry about what we'd do with the photos on our old phone in case we buy a new mobile phone. The account that is linked to cloud does all the backing up and transferring of the photos and videos to the new phone as well. The photographs are so well backed up that years down the memory lane, Google reminds us where we were, with whom we were and what we were doing back then. To add to the nostalgia, it also gives us an option of viewing more photographs from that month of that particular year and be in the fantasy of it forgetting about where we are now and what we are currently doing. Probably one major reason for us to miss our old friends, college life, bunking, chit-chatting, etc. Also, if we find a particular snap very interesting, we take a screenshot of that and put it as our status on WhatsApp. Now this screenshot could be a snapshot of the original pic or of another snapshot too. After taking this snapshot, since it's a new photograph in our smartphone, 'Google Photos' backs up this new snapshot too. Now an interesting thing to notice about this is that there are repeated pictures being saved in the cloud. Taking undue advantage of the storage space that is available and being offered we load everything in this huge cloud. Food for thought here is that while taking a snapshot of the original picture or snapshot of the snapshot if Google had told us that, that particular picture already exists in the cloud, it'd save us lot more space and avoid a duplication called deduplication. This is the current problem faced by majority of the organizations using cloud for various purposes. A deduplication [13] check could be done at various levels. For example, file level, where it checks if the filename is the same, or block level, where it checks if the content of the files is the same, etc. The following literature survey shows the research work done in this field to know what are the solutions fund till date to address this problem. Hence, having enormous space to save the files is not just enough but to use this space efficiently is of paramount importance in the present scenario. Also being safe with what data is shared is also very crucial. Afterall its better to be safe than sorry! The later sections elaborate on the proposed solution to this emerging problem and the future scope as to what else could be added to the current research work.

II. RELATED WORK

In [1] Cloud based attacks and vulnerabilities are collected and classified with respect to their cloud models. It also presents a taxonomy of cloud security attacks [12] and potential mitigation strategies with the aim of providing an in-depth understanding of security requirements in the cloud environment. [1] For example, the Authentication Attack, Password Reset Attack, Man-In-the-Middle Attack and Cloud Malware-Injection Attack. They also [1] highlighted the importance of intrusion detection and prevention as a service. [2] The outsourced cloud storage is not fully trustworthy; it raises security concerns. [2] Specifically, aim at achieving both data integrity and deduplication in cloud by proposing two secure systems, namely SecCloud and SecCloud+. [2] SecCloud introduces an auditing entity which helps clients generate data tags before uploading as well as audit the integrity of data having been stored in cloud. [2] SecCloud+ is designed motivated by the fact that customers always want to encrypt their data before uploading, and enables integrity auditing and secure deduplication on encrypted data. [3] Implementing cloud computing empowers numerous paths for Web-based service offerings to meet diverse needs. [3] Loss of sensitive data has increased users' anxiety and reduces the adoptability of cloud computing in many fields, such as the financial industry and governmental agencies. The proposed approach in [3] divides the file and separately stores the data in the distributed cloud servers. [3] The proposed scheme is entitled 'Security-Aware Efficient Distributed Storage (SA-EDS) model', which is mainly supported by proposed algorithms, including 'Alternative Data Distribution (AD2) Algorithm', 'Secure Efficient Data Distributions (SED2) Algorithm' and 'Efficient Data Conflation (EDCon) Algorithm'. [4] To protect the confidentiality of sensitive data while supporting deduplication, the convergent encryption technique has been proposed to encrypt the data before outsourcing. [4] To better protect data security, this paper [4] makes the first attempt to formally address the problem of authorized data deduplication. [4] Different from traditional deduplication systems, the differential privileges of users are further considered in duplicate check besides the data itself. [4] Security analysis demonstrates that our scheme is secure in terms of the definitions specified in the proposed security model. [4] This model shows authorized duplicate check scheme incurs minimal overhead compared to normal operations. [5] Gives details of the vulnerabilities in cloud computing [14]. It's a survey paper which surveyed on the various techniques used till date for cloud computing, what are the issues in doing so, how they can be combated, etc. [6] Talks about an efficient deep learning model proposed to predict the overload on the cloud. they also work on virtual machines on the cloud. results obtained show that there is a good prediction and it's a good learning model which can be used by the industries. [7] For data security a hashing algorithm is used to generate an immediate cipher txt which will be combined with other offline cipher texts to get the actual cipher text. The proposed work proves data integrity without any doubt. [8] Is a survey paper giving insights about what exactly is cloud computing, how exactly things work in cloud computing [11], how are these various computations done, what are the risks involved in doing so, etc. [9] in this paper they have made use of amazon web services- EC2 for their computations and study the services the cloud can offer. [10] In this paper the problems of data not being in encrypted form in cloud is studied.

III. PROPOSED SYSTEM

This is an approach to avoid duplication of data in the cloud called 'deduplication'. In this approach, the deduplication check happens at different levels. One such level is the 'file level', where it checks if the file of the same name is being uploaded as it is in the cloud already. For example, if user A uploads a file called 'document.jpg', and another user or the same user also wants to upload 'document.jpg' to the cloud again. Due to deduplication, the attempt to upload the same file to the cloud is stopped, i.e., deduplication is efficiently checked at the file level by saying 'file with this filename already exists. Try uploading a different file.' Another such level is the 'block level', where it checks if the file uploaded and the file to be uploaded have the same file contents or not. For example, if a user A uploads a file 'document.jpg' with a scanned copy of the heart and another user or the same user also wants to upload 'heart.jpg' also having a scanned copy of the heart to the cloud again. Due to deduplication, the attempt to upload the file contents to the cloud is stopped, i.e., deduplication is efficiently checked at the block level by saying 'File contents of this file is already present in the cloud. Try uploading a different file.' These are examples of how exactly the deduplication is being checked in the proposed model. How exactly this works is by making use of an open private server to maintain private cloud data, user, private cloud, public cloud and a hybrid cloud. The unique encryption technique used is that of the AES (Advanced Encryption Scheme) algorithm to secure the data shared. Dropbox is used to upload the encrypted file to the cloud. each time a trusted user wants to upload the file a unique ID (identification key) is given to upload. The user is identified as trusted or not by first registering with the cloud. Then using the user credentials, he can upload files which are encrypted to the cloud. To better protect data security, this paper [1] makes the first attempt to formally address the problem of authorized data deduplication. Different from traditional deduplication systems, the differential privileges of users are further considered in duplicate check besides the data itself. In this research work [2], Cloud based attacks and vulnerabilities are collected and classify with respect to their cloud models. The proposed approach [3] divides the file and separately stores the data in the distributed cloud servers. Propose two secure systems, namely SecCloud and SecCloud+. [4] SecCloud introduces an auditing entity which helps clients generate data tags before uploading as well as audit the integrity of data having been stored in cloud. [5] Results indicated that the projected model achieves a better coaching efficiency and employment prediction accuracy. The contents above summarize in detail about each research paper that was studied in order to carry out the work proposed in this report. An exhaustive research was carried out in order to successfully achieve the results shown.

IV. IMPLEMENTATION

This is an approach to avoid duplication of data in the cloud called 'deduplication'. In this approach, the deduplication check happens at different levels. One such level is the 'file level', where it checks if the file of the same name is being uploaded as it is in the cloud already. For example, if user A uploads a file called 'document.jpg', and another user or the same user also wants to upload 'document.jpg' to the cloud again. Due to deduplication, the attempt to upload the same file to the cloud is stopped, i.e., deduplication is efficiently checked at the file level by saying 'file with this filename already exists. Try uploading a different file.' Another such level is the 'block level', where it checks if the file uploaded and the file to be uploaded have the same file contents or not. For example, if a user A uploads a file 'document.jpg' with a scanned copy of the heart and another user or the same user also wants to upload 'heart.jpg' also having a scanned copy of the heart to the cloud again. Due to deduplication, the attempt to upload the file contents to the cloud is stopped, i.e., deduplication is efficiently checked at the block level by saying 'File contents of this file is already present in the cloud. Try uploading a different file.' These are examples of how exactly the deduplication is being checked in the proposed model. How exactly this works is by making use of an open private server to maintain private cloud data, user, private cloud, public cloud and a hybrid cloud.

The unique encryption technique used is that of the AES (Advanced Encryption Scheme) algorithm to secure the data shared. Dropbox is used to upload the encrypted file to the cloud. each time a trusted user wants to upload the file a unique ID (identification key) is given to upload. The user is identified as trusted or not by first registering with the cloud. Then using the user credentials, he can upload files which are encrypted to the cloud.

So, to begin with first the user has to open the private server and run all the services. He then has to navigate to eclipse and run the code. Upon running the code, the credentials are asked. If a trusted user, credentials are entered and now a unique access ID is generated. He now has access to the drop box. He uploads whichever file he wants and if another user wants to upload the same file, i.e., file with the same name or the same file content, be it a file of any file format, the cloud says 'No. I already have this file. Please upload a new file'. The python code is run to show this message. Hence, an integration of java and python is made use of to execute the proposed system. The system architecture of the proposed system is as shown in the figure below.

A deduplication [13] check could be done at various levels. For example, file level, where it checks if the filename is the same, or block level, where it checks if the content of the files is the same, etc. The following literature survey shows the research work done in this field to know what are the solutions fund till date to address this problem. Hence, having enormous space to save the files is not just enough but to use this space efficiently is of paramount importance in the present scenario. Also being safe with what data is shared is also very crucial. Afterall it's better to be safe than sorry! The later sections elaborate on the proposed solution to this emerging problem and the future scope as to what else could be added to the current research work.

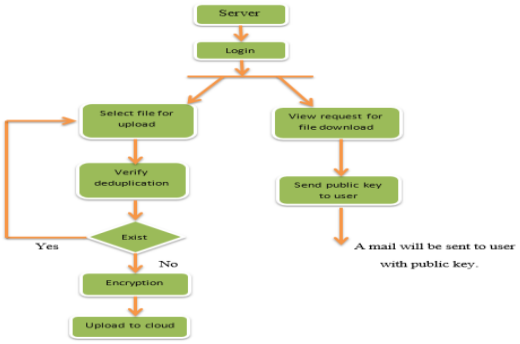

Fig. 1 System architecture

The above figure shows the system architecture of the proposed system where the server allows to login. Further after logging in, either user needs to choose the files to be uploaded or view request for file download. If viewed request for downloading file, then the public key will be sent to the user via mail. If user chooses files needed to be uploaded, the deduplication verification happens. If it exists then user is asked to choose another file to upload to cloud else the file chosen is encrypted using AES algorithm and uploaded to cloud. the below figure is a flowchart showing the user flow.

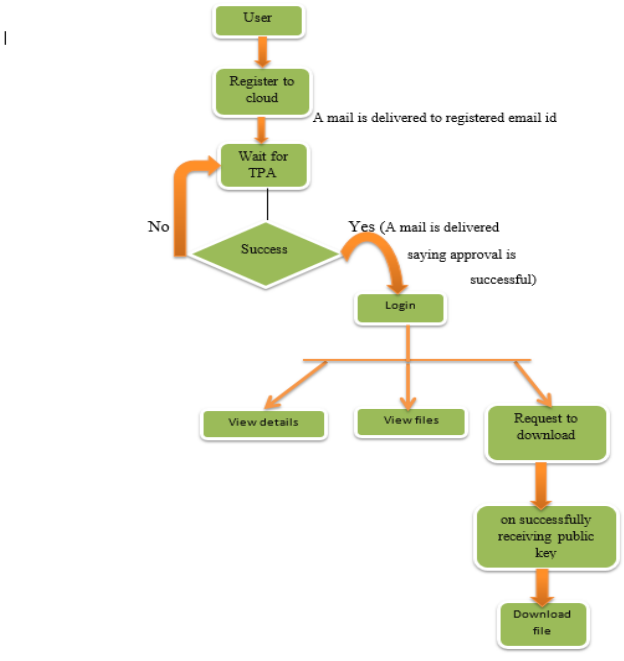

Fig. 2 (a) User flow

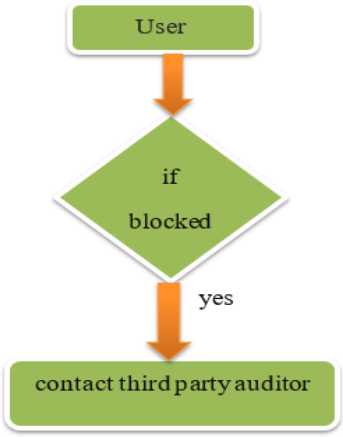

Fig. 2 (b) User flow confirmation

The above figure shows the steps the user has to follow to upload a file to the cloud. Fig. 2 (a) shows that the user has to register to the cloud and then a mail will be sent to the registered email id. The user should then wait for the TPA (Third Party Auditor). If received, then the mail is received that there is a successful login, else continue to wait for the TPA. Upon logging in, the user can view files or view details or request to download. Further, on successfully receiving the public key, the file can be downloaded. The below figure shows details of the TPA work flow.

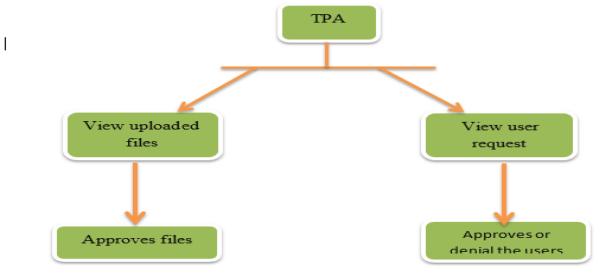

Fig. 3 TPA work flow

The above figure shows details of the TPA work flow. This has a broad classification as either to view the uploaded files or view the user request. If chosen to view the uploaded files, files can only be approved. If chosen to view the user requests, users can be approved or denied. This is how the proposed model exactly works. The next section deals with the results obtained upon implementing the proposed work.

V. RESULT ANALYSIS

The proposed model was implemented successfully. Deduplication was checked efficiently and only the files being uploaded to cloud are encrypted. Hence the data is completely safe in the cloud because its in the encrypted form. So, any search operation done would be on the encrypted data. The below screenshots give details of the results obtained on implementing this proposed model.

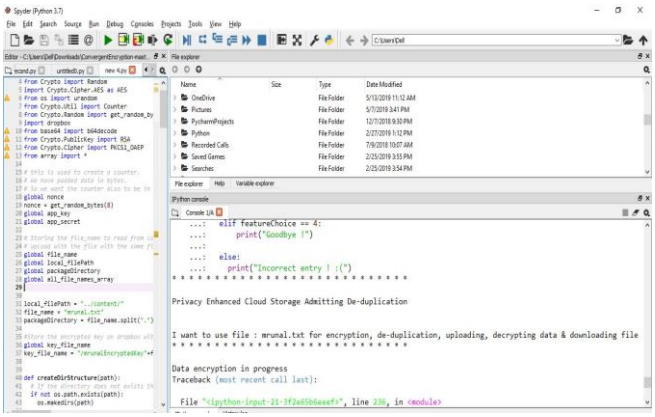

Fig. 4 Python code screenshot

The above figure shows the python code screenshot. This code when run checks for deduplication of files selected to be uploaded to cloud. the below figure shows details of how exactly the cloud looks when a file is uploaded to it.

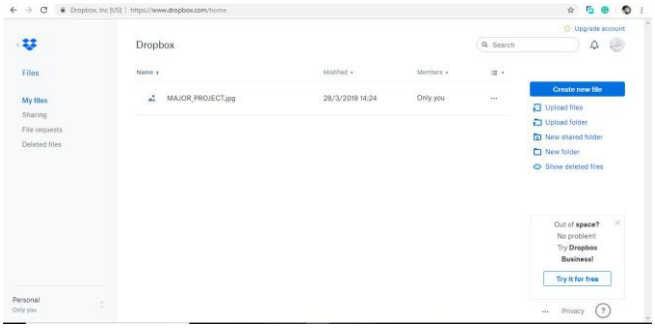

Fig. 5 Screenshot of files in Dropbox

The above figure shows details of the files uploaded in drop box. Before uploading to drop box, the user has login with the credentials provided. If logged in, file chosen is first checked for deduplication. If it exists the user is asked to choose another file to upload, if not the chosen file is encrypted and uploaded to cloud.

VI. CONCLUSION

We did an investigative study on the available techniques of avoiding duplication of data saved in different names/file formats called deduplication in the cloud. The available techniques just allow to upload any type of files to a private cloud or public cloud. No one has tried to read the data that has been uploaded to the cloud and save it from additional storage space by allowing multiple uploads of the same contents of the file in just different file formats. Hence after an elaborate and exhaustive research, we conclude that the cloud is now free from deduplication of data and there is an efficient utilization of storage space in the cloud. The cloud can now restrict the user from uploading the same file contents saved in a different file name or file format to the cloud. Thus, utilizing the storage space it has also in a much

better and efficient manner. Also, the data uploaded is secure. Hence proving no multiple files with same file contents uploading to cloud, efficient utilization of storage space and secure way to share data over the internet. The future work includes to further improve the efficiency of medical data security even more. It also aims to provide deduplication for image, PDF, etc. and reducing to delay required to send public key with automatic servers. Another important future enhancement includes to use the private server itself as a cloud.

REFERENCES

[1] Iqbal, Salman, Miss Laiha Mat Kiah, Babak Dhaghighi, Muzammil Hussain, Suleman Khan, Muhammad Khurram Khan, and Kim-Kwang Raymond Choo. "On cloud security attacks: A taxonomy and intrusion detection and prevention as a service". *Journal of Network and Computer Applications* 74 (2016): 98-120.

[2] Li, Jingwei, Jin Li, Dongqing Xie, and Zhang Cai. "Secure auditing and deduplicating data in cloud". *IEEE Transactions on Computers* 65, no. 8 (2016): 2386-2396.

[3] Li, Yibin, Keke Gai, Longfei Qiu, Meikang Qiu, and Hui Zhao. "Intelligent cryptography approach for secure distributed big data storage in cloud computing". *Information Sciences* 387 (2017): 103-115.

[4] Li, Jin, Yan Kit Li, Xiaofeng Chen, Patrick PC Lee, and Wenjing Lou. "A hybrid cloud approach for secure authorized deduplication". *IEEE Transactions on Parallel and Distributed Systems* 26, no. 5 (2015): 1206-1216.

[5] Ali, Mazhar, Samee U. Khan, and Athanasios V. Vasilakos. "Security in cloud computing: Opportunities and challenges". *Information sciences* 305 (2015): 357-383.

[6] Zhang, Qingchen, Laurence T. Yang, Zheng Yan, Zhikui Chen, and Peng Li. "An efficient deep learning model to predict cloud workload for industry informatics". *IEEE Transactions on Industrial Informatics* 14, no. 7 (2018): 3170-3178.

[7] Li, Jin, Yinghui Zhang, Xiaofeng Chen, and Yang Xiang. "Secure attribute-based data sharing for resource-limited users in cloud computing". *Computers & Security* 72 (2018): 1-12.

[8] Chen, Deyan, and Hong Zhao. "Data security and privacy protection issues in cloud computing". In *2012 International Conference on Computer Science and Electronics Engineering*, vol. 1, pp. 647-651. IEEE, 2012.

[9] Iosup, Alexandru, Simon Ostermann, M. Nezih Yigitbasi, Radu Prodan, Thomas Fahringer, and Dick Epema. "Performance analysis of cloud computing services for many-tasks scientific computing". *IEEE Transactions on Parallel and Distributed systems* 22, no. 6 (2011): 931-945.

[10] Duncan, Adrian, Sadie Creese, Michael Goldsmith, and Jamie S. Quinton. "Cloud computing: Insider attacks on virtual machines during migration".In *2013 12th IEEE International Conference on Trust, Security and Privacy in Computing and Communications*, pp. 493-500. IEEE, 2013.

[11] Kodumru, Nagasai Lohitha, and M. Supriya. "Secure Data Storage in Cloud Using Cryptographic Algorithms". In *2018 Fourth International Conference on Computing Communication Control and Automation (ICCUBEA)*, pp. 1-6. IEEE, 2019.

[12] Supriya, M., K. Sangeeta, and G. K. Patra. "Comparison of AHP based and Fuzzy based mechanisms for ranking Cloud Computing services". In *2015 International Conference on Computer, Control, Informatics and its Applications (IC3INA)*, pp. 175-180. IEEE, 2015.

[13] Supriya, M., K. Sangeeta, and G. K. Patra. "Comparison of cloud service providers based on direct and recommended trust rating". In *2013 IEEE International Conference on Electronics, Computing and Communication Technologies*, pp. 1-6. IEEE, 2013.

[14] Deeksha Vimmadisetti, Tushar Sharma, Ashwini Bhaskar, Kavitha C.R., "Data Security on Cloud: A survey, Research issues and Challenges", IJAER International Journal of Applied Engineering Research), ISSN 0973-4562 Volume 10, Number 11, July 2015, pp: 28875-28887.

Proceedings of the Fourth International Conference on Communication and Electronics Systems (ICCES 2019)
IEEE Conference Record # 45898; IEEE Xplore ISBN: 978-1-7281-1261-9

Smart Sugar Cane Grower Inquiry and Plotting Using Android Application

Apoorv Kansal and Pradeep Kumar
Department of Electronics & Communication Engineering
Amity University Uttar Pradesh, Noida, India
appuavi2012@gmail.com, pkumar4@amity.edu

***Abstract*— This paper presents the development of Sugarcane Grower Enquiry and Survey Application(Android) that would be a Grower Enquiry Mobile Application so that the Growers could know about their Basic Quota, Cane Area, Survey, Purchy, Calendar, Weighment , Payment, Loan Details and Bank Details of their Sugarcane crop produced and provided to Sugarcane Factories. The proposed Paper would also serve to show the plots of each Growers via Google Map. Moreover there will be 8 Main Options which contain 10 Activities/ Screens.**

Keywords*— *Android, Grower Enquiry, Sugarcane factories, SOAP API, XML Pull Parsing, Android Studio.

I. INTRODUCTION

In recent years, researchers have developed applications and systems for precision agriculture based on current resources and future possibilities to improve profitability [1-5]. The concept of smart farming using IoT and advanced sensors has been also developed [6-8]. A novel methodology for the monitoring of the agricultural production process based on wireless sensor networks has been proposed [9]. Wireless sensor networks for agriculture: The state-of-the-art in practice and future challenges and Nb-IoT system for M2M communication were developed [10-11]. Optimized algorithm of sensor node deployment for intelligent agricultural monitoring has been described [12]. Some websites are created by different IT Companies so that farmers could view the details of their sugarcane crops produced and delivered to different sugarcane factories. By visiting these websites and logging in to their accounts, they are able to view the quality of crops produced by them, the status and variety of their crops. They get to know about the details of the amount of money they have taken as loan from the sugarcane factories to grow the required amount of sugarcane, the amount of money they have been paid in return by the sugarcane factories for the quantity of sugarcane delivered to the factories. Up till now in India the entire data of the Farmers' sugarcane fields and crops are updated on Computer Systems only. Describing the process and the data that is displayed on these websites, basically what happens is that factories provide welfare schemes such as pesticides, urea, seeds etc. on loan. If a grower requests for some initial money as a loan to grow crops or to buy seeds as per his requirement, then sugarcane factories come forward to provide the necessities to the farmers. Eventually, the factories want good quality of sugarcane to be produced by the farmer in return so that they can produce sugar out of them. Some factories even have research labs to produce and invent Sugarcane seeds of new types and quality so that more amount of cane could be produced at minimum cost and minimum amount of land is required by the farmers. Modern types of seeds are distributed to the farmers. By doing this, quantity of crop produced could be increased by such loans and sugar would be produced more. So loans for producing new variety of sugarcane crops from the seeds are given to the farmers. In this way, Sugarcane factories and farmers both are at profit. It is noticed that by distributing modern seeds, quantity of sugarcane produced was doubled. In this proposed paper, we have focused on helping the farmers with advancement in Technology to modify and optimize the way Farmers and Sugarcane Industries are used to deal with their data. Since the advancement of Android Application Development, some IT Companies related to Sugarcane Industries are trying to fulfill the need of farmers and sugarcane factories to develop user friendly Android Applications so that farmers don't require to go to Cyber Cafes for viewing the details of their crop field plots. With the proposed Paper a user-friendly Android App has been developed for the farmers keeping in mind their need of viewing their credentials and details. Hindi Language is used for displaying the different options and details so that the famers and local people working in Sugarcane Factories could easily access it accordingly. Each farmer has some sugarcane plots which produce thousands of quintals of sugarcane crop. So one can easily estimate the use of this Application such that this Application would serve to thousands of farmers at the same time very easily. The main purpose of this App is to run 8 options for the farmers. They are : Grower Enquiry, Loan Details, Grower Account Details, Survey, Calendar ,Cane Payment, Weighment , Purchy Details.

The organization of this paper is as follows: This section presents the brief introduction of sugar cane smart farming and precision agriculture using various techniques. Section 2 gives the overview of the android application description. Section 3 gives the details description of the android application implementation and results. Conclusion is given in section 4. At last related references are given.

II. ANDROID APPLICATION DESCRIPTION

The Application requires a proper co-ordination between the Web-Service which takes the data from the main Server and retrieves the required data in key-value pairs back to Android App End. The Android App is developed in Android Studio

Software using Java Programming. Further, the App is divided into 2 sections: Front End and Back End developed using XML files and Java classes respectively. The primary goal of developing this Android Application is to provide relief to the farmers and local staff of Sugarcane factories so that they don't require to go to the cyber cafes to look for their credentials and details related to any plot. Therefore, keeping this in mind we are developing such Application which could run on every smart phone whether it is an old one consisting of Android Jellybean or even the Latest Oreo 8.1. The App is compatible to every Android SDK Versions. That's why minimum SDK Version taken is 15. The App is made user-friendly in the sense that the default language of all the options, buttons and menu are set in Hindi to connect to those people as well who are not much educated.

Moreover, the Application's Main Menu consists of 9 items or options. The Main Page Activity basically consists of Grid View Layout which internally consists of 9 items. Each item or option is linked with subsequent image. The image describes the option name so that a farmer could easily know what the option is all about. So the images would help the farmers to use the App easily. The Front End is developed in such a way that the App looks easy to access and the farmers shouldn't find any difficulty while using it. The UI has a theme consisting of 2 colors: green and white to make it look simple and sober. Green color signifies agriculture basically Sugarcane crops. Each farmer is associated with a farmer code and its village with a village code. Every factory is allotted a unit code. When the application is run by any user, a Splash Screen is shown first reflecting the name of the company and the image depicting sugarcane. Then a Screen arises which asks the user to select any 1 of the 10 sugarcane factories. After choosing the concerned factory, next screen is the Main Page Activity screen where the grower is asked to write his Village Code and Grower Code. Only them he could use the provided 9 Options that are Grower Enquiry, Loan Details, Grower Account Details, Survey, Calendar ,Cane Payment, Weighment, Purchy Details and Log Out. Actually, the Android Application needs Year, Unit Code, Grower Code and Village Code so that these values are taken by Web Service and then the Web Service connects with the Server and checks for the credibility of these 4 codes. If the codes are accepted by the Server, then subsequent method is called and then the Web Service returns the details that need to be displayed on the Screen. This Web Service is called via Soap API i.e using ksoap2. Every Item or Option is connected with some Method which is created at the back end of Web Service. The particular method returns the data as the key-value pairs to the Web Service which in turn connects with the Android Backend and Frontend to display the required details on the Screen of the Grower in tabular form. Grower Enquiry details option includes farmer's name, father's name, village name, centre name, mobile number, total land, average yield, mode of cane delivery, crushing year and society. Loan Details option consists of Loan Type, Loan Description, Loan Amount, Received Amount, Balance Loan and Loan Date. Grower Account Details option includes Bank Name, Bank Branch Name and Grower Account Number. Survey Option includes details like Is Survey, Plot Serial, Plant/Tree type, Village Name, Variety Name, Latitudes and Longitudes of North-East, North-West, South-East, South-West Directions, Plot Area of each of the plots of every farmer, Cane Type. Moreover one can see any plot on Google Maps. Plots are drawn as polygons via Google Map API. Calendar Option consists of the crop details of every farmer. Calendar displays 12 Fortnights. Each Fortnight has 15 days. So as a whole Calendar represents the Purchy(Indent) Details of sugarcane produced and delivered to the respected Sugar Mills in 180 Days of an year. Cane Payment Option includes details like Payment Date, Purchy No., Final Weight, Due Amount, Deducted Amount, Paid Amount, Bank Name, Branch Name, Account Number, Payment Sheet Number. Weighment Option includes details like Mill Purchy Number, Tare Date, Gross Weight, Tare Weight, Net Amount, Indent Slip Number and Mode. Purchy Details(Indent) option includes details like Mill Purchy Number, Fortnight, Day of Fortnight, Variety, Delivery Mode Name, Purchy Issue Date and state of purchy.

III. ANDROID APPLICATION IMPLEMENTATION AND RESULTS

The aim is to not to store any kind of information inside this Application as a local storage. So "SQLite" is not used so that in case a Virus or a Hacker tries to hack the Application, he would not find any private information related to any farmer since this Application gets the details of Bank, Aadhar Card Number etc from the Server which is accessible by the registered devices only. The splash screen of the developed android application is shown in figure 1.

Fig. 1: Splash Screen(First Screen)

Constraints include doing Research in handling SOAP WEB API i.e "ksoap2". Soap API is a connecter which calls the Web Service. Soap API gives the Unit Code, Grower Code, village code and Year to the Web Service to check for the credibility of the data entered by the user. This data is sent to the Server by the Web Service and then the Server responds the appropriate messages back to the Web Service. The Web Service returns the message back to the Soap Calling into the variable declared as "message". This variable could contain entire table. Soap Objects are created which stores the result sent by the Server. When the Soap API is ready with the required data that is asked by the Grower, then comes the role of Parsing. Xml Parsing includes different tags. Each Tag represents a Column of the table. When Server sends back the data, it sends the entire table of the corresponding method

which is created on the Server. Each Activity is connected to its corresponding separate method on Server. So if the grower wants to have a look on it Grower Enquiry Details, so Soap API would have to connect with the Web Service and retrieves the data from "getGrowerDetailsEnquiry" method created at the WebService Backend Database. The data is send back to the Soap call and stored in “message” object. So only then XML Pull Parsing comes into force and different columns are extracted in terms of different tags.

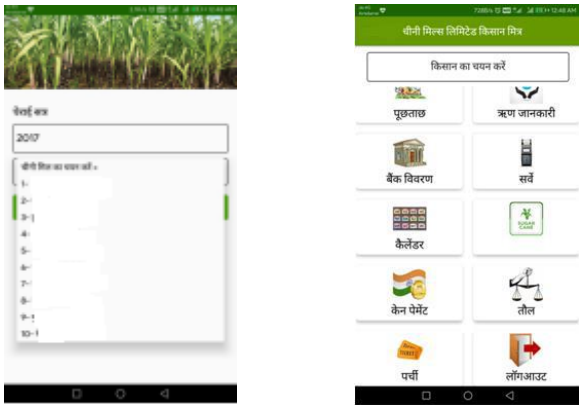

(a) (b)

Fig. 2: (a) Main Activity depicting Spinner, (b) Main Page Activity

Under “MainPage” Activity shown in figure 2, one of the most important task performed is getting the IMEI NUMBER given in figure 3 of the device on which the app is running. This is done for security purposes, as only those devices which get registered on the Server are allowed to use this app. That means if the non-registered device tries to access this app, then it won’t run on the suspected device.

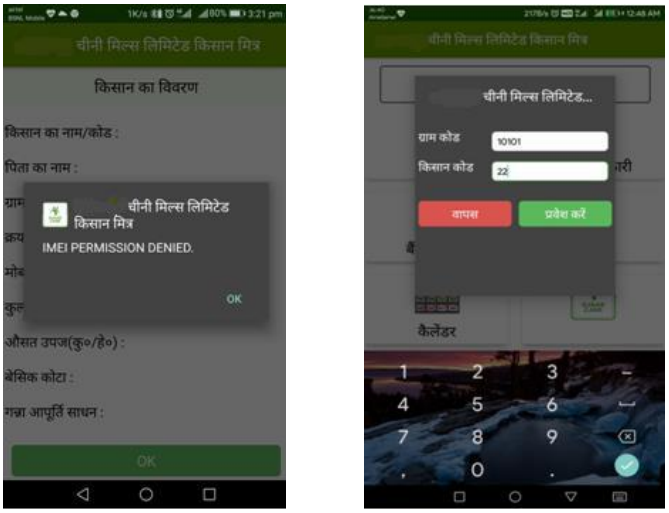

(a) (b)

Fig.3: (a) IMEI Permission Denial, (b) Bootstrap Dialogue Box

The 8 Options are Grower Enquiry Activity shown in figure 4, Loan Details, Grower Account Details, Survey Activity, Calendar Activity, Cane Payment Activity, Weighment Activity and Indent(Purchy) Activity. Last Option is Log Out.

A. Grower Enquiry Details

In Grower Enquiry Activity, details include Grower Name, Father’s name, Village name, center name, mobile number, total land, average yield, mode of cane delivery, crushing year and society name are displayed for the farmers.

Fig.4: Grower Enquiry Activity

B. Loan Details

Loan Details Activity shown in figure 5 includes Loan Type, Loan Description, Loan Amount, Received Amount, Balance Loan and Loan Date. Moreover, Loan Amount in Loan Details activity denotes the amount of money taken in advanced by the grower from the sugarcane factory for buying pesticides or urea or may be seeds. Received Amount tells about the amount of money received by the grower when he supplied the sugarcane factory with the sugarcane. Deducted amount is the difference of the final amount to be received by the farmers and the loan that farmer took from sugarcane factories.

Fig.5: Loan Details Activity

C. Grower Account Details

Fig.6: Grower Account Details Activity

Grower Account Details given in figure 6 include village name, grower name, father's name, center name, bank name, bank branch name and bank account number. Method of the web service published to which this Activity is connected to is "getGrowerDetailsEnquiry",

D. Weighment Activity

Weighment Option shown in figure 7 includes details like Mill Purchy Number, Tare Date, Gross Weight, Tare Weight, Net Amount, Indent Slip Number and Mode. Method of the web service published to which this Activity is connected to is "getWeighmentDetails".

Fig. 7: Weighment Details

E. Survey Activity

Survey Option shown in figure 8 & 9 includes details like Is Survey, Plot Serial, Plant/Tree type, Village Name, Variety Name, Latitudes and Longitudes of North-East, North-West, South-East, South-West Directions, Plot Area of each of the plots of every farmer, Cane Type. Moreover one can see any plot on Google Maps. Plots are drawn as polygons via Google Map API.

Fig. 8: Survey Activity (first half of the screen)

Fig. 9: Survey Activity (second half of the screen)

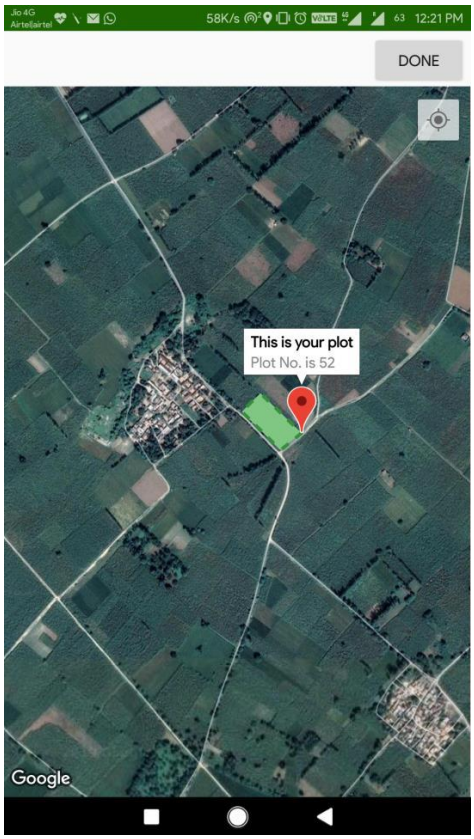

Fig. 10: First Plot of a farmer shown on Google Maps via Google API

Each plot is drawn shown in figure 10 as a polygon and its boundaries are marked accordingly by taking the co-ordinates of latitude longitude of each of its 4 corners. Each crop field plot of sugarcane is shown on the map (figure 11) when the farmer taps on "Yes" TextView box corresponding to each plot. 2 "Bean Classes" are used to use the concept of encapsulating many objects into a single object. Method of the web service published to which this Activity is connected to is "getGrowerSurveyDetails". A bean class implements Serialization concept and has public getters and setters methods. One of the bean classes created is "PlotLatLng" class and other one is "SurveyData" class.

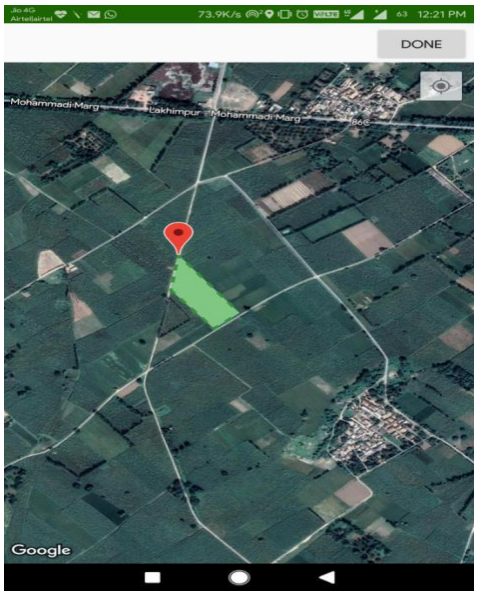

Fig. 11: Second Plot of a farmer shown on Google Maps via Google API

Map Activity Class is opened along with sending "plotLatLng" object in the bundle as serialized and also the plot serial number of each plot of the farmer is also sent with the bundle as well (figure 12).

Fig. 12: All plots of a farmer shown on 1 screen of Google Maps along with the required information of each plot

To see all the plots of the farmer, All Plots Activity Screen is executed from Survey New Activity. "SurveyData" bean class is used.

F. Calendar Activity

Calendar Option shown in figure 13 consists of the crop details of every farmer. Calendar displays 12 Fortnights. Each Fortnight has 15 days. So as a whole Calendar represents the Purchy(Indent) Details of sugarcane produced and delivered to the respected Sugar Mills in 180 Days of an year. Method of the Web Service published to which this Activity is connected to is "getCalenderDetails". "showSummary" function is called and executed. "LayoutParams" attribute of "TableRow" layout is used to draw and map the table.

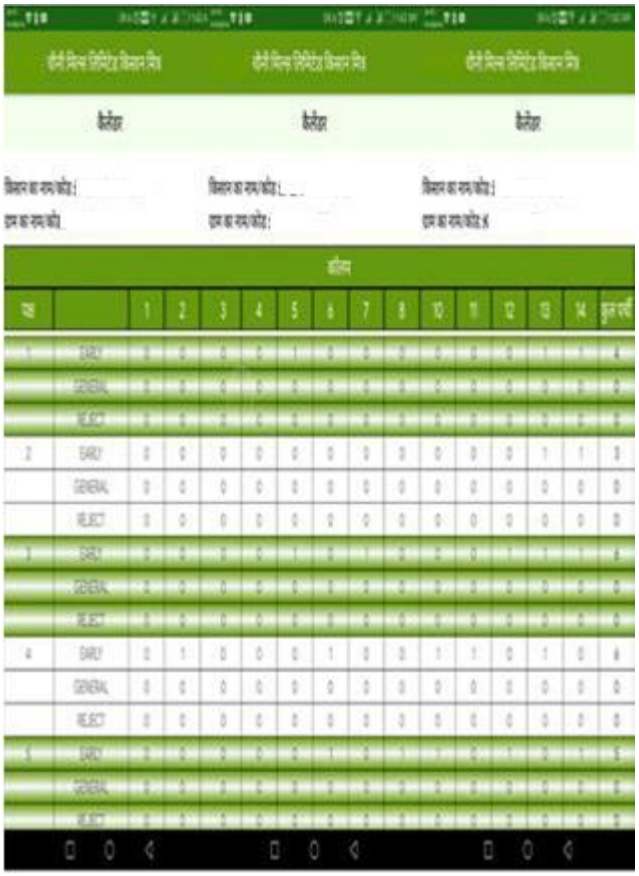

Fig.13: Calendar Activity for 12 Fortnights

G. Payment Activity

Cane Payment Option shown in figure 14 includes details like Payment Date, Purchy No., Final Weight, Due Amount, Deducted Amount, Paid Amount, Bank Name, Branch Name, Account Number, Payment Sheet Number. Method of the Web Service published to which this Activity is connected to is "getPaymentDetails".

Fig.14: Payment Activity for 12 Fortnights consisting a total of 168 days of an year

H. Indent Activity

Purchy Details(Indent) shown in figure 15 option includes details like Mill Purchy Number, Fortnight, Day of Fortnight, Variety, Delivery Mode Name, Purchy Issue Date and state of purchy. Method of the Web Service published to which this Activity is connected to is "getPurchyDetails"

1609348	1	9	Early	CART -20	CART -20	17/11/2017	22/11/2017	
1621194	2	13	Early	CART -20	CART -20	10/12/2017	14/12/2017	
1628915	3	5	Early	CART -20	CART -20	24/12/2017	28/12/2017	
1631042	3	12	Early	CART -20	CART -20	29/12/2017	02/01/2018	
1630958	3	14	Early	CART -20	CART -20	29/12/2017	02/01/2018	
1640846	5	6	Early	CART -20	CART -20	21/01/2018	25/01/2018	
1642788	5	10	Early	CART -20	CART -20	26/01/2018	30/01/2018	

Fig.15: Indent Activity(Sugarcane Purchy Details)

IV. CONCLUSION

In this paper, we have focused on helping the farmers with advancement in technology to modify and optimize the way of farming and Sugarcane Industries are used to deal with their data. With the proposed paper a user-friendly Android App for the farmers has been developed, keeping in mind their need of viewing their credentials and details. Hindi Language is used for displaying the different options and details so that the famers and local people working in Sugarcane Factories could easily access it accordingly.

REFERENCES

[1] Zhang, Chunhua & Kovacs, John "The application of small unmanned aerial systems for precision agriculture: A review" Precision Agriculture 13(6): 693-712, 2012.
[2] Beeri, O., & Peled, A. "Geographical model for precise agriculture monitoring with real-time remote sensing" ISPRS Journal of Photogrammetry and Remote Sensing, 64, 47–54, 2009.
[3] Lambert, D., & Lowenberg-Deboer, J. "Precision agriculture profitability review" Purdue, USA: Site Specific Management Center, pp. 154, 2000.
[4] McBratney, A., Whelan, B., & Ancev, T. "Future directions of precision agriculture" Precision Agriculture, 6, 7–23, 2005.
[5] Stafford, J. V. "Implementing precision agriculture in the 21st century" Journal of Agricultural Engineering Research, 76, 267–275, 2000.
[6] Maria Aleksandrova "IoT in Agriculture: Five Technology Uses for Smart Farming and Challenges to Consider" June 10, 2018.
[7] Anderson, Chris. "Agricultural Drones: Relatively cheap drones with advanced sensors and imaging capabilities are giving farmers new ways to increase yields and reduce crop damage." MIT Technol. Rev 17: 3-58, (2014).
[8] McNairn, H., & Brisco, B. "The application of C-band polarimetric SAR for agriculture: A review" Canadian Journal of Remote Sensing, 30, 525–542, 2004.
[9]Díaz, S.E.; Pérez, J.C.; Mateos, A.C.; Marinescu, M.-C.; Guerra, B.B. A novel methodology for the monitoring of the agricultural production process based on wireless sensor networks. Comput. Electron. Agric. 2011, 76, 252–265.
[10] Ojha, T.; Misra, S.; Raghuwanshi, N.S. Wireless sensor networks for agriculture: The state-of-the-art in practice and future challenges. Comput. Electron. Agric. 2015, 118, 66–84.
[11] Ratasuk, R.; Vejlgaard, B.; Mangalvedhe, N.; Ghosh, A. Nb-IoT system for M2M communication. In Proceedings of the IEEE Wireless Communications and Networking Conference, Doha, Qatar, 3–6 April 2016; pp. 1–5.
[12] Sai, Z.; Fan, Y.; Yuliang, T.; Lei, X.; Yifong, Z. Optimized algorithm of sensor node deployment for intelligent agricultural monitoring. Comput. Electron. Agric. 2016, 127, 76–86.

Proceedings of the Fourth International Conference on Communication and Electronics Systems (ICCES 2019)
IEEE Conference Record # 45898; IEEE Xplore ISBN: 978-1-7281-1261-9

Landslide detection system using computer vision approach and Raspberry Pi

Praveen Kumar Mishra
Defence Terrain Research Laboratory
Defence Research & Development Organization
Delhi, India
praveenmishra1109@gmail.com

Sunil Dhar
Defence Terrain Research Laboratory
Defence Research & Development Organization
Delhi, India
sunildhar21@hotmail.com

M K Kalra
Defence Terrain Research Laboratory
Defence Research & Development Organization
Delhi, India
kalramk@rediffmail.com

Abstract--- Landslide is a natural hazard, which badly affects people's safety and property. Continuous monitoring of such a disaster may lead to reducing of losses of human lives. With this aim, in this paper, we have proposed a surveillance system for real time landslide monitoring using computer vision algorithms. Here we have used a video camera to acquire live view of landslide site and a small computer board 'raspberry Pi' to run the algorithm we will introduce here. When landslide is detected SMS text messages are transmitted using a GSM modem. Due to video camera and Raspberry Pi, this method is inexpensive yet efficient and also requires low power, therefore this method can be used in any region. We have used median filtering to remove noise present in the detection algorithm. Here we have also proposed a new implementation method for median filtering using a linked list and parallel processing which is very time efficient.

Keywords—computer vision, camera, raspberry pi, motion detection, background subtraction, video, entropy, landslide, median filtering, image processing, artificial intelligence

I. INTRODUCTION

The term landslide describes gravitational movements of soil or rock down slopes. Landslide is a geological disaster which is the major cause of damage to life, human settlements, and public utility [1]. Landslide is a serious problem in mountainous terrain like Himalayan states of India [2]. Therefore in these regions, there is an urgent requirement to establish a system for landslide monitoring to save human lives and properties. There is a need to establish landslide monitoring and detection systems which can provide alarms at the moment when a landslide occurred. These systems may save human life and property by generating alarms at critical moments [3].

Several measurement methods have been developed for slope instability and landslide risk estimation [4]. For example map analysis and remote sensing are used for landslide risk estimation based on terrain information and geological information. But these methods are costly, labor intensive and highly subjective.

One approach for landslide monitoring is by installing various geotechnical instruments such as inclinometers, extensometers or piezometers on the slop. Various geotechnical instruments based landslide monitoring systems have been discussed [5]. But these types of systems are very costly and require continuous maintenance.

In this work, we have introduced a low cost and low power consumption system for landslide detection and monitoring. For this work, we have used a web camera, and a single board computer raspberry pi to detect landslide events using motion detection technique and median filtering.

Landslide detection in a video stream can be thought about detecting moving objects in a video. There are various techniques existing for detecting moving objects in a video. One of them is temporal differencing which uses pixel wise difference between 2 consecutive frames in a video. This method is sensitive to noise, cannot handle complex background and still object detection [6].

The second method is Optical flow [7] which is very complex and time inefficient therefore cannot be used in real time application. Gaussian mixture model based background subtraction is another method for moving object detection [8]. However, this method cannot handle multimodal background.

In this work, we have used Visual Background Extractor (ViBe) [9]. This method has high accuracy, requires less memory space and is time efficient. The Vibe can handle complex background and small camera movement.

Median filter is used to reduce impulse noise. Various methods have been discussed in the literature [10] [11] for conventional median filtering. In [12] various algorithms have been proposed for fast median filtering with time complexity from $O(n^2)$ to $O(n \log n)$. Here we have used linked list and parallel processing to reduce time complexity.

We have used entropy threshold technique [13] as an index to determine down slope motion of large area i.e. landslide or small object's motion.

The research paper is divided as follows. In Section **II** we present a system diagram and give an overview of hardware components used in the proposed landslide detection system. In Section **III** we shortly describe the methodology and about the developed algorithm for landslide detection. In Section **IV** we present the achieved experimental results. Finally, in section **V** we conclude the research paper and discuss about the future work.

II. Proposed system

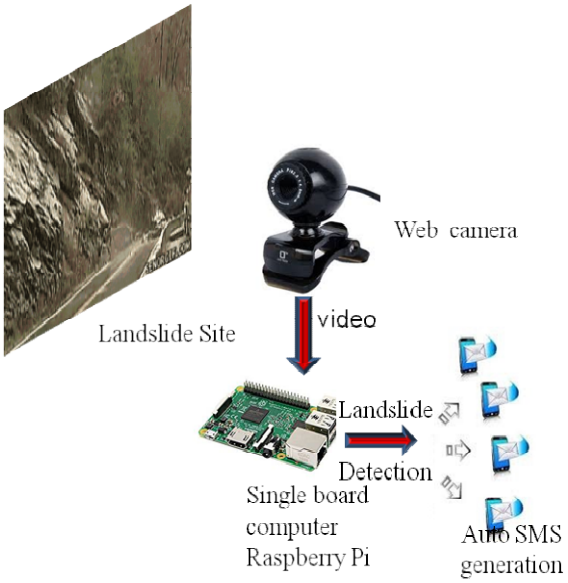

Figure 1: System Diagram

System diagram of the proposed system is given in figure 1. Following hardware components are used:

- Video camera: a digital video camera is used to capture live view of landslide vulnerable site. Video camera feed is basic input to our system. OpenCV library is used by single board computer raspberry PI to capture video from web cam and accessing video frames.
- Raspberry Pi: Raspberry Pi is a low cost, powerful and portable computer board having dimension of a credit card, developed by the Raspberry Pi Foundation. Raspberry pi is a central processing unit of our landslide detection system. We have used a third generation the Raspberry Pi 3model B and raspbian operating system. The selected Raspberry Pi 3 model B includes 64 bit Quad Core 1.2GHz Broadcom BCM2837 processor and 1GB RAM.
- GSM modem: GSM modem is a wireless modem that uses a SIM card and operates over a cellular network. GSM modem is connected to raspberry PI through a serial cable. GSM modem is programmed using AT commands for Automatic SMS generation to send an alert message when a landslide occurs. Here GSM modem is programmed to send a landslide alert message as Flash SMS.

III. METHODOLOGY

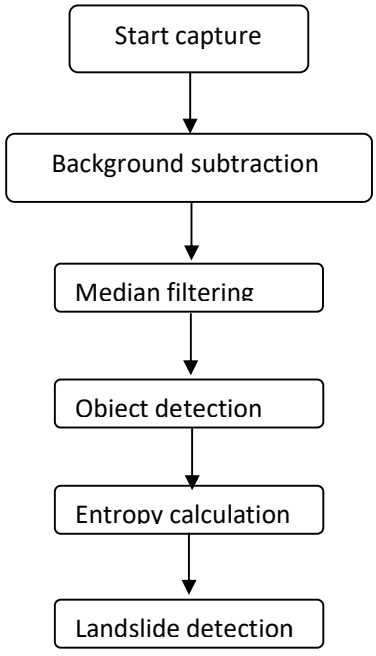

Figure 2: Flow diagram of methodology

A. Background Subtraction

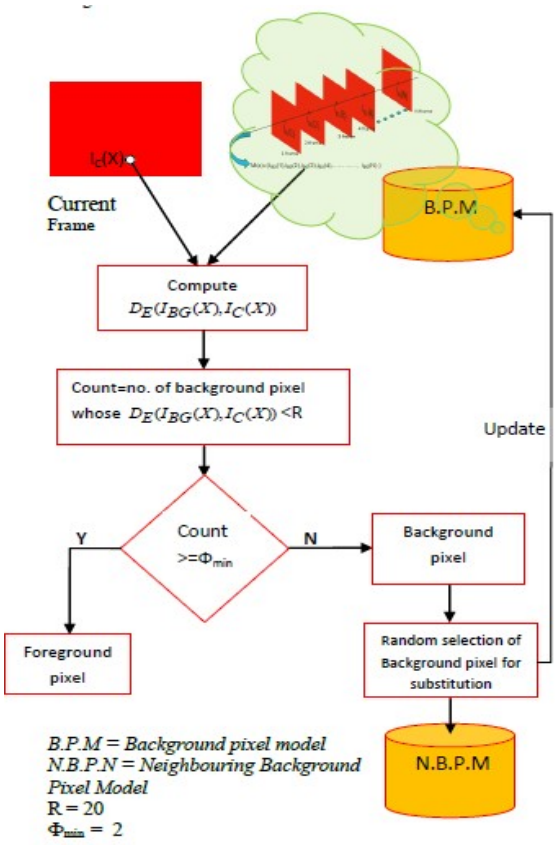

Figure 3: Flow Diagram of Visual Background Extractor

Background subtraction is the second step of the flow diagram of methodology shown in figure 2. Background subtraction detects moving objects from static cameras. Here we have used Visual Background Extractor (ViBe) [9]. This method, has high accuracy, requires less memory space and is time efficient. The Flow diagram of Visual Background Extractor (Vibe) is shown in Figure. 3. The ViBe is pixel based background subtraction approach. Here each background pixel model is set of previously observed background pixel values instead of estimating probability density function like in GMM based approach. Each pixel value is compared to closest value of its background pixel model. Background pixel models are initialized by a single frame using pixel values of their spatial neighborhood. Consequently Vibe starts background subtraction from second frames. The Vibe can handle sudden illumination changes. Vibe has a unique property of spatial diffusion where each background pixel updates one of its spatial neighbouring background pixel model chosen randomly. This feature makes Vibe to handle small camera movement and slowly evolving structure.

Each background pixel model is updated with each new incoming frame by using a conservative update policy. This update policy has 3 important properties

1) Memory less update policy
2) Random time sub sampling
3) Spatial temporal update policy

B. Median Filtering

Outcomes of visual Background extractor are binary images which contain salt and pepper type noise. This type of noise can be effectively removed by using a median filtering . We propose a fast median filtering algorithm for smoothing the output of background subtraction. The median filter is the well known method in image processing for reducing the impulsive noise. However, it has a problem that execution speed is slow because it uses a sorting algorithm to obtain the median value. So, a fast median filtering algorithms has been discussed here for real time landslide detection.

Median filter is a nonlinear filter which replaces value of each pixel by median, of all pixel values in its spatial neighbourhood. For computation of median filtering, pixel values covered by kernel, are sorted. If the kernel size is odd, then the median is just the middle value of a sorted array. For even size kernel, median is average of two middle values. There are various sorting algorithms like quick sort and heap sort whose time complexity can have significant variations, depending on the kernel size and can increase with the kernel size. Each time, kernel is moved to cover new pixel values and old values from kernel are discarded. Now new pixel values in the kernel are sorted into numerical order to compute median value. This process is repeated until whole image is covered. This is very time inefficient.

We have proposed a new implementation of median filtering where we never have to re-sort the running kernel; the operations are designed so that the array will remain sorted after each deletion and addition. All pixel values of the window are not discarded and also sorting algorithms are not used in every time. Pseudo code of the proposed median filtering algorithm is shown in **Algorithm: proposed median filtering algorithm** for kernel slide horizontally. Since insertion and deletion operation of pixel values are fast in a linked list, therefore we have used linked list data structure.

Here we have used parallel processing to compute median filtering. Since our used raspberry pi 3 model B has 4 cores, video frames are subdivided into 4 equal segments. We divide the 340x480 frame size into 4 equal parts and each of 4 segments is given to each core. Each core performs median filtering simultaneously to reduce time complexity. Now the output of all core are recombined to get final result. For median filtering computation, the following steps are followed:

- First time, linked list is sorted using pixel values in the kernel.
- In next time (window slides to the next location), from the sorted linked list, delete node corresponding to the first row or first column depending on whether video frame is scanned horizontally or vertically as shown in figure 4 and figure 5.
- For all new value in the window to be added, use a linear search to find their position in the sorted array. Add the new values in those positions.
- Note that the linked list is still sorted. The median will be in the middle of the linked list (assuming window size is odd) or the average of two median values (window size is even).

Algorithm: proposed median filtering algorithm

Input: Image X of size M×N, kernel size n
Output: Image Y of the same size as X
Initialize Linked list L with special neighbourhood of $X_{1,1}$
for i= 1 to M do
for j= 1to N do
for k= -n/2 to n/2 do
Remove $X_{i+k,j-n/2}$ from Linked list L
Add $X_{i+k,j+n/2}$ to L using lenear search
end for
$Y_{i,j}$ ← median (L)
end for
end for

In a brute-force way, the time complexity per pixel is $O(n^2 \log n)$ when applying a quick sort to a median filter with a window size of n. As shown in pseudo code of our proposed algorithm, for kernel size of **n×n**, n addition and n deletion are required to update the linked list. So our proposed method has time complexity of $O(n)$ and also space complexity of $O(n)$ per pixel for kernel size **n×n**. This method is easy to implement in hardware

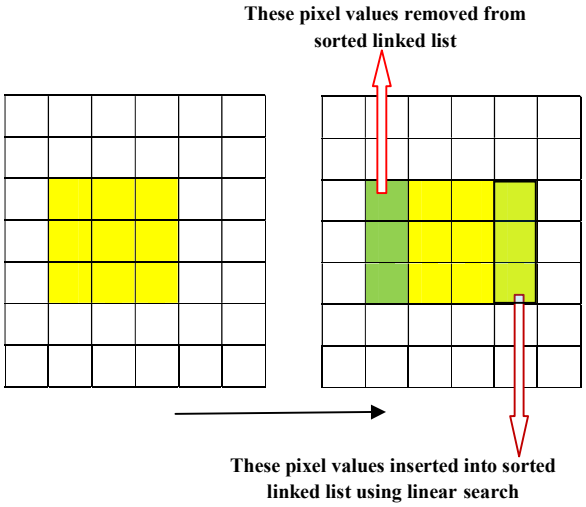

Figure 4: Removal of linked list node when window slide horizontally

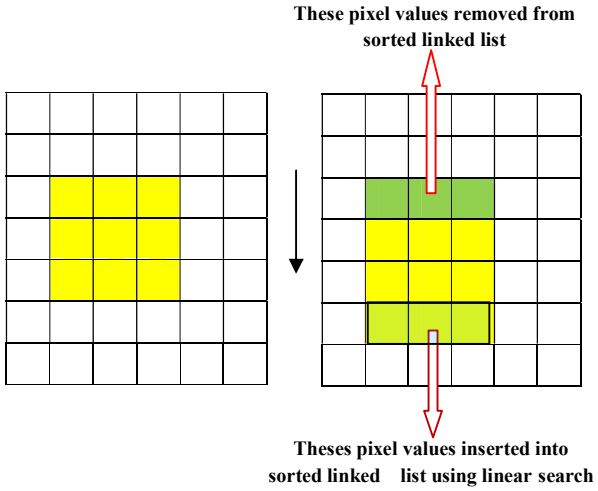

Figure 5: Removal of linked list node when window slide vertically

.

C. Object Detection

Result of median filtering is a binary image where all white pixels belong to the moving objects. These white pixels can be grouped by using pixel connectivity process where pixels having similar intensity values and connected in some way to each other form a group. Now these groups can be labeled by assigning grey values to each group.This labeling technique is called connected component labeling. There are various proposed algorithms for connected component labeling. For this work we have chosen one pass algorithm because it requires

less computational time. Now these labeled groups belong to moving objects.

D. Entropy Calculation

After background subtraction and noise removal using median filtering, landslide detection is possible but still there is need of a threshold to determine whether it is down slope motion of large area i.e. landslide or small object's motion. Entropy [14] is used to measure the amount of disorder or randomness in a frame. As shown in figure 6 (a), the frame is perfectly ordered so its entropy is zero. Figure 6(b) shows a disordered frame so its entropy is higher than figure 6 (a). Finally frame in figure 6(c) is highly disordered so its entropy is highest. Consequently entropy thresholding can be used to find landslide movement. The Entropy of a frame can be calculated by the following formula

$$H = -\sum_{k=1}^{n} P_k \log_2(P_k)$$

k is no. of gray levels and P_k is probability of gray level k. For our work, this entropy threshold is set to 0.8.

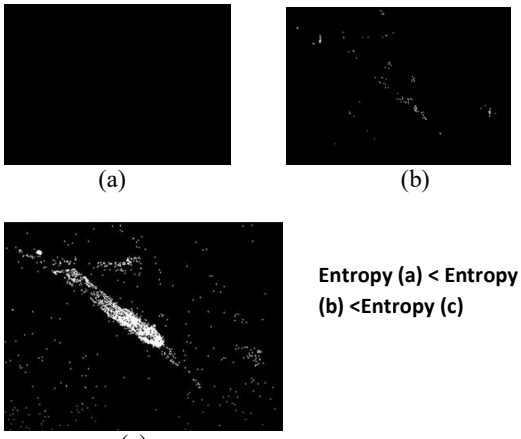

Figure 6: Illustration of Entropy in different frame

IV. RESULTS

All the operations, we have discussed in the methodology section, are applied on each individual frame of a video stream. Here we have used openCV library for accessing video frames and for changing frame rate. We have developed a GUI for this work whose screenshot is shown in figure 7. There are two fields in GUI first is ROI (region of interest) and second is window size of median filtering. ROI is used to select a portion of live view on which the proposed algorithm is performed. ROI is can be defined by regular polygon or freestyle.

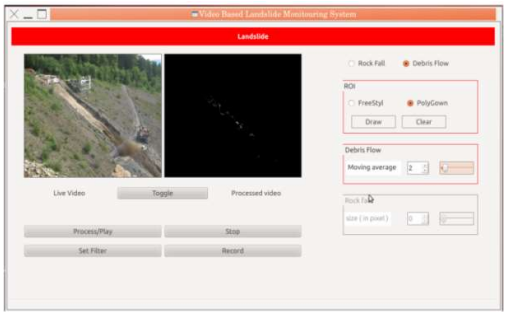

Figure 7: Snapshot of developed GUI

We have tested our proposed algorithm on prerecorded footage of debris flow landslide. The footage is of 52 seconds and frame size is 340x480. Actual landslide occurs after 7 second and our proposed landslide detection system detects it at 7 second and generates an alarm message. Our proposed algorithm works similar on the video if frame rate of the video increases upto 40 fr/seconds. This algorithm will work the same in case of live streaming from the web cam.

Result of the proposed algorithm is shown in fig 8. As a landslide occurs, a message "LANDSLIDE DETECTION" is flashed in red colour at top most window and test SMS is sent to the local authority.

For this result, we have selected a third generation of Raspberry Pi 3 model B and raspbian operating system. Raspberry Pi 3 model B includes 64 bit Quad Core 1.2GHz Broadcom BCM2837 processor and 1GB RAM. Above mentioned raspberry Pi with a USB web-camera of 5MP and a GSM modem is hardware components used in the proposed system.

Figure 8: Result of developed algorithm

V. CONCLUSION & FETURE WORK

The research work has been introduced a landslide monitoring and detection system which detect landslide in real time. Hare, we have used a Raspberry Pi 3 B and webcam which requires less power and is very economical therefore it is suitable to use in remote areas. Our proposed

system provides an innovative and economical system for landslide detection. When landslide occurs our system can detect the event and can inform concerned authority by real time SMS text message. Concerned authority can take necessary steps to divert the traffic and to protect property and lives living in landslide vulnerable areas. We have proposed a fast implementation method for median filtering using linked list data structure which has time complexity of $O(\sqrt{n})$. In the future, we can incorporate deep learning and convolution neural network to detect landslide.

VI. REFERENCES

[1] Margottini, C.; Canuti, P.; Sassa K. Landslide Science and Practice. *Proc. of the Second World Landslide Forum, Rome, Italy,* 2011, Vol. 2.

[2] Chaturvedi, P., Jaiswal, B., Sharma, S., & Tyagi, N. Instrumentation Based Dynamics Study of Tangni Landslide near Chamoli, Uttrakhand. *International Journal of Research in Advent Technology*, Vol.2, No.10, October 2014 E-ISSN: 2321-9637

[3] Hung-Ming Kao; Hsuan Ren; Chao-Shing Lee; YenLiang Chen; Yen-Shuo Lin and Yeng Su. "Monitoring Debris Flows Using Spatial Filtering and Entropy Determination Approaches", Terrestrial, Atmospheric & Oceanic Sciences, 2013.

[4] Lynn, M. and Bobrowsky, P. (2008). The landslide handbook - A guide to understanding landslides, Reston, Virginia, U.S. Geological Survey

[5] Haritaoglu, I., Harwood, D. & Davis, L.S., (2000). " W4: real-time surveillance of people and their activities". IEEE Trans. Pattern Anal. Mach. Intell. 22, pp 809–830.

[6] Singer, J. and Thuro, K. (2006). "Development of continuous 3D-monitoring system for unstable slopes using Time Domain Reflectometry", Proceedings of the 10th IAEG International Congress, Nottingham, UK

[7] Horn, B. K. P. and B. G. Schunck, 1981: Determining optical flow. Artif. Intell., 17, 185-203.

[8] Stauffer, C. and W. E. L. Grimson, 1999: Adaptive background mixture models for real-time tracking.IEEE Comput. Soc. Conf. Comput. Vis. Pattern Recogn.,2, 246-252,

[9] Barnich, O, and M Van Droogenbroeck. "ViBe: A Universal Background Subtraction Algorithm for Video Sequences", IEEE Transactions on Image Processing, 2011.

[10] Guohong Liu, Wenming Guo, "Application of improved arthmetic of median filterin denoising, Computer Engineering and Applications," 2010, vol.46, no.10, pp.187-189

[11] Xiaokai Wang, Feng Li, "Improved adaptive median filtering," Computer Engineering and Applications, 2010, vol.46, no. 3, pp. 175-176

[12] Qinghua Huang, Heqin Zhou, Huanqing Feng, "A fast and effective algorithm of pulse noise filtering for imaging data" Computer Engineering and Applications, 2002, no. 17, pp. 113- 114, 210.

[13] Pun, T. (1981). Entropic thresholding, a new approach. Computer Graphics and Image Processing, 16(3), 210-239

[14] Shannon, C. E., & Weaver, W. (1963).University of Illinois Press Urbana, IL.sec.

Proceedings of the Fourth International Conference on Communication and Electronics Systems (ICCES 2019)
IEEE Conference Record # 45898; IEEE Xplore ISBN: 978-1-7281-1261-9

A Survey of Recent Advances in Crowd Density Estimation using Image Processing

Komal R Ahuja
(Electronics and Tele Comm.)
V.E.S. Institute of Technology
Mumbai, India
Email: 2017komal.ahuja@ves.ac.in

Nadir N. Charniya
Professor, Electronics and Tele Comm.
V.E.S. Institute of Technology
Mumbai, India
Email: nadir.charniya@ves.ac.in

Abstract- Crowd analysis is an essential topic of research in artificial intelligence. There are several applications on crowd analysis, such as, environmental management, urban planning and public safety. This paper presents review of different methodologies those have been implemented for estimating crowd. This paper covers several methods of crowd density estimation, such as, image processing techniques, machine learning and deep learning based technique, and smartphone based technique.

Keywords—Image processing methods, direct method, indirect method, location based smartphones for crowd counting, machine learning and deep learning based crowd classification.

I. INTRODUCTION

With the increase in human population, crowd gathering takes place at many public places such as rail, maglev, metro, stadium, marathon etc. So there is a risk of stampedes. Various incidents took place because of overcrowd such as in 2005, more than 640 people died in Religious procession at Baghdad, In 2013, 115 people died in Hindu Festival at Datia District, in 2014, during Dussehra festival in India around 32 people died and in 2017, 23 people died at Elphinston Road Mumbai [1], [2]. Due to such incidents, there is a requirement of some efficient and effective crowd density estimation and crowd management techniques. Estimating crowd density is of great importance, as it can prevent stampede. Traditionally, human operators were required for continuously monitoring the CCTV cameras installed for identifying any suspicious or unusual action of the crowd. Analyzing and observing such huge information originating from different view-points and various angles is critical job for the human operators and would be costly. Also, if a very small team is appointed for crowd monitoring task then it may lead to improper analysis and they may miss any unusual event within the crowd. For better accuracy of crowd density estimation advanced computer vision techniques are being deployed recently to automate crowd monitoring system. This would reduce the need of human operator significantly and hence the cost involved in employing the security persons would also reduce. Various methods adopted for crowd density estimation are reviewed in this paper.

Conventional Image Processing have been widely used for crowd density estimation is studied in this paper. It involves two approaches first is direct approach which is also known as detection based method in which individuals are directly segmented from the crowded scene and then number of people are detected. The other approach is indirect based which is also knows as feature based method in which features are learned by using some learning algorithm. The other method is by using location based smartphone for people counting is reviewed in this paper. One more method is by using Machine Learning and Deep Learning algorithm to classify images as low crowd, high crowd, moderate crowd, extremely dense crowd. In deep learning, various algorithms are available such as Artificial Neural Network (ANN), Convolutional Neural Network (CNN), and Recurrent Neural Network (RNN).

II. RELATED WORK

[1] proposed two approaches direct based and indirect based. Both approaches have some limitations. Various methods have been proposed by many researchers for crowd counting in public areas. [17] proposed ROI (Region of Interest) based crowd counting This method is based on human detection or any regression method. The main important step in this method is background subtraction and then mapping the foreground shape with the human shape. This method is not suitable for highly dense crowd or in occluded area. Various other researchers implemented

Markov Random Field (MRF) for foreground subtraction [28]. Recently computer vision techniques are adopted for crowd analysis.

III. Crowd density estimation using Conventional Image Processing Techniques

Crowd density estimation using conventional image processing technique is categorized as: Direct and indirect approaches [1].

A. Direct approach for crowd density estimation

Direct approach aims to estimate number of people by segmenting each individual from images and it also locate their position. This method is applicable only in low crowd scene. In high crowd scenario or in high occlusion scene, detecting each individual is difficult task. This approach is further improved by using part based detection such as head detector and omega shape detector which is formed by head and shoulder, pedestrian detector. However, this part based detection is not suitable for very high crowd. Further Direct approach is of two types Model based approach and Trajectory based approach [1].

In model based method each individual is segmented and counted with the help of some model or appearance of human shape. This method is used for counting problem. In trajectory based approach, every pedestrians motion is tracked using interest based points. After detecting peoples position counting can be carried out.

B. Indirect approach for crowd density estimation

Indirect approach aims to extract local and global features from images. As detecting features is much easier task then detecting people in high crowd situations. In the literature foreground and background subtraction technique were used to estimate crowd and edge based features was extracted for crowd analysis. However, foreground and background subtraction is very difficult in highly crowded areas are the limitations of this approach. Edges like features are incorrect in complicated background and occluded areas. [1], [15]. To overcome such problems more methods are proposed and they are discussed in the succeeding subsections.

a. Pixel Based Method

Pixel based method [1] extract very local features to estimate crowd. The first step in pixel based is to remove background by using some background subtraction techniques; the next step is to extract features by using edge detection method. These features are the input to back propagation neural network. This method is 100% accurate in very low to low crowd situations. However, due to high occlusion false information could be captured by this pixel based method.

b. Texture based method

Texture feature extraction is proposed by many researchers as it is highly efficient method for feature extraction which is used for many image processing applications. Texture gives the detailed information about all the regions of an image. Texture extraction is more robust than pixel based method. Marana proposed images of low crowd exhibit coarse pattern while images of high crowd exhibit fine pattern. In their work, researchers proposed Gray-Level Co-occurrence Matrix (GLCM) features for crowd density estimation. Four GLCM features, such as, Contrast, Energy, Homogeneity, and Entropy for estimating crowd were extracted. These features were applied to the input of neural network for crowd classification. However, this method needs more time for crowd classification. The other recent methods are based on Local Binary Pattern (LBP) and Gabor Features [4], [10].

1. Local Binary Pattern

LBPs are texture descriptor proposed by Ojala et al [5] It simply describes the local information. The calculation of LBP involves the subsequent steps. The first step is to convert the color image into the gray scale image. Then the gray scaled pixels are computed for 8 neighborhood pixels with the central pixel. [3], [4]. If the intensity of the pixel to be converted to grayscale is greater or equal to its neighbour's pixel value than it is set 1 or else, it is set to 0. A similar procedure is done for all the pixels in the image to generate a gray image.

LBP is defined as follows: [4]

$$\text{LBP} = \sum_{i=0}^{P-1} s(P^i - P^c)\, 2^i \qquad (1)$$

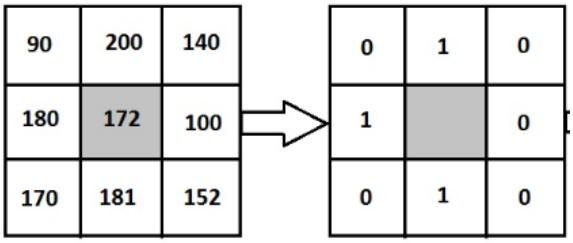

Fig. 1. Converting into a gray scale image in LBP [5]

where P is the number of neighbors; P^C denotes the central pixel; P^I denotes the other pixel around P^C. S(x) is defined as:[6]

$$S(x) = \begin{cases} 1, & x \geq 0 \\ 0, & x < 0 \end{cases} \quad (2)$$

The next step in calculation of LBP is to take any neighbourhood pixel value and traversing the LBP code in clockwise or anticlockwise. This will result into 8-bit binary pattern, [7]

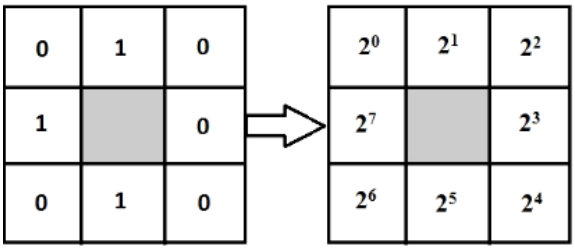

Fig. 2. Converting grayscale into decimal representation in LBP [5]

The final step in LBP is converting the binary into decimal number. This value is stored in output array.

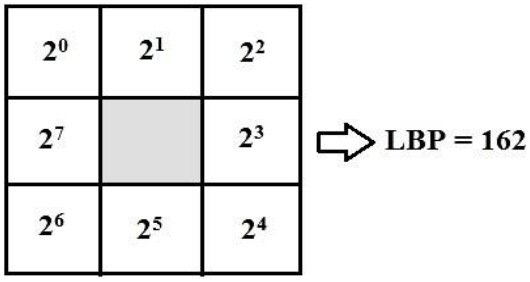

Fig. 3. Converting binary to decimal and storing the LBP value in output array [5]

The process of converting to grayscale and obtaining the output decimal value in the LBP array is repeated for each pixel in the image. Fig. 4 shows the LBP of an image.

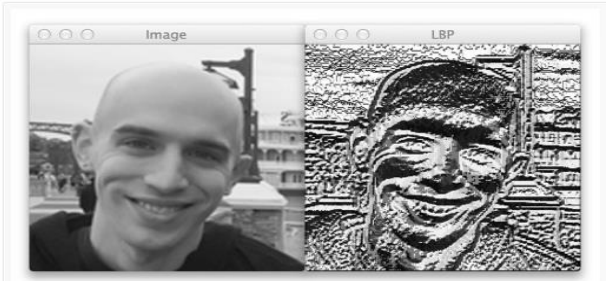

Fig. 4. Original image (left) and its LBP (right) [5]

Finally, the histogram is computed from the output array. The patterns obtained from a 3 x 3 neighbourhood are 2 ^ 8 = 256. Thus the final feature vector is 256 bin histogram of LBP 2D array. The advantage of using LBP in image processing technique is that it provides detailed information of the images.

2. Gabor Features

Gabor features find their uses in image classification, image segmentation. Gabor features are represented by using different scale and different orientations. Gabor filter are set of linear filter which are efficiently employed for edge detection and texture feature extraction. Gabor filters are those filters which allows certain range of frequencies and rejects the unwanted frequencies. The images are filtered by gabor filter with a specific frequency and orientation and feature vector is created. This feature vector is input to segmentation or classification problem. A 2D gabor filter is a sinusoidal Gaussian filter with a preferred frequency and orientation. Two-Dimensional gabor filter is as given in the Fig. 5.

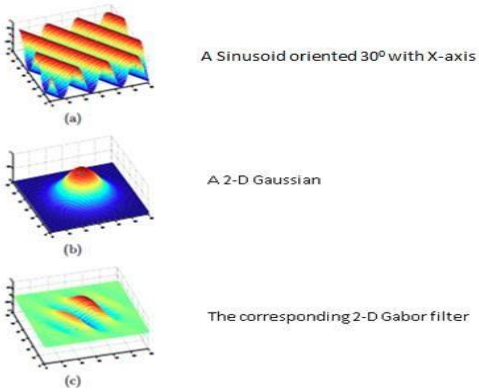

Fig. 5. Two-Dimensional Gabor filter

Two-dimensional Log-Gabor filter involves radial and angular filter components. The frequency

response of a 2-D Log-Gabor filter is given in eq.(3)[9]

$$G(r,\theta) = \exp\left(\frac{-[\ln(\frac{r}{f_o})]^2}{2[\ln(\frac{\sigma_r}{f_o})]^2}\right) \exp\left(\frac{-(\theta-\theta_0)^2}{2{\sigma_\theta}^2}\right) \quad (3)$$

where (r, θ) represents the polar coordinates, the central frequency of the filter is given by f_0, the orientation of filter is denoted by θ_0. σ_r and σ_θ are the scale and angular bandwidths respectively. By using different values of frequency and orientation, a bank of Gabor filter is created. Then each feature is convolved with discrete time Fourier transform of the input image. The two features are extracted using Gabor are:

Local Energy = $\sum i \sum j |G(i,j)|2$ (4)
Mean Amplitude = $\sum i \sum j |G(i,j)|$ (5)

List of different Gabor filters are obtained by using different values of frequency and orientations.

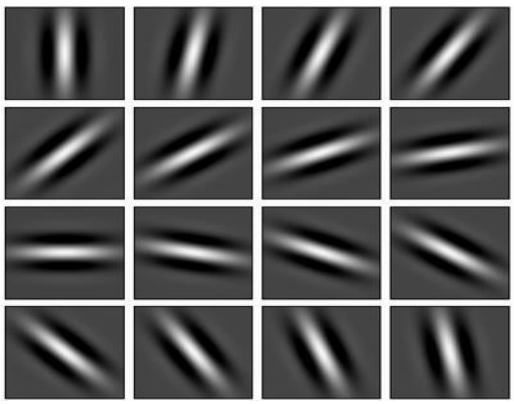

Fig. 6 A bank of 16 Gabor filter [8]

3. Gray Level Co-occurrence Matrix

GLCM is a mathematical and statistical tool for image texture feature analysis. It gives the relationship between the adjacent pixels. The main image texture features used for crowd density estimation are contrast, energy, entropy, homogeneity. GLCM takes the relation between two pixels reference pixel and neighbour pixels. GLCM is prepared by using Gray pixel values and it will calculate how often the pixel occurs horizontally, vertically, and diagonally. The GLCM example is given below [11], [12], [13].

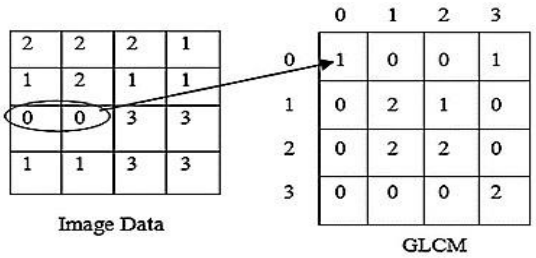

Fig.7. GLCM example

The four important features are given by the equations (3) to (6) [11]

Contrast: Contrast estimates the magnitude of intensity between a pixel and its neighboring pixel for the entire image.

The formula for contrast is gives below:

Contrast = $-\sum_i\sum_j (i-j)^2 P[i,j]$ (6)

Energy: restores the addition of squared components in the GLCM.

The formula for Energy is given below:

Energy = $-\sum_i\sum_j P^2[i,j]$ (7)

Entropy: Entropy provides the necessary information of images which are requires for various image compression techniques.

The formula is given as:

Entropy = $-\sum_i\sum_j P[i,j] log P[i,j]$ (8)

Homogeneity: Gives the value which provides the information of closeness distribution of all elements of GLCM with the GLCM diagonal elements The formula is given below:

Homogeneity = $\sum_i \sum_j \frac{P[i,j]}{1+(i-j)^2}$ (9)

IV. Crowd Monitoring Through Location Based Smart phones Wi-Fi Probes

In this method sensing approach is proposed using phones in which people will participate and share their location. This method proposed the moving speed of individuals in the crowd is the main important factor for crowd density estimation. To determine the crowd, the exact location of people is an important issue. There are two main approaches for obtaining the location of smartphones In-network localization and In-phone localization. In-network localization method explains the fact that at every time the smart phone is

connected to the base station in the network. The entire information about which phone is connected to which base station is stored in the database and automatically it updates the databases. As the location of all the base stations are known, estimation of position of smart phone can be localized and hence location of people can be obtained. From this information people count can be estimated [26] [27] [28].

The other method is by using Wi-Fi signals. With the growing technology, Wi-Fi enabled smartphones are used by every individual. Smartphones send request periodically for connecting to the existing network. This method is applied for counting number of individuals by counting the devices who share the network.

V. Crowd density estimation using Machine Learning and Deep Learning

Machine Learning and Deep Learning are recent techniques for crowd density estimation. They involve the following steps shown in fig.8. The first step is to acquire features for various density levels using several feature extraction algorithms and the next step is use classifier for classification into various density levels such as low crowd, high crowd, moderate crowd and extremely dense crowd.

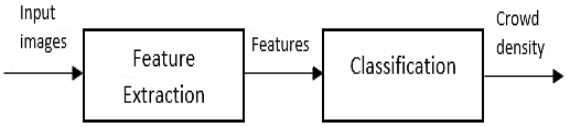

Fig. 8. Machine Learning Architecture

In Deep Learning feature extraction is carried out by hidden layer and it compute feature vector. This feature vector will help to compute classification. Convolutional Neural Network is popular Deep Learning algorithm for many image processing applications. CNN consist of input layer, output layer, and many hidden layers as shown in the Figure 9. CNN receives data through input layers and sends the data to hidden layers. Each hidden layer consists of neurons. The final output layer is a dense layer also known as fully-connected layer which performs deep learning classification task. Thus, the network calculates output by adjusting weights and bias. Hidden layers are Convolution Layer, Pooling layer and many nonlinear layers,

Each convolution layer contains many kernels and these kernels are convolved with input images and generate corresponding feature map.

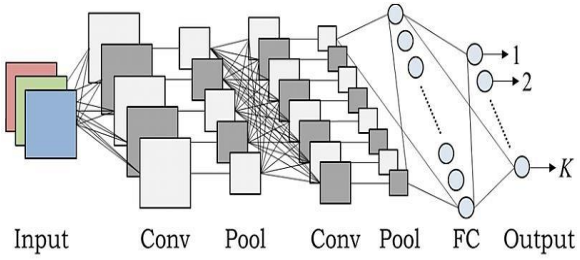

Fig. 9. Deep Learning Architecture [16]

Assume the input I is (*n x n)* matrix, convolution kernel k is a (*k x k)* matrix, bias is b_1, then we could get a (*n-k+1*) *x* (*n-k+1*) feature map after convolution. The computation is shown in Equation [14].

$$F_{ij} = S(\sum_{i=1}^{k} \sum_{j=1}^{k} (I_{ij} K_{ij} + b_1)) \qquad (10)$$

where F_{ij} is feature matrix and S is motivation function. In convolution, input images are passed through a set of convolutional filters from which various features are calculated.
Consider the following (5x5) image matrix whose pixel values are only 0 and 1

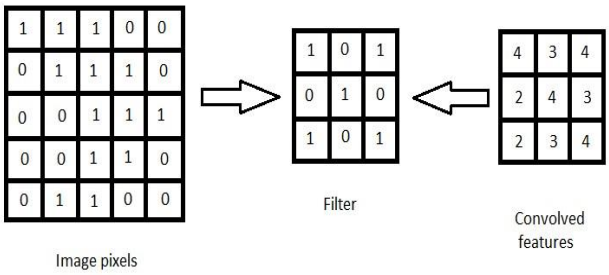

Fig.10. Convolution Example

To detect patterns, compute the dot product by sliding matrix over the image.

In CNN architecture, the Pooling layer is placed between two successive convolutions. Pooling layer reduces the dimensions of the features of input images. It is of two types: One is Max pooling and other is average Pooling. In Max Pooling operation it accepts the largest value from the region and in average Pooling, it takes the average of the region.

The last layer is Fully Connected layer. In this layer, the neurons have complete connection to all the activations from the previous layers. The output of

Fully Connected layer is K vector in which K represents the number of classes depending upon the classification task.

VI. Comparison Of Various Methods For Crowd Density Estimation [1].

Various methods for crowd density estimation have been compared in Table I.

TABLE I. DIFFERENT METHODS FOR CROWD DENSITY ESTIMATION

Methods	Objective	Limitation
Direct Method		
Model based method	Segmenting people from crowded scene using some model or appearance of human shape and counting them.	Accurate results in low or moderate crowd but less accurate in dense crowd situation
Trajectory based method	Individual's position is tracked using some interest point and counting is carried out.	It gives good results in sparse crowd but when the crowd is occluded then this method is not reliable.
Indirect Method		
Pixel based method	Determination of foreground pixels	It is simple but gives false result in highly occluded and cluttered areas. Sensitive to light changes
Texture based method	Explores detailed information of the image patches.	Detecting individual in crowded scene is easier in this method but detecting texture based features is time consuming
Smartphone based approach	Counting is carried out by detecting smartphones position or by localizing wi-fi signals.	This method is not suitable when the peoples cell phones are not working or it are switched off.
Deep Learning and Machine Learning based approach	It is neural networks training based approach and is data dependent.	Accurate but time consuming when the dataset required is too large.

VII. Conclusion And Future Scope

Crowd analysis such as crowd management, people counting and estimating crowd density is an important problem for public security. Different computer vision techniques or methodologies that are recently adopted for crowd density estimation are reviewed in this paper. Different methods used for crowd density estimation are an image processing based technique that is further classified into Direct method based on model and trajectory and Indirect method based on pixel counting and texture based analysis. Machine Learning and Deep Learning based methods are based on training of neural network models those are accurate but needs exhaustive training on data. Smartphone based method needs the cell phones of the people in the crowd active so as to be detected by Wi-Fi signal. Crowd density estimation on public gathering is demanding task to prevent stampede. By estimating crowd any unusual and abnormal activity or action within the crowd can be identified. These techniques of crowd monitoring can be used to estimate the number of people in railway compartments so that the people on the platform will come to know about the crowd density in the compartment before the train arrives. This would help the passengers to board the suitable low or medium crowd compartment.

References

[1] Saleh, Sami Abdulla Mohsen, Shahrel Azmin Suandi, and Haidi Ibrahim. "Recent survey on crowd density estimation and counting for visual surveillance." Engineering Applications of Artificial Intelligence 41, 2015: 103-114.

[2] Gad, Ahmed F., Ahmed M. Hamad, and Khalid M. Amin. "Crowd density estimation using multiple features categories and multiple regression models." 2017 12th International Conference on Computer Engineering and Systems (ICCES). IEEE, 2017

[3] Lamba, Sonu, and Neeta Nain. "A Large Scale Crowd Density Classification Using Spatio-Temporal Local Binary Pattern.", 13th International Conference on Signal-Image Technology & Internet-Based Systems.2017

[4] Wang, Zhe, et al. "Crowd density estimation based on local binary pattern co-occurrence matrix." IEEE International Conference on Multimedia and Expo Workshops. 2012.

[5] Local Binary Pattern (LBP) Available at https://www.pyimagesearch.com/2015/12/07/local-binary-patternswithpython-opencv/ accessed on January 2019

[6] Ma, Yan. "Number local binary pattern: An extended local binary pattern."International Conference on Wavelet Analysis and Pattern Recognition. IEEE, July 2011

[7] Meena, K., and A. Suruliandi. "Local binary patterns and its variants for face recognition." IEEE International Conference on Recent Trends in Information Technology (ICRTIT). 2011

[8] Gabor Features Available on https://medium.com/@anuj_shah/through-the-eyes-of-gabor-filter-17d1fdb3ac97 accessed on December 2018

[9] Pai, Abhilash K., A. K. Karunakar, and U. Raghavendra. "A novel crowd density estimation technique using local binary pattern and Gabor features." 14th IEEE International

Conference on Advanced Video and Signal Based Surveillance (AVSS). 2017.

[10] Wu, Xinyu, et al. "Crowd density estimation using texture analysis and learning." 2006 IEEE international conference on robotics and biomimetics. 2006.

[11] Eleyan, Alaa, and Hasan Demirel. "Co-occurrence matrix and its statistical features as a new approach for face recognition." Turkish Journal of Electrical Engineering & Computer Sciences 19.1, 2011: 97-107.

[12] Fagette, Antoine, et al. "Unsupervised dense crowd detection by multiscale texture analysis." Pattern Recognition Letters 44, 2014: 126-133.

[13] Saqib, Muhammad, Sultan Daud Khan, and Michael Blumenstein. "Texture-based feature mining for crowd density estimation: A study." IEEE International Conference on Image and Vision Computing New Zealand (IVCNZ). 2016.

[14] Pu, Shiliang, et al. "Estimation of crowd density in surveillance scenes based on deep convolutional neural network." Procedia computer science 111, 2017: 154-159.

[15] Sindagi, Vishwanath A., and Vishal M. Patel. "A survey of recent advances in cnn-based single image crowd counting and density estimation." Pattern Recognition Letters 107, 2018: 3-16.

[16] Deep Learning available at http://cs231n.github.io/convolutional-networks / accessed on March 2019

[17] Cao, Lijun, et al. "Large scale crowd analysis based on convolutional neural network." Pattern Recognition 48.10, 2015: 3016-3024.

[18] Zhang, Youmei, et al. "Multi-resolution attention convolutional neural network for crowd counting." Neurocomputing 329, 2019: 144-152.

[19] Hu, Yaocong, et al. "Dense crowd counting from still images with convolutional neural networks." Journal of Visual Communication and Image Representation 38, 2016: 530-539.

[20] Sindagi, Vishwanath A., and Vishal M. Patel. "Cnn-based cascaded multi-task learning of high-level prior and density estimation for crowd counting." 14th IEEE International Conference on Advanced Video and Signal Based Surveillance (AVSS). 2017.

[21] Fu, Min, et al. "Fast crowd density estimation with convolutional neural networks." Engineering Applications of Artificial Intelligence 43, 2015: 81-88.

[22] Sang, Jun, et al. "Improved Crowd Counting Method Based on Scale-adaptive Convolutional Neural Network." IEEE Access 2019.

[23] Li, Baiping, Xinyi Han, and Dongmei Wu. "Real-Time Crowd Density Estimation Based on Convolutional Neural Networks." IEEE International Conference on Intelligent Transportation, Big Data & Smart City (ICITBS). 2018.

[24] Saqib, Muhammad, et al. "Crowd Counting in Low-Resolution Crowded Scenes Using Region-Based Deep Convolutional Neural Networks." IEEE Access 2019: 35317-35329.

[25] Cho, Siu-Yeung, Tommy WS Chow, and Chi-Tat Leung. "A neural-based crowd estimation by hybrid global learning algorithm." IEEE Transactions on Systems, Man, and Cybernetics, Part B (Cybernetics) 29.4, 2009: 535-541.

[26] Yuan, Yaoxuan, et al. "Estimating crowd density in an RF-based dynamic environment." IEEE Sensors Journal 13.10, 2013: 3837-3845.

[27] Yuan, Yaoxuan, et al. "Estimating crowd density in an RF-based dynamic environment." IEEE Sensors Journal 13.10, 2013: 3837-3845.

[28] Tang, Xiaoyong, Bin Xiao, and Kenli Li. "Indoor crowd density estimation through mobile smartphone wi-fi probes." IEEE transactions on systems, man, and cybernetics: systems 99, 2018: 1-12.

[29] Wirz, Martin, et al. "Probing crowd density through smartphones in city-scale mass gatherings." EPJ Data Science 2.1, 2013.

[30] Gupta, Gaurangi, et al. "Device-Free Crowd Count Estimation using Passive UHF RFID Technology." IEEE Journal of Radio Frequency Identification, 2018.

Proceedings of the Fourth International Conference on Communication and Electronics Systems (ICCES 2019)
IEEE Conference Record # 45898; IEEE Xplore ISBN: 978-1-7281-1261-9

Smart City Management System using IoT with Deep Learning

Shubham Jain[1], Aman Jatain[2], Shalini Bhaskar[3]

Amity School of Engineering and Technology

Amity University Gurugram, Haryana, India

[1]shubham.sjain.jain@gmail.com, [2]amanjatainsingh@gmail.com, [3]sbbjaj@ggn.amity.edu

***Abstract*— The project aims to model implementation of an advanced Smart City system that consists of Smart Home equipped with security features, Smart Waste Management System and automated street lights. Because of the increasing instance of gun violence in the country as well as abroad, we have added the feature of detecting guns outdoors using neural networks, image classifier and object detection. The system is designed by merging the concept of the Internet of Things that control various components of the Smart City ranging from energy efficient Smart Home along with its security measures to identifying a gun from closed-circuit television (CCTV) footage to detect danger on streets of the city achieved by creating an image classifier by training a neural network. As there is no sensor currently available that can detect the presence of an object in a photo, an image classifier is used to detect guns in the photos taken by the CCTV camera.**

***Keywords*— Internet of Things (IoT), Deep Leaning, Smart City, Smart Home, Smart Waste Management System, Smart Streets, Intelligent CCTV, Object Detection, Neural Network, Supervised Learning, PyTorch.**

I. INTRODUCTION

Presently, even though devices can communicate to different machines by the power of IoT, they still don't natively have the ability to detect an object from the images captures by a camera (CCTV in case of Smart City) that can have a vast number of applications. The proposed system has the capability to detect a gun from an image acquired from closed-circuit television by processing it using a trained neural network as the implementation of deep learning and generate an alert to notify of potential gun violence. The paper attempts to fill the gap in IoT enabled devices and Object Detection, allowing more room for new possibilities and applications [20]. The implementation of Smart City [17] will contain three major components. First, one is the Smart Home that includes automated lighting that is configured in conjunction with light sensors (LDR, that is, light dependent resistor) and can also be controlled via a mobile application. Aside from lighting, the smart home monitors humidity and temperature and automatically switches on an air conditioner to regulate and maintain the preferred temperature conditions as per the user's needs.

Due to the rapid development of deep learning, a variety of research areas have achieved remarkable results that are accompanied by the continuous improvement of neural networks, their architectures, algorithms, computer vision has arrived at a new peak [3]. IoT has gained importance and popularity in recent years. But there is no sensor available that can directly detect an object in an environment. Object detection can play a vital role in this task and act as a sensor replacement. Object detection as one of the important applications in the field of computer vision has been the focus of research, and convolution neural network has made great progress in object detection. Object detection is developing from the single object recognition to multi-object recognition [13]. On the other hand, IoT plays the role of raising a high-risk alert. The smart home is also equipped with security features that can detect the presence of an intruder, take a photograph and send it via email to the owner as well as nearest concerned authorities. The second component is the Smart Waste Management System which enables Municipal Corporation to track waste, the location of bins, the release of any toxic gas and monitors waste better. The third feature of the smart city is Smart Streets that have efficient street lights which are integrated with an autonomous system that can help control traffic flow by sensing the traffic density. Along with the above-mentioned functionalities, motion sensors are also calibrated to turn on the street lights for a duration in the surrounding sectors on detecting motion in presence of low natural light, thereby resulting in a more efficient and energy-saving environment [16].

II. RELATED WORK

The Internet of Things (IoT) has acquired popularity in recent years and progresses towards becoming part of our everyday life in the near future. It contains objects of day-to-day life that are able to communicate closely with one another and users by equipping them with sensors and the ability to exploit the vast domain provided by the Internet [1]. They are optimized by specially configured protocols that make the communication process efficient and reduces the overall latency. By enabling access to a wide bouquet of devices such as, home appliances, smart wearables, surveillance cameras, healthcare systems, monitoring sensors, actuators, displays, vehicles, and many more.

Machine Learning is a method of teaching computer something by feeding a large amount of data into it. Image classifier is basically an algorithm created using neural network and deep learning to detect features and objects in images and classify them into categories accordingly. We can teach our computer to see things using image classifier. We first train it on images whose category is known and then export the trained classifier as an application. To ensure the classifier is good at generalization and detecting objects in images it hasn't previously encountered, image augmentation and dropout are used. A more robust classifier is created by training it on flipped, cropped and rotated images. In this project, we are integrating Image Classifier with IoT to create a Smart City Management System with features for gun detection and violence control. With the increasing instances of gun-related violence in the country and abroad, it is important to detect such mishaps before they can take place. For that, it is important that the usual delay involved in manual surveillance is eliminated. That can be done by replacing human eyes with artificial intelligence. As soon as an image is captured by the CCTV surveillance camera, it is sent to the image classifier which determines whether or not the image contains a gun. If it does, a high alert is sent to the authority. Otherwise, the image is discarded.

Some of the Convolutional Neural Network models are AlexNet, ResNet, and Vgg etc. These models are several layers deep and the pre-trained models can be suited to any given project by simply replacing its classifier or last layer. Then,

instead of training the whole network, only the classifier needs to be trained. The parameters of the classier are chosen to best suit the needs of the application. This type of learning is called "Transfer Learning" as a trained model is used to detect features and those features are then used to train the classifier. Extensive research has been done in the field of deep learning, object detection and computer vision. It ranges from detecting anomalies in red blood cells to detecting the species of flower via a mobile phone using a simple app. The level of training and testing done is according to its application. Deep Learning and Home/City automation have never been combined at a large scale even though they are perfectly suited for each other. A large amount of manual labour is employed currently that can be utilized more efficiently in other areas, for example in actual gun control, if the detection part is automated.

Clement et al. (2017) [23] in their Service-Oriented Reference for Smart City discusses the trends of shifting existing cities into IoT enabled smart cities with the objective of creating an autonomous and integrated system by bringing together the technology of different domains. They also mention the extensiveness of cities and propose a service-oriented architecture that binds different aspects of the smart city such as intelligent traffic management, smart grids and autonomous vehicles managed by smarter versions. It further highlights the critical integration between environmental factors, logistics, infrastructure and the human layer to provide a concrete platform.

Betis et al. (2018) [15] mentions the expected increasing number and type of services provided for citizens so as to achieve goals such as energy saving, sustainability and quality of life. It suggests that upgrading a city's organization doesn't merely include infrastructure, it rather requires drastic changes and large-scale implementable innovations that include relevant new technologies. It addresses the issues of smart/sustainable energy systems (smart grids), e-health, social factors and general involvement of citizens. It supports the argument that smart city paradigm can be achieved with local government, industrial developers and non-governmental organizations (NGOs) working together towards a common goal.

Li et al. (2012) [11] describes the principle and framework by suggesting the use of IoT protocols for Machine-to-Machine (M2M) communication in coordination with sensor network that can include infrared sensors, GPS, Radio Frequency Identification (RFID) and other devices by connecting them to the internet or mobile telecom network. It proposes a multi-layer framework that consists of a sensing layer, network layer and application layer.

The sensing layer mainly realizes physical information collection from the real-world which is then converted to digital information that can further be used to process and analyse data. Since objects themselves do not have the capability to communicate, sensors, executors and intelligent devices through RFID can interchange information utilizing communication module in the communication sub-layer. The network layer includes a variety of wireless networks and cable-connected gateway providing access to the core network and mainly realizing bidirectional transmission, route and control of sensor layer data and relevant information. The application layer provides support for sub-layers and kinds of practical IoT applications with the ability to interface between industrial and public domains having a vast number of applications.

Brand et al. (2018) [22] briefed that a smart city should be an open platform where the city is willing to share experience and resources are planned or available in an efficient manner. The smart city initiative can be served as a collaboration platform for the global community of professionals, academia and local government to overcome the challenges associated with IoT, big data and related technologies. It presents the use of smarter protocols for communication and the pressing social and ethical issues regarding the development of Artificial Intelligence and Autonomous Systems. The IEEE can provide solutions for both technical and ethical standards that transcend technology of different domains such as Big Data, IoT, Cyber Security, Deep Learning and many such more into an integrated system where devices can closely communicate in real-time.

Darbari et al. (2015) [10] in their Intelligent Traffic Monitoring Using Internet of Things (IoT) with Semantic Web describes the need for an intelligent traffic monitoring system due to the sudden rise in vehicle demand and population resulting in heavy traffic especially on certain routes and hence, the need to control them. It suggests that this objective can be achieved by Hierarchical Cluster Analysis based on the assumption that every object in the entire universe is associated with some information that can be used to help in forming clusters. Web services can be used as a medium to communicate between heterogeneous environments. XML can be customized accommodating special tags for spatial locations and sensor networks. Fuzzy logic can be used to implement the decision-making aspect of traffic monitoring by Fuzzy Inference System to dynamically allocate traffic light timers to manage the flow of the same more effectively thereby resulting in smarter management of streets in the smart city and significant reduction in heavy traffic that has increased over recent years.

Zhao et al. (2017) [12] in their Object Detection with Deep Learning mentions the close relationship of object detection with image understanding and video analysis which has attracted research attention in recent years. The traditional object detection methods are based on selective and limited features that have relatively rigid architecture thereby not being flexible enough to be able to learn new semantic. Deep learning can be used to train the neural networks that permit detection of deeper features using classifiers and usage of more powerful tools. The focus on generic object detection architectures with some modifications to improve the performance of detection classifiers is also suggested. It has several relevant applications

such as facial detection and recognition by cross-referencing the image with the pre-configured dataset. It demonstrates the progress in the development of neural network algorithms and their impact on object detection techniques that can be considered as learning systems.

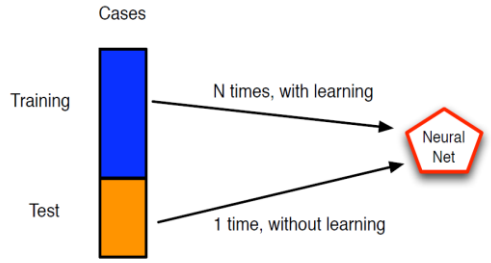

Fig. 1 The essence of the Backpropagation Algorithm [19]

Tang et al. (2017) [21] describes the most typical methods used nowadays in object detection via deep learning. It not only discusses the difference between classical methods and deep learning methods in object detection but also the challenges faced in object detection based on deep learning along with proposing some solutions. It focuses on the framework design and the working principle of models as well as the analysis of performance in real-time and accuracy of detection by keeping track of false acceptance rate (FAR) and false rejection rate (FRR). It highlights the faster recognition rates obtained by using deep neural networks (DNN) and demonstrates the effective object detection even after the crop and warp operations. The classifier can be trained by using an appropriate dataset that can then be further optimized by adjusting the weights and following the approach of supervised learning to achieve the target goal.

Alex Krizhevsky et al. (2014) [24] devised a new method of training a convolution neural network by parallelizing it over various GPUs. This method scales much better than any other method when applied to modern convolution network that is deeply layered. Convolution Neural Networks are big networks that are trained on a large amount of data. The parallelizing of their training can be done in two ways:

1. Different workers train different part of the model (Model parallelism)
2. Different workers train on different data examples (Data Parallelism)

In model parallelism, the input and output of different parts must synchronize. In data parallelism, the model parameters must synchronize to ensure the trained model is consistent. Ideally, both type of parallelism should be exploited as none is better than the other. Model parallelism is more efficient in case of high computation per neuron. Data parallelism is more efficient in the case of higher computation per weight. Batch size is another factor that affects the preference.

There are two types of layers in modern convolution neural networks:

1. Convolution layers: contain 95% of computations but only 5% of parameters, have large representation.
2. Fully-connected layers: contain 5-10% of the computation but 95% of the parameters, have small representation.

A different way of parallelizing looks more attractive for the two types of layers. Data Parallelism suits convolution layers better whereas model parallelism suits fully connected layers better. This is what Alex Krizhevsky proposed in the paper.

One way of doing this is that each worker is assigned a certain amount of data in the beginning when they are training the convolution layers. The workers use this data to train the layers using data parallelism. They must also synchronize the weights. When the time comes to train the fully connected layers, the workers switch to model parallelism.

The backpropagation depends on which of the method was used in feed-forwarding. Previously, the neural networks were trained on a GPU cluster. The network was locally connected but not convolutional. The workers were distributed spatially across the image and only neuron activation near the edges of workers area of responsibility needed to be communicated. In case of using this scheme in convolution networks, the weight needed to be synchronized as well. It would require synchronization at every convolution level. Also, with eight or more workers, the area of responsibility of each worker will be very small making computations inefficient. The scheme proposed by Alex Krizhevsky seemed like a better way of parallelizing the training of neural networks as it even works on architecture that has not been adapted to multi- GPU setting.

Shuiwang et al. (2013) [25] developed a 3D CNN model to detect human action in surveillance videos. This kind of analysis finds its application in domains like intelligent video surveillance, customer behaviour analysis etc. An accurate and precise analysis is difficult due to cluttered backgrounds, viewpoint variation etc. Most of the models employed formerly made certain assumptions about the condition in which the video was taken. Also, they followed a two-step approach: in the first step, the features were computed from raw data frames. In the second step, the detected features were used to train a classifier. However, this method was not practical as features are rarely important in detecting human actions as they may appear drastically different in terms of their appearance and motion patterns. Convolutional neural networks can work directly on raw data, hence not needing to build classifiers based on complex handcrafted features. Deep learning is more efficient at learning as it builds high-level features from low-level ones and can be trained using supervised or unsupervised learning methods and they have been shown to give an excellent result in domains like natural language processing, image restoration, human tracking etc. CNN's have been shown to be unaffected by variations such as poses, lightening and surrounding clutter.

CNN models, however, are currently limited to handling 2D inputs (images). Here they developed a novel 3D model for action recognition in videos that extracts information from both: the spatial dimension as well as the temporal dimension, by performing 3D convolutions. A simpler approach would have been to recognize action at every single frame, failing to

recognize the motion information encoded in a series of frames. It captures the motion information encoded in a series of frames. Multiple channels of information are created from the input frames and the final representation combines information from each channel. By performing multiple distinct convolution operation at a single frame, different types of information can be extracted. Regularization of output and combining the output from various models is done to further boost the performance.

This model was used in a practical situation of analysing airport surveillance videos and it achieved better performance than formerly employed methods. The model was evaluated on TRECVID data, which consists of data from surveillance video footage at London Gatwick Airport. The model achieved the best performance at all the specified categories. It also achieved competitive performance on the KTH data. Key contributions of their work are:

1. Proposal for applying 3D convolution to extract multiple information (both spatial as well as temporal features).
2. 3D convolution architecture developed based on the 3D convolution feature extractors.
3. Auxiliary outputs computed at high-level motion features used to augment the output of the model.
4. The 3D model evaluated.

Kalchbrenner et al. (2014) [26] proposed DCNN (Dynamic Convolution Neural Network) that has the ability to accurately represent sentences. It is adapted for the semantic modelling of sentences for purpose of classification or generalization. The sentence modelling problem is the core of many tasks involving a degree of natural language comprehension including sentiment analysis, paraphrase detection etc. Individual sentences are rarely observed. A sentence must hence be represented in terms of frequently observed n-grams in the sentence and features.

The model employs a global pooling operation over linear sequences called k-Max Pooling. Long- and short-range relations is explicitly captured. The network does no use a parse tree and hence can be easily applied to any language. The model performs significantly better than the strongest baselines in domains like small case binary and multi-class sentiment predictions, six-way question classification and twitter sentiment predictions.

The gap in the literature and proposed model is bridged by integration between the IoT aspects of project and the trained neural network that is used to classify whether image captured from the PiCamera (acting as CCTV) contains a gun leading to potential high-risk activity that could lead to violence thereby generating an alert as well as providing pathway to analyse the gun-related violence rates in the city. Image Classifier can be successfully integrated with IoT to create a system that detects guns (or any other object) in the surrounding and create an alert for it. Other cases for which this system can be applied are accidents, unaccounted baggage, missing kids, stray trash etc. With the growing need for automation and data-centric computations, IoT and Deep Learning can complement each other and fill in the gaps wherever needed.

III. Proposed Work

The smart city comprises of three major components, smart homes that come with special features, smart waste management system and smart streets equipped with intelligent CCTV. Various sensors are placed inside smart homes to detect motion and lighting conditions. Cameras are placed for security purposes. Following are key features of the proposed system:

- The lighting of Smart Home can be controlled remotely via smartphone, and if a room is vacant for a relatively long time then lights are automatically switched off to save energy. Ambient light has also been added.
- Humidity and temperature sensors are used to monitor environmental conditions inside the house. Temperature is regulated by the use of an air conditioner.
- Flame sensor senses if there is a fire outbreak and sends a signal to sound alarms and alert to Smart Home owner's mobile phone in case of a critical condition.
- If an intruder is detected, the image is captured and a copy of it is sent to the owner's email address as well as to the authorities with an alert message.
- Smart Waste Management is implemented in the smart city. The system will keep track of completely filled trash/waste bins that can be used by the State Municipality. Their real-time status can be seen via web-page on the internal server for efficient route planning.
- The streets are made smart as well. The street lights are switched on for specified duration upon detection of motion in its proximity only if natural light is less than threshold and motion is detected in the neighbouring area.
- The PiCamera is used as a CCTV on the streets to capture images at regular intervals along with the location. The images are then sent to an image classifier to detect the presence of guns in them.

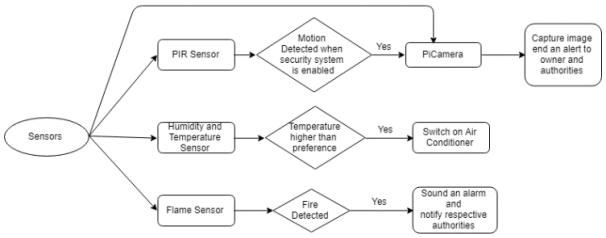

Fig. 2 Control Flow of Smart Home

The control flow of the Smart Home is illustrated in figure 2. It outlines the basic data flow of how aside from smart lighting and control of various components of the smart home, the humidity and temperature inside the house is monitored using the DHT11 sensor and autonomously triggers an action to switch on the air-conditioner if the temperature is higher than the preferred preset. The smart home also has safety and security features. The intrusion detection system uses motion sensors and camera to detect an intruder, take a photograph and

send it to the owner as well as nearest authority alongside generating an alert on the resident's mobile phone [18].

In the presence of natural light is below the threshold, the system checks for the detection of motion. Upon satisfaction of both the conditions, the street lights in the neighbouring area are switched on. After a particular duration, the conditions are checked again and if they are not fulfilled then the lights are switched off to save energy.

Convolutional Neural Networks (CNN's) have a vast number of applications in computer vision, image and video recognition and natural language processing. However, the basic concept at its core remains the same and can be applied to other use-cases as well. CNN's are made up of neurons, like neural networks, and are learnable by adjustable weights and biases. Each neuron receives multiple inputs, performs a weighted sum over them which is then passed through an activation function to obtain an output. However, unlike neural networks, the input in CNN is a multi-channelled image instead of traditional vector input. It can be said that CNN's operate over volumes. The convolutional layer contains a set of independent filters where each of them is independently convolved with an image. These filters are initialized randomly and become our parameters which will be learnt by the network.

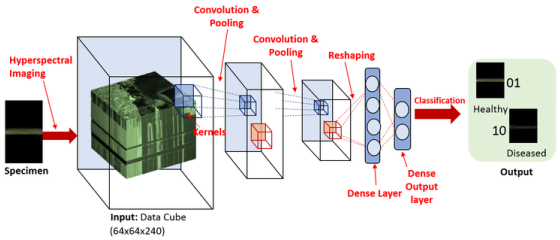

Fig. 3 Architecture of 3D Convolutional Neural Network [27]

The architecture for said Convolutional Neural Network is illustrated in figure 3. The function of Pooling Layer is to progressively reduce the spatial size of representation to thereby reduce the number of parameters and amount of computation. Pooling layer operates on each feature map autonomously. Max Pooling is the most common approach used in pooling.

The Images classifier is built using pre-trained neural networks with a custom classifier layer. The classifier is trained on a dataset comprising of images with the known output by using PyTorch. The working of classifier comprises of following steps:

1. The dataset is divided into training and testing dataset.
2. Data augmentation is done so that the trained classifier performs better at generalizing. The model is tested on the testing dataset.
3. Sufficient accuracy is reached by tweaking network training parameters like learning rate.
4. The network attributes are saved.
5. The classifier used to detect the presence of guns in images sent by the CCTV.
6. If a gun is detected in an image, a high-risk alert is created for that location and is sent to the authorities.

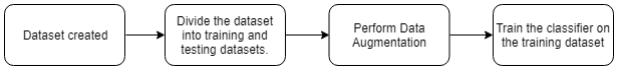

Fig. 4 Training Image Classifier

The classifier training by using a neural network is demonstrated in figure 4. The supervised learning [14] approach is used for training the classifier. It is attained by using the training dataset to present positives and negatives for the target object in the object detection algorithm. After the successful training of the neural network, the test dataset is used to determine if desired results are achieved [4]. If the result of test data is not satisfactory then the training process is repeated for adjusted weights and classifier is thus obtained.

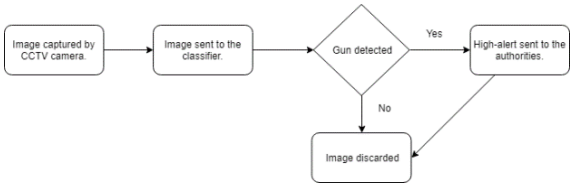

Fig. 5 Detecting High-Risk using Image Classification

As demonstrated in figure 5, the classifier is used to detect gun from an image acquired from CCTV. The classifier checks for the presence of a gun in the image. If a gun is detected, then a high-risk alert is generated and sent to authorities with the location of the potential incident, otherwise, the image is discarded after a preset time span.

Fig. 6 Model of Smart City

The model of Smart City equipped with various sensors is demonstrated in figure 6, having major components as Smart Home, Smart Street Lights and Smart Waste System.

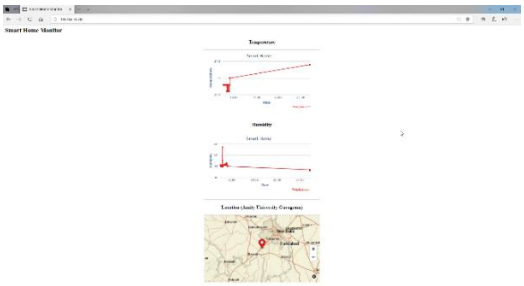

Fig. 7 Web page to monitor humidity and temperature of Smart Home

As represented in figure 7, the web page that can be accessed by the local server which displays a graph for temperature and humidity that is updated in real-time at regular intervals along with the location of Smart Home.

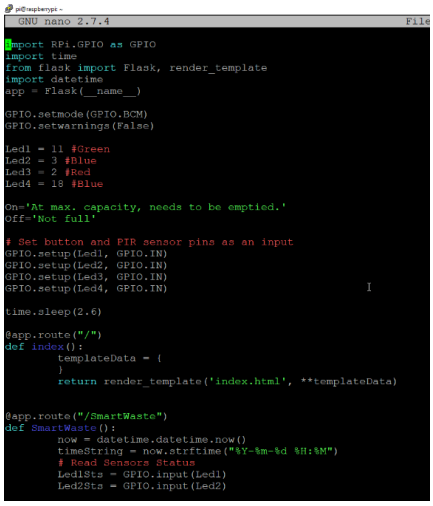

Fig. 8 Flask server

As shown in figure 8, the Flask Server has been used to provide dynamic web-functionalities such as real-time Smart Home monitor and live Smart Waste Management. It is based on Python and allows users to define dedicated functions to handle the web-page requests.

Fig. 9 Example of an image in training and testing dataset

A sample of images that were used to train and test the Image Classifier as demonstrated in figure 9 and were taken from the PiCamera.

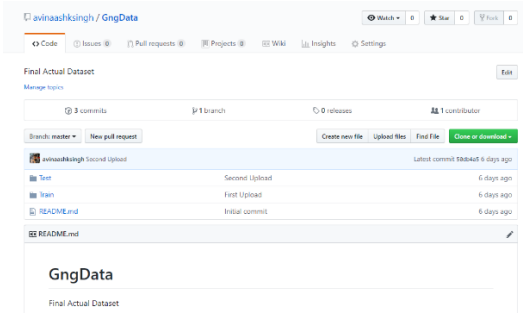

Fig. 10 Dataset on GitHub

As illustrated in figure 10, since files cannot be directly loaded into google Colab, there are certain code snippets available to include files either from a local machine or from Google Drive. These code snippets temporarily load the file. The files get deleted at the end of every session. To go around this problem, the dataset is first organized and then uploaded on GitHub. Then the GitHub repository is cloned in the colab project file. This way, the dataset is cloned in every session whenever the command is run.

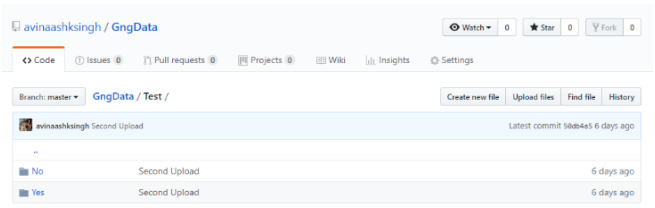

Fig. 11 Organized Dataset

As demonstrated in figure 11, the pre-trained models require the dataset to be organized in a definite structure. The root folder must contain the Training and the Testing set in separate folders. These folders then contain the folders for different categories. While training and testing, the labels are derived from the name of these folders. The pathname of every directory is passed while creating the testing and training dataset.

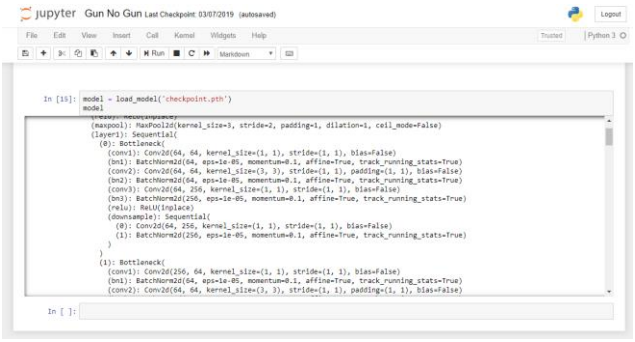

Fig. 12 Convolutional Layers

As shown in figure 12, after loading the pre-trained model from the checkpoint, the model architecture can be displayed. Even though the various layers are beyond the understanding of a newbie, but it is still fascinating to see the amount of work that goes into feature detection and analysis.

IV. Result Analysis

Upon powering the project, Raspbian OS is booted up. The Python scripts for various components are executed at start-up. The calibrated sensors become active, constantly sensing for trigger action. The cloud-based services such as Flask and Blynk are initiated. The integration and resolution of dependencies among the vast number of sensors has been done so they don't conflict when accessing the same GPIO pin. Ideal delays have been introduced for appropriate calibration of sensors to achieve proper functioning. The lighting of Smart Home can be controlled via mobile application. Ambient light

is switched on automatically in the presence of low natural light. The flame sensor constantly checks for a fire outbreak. In case of fire, an alarm is sounded along with a generation of push notification on a mobile phone. Humidity and temperature conditions are monitored whose status and location can also be viewed from a web-page on an internal server. The room's light is switched on for specified time on detection of motion. Aside from the above, the Smart Home also has an intruder detection system. The PiCamera is used to capture an image when the house is vacant and protocol is activated from the remote control. The image is then sent to the owner's email address along with an alert message. The street's lighting is automated to switch them on for specified time upon detection of motion under low natural light. Smart Waste Management System consists of Smart Bins which have a notification light that switches on if the bin is at near-full capacity. The status of bins can be viewed from a remote location by accessing the web-page on the internal server, thereby allowing efficient route planning for cleaning municipality.

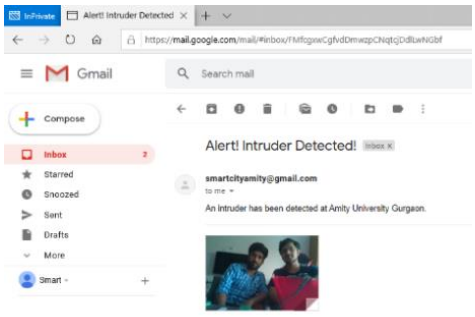

Fig. 13 Email with an image captured by camera upon detection of Intruder

As shown in figure 13, the functioning of the Intruder Protocol. Upon detection on the intruder, an image is captured by PiCamera and emailed to the user with an alert message. It can also be configured to inform authorities about the intruder break-in.

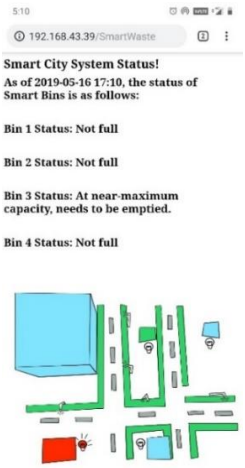

Fig. 14 Webpage for status of Smart Bins in various sectors across the City

As illustrated in figure 14, the web page displays the current date and time along with the status of the Smart Bins location in different sectors of the Smart City. It allows the Municipal Corporation responsible for cleaning the trash to view in advance which bins are close to max capacity and hence, the driver can plan the route accordingly thereby providing better waste management facility.

The PiCamera (acting as CCTV) takes images of the surrounding at regular interval. The images are sent to the image classifier where they are analyzed whether they contain a gun. Whenever the shooter/gun is in its field of vision, an alert is created and sent to the authority (in this case, to the email). The model is full-proof because it gave 86% accuracy during testing. The model was tested during the training phase and also after its final implementation.

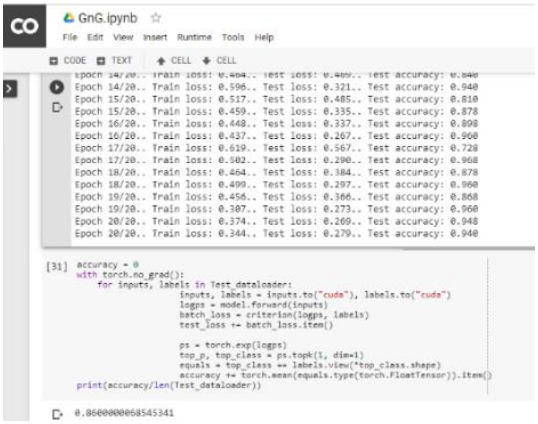

Fig. 15 Training of network

As demonstrated in figure 15, epochs at the time of training the neural network on the created dataset. The network processes and detects features from all the images once in every epoch. The number of images in the network is parsed at one time depending on the batch size. The final training accuracy obtained was 94% and the final testing accuracy was approximately 87%.

Fig. 16 Python script for Gun Detection

The python code for detecting the presence of a gun in the image is demonstrated in figure 16. The normalizing parameters for the classifier based on a neural network used in the system can also be seen. PyTorch, Numpy and TorchVision have been used for the implementation of the classifier as a python script.

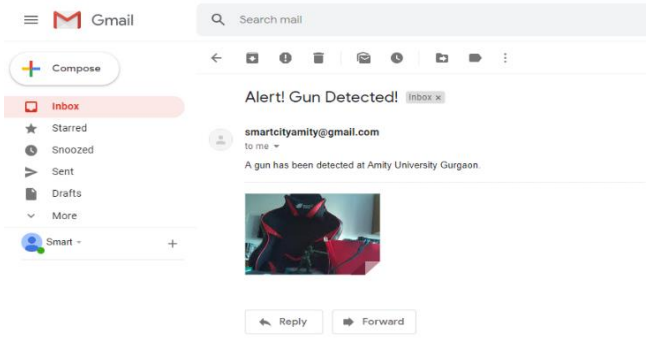

Fig. 17 Alert created by Image Classifier

As shown in figure 17, the alert that is sent to the authority once a gun is detected. The mini-soldier has been used as a gun for training the classifier. The alert is sent in the form of an email with the image attached.

V. Conclusion

It can be concluded that Smart City envisions a far more integrated, autonomous and efficient system than the traditional cities. The smart home provides a much more convenient residential environment that allows residents to possess massively more control than the conventional ones. Other than basic monitoring and control systems, the integration between safety and security module provides better peace of mind to the people of the city. The smart streets can allow the city to be energy efficient, monitor and regulate the traffic to avoid heavy traffic density on common routes. The object detection integrated with IoT is the highlight as presently, no standalone sensor is capable of detecting a target object (gun in this case). Due to the rise in gun-violence rate over recent years, it is an essential feature to be included in the smart city. The system is designed by merging the concept of the Internet of Things that controls several components of Smart City with an image classifier developed by training a neural network. Large-Scale implementation of the proposed work can hence aid in a more energy-efficient ecosystem along with providing some necessary security features.

References

[1] Zanella, A., Bui, N., Castellani, A., Vangelista, L., & Zorzi, M. Internet of Things for Smart Cities. IEEE Internet of Things Journal, 1(1), 22–32. (2014).
[2] Harmon, R. R., Castro-Leon, E. G., & Bhide, S. Smart cities and the Internet of Things. 2015 Portland International Conference on Management of Engineering and Technology (PICMET). (2015).
[3] Zhou, X., Gong, W., Fu, W., & Du, F. Application of deep learning in object detection. 2017 IEEE/ACIS 16th International Conference on Computer and Information Science (ICIS). (2017).
[4] Shah, M., & Kapdi, R. Object detection using deep neural networks. 2017 International Conference on Intelligent Computing and Control Systems (ICICCS). (2017).
[5] Erhan, D., Szegedy, C., Toshev, A., & Anguelov, D. Scalable Object Detection Using Deep Neural Networks. 2014 IEEE Conference on Computer Vision and Pattern Recognition. (2014).
[6] Giaffreda, R., Caganova, D., Li, Y., Riggio, R., Voisard, A. Internet of Things and IoT Infrastructures. First International Summit, Rome, Italy (2014).
[7] Wan, Jiafu, Humar, Iztok, Zhang, Daqiang. Industrial IoT Technologies and Applications. International Conference, Industrial IoT 2016, GuangZhou, China (2016).
[8] Ding, B., Luo, F.-L., Sun, X.-L.: Research on Application Strategy of RFID in Discrete Manufacturers. Chinese Journal of Management Science 16(2), 76–82 (2008).
[9] Liu, Q., Cui, L., Chen, H.: Key Technologies and Applications of Internet of Things. Computer Science 37(6), 1–10 (2010)
[10] Manuj Darbari, Diwakar Yagyasen, and Anurag Tiwari. Intelligent Traffic Monitoring Using Internet of Things (IoT) with Semantic Web. Volume 1, Advances in Intelligent Systems and Computing. (2015).
[11] Tong Li and Liping Chen. Principle, Framework and Application. Vol. 144. Springer, Berlin, Heidelberg. (2012).
[12] Zhong-Qiu Zhao, Peng Zheng, Shou-tao Xu, and Xindong Wu. Object Detection with Deep Learning. Journal of Latex Class Files, Vol. 14, No. 8. (2017).
[13] Christian Szegedy, Alexander Toshev and Dumitru Erhan. Deep Neural Networks for Object Detection. Advances in Neural Information Processing Systems (NIPS 2013).
[14] Avital Oliver, Augustus Odena, Colin Raffel, Ekin D. Cubuk & Ian J. Goodfellow. Realistic Evaluation of Deep Semi-Supervised Learning Algorithms. 32nd Conference on Neural Information Processing Systems (NeurIPS 2018), Montréal, Canada. (2018).
[15] Gilles Betis, Christos G. Cassandras and Carlo Alberto Nucci. Smart Cities. IEEE Vol. 106, No. 4 (2018).
[16] Carlo Ratti and Fábio Duarte. Smart cities, Big Data and Internet of Things. Vol. 6 Issue 4, IEEE Standards University. (2016).
[17] Carlos E. Jiménez. The Making of Smart Cities: Working Together. IEEE Computer Society Smart Cities Committee. (2014).
[18] Rodger Lea. Smart Cities: An Overview of the Technology Trends Driving Smart Cities. IEEE Technical Article. (2017).
[19] www.idi.ntnu.no/emner/it3105/materials/neural/learn-sup.pdf
[20] Saraju and Mohanty. Smart Cities. IEEE CE Society Webinar. (2017).
[21] Cong Tang, Yunsong Feng, Xing Yang, Chao Zheng, Yuanpu Zhou. The Object Detection Based on Deep Learning. 4th International Conference on Information Science and Control Engineering, China. (2017).
[22] Hermann Brand. IEEE an Open Platform for Smart Cities. ITU Workshop, Belgium. (2018)
[23] S.J. Clement, D.W. McKee, Jie Xu. Service-Oriented Reference Architecture for Smart Cities. IEEE Symposium on Service-Oriented System Engineering, San Francisco, California, USA. (2017).
[24] Alex Krizhevsky, Ilya Sutskever, Geoffrey E. Hinton, ImageNet Classification with Deep Convolutional Neural Networks, 2012
[25] Shuiwang Ji, Wei Xu, Ming Yang, Kai Yu, 3D Convolutional Neural Networks for Human Action Recognition, NEC Laboratories America, Inc., Cupertino, CA 95014, USA
[26] Nal Kalchbrenner, Edward Grefenstette, Phil Blunsom, A Convolutional Neural Network for Modelling Sentences, Department of Computer Science, University of Oxford, 2014
[27] https://www.researchgate.net/figure/3D-Convolutional-Neural-Network-Architecture-for-Classification_fig2_324744613

Proceedings of the Fourth International Conference on Communication and Electronics Systems (ICCES 2019)
IEEE Conference Record # 45898; IEEE Xplore ISBN: 978-1-7281-1261-9

Microcontroller rooted collaborative functioning system in Vehicles

P. Tarun, T. Pradeep Chandra, G. Anil Kumar and Sudha Yadav

***Abstract*— Automobile industry is growing vast throughout the world. The cost of the vehicles are also moderate. There are a large number of personal vehicles. Due to the surge, road accidents are the major problem. It is not only the duty of the person who drives, but also of the vehicle's manufacturer to ensure more preventive systems suitable for our daily routine. Automobile industry had been taking a few safety steps over the last two decades. Few more safety measures are being added to make the system more versatile. There is a large void in post-accident emergency facilities. If emergency services with definite accident location are provided in time, many lives can be hoarded. In this paper, a novel approach is proposed for this issue and adds some safety measures. Our system will not allow drunken people to drive the vehicle; A help request is sent to helpline Centre with accident location when an accident happens; Vehicle stops automatically if there is any leakage of fuel gas; Driver will be alerted if he/she is in drowsiness state and stops the vehicle if continues to drive in drowsiness state.**

***Index Terms*— Real time accident detection system, road accidents, Prevention of accident, Immediate rescue system, Gas leakage detection, Drowsiness detection.**

I. INTRODUCTION

In the introduction, It is briefed about the accidents and the statistics of the deaths in the past decades. And about, how are accidents happening, what are the major causes of the accidents, what plays the major role in saving a life. Later, we will be comparing our system with the previous, existing and proposed systems. In the next part, It would be described about the sensors used in our system along with their working and some sensor description. In this part, we can find the block diagram of the system and its working. And the next part shows us the flowcharts and gives a brief about the algorithm. Followed by a demo of the system in the pictures and the sample outputs. Lastly the results initiated and the conclusion followed with the references for the whole system.

According to world health organization (WHO) "Global status report on road safety", approximately a million people is losing their valuable life's and 20-30 million people are being injured due to road accidents every year. Among these, 30% of deaths are due to delay in contact with emergency services and 17% of deaths are due to drunken driving [1,6].

In general, when an accident occurs, one has to manually contact the emergency services. Sometimes no one voluntarily comes forward neither to help nor to inform helpline services and wait for others to do, that leads in loss of time which eventually leads to a death of the victim. Many times we do not find any automated systems that could directly intimate helpline services or our close members. Now a days some systems have an option called SOS (Save Our Souls), which also has to be functioned by a person manually.

Chances are evidently high, for those who drink and drive in making an accident. Alcohol slows down one's brain and body responses, which leads to impair our vision and hearing, make one loose his concentration and feel drowsy. A medical report says, for those who drink and drive, night vison will be reduced by 25%. Blood Alcohol Concentration (BAC) is the measure of amount of alcohol present in 100ml of blood. The permissible alcohol limit is 30 mg/100 ml of blood. Right now, There is not any system present in vehicles which prevents drunken people to drive.

As our future is about to be completely on electric cars, LPG and LNG fueled cars. The government of India has announced plans to set up 10,000 CNG distribution stations by 2030 to decrease the usage of diesel and petrol. The risk for LPG and LNG leakage is very high. There is not any system present in vehicles which detects the leakage of LNG/LPG and take preventive measures accordingly. There had been many cases registered over the LPG leakage in cars. LPG is a propane or a butane. LPG leakage results in explosion either in household goods or in vehicles, they also causes irritation when comes in contact with eyes and skin. When LPG leakage occurs, the smell is due to a stench of other chemical called Ethyl Mercaptan, which when inhaled causes dizziness, light headedness, coma and death. They are also hazardous to liver and kidneys. The most dangerous property of this Ethyl mercaptan is Highly inflammable [3].

Sleep deprivation, the term used to mention the drowsiness, is one of the highest risk factor for the car accidents. A survey

P Tarun, Student, Department of Electrical & Electronics Engineering, Amrita School of Engineering, Bengaluru, Amrita Vishwa Vidyapeetham, India, potluritarun30@gmail.com

G Anil Kumar, Student, Department of Electrical & Electronics Engineering, Amrita School of Engineering, Bengaluru, Amrita Vishwa Vidyapeetham, India, anilchanti1050@gmail.com

T Pradeep Chandra, Student, Department of Electrical & Electronics Engineering, Amrita School of Engineering, Bengaluru, Amrita Vishwa Vidyapeetham, India, pradeept1997@gmail.com

Sudha Yadav, Assistant Professor, Department of Electrical & Electronics Engineering, Amrita School of Engineering, Bengaluru, Amrita Vishwa Vidyapeetham, India, sy_sudha@blr.amrita.edu

in United States says, about 20% of the car accidents are due to sleep deprivation. As night rides are more often to the transport vehicles containing heavy goods, the after effects of an accident are very devastating, resulting mostly in on spot deaths and in these cases sleep deprivation plays a major role. Here, delay in immediate interaction with helpline services also costs a life.

To overcome these, a few rescue systems exist whose responses are partly delayed from the emergency services and are less effective in safety and preventive measures. Our model is made in consideration with various causes of accidents. So we came up with a real time alternative which upgrades the safety in the system and decreases the delay in responses.

II. RELATED WORKS

The literature survey for the work is discussed in this section. Accidents are being detected by piezo electric sensors [6]. Based on the impact, a corresponding voltage is generated between plates, which is read by micro controller. There is a chance that piezo electric sensor doesn't detect the accident, for example it is difficult for piezo electric sensor to detect a sideswipe collision. Some set of EEG signals from brain are taken and studied to detect whether driver had alcohol [4]. Gas sensor MQ6 is used for detecting any leakage of LPG gas from the gas cylinders in home and turns off the regulator if system detects any LPG [3]. Eye blink sensor is used in controlling home appliances [5].

In our proposed system, we used an eye blink sensor for detecting drowsiness based on the eye blink length, Vibration sensor SW420 for detecting accident, MQ3 gas sensor for alcohol level detection, MQ6 gas sensor for detection of leakage of fuel gasses.

III. SYSTEM DESCRIPTION AND DESIGN

Our system uses Arduino MEGA 2560 as micro controller, gas sensor MQ3 for detecting the alcohol content, vibration sensor SW420 to detect an accident, H bridge for controlling the motor drive. Eye blink sensor for detecting drowsiness. MQ6 for detecting any leakage of LPG fuel or any smoke. GPS module to get the co-ordinates of a place where accident occurred and a GSM module for sending a help request to emergency services.

A. Arduino MEGA 2560

Arduino MEGA has following :
Operating Voltage – 5v
Input Voltage (recommended) 7-12v
Digital I/O Pins – 54
Analog Input pins – 16
DC current per I/O pin – 40 mA
Flash Memory 256 KB
SRAM – 8 KB
Clock Speed – 16MHz
UART'S – 4

The Arduino ATMEGA 2560 is powered using USB or with an external constant DC power supply. External supply should be constant DC of 7-12 V. It can be supplied by using an AC-DC adapter or by using a DC battery. Arduino ATMEGA 2560 has a 2.1 mm power jack. If we use constant battery The positive terminal is connected to Vin pin of Arduino and the ground to GND pin of Arduino. The input supply to Arduino should not exceed 12V, if exceeds the regulator overheats and damages the board. If input supply is less than 7V, the board becomes unstable. The Arduino ATMEGA 2560 differs from other Arduino boards in, it do not use the FTDI USB to serial drive chip instead, it uses an ATMEGA8U2 as a USB to Serial converter.

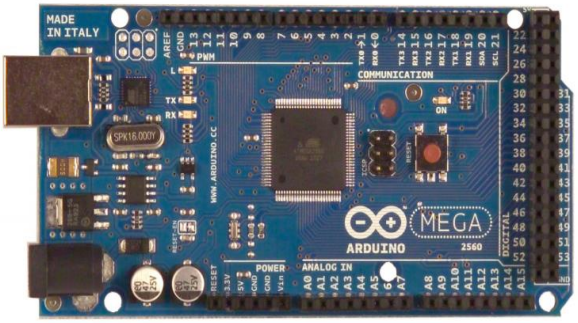

Fig 1. Arduino ATMEGA 2560.

Communication of Arduino ATMEGA 2560 with other modules like computers, micro controllers, etc.… can be done in different ways. It has a total of four UART's (Universal Asynchronous Receiver Transmitter) for TTL (transistor-transistor logic) serial communication. The Arduino software contains a serial monitor which makes the simple textual data from the board. The Receiver and Transmitter pin LED's will be flashing when the data is being transmitted via the ATMEGA8U2 chip and a USB connection to the computer. Arduino ATMEGA 2560 has a reset button on board. The Arduino ATMEGA 2560 is designed such that reset can be done by running in software of a connected computer. Each time when we connect Arduino ATMEGA 2560, it resets the data that is present in the micro controller.

B. Gas sensor MQ3 & Vibration Sensor SW-420

This sensor contains a sensitive material that is less conductive in nature. The sensor's conductivity increases as the concentration of the alcohol gas in air increases. The output signal strength depends on the concentration of the gas with the help of a simple electro circuit. This MQ-3 gas sensor has high sensitivity to alcohol, and has a good resistance against the disturbance of gasoline, smoke and vapour. This sensor is used to detect the alcohol at different concentrations and it is cost effective too and also suitable for various applications.

Fig 2. MQ-3 gas sensor.

It has high sensitivity and fast response time. Sensor provides an analog resistive output based on alcohol concentration.

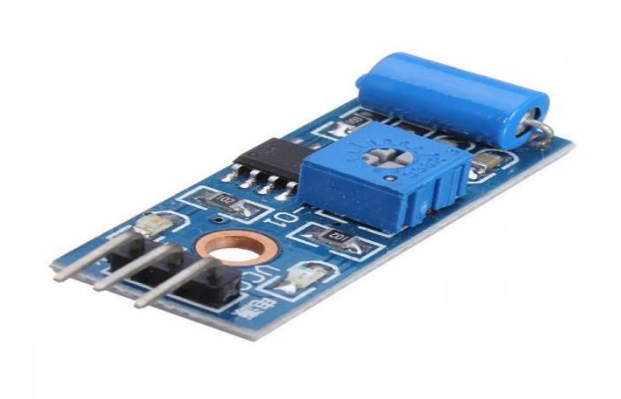

Fig 3. Vibration sensor SW420.

It is a highly sensitive non-directional vibration sensor. It's working can be described as, if the module is stable, the circuit is turned on and the output will be high. If some vibration or any movement occurs in the module, the circuit will be disconnected and the output will be low. Advantage of this module or sensor is that, the sensitivity of the module can be adjusted accordingly to our own needs. The working bias of the circuit is between 3.3V to 5V DC.

C. H- Bridge L298N

It is defined as a bridge circuit built of four switches, which can be used to control the flow of current to the load. It is interfaced with Arduino and controlled using Control pins. Based on the digital values given to the control pins, operation varies.

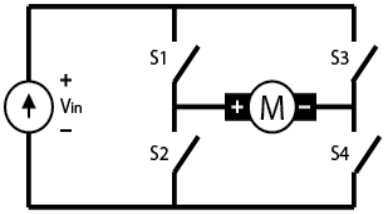

Fig 4. H-bridge circuit.

- If switches S1 and S4 are closed, then the current will flow from the left to the right and results in forward operation of the motor.
- The current in the circuit will flow from the source, through switch S1, and then through the load, then through switch S4.

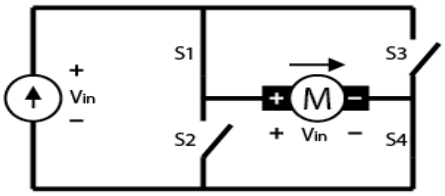

Fig 5. Forward operation.

- If switches S2 and S3 are closed, then the current will flow from the right to the left and results in reverse operation of the motor.
- The current will flow from the source, through the switch S3, and then through the load, then through switch S2.

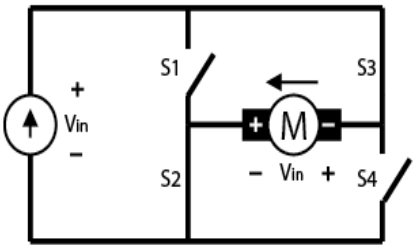

Fig 6. Reverse operation.

It is very cautious that when working with the H-bridges, check carefully while switching, short circuiting should never happen so that, it may damage the load and results in burning of the bridge circuit.
The below case is seen when switch S1 and switch S2 (or) switch S3 and switch S4 are closed.

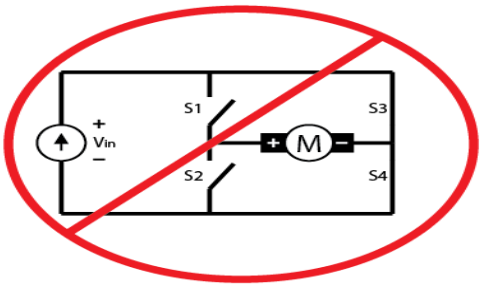

Fig 7. Cautious operation.

D. GSM and GPS module

The SIM800 is a quad band GSM module which can be implanted straightforwardly by the user. AT stands for ATTENTION. Attention commands are used for setting UP and controlling the module. There are some Attention commands in making a phone call and delivering a message.

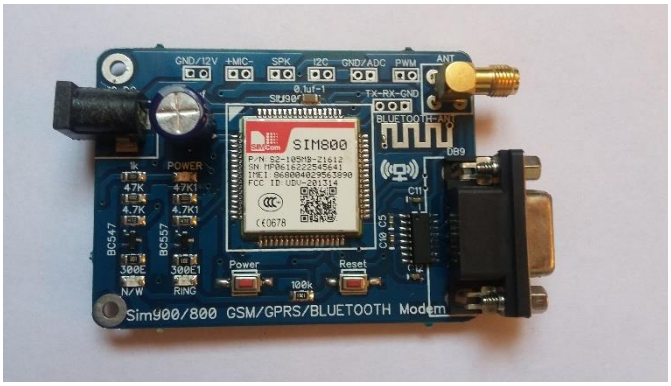

Fig 8. GSM SIM800 module

The NEO-6M GPS module is a well dressed GPS receiver with an integrated 25 x 25 x 4mm ceramic antenna, which gives a robust satellite tv for pc search capability. With the power and signal indicators, it could extol the clever working of the module. The facts backup battery, the module can store the facts, if the main energy gets shut downed accidentally.

Fig 9. NEO 6M GPS module

E. Eye blink sensor

The eye is irradiated by an IR led, that is powered with a +5V DC from the energy supply and the reflected light is detected by an IR photo diode. The variant throughout the eye will vary as per the eye blink. The precise functionality relies significantly upon the arrangement and the aiming of emitter and detector with the eye. If the eye is shuttered, then the output is high and if not, the output is low. This is to check whether the attention is downing or in establishing the position. This output is given to common sense circuit (logic circuit) to indicate the alarm.

Fig 10. Eye blink sensor

F. Block diagram

The block diagram represents the overall system. The sensors involved in the system are Gas sensor MQ3, Vibration sensor SW420, Gas sensor MQ6 and an eye blink sensor. For controlling the motor we used the H-bridge. For communicating an accident occurred, we used a GSM 800C and for getting the accident co-ordinates we used a NEO-6M module. The micro controller we used in this system is Arduino ATMEGA 2560.

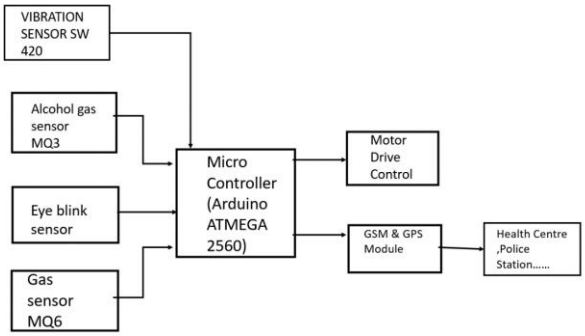

Fig. 11. Block diagram

MQ3 gas sensor gets the alcohol content that is present in the driver's body and compares it to the threshold value. If it exceeds the threshold value, vehicle engine will not start. If the alcohol content is within the prescribed limits, the vehicle starts. Once the vehicle is started, it continuously checks for the eye blink length from the eye blink sensor. In general, the closing eye blink length is 300-500 milli seconds. We kept a threshold value for eye blink length as one second. If it exceeds, buzzer turns ON and count will get incremented by one. If the count equals five, the buzzer will turn on and the vehicle stops. There may be chances for the driver closing eyes for more than one second if there is any dust or if he/she gets some dust irritation. To overcome this issue, we used this count command as mentioned.

There are two interrupts present in our system, one is when an accident occurs and the other is when there is any leakage in the LNG /LPG in the engine cabin. System continuously checks for the eye blink length but if any interrupt comes, it stops checking the eye blink length and proceeds further for the required actions on the necessity of the interrupts.

If MQ6 gas sensor detects any leakage of LNG/LPG in the engine cabin, then the interrupt comes in and stops the main

program. The required action, if there is any leakage of LPG/LNG in the engine cabin, is to turn on the buzzer and further stopping the vehicle.

If an accident occurs, Vibration sensor SW 420 detects and asks for an interrupt service routine. The main program is stopped and required action for the accident is proceeded. It checks for the accident and then the Arduino gets the geo coordinates from NEO 6M module and a help message is sent to help Centre with the location coordinates (latitude and longitude) link.

IV. FLOW CHART

The below schematic flow charts will explain the work flow process of the system. Interrupt occurs in two ways, one when an accident occurs and other when there is any leakage of LPG/CNG fuel gas. Main program always checks for drowsiness detection. The below flowchart is the main program work flow.

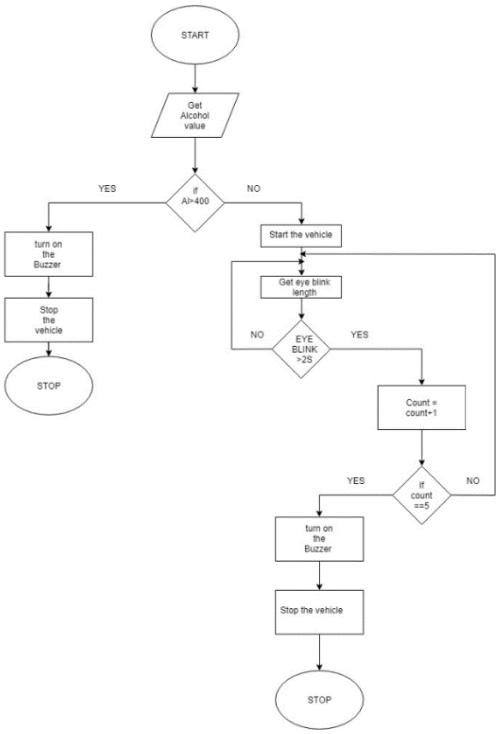

Fig 12. Main program flow chart

When driver starts the vehicle, MQ3 sensor will activate. The MQ3 gas sensor gets the value of the alcohol content that is present in the driver's body by the exhaled air in the driver's cabin and transfer that data to micro controller Arduino ATMEGA 2560.

The value is compared with the threshold value, if it exceeds the vehicle will not start and the buzzer gets turned ON indicating that driver is drunken and not allowing him to drive the vehicle. If the value is present within the limits, the vehicle starts, and eye blink sensor activates. The eye blink length is continuously checked with the threshold value. If it exceeds, a buzzer will turn ON and sounds with low pitch to help driver to get rid of drowsiness and a count will get incremented every time when it exceeds. If the count exceeds the threshold value then the buzzer turns ON and sounds with high pitch and stops the vehicle.

In our system we used a motor instead of an engine. So, for turning ON of engine is turning ON of motor and vice versa. H-bridge is used to control the motor. H - bridge can be interfaced with Arduino ATMEGA 2560. It can be controlled using control pins of H-bridge.

The below flowchart (fig 13) shows the work flow process, whenever an accident occurs, an interrupt service routine comes and pauses the main program. Accident is detected by the vibration sensor SW420. When an accident occurs, vehicle will have heavy vibrations at the colliding instant. Whenever there is a massive vibration, the SW 420 sensor senses it and asks for interrupt service routine. Whenever interrupt comes in, the main program is kept on hold and required action takes place for the accident. The location coordinates of the accident are given to the micro controller through the GPS NEO 6M module. Using GSM 800 module, a help message is forwarded to the helpline center's with the accident location coordinates.

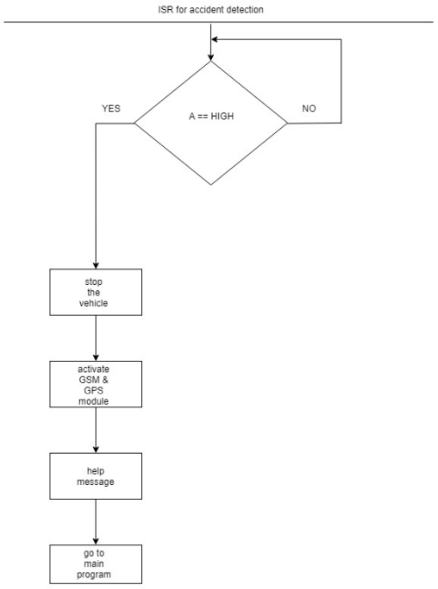

Fig 13. Accident detection interrupt flow chart.

The below flowchart (fig 14) is the work flow process when there is any leakage in the fuel gas. MQ6 gas sensor is used for detecting any fuel gas (LPG/LNG) in the engine cabin. If it detects any leakage gas, it calls for an interrupt service routine. The main program is paused and required interrupt function executes. The vehicle shut downs, buzzer will turn ON, LED turns on indicating there is a leakage of fuel in the vehicle.

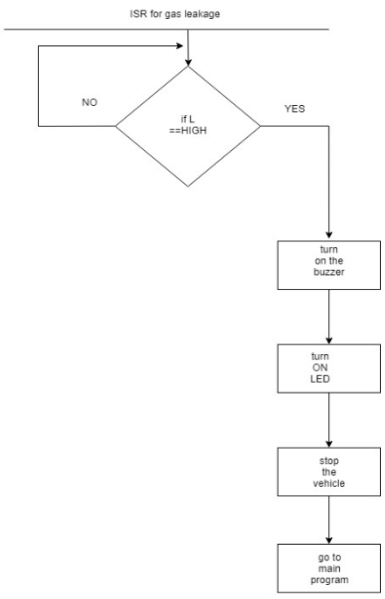

Fig 14. Gas leakage interrupt flowchart.

The flowchart in (fig 15) shows the representation of the entire work flow process of the system. Whenever an accident occurs, corresponding action takes place. The system uses interrupts for accident and gas leakage detection. Eye blink rate is continuously assessed in the main program. If any interrupt comes, required action takes place. The interrupt flowcharts and main program flow chart are explained in detail in the above sections.

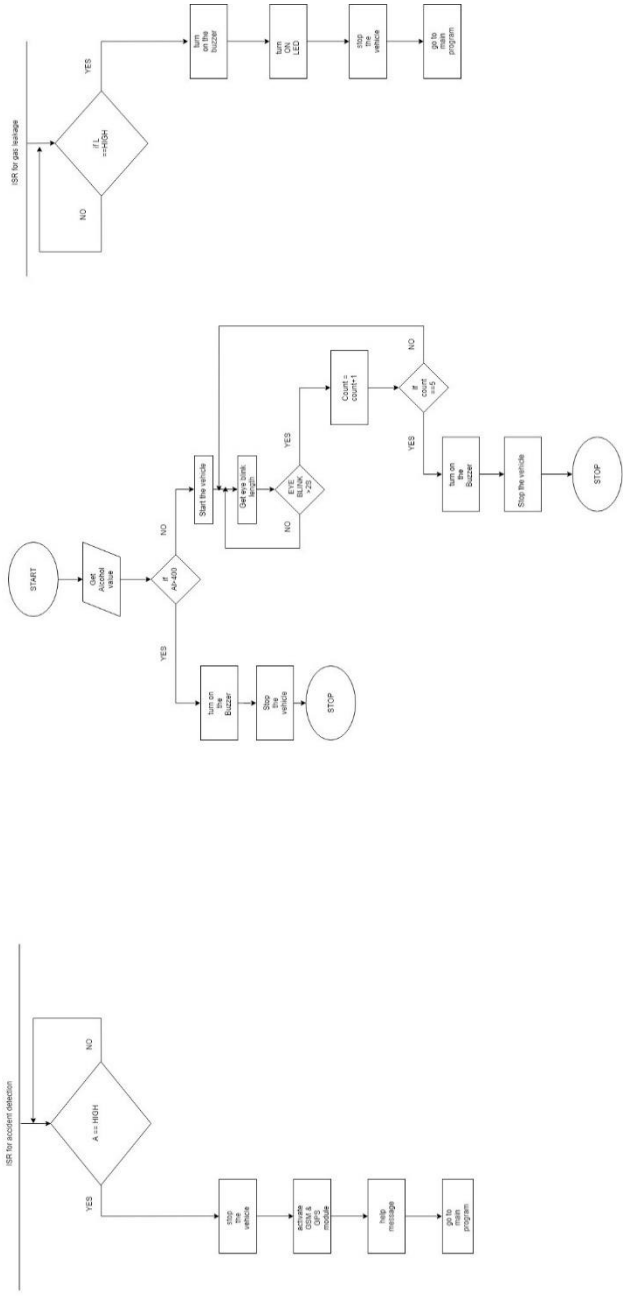

Fig 15. Entire flow chart.

V. HARDWARE SETUP AND RESULT

Connecting our system accordingly with the vehicle's central Electronic Control Unit(ECU), so that it co-ordinates with the unit adaptively.

Main burden arises in positioning of the sensors i.e., as of our knowledge:

a)Alcohol detection sensor is placed at the nearest point to the driver's face.

b)Gas detection sensor is placed in the exhaust chamber near the engine.

c)Vibration sensor is located at a stable position, where minute vibrations cannot disturb the sensor's output. And the remaining

module of it is hoarded with the Arduino near the ECU.
d)Eye blink sensor is located in the glasses, These has to be worn by the driver only while driving.
e) A buzzer has to be located on the dashboard.

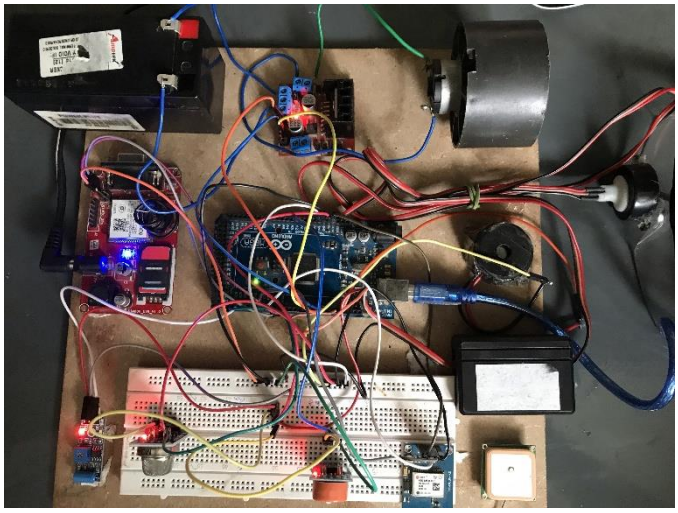

Fig 16. Entire setup

The above picture is the entire set up of our system. We connected the sensors : MQ3 gas sensor, MQ6 gas sensor on bread board and vibration sensor on bottom left. A buzzer which is present beside the motor turns ON when driver goes to drowsiness state or if the driver is in alcoholic state. Motor stops resulting in stopping the vehicle, when there is a leakage of LPG in the system.

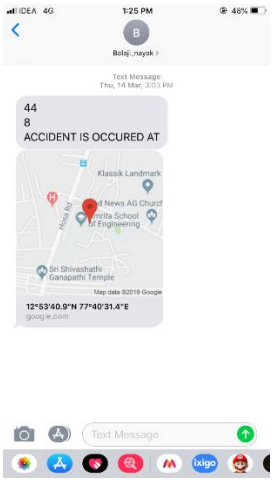

Fig 17. Help request message.

The above figure is the help request that is sent automatically by our system when an accident occurred. The help request will be having the co-ordinates of the accident's location.

Fig 18. Location coordinates of the accident.

The above figure is the location coordinates of the accident occurred. The red pin mark indicates the accident location and the blue mark indicates our location. The request message sent with the location co-ordinates of the accident helps to fasten the rescue process.

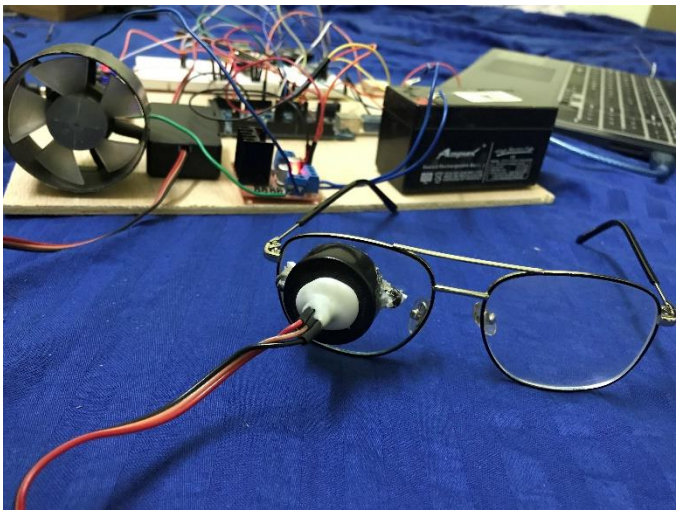

Fig 18. Eye blink sensor.

The entire setup with eye blink sensor. The eye blink length is continuously cross checked with the microcontroller. If any mismatch occurs (drowsiness), it buzzes for one second duration and if it continues, vehicle (motor) stops and a buzzer with high pitch sounds.

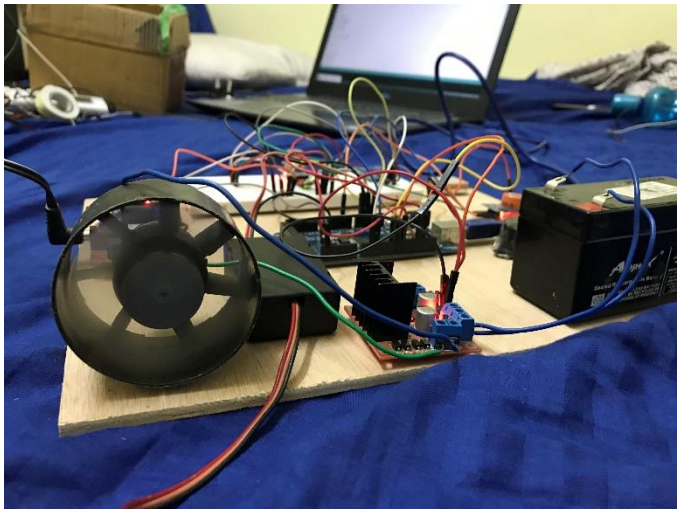

Fig 19. Normal condition.

From the above image we can observe the motor is in ON condition indicates everything is normal which includes

- Driver is not drunken.
- No leakage of fuel gas.
- Driver is not in drowsiness state.
- No accident occurred.

The entire setup ensures a faster rescue operation for accidents and also warns the driver on certain stances such as over speeding, while going to drowsiness state and if any leakage of LPG in the system.

On a whole, this system helps in a better and a faster way of rescue in lone stances, this helps in reducing the risk of losing lives by establishing some rescue in a minimal time.

VI. OBJECTIVES ACHEIVED

Our prototype is aimed to be designed and implemented by the automobile manufacturers in the vehicles. As it locates an accident and prevents the driver in undergoing an accident at typical times. The objectives achieved from the proposed model are summarized below:

- Mediate the Sensor information and locate the accident location using GPS for help and rescue.
- In case of any gas leakage(LPG) , it alerts the driver.
- In case of any drowsiness, it alerts the driver as a threatening call (vibration /Buzzer).

VII. CONCLUSION

The Proposed system makes use of various sensors to detect an accident, leakage of fuel gas, level of alcohol present and drowsiness. prevents drunken people to drive the vehicle, Alerts driver when he/she goes to drowsiness state, Stops the vehicle when it detects any leakage of CNG/LPG in the engine cabin and detects an accident on real time system and inform the supervisory with the accident location.

As a further extension, the Drowsiness of the driver can be precisely detected using image processing and based on the state of drowsiness, command will be initiated with an alert and the vehicle will automatically slows down and stops. Fire Extinguishers will be automatically sprayed if there is any fire in the vehicle. Accident detection can be linked directly to the air bag system in vehicles, It makes more simpler reducing the complexity.

VII. REFERENCES

[1] Usman Khalil, Adnan Nasir, S.M. Khan, T. Javid, S.A. Raza, A. Siddiqui "Automatic Road Accident Detection using Ultrasonic Sensor," IEEE 21st International Multi-Topic Conference (INMIC) 2018.

[2] Sahil Haria, Vaibhav Gala, Shubham Anchaliya, Tina Maru, "Car Crash Prevention And Detection System." Second International Conference on Intelligent Computing and Control Systems. (ICICCS 2018)

[3] Ajay Kumar, Mukesh Kumar, Balawinder Singh, "Designing and Implementation of Smart LPG Trolley with Hoe safety". 2016 2nd international conference on next generation computing technologies (NGCT 2016)

[4] Prajnyajit Mohanty, Pallem Siddharth, Kunja Bihari Swain, Rakesh Kumar Patanaik, "Driver Assistance for the Detection of Drowsiness and Alcohol Effect," 2017 IEEE 3rd International Conference on Sensing, Signal Processing and Security (ICSSS)

[5] B.S.Sourab, Ranganatha Chakravarthy H.S, Sachith, " Implementation of Home Automation Using Eye Blink Sensor," 2014 International Conference on Electronics, Communication and Computational Engineering (ICECCE)

[6] Nagarjuna R Vatti, Prasanna Lakshmi Vatti, Rambabu Vatti, Chandrasekhar Garde, "Smart Road Accident Detection and Communication System," 2018th International Conference on Current Trends toward Converging Technologies, Coimbatore, India.

[7] Arjit Banik, Bodhayan Aich, Suman Ghosh, "Microcontroller based low gas leakage detector with SMS," 2018 Emerging Trends in Electronic Devices and Computational Techniques (EDCT)

[8] Zheng Xu Hou, Yiping Chen," A Real Time Vehicle Collision Detecting and Reporting System Based on Internet of Things Technology," 2017 3rd IEEE International Conference on Computer and Communications.

[9] Parag Parmar, Ashok M. Sapkal, " Real Time Detection and Reporting of Vehicle Collision," International Conference on Trends in Electronics and

[10] Jan Kubicki, Jaroslaw Mlynczak, Jadwiga Mierczyk, Krzysztof Kopczynski," Optoelectonic system for stand-off detection of alcohol vapours," 2018 Baltic URSI Symposium(URSI).

[11] Anand kumar, N Anusha ,B Sai Srinivasa Prasad," Automatic Toll Payment, Alcohol Detection, Load and Vehicle Information Using Internet Of Things and Mailing System," 2017 international conference on intelligent computing and control(I2C2'17) .

[12] Hossam M. Sherif, M. Amer Shedid , Samah A. Senbel, "Real time traffic accident detection system using wireless sensor Network," 2014 6th international conference of soft computing (SoCPaR), Tunis, Tunisia.

Proceedings of the Fourth International Conference on Communication and Electronics Systems (ICCES 2019)
IEEE Conference Record # 45898; IEEE Xplore ISBN: 978-1-7281-1261-9

A Review on Various Inter Cluster Multi-hop Routing Protocols in Wireless Sensor Network

Sanjeev Kumar
ECE Department, NIT KKR
Kurukshetra, India
sanjeev_31705120@nitkkr.ac.in

Dheeraj Kumar Sharma
ECE Department, NIT KKR
Kurukshetra, India
sharma986dheeraj@nitkkr.ac.in

Abstract - Over the last few years, WSNs has attracted tangible involvement in many real time applications. They are composed of small, low cost sensor nodes and these nodes having limited power. After consumption of power, sensor nodes become dead and the life period of WSNs depends on life of sensor nodes present in the network. Sensor nodes are generally deployed in remote area where recharging or replacement of battery is not possible. Hence, it is compulsory to develop some the techniques to improve the life of the nodes and life-time of the network. Clustering protocol is used to increase the lifetime of the wireless sensor networks and for long distance data transmission; Multi hop roughing protocol are preferred. MH technique reduced the energy cost of every node which lies in path. This paper describes various inter cluster multi hop routing protocols in WSNs.

Keywords - ***Wireless Sensor Network, cluster, multi-hop and energy efficient routing protocols.***

I. Introduction

Wireless sensor networks are formed by small, compact, low energy, low cost, multifunctional sensor nodes which are placed in the wanted region. Each node can sense the physical condition of environment surrounding it and also can transmit and receive the data. Currently, WSNs have been broadly used for the tracking and surveillance, environmental monitoring, medical care, infrastructure management, and many other areas [1]. WSNs are usually used in military operations [2]. However, sensor nodes are generally spread out in the precipitous and hostile domain where it is tough to reach and power availability is restricted. Therefore, sensor nodes may be faulty and unreliable. Generally, hardware fault and software fault are the two types of fault mainly occurring in WSN. The fault in hardware is usually due to damage of sensor nodes or due to low energy, and then those nodes cannot collect and transmit the data. Hence, energy is the major issue in the WSNs. Efficient use of nodes' available energy can solve low energy problem in WSNs. By using routing process in the network, we can utilize the available energy of node efficiently. Hence, all researchers target the energy-efficient and reliable routing protocol.

According to structure of network, all the routing techniques in WSN mainly divided into two categories: 1) hierarchical routing, 2) flat routing [3]. Architecture of hierarchical routing technique helps to get high scalability and efficiency in the network. In this routing all nodes perform different works. Entire area of network is portioned into different clusters and every cluster contains member nodes and cluster head. In flat routing protocols, same type of work is performed by all the nodes in the network.

Data transmission between nodes and base station can transmit in mainly two ways: 1) Direct transmission, 2) Multi-hop transmission [4] [5]. In direct transmission, each sensor nodes transmit sensed data to base station without using any intermediate nodes. So, it use large amount of energy to transmit the data for the far nodes. To solve this issue, we use MH transmission. In this, all nodes work cooperatively to relay data to the base station; as a result the total distance is divided into small distances. Also multi-hop technique uniformly distributed the energy cost of network between the all nodes but it is not guaranteed that overall energy consumption along the path is minimized. So, it may possible that total cost in multi-hop transmission is greater than direct transmission.

Clustering is used to improve the life duration of the WSN and Multi-Hop (MH) techniques are preferred in long distance transmission reduce the energy cost every node which lies in path. So, for long distance, multi-hop communication is adopted among CHs. Figure 1 shows the multi-hop routing among CHs of clusters. This paper provides a review on different multi-hop routing techniques in clustering protocol.

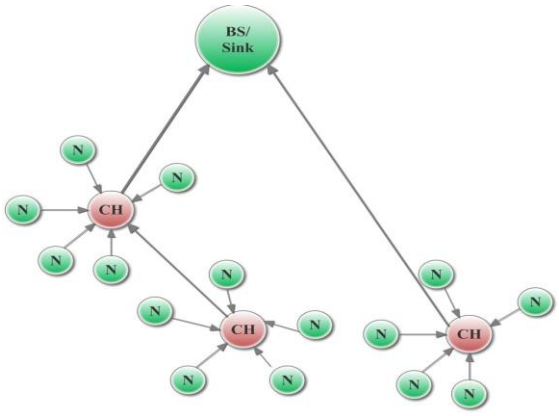

Fig. 1: Multi-hop in clustering protocol

II. Inter-cluster multi-hop routing protocols

1) Multi-hop-LEACH

In WSNs energy consumption is determine by radio energy model. According to this, energy consumption depends on

the distance from cluster head to base station. If distance between it is more than a threshold value, then energy consumption is directly proportional to d^4 (d=distance). In large area of network, distance between base station and some cluster heads are greater than threshold value. So, these cluster head dissipate their energy very rapidly and become dead. Such type of problem cannot be handles by basic LEACH. So, we use MH LEACH [6] which handles such type of problem. This routing technique improves the performance of network by choosing MH communication between base station and cluster heads. In multi hop leach protocol, set-up stage is same as to the LEACH protocol but in steady stage, CHs which distance is greater than threshold value are selected as hoping nodes via which transmitted data goes to the destination or BS. The CHs which distance is less than threshold distance from the BS, they transmit their information directly (single hop communication) to base station.

Multi-hop LEACH is scalable and energy efficient but it is more complex and it increase network overhead because of MH transmission via relay nodes.

2) Energy-LEACH

E-LEACH [7] technique is based upon the residual or remaining energy of nodes. Cluster head selection is in this technique is depending upon the energy left in the nodes but working principal of it is same like LEACH. In this technique, any node become a CH in first round because initially all nodes have same energy, so each nodes have the same probability select as a CH in the first round. Randomly, $N_{CH} = p$ x N_t number of nodes are chosen as the cluster heads. Where N_{CH} denotes the number of CHs in the 1st round and other notations are as usual. In 1st round each node consume different amount of energy, so energy left in each nodes are different after finishing of 1st round. So, the nodes in which left energy (residual energy) have more, that nodes have more probability to select as cluster heads and remaining are member nodes.

In E LEACH protocol, always higher energy nodes are selected as cluster heads in every round that improved the overall life of the WSNs. This protocol only worried about the residual energy of the nodes it is not worries about optimal path. By selecting optimal path, more energy can be saved. So, this protocol is not overall energy efficient.

3) WST LEACH

WST LEACH [8] protocol is solving the following two problem of basic LEACH, first is, cluster head selection and second is, in which way CHs and base station communicate. In this protocol, CH selection process is different for forming a weighted spanning tree. For this protocol, a new modified $T(n)$ formula is given by equation 1 for CH selection. In Equation 1, the coefficients are denoted by c_1, c_2 and c_3, node n residual energy is denoted by *'e'*, initial energy is denoted by 'E_0', '*Nb'* denotes the *n* neighbor's node, '*N'* denotes the total nodes present in the WSN, *'d'* denotes the distance and probability of node n selected as CH is denoted by '*p'*.

$$T(n) = \frac{P}{1 - P * (r \; mod(\frac{1}{p}))} * \left[c_1 * \left(\frac{e}{E_0}\right) + c_2 * \frac{Nb}{p * N}\right) + c_3 * (1/d)] \quad (1)$$

In this protocol, CHs communicates with base station by multi-hop communication. Each CH assigned with some weight. According to this weight spanning tree is formed. Weight formula is given by equation 2.

$$W(j,k) = \frac{e(j)}{E_0} * \frac{N}{M(j)} * \frac{1}{d(j,k)^i} \quad (2)$$

Where, 'W (j,k)' is weight of jth and k^{th} cluster head and whichever is higher magnitude between *i* and *j* cluster heads that include in the spanning tree. '*e(j)'* denotes remaining energy of jth cluster heads. CHs having highest weight are joining spanning tree.

By using WST LEACH protocol, communication path is optimized. So, it is more energy efficient and also it can improve the life of the network but it has some issues of scalability and control packets overheads.

4) Multi-hop Routing-LEACH

The target of MHR-LEACH [9] is to reduce the power utilization by the network and increase the life of network. In this protocol, the entire areas are divided into many layers and make sequence of various layers of clusters and all these clusters having equal size in every layer. It means that any member nodes of cluster transmit their information to base station in same no. of hops. By the help of TDMA scheduling, base station allot a time slot for each cluster head and according to it, each cluster heads allot a time slot for own cluster member . In this protocol, the node having highest residual energy can select as a cluster head.

MHR-LEACH protocol is increase the life of the network and it is highly scalable but hotspot problem the main issue with it.

5) LEACH D

LEACH-D [10] protocol is used to achieve better network lifetime. It is achieved in the three ways. 1st approach is CHs selection. It is depend upon energy left in the nodes and the nodes density distribution. In this protocol, nodes which located in high density and having more remaining energy are chosen as cluster head. Second approach is based upon distance to base station and degree of connectivity. In this cluster head decide and calculate the cluster radius. Cluster is form by nodes join the CH according to distance from the CH to the BS and energy of cluster head. The cluster head reduces energy consumption by adopting this approach. In third approach, multi-hop transmission is uses among CHs to send information from member nodes to base station.

In LEACH D, CH is selected by threshold value which is calculated by help of energy and connectivity density factor. This technique increases the scalability and energy efficiency of the network but hotspot problem arises in it.

6) C-LEACH

In Cell LEACH [11] protocol, total area is divided into some hexagonal cells and each cell having some sensor nodes. A cluster is formed by seven nearby cells. A special node is present among the nodes present in the cells which called cell head and other nodes are called as member nodes and every cluster having a cluster head and they are changing randomly in each round. According to TDMA, time slice is allotted by cell head to the cell members and the data transmission by cell member during its allotted time slice. In this protocol, when member nodes transmit their information to cell heads, all other nodes are off, after that cell head send the all received information to own cluster head and then cluster head send it to base station by choosing the smallest path between them.

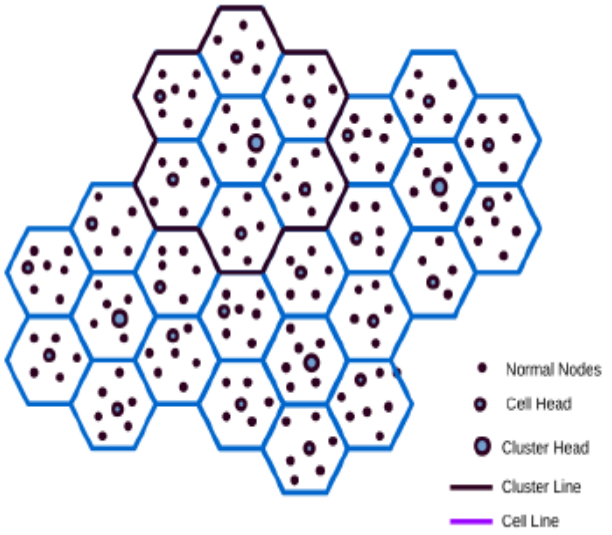

Fig. 2: Cells and Cluster.

Figure 2 shows the cells and clusters which form by seven cells.

C LEACH improves scalability and energy efficiency and it provide very good network coverage but overhead and complexity are increased.

7) Enhanced-LEACH

In E-LEACH [12] protocol, sufficient number nodes selected as cluster heads and round time is varied in each round to improve the life of network and distribute energy equally. To calculate the power used, this protocol add the power consume by each node of the network to send the data. In this protocol, two conditions are there for the selection cluster head and these conditions are following in every round. 1st is energy left in the nodes and 2nd is amount of energy required to send information to base station. The main benefit of following these two conditions is that energy distribution in the network is uniformly distributed. In this protocol, CH selection is depending upon remaining energy of node and power required to transmit information from cluster head to base station.

The E-LEACH protocol is energy efficient and highly scalable but packet overhead and delay in the transmission are the issue with it.

8) EEMH-LEACH

EEMH-LEACH [13] protocol is use to minimize the problem of direct communication between cluster head to base station and selection of cluster head in basic LEACH. Three different approaches have been used in this protocol. First one is average energy remaining energy are used for the selection of cluster heads, second one is finding a path between cluster head and base station for communication and in this path energy cost should be minimum, third one is direct communication between base station and nodes which are nearer to it. For selection of cluster head, we have required to calculate the a threshold value *TH*(*n*) similar to LEACH. But it have one extra parameter which is energy remaining. It is denoted by *E(Re)*. New threshold *TH*(*n*) and *E(Re)* are given by eq. 3 and 4.

$$TH(n) = \begin{cases} \dfrac{P}{1 - P * (r \bmod (\frac{1}{P}))} * E(Re) & : if\ n \epsilon G \\ 0 & : otherwise \end{cases} \quad (3)$$

$$E(Re) = \begin{cases} \dfrac{E_{res} - E_{avg}}{E_{res}} & : if\ E_{res} > E_{res} \\ 1 - E_{avg} & : otherwise \end{cases} \quad (4)$$

When cluster head receives CH message from the cluster head or base station they computes communication cost matrix *b* and it is calculated by help of eq. 5.

$$b = \begin{cases} C(m) + d_{mn}^4 & : d_{mn} \geq d_0 \\ C(m) + d_{mn}^2 & : d_{mn} < d_0 \end{cases} \quad (5)$$

Where *C*(*m*) denotes the communication cost matrix of node *m* & d_{mn} denotes the displacement between nodes *m* & *n*. using equation 5 and 6 we can calculate the cost metric of node *n*.

$$C(n) = \min(C(n), c) \quad (6)$$

Using cost matrix of *m* we can find data sending path between cluster head and base station.

EEMH-LEACH technique uses multi-hop and single hop to send data between clusters and BS. So, it saves significant energy and also good in packet delivery but delay in the packets transmission is increased.

9) Orphan-LEACH

In WSNs some nodes are there for which no cluster head are assigned. These nodes are called orphan nodes which are consider in O-LEACH [14]. This protocol is discussed in two situations. In 1st situation, a member nodes work like a gateway of orphan nodes and the orphan nodes transmit own information to the gateway by joining it. After that, it collects the information and transmits them to base station. In 2nd situation, nodes which lie in an unclosed region are called orphan nodes and they create a sub cluster. Cluster head selection is based upon the distance from gateway nodes.

This protocol is use to get large coverage area rate of connectivity. It is more energy efficient and scalable. The issue with it is searching of orphan nodes and knowledge about it.

.

10) Cross Layer-LEACH

Cross layer method is used in CL-LEACH [15] to increase life of network. Entire function of CL-LEACH is partition in four different parts. First one is making of cluster, in which every node in the cluster choose own cluster head according distance between cluster head and base station and energy. In second part, routing process achieve in two steps: (i) distance calculation and (ii) route discovery. Distance between two nodes is calculated by eq. 7.

$$D = \sqrt{(p_2 - p_1)^2 + (q_2 - q_1)^2} \qquad (7)$$

Where, (p_1, q_1) is coordinates of first node and (p_2 , q_2) is coordinates of second node. In the route discovery, first node always checks the cache in the route before transmitting the information to next node, if any route cache present in the path then information is not transmitted otherwise transmitted. In CL-MAC model if remaining energy of node is more than threshold value then this node works like a relay node in MH communication. Brocken link along the path is detected by route maintenance and they are maintaining by adding new paths line in pre-existing path.

CL-MAC protocol is energy efficient, it has low message cost and live nodes present in the network are more, although it have complexity and message overhead.

11) DHL-LEACH

DHL-LEACH [16] technique resolves the problem which created due to double hop transmission structure. The sensor node nearer to base station lives in lower most layer of network. According to consumption of power, entire area is portioned in some layers. In data sending period, nodes present in the lower most layers measure their distance from cluster head and base station and compare it. If BS distance is shorter than to CH then that nodes directly transmit their sensed information to base station else they transmit them to cluster head. So, the nodes which lies away from base station, they transmit their information to cluster head, after that cluster head transmit them to base station.

DHL LEACH technique is better in terms of power utilization but in large scale networks it is suffers from short node lifespan problem.

12) Improved MHT-LEACH

In IMHT-LEACH [17] divides the all cluster heads into many levels, instead of dividing in only two levels like in MHT-LEACH. This protocol gives a different way to route the information to BS via different the levels. It reduces the data transmission cost when network area is large. In this protocol, all the cluster heads are separated into levels according to distance from the base station and *do/2* is the length of each level. This protocol has four stages to set a route between cluster head and base station: (i) Setup phase (ii) Announcement Phase (iii) Routing Phase and (iv) Redundancy Phase.

IMHT-LEACH technique improves the life of the network, stability and throughput WSNs.

13) EACBM

The basic operation of EACBM [18] is clustering and multi-hoping. It has three level heterogeneous clusters and three types of sensor nodes (SNs): (i) normal sensor nodes, (ii) intermediate sensor nodes and (iii) advance sensor nodes. These all nodes randomly deployed in the network area. In this technique, selection of cluster head is depend upon the probabilistic equation and its count is fixed. In this protocol, the nodes which are not attach to any cluster head or they not comes under the sensing range of cluster head are created a sub cluster because it is compulsory to gather information from every nodes of network. Cluster head gather information from member node and transmit them to base station by MH communication. Working diagram of EACBM shown by figure 3.

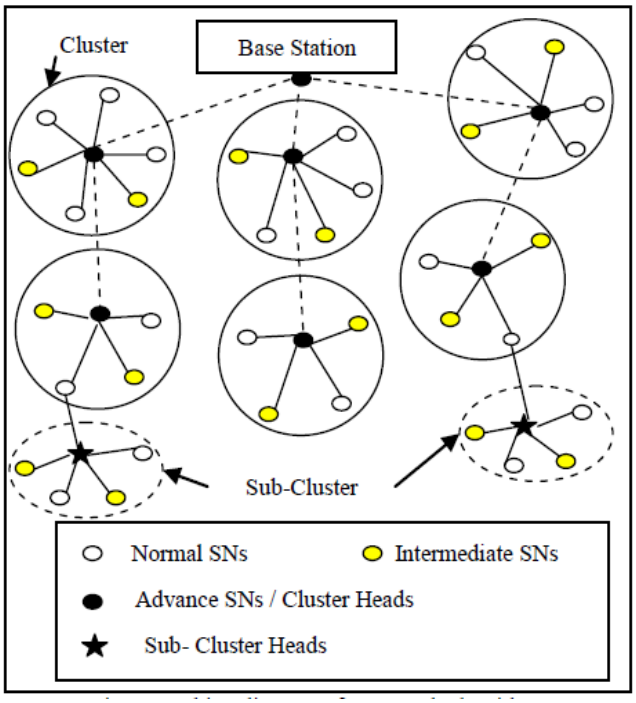

Fig. 3: Working diagram of EACBM protocol

EACBM protocol increase stability and life of the network and provide a stabilized model for WSNs.

14) ECMR

ECMR [20] is very new technique on cluster bases which improved the energy efficiency successfully by using multi hop routing protocol. This technique combines the two different technique which are clustering and Dijkstra routing technique. The total left energy of each CH along with total transmit power is used to calculate the weight load. CHs which have highest remaining energy and lower transition power having high probability to join the shortest path communication. Dijkstra algorithm use weight factor

to find the shortest path between source node to sink node or BS in ECMR.

Out of ECMR and LEACH protocols, the performance of ECMR is good in terms of life time of network and packet received at target node or BS.

III. Comparison between different Inter-cluster multi-hop routing protocols

The comparison of different inter cluster multi hop routing in clustering protocol is presented in Table 1. The comparison is done on the basis of their energy efficiency, scalability, complexity, overhead and delay.

.

Table 1: Comparison of different inter-cluster multi-hop routing techniques.

Routing protocols	Energy Efficiency	Scalability	Complexity	Overhead	Delay
Multi-hop LEACH	High	High	High	Moderate	High
Energy LEACH	High	High	High	Moderate	High
WST LEACH	Very high	High	Moderate	High	Small
MHR LEACH	High	High	High	High	High
LEACH D	Very high	Very high	Very high	High	Low
CELL LEACH	Moderate	Very high	Very high	Very high	Moderate
E LEACH	High	Very high	High	High	High
EEMH LEACH	Very high	Moderate	Very high	High	Small
O LEACH	High	High	High	High	High
CL LEACH	High	Moderate	High	High	High
DHL LEACH	High	High	Low	Moderate	Moderate
IMHT LEACH	Very high	Very high	High	Moderate	Moderate
EACBM	High	Very high	High	Moderate	Moderate
ECMR	Very high	High	Very high	Moderate	High

IV. Conclusions

In this paper, the several inter cluster multi-hop routing protocols are discussed in which IMHT LEACH and EACBM protocol are better in term of scalability, LEACH-D have low delay and the ECMR routing technique is better than other protocol in terms of energy efficiency. It is also good in terms of overhead but it is more complex. All discussed protocols mainly consider the problem of energy consumption and at some extent they overcome it. By balancing the load of nodes, we can save the energy consume by the nodes and increase the life of the network.

References

[1] Yick, J., Mukherjee, B., Ghosal, D.: "Wireless sensor network survey", *Comput. Netw.*, 2008, 52, (12), pp. 2292-2330.

[2] Li. Y. Thai, M.T.: "*Wireless sensor networks and applications*" (Springer Science & Business Media, 2008).

[3] Al. Karaki, J.N., Kamal, A.E.: "Routing techniques in wireless sensor networks: a survey", *IEEE Wirel. Commun.*, 2004, 11, (6), pp. 6-28

[4] Heinzelman, W.R., Chandrakasan, A., Balakrishnan, H.: 'Energy-efficient communication protocol for wireless microsensor networks'. Proc. 33rd Annual Hawaii Int. Conf. System Sciences, 2000, p. 10

[5] Wang, J., Cho, J., Lee, S., *et al.*: "Hop-based energy aware routing algorithm for wireless sensor networks", *IEICE Trans. Commun.*, 2010, 93, (2), pp. 305-316

[6] Y. Lei, F. Shang, Z. Long, and Y. Ren, "An energy efficient multiple-hop routing protocol for wireless sensor networks," in *Proc. 1st Int. Conf. Intell. Netw. Intell. Syst. (ICINIS)*, Nov. 2008, pp. 147-150.

[7] F. Xiangning and S. Yulin, "Improvement on LEACH protocol of wireless sensor network," in *Proc. Int. Conf. Sensor Technol. Appl.*, Oct. 2007, pp. 260-264.

[8] H. Zhang, P. Chen, and S. Gong, "Weighted spanning tree clustering routing algorithm based on LEACH," in *Proc. 2nd Int. Conf. Future Comput. Commun. (ICFCC)*, vol. 2. May 2010, pp. V2-223-227.

[9] M. O. Farooq, A. B. Dogar, and G. A. Shah, "MR-Leach: Multi-hop routing with low energy adaptive clustering hierarchy," in *Proc. 4th Int. Conf. Sensor Technol. Appl. (SENSORCOMM)*, Jul. 2010, pp. 262-268.

[10] Y. Liu, K. Xu, Z. Luo, and L. Chen, "A reliable clustering algorithm base on LEACH protocol in wireless mobile sensor networks," in *Proc. 2nd Int. Conf. Mech. Electr. Technol. (ICMET)*, Sep. 2010, pp. 692-696.

[11] A. Yektaparast, F. H. Nabavi, and A. Sarmast, "An improvement on LEACH protocol (cell-leach)," in *Proc. Adv. Commun. Technol. (ICACT)*, Feb. 2012, pp. 992_996.

[12] J. Xu, N. Jin, X. Lou, T. Peng, Q. Zhou, and Y. Chen, "Improvement of LEACH protocol for WSN," in *Proc. 9th Int. Conf. Fuzzy Syst. Knowl. Discovery (FSKD)*, May 2012, pp. 2174-2177.

[13] A. Antoo and A. R. Mohammed, "EEM-LEACH: Energy efficient multi-hop LEACH routing protocol for clustered WSNs," in *Proc. Int. Conf. Control, Instrum. Commun. Comput. Technol. (ICCICCT)*, Jul. 2014, pp. 812-818.

[14] W. Jerbi, A. Guermazi, and H. Trabelsi, "O-LEACH of routing protocol for wireless sensor networks," in *Proc. 13th Int. Conf. Comput. Graph, Imag. Vis (CGiV)*, Mar. 2016, pp. 399-404.

[15] P. Marappan and P. Rodrigues, "An energy efficient routing protocol for correlated data using CL-LEACH in WSN," *Wireless Netw.*, vol. 22, no. 4, pp. 1415-1423, May 2016.

[16] J. Y. Lee, K. D. Jung, S. J. Moon, and H. Y. Jeong, "Improvement on LEACH protocol of a wide-area wireless sensor network," *Multimedia Tools Appl.*, vol. 75, pp. 1-18, Jul. 2016.

[17] Hui Chen, Feng Wang and Mu Zhang "An improved inter-cluster multi-hop LEACH protocol oriented reliable transmission in WSNs," *3rd IEEE Int. Conf. Computer application*, 2017, pp. 193-197.

[18] Amanjot Singh Toor and A. K. Jain "A new energy aware cluster based multi-hop energy efficient routing protocol for Wireless Sensor Networks" *6th IEEE Int. Conf. on Smart Energy Grid Engineering*, 2018, pp. 133-137.

[19] Thong Nhat Tran, Toan Van Nguyen, Vo Nguyen Quoc Bao and Beongku An, "An energy efficiency cluster-based multi-hop routing protocol in wireless sensor networks" *Int. Conf. on Advanced Technologies for Communications*, 2018, pp. 349-353.

Proceedings of the Fourth International Conference on Communication and Electronics Systems (ICCES 2019)
IEEE Conference Record # 45898; IEEE Xplore ISBN: 978-1-7281-1261-9

Design of Microstrip Bandpass Filter Based on Genetic Optimization

Navin Baaskar E V, Harshini R, Poornima T, Natarajamani S
Department of Electronics and Communication Engineering
Amrita School of Engineering, Coimbatore
Amrita Vishwa Vidyapeetham, India
E-mail: s_natarajamani@cb.amrita.edu

***Abstract*—In this paper, Structural optimization based microstrip bandpass filter design is discussed. Conventional optimization mainly focuses on the dimensional optimization of the filter. Here, the focus is to design a bandpass filter using rectangular patch-based resonator. The obtained result is then optimized using Genetic Algorithm which is part of Evolutionary algorithm. In order to obtain an optimized result, we define a fitness function in terms of S_{11} (dB) and S_{21}(dB) parameters. The final design of the filter will possess maximum transmission co-efficient and minimum reflection co-efficient.**

***Index Terms*—Microstrip bandpass filter, genetic optimization, narrow band frequency response, patch resonator.**

I. Introduction

In wireless technologies, bandpass filters are widely used in transmitters and receivers. These filters are main components at the front end of these devices. It plays an important role in limiting the bandwidth of the output signal to the minimum of transfer information at desired speed. Narrowband microwave bandpass filters with high performance are the most preferred ones for the modern wireless communication systems [1]. A balanced patch type resonator has the advantage of having high resistance to outside noise compared to the unbalanced structures [2]- [4]. Evolutionary algorithm can be used to obtain optimum solution by selection and evaluation of various designs [5]- [6]. The patch based resonator is a good contender for the bandpass filter because it is easy to remove cells from the patch to reduce insertion loss and thus improve transmission [7] - [9].

In this paper, the genetic algorithm(GA) has been used to design bandpass filter with higher performance. We propose a GA-optimization method which introduces a fitness function estimating the S-parameters in a passband. The fitness function is defined in a way that increases transmission coefficient and decreases reflection coefficient. The GA-optimization method used here involves the following processes Representation, crossover and mutation. Finally, the best solution is returned as the final output.

II. OPTIMIZATION DESIGN

Fig.1. shows a design of microstrip bandpass filter. It consists of a substrate with dielectric constant ϵr = 10.2. The substrate used in this analysis is Rogers RT/Duroid 6010. The dimensions of the substrate are length L_1=15mm, width W_1 = 12mm and thickness H_1 = 1.27mm. The dimension of the conductor are L_2 = 9mm, L_3 = 2.7mm, W_2 = 0.6mm, W_3 = 8.4mm. The dimensions of each cell of the square patch resonator are length P = 1mm and width Q = 1mm.

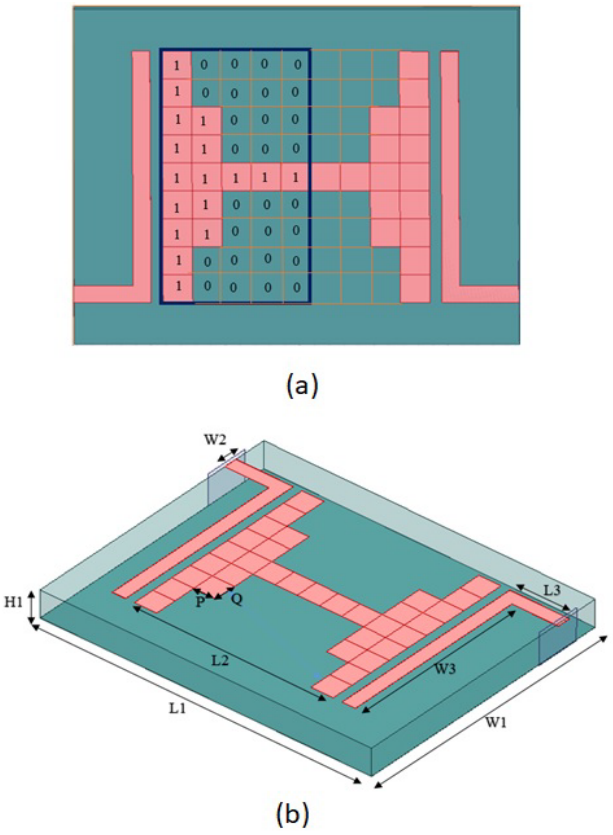

Fig. 1. GA optimized filter (a) top view and (b) Bird view

In the GA, the circuit is described by binary code as the conducting cells of the square patch resonator are 1 and other cells are 0.The geometry of the circuit is organized in such a way that it is symmetrical about y axis. The input and output ports are placed at inverted L shaped feed lines.

A. Fitness Function

The fitness function used for reflection coefficient and transmission co-efficient are taken into consideration. It is expressed as follows:

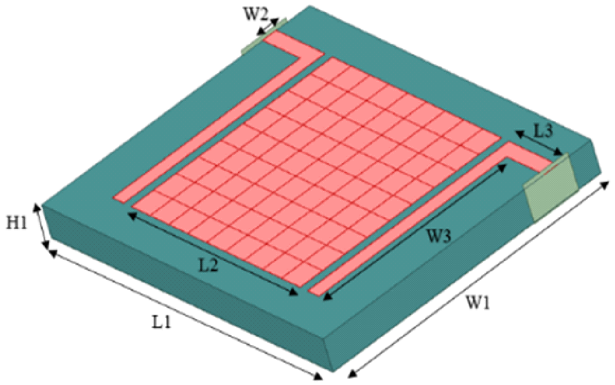

Fig. 2. Initial structure of filter

$$F = \{S_{21}(dB)/S_{11}(dB)\}\ at\ 2.5GHz \leqslant f \leqslant 4.5GHz \quad (1)$$

Reflection coefficient (S_{11}) of the filter was chosen because it describes the impedance matching which in turn shows how well the filter is capable of making use of the input power that is being provided from the feed. Transmission coefficient (S_{21}) of the filter was chosen because it shows how well the input power is being transmitted to the output port without getting attenuated. The transmission co-efficient has to be maximized and the reflection co-efficient has to be minimized. Thus the fitness function is maximized in the passband to obtain an optimal solution.

III. Filter Design

Fig.2. shows the initial design of the bandpass filter using patch resonator. Using GA, the cells are removed uniformly from the resonator. The initial population is created randomly with symmetry along the y axis. The fitness function of the initial population is calculated and stored

A. Crossover

The crossover is designed in such a way that it combines the genetic information into two parents to generate new off springs. The crossover population is generated from the initial population. Two parents (initial matrix) are taken at a time and are combined together to produce a progeny (crossover matrix).

B. Mutation

The crossover population is mutated to obtain a new set of pro-genies. Mutation is more powerful in the sense that it has the capability to give birth to a more distinct variety of children.

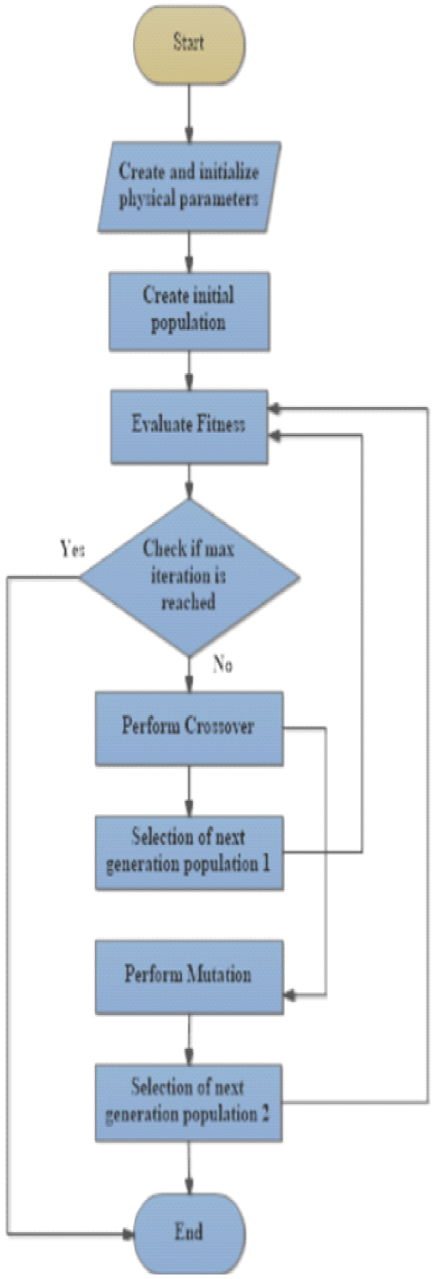

Fig. 3. Flowchart of algorithm

IV. Result and Discussion

A. Selection

The fitness function of the initial population, crossover population and mutated population are calculated. These fitness function values are compared to obtain the best population set. This set is stored as the initial population for the next generation. This process is repeated for the given number of iterations. After the final iteration, the best solution (Fig.1.) is obtained.

The initial design (Fig.2.) has the passband centre frequency

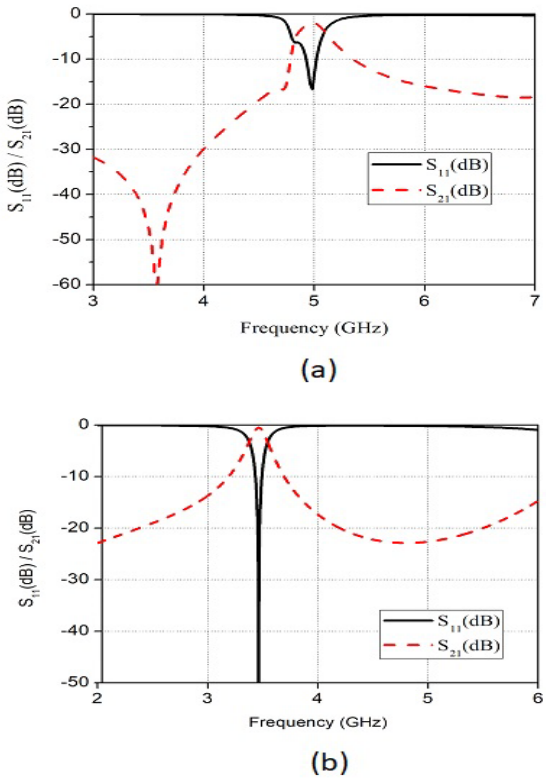

Fig. 4. (a) S parameters Vs Frequency for Fig. 2 (b) S parameters Vs Frequency for Fig. 1

located at 5GHz.The S-parameter values obtained at the centre frequency are S_{11}= -16.12(dB) and S_{21}= -1.92(dB). The GA-optimized design (Fig.1.) has improved transmission performance with lesser S_{11} and higher S_{21}.The passband centre frequency is shifted to 3.3GHz and the values of S-parameters are S_{11}= -25.13(dB) and S_{21}= -0.52(dB).

V. CONCLUSION

In this paper, the Bandpass filter has been structurally optimized using evolutionary algorithm. From the generation of the initial population to performing the genetic operations on subsequent population, measures were taken to ensure that genetic diversity was maintained. The output of the evolutionary algorithm iterations is quite satisfactory. The added advantage of the structurally optimized designs is that the area occupied by the optimized designs is much lesser than the base design. Transmission performance has been improved to a greater extent in the passband.

REFERENCES

[1] Y. S. Mezaal and H. T. Eyyuboglu, "A new narrow band dual-mode microstrip slotted patch bandpass filter design based on fractal geometry," 7th International Conference onComputing and Convergence Technology (ICCCT), pp. 1180-1184, 2012.

[2] Liu, Qianwen Wang, Jianpeng Yixuan, "The Compact balanced bandpass filter using isosceles right triangular patch resonator," Electronics Letters, vol.53, pp.253-254, Feb 2017.

[3] Mezaal, Dr.Yaqeen Al-zayed, Ayman, "Design of Microstrip Bandpass Filters Based on Stair-Step Patch Resonator," International Journal of Electronics, vol. 3, pp.477-490, Nov 2018.

[4] V. Radonic and V. Crnojevic-Bengin, "Cross-coupled microstrip filter using grounded patch resonators," 41st European Microwave Conference, Manchester, pp. 763-766, 2011.

[5] T. Nishino and T. Itoh, "Evolutionary generation of microwave line-segment circuits by genetic algorithms," IEEE Transactions on Microwave Theory and Techniques, vol. 50, no. 9, pp. 2048-2055, Sept. 2002.

[6] R. Sushmeetha and S. Natarajamani, "Compact Tunable Dual-band Bandpass Filter using Edge-open Split Ring Resonators for X-Band Applications," International conference on advances in computing communications and information, pp.1624-1626, 2018.

[7] M. Chang and W. Weng, "A dual-band slot antenna design using particle swarm optimization," International Applied Computational Electromagnetic Society Symposium (ACES), pp. 1-2, 2017.

[8] K Kavitha, M Jayakumar, "Design and Performance Analysis of Hairpin Bandpass Filter for Satellite Applications," Procedia Computer Science, vol. 143, pp. 886-891, 2018.

[9] Akinori Kido, Hroyuki Deguchi, Mikio Tsuji and Masataka Ohira, "Multi-Resonator Generation in Arbitrarily-Shaped Planar-Circuit Filters by Genetic Optimization," European Microwave Integrated Circuit Conference, pp. 443-446, 2007.

Proceedings of the Fourth International Conference on Communication and Electronics Systems (ICCES 2019)
IEEE Conference Record # 45898; IEEE Xplore ISBN: 978-1-7281-1261-9

Support Vector machines based gender detection by using Gait Energy image Projections

Hema M[1], K Esther Rachel[2]
1. Assistant Professor, Dept., of ECE ,JNTUK University College of Engineering, Vizianagaram, India
2. JNTUK University College of Engineering, Vizianagaram, India
hema.asrith@gmail.com, rachel.kathi@gmail.com

***Abstract*— Determining the gender of a person has a prominent role in many social interactions. Recognition of gender will be beneficial in certain applications like interaction of human and computer, scrutinizing systems, Demographic research. Identification of gender can be made by using different sources such as through voice, facial expressions and gait. Due to the distinctive advantages of gender perception based on gait, such as non-invasive, non-contact and obtained easily at a distance, there is an increase in the interest of researchers in the classification of gender-based on gait. In the proposed work, there are 2 stages of methodology. The first stage consists of determining Gait energy image projection model(GPM) which is our new proposed descriptor for gender perception and in the second stage; the proposed descriptors are merged with the better existing ones such as GEI, Gait Entropy Images, Dynamic Gait Energy Image (D-GEI), Gradient Gait Energy Image (GGEI) to enhance the performance. Finally ,for classification, SVM classifier is given to the proposed descriptors for determining the gender. The OU-ISIR database and CASIA datasets are considered for the gender evaluation and comparison of different performance metrics like Accuracy, Precision, Recall and Error rate.**

Keywords*— *Gait Energy Image Projection Model (GPM), Gait Analysis, Gender recognition

I. INTRODUCTION

The recognition of gender has an eminent role in social communication. Many biological features were applied for gender identification such as footprints, sound, face and gait. Perception at a great distance can be handled with gait when compared with voice (or) face[1]. Nonaggression, accessible collection and non-contact are some of the advantages of gait. Due to this, gait has an incomparable place in gender recognition. Biometric systems, surveillance systems are some examples to explain the benefits of gait.

Generally, for the confirmation of a person, reliable person recognition schemes are required. The key role of such recognition systems is to confirm that, the services are done only by the authorized users and not by any other persons. Accessing of computers, laptops, ATMs are the familiar examples for the secure access.

With the advancements of biometrics, it is easy for the establishment of person's identity based on "who he/she is" rather than " what he/she possess". In the 19th century beginning, biometrics are used for the criminal identification. Later, biometrics extended its applications from forensics, convicts and prisoners identification to person identification in many civilian applications.

Gait is an essential way of human locomotion [2]. In the present days, there are two significant categories of gait approaches. They are Model dependent approaches and Silhouette dependent approaches. To obtain the static and dynamic parameters in series, we will go with the model-based methods which establish a mathematical model that represents dynamic changes in walking. In the silhouette based method, to recognise the gender, the silhouettes of gait sequence characteristics are considered because of their low computational complexity and noise reduction.

Estimating human gender at a farther distance has several applications and also found solutions for face-based approaches disadvantages. Hence, in present paper, the highlighted concepts are different gender features on human gait which cited some great work dealing with gender classification based on gait at the beginning[3]. For the underscore of the relevant gender gait features, we introduce the proposed descriptor. As the estimation of gender by gait is a tough job, the idea of fusion is introduced that can improve recognition performance. Many of the recent works in the fusion of information explained that the several features fusion achieves better performance and robustness. It overcomes the individual feature based identification method in many applications. The experimentation also showed that the descriptors fusion had given splendid results when compared with the individual features recognition rate.

The preceding of paper is described as below; In section II, the work that is performed in previous research is described. In Section III, procedural steps of the identification method is described. Next, the methodology of proposed work and different features is described for gender recognition is given. In the former part of the paper, the fusion of descriptors is explained. Based on highly populated OULP database [4] and CASIA B database, the experimental study and results analysis of our proposed descriptor is presented in Section VI. A relative study of the put forth descriptor with the existing features and fusion of descriptors regarding performance like the Correct Classification Rate (CCR) along with the precision, recall and Error rate is presented. Finally, the conclusion of current paper is described in section VII.

XXX-X-XXXX-XXXX-X/XX/$XX.00 ©20XX IEEE

II. RELATED WORK IN GAIT ANALYSIS

Basically, humans have the capability of determining the age and gender on seeing a person. But , there are some cases, where the person is not clearly seen (or) observed through the human eyes. For example, in scrutinizing systems (or) in monitoring systems , a person is observed and captured through a camera. When the resolution of the captured image is low, then the person's details like gender (or) age can't be identified easily. To resolve this problem, we come across the gait analysis.

Gait has two modes of approaches for performing the analysis in recognizing a person's features. They are Model independent and Model dependent approaches. In the Model independent approach, pre-defined model will be absent. There are no assumptions on the description of model. Moving on to the model dependent approaches, the assumptions are made on the past research work and modelling of model is done based on the assumptions. Generally, model independent approaches are highly preferable than the model dependent approaches.

In the past days, by using the face features such as shape of the individual's face, its geometry and its appearance, the age and gender can be determined. In one of the research work , based on the face based features, age and gender is determined. Gender and age estimation can be done by observing the eyebrows, the way of clothing, the hair style and body shape. Static body features[5] and Dynamic body feature are the most appropriate features for the determination of gender of a person. Many research works are done[6] based on these features and gained good accuracy in gender recognition[7].

In the case of age prediction, the images of the faces that are taken at low resolution are not that suitable and analysis of such images is also not possible. Hence, the approaches using gait came into existence for determining both the age and gender of person as it is best suited for analysing low resolution images. As gait is referred to as the human walking, many of the age and gender related parameters like stride length, cadence speed will be different for different persons.

There are some research works done by researchers in the literature. For the calculation of contour-based information for the extraction of gait features,[8] showed age classification by using the descriptors such as FED, HMM[9] which gave some improvement in the recognition. A work is done in the age and gender classification for the finding of gait differences. For the extraction of gait features, silhouette is used and it is described in frequency domain. Depending on this work, many parameters in connection to gait are clearly demonstrated which differentiate the younger and elder.

The research work is also done based on the apparel features of a person for age and gender prediction by using footwear and clothing conditions and obtained better outcomes in gender prediction. There are some other features for this work such as Gait energy image which is generally used in age and gender perception and gave splendid results in its performance. Many research works are done based on GEI which is obtained from silhouettes to extract the spatial information and temporal information. But, there are some failures in using the GEI , that is, there is some unwanted information which occupies more amount of storage space.

Some of the authors suggested a new approach using the Gabor filters for the feature extraction which is suited for orienting the body shapes of the silhouettes. Many research works are performed based on the silhouettes, which is the important tool required for extracting any feature based on the applications.

In the gait analysis, determining age and gender is a complicated task. To overcome this problem, the concept of fusion is introduced. With the fusion of different gait features, the accuracy is enhanced and performance of the descriptors will also be increased. So, the concept of fusion is introduced for the proposed and existing descriptors.

Research works are done on biological features for identifying the gender and age of a person. By analysing the biological features such as speech given by person, based on fingerprints, based on the voice, the determination of a person is done. But, the biological features are noise sensitive and the information may be corrupted. As a result, the results produced from this noisy information may not be correct. So, gait analysis is considered as the best suitable solution for the age and gender prediction.

III. OVERVIEW OF THE METHOD

In the framework of the gender detection, there is some sequence of steps that have to be implemented and the same demonstrated in Fig.1

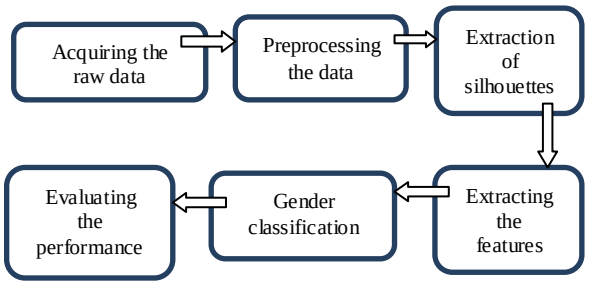

Fig 1. Gender classification taxonomy

IV. METHODOLOGY OF PROPOSED WORK

In the proposed work, two stages have to be implemented to classify the gender. In the first step, the Gait Energy Image Projection Model (GPM) is introduced which presents the vital gender-related parameters such as body size, head pitch, arm swing and stride length variations that characterise the gender in the respective gait cycle shown in Fig 2.

Two projections are present in GPM. They are Gait Energy Image longitudinal projection (GLP) and Gait Energy Image transverse projection (GTP). The GLP explains the stride length and body size whereas the GTP

gives the details regarding the head pitch, hunched posture and arm swing of the GEI image sequences given in Fig. 3.

In this paper, by using GLP and GTP, a new method is proposed and in parallel, we are highlighting the gender-related gait features. GPM combines both GLP and GTP by the use of the concatenation technique

$$GPM=\{GLP_{cycle}\ U\ GTP_{cycle}\} \quad (1)$$

Mathematically, GLP_{cycle} is defined as equation(2)

$$GLPcycle = \frac{1}{M}\sum_{i=1}^{M} GLPi \quad (2)$$

Here, M defines number of frames ; GLP_i defines *i*th frame vector of GLP.
And GTP_{cycle} is defined as equation(3)

$$GTPcycle = \frac{1}{M}\sum_{i=1}^{M} GTPi \quad (3)$$

M defines number of frames ; GTP_i defines *i*th frame vector of GLP.

Gait energy images (GEI): GEI represents the spatiotemporal information of silhouette images from entire gait cycle. Averaging the silhouette from the entire gait cycle gives energy image.

The D(x,y) represents GEI and calculated by using equation (4)

$$D(x,y) = \frac{1}{N}\sum_{t=1}^{N} Bt(x,y) \quad (4)$$

Where N defines number of gait cycle images; x and y are the coordinates of every image B.

Gait entropy images (GEnI): It is obtained from normalised silhouettes. From gait cycle, the calculation of Shannon entropy is performed for individual pixels of silhouette images.

Uncertainty associated with any random variable is given by Shannon entropy. With the use of Shannon entropy, the randmoness of the pixel is evaluated.

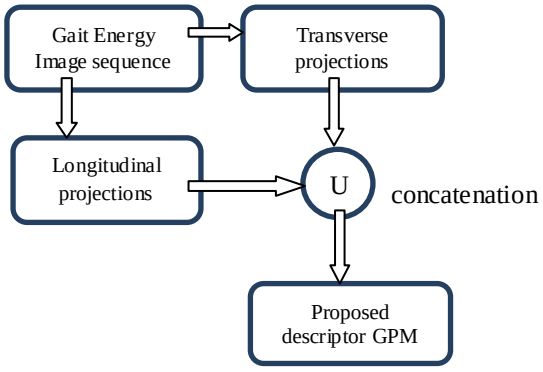

Fig .2 Proposed descriptor

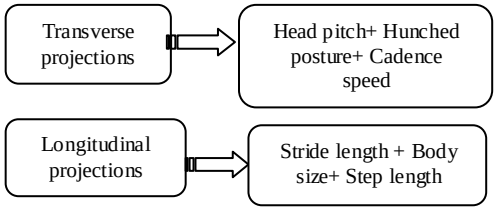

Fig. 3 Projections of GEI

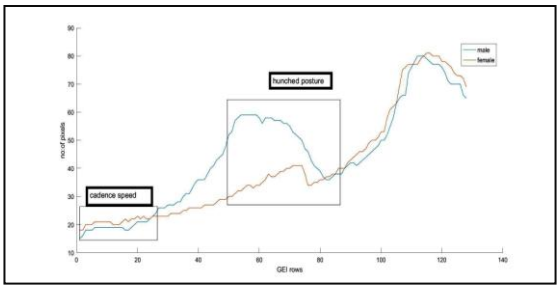

Fig. 4 GTP representation for male and female

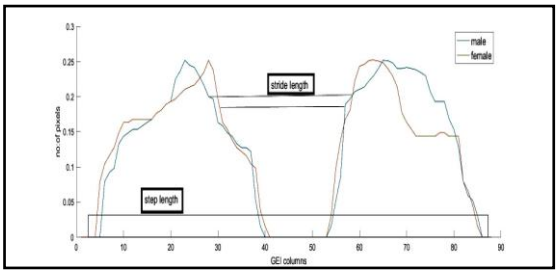

Fig. 5 GLP representation for male and female

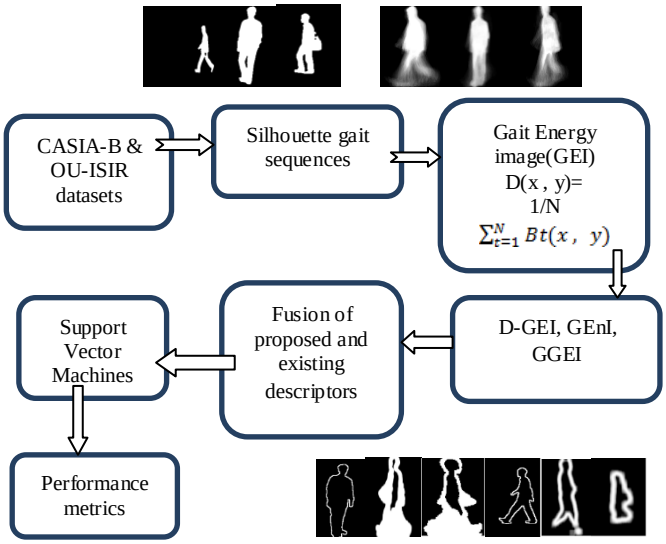

Fig. 6 Flow chart of the proposed methodology

The entropy of the fixed pixel location intensity value from a gait cycle is given by

$$H(x,y) = -\sum_{k=1}^{K} pk(x,y)\log 2pk(x,y) \quad (5)$$

Where x, y defines pixel coordinates & p_k (x, y) gives the probability that the pixel considers kth value.
Here, silhouettes represents binary images and hence K=2.
Then, using scaling operation and discretising operation for H(x,y), the obtained gait entropy image G(x, y) is as

$$G(x,y)=\frac{(H(x,y)-Hmin)*255}{(Hmax-Hmin)} \quad (6)$$

Where $Hmin=\min(H(x,y))$ and
$Hmax=\max(H(x,y))$

Dynamic Gait Energy image (D-GEI): There are three steps in the extraction of D-GEI.
The first step is to get GEI dynamic region,

$$I'gei(x,y)=\begin{cases}0 & \text{if } Igei(x,y) > 220\\ 1 & \text{if } Igei(x,y) \cong 0\end{cases} \quad (7)$$

The second step is logical 'and' operation is present with a dynamic part of GEI to the dynamic area of the frame.

$$F'(x,y) = F(x,y) * I'gei(x,y) \quad (8)$$

Where I'gei(x, y) defines dynamic part of GEI
F(x, y) gives frame in the gait cycle; F'(x, y) defines dynamic region of the frame.
Gradient Gait Energy Image (GGEI): GGEI is obtained by applying the computation procedure called neighbourhood gradient computation procedure which results in the subtraction of each of the pixel to the next 3*3 area from the centre pixel.

V. DESCRIPTORS FUSION

Identifying the gender automatically is a crucial task. Hence, an approach is proposed called the descriptors fusion approach to address the gender estimation problem. Recent advances proved that multiple features fusion [10], [11] achieves better performance and robustness and gives the recognition rate when compared to a single-feature recognition rate.

Generally, gender-related parameters are complementary and overlap. Hence, by the fusion of gait features, gender classification performance can be improved. Therefore, GPM, GEI, GEnI, D-GEI and GGEI should be merged.

$$GGGDG=\{GPM \cup GEI \cup GEnI \cup D\text{-}GEI \cup GGEI\} \quad (9)$$

Then, the features that are computed for the considered datasets are given to the classification algorithm for the gender recognition which is represented in Fig .6

VI. EXPERIMENTS AND ANALYSIS

A. Classifier

Gender identification is a binary case. So, for the classification process, SVM algorithm [12], [13] is suitable which separates data points in each class by the use of the best hyperplane. Different kernels for example polynomial, linear are applied for classification purpose and among the kernels; linear function gave the better results when compared to other kernels as our data is separable in a linear manner to discriminate male and a female.

B. Experiments and Results

The experimental study is conducted on two datasets namely CASIA B [14] and OULP datasets shown in Table 1.

Firstly, we test the performance of the descriptors individually. Secondly, we test the fused descriptors performance to illustrate the performance.

TABLE 1. DATASETS USED IN PROPOSED METHODOLOGY

Type of dataset	Number of persons	Number of image sequences	Variations
CASIA B dataset	124 persons	13640 image sequences	11 view angles
OULP dataset	4007 persons	2135 men 1872 women	1 to 94 years of variation

Here, we designed a test protocol for five cross-validations. We considered an equal number of persons for gender classification because it is a two-class problem. For the experiments, we selected 30 subjects (15 female and 15 male) randomly for the training phase. Next, 60 persons (30 male and 30 female) are selected for the testing phase.

TABLE 2. THE RESULTS OF INDIVIDUAL DESCRIPTORS OF CASIA B DATASET

Descriptor	Recall (%)		Precision (%)		CCR (%)
	Male	Female	Male	Female	
GPM	**99.89**	**89.47**	33.33	**99.92**	**90**
GEI	85.71	78.26	54.54	94.73	80
GEnI	66.66	80.95	60	85	76.6
D-GEI	83.33	71.42	55.55	90.9	75
GGEI	72.72	73.68	**61.53**	82.35	73.3

For every individual descriptor extracted from the GEI images, different number of subjects are considered for evaluating the performance and for the fused descriptors, another set of images are taken from the training phase for evaluation and the results are tabulated.

TABLE 3. THE RESULTS OF INDIVIDUAL DESCRIPTORS OF OULP DATASET

Descriptor	Recall (%)		Precision (%)		CCR (%)
	Male	Female	Male	Female	
GPM	**99.92**	**94.44**	66.66	**99.89**	**95**
GEI	99.89	84.21	25.00	**99.89**	85
GEnI	75	88.88	**81.81**	84.21	83.33
D-GEI	75	83.33	75	83.33	80
GGEI	75	77.27	54.54	89.47	76.66

TABLE 4. THE RESULTS OF FUSED DESCRIPTORS OF CASIA B AND OULP DATASETS

Fused descriptors	Accuracy (%)	
	CASIA B	**OULP**
GPM U GEI U GEnI U D-GEI U GGEI	**96**	**98**
GPM U GEI U D-GEI U GEnI	94.33	95.66
GPM U GEI U D-GEI U GGEI	93.01	94.85
GPM U GEI U D-GEI	91	93.48
GPM U GEI	90	92.81

C. Analysis

From Table 2 and 3, it is clearly shown that the put forth descriptor GPM has given better results when compared to that of the existing descriptors. In the proposed descriptor, we consider the longitudinal projections and transverse projections of an image, and hence, the gender-based parameters can be easily observed and hence the discrimination rate is enhanced to that of the existing ones. The results are highlighted in Table 2, 3 for both CASIA B and OULP datasets.

It is observed through Table 4 that, fusion of different descriptors performs better when compared with the individual descriptors performance. The features fusion is the union of different frames and the features that are not highlighted in any of the images can be observed in the fused frames. Hence, the classification performance will be high and hence the recognition performance will be better when compared to individual descriptors performance. The OULP large population set gives better performance when compared to that of the CASIA B sets which gives 95% accuracy because of its excellent gender balance and it is useful for all tests. The error rate is also reduced in OULP dataset when compared to CASIA dataset. The 90^0, 180^0 and 0^0 view angles gave the best outcomes in contrast to the other view angles in CASIA B dataset for all 124 persons with all the three variations like cloth , bag and normal walking.

GPM descriptor gave the best results in contrast with other existing descriptors because in GPM descriptor, both the transverse projection and the longitudinal projection which highlight the critical parameters for gender recognition whereas, in other features, the static and dynamic information is only represented. Some gender-related parameters [15] are not seen clearly in some existing descriptors which reduce the prediction accuracy.

There are some constraints to this method. Such as precision value is less in some cases for males. Because the trunk component and head component for the slim and fat persons can't be easily identified especially for female and male cases, the hairstyle is outstanding dissimilarity for male and female. So, precision is less for a male in very few cases. We obtained optimal outcomes only in three view angles for 0^0, 90^0 and 180^0 in CASIA B dataset.

VII. CONCLUSION

Gait based gender perception is a peculiar and fascinating topic of present days. The put forth method gives good results and accuracy is also higher when compared with features that are generally used for gender identification. As a result, it proved that gait analysis is best suited for gender perception at a greater distance.

In our prescribed method, both the temporal and static features are used for the classification of gender and their fusion is performed and achieved better results when compared to individual features. In future, we will try to classify the gender using the different classifiers and also other factors that affect the gender classification to determine cross-gender classification using the different descriptors and their combinations.

ACKNOWLEDGEMENT

The authors are sincerely thanking the efforts of CASIA B dataset and OULP dataset providers to carry out our research work.

REFERENCES

[1] Haur tay, Choon boon ng ,."Vision based human gender recognition" ; survey arXiv:1204.1611,preprint.

[2] L. Lee, Grimson, "Gait analysis for classification and recognition", international conference in Gesture and face recognition, IEEE Washington,.pp 155-162.

[3]R chellappa, T tan, Nixon M S, "Human identification on gait". international biometric series. Springer, Dec. 2005.

[4] Briani1, R.V., Taborda, B., Martines, É.C.C., et al.: "Comparison of temporal and kinetic walking parameters among young people and falling and elderly persons", Rev. Bras. Geriatria Gerontologia, 2015, 18, (4), pp. 761–768

[5] Shiqi, Tieniu Tan, Kaiqi Huang, Kui , and Xinyu . "A study in gait based gender classification" . Image Processing, IEEE Transactions on, 18(8):1905–1910, 2009.

[6] J Richard Udry. "The nature of gender". Demography, 31(4):561–573, 1994

[7] Makihara , Okumura; Iwama. H .: "The OU-ISIR gait database: large population dataset , comprising evaluation of gait recognition",, pp. 1511-1521 , iwama, okumura

[8] Han ,.b bhanu. "Individual recognition using gait energy image",. 28(2):316- 322, 2006.

[9] Zhang, D., Wang, Y., Bhanu, B.: "Age classification based on gait using HMM". Int. Conf. Computer Society, Istanbul-Turkey, August 2010, pp. 3834–3837

[10] Mansouri , aouled sIssa, M., ben jemaa, : "Gait fusion of features for efficient age classification", IET Biometrics, 2017, , Vol. 12 Iss. 1, pp. 69-75

[11] Wang, huang, "Gender classification on the fusion of multiview gait sequences", Pro conference in asia. Computer Vision, , pp. 462-471,2007

[12] Nixon,hwang and yoo, "Gender recognition using gait by support vector machine", concepts in advanced in Intelligent Vision Systems, Belgium, Sep. 2005, pp. 138-145.

[13] R. Begg. "Support vector machines in gait classification". IEEE. in Biomedical Engineering, May 2005,52(5):828-838

[14] Yagi, makihara and mannami Y.: "Gait analysis for age and gender with a large scale multiview database". queenstown, New Zealand, November 2010, pp. 440-451

[15] X. Li, S. J. May bank, S. Yan, D. Tao, and D. Xu, “Gait component and applications to gender recognition,” IEEE Transactions. Systems.,, Appl. Rev., volume. 38,. 2008 .,pp. 145-155

Proceedings of the Fourth International Conference on Communication and Electronics Systems (ICCES 2019)
IEEE Conference Record # 45898; IEEE Xplore ISBN: 978-1-7281-1261-9

Design of Knee Exoskeleton using Electromyography Sensor

P. Jain[1], G. Himanshu[1], M. Bhupendra[1], Y. Dharmendra[1], V. Aditya[1], D. Kumar[1] and T. K. Bera[1]
[1]Mechanical Engineering Department, Thapar Institute of Engineering and Technology, Patiala

***Abstract*—With an increase in number of knee problems in patients, the demand for the rehabilitation has increased. Most of the rehabilitation trainings are expensive and time consuming. So, the need for personalized treatment in rehabilitation is increasing. The knee exoskeleton is one of such solutions to assist the patients suffering from weal knee, paraplegia and hemiplegia. These exoskeletons meet the patient's expectation in terms of assistance required and wearing comfort. These are relatively more portable than lower body exoskeletons owing to their lighter weight. These can either be used for gait rehabilitation, providing assistance during sit to stand motion, normal walking and running, for load carrying augmentation or for performing activities of daily living. In this work, a knee exoskeleton consisting of a linear actuator and surface Electromyography sensor is designed and fabricated. Experiments are performed to validate the results with those of theoretical one. The developed knee exoskeleton is found to be well suited for assisting the wearer during the rehabilitation.**

Keywords—knee exoskeleton; linear actuator; EMG sensor; four bar mechanism; rehabilitation; joint angle; joint torque.

I. INTRODUCTION

The world's population is ageing—essentially each country is experiencing growth in the number of elderly people in the population. Globally, the population aged 60 years or above is growing faster than other age groups. Figure 1 describes the ageing population trend.

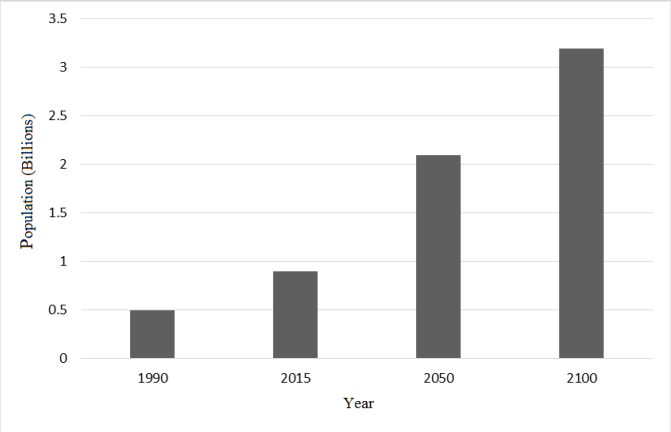

Fig.1 Projected global ageing population (60 years and above)

Owing to the aging population, large number of people suffer from neurological sicknesses such as stroke, central nervous system syndrome, spinal cord injury etc. The manual therapy for patients suffering from such diseases is very much physically demanding. To overcome such problems robotic exoskeletons have been developed. In comparison to the manual therapies, these exoskeletons are physically very less demanding.

The Exoskeleton that are used for rehabilitation could be classified into various categories. Depending on the body parts, they can be classified into full body, upper extremities such as arms and torso and lower extremity exoskeleton such as legs. The upper extremity exoskeletons could be further broken down to specific areas such as wrist, fingers, shoulders and elbow joints. Based on the input power, they can be classified into powered, passive, pseudo-passive and hybrid exoskeletons. The powered exoskeletons make use of batteries and electric cables for running the sensors. The actuators are required to be switched on every time. This is due to the fact that the device needs to maintain its shape. These exoskeletons can further be broken down to static and dynamic exoskeletons. The passive exoskeleton doesn't contain any power sources. These are generally used for weight redistribution, energy capturing, dampening and locking. The springs and locking mechanism diverts the weight of the object around the wearer's body. The spring damper exoskeletons are used to charge the batteries. The pseudo passive exoskeletons aren't meant for actuation purpose. These exoskeletons find their application in controlling a variable damper in the knee. The hybrid exoskeletons consists all the controllers and sensors of powered exoskeleton. On the basis of the mobility, exoskeletons are classified as fixed, supported and mobile. The fixed device is usually tethered, wall attached or suspended from the air by fixed hook and harness. Based on the control mechanism, the exoskeleton can be controlled using joysticks, buttons or control panel, mind controlled, using sensors or there is no control. The supported exoskeletons are normally supported by the moving frame or by a wheeled robot. With mobile robot, the user and the exoskeleton could move around freely. The joystick provides complete energy that is required for the wearer's motion. Using buttons or controlled panels, the exoskeletons operate in pre-programmed mode. Electrode skull caps are used when there is a control using signals generated by brain.

In this work, an attempt has been made to design and fabricate a knee exoskeleton. This device is based on four bar mechanism that could assist the wearer during the rehabilitation stage. A (sEMG) sensor is used to detect the user's intention. Goniometer is used to measure the joint angle and force sensitive resistor (FSR) is used to measure the force developed

by the linear actuator. A mathematical model of the exoskeleton design is presented along with the experimental results

This paper is organized in five sections. The introduction of the present work is included in Section-I. Section-II discusses the work related to the design and control of knee exoskeleton. Section-III discusses the mathematical model of the proposed knee exoskeleton design followed by the calculations for joint torque, joint angle and the experimental details. Section-1V consists of the results and discussions, followed by the Section-V which concludes the current work and discusses the scope for future work.

II. Related work

A knee exoskeleton could be remarkable for people suffering from weak knee. This is due to the fact that a human knee produces large peak torques and absorbs impact during the motion. The knee experience between 5 and 10 degrees of external rotations automatically as the leg extends [1]. A knee exoskeleton consisting of a motorized mechanism was presented [2]. The effects of different exoskeletons designed on the joint internal forces were studied [3]. An adaptive device was proposed that could assist both the translational and rotational motion of the kinematic chain. An EMG based model of the human knee that could anticipate knee movements was presented [4]. A control scheme for powered knee based device was proposed. It is based on real time estimation of EMG signals that are captured based on user's intention from the leg's muscles [5]. A tele-impedance based control strategy was stated to identify detect the user intention of motion to generate assistive torques at knee joints for performing various task [6].The human motion intention was evaluated based on electroencephalogram **(**EEG) and surface electromyography sEMG signals. The signals were used to control the knee joint and were meant for sit stand flexion extension motion of the knee [7]. A proxy sliding based controller was used to control the knee joint position. In addition, the response of the system at zero torque condition was also noted experimentally [8]. A parallel elastic exoskeleton was proposed. It consists of a clutch for disengaging the spring placed in parallel to the leg. This leads to the motion not getting restricted during the swing phase [9]. A modular knee exoskeleton where the user intention is determined by force-sensitive resistors (FSRs) which have been put on the user's foot. The torque sensor is attached to the knee joint and an encoder which is fitted inside the motor. The device is tested on standing, walking and sitting motion controls [10]. An analysis of different mechanisms based on combinations of passive and active actuators was demonstrated. A knee exoskeleton was thus proposed to support the worker's body weight during sit to stand for various seated positions [11]. A prosthetic knee that mimics the biomechanics of human knee joint was proposed [12]. The spring parameters and its effectiveness were determined in a novel knee joint exoskeleton by using dynamic study and simulations. The analysis includes forward kinematics using Lagrangian dynamics followed by simulations using ADAMS. The parameters of the hydraulic dampers used were found to satisfy the real requirements [13].

III. Proposed Knee exoskeleton Design

A knee exoskeleton consisting of linear actuator is proposed. It is based on four bar mechanism. The rigid links AE, ED, DCB and AB constitutes the four bars of the mechanism. Link AB is the fixed link, whereas the link DCB acts as a rigid binary link attached with the joints D and B in the mechanism. This planar four bar linkage is a rocker-rocker mechanism as the sum of the shortest and the longest link is greater than the sum of the length of other two links.

The schematic drawing of the proposed exoskeleton and its cad design is shown in Fig. 2 and Fig. 3, respectively.

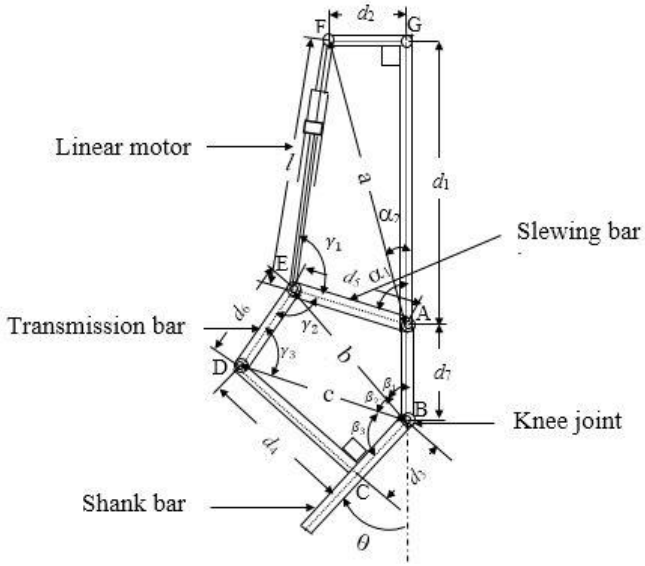

Fig. 2 Schematic drawing of the proposed design

Fig. 3 CAD model of the proposed knee exoskeleton design

A. *Mathematical Model of the proposed design*

Figure 2 depicts the schematic drawing and kinematic parameters of the knee exoskeleton. When the actuator pushes the link d_5, the force is transmitted to the shank link through the link d_6. The force generates the joint torque. The transmitted force F_3 and the torque changes with the knee joint angle. The joint angle (θ) can be expressed as

$$\theta = 180\text{-}\beta_1\text{-}\beta_2\text{-}\beta_3 \quad (1)$$

where $\beta_1 = \cos^{-1}\left(\frac{b^2+{d_7}^2-{d_5}^2}{2bd_7}\right)$, $\beta_2 = \cos^{-1}\left(\frac{b^2+{d_3}^2+{d_4}^2-{d_6}^2}{2b\sqrt{({d_3}^2+{d_4}^2)}}\right)$ and $\beta_3 = \tan^{-1}\left(\frac{d_4}{d_3}\right)$.

$$b = ({d_5}^2 + {d_7}^2 - 2d_5d_7\cos(180 - \alpha_1 - \alpha_2))^{\frac{1}{2}} \quad (2)$$

where $\alpha_1 = \tan^{-1}\left(\frac{d_4}{d_3}\right)$, $\alpha_2 = \cos^{-1}\left(\frac{{d_1}^2+{d_2}^2+{d_5}^2-l^2}{2al_5}\right)$.

The joint torque due to actuators can be derived as follows:

$$\tau_{\text{joint torque}} = F_3.\sqrt{{d_3}^2 + {d_4}^2}.\sin\gamma_3 \quad (3)$$

Where $F_3 = \frac{F_1.\sin\gamma_1}{\sin\gamma_2}$, $\gamma_1 = \cos^{-1}\left(\frac{l^2+{d_5}^2-{d_1}^2-{d_2}^2}{2ld_5}\right)$,

$\gamma_2 = \pi - \alpha_1 - \alpha_2 - \beta_1 - \beta_2 - \gamma_3$ and $\gamma_3 = \cos^{-1}\left(\frac{{d_3}^2+{d_4}^2+{d_6}^2-b^2}{2d_6\sqrt{({d_3}^2+{d_4}^2)}}\right)$.

F_3 is the transmitted force along ED and F_1 is the force developed by the linear actuator along FE.

B. Experimental setup

The aluminium bars of grade 2000 were used to build the basic four-bar structure along with the extra links to fasten and clamp the actuator. A linear actuator of 12V DC supply is mounted with the aid of cotter pins. A 7-12 V input voltage Arduino UNO microcontroller was used for the control purpose. EMG sensor was placed at three locations on the leg as shown in Fig. 4 to get the input signal from the user to initialize the actuator. The EMG sensor ensures maximum safety because it works according to the user's intentions. A force surface resistor was used to measure the force developed by the actuator. A goniometer was used to measure the joint angle rendered by the device on the subject's knee. Strapping was custom-made according to the user's need with its one strap fastening around the user's waist and thigh while the other around the subject's calf.

C. Experimentation

The values of the link lengths of the proposed design are mentioned in Table I and the calculated parameter values are stated in Table II.

TABLE I Link lengths

Parameter	Values (m)
d_1	0.3104
d_2	0.1158
d_3	0.1750
d_4	0.0200
d_5	0.1950
d_6	0.0450
d_7	0.0507
l_{max}	0.381
l_{min}	0.275

The knee exoskeleton is used for a healthy male who is free from musculoskeletal and neurological injuries. The weight of the person is 63 kg and the height is 1.6 m. Figure 4 shows the the prototype of the knee exoskeleton being wore by the subject. The control flow diagram of the knee exoskeleton prototype is shown in Fig. 5. Two batteries of 18 V and 12 V are used for the power supply. The current flows through 2 channel 5 V relay to the linear actuator. The power from the 18 V battery flows through the FSR, the controller, the 5 V channel to the actuator. Figure 7(a)-7(d) shows the images of the person's shank in flexion and extension motion at various values of joint angle. The experimentation was performed for two cycles. Each cycle comprises of the flexion and extension motion of the persons' shank.

TABLE II Design parameters

Parameters	Values for l_{max}	Values for l_{min}
$\gamma_1 = \cos^{-1}\left(\frac{l^2+{d_5}^2-{d_1}^2-{d_2}^2}{2ld_5}\right)$	52.43°	23.53°
Force along $FE, F_1 = \frac{\tau_{motor}}{d_5\,sin\gamma_1}$	87 Nm	87 Nm
$\alpha_2 = \tan^{-1}\left(\frac{d_2}{d_1}\right)$	114.27°	47°
$a = \sqrt{({d_1}^2 + {d_2}^2)}$	0.33 m	0.33 m
$\alpha_1 = \cos^{-1}\left(\frac{{d_1}^2+{d_2}^2+{d_5}^2-l^2}{2ad_5}\right)$	20.46	20.46
$b = \sqrt{{d_5}^2 + {d_7}^2 - 2d_5d_7\cos(180-\alpha_1-\alpha_2)}$	0.21 m	0.12 m
$\beta_1 = \cos^{-1}\left(\frac{b^2+{d_7}^2-{d_5}^2}{2bd_7}\right)$	103.93°	45.45°
$\beta_2 = \cos^{-1}\left(\frac{b^2+{d_3}^2+{d_4}^2-{d_6}^2}{2b\sqrt{({d_3}^2+{d_4}^2)}}\right)$	24.31°	28.93°
$\gamma_3 = \cos^{-1}\left(\frac{{d_3}^2+{d_4}^2+{d_6}^2-b^2}{2d_6\sqrt{({d_3}^2+{d_4}^2)}}\right)$	28.39°	81.87°
$\gamma_2 = 180 + (\alpha_1+\alpha_2) - (\beta_1+\beta_2) - \gamma_3$	158.08°	91.27°
$F_3 = \frac{F_1.\sin\gamma_1}{\sin\gamma_2}$	184.78 N	76.76 N
$\tau_{\text{joint torque}} = F_3.\sqrt{{d_3}^2 + {d_4}^2}.\sin\gamma_3$	10.34 Nm	8.94 Nm
$\beta_3 = \tan^{-1}\left(\frac{d_4}{d_3}\right)$	44.31°	6.52°
Joint angle$(\theta) = 180 - (\beta_1+\beta_2+\beta_3)$	7.44°	61.32°

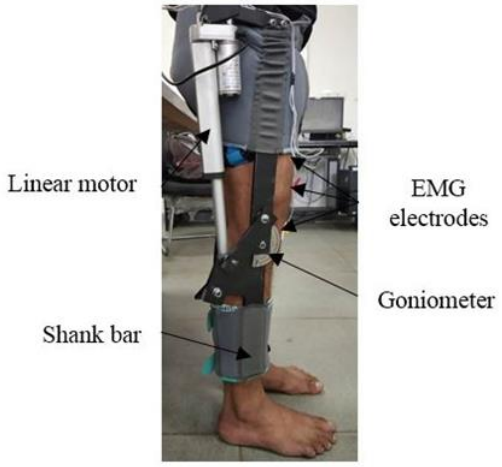

Fig. 4 Prototype of the knee exoskeleton

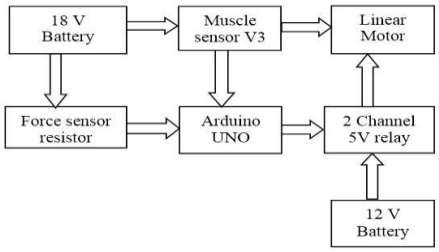

Fig. 5 Control flow diagram

Table III FSR output voltages

Force (N)	FSR resistance (kΩ)	Voltage across resistor (V)
0.2	30	1.3
1	6	3.1
10	1	4.5
100	250	4.9

The output voltage corresponding to the FSR was approximately 4.8V. It is concluded from Table III that, the force developed by the linear actuator being measured by FSR is 87 N.

Figure 6 shows the location of the FSR below the poston rod. Figure 7(a)-7(d) show the shank position at different joint angle values.

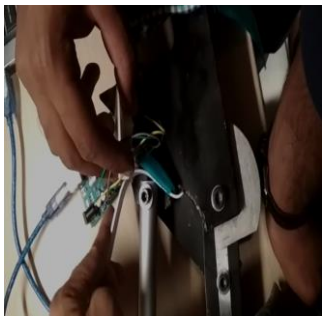

Fig. 6 FSR reading

(a) (b)

(c) (d)

Fig. 7 Shank positions at (a) θ=7.7°, (b) θ=30°, (c) θ=45° and (d) θ=62.9°

III. RESULTS AND DISCUSSIONS

The cycle starts when the person is at the standing position. The EMG sensor detects the wearer's intention by sensing the muscle activity. The contraction and the relaxation of the muscles is reponsible to drive the actuator. The muscle sensor provides signals to actuate the linear actuator.

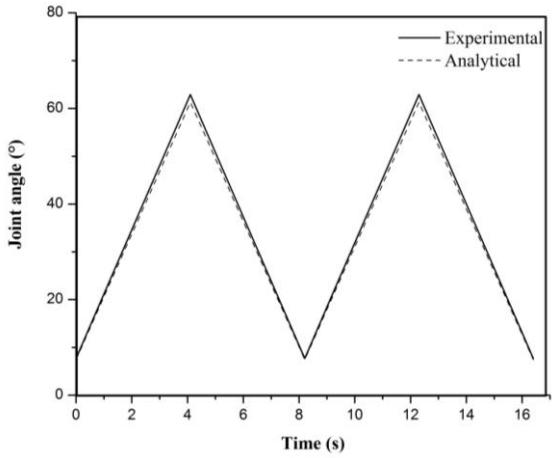

Fig. 8 Plot for joint angle with time

Figure 8 shows the variation of joint angle (θ) with time for both experimental and analytical analysis for two cycles of flexion and extension motion of shank. It is clear that, as the shank starts to flex in the clockwise direction direction, the joint angle increases and reaches to its maximum value. The maximum value of joint angle (θ) measured by the goniometer is 62.9° while the analytical value is 61.3°. The EMG sensor now detects the user intention to provide the shank's extension in the counter clockwise direction. Due to the muscle activity, when the shank starts to rotate in clockwise direction, the joint angle decreases to 7.7° experimentally. The theoritical value of the minimum joint angle (θ) is 7.4°.

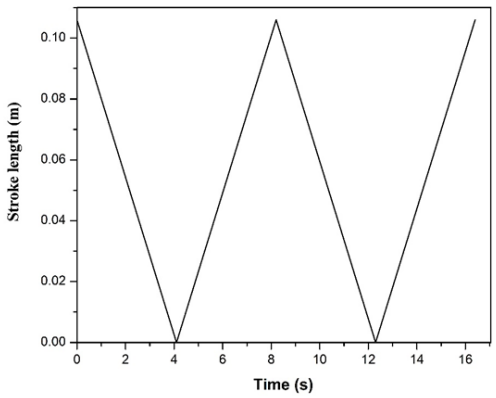

Fig. 9 Plot for stroke length with time

Figure 9 shows the measure of the piston stroke length with time. The piston stroke length is maximum and minimum at the start of flexion and extension movemen, respectively. The cycle time is approximately 8.2s.

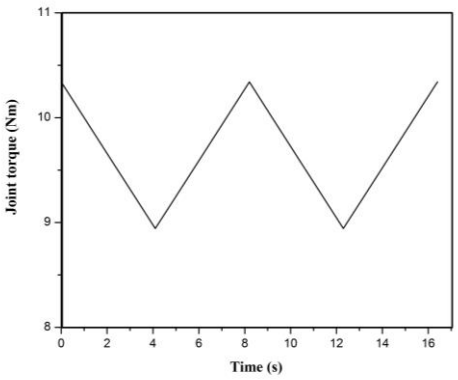

Fig. 10 Plot of joint torque with time

Figure 10 depicts the joint torque values required for performing the flexion and extension motion with time. Joint torque is the torque generated by linear actuator at point B. The value of the joint torque due to the actuator for performing flexion and extension motion is 10.34 Nm and 8.94 Nm, respectively.

Figure 11 shows the experimental and analytical values of the angular velocity of shank for the two cycles of flexion and extension motion with respect to time.The experimental value of the angular velocity of the shank is 0.235 rad/s while the analytical value is 0.229 rad/s.

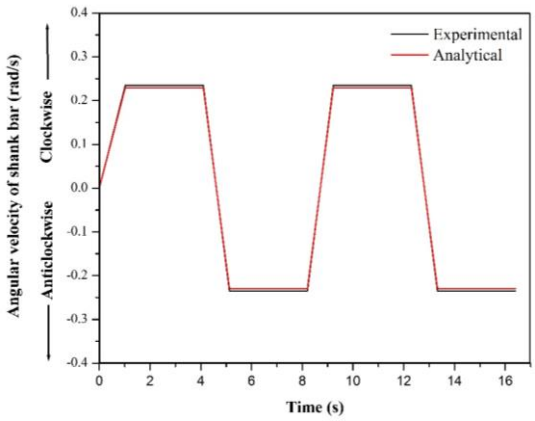

Fig. 11 Plot for shank angular velocity with time

IV. CONCLUSION

The design and fabrication of a surface electromyography sensor based knee exoskeleton consisting of a linear actuator are proposed. The prototype is fabricated and the experiments are performed. The experimental and theoretical values of the joint angle and shank's angular velocities are validated for the kinematic design of the proposed knee exoskeleton. Thus, the flexion and extension motions of the lower limb through the proposed design are well suited for the rehabilitation of the knee joint.

The future work is focused on optimizing the design parameters of the four bar mechanism in order to maximize the joint range of motion. In addition, the focus would also be on designing the exoskeleton for assisting the patients in performing the activities of daily living (ADL).

ACKNOWLEDGMENT

The project was supported by the Mechanical Engineering Department, Thapar Institute of Engineering and Technology, Patiala, India.

The author would like to express sincere thanks to the members of the Mechatronics laboratory at TIET Patiala, India who are associated with this project.

REFERENCES

[1] Y. Liao, Z. Zhou, and Q. Wang, "BioKEX: A bionic knee exoskeleton with proxy-based sliding mode control," *Proc. IEEE Int. Conf. Ind. Technol.*, vol. 2015–June, no. June, pp. 125–130, 2015.

[2] G. Elliott, A. Marecki, and H. Herr, "Design of a Clutch–Spring Knee Exoskeleton for Running," *J. Med. Device.*, vol. 8, no. 3, p. 031002, 2014.

[3] S. Hirokawa, "Three-dimensional mathematical model analysis of the patellofemoral joint," *J. Biomech.*, vol. 24, no. 8, pp. 659–671, 1991.

[4] M. Machado *et al.*, "Development of a planar multibody model of the human knee joint," *Nonlinear Dyn.*, vol. 60, no. 3, pp. 459–478, 2010.

[5] A. M. Dollar and H. Herr, "Design of a quasi-passive knee exoskeleton to assist running," *2008 IEEE/RSJ Int. Conf. Intell. Robot. Syst. 22-26 Sept. 2008*, pp. 747–754, 2008.

[6] H. Fu *et al.*, "A novel prosthetic knee joint with a parallel spring and damping mechanism," *Int. J. Adv. Robot. Syst.*, vol. 13, no. 4, pp. 1–9, 2016.

[7] C. Fleischer, "Controlling Exoskeletons with EMG signals and a Biomechanical Body Model," *Diss. TU Berlin*, p. 161, 2007.

[8] N. Karavas, A. Ajoudani, N. Tsagarakis, J. Saglia, A. Bicchi, and D. Caldwell, "Tele-impedance based assistive control for a compliant knee exoskeleton," *Rob. Auton. Syst.*, vol. 73, pp. 78–90, 2015.

[9] A. C. Villa-Parra *et al.*, "Control of a robotic knee exoskeleton for assistance and rehabilitation based on motion intention from sEMG," *Res. Biomed. Eng.*, vol. 4740, 2018.

[10] J. H. Kim *et al.*, "Design of a Knee Exoskeleton Using Foot Pressure and Knee Torque Sensors," *Int. J. Adv. Robot. Syst.*, vol. 12, no. 8, 2015.

[11] J. Noh, J. Kwon, W. Yang, Y. Oh, and J. H. Bae, "A 4-bar mechanism based for knee assist robotic exoskeleton using singular configuration," *IECON Proc. (Industrial Electron. Conf.*, pp. 674–680, 2016.

[12] R. R. Torrealba, S. B. Udelman, and E. D. Fonseca-Rojas, "Design of variable impedance actuator for knee joint of a portable human gait rehabilitation exoskeleton," *Mech. Mach. Theory*, vol. 116, pp. 248–261, 2017.

[13] L. Fan, L. Yan, J. Xiao, and F. Wang, "Dynamics analysis and simulation verification of a novel knee joint exoskeleton," *J. Vibroengineering*, vol. 19, no. 4, pp. 3008–3018, 2017.

Proceedings of the Fourth International Conference on Communication and Electronics Systems (ICCES 2019)
IEEE Conference Record # 45898; IEEE Xplore ISBN: 978-1-7281-1261-9

Designing of Microcontroller based Energy Meter (Smart Energy Meter) for Energy Preserving

K. V. Jyothi Prakash
Department of E&C Engineering
Siddaganga Institute of Technology
Tumakuru, Karnataka, India
jyothiprakashkv@sit.ac.in

Chethana N S, Fariya Tamkeen, Kala C S, Kavya N R
Department of E&C Engineering
Siddaganga Institute of Technology
Tumakuru, Karnataka, India

***Abstract*— Electricity is one of the basic requirements of human beings since it is very widely used for domestic, industrial and agriculture applications [1]. In most of the developing countries the energy generated is less than the requirement hence there is scarcity of energy, therefore effective utilization of energy is very important. In the existing system there is no any indication of the energy used to the consumer at regular intervals, only by the end of the month when the bill is received the consumer will come to know the energy used by him. Further the meter reading at present is also manual which needs lot of man power. In this paper a smart energy meter is proposed with which the consumer will be notified the amount of power consumed by the end of the day such that he can plan the consumption of power. Also the power consumed by the consumer will be notified to the distributor as well as consumer such that no manpower is necessary for meter reading.**

Keywords—Smart power meter, electricity, consumer, distributor, microcontroller, GSM, WIFI

I. INTRODUCTION

Electricity has become very important to human survival and progress. Along with new techniques of power generation to meet the increased demand, automation in the energy distribution is also necessary to enhance people's life standard. The manual meter reading is not that efficient and requires lot of man power hence, there is increased demand for Smart electronic meter systems which will send the meter readings to the distributor without any human interventions.

The electricity distributer has made rules in the billing system based upon the number of power units used where, the consumer will not be aware of his usage. Keeping this in consideration the smart energy meter will help in knowing the number of power units consumed and the amount that needs to be paid. If the usage is going beyond normal, consumer can control the operation of electric devices and can reduce the power consumption. The cost of power consumed will be calculated by reading the pulses generated by the meter. The calculated amount for a month is then sent to consumer and distributer and will also be displayed on the LCD to the consumer on daily basis. In existing system either an electronic energy meter or an electro-mechanical meter is fixed in the premise for measuring the usage which is capable of recording kWh units which is then have to be read by meter readers monthly. The cost for the recorded data will be generated according to the present tariff whereas, in smart electronic meter the meter reading need not be read. Both consumer and distributer will be sent the information which includes the details of their power consumption and the cost with time. Since the consumer already have prior knowledge about their usage and the cost for the power consumed they can cut down their consumption of power and save it.

This paper consists of introduction to the smart energy meter, existing energy measurement system, proposed system with additional features, Implementation of the system, block diagram, methodology, flowchart, results, conclusion, future scope and references are discussed.

II. EXISTING SYSTEM

In the existing system, a mechanical or an electronic energy meter will be fitted at every consumer point which will record the amount of power consumed by the consumer. At the end of every month a meter reader has to visit every consumer and should issue the bill, hence lot of man power is required. In this existing system there is no any alert message given to the consumer about how much power they have consumed every day so that they can plan and effectively utilize the electric appliances and cut down the electricity bill. Only at the end of the month the consumer will come to know the electricity bill. Further in the existing system if any faulty electrical appliances are consuming more power than their rated power the consumer will come to know only at the end of the month.

III. PROPOSED SYSTEM

In the proposed system along with the mechanical or electronic energy meter optocoupler, Arduino UNO microcontroller, real time clock (RTC), liquid crystal display (LCD), WIFI module and GSM module will also be connected. This smart energy meter will not only record the amount of power consumed by the consumer but also will send the alert message to the consumer through GSM about the amount of power consumed and the cost of the power consumed at regular intervals. Hence a smart consumer can plan the power consumption and can cut down the power consumption by properly using the electric appliances. Along with this since the WIFI module is connected, the bill

generated at the end of every month can be sent to the distributer as well as a copy to the consumer such that the man power required for reading the meter for generating the bill can be avoided.

IV. IMPLEMENTATION

A. Block Diagram

The Block diagram of smart energy meter is shown in Fig. 1.

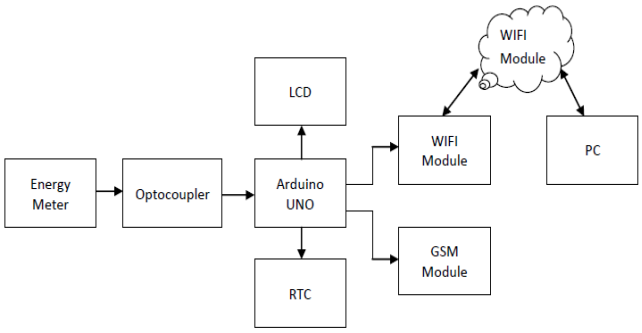

Fig. 1 Block Diagram of Smart Energy Meter

The smart energy meter consists of an electronic energy meter, optocoupler, Arduino UNO microcontroller, real time clock (RTC), liquid crystal display (LCD), WIFI module, GSM module and PC.

Energy Meter
An energy meter is a device which measures the amount of power consumed by the electrical appliances. Electric distributer uses energy meters which are installed at consumer's premises to record the power consumption for billing purposes. The calibration LED present in the energy meter will indicate the real time power consumption by the consumer and by recording the number of blinking of the LED the power consumption is calculated.

Optocoupler
The optocoupler is a light sensitive device which senses the light from the calibration LED and generates a pulse which will be applied to Arduino controller. Optocoupler is used to provide isolation.

Real Time Clock (RTC)
The RTC is used to keep track of date and time to generate bill at regular intervals, it is interfaced to Arduino to initiate the GSM and WIFI module for sending information to consumer and distributor.

Arduino UNO
Arduino UNO is a microcontroller used to interface optocoupler, LCD, RTC, WIFI module and GSM module. Arduino will count the pulses given by optocoupler which is the real time power consumption by the consumer and calculate the cost for the power consumed. The power consumed and the cost will be displayed on the LCD and at regular interval initiated by RTC the details will be sent to consumer through GSM and to the distributor using WIFI module [2] [3].

Liquid Crystal Display (LCD)
A 16×2 LCD is used to display the power consumed by the consumer and cost of the power consumed at the user end.

Global system for mobile communication (GSM):
GSM is used to send the calculated power consumed and the cost to the consumer through SMS [4].

WIFI Module
WIFI is used to connect the PC at the distributor end to the consumer point. The power consumed and the cost will be updated in the PC at the distributor end using WIFI.

B. Design

For every 1 Unit (1KWh) of power consumption the calibration LED in the energy meter will blink 3200 times which will be converted as 3200 pulses by optocoupler. These pulses will be counted by the Arduino and calculate the power as per the current tariff. At regular interval the RTC will initiate the process to send the details power consumption and the cost to the consumer and distributor.

C. Methodology

The methodology of implementation of smart energy meter is shown in Fig. 2.

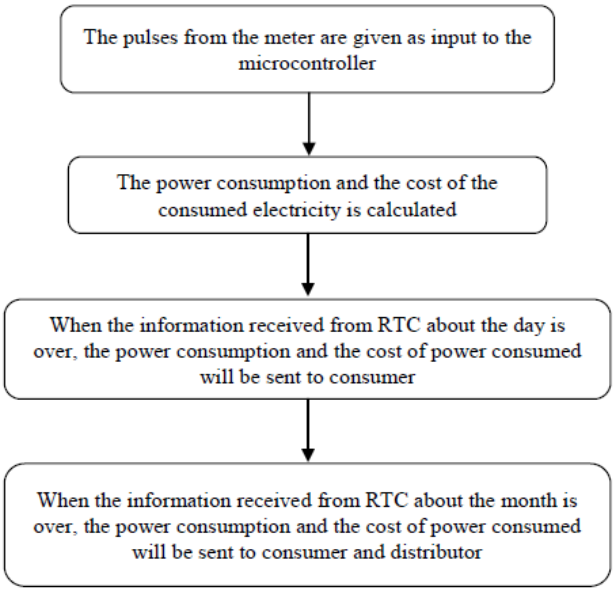

Fig. 2 Methodology of implementation of smart energy meter

The pulses generated in the energy meter as per the consumption of power by the consumer will be read by the Arduino microcontroller. The microcontroller will calculate the power consumed by the customer and the cost for the

consumed power in a day. At the end of the day the microcontroller will send the information about the power consumed and the amount for the consumed power to the customer through GSM. At the end of the month the information about the power consumed and cost of the consumed power will be sent to both consumer and distributor.

D. Flowchart

The flowchart of smart energy meter is shown in Fig. 3. The pulses are counted from the energy meter by the microcontroller and the power consumed by the consumer will be calculated by incrementing the counter. The power consumed and the cost of power consumed will be displayed on LCD. After receiving the signal from RTC about the end of the day a message will be sent to the consumer about the power consumed and amount for the consumed power. Once the RTC sends the information about end of the month message will be sent to the consumer and the distributor about the power consumed and amount for the consumed power.

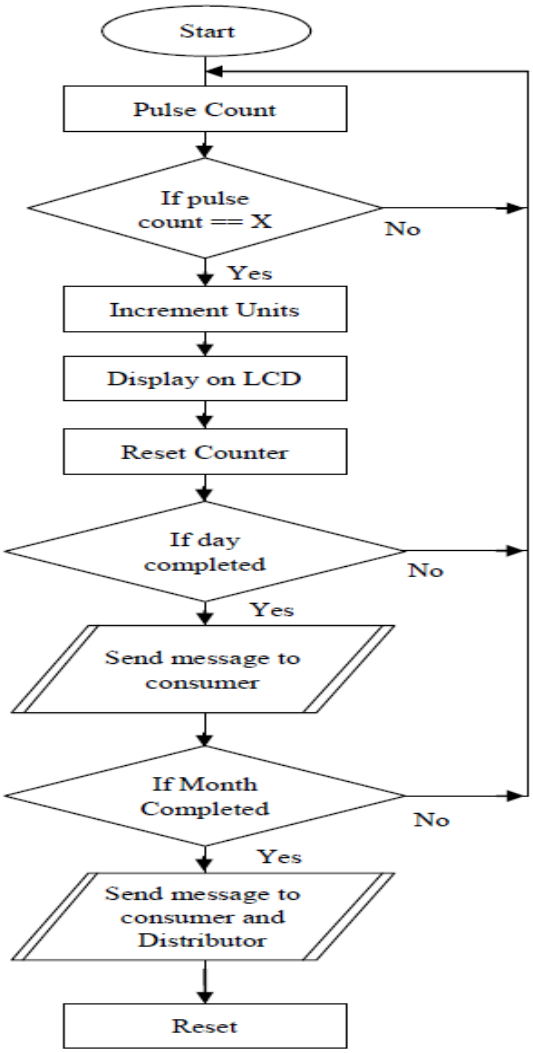

Fig. 3. Flowchart of smart energy meter

V. RESULTS AND CONCLUSION

A. Results

The working model of the smart energy meter is shown in Fig. 4.

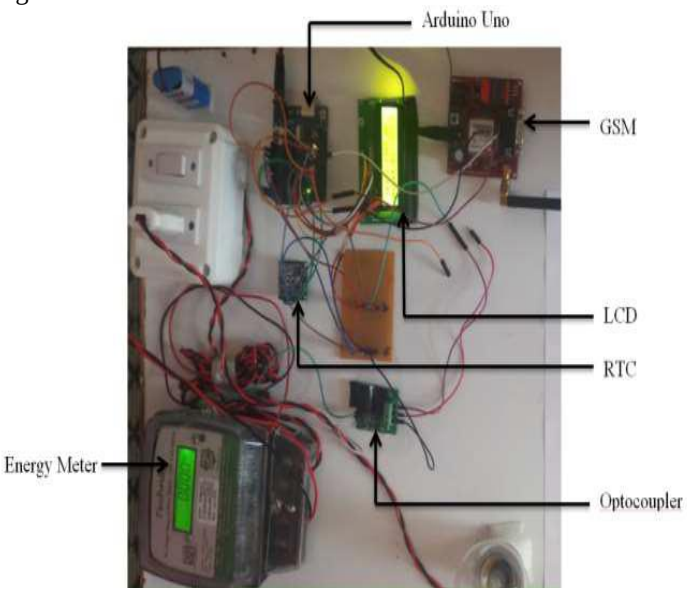

Fig. 4. Working model of smart energy meter

The display of power consumed and the amount for the power consumed on LCD is shown in Fig. 5.

Fig. 5 Display of power consumed and the amount for the power consumed on LCD

The message sent to the consumer about the power consumed and the cost of the power consumed is shown in Fig. 6.

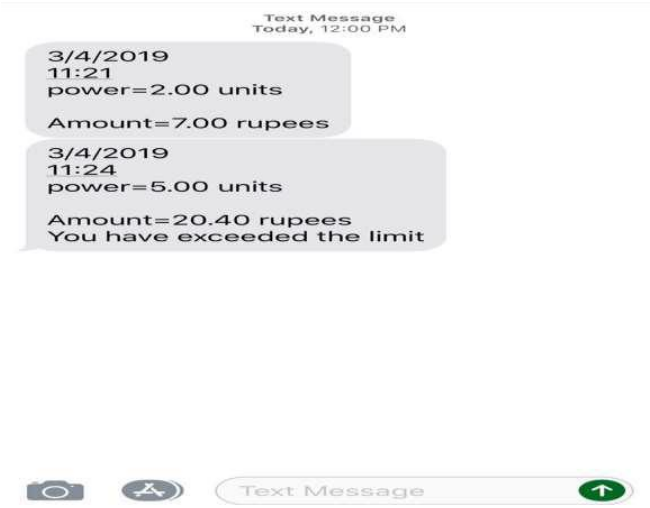

Fig. 6. Message sent to the consumer about the power consumed and the cost of the power consumed

B. Conclusion

The Smart Energy Meter is successfully designed, which sends the message of power consumption along with cost to both consumer and distributer using GSM at the end of each month. It also sends the alert message to consumer about the amount of power consumed and the cost for the power consumed at regular interval of time. The automation of billing system eliminates the human involvement hence it is more reliable. Smart Energy Meter will bring the solution of creating awareness of unnecessary usage of power and will tend to reduce the wastage of power.

C. Future Scope

The smart energy meter can be further improved by including IOT such that the database can be maintained for a long period. Further the energy meter can be made a prepaid energy meter such that when there is overdue of the bill the power can be disconnected. A mobile app can also be developed such that the consumer can contact the distributor through app for any additional power allocation required during some rare occasion or can complaint to the distributor regarding any problems he is facing.

REFERENCES

[1] Bharath P, Ananth N, Vijetha S, Jyothi Prakash K.V, “Wireless automated digital Energy Meter”, International Conference of E-Society, E-Education and E-Technology (ICSET), 2008.

[2] Win Adiyansyah Indra, Fatimah Bt Morad, Norfadzlia Binti Mohd Yusof, Siti Asma Che Aziz, “GSM Based smart Energy meter with Arduino”, International Journal of Applied Engineering Research, Malaysia, 2015.

[3] Sneha Chaudhari, Purvang Rathod, Ashfaque Shaikh, Darshan Vora, Jignesha Ahir, “Smart energy meter using Arduino and GSM”, International conference on Trends in Electronics and Informatics (ICEI), 2017.

[4] S. Vougioukas, M. Roumeliotis, “A system for basic-level network fault management based on the GSM short message service (SMS)”, International Conference on Trends in Communications, 2001.

Proceedings of the Fourth International Conference on Communication and Electronics Systems (ICCES 2019)
IEEE Conference Record # 45898; IEEE Xplore ISBN: 978-1-7281-1261-9

FLOOD AND EARTHQUAKE DETECTION AND RESCUE USING IOT TECHNOLOGY

Venita Babu
Department of Electronics and Communication Engineering
Sahrdaya College of Engineering and Technology
Thrissur, India
venitababu51@gmail.com

Dr.Vishnu Rajan
Department of Electronics and Communication Engineering
Sahrdaya College of Engineering and Technology
Thrissur,India
vishnurajan@sahrdaya.ac.in

***Abstract* – Flood and earthquake are one of the most devastating natural disasters in the world. Such natural disasters deleteriously affect the environment, lives of human, etc. which indirectly affect the economy of the country. Due to such natural disasters, there is a decline in the death rate of the human and fauna. So we should have a monitoring and observatory flood and earthquake detection system. The proposed system based on IOT technology gives a real-time analysis of flood and earthquake and so that the authority can monitor flood and earthquake affected areas. This paper highlights the Flood and earthquake Observatory System as a warning and alert system to efficiently monitor the critical flood prone and earthquake areas in real time basis baring the cost and safety measures. The proposed system also alerts the authority regarding the presence of a human in the area. It also provides backup supply for emergency situations using solar energy. Design of the proposed system includes integrating sensors to the microcontroller, RF transmitter, and receiver for long-range communication, and Thing Speak IOT platform for examining and visualizing sensor values which have been uploaded.**

***Keywords*—SmartCity, Water Quality Monitoring, WSN, LoRa, LoRaWAN, IoT, LPWAN**

I. INTRODUCTION

Natural disasters are a worldwide phenomenon. Recently hurricanes, floods, tides, etc. have illustrated along with the differences in the effects of disasters on developed compared to developing countries like India [1]. An effective solution to such natural disasters is by giving people adequate time to evacuate and protect their property. If people knew about the flood was coming, many lives and property could be saved.

Flood and earthquake are crucial disasters in the world affecting the economic status of the country in the form of natural resources, lives of human and fauna, economic properties, environment, and other infrastructure [2]. The extent of flood and earthquake damages depends on the certain measures and steps taken by the responsible authorities especially government officials during such a critical period.

Internet of things (IoT) is emerging technology that Connects anything and everything to the Internet[3]. IoT is the technology rapidly widens according to the usage. This technology brings out new technology such as natural disaster monitoring. IoT technologies in detecting the activity of natural disasters like flood and earthquake helps to rescue the lives of people

Natural disasters such as flood and earthquake that occurs in different places around the world which has become a critical problem[4]. Thus there is a need for a Flood and earthquake observatory and warning system which can save lives of human, environment, an economy of the country. Recently Kerala faced dangerous floods which resulted in deaths of human, fauna and destroyed the environment of the state which reduced the economic status of the state. To solve such issues and creating a remedy such as introducing early warning, detection, and rescue system of flood and earthquake.

Even though significant progress has been made during the last decade in the field of developing and implementing efficient flood and earthquake observatory and warning system, there are a lot of challenges faced by the researchers. There is a need for an intelligent flood and earthquake observatory and warning system which is fast, efficient, simple and accurate. Flood and earthquake observatory and warning system using IOT is a new technology to implement an efficient flood and earthquake observatory and warning system with high security and researchers are showing great interest in this technology. Also, this can develop and implement flood and earthquake observatory and warning system that will help to save lives of society, and the economy of the country.

The first section in this paper gives a general idea about the flood and earthquake detection system and its associated problems and find out a general solution to it.Second section explains about the proposed system which is explained through block diagram having pole unit and home unit. Third section explains about the technical descriptions of various modules used in the proposed system. Fourth section explains about the result analysis through proteus simulation and hardware interfacing of the proposed system. Last section includes conclusion and future scope

II. PROPOSED SYSTEM

The proposed system is a warning and alert system to monitor efficiently critical flood prone and earthquake areas in real time basis. The system includes a water level sensor (float sensor) which detects water level intensity and gives alert to house member. There are 4 types of alert given i.e.; green bulb indicates no danger, orange bulb-low level danger, blue bulb- medium danger, red bulb – high danger. Each color bulb is on in each alert. When water level increases to mid-level itself (blue bulb turns on), through hooter dangerous siren is alerted and alert the authorities by providing messages through GSM, and even nearby house member will also be alerted. The system even detects an earthquake by using a vibration sensor (accelerometer/ gyroscope) and provide alert to authorities through GSM. In such flood-prone areas, they may not be the current supply. So we provide solar energy through the solar panel to charge the whole system and provide a slot to charge our mobiles. Through RF transmitter wirelessly communicate to the pole unit section through RF receiver, a dangerous siren(hooter) is alerted in pole section indicating blue bulb on, so that other human near to pole unit can try out to help the people affected by a flood. Presence of rain can be detected by the rain sensor. The gateway here is ESP Wi-Fi module. The gateway then transmits the sensor data packets to the ThingSpeak cloud server over internet protocol and we can monitor the sensor values in ThingSpeak API and also in internet-enabled devices and through GPS(location tracking) is possible which helps them to locate and trace people who are affected by flood and earthquake.

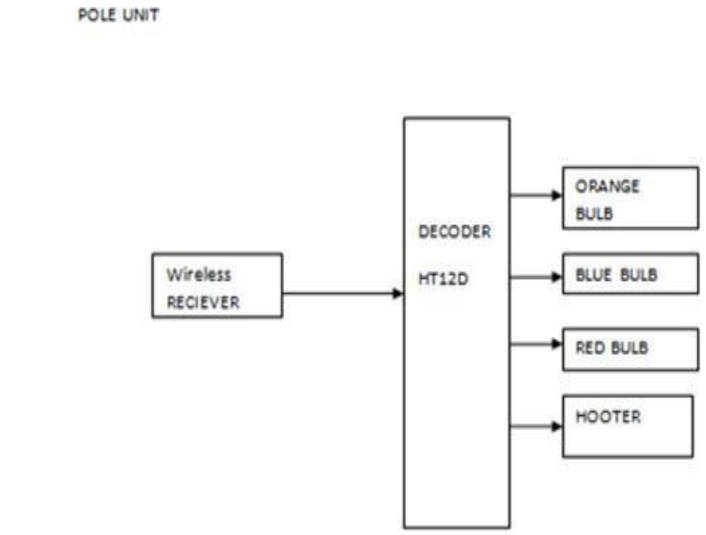

Figure 1: Pole unit of proposed system

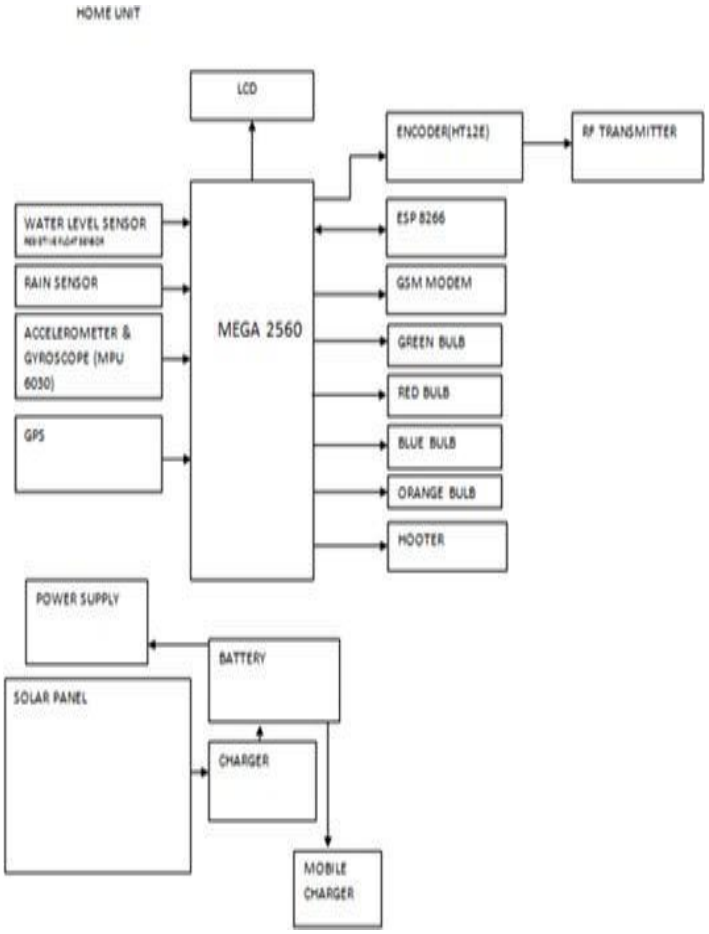

Figure 2: The Proposed Flood and earthquake detection and rescue using IOT technology Home unit

III.TECHNICAL DESCRIPTIONS

3.1. Arduino Mega2560

Arduino Mega 2560 is used for projects that contain more input/output pins, RAM (random access memory and more memory space [5]. It is used in many robotics projects. It contains 54 digital I/O pins (14 can be used as PWM outputs) and 16 analog inputs. It is programmed using Arduino software (IDE-integrated development environment) using C language. It also consists of 4 UARTS (serial ports), USB connection, a power jack, ICSP header, reset button,16MHZ crystal oscillator and can be simply connected to the computer with USB cable or power it with AC-to-DC adapter

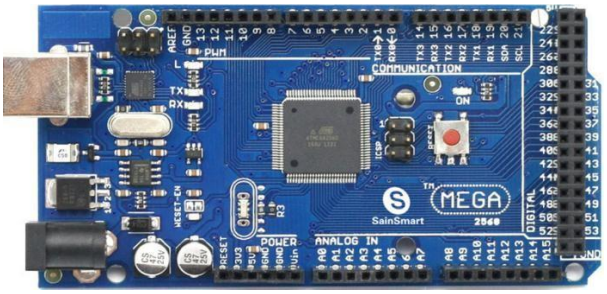

Figure 3: Arduino Mega2560

3.2. Water level sensor

Water level sensor is also known as float sensor to detect the water level increased or decreased in terms of resistance varying. It consists of float connected to potentiometer.

Figure 4: Water level sensor

3.3.Rain sensor module

Presence and intensity of rainfall are detected by the rain sensor module [6]. When raindrop falls on raining board, module act as a switch. It contains features such as potentiometer (to adjust sensitivity), LED (power indicator). Here rain board and control board are separate for convenience. It produces the analog output. The module is connected to the 5V power supply. When the induction board has no raindrop, LED turns on i.e.; Do output is high. When it has a little number of raindrops, Do output is low.

Figure 5: Rain sensor module

3.4. MPU6050 - Accelerometer and Gyroscope

Micro-Electro-Mechanical Systems (MEMS)-MPU6050 consists of a 3-axis Accelerometer and 3-axis Gyroscope inside it [7]. It measures acceleration, velocity, orientation, displacement, and other motion- related parameters .to perform complex calculation, DMP(digital motion processor) is used which is present inside the module.MPU6050 sensor can be interfaced to the microcontroller using AD0 pin.

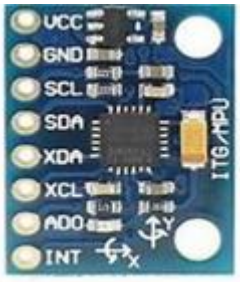

Figure 6: MPU6050-Accelerometer and Gyroscope

3.5. GPS-Global positioning system

GPS is known as global positioning system which transmits microwave signals [8]. It determines position i.e.; location in terms of latitude and longitude

Figure 7: GPS-Global positioning system

3.6. GSM Modem

A **GSM modem** performs like a mobile phone consisting of SIM card (subscriber identity module) [9].It is used for sending and receiving messages to regarding persons or authorities

Figure 8: GSM Modem

3.7. LCD-Liquid crystal display (16*2)

It is an electronic display module .These modules are preferred over seven segments.LCD's are economical and easily programmable. It can display 16 characters

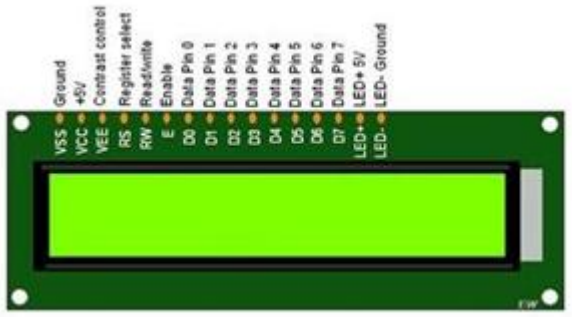

Figure 9: Liquid crystal display

3.8. RF TRANSMITTER AND RECEIVER

The RF module operates at Radio Frequency (30 kHz & 300 GHz)[10]. If there is an obstruction between transmitter & receiver, radio frequency signals can travel. Radio frequency signals are more strong and reliable than the Infrared signals. RF module consists of two devices known as RF Transmitter and RF Receiver. The transmitter/receiver (Tx/Rx) pair has an operating frequency of about 434 MHz. The RF module consists of a pair of encoder/decoder. HT12Eis used for encoding parallel data transmission while the reception is decoded by a HT12D.

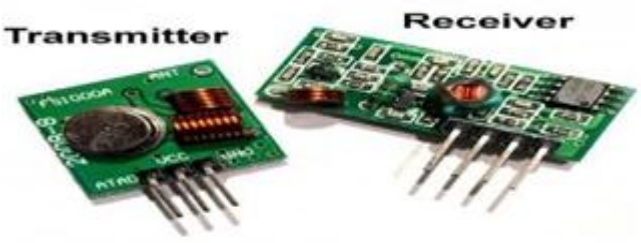

Figure 10: RF transmitter and receiver

3.9. SOLAR PANEL

Solar panels that generates power from the sun which converts sunlight to electricity [11].12-volt panel size of about 25 inches by 54 inches contains 36 cells which are wired in series connection to produce about 17 volts output

Figure 11: Solar panel

3.10. ESP8266 Module

ESP8266 is power-packed module and capable of onboard processing and storage capability that can be integrated with the sensors and other specific devices through its general purpose input/output pins with minimum development up-front and minimum loading during runtime [12].This module is pre-programmed by AT command. By simply connecting this to your arduino device and get about as much Wi-Fi ability

Figure 12: ESP8266 Module

3.11. LM317 Circuit

Solar charger circuit is used to charge lead-acid batteries or Ni-Cd using solar power. This Circuit harvests solar energy to charge a 12- volt 1. 2Ah battery for various applications. The charger circuit has voltage and current regulation cut-off facilities. While adjusting the adjustment pin, voltage and output current can be regulated

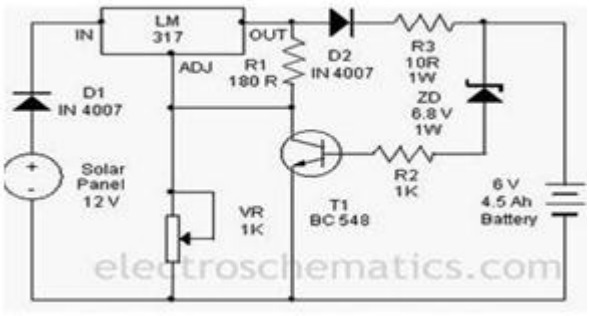

Figure 13: solar charger with current regulation and cutoff

3.12.Power supply

The input to the circuit is obtained from the regulated power supply. Normally devices work in dc supply, so here diodes are used for rectification purpose to convert incoming ac supply to dc supply and and voltage regulator (7805) is to convert incoming dc supply of 12V 12V to 5V and capacitors is used to pure dc voltage

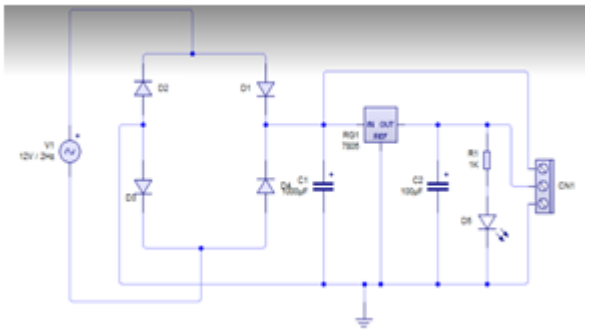

Figure 14: Power supply

IV.RESULTS AND DISCUSSIONS

The Flood and earthquake detection and rescue using IOT technology system presented a good performance. Simulation of the project is done in Proteus. The simulation result is shown in the figure 14. Accelerometer sensor, Rain sensor, and Water level sensor (Float sensor) values displaying on LCD have been included in the simulation. Messaging to authorities is done through GSM and its commands displayed on virtual window in Proteus.The PCB design of the system is done in Proteus ARES.

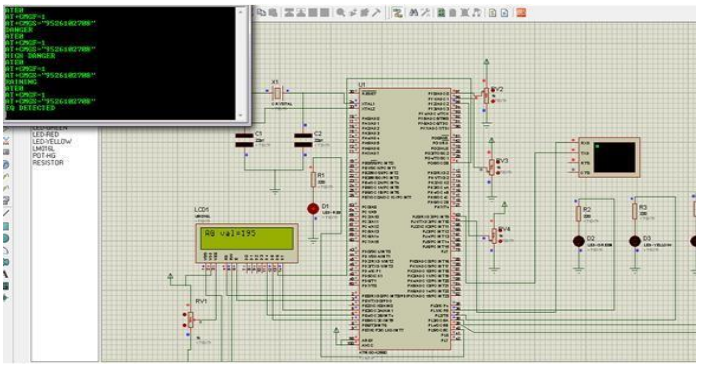

Figure 15: Simulation of the Project

In above simulation, there is also alert system showing 4 types of LED (green-normal, yellow and blue-midlevel, red-danger level) are shown in Proteus.

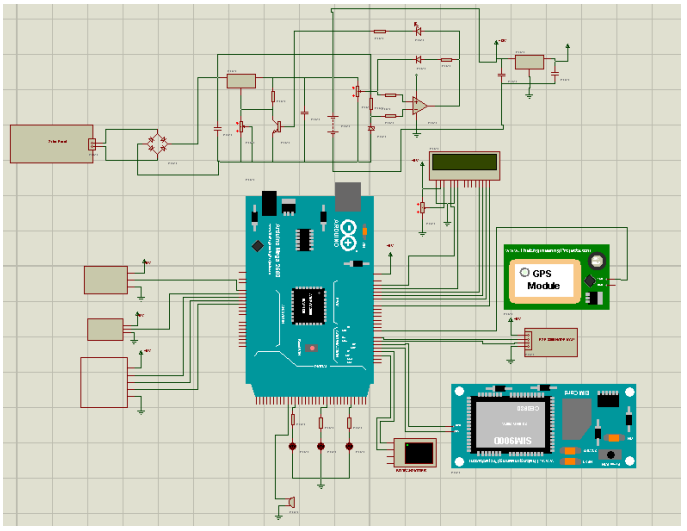

Figure 16: Schematic layout of the Project done in Proteus

Figure 17: PCB output of LM317 CIRCUIT

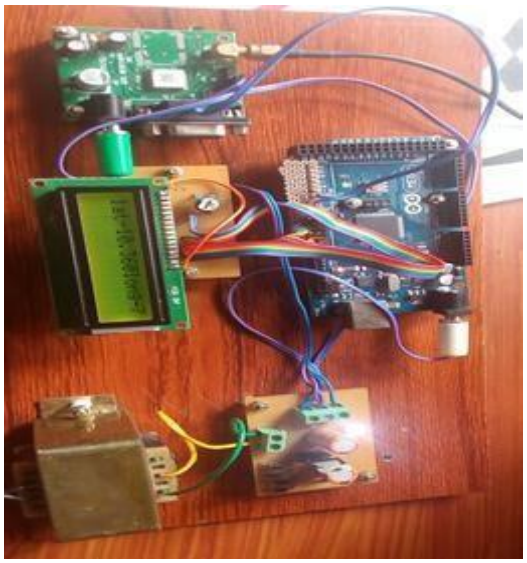

Figure 18: PCB output of GPS showing latitude and longitude

The above figure explains about GPS hardware interfacing to arduino mega 2560 microcontroller and LCD displaying latitude and longitude values

.

Figure 19: Final PCB output of Flood and earthquake detection and rescue using IOT technology

The sensor data packets from the RF receiver are picked up by the gateway ESP Wi-Fi module. Sensor nodes and the base stations (gateway) communication goes over the wireless channel utilizing the RF technology. Gateways connect to the internet and relay messages to the central network server using the standard IP protocol. Here the network server is ThingSpeak cloud-based platform. It provides live visualizations of data measured by sensors. We can send our data to be stored, to a ThingSpeak channel. Each channel can store up to 8 fields of data. We can monitor data from the phone, laptop or any other internet-enabled devices by login to ThingSpeak account.

V. CONCLUSION AND FUTURE SCOPE

Designing and implementation of Flood and earthquake detection and rescue using IOT technology is successfully completed. The system is able to monitor the water level sensor, accelerometer sensor, rain sensor to detect the presence of flood and earthquake to alert house hold members and authorities. The system performed well as per the design. By analyzing various technologies it is better understood that IOT.. The future work includes visualizing the location of flood and earthquake affected area in ThingSpeak IoT platform and monitoring those data on internet enabled devices. Also, the system can be extended to IoT based other natural disaster detection system

REFERENCES

[1] Elizabeth Basha, Daniela Rus, "Design of Early Warning Flood Detection Systems for Developing Countries", IEEE 2007

[2] Rifaat Abdalla , Keith Niall, "WebGIS-based Flood Emergency Management Scenario", International Conference on Advanced Geographic Information Systems & Web Services,2009

[3] Mohamad Nazrin Napiah, Mohd Yamani Idna Idris,Ismail Ahmedy,Md Asri Ngadi, "Flood Alerts System with Android Application", ©2017 IEEE

[4] Z.N. Khalil Wafi , Mohd Fareq Abd.Malek, Sateaa Hikmat alnajjar, R.Badlishah Ahmad , "Early warning system for Disaster management in rural area", International Symposium on Technology Management and Emerging Technologies (ISTMET), August 25 - 27, 2015,Langkawi, Kedah, Malaysia,2015

[5] www.smarter.com/Arduinos/look here

[6] www.answersite.com/rainsensors/search no more

[7] components101.com/sensors/mpu6050 module

[8] www.smarter.com/GPS satellites/look no further

[9] www.nowsms.com/faq/what-is-a gsm-modem

[10] in.zapmetasearch.com/rf modules

[11] www.teoma.co.uk/solarpanels/seenow

[12] www.teoma.co.uk/about wifi/search no more

Proceedings of the Fourth International Conference on Communication and Electronics Systems (ICCES 2019)
IEEE Conference Record # 45898; IEEE Xplore ISBN: 978-1-7281-1261-9

Feature Selection based Classification of Spams Using Fuzzy Support Vector Machine

Lovely Bansal
Dept. of CSE & IT
SRCEM
Gwalior, India

Dr. Nirupama Tiwari
Dept. of CSE & IT
SRCEM
Gwalior, India

Abstract*—E-mail is the secure way for the online form of communication as well as for transferring of data or messages through web. A day to day increase in the popularity, which give rapid growth to unsolicited mails in bulk amount. To filter the data, various methods present which is to detect automatically as well as eliminate such untenable messages. There are large number of technique for email spam filtering such as Clustering techniques, Learning based technique, Knowledge-based technique, Heuristic processes & many more. Given paper is on the research of spam filtering by using the feature selection through Relief feature selection technique & then classifies data by using Fuzzy support vector machine so as to deal with the factors of uncertain type. The experimental outcome illustrate that given algorithms can improve filtering rate parameters & spam filtering speed more efficiently.

Keywords— Spam, Fuzzy support vector machines, Relief feature selection, Polynomial kernel.

I. INTRODUCTION

E-mail is a major form of revolutionary which is taking place over the conventional communication systems which is because of its fast, convenient to use, easy, as well as economically cheaper to use. A key bottleneck in the E-communications is huge diffusion of emails which is unwanted & dangerous in nature so named as spam emails. A key concern is for developing of suitable filters which can capture those emails in sufficient amount and get high rate of performance. Researchers of Machine learning (ML) have developed number of approaches which is to deal with similar problem. in the machine learning framework, support vector machines (SVM) have maintained a large part to spam email filtering development . Based on SVM different scheme been designed through the approaches of text classification (TC). A major issue when we use SVM is the kernels selection as it affects openly by the partition of emails in quality space [1]. In this section figure (1) shows the brief process of filtering the spam. Here the first step is of preprocessing in which we remove redundant messages, conversion of lower case, tokenization as well as streaming is done in this step, next is feature selection & weighted feature where information gain methods we also select the feature size in this step ,next is representation of features is performed after selecting the required features, at last dataset is divided in train & test set in which learning & testing on models performed respectively, then classification is done to get the evaluated result, after this step the process ends.

Several types of researches have been performed on email filtering, some acquired good accuracy and some are still going on. Spam filtering is a process to detect unsolicited massage and prevent from entering into user's inbox. Now days, various systems have been existed to generate anti-spam technique for preventing unsolicited bulk email. Most of the anti-spam methods have some inconsistency between false negatives (missed spam) and false positives (rejecting good emails) which act as a barrier for most of the system to make successful anti spam system. Therefore, an intelligent and effective spam-filtering system is the prime demand for web users. [2]

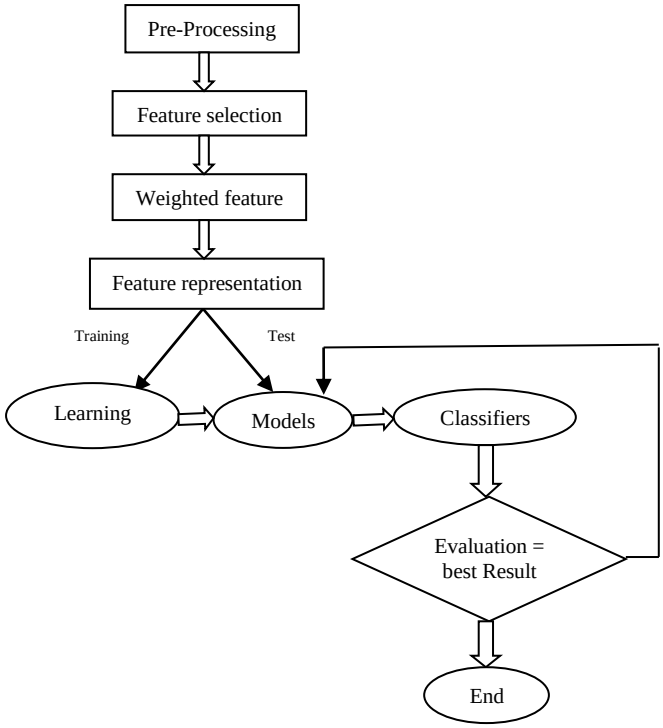

Figure 1: Process of Spam Filtering. [2]

Spam is making use of electronic messaging systems (by including the most of broadcast media, digital form of delivery systems) to transfer the unsolicited messages in bulk indiscriminately [3]. E-mail spam, also termed as e-mail in junk form / unsolicited bulk e-mail (UBE), it's a subset of spam which consist of nearly similar messages delivered to many recipients by the e-mail [4].

Several studies took place in this field and published the ways on how to get rid of spam mails , some of these are Rule Based Spam Filtering, Content Hash Based Filtering, Support Vector Machines (SVM), Machine Learning techniques, Content- Based Filtering (CBF) and many more [5]. From all above methods, CBF has been used widely as anti-spam solution because it's available in easy way with its full implementations in commercial form [6].

XXX-X-XXXX-XXXX-X/XX/$XX.00 ©20XX IEEE

FCM is to reduce feature set at the time of training phase and the membership degree is in use at time of clustering, which is performed among data and clusters centers have been included during system training. The given degree of membership is then required as box constraint when the incorporation of training phase with fuzzy SVM based classifier. In our work, FSVM based classifier is being used in place of SVM classifier to get better performance of system at time of classification.

The rest of the paper is organized as follows. In Section 2, feature selection technique a relief feature selection algorithm been described. In Section 3 other related researches performed till yet been discussed in literature review. In Section 4 flow of work done in our research area with brief review on methods used in research is discussed. In section 5 the experimental results being discussed where results obtained on various threshold values and comparisons of our work with past research is discussed. At last the conclusion of the work is presented in section 6

II. RELIEF FEATURE SELECTION

Relief is said to be feature weight based algorithm which is inspired from the learning of instance based [researcher Aha, Kibler, Albert year 1991 & Callan, Fawcett dz & Rissland year 1991]. Here the training data denoted as §, size of sample is denoted as m, and relevancy threshold is denoted by α , Relief take only those features those are appropriate to the target concept in statistical manner. A threshold is to encode as ($0 \leq \alpha \leq 1$). We also let scale of each feature which can either be nominal (take only Boolean) else numerical (which take only integer / real) values of feature. Difference among 2 instances X & Y is used are given functional diff.

When X_k , Y_k are the nominal,

Diff (X_k and Y_k) ={0 <if X_k and Y_k are the same>

1 <if X_k and Y_k are the different >

When Xk and yk are numerical,

diff(X_k and Y_k) = (X_k and Y_k)/nu_k

where nu_k is a unit of normalization to normalize given values of diff within the interval [0, l].

Algorithm representation of Relieff Feature Selection

1. Relief(§,m, α)
2. Separate § into § + = { instances of positive type] and
   §- = (instances of negative type)
3. w = (O,O, . . . * 0)
4. For i= 1 to m
5. Select randomly the instance X € S
6. Select randomly one instance of positive type near to the X, Z+ € § +
7. Select randomly one instance of negative type near to the X, Z- € S
8. if (X will be positive form of instance)
   Then Near-hit equal to Z+; Near-miss equal to Z-
   Else Near-hit equal to Z-; Near-miss equal to Z+
9. weight updated (W, X, Near-hit, Near-miss)
10. where Relevance is (l/m)W
11. For i = 1 to p
    if the value of (relevance i ≥ t)
    then fi is feature of relevant form
    else fi is irrelevant
12. Again weight is updated
13. For i= 1 to p
    Wi = Wi – diff (xi, near-hit i)2 + diff(xi, near-miss i)2

Relief select a sample which is m composed by no: of triplets of instance X, its instance for Near-hit is 1. Relief makes use of the p-dimensional formula of Euclid distance for choosing Near-hit as well as Near-miss. Relief each time make a calls for routine which is for updating W which stands for the vector for feature weight for each triplet sample & to determine the relevance of average weight. At last, Relief selects only such features which have average weight called (**'relevance level'**) above w.r.t given value of threshold α .[7]

III.LITERATURE REVIEW

Yuksel et al. [8] [2017] use Support Vector Machine and Decision tree for spam filtering. The Decision tree used in data mining and the support vector machines as a supervised learning model which can analyze the data for spam classification. First data was divided into two sections; one is training and other is test data, then the algorithm was trained and evaluated through Microsoft Azure platform which provides tools for machine learning and compared results with decision tree and support vector machine algorithm. The result of SVM method was 97.6% and for Decision tree the result was 82.6%. The result estimate that, SVM classifier performed better than DT.

Choudhary et al. [9] [2017] presented a novel approach using machine learning classification algorithm for finding and classifying SMS spam by using Short Message Service (SMS). The first step in this approach is feature selection and for that, they work on presence of mathematical symbols: UGLs, Dots, special symbols, emotions, Lowercased words and Uppercased words, mobile number, keyword specific and the message length in the SMS. After that they created a system design and collected a dataset which contained2608 emails out of 2408 collected SMS Spam Corpus.

Verma et al. [10] [2017] proposed a method for spam detection using Support Vector Machine algorithm and feature extraction. This methodology works through several steps such as Email collections, preprocessing, feature extraction, SVM training, test classifier, top word predictors, test email and result. First they take a dataset from Apache Public corpus. In preprocessing section, they remove all special symbol, URL and HTML tags and also unnecessary alphabet. Then they mapped all word from the dictionary using Vocab file. SVM classifier applied on the training dataset. The Accuracy of the system was 98%.

Rusland et al. [11] [2017] perform the analysis using Naïve Bayes algorithm for email spam filtering on 2 datasets those are evaluated on the basis of the accuracy, recall, precision and F-measure. Naïve Bayes algorithm is a probability-based classifier and the

probability is counting frequency as well as values combination in dataset. This research performed through three phases such as pre-processing, Feature Selection, and implementation through Naïve Bayes Classifier.

Sah et al. [12] [2017] proposed a method for detecting of malicious spam through feature selection and improve the training time and accuracy of malicious spam detection system. They also showed the comparison of difference classifier as Naïve Bayes (NB) and Support Vector Machine (SVM) based on accuracy and computation time. The proposed approach completed by $f(x) = a_0 + \sum_{n=1}^{\infty} \left(a_n \cos\frac{n\pi x}{L} + b_n \sin\frac{n\pi x}{L}\right)$ steps such as preparing the text data, creating word dictionary, Feature extraction process and training the classifier.

Singh et al. [13] [2018] discussed the solution and classification process of spam filtering and presented a combining classification technique to get better spam filtering result. With the help of Data mining, they collected several information of failures of previous papers, success with recent issues of spam filtering. In this method, researchers used binary value where 1 is for spam email & 0 for ham.

Abdulhamid et al. [14] [2018] discussed a performance analysis based approach by using some classification techniques such as Bayesian Logistic Regression, Hidden Naïve Bayes, Rotation Forest, REP Tree, Naïve Bayes, Radial Basis Function (RBF) Network, Voted Perceptron, Lazy Bayesian Rule, Multilayer Perceptron, Random Tree and J48. The competence of these techniques classified through Accuracy, Precision, Recall, F-Measure, Root Mean Squared Error, Receiver Operator Characteristics Area & Root Relative Squared Error using Spam base dataset and WEKA data mining tool.

IV.PROPOSED METHODOLOGY

In our propose work spam-filtering techniques is based on the statistics which is focusing on how to improve the recognition parameters of spam, where, the recognition time of execution will depend on no of samples which are randomly selected each time and how much amount of system memory is free at the time of execution . E-mail is easy, fast and cheap method of communication, which may cause unpredictable consequences for users, if sent information is not arrive in time. This paper proposes an algorithm on fast content-based spam filtering with proposed technique of feature selection and fuzzy-SVM.

Here from large part of original data, the fixed size of training set, the fixed size of the test set is randomly selected. First, training set is being required to train classifier, and then test set is needed to test the classifier, process is required to calculate performance level of proposed classifier. With the help of precision and recall parameters. Threshold value of 70% and 50% is used to extract the relevant features or attributes and discard the rest of it with the help of feature selection technique.

As evaluation of filtering method of feature selection, Relief is use to calculates a proxy statistic for every feature (attributes in our paper) from the sample of dataset that is then used to estimate or to calculate the 'quality of feature' or 'rank' to target concept. These types of feature statistics are known to be as the feature weights is within rank (W[A] is the weight of feature 'A'), or much casually as the 'rank' of feature. When the number of attributes which are 57 multiplied by used threshold value (say 0.7) the value is generated, if the rank is greater than or equal to attribute value/ weights of feature then attribute is extracted or else it's discarded .
Here, we apply clustering algorithm fuzzy c means to get the membership degree. With the help of SVM with polynomial kernel function the required model is classified. This is generated FSVM which is suitable for the uses in which data points consist of unmodelled characteristics.[15]

After the achieved train FSVM classification model. This is suitable for non linear problems and to deal with uncertain factors. So, this paper uses the modified classification technique of SVM into FSVM through polynomial kernel and clustering algorithm fuzzy c means. The dissimilarity in both the classifier is FSVM and SVM is, in FSVM, each data sample make use of degree of membership to which dataset belongs to from 2 distinct classes. The main part of proposed technique is to find out the best possible separating hyper plane so as to segment / distribute the set of data to complete the classification.

Generating the Fuzzy Memberships

To select fuzzy memberships of appropriate type in a given condition is much easy. Firstly, the lowermost bound of the fuzzy memberships need to be defined, & secondly, we require choosing those property of data set which helps to establish the connection among set of data and fuzzy memberships function. [16]

Assume that we have to perform the sequential learning problem. Where First thing is to choose, $\boldsymbol{\sigma} > 0$ because lower bound of the membership function. In second step , we identify ,time which is the major property of given kind of situation which then make s_i stand for fuzzy membership which is a function of time t_i

$$s_i = f(t_i)$$

where $t_1 \leq \ldots \leq t_l$ *is* time the arriving time of point in system. We choose $s_t = f(t_1) = 1$, and make use of first point to be the least essential and choose $s_1 = f(t_1) = \boldsymbol{\sigma}$.

By applying conditions for boundary, we get t_l

$$s_i = f(t_i) = \frac{1-\sigma}{t_l - t_1} t_i + \frac{t_l\sigma - t_l}{t_l - t_1}$$

The polynomial kernel not only takes care of given features of i/p samples which is to know their similarity, but also combinations of these. In context of regression analysis, such type of combinations is c/d interaction features.

$$K(\vec{x}, \vec{z}) = (\vec{z}^T \vec{x}_+ C)^n$$

Where n is "order" of kernel, and C is constant which permit to trade off influence of higher order & lower order of terms. Quadratic kernels are much popular form of the Polynomial kernel, Higher order kernels be likely to "over fit" training data so, thus don't generalize well. [17]

Here we, use k no of samples which is to train then get FSVM classification model. We achieve classification o/c after placing data for characterizing the mail in the model.

In this research we have Train classification model with FSVM. The data samples for this paper is from, famous UCI Machine Learning Repository having the spam base data unit. Randomly choose 300 no: of samples of the positive (ham) and 300 samples of negative (spam), having total of 600 used samples. Now from 300 positive samples, 200 no: of samples were chosen as the training set & 100 for testing set for both category of email and similarly performed with 300 negative samples

Pseudo code of FSVM& Polynomial kernel

Step 1. Start
Step 2. Load Spam base dataset
Step 3. Select randomly 600 samples of data
Step 4. Now categorize the 600 samples as 300 ham (+) and 300 spam (-)
Step 5. Now Divide samples 200 training and 100 testing for individually ham and spam.
Step 6. Divide the training data into sets
$D_1 = \{(x_1, 1), (x_2, 1) \ldots (x_n, 1)\}$
$D_2 = \{(x_{\frac{\pi}{2}+1}, -1), (x_{\frac{\pi}{2}+2}, -1), \ldots (x_n, -1)\}$

Step 7. Apply Relief feature selection strategy on training samples and calculate w[A]
$w[A] = w[A] - \sum_{j=1}^{k} \frac{diff(A,ri,hj)}{(m,k)}$

Step 8. Apply fuzzy-c-means (on equal attributes on training & testing) to calculate membership degree s_i
Step 9. Classify obtained model using SVM
Step 10. Using Polynomial kernel function to make kernel in commutation
$$K(\vec{x}, \vec{z}) = (\vec{z}^T \vec{x}_+ C)^n$$

Step 11. Obtain the trained model of Fuzzy Support vector machine
Step 12. Result obtained (ham and spam mails)
Step 13. Process ends.

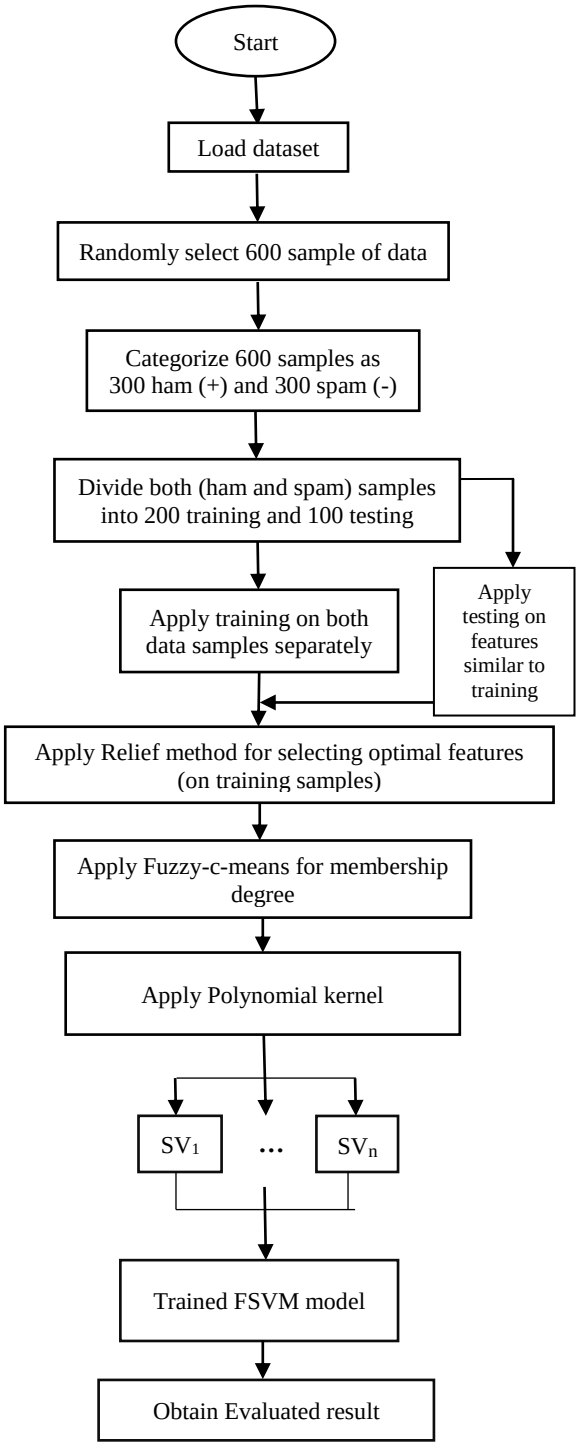

Figure 2 Flow diagram of FSVM using relief feature selection& polynomial kernel

V. EXPERIMENTS RESULTS AND DISCUSSION

The research work is implemented on MATLAB simulation tool. The given screenshot is to show the used train dataset sample from the "spam base data unit".

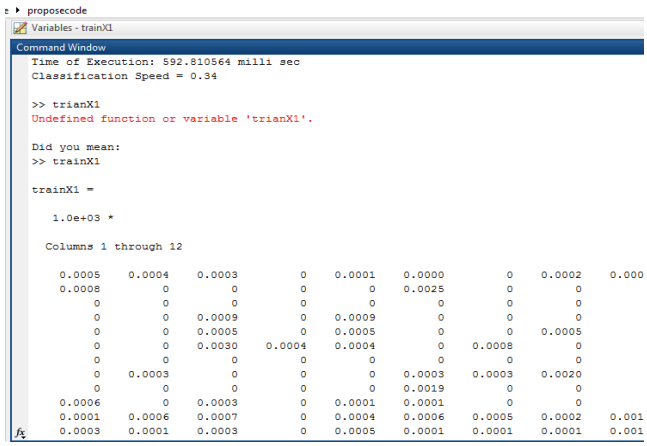

Figure 3train data set sample screenshot.

The performance of this research model is based on some specific criteria that is precision (p), recall rate (R) and speed of classification (*v*), time of execution (t). The higher is speed less is classification time taken for processing.

1) R =. $\frac{TP}{TP+FN}$, the recall rate shows discovering no of spam ability. The higher value of R, less is no: of spam evading arrest.
2) P =. $\frac{TP}{TP+FP}$, is identified as the % of real errors among all encounters that were classified as errors.
3) $v = \frac{N}{t}$, v stands for speed of classification.

Table 1: illustrate that FSVM using relief feature selection is comparatively generating better value of recall and precision on different threshold value then the FSVM using k-means clustering algorithm. Graphical representation is performed on 50% value and 70% value of threshold on a separate basis.

Table 1 Comparison of existing and proposed work with threshold value of 50% and 70%.

Algorithms	Recall		Precision	
	50%	70%	50%	70%
K-means& FSVM	85.94%	85.29%	91%	90%
Relief & FSVM	89.23%	92.59%	93%	94%

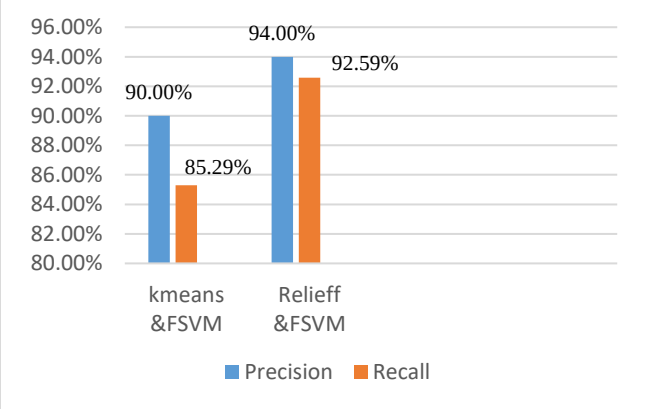

Figure 4 Recall and Precision of FSVM using k means and FSVM using Relief feature selection with threshold 70%

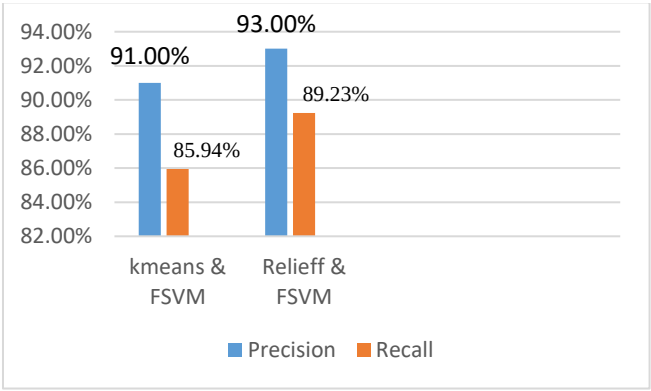

Figure 5 Recall and Precision of FSVM using k means and FSVM using Relief feature selection with threshold 50%

As shown in Table 2, the comparison of proposed method with those of other existing method is generating much better results, when comparison is performed on recall and precision values.

Figure 2 Comparison of proposed technique with other existing methods

Reference	Classifier used	Precision	Recall
Alsmadi, I [15]	NGram	83.6%	88.4%
Etaiwi, W.[16]	Naïve Bayes	51.8%	86.8%
Shengnan Wang, [17]	k-means & FSVM	90%	85.29%
Proposed method	Relief & FSVM	94%	92.59%

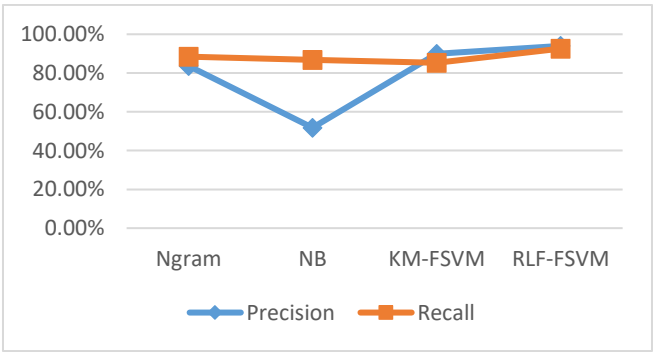

Figure 6 Graphical comparisons of various existing methods with proposed technique

As shown in Table 3, the classification speed and time of execution. The result obtained shows a huge difference between existing and proposed work. **As we are achieving high speed of classification and time of execution is reduced from the base work.** As this is the desired result so far.

Table 3 Comparison of Time spent & Speed of the classification from base work to propose work

ALGORITHMS	Base work	Propose work
	FSVM(K-means & RBF)	FSVM(Relief &Polynomial)
Classification Speed	0.71	2.21
Time of Execution	283.590212	90.629472

VI.CONCLUSION

Spam also called unsolicited bulk mails. E mail is undoubtedly a very effective, economically cheaper and also easy method of communication for ongoing time. But, as social networks and advertisers, have evolved their business worldwide with the help of emails , which contain unwanted information called spam.

This research paper is based on Fuzzy support vector machine (FSVM) classifier with Relief feature selection method which is required to extract features in form of attributes. In this research relief works on rank of the attributes, the rank is dependent on the value of threshold and number of attributes used. Here FSVM is required to train the classification model, with the help of membership degree which is to show the degree of similarity as the proposed model is much better for working on uncertain factors. Proposed experiments have shown that it is the improved form of spam filtering algorithm from other work by two aspects of reducing the time of execution & maximizing the speed of classification. How to improve filtering parameters in feature selection technique so as to achieve improved filtering results is significant topic for the future work.

REFERENCES

[1] J. V. Chandra, N. Challa, S. K. Pasupuleti, “A practical approach to Email spam filters to protect data from advanced persistent threat,” Circuit, Power and Computing Technologies (ICCPCT), Nagercoil/ India, 2016.

[2] Prabha Pandey1 , Chetan Agrawal2 , Tehreem Nishat Ansari, “A Hybrid Algorithm for Malicious Spam Detection in Email through Machine Learning” , International Journal of Applied Engineering Research ISSN 0973-4562 Volume 13, Number 24 (2018) pp. 16971-16979 © Research India Publications.

[3] N. Agrawal, S. Singh, “Origin (dynamic blacklisting) based spammer detection and spam mail filtering approach,” Digital Information Processing, Data Mining, and Wireless Communications (DIPDMWC), Moscow/Russia, 2016.

[4] W. Hu, J. Du, Y. Xing, “Spam filtering by semantics-based text classification,” Advanced Computational Intelligence (ICACI), Chiang Mai/Thailand, 2016.

[5] M. Rajalingam, V. Raman, P. Sumari, “Implementation of vocabularybased classification for spam filtering,” Computing Technologies and Intelligent Data Engineering (ICCTIDE), Kovilpatti/India, 2016.

[6] S. Rane, G. Moholkar, K. Yerunkar, N. Nikam, “The Detection of Suspicious Email Based on Decision Tree,” International Research Journal of Engineering and Technology (IRJET), 2017

[7] Kira, Kenji and Rendell, Larry (1992). The Feature Selection Problem: Traditional Methods and a New Algorithm. From: AAAI-92 Proceedings. Copyright ©1992, AAAI (www.aaai.org). All rights reserved

[8] Yüksel, A. S., Cankaya, S. F., & Üncü, İ. S. (2017). “Design of a Machine Learning Based Predictive Analytics System for Spam Problem”. Acta Physica Polonica, A., 132(3).

[9] Choudhary,N., & Jain, A. K. (2017). “Towards Filtering of SMS Spam Messages Using Machine Learning Based Technique. In Advanced Informatics for Computing Research”, (pp. 18-30). Springer, Singapore.

[10] Verma, T. (2017). “E-Mail Spam Detection and Classification Using SVM and Feature Extraction”.

[11] Rusland, N. F., Wahid, N., Kasim, S., & Hafit, H. (2017, August). “Analysis of Naïve Bayes Algorithm for Email Spam Filtering across Multiple Datasets”. In IOP Conference Series: Materials Science and Engineering (Vol. 226, No. 1, p. 012091). IOP Publishing.

[12] Sah, U. K., &Parmar, N. (2017). “An approach for Malicious Spam Detection in Email with comparison of different classifiers”.

[13] Singh, V. K., & Bhardwaj, S. (2018). “Spam Mail Detection Using Classification Techniques and Global Training Set. In Intelligent Computing and Information and Communication” (pp. 623-632). Springer, Singapore.

[14] Shafi’i Muhammad Abdulhamid, M. S., Osho, O., Ismaila, I., &Alhassan, J. K. (2018). Comparative Analysis of Classification Algorithms for Email Spam Detection.

[15] Alsmadi, I., & Alhami, I. (2015). “Clustering and classification of email contents”. Journal of King Saud University - Computer and Information Sciences, 27(1), 46–57.

[16] Etaiwi, W., & Naymat, G. (2017), “The Impact of applying Different Preprocessing Steps on Review Spam Detection”. Procedia Computer Science, 113, 273–279.

[17] Shengnan Wang, Xiaoyong Zhang, Yijun Cheng, Fu Jiang, Wentao Yu, Jun Peng, “A Fast Content-based Spam Filtering Algorithm with Fuzzy-SVM and K-means” 2018 IEEE International Conference on Big Data and Smart Computing.

Proceedings of the Fourth International Conference on Communication and Electronics Systems (ICCES 2019)
IEEE Conference Record # 45898; IEEE Xplore ISBN: 978-1-7281-1261-9

Analytical Study of PV Array with 3-Phase 3- Level Z-source inverter and VSI inverter

Kailash Baindara[*1],Seema Agrawal[*2],Tanushree Samaria[3], Mahendra Lalwani[4]
Department of Electrical Engineering
Rajasthan Technical University, Kota-324010, INDIA
[1]kbaindara000@gmail.com, [2]seema10dec@gmail.com, [3]tanusamariya@gmail.com, [4]mlalwani@rtu.ac.in

***Abstract*- In proposed article comparative study and simulation of PV system connected with Z-source and conventional inverters output are analyzed. A perturb and observe MPPT technique incorporated for maximizing output power of PV panel. Inverters is used in our system are receiving power input (DC) from PV system and inverters output is controlled by various triggering by space vector pulse width modulation technique (SVPWM). Respectively output voltages of both types of inverters are compared in respect of total harmonic distortion (THD) and obtain simulation results are gives effectiveness of Z-source inverter as compare to conventional inverter. In both cases inverters are able to calculate distortion factor according to IEEE standard. Projected model is intended under MATLAB/SIMULINK platform 2016(b).**

Keywords: Space vector pulse width modulation (SVPWM), photovoltaic (PV), Z-source inverter (ZSI),total harmonic distortion (THD).

I. INTRODUCTION

Electricity utilization is growing day by day. The use of renewable energy is become trendy because of lower availability in fossil fuel. Also conventional power generation methods are harmful for environment as compared to renewable energy source. Generation of energy through renewable sources is recommended pollution free energy. [1-2].

Main sources of renewable energy are hydro, bio-fuel, wind and photovoltaic [3]. Most beneficial and popular sources are PV and wind. Power generation using sunlight has growing rapidly in last few decades in India because power generation using sunlight provide various benefits such as less cost, pollution free, less maintenance charges and uninterrupted accessibility during day.

PV panel supplied regular DC power for get better efficiency of PV system, MPPT methods is extremely important [4]. Various methods of MPPT are Perturbation and Observation (P&O), Fractional Short-Circuit Current, fuzzy logic control, Incremental conductance, Ripple Correlation Control and Fractional Open-Circuit Voltage technique. Extraction of maximum power from PV is varied with solar irradiance and cell temperature. As a result to extract the maximum power from PV system on- line tracking of MPP is necessary [5, 6].

For MPPT perturb and observe (P&O) is usually used because its implementation is simple. P&O algorithm provides maximum power output by increasing or decreasing output voltage of PV panel.

PWM technique is usually used in DC to AC converter [7-9]. The PWM technique is extremely useful, in this method width of gate pulses are composed by different phenomena. In PWM based inverter output voltage is kept equal to rated voltage regardless of load. Output voltage in traditional inverters fluctuates according to variation in load.

The Z-source converter can convert and enhance voltage quality in single stage, but when it is supplied from conventional sources boosting factor is low. In a Z-source inverter an impedance circuit is used it provides connection between power source and inverter circuit [10]. The only difference between Z-source inverter and PWM based conventional inverter is use of impedance circuit in ZSI.

II. SYSTEM DESCRIPTION

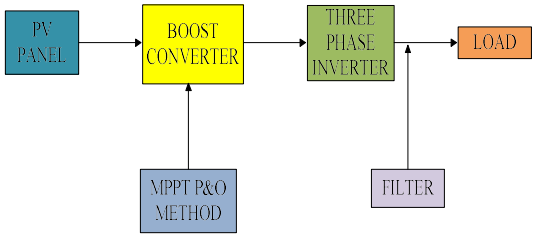

Fig.1. Basic arrangement of proposed scheme.

Fig.1 displays the basic arrangement of PV system. It has a PV panel connected with DC to DC boost converter.The Sun light in the form of photons incidence on PV array which generates electricity.PV panel output is controlled by MPPT technique (P&O) through boost converter. Three phase inverter is directly supplied by DC output of boost converter and provides AC voltage to load through a LC filter.

A. PV Modeling

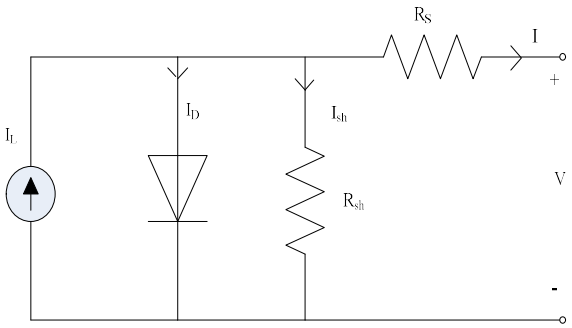

Fig.2. One diode model of PV cell.

Fig.2 represents one diode model of PV cell.

Here,
I_L = Cell current produce by light
I_D =Diode current
I_{sh}= Current lost in shunt resistance

$$I_D = I_O[\exp\left(\frac{V + IR_S}{\eta V_T}\right) - 1] \quad (1)$$

η = Diode ideality factor
I_0 = Saturation current
V_T = Thermal voltage
Thermal voltage given by:

$$V_T = \frac{kT_C}{q} \quad (2)$$

k = $1.381*10^{-23}$J/K
q = $1.602*10^{-19}$C
Complete governing equation for single diode model:

$$I = I_L - I_O[\exp\left(\frac{V + IR_S}{\eta V_T}\right) - 1] - \frac{V + IR_S}{R_{sh}} \quad (3)$$

Fig.3 and Fig.4 represent current-voltage and power-voltage curve of PV panel and different waveform obtained from PV panel.

Different parameters value of PV panel is illustrated in Table 1.

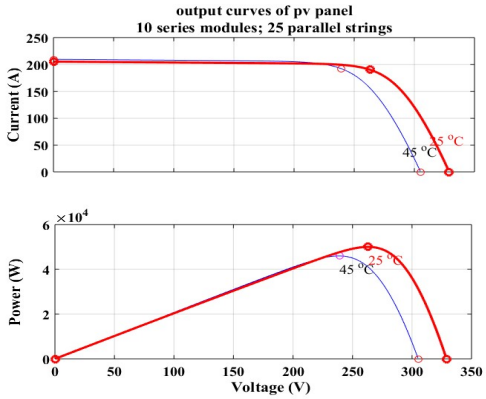

Fig.3. I-V & P-V curves of PV panel.

TABLE I. PV panel parameters used in represented model

Name	200W panel
Maximum Power(P_M)	200 W
Voltage at MPP	26.3 V
Current at MPP	7.61 A
Short circuit current (I_{sc})	8.21 A
Open circuit voltage (V_{oc})	32.9 V
Temp coefficient of V_{OC}	-0.36099 %/DegreeC^0
Temp coefficient of I_{SC}	0.102 %/DegreeC^0
No of parallel strings	25
Series module per string	10

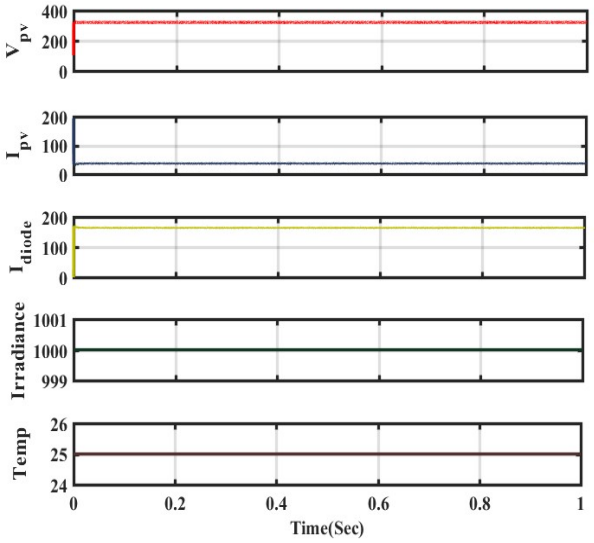

Fig.4. waveform of PV array (i) Voltage (ii) Current (iii) Diodecurrent (iv) Irradiance (v) Temperature.

B. *Maximum power point tracking*

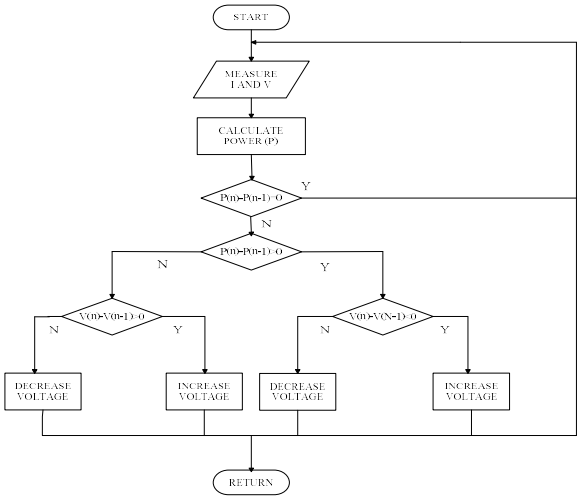

Fig.5. P&O algorithm.

C. *Inverter*

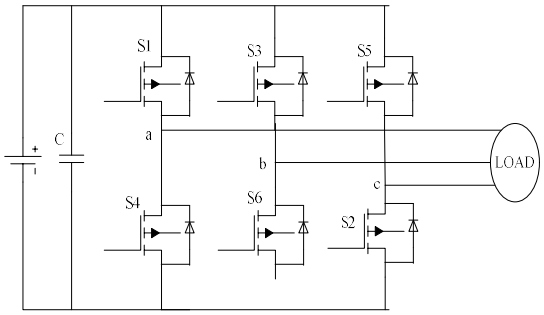

Fig.6. Basic diagram of a three phase three level inverter

Switches either IGBT or MOSFET are connected as shown in above figure 6. We can get ac output from dc input by specified triggering of switches.

D. *Z-source inverter*

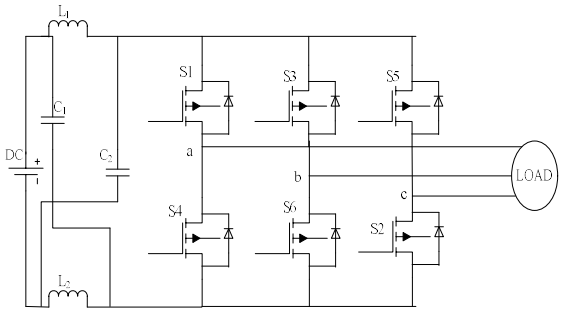

Fig.7. Circuit representation of Z- source inverter.

Circuit representation of Z-source inverter is shown in figure 7. In a Z-source inverter two inductors and two capacitors of equal values are connected in the form of Z.

Z-source inverter parameters are represented in Table II.

TABLE II: Parameters of Z- source inverter

S. No.	Parameters	Value
1	Voltage	320V
2	L_1, L_2	45mH
3	C_1, C_2	200µF

E. *Filter*

Passive LC filter as fig. 8 is used to reduce the harmonics of output signal of inverter.

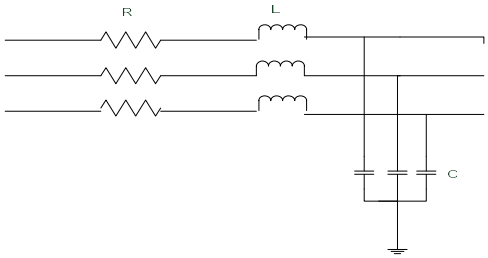

Fig.8. LC passive filter.

TABLE III parameters of LC filter

S.No.	Parameters	Values
1	R	10ohm
2	L	97mH
3	C	80µF

III. SIMULATION RESULT

A. *VSI inverter results*

Fig. 9 to Fig. 14is illustrated waveform obtained from VSI inverter.

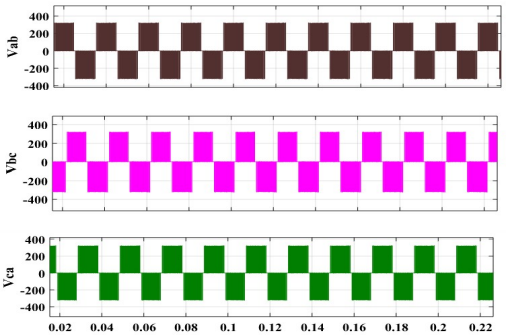

Fig.9. Line to line output voltage of VSI inverter.

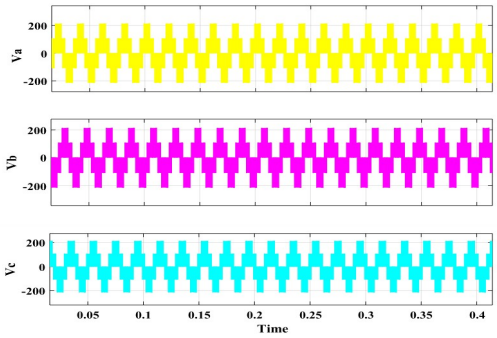

Fig.10. Phase to ground output voltage of VSI inverter.

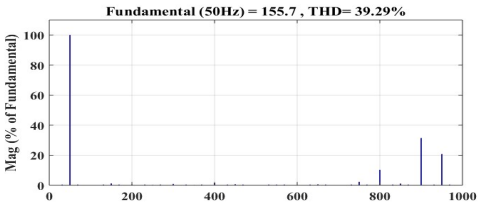

Fig.11. THD of VSI inverter output

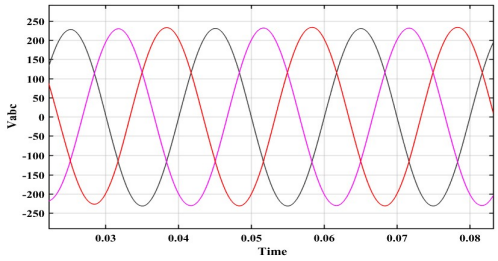

Fig.12. Output voltage of VSI inverter after filter

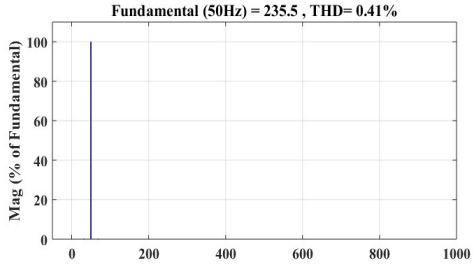

Fig.13. THD of VSI output AC voltage after filter.

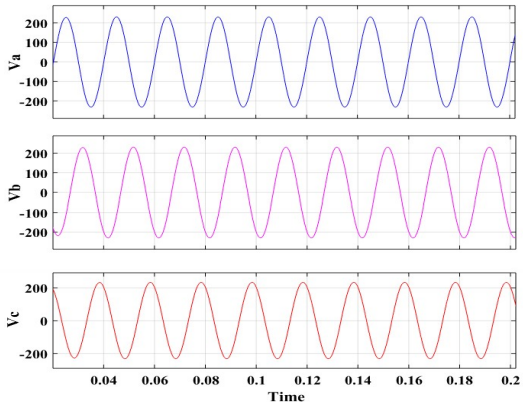

Fig.14. Output waveform of voltage VSI after filter

B. Z-source inverter results

Fig. 15 to Fig. 21 show waveform obtains from Z-source inverter.

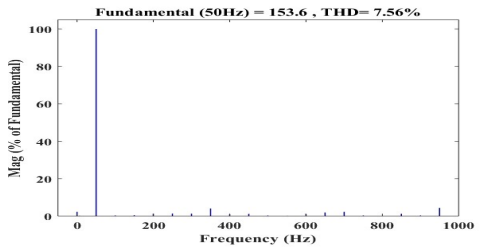

Fig.15. THD of ZSI output.

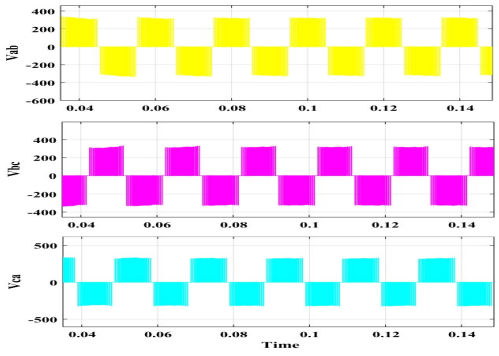

Fig.16. Voltage between two phases of ZSI.

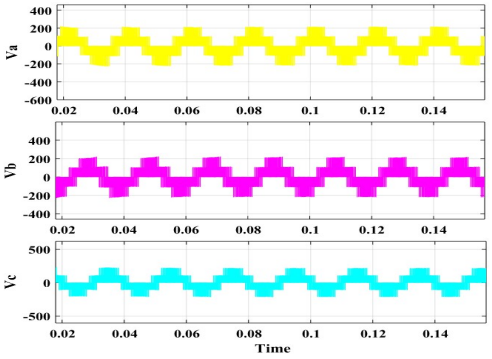

Fig.17. Phase to ground voltage of ZSI.

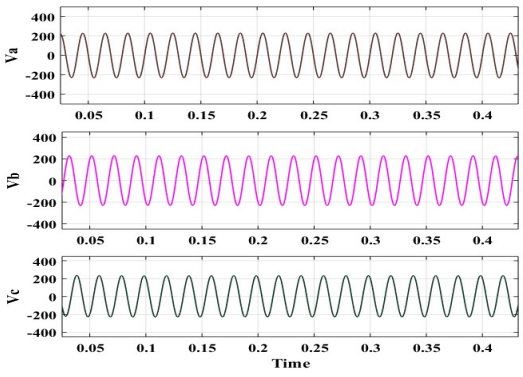

Fig.18. Z-source inverter output waveform of voltage after filter.

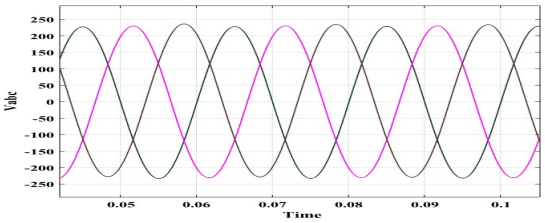

Fig.19. Output three phase waveform of Z-source inverter.

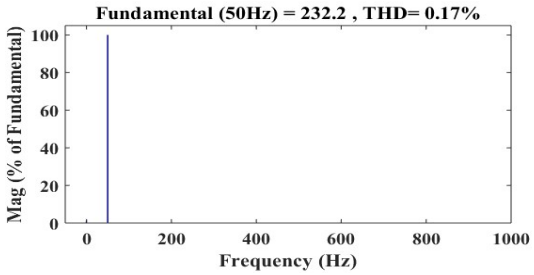

Fig.20. THD of output signal from Z-source inverter after filter.

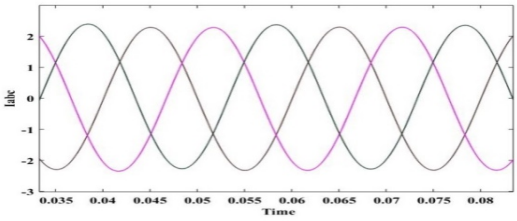

Fig.21. Output current waveforms of Z-source inverter Result.

IV. CONCLUSION

In proposed model, conventional and Z-source based PV connected have been investigated and compared. The proposed z-source inverter has shown better performance than conventional SVPWM based inverter. From the result it is clear that z-source inverter provides 7.56% THDwhereasSVPWM based conventional VSIinvertergives 39.29% voltage harmonics. It has been shown that high quality waveform at output of Z-so-urce based inverter can be reached by using suggested method.

REFERENCES

[1] Maria A. Usova, Vladimir I. Velkin,"Possibility to Use Renewable Energy Sources for Increasing the Reliability of the Responsible Energy Consumers on the Enterprise"17th International Ural Conference on AC Electric Drives (ACED),2018.

[2] Shyam.B, P. Kanakasabapathy, "Renewable Energy Utilization in India–Policies, opportunities and challenges" IEEE International Conference on Technological Advancements in Power and Energy (TAP Energy) 2017.

[3] Seema Agrawal, Seemant Chourasiya, D.K Palwalia, "Hybrid Energy Management System design with Renewable Energy Sources", IJSET, Vol. 6, No. 3, 2018.ISSN 2277-1581 impect Factor 1.632 pp.174-177 DOI : 10.5958/2277 1581.2017.00104.8

[4] Ranita Sen , Anjali Garg , Alka Singh, "Modeling of PV array using P&O algorithm in Boost Converter," International Conference on Computing and Communication Technologies for Smart Nation (IC3TSN), 2017.

[5] Sriramalakshmi Palanidoss, Vishnu Theja. V S, "Experimental Analysis of Conventional Buck and Boost Converter with Integrated Dual Output Converter," International Conference on Electrical, Electronics, Communication, Computer and Optimization Techniques (ICEECCOT), 2017

[6] Aishwarya V. Magar,Sanjay G. Kanade, Ashish P. Kinge, "Transformerless Buck-Boost DC-DC Converter," IEEE Global Conference on Wireless Computing and Networking (GCWCN), 2018.

[7] Karima Boudaraia ,Hassane Mahmoudi , Ahmed Abbou , and Mohamed Hilal, "Buck Converter MPPT Control of a Photovoltaic System," 5th International Conference on Multimedia Computing and Systems (ICMCS), 2016.

[8] Ravi Kant Sharma, Shivam, "Performance Analysis of Multilevel inverter based on SVPWM for Renewable Energy Sources", 6th International Conference on Signal Processing and Integrated Networks (SPIN),2019. .

[9] R. K. kumawat, Seema Agrawal, Seemant Chourasiya, D.K. Paliwalia, "Modeling & Simulation of PV ARRAY with Single Phase Reduced Switch Count Five Level PWM Inverter for Renewable Energy Applications", APGRES June, 2015.

[10] Khushboo gupta, Seemant Chourasiya, R. K. kumawat, Seema Agrawal, D.K.Paliwalia, "A Review : Modulation Techniques for Neutral Point Clamped Inverter" ICATETR June, 2015.

Proceedings of the Fourth International Conference on Communication and Electronics Systems (ICCES 2019)
IEEE Conference Record # 45898; IEEE Xplore ISBN: 978-1-7281-1261-9

Voice Activity Detection Using Novel Teager Energy Based Band Spectral Entropy

Raveesh Hegde
Dept. of Telecommunication Engineering
CMR Institute of Technology
Bengaluru-560037, India
raveesh.h@cmrit.ac.in

R. Muralishankar
Dept. of Electronics and Communication Engineering
CMR Institute of Technology
Bengaluru-560037, India
muralishankar@cmrit.ac.in

***Abstract*—there are many features proposed in the literature for voice activity detection (VAD). Shen et al. [20] first used a spectral entropy-based feature to detect regions of speech spurts under noisy conditions. However, VAD employing this feature was unreliable when the noise level greatly exceeds the speech level. To improve the performance of spectral entropy based VAD under low signal-to-noise ratios (SNRs), spectrum of a signal over a frame is divided into sub bands and spectral entropy is computed over these bands. Later, these spectral entropies are weighted and summed to obtain the entropy. Based on the amount of noise in each band, weights were found empirically. This approach was named as banded spectral entropy (BSE) [21]. In [24], deviation threshold computed from approximate ramp line and the sorted spectral coefficients of the band are adopted to decide useful/useless bands. In this paper, we propose a novel Teager Energy Band Spectral Entropy (TE_BSE) feature for VAD. Here, we carryout enhancement of spectral peaks employing Teager energy of each frequency transformed speech frame. This is followed with dividing of spectrum into sub bands and entropy computation over each band. The summing of entropy from each useful band is done to get TE_BSE feature. We identify useful/useless bands following [24]. Later, we present the performance of our proposed VAD in terms of probability of detection (P_D), probability of false alarm (P_{FA}) and probability of error under different noises and SNRs. Finally, from the VAD results on real-world sample, proposed VAD outperforms statistical based VAD by Sohn et. al. [8] with improved P_D not at the cost of increase in P_{FA}.**

Keywords—Voice Activity Detection; Spectral Entropy; Band Spectral Entropy; Teager Energy Operator;

I. INTRODUCTION

A process of marking the boundaries or classifying between speech and non-speech (silence, background noise etc.) segments of a digital speech signal is popularly known as voice activity detection (VAD)**.** Speech/non-speech detection as a preprocessing step, enhances the performance of applications including robust speech recognition [1,2], discontinuous transmission [3,4], real-time speech transmission on the Internet [5] or combined noise reduction and echo cancellation schemes in telephony [6,7]. Speech/non-speech classification task is not as trivial as it appears; indeed, most VAD algorithms fail when the background noise increases. Numerous researchers have proposed different schemes for detecting speech regions in a noisy speech signal [8-11].

The different VAD methods include those based on energy thresholds [13], pitch detection [16], spectrum analysis [15], zero-crossing rate [3], periodicity measure [17], higher order statistics in the Linear Predictive Coding (LPC) residual domain [18] or combinations of different features [3,4,19]. Shen et al. [20] first used a spectral entropy-based parameter to detect regions of speech spurts under noisy conditions. However, their method is unreliable when the noise level greatly exceeds the speech level. Additionally, the spectral entropy relies on the variance of spectral magnitude to distinguish speech from noise, but the variance of spectral magnitude in turn strongly depends on the nature of noise.

One can improve the robustness of spectral entropy by exploiting banded structure of speech spectrogram and discarding bands dominated by noise, thereby enhancing the banded nature of speech spectrogram. Spectral entropy thus computed is called the banded spectral entropy (BSE) [21]. However, BSE does not sufficiently specify the organization of the banded nature on the spectrogram. Therefore, in [21], Wu and Wang have proposed a set of weights to compensate for this drawback. These weights have been found empirically by the authors [21] to sufficiently characterize the speech signals rather than by simply computing spectral entropy of each sub-band [20]. Although the weighted BSE remains a good feature parameter, the detection sometimes fails at very low SNRs. The question that needs to be addressed is the following: *How is one to discard the noisy bands and hence, effectively retain only the useful bands*?

In [22], it was shown that the number of noisy bands (or useful bands) is related to the background noise level. A Minimum Mel-scale frequency Band (MiMSB) parameter proposed in [23] has been used in [21] to estimate the varying noise levels by adaptively choosing one band with minimum energy. A Normalized Minimum Band Energy (NMinBE) parameter has been proposed to accurately decide the number of useful bands. The authors in [21] have used the number of useful bands empirically derived from the knowledge of NMinBE. Further, it has been assumed in [21] that a short window of non-speech interval exists prior to the commencement of the input signal and the mean and variance of the logarithmic Adaptive BSE (ABSE) has been initialized on the estimates computed from this window. Successively, the relative mean and variance of the logarithmic ABSE values are updated during non-speech periods.

In contrast, our proposed band selection scheme is easy to setup and has too less empirical parameters as part of the initialization. This scheme exploits the banded structure available in noisy speech spectrum and selects those sub-bands where speech dominates over noise. We examine the banded structure on speech spectrogram to detect speech/non-speech regions as used in [21], but differ from it in terms of selection of useful/useless bands. Our band selection scheme depends not exclusively on the statistical behaviour of speech, but also on speech contaminated by noise in sub-bands. Specifically, we exploit the well-known fact that the formants play a major role in modelling speech signals in a compact way, and that the first three formants are sufficient to synthesize intelligible speech. Therefore, the detection of speech/non-speech is equivalent to identifying the presence or absence of formants.

In this paper, we adopt band spectral entropy (BSE) in [21] to compute the entropy. However, our approach is different on two counts (i) Selection of useful/useless bands in a spectrum employing deviation between coefficients that approximate ramp line (ARL) and sorted spectral coefficients (ii) Enhancement of spectral peaks employing Teager energy operator (TEO) on the signal spectrum such that the spectral peaks are enhanced. This is followed with the smoothening of present spectral estimates with past spectral estimates. Further, our work deviates from [24] on second count. In section, II we discuss spectral peak enhancement and smoothening employing TEO and later computation of BSE. We name this new feature as Teager energy band spectral entropy (TE_BSE). Section, III presents theory behind the selection of useful/useless bands proposed in [24]. In section, IV we present experimental setup in extracting TE_BSE feature followed with performance analysis this feature under (i) Stationary noise (ii) Non-stationary noise and (iii) Non-stationary heavy noise environments. Finally, we present the VAD output employing proposed feature and compare with statistical based VAD by Sohn et. al. [8]. This followed with concluding remark and some vistas for future.

II. BAND SPECTRAL ENTROPY

We now review the procedures in [20, 21] in some more detail. The entropy measures the randomness of the signal $x(.)$ with the defined probability density function $f(x)$as

$$H(x) = -\int f(x)\log\big(f(x)\big)\,dx. \tag{1}$$

Shen et al. [20] employed it to discriminate speech from non-speech signals as part of ED. The speech signal is observed over a frame of length, N. The Short-Time Fourier Transform (STFT) of lth frame, $s(n,l)$, is given by

$$S(k,l) = \sum_{n=0}^{N-1} w(n)\, s(n,l)\exp\left(-\frac{j2\pi kn}{N}\right), \quad k = 0,\dots,N-1, \tag{2}$$

where$|S(k,l)|$ represents the spectral magnitude of the kth frequency bin of the lth frame, N being the total number of frequency bins and $w(n)$, a Hamming window. Excluding the symmetry and squaring each of$|S(k,l)|$, let

$$S_{msq}(k,l) = |S(k,l)|^2, k = 0,\dots,\frac{N}{2}-1. \tag{3}$$

Then, the probability associated with each $S_{msq}(k,l)$ component $P(j,l)$ can be estimated by normalizing

$$P(j,l) = \frac{S_{msq}(k,l)}{\sum_{k=0}^{\frac{N}{2}-1} S_{msq}(k,l)}, 0 \le j \le \frac{N}{2}-1. \tag{4}$$

The corresponding spectral entropy over a frame is

$$H(l) = \sum_{j=0}^{\frac{N}{2}-1} P(j,l)\log\big(1/P(j,l)\big). \tag{5}$$

Spectral entropy depends on the variation of the spectral energy but not on the amount of spectral energy. Consequently, spectral entropy, and hence the performance of VAD, are robust to the changing noise levels [20]. However, the magnitude associated with each point in the spectrum is affected by noise and, therefore, VAD performance would degrade severely at low SNRs. Further, the observation in [21] about 'effect of noise in the spectrum' was primarily restricted to a few sub-bands instead of a full band. This naturally suggests multiband analysis and necessitates the entropy computation for each of the sub-bands [21]. The sub-band energy of a given frame is computed as follows:

$$E_{SBE}(m,l) = \sum_{k=(m-1)*(N/2N_b)}^{\left(\frac{N}{2N_b}\right)-1+(m-1)*(N/2N_b)} S_{msq}(k,l), \quad 1 \le m \le N_b, \tag{6}$$

where N_b is the total number of sub-bands for each frame ($\mathrm{N_b} = 32$) and represents the energy of the sub-band. Again, we define the probability associated with each sub-band as

$$P_{SBE}(m,l) = \frac{E_{SBE}(m,l)}{\sum_{k=1}^{N_b} E_{SBE}(k,l)}, 1 \le m \le N_b. \tag{7}$$

The BSE parameter, $H_{SBE}(l)$, is now computed as

$$H_{SBE}(l) = \sum_{m=1}^{N_b} P_{SBE}(m,l)\log\big(1/P_{SBE}(m,l)\big). \tag{8}$$

Further, in [21], a set of weights is proposed to compensate for this drawback. These weighting factors are found empirically to characterize speech signals more effectively than by simply computing spectral entropy of each sub-band. Although the weighted BSE remains a good feature, the detection sometimes fails at very low SNRs. Therefore, it is required to discard the noisy bands and retain others.

A. BSE using Teager Energy Operator

Formant tracking using the Teager energy operator (TEO) has been proposed by many researchers [25-28]. In [28], multiband approach along with TEO is employed in formant tracking. We are motivated by the efficacy of TEO in formant estimation and have adopted it in our approach. A discrete version of TEO on a time domain signal, $x(n)$is given by

$$E_{Teager}\big(x(n)\big) = x^2(n) - x(n-1)x(n+1), \forall n. \tag{9}$$

To enhance peaks in the spectrum, and thereby to track the formants, we employ TEO on $S_{msq}(k,l),\ k=0,\dots,-1,$ in (3). This results in $S_{Tmsq}(k,l)$. However, this enhancement comes at the cost of enhancing spurious peaks in $S_{msq}(k,l)$ due to the difference operation in TEO (refer (9)). To derive the benefits of TEO and minimize spurious peaks, we use convex combination of S_{msq} and S_{Tmsq} as follows.

$$E(k,l) = \alpha S_{msq}(k,l) + (1-\alpha) S_{Tmsq}(k,l), \quad k = 0,\dots,(N/2)-1. \tag{10}$$

Here, $0 \le \alpha \le 1$. To find the probability associated with lth frame, we use (4) and replace $S_{msq}(k,l)$ by $E(k,l)$ as

$$P_T(j,l) = \frac{E(k,l)}{\sum_{k=0}^{\frac{N}{2}-1} E(k,l)}, 0 \le j \le \frac{N}{2}-1. \tag{11}$$

The corresponding spectral entropy is computed as follows:

$$H_T(l) = \sum_{j=0}^{\frac{N}{2}-1} P_T(j,l) \log\left(\frac{1}{P_T(j,l)}\right), 0 \le j \le \frac{N}{2}-1. \tag{12}$$

We observe that the dominance of formants in sub-bands introduces sparseness (presence of structure) and the absence of formants or noise contamination introduces denseness (absence of structure). We attempt to detect formants by utilizing banded structure of speech signals [21]. From $E(k,l)$, we compute the sub-band energy, sub-band probability and associated entropy using (6), (7) and (8). Thus,

$$E_{SBE}^{T}(m,l) = \sum_{k=(m-1)*(N/2N_b)}^{\left(\frac{N}{2N_b}\right)-1+(m-1)*\left(\frac{N}{2N_b}\right)} E(k,l), 1 \le m \le N_b, \tag{13}$$

$$P_{SBE}^{T}(m,l) = \frac{E_{SBE}^{T}(m,l)}{\sum_{k=1}^{N_b} E_{SBE}^{T}(k,l)}, 1 \le m \le N_b \tag{14}$$

and

$$H_{SBE}^{T}(l) = \sum_{m=1}^{N_b} P_{SBE}^{T}(m,l) \log\left(1/P_{SBE}^{T}(m,l)\right). \tag{15}$$

III. Selection of Useful/Useless Spectral Bands

In [20], weighted BSE is supported with useful/useless band selection using NMinBE parameter under low SNRs. We differ from [20, 21] in the selection of useful/useless sub-bands. Here, we examine each frame by equally partitioning $P_T(j,l), 0 \le j \le \left(\frac{N}{2}\right)-1$, into N_b sub-bands as $P_T^b(m,l)$, where $b = 1,\dots,N_b,$ and $m = \left(\frac{(b-1)N}{2N_b}\right),\dots,\left(\frac{bN}{2N_b}\right)-1$. The presence/absence of structure in sub-bands is equivalent to the presence/absence of formants in the sub-bands. We argue that the presence of formant amounts to sparseness and that their absence, due to the presence of noise, yields denseness. This provides a basis to measure sparseness or denseness via the deviation of an approximate ramp line (ARL) [24] from the sorted $P_T^b(m,l)$ coefficients. The sorted $P_T^b(m,l)$ coefficients are henceforth denoted as $\tilde{P}_T^b(m,l)$. We connect the first coefficient of $\tilde{P}_T^b(m,l)$ to the last coefficient to generate ARL. Subsequently, we sample ARL with uniform intervals between samples. Here, ARL is computed for each sub-band in the frame of a given speech signal.

We observe that for the sub-band, the $\tilde{P}_T^b(m,l)$ coefficients are closer to ARL when non-speech/noise dominates over speech and that they are relatively removed from it otherwise. Closeness to ARL is computed by taking sum of square difference between samples of ARL and $\tilde{P}_T^b(m,l)$ coefficients as

$$CL^b(l) = \sum_{m=\frac{(b-1)N}{2N_b}}^{\frac{bN}{2N_b}} \left(ARL^b(m,l) - \tilde{P}_T^b(m,l)\right)^2. \tag{16}$$

We present some features of the proposed scheme.

- When speech formants dominate over noise in a sub-band, the deviation of $\tilde{P}_T^b(m,l)$ coefficients from ARL is higher than otherwise. This accounts for correct performance.
- When noise dominates over speech formants in all the sub-bands, speech sub-bands may be identified as non-speech, thus resulting in Missed Detection (MD). This occurs when speech is completely masked by the noise under very poor SNR conditions.
- Noise induced spectral peak in the sub-bands results in false alarm (FA) in the event of sub-bands having no speech signal. This occurs when a non-stationary narrow band noise in non-speech region presents itself a peak within sub-band. Then, any appreciable deviation generated by this noisy spectral peak away from ARL will result in a non-speech packet being detected as a speech packet.

The nature of ARL and $\tilde{P}_T^b(m,l)$ coefficients under additive babble noise during speech/non-speech frames for the SNRs, $0, 5$ and 15dB is presented through Fig. 1 – Fig. 3. Here, the sub-band b is fixed and $\tilde{P}_T^b(m,l)$ coefficients from (i) Speech plus babble noise frame; and (ii) Babble noise only frame are used to obtain ARL and plot of sorted coefficients of $\tilde{P}_T^b(m,l)$, respectively. Conclusions drawn from these plots are summarized as follows:

- When SNR is at 0 dB, the difference in the range of $\tilde{P}_T^b(m,l)$ for speech and non-speech frames is not so pronounced. However, large deviation of $\tilde{P}_T^b(m,l)$ from ARL can be noticed for the speech frame than for non-speech frame. This helps in deciding *speech/non-speech* sub-bands in a frame and to the computation of SBE when a sub-band is declared as *speech*. As SNR increases, $\tilde{P}_T^b(m,l)$ range increases/decreases for speech/non-speech frames as also the deviation from ARL.

A Deviation Threshold (DT) is selected empirically to achieve minimum MD and restrict FA to an allowable range. Each sub-band is checked for the presence or absence of formants based on the deviation achieved and compared with the DT. This refined adaptive band selection scheme will adapt quickly to change in signal and noise conditions. Thus,

the proposed approach has less parameters to setup arbitrarily than in [21]. Threshold for BSE is initialized assuming first 200ms as non-speech region. We differentiate speech regions from non-speech regions using the BSE feature computed from useful sub-bands. A simple hangover scheme is employed to minimize fast switching between speech and non-speech and vice versa.

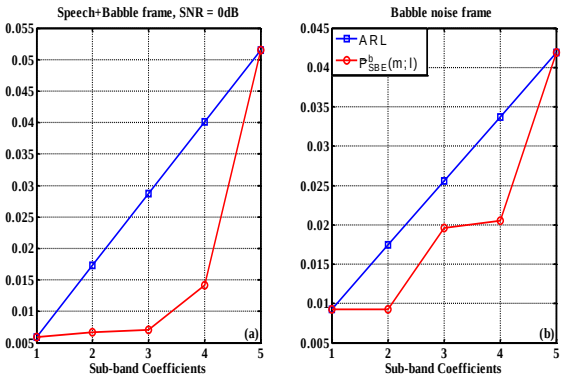

Fig. 1.Plot showing ARL and $\widetilde{P}_T^b(m,l)$ under babble noise with 0dB SNR (a) Speech plus noise (b) noise only frame.

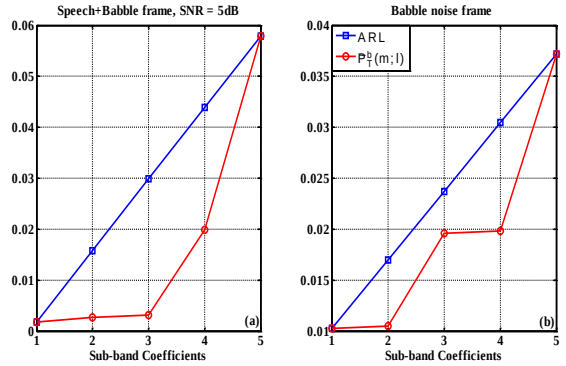

Fig. 2. Plot showing ARL and $\tilde{P}_T^b(m,l)$ under babble noise with 5dB SNR (a) Speech plus noise (b) noise only frame.

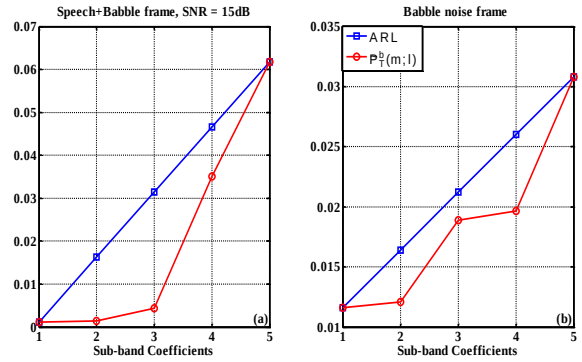

Fig. 3. Plot showing ARL and $\tilde{P}_T^b(m,l)$ under babble noise with 15dB SNR (a) Speech plus noise (b) noise only frame.

IV. Experimental Setup and Result Analysis

We evaluated our VAD scheme by considering clean and noisy speech signals that are sampled and digitized. Sampling frequencies of 8 and 16 kHz are considered in our evaluation. Then, sampled and digitized speech signals are framed such that the successive frames do not overlap. Here the frame length is chosen to accommodate 320 speech samples. The number of sub-bands, N_b is fixed to 32. In computing $E(k,l)$ using (10), we set α to be 0.3. To simulate the noisy speech with SNRs from $0-40$ dB, speech signal is added with 13 different noises: Babble, F16, Tank, Factory, Car, Subway, Fan, Pink, HFchannel, Machine Gun, Destroyer Engine, Military Vehicle, Jet Cockpit and White.

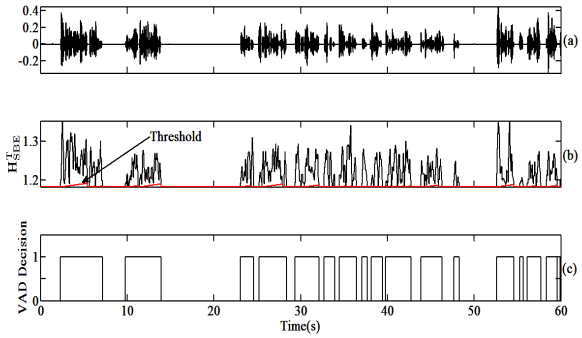

Fig. 4. Result of VAD under clean signal (a) Speech signal (b) Band Spectral Entropy and Threshold (c) VAD Decisions (Speech = 1;Non-speech = 0).

The SNR is varied in steps of 5dB. The results of VAD using proposed scheme under clean and noisy conditions are presented (refer Fig. 4). Here, Fig. 4(a) is speech sample under clean conditions. Figure 4(b) shows H_{SBE}^T and the threshold computed for the speech signal in Fig. 4(a). The corresponding

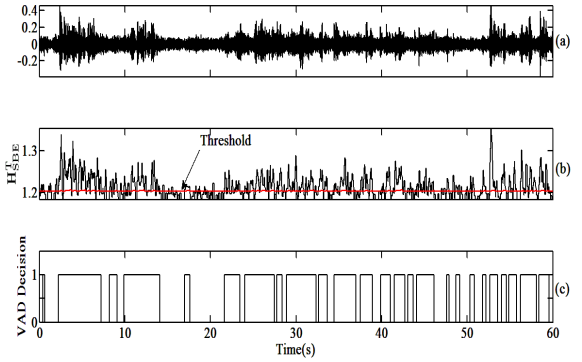

Fig. 5.Result of VAD under Babble noise with SNR = 0dB (a) Speech signal (b) Band Spectral Entropy and Threshold (c) VAD Decisions (Speech = 1; Non-speech = 0).

VAD decisions are in Fig. 4(c). In Fig. 5 – Fig. 7, we added Babble, Jet Cockpit and Subway noises to the speech in Fig. 6(a) to simulate respective noisy speech signals where the SNR is maintained at 0 dB. Parts (c) of Fig. 5 – Fig. 7 show VAD decisions with the proposed approach. We observe from Fig. 5(c) that in the presence of speech-like noise, such as Babble, FA errors are more pronounced than MD errors under low SNR conditions. However, the VAD decisions presented in Fig. 6(c) and Fig. 7(c) are for non-speech like noises such as Jet Cockpit and Subway noises where it can be observed

that FA and MD errors are minimal for the same SNR setup. This is attributed to the robustness of the proposed speech /non-speech band selection scheme under additive non-speech like noises as against Babble noise.

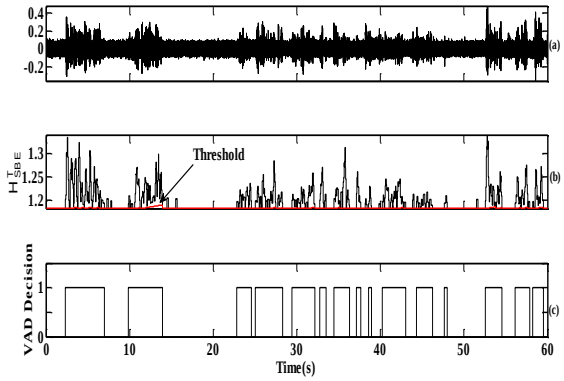

Fig. 6. Result of VAD under Jet Cockpit noise with SNR = 0dB (a) Speech signal (b) Band spectral entropy and threshold (c) VAD Decisions (Speech = 1; Non-speech = 0).

We evaluate the proposed scheme considering more than 46 speech samples from the *Switchboard Corpus*, a corpus of spontaneous conversations by multiple speakers over telephone [29]. In the performance evaluation that follows, we compare VAD results from our scheme with the manually segmented speech/non-speech information provided with the database. The results are presented for the SNRs from -10 to 40dB. Here, speech with additive noises is broadly classified under three categories: (i) Non-stationary Noisy Speech (NsNS) (ii) Non-stationary Heavy Noisy Speech (NsHNS); and (iii) Stationary noisy speech (SNS).

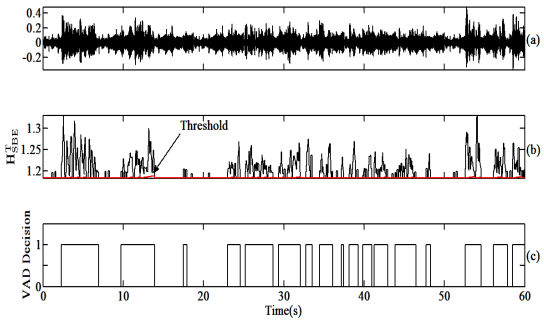

Fig. 7.Result of VAD under Subway noise with SNR = 0dB (a) Speech signal (b) Band spectral entropy and threshold (c) VAD Decisions (Speech = 1; Non-speech = 0).

Analysis of the performance of our scheme under these three noisy conditions averaged over the number of speech samples is presented as follows:

- P_D^S represents the ratio of the number of speech packets correctly recognised to the total number of speech packets. In Fig. 8(a) P_D^S is more than 0.8 for the SNRs greater than or equal to 0 dB. Under NsHNS conditions (see Fig. 8(b)), we achieve similar performance as in the Fig. 8(a) except for the case of Destroyer Engine noisy conditions. However for SNS conditions as presented in Fig. 8(c), similar performance of Fig. 8(a) is achieved except for the case of additive Car and Fan noisy conditions. This is due to the effect of these noises on the banded structure of speech; consequently, DT fails to detect the speech bursts.
- However, the corresponding Probability of False-alarm (P_{FA}) presented in Fig. 9(c) is lower than the achieved P_{FA} for NsNS and NsHNS conditions (see Fig. 9(a) and Fig. 9(c)). The trade-off is significant.
- Probability of Error, (P_E), combines both the errors P_{FA} and P_{MD}--upon multiplying with the prior probabilities,i.e. probability of speech packets and probability of non-speech packets for a given test speech sample. Thus, P_E represents the total error vis-à-vis speech - non-speech detection and the goal is to achieve lower P_E under different noisy conditions. Fig. 10 presents P_E for the three noisy conditions. Under SNS conditions,P_E is lower than 0.1 for SNRs greater than 0 dB, except the Car and Fan noises. This is due to higher P_{MD} even though P_{FA} is less than 0.2. For NsNS & NsHNS conditions, P_E is less than 0.2 for SNRs greater than 0 dB except Babble, Destroyer Engine and Military Vehicle noises, as shown in Fig. 10(a) and Fig. 10(b). We know that the Babble noise is speech like and as expected, P_{FA} is higher, and hence,higherP_E.

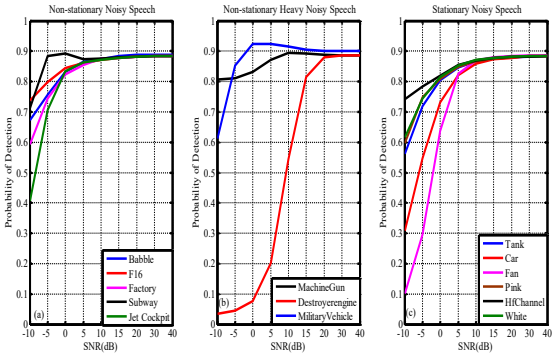

Fig. 8.Probability of speech detection (P_D^S) vs. SNRs in dB (a) Non-stationary noisy speech (b) Non-stationary heavy noisy speech (c) Stationary noisy speech.

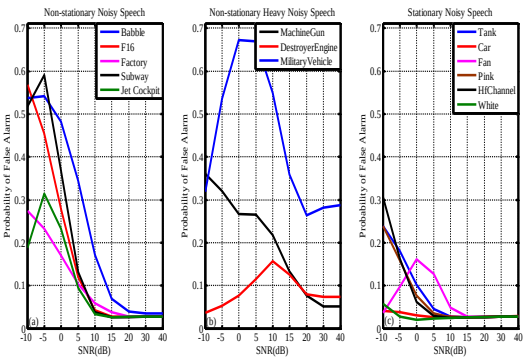

Fig. 9.Probability of False-alarm (P_{FA}) vs. SNRs in dB (a) Non-stationary noisy speech (b) Non-stationary heavy noisy speech (c) Stationary noisy speech.

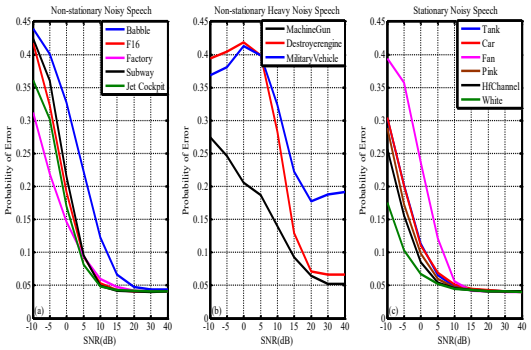

Fig. 10. Probability of Error (P_E) vs. SNRs in dB (a) Non-stationary noisy speech (b) Non-stationary heavy noisy speech (c) Stationary noisy speech.

We present VAD of our scheme in Fig. 11 for a real world speech sample having background noise and low fidelity. Result thus obtained is compared with the popular scheme proposed by Sohn et. al. [8]. For the P_D^S under both schemes are similar with minimal P_{MD} in favour of our scheme. It is important to note that this performance also comes with minimal P_{FA}. However, it is not true for VAD in [8]. Further, perceptual and statistical tests on VAD results corroborate good performance of our scheme over [8].

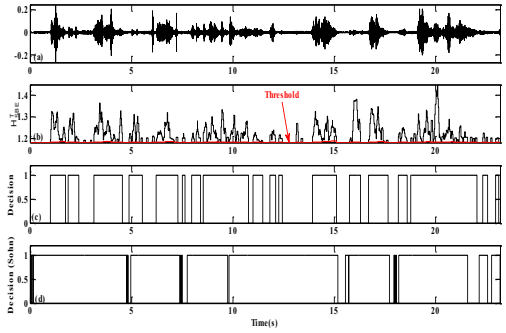

Fig. 11. VAD for a real world speech sample (a) Non-stationary noisy speech (b) Band spectral entropy and threshold (c) VAD Decision using proposed scheme (d) VAD decision using scheme proposed by Sohn et. al. [8].

CONLUSION

In this paper, we proposed a novel Voice Activity Detection (VAD) using Teager Energy based Band Spectral Entropy (TE_BSE). We segmented the input speech signal into non-overlapping frames. For each frame,we compute the entropy via normalized frame signal energy obtained for each sub-band. However, this parameter was seen to be sensitive to noise. We recognized that the signature of speech signal is embedded in a formant structure. We employed the Teager Energy Operator (TEO) to enhance formant peaks of the sub-band spectrum. This comes at the cost of enhancing high frequency regions of the spectrum under low SNRs. To exploit the benefits of normalized signal energy and TEO, we employed them under convex combination. Using the approach in [24], to obtain deviation threshold to declare each sub-band as useful or useless. Useful sub-bands are used to compute spectral band entropy. We differentiated *speech regions* from *non-speech regions* using the SBE feature computed from useful sub-bands. Finally, we evaluated the proposed scheme under simulated noisy (NsNS, NsHNS and SNS) and real world conditions to assess the robustness in providing accurate VAD decisions. The enhanced performance of the proposed schemes under varying noise conditions as claimed through the simulation studies is actually borne out in the implementation on real world speech signals.

The schemes proposed and analyzed in this work may readily be gainfully employed for cleaning up several speech signals when contaminated by various types of noise from the environment. One of the very promising applications of the VAD studied here can be in speech compression for transmission in the context of audio conferencing over the VoIP such as in Skype.

References

[1] L. Karray, and A. Martin, “Toward improving speech detection robustness for speech recognition in adverse environments”, Speech Communication, no. 3, pp. 261–276, 2003.

[2] J. Ramírez, J. C. Segura, C. Benítez, A. de la Torre, A. Rubio, “A new adaptive long term spectral estimation voice activity detector”, Proc. EUROSPEECH 2003, Geneva, Switzerland, pp. 3041–3044.

[3] ITU-T Recommendation G.729-Annex B, A silence compression scheme for G.729 optimized for terminals conforming to recommendation V.70, 1996.

[4] ETSI EN 301 708 Recommendation, Voice Activity Detector (VAD) for Adaptive Multi-Rate (AMR) Speech Traffic Channels”, 1999.

[5] A. Sangwan, M. C. Chiranth, H. S. Jamadagni, R. Sah, R. V. Prasad, and V. Gaurav, ``VAD Techniques for Real-Time Speech Transmission on the Internet”, Proc. IEEE International Conference on High-Speed Networks and Multimedia Communications, pp. 46-50. 2002.

[6] F. Basbug, K. Swaminathan, and Nandkumar, “Noise reduction and echo cancellation front-end for speech codecs”, Proc. IEEE Trans. Speech Audio Processing, vol. 11, no. 1, pp. 1–13, 2004.

[7] S. Gustafsson, R. Martin, P. Jax, and P. Vary, “A psychoacoustic approach to combined acoustic echo cancellation and noise reduction”, Proc. IEEE Trans. Speech and AudioProcessing, vol. 10, no. 5, pp. 245–256. 2002.

[8] J. Sohn, N. S. Kim, and W. Sung, “A statistical model-based voice activity detection”, Proc. IEEE Signal Processing Letters, vol. 16, no. 1, pp. 1–3, 1999.

[9] Y. D. Cho, and A. Kondoz, “Analysis and improvement of a statistical model-based voice activity detector”, Proc. IEEE Signal Processing Letters, vol. 8, no. 10, pp. 276–278, 2001.

[10] S. Gazor, and W. Zhang, “A soft voice activity detector based on a Laplacian-Gaussian model”, Proc. IEEE Trans. Speech Audio Processing, vol. 11, no. 5, pp. 498–505, 2003.

[11] L. Armani, M. Matassoni, M. Omologo, and P. Svaizer, “Use of a CSP-based voice activity detector for distant-talking ASR”, Proc. EUROSPEECH 2003, Geneva, Switzerland, pp. 501–504, 2003.

[12] R. L. Bouquin-Jeannes, and G. Faucon, “Study of a voice activity detector and its influence on a noise reduction system”, Speech Communication, vol. 16, pp. 245–254, 1995.

[13] K. Woo, T. Yang, K. Park, and C. Lee, “Robust voice activity detection algorithm for estimating noise spectrum”, Electronics Letters, vol. 36, no. 2, pp. 180–181, 2000.

[14] Q. Li, J. Zheng, A. Tsai, and Q. Zhou, “Robust endpoint detection and energy normalization for real-time speech and speaker recognition”, Proc. IEEE Trans. Speech Audio Processing, vol. 10, no. 3, pp. 146–157, 2002.

[15] M. Marzinzik, and B. Kollmeier, “Speech pause detection for noise spectrum estimation by tracking power envelope dynamics”, Proc. IEEE Trans. Speech Audio Processing, vol. 10, no. 6, pp. 341–351, 2002.

[16] R. Chengalvarayan, “Robust energy normalization using speech/non-speech discriminator for German connected digit recognition”, Proc. EUROSPEECH 1999, Budapest, Hungary, pp. 61–64, 1999.

[17] R. Tucker, “Voice activity detection using a periodicity measure”, Proc. Inst. Elect. Eng., vol. 139, no. 4, pp. 377–380, 1992.

[18] E. Nemer, R. Goubran, and S. Mahmoud, “Robust voice activity detection using higher-order statistics in the lpc residual domain”, Proc. IEEE Trans. Speech Audio Processing, vol. 9, no. 3, pp. 217–231, 2001.

[19] S. G. Tanyer and H. Özer, “Voice activity detection in nonstationary noise”, Proc. IEEE Trans.Speech Audio Processing, vol. 8, no. 4, pp. 478–482, 2000.

[20] J. L. Shen, J. W. Hung, and L. S. Lee, “Robust entropy-based endpoint detection for speech recognition in noisy environments,” Proc. ICSLP, 1998.

[21] B. F. Wu and K. C. Wang, “Robust endpoint detection algorithm based on the adaptive band-partitioning spectral entropy in adverse environment”, Proc. IEEE Trans. Speech Audio Processing, Vol. 13, No. 5, pp. 762-775, 2005.

[22] G. D. Wu and C. T. Lin, ``Word boundary detection with mel-scale frequency bank in noise environment,” IEEE Trans. Speech Audio Process., vol. 8, no. 3, pp. 541-554, May 2000.

[23] C. T. Lin, J. Y. Lin, and G. D. Wu, "A robust word boundary detection algorithm for variable noise-level environment in cars,” IEEE Trans. Intell. Transp. Syst., vol. 3, no. 1, pp. 89-101, March 2002.

[24] H. N. Shankar and R. Muralishankar, “Recognition of boundaries between silence and speech”, Proc. ICPRAT 2013, pp 48-55, March 2013.

[25] Shan Lu and Peter C. Doerschuk, "Nonlinear Modeling and Processing of Speech Based on Sums of AM-FM Formant Models,”IEEE Transactions on Signal Processing, vol. 44, pp. 773-782, April 1996.

[26] Alan C. Bovik, Petros Maragos, and Thomas F. Quatieri, "AM-FM Energy Detection and Separation in Noise Using Multiband Energy Operators,”IEEE Transactions on Signal Processing, vol. 41, pp. 3245-3265, December 1993.

[27] RidhaHamila, MarkkuRenfors, MoncefGabbouj, and JaakkoAstola, "Time-Frequency Signal Analysis Using Teager Energy,”Proc. Fourth International Conference on Electronics, Circuits and Systems, (Cairo, Egypt), pp. 911-914, December 1997.

[28] Alexandros Potamianos and Petros Maragos, "Speech Formant Frequency and Bandwidth Tracking Using Multiband Energy Demodulation," in Proc. IEEE ICASSP-95, (Detroit, Michigan), pp. 784-787, May 1995.

[29] http://www.ldc.upenn.edu/Catalog/readme_files/switchboard.readme.html

Proceedings of the Fourth International Conference on Communication and Electronics Systems (ICCES 2019)
IEEE Conference Record # 45898; IEEE Xplore ISBN: 978-1-7281-1261-9

AGRI SUCCOR : Mobile Application for Agriculture

Mrs. J. Jayachitra[1],
Department of IT,
IFET College of Engineering,
Villupuram, Tamilnadu
India
jayachitraifetit@gmail.com

M. Madhu[2] , S.D. Shaik Mohammed Faruk[3]
Deaprtment of IT,
IFET College of Engineering
Villupuram, Tamilnadu
India
Madhumathan155@gmail.com
Faruk140660@gmail.com

***Abstract*—India is an agricultural country with the staple food being rice and wheat. The farmers serve as a backbone to our nation. But, the livelihoods of the agriculturists are at stake. They incur heavy losses due to crop failure and natural calamities. The emerging technology has provided many solutions to upgrade their lifestyle, but still there are challenges. Our main motive is to design a farmer friendly application- Agri Succor to sell their commodities directly to the customers at a reasonable market value without any mediator with the help of volunteers. For the efficient utilization of our mobile application by the farmers, we have incorporated features like information in regional language, crop-disease identification and sell their products directly. This application will emerge out as an essential productivity tool for the farmers if implemented in future**

Keywords—Farmers, Agri Succor, crop disease identification, mobile application

I. INTRODUCTION (*HEADING 1*)

We all are much aware of the fact that India is an agricultural country and tea, cotton and spices are the main exports. Rice and wheat are the most important crops in India because they are the staple food. However, our country, especially Tamil Nadu does not have an accessible agricultural information system for the farmers to gain knowledge on any of the agriculture related problems and solutions. So, there is not much scope in promoting agricultural activities to farmers who serve as a backbone to our nation. But for the past decade or so the lives of the farmers are at stake due to losses incurred during the land cultivation, harvest and natural calamities. The field of information technology has a huge impact on people nowadays and hence, there are many solutions commercially made available for the upliftment of the farmers. Yet, none of them proved to be such helpful in improving their livelihoods. There are also many mobile applications that are specially designed for farmers. Most of these apps mainly focus on only one particular feature like crop management, usage of pesticides, etc. Still, such applications lacked in some aspects as the farmers are unaware about the existence of such applications. Even if they are aware about those applications, the farmer does not know how to access it even though it is in his native language as he might be illiterate.

Our proposed project provides an ultimate solution to all the problems above mentioned. With the assistance of the Tamil Nadu Agritech portal[1], we will handle this situation by establishing a buy-sell platform exclusively for the farmers welfare with almost all kind of facilities.

The main objective of our application is to design a farmer friendly mobile application. So, we have named our app as 'Agri Succor'- Agriculture Helper. The proposed app is interlinked to the TNAU Agritech portal [1] for getting authentic information. Through this application, the farmers can sell their products produced on their farmlands directly to buyers at a reasonable market price. This application bridges the gap between the farmers and consumers through the most crucial role players- the volunteers. There is no intermediate involved in this process. The most astonishing feature of our application is that it is available in the regional language. We also provide another important characteristic – voice to text conversion. As a result, the farmer can enter the details either in text or in speech format. The farmers can get agriculture related information from other fellow farmers or volunteers connected through this application. The solutions for the farm related problems are extracted from the Tamil Nadu Agricultural Agritech application. An additional aspect is employability is created for the volunteers.

First of all, we discuss about the related works about the existing mobile applications on agriculture. Then, we explain about our proposed system which includes the architecture, methodology, as well as the implementation of the Agri Succor application. It is followed by the advantages of the application.

II. RELATED WORKS

A. CCMobile App: CC stands for Connected Crops[2]. User can read the environment metrics like temperature, humidity, etc. Sensor readings are available through SMS or email alerts, graphing and the climate factor historical data. It optimized crop management but it covered only the climate factor

B. Spray Guide: Spray Guide[3] calculates the amount of solute, the amount of solvent, the mixing time and the spraying areas ,etc. Users can share their experience together with data and results to others over their social accounts.by using the this app ,produce quality product but this is not supported crop diseases detection.

C. IFFCO Kisan: It is offered by Indian Farmers Fertiliser Cooperative Limited (IFFCO). IFFCO Kisan[4] seeks advice from the agricultural experts and scientists about crops, agriculture cycle, etc. It is used to provide good Water management but not in the regional language

D. Mandi Trades: Mandi Trades[5] is a buying or selling platform by marketing of farm products. It Uses location intelligence to get a map-based view of both buyer and seller info, along with the geographical proximity. This app eliminates middlemen but it is not ensure the quality check.

E. myRML Farmer: Farm and crop specific precision solutions built with the help of India's top most agriculturists. myRML[6] Works by using specific tools it was designed to analyze or provide information on different aspects of farming habits. It provides high level guidance but there is no provision for weather forecast.

F. AgriSync: AgriSync[7] enables farmers and advisors to connect and resolve support issues using a mobile video customer service platform. It allows the advisor's organization to see open cases, resolution status and farmer feedback in real-time.

G. RainbowAgri Market: RainbowAgri[8] helps in digitizing and branding agriculture. It is a simple mobile and web based tool to profile the farmers, organize and manage farming communities.

III. PROPOSED WORK

The proposed system is designed to provide a friendly interface especially to the farmers. The three main roles of our application are farmers (sellers), volunteers and buyers. The personal details of all the users are highly confidential and secure. In this mobile app, the farmers can provide details about their farmlands and groceries that are being cultivated in their land. The information can be entered either in text or voice format that too in his/her own language. Once the crop has been harvested, the farmer can upload the image of the plant. The plant is checked for the pesticides level and the disease is identified in the app. The recovery solution for the same is provided either in video, audio or text format which are obtained from the Tamil Nadu Agritech application. Once the plant is quality checked, it can be viewed by the buyers who can purchase them at an affordable market price and delivered with the help of the volunteers. Hence all the facilities are available under one roof.

The architecture of the proposed system is shown in Fig.1. The architecture depicted below shows the overall structure of our project. The database plays a major role in gathering and retrieval of data.

a. Collection of Data: The input can be given as text, voice or else as image when the crop is diagnosed for any disease with the help of TNAU application. The interested buyers and sellers can register in this app using the buy- sell platform. The interested volunteers can enroll themselves for uploading the agriculture related news, new government schemes for the betterment of the farmers.

b. Retrieval of Data: The farmers can get the authentic information on crop disorders, recommended pesticides, buyer & seller information, product details and recovery solutions in text, voice and video formats in the corresponding native language. The data which is gathered need to be organized as a report. Using crucial strategies, the data is converted to report before sending them to the farmers, volunteers and consumers. This result can be either in the form of text or voice as per the wish of the user. Data retrieval is the defined as the process of identifying and extracting data from a database, based on a query provided by the user or application. It is achieved through the usage of SQL Processing.

All the features in the architecture are realized through the implementation process

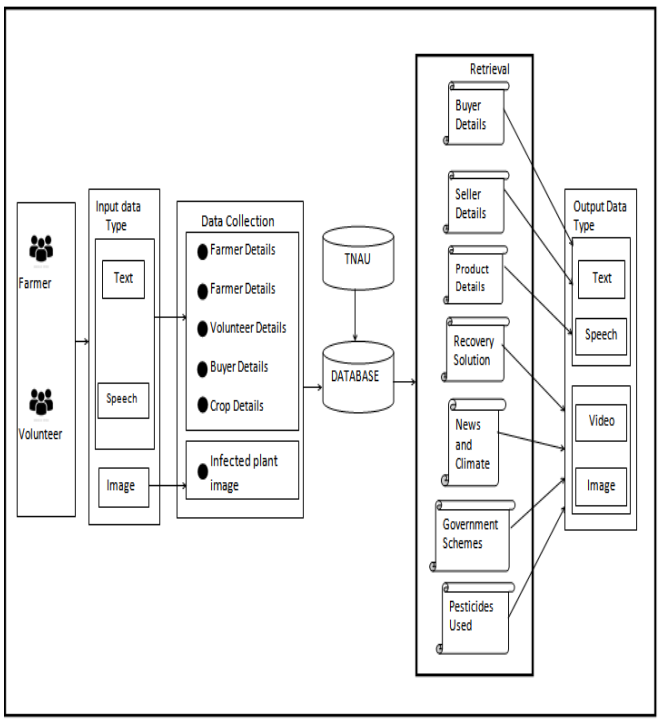

Fig.1. Architecture of the proposed system

A. IMPLEMENTATION

The implementation of the Agri Succor app is divided into three sections:

1. **Interface design:** It consists of three form designs for the use of farmers, volunteers and buyers.

Designing the interface of the application involves three main modules:

a. ***Farmers login***: The farmer login is shown in Fig.2.It consists of the entire details of the farmer including his location, type of crops cultivated in his farmland, price of his farm products, etc. given as text or voice with the option for regional language if required. This information is stored in the database. The farmer can even upload images of his commodities to check the level of pesticides used as well as check for any crop related disorders. He can have access to remedial measures for the crop diseases. In addition to this, he can keep a tab on the agriculture related news and schemes. He can even provide suggestions for the crop diseases to assist other fellow farmers. He can sell his produces to the consumers directly with no intermediary between them.

b. ***Volunteers login:*** The Volunteers login is shown in the Fig.3.The regular updates regarding agricultural schemes, climate and suggestions on crop cultivation are provided by the volunteers. Their main duty is to create awareness among the farmers regarding all kind of agricultural information. The much needed employability is given to these volunteers for their dedicated work. The delivery of farm products to the customers are done with the help of these volunteers

Fig.2. Farmers login

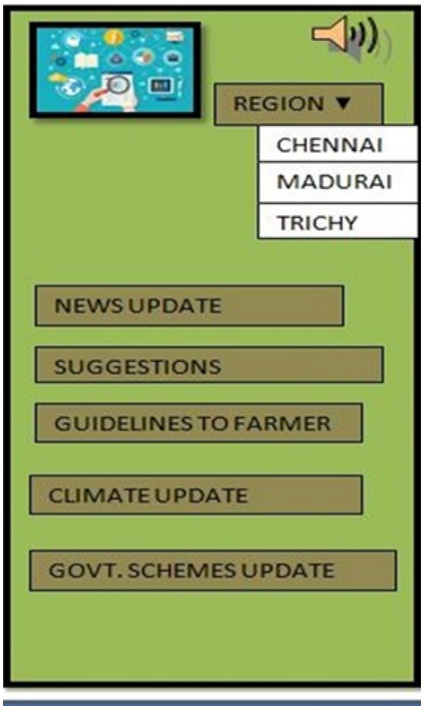

Fig. 3. Volunteers login

c. ***Buyers login***: The Buyers login is shown in Fig.4. The consumers who are willing to buy the farm products directly from the farmers need to enter their information. Once they select the items of a specific farmer, notifications are sent to the respective farmer. The ordered items are safely delivered to the customer.

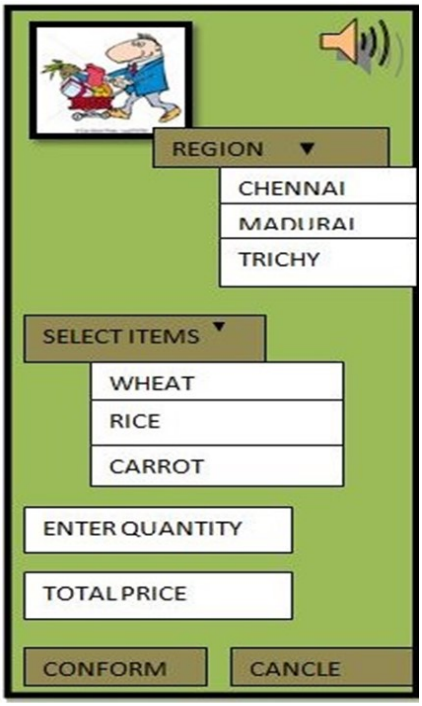

Fig. 4. Buyers login

2. **Voice to text conversion:** For extraction of voice signal, we use Mel-Frequency Cepstral Coefficient algorithm [9] and Minimum Distance Classifier. Support Vector Machine methods are used for speech classification. These techniques are highly efficient in converting the speech to text and vice versa.

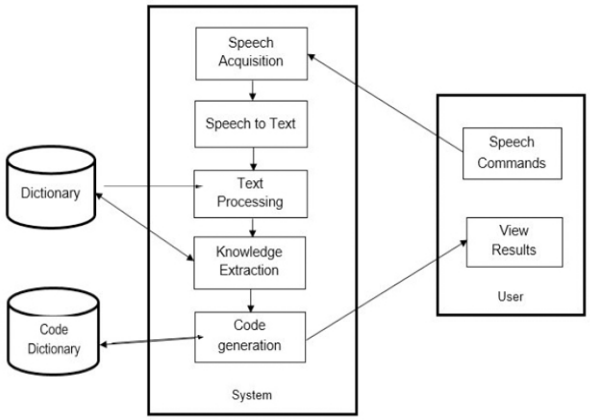

Fig.5.Voice to text conversion

3. **Disease identification:** Crop disease identification is done with the help of suitable image processing techniques. The procedure involves classification, feature extraction, multi-scale signal analysis, pattern recognition and projection

IV. BENEFITS

The Agri Succor will indeed be beneficial in almost all aspects. Some of the most important advantages of the proposed system are listed below:

a. Through the use of the application, both the standards of agriculture and farmers can be raised up.
b. The details can be given as voice or text input.
c. It also increases the job opportunities for the unemployed youth.
d. The commodities are freshly handpicked and delivered to the customers at a reasonable market value.
e. The application can be accessed in the regional language.
f. Instant updates on agricultural schemes, climate, crop diseases and their solutions are provided by the farmers and volunteers.
g. Quality check of the farm products before marketing them ensures that only disinfected items are sold.
h. The remedial measures for the crop diseases are provided in terms of text, voice and video. Considering the above pros of our application, we hope that this project will truly enhance the lifestyle of the farmers.

V. CONCLUSION

Through this mobile application, most of the problems faced by the farmers are provided immediate solutions and guidelines. If this initiative will be implemented in future, unemployability will be reduced to a considerable extent. Moreover, the betterment of the farmers could surely be realized. This application will emerge out as an essential productivity tool for the farmers.

REFERENCES

[1] http://agritech.tnau.ac.in/
[2] https://www.farms.com/agriculture-apps/crops/ccmobile-app
[3] http://www.simplot.com/farmers/products/specialty_products/spray_guide_app
[4] http://www.iffcokisan.com/
[5] http://www.manditrades.com/
[6] http://app.rmlglobal.com/
[7] https://www.agrisync.com/.
[8] http://www.rainbowagri.com/
[9] Zaidi Razak,Noor Jamilah Ibrahim, emran mohd tamil,mohd Yamani Idna Idris, Mohd yaakob Yusoff,Quranic verse recition feature extraction using mel frequency ceostral coefficient (MFCC),Universiti Malaya.

Proceedings of the Fourth International Conference on Communication and Electronics Systems (ICCES 2019)
IEEE Conference Record # 45898; IEEE Xplore ISBN: 978-1-7281-1261-9

A Survey on Energy Efficient Routing Protocol for IoT Based Precision Agriculture

T. Aishwarya Lakshmi, Balaji Hariharan, Rekha P
Amrita Center for Wireless Networks & Applications (AmritaWNA)
Amrita School of Engineering, Amritapuri
Amrita Vishwa Vidyapeetham, India
aishulakshmi18@gmail.com, balajih@am.amrita.edu, rekhap@am.amrita.edu

***Abstract*— Wireless Sensor Network (WSN) is widely used in Internet of Things (IoT) based Precision Agriculture (PA) to increase the crop productivity and yield. Parameters like pH, temperature, soil moisture, air humidity are measured in PA for monitoring the field remotely. The nodes used for WSN's are low-cost tiny sensor node that monitors the environmental parameters and collects the data and transfers these data to sink. These nodes are energy constraint as they are placed remotely and are equipped with batteries which have limited power. Minimizing the energy usage and maximizing the lifetime of the network are the major challenge faced by the sensor nodes. In this paper, we address some of the existing energy efficient routing protocols for precision agriculture.**

Keywords — Energy efficiency; Routing Protocol; Sensor Networks; Precision Agriculture; IoT

I. INTRODUCTION

A Wireless sensor network (WSN) is a network of low-cost tiny sensor nodes deployed over a certain area. The nodes sense, process and transmit data using wireless medium. WSN with IoT is widely applied in diverse areas such as agriculture [8] [9], medical care [10] [11], disaster management, industrial control, national defence, etc. In precision agriculture WSN is used to increase the productivity and yield of the crop by continuously monitoring the field for environmental data.

In precision agriculture, parameters like air temperature, soil moisture, pH, air humidity, etc. are measured to continuously monitor the field without human interaction [8]. The sensor node senses the environmental condition and transfers these sensed data to the sink or the base station or cluster head. The sensor node comprises of units for sensing, processing, transmitting and supplying energy. The sensing unit senses the environmental parameters, the processing unit process the data. The radio unit is utilized for transmitting and receiving the data and power unit provides power to the node.

Sensor nodes interact with each other and the sink using the routing protocol. Classification of the routing protocol is based on the network structure.

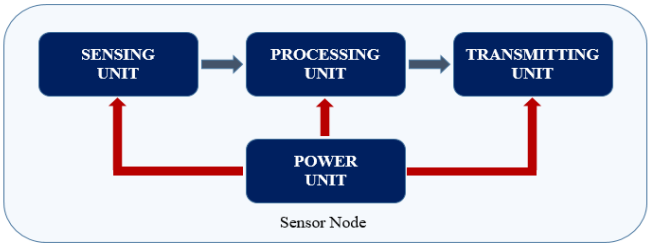

Fig. 1. Components in a sensor node

Transmission of data over a long distance consumes more energy compared to sensing and processing [1]. Minimizing energy usage is needed as power is a restricted entity for these sensor nodes as replacing or recharging the battery after deployment is not simple. Minimizing consumption of energy improves the life of the network. The key problems are energy consumption and network's lifespan. In this paper, multiple routing protocols are addressed using wireless sensor network to minimize power consumption for IoT-based Precision Agriculture (PA).

Agriculture is usually done in hectors of land, so monitoring the land manually increases the labour cost, the texture of soil varies in each region of the agricultural field. The precision agriculture concept has overcome the traditional agricultural methodology. In precision agriculture, monitoring of the agricultural land is supported using drones, tractors, sensors, etc. Maximum agricultural land coverage, sensor node energy, and routing protocol scalability are the few elements that influence the WSN implementation in precision agriculture. It is also necessary to update the farmer on environmental conditions on a continuous basis.

The paper is structured as follows: the associated study is given in Section II. Section III introduces the challenges faced during a routing protocol design. In Section IV, classification of routing protocols in WSN is presented. Section V addresses various energy-efficient routing protocols for precision agriculture. Section VI outlines discussion and open subjects for future studies. Finally, the paper is concluded in Section VII.

TABLE I. CHALLENGES RESOLVED BY EXISTING ROUTING PROTOCOL

Protocol	Limited power	Limited memory and storage	Deployment	Scalability
EETF	Transmit only useful information	Once data has been transmitted, it is discarded	Deterministic	No
SOUL	Using energy computer software components	The sensed data is stored for 4 hours and then discarded.	Deterministic	No
PTSR	Using heterogeneous nodes and region based deployment	Only stores information about the elected cluster head	Deterministic	Yes
IMR	Hierarchical routing based on tiers	Only store information regarding its level	Deterministic	No
EEZRP	Nodes energy level is considered	Store route data in the routing table and discards after completion of the round	Random	Yes
IEE AODV	Each nodes energy level is considered while selecting the path	Store route data in the routing table and discards after completion of the round	Random	Yes
EEHC	Using heterogeneous nodes and efficiently selecting the cluster head	Only stores information about the elected cluster head	Random	Yes

II. RELATED WORKS

In our related routing protocol research, WSN routing protocols may differ depending on application (based on protocol operation) and network architecture (based on network structure). Many researchers have carried out their research on routing protocols.

Design of routing protocols can be classified as proactive, reactive and hybrid protocols. All nodes maintain the knowledge about its next hop node in the proactive protocol. All nodes relay on its neighbouring nodes to send data. The data are only sent after mutual agreement between the two nodes. Reactive protocol, or demand routing protocol is based on query reply. The route is only established when a data needs to be sent. Hybrid protocol is a protocol based on distance vectors that contains the features and benefits of the link state protocol.

The operation of the routing protocol can be categorized based on multipath, query, negotiation, and Qos. Multipath-based protocol utilizes various routes rather than a single route to improve network performance. By keeping various routes between source and destination, fault tolerance can be improved, but it increases the energy usage and data traffic. The recipient nodes propagate a request for information from a node through the network in the query-based protocol. When a request is received, the node sends the data. Negotiation-based protocol utilizes negotiation to eliminate the transfer of redundant data. The decision on data transmission and reception is made based on the availability of the resource. Qos-based protocol balances energy consumption and information quality by providing data with relevant QoS metrics such as delay, power or bandwidth.

III. CHALLENGES FACED DURING A ROUTING PROTOCOL DESIGN

The wireless sensor nodes face many challenges as they are deployed remotely in the field. So when designing a sensor node these challenges needs to be considered as this can cause failure of the node [13]. The challenges faced by the wireless sensor nodes are discussed in this section. Table I discusses the challenges resolved by some of the routing protocol.

A. Limited power

The nodes are placed remotely in the field and they are subjected to failure due to depletion of the battery and due to the environmental changes. Minimizing the nodes' power usage as they are deployed remotely is the biggest constraint for wireless sensor nodes. For a prolonged period of time, these nodes need to operate remotely in a field and the battery cannot be replaced or recharged once deployed. Once the node's energy level reaches its minimum, the node becomes faulty and this effectively impacts system efficiency. A WSN routing protocol should minimize power usage and maximize the lifetime of the network.

B. Limited memory and storage

The sensor nodes have limited processing and memory capabilities. The sensor node has an internal memory of 2 KB to 256 KB and internal storage of 48KB to 2GB. An efficient algorithm needs to be designed in order maintain a trade-off between storage, bandwidth and computational complexity.

C. Deterministic or random deployment

Based on the application requirement, the sensor nodes can be implemented deterministically or randomly in WSN. Large-scale applications such as forest fire detection, etc. random deployment is used and sensor node determinist deployment is done for applications such as water leak detection, etc. deterministic deployment of sensor nodes is

done. The sensor nodes deployed in large area have no prior knowledge regarding their position and this makes the network more complicated as location-based protocol needs to be introduced.

D. Scalability

Sensor nodes in WSN can be deployed in large area randomly, and the designed routing protocols should be capable of scaling within the network. The communication connections between sensor nodes and sensor nodes and sink established for data transmission may not be direct. The routing protocol should, therefore, be able to identify the most effective communication path between the nodes.

IV. CLASSIFICATION OF ROUTING PROTOCOLS IN WSN

WSN routing protocols are categorized based on their network structure. It is classified as data-centred, hierarchical, and location-based [12].

A. Data-Centred protocols

Data-Centred also knows as the flat algorithms are based on query mechanisms. Here, the sink node sends a request for obtaining the data, this mechanism prevents continuous data transmissions and also saves the energy consumed. Directed Diffusion and SPIN (Sensor Protocols for Information via Negotiation), are some of the flat algorithm paradigms.

B. Hierarchical protocols

Hierarchical protocols use a cluster-based system in which nodes are split into tiny clusters and the role or function of nodes in a cluster varies. The energy of the nodes can be conserved by aggregating data with cluster heads (CHs). TEEN (Threshold-Sensitive Energy-Efficient Sensor Network Protocol) and LEACH (Low-Energy Adaptive Clustering Hierarchy) are some of the hierarchical algorithm paradigms.

C. Localization - Based protocols

Localization-based or geographic protocols are used when the position of the nodes is unknown. The position information is used to route the data to the required areas of interest. In this case, data flooding is restricted to save the network's energy. GAF, GEAR are some of the geographic algorithm paradigms.

V. ENERGY EFFICIENT ROUTING PROTOCOLS IN WSN FOR PRECISION AGRICULTURE

A routing protocol is used for transferring data between two sensor nodes or sensor node and sink. Routing protocols designed for WSN are desired to meet few parameters such as efficiency in energy consumption, scalability in a field, robustness and convergence. Reliable communication and choosing an energy-efficient routing, route and reducing the consumption of energy of the network as a whole is the main criteria that the designed routing protocol must satisfy. The major factor affecting the energy consumption is a continuous retransmission of data. The transmission of the data consumes

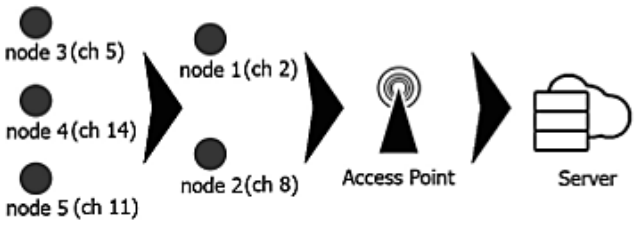

Fig. 2. Sensor topology of EETF [1]

Some of the energy efficient routing protocols which can be applied to precision agriculture are discussed in later section.

A. An Energy-Efficient Transmission Framework

Energy-Efficient Transmission Framework (EETF) is a data-driven algorithm based on greedy method which minimizes the energy consumption with lower complexity [1]. The algorithm focuses on energy efficient data transmission, which minimizes the energy consumption and guarantees data transmission rate. The algorithm is intended to discover the ideal route for transmission of the collected data with less transmission energy between the sensor nodes and the sink. The sensor node captures the data from the field and when useful data are available on sensor node, the sensor node finds the neighbouring node and transmits the data (Fig. 2).

The energy efficient transmission framework is divided into five modes: listen, collection of data, transmission of data, sleep and idle mode. The nodes are located sparsely in the field so that they can rely on the nearby node for the transmission of data to the sink. The sensors sense the data and stores in the buffer during the collecting data mode. After collecting the useful data, the sensor transmits the data in transmitting mode. It is said that the energy-efficient transmission algorithm effectively minimizes the energy consumption of the sensor nodes and also ensures secure transmission. The algorithm is compared with SPIN and ESPIN protocols.

B. SOUL

Sensor nodes' system for data acquisition of Long range (SOUL) is a theoretical framework in which designed sensor node hardware and software focuses on managing energy consumption and message grouping to enhance the lifetime of sensor nodes. SOUL is designed with five hardware components: microcontroller, Real Time Clock (RTC), power unit, acquisition unit and communication unit. The hardware has an energy control unit which switches ON/OFF the transducers.

The Sensor node software deals with minimizing the energy consumption while sensing, processing, transmission and reception of data. The algorithm monitors the sensor's energy level and a data system is used for packet transmission. The energy management model deals with computer software components (CSC). Energy monitoring CSC, which is used to estimate the nodes energy level after each round (a round has data acquisition, processing, transmission, and sleep mode). Sensor node management CSC deals with acquiring the data, grouping and transmission of data and also deals with confirming the transmission of data using acknowledgement

packet. Quality monitoring CSC ensures that the nodes are in line-of-sight with the coordinator. Transmission window is created in order to avoid collision during packet transmission.

C. Periodic Threshold Sensitive Routing Protocol

In PTSR [4] authors considered a square field which is further divided into nine sectors as shown in Fig. 3. Type-1, type-2 and type-3 heterogeneous sensor nodes are considered for the acquisition and transmission of environmental parameters. These sensors vary in their initial energy level. The energy level of Type 3 sensor is more than type 2, and type 2's energy level is more than type1. Type 1 sensor nodes are placed in the innermost region followed by type 3 then type2. Type 3 is placed in the middle region to eliminating coverage hole in the field. The base station selects the cluster heads for the middle and outermost area. The Type 1 sensor node transmits the information straight to the base station, while the Type 2 and Type 3 node relays on their cluster heads to transmit the information. Type 2 cluster head transmits the information to a cluster head of type 3 that reaches the base station further. The sensor node transmits data only when the set threshold is reached.

D. IMR

Integrated MAC and Routing protocol (IMR) [3] has a hierarchical architecture in which the network is divided into three tiers. The node who has the data broadcasts RTR packet, and the node whose level is less than senders tier responds with CTR packet. After receiving data, the node sends back ACK packet, and now receiver becomes the sender and the process continues. IMR is compared with protocols such as DSR, AODV and AOMDV and it is found that IMR is proven to perform better compared to DSR, AODV and AOMDV in terms of average network lifetime. The results are simulated using NS2.

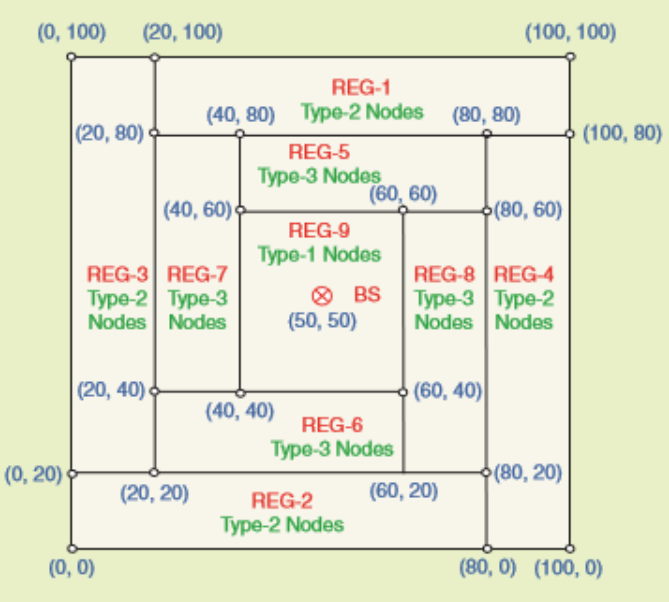

Fig. 3. PTSR network architecture [4]

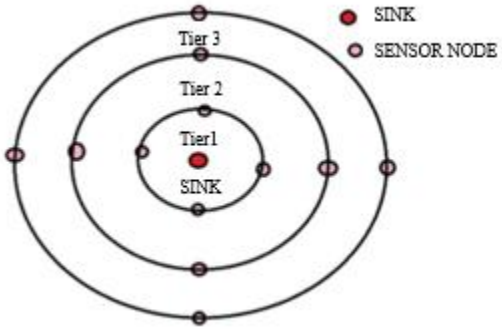

Fig. 4. IMR architecture [3]

E. EEZRP

In the Energy Efficient Zone-based Routing Protocol (EEZRP) [5] the nodes are localized using RELMA localization approach. The nodes are allocated areas depending on their number of base station hops. Based on the sensing range, the region is split into squares and is presumed to be twice the square's side length. Each cell is assumed to be either covered by one node or by the active node in the neighbouring square. This eliminates the sensing hole issue. The parameters used for selecting the active nodes are residual energy, distance, buffer size and sleep rounds. For determining the path distance and available energy of the nodes are considered. Subscribe or publish paradigm is used to achieve fault tolerance. The EEZRP protocol works better in terms of network life than the current LEACH and DSC protocols.

F. IEE AODV

IEE AODV [6] is an energy efficient AODV in which the energy efficiency is considered along with choosing the optimal path. Reactive protocols such as AODV, nodes select the best path to transfer the data. In traditional AODV energy was not considered as a major factor. IEE AODV integrate drain count into the traditional AODV, i.e. measuring the energy level of each node in the path and incrementing the drain count value by 1 if the energy has reached its threshold. The path which has the least value of drain count and with shortest distance is selected. If the drain count for more than one path is same, then min hop count is considered. If more than one path has same min hop count, then, the path where node's transmission power is least is considered. IEE AODV obtains a better network lifetime as compared to the traditional AODV. Link failure is managed by choosing an alternate path, the path related information's are stored in the destination during the route discovery period.

G. EEHC

The Energy Efficient heterogeneous clustered protocol [7] deals with heterogeneous nodes, which vary in their initial energy level. The benefits of using heterogeneous nodes over homogeneous nodes are that they help extend the network's lifetime, enhance the effectiveness of data transmission and

TABLE II. ENERGY EFFICIENCY ACHIEVED BY THE ROUTING PROTOCOL

Protocol	Energy efficiency achieved by the routing protocol
EETF	81.53% more efficient than SPIN and 36.84% more efficient than ESPIN
SOUL	56.9% more efficient in best case and 40% more efficient in worst case compared to normal sensor node.
PTSR	62% more efficient than EEHC protocol.
IMR	15% more energy efficient than AODV.
EEZRP	2.5% more efficient than LEACH protocol
IEE AODV	6.5% more efficient than AODV
EEHC	10% more efficient than LEACH with same power module.

decrease data transmission latency. The EEHC utilizes three kinds of heterogeneous nodes that differ in their initial level of energy. Nodes with β and α times energy compared to normal nodes are categorized as super-nodes and advanced nodes respectively, and few are normal nodes. These nodes are deployed uniformly over the field. EEHC protocol is an enhanced LEACH protocol. The selection of cluster head in EEHC protocols is defined so that each set of nodes has different probabilities and the node with maximum power level is selected as the head of the cluster. EEHC protocol performs better compared to the existing LEACH protocol with homogeneous node and LEACH with heterogeneous nodes. As the energy consumption of this protocol is less it can be used in the agricultural domain.

VI. CONCLUSION AND FUTURE RESEARCH

The sensor nodes sense the environmental condition in wireless sensor networks and transmit the information to the head of the cluster or the sink. Continuous data transmission consumes more energy than processing and sensing. The major issues and challenges faced by the routing protocols are energy efficiency, reliability, scalability, etc. these issues still exist and needed to be solved in the sensor networks. In this paper we have discussed some of the routing protocol which can be applied to IoT based precision agriculture. The protocol should minimize the use of energy and maximize the lifetime of the network. The energy efficiency achieved in each protocol is shown in Table II. None of the protocols discussed are best suited for IoT-based precision agriculture. PTSR protocol relatively performs better than others as it satisfies full coverage of the agricultural land and also continuously updates the user regarding the same. A Routing protocol needs to be designed which satisfies all the requirements in IoT based precision agricultural domain.

VII. ACKNOWLEDGEMENT

We would like to express our immense gratitude to our beloved Chancellor Sri. Mata Amritanandamayi Devi (AMMA) for providing the motivation and inspiration for doing this research work. The authors would like to thank everyone who was instrumental in doing this research work.

REFERENCES

[1] Lerdsuwan, Peerapak, and Phond Phunchongharn. "An energy-efficient transmission framework for IoT monitoring systems in precision agriculture." In International Conference on Information Science and Applications, pp. 714-721. Springer, Singapore, 2017.

[2] Vieira, Ricardo Godoi, Adilson Marques Da Cunha, Linnyer Beatryz Ruiz, and Antonio Pires De Camargo. "On the design of a long range WSN for precision irrigation." IEEE Sensors Journal 18, no. 2 (2018): 773-780.

[3] Balamurali, R., and K. Kathiravan. "An analysis of various routing protocols for precision agriculture using wireless sensor network." In Technological Innovation in ICT for Agriculture and Rural Development (TIAR), 2015 IEEE, pp. 156-159. IEEE, 2015.

[4] Maurya, Sonam, and Vinod Kumar Jain. "Energy-efficient network protocol for precision agriculture: using threshold sensitive sensors for optimal performance." IEEE Consumer Electronics Magazine 6, no. 3 (2017): 42-51.

[5] Karim, Lutful, Nidal Nasser, and Tarek El Salti. "Efficient zone-based routing protocol of sensor network in agriculture monitoring systems." In Communications and Information Technology (ICCIT), 2011 International Conference on, pp. 167-170. IEEE, 2011.

[6] Kumar, Dilip, Trilok C. Aseri, and R. B. Patel. "EEHC: Energy efficient heterogeneous clustered scheme for wireless sensor networks." Computer Communications 32, no. 4 (2009): 662-667.

[7] Patil, Annapurna P., B. Varsha Chandan, S. Aparna, R. Greeshma, and H. P. Akshatha. "An improved energy efficient AODV routing protocol for MANETs." In 2014 Eleventh International Conference on Wireless and Optical Communications Networks (WOCN), pp. 1-5. IEEE, 2014.

[8] Rekha, P., Venkata Prasanna Rangan, Maneesha V. Ramesh, and K. V. Nibi. "High yield groundnut agronomy: An IoT based precision farming framework." In 2017 IEEE Global Humanitarian Technology Conference (GHTC), pp. 1-5. IEEE, 2017.

[9] Prabha, Rekha, Emrick Sinitambirivoutin, Florian Passelaigue, and Maneesha Vinodini Ramesh. "Design and development of an IoT based smart irrigation and fertilization system for chilli farming." In 2018 International Conference on Wireless Communications, Signal Processing and Networking (WiSPNET), pp. 1-7. IEEE, 2018.

[10] Krishnan, Rahul, and Maneesha Ramesh. "A low cost remote cardiac monitoring framework for rural regions." In Proceedings of the 5th EAI International Conference on Wireless Mobile Communication and Healthcare, pp. 231-236. ICST (Institute for Computer Sciences, Social-Informatics and Telecommunications Engineering), 2015.

[11] Pathinarupothi, Rahul Krishnan, Bithin Alangot, Maneesha Vinodini Ramesh, Krishnashree Achuthan, and P. Venkat Rangan. "H-plane: intelligent data management for mobile healthcare applications." In International Conference on Mobile Web and Information Systems, pp. 283-294. Springer, Cham, 2016.

[12] Vhatkar, Sangeeta, and Mohammad Atique. "Design issues, characteristics and challenges in routing protocols for wireless sensor networks." International Journal of Computer Applications 975 (2013): 8887.

[13] Biradar, Rajashree V., V. C. Patil, S. R. Sawant, and R. R. Mudholkar. "Classification and comparison of routing protocols in wireless sensor networks." Special Issue on Ubiquitous Computing Security Systems 4, no. 2 (2009): 704-711.

Proceedings of the Fourth International Conference on Communication and Electronics Systems (ICCES 2019)
IEEE Conference Record # 45898; IEEE Xplore ISBN: 978-1-7281-1261-9

Beamforming Based Underwater Wireless Optical Communication Systems

Sajmath P. K.
Dpt.of Electronics and Communication
MEA Engineering College,Perinthalmanna
Malappuram,Kerala,India
sajmathp.k@gmail.com

Renjith V. Ravi
Dpt.of Electronics and Communication
MEA Engineering College,Perinthalmanna
Malappuram,Kerala,India
renjithravi.research@gmail.com

***Abstract*—The beamforming based underwater wireless optical communication (UWOC) systems with phase shift keying (PSK) modulation is elucidated in this work. UWOC is a powerful technology which is used for large speed underwater communications. Turbulence is the main mortifying factor of underwater, when light waves are propagating through underwater. For mitigating the turbulence spatial diversity technique is used. The belongings of absorption and scattering are measured here. For calculate the system BER, the sum of log-normal random variables are used. Transmit beamforming is a method to minimize the channel interference. By using transmit beamforming technique the spatial separation between symbols are increased. Study the enactment of UWOC PSK with beamforming and without beamforming. Also compared the enactment of each configuration with existing one. Here, we can analyse that the numerical result of UWOC PSK with beamforming shows a better result than the conventional method, i.e, the BER of UWOC PSK with beamforming is less than that of UWOC OOK.**

***Index Terms*—MIMO, Underwater wireless optical communication, Log-normal fading channel,Optimal combining, Transmit beamforming.**

I. INTRODUCTION

The data transmissions through water environment without guides are known as Underwater wireless communication (UWC) in [1]. The operation is based on wireless carriers, the carriers may be acoustic waves,radio-frequency (RF) waves, or optical waves. Underwater wireless optical communication (UWOC) has smart and upcoming alternative. In current years light can be used for wireless communication. The visible light is subjected to attenuation in seawater and also the information of aquatic optics is limited, because of these reasons the initial progress of UWOC is not much better than the earlier terrestrial free-space optical communications. The initial applications of UWOC are limited one and they are generally used for military purpose. Comparing to the previous works the optical transmission shows that it has larger bandwidth, high security, and the time latency is very less. The UWOC is a promising technology and it have been used in several applications, due to its properties like reliability, scalability and flexibility. Because of this advantage UWOC used as a prevailing technology as in imaging, high-throughput sensor networks, etc. Because of the degrading factors of channel i.e., absorption, scattering, and turbulence the UWOC channel, is currently used for short-range communications [2]. If we can overcome these three impairments, we may use the UWOC in more applications. In previous years there has been number of experiments are done for characterizing the impairing effects for different water types.

In this paper, UWOC PSK with beamforming is elucidated. For combining the optimal combiner (OC) technique is used. To obtain the absorption, scattering and their belongings into account, the Double Gamma function model is used. Which is based on channel impulse response are taken in to account. Fading coefficients are modeled by log-normal random variable. Then multiply the fading coefficient with the above impulse response. By using beamforming the spatial separation between the symbols are increased.

II. UWOC CHANNEL

UWOC is one promising technologies. Along with its advantages it has lots of limitations since its medium having main three impairing effect. They are absorption,scattering and turbulence.

A. Absorption and Scattering

The optical beam's propagation through the underwater makes collaborations of photons and seawater particles. The photons are loss their energy if it is passing through the water, because there are enormous particles are there at the medium. which is termed as absorption and which is an lasting process. In scattering the photon's are transmitted to different [3]. It produces loss to the system, only few lights are reached at the receiver. The distortion due to these two are modeled by using $u(\lambda)$ and $v(\lambda)$ where $u(\lambda)$ is the absorption coefficient and $v(\lambda)$ is the scattering coefficient, and λ denotes the wavelength of that propagating light. Moreover, $w(\lambda)$ is total effects and can be measured as $w(\lambda) = u(\lambda) + v(\lambda)$. The value of these coefficients can be alter with λ and types of water. [4] shows that at the wavelength interval $400nm < \lambda < 530nm$ the presence of absorption and scattering is less. So to understand the data communication UWOC systems mainly used the blue/green region in the spectrum. The channel impulse response has been simulated, by using the above two degrading effects [5]. $h_{0,ij}(t)$ is the impulse response between transmitter and receiver. Here it is fading free and the data is

transmitted between i^{th} transmitter at the transmitter side and j^{th} receiver. The link distance and angle of divergence are important parameter. When increases the channel introduces more loss. This behaviour is unobserved in clear water, the water turbidity and multiple scattering can also affect the system performance,they are ostensible. As increasing this two the performance become decreases. The above difficulties can be avoided by increasing the angle of pick up and the receiving cross section.

B. Turbulence

Absorption and scattering effects and how they are characterized are explained in the above section. [6] here the effect of turbulence is taken into account, multiply the fading-free impulse response with multiplicative fading coefficient i.e., multiply $h_{0,ij}(t)$ with α_{ij}^2 with log-normal distribution. [7] which include the weak oceanic turbulence cases. Turbulence is another fading reason which can be introduced by log normal distribution of UWOC. Due to the intelligibility of background noise of underwater UWOC system typically employ large receiving aperture, thus reduces the turbulence effects [8]. Although the links is modeled by a RV, and due to the highly-scattering nature of UWOC channels and for simplicity, the perfect arrangement are there in this system. [9], for modeling the turbulence-prompted dwindling let $\alpha = \exp(X)$ which is the fading amplitude of the channel with log-normal probability density function (PDF)

$$f_\alpha(\alpha) = \frac{1}{\alpha\sqrt{2\pi\sigma_X^2}}\exp\left(-\frac{(\ln(\alpha) - \mu_X)^2}{2\sigma_X^2}\right). \quad (1)$$

Where the fading log-amplitude X which is having a Gaussian distribution with mean(μ_X) and variance (σ_X^2) this can normalize by fading amplitude in such a way that E[α^2]=1 which implies μ_X=σ_X^2.

III. IMPULSE RESPONSE MODELING

The modeling of impulse response are important aspects. The impulse response modeling is based on Monte Carlo (MC) [10]. The below described the Double gamma function model how they related to MC.

A. Double Gamma Function model of impulse response

The viable form of the UWOC link's impulse response is presented here. The optical thickness can be written as τ = zr where z is the extinction coefficient and r is the link range. In Beer's law the path loss versus τ is considered. [3], the absorbance of light depend upon many parameters, and the multiple scattering of light induces path loss. In this work, there main aim is the modeling of UWOC channel. In [11] includes the initial usage. Which is based on clouds. The seawater and clouds have different channel properties, it is inspired by the dispersing nature . For modeling the UWOC links this modeling can be apply with relatively large value of τ where multiple scattering light may dictated [12]. The expression of the double Gamma functions is,

$$h(t) = A_1\Delta t e^{-A_2\Delta t} + A_3\Delta t e^{-A_4\Delta t}, (t \geq t_0) \quad (2)$$

where A_1, A_2, A_3 and A_4 and $\triangle t = t - t_0$. The four parameters are to be solved, t is called as the time scale and $t_0 = L/v$ is called as the propagation time. The parameter set (A_1, A_2, A_3, A_4) in (2) can be calculated from the simulation results of Monte Carlo (MC) method using nonlinear least square criterion as,

$$(A_1, A_2, A_3, A_4) = \arg\min\left(\int [h(t) - h_{mc}(t)]^2 dt\right) \quad (3)$$

In (3) the $h(t)$ and $h_{mc}(t)$ are the simulation results of impulse response. The $h(t)$ is the double Gamma functions model and $h_{mc}(t)$ is the MC model. To return the argument of the minimum the $argmin(\cdot)$ is used. By using curve fitting approach the (3) can be solved.This can be done by software such as MAT LAB. The multiple scattering effect is studied by using SPF. The energy distribution is also described by this scattering phase function (SPF). The SPF can be in the form $\beta(\theta, \lambda)$

$$1 = 2\pi\int_0^\pi \beta(\theta, \lambda)\sin\theta d\theta \quad (4)$$

The scattering phase function is similar to that of Rayleigh scattering. The system mainly focused blue/green region of visible light.

IV. UWOC PSK SYSTEM MODEL

An UWOC PSK with beamforming system is considered here. In the earlier case UWOC with OOK modulation is taken in account. Both equal gain combining and optimal combining are taken in [2]. The possibilities of underwater wireless communication is carried out their along with its limitations. Here beamforming properties and PSK modulation are taken along with UWOC, thus it outperform the conventional system performance. Here the beamforming based UWOC with PSK modulation is taken instead of UWOC OOK. The input signal is transmitted through the channel and combined using optimal combining at the receiver side. As it mentioned in Fig. 1, signal are propagated from transmitter to receiver through the channel,channel containing the impairing effects. $h_{0,ij}(t)$ is for absorption and scattering of ith transmitter to j^{th} receiver and the turbulence is modeled as a multiplicative fading coefficient α_{ij}^2, which is a log-normal distribution. The distribution is based on weak oceanic turbulence. The aggregated impulse response both at the transmitter and receiver is $h_{i,j}(t) = \alpha_{ij}^2 h_{0,ij}(t)$. The transmitted signal s(t)

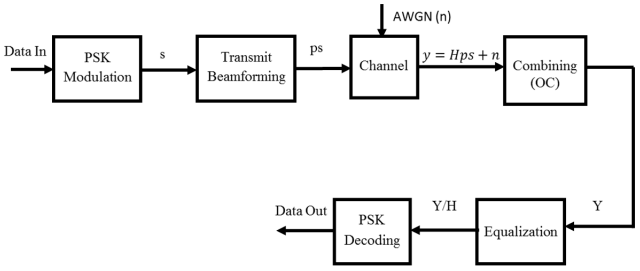

Fig. 1. UWOC with PSK and Transmit Beamforming

$$S(t) = \sum_{k=-\infty}^{\infty} b_k P(t - kT_b), \quad (5)$$

In this the $b_k \epsilon(-1, 1)$, and $\Gamma(t) = h_0(t) * P(t)$, the * is the operator named as convolution. In the earlier case the $b_k \epsilon(0, 1)$. $y(t)$ is the received optical signal. This can be expressed as,

$$y(t) = S(t) * \alpha^2 h_0(t) = \sum_{k=-\infty}^{\infty} b_k \alpha^2 \Gamma(t - kT_b) \ , \quad (6)$$

Equal power are allocated to all the transmitters. The transmitters and receivers are located in an random manner. The general impulse response expression is $h_{i,j}(t) = \alpha_{ij}^2 h_{0,ij}(t)$. The Fig.1 shows the simple UWOC PSK with beamforming block diagram where the data to be transmitted is passing to PSK modulation. The modulated data x is multiplied with beamformer matrix to avoid interference. In the earlier case containing an OOK modulation after it passes through the channel. Here by using the beamformer matrix interference can be minimized. The output of transmit beamformer ps is transmitted through the channel. They subjected to the underwater impairing effects and noise. The output of the channel is $y = Hps + n$. The optimal combining technique is used in the receiver side. Then the out is Y/H. By using PSK demodulation the data is demodulated. UWOC channel with all the three impairing effects are shown in Fig.2. Where $h_{0,ij}(t)$ is the combined effect of absorption and scattering. Then multiply this with turbulence. Convolution in time domain is similar to multiplication in frequency domain, FFT (Fast Fourier Transform) is used for that purpose. In the proposed work there we consider different configurations like SISO, SIMO, MISO and MIMO.

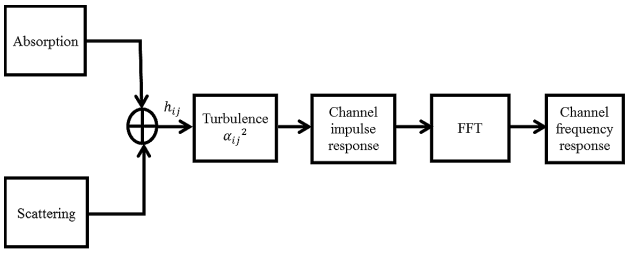

Fig. 2. UWOC Channel

V. Simulation Results

The simulation results for the BER enactment of UWOC PSK with Beamforming system in various scenarios are presented here. For channel fading statics consider log-normal distribution, equal power are distributed between the transmitters and the fading statistics are similar for all links. Aperture area at the receiver side are similar for all the receivers. The impulse response is based on MC method. The result is compared with an threshold to measure the received signal for to ensuring the transmitted data. Before reaching signal on the receiver side the input are added by the noise. At last, the received data is compared with the transmitted data for determining the BER value. This is based on a particular transmitted power. The different MIMO configurations are carried out here. Their performance comparison also considered, of them MISO gives a better performance than that of others.The performance of UWOC OOK is compared with UWOC PSK with beamforming and without beamforming. Firstly taken SISO transmission which is considered in a

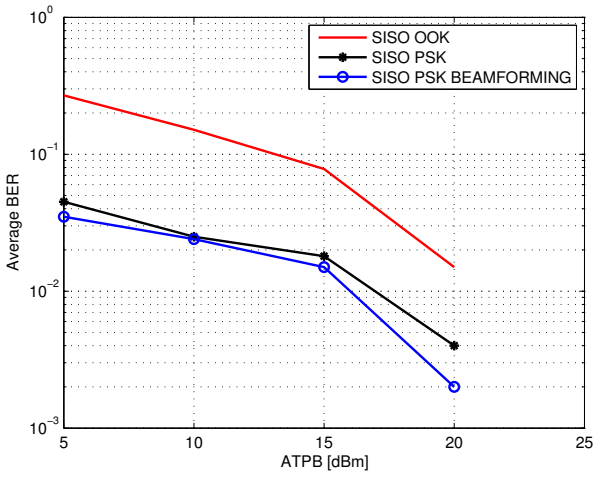

Fig. 3. SISO Configuration

coastal water link with 25m distance ie, UWOC PSK with beamforming and without beamforming is compared in Fig.3. Also compared this results with UWOC OOK modulation. The UWOC PSK with beamforming outperforms than other two. The beamforming technology is introduced to minimize the interference, thus to improve the enactment of the system. In the graph x-axis indicates the ATPB (Average Transmitted Power per Bit) and y-axis indicates the average BER (Bit Error Rate).

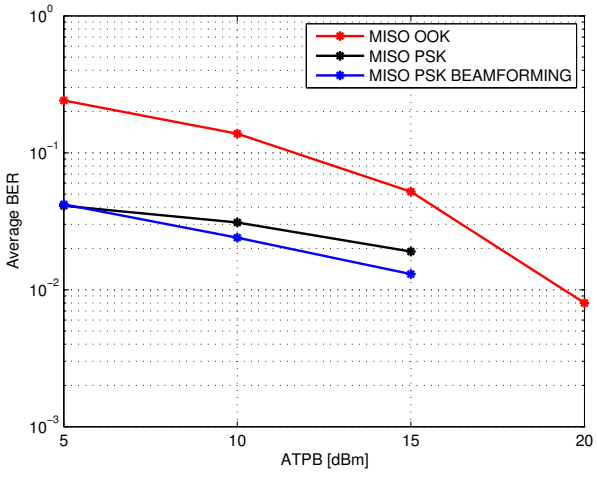

Fig. 4. MISO Configuration

Fig. 4 depicts the BER of coastal water with 25m distance.The performance of MISO with OOK is much better

than that of other configuration. The proposed work shows that the PSK UWOC with beamforming gives better result than that of PSK UWOC and OOK UWOC. The spatial separation between the symbols are increased by beamforming. The

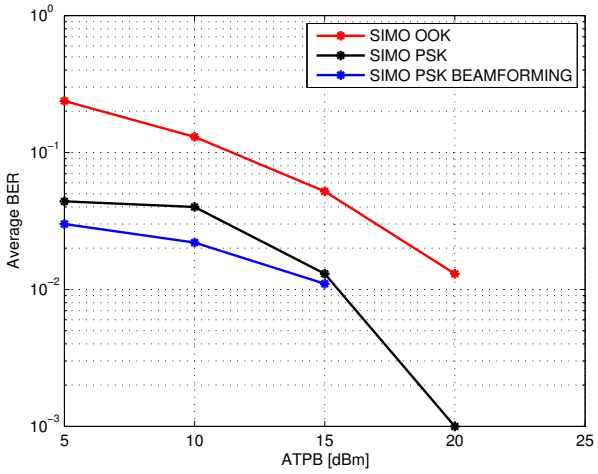

Fig. 5. SIMO Configuration

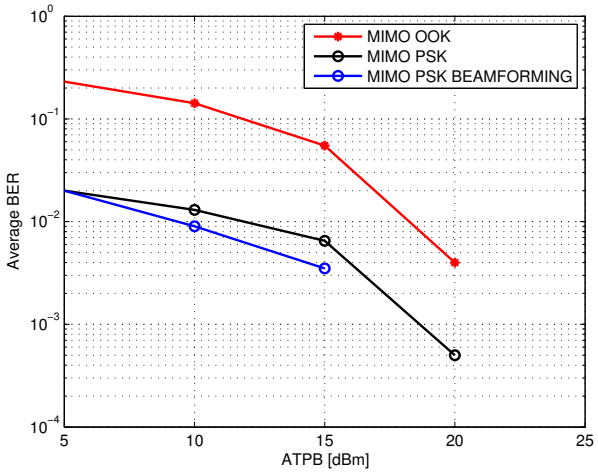

Fig. 6. MIMO Configuration

Fig. 5 and Fig. 6 shows different configuration's performances i.e, SIMO and MIMO. In all these cases UWOC PSK with beamforming shows less BER than that of other two cases. For transmit beamforming the channel phase is estimated and angle is estimated. This angle effect is eliminated by beamforming technique. The above all cases the comparison of conventional method and proposed work are considered, that shows the importance of proposed work. The Fig. 7 shows the comparison of UWOC OOK and Beamforming based UWOC PSK in its absorption and scattering effects. The UWOC with PSK and Beamforming gives a better BER performance than that of conventional UWOC OOK.The Fig. 8 shows the turbulence comparison of proposed and conventional method. Their

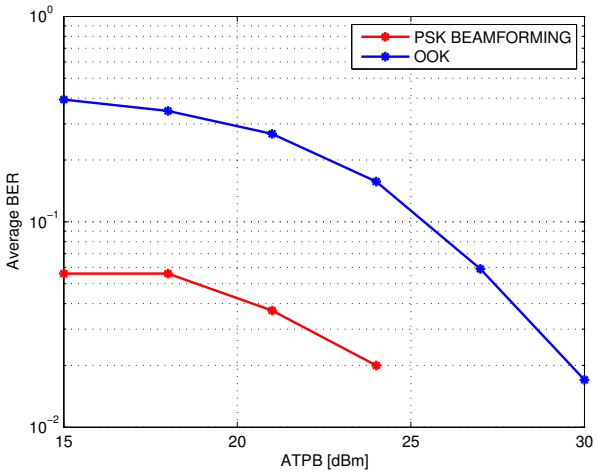

Fig. 7. Absorption and Scattering Effects

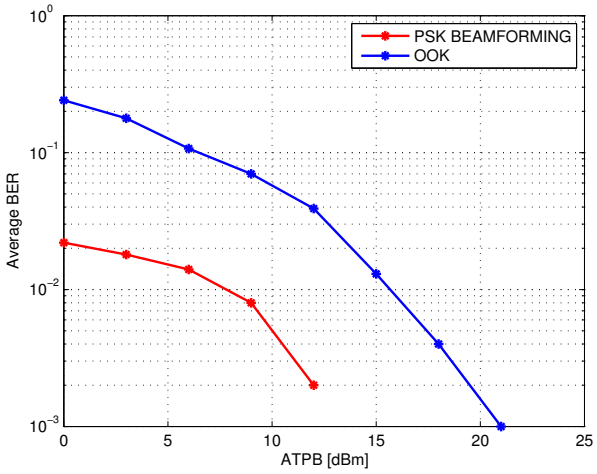

Fig. 8. Turbulence Effect

also proposed work shows less BER than that of conventional one.

VI. CONCLUSION

The beamforming based UWOC PSK are studied in this work. Channel modeling takes all the impairments into account. The impulse response are obtained by using MC simulations. The numerical results indicates that the performance beamforming with PSK gives better result than that of conventional method. By beamforming the channel separation between the symbols are increased. Transmit beamforming is used here to improve the performance. The turbulence have important roll in UWOC systems, the performance of UWOC increases with decreasing the turbulence value. The individual turbulence effects and absorption and scattering effects are also shown there, in order to specify the importance of proposed work. The proposed work shows that beamforming based UWOC PSK outperform that of UWOC OOK.

REFERENCES

[1] Z. Zeng, "A survey of underwater wireless optical communication," Ph.D. dissertation, University of British Columbia, 2015.

[2] M. V. Jamali, J. A. Salehi, and F. Akhoundi, "Performance studies of underwater wireless optical communication systems with spatial diversity: Mimo scheme," *IEEE Transactions on Communications*, vol. 65, no. 3, pp. 1176–1192, 2016.

[3] C. D. Mobley, *Light and water: radiative transfer in natural waters*. Academic press, 1994.

[4] C. F. Bohren and D. R. Huffman, *Absorption and scattering of light by small particles*. John Wiley & Sons, 2008.

[5] W. C. Cox Jr, *Simulation, modeling, and design of underwater optical communication systems*. North Carolina State University, 2012.

[6] S. M. Navidpour, M. Uysal, and M. Kavehrad, "Ber performance of free-space optical transmission with spatial diversity," *IEEE Transactions on wireless communications*, vol. 6, no. 8, pp. 2813–2819, 2007.

[7] H. Gerçekcioğlu, "Bit error rate of focused gaussian beams in weak oceanic turbulence," *JOSA A*, vol. 31, no. 9, pp. 1963–1968, 2014.

[8] X. Yi, Z. Li, and Z. Liu, "Underwater optical communication performance for laser beam propagation through weak oceanic turbulence," *Applied Optics*, vol. 54, no. 6, pp. 1273–1278, 2015.

[9] M. Safari and M. Uysal, "Relay-assisted free-space optical communication," *IEEE Transactions on Wireless Communications*, vol. 7, no. 12, pp. 5441–5449, 2008.

[10] C. Gabriel, M.-A. Khalighi, S. Bourennane, P. Léon, and V. Rigaud, "Monte-carlo-based channel characterization for underwater optical communication systems," *Journal of Optical Communications and Networking*, vol. 5, no. 1, pp. 1–12, 2013.

[11] G. C. Mooradian and M. Geller, "Temporal and angular spreading of blue-green pulses in clouds," *Applied optics*, vol. 21, no. 9, pp. 1572–1577, 1982.

[12] M. Karimi and M. Nasiri-Kenari, "Free space optical communications via optical amplify-and-forward relaying," *Journal of Lightwave Technology*, vol. 29, no. 2, pp. 242–248, 2011.

Proceedings of the Fourth International Conference on Communication and Electronics Systems (ICCES 2019)
IEEE Conference Record # 45898; IEEE Xplore ISBN: 978-1-7281-1261-9

Improving GPS based distance measurement accuracy using Machine Learning: an empirical study

Rishish Kumar Naik, Binoy B. Nair
Department of Electronics and Communication Engineering,
Amrita School of Engineering, Coimbatore,
Amrita Vishwa Vidyapeetham, India
kumar.rishish@gmail.com, b_binoy@cb.amrita.edu

***Abstract*— Shortage of workforce is one of the most critical issues facing agriculture today. Automation of farm machinery can mitigate this to an extent, however, in a middle-income country like India, the cost of automation has to be minimized in order to encourage wider adoption. An attempt has been made in this study to design a machine learning based system to to improve the distance measurement accuracy of a low-cost GPS receiver deployed for vehicle localization and tracking in an autonomous harvester designed for harvesting onion. Nine different machine learning based models are evaluated for their effectiveness in improving the distance measurement accuracies for step sizes ranging from 2-10 meters. Results indicate that machine learning based system proposed is capable of improving the measurement accuracy of GPS system under test.**

Keywords— Global Positioning System (GPS), Accuracy, Machine Learning.

I. INTRODUCTION

Agriculture has traditionally been one of the major sources of employment and a major contributor to the GDP of most of the developing countries over the past half century. However, this share has been declining over the years as more and more people give up agriculture for other occupations. Considering India as example, the percentage of males employed in agriculture has decreased from 57.72 in 1991 to 37.2% in 2018[1] . Similarly, female employment in agriculture as a part of the total workforce has dropped from 76% in 1991 to 55.38% in 2018[1]. The only solution under such circumstances is to introduce automation in agriculture. This has been attempted widely in developed countries[2], however, in developing countries like India, the cost of employing such machinery is prohibitively expensive. Development of low-cost alternatives for automation of agricultural machinery is essential under such circumstances. An attempt in this regard has been made in [3]. A prototype autonomous onion harvester has been developed [3] with autonomous navigation within the field to be harvester, as one of its major features. Global Positioning System (GPS) has been employed to identify the location of the harvester and for the measurement of distance the vehicle has covered. However, high precision GPS module were observed to be too costly and hence, an alternative approach of choosing a low-cost, lower accuracy GPS and then augmenting its distance measurement accuracy using machine learning was taken. The autonomous onion harvester prototype and the GPS module under test (uBlox Neo 6M) are presented in Fig. 1.

Section 2 presents the literature in the area, the methodology is presented in section 3, results are presented in section 4 and the conclusion in section 5.

II. LITERATURE SURVEY

There have been several studies on augmenting the accuracy of GPS systems. In[4], a navigation system has been designed using GPS for an autonomous car in which GPS provides the data for the current location of the car and the target location details are taken from a map. A compass is used for getting the heading of the car, which helps in getting the required correction in heading for its navigation. In[5], design of a school bus tracking system, in which GPS position data is used for its tracking and Kalman filter has been used for efficiently predicting the arrival time of bus by taking its speed, distance to travel(from GPS coordinates) as input for the system is presented. In[6], the precision of two different GPS(SPI-Pro, GPS-5 Hz and MinimaxX, GPS-10 Hz module for distance calculation in high-speed mode has been compared. It is observed that GPS-10 Hz has better accuracy to calculate the distance in high-speed mode. In[7], accuracy of distance measurement for three different GPS modules has been computed. Overall error in the distance accuracy varies from 3.3 to 18.53% depending upon the device selection. A tracking system has been designed in[8], using dead reckoning and a GPS module for tracking animals which also calculates distance travelled and improve the life of tracking collar which are used to collect data. [9]presents the design of a system to improve the accuracy of vehicle attitude estimation for low-cost INS/GPS integration by using the GPS measured course angle. In[10], a system design for positioning of tractors by improving the precision of low-cost GPS is presented. A model for localization of the vehicle in an urban city by using SVM to overcome the limitations of extended Kalman filter is presented in[11].

It is observed from the surveyed literature that machine learning can be an effective means to address the error in measurement produced by GPS systems. In the subsequent

section, the methodology employed to realize such a system is presented.

Fig. 1 Autonomous onion harvester prototype (GPS module under test inset)

III. METHODOLOGY

A. Data Collection and analysis

The first step in the process is to collect the data. In the present study, the GPS receiver employed is uBlox NEO-6M[12]. This receiver has 50 channels. It has time to first fix during cold start of 27 seconds and during hot start is 1 second. It has a maximum navigation update rate of 5Hz and its horizontal position accuracy is 2.5 meter. For data collection, the GPS setup was installed at a fixed location. uBlox GPS was interfaced with an Arduino Mega microcontroller board and the received latitude and longitude data was logged.

To collect data from the GPS receiver, the data collection setup was moved in the pattern shown in Fig 2. In the figure, each arrowhead represents one completed movement step. Hence, it can be seen that there are total of fourteen steps (or locations) in the movement path. Approximately 100 latitude-longitude values were collected for the GPS receiver at each location before the movement to next location was made. In Fig 2, data collection started from the rightmost point at the eastern side and ended at the leftmost point at the western side. Data has been collected following the same pattern for movement step sizes of 2-10 meters, i.e. total of nine sets of readings, each comprising of fourteen locations, were taken.

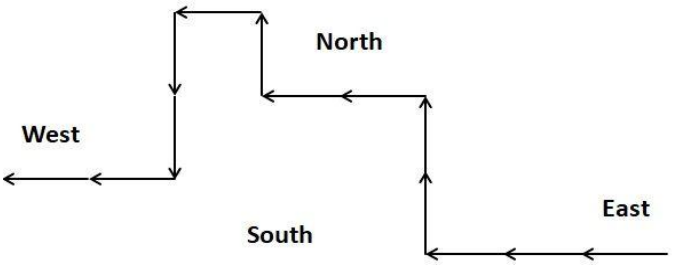

Fig. 2 Movement pattern for Data collection

The latitude-longitude value detected by the GPS at a fixed location is found to be continuously fluctuating. An example is presented in Fig. 3, where the location readings produced by the GPS module when stationary after the 4th step with step size of 2 meters, is shown. A total of 100 location readings were logged, and it is observed that the position readings were non-stationary in nature.

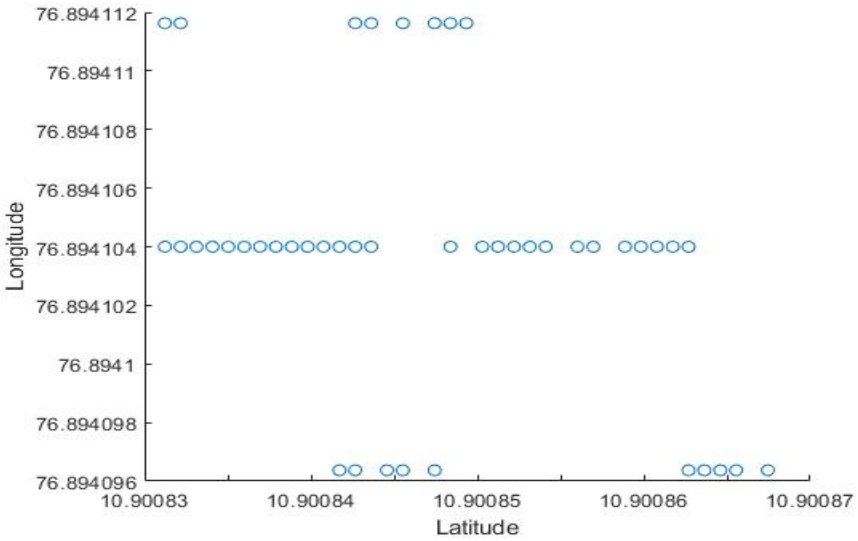

Fig. 3 Scatter plot of position detection readings from GPS for a fixed location

Consider the *i*-th reading logged by the GPS module to be denoted by:

$X_{ij} = \{\varphi_{ij}, \lambda_{ij}\}$ where φ_{ij} and λ_{ij} are the latitude and longitude respectively for the *j*-th location reading at the *i*-th location. To analyze the variation in the collected data, mean, median, mode, standard deviation, maximum value and minimum value was calculated for all the sets of data. Then the distance between all the consecutive fixed locations was calculated by considering the mean, median, mode, mean + standard deviation, mean - standard deviation, minimum value, maximum value and the average of maximum & minimum value using the Haversine formula in (1).

$$d = 2r\mathrm{Sin}^{-1}\left(\sqrt{\mathrm{Sin}^2\left(\frac{\Phi_2-\Phi_1}{2}\right)+\mathrm{Cos}(\Phi_1)\,\mathrm{Cos}(\Phi_2)\,\mathrm{Sin}^2\left(\frac{\lambda_2-\lambda_1}{2}\right)}\right) \quad (1)$$

d = distance between two points
r = radius of earth
Φ_1, Φ_2 =latitude of the two points
λ_1, λ_2 =longitude of the two points

Then the error in the calculated distance has been calculated by comparing it with the actual distance taken between consecutive fixed locations. The results are graphically represented in Fig. 4.

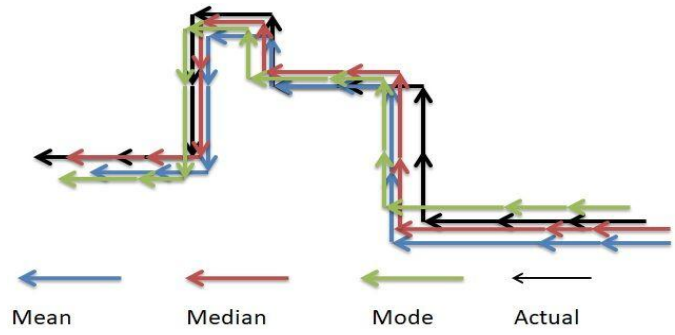

(a)

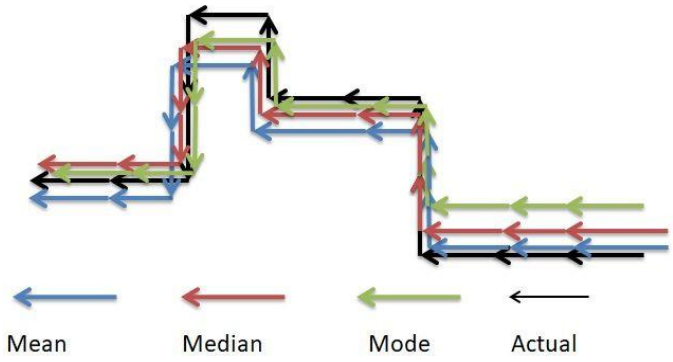

(b)

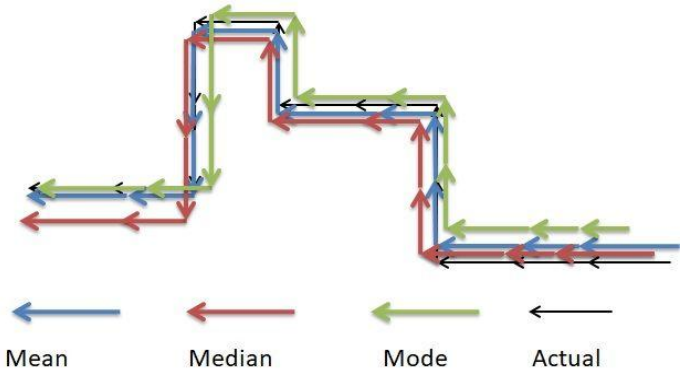

(c)

Fig. 4. Actual vs calculated distance using mean, median and mode of the location coordinates for step sizes of (a) eight meters, (b) nine meters and (c) ten meters

The algorithm to find the distance between fixed locations and error in the calculated distance is given below:

```
Input: Location //(Lat,Lon) array for
all locations

Begin

1. min_step ← 2  // minimum step size is
2 meters

2. max_step ← 10  // maximum step size
is 10 meters

3. step_count ← 14 // total 14 steps for
each step size

4. FOR j = min_step : max_step

    FOR k = 1 : step_count


summ_stats{j,k,1}←mean(Location{j,k})


summ_stats{j,k,2}←median(Location{j,k})


summ_stats{j,k,3}←mode(Location{j,k})


summ_stats{j,k,4}←std.deviation(Location
{j,k})


summ_stats{j,k,5}←summ_stats{j,k,4}+
summ_stats{j,k,1}

summ_stats{j,k,6}← summ_stats{j,k,4}-
summ_stats{j,k,1}

      summ_stats{j,k,7}←max(Location
{j,k})
```

```
      summ_stats{j,k,8}←min(Location
{j,k})]
          IF k > 1
            Distance{j,k-1}←
Fn_distance(summ_stats{j,k},summ_stats{j
,k-1})
          // Fn_distance gives distance
between all the consecutive locations
using Haversine formula.
          Error{j,k-1} ← j-Distance{j,k-
1} //Subtracts all the distances from
the step size.
          END IF
     END FOR
END FOR
END Algorithm
```

Function to calculate distance between two GPS coordinates:

Input: latlon1 = Latitude and longitude of 1st location, latlon2 = Latitude and longitude of 2nd location.

Begin

```
1. radius ← 6371;
2. lat1 ← latlon1(1)*pi/180;
3. lat2 ← latlon2(1)*pi/180;
4. lon1 ← latlon1(2)*pi/180;
5. lon2 ← latlon2(2)*pi/180;
6. deltaLat ← lat2-lat1;
7. deltaLon ← lon2-lon1;
8. a=sin((deltaLat)/2)^2 +
cos(lat1)*cos(lat2) *
sin(deltaLon/2)^2;
9. c=2*atan2(sqrt(a),sqrt(1-a));
10. d_km=radius*c;
```

end Function

B. Machine learning models considered

To minimize the error in measured distances, machine learning models were employed. Nine models based on three different machine learning techniques were evaluated for their effectiveness, namely, multiple linear regression, regression tree and Support Vector Regression (SVR).

1) Multiple linear regression: It is a type of Linear Regression which works with more than one number of predictor variables. The objective of this algorithm is to design the linear relationship among the independent(all features of the system) variables and dependend(output of the system) variable. Multiple linear regression based models are the simplest of models used for regression analysis. The general expression for the output of a multiple regression model is presented in (2).

$$\hat{y} = a_0 + a_1 x_1 + a_2 x_2 + \cdots + a_n x_n \quad (2)$$

Here, $x_1, x_2, \cdots, x_n$ are the features (or explanatory variables) and $\hat{y}$ is the estimated output. Linear regression based models are relatively simple and easy to train, and highly suitable for modeling linear relationships. Hence, multiple linear regression is considered as the benchmark model in this study

2) Regression tree: Regression trees behave in a fashion similar to the classification trees in which the algorithm attempts to successively partition the dataset into subsets that results in the minimum sum squared error(SSE)[13]. For a regression tree T, the SSE is defined as per (3)[13]

$$S = \sum_{c \in leaves(T)} \sum_{i \in c} (y_i - m_c)^2 \quad (3)$$

Where: $m_c = \frac{1}{n_c} \sum_{i \in c} y_i$ is the prediction for leaf *c*

The attribute or feature, splitting using which results in the maximum reduction in *S* is taken as the splitting attribute. The splitting process continues till the termination conditions of $S < \delta$ (usually the threshold δ is a small number, here, its 10^{-6}) or $n_c < minsamples$ ($minsamples$ is the minimum number of samples in the node) is reached.

3) Support Vector Regression (SVR): SVR has been widely used for solutions to nonlinear regression problems. SVR is used to fix the error within a limit whereas simple regression technique is used to reudce the rate of error. A detailed treatment of SVR has been provided in[14]. Three kernel functions are considered in this study, linear, quadratic and Gaussian. The functions are presented in (4),(5) and (6).

$$k(x, y) = x^T y + c \quad (4)$$

$$k(x, y) = (x^T y + c)^2 \quad (5)$$

$$k(x, y) = \exp\left(-\frac{\|x-y\|^2}{2\sigma^2}\right) \quad (6)$$

Here, *x* and *y* are the feature vectors and σ is the standard deviation.

C. Tracking System of Harvester

An android application has been developed for remotely tracking of the Onion Harvester which takes location information from an open source cloud platform namely, ThingSpeak. For the tracking system uBlox NEO-6M GPS module, NodeMCU board which is having inbuilt Wi-fi module and ThingSpeak open source cloud platform has been used. Block Diagram of the Tracking System of Harvester is presented in Fig. 5.

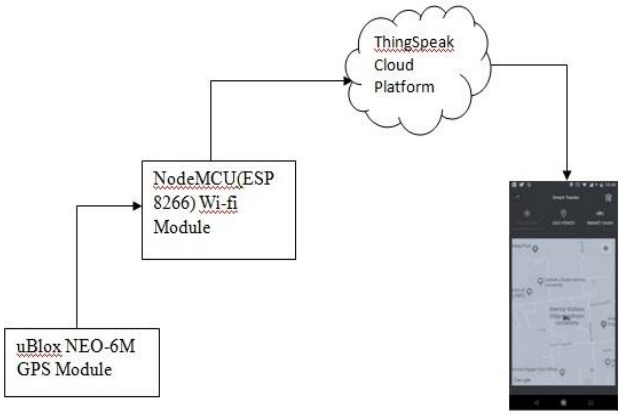

Fig. 5 Block Diagram of the tracking System

GPS module has been interfaced with the NodeMCU board. After receiving the location information(latitude and longitude value) GPS module transmit it to the NodeMCU board using serial communication and then NodeMCU uploads the GPS coordinates to the ThingSpeak cloud platform by using the mobile data connecting to the hotspot facility of the mobile. After getting uploaded to the cloud platform android application will fetch the GPS coordinates from the cloud. Then it will show the GPS coordinates on the android application as an overlay of google map to display the navigation of the vehicle.

IV. Results and Discussion

A ten-folds cross validation approach was taken to evaluate model effectiveness. The performance of the proposed system was evaluated on three parameters, namely the Root Mean Squared Error (RMSE), Mean Squared Error(MSE) and Mean Absolute Error (MAE). The results are presented in Table 1. The parameters were selected using trial and error.

TABLE 1 DISTANCE MEASUREMENT ACCURACY

ML algorithm	Parameters	RMSE (m)	MSE (m)	MAE (m)
Linear Regression		1.57	2.47	1.26
Regression Tree	min. leaves: 4	1.74	3.02	1.34
	min leaves: 12	1.62	2.63	1.29
	min leaves: 36	1.88	3.55	1.59
SVR	Linear	1.62	2.68	1.27
	Quadratic	1.66	2.77	1.23
	Gaussian ($\sigma = 0.66$)	1.68	2.83	1.33
	Gaussian ($\sigma = 2.65$)	**1.42**	**2.03**	**1.10**
	Gaussian ($\sigma = 10.58$)	1.46	2.12	1.19

It is seen from Table 1 that SVR based systems are better capable of reducing the error in measurements. The performance of the best performing system (SVR with $\sigma = 2.65$**)** is presented in Fig. 6.

In Fig. 6, the x-axis represents the step size and the y-axis represents the residuals. It can be seen form the figure that for smaller step sizes, the performance of the proposed system is poorer when compared to larger step sizes. However, it is also clearly visible from the boxplots that the mean of the estimations are accurate to a large extent and accuracy of measurements becomes better and the deviations in the estimation also reduce for larger step sizes.

V. CONCLUSION

A novel, machine learning based technique to improve the accuracy of a commercial low-cost GPS module has been presented in this work. Nine models based on three different

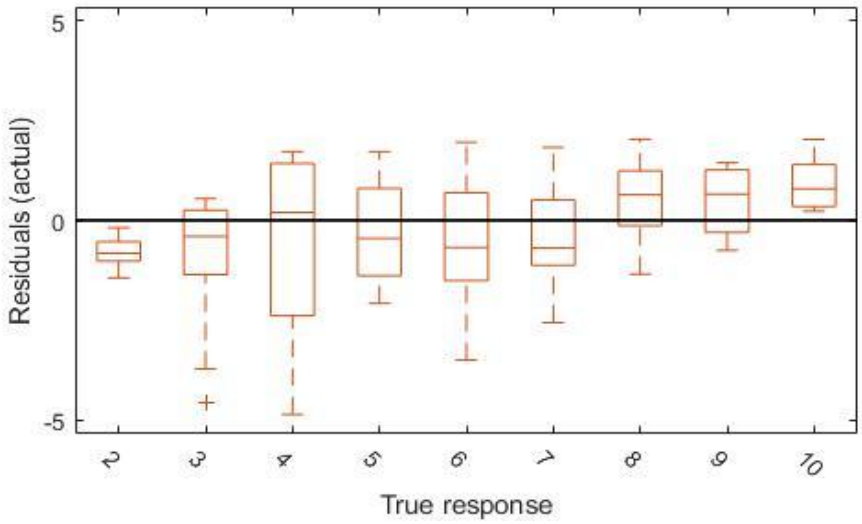

Fig. 6 Residual boxplot for SVR ($\sigma = 2.65$)

machine learning techniques were evaluated for their ability for compensating the variations in the readings produced by the GPS module. It can be seen from the results that the proposed system is well capable of reducing the distance measurement errors. It is also observed that SVM based system is ideally suited for the purpose, resulting in RMSE measurement error of 1.42 meters. Effectiveness of the proposed system can be further improved by taking more number of readings at each location and by employing deep learning based models, both of which could be considered as future extensions of this work

REFERENCES

[1] "Agriculture & Rural Development.". Available: https://data.worldbank.org/topic/agriculture-and-rural-development?locations=IN&page=2.

[2] J. Dvorak, "An Autonomous, Solar-Powered Tractor," p. 23.6 (2016): 24-26, 2016.

[3] "FISITA 2018," 2018. .

[4] P. G. Parakkal and V. V. Sajith Variyar, "GPS based navigation system for autonomous car," in *2017 International Conference on Advances in Computing, Communications and Informatics, ICACCI 2017*, 2017, vol. 2017–Janua, no. 1, pp. 1888–1893.

[5] R. C. Jisha, A. Jyothindranath, and L. Sajitha Kumary, "IoT based school bus tracking and arrival time prediction," in *2017 International Conference on Advances in Computing, Communications and Informatics, ICACCI 2017*, 2017, vol. 2017–Janua, pp. 509–514.

[6] M. Fiorenza *et al.*, "Accuracy of GPS Devices for Measuring High-intensity Running in Field-based Team Sports," *Int. J. Sports Med.*, vol. 36, no. 01, pp. 49–53, 2014.

[7] C. Powell, A. Donnelly, M. Lyons, and R. Anderson, "An examination of the accuracy and reliability of three GPS devices," in *ICAMPAM 2015*, 2015, no. June.

[8] O. P. Dewhirst, H. K. Evans, K. Roskilly, R. J. Harvey, T. Y. Hubel, and A. M. Wilson, "Improving the accuracy of estimates of animal path and travel distance using GPS drift-corrected dead reckoning," *Ecol. Evol.*, vol. 6, no. 17, pp. 6210–6222, 2016.

[9] Z. Wu, M. Yao, H. Ma, and W. Jia, "Improving accuracy of the vehicle attitude estimation for low-cost INS/GPS integration aided by the GPS-measured course angle," *IEEE Trans. Intell. Transp. Syst.*, vol. 14, no. 2, pp. 553–564, 2013.

[10] J. Gomez-Gil, R. Ruiz-Gonzalez, S. Alonso-Garcia, and F. J. Gomez-Gil, "A Kalman filter implementation for precision improvement in Low-Cost GPS positioning of tractors," *Sensors (Switzerland)*, vol. 13, no. 11, pp. 15307–15323, 2013.

[11] I. Belhajem, Y. Ben Maissa, and A. Tamtaoui, "Improving Vehicle Localization in a Smart City with Low Cost Sensor Networks and Support Vector Machines," *Mob. Networks Appl.*, vol. 23, no. 4, pp. 854–863, 2018.

[12] "UBLOX: NEO-6 GPS Modules Datasheet," 2011.

[13] C. R. Shalizi, *Regression Trees. In: Advanced data analysis from an elementary point of view*. 2013.

[14] A. J. and B. S. SMOLA, "A tutorial on support vector regression*," *Stat. Comput. 14*, pp. 199–222, 2004.

Proceedings of the Fourth International Conference on Communication and Electronics Systems (ICCES 2019)
IEEE Conference Record # 45898; IEEE Xplore ISBN: 978-1-7281-1261-9

Design and development of fuel level measurement technique for automotive application.

Mr. Kiran Patil
Dept. Of Instrumentation & Control
College of Engineering, Pune
Pune, (MH) India
patilkb17.instru@coep.ac.in

Prof. Dr. C. Y. Patil
Professor of
Dept. Of Instrumentation & Control
College of Engineering, Pune
Pune, (MH) India
cyp.instru@coep.ac.in

Mr. Sujit Barhate
Program Manager
HELLA India Automotive Pvt. Ltd.
Pune, (MH) India
sujit.barhate@hella.com

***Abstract*— In day to day life use of vehicle is continuously increasing among all the countries, and as a most important part of vehicle, usage of fuel is increasing and not it is becoming critical problem. So, for accurate measurement of fuel level becomes extremely important. The design and development of Capacitive sensor is some contribution towards the accurate fuel level measurement in automotive sector. Wide variety of existing fuel level sensors are available such as mechanical float type, load cell, ultrasonic trans-receiver based and Capacitive plate sensors. Nowadays all the vehicle has digital display (Dashboard) units, so fuel bunks occurring chances are more compare to other because of the digit roundoff. When we refill the fuel, we don't know the exact amount of fuel added is same as that to the amount paid by us. So here the fuel level measurement sensor plays vital role for customers, at the same time it improves performance and safety aspects related to the vehicle. Currently the capacitive fuel level measurement sensors are used in Aircrafts, where fuel level is considered as most critical parameter. That implies the capacitive level sensor construction is costly for small vehicle. So, the main objective of this paper to working towards the development of low-cost capacitive fuel measurement sensor for 2W/3W vehicles.**

Keywords— 2W/3W, ASIC, Automotive, Fuel level sensor, Capacitive sensor.

I. INTRODUCTION

First digital fuel level indicator was introduced in India by Varun digital indicator, there intentions were better understanding to the driver about amount of fuel available in the tank. They were providing this sensor with up to three-digit resolution. Initially this development was done for commercial and passenger vehicle application, because of long distance travelling with heavy duty load carrying. This measurement system was developed with sensor and digital signal processing to display it on dashboard [11]. At the same time measured amount of fuel level is used in mileage and performance estimation of the vehicle.

Most of Fuel bunk incident happens in India during fuel filling at the petrol pump, because of the accuracy of the fuel level measuring sensor and unawareness of the customer. Practically if you see when we fill the petrol, we don't know how much petrol he filled in the tank independent of amount of fuel said by us. So, for authentication the fuel level sensor becomes extremely important. This day the fuel cost is continuously increasing, so OEM started working on improving efficiency and hence everyone comes up with different efficiency improving techniques. And EFI is one of them which continuously monitor the fuel injected by fuel pump in the engine and corresponding power generated by the engine [12].

In old fuel level measuring technique such as float type resistive potentiometric, pressure sensor based. There intention of the sensor was only to display amount of fuel present in the tank.

Usual methodology of measuring fuel level uses the different principle of operation, where its contribution in using, completely depends on the accuracy and the cost of the sensor. Because of the cost volume of utilization in actual vehicle makes impact [2].

II. RELATED WORK

At the point of time, the fuel level in the tank varies. It results, the change in dielectric constant of the sensor measuring plate so which results in effective change in capacitance of the sensor. At the point when we got capacitance value, a straightforward numerical preparing can without much of a stretch illuminate the height of the fuel. If we consider coaxial link type structure [7], so the internal electrode radius is r and R gives the range of the outside terminal. In construction of the sensor, its height is 'L' and fuel level is 'h'. In the condition when there is no fuel in the tank, Ɛ0 speaks to the dielectric consistent in the vacuum 8.8542x10-12 F/m; then the capacitance C_0 *is* expressed as:

$$C_0 = \frac{2\pi\varepsilon_0}{\ln(R/r)}L \qquad (1)$$

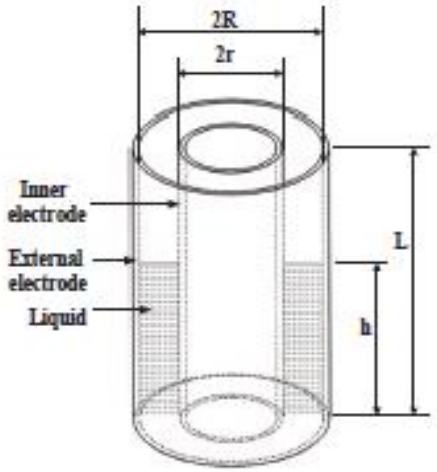

Figure. 1. Fuel level sensor structrure

In the above figure capacitive sensor structure is shown, where fuel level is expressed as 'h', to estimate the fuel level in terms of capacitance. It underneath the level influenced by the relative dielectric Steady, of the air (1.0058). alludes to the dielectric steady of the fuel level 'm'. In the sensor output estimation procedure comprises main ingredient which is separated by two different medium such as air and fuel [1]. The capacitance estimated by both the medium are different, below expression.

$$C_o = \frac{2\pi\varepsilon_1\varepsilon_0(L-h)}{\ln(R/r)} + \frac{2\pi\varepsilon_r\varepsilon_0 h}{\ln(R/r)} \qquad (2)$$

The deliberate capacitance measures by the senor is 'C_0', it is directly proportional to the level indicated by fluid, which changes in real time while continuously level varies. however, the general permittivity of the fuel and the air are unique. In view of the direct connection of capacitance, which is result of change in capacitance and fuel level 'h'.

which in turns to the actual level of the fuel.

Initially when the tank contains no fuel, the medium between both the plates is air. So, it defines the capacitance between the both plates represented as C_0.

$$C_0 = \frac{2\pi\varepsilon_1\varepsilon_0 L}{\left[\ln\left(\frac{R}{r}\right)\right]} \qquad (3)$$

Keeping equation (3) in equation (2),

$$C = C_0 + C_0(\varepsilon_r - \varepsilon_1)\frac{h}{\varepsilon_1 L} \qquad (4)$$

Equation (4), shows that capacitance is comparing to the dielectric steady, and fluid dimension changing in the fuel tank will incite substance relative change between the both the plates. For alteration of the sensor. Notwithstanding the steady and, and moreover fixed characteristics. The capacitance will augment as a component of the liquid stature h. By evaluating the capacitance of the two plates, the fuel level in the tank can be resolved. Equation (4) shows C reaches a maximum at C_{max} when h equals to L.

$$C_{max} = C_o + C_o\left(\frac{\varepsilon_r}{\varepsilon_1} - 1\right) \qquad (5)$$

Other than the construction and operating behavior of the sensor, it is also mandatory to consider the other operating conditions. Because this sensor is being installed inside or on the tank. So, sensor will directly come in the contact with all type of fuel, even the owner is not sure about the adulteration of the fuel and many other things [1].

Even the environmental conditions like Sunlight, rain will contribute to the change in performance of the sensor, which might be in turns the degradation of the sensor life and in the outcome accuracy of sensor will be changed. So, all OEM's will do the analysis on the sensor before installing on actual vehicle, even as organization who will develop as actual sensor will also do deep analysis for performance to insure all the major aspects before going to the customers [1-4].

III. PROPOSED SYSTEM

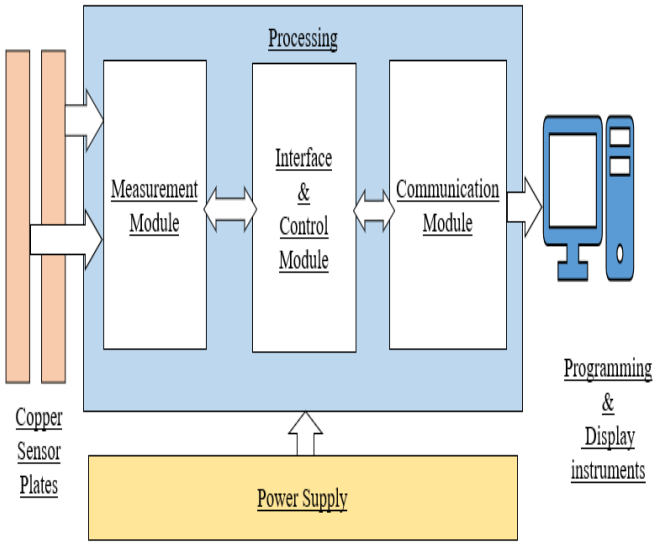

Figure. 2. Fuel level sensor block diagram

Block diagram has all the blocks, which are used for measurement of capacitance. Measurement system contains four major section, i.e. Sensor plates, Processing Power supply and display section. Sensor's measured raw data is sent to the measurement module, this data has been converted from capacitance to level corresponding to the tank using capacitance to digital converter IC. Some additional calculations and for calibration and level matching are done under the same block. Communication blocks providing the data to displaying. Power supply module is universal to all the modules and providing constant supply of 5V to all modules. Programming and display module used for data calculation and calibration using the programming. To display result Serial communication window is used [8].

The two sensor plates are placed o the tank, from outsied so it will not have direct contact with fluid,these plates measures the change in capacitance, and prosesed

capacitance by obove system is corrosponds to the level in the tank [6].

IV. Results analysis

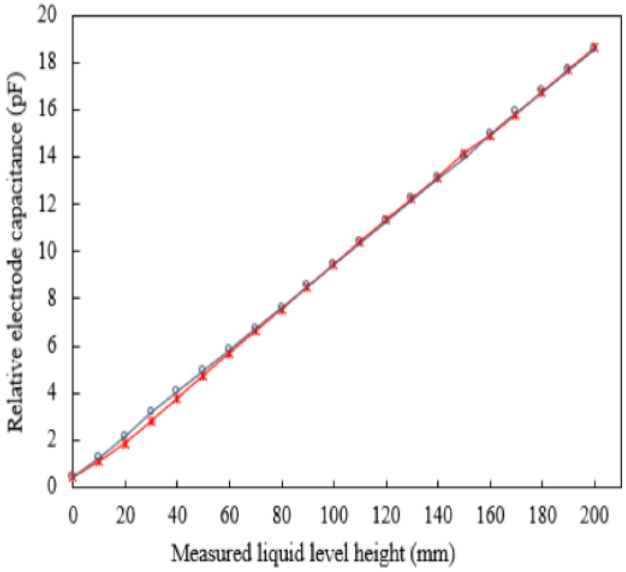

Figure 3. Relationship between fluid level and output capacitance.

When the measured fuel level is stable, the relationship between the sensor output capacitance and measured fuel level is linear. The input and output curves of the sensor were measured during the experiment and then fitted and linearized.

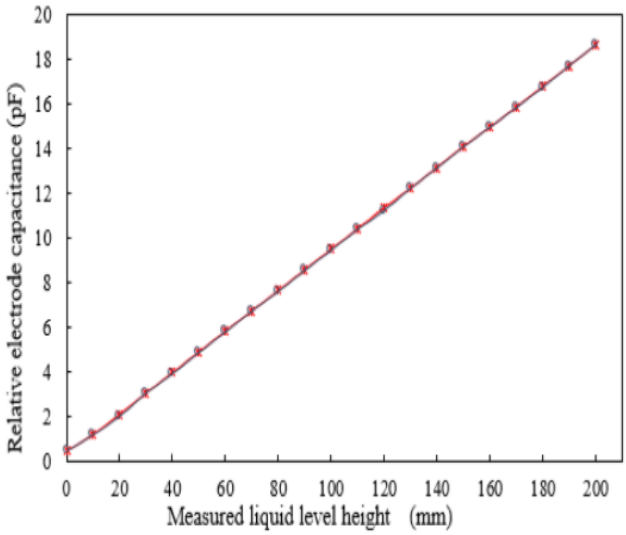

Figure11 4. Relationship between fluid level and average output capacitance

The relationship between the fluid level and output capacitance is shown in above figure, the experimental results show that the capacitances measured from reference electrode and measuring electrode with respect to each other. Level electrode measures actual level of amount of liquid present in the tank, capacitance proportional to the fluid height and reference electrode measures for fluid type and temperature variations.

V. Conclusion

This paper expounds efficiently the general plan of implanted fuel sensor and shows the practicality from the structure to the naturally sheltered circuit structure. The proposed thought which comprises of capacitive sensor fuel estimation framework that obtains the deliberate fluid level and this information is given to the vehicle parameter indication display to indicate actual level. The processor handled the information by computing height in the liters that data is conveyed to the controller section to give other functionality like SMS, connectivity such as uploading data on clouds. Also, during meantime controller conveys the information to the owner using connectivity. In this way, this stays away from the fuel burglary events while fuel filling and in parking also. At the same time system can also useful in leakage detection.

VI. Future scope

As the fuel monitoring system is real time application, and level is monitored continuously we can implement fuel theft detection, whenever there is large decrease in fuel level in tank the system is activated giving the owner the precise indication of fuel content. So, this can be extended to tracking system where the vehicles fuel data can be directed to a database were each vehicle can be tracked easily by the owner. There is a scope for developing low cost sensors and implementing data acquisition system for storing the data of fuel fillings per month or per week as it is monitored continuously.

Refrences

[1] Zhang, Qingliang. "Design of a capacitive liquidometer applied in automobile." In *2015 International Conference on Estimation, Detection and Information Fusion (ICEDIF)*, IEEE, 2015, pp. 229-232.

[2] Toth, Ferry N., and Gerard CM Meijer. "A new capacitive precision liquid-level sensor." In *Proceedings of 20th Biennial Conference on Precision Electromagnetic Measurements*, IEEE, 1996, pp. 356-357.

[3] Yuan, Mei, Zhaohua Zhang, Shaopeng Dong, and Sufang Xue. "Design of embedded fuel sensor based on intrinsically-safe circuit." In *2017 Chinese Automation Congress (CAC)*, IEEE, 2017, pp. 4666-4671.

[4] Kandlbinder, Christoph, Alice Fischerauer, Tristan Zürl, Tobias Helling, Gerhard Fischerauer, Martin Siegl, and Jens Gerstmann. "Observation of bubbles inside cryogenic liquids using capacitive multi-electrode sensors." In *2016 13th International Multi-Conference on Systems, Signals & Devices (SSD)*, IEEE, 2016, pp. 141-146.

[5] Loizou, Konstantinos, and Eftichios Koutroulis. "Water level sensing: State of the art review and performance evaluation of a low-cost measurement system." *Measurement* 89 (2016): 204-214.

[6] Hamanaka, Marcelo Eustaquio, Alan Kardek Rego Segundo, and Sàvio Augusto Lopes da Silva. "Portable non-invasive capacitive transducer for measuring fuel level." In *2017 IEEE SENSORS*, IEEE, pp. 1-3, 2017.

[7] Bommer, Jason, Andy Robb, René Martinez, Shashi Ramamurthy, Jason Harrigan, Harikiran Muniganti, Vivekanand Mannangi, and K. J. Vinoy. "Wireless aircraft fuel quantity indication system." In *2014 IEEE Sensors Applications Symposium (SAS)*, IEEE, 2014, pp. 305-310.

[8] Petlach, Petr, and Michal Dub. "Possibilities of COTS ultrasonic fuel quantity measurement." In *2016 IEEE/AIAA 35th Digital Avionics Systems Conference (DASC)*, IEEE, 2016, pp. 1-6.

[9] Ma, Shiyong. "Oil tank system for automatic measurement and stocktaking." In *2011 International Conference on Electric Information and Control Engineering*, IEEE, 2011, pp. 1502-1505.

[10] Sartori, Davide, and Davide Brunelli. "A smart sensor for precision agriculture powered by microbial fuel cells." In *2016 IEEE Sensors Applications Symposium (SAS)*, IEEE, 2016, pp. 1-6.

[11] Yu, Jing, Hang Yu, and Dongsheng Li. "Design and Characteristic Analysis of Cross-Capacitance Fuel-Level Sensor." *Sensors* 18, no. 3984, 11 (2018):.

[12] Kandlbinder, Christoph, Alice Fischerauer, Tristan Zürl, Tobias Helling, Gerhard Fischerauer, Martin Siegl, and Jens Gerstmann. "Observation of bubbles inside cryogenic liquids using capacitive multi-electrode sensors." In *2016 13th International Multi-Conference on Systems, Signals & Devices (SSD)*, pp. 141-146. IEEE, 2016.

[13] Fleming, William J. "Overview of automotive sensors." IEEE sensors journal 1, no. 4 (2001): 296-308.

[14] Terzic, Edin. "Capacitive fuel level sensor development in automotive applications." (2012).

[15] Divakar, Vinay. "Fuel gauge sensing technologies for automotive applications." International Journal of research in Computer Engineering and technology (IJARCET) 3, no. 1 (2014)

Proceedings of the Fourth International Conference on Communication and Electronics Systems (ICCES 2019)
IEEE Conference Record # 45898; IEEE Xplore ISBN: 978-1-7281-1261-9

A Card Emulation Technique based Secure Framework for Internet of Things (IoTs) Applications

B. B. Gupta
Department of Computer Engineering
NIT Kurukshetra
Gupta.brij@gmail.com

Shaifali Narayan
Department of Computer Engineering
NIT Kurukshetra
Shaifalinarayan1993@gmail.com

***Abstract* – IoT (Internet of Things) enables the devices to be smartly connected with each other to share the data and collect it for future analysis. With the expansion of time, the applications of IoT are increasing in every sector of society like homes, devices, vehicles, health sector, and many more. The wireless communication in IoT makes use of different wireless communication protocol, one such protocol is NFC. The card emulation technique in NFC is widely used in payment sector and research is in progress to enhance its application area. Smart cards in IoT are used to store the keys and user identification information to provide an easy way to authenticate users and provide them the service. In this paper, we will represent a communication protocol between an IoT device and the user smart phone using card emulation technique that can be used in many sectors of IoT. The protocol will eliminate the use of smart cards in IoT by providing users with virtual cards that can be stored and accessed with smart phone. The protocol provides an authorization facility of user, and controls the access of illegitimate user.**

Index Terms – Internet of Things, NFC, card emulation, authorization, smart phone.

I. INTRODUCTION

With the increased use of internet in the past few years, several new ways technologies discovered that uses the internet and provide ease to users in their daily life. One such technology is Internet of Things (IoT), which is used for transferring the information among the devices connected and humans. IoT is a network of intelligent objects which have the capability to share the collected data with the other connected device, store it for future analysis and allow them to take any action on behalf of the owner in the environment [1], [2]. With the large number of devices present in IoT environment, it allows the companies to keep the record of the items produced, and secure them from theft, produce the items according to its consumption in the market, and can incorporate the changes in the items accordingly. The consumers can control the IoT devices with their smart phone through application, which provides ease to them in their daily life.

For communication in IoT protocols used are- short range network and low power wide area network [3]. The short range communication network will include the Bluetooth, Near Field Communication (NFC), RFID, ZigBee, and Z-Wave. The low power wide area network will include SigFox, which is a wireless communication technology for objects with low energy consumption like sensors and machine to machine applications. In addition, the other category is cellular technology that makes use of GSM, 3G/4G for communication and are used by applications which require large distance for operation.

NFC which is a short range communication protocol has gained a lot of attention in the past few years, after its effective use in smart phones for transferring the data and making payments. NFC is used in IoT as it provides easy data sharing and network access and provides multi-level data security. NFC works in three modes – reader/writer mode, card emulation mode and peer to peer mode [4]. The IoT applications are mainly based on the peer to peer mode of NFC.

The applications of IoT are increasing with the time to provide ease to users in the daily life by controlling the objects with smart phones. These applications are based on peer to peer mode of NFC. Some of the examples are described further. A smart library system which was based on IoT, make use of NFC for tracking the books [5]. A smart parking system which is based on the protocols used in IoT and make use of NFC for peer to peer mode for information transfer and e-wallet for payment [6]. Other examples include authorization facility for public health devices [7], an IoT based vehicle location detection system which makes use of NFC tags and readers for gathering the information [8]. Other than NFC, IoT systems are also proposed which works on Raspberry pie and are used for home automation and surveillance system [9].

For the ease in user authentication, security or authentication tokens are used which is a physical device. To verify a user identity- keys, passwords and biometric data are stored on the pocket sized smartcards which are a type of authentication token [10]. To authenticate the user smart cards are also used in IoT with multi–server environment [11] and distributed cloud computing service [12]. The protocol allows a user to login to the authentication server using a smart card which verifies the user and the authentication server by generating the same session key. Other than this, IoT is also combined with the smart card- HSM, to protect the cryptographic keys and the enrolling certificates on an IoT device [13]. Smart card-HSM is a lightweight hardware security module, in a smart cards, USB or MicroSD form, to secure the ECC and RSA keys in a key store which is remotely managed. The security to the keys is provided by

the secure element which offer tamper resistant runtime environment to store cryptographic keys and the codes.

For accessing the different applications, the user needs to carry different smart cards with them. The cards can be used for different purpose like authentication of user, providing access to certain applications, storing the keys and code, identification purpose, etc. To eliminate the carrying of number of cards and to provide ease in usage to the customer, card emulation technique was proposed. Host card emulation technique enables a NFC enabled smart phone to emulate a contactless smart card [14]. It is much popular in payment application which allows a user to pay through their smart phone by emulating them as a payment card.

In this paper we will present a protocol for authenticating the user to the IoT applications and devices by using the card emulation technique. The user instead of using the smart cards for accessing the IoT device and application will use the smart phone which will emulate as the smart card and provide access. This will eliminate physical carrying of cards and provide an ease to the user to access the applications using their smart phones by making use of NFC.

Further, the paper is organized as follows. Section II describes the background details. Section III describes the related work. In addition, Section IV describes the proposed system and section V shows the results of simulation which is then followed by section VI as conclusion and then acknowledgment and references.

II. BACKGROUND

The Secure Element (SE) is a union of hardware component, software, medium, and the use of protocols which are used in a smart phone to provide secure storage [15]. SE enables a user to securely execute the application and store the keys, data, and codes related to the application in a secure area. SE is also used for authentication process in the application which needs secure system for execution. SE is available in three forms – removable SE, inbuilt SE and cloud based SE [15], [16].

A. Removable SE

Removable secure elements are the one that can be removed from the mobile device when necessary. MicroSD cards [17] and Universal integrated circuit cards (UICCs) [18] are the types of removable SE. UICC are the new generation SIM cards which are present in the mobiles, laptops that are used for the high speed network. It is a type of smart card which has its microprocessor, softwares and storage units. It is advancement to the SIM cards. UICC can support multiple applications over it and it communicates through Internet Protocol (IP). It is also capable of supporting multiple PIN codes to prevent misuse of personal data.

MicroSD card secure element is advancement to the technology where the mobile device turns into the NFC enabled device by inserting a micro SD card. It offers low risk, and issuer centric storage type for a fast implementation and high control.

B. Inbuilt SE

Inbuilt SE is secure element which is built in the mobile system and works in the same manner as the removable SE. SE is used to store secret keys and provide a secure storage to the mobile device. It is non detachable and supports multiple application to execute. It needs high level of security as compare to removable SE and works with all smart card standards. The working of the chip and the NFC controller is based on the pre-defined protocols.

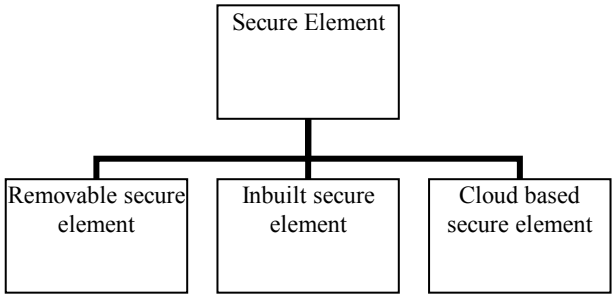

Fig. 1 Types of secure elements

C. Cloud based SE

With the physical SE, it was difficult to integrate them with the mobile devices because of the interdependencies which were needed to create relationship between the two components. To overcome such difficulties, industries moved towards the cloud based or remote SE. Cloud based SE reduced the complexity and cost of maintaining the physical SE. The cloud based SE requires a proper level of security to the stored data.

III. RELATED WORK

There are some IoT based systems that were earlier proposed to increase the IoT application area. These systems are based on communication protocol NFC which is used in IoT.

Brian et al. [5] proposed a smart library system which is based on IoT and provides book tracking by the use of NFC. The system provides facility to the user to get a book from its place through NFC tags and Local Positioning systems (LPS) based on Wi-Fi. The physical entry of the user to library needs biometric finger prints and user device authentication is performed to authenticate the device before accessing the services. LPS allows a user to track the book to a rack or to a user and the books are embedded with NFC tags and the racks are embedded with NFC reader.

Mainetti et al [6] proposed an IoT based parking system, using heterogeneous sensor network including RFID and light sensors. The system made us of the cloud platform and IoT gateway along with user interface provided by DriverApp and TrafficApp. To exchange the information between different entities, RESTful communication was used. The proposed system is time consuming as the involved procedures takes lot of time.

Lee [7] proposed NFC peer to peer based authorization protocol that is used between public health devices and mobile including NFC P2P facility. The protocol uses NFC data exchange format and Record Type definition for sharing data over NFC standards. It performs IoT device and user registration to the server.

Sukumar [8] proposed a vehicle location system helpline system based on IoT. The system uses NFC tags and readers to achieve the objective. NFC tags are used on the bus and the NFC readers are installed on every bus stop to update the IoT about the last stoppage location of the bus. The system is only proposed for bus facility.

IV. PROPOSED SYSTEM

This section will present the proposed protocol for authenticating the user to the IoT applications through the smart phone by using card emulation technique. This section will cover the system entities, phases of protocol and working. The protocol will be proved with the help of the sequence diagram. The proposed model is shown in Fig. 2.

A. System Entities

1) *User/User device:* The user who is willing to use the IoT application and will be able to access it through the smart phone which is the user device.

2) *NFC terminal/reader:* The NFC based terminal where the user will share his credentials by using the NFC based smart phones. The terminal will be used to read the data from the user device and provide the service to the user if authenticate them successfully by servers.

3) *Card Service Provider (CSP):* This is a cloud based secure element which will be needed to store the authentication keys and its original id that will be required while accessing the application. The server will be verified by the IoT service provider.

4) *Authentication Server (AS):* The server will be used to authenticate the user by its id and pin. The id stored on AS will be the virtual id, which will be mapped to original id in CSP. The server will be verified by the IoT service provider.

5) *IoT service provider:* The service provider who will provide the access to the IoT application by smart phones. The application running on user mobile to access the IoT device by card emulation will be hosted by the IoT service provider.

B. System Phases

The system is divided into six phases – Registration phase, enrolling phase, Card & Key generation phase, Encryption phase, Verification Phase and Access phase.

1) Registration Phase: This phase will deal with the registration of the user to the application running in the mobile device to access the IoT device. The user will enter the required details to the registration page and a user account will be created through which the user can access the IoT devices. The user will get a user id and a password for accessing the account.

2) Enrolling Phase: This phase will deal with enrolling the user to the required IoT application, for example- IoT based car parking system, library management etc. The user will enter his details to get a virtual smart card which can be used by user to access the particular application. The original user id will be stored at CSP and a virtual id will be stored at AS for verifying the user.

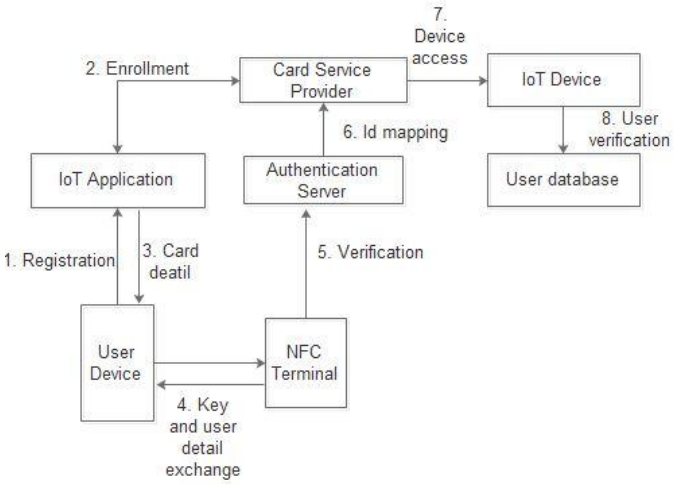

Fig. 2 Proposed Model

3) Card & Key generation phase: This phase deals with generating the card details for the user like the user virtual id and its pin which will be used to access the IoT application. It will also include the generation of keys which will be used for securing the data transmission. The keys will securely get stored in the cloud secure element for maintaining the privacy of the keys, and will not be stored on user device.

4) Encryption Phase: After card generation when the user will access the IoT based application, the data transmitted between the user device and the terminal will be encrypted by a symmetric key to bind the generated data to a particular terminal. This will avoid the sniffing attack which is common in NFC. The symmetric key will be generated by Diffie-Hellman algorithm.

5) Verification Phase: In this phase the data received by the terminal will be decrypted by the symmetric key and will be send to the AS for authenticating the card details send by the user. The AS on successful authentication will send the user virtual id to the CSP.

6) Access Phase: The CSP on receiving the virtual user id from AS, will map it to the original user id to get the selected user keys. The keys and virtual id will then be shared with the IoT device for communication and storing the user data that accessed the IoT based application.

C. *Working*

Fig. 3 represents the flowchart of the proposed system and describes how the system will work from initial stage to the final stage. To secure the user access, the application will take user fingerprint as the initial authentication at device level. The user id and pin will be used for authentication at application access level.

Fig. 4 and Fig. 5 describe the working of the proposed system. Fig. 4 shows the registration phase, enrolling phase and card & key generation phase. After the completion of these three phases, the user will be provided with a virtual card that will be securely stored on the user device. Fig. 5 shows the working of the system after the generation of the card, which includes the encryption phase, verification phase and access phase. The completion of these phases will provide authenticate user to access the IoT devices.

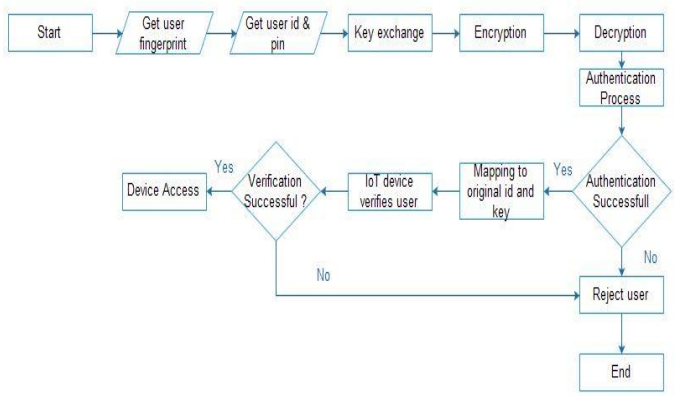

Fig. 3 Flowchart of the system

The protocol provides an authorization facility of user, and controls the access of illegitimate user. To access the application, the user needs to verify its biometric credentials which will be stored in smart phone memory. Once the user access the application, using the virtual cads provided to the user can access the IoT application.

D. *Mathematical Representation*

To access the service, the user device and the NFC terminal will perform initial communication to exchange the symmetric key K_i generated by Diffie – Hellman algorithm. The IoT application will encrypt the user credentials virtual user id V_i and pin with K_i.

$$v = g^x \bmod p$$

$$u = g^y \bmod p$$

Where p is a prime number and g is co-prime to p. x and y are the random numbers chosen by the user and the terminal.

$$K_{i=}(g^x)^y \bmod p \text{ and } (g^y)^x \bmod p$$

The key K_i will encrypt the V_i and pin using the symmetric key algorithm.

$$\text{Encrypt } \{V_i, \text{pin}\}\ K_i$$

The terminal on receiving the encrypted data will decrypt it with K_i and forward V_i and hashed pin *h*(pin) to AS, for authenticate the credentials.

$$\text{Decrypt } \{V_i, \text{pin}\}\ K_i$$

$$Z_i = \{V_i, h(\text{pin})\}$$

AS will receive Z_i and check if the user is registered or not by using V_i. On successful authentication, AS will forward the V_i and S_i to the CSP.

$$S_i = h(V_i)$$

CSP will verify the user by V_i and on successful verification will map V_i to the original id and communication key KEY_i. CSP will forward the encrypted V_i and KEY_i to IoT device for access to the user. The V_i and KEY_i will be encrypted by a shared key K_Z to secure the id and keys from key stolen attack.

$$\text{Encrypt } \{V_i, KEY_i\}\ K_Z$$

The IoT service will be maintaining a database of authorized user, which will be created during user registration. The data received will be decrypted by K_Z and if V_i matches in the database the user will get access to the device by the use of Keys.

$$\text{Decrypt } \{V_i, KEY_i\}\ K_Z$$

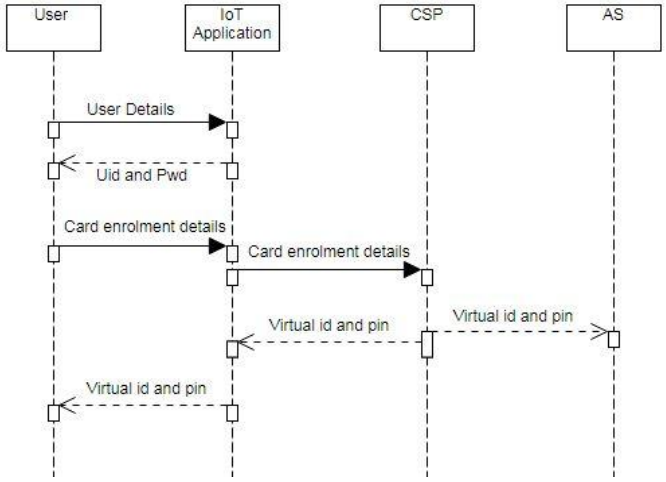

Fig. 4 Registration, Enrolling and Card & key generation phase.

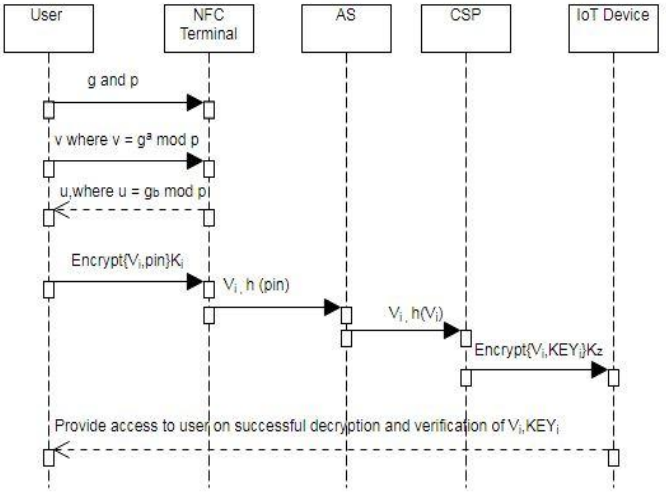

Fig. 5 Encryption, Verification and Access phase

V. RESULTS

The proposed system is implemented on AVISPA tool and is verified on the same platform. AVISPA stands for Automated Validation of Internet Security Protocol and Application [19]. It is a tool which can be used to analyse the large scale sensitive and internet security based applications and protocols. The tool can be used to find the attacks over protocol proposed. Fig. 6 shows the message sequence chart for the proposed system in AVISPA and Fig. 7 shows the security of the protocol under attack searcher (ATSE) in AVISPA tool.

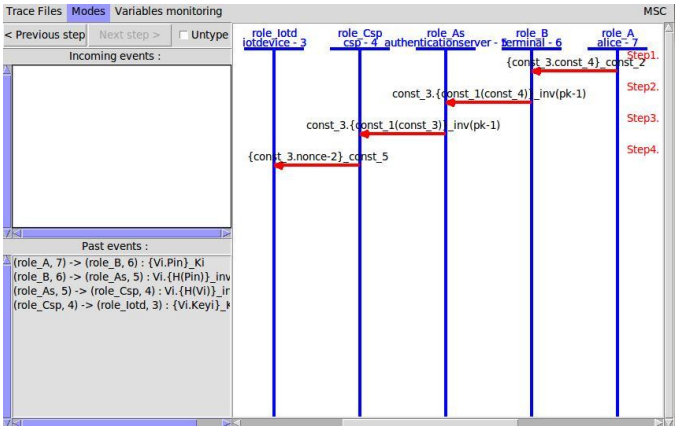

Fig. 6 Message sequence diagram in AVISPA

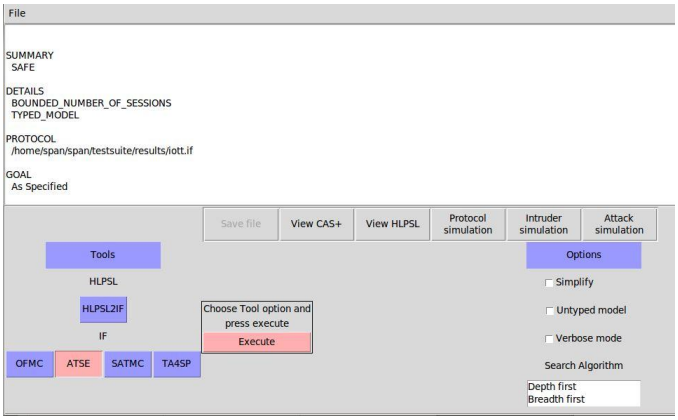

Fig. 7 Simulation result under ATSE model

VI. CONCLUSION

In the last few years, IoT has increased its use and the application area. Every industry in the current time depends on data and IoT improves and enlarge this data by connecting many devices that are capable of decision making. In this paper, we proposed a system that eliminates the use of smart cards in IoT system for authentication, and storing keys. To replace the smart cards we made use of card emulation technique and cloud based secure element to store the keys securely. The model can be used for authentication purpose, accessing any IoT device, and storing the communication keys. The model only allows the registered users to access the services. The paper has discussed few of the previously proposed systems for IoT making use of NFC for their access. In addition, the simulation result of protocol on AVISPA is also included.

ACKNOWLEDGMENT

This publication is an outcome of the R&D works undertaken under the YFRF project under Visvesvaraya Ph.D. Scheme of Ministry of Electronics & Information Technology, Government of India and being implemented by Digital India Corporation.

REFERENCES

[1] Madakam, S., Ramaswamy, R., & Tripathi, S. (2015). Internet of Things (IoT): A literature review. Journal of Computer and Communications, 3(05), 164.
[2] Gupta, B. B., & Quamara, M. (2018). An overview of Internet of Things (IoT): Architectural aspects, challenges, and protocols. Concurrency and Computation: Practice and Experience, e4946.
[3] Al-Sarawi, S., Anbar, M., Alieyan, K., & Alzubaidi, M. (2017, May). Internet of Things (IoT) communication protocols. In 2017 8th International Conference on Information Technology (ICIT) (pp. 685-690). IEEE.
[4] Coskun, V., Ozdenizci, B., & Ok, K. (2013). A survey on near field communication (NFC) technology. Wireless personal communications, 71(3), 2259-2294.
[5] Brian, A. L. A., Arockiam, L., & Malarchelvi, P. D. S. K. (2014). An IOT based secured smart library system with NFC based book tracking. International Journal of Emerging Technology in Computer Science & Electronics (IJETCSE), 11(5).

[6] Mainetti, L., Patrono, L., Stefanizzi, M. L., & Vergallo, R. (2015, December). A Smart Parking System based on IoT protocols and emerging enabling technologies. In 2015 IEEE 2nd World Forum on Internet of Things (WF-IoT) (pp. 764-769). IEEE.
[7] Lee, B. M. (2015). Authorization Protocol using a NFC P2P mode between IoT device and Mobile phone. Advanced Science and Technology Letters, 94, 85-88.
[8] Sukumar, P., & Ravi, D. S. (2016). Iot based efficient vehicle location help line system using nfc. International Journal of Emerging Technologies in Engineering Research (IJETER), 4(5), 10-13.
[9] Quadri, S. A. I., & Sathish, P. (2017, June). IoT based home automation and surveillance system. In 2017 International Conference on Intelligent Computing and Control Systems (ICICCS) (pp. 861-866). IEEE.
[10] Crossman, M. A., & Liu, H. (2015, April). Study of authentication with IoT testbed. In 2015 IEEE International Symposium on Technologies for Homeland Security (HST)(pp. 1-7). IEEE.
[11] Bae, W. I., & Kwak, J. (2017). Smart card-based secure authentication protocol in multi-server IoT environment. Multimedia Tools and Applications, 1-19.
[12] Gupta, B. B., & Quamara, M. (2018). An identity based access control and mutual authentication framework for distributed cloud computing services in IoT environment using smart cards. Procedia computer science, 132, 189-197.
[13] https://www.smartcard-hsm.com/2017/02/14/IoT_Devices_with_SmartCard-HSM.html Accessed 10 April 2019
[14] Alattar, M., & Achemlal, M. (2014, August). Host-based card emulation: Development, security, and ecosystem impact analysis. In 2014 IEEE Intl Conf on High Performance Computing and Communications, 2014 IEEE 6th Intl Symp on Cyberspace Safety and Security, 2014 IEEE 11th Intl Conf on Embedded Software and Syst (HPCC, CSS, ICESS) (pp. 506-509). IEEE.
[15] Reveilhac, M., & Pasquet, M. (2009, February). Promising secure element alternatives for NFC technology. In 2009 First International Workshop on Near Field Communication (pp. 75-80). IEEE.
[16] https://www.rambus.com/blogs/what-is-a-secure-element/ Accessed 15 April 2019
[17] http://siriushellas.gr/nfc-microsds-secure-elements/ Accessed 15 April 2019
[18] https://www.justaskgemalto.com/en/what-uicc-and-how-it-different-sim-card/ Accessed 15 April 2019
[19] http://www.avispa-project.org/ Accessed April 20, 2019

Proceedings of the Fourth International Conference on Communication and Electronics Systems (ICCES 2019)
IEEE Conference Record #45982; IEEE Xplore ISBN: 978-1-7281-1261-9

Software Defined Networking (SDN) based Secure Integrated Framework against Distributed Denial of Service (DDoS) Attack in Cloud Environment

Dr. B. B. Gupta
National Institute of Technology Kurukshetra, India
gupta.brij@gmail.com

Chhavi Chaturvedi
National Institute of Technology Kurukshetra, India
chhavi.chaturvedi1995@gmail.com

***Abstract*— Cloud computing is nowadays developed as a scalable and cost-effective technique. It facilitates many features in the computing environment like resource pooling, multi-tenancy, virtualization etc. In order to avoid resource maintenance, computing has been done on the service provider's infrastructure. Data security is the main concern in cloud computing because it is stored in data centers provided by service providers. DDoS attacks are rapidly growing in the cloud environment and have become a serious threat to cloud consumers. SDN is used to identify and prevent DDoS attacks in the cloud and it simplifies network complexity. In this paper, we have proposed a method that detects and mitigates DDoS attacks in cloud computing using the features of SDN with high accuracy and low computational cost. The proposed system is able to block the illegitimate users and allow only legitimate users to access the cloud services. The results are calculated by simulation experiments.**

Keywords*— *Cloud computing, SDN- based cloud, Software-defined networking, DDoS attack, OpenFlow.

I. INTRODUCTION

Cloud computing originates new era of computing and it has grown rapidly, not only in industries but also in academia due to the important characteristics provided by it, like - pay as per usages, on-demand self-service, rapid elasticity, broad network access and resource pooling. The basic services offered by the cloud are - infrastructure as a service (IaaS), platform as a service (PaaS) and software as a service (SaaS), which attracts great interest of users and provide advantages like reducing the operational and overall cost [1].

In the area of computer networking, a new technology is drawing attention is software-defining networking (SDN). It leverages the lack of programmability in existing networking architecture. The conventional networking architecture is simplified through SDN by decoupling network control plane from infrastructure plane and facilitates new features of networking. The logically centralized control plane provides programmability that allows writing new software logics for implementing new control functionalities and these control logics deploy in the data forwarding plane. Many companies like HP, IBM, and CISCO, etc. provides the platform based on SDN technology and many companies including Google, Amazon, and Microsoft uses SDN platforms for their data centers and public clouds platforms which shows the scope of SDN in the IT industry.

Therefore, implementing SDN in the cloud can simplify the operational complexity of cloud and can enhance its performance based on parameters like routing, switching, monitoring, virtualization, network traffic engineering, and most importantly load balancing. . The integration of SDN and cloud leads to the development of SDN based clouds where the SDN controls network infrastructure and extends cloud services with Networking as a Service (NaaS) [2]. SDN provides new opportunities to ensure the security of cloud computing environment through networking [3] by detecting and preventing the threats that target cloud environment. Among all security requirements, availability of data and services is essential for implementing core operations i.e. providing cloud services and implementing on-demand self-service feature. Cloud services and data availability is mainly damaged due to DDoS attack by making them unavailable for its intended users and targets the service providers to degrade their services and breach the trust between the service provider and its customers [4]. The DDoS attack is performed by more than one machine or bots where a bot is a compromised machine developed when a malware code is injected in the machine and follows the instructions given by the attacker and the group of compromised machines is known as a botnet. SDN provides i) centralized control to the network and ii) open programming that provides real time implementation and modification of detection algorithms in network devices.

Apart from these benefits, the SDN-based cloud may also introduce potential security risks like separating the data and control plane may introduce a new attack surface for the attacker. SDN itself is a target of DDoS attack and also an attacker can take advantage of its features to perform the attack. The hardware devices – forwarding switches and controllers are supported by data plane and control plane respectively and possible vulnerabilities in the hardware devices can lead to attack in SDN. Security threats to SDN include unauthorized access (at controller and application plane), data leakage (side channel attack at data plane and forwarding policy discovery), data modification, fraudulent rule insertion at the control plane, and controller-switch communication flooding (Denial of Service). Although all the security threats degrade the performance of SDN- based cloud but DDoS is a major threat which has a disastrous effect on the whole cloud environment.

In this paper, we present a methodology that is able to detect DDoS attack in cloud environment by implementing detection method on the controller of control layer. After detecting an attack packet, the system will block the malicious packet and also remove the malicious entries from the switches flow table.

The organization of this paper is as follows: - Section 2 describes the basic features of cloud computing, SDN and DDoS attack. Section 3 presents an overview of existing methods to prevent DDoS attacks in the SDN based cloud environment. In Section 4 provides an architectural description of the proposed model along with implementation. Experimental analysis and performance assessment of our proposed approach is in Section 5.

Section 6 concludes the paper followed by acknowledgment and references.

II. BACKGROUNG

Cloud computing is defined as "*a model for enabling convenient, on-demand network access to a shared pool of configurable computing resources (e.g., networks, servers, storage, applications and services) that can be rapidly provisioned and released with minimal management effort or service provider interaction*"[1], according to NIST (National Institute of Standards and Technology).

Many companies provide cloud services like –

- IaaS - Google Compute Engine (GCE), Digital Ocean, Rackspace, Microsoft Azure, Cisco Metapod, Amazon Web Services (AWS), etc.
- PaaS - Windows Azure, AWS Elastic Beanstalk, Apache Stratos, Google App Engine, OpenShift, Force.com etc.
- SaaS - Salesforce, Google Apps, Concur, Dropbox, Cisco WebEx, GoToMeeting, etc.

In the cloud computing architecture basic delivery models are public, private, hybrid and community cloud. Cloud computing provides flexibility, adaptability, and scalability according to various user demands by using virtualization functionality in its core. The cloud computing architecture is depicted in Fig.1.

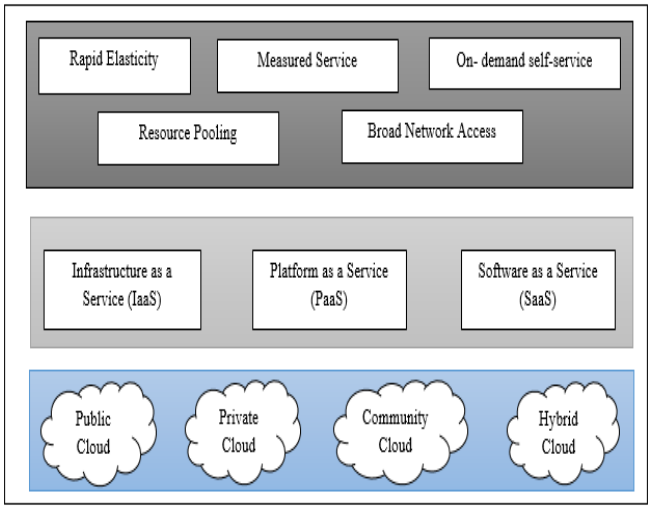

Fig.1 Cloud computing architecture

The framework of SDN is comprised of three layers: - infrastructure layer (data plane), control layer (control plane) and application layer, shown in Fig.2. Forwarding switches which are present in the data layer can be physical or virtual that can be used to forward the packets as per the entries defined in the flow table. The incoming and outgoing services for the packet are provided at the infrastructure layer in SDN environment. The control layer is responsible for formulating the forwarding rules for the packet by analyzing them and it also manages the infrastructure layer. Controllers are the software that communicates with forwarding devices using southbound API interface and networking applications using northbound API interface and are used to provide programmability and network monitoring. Controllers communicate with each other through the eastbound/ westbound API interface. The standard interfaces like southbound APIs such as OpenFlow, ForCES, PCEP, etc. are used to connect the infrastructure and control layer. Control plane provides hardware abstraction for SDN applications. The application layer has various networking applications for network security, network monitoring and analysis, network virtualization, mobility management, and policy implementation. The controllers communicate with applications or software in application plane using northbound APIs [5].

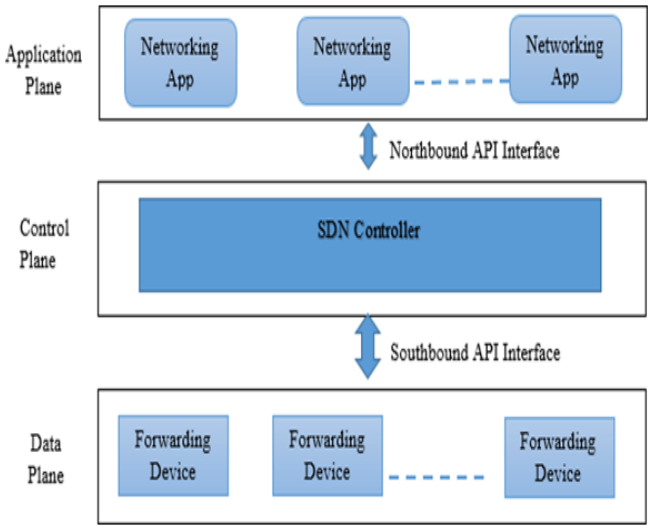

Fig.2 SDN Architecture

The evolution of SDN- based cloud has drawn attention from companies and as well as researchers in recent years. Existing cloud networking architecture follows the single policy method for all cloud users such as single security policy applied on all the cloud services does not provide quality of service (QoS) to the user for some cloud services. SDN has a feature of open programmability that provides the privilege to modify or redesign the existing algorithm or method in real time and due to logically centralized feature of SDN it will be reflected to all devices connected in the network. SDN provides network function virtualization which guarantees stable network performance in SDN-based cloud environment. Advantages provided by SDN based clouds over conventional cloud include quality of service (QoS), server virtualization, storage centralization, network centralization, security, etc.

The security of SDN based cloud increased due to features of SDN. Although SDN based cloud has several advantages, it experiences many challenges such as –

- Performance: the controller cannot handle large amounts of traffic.
- Availability: Controller failure affects network availability
- Scalability
- Security

III. RELATED WORK

In this section, we will review the currently available solutions to detect and prevent DDoS attacks in a cloud computing environment based on the SDN. Braga et al. [6],

presented a lightweight method for DDOS attack detection on the basis of flow analysis and centralized control mechanism and made use of self-organized maps (SOM) for traffic classification. The process occurred in three stages: - flow collection, feature extraction and classification. Giotis et al. [7], used sFlow's packet sampling feature to improve scalability and reduced the communication between the forwarding switch and open flow (OF) controllers. It also used the SDN's dynamic rule update and traffic analysis feature. Passito et al. [8] exploits the abstraction feature of SDN and proposed a framework for the formation of cooperative SDNs is AgNOs and expended its domain beyond the enterprise network. Shin et al. [9], proposed a mechanism named AVANT- GUARD that enhanced the functionality of the OpenFlow enabled switches to prevent malicious flows for the controller. Wang et al. [10], proposed a mechanism for DDoS attack prevention after examining the impact of SDN in DDoS defense and observed that SDN can be useful for DDoS attack detection and mitigation. Therefore, they provide DDoS attack detection and mitigation architecture "DaMask". It is divided in two components: DaMask-D and DaMask- M. DaMask- D is based on anomaly detection system and DaMask- M is a DDoS mitigation system that immediately responds to the attack.

Cui et al. [11], has presented a mechanism, SD Anti-DDOS, which detects DDOS attack with the aim of reducing reaction time to mitigate the attack. It consists of four module architecture in which data stream unusual traffic detection algorithm is used for attack detection and blocking the packets from the source and release the space occupied by the malicious packets in flow table to mitigate the attack. If the response time is large, the SDN controller is forced to process a large number of traffic packets, which increases the possibility of controller failure. Sahay et al. [12], proposed an autonomous DDoS attack mitigation scheme *ArOMA,* which works to coordinate different types of DDoS mitigation systems from the ISPs and its users systematically and exploits SDN programmability and centralized control features. Yan et al. [13], has presented a SDN controller scheduling algorithm which uses multiple queues and utilizes different time slicing approaches according to intensity of DDoS attack.The algorithm provides a gradient for the normal SDN switch by processing the flow request process using other switches during the attack. Xing et al. [14], presented a system, SnortFlow which is an intrusion prevention system (ISP) based on Snort and OpenFlow. It detects intrusion and reconfigures SDN to provide security to the cloud from intrusions. The system uses Snort's intrusion detection functionality and OpenFlow's flexible network reconstruction functionality. Bhushan et al. [15], proposed an algorithm to reduce the DDoS attack while modeling the flow-table space. When a switch cannot handle the incoming flow request because the flow table is not empty, then approach analyze the status of other switch's flow table to recognize the appropriate switch to handle traffic and also discard the less usage and attack traffic flow rules.

IV. PROPOSED ARCHITECTURE AND METHOD

The current cloud architecture is not able to provide clear and effective security policies against DDoS attack and the security policies has been generalized to each user, due to which some of the organizations are in dilemma that adaption of public cloud is beneficial for their organization or not. Thus, in this research work, we propose a solution for the above problem using SDN architecture in the cloud environment. The logically centralized architecture and programmability feature of SDN provides the analysis of network traffic towards the cloud more effectively. Our proposed approach will be able to detect the DDoS attack and mitigate the attack by blocking and extracting malicious flow entries from the flow table. The framework of SDN based cloud is depicted in Fig.3.

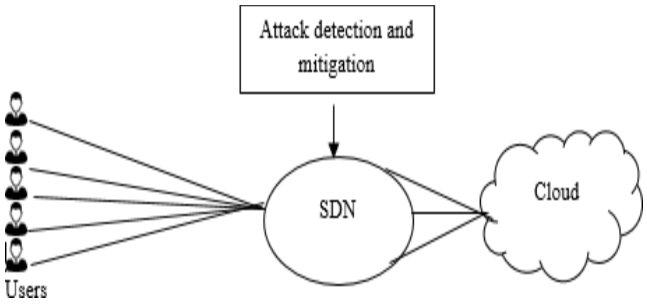

Fig.3 SDN- based cloud

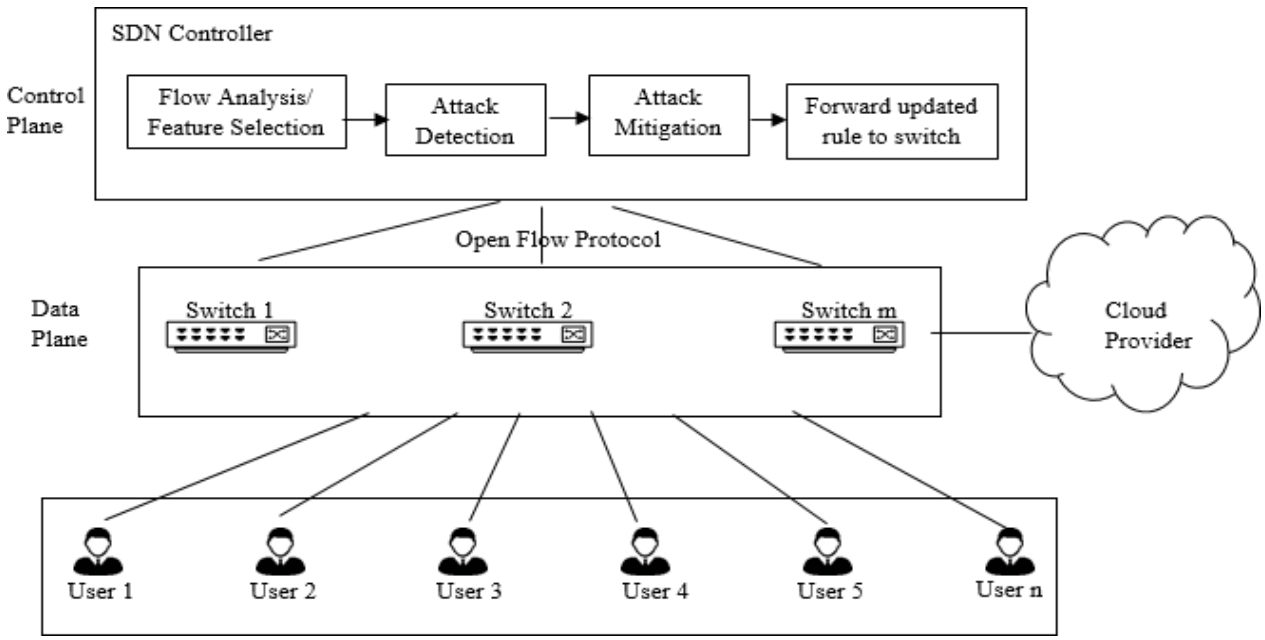

Fig.4 Architecture of proposed approach

A. *Proposed Architecture*

The proposed scheme is described in Fig.4.

- SDN Switches: A switch is a packet forwarding device based on flow table rules. The flow tables are stored at the switch and have limited memory space. The switches are responsible for collecting the client's requests and send it to the controller and update the flow table entry according to the controller's response. The OpenFlow (OF) protocol is used to provide communication between the switch and the controller.
- SDN Controller: A controller is responsible for packet forwarding by the switch and is the backbone of entire network. Attack detection and mitigation algorithm are implemented on the controller. The SDN controller receives flow entries from switches and the controller performs various functioning (data collection, flow analysis, attack detection, and mitigation) to achieve the objective.
- Cloud Users: This entity uses cloud services provided by a cloud service provider.
- Cloud provider: This unit provides many services for cloud users

B. *Attack Detection and Mitigation Approach*

Our attack detection approach is based on artificial neural network. Using neural network algorithm's features, the DDoS attack detection system can identify normal traffic and malicious traffic. In the attack detection system, the controller collects the flow entries from switches and uses principal component analysis (PCA) approach to generate eigenvalues of the flow and is forwarded to trained neural network systems to determine normal traffic packet or a malicious traffic packet. To analyze the data, a dimensionality reduction approach PCA is used. It modifies correlated variables into linearly unrelated variables (principal components) using orthogonal transformation. The nth principal component of transformation is the linear combination of original variable and orthogonal to $(n-1)^{th}$ principal component and has n^{th} highest variance. The resulting vectors contain uncorrected and orthogonal set of values. For a reduction in dimensions of data, consider only a few initial principal components as it has large variance data of the original data set and there is a negligible variance in others, hence the variance loss is minimal. Steps follow to perform transformation:-

- Consider a set of information or data $X_1, X_2, X_3, X_4, X_5, \ldots\ldots, X_n$, where each information has vector length p. The data matrix $X_{n \times p}$, where each n row represents the set of observations and the p columns represents features.

$$\mathbf{X} = \begin{bmatrix} x_{11} & x_{12} & \cdots & \cdots & x_{1p} \\ x_{21} & x_{22} & \cdots & \cdots & x_{2p} \\ \vdots & \vdots & \vdots & \vdots & \vdots \\ \vdots & \vdots & \vdots & \vdots & \vdots \\ x_{n1} & x_{n2} & \cdots & \cdots & x_{np} \end{bmatrix}$$

$$X = [X_1 \quad X_2 \quad \ldots \quad \ldots \quad X_p] \tag{1}$$

- Calculate the empirical mean observation:-

$$\mu = \frac{1}{p}\sum_{i=1}^{p} X_i \tag{2}$$

- Find experimental mean with each column j = 1 to *p*.
- Construct an experimental mean vector **u** of dimension p x 1 from calculated mean values

$$u_j = \frac{1}{p}\sum_{i=1}^{p} X_{ij} \tag{3}$$

- Calculate the deviation from mean:

$$A_{n\times p} = X - u \tag{4}$$

- Calculate covariance matrix:

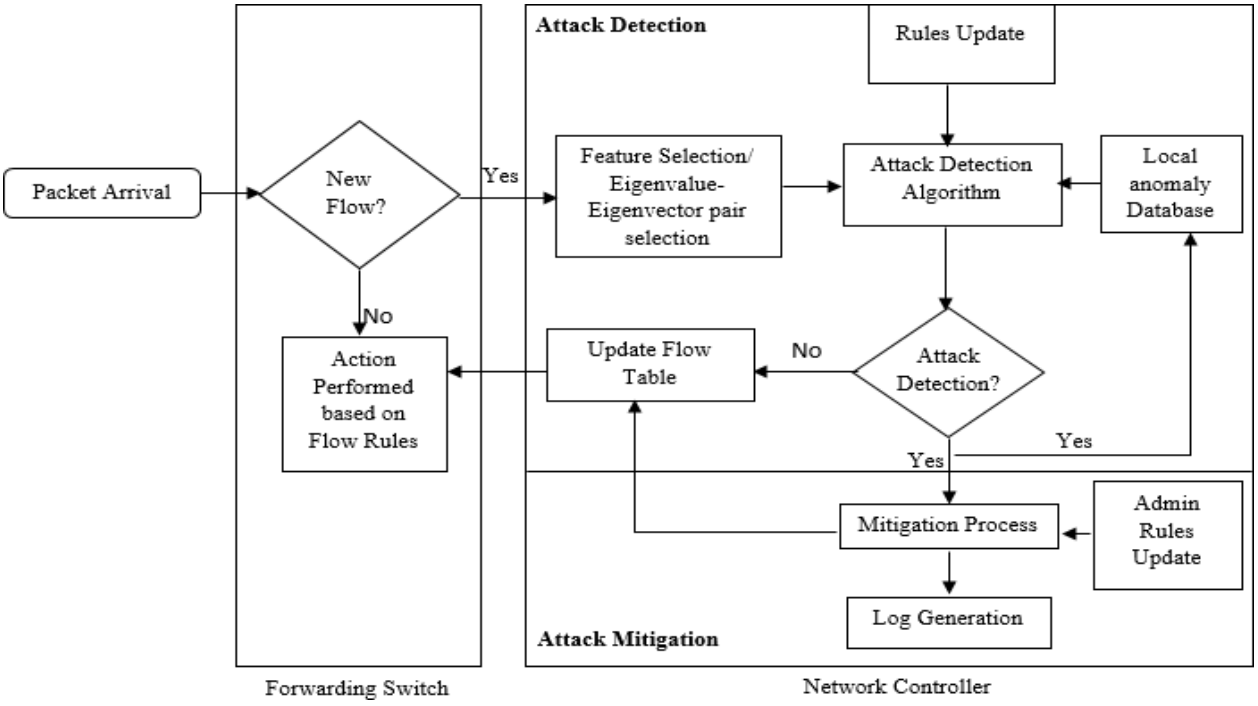

Fig.5 Flowchart of proposed model

$$C_{p\,x\,p} = \frac{1}{n} AA^{T} \quad (5)$$

- Find the Eigen values and eigenvectors of the covariance matrix: - The eigenvalue - eigenvector pairs are calculated by Singular value decomposition (SVD) method and suppose (λ_1, v_1), (λ_2, v_2), $(\lambda_3, v_3)\ldots$ (λ_p, v_p) are eigenvalues - eigenvector pairs of covariance matrix C. Select k inherent dimensionality subspace eigenvectors which has highest eigenvalues. The dimensionality k can be calculated by:-

$$\frac{\sum_{i=1}^{k} \lambda_i}{\sum_{j=1}^{p} \lambda_j} \geq \beta \quad (6)$$

Here β is the ratio of the amount of information contained in the subspace to the total amount of information. We construct a matrix $U_{p\,x\,k}$ from k eigenvector and each eigenvector contains p Eigen values.

The attack detection consists of two stages: training and testing. During the training phase, neural network is formed on a predefined training dataset. In the system, the extracted flow is taken as the input parameter and the target value as the output parameter. Target values for normal traffic and malicious traffic are assigned as 0 and 1, respectively. We used a multilayer perceptron (MLP) algorithm which is a feed-forward neural network that classifies network traffic as normal or malicious traffic. Fig.5 describes the complete flow of our proposed scheme.

To detect the attack, the packet flow is captured and preprocessed to remove the features (eigenvalues) and then transferred as the input of the MLP to detect whether it is a normal flow or malicious flow. If it is found in the form of normal flow then the normal forwarding rules will be implemented in the flow table, but if it is found as a malicious flow, then the mitigation of the attack is necessary. For the attack mitigation, we have identified the switch that sends the request to the controller for malicious flows and adds a blocked rule for that particular source and destination IP address pair. The blocking rules have the highest priority among all flow rules and drop packet operations are used to block the malicious flow. The mitigation architecture is shown in Fig. 6.

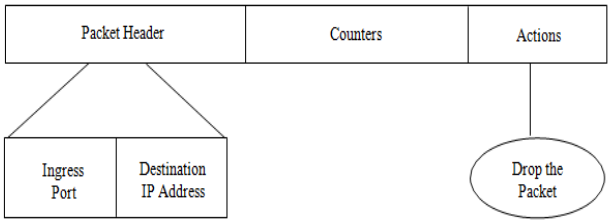

Fig. 6 Mitigation approach

V. EVALUATION

The proposed system uses Mininet, a SDN simulation tool and implemented on a python based open source platform for SDN applications - POX controller. The proposed system contains six hosts (h1, h2, h3, h4, h5, h6) where h1 is a cloud server. The normal traffic is generated using Scapy tool which is a packet manipulation tool and it helps to produce TCP, UDP, ICMP, SCTP traffic. "Low Orbit Ion Canon (LOIC)" tool is used to generate DDoS attack traffic in this paper, which is popular and also able to generate different types of attack: - TCP/SYN, UDP, and HTTP flood attacks. Normal traffic is generated from host h3 and h4 and host h2, h5 and h6 have generated malicious traffic. Normal traffic includes TCP, UDP and ICMP protocol data, and the traffic of the attacks includes TCP floods and UDP floods. The parameters of the MLP model used in this approach are shown in Table 1.

TABLE I. MLP parameters

Parameter	Value
Total layers	3
Hidden layer neurons	5
Rate of learning	0.2
Momentum	0.2
Maximum no. of epochs	500

In order to mitigate the attack, we need to detect the malicious traffic and for attack detection, we have trained the detection system in advance with the predefined dataset. We used OpenFlow controller to mitigate the attack. When new flow arrives, the switch sends a request to controller and controller replies with appropriate actions such as Forward, Drop and Modify-fields. In this paper, we examine the network traffic and classify normal traffic and malicious traffic, if the detection system has identified malicious packet, it sends to the attack mitigation system.

Fig. 7 describes the controller's network load with time and Fig. 8 shows the utilization ratio of the CPU of the controller.

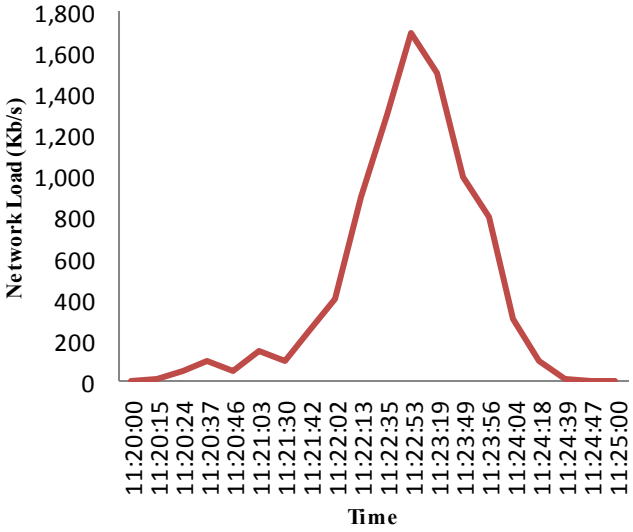

Fig.7 Controller's network load with time

The mitigation system initiates a flow to the switch for mitigating the attack. The new flow contains the source IP address of the malicious packet and attaches a Drop action in the action field with the highest priority. The flow rules are added in the flow table of the switch and if a new packet

comes from the same source IP address it will dropped by the switch. The accuracy (rate of correctly classified instances for every class) of the attack detection is driven by:

$$\text{Accuracy} = \frac{\text{TN} + \text{TP}}{\text{TN} + \text{TP} + \text{FN} + \text{FP}}$$

- Precision is a positive predicate and calculated by:

$$\text{Precision} = \frac{\text{TP}}{\text{TP} + \text{FP}}$$

- A recall is a positive sensitivity value and determined by:

$$\text{Recall} = \frac{\text{TP}}{\text{TP} + \text{FN}}$$

In this paper, we calculate the accuracy, precision and recall values and have achieved overall accuracy is 99.97%, precision is 0.99 and recall is 1.

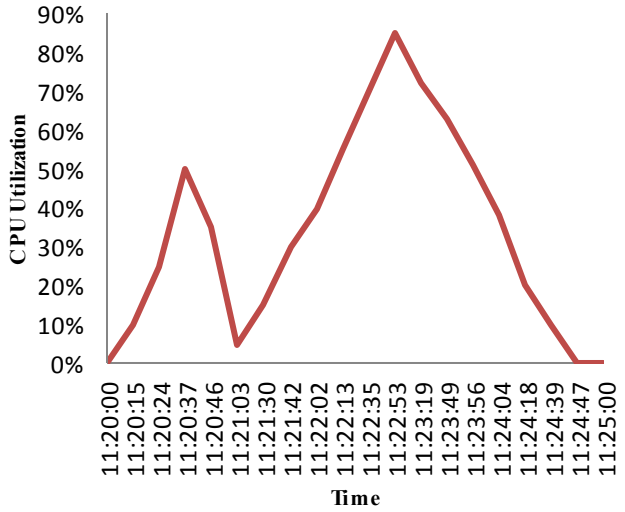

Fig.8 Controller's CPU uses over time

VI. CONCLUSION

Cloud computing and SDN have gained popularity, but DDoS attacks are a major threat to cloud computing environments. However, the collaboration between SDN and cloud computing technology effectively prevents DDoS attacks. The SDN has many features that help in designing an effective DDoS attack mitigation approach. Our proposed approach allows traffic collection and analysis, followed by DDoS attack prevention algorithm in SDN which is implemented on POX controller in Mininet simulator that allows legitimate flow to access the cloud computing environment. The accuracy, precision, and recall have been evaluated in this paper which provides very less false positive. Apart from this, in this paper we also discussed some of the previously proposed schemes for DDoS attack prevention in cloud environment using SDN. Our future work consists of studying new techniques of detecting vulnerabilities and attack in SDN-based clouds and working on on-demand security as a service in SDN-based cloud.

ACKNOWLEDGMENT

This publication is an outcome of the R&D works undertaken under the YFRF project under Visvesvaraya Ph.D. Scheme of Ministry of Electronics & Information Technology, Government of India and being implemented by Digital India Corporation

REFERENCES

[1] Mell, P., & Grance, T. (2011). The NIST definition of cloud computing.

[2] Azodolmolky, S., Wieder, P., & Yahyapour, R. (2013, June). SDN-based cloud computing networking. In 2013 15th International Conference on Transparent Optical Networks (ICTON) (pp. 1-4). IEEE.

[3] Jarraya, Y., Madi, T., & Debbabi, M. (2014). A survey and a layered taxonomy of software-defined networking. IEEE communications surveys & tutorials, 16(4), 1955-1980.

[4] Kandukuri, B. R., & Rakshit, A. (2009, September). Cloud security issues. In 2009 IEEE International Conference on Services Computing (pp. 517-520). IEEE.

[5] Xia, W., Wen, Y., Foh, C. H., Niyato, D., & Xie, H. (2015). A survey on software-defined networking. IEEE Communications Surveys & Tutorials, 17(1), 27-51.

[6] Braga, R., de Souza Mota, E., & Passito, A. (2010, October). Lightweight DDoS flooding attack detection using NOX/OpenFlow. In LCN (Vol. 10, pp. 408-415).

[7] Giotis, K., Argyropoulos, C., Androulidakis, G., Kalogeras, D., & Maglaris, V. (2014). Combining OpenFlow and sFlow for an effective and scalable anomaly detection and mitigation mechanism on SDN environments. Computer Networks, 62, 122-136.

[8] Passito, A., Mota, E., Bennesby, R., & Fonseca, P. (2014, May). AgNOS: A framework for autonomous control of software-defined networks. In 2014 IEEE 28th International Conference on Advanced Information Networking and Applications (pp. 405-412). IEEE.

[9] Shin, S., Yegneswaran, V., Porras, P., & Gu, G. (2013, November). Avant-guard: Scalable and vigilant switch flow management in software-defined networks. In Proceedings of the 2013 ACM SIGSAC conference on Computer & communications security (pp. 413-424). ACM.

[10] Wang, B., Zheng, Y., Lou, W., & Hou, Y. T. (2015). DDoS attack protection in the era of cloud computing and software- defined networking. Computer Networks, 81, 308-319.

[11] Cui, Y., Yan, L., Li, S., Xing, H., Pan, W., Zhu, J., & Zheng, X. (2016). SD-Anti-DDoS: Fast and efficient DDoS defense in software-defined networks. Journal of Network and Computer Applications, 68, 65-79.

[12] Sahay, R., Blanc, G., Zhang, Z., & Debar, H. (2017). ArOMA: An SDN based autonomic DDoS mitigation framework. Computers & Security, 70, 482-499.

[13] Yan, Q., Gong, Q., & Yu, F. R. (2017). Effective software-defined networking controller scheduling method to mitigate DDoS attacks. Electronics Letters, 53(7), 469-471.

[14] Xing, T., Huang, D., Xu, L., Chung, C. J., & Khatkar, P. (2013, March). Snortflow: A openflow-based intrusion prevention system in cloud environment. In 2013 Second GENI Research and Educational Experiment Workshop (pp. 89-92). IEEE.

[15] Bhushan, K., & Gupta, B. B. (2018). Distributed denial of service (DDoS) attack mitigation in software defined network (SDN)-based cloud computing environment. Journal of Ambient Intelligence and Humanized Computing, 1-13.

Proceedings of the Fourth International Conference on Communication and Electronics Systems (ICCES 2019)
IEEE Conference Record # 45898; IEEE Xplore ISBN: 978-1-7281-1261-9

Modeling and Simulation of gird connected hybrid power system integrated with solar PV/Wind and controlled by Voltage Regulator

Vandana chaudhary*[1], Annapurna Bhargava[2] ,Swati Bhasin[3]

Department of Electrical engineering

Rajasthan technical university

Kota, INDIA

[1]V30chaudhary@gmail.com,[2]Abrtu2006@gmail.com,[3]swatibhasin68@gmail.com

Abstract **- Due to hike in price of conventional source of energy we attentive toward non -conventional source of energy. This paper with present of a hybrid solar-wind energy system with gird connected. Hybrid solar-wind system consist wind , solar source and ac loads. In solar dc output system is raised by boost converter. MPPT technique is used to maximize the output of solar system. The wind subsystem is made of a permanent magnet synchronous generator and rectifier, boost converter for maximum output. Voltage regulator is used for controlling the hybrid solar & wind system. Modeling of hybrid PV and wind turbine which is controlled by voltage regulator is explained. To increase reliability & reduce reliance on one single source we connected these two systems.**

Keywords-MPPT, Hybrid System, Voltage Regulator

I. INTRODUCTION

Over the last few years because of growing the evaluate of fossil fuel to making the electricity, high depletion of non - renewable energy and environment anxiety so we turn to focus toward on non-conventional source of energy.[1] Right now the renewable energy source are come essential throughout the world. Modernity utilization of dissimilar renewable sources alike sun ,wind & hydro is made use to produce the power & it is fateful for human life.it can be detract of requirement of electricity & abate the pollution impact[1]

Conjunction of two and more renewable source energy is hybrid power system. PV –fuel cell, PV-Biomass, wind – PV etc. are hybrid energy source[16]. Due to ecological abate the cost and fit for rural usage. A hybrid system of PV-wind power are cost effective energy solution with elevate reliability and power characteristics [3,4].Aim of this paper is modeling of hybrid solar PV/Wind power system. All the essential main parameter of this model can be improved and impact the working on hybrid power system. The introduce model made of PV array , wind conversion system ,DC/DC converter, battery, voltage regulator[16,17]. Here Voltage regulator is used for control hybrid system. .Matlab/Simulink is used for PV/Wind simulation model.

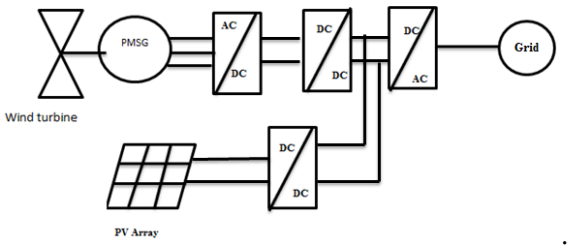

Fig.1 block daigram of hybrid system

Fig. 1 shows a hybrid power system which is comprise PV array and wind energy system which is associated to grid through different converters [5].

II. MODELING OF PV CELL

PV cell is fundamental element of PV system. To attain needed voltage and current no. of PV cell connected in series and parallel. PV cell is a semiconductor diode consist with p-n junction which is spark the light. Simulation of mathematical model of PV cell is helpful to show voltage, current& power conduct at different operating condition [6]. In a PV cell series resistance (Rs) is linked in series along with parallel conjunction with photocurrent source (Iph), grandstand diode (D) and shunt resistance (Rsh). Fig.2 shows corresponding circuit of PV cell.

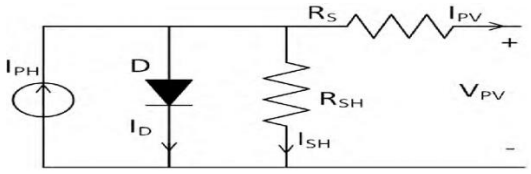

Fig.2 Solar cell basic circuit

Current source of solar cell, current of diode ,current shunted diode display by *Iphs* ,*Ids* ,*Ishd*

$$Ipvs = Iph - Ids\left(e^{q(Vphs+Ipvs*Rs)/nKT)} - 1\right) - \frac{Vphs + Ipvs * Rs}{Rs} \quad (1)$$

Where

Iph = induced solar current

Ids= diode saturation current

qs=electron charge

ks =Boltzmann's constant

ns=ideality factor

Ts=temp ^{o} k

By changing the value of solar irradiation level& working temp. we can change the value of induced solar current

$Iphs = Ishc + Kj(Tct - Trt) * Irs/1000$

Ishc= cell short circuit current

Kj= temp coefficient

Tct, *Trt*=reference and working temp.

III MPPT TECHNIQUE

Results of output power of PV modules are fluctuating according to their environmental condition.so we need to use control technique which help to get high power regardless environmental condition alike temp. & irradiance.

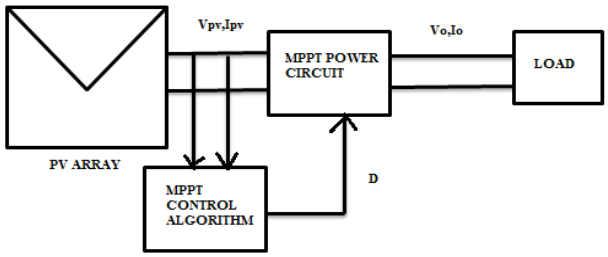

Fig.3 Block diagram of MPPT control

Fig. 3 shows block diagram of MPPT control .There is have to existence a maximum power point because PV cell has nonlinear relationship that is hold on growing with atmosphere condition ,temp.& irradiance level. In this paper perturb and observe (P&O) technique is applied for tracking maximum power at varying temp.& irradiance. It conducts by continually evaluate the terminal voltage and current of PV array, then continually perturbing the voltage by addition small interrupt ,then observing the modification of power to find control signal. Variation developed by variable switching duty cycle. Duty cycle is control by perturb & observation (P&O) MPPT algorithm [6]. DC-DC boost converter is used to convert dc to high level DC output voltage.

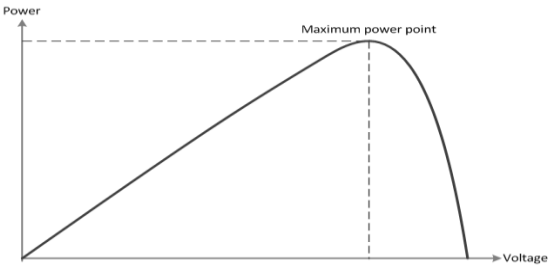

Fig.4 MPPT graph

Fig. 4 shows MPPT graph with respect to power and voltage.

By varying duty cycle converter output voltage is preserve constant .the solar PV array output show

$$Vpv = (1 - D)Vout \quad (2)$$

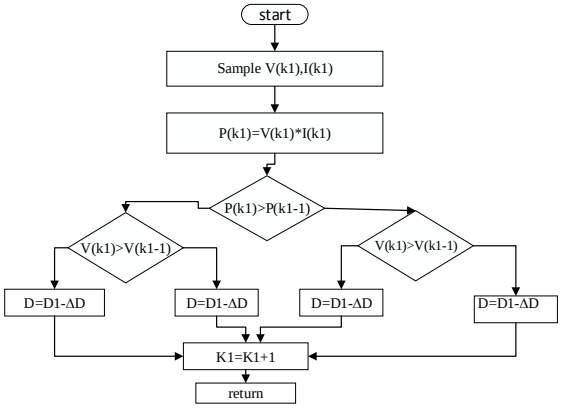

Fig. 5 MPPT flow chart

Expressed variation in output voltage of PV array with different level of solar irradiation and temperature [7,8].

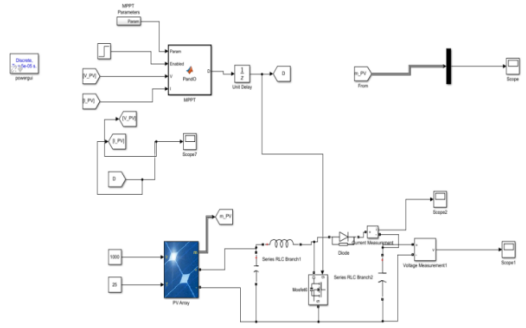

Fig.6 PV panel with MPPT (P&O) technique.

Fig. 5, 6 show MPPT flow chart and simulation of PV array with MPPT technique.

IV WIND MODEL

The arrangement which convert wind energy to mechanical energy called wind turbine. The power occupy by wind system is represent by this equation [9]

$$Pmechp = \frac{Cpc(\alpha,\gamma)\rho A}{2} \qquad (3)$$

Fig 7 shows a wind turbine system model which gives 3 phase AC power then rectifier is used for convert AC power to DC power. For coupling both systems we need convert AC power to DC power with same magnitude. Here we used PMSG synchronous machine because PMSG work is raised reliability of wind turbine. It is an electrical rotating machine in which field excitation is composed by permanent magnets .There is no need reactive magnetizing current. Synchronous generator has many merits corresponding low burden, compact design, & advance capability [10].

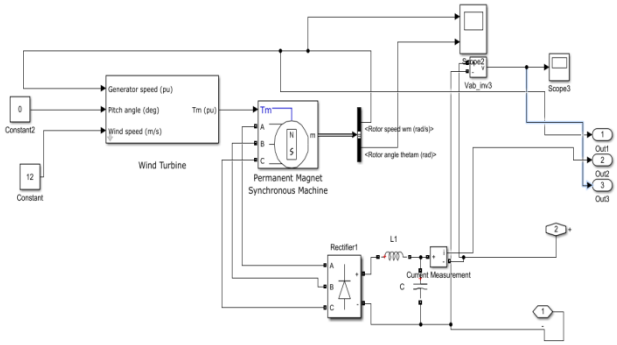

Fig.7 modeling of wind turbine

V BATTERY SUBSYSTEM

Fig. 8 display battery MATLAB model, in which by using three phase inverter battery connected with main supply. Battery system is charged when system run without any problem and used battery power when system is run abnormal condition [2,15].

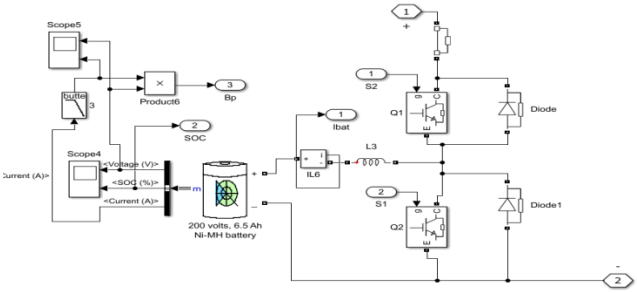

Fig.8 modeling of storage system

VI VOLTAGE REGULATOR

Fig.9 shows an inverter transforms DC to AC power at desired frequency which is controlled by voltage regulator. In voltage regulator generated DC transform into three phases AC by PWM signals. The PWM signals comprise three sinusoidal signals with 120^0 phase shift, compared vector control signals with high frequency carrier signal and produce needful pulse for operation [15]. Due to 120^0 Phase to neutral voltage Vph at the fundamental frequency shows as

$$Vphs = \frac{(2\sqrt{2})}{\pi}\cos\left(\frac{\pi}{6}\right)Vdcs \qquad (4)$$

Where Vph is the generated phase voltage at the terminals, and Vdc is the input voltage of the inverter. The PID control PWM technique is applied to produce desired pulses for the inverter [13].

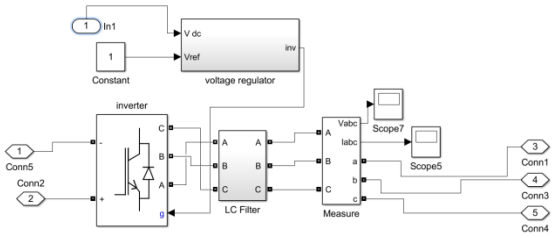

Fig.9 modeling of inverter with voltage regulator

VII RESULTS AND SIMULATION

Fig.10 is represent simulation of hybrid system which is comprise solar and wind sources and energy user block and control by voltage regulator. Solar irradiance and wind speed is taken for simulation. Fig.10 shows output of solar and wind generation system. Hybrid system is run for 0.3 sec in Matlab/Simulink software. Fig.11,12show DC voltage after using boost converter which is boost PV array voltage to a high level dc voltage with MPPT technique & wind turbine output in which PMSG wind turbine produce AC voltage and then rectifier transform AC to DC voltage , Fig.13 show dc boost voltage after coupling both PV/Wind subsystem. Fig.14, 15 show three phase AC voltage after using inverter which is not in pure sinusoidal form & three phase AC voltage without any fluctuation when we connected system to grid respectively.

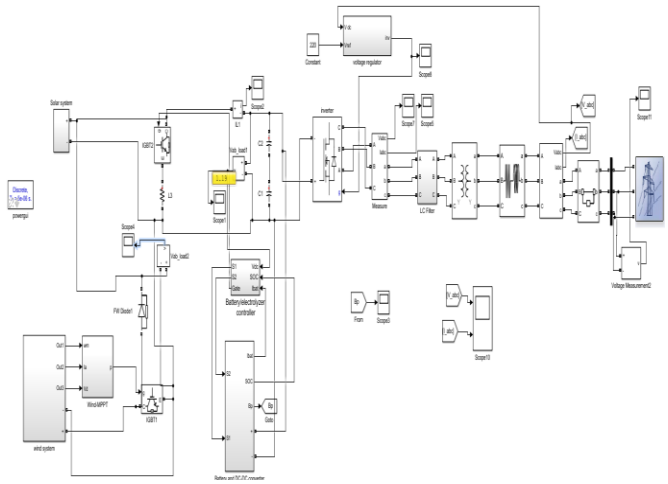

Fig.10 modeling of hybrid PV/wind/battery system controlled by voltage regulator

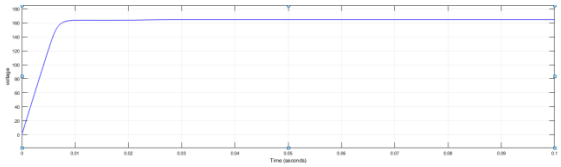

Fig 11 solar output voltage

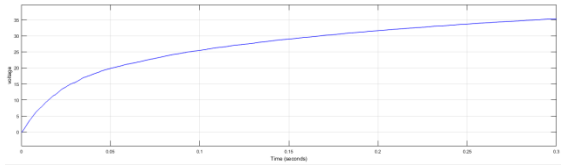

Fig 12 wind output voltage

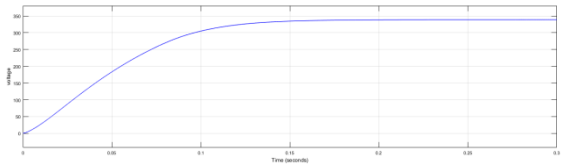

Fig 13 hybrid solar and wind voltage

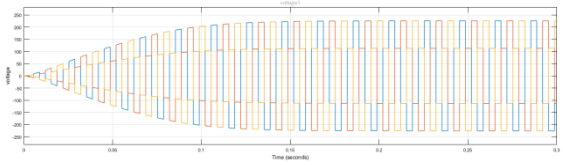

Fig 14 output voltage after inverter

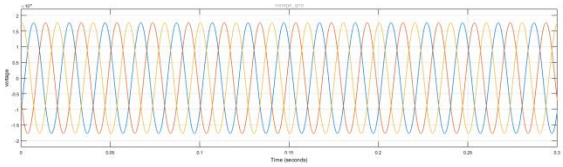

Fig 15 output voltage when hybrid system connected to grid

VII CONCLUSION & FUTURE SCOPE

This paper represents a hybrid system which is comprised solar and wind generation system and controlled by voltage regulator. By using MATLAB software simulation was controlled .The operation of system is evaluate at various wind speed and irradiance stages. The introduce hybrid system is examine wind speed at 12m/s and solar PV panel at irradiance 1000w/m^2 and temp 25^0 form t= 0 to t=0.3sec. is applied then coupled both DC voltage to DC link is controlled by voltage regulator and performance is evaluate & improved. To fulfill the requirement of electricity in a remote area hybrid system is used. The developed system working is performed in Matlab/Simulink software and results are displayed .Other renewable energy sources is used for hybrid system instead PV/Wind energy sources and to get more reliable and satisfied results several control technique is used for inverter in place of voltage regulator.

REFERENCES

[1] J.Godson,M.Karthick,"Solar PV-Wind hybrid power generations system" Vol. 2, Issue 11, November 2013

[2] Dr. Swapnil B. Mohod, Vikramsingh R. Parihar," Hybrid Power System with Integration of Wind Battery and Solar PV System" 978-1-5386-0814-2/17/2017 IEEE.

[3] Anjali Rana, Mohammand Ilyas" Implementation of WIND/PV Hybrid system using matlab"IJAREEIE Vol. 4, 10-15662 Issue 7, july 2015.

[4] Mubashar Yaqoob Zargar,Mairaj-ud-din Mufti,"Modelling and control of wind solar hybrid system using energy storage" 978-1-5090-1666-2/16/2016 IEEE.

[5] Prachi P.Chintawar,M.R.Bachwad,"Power quality imrovement Wind/PV hybrid system by using facts device" vol 4 issue 6,june 2015.

[6] N. Mendalek and K. Al-Haddad "Photovoltaic System Modeling and Simulation" vol 2. 978-1-5320-9 2017 IEEE.

[7] Oladimeji Ibrahim,Nor Zahir Yahaya, Bandar Seri Iskandar" Matlab/Simulink Model of Solar PV Array with Perturb and Observe MPPT for Maximising PV Array Efficiency" vol 3 issue Dec IEEE 2015.

[8] Mukesh Kumar, Mohit Kachhwaya, Bhavnesh Kumar" Development of MATLAB/Simulink based model of PV System with MPPT" 978-1-5090-4530-2016 IEEE.

[9] Rim ben ali, Horst schulte, Abdelkader mami "modeling and simulation of a small wind turbine system based on pmsg generator" in Evolving and Adaptive Intelligent Systems 978-1-5090-6444-1/17/$31.00 ©2017 IEEE

[10] Raghuvendra Kumar Tiwari, Krishna Kant Sharma" Simulation and Modeling of Wind Turbine using PMSG" In International Journal of Recent Research 2016.

[11] Ahmed Chaib,Djalloul Achour,Mohamed Kesraoui,"Control of a Solar PV/Wwind hybrid energy system", international scientific conference "Enviromental and climate Technologies"14-16 october 2015.

[12] Prajapati bhavna, Vaishali y. Patel, Madhusudan v. Gohil "simulation of a solar-wecs hybrid renewable energy conversion system using matlab/simulink" International Journal For Technological Research In Engineering Volume 2, Issue 8, April-2015..

[13] Neha Adhikari, Bhim Singh, A. L. Vyas, Ambrish Chandra, Kamal-Al-Haddad, "Analysis, Design and Control of a Standalone HybridRenewable Energy Conversion System" IEEE.

[14] Qi Zhiyuan, "Coordinated Control for Independent Wind-SolarHybrid Power System" vol 7,978-1-4577- 0547-2/12/2012 june IEEE.

[15] Partha Sarothi Sikder, Nitai Pal," Modeling of an intelligent battery controller for standalone solar-wind hybrid distributed generation system 1018-3639/ 2019

[16] B.Kanagasakthivel ,Dr. D. Devaraj "Simulation and performance anyasis of solar PV-wind hybrid energy system using Matlab/Simulink" 978-1-4799-7633-2,2015 IEEE.

[17] Abeer A. M. EI-Hany,Shawky H.Arafa, Maged N.F.Nashed, "modeling and simulation for hybrid of PV-Wind system." In international Journal of Engineering Research volume No 4, issue No 4, pp: 178-183

Proceedings of the Fourth International Conference on Communication and Electronics Systems (ICCES 2019)
IEEE Conference Record # 45898; IEEE Xplore ISBN: 978-1-7281-1261-9

Analysis of Z-Source Based Single Stage Three-Port Converter for PV Renewable Energy System

Mohit Sharma
Department of Renewable Energy Technology
University Department
Rajasthan Technical University, Kota
Kota, Rajasthan, India
mohitsharma851995@gmail.com

Dr. Ashok Kumar Sharma
Department of Electrical Engineering
University Department
Rajasthan Technical University, Kota
Kota, Rajasthan, India
aksharma@rtu.ac.in

Anshul Gautam
Department of Electrical Engineering
University Department
Rajasthan Technical University, Kota
Kota, Rajasthan, India
anshul941@gmail.com

Dolly Murodia
Department of Electrical Engineering
University Department
Rajasthan Technical University, Kota
Kota, Rajasthan, India
dolmurodia@gmail.com

Prerna Saxena
Department of Electrical Engineering
University Department
Rajasthan Technical University, Kota
Kota, Rajasthan, India
prernasaxena2@gmail.com

***Abstract* - Solar power unit is needed to increase the lesser voltage of solar panels to the voltage of the power grid; thus, converter should have an immense voltage gain with few switches otherwise it leads to system complexity. A three-port converter with enhanced topology for renewable power utilizations based on Z-Source network is suggested to fix these issues well. This Z-Source network symbolize the suggested converter's distinctive characteristics. One port of energy storage system for energy storage and supplying, and the last one is for loads. It is followed with new topology design and output analyses by MATLAB.**

Keywords— Five-terminal, impedance network, renewable energy systems, three-port converter, MATLAB Simulink.

I INTRODUCTION

In the interest of clean, immense suitability, and sustainable benefits of renewable energy schemes such as photovoltaic panels and wind turbine generators Use a big percentage of electricity production to replace traditional expensive, lesser-efficiency and polluted production of electricity [1][2]. However, there is a significant disadvantage of renewable energy systems, i.e. wind or solar are linked to climate and this difficult or intermittent feature extended the intricacy of grid implementation. [3], [4]. One solution issue of energy storage system for stabilizing output of energy storage systems[5]. An instance of a solar energy conversion system with energy storage scheme is displayed in Fig.1, where solar power units are needed to increase the lesser voltage of solar panels, so it takes a high voltage boost converter [6], In addition, the bidirectional energy storage unit combines renewable energy systems to balance output. In order to link the PV and output of load, it required minimum two converters [7]. The diagram shows that power converters are used to bridge various renewable energy systems and energy storage systems into a sub-scheme and to track power transformation and storage to match outputs [8].

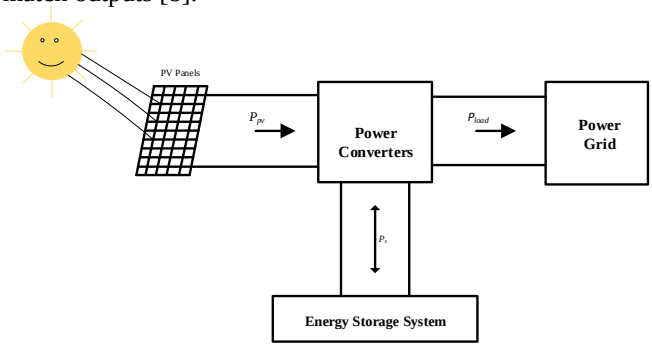

Fig. 1 Solar energy conversion system with energy storage unit.

For this purpose, Multi-stage converter with multiple ports are better to operate conversion of power and grid assimilation for variety of sources. For example, for matching renewable resources, energy storage and utility grids, various phases of power converters are incorporated as shown in Fig. 2

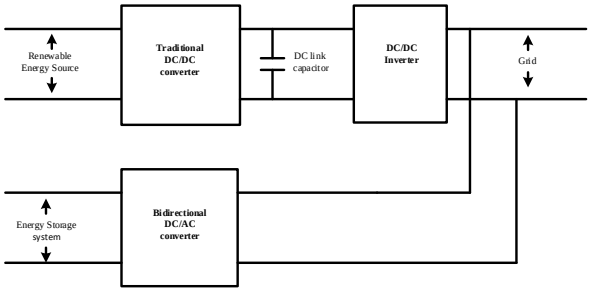

Fig. 2 Multi-port conversion system

Therein, three converters This results in low system effectiveness and high system costs [9]. Existing switches

also enhance the complexity of the system [10], and Such converters ' control policies, reduce stability [11], To resolve issues of renewable energy and energy storage applications a multi-port single stage converter is introduced. A three-port DC to DC converter is designed in [12][13]. Not only did the converter provide higher voltage yield but also provide multiple modes of operation. However, therein Many switches and complicated control strategies are still available, due to this, it increases the system instability[14]-[17]. A single-stage converter with multiple ports is therefore necessary which is based on impedance networks with these characteristics.

- Component ports for renewable resources connecting
- Assimilation of the scheme for storage of energy.
- Huge increase in voltage output.
- Issues related to shoot-through is nullified.
- Immense performance and flexibility, small size, less price.

Impedance networks are known to have the benefits of immense voltage yield, resistance to shoot through problem [18]-[20]. by using impedance networks technique, an impedance network with two quasi z-source is designed[21], A converter with three ports is suggested here.

This paper coordinated as follows: Section II presents Multi-terminal Z-Source Impedance Network. Section III and IV represents system design and analysis and modes of operation respectively. In Section V, simulation model and verification are displayed. Parameter designs are displayed in section VI and conclusion in Section VII.

II MULTI-TERMINAL Z-SOURCE IMPEDANCE NETWORK

Second fundamental network is continues current qZS network. The difference between basic Z-Source network and continues-current qZS network is only a diode in forward direction is placed in continues-current quasi Z-Source network between the inductor in cascade format, and capacitors are placed in different parallel portion via inductor [15]. The resultant output of current by continues - current qZS network has zero fluctuations or constant current is to be shown so this network is called continues-current qZS network, which is displayed in Fig.3(a). Third fundamental network is discontinues-current qZS network, which is displayed in Fig.3(b). In this network (discontinues current qZS network) has two sets of inductors and capacitors are parallelly connected and a diode is placed between them.

Discontinues-current qZS network's output has Intermittent current and fluctuations present in current, so it is called discontinues-current qZSource network.

As displayed in Fig.4, a distinctive converter with three ports is designed., therein, two qZS impedance networks as represented in Fig. 3(c).

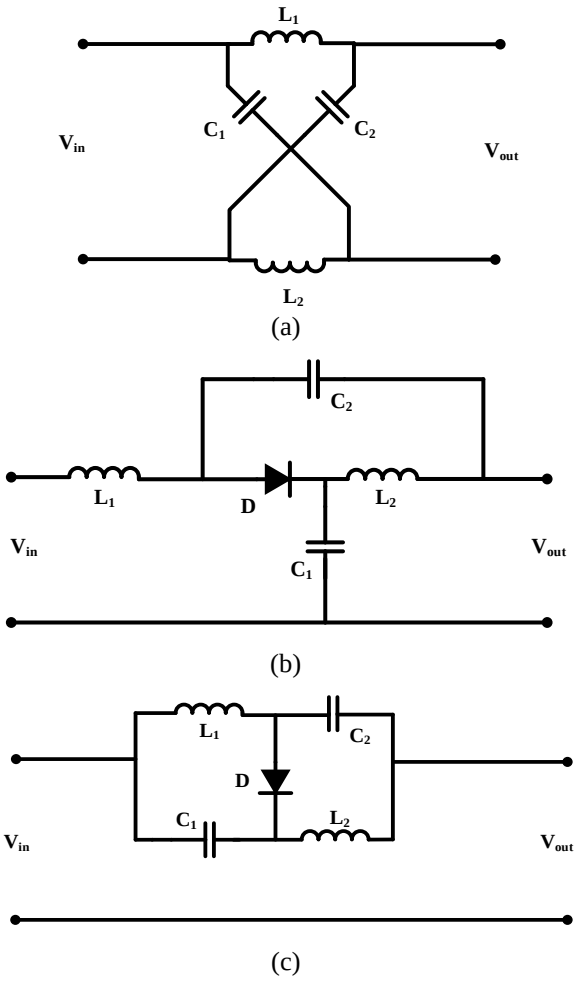

Fig.3 (a) Basic Z-Source network, (b) Continuous-current qZS Circuit, (c) Discontinuous-current qZS network

III SYSTEM DESIGN AND ANALYSIS

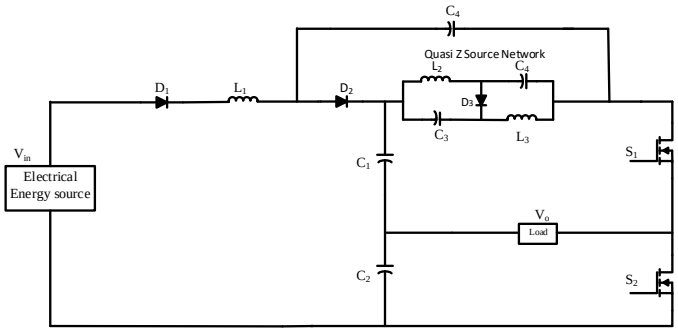

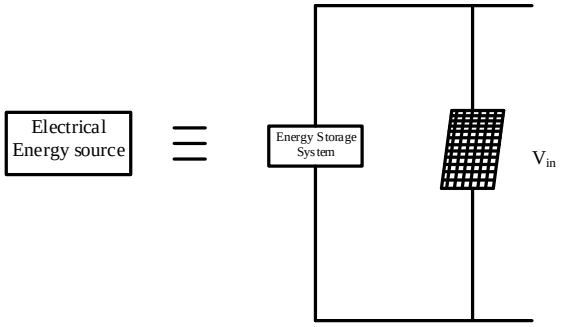

Fig.4 Schematic of the proposed converter

The proposed converter consists of diodes D_1, D_2 and D_3 two switches, S_1, S_2, and a two quasi z-source impedance network composed by three capacitors C_1, capacitors C_2, capacitors C_3, and three inductors, L_1, inductors L_2. The distinctive characteristics of the design are as follows, such as just two three-port switches, few elements, High performance, small size, low price, and high flexibility.

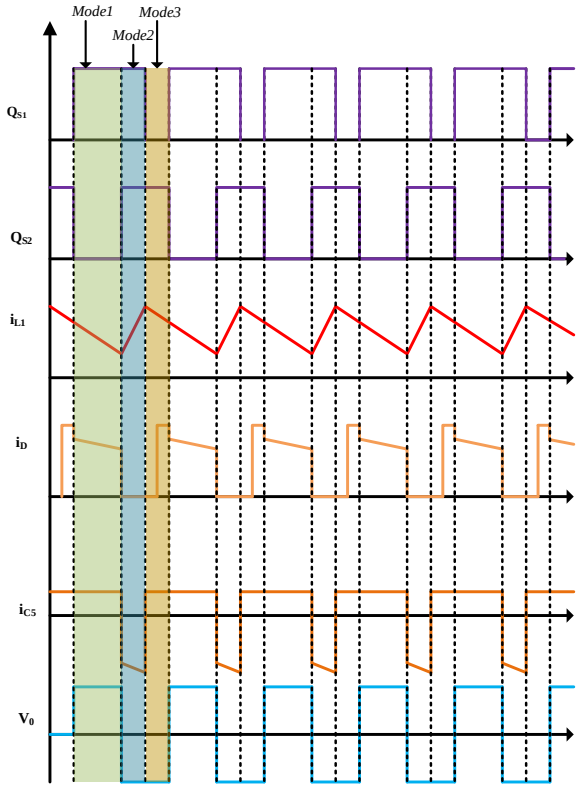

Fig.5 Key waveforms of $d_1 = 0.8$, $d_2 = 0.5$

In all renewable energy instances, the suggested converter can work. The energy from sun that is solar energy can be used as an example for all cases.

- In shiny day when solar energy is generous, it is used to charge the unit.
- When clouds are there and solar energy is limited, the energy from the storage unit is transferred to the load.
- During night time or in rainy days that is in absence of solar energy, the energy from the storage unit is transferred to the load.

Consider that in every case the input is constant by the PV penal or by the energy storage systems.

There are three modes shown in Figs. 6(a), 6(b), and 6(c). Denote d_1, d_2 as the duties of the switches S1 and S2. Assume d1 ≥0.5 and d2 =0.5. Fig.4. Key waveforms of are shown in Fig.5.

IV Modes of Operations

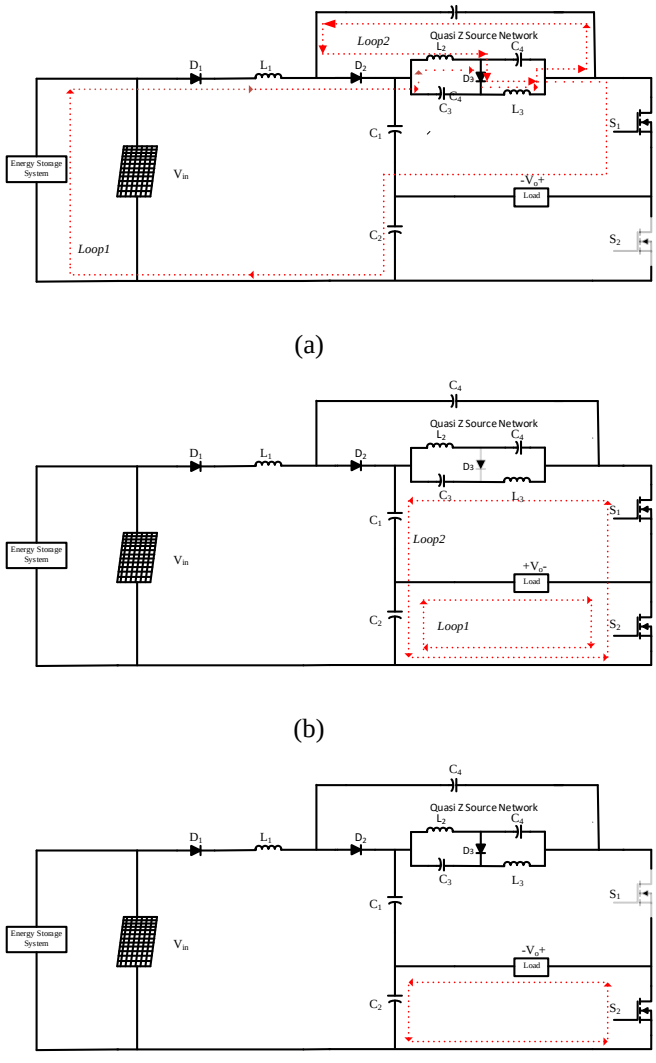

Fig. 6 Equivalent circuits (a) Mode I: S_1 on, S_2 off; (b) Mode II: S_1 on, S_2 on; and (c) Mode III: S_1 off, S_2 on.

- Mode 1: (Fig. 6(a)): S_1 "ON" and S_2 "off" current flow through C_1, load, S_2. In loop2 current is reversed and flow through D_2, L_2, D_3, and L_3 in this mode inductor L_2 and L_3 are charged and discharged simultaneously.
- Mode 2: (Fig. 6(b)): S_1 and S_2 are "ON" C_2 is discharged in loop1 and current flow through D_1, D_2, L_2, D_3, L_3, S_1 and load in loop1. In loop2 C_1 is discharged and current is flow through C_1, C_3, L_3, S_1, S_2 and C_2.
- Mode 3: (Fig. 6(c)): S_1 and S_2 are "ON" C_2 is discharged in loop1 and current flow through D_1, D_2, L_2, D_3, L_3, S_1 and load in loop1. In loop2 C_1 is discharged and current is flow through C_1, C_3, L_3, S_1, S_2 and C_2.

V SIMULATION MODAL AND VERIFICATIONS

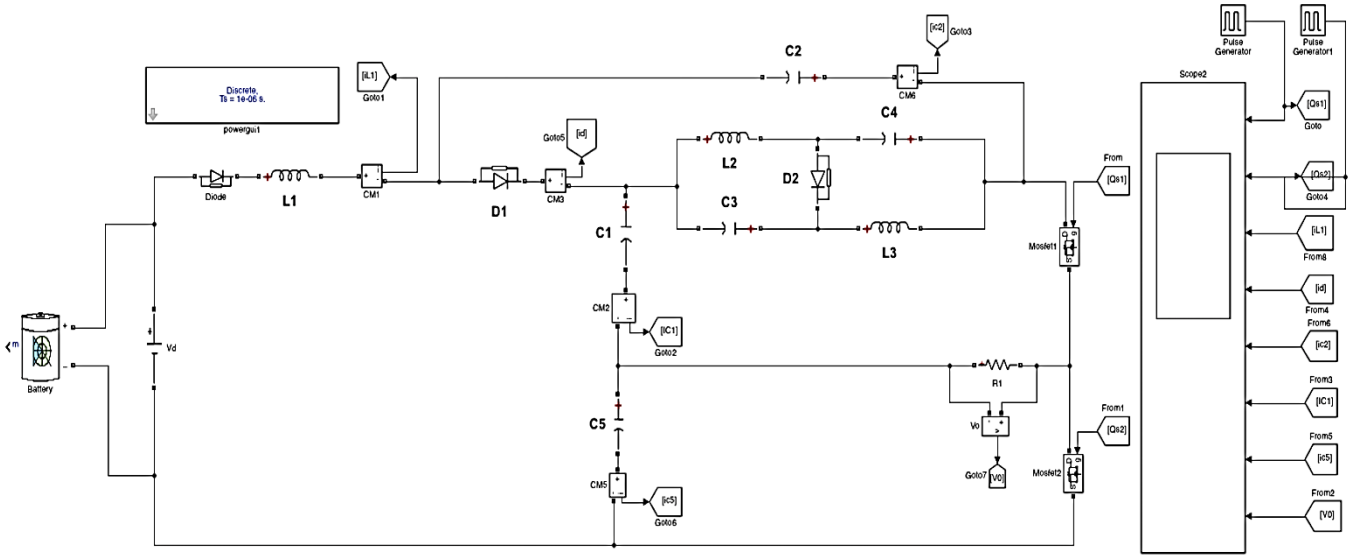

Fig. 7 Simulation model of proposed converter

MATLAB software is used for verification to check the validity and feasibility of the suggested converter and the parameters of simulation are displayed in TABLE 1. Simulation results are represented in Fig.8(a) and Fig. 8(b), Which are compatible with the Figs 4 theoretical evaluation. The duty ratio of given switches Q_{s1} and Q_{s2} is d_1=0.8 and d_2=0.5. Output voltage v_0 is symmetric with about ±400V as displayed in fig. 8(a),(b).

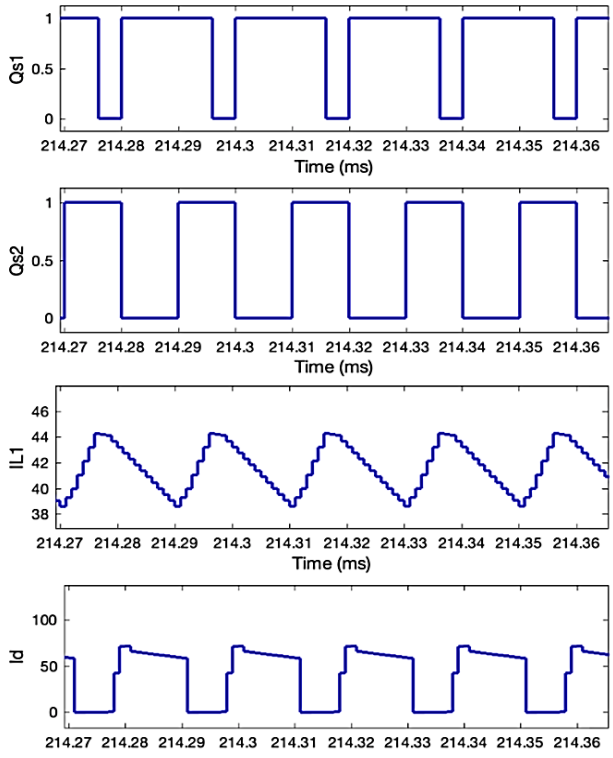

(a)

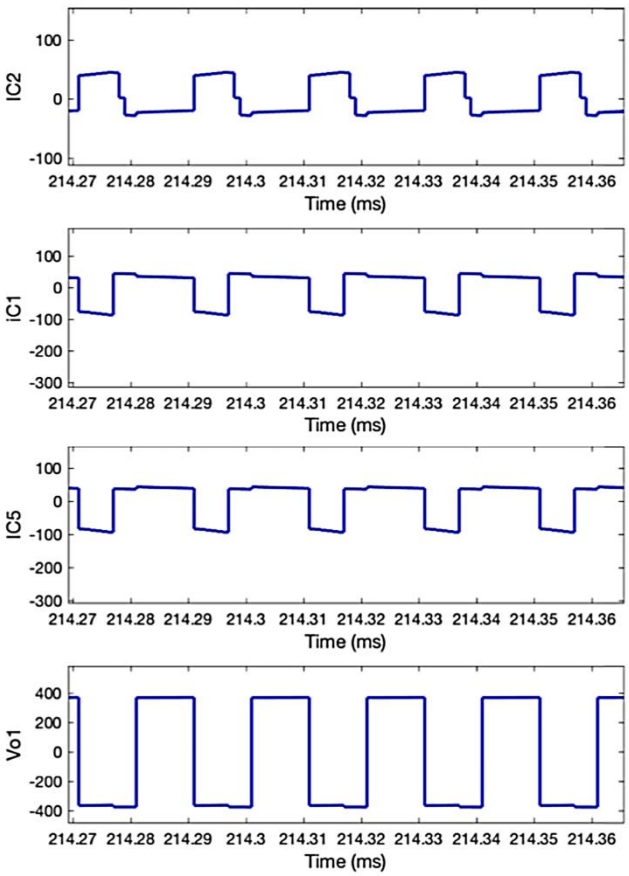

(b)

Fig. 8 Simulation results.

These eight figures depicted in Fig. 8show the driven signals of S1 and S2, currents of D, $L_1(L_2)$, C_1, and C_3, output voltages of V_{o1}

VI Simulation Parameters

Input voltage V_d Switching frequency fs	100V 50khz
Inductors L_1, L_2, & L_3	470µH
Capacitor C_1, C_2& C_3	330µF
Load	50Ω
Active Switch	Power MOSFET
Diodes	PN Junction

VII Conclusion

This paper developed a new topology framework of renewable power applications and power storage units bridging three-port converters. The distinctive topology is defined by a few numbers of elements and a distinctive impedance network structure. It can not only achieve distinct circumstances for the harvesting of renewable energy, but also boost the gain in output voltage with high power storage unit's stability. In order to understand This new topology and its benefits are provided with a thorough assessment. Then, small-signal model is Carried out for converters stable operation. Finally, comprehensive simulation checks are performed. The future scope of proposed model can be extended using voltage stabilizer which gives constant input to the system when the weather conditions changes. It can explore to hardware implementation for boost mode also and can be analyzed for various topologies as unidirectional converter.

References

[1] Zhang, G., Li, Z., Zhang, B., & Halang, W. A. (2018). "Power electronics converters: Past, present and future". *Renewable and Sustainable Energy Reviews*, *81(April)*, *2028–2044*.

[2] Yu, S., Chau, T. K., Fernando, T., Savkin, A. V., &Iu, H. H. C. (2017). "Novel Quasi-Decentralized SMC-Based Frequency and Voltage Stability Enhancement Strategies Using Valve Position Control and FACTS Device". *IEEE Access*, *5*, 946–955.

[3] Kerdphol, T., Rahman, F. S., Mitani, Y., Watanabe, M., & Kufeoglu, S. (2018) "Robust Virtual Inertia Control of an Islanded Microgrid Considering High Penetration of Renewable Energy". *IEEE Access*, *6*, 625–636.

[4] Talari, S., Shafie-khah, M., Osório, G. J., Aghaei, J., & Catalão, J. P. S. (2018). "Stochastic modelling of renewable energy sources from operators point-of-view: A survey". *Renewable and Sustainable Energy Reviews*, *81*(May), 1953–1965.

[5] Al Haj Hassan, H., Pelov, A., & Nuaymi, L. (2015). "Integrating cellular networks, smart grid, and renewable energy: Analysis, architecture, and challenges". *IEEE Access*, *3*, 2755–2770.

[6] Zhang, G., Wang, Z., Iu, H. H. C., Chen, S. Z., Ye, Y., Zhang, B., & Zhang, Y. (2018). "Unique Modular Structure of Multicell High-Boost Converters with Reduced Component Currents". *IEEE Transactions on Power Electronics*, *33*(9), 7795–7804.

[7] Zhu, H., Zhang, D., Zhang, B., & Zhou, Z. (2015). "A Nonisolated Three-Port DC-DC Converter and Three-Domain Control Method for PV-Battery Power Systems". *IEEE Transactions on Industrial Electronics*, *62*(8), 4937–4947.

[8] Morstyn, T., Savkin, A. V., Hredzak, B., & Agelidis, V. G. (2018). "Multi-agent sliding mode control for state of charge balancing between battery energy storage systems distributed in a DC Microgrid". *IEEE Transactions on Smart Grid*, *9*(5), 4735–4743.

[9] Mira, M. C., Zhang, Z., Knott, A., & Andersen, M. A. E. (2017). "Analysis, Design, Modeling, and Control of an Interleaved-Boost Full-Bridge Three-Port Converter for Hybrid Renewable Energy Systems". *IEEE Transactions on Power Electronics*, *32*(2).

[10] Al Busaidi, A. S., Kazem, H. A., Al-Badi, A. H., & Farooq Khan, M. (2016). "A review of optimum sizing of hybrid PV-Wind renewable energy systems in oman". *Renewable and Sustainable Energy Reviews*, *53*.

[11] Morstyn, T., Hredzak, B., & Agelidis, V. G. (2018). "Control Strategies for Microgrids with Distributed Energy Storage Systems: An Overview". *IEEE Transactions on Smart Grid*, *9*(4),

[12] N. Zhang, D. Sutanpo, K. M. Muttaqui, "A review of topologies of three port dc-dc converters for the integration of renewable energy and energy storage system". *Renewable. Sustain. Energy REV., vol. 56, pp. 388-401. Apr 2016.*

[13] Zhang, G., Zhang, B., Li, Z., Zhang, Y., & Chen, S. Z. (2017). "A Novel Single Input Dual Output Impedance Network Converter". *IEEE Journal of Emerging an d Selected Topics in Power Electronics*, *5*(3).

[14] Duarte, J. L., Hendrix, M., Simões, M. G., & Member, S. (2007). "Three-Port Bidirectional Converter for Hybrid Fuel Cell Systems", *IEEE Transactions on Power Electronics*, *22*(2), 480–487.

[15] Zhang, P., Chen, Y., & Kang, Y. (2017). "Nonisolated wide operation range three-port converters with variable structures". *IEEE Journal of Emerging and Selected Topics in Power Electronics*, *5*(2), 854–869.

[16] Hu, Y., Xiao, W., Cao, W., Ji, B., & Morrow, D. J. (2015). "Three-port DC-DC converter for stand-alone photovoltaic systems". *IEEE Transactions on Power Electronics*, *30*(6), 3068–3076.

[17] Duarte, J. L., Hendrix, M., Simões, M. G., & Member, S. (2007). "Three-Port Bidirectional Converter for Hybrid Fuel Cell Systems." *IEEE Transactions on Power Electronics, 22(2), 480–487.*

[18] Jang, M., Ciobotaru, M., & Agelidis, V. G. (2011). "Grid-connected fuel cell system based on a boost-inverter with a battery back-up unit". *8th International Conference on Power Electronics - ECCE Asia: Green World with Power Electronics, ICPE 2011-ECCE Asia, 1637–1644.*

[19] Piris-Botalla, L., Oggier, G. G., & García, G. O. (2017). "Extending the power transfer capability of a three-port DC–DC converter for hybrid energy storage systems". *IET Power Electronics, 10(13), 1687–1697.*

[20] Hu, Y., Xiao, W., Cao, W., Ji, B., & Morrow, D. J. (2015). "Three-port DC-DC converter for stand-alone photovoltaic systems". *IEEE Transactions on Power Electronics, 30(6), 3068–3076.*

[21] A. Gautam, A. K. Sharma, A. Pareek and R. Singh, "Analysis of Combined Z-Source Boost DC-DC Converter for Distributed Generation Systems," *2018 International Conference on Inventive Research in Computing Applications (ICIRCA), Coimbatore, 2018, pp. 1162-1167.*

Proceedings of the Fourth International Conference on Communication and Electronics Systems (ICCES 2019)
IEEE Conference Record # 45898; IEEE Xplore ISBN: 978-1-7281-1261-9

Direction of Arrival and Channel Estimation using Machine Learning for Multiple Input Multiple Output System

Sruthi Ravindran
P.G. Scholor, ECE Dept.
RIT (Govt. Engg. College), Kottayam

Dr. Renu Jose
A. P. , ECE Dept.
RIT (Govt. Engg. College), Kottayam

***Abstract*—The massive multiple input multiple output (MIMO) system is a prodigious method that could improvise a communication system's capacity with the aid of an increased number of antennas. The fundamental challenges of massive MIMO system are complicated channel modeling, high dimensional channel state information (CSI), and narrow radio frequency chains (RF chains), etc. For solving this problem we introduce deep neural network (DNN) framework for direction of arrival estimation (DOA estimation). Using the information obtained about DOA and gain that is complex, the channel is estimated and mean square error (MSE) performance is evaluated for both DOA and channel estimation.**

***Index Terms*—MIMO, CSI, RF, DNN, DOA, MSE**

I. Introduction

The increase of visualization network infrastructure and the necessity of efficient and sustainable utilization of energy are the key requirements of next generation communication systems. The highly increasing data traffic growth will be the greatest challenge for designing 5G communication networks. [1]. Massive MIMO (m-MIMO) systems can improve a communication system's capacity with the aid of an increased number of antennas [8]. The complex channel modeling, the high dimensional CSI and large number of accessing users, etc [7] are some of the practical challenges faced by m-MIMO. Without introducing efficient schemes, the performance of the system will degrade.

In recent years, various techniques were developed to enhance the capacity of m-mimo. In [4] a full space spatial spectrum sharing strategy is introduced by using two cognitive radio base station (CBS) at adjacent sides of a single cell. A 2-D spatial basis expansion model (2D-SBEM) is used to represent channel vectors, which helps in mitigating pilot contamination and training overhead problem. Then [10] provides several beam selection techniques for beam-space MIMO (B-MIMO) that helps in reducing radio-frequency (RF) complexity of millimeter wave transmitters. In previous researches, deep learning has been proved to be effective for Channel State Information (CSI) localization, channel equalization, and channel decoding. Network traffic control is an essential component for delivering a variety of services and experiences to users in a mobile-centric heterogeneous networks. [5] shows an effective method of deep learning neural networks to significantly improve heterogeneous network traffic control. [16] shows how a Bayesian framework is used in orthogonal frequency division multiplexing (OFDM) systems for joint channel estimation and sampling frequency offset.

This paper organization methodology is described below. Section II outlines the review of literature regarding the earlier researches on the topic. The massive MIMO and deep learning model used is described on section III. Simulation results are presented on section IV and the paper is concluded in section V.

II. Literature Review

The basic MIMO system, its design, architecture, advantages, disadvantages, future scope etc., are explained in [7]. The main advantage of MIMO system is increased data rate by many folds, without any extra bandwidth.

[14] describes how the channel estimation of a m-MIMO system can be done using 1-Bit Quantization. In this system, the Expectation-Maximization(EM) algorithm combined with a sparse recovery method yields better results. In a m-MIMO system a low rank channel estimation is done where the sparse properties of channel environment are exploited is reviewed in [9]. Based on the signal model in [6], for sparse channel estimation, a region of received signal free from interference is used. It yields an estimator which has low complexity and the received signals used on a small scale for estimation.

[8] analyses the performance of Up-Link (UL) and Down-Link (DL) in cellular networks using m-MIMO system. The total number of antennas required to attain maximum efficiency with minimum Mean Square Error (MSE) and Regularized Zero Forcing (RZF) are also derived. The performance analysis using factor analysis is given in [2].

A novel mm-wave frequency transmission scheme exploiting both the concepts of Beam-space MIMO communications and beam selection are discussed in [10]. It resulted in higher power efficiencies than a full system with significant reduction in RF complexity. [11] shows joint estimation of channels and carrier frequency offset in OFDM systems using a statistical framework. Main defect of a MIMO-OFDM system is time ambiguity with channel fading and phase noise. [3] introduces how joint Bayesian estimator and bounds estimated can be used to reduce these defects.

[15] describes the effect of missing sensors in estimating the DOA of the signal using Multiple signal classification (MUSIC) method. It was found that the missing sensors significantly degraded the accuracy of MUSIC. [12] performs a 2-D estimation of DOA using a less complex Unitary Estimation of Signal Parameters via Rotational In-variance Techniques algorithm. It was concluded that estimated accuracy depended on the array configuration and incident directions of the signal.

The channel characteristics of m-MIMO systems are very complicated, so the traditional methods are not capable of recording the real-time changes of channel condition. Because of sharp variations in channel characteristics, the DOA and channel performances are degrading.The CSI of a m-MIMO system can be auto-detected using a machine learning (ML) technique. In 2006 a new technique called deep learning, which can take care of big data and solve complex nonlinear problems effectively was proposed [1], [13].

III. System Description

The three stages of DOA and channel estimation using machine learning for MIMO system - massive MIMO system model, deep learning based estimation for DOA, and deep learning based channel estimation. Fig. 1 shows an up-link model for a massive mimo system, where the base station consists of M number of receiver antennas and a K number of user equipment(UE) where each has a single antenna is used and H is the channel matrix.

A. Model of the System

Here we consider a system model with M number of antennas arranged in a uniform linear array fashion in one base station and K number of UE. The assumption made here is that BS has zero information based on each path of the user. Now the up-link model of user K is shown below [17]

$$\mathbf{h}_K = \sum_{i=1}^{J} g_{K,i}\mathbf{a}_t(\theta_{K,i}) = \mathbf{A}_{t,K}\mathbf{g}_K, \tag{1}$$

where J is denoted as the number of resolvable path and $g_{K,i}$ is the complex gain. Physical DOA of i-th path can be represented as $\theta_{K,i}$ and $a_t(\theta_{K,i})$ is defined as the steering vector. The up-link channel matrix can be denoted as $H = [h_1, h_2, ..., h_k]$.

A precoding based on zero forcing is used here to reduce user to user interface [1], [17].

$$\mathbf{x} = Ps \tag{2}$$

where s is the source code and P is precoding.Then, the received signal is

$$\mathbf{Y} = H\mathbf{x} + N \tag{3}$$

where N is Additive White Gaussian Noise (AWGN).The channel gain and the information about DOA are key characteristics of channel modeling.

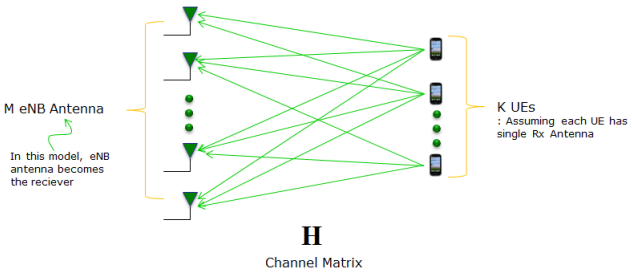

Fig. 1. Massive MIMO up-link model

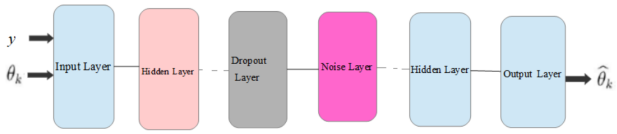

Fig. 2. Framework for DOA estimation based on deep learning

B. DOA Estimation Using Deep Learning

This section illustrates a framework of the massive MIMO system for DOA estimation based on deep learning. Deep learning neural network (DNN) through nonlinear operations and propagation aids for the high computational complexity of massive MIMO system [1].

DNN is the profound form of artificial neural network (ANN). Multiple hidden layers are present in DNN, and each hidden layer consists of a large number of neurons. In the output layer, the nonlinear function uses the weighted sum of all neurons. The sigmoid function and the another function known as ReLU function are the most commonly used nonlinear functions.

$$f_{\text{Sigmoid}}(q) = \frac{1}{1+e^{-q}} \tag{4}$$

$$f_{\text{ReLU}}(q) = \max(0, q) \tag{5}$$

where q is the argument of function.

A framework for DOA estimation based on deep learning is being shown in Fig. 2. There are two stages for the DNN one is for training the DNN i. e., offline learning scheme and the other is online deployment for testing. The so obtained received signal vector Y is obtained depending on a fixed channel matrix H is used as training samples. The received signal Y from all directions is collected based on different channels. The θ_k is generated randomly, which is used as a training set along with Y (i.e., training samples used in DNN). The next stage is online deployment where DOA is estimated and a specific channel model is obtained.

The mean square error for the estimation of DOA parameters can be calculated as

$$MSE = \frac{1}{n}\sum_{j=1}^{n}\left\|\theta_k - \widehat{\theta}_k\right\|^2 \tag{6}$$

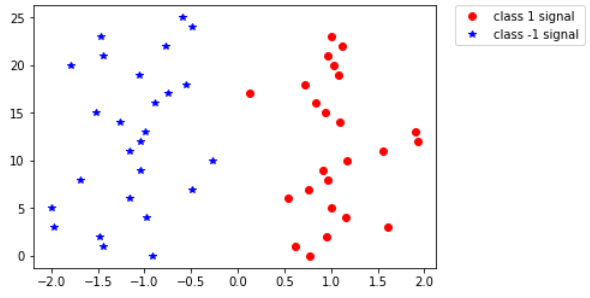

Fig. 3. BPSk in AWGN channel using simple perceptron

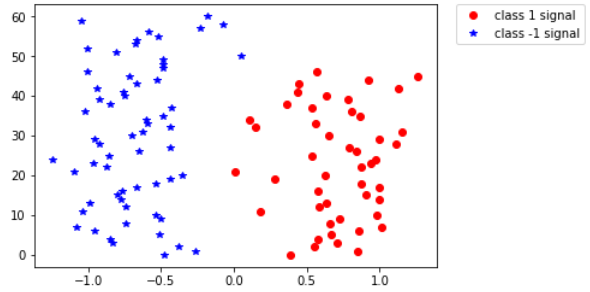

Fig. 4. QPSk in AWGN channel using simple perceptron

where n is the number of samples, and $\widehat{\theta}_k$ is the prediction. For obtaining estimated θ_k, a loss function which is calculated using MSE is as follows

$$L = \frac{1}{K}\sum_{k=1}^{K} MSE \tag{7}$$

The loss function that follows as a part of the DNN framework is calculated using the gradient decent algorithm.

C. Channel Estimation Based on Deep Learning

For obtaining the channel matrix characteristics, a deep learning method is introduced in this section while considering a massive MIMO system. Here, the co-variance of channel matrix having low rank is considered [9]. The channel matrix can be obtained by using DOA information from the previous section and the complex gain. Let us assume that, $\widehat{Y}$ is the output signal vector that is estimated. Loss function, l_1 can be expressed using the following equation:

$$l_1 = \frac{1}{n}\sum_{j=1}^{n}\left\|x_j - \widehat{Y}_j\right\|^2 \tag{8}$$

where x_j is the j-th transmitted signal. Our main aim is to minimize the gap or variation between output of the DNN and the signal that has been transmitted. The performance analysis of channel estimation based on deep learning can be evaluated by using MSE concept.

$$MSE = \frac{1}{Kn}\sum_{j=1}^{n}\sum_{k=1}^{K}\frac{\left\|h_{k,j} - \widehat{h}_{k,j}\right\|^2}{|h_{k,j}|^2} \tag{9}$$

IV. EXPERIMENTAL RESULTS

The performance of DOA and channel estimation is being analyzed in this section. The simulations have been done in Python 3. 6. Tensorflow is used to design and process DNN. A massive MIMO system was taken into consideration, where the base station consists of $M = 128$ antennas and $K = 128$ is the number of single antenna users. They are connected by $P = 5$ resolvable paths. DOA $\theta_{k,i}$ is randomly distributed in space $[-\frac{\pi}{2}, \frac{\pi}{2}]$, and the distance between antennas $d = \frac{\lambda}{2}$. The collected signals from all direction were used as training samples and the sampling interval is $0.01°$.

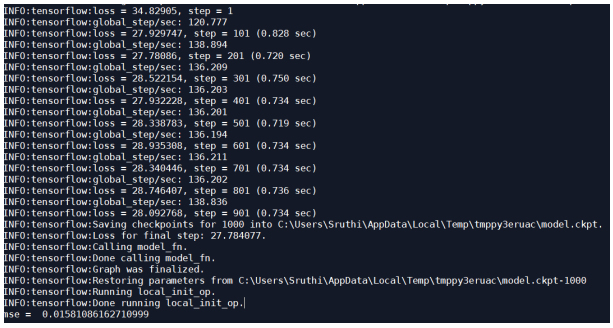

Fig. 5. MSE calculated for DOA estimation when $M = 1$ and $K = 10$ is used

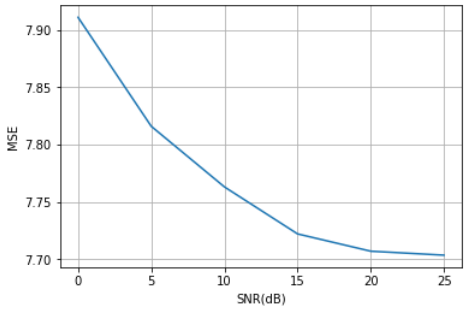

Fig. 6. Mean square error for estimation of DOA parameters when $M = 128$ and $K = 128$

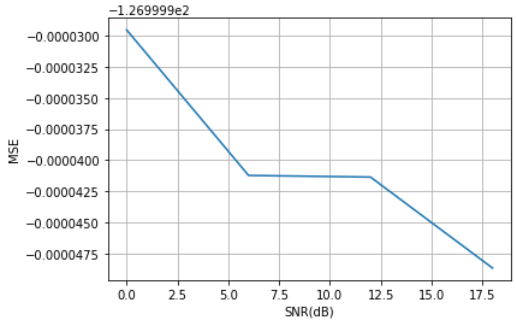

Fig. 7. Mean square error for estimation of channel parameters

In Fig. 3 and Fig. 4 a binary phase shift keying(BPSK) and a Quadrature Phase Shift Keying (QPSK) modulated signals passed through a AWGN channel is classified using a simple perceptron. The number of epochs taken is 1 for BPSK and 10 for QPSK when SNR is 4 and the BER obtained is 0. It is observed that as the SNR value is increased the signal is classified correctly and for small SNR values the classification is not perfect. Fig. 5 shows the mse calculated for DOA estimation. Here a single transmitter antenna is used, and the number of single antenna users $K = 10$. Number of iterations used is 1000 and it is observed that the MSE calculated is 0.0158.

The performance is illustrated in Fig. 6 by plotting the MSE for the estimation of DOA parameters against SNR using the DL technique where $M = 128$, $K = 128$ and here we consider length as $L = 10$ for the training sequence. It could be noticed that MSE value for the estimation of DOA parameters is decreasing gradually when SNR value is increased.

Again, Fig. 7 illustrates the MSE for estimation of channel parameters against SNR using DL method. The number of iterations carried out is 20, the learning rate is set as 0.01 and the batch size taken is 5. It is observed that the MSE first reduces steadily and then it remains constant upto 12dB and then it reduces steadily as the SNR value increases. That means Fig. 7 yields a poor BER rate. The performance could be improved by increasing the count of iterations, batch size and increasing number of training and testing samples. In this simulation the training set comprises 100 examples and for testing we use 20 samples.

V. CONCLUSION

The massive MIMO system is implemented using a deep learning scheme in this paper, where additional antennas are used at the base station and DNN is integrated into single antenna users. At first a massive MIMO system model is constructed and then a DNN is developed, in which many hidden layers are included to increase the ability of representation. This novel DNN is used for DOA estimation and the information thus obtained along with the complex gain information is used for channel estimation. The MSE performance against SNR is obtained for DOA and channel estimation.

In the future, the deep learning model can be further developed to reduce the number of required pilot DOA. Hence, the computational complexity in massive MIMO channel estimation will decrease.

REFERENCES

[1] H. Huang, J. Yang, H. Huang, Y. Song and, G. Gui, "Deep Learning for Super-Resolution Channel Estimation and DOA Estimation based Massive MIMO System," *IEEE Trans. Veh. Technol.*, VOL. 3, NO. 1, MAR. 2018.

[2] X. Wei, W. Peng, D. Chen, R. Schober, and T. Jiang, "Uplink Channel Estimation in Massive MIMO Systems Using Factor Analysis," *IEEE*, 2018.

[3] R. Jose and K. V. S. Hari,"Bounds and joint estimators for channel, phase noise, and timing error in communication systems using statistical framework," *Elsevier publication,* vol. 72, pp. 431-442, Nov. 2018.

[4] H. Xie, B. Wang, F. Gao, and S. Jin "A Full-Space Spectrum-Sharing Strategy for Massive MIMO Cognitive Radio Systems", *IEEE J. Sel. Areas Commun.*, vol. 34, no. 10, pp. 2537-2549, Oct. 2016.

[5] N. Kato, Z. M. Fadlullah, B. Mao, F. Tang, O. Akashi, T. Inoue, and K. Mizutani," The Deep Learning Vision for Heterogeneous Network Traffic Control: Proposal, Challenges, and Future Perspective", *IEEE Wireless Commun.*, Vol. 24, no. 1, pp. 154-160, Feb. 2018.

[6] R. Jose, G. Pavithran and Aswathi. C," Sparse channel estimation in OFDM systems using compressed sensing techniques in a Bayesian framework,"*Elsevier publication,* vol. 61, pp. 173-183, Jul. 2017.

[7] P. Vardhan, M. Gupta, A.Kumar"Massive-MIMO- Past, Present and Future: A Review," *Indian Journal of Science and Technology (ISSN)*, vol. 9, no. 48, Dec. 2016.

[8] J. Hoydis, S. ten Brink and M. Debbah,,"Massive MIMO in the UL/DL of Cellular Networks: How Many Antennas Do We Need?," *IEEE J. Sel. Areas Commun.,* vol. 31, no. 2, Feb. 2013.

[9] H. Xie, F. Gao, and S. Jin, "An Overview of Low-Rank Channel Estimation for Massive MIMO Systems," *IEEE Access*, vol. 4, pp. 7313-7321, 2016.

[10] P. V. Amadori and C. Masouros," Low RF-complexity millimeter-wave beamspace-MIMO systems by beam selections," *IEEE Trans. Commun.,* vol. 63, no. 6, pp. 2212-2223, Jun. 2015.

[11] R. Jose," Estimation of Channel and Carrier Frequency Offset in OFDM Systems using joint statistical framework," *Elsevier publication,* vol. 25, pp. 139-147, Dec. 2017.

[12] T. Wang, B. Ai, R. He, AND Z. Zhong,"Two-Dimension Direction-of-Arrival Estimation for Massive MIMO Systems," *IEEE Access,* Nov 2015.

[13] Hinton, Geoffrey E., S. Osindero, and Y. W. The, "A Fast Learning Algorithm for Deep Belief Nets," *Neural Computation*, VOL. 18, 2006

[14] C. Stockle, J. Munir, A.Mezghani and J. A. Nossek," Channel Estimation in Massive MIMO Systems Using 1-Bit Quantization", *IEEE*, 2016.

[15] L. Gupta, and R. P. Singh,"Array Signal Processing: DOA Estimation for Missing Sensors," *IEEE,* 2010.

[16] R. Jose and K. V. S. Hari ," Joint statistical framework for the estimtion of channel and SFO in OFDM systems ," *IET Signal Process,* vol. 11, pp. 780-787, Sep. 2017.

[17] D. Tse, and P. Viswanath," Fundamentals of Wireless Communication," Cambridge University Press, 2004.

Proceedings of the Fourth International Conference on Communication and Electronics Systems (ICCES 2019)
IEEE Conference Record # 45898; IEEE Xplore ISBN: 978-1-7281-1261-9

FPGA Implementation of 8-bit SSA Multiplier for designing OFDM Transceiver

Mallapareddi Sagar and Ganapathi Hegde
Department Electronics and Communication Engineering
Amrita School of Engineering, Bengaluru
Amrita Vishwa Vidyapeetham
India

***Abstract* —— In recent technology of digital signal processing applications, we have number of modulation and demodulation techniques. In this domain multiplexing technique is having greatest importance as it has a transmission and reception part with secure systems for communication. Thus orthogonal frequency division multiplexing (OFDM) is superior to other multiplexing techniques, which has multiple carriers with very much robust frequency selective distorted channels. OFDM will have a number of modules such as serial to parallel converter, modulator, IFFT, FFT, demodulator and so on. The Proposed work will concentrate on arithmetic operations in OFDM with re-modified technique using large integer values such as addition, and multiplications. This large integer based arithmetic operation technique were designed using Schönhage–Strassen algorithm (SSA). Thus the proposed method will focus on this SSA algorithm based arithmetic operations with Number Theoretic Transform (NTT) and Inverse Number Theoretic transform (INTT) method. Proposed method of OFDM will replace FFT-IFFT to NTT-INTT method and this application is developed in Verilog HDL and synthesized in Xilinx vivado 15.4. It proved better results in terms of area and delay when compared with conventional design.**

Keywords—SSA,NTT,INTT,FFT,IFFT,Orthogonal frequency division multiplexing(OFDM).

I. INTRODUCTION

In the digital communication technique multi-carrier transceivers is increasing in recent digital world. In this type of communication high speed and secure communication is required to transfer and receive the message [1]. The telecommunication system have multiple signals to disturb a communication bandwidth in series of over-lapping and non-over-lapping bands, thus multiplexing based communication is required to reduce this disturbance which ensures data privacy on un-trusted communications [2]. Thus a statistical multiplexing of variable bandwidth communications is introduced, in this area orthogonal frequency division multiplexing (OFDM) is a high priority one, to transfer and receive the data in high secure communication with multi carrier bandwidth, and it has a capability to divide higher data rate stream into number of lower data rate stream over multiplexed orthogonal subcarriers [3]. OFDM contains QAM or QPSK modulator/demodulator (depending on spectral frequency), FFT/IFFT module, serial to parallel/parallel to serial converter.

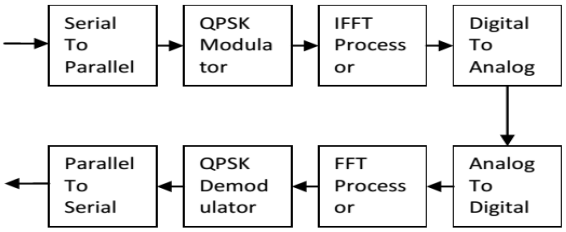

Fig. 1. Basic design of OFDM Blocks.

In the implementation of OFDM technique, it has a lot of arithmetic operations such as additions, subtractions, multiplications and divisions. For more secure communications system will requires a arithmetic operations for data privacy on un-trusted servers. Thus proposed area of arithmetic operations will have efficient schemes to handle large integer multiplications on Schönhage–Strassen algorithm (SSA) [4], [5]. This algorithm proved better results in asymptotic complexity of million bit multiplications in number theoretic transforms (NTT) [6], compared to existing multiplications method of Karatsuba algorithm [7]. This Number theoretic transform (NTT) method is compared to Fast Fourier Transform (FFT) to recognize as viable solution for occupying less area in larger size of multiplications with traditional and different set of twiddle factors. Thus, a NTT/INTT method will have a capability to replace FFT/IFFT in OFDM technique with same modulation and demodulation technique [8]. Following manner the remaining portion of the paper is configured. Section II reviews the SSA algorithm with using NTT and INTT method. Section III describes the proposed method OFDM with INTT/NTT Integration with QPSK Modulation and Demodulation. Section IV gives the detailed results and experimental implementations. Finally Section V gives the conclusion of this paper.

II. RELATED WORK

The SSA Algorithm is best one for multiplying operands which has maximum word length close to few million bits [9]. Traditional multiplication methods, Karatsuba-Ofman method, Toom [10] -cook [11] method is not going to work as the word length increases. Thus, this SSA algorithm of large integer multiplications [12] achieved through NTT/INTT method, which is described in Algorithm 1.

Algorithm 1 : Schönhage – Strassen algorithm

// Inputs :P (multiplicand, u bits), Q(multiplier, u bits), B(base=2^b)
// Output : Z=P x Q
{

1. Initialization: Decompose P and Q, respectively, into a sequence of digit p_n and q_n, $0 \le n < M$, using base B. Then assign $p_n=0$ and $q_n=0$ by zero padding for $M \le n < 2M$.
2. $P_k = NTT(p_n)$, $Y_k = NTT(q_n)$;
3. $Z_k = P_k \otimes Q_k$; // point-wise multiplication
4. $Z_k = INTT(Z_k)$;
5. carry = 0;
6. for i =0 to 2M-1 { // resolving carries computation
7. sum = z_i + carry;
8. sb_i= sum mod B; carry = |sum/B|;
9. }
10. return $Z= \sum^{2M-1} sb_i \times 2^{ib}$;
11. }

Algorithm 1 describes complexity of two integer multiplication of X and Y and output Z with respect to 2^b. Once initialization of decomposed input bits X and Y into the sequence of digit X_n and Y_n with respect to modulo M. This inputs will convert it to X_k and Y_k as per NTT and INTT method of Frequency to time conversion and time to frequency conversion, the output data will come from point wise multiplications, and finally resolving this carries computations by using modulo 2M-1, and return the output value in Z .

III. PROPOSED METHOD OF OFDM WITH NTT/INTT

In this Proposed method of orthogonal frequency division multiplexing (OFDM) [13] technique which carries a number of frequency bands, in a single band of subcarrier, which carries a user information in differentiating form of various spread spectrum technique such as FDM, OFDM, COFDM, VOFDM, WOFDM, and so on. This OFDM technique will has a multiple access and multiplexing method of user data streams onto downlink and uplink in sub-channels.

A. OFDM Transmitter

In this OFDM Modulation Technique started from Serial to parallel converter, this converter will convert the user data of multi-bit into single bit, then the second step needs some modulation and demodulation technique, here this design will have QAM-QPSK 4 Quadrant Modulation and Demodulation will integrated, The output of QPSK data will give to NTT-INTT module as per real and imaginary conversion through fading block to added error signal, then output of INTT module which gives a modulated data is given to DAC module to transmit the modulation signal. In this Fig.2 block diagram will describe this flow of OFDM modulation.

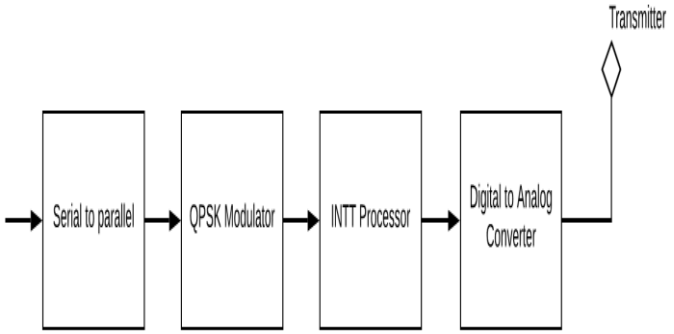

Fig. 2. Block diagram of basic baseband OFDM transmitter with using INTT.

In this QPSK modulation is a variation method of BPSK modulation, it will have a Double side band suppressed carrier modulation scheme, here it will describe in 4 Quadrant with using quadrant phase angle method. Output of serial to parallel conversion block will alienated into two signal such as SIN and COS wave, it will multiplied with encode TX module with respect to carrier Oscillator, and finally added with this two output of SIN and COS, these modulation signal will be taken from here, Fig.3 will show this flow of QPSK modulation.

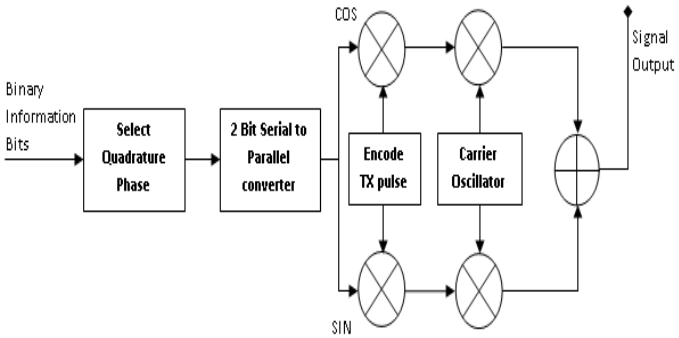

Fig. 3. QPSK Modulation.

B. OFDM Receiver

In this OFDM Demodulation[14] Technique ,it receives the input from transmitter and it is given to analog to digital converter, this digital data will process in NTT block with same in the method of IFFT its regarding frequency to time, this output data will give to QPSK demodulation to split and identified the quadrant to take a digital values, these digital n-bit value will give to parallel to serial converter, and these final data will checked in Bit Error Rate (BER), Fig.4 will describe a OFDM Demodulation.

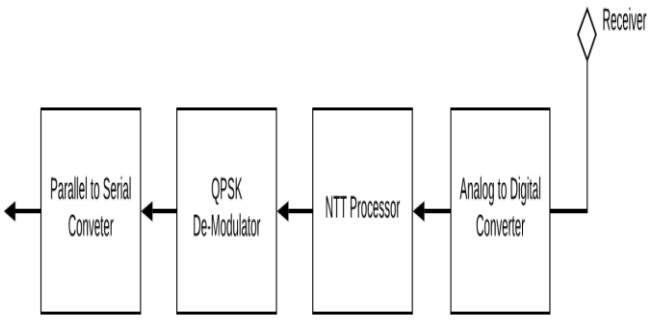

Fig. 4. Block diagram of basic baseband OFDM receiver with using NTT.

In this block of Fig.4 will have a QPSK demodulation after the NTT Processor with frequency to time conversions, in this QPSK demodulator will determine the phase changes from the modulation of SIN and COS, and it will identified four possible states such as 0, π, +π/2, -π/2. Fig.5 will describe this quadrant phase shifting method in π/4.

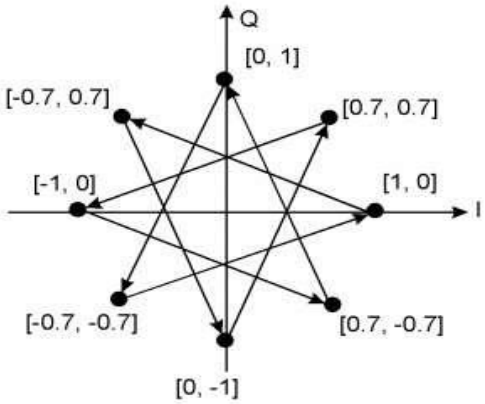

Fig. 5. π/4 shifter QPSK Constellation.

As per this Quadrant phase shifting QPSK demodulation will consider and recover the original input information's with help of Carrier recovery module, low pass filter, symbol timing recovery, decision circuits, multiplexer, Fig.6 will describe this in details, how this demodulation will happen in QPSK. As shown in Fig.6, the input signal of modulation will received to BPF (Band Pass Filter), it will reduce the noise in upper and lower range of input signal, and the signal will pass through carrier recover circuit, such as the numerical control oscillator will take to correct the error signal and generate the high frequency noise using COS and SIN multiplier, after multiplier the output signal will give to low pass filter (LPF), and we get the noise reduction output, it will give as a input of decision circuit, the decision circuit will find the range of frequency changes as per the modulation and generate the differential signal, those differential output will multiplexed and taken as a output in recovered signal.

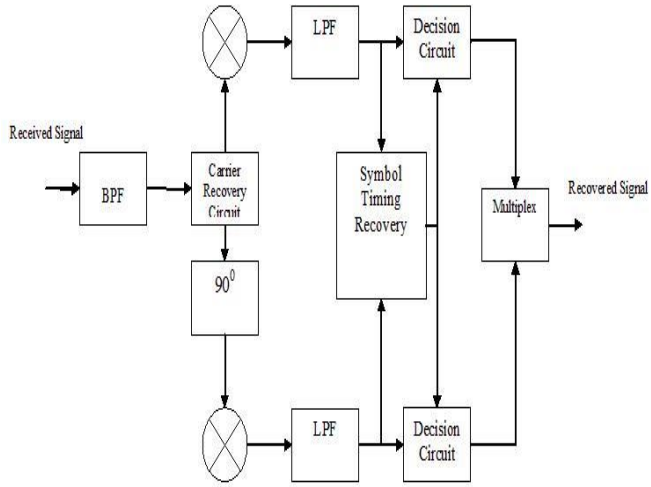

Fig. 6. Block diagram of QPSK Demodulator.

IV. RESULTS AND EXPERIMENTAL IMPLEMENTATION

Implementation of this OFDM transmitter and receiver using NTT-INTT module and QPSK 4-Qudrant modulation is done separately and tested on FPGA, and then both the system were integrated to form single system. Here we have given a input data in a .hex file, its having some hexadecimal data, it will readout from file reading code and given into QPSK8_NTT_MOD at 8-bit with including carrier signal generation from voltage control oscillator, this file reading method and carrier signal generation given in test bench of this code.

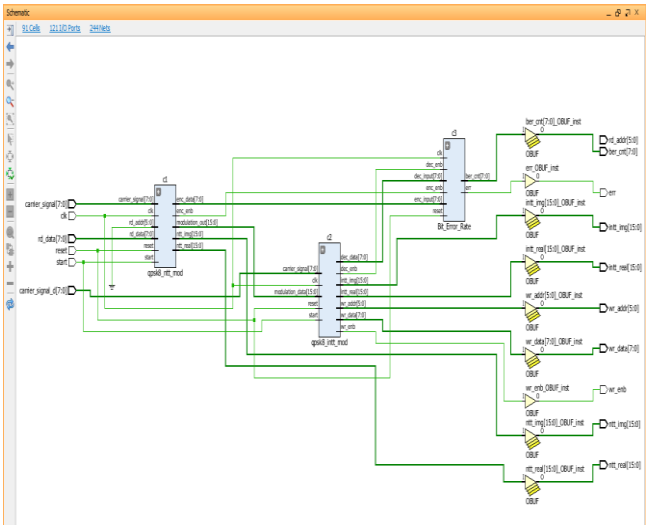

Fig. 7. OFDM Transmitter and Receiver Top module.

The top module of OFDM transmitter and Receiver as shown in the Fig.7 it contains QPSK8_NTT_MOD, QPSK8_INTT_MOD and BER Testing.

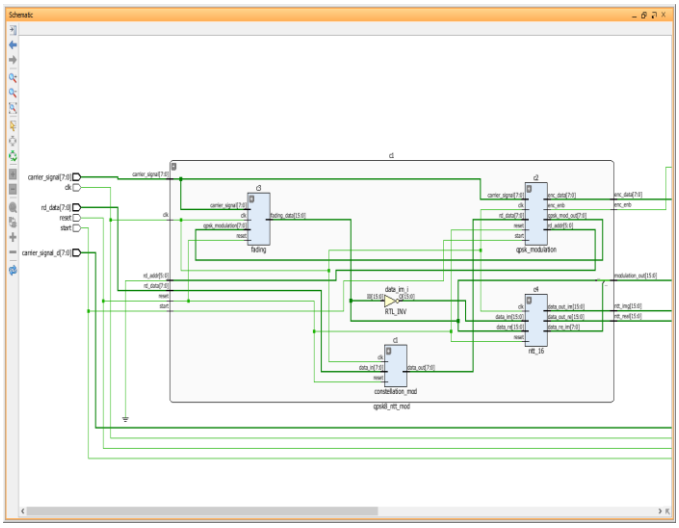

Fig. 8. OFDM Modulation.

As shown in Fig.8 the QPSK8_INTT_MOD block will contain constellation modulation, QPSK modulation, NTT_16 point and Fading code for adding the errors. Fig.9 shows QPSK8_NTT_MOD block will contain INTT_16 point, QPSK Demodulation, Constellation Demodulation, this modulation and demodulation code will give a data to Bit Error Rate code, this bit error rate will receive this data, and sampled as per the demodulation time, then it will compare both modulation and demodulation data and given the error output for testing.

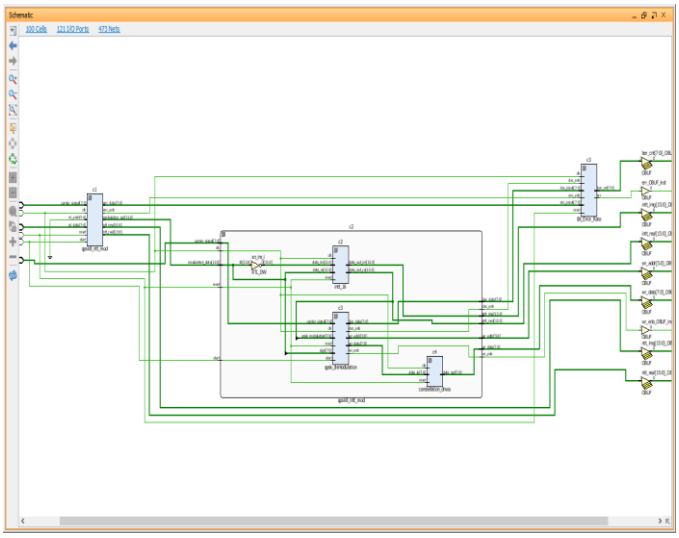

Fig.9. OFDM Demodulation.

This system is designed completely on Verilog HDL and Synthesized on Xilinx vivado 15.4.An extended work of SSA multiplication is done separately and the simulation result including the synthesized diagram of SSA multiplier is shown in Fig.10 and Fig.11 respectively. In SSA multiplier output as shown in the Fig.10 we have taken two numbers a=98 and b=2 and the multiplied output is 73mod123.

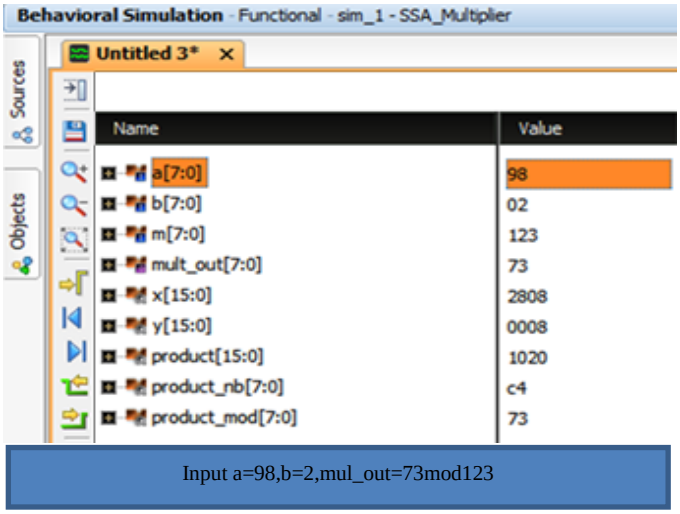

Fig. 10. SSA MULTIPLIER simulation results.

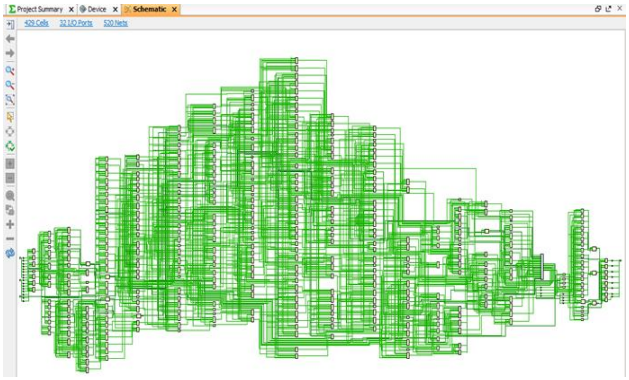

Fig. 11. SSA MULTIPLIER synthesized design.

Table I. Area and Delay Comparison

Parameters	Number of slices	Number of LUTs	Delay(ns)
16 Point NTT	969	1636	25.847
16 Point INTT	907	937	24.503
SSA MULTIPLIER	2107	1301	63.9211
Proposed OFDM system	2557	4717	77.268

Table II. Area and Delay Comparison

Parameters	Number of slices	Number of LUTs	Delay(ns)
16 Point FFT	1168	2304	30.687
16 Point NTT	969	1636	25.847

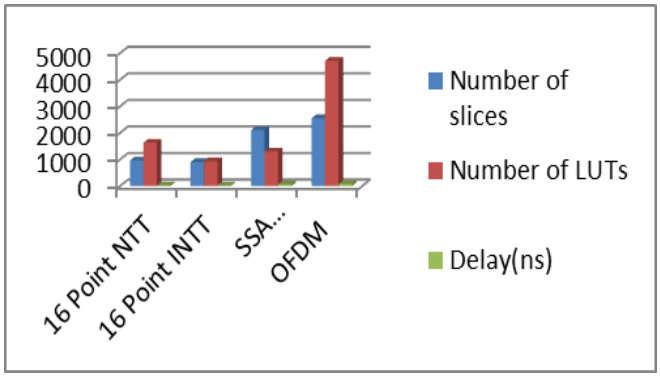

Fig. 12(a). Area and Delay Comparision.

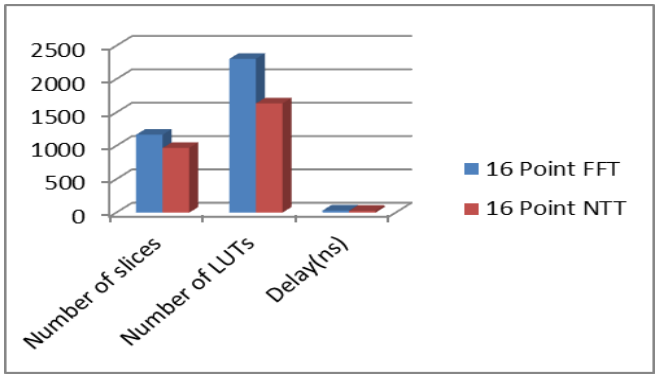

Fig. 12(b). Area and Delay Comparision.

In the Table I the delay and area comparison of entire proposed OFDM system is given. Table II clearly shows that NTT consumes 29% less LUTs and 15.77% less path delay as compared to FFT [15]. The bar graph shown in the Fig.12 (a) and Fig.12 (b) for the Table I and Table II respectively. This certainly shows that the overall OFDM area and delay can be reduced using the proposed method and also provides more computational features.

V. CONCLUSION AND FUTURE SCOPE

In this research work, we explored feasible solution of OFDM modulation and demodulation technique with low complexity SSA based multiplication of large integer focusing on FPGA implementation . We have designed and proved the performance of QPSK 4 Quadrant modulation and demodulation technique with NTT-INTT modulation and demodulation in OFDM using SSA algorithm. Finally proposed method shows that NTT consumes 29% less LUT's and 15.77% less path delay as compared to conventional method of FFT.

Future research may include more optimization of design using advanced algorithms to reduce overall power and delay. Thus this OFDM methodology is suitable for all digital signal processing applications for transmission and reception of large data with less bit loss in high speed communications.

REFERENCES

[1] K. Vrinda, Dr. N.S. Murty, and Dr. Dhanesh G. Kurup, "Performance of Vector Fitting Algorithm Applied to Bandpass and Baseband Systems," Circuits, Systems, and Signal Processing, pp. 1-18, 2018.
[2] R. Bhaskar, Hegde, G., and Vaya, P. R., "An efficient hardware model for RSA encryption system using Vedic mathematics," in Procedia Engineering, Coimbatore, 2012, vol. 30, pp. 124-128.
[3] Chu Yu ; Mao-Hsu Yen ; Pao-Ann Hsiung ; Sao-Jie Chen , "A low-power 64-point pipeline FFT/IFFT processor for OFDM applications," IEEE Transactions on Consumer Electronics.
[4] Jheng-Hao Ye, Ming-Der Shieh, Member IEEE, "Low Complexity VLSI Design of Large Integer Multipliers for Fully Homomorphic Encryption," IEEE, 2018.
[5] A. Schönhage and V. Strassen, "Schnelle multiplication großer Zahlen," IEEE Transactions on Consumer Electronics A Computing, vol. 7, nos. 3–4, pp. 281–292, 1971.
[6] Xiang Feng, Shuguo Li, "Design of an Area Efficient Million Bit Integer Multiplier Using Double Modulus NTT," 2017, IEEE.
[7] A. Karatsuba and Y. Ofman, "Multiplication of multi digit numbers on automata," Soviet Phys. Doklady, vol. 7, no. 7, pp. 595–596, Jan. 1963.
[8] A. Cortes ; I. Velez ; J.F. Sevillano ; A. Irizar , "An approach to simplify the design of IFFT/FFT cores for OFDM systems ".
[9] W. Wang, X. Huang, N. Emmart, and C. Weems, "VLSI design of a large-number multiplier for fully homomorphic encryption," IEEE Trans. Very Large Scale Integr. (VLSI) Syst., vol. 22, no. 9, pp. 1879–1887, Sep. 2014.
[10] A. L. Toom, "The complexity of a scheme of functional elements realizing the multiplication of integers," Soviet Math. Doklady, vol. 3, no. 4, pp. 714–716, 1963.
[11] S. A. Cook, "On the minimum computation time of functions," Ph.D. dissertation, Dept. Math., Harvard Univ., Cambridge, MA, USA, 1966.
[12] C. Gentry, "Fully homomorphic encryption using ideal lattices," in Proc. 41st Annu. ACM Symp. Theory Comput., 2009, pp. 169–178.
[13] Anshul C.Gurve1, S.S.Wasnik2, A.D.Bijwe3 Ashwini S. Yerlekar4, Nilesh Chide, "Study of OFDM Variants and Implementation of OFDM Using fft / ifft", International Journal of Advanced Research in Computer and Communication Engineering,2014.
[14] Ananta S. Chavan and Sidhant S. Kulkarni ,"Effect of Number of Subcarriers on Implementation of OFDM Transceiver on FPGA ," International Journal of Innovative Research in Electronics and Communications (IJIREC),2015.
[15] Surabhi Kudeshia and Dr.(Mrs.) Anjali Ashish Potnis "Novel Design of FFT using High Radix Butterfly of Complex Valued Data," International Conference on Computer Communication and Informatics (ICCCI-2017).

Proceedings of the Fourth International Conference on Communication and Electronics Systems (ICCES 2019)
IEEE Conference Record # 45898; IEEE Xplore ISBN: 978-1-7281-1261-9

Location Module for 5G Base Station to Support Mobility Management of Drones

Nithin P S, Sai Shibu N B, Sree Lakshmi S, Seshaiah Ponnekanti
Amrita Center for Wireless Networks & Applications (AmritaWNA),
Amrita School of Engineering, Amritapuri
Amrita Vishwa Vidyapeetham
India
Email: psnithin93@gmail.com, saishibunb@am.amrita.edu, sslekshmi@am.amrita.edu,
seshaiah.ponnekanti@gmail.com

***Abstract*—In the last few years, information and communication technology market has been witnessing rapid growth. In future, 5G Service Based Architecture (SBA) with a multitude of key enabling technologies are expected to provide a wide range of services such as rapid emergency response, virtual hospital kiosks, wearable devices, autonomous vehicles, etc. With the proliferation of tiny IoT devices and drones, it is envisioned that the network densification will take place in future 5G networks. This paper provides an overview of location module co-located at the 5G gNodeB (gNB-Base Station) to deliver location information in the dense 5G network. The location module provides opportunities to deliver effective location information from the network side together with popular navigation tools and applications like Google maps. The paper also addresses the design of an example use case and developed proof of concept of Platform as a Service (PaaS) for drone operations in 5G.**

***Index Terms*—5G, 5G SBA, DoA estimation, API, Platform, Drone Services.**

I. Introduction

Nowadays location-based services and technologies are rapidly increasing but applications such as autonomous cars, telemedicine and emergency services need precise location services [1]. Currently, these location data are obtained from the Global Positioning System (GPS) and then provided to the Over-The-Top (OTT) Applications. This information is used to provide several location-based services including navigation and route suggestions etc. Service Providers (SPs) or Network Operators use the information from the GPS through the network signaling procedures to cater to the needs of emergency calls [1].

In future, the 5th generation communication technology (5G) will transformation in to a new set of technology and service capabilities for a wide variety of vertical industries such as automotive, healthcare etc. 5G will become unified network to provide new applications and services across different vertical sectors. In recent years, there has been significant attention gained in developing a vertical for smart cities. In urban scenario, sources are denser, tightly coupled and always connected to the internet. Ubiquitous coverage in an ultra-dense environment is provided with the help of the densely deployed small cells and macro cells [2]. Fig. 1 explains the current location techniques and the requirements for delivering location information in 5G networks.

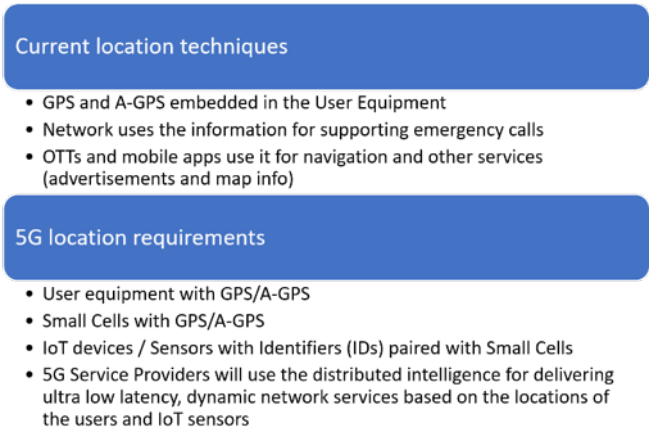

Fig. 1. Existing Location Techniques and 5G Location Requirements

From the service point of view, the 5G Core Network (CN) is more important because it provides functions such as mobility, authentication, security and session management. Now that the 3rd Generation Partnership Project (3GPP) standardized the core network to SBA [3]. The SBA enables globally connected services and platforms to meet the demands of different vertical industries.

The paper is organized as follows: Section II of the paper explains 5G key enablers and background on the location module. Section III explains about the utilization of API in 5G SBA. Section IV explains the architecture of the location module in the network. Finally, 5G SBA Platform as a Service (PaaS) use case has been outlined followed by summary and section V cover the paper conclusions.

II. 5G Enablers and Background on the Location Module

The key enablers in 5G are Network Function Virtualization (NFV), Mobile Edge Computing (MEC), Software Defined Networking (SDN) and Application Programming Interface (APIs) [4]. Fig. 2 shows the illustrations of key enablers in 5G.

- **NFV** mainly transform the functional modules of a network into network function software and instantiates at the right time when needed.

- **MEC** is introduced in the 5G core network to improve the service environment and the user experience by virtualized server platforms for reducing the network traffic and signal load in the core network [4].
- **SDN** is a foundation layer that enables SPs to move workloads in a virtualized network. SDN provides agility, flexibility and availability thereby offering the ability to spin-up new services dynamically.
- **APIs** plays a vital role in the delivery of services to the 3rd party with the help of Network Exposure Function (NEF).

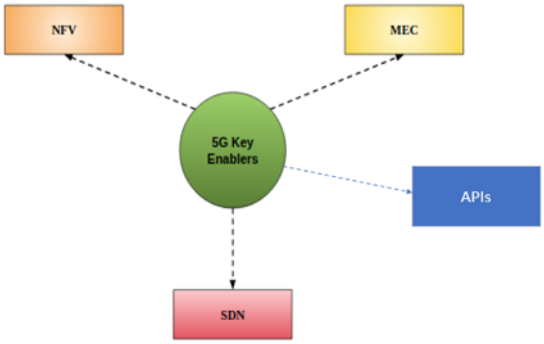

Fig. 2. Key enablers in 5G

A. Background to the Location Technologies

OTT provides applications to offer services such as navigation, messaging, teleconferencing, video and music streaming, etc. OTTs are the stakeholders in SP network. OTTs need user location to offer better services like video recommendation, route suggestions, automated call and video quality improvement. These OTT use GPS modules available on the devices for location information. GPS based locations are accurate only up to 8m [5].

Fig. 3 explains how the OTT collects the location data from devices using the GPS module. Let M1 and M2 be two mobile handsets with GPS module. Consider that the user of M1 device is searching for a video in the OTT application. The OTT application will request the built in GPS module for the location and time data. The module receives the beacon signal from at least four satellites and these beacon signals are used to extract the location coordinates and current time [6]. The location coordinate and time data will be given to the OTT server. The OTT server has algorithm to sort the video as per the user request, location, date of upload and the users interest from his recently watched videos. The user gets to see video that is more relevant to him [7].

OTT can provide the service through the network but they cannot assure any quality in the services. The quality in the services is handled by the SP. It depends on the signal quality, bandwidth availability, etc. 5G technology will utilize Internet of Things (IoT) devices deployed for different applications such as Smart City air quality monitoring, Smart Healthcare wearables, Telemedicine Kiosks, Emergency Response services, Surveillance Cameras, Traffic Signals, Point

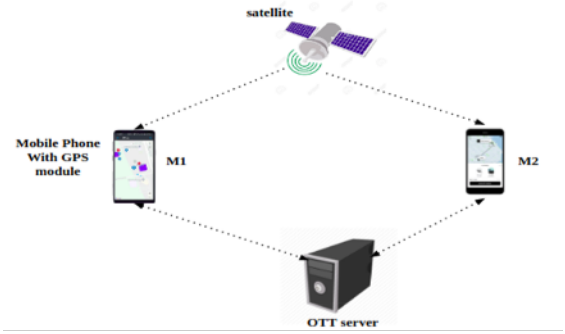

Fig. 3. GPS based location services used by OTTs

of Sale machines. Locating these devices using GPS is near impossible activity. The tiny IoT sensors may not have the hardware capability to host GPS receiver. To overcome these challenges, distributed location management is required from the 5G network side. The paper proposes a location module to improve the location services delivered by the OTT. The Location module is co-located on the 5G Base Station servers (gNB) and Sensor Gateways.

III. Utilization of APIs in 5G SBA

Currently, 3rd Party applications communicate with the network server using the APIs. As shown in Fig. 4, in the 5G network, APIs are expected to be used widely at the remote cloud and edge of the network. The APIs are central in the overall service delivery and bridge the developers to the network capability and provide secure access to the SP database [8].

Representational State Transfer (REST) and Simple Object

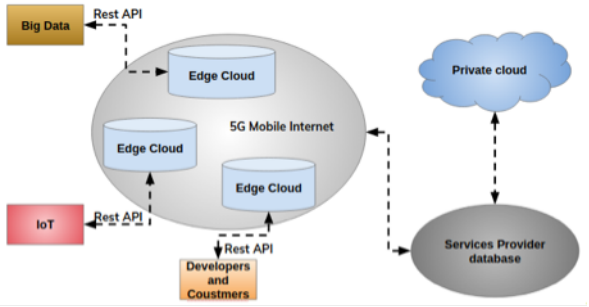

Fig. 4. Role of APIs in 5G SBA

Access Protocol (SOAP) are the most commonly used API services. REST API will provide functionality to handle and deliver the data. The client application can create, obtain, list, or modify the server data by using the HTML protocols such as GET, PUT, POST and DELETE. XML and JSON are the most commonly used data format in APIs. XML is a markup language that is capable to display text data. JSON is more human-readable format which deliver the data more in the form of data structure in the modern programming language [8]. In 5G, the APIs will play a vital role in the service delivery.

IV. Architecture for Location Module in 5G SBA

Location module supports the functionality of localization engine which can deliver more accurate location compared to the other localization techniques that uses GPS. The location module co-operates with a direction finding and beamforming module within the 5G gNB. The super-resolution techniques provide the directions of the users as well as the small base stations. It is also anticipated that the small cells within the network provide their own locations using embedded GPS module. The IoT devices within the proximity of small cells will be coupled with the sensor identifiers (IDs). The overall locations are collected by the network and converted into detailed location map which will include IoT devices and sensors deployed in the network. All information are stored in SP database to generate intelligent maps. Fig. 5 gives an overview of location engine architecture in 5G SBA. Location engine is enabled by the following:

- **GPS Info:** Collect location information with GPS and provide to the OTTs.
- **Radio Resource Management (RRM):** RRM coupled with network intelligence will map sensor IDs to small cell locations.
- **API and NEF:** APIs interacts through NEF to securely provide location information to 3rd party applications.
- **Beamforming / Direction Finding:** Helps to estimate angles of arrival of different sources in the network.

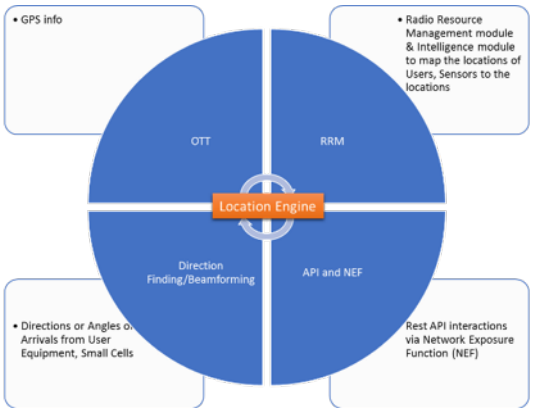

Fig. 5. Location Module Architecture in 5G SBA

The software architecture of the location module for 5G SBA in described in Fig. 6. The software design is done using the Python programming language. It consists of 3 major parts such as Location data storage , Location generator, REST API, Visualization Dashboard.

- **Location Generator:** In the location generator the angels and distances of user equipment estimated from the small cell will be converted to the latitude and longitude of the of the user equipment .
- **Location Data Storage:** The coordinates of the devices as obtained from the location generator, device id, base station to which the device is connected is stored to the database at MEC.

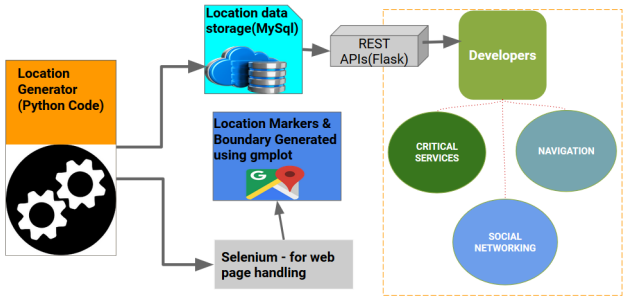

Fig. 6. Software architecture of the location module

- **Visualization Dashboard:** Visualization dashboard at the SP side will help the operator to track the users or devices in real time.
- **REST API Services:** The REST API provides the location data from the database to the 3rd party applications. 3rd party application developers use the APIs to improve the location accuracy in their Applications.

The following section explain the proof of concept and use case developed to showcase the functionality of the 5G SBA and Location module in drone rental application

V. 5G SBA Platform: Use Case and Proof of Concept for Drone Rental Services

Platforms are one of the key enablers in 5G to support applications and provide different services on the cloud. Platforms are scalable, flexible and dynamically programmable where many network functions are built, configured and deployed based on the network, traffic and use case dependencies to enable service [9]. Platforms offer APIs to provide Platform as a Service (PaaS) to deliver real-time location information, which is reasonably challenging. This paper designed an example use case and developed proof of concept for 5G SBA Platform which can be utilized by drone operators.
Drone or quad copter is a lightweight and flying object that can be used in various applications such as on air seed sowing for the large cultivation field, remote monitoring the cultivation field, cargo delivery in e-commerce, emergency response etc. With the current generation of communication, drone services are not widely established mainly due to the poor coverage and connectivity [10]. The drone services will become a reality with 5G enabling deeper coverage and connectivity [11]. Fig. 7 shows the proof of concept architecture developed for the drone rental service in 5G.

A. Drone Rental SP Infrastructure

The service provider infrastructure consists of an application server and a dashboard. The server handles the user information and location data of each drone given to the users. The dashboard, displays the live location of the drones for tracking and health status of individual drones.

B. 5G SBA providing NEF capabilities to APIs

5G SBA consist of NFV which enables different services such as enhanced Mobile Broadband (eMBB), massive Machine Type Communication (mMTC) and ultra-Reliable Low

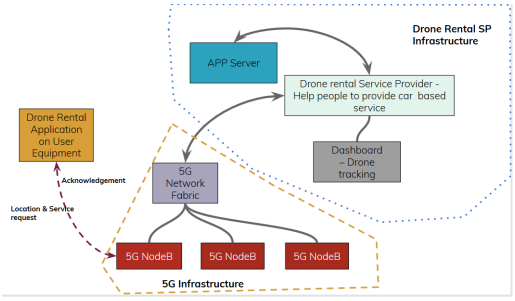

Fig. 7. Architecture developed for Drone Rental Service

Latency Communication (uRLLC) to the 3rd parties [12]. Each drone will be connected to the network using 5G small cells. By using the location engine, the location of each drone is estimated and the data is stored to the database. As shown in the Fig. 8 by using the SPs APIs, the drone can be tracked more precisely with data stored in the SP database. REST API provides location data from the database to 3rd party applications securely via NEF.

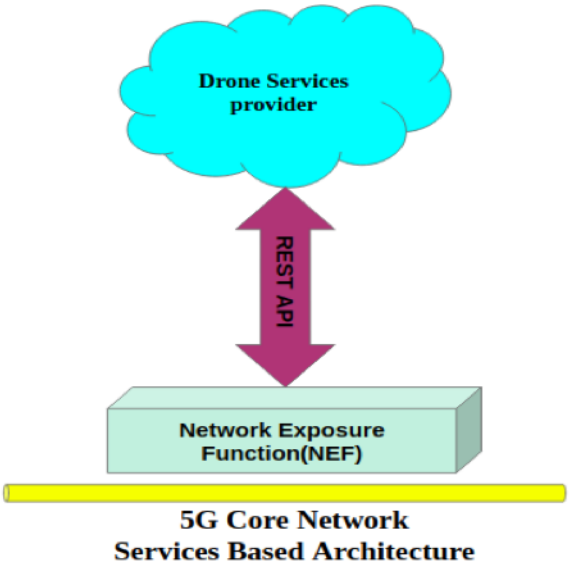

Fig. 8. Service Provider Infrastructure

C. User Interface for real time tracking

It is expected that all the drones are tracked by the SP using the location engine explained previously in this paper. The client application in the User Equipment (UE) will receive the location of the drone through the REST APIs from the drone SP database. This will help the owner of the drone to locate it, get the state of charge, remaining flight time, etc. The client application also offers drone service request, payment and reservation. Apart from the mobile application, the website offers drone services for the drone users to check the availability and reserve drones online. The web page also supports payment option. The web page was designed using the HTML and PHP. Snapshot of the web page is shown in Fig. 9. The page to locate the drone was generated using the location module that co-located with the 5G Base station. Fig. 10 shows the mobile application developed as a proof

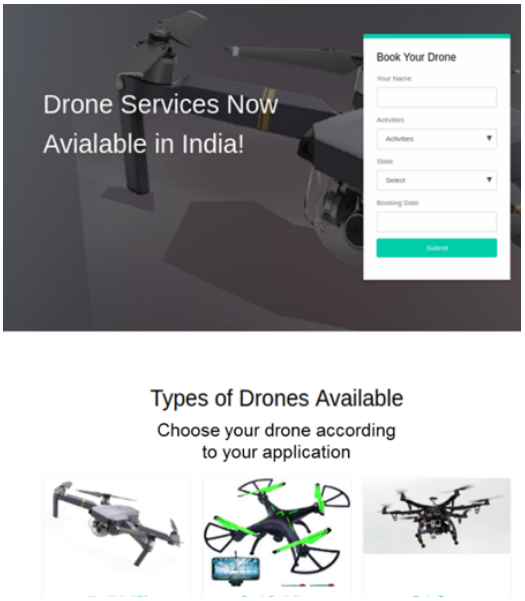

Fig. 9. Webpage provided by the drone rental company

of concept to demonstrate location tracking of drone. The blue markers represent the drones, the red marker represents the base station to which the drones are connected and the blue layers represents the coverage of the base station. Drone owners can use this application to track the drones by using the APIs provided by the SP. Third party applications can use the APIs to offer additional services to the customers along with the services offered by the drone provider.

The location services play a vital role in tracking the drones

Fig. 10. Mobile Application for real time tracking of Drones

and monitoring its health. Platforms allow users to remotely control the drone operation using the client application. Advanced Machine Learning algorithms can be applied to automate various services such as autonomous address discovery, navigation and product delivery. Fig. 11 shows the example

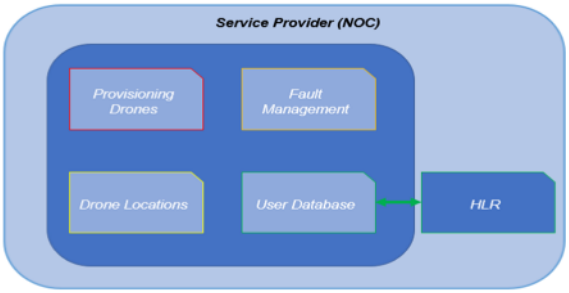

Fig. 11. Example SP dashboard operational aspects

SP dashboard at the Network Operation Center (NOC). The SP dashboard has the following modules:

- **Home Location Register** (HLR) is the primary database that holds the information of the subscribers. HLR is maintained by the 5G SP and it contains user information such as name, address, account details, data balance and settings.
- **User Database** is managed by the drone service provider to store details of the users. Details such as name, address, type of service requested, history of service opted, payment details and
- **Drone Locations** is provided by the location module in real time.
- **Fault Management** module frequently checks for the health of the drones and reports it to the NOC.
- **Provisioning Drones** module initiates the licensing and monitors the consensus of the user agreement. If any violation is observed, it initiated auto return function where the drone is returned back autonomously to the service provider.

VI. Conclusion

This paper proposes a location module for 5G communication technology. The proposed module supports the 3rd party mobile applications and OTT Services by providing enhanced location data of the user or IoT devices. By using the location modules APIs, the OTTs or applications can get the accurate location data for devices from the SPs. By using this method, it is ensured that the personal details of the devices or consumers are protected by the SPs. The paper concludes by showing example APIs and Platform framework that can be utilizing the 5G SP. It is anticipated that the proposed SP based location framework will help the OTTs to provide more secure location based services without exposing the user identity.

References

[1] A. M. Kunz, L. Nkenyereye, and J. Song, "5g evolution of cellular iot for v2x," *2018 IEEE Conference on Standards for Communications and Networking (CSCN)*, pp. 1–6, 2018.
[2] P. Sarigiannidis, T. Zygiridis, A. Sarigiannidis, T. D. Lagkas, M. Obaidat, and N. Kantartzis, "Connectivity and coverage in machine-type communications," in *2017 IEEE International Conference on Communications (ICC)*, pp. 1–6, May 2017.
[3] 3GPP, "Release 15." https://www.3gpp.org/release-15. Accessed: 2019-05-27.
[4] F. Z. Yousaf, M. Bredel, S. Schaller, and F. Schneider, "Nfv and sdnkey technology enablers for 5g networks," *IEEE Journal on Selected Areas in Communications*, vol. 35, pp. 2468–2478, Nov 2017.
[5] E. Wang, W. Zhao, and M. Cai, "Research on improving accuracy of gps positioning based on particle filter," in *2013 IEEE 8th Conference on Industrial Electronics and Applications (ICIEA)*, pp. 1167–1171, June 2013.
[6] R. Singh, M. Guainazzo, and C. S. Regazzoni, "Location determination using wlan in conjunction with gps network (global positioning system)," in *2004 IEEE 59th Vehicular Technology Conference. VTC 2004-Spring (IEEE Cat. No.04CH37514)*, vol. 5, pp. 2695–2699 Vol.5, May 2004.
[7] Y. Song, Y. Zhang, J. Cao, T. Xia, W. Liu, and J. Li, "Web video geolocation by geotagged social resources," *IEEE Transactions on Multimedia*, vol. 14, pp. 456–470, April 2012.
[8] S. Kumari and S. K. Rath, "Performance comparison of soap and rest based web services for enterprise application integration," in *2015 International Conference on Advances in Computing, Communications and Informatics (ICACCI)*, pp. 1656–1660, Aug 2015.
[9] I. Afolabi, T. Taleb, K. Samdanis, A. Ksentini, and H. Flinck, "Network slicing and softwarization: A survey on principles, enabling technologies, and solutions," *IEEE Communications Surveys Tutorials*, vol. 20, pp. 2429–2453, thirdquarter 2018.
[10] X. Foukas, M. K. Marina, and K. Kontovasilis, "Orion: Ran slicing for a flexible and cost-effective multi-service mobile network architecture," in *Proceedings of the 23rd Annual International Conference on Mobile Computing and Networking*, MobiCom '17, (New York, NY, USA), pp. 127–140, ACM, 2017.
[11] L. Rajagopal and D. Raj, "Study of synchronization facets for 5g small cell use case scenario," in *2017 2nd International Conference on Communication and Electronics Systems (ICCES)*, pp. 529–534, Oct 2017.
[12] S. Swetha and D. Raj, "Optimized video content delivery over 5g networks," in *2017 2nd International Conference on Communication and Electronics Systems (ICCES)*, pp. 1000–1002, Oct 2017.

Proceedings of the Fourth International Conference on Communication and Electronics Systems (ICCES 2019)
IEEE Conference Record # 45898; IEEE Xplore ISBN: 978-1-7281-1261-9

Comparison between Hybrid AMI and Duobinary–VLC (Visible light Communication) using WDM (Wavelength Division Multiplexing)–PI (Polarization interleaving) Transmission System

Chetna Verma
Department of Electronics and Communication Engineering
Government Women Engineering College, Ajmer
Rajasthan-305002, India
chetnaverma44@gmail.com

Chetan Selwal
Department of Electronics and Communication Engineering
Government Women Engineering College, Ajmer
Rajasthan-305002, India
selwal.chetan@gmail.com

***Abstract*—VLC is need of high-speed data rate transmission for next-generation networks. LOS communication is a must for a high-speed VLC communication system. In the VLC system, we have formed a high-speed Visible light communication system utilizing WDM, and PI scheme for broadcast information in the visible form of eight channels, each one bear 10 Gbps data accomplished by the VLC link of 160 m. We have compared performance improvement using AMI coding and duo binary coding. The bit rate of 10 Gbps up to 160m has been investigated using Q factor in eye diagrams and bit-error-rate (BER) which is targeted to achieve the value greater than 7 and less than 10-9 respectively. VLC system simulation is done on Optisystem 15.**

Keywords—Alternate mark inversion; Duobinary, Wavelength-division multiplexing; Polarization interleaving; VLC communication

I. INTRODUCTION

Visible light communications (VLC) systems is a data communication which uses visible light between 400-800THz (780-375nm) ranges in the electromagnetic spectrum[1]. In this paper, the laser diode is used as a source in the WDM (Wavelength division multiplexing) PI (polarization interleaving) Visible light communication system[2]. VLC (Visible light Communication) using WDM (Wavelength Division Multiplexing)–PI (Polarization interleaving) Transmission System for long distance transmission and high-speed data LASER is used[1]. A LASER pointer, with alternate mark inversion and Duo binary Coding, has better accomplishment in VLC systems due to the high distance along with luminous beam concurrence. High-speed and Long-reach Hybrid AMI-WDM–PI is used in VLC communication system [3]. In this paper, we compare AMI Coding and Duobiny coding with the help of WDM-PI VLC system [4-6]. In this paper, we compare between AMI (alternate mark inversion techniques) and Duobinary techniques using WDM (Wavelength Division Multiplexing)–PI (Polarization interleaving) Visible light communication System.

1) Coding

In this paper, we compare two coding techniques, Alternate Mark Inversion (AMI) and Duo binary coding with the help of WDM-PI VLC system. These two techniques are

A. AMI Coding

AMI is Line coding techniques. AMI is a bipolar encoding in which if 0 is generated then it touches reference line means neutral (zero) voltage represents binary 0 and if 1 is generated then alternating positive and negative voltages show binary 1 [7].

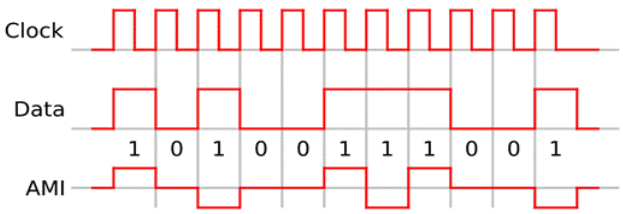

B. Duobinary Coding

In communication, Duobinary is also a return-to-zero (RZ) line coding and duobinary coding is also bipolar encoding techniques, in which three values are used which are +,- and zero in which two are nonzero values. this type of signal is the duo binary signal [7-8].

2) Wavelength Division Multiplexing:

- WDM is an analog multiplexing technique to combine the optical[8] signal.
- Light has a property that keeps it from mixing and allows it to be separated into its wavelength.
- To utilize the high data rate capability of FSO, WDM has been devised.

• Wavelength division multiplexing method used to increase the capacity of the system[9].

II. SYSTEM DESCRIPTION

The integrated VLC WDM–PI technique designed is displayed in Fig 1 and architecture is simulated using OptiSystem™15 software.

1) AMI System:

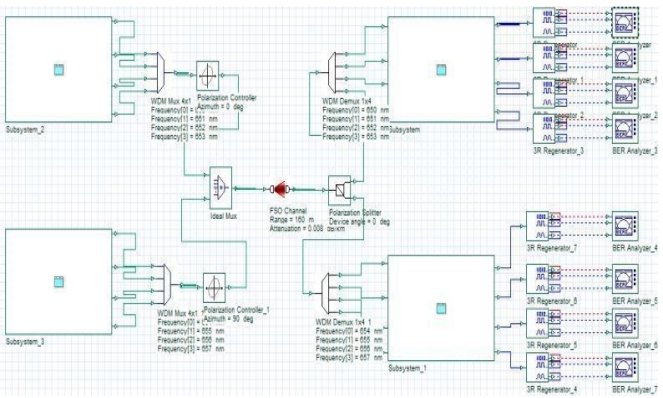

Fig. 1. Proposed 10 Gbps AMI–WDM–PI VLC communication system.

B. Transmitter

Implementation of Tx stage of AMI FSO Visible Light Communication System using AMI-WDM-PI is shown below in figure 2[3,9]. In the transmitter side firstly bit sequence generator is present which transmit the bit sequence after that dual port Mach-Zehnder modulator is present which modulated the binary sequence. In the block diagram, signal modulates over illuminated sources of 0 dBm and wavelength of 650 nm along with 1 nm separation. Delay-and-add and subtract procedures are used to produce AMI line codes [2]. Data are transmitted through NRZ pulse generator, as in on–off keying [10-11].

In the below block diagram even and odd channels are present in the form of data channels and this even and odd channels are individually multiplexed[2]. Polarization controller maintained the two multiplexers output. This two polarization output give to ideal MUX input and this MUX output combined with the channel in the form to switch the azimuth specification of the even and odd channel to orthogonal signals[2].

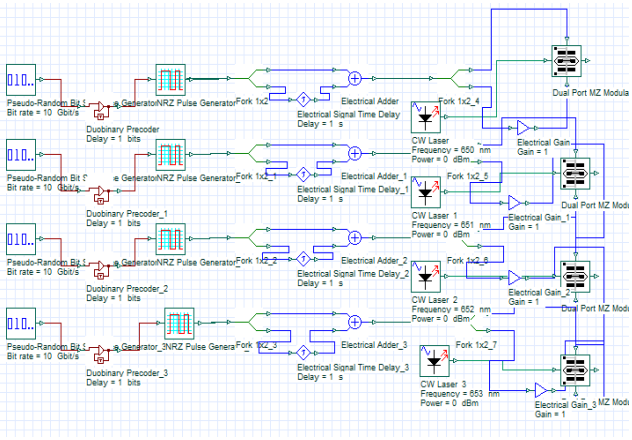

Fig. 2. Implementation of Tx stage of AMI FSO VLC.

C. FSO channel

• The FSO channel[3] includes a Tx and an Rx antenna.

• In the free space wireless channel (FSO) even and odd channels are present in the form of data channels and this even and odd channels are [2] individually multiplexed with the help of WDM multiplexer. the polarization controller maintained the multiplexer output. [11].

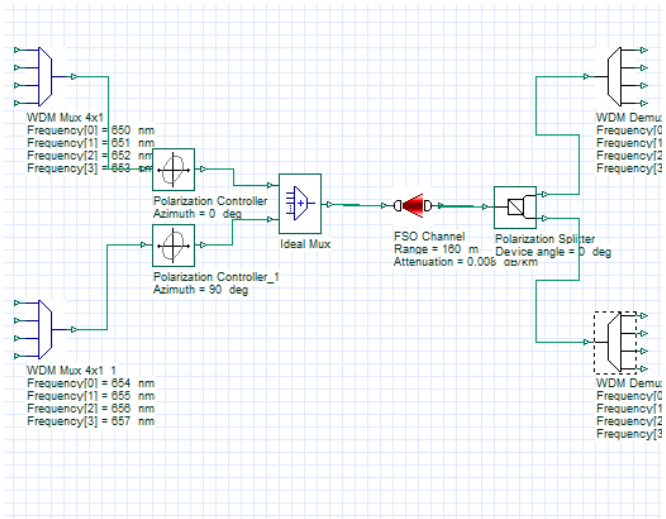

Fig. 3. Channel operation in VLC System

D. Receiver

In VLC system at the receiver [5], side contains polarization splitter (PS) which split the FSO Channel signal output, give approval polarization stage, this signal split into even and odd signals. The polarization splitter output is later recognized by a photodiode PIN for demultiplexing, signal filter by the Bessel low pass filter[2].

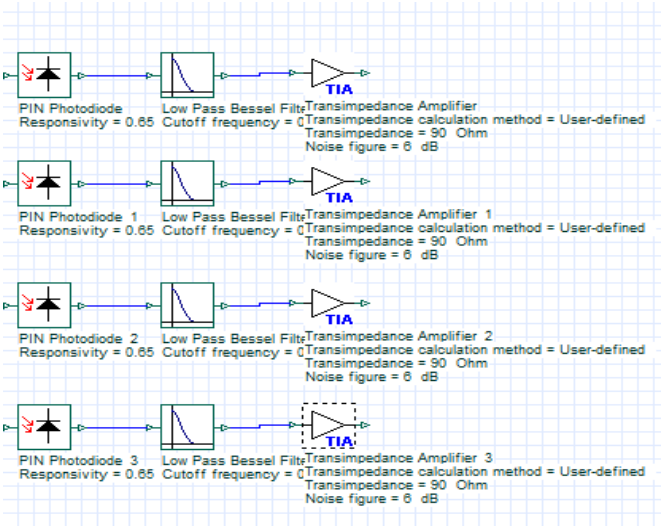

Fig. 4. Receiver operation in FSO VLC System

D. Duobinary

- The Duo binary was produced by first generating an NRZ duo binary signal utilizing a precoder and a duo binary pulse generator[12].
- Figure1 shows a system transmitting a Duo binary signal at 10 Gb/s.
- The duo binary precoder used in this place was composed of a Binary not gate along a delayed feedback path.
- AMI and Duobinary transmitter side are same except Duobinary transmitter side have binary NOT before Duobinary precoder.

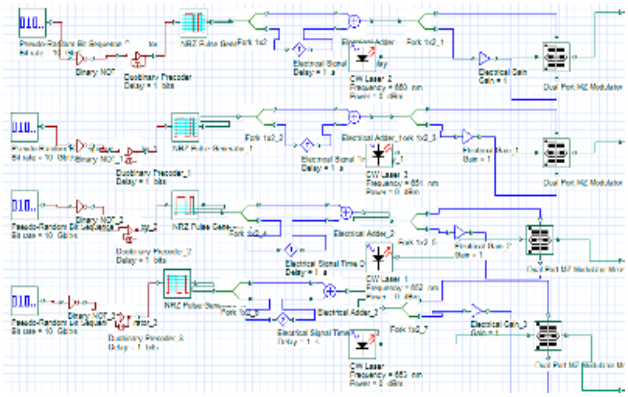

Fig. 5. Implementation of Transmitter stage of Duobinary VLC System.

III. RESULTS AND DISCUSSION

A. Figures and Tables

1) Positioning Figures and Tables: The specification value details of this system are specified in Table 1.

Table Head			
	Parameters	***Value***	***Subhead***
1	Bitrate	10	Gbps
2	Distance	160	m
3	Operating wavelength	650-657	nm
4	Time window	12.8-009	s
5	Sample rate	640e+009	Hz
6	Sequence length	1024	bits
7	Sample per bit	32	
8	Number of samples	32768	
9	Symbol rate	10e+009	Symbol/s
10	Transimpedance amplifier	90	Ohm
11	Noise Figure	6	dB

A. *AMI–WDM–PI*

Figure 6 performs the efficient estimation of the planned AMI–WDM–VLC communication system in the form of Q factor and BER[14]. In this system, we used channel distance 160 m with 10 Gbps bit rate sequence. Channel 1 and Channel 8figure 6 shows accomplishment evaluation of the planned transmitter, channel and receiver respectively. The Q-factor for channel 1 is 7.52929 dB for link length 160 m whereas for channel 8 it is noted as 7.00885dB at FSO.likewise, channel 1 BER value is recognized as 2.45736e-014whereas channel 8, it is noted as 1.19991e-012 at FSO transmission of 160m, respectively.

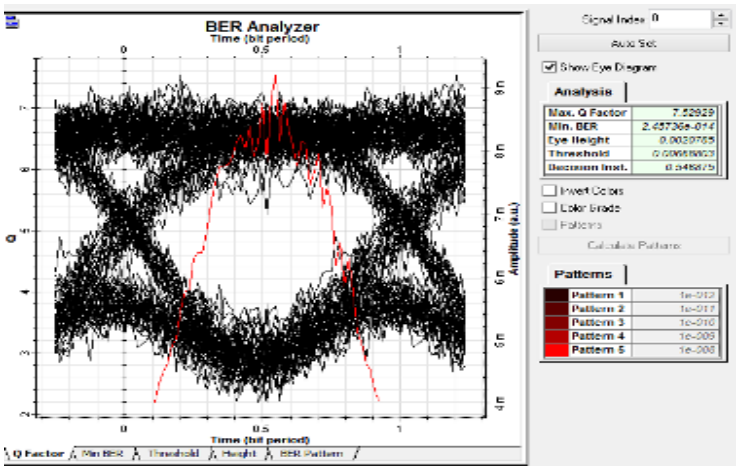

(1) Channel 1eye diagram for AMI system

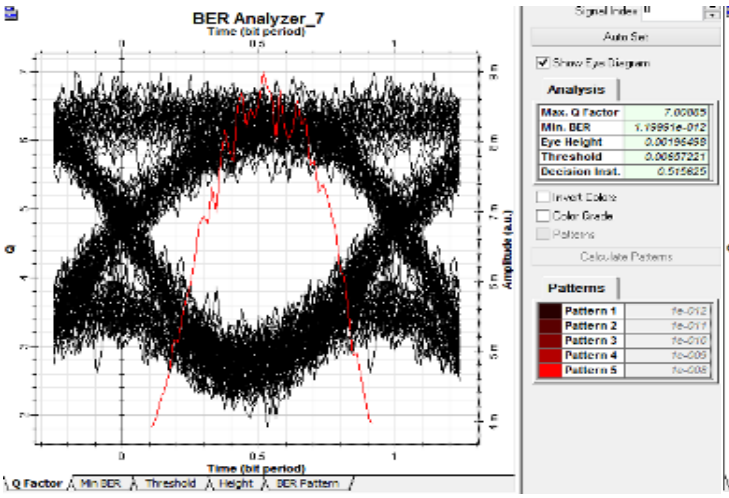

(2) Channel 8 eye diagram for AMI System

Fig. 6. Eye diagram analysis for channel 1 and channel 8 at the receiving end of 160m

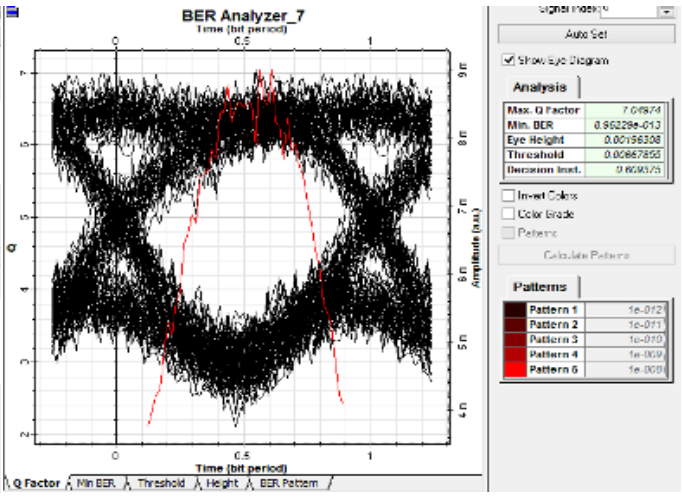

(b)Channel 8 eye diagram for Duobinary system

Fig. 7. Eye diagram analysis for channel 1 to 8 at the receiving end of 160m

B. Duobinary–WDM–PI

Figure 5 performs the efficient estimation of the planned Duo binary–WDM–VLC communication system in the form[13] of Q factor and BER[14]. In this system, we used channel distance 160 m with 10 Gbps bit rate sequence. Figure 5 shows the accomplishment evaluation of the planned Duo binary system respectively. We get channel 1 Q-factor is 5.27457 dB for link length 160 m whereas for channel 8 it is noted as 7.04974dB at FSO. likewise, channel 1 BER value is recognized as 6.65303e-008 whereas channel 8, it is noted as 8.96229e-013 at FSO transmission of 160m, respectively.

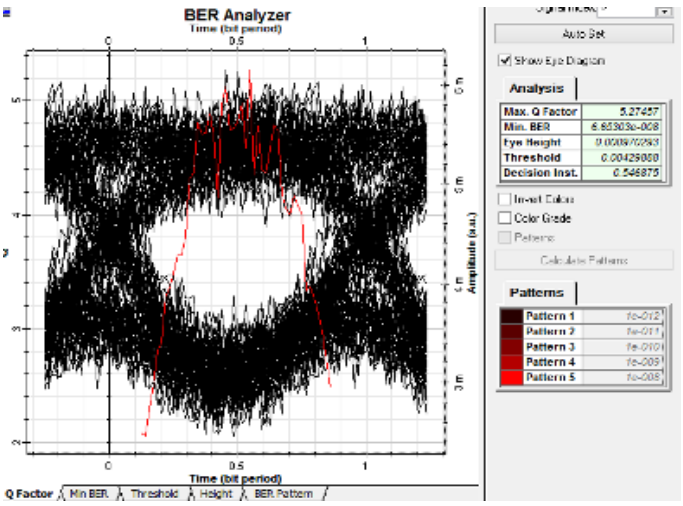

(a) Channel 1 eye diagram for Duobinary System

IV. CONCLUSION

We compared between AMI scheme and Duo binary using WDM–Polarization interleaving Visible light communication system. The whole designing structure is based on FSO optical link of 160 m with the 10 Gbps data. The results are stated in forms of eye diagrams that demonstrate that entire eight channels, each one accomplish10 Gbps AMI-encoded data and Duo binary data, are transmitted and retrieved well with adequate BER, and Q Factor. It has been observed that the AMI is better than Duo binary encoding scheme in the form of Q factor as well as BER which is targeted to achieve the value greater than 7 and less than 10-9 respectively[14].

References

[1] Chetna Verma, Chetan Selwal. "4QAM OFDM Visible Light Communication using Laser", 2018 7th International Conference on Reliability, Infocom Technologies and Optimization (Trends and Future Directions) (ICRITO), 2018

[2] Abdallah Ahmad Shatnawi, Mohd Nazri Bin Mohd Warip. "High-speed and Long-reach Hybrid AMI–WDM–PI Inter-satellite Communication System", Journal of Optical Communications, 2017

[3] Chetna Verma, Chetan Selwal. "Visible light communication system(VLC) Using Diversity Technique with 4 QAM OFDM FSO Link", 2018 2nd International Conference on I-SMAC (IoT in Social, Mobile, Analytics and Cloud) (I-SMAC)I-SMAC (IoT in Social, Mobile, Analytics and Cloud) (I-SMAC), 2018 2nd International Conference on, 2018.

[4] Bansal U, Kaur K, Chaudhary S. "Role of laser linewidth in high- speed DWDM system by incorporating duobinary modulation scheme". Int J Comput Appl 2015;109(15):30–2.

[5] Kamal Kishore Upadhyay, Saumya Srivastava, N. K Shukla, Sushank Chaudhary. "High-Speed 120 Gbps AMI-WDM-PDM Free-Space Optical Transmission System", Journal of Optical Communications, 2017

[6] Manisha Prajapat, Chetan Selwal. "Free Space Optical link performance simulation under different atmospheric conditions and diversity", 2017 International Conference on Computer, Communications and Electronics (Complex), 2017

[7] an-dollar-touches-smh.com.au

[8] mickygantengepol.blogspot.com

[9] en.wikipedia.org

[10] Dailey JM, Power MJ, Webb RP, Manning RJ. “High-bandwidth generation of duobinary and alternate-mark-inversion modulation formats using SOA-based signal processing”. Opt Express 2011;19(27):25954–68.

[11] Sushank Chaudhary, Priyanka Chauhan, Abhishek Sharma. "High Speed 4 × 2.5 Gbps-5 GHz AMI-WDMRoF Transmission System for WLANs", Journal of Optical Communications, 2017

[12] Utpal Das, P. K. Sahu, Bijayananda Patnaik. "Chapter 18 Ultra High Bit-rate Fiber Optic Hybrid (WDM and TDM) Communication System Design and Simulation", Springer Nature, 2014

[13] www.ijcaonline.org

[14] Guddan Kumari, Chetan Selwal. "Performance optimization of return-to-zero DPSK modulation in inter-satellite optical wireless communication", 2016 International Conference on Recent Advances and Innovations in Engineering(ICRAIE), 2016

Proceedings of the Fourth International Conference on Communication and Electronics Systems (ICCES 2019)
IEEE Conference Record # 45898; IEEE Xplore ISBN: 978-1-7281-1261-9

Remote Vehicle Data Logging system for Off Highway Mining Equipment's

Hifza shaima
Dept of E&C, JSS Science and Technology
University Mysore-570006 Karnataka India
hifzashaima4@gmail.com

Yashwanth S D
Dept of E&C JSS Science and Technology
University Mysore-570006 Karnataka India
yashwanth@sjce.ac.in

E K Ratna Kanth
Dept of E&E, Assistant Manager, BEML
Limited Mysore Karnataka India
ratnakanthek@gmail.com

Abstract: **The automotive industry is increasingly focused on specialization and customization. The goal is to optimize product features with regard to transport effectiveness, safety, quality and environmental impact leading to a minimized lifetime cost for the vehicle. But one piece in the puzzle is to have better understanding of how the vehicles actually are used, through the sensor data available in the vehicles. Here we develop a data logging system for off highway mining equipment's. The GSM, GPRS and Ds3231 RTC modules are used for this data logging system. The different parameters readings from the sensors are stored and uploaded to server if some errors are diagnosed. This error data is saved in SD card and the error diagnosed data is logged to cloud through network. from the server the data can be easily opened in monitoring desktop or phone. For further fault analysis and research, can be done in manufacturing service center.**

Keywords: GPRS/GSM; SIM900a; DS2331 RTC Module; Data logger and Arduino Mega

I. Introduction

As society is making lighting up the transportation needs of the world is a tremendous issue with wide effects on nature and on human lives. One way of making the transportation solutions more effective is to use a specially tailored vehicle for the intended usage. The automotive industry is increasingly focused on specialization and customization. The goal is to optimize product features with regard to transport effectiveness, safety, quality, and environmental impact leading to a minimized lifetime cost for the vehicle.

Present day trucks are perplexing electro-mechanical frameworks with many arranged Electronic Control Units (ECUs). Sensors are placed throughout the system. This connectivity makes it possible to access sensor signals, which give a view of the state of the vehicle and its components and subsystems. The available information is of interest to a number of different stakeholders, as for example development, fleet owners, and traffic accident researchers [2]. The stakeholders want to optimize the vehicle and its functionality, which leads to a need for various types of information, as for example driver behavior and vehicle usage Developers want to know how the vehicle is performing, to get errors, faults, and abnormal behavior [8], in order to improve the vehicle and understand when and why components fail [3]. Fleet owners are able to plan for maintenance to minimize the risk of vehicles breaking down and missing scheduled runs. Drivers, fleet owners, automotive companies, and insurance companies are all concerned in on-board information from the vehicles.

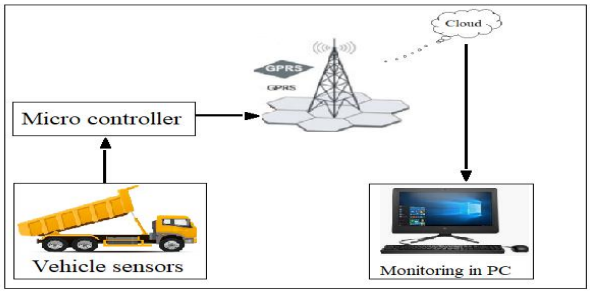

Fig 1. The structure of data logging system.

As we are using the internet the structure pushes toward getting to be confirmed and constant data watching and real time data monitoring is also possible using GSM/GPRS system [9]. In this paper we have designed a real time data logging system for off highway mining equipment. Here the data is recorded through sensors whenever any error takes place in the equipment, this data is logged and saved in SD card and from server it can be easily monitored in PC or phone. For further analysis the structure of this system is shown in the above Fig 1. To build this we are using Arduino Mega microcontroller here the data can be logged at any interval of time to maintain the date and time [7] we are using RTC module DS3231 and get the temperature, speed and current readings [6].

The rest of this paper is composed this way. In area II we have examined the past work accomplished for this undertaking. In segment III proposed work, we

have made an analysis of technologies used and the overall system architecture of the system is discussed. In section IV, we have analyzed the raw sensors data. In section V, we have represented the flow chart of the work. In section VI we have wind up the paper by showing outcomes. Lastly in section VII we concluded the paper and the future work.

II. Previous work

In the field of vehicle data acquisition and logging study there exists both fully ready products, research ideas and prototypes [4].

There are many telematics products created on vehicle data [10]. Volvo Trucks has a fleet and vehicle supervision system called Dynafleet, where available info is, for example, vehicle position, driver rest times, fuel consumption and service intervals. General Motors has a system called OnStar, which has almost the same services. Part of this system is vehicle diagnostics, which uses the diagnosing errors for the different systems. Some other companies also have similar products. The work in this project concentrates on the on-board analysis. The aim in this project is also to extend the available information from the vehicle and describes different research solutions to vehicle data logging and analysis.

III. Proposed work

A. Internet of things (IoT)

Earlier, the internet comes to be used for in truth getting to locations to speak with each special. anyhow, with the development of improvement, the internet is used for interfacing machines with higher limits and occasional strength usage to the cloud. further, in recent times huge affiliation of sensors that would benefit and way records may be made with those devices. Additionally, a tiny bit at a time went with this came the likelihood of "Internet of things" with the help of which PC can accumulate information about any substance.[1]

B. Vehicle logging

The modern trucks are complex mechatronic system containing several distributed and networked ECUs. The different ECUs are specialized to handle specific subsystems and their functionality, for example an Engine Control Module or Gearbox Control Module. Each ECU receives and transmits messages on the different networks using CAN protocol. The ECU controls the specific subsystem, by getting the input from the sensors and sends the output signal to the actuators. In the event of faults Diagnosing the Trouble Codes are set and The On-board Diagnostics [14] connection is the legally defined standard for the connection through which diagnosed errors can be studied at manufacturing service-centers [11].

C. The system architecture and specifications

Here the gateway is made of GPRS,GSM sim900a module, DS3231 RTC module, SD card and Arduino Mega microcontroller.

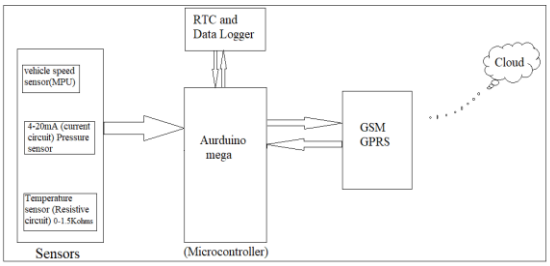

Figure 2: system architecture of logging system

The sensors of the dumper truck measures such as eingne oil temperature, eingine oil pressure and speed of the vehicle are programmed by microcontroller and the data is logged. The system architecture of logging system is as shown in Figure 2.

D. Arduino Mega

The Arduino Mega-2560 is a microcontroller board (ATmega2560). It has 54 digitals enter and output pins (in which 15 can be used as PWM outputs), 16 analog inputs, four UARTs (hardware serial ports), a 16 MHz crystal oscillator, a USB connection, an electricity jack, an ICSP header, and a reset button. The information and yield pins are utilized for developing the placing for composing packages for the board. This device makes a level to structure our framework. With the assistance of this current gadget's exhibition which can be utilized to connect to IoT.

E. Pressure transducer:

- Make: ADZ (made in Germany)
- Pressure rating: (0-400PSI) (0-27.5bar)
- Electrical rating: (10-32V) (4-20mA)
- Minimum 10V is required to drive the current through channel.
- Requires two port pins for communication.
- This is current type sensor.

F. Temperature sensor:

- Make: ADZ (made in Germany)
- Temperature rating: (0-400PSI) (0-1500Ω)
- Electrical rating: (10-32V) (4-20mA)

- Minimum 10V is required to drive the current through channel.
- This is resistive type sensor.

G. Speed sensor:

- The inductive impact in the sensor's curl is creating the wavering voltage, for example, one sort of sinusoidal waveform signal (~ AC voltage).
- The voltage sign created by the sensor relies upon the speed of the flywheel and the number of turns in the curl. The yield voltage could be likely somewhere in the range of 1V and 5V
- When the fly(gear) wheel with the teeth goes in enough close separation to the shaft stick of the sensor, the attractive field encompassing the loop is changed. Because of the adjustments in the attractive field, and the voltage is prompted in the loop, which is relative to the quality and rate of progress of the attractive field. One completely complete swaying is created for every tooth that goes adjacent to the sensor post stick.

H. GPRS/GSM sim900a

- Single supply voltage: 3.4V – 4.5V
- Supports UART interface
- Supports a solitary SIM card
- Firmware redesign by investigating port
- Communication by utilizing AT directions
- Power sparing mode: Typical power utilization in SLEEP mode is 1.5mA
- Frequency Group: SIM900A Dual-band: EGSM900, DCS1800. The SIM900A can look through 2 frequency band groups consequently.
- Dual-Band GSM/GPRS 900/1800 MHz.
- RS232 interface for direct correspondence with PC or MCU unit.
- Configurable baud rate.

H. DS3231 RTC module

The DS3231 is ease, amazingly particular real Time Clock that can maintain hours, minutes and seconds, simply as, day, month and three hundred and sixty-five days. Likewise, it has programmed recompence for bounce years and for a substantial duration of time with underneath 31 days.

- Accuracy ±2ppm from 0°C to +40°C
- Accuracy ±3.5ppm from -40°C to +85°C
- Digital Temp Sensor Output: ±3°C Accuracy
- Register for Aging Trim
- RST Output/Pushbutton Reset Debounce Input
- Two Time-of-Day Alarms
- Programmable Square-Wave Output Signal
- Simple Serial Interface Connects to Most Microcontrollers
- Fast (400kHz) I2C Interface
- Battery-Backup Input for Continuous Timekeeping
- 3.3V Operation

IV. Analyzing the raw data of sensors

A. Pressure sensor (Engine oil pressure)

Precision of analog channel A1 = 5/1023=0.0048875V or 4.88mV

The resulted curve of pressure sensor obtained is a straight line, not passing through origin and cutting the Y-axis. It is shown in the fig below in result section

Considering Y= mx+c, standard equation of a straight line.

Where,

Y= Current(mA) output of transducer

m= Slope i.e. (mA/bar) = (current/pressure)

x= pressure applied to the transducer

c= offset current output of transducer when no pressure is applied

Therefore, the slope value obtained by calculating is m = 0.56mA/bar

Y=current in mA	M=slope	x=pressure in bar	C=offset current
4	M0=0	0	4
5.1	M1=0.56	2	4
6.8	M2=0.56	5	4
7.4	M3=0.56	6	4
9.7	M4=0.57	10	4
	Mavg=0.56		

Table 1: Average Slope calculation

B. Temperature sensor (Engine oil temperature)

Raw data of sensor resistance R_s raw = Analog read A_0

Voltage V_{in} = 5V

R_c buffer = R_s raw * V_{in}

Voltage across resistance R_c, $V_{RC} = R_c$ buffer / 1023°C

R_S buffer = $((V_{in} / -V_{RC}) -1)$

C. Speed sensor (Engine crankshaft speed)

Fly wheel is a geared wheel which has 118 teeth's, and the Coil winding is concentrated at the tip in which magnet is cylindrical in shape

When the tip of sensor faces the teeth of a flywheel flux converges closely increasing flux density as shown in Figure 3.

When the tip of sensor faces the gap between teeth's (during normal time) the flux is distributed as shown in Figure 4

Therefore, as flux converges and redistributes the coil in that region feels the changing flux and generates the EMF

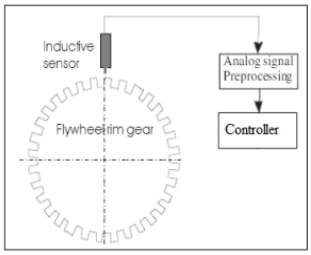

Figure 3: Schematic representation of speed sensor

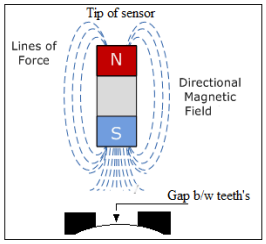

Figure 4: when sensor tip coincides the gap

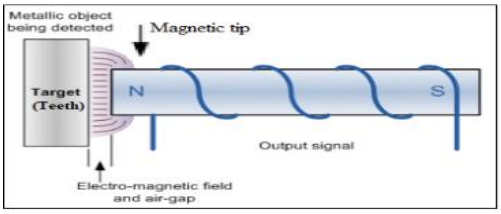

Figure 5: when teeth coincides with sensor pin

If number of teeth counts is 118, one rotation is completed

If in a minute number of counts=N

Then, N/118 give number of rotations in a minute i.e.=(N/118) RPM

V. Flow chart of the project work

The figure 6. below shows flow of the proposed project. With the help of Arduino Mega-2560, DS3231 RTC module, GSM/GPRS module as shown in figure 2 above. After accumulating information of temperature, pressure, and speed from sensors. The data is uploaded to the server. And monitored in PC or phone.

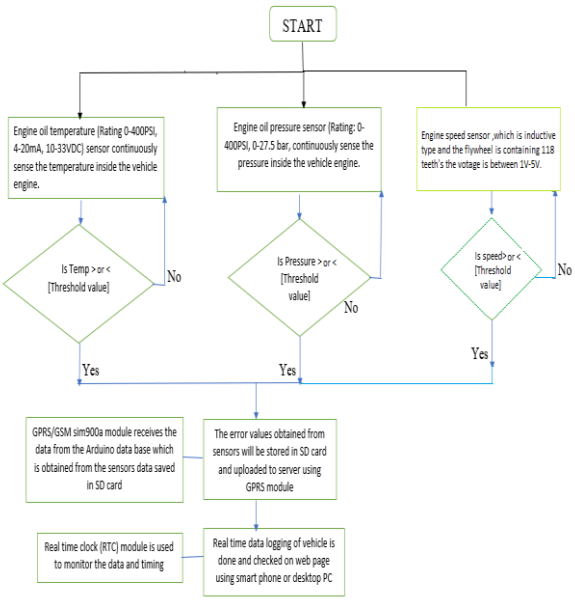

Figure 6: flow diagram of our project

VI. Result and discussion

With the assist of Arduino Mega-2560, DS3231 RTC module, GSM/GPRS module as verified in figure 2. After accumulating information of temperature, pressure, and speed from sensors [6]. The data is uploaded to the server. And monitored in PC or phone. Figures 7,8,9,10 and 11 and Table 2 and 3 depict the results.

We have taken the Engine transmission oil temperature and air pressure raw data were temperature sensor is resistive type, as a result current and temperature linearly increases as shown in the Figure 9. Resistive curve which is nonlinear in nature [5], were the pressure sensor is current type of sensor, as the result there is a change in pressure which is shown in the Figure 8, Current v/s Pressure curve which is linear in nature is as shown in Figure 11.

Current in (4-20mA)	Pressure in bar	Pressure in KPa
4	0	0
5.1	2	200
6.8	5	500
7.4	6	600
9.7	10	1000

Table 2: Data obtained from pressure sensor

1bar = 100KPa

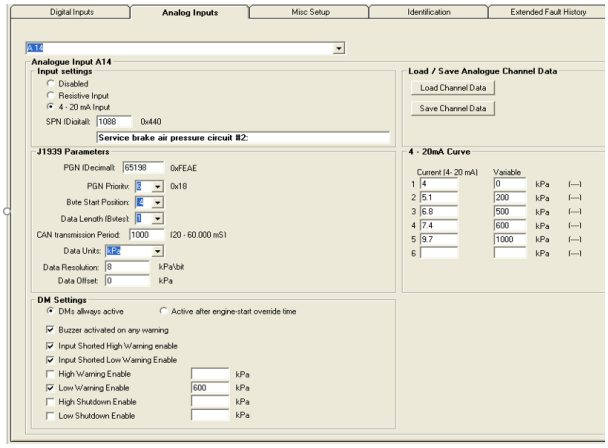

Fig. 7: The data logged by pressure sensor is monitored in PC

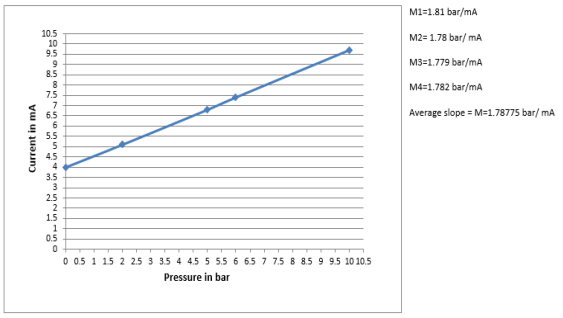

Fig. 8: Resultant curve of current v/s pressure

Resistance in K	Temperature in ℃
1029	40
460	60
164	90
74	120
40	140

Table 3: Data obtained from temperature sensor

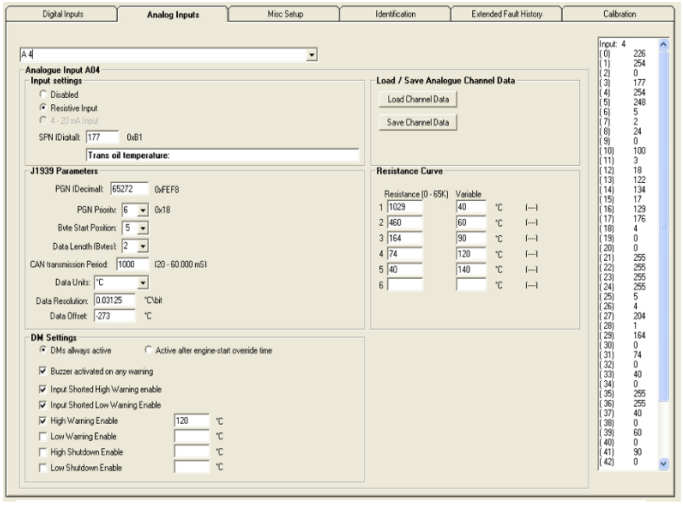

Figure 9: data logged by temperature sensor is monitoring in PC

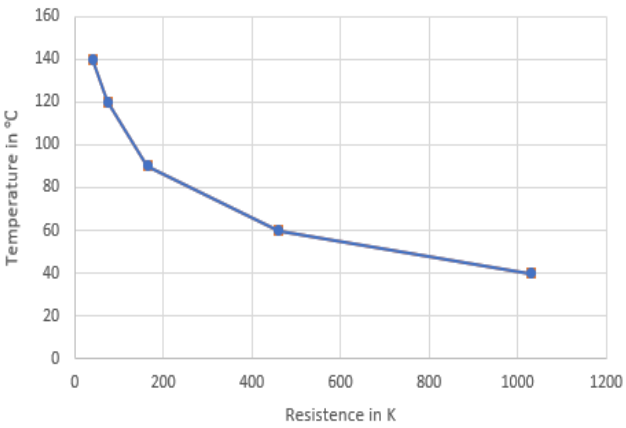

Figure 10: resultant curve of temperature V/s resistance

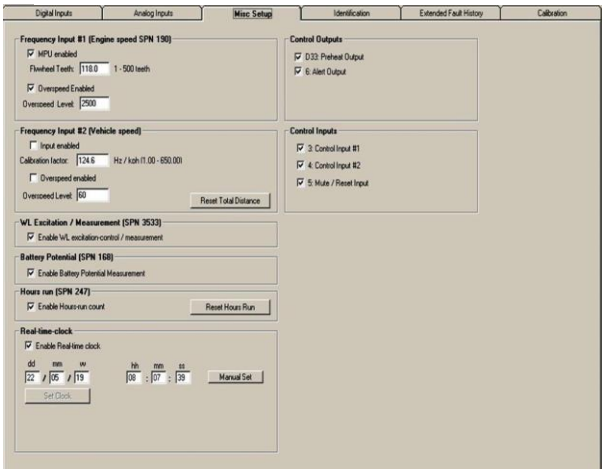

Figure 11: data logged by engine speed sensor is monitoring in PC

VII. Conclusion and Future work:

This project work provides the error information to the driver as well as the manufacturer which would help in a well-operational configurable on-board vehicle data system. Present day trucks are unpredictable electro-mechanical frameworks with many arranged Electronic Control Units and Sensors are put all through the framework. This connectivity makes it possible to access sensor signals, which give a view of the state of the vehicle and its components and subsystems. The results of remote vehicle data logging system for off highway mining equipment's is shown in the result and discussion section.

The next step would be to run the created hardware unit on actual vehicle. This would give the opportunity to determine the resource usage in detail. In this project, tests were conducted where the analysis gave useful results for monitoring engine pressure, engine crankshaft speed performance, and vehicle engine temperature, but there are many more other settings in the vehicle where the study is likely

to be applicable. Appropriate areas could be opted to monitor and detect between different driver behavior or to monitor definite subsystems as the engine, transmission, or air suspension.

References

1. Ananya Roy, Prodipto Das, Rajib Das, “Temperature and humidity monitoring system for storage rooms of industries” Dept of Computer science, Assam University, silchar.
2. Jin Wang, Guofeng Li, Yiy Liu, “ Vehicle supervision system based on MEMS geomagnetic sensor” Department of Electronic Science and Technology, Nankai University, Tianjin, China, 300071
3. S. Fryk and P.-O. Edlund, "The Right Truck for the Job with Global Truck Application Descriptions," in SAE Commercial Vehicle Engineering-Congress and Exhibition, Chicago, Illinois, 2004.
4. J. Olsson and H. H. Bosch, "Towards Data-Driven Product Development: A Multiple Case Study on Post-Deployment Data Usage in Software-Intensive Embedded Systems," in In Proceedings of Lean Enterprise Software and Systems Conference (LESS), Galway, Ireland, 2013
5. A. Mosallam, S. Byttner, M. Svensson and T. Rognvaldsson, "Nonlinear Relation Mining for Maintenance Prediction," in Aerospace Conference, 2011 IEEE, Big Sky, MT, 5-12 March 2011.
6. Research of Electric Vehicle Security Assurance and Monitoring System LiHaiying, ZhangDan, JiaYongli , QiuXinhong School of Metallurgyand Energy, HebeiUnited University, Tangshan,China, ITEC Asia-Pacific 2014 1569949785.
7. Minso Ryu, Jungkuen park, “Timing constraint remapping to avoid time discontinuities in distributed real-time systems” fifth IEEE conference.
8. Catarina C. Rolim, Gonçalo N. Gonçalves, Tiago L. Farias, Óscar Rodrigues. Impacts of Electric Vehicle Adoption on Driver Behavior and Environmental Performance, Procedia - Social and Behavioral Sciences 2012;706-715.
9. Design and Implementation of Vehicle Monitoring System Based on GSM/GIS/GPS Hui Tan Department of Business Management, Nanjing Institute of Industry Technology, Nanjing, Jiangsu, 210046, P.R.China, 2010 Second International Conference on Information Technology and Computer Science.
10. Tan Hui. “Application of GPS vehicle monitoring and dispatching system in logistis industry”, logistis technology (in Chinese), Nov 2007, vol. 26, pp.185-187.
11. “Vehicle Localization Integrity Based on Trajectory Monitoring” Olivier Le Marchand, Philippe Bonnifait, Javier Ibañez-Guzmán1, David Bétaille Renault SA, Guyancourt, France Heudiasyc UMR 6599, Université de Technologie de Compiègne, France Laboratoire Central des Ponts et Chaussées, Nantes, France, The 2009 IEEE/RSJ International Conference on Intelligent Robots and Systems October 11-15, 2009 St. Louis, USA.
12. G. Schroth, A. Ene, J. Blanch, T. Walter, and P. Enge, “Failure detection and exclusion via range consensus,” in Proc. of the European Navigation Conference GNSS, Apr. 2008
13. H. Durrant-Whyte, D. Pagac, B. Rogers, M. Stevens, and G. Nelmes, “An autonomous straddle carrier for movement of shipping containers,” IEEE J. Robot. Automat., vol. 14, pp. 14–23, Sept. 2007
14. O. Le Marchand, P. Bonnifait, J. Ibaï£¡ez-Guzmï£¡n, F. Peyret, and D. Bï£¡taille, “Performance evaluation of fault detection algorithms as applied to automotive localization,” in Proc. of the European Navigation Conference GNSS, Apr. 2008

Proceedings of the Fourth International Conference on Communication and Electronics Systems (ICCES 2019)
IEEE Conference Record # 45898; IEEE Xplore ISBN: 978-1-7281-1261-9

Interference in Large Scale wireless networks: A Case Study with LoRa (Long Range WiFi) and LTE (Long Term Evolution)

Adwitiya Mukhopadhyay[1], Ashish Sunil Thomas[2], Rekha Ramakrishna Hegde[3]
Department of Computer Science
Amrita School of Arts and Sciences, Mysuru
Amrita Vishwa Vidyapeetham, India
m_adwitiya@asas.mysore.amrita.edu, ashishthomas1995@gmail.com, rekharjaji@gmail.com

***Abstract* — Advancement in communication systems has resulted in the increase of services of different wireless technologies such as WiFi (Wireless Fidelity), LoRa (Long Range WiFi), LTE (Long Term Evolution), WiMAX (World Wide Interoperability for Microwave Access), etc. 4G wireless technology gives all enhanced features such as cost-effectiveness, high data transfer rate and provides direct communication. LoRa also provides mobility feature and portability feature. Installation and implementation of these networks are easy. LoRa and LTE wireless networks give high data transfer rates and better service when compared to other networks like 1G, 2G, 3G etc. and these networks are heavily used by the users for communication. LoRa caters to long-range communication. The other technologies such as WiMAX is not widespread across India. Bluetooth technology has disadvantages like short-range, slow data speed, poor data security when compared to LoRa and LTE. This paper provides related work on LTE and LoRa performance-based simulations. In our Simulation, we have shown how LTE and LoRa work with different node densities such as 25, 50, 100, 150 and 200. PLR (Packet Loss Ratio) is calculated as nodes increase with increased traffic. PLR is compared between LTE and LoRa. The experiment is done using OMNET++ tool. Performance of LTE and LoRa is tested separately. Simulation results have shown that performance of the LoRa is better when compared to LTE because PLR is high on LTE network with increased node density and increased traffic compared to LoRa.**

Keywords— LTE, LoRa, PLR, PGW, D2D (Device to Device)

I. INTRODUCTION

Transfer of data between two or more points that are not physically connected is termed as wireless communication. The distance is short, like a few meters for remote television control, or thousands or even millions of kilometers. It includes multiple types of fixed, mobile and portable two-way radios, cell phones and radio access networks. Usage of these wireless networks is increasing day by day. As traffic demand grows exponentially, users are facing problems with loss of data and increasing latency. Different technologies are used in the 21st century to support efficient data transfer such as WiFi, Bluetooth, Infrared and D2D (Device to Device) in cellular networks. [1]. The users of any wireless technology expect always the best connection at any time with high-speed data transfer. In order to meet the user requirement, technology is growing day by day and the capacity of the cellular networks has been increasing with advanced technology such as 3G and 4G. Still, there exists a demand for higher network capacity and faster traffic. LTE (Long Term Evolution) and LoRa (Long Range WiFi) networks are widely used by the users.

LoRa is used for low cost and unregulated point to point network connectivity. Features of Long Range WiFi (LoRa) are:

- Maximum output power 2000mW
- Data transfer rate: 300 Mbps
- Frequency: 2.4 GHz IEEE 802.11 b/g/n
- It works with indoors and outdoors

Long Term Evolution introduces an omnipresent network concept. LTE also offers higher data rates for many previously unavailable services and applications. This facilitates global roaming among different types of mobile access networks. LTE supports various scalable bandwidths from 1.4 MHz to 20 MHz [2]. Few LTE features are listed here:

- Increased data rate, DL 3Gbps, UL 1.5Gbps
- Improved performance at cell edges
- Range up to 20 Km.
- Bandwidth from 1.4 MHz to 20 MHz
- Supports equally TDD (Time Division Duplexing) FDD (Frequency Division Duplexing)

In order to find the most suitable and the best network to send data as the traffic flow increases, simulation is done with different node densities and traffic flows. The proposed work is done with the OMNeT ++ simulation tool. Performance of the network is evaluated by PLR (Packet Loss Ratio). PLR is evaluated by adding interference that modifies the signal in an abnormal way. The interference of data is evaluated by using LoRa and LTE network.

This paper presents an analysis of PLR (Packet Loss Ratio) with LoRa WiFi and LTE technologies. This paper contains following sections: Section II summarizes the Related Works, Section III has the Comparison of Technologies, Section IV has Experimental Design and Section V has Results and Analysis.

II. RELATED WORKS

Shihab Jimaa et al [3] present a futuristic approach about LTE in Cloud Radio Access Network, Multihop Wireless Networks and MPLS (Multi-protocol label switching). Here, LTE uses uplink and downlink transmission based on multiple access technologies. This paper focuses on the LTE requirements and multiple access technologies used in LTE. According to the results observed, uplink and downlink used for peak bit rate with

the help of High-Speed Packet download Access (HSDPA) and High-Speed Packet uplink Access (HSUPA).

Zeeshan Hameed Mir et al [4] appraise two Communication standards namely 802.11p by IEEE (Institute of Electrical and Electronics Engineers) and LTE (Long term evolution) by 3GPP for vehicular networking. This has a variety of parameters such as vehicle density and average speed. The standards of communication are compared in different scenarios with delay, scalability and mobility. As per the results, LTE has higher network capacity and supports mobility. It was also observed that delay increases as the network load decreases. Results show that IEEE802.11p provides end-to-end delay of less than 100ms and a 10-kbps throughput.

Abhijeet Bhorkar et al [5] presented analytical expressions of LTE-U throughput in the presence of WiFi. Paper shows the results with the help of threshold and transmission power during the usage of LTE-U and WiFi. It also compares the performance of WiFi and LTE-U. In some scenarios, transmission power of LTE-U and WiFi is reduced to 30dbm when transmission power is 20dbm, it improved the WiFi throughput. So, LTE-U is better with WiFi in terms of throughput.

Tauseef Ahmad et al [6] proposed the wireless network performance where LTE is used in Medium Access Control (MAC) layer. Traffic in User Datagram Protocol (UDP) is considered for evaluation. Throughput, end-to-end delay and jitter parameters have been evaluated. For downlink scenarios, parameters such as bandwidth and packet size were considered. As per the results, bandwidth and throughput were increased, but delay and jitter were decreased. This is implemented with NS2.

Dong Hyun Kim et al [7] proposed the communication of WiFi and LoRa technologies with the help of Long-Range, low-power and a large amount of data transmission. To provide efficient data transmission, WiFi and LoRa technologies are used. It also finds the distance between WiFi and LoRa. It is implemented with WiFi, LoRa gateway and an end device which is to test the performance of developed device. RSSI (Received Signal Strength Indicator) has valuated according to the distance and data rate. Based on the results obtained, LAN can communicate with high transmission rate and LoRa can communicate with low power and long-distances.

Martin Bor et al [8] describe the impact of the selection of parameters that define LoRa transmission based on performance of communication. This work developed a link probing regime that helps to find transmission parameters, which satisfy functional requirements. So, the method for LoRa transmission deploys the LoRa wireless network. Here, every transmission parameter is tested based on the performance impact. Based on the results obtained, a good transmission parameter suitable for a stronger network operation and balanced energy utilization is identified.

R.Bosisio et al [9] proposed a multi-antenna E-UTRA which conforms to 3GPP recommendation. The downlink is used in the system performance. Here, the users' scheduling and interference mitigation (like interference coordination and interference randomization) is proposed in terms of E-UTRA and compares the performance between the interference. According to the results, method is efficient for the traffic load because of the randomization of coordination and interference.

Mahmudur Rahman et al [10] proposed the interference avoidance method for LTE downlink. The proposed method is evaluated with simulation and it is compared with number of references mechanisms. It also attains the higher performance. Cell edge and throughput are compared to the previous methods. Here the mechanism is used in various scenarios. In terms of results, it shows that static mechanisms achieved improved cell-edge throughput.

Si WEN et al [11] proposed several interferences in coordination mechanism that includes centralized power control, resource allocation, mode selection strategy and distributed self-optimization schemes. These schemes provide, routine of D2D communication enabled network and evaluate the effect of local service ratio and user density. It also analyzes the efficiency of single cell assessment and multi-cell simulation. Based on these analyses, the results are observed that Device to Device communication increases the capacity of the cellular network.

Muhammad Usman Memon et al [12] provides a comprehensive assessment of the WIFI and ZigBee technology interference. Paper shows that how results are analyzed which gives the deployment information used in radio access technologies to avoid common interference. Here, the results show the ZigBee communication with various frequency offsets and distance respectively in the two scenarios. The ZigBee and WiFi investigated with the help of experiments and tests and the results were used in distance and frequency offsets between both the technologies.

Rongqing Zhang et al [13] proposed a scheme which make a network corresponding to the ideal resource sharing. They also introduced an interference-aware graph-based resource sharing mechanism which is more effective in allocating the resource at the base station with the less difficulty in computation. With the respective results, it analyzes two resource sharing schemes. Performance is more about network data rate that confirms the effectiveness of communication and the D2D communication underlays traditional cellular networks.

Thiemo Voigt et al [14] examine the use of directional antennae and more number of base stations with internetwork interference. Here, directional antennae signal strength at receiver side is evaluated without increasing transmission energy cost. According to this paper, both the methods improves the LoRa network performance in the interference settings. Based on the results, the directional antennae and several base stations have improved the performance.

Charalampos Orfanidis et al [15] examine the interference interactions between LoRa and IEEE 802.15 4g networks. It shows LoRa receives high packet rate with IEEE 802.15 4g interference. Paper shows the evaluation of protocols for both radio access networks. According to the results, LoRa is much better under interference than IEEE 802.15 4g and radio configuration of LoRa is important for degree of tolerance. Here the main significance of results comes in both the radio platforms where there are collision avoidance mechanisms, reliability and robustness in the higher layers.

Salah Eddine Elayoubi et al [16] proposed a model of inter-cell interference for the distribution of collisions which takes an effect of power control. Proposed model calculates the power in terms of Markovian Analysis. Paper compares different interference mitigation schemes. Based on the results, the two frequency planning schemes (reuse1 and reuse3) are compared, although reuse3 decreases interference and overall throughput because of the loss of resources.

Klaus Doppler et al [17] presented the for D2D communication method and events in LTE network. Here the D2D communication analysis provides feasibility in system simulations and in terms of traffic, the buffered traffic holds cellular and D2D connections. In terms of throughput, it reduces the D2D peers where it is not located in the same room. According to the results, D2D communication works under the cellular network. So, the throughput will increase to 65% compared to D2D traffic which is relayed on a cellular network.

Cenk M. Yetis et al [18] classified the problems of signal space interference as proper and improper based on various equations. With the help of Bernshtein's theorem, it finds the feasibility analysis by using MIMO interference channels. It has observed that when the system is improper, then it is infeasible in other systems.

Pengcheng Bao et al [19] described the problem in the D2D communication which underlays cellular networks. Some of the concepts such as accessible region and reusable region are used. It calculates boundary of both accessible and reusable region. With the help of this scheme, it effectively increases the interference between both regions.

Jaeyoung So et al [20] describe the LoRa network server(LNS) implementation on OpenStack. Experiment is done using open sources for LoRa terminal, LoRa gateway and OpenStack. According to the results, the operations on LNS has classified as four blocks: the gateway agent, application server agent, LoRa data and LoRa Agent. It also improves the scalability and maintainability and conform to system design.

Giriaja CV et al [21] provided a SNR based Master-Slave Dynamic D2D Communication Algorithm (SMSDCA). Algorithm increases the resource utilization and also provides better QoS. D2D channel is assigned by the base station. The proposed method considers the SNR, energy, and movement of the device. This is implemented in a MATLAB simulation. Result shows the throughput and count of users served in D2D communications. According to the results, the interference in the D2D communication is decreased by assigning the transmission power.

III. COMPARISON OF TECHNOLOGIES

TABLE I Comparison of LoRa and LTE

Features	LoRa	LTE
Modulation	SS Chirp	OFDMA
Bandwidth	500-125kHz	200MHz
Data Rate	300 Mbps	DL 3Gbps UL 1.5 Gbps
Output power	20 dBm	23-46 dBm
Range	15 Km	Up to 20 Km
Cost	Low	High
Power consumption	Low	High

IV. EXPERIMENTAL SETUP

A. Experimental setup for LTE

The performance of LTE is evaluated by sending 500B of data using OMNET++. LTE is a network for high-speed data communication. ENodeB and UE nodes represent the LTE network. The experiment is done with different node densities. eNodeBs are base stations in the LTE network. UE is a device used by the end-user for communication. UE uses the PGW (Packet Gateway) for communication. PGW that acts as an interface between various technologies. Fig.1 shows the experiment was done in 3000 * 3000 simulation area where various node densities such as 25, 50, 100, 150, and 200 and with different traffic flows such as one flow, two flow, three flow, four flow and five flow for each node densities. The packet interval is sent in 100ms with the linear mobility model. These simulation parameters and values are shown in the table II. One flow represents the main flow and two flow is adding interference to the main flow and it goes on up to four interference.

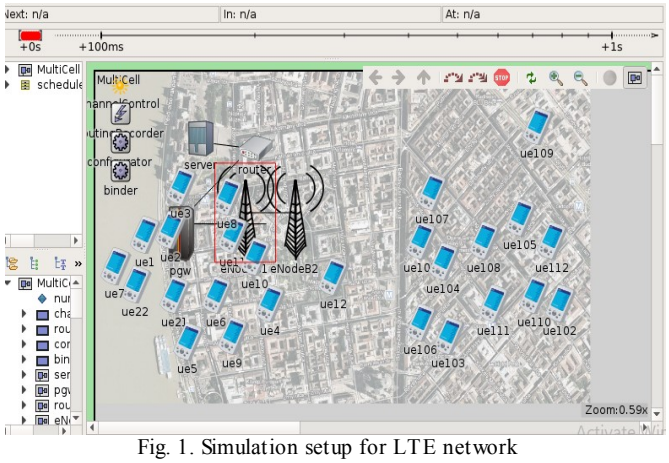

Fig. 1. Simulation setup for LTE network

TABLE II Simulation parameters and values

Parameters	Values
Simulator	OMNeT++
Node Density	25, 50,100, 150, 200
Flows	1,2, 3,4 5 flows
Packet Interval	100ms
Mobility Model	Linear Mobility Model
Simulation Area	3000*3000

B. *Experimental setup for LoRa*

The performance of LoRa is evaluated by sending 500B of data using OMNET++ and compared with LTE. Fig.2 shows the simulation was done in 3000 * 3000 simulation area where different node densities as 25, 50, 100, 150, and 200 and with different traffic flows as one flow, two flow, three flow, four flow and five flow for each node densities. The packet interval is sent in 100ms with the linear mobility model. These simulation parameters and values are shown in the table III. One flow represents the main flow and two flow is the main flow with adding interference to the main flow and it goes on up to four interferences.

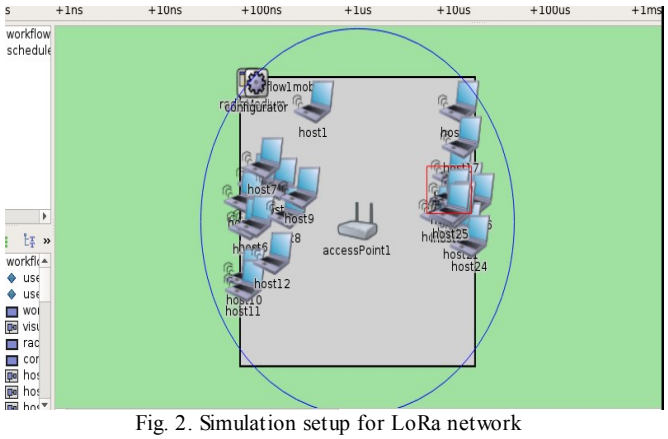

Fig. 2. Simulation setup for LoRa network

TABLE III Simulation parameters and values

Parameters	Values
Simulator	OMNeT++
Node Density	25, 50,100, 150, 200
Flows	1,2, 3,4 5 flows
Packet Interval	100ms
Mobility Model	Linear Mobility Model
Simulation Area	3000*3000

V. RESULTS AND ANALYSIS

A. *LTE Network*

Table IV shows the PLR (Packet Loss Ratio) for LTE network as traffic increases by one flow up to five flows.

TABLE IV. PLR for LTE network.

Flows	PLR				
	Node Count				
	25	50	100	150	200
1	0.2	0.2	17.6	19.6	19.6
2	11.6	19.6	30.2	37.4	39
3	15.6	26.4	36	40.2	57.2
4	17.8	36	48	48	59.4
5	19.6	48	77.6	77.6	81

Fig.3 shows the PLR ratio for LTE network with different node densities 25, 50, 100,150 and 200 with different interference - one flow, two flow, three flow, four flow and five flow.

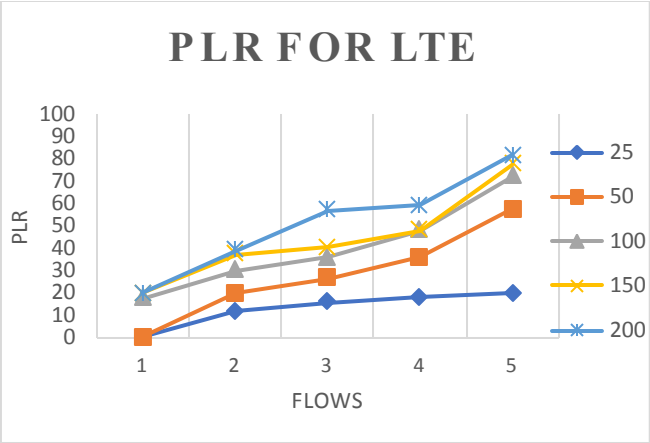

Fig. 3. PLR for LTE with various node densities and interference

In the above experiment, PLR is calculated by using the formula as follows:

$$PLR = (No\ of\ lost\ packet / No\ of\ sent\ packet) * 100 \quad (1)$$

The simulation results show that as traffic flow increases for increased node densities, packet loss ratio also increases. PLR is high with 200 node density for all the traffic flow when we compared to other node densities 25, 50, 100, and 150. PLR is less with 25 node densities when compared to other node densities 50,100 and 200.

B. LoRa Network

Table V shows the PLR (Packet Loss Ratio) for LoRa network as traffic increases by one flow up to five flows.

TABLE V. PLR for LoRa Network

Flows	PLR				
	Node Count				
	25	50	100	150	200
1	0	0	0	0	0
2	0.6	1.6	1.6	1.8	3/39
3	1.6	5	7.4	8.8	10.4
4	7.2	7.6	8	9	13.8
5	8.6	9.4	15.8	16.2	17.8

Fig.4 shows the PLR ratio for LoRa network with different node densities 25, 50, 100,150 and 200 with different interference one flow, two flow, three flow, four flow and five flow.

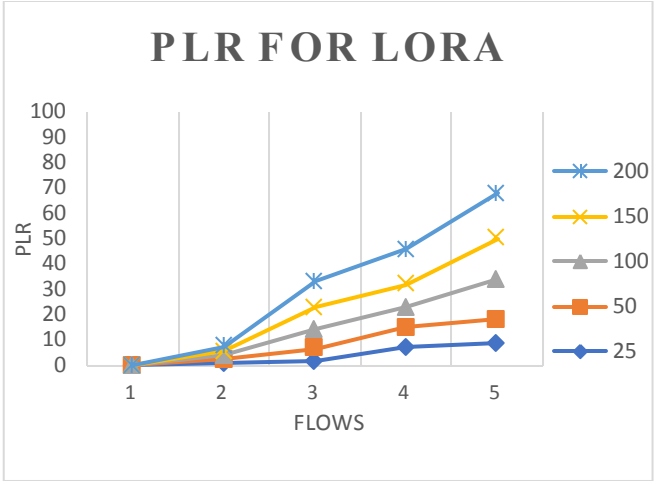

Fig.4. PLR for LoRa WiFi with various node densities and interference

Simulation results proved that the performance of LoRa is better, i.e. PLR is less when compared to LoRa WiFi. Results have shown that as traffic increases, PLR also increases and it is decreased with less traffic flow. PLR is high in LTE when there is the same traffic in both LTE and LoRa. So, the performance of LoRa is better than LTE with different node densities and traffic flows.

VI. Conclusion

The overview of this paper explains on LoRa WiFi and LTE wireless networks provide high data rates and better service when compared to other networks like 1G, 2G, and 3G etc. These networks are heavily used by the users for communication. In our Simulation, we have shown how LTE and LoRa work with different node densities 25, 50, 100, 150 and 200. PLR is calculated as nodes increases with increased traffic. PLR is compared between LTE and LoRa. The results of the simulation showed that the performance of LoRa is better when we compared to LTE because PLR is high in LTE network with increased node density and increased traffic compared to LoRa.

References

[1] U. S. Vaishnav and M. Panda, "Resource Allocation for Device-to-Device (D2D) Communication in Underlaying Cellular Network," pp. 1424–1430, 2017.

[2] A. Mohammed, A. Algader, A. Gasimelsid, and A. B. A. Nabi, "Vertical Handover in Long Term Evaluation (LTE)," vol. 4, no. 8, pp. 2013–2016, 2015.

[3] S. Jimaa, "LTE-A an Overview and Future Research Areas," pp. 395–399, 2014.

[4] Z. H. Mir and F. Filali, "LTE and IEEE 802 . 11p for vehicular networking : a performance evaluation," pp. 1–15, 2014.

[5] A. Y. Ding, P. Hui, M. Kojo, and S. Tarkoma, "Enabling energy-aware mobile data offloading for smartphones through vertical collaboration," *Proc. 2012 ACM Conf. Conex. student Work. - Conex. Student '12*, p. 27, 2012.

[6] T. Ahmad, "Behavior of UDP Traffic over LTE Network," vol. 137, no. 3, pp. 1–6, 2016.

[7] D. H. Kim, J. Y. Lim, and J. D. Kim, "Low-Power, Long-Range, High-Data Transmission Using Wi-Fi and LoRa," in *2016 6th International Conference on IT Convergence and Security (ICITCS)*, 2016, pp. 1–3.

[8] M. Bor and U. Roedig, "LoRa Transmission Parameter Selection," in *2017 13th International Conference on Distributed Computing in Sensor Systems (DCOSS)*, 2017, pp. 27–34.

[9] R. Bosisio and U. Spagnolini, "Interference Coordination Vs.

Interference Randomization in Multicell 3GPP LTE System," in *2008 IEEE Wireless Communications and Networking Conference*, 2008, pp. 824–829.

[10] M. Rahman, H. Yanikomeroglu, and W. Wong, "Interference Avoidance with Dynamic Inter-Cell Coordination for Downlink LTE System," in *2009 IEEE Wireless Communications and Networking Conference*, 2009, pp. 1–6.

[11] S. Wen, X. Zhu, Z. Lin, X. Zhang, and D. Yang, "Optimization of interference coordination schemes in Device-to-Device(D2D) communication," *2012 7th Int. ICST Conf. Commun. Netw. China, CHINACOM 2012 - Proc.*, pp. 542–547, 2012.

[12] M. U. Memon, L. X. Zhang, and B. Shaikh, "Packet loss ratio evaluation of the impact of interference on zigbee network caused by Wi-Fi (IEEE 802.11b/g) in e-health environment," in *2012 IEEE 14th International Conference on e-Health Networking, Applications and Services (Healthcom)*, 2012, pp. 462–465.

[13] Rongqing Zhang, Xiang Cheng, Liuqing Yang, and Bingli Jiao, "Interference-aware graph based resource sharing for device-to-device communications underlaying cellular networks," in *2013 IEEE Wireless Communications and Networking Conference (WCNC)*, 2013, pp. 140–145.

[14] T. Voigt, M. Bor, U. Roedig, and J. Alonso, "Mitigating Inter-network Interference in LoRa Networks," no. 1, pp. 1–6, 2016.

[15] C. Orfanidis, L. M. Feeney, M. Jacobsson, and P. Gunningberg, "Investigating interference between LoRa and IEEE 802.15.4g networks," in *2017 IEEE 13th International Conference on Wireless and Mobile Computing, Networking and Communications (WiMob)*, 2017, pp. 1–8.

[16] S. E. Elayoubi and O. Ben Haddada, "Uplink intercell interference and capacity in 3 G LTE systems," *ICON 2007 - Proc. 2007 15th IEEE Int. Conf. Networks*, vol. 2, no. 3, pp. 537–541, 2007.

[17] N. R. C. Klaus Doppler, Mika Rinne, Carl Wijting, Cássio B. Ribeiro, and Klaus Hugl, "Device-to-Device Communication as an Underlay to LTE-Advanced Networks," no. December, pp. 42–49, 2009.

[18] C. M. Yetis, Tiangao Gou, S. A. Jafar, and A. H. Kayran, "On Feasibility of Interference Alignment in MIMO Interference Networks," *IEEE Trans. Signal Process.*, vol. 58, no. 9, pp. 4771–4782, Sep. 2010.

[19] P. Bao, G. Yu, and R. Yin, "Novel Frequency Reusing Scheme for Interference Mitigation in D2D Uplink Underlaying Networks," no. July 2013, pp. 491–496, 2013.

[20] J. So, D. Kim, H. Kim, H. Lee, and S. Park, "LoRaCloud: LoRa platform on OpenStack," in *2016 IEEE NetSoft Conference and Workshops (NetSoft)*, 2016, pp. 431–434.

[21] Giriraja C V and T. K. Ramesh, "SNR Based Master-Slave Dynamic Device to Device communication in underlay cellular networks," in *2015 International Conference on Advances in Computing, Communications and Informatics (ICACCI)*, 2015, pp. 2114–2117.

[22] M. Pushpalatha, N. V. Shruthi, T. K. Ramesh and S. K. Konda, "Efficient Multicast Algorithm for Dynamic Intra Cluster Device-to-Device communication for small world model paper," *2015 International Conference on Advances in Computing, Communications and Informatics (ICACCI)*, 2015, pp. 1782-1786

[23] S. Unni, D. Raj, K. Sasidhar and S. Rao, "Performance measurement and analysis of long range Wi-Fi network for over-the-sea communication," *2015 13th International Symposium on Modeling and Optimization in Mobile, Ad Hoc, and Wireless Networks (WiOpt)*, 2015, pp. 36-41.

[24] U. S. H. Varma, M. V. S. Nikhil, G. S. S. K. Manikanta, T. B. S. Kiran and S. Kirthiga, "Cooperative MIMO with relay selection for LTE advanced system," *2017 International Conference on Circuit ,Power and Computing Technologies (ICCPCT)*, 2017, pp. 1-6.

Proceedings of the Fourth International Conference on Communication and Electronics Systems (ICCES 2019)
IEEE Conference Record # 45898; IEEE Xplore ISBN: 978-1-7281-1261-9

Implementation On High-Performance Quasi-Z-Source Series Resonant DC To DC Converter for Photovoltaic Module Level Power Electronics Applications

Tejashri S .Wable
Department of Electrical
G. H. Raisoni Institute of Engineering And Technology
wabletejashri@gmail.com

V. M.. Panchade
Department of Electrical
G. H. Raisoni Institute of Engineering And Technology
vmpanchade@gmail.com

Abstract— The superior semi Z-source arrangement resounding DC to DC converter as a hopeful topology for the PV module level power gadgets applications. The converter includes a wide information voltage and burden guideline go on account of the multi-mode task, for example at the point when the shoot-through heartbeat width balance and stage move tweak are joined in a solitary changing stage to understand the lift and buck working modes, separately.

Keywords: solar photovoltaic; resonant converter; DC to DC converter; quasi Z-source converter; renewable energy; MIC

I. INTRODUCTION

A two-organize topology is proposed, which comprises of a lift converter and a SRC. The lift converter steps the changing PV voltage VPV to a halfway steady voltage transport VDC, mid. The SRC converter is worked at fres,1 fifty-fifty cycle broken conduction mode (HC-DCM). This empowers an exceptionally effective voltage change by using the transformer spillage inductance as reverberation inductance and the charging current in mix with the parasitic yield capacitances of the full-connect MOSFETs for ZVS switching. A DC-to-DC converter is an electronic circuit which changes over a wellspring of direct current (DC) starting with one voltage level then onto the next. It is a class of intensity 8 converter. The DC yield voltage is constrained by fluctuating obligation cycle. There are three essential kinds of DC – DC converters considered for DC control transformation. These circuits are structured by utilizing a semi directing switch, for example, a thyristor, IGBT, GTO. The switch is turned on by an entryway beat (obligation proportion). The switch is associated in arrangement with the heap to a DC supply, or a positive voltage is connected between the terminals. At the point when the turn is killed, the present stream diminishes which is considered as underneath holding current, or an invert (negative) voltage is connected among anode and cathode terminals. Along these lines, legitimate entryway beats are required for acquiring the ideal converter yield. The impedance arrange gives a proficient outcome the power change Different topologies and control strategies utilizing distinctive impedance-source systems have been displayed in the writing, e.g., for flexible speed drives, uninterruptible power supply (UPS) disseminated age, (energy component, photovoltaic (PV), the breeze, and so on.) battery or super capacitor vitality stockpiling electric vehicles. The general square graph for impedance arrange is appeared in figure1. With the exchanging design, it is feasible for electrical power change application.

By and large, the Z-source converters are ordered into two fundamental sorts: one is voltage-encouraged another is a current-sustained inverter. Notwithstanding, ZSI gives the support between the source and inverter extension and it effectively makes the short and an open-circuit whenever relying upon the method of activity. Accordingly, the customary VSI/CSI based impedance arrange experiences following issues like broken info current in the lift mode for the voltage-encouraged ZSI. The improved exhibition creates the answer for this issue which has equipped for bidirectional power stream and buck– help activity, despite the fact that the changes must be turn around blocking gadgets. This topology is for the most part conceivable in sustainable power source age and basic engine drives applications.

II. LITERATURE SURVEY

Zambra, D. A. B., et al., (2010) proposed "Examination of NeutralPoint-Clamped, Symmetrical, and Hybrid Asymmetrical Multilevel Inverters." This paper presents execution files, for example, complete symphonious bending, first-request mutilation factor, second-request twisting variable, normal mode voltage, semiconductor control misfortune circulation, and warmth sink volume. Staggered inverters are intended to exhibit 99% productivity at the ostensible working point [1]. Fundamentally, these kinds of structures require countless. Qian, W., et al., (2011) proposed "Trans-Z-source inverters." The proposed inverter is developed by utilizing two inductors and capacitors 64 interfaced with DC source and the inverter connect [2]. This is workable for both buck and lift activity expanded voltage gain and the voltage worry in the yield waveform. It is another bidirectional power stream based diode - impedance organize for building up the switch blocking IGBT. In this way wide scope of voltage is acquired from different applications, for example, half and half/electrical vehicles to other engine applications.

Trinh, Q. N., et al., (2012) proposed "another Z-source Inverter Topology with High Voltage Boost Ability." This paper proposes the voltage gain proportion of SL inverter is high and little shoot - through obligation proportion. The volume and cost of the framework are practically same as those of the regular one. Symphonious current is delivered over the inductor with inverter side. Huge channels are required.[3]

Nguyen, M. K., et al., (2013) proposed "TZ-Source Inverters." This paper proposes a solitary stage high-advance up lift voltage inverter dependent on transformers, called TZ-source inverters. This inverter creates an exceptionally high lift voltage gain when the turn proportion of the transformer is bigger than one. This decreases the transformer's size and weight while delivering a similar yield voltage gain yet the transformer windings produce voltage stresses.[4]

Tang, Y., et al., (2013) proposed "Z-source AC-AC converters taking care of compensation issue." In this paper, a Z-source AC-AC converter is displayed to improve the buck-support capacity, which incorporates four switches in single stage and six switches in three stages. For wellbeing reason, another correspondence technique is utilized without utilizing any snubber circuits. The outcomes are confirmed both by recreation and trial bad habit. These converters have more points of interest and accomplish low exchanging misfortunes and less number of switches, thusly high effectiveness and extraordinary unwavering quality were accomplished.[5]

Reddy ,T. S., et al., (2013) proposed "Novel DC-DC Converter for PV framework with High Voltage Gain." This paper exhibits another group of dc– dc converters real points of interest of this topology are the info current is ceaseless with low swell; the information inductor is intended for double the exchanging recurrence, with resulting weight and volume decrease; the voltage worry over the switches is lower than half of the yield voltage, and normally cinched by one yield channel capacitor. As a weakness, a little snubber is vital for each switch and one extra winding for every cell is required for the autotransformer.

Zengin, S.J, et al., (2013) proposed "Decoupling Capacitor Selection in DCM Flyback PV Micro inverters Considering Harmonic Distortion" [6]. This paper centers around the choice of least decoupling capacitor esteem for the best possible task of irregular conduction mode by thinking about the all out symphonious twisting (THD) and PV control usage proportion [11]. A decoupling capacitor choice strategy for single-stage and two-organize flyback inverters is proposed. For single-arrange inverters, the decoupling capacitor is set over the PV yield terminals, and ought to be estimated by the ideal THD limit. For two-organize inverters, the control strategy for the dc– dc converter decides the phase where the decoupling capacity happens. 66 Thus, the PV side decoupling capacitor ought to be dimensioned by the PV control usage proportion, and the inverter side decoupling capacitor ought to be chosen by the ideal THD confinement. It is noted from the proposed framework yield reaction of the information voltage module, channel to source voltage and exchanging beat, transformer essential voltage and auxiliary voltages, input current, transformer optional side current, yield voltage, yield current, and yield voltage are decreased [12].

Beriber,D., et al., (2013) proposed "MPPT Techniques for PV Systems." This paper proposes another plan to expand the yield control from dc interface sun oriented board [7]. Consequently the converter requires MPPT circuit. The lift converter is utilized to venture up the vitality level just as to coordinate the 50 load voltage. There are three MPPT procedures for reviewing power creating application, for example, Perturb and Observe, Incremental Conductance, fluffy rationale based following method. The P&O and Incremental Conductance are extremely old model calculations and it has more downsides. The unfaltering state working point wavers greatest area, it might be the wastage of intensity from the PV board. However, the fluffy rationale controller gives quick and stable following most extreme power as contrasted and other control procedures. The significant bit of leeway of this plan is that it quantifies the PV

current flawlessly. Das, M., et al., (2014) proposed "A Novel Control Strategy for Standalone Solar PV Systems with Enhanced Battery Life." another control plot ABC (three stage) to DC is proposed for an independent PV application [8]. There are two power changing over stages utilized for high increase DC– DC activity, which is trailed by three stage converter. The responsive power load is considered for PV based independent application and the dynamic power request is constrained by controlling the dc connect voltage. Besides, the responsive power is constrained by shifting the inverter yield voltage size. The greatest power tracker is consolidated with the controller. The MPPT give control at the season of sun powered power request and improve the battery lifetime. However a dump load isn't required for overabundance vitality charging and load generation. The bidirectional converter is utilized to understand the DC interface based battery association.

III. PROPOSED SYSTEM

The galvanically bound semi Z-source game plan full DC-DC converter is assessed as a cheerful methodology for Photovoltaic applications [9]. This control system contains the qZS sort out (LqZS1, LqZS2, CqZS1, CqZS2, SqZS), a full-interface inverter (S1… S4), the voltage doubler rectifier (D1, D2, C1, C2) and a phase up isolation transformer TX.

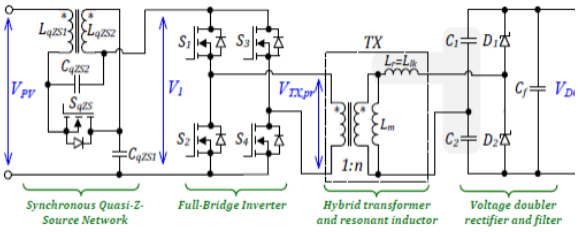

Fig 1. Block diagram of proposed system

The voltage range information is accessible. no matter what voltage, current knowledge incorporate. From above estimated structure the input is from pv panel which is 11.33 V (from fig 4). After Using full bridge inverter this 11.33V DC is converted to ac which is as input to to the transformer which having ratio 1: 230. Using VDR we get the increased voltage in dc form whicg is near to 30V (From fig 5)

Table I Specifications of Components used in the Hardware

Component	Specifications
S_1, S_2, S_3, S_4	MOSFET IRF 540
S	MOSFET CZ01B508
D_1, D_2	UF 5408, 4Amp, 250V
C_f	0.1uF ac 400Vac
L_f	1.2mH 4Amp

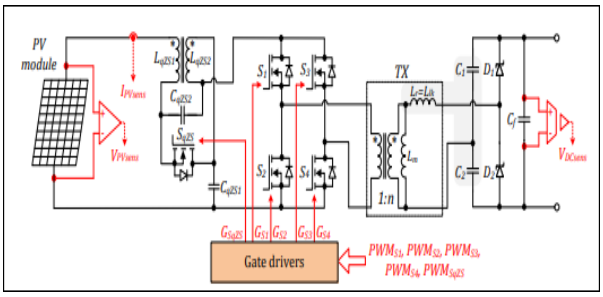

Fig 2 Block diagram of the control system

The proposed control framework is very basic since it doesn't control the DC-connect voltage. In many appropriated age applications, the DC-interface voltage is adjusted by the power utilization of the heap, for example inverter, vitality stockpiling, and so forth. On the off chance that the DC link voltage surpasses the cut off points characterized for the typical task, the insurance calculation will cripple the converter activity.

IV. RESULT

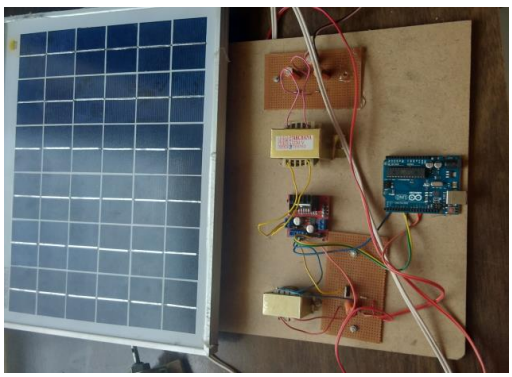

Fig 3. Hardware model of proposed system

Fig . 4. Input voltage from PV panel.

Fig 5. Output voltage from voltage doubler rectifier side

V. CONCLUSION

An unusual single-sort out galvanic in nature withdrawn huge development in DC-DC converter. Because of the different mode operation the results from the output are with increased in voltage range and this is our main aim for this methodology. Course of action reverberating tank consolidated to the helper bit of converter incorporates a extensive voltage data and weight rule expand. Let the above defined system gives the results which having high inclination with above methodology, believing upon the working condition we get desire results.

For future work we will develop it for the aircraft technology as well as for distributed power generation which will generate from renewable as well as non-renewable sources.

REFERENCES

[1] Zambra, D. A. B., Rech, C., &Pinheiro, J. R. (2010). Comparison of Neutral-Point-Clamped, Symmetrical, and Hybrid Asymmetrical Multilevel Inverters. IEEE Transactions on Industrial Electronics, 57(7), 2297–2306.

[2] Qian, W., Peng, F. Z., & Cha, H. (2011). Trans-Z-Source Inverters. IEEE Transactions on Power Electronics, 26(12), 3453–3463.

[3] Trinh, Q.-N., Lee, H.-H., & Chun, T.-W. (2011). A new Z-source inverter topology to improve voltage boost ability. 8th International Conference on Power Electronics - ECCE Asia.

[4] Nguyen, M.-K., Lim, Y.-C., & Kim, Y.-G. (2013). TZ-Source Inverters. IEEE Transactions on Industrial Electronics, 60(12), 5686–5695.

[5] Tang, Y., Zhang, C., & Xie, S. (2007). Z-Source AC-AC Converters Solving Commutation Problem. 2007 IEEE Power Electronics Specialists Conference.

[6] Zengin, S., Deveci, F., &Boztepe, M. (2013). Decoupling Capacitor Selection in DCM Flyback PV Microinverters Considering Harmonic Distortion. IEEE Transactions on Power Electronics, 28(2), 816–825.

[7] Beriber, D., &Talha, A. (2013). MPPT techniques for PV systems. 4th International Conference on Power Engineering, Energy and Electrical Drives.

[8] Das, M., &Agarwal, V. (2014). A novel control strategy for stand-alone solar PV systems with enhanced battery life. 2014 IEEE Applied Power Electronics Conference and Exposition - APEC 2014.

[9] Vinnikov, Dmitri, Andrii Chub, Elizaveta Liivik, and Indrek Roasto. "High-Performance Quasi-Z-Source Series Resonant DC-DC Converter for Photovoltaic Module Level Power Electronics Applications", IEEE Transactions on Power Electronics, 2016.

[10] Reddy ,T. S., et al., (2013) proposed "Novel DC-DC Converter for PV framework with High Voltage Gain.

[11] Sinan Zengin, Fırat Deveci, Mutlu Boztepe. "Decoupling Capacitor Selection in DCM Flyback PV Microinverters Considering Harmonic Distortion", IEEE Transactions on Power Electronics, 2013

[12] Andrii Chub, Dmitri Vinnikov, Roman Kosenko, Elizaveta Liivik. "Wide Input Voltage Range Photovoltaic Microconverter With Reconfigurable Buck–Boost Switching Stage", IEEE Transactions on Industrial Electronics, 2017

Proceedings of the Fourth International Conference on Communication and Electronics Systems (ICCES 2019)
IEEE Conference Record # 45898; IEEE Xplore ISBN: 978-1-7281-1261-9

MODIFIED BUCK BOOST CONVERTER WITH REDUCED CURRENT RIPPLE USING DELTA TO STAR IMPEDANCE NETWORK

SANJU B
EEE DEPARTMENT
ASIET
KALADY,INDIA
sanjutnj@gmail.com

Dr.JENO PAUL
EEE DEPARTMENT
ASIET
KALADY, INDIA
jeno.eee@adishankara.ac.in

SREEHARI S
EEE DEPARTMENT
ASIET
KALADY, INDIA
sreehari.eee@adishankara.ac.in

REJOICE THOMAS PAUL
EEE DEPARTMENT
ASIET
KALADY, INDIA
rejoicetthannikott@gmail.com

KRISHNAPRIYA VINOD
EEE DEPARTMENT
ASIET
KALADY, INDIA
krishnapriyavinodt@gmail.com

ABSTRACT **- The paper presents a Buck-Boost converter with reduced ripple current based delta star network. The main objectives are to reduced current ripples and improve Efficiency of the Conventional Buck Boost Converter. A delta to star impedance network using converter input side .The proposed system consists of the Buck Boost Converter's inductor, a Coupled based inductor, Resonant inductor & capacitor. The buck boost converter efficiency is poor for high gain and Current ripple high.so, proposed Buck Boost Converter ripple current can be Reduced and efficiency can be improved. Hence the Buck Boost Converter with delta to star network is used to improve the above mentioned-parameters.**

The existing and modified system is verified using MATLAB simulink software and results proves the above mentioned parameters.

Keywords – Impedance network, Buck Boost Converter, Ripples Reduction

I INTRODUCTION

Current scenario Different delta to star techniques have been developed & studied in the literature survey to be adopted in the circuit to increase converter's o/p performance, that is the Conversion ratio, to different benefits like the Distributed systems powered by renewable sources. Examples, WIND power system, & SOLAR system .then commonly used as LED driver, used for power factor corrections ,used in HVDC system ,and used in hybrid electric vehicles[1] – [5] .But , some papers have been put into improve converter's input side performance, that is the current ripple of the input side, using delta star networks.

Very unique from way to deal with the ripples problem of the buck boost by converter using proposed network in input side of the boost converter disadvantages are Lower Dynamic Response of the circuit & make the boost circuit un necessarily big and decreasing the efficiency , using the coupled based delta star technique is one of the final solution.[6] but, most technologies are implemented by replacing the converter's input side inductor with coupled based delta star Network.[7] which may not be an convenient applications in industrial benefits as it required to improve the real circuit of the conventional converter.[9]-[12] currently, one another coupled based delta star network has been proposed in to reduce the i/p side ripples without the value to replace the Converter's Inductor. but, two capacitor pair are needed in this type of

method & the Resonant Inductor is required to be comparatively high.

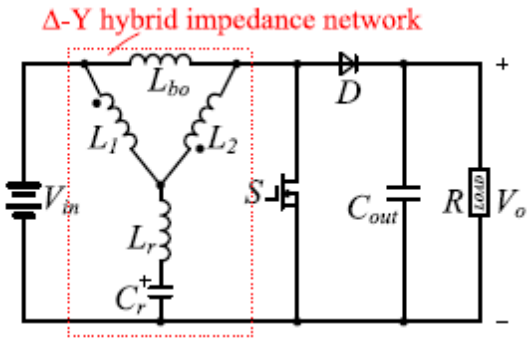

Figure 1.Conventional boost converter with impedance network

Figure 1 Shows the structure of conventional boost converter. This work propose a delta star technique based conventional converter to work with the ripple problem for the bst converter . delta star network consists of a main inductor, a L1,L2 (coupled) inductor, and a Lr inductor & two capacitor. The existing system remains the conventional converter's original circuit and voltage conversion advantage reduce the ripples & the improve efficiency of the conventional converter.

The paper presents a structure for effectively reduced ripple current with high efficiency ,but no help for minimized the Average Current of the buck-boost circuit's inductor.in this case we are using delta to star network based modified Buck Boost Converter with reduced input ripples. Active solution can adopted to reduce the input side ripples for conventional boost converter. The most attractive and typical solutions is to merge other power converters using an Interleaved Converter. the i/p current distributed to Inductor in other power converter and i/p side ripples can simultaniously reduced by normally controlling other power converters. and, the stress of current on each other normal power converter's inductors can be distributed at same time. But, this technique may high to the cost increases and very complex of the existing system as more passive & active component are needed.

II PROPOSED SYSTEM

A Buck Boost circuit

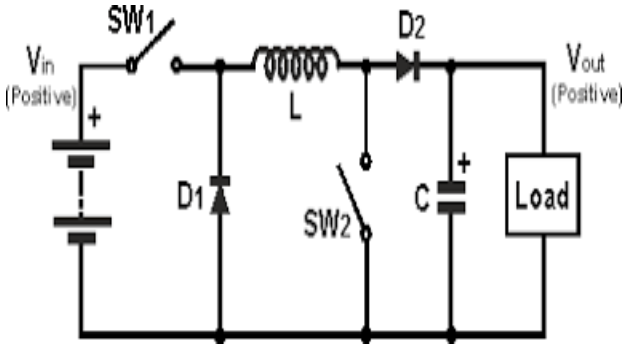

Figure 2.Buck boost structure

Figure 2.shows the circuit of the Conventional Buck Boost converter is greater than or less than the I/P voltage. A circuit having the two main switches, two different diodes, inductor, and output capacitor. The voltage of the magnitudes depends upon the main duty cycle. these converter also known as the Step down & Step up transformers. The i/P voltage is step down/up to some level of less than or more than the input voltages, by using the lower conversion level, the output power is equal to the input.

B.Modified system

This paper proposes delta star network based Buck-Boost converter with current ripple reduced The fig 3. Shows the proposed circuit.

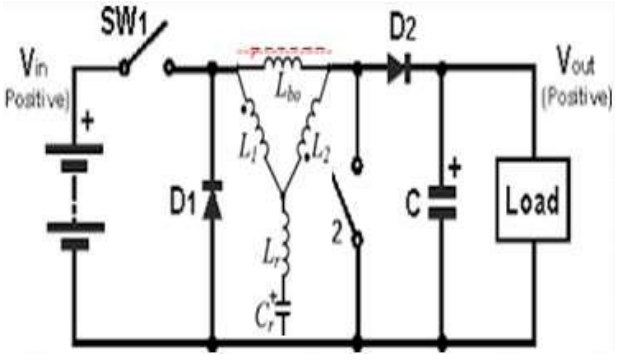

Figure.3.Proposed Converter

The Buck-Boost structure consists of two main MOSFETs S1 & S2,and two converter diodes D1 & D2 & the delta star network consists of a Lbo main inductor , L1 and L2 Coupled Inductor (*L*2 is the secondary and *L*1 is the primary sides),and a additional inductor Lr and two capacitor Cr. The modified converter remaining the Buck Boost Converter's original circuit and Δge conversion advantage reduce the ripple current input side and the current of the inductor.

To modify the equations of the working principle, two assumption are as follows:

i) All components are ideal
ii) Two capacitor size is large that the switching Δge across each capacitor is considered.

C.Modes of operations

The circuit has 4 modes of operation in both discontinuous & continuous modes of the inductor.

Mode1 : In this mode S1 is ON condition, and converter diode D2 turned ON, Diode D1 reverse bias condition, switch S2 is OFF, current is flowing through the load via the main inductor and current in the load and the charge on output capacitor builds up gradually during the ON period.

Mode 2 : Switch S2 is ON and S1 still ON & the D2 diode is reversed current by the voltage of the output, The Inductor is charged by the Δge of the i/p V & I increases. and The current through the La inductor & the current through the *Lb*(*iLb*) inductor is Increasing from *iLa* is bigger than *inductor 2 current*, The current through the Lc inductor (*iLc*) is +ve. the is store the energy. As to the increase the value in *iLbo*, The maximum of the ripple eliminated in this case.

Mode 3 :The switch is OFF & the D1 and D2 is same time conducting. the initial source of current now the inductor. The Lbo inductor is and energy releasing & current decreasing. current inductor via (*iLa*) is increasing & current flow in the next *Lb*(*iLb*) is decreasing. *iLb* is bigger than *iLa*, current flowing the *Lc*(*iLc*) is not +ve & the *Cr* is energy releasing. In this mode4, the value is increased in *iLa* can balance the amount is decreased in *iLbo*, the inductor input side current ripple reduced.

Mode 4 : in this mode switch S1 conducting and diode D2 still conducting, diode D1 reversed biased, switch S2 is turned OFF, current is flowing through the load from the converter inductor and the output Co charged,D2 is now forward bias.

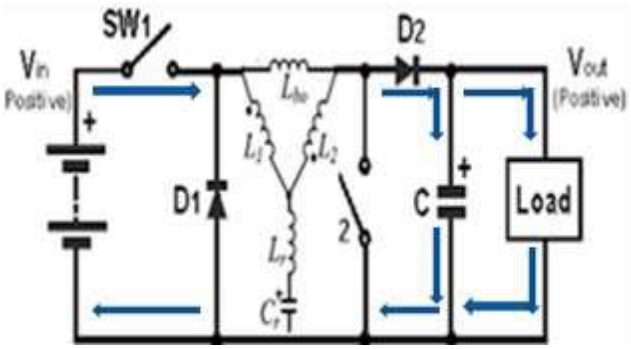

(a)

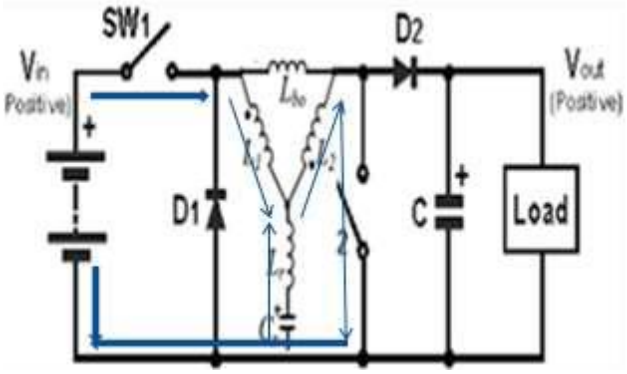

(b)

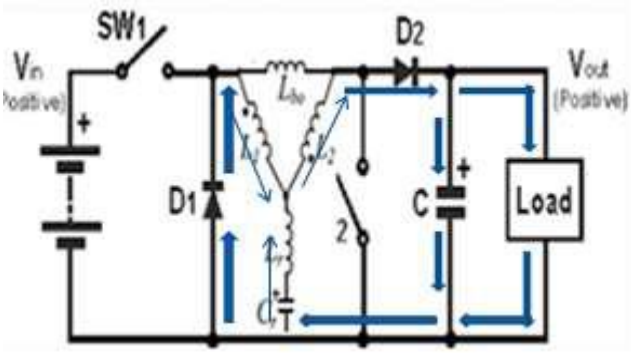

(c)

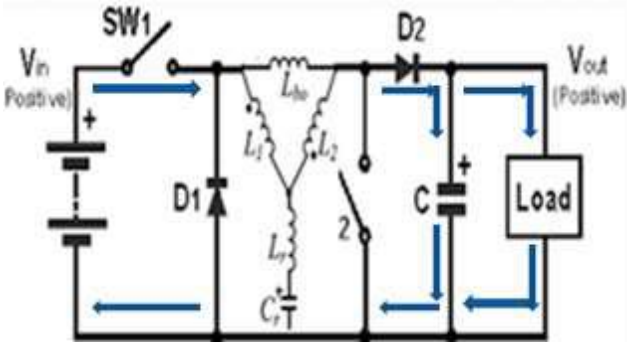

(d)

Figure .4 Modes of operation (a) Mode I (b) Mode II (C) Mode III (d) Mode IV

D.Design equations

converter having the Lbo inductor, two switches S1,S2,Cout capacitor & load. Modified circuit having L1,L2 inductor, Cr inductor, resonant capacitor . By using Kirchof law,

La = inductor 1 + M
Lb= inductor 2 +*M*
Lc= Resonant inductor (1)

where inductor 1 & inductor *2* of the Coupled Inductor and Equivalent inductor is the inductor 3, *M mutual inductor*

Dutyratio

D =Ton/T (2)

Output voltage

Average voltage across the main inductor is zero,

Vo = Dvin / (1 – D) (3)

To design capacitor & inductor of the Buck Boost Converter

Lo = (1-D)Vo/(ΔILO)fs (4)

Output capacitor

Co=D/ (Rfs) (ΔVco/ vo) (5)

The avg current of the conventional converter inductor Lbo, equation given below

IAvg-D=Iin (1- D) (6)

IAvg-s=IinD (7)

Using kirchoff's circuit law for input current

Iin=ILbo + ILa (8)

The i/p side ripples current of the modified converter can be derived as

ΔIin=ΔILbo + ΔILa (9)

III SIMULATION RESULTS

The MATLAB simulation results of the existing & .proposed converter results are obtained and verified. Fig.5 shows the voltage current across the switch and fig 6 output diode voltage and current .

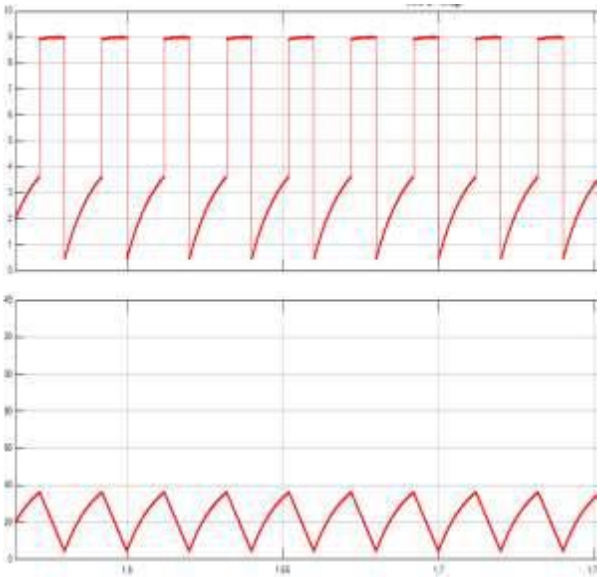

Figure .5 Input current & voltage of the conventional boost converter

Figure 5.shows the inductor current ripple . To reduce the inductor ripple current using the delta to star network & figure 6.diode voltage and current.

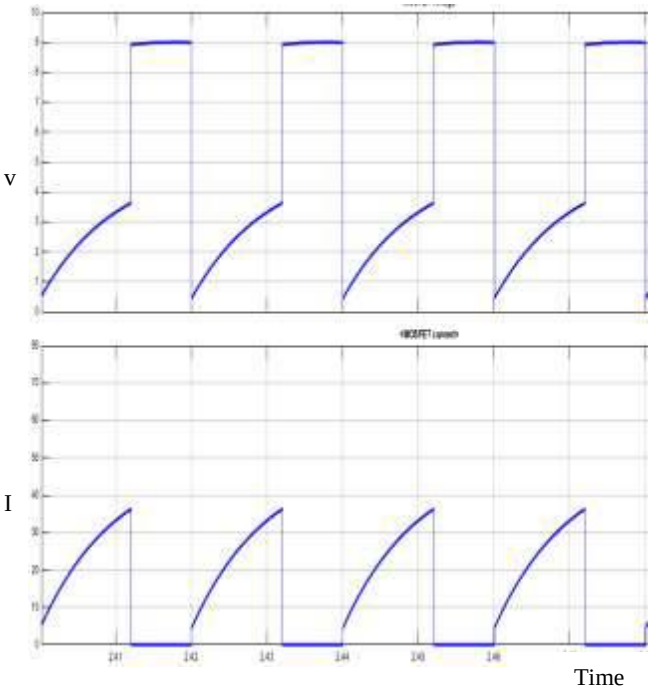

Figure .6 Diode V and I of the boost Converter

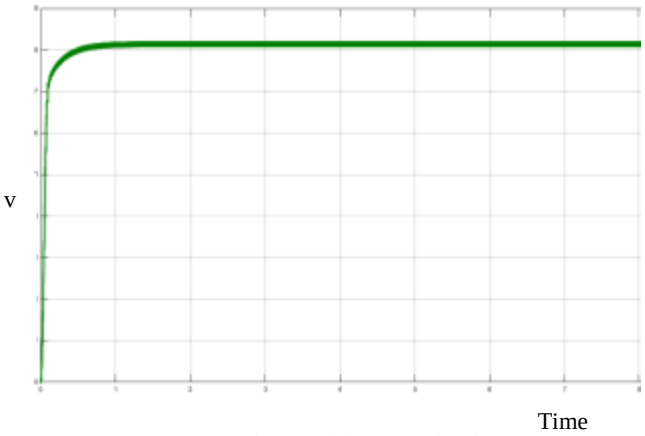

Figure .7 O/P Δge of the conventional boost converter

Figure 5 shows switching across the voltage and current(I) of the boost converter and the ripple (I)current is identified in the traditional converter. Fig7 shows output voltage of the traditional converter.

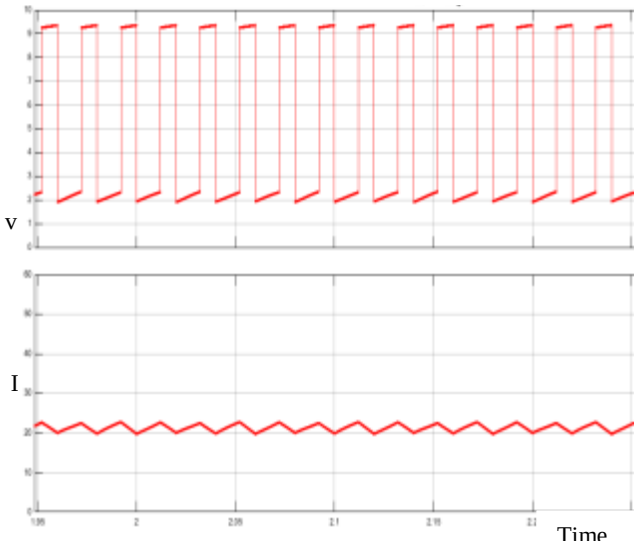

Figure .8 Inductor current and switching voltage of the existing System

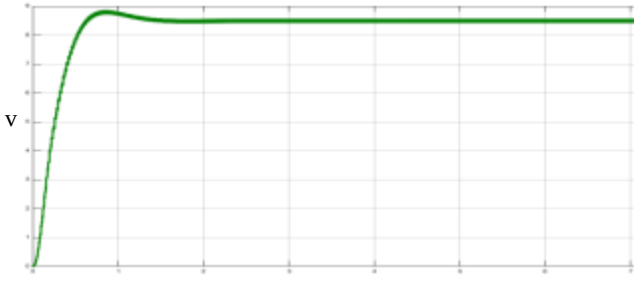

Fig .9 Output voltage of the existing system

Fig 8 shows switching across the voltage and current of the existing circuit, the ripple current can be reduced compared to the traditional converter. Fig 9 shows output voltage of the existing circuit.

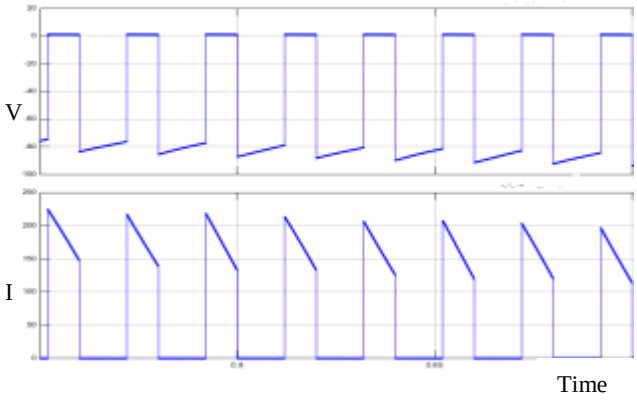

Figure .10 Diode V and I of the modified system

figure 10 diode voltage and current of the modified system. figure 11 shows the inductor current and switching voltage of the modified system.

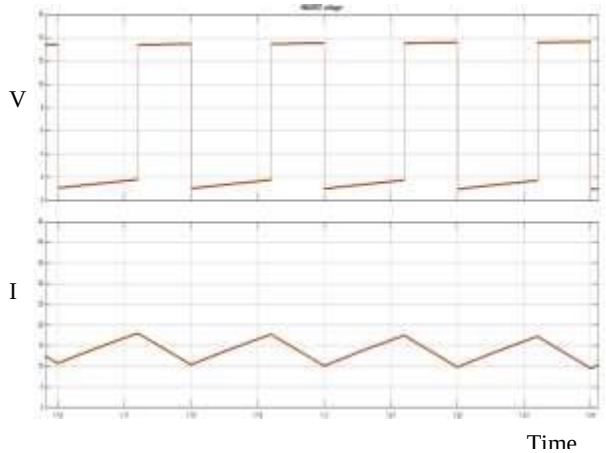

Fig .11 Inductor current and the MOSFET voltage of the modified system

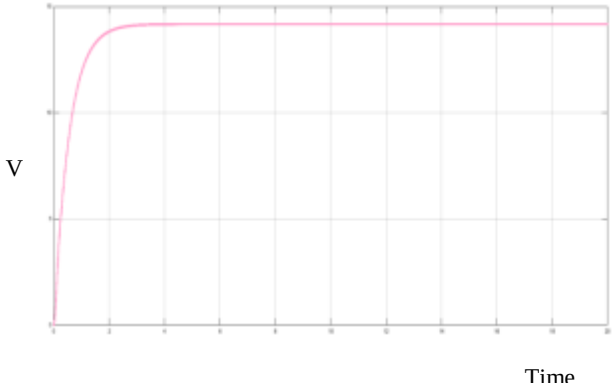

Fig .12 Output voltage of the modified system

Fig 11 shows switching across the voltage and current of the modified circuit, the ripple current can be reduced compared to the traditional converter. Fig12 shows output voltage of the existing circuit.

IV CONCLUSION

The Buck Boost Converter having a star to delta impedance network with reduce input current ripple and improves efficiency. The converter with coupled inductor reduces the ripple current and average current. The delta star network based Buck Boost converter in the main inductor to reduce the ripple current. which apply the delta star network to replace the Inductor in the Buck Boost Converter. The ripple is reduced comparing to the conventional converter .and also improved the efficiency comparing to the conventional converter. The proposed system is used in telecom and computer applications and also used in electric vehicles photovoltaic cells & satellites

V REFERENCES

[1] YP.Siwkoti, PC.Lo, .Blabjerg, S.. Andrasen, & E.Town, For distributed generation using impedance network bst converter,' *Trans of IEEE.,Indu. Electrons.*,volume.60,number2, P.1060 to 1069,February-2015.

[2] YP. Siwkoti, Blabjerg, & PC. Lo, 'Qusi Y source bst circuit,'*Transn of IEEE. Power Electrons.*,volume-30, number-12, P.6514 to 6519,Dec2015.

[3] Zang, HHC.Lu, Zang, Y.Li, Chenn, & B.Zang, ' High gaim with delta star nwk conventional bst converter ' *Transn . Electroni.*, volume.33, number.9, P. 6661to6665,Sep2017.

[4] R.Ericson & .Maksiovc, '*Fundamental of Power Electrons'*,2 nd . Bostton, MA, United states of America ,Kluweer-2001.

[5] JM.Simneli & A.Torey, 'For bst derived high power factor converters with design consideration,' in *Procs. 7th Int.Confe.IEEE Appl. Electron.*, 1992,vol.2,pp.186 to 192.

[6] WT. Fn, K.F.Yen, H.S.Chng, ' Semi conductor filter use of series devices for filtering harmonics,'*Transan of IEEE Electronics.*, volume.31 ,number.3,2053 to 2067,March-2016.

[7] Bedjajev,.Letla, & Zais, 'Impact of components losses of the capacitor filter dual bridge for the isolation of power electronics transformer,' in *Procs. 8Th Inter. Confe. Power Electronics.*,Junuary-2013, P.132to137.

[8] J.Wag, WG.Dnford, K.Much, ' Discontinuous characteristics with design of a ripples free conventional bst converter,' *Transn of IEEE. Electronics* .volume.12,number.4, p. 685 to 694,July-1997.

[9] Diz, Menses, JA.Oliver, Garsia, B.Alo, JA.Coboss,' Ripples cancellation nwk with analysis of a conventional power(boost) circuit,' *Transa.of IEEE Electroni.*, volumel.24,number.12,,p.2769, December-2009.

[10] YP.Siakoti, .Z.Pengg , Blaabjerg, PC.Loh, & G.Town,' For power conversion I, topological review with

delta star netwks' *Transn of IEEE. Power Electrons.*,volume.30,number.2,p.700 to 716,Februry-2015.

[11] RS Balogg & PT.Kren, 'Basic filter block with coupled inductor,' *Transac of IEEE. power Electrons*, volume-28., number-1, P. 536to546., January-2013.

[12] BR Linn & L. Hang, ' current ripple reduction with ZVS switch interleaved circuit,'*Transaction of IEEE. Indu. Electrons.*, volume-55, number-4, P. 1576to1585,April-2008.

Proceedings of the Fourth International Conference on Communication and Electronics Systems (ICCES 2019)
IEEE Conference Record # 45898; IEEE Xplore ISBN: 978-1-7281-1261-9

Prediction of Bug Severity by Classification of Bug Reports

Sarbjeet Kaur
Department of computer science and engineering
National Institute of Teacher Training and Research
Chandigarh, India
sarbjeet.cse@nitttrchd.ac.in

Maitreyee Dutta
Department of computer science and engineering
National Institute of Teacher Training and Research
Chandigarh, India
d_maitreyee@yahoo.co.in

Abstrac-- With the continued demands of software organizations, the rate of defect offered in the software cannot be ignored. In the essential process of bug-tracking, software maintenance has been found in the previous findings to improve the security and bug-fixing process by forecast the 'bug quality' of the software project. For this reason, many classifications / forecasting approaches have been created in the year to provide an automated argument on the severity classes.Bug interpretation of bug reports certainly decreases concert of bug prediction models. Manual testing can help lower the sound but brings substantial loads for the development. Bug fixes enable software developers to resolve software problems.

Index Terms: Bug Triaging, Bug Severity, Bug Forecasting, Classification,

I. INTRODUCTION

As recently as promotion in software technology, software organizations are coming up with the latest software development at the latest rates. These are large pieces of software size that contain many lines of code, which results in defects and drawbacks. Today, we are in a situation where the likelihood of flaws in the software is being highlighted, which leads to a lot of speed, which leads to effective failure. This is due to an ever increasing size of new developed software to meet the demands of the people. The beginning of a fault in software is an inevitable event that we can not survive. So, there is only one solution that has been left for us, to find out the fault and after this, as soon as possible, to prepare some methods and tools to remove these defects from the software [1]. Bug fixing system (BTS) reports these defects. These bug tracking systems normally maintain databases for collecting and maintaining bug reports. BTS tracks bugs in a large number of bugs. Therefore, to fix the bugs at slowness time and assets and to find out which should be sort out soon, it becomes a challenging task for the triaging [2]. Preferring bug reports helps developers better manage bugs triggered process. The main bug is instruction book and takes time. The bug report should allow users to compare the information given in new bug reports to the current education, and determine the level of priority [10].

Different Levels for Bug Priority and Severity

1. High severity & High Priority: The decline in all important business cases automatically gets promoted to the current category.

2. High Priority & Low Severity: Any small serious bugs that directly affect the user's expertise are automatically promoted in the current class.

3. High Severity & Low Priority: The defects need to be mounted, though not directly. This will be especially during the ad hoc testing. This implies that practicality is affected to an extent, although it suggests that only some unusual input parameters are used

4. Low Severity & Low Priority: No Writing System Mistakes / Font Cover / Not Applicable within the paragraphs of the third or fourth page of the arrangement and within the main or front page / title. Usually the dimensions of the cell in cosmetic errors or in a table on the UI are classified here.

In order to assist in bug fixing, it have a tendency to introduce a new automatic approach to suggesting the level of priority of the bug report. To do this, we have a tendency to leverage the data within the bug report. A simultaneous and lengthy interpretation of bug reports, in which users can encounter the default. These are the people who are complex, the grate counting bugs and many more. We want to take advantage of this data to foretell the priority level of the bug report [11].

Bug Report Format: Today the use of jira and bugzilla bug trackers for different types of bug tracking system is used to compare bugs. The severity of the bug is an main element in deciding the priority of the bug because the number of bugs is usually high. A bug is basically a description in which software engineers mention the position of a fault in the software system[11].

Table1: Bug report Content[11]

Field	Description
Summ	Summary: This field contains a short description and contains only a few words.
Desc	Description: This field contains a detailed explanation of the bug and information like how a bug has reproduced an error in the output when the bug will occur.
Prod	Product: It is the product affected by a bug.
Comp	Component: It is the component affected by a bug.
Sev	Severity: It is basically the level which is assigned to the bug according to its impact on the software. The severity level for the bugs are the following: • Critical • Major • Moderate • Trivial

*BUG SEVERITY***:** It is the degree to which the error can influence the software. As such, it characterizes the effect that a given error has on the frame. For example: if an application or page fails when a remote connection is clicked, for this situation touching the remote connection of a client is uncommon, however, the effect of the destruction of the use is serious. Then, the severity is high but the need is low [1]. For the most part, the bug reporter does not know how to handle severity, so the standard is assigned in the severity value and discussed below.

(i) Critical: The bug that outcomes at the end of the entire framework or at least one part of the framework and causes broad defilement of the information. The fizzled work is unusable and there is no worthy option strategy to accomplish the required outcomes then the severity will be expressed as critical.

(ii) Major: The bug affects the main function or the main data. This is the solution, but it is not clear and it is difficult. Example: A feature is not a functioning function of a module but it is possible if 10 complex indirect steps are applied in more modules.

(iii) Moderate: The bug that does not bring about the end, but rather makes the framework deliver mistaken, fragmented or conflicting outcomes then the severity will be expressed as moderate.

(iv) Minor: The bug that does not cause the end and does not harm the convenience of the frame and the coveted results can be acquired without effort when solving the bugs and then the severity is expressed as minor.

(v) Cosmetic: The bug that is identified with the improvement of the framework where the progressions are identified with the look and feel of the application then the severity is expressed as cosmetic.

Manual Bug Testing: Bug life is a special set of bicycle states that goes from detection to faultless stability. The number of states that differs from project to defective project. Below Figure 1 are the manual steps taken to diagnose bugs.

- *New:* When a latest fault is logged and posted for the first time, it has been decided as a new status.
- *Assigned:* Once tester post the bug, the forefront of the tester agreed to the bug and allot the bug to the developer team.

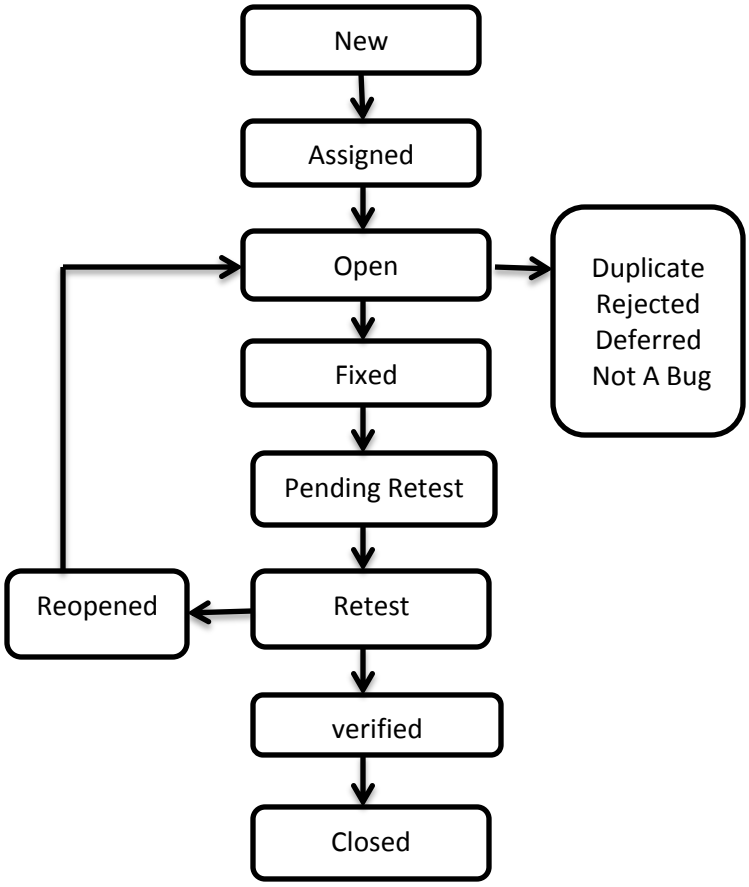

Figure1. Manual Bug Testing

- *Open:* The developer inception analysing and works on fault resolve.
- *Fixed:* When a developer changes the preferred code changes and substantiates the change, he may "fix" the bug situation.
- *Pending retest:* Once the fault has been fixed, the developer gave the code a special code to reassign the code to the tester. Because the software test is left over from the end of the tester, the status represented is "pending request".
- *Retest:* To check whether the developer has made a fix or not and the "re-investigation" to investigate the situation, the investigator reviews the code at this stage.
- *Verified:* Backups the tester bug after the developer define if a bug is originated in the software, the bug has been corrected and the set to status is "verified".*Reopen:* If the bug is still pending, the developer has firm the bug, then the lawmaker has changed the situation to "reopening" again the bug proceed through the lifecycle.
- *Closed:* If the bug is not present then the tester directs the position "closed".
- *Duplicate:* If the defect is frequents twice or the fault matches the same fundamental of the bug, then the situation is "duplicated"
- *Rejected:* If the developer perceives the defect is not authentic defect then it changes the defect to "rejected."
- Deferred: If the current bug is not a prime concern and if it is expected to come in the next freeing, such bugs are evaluated "deferred".
- Not a bug: If this does not affect the functionality of the employment then the given situation in the bug is "no bug".

II. LITERATURE SURVEY

Jindal, Rajni et al. [1] presented a defect severity prediction model by mining the software reports. This model has the ability to predict the severity level of the bug in the bug reports. The defects reports used in this are from the PITS dataset. This data set is popular because it is used by the NASA. Data mining approach is involved to extract the data from the reports and then used by the prediction model. The concept of logistic regression, multi-layer perceptron, and the decision tree is used in this model. The outcomes of the decision tree are best among all when it is compared in the analysis process.

Heena Singla et al. [2] proposed the bug tracking system which identifies the bugs. Physical method is different from software which inputs are accepted and outputs are generated. Any change in the software is usually requested while developing any software system. Mainly, the request is related to software maintenance. The cost of the software is usually spent on software maintenance. The BTS is manually assigned to a respected developer for fixation.

Kwanghue Jin et al. [3] proposed a new programming framework, developed and used as a part of the quality of the fields. Along these lines, bugs ought to be settled accurately to their seriousness levels since they have to isolate seriousness levels. Subsequently, rectify expectation of bug seriousness is required for effective programming improvement and support that designers can know which bug requires to be settled promptly. Prior investigations utilized just content data of the bug report for their forecast systems. In this manner, so as to build up the bug settling, initialize a solid procedure of bug seriousness expectation that additional the Description and Reporter fields since bug columnists record content qualities of the report.

Zhou et al. [4] proposed method of multilingualism by unloading material for computerizing the process of prophecy and adding information mining strategies. The main stage uses the content generation tools to cut down the body parts of the bug reports and perform at the potential three levels. Information connecting strategies are used to connect to two phases. Trials related to previous reviews of similar information - three projects - Reliable get a better upgrade; they have achieved their best results according to overall performance. Seven other well-known open source framework's past reviews have confirmed the searches.

Hans Hansson et al. [5] presented compassionate the dissimilarity between severability bugs and other bugs, in addition to the different severity bugs of their intensity and fixing time period, is a pragmatic study. The introduction of multicore and other parallel designs, there is an expanded necessity for adequate and viable treatment of programming executing on such structures. A huge angle in this setting is to comprehend the bugs that happen because of parallel and simultaneous execution of programming.

Fairuz Amakina Narudin et al. [6] proposed An optional answer to a bug-searching survey by using random training access to machine learning classifiers. Among the diverse system, activity

includes, the four arrangements picked are fundamental data, time-based, content-based, and association based. The approach uses two datasets: open that is MalGenome and private that is self-accumulated. In light of the evaluation comes to fruition, both the Bayes system and irregular woodland classifiers conveyed more precise readings, with a 99.97% genuine positive rate (TPR) instead of the multi-layer perceptron with only 93.03% on the MalGenome dataset.

Fabio Palomba et al. [7] presented the process of estimating bugs about a particular bug. In particular, it evaluate the commitment of a measure of the severity of the odors of the code (i.e, the intensity of the code warning) by looking at the new model's results in conjunction with the current bug reports model and the pattern shown. Results show that the accuracy of error forecasting increases by including the code warning magnitude as an indicator. It also evaluates the actual pick-up given by the intensity list in terms of alternative measures in the model, counting those used to record the intensity of the code warning. They see that the intensity list is much more vital when compared to the different measurements used to anticipate the bugginess of the doubtful classes.

John Anvik et al. [8] proposed automated bug assignments using time-metadata in tf-idf . In this technology, the interest of the developer to use the word is considered to determine the value of the developer skill. It raises the accuracy of bug assignment approach. This term improves the metadata of the word in the automatic bug assignment as an effective parameter in the form of commodity technology.

Yuan Tian et al. [9] presented the concept of multi-factor analysis for bug report prediction. This work is based on machine learning and factors like temporal, textual, author, and bug reports. These factors are considered as a feature and used for the training of the discriminative model using the classification algorithm. This classification algorithm handles the imbalanced data and ordinal class. The proposed model improves the f-measure in the outcomes.

Xiaohu Yang et al. [10] presented software bugs are regular in all phases of the product advancement and upkeep lifecycle. To deal with the report of programming bugs, every one of the engineers utilized following framework in programming bugs. In light of the most vital of programming bugs, countless systems have been intended to oversee and decrease the effect of programming bugs. These systems incorporate bug triaging and designer suggestion bugs need. In regular bug settling strategy, an analyzer or a client distinguishes a bug and presents a bug answer to clarify the bug in bug following frameworks.

Shruti Gujral et al. [11] proposed a calculation of bug severity arrangement which can further enhance the execution of the programmed procedure of bug severity arrangement. The calculation incorporates making a lexicon of condemnatory terms that assistance in choosing severity level naturally. These condemnatory terms are accumulated in the wake of pre-processing of bug reports.

Adhiselvam et al. [12] proposed the concept of the MRTBA in which edge weight is used to take the information and procces calls the program. Here every hub speaks to strategy and each edge speaks to a technique called. The calculation goes into recognition of flawed hubs. The approach mines all hubs at the same level, as well as the hubs, exhibit at various levels. In this approach MRTBA, bug restriction approach has been introduced for dynamic control stream. This work can be enhanced by stretched out with the proposition of steps includes in associating same hubs at various levels. It likewise additionally upgrades to discover aberrant recursions for both the non-trivial and trivial map lessening in programming bug limitation.

Cheng-Zen Yang et al. [13] proposed a method to improve severity prediction of software bug reports suing four quality indicators. Classification of the bug report is based on the Multinomial Naive Bayes (MNB) classifier; where first of all, the preprocessing of bugs is performed then structural information extraction for quality indicator then this data goes to the prediction model and severity is predicted with incoming defect reports also. The outcomes of this approach improved from the existing approaches.

Ali Feizollah et al. [14] presented the 5 machine learning algorithm on the malware data samples collected from the android based genome project. The work is based on the network characteristics by using parameters that are duration of a connection, TCP size, and GET/POST parameters. The performance evaluation is done on the basis of outcome comparison and found that the KNN (K-nearest neighbor) provides the optimal and effective results among 5 classifiers.

Yang et al. [15] proposed a method of severity prediction and bug triage of bug. In this firstly bug reports are take out from the bug repository it gives

the complete information related to the bug. In this method firstly fix the bug and then predicts its severity. The result of the proposed paper shows that this is very effective to fix and predict the bug.

Nivir Kanti Singha Roy et al. [16] proposed the concept of text mining with bi-grams and highlights the determination to make better the order of the bugs in the serious / non-extreme classes. They adopt the NB classifier taking into account the Mozilla and Eclipse datasets commonly used in related work. The outcome is independently subordinate because sometimes the expansion of the bi-grams can aggravate the execution.

N. K. Nagwani et al. [17] focused on the prediction at the granularity of files. This work investigates the respond of the developers on the bug prediction algorithm by using the research question. The purpose of the research objective is to inform informal discussions and third party solutions to informal user studies, data gathered from Google tools and other questions. The outcomes show that there is no notable change in the developer's conduct after using bud prediction algorithm.

Table2: Summary of Literature Survey

S.No	Author	Year	Data Set	Parameter Used	Basic Methodology/Algorithm	Future Scope
[1]	Jindal et al.	2017	PITS dataset	• Sensitivity • Cutoff Point • Area under Curve	-Logistic Regression -Multi-Layer Perceptron -Decision Tree	These 3 models have shown a truly sensible achievement for estimating the high level of flaws. However, because the medium, low and indeed low-level fault level estimation, only the DT model is appropriate.
[3]	Jin, Kwanghue, et al.	2016	Eclipse and Mozilla Dataset	• Precision • Recall • F-measure	-Multinomial Naïve Bayes	Bugs submitted by reporters it do thus for initial time, the accuracy might decline as a result of solely the component applied is employed for prediction, Since no past report former time exists.
[4]	Zhou, Yu, et al.	2016	Bug Report Corpus	• Precision • Recall • F-measure	-Multinomial Naïve Bayes	How many training e.g. are needed in every stage to provide stable prediction result? A mix of independent models will increase performance.
[6]	Narudin, FairuzAmalina, et al.	2016	MalGenome Dataset	• Precision • Recall • F-measure	-Naïve Bayes -Random Forest	The larger the scale of the dataset, the higher is that the time interval to make the detection model and increase the precision, recall and f-measure value.
[11]	Tian, Yuan, et al.	2015	Bug Repository of Eclipse	• Precision • Recall • F-measure	-Gray classification Engine - Linear Regression	Plan to combine there tool with bugzilla or other bug tracking system.
[12]	Xia, Xin, et al.	2015	An open dataset of 6 bug blocker	• Precision • Recall • F-score	-Bagging -Random Forest	The performance of ElBlocker is not perfect. To Enhance the performance ELBlocker need to apply some information retrieval and text mining technique.
[15]	Gujral, et al.	2015	Bug-Zilla repository	• Precision • Accuracy	-Dictionary Based Approach -Multinomial Naïve Bayes	To improve bug classification have to be compelled to add wordbook of terms.
[16]	Adhiselvam et. al.	2016	Input Programs	• Dynamic Control Flows	-Map Reduce Apriori Algorithm	Interlacing ditto node at totally disparate level, self-recursions method to urge the utmost variety of minimum map scale back nodes.

Shadi Banitaan et al. [18] proposed TRiaging Approach utilizing bug reports Metadata.. They perform test assessment on open-source extends to be a specific Free desktop, NetBeans, Eclipse, and Firefox. The comes about to demonstrate that TRAM beats existing machine learning based approaches as far as characterization exactness.

Kim Herzig et al. [19] proposed comprehensive issues with the division of bugs and non-bugs in programming chronicles, which can greatly affect the

accuracy of the equipment and focus that use such information. Methodologies depending on bug *datasets ought to be gone before by a watchful manual approval of information quality; in any event of a noteworthy specimen. Information quality ought to be talked about as a danger to legitimacy. Bug prediction models prepared and assessed on one-sided informational indexes are debilitated to anticipate changes rather than bugs. Sifting through non-bugs while evaluating code quality may even enhance comes about. The arrangement of bug reports is reliant on the point of view of the spectator. Methodologies utilizing bug informational collections ought to approve whether the point of view of the prediction display coordinates the point of view of the bug maker

Xin Xia et al. [20] studied the impact of the misclassification in the bug prediction. It is a bug report of 5 open source projects in which misclassified bug reports have also occurred in which bugs are considered as a feature. The misclassification introduces the bias in the prediction model makes confusion between bugs and features.

Fischer et al. [21] presented the Discharge History is a way to create a database that collects bug information and contains hidden information that is not protected by the wireless control framework, for example, the combination Focus. At that time, fundamental questions can be integrated with organized information to achieve the important perspectives that highlight the development of a product enterprise. Such perspectives enable more accurate thinking about the angle of development and encourage the development of programming. They showed access to Mozilla's vast open source project which offers unique possibilities to look for and approves access.

Malhi et al. [22] Enforcement of Elementary Integrity Check (PCA) strategy in the light of an element of planning. The eligibility of the plan was confirmed on one direction test bed, which uses both direction and unsafe perfection order in both ways. The goal of the examination was to recognize the seriousness of producing imperfection, where there was no access from the beginning of the disorder conditions. The proposed plot has already appeared to present an order of more correct behavior, with lesser fact contribution than using the most importantly watched points. As a result, the machine certifies its usefulness as a powerful tool to evaluate fitness.

III. CONCLUSION

In this paper, bug severity classification has been utilized i.e. a problem related to software engineering for forecasting the most suitable level of a subject that could be helpful in activities like bug schedules. Software bug fixing is a crucial step for open source and business software, so bugs have their severity level [16]. Many attempts have been made to classify defect severity. The text information used for the preview is also the purpose. More searches in this way determine the purpose of predicting the severity of the bug.

REFERENCES

[1] R.Jindal, R.Malhotra and A.Jain, "Prediction of defect severity by mining software project reports," *International Journal of System Assurance Engineering and Management*, vol. 8, no. 2, pp. 334-351, 2017,.

[2] H.Singla, G.Sharma, and S.Sharma, "Domain Specific Automated Triaging System for Bug Classification," *Indian Journal of Science and Technology*, vol. 9, no. 33, 2016.

[3] K.Jin, A.Dashbalbar, and G Yang, "Bug Severity Prediction by Classifying Normal Bugs with Text and Meta-Field Information," *Advanced Science and Technology Letters*, vol. 129, pp. 19-24, 2016.

[4] Y Zhou, Y Tong, R Gu, H Gall, "Combining text mining and data mining for bug report classification," *Journal of Software: Evolution and Process*, IEEE, vol. 28, no. 3, pp. 150-176, 2016.

[5] A.Asadollah, D.Sundmark, S.Eldh, H Hansson, "A Study on Concurrency Bugs in an Open Source Software, "IFIP *International Conference on Open Source Systems,"* pp.16-31, year.2016.

[6] FA.Narudin, A Feizollah, NB Anuar, A Gani, "Evaluation of machine learning classifiers for mobile bug detection," *Springer Soft Computing*, vol. 20, no. 1, pp. 343-357, 2016.

[7] F.Palomba, M.Zanoni, FA. Fontana, "Smells like teen spirit: Improving bug prediction performance using the intensity of code smells, " *International Conference on Software Maintenance and Evolution (ICSME), IEEE*, pp. 244-255, 2016.

[8] R Shokripour, J Anvik, ZM Kasirun, S Zamani " A time-based approach to automatic bug report assignment," *Journal of Systems and Software*, Elsevier, vol. 102, pp. 109-122, 2015.

[9] Y.Tian, D.Lo, X.Xia, C.Sun "Automated prediction of bug report priority using multi-factor analysis," Springer *Empirical Software Engineering*, vol. 20, no. 5, pp. 1354-1383, 2015.

[10] X.Xia, D.Lo, E.Shihab, X.Wang, X.Yang, "Elblocker: Predicting blocking bugs with ensemble imbalance learning," *Information and Software Technology*, Elsevier, vol. 61, pp. 93-106, 2015

[11] S.Gujral, G.Sharma, S.Sharma, "Classifying bug severity using dictionary based approach." *International Conference on Futuristic Trends on*

Computational Analysis and Knowledge Management (ABLAZE), IEEE, pp. 599-602, 2015.

[12] A.Adhiselvam, E.Kirubakaran, R.Sukumar, "An Enhanced Approach for Software Bug Localization using Map Reduce Technique based Apriori (MRTBA) Algorithm." *Indian Journal of Science and Technology* vol. 8, no. 35, 2015.

[13] Yang, Cheng-Zen, et al. "Improving severity prediction on software bug reports using quality indicators," *International Conference on Software Engineering and Service Science (ICSESS)*, IEEE, 2014.

[14] Feizollah, Ali, et al. "A study of machine learning classifiers for anomaly-based mobile botnet detection," *Malaysian Journal of Computer Science*, Scopus, vol. 26, no. 4, 2014.

[15] G.Yang, T.Zhang, B.Lee. "Towards semi-automatic bug triage and severity prediction based on topic model and multi-feature of bug reports," *Computer software and applications conference (COMPSAC)*, IEEE, pp. 97-106, 2014.

[16] NKS.Roy, B.Rossi, "Towards an improvement of bug severity classification." *Software Engineering and Advanced Applications (SEAA)*, IEEE, pp. 269-276, 2014.

[17] Lewis, Chris, et al. "Does bug prediction support human developers? findings from a google case study." *International Conference on Software Engineering*. IEEE Press, 2013.

[18] NK.Nagwani, S.Verma, KK. Mehta, "Generating taxonomic terms for software bug classification by utilizing topic models based on Latent Dirichlet Allocation." *International Conference on ICT and Knowledge Engineering (ICT&KE)*, IEEE, pp.1-5, 2013.

[19] S.Banitaan, M.Alenezi, "Tram: An approach for assigning bug reports using their metadata." *Communications and Information Technology (ICCIT)*, IEEE, pp. 215-219, 2013.

[20] K.Herzig, S.Just, A.Zeller, "It's not a bug, it's a feature: how misclassification impacts bug prediction." *International Conference on Software Engineering*, IEEE , pp. 392-401, 2013.

[21] M.Fischer, M.Pinzger, H.Gall, "Populating a release history database from version control and bug tracking systems." *International Conference on Software Maintenance ICSM*, IEEE, pp. 23-32, 2003.

[22] A.Malhi, RX.Gao, "PCA-based feature selection scheme for machine defect classification." *IEEE Transactions on Instrumentation and Measurement*, IEEE, vol. 53, no. 6, pp.1517-1525, 2004.

Proceedings of the Fourth International Conference on Communication and Electronics Systems (ICCES 2019)
IEEE Conference Record # 45898; IEEE Xplore ISBN: 978-1-7281-1261-9

Data Modelling for Thing Prediction in Station-of-Things Environment

Soumya Saha [1], Tejashree M. Bhave [2], Manisha J. Nene [3]
Department of Applied Physics [1,2], Department of Computer Science and Engineering [3]
Defence Institute of Advanced Technology
Pune, India
soumyasaha@live.in [1], tejashreebhave@diat.ac.in [2], mjnene@diat.ac.in [3]

***Abstract*—The study in this paper uses the concept of Internet-of-Things (IoT) to represent a station containing a thing of interest termed as Station-of-Things (SoT). Research in communication, computation and sensors innovation has enabled to build intelligent SoT environment. This SoT environment is applicable to numerous situations to identify the inhabitance of chairs in a study hall, seats in a theatre or auditorium, cars in parking-lot, books in a bookshelf, and so forth. In this paper, the proposed communication model, network model and test results show the value of the work which establishes a framework to gauge and assess the inhabitance of the thing in a station. Further, the sensor network enables the capturing of dimensional-data. This data is utilized by a machine learning model to infer the type of a thing. Hence, the study demonstrates a preliminary data model to predict the type of thing in SoT environment.**

Keywords—Station-of-Things (SoT); Smart Parking System; Intelligent Parking System; Wireless Sensor Networks (WSN); Internet-of-Things (IoT); Ultrasonic Sensor; Infrared Sensor; Radio Frequency Identification (RFID) Sensor; Machine Learning (ML); Artificial Intelligence (AI)

I. INTRODUCTION

With the development of innovation and the accuracy of the Moore's law [1], there has been a pattern to advance an intricate microchip to satisfy the necessity of smaller yet powerful cost-effective miniaturized devices. Numerous gadgets these days are outfitted with exceptional registering power, conceivably including additional usefulness and in this manner, it appears to be normal to interconnect gadgets in the period of web innovation. Such availability, upheld by the consolidation of asset compelled gadgets including sensors and actuators, empowers savvy frameworks that acquire data from the physical world, procedure such data, and may perform activities on the physical world appropriately has stressed to build smart environments around us.

Advantages of web innovation include efficient resource management, upgraded profitability and expanded personal satisfaction for human populaces [2]. The joint inspiration fundamental in all exploration fields is to explore how "shrewd innovation" may improve our private and expert life, and how that innovation can be figured it out. To land at our ideal objective, a few disciplines need to contribute, going from specialized disciplines required with sensors and systems to artificial intelligence and human-PC cooperation, and beyond. A system has always been classified as smart [3] system whenever sensors have been used to perceive, interpret the perception and yield wise decisions beyond perceive-act rules. However, intelligent systems are combined with perception and action to derive methods that emphasize refined handling strategies that are driven by technological innovations. Artificial intelligence is a composite of both smart and intelligent systems and relates how the perception can be co-related to the human like actions.

Human portability is a need and without it, individuals will battle to get to the administrations and merchandise and meet social and financial prerequisites expected to satisfy a solid life. A quickly developing worldwide populace, expanding prosperity, urban spread and declining transport costs are pushing this interest for versatility upwards further and further. For example, the number of vehicles sold in the recent years worldwide has consistently risen. Transport is a human asset and a vitality escalated, for instance, which is likewise in charge of a sizable offer in worldwide ozone harming substance outflows. Car is the mostly used land transport. Stopping and traffic blockages keeps down monetary efficiency. Car parking techniques differ and has advanced in the course of recent years with respect to the varying organization needs. They are the consequence of incorporation of different techniques and proliferations in communication, computing and sensing technologies. These techniques have evolved with generation of voluminous data sets challenging to manage.

II. RELATED WORK

The most recent two decades have been caution of the dynamite examination to determine the parking mess. Authors have introduced and proposed different methodologies to implement smart parking. Smart parking is the combination of technology and human innovation to reduce human effort for the parking of vehicles. The smart parking methodologies differ from each other in the detection mechanism used to detect the presence or absence of a car in a parking space, how the occupancy status of parking space is reported to the next base station or server, the communication protocol and architecture in use, the flow of data architecture, hardware and

software that work hand in hand as a standalone system, and so forth.

The researchers have proposed parking models where each parking space is monitored with the deployment of a parking node at each parking space. In [4], the author proposed a GSM (Global System for Mobile) network-based parking reservation system, which allows the driver to pre-book the available parking spaces through SMS (Short Messaging Service). A similar system has been proposed in [5] however, it requires Internet connectivity to pre-book the parking space. The system utilizes light and vibration sensors, that are installed in each parking space to collect occupancy information. In [6], RFID (Radio Frequency Identification) tags are placed at each parking space. The battery that controls the RFID is supplanted by a sunlight-based cell. As the vehicle consumes a parking spot, its shadow will block the sunlight-based light, and subsequently the RFID label won't be fueled, making it stop transmission of information to the reader put at some separation. In any case, this system is faulty, on the off chance that the shadow does not falls on the RFID tag or the sunlight-based cell in the RFID tag is impeded by the motor oil, that may spill from a vehicle may trigger false detection of a car. In [7], the author proposed a WSN (Wireless Sensor Network) based parking system, where the wireless nodes are installed at each parking space, and they report parking availability information to the next base station.

The study has evolved further where the authors have proposed smart parking spaces that can be collectively monitor multiple parking spaces without the requirement of installation of parking node at each parking space. In [8], a camera sensor captures a series of images to analyse time variant parking status, however the system does not have a mechanism to report the occupancy status to the user. The proposed work in [9] is inspired by [8] where in circles are drawn on each parking space. If a car has occupied a parking space, the circle will not be visible by the camera, and system will understand that the parking space is occupied; if the circle is visible, system will consider the parking space to be unoccupied. In [10], the author proposed a parking lot surveillance system that incorporates microphone sensor nodes to detect an acoustic event to improve the performance of camera-based system proposed above.

The efforts of researchers have progressed and they have proposed parking systems that use the combination of two or more technologies for reliable performance. In [11], computer vision is used to extract vehicle information from the license plate, at the entry of the parking lot itself. In [12], the author proposed an IoT (Internet-of-Things) based system inspired by [11], where each parking space is also monitored by a Pi camera and an ultrasonic module. As the driver parks the car in the parking space, the camera at the parking space will match the information collected at the gate. In [13], the author proposed a smart parking framework that uses the integration of both WSN and RFID. RFID readers are placed at the entry and exit of the parking lot. The WSN monitor the status of the parking spaces and the RFID monitors the entry and exit of vehicles from the parking lot. In [14], the author proposed a RFID and GSM based solution to prevent theft of vehicles from an organization. In [15], the author proposed a smart parking system based on the integration of WSN, RFID, ad-hoc network and IoT. It mainly addresses the cyber security issues that may possess a threat to the smart parking network and presents a basic model of cryptographically tackle them.

The work in this paper aims to digitally detect the occupancy of a *station* along with the ability to predict the *thing* type that occupies the *station*. The paper is organized into seven sections. Section III introduces the notion and case-study of *SoT (Station-of-Things)* contemplated in this paper. It also presents the logical, physical and data exchange interpretation of the *SoT* model. Section IV describes the firmware required for the implementation of *SoT* model. Section V presents the *SoT* model for implementation. Section VI depicts the results and the challenges associated. Section VII concludes the work and proposes the future work.

III. STATION-OF-THINGS MODEL

The work in this paper presents a notion to represent the state of a *station* containing an object or a *thing* of interest together constitute *SoT* [16]. Occupancy of benches in a classroom, books on a book-shelf, seats in an auditorium, cars in a parking lot, they all exemplify *SoT*. The use of occupancy of a *thing* and its *size* in a *station* leads to the generation of information useful to derive intelligence in the *SoT* environment.

A. Assumptions

In this paper, a car parking space represents a scenario of *SoT*. The parking space is the effective area required to *station* a car. Ref Fig. 1. the parking space for the implementation of *SoT* model is a semi-closed type, with a tin shed at the top, that serves as the roof and provides shelter to the car with the following dimensions: 450 cm (L) x 350 cm (B) x 300 cm (H). The height of the car is denoted by 'h'. The parking space is within a Wi-Fi (Wireless Fidelity) enabled ecosystem and has provision to provide 220 V power supply. Alternatively, direct solar can be an option, however, it lies outside the scope of the paper.

S1 and S2 are the output of the Sensor_1 (Ultrasonic Sensor) and Sensor_2 (Infrared Sensor) respectively. A and B are the lower and upper thresholds set for the prediction of a car. C and D are the lower and upper thresholds set for the prediction of a Hatchback/Sedan type car. E and F are the lower and upper thresholds set for the prediction of a Crossover type car. G and I are the lower and upper thresholds set for the prediction of a SUV type car.

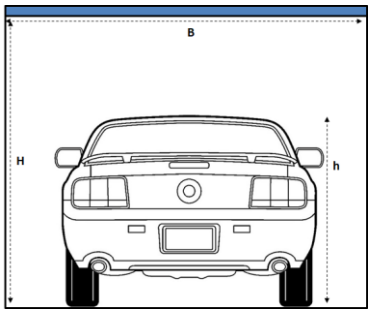

Fig. 1. Data Parameters for Station-of-Things Model: Parking Space

B. *Network Model*

The details of the network models to enumerate network architecture type I and II, Ref Fig. 2. of the *SoT m*odel is as follows: -

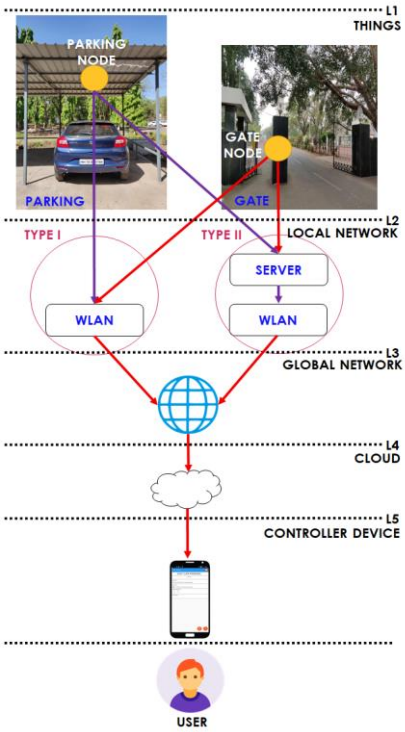

Fig. 2. Station-of-Things: Proposed Network Model

The type I architecture where in layer L1 takes in the deployed nodes (parking node at each parking space and gate node at the common entry cum exit gate of the parking lot) comprising of the microcontroller board and sensor modules, layer L2 is the interconnection of these nodes within a local network such as an organization network, represented as 'WLAN' that enables the flow of data, subsequently layer L3, to allow flow of data from a local network to another local network that is connected to a common global network. Layer L4 is an online service platform to decipher the sensor gathered data, on which layer L5, a controller gadget sits and is overseen by a user.

Layer execution remains the same for type II architecture as in type I. The type II architecture provides a mechanism where most of the data generated within the organization is retained and is not pushed to the cloud. The choice of retaining data will differ from one organization to another. This architectural design is future proof in discrepancies that may occur in Internet dependent networks. The study in this paper progresses with the type II network architecture.

C. *Communication Model*

Ref Fig. 3. is the interpretation how the miniaturized devices with constraint computation is required to communicate with heterogeneous devices connected to the web. There is a prerequisite of a convention that aides and supports such correspondence between heterogeneous gadgets that contrast on preparing, memory and capacity abilities. MQTT (Message Query Telemetry Transport) is a messaging based publish-subscribe protocol [17] that supports such heterogeneity. This protocol has been intended to work in restricted transmission capacity systems to interface with constrained CPU's and with a next to no overhead. The MQTT framework comprises of the clients (nodes) that speak with a server, regularly called a broker. The client can be classified based on the work it performs – a publisher or a subscriber.

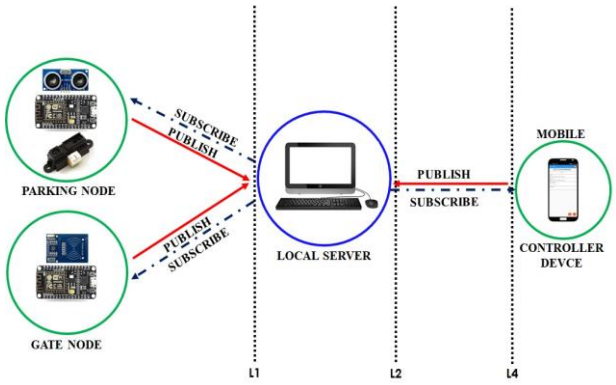

Fig. 3. Station-of-Things: Proposed Communication Model

IV. Data Modelling For Thing Prediction: Firmware

To enable the *thing* prediction using data models i.e. the data generated using the sub-systems, the hardware and software termed as firmware is described below.

A. *Hardware*

The framework equipment is sorted into four principle segments to be specific: parking node, gate node, local server and a mobile.

The parking node comprises of the Node MCU (Microcontroller Unit) [18] which is a solitary board microcontroller dependent on minimal effort ESP8266 Wi-Fi chipset, HC-SR04 US (Ultrasonic) sensor module and the SHARP GP2Y0A02YK IR (Infrared) sensor module. The HC-SR04 sensor module incorporates the transmitter and collector and has the accompanying particulars: 400 cm maximum radius for detection, 3 cm dead zone and 0.3 cm resolution with a beam angle of 30°. The US sensor works on the rules of SONAR (Sound Navigation and Ranging) and RADAR (Radio Detection and Ranging). The GP2Y0A02YK IR [19] sensor module is an active sensor based on the hypothesis of optical triangulation. It is equipped with an IR transmitter and a position sensitive device.

The gate node comprises of the Node MCU that houses RC 522 sensor module which is a passive RFID sensor that works at 13.56 MHz and can detect RFID tags in the similar recurrence from a most extreme separation of 3 cm.

An android OS (Operating System) based mobile application is used to obtain parking information which also supports booking of a parking space. The development of parking application is outside the scope of this paper.

The local server is deployed with storage and computational power.

The 5V/1.5A power adapter is an AC to DC converter, and is used to energize the parking nodes and gate nodes.

B. Software

The Arduino IDE (Integrated Development Environment) is a C language-based programming environment to write and upload the programs to the Node MCU.

C. Power Rating Ajustments

The GPIO (General Purpose Input Output) pins of the Node MCU can supply most extreme +3.3V, however the HC-SR04 US sensor and the SHARP IR sensor is rated at +5V. Supplying +5V to the US and IR sensor was an option, however it could damage the microcontroller board. To avoid this, a potential divider circuit was used to lower the sensor output voltage to a range that can be handled by the Node MCU.

V. DATA MODELLING FOR THING PREDICTION: IMPLEMENTATION

A. Parking Node : Sensor Mounting

Ref Fig. 4. and 5. the sensors can be mounted either on the top (below the shelter) or at the bottom (ground level). Sensors mounted underneath the car are prone to fluids such as oil and water, which may influence their discovery execution. To avoid that, we favored to mount the sensors on the top. This will certainly expand the life of the sensor and decrease its climate affectability.

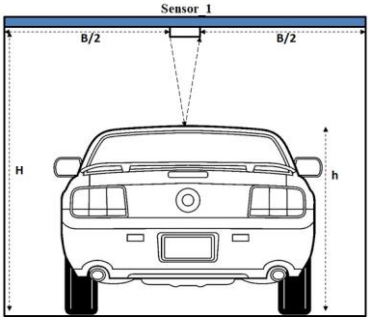

Fig. 4. Station-of-Things: Parking Node Sensor Mounting Type I

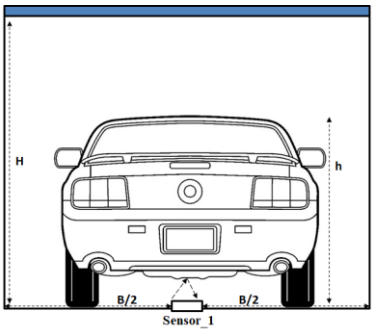

Fig. 5. Station-of-Things: Parking Node Sensor Mounting Type II

Ref Fig. 6. each car parking space is equipped with a two-sensor combination which can detect the inhabitance of a car as well as the data component (height of car) to bring intelligence by deriving information about the type of car parked in the parking space. A parking node collects periodically this information using Wi-Fi. When the status of a car parking space is changed, information about it will be pushed by the node to the further base-station/local server as designed in the communication model; either to the server/cloud/mobile.

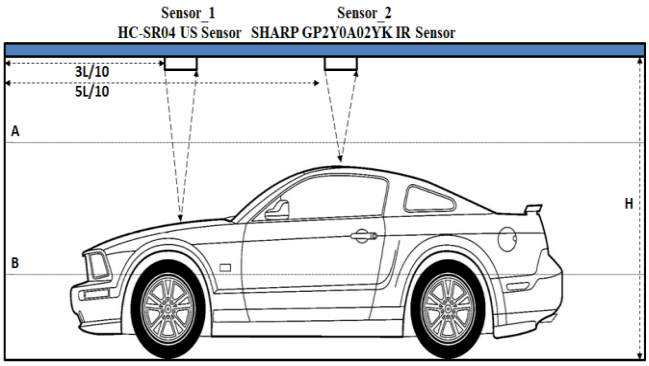

Fig. 6. Station-of-Things: Parking Node Sensors Mounting

B. Parking Node : Sensing Scheme

Table 1. lists the *height* (data component) features of the various car types and models that are pre-fed into the system.

TABLE I. REFERENCE TABLE CONTAINING PRE-FED HEIGHT OF CARS

Car Type	Model	Height 'h' (in cm)	Parameters (Ref Fig. 9.)
Hatchback	Maruti Suzuki Alto 800	147.5	C,D
	Renault Kwid	147.8	
Sedan	Maruti Suzuki Ciaz	148.5	
	Hyundai Elantra	146.5	
SUV	Honda CR-V	168.9	E,F
	Renault Duster	169.5	
Crossover	Hyundai i20 Active	155.5	G,I
	Maruti Suzuki S-Cross	159.5	

C. Parking Space Occupancy Scheme

Ref Fig. 6. and Fig. 7., the values read by sensors S1 and S2 form the input to the algorithmic steps employed to assess the inhabitance of a car in a parking space is as follows:

```
1. Read S1
2. If ((S1≥B)and(S1≤A))
3.      {
4.      Read S2
5.      If ((S2≥B)and(S2≤A))
6.              Output "Car Detected"
7.      Else
8.              Output "Can't Say, Car Detected!"
9.      }
10. Else
11.     Output "Car Not Detected"
```

Fig. 7. *Station-of-Things*: Car Occupancy Heuristics

D. Neighbourhood Hightlights Extraction Scheme

Ref Fig. 8. and Fig. 9., the values read by sensors S1 and S2 form the input to the algorithmic steps employed to assess the prediction of a car type in a parking space is as follows:

```
1. Read S2
2. If ((S2≥B)and(S2≤A))
3.      {
4.      If ((S2≥D)and(S2<=C))
5.              Output "Hatchback_Sedan_Type Car"
6.      Else If ((S2≥F)and(S2≤E))
7.              Output "Crossover_Type Car"
8.      Else If ((S2≥I)and(S2≤G))
9.              Output "SUV_Type Car"
10.     Else
11.             Output "Unknown_Type Car"
12.     }
13. Else
14.     Output "Can't Say, Car Detected!"
```

Fig. 8. *Station-of-Things*: Car Type Prediction Heuristics

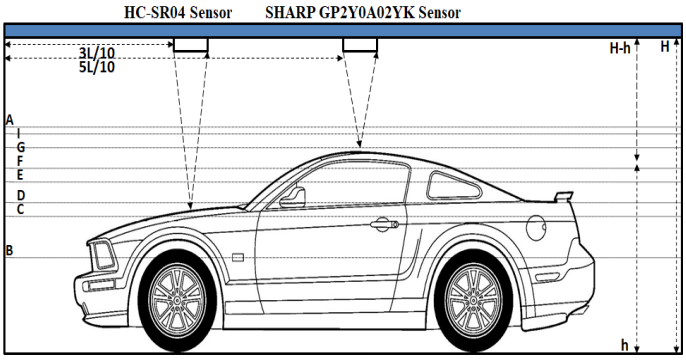

Fig. 9. Station-of-Things: Car Type Prediction Scheme

E. Parking Lot Occupancy Scheme

The gate node is mounted at the common entry way/exit way of the parking lot to monitor the number of cars entering and exiting the parking lot. Ref Fig. 10. describes the RFID sensing scheme employed. At any point of time, the occupancy status of a parking lot is computed as: Available Parking Slots (A) = Total Parking Slots (T) - Checked In Cars (C.I) + Checked Out Cars (C.O).

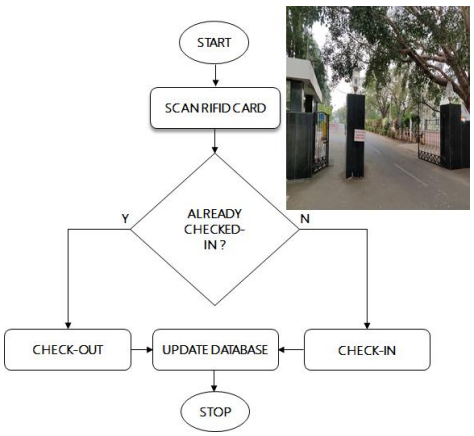

Fig. 10. Station-of-Things: RFID Sensing Scheme

F. Mobile Application Development

Ref Fig. 11. is the android based mobile application interface that is developed and installed in the security staff's device to provide real time parking information, reservation and manage check-in and check-out of cars.

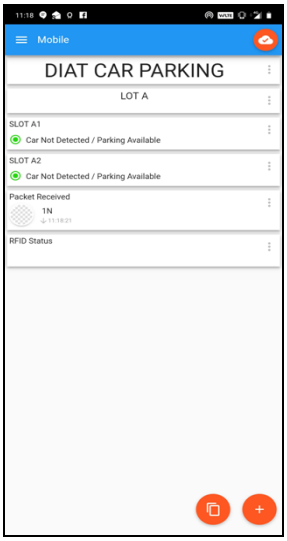

Fig. 11. Station-of-Things: Mobile Application Screenshot

VI. Results & Challenges

The proposed deployment model for *SoT*, Ref. Fig. 9. along with the occupancy detection of the *station*, also enables the prediction, Ref. Table II. The ability to estimate the dimension parameter demonstrates the merit of the work which lays a foundation to estimate the size-parameters of a *thing* in a *station*, Ref. Table II.

Here, the remote estimation of the neighborhood highlights in a parking space (*station*) such as the stature (height) for the extraction of the global features, for example, to anticipate the car type. In the long run, such information parameters inferred utilizing sensor hubs at right position in the *station* show the possibility to forecast the car type and car model. These sensor-hub created information nourishes to give the essential information types to improve machine learning models to enable artificial intelligence.

The difficulties associated here is the placement of sensors to quantify the useful parameters, sensitivity factor of a sensor-hub and ecological factors that affect the rightness in the readings. Deployment of such systems are prone to generation of lot of data leading to big data and hence employing suitable data analytics tools plays a major role to bring intelligence and correct predictions.

TABLE II. RESULTS CONTAINING HEIGHT BASED PREDICTION CAR TYPE

Model	Predicted Car Type
Maruti Suzuki Alto 800	Hatchback/Sedan
Renault Kwid	
Maruti Suzuki Ciaz	
Hyundai Elantra	
Honda CR-V	SUV
Renault Duster	
Hyundai i20 Active	Crossover
Maruti Suzuki S-Cross	
Jeep Wrangler	Unknown
Tata Nano	

VII. CONCLUSION & FUTURE WORK

With the approach of IoT and WSN, the research on building the smart parking systems has advanced rapidly. Variety of smart parking systems exist. A smart parking solution contributes to bring effectiveness in human-endeavors. In areas and regions where installation of cameras to detect a *thing* is prohibited such techniques form a base, to enable identification of a *thing* which occupies a *station*.

The study in this paper proposes a concept of *SoT*, here a parking lot represents a s*tation* and a car represents a t*hing*. The study proposes a technique which utilizes ultrasonic and infrared sensors to detect the desired parameters. A deployment model, network and communication model for *SoT* to the requirement is proposed, Ref. Fig. 9. which predicts the occupancy of the s*tation*, along with the capturing of the dimensional-data parameters for the prediction of the type of *thing*, Ref. Table II, establishing a framework to assess the *size*-parameters of a *things* in a s*tation*. Such systems are prone to push and generate lot of data leading to big data where the rule base data models to map and predict a *thing* becomes the need of an hour which can form a base to advance machine learning models to derive intelligence artificially.

The future work is to study big data modelling and analysis techniques which can accommodate voluminous data.

REFERENCES

[1] Moore GE (1965) Cramming more components onto integrated circuits. Electronics 38:114–117

[2] C. Gomez, J. Paradells, C. Bormann and J. Crowcroft, From 6LoWPAN to 6Lo: Expanding the universe of IPv6-supported technologies for the Internet of Things, IEEE Communications Magazine 55(12) (2017), 148–155.

[3] Wolter, D. & Kirsch, A. Künstl Intell (2017) 31: 231. https://doi.org/10.1007/s13218-017-0498-4

[4] N. H. H. Mohamad Hanif, Mohd Hafiz Badiozaman and H. Daud, "Smart parking reservation system using short message services (SMS)," 2010 International Conference on Intelligent and Advanced Systems, Manila, 2010, pp. 1-5.

[5] Hongwei Wang and Wenbo He, "A Reservation-based Smart Parking System," 2011 IEEE Conference on Computer Communications Workshops (INFOCOM WKSHPS), Shanghai, 2011, pp. 690-695.

[6] P. Šolić, I. Marasović, M. L. Stefanizzi, L. Patrono and L. Mainetti, "RFID-based efficient method for parking slot car detection," 2015 23rd International Conference on Software, Telecommunications and Computer Networks (SoftCOM), Split, 2015, pp. 108-112.

[7] J. Yang, J. Portilla and T. Riesgo, "Smart parking service based on Wireless Sensor Networks," IECON 2012 - 38th Annual Conference on IEEE Industrial Electronics Society, Montreal, QC, 2012, pp. 6029-6034.

[8] Al-Kharusi, Hilal& Al-Bahadly, Ibrahim. (2014). Intelligent Parking Management System Based on Image Processing. World Journal of Engineering and Technology. 02. 55-67.

[9] S. Banerjee, P. Choudekar and M. K. Muju, "Real time car parking system using image processing," 2011 3rd International Conference on Electronics Computer Technology, Kanyakumari, 2011, pp. 99-103.

[10] K. Na, Y. Kim, and H. Cha.: Acoustic sensor network-based parking lot surveillance system. In: Proceedings of the 6th European Conference on Wireless Sensor Networks, EWSN '09, pages 247–262, Berlin, Heidelberg, (2009). Springer-Verlag.

[11] S. Rane, A. Dubey and T. Parida: Design of IoT based intelligent parking system using image processing algorithms. In: 2017 International Conference on Computing Methodologies and Communication (ICCMC), pp. 1049-1053, Erode (2017).

[12] R. Lookmuang, K. Nambut and S. Usanavasin, "Smart parking using IoT technology," 2018 5th International Conference on Business and Industrial Research (ICBIR), Bangkok, 2018, pp. 1-6.

[13] E. Karbab, D. Djenouri, S. Boulkaboul and A. Bagula, "Car park management with networked wireless sensors and active RFID," 2015 IEEE International Conference on Electro/Information Technology (EIT), Dekalb, IL, 2015, pp. 373-378.

[14] L. Kumar, M. H. Khan and M. S. Umar, "Smart parking system using RFID and GSM technology," 2017 International Conference on Multimedia, Signal Processing and Communication Technologies (IMPACT), Aligarh, 2017, pp. 180-184.

[15] O. Abdulkader, A. M. Bamhdi, V. Thayananthan, K. Jambi and M. Alrasheedi, "A novel and secure smart parking management system (SPMS) based on integration of WSN, RFID, and IoT," 2018 15th Learning and Technology Conference (L&T), Jeddah, 2018, pp. 102-106.

[16] Soumya Saha, Tejashree Bhave, Manisha Nene, "Intelligence in Station-of-Things," Proceedings of the International Conference on Internet of Things and Connected Technologies, MNIT Jaipur, May 2019, Springer Publication. In press.

[17] MQTT Documentation http://mqtt.org/documentation.

[18] NodeMcu -- An open-source firmware based on ESP8266 wifi-soc, http://www.nodemcu.com/index_en.html.

[19] SHARP GP2Y0A02YK IR Sensor Datasheet.

Proceedings of the Fourth International Conference on Communication and Electronics Systems (ICCES 2019)
IEEE Conference Record # 45898; IEEE Xplore ISBN: 978-1-7281-1261-9

Performance Analysis of Immense Preference Data Forwarding (IPDF) Scheme incorporated with Constructive Time Slot Allocation in IEEE 802.15.4 for Wireless Body Area Networks

Sindhuja Banu.S
Department of Electronics and Communication Engineering, Sri Shakthi Institute of Engineering and Technology,
Coimbatore, Tamilnadu, India.
e-mail: sindhujabanu16@gmail.com

Dr. Baskaran.K
Department of Electrical and Electronics Engineering
Alagappa Chettiar College of Engineering and Technology
Karaikudi, Tamilnadu, India
e-mail: drbaskaran@gct.ac.in

Abstract— A large time delay during emergency data transfer in WBAN is a challenging task since it involves transmission of time sensitive crucial information to the receiver for immediate treatment of the patient. This paper aims in providing an efficient transmission of Immense Preference Data (IPD) to the respective end user with minimal delay and energy consumption. IEEE 802.15.4 MAC superframe was altered within permitted standards and IPDF Routing Scheme was designed and implemented in which, time slots were efficiently allocated according to data type. Guaranteed Time Slots (GTS) in Contention Free Period (CFP) was allocated to IPD of the slot's possessor and the non-possessor node at t0 and t1 respectively. This provides an immediate and guaranteed transfer of data without any further delay and unnecessary waiting time for channel contention at Contention Access Period (CAP) was also reduced, so as to add to the minimization of power consumption and latency. CAP was further divided into two phases for transmitting Minor Preference Data (MPD) of possessor and non-possessor which minimizes collision of data packets that further decreases delay and power consumption of MPD. Simulations and performance analysis of IPDF scheme were carried out in NS2. Delay and power consumption minimization and PDR and throughput maximization for IPD in comparison to IEEE 802.15.4 MAC standard and PA-MAC was achieved.

Keywords— IEEE 802.15.4 MAC Superframe, MAC Routing Scheme in WBAN, Emergency data handling, time slot assignment, and energy - delay trade – off.

I. INTRODUCTION

IEEE 802.15.4 was chosen as a better standard for WBAN because of its low power consumption and data rate for wireless connection that involves mobile, stationary and portable devices. Also, it consumes less battery power and covers a distance within the range of 10 m which is ideally suited for WBAN. The standard supports 16 channels in 2.45 GHz band, 30 channels with 915 MHz band and 3 channels in 868 MHz band. It has an optional CFP. Also, CAP operation is based on CSMA/CA. It operates with a star or peer – peer topology. MAC management integrating the MAC Layer Management Entity (MLME) Service Access Point (SAP) and data service supporting forwarding and receiving the MAC Protocol Data Units (MPDUs) are carried out by the MAC layer.

The CSMA/CA mechanism at the CAP in IEEE 802.15.4, makes the node to wait for a random back off period until the channel becomes free. Also, there is a response wait time when the node requests for a time slot. Before accessing the channel, the device waits for a random period called back off delay represented by Back off Exponent (BE). A device should wait for a time between 0 to 2^{BE}-1. This expends listening mode energy alone. Contention Window (CW) is the number of back off time periods where the medium has to be sensed to be idle before transmitting the data [10] and [11].

The Beacon Interval,

$$BI = \text{a base superframe duration} * 2^{BO} \text{ symbols} \quad \text{for } 0 \leq BO \leq 14. \tag{1}$$

The active period which is Superframe Duration,

$$SD = \text{a base superframe duration} * 2^{SO} \text{ symbol} \quad \text{for } 0 \leq SO \leq BO \leq 14. \tag{2}$$

Beacon Order (BO) implies the period at which the coordinator has to transmit the beacon. Superframe Order (SO) implies the active period of the superframe.

$$\text{The Duty Cycle, } DC = SD / BI = 2 (SO – BO) \tag{3}$$

When the duty cycle is low, it implies that there is a high sleep time. So altering the SO or BO will have affect the DC. To reduce the DC, BO has to be increased by keeping SO as a constant or decreasing SO by keeping the BO as a constant. So it reduces the energy consumption. But, a shorter CAP length would lead to transmission of pending data at the initiation of the successive superframe resulting in high collision and retransmission. This again leads to increase in power consumption. Retransmission enhances the reliability but, contributes to the packet delay. Decreasing the delay by

sending and receiving the packets in the same superframe contributes in faster medium access and avoids additional delay caused by sleep time. At the same time, the energy – delay trade – off has to be taken into account while designing the routing scheme. The macMinBE and macMaxBE values as fixed by the standard are 3 and 5 respectively. When these values are decreased, the waiting time of a node decreases, thereby increasing the throughput. But at the same time, when the traffic increases, the node tries to access the channel with more probability within a shorter time period. This may lead to several collisions that again results in delay and throughput reduction and vice versa. Therefore, the BO, SO, Number of Back offs (NB), macMinBE, macMaxBE and CW size are the major parameters under concern to improve the network performance.

The primitive traits of MAC layer are to provide and perpetuate the beacon maintenance, GTS operation, medium access mechanism, frame verification and affirmation and association and disassociation of frames [10] and [11]. It has been a challenging task to balance out the energy – delay trade – off during data transmission. When an IPD occurs, the data has to be transmitted immediately due to high time sensitivity of the emergency datum. The contention taking place in CAP for time slot allocation and data forwarding, efficient routing of data according to its priority level and effective bandwidth usage are the primary factors considered in the design of MAC superframe structure of IEEE 802.15.4. Fig. 1 shows the general IEEE802.15.4 superframe structure. The three important parameters namely, delay, throughput and energy consumption, while dealing with IPD were under research and various analyses to bring down the energy consumption and latency, at the same time, increasing the throughput were laid out. The superframe structure was modified according to the aforementioned requirements and further researches were done and a routing scheme was proposed to improvise the above mentioned QOS parameters. An efficient routing scheme on the MAC layer extends in improving the data delivery and reducing the latency.

The paper is organized as follows: Section 2 discusses literature on MAC protocol along with their routing schemes. Section 3 explains the proposed routing scheme in the superframe structure and its operation. Section 4 presents the simulation parameters and discusses the results and finally Section 5 concludes the paper.

II. RELATED WORK

As proposed in [1]: A Modified IEEE 802.15.4 Superframe Structure for Guaranteed Emergency Handling in Wireless Body Area Network, the superframe structure was modified by utilizing the inactive period for emergency data transmission. The inactive period was divided into Emergency Reporting Period (ERP), Emergency Beacon (EB) for notification of an emergency datum and Emergency Transmission Period (ETP) for transmission of the emergency data. The channel was accessed by two mechanisms namely, CDMA based access based on codes and random back off access that uses a time based back off window. CDMA based access mechanism provides higher throughput and lesser delay since; length of the ERP is shorter comparatively. An Improved IEEE 802.15.4 Superframe Structure with Minimum Delay and Maximum CFP Link Utilization [2] supports the maximum GTS utilization by the request nodes. The CFP is divided into 14 slots which is equal to one half of the CAP slot without violating the minimum length of the slot requirement. Also, the CFP is placed next to the beacon when there are GTS requests. Else, CAP follows the beacon frame. This helps in reducing the packet delay since, the node requests are accessed immediately and the data are transmitted immediately without waiting for a long time during contention. Also, many node requests can be processed due to further extension in number of GTS slots, thereby, accommodating in efficient bandwidth utilization in all the three frequency band ranges as laid in the IEEE 802.15.4 standard. The interrupt MAC was proposed in [3]: A MAC Routing scheme for Medical Monitoring Applications of Wireless Body Area Networks, where, frequent interrupts are introduced in between when emergency data arises instead of beacons. This reduces the unnecessary beacon transmission. The interrupt slots are inserted in between the GTS when emergency data arises. But, IMAC superframe structure requires a long beacon length than that is present in the current superframe. So the system is more complex than the conventional superframe of IEEE 802.15.4. When there is less frequent urgent data, this proposal provides better time utilization and energy efficiency. But, when the urgent data frequency is high, IMAC is not a wiser option. The DRT (Delay, Reliability and Throughput) profile was dealt in [4]: Delay, Reliability, and Throughput Based QoS Profile: A MAC Layer Performance Optimization Mechanism for Biomedical Applications in Wireless Body Area Sensor Networks. The optimization of certain QOS parameters with respect to time were carried out and the results show that, reduced delay was obtained during high data rates and frequencies and high delay was achieved at lower data rates and frequencies. A more reliable system at a permissible delay and data rates was achieved using the DRT parameters. The DRT parameters are based on CSMA / CA mechanism while taking IEEE 802.15.4 and IEEE 802.15.6 into concern. The proposed MAC algorithm in [5]: D-MAC: A Dynamic MAC Algorithm for the Body Area Sensor Networks Based on IEEE 802.15.4 deals with dynamically changing BO and SO values in the MAC superframe structure. The BO and SO values in the conventional standard are fixed. But, in the proposed algorithm, the BO ad SO values keeps changing dynamically according to the traffic load so that, Duty Cycle (DC) can be adjusted to the desired values, so as to increase the throughput and decrease the latency and energy consumption. The various traffic adaptive schemes were studied in [6]: Traffic Adaptive MAC Routing Scheme in Wireless Body Area Networks. During high traffic, the number of nodes increase which leads to higher collision due to more channel contention. This leads to packet loss or retransmissions. This affects the delay, throughput, energy consumption and PDR. Therefore, relatively better traffic adaptive routing scheme are necessary to enhance and achieve a balance between energy and delay

factors, maximizing the throughput and PDR. This provides a better system in timely data processing and packet reception with a balance over energy – delay trade – off. In [7]: IEEE 802.15.4 Frame Aggregation Enhancement to Provide High Performance in Life-Critical Patient Monitoring Systems, the frame aggregation technique was proposed. The signals transmitted by the WBAN nodes are a number of small packets within a short time span. This does not utilize the maximum channel capacity as, only the packets that contend and get the channel for transmission are forwarded whereas, the nodes that are not allocated with the slots have to wait for certain time period and again contend the medium for slot allocation and then transmit once it is allocated with the time slot. Therefore, a maximum packet size of about 17 bytes is only getting transmitted in the medium. But the actual capacity of packet size that can be transmitted is 127 bytes. Therefore, it does not utilize the channel to its maximum. So, frame aggregation which uses many MAC frames under a single Physical header are sent within a successful medium access. The performance analysis of frame aggregation technique has shown a tremendous improvement on delay performance and throughput. As proposed in [8]: Priority-based Service Differentiation Scheme for IEEE 802.15.4 Sensor Networks, the CW size and BE are important parameters in designing a MAC routing scheme because, when the CW size is affects the throughput factor and BE affects the delay factor during packet transmission. This leads to adjusting the CW size for enhancing the throughput of the device and BE for decreasing the delay. In [9]: An Emergency Handling Scheme for Superframe-Structured MAC Protocols in WBANs, the authors proposed a scheme for handling urgent data where a Mixed Period (MP) and an Extended Period (EP) were inserted in the MAC superframe of IEEE 802.15.4. The CAP slots were placed in the MP prior to the CFP for transmitting the urgent data at once without any supporting for any further delay. The EP is allotted with a Extended Request Period (ERP), a CFP and an additional CAP for supporting the transmission of those slots that have not been successful during the MP. This EP provides guaranteed transmission of the data. The results show that, the delay provided by the proposed scheme was reduced while handling the urgent data to a great extent. The three algorithms following the three approaches namely, offline computation, model-based adaptation and measurement-based adaptation respectively were compared in [12]: Strategies for Optimal MAC Parameter Setting in IEEE 802.15.4 Wireless Sensor Networks: a Performance Comparison, in order to come up with optimization of IEEE 802.15.4 in terms of maximum reliability and minimum energy consumption. The results validate that the performance of adaptive algorithms are better than the model-based algorithms. This is because the model-based approach does not work well while operating during varying time period in real time scenarios. But, the measurement – based approach works well without the aforesaid limitations. So, the performance analysis of the third approach was laid out and proved. The algorithm proposed in [13]; Modeling and Optimization of the IEEE 802.15.4 Protocol for Reliable and Timely Communications, provides minimum energy consumption during mobile and immobile situations. When the load increases, the algorithms proposed by the authors give better medium access solutions. Under dynamic scenarios, the algorithms supports in quickly making out the errors.

The above literature clearly indicates that, the handling of immense data or urgent data is of vital importance and a proper channel allocation schema is required for efficient data transmission. The data handling, routing of emergency datum with minimal time and delay and maximum throughput and PDR is of primitive concern. Therefore, this paper contribute to modification of the IEEE 802.15.4 superframe structure and proposing a MAC routing scheme to efficiently handle the immense data and allocating the time slots in such a way that, the channel is utilized better with increased PDR and throughput and at the same time, minimizing the delay and energy consumption.

III. PROPOSED SCHEME

Fig.1 shows the MAC superframe structure of IEEE 802.15.4 in beacon mode. Since we operate in 2.4 GHz band with 250 Kbps rate of 16 slots, where, it commences with the beacon period for network synchronization and association at slot 0 and has a Beacon Extension Period (BEP) followed by Contention Access Period (CAP) from slot 1 to 8 where CSMA/CA contention for the channel access takes place. Contention Free Period (CFP) provides Guaranteed Time Slots (GTS) for the IPD requiring immediate data transfer, followed by the inactive so called, sleep period. We can extend or compress the inactive period according to the requirement as per the standard. So according to the customary standard, the IPD would suffer packet loss when it is sent in CFP which is placed after the CAP. When the packet size is more or when CFP in the current superframe is unable to transmit the data completely, it would be stored as pending data and it has to wait until the CFP of the next superframe which would increase the packet delay and sometimes, packet loss when the next superframe is also busy. Since, the medical arena permits a maximum delay of 125ms and 250 ms for IPD and MPD respectively, the average end to end delay becomes an important criteria during data transmission.

Therefore, the proposed routing scheme (IPDF) modifies the IEEE 802.15.4 MAC superframe structure to reduce the delay and power utilization resulting in increased throughput. Superframe ranges intervening both the beacons along with the active and inactive periods and is called as Beacon Interval (BI). Superframe Duration (SD) is time span of an active period. SD and BI rely on aBaseSuperFrameDuration (BSFD), Superframe Order (SO) and Beacon Order (BO). Anyhow, BSFD rely on aBaseSlotDuration (BSD) & aNumSuperframeSlot (NSS). BSFD is dependent on transmission capacity or the bandwidth of the network and it's a constant value which is equal to 960 symbols.

Fig.2 shows the modified superframe structure. The frame is initialized with a beacon following an additional Data Preference Notification Beacon (DPNB) to notify the preference of the arriving data. So BEP in the frame's standard is utilized which does not violate the permissible limit. Also, CFP can be extended, provided, the minimum CAP length has to be 440 symbols. The CFP is placed after the DPNB with 7 slots allowed in the standard. They are GTS allocated only for the IPD. The GTS can have more than 1 slot as per the standard. In IPDF SCHEME, the GTS operates in t_0 and t_1 for the IPD of the possessor and non-possessor respectively. Therefore, the CFP is also modified without violating the permissible criteria as per the given standard. Then follows the CAP, which operates in two phases namely Phase (P1) and Phase 2 (P2), used for transmitting MDP of the possessor and non-possessor respectively. Finally, the inactive period follows the CAP where the node enters the sleep mode when there is no data for transmission. Fig.3 depicts detailed flowchart on the Packet Preference Selection, Channel Allocation and data transmission procedure for IPDF Scheme.

A. Operation of IPDF Routing Scheme

When the data arrives, the beacon initializes the data transmission. The DPNB notifies the preference of the arriving data. If the arriving data is the IPD and it is the slot's possessor, t_0 is allocated immediately in CFP and the data is transmitted at once without any delay. If it is the slot's non-possessor, the node has to wait till the duration of t_0 and only then allocated with t_1 slot. This avoids any collision or unwanted delay of prioritized data as per the medical requirement of <125ms. When the DPNB identifies MPD arriving, then, it makes the node to access the CAP without waiting during CFP thereby, reducing the delay of MPD as well, which has to be <250ms. But, CAP- P1 allows only the possessor's MPD to be transmitted and CAP – P2 allows non-possessor's MPD to be transmitted. During CAP access, the MPD have to follow the CSMA/CA mechanism in order to access the medium while contending, when the medium is busy. The IPDF algorithm explains the aforementioned operation during channel access.

The proposed scheme involves the CAP segmentation into dynamic phases that leads to prevention of bandwidth wastage during channel contention, thereby, utilizing the same, efficiently by priority based transmission of medical data. The length of individual dynamic phase in the CAP can be estimated as,

$$L_n = \sum_{i=0}^{n-1} l_i + L * (N_n / N) \quad (4)$$

where, L is the length of individual phase in the CAP with n taken from 1, during initialization of each phase, N_n is the entire nodes with load grouping based on packet preference and N being consummated count of nodes.

IPDF Algorithm for Accessing the Channel

```
If (Immense Preference Data)
        Access CFP
                If (Possessor node)
                        Allocate a slot at t0
                        Transmit Data immediately at t0
                Else
                        Wait till t0
                        At t1, allocate a slot
                        Transmit Data in t1
                End if
Else
        Access CAP
                If (Possessor node)
                        Phase 1 (P1): Allocate a slot and
                        transmit data
                Else

                        Phase 2 (P2): Channel Contention
                        according to CSMA/CA Procedure
                End if
```

The MPD is inclusive of the entire data traffic excluding crucial data traffic. So, the normal and low preference data packets that is to be sent from the human body continuously for regular monitoring that is not very much time sensitive when compared with the emergency packets, would get into channel contention at CAP.

B. Significant Advancements of IPDF Routing Scheme

The proposed routing scheme brings forth the consecutive significant advancements:

1. A routing scheme with Immense Preference Data Forwarding incorporated with Constructive Time Slot Allocation Scheme was contemplated to maximize throughput, minimize overall delay and utilization of energy by a sensor node thereby, increasing its PDR and lifetime.
2. Since there is a faster access to the channel and possessor data, non-possessor IPD and MPD are transmitted efficiently as explained in the operation of the routing scheme, thereby, decreasing the back off time period leading to reduction in the response wait time.
3. Since the redundant contentions cause unwanted wastage of energy and bandwidth, the proposed scheme greatly overcomes it by efficiently transmitting their absolute data of the possessors in the CFP itself. Only the non-possessors contend for the CAP according to the preference of the data.
4. This results in decrease in Duty cycle which decreases the end to end delay as we transmit and receive the absolute data within that superframe itself and at the same time, circumventing the added delay due to data storage in the coordinator amid the sleep time.

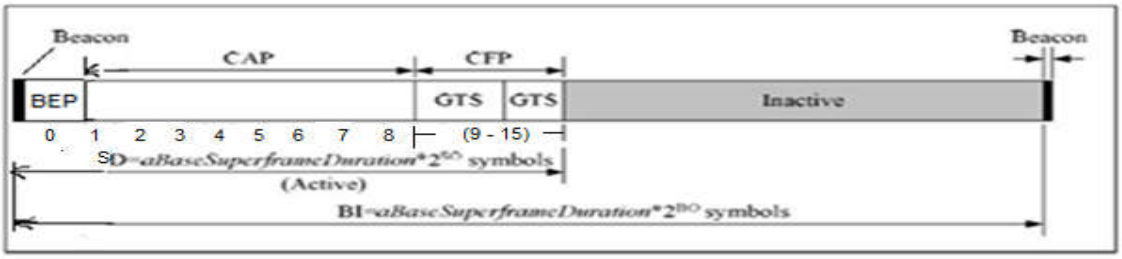

Fig. 1 Superframe structure of IEEE 802.15.4

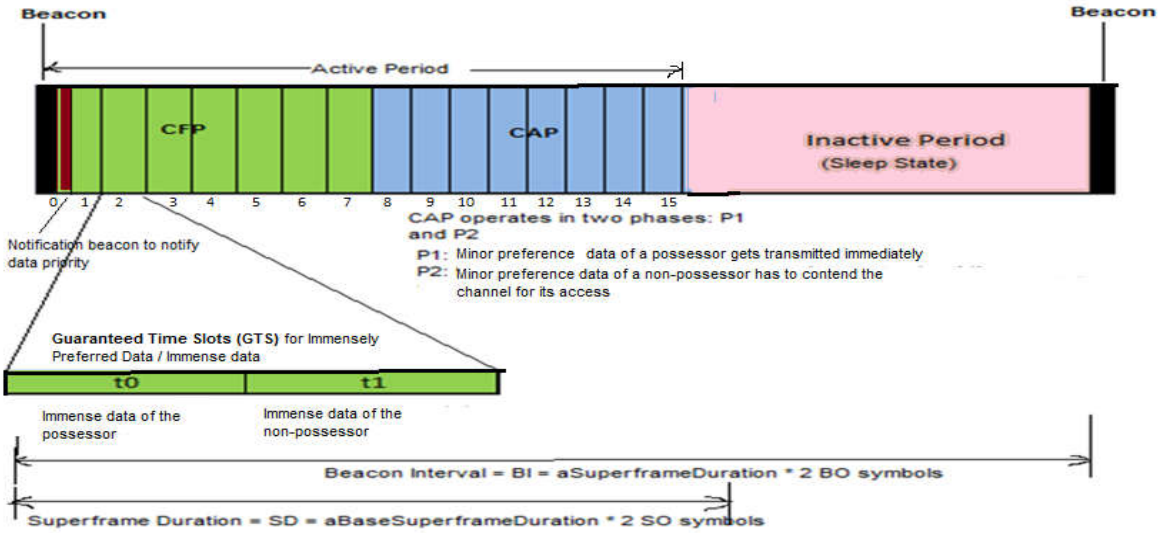

Fig. 2 Modified Superframe structure for IPDF Scheme

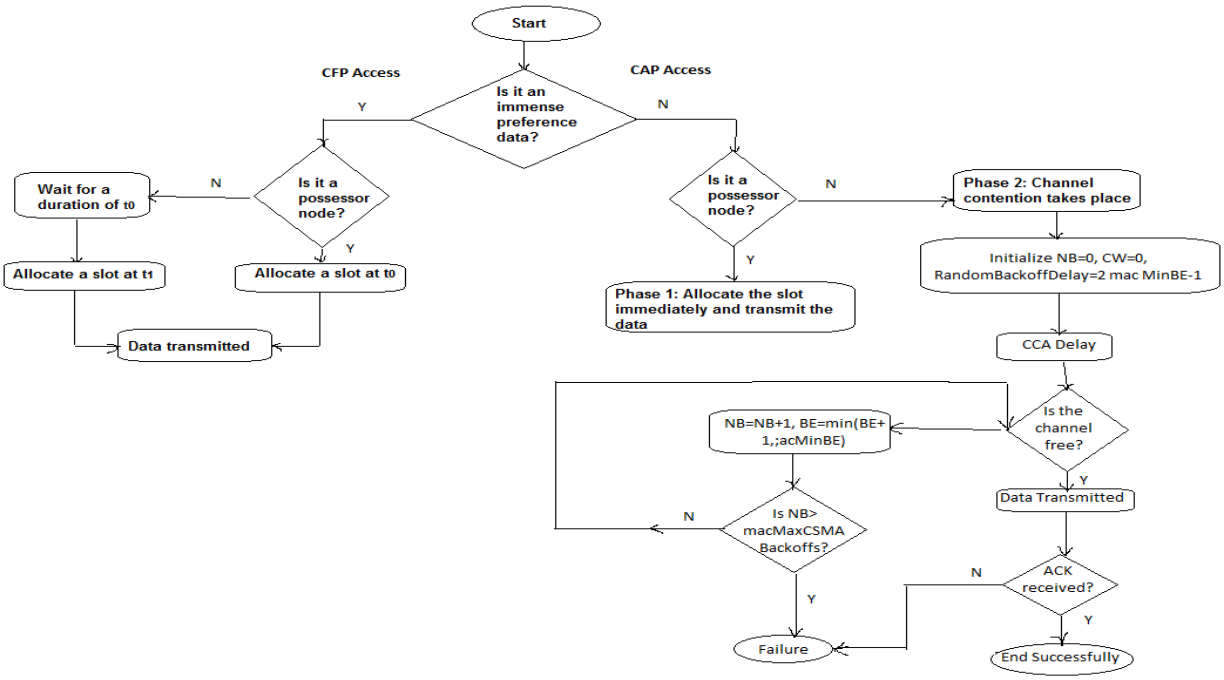

Fig. 3 Flowchart for Packet Preference Selection, Channel Allocation and data transmission for IPDF Scheme

IV. PERFORMANCE ANALYSIS

The IPDF scheme was evaluated using Network Simulator 2 (NS-2). A single hop data transmission with star topology was utilized with assumption that, all the biosensors were affixed to the body with random deployment of the nodes surrounding the coordinator with radius of 4m.

TABLE I. SIMULATION PARAMETERS

Parameter	Value
Area	500 m x 500 m
Routing Protocol	AODV
Physical / Mac layer	802.15.4
Channel type	Wireless
Radio Propagation mode	Two Ray Ground
Network Interface type	Phy / Wireless Phy
Interface queue type	Drop Tail / PriQueue
Antenna Model	Omni directional Antenna
Link Layer type	LL
Traffic type	CBR
Network Topology	Star
Channel Rate	250 Kbps
Frequency band	2.4 GHz
Pt = Power of radio transmission	36.5 mW
Pr = Power of radio reception	41.4 mW
Pi = Power of idle listening	41.4 mW
aBaseSuperframeDuration	960 symbols (15.36 ms)
macBeaconOrder (BO)	4
macSuperframeOrder (SO)	3
Beacon Interval (BI)	245.76 ms
aNumSuperframeSlots	16
UnitBackoff Period	20 symbols (0.32 ms)
aMaxSIFSFrameSize	18 octets
aTurnaroundTime	12 symbols (0.196 ms)
macAckWaitDuration	54 symbols (0.864 ms)
macMinBE	3
macMaxBE	5
macMaxCSMABackoffs	4
macMaxFrameRetries	3
CCA	8 symbols
SIFS	12 symbols (0.192 ms)
LIFS	40 symbols (0.64 ms)
Notification Beacon	40 bytes (1.28 ms)

The assumptions made during simulation were that, the data traffic was assumed to be 20 % of Immense Preference Data, 40 % Medium Preference Data and 40 % Minimum Preference Data, the entire nodes operated within the coordinator boundary limit without any intricacies from the neighboring networks. The simulation results for the proposed scheme were evaluated and compared against IEEE 802.15.4 and PA-MAC.

From Fig.4, the contention during CAP was greatly reduced in IPDF scheme, thereby reducing delay, compared to the customary IEEE 802.15.4 standard and PA-MAC, due to limited access in the data traffic load in the intervening CAP phases, by providing a rapid access for IPD and LPD in the channel. In PA-MAC, there was an uncontrolled contention of variable traffic in various phases of CAP and there exists no traffic prioritization in IEEE 802.15.4 MAC during the ingress to the medium resulting in huge delay in the entire network.

Fig. 4 Delay Performance with respect to Node Count

It was observed from Fig.5 that, delay for variable packet volume was very small (<125 ms) as necessary for the medical real time traffic utilization, compared to the customary IEEE 802.15.4 and PA-MAC.

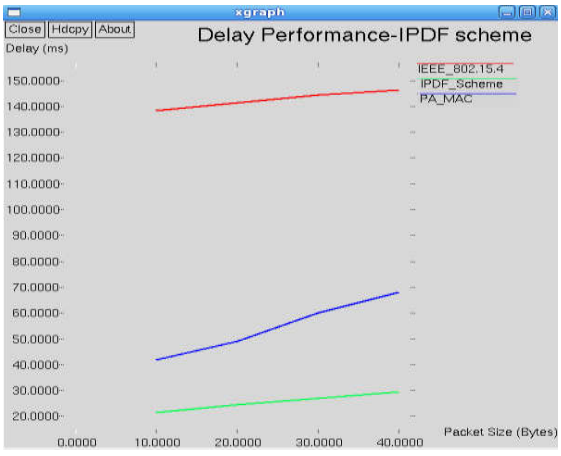

Fig. 5 Delay Performance with respect to Packet Size

When there exists a huge volume of data traffic, only a certain amount of nodes could be accommodated in the system that results in large collision. Whereas, the channel access is confined based on traffic preference in IPDF scheme (IPD in CFP and LPD in CAP, restraining only for LPD traffic). This results in decreased collision, providing a better channel access and thereby, improving the throughput of the network as depicted in Fig.6.

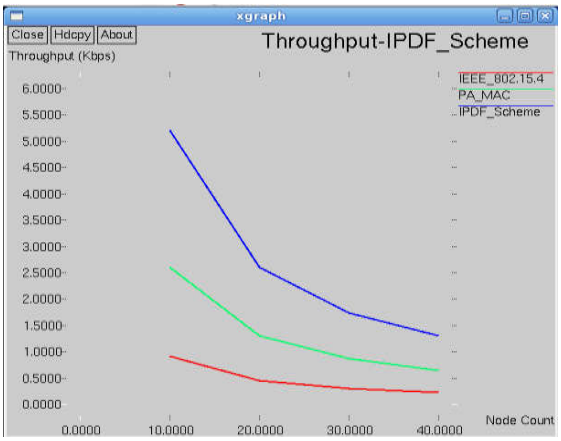

Fig. 6 Throughput Inquiry with respect to Node Count

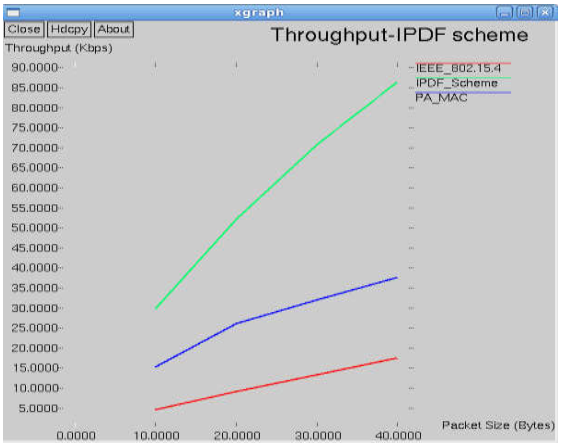

Fig. 7 Throughput Inquiry with respect to Packet Size

Fig. 7 shows that, the throughput of IPDF scheme increases gradually with packet size. When the node count boosts up, the exhausted energy also shoots up due to collision upsurge and therefore, packet retransmits.

From Fig. 8, the PA-MAC and customary IEEE 802.15.4 consumes energy of approximately 10.5 mJ and 10 mJ respectively with 20 nodes, whereas, IPDF scheme uses 9.5 mJ of energy, because, there was a constrained medium access in CAP and CFP was entirely dedicated only for IPD. Due to the CAP phase distinction, the energy consumed was greatly reduced in IPDF scheme due to unnecessary contentions leading to energy exhaustion.

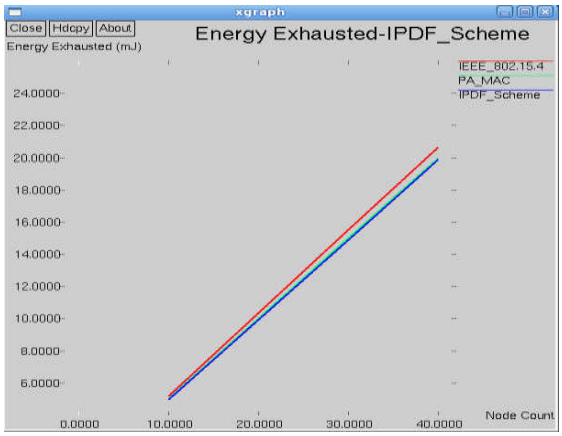

Fig. 8 Energy Exhausted with respect to Node Count

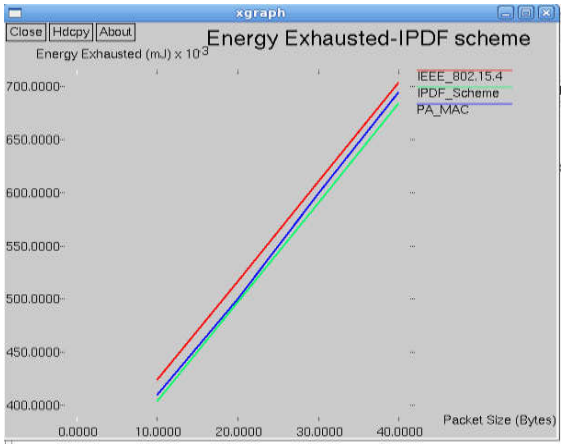

Fig. 9 Energy Exhausted with respect to Packet Size

From Figure 9, IPDF scheme consumes energy equivalent to PA-MAC but, lesser than the customary IEEE 802.15.4, that could transmit IPD and LPD within a short time period compared to the customary protocol and PA-MAC.

V. CONCLUSION AND FUTURE WORK

The Immense Preference Data Forwarding (IPDF) Scheme was designed and implemented with a modified MAC superframe structure in IEEE 802.15.4, by allocating maximum priority IPD of the possessor and non-possessor to t_0 and t_1 in CFP respectively, for immediate data transfer, to minimize the delay associated with IPD traffic. The MPD of the possessor and non-possessor are routed through the P1 and P2 phases in the CAP respectively, to handle the MDP traffic as well. The performance analysis of the proposed Scheme was carried out. The throughput showed a significant increase and delay and energy consumption showed a significant reduction for IPD and MPD of IPDF SCHEME when compared to PA-MAC and customary IEEE 802.15.4 standard. In future, an equitable contention ingress scheme for both medium and low preference data with maximum channel utilization would be considered.

REFERENCES

[1] Jay Shree Ranjit, Seokjoo Shin, "A Modified IEEE 802.15.4 Superframe Structure for Guaranteed Emergency Handling in Wireless Body Area Network", Network Protocols and Algorithms, vol. 5, No. 2, 2013.

[2] Ahmad Naseem Alvi, M. A. Yaqub, Nadeem Javaid, Syed Hassan Ahmed, Safdar Hussain Bouk, Dongkyun Kim, "An Improved IEEE 802.15.4 Superframe Structure with Minimum Delay and Maximum CFP Link Utilization", Ad Hoc & Sensor Wireless Networks, March 2015.

[3] Minglei Shu, Dongfeng Yuan, Chongqing Zhang, YinglongWang and Changfang Chen, "A MAC Protocol for Medical Monitoring Applications of Wireless Body Area Networks", Sensors, vol. 15, pp 12906 – 12931, June 2015.

[4] Muhammad Sajjad Akbar,Hongnian Yu, and Shuang Cang, "Delay, Reliability, and Throughput Based QoS Profile: A MAC Layer Performance Optimization Mechanism for Biomedical Applications in Wireless Body Area Sensor Networks", Journal of Sensors, vol. 2016.

[5] Arshad Farhad, Yousaf Zia, Sajid Farid, and Faisal Bashir Hussain, "D-MAC: A Dynamic MAC Algorithm for the Body Area Sensor Networks Based on IEEE 802.15.4", (International Journal of Computer Science and Network Security, vol. 16, May 2016.

[6] Farhan Masud, Abdul Hanan Abdullah, Gaddafi Abdul-Salaam and Fasee Ullah, "Traffic Adaptive MAC Protocols in Wireless Body Area Networks", Wireless Communications and Mobile Computing, vol. 2, pp. 1-14, 2017.

[7] Muhammad Sajjad Akbar, Hongnian Yu and Shuang Cang, "IEEE 802.15.4 Frame Aggregation Enhancement to Provide High Performance in Life-Critical Patient Monitoring Systems", Sensors, vol. 17, 2017.

[8] Eui-Jik Kim, Meejoung Kim, Sung-Kwan Youm, Seokhoon Choi, Chul-Hee Kang, "Priority-based Service Differentiation Scheme for IEEE 802.15.4 Sensor Networks", International Journal of Electronics and Communication vol. 61, pp 69-81, February 2007.

[9] Beom Seok KIM, Jinsung CHO, Dae- Young KIM, "An Emergency Handling Scheme for Superframe-Structured MAC Protocols in WBANs", IEICE Transactions on Communications, vol. 9, pp 2484-2487, 2011.

[10] IEEE Std. 802.15.6-2012, "Part 15.4: Wireless Medium Access Control (MAC) and Physical Layer (PHY) Specifications for Low-Rate Wireless Personal Area Networks (WPANs)". https://standards.ieee.org/about/get/802/802.15.html.

[11] IEEE 802.15 WPAN Task Group 6 Body Area Networks (BAN). http://www.ieee802.org/15/pub/TG6.html

[12] Simone Brienza, Domenico De Guglielmo, Giuseppe Anastasi1, Marco Conti, Vincenzo Neri, "Strategies for Optimal MAC Parameter Setting in IEEE 802.15.4 Wireless Sensor Networks: a Performance Comparison", Computers and Communications (ISCC), 2014.

[13] Pangun Park, Piergiuseppe Di Marco, Carlo Fischione, Karl Henrick Johansson, "Modeling and Optimization of the IEEE 802.15.4 Protocol for Reliable and Timely Communications", IEEE transactions on Parallel and Distributed Systems, vol. 24, March 2013.

Proceedings of the Fourth International Conference on Communication and Electronics Systems (ICCES 2019)
IEEE Conference Record # 45898; IEEE Xplore ISBN: 978-1-7281-1261-9

Automated Library System Using Robotic Arm

K. V. Jyothi Prakash
Department of E&C Engineering
Siddaganga Institute of Technology
Tumakuru, Karnataka, India
jyothiprakashkv@sit.ac.in

K M T Tejaswi Kumar, K Punyadeep,
Kamsala Ravi Theja, Gopala Krushna
Department of E&C Engineering
Siddaganga Institute of Technology
Tumakuru, Karnataka, India

***Abstract* — A library is a collection of information resources and provides invaluable services to its users for reference and borrowing of books and documents. As the library grows in size, the problem associated with the maintenance of the books also grows. Searching a book in the library manually is a tedious process and if there is any misplacement of the book either intentionally or unintentionally then it consumes more time and more effort to search the book. To overcome this problem an attempt is made to introduce automation of library for fast searching of books and to pick or place the book in a particular rack. A robot with an arm is developed which is able to find the book at particular position and then pick or place in a particular rack in the library.**

Keywords —— Library, robot, robotic arm, Arduino, infrared sensor, WIFI module.

I. INTRODUCTION

International Federation of Robotics (IFR) defines a service robot as a robot which operates semi or fully autonomous to perform services useful to the well-being of humans and equipment, excluding manufacturing operations. Robotic arm is a mechanical arm which is manually controlled through wired or wireless systems to perform the desired task in various fields of application such as military tasks, hospital operations, dangerous environment and agriculture.

The main aim here is to build a robotic arm that is capable of picking the particular book and in case of any misplacement of the book the robotic arm should be capable of picking the particular book required by the user. The system that is built has two circuits namely Arduino circuit with Wi-Fi module for control operation and motor driver circuit to drive the DC motor. A robot with an arm is developed which is capable of searching the book at particular slot and then pick or place the book in a particular rack in the library. To create a systematic, faster and efficient operation, Arduino will be used which will process the input received from the WIFI module and perform the programmed action. This system proposes a database that provides a way of searching the required book to pick or place, to find the misplaced book and to get the information about the status of the book. A GUI is developed on visual basic platform. The GUI has icons such as add book, search book and reset. The hardware of the system consists of line follower robot that navigates in the library and detects the exact location of the required book. The visual basic platform is interfaced through WIFI module with the robot to pick or place the book in the designated position as per the instructions of the user.

II. EXISTING SYSTEM

In the library the books will be placed in the designated position of racks and if any user needs a particular book will first check the availability of the book and search the book in that designated position. But the problem is if someone by mistake or purposefully places the books in wrong positions then it is very difficult to locate the book. The user or the library staff has to search all the racks to locate the book which will be either time consuming or sometimes it may not be possible to locate the book at all.

III. PROPOSED SYSTEM

In the proposed system a robot with an arm is developed such that whenever a user wants to borrow a book will first search for the availability of the book. If the book is available then the user will press a button to inform the robot to bring that book. The position of the book will be sent to robot through WIFI module and the robot will move and bring the book. The advantage of this system is even if the book is misplaced the database will be updated to the new position of the book so that robot will search the book and pick it. Further in this proposed system whenever a book is returned back by the user, the robot will be intimated to place the book in designated position and that position details will be updated in the database.

IV. IMPLEMENTATION

A. Block Diagram

The Block diagram of automated library system using robotic arm is shown in Fig. 1. The automated library system consists of IR sensor, Arduino, robotic arm, WIFI module, DC motors and motor drivers and PC. It has two sections: a transmitter section and a receiver section. Transmitter section consists of PC for sending the commands to the robot through WIFI module. Receiver section consists of microcontroller to process the signals received through WIFI module.

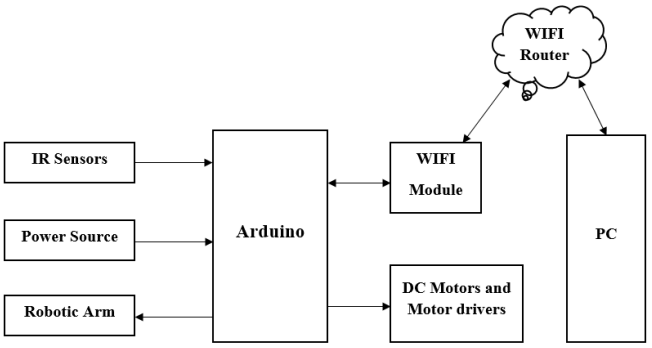

Fig. 1 Block Diagram of Automated Library System using Robotic Arm

The automated library system is concerned with the implementation of pick and place task using Arduino board. Instructions from user are sent from PC via WIFI module to the Arduino and the protocol used for communication between PC and controller is serial UART. The received data is processed and corresponding output is sent to the motor driver which enables the DC motors for the movement of robotic arm and line follower robot.

Arduino

Arduino is a software and user community that design and manufacture computers. It is a open source software and microcontroller based kit for building digital devices and interactive objects that can sense and control physical devices. Here Arduino controller is used to process the commands required for the movement of motors, line follower robot and to control all other peripherals.

DC Motor

The DC Motor is a class of rotary electrical machines that converts electrical energy into mechanical energy. The common type of motor work on the force produced by the magnetic fields. The speed of the DC motor can be controlled using either a variable supply voltage or by changing the strength of the current in its field windings. DC motors are used for the movement of the robot and also for the movement of grippers.

Motor Driver(L293D)

The L293D motor driver is used to provide user with ease and user friendly interfacing for embedded application. The L293D is a dual H-bridge driver that can drive up to 1 Amp per bridge with supply voltage up to 24V. In automated library system using robotic arm two motor drivers is used to drive four DC motors.

Robotic arm with gripper

Robotic arm is an anthropomorphic structure which resembles human arm. In this project DC motors of 30RPM are used for the movement of the robotic arm and also for opening and closing of the gripper. Robotic arm with gripper is used to pick or place the book in to the rack.

IR Sensors

IR sensor uses the light sensor to detect specific light wavelength in the infrared (IR) spectrum by using an IR LED and it works on the principle of obstacle detection. The IR transmitter continuously emits the light, whenever the book is detected by the IR transmitter then the light gets bounces back to the IR receiver which indicates that the book is present in the rack and also used for line tracking of the robot.

Power Source

The battery is used to deliver required amount of power to all the components in the project. In this project line follower robot is energized using a 12V and 7.2A battery and all other components like IR sensors, Arduino, WIFI module and motor driver are energized using 12V and 1.2A battery.

Liquid Crystal Display (LCD)

A 16 X 2 LCD can display 16 characters per line and there are 2 such lines and each character is displayed in 5 X 7 pixel matrix. LCD is used to display the commands sent from the PC.

B. Algorithm and Flowchart

The algorithm used in the automated library system using robotic arm is:

- Configure WIFI module and Arduino.
- Set or define the input and output port.
- Set the baud rate as 9600 and enable the transmission pins for communication.
- Initialise LCD.
- Send the appropriate input from the PC to the Arduino through the WIFI module.
- Commands from PC are processed in the Arduino.
- The processed input from Arduino (i.e. book number) is sent to motor driver which runs the appropriate motors.
- If valid book number is entered, Robot moves towards the defined book position.
- If the book is found the robot pick the book and returns it to the destination.
- If the user wants to return the book, the robot pick the book from the user and moves towards the predefined position and places it.

The flowchart of Automated Library System is using Robotic Arm is shown in Fig. 2.

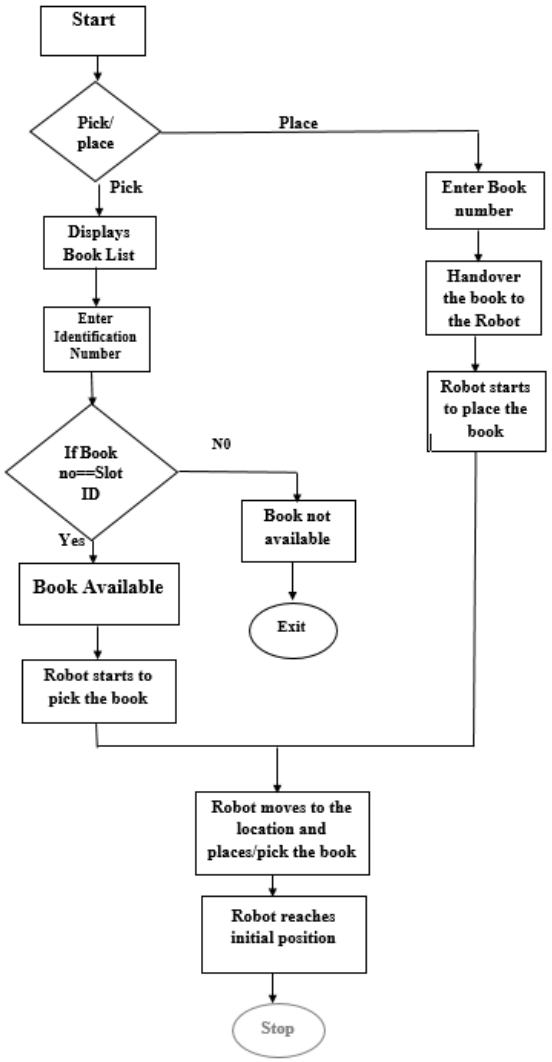

Fig. 2. Flowchart of Automated Library System

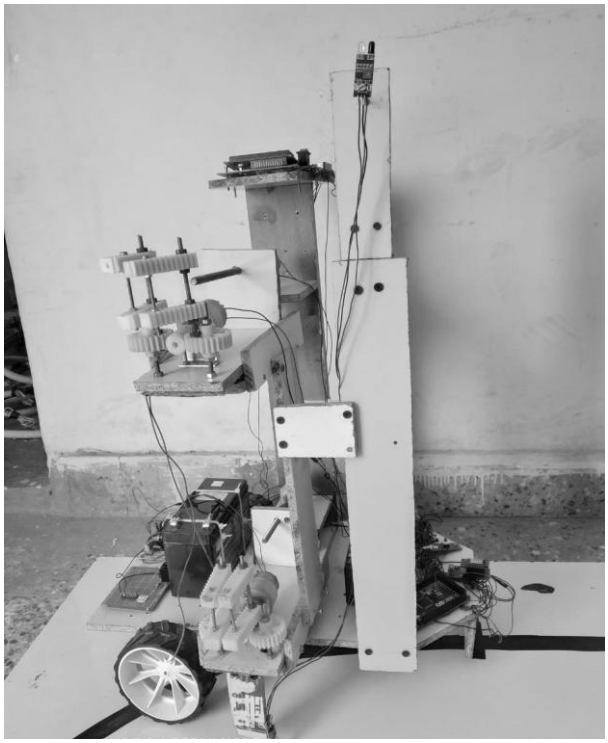

Fig. 3. Working model of smart energy meter

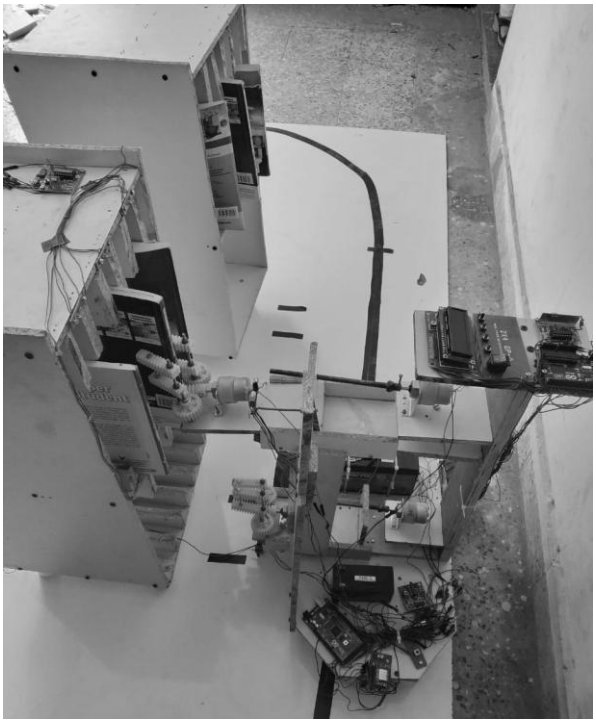

Fig. 4. Robot picking the book at a particular slot

V. RESULTS AND CONCLUSION

A. Results

The working model of the Automated Library System is shown in Fig. 3. The hardware of the automated library system using robotic arm consists of gripper and triangular bars to hold the book firmly. The system uses four DC motors each of 30 RPM and two Johnson motor each of 30 RPM with 6 to 7 kg torque is used. Motor drivers converts lower currents into higher currents that are used to drive the motors. Motor driver can drive two DC motors simultaneously. The system uses RF transmitter and receiver to communicate between Arduino and obstacle detectors. IR sensors are used to detect the book i.e. whether the book is present in the slot or not and they are also used for line follower robotic vehicle and make the robotic vehicle to stop at particular slot to pick as shown in the Fig. 4 or to place the book as shown in the Fig. 5

.

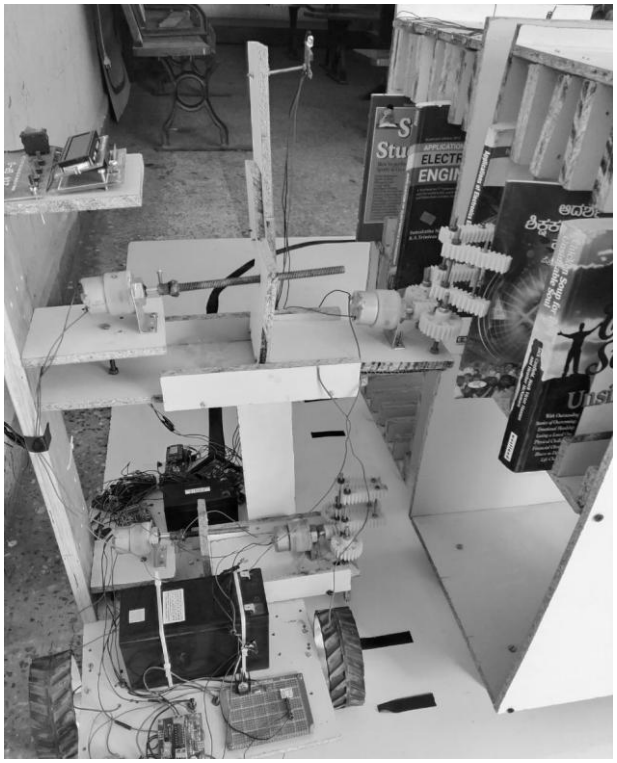

Fig. 5. Robot placing the book at a particular slot

The visual basic window of the automated library system using robotic arm uses VBA (Visual Basic for Application) language. The interface of the visual basic window is provided with different type of icons such as add book, search book, reset and close icons. The visual basic window of the automated library system using robotic arm is shown in Fig. 6.

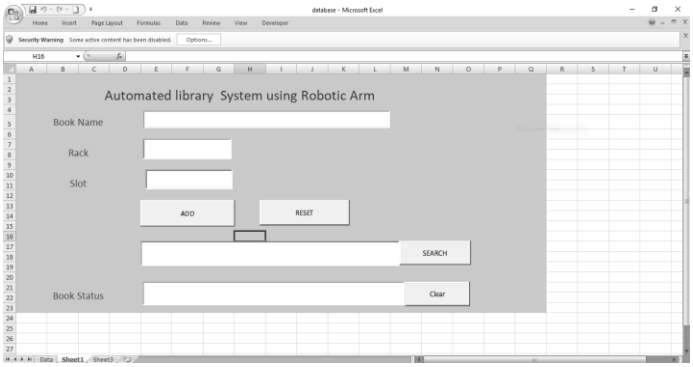

Fig. 6. Visual basic window of the automated library system using robotic arm

The search icon is used to search a particular book in the library. The result of searching the particular book in the library is shown in Figure. In this visual basic platform search option is used to search a book. In this comport the details such as book name is entered. This comport shows whether the book is available or not in the slot of the rack in the library. If the book is available then the robot moves to the predefined position to pick the required book and returns it to the destination as shown in Fig. 7. If the book is not available in the library the PC shows the comment in the comport as Book not available as shown in Fig. 8. The add book icon is used to add new book to the XL Macro database used in automated library system using robotic arm. Whenever we want to add new book to the database as shown in Fig. 9, the name of the book that is adding should be written in the comport and then press the add icon as shown in Figure. The reset icon is used to reset the visual basic window.

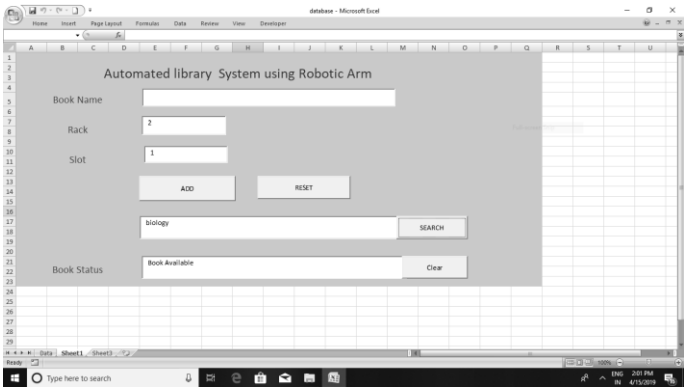

Fig. 7. The book selected is available in the rack

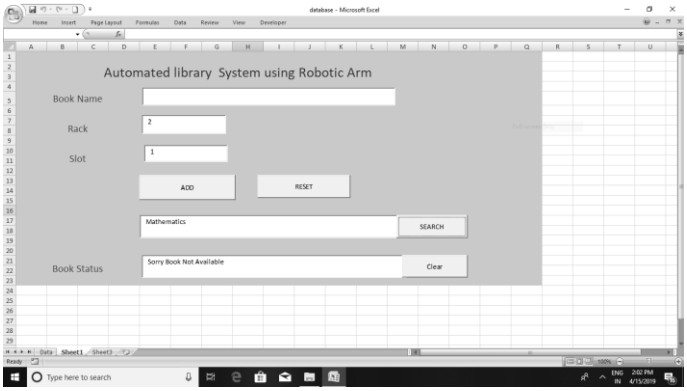

Fig. 8. The book selected is not available in the rack

	A	B	C	D
1	Serial No.	Book Name	Rack No.	Slot No.
2	1	Microelectronics	1	1
3	2	Network Analysis	1	2
4	3	Signals and Systems	1	3
5	4	Power Electronics	1	4
6	5	Antenna and propagation	2	1
7	6	Wireless Communication	2	2
8	7	Embedded System	2	3
9	8	Digital Signal Processing	2	4

Fig. 9. Database to display the book numbers

B. Conclusion

The main objective was to overcome the problem of searching the books in the library and provide automation in a user friendly manner. The robot with an arm is designed which can search the required book, pick the book from the rack and deliver the book to the issue counter. It can also place the book in its designated slot once the book is returned by the

borrower. The hardware and software required for automated library system using robotic arm has been designed and tested successfully.

C. Future Scope

The robot can be made more efficient by incorporating image processing technique to identify the books and book slot to pickup or place the books.

REFERENCES

[1] Bin Abdullah, Shah Alam, Ismail, Ibrahim, Hakim Bin Noor, "Library shelf management system using RFID technology", IEEE International Conference on System Engineering and Technology (ICSET), 2011.
[2] Dong Zhang, Xiling Shi, "Self- service management platform design for library based on RFID", 2nd International Conference on Artificial Intelligence, Management Science and Electronic Commerce (AIMSEC), 2011.
[3] Tetsuo Tomizawa, Akihisa Ohya and Shinichi Yuta, "Book Browsing System using an Autonomous Mobile Robot Tele-operated via the Internet", In Proc. of the IEEE Int.Conf. on Intelligent Robots and Systems, 2008.
[4] Muhammed Jabir N. K, Neetha John, Muhammed Fayas, Midhun Mohan, Mithun Sajeev, Safwan C. N, "Wireless Control of Pick and Place Robotic Arm Using an Android Application", International Journal of Advanced Research in Electrical, Electronics and Instrumentation Engineering, Vol. 4, Issue 4, April 2015, Kothamangalam, Kerala, India.
[5] Pedro Neto, J. Norberto Pires and A. Paulo Moreira, "Remote based control of an industrial robotic arm", The 18th IEEE International Symposium on Robot and Human Interactive Communication, 27 Sept.-2 Oct. 2009, Toyama, Japan.

Proceedings of the Fourth International Conference on Communication and Electronics Systems (ICCES 2019)
IEEE Conference Record # 45898; IEEE Xplore ISBN: 978-1-7281-1261-9

Controllability Intelligence of Lightning Protection System due to 110kV Transmission line

Mohammed Abdaldaim Ibrahim
School of Electrical and Electronic Engineering
North China Electric Power University
Beijing, China
1164300022@ncepu.edu.cn

Lin Li
School of Electrical and Electronic Engineering
North China Electric Power University
Beijing, China
lilin@ncepu.edu.cn

Ping Wang
School of Electrical and Electronic Engineering
North China Electric Power University
Baoding, China
Pingwang0501@163.com

***Abstract*: A lightning protection system (LPS) of an urban 110 kV substation is designed and analysed according to NFPA 780 and IEC 62305-3 standards. The analysis of the LPS is based on the value of risk assessment. The total area of the plant is described by one soil layer with uniform resistivity. This study aims to improve the understanding of unexpected attitude of the grounding grid system under lightning strike currents by explaining the basic notion of the lightning protection level. The program is integrated with the CDEGS software, which provides effective geometrical modeling with object and result visualization. Furthermore, module and automated fast Fourier fransform is implemented in this study to simulate electromagnetic fields in the period and frequency scope. These current values are compared to the desired protection levels within the standards. The study results show that for the improved protection of the system against lightning, the total power grid must be considered as a source of improvement for studying shielding influence and the protection levels provided inside this substation.**

***Keywords- LPS;NFPA780; shielding failure; CDEGS software; step voltage*.**

I. INTRODUCTION

A lightning protection system (LPS) is an extremely controversial subject. It is difficult to obtain realistic information on the capacity of the system even if precautions are accurately calculated. Lightning is a natural phenomenon that cannot be controlled by humans, but LPSs are not. Lightning protection provides a path to direct high energy into the soil, which is achieved by a grounding grid under the area to be protected. Lightning strike causes large potential differences in the electrical systems that are distributed one by one in the substation grounding grid. In this study, a 110 kV substation is designed, and the lightning voltage and current, and the LPS protection of the substation during a thunderstorm are calculated. The designed LPS results in reduced impact of lightning disturbances and improved robustness of the grid substation. The assessment of the LPS is performed using traditional techniques from the literature [1]. Lightning generates considerable voltage anomaly in high transmission and distribution grid systems in direct strikes. These considerable voltage anomalies lead to line power failure. New evolution have made it prospective to expand a solution to lightning problems, and also to decrease the total cost of the substation grid design [2].These studies and analyses are carried out to provide high protection for this substation. This model proposes a new design of electrical stations and is accomplished by modeling simulation using the CDEGS software shown in Fig. 1. In some cases, lightning affects the upper part of the substation, which does damage to most of the equipment inside the substation, leading to a complete cessation of all parts of the substation. Insulation flaw on 110kV transmission line in front of the substation can get short circuit currents with high magnitude [3]. Electrical grid substations can be abnormal to different forms of voltage deflection. Through the design point, the engineer should select the risk scale for which the substation is designed according to the risk standard, is common, attached to the basic insulation level chose. To reduce the occurrence of such specific risks copper was added to the top of one corner of the substation [4]. In the present paper, a new analytical implementation of lightning is presented. The primary circuit arrangement is the same as in [5]. However, the present implementation was extended to include lightning surges on a 110 kV urban substation. To estimate a performance in the first moments of a lightning pulse, the high frequency content of the lightning current stroke is used as an approximation of the first strike. The time domain waveform is transferred to the frequency domain by using rolling sphere method [6]. LPS is designed by the keraunic scale at the material position of grid substation, that is defined accordingly the average number of thunderstorm days per year, and is related to the density and quantity of flashes to the ground [7]. A substation was designed and studied according to the yearly average flash density in the region Ng=10(f/km square/ye) reliance on the global map of the lightning frequency –strike. In this study, three-dimensional 110 kV ground grid substations are applied, and transient responded simulations in the CDEGS software and the assessment of the lightning performance of the substation was performed. All calculations were

conducted and analyzed according to the international standards for the design of 110 kV substations. Moreover, the plan was built on the full frames that provide high protection of the substation. For modeling, the lightning current flowed into the ground.

II. SYSTEM CHARACTERISTICS

This paper describes the Controllability of a grounding grid system for a 110 kV urban substation by MALT model using the CDEGS software. The size of the substation is 58.5 x 36 m2, and the soil resistivity is uniform layers. The depth of the layer is 3 m, and the assessment of the soil resistivity is 2000 Ω.m. The intelligent designing of the substation grounding grid is represented in Fig. 1. When lightning strikes this substation, a part of the lightning strikes current flows to the soil through the down conductor and its grounding system. However, if the lightning strike current is high, the insulator would be flashover, and a side of the lightning current invades this station. Therefore, this model was developed to handle the problems resulting from lightning strikes. We relied on optimal measurements to obtain the protection parameters like the touch and step voltages. We analyzed the basic rules to get high protection for the substation. We also discussed if the substation needs an LPS.

A. Ligthning Protection System(LPS)

An LPS consists of an air_termination system (ATS) for the above upper-most parts of the construction with down-conductors and an earth_termination system. For controllability protection level selection, the IEC standard point out to the assessment of the risk mentioned in [8, 9]. Four lightning protection levels (LPLs) for the models are realized to fulfill the desired LPL performance class. For each LPL, a set of maximum and minimum lightning strikes current parameters is fixed. Each set contains level-dependent and level-independent construction rules. Four classes of LPSs (I, II, III, and IV) are defined as a set of building rules, based on the identicaling LPL. We used the risk assessment to determine the class of the LPS. If Nd ⩽ Nc the system does not need an LPS, and if Nd > Nc, otherwise. Risk assessment depends on the parameters shown in Tables 1 and 2. The main risks of lightning are studied extensively using mathematical modeling and simulations. The structure of the substation is designed by the CDEGS software explained in Fig. 1, and all calculations of risk assessment are explained in the following.

B. Lightning Risk Assessment

The risk assessment is performed to determine if the substation needs an LPS. For this, the lightning strike frequency (Nd) should be compared to the tolerable risk factors (Nc). The comparison is conducted by the ratio between the acceptable risk and the lightning strike frequency. If the calculated rate is 1.0 or higher, then an LPS is required, and if it is lower than 1.0, then there is no need

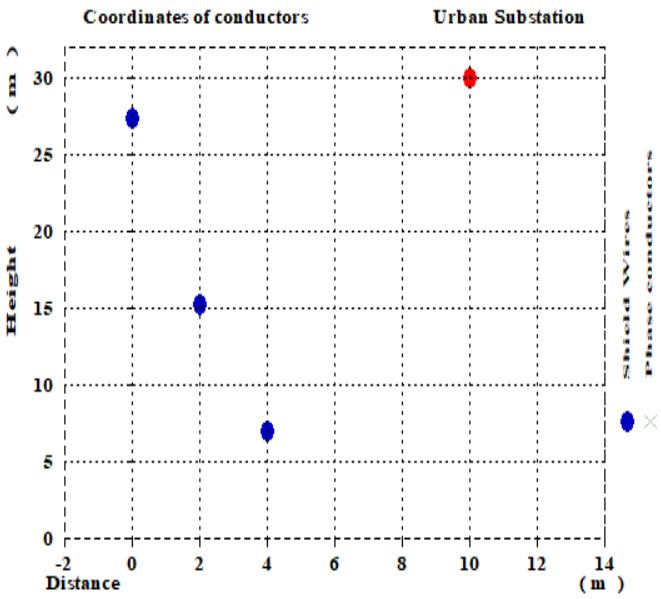

Fig.1 110kV substation grounding grid using CDEGS software.

for an LPS. The application is through NFPA 780 - 2008 edition [10]. The lightning strike frequency to the system can be calculated as Eq. (1):

$$Nd=Ng*C1*Ae*10^{-6} \quad (1)$$

The lightning strike frequency (Nd) consists of the common area of the facility (Ae), its surrounding environment (environmental coefficient C1), and the lightning flash density (Ng) of the city. The common area of the substation structure can be obtained as

$$Ae=L+W+6H(L+W)+9*3.14H^2 \quad (2)$$

Where L, W and H are the length, width and height of the structure, respectively. At this substation, the surrounding environment of the facility has an integral effect, so the designed external structure is critical to avoid the impact of lightning strikes, and all factors indicate that the high protection of the station leads to full stability of all parts of the substation [11]. The tolerable risk of the facility (Nc) is determined by Eq. (3) and is dependent on the structure coefficient (C2), contents within the structure (C3), structure occupancy (C4), and lightning consequence coefficient structure (C5).

$$Nc=C1*(10^{-3})/C2*C3*C4*C5 \quad (3)$$

Equation (1) and (3) are used to locate the distribution of lightning strike current capacity that below the shield wire. The structure is metal, and the coefficients are shown in Table 1, according to NFPA-780. Furthermore, after applying Eqs. (1) and (3) and Table 1, the result of the lightning risk assessment will determine whether an LPS should be installed. From the results in Table 2, we find that an LPS should be fixed because Nd>Nc or the ratio of Nd/Nc is greater than 1. Three LPLs used in this study are based on the standards. Commonalty lightning parameters are primary input variables for determining the effectiveness of voltage-

TABLE 1. C COEFFICIENT SPECIFICATION

Symbol	Relative Structure Location	value
C1	Isolated structure	1
C2	Metals	0.5
C3	High value	2
C4	Risk of panic	3
C5	Consequences to the environment	10

TABLE 2. MODEL CALCULATION OF THE LPS PARAMETERS

Symbol	Computation result of the parameters
Ae	16936.88 m2
Nd	0.16937
Nc	0.00005

protection. More recent lightning strike measurements were obtained by SES-shielded -CDEGS software.

III. LPS

There are four part of LPSs (I to IV), as shown in Table 3. The qualities of an LPS are determined by the characteristics of the model to be protected and by the considered LPL. The standard corresponding to LPLs defined in IEC 62305-1. After that, to determine the protection level class, the efficiency protection (E) is calculated to be 99% according to Eq. (4). A lightning strike is uncontrollable However, it can be discovered and lightning be tracked [12, 13].

$$E \geq 1\text{-}Nc/Nd \quad (4)$$

A. ATSs

An ATS is designed to prevent lightning damage to the substation. It should be designed to avert uncontrolled lightning strikes to the protected structure ATSs can consist of rods, spanned wire cables, meshes, conductors in the substation grounding grid.

We used air-termination rods according to [14] when the surface requires some rod air terminal units, we determine the air termination dependence as Eq. (5).

$$d = 2 \text{ sq. } (2*r*h\text{-}h\text{^}2) \quad (5)$$

Where d is the distance between two rods (m), r is the radius of the rolling sphere (m), and h is the height of the rods (m). At all events, earth-termination system designs with a considerable area between conductors and the soil buried deeply in the ground lead to lower step-voltages on the surface than those that are less deeply buried or have shorter conductors.

TABLE 3. CLASS OF LIGHTNING LEVEL AND EFFICIENCY IN IEC 62305-1[3]

Class of Protection level	LPS efficiency
I	98%
II	95%
III	90%
IV	80%

For determining the placement of the air termination system for changeable surfaces: the first one is the covering angle method for the height variation between two plan surfaces and the second is the rolling sphere method for the height between more surfaces in the situation of frame with complex spheral size. According to the standard DEHN shield, the determined height of the air-termination rods h (m) is presented in Fig. 2(a). The intelligence depth of the rolling sphere is controlled by the generality significant distance of the air termination rods from each other [15]. Air-termination rods are used to protect the surface of the substation on the roof against a direct lightning strike. The maximum lightning current depending on the value of the rod is shown in Table 4.

B. Down-conductor systems

We hope to minimize the damage caused by lightning to this substation. It is necessary to use a down-conductor system for the LPS. Exemplary estimation of the distance between down conductors and LPS are shown in Table 5. All values are given by IEC 62305-3 [16]. In this system the down-conductors are placed in one of the corners of the 110kV substation; they are distributed around the perimeter. The down-conductors are connected directly to the substation. They are installed directly onto the structure because of the temperature increase phenomenon during a lightning strike to the LPS. If the wall is made of an ordinarily inflammable material, the all value down conductors may be installed directly on or in the wall, as shown Fig. 1

C. Earth-termination systems

Earth-termination systems are an essential bit of LPSs. They must be designed to ensure safe lightning current transition into the ground grid wanting make step voltages on the surface of the soil, which would be serious to human beings. The attitude of an earth-termination system under high lightning currents was studied to minimize hazardous overvoltages.

TABLE 4. VALUE OF THE RODS AND MAXIMUM CURRENT DEPENDENCE FOR LEVEL I

Symbol	Computation result of the Parameters
r (m)	20
h(m)	10
Angle α	45
Maximum lightning Current(KA)	200

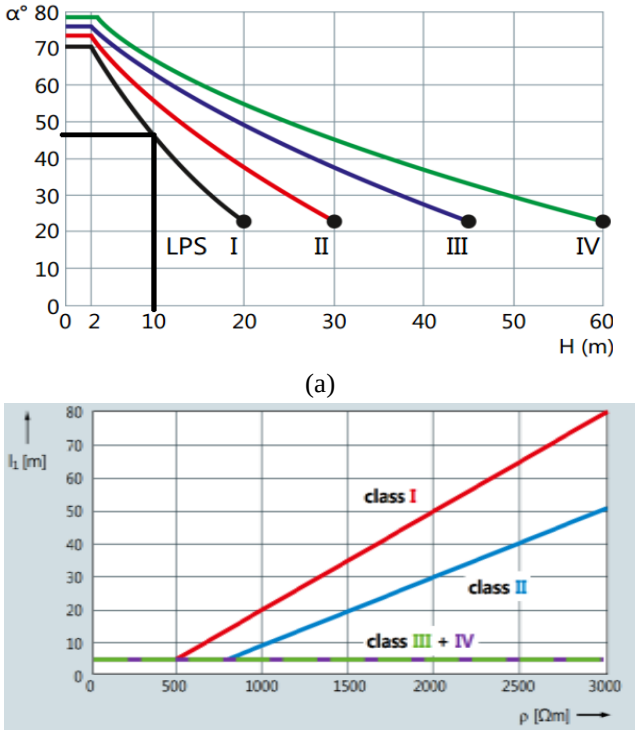

Fig. 2. Model of the LPL [15]. (a) Description of the resulting value of the LPS between angle α and H (m), (b) Minimum length of each earth electrode according to the resistivity and the LPS class.

This was performed by many authors theoretically both in the frequency and time domains [10]. In an earth-termination system, the length of earth electrode should be calculated according to the class of the LPS to determine the soil resistivity layer. For class I, the ρ = 2000 Ω.m and the length of the electrode is 50m, as shown Fig. 2(b).

IV. PEAK LIGHTNING CURRENT

Lightning currents that can pass during a direct lightning stroke can be simulated with the surge current of a waveform of 10/350 μs in IEC 62305-1. For class I, the peak value current is 200kA, conformable to the first short strike LPS. The lightning surge current can be jointly outlined by the attached double exponential-type function in Eq. (6) and Fig. 3.

$$i(t) = I/\eta * \exp^{\wedge}(-\alpha t) - \exp^{\wedge}(-\beta t) \quad (6)$$

Where I is the peak current, η is the correction factor, t is the time variable, and α and β are time constants. In this system, to calculate the lightning surge, we also used the Heidler representation of the lightning surge

TABLE 5. CLASS OF LIGHTNING LEVEL AND EFFICIENCY IN IEC 62305-1[3]

Class of the protection level	Typical down-conductor distances (m
I	10
II	10
III	15
IV	20

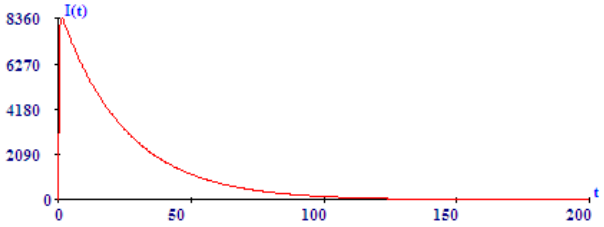

Fig. 3. Double exponential-type function of the lightning surge using FFTSES

and subsequent current pulse wave as one of the most widely used surge models for the lightning surge propagation in the transmission line and grounding system. The Heidler surge function value is described in Table 6. The field methods are mostly more accurate than circuit or substation approximation, but they take into account all electromagnetic phenomena. The calculation is carried out for conductive structures with single earth electrodes in the earth with 2000 Ω.m. The surge current distribution in the vertical and horizontal elements of the LPS is calculated during a lightning strike to the corner of the substation. In this study, the effectiveness of high current density that progresses the grounding realization is not taken into account that is a path adopted by many researchers [9-12]. In high lightning currents, the electric field at the ground electrodes may be larger than the electric force of the soil, resulting in collapse. This generally get better the grounding performance especially in lower resistivity soil. There is no unanimity on the simple formularization that takes into account the influence of this complex and patchy process as they are forced by the necessary underlying simplifications and proposition.

V. COMPUTATION RESULTS

The computation step is mostly based on the use of the well-known SES shield to design the substation according to the lightning specification, striking distance, and ground flash density. The probability for a stroke current smaller than 12.52 kA is 15.571%. Additionally, the likelihood that there will be one failure per year is 1 per 0.0033%. All substation characteristics, critical and intermediate values, are computed by the CDEGS software, as shown in Tables 7, 8 and Fig. 4. From the result of the risk assessment

using the CDEGS software, the collection area of direct strikes to the structure (58.5 x 36 m2) is 2.229 m and the overhead lines from direct strikes are 34.05 m. The CDEGS software firstly utilized the fast Fourier transform to draw the time domain lightning surge zone. The 110 kV substation need to perform to reform the faults and the past studies indicate the possibility of variable current depending on the grounding potential rise. In this study, we attempted to find reasonable solutions to solve the problems resulting from the chosen values of the soil resistivity and the quality of the conductors. All the resulted in this paper indicated positively solutions to help their implementation. By far, the maximum cost-effective control of the assessment of high-transmission lines under a lightning is the optimization of the shielding angle and the decrease of the grounding resistance. Furthermore, for the 110 kV substation, the standard was updated using the CDEGS software to improve the spacing rods.

TABLE 6. PARAMETERS FOR EQ. (6)

10/350 µs waveform	
I	200 kA
η	0.5
α	53798.93
B	499449.6
t	200 µs

.

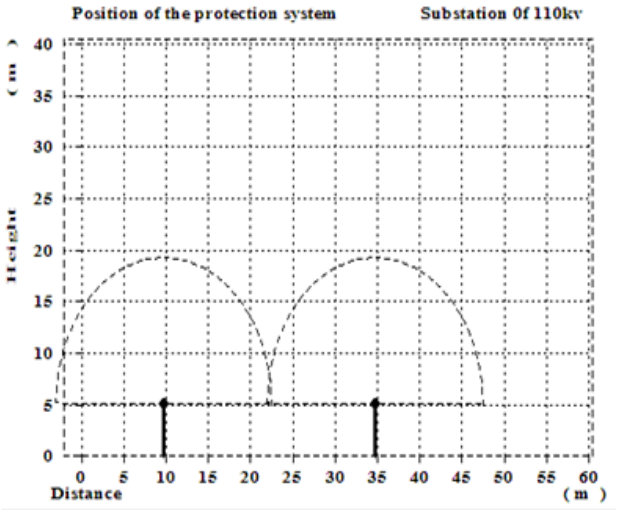

Fig.4. Risk assessment for lightning protection in the 110kV substation

TABLE 7. SUBSTATION CHARACTERISTICS USING THE SES SHIELD

Parameters	value
Voltage phase	110 kV
Basic impulse	1850 kV
Mid-span height	26 m
Outer diameter of the conductor	25.4 mm
Bundle spacing	0.460 m

TABLE 8. INTERMEDIATE AND CRITICAL VALUES USED IN THE SES-CDEGS SOFTWARE.

Parameters	value
Withstand insulator voltage VC	1850 kV
Equivalent bundle radius R0	0.204 m
Surge impedance Zw	499449.6 Ω
Critical current Ic	12.527 kA
Critical distance Sc	41.370 m
Height of the protection system Hg	58.5 m
Lightning surge per year	1 per -30594 y

Based on the results represented in this paper and according to all international standards for the protection of high- voltage substations, it was concluded that the effects of lightning can be reduced using LPSs. In addition, Fig. 5(b) shows the summary of the study in terms of the optimal representation of the calculation of top step and touch voltages in the protection of the human elements and equipment and all various types of 110 kV substations. This study indicates out that the process of the analysis and follow-up effects of lightning can be made with four levels of protection algorithms, but level 1 is preferred for the use as it is good for efficient treatment of the effects. Furthermore, in this paper, we explained the analysis by the CDEGS software that can process the problems and in turn should be implemented by subsidiary stations depending on LPS mechanism. According to the IEC standard of LPLs, the attachment between the substation top and the grounded structure takes place for lightning strikes at a critical distance from the structure. This distance is fixed as the radius of the level used in the rolling sphere model of locating lightning down conductors on the structures. The analysis was applied according to [8].

TABLE 9. FINAL RESULTS FOR THE SYSTEM USING THE CDEGS SOFTWARE

Status	Maximum value	Computed value	Grounding grid status
Potential rise	5000 V	498.3626 V	Acceptable
Touch voltage	1005.2 V	252.8969 V	Acceptable
Step voltage inside the grid	3553.1 V	10.4823 V	Acceptable
Step voltage outside the grid	3553.1 V	13.0001 V	Acceptable

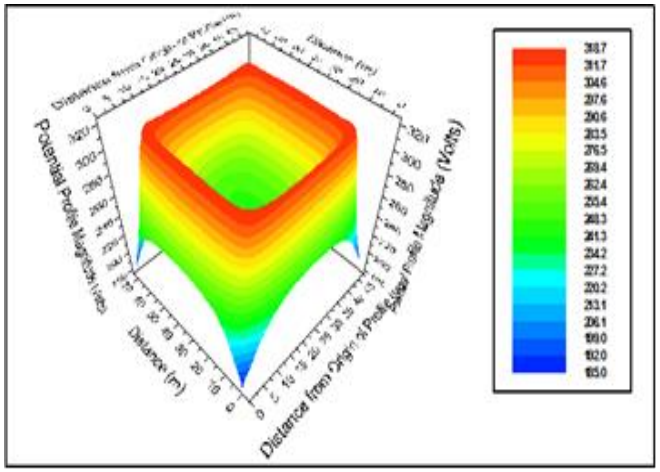

(a)

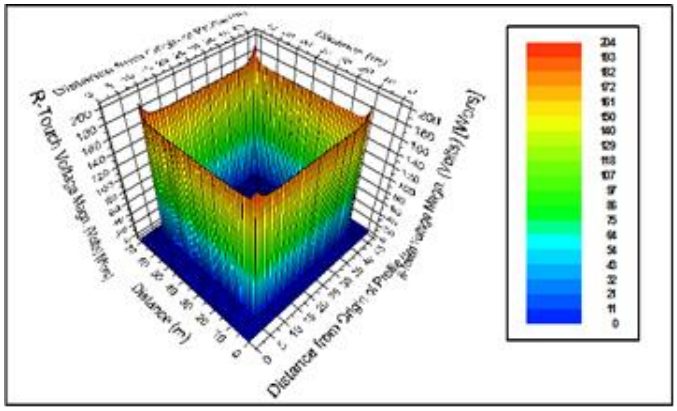

(b)

Fig.5. (a) 3D-system model of step voltage, (b) 3D-touch voltage for the 110 kV substation using the SES-CDEGS software.

VI. CONCLUSION

In this study, a new design for a 110 kV urban substation is proposed. According to the optimization process, the LPS is calculated to be placed in one corner of the substation. The stepwise procedure for designing the earth grid was presented. The design parameters were obtained from the risk assessment using the SES shield in the CDEGS Software. The results of this study show that the representation of the substation includes the calculation of all parameters things that lead to the occurrence of any risks, which considered correctly according to the international standards. The grounding grid was also computed against any hazards considered in this study. A substantial analysis whether an LPS should be applied is performed by the designer when a new substation is designed or an existing structure is updated. Lightning risk assessment is a tool that can be used to determine whether an LPS is required. Touch and step voltages were estimated and considering the human body presence on the soil surface. The results show that the approximate mode in this study is suitable for determining lightning-caused voltage peaks considering the horizontally stratified ground with acceptable accuracy.

REFERENCES

[1] J. He, X. Wang, Z. Yu, and R. Zeng, "Statistical analysis on lightning performance of transmission 284 lines in several regions of China," IEEE Transactions on Power Delivery, vol. 30, pp. 1543-1551, 2015.

[2] C.A. Christodoulou, L. Ekonomou, G.P. Fotis, V. Vita, and P.M. Kyrtsopoulos, "Computation of the injected energy to medium voltage surge arresters for the Hellenic distribution network", 9th WSEAS Int. Conf. on Power Systems (PS '09), Budapest, Hungary, pp. 142–145, 2009.

[3] Bojan Franc, Bozidar Filipovic, Viktor, "Lightning overvoltage performance of 110 kV air-insulated substation". Electric Power Systems Research, vol.138, pp. 78–84, 2016.

[4] Roy B. Carpenter, Jr, R. A. Auer, "Lightning and Surge Protection of Substations". IEEE Trans. On Industry Applications, Colorado 80303. PpB6-1, 1991.

[5] Roy B. Carpenter, Jr "Lightning Surge Characteristics on Inclined Incoming Line to Substation based on Reduced-scale Model Experiment". IEEE Trans. On Dielectrics and Electrical Insulation, pp739-744, June 2013.

[6] Leonid Grcev, "Modeling of Grounding Electrodes under Lightning Currents". IEEE Trans. on Electromagnetic Compatibility, pp559-569, August 2009.

[7] C. Ndungu, J. Nderu, L.Ngoo, P.Hinga, "Lightning Protection of Hv Substations at Coastal Region and Enhanced Earthing System- Case Study". IEEE African 2017 Proceedings, pp1319-1324, 2017.

[8] DES Oiseaux, Laval, and Quebec, "A simple substation grounding grid analysis". Safe Engineering Services & Technology Itd, pp.1-101, January, 2012.

[9] Giuseppe Parise, Luigi Martirano., Mario Lucheroni, "Level, Class, and Prospected Safety Performance of a Lightning Protection System for a Complex of Structures (LPCS)". IEEE Trans. On Industry Applications, pp2106-2110, 2010.

[10] NFPA-70-, MA USA "National Fire Protection Association", 2011.

[11] Krider, E. P, Noggle, R. C, Pifer, A. E, and Vance, D. L, "lightning direction-finding systems for forest fire detection". Bull. Am. Meteorol.Soc, pp. 980-986,1998.

[12] Chong Tong., Yuan Goa. Minguang Tong, Junping Luo., Lingyu Zhang, "Dynamic Lightning Protection of Smart Grid Transmission System". Proc. Int. Conf. on Lightning Protection (ICLP), Vienna, Austria, pp.1-10, 2012.

[13] DEHN, SÖHNE, "lightning Protection Guide". DEHN protects, 3rd updated Edition, pp.63, 2014.

[14] Giuseppe Parise., Luigi Martirano, "The Lightning Protection of a Complex of Structures (Lpcs)". IEEE Systems Technical Conference on Industrial and Commercial Power 2005. Italy, 2005, pp.99-105.

[15] BS EN/IEC 62305, "lightning protection standard". pp. 1-16, 2016.

[16] Vernon Cooray, "Lightning Protection". Electronic books. Institution of Engineering and Technology (IET Power and Energy Series 58), London, pp 330, 2010.

Proceedings of the Fourth International Conference on Communication and Electronics Systems (ICCES 2019)
IEEE Conference Record # 45898; IEEE Xplore ISBN: 978-1-7281-1261-9

Analysis of Single Phase Pulse Width Modulation (PWM) AC to AC Step-Up Converter Based on SC Structure

Priyanka Nehra
Department of Electrical Engineering
Rajasthan Technical University, Kota
Kota, INDIA
Priyankanehra769@gmail.com

Ashok Kumar Sharma
Department of Electrical Engineering
Rajasthan Technical University, Kota
Kota, INDIA
aksharma_eck@hotmail.com

***Abstract*— This article describes a new topology of single-phase pulse width modulation (PWM) AC to AC converter, the designed converter does not need to follow the duality of the input voltage for secure switching and requires one of two techniques which is a smooth switching or lossy RC snubber strategy. In this recommend work the usual phase support of PWM AC to AC converter is supplanted with the switching cell framing and coupled inductor hence, the Step-Up type pulse width modulation (PWM) AC to AC converter is formed. The simulation presented in the setting of MATLAB-2016 b.**

Keywords—AC-AC Converter, Boost inductor, Pulse width modulation (PWM), Switching cell (SC), Commutation problem.

I. INTRODUCTION

For AC-AC energy power conversion requiring varying output voltage and variable frequency, the most common configuration is the dc-linked voltage source inverter, like pulse width modulation (PWM) inverter. This approach shows a multiple mode of operation for single-phase grid converter (SPMC) topology [1]. New zero-voltage transition, energy factor, three phase ac-ac converter with high frequency single-phase connection in many applications where the voltage regulation is needed, it is used [2],[3],[4]. topology of a single-phase ac -ac converter capable of producing voltage output to buck or increasing topology design mode uses a minimum of two segment overlapping controlled switches in each input cycle. this topology is easy, low cost and minimum numbers of devices [5]-[6]. A dynamic voltage restorer (DVR) type technique is also used switching cell structure so DVR has no switching issue and therefore does not need to sense the input voltage duality [7]-[8]. In conventional approach commutation problems arise, damaging switching elements so eliminating these problems using switching cell structure and coupled inductor with boost inductor which increasing high efficiency and low cost [9]. In this paper, the solid AC-AC converters link with PWM of z phase connection is implemented without the issue of commutation. For practical applications and highly attractive by means of magnetic integration of the discrete coupled inductor with boost inductor in single phase ac converter [10]. Fig. (1) shows implementation of stage-legs this structure can produce a wide frequency range without taking into account the input frequency. Which proposes a single-phase ac-ac converter with a diode-clamped neutral point system [11]. Noise from EMI is one of the main problems during grid tied power converter construction [12]. In this topology, the number of switches is reduced to just four, resulting in reduced losses and higher efficiency compared to earlier topologies.

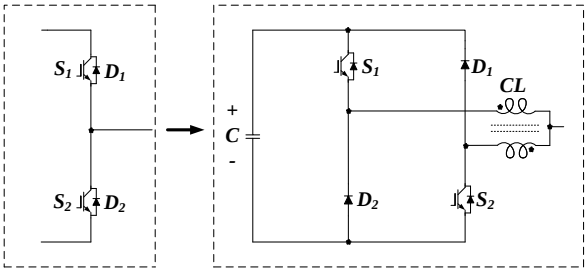

Fig. (1) implementation of stage legs

II. CONSTRUCTION OF DESIGNED CONVERTER

In this construction of proposed converter switching cells, a filtering inductor, two capacitors and load are employed. This Converter approach is introduced with two switching cells, P-type and N-type, having their intimations and demands in electronic circuits. Basic cell structure is introduced in this paper having a switching segment (IGBT) and a diode.

The P-type is a reflector circuit of N-type and vice-versa. The topology of Proposed PWM AC-AC converter has been depicted in Fig. 2. that mainly consists four bidirectional IGBT switches, Sw_1-Sw_4, and coupled inductor with boost inductor [13]. There are many problems arise in conventional approach so reduce all them using switching cell structure with boost inductor. The step-up type converter is displayed in Fig 1[14]. With this configuration, the proposed converter can bear both dead and overlap time without harming equipment for switching. This design can prevent the shoot through issue created problem such as door miss triggering signals. Thus, it is possible to design an externally secure and durable scheme. So, Fig.2. conventual shown as below-

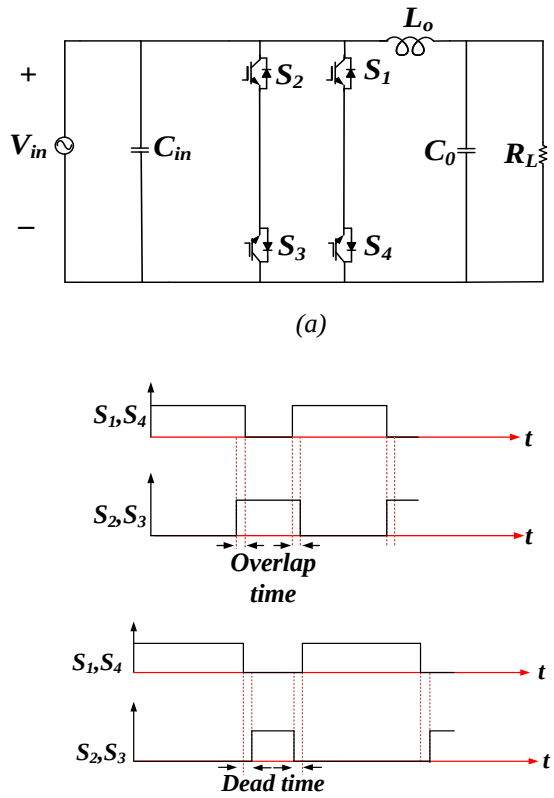

Fig.2. problems of switching in conventional ac-ac PWM converters.[15].

III. Performance Of The Proposed Converter

Fig.3 indicates the operation of proposed converter. In this figure current is flowing between the switching legs, boost inductor and the couple inductor. Only the positive half cycle of voltage input is considered Similarly, negative can be analyzing because the structure is symmetric between the upper side and lower side leg. The center recognized as ground potential between these legs and known as and inductor connection terminals is marked as 'A' and 'B'. Figure indicates the proposed converter's operational waveforms when D<0.5. Since there are four continuous modes for conduction and 3 level unipolar voltage for top and bottom leg depending on the duty cycle.

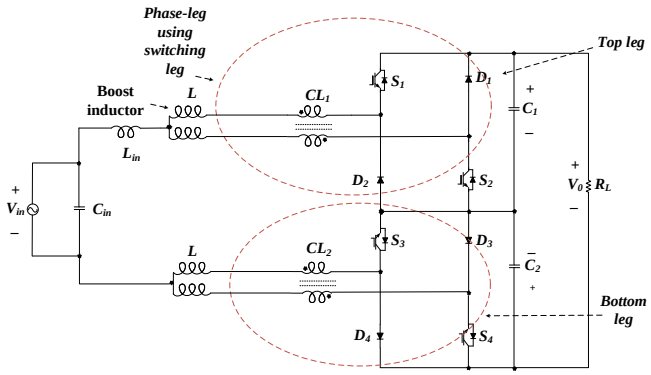

Fig.3.Proposed Step-Up converter with SC, coupled inductor and boost inductor

In the document, it is presumed that the two binding inductors are identical with each other and it is presumed that the coupling coefficient is near to infinity. then fig.4 shows modes operation boost ac-ac converter and modes are following as:

1. Mode A

The switches S_1, S_4 are all switched on in this operating mode and the diodes D_1, D_4 are all switched off. The input inductor which is a coupled inductor is denoted as L_{in} that stores the energy of the input and L_s is the self-inductance and voltage are as follows:

$$v_A = \frac{v_{C_1}}{2} \quad ; \quad v_B = \frac{v_{C_2}}{2} \tag{1}$$

$$v_{AB} = v_A - v_B = \left(\frac{vC_1}{2} - \frac{vC_2}{2}\right) = \frac{v_o}{2} \tag{2}$$

$$vL_{in} = v_{in} - v_{AB} = v_{in} - \frac{v_o}{2} \tag{3}$$

$$\frac{di_{L_{in}}}{dt} = \frac{vL_{in}}{L_{in}} = \frac{v_{in} - {}^{v_o}/_2}{L_{in}} \tag{4}$$

$$\frac{di_{cm1}}{dt} = \frac{vc_1}{4L_s} \tag{5}$$

$$\frac{di_{cm_2}}{dt} = \frac{v_{C_2}}{4Ls} \tag{6}$$

2. Mode B

The switches *S*2 and *S*3 turn OFF in this mode of operation while *S*1 and *S*4 remain ON. The diodes *D*1 and *D*4 turn ON cause of freewheeling action and *D*2 and *D*3 remain OFF. The energy stored in the L_{in} is transmitted through S_4, D_1 to the output. The relationships between current and voltage are as follows:

$$v_A = v_{C_1}, v_B = v_{C_2} \tag{7}$$

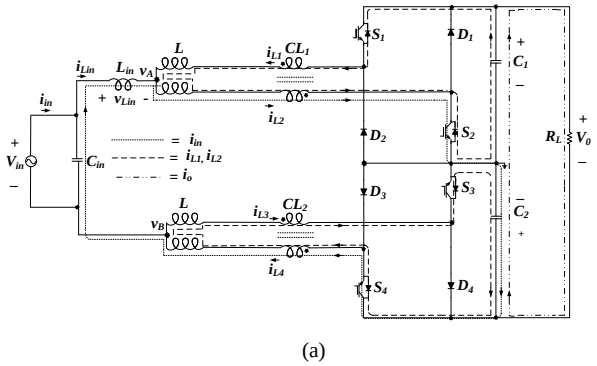

(a)

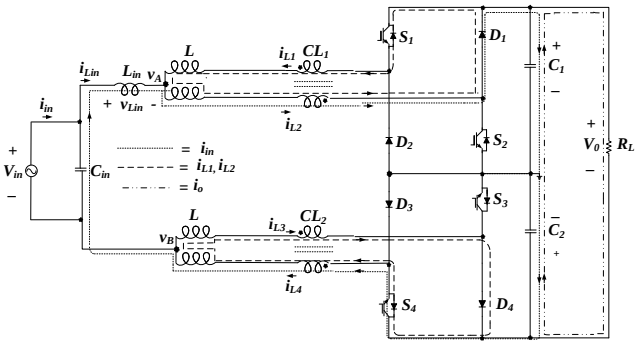

(b)

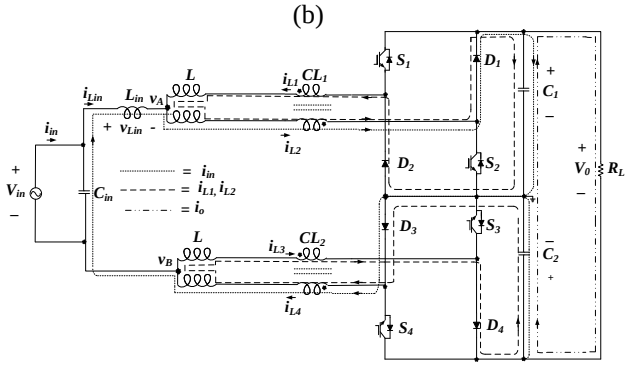

(c)

Fig.4 proposed converter's operating modes when (D<0.5). 1. Mode A *(0 ~ DTs)* 2. Mode B *(DTs ~ 0.5Ts)* 3. Mode C *(0.5Ts ~ (0.5 + D) Ts)* 4. Mode D *((0.5 + D) Ts ~ Ts)*

$$v_{AB} = v_A - v_B = v_{C_1} - v_{C_2} = v_0 \quad (8)$$

$$v_{L_{in}} = v_{in} - v_{AB} = v_{in} - v_0 \quad (9)$$

$$\frac{di_{L_{in}}}{dt} = \frac{v_{L_{in}}}{L_{in}} = \frac{v_{in} - v_0}{L_{in}} \quad (10)$$

$$\frac{di_{cm_1}}{dt} = \frac{di_{cm_2}}{dt} = 0. \quad (11)$$

Voltage across capacitor C1 is denoted by Vc1 as similar C2 capacitor is shown by Vc2.

3. Mode C

Mode 1 is repeated in this mode again, but all are switched off with a differencethat switches S1 to S4 and D1 to D4 are all s witched ON. Input power is again stored in L_{in}.

$$\frac{di_{cm_1}}{dt} = -\frac{v_{C_1}}{4L_S} \quad (12)$$

$$\frac{di_{cm_2}}{dt} = -\frac{v_{C_2}}{4L_S} \quad (13)$$

4. Mode D

The difference in this mode is that V_A and V_B will be z ero instead of V_{C1} and V_{C2} during periods B and D.Equation 14 shows the voltage gain of proposed step-up converter with boost inductor.

$$\frac{v_0}{v_{in}} = \frac{1}{1 - D} \quad (14)$$

Fig.5 shows the Step-Up ac-ac converter main operational waveforms when D (Duty ratio) value is less than 0.5

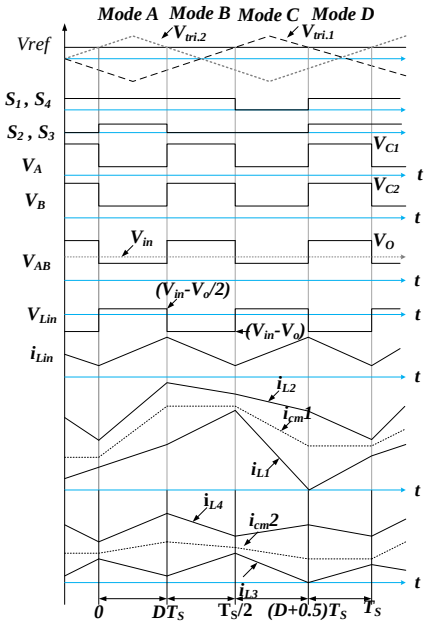

Fig.5. Single -phase PWM boost AC-AC converter key operational waveforms

IV. Simulation Of The Proposed Boost Converter Based On Switching Cell Structure

The simulation model by MATLAB 2016b of the single-phase PWM (pulse width modulation) proposed Step-Up converter is shown below in Fig.6. based on switching cell structure, coupled inductor with boost inductor. Parameters are input voltage (v_{in}=110v_{rms}) and capacitor (C_{in},C_1,C_2=2.2μf) and switching frequency (f=50 kHz) as follow:

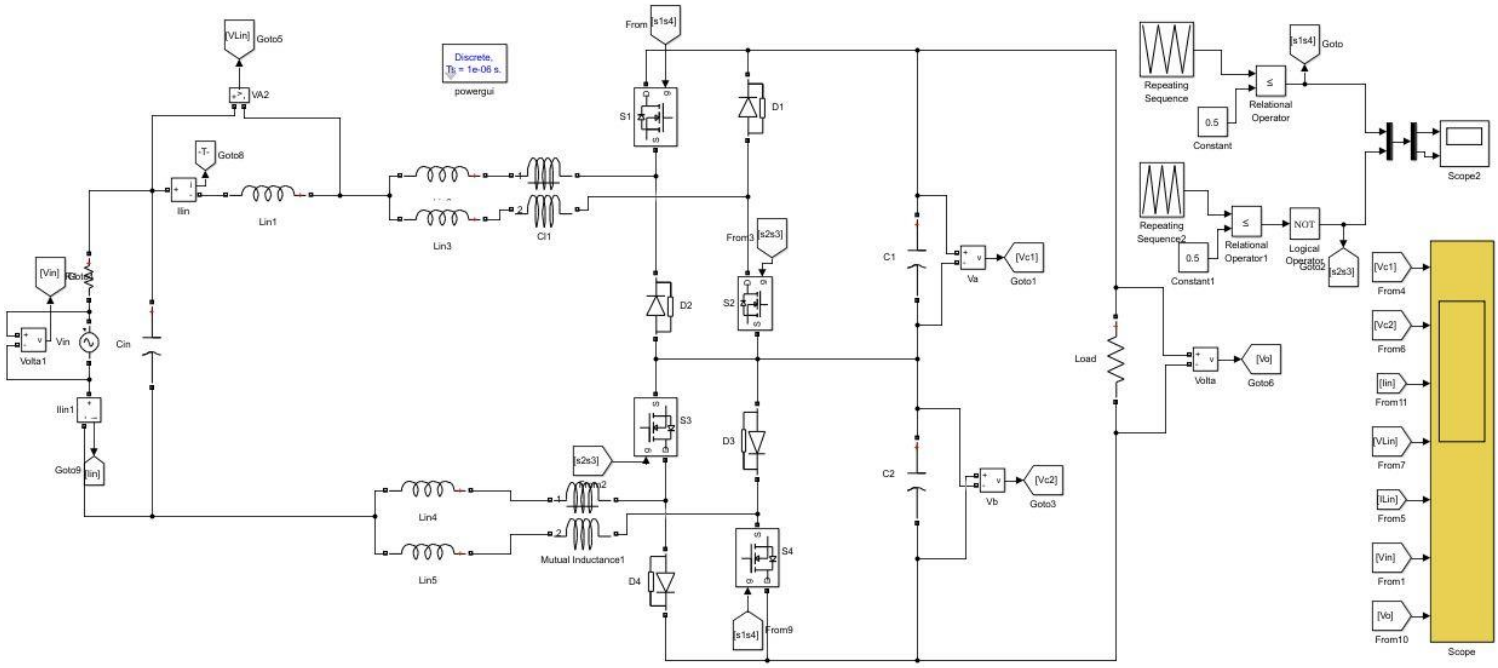

Fig.6.Matlab Simulation Model of Proposed Boost Converter based on switching cell structure

V. SIMULATION RESULTS

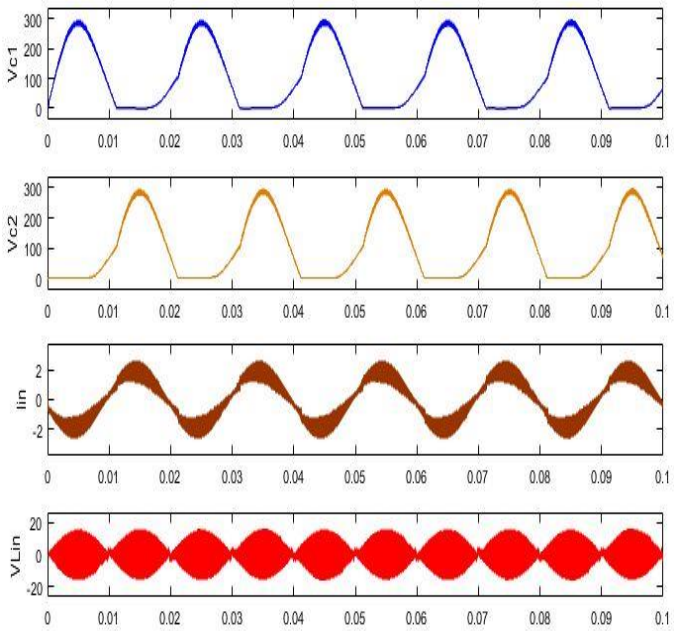

(a)

Fig.(a) shows voltage waveform of C1, C2,. Input inductor voltage and input current also.

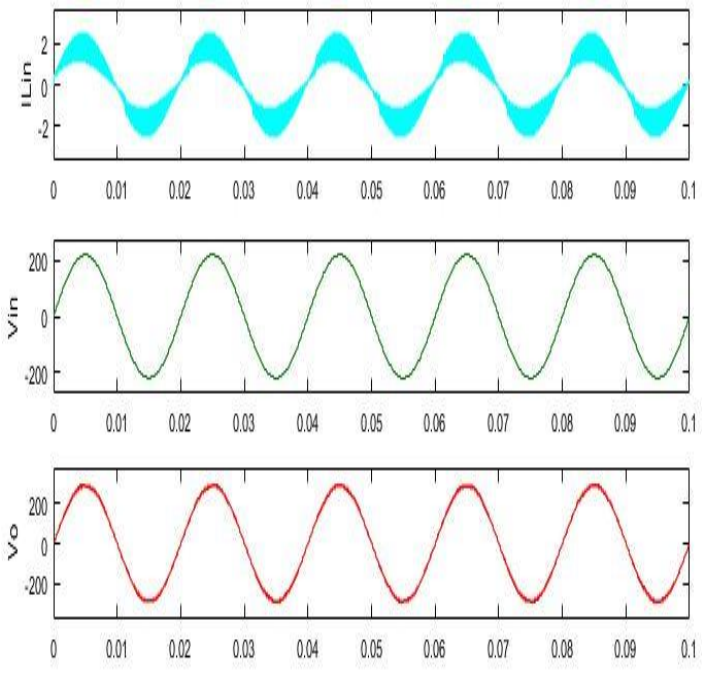

(b)

Fig.(b) shows input inductor current, input voltage, output voltage

Fig.7. MATLAB simulation result

Fig.7 represents the simulation of the proposed converter. According to the parameter design simulation parameters are selected input voltage (v_{in}=110 v_{rms}), output voltage (v_o=220v_{rms}), output power (p_o=200 w) and D =0.4.

The ac to ac converter step-up operation is obtained from the MATLAB setting. Fig.8. indicates the 50 Hz variable output frequency output voltage and % THD (Total harmonic distortion).

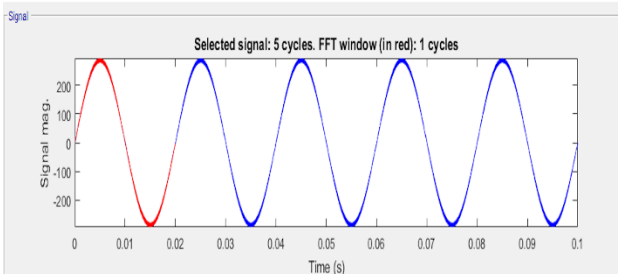

(a)

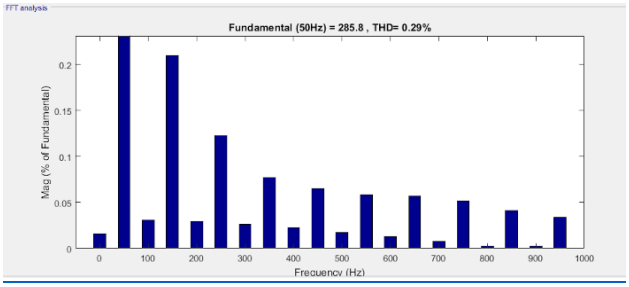

(b)

fig.8. shows (a)output voltage and its (b) THD (total harmonic distortion)

VI. Conclusion

In this paper, step-up ac to ac converter has been created for single-phase pulse width modulation (PWM), which detects the switching issue in a single-phase direct PWM ac-ac converter without detecting the duality of input voltage. This step-up ac-ac converter uses the basic structure of the SC and the coupled inductor to allow it to be opened and shortened without damaging the switching devices. It is possible to replace IGBT with MOSFET for the primary power device for better outcomes. The suggested converters are used in industrial applications and also can be implemented for future research work. With the use of coupled inductor and switching cell higher efficiency can be achieved.

References

[1] S. B. Mohite and P. K. Gujarathi, “A design and implementation of a novel multimode single phase matrix converter,” *SPEEDAM 2010 - Int. Symp. Power Electron. Electr. Drives, Autom. Motion*, pp. 1227–1230, 2010.

[2] T. H. Abdelhamid and A. Sabzali, “Factor Corrected,” pp. 1–6, 2006.

[3] N. A. Ahmed, M. Miyatake, H. W. Lee, and M. Nakaoka, “A novel circuit topology of three-phase direct AC-AC PWM voltage regulator,” *Conf. Rec. - IAS Annu. Meet. (IEEE Ind. Appl. Soc.*, vol. 4, no. c, pp. 2076–2081, 2006.

[4] M. Jiag, “A Novel High Input Power Factor Single-Stage,” pp. 1–5, 2006.

[5] S. Kitcharoenwat, M. Konghirun, and A. Sangswang, “A novel single phase AC-AC converter with power factor control,” *Trans. Electr. Eng. Electron. Commun.*, vol. 11, no. 1, pp. 17–23, 2013.

[6] S. H. Hosseini, J. Nabati, and A. Mirlou, “Generalized single phase Z-source matrix converter,” *2011 IEEE Electr. Power Energy Conf. EPEC 2011*, pp. 404–408, 2011.

[7] H. F. Ahmed, H. Cha, and A. A. Khan, “Design of dynamic voltage restorer for voltage sag and swell compensation using high-frequency-isolated direct AC-AC converter without commutation problem,” *2015 17th Eur. Conf. Power Electron. Appl. EPE-ECCE Eur. 2015*, 2015.

[8] S. Kim, H. G. Kim, and H. Cha, “Dynamic voltage restorer using PWM AC-AC Converter with switching cell structure,” *9th Int. Conf. Power Electron. - ECCE Asia "Green World with Power Electron. ICPE 2015-ECCE Asia*, pp. 946–951, 2015.

[9] B. T. Deshmukh, “a Novel Single Phase Multimode Matrix,” no. Ictes, pp. 196–199, 2007.

[10] A. A. Khan, H. Cha, and H. G. Kim, “Magnetic integration of discrete-coupled inductors in single-phase direct PWM AC-AC converters,” *IEEE Trans. Power Electron.*, vol. 31, no. 3, pp. 2129–2138, 2016.

[11] B. R. Lin, Y. C. Lee, and D. J. Chen, “Implementation of a single-phase AC/AC converter with neutral-point-clamped scheme,” *Proc. IEEE Int. Conf. Ind. Technol.*, vol. 2, pp. 780–785, 2002.

[12] M. H. Hedayati and V. John, “Filter Configuration and PWM Method for Single-Phase Inverters with Reduced Conducted EMI Noise,” *IEEE Trans. Ind. Appl.*, vol. 51, no. 4, pp. 3236–3243, 2015

[13] A. A. Khan, H. Shin, H. Cha, and H. G. Kim, “Novel three-phase PWM AC-AC converters solving commutation problem,” *2014 Int. Power Electron. Conf. IPEC-Hiroshima - ECCE Asia 2014*, pp. 110–116, 2014.

[14] S. Kim, H. G. Kim, and H. Cha, “A novel single-phase cascaded multilevel AC-AC converter without commutation problem,” *2014 IEEE Energy Convers. Congr. Expo. ECCE 2014*, pp. 556–562, 2014.

[15] H. H. Shin, H. Cha, H. G. Kim, and D. W. Yoo, “Novel single-phase PWM AC-AC converters solving commutation problem using switching cell structure and coupled inductor,” *IEEE Trans. Power Electron.*, vol. 30, no. 4, pp. 2137–2147, 2015.

[16] M. Jiang, Y. Chien, B. Shih, and T. Liu, “Converter,” pp. 13391343, 2014.

Proceedings of the Fourth International Conference on Communication and Electronics Systems (ICCES 2019)
IEEE Conference Record # 45898; IEEE Xplore ISBN: 978-1-7281-1261-9

Deep learning based Customized Model for Features Extraction

[1]Akshya Reghunath, [2]Shalini Vanaja Nair, [1]Jalpa Shah
[1]Dept. of Electronics and Communication Engineering, Amrita School of Engineering, Bengaluru, Amrita Vishwa Vidyapeetham, India
[2]Ennoventure Inc, Washington DC, USA

***Abstract*—In the last few years, deep learning is one of the powerful technique, used for image recognition. Among the various kinds of deep neural networks, Convolutional Neural Network (CNN) nowadays has been widely used for the purpose of image recognition. In this work, we present the customized model developed for feature extraction of medical packages. Now a days, it is difficult to distinguish an original medicine from counterfeit. The proposed model based on CNN can be useful in identifying the original medicine which forms the first step in the process to identify counterfeits. The medicine images are used as dataset for feature extraction and image classification. Medicine package shape, edges and colour are used for feature extraction of customized model. Classification is done to distinguish medicines which is of same colour and differs in their name, printed text, barcode and the company logo. One of the popular pre-trained CNN architecture model VGG-19 is used for comparing the results of developed customized model. Customized model consists of only five layers convolution layer, maxpooling layer, dropout layer, flatten layer and dense layer. In comparison to pre-trained VGG-19 model customized model reduces number of layers from 19 to 5. Number of layers are reduced to 5 because increasing the number of layers were not showing much improvement in the testing results for given dataset. Training accuracy of 93.17% , validation accuracy of 88.68% and testing accuracy of 76.67% is obtained for the customized model. The results can be made more precise and accurate by optimizing the number of layers in the model. In the proposed model we have used 5 layers. The optimization of number of layers is done based on the prediction accuracy. The accuracy of less than 50% was achieved using 3 layers and it is increased up to 76% with 5 layers. No further improvement in the prediction accuracy was observed by increasing number of layers to 6 or 7, so for the proposed model 5 layers are selected.**

***Index Terms*—Convolutional Neural Network; Deep learning; VGG-19; Medicine Package; Identification; Feature Extraction**

I. Introduction

Nowadays, deep learning has become one of the most popular technique which has now found its adoption in various fields [1]. After a great development deep learning became a growing area especially in the region of Artificial Intelligence (AI) and Machine Learning (ML). Various frameworks and libraries [2, 4] which are existing for research and development in deep learning such as Tensorflow, Theano, Caffe and Keras. Out of the many deep learning architecture techniques few of them are Convolutional Neural Network (CNN), Recurrent Neural Network (RNN), Long Short-Term Memory (LSTM), Deep Belief Networks (DBNs), Deep Stacking Networks (DSNs) and Generative Adversarial Networks (GANs). Since, object Recognition has become a critical area of research in the field of Machine Learning as it forms a crucial part of the intelligence system related to Computer Vision, Robotics and Autonomous Vehicles. Extracting the variant features found in the input images is always the most challenging area in object recognition. Convolutional object recognition uses neural networks to predict decisions about the object recognition based on features which is being extracted from the images. The best known deep learning architecture is CNN [4]-[5] for the purpose of image and object recognition. CNN includes a service of layers which includes convolutional layers, pooling layers, the rectified linear unit layers, softmax layers and fully connected layers. CNN is defined as a category of deep neural networks widely used for analyzing visual imagery. CNN have been inspired from the biological processes in which the connectivity pattern between the neuron looks like the organization of animal visual cortex. Each cortical neuron stimulates only in a predefined region of the visual field. This field is known as the receptive field. The receptive field consists of various neurons that are not fully overlapped. CNNs use less pre-processing technique compared to any other image classification algorithms. The learning of CNN from the given features without human intervention, considered as one of the advantage.

The basic architecture of CNN has been shown in Fig. 1. The CNN consists of input layers, output layers and hidden layers. The hidden layers comprises of convolutional layer, pooling layer and fully connected layer. Convolutional layer will apply a convolution technique to the inputs. The CNN may consists of global or local pooling layers, that joins the outputs of each neuron clusters into a single neuron at the next layer. There are two types of pooling layers: one is maxpooling layer which uses the maximum value from every cluster of neurons from the previous layer and second is average pooling layer which uses average value from each of cluster of neurons obtained from previous layer. The output of pooling layer act as a input for fully connected layers. The classification of inputs is done by fully connected layers. Each of neuron in CNN has activation function which process the input and provides appropriate output. The activation function consists of vector of weights and a biases. Improvement in the learning of a neural network depends on incremental adjustments to the biases and weights. The combination of weights and bias is known as filter. The important fact of CNN is that many of

the neurons share the same kind of filter.

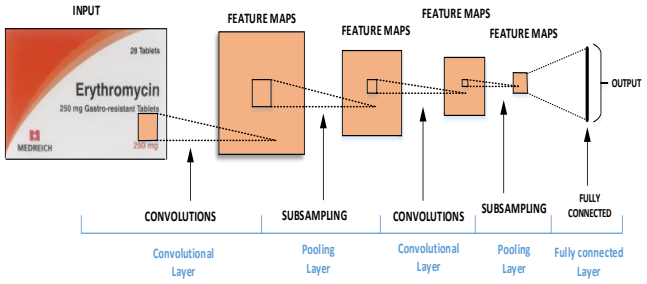

Fig. 1. Basic CNN Architecture

The main objective behind training the CNN is to identify the correct weights with the help of multiple iterations. When CNN is trained using dataset, the network obtains knowledge from this dataset refereed as weights of the network. Thus the weights obtained can be given to any other CNN, rather than training it from the beginning. The pre-trained model can be used for the same purpose after training through large dataset. The pre-trained model may not be able to give 100% accuracy, but it helps to save huge efforts required for training from scratch. We can transfer the weights of pre-trained model for any untrained CNN model, which is known as transfer learning. By doing this we are actually transferring the learning part of the pre-trained model to another model.

In the proposed work, the dataset is created by capturing front and sideview images of various medical packages which contains the information about the features. Cropped images of around 688 medical packages are used. With the help of image augmentation, horizontal, vertical flips and rotation are also used in the dataset. We have used pre-trained CNN model VGG-19, which is found most appropriate to extract features from our dataset. With the help of the pre-trained CNN model for feature extraction, we are exploiting the learning capabilities of the pre-trained model acquired through lengthy training time on very huge datasets.

This paper is organized as follows. Section II presents the review related to features extraction and image classification. Our proposed model is discussed in Section III. Comparison results related to pre-trained model and proposed model are presented in Section IV. Section V concludes this paper and provides some prospective on possible future work.

II. Literature Survey

Image recognition technique is the ability of the software to identify objects and places in images. Human brains can recognize objects without any difficulty and can easily classify them but for a software to recognize, deep machine learning is a necessity. This feature of image recognition for a software was found best with CNN. Image recognition algorithms works by the use of comparative 3D models. The following are the networks which are the most popular ones.

A. AlexNet

AlexNet was the first deep neural network to provide a better accuracy for ImageNet classification with a significant improvement compared to any traditional network. It consists of a total of 5 convolutional layers which is being further followed by 3 fully connected layers. This network uses ReLU activation function which helps in faster training [9]. The ReLU actiation function is placed after after each and every convolutional and fully connected layers. Convolution layer is built using kernel filters. AlexNet also overcomes the problem of overfitting with the use of dropout function.

B. VGG-16

The VGG-16 network uses more smaller sized kernel filters compared to AlexNet. Multiple smaller stacked filters are better than the one with the larger size because it helps in learning more complex features. In the VGG-16 architecture concept of blocks is introduced, where blocks with same filter size applied multiple times in every layer and helps in extracting more complex features.

C. VGG-19

VGG-19 architecture is different from VGG-16 only in depth of layers. The VGG-19 contains three layers more compared to VGG-16. These layers understand detailed patterns of images for effective training. In earlier research work it has been found that by using multi-scale testing VGG-16 reduced the error rate from 8.8% to 8.7% similarly VGG-19 reduced the error rate from 8.7% to 8.6%.

D. GoogleNet/Inception

By comparing VGG network with GoogleNet it has been found that GoogleNet using 7-nets has an error rate of 6.7%, while VGGNet using 2-nets has an error rate of 6.8% which is really competitive. GoogleNet has developed a inception module which approximates CNN with a normal dense construction so that only few members of neurons are used and the width or the number of convolutional filters are always kept small. It has bottleneck layer which helps in reducing the computation requirement.

In the earlier research work [7]-[8] performance of two classifiers methods is evaluated. The two classifiers Linear SVM and Quadratic SVM were used. Results shows pre-trained model AlexNet provides better accuracy on both the classifiers compared to traditional method of features extraction. According to the result it has been found that the pre trained model AlexNet had better accuracy on both the classifiers. Even though both the classifiers have performed similarly but Quadratic SVM gave better results than linear SVM [9]. In [10] to check the quality of leather material using leather images AlexNet CNN model is used. Tanning leathers are having different textures in the same category which is caused due to process of tanning or the skin were being taken from various part of the animal body. Better results are obtained using pre-trained CNN model compared to hand crafted features extraction method. Machine learning

is also used to classify the food categories [11]. Classification was done using Linear SVM and AlexNet. In [12] for original fingerprint identification VGG-19 and AlexNet is used. comparison results show VGG-19 has better accuracy than AlexNet. As VGG-19 produce better accuracy results compared to other networks, in the proposed work we have used VGG-19 for comparison [12].

III. Proposed Model

From the earlier research work it was found that VGG-19 is one of best pre-trained model for object recognition. So, before developing customized model, pre study on our medicine related database is performed using VGG-19. Fig. 2 describes the standard steps followed during training and validation of VGG-19 for features extraction. The dataset is created using front and sideview images of various 688 medical packages which contains the information about the features. Using image augmentation, horizontal, vertical flips and rotation of images are also used. The data set is divided into two parts in which 80% of data set is used as training dataset and 20% of dataset is used as validation dataset. The training and validation of the model is executed for 30 epochs. Each epoch allows one pass through the dataset, within each epoch the corresponding features and labels are extracted. Using extracted features model makes prediction about medical package. The same process repeats for every epoch. Similar process will be repeated in validation using validation dataset. After validation process, cross-entropy loss is calculated to in terms of percentage to determine how accurately the prediction of the medical packages is done. The input images are resized so that it can fit into CNN input layer. Features are extracted after the training and validation of VGG-19. At the end of training and validation different classes of images will be predicted. We have used VGG-19 of 3×3 convolutional layers to classify images into 32 objects. The size of output images from convolution layer are resized with the help of max-pooling layer. There are two fully connected layers having 4096 nodes each are followed with a softmax classifier that helps in the extraction of various features which are being used for classifying the products. The accuracy of classification can be improved by increasing the depth of VGG-19. As an input dataset, medicine package images are used of the size 224×224. The input dataset of 688 different medicine images is used out of which 510 images have been used as the training dataset and 178 images have been used for the purpose of validation dataset. The testing is performed using unseen dataset of 150 different medicine images.

To train the model, we have used an open source software library called Keras-Tensorflow, developed for faster experimentation of CNNs and recurrent networks. We have included few predefined packages such as numpy, pandas, keras etc. Then loading of VGG-19 is done. The last layer of VGG-19 is replaced with 32 classes of our dataset. For learning of complex functions present in the images, ReLu activation function is added to the dense layers and the softmax function is added to the last layer. Next step is loading the ImageGenerator which is inbuilt in keras to train our model.

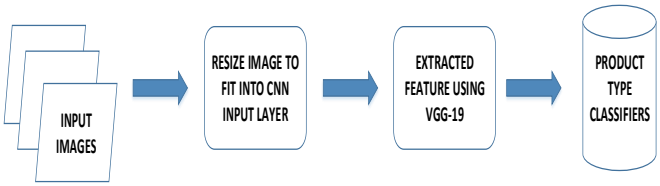

Fig. 2. Training and Validation steps for features extraction

During the training, validation and testing, the performance of the pre-trained VGG-19 model is evaluated based on accuracy. Accuracy is defined as from the given dataset of images how many images are classified correctly by model. Accuracy is represented in terms of percentage. The training accuracy gives an idea about what percentage of images in the current training dataset are correctly classified. Similarly the testing accuracy provides us the percentage of how well model is able to classify new images that does not belong in training dataset. The validation accuracy is used to understand whether the model is under-fitting or over-fitting. The results showed an accuracy of 98% during testing with epochs of 30.

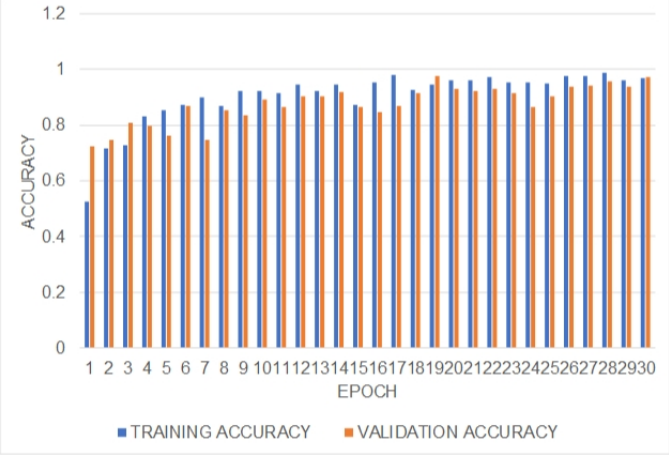

Fig. 3. Training accuracy vs Validation accuracy

TABLE I
Performance Results of VGG-19

	Number of Images	Accuracy
Training	510	97.08%
Validation	178	97.42%
Testing	150	93.33%

The Fig. 3 shows the comparison between the training and the validation accuracy. It has been plotted for 30 epochs. At the beginning huge difference in the values of training accuracy (52.5%) and the validation accuracy (72.5%) is observed. But at the end of 30 epochs training accuracy and validation accuracy are close to each other. The training

accuracy of 97.08% ,validation accuracy of 97.42% and testing accuracy of 93.33% is obtained as shown in Table I.

A. Custom Model

In the VGG-19 number of layers used are 19 which are reduced to 5 in the customized model which helps in reducing computational time and complexity. The custom model is created without the use of any pre-trained network weights. Fig. 4 represents the layers of the customised model. In each convolutional layer, a filter of size 5×5 has been taken and then the filter is being moved across the image to perform convolutional operations. Convolution operations are nothing but summation of element-wise matrix multiplication of the filter values and the pixels in the image. The output of the convlutional layers is given to the pooling layers. Pooling layers are used to downsample the images. The image would contain a lot of pixel values and it is easy for the network to learn the features if the image size is progressively reduced. Pooling layers helps to reduce the number of parameters required and hence, this reduces the computation required. For the proposed model max-pooling layers are used. The output obtained from the pooling layers is then sent to the dropout layer which uses a regularization technique to prevent overfitting. Thus the result obtained after dropout layer will be pooled feature maps which will be converted in to a long vector of data with the help of flatten layer. Next is the dense layer which is the fully connected layer whose function is to classify input images based on features extracted from the convolution and pooling layers. is The custom model analytics are shown in Table II.

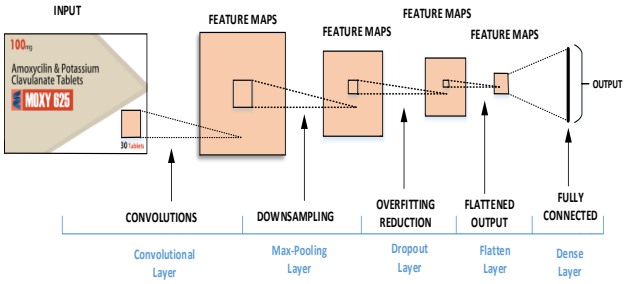

Fig. 4. Layers of custom model

.

The input dataset consists of medical package images as shown in Fig. 5. These input dataset images are resized into size of 116×116. The input dataset contains 1644 medicine package images from which 1304 are used for the purpose of training dataset and 340 images are used for the purpose of validation dataset. The training and validation dataset consists of augmented images of various medicine packages. Augmentation includes rescaling, horizontal flip, width shift range, height shift range and zoom range. In the proposed work categorical cross-entropy loss function and adam optimizer is used. The training is done for 30 epochs. The unseen

TABLE II
CUSTOM MODEL ANALYTICS

Layer	Output Shape Size	Param#
conv2d_3(Conv2D)	116 × 116	2280
max_pooling2d_3(MaxPooling2)	58× 58	0
conv2d_4(Conv2D)	56× 56	4065
max_pooling2d_4(MaxPooling)	28× 28	0
dropout_2(Dropout)	28× 28	0
flatten_2(Flatten)	11760	0
dense_4(Dense)	128	1505408
dense_5(Dense)	50	6450
dense_6(Dense)	17	867
	Total params:	1,519,070
	Trainable params:	1,519,070
	Non-Trainable params:	0

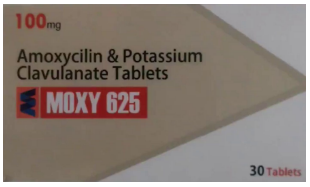

(a) Amoxy front

(b) Amoxy shortside

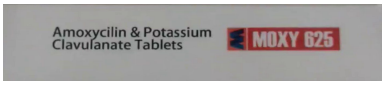

(c) Amoxy longside

Fig. 5. Example of Input Dataset

dataset of size 150 is used for testing the performance of the customized model. The Fig. 6 shows the comparison between the training and the validation accuracy. At the end of 30 epochs training accuracy and validation accuracy are close to each other. The training accuracy of 93.17% ,validation accuracy of 88.68% and testing accuracy of 76.67% is obtained as shown in Table III. Further training with epochs of 40 shows training, validation and testing accuracy 96.28%, 91.13% and 79.19% respectively, which is approximately 3% more than epochs of 30. With 50 epochs the results further improved to 97.12%, 92.23% and 81.2% respectively which is 4% more than the epochs of 30. On further increase in epochs to lead to degradation of the accuracies.

TABLE III
PERFORMANCE RESULTS OF CUSTOMIZED MODEL

	Number of Images	Accuracy
Training	1304	93.17%
Validation	340	88.68%
Testing	150	76.67%

IV. Results

Results of the Custom Model

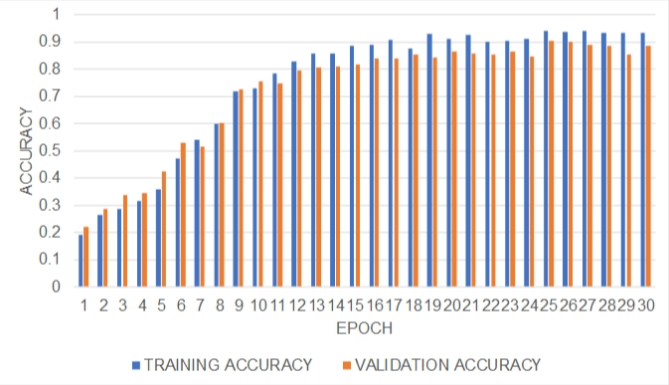

Fig. 6. Training Accuracy vs Validation Accuracy

The comparison results of VGG-19 and Custom Model are presented in Table IV. In the VGG-19 138 Million parameters are used for training the model and 150,000 parameters are used for training the customized model. The training and validation accuracy of both the models are comparable. The difference in testing accuracy of both the models can be minimized further by increasing number of layers, parameters of the customized model.

TABLE IV
Convolutional Neural Network Architecture

Architecture	Parameters	Training Accuracy	Validation Accuracy	Testing Accuracy
VGG-19	138 Million	97.08%	97.42%	93.33%
Customized CNN	150000	93.17%	88.68%	76.67%

V. Conclusion and Future Work

Identification of original medicine packages is difficult through human eye as it looks very similar in view. The proposed work presents customized CNN model which can be used to classify medical packages that looks very similar. The pre-trained model VGG-19 is used for comparing the results of customized model. The number of parameters and layers are reduced in customized model in compression to VGG-19. Customized model results show training accuracy of 93.17% ,validation accuracy of 88.68% and testing accuracy of 76.67%. The model was also tried by adding two more layers to the original layers of Custom Model, still same accuracy result was achieved, but the accuracy can be improved if more number of layers are added, and by changing the value in parameters and it has been left as a future work. The proposed customized model can be used for identifying the original medicine packages.

References

[1] Khan Hamayun A., "DM-L Based Feature Extraction and Classifier Ensemble for Object Recognition", *Journal of Signal and Information Processing*, vol 9, pp. 92-110 2018
[2] Buduma Nikhil, "Fundamentals of deep learning", *O'Reilly Media, Inc., 1005 Gravenstein Highway North, Sebastopol, CA 95472.*, vol 521, pp. 85-109 2017
[3] Goodfellow Ian, Bengio Yoshua, Courville Aaron, "Deep Learning", *MIT Press, Cambridge*, vol 13, pp. 326-365 2016
[4] Nielsen, Michael A., "Neural Networks and Deep Learning", *www.cs.wisc.edu/ dpage/cs760/*, vol 3, pp. 875-936 2015
[5] Lecun, Yann and Bottou, Leon and Bengio, Yoshua and Ha, Patrick, "Gradient-Based Learning Applied to Document Recognition", *Proceedings of the IEEE*, vol 5, pp. 2278-2324 1998
[6] Gu, J., Wang, Z., Kuen, J., Ma, L., Shahroudy, A., Shuai, B. and Wang, G., "Recent Advances in Convolutional Neural Networks", *Neurocomputing*, vol 323, pp. 37-51, 2017
[7] Chung, Clement and Patel, Shital and Lee, Rosetta and Fu, Lily and Reilly, Sean and Ho, Tuyet and Lionetti, Jason and George, Michael D. and Taylor, Pam, "Implementation of an integrated computerized prescriber order-entry system for chemotherapy in a multisite safety-net health system", *American Journal of Health-System Pharmacy*, vol 75, pp. 398-406 2018
[8] Suah, Faiz Bukhari Mohd, "Preparation and characterization of a novel Co(II) optode based on polymer inclusion membrane", *Analytical Chemistry Research*, vol 12, pp. 40-46 2017
[9] Abdullah and Hasan, Mohammad S., "An application of pre-trained CNN for image classification", *20th International Conference of Computer and Information Technology, ICCIT 2017*, vol 2018-jan, pp. 1-6 2018
[10] Winiarti, Sri and Prahara, Adhi and Ismi, Dewi Pramud, "Pre-Trained Convolutional Neural Network for Classification of Tanning Leather Image", vol 9, pp. 212-217 2018
[11] Farooq, Muhammad and Sazonov, Edward, "Feature Extraction Using Deep Learning for Food Type Recognition", vol 10813, 2018
[12] Rodrigo Frassetto Nogueira, Roberto de Alencar Lotufo, and Rubens Campos Machado,"Fingerprint Liveness Detection Using Convolutional Neural Networks" vol 11, pp 1206-1214, 2016
[13] Lu L., Shin H., Roth H. R., Gao M., Lu L., Member S., Xu Z.,Nogues I., Yao J., Mollura D., and Summers R. M., "Deep Convolutional Neural Networks for Computer-Aided Detection : CNN Architectures , Dataset Characteristics and Transfer Learning Deep Convolutional NeuralNetworks for Computer-Aided Detection : CNN Architectures , Dataset Characteristics and Transfer," IEEE Trans. Med. Imaging, vol. 35, no. 5, pp. 1285–1298, 2016.
[14] Griffin, G., A. Holub, and P. Perona. "The caltech 256 dataset." TR-2007-001 (2006).
[15] Athiwaratkun B., "Feature Representation In Convolutional Neural Networks" pp. 6-11, 2015.
[16] Burges C. J. C. , "A Tutorial on Support Vector Machines for Pattern Recognition," vol. 43, pp. 1–43, 1997.
[17] Bengio, Y., Lamblin, P., Popovici, D., Larochelle, H "Greedy layer-wise training of deep networks" in *NIPS*, pp. 153–160 (2007).
[18] Ciresan, D.C., Meier, J., Schmidhuber, "Multi-column deep neural networks for image classification". in *CVPR* (2012).
[19] Hinton, G.E., Osindero, S., Teh, Y., "A fast learning algorithm for deep belief nets. Neural Computation" vol. 18,pp. 1527–1554 (2006).
[20] Howard, A.G., "Some improvements on deep convolutional neural network based image classification" *arXiv* 1312.5402 (2013).
[21] Oquab, M., Bottou, L., Laptev, I., Sivic, "Learning and transferring mid-level image representations using convolutional neural networks" in *CVPR* (2014).
[22] Simonyan, K., Vedaldi, A., Zisserman, "Deep inside convolutional networks: Visualising image classification models and saliency maps" *arXiv* (2013).
[23] Haralick R. M., Shanmugam K., and Dinstein I., "Textural Features for Image Classification," *IEEE Trans. Syst. Man. Cybern.*, vol. SMC-3, no.6, pp. 610–621, Nov. 1973.
[24] Krizhevsky, A., Sutskever, I., Hinton, "Imagenet classification with deep convolutional neural networks" in *Advances in Neural Information Processing Systems*, pp. 1097–1105 (2012).
[25] Pan, S.J., Yang, "Survey on transfer learning" *IEEE Trans. Knowl. Data Eng.* 22, 1345–1359 (2010).

[26] Bharadwaja V, Ananmy R, Nikhil S, Vineetha KV, Shah J, Kurup DG, "Implementation of Artificial Neural Network on Raspberry Pi for Signal Processing Application", *International Conference on Advances in Computing, Communications and Informatics (ICACCI)*, pp. 1488-1491 (2018).

[27] Ramachandran, R., Rajeev, D.C., Krishnan, S.G., Subathra, P., "Deep learning – An overview", *International Journal of Applied Engineering Research, 10 (10)*, pp. 25433-25448 (2015).

Proceedings of the Fourth International Conference on Communication and Electronics Systems (ICCES 2019)
IEEE Conference Record # 45898; IEEE Xplore ISBN: 978-1-7281-1261-9

Non Orthogonal Multiple Access in Cooperative Relay Sharing with Randomly Deployed Users

Dr. Ankur Bansal
Division of Electronics and Communication Engineering
Netaji Subhash University of Technology
New Delhi :- 110078
email :- bansal.ankur143@gmail.com

Avinav Joshi
Division of Electronics and Communication Engineering
Netaji Subhash University of Technology
New Delhi :- 110078
email :- joshiavinav04@gmail.com

***Abstract*— We have investigated and proposed a cooperative communicating strategy using non-orthogonal multiple access (NOMA) in which the users are randomly deployed. In this technique there are two randomly deployed sources which share or exchange information with their respective destinations parallely over the same range of frequency through a common shared relay. Further in this strategy, after the symbols are received they are transmitted simultaneously in parallel by both the sources with different powers allocated, the relay sends a coded complex signal super-positioned using NOMA-RS to the respective destinations. The most important benefit of NOMA-RS is that same relay can be shared by two sources. Through the mathematical calculations and simulations, we demonstrate the efficiency of the suggested strategy in terms of outage probability of two source and destination pairs.**

Keywords*— *Outage Probability, successive interference cancellation , relay sharing, non-orthogonal multiple access

I. INTRODUCTION

In order to deliver an overall strong network to a very large number of users and to achieve high signal to noise ratio (SNR), Non - Orthogonal Multiple Access (NOMA) is considered as the most important applicant of 5G because of its highly spectral proficient characteristics [1]. For additional improvement of the effectiveness of NOMA network, cooperative Non Orthogonal Multiple Access with relay sharing (NOMA-RS) using decode-and then forward (DF) technique is presented in the paper [2]–[4], where committed users or relays work together to enhance the system performance by making use of spatial diversity. NOMA-RS, where users who have comparatively better channel level act as a cooperating relay for users that are having low channel level, is presented in [2]. The analysis of capacity of a cooperating relay scheme (CRS) with help of NOMA for spatially multiplexed systems is investigated in [4]. Downlink process of NOMA, employing the amplifying-and-forwarding strategy is explained in [5] and [6]. Furthermore, cooperative NOMA that is introduced in [2]–[6] only considers perfectly implemented successive interference cancellation (SIC).

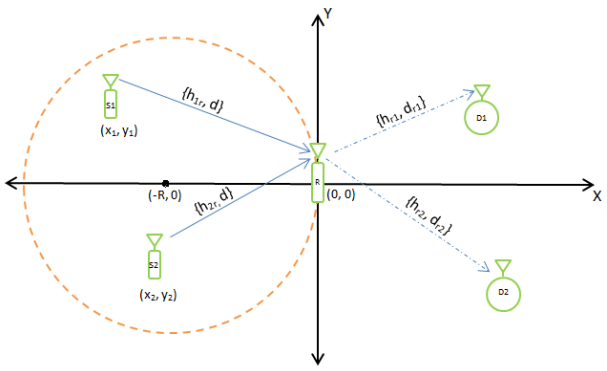

Fig. 1 Model of the System

Based on the already existing theory based on cooperative relay sharing making use of NOMA, there exists a great scope for designing plans that can additionally improve gains in capacity of the proposed system and can deliver great connectivity to very large number of users. In this research paper, we have investigated the effect of the relay sharing (RS) on the characteristics of cooperative NOMA when the users are randomly deployed. Important work of this paper is defined as follows:

1) We have investigated and proposed a cooperative relay sharing technique with the help of NOMA where two or more than two random users are transmitting symbols simultaneously at the same time, and then their symbols are detected and interpreted at relay which are again authorized to be forwarded simultaneously.
2) The analytical outage probability (P_{out}) of NOMA relay has been derived and then analytical results have been

verified by comparing them with simulation results.

II. System Models

We are considering here a dual-hop cooperative relay allocation system as illustrated in Fig.1, where there are two randomly deployed source-destination pairs S_1-D_1 and S_2-D_2 which uses a common relay R which is half duplex engaging DF strategy. Every node is provided with an antenna. It is presumed that there are no straight connections from S_1 to D_1 and S_2 to D_2 due to inadequate channel conditions and physical obstacles. In such situation, both the sources S_1 and S_2 entirely dependent on relay R to exchange information concurrently with their respective recipients D_1 and D_2. This presumption can be explained by taking an example of metropolitan cities where S-D pairs are isolated from each other and there is no line of sight communication available and is also in line with previous works.

As illustrated in Fig. 1, the information is transmitted from sources to destinations over two transmission phases through a common relay R. The two phases, I and II of NOMA-RS are alike to uplink and downlink NOMA respectively. In cellular networks, the bit rate of users over uplink does not rely on the bit rate of downlink and the converse is also true. Besides, it is widely known in research that the rate at which data transfers of the user executing SIC profitably in NOMA system, grows linearly with an increase in transmitted signal-to-noise ratio (SNR) γ_o. On the contrary, the channel capacity of the user that does not execute SIC, almost begins to be persistent when γ_o increases because of the intrusion of other users. If distinctive users execute SIC in uplink as well as in downlink, then users will not be able to get actual advantage from SIC in case of NOMA system. Therefore, the spectral effectiveness of this network will not be enhanced as assumed, as in cooperative systems, the rate at which data is transferred by the user is influenced by the most weak connection.

Consequently, in NOMA-RS, the network is examined accordingly that SIC is executed by the identical user in both uplink as well as downlink, such that the network get benefit from both NOMA as well as shared diversity. The S_1-D_1 as well as S_2-D_2 sets can be thought of as users with high and low bit rate needs, respectively. For our system model we consider d to be random distance which is defined as the distance between the uniformly generated points (sources) inside a circle and the relay which is placed at the circumference of the circle. The coefficients of the channel are defined as $h_{1r} \sim CN(0, \lambda = d^{-v})$, $h_{2r} \sim CN(0, \lambda = d^{-v})$, $h_{r1} \sim CN(0, \lambda_{r1} = d_{r1}{}^{-v})$ and $h_{r2} \sim CN(0, \lambda_{r2} = d_{r2}{}^{-v})$ for links $S_1 \rightarrow R$, $S_2 \rightarrow R$, $R \rightarrow D_1$ and $R \rightarrow D_2$, respectively where v represents path loss.

Considering a circle of radius R centered at (0, 0), the cumulative dustribution function (CDF) of the distance d between two uniformy distributed random points, one located at (R, 0) and other located anywhere on or inside the circle, [11, eq. (21)] is given by,

$$F_d(r) = \frac{1}{\pi R^2}\left[r^2 \cos^{-1}\left(\frac{r}{2R}\right) + R^2 \cos^{-1}\left(\frac{2R^2 - r^2}{2R^2}\right) - \frac{r}{2}\sqrt{4R^2 - r^2}\right]; (0 < r < 2R) \quad (1)$$

Similar results are found for the case when the origin of the circle is shifted to (-R, 0) and the random point at the circumference is located at (0, 0). Therefore, the probability distribution function (PDF) of the distance d is found to be

$$f_d(r) = \frac{2r}{\pi R^2}\cos^{-1}\left(\frac{r}{2R}\right); (0 < r < 2R) \quad (2)$$

The distance between the relay and the destinations namely d_{r1} and d_{r2} are assumed to be constant. The transmission of data in two phases is described as follows.

A. Ordered Statistics

As we have randomly deployed points at the source end of the system we make use of ordered statistics for computing the PDFs of the square of absolute value of channel coefficients namely $|h_{1r}|^2$ and $|h_{2r}|^2$. According to ordered statistics, the channel with worse user *i.e.* the user whose distance to the relay is maximum will always be assigned the channel coefficient as h_{1r}. Given any random variables $X_1, X_2, X_3, \ldots, X_N$, the ordered statistics $X_{(1)}, X_{(2)}, X_{(3)}, \ldots, X_{(N)}$ are also random variables which are described by arranging the values of $X_1, \ldots, X_N$ in ascending sequence. For an unordered cumulative distribution function (CDF), $F_X(x)$, the ordered CDF for that sample has distributions as follows

$$F_{X_{(r)}}(x) = \sum_{j=r}^{N}\binom{N}{j}[F_X(x)]^j[1 - F_X(x)]^{N-j} \quad (3)$$

where r = 1,2,3,…,N. Therefore if we have a channel $h \sim CN(0, \lambda)$, having the CDF of square of absolute of channel coefficient as $F_{|h|^2}(x)$ then for n=1, 2, 3…, N the Power Density Function of ordered variables can be defined as follows

$$f_{|h_{nr}|^2}(x) = \frac{N!}{(n-1)!(N-n)!}\left(F_{|h|^2}(x)\right)^{n-1} \times \left(1 - F_{|h|^2}(x)\right)^{N-n} f_{|h|^2}(x). \quad (4)$$

Therefore for N=2 (after ordering), the PDFs of two channel coefficients can be defined as

$$f_{|h_{1r}|^2}(x) = \frac{2}{\lambda} exp\left(\frac{-2x}{\lambda}\right), \quad (5)$$

and

$$f_{|h_{2r}|^2}(x) = \frac{2}{\lambda}\left(1 - exp\left(\frac{-x}{\lambda}\right)\right) exp\left(\frac{-x}{\lambda}\right). \quad (6)$$

B. Transmission Phase-I

This phase is similar to uplink NOMA. During phase I both the sources S_1 and S_2 concurrently send symbols s_1 and s_2 with powers $\Psi_1 P_T$ *and* $\Psi_2 P_T$, where P_T is the total transmitter power available and $\Psi_1 + \Psi_2 = 1$ is defined as total transmit power constraint $\Psi_1 + \Psi_2$ are representing the power allocating coefficients. We have presumed that S_1 and S_2 have some kind of cooperation depending on which, power is being spread among the sources to fulfill the overall requirement of transmitting power. It is to be noted that the requirement of total transmission power is essential for many real scenarios [7]. Furthermore, we have assumed perfect synchronization of time between the sources S_1 and S_2, so that symbols s_1 and s_2 reach at relay R simultaneously. We have made an assumption that the worse symbol will be denoted by s_2. In this technique R first deciphers the comparatively finer user symbol by assuming the worse user symbol as noise. Then, relay R performs successive interference cancellation to secure symbol of worse user. Therefore, the received signal-to-interference noise ratio for better symbol can be defined as

$$\gamma_{S_1}^I = \frac{\Psi_1 \gamma_o |h_{1r}|^2}{\Psi_1 \gamma_o |h_{2r}|^2 + 1} \quad (7)$$

where $\gamma_o = \frac{P_T}{\sigma^2}$ and σ^2 signifies the variance of noise. Further by considering imperfect SIC, the signal to interference noise ratio (SINR) received for weaker symbol is computed as

$$\gamma_{s_2}^{I} = \frac{\Psi_2 \gamma_o |h_{2r}|^2}{\Psi_1 \gamma_o |g_{1r}|^2 + 1} \quad (8)$$

where, $g_{1r} \sim CN(0, \xi_1 \lambda_{1r})$, and the variable ξ_1 $(0 < \xi_1 < 1)$ is denoting the residual interference level due to the imperfect SIC present at relay.

C. Transmission Phase-II

This phase is similar to downlink NOMA. During phase II, the relay R transmits a superimposed composite symbol $z = \sqrt{\Psi_3 P_r}\, s_1 + \sqrt{\Psi_3 P_r} s_2$, where s_1 and s_2 are the symbols rejuvenate at relay R amid I. P_r is the total power of transmission at R. Ψ_3 and Ψ_4 represent power allocation coefficients and $\Psi_3 + \Psi_4 = 1$. According to the protocol of NOMA, the SINR received at D_1 for symbol s_1 is given by

$$\gamma_{s_1}^{II} = \frac{\Psi_3 \gamma_o |h_{r1}|^2}{\Psi_4 \gamma_o |h_{r1}|^2 + 1} \quad (9)$$

where $\gamma_o = \frac{P_R}{\sigma^2}$. Similarly to phase-I D_2 is performing SIC to interpret its symbol s_2. For performing successive interference cancellation, D_2 interprets high strength symbol s_1 first by considering its own symbol s_2 as noise and then using SIC cancels it to get its own symbol s_2. Therefore, the SINRs received for the symbols s_1 and s_2 are respectively computed as

$$\gamma_{s_1 \to s_2}^{I} = \frac{\Psi_3 \gamma_o |h_{r2}|^2}{\Psi_4 \gamma_o |h_{r2}|^2 + 1} \quad (10)$$

$$\gamma_{s_2}^{II} = \frac{\Psi_4 \gamma_o |h_{r2}|^2}{\Psi_3 \gamma_o |g_{r2}|^2 + 1} \quad (11)$$

where, $\gamma_{s_1 \to s_2}^{I}$ represents SINR that we require at D_2 to interpret s_1, $g_{r2} \sim CN(0, \xi_2 \lambda_{r2})$ and ξ_2 represents the level of remaining noise at D_2.

III. Outage Probability Analysis

This segment explores the outage probability of NOMA – RS over independent Rayleigh faded channels.

A. CDF of S_1-D_1 Pair

Considering (7), (9) and (10), the possible SINR related with symbol s_1 is represented as

$$\text{SINR} = \min(\gamma_{s_1}^{I}, \gamma_{s_1}^{II}, \gamma_{s_1 \to s_2}^{I}). \quad (12)$$

Let $X = \gamma_{s_1}^{I}$ and $Y_1 = \min(\gamma_{s_1}^{I}, \gamma_{s_1}^{II}, \gamma_{s_1 \to s_2}^{I})$.Then using (5), (6) and (7), CDF of X can be represented by

$$F_X(x|d) = 1 - \left(\frac{\Psi_1^2}{(\Psi_1 + \Psi_2 x)(\Psi_1 + 2\Psi_2 x)}\right) \exp\left(\frac{-2x}{\Psi_1 \gamma_o \lambda}\right) \quad (13)$$

Using (12) and the cumulative distribution function of minimal of two exponentially distributed random variables, Cumulative Distribution Function of Y_1 conditional on distance, is computed as

$$F_{Y_1}(y|d) = 1 - \left[\left(\frac{\Psi_1^2}{(\Psi_1 + \Psi_2 y)(\Psi_1 + 2\Psi_2 y)}\right) \times \exp\left(\frac{-2y}{\Psi_1 \gamma_o \lambda} - \frac{-y}{(\Psi_3 - \Psi_4 y)\gamma_o \lambda_{r1}} - \frac{-y}{(\Psi_3 - \Psi_4 y)\gamma_o \lambda_{r2}}\right)\right]. \quad (14)$$

Further the average CDF of Y_1 can be found by integrating (14) with $f_d(r)$ such as

$$F_{Y_1}(y) = \int_0^{2R} F_{Y_1}(y|r) f_d(r) dr\,. \quad (15)$$

Using (1), (14), (15) and utilizing MATHEMATICA, we get

$$F_{Y_1}(y) = 1 - \left[\left(\frac{\Psi_1^2}{(\Psi_1 + \Psi_2 y)(\Psi_1 + 2\Psi_2 y)}\right) \exp\left(\frac{-y}{(\Psi_3 - \Psi_4 y)\gamma_o}\left(\frac{1}{\lambda_{r1}} + \frac{1}{\lambda_{r2}}\right)\right) \times \left(\frac{\Psi_1 \gamma_o}{4R^2 y}\right)\left(1 - \exp\left(\frac{-4R^2 y}{\Psi_1 \gamma_o}\right) I_0\left(\frac{4R^2 y}{\Psi_1 \gamma_o}\right)\right)\right]. \quad (16)$$

where $I_0(x)$ is the improved Bessel function of first order .

B. Outage Probability of S_2-D_2 Pair

Considering (8) as well as (11), the possible SINR related with symbol s_2 is represented as

$$\text{SINR} = \min(\gamma_{s_2}^{I}, \gamma_{s_2}^{II}) \quad (17)$$

Let $U = \gamma_{s_2}^{I}$, $V = \gamma_{s_2}^{II}$ and $Y_2 = \min(\gamma_{s_2}^{I}, \gamma_{s_2}^{II})$. Then CDFs of U and V are given by,

$$F_U(u|d) = 1 - \left[\frac{4\Psi_2}{2\Psi_2 + \Psi_1 \xi_1 u} exp\left(\frac{-u}{\Psi_2 \gamma_o \lambda}\right) - \frac{\Psi_2}{\Psi_2 + \Psi_1 \xi_1 u} \exp\left(\frac{-2u}{\Psi_2 \gamma_o \lambda}\right)\right], \quad (18)$$

and

$$F_V(v) = 1 - \left(\frac{\Psi_4}{\Psi_4 + \Psi_3 \xi_2 v}\right) \exp\left(\frac{-v}{\Psi_4 \gamma_o \lambda_{r2}}\right), \quad (19)$$

Now CDF of Y_2 conditional on distance can be found using

$$F_{Y_2}(y|d) = 1 - (1 - F_U(y|d))(1 - F_V(y)). \quad (20)$$

which represents the Cumulative Density Function of minimal of two random variables. Further the CDF of Y_2 can be computed as

$$F_{Y_2}(y) = 1 - \left[\left(\left(\frac{4\Psi_2 \Psi_4}{(2\Psi_2 + \Psi_1 \xi_1 y)(\Psi_4 + \Psi_3 \xi_2 y)}\right) \Phi(y, R) - \left(\frac{\Psi_2 \Psi_4}{(\Psi_2 + \Psi_1 \xi_1 y)(\Psi_4 + \Psi_3 \xi_2 y)}\right) \Phi(y, R\sqrt{2})\right) exp\left(-{}^{y}/_{\Psi_4 \gamma_o \lambda_{r2}}\right)\right], \quad (21)$$

where,

$$\Phi(y, \alpha) = \left(\frac{\Psi_2 \gamma_o}{2\alpha^2 y}\right)\left(1 - \exp\left(\frac{-2\alpha^2 y}{\Psi_2 \gamma_o}\right) I_0\left(\frac{2\alpha^2 y}{\Psi_2 \gamma_o}\right)\right), \quad (22)$$

C. Outage Probability of S_1-D_1 and S_2-D_2 pair

The outage probability of S_1-D_1 can be found by substituting $y = \gamma_{th}$ in (16), i.e.

$$P_{out}^{S_1 - D_1} = F_{Y_1}(\gamma_{th}) \quad (23)$$

Similarly, the outage probability of S_2-D_2 can be found by substituting $y = \gamma_{th}$ in (21), i.e.

$$P_{out}^{S_2 - D_2} = F_{Y_2}(\gamma_{th}) \quad (24)$$

where, γ_{th} is some threshold SNR.

IV. Results And Discussions

In this section we have discussed the results and compared the analytical and simulation results to validate our work. Fig. 2 represents the outage probabilities of the proposed Non Orthogonal Multiple Access Technique with respect to (w.r.t) SNR, γ_o for S_1-D_1 and S_2-D_2 pairs of source and destinations. For our analysis we have taken the values of $d_{r1} = 1$ and $d_{r2} = 1$ and the path loss exponent $v = 2$. The close consistency between the simulation and analytical results for the outage probability of NOMA-RS validates the precision of our result.

We have taken the value of threshold SNR, γ_{th} to be -5dB. Also we have assumed the power allocation coefficients, Ψ_1 = 0.6, Ψ_2 = 0.4, Ψ_3 = 0.9 and Ψ_4 = 0.1 and the values of residual interferences namely $\xi_1 = \xi_2 = (0.02)^3$. The plot infers that with the increasing value of SNR the outage probability decreases.

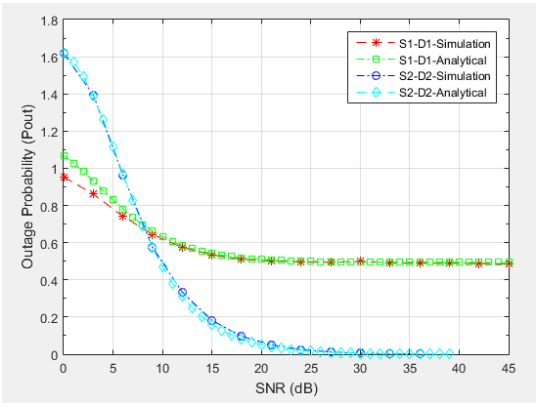

Fig. 2. Outage probability of S_1-D_1 and S_2-D_2 pair w.r.t γ_o, Ψ_1 = 0.6, Ψ_2 = 0.4, Ψ_3 = 0.9 and Ψ_4 = 0.1, $\xi_1 = \xi_2 = (0.02)^3$, γ_{th}= -5dB

Fig.3 represents the outage probabilities of S_1-D_1 and S_2-D_2 pair w.r.t the threshold SNR. The plot confirms the fact that the outage probability increases with the increase in threshold SNR.

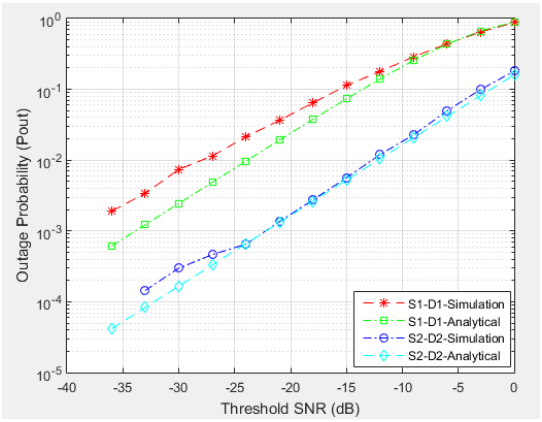

Fig. 3. Outage probability of S_1-D_1 and S_2-D_2 pair w.r.t γ_{th}. Ψ_1 = 0.6, Ψ_2 = 0.4, Ψ_3 = 0.9 and Ψ_4 = 0.1, $\xi_1 = \xi_2 = (0.02)^3$, γ_o=20dB

V. Conclusions

We have investigated and proposed a common relay system for NOMA where the two randomly deployed sources with uniform distribution can exchange information with their respective destinations simultaneously in parallel. We have attained the outage probability of NOMA-RS analytically. We found that the outage probability of NOMA-RS technique significantly depends on the SNR. As the SNR is increased in value, the outage probability decreases. Also the outage probability increases with increase in the value of threshold SNR. It is to be noted that power allocation coefficients have a considerable amount of effect on outage of NOMA-RS. Besides this the benefit of NOMA-RS is that can be serve a large number of devices or users at a given period of time.

References

[1] F.-L. Luo and C. Zhang, *Non-Orthogonal Multiple Access (NOMA): Concept and Design*. Hoboken, NJ, USA: Wiley, 2016, pp. 143–168.

[2] Z. Ding, M. Peng, and H. V. Poor, "Cooperative non-orthogonal multiple access in 5G systems," *IEEE Commun. Lett.*, vol. 19, no. 8, pp. 1462–1465, Aug. 2015.

[3] Z. Ding, H. Dai, and H. V. Poor, "Relay selection for cooperative NOMA," *IEEE Commun. Lett.*, vol. 5, no. 4, pp. 416–419, Aug. 2016.

[4] J.-B. Kim and I.-H. Lee, "Capacity analysis of cooperative relaying systems using non-orthogonal multiple access," *IEEE Commun. Lett.*, vol. 19, no. 11, pp. 1949–1952, Nov. 2015.

[5] J. Men, J. Ge, and C. Zhang, "Performance analysis of non-orthogonal multiple access for relaying networks over Nakagami-m fading channels," *IEEE Trans. Veh. Technol.*, to be published. [Online]. Available:http://ieeexplore.ieee.org/stamp/stamp.jsp?tp=&arnumber=7748569&isnumber=4356907, doi: 10.1109/TVT.2016.2630706.

[6] J. Men and J. Ge, "Performance analysis of non-orthogonal multiple access in downlink cooperative network," *IET Commun.*, vol. 9, no. 18, pp. 2267–2273, Dec. 2015.

[7] Z. Yang, Z. Ding, P. Fan, and N. Al-Dhahir, "A general power allocation scheme to guarantee quality of service in downlink and uplink NOMA systems," *IEEE Trans. Wireless Commun.*, vol. 15, no. 11, pp. 7244–7257, Nov. 2016.

[8] S. C. Liew, L. Lu, and S. Zhang, "A primer on physical-layer network coding," *Synth. Lectures Commun. Netw.*, vol. 8, no. 1, pp. 1–218, 2015.

[9] C. Zhong and Z. Zhang, "Non-orthogonal multiple access with cooperative full-duplex relaying," IEEE Commun. Lett., vol. 20, no. 12, pp. 2478–2481, Dec. 2016.

[10] H. Wang, J. Lee, S. Kim, and D. Hong, "Capacity enhancement of secondary links through spatial diversity in spectrum sharing," IEEE Trans. Wireless Commun., vol. 9, no. 2, pp. 494–499, Feb. 2010.

[11] Z. Khalid and S.Durrani, "Distance Distributions in Regular Polygon," IEEE Transactions on Vehicular Technology, vol, 62, no. 5, pp. 2363-2368, Jun. 2013.

[12] A. Sang, X. Wang, M. Madihian, and R.D. Gitlin, "A flexible down-link scheduling scheme in cellular packet data systems," *IEEE Trans. Wireless Commun.*, vol.5, no.3, pp.568–577, March 2006.

Proceedings of the Fourth International Conference on Communication and Electronics Systems (ICCES 2019)
IEEE Conference Record # 45898; IEEE Xplore ISBN: 978-1-7281-1261-9

Building Detection from LIDAR Point Cloud Data

Mayura N P[1], Veni S[2]
Department of Electronics and Communication Engineering
Amrita School of Engineering, Coimbatore
Amrita Vishwa Vidyapeetham
India
mayuranp27@gmail.com[1], s_veni@cb.amrita.edu[2]

***Abstract*—LiDAR (Light Detection and Ranging) is an emerging technology now and has proved to be one of the best techniques for 3D city modeling. Building detection is an important aspect of 3D city modeling as it can help in urban planning, utility services, disaster management, traffic management, environmental monitoring and many other applications. In this paper we propose a method in which building structures can be accurately discriminated from vegetation. Pre-processing of the data is done using a remote sensing tool called Las Tools. The data is structured using kd tree and then further segmented using Euclidean distance clustering. Then we process this data using another open-source remote sensing tool called CloudCompare. This paper will help in imparting a clear idea of how efficiently and accurately building detection can be performed with the help of these open-source tools without deploying much complex algorithms.**

Keywords—LiDAR, kd tree, Euclidean distance clustering, LAStools, CloudCompare

I. INTRODUCTION

LiDAR is an evident technology in the field of remote sensing and has proved to be one of the best methods to efficiently and accurately classify data using it's 3D information. Previously data acquisition was done using hyperspectral and multispectral imaging techniques [1]. Though spectrally rich these datasets demands a huge memory for processing. LiDAR datasets also require quite a bit of memory to process, but they are more accurate and reliable than multipectral and hyperspectral imaging techniques as it contains the 3D information about the data. We know LiDAR stands for Light Detection and Ranging. Like the name suggests it uses pulsated laser pulses which are send to the ground from terrestrial, airborne or spaceborne sensors. This laser pulse travels a huge distance until it hits a target and is reflected back to the source producing highly accurate x,y,z measurements. Thus the range distance R from the source and the destination in LiDAR is found using the formula:

$$R = C\,(t/2) \qquad (1)$$

Where C is defined as the speed of light and t is the time taken for the sending pulse to return back to the destination. This data accounts for LiDAR's z axis which has the height information. The other two axis contains latitude (x-axis) and longitude (y-axis). Thus along with this highly georeferenced coordinates the LiDAR data may also contain GPS time, point classification values, intensity, scan direction, number of returns, return number, RGB (red, green, and blue) values, points that are at the edge of the flight line and scan angle. The LiDAR point cloud is basically a collection of 3D elevation points. A single pulse emitted from the sensor might have one or multiple returns of which first return is the most important one. It contains the top most elevation points of trees or buildings and the last returns are the most insignificant one as it mostly refers to ground data. But the last returns will turn out to be important in cases which only require ground information.

Building detection and extraction plays an important role in 3D city modeling, urban planning, in geographic information systems database and in environmental monitoring. It has become an emerging topic for research in remote sensing and photogrammetry. The data acquired from advanced pre-processing techniques and new sensors is used in this technique. Though technologies are highly developed, it is still a challenge as urban scenes are complex. Building extraction is an important aspect of 3D city modelling as we need to identify and model buildings separately. The height factor of LiDAR data is extracted using Canopy Height Models for urban planning [2]. But while doing so, some misinterpretation takes place where the systems misclassify trees as buildings. Moreover the building boundaries are less regularized and more false positives arise during classification. As the building scenes are becoming more complex new algorithms have to be employed to extract building points from other non-building points.

The main objective of this project is to accurately extract building points and its boundaries from LiDAR point cloud data by employing new feature calculation techniques. This project also aims at eliminating misclassification of trees as buildings which will help us distinguish buildings from trees. Pre-processing of the dataset is performed where we tile the data, remove noise and classify it into ground and non-ground points. Then we have employed mainly two methods for clustering and segmentation of data and then the output obtained is processed using an open source remote sensing tool and the results are checked for accuracy of building points.. Building detection and extraction from LiDAR point cloud data is widely deployed in Urban Planning Visualization, Traffic Management, Utility Services Drainage Calculations, 3D city modeling and several other applications [3].

This paper is organized as follows. The related work and the data description is detailed in section II and III respectively. Proposed work and the result analysis is discussed in section

IV and V respectively. Finally the paper is concluded in section VI.

II.RELATED WORK

The building extraction methods are classified according to the type of data used. Each method has different techniques employed for building extraction. These are broadly categorized as follows:

i. Building Extraction using 2D information

ii. Building Extraction using fusion of 2D and 3D information

iii. Building Extraction Using 3D LiDAR data

A. Building Extraction Using 2D data

The data is obtained using space borne and air borne images. Various techniques like colour invariance specifications, shadow information and corner detection are used to find and distinguish rooftops [4]. And also various energy based algorithms like level-set curve and box-fitting algorithms are employed for accurate building extraction [5]. Though reliable, these techniques have produced shadows and blockage in complex scenes which resulted in erroneous image extraction.

B. Building Extraction using fusion of 2D and 3D information

A 2D-3D fusion based method in which the input data sources can be divided into two, photogrammetry and Light Detection and Ranging (LiDAR). Generally three colour channels are present for photogrammetry, sometimes with an additional infrared channel as well. Mainly height information is contained in LiDAR data. By fusing these two datas the accuracy of automatic building extraction can be improved significantly [6]. But due to the different characteristics of LiDAR and image data the fusion of the two may result in an erroneous output. The concept of image fusion becomes difficult due to the varying characteristics of both the data. The data sets must be arranged at one pixel-level to fully exploit data fusion from multiple sensors. Even a small error in image registration can cause error in the output data. In particular, due to error in image registration in building extraction some trees were misinterpreted as buildings [7]. Secondly the spatial resolution of LiDAR data is low compared to photogrammetry. Both LiDAR and image data may not be available together for certain regions. Optical muti-view imagery was proposed in 2013 [8]. Two main steps are involved one is the segmentation of the roof top and the other is the reconstruction of the 3D roof model. The roof is initially segmented using point-based method using normal estimate and then a shrink and expand technique is used for refinement of the segmented regions. Finally a 3D step line is determined by integrating the optical multi-view image with the points of the segmented rooftop to reconstruct a 3D rooftop model. But this method needs to be further improved to be fully automated.

An automated method to integrate the 3D data with ground view image of facades using projective trajectory is proposed [9]. A feature extraction method in which the input image is segmented. It also combines global feature extraction on a local region segmentation method and an adaptively tessellated Gaussian Sphere with Hough transform [10]. Lines having a common vanishing point are clustered and building facade regions are detected using spatial locality of horizontal and vertical line clusters. The position of the camera is estimated using the roof corners of the facade regions extracted. To automate camera pose several 3D to 2D correspondences are derived using multiple hypothesis. A Hough transform and an M-consensus sample estimator is used to find the correspondence between 3D model and images. The camera parameters obtained earlier are refined by using the 2D corner matches using Lowes algorithm.

C. Building Extraction Using 3D LiDAR data

1) Supervised Model: In supervised model we employ detection algorithm based on features like radiometry, geometry, echo characteristics and topology [11]. Support Vector Machines (SVMs) are used in-order to classify the data. We feed the data into an SVM classifier which will categorize the data into different classes based on the given features and algorithms. SVMs are said to produce promising results if they are trained properly. But in supervised model a lot of training samples must be given to train the SVM classifier to accurately model the data to find the endmost target classes .

2) Unsupervised Model : As supervised models require the adoption of machine learning techniques and are dependent on training samples many experiments have been performed to develop to unsupervised models. It does not require any training data set [12]. Many algorithms such as fitting algorithm, morphological filtering and region growing has been proposed in this method. Fitting algorithm is based on RANSAC (Random Sample Consensus) and Hough Transform [13]. However, due to oversampling in RANSAC unwanted planes in vegetations are extracted. Morphological filtering is based mainly on geometric properties.

A segmentation based building detection approach which gives a performance comparison between the open source point cloud library (PCL) and the commercially available software Terrasolid has been proposed [14]. This novel method adopts a surface based filtering approach along with data structuring using kd tree algorithm. A Euclidian distance based segmentation technique is used to segment the LiDAR point into different clusters. The segmentation is done based on the distance of one point from every other point. In order to reconstruct the buildings the building clusters is separated from non-building clusters by using the histogram of the local normal points of all clusters. The statistical parameters like mean, variance and standard deviation of these histograms does not vary much for a building whereas it varies greatly for trees. This way building points can be reconstructed after segmentation. As the number of clusters are to be defined it will make this process a semi-automatic one.

Building boundary tracing and regularization methods has also been proposed [15]. In this work data gathering is performed as the initial step and the gathered LiDAR point cloud data is separated into ground and non-ground points. These points are then segmented to obtain LiDAR building points. These points are then processed to get a regularized boundary for the pre-processed building points. The main processes involved here are initial boundary detection, boundary tracing and boundary regularization. Initial boundary detection has two parts plane detection and hole detection followed up by boundary tracing. Boundary regularization is done by corner detection and line extraction. Then the footprints of the buildings are generated by using the extracted corners and lines.

Another work proposed in 2014 follows a rule based approach for extraction of roof planes automatically [16]. The LiDAR data is pre-processed to obtain a Digital Elevation Model (DEM). The obtained data is divided into two categories, ground and non-ground. A building mask is generated using ground points where the black areas are used to represent ground which suggest the last returns. Planar roof points are obtained by segmenting non-ground points. The building mask is made into small grids and the cells having the black pixels clustered in away such that each cluster represents an individual tree or a building. Segmentation of the non-ground points within the cluster is done based on neighbourhood relations and co-planarity. Refinement of the planar segments using a rule based approach is done and also another rule based approach is also employed for tree detection and elimination of small random trees in the LiDAR point cloud.

Several other non-analytical approaches based on shape, size, height, structure of the building element and difference between the first and last return were proposed. To differentiate buildings accurately from vegetation many point based and grid based features have been developed [17]. This comprises of point-based features such as normal distribution, flatness and grid based features such as GLCM (Grey-Level Covariance Matrix) homogeneity, roughness and gradient methods. This work aims at using solely LiDAR data by fusing point and grid based features for automatic building extraction. Point-based and grid-based features are employed in order to accurately classify building structures. A point features based on the normal vector variance is proposed. After extracting the features a graph cuts algorithm is employed to accurately distinguish building points. This algorithm combines the features extracted along with the neighbourhood contextual information and thus provides an automatic robust building detection mechanism. A DSM interpolation with feature retention is also performed.

There are several techniques involved in building detection. Though many methods has proved to be efficient there are still some drawbacks that we needs to surpass. Building detection can be performed using 2d data, fusion of 2d-3d data and 3d data alone as well. Building detection using 2d data is more complex and yields less results as compared to the latter two. The fusion of 2d-3d data has shown promising results but are prone to more errors. It can be seen that using 3d data alone is much more efficient and reliable. So here we are solely working on 3d data.

III.DATA DESCRIPTION

The dataset taken for this study is ISPRS Test Project on Urban Classification and 3D Building Reconstruction dataset of Vaihingen city, Germany [18]. Each region in the city is characterized by different styles and the two test areas taken in this project has 35 and 14 buildings respectively with each building larger than 2.5 m^2 in total. Test Area 1 is classified as inner city where there are many complex structured buildings and Test Area 2 consists of High riser buildings of residential area (Fig.1.). The mean point density of the dataset is given as 4 points/m^2 and the median point density is 6.7 points/m^2.

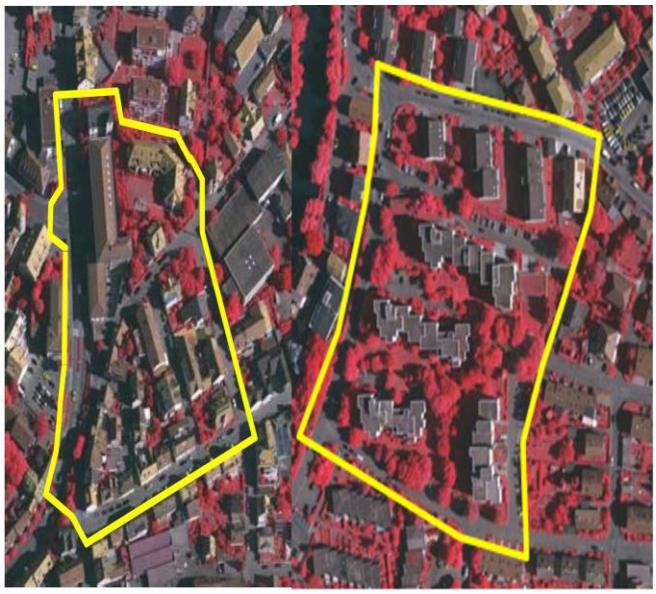

Fig.1. Aerial imagery of Test Area 1 and 2 taken from ISPRS [18]

IV.PROPOSED WORK

The data collected is processed in the following way. Necessary pre-processing techniques are performed using LAStools. The main steps involved in the pre-processing are

A. Pre-processing using LAStools

Firstly tiling of the data is done in order to get specific areas of interest in the dataset. We have to set a buffer while tiling so that that data at the edges is not lost. Here we have used a tile size of 500 and the buffer size of 30. The whole dataset is segmented to obtain a test area and the whole process is applied to this test data.

1) Estimating the ground points: The ground points in the dataset or the bare earth points are estimated (Fig.3). Mostly the last returns will be classified as ground points. This is performed using lasground feature in LASTools.

2) Estimating the Height of non-ground points: This mainly gives the top most elevations of the data or the first returns. The lasheight feature in LASTools helps in obtaining the height model of the building points obtained after

classification. The z-axis of the LiDAR data is replaced with this height.

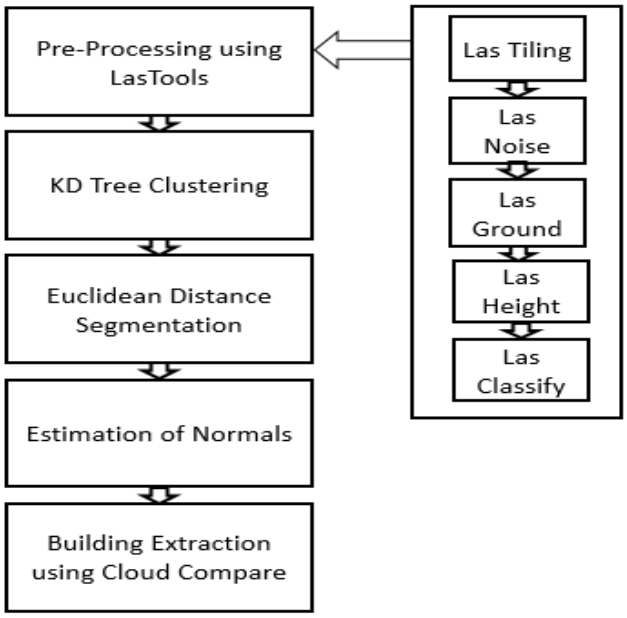

Figure 1. Proposed work block diagram

3) Classification: After classifying the ground and non-ground points we use another classification method called LasClassify by which we eliminate the classified ground points. The non-ground points are then taken and further processed to obtain the desired results. Thus the ground points are completely eliminated

B. Data Structuring

The LiDAR point cloud data is highly unorganized and discrete in nature. This is because the pattern in which the points in LiDAR data is stored is same as the scanning mechanism. So the boundary points of a LiDAR data are random and cannot be fit into a grid which in turn makes LiDAR data difficult to work with. Hence a hierarchical structuring of the data is done using kd tree clustering to make the dataset an organized one.

C. Euclidean distance clustering

Spatially isolated points can be separated using Euclidean Distance clustering [14]. Here the data is classified according to the distance between each point. A certain threshold is determined first and if the point exceeds falls within the threshold it is placed in the cluster and if the point exceeds the threshold it is kept in another cluster. The number of clusters formed can vary for different datasets depending on the minimum and maximum number of points set in the clustering algorithm. This was performed using the open-source library PCL (Point Cloud Library - http://pointclouds.org) in Visual Studio C++.

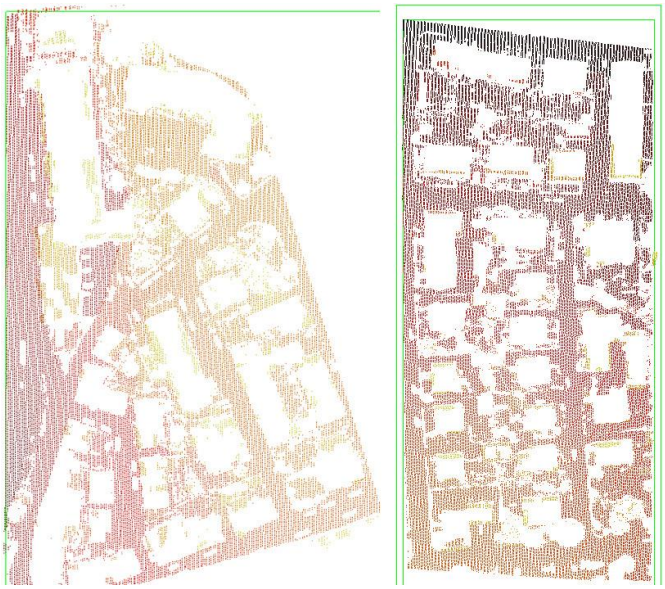

Fig.4. Data points of Test Area 1 and 2 classified as ground

The obtained data (Table. I) is processed to extract building structures. For this we have used another open-source remote sensing tool called CloudCompare. The results thus obtained are checked for accuracy.

TABLE I. RESULTS OF EUCLIDEAN DISTANCE CLUSTERING

Results of Euclidean Distance Segmentation	**Parameters for Test Area 1**	**Parameters for Test Area 2**
Cluster Tolerance (dth)	1 m	0.75m
Min/Max no. of points in the cluster	50-5000	30-3500
Number of Clusters	34	12
No. of buildings in the survey area	37	14
No. of buildings identified	37	14

D. Processing using CloudCompare

1) Estimation of Normals: Building structures are characterized by normals and normal estimation plays an important part in building point detection (CloudCompare 2.6.2, 2019).

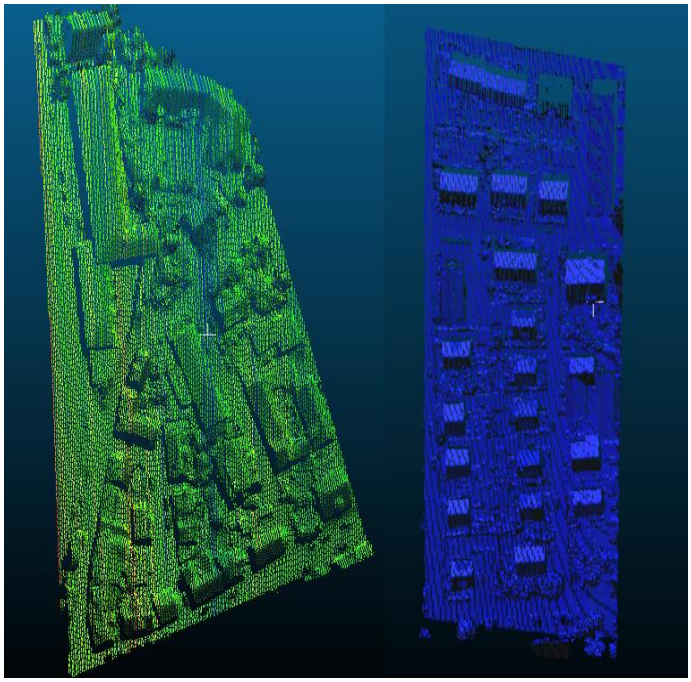

Fig.5. Estimation of building Normals from the data for Test Area 1 and 2

2) Filtering of ground points small shrubs: The filter by value tool is set to efficiently remove the unwanted points below a certain limit.

3) CANUPO Plugin: Further a plugin tool called CANUPO Plugin is used to classify building and tree points [19] .

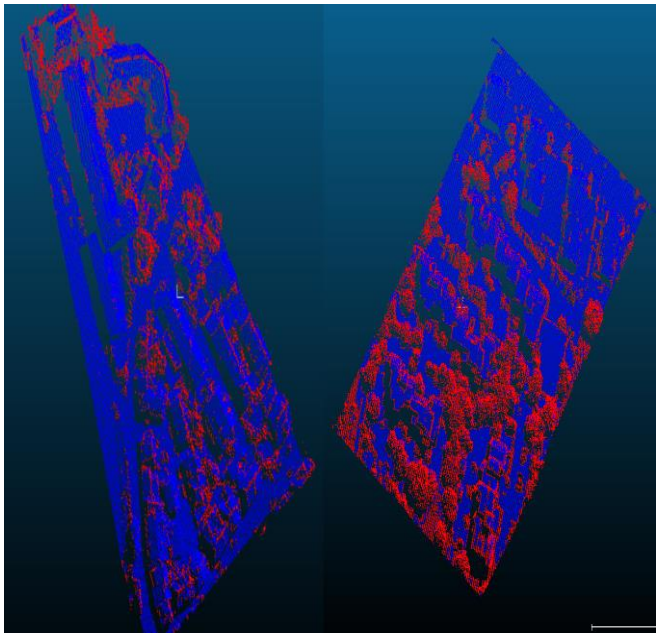

Fig.6. Final classified output for Test Area 1 and 2, where building points are classified as blue and tree points as red. (3D View)

The tool is first trained using building and tree data sets separately and this training data is applied to the test data to obtain well classified tree and building points (Fig.5).

V.RESULT ANALYSIS

The dataset of Vaihingen city, Germany is taken. The whole dataset is divided and two test areas are selected for easy processing and identification of building points. The collected data is filtered and the noise is removed. In LASTools we first classify the ground points and the non-ground points. This output is used to estimate the height of the non-ground points and the z axis which gives the height is replaced by this value thus eliminating the ground points. The non-ground points obtained are classified to buildings, trees etc. by appropriate processing techniques. Data structuring is performed on this filtered output after which Euclidean distance clustering is carried out and the results are shown in Table I. The data is then processed using an open-source software called CloudCompare. First the normals in the dataset are estimated as building are characterized by normals. Small shrubs and trees are filtered out by filtering the points above a particular value. Then we use CANUPO Plugin to discriminate the trees from buildings. For training we feed building data points as well as tree data points separately by segmenting these data points from the dataset. The training data is collected from the dataset by extracting only the target points from the whole data. The training data obtained is applied to the original test data. Now the buildings and the trees are classified into two separate classes. For Test Area 1, a total of 30 buildings are classified separately out of 37 buildings. The number of partially detected buildings and overlapping buildings are 5. And the total number of fully detected building structures are 20 and for the Test Area 2 a total of 11 buildings are classified separately out of 14 buildings. There are no partially detected buildings and the number of overlapping buildings are 2. An overall accuracy of 81% and 78.5% is obtained for test area 1 and 2 respectively depicted in Table II. The overall accuracy is calculated using equation (2).

$$Overall\ Accuracy = \left(\frac{\text{Total no. of buildings detected}}{\text{Total no. of building present}}\right) 100 \qquad (2)$$

The class with the blue colour indicates the buildings and the red ones indicate the trees. A true orthophoto obtained from ISPRS Dataset is superimposed over the DSM (Digital Surface Model) of the output data to identify the number of buildings detected. The total number of buildings detected is calculated for both the test areas and has given promising results. Though some roof top boundary points are misclassified as tree points, this can be avoided by fully exploiting the CANUPO Plugin tool by adjusting the filter values.

TABLE II. BUILDING DETECTION FINAL RESULT

Dataset	Test Area 1	Test Area 2
Total No. of Buildings Present	37	14
Total No. of buildings detected	30	11
No. of Overlapping buildings identified	5	0
Partially Detected Buildings	5	2
Fully Detected Buildings	20	9
Overall accuracy	81%	78.5 %

VI.CONCLUSION

This paper detects building structures from LiDAR point cloud data. The data has been processed with the help of python software, PCL library and two open-source remote sensing tools LASTools and CloudCompare respectively. The data is pre-processed, filtered, structured, clustered and finally classified into two different classes. We can see that structuring along with clustering of data helps to segment the dataset more precisely. This paper has also shown that applying feature based extraction techniques can yield good results. The total number of buildings detected for test area 1 is 30 out of 37 in total and for Test Area 2 is 11 out of 14. An overall accuracy of 81% can be observed for the inner city for test area 1, where there are complex structures and historic buildings. The Test Area 2 shows an overall accuracy of 78.5% for the high riser residential areas. It can also be observed that these open source tools have been instrumental in detecting the building structures without employing complex algorithms. These results can be further improved by exploiting more features of these tools. Here we have given a two-class classification as a final output where we discriminate trees and buildings separately. Several other objects like roads, cars, power lines etc. in urban scenes can be detected easily using these open-source softwares which is the future scope of this project.

REFERENCES

[1] Anand, R., S. Veni, and J. Aravinth. ”Big data challenges in airborne hyperspectral image for urban landuse classification.” 2017 International Conference on Advances in Computing, Communications and Informatics (ICACCI). IEEE, 2017.

[2] Lavenya, R., et al. ”Estimation of Peaks and Canopy Height Using LiDAR Data.” 2018 International Conference on Communication and Signal Processing (ICCSP). IEEE, 2018.

[3] Biljecki, Filip, et al. "Applications of 3D city models: State of the art review." ISPRS International Journal of Geo-Information 4.4 (2015): 2842-2889.

[4] Chen, Renxi, Xinhui Li, and Jonathan Li. "Object-based features for house detection from rgb high-resolution images." Remote Sensing 10.3 (2018): 451.

[5] Dini, Gholam Reza. Toward an Automatic Solution for Updating Building Databases Using Space-borne Stereo Imaging. Diss. Technische Informationsbibliothek und Universitätsbibliothek Hannover (TIB), 2014.

[6] Lee, Dong Hyuk, Kyoung Mu Lee, and Sang Uk Lee. "Fusion of lidar and imagery for reliable building extraction." Photogrammetric Engineering & Remote Sensing 74.2 (2008): 215-225.

[7] Cho, Moses Azong, et al. "Mapping tree species composition in South African savannas using an integrated airborne spectral and LiDAR system." Remote Sensing of Environment125 (2012): 214-226.

[8] Cheng, Liang, et al. "Integration of LiDAR data and optical multi-view images for 3D reconstruction of building roofs." Optics and Lasers in Engineering 51.4 (2013): 493-502.

[9] Frueh, Christian, Siddharth Jain, and Avideh Zakhor. "Data processing algorithms for generating textured 3D building facade meshes from laser scans and camera images." International Journal of Computer Vision 61.2 (2005): 159-184.

[10] Lee, Sung Chun, Soon Ki Jung, and Ram Nevatia. "Automatic integration of facade textures into 3D building models with a projective geometry based line clustering." Computer Graphics Forum. Vol. 21. No. 3. Oxford, UK: Blackwell Publishing, Inc, 2002.

[11] Zhang, Jixian, Xiangguo Lin, and Xiaogang Ning. "SVM-based classification of segmented airborne LiDAR point clouds in urban areas." Remote Sensing 5.8 (2013): 3749-3775.

[12] Mongus, Domen, Niko Lukač, and Borut Žalik. "Ground and building extraction from LiDAR data based on differential morphological profiles and locally fitted surfaces." ISPRS Journal of Photogrammetry and Remote Sensing 93 (2014): 145-156.

[13] Tarsha-Kurdi, Fayez, Tania Landes, and Pierre Grussenmeyer. "Hough-transform and extended ransac algorithms for automatic detection of 3d building roof planes from lidar data." ISPRS Workshop on Laser Scanning 2007 and SilviLaser 2007. Vol. 36. 2007.

[14] Ramiya, Anandakumar M., Rama Rao Nidamanuri, and Ramakrishan Krishnan. ”Segmentation based building detection approach from LiDAR point cloud.” The Egyptian Journal of Remote Sensing and Space Science 20.1, : 71-77, 2017.

[15] Varghese, Viji, Dimple A. Shajahan, and Aneesh G. Nath. "Building boundary tracing and regularization from LiDAR point cloud." 2016 International Conference on Emerging Technological Trends (ICETT). IEEE, 2016.

[16] Awrangjeb, Mohammad, Guojun Lu, and C. Fraser. "Automatic building extraction from LiDAR data covering complex urban scenes." The International Archives of Photogrammetry, Remote Sensing and Spatial Information Sciences 40.3 (2014): 25.

[17] Du, Shouji, et al. ”Automatic building extraction from LiDAR data fusion of point and grid-based features.” ISPRS Journal of Photogrammetry and Remote Sensing 130, 294-307, 2017.

[18] https://www.isprs.org/

[19] Brodu, Nicolas, and Dimitri Lague. "3D terrestrial lidar data classification of complex natural scenes using a multi-scale dimensionality criterion: Applications in geomorphology." ISPRS Journal of Photogrammetry and Remote Sensing 68 (2012): 121-134.

Proceedings of the Fourth International Conference on Communication and Electronics Systems (ICCES 2019)
IEEE Conference Record # 45898; IEEE Xplore ISBN: 978-1-7281-1261-9

Eye Movement Based Cursor Control and Home Automation for Disabled People

Sharon Mathew
Dept. of ECE
RSET
m.sharon978@gmail.com

Sreeshma A
Dept. of ECE
RSET
sreeshmaavikkal274@gmail.com

Theresa Anitta Jaison
Dept. of ECE
RSET
tanitajaison@gmail.com

Varsha Pradeep
Dept. of ECE
RSET
varshavijayas97@gmail.com

S Santhi Jabarani
Assistant Professor
Dept. of ECE RSET
santhij@rajagiritech.edu.in

***Abstract*—Access to computer technology is of vital importance to people with disabilities. Eyes can be regarded as one of the organs that can help a paralyzed person to communicate suitably. This paper provides a novel idea to control home appliances for disabled people who cannot move anything except their eyes by controlling the computer mouse cursor through their eye movement. The proposed method here uses an eye tracking method for eye movement acquisition, further following a simple circuitry. This system is very helpful for solving the HMI problems of the disabled.**

Keywords - Eye Tracking, Image Processing, Facial Land-mark, Eye Aspect Ratio, Home Automation, MQTT.

I. INTRODUCTION

Nowadays computers have become the most usable devices. They are used for communication, education, entertainment and scientific research. Unfortunately, paralyzed, elderly, and those with restricted upper limb movement find difficulty to use them. This project focuses on hands free computing and an eye controlled home automation for the disabled [1].

This project is a real time eye tracking system that will control the cursor movement by tracking the eye movements of the user and mapping it to the computer screen [2]. Real time execution is obtained by running a web cam (video streaming) and capturing continuous frames of images. Haar cascade algorithm [3] is applied in each frame to detect all the faces in the image. Next, facial landmark detector is applied in each face detected to obtain facial features like eyes, eyebrows, nose, mouth etc. Specific region of interest, eyes in this case, is considered and some image processing techniques are applied for better performance in eye tracking. Eye tracking is done by tracking the position of limbus whenever the users gaze changes. Cursor can be controlled by specific functions in the Python library. A delayed eye blink performs the click action on the device.

As shown in Fig 1. using web cam frame by frame images of the patient is captured continuously (Image capturing). Face and eyes of the patient is detected from the image using Facial Landmark Detection. Using Facial Landmark Detection eye coordinates are obtained and by using those coordinates we are able to track the eye movements. Then by mapping those coordinates with the computer cursor coordinates, cursor control can be achieved. A small delay is established such that if the blink time is equal to the delay time click action is performed.

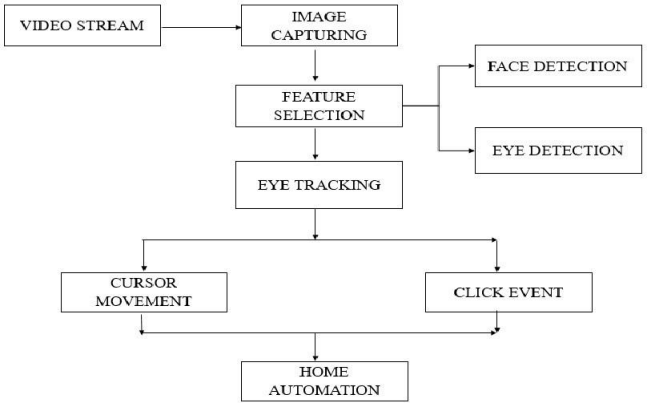

Fig. 1. System Block Diagram

The project not only enables the full control of the device with eyes but also enables home automation using the same concept for the disabled. It includes basic day to day operations like switching on and off an appliance or increasing the speed of fan.

A. ORGANIZATION AND SUMMARY

The remainder of this paper is organized as follows: Literature Survey in Section II, Face and Eye Detection in Section III. Section IV contains the proposed algorithm for Cursor Movement, Blink Detection in Section V, Section VI shows the Home Automation section of the project, Experimental Results obtained in Section VII and Section VIII includes Con-

clusion and at last Future Expansion followed by References respectively.

II. LITERATURE SURVEY

The interaction between humans (the users) and computers plays an important role in today's life. Input devices such as keyboard, mouse etc. are the normally used devices to interact with digital instruments, this devices cannot be operated by disabled peoples. For paralyzed people for whom eye movements and blinks are the only way to communicate with the outside world, an eye movement based cursor control and home automation is proposed in this paper. There are many related works based on this concept:

- Voice Based Method: In this method, voice of the user is analyzed and it is converted to digital form [7]. Based on the user's voice the computer cursor is controlled. But the drawback of this system is that background noise can affect the system.
- Motion Based Method: Normal movement of different organs such as head, foot, hands, etc. is utilized and given as input to the computer. There are many motion based devices such as head tracking system in which cursor control and click event is achieved based on the motor abilities of the head region [8].
- Hand Gesture Based Method: Identifying specific human hand gestures and using them to convey information or for controlling device [9]. The gestures are given as input to the computer system, the system then performs its corresponding task which is already predefined as per the application. Based on color, the hand location is traced and with the help of trained classifiers different gestures are classified.
- SMS Based Home Automation System: A basic home automation system based on SMS (Short Message Service) technology. The system consists of mainly two components: the GSM (Global System for Mobile communications) modem and a micro controller. Here SMS technology is used to exchange data through the GSM module and thereby connecting the user and home automation system. The micro controller acts as the bridge between the user and sensors and actuators of home automation system [10]. This system can supports a wide range of home automation devices such as security, home appliances and telecommunication devices.

III. FACE AND EYE DETECTION

Feature Selection is an important part of this project. The features such as face and eyes detected should be accurate and real time. The chance of obtaining false detection such as detecting chin as eye is very high in case of some detection technique. This can totally affect the output of the system.

In this project Face and Eye features are detected using Facial Landmark detection [4]. Facial landmark detection is a two-step process:

- Localization of face and eyes in the image using Haar Cascades.
- Detection of key facial structures on the face ROI(Region of Interest).

Facial Landmark Detector consist of pre-trained models. To estimate the location of 68 coordinates (x, y) that map the facial points on a person's face, dlib library in Python is used. The dlib library contains pre-trained facial landmark detector. Using Haar cascade face and eyes of the image is detected. The original image and the detected face rectangles is passed as input to the facial landmark detector. The output of the face detector is a vector of rectangles that contain one or more faces in the image. We get 68 landmarks for every face detected and they are stored in a vector of points. The 68-point detector localizes regions along the eyes, nose, mouth, eyebrows and jawline. Using Haar cascade alone may result in less accurate output, landmarks improves face recognition and from the obtained facial landmarks, we can also find the direction of the face using landmark coordinates.

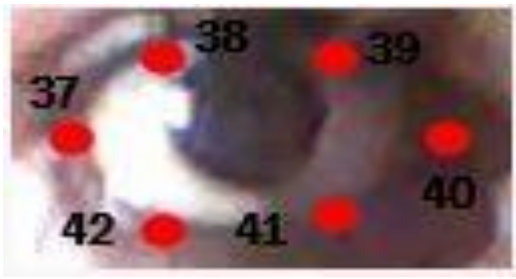

Fig. 2. Eye Coordinates from Facial Landmark

Eye coordinates obtained from Facial Landmark Detection shown in Fig 2 is used for computing cursor control and for estimating EAR which is explained in Section V. By using this coordinate's, eye tracking which is used for cursor control and blink detection is implemented first. There are different methods for Eye Tracking such as Limbus Tracking, Pupil Tracking etc. Here we are using Limbus Tracking. Limbus is the border of the cornea and the sclera (the white of the eye).

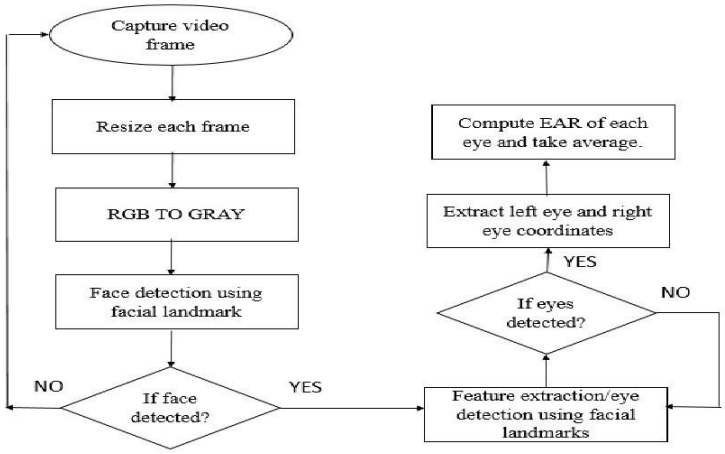

Fig. 3. Algorithm for Eye Tracking

IV. CURSOR CONTROL

Using color tracking method by setting a threshold, Limbus can be differentiated from the white region of eyes. The default position of eyes (pupil at the centre) is stored as initial array. Array obtained by the movement eyes is compared with the initial array and based on this the cursor is mapped. The algorithm for cursor control is shown below:

Algorithm

1) Detection eyes in the image using facial landmark detection and extraction of eye coordinates obtained from facial landmark detection.
2) Convert RGB image of eyes to HSV.
3) Color tracking by setting threshold.
4) Limbus detection using convexhull() in Python.
5) Get eye as array of values.
6) Track the movement of eye by the change in values of array.
7) Compare the newly obtained array with the initial array.
8) Map the array values to the cursor coordinates.

V. BLINK DETECTION

For the application of controlling home appliances, eye blink signals of the user is used which is a natural source of input. After detecting eye coordinates using facial landmark detection, Eye Aspect Ratio (EAR) is computed [5]. EAR is used as an estimate for eye opening state. Here eye is represented by 6 (x, y)-coordinates, starting at the left-corner of the eye and around in a clockwise direction. When the eyes are open EAR is always a constant value and zero when eyes are closed. The ratio falls rapidly to 0 when eyes are closed.

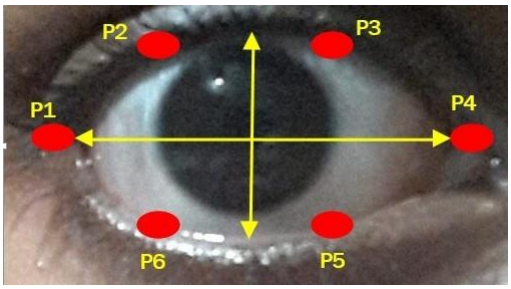

Fig. 4. Calculation of EAR when Eye is in Open state

Steps:

1) Compute the Euclidean distances between the two sets of vertical eye landmarks (x, y)-coordinates (*p2,p6*) and (*p3,p5*)
2) Then compute the Euclidean distance between the horizontal eye landmark (x, y) - coordinates: (*p1, p4*).
3) EAR can be calculated by:

$$EAR = \frac{\|p2 - p6\| + \|p3 - p5\|}{2\ \|p1 - p4\|} \quad (1)$$

VI. HOME AUTOMATION

Automation of household activity such as control of light, fan, other home appliances and security systems in order to provide more convenience, comfort and ease of access for disabled people.

There are mainly three sections in this system:

- Eye blink signal.
- Controller.
- Driver circuit

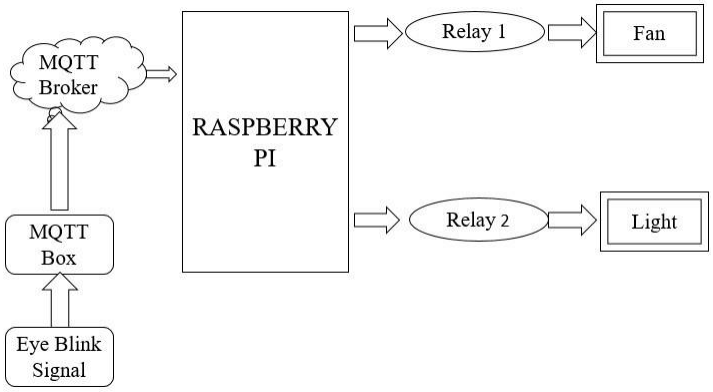

Fig. 5. Block Diagram of Home Automation

The home automation system will control fan, light and other home appliances. The eye blink signal acts as input in real time and send appropriate control signal to the controller. The controller takes appropriate decision based on various sets of inputs and the output of the controller is used to control the appliances. [11]

Program algorithm for initializing the controller- Raspberry Pi

1) Define and declare the output pins connected to Raspberry Pi.
2) Check whether the connection is set and print SUCCESS if set.
3) Create MQTT client with client address, subscription id etc.
4) Subscribe to the topic.
5) Once connection is set receive the payload as inputs.
6) Compare the Payload with a set of predefined strings.
7) Make the two output pin High or Low according to the Payload.
8) If connection is lost print Failed to connect message and display the message and cause.

MQTT (Message Queuing Telemetry Transport) is the communication protocol used [6][12]. MQTT is connectivity proto- col used for IoT applications. It is a publish-subscribe communication protocol. MQTT is used for transmitting short messages at high speed. Here home appliances can be controlled using the MQTT protocol. To connect via MQTT two process should take place Publish and Subscribe.

In this project, the MQTT box acts as the Publisher which publish the message (control signal) to the MQTT broker. The

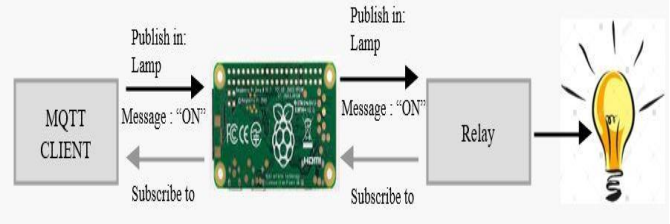

Fig. 6. MQTT Process

received control signal is send to the MQTT client (Relay) and thereby controlling home appliance. Both MQTT Broker and client should be subscribed to the same topic as shown in Fig. 6.

The whole screen divided into two parts (incremented with the no. of application) acting as buttons. When the cursor moves to any one of the buttons and performs the click action by blinking, an event alert pops up for confirmation. Once confirmed, the message lamp on/off or fan on/off is passed accordingly to the server via MQTT.

To publish a message via MQTT:

- Create the client object.
- Create the client connection.
- Publish the message.
- For the publish request, examine the return code.
- Examine the required output in the hardware i.e. Home appliances.

The topic and the payload are the only parameters that are needed to be supplied.

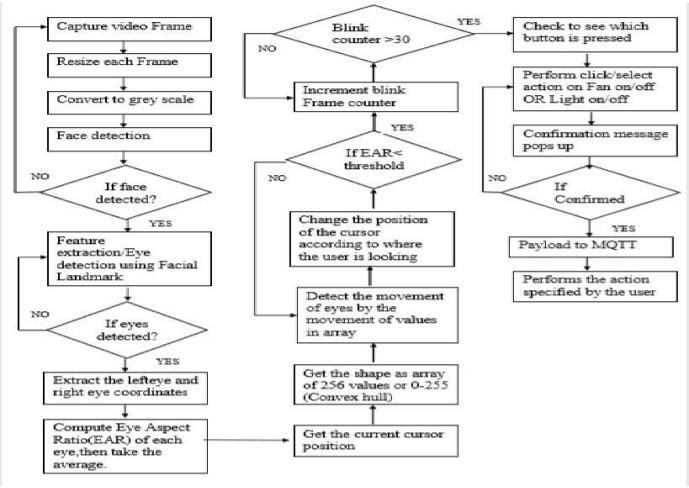

Fig. 7. Algorithm

The overall algorithm of the project is shown in the above figure fig. 7. The project can be divided into mainly three sections:-

- Eye Tracking.
- Cursor Control.
- Interfacing with Home Automation.

According to our application the number of home appliances can be increased and by using MQTT Box it can be controlled from anywhere and at any time.

VII. EXPERIMENTAL RESULT

The system was primarily developed and tested on a Windows 10 PC with an Intel Core i5- 6200U CPU 2.40 GHz processor and an 8 GB RAM. The video was captured with the built-in camera of the laptop. The video was captured at 30 frames per second. The code was written in Python and the code for controller was written in C in Raspbian OS.

Fig.8. shows the face and eye detected image using Facial Landmark Detection. Accurate and real time detection of face and eyes is obtained even if the head is tilted.

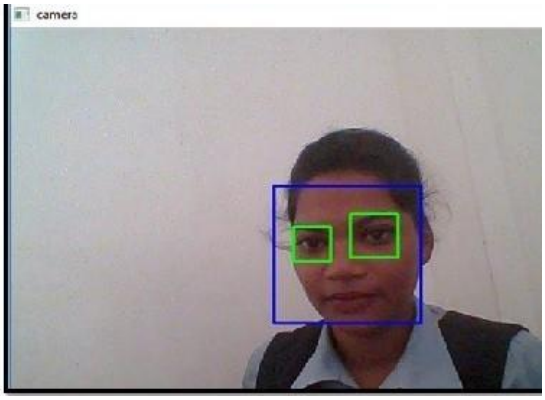

Fig. 8. Face and Eye Detected Image

The Fig.9. shows the result obtained using Facial Landmark. Here by specifying the region of interest i.e. our eyes, contours are drawn using the 6 coordinates obtained in facial landmarks of the eye. By setting a color threshold we can easily track the movement of Limbus and followed by implementing cursor movement.

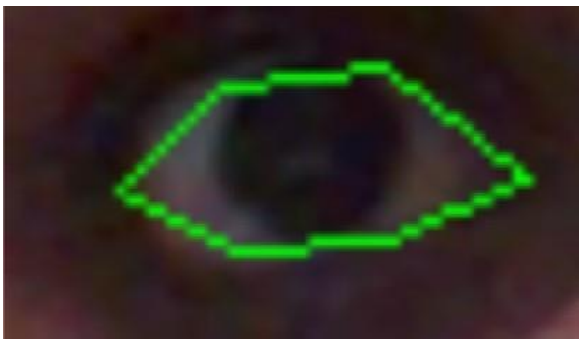

Fig. 9. Eye Contour after Detecting Eyes using Facial Landmark

The following figure is a screen-shot of the MQTTBox. It is a helper program to develop and load test MQTT based clients. The input to the MQTT is the eye blink signal and the advantage of using MQTTBox is that we can enter input manually from anywhere by subscribing the same topic. History of published/subscribed messages for each topic can be

seen through MQTTBox. Thus information's can be accessed from anywhere at any time.

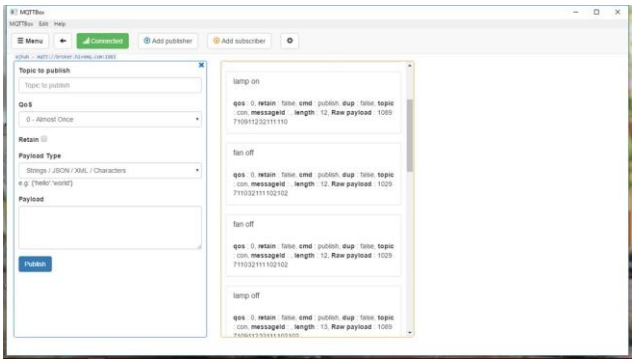

Fig. 10. MQTT Box

The cursor is controlled by tracking the eye movements, blinking performs the click action enabling a pop up message for confirmation. Fig. 11. shows the pop up message for confirmation when a blink is detected.

Fig. 11. Blink detected and select action performed

Finally, when confirmation is given, the payload is published in MQTT and control system responds accordingly.

VIII. CONCLUSION

This paper has presented eye controlled home device for patients where mobility is a point of concern. It is a low cost device for controlling the home appliances using eye movements. The device is based on the acquisition of eye blink signals by the computation of eye aspect ratio. For eye detection, Facial Landmark detection is used which gives more accurate detection than Haar cascade classifiers. This device incorporates the activation and deactivation of Fan and light controlled (can increase the number of home appliances) by eye blink signals.

The main challenge involved in the implementation of the system is the development of a real time eye tracking system. By using the coordinates obtained from Facial Landmark eye tracking was able to implement more accurately and real time processing was also easy.

IX. FUTURE EXPANSION

The project can be extended for detecting emotions and thereby displaying a message or quote to cheer up the user. It can also be used to detect the drowsiness of the user, so that an alarm can be set for safe driving. The project can also be expanded by the implementation of a soft keyboard. By the control action using eye movements, video game can also be played using eye.

REFERENCES

[1] Prashant Salunkhe, Ashwini R. Patil, "A Device Controlled Using Eye Movement" IEEE Trans. Vol. 13, no. 9, pp. 3421-3429, September (2016).

[2] Joseph K George , Subhin K B , Arun Jose ,Hima, "Eye Controlled Home Automation for Disables" IOSR Journal of Electrical and Electronics Engineering (IOSR-JEEE) e-ISSN: 2278-1676,p-ISSN: 2320-3331.

[3] N. L. Fitriyani C. K. Yang and M. Syafrudin, "Real-time eye state detection system using haar cascade classifier and circular Hough transform", IEEE 5th Glob. Conf. Consum. Electron. GCCE, pp. 57, 2016.

[4] Pandey M., Chaudhari K., Kumar R., Shinde A., Totla D., Mali N.D, "Assistance for Paralyzed Patient Using Eye Motion Detection",2018 Fourth International Conference on Computing Communication Control and Automation (ICCUBEA) 2018.

[5] Chatterjee I., Isha Sharma A. (2018). "Driving Fitness Detection: A Holistic Approach For Prevention of Drowsy and Drunk Driving using Computer Vision Techniques",South-Eastern European Design Automation, Computer Engineering, Computer Networks and Society Media Conference 2018.

[6] Upadhyay Y., Borole A., Dileepan D." MQTT based secured home automation system", Symposium on Colossal Data Analysis and Networking (CDAN) 2016.

[7] Djoko Purwanto, Ronny Mardiyanto, Kohei Arai. "Electric wheelchair control with gaze direction and eye blinking", Artif Life Robotics, 14:397400, May 18, 2009.

[8] Akshai P Sajeev, Arshin Salim, Unnikrishnan. R, Aby Abahai T."Cursor Control Using Head and Hand Movement", IJSRSET, Vol 2, Issue 3, P-ISSN : 2395-19902016, 2016.

[9] Gergely Sziladi, Tibor Ujbanyi, Jozsef Katona, Attila Kovari."The analysis of hand gesture based cursor position control during solve an IT related task", 8th IEEE International Conference on Cognitive Infocommunications (CogInfoCom 2017) September 11-14, 2017

[10] Elkamchouchi, Hassan M. and Ahmed M. Elshafee. "Design and prototype implementation of SMS based home automation system." 2012 IEEE International Conference on Electronics Design, Systems and Applications (ICEDSA) (2012): 162-167.

[11] H. Bharathi, U. Srivani, M. D. Azharudhin, M. Srikanth and M. Sukumarline, "Home automation by using raspberry Pi and android application,"2017 International conference of Electronics, Communication and Aerospace Technology (ICECA), Coimbatore, 2017, pp. 687-689.

[12] J. Prabaharan, A. Swamy, A. Sharma, K. N. Bharath, P. R. Mundra and K. J. Mohammed, "Wireless home automation and security system using MQTT protocol," 2017 2nd IEEE International Conference on Recent Trends in Electronics, Information Communication Technology (RTEICT), Bangalore, 2017, pp. 2043-2045.

Proceedings of the Fourth International Conference on Communication and Electronics Systems (ICCES 2019)
IEEE Conference Record # 45898; IEEE Xplore ISBN: 978-1-7281-1261-9

STAVI : Smart Travelling Application for the Visually Impaired

Prerana V
Department of ISE
BMS Institute of Technology & M
Bangalore, India
preranav.11@gmail.com

S Tejaswini
Department of ISE
BMS Institute of Technology & M
Bangalore, India
tjjjaswini@gmail.com

Jasmine Manandhar
Department of ISE
BMS Institute of Technology & M
Bangalore, India
jazz.mdr@gmail.com

Santhosh T K
Department of ISE
BMS Institute of Technology & M
Bangalore, India
kalliguddi.santhosh@gmail.com

Pushpa S K
Professor, Department of ISE
BMS Institute of Technology & M
Bangalore, India
pushpa.sk@bmsit.in

Manjunath T N
Dean, External Relations
BMS Institute of Technology
Bangalore, India
manju.tn@bmsit.in

***Abstract*— The main objective of this paper was to develop a software application for smart phones to help the visually impaired in assisting their daily activities. The approach focused on helping the visually impaired to navigate from a source to destination without any hassle and to avoid multiple rerouting. The above approach was used to ensure that the users no more faced the issues of re-routing and also provides a voice-based feedback system giving information about their surroundings. Furthermore, the proposed approach was carried out with a single voice assisted application where different features such as calling, messaging, emergency help, landmark and bus stop detection along with the main navigation without rerouting. Hence this helped to provide a single interface voice-based system for the visually impaired to perform basic functionalities on a Smart phone efficiently without depending on another human being for constant assistance.**

Keywords—navigation, voice-based, smart phone, calling, emergency, help, landmark detection, bus stop assistance

I. INTRODUCTION

Blindness obstructs an individual from being able to do general day to day activities. The tasks carried out by human with proper eyesight, even the simplest ones can be considered as a complicated task for them that causes inconvenience in daily and social life.

A number of guidance devices were developed to make their life easier. Initially they walked around along with a dog that helped them to guide their way to the destination. Advances in wearable computing, voice recognition, wireless communication, GIS and GPS (Global Positioning System) have made possible to address the visually impaired and disabled navigation problem. There are many electronic devices that are designed to help the visually impaired to navigate safely and independently. Several devices that provide guidance to a remote location that are available currently are either expensive or too difficult to handle.

In today's world, every single person depends on a smart phone in their day to day life for any simple means. But since there are many applications in a smart phone and the person might need to switch in between applications, this project is concerned with a single voice assisted application where in different features are installed that will help the visually impaired. This project is an approach to help the blind people to make their life easier by providing them an application called STAVI that helps them to call, message, seek help, identify landmarks around, navigate without rerouting etc. just by giving voice input commands. The application provides necessary output for the blind in case of a wrong route thus helping them navigate easily.

II. LITERATURE SURVEY

[1] Proposed an effective algorithm to classify the captured into various classifiers and to implement extraction schemes to detect the same. The final implementation is done through ORB – using FAST as detector and BRIEF as descriptor. However, the use of FAST and BRIEF algorithms is not robust when compared to SIFT and SURF algorithms. Effective only image recognition, no mention of voice-based approach to convey the same to the blind. Future Enhancement of the project included currency note identification but was not effective and did not produce results for torn notes. No mention of the way the input was received. Overall the algorithm is focused onto implement object identification but doesn't integrate various functionalities. [2] proposed an application where various modules have been implemented that includes phone battery information, calling, OCR Recognition, GPS module and indoor guidance activity. The power source for the android application is derived through phone battery and the power source for external modules is obtained through a high capacity solar battery. [3] Proposed a system that can be deployed only for OCR and object identification. The same auditory and video interface can be implemented for various purposes like bus stop detection and assistance to cross roads. The system is highly efficient to implement a single module but can be extended to various domains for future enhancement like navigation etc. [5] proposed an android application that enables to call, send and receive texts with the help of an available phone book. It also makes use of the positioning and battery monitoring. When the app is launched, there are 4 main processes. Two of the processes

are for listening for notifications about new text messages and concerning the battery level as well as the process linked with acquiring geographical coordinates. Speech recognizer helps to access the Google Speech recognition module. The TexttoSpeech class monitors the synthesis of the text to speech. The application has a dedicated phone number contact list besides the already available smart phone book. New additions or deletions can be made with the respective voice command. Similarly, calls can be made with notifications about the new incoming messages. However, it doesn't implement GPS navigation would help the person to travel. [6] proposed an application that is based on object analysis and comparison of the scanned objects stored in the file of mobile application using Image Processing and Artificial Neural Network. ADT-Bundle-windows-x86 software is the software used in order to develop this application.

METHODOLOGY:

Understanding the issues present in the existing approach, there was a need to develop an application embedded over a single system. The modules in our system include Calling, Messaging, Map based Navigation, Volunteer assistance in case of an emergency, Landmark detection and Bus Stop detection. In our application, we help the VI navigate from place to another through voice commands. In case the user takes a wrong turn, instead of rerouting through a new route which might be longer, the application's feature states that it is a wrong turn. Also, for the ease of user, landmarks around the current location such as a departmental store or bus stand are constantly given out as voice commands with certain time interval. The application allows the visually impaired to call someone through voice calling. The next feature is when the user has to send a message to anybody in his/her contact list, the user prompts "SMS" and the contact name, the application reverts back asking what the message is and the user can give his/her voice input. When the application is running, it also reads the incoming messages to the user through voice commands. When the user is in danger, the user can give a voice input of help, the nearest volunteer receives a message giving in the user's current coordinates. This provides an extensive and improved methodology to customize to the needs of the visually impaired and hence achieves the objective of the project.

III. IMPLEMENTATION

The Android application is built with a simple UI to avoid complexities and overlapping of layers within the application. The system architecture shown in Fig 3.1 consists of an Android layer, a server to communicate the data between the front end and backend and a database layer that stores the real time values that is retrieved continuously. The system is built on Android operating system and can be implemented on any latest OS versions. The android front-end layer consists of a button that listens to commands provided by the user. The backend is made of an API that takes the required real time values from the system. The communication between the API and the Outer layer occurs through a Server hosted in a domain. To understand the working of the same, the Server can be hosted locally to test the functionalities and the same can be migrated on a cloud platform in future. To push the real time value from the API and to store the data, a database layer implemented using MySQL is used. The server-side script handling and connections to the database is made using Java which runs on the NetBeans IDE.

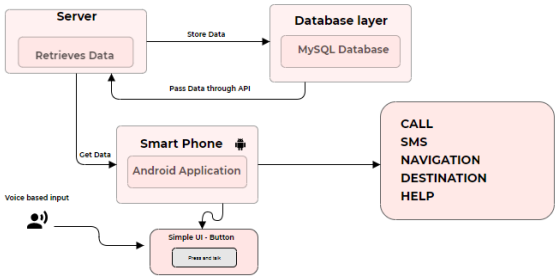

Fig 3.1: System Architecture

MODULE 1: CALLING

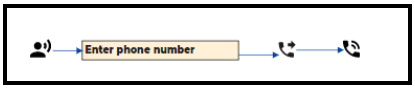

Fig 3.2: Module Architecture – Calling

The UI in Fig 3.2 consists of a Press button that listens to the voice input provided by the user. The user has to configure permissions to the android application that enables the application to access the contacts stored in the phone. Once the user inputs the command "CALL" followed by the number, the Call is automatically redirected to the following person. The voice command is first converted to text and if the text matches the string CALL, the system waits for the user to input the name of the contact and once the command is complete, Call Intent API is used to place a call to the required user. The system checks for the validity of string and only when the string matches the same, Call Intent is invoked. This API places a call from the Android system itself thus providing customization through the STAVI application.

```
(task.startsWith("call")) || (task.startsWith("Call")))

String s[]=task.split(" ");
to=s[1];
for(int i=0;i<StoreContacts.size();i++ )
{

   if(StoreContacts.get(i).toString().startsWith(to))
   {
      String d[]=StoreContacts.get(i).toString().split("\n");
      to=d[1];
      break;

   }

}
call(to);
```

Fig 3.3: Code Snippet – Call

MODULE 2: MESSAGING

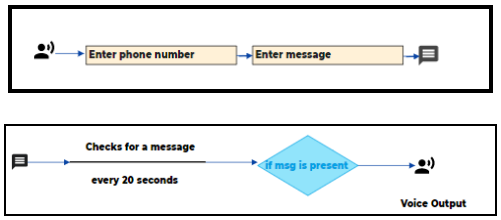

Fig 3.4: Module Architecture – Messaging

The application UI in Fig 3.4 is same as the Calling Feature and it requires a command from the user called "SMS" followed by the number to which the SMS has to be sent. Once the contact details are identified, the system returns with a callback that instructs the user to input the message that needs to be sent. The user then has to prompt the command "MESSAGE" followed by the message. For e.g. to send a message to Alice, the user inputs, SMS ALICE followed by "MESSAGE HOW ARE YOU?"," How are you" is sent to Alice with the same number that is configured to send messages in the android settings. Apart from this, a function call keeps invoking the android system to check if there any messages obtained on the phone at delay of 20s. If a message is obtained during this time interval, the listener detects the change in the event, opens the message and reads the message aloud to the user. To implement the same in android, SEND_SMS permission has to be granted in the application settings. SMS Manager API is used to invoke the Intent that sends the required SMS to the user. The Event Listener that is running in the background checks for the new messages and once the event is invoked, the TTS API is used to convert the message to speech through which the message is read to the user.

```
class check_msg extends AsyncTask<String, Void, String> {
public void onPreExecute() {
}

public String doInBackground(String... args0) {
    try {
        File pictureFileDir =   new File(Environment.getExternalStorageDirectory(), "A");  // getDir();

        String numbers="";
        File f=new File(pictureFileDir + "/msg.txt");
        if(f.exists())
        {
            FileInputStream fis1 = new FileInputStream(pictureFileDir+"/msg.txt");
            byte b1[]=new byte[fis1.available()];
            fis1.read(b1);
            String s1=new String(b1);
            numbers=s1;


        }

        return numbers;
    } catch (Exception e) {
        return new String("");
    }
}
```

Fig 3.5: Code Snippet – Messaging

MODULE 3: VOLUNTEER ASSISTANCE

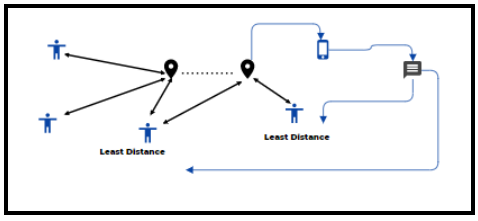

Fig 3.6: Module Architecture -Volunteer Assistance

This feature helps the visually impaired to reach out to a human assistance in case of a medical emergency or travel assistance as shown in Fig 3.6. The database has details of the nearest volunteers or the NGO's present in every geographical area. When the user inputs the command "HELP", the appropriate function call is made, that further queries the database for the nearest volunteer available. Distance formula is used to find the closest distance between the source and volunteer's location. This can be optimized by using Dijkstra's Algorithm. Once the single source shortest path is obtained the distance calculated in the distance formula is pushed on to the tree structure. If a new volunteer is available, the new distance is calculated and compared along with the earlier distance and this new data is pushed to the tree. Once the volunteer details are obtained, an SMS containing the current location is sent along with a default message containing the details of the visually impaired. By this approach the volunteer can access the location of the user and thereby can assist the blind accordingly. To access the location, suitable permissions have to be provided during the configuration settings. A locationManager is set up that invokes Location service. The Location Manager code snippet shown in Fig 3.7 requests the service to get updates of a current location through the service and a Location_Listener is used to update the latitude and longitude accordingly. This updated value is shared across the message to the volunteer.

```
public class  help extends AsyncTask<String, Void, String> {
    public void onPreExecute() {
    }

    public String doInBackground(String... args0) {
        try {

            URL url = new URL(Global.url + "help");
            JSONObject json = new JSONObject();
            json.put("lat",GPSTracker.latitude+"");
            json.put("lon",GPSTracker.longitude+"");
            String response = HttpClientConnection.HttpExecute(url, json);
            String status=response;

            return status;

        } catch (Exception e) {
            return new String("Exception: " + e.getMessage());
        }
    }
```

Fig 3.7: Code Snippet – Help

MODULE 4: BUS STOP DETECTION

Fig 3.8: Module architecture – Bus Stop Detection

The visually impaired often find it difficult to travel in public transport due to lack of information regarding the nearest bus stand and distance between the current location and the nearest bus station. Even after retrieving the bus station information, the visually impaired find it difficult to locate how far the final destination is from the present location. In such cases, the visually impaired usually miss

their destination and find it difficult to reach back to their destination. Therefore, the bus stop feature in our approach helps us to solve this issue as depicted in Fig 3.8. The Bus Stop API takes in values of all the nearest bus stop from the local API, and stores it in the database. A listener in the background provides and audio prompt about the nearest bus stop and how far is the user from the nearest bus stop. Once the user sits inside a bus, he commands the app for "DESTINATION USER_DESTINATION". On checking the destination, the API fetches all the data from maps API regarding all the bus stops on the way to the destination. By doing this the user is aware to when he has to get down.

MODULE 5: NAVIGATION AND LANDMARKS

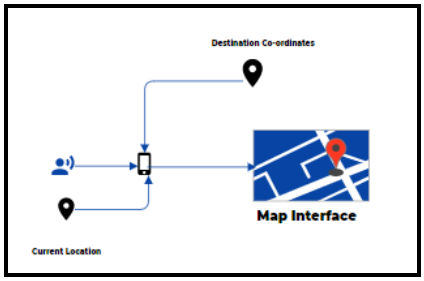

Fig 3.9: Module Architecture: Navigation Assistance

On survey of issues faced by the visually impaired, results of the survey depicted issue regarding navigation with no rerouting. When Google Maps in-built API is used, and the user has to travel from a source to destination, the results are retrieved with multiple routes to the same destination. Once the user starts to travel along a single path and due to circumstances, he moves out of the path, the Google API automatically reroutes itself finding a new path to the same destination. This approach turns out to be disadvantageous for the visually impaired as they are not aware of the routes and if the routes are changed, then they keep rerouting along a new path and often travel longer and tedious routes to reach the destination. In some cases, they end up moving far away from their original destination. Hence a new approach was designed in order to fix a single path between the source and the destination and notify the user when the user takes a wrong route. In order to implement this, the app uses MapMyIndia API that sets a single path from source to destination. The http request shown in Fig 3.10 also has parameters that can specify multiple or single route. If single route is selected, the map sets a single route from source to destination. The source and destination co-ordinates are initially sent to a geocoder function that converts the destination details into map co-ordinates. This is sent along with the Http request made to the API. The API returns with a single route as shown in the Fig 3.11. With this data, the User is prompted continuously providing the details regarding the navigation. In case the user's path does not match the path in the database server, the User is notified with an alert message informing him that it is a wrong route and he has to move back to the old path. The input parameters will be supported in the Route / Driving Directions API request are as below:

1. ***license_key**: the REST API license key allocated to you by signing into our services and registering yourself as a developer (28 Char Alphanumeric).

2. ***Start**: the start (departure) point of the route in WGS-84 coordinates, formatted as (latitude, longitude).

3. ***destination:** the destination of the route in WGS-84 coordinates, formatted as formatted as latitude, longitude.

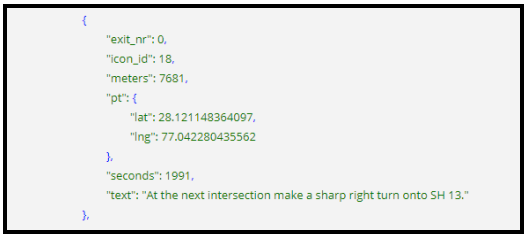

Fig 3.10: JSON format of Http response

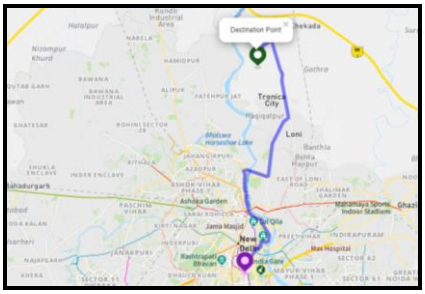

Fig 3.11: Single route selection between source and destination

There is also a continuous feedback provided regarding the nearby landmarks and grocery store to the user. The nearest landmark to the user is retrieved and prompted to the user accordingly.

IV. RESULTS

The application prototype was first developed in Adobe XD to obtain an idea about the working of the project. Using the prototype as the reference, the final application was developed in Android by importing and implementing suitable libraries and packages.

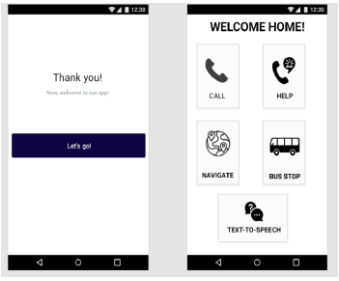

Fig 4.1: Home Page - Prototype

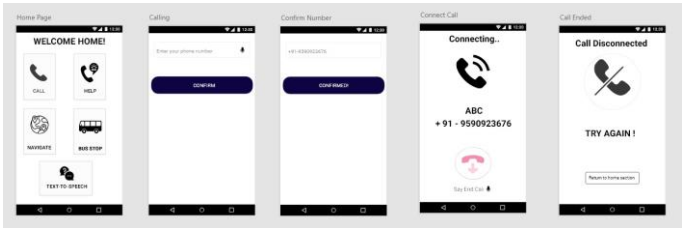

Fig 4.2: Calling - Prototype

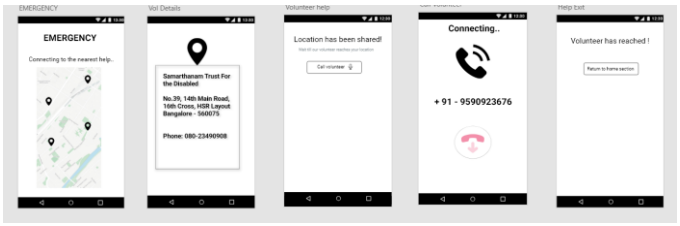

Fig 4.3: Help – Prototype

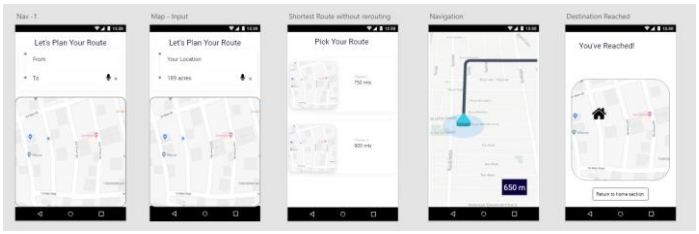

Fig 4.4: Navigation – Prototype

On the basis of the prototype, the final system was developed and the given below are the implementation details of the final system.

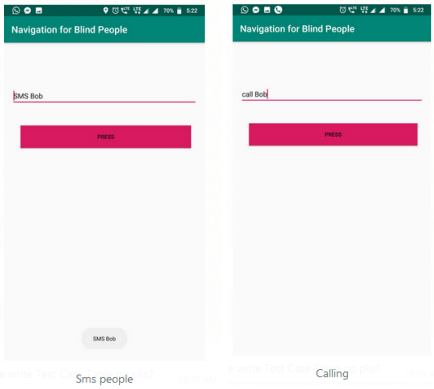

Fig 4.5: SMS and Call features in STAVI

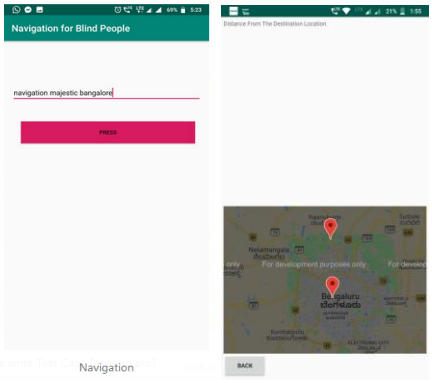

Fig 4.6: Navigation features in STAVI

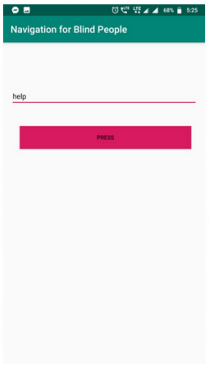

Fig 4.7: Help feature in STAVI

The Fig 4.8 below shows comparative study that STAVI provides variable number of features when compared to other applications.

Lazarillo is an android application that helps the blind to explore the places around and helps to search for category specific locations. This application also helps with navigation of the blind. This application is not efficient and user friendly. The server suddenly stops working.

TapTapSee is an application for the blind which mainly focuses on image identification. It does not provide any help with navigation and travel.

Eye-D provides landmark detection, read text from a document, to live chat with another user. This application is not voice controlled and hence does not help the visually impaired to communicate easily.

Blind Communicator is a communication-based application mainly focusing on SMS, Call, Contact search and Recording facilities. This doesn't not provide any navigation help.

Visually Impaired has 5 basic features: Bluetooth, Call, to run social media applications, Accessibility options and Flashlight none of which help in overall navigation and travel and thus not helpful.

Considering the drawbacks from the above applications, we extract the features that are considered useful for the blind. Thus, STAVI helps to integrate various number of features in a single application and helps to implement the same efficiently.

Applications	Features
Lazarillo	3
TapTapSee	3
Eye-D	5
Blind Communicator	5
Visually Impaired	5
STAVI	6

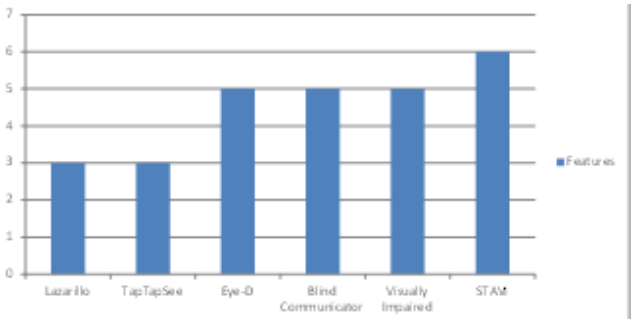

Fig 4.8: Comparison of different applications with STAVI

V. CONCLUSION

Blindness or even partial blindness can cause tremendous difficulties in an individual's life. Even the blind use smartphones to connect to people. With the same idea, the application we have created is focus on helping the visually impaired with the help of smartphones. The application incorporates the use of voice commands to perform different tasks like calling someone or sending an SMS. With the help of this application, the blind can benefit to travel places through voice navigation, gain knowledge about the nearby landmarks and even detect the bus stops when in a bus. The navigation feature also specifies no rerouting function that makes it easier to travel places thus achieving the objective of the project.

Thus, elaborating the comparative study as discussed in the previous sections, STAVI proves to be more efficient with varied number of functionalities when compared to other currently available applications.

VI. REFERENCES

[1] Nada N. Saeed, Mohammed A.-M. Salem, Alaa Khamis, "Android-Based Object Recognition for the Visually Impaired" – 2013 IEEE 20th International Conference on Electronics, Circuits and Systems (ICECS)

[2] Laviniu Tepelea, Ioan Gavrilu, Alexandru Gacsádi , "Smart Phone Application to assist visually impaired people" - 2017 14th International Conference on Engineering of Modern Electric Systems (EMES)

[3] Jing – Zhong Wang , Xiao Hui Guo, Ke Xiao, "Research and implementation of blind reader system on an Android Based Platform" – IEEE 2016 13th International Conference on Wavelet Active Media Technology and Information Processing. (ICCWAMTIP)

[4] Kasthuri R, Nivetha B, Shabana S, Veluchamy M, Sivakumar S, "Smart Device for visually impaired people"- 2017 IEEE Third International Conference on Science Technology Engineering & Management (ICONSTEM)

[5] Piotr Kardyś, Adam Dąbrowski, Marcin Iwanowski, Damian Huderek, "A new Android application for blind and visually impaired people" – IEEE Conference on Signal Processing Algorithms, Architecture, Arrangements an Applications

[6] Shruti Parkhi, Dr.S.S.Lokhande and N.D.Thombare, "Vocal Vision Android Application for Visually Impaired Person" - International Journal of Science, Engineering and Technology Research (IJSETR) Volume 5, Issue 6, June 2016

[7] Jin-hee Lee, Sang-Chul Lee, Kyeongyul Kim, and Byeong-Seok Shin, "Smart Backpack for Visually Impaired Person" - International Conference on ICT for Smart Society-IEEE, June 2013.

[8] Zewen Li, Gang Luo and Shrinivas Pundlik, "Stabilization of Magnified Videos on a Mobile Device for Visually Impaired", IEEE Conference on Computer Vision and Pattern Recognition Workshops, 2013.

[9] Varit Prudtipongpun, Thorntita Rattanapongsen, Wirawan Buakeaw and Mingmanas Sivaraksa, "Indoor Navigation System for Vision-impaired Individual", IEEE-International Conference on Signal-Image Technology & Internet-Based Systems (SITIS), 2015.

[10] David Zhou, Hanbing Yan and Yonggao Yang,"A smart "virtual eye" mobile system for the visually impaired", IEEE Potentials, 2016.

[11] Yong CHUNG, Kang Hyeon RHEE and Sanghag Kim," The Smart Cane Utilizing a Smart Phone for the Visually Impaired Person", IEEE 3rd Global Conference on Consumer Electronics (GCCE), 2014.

[12] Eduardo Ghidini, Isabel H. Manssour, Wagner D. L. Almeida and Milene S. Silveira," Developing Apps for Visually Impaired People: Lessons Learned from Practice", 49th Hawaii International Conference on System Sciences, 2016.

Proceedings of the Fourth International Conference on Communication and Electronics Systems (ICCES 2019)
IEEE Conference Record # 45898; IEEE Xplore ISBN: 978-1-7281-1261-9

Location Based Cluster Head Selection for Wireless Sensor Networks

Rudramurthy V C
Asst Prof, Dept of CSE
Global Academy of Technology
Bengaluru, India
murthyvc.83@gmail.com

Dr. R Aparna
Professor, Dept of ISE
Siddaganga Institute of Technology
Tumakuru, India
raparna@sit.ac.in

***Abstract*-- A state-of - the-art computer network innovation is the Wireless Sensor Network (WSN). Collection of antenna nodes is known as sensor networks. These nodes co-operatively send detected statistics to base station (BS). Thousands of tiny sensor nodes are present in these networks. The WSN networks are controlled with power, memory and computing. In WSNs mainly testing chore is life time of the nodes. The exchange of information from source node to a destination through correspondence channel assumes a noteworthy job in the lifetime of the nodes. So with the help of proper routing protocol, we can boost the survival of the network. Clustering is a type of routing algorithm. By means of clustering, we can prolong the liveliness intensity of the sensor nodes. This increases the lifetime of the sensor nodes. In many clustering algorithms, the selection of the cluster head will play a very vital role and also the location of the cluster head within the cluster plays a foremost role. In this paper, we are proposing a system for choosing a cluster head from a particular location within the cluster that helps other nodes to communicate with the cluster head without consuming much energy. The proposed technique is contrasted and the current strategy with the assistance of simulation.**

Keywords*—*Wireless Sensor Networks, Cluster, Cluster Head, Vice Cluster Head.

I. INTRODUCTION

A Wireless Sensor Network (WSN) is a remote system comprising of spatially dispersed independent contrivances utilizing sensors [1]. These sensors are used to examine physical or ecological conditions. Figure 1 shows simple WSN.

Nodes are conveyed intently in the remote land arrange. Each sensor node is characterized by a set of limited resources.

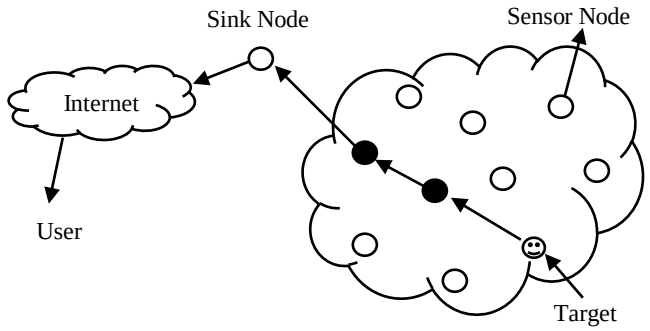

Figure 1 Wireless Sensor Networks

They will sense the surroundings and collect the data from the environment based on the sensing device configuration. Radio sign are utilized to convey with the sensor in the remote sensor arrange. The sensor nodes will process the sensed data and transmit the same thing towards the Sink Node (SN) or Base Station (BS). The main constraints of the WSN are energy, the network bandwidth and routing. These sensor nodes are fueled by batteries. The recharging of the batteries of sensor nodes is not possible, since they are deployed in remote and unattended geographical locations. So energy plays a very imperative part in the existence of the sensor nodes. Energy efficiency is significant to boost the lifetime of WSNs, much more should be focused on energy consumption and the energy utilization must be balanced among sensors. Different techniques have been used in WSN in order to resolve not all constraints together, but one specific constraint at a time. Much research work has been going to decrease the energy consumption in sensor nodes. In such manner, there is a need of better convention which chips away at vitality protection idea and accordingly builds the general lifetime and execution of the system required.

In this paper, we are proposing a cluster head selection technique for a cluster without consuming much energy.

QUALITIES OF WSN

The primary qualities of WSN include:

- Power use imperatives for sensor nodes utilizing batteries.
- Nodes mobility
- Heterogeneity in nodes
- Capacity to endure cruel ecological conditions
- Usability
- Scalability to large scale of consumption
- Capacity to adapt to hub failures
- Production Costs

APPLICATIONS OF WSN

WSN has numerous different applications [3].

- Monitoring the traffic
- Detection of fire
- Nuclear reactor control
- Environment monitoring

- Acoustic recognition
- Military observation
- Monitoring in medical area
- Environmental air, water and soil tracking
- Industrial machine tracking
- Asset tracking
- Building and bridge structural surveillance

The rest of the paper is sorted out as pursues. Division 2 explains the obstacles and design issues in WSNs. The clustering is described in division 3. Literature survey is explained in sector 4. Segment 5 discusses the proposed technique for the cluster head selection. The simulation results are discussed in part 6. The conclusion of the paper clarified in sector 7.

II. Obstacles and Design issues in Wsn

Many margins are in WSNs compared to other networks. The restrictions while designing the WSN are as follows [4]-[6].

- **Wireless in standard**: The wireless medium is in nature fewer secure. The remote medium enables an assailant to just catch any legitimate parcels and effectively embed the malevolent ones.
- **Restricted Resources**: All safety efforts require an exact measure of belongings for the attainment, together with information memory, system space, and vitality to manage the sensor gadgets.
- **Power Limitation**: Energy must be preservedin the sensor nodes after deployment to improve the duration of the individual sensor nodes.
- **Managed Remotely**: detection of the physical tampering in the sensor network is practically impossible due to remote supervision.

There are some problems present during designing the WSN. They are listed below

- **Data Integrity**: Ability to watch that the message has not been adjusted while it was on the framework.
- **Data originality**: Ability to receive the new messages not the old ones.
- **Data Confidentiality**: Secrecy guarantees that a given message can't be comprehended by anybody other than the favored beneficiaries.
- **Self-Organization**: Fixed infra-structureis not available in sensor network to manage effectively.

Energy utilization is the most noteworthy aspect to decide the existence of a sensor organizes on the grounds that generally nodes are driven by battery. The streamlining should be possible by having vitality cognizance in each part of plan and activity.

Various sorts of calculations and conventions are being concentrated to diminish the generally energy use of the sensor networks.

Nodes talk by methods for remote, lossy lines with no establishment. An additional go up against is identified with the confined, as a rule non-reasonable power source supply of the nodes. To construct the lifetime of the framework, the shows ought to be organized from the most punctual beginning stage with the ultimate objective of profitable supervision of the essentialness resources. The wireless protocol we select depends on the purpose necessities.

III. Clustering in WSN

Distribution of nodes to make into teams is thought as clustering [Figure 2]. There are so many clustering algorithms already present [7, 8].The group of sensors is cluster. The cluster is headed by a node is called Cluster Head (CH). The CH is in charge for collecting the cluster members ' information along with transferring the full information to the Base Station (BS). A number of variables influence the efficiency of the cluster, namely energy, network lifetime, delay in electing the cluster head and so on. Network's lifetime relies on the power of the sensors. The power will be utilized for data processing and transfer. If many nodes are sending the same data, there will be lot of redundant data in the network. By using the concept of the Aggregation, redundancy can be eliminated.

Advantages of using Clustering concept

- Redundancy can be decreased using data aggregation.
- Automatic recovery from failure.
- Channel contention and packet collision can be scale down by using clustering.

Disadvantages

- Determination of cluster head in each round.
- Energy consumption for forming a cluster.
- Sensor nodes close to BS lose their power very soon.

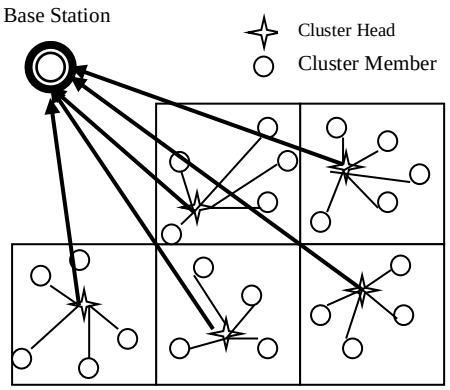

Figure 2: Clustering in WSN

Cluster routing technology has lot of advantages against other routing techniques. Because of this, it is used in most routing techniques in WSN. Clustering can decrease the energy consumption by localizing the statistics traffic.

The CH will accomplish the group information aggregation. CH will take the data from the nodes present in the group. This CH will total the data got from sensors. The aggregated information is sent to the BS. The reliability of the network depends on the CH functionality. In the event that the CH isn't working fine, it influences the entire system execution.

IV. LITERATURE SURVEY

There are many benefits from Clustering of sensor nodes. Clustering promotes network-wide sharing of control. Clustering uses the region of communication to condense the power used in the network. Sensor nodes communicate their information over nearest cluster head. The cluster head will aggregate the information and forwards to the BS.

Sabrine-Khriji et al. [9] have proposed a REDA predicated on the idea of prototype production. The model is precise to the data sensed and utilizes conditional data collected from nodes in consecutive iterations. The REDA wipes out the dissemination of the superfluous information from the sensor hub to group head.

J.K.Deepak Keynes et al. [10] have proposed a cross energy proficient scattered clustering method (CC-LEACH) for crowded WSN. The CC-LEACH demonstrates a lessening in packet fall, power burning up and end-to-end latency for thick WSNs. The simulation findings indicate an increase in the performance, packet shipping ratio with quantity of packets acknowledged at the BS.

Kushal B Y et al. [11] have proposed to enhance the vitality dissemination by altering the group head choice methodology in LEACH calculation and evade the vitality opening issue considering versatility to the sink hub which draws out the lifetime of whole system.

Yasha Istwal et al. [12] proposed the twin CH routing practice with super node having CH with four levels of heterogeneity to pick up the lifetime of a WSN. The goal is to lessen the quantity of choice of CH with the goal that vitality utilization can be limited. The outcome demonstrates the improvement in the lifetime of the system by utilizing the changed LEACH technique.

Lohit B.Dalal [13] proposed an Efficient Dynamic Deputy Cluster Head Selection [EDDCH] that is used to solve the problem of difficult cluster head selection. Efficient vibrant deputy cluster head selection is performed in view of energy level of the node. The node with upper vitality level is picked as cluster head and node with next dimension is delegate group head. Group head gathers the data from part nodes and deputy cluster head moves this data to BS. The simulation examination describes that the projected technique will overcome the imbalance of energy usage, thereby improves the network lifetime.

In [14] Vipin et al, projected a straight forward and well-organized CH selection called SCHS. In SCHS, the territory is isolates into two sections, periphery and internal zone. The hubs present in the internal region will take part in the cluster head determination. SCHS diminishes the intra-group correspondence separation and subsequently improves the vitality adequacy of cluster.

Zhang Ming [15] proposed an associate CH clustering technique based cluster grading (ACHC-CG) in WSNs. The There are three characteristics of ACHC-CG. Initially, divide cluster into grades based on density of the nodes. Secondly, the assistant CH generated based on the created dependent on the rest of the vitality and transmitting separation. This CH is accountable for exchange data between neighbors CH, while main CH is liable for getting sensing data in cluster and processing to diminish energy exploitation of head to drag the lifetime of the network. The simulation result shows prolonging the network lifetime.

K.R.Anu Priyanka et al. [16] proposed a dynamic cluster head election mechanism in which each sensor node compares its residual energy with other nodes. Depending on the left over energy, CH is selected. The simulation shows the increasing the overall lifetime and throughput compared to single level of clustering.

Hai Lin et al. [17] proposed a latest clustering method called DDEC to advance the network efficiency. The DDEC scheme divides the structure into groups with a similar amount of parts to adjust the burden. The group head is chosen in the bunch dependent on residual vitality, separation and thickness. This strategy accomplishes to reduce the intra-group correspondence cost and broadens the system lifetime.

V. PROPOSED APPROACH

Energy efficiency in wireless sensor networks is very important while routing. An opportunistic routing protocol in any network is one of the solutions to increase network lifetime through the use of dynamic routing decision. They will route the network by taking dynamic decisions based on the network conditions.

In Cluster based routing approach, CH selection will play an imperative role for power competence of clustering algorithms. Intra-cluster correspondence relies upon the situation of the cluster head and correspondence vitality relies upon the separation factor. Intra-cluster correspondence includes every one of the nodes and thus much vitality is required for intra-cluster correspondence.

An efficient CH selection technique is required for energy competent communication in cluster. Sensor nodes in nature have small storage circuitry. Computing sensors is highly energy-intensive.

The proposed model protocol has some assumptions. All sensor hubs are homogenous and are stationary. These hubs are area mindful. Just one BS is available exterior the field.

Nodes are unilaterally installed in the field. The complete field is split into two divisions in the suggested system [14]. One is outside, and the other is inside. The division of cluster is revealed in figure 3. Let‘d’ is the distance for partition of pasture. Zone beginning from limit of the field up to the distance'd' is border area and left over zone is called inner area. The number of nodes present in the inner area and border area depend on the value of‘d’. The nodes in the boundary region will not take room in the choice of CH. For CH choice, the nodes in the internal area will be identified. The boundary

zone nodes in each round are always aspect of the participant nodes. The CH is always taken from the nodes' internal region. Ergo, the CH will always be proximate to the core of the cluster. This technique will use less energy for intra-cluster communication.

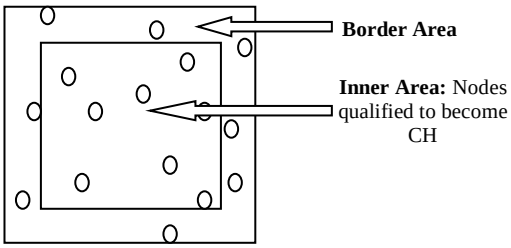

Figure 3: Division of Cluster

In many clustering calculations, the race of the cluster head is done enthusiastically dependent on the remaining vitality. Another CH must be substituted when the CH energy crosses the limit level. Selecting a fresh CH involves lot of power utilization. To lessen the overhead of choosing another cluster head, a reinforcement node must be available in the group which can go about as a cluster head. The backup cluster node is known as ***Vice Cluster Head (VCH).***

In the existing methods, the assistant/vice CH [13, 15] is elected while electing CH. Every cluster will have the CH and assistant / vice CH in this idea. In this concept, any node in the cluster may contest for CH or assistant/vice CH selection process. If the node is present in the border of the cluster, all member nodes have to communicate with the cluster head which leads to more energy consumption due to distance issue.

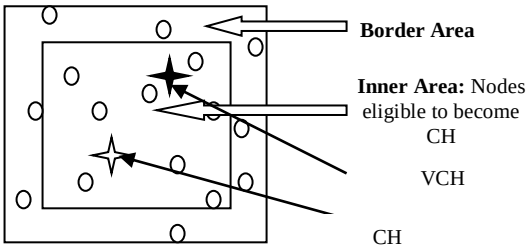

Figure 4: Selection of CH

This can be overcome by limiting the nodes based on node location in the clusteras shown in figure 4. So as to constrain the nodes taking an interest in cluster head choice procedure, we can permit just those nodes inside the internal zone to take part in cluster head choice procedure. Only nodes present in the inner area of the cluster will get chance to become cluster head. Same tactic can be used for the choice of the vice cluster head. If we select the CH / vice CH from the inner area, they will always be nearer to center of the cluster. This decreases the quantity of energy that other nodes need to interact with the cluster head, as all nodes in the cluster are nearly equidistant from the CH.

VI. Simulation Results

A sensor network is used for simulation purposes. The sensor network consists of ***n*** nodes and they are randomly dispersed. All the sensor hubs are considered to have equivalent measure of vitality at first. NS-2[19] is used for the simulation purpose. The location of the sink node is outside the sensing field. Only one sink node is present in the network.

The area used for simulation is 1000X1000 m^2, 1000 sensor nodes are used for simulation. preliminary energy of each node is considered as100J and sensing power is 0.0175J. The power used for transmitting and receiving is 0.9J and 0.8J respectively.

The proposed scheme is compared with the Dynamic Cluster Head Selection Method (DCHSM) [18]. Figure 5 shows the comparison of the planned scheme with DCHSM scheme with respect to packet delivery ratio.

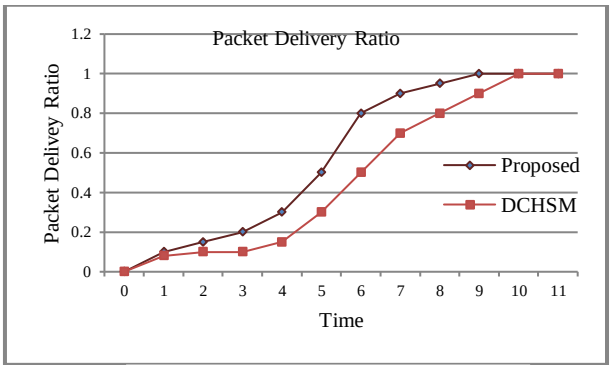

Figure 5: Packet Delivery Ratio

Throughput is defined as successful packet delivery rate in bits per seconds. Figure 6 demonstrates the comparison of the suggested method's performance with DCHSM [18]. Figure 7 demonstrates the comparison between the technique proposed and DCHSM [18] with the amount of active nodes in distinct rounds.

The visualization analysis shows that the packet delivery ratio is enhanced in the suggested proposal as all nodes in the cluster are almost equitable to the CH. Since energy consumed for transmitting and receiving the data is less as compared to the scheme proposed in [18], there will be more nodes active for longer duration than the nodes in the scheme proposed in [18] and also cluster head selection process is not carried out frequently as vice cluster head is available to act as cluster head

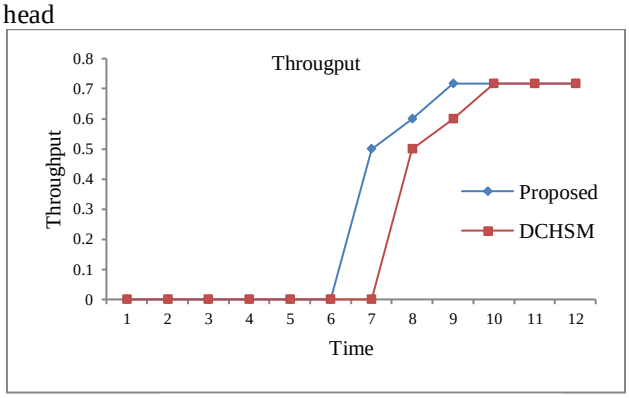

Figure 6: Throughput

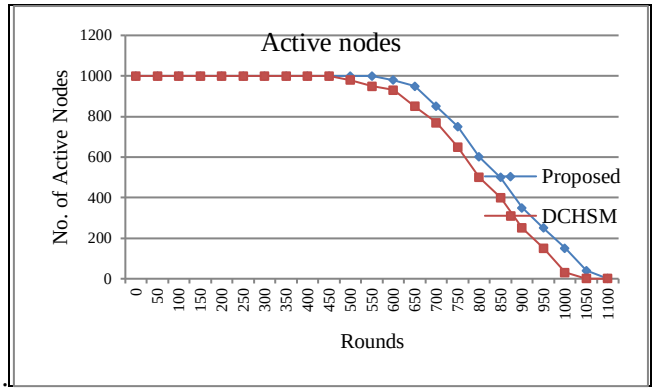

Figure 7: Active nodes

VII. CONCLUSION

Wireless Sensor Network (WSN) is possible future for many applications. This paper discussesthe advantage of selecting a vice cluster head along with a cluster head and the routing concepts in WSN. It is observed that the clustering routing technique can be strengthened. CH choice is a major problem for clustering schemes' power effectiveness. In this paper, the cluster area is alienated into border area and inner area. The CH and VCH choice is held for the nodes present in the internal zone of the cluster. This allows only the nodes current in the cluster middle to become a CH and in turn decreases the energy level needed for other nodes in the cluster to interact with the CH. The results of the simulation display that the packet delivery ratio is strengthened and the energy demand for transmitting the data is lowered relative to the Dynamic Cluster Head Selection Method.

REFERENCES

[1] Akyildiz, I.F. Weilian Su Sankarasubramaniam, Y. Cayirci, E. Georgia , "*A survey on sensor networks*", IEEE communication magazine,Vol.30,No.8,pp. 102 – 114, 2002.

[2] D. Estrin, R. Govindan, J. Heidemann, S. Kumar, "*Next century challenges: scalable coordination in sensor networks*", ACM MobiCom'99, Washington, USA, 1999, pp. 263–270.

[3] Dr. Manoj Kumar Jain,"*Wireless Sensor Networks: Security Issues and Challenges*", Volume 02, Issue 01, Manuscript Code: 110746, IJCIT,2011.

[4] Yong Wang, GarhanAttebury, and Byrav Ramamurthy, "*A Survey Of Security Issues In Wireless Sensor Networks*", IEEE Communications Surveys & Tutorials, Volume 8, No. 2, 2nd Quarter 2006.

[5] Idrees S. Kocher, Chee-Onn Chow, Hiroshi Ishii, and Tanveer A. Zia, "*Threat Models And Security Issues In Wireless Sensor Networks*", International Journal Of Computer Theory And Engineering, Vol. 5, No. 5, October 2013.

[6] Jyoti Shukla, BabliKumari, "*Security Threats and Defense Approaches In Wireless Sensor Networks: An Overview*", International Journal Of Application Or Innovation In Engineering & Management (IJAIEM), Volume 2, Issue 3, March 2013.

[7] A. Abbasi and M. Younis, "*A Survey on Clustering Algorithms for Wireless Sensor Networks*",Computer Communication, Vol. 30, No. 14-15, 2007, pp. 2826-2841.

[8] D. Wei and H. Chan, "*Clustering Ad Hoc Networks: Schemes and Classifications*",Proceedings of the 3rd Annual IEEE communications Society on Sensor and Ad Hoc Communications and Networks, Reston, 28 Septem-ber 2006, pp. 920-926.

[9] SabrineKhriji, GuillemVinasRaventos, Ines Kammoun and OlfaKanoun, "*Redundancy Elimination for Data Aggregation in Wireless Sensor Networks*", 2018 15th International Multi-Conference on Systems, Signals & Devices (SSD), YassmineHammamet, Tunisia, Tunisia.

[10] J. K. Deepak Keynes and Dr. D. ShaliniPunithavathani, "*Clustering Methodology to Prolong Lifetime in Wireless Sensor Networks*", International Conference on Information, Communication and Embedded Systems (ICICES 2017).

[11] Kushal B.Y and Chitra M." *Cluster based routing protocol to prolong network lifetime through mobile sink in WSN*", 2016 IEEE International Conference on Recent Trends in Electronics, Information Communication Technology (RTEICT), pp. 1287–1291 (2016).

[12] Yasha Istwal and Shashi Kant Verma, "*Dual Cluster Head Routing Protocol with Super Node in WSN*" Wireless Personal Communications, January 2019, Volume 104, Issue 2, pp 561–575

[13] Lohit B. Dalal, "*An Efficient Dynamic Cluster Head Selection Method for Wireless Sensor Networks*" International Research Journal of Engineering and Technology (IRJET), Volume 05, Issue 12, Dec 2018.

[14] Vipin Pal, Girdhari Singh and Rajender Prasad Yadav, "*SCHS: Smart Cluster Head Selection Scheme for Clustering Algorithms in Wireless Sensor Networks*", Wireless Sensor Network, 2012, 4, 273-280, http://dx.doi.org/10.4236/wsn.2012.411039 Published Online November 2012.

[15] Zhang Ming, "*Assistant Cluster Head Clustering Algorithm based on Cluster Grading in Wireless Sensor Networks*", Journal of Applied Sciences, vol. 13, issue 10, pp. 1858-1864

[16] K.R.Anu Priyanka and R. Jaya, "*Improved Dynamic Cluster Head Election using Wireless Sensor Network*", International Journal of research in Engineering, Science and Management, Vloume 2, Issue 1, January 2019.ISSN (Online):2581-5792.

[17] Hai Lin, RongXie and Lanning Wei, "*Density, Distance and Energy based Clustering Algorithm for Data Aggregation in Wireless Sensor Networks*", 2017 IEEE/CIC International Conference on Communication in China (ICCC).

[18] DongyaoJia, Huaihua Zhu, Shengxiong Zou, and Po Hu, *"Dynamic Cluster Head Selection Methodfor Wireless Sensor Network",* IEEE Sensors Journal, Vol. 16, No. 8, April 15, 2016, pp 2746-2754.

[19] K. Fall and K. Vardhan, "*The Network Simulator NS-2*". http:// www.isi.edu/nsnam/ns/

Proceedings of the Fourth International Conference on Communication and Electronics Systems (ICCES 2019)
IEEE Conference Record # 45898; IEEE Xplore ISBN: 978-1-7281-1261-9

Analysis of Single-Stage Boost Inverter for Renewable Energy Generation System(REGS) in Discontinuous Conduction Mode(DCM)

Dolly Murodia
Department of Electrical Engineering
Rajasthan Technical University
Kota (Raj.)
dolmurodia@gmail.com

Dr. Ashok Kumar Sharma
Department of Electrical Engineering
Rajasthan Technical University
Kota (Raj.)
aksharma@rtu.ac.in

Sawan Singh
Department of Electrical Engineering
Rajasthan Technical University
Kota (Raj.)
sawansingh19@gmail.com

Abstract: **New technologies are expected to lower the investment and reduce cost. Fuel cell generation technologies are now on the verge of being introduced commercially and delivered to market and it might become eminently fuel-efficient and more economical to generate electricity than present utility grid. Unluckily, comprising the systems for power generation from fuel cell have single-phase inverters which draw low-frequency current ripple at twice the output frequency from the fuel cell which may create instability, low efficiency, and lifetime duration of fuel cell stack is shorten. Research in this paper focused on single-stage boost inverter topology with the function of low frequency current ripple (LFCR) reducing to recognition quantity. In addition, present system consists of hybrid switched-inductor step up converter and full bridge inverter which shares a bridge-arm with the converter. The current of boost inductor is designed to work with discontinuous conduction mode (DCM) and analyzed the LFCR in fuel cell output current. The circuit layout, simulation results and performance analysis of 1.26kW/24Vdc, 12kHz are shown to demonstrate theoretical study.**

Index-Terms:-Hybrid-Switched-inductor,Single-stage,Low frequency current ripple(LFCR), Discontinuous conduction mode.

I. INTRODUCTION

Consumption of conventional energy is rising rapidly but sometimes it exhibit uncertainty and discontinuity and also give direct effect on utility grid, if the grid couple inverter used in REGS. Concept of microgrid put forward by researchers which can improve reliability, safety, stability and power supply quality.

Energy storage devices such as fuel cells have various advantages as compared to conventional sources. The direct methanol fuel cell (DMFC) and proton exchange membrane fuel cell (PEMFC) have low-temperature, low heat transmission which makes them ideal for various application [1],[2]. By considering cost issues, the fuel-cell voltage is gradually lesser than 40Vdc and it is boosted up to high voltage of 180-200Vdc for DC to AC inverter [3].

The utmost voltage ratio is broad to 10 times in this state. The orthodox boost converter cannot encounter this requirement owing to the fact that the set off duty ratio in boost converter is close by 1 and urge to high current ripple with less effectiveness.

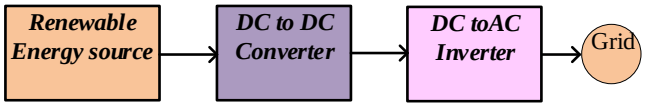

Fig.1 Block diagram of traditional two-stage conversion system

For distribution of power, a grid coupling converter is required for fuel cell system to supply power to grid but having one snag is that the lifetime duration of fuel cell stack is shorten with the ripple current. Thus, in sequence to expand the life duration, the fuel cell ripple current obliged to be diminish in the grid coupling converter [4]. There are various methods to mitigate the current ripples such as by improving control methods like use of active control methods with dual-loop control or with adding hardware circuit [5]. One more method is available to reduce LFCR is through waveform control method [6]. There are several disadvantages of these types of method. Sometime its hard to design the closed control loop which leads to complicate the circuit. Different topologies are mentioned like two-stage power conversion where the front stage is DC to DC converter and the later one is a full bridge inverter [7],[8] which leads to lower the efficiency and controllers are also hard enough to design. The LCL filters are

used in grid couple inverter utilization and is a third order filter which furnished more dense and streamlined designs[9],[10].

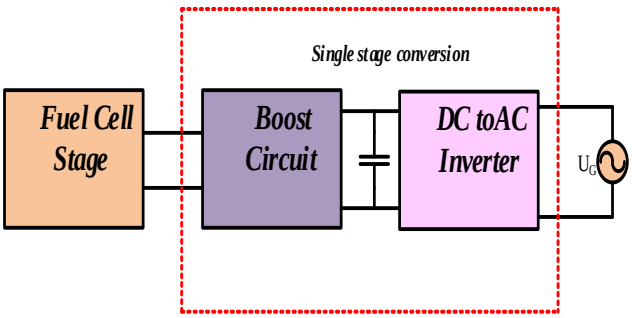

Fig.2 Block diagram of fuel cell based single-stage system connected to grid

Therefore, A new topology where a single-stage boost grid tied full bridge inverter with hybrid switched inductor for fuel cell power generation in discontinuous conduction mode is introduced. The main objective of the proposed inverter is to reduce the current ripple at dc side. It is clearly exemplified in this paper that the projected inverter overall improves the performance of the system.

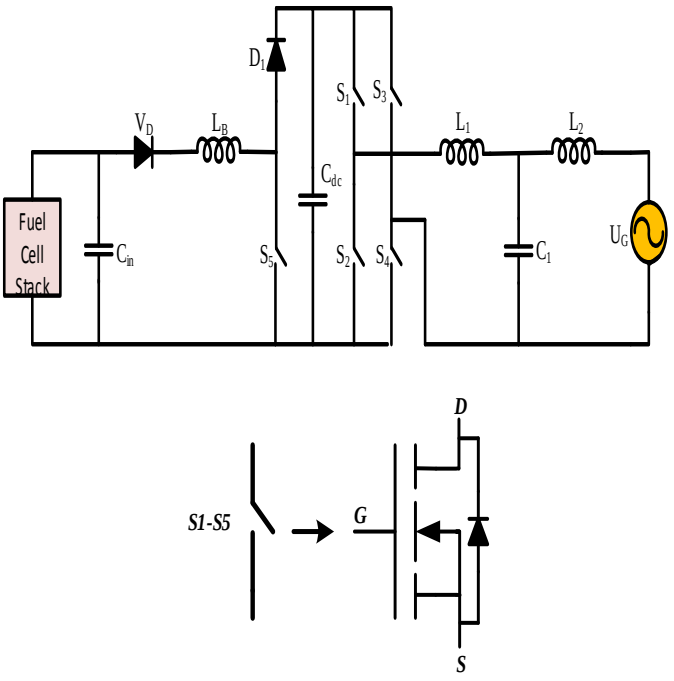

Fig.3 Classical two-stage inverter

This paper is straightened out as follows: Section II furnish the topology of projected inverter. Section III displays the control strategy of system. Parameters design is presented in section IV. In Section V simulation model and verification is displayed. Finally, conclusion and future scope of projected inverter is subsidized in Section VI.

II. SINGLE-STAGE TOPOLOGY

A. *Topology of the projected inverter*

Fig. 1(a) shows a two-stage traditional topography for renewable energy generation system (REGS), such as fuel cell, where the slightest input voltage U_{in} is not so much than the grids peak voltage.

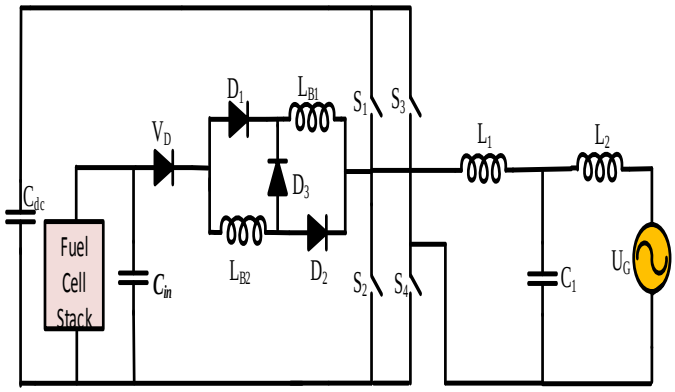

(a)

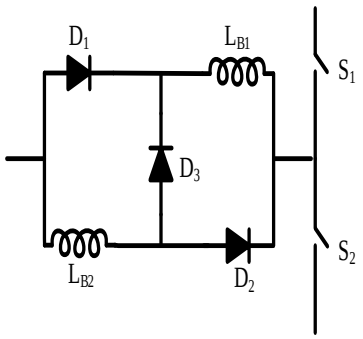

(b)

Fig.2 Proposed topology: (a) Proposed boost inverter (b) Hybrid switched inductor

The first stage is boost converter & the later stage is inverter with full bridge topology which consist of four MOSFET switches S1-S4. The advantage of conventional two-stage is that it can be controlled easily & separately but has one disadvantage of low efficiency. In proposed topology, the system consists of single stage power conversion where the fuel cell stack used as a DC source, hybrid switched inductor IL_{B1} and IL_{B2} is connected to one leg of full bridge inverter which consist of MOSFET switches. This topology is used as it helps to decrease the cost of the system & also increases efficiency as compared to the traditional two stage conversion system. The current across the fuel cell that is input LFCR is also reduced to minimum limit by the control method.

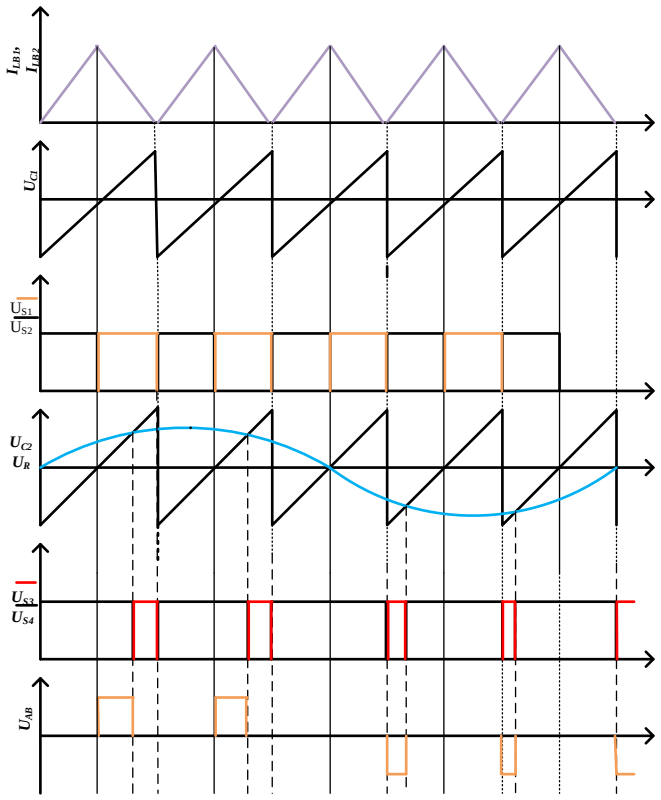

Fig.3 Main waveforms of switches and inverter output

In fig.3, main waveforms of switches are displayed where switching of Switch S_1 and Switch S_2 are retrieved by $U_{cr(carrier\ wave)}$ while switching of another 2 switches are retrieved by comparing U_{cr} with $U_{r(sine\ wave)}$. U_{AB} is the output waveform of inverter.

The boost inductors current IL_{B1} & IL_{B2} should be controlled to reduce current ripple at low frequency. There are several methods to decrease current ripple such as designing resonant controller, waveform method etc. The main disadvantage of these methods is it is so complicated to design. Hence to avoid this, the foresight time of switch S1 and switch S2 is set to half of the switching cycle. The duty ratio of boost circuit is 0.5. The output current of inverter is controlled by SPWM (Sinusoidal Pulse Width Modulation) [12]. The signals for switch S3 &S4 are given by comparing carrier signal U_c & reference sine signal U_r. The output voltage of proposed inverter is also obtained as unipolar SPWM.

The grid current should be in resonant condition with the grid voltage for steadiness purpose. It can be represented for different conditions. Here, $I_{L1}<0$, $U_g<0$ is taken.

For simplification commutation time and dead time of switches are ignored. The key waveforms of operation is shown in fig(4).

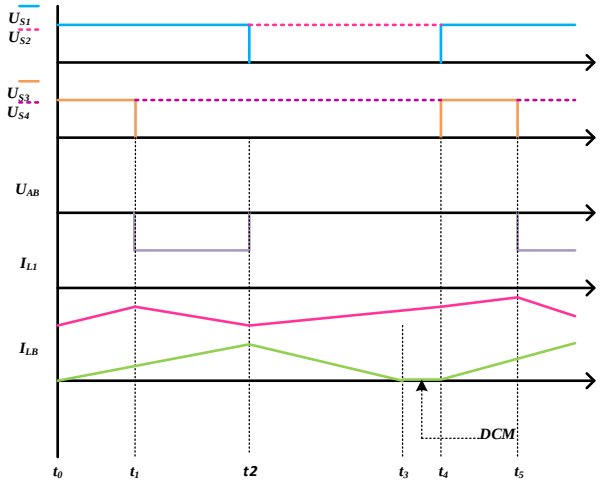

Fig.4 Operation waveforms when $IL_{1<}0, U_{g<}0$

III. CONTROL STRATEGY OF SYSTEM

The control strategy consists of following blocks as shown in fig.5

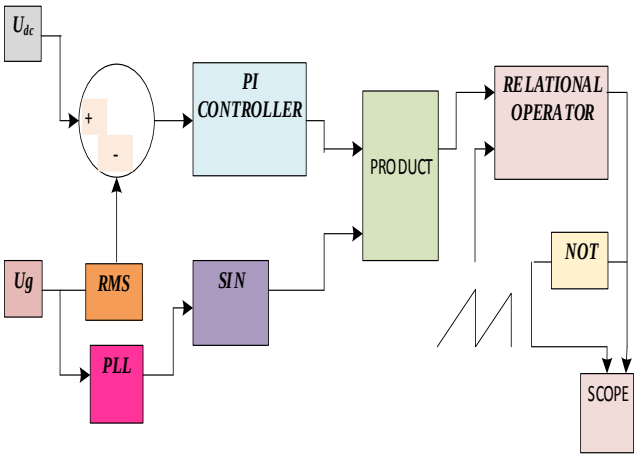

Fig.5 Control strategy of proposed inverter

The two variables, boost voltage at output U_{dc} and grid current I_g need to be controlled. U_{dc} is restrained by PI Controller while U_g is given to PLL block and further compared with output of PI controller that is U_{dc}. Phase locked loop is a kind of feedback loop which is used to lock different waveforms shifted in phase but at same frequency. The reference values of U_{dc} and U_g are taken and further given to gate drive signals of inverter as displayed in fig.5.

IV. PARAMETERS DESIGN

A. *Calculation of boost inductor*

Conforming to paper,boost inductor is designed to work with DCM [12]. The boost inductor can be given by

$$I_{L_{B1,2}} = 0.5 \times \Delta i_{L_{B1,2}} \times (D + \Delta D) = \frac{D^2 T_S U_{in} U_{DC}}{2L_{B1,2}(U_{DC} - U_{in})} \quad (1)$$

$$L_{B1,2} \leq \frac{0.125 \times T_S U_{in}^2 U_{DC}}{P_{FC}(U_{DC} - U_{in})} \quad (2)$$

The fuel cell output pulsation also demands on calculation of final value of boost inductor. The immense P_{fc} requires lesser L_b value.

B. *Power of fuel cell*

The power of fuel cell P_{fc} can be determined by following given equation-

$$P_{FC} = P_{in} = \frac{D^2 T_S U_{in}^2 U_{DC}}{2L_{B1,2}(U_{DC} - U_{in})} \quad (3)$$

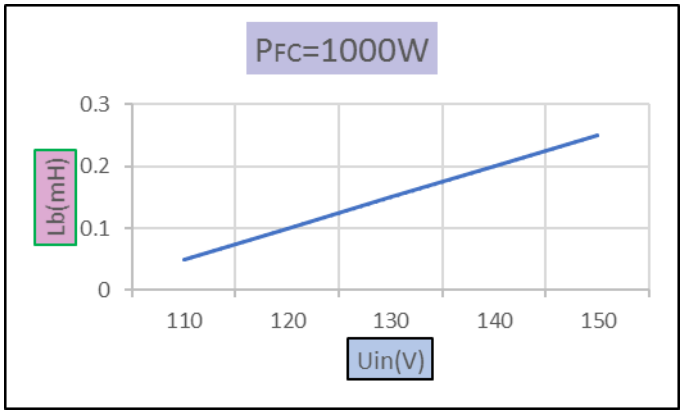

Fig.6 Graph between boost inductor (L_b) v/s input voltage (U_{in})

Formerly, the P_{FC} and switching frequency is monotonous, boost inductor (L_b) can be influenced by U_{in} as displayed in fig.6.

C. *Grid voltage and current*

The grid voltage is given by

$$u_G = \sqrt{2} U_G \sin \omega t \quad (4)$$

Where U_G is the value of grid voltage RMS.
Grid current can be given as

$$i_G = \sqrt{2} \frac{P_{in}}{U_G} \sin \omega t \quad (5)$$

D. *Selection norms for capacitor in input side*

The main advantages of present inverter is that the current ripples can be sensed without any closed loop technique. Cdc acts as a filter capacitor and current across it is consist of two parts that is $I_{DC\text{-}B}$ and $I_{DC\text{-}I}$. C_{DC} is inversely proportional to low- frequency current ripples. The value C_{DC} is taken high with the reference of alpha (percentage of double frequency line). Therefore, three electrolytic capacitors are chosen as boost filter in output side of converter.

S.no	Parameters	Values
1	Input voltage (Uin)	110-180 V
2	Boost capacitor (C_{DC})	400µF
3	Boost output voltage (U_{dc})	360 V
4	VD & D1-3	MUR1540
5	Grid Voltage (u_g)	110/50Hz
6	LCL filters(L1,L2,C1)	L1=4mH, L2=0.5mH, C1=5Mf
7	Switching Frequency (F_{SW})	12kHz
8	Boost Inductors (L_{B1} & L_{B2})	L_{B1}, L_{B2}=1e-4
9	Fuel cell stack	1.26kW

Fig.7 Configuration parameters of the proposed system

V. SIMULATION MODEL AND VERIFICATION

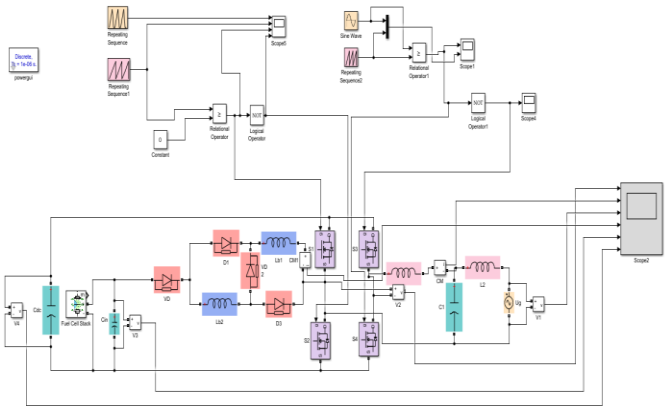

Fig.8 Simulation model (open loop)

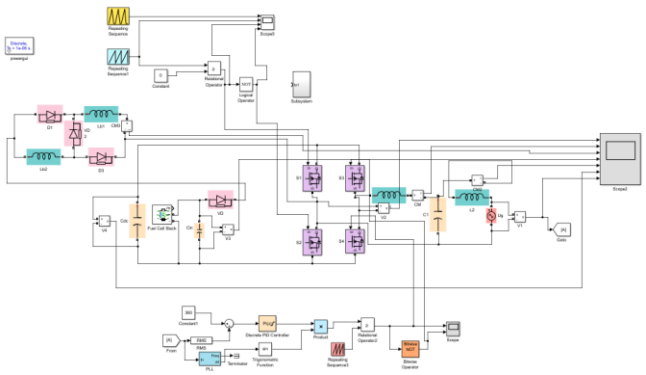

Fig.9 Simulation model with control strategy

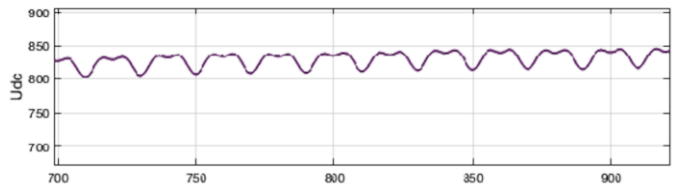

(a)

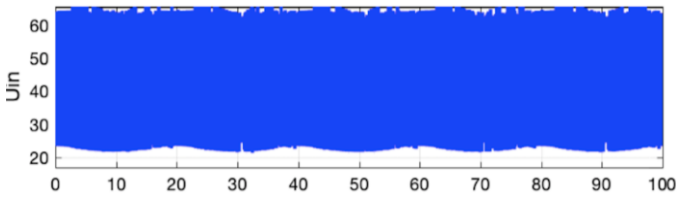

(b)

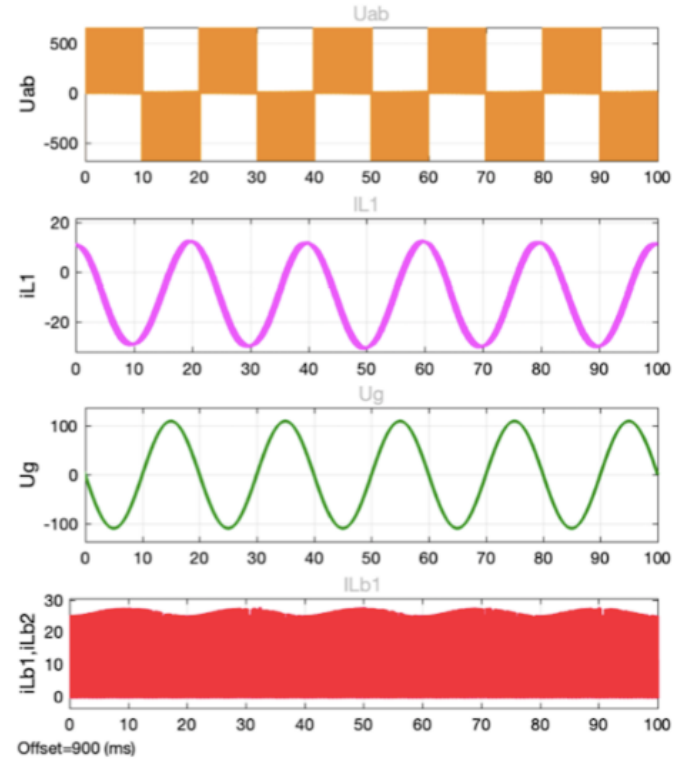

(c)

(d)

Fig.10 Simulation results of the projected inverter

The open loop and closed loop simulation models of projected inverter are displayed in fig.8 and fig.9. The waveforms of projected inverters are displayed in fig.10, where voltage across U_{dc} is presented in Fig.10(a). The voltage U_{ab} is SPWM wave which is used for grid coupled filter design. Fig.10 (c) displayed various waveforms such as output current $IL_{1,}$ boost inductors IL_{b1} IL_{b2} which all shows that the projected inverter is endowed for fuel cell power generation. The retrieved waveform of IL_{b1} IL_{b2} are in DCM as displayed in fig.10(d).

VI. CONCLUSION

This paper presents a single stage boost inverter topology for REGS with reduced current ripples at low frequency as compared to the traditional conversion system. A control technique is also proposed for the better efficiency. A single stage conversion system reduces cost and improves the reliability and the hybrid inductor switch are designed in DCM mode in order to reduce current ripples in input side of the system. In order to understand this topology simulation concludes that the inverter has satisfactory performance as compared to traditional conversion methods. In future, the FC technology is protractible to develop automated fuel cell and can also be explore for CCM instead of DCM. It can be considered for stand-alone application system and backup system. FC stacks integration with various topology of DC to DC converter can be explore and study of a closed loop controller can se analyzed. It can also have applications such as transportation, portable uses as well as for stationary installations.

REFERENCES

[1] R. S. Gemmen, “Analysis for the effect of inverter ripple current on fuel cell operation condition,” *journal of fluid mechanics*, vol.125, no. 3, pp. 576–585, Mar. 2003.

[2] Y. Ohnuma, K. Orikawa and J. Itoh, “A Single-phase Current Source PV Inverter with Power Decoupling Capability using an Active Buffer,”*IEEE Trans. Ind. App.*, vol. 50, no. 12, pp. 4000–4008, Dec. 2013.

[3] Y. Tang, D. Fu, T. Wang and Z. Xu, "Hybrid Switched-Inductor Converters for High Step-Up Conversion," in *IEEE Transactions on Industrial Electronics*, vol. 62, no. 3, pp. 1480-1490, March 2015.

[4] Liu C, Lai J S, “Low frequency current ripple reduction technique with active control in a fuel cell power system with inverter load,”*IEEE Trans. Power Electron.*, vol. 22, no. 4, pp. 1429-1436, Apr.

[5] J. Kan, S. Xie, Y. Wu, Y. Tang, Z. Yao and R. Chen, "Single-Stage and Boost-Voltage Grid-Connected Inverter for Fuel-Cell Generation System," in *IEEE Transactions on Industrial Electronics*, vol. 62, no. 9, pp. 5480-5490, Sept. 2015.

[6] G. Zhu, S. Tan, Y. Chen and C. K. Tse, "Mitigation of Low-Frequency Current Ripple in Fuel-Cell Inverter Systems Through Waveform Control," in *IEEE Transactions on Power Electronics*, vol. 28, no. 2, pp. 779-792, Feb. 2013.

[7] C. Liu and J. Lai, "Low Frequency Current Ripple Reduction Technique With Active Control in a Fuel Cell Power System With Inverter Load," in *IEEE Transactions on Power Electronics*, vol. 22, no. 4, pp. 1429-1436, July 2007.

[8] J. Itoh and F. Hayashi, "Ripple Current Reduction of a Fuel Cell for a Single-Phase Isolated Converter Using a DC Active Filter With a Center Tap," in *IEEE Transactions on Power Electronics*, vol. 25, no. 3, pp. 550-556, March 2010.

[9] A.Reznik,M.G Simoes,A.al-durra and S.M. Muyeen,"LCL Filter design and Performance analysis for Grid-Interconnected System" *IEEE Trans. Ind.Appli*.,vol.50,no.2,pp.1225-1232,Mar./apr.2014

[10] N. Altin, S. Ozdemir, H. Komurcugil, I. Sefa and S. Biricik, "Two-stage grid-connected inverter for PV systems," *2018 IEEE 12th International Conference on Compatibility, Power Electronics and Power Engineering(CPE-POWERENG 2018)*, Doha, 2018, pp. 1-6.

[11] J. Kan, S. Xie, Y. Wu, Y. Tang, Z. Yao and R. Chen, "High-Frequency-Link Inverter Using Combined Synchronous Rectifiers," in *IEEE Transactions on industrial Electronics*,vol.61,no.12,pp.6769-6777,Dec.2014

[12] K.R Sekhar and S. Srinivas ,"Discontinuous Decoupled PWM's for Reduced Current Ripple in a Dual Two-Level Inverter fed Open-End Winding Induction Motor Drive" *IEEE Trans. Power Electron*., vol. 28, no.5, pp.2493-2502, May.2013.

.

Proceedings of the Fourth International Conference on Communication and Electronics Systems (ICCES 2019)
IEEE Conference Record # 45898; IEEE Xplore ISBN: 978-1-7281-1261-9

Gain Enhancement of Compact UWB Antenna Using Planar Reflector

Mahadu A. Trimukhe
EXTC Department
TPCT's Terna College of Engineering, Nerul
Mumbai, India
mahadu2005@gmail.com

B. G. Hogade
Electronics Department
TPCT's Terna College of Engineering, Nerul
Mumbai, India
bghogade@gmail.com

***Abstract*— This paper present, a enormous gain Ultra wideband (UWB) printed patch antenna by a planar reflector is offered. The reflector is located lower the ground plane with a 15mm distance. By using a reflector, the gain of the antenna have been improved. A determined gain of 6.4 dBi with gain deviation < 2.2 dBi through 3.1 to 10.6 GHz frequency band. A proposed antenna with an overall size 20 × 20 mm^2 fabricated on FR 4 substrate. The simulated results is good contract with the tested results.**

Keywords*— *Compct UWB, Gain Enhancement, Corner Planar Reflector, Radiation pattern.

I. INTRODUCTION

In year 2002, the Federal Communications Commission (FCC) permitted the usage of unrestricted UWB spectrum from 3.1 to 10.6 GHz [1]. UWB antennas are used in many communication applications, viz. imaging, radar, space communication system, etc. [2]. The UWB communication system offers many types of benefits such as wide bandwidth, high-speed data rate capacity for wireless transmission and very low power consumption. Proposal of a small size UWB antenna is a significant challenge owing to some fundamental limitation intended for electrically small antennas [3]. With the comprehensive research on UWB antennas over the past decade, miniaturization of UWB antennas has attracted the researcher's attention. Recently, various compact UWB antennas have been proposed which provide an omnidirectional emission shape through gain of 3-5 dBi [4-8]. However, reducing the dimension of the antenna directly affects the degradation gain and the limitation of the current path [9-10]. In [11-15], improvement of gain has been described using various types of reflectors, including planar, frequency selective surface (FSS), FSS reflector, multilayer FSS, angular, corner and a parabolic reflector. In [11] using FSS layer reflector gain is improved 8- 9.7 dBi over 3.1-6 GHz frequency. Using planar reflector gain is enhanced from 7.5-10.2 dBi over 4.1-10.6 GHz frequency [12]. A gain of curved UWB antenna is improved to 8 dBi in excess of 3.5-10 GHz in [15]. However, antenna structures and reflectors in [11-15], have large dimensions.

Now this article, gain enhancement of a slotted meandering line for compact UWB antenna [10], by a planar reflector is anticipated. The antenna deals omnidirectional radiation shape with less cross polarization < -20dB. The gain differs from 2.2 - 6.4 dBi done 3.1 to 10.6 GHz frequency group. The proposed antenna manufactured and verified, simulated results approve with measured significances.

II. GEOMETRY OF THE ANTENNA AND CORNER PLANAR REFLECTOR

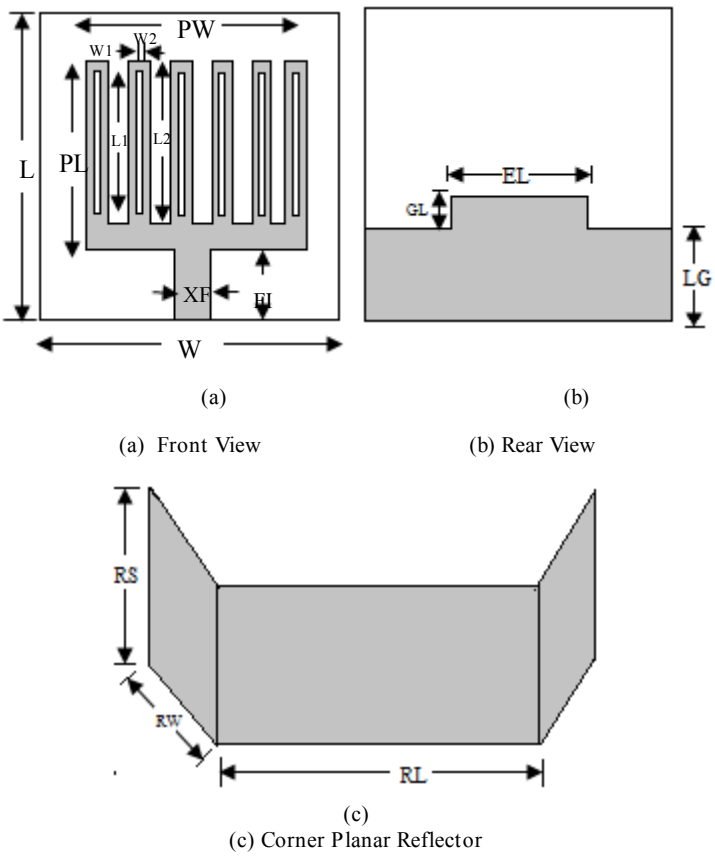

(a) (b)

(a) Front View (b) Rear View

(c)
(c) Corner Planar Reflector

Fig. 1. Structure of offered UWB antenna with Reflector

Elevated consideration of the offered antenna are L= 20mm, W= 20mm, PL= 9.8mm, PW= 12mm, XF= 2.2mm, LG=

5.5mm, RW= 12mm, FI= 5.5mm, L1= 6.6mm, L2= 8.8mm, W1= 0.4mm, W2= 1.2mm, RL= 20mm, RS= 7mm, EL= 8mm, GL= 0.1mm.

The structure of the offered antenna with design parameter is presented in Figure 1. The antenna is intended using FR 4 substrate with an size of 20 × 20 mm^2 having dielectic constant and loss tanget of 4.4 and 0.02 correspondingly. Provide 50Ω microstrip line to the antenna. Impedance matching bandwidth of 7.6 GHz (3.1 to 10.6 GHz) for reflection coefficient <-10 dB is achieved after modification of the finite truncated ground plane using reflector. The distance between reflectors from ground plane is most important for wave reflected from the reflector to be in practical phase with the wave radiated from the radiating patch. Return loss variation of distance between reflector and antenna is shown in Figure 2. A 15mm distance from antenna to reflector is elevated to achieve the extreme gain of an antenna. Dimension of a reflector are optimized for obtaining the high gain as well as the desired radiation patterns. Table I shows the effect of distance between reflector and UWB antenna. The projected antenna is enriched by using the High Frequency Structure Simulator (HFSS) simulation software.

Table I. Comparison table of effect distance of reflector

Sr.No.	Effect of d	Freq range (GHz)	Return loss (db) peak	BW (%)
1.	15 mm distance	3.1-10.6	-40	109.4
2.	25 mm distance	3.2-10.7	-25	107.9
3.	35 mm distance	3.2-10.7	-25	107.9

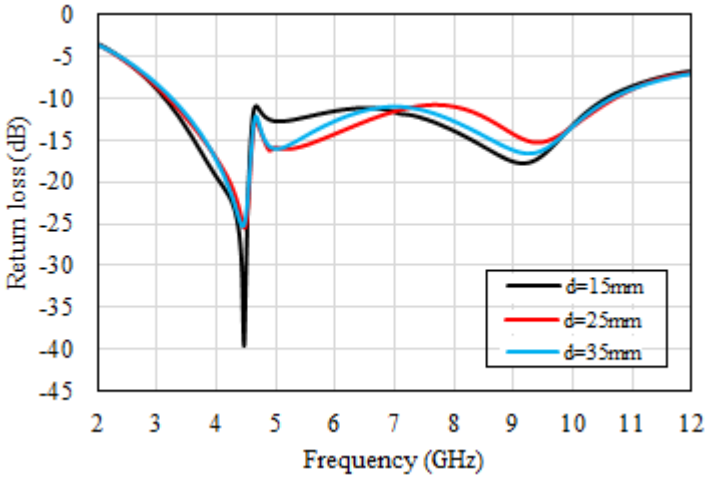

Fig. 2 Retun loss variation of distance between reflector and antenna

III. RESULTS AND DISCUSSION

The proposed antenna geometry is made-up and verified. The photography of invented antenna with reflector is displayed in Figure 3. The return loss is measured using Agilent VNA (8722ET). The simulated and measured return coefficient of proposed UWB antenna is shown in Figure 4.

The antenna operates in UWB band from 3.1 to 10.6 GHz frequency with its input reflection coefficient below -10 dB. The simulated and tested results are in decent promise with each other.

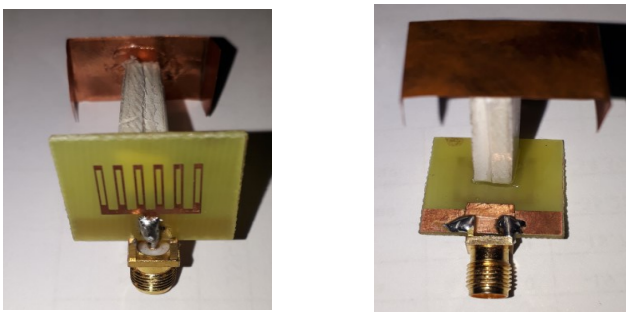

(a) (b)

Fig. 3. Invented antenna a) Front View with reflector b) Back View with reflector

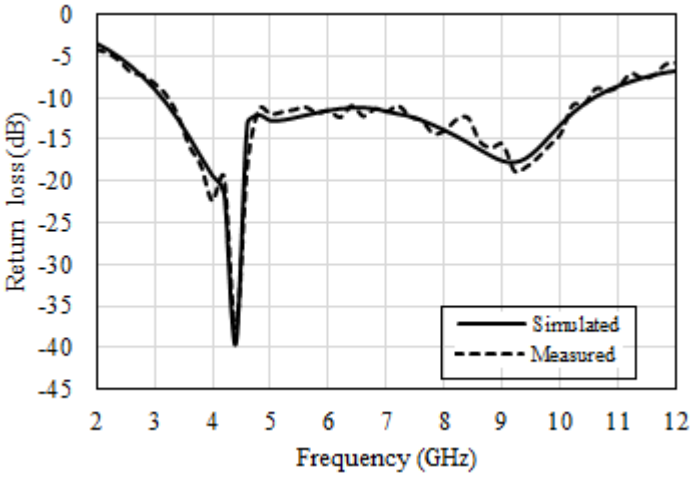

Fig. 4. Simulated and tested return coefficient of anticipated antenna

Fig. 5. Frequency vs. Gain plot with and without reflector.

Figure 5 shows a frequency vs. gain plot with and without reflector in the 3.1 to 12 GHz frequency band. The gain is increased by 2.2 to 6.4 dBi over 3.1 to 10.6 GHz with the use of a reflector, the highest gain is 6.4 dBi. The gain of proposed antenna is high compares to without corner reflector antenna with maintaining UWB band.

The simulated 2D radiation configurations for the offered antenna by co-polar and cross-polar at 4 GHz, 6 GHz and 8 GHz is displayed in Figure 6. The co-polar H-plane radiation shape be there purely omnidirectional at the given frequencies. Similarly monopole antenna in E plane

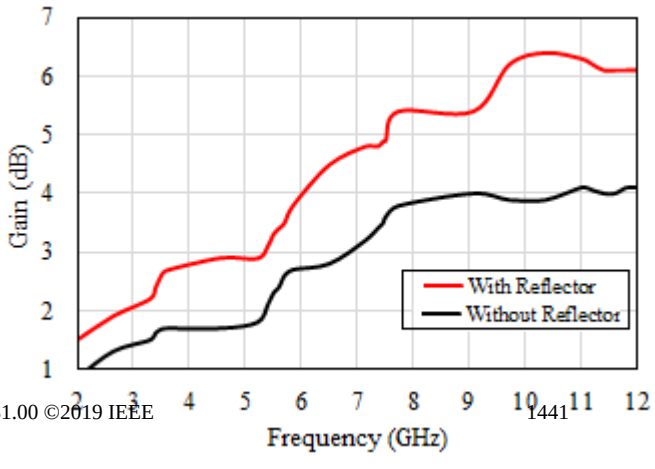

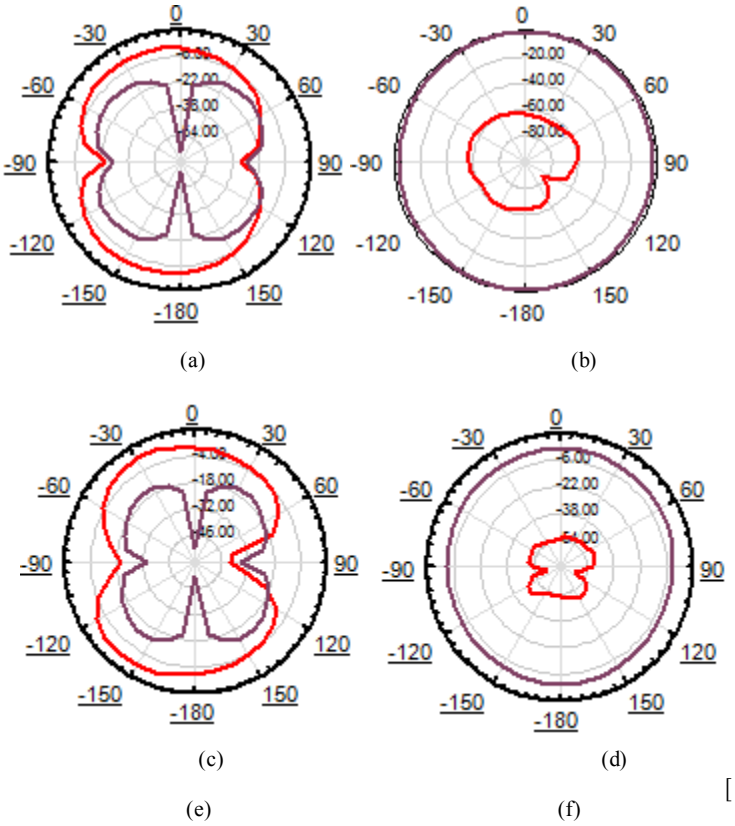

Fig. 6. Radiation configurations for the anticipated antenna with co-polar and cross-polar E-plane and H-plane at resonant frequencies. (a) and (b) at 4 GHz, (c) and (d) at 6 GHz. (e) and (f) 8 GHz.

IV. CONCLUSION

Small size of UWB antenna using Corner Reflector is proposed. The antenna is simulated and fabricated on the low-cost material of a FR 4 substrate. The proposed corner reflector antenna

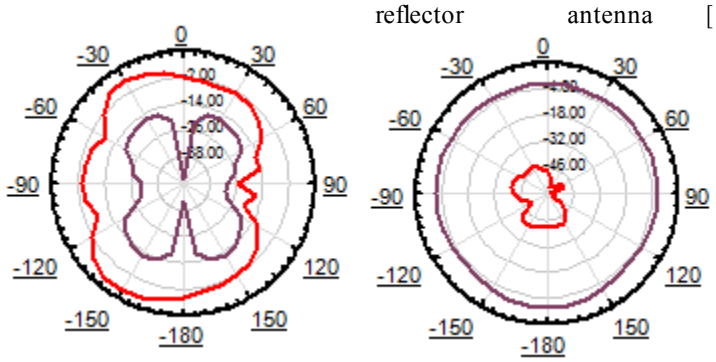

enhanced the gain by 2.2 to 6.4 dBi over the impedance bandwidth of 3.1 to 10.6 GHz. The proposed structure remain wide bandwidth, high gain, low profile and light weight which will be useful in UWB wireless application.

REFERENCES

[1] First order and report: Revision of part 15 of the Commission's rules regarding UWB transmission systems, Federal Communications Commission, Apr. 22, 2002.

[2] K. Siwiak and D. McKeown, Ultra-wideband Radio Technology, Wiley & Sons, 2004.

[3] Balanis, C.A.: 'Antenna theory analysis and design' (John Wiley & Sons, Hoboken, NJ, 2005, 3rd edn.)

[4] Guo L., Wang S, Chen X, Parini C.G. "A small printed quasi self-complementary antenna for ultrawideband systems," IEEE Antennas Wirel. Propag. Lett., vol 8, pp.554–557, Mar. 2009.

[5] Abbosh A, Bialkowski M, Jacob M, Mazierska J., "Design of a compact ultra-wideband antenna," Micro. Optical Tech. Lett., vol. 48, pp.1515–1518, 2006.

[6] Mahadu A. Trimukhe and Balaji G. Hogade, "Miniature low profile UWB Antenna with defective ground plane," in proc. IEEE Int. Conference on Inventive Communication and Computational Technologies, Sept. 2018, pp. 111-114.

[7] Guo, L., Wang, S., Chen, X., and Parini, C.G., "Study of compact antenna for UWB applications," Electron. Lett., vol. 46, (2), pp. 115–116, Jan. 2010.

[8] Bekasiewicz, A., and Koziel, S., "Structure and computationally-efficient simulation-driven design of compact UWB monopole antenna," IEEE Antennas Wirel. Propag. Lett.,vol. 14, pp. 1282–1285, Feb. 2015.

[9] Bekasiewicz, A., Koziel, S.: 'Compact UWB monopole antenna for internet of things applications', Electron. Lett., vol. 52, (7), pp. 492–494, Mar. 2016.

[10] Mahadu A. Trimukhe, Balaji G. Hogade "Design and Simulation of effects corresponding to Reduced conducting area using Slotted Meandering Line for Compact Ultra -Wideband (UWB) Antenna," *Journal of Communication,* vol. 14, no.4, pp. 318-323, April 2019.

[11] Snehal Patil, Rajiv Gupta and Shilpa Kharche, "Gain Improvement of Lower UWB Monopole antenna using FSS Layer," IEEE Int.Conf. on Nascent Technologies in the Engineering Field (ICNTE), Mumbai 2017, pp. 1-5.

[12] S. Kharche, G. S. Reddy, J. Mukherjee and R. K. Gupta, "Parallel metal plated high gain ultra-wideband antenna with unidirectional radiation pattern," IEEE Int. Conf.on Electronics, Computing and Communication Technologies (IEEE CONECCT), Bangalore, 2014, pp. 1–5.

[13] H.-Y. Chen and Y. Tao, "Bandwidth Enhancement of a U-Slot Patch Antenna Using Dual-Band Frequency Selective Surface With Double Rectangular Ring Elements," Microw. Opt. Technol. Lett., vol. 53, no. 7, pp. 1547–1553, Jul. 2011.

[14] Pirhadi, H. Bahrami, and J. Nasri, "Wideband High Directive Aperture Coupled Microstrip Antenna Design by Using a FSS Superstrate Layer," IEEE Trans. Antennas Propag., vol. 60, no. 4, pp. 2101–2106, Mar. 2012.

[15] Y. Ranga, K. P. Esselle, L. Matekovits, S. G. Hay , "Increasing the gain of a semicircular slot UWB antenna using an FSS reflector, IEEE Conference on Antennas and Propagation in Wireless Communications, APWC), pp. 478–481, 2012.

Proceedings of the Fourth International Conference on Communication and Electronics Systems (ICCES 2019)
IEEE Conference Record # 45898; IEEE Xplore ISBN: 978-1-7281-1261-9

A novel systematic approach for Residential Smart Grid

Naveen Ananda Kumar J
Institute of management
Christ (Deemed to be University)
Bengaluru, India
jnaveens@icloud.com

Shubashree S
Institute of management
Christ (Deemed to be University)
Bengaluru, India
Shreesivakumar96@gmail.com

***Abstract*- Power shortage is a very common problem faced by every home and there is no solution to completely eradicate this from its roots. However, with Internet of Things, this problem can be controlled to an extent where people do not have to suffer without electricity for their basic needs such as lights and fans. In our paper, we propose the implementation of a network enabled processing unit in every home (multi-processing unit) that can communicate with a common centralized gateway (Universal Home Gateway) thereby gathering real time data about the demands of the consumer. Also, we propose an installation of two wiring system at each household which is connected only to necessary loads that will have power all the time. Whereas the other connected to heavy (luxury) loads that gets cuts off when demand rises more than supply. Thereby, giving electricity to cater consumer's basic needs all the time. This helps in real time demand side management.**

Keywords- IoT, Smart grid, Customer centric grid and Real time demand management.

I. INTRODUCTION

In Smart Grid, the meters that are installed with the system has a multipurpose role with smart capabilities in order to meet the consumer's demand and needs [1]. The smart meter thus installed can measure real-time electricity usage and communicate data. This enables remote real-time monitoring and control power usage. Thus, consumers are provided with real-time pricing and can analyze the real-time usage information. In this connection Demand Side Management (DSM), Dynamic pricing and Demand Response Management (DRM) programs are applied by utility companies to regulate the energy consumption in homes by connecting the smart meter with many DSM properties and Home energy management system is also applied for the same cause. [2]

The smart meter in each and every household is connected to the internet along with a remote control is made possible [3]. The households are provided with two lines- one connected to heavy loads such as Air conditioners, washing machine, microwave oven etc., and other to only necessary loads such as light, fan, Wi-Fi etc., During the time of power deficit, instead of cutting power to the entire house, the line for the heavy load alone is turned off thereby providing uninterrupted power to the basic necessary loads. [4] This improves load scheduling and service to the customers. With a development in cloud infrastructure and improvement in mobile communications, the forthcoming Smart grids will likely to be more combined with the cyber infrastructure for sensing, control, scheduling, dispatch, and billing. A framework model that can forecast power dissipation profiles for every household as well as increasing per-area-consumption can also be made possible.

II. PRESENT SCENARIO

The existing system is distributed centric and demand response management is very poor, real time data gathering for individual homes is not possible [5]. In case of power deficit, there is a need to cut entire house power supply. Draw backs in the existing system

- Distributer oriented grid design. [6]
- Greater chance of power theft and Poor load scheduling. [7]

III. PROPOSED SYSTEM

We propose the implementation of a network enabled processing unit at every home (multi-processing unit) that can communicate with a common centralized gateway (Universal Home Gateway) thereby gathering real time data about the demands of consumer. [8] Also, the proposal includes an installation of two wiring system at each household one connected only to necessary loads that will have power all time and other connected to heavy(luxury) loads that gets cuts off when demand rises more than supply thereby giving electricity to cater consumer's basic needs all the time. [9]

A. Hardware used

- Ardunio Uno
- Hall effect current sensor
- Node MCU
- LCD 2004

- LCD i2c controller
- Rectifier circuit
- Logical level shifter
- Relay and Load

B. Software used

- Ardunio C ide
- DeviceHub
- ThingSpeak

C. System design

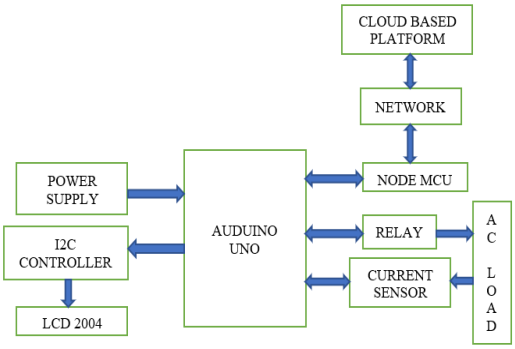

Figure 1.1 Block diagram of the circuit

The fig1.1 explains the block diagram of the proposed system, the 230 voltage AC main electricity supply is converted to 5V DC using a regulated power supply system. LCD 2004 display is interfaced to Arduino Uno using I2C controller. The Hall effect current sensor is used to measure the electricity used from the AC load through the Ardunio Uno. A relay is controlled by Ardunio Uno to switch on/off the AC load based on the signals received from the Ardunio Uno. Node MCU is used to connect system with the network, transfer and receive the data from the cloud through the network.

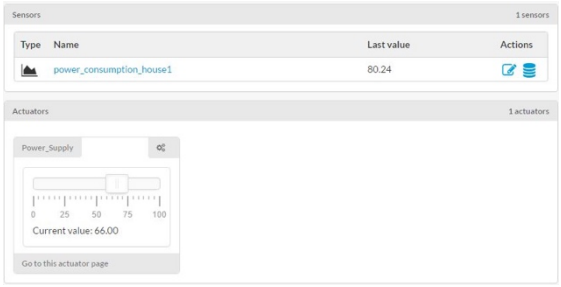

Figure 2.1 The producer side user interface for setting the power limit

Here the Wi-Fi is used as the network for connecting the network with the cloud [12].

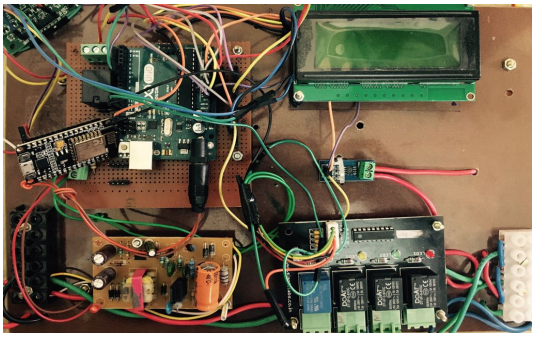

Fig 1.2 shows the hardware components in the IoT based kit

D. Working process

Each household wiring is separated into two wiring systems. (i) Basic needs – it powers the basic lighting, fans and other necessary appliances. (ii) Luxury needs – it powers air conditioning, refrigerator, washing machine and other luxury appliances which does not include under basic needs. When there is a power shortage, there is no need of shutting down the entire system instead only the luxury needs are turned off until the power shortage is rectified. With installing our proposed IoT based kit, we can make this selected power cut possible without majorly interrupting the existing system. The IoT based kit proposed by us is a wireless model which outcomes the disadvantages of the existing power supply models which cuts down the power entirely.

In our model, we have developed a user interface using DeviceHub platform where the producer can check the real time demand and can allocate power limit to every household based on the power produced. Once the usage exceeds the defined limit, it turns off the power to the entire home. But if they manage the use of power by switching off the excess load which falls within the defined limit, it turns on automatically and there is continuous uninterrupted power supply. The consumers can also check the power used by them in their house space in real time through ThingSpeak platform used in this model.

E. Advantages of our model

- Continuous intersection of combined smart grid in same arrangement with smart home applications [10]
- Data collection from multiple sources that constitutes varied communication sensors for customized data access. [11]

Figure 2.1 shows the producer side user interface for setting the power limit for each and every household. shows the real time power consumed based on the usage of power consumed by the customers which was developed using devicehub.net.

F. DeviceHub platform

DeviceHub is a platform used by the young developers to develop an insightful future. Joining hardware and web-based technologies, has always been a challenge. This platform gives a solution with the help of IoT and Cloud integration. DeviceHub platform provides data collection, remote control, cloud services and analytical gateway for new developers. To help the SMEs and other individual developers, PaaS (Platform as a Service) [12], a user-friendly platform, is used to connect the mobile application developers to other electronic devices such as sensors. This PaaS is used in the project to develop the real time data transfer for demand forecast and consumption in real time [13].

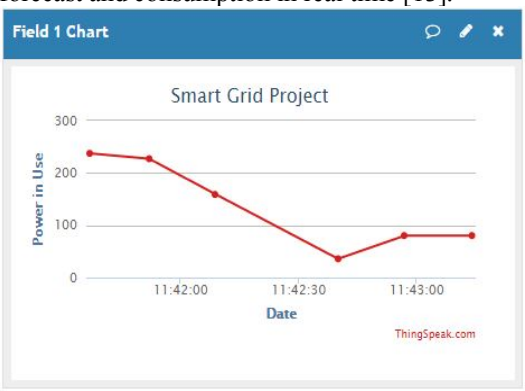

Fig 3.1 Graph showing power in use from Thing Speak

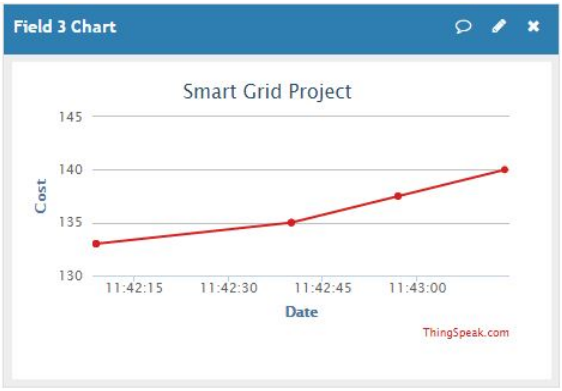

Fig 3.2 Graph showing cost per wh from thing speak

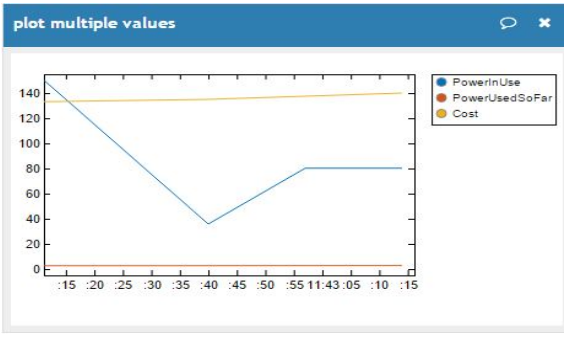

Fig 3.3 Graph showing all values in single graph

G. ThingSpeak platform

Data collection and storage is an important part for any developer. With data usage growing at a faster pace, it is important to have a platform to collect and store the data along with other cloud applications. [14] ThingSpeak is an IoT integrated platform that is used for efficient data storage and collection. This is utilised for analysing and visualizing the data used by the consumers [15]. Sensor data which is widely used can also be redirected to ThingSpeak from Arduino and other hardware appliances that are applicable. [16]

Figure 3.1 shows the consumer side user interface which shows the power in use. Figure 3.2 shows cost per watt hour (Wh). Figure 3.3 shows consolidated graph values of Power in use, Cost and Power used so far in a single graph through Thing Speak platform.

IV. FUTURE SCOPE

Using different types of Information Technology, communication devices and automated checks, power grid is converted to a Smart Grid with combining advanced tools and technologies [17]. With different ideas and developments booming, usage of the smart grid is the key reason for India to be in the front. Despite of facing numerous problems in the smart grid, India is still in the third position for transmitting and distributing network in the world. The few problems currently faced by India are shortage in electricity supply, lack of network access in all the places, demeaning quality and dependability and theft that is widespread[18]. The need to eradicate the above-mentioned problems in a well-organized, reliable and safe environment is vital and this can be achieved by advanced developments in Smart Grid, which in turn will lead to less power fall and power access for all [19].

V. CONCLUSION

The smart grid developed by us reduces the possibility of power shortage and power cuts. The users have the privilege of not suffering even without basic needs during their day to day activities. A smart grid distributes electricity from providers to customers using two-way digital technology to regulate appliances at customers' homes to save energy, decrease costs and increase dependability and transparency. Information and net metering system are used to avoid overlapping of the power distribution and electricity travels from the power plant to home through a remarkable system called the power grid. A modernized electricity network is being promoted by multiple governments, including the Government of India as a way of addressing energy independence, global warming and emergency resilience issues.

ACKNOWLEDGMENT

We thank our friends Praveen Kumar P and Rahaman Basha from Kingston college of engineering and colleagues from Institute of management, Christ (Deemed to be) University who provided us with insights which was a great assistance in shaping our research. We would like to express our gratitude to family, faculties and colleagues of Institute of management, Christ (Deemed to be) University.

REFERENCES

[1] Logenthiran, T., Member, S., Srinivasan, D., Member, S., & Shun, T. Z. (2012). Demand Side Management in Smart Grid Using Heuristic Optimization, 3(3), 1244–1252.

[2] Li, L., Xiaoguang, H., & Ke, C. (2011). The Applications Of WiFi-based Wireless Sensor Network In Internet Of Things And Smart Grid, 789–793.

[3] Science, C. (2013). A cloud-based architecture for Big-Data Analytics in Smart Grid : A Proposal.

[4] Samadi, P., Schober, R., Wong, V. W. S., & Jatskevich, J. (n.d.). Optimal Real-time Pricing Algorithm Based on Utility Maximization for Smart Grid.

[5] Li, L., Ota, K., & Dong, M. (2017). When Weather Matters : IoT-Based Electrical Load Forecasting for Smart Grid, (October).

[6] Gungor, V. C., Lu, B., Member, S., Hancke, G. P., & Member, S. (2010). Opportunities and Challenges of Wireless Sensor Networks in Smart Grid, 57(10), 3557–3564.

[7] Rahimi, F., Member, S., & Ipakchi, A. (2010). Smart Grid Paradigm, 1(1), 82–88.

[8] Zanella, A., Member, S., Bui, N., Castellani, A., Vangelista, L., Member, S., & Zorzi, M. (2014). Internet of Things for Smart Cities, 1(1), 22–32.

[9] Viswanath, S. K., Yuen, C., Tushar, W., Hu, K., Chen, C., & Centre, I. D. (2016). S ystem D esign of the I nternet of T hings for R esidential S mart G rid, (October), 90–98.

[10] Wong, V. W. S., Member, S., Jatskevich, J., Member, S., Schober, R., & Leon-garcia, A. (2010). Autonomous Demand-Side Management Based on Game-Theoretic Energy Consumption Scheduling for the Future Smart Grid, 1(3), 320–331.

[11] Metke, A. R., & Ekl, R. L. (2010). Security Technology for Smart Grid Networks, 1(1), 99–107.

[12] Diamantoulakis, P. D., Kapinas, V. M., & Karagiannidis, G. K. (2015). Big Data Analytics for Dynamic Energy Management in Smart Grids, 2(3), 94–101.

[13] Fadlullah, Z., Member, S., Fouda, M. M., & Member, S. (2011). Towards Intelligent Machine-to-Machine Communications in Smart Grid, 49(4), 60–65.

[14] Kim, H., Kim, Y., Yang, K., Thottan, M., Labs, B., & Hill, M. (n.d.). Cloud-based Demand Response for Smart Grid : Architecture and Distributed Algorithms.

[15] Simmhan, Y., Aman, S., Kumbhare, A., Liu, R., Stevens, S., & Zhou, Q. (n.d.). C - s p d -d s g m.

[16] Elisa Spano, Luca Niccolini, Giuseppe Iannaccone, Stefano Di Pascoli Last-Meter Smart Grid Embedded in an Internet-of-Things Platform

[17] Jianli Pan, Member, IEEE, Raj Jain, Fellow, IEEE, Subharthi Paul,Member, IEEE, TamVu, Member, IEEE, Abusayeed Saifullah,Member,IEEE, and Mo Sha, Member, IEEE(2015). IEEE internet of things,journal, vol. 2, no. 6, december 2015

[18] Jianli Pan, Member, IEEE, Raj Jain, Fellow, IEEE, Subharthi Paul,Member, IEEE, TamVu, Member, IEEE, Abusayeed Saifullah,Member,IEEE, and Mo Sha, Member, IEEE(2015). IEEE internet of things,journal, vol. 2, no. 6, december 2015

[19] Jinghuan Ma, He (Henry) Chen, Student Member, IEEE, Lingyang,Song Senior Member, IEEE, and Yonghui Li, Senior Member, IEEE.(2016) Residential Load Scheduling in Smart Grid. A Cost EfficiencyPerspective

[20] Boobalan, J., Jacintha, V., Nagarajan, J., Thangayogesh, K., & Tamilarasu, S. (2018). An IOT based Agriculture Monitoring System. 2018 International Conference on Communication and Signal Processing (ICCSP), 594–598. [21]Spanò, E., Niccolini, L., Pascoli, S. Di, Iannaccone, G., & Member, S. (2015).

[21] Last-Meter Smart Grid Embedded in an Internet-of-Things Platform. IEEE Transactions on Smart Grid, 6(1), 468–476. https://doi.org/10.1109/TSG.2014.2342796
Subhash, B. (2014). Overview of Smart Metering System in Smart Grid Scenario, (Pestse).

Proceedings of the Fourth International Conference on Communication and Electronics Systems (ICCES 2019)
IEEE Conference Record # 45898; IEEE Xplore ISBN: 978-1-7281-1261-9

Survey on Classification Techniques Applied to Intrusion Detection System and its Comparative Analysis

Ritumbhra Uikey
Department of Computer Science and Engineering
Maulana Azad National Institute of Technology
Bhopal, India
rituikey20@gmail.com

Dr. Manasi Gyanchandani
Department of Computer Science and Engineering
Maulana Azad National Institute of Technology
Bhopal, India
manasi_gyanchandani@yahoo.co.in

***Abstract*—Network security is the process of preventing and protecting against unauthorized access from the Internet. Intrusion detection is a basic part of security tools e.g., intrusion detection systems, adaptive security appliances, firewalls and intrusion prevention systems. There are several types of intrusion Detection System (IDS) exists e.g. Network IDS (NIDS), Host IDS, signature-based IDS, Anomaly based IDS. As huge amount of information in the form of packet flow across network may contains vulnerable information which lead to security threats. Many standard IDS datasets are available for researchers to measure their attack type detection/classification method's performance. In this paper we have done survey on classification methods applied on KDD99 and NSL-KDD. Most of the existing work focused on performance of classifier based on time and overall accuracy. we have shown the results of these papers to do collective study. The detection rate of majority classes (DoS and Probe) are good but not the same case with minority classes (U2R and R2L) when base classifier are used alone. It has been studied that there is as improvement in minority classes detection rate with pre-processing or hybrid classifier. By doing comparative study on results given by existing research papers shows that ABC-AFS [25] perform best among all.**

***Index Terms*—Feature Selection, NSl-KDD, KDD99, Class Imbalanced Data, Detection Rate (DR)**

I. Introduction

From past years, Internet or group of networks is spread around the world connecting large number of users. These networking are used by many organizations to perform information exchange or data transfer. The vast amount of attacks over the Internet makes computer users and many organizations under risk taking and the potential violation of security. The concept of intrusions detected in the system can be expressed as an attempt to invade a system and spread the following aspects which affect the major part of the system such as integrity, availability, confidentiality or the quality of the services in the system. In today's scenario, several information security techniques are available to protect information systems against un-authorization accessibility to the user, duplication of data, alteration, destruction and virus attacks detected. Intrusion is an extreme issue in security, network data can be effected by a single instance of intrusion can which will lead to breach in security in almost no time. The network connections are basically categorized into host-based data also named as an audit data [8] and network-based data (i.e., tcpdump) [9].

A. IDS Dataset

Some publicly available network traffic datasets are as follows:

1) **KDD99**:This data set is an upgraded version of DARPA98 dataset and used in "The Third International Knowledge Discovery and Data Mining Tools Competition". The goal of competition was to develop a network intrusion detector also can say a predictive model should have the capability to differentiate between normal and attack connections in the network.
2) **NSL-KDD**: The "Network Security Lab - Knowledge Discovery and Data Mining" is derived from the KDD99 dataset to overcome its limitation of containing large number of redundant instances. The NSL-KDD contains non-redundant and reasonable number of instances so that accuracy, performance of the classifier can be enhanced [2].
3) **KYOTO 2006+**: This dataset includes network data from Kyoto University's "Honeypots" [14].
4) **ADFA** : This Intrusion Detection Dataset developed to perform experiments by Host IDS. [10].
5) ISCX 2012: The dataset was created by "Information Security Centre of Excellence at University of New-Brunswick". Overall 2450324 network flows for a week is included in this dataset [3].
6) **CICIDS2017**: It also consists of network data as labeled flows consists of the timestamp, protocols, IPs and ports of both source and destination as well as attacks evaluated using CICFlowMeter [16].
7) **UNSW-NB15**: It contains combination of benign and synthetic attack behaviours which is generated by the "IXIA PerfectStorm" tool in the Cyber Range Lab of the "Australian Centre for Cyber Security (ACCS)" [18], [19].

B. KDD99 and NSL-KDD

In this papers, we will discuss about results of different classification techniques on KDD99 and NSL KDD. The dataset contains 39 attack types which are broadly classified into 4 attack type i.e. Probe, Denial of Service (DoS), Root to Local (R2L) and User to Root (U2R) as shown in Table1 [36] . The test set contains additional attack which are shown in bold font.

1) **DOS**- In this, an intruder try to make network resource unreachable by temporarily or indefinitely interrupting service of the host in network. Some examples of DOS attacks are mail bomb, teardrop, back, Ping of Death (pod), smurf, Neptune, land etc.
2) **U2R**: An unauthorized individual/party try to access the system using authorized account and make attempts to misuse vulnerabilities in the system to have root user privileges. Some example of U2R attack are rootkit, xterm, perl etc.
3) **R2L**: An intruder seeks to get the right of sending packets over targeted network by gaining local access as a user of the network. It is also known as Root to user (R2U) attack.
4) **Probe**: In this, the information about targeted host or network is collected so that state of the network can be learned and more formally for renaissance purpose.

TABLE I
ATTACK TYPES [44]

S.no.	Attack Category	Attack Types
1	DoS	**Apache2**, **Processtable**, Neptune, Land, Pod, Teardrop, **Mailbomb**, Smurf, **UDPstorm**, Back
2	Probe	Satan, Portsweep, **Saint**, Nmap, **Mscan**, Ipsweep
3	R2L	**Xterm**, **Httptunnel**, Rootkit, **Ps**, Buffer_Overflow, Perl, LoadModule, **SQLattack**
4	U2R	Imap, Spy, WarezMaster, Guess_Password, Warez-Client, MultiHop, Ftp_Write, **Named**, **Sendmail**, **Xlock**, **SnmpGuess**, **Xsnoop**, **Worm**, **SnmpGetAttack**, Phf

In section 2, discussion on different machine learning techniques are applied to KDD9 and NSL KDD dataset are provided. In section 3 we will discuss the outcome of these techniques and the comparative analysis has been done which is shown in table 2.

II. RELATED SURVEY

A study by Jim Anderson [1] based on one of the earliest works on intrusion detection and recommended number of ways for analyzing audit data of system. His methods utilize gathered an audit data for analysis of performance and were designed for batch mode processing, means collected data of complete day would be examined at the end of the day.

The classification problem in intrusion detection area has been examined for quite a long time using existing machine learning techniques comprising conventional classification techniques e.g., Decision Trees (DTs), k-NN, Bayesian, SVM, Self-Organized Maps (SOMs), Genetic Algorithm (GA), Artificial Neural Networks (ANNs), hybrid classifiers (combination multiple machine learning techniques) and fuzzy logic. A survey on utilization of these methodologies and 55 research articles reports its statistics during the period 2000-2007 was given in [15]. The survey demonstrates that K-NN and SVM were the most widely used methods while there is an increment in utilization of hybrid methods after 2004. Another recent survey [17] provides in-depth review of intrusion detection by using computational intelligence which includes the description of Swarm Intelligence methods and classification algorithms. Recently, incorporation data mining techniques with "On Line Analytical Processing (OLAP)" tools is introduced [20]. It has been shown that this collaboration provide a good solution to handle problem in IDSs, for example low detection rate and high false alarm rate.

As huge amount of network traffic data is generating by organizations, to handle such data Extreme Learning Machine (ELM) is used in [13]. Comparison of ELM has been done with Random Forest(RF), SVM(Linear) and SVM(RBF) based on three parameters (Accuracy, Recall and Precision). Experiments were performed on NSL-KDD training dataset which are randomized then partitioned into three parts (full, half and one-forth). Mostly, researchers evaluate performance of presented IDS in the context of data mining by utilizing the standard KDD Cup 1999. However, the imbalanced distribution of class in the data set causes minority class problem which leads low detection rate of such classes. Two commonly used sampling methods (over-sampling and under-sampling) to alleviate the minority class problem were examined in this research. However, these methods are less effective to resolve the problem is shown in [53].

The RF algorithm is applied in anomaly, misuse and hybrid detection. The hybrid approach is proposed for detection of both misuse and anomaly attacks [7]. The framework consists of two phases, phase1 the misuse detection is applied so that known intrusions are filtered out from the datasets then in phase2 entering the anomaly detection component to enhance the performance of the approach. Feature selection algorithm are applied which select 34 attributes based on its importance. Thorough examination of four important techniques for anomaly detection which comprises statistical, classification, clustering and information theory provided in [11].

A new hybrid feature reduction technique has been proposed for classification by combining the approaches of both PCA and IG with an ensemble classifier based on SVM, multilayer perceptron (MLP) and Instance-based learning algorithms (IBK). The evaluation of IG-PCA's performance done on three standard datasets, namely Kyoto2006+, NSL-KDD and ISCX 2012. The reduction in computational cost of the proposed method significantly among all experiments is shown [5].

Another new hybrid classification technique based on approaches of Artificial Fish Swarm (AFS) and Artificial Bee Colony (ABC) algorithms is proposed. Removal of irrelevant features performed using Correlation-based Feature Selection

(CFS). "Fuzzy C-Means Clustering (FCM)" applied to partition the training dataset. This hybrid method was performed on UNSW-NB15 and NSL-KDD datasets. The size of feature set after reduction is 6 for both these dataset [25]. Intrusion detection using AdaBoost has been presented [12] in which decision stump is selected as a weak classifier. Versatile initial weights and a simple strategy (described in section D) are adopted to enhance the algorithm's performance and avoid over-fitting. The algorithm is performed on KDD99 dataset. The "Feature Selection, Weight, and Parameter Optimization of SVM using GA (FWP-SVM-GA)" based on the features of both SVM and GA algorithm is proposed in [6]. Experiments were performed on standard KDD99 dataset and dimensionality reduction (selection of 19 features) has been done using GA and SVM.

A. Class Imbalanced Data

In-depth review of modeling techniques includes classification algorithms, model evaluation and data preprocessing. Authors have reviewed 527 papers related to imbalanced data from practical as well as technical point of view [38]. Some basic techniques for imbalance learning are as follows:

1) **Pre-processing**
   a) **Resampling**: The number of instances are randomly selected from the original data sample with replacement in such a way that number of instances in each drawn sample are approximately equal to the original data sample. Because of replacement, the selected number of samples consists of redundant cases are used by resampling methods. Mostly used resampling methods (three hybrid, eight undersampling and nine oversampling methods) e.g. SMOTE, SMOTE-ENN, SPIDER, AHC, RUS, OSS etc are discussed in [21].
   b) **Feature Selection and Extraction**: The process of selecting subset of attributes to improve classifier's performance is known as Feature selection. It has three methods (filters, wrappers, and embedded) [37]. Unlike Feature selection, new features space is created from the original feature space by utilizing functional mapping in feature extraction [33], [35].
2) **Cost-Sensitive Learning**: In this kind of learning, misclassification of rare class samples is assumed higher cost related to majority classes. Such learning can be incorporated at data as well as algorithmic level [39].
3) **Ensemble Classifiers** [43]: Following method to create ensemble classifier
   a) **Bagging**: It is the abbreviation of Breiman's bootstrap aggregating method provides flexible and straightforward ways of accomplishing a high accuracy [45]. In this method, various subset of connections are randomly taken from the complete training dataset with replacement. More than one classifiers of the same category are trained using newly created subset. By using majority voting, combination of particular classifiers are achieved.
   b) **Boosting**: In 1997, Freund and Schapire presented a boosting algorithm called as "Adaptive boosting" in short "AdaBoost". The technique develop a set of hypothesis and particular hypothesis determines weighted majority voting of the classes to combine decisions [47].
   c) **Stacking**: The outcomes of classifier's ensemble provided as input to next 2nd level meta classifier possess capability of learning the mapping between ensemble outputs and actual classes [46].
4) **Modification in Algorithmic Classifier**: The learning capability of an existing classification methods should be improved in order to enhance classification accuracy for imbalanced dataset. Some common techniques to improve decision tree, Naive Bayes, K-NN, SVM, ELM and rule-based classifer are discussed in table 5 in [38].
5) **Multi-Class imbalanced learning**: In [40], ad-hoc learning algorithms, "One-Versus-All (OVA)" approach and "One-Versus-One (OVO)" approach decompositions for addressing learning problems in multi-class imbalance data has been studied. OVO outperforms OVA is shown in their experimental results but OVA requires less decomposition (i.e. time efficient) that's why still popular than OVO.

III. Comparative Analysis

In [48], an optimal decision forest known as Kernel Miner which won second place in the competition of "KDD'99 Classifier Learning Contest" held in August 1999 has been used. The tool works with more number of databases e.g. as Oracle, MS Access, dBase, SQL Server etc through or directly OLEDB/ODBC and basically developed for Windows 95/98/NT.

In [29], feature subset merit measure and feature correlation metric has been introduced to quantify the relevancy and correlation among features for the efficient feature reduction. Authors have proposed new learning classifier algorithm.

In [50], an appropriate classifier are selected by performing experiments using different classifiers (Naive bayes, Best-First tree, MLP, Random Forest Tree) on NSL KDD dataset. To perform effecient classification, 26 features are selected using SFFS [51]. The classfication of test set was done using both 20% train set and whole train set. Their result shows that Naive bayes Performance is better compared to remaining classifiers.

In [30], a model for "Fast Learning Network (FLN)" based on "Particle swarm optimization (PSO)" is presented namely, PSO-FLN. For training FLN and ELM classifer, the comparison of developed model has been done with number of meta-heuristic algorithms.

Comparison of various methods for creating a multi-class SVM classifier using a set of binary SVM classifiers and aim to determine best multiclass SVM model [52]. WOAR SVM has been proposed and Differential Evolution (DE) model selection is used to get an optimal set of SVM hyperparameters. The

WOAR SVM is compared with (OAO, OAR, DAG, ADAG, ECOC) SVM.

A new hybrid approach is proposed on the basis of Binary Classifiers (BC) and K-NN for improvement and reduction in performance and bias towards majority classes respectively. In step 1, various BCs are employed and one composite module to efficiently identify the actual class. Further, the connections/instances with uncertain classes are transferred to step 2 to identify their classes using k-NN. Experiments were performed on two test set ($KDDTest^{+}$ and $KDDTest^{-21}$) [49]. we have shown experimental results on $KDDTest^{+}$ in table 2.

The SVM method is combined with Clustering based on "Self-Organized Ant Colony Network (CSOACN)" to take the characteristics of "Combining Support Vectors with Ant Colony (CSVAC)". A consistent as well as uniform train set and two test set namely (t_1 and t_2) are created from 10% KDD99 dataset on which algorithm is implemented and evaluated. Experiments show that CSVAC performed better than SVM and CSOACN alone with respect to DR and execution time efficiency [32]. For simplicity, result on t_2 test set is shown in Table 2.

In [42] a new method which is an association of DGSOT and SVM is presented, starts with an original training set and expanded gradually with the help of clustering structure which is generated by DGSOT. Comparison of their method with the random selection and Rocchio Bundling techniques with respect to accuracy improvement and training time gain has been done on benchmark DARPA 1998.

In [41], a method comprising of filtering, discretization and classification methods to maintain the classifier's performance results with a reduced features set of KDD99 has been presented. The new reduced training set is created using two class binarization techniques [34](One vs Rest and One vs One). The process of creating reduced training data using 3 different manner described in section 7.3 [41]. In all these 3 newly subset, original training set containing 494,021 connections are reduced to 46,093, 494,021 and 46,093 connections.

Classification on KDD99 dataset have been done using functional network and performed comparison with other techniques (Different SVM models, ANOVA ensemble and linear perceptrons) [23]. Basically functional networks are general form of neural networks which consists of input layer, output layer and one or more computing layer as well as contains knowledge about structure of the problem and data [24]. Implementation has been done using polynomial, Fourier and exponential functions.

In [26], a new hybrid learning method is presented on the basis of features such as density, cluster centers, and nearest neighbors (DCNN). The number of features has been selected using Fisher Scores and SVM are 19 which is similar to work in [27]. And performed comparison of DCNN with CANN [31] and k-NN with k=21.

In [4], another model based on CNN-IDS is proposed. The original connection/traffic vector is converted into an image format to reduce computational cost and performance of proposed CNN model is examined on KDD99 dataset. Feature reduction is done using PCA and Auto Encoder (AE). CNN also used in [22] and shows approximately similar result.

A wrapper method uses GA and Logistic Regression (GA-LR) as a search strategy and a learning algorithm respectively for network IDS to perform good feature selection has been presented [28]. Three decision tree (NBTree, RF and C4.5) are used for classification. The experiment was conducted on two standard KDD99 and UNSW-NB15 dataset. Different subset of attributes are created using GA-LR of size 15, 16, 17, 18, 20 and 22 from NSL-KDD among which best subset is selected of size 18. Similarly with UNSW-NB15 (Size of best subset selected is 20). As scope of this paper is within KDD, result of C4.5 with reduced attribute is shown in table 2. The symbol '-' in table 2 indicates value is not provided in the corresponding paper.

IV. Conclusion and Future Work

In this paper, comparative analysis of different classifiers based on the recall of each five class from different research papers with overall accuracy is shown in table 2. Most of these researches mainly focus on overall classifier accuracy, time complexity etc. Classifier accuracy is affected due to majority classes. As R2L and U2R are minority classes so their detection rates are not very good when base classifiers such as kernel Miner in [48], J48 or C4.5 and NB in [50], (J48, RF, KNN, NB) in [49], pure SVM in [42] are used as shown in table 2. Also variation in SVM (OAR, OAO, DAG, ADAG, ECOC, combine with Rocchio Bundling) unable to give good DR of R2L and U2R [42], [52] but its proposed method gives better result . In some research papers Neural Network has been used for classification such as functional Networks in [23], CNN in [4] does not provide good solution for minority. Performance of classifier should be evaluated not only based on overall accuracy but also with respect to DR of each class in dataset. With an appropriate pre-processing or combining some technique to base classifiers such as C4.5, SVM+DGSOT, DCNN, BC+k-NN provides some improvement to U2R and R2L DR [26], [28], [41], [42], [49]. ABC-AFS gives best result compared to all other classifers.

The false detection of minority class will lead to many discrepancies in IDES. There are a lot of techniques exists that enhanced classifier accuracy by improving majority class detection rates. We should explore also techniques to correctly detect rare events or minority classes without effecting detection of majority classes which will cause classifier un-biased and add on its enhancement. Also will evaluate ABC-AFS on other imbalance dataset.

References

[1] Anderson, James P. "Computer Security Threat Monitoring and Surveillance," Technical Report, James P. Anderson Company, 1980.

[2] Tavallaee, Mahbod, Bagheri, Ebrahim, Lu, Wei, Ghorbani, Ali A, "A Detailed Analysis of the KDD CUP 99 Data Set," 2009 IEEE Symposium on Computational Intelligence for Security and Defense Applications," pp. 1–6, 2009.

TABLE II
DETECTION RATE OF EACH CLASS

Dataset	Pre-Processing, Selected Attribute	Classifer	Normal (%)	DoS (%)	Probe (%)	U2R (%)	R2L (%)	Accuracy (%)
In [48]KDD99	41	Kernel Miner	99.42	84.52	97.47	11.84	7.32	92.92
In [23]KDD99	41	5FNs_poly	-	96.77	85.96	8.33	29.43	92.45
In [23]KDD99	41	5FNs_fourier	-	96.86	85.74	10.97	23.75	92.72
In [23]KDD99	41	5FNs_exp	-	96.85	85.60	13.60	23.77	92.75
In [41]KDD99	P+C, 7	C4.5	97.08	86.08	73.62	25	8.12	94.08
In [41]KDD99	E+I, 16	C4.5	96.36	94.07	79.48	19.3	32.87	91.81
In [26]KDD99	Fisher Scores+SVM, 19	CANN	89.97	89.65	90.83	63.16	80.42	89.79
In [26]KDD99	Fisher Scores+SVM, 19	K-NN	88.83	76.38	90.77	51.92	45.38	84.36
In [26]KDD99	Fisher Scores+SVM, 19	DCNN	98.69	93.20	97.44	67.31	86.55	96.74
In [4]KDD99	41	CNN	99.47	98.1	83.53	20.61	18.96	94
In [30]KDD99	41	PSO-FLN	99.78	98.37	90.77	93.63	63.64	98.92
In [28]KDD99	GA-LR, 18	RF	99.97	99.98	98.43	95.48	52.17	98
In [29]KDD99	9	Learning Classifier	98.45	99.93	99.91	75.34	41.34	-
In [32]KDD99	41	CSVAC	96.9	94.84	53.25	44.23	87	94.86
In [50] NSL-KDD	SFFS, 26	J48	-	77	57	9.2	5.5	61.06
In [50] NSL-KDD	SFFS, 26	Naive Bayes	-	61	59	4.5	31	70.08
In [49] NSL-KDD	41	J48	-	75.64	67	7	2	81.01
In [49] NSL-KDD	41	RF	-	79.24	69.14	3	0.15	77.06
In [49] NSL-KDD	41	KNN	-	77.18	60.26	2.50	3.01	76.70
In [49] NSL-KDD	41	NB	-	64.16	89.76	5	19.86	77.75
In [49] NSL-KDD	41	BC+KNN	-	91.10	87.44	55.5	61.26	94.92
In [52] NSL-KDD	41	ECOC SVM	92.41	75.65	74.53	19.05	21.2	76.15
In [52] NSL-KDD	41	OAR SVM	93.32	75.3	77.08	9.52	17.7	77.06
In [52] NSL-KDD	41	DAG SVM	91.71	80.72	48.3	0	43.83	68.78
In [52] NSL-KDD	41	ADAG SVM	93.15	80.51	43.33	4.76	17.59	64.59
In [52] NSL-KDD	41	OAO SVM	93.93	78.25	78.49	11.9	12.51	77.53
In [52] NSL-KDD	41	WOAR SVM	89.29	89.23	84.21	33.33	30.05	80.65
In [25] NSL-KDD	CFS, 6	ABC-AFS	94.3	94.4	97.1	94.4	93.7	99
In [42] DARPA	41	Pure SVM	98	84	88	0	18	57.16
In [42] DARPA	41	SVM+Rocchio Bundling	98	34	88	11	27	51.6
In [42] DARPA	41	SVM+DGSOT	95	97	91	23	43	69.8

TABLE III
ABBREVIATIONS

ADAG	Adaptive Directed Acyclic Graph
CNN	Convolutional Neural Network
k-NN	k - Nearest Neighbour
WOAR	Weighted One Against Rest
OAO	One-Against-One
OAR	One-Against-Rest
DAG	Directed Acyclic Graph
ECOC	Error-Correcting Output Code
DGSOT	Dynamically Growing Self-Organizing Tree
P+C	Proportional k-Interval Discretization(PKID)+Consistency-based filter
SVM	Support Vector Machine
E+I	Entropy Minimization Discretization + Interact(EMD+INT)
IG	Information Gain
PCA	Principle Component Analysis
RBF	Radial Basis Function
MLP	Multi Layer Perceptron
SFFS	Sequential Floating Forward Selection

[3] Ali Shiravi, Hadi Shiravi, Mahbod Tavallaee and A.A. Ghorbani, "Toward Developing a Systematic Approach to Generate Benchmark Datasets for Intrusion Detection," Computers & Security, Elsevier, vol. 31, pp. 357–374, 2012.

[4] Yihan Xiao, Cheng Xing, Taining Zhang and Zhongkai Zhao, "An Intrusion Detection Model Based on Feature Reduction and Convolutional Neural Networks," IEEE Access, vol. 7, pp. 42210–42219, 2019.

[5] Fadi Salo, Ali Bou Nassif and Aleksander Essex, "Dimensionality Reduction with IG-PCA and Ensemble Classifier for Network Intrusion Detection," Computer Networks, vol. 148, pp. 164–175, 2019.

[6] P. Tao, Z. Sun, and Z. Sun, "An Improved Intrusion Detection Algorithm Based on GA and SVM,"IEEE Access, vol. 6, pp. 13624–13631, 2018.

[7] J. Zhang, M. Zulkernine and A Haque, "Random-Forests-Based Network Intrusion Detection Systems," IEEE Transactions on Systems, Man, and Cybernetics, Part C (Applications and Reviews), vol. 38, pp. 649–659, 2008.

[8] S. Freeman, A. Bivens, J. Branch and B. Szymanski, "Host-Based Intrusion Detection Using User Signatures," Proceedings of the Research Conference. RPI, Troy, NY, pp. 2005–2014, 2002.

[9] David J. Marchette, "A Statistical Method for Profiling Network Traffic,"Workshop on Intrusion Detection and Network Monitoring, pp. 119–128, 1999.

[10] G. Creech and J. Hu, "A Semantic Approach to Host-Based Intrusion Detection Systems Using Contiguous and Dis-contiguous System Call Patterns," IEEE Transactions on Computers, vol. 63, pp. 807–819, 2013.

[11] M. Ahmed, A.N. Mahmood and Hu, Jiankun, "A Survey of Network Anomaly Detection Techniques," Journal of Network and Computer Applications, Elsevier, vol. 60, pp. 19–31, 2016.

[12] Weiming Hu, Wei Hu and Steve Maybank, "Adaboost-Based Algorithm for Network Intrusion Detection," IEEE Transactions on Systems, Man, and Cybernetics, Part B (Cybernetics), vol. 38, pp. 577–583, 2008.

[13] I. Ahmad, M. Basheri, M.J. Iqbal and A. Rahim, "Performance Comparison of Support Vector Machine, Random Forest and Extreme Learning Machine for Intrusion Detection," IEEE Access, vol. 6, pp. 33789–33795, 2018.

[14] J. Song, H. Takakura, Y. Okabe, M. Eto, D. Inoue and k. Nakao, "Statistical Analysis of Honeypot Data and Building of Kyoto 2006+ Dataset for NIDS Evaluation," Proceedings of the First Workshop on Building Analysis Datasets and Gathering Experience Returns for Security, ACM, pp. 29–36, 2011.

[15] C.F. Tsai, Y.F. Hsu, C.Y. Lin, and W.Y. Lin, "Intrusion Detection

by Machine Learning: A Review," Expert Systems with Applications, Elsevier, vol. 36, pp. 11994–12000, 2009.

[16] I. Sharafaldin, A.H. Lashkari, A.A. Ghorbani, "Toward Generating a New Intrusion Detection Dataset and Intrusion Traffic Characterization," ICISSP, pp. 108–116, 2018.

[17] S.X. Wu, and W. Banzhaf, "The Use of Computational Intelligence in Intrusion Detection Systems: A Review," Applied Soft Computing, Elsevier, vol. 10, pp. 1–35, 2010.

[18] N. Moustafa and J. Slay, "UNSW-NB15: A Comprehensive Data Set for Network Intrusion Detection Systems (UNSW-NB15 Network Data Set)," 2015 Military Communications and Information Systems Conference (MilCIS), pp. 1–6, 2015.

[19] N. Moustafa and J. Slay, "The Evaluation of Network Anomaly Detection Systems: Statistical Analysis of the UNSW-NB15 Data Set and the Comparison with the KDD99 Data Set," Information Security Journal: A Global Perspective, Taylor & Francis, vol. 25, pp. 18–31, 2016.

[20] H. Brahmi, I. Brahmi and S.B. Yahia, "OMC-IDS: At the Cross-Roads of OLAP Mining and Intrusion Detection," Pacific-Asia Conference on Knowledge Discovery and Data Mining, Springer, pp. 13–24, 2012.

[21] O. Loyola-González, J. Martínez-Trinidad, J.A. Carrasco-Ochoa and M. García-Borroto, "Study of the Impact of Resampling Methods for Contrast Pattern Based Classifiers in Imbalanced Databases," Neurocomputing, Elsevier, vol. 175, pp. 935–947, 2016.

[22] K. Wu, Z. Chen and W. Li, "A Novel Intrusion Detection Model for a Massive Network Using Convolutional Neural Networks," IEEE Access, vol. 6, pp. 50850–50859, 2018.

[23] A. Alonso-Betanzos, N. Sánchez-Maroño, F. Carballal-Fortes, J.A. Suárez-Romero, and B. Pérez-Sánchez, "Classification of Computer Intrusions Using Functional Networks. A Comparative Study," ESANN, vol. 7, pp. 25–27, 2007.

[24] E. Castillo, A. Cobo, J.A. Gutierrez and R.E. Pruneda, "Functional Networks with Applications: A Neural-Based Paradigm," Springer Science & Business Media, vol. 473, 2012.

[25] V. Hajisalem and S. Babaie, "A Hybrid Intrusion Detection System Based on ABC-AFS Algorithm for Misuse and Anomaly Detection," Computer Networks, Elsevier, vol. 136, pp. 37–50, 2018.

[26] X. Wang, C. Zhang and K. Zheng, "Intrusion Detection Algorithm Based on Density, Cluster Centers, and Nearest Neighbors," China Communications, IEEE, vol. 13, pp. 24–31, 2016.

[27] Z. Xue-qin, G. Chun-hua and L. Jia-jun, "Intrusion Detection System Based on Feature Selection and Support Vector Machine," First International Conference on Communications and Networking in China, IEEE, pp. 1–5, 2006.

[28] C. Khammassi and S. Krichen, "A GA-LR Wrapper Approach for Feature Selection in Network Intrusion Detection," Computers & Security, Elsevier, vol. 70, pp. 255–277, 2017.

[29] G. Qu, S. Hariri and M. Yousif, "A New Dependency and Correlation Analysis for Features," IEEE Transactions on Knowledge and Data Engineering, vol. 17, pp. 1199–1207, 2005.

[30] M.H. Ali, Bahaa Abbas Dawood Al Mohammed, A. Ismail and M.F. Zolkipli, "A New Intrusion Detection System Based on Fast Learning Network and Particle Swarm Optimization," IEEE Access, vol. 6, pp. 20255–20261, 2018.

[31] Wei-Chao Lin, Shih-Wen Ke and Chih-Fong Tsai, "CANN: An Intrusion Detection System Based on Combining Cluster Centers and Nearest Neighbors," Knowledge-Based Systems, Elsevier, vol. 78, pp. 13–21, 2015.

[32] W. Feng, Q. Zhang, G. Hu and J.X. Huang, "Mining Network Data for Intrusion Detection through Combining SVMs with Ant Colony Networks," Future Generation Computer Systems, Elsevier, vol. 37, pp. 127–140, 2014.

[33] H. Motoda and H. Liu, "Feature Selection, Extraction and Construction," Communication of IICM (Institute of Information and Computing Machinery, Taiwan), vol. 5, pp. 67–72, 2002.

[34] N. Yukinawa, S. Oba, K. Kato and S. Ishii, "Optimal Aggregation of Binary Classifiers for Multiclass Cancer Diagnosis using Gene expression profiles," IEEE/ACM Transactions on Computational Biology and Bioinformatics, vol. 6, pp. 333–343, 2008.

[35] L. Yijing, G. Haixiang and L. Xiao, L. Yanan and L. Jinling, "Adapted Ensemble Classification Algorithm Based on Multiple Classifier System and Feature Selection for Classifying Multi-Class Imbalanced Data," Knowledge-Based Systems, Elsevier, vol. 94, pp. 88–104, 2016.

[36] S. Mukkamala, and A.H. Sung and A. Abraham, "Intrusion Detection using an Ensemble of Intelligent Paradigms," Journal of Network and Computer Applications, Elsevier vol. 28, pp. 167–182, 2005.

[37] i. Guyon and A. Elisseeff, "An Introduction to Variable and Feature Selection," Journal of Machine Learning Research, vol. 3, pp. 1157–1182, 2003.

[38] G. Haixiang, L. Yijing, J. Shang, G. Mingyun, H. Yuanyue and G. Bing, "Learning from Class-Imbalanced Data: Review of Methods and Applications," Expert Systems with Applications, Elsevier, vol. 73, pp. 220–239, 2017.

[39] V. López, A. Fernández, J.G. Moreno-Torres and F. Herrera, "Analysis of Preprocessing vs Cost-Sensitive Learning for Imbalanced classification. Open Problems on Intrinsic Data Characteristics," Expert Systems with Applications, Elsevier, vol. 39, pp. 6585–6608, 2012.

[40] A. FernáNdez, V. LóPez, M. Galar and M. Del Jesus and F. Herrera, "Analysing the Classification of Imbalanced Data-sets with Multiple Classes: Binarization Techniques and Ad-hoc Approaches," Knowledge-Based Systems, Elsevier, vol. 42, pp. 97–110, 2013.

[41] V. Bolon-Canedo, N. Sanchez-Marono and A. Alonso-Betanzos, "Feature Selection and Classification in Multiple Class Datasets: An Application to KDD Cup 99 Dataset," Expert Systems with Applications, Elsevier, vol. 38, pp. 5947–5957, 2011.

[42] L. Khan, M. Awad and B. Thuraisingham, "A New Intrusion Detection System using Support Vector Machines and Hierarchical Clustering," The VLDB journal, Springer, vol. 16, pp. 507–521, 2007.

[43] A.A. Aburomman and M.B.I Reaz, "A Survey of Intrusion Detection Systems Based on Ensemble and Hybrid Classifiers," Computers & Security, Elsevier, vol. 65, pp. 135–152, 2017.

[44] M. Latah and L. Toker, "Towards an Efficient Anomaly-Based Intrusion Detection for Software-Defined Networks," IET Networks, IET, vol. 7, pp. 453–459, April 2018.

[45] L. Breiman, "Bagging predictors," Machine Learning, Springer, vol. 24, pp. 123–140, 1996.

[46] D.H. Wolpert, "Stacked Generalization," Neural Networks, Elsevier, vol. 5, pp. 241–259, 1992.

[47] R.E. Schapire, "The Strength of Weak Learnability," Machine learning, Springer, vol. 5, pp. 197–227, 1990.

[48] I. Levin, "KDD-99 Classifier Learning Contest: LLSoft's Results Overview," SIGKDD Explorations, vol. 1, pp. 67–75, 2000.

[49] L. Li, Y. Yu, S. Bai, Y. Hou and X. Chen, "An Effective Two-Step Intrusion Detection Approach Based on Binary Classification and k-NN," IEEE Access, vol. 6, pp. 12060–12073, 2017.

[50] A.S.A. Aziz, EL Sanaa and A.E. Hassanien, "Comparison of Classification Techniques Applied for Network Intrusion Detection and Classification," Journal of Applied Logic, Elsevier, vol. 24, pp. 109–118, 2017.

[51] A.S.A. Aziz, A.T. Azar, M.A. Salama, A.E. Hassanien and S.E. Hanafy, "Genetic Algorithm with Different Feature Selection Techniques for Anomaly Detectors Generation," Federated Conference on Computer Science and Information Systems, IEEE, pp. 769–774, 2013.

[52] A.A. Aburomman and M.B.I. Reaz, "A Novel Weighted Support Vector Machines Multiclass Classifier Based on Differential Evolution for Intrusion Detection Systems," Information Sciences, Elsevier, vol. 414, pp. 225–246, 2017.

[53] K. Khor, C. Ting and S. Phon-Amnuaisuk, "The Effectiveness of Sampling Methods for the Imbalanced Network Intrusion Detection Data Set," Recent Advances on Soft Computing and Data Mining, Springer, pp. 613–622, 2014.

Proceedings of the Fourth International Conference on Communication and Electronics Systems (ICCES 2019)
IEEE Conference Record # 45898; IEEE Xplore ISBN: 978-1-7281-1261-9

An Efficient Approach for Multiclass Student Performance Prediction based upon Machine Learning

Abhinav Jain
Research Scholar,CSE Department
NITTTR,Chandigarh
INDIA
navjainabhi@gmail.com

Shano Solanki
Assistant Professor,CSE Department
NITTTR,Chandigarh
INDIA
s_solanki_2000@yahoo.com

***Abstract*— The field of educational data mining has enabled the researchers, educators to predict the student's pass rate, failure rate, dropout rate etc. The main reason for dropouts of the student is the failure of students. Several researchers have proposed various educational data mining techniques for predicting the student performance and analyzed existing techniques on educational datasets. In this paper, we have analyzed the performance of four machine learning algorithms on educational dataset used for the early prediction of student performance. While there is a rich literature survey in student performance prediction, our work differs from existing works as follows:(i) Our prediction is not limited to binary classification of pass and fail but we have used a multiclass classification in which student are divided into three classes namely poor, average, good performing students;(ii) We have used data preprocessing, feature extraction, fine tuning of parameters of algorithms to build the model which is not focused by many researchers;(iii) We have built a more accurate model with 95% accuracy and lesser execution time;(iv) We have studied the relationship between various attributes through a correlation heatmap. This paper will elaborate on student performance prediction techniques and give a comparative study among them.**

Keywords—data mining; educational data mining; student performance prediction; prediction analysis; dropouts

I. INTRODUCTION

Over the last few years, the field of educational data mining saw a huge increase in number of researchers. Educational Data Mining can be applied in several areas such as user grouping, student performance prediction, user modeling or profiling, trend analysis [1]. New statistical methods, machine learning algorithms are being developed by the researchers to mine the educational data for a better understanding of students, teachers and their different attributes [2]. The inspection of educational data to upgrade performance of students and teachers is not a very new thing [5]. Due to the latest advancements in institutes, expansion in computing facilities and web-based learning has attracted researchers to create new techniques for examining the educational data [3]. The data can be taken from the admission system, registration system, and library management system, syllabus management and course management systems [4]. Data can be used to predict student performance [6].

Educational Data Mining used in this research, predict the students' performance by using four machine learning techniques namely decision tree, random forest classifier, gradient boosting classifier and extreme gradient boosting classifier. There are various classification techniques applied by researchers to predict student performance [7]. Only few of them addressed multi-class classification with good accuracy and lesser execution time. Also, very few existing works studied the relationship between attributes and only few considered selection of relevant attributes as an essential step to predict student performance and fine tuning of algorithm parameters. This research will give a more accurate model by which the teachers or administrator not only predict the failure of the students but also categorizes them according to their levels. Necessary steps can be taken by administrator, teachers and students to prevent failure and to improve performance. This will act as alarming system to students reflecting their drawbacks [8].

The rest of the paper is organized as follows. Section II describes the existing works related to this research. Section III describes the dataset, feature extraction process, and gives the relation between attributes through a correlation heatmap. Section IV describes proposed methodology to build our prediction model. Section V discusses the result achieved by the model. Section VI summaries the paper by giving a conclusion and discuss the future work.

II. RELATED WORK

Number of researchers had proposed various prediction models for the prediction of students. This section elaborates some of the related works.

In [9], the authors proposed a bilayered structure which consists of ensemble predictor and base predictor using which student's performance in degree program was predicted. The dataset was collected from University of California after examining the undergraduate students over 3 years. There was diversity in datasets as major, culture and specialization of students was different. The courses which were relevant for

student performance taken for student performance were chosen by probabilistic matrix factorization. The research work was only confined to courses which were mandatory but did not consider elective courses for prediction.

In [10], a predictive model was proposed by the authors to predict the academic performance of students. Three classifiers namely J48, PART, RIPOR were modeled on the dataset of 932 students of a University in Columbia to analyze and evaluate their performance. It was found in the research that after four iterations, J48 performed the best among three classifiers which were used. Highest accuracy which was achieved by J48 classifier after 4th iteration is 86.4%. Data preprocessing, attributes selection had a significant effect on accuracy of the model.

In [11], the authors proposed a K-means clustering analysis on student data through which students were clustered into different clusters as a good or bad performer. During the placement and admission process, this analysis was found to be helpful. The internships, projects, skill sets, SSC, HSC, and B.E. marks were few parameters included for this analysis. The implementation was very easy. However, there is need to involve socio-economic attributes in student data. In future, other efficient clustering techniques like Fuzzy C-Means should be applied to improve efficiency.

In [12], the authors predicted the passing rates of the students using support vector machine (SVM) and decision tree (DT). While the others authors predicted the passing rate using simple algorithms, the authors in this research work predicted using optimized support vector machine decision which was optimized using grid search. The results had shown better accuracy. Around 92% accuracy is achieved by using the optimized support vector machine and this also proves that the parameter tuning of algorithms has significant impact on performance of algorithms. The dataset taken was from UCI data repository which included the performance of secondary school students in the subject of Mathematics and Portuguese language.

In [13], the authors preprocessed the student data to perform feature extraction on the basis of Bloom's taxonomy and category. The data of students was gathered in a serious game to perform extraction on the basis of Bloom's Taxonomy and category. It was seen that there was decrease in execution time and there was improvement in level of accuracy. With comparison to traditional Fuzzy C-Means, execution time was 2.2-2.7 seconds lesser for the proposed FCM approach and the level of accuracy was improved up to 2.3-4.7%. Also, in comparison to traditional Fuzzy C-Means approach, the performance was enhanced when the features were extracted using Bloom's taxonomy-based extraction and Category-based extraction. Weights were added to features for improving the proposed methods.

In [14], the authors presented a comparison among four techniques namely neural networks, decision tree, support vector machine and naive bayes and their performance was analyzed using F-measure performance metric. The authors had firstly studied the effects of data preprocessing on the algorithms and compared them with the results achieved without data preprocessing. Secondly, the authors had studied the effects of fine tuning of parameters of algorithms on the classification techniques and comparing them with the results achieved without fine-tuning of parameters of algorithms. It was found that support vector machine performs well in both the cases and there is a significant effect of both fine-tuning and data preprocessing on the performance of the algorithms. The students who were enrolled in introductory programming courses in Brazilian Public University by distance learning and by on-campus courses were considered as the dataset and on these datasets the performance of algorithms is tested.

In [15], the author proposed a knowledge flow model using all five different classifiers namely REPTree, J48, SMO, MLP, Naïve Bayes. The analysis was done on the basis of prediction accuracy. It was seen that around 93% of accuracy was reached in case of Multilayer Perceptron (MLP). All the analysis was done on WEKA tool. The attributes didn't consider socio-economic attributes of students. The performance of Multilayer Perceptron was greater among all the five classifiers used in this research. The model could be useful for the students who are new to the introductory programming so that they can be helped with special attention.

In [16], the authors studied the performance of undergraduate students by utilizing data mining techniques. There was a detailed focus on the two important aspects of the performance of students. The academic achievement of the students was predicted at the end of 4 years of study program initially. Further, the typical progressions were studied and the prediction results were combined along with them secondly. Low and high achieving students were the two important groups of students that had been recognized. A timely warning was provided and low achieving students were supported so that their performance could be improved by focusing on fewer numbers of courses which were affecting performance.

In [17], the authors proposed and validated a predictive GPA model by Maximum Weight Dependency Tree. A relatively small-sample experiment was used for determining the set of self-regulatory learning behaviors. For every constituent of the generated model, the predictability was quantified and its relevance was calculated. Utilizing the constructed models for designing the intervention strategies that helped students when the academic failure was at risk was the major objective of grade prediction. The basic interventions were defined and the interventions which were of help to students having minimum GPA were identified by this application framework. Around 65% of accuracy was achieved by the proposed algorithm.

In [18], the authors analyzed the progress of students, their performance and their potentials using the multiple analysis tools. Initially, Student Attribute Matrix (SAM) formulated the student model. The analysis performed further could be utilized as the student attributes quantified by SAM. The BP-NN algorithm was applied secondly, for providing student performance estimation tools. The prior knowledge of students and their performance attributes were used to estimate the attributes of students further. For describing the progress of students related to different aspects along with the casual relationships, the BP-NN was used to propose the student progress indicators and attributes thirdly. The level at which a

factor would affect the performance of student could be known by these indicators and predictor. It was thus possible to train up the students. For the evaluation of student achievement and development, a student potential function was proposed at the end of this paper. The real academic performance data which was gathered from 60 high school students was used to check the performance of these analysis tools. Correct and highly accurate results were achieved by applying the proposed tools as per the evaluation results.

III. Dataset Preprocessing and Feature Extraction

In this section, we have described the dataset used in this research, hardware and software used, process of data preprocessing and relevant attributes selection using Exploratory Data analysis.

A. Dataset Description

After exploring various data sources, the dataset is taken from UCI data repository. The dataset consists of performance of secondary school students of two Portuguese schools in the subject of mathematics [19].The dataset includes various attributes related to students such as mother's education, father's education, previous period grades and other social, demographic attributes [20].There is 32 attributes in the dataset and the dependent or response variable is G3 and it has a strong correlation with G1 and G2 i.e. period 1 and period 2 scores. There are in total 395 records of different students in the dataset. All the attributes which are present in the dataset is shown in the Table I.

TABLE I. Attributes Description of Student Performance Dataset

Attribute	Description (Domain)
sex	student's sex (binary: female or male)
age	student's age (numeric: from 15 to 22)
school	student's school (binary: *Gabriel Pereira* or *Mousinho da Silveira*)
address	student's home address type (binary: urban or rural)
Pstatus	parent's cohabitation status (binary: living together or apart)
Medu	mother's education (numeric: from 0 to 4[a])
Mjob	mother's job (nominal[b])
Fedu	father's education (numeric: from 0 to 4[a])
Fjob	father's job (nominal[b])
guardian	student's guardian (nominal: mother, father or other)
famsize	family size (binary: ≤ 3 or > 3)
famrel	quality of family relationships (numeric: from 1 – very bad to 5 – excellent)
reason	reason to choose this school (nominal: close to home, school reputation, course preference or other)
traveltime	home to school travel time (numeric: 1 – < 15 min., 2 – 15 to 30 min., 3 – 30 min. to 1 hour or 4 – > 1 hour).
studytime	weekly study time (numeric: 1 – < 2 hours, 2 – 2 to 5 hours, 3 – 5 to 10 hours or 4 – > 10 hours)
failures	number of past class failures (numeric: n if $1 \leq n < 3$, else 4)
schoolsup	extra educational school support (binary: yes or no)
famsup	family educational support (binary: yes or no)
activities	extra-curricular activities (binary: yes or no)
paidclass	extra paid classes (binary: yes or no)
internet	Internet access at home (binary: yes or no)
nursery	attended nursery school (binary: yes or no)
higher	wants to take higher education (binary: yes or no)
romantic	with a romantic relationship (binary: yes or no)
freetime	free time after school (numeric: from 1 – very low to 5 – very high)
goout	going out with friends (numeric: from 1 – very low to 5 – very high)
Walc	weekend alcohol consumption (numeric: from 1 – very low to 5 – very high)
Dalc	workday alcohol consumption (numeric: from 1 – very low to 5 – very high)
health	current health status (numeric: from 1 – very bad to 5 – very good)
absences	number of school absences (numeric: from 0 to 93)
G1	first period grade (numeric: from 0 to 20)
G2	second period grade (numeric: from 0 to 20)
G3	final grade (numeric: from 0 to 20)

a 0 – none, 1 – primary education (4th grade), 2 – 5th to 9th grade, 3 – secondary education or 4 – higher education.
b teacher, health care related, civil services (e.g. administrative or police), at home or other.

B. Hardware & Software

We have used the Python language version 3.7.0 to carry out the whole research work. The IDE on which work is carried out is Jupyter Notebook version 4.4.0. The processor is Intel Pentium N3710 with 4GB random access memory and 64-bit operating system.

C. Data Preprocessing

After appropriate dataset selection, the data pre-processing is an important step in making machine learning model. Firstly, dataset is loaded as a comma separated values file. Then, null values are checked. After that the final score which is a numeric variable is converted into categorical variable. For the students who scored marks in the range of 15 to 20 are categorized as good performing students, students who scored marks in range of 10 and 14 are categorized as average performing students and students having marks less than or equal to 9 are categorized as low performing students. Student's final grade after categorization is shown in Fig. 1. All the nominal attributes such as mother's occupation, father's occupation etc. were converted into numeric attributes through 1-hot-encoding technique.

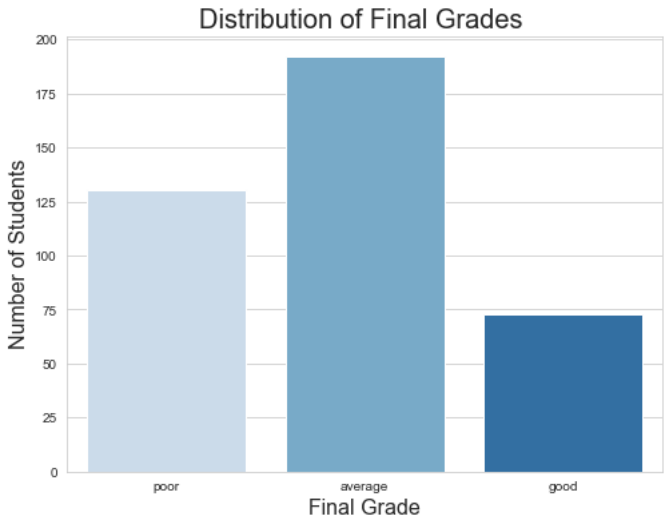

Fig. 1. Distribution of final grades.

D. Attributes Selection

The selection of relevant attributes which are affecting the prediction result is done using exploratory data analysis. The seaborn library of python is used to generate the correlation heatmap. The range varies from -1 to 1. The attributes which are having negative value has a negative correlation with other variable and attributes which are having positive value has a positive correlation with another variable. Positive correlation can be explained through an example in our dataset, if mother's education is high then there is a high chance that final grade of student is higher. Negative correlation can be explained through example of failures in our dataset. For example, if failures of a student increase, then there is a high chance that final grade of that student decreases. The correlation heatmap of our dataset is shown in Fig. 2. The values which are close to zero whether positive or negative has no significant correlation with other variables. These attributes can be dropped from the dataset without any loss in performance. After analysing the correlation heatmap, the feature which is selected for model is as follows: failures,

desire of getting higher education, mother's education, father's education, weekend alcohol consumption, absences, first period score, second period score and the target variable final score. All the other attributes are dropped out from the dataset.

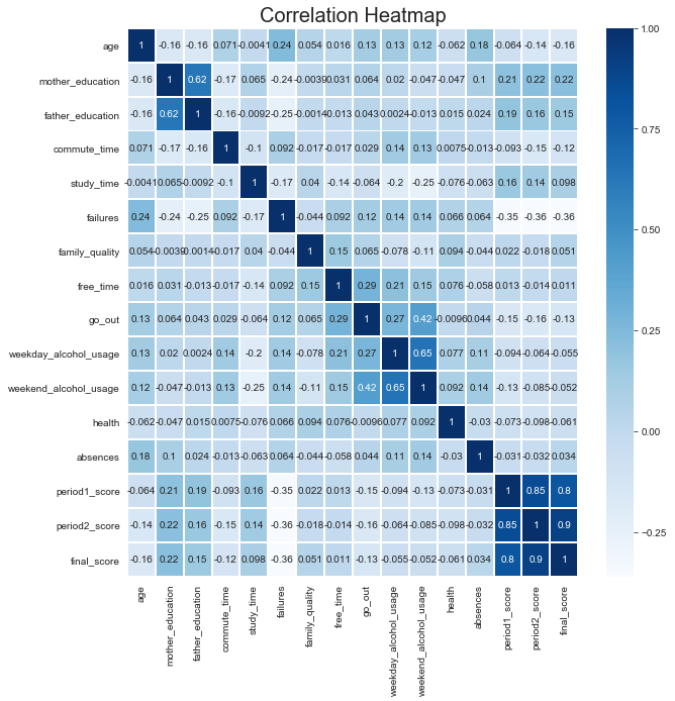

Fig. 2. Correlation Heatmap

IV. Proposed Methodology

Machine learning tasks can be divided into broadly three categories namely supervised learning, unsupervised learning and semi-supervised learning. In this research work, supervised learning is used to build the model as multiclass classification of student performance is done in this research work. In supervised learning, a mathematical model is built by the algorithm from a set of training data that contains both the inputs and the desired outputs. For example, in this research work the task is to determine whether the student is a good performer, average performer or poor performer, the training data includes each student record with all the student related attributes and output variable i.e. the performance of students. The screenshot of training dataset is shown in the Table II. After building the model through supervised machine learning approach, the model is tested by giving new student records without giving the output label i.e. performance of students and their performance is predicted. After that performance of applied algorithms is evaluated. The proposed methodology is shown in Fig. 3.

Appropriate attributes selection is done through correlation heatmap and preprocessing of data is also done by converting output variable into categorical value and by checking for null values, the next step is to split the data in to training and testing. Then different algorithms are fine-tuned with respect to certain parameters. The process of fine tuning and training the algorithms is discussed below with respect to every algorithm:

A. *Decision Tree*

Decision Tree Classifier uses a decision tree to get a decision about the target value. Tree based learning are consider to be one the best and mostly used supervised machine learning algorithms. Firstly, decision tree classifier is trained using the training data then the performance of the classifier is checked using testing data as shown in Table III. Then the decision tree classifier is tuned with respect to minimum samples leaf and applied on extracted features, the dataset obtained in the previous step. Again, tuned classifier is trained using the features extracted data and accuracy is calculated with respect to testing data. Minimum samples leaves specifies the minimum number of samples required to be at a leaf node. The result has shown a significant improvement in terms of accuracy and weighted average of precision, recall, F-measure and decrease in execution time as shown in Table IV.

B. *Random Forest Classifier*

Random forest classifier is a special type of Bootstrap Aggregation. Random forest classifier generates a set of decision trees from randomly selected subset of training set. The final class of the test object is found out by aggregating the votes of different decision trees. Random forest classifier is trained using the training data and then the accuracy of the classifier is checked using testing data as shown in Table III. After this, the random forest classifier is tuned with respect to minimum samples leaf, number of estimators and tuned classifier is applied on extracted features dataset obtained in the previous step. Again, tuned classifier is trained using the dataset consisted of extracted features and accuracy is checked with respect to testing data. Minimum samples leaves specifies the minimum number of samples required to be at a *leaf* node while number of estimators controls the number of trees to be used in the forest. The result has shown a significant improvement in terms of accuracy and weighted average of precision, recall, F-measure and decrease in execution time as shown in Table IV.

TABLE II. Screenshot of Training Data

	school	sex	age	address	family_size	parents_status	mother_education	father_education	mother_job	father_job	...	free_time	go_out
0	GP	F	18	U	GT3	A	4	4	at_home	teacher	...	3	4
1	GP	F	17	U	GT3	T	1	1	at_home	other	...	3	3
2	GP	F	15	U	LE3	T	1	1	at_home	other	...	3	2
3	GP	F	15	U	GT3	T	4	2	health	services	...	2	2
4	GP	F	16	U	GT3	T	3	3	other	other	...	3	2

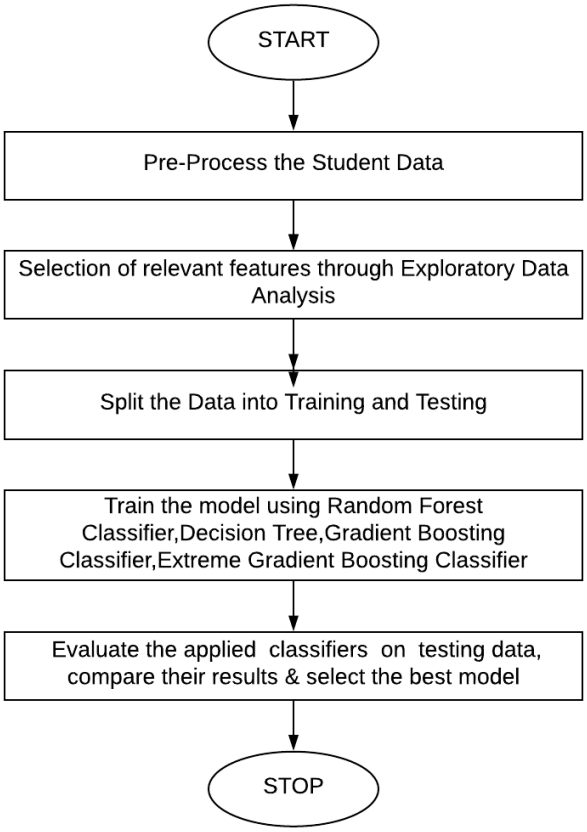

Fig. 3. Proposed Methodology

C. Gradient Boosting Classifier

Gradient Boosting Classifier is an ensemble method of combine's weak learners into strong learners. Gradient boosting helps in automatically reducing the bias. Gradient boosting classifier is trained using the training data then the accuracy of the classifier is checked using testing data as shown in Table III. Then the gradient boosting forest classifier is tuned with respect to minimum samples leaf, number of estimators and tuned classifier applied on featured extracted dataset obtained in the previous step. Again, tuned classifier is trained using the feature extracted data and accuracy is checked with respect to testing data. However, after parameter tuning and feature extraction significant increase in terms of performance parameters is not shown in case of gradient boosting classifier as shown in Table IV. The classifier parameters are tuned with respect to two parameters i.e. minimum sample leaf and n estimators. Number of estimators specifies the number of boosting stages to perform. Gradient boosting is fairly robust to over-fitting so a large number usually results in better performance. Minimum samples leaf specifies the minimum number of samples required to be at a leaf node.

TABLE III. PERFORMANCE METRICS WITHOUT FINE TUNNING AND ATTRIBUTE SELECTION

Prediction Technique	**Performance Metrics**				
	Accuracy	***Precision***	***Recall***	***F-measure***	***Execution Time (in second)***
Decision Tree	84	84	84	84	0.249
Random Forest	73	75	73	73	1.5
Gradient Boosting	92.4	92	92	92	1.256
Extreme Gradient Boosting	**91.6**	**92**	**92**	**92**	**0.70**

D. Extreme Gradient Boosting Classifier

Extreme gradient boosting classifier is designed to increase the speed of gradient boosting classifier and it has inbuilt cross validation feature. It is a faster version of gradient boosting classifier in which cross validation is inbuilt. Without any parameter tuning and feature extraction this classifier outperforms all other classifiers when both accuracy and execution time are considered as shown in Table III. Extreme gradient classifier is faster in terms of execution time. After, parameter tuning and feature extraction significant increase in terms of performance parameters is not shown in case of extreme gradient boosting classifier as shown in Table IV. Two parameters were tuned i.e. minimum sample leaf and number of estimators. Number of estimators specifies the number of boosting stages to perform. Gradient boosting is fairly robust to over-fitting, so, a large number usually results in better performance. Minimum samples leaves specify the minimum number of samples required to be at a leaf node.

TABLE IV. PERFORMANCE METRICS WITH FINE TUNNING AND ATTRIBUTE SELECTION

Prediction Techniques	***Performance Metrics***				
	Accuracy	***Precision***	***Recall***	***F-measure***	***Execution Time (in second)***
Decision Tree	92.4	93	92	93	**0.015**
Random Forest	**95**	**95**	**95**	**95**	**0.20**
Gradient Boosting	93.27	94	93	93	0.420
Extreme Gradient Boosting	**93.27**	94	93	93	**0.111**

V. RESULTS & DISCUSSION

The four algorithms were evaluated on various performance metrics like accuracy, precision, recall, F-measure and execution time. Accuracy is the ratio of correctly

predicted class to the total number of observations. A comparison of accuracy of different techniques with and without parameter tuning and attribute selection is shown in Fig. 4. Precision is the ratio of correctly predicted positive observations to the total predicted positive observations. Recall can be defined as the ratio of correctly predicted positive observations to the all observations in actual class. F1 Score is the weighted average of Precision and Recall. Therefore, this score takes both false positives and false negatives into account. Execution time is the time required for the algorithm on training and testing data. Results have shown that without any parameter tuning and feature extraction, extreme gradient boost outperforms all other classifiers in terms of accuracy and execution time. But after fine tuning and feature extraction, random forest outperforms all other classifier in terms of accuracy, precision, recall, F-measure with respect to other prediction techniques.

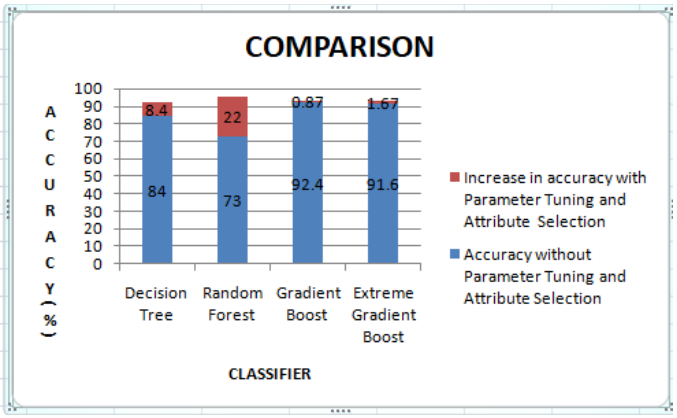

Fig. 4. Comparison of accuracy of different techniques with and without parameter tuning and attribute selection

VI. Conclusion & Future Work

It has been concluded from the research work that proposed machine learning approaches is better in terms of accuracy and other performance parameters when parameter tuning and attributes selection is done. Random forest classifier outperforms all the applied classifiers. Also, the multiclass analysis will give a better analysis to teachers, students, administrators to classify students on the basis of their performance and they can take necessary steps to help students to improve their performance. This prediction models will act like an alarming system to the students. Also, dataset includes not only the academic attributes but also socio-economic attributes. In the future work, a more enhanced dataset including behavioral attributes also along with other student attributes can be considered and parameter tuning can be applied on other algorithms to further increase the accuracy.

References

[1] S.L. Prabha, A.R. Mohamed Shanavas, "Educational Data Mining Applications", *Operations Research and Applications: An International Journal (ORAJ)*, vol. 1, no. 1, pp. 23–29, August 2014.

[2] R. Baker, K. Yacef, "The State of Educational Data Mining in 2009: A Review and Future Visions", *Journal of Educational Data Mining*, vol. 1, no. 1, pp. 3-17, 2009.

[3] C. Romero and S. Ventura, "Educational Data Mining: A Review of the State of the Art", *IEEE Transactions on Systems Man and Cybernetics Part C (Applications and Reviews*), vol. 40, no. 6, pp. 601–618, 2010.

[4] C. Silva, and J. Fonseca, "Educational Data Mining: A Literature Review", *Advances in Intelligent Systems and Computing*, vol. 520, pp.87-94, 2016.

[5] A. B. E. D. Ahmed and I. S. Elaraby, "Data Mining: A prediction for Student's Performance Using Classification Method", *World J. Computer. Appl. Technol.*, vol. 2, no. 2, pp. 43–47, 2014.

[6] Brijesh Kumar Baradwaj, Saurabh Pal, "Mining Educational Data to Analyze Student's Performance", *International Journal of Advanced Computer Science and Applications*, vol. 2, no. 6, 2011.

[7] S.Archana, Dr. K.Elangovan, "Survey of Classification Techniques in Data Mining", *International Journal of Computer Science and Mobile Applications*, vol.2, no. 2, pp. 65-71, 2009.

[8] S. B. Wadkar, S. C. Dharmadhikari, and S. K. Dwivedi, "A Survey on Performance Evaluation and Prediction of Teachers'', *Students' Performance Using Data Mining Techniques*," Int. J. Adv. Res. Comput. Commun. Eng. ISO Certif., vol. 3297, no. 1, pp. 281–285, 2017.

[9] Jie Xu, Kyeong Ho Moon, and Mihaela van der Schaar, "A Machine Learning Approach for Tracking and Predicting Student Performance in Degree Programs", *IEEE Journal of Selected Topics in Signal Processing*, vol.11, no. 5, pp. 742–753, 2017.

[10] S. M. Merchán, and J. A. Duarte, "Analysis of Data Mining Techniques for Constructing a Predictive Model for Academic Performance", *IEEE Latin America Transactions*, vol. 14, no. 6, pp. 2783–2788, 2016.

[11] I. Singh, A. S. Sabitha, A. Bansal, "Student Performance Analysis Using Clustering Algorithm", IEEE *6th International Conference on Cloud System and Big Data Engineering*, pp. 294–299, 2016.

[12] X. Ma, Z. Zhou, "Student pass rates prediction using optimized support vector machine and decision tree", *2018 IEEE 8th Annual Computing and Communication Workshop and Conference (CCWC)*, pp. 209-215, 2018.

[13] Y. Yamasari, Supeno M. S. Nugroho, I N. Sukajaya, Mauridhi H. Purnomo, "Features Extraction to Improve Performance of Clustering Process on Student Achievement", IEEE *International Computer Science and Engineering Conference (ICSEC)*, pp. 2–6, 2016.

[14] Evandro B. Costa, Baldoino Fonseca, Marcelo Almeida Santana, Fab-rlsia Ferreira de Arajo, Joilson Rego, "Evaluating the effectiveness of educational data mining techniques for early prediction of students' academic failure in introductory programming courses", *Computers in Human Behavior*, pp. 247-256, 2017.

[15] M. Sivasakthi, "Classification and Prediction based Data Mining Algorithms to Predict Students' Introductory programming Performance", *IEEE International Conference on Inventive Computing and Informatics (ICICI)*, pp. 1–5, 2017.

[16] R. Asif, A. Merceron, S. A. Ali, and N. G. Haider, "Analyzing undergraduate students' performance using educational data mining", *Computer & Education*, vol. 113, pp. 177–194, 2017.

[17] A. Zollanvari, R. C. Kizilirmak, Y. H. Kho, and D. Hernandez-Torrano, "Predicting Students' GPA and Developing Intervention Strategies Based on Self-Regulatory Learning Behaviors", *IEEE Access*, vol. 5, pp. 23792–23802, 2017.

[18] Fan Yanga, Frederick W.B. Li, "Study on student performance estimation, student progress analysis and student potential prediction based on data mining", *Computers & Education, vol. 123*, pp. 97–108, 2018.

[19] "UCI Machine Learning Repository:Student Performance Data Set",2008.[Online].Available:https://archive.ics.uci.edu/ml/datasets/student+performance#. [Accessed: 14-Apr-2019].

[20] P. Cortez, A. M. G. Silva, "Using data mining to predict secondary school student performance", *in Proceedings of 5th Future Business Technology Conference*, 2008, pp. 5-12.

Proceedings of the Fourth International Conference on Communication and Electronics Systems (ICCES 2019)
IEEE Conference Record # 45898; IEEE Xplore ISBN: 978-1-7281-1261-9

Extracting Primitive Tasks from Procedural Videos using Machine Learning

Amulya Shivanath
Dept. ISE
Ramaiah Institute of Technology
Bengaluru, India
amulyashivanath3897@gmail.com

Dr.Sumana M
Associate Professor, Dept. ISE
Ramaiah Institute of Technology
Bengaluru, India
Sumana.a.a@gmail.com

***Abstract*— Narrated instructions videos are the rich source of information. The problem of automatically extracting the procedures that are narrated in the video and to summarize the important steps to reduce the time and provide the information to the user is addressed. Natural Language Processing Technique is used for extracting the summarization of the narrated task in the given video. The input video dataset contains real world interactions between a human and machine to explain the procedure to complete a certain task. The given data set is analyzed, processed, and finally a list of important steps are extracted which will help in achieving the given task. Procedure identification or Procedure Extraction is useful for a variety of applications including intelligent tutoring systems, representation learning, transfer learning and video understanding.**

Keywords— video data set; procedure extraction; Natural Language Processing; Summarized instructions; Achieve the given task.

I. INTRODUCTION

Procedural videos are the narrated instructional videos that guide the viewer to tackle an unfamiliar situation. Internet remains a huge source of information media. It provides a large number of videos for a particular task. These videos are made with an intention to teach viewers about the task. Example if a viewer needs to know how to make a coffee as he is new to the field he will seek the help of internet to tackle his situation. We get a lot of results for the phrase "How to make coffee" out of which the best one which explains in a easy understandable way and to the fullest need to be chosen.

This task can be made less time consuming by summarizing the necessary steps to a easy readable format. The proposed work deals with this intention. Unsupervised machine learning technique is followed to retrieve the summary. The challenging task was to deal with the linguistic expressions that are the way the information is conveyed through the language. Even though we considered only English subtitle videos we could find people using different phases to convey information. Example "put coffee, pour coffee, serve coffee all mean the same but used in different videos . But we cannot just neglect them though they mean the same .There is a situation that some videos may vomit some steps thinking it is minor, but it also should be considered for a full information delivery.

In this work we use clustering of text to automatically identify sequence of steps .Videos and its subtitle files are studied to identify keywords to automatically build a Annotation file which is the input for the clustering algorithm which will filter the duplicates and align the text to form sequence.

II. Related work

Procedural Knowledge is also known as imperative knowledge is the knowledge exercised in performing a task according to cognitive science [1]. Processing the images and videos automatically to describe their contents to the viewer more clearly has become popular in recent years using natural language processing [2]. Usually a procedural video is guided by human experts who demonstrate a way to accomplish a task e.g. A woman who could be a beautician can demonstrate steps of applying a makeup, A lecturer teaching steps to solve a problem or a Chef instructing for a tasty recipe preparation. Observing the similarities in the demonstrations and recording them remains a key step in building a model is a challenging problem [3]. Video Captioning problem had a rapid progress due to the availability of large-scale of dataset on the internet [4][5].

Most Recently "flipped" classroom have become very popular , it believes that videos remain a effective approach to teach imperative knowledge as long as the content is proper[6][7].Video demonstrations can be used to create a model that will learn from human explanation. But automatic learning of tasks is a challenge as it requires the pre-learning of the relation between tasks and which steps remain important for the final result summarization.

In this work we have concentrated on finding a way to retrieve the main steps first through the text and then through the video. The main steps are summarized after applying the clustering method repeatedly till all the steps are obtained. Unsupervised machine learning approach is used as we could

not label the classes as the videos may differ in using the sentences even though they are meaning or explaining the same task. In this work, we learn the flow in which we can extract sequence of events from a set of narrated instruction videos of a task on the Internet. Such data contains the detailed descriptions of the event they are illustrating but is not structured and contains more amount of noise and disturbance when compared to the original set [15, 16]. Interpretation of a narrated instruction video set has been recently addressed in the following reference [17]. From the related work we were able to find that we could complete our paper in two different ways one, is to read from subtitles file and other is to go through the Annotation files. Going through the Annotation files is better as compared to the subtitles files as the English usage differ from video to video in the given set. If we go for subtitles file it will not be as effective as it could be hence we decide on doing with Annotation file.

III. PROPOSED WORK

A. *Obtaining the Dataset*

The dataset being used is collected by searching through the YouTube with a specific keyword say "making coffee" or "changing tire". As we all know that over internet we can find a lot of things as in these days internet is a very large source for finding any information that is required, this is the reason we get ample amount of options if we search for a thing over any internet platform. In the same way we were listed up with too many videos for the search we made relating to a particular task. The top 30 videos having English subtitles are chosen. The selection of videos are done on the basis of 2 important things, one is that the subtitles are clearly visible to the user seeing them, and the other is that, in all videos there is a human present physically present who is explaining the steps he has been performing in the video to achieve the specified task. These 30 videos set having the aim of making coffee and changing tire are considered as the data set for this paper. The subtitles are extracted from these videos present in YouTube using automatic speech recognition system (ASR). The extracted subtitles are once manually checked to verify there are no spelling mistakes. The average length of each videos considered in the set is about 2 minutes approximately.

B. *Obtaining a Annotation file*

Once the textual data from the videos are extracted and stored as a text file now the next step in the paper is to analyze the subtitles file to extract important steps from it. The extracted words are written on a new file. This new file can be used to create an annotation file. An annotation file is a text file consisting of important steps – that are extracted from subtitles – along with the number of subtitle files in which that particular step has been mentioned in the given set of subtitles.

Obtaining the annotation file stands as the preprocessing work relating to this paper. An Annotation file is a text file containing the set of important steps that are considered after analyzing the video files. As it may seem what is the use of important steps when that whole set of instructions are readily available with us in the subtitle files. Yes the whole set of instructions are available but as said earlier the videos are considered from YouTube. Even though, the task each narrator is planning to achieve is the same at last, the set of words used to one of the narrators in one video can be different from the words used by other narrator. For example assume the task to be state as "raise the car by using Jack", this step can be explained by one narrator as "place the jack under car and raise the car". The other narrator can say it like "Use the jack to raise car". In both the steps the narrator wants the user to raise the car up, but the sentences used are different. Hence the important step that can be extracted from here is that "put jack", "place jack", "raise car", "use jack" and so on.

The steps are noted down on a separate text file. This text file is an input file to an automation tool that is being used in this paper. The automation tool that we are using is a free license automation tool called as the AutoIT. The automation tool takes in 2 input files, one is the file that we recently created which contains the important steps, and the other file is the subtitle file.

Fig 1: The obtained annotation file.

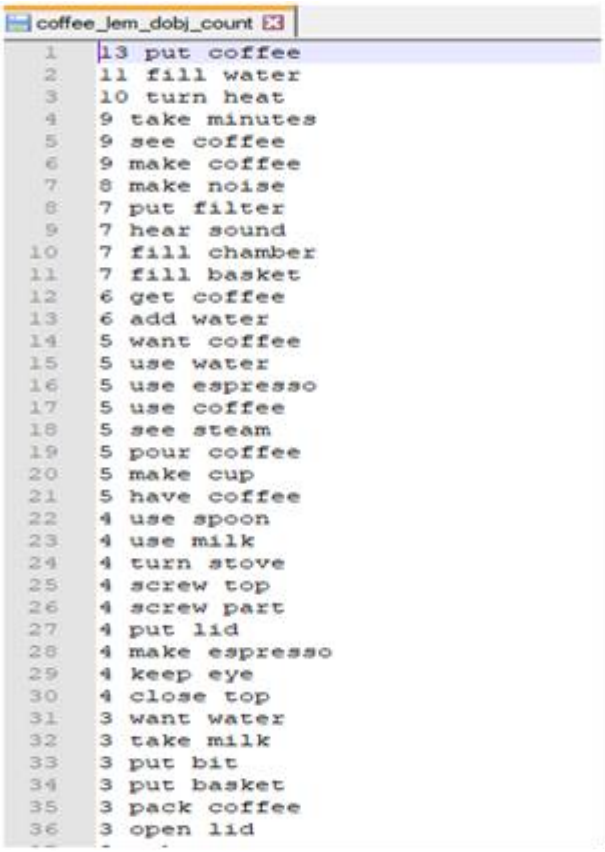

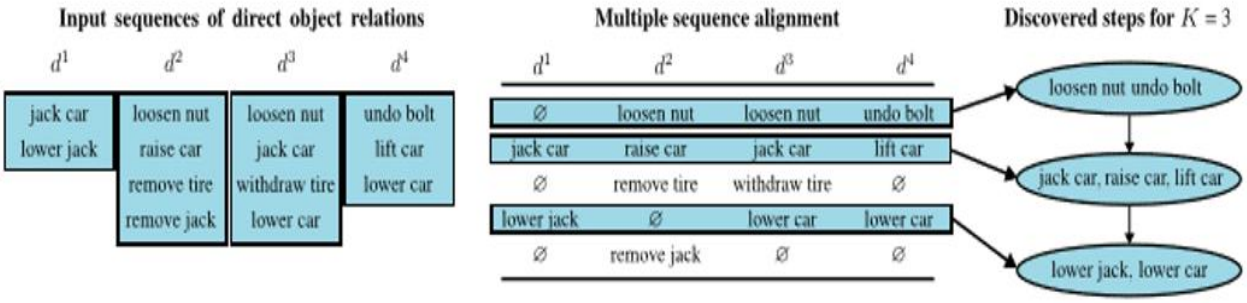

Figure 2: This shows the process of analyzing and clusters of data into groups.

The automation tool works as follows, it reads the data line by line from the file containing the important steps, compares the words with the data present in the subtitles file. Whenever there is a match of words in both the files a counter is incremented. The AutoIt tool will scan over all the 30 subtitle files and finally will give us the result which contains the total number of files that contains the given important step. This number is appended with the specified step and both are written on to a new file.

This newly generated file is named as the annotation file in this paper. Consider an example as shown in figure 1. This is the annotation file that has been created for the task of making coffee. It can be seen that in line 6 the important step that is noted down as "make coffee" is appended with a value 9. This means to state that the step "make coffee" is used in 9 files among the given set of 30 files. Similarly consider line 13 as seen in figure 1, the step is "add water" this has been appended with 6 which indicates that the step "add water" is present in 6 subtitle files.

Figure 3 shows the input file that is given to the AutoIt tool that will be compared with the subtitles files to give an annotation file similar to the figure as shown in Figure 1.

The point to note down here is that the step "add water" could have been used in the subtitle files in many ways say for example: "then add little water", "now we will add little bit of water to vessel", "we are adding water now", and so on.

In the similar fashion the annotation file is created inclusive of all the important steps.

C. Processing the Annotation file

Once the annotation file is received, move to the next step in the paper processing the received annotation file. In this step we analyze the annotated file in order to group the similar important steps.

The Annotation file is processed through a Natural Language Processing (NLP) algorithm. "Matlab" software is used for the processing of the annotation file and for clustering of the similar steps. It takes some iterations to completely sort all the necessary steps and give a summarized form. In the paper the maximum numbers of iterations are taken to be 15. This can be any number but after some trial and error methods we summed the number of iterations to be 15. The Annotation file contains raw information as discussed in the previous section. The instructions may contain repeated keyword for example say 'lower car', 'lower jack' both points to the same operation of lowering the car. This does not mean that we can consider one of the two and neglect the other. Both are equally important. In such a case both the steps are combined together and written under same step.

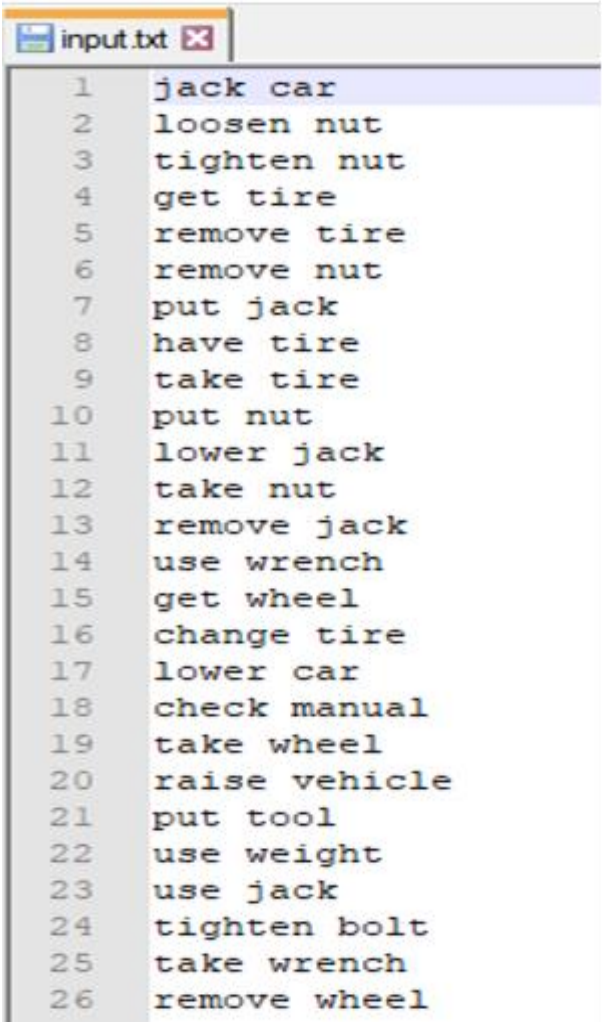

Figure 3: The input file that is given as input to AutoIt automation tool.

The processing of the same can be seen in figure 2. Multiple sequence alignment is done to cluster the similar text. The steps are recognized as a direct object relation which means we consider the steps by a pair of a verb and a object. Example Under step 3 it can be seen that the steps "loosen nut", "undo bolts" have been considered. The algorithm implemented will cluster the text based on the similarity between the keywords as shown in the middle part of figure 2 which is later clustered onto a single step say A1. Similarly "jack car", "raise car" and "lift car" onto group A2.

This clustering of files take part under different iterations and finally as described at the iteration number 15 we get the complete list of sorted summarized steps for achieving the given task.

IV. Results

The primary goal that this paper is trying to portray is on clustering of verbal descriptions present in any of the video set into a sequence of necessary important steps required to achieve the specified task. From the obtained results of the above processing can now be used to analyze the steps for the given task. In our case the given tasks are "Making coffee" and "Changing a tire".

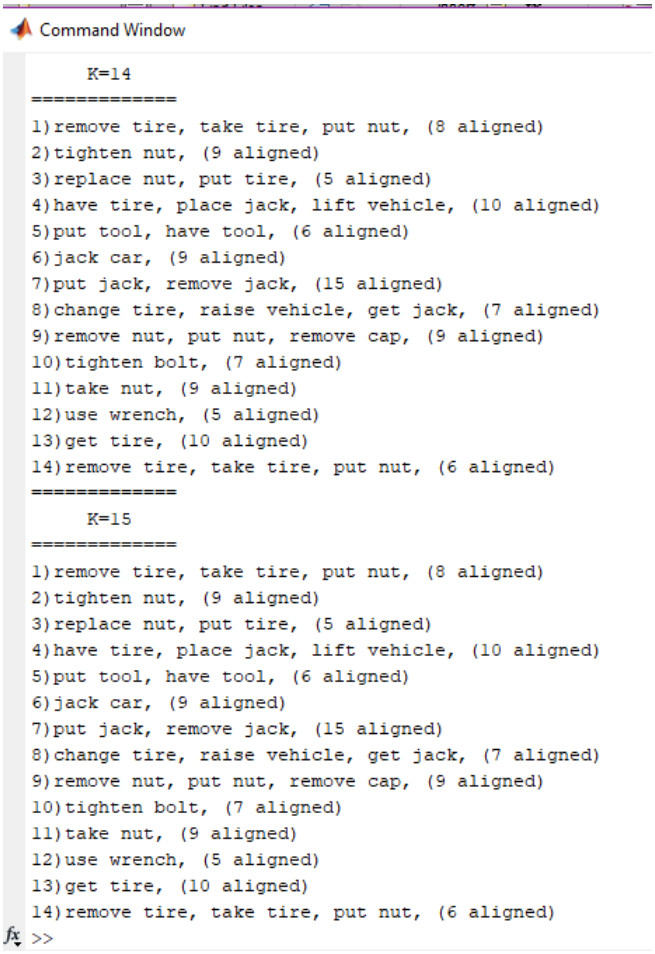

Figure 4. The obtained result after the data is sorted for "Making Coffee".

Now a days people prefer referring to the summarized data rather than going through the whole content. In such a case this procedure can be used to summarize the contents into steps.

The process that is addressed in this paper can be state as multiple sequence alignments problem. In the paper an approach of trying to align a set of instructions present in the given set of data into a set of steps which can be referred instead of going through the whole video.

Figure 4 and figure 5 explains the result that was obtained for 2 data sets. As seen in figure 4 the final output shows the sequence obtained for "Making coffee". Similarly the figure 5 shows the necessary steps when any one wants to change the flat tire of a car. The steps are so clear to understand.

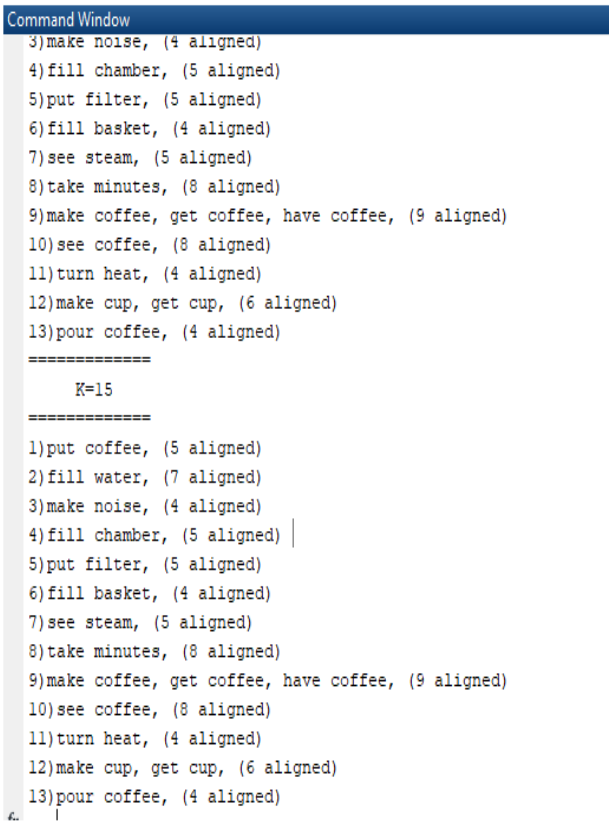

Figure 5: The obtained result after the data is sorted for "Changing Tire".

V. Conclusion

The goal of the arriving at the summary of the important steps of a procedural videos is achieved finally by the use of clustering of data. Before clustering the input is to be clear for this purpose pre-processing was done on the dataset which was a set of videos from the dataset obtained by taking into account that the videos should involve the live demonstration from a human and should include steps to achieve the task and care was also taken to get the videos all explaining the same task with a length not more than 2 minutes. The dataset involved the subtitles file was also the main observation done through which it will be able to pick important keywords easily and done as a text file. This text file is input to automation tool to know the

number of occurrences of each keyword in the videos which further helped us in alignment of the steps in sequence. The output file of the automation is the input for the algorithm which automatically gives us the summary of steps. This work could be further extended to integrate with videos and make the final presentation more colorful and justified.

REFERENCES

[1] Duane F Shell, David W Brooks, Guy Trainin, Kathleen M Wilson, Douglas F Kauffman, and LynneMHerr. Theunifiedlearningmodel. InTheUnifiedLearningModel,pages1–4.Springer, 2010W.-K. Chen, *Linear Networks and Systems* (Book style).Belmont,CA:Wadsworth, 1993, pp. 123–135.

[2] Krishna, Ranjay, Kenji Hata, Frederic Ren, Li Fei-Fei, and Juan Carlos Niebles. "Dense-captioning events in videos." In *Proceedings of the IEEE International Conference on Computer Vision*, pp. 706-715. 2017.

[3] Dennen, Vanessa P., and Kerry J. Burner. "The cognitive apprenticeship model in educational practice." *Handbook of research on educational communications and technology* 3 (2008): 425-439.

[4] Rohrbach, Anna, Marcus Rohrbach, Niket Tandon, and Bernt Schiele. "A dataset for movie description." In *Proceedings of the IEEE conference on computer vision and pattern recognition*, pp. 3202-3212. 2015.

[5] Russakovsky, Olga, Jia Deng, Hao Su, Jonathan Krause, Sanjeev Satheesh, Sean Ma, Zhiheng Huang et al. "Imagenet large scale visual recognition challenge." *International journal of computer vision* 115, no. 3 (2015): 211-252.

[6] Guo, Philip J., Juho Kim, and Rob Rubin."How video production affects student engagement: An empirical study of MOOC videos." In *Proceedings of the first ACM conference on Learning@ scale conference*, pp. 41-50. ACM, 2014.

[7] Milman, Natalie B. "The flipped classroom strategy: What is it and how can it best be used?." *Distance learning* 9, no. 3 (2012): 85.

[8] Sermanet, Pierre, Corey Lynch, Yevgen Chebotar, Jasmine Hsu, Eric Jang, Stefan Schaal, and Sergey Levine. "Time-Contrastive Networks: Self-Supervised Learning from Pixels."(2017).

[9] Merel, Josh, Yuval Tassa, Sriram Srinivasan, Jay Lemmon, Ziyu Wang, Greg Wayne, and Nicolas Heess. "Learning human behaviors from motion capture by adversarial imitation." *arXiv preprint arXiv:1707.02201* (2017).

[10] Goel, Karan, and Emma Brunskill. "Unsupervised Learning of Procedures from Demonstration Videos."

[11] Redondo-Cabrera, Carolina, and Roberto Lopez-Sastre. "Unsupervised learning from videos using temporal coherency deep networks." *Computer Vision and Image Understanding*179 (2019): 79-89.

[12] Zhou, Luowei, Chenliang Xu, and Jason J. Corso. "Towards automatic learning of procedures from web instructional videos." In *Thirty-Second AAAI Conference on Artificial Intelligence*. 2018.

[13] Lin, Xiaozhu, Qin Jin, Shizhe Chen, Yuqing Song, and Yida Zhao. "iMakeup: Makeup Instructional Video Dataset for Fine-Grained Dense Video Captioning." In *Pacific Rim Conference on Multimedia*, pp. 78-88. Springer, Cham, 2018.

[14] De Marneffe, Marie-Catherine, Bill MacCartney, and Christopher D. Manning. "Generating typed dependency parses from phrase structure parses." In *Lrec*, vol. 6, pp. 449-454. 2006.

[15] Frermann, Lea, Ivan Titov, and Manfred Pinkal. "A hierarchical bayesian model for unsupervised induction of script knowledge." In *Proceedings of the 14th Conference of the European Chapter of the Association for Computational Linguistics*, pp. 49-57. 2014.

[16] Regneri, Michaela, Alexander Koller, and Manfred Pinkal. "Learning script knowledge with web experiments." In *Proceedings of the 48th Annual Meeting of the Association for Computational Linguistics*, pp. 979-988. 2010.

[17] Malmaud, Jonathan, Jonathan Huang, Vivek Rathod, Nick Johnston, Andrew Rabinovich, and Kevin Murphy. "What's cookin'? interpreting cooking videos using text, speech and vision." *arXiv preprint arXiv:1503.01558* (2015).

Proceedings of the Fourth International Conference on Communication and Electronics Systems (ICCES 2019)
IEEE Conference Record # 45898; IEEE Xplore ISBN: 978-1-7281-1261-9

Design of Beam Steering Antenna for ISM Band III Using Corporate Feed Network

Amit Abhishek[1], Ankur Utsav[2], Ritesh Kr. Badhai[3], P. Suraj[4]

[1,2,3,4]Department of Electronics and Communication
Birla Institute of Technology, Patna Campus - 800014, India
[1]abhi.amit814@gmail.com [2]ankur.utsav007@gmail.com [3]riteshkbadhai@bitmesra.ac.in [4]psuraj@bitmesra.ac.in

***Abstract*— In this paper a single band beam steering antenna is designed using corporate feed network and feed this network at the output ports of the branch line coupler and it obeys the property of phase shifting of the radiation pattern in both positive and negative direction. A microstrip patch antenna is designed at Industrial Scientific and Medical ISM Band III (24 GHz) which is an unlicensed band and at the same resonance frequency coupler is also designed using Roger RT-Duroid 5880 substrate having relative permittivity (ϵ_r) of 2.2 and its dissipation factor (tanΔ) is 0.0009. After feeding the corporate feed network at output ports of coupler the phase of the beam is varying to ± 55° after feeding excitation at port 1 and port 2 simultaneously. All design and simulations have performed in HFSS software tools.**

Keywords*— Beam Steering, Corporate Feed Network, Branch Line Coupler (BLC), Antenna Array, ISM Band III.

I. INTRODUCTION

Beam steering is all about changing the pattern of the beam at the respective phase angle. It is achieved by different methods such as by using a phase shifter method and switching it by using PIN diode[1], by using branch line coupler beam forming network i.e. BFN [2] is designed and assigning feed at input port one by one and phase is varying at some extent angle. The Beam also steer mechanically by implementing drivers and motors in the system which steers the antenna and beam starts steering respectively in earlier days. Now we design the system which steers the beam electronically where driver elements are used to steer the beam. A new approach to create beam steering for the circularly polarized (CP) antenna array without phase-shift circuits is recommended [3]. It is found that in a spherical coordinate system (r, θ, φ), for any constant r and θ, as φ varies from 0 to 2π, the phase of the CP antenna's co-polarized far field will progress linearly by 2π, and the magnitude is constant [3]. All-metal beam steering antenna founded on the concept of Risley prism is presented in this communication. The antenna is composed of a feed antenna and two metal lenses. A Mechanically rotate two lenses along the same axis independently can steer the radiation beam in both azimuth and elevation planes [4]. If we design an antenna for a band and by changing the size of the patch at different frequencies it will operate, so we steer the beam by this method also [5]. The circular array beam steering scheme using Orbital Angular Momentum (OAM) to resolve the different challenges by providing means to steer an axial beam using RF phase-shifters and RF hybrid couplers [6].The beam is also steered by using Linear Polarized (LP) metalines and Circular Polarized (CP) metalines for discerning the LP beam steering antenna and CP beam steering antenna [7]. Without using phase shifter beam steering is also possible by using three-element phase array antenna, the center or driven patch is fed by an RF source and two neighboring antennas are excited through the mutual coupling from the center antenna [8]. Silicon based electronic integrated circuits (EICs), Photonic integrated circuits (PICs) and antenna-on-chip (AoC) is another advanced process involves in beam-steering [9].

In this paper, we design a rectangular microstrip antenna which operates at 24 GHz and a Branch Line Coupler at the same band. Basically, we need to steer the beam so we design a beam forming network. The designed antenna is used to form a corporate feed network and at the output ports of the coupler is feeded. Different phase is obtained by exciting each port alternatively. Beam steer antenna is broadly used in a current communication network such as Radar network, point to point or multipoint networks and as well as in satellite communication. This beam steering antenna is highly efficient for the ISM Band III applications.

II. ANTENNA DESIGN

As the defined band is ISM band III i.e. 24 GHz and at that frequency, we proposed an antenna which is a rectangular microstrip patch antenna having feed line and its dimension is calculated at 50 ohm impedance value.

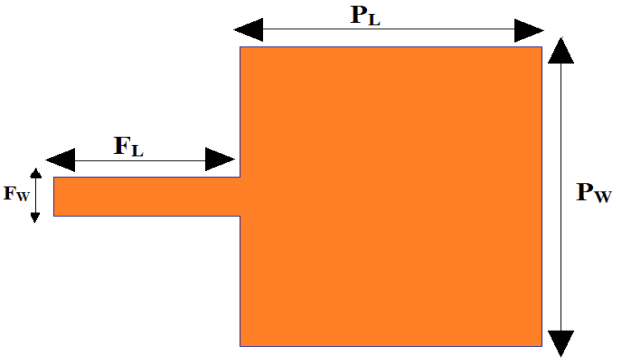

Fig. 1. Designed antenna for ISM Band III

The proposed antenna is shown in Fig 1.with its simulated response in Fig 2. The detailed dimension of the proposed antenna parameters are tabulated Table I. The radiation pattern for the designed antenna is shown in Fig.3 at phi =0 deg. The reflection coefficient (|S11|) for the designed antenna is -46.07 dB and total dimension of the antenna is 5.74mm × 3.9mm (L × W) and designed at the height of 0.79 mm using Roger RT-Duroid 5880substrate. The peak Gain

TABLE I. ANTENNA PARAMETERS

Parameter	Values
P_l	3.55mm
P_w	3.9mm
F_l	2.19mm
F_w	0.5mm

of the single feed antenna is 7 dB and beamwidth of single feed antenna is 58.45° at -3dB down.

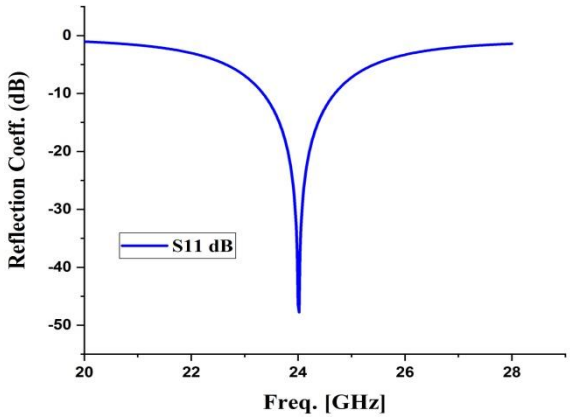

Fig. 2. Simulated response of the designed antenna

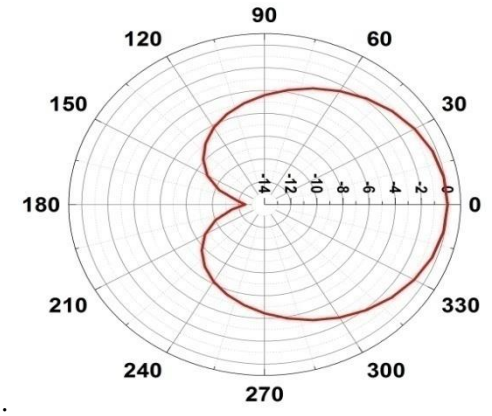

Fig. 3. Radiation Pattern for the designed antenna

III. BRANCH LINE COUPLER DESIGN

Branch Line Coupler is also called the quadrature coupler and having one input port, two output port, and an isolated port as shown in Fig. 4. As branch line coupler has two output ports and there is a phase shift of 90° so, it is used to shift the phase of the beam at some angle. The Coupler is designed at the ISM Band III for proper matching with antenna and it is shown in Fig. 5. The parametric table for this coupler is shown in Table II and all values derive at 50 ohm characteristic impedance (Z_0) value. The value that we calculated for the performed mode of Coupler design for 9 GHz which also resonate of higher order mode at 24 GHz because Coupler having large Bandwidth (B.W) so we design any coupler at lower band and make it also to resonate at a higher frequency. The reason to do so because when we calculate the values of arms of the coupler at 24 GHz it becomes very small and there is an overlap between the arms. We simulate the Coupler at 9 GHz and its simulated result in Fig. 8(a) and after switching it to 24 GHz the

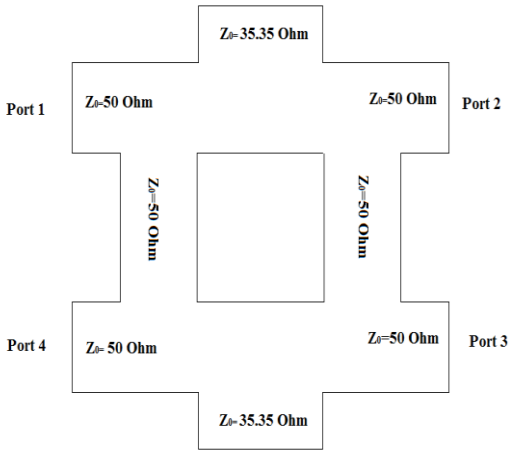

Fig. 5. The basic structure of Branch Line Coupler.

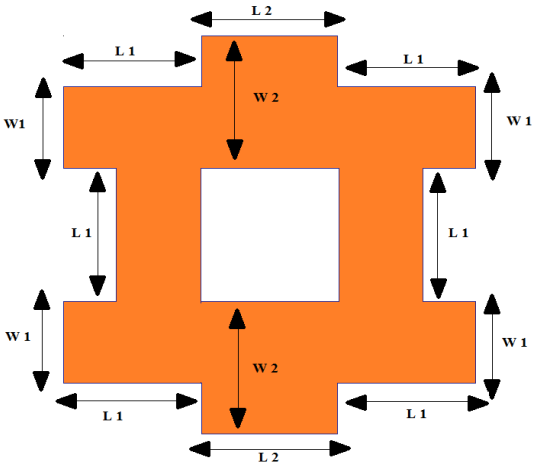

Fig. 6. Designed Branch Line Coupler for ISM Band III.

simulated result is shown in Fig. 8 (b). The phase shift occurs at output ports i.e. Port 2 and port 3 and simulated phase changes is shown in fig. 7 with |S21| for port 2 and |S31| for port 3 respectively. The simulated response for the same coupler at 9 GHz and 24 GHz is not similar, the response of coupler at 9 GHz obeys the defined characteristic of the coupler means at output ports transmission coefficient is same as |S21| and |S31| as shown in Fig. 7(b) and for 24 GHz |S21| and|S31| are totally different from the simulated response for 9 GHz and it happens because the higher frequency is putting at a lower frequency designed coupler.

TABLE II. COUPLER PARAMETERS

Parameter	Values
Length [L1] (Z_0= 50Ω)	4.49mm
Width [W1] (Z_0= 50 Ω)	2.34mm
Length [L2] ($Z_0/\sqrt{2}$ =35.35Ω)	4.41mm
Width [W2] ($Z_0/\sqrt{2}$ =35.35Ω)	3.81mm

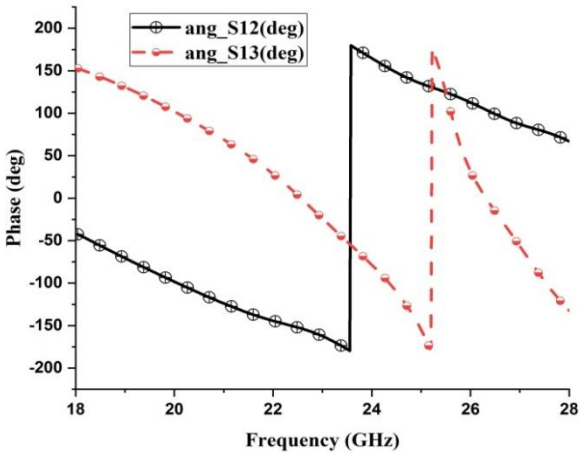

Fig. 7. Phase Vs Freq response at port 2 and port 3.

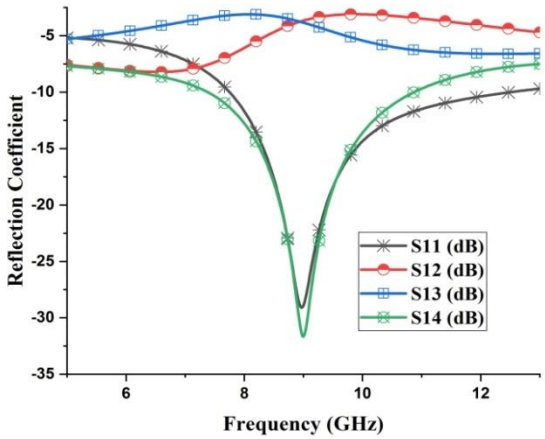

Fig. 8 (a). Simulated response at 9 GHz.

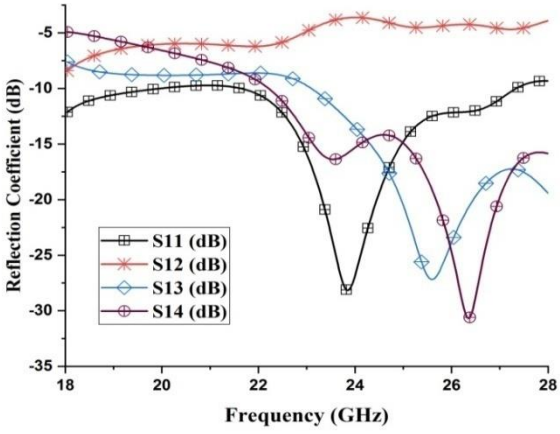

Fig. 8 (b). Simulated response at 24

IV. RESULTS AND DISCUSSIONS

By using branch line coupler and 2×4 corporate feed networks a beam forming network is designed with different feed lines. At Z_0=50Ω a feed line is designed and another one is designed at Z_0=70.7Ω.The designed beam forming network is shown in fig.9. At port 1 excitation is given and

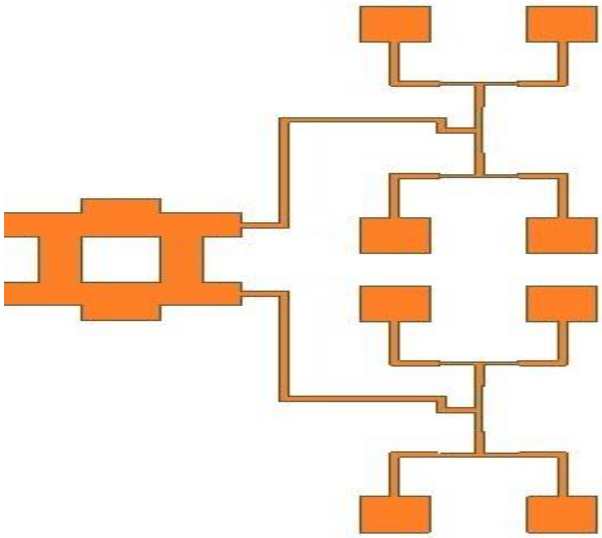

Fig. 9. Beam forming network design

terminating the port 2 the radiation pattern is formed at +55°. After exciting port 2 and terminating port 1 the beam is forming at -55°. The simulated reflection coefficient for each port is similar and it is shown in fig.10. The simulated value of S11 is -14.86dB for port 1 and port 2 respectively. The single microstrip antenna can also feed at the output ports and beam-steering may occur but the gain of the antenna is also desirable. The simulated response at each port is not wide means bandwidth is narrow. The purpose to design this beam forming network is to increase the antenna gain and increase the bandwidth. Without corporate feed network antenna's peak gain is 7dB but with corporate feed network antenna's peak gain is 11 dB. The radiation pattern at port 1 is shown in fig.11 (a) and at port 2 is shown in fig.11 (b).

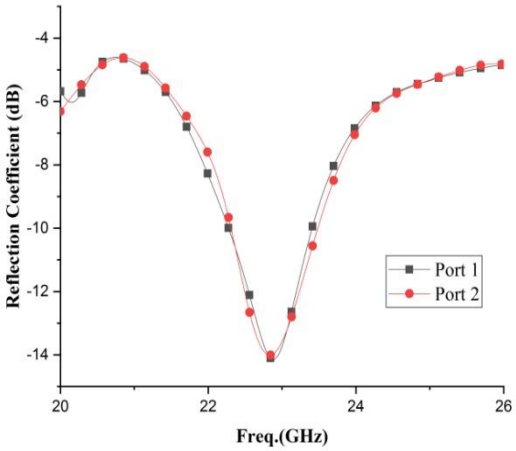

GHz Fig.10. Simulated reflection Coefficient at each port

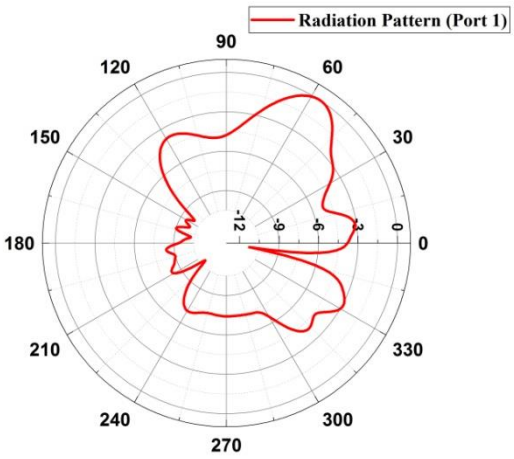

Fig. 11 (a). Radiation pattern at port 1

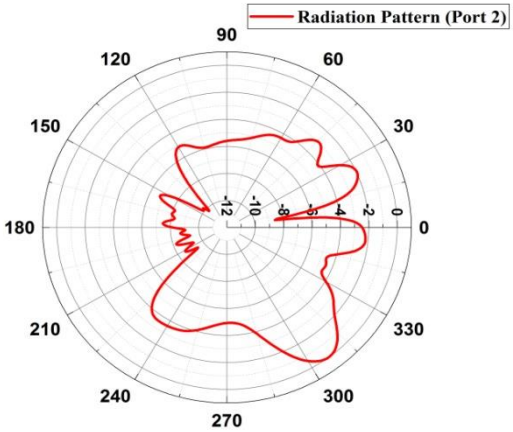

Fig.11(b). Radiation pattern at port 2

The current density distribution at each port is observed at designed network. For port 1 simulated response of current distribution is shown in fig. 12(a) and for port 2 is fig. 12(b). The current density distribution shows the intensity of current flowing from excited port to the feeded antennas. At each port the intensity of current is good and it shows the distributed power in the designed beam forming network.

CONCLUSION

In this paper a novel, innovative, new beamforming network using corporate feed is proposed. For achiveing radiations at particular directional its always difficult to move antenna every time. So we use beam forming networks. Here also our beams are stearing from +55° to -55 ° after exitation of port 1 and port 2 respectively.The dimension of the proposed system is also very small and with good impedence matching, high peak gain and very directive radiation pattern at different angles are achived.We can apply beamforming in different applications like satelite communication, Telecommunication and in radar technology.

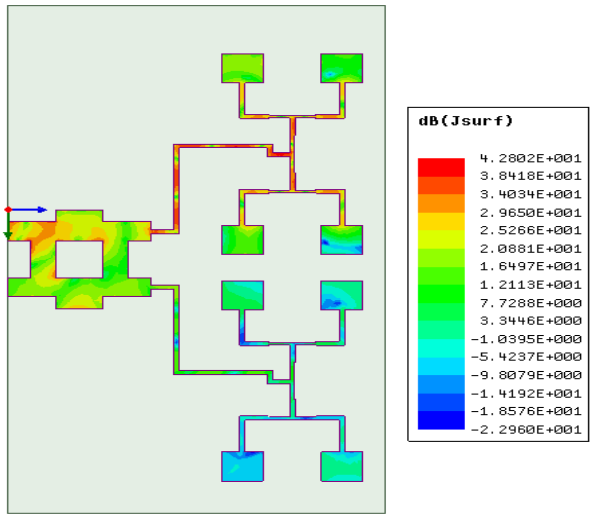

Fig.12(a). Current density distribution at port 1

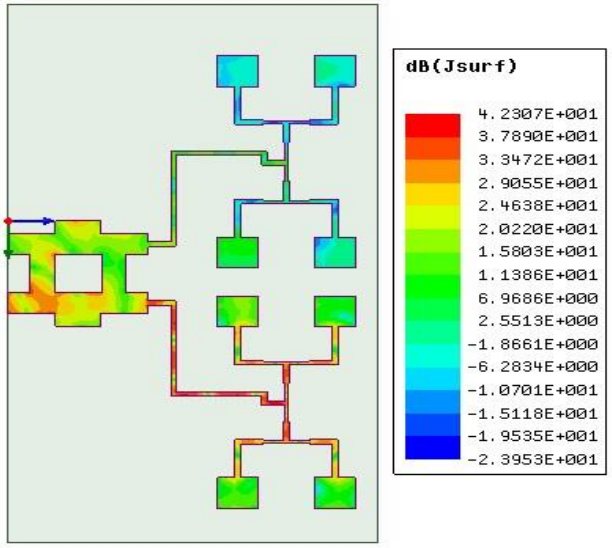

Fig.12(b). Current density distribution at port 2

REFERENCES

[1] Hayat Eriffi, Abdemnaceur Baghdad, Abdelmajid Badri, "Electronically Reconfigurable Beam Steering Array Antenna using Switched Line Phase Shifter", IEEE,978-1-5386-2123-3/17,2017.

[2] G.Rosati and J.Munn, " Fast Prototyping of an 8*8 Butler Matrix Beamforming Network for 5G Applications", IEEE, 978-1-5090-4451-1/17,2017.

[3] Ya-Li Yao, Fu-Shun Zhang, Fan Zhang, " A New Approach to Design Circularly Polarized Beam Steering Antenna Arrays Without Phase Shift Circuits." , DOI 10.1109/TAP.2018.2811839; IEEE Transactions on Antenna and Propagation.

[4] Xuelong Zhao, Chengwei Yuan, Lie Liu, Shengren Pen, Qiang Zhang, Long Zhou Yu, and Yunfei Sun, " All-Metal Beam Steering Lens Antenna for High Power Microwave Application", IEEE TRANSACTIONS ON ANTENNA AND PROPAGATION, vol.65, No. 12, December 2017.

[5] Mohammad Mantash and Tayeb A.Denidni, " Millimeter-Wave Beam Steering Antenna Array For 5G Applications", IEEE, 978-1-5386-3531-5/17, 2017

[6] Mark Klemes, Halin Boutayeb, and Fayez Hylazie, " Orbital Angular Momentum (OAM) modes for 2-D Beam-Steering of Circular Arrays," 2016 IEEE Canadian Conference on Electrical and Computer Engineering (CCECE), 978-1-4673-8721-7

[7] Hisamatsu Nakano, Tomoki Abe, and Junji Yamauchi, "Beam-Steering Antenna Using Metalines", 978-1-5386-0465-6/17 2017 IEEE.

[8] Yazid Yusuf, Xun Gong, "A Low-Cost Patch Antenna Phased Array With Analog Beam Steering Using Mutual Coupling and Reactive Loading", IEEE ANTENNAS AND WIRELESS PROPAGATION LETTERS, VOL., 7,2008.

[9] Zizheng Cao, Qian Ma, Adrianus Bernardus Smolders, Yuqing Jiao, Michael J. Wale, Chin Wan Oh, Hequan Wu, and Antonius Marcelues Jozef Koonen, “Advanced Integration Techniques on Broadband Millimeter-Wave Beamsteering For 5G Wireless Network and Beyond”, IEEE JOURNAL OF QUANTUM ELECTRONICS, VOL., 52, NO. 1, JANUARY 2016.

Proceedings of the Fourth International Conference on Communication and Electronics Systems (ICCES 2019)
IEEE Conference Record # 45898; IEEE Xplore ISBN: 978-1-7281-1261-9

A DECODER-MUX BASED ARBITER PHYSICAL UNCLONABLE FUNCTIONS FOR LOW COST SECURITY APPLICATIONS

Anil Kumar.Kurra
Ph.D Scholar, ECE
VFSTR(Deemed to be university)
*V*adlamudi,India-522213
kakumar94@gmail.com

Usha Rani.Nelakuditi
Professor, ECE
VFSTR(Deemed to be university)
*V*adlamudi,India-522213
usharani.nsai@gmail.com

Abstract— Physical Unclonable Functions (PUFs) are extensively used to generate the cryptographic keys from the Integrated circuits(ICs),by utilizing the uncontrollable and unavoidable process variations during fabrication process. Arbiter PUFs are emerged to be a one of the strong delay based PUFs having exponential number of challenges and used in commercial and critical security applications. In this paper we proposed 8-stage decoder-multiplexer based arbiter PUF, simulated on cadence spectre using CMOS 90nm technology and measured its security metrics such as reliability(92.56%), uniqueness(48%) and uniformity(47.36%) respectively.

Keywords— Physical Unclonable Functions(PUFs),Arbiter PUF, Hardware security, machine learning attacks.

I. INTRODUCTION

As a continuous growth of the complex digital devices, it is very much necessary to enhances the authenticity, confidentiality, and trustworthiness of each and electronic device. Over the past decade in the field of intrinsic security, several methods being developed to generate the secret keys such as True Random Number Generator(TRNG),pseudo random number generator(PRNG) etc and stored in Non-Volatile Memories(NVMs). Storing the confidential keys in Non-volatile memories are vulnerable to side-channel attacks and also occupies the huge area. Hence to mitigate the above problem Physical Unclonable Functions (PUFs) are emerged to be a one of the promising hardware cryptographic primitive.PUF is a small piece of an electronic circuit which generates an efficient and reliable volatile secret keys by utilizing the unavoidable semiconductor process variations during the manufacturing process[1]. Therefore, these random variations will make each IC will acts as an individual physical fingerprint. The response of a PUF is always the function of the input challenge and random structure of the electronic circuit. Typically, the applied challenge and resulting response are termed to be a Challenge-Response pair(CRP), it can be expressed as Response=PUF(Challenge). Due to its inherent nature and intractably behavior, each challenge can trigger an unpredictable response.Fig.1,depicts an outline of the PUF[2][3]. The generated set of responses from an IC is mainly dependent on two statistical sources such as global mismatches and local mismatches[4](Fig.2,). Global mismatches occur during the fabrication process and factors which are mainly due to oxide thickness, channel length, diffusion depth, impurity concentration, etc, are significantly responsible for on-chip secret keys. On the other hand local mismatches such as supply voltage, temperature, aging can affect the performance of the PUF circuit. The outcome of any PUF circuit is a combination of these mismatches and it can be expressed by (1).

$$M_{Total} = M_{Global} + M_{Local} \quad (1)$$

The rest of the paper is organized as follows in section 2 describes the background and preliminaries of strong PUFs(ring oscillator and arbiter PUF). Section 3 delivers the proposed decoder-mux based arbiter PUF and its results. Finally, section 4&5 describes the conclusion and future scope.

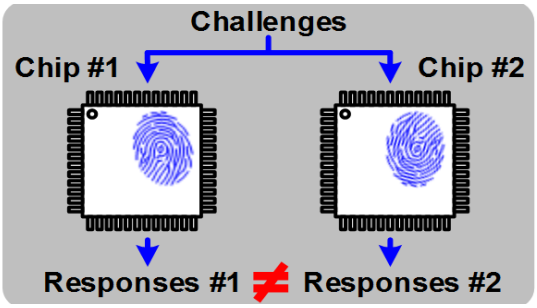

Fig. 1,Challenge response behavior of PUF circuit.

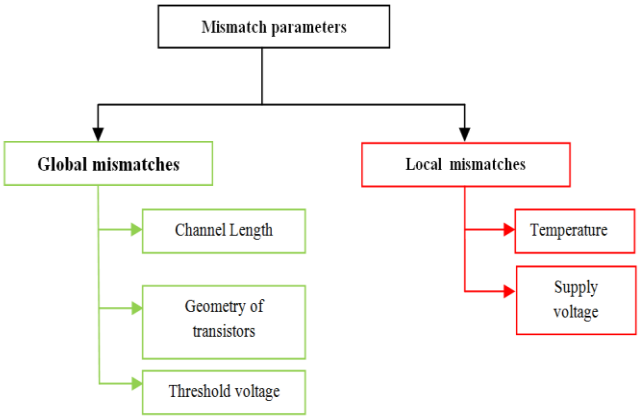

Fig. 2, Classification of mismatches for CMOS PUFs.

II. BACKGROUND AND PRELIMENRARIES

By taking advantage of the mismatches occurred in CMOS ICs, Many constructions have been performed. Depending upon the number of CRPs researchers can be broadly classified PUFs into two categories such as strong PUFs and weak PUFs[5][6]. Weak PUFs are the PUFs having a limited number of CRPs, Signatures obtained from PUF are stable and robust against the environmental variations. Responses are highly unpredictable and strongly depends on fabrication process variations. Weak PUFs such as SRAM PUF, butterfly PUF, etc. On the other hand, strong PUFs differ from weak PUFs, the properties acquired by strong PUFs such as a large set of CRPs, responses can be stable over a wide range of temperatures. Strong PUFs such as arbiter PUFs, ring oscillator PUFs, etc. Depending upon type of application different PUFs being used in each scenario. The main objective of this paper is to discuss the different types of strong PUFs (Multiplexer based PUFs)

corresponding advantages and relatively compare the performance metrics with the proposed PUF. Basically there two different types of strong PUFs are widely used in the device authentication and cryptography such as ring oscillator PUF and arbiter PUF respectively.

A. Ring oscillator PUF

The basic architecture of the ring oscillator PUF as shown in Fig.3, It consists of N-identical delay loops (ring oscillators) are placed on the silicon-Chip[7][8][9]. The minute fabrication variations in the silicon layers of the semiconductor device can results, a slit frequency difference in each pair of delay loops. when a set of input challenge being applied to the PUF circuit depending upon a fixed set of frequency oscillations and process variations can produce the response either '1' or '0' respectively. Researchers have been proposed the several types of ring oscillators in order to improve the performance metrics of the PUF, out of those configurable ring oscillator is one type of the PUF, which enhances the reliability of the PUF.

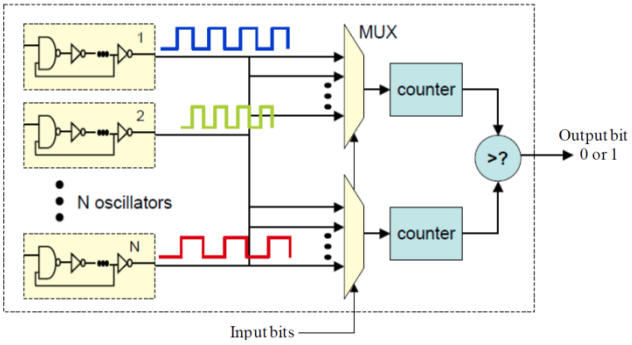

Fig. 3, Ring oscillator PUF.

B. Arbiter PUFs

Arbiter PUF can be coined as one of the strong delay-based PUF. It consists of N stages and two multiplexers are connected at the top and bottom of each stage. A pulse signal is applied as an input of the first stage and selection lines in each stage of the multiplexer will act as a challenge. Depending upon a set of challenges and intra-die variations lead to generate a unique set of responses. The last stage of two multiplexers is connected to the arbiter (DFF) which determines the final response '0' or '1' based on analogy delay difference. For an N-stage arbiter PUF having 2^N number of symmetrical paths and N-challenges. Fig. 4, depicts the linear arbiter PUF architecture [10][11]. One of the biggest issue associated with classical arbiter PUF relatively suffers from reliability and linearity. In order to overcome the above-mentioned issues researchers[12] have proposed several Non-linear arbiter PUFs such as feed-forward arbiter PUF, feed-forward cascade PUF, feed-forward separate, buffer-based PUFs, etc.

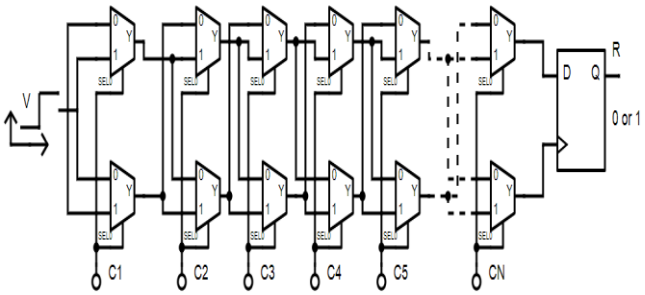

Fig. 4, Schematic of the linear N-stage arbiter PUF[13].

III. PROPOSED DECODER BASED ARBITER PUF

3.1 Operation of decoder PUF

Fig .5, depicts the basic block diagram of the decoder-mux based arbiter PUF. The architecture mainly consists of two stages such as delay network and arbiter network. Each individual stage of the delay network having two switching elements such as 2-4 decoder and transmission gate based multiplexer respectively. A pulse signal is applied as stimulus for the first stage of the delay network and selection lines of the top and bottom multiplexer will acts as the challenges for the first stage of the delay network. Depending upon the input challenges and minute process variations makes significant delay variations in each and individual stage. This process will be continuous until final stage of the delay network and Last stage of the delay network is fed to the arbiter(DFF),which decides the final response based on arrival of the signal. Fig.6 depicts the 8-stage decoder-mux based delay network and fig.7, represents Schematic of the arbiter.

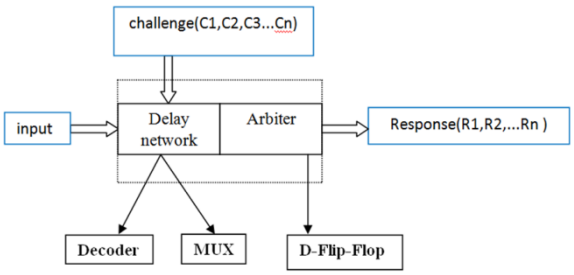

Fig. 5, Block diagram of decoder-Mux based PUF structure.

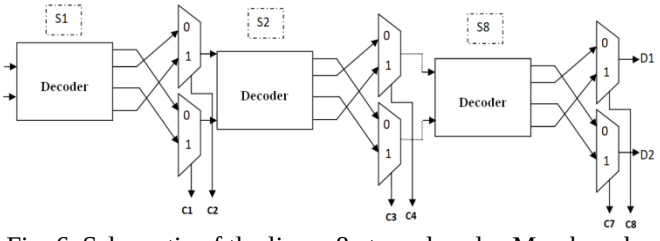

Fig. 6, Schematic of the linear 8-stage decoder-Mux based delay network.

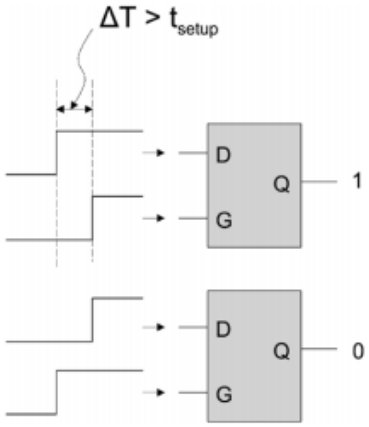

Fig. 7, Detection of final response by an arbiter with respect to delay difference

3.2 Simulation setup and Results

The proposed 8 stage decoder-MUX based PUF architecture being implemented and characterized using cadence spectre. The technology library used as CMOS 90nm process nodes. To study the effect of the process variations and environmental variations performed the Monte-Carlo (MC) simulation to analyze the statistical variations over 200 iterations and 150 samples. From the estimated results measured the security metrics and analyzed the final yield of the proposed PUF based on mean and standard deviation. The yield can be enhanced by each design by tweaking process variations. For any PUF architecture the performance can be estimated by using a set of metrics such as uniqueness, reliability, and uniformity. This can be discussed in a detailed manner in the below discussion.

A. uniqueness:

It is one of the important metric, which can be used to assess the similarity of the PUF responses over different instances. This can be measured by using the Inter-Hamming Distance(HD_{inter}), for any PUF the uniqueness should be very high, otherwise, the response could be predictable and not used for security applications. The ideal value for HD_{inter} is 50%. There are several measurements are employed to estimate the PUF response and most commonly used metric can be expressed by (2).

$$\text{uniquness} = \frac{2}{k(k-1)} \sum_{k}^{k-1} \sum_{j=i+1}^{k} \frac{HD(R_i, R_j)}{N} \times 100\% \quad (2)$$

'N' is the total number of PUF instances, R_i, R_j -is two dissimilar chips i and j.

In order to estimate the uniqueness of a PUF applied the MC analysis over 200 iterations and 25 random challenges. And measured Its mean and standard deviation from 3-sigma plot. The response could be taken at 25^0C and 1v.To achieve better uniqueness varied the threshold voltage(Vt) of the MOSFET were varied and measured its final response ate different intravels. The uniqueness could be measure at different corners such as typical typical(TT),slow slow(SS),slow fast(SF),fast slow(FS) and fast fast(FF). From the obtained results we estimated the maximum uniqueness could be 48% at TT corner. Fig 8(a),(b),(c),(d)and (e) depicts inter die HD variations at different corners.

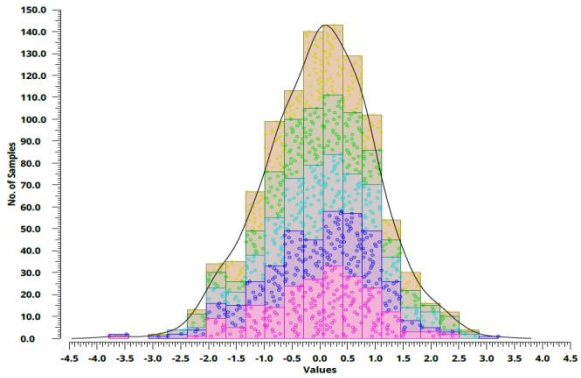

(a)

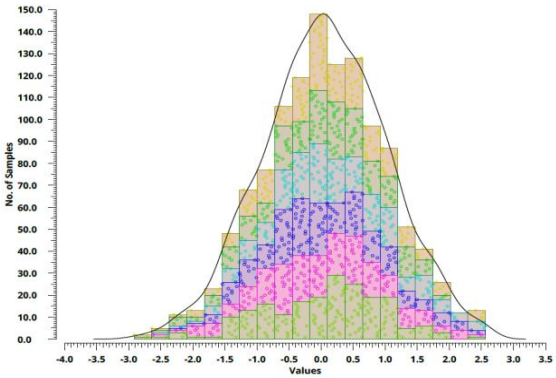

(b)

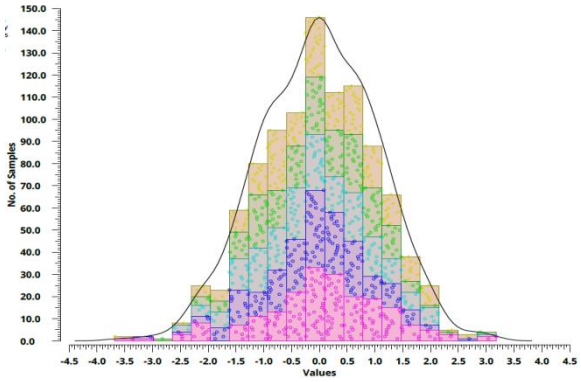

(c)

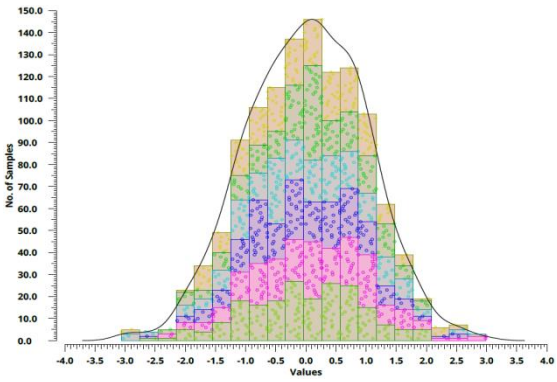

(d)

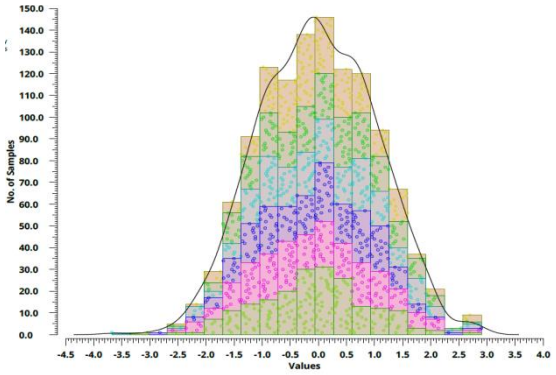

(e)

Fig. 8,Distribution of Hamming Distance at different corners(a)TT,(b)SF,(c)FS,(d)SS,(e)FF.

B. Reliability

The ability of PUF which can recreates the same response under different environmental conditions such as temperature, voltage and ageing etc. Due to these effects the response of the PUF should be flipped. The ideal value of the reliability is 100%.This metric can be measured using Intra Hamming Distance(HD_{intra}).Mathematically it could be expressed by (3).

$$\text{reliability} = \frac{1}{s}\sum_{t=1}^{s}\frac{HD(R_i, R_{i,t})}{N} \times 100 \quad (3)$$

In order to estimate the reliability of the PUF, chosen as a reference response/golden response at 1v and 25^0c, then collected a set of 25 random challenges and measured its reliability by varying temperature from -20^0c to -55^0C and supply voltage ranging from 0.9V to 1.5V respectively. This process can be done for 200 iterations over 150 samples at each iteration. From the results we observed the maximum reliability 92.56% and minimum reliability is 89.36%. Fig 9(a) and (b) represents the reliability of proposed PUF at different nodes of voltage and temperature at different instances.

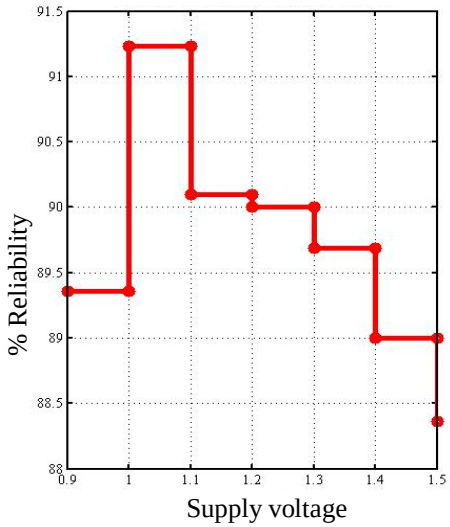

(a)

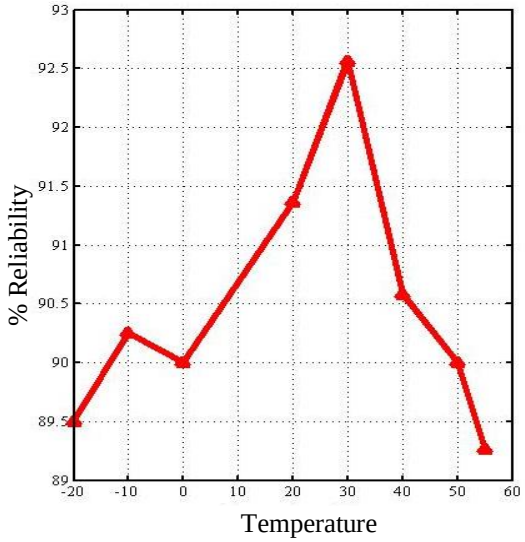

(b)

Fig. 9, % Reliability with respect to (a) Supply voltage and (b) temperature.

C. uniformity

It is a measure of unpredictability of the PUF response, even with the prior knowledge of circuit the generated response could be unpredictable for each and every challenge. The ideal value of the uniformity is 50%. This indicates that response having equal proportion of '1' and '0' respectively. Mathematically it could be expressed by equation (4).

$$\text{uniformity} = \frac{1}{n}\sum_{i=1}^{n} R_{i,l} \times 100\% \quad (4)$$

Fig.10, represents the distribution of the response of the PUF response over 150 number of samples. The test results indicates that maximum mean could be 47.36% respectively.

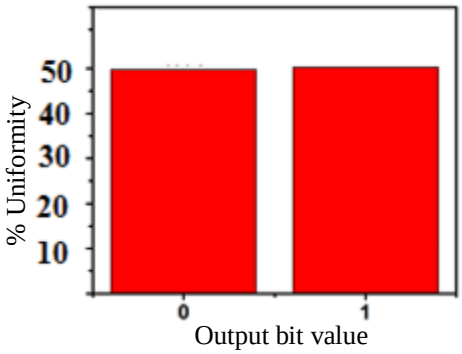

Fig. 10, Estimation of uniformity (% '0' and '1').

IV. CONCLUSION

In order to enhance the security of the PUF and avoided invasive, semi-invasive and side channel attacks proposed a non-linear complex decoder-mux based arbiter PUF. This architecture can satisfy the security metrics and suitable for the device authentication, identification, and IoT environment. The proposed architecture can be tested over the wide range of voltage and temperatures to estimate its reliability, uniqueness, and uniformity. It was observed that these values are very close to the ideal values. And there is

an improvement of reliability with respect to the non-linear MUX based PUFs

V. FUTURE SCOPE

Fabrication of proposed and thoroughly tested decoder-mux based strong PUF architecture can be considered for future work since it can be used in many real-time IoT authentication applications.

REFERENCES

[1] B. Gassend, D. Clarke, M. Van Dijk, and S. Devadas, "Silicon physical random functions," in Proc. 9th ACM Conf. Compute. Security,2002, pp. 148–160.

[2] M. Rostami, F. Koushanfar, and R. Karri. A primer on hardware security: Models, methods, and metrics. Proceedings of the IEEE, 2014.

[3] D. Lim, J. W. Lee, B. Gassend, G. E. Suh, M. van Dijk, and S. Devadas, "Extracting secret keys from integrated circuits," IEEE Trans. Very Large Scale Integr. (VLSI) Syst., vol. 13, no. 10, pp. 1200–1205, Oct. 2005.

[4] B. Gassend, D. Clarke, M. van Dijk, and S. Devadas, "Silicon physical random functions," in Proceedings of the 9th ACM Conference on Computer and Communications Security, ser. CCS '02. NewYork, NY, USA: ACM, 2002, pp. 148–160.

[5] D. Forte and A. Srivastava, "Manipulating manufacturing variations for better silicon-based physically Unclonable functions," in 2012 IEEE Computer Society Annual Symposium on VLSI, Aug 2012, pp. 171–176.

[6] R. Kumar, S. N. Dhanuskodi, and S. Kundu, "On manufacturing aware physical design to improve the uniqueness of silicon-based physically Unclonable functions," in 2014 27th International Conference on VLSI Design and 2014 13th International Conference on Embedded Systems, Jan 2014, pp. 381–386.

[7] J. W. Lee, D. Lim, B. Gassend, G. E. Suh, M. van Dijk, and S. Devadas, "A technique to build a secret key in integrated circuits for identification and authentication applications," in VLSI Circuits, 2004. Digest of Technical Papers. 2004 Symposium on, June 2004, pp. 176–179.

[8] Mingze Gao, Khai Lai, and Gang Qu. A highly flexible ring oscillator PUF. In DAC '14, 2014.

[9] M. Young, The Technical Writer's Handbook. Mill Valley, CA: University Science, 1989. [10] Y. Hori, T. Yoshida, T. Katashita, and A. Satoh, "Quantitative and Statistical Performance Evaluation of Arbiter Physical Unclonable Functions on FPGAs," in Proceedings of the International Conference on Reconfigurable Computing and FPGAs, 2010, pp. 298–303.

[10] M. Cortes, G. Araujo, and J. Capovilla, "Improving the statistical variability of delay-based physical Unclonable functions," in 2015 28th Symposium on Integrated Circuits and Systems Design (SBCCI), Aug 2015, pp. 1–7.

[11] Y. Lao and K. K. Parhi, "Statistical analysis of MUX-based physical Unclonable functions," IEEE Transactions on Computer-Aided Design of Integrated Circuits and Systems, vol. 33, no. 5, pp. 649–662, 2014

[12] V. P. Klybik and A. A. Ivaniuk, "Use of arbiter physical Unclonable function to solve identification problem of digital devices," Auto. Contr. and Comput. Sci. , vol. 49, no. 3, pp. 139–147, 2015.

Proceedings of the Fourth International Conference on Communication and Electronics Systems (ICCES 2019)
IEEE Conference Record # 45898; IEEE Xplore ISBN: 978-1-7281-1261-9

Memory Optimizing Algorithms for Data Acquisition in Electric Drive of Hybrid Electric Vehicles

Gopika Rajan
Department of Electrical and Electronics Engineering
Federal Institute of Science and Technology
Ernakulam, India
gopikarajan4@gmail.com

Vinoth Ramalingam
Electric and Hybrid Vehicles
Robert Bosch Engineering and Business Solutions Pvt. Ltd
Coimbatore, India
Vinoth.Ramalingam@in.bosch.com

***Abstract*—Data acquisition of electric drive is very much relevant in the context of electric vehicles. Different data like IGBT temperature, diode temperature, coolant temperature, electric machine coolant temperature, motor torque, electric machine speed data etc. have to be acquired and analyzed in electronic control units. Data samples are processed in RAM using various algorithms and relevent information is extracted and transferred to ROM as various maps. These information are useful in life time estimation, failure analysis and optimum design of various electric drive components. Histograms and rainflow counting are conventionally adopted methods in data acquisition. Histograms may include irrelevant information and also require large memory space. Normal offline rainflow counting also demands large memory, which necessitates the need for an optimum memory consuming data acquisition algorithm. An online rainflow counting algorithm based on three point method can minimize the RAM space consumption by significant amount. The data counts remains same as in offline rainflow algorithm. Instead of using histograms for data like electric machine speed, data counts for only the relevant operating range can be stored, which minimizes memory requirement. Also level crossing counting is another algorithm which can be adopted where we are interested only in threshold crossings of the parameter acquired, for example the threshold crossing of inverter phase currents, which can cause serious damage to the system. Memory requirement minimization achieved by the above mentioned algorithms are validated by simulation.**

***Index Terms*—offline rainflow algorithm, online rainflow algorithm, level crossing counting, histograms.**

I. Introduction

Different data acquisition algorithms are used for processing and storing electric drive data. Histograms are conventionally used storage method, which consumes large memory space. Other advanced counting methods are used for filtering and storing input data without losing much granularity. Level crossing counting, as per ASTM standards is implemented, where preset threshold crossing information of acquired data is required[2]. In peak counting the peaks and valleys are counted based on a preset level. Peaks higher than the reference level and valleys lower than the reference level are counted[2]. Simple range counting and maximum edge counting are other conventionally used cycle counting methods[2].Rainflow counting is another widely implemented algorithm in cycle counting and fatigue analysis. Different variants of this algorithm is used. Rainflow algorithm based on pagoda roof analogy proposed by Endo and Matsuishi is the basis for all rainflow varients[3]. One of the most widely implemented rainflow algorithm was proposed by Downing and Socie. This three point algorithm was specified in ASTM E 1049-85[2]. Rainflow cycle counting algorithms provide means for comparing obtained variable amplitude load history with constant amplitude load pattern. Rainflow algorithm identifies closed hysteresis loops in the stress - strain plane and provides a method for treating open loops[4]. Other modern methods like Moshrefifar and Azamfar counting were later proposed, but rarely adopted due to complexity in the procedure[5]. In the above method rainflow counting is widely adopted and efficient method, but consuming lot of memory. An online rainflow counting based on the three point algorithm can considerably reduce the RAM consumption[6]. The input data samples are filtered and processed and relevant data is extracted at the instant when the input samples are obtained and the samples are discarded, reducing RAM memory consumption. The online three point rainflow algorithm can be used in data acquisition of various electric drive parameters like IGBT temperature, diode temperature, coolant temperature, electric machine speed etc. in the electric drive.

II. Offline Rainflow Algorithm

A. Algorithm

For a sample load-time history as in Fig. 1, let 'X' be the current range, 'Y' be previous range adjacent to 'X' and S be the Starting point in the history. The three-point offline algorithm as per ASTM E 1049-85[2] is specified below,

A) Read next valley or peak. If end of data then go to step F.
B) If the number of turning points is less than three then go to step A. Update X and Y with three most recent valleys & peaks that are not eliminated.
C) Check the magnitude of ranges Y & X.
    A) If X<Y, go to step A.
    B) If X>=Y, go to step D.

D) If Y includes S them go to step E, if not count Y as a full cycle and remove the turning points in Y & go to step B.
E) Range Y is counted as a half cycle and remove the initial point in Y and set next point in Y as starting point and go to step B.
F) Count remaining ranges as half cycles.

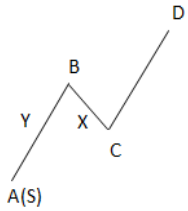

Fig. 1. Sample load history showing ranges and starting point.

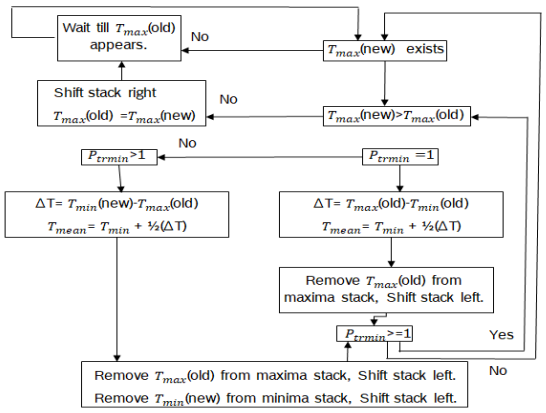

Fig. 2. Online Rain-Flow counting algorithm working on maximal values.

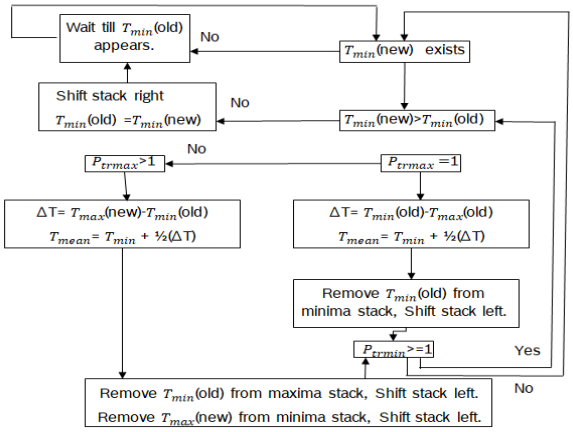

Fig. 3. Online Rain-Flow counting algorithm working on minimal values.

B. Challenges in implementing offline rainflow algorithm

The offline rainflow algorithm is not suitable for real time applications. The load history for significant time should be stored for proper cycle formation from the data. The algorithm cam be applied only on a stored load history. It have a buffer which accommodates the consequent turning points (minima & maxima). The buffer size should be determined before the algorithm is executed. For this the duration between successive usage of the rainflow algorithm, should be predetermined before the algorithm execution. The buffer should have the capacity of holding the entire loading range of the system under consideration. This involves large quantities of data demanding substantial computational resource to process the data during algorithm execution. In real-time applications, coding should be carefully done so that other real-time activities of the ECU are not interrupted.

III. Memory Optimizing Algorithms

A. Online Rainflow Algorithm

The turning points are processed as it occurs. Two buffers are used for this purpose. After processing, the turning points are discarded thus minimizing memory consumption. The load-time history need not be stored. Half and full cycles are extracted in a recursive manner, depending on the buffer contents. The procedure used for obtaining the full and half cycles is similar to the one used in offline rainflow method, and the cycle counts are therefore same for same loading sequences. Pre-ordering of input data points in ascending or decending order as in offline rainflow is not required. The online three point algorithm is depicted in fig. 2 and fig. 3, where, T_{max}-Element of maxima stack, T_{min}-Element of minima stack, P_{trmin}-Element of minima stack elements, P_{trmax}-Element of maxima stack elements. The MATLAB simulation of both online and offline three point rainflow on IGBT temperature input in the range, [20^oC-120^oC] and coolant tempearture input in the range, [20^oC-120^oC] gives similar maps, shown in fig. 4 and fig. 5 respectively, which implies there is no loss of data in the online method.

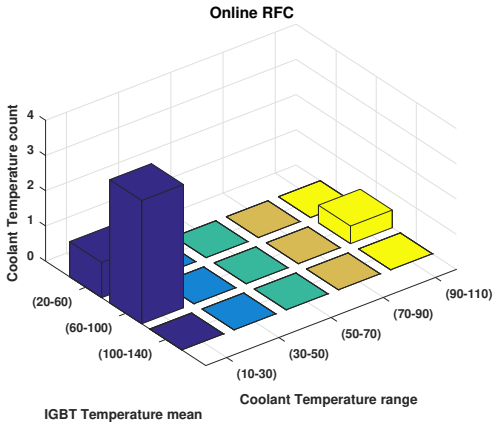

Fig. 4. Online rainflow counting(3D map).

B. Histograms

Histograms are used to represent the distribution of normal data accurately. It is the probability distribution estimate of a continuous variable (quantitative variable). For constructing

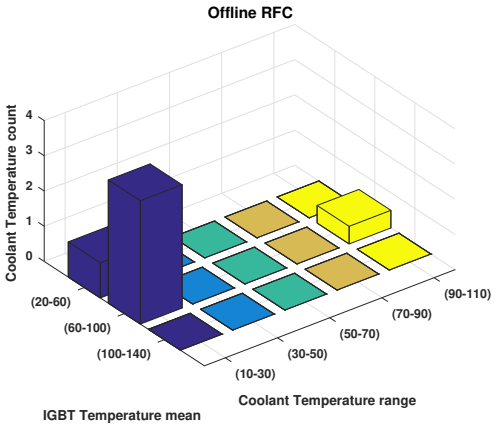

Fig. 5. Offline rainflow counting(3D map).

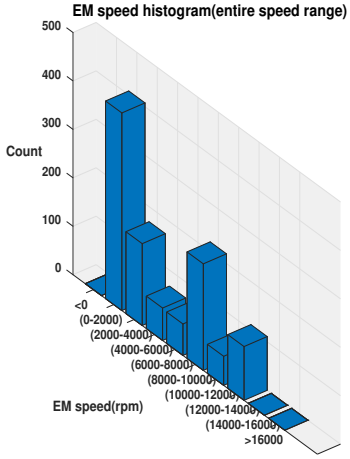

Fig. 7. EM speed histogram for entire speed range(1D).

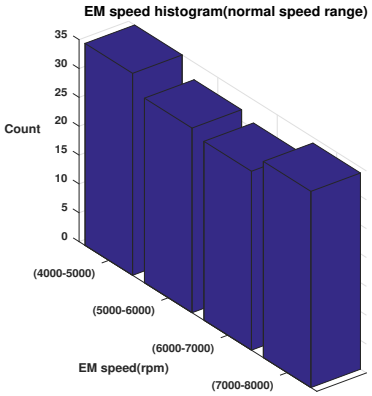

Fig. 8. EM speed histogram for entire speed range(1D).

histograms, the initial step is to make bins of input parameter's value ranges. This means, dividing full operating range of values to series of intervals and then counting how many values is lying in each interval. The bins should be consecutive and non - overlapping. Considering the electric motor speed histogram, the speed may be divided into ten sections as depicted in fig. 6, each section may require a four byte for the count. Thus a total of 40 bytes will be required for the entire histogram in the memory. For the normal driving speeds(40Kmph-160Kmph), the EM speed will be a factor (gear ratio) times the driving speed. This lies between a specific rpm range say, 4000rpm-8000rpm. Histogram for entire EM speed range will be having more sections than this one. Thereby the memory requirement is minimized and also the granularity of the map is now increased as depicted in fig. 6. Only four sections are present in this map. So for each sections of 4 bytes, a total of 16 bytes will only be required, saving 24 bytes of memory. Simulation results for electric motor speed inputs for three minutes are given in fig. 7 and fig. 8.

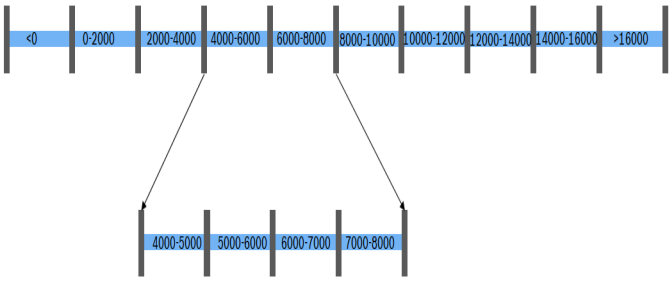

Fig. 6. EM speed histogram sectors for entire speed & normal speed ranges(rpm).

C. Level crossing counting

In level crossing counting, counts are registered when the input data exceeds preset levels. This method can be adopted where we are interested only in threshold crossings of a parameter, which may can have serious effect on the system under consideration. For example, Consider the scenario of a vehicle moving down hill, the electric motor's speed may increase beyond its rated limit which can have adverse effect on the machine. So recording such threshold crossings are of much significance. For such an application the level crossing counting can be used instead of recording a complete histogram. Simulation results of electric motor speed crossing of the rated limit, 16,000rpm for speed inputs for three minutes given in fig. 6 shows that it may require only a byte or two for storing the level crossing counts. Thus the memory requirement can be minimized by a considerable amount than in the case of storing the entire motor speed histogram which may be requring number of sections, having a larger memory requirement say, 4 bytes each.

IV. Conclusion

Different memory optimizing methods were identified for acquiring electric drive parameters. An online rainflow algorithm which minimizes the RAM memory requirement by

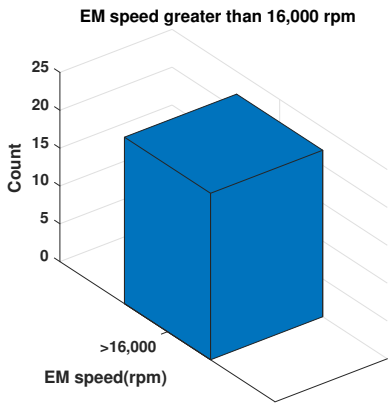

Fig. 9. Offline rainflow counting(3D map).

avoiding the requirement of load history storage can be used in storing parameters like IGBT temperature, diode temperature, coolant temperature etc. Instead of histograms for entire operating ranges , storing only map for normal operating ranges for parameters like electric motor speed memory requirement can be considerably minimized. Level crossing counting can be adopted where only threshold crossings of the acquired parameters are of interest, saving memeory space.

Data acquisition is very much relevant not only in automotive field but also in all areas where a stress cycle analysis is required, as in life time estimation of wind turbine parts, fatigue analysis of mettalic parts of different machines etc. In hybrid electric vehicles the data acquisition functionality will be handled by a particular electronic control unit (ECU) which will be handling other real time electic drive functionalities say, controlling the gate circuit of the electric motors inverter. For such other important real time functions to be performed un - disturbed and efficiently, sufficient memory should be free. So for a functionality like data acquisition, which take up large RAM and EEPROM space, the data acquiring algorithm should be carefully selected. Algorithms should be selected such that the acquired data should maintain maximum possible granularity and consuming minimum memory possible. So techniques with optimum memory usage in data acquisition is of great future scope.

REFERENCES

[1] S. D. Downing and D. F.Socie, " Simple rainflow counting algorithms, " *International Journal of Fatigue*, vol. 4, no. 1, pp. 3140, 1982.

[2] "*Standard Practices for Cycle Counting in Fatigue Analysis, "Annual Book of ASTM Standards*, ASTME 1049-85 (Reapproved 1997), 1999, vol. 03.01, Philadelphia, USA.

[3] M. Matsuishi and T. Endo, Fatigue of metals subjected to varying stress, *Japan Soc. Mech. Engineering*, 1968.

[4] C. H. McInnes and P. A. Meehan, "Equivalence of four-point and three-point rainflow cycle counting algorithms,"*International Journal of Fatigue* 30 (2008) 547-559.

[5] M. Azamfar and M. Moshrefifar, "Moshrefifar and Azamfar method, a new cycle counting method for evaluating fatigue life, " *International Journal of Fatigue* 69 (2014) 2-15.

[6] M. Musallam and C. M. Johnson, "An efficient implementation of the rainflow counting algorithm for life consumption estimation, " *IEEE Transactions on Reliability*, vol. 61, no. 4, December 2012.

[7] M. Musallam and C. M. Johnson, "Real-time compact thermal models for health management of power electronics, " *IEEE Power Electronics Trans.*, vol. 25, no. 6, pp. 14161425, 2010.

[8] M. Musallam, M. Johnson, C. Yin, C. Bailey, and M. Mermet-Guyennet,"Real-time life consumption power modules prognosis using on-line rainflow algorithm in metro applications, " in *IEEE Energy Conversion Congress & ExpoECCE*, Atlanta, Georgia, USA, September 1216, 2010.

[9] I. Rychlik, "A new definition of the rainflow cycle counting method, " *International Journal of Fatigue*, vol. 9, no. 2, pp. 119121, 1987.

[10] M. Meggiolaro and J. Pinho de Castro, "An improved multiaxial rainflow algorithm for non-proportional stress or strain histories, " *International Journal of Fatigue*, vol. 42, pp. 194206, 2011.

[11] "*ASCET V5.2 Reference Guide*, " Document EC010005 R5.2.2 EN, ETAS GmbH, Stuttgart. algorithm for non-proportional stress or strain histories, " *International Journal of Fatigue*, vol. 42, pp. 194206, 2011.

[12] K. L. Singh and V. R. Ranganath, "Cycle counting using rainflow algorithm for fatigue analysis, " in *15th National Conference on Aerospace Structures*, Coimbatore, Tamil Nadu, India, October 1516, 2007.

Proceedings of the Fourth International Conference on Communication and Electronics Systems (ICCES 2019)
IEEE Conference Record # 45898; IEEE Xplore ISBN: 978-1-7281-1261-9

Real-Time Vehicular Traffic Analysis using Big Data Processing and IoT based Devices for Future Policy Predictions in Smart Transportation

Ramesh R[1], Divya G[2], Dr. M A Dorairangaswamy[3], Unnikrishnan K N[4], Aleena Joseph[5], Asha Vijayakumar[6], and Arun Mani[7]
[5, 6, 7] Student, Department of Information Technology
[1, 2, 4] Assistant Professor, Department of Computer Science and Engineering
[3]Professor, Department of Computer Science and Engineering
Adi Shankara Institute of Engineering and Technology

Abstract: **- The primary objectives of the project are "Node Congestion Management" and "Policy Settings". The secondary objective is to assess the congestion nodes and construct a graph based output so as to analyze the trends in traffic flow of Ernakulam district during 2 peak hours that is first peak hour from 7.00 am to 8.30 am and second from 4.00 pm to 6.30 pm. The traffic management and public works department under state government of Kerala can get various insights related to congestion nodes. One important intelligence that this project provides is the change in congestion rate of various congestion points with respect to a single road infrastructure project. Even a road-hump or a speed breaker would affect the congestion rate at various congestion points far away. This automated analysis based on machine learning would save public funds by preventing unnecessary allocation of funds. Also this system justifies allocation of funds for various useful projects. The traffic monitoring helps in long term decision making especially while formulating transport policies and budgets. It also guides the law enforcement agencies to properly understand the variations of such traffic and properly take precautionary measures like installation of security cameras and other control measures.**

Keyword: Smart city, smart transportation, IoT sensors, Big Data processing, Traffic congestion;

I INTRODUCTION

One of the desired outcomes while designing a Smart City [4], [13] [14], [15], [16], [19], [20] is to develop cities that provide necessary infrastructure and quality of life to citizens. It also promotes a clean and sustainable environment and application of 'smart' solutions. But the Smart Cities Mission announced by government of India still has its own challenges to face. Some of the difficulties are discussed below.

Smart Traffic management [9], [22] is very important for the success of smart city concept. With the low cost vehicle sensors and smart traffic management systems real-time monitoring and alert systems can be deployed to provide travelers better service. With the proper integration of IoT services, real-time Big Data analysis of traffic details and mobile applications for alerts, city planners can provide the citizens with effortless traffic service in the near future.

Internet of Things (IoT) has gained significant traction, leading to development of various types of sensors that are connected to the broad internet with the help of wired or increasingly wireless technologies. In the recent past, IoT devices have become extremely cheap even from developing world standards. This has enabled widespread deployment capabilities. The high levels of deployment have enabled collection of large amounts of data with the help of sensors connected to the internet. This data can be leveraged using latest data analytical techniques to extract useful information. Big Data from heterogeneous sources with high-volume with distributed and decentralized control, seeks to explore complex relationship among data. The infrastructure involving the combination of big data, cloud computing and internet of things (IoT) is utilized in the proposed paper. Currently there is increasing focus on using combination of these technologies to improve quality of life of common man [17], [23].

It has been recognized that urban cities are the focus for expansion and are drawing a million people every minute from rural areas. Based on expert opinion, [4] global urban population would double by 2050 as more and more people are moving towards cities at a steady pace every single day. It means adding an equivalent 7 New Delhi cities every single year.

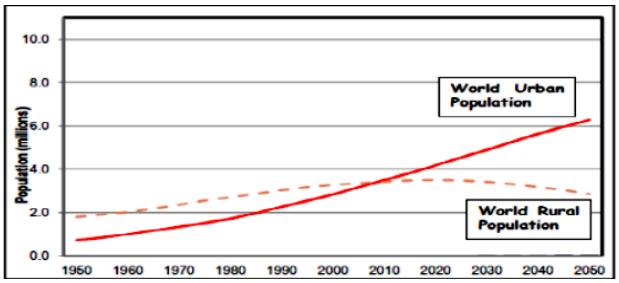

Fig.1 Urbanization trend (Source: [13])

Compared to China which has over 160 cities each with population above one million, India possess only 40 such cities. To meet these challenges drastic increase in the number of cities should be proposed. To support the development of newer cities challenges of urban transportation and mobility needs to be addressed immediately. A comprehensive and support policy framework for urban transportation needs to be developed for establishing new smart cities with sustainable urban spaces. Based on the report from the High Power Expert Committee on Investment Estimates in Urban Infrastructure [39], around Rs 44 thousand crores is the predicted cost to be earn-marked by the government for a period of twenty years. In the following sessions we propose an intelligent transportation system for arrival time prediction. Section II

analyses various existing systems related to vehicular traffic management. The limitations of the existing systems and the important current players in the area of smart transportation are discussed in section III. Section IV deals with the problem faced and motivations for the proposed system. The proposed architecture working is evaluated in Section V and the corresponding cluster analysis of congestion nodes in Section VI.

II RELATED WORKS

In today's world, In order to continued business success and growth automation and data are essential. Vehicle counters [2], [9] solve the issue of collecting both vehicle information and vehicle counting. Most companies and organizations have a general idea of the traffic in and out of their facilities, but they facing a big issue for make strategic decisions according the huge number. Sales and activity which help us to get a huge idea about what has happened throughout the day, week or month, but if we want to know about the traffic with the vehicle counters and analytics software, you must want to capture some knowledge on pattern, trends and opportunities.

Manual counts

One of the simplest methods is manual counting [10] of pedestrians and vehicles. It is a simple and accurate method of traffic counting, which comprises people manually counting vehicles. In this method the people who stand at the side of the road takes count using an electronic hand held counter or record data using tally sheet. Also most of them watch the recorded video and take the counting from that. A small sample data is collected over less than a day. For getting data over a season or year it is extrapolated. It provides 99% accuracy.

Video Vehicle Detection

Manual intensive is a major drawback of manual count method. There are number of systems which are used to analyze the video and detecting cars with a similar accuracy to that of people watching the video. This process automates the counting of vehicles. This method is not only cost effective, but it can also count vehicles in any direction. One of the advantages of this process is that it requires only one camera for several lanes.

Video is analyzed locally to get the count of vehicles and the count can be uploaded online. So, the bandwidth is minimized. The historical data is typically available online. It can be done throughout the year and hence we can get a precise count.

Pneumatic Road tube counting

Pneumatic road tube counting is a popular method used for vehicle sensing for many years. More than one rubber tubes are stretched across the road. One end of the rubber tube is connected to a data logger and other end is sealed. The air pressure in the tube is squashed when the vehicle hits the tube. The data logger records the time of the event.

Direction can be determined by identifying the first tube that was hit. It two vehicles hit simultaneously then the direction cannot be determined accurately. This is the drawback of this method.

Piezoelectric Sensor

Piezoelectric Sensor converts mechanical energy to electrical energy. This concept is used to collect information about the traffic. A groove is cut on the surface of the road and piezoelectric sensor [2] is mounted. The sensor is squeezed when a car drives above it. This mechanical pressure is converted to electrical voltage. The change in voltage levels can be detected and count can be recorded. The counting can be performed in this way. These sensors can be connected to a device which uploads the count to a database locally or to a cloud.

Inductive Loop

Inductive loop will detect moving magnet or alternating current. The principle is that an electric current is induced when a magnetic field is detected near an electric conductor. Vehicle acts as a magnetic field. The inductive loop placed on roads acts as conductor. When current is generated in the inductive loop, the count of the vehicle can be recorded.

Magnetic Sensor

Magnetic sensor detects the change in earth's magnetic field. The vehicle acts as a magnetic field and when it passes over the sensor there is change in magnetic field. This change is detected and vehicle count is updated. The sensor may be inserted on the road or kept on the roadside. The only drawback is that the vehicle close by each other cannot be detected clearly.

Acoustic detector

As the vehicle passes, a sound is created and the acoustic detector detects this sound and counts the vehicle. Acoustic detector is placed in such a way on the roadside poles so that they point towards the traffic. The benefit is that it can be used for different lanes. These detectors can communicate their counts wirelessly.

Passive Infrared

Passive Infrared Sensor detects the radiation, radiating from an object that comes in its view. Vehicle can be detected using this sensor. There is change in the radiation when a vehicle passes by and hence the count is increased. The limitation is that only one or two lanes can be detected.

Doppler and Radar Microwave Sensors

Doppler and Radar Microwave Sensor will transmit low-energy microwave signal. There is change in frequency, if there is vehicle in motion in its detection area. Hence moving vehicles can be detected.

Radar is capable of determining the position by detecting distant objects and speed of movement. The time delay of the return signal will be used to calculate the distance to the vehicle.

In the arrival time prediction system, Big Data analysis plays crucial role in producing real-time data. Some of the research works carried out in the segment of smart transportation is as follow. Big data for social transportation [28] is one of the major contributors for smart transportation

solutions. A study conducted by University of California [18] for traffic monitoring shows that a 2-3% penetration of GPS enabled mobile phones is enough for finding the speed of vehicular traffic. Other studies on GPS data were conducted by taxi calling service providers (UBER, Didi Taxi etc) while developing their software. The modeling employed for visualizing human mobility details is based on Origin destination (OD) matrix. Researchers can make use of existing traffic allocation patterns with OD matrix developed to reach out useful conclusions. Another source of datasets used for creating OD matrix is mobile phone data [12].

In China, to make sure maximum travelers reach the mega event- Shanghai World Expo 2010, a traffic prediction system based on mobile phone data was developed to broadcast to travelers the real-time traffic congestion information so that they can plan their trips accordingly. Crowdsourcing and data from public domains of social media websites are also good source for social transportation scheme.

In another related research which focused on improving the accuracy of arrival time prediction of buses [26], bus scheduling dataset, time point dataset, real-time transit feeds and crowd sourced data feeds were utilized. The proposed system employed clustering analysis and kalman filtering techniques for developing the prediction model. The arrival time prediction can be reduced by 25% if predicted an hour before and by 47% if predicted before 15 minutes.This is one of few research works where shared route segment is taken into account while calculating the arrival delay.

Graph-oriented smart ITS solutions [25] finds popularity among researcher in the field of smart city solutions. The system employed Giraph and Spark tool above Hadoop architecture to generate and process graphs. The traffic dataset is modeled on a directed and weighted road graph with three types of weights- distance between two vertexes (intersections), average speed of all vehicles from one intersection to another intersection and number of vehicles going from one intersection to another intersection. Decisions are made by parallel processing of sub-graphs. By analyzing the real-time traffic conditions the quickest road is found out by the proposed system.

A framework [24] for Smart Transportation using Big Data is proposed. The framework consists of 4 layers: Input layer, storage layer, analysis layer and communication layer. Input layer deals with all kinds of data read from sensors like RFID, GPS etc. The data in Storage layer is collected from heterogeneous sources. Data will be fetched from storage layer to analysis layer for analysis using different tools. Big Data technology can be used in smart transportation systems. Another study was conducted on smart transportation using Bluetooth devices in bus rapid system, Colombia [23]. The analytics was focused on the planning of bus rapid transit systems by using OD matrix using Bluetooth signals presents in the BRT systems. It is used by the administrative authorities for planning of BRT systems and utilized the NoSQL approach for storing the database in cloud. The system offers web based and mobile app based interaction with the clients. It also offers a reduced cost, high scalable, reliable and fast deployment platform for collecting reliable data for processing.

III CURRENT PLAYERS

- **CISCO**: report pointed out that the devices connected to Internet exceeds number of people on earth and it will reach 50 billion in 2020.
- **Redhat**: Fleet telematics solution (Italy), Smart toll collection system (EU roadway system).
- **Sensys Networks** developed a magnetic sensor based system and micro radar sensor systems for use in traffic intersections.
- **MIT and University of Sri Lanka**: Wireless sensors used to monitor the state of road surfaces.
- **Moovit app**: provides more accurate and live information regarding timing and routes. Other Apps: Offi, Bosch City App.
    - **Japan's broadband access**provides the facility of communication between people, people and devices, and devices to devices.
    - **South Korea's smart home** enables their people to access things remotely.
    - **FASTag (ICICI, AXIS bank and NHAI):** Itis part of **National Electronic Toll Collection** (NETC) enables automatic deduction of toll charges and hassle free trip on national highways.
    - **Delhi Integrated Multi-Modal Transit System Ltd:** Wireless Traffic Signal Controller (Wi-TraC) and Red Light-Stop Line Violation & Detection System.
    - **Some examples of Vehicular counting tools:**
    - The **COUNT cam** will record 360 hours of video without charging. It counts car, bikes, and pedestrians (Starting price $1000).
    - **Video Turnstile** people and vehicle traffic counting system: Using this system we can count vehicles moving in different directions.
- **PureTech's** Video-Based Vehicle Counting.

At present, traffic information is commonly shared between different traffic agencies by means of voice or data communications. For such data communication between management centers, a common language and a frame of reference is required. There are many possible ways to analyze traffic data like manually counting each vehicle or through image processing, video analytics and so on. Manual counting involves a team to count each vehicle travelling on the road and update the statistics and a separate team is required to analyze these results of statistics.

Limitations of the Existing System

- Requires very huge man power.
- Time consuming and cumbersome.
- Create unmanageable traffic jams.
- If there is no traffic, the team personnel still need to wait at junctions.

- Lack of traffic details to users: Present traffic systems fail to provide traffic information including busy/idle time and number of accidents happening.
- The expense involved in maintaining the field components used is also high.
- Setting up the framework initially is also difficult.

IV MOTIVATION

There are so many hurdles going to be faced to make the public transportation smarter. Presently there is lack of public domain data related to transportation in India. Researchers often finds hard to get human mobility details to perform data analytics. Few short comings in smart transportation in India are:

1.) No real-time arrival time predictor: Smart management of the traffic system with the provision of real-time information to the citizen based on the current traffic situation has a major impact on the citizen life.

2.) No major Intelligent Transportation System [ITS] in Kerala and other Tier-1 and tier-2 cities in India: The big data generated by the vehicular network and traffic system should be utilized to analyze different aspects of smart transportation to obtain smart city.

3.) Relationship between various congestion nodes needs to be analyzed before planning an infrastructure or after it's been installed. Consider a route segment which consists of n congestion nodes. Many research works been conducted for evaluating factors affecting congestion nodes. But due to lack of study on how different congestion nodes are related, either regression based or correlation, deteriorates the scope of enhancement of ITS.

4.) Difficulty in making algorithm for smart phone based application.

5.) Lack of research about last mile connectivity issues.

V PROPOSED ARCHITECTURE:

The proposed system uses big data analytics tools like Hadoop version 3 for studying stored historical data and Apache Spark for real-time data analytics. Apache spark and Apache Hadoop offers flexibility of using various programming languages like Java, Python and Scala etc. The proposed system emphasizes the importance of Big-data processing using Hadoop in IoT based applications. The combination of big data, cloud computing and internet of things (IoT) is utilized in the proposed design. Currently there is increasing focus on using combination of these technologies to improve quality of life of common man. Availability of cheap IoT devices has enabled collection of large amounts of data with the help of sensors connected to the internet. This data can be leveraged using latest data analytical techniques to extract useful information. Big data with large-volume, heterogeneous, autonomous sources with distributed and decentralized control, seeks to explore complex and evolving relationship among data. We initially propose to collect our data using RFID mechanism and GPS. With the substantial growth of location data, data analytics plays a significant role in analysing the data and in solving emerging problems in traffic management. We are planning to implement RFID and GPS modules in our college bus fleet and store the data using IoT module. The digital location data obtained from IoT module or GPRS module can be collected in real-time using a publicly accessible server. For this we need to put a server OS instance in listening mode linked with a public IP. The collected data can be used for performing various machine learning techniques. The storage data structure preferred is either multi-dimensional matrix or graphical representation.

The proposed system evaluated various congestion nodes in 4 bus routes (Table-1). The congestion nodes are then evaluated for 2 month period from March 1st 2019 to April 30th 2019. The proposed system helps in proper scheduling of buses. The graphical analysis helps to take decisions for deciding whether or not speed breakers or road bumpers are required by correlating the accident information with the day to day traffic analysis. The processed and analysed data shows interesting patterns of traffic. During Haj season, the traffic towards airport has spiked but other lane traffic remains almost constant. During Sabarimala season, the traffic towards Kottayam district and Thodupuzha district increased exponentially. The data collected helped local traffic officers better understand the traffic during day time and during various months. The proposed system gives directed design plans for laying funds in future infrastructure projects. The government agencies like public works department can get the fund allocated with authentic data without delays. The policy makers make use of such automated data collection system to get better idea about developing predictable models. The system can be effective if it can be integrated with cloud platform like Ubidot. Ubidot or other cloud platforms act as one of the future extension to the predictive automated counting system. Such integration gives better analytical decision making data in time for policy makers.

The data obtained from Ubidot is collected and analysed for getting a better idea about the daily as well as day to day traffic details. The sensor data collected are processed using Hadoop system to get further analytical information regarding future traffic prediction. R programming can also be employed for getting more futuristic analytical information regarding future traffic patterns.

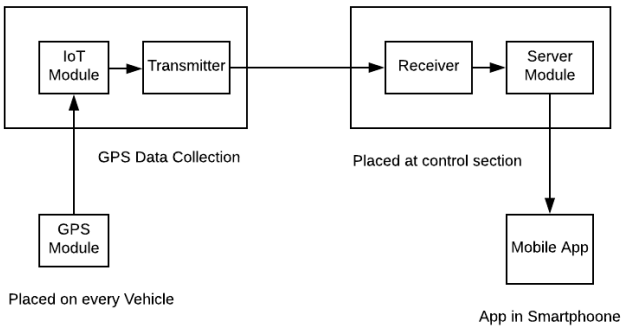

Fig.2 Proposed Smart Transportation System Architecture

Basically the proposed system consists of four modules:

- GPS module
- IoT module for GPS data collection.
- Server module for receiving data.
- Mobile App Development module

- The system will consist of a GPS module installed on every vehicle and receiver module installed on every control section.
- The data generated for a period of time is collected and analysed to discover the usual congested routes.
- Transmitter module transmits this information to control section. Control section along with software section processes the data.
- It assesses the congestion nodes and constructs a graph based output so as to analyse the trends in traffic flow.
- The useful information is made available to the end user through a mobile application.

VI. RESULTS:

The real-time datasets are provided by VTS (Vehicular Tracking System) systems implemented at Adi Shankara Institute of Engineering and Technology. We have evaluated four bus routes for our study covered by bus numbers: 10, 11, 12 and 13. The details of the route are shown in the table-1. The test dataset for neural network analysis is collected from the month of February and the training dataset is fetched from the month of March. Figures 3, 4, 5 and 6 reveals the congestion points (Heat maps) during peek traffic hours from 7:30 AM to 8:30 AM and from 4:00 PM to 6:30 PM. Red region represents heavy traffic, yellow regions represents moderate traffic and green regions represent normal traffic. The figures identified heavy congestion points at “Mattoor junction”, “Aluva bridge”, “Maradu junction”, “Kochi”, “Vytilla junction” and “Fort Kochi”. Our study identified moderate congestion points are “Aluva Metro Station” and “Kochi International Airport road”. We also extended our study using 4 bus routes as shown in figure-9.

The system we modelled using the VTS datasets can be automated bye connecting the VTS database with machine learning front-end application. The front-end can be easily programmed using Python machine learning libraries which gives real-time graphical output related to various congestion nodes and clusters so that decision makers in government level can make use of these evaluated results when making fund allocation as well as resource allocation. The proposed system when evaluated over a period of months starts producing real-time outputs in the google map showcasing whether signal light timings placed in one location needs to be decreased or not.

Table.1 Bus routes taken for neural network analysis

Bus no.	Route
10	Old NH47,Kumbalam north, Thoppumpadi to ASIET
11	Bypass road, Irinjalakuda, Thrissur to ASIET
12	Mulanthuruthy, Ernakulam to ASIET
13	Kochi - Madurai - Dhanushkodi Road to ASIET

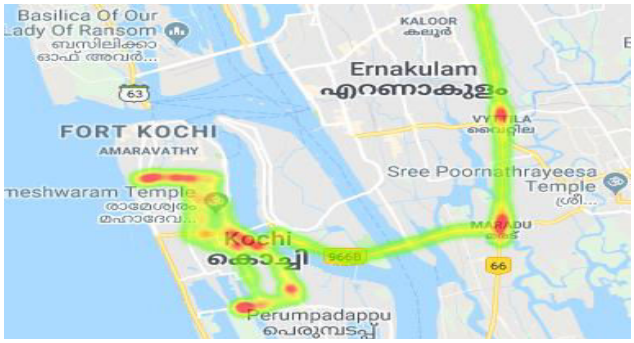

Fig.3 Ernakulam congestion analysis

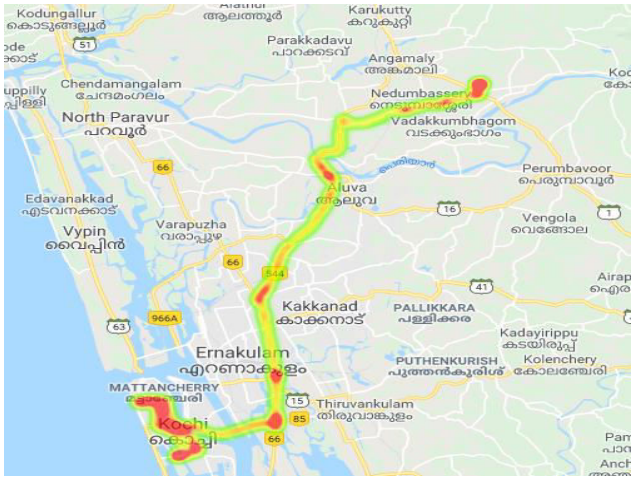

Fig.4 Ernakulam bus route congestion analysis

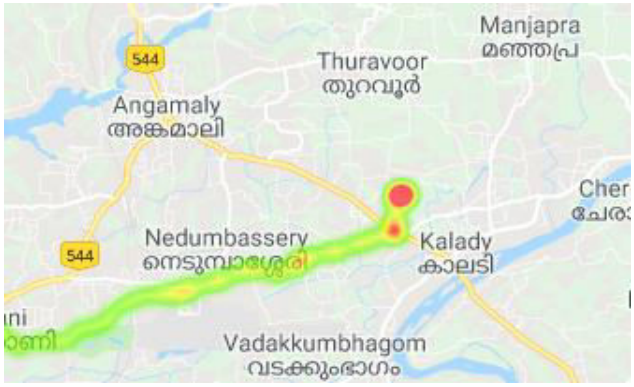

Fig.5 Kochi Airport congestion analysis

Fig.6 Aluva congestion analysis

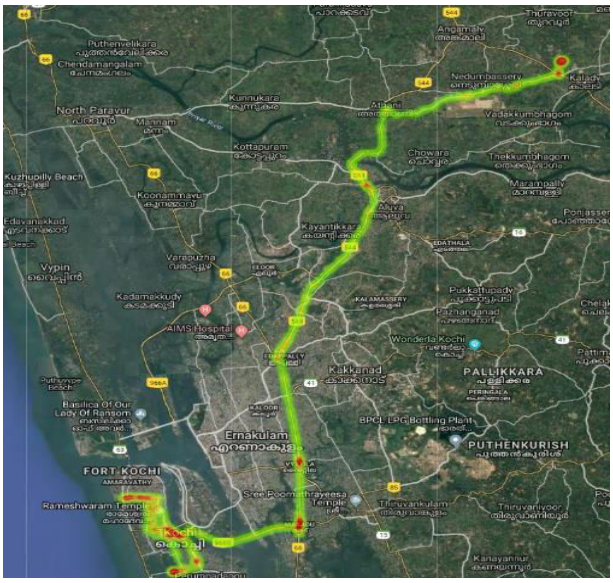

Fig.7 Ernakulam bus route congestion analysis

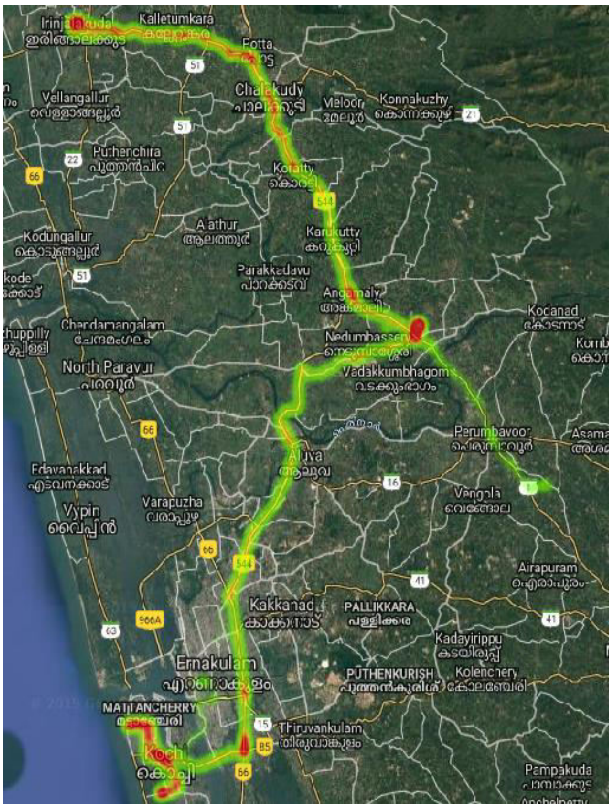

Fig.9 4 bus routes congestion analysis

VII. CONCLUSION

The proposed Machine learning based congestion prediction algorithm that used Logistic Regression gives a simple, accurate and early prediction of the traffic congestion for a given static road network which can be considered as a graph. The complexity of the algorithm mentioned above would be constant. So, this is can be effectively used by any devices which has a less computation capability and with less resources. As a future direction the traffic congestion prediction can be predicted using various Hybrid techniques which can give high accurate results.

Acknowledgement: We thank Management, Principal and Head of the Department-CSE & IT of Adi Shankara Institute of Engineering and Technology for giving permission to access database of college's vehicle monitoring system. We would like to extend our sincere thanks to all staff coordinators of Data Analytics Research Lab, ASIET, for providing all computing resources and for their whole-hearted efforts put in for the completion of our work.

REFERENCES:

[1] J. Dean and S. Ghemawat, "Mapreduce: simplified data processing on large clusters," Commun. ACM, vol. 51, pp. 107–113, Jan. 2008.
[2] Chris Sweeney, Liu Liu, Sean Arietta and Jason Lawrence, "HIPI: A Hadoop Image Processing Interface for Image-based MapReduce Tasks", University of Virginia, 2011.
[3] Arto Heikkinen, Jouni Sarvanko, Mika Rautiainen and Mika Ylianttila (2013) Distributed Multimedia Content Analysis with MapReduce, IEEE.
[4] Chenwei Song, Wenfeng Shen, Lianqiang Sun, Zhou Lei and Weimin Xu (2014) Distributed Video Transcoding Based on MapReduce, IEEE ICIS.
[5] Chungmo Ryu, Daecheol Lee, Minwook Jang, Cheolgi Kim and Euiseong Seo (2013) Extensible Video Processing Framework in Apache Hadoop, IEEE International Conference on Cloud Computing Technology and Science.
[6] Frank J. Seinstra, Jan-Mark Geusebroek, Dennis Koelma, Cees G.M. Snoek, Marcel Worring, and Arnold W.M. Smeulders (2007) High-Performance Distributed Video Content Analysis withParallel-Horus, IEEE.
[7] J. Dean and S. Ghemawat (2008) Mapreduce: simplified data processing on large clusters, Commun. ACM, vol. 51, pp. 107113, Jan.
[8] Ke-yan Liu, Tong Zhang and Lei Wang (2010) A New Parallel Video Understanding And Retrival System, ICME.
[9] Ramesh. R, Dr. Murali P, Divya G, Gigy Johnson, "Integrated Statistical Approach for Smart City in India Using IoT, A Case Study", ISSN (Print): 2393-8374, (Online): 2394-0697, Volume-4, Issue-5, 2017.
[10] An Investigation on the Manual Traffic Count Accuracy, Procedia - Social and Behavioral Sciences 12/2012;43: 226-231.DOI: 10.1016/j.sbspro.2012.04. 095
[11] Accuracy of Pneumatic Road Tube Counters. McGowen and Sanderson. A report prepared for the 2011 Western District Annual Meeting Institute of Transportation Engineers Anchorage, AK May 2011.
[12] ITSChina. Last visit: May 15, 2015. [Online].Available:http://www.itschina.org/article.asp?articleid\protect$\relax =$2259.
[13] India. Ministry of Urban Development, Draft Concept Note on Smart City Scheme, p.1.
[14] H. Schaffers N. Komninos M. Pallot B. Trousse M. Nilsson A. Oliveira "Smart cities and the future internet: Towards cooperation frameworks for open innovation". The Future Internet Lect. Notes Comput. Sci. vol. 6656 pp. 431-446 2011.
[15] M. Dohler I. Vilajosana X. Vilajosana J. Llosa "Smart Cities: An action plan", Proc. Barcelona Smart Cities Congress pp. 1-6 Dec. 2011.
[16] J. M. Hernández-Muñoz J. B. Vercher L. Muñoz J. A. Galache M. Presser L. A. Hernández Gómez J. Pettersson "Smart Cities at the forefront of the future Internet". The Future Internet Lect. Notes Comput. Sci. vol. 6656 pp. 447-462 2011.

[17] N. Bui M. Zorzi "Health care applications: A solution based on the Internet of Things" Proc. ISABEL pp. 1-5 Oct. 2011.
[18] S. Amin et al., “Mobile century using GPS mobile phones as traffic sensors: A field experiment,” in Proc 15th World Congr. Intell. Transp. Syst., 2008, pp. 16–20.
[19] URL: http://smartcities.gov.in/content/
[20] http://www.mospi.gov.in/statistical-year-book-india/ 2016/190
[21] Chungmo Ryu, Daecheol Lee, Minwook Jang, Cheolgi Kim and Euiseong Seo (2013) Extensible Video Processing Framework in Apache Hadoop, IEEE International Conference on Cloud Computing Technology and Science.
[22] S. W. Turner and S. Uludag, "Intelligent transportation as the key enabler of smart cities," NOMS 2016 - 2016 IEEE/IFIP Network Operations and Management Symposium, Istanbul, 2016, pp. 1261-1264.
[23] L. F. Herrera-Quintero, K. Banse, J. Vega-Alfonso and A. Venegas-Sanchez, "Smart ITS sensor for the transportation planning using the IoT and Bigdata approaches to produce ITS cloud services," 2016 8th Euro American Conference on Telematics and Information Systems (EATIS), Cartagena, 2016, pp. 1-7.
[24] S. Shukla, Balachandran K and Sumitha V S, "A framework for smart transportation using Big Data," 2016 International Conference on ICT in Business Industry & Government (ICTBIG), Indore, 2016, pp. 1-3.
[25] M. M. Rathore, A. Ahmad, A. Paul and G. Jeon, "Efficient Graph-Oriented Smart Transportation Using Internet of Things Generated Big Data," 2015 11th International Conference on Signal-Image Technology & Internet-Based Systems (SITIS), Bangkok, 2015, pp. 512-519.
[26] F. Sun, Y. Pan, J. White and A. Dubey, "Real-Time and Predictive Analytics for Smart Public Transportation Decision Support System," 2016 IEEE International Conference on Smart Computing (SMARTCOMP), St. Louis, MO, 2016, pp. 1-8.
[27] Chenwei Song, Wenfeng Shen, Lianqiang Sun, Zhou Lei and Weimin Xu (2014) Distributed Video Transcoding Based on MapReduce, IEEE ICIS.
[28] Xinhu Zheng, Wei Chen, Pu Wang, Dayong Shen, Songhang Chen, Xiao Wang, Qingpeng Zhang, and Liuqing Yang, “Big Data for Social Transportation”, IEEE Transactions on Intelligent Transportation Systems, Vol.17, No.3, March 2016.
[29] J. Dean and S. Ghemawat, “Mapreduce: simplified data processing on large clusters,” Commun. ACM, vol. 51, pp. 107–113, Jan. 2008.
[30] Chris Sweeney, Liu Liu, Sean Arietta and Jason Lawrence, ”HIPI: A Hadoop Image Processing Interface for Image-based MapReduce Tasks“, University of Virginia, 2011.
[31] Arto Heikkinen, Jouni Sarvanko, Mika Rautiainen and Mika Ylianttila (2013) Distributed Multimedia Content Analysis with MapReduce, IEEE.
[32] Koushalya Bijjaragi , Poonam Tijare, “ Big Data Approach for Secure Traffic Data Analytics using Hadoop”, International Journal on Recent and Innovation Trends in Computing and Communication ,Volume: 4 Issue: 5,May 2016
[33] Suguna Devi, T. Neetha, “Machine Learning based traffic congestion prediction in a IoT based Smart City” , International Research Journal of Engineering and Technology (IRJET) , Volume: 04 Issue: 05 | May -20170
[34] P.S. Saarika, K. Sandhya,T. Sudha, “Smart transportation system using IoT”, International Conference On Smart Technologies For Smart Nation (SmartTechCon),2017,IEEE.
[35] J.Sherly, D.Somasundareswari, “INTERNET OF THINGS BASED SMART TRANSPORTATION SYSTEMS”, International Research Journal of Engineering and Technology (IRJET), Volume: 02 Issue: 07 | Oct-2015
[36] Dr.Khalifa A. Salim, Ibrahim Mohammed Idrees, "Design and Implementation of Web-Based GPS-GPRS Vehicle Tracking System”, IJCSET | December 2013 | Vol 3, Issue 12, 443-44.
[37] https://www.technavio.com/blog/intelligent-transport-system-iot-promote-smart-safe-urban-mobility.
[38] Parag Gawade, Prof.Meeankshi A , “IOT Based Smart Public Transport System”, International Journal of Scientific and Research Publications, Volume 7, Issue 7, July 2017.
[39] https://data.gov.in/catalog/estimates-urban-transport-investments-high-powered-expert-committee-hpec.

Proceedings of the Fourth International Conference on Communication and Electronics Systems (ICCES 2019)
IEEE Conference Record # 45898; IEEE Xplore ISBN: 978-1-7281-1261-9

Reliable Machine Learning Approach to Predict Patient Satisfaction for Optimal Decision Making and Quality Health Care

G.Sabarmathi[1] , Dr.R.Chinnaiyan[2]
[1]Research Scholar, Asst.Professor, Computer Science, Christ Academy, Institute for Advanced Studies, Bangalore
sabarganesh@gmail.com
[2]Associate Professor, Department of Information Science and Engineering, CMR Institute of Technology, Bengaluru
vijayachinns@gmail.com

Abstract: **In this paper a unique approach towards decision making process and better quality care through Machine Learning (ML) concepts as an alternative mode by identifying the characteristics and patient satisfaction (PS) in health care system is proposed. Extracting the information from raw data using some algorithmic approach is known as Data mining. In this a ML approach is used in determining the patient satisfaction in health care sector. Applied regression models to determine the patient satisfaction and also correlation methods is identified as an important attribute to be considered in determining the better quality in health care sets. The data set is taken based on the opinion on three types of data such as a) patient opinion towards hospital care b) nurse opinion towards workplace and c) Administrative aspects of healthcare. Our findings revealed high accuracy in Regression (88%), that helps in concluding by considering the administrative and workplace attributes related to patient satisfaction. The results are validated using traditional statistical methods like binomial correlation and linear regression.**

Keywords: Patient Satisfaction (PS), Machine learning(ML), Healthcare, Regression, correlation

1. INTRODUCTION

The recent trend in service sector evaluation is to consider end user satisfaction as one of the key constraint, as it is associated with satisfaction level in performance of business. In case of healthcare sector patient satisfaction plays a key role in evaluating the quality of service they provide. So far there is no clear picture on pre-defined data sets that has to be considered in evaluating the patient satisfaction, however each healthcare sector follows their own metric in evaluating this. Patient satisfaction is considered to be one of the key metric in evaluating quality of healthcare services and their decision making process, In turn this helps them to improvise their services in health care based on their marketing strategy and eventually targeting the patient satisfaction [1].

Pati

Patient satisfaction is considered to be one of the excellence that is linked with excellence of health care [2], as it is considered that mollified patient will have faith in the recommended cure that improves their life amongst others. The opinion from the patient helps the health care sector administration to measure and relate various departments, in progressing their existing services that they offer. The opinion also helps the doctors to treat the patients in a better way [3].

In various works different metrics are considered that predicts patient satisfaction in an incorrect mode as it is not directly related with quality of healthcare. The metrics that are considered in evaluation are communication with physician and nurses, waiting time, [4] timely services, access to the services [5]. Patient nurse ratio, working nature of attenders all related with the good quality of healthcare services that is associated with patient satisfaction. Maximum research works studies patient satisfaction using traditional statistical methods [5, 6]. Where there is limited data mining techniques are used in discovering healthcare services relating with patient's view. To understand patient healthcare choice it is better to compare the old methods with new data mining concepts. [7]

Data mining concepts is used to extract the needed information from big data that helps in decision making process both at organizational and medical fields. The main task in using this data mining technique is its type and diversity nature of the data along with omitted data. As many data is not available in the format needed for processing, it has

to be preprocessed to make it in a usable form (electronic form).

But this problem is reducing in recent days as many of the health care sector became digitalized with their data in both medical and organizational levels. In this paper we access three data sets like patient view towards health care, nurse view towards workplace and Managerial aspects of healthcare. Data mining techniques are applied to extract the information about patient satisfaction in different ways. We try to implement machine learning techniques as an alternative method in extracting managerial and operative features which affect the views of patients. The resulted information can be considered for decision making and deriving hypothesis [8, 9]. In healthcare sector it provides support in decision making for both administrative and clinical cure to improve the service that they offer. [10]

2. PATIENT SATISFACTION AND DECISION MAKING

This section is going to discover the factors related to patient satisfaction and the analysis of their results to administrative tactics for a health care services.

2.1 Patient Satisfaction:

When we think about patient care in health care sector, data plays a major role in analyzing personal experience factors that relates with patient satisfaction. Hush et al [11] mentioned in his work that the researchers used least squares regression models to evaluate the correlation between various parameters, like issues related to various facilities available and the way they communicate in obtaining patient satisfaction among different patients who had taken care during the past five years. Patient satisfaction is measured to be decidedly correlated to personal experiences as well as hopes. Further studies show that the relations of the therapist with the patient as well as his/her complete experience correspondingly contributing factor that is considered to be significant than the real consequence of the treatment [11].

2.2 Organization and Consumer Satisfaction healthcare sector is considered as a service oriented and the patients as consumer the organization tactics is tested to yield the satisfaction. By assuming this model, various administrations are inspiring the customers that it is based on the choice satisfaction. [12]. Many research has conveyed the message that more personalized communication between the consumer and the administration leads to more satisfying experience.

Additionally there is a demand from consumer related to the services offered has increased research area. Satisfaction plays a vital role in health care sector in determining their objectives related to both administrative and clinical aspects. The data obtained is used to decide and update the changes required in quality of service.

3. PROPOSED METHOD0LOGY

To obtain patient satisfaction from the given data sets we applied the known machine learning techniques. It is used to analyze huge data sets and their relationship between the data in turn it provides the meaningful information [13]. In this study we use Machine learning concepts which is dived into two categories as supervised and unsupervised learning. In supervised learning includes classification, regression prediction and time series analysis that helps in forming models that is used to classify new and unknown information. In unsupervised learning we use clusters in determining the different patterns and similarity between the data [14]. For our studies we used Regression concepts for analyzing the data the results are validated by linear regression and binomial correlation using traditional statistical method.

3.1 Regression:

Regression is a task used to predict the number such as Age, height, Income distance etc., It predicts the data where the target data is unrevealed. It is done by the statistical team by measuring the difference between the predicted and expected values. [15]

Most widely used statistical technique that estimates the relationship between the variables is Regression. This model provides easy structure for describing and testing the hypothesis between the explanatory variable and a response variable

Normally, a regression analysis is applied for (1) modeling the relationship between variables. (2) Predicting the target variable (forecasting). (3) Testing the hypotheses. Linear model is the very basic in regression analysis. It can be obtained by having n sets of observations {X1i, X2i, ..., Xpi, Yi}, i = 1, ..., n, that represents random sample from large dataset. It is expected that these observations satisfy a linear relationship

$Yi = \beta 0 + \beta 1X1i + \beta 2X2i + ...\beta pXpi + \varrho i$, $i = 1, \ldots, n$ where the β coefficients of unknown parameters, and the ϱi are random error terms.

3.2 Prediction is a method used in predicting the outcome based on available data by incorporating with unavailable data sets of future

4. RESULT ANALYSIS

The main objective of this study is to examine the parameters of patient satisfaction and to study the above objective, response from 80 respondents that collected through online source.

The opinion attitude towards Patient satisfaction consists of 5 determinants. These constructs are determined using Likert scale of 1 to 5 where 1 denotes strongly disagree and 5 denotes strongly agree. The descriptive statistics of predictive statistics are depicted from the table 1 and table 2.It is denoted by chart in Figure1 and figure 2.

The parameters of patient satisfactions (PS) are

1. PS1- Patient level of education
2. PS2- Patient care from nurses
3. PS3- Patient care from doctors
4. PS4- Patient opinion on hospital environment
5. PS5- Patient opinion during discharge.

Descriptive Statistics	PS1	PS2	PS3	PS4.	PS5
Mean	3.8250	3.9750	3.5125	3.7875	4.0250
Median	4.0000	4.0000	4.0000	4.0000	4.0000
Mode	4.0000	4.0000	4.0000	4.0000	4.0000
Std. Deviation	0.7424	0.7951	1.1691	1.0150	0.8855

Table 1. Descriptive Statistics of Patient Satisfaction

Predictor	Beta	Sig
PS1	0.093	0.00
PS2	0.193	0.00
PS3	0.245	0.00
PS4	.097	0.00
PS5	.490	0.00

Table 2. Predictive Statistics of Patient Satisfaction

Figure 1. Descriptive Statistics of Patient Satisfaction

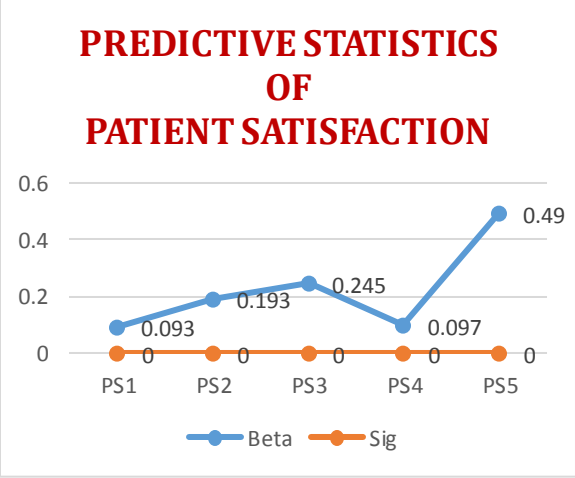

Figure 2 Predictive Statistics of Patient Satisfaction

From the correlation matrix it is evident that patient satisfaction is positively correlated with patient care from nurses, patient care from doctors and patient opinion during discharge. The correlation is significant from the above table. Linear regression is applied with dependent variable patient satisfaction and patient level of education, patient care from nurses, patient care from doctors, and patient opinion on hospital environment and patient opinion during discharge as predictor variable.

PARAMETERS	Pearson Correlation	Sig. (2-tailed)
Patient Satisfaction	1	0
PS1	0.093	0.411
PS2	0.193	0.086
PS3	0.245*	0.028
PS4	0.097	0.392
PS5	0.490**	0.000

Table 3. Prediction of Output Variable

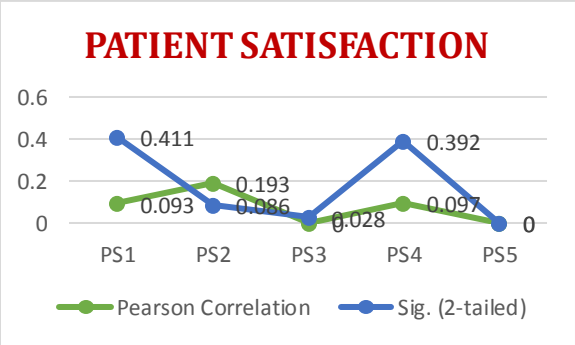

Figure 3. Prediction of Output Variable

From the Table 3 and Figure 3 it is evident that the r egression model statistically predicts the outcome var iable that is Patient satisfaction as p value is less than 0.05.Therefore we can conclude that the relationship between Patient satisfaction and different predictor v ariables is significant. Therefore we can conclude tha t there is linear relationship between patient satisfacti on and five predictor variables

5. CONCLUSION:

In this paper we discussed various parameters that is related to patient satisfaction in a hospital environment, from the perception of a consumer service model. In this we used the data available from various consumers to provide a valid view point to the organization in setting the services related to patient satisfaction. Here regression technique is used to derive the correlation factor using correlation the results are predicted with predicted variable by obtaining the significant result. It is thus concluded that the linear relationship is obtained between patient satisfactions correlating with predicted variable. In this we try to give a model that will help in decision making process of the organization focusing on the parameters specified in turn which builds a safe and support healthcare environment

7. REFERENCES

[1]. Lis CG, Rodeghier M, Gupta D, Distribution and determinants of patient satisfaction in oncology: A review of the literature, 2009, 3(3):287-304
[2]. Mpinga EK, Chastonay P, Satisfaction of patients: a right to health indicator? Health Policy. 2011, 100(2-3):144-50
[3]. Wagner D, Bear M, Patient satisfaction with nursing care: a concept analysis within a nursing framework, J Adv Nurs. 2009, 65:692–701.
[4]. Marton KI, Sox HC, Alexander J and Duisenberg CE, Attitudes of Patients toward Diagnostic Tests: The Case of the Upper Gastrointestinal Series Roentgenogram, Medical Decision Making, 1982, 2:439-448
[5]. O'Toole RV, Castillo RC, Pollak AN, MacKenzie EJ, Bosse MJ, LEAP Study Group. Determinants of patient satisfaction after severe lower-extremity injuries. J Bone Joint Surg Am. 2008, 90(6):1206-11.
[6]. Aiken LH, Sermeus W, Van den Heede K et al, Patient safety, satisfaction, and quality of hospital care: cross sectional surveys of nurses and patients in 12 countries in Europe and the United States, BMJ, 2012, 344.
[7]. Liu SS, Chen J, Using data mining to segment healthcare markets from patients' preference perspectives. Int J Health Care Qual Assur, 2009, 22(2):117-34.
[8]. Yoo I, Song M, Biomedical ontologies and text mining for biomedicine and healthcare: a survey, Journal of Computing Science and Engineering 2(2):109–36, 2008.

[9]. Richards G, Rayward-Smith VJ, Sönksen, PH, Carey S and Weng C, Data mining for indicators of early mortality in a database of clinical records. Artif. Intell. Med., 2001, 22:215–231.
[10]. J. L. Lebow, Consumer Assessments of the Quality of Medical Care, Medical Care 12 (1974): 328-337
[11]. Hush JM, Cameron K, Mackey M, Patient satisfaction with musculoskeletal physical therapy care: a systematic review, Phys Ther, 2011, 91(1):25-36
[12]. Cleary PD, McNeil BJ, Patient satisfaction as an indicator of quality care, Inquiry, 1988, 25(1):25-36.
[13]. Hand D, Mannila H, Smyth P, Principles of data mining, MIT, 2001
[14]. Dunham M, Data mining-Introductory and advanced topics, Pearson Education, 2003.
[15]. http://www.comp.dit.ie/btierney/Oracle11gDoc/datamine.111/b28129/regress.htm
[16]. Jerome H. Friedman, Department of statistics, Stanford Linear Accelerator Center, Stanford University, Stanford, CA 94305.
[17]. R.Chinnaiyan, S.Somasundaram(2010) "Evaluating the Reliability of Component Based Software Systems " ,International Journal of Quality and Reliability Management , Vol. 27, No. 1., pp. 78-88
[18]. R.Chinnaiyan, S.Somasundaram(2009) "Reliability of Object Oriented Software Systems using communication variables – a review " ,International Journal of Software Engineering, Vol.2, No.2,PP.87-96
[19]. R.Chinnaiyan, Dr.S.Somasundaram, "Reliability Assessment of component based software systems using Test Suite - A Review", Journal of Computer Applications, Vol – 1, No.4, Oct – Dec 2008.
[20]. R.Chinnaiyan, Dr.S.Somasundaram, "An Experimental Study on Reliability Estimation of GNU Compiler Components – A Review", International Journal of Computer Applications (0975 – 8887) Volume 25– No.3, July 2011.
[21]. R.Chinnaiyan, Dr.S.Somasundaram, "Reliability of Component Based Software With Similar Software Components - A Review", i-Manager's Journal on Software Engineering; Nagercoil5.2 (Oct-Dec 2010).
[22]. R Chinnaiyan, S Somasundaram, "Monte Carlo Simulation For Reliability Assessment of Component Based Software Systems", i-Manager's Journal on Software Engineering, 2010.
[23]. S.Kayalvizhi et al., "An Intelligent Application for Determine Patient Satisfaction using Data Mining Techniques" IJRDO - Journal of Computer Science and Engineering, ISSN: 2456-1843
[24]. Dr Kee Yuan Ngiam et al.," Big data and machine learning algorithms for health-care delivery", vol 20, ISSUE 5, PE262-E273, MAY 01, 2019.
[25] G. Sabarmathi, R. Chinnaiyan, Big Data Analytics Research Opportunities and Challenges - A Review, International Journal of Advanced Research in Computer Science and Software Engineering(IJARCSSE), Volume:6, Issue :10, pp. 227-231.
[26] G. Sabarmathi, R. Chinnaiyan, Investigations on big data features research challenges and applications, IEEE Xplore Digital LibraryInternational Conference on Intelligent Computing and Control Systems (ICICCS 2017) , IEEE Xplore Digital Library, pp. 782 – 786
[27] G. Sabarmathi, R. Chinnaiyan, Reliable Data Mining Tasks and Techniques for Industrial Applications, IAETSD JOURNAL FOR ADVANCED RESEARCH IN APPLIED SCIENCES(IAETSD-JARAS 2017), Volume:4, Issue:7, pp.138-142

Proceedings of the Fourth International Conference on Communication and Electronics Systems (ICCES 2019)
IEEE Conference Record # 45898; IEEE Xplore ISBN: 978-1-7281-1261-9

Application of Tree Data Structures for Improving Energy Efficiency & Life Time Of Wireless Sensor Networks(WSN): A Critical Study of the State-of-the-Art and Feasibillity For Further Research

Pranesh*, Santhosh L Deshpande**

*Research Scholar, VTU-RRC, VTU, Belgaum, Karnataka, India

**Professor, Department of Post Graduate studies, Visvesvaraya Technological University (VTU), Belgaum, Karnataka, India

praneshvkallapur@yahoo.co.in, sld@vtu.ac.in

***Abstract*— Wireless Sensor Networks(WSN) are characterized by highly application specific nature, stringent resource constraints, self-organizing, spatio-temporal traffic, and large dynamic topology with several contradicting design goals. Of these design goals, network life time and energy efficiency are considered as of paramount importance. Many existing research works have stressed on developing techniques to extend the network life time and achieve energy efficiency of WSN. Some of these techniques include the application of Tree as a data structure. The authors of this paper has made an attempt to present a critical study of research works which have applied different variants of Trees for extending network life time and energy efficiency. Also, the paper mainly tries to present the theoritical discussion on performance implications of application of variants of trees, advantages, and disadvantages alogn with the causes.. The paper further tries to articulate the possible feasibility of the application of Red Black Trees (RBL) in WSN and explain the major constriants in WSN which may bring issues in applying the concepts of RBLs in their original form.**

***Keywords*— Wireless Sensor Network (WSN), Tree Based Approaches, Red Black Tree, Network Life Time, Energy Efficiency**

I. INTRODUCTION

Wireless Senor network(WSN) is composed of thousands of sensor nodes spread across large geography, possibly, for monitoing phenomenon of the interest. Applications of WSN range from home automation to industrial and very specific uses like defence applications etc. However, WSN are characterized by serveral unique features like contradicting design goals, stringent resource constraints, and highly application specific nature. Due to these wide varying applications WSN are evolving as a new paradigm for information processing [1][2].

The contradicting constraints on resources lead to two very important design goals: improving network life time and energy efficiency.

The large number of sensor nodes and associated unique features & constraints make these wireless sensor networks to be unable to adapt to any kind of global addressing mechanisms and/or comon solutions [1].

In this regard, a novel architecture & design of WSN, its protocol stack, layer wise open issues have been discussed in detail, along with description of some of the existing WSN specific protocols as solutions to some of the open issues, in [1]. The need for self-organization and some solutions for the same have been presented elaborately in [3].

Thus, with the above general background about WSN, the motivation of this paper is to attempt to present a detailed survey of the various existing works which proposed application of Tree as a data structures and Chain concept from discrete mathematics for achieving energy efficiency and extended the network life time. For details on Chains one can refer to [53] or [54].

Further, the organisation of this paper is as follows: section II presents the detailed literature survey of research

works, the theoritical discussion on the implications of application of tree data structures is presented in section III, section IV presents discussion on feasibility & limitations in case of applying Red Black Trees in WSN, and the paper will be concluded in section V mentioning the scope for future research using red black trees.

II. Literature Survey

Wendi et al have proposed a work involving clustering for energy efficient communication resulting in severn times efficiency in energy [4]. Huang et al proposed an energy efficient routing scheme for WSN based on clustering with the use of minimum spanning trees degree constrained(CMST-DC)[6].

Z. Han et al proposed an efficient routing by constructing routing tree (GSTEB)[5]. Weighted Spanning Tree variant of LEACH (WST-LEACH) was proposed in [7] . Geographic and Energy Aware Routing (GEAR) algorithm, claimed to perform noticebaly better than any non-energy aware routing algorithms[8].

B. Krishnamachari et al[9] have discussed in detail about the infulence of source-destination placement, communication network density, and the energy costs on each other.

A. Boulis [12] proposed distributed estimation algorithm to explore energy-accuracy subspace for subclass of periodical data collection problems.

Y. Yu et al [13] explores energy-latency trade off to a great deal.

H. O. Tan and I. Korpeoglu[14] proposed a new work consisting of two new algorithms, with power efficiency as their major design goals, called as “Power Efficient Data gathering and Aggregation Protocol(PEDAP)”.

A near-optimal chain-based protocol with energy efficeint as its primary design goal, called Power-Efficient GAthering in Sensor Information Systems (PEGASIS), was proposed by [15]. Joanna Kulik et al [16] proposed Sensor Protocols for Information via Negotiation(SPIN) family of protocols , claiming 75% energy efficiency but incurr lot meta-data usage. T. He et al [17] proposed a research work by using feedback between sensor nodes.

Nahdia Tabassum et al[18] proposed a work which is energy aware version of periodical data collection. Further the same authors present two more improved works in [19] [20] which are based on ‘chain’ concept and claim to achieve 15-30% extended network life time and 90-95% energy efficiency K. Du et al [21] also present a similar chain-based improved algorithm for data gathering, called 'Chain Oriented SEnsor Network' (COSEN).

Heuristics based aggregation tree construction for data gathering had been discussed in detail in [22].

K. Kalpakis et al [23] attempted to propose a novel solution for extending life time of network for data gathering purposes. Another work intending to extend the life time of network for data aggregation is presented by B. Hong and V.K. Prasanna [24].

N. Sadagopan et al [25] focused on maximizing the data collected than so far considered parameters. However, F. Ordonez et al [26] presented a more interesting work concerning the same maximization of data collection but amidst of energy constraints while providing flexibility to choose trade off depending upon the design requirements.

Another research work intending to extend the life time of the network for data aggregation was presented by Y. Xue et al [27].

Kyung tae kim et al [28] proposed an idea of construction of trees for the purpose of data collection, which was termed by authors as Tree-Based Clustering (TBC). Further, authors claim that the proposed work outperforms when compared to PEGASIS and LEACH.

P. Parthasarathy and R.Karthickeyan [29] presented a research work to improve the life time of the network for data aggregation purposes.

Mohammad Abdus Salam and Tanjima Ferdous [30] present a detailed survey of Tree-based data aggregation works for WSN in detail. Dreef et al [31] focused on the

application of Tree as a data structure to achieve improved security.

Hussain, S et al [32] proposed a work for hierarchical clusters operating in distributed fashion. It was a modified version of Kruskal's minimum spanning tree (MST).

Gupta, S et al [33] analysed the issues with broadcast and convergecast trees and attempted to provide improved solution. Application of Spanning trees for energy-aware data aggregation was considered in the work by M. Lee et al [34].

Genetic Algorithms were also considered for the benefit of data aggregation with trees being used data structures in the works like [35] and [36].

The network life time maximization was attempted as an Linear Programming problem in[37] and was interested in studying the impact of multiple sinks.

Another application of tree data structure was found in the research work by OmPrakash Gnawali et al [38]. Further, two more improvements were suggested to the original CTP as presented in [41] and [42]. Research work presented in [43] attempts to evaluate the performance of CTP and other variants of it using Castalia simulator. Further, some improved versions of CTP were published in the works [44] & [45] .

III. Advantages, disadvantages, & Performance implications of application of tree data structures in WSN

Main advantage of MST and BST variants of trees is that they are easy and simple to implement. But, at the same time they have several disadvantages. In case of minimum spanning trees, they have varying path lengths along with many instances being applicable. Most frequently followed algorithms for constructing minimum spanning tree have been shown to run with complexity of O(m log n) where 'm' is the number of edges in the resultant spanning tree and 'n' is the number of nodes. Any other variants of binary trees are also having varying depths and operational costs (time complexity) depending upon the circumstances. For example, simple binary search tree may often show the performances for best case as *O(log n)* and for worst case can degrade to *O(n)* when it becomes unbalanced, where 'n' is the number of nodes in the tree. Thus, the time taken to perform operations is less if the height of the search tree is small; but if its height is large, their performance may be no better than with a linked list.

* highlight the issues of this delay in wsn.

Further, AVL trees impose rigid balance on the tree structure leading to slow and costly operations.

But, all the above discussed variants of tree data structure are not well suited for application in WSN. Major reasons for such infeasibility come from two aspects. First aspect of such infeasibility is that most often applied tree variants in the existing works are going to demonstrate the worst performance in case of frequent insert, delete and lookups in trees with arbitrarliy longer depths.

Second aspect of such infeasibility stems from some important unique features of WSNl ike highly dynamic topologies, frequent need for self-reconfiguration etc.

Further, normal datastructure algorithm for trees is different than trees in WSN. Because, in normal datastructure single system handles insertion, deletion of node along with building the tree. But in WSN, many things happens in parallel. For example, all nodes in one hop distance to sink node, may join sink node, sequentially, one after the other. For example, if 4 nodes are there in one hop distance to sink then it may take 4 x time required to join one node to sink, as the total time. However, the nodes in 2 hop distance to sink, will join the one hop nodes and it can happen parallelly. So the time calculation or algorithm complexity, in fact, varies depending on these parallel activities happening. It also varies based on sink position. Most often, many of these parallel activities will be affecting a particular parent in localized fashion. And, most influencing factor in WSN, while applying Tree data structures, is the number of hops or reachability to sink than hieght/length of tree/path.

IV. Red Black Trees(RBL): Feasibility, Potentials, and limitations for Application in WSN

Red Black Trees are a variant of self-balancing trees. The nodes in RBL are differentiated as red and black nodes. Further, every path in RBL from root to leaf has same number of black links. In RBL at most one red link in-a-row or path from root to leaf is permissible. Height of tree in case of RBL is less than *2 log (n + 1).*

These RBL trees have been proven to show best and constant performance where insertion, deletion and lookups are frequently performed. Because of this reason it may seem that the RBL are well suited for WSN where topological changes bring in frequent node insertion, deletion, and lookup. The only disadvantage is that they are comparatively difficult to be implemented. More details on these Red Black Trees can be found in references like [47][48][53].

However, RBL trees put a restriction that all parent nodes must have same number of leaf nodes. This restriction puts a difficulty in WSN, as the nodes can be deployed randomly which makes meeting this restriction infeasible most often. Additionally, in WSN topology creation depends on communication range too. Thus, several unqiue aspects of WSN may expect some variant of RBL, but not exactly the original RBL concept, to be applicable for improving network life time & energy efficiency. More research need to take place with focus on exploting the benefits of RBL towards improving the performance of WSN while circumventing the limitations imposed by RBL on WSN.

V. CONCLUSIONS

WSN have found wide spread application in different domains. The WSN are also characterised by peculiar features and conflicting design goals making them different from other types of networks. Various techniques like application of data structures etc have been considered in the earlier research works to improve the overall performance and specifically energy efficiency and network life time. In this regard, this article made an attempt to present, as far as possible, a critical study of existing research works which applied tree data structures for improving the energy efficiency and extending the network life time of WSN. Further, the theoritical discssion on the implications of applying different types of tree data structures on the overall performance and specifically towards the energy efficiency & network life time was also presented. Also, this artcile presented a brief discussion on the possible potentials for application of Red Black Tree as data structures for improving energy efficiency and network life time along with mentioning the design issues likely to be manifesting on the way in such attempt. The paper is concluded with stress on need for elaborated research in future in this regard. Authors of the paper are making research on the different novel approaches of using Red Black Trees in WSN and hopeful of presenting the research reseults to the research community soon.

REFERENCES

[1] F. Akyildiz, W.Su, Y. Sankarasubramaniam and E. Cayirci, “Wireless sensor networks: A Survey”, *Computer Networks*, Vol 38, Issue 4 , 393-422, 2002.

[2] Feng Zhao and Leonidas J. Guibas, “Wireless Sensor Networks: An Information Processing Approach”, Elsevier Publications, 2007

[3] K. Sohrabi, J. Gao, V. Ailawadhi & G.J. Pottie, “Protocols for Self Organization of a Wireless Sensor Network”, IEEE Personal Communication, Vol. 7, Issue 5, pp. 16-27 (October 2000)

[4] Wendi Rabiner Heinzelman, Anantha Chandrakasan and Hari Balakrishnan, “Energy-Efficient Communication Protocol for Wireless Micro Sensor Networks”, Proc. International Conf. System Sciences, 2000.

[5] Z. Han, J. Wu, J. Zhang, L. Liu, and K.Tian, "A General Self-Organized Tree-Based Energy-Balance Routing Protocol for Wireless Sensor Network ", 2014

[6] Huang, Y., Lin, J., and Liang, C. "An energy efficient routing scheme in wireless sensor networks", 22nd International Conference on Advanced Information Networking and Applications Workshops, IEEE, pp.916-921, 2008.

[7] Chen, P., Gong, S., Zhang, H. "Weighted spanning tree clustering routing algorithm based on LEACH ", 2nd International Conference on Future Computer and Communication (ICFCC'10), IEEE, pp. V2-223 – V2-227, 2010.

[8] Yan Yu, Ramesh Govindan, Deborah Estrin, “Geographical and Energy Aware Routing: A Recursive Data Dissemination Protocol for Wireless Sensor Networks”, 2001

[9] B. Krishnamachari, D. Estrin, and S. Wicker, “The impact of data aggregation in wireless sensor networks”, Proc. 22nd International Conference on Distributed Computing Systems Workshops, July 2002, pp. 575-78.

[10] E.J. Duarte, Melo, and M. Liu, “Data-gathering wireless sensor networks: organization and capacity”, Computer networks: The International Journal of Computer and Telecommunications Networking , vol. 43, no. 4, Nov. 2003.

[11] K. Vaidhyanathan, S. Sur, S. Narravula, P. Sinha, “Data aggregation techniques sensor networks”, Technical Report, OSU-CISRC-11/04-TR60, Ohio State University, 2004.

[12] A. Boulis, S. Ganeriwal and M. B. Srivastava, “Aggregation in sensor networks: An energy-accuracy tradeoff”, 1st IEEE International Workshop on Sensor Network Protocols and Applications , USA, May 2003.

[13] Y. Yu, B. Krishnamachari, and V. K. Prasanna, “Energy-latency tradeoffs for data gathering in wireless sensor Networks”, IEEE INFOCOM, March 2004.

[14] H. O. Tan and I. Korpeoglu, “ Power efficient data gathering and aggregation in wireless sensor networks”, SIGMOD Record , vol. 32, No. 4, December 2003, pp 66-71.

[15] S. Lindsey, C. Raghavendra, and K.M. Sivalingam, “Data gathering algorithms in sensor networks using energy metrics”, IEEE Trans. Parallel and Distributed Systems , vol. 13, no. 9, September 2002, pp. 924-935.

[16] Joanna Kulik, Wendi Rabiner, Hari Balakrishnan, “Adaptive Protocols for Information Dissemination in Wireless Sensor Networks”, Proceedings of 5th ACM/IEEE Mobicom Conference, Seattle, WA, August 1999

[17] T. He, B.M. Blum, J.A. Stankovic, and T. Abdelzaher, “AIDA: Adaptive application- independent data aggregation in wireless sensor networks,” ACM Transactions on Embedded Computing Systems , vol. 3, no .2, May 2004, pp. 426-457.

[18] Nahdia Tabassum, Quazi Ehsanul Kabir Mamun and Yoshiyori Urano, “An Energy aware Protocol for periodical data collection in wireless sensor networks”, 2007

[19] Nahdia Tabassum, Quazi Ehsanul Kabir Mamun, A K M Ahsanul Haque, Yoshiyori Urano, “ A Chain Oriented Data Collection Protocol for Energy-Aware and Delay Constrained WSN”, African Journal of Information and Communication Technology. Vol 2 No. 3, Sept '06, 126-136 (2006).

[20] Nahdia Tabassum, Quazi Ehsanul Kabir Mamun, Yoshiyori Urano, “COSEN: A Chain Oriented Sensor Network for Efficient Data Collection”, Third International Conference on Information Technology: New Generations (ITNG'06) , 2006

[21] K. Du, J. Wu and D. Zhou, “ Chain-based protocols for data broadcasting and gathering in sensor networks,” International Parallel and Distributed Processing Symposium , April 2003

[22] M. Ding, X. Cheng and G. Xue, “Aggregation tree construction in sensor networks,” 2003 IEEE 58th Vehicular Technology Conference, vol.4, No.4, October 2003, pp 2168-2172.

[23] K. Kalpakis, K. Dasgupta and P. Namjoshi, “Efficient algorithms for maximum lifetime data gathering and aggregation in wireless sensor networks,” Computer Networks , vol. 42, no. 6, August 2003, pp.697-716.

[24] B. Hong, V.K. Prasanna, “Optimizing system lifetime for data gathering in networked sensor systems,” Workshop on Algorithms for Wireless and Ad-hoc Networks (A-SWAN), August 2004, Boston.

[25] N. Sadagopan, and B. Krishnamachari, “Maximizing data extraction in energy-limited sensor networks,” INFOCOM 2004 , vol.3, March 2004, pp. 1717-1727

[26] F. Ordonez, and B. Krishnamachari, “Optimal information extraction in energy-limited wireless sensor networks,” IEEE Journal on Selected Areas in Communications , vol. 22, no. 6, August 2004, pp. 1121-1129.

[27] Y. Xue, Y. Cui and K. Nahrstedt, “Maximizing lifetime for data aggregation in wireless sensor networks”, ACM/Kluwer Mobile Networks and Applications (MONET) Special Issue on Energy Constraints and Lifetime Performance in Wireless Sensor Networks , Dec. 2005, pp. 853-864.

[28] Kyung tae kim, chang hoon lyu, sung soo moon,” TBC for energy efficient WSN”, Proc. Int’l Con. Advanced Information Networking and Application Workshop,2010.

[29] P. Parthasarathy, R.Karthickeyan , “Tree Based Data Aggregation Algorithm to Increase the Lifetime of Wireless Sensor Network”, International Journal of Innovative Research in Science, Engineering and Technology(IJIRSET), Volume 3, Special Issue 1, February 2014,

[30] Mohammad Abdus Salam, Tanjima Ferdous, “Tree-based Data Aggregation Algorithms in Wireless Sensor Networks: A Survey”, Proceedings of the 2012 International Conference on Industrial Engineering and Operations Management Istanbul, Turkey, July 3–6, 2012

[31] Dreef, D., Sun, B., Xiao, Y., and Wu, K. "Secure data aggregation without persistent cryptographic operations in wireless sensor networks", 25th IEEE International Performance, Computing, and Communications Conference (IPCCC'06), IEEE,pp. 635-640, 2006

[32] Hussain, S., Yang, L., and Gagarin, A., "Distributed search for balanced energy consumption spanning trees in wireless sensor networks", International Conference on Advanced Information Networking and Applications Workshops, IEEE, pp. 1037-1042, 2009.

[33] Gupta, S., Schwiebert, L., and Annamalai, V. "On tree-based convergecasting in wireless sensor networks", IEEE Wireless Communications and Networking (WCNC), pp. 1942-1947, 2003

[34] M. Lee and V.W.S. Wong, “An Energy-aware Spanning Tree Algorithm for Data Aggregation in Wireless Sensor Networks,” IEEE PacRrim 2005, Victoria, BC, Canada, Aug. 2005.

[35] O. Islam and S. Hussain, “Genetic Algorithm for Data Aggregation Trees in Wireless Sensor Networks”, 3rd International Conference on Intelligent Environments, Ulm, 24-25 September 2007, pp. 312-316, doi:10.1049/cp:20070386

[36] Ali Norouzi, Faezeh Sadat Babamir, Zeynep Orman, “A Tree Based Data Aggregation Scheme for Wireless Sensor Networks Using GA”, Wireless Sensor Network Journal (Scientific Research Publication), 2012, 4, 191-196

[37] Y. Xue, Y. Cui, K. Nahrstedt, “Maximizing lifetime for data aggregation in wireless sensor networks,” ACM/Kluwer Mobile Networks and Applications (MONET) Special Issue on Energy Constraints and Lifetime Performance in Wireless Sensor Networks , Dec. 2005, pp.853- 864.

[38] OmPrakash Gnawali, Rodrigo Fonseca, Kyle Jamieson, David Moss, and Philip Levi, “ Collection Tree Protocol”, In Proceedings of the 7th ACM Conference on Embedded Networked Sensor Systems (SenSys2009), Berkeley, CA, USA, November 2009.

[39] Ugo Colesanti and Silvia Santini, “The Collection Tree Protocol for the Castalia Wireless Sensor Networks Simulator”, Technical Report 729, Department of Computer Science, ETH Zurich, Zurich, Switzerland, June 2011

[40] Ugo Colesanti and Silvia Santini, “ A performance evaluation of the collection tree protocol based on its implementation for the Castalia wireless sensor networks simulator”, Technical Report 681, Department of Computer Science, ETH Zurich, Zurich, Switzerland, August 2010.

[41] Jingjing Zhang, Zhenqi Yang, Baowei Wang,Huiyu Sun and Xingming, “E-CTP: An Energy-balanced Collection Tree Protocol for Power Constrained Wireless Sensor Networks, International Journal of Grid and Distributed Computing.Vol.7, No.2 (2014), pp.115-126

[42] Fariborz Entezami, Martin Tunicliffe, and Christos Politis, “RCTP: An Enhanced Routing Protocol Based on Collection Tree Protocol”, International Journal of Distributed Sensor Networks, Volume 2015, Article ID 363107

[43] Pranesh V Kallapur, Vibha Prabhu, “Performance Analysis of LEACH, CTP, E-CTP Using Castalia Simulator”, International Journal of Computer Networks and Wireless Communications(IJCNWC), Vol. No. 5, Issue No. 3, June 2015

[44] Pranesh V Kallapur, Vibha Prabhu, “Improved Variant of CTP for Enhanced Data Delivery Ratio and Reduced Computation Overhead”, IEEE International Conference On Applied and Theoretical Computing & Communication Technology(ICATCCT-2015), 29-31 October, 2015, India, DOI : 10.1109/ICATCCT.2015.7456984

[45] Pranesh V Kallapur, Vibha Prabhu, “Enhanced Variants of CTP for Improved Data Delivery Ratio and Energy Consumption”, IEEE International Conference On Applied and Theoretical Computing & Communication Technology(ICATCCT-2015), 29-31 October, 2015, India DOI:10.1109/ICATCCT.2015.7456976

[46] Liehuang, Z., Yuanda, C., Dazhen, W., and Hong, T., "A novel tree-based authenticated dynamic group key agreement protocol for wireless sensor network ", International Symposium on Electronic Commerce and Security , IEEE, pp. 540-544, 2008

[47] https://www.cs.cmu.edu/~fp/courses/15122-f10/lectures/17-rbtrees.pdf, Lecture Notes on Red/Black Trees, Frank Pfenning, CS Department, CMU

[48] https://dspace.mit.edu/bitstream/handle/1721.1/37150/6-046JFall-2004/NR/rdonlyres/Electrical-Engineering-and-Computer-Science/6-046JFall-2004/B3727FC3-625D-4FE3-A422-56F7F07E9787/0/lecture_01.pdf, Erik D. Demaine and Charles E. Leiserson, 2015, MIT

[49] Athanassios Boulis et al., “Castalia: A Simulator for Wireless Sensor Network”, http://castalia.npc.nicta.com.au/

[50] Castalia User's Manual - http://castalia.npc.nicta.com.au/documentation.php

[51] Pediaditakis D, Tselishchev Y, Boulis A, “Performance and Scalability Evaluation of the Castalia Wireless Sensor Network Simulator”, Proceedings of the 3rd International ICST Conference on Simulation Tools.

[52] Fei Yu, “A Survey of Wireless Sensor Network Simulation Tools”, http://www1.cse.wustl.edu/~jain/cse567-11/ftp/sensor/index.html

[53] https://www.cs.princeton.edu/courses/archive/fall06/cos226/lectures/balanced.pdf

[54] Discrete Mathematical Structures, Bernard Kolman, Robert C Busby, Sharon Cutler Ross

[55] http://textofvideo.nptel.iitm.ac.in/106106094/lec40.pdf

Proceedings of the Fourth International Conference on Communication and Electronics Systems (ICCES 2019)
IEEE Conference Record #45898; IEEE Xplore ISBN: 978-1-7281-1261-9

A Survey of Privacy Leakage and Security Vulnerabilities in the Internet of Things

Amit Kumar Tyagi [0000-0003-2657-8700]
School of Computing Science and Engineering
Vellore Institute of Technology, Chennai Campus,
Chennai, 600127, Tamilnadu, India.
amitkrtyagi025@gmail.com

Deepti Goyal
Department of Computer Science and Engineering,
Lingaya's Vidyapeeth, Faridabad - 121002,
Haryana, India
deeptigoyal1994@gmail.com

Abstract. ***Due to recent development in technology, today's we are insisted to connect every object (device) with updated technology (i.e., which can run through connected via internet). Some examples like smart agriculture, smart homes, smart city, etc., are some applications of advancement in integration of Internet of Things together. Today's Internet of Things (IoT) or Internet Connected Things (ICT) are connected everywhere, with every-applications which is used to build a smart environment (with physical world). In general, these internet-connected devices (in integration) provide efficient services to users/ human. In other words, people life becomes easier to live with such devices in different applications (like smart transportation, smart cities, smart homes, smart grid, etc.). But, using these devices in their daily life, people are very much concern about "their personal information" or "their co-ordination/ location". So a question raised here: "Is it (personal information) safe with these (such) devices"? Do we know what is coming to our life/ in near future via leaking of privacy (or tracking our footprints) by these smart devices? When these devices are connected together, they build an ecosystem together for human being/ for many applications. A lot of data is being captured and transformed into valuable forms, which is used in future for increase productivity by firms/ organisation (in many application areas), ranging from automated home appliances, smart grids and high-resolution assets, to product management. This captured and collected data creates several issues, so it requires new/ useful strategies of enhancing the present status of IoT by incorporating (or overcoming) security and privacy into its current design, structure and implementation. Hence, this article explains such issues (in IoT) like privacy breaches, security vulnerability etc., in clear manner.***

Keywords **–** Internet of Things (IoTs), Internet Connected Things, Privacy, Security, Cyber- Attacks, and Internet of Thing's Applications.

I. Introduction

In the past decade, several security vulnerabilities are being found in Internet of Things/ Cyber-Physical Systems like robotics/ electronic power grid, intelligent transportation systems, and medical devices, and so on. The term 'Internet of Things (IoTs)' was first coined by the cofounder and Executive Director of MIT's Auto-ID lab, Kevin Ashton in the mid-1990s [1]. There are salient attributes across array of definitions, such as sensors, things, people, process, automation, data, network, connectivity, convergence, and intelligence. Hence, Internet of Things (or Internet Connected Things or Smart Things) can be defined as "Intelligent interactivity between human and things to exchange information and knowledge for new value creation". Billions and billions of devices are getting connected to the internet everyday as hardware is getting cheaper and smaller to fit into even the tiniest object. Manufacturers are connecting even the mundane kitchen gadgets to the internet to do some little work. Over a period of time, it is possible to turn the dumbest thing into a smart device. For example, a washing machine manufacturer collecting data to understand the product's wear and tear to build a better version in future (i.e., for future customers). However, a customer is always unaware from this kind of strategy of manufactures. So, in future we may expect a device to be unexpectedly smart. This scenario is the outcome of industries who are just thinking ways to make a device IoT enabled rather than thinking whether they should make a device IoT enabled or not. Interestingly it is not the consumer but the manufacturer who is benefitting by collecting data. Every manufacturer's primarily intention is to digitalize things to collect data. Manufacturer first aim is to attract many customers (with putting security risks at side), to make maximum profits and to stand in competitive market. Also, the customers wanted themselves to be updated with the latest technological innovations and are ignoring the associated security risks. A lot of data (called Big Data) is being generated by internet of Things (internet) and its integration. Also, this generated data is being collected on a cloud. On another side, cloud is the backbone for the Internet of Things, through which we can share resources anywhere, anytime. As IoT devices or this technology evolves, human being become more familiar with smart things/ these devices. So, we use these internet connected/ IoT devices for solving some real world's problems/ tasks related to real-time scenarios like self-driving cars or health care, etc. But as the data becomes more critical, we need more useful, sufficient analytics tool (approaches) to manage, store, secure and process information. Note that as data changes from critical to hyper-critical, we require more advanced security protocol systems. But a serious question arises here, who will fix these security issues in devices and at which level/ layer of communication/ implementation?

Internet of Things provides several benefits to users, and has the potential to change the ways that user's interact with technology. In near future, the Internet of Things is being integrating with virtual world with physical world (together), which is difficult to protect. From a security and privacy perspective, the predicted pervasive introduction of sensors and devices into currently intimate spaces like home, car, and with wearables and ingestible, even the body, it poses particular challenges. As physical objects are increasing in our daily life (according to our needs), then in future, detection and sharing of observations about us (by devices) will be increased automatically, i.e., we will require to protect our privacy. The IoT has the potential to connect 10X as many (28 billion) "things" to the Internet by 2020, ranging from bracelets to cars (in near future). Note that the Internet of Things (IoT) is emerging as the third wave in the development of the Internet, in 1990s' Internet wave was the first one, whereas in 2000s', mobile wave was the second one [2]. With decreasing prices/ cost of sensors, processing power and bandwidth to connect devices are enabling ubiquitous connections right now. Pervasive computing follows 6A's, authorized access to anytime-anywhere-any device-any network-any-data. Internet of Things (IoTs) makes a smart environment in integration of together [3], in this smart environment several smart things works together smartly, security, and efficiently. In the development of the Internet of Things (IoT) devices/ smart things, several issues like security, privacy, scalability, lack of standards, etc., (already) has been raised. Loopholes in security (badly configured devices) may provide a backdoor to unknown/ malicious users/hackers. Internet of Things devices are becoming more attractive to human beings (now days) than any other technologies (e.g., mobile phones), which access user's most sensitive information/ personal data, i.e., social security numbers and banking information. This is an essential issue overcome/ to received attention from research community.

A. Component of Internet of Things

With knowing total number of connected devices with Internet of Things (IoTs), we can derive the phenomenon of a network/ understand a network clearly (for which application IoTs are working). Here, IoT is "a complex eco-system encompassing all aspects of the Internet, including analytics, the cloud, application, security and much more" [1, 3]. In technical words, connecting

978-1-7281-1261-9/19/$31.00 ©2019 IEEE

devices/ Things with Internet connected devices/ IoTs are the main causes in generating a lot of components, i.e., physical devices with sensors/ connected things, connection and infrastructure, and analytics and applications). The following enabling technologies with Internet of Things are included as:

- Radio-Frequency IDentification (RFID): They help in automatic identification of anything they are attached to acting as an electronic barcode.
- Wireless Sensor Networks (WSN): A sensor network consisting of a large number of intelligent sensors, enabling the collection, processing, analysis and dissemination of valuable information, gathered in a variety of environments. The components that make up the WSN monitoring network include: WSN hardware, WSN communication stack, Middleware and Secure Data aggregation.
- Addressing Schemes: Internet Protocol version 6 (IPv6) is used for identifying the IoT devices uniquely as it is a key aspect for controlling and monitoring the devices.
- Data Storage and analytics: Billions and Billions of IoT devices are producing continuous streams of data. In order to process the data collected and gain knowledge we require AI based machine learning algorithms. These algorithms need to be interoperable and adaptive.
- Visualization: Visualization is the key to the success of any IoT application. Visualization techniques help the end users in making quick decisions.

An IoT device can be classified further into two categories, i.e., Physical objects (i.e., smartphone, camera, sensor, vehicle, drone, and so on), and Virtual objects (i.e., electronic ticket, agenda, book, wallet, and so on). In simple terms, IoT is a combination of embedded technologies including wired and wireless communication sensors and actuator device and physical objects connected to the internet. An IoT system has four major constituents: a). Sensors that collect data from smart devices b). Input which activates the sensors c). Data analysis that is performed to extract useful information. d). A monitoring system for ensuring security and privacy of the information.

Hence, this section discusses about several things likes introduction and essential components of IoTs. Further, the organization of this paper is discussed as: Section 2 discusses a vision for future, i.e., how near future can be changed/ will be with Internet of Things and Machine Learning or intelligence together. Further, section 3 discusses about some current trends in IoTs technologies. Then several Threats to Internet of Things Ecosystem like human and cyber-attacks (also some vision of IoTs in future) are being discussed in section 4. Further, we will secure an IoT ecosystem using some preventive and cryptographic mechanisms in section 5. Then, security and Privacy Goals with internet of Thing's Devices (via a 360^0 view) have been discussed in section 6. Before conclusion, some challenges in IoTs devices/ with internet connected things have been discussed in section 7. In last, this work is concluded with some future work (scope) in section 8. Note that in this work, we have used terms 'Internet of Things' with 'Internet Connected Things' or 'Smart Things' interchangeably.

II. How Internet of Things is affecting User's Privacy?

Generally, Internet of Things enabled devices are physical gadgets with built-in Internet connectivity that allow data transmission [10]. But, a user is unaware what is happening in the background, i.e., a user have no indication that anything is happening in back-send. Are these devices are supporting users in a positive ways or in negative ways? For example, a movie named "Spy in the sky" was released in 2015.In this movie, user's location or movement was getting traced by drones (in form of/ like a bird). Such incidents are possible in real-world also. As another example, a hacker or antivirus companies have added some patches with their antivirus update, to get end-user activities. Even hackers can send malicious files to an end user which may control end user's systems/devices entirely. As discussed above, increases in data. Also, using devices by several people without knowing such technology/ device or having low security in respective devices are the main reason of losing their footprints to other users/ attacker/ hacker. IoTs are much helpful in building Cyber Physical Systems (CPSs), but providing automation to machines or every work may harm to society/ people via tracing their movements (or footprints). These are is no guarantee that these devices will not track user's movements or reveal this collected information to other user/ outside world. Internet of Things device are being used in several applications like industries/ industrial intent, personal medical devices, smart home, wearable, smart city, smart grid, connected car, smart retail, smart supply chain, smart farming, etc. [2]. Apart that, today's IoT devices are resilience to several attacks like TREsPASS attack, Distributed-Denial-of-Service, Falsification attack, Man-in-Middle attack. Hence, with such attacks, hacker/ attacker breach or track or interfere into user's personal life/ daily life. In summary, a user may be traced in public places by several devices or by his own devices (like smart phone, laptops, or nay internet connected devise, etc.). Also, he/ she can be traced by hackers/ machines/ robots (i.e., a cyber-physical system) in his/ her home. A robot can look to his owner, i.e., at what time which work he/ she is doing and so on. According to that, machine/ robot may use this information/ traces/ patterns against his owner (in future) only. For example, in a movie named "Edward Snowden" which was made on true incident. In respective movie, Central Intelligence Agency (CIA) looks into its citizen's life and traces every movement of its citizens. Together this, CIA read all messages through mails, phones, etc., of its citizens (also put surveillance on its citizens). Hence, there was no privacy protection mechanism, even companies made to bind to share their user's data with the respective government. As another example, in China (now a day) mobile companies have to share its user's data with respective governments (as a mandatory rule). Such examples are complete violation of personal privacy. Basically, a user's privacy need to be protected and kept preserved, because privacy a fundamental right for citizens of a country (e.g., India, USA, etc.).

Hence, major security issues in IoTs/ Internet Connected Devices are: handling data encryption, data authentication, IoT hardware issues, hardware testing (as inevitable), and managing updates (in devices). Also, major trust issues in IoT are: lack of security, leaking of privacy/ tracking footprints of users, safety (smart locks, etc.). To overcome such raised issues in IoTs, we need to fulfil some goals with respect to privacy and trust. Primary security goals in IoT are confidentiality, integrity, authentication and authorization, availability, accountability, auditing, non-repudiation. On the other hand, privacy goals in IoTs are: privacy in devices, privacy during communication, privacy in storage, privacy in processing, identity privacy and location privacy and building trust with respect to respective service provider (who own IoTs devices). Hence, this section discusses about how internet connected devices may affect user's privacy in a crowd places and non-crowded places. Now how IoTs can be useful to a human being can be discussed via two scenarios (see figure 1). Here, we need to discuss one day of a user with two different scenarios [4, 5], in that we are finding that intelligence or machine learning are much helpful/ in helping them to get ready for next day (for job/ work). Hence, what we noticed from the discussed scenarios (discussed in [4]]). We learned here, differences among life living with and without intelligence, and importance of Machine Learning or intelligence/ artificial intelligence in near future. For new users, no matter when a user gets up, shower and coffee are being ready without ever-getting the chance to waste water or warm or cold using intelligence with (in) IoTs devices. Smart things keep/ perform event in flow/ in manner (see figure 1). Above all tasks which were done by user only (in scenario 1), can be done in sequential or in parallelized way with Intelligence. But, depending more on technology also creates several problems like leaking of privacy/ personal information, storing information without user's permission, trust, safety, etc.

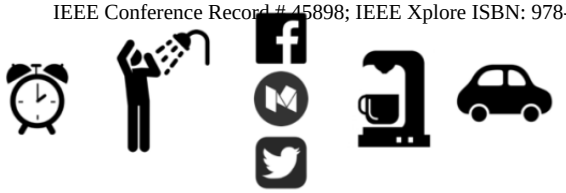

Figure 1: Flow of Events with Internet of Things and new Technology like Machine Learning, or Deep Learning [4]

Hence, this section discusses about internet connected things, i.e., how they (IoTs) are changing human's being life or making their life better. Later, this section also discusses uses of IoTs (with intelligence or machine learning) in human's being life with an example (i.e., with two scenario). Now next section will discuss about the technologies which are trending now and in near future.

III. Technologies Trending Now and in Near Future

As discussed above, most of the benefits (from cloud based IoTs) are coming with huge risks, like losing of privacy loss and security breaches. To secure the IoT devices (also to preserve privacy of user in IoTs), several novel ideas/ proposed work have been proposed by many researchers [6]. The Internet is the main backbone for making a communication among devices/ machines, also a platform to reveal people's information to malicious users/ hackers. In 1990, internet/ worldwide web (a method of publishing information on the Internet) created by Tim Berners-Lee [7, 8]. Today's Internet users are in billions, it is being in maximum devices (i.e., interlinked human and creates new generations of interactive experiences). In near future, Internet will be used with billions of IoTs/ IoT ecosystems (a world of networked smart devices equipped with sensors, connected to the Internet, all sharing information with each other without human intervention). It is because today Internet has a lot of information (due to having a large network of information). In simple terms, Internet became a bigger platform/ source of information (also it is due to large number of websites available on it).

Value Propositions: With the rise of internet connected devices and connected individuals, technology experts forecast four components like Big data, cloud, social media, and mobile devices/ things [4]. Interaction of these components (together) will fuel and shape the IoT to a new level. The 'Internet of Things' generate a lot of data (called as 'Big Data'), which is used by data scientists, researchers or organisations (or manufacturer) to do prediction/ make some decision for future. The volume of data attributable to the 'Internet of Things' is substantial. As sensors (embedded in IoTs) interact with the other things (or devices), 'Things' such as RFID tags generates huge and huge of data. In result, traditional tools fail to handle this large amount of data. Today's digital processing becomes a requirement of feasibility. The velocity of data associated with the 'Internet of Things', is compared with traditional transaction processing, explodes as sensors can continuously capture data. The variety of data is generated by 'Internet of Things' is also increasing/ changing frequently (due to using different types of sensors in different applications). The veracity of data in the 'Internet of Things' may also be improving as the quality of sensor and other data improves over time. For example, use of Radio Frequency Identification (RFID) tags generates much more reliable information than a decade ago. Such high volumes of data, coupled with an increasing velocity of data, along with an increased variety of data, illustrate the push by the 'Internet of Things' to generate 'Big Data'. Hence, a 360^0 view of IoTs Things/devices can be discussed in following applications:

- IoTs for manufacturing
- IoTs for retail
- IoTs for electronics
- IoTs for automotive
- IoTs for energy and utilities
- IoTs for insurance
- IoTs for industrial
- IoTs for aviation

Above discussed point and uses of IoTs in several applications has been discussed in [3]. Hence, this section discusses trending technology of Internet of Things (IoTs) in several applications. Now, next section will discuss several raised threat in an IoT ecosystem.

IV. Potential Threat to Internet of Things Ecosystem

As discussed in [1, 4], 'Internet of Things' Generates 'Big Data', above discussed points are four pillars (of technology), which are interconnected with each other and work efficiently (with respect to cost and accessing to find/ search records over records or a database). But, IoTs have different views/ aspects for these pillars, i.e., tracking or leaking information of user to malicious users (by malicious systems/ devices, for example, in a Hollywood movie "Eagle Eye", released in 2008, in that computer systems or army personal track a user or its location everywhere with the help of small drone) [4]. As many as devices are being with other smart devices (IoT), researchers require to test several security, scalability, critical concerns etc. Through this, researcher tells to world about possible security vulnerabilities (or key threat) in IoTs, i.e., not having proper *security measures for large network of IoTs*. The key threat vectors explained in [11], also discussed here in brief:

a) Threat Posed by Compromised Devices: As we all know IoT devices contain information and the attacker have the potential target to exploit that information, for example, User installs a security camera, it could expose personal information of user. This information can be hacked easily and the attacker can control and manage it [4, 11]. Can we put trust on these devices? If yes, then how much? This question is really a tricky one.

b) Threat over Communication Link: A network of connected IoT devices transmits a lot of data, during this transmission lots of attacks are possible which is too dangerous. Note that this communication can be intercepted, captured, or manipulated (or shared with others/ unknown users) during transmission. For example, an attacker may trace the footprints of a user via his/ her communication, on the other side, attacker may track energy usage to plan an attack on the entire smart system. Here, successful attacks may affect trust among user, devices, firms and manufactures (of such devices) with respect to data transmitted in IoT infrastructure.

c) Threat on the Master: This threat is against manufacturer and Cloud Service Provider (CSP) raises issues like safety, trust and privacy. Manufacturers and IoT cloud both contain trillions amount of data which is highly sensitive and a strategic asset because it is determined by analytics process. Note that this has higher competitive information in view of underground APT (Asia-Pacific Tele-community) group, if leaked/ intercepted. If the Master is compromised, it gives opportunity to an attacker to manipulate many devices at once, some of which may have already been deployed in the field.

Besides all the IoT application benefits, several security threats in IoTs are observed and discussed in [4, 11]. Note that the internet connected devices (or internet of things) or machines are extremely valuable to cyber-attackers for several reasons:

i. Most Internet Connecting (IoT) devices are operating by the users who have less knowledge of cybercrimes. Then, it is easy to gain physically access to smart device by an intruder (attacker).

ii. Most IoT components communicate over wireless networks where an attacker could obtain confidential information by eavesdropping.

iii. Most IoT components cannot support complex security schemes due to low power and computing resource capabilities.

a. Human Threats

Malicious human activity always a dangerous threat to our systems/ computing device, for example, an employee (of an organisation) may try to tamper with or destroy or leak data [12]. Human is constantly trying to find new ways to annoy, steal, and harm. Human threats are categorized into the following:

- Unstructured threats consist of users which are less experienced and hack the data by using available hacking tools.
- Structured threats consist of users who can understand, develop and can exploit codes and scripts for example, structured threat, i.e., Advanced Persistent Threats (APT) [13]. Here, APT is defined as "a sophisticated network attack targeted at high-value information in business and government organizations, such as manufacturing, financial industries and national defense, to steal data" [14].

Hence due to weaknesses in security vulnerabilities or Rogue security software, malicious users can enter in another user's system and can steal their data.

b. Common Cyber-Attacks

Using malicious code, i.e., in form of worms, virus, etc., Cyber-attacks are being done to harm users or their data (which is a cybercrime due to stealing of information and identity theft of users). In general terms, Cyber-attack is an attack is "any attempt to expose, alter, disable, destroy, steal or gain unauthorized access to or make unauthorized use of an asset" [15]. Generally, cyber-attacks are socially or politically motivated on internet-connected systems/ things, i.e., stealing, altering, or damaging someone information on an internet connected system/ things. Today's several attacks have been performed or formed one thing/ computer (system) to another things/ computer (systems). Many attacks on these things (internet connected devices) have been detected in the past decade. Some of these Cyber-Attacks on IoTs are listed here as:

1. Physical attacks**:** It is the subset of physical threats. Attack means that there is some attacker and his intention to do attack and tempers with hardware components. Most of the devices typically operate in outdoor environments, which are highly vulnerable to physical attacks.
2. Reconnaissance attacks: It is unauthorized discovery and mapping of systems, services, or vulnerabilities, for example, scanning network ports [16], packet sniffers [17], traffic analysis, and sending queries about IP address information.
3. Denial-of-Service (DoS): A Denial of Service (DoS) attack happens when a service that would usually make a machine or network resource unavailable to its intended users. In this attack , the attacker (hacker) sends excessive messages asking the server to authenticate requests that have invalid return addresses
4. Access attacks: The attacker wants to gain to a system network, where the intruder has to find out the vulnerabilities or weaknesses in the network authentication, i.e., FTP and web services. This attack is of two types: Physical access and Remote access.
5. Attacks on Privacy: Privacy protection in Internet connecting things (like autonomous vehicles, intelligent/ smart vehicles, etc.) is always a challenging task in IoT because of the huge information is easily available (being collected by smart devices) through remote access. The most common attacks on user privacy are:
    - Data mining: The attacker can extract useful information and patterns from data in large databases.
    - Cyber espionage: The attacker use malicious software and cracking techniques to steal the secret information of the individuals, organizations or the government.
    - Eavesdropping: listening to a conversation between two parties [20].
    - Tracking: The attacker can track the movements of the user with the help of devices Unique Identification Number (UID), for example, mobile number.
    - Password-based attacks: Such attacks attempts by malicious users to duplicate a valid user password into two different ways via dictionary attack (making possible combinations of letters and numbers, i.e., guessing user passwords) and brute force attacks (using some hacking/ cracking tools to try all possible combinations of passwords to break user passwords).
6. Cyber-crimes: Now days, these smart devices are being used (using internet) for other uses rather on their actual uses, i.e., used to exploit users and data for materialistic gain, such as intellectual property theft, identity theft, brand theft, and fraud [18, 19, and 21].
7. *Destructive attacks: Space is used to create large-scale disruption and destruction of life and property. Examples of destructive attacks are terrorism and revenge attacks.*
8. *Supervisory Control and Data Acquisition (SCADA) Attacks: As any other TCP/IP systems, the SCADA [22] system is vulnerable to many Cyber-attacks [23, 24]. The system can be attacked in any of the following ways: i) Using denial-of-service to shut down the system. ii) Using Trojans or viruses to take control of the system. For example, in 2008 an attack launched on an Iranian nuclear facility in Natanz using a virus named Stuxnet [25].*

Some other cyber-attacks are: Phishing. Man-in-the-middle attack, Denial-of-service attack, SQL injection, Zero-day exploit, etc. We need to remember here that as the number of IoT devices are integrating together and becoming a reality to user's life, and then obviously several security threats also will be occurred. Everyday unfortunately, IoT devices are getting new attacks (with new mechanisms, code).

c. Vision of the Internet of Things

As discussed IoTs are being used everywhere now days. Also we find that several threats have been mitigated on IoTs devices. So, a manufacturer (of these devices) needs to build these devices in future with considering issues like privacy, safety, and quality of life (for other user/ firm, which will use it in a distributed multi-user system with internet). Internet of Things is being look at outer world in the following way

a) Large Scale Ubiquitous and Pervasive Connectivity: Today's in vision of the IoT, these devices are using in creating smart environments, i.e., to makes energy, transport, cities, etc., more intelligent [29]. Integration of IoTs makes an environment which provides efficient services to users anytime, anyplace (using optimal path). IoTs in near future will be used in several areas like businesses and industrial Internet (with creating an open, global network of people, data, and things).
b) Context-Aware Computing: It requires most in Internet of Things, i.e., users require awareness of the computing elements (to optimize their performance and to enable services customization). Also, creation of smarter environments, entertainment and business applications (which are beneficial to users) would require acquiring, analysing and interpreting important context information about users.
c) Seamless Connectivity and Interoperability: Internet Connected Things or IoT requires seamless connectivity and Interoperability, so that context information can be shared among heterogeneous devices.
d) Network Neutrality: Network neutrality (a part of vision of IoTs) states that "no bit of information should be prioritized over another". So the principle of connecting any device to other devices from anywhere at any-time

make most optimal physical path between sender and
IEEE Conference Record # 45338; IEEE Xplore ISBN: 978-1-7281-1261-9
the recipient in a network/ communication.

Hence, this section discusses about several threats notified in the IoT ecosystem. Also, this section discusses about human and cyber-attacks (including vision of IoTs things) in detail. Now, next section will discuss some mechanism to secure an IoTs ecosystem in detail.

V. Securing Internet Connecting Things Ecosystem

As we all know, IoT will be a game changer for the applications and business but it will raise issues like security and privacy on a large scale and requires attention from manufacturer. In general, IoT security depends on the ability to identify devices, protecting IoT hosting platform, and protecting data (collected by smart/ IoT devices) and share this data with Trusted IoT Device (a trusted device is required to be reliably identifiable and associated with a manufacturer/ provider. Sharing information with trusted entities only increase trust among users and on technology. Now, here we are discussing all necessary tasks/ components to require/ secure an IoT ecosystem.

a. Maintaining Data Integrity with Internet of Things/ Internet Connected Things

Internet of Things promises to open up new opportunities for businesses to offer exciting services. These days insurance companies are installing IoT devices in the vehicles to collect the data about health and driving details of user to take decisions about the insurance claims. To prevent the data from the malicious user, the data should be encrypted at network layer. Blockchain Technology (first time used in Bit coin: A Crypto- currency [30], in 2009) can be used to fulfil this wish, i.e., can provide higher security to a distributed, decentralized and centralized system.

b. Establishing Trusted Identity Internet of Things

As discussed above, Internet of Things is built on a network of uniquely identifiable devices, whereas, public key cryptography plays a biggest role in establishing trusted identities (in IoTs). Public key cryptography used a concept of using two different keys to share any information among systems/ users. Where one of the key is made public (i.e., public key) and the other is kept private (i.e., private key). Information can be read if both of the keys apply correctly on encrypted information. This process is done by a Certification Authority (CA). Also, trust can be built via creating blocks and storing encrypted information in blocks with consisting information with respect to previous and next block's records (i.e., a Blockchain concept) in an IoT environment.

c. Establishing a Public Key Infrastructure for Internet of Things

As discussed above, identity infrastructure is built on both/ combination of public and private keys. If a private key is not kept secure/ private, then credibility of respective key may get compromised. The secure generation and storage of these keys is paramount. Public Key need to be secured by a novel propped solution (which is properly implemented with some real world attacks) against tamper-resistant hardware / to protected stored data. Using this mechanism, we can easily mitigate an attacker/ attack in a network.

d. Protecting Aggregated Big Data with Encryption

The data collected, transmitted, and stored in clouds/ IoT can be protected using encryption mechanisms. We can use Blockchain technology to secure this data, i.e., storing this data in blocks (after encrypt) then make a connection with next blocks (according to data/ information). A data is situated in two forms (in a cloud/ IoTs communication) like data at rest (static) and data in motion (dynamic).

- Protection of Data at Rest: When IoTs devices are communicating, then they generating a lot of data, which is stored at several locations with secure mechanisms. Encrypting this data and keeping it at server side provides scalable, cost effective storage, and fast processing in near future. These encryption mechanisms provide availability, integrity and usage of respective collected data (i.e., accessible all time to users). Storing this data with protected manner and avoiding any possible entry point to any malicious users/insider is an essential issue to overlook/ focus in near future. To overcome this issue of protecting stored data, firms/ organizations need to use sufficient encryption mechanism (after compression of data)/ lock down sensitive data at rest in big data clusters (without affecting systems/ devices performance). For that, it requires transparent and automated file-system level encryption that is capable of protecting sensitive data at rest on these distributed nodes.
- Protection of Data in Motion: Encrypting communicated data presents a unique challenge because it has a high variety and increasing at a higher rate. As data moves from one location to another, it is highly vulnerable to attacks like fibre tapping attack, man in middle attack, etc. Note that an attacker can listen a communication (which is being with two parties/ devices) with tempering/ attaching a cable (with fibre coupling device) and no device (or mechanism) can detect it. In this, attacker can record all activity that runs across a network, and data is captured and stolen without the owner's knowledge (even sender and receiver's knowledge). In worst case, this type of attack can also be used to change data, and has potential to override the controls on the entire system. Note that encryption is also required at the back-end infrastructure level of manufacturers, cloud service providers, and IoT solution providers.

A data can also be protected using Blockchain concept. Security can be provided to any types of data via creating blocks and storing encrypted data/ information in blocks with consisting information with respect to previous and next block's records. This process is clearly impossible to compromise (except in case of covering majority of blocks) by any attacks. Note that Physical security is probably more of an issue, since these devices are usually out in the open or in remote locations and anyone can get physical access to it. Once someone has physical access to the device, the security concerns rise dramatically. Hence this work presents several suggestions or techniques to (provide security) securing an IoT or Cloud based IoT ecosystem. Now, next section will discuss several security and privacy required in IoTs (via 360^0 view).

VI. Security and Privacy Goals with internet of Thing's Devices (via a 360^0 view)

In above discussion (in section 5), storing or learning patterns of user's daily activities is ok, but it is critical when it is shared with unknown device/ users. It is a major and essential challenge (issue) to overcome. Privacy is a fundamental right, which needs to be protected. It can be protected with complete isolation from outside world/ Internet-world. A user starts to interact with other devices/ people; he/she starts sharing/ is willing to share information about itself with others. Hence, some privacy goals in IoT based Cloud are included as:

- Privacy in devices: When a user sends information from one device to another, then this personal/ sensitive information of users may be leaked to other devices (or users). It (privacy breaching) is also possible in case of device's theft or loss. In summary, it depends on physical and commutation privacy.
- Privacy during communication: When a device is connected to another device, it depends on availability, integrity and reliability of a device to reveal its service to another device. Here to reduce the breaching of

with devices only when there is a need.

- Privacy in storage: In this, a device which is not in use or in its ends of life, then storage information in such devices (or IoTs) needs to be protected from reaching in hands of illegal users. Such information may use by attacker to blackmail the respective users (in future). It means data should be protected which is stored in such devices. Hence, a proper deletion and wipe off (of storage) of devices is required for avoiding any kind of attack.
- Privacy in processing: It depends on device and communication integrity [26]. Data (or information) should be disclosed to or retained from third parties without the knowledge of the data owner.
- Identity privacy: Every device has some unique identity which should be identified by the authorized person/ device only (to avoid any attacks like privacy breaching, etc.).
- Location Privacy: It is the geographical position of relevant device should only discovered by authorized entity (human/device) [27, 28].
- A user consists data, information, identity, location and genomic types of privacy in communication of/ with internet of things. Such types of privacy contain valuable and sensitive information, which require protection against malicious users. Similarly, some security protection required with IoTs as:
- Security of IoT devices: Security of IoT ecosystem need to be provided physically. When an IoT ecosystem is being like smart grid, then from we require some manpower/ human being to take care that site, i.e., protection site against any kind of damages. For example, organisations are hiring persons for taking care of their infrastructure (i.e., in telecom industry).
- Security in IoT devices: Proper encryption mechanism, efficient algorithms to collect data in a database, access control to known users, etc., are some essential components need to include when IoTs devices is being used.

Hence, this section discusses several security and privacy goals with respect to internet connected things via 360^0 view. In this, we find that privacy of information stored/ communicated in devices should be persevered and protected, also security of devices and enough level of security need to be provided in IoTs. Now, next section will discuss about some challenge in IoTs.

VII. Issues and Challenges in Internet Connected Things

In the past decade, several challenges have been investigated in IoTs. We need to focus on these challenges to encourage higher growth rate of IoT (in near future), and to provide opportunities to future researchers to do their research work. Industry also can consider these challenges to capture new competencies and capacities. These challenges (investigated in an IoT ecosystem) can be discussed as:

- Infrastructure: An Infrastructure is an environment which is interoperable, trustable, mobile, distributed, valuable, and powerful for provide services to human beings. An IoT ecosystem consist several emerging applications in it, i.e., like Smarter Cities, Smart Grid, Smart Building, Smart Home, Intelligent Transport Systems, and ubiquitous healthcare, etc. Due to that, large numbers of address schemes are required to provide address to each and every connected IoTs (to offer offers scalability, flexibility, tested, extended, ubiquitous, open, and end-to-end connectivity). Note that Addressing schemes are used to identify with respect to identify sender's identification/ location, to provide security to devices.
- Data and Information: Lots of data is being generated with these devices (in integration), which is a major challenges to handle, and analysis. Modern analytic tools/ new big data solutions are required (by service providers) to analyse data, and discover relevant trends and patterns for future purpose.
- Security and Privacy: The smart devices connected to the internet connected devices (ICD) helps consumers, or industries or service providers (in many ways) to increase business (or solve queries of users). Smart devices transmit data, with compiling it (in shorter form) to end users. Third parties users like researchers, health care providers, etc., can use this information for their research purpose. But again, leaking of privacy or breaching of privacy, trust issues will be arises in an IoT ecosystem.
- Ecosystem: The IoT revolution is on peak. Each city or machine is being embedded with smart devices or internet of things. 'Things' already have a lot of information of users. This information is being used to produce new facts/ information, communicate, and to become an integral, essential part of the Internet. In near future, the market for IoT will reach approximately £200bn a year (worldwide) with new and innovative business models, applications and services developing across different sectors of the economy. Such smart innovation in several areas will improve growth of respective areas (using efficient, better wireless connectivity, system integration and decision-support tools).

A. Challenges in Internet of Things

A key challenge in machine learning is "How to represent the Input Data and what are possible Security Attacks and System Vulnerabilities"? There has been a lot of work done in the scenario of IoT security up till now. The related work can be divided into system security, application security, and network security. Some few problems in this regard can be included as:

a) Design of Service oriented Architecture (SoA) for IoT: SoA needs to handle a large number of devices connected to the system which phrases scalability issues. Here in this challenges like: data transfer, processing, and management become a matter of burden.
b) Heterogeneity: IoTs is having a complicated heterogeneous network platform. This, in turn enhances the complexity among various types devices through various communication technologies showing the rude behaviour of network to be fraudulent, delayed, and non-standardized. The management of connected objects by facilitating through integration between devices, for example, hardware components and/or software services, and administering them after providing addressing, identification, and optimization at the architectural and protocol levels is a serious research challenge.
c) Lack of Service Description Language (SDL): In network services, a lack of a Service Description Language makes the service development, deployment, and resource integration difficult by extending the product dissemination time (due to/ causing loss in market). A Novel SDL may and change or solve several problems like product dissemination. We must identify a commonly accepted SDL, so powerful service discovery methods and object naming services need to be implemented.
d) Lack of a Unified infrastructure: IoT is designed with a traditional network/ IoT makes CT environment. This environment is affected by its connection. So, we require a unified information infrastructure to connect large number of IoTs devices (to produce real-time data).
e) Handling Large Data base: Today's existing/ Traditional Data Base Management System (DBMS) cannot handle the originated data, because of the huge data (generated or collected). The current fault tolerance system is in capable of managing the high speed generated data. A new IoT based data centric architecture need to be proposed to tackle this issue.

IEEE Conference Record #45982; IEEE Xplore ISBN: 978-1-7281-1261-9

f) Efficient of Data generated by IoTs: The data generated from IoTs devices (connected through internet) will be in present in different volume, variety and formation. So big data/ IoTs generated data specific design should be invented to handle these types of data.

B. Issues in Internet of Things

IoT system includes large number of nodes which should be identified uniquely in the network configuration. Since the IPv4 numbered addresses are about to exhaust, so we have to find a new addressing scheme like IPv6 to configure all IoTs devices. Further, different devices use different protocols to handle hardware/ software compatibility, this is also a major issue with IoTs. Hence, the lack of standardised tools for security, communication and identification need to be developed to make the IoT ecosystem efficient, accurate and safe (privacy preserved). In summary, information security and data privacy protection are two major concerns in IoT. Having highly complex, deployment, mobility and heterogeneous in nature, IoT always faces severe security and privacy threats. From [4] and above discussion, we conclude that "privacy protection in IoT environment is more vulnerable than in traditional Information and Communications Technology (ICT) network due to the large number of presences of attack vectors on IoT entities". A popular example can be discussed as: "IoT based health care monitoring system will collect patient's data (e.g., heart rate, pulse, body temperature, respiration, etc.) and later on send this information directly to the doctor's office or hospital via network (Internet)". As the time of data transfer over the network, if patient's data is stolen or misplaced serious risk may arise which can cause even death to the user. In such situation, it is noticed that most of the architectures do not include privacy, and security aspects into the respective concept which is drawback that needs to be clarified. Hence, as we have discussed in above sections that Data is collected or produced in raw form, i.e., consist non-relevant handouts. And this generated data is too helpful in decision making in several applications. The value of this collected/ generated data is only possible after analysis/ filtering process. So efficient and modern tools to analysis this collected data needs to developed. Also a commonly accepted service description language (which is compactable with different communication and implementation) must be identified to make the development process easier.

Hence, this section discusses several challenges in internet of things like heterogeneity, lack of unified infrastructure, lack of unified standards, huge data base, huge consumption of energy, etc. Some more work towards IoTs devices has been discussed in Table 1 (in appendix A). Hence, these issues, challenges can be considered as future work in near future from/ by respective interested researchers/ research community. Now, next section will conclude this work in brief (with some future scope of this work for future).

VIII. Conclusion and Future Scope

Today's internet of things are being used everywhere, i.e., in many applications (like smart home, smart transportation, smart farming, etc.) to make human life easier. Even some countries are insisting their citizens to use these devices, for example, in India, Amravati (new capital of Andhra Pradesh state) will be first smart city. Similarly, Dubai will work completely on smart things, i.e., as a smart city before 2022. So, as uses of these devices are increasing, attacks will also be increased in near future. This work provides a detail description of internet connected things. It also discusses some serious concerns and challenges in IoTs in near future. These investigated issues, challenges need to be overcome or require attention from research community. Also, major limitations of IoTs like Battery life extension and Lightweight Computation are also needed to be improved (for providing efficient, smart, and secure services for a longer-time). Hence, security at the device level, protecting the master-device, encrypting information/ communication links are critical to perform secure operations (among IoTs). In summary, we should improve existing methods to secure IoTs/ IoT ecosystem instead of searching for a new method. As future work, we should focus on delivering the current state-of-the-art security controls, and optimise the new and complex embedded applications to drive the further adoption of IoT (because integration of IoTs in several applications and in many counties is growing exponentially).

References

[1] TELEFÓNICA I+D: Internet of Things + Internet of Services (2008).
[2] Simona Jankowski, et al., The Internet of Things: Making sense of the next mega-trend, Goldman Sachs Global Investment Research's report, Sptemmber 3, 2014.
[3] Amit Kumar Tyagi, Nandula Anuradha, G. Rekha, Sonam Sharma, and Sreenath Niladhuri, How a User will look at the Connection of Internet of Things Devices?: A Smarter Look of Smarter Environment, ICACSE: 2019: 2nd International Conference on Advanced Computing and Software Engineering, KNIT Sultanpur, 2019, India, 8-9 February 2019.
[4] Amit Kumar Tyagi, and M.Shamila, Spy in the Crowd: How User's Privacy is getting affected with the Integration of Internet of Thing's Devices, SUSCOM-2019: International Conference on Sustainable Computing in Science, Technology & Management (SUSCOM-2019). Amity University Rajasthan, India, 26-28 February 2019.
[5] https://towardsdatascience.com/iot-machine-learning-is-going-to-change-the-world-7c4e0cd7ac32
[6] Arbia Riahi, Sfar Enrico Natalizio,Yacine Challal, Zied Chtourou, A roadmap for security challenges in the Internet of Things, Digital Communications and Networks, Volume 4, Issue 2, April 2018, Pages 118-137.
[7] https://en.wikipedia.org/wiki/Tim_Berners-Lee
[8] https://www.w3.org/People/Berners-Lee/
[9] https://impact.com/marketing-intelligence/7-vs-big-data/
[10] https://www.optimusinfo.com/blog/understanding-the-7-vs-of-big-data
[11] Amit Kumar Tyagi, G. Rekha, and N. Sreenath, Beyond the Hype - Internet of Things Concepts, Security and Privacy Concerns, 22-23 March 2019, in Proceeding of Springer/ International Conference on Emerging Trends in Engineering, College of Engineering (ICETE), Osmania University, Hyderabad, Telangana, India.
[12] http://online-passport.info/comsecpriv/?page_id=41
[13] C. Tankard, Advanced persistent threats and how to monitor and deter them, Network security, vol. 2011, no. 8, pp. 16–19, 2011.
[14] F. Li, A. Lai, and D. Ddl, Evidence of advanced persistent threat: A case study of malware for political espionage, in Malicious and Unwanted Software (MALWARE), 2011 6th International Conference on. IEEE, 2011, pp. 102–109.
[15] American Government, Power and Purpose: Political science, Political science, book, CTI Reviews – 2016.
[16] S. Ansari, S. Rajeev, and H. Chandrashekar, Packet sniffing: a brief introduction, Potentials, IEEE, vol. 21, no. 5, pp. 17–19, 2002.
[17] M. De Vivo, E. Carrasco, G. Isern, and G. O. de Vivo, A review of port scanning techniques, ACM SIGCOMM Computer Communication Review, vol. 29, no. 2, pp. 41–48, 1999.
[18] B. Schneier, Secrets and lies: digital security in a networked world. John Wiley & Sons, 2011.
[19] J. M. Kizza, Guide to Computer Network Security. Springer, 2013.
[20] I. Naumann and G. Hogben, Privacy features of european eid card specifications, Network Security, vol. 2008, no. 8, pp. 9–13, 2008.
[21] C.Wilson, Botnets, cybercrime, and cyber-terrorism: Vulnerabilities and policy issues for congress." DTIC Document, 2008.
[22] A. Daneels and W. Salter, What is SCADA, in International Conference on Accelerator and Large Experimental Physics Control Systems, 1999, pp. 339–343.
[23] A. Nicholson, S. Webber, S. Dyer, T. Patel, and H. Janicke, Scada security in the light of cyber-warfare, Computers and Security, vol. 31, no. 4, pp. 418–436, 2012.
[24] V. M. Igure, S. A. Laughter, and R. D.Williams, Security issues in scada networks, Computers & Security, vol. 25, no. 7, pp. 498–506, 2006.
[25] M. Kelleye, Business Insider. The Stuxnet attack on Irans Nuclear Plant was Far more Dangerous Than Previously Thought, http://www.businessinsider.com/stuxnet-was-far-more-dangerous-thanprevious-thought-2013-11/,2013, [Online; accessed 03-Sep-2014].
[26] C. P. Mayer, Security and Privacy challenges in the internet of things, Electronic Communications of the EASST, vol. 17, 2009.
[27] A. R. Beresford, Location privacy in ubiquitous computing, Computer Laboratory, University of Cambridge, Tech. Rep, vol. 612, 2005.
[28] Amit Kumar Tyagi, N. Sreenath, Future Challenging Issues in Location Based Services, International Journal of Computer Applications (ISSN: 0975 –8887), Volume 114, No. 5, pp.51-56, March 2015.
[29] Misra, Sridipta, Maheswaran, Muthucumaru, Hashmi, Salman, Security Challenges and Approaches in Internet of Things,Engineering Signals & Communication, 2017 (Available at: https://www.springer.com/in/book/9783319442297#rev1502).

978-1-7281-1261-9/19/$31.00 ©2019 IEEE

[30] S. Nakamoto, "Bitcoin: A peer-to-peer electronic cash system," 2008. [Online]. Available: https://bitcoin.org/bitcoin.pdf

Appendix - A

Table 1: Challenges, Issues and Cyber-Attacks including Solutions in Internet of Things

S.No	Challenges	Issues	Cyber Attacks	Overcoming Solutions
1.	Security	As the IoT connected devices increases it will also increases the opportunity to exploit security vulnerabilities for an attacker	-	A collaborative approach to security will be needed to resolve this issue
2.	Privacy	The collection of this information exposes legal and regulatory challenges facing data protection and privacy law.	-	Strategies will need to be developed to respect individual privacy choices across a broad spectrum of expectations, while still fostering innovation in new technologies and services.
3.	Standards	Absence of the standards can enable stupid behaviour by IoT devices.	-	It requires a thoughtful design and standardization of configuration tools, methods, and interfaces, coupled with the adoption of IPv6, will be essential in the future.
4.	Home Invasions	IP address can be easily exposed easily, later location of residential address also can be leaked.	Hackers sold this information to the underground websites, to use this information for their business	-
5.	Remote Vehicle access	Car Hijack can be done easily	-	-
6.	Easy exposure	IoT devices are not resilient to third-party exposure — they either lay open or easily accessible to anyone.	This means that an intruder can either easily steal the device, connect the device to another device containing harmful data, or try to extract cryptographic secrets, modifying the programming or even replacing those devices with malicious ones in which the intruder has complete control.	-
7	Infrastructure	It requires large number of address schemes. Addressing schemes are used to identify with respect to identify sender's identification/ location, to provide security to devices.	-	-
8.	Data and Information	To handle and anlayze the data generated by the devices	-	Analytic tools is required
9.	Security and Privacy	Privacy related to personal data, and data sharing	-	-
10.	Ecosystem	It stimulate innovation and growth in areas such as components, devices, wireless connectivity, system integration and decision-support tools	-	-

Proceedings of the Fourth International Conference on Communication and Electronics Systems (ICCES 2019)
IEEE Conference Record # 45898; IEEE Xplore ISBN: 978-1-7281-1261-9

A Performance analysis of Medical Image Transmission Based on Compression and Parallelism

Abstract:

In the period of creating advanced imaging system, it for the most part centres to improve demonstrative translation and computerized picture the executives. The advanced picture the executives include different handling steps: picture obtaining, picture preparing, and image storage and picture transmission. In the human services condition, computerized picture securing modalities particularly processed tomography and attractive reverberation imaging system produces complex experiences as far as picture stockpiling and picture transmission. This examination paper tends to these issues by proposing a picture pressure procedure alongside parallel transmission control convention which sets up relationship between two application elements.

An objective single compression ratio may not be suitable for CT and MRI datasets because of their different mode of image generation and bit depth and contrast resolution. From the results, it can observed that experiments over Local Area Network (LAN) and Wide Area Network (WAN) using parallel connection, transmission time is improved linearly to the maximum value and decreases to some extend and it reaches flat. The transmission time is highly influenced by use of type of networks. In this research, it can be concluded that for 10 parallel WAN connections achieves maximum speedup compared to LAN for the four datasets.

Keywords: Image storage, image transmission, transmission time, Compression ratio and parallelism

Research Background

Telemedicine is an interactive communication tool which is widely used by doctors to remotely monitor the health status of the patients. Today, almost all healthcare providers depend on high-quality digital images from digital image acquisition modalities for diagnostic interpretation. The image acquired from the computed tomography (CT) and magnetic resonance imaging (MRI) frameworks are digitized and transmitted to advanced PCs for picture preparing. The consequences of the prepared pictures are exhibited to the radiologists for screening and indicative translation [1, 2].

In a multispecialty emergency clinic,a standard Brain CT and Chest CT may create around 250 to 350 pictures and a normal Brain MRI and Spine MRI may likewise deliver 300 to 400 pictures. To store a CT or MRI picture, it requires a high extra room as far as Mega Bytes (MB). So as to store and spare every one of these pictures, it requires monstrous extra room which isn't monetarily plausible. In this manner, it is important to pack the picture so as to lessen the limit of capacity and diminishing the transmission time. Further, Computer systems have been broadly used to convey the computerized pictures to remote spots [3]. In a multispecialty emergency clinic, a normal brain CT and Chest CT may create roughly 250 to 350 pictures and a standard Brain MRI and Spine MRI may likewise deliver 300 to 400 pictures. To store a CT or MRI picture, it requires a high extra room as far as Mega Bytes (MB). So as to store and spare every one of these pictures, it requires tremendous extra room which isn't monetarily attainable. Thusly, it is important to pack the picture so as to diminish the limit of capacity and diminishing the transmission time.Further, Computer systems have been broadly used to convey the computerized pictures to remote spots [3]. In Image processing, there are two types of image data compression: a) Lossless or reversible, b) lossy or irreversible

compression. In lossless compression method, to provide the compressed image involves image transformation and encoding. In lossy compression method, to provide compressed image involves image transformation, quantization and encoding [4, 5]. Ramakrishan et al. [6] presented an approach to improve the speed of data transmission between DICOM application entities using progressive transmission. In this paper, a wavelet based set partitioning in hierarchical trees coder has been used which consumes minimum bandwidth than variants of JPEG. Standard compression techniques that were used for clinical is Joint Photographic Experts Group which was developed based on irreversible compression technique. Each compression techniques performance depends on mode of image generation and contrast resolution [7]. Kalyanpur et al. [8] determined that for a lossy 10:1 compression was most suitable for CT image transmission. The author has not estimated compression ratio for MRI images.

Maani et al. [9] proposed parallel connection between two DICOM application entities. Two interfaces were used for parallel data transmission. The results indicate that transmission time is accelerated to 14 times for WAN. The author has not concentrated to decide the ideal number of parallel associations and picture pressure systems. Maani et al. [10]

This research paper addresses these issues by proposing an image compression technique along with parallel transmission control protocol which establishes association between two application entities. Further to determine the optimum number of parallel connections over the LAN and WAN for the BREBIX and CARCINOMIX datasets.

This paper has been classified into four segments, first introduction, second discusses about the proposed method in this paper, third about experimental setup and results, and finally the work is concluded with future work.

DICOM PROTOCOL

The Digital Imaging and Communications in Medicine (DICOM) Standard specifies a non-proprietary data interchange protocol, digital image management format, and file structure for biomedical images. It defines the form and flow of the electronic messages that convey biomedical images and related information between two computers [11]

Fig. 1 DICOM as an application layer protocol

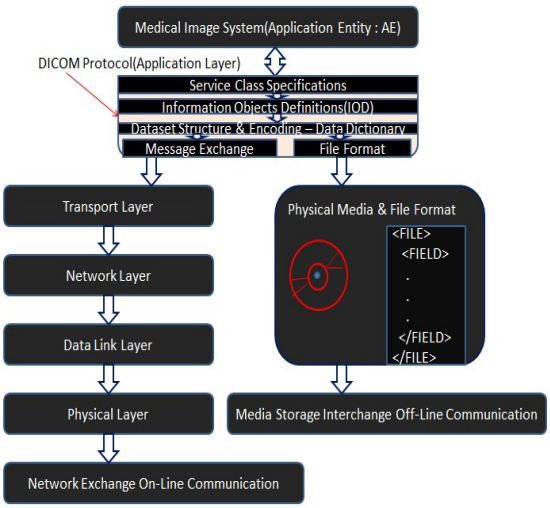

Fig 1

DICOM is an application layer convention and it's been related with TCP/IP convention suite that can be effectively utilized over the web is appeared in the figure 1.AE (application substance) is the application utilizing with the help of DICOM, AE can ask for or give administration rely upon the situation, SCU(serviceclassuser) means AE requesting services ,SCP(service class Provider) implies AE giving administrations to other applications. For

occurrences if DICOM application needs to discover picture in DICOM server. DICOM Application become SCU,DICOM server become SCP and DICOM FIND administration is the administration class.

The item occurrence by and large alluded data object definition(IOD) (e.g., a CT picture). The capacity or administration for the article (e.g., capacity) is called DICOM message administration component (DIMSE). Since each administration class called as an administration combined with an item, that is alluded as a Service–Object Pair(SOP).Sometimes two AE willing to begin imparting, that must be built up session. By and large session alluded as affiliation. After setup of affiliation the SCU sends solicitation to SOPs from the SCP. Once the SOP solicitation finished the affiliation is ended consequently.

PACS (Picture Archiving and Communication Systems) are restorative systems comprising of essential equipment and programming structured and used to run computerized therapeutic imaging. They contain computerized picture obtaining gadgets (modalities –, for example, figured tomography (CT) scanners, or ultrasound), advanced picture documents (where the gained pictures are put away), and workstations (where radiologists see the pictures). When you play with your advanced camera (methodology), store the pictures on your PC (document), and send them to your companions (analysts), you utilize precisely the same model. Obviously, PACS take the model to a significantly more mind boggling level as appeared in the figure. 2Fig 2 PACS Architecture

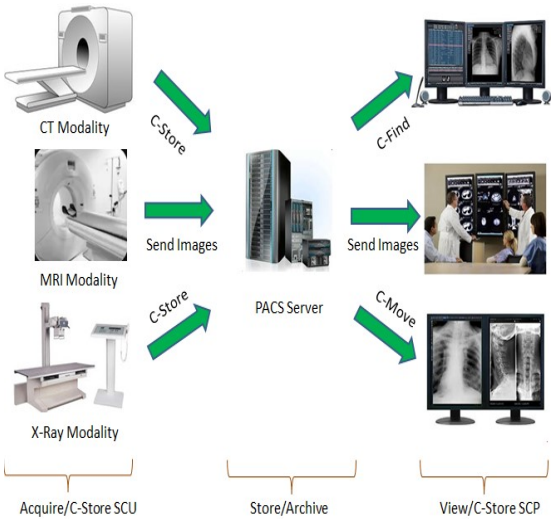

Fig 2

Data Image Compression

Because of their large volume of CT and MRI images, efficient compression techniques are necessary to reduce storage and bandwidth costs of medical systems. In this research, we modified the work of Zixiang Xiong et al. [2003]. In their exploration, proposed 3-D whole number wavelet change structure pursued by legitimate movements which accomplishes best execution as far as lossy and lossless pressure. In our examination we utilized blend of Integer wavelet change and 3-D set parceling in various leveled trees. To expand the coding effectiveness of 3-D SPIHT, every hub in the spatial-fleeting direction tree speaks to a gathering of wavelet coefficients. For a fixed picture measure, expanding the deterioration levels improves the pressure execution with wavelet change and 3-D SPIHT coding. The proposed pressure calculation of half breed blend of 3-D whole number wavelet change and 3 D SPIHT coding has connected to four diverse datasets; two distinctive CT pictures and two diverse MRI images[13-15]

Dataset Description:

In this research, we used four standard datasets for the evaluation of the proposed compression algorithm and image transmission. The description of the dataset is shown in the Table 1. In the

Table 1, it consists of four datasets namely, BREBIX,CARCINOMIX, MR BODY and MR BRAIN. The datasets BREBIX and CARCINOMIX consists of 1075 CT images and 539 MB uncompressed image data.

Table 1 Description of the experimental dataset

S. No	Name of the dataset	Type of Modality	Total number of images	Total volume of uncompressed data (MB)
1	BREBIX	CT	638	320
2	CARCINOMIX	CT	437	219
3	MR BODY	MRI	218	34
4	MR BRAIN	MRI	140	61

Table 1

Similarly, the datasets MR BODY and MR BRAIN consists of 358 MRI images and 95 MB volume uncompressed data images. The total dataset consist of 1433 images and 634 MB volume of uncompressed data images.

Data transmission using parallelism:

System Description

In this exploratory setup, LAN and WAN has been utilized to investigate the presentation of the system. So as to decide the ideal number of parallel associations, aggregate of 50 associations were consolidated in the examination. To find the mean speedup time, the experiments were repeated for 50 times on LAN and WAN. A sender system arranged with Pentium Quad center CPU and 8 GB of RAM running Linux Ubuntu. The recipient framework designed with a 4 Quad center CPU and 8 GB of smash running on Ubuntu OS.

Two interfaces are using for parallelize data transmission; each interface is located exactly where AE is located. Storage device carried out by interfaces; moreover only single connection existing between the AE and the interface. This method allows maintaining single association between the interface and AE that gives freedom to parallelize connection without increasing associations. The computer has both AE and interface and two interfaces are working using parallelism method, this can make use of available network bandwidth effectively, so we can easily increase the data transmission speed.

In many cases two interfaces using only one DICOM connection until otherwise AE sends storage SOP request. Here AEs plays either SCU or SCP at a time, but interface plays SCP or SCU based on sending or receiving data. For example AE1 request a MR image from interface1.AE1 is a SCU and Interface 1 is a SCP consequently interface 1 transfer the request to interface 2.Now interface 1 is SCU and interface2 is a SCP.Finally particular request is transferred to AE2 from interface 2.Here interface 2 is a SCU and AE2 is SCP.

In this paper Interfaces are implementing by using java language. Dcm4che is an open-source, which is used to implement DICOM protocol. The thread pool which is used to make TCP connections, but user must identify the size of the pool,(i.e.,)whenever an interface receives a message from the sender,type of sender must be checked. Generally interface has five main components receiver, sender to AE, and sender to interface, message interpreter, and thread pool**.**

Experiments on LAN and WAN

For the BREBIX dataset, this consists of only CT images, by adding six parallel connections to LAN, the transmission time has been improved for about 2.5 times. For the CARCINOMIX dataset, this consists of only CT images, by adding eight parallel connections to LAN, the transmission time has been improved for about 3 times. For the MR BRAIN dataset, this consists of only MRI

images, by adding four parallel connections to LAN, the transmission time has been improved for about 3.5 times. For the MR-BODY dataset, this consists of only MRI images, by adding ten parallel connections to LAN, the transmission time has been improved for about 4.5 times. By varying the parallel connections using trial and error method, it can be fixed optimum level of 6 parallel connections for LAN which reports mean transmission time about 2.5 times.

For the BREBIX dataset, this consists of only CT images, by adding fifteen parallel connections to WAN, the transmission time has been improved for about 19 times. For the CARCINOMIX dataset, this consists of only CT images, by adding 13 parallel connections to WAN, the transmission time has been improved for about 16 times. For the MR BRAIN dataset, this consists of only MRI images, by adding twelve parallel connections to WAN, the transmission time has been improved for about 8 times. For the MR-BODY dataset, this consists of only MRI images, by adding eighteen parallel connections to WAN, the transmission time has been improved for about 9.5 times. By varying the parallel connections using trial and error method, it can be fixed optimum level of twelve parallel connections for WAN which reports mean transmission time about 10 times.

Draw graph here

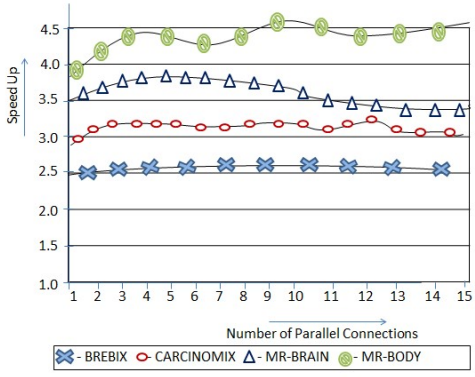

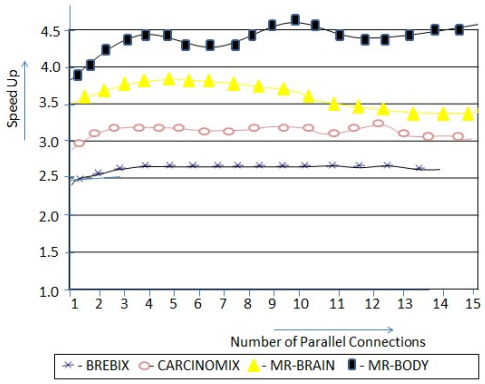

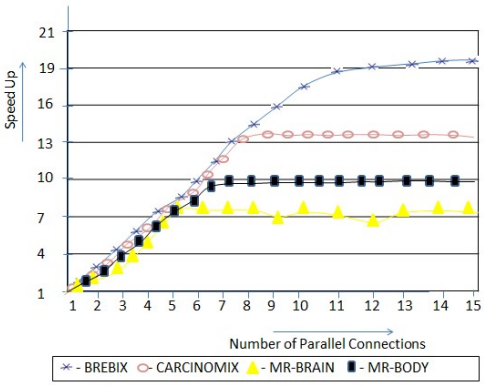

Results and Discussion

From the test results, it tends to be exhibited that straightly expanding the quantity of parallel associations, the speedup factor does not directly increments. In the wake of achieving an immersion level, speedup achieves level.When the number of parallel connections reaches almost constant and does not support to increase the speedup time, optimum use of parallel connections can be determined. Further, by increasing the number of parallel connections, both LAN and WAN adds overhead and reaches saturation and tends to decreases the speedup. From the results, it can be observed that compare with LAN, WAN uses relatively large number of parallel connections. It can also be observed that WAN performs better in terms of speedup. Maani et al [9] revealed the exhibition of the strategy for the long separation association on WAN was amazing and quickened the transmission time to around multiple times for the given dataset.

Further, Maani et al [10], reported the higher speed up for about LAN using parallel connection.

In this research work, we proposed an image compression technique along with parallel transmission control protocol which establishes association between two application entities. By using the combination of parallelism and compression, there is a relatively large improvement in the transmission speed up. By employing hybrid compression algorithm, it reduces storage space and network transmission time in both LAN and WAN.

Conclusion

In this exploration work, proposed a half and half pressure calculation alongside parallelism to improve transmission time of CT and MRI information picture. Structure the outcomes, it was shown that mix of half and half pressure calculation alongside parallelism improves moderately transmission time over both LAN and WAN. The speedup was about 2.5 for CT picture datasets and was around 10 for the two MRI picture datasets. From results, it demonstrates that there is a deviation of speedup in view of the CT pictures and MRI pictures. It can likewise be confirm that the methodology type assumes basic job in by and large speedup.

Mr.P.Sreenivasulu ,
Research Scholar,ECE Department
SVUCE,Tirupati,sreenu306@gmail.com

Dr.S.Varadarajan ,
Professor in ECE Department
SVUCE,Tirupati,
varadasouri@gmail.com

References

1. Baxes GA. Digital image processing-principles and applications, New York: John Wiley & Sons Inc.; 1994.
2. Dreyer K.J., Mehta A., Thrall J.H., "PACS: A guide to the digital revolution", 2nd ed., Springer-Verlag, New York, NY (2005).
3. Huang HK. PACS and imaging informatics: basic principles and applications. New Jersey: John Wiley & Sons, Inc.;2004. p. 119-152.
4. Erickson BJ, et al. Evaluation of irreversible compression of digitized posteriori anterior chest radiographs. Journal of Digital Imaging Aug 1997;10(3):97e102.
5. Erickson BJ. Irreversible compression of medical images. Journal of Digital Imaging March 2002; 15(1):5e14.
6. Ramakrishnan B, Sriraam N: Internet transmission of DICOM images with effective low bandwidth utilization. Digital SignalProcessing. 16(6):825–831, 2006
7. Iyriboz TA, Zukoski MJ, Hopper KD, StagPL. A comparison of wavelet and Joint Photographic Experts Group lossy compressionmethods applied to medical images.J Digit Imaging 1999; 12:14–17.

8. Kalyanpur A, Neklesa VP, Taylor CR, Daftary AR, Brink JA: Evaluation of JPEG and wavelet compression of body CT images for direct digital teleradiologic transmission. Radiology. 217

(3):772–779, 2000

9.Sung MM, Kim HJ, Yoo SK, Choi BW, Nam JE, Kim HS, Lee JH, Yoo HS: Clinical evaluation of compression ratios using JPEG2000 on computed radiography chest images. Journal of Digital Imaging: The Official Journal of the Society for Computer Applications in Radiology. 15(2):78–83, 2002

10. Erickson BJ: Irreversible compression of medical images. Journal

of Digital Imaging: The Official Journal of the Society for Computer Applications in Radiology. 15(1):5–14, 2002

11. Amor NB, Essoukri N and Amara B: DICOM image compres-

sion by wavelet transform. In: Systems, Man and Cybernetics, 2002 IEEE International Conference on, 2002, vol. 2, pp 553– 557

12. Seeram E: Irreversible compression in digital radiology. A literature review. Radiography. 12(1):45–59, 2006

13. Sung M-M, Kim H-J, Kim E-K, Kwak J-Y, Yoo J-K, Yoo H-S: Clinical evaluation of JPEG2000 compression for digital mam-mography. IEEE Transactions on Nuclear Science. 49(3):827– 832, 2002

14. Logeswaran R: Compression of medical images for tele-radiology, Teleradiology. Springer, Berlin Heidelberg, 2008,

pp 21–31

17. Pianykh OS: Digital imaging and communications in medicine: A practical introduction and survival guide. Springer Publishing Company, Incorporated, Leipzig, Germany, 2008

18. Maani R, Camorlinga S, Arnason N, Eskicioglu R: A practical fast method for medical imaging transmission based on the DICOM protocol, Medical Imaging 2010. Advanced PACS-based Imaging Informatics and Therapeutic Applications, San Diego, USA, 2010, p 76280M

19. National Electrical Manufacturers Association, DICOM Official Website. http://medical.nema.org/. Accessed in December 2009.

20. Vossberg M, Tolxdorff T, Krefting D: DICOM image communi-cation in globus-based medical grids. Information Technology in Biomedicine, IEEE Transactions on 12(2):145–153, 2008

Proceedings of the Fourth International Conference on Communication and Electronics Systems (ICCES 2019)
IEEE Conference Record # 45898; IEEE Xplore ISBN: 978-1-7281-1261-9

Lane-Finding Based on Structure Analysis of Lane and Computer Vision

Shashank Gupta
M.Tech Research Scholar, Dept. of Computer Science & Engineering.
MMMUT,
Gorakhpur (U.P.), India.
shashankgupta451@gmail.com

Divakar Yadav
Associate Professor, Dept. of Computer Science & Engineering.
MMMUT,
Gorakhpur (U.P.), India.
dsycs@mmmut.ac.in

***Abstract*- Advanced driver-assisting systems (ADAS) performs a crucial role for the safety and ease of transportation. Finding of lane markings is an essential step of ADAS. For the protection of automated vehicles, the precise results of lane detection are compulsory. In this study, we present an innovative approach based on structural analysis of lane and Computer Vision Technique such as Hough Transform (HT) for the detection of lane markers. Firstly, a stage of preprocessing is applied to remove the pavement area that develops the lane markings background. Next, an edge detection technique is applied to generate the map of the edge and masking is performed to obtain edges in our region of interest (ROI). Then, using HT to find lanes, important lines are analyzed in the area of interest. In end, the concept of vanishing point used to predict lane has been explained. Experimental result states that the proposed system can find boundaries of the lane and exact lane departure alert in the existence of several image artefacts, such as light change, bad lane mark. The proposed technique displays more efficiency.**

Keywords- Advanced driver-assisting system, lane-finding, image preprocessing, ROI making, Hough transform.

I. INTRODUCTION

As per the report of World Health Organization [1], approximately 1.32 millions people die in traffic accident each year i.e., on average 3,288 deaths in a day [2]. Additionally 21-50 millions are disabled or injured. In India, at least 201,050 peoples dies every year as an outcome of vehicle accidents on the road acc. to the WHO [1]. Valued efforts should be build-up to promote the adoption of deed for road safety enhancement. The advanced driver-assisting system (ADAS) has caught the attention of several security/safety divisions and related researches nowadays. Using different variety of detectors install on vehicles to gain relevant facts from the inner and outer of vehicle. These facts are used to perform tracking, identification of dynamic object and various processing jobs. These systems permits driver to find out the probable danger so quickly, thereby increasing the safe driving. The precise detection of road lanes is a critical problem. Lane boundaries empower vehicles to remain into the right lane and to avert crashes or collisions.

A. Lane Detection

Lane detection, one of the most important areas of Computer Vision, finds its applications in driver support systems and autonomous vehicles. The lane marker is a traffic signal that looks for the car's primary driving specifications. A lane has well-defined geometry and when the road becomes clear, then detection of the lane can be trivial. However, lane marks in the natural environment are not always obvious. The factors that affect the clarity in lane detection include environmental and human factors like shadow of trees, poor weather conditions, bad road conditions or even poorly painted lane markings. Identifying road routes is a daunting action, especially in the existence of poor light situation. The lane finding plays a crucial role in both current unmanned driving and traditional assistant driving. To reduce the issue of detecting poor lane mark, robust lane finding and lane departure techniques should be used. The system of lane finding must be able to detect all type of markings from disorganized roadways and these markers should be filtered to produce reliable estimation of vehicle trajectory and position with respect to the lane.

B. Advanced Driver-Assisting Systems (ADAS)

Advanced driver-assisting systems (ADAS) are system that assist the driver in avoiding collisions and unwanted accidents by providing alerts and/or warnings whenever required, which enhance the well-being of vehicles. The development of autonomous or self-driving vehicles depends on the development of ADAS. ADAS has caught the attention of several security/safety divisions and related researches nowadays. Using different variety of detectors install on vehicles to gain relevant facts from the inner and outer of vehicle. These facts are used to perform tracking, identification of dynamic object and various processing jobs. These systems permits driver to find out the probable danger so quickly, thereby increasing the safe driving.

In this study, we present an innovative approach based on structural analysis of lane and Computer Vision Technique such as HT for the detection of lane markers. Firstly, a stage of preprocessing is applied to remove the pavement area that develops the lane markings background. Next, an edge

detection technique is applied to generate map of an edge and ROI masking is performed to obtain edges only in our region of interest. Then, using HT to find lanes, important lines are analyzed in the area of interest. In the end, the concept of vanishing pt. used to predict lane has been explained.

This paper is organized as follows. In Section II, we presents the related work. In Section III, we describe the proposed work. In Section IV, we present the simulation of proposed system and its results. Finally, in Section IV we presents the conclusion and future scope of the paper.

II. Related Work

Identifying road routes is a daunting task, the lane marker is a traffic signal that looks for the car's primary driving specifications. In the existence of diverse environmental and light conditions, strong lane finding and the lane departure technics should be applied to diminish the issue of detecting bad lane marks. Lane markers are shiny from the surface of the road, using this feature [5] propose the technique of finding lanes on the basis of horizontal {black, white and black} arrangement. Chiu and Lin [6] used colour-based partition to find out the edges that offer strong performance in the existence of noise, which disrupts the lane notation by the preceding vehicle. Depending on the angle information of the lane, the Lane Departure Identification (LDI) does not give less false warning ratio. In such a situation, different noise aspects [9] can affect its performance. Lane markings visibility is influenced by endangered. Lee et al. [10] introduced a lane boundary pixel extractor approach that maximize the durability of lane identification, that finding pixels to increases the LDI which are potentially component of the lane limitation. However, the optical center of the installed camera on a vehicle coincide with the centre of lane, which is an important condition. The main drawback of this approach occurs when the vehicles are presents infront of the camera that results more false output signals.

Many researchers suggest different image preprocessing techniques that are used to improve the accuracy of identifying lanes. These techniques are the examples of morphological processing to reduce noise; and to modify an image for the hue-saturation-value [12]. Canny edge detection technique [3] is used for histogram equalization [14], to produce single pixel wide edges [13], grayscale conversion and the application of a Gaussian low-pass filter to remove noise [16], filtering [8], clustering and polyline extraction [15], splitting, and smoothing of an image [17].

Parajuli et al. [21] using good local shield features and obtained good results. But, in the shadow this approach attains poor performance and generate less correct warnings. To recognize any arbitrary shape, HT is used which results strong performance in the various situation [18]. In this paper, HT is applied to find the lane lines derived from binary images [11]. The computation complexity of HT is optimal. Chi-Feng et al. [20] suggest the lane departure technology based on the angular relationship of lane boundaries, but it suffer from failure of proper identification and therefore, results less accurate. C. Mu et al. [22] propose lane identification technique on the basis of piecewise fitting and object segmentation. There is a problem of detecting false lanes in their study. In our methodology, HT technics is used for finding lane marker of road. While Euclidean's distance is applied to evaluate the parameters respective to the lane. On basis of those parameters lane departure recognition is gone through it.

III. Proposed Work

Most of lane markers are basically straight on the road, and there are some sharp tilt in the turn of the road. Therefore, in locating and tracking the lane, HT technique is employed for detecting the line and depict the lane's estimated position. Basically, there are 5 parts in our proposed method: Image Preprocessing, Edge Detection, ROI masking, Lane Detection, and Lane Departure Recognizer.

A. Block Layout

The block layout of our proposed methodology is described below in Fig.3.1.

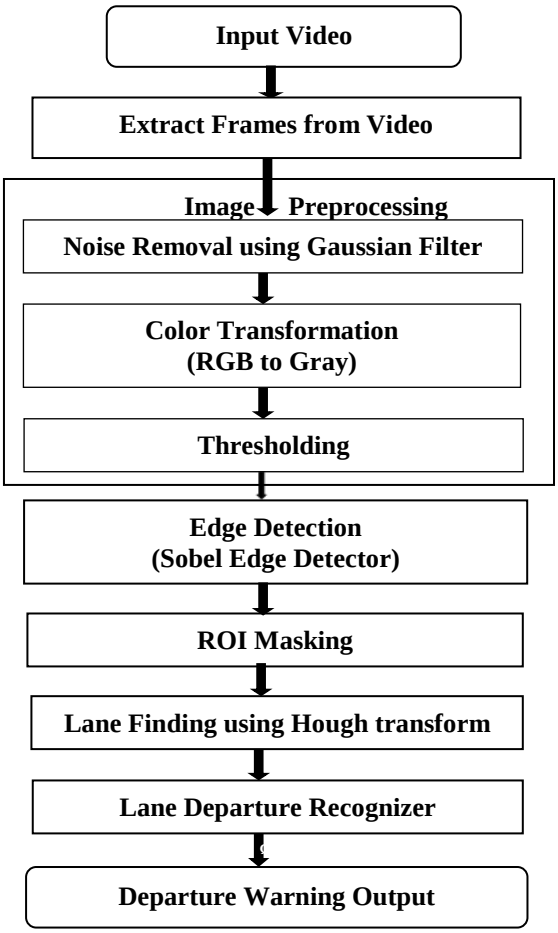

Fig. 3.1: Block Layout of Proposed method

B. Image Preprocessing

Pre-processing of the image is primarily to suppress the interference and to gain the meaningful information of image. In order to preprocess the image taken by the camera in actual time, primarily to remove the different noise of the image, color transformation technique like RGB to Gray, etc. includes.

1) Noise Removal using the Gaussian Filter

Firstly, the smoothing of input image is to be performed to diminish noise in the image. Image de-noising ensures that that in the image, noise does not interfere in any image processing in the future. To convert the input video frame to a filtered RGB image, use of the standard Gaussian filter in MATLAB having function imgaussfilt3() has done with the default sigma value of 0.5.
Here, comparison of before and after filtering shown below.

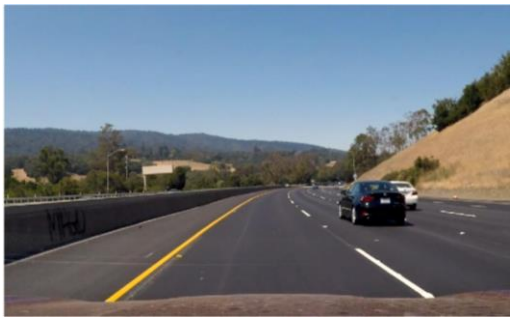

Fig. 3.2: Image before filtering

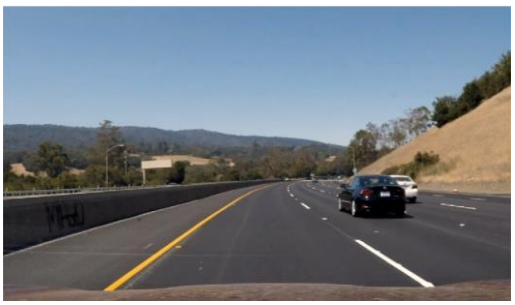

Fig. 3.3: Image after filtering

2) Color Transformation

Since the lane markers are tinted with yellow or white colour on the black road surface, it can easily be distinguished by the contrast between the border and the surface of the road. Therefore, while locating the lane marker, only Gray level components is to be considered. To transform the filtered RGB image into grayscale image, RGB to GRAY colour transformation function is employed. It alters the values of RGB image into grayscale by performing the weighted sum of R, G and B components is given by:

$$Y = (0.299 * R) + (0.588 * G) + (0.114 * B) \quad (1)$$

In addition, it must be taken into account that a mapping function has been configured essentially for grayscale images from RGB. Color component is more sensitive as compared to the Human vision system and the impaired critical information of visually is expressed by the luminance component(Y). The gray balance step on filtered RGB image as shown below:

Fig. 3.4: Grayscale Image

3) Thresholding

Once the grayscale image has been acquired, we do thresholding to create a binary image that improves the accuracy and speed of the lane finding system. This is done because the edge detector needs to have an input intensity image or binary image. We set any value higher than the pixel intensity of 180 (value obtained from test and error) to 0 (white). Thresholding helps in sections of the road made especially with concrete.

Fig. 3.5: Image after Thresholding

C. Edge Detection

The boundaries of the lane are marked with the edge. So, the edge detection is a fundamental step of lane finding system. In this step, output of the initial image processing is taken as an input in the edge detection technique. Now, we are ready to discover the edges in our image. There are many strong edge detectors namely sobel edge detector, canny edge detector, etc. available for detecting the edge. In this paper, use of Sobel Edge Detector to obtain map of the edges. The advantage of using the Sobel Operator, apart from the fact that it is computationally expensive, is that it can seek edges in the particular direction. This is more helpful for us because our lanes are vertically oriented in the image. Fig. 3.6 demonstrate the image obtain from the Sobel Edge Detector appears as an outline of the threshold image.

Fig. 3.6: Sobel Edge Detector Output

D. ROI masking

Applying edge detection on the entire image results in several extraneous edges which may hamper the lane detection when we later apply the Hough Transform. To deal with this we select a polygonal region right in front of the car as that's the region which we are interested in. We create a mask such that all the values within this are set to 0 and all values outside it are set to 1.

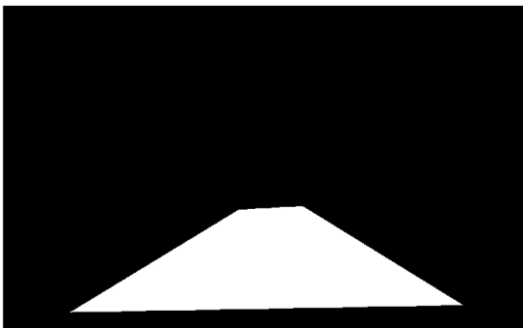

Fig. 3.7: Selected ROI mask

Now we apply this mask on our edge detection output to obtain edges only in our region of interest. Following, this we obtain edges only in our region of interest.

Fig. 3.8: Image after ROI masking

E. Lane Detection

Once we have our edges in the region of interest we can go ahead and find lines in that area using the Hough Transform. We used the Hough transform (HT) to find the lane because this technique is tolerant towards the interval in the feature boundary (such as partial blockage) and image noise. HT technique is applied to find the parameters of lane marking, which best fits to a set of pixels obtains from the detection of an edge [7]. Implementation of HT is given by [19]:

$$d = x_i \cos\theta + y_i \sin\theta \quad (2)$$

Where, θ = Angle between the normal line and the x-axis. And the range of theta is between 0° and 90°.

(x_i, y_i) = coordinate position of the ith pixel.

d = Distance of the fitted line from the x-axis.

Hough transform is applied to a set of edge points (x_i, y_i) results in a 2-D function P(d, θ) which represents the number of edge points satisfying the (2) [19]. Whenever, equation (2) is computed for e, the value associated with the cell of the accumulator array determined by θ and resulting d are added by 1. The local maxima of P(d, θ) can be used to detect straight line segments passing through edge pixels. The below Figure 3.9 shows that detection of lane line and highlighting lane on the road using Hough Transform technique.

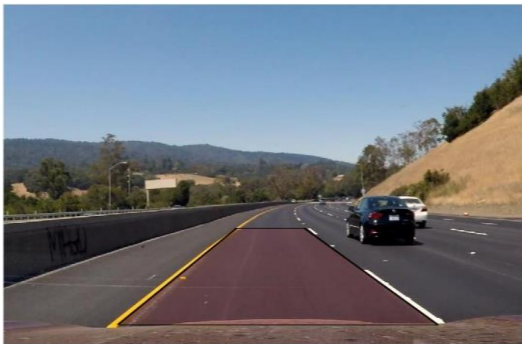

Fig. 3.9: Detection of Line and highlighting lane on the road

F. Lane Departure Identification Recognizer

1) Calculate Vanishing Point

We utilize the concept of vanishing point to predict if the lane is curving towards right or left, or going straight as shown in figure 3.10. We calculate the vanishing pt. by finding the point of intersection of our two lanes. Note that we only need the x coordinate of the vanishing point. This is done again by using simple geometry. By finding the equations of lines in point-slope form and equating them to obtain x. Our strategy will be to analyse the location of vanishingPoint of the image. If the vanishingPoint is close to centre of the image then the road ahead is straight, if it is on the left half on the image, then the road is curving right and if it is in the right-half of an image, then the road is curved on the left side. There's of course some thresholding to be applied as the car might not always be traveling at the centre of the road.

After trial and error, the following scheme was developed:

```
if vanishingPoint > 530
lanePrediction = "Right Curve Ahead"
else if vanishingPoint < 515
lanePrediction = "Left Curve Ahead"
else
lanePrediction = "Straight Ahead"
end.
```

Fig. 3.10: Lane Departure Identification Image of Input frame

2) Buffer of Vanishing Points

Simply using the vanishing point calculated at each frame to do lane prediction may not always give desirable results as there may be some frames where the lane prediction is a little tilted which hampers the calculation of vanishing point. To do this, a circular buffer was implemented which stores the vanishing points of the last 25 frames and calculates their average. This average value of vanishing points is then used to predict the direction of the lane. However, lane prediction on the patch where the road is not dark takes a hit.

IV. SIMULATION AND RESULTS

The simulation of our proposed methodology has been done using MATLAB R2017a environment. MATLAB stands for Matrix Laboratory and it is a very effective tool used by several researchers for simulation purposes. We simulated the basic lane finding system can find/detect boundaries of lane in the presence of various image artefacts, such as bad lane mark, light change and shadow of trees, and it demonstrate the exact departure alert for lane in small intervals. The comparison will be done based on higher detection and lower false alarm rates. The proposed system of working demonstrate higher efficiency percentage with almost all original input videos and produces higher detection and lower false alarm rates.

A. Simulation Parameters

The proposed methodology is implemented on the Intel based Core-i5 processor with CPU M3230 and 2.60GHz processing rate. Acquisition of data is being taken out using an input video sample and stable images in the real time scenario to examine the proposed system. Simulator platform specification details are given in the Table 4.1.

Table 4.1 Platform Information

Processor	Intel(R) Core(TM)-i5 CPU 3230M @ 2.60GHz
Processor cores	2
Memory	4 GB DDR III RAM
Compiler	Borland C++ Builder 6.0
Software tool	MATLAB
Resolution	1280 pixels × 720 pixels
Operating System	Windows 8
System Type	64 bit operating system
Frame Rate	30

There were a total of 1250 frames in the input video, whose resolution was 1280px × 720px and the speed of frame was 30frames / second. The size of the video input sample was 24.0 MB with the data rate of 4037kbps. This video contains several type of straight and curved lane regions.

B. Simulation Results

We simulated lane finding using lane structural analysis and Hough transformation technique in MATLAB simulation environment according to the parameters listed above in the table 4.1. The results are shown with the help of snapshots taken after simulation.

1) Input Frame Images

Figure 4.1 shows a set of original frame of video passed as input images of different types.

Fig. 4.1: A set of original frame of video passed as input images of different types.

2) Colour Transformation Result

Figure 4.2 shows the colour transformation result of filtered RGB images into grayscale images.

Fig.4.2: Colour change result of filtered RGB images in grayscale images

3) Thresholding Output

Figure 4.3 shows a set of images after applying thresholding operation on grayscale images.

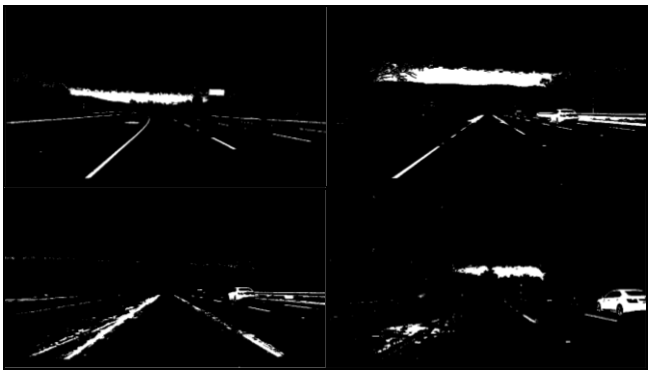

Fig. 4.3: Set of images after applying thresholding operation on grayscale images.

4) Deployment of Sobel Edge Detector

Images obtained from the Sobel Edge Detector are shown in Figure 4.4 which appear as the outlines of threshold images.

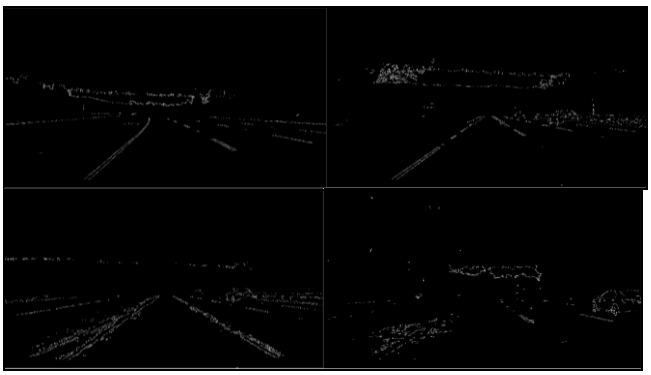

Fig. 4.4: Output images obtained from the Sobel Edge Detector

5) Masking with Selected ROI mask

Figure 4.5 shows a set of images after applying ROI masking on the output images of our Sobel Edge detector.

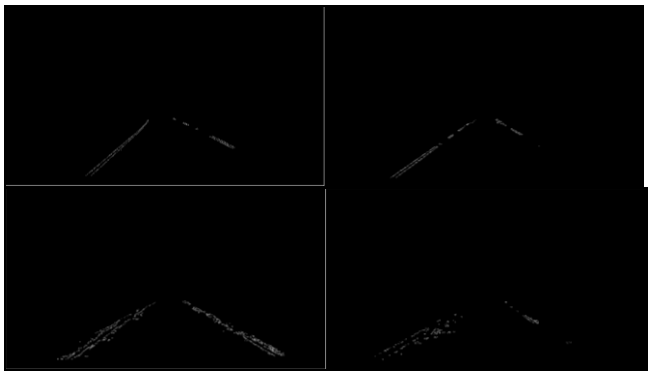

Fig. 4.5: A set of images after applying ROI masking

6) Lane Detection Output

Figure 4.6 shows a set of final outputs with lane finding and departure identification of original video frames passed as input images of different types.

Fig. 4.6: A set of final outputs with lane finding and departure identification of original frame

It has been shown that the proposed system identifies the lane signs correctly and in various cases issuing lane departure alert to the driver. Table 4.2 illustrates the false-alarm rate and lane detection rate by the proposed system for various input video.

Table 4.2 Experimental result of proposed system

Parameters		***Case 1***	***Case 2***	***Case 3***
Input Frame Resolution		1280 x 760	1280 x 760	1280 x 760
No. of Output frames		212	526	1250
No Departure		0	131	353
Left Departure		212	405	501
Right Departure		0	0	396
Lane detection	***True***	212	524	1024
	False	0	2	26
False Warning		0	35	103
True Warning		100%	93.35%	91.76%

The given system is compared to the lane departure identification (LDI) technique presented by Gaikwad and Lokhande [11]. According to the Euclidean distance based departure, LDI is introduced. Table 4.3 shows the comparison of these two techniques on the basis of average lane detection rate and false warning rate for day-time, night-time.

Table 4.3 Comparison of LDW technique presented by [11] with the proposed system.

	Proposed System		***LDW by [11]***	
	Day-time	***Night-time***	***Day-time***	***Night-time***
True Lane Detection	97.92%	99.97%	87.9%	94.1%
False Lane Detection	2.08%	0.03%	12.1%	5.9%
True Warning	94.9%	97.8%	90.4%	96.4%
False Warning	5.1%	2.2%	9.6%	3.6%

From the above Table 4.3, it is concluded that we can attains false-warning ratio is low and true lane detection is high with the proposed system.

V. CONCLUSION AND FUTURE SCOPE

This paper describes an innovative lane departure alert model based on the Sobel Edge Detector and Computer Vision Technique such as Hough Transform. Hough line recognition technique is simple as well as accurate; with this after adding the tracking algorithm the curve can be detected. To enlarge the contrast of input frame, Histogram equalizer method is applied in this proposed method. In Hough transform (HT) technics, there is an independent extraction of lane marking on the left and right side of the ROI subdivision. This will minimizes the time of computation needed to recognize the lane.

Practical outcomes show that the submitted lane-finding system provides the lane identification rate is high, 97.92 percent and the rate of false warning is low, approximately 5.1 percent. The whole system performs superb under various environmental situations such as night time, bad weather, and shade from trees or vehicles, however its functioning is mostly depends upon the road-lane markers visibility. When the vehicle direction gets distracted from its disappearing pt., then the driver is reminisce to take appropriate actions to receive the lane departure alert that can effectively prevent the happening of the accident. The biggest disadvantage is that the demonstration of lane identification is affected by the vehicle or other objects obstructing the lane markers in front of the vehicle and may be suffer from several interference. That's why, the identification of lane lines should be adaptable to different conditions.

In the future, more research is requisite to select the region of interest's (ROI). To detect the turns, we can also try to enhance the identification capability of the different curves by adding fitting technique. So, further research work on this should be done to build a more accurate lane finding system.

REFERENCES

[1] "World Health Organization (WHO)". Available at http://gamapserver.who.int/gho/interactive_charts/road_safety/road_traffic_deaths/atlas.html, accessed October 2018.
[2] "Association for Safe International Road Travel (ASIRT)". Available at https://www.asirt.org/safe-travel/road-safety-facts/, accessed October 2018.
[3] Sandip N. Pawar, and S. M. Mukane. "A Driver Assistance System Using ARM Processor for Lane and Obstacle Detection.", Techno-Societal 2016, ICATSA, Springer, 2016, pp 303-313.
[4] S. Jung, J. Youn, S. Sull, "Efficient Lane Detection Based on Spatiotemporal Images," IEEE Trans. on Intell. Transportation Syst., 2016, vol. 17, no. 1, pp. 289-295.
[5] M. Bertozzi and A. Broggi, "GOLD: A Parallel Real Time Stereo Vision System for generic obstacle and lane detection", IEEE Trans. On Image processing, January 1998, vol. 7, no. l, pp. 62-81.
[6] K.Y. Chiu, S. F. Lin, "Lane detection using color base segmentation", IEEE Proc. Int. Vehicles Symp., June 2005, pp.706-711.
[7] S. P. Narote, P. N. Bhujbal, A. S. Narote, and D. M. Dhane, ``A review of recent advances in lane detection and departure warning system," Pattern Recognit., Jan. 2018, vol. 73, pp. 216-234.
[8] U. Ozgunalp, R. Fan, X. Ai, and N. Dahnoun, ``Multiple lane detection algorithm based on novel dense vanishing point estimation," IEEE Trans. Intell. Transp. Syst., Mar. 2017, vol. 18, no. 3, pp. 621-632.
[9] J. W. Lee, "A machine vision system for lane-departure," Comput. Vis. Image Understanding, Apr. 2002, vol. 86, no. 1, pp. 52–78.
[10] J. W. Lee and U. K. Yi, "A lane-departure identification based on LBPE, Hough transform, linear regression," Comput. Vis. Image Understanding, Sep. 2005, vol. 99, no. 3, pp. 359–383.
[11] V. Gaikwad and S. Lokhande, "Lane Departure Identification for Advanced Driver Assistance," IEEE Trans. on Intelligent Transportation systems, September 2014, vol. l6, no. 2, pp. 910-918.
[12] F. N. Bush and J. M. Esposito, "Vision-based lane detection for an autonomous ground vehicle: A comparative field test," in Proc. 42nd Southeastern Symp. On Syst. Theory, 2010, pp. 35–39.
[13] M. Oussalah, A. Zaatri, and H. Van Brussel, "Kalman filter approach for lane extraction and following," J. Intell. Robot. Syst., June 2002, vol. 34, no. 2, pp. 195–218.
[14] H. Chen and Z. Jin, "Research on real-time lane line detection technology based on machine vision," in Proc. Int. Symp. On Intell. Inf. Process. And Trusted Comput., 2010, pp. 528–531.
[15] M. Felisa and P. Zani, "Robust monocular lane detection in urban environments," in Proc. IEEE Intell. Veh. Symp., 2010, pp. 591–596.
[16] C. Nuthong and T. Charoenpong, "Lane detection using smoothing spline," in Proc. 3rd Int. Congr. On Image and Signal Process., 2010, vol. 2, pp. 989–993.
[17] P.-Y. Hsiao, C.-W. Yeh, S.-S. Huang, and L.-C. Fu, "A portable visionbased real-time lane departure warning system: Day and night," IEEE Trans. Veh. Technol., May 2009, vol. 58, no. 4, pp. 2089–2094.
[18] W. Yue, E. K. Teoh, and D. Shen, "Lane detection and tracking using B-Snake," Image Vis. Comp.., Apr. 2004, vol. 22, no. 4, pp. 269–280.
[19] Bhujbal, P.N. and Narote, S.P., "Lane departure warning system based on Hough transform and Euclidean distance," IEEE Proc. Third Int. Conf. on Image Information Process. (ICIIP), 2015, pp. 370-373.
[20] W. Chi-Feng, C.-J. Lin, and C.-Y. Lee, "Applying a functional neurofuzzy network to real-time lane detection and front-vehicle distance measurement," IEEE Trans. Syst., Man, Cybern. C, Appl. Rev., Jul. 2012, vol. 42, no. 4, pp. 577–589.
[21] A. Parajuli, M. Celenk, and H. Riley, "Robust lane detection in shadows and low illumination conditions using local gradient features," Open J. Appl. Sci., Mar. 2013, vol. 3, no. 1B, pp. 68–74.
[22] C. Mu and X. Ma, "Lane detection based on object segmentation and piecewise fitting," TELKOMNIKA Indonesian J. Elect. Eng., May 2014, vol. 12, no. 5, pp. 3491–3500.

Proceedings of the Fourth International Conference on Communication and Electronics Systems (ICCES 2019)
IEEE Conference Record # 45898; IEEE Xplore ISBN: 978-1-7281-1261-9

A Distributed Minimum Spanning Tree Based on all Best Swap Edges in CRN

Deepak Rohilla
Department of Computer Engineering
National Institute of Technology
Kurukshetra, India
acerohilla1995@gmail.com

Mahendra Kumar Murmu
Department of Computer Engineering
National Institute of Technology
Kurukshetra, India
mkmurmunitkkr@gmail.com

Abstract*— The minimum spanning tree is a fundamental problem in distributed networks. We wish to extend this problem into cognitive radio networks. In general, a tree spanner is minimum spanning tree T which has a real-weight with n vertex (or secondary user (SU)) and m edges. It approximately preserves distances to multiple stretch factor σ in graph G. A tree spanner with good stretch factor may be useful to find the applications in distributed system, communication network, and network design. However, to find valuable tree spanner in CRN is very tough computational task. If we face an edge failure due to randomly appearance of primary user (PU) in cognitive radio network (may be minimum spanning tree), the effort must be afforded to reconstruct a new minimum spanning tree can be excessive. To avoid this drawback, we propose an efficient algorithm in CRN. The method aims to lists all finest feasible edge and applies swapping of edges in order to find MST in CRN. Moreover, the article acquainted and resolved issues related to all finest swap edges of MST in a cognitive radio network.

Keywords*— MST, SU, PU, Cognitive Radio Network (CRN).

I. INTRODUCTION

Cognitive radio network (CRN) is a rising area of research in the wireless network. A cognitive radio is a creative communication system that senses it around and accommodate its internal seats for the statistical change within incoming radio frequencies signals by building comparable changes in a conversed operating parameter in a real time. The nodes present in a cognitive radio network are classified into two components: licensed user or primary user or PU and unlicensed users (secondary users or SU). The primary user node holds a license of a spectrum. The secondary users always cooperate the environment while came in influence on other using a white hole or free spectrum of primary user(s). The networks formed by SU nodes are temporarily available. The minimum spanning tree (MST) is a classic problem for efficient data communication in all the networks types. In CRN, the minimum spanning tree is maintained by SU nodes. In this, if some link fails then it may destroy tree, so we have to find the alternate link(s) to update or maintain the MST. A problem for evaluating the best swap edge for minimum spanning tree in cognitive radio network had a rich algorithm culture. Let suppose, $G = (V, E, w)$ represent a MST having n vertices and m edges (links between SU nodes) and a 2-way edge connected graph which is undirected and having a positive real number as edge weight. The problem is about computing a swap edge for every edge belongs to minimum spanning tree in a cognitive radio network. The edge e belongs to MST and f belongs to CRN (not belongs to MST). We intend to accomplish the edge swap between edge e with edge f in T throughout all the possible swap trees. In this context, the basic principles of all the best solutions based on switching edge are as follows. The edge swap operation is usually performed (possibly optimal) when a spanning tree for each time an edge failure occurs and hence a corresponding optimal switching edge is inserted. The approach may help us to reestablish the connection in minimum spanning tree in faster way.

The article is focuses on the elusive spanning tree structure that have all the best swap edge problem with the tree spanner. The purpose of building a tree spanner is to maintain the distance from each node to all other nodes in CRN. In fact, the stretch factor of a MST T in a cognitive radio network is define as $dT(u, v)/dG(u, v)$, where, u and v are SU nodes and dT and dG denoting the distance in T and G, respectively. Thus, a tree spanner which is optimal will show the smallest stretch factor for every spanning tree in CRN. However, finding best tree spanner is a typical task. Thus, if a given solution experience a temporary edge failure, recalculating from best solution is not easy.

Therefore, swapping edges in minimum spanning tree is more interesting and appealing, in general, and absolutely the all best swap edges-TS problem. The author derived two solution for the weighted and unweighted graph that are executing in $O(m^2 \log n)$ and $O(n^3)$ time, $O(m)$ and $O(n^2)$ space complexity, respectively. We presents to explore a latest algorithm that solves ABSE-TS (all best swap edges - tree spanner) problem in $O(n^2 \log^4 n)$,$O(n^2 + m\log^2 n)$ time and space respectively. The solution given by the authors improves time complexity of both the algorithm given [3] for weighted and unweighted graph whenever as $m = (n \log^3 n)$. The most important for the dense graph which is weighted, improvement is about quadratic in n. Moreover, the extensive analysis of cost has been focused in the literature [10]. For example, in CRN, if a given edge e fails, a single switching edge f results O (m) evaluation time cost in each pairs of CRN. The collection of tree edge can be used for the swapping purposes. In addition, one of the important advantages of edges f is that it elongates the availability of vertices and increases stretch width. Hence, both the previous approaches take (m^2) time.

To avoid cost related bottlenecks, the total number of vertices' optimal replacement edge may be greatly reduced by

the number of critical edge, if used. More specifically, for every *n*-1 edges in *T*, *O*(nlogn) is successfully reduce to the number of optimal swap edges candidate, and for each of them O ($\log^2 n$) check the possible critical. The main factors to achieve this goal are:

The centroid decomposition of spanning tree *T* consist of a logarithmic decomposition of all vertex of *T*. Using the decomposition, carefully, we combined with the series of preprocessing steps to accomplish all information with the all the nodes of tree. It helps to reduce the corresponding best swap critical edge candidate.

From the literature view, we noticed that the best use of decomposition to solve best swap link (edges) problem for a MST in CRN useful like in other environments. The stretch factor function is associated with an edge which are not belongs to MST. If an edge fails, the stretch factor activates the any other one from non-tree edges. The resultant edge is optimal that is used for edge swapping. A simple illustration of the centroid decomposition of a tree *T* corresponding to the first vertex of *T* are shown in figure 1. Thus, when we find the critical edges, candidate optimally rectified edge *f*, we must evaluate the maximum value of all functions in *f*. The given below figure 1 explains geometric view. We maintain the upper bound envelope of the series of function. Furthermore, for consistency, the series of functions need to be correctly grouped give to basic centroid decomposition. All these groups are dynamic, and they are completely interdependent. At the end of the tree decomposition, the networks find MST in CRN.

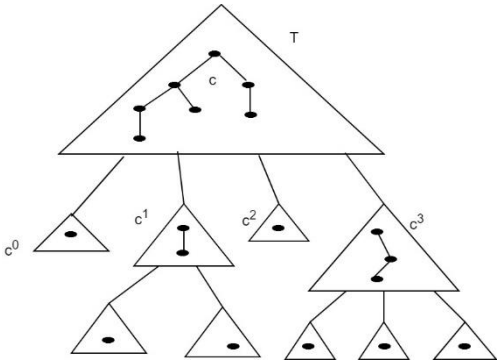

Fig 1. Centroid Decomposition of tree T

II. RELATED WORK

The explorations on these tree spanners are appropriately operative and strongly linked to extensive literature on spanner, where the distance of CRNs is largely conserved by some sparse spanning trees. As indicated earlier, finding the best tree spanner is very difficult problem. More accurately, if CRN does not tolerate tree 1-spanners on the weighting graph (i.e., if spanning tree having stretch factor = 1 must be built in polynomial time [9]). It is not approximated good than $\sigma = 2$ unless P = NP [16]. We propose a new algorithm for solving the Best_Swap_edges-TS problem in O ($n^2 \log^4 n$), O ($n^2 + m \log^2 n$) time and space respectively.

Thus, when $m = \Omega (n \log^3 n)$, our algorithm improves the execution of the two algorithms on time complexity explained in [3] applicable for both weighted and unweighted graphs. In order to focus on our results, observed in [10], evaluation of the expansion of exchange tree caused by a single exchange edge f is G in principle will need to be evaluated. An extension of the node pair associated with *O*(m), that is, all non-tree edge endpoints that can be used as replacement edges of e except f. Data structures that show effective solutions to all optimal exchange edge problems include Power Heap [6], Top Tree [3], Mergeable Heap [18], and many other issues. In fact, the Best_Swap_Edge-TS problem is analyzed in [10], and the authors used O ($m^2 \log n$) and O to design two solutions, weighted and unweighted uses the space of O(m) and O(n^2) respectively. For approximations there is no significant upper bound other than the O (n) coefficients returned by the G.

If CRN is not weighted, stuffs will get better. High accurately, in this area the problem approximately an *O*(log n) and problem is inaccessible with the addition of O(n) unless P = NP [11]. Furthermore, the determination of whether CRN tolerates the corresponding tree spanner and stretch factor tree decision problems is NP complete for each fixed stretch factor greater than 4 or equal to 2 may be resolve in polynomial time [9], and for stretch factor 3, problem is open till now. Decisively it is well known observe about constant stretch tree spanner that is found for some different categories of graphs (unweighted), such as strong strings, spacings, displacement maps, etc. ([7] and See the references in). With regard to the exchange problem in the exchange tree, this is drawing great attention from the algorithm community. In fact, there are series of papers that solve the swap edge problem from various types of spanning trees in CRN. In addition to MST we remember MDST (minimum diameter spanning tree), MCSRT (minimum routing costs spanning tree), and a single source SPT (shortest path tree) to name a few for MDST the best exchange is to minimize the end of the diameter of replacement tree [13] and [17], and the bests solution is to perform in $O(m \log \alpha (m,n))$ time [6]. For MRCST, the good exchange is absolutely an advantage to minimize the cost of switch tree [23] and a good solution to solve this type of problem in [5].

The authors propose two new standards to replace the SPT associated with this paper which minimize, maximum and average the stretch factors from roots for which they are valid in O($mn + n^2 \log n$) and O($mn \log \alpha(m),n)$) time solutions. In last, for well-being of completeness, reference is made to the notion of mean tree sigma spanner focusing on mean tree stretch. It is shown that each graph allows the mean tree O (1) spanner [1].

III. SYSTEM MODEL

We are assuming a cognitive radio network (considered graph G) having *V* nodes, *E* edges and weight w, which is 2 edges connected, weighted and undirected with a given cost belongs to real positive numbers. If edge *e* belongs to *E*, then we may stand for by $G - e$ achieved from *G* by eliminating the same edge. Alike, if vertex *v* belongs to *V* (*G*) then we may denote by $G - v$ achieved from *G* by eliminating the same vertex and its incident edges. With edge *e* belongs to *E*(*T*) we are assuming *S*(*e*) is the set of all the swap edge for *e* having

endpoint substitute in two distinct components (connected) of $T - e$. Let $T_{e/f}$ stand for *swap tree* obtained from T by exchanging edge e to edge f. Let node i, j belongs to V so distance between node i and j in CRN is represented by $dG(i, j)$. We are defining the *stretch factor* of pair (i, j) with respect to graph G and minimum spanning tree T as $\sigma_G(T, i, j) = dT(i,j)/dG(i,j)$. Where σ represent stretch factor and dG(i,j) represent distance between node a and b.

Notation	Detail
V and E	Set of vertices and edges respectively
S(e)	Swap edges of e
$T_{e/f}$	Tree after exchanging edge e by f
σ	Stretch Factor
ϕ	Objective function
T	Subtree of graph G
U_e	Containing all vertices of T-e including root of T
D_e	Containing all vertices of T-e excluding root of T
¬	NULL

IV. ALGORITHM DESCRIPTION

We consider minimum spanning tree T a rooted at any vertex which is useful and assuming that tree T is binary. Absolutely, if spanning tree T is not a binary it may be possible by using standard techniques to convert G and spanning tree T into its equal graph Q' and corresponding spanning tree S' (binary tree) with vertices and edges in Q' are n and m respectively such that a best swap edges for some edge of given spanning tree T is associated with best swap edge for a corresponding edge of corresponding T'. According to preprocessing steps we are computing a *centroid* of spanning tree T. A centroid of tree (n vertices tree) is a vertex by deletion of this vertex tree divided into subtrees of a size maximum $n/2$. In $O(n\log n)$ time centroid decomposition of T may be computed and it should be defined by tree T with height $O(\log n)$ whose vertices are indeed subtree. The root of T is T.

Algorithm: Best_Swap_Edges-TS(G,T)

1. $T \leftarrow$ Centroid of T;
2. foreach edge e belongs to E(T) **do**
3. $U_e \leftarrow$ all vertices of T – e;
4. $f^* \leftarrow$ random edge;
5. foreach v belongs to U_e **do**
6. compute v-Best_Swap_edges f for e;
7. if $\sigma_{G\text{-}e}(T_{e/f}) < \sigma_{G\text{-}e}(T_{e/f^*})$ then $f^* \leftarrow$ f;
8. return f^* as the best swap edge for e and continue.

Let $\mathcal{T}$ is a simple node of minimum spanning tree T (subtree of T) so that $\mathcal{T}$ contain higher in compare to single vertex and we are assuming c be the centroid of subtree $\mathcal{T}$. After-all T is binary and forest $\mathcal{T} - c$ contains not more than 3 tree that we may call T^1_c, T^2_c, and T^3_c (if $T - c$ generate not more than 3 subtrees then we may allow some T^i_c empty tree). Furthermore, assuming T^0_c is the subtree of T that contains a vertex c. Then, $\mathcal{T}$ will be in tree T a child for every subtree T^2_c, $i = 0$ to 3. In linear we can found the centroid of n vertex tree then the complete procedure desire $O(n\log n)$ complexity and looks simple to analyze tree height is $O(\log n)$. In this paper, solution (observe algorithm all best swap edges-TS) work in $n - 1$ phase for every tree edges considered in preorder with respect to T and at last of each phase return a best swap edge for the same edge. Let edge e belongs to $E(T)$ is recently considered edge. Our authors crack down each and every of the phase into $O(n)$ extra sub phase: where edge e is in the condition of failing, we favor all vertices that belongs to T-e tree, and for every vertex v. Edge f belongs to set of vertices form T-e and having the minimum stretch where stretch factor is $\sigma_{G-e}(T_{e/f})$.To resolve this approach of special cases any time we conclude that f is a random edge and stretch factor is infinite(+ve). As in the remaining part of this paper, basis of our algorithm is applicable for the evaluation of v-Best_Swap_Edges and for the stretch factor also. That is completely through an adept selection of the set of *candidates* v-Best_Swap_Edges as we should discuss in brief description in the next. Formerly all v-Best_Swap_Edges for edge e are computing some best swap edges that can observed as one that minimize a associated stretch factor. A best swap edge for e (v-best cut edge) is an edge f minimizing $\max g \in s(e) \phi(f,g)$.

Procedure: Find_v-Best_Swap_edges(x) // x is a subtree of T

1. If |V(x)| = 0 then return (¬,¬);
2. C← the Centroid of x;
3. if C belongs to U_e then;
4. $\mathcal{T} \leftarrow$ *distinct child of* x in T that consists all vertex common in x and D_e;
5. return Find_v-Best_Swap_edges($\mathcal{T}$);
6. else
7. f = minimize $w(f) + d_T(u,c)$; //c belongs to D_e;
8. g1 = evaluate a critical edge function for f;
9. $\mathcal{T} \leftarrow$ NULL or it is a child x in T;
10. $(f', g_2) \leftarrow$ Find_v-Best_Swap_edges(subtree x);

if $\phi(f,g_1) <= \phi(f',g_2)$ return $\phi(f,g_1)$; else return $\phi(f',g_2)$;

Now, we will resolve critical edge function in $O(\log^2 n)$ which find the critical edge for a given edge. If vertices in a subtree is only one, then the only vertex invokes critical candidate function which return a critical edge. If vertex is greater than one, then we differentiate two instances depending upon the centroid position of subtree x. if centroid of subtree x is belonging to D_e then it is noticed that critical edge for f should be incident to any of these tree (T^1_c, T^2_c, and T^3_c). Let j be a index selected from 0 to 3 and not belongs to i in (T^i_c) then critical candidate function return a critical edge g1 otherwise invoke the algorithm recursively and return critical edge for f.

V. CONCLUSION

The all best swap edges approach has been used to develop MST in CRN. The proposed algorithm allows minimum spanning tree to find all the replacement of links that may fails and maintain minimum-cost spanning trees in cognitive radio network. An effective solution for link failure issue runs in $O(n^2 \log^4 n)$ time which impacts definitely while swapping the failure edges in a minimum spanning tree. Moreover, the complete transmission structure of algorithm is relatively straight-forward. An attractive problem is open to find out whether it is possible to improve the space complexity of this algorithm.

REFERENCES

[1] Davide Bilò, Feliciano Colella, Luciano Gualà,Stefano Leucci, Guido Proietti. "An ImprovedAlgorithm for Computing All the Best Swap of a Tree Spanner", Algorithmica, 2019.

[2] Bilò, Davide, and Kleitos Papadopoulos. "A Novel Algorithm for the All-Best-Swap-Edge Problem on Tree Spanners." arXiv preprint arXiv:1807.01260 (2018).

[3] Davide Bilò, Feliciano Colella, Luciano Gualà, Stefano Leucci, and Guido Proietti. Effective edge-fault-tolerant single-source spanners via best (or good) swap edges. In Shantanu Das and Sébastien Tixeuil, editors, Structural Information and Communication Complexity - 24th International Colloquium, SIROCCO 2017, Porquerolles, France, June 19-22, 2017, Revised Selected Papers, volume 10641 of Lecture Notes in Computer Science, pages 303–317. Springer, 2017. doi:10.1007/978-3-319-72050-0_18.

[4] M.K Murmu, A.M Firoz,Sandeep,Shubham," A Distribured Minimum Spanning Tree for Cognitive Radio Networks", IMCIP Procedia Computer Science Volume 89, Pp 162-169,Elsevier, 2016

[5] Stephen Alstrup, Jacob Holm, Kristian de Lichtenberg, and Mikkel Thorup. Maintaining information in fully dynamic trees with top trees. ACM Transactions on Algorithms, 1(2):243–264, 2005. doi:10.1145/1103963.1103966.

[6] Davide Bilò, Feliciano Colella, Luciano Gualà, Stefano Leucci, and Guido Proietti. A faster computation of all the best swap edges of a tree spanner. In Proc. of the 22nd Intl. Colloquium Structural Information and Communication Complexity, pages 239–253, 2015. doi:10.1007/978-3-319-25258-2_17.

[7] Davide Bilò, Feliciano Colella, Luciano Gualà, Stefano Leucci, and Guido Proietti. Effective edge-fault-tolerant single-source spanners via best (or good) swap edges. In Proc. of the 24th Intl. Colloquium Structural Information and Communication Complexity, in press.

[8] Davide Bilò, Luciano Gualà, and Guido Proietti. Finding best swap edges minimizing the routing cost of a spanning tree. Algorithmica, 68(2):337–357, 2014. doi:10.1007/ s00453-012-9674-y.

[9] Davide Bilò, Luciano Gualà, and Guido Proietti. A faster computation of all the best swap edges of a shortest paths tree. Algorithmica, 73(3):547–570, 2015. doi:10.1007/ s00453-014-9912-6.

[10] Andreas Brandstädt, Victor Chepoi, and Feodor F. Dragan. Distance approximating trees for chordal and dually chordal graphs. J. Algorithms, 30(1):166–184, 1999. doi:10.1006/jagm.1998.0962.

[11] Gerth Stølting Brodal and Riko Jacob. Dynamic planar convex hull. In Proc. of the 43rd Annual IEEE Symposium on Foundations of Computer Science, pages 617–626. IEEE, 2002.

[12] Leizhen Cai and Derek G. Corneil. Tree spanners. SIAM J. Discrete Math., 8(3):359–387, 1995. doi:10.1137/S0895480192237403.

[13] Shantanu Das, Beat Gfeller, and Peter Widmayer. Computing all best swaps for minimum-stretch tree spanners. J. Graph Algorithms Appl., 14(2):287–306, 2010.

[14] Yuval Emek and David Peleg. Approximating minimum max-stretch spanning trees on unweighted graphs. SIAM J. Comput., 38(5):1761–1781, 2008. doi:10.1137/060666202.

[15] Harold N. Gabow. A scaling algorithm for weighted matching on general graphs. In Proc. of the 26th Annual Symposium on Foundations of Computer Science, pages 90–100, 1985. doi:10.1109/SFCS.1985.3.

[16] Giuseppe F. Italiano and Rajiv Ramaswami. Maintaining spanning trees of small diameter.Algorithmica, 22(3):275–304, 1998. doi:10.1007/PL00009225.

[17] Hiro Ito, Kazuo Iwama, Yasuo Okabe, and Takuya Yoshihiro. Polynomial-time computable backup tables for shortest-path routing. In Proc. of the 10th Intl. Colloquium Structural Information and Communication Complexity, pages 163–177, 2003.

[18] Camille Jordan. Sur les assemblages de lignes. J. Reine Angew. Math, 70(185):81, 1869.

[19] Christian Liebchen and Gregor Wünsch. The zoo of tree spanner problems. Discrete Applied Mathematics, 156(5):569–587, 2008. doi:10.1016/j.dam.2007.07.001.

[20] Enrico Nardelli, Guido Proietti, and Peter Widmayer. A faster computation of the most vital edge of a shortest path. Inf. Process. Lett., 79(2):81–85, 2001. doi:10.1016/ S0020-0190(00)00175-7.

[21] Enrico Nardelli, Guido Proietti, and Peter Widmayer. Nearly linear time minimum span-ning tree maintenance for transient node failures. Algorithmica, 40(2):119–132, 2004. doi:10.1007/s00453-004-1099-9.

[22] Seth Pettie. Sensitivity analysis of minimum spanning trees in sub-inverse-Ackermann time. In Proc. of the 16th Intl. Symposium on Algorithms and Computation, pages 964–973, 2005. doi:10.1007/11602613_96.

[23] Guido Proietti. Dynamic maintenance versus swapping: An experimental study on shortest paths trees. In Proc. of the 4th Intl. Workshop on Algorithm Engineering, pages 207–217, 2000. doi:10.1007/3-540-44691-5_18.

[24] Aleksej Di Salvo and Guido Proietti. Swapping a failing edge of a shortest paths tree by minimizing the average stretch factor. Theor. Comput. Sci., 383(1):23–33, 2007. doi: 10.1016/j.tcs.2007.03.046.

[25] Robert Endre Tarjan. Sensitivity analysis of minimum spanning trees and shortest path trees. Inf. Process. Lett., 14(1):30–33, 1982. doi:10.1016/0020-0190(82)90137-5.

[26] Bang Ye Wu, Chih-Yuan Hsiao, and Kun-Mao Chao. The swap edges of a multiple-sources routing tree. Algorithmica, 50(3):299–311, 2008. doi:10.1007/s00453-007-9080-z.

Proceedings of the Fourth International Conference on Communication and Electronics Systems (ICCES 2019)
IEEE Conference Record # 45898; IEEE Xplore ISBN: 978-1-7281-1261-9

A Robust Code for MBU Correction Till 5-Bit Error

K. Sai Karan, N. Srikanth, Sonali Agrawal
Department of Electronics and Communication Engineering
Amrita School of Engineering, Bengaluru
Amrita Vishwa Vidyapeetham
India
{ksaikaranreddy, nimmagaddasrikanth1998}@gmail.com, a_sonali@blr.amrita.edu

***Abstract*—Memory is a component, playing a significant role in electronic systems. The use of static random access memories (SRAMs) is increasing in multimedia and system on chip applications. The key challenge faced by SRAMs is soft errors induced by the radiation that cause the change of values in memory cells. Error correction codes (ECCs) are used to face this challenge. As the technology is scaling down the chances of multiple bit upsets(MBUs) is increasing. So ECCs with higher correction ability are needed. Many ECCs have been proposed to face the challenge of MBUs. Some of them are SEC-DED codes, QAEC codes, FUEC-QUAEC codes. In this paper, we are presenting ECCs that has same redundancy as recently proposed FUEC-QUAEC codes [1] and can correct all the errors till 5-bit adjacent error. The procedure for encoding and decoding of proposed codes is presented. The encoder and decoder have been implemented using 45nm library and compared with QAEC codes, showing that proposed codes have better error correction capability with moderate delay over head and low power consumption than QAEC codes.**

***Keywords*—Static random access memory (SRAM), Error correction codes (ECCs), Multiple bit upsets (MBUs), 5-bit adjacent error**

I. INTRODUCTION

In reliability of memories, Soft errors plays the most prominent role. Soft error don't cause any harm to hardware, but instead they will corrupt the data which is being streamed. Soft errors are detected and corrected by using ECCs. Computer memories are very delicate to the soft errors, which reduces system reliability. Cells in memory may be corrupted by alpha particles projected from IC package material or high-energy neutron from terrestrial atmosphere [2].

When memories are continuously concatenated with electronic systems or even when CMOS technology scales down, the occurrence rate of soft errors in memory cells is abruptly increasing, mainly with the memories that operate in space applications [3] [4] and are caused from ionizing effects of atmospheric neutron [5], cosmic rays [6] and alpha-particle [7]. More importantly, SRAM memory failures are significantly increasing, which is leading to exposure of major reliability concern for most of the applications. Single bit upset(SBU) and multiple bit upsets (MBUs) both have became major reliability concern in memory based applications [8]. Therefore, error correction codes (ECCs) are used in improving the memory protection to make memory fault free.

Many methods are available to secure memory from soft errors. To keep away soft errors of single bit, Single Error Correction (SEC) codes are usually used. Moreover, as technology scales down, a single particle hit have the chance of changing multiple memory cells that are adjacent more commonly. This phenomenon leads to Multiple Bit Upset.

Based on this, we can say that adjacent bit corruption are most common error patterns in the set of multiple bit errors. So, the adjacent bit correction has become more popular in the memory based designs. Different codes have been presented, that have calibre of correcting adjacent bits errors like double bit adjacent error correction (DAEC), triple bit adjacent error correction (TAEC), 3-bit random error-correction, Quadruple adjacent error correction (QAEC) codes.

For example, codes designed for SEC-DAEC and 3-bit BEC are presented in [9] [10] and codes designed for QAEC are presented in [11]. Codes that are more advanced in terms of correction ability are required. So, extension of the ECCs to correct all errors till 5-bit adjacent errors is of interest. It can be done by adding two parity bits to the codes presented in [11] and with same redundancy to the codes presented in [1]. As we concentrate on increasing error correction capability, there will be trade-off between performance parameters [12].

In this paper, we present codes that can correct all errors till 5 bit burst error by making changes in the QAEC codes [11]. The conditions used for the construction of the parity check matrix and the algorithm used for the construction of the parity check matrix are specified. The codes are presented for data size of 16, 32 and 64. Encoding and decoding simulations are done in Verilog HDL and the synthesis is done in Cadence 45nm library. The proposed codes are compared with respect to area overhead, delay overhead and power overhead with QAEC codes [11] to show that the proposed codes have error correction ability for more number of bits with less power consumption and slightly high delay .
This paper is split into the VII sections. In sections II, linear binary block code is introduced. In section III, design rules for the proposed error correction codes are discussed. Algorithm used to construct the H-matrix is shown in section IV. In section V, proposed codes are presented for 16, 32, 64 bit data, encoding and decoding procedure is also discussed. In section VI, the proposed codes are compared with QAEC codes [11] with respect to area ,power ,delay overheads. In section VII, the conclusion and scope are presented.

II. DESCRIPTION OF LINEAR BINARY BLOCK CODES

In linear binary block codes there are two types- systematic and non systematic. The only thing differentiating them is that there will be an unit matrix at the beginning or the ending of the generator matrix in systematic linear binary block codes but there is no identity matrix in non systematic codes.

In a linear binary block code of size (n,k) there will be r redundant bits (r=n-k). Here n and k represents number of bits in the codeword and number of bits in the data respectively.

To convert data to codeword we use the generator matrix

$$G = [P, I_{k\times k}]_{k\times n} \tag{1}$$

Where I is unit matrix and P is some binary matrix of size kx(n-k). If D represents data and C represents codeword then

$$C = D_{1\times k}.G_{k\times n} \tag{2}$$

To convert the received codeword(R) to data we find syndrome using a parity check matrix H.

$$H = [I_{n-k\times n-k}, P^T]_{n-k\times n} \tag{3}$$

$$S^T = H.R^T \tag{4}$$

Where S represents syndrome and er is error vector.

$$R = C + er \tag{5}$$

$$S^T = H.(C + er)^T$$

$$S^T = H.er^T \quad (H.C^T = 0) \tag{6}$$

So by finding syndrome we will be able to find the error positions and correct the received codeword.

III. BASE FOR THE PROPOSED CODES

In this section we are going to discuss about syndromes.To correct errors, how many syndromes are required and what should be the characteristics to correct required errors.

A. Syndromes required:

Let us assume a codeword of size n in which data size is k and r is no of redundant bits-

$$n = k + r \tag{7}$$

In a code word of length n there will be n possible SBUs(—1—), (n-1) adjacent double bit errors(—11—), (n-2) adjacent triple bit errors(—111—), (n-2) 3 bit almost adjacent errors(—101—) and so on. similarly for a error of window size q there will be (n-q+1) possibilities of that type of errors in that code word.

In the proposed codes we are correcting all the errors till window size four and five bit burst errors. One type of error of window size 1, one type of errors of window size 2, two types of errors of window size 3, four types of errors of window size 4 and a five bit burst error fall into the above mentioned categories. To find each error we need one syndrome. So total no of syndromes required is

n+(n-1)+2.(n-2)+4.(n-3)+(n-4)

$$\text{total syndromes required} = 9(n) - 21 \tag{8}$$

TABLE I: CHECK BITS AND SYNDROMES NEEDED FOR PROPOSED CODES

Data Bits	Check Bits	Total Bits	Syndrome needed
16	9	25	204
32	10	42	357
64	11	75	654

B. Characteristics of syndromes:

In order to differentiate one error from another all the syndromes should be unique. Another important thing about syndromes is that, no syndrome representing an error that need to be corrected, should not be equal to zero. Because no error condition will give a syndrome equal to zero. This can be understood by getting the idea on how syndromes in the syndrome set are generated.

The syndromes are generated by XOR operation of the columns corresponding to the error positions. Let S(a) represents syndrome for an error at position a in the codeword, S(a,a+1) represent errors at position a and a+1, S(a,a+1,a+2) represent errors at position a, a+1 and a+2. The syndrome equations that are used in this paper are

$$S(a) = H(a) \tag{9}$$

$$S(a, a+1) = H(a) \oplus H(a+1) \tag{10}$$

$$S(a, a+1, a+2) = H(a) \oplus H(a+1) \oplus H(a+2) \tag{11}$$

$$S(a, a+2) = H(a) \oplus H(a+2) \tag{12}$$

$$S(a, a+1, a+2, a+3) = H(a) \oplus H(a+1) \oplus H(a+2) \oplus H(a+3) \tag{13}$$

$$S(a, a+3) = H(a) \oplus H(a+3) \tag{14}$$

$$S(a, a+1, a+3) = H(a) \oplus H(a+1) \oplus H(a+3) \tag{15}$$

$$S(a, a+2, a+3) = H(a) \oplus H(a+2) \oplus H(a+3) \tag{16}$$

$$S(a, a+1, a+2, a+3, a+4) = H(a) \oplus H(a+1) \oplus H(a+2) \oplus H(a+3) \oplus H(a+4) \tag{17}$$

The conditions for the syndromes are-

$$S(a) \neq S(a, a+1) \neq S(a, a+1, a+2) \neq S(a, a+2) \ldots. \neq S(a, a+1, a+2, a+3, a+4) \tag{18}$$

$$S(a) \neq S(b) \tag{19}$$

$$S(a, a+1) \neq S(b, b+1) \tag{20}$$

$$S(a, a+1, a+2) \neq S(b, b+1, b+2) \tag{21}$$

.....

$$S(a, a+1, a+2, a+3, a+4) \neq S(b, b+1, b+2, b+3, b+4) \quad (22)$$

where a$\neq b \forall a, b \in [1, n]$

IV. CONSTRUCTION OF PARITY CHECK MATRIX FOR THE PROPOSED CODES

Parity check matrix, H matrix is a matrix which describes the linear relations to find the elements of a codeword. In order to construct H matrix for (n,k) systematic linear binary block code, initially we need to consider an unit matrix of size (n-k) as the H-matrix. So, there will be $((2)^{n-k})$ possible column vectors. Since we have already used (n-k) column vectors of weight one in construction of the initial columns of the H-matrix and cannot use zero column vector in the construction of the H-matrix. So, finally there will be $((2)^{n-k}$-(n-k)-1) column vectors remaining to choose other k column of the matrix. In order to reduce the complexity of the code, we need to reduce the number of ones in H matrix. So to do that, while selecting a column, we start checking whether that column vector is suitable or not from lower weight column vectors. We start checking vectors with weight two and once all the column vectors with weight two are checked, we move to weight three and once all them are checked and then we increment weight by one. This process happens at the selection of each column for the H-matrix. In order to verify whether a column vector is suitable for that position or not, we need to find the syndromes that will be generated for the corresponding column vector at that position and compare the resultant syndromes with the syndrome set. If none of the resultant syndromes generated by adding column to H-matrix are not present in the syndrome set, then that resultant syndromes will be added to the syndrome set and fix the position of the corresponding column in the H-matrix and move to find the next column of the H-matrix. While search for a^{th} column of H-matrix, if all the column vectors are failing to satisfy the satisfiability condition then we remove the $(a-1)^{th}$ column of the H-matrix and all the syndromes corresponding to $(a-1)^{th}$ column will be removed from the syndrome set and Again searching for the $(a-1)^{th}$ column starting from column weight two.

The search process here will be similar to other column vector search except that it doesn't consider the previously used column vector at that position. once it finds a column

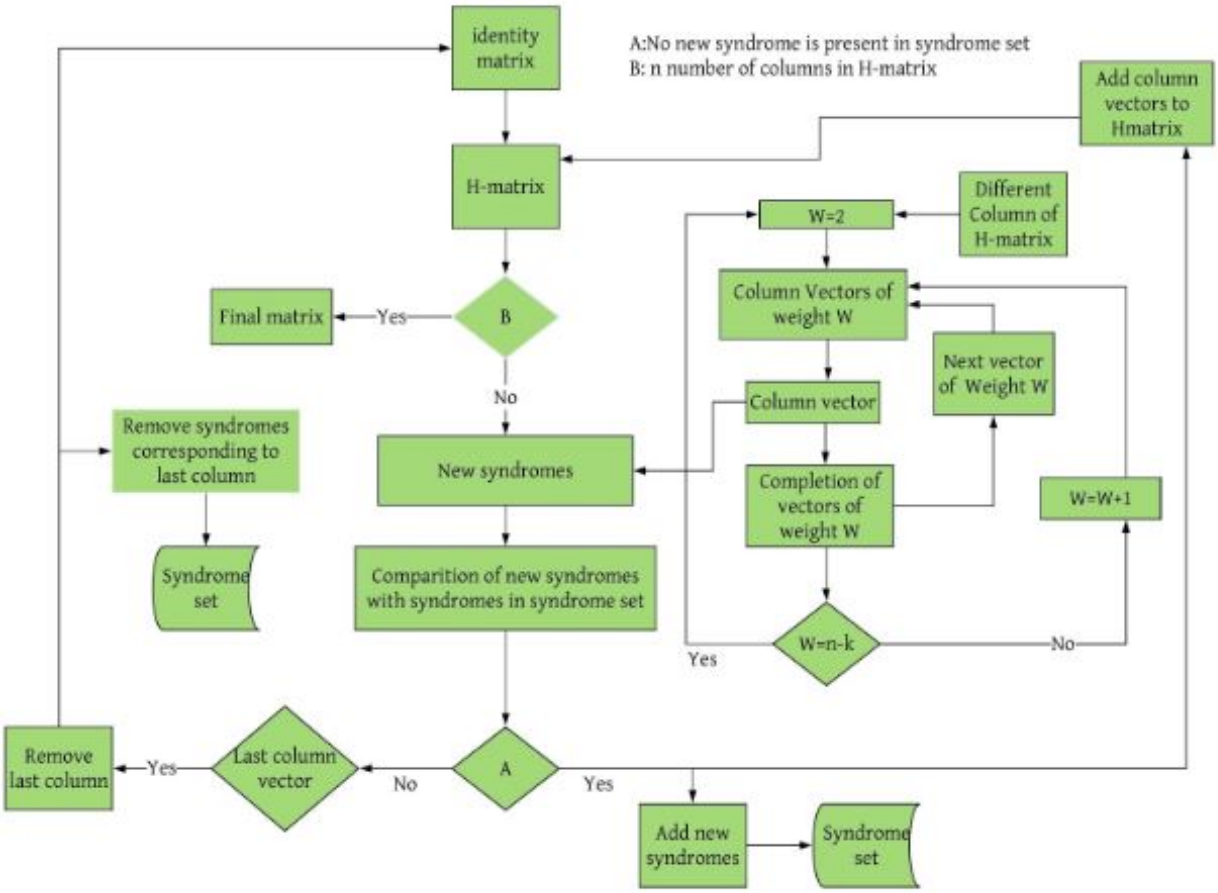

Fig. 1: Flow chart for generation of H-matrix

TABLE II: PERFORMANCE OF PROPOSED CODES W.R.T TOTAL NO OF ONES AND HEAVIEST ROW

Code	(n,k)	Total no of ones	Heaviest row
Proposed codes	(25,16)	51	8
QAEC Codes [11]	(23,16)	54	9
Proposed Codes	(42,32)	91	12
QAEC Codes [11]	(40,32)	96	14
Proposed Codes	(75,64)	178	25
QAEC Codes [11]	(73,64)	186	22

vector and adds its syndromes to the set then it moves to the ath column and continue this process until H-matrix has n columns. The flow chart of this process is shown in Fig.1

The total ones in a parity check matix gives how complex the circuit used for encoding and decoding are, the heaviest row indicates the highest time taken to find a checkbit.

From the above TABLE II, We notice that the proposed codes have less no of total ones than the QAEC codes and the size of the heaviest row of proposed codes are also less compared to the QAEC codes except for the 64 bit data. So the circuit of the proposed codes is less complex when compared with QAEC codes.

V. ENCODING AND DECODING FOR THE PROPOSED CODES

By using the procedure mentioned in section IV, we have found codes that can correct single bit (..,1,..), double adjacent (...,11,...), triple adjacent (...,111,...), 3-bit almost adjacent (...,101,...), four bit adjacent (...,1111,...) and other 3 patterns with window size 4 [(...,1001,...), (...,1011,...), (...,1101,...)] and 5-bit adjacent (...,11111,...) error patterns for 16, 32, 64 bit data.These patterns represent a stream of data, where 1 represents the error of the data at that position. The H matrix for (25,16), (42,32) and (75,64) codes are given in Fig.2, Fig.3, Fig.4 respectively.

$$H = \begin{bmatrix}
1000000000000010001000100\\
0100000001000010001000001\\
0010000001000010001100010\\
0001000000010000000010100\\
0000100000001000100010001\\
0000010001000000010100011\\
0000001000100010001100100\\
0000000100010001100001111\\
0000000010001100101010001
\end{bmatrix}$$

Fig. 2: Best parity check matrix for (25,16)

$$H = \begin{bmatrix}
10000000000000000100010001000100000100010\\
01000000000000100000001000010000100001000\\
00100000001000010001000000100000011000111\\
00010000000100001000100000000001001100001\\
00001000000010000010000010000011000010100\\
00000100000001000000000100001100010110001\\
00000010001000000100100000010010001001010\\
00000001000100010001100011001000100000010\\
00000000100010001000001100100010010000110\\
00000000010001100011010110001001000010000
\end{bmatrix}$$

Fig. 3: Best parity check matrix for (42,32)

To explain how encoding and decoding works, Let us consider a data $D(D_1\ D_2...D_{15}\ D_{16})$ of size 16. First we need to find check bits for the given data D.

From the H-matrix shown in Fig.2, we get the following equations to find the check bits for 16 bit data

$$C_1 = D_5 \oplus D_9 \oplus D_{13} \tag{23}$$

$$C_2 = D_1 \oplus D_6 \oplus D_{10} \oplus D_{16} \tag{24}$$

$$H = \begin{bmatrix}
100000000000000000000100001000001000100000001000000000001000000100010001001\\
010000000000000000010000010000100001000001000001000010000010000100010000000\\
001000000000000010000001000001000000000010000010000100010001100001000010000010\\
000100000001000010000100000010000000000000010000010010000100100001001011100000\\
000010000000100001000001000000000010001001000000100000100000001010000000110000\\
000001000000010000001000000000001100010001000111010001000000110000100110010000\\
000000100000000100000000001010001000001100000010001000001000010011001000000001\\
000000010001000000100010000000011000100010100001010000110011000000100001000000\\
000000001000100010000000010001100100001001000001101000101000011000110000001100\\
000000000100011000110010011001000000100111001000001111001010000011000010110
\end{bmatrix}$$

Fig. 4: Best parity check matrix for (75,64)

TABLE III: COMPARISON OF PROPOSED CODES TO QAEC CODES

		Encoder			Decoder		
Data Size	Code	Area(nm^2)	Delay(ps)	Power(mW)	Area(nm^2)	Delay(ps)	Power(mW)
16	Proposed Codes	127	689	0.011	1171	4899	0.081
16	QAEC Codes [11]	123	1124	0.013	797	4184	0.089
32	Proposed Codes	252	1091	0.026	2243	5440	0.174
32	QAEC Codes [11]	269	1316	0.032	1695	5030	0.181
64	Proposed Codes	521	1761	0.069	4314	6002	0.371
64	QAEC Codes [11]	522	1373	0.077	2850	5808	0.366

$$C_3 = D_2 \oplus D_7 \oplus D_{11} \oplus D_{12} \oplus D_{15} \quad (25)$$

$$C_4 = D_3 \oplus D_{12} \oplus D_{14} \quad (26)$$

$$C_5 = D_4 \oplus D_8 \oplus D_{12} \oplus D_6 \quad (27)$$

$$C_6 = D_1 \oplus D_9 \oplus D_{11} \oplus D_{15} \oplus D_{16} \quad (28)$$

$$C_7 = D_2 \oplus D_6 \oplus D_{10} \oplus D_{11} \oplus D_{14} \quad (29)$$

$$C_8 = D_3 \oplus D_7 \oplus D_8 \oplus D_{13} \oplus D_{14} \oplus D_{15} \oplus D_{16} \quad (30)$$

$$C_9 = D_4 \oplus D_5 \oplus D_8 \oplus D_{10} \oplus D_{12} \oplus D_{16} \quad (31)$$

By using the above equations we find the check bits and add them in the front part of the data to form a codeword $C(C_1\ C_2...C_9\ D_1\ D_2...D_{15}\ D_{16})$ and the code word will be stored in the memory.

When a alpha particle hits the memory, the content of some bits will get flipped [13]. Let us assume that the data is flipped at positions 8, 9, 10, 11 and 12 in codeword. When we are retrieving data from the memory cell, we receive the codeword as $R(C_1\ C_2...C_7\ C_8^{'}\ C_9^{'}\ D_1^{'}\ D_2^{'}\ D_3^{'}\ D_4...D_{15}\ D_{16})$

Next we find syndrome $S(S_1\ S_2...S_8\ S_9)$

$$S_1 = C_1 \oplus D_5 \oplus D_9 \oplus D_{13} \quad (32)$$

$$S_2 = C_2 \oplus D_1^{'} \oplus D_6 \oplus D_{10} \oplus D_{16} \quad (33)$$

$$S_3 = C_3 \oplus D_2^{'} \oplus D_7 \oplus D_{11} \oplus D_{12} \oplus D_{15} \quad (34)$$

$$S_4 = C_4 \oplus D_3^{'} \oplus D_{12} \oplus D_{14} \quad (35)$$

$$S_5 = C_5 \oplus D_4 \oplus D_8 \oplus D_{12} \oplus D_{16} \quad (36)$$

$$S_6 = C_6 \oplus D1^{'} \oplus D_9 \oplus D_{11} \oplus D_{15} \oplus D_{16} \quad (37)$$

$$S_7 = C_7 \oplus D_2^{'} \oplus D_6 \oplus D_{10} \oplus D_{11} \oplus D_{14} \quad (38)$$

$$S_8 = C_8^{'} \oplus D_3^{'} \oplus D_7 \oplus D_8 \oplus D_{13} \oplus D_{14} \oplus D_{15} \oplus D_{16} \quad (39)$$

$$S_9 = C_9^{'} \oplus D_4 \oplus D_5 \oplus D_8 \oplus D_{10} \oplus D_{12} \oplus D_{16} \quad (40)$$

Syndrome generated : $S_1\ S_2\ S_3\ S_4\ S_5\ S_6\ S_7\ S_8\ S_9$.
Now the syndrome will be compared with XOR operation of different combinations of columns of H matrix and when they match, it takes the position of the columns that gave XOR operation equal to syndrome, as the error position in the given codeword and flip the bits at the position and take last 16 bits of codeword as data. Received codeword after decoding is $R(C_1\ C_2...C_7\ C_8\ C_9\ D_1\ D_2\ D_3\ D_4...D_{15}\ D_{16})$. so data is $D(D_1\ D_2...D_{15}\ D_{16})$.

VI. EVALUATION AND COMPARISON

The proposed codes are compared with QAEC codes presented in [11] and the potential benefits of the proposed codes are discussed in this section. The modeling of encoder and decoder is done in Verilog and synthesized in Cadence 45nm library.

The comparison of the codes is done on the basis of redundancy and complexity, area, delay and power overhead. The TABLE III shows the comparisons on area, delay, power overhead.

In terms of redundancy the proposed codes has redundancy greater than QAEC codes [11] by 2 but the complexity of the proposed codes is less than the QAEC codes [11]. Which can be seen from the total no of ones and heaviest row in H matrix in TABLE II.The proposed codes can detect and correct all the errors till window size of 4 and 5 bit adjacent errors but the QAEC codes given in paper [11] can only detect and correct all the errors till window size of 3 and 4 bit adjacent errors.

With respect to other performance parameters For 16 bit data the area on the encoder side is increased by 3.25% and decreased by 6.31% and 0.19% in 32 and 64 bit data respectively. While the area on decoder side have increased by large percentage for the proposed codes by 46.924%, 32.3%, 51.36% for 16, 32, 64 bit data respectively. On the encoder side the delay of the proposed codes have decreased by 38.7% and 17.09% for 16,32 bit data respectively but increased by 28.25% for 64 bit data and on decoder side the delays have been increased by 17.08%, 8.15%, 3.34% for 16, 32, 64 bit data respectively. The power consumption of the proposed codes is decreased by 15.38%, 18.75%, 10.38% for 16, 32, 64 bit data respectively on encoder side and decreased by 8.9% and 3.864% on decoder side for 16, 32 bit data respectively but increased by 1.36% for 64 bit data. The above percentage changes are with respect to QAEC codes [11].

As summary, the codes with advanced correction ability presented in this paper comes at the cost of increased redundancy but the complexity on the encoder and decoder side is decreased as the total number of ones in the parity check matrix of proposed codes is less than that in the QAEC codes [11]. And as for area, it has increased but since the Area of ECC is much small when compared with total memory, the increase of ECC area is not much significant. From the percentages comparisons made in the above paragraph we

can clearly see that overall delay of proposed is slightly higher and the power consumption of proposed codes is less when compared with QAEC codes [11].So the proposed codes correct more errors and consume less power with moderate increase in delay when compared with QAEC codes [11].

VII. CONCLUSION AND SCOPE

This paper proposes new error correction codes that can correct all errors till 5 bit adjacent error by which reliability is increased. The proposed codes have a redundancy greater than the QAEC codes by two. The codes for the 16,32,64 data bits have been presented.The proposed codes are enforced in Verilog and synthesized in Cadence for 45nm library. The addition of ECCs means introducing delay, power and area overheads. The area overhead of proposed codes is almost same as that of the QAEC codes [11] on the encoder side but they have increased on the decoder side. While the delay overhead of the proposed code is much less on encoder side but it has slightly increased on the decoder side when compared to the QAEC codes [11]. The power consumption of the proposed codes is less than the QAEC codes [11]. Therefore the propounded codes can be used to correct MBUs in application where the power consumption, reliability and delay are the major factors. The proposed scheme can be extended to correct more conditions in 5 bit errors patterns without increasing the redundancy.

REFERENCES

[1] J. Gracia-Morán, L. J. Saiz-Adalid, D. Gil-Tomás, and P. J. Gil-Vicente, "Improving error correction codes for multiple-cell upsets in space applications," *IEEE Transactions on Very Large Scale Integration (VLSI) Systems*, no. 99, pp. 1–11, 2018.

[2] R. Baumann, "Soft errors in advanced computer systems," *IEEE Design and Test of Computers*, vol. 22, no. 3, pp. 258–256, May,2005.

[3] D. F. Heidel, P. W. Marshall, J. A. Pellish, K. P. Rodbell, K. A. LaBel, J. R. Schwank, S. E. Rauch, M. C. Hakey, M. D. Berg, C. M. Castaneda, *et al.*, "Single-event upsets and multiple-bit upsets on a 45 nm soi sram," *IEEE Transactions on Nuclear Science*, vol. 56, no. 6, pp. 3499–3504, 2009.

[4] R. Schrimpf and D. Fleetwood, "Radiation effects and soft errors in integrated circits and electronic devices," *World Scientific*, 2004.

[5] G. Tsiligiannis, L. Dilillo, A. Bosio, P. Girard, S. Pravossoudovitch, A. Todri, A. Virazel, H. Puchner, C. Frost, F. Wrobel, *et al.*, "Multiple cell upset classification in commercial srams," *IEEE Transactions on Nuclear Science*, vol. 61, no. 4, pp. 1747–1754, 2014.

[6] S. Shamshiri and K.-T. Cheng, "Error-locality-aware linear coding to correct multi-bit upsets in srams," in *2010 IEEE International Test Conference*, pp. 1–10, IEEE, 2010.

[7] G. Cardarilli, A. Leandri, P. Marinucci, M. Ottavi, S. Pontarelli, M. Re, and A. Salsano, "Design of a fault tolerant solid state mass memory," *IEEE Transaction on Realiablity*, vol. 52, pp. 476–491, Dec,2003.

[8] A. D. Tipton, J. A. Pellish, R. A. Reed, R. D. Schrimpf, R. A. Weller, M. H. Mendenhall, B. Sierawski, A. K. Sutton, R. M. Diestelhorst, G. Espinel, *et al.*, "Multiple-bit upset in 130 nm cmos technology," *IEEE Transactions on Nuclear Science*, vol. 53, no. 6, pp. 3259–3264, 2006.

[9] Z. Ming, X. L. Yi, and L. H. Wei, "New sec-ded-daec codes for multiple bit upsets mitigation in memory," in *IEEE/IFIP 19th International Conference on VLSI and System-on-Chip*, pp. 254–259, 2011.

[10] L.-J. Saiz-Adalid, P. Reviriego, P. Gil, S. Pontarelli, and J. A. Maestro, "Mcu tolerance in srams through low-redundancy triple adjacent error correction," *IEEE Transactions on Very Large Scale Integration (VLSI) Systems*, vol. 23, no. 10, pp. 2332–2336, 2015.

[11] J. Li, P. Reviriego, L. Xiao, C. Argyrides, and J. Li, "Extending 3-bit burst error-correction codes with quadruple adjacent error correction," *IEEE Transactions on Very Large Scale Integration (VLSI) Systems*, vol. 26, no. 2, pp. 221–229, 2018.

[12] N. Sowjith, K. S. Sandeep, M. Sumanth, and S. Agrawal, "Low power vlsi architecture for combined fmo/manchester encoder for reusability and fmo/manchester codecs," in *IEEE International Conference on Computational Intelligence and Computing Research (ICCIC)*, pp. 1–5, 2016.

[13] S. Manoj and C. Babu, "Improved error detection and correction for memory reliability against multiple cell upsets using dmc & pmc," in *IEEE Annual India Conference (INDICON)*, pp. 1–6, 2016.

Proceedings of the Fourth International Conference on Communication and Electronics Systems (ICCES 2019)
IEEE Conference Record # 45898; IEEE Xplore ISBN: 978-1-7281-1261-9

Enhanced Security through Cloud-Fog Integration

Rose K Johney
Dept. of Information Technology
Government Engineering College,
Idukki, Kerala, India
Email: rosekjohny@gmail.com

Elizabeth Shelry
Indian Institute of Information
Technology and Management-Kerala
Thiruvananthapuram
Email: rsherly@iiitmk.ac.in

K R Remesh Babu
Dept. of Information Technology
Government Engineering College,
Idukki, Kerala, India
Email: remeshbabu@yahoo.com

Abstract: Moving data and computation to the cloud is a promising technology in recent years. As the device density increases in the connected world, proper storage in the traditional cloud without security threats is a cumbersome task. Modification and leakage of data is the major threat in adopting cloud computing. Intelligent technologies are needed to safeguard against cyber-attacks. Fog paradigm enables users for data storage, management and network functions closer to them. Fog server introduced as a middle layer between user devices and the cloud to provide more security for uploaded data. It collects and transfers the encrypted data from the user, and apply reed Solomon code for error detection and MD5 hashing for malicious message detection to ensure more security and integrity. This data will be stored in different cloud servers and respective user's fog devices. Thus the combination of cloud with fog computing will ensure integrity, availability and confidentiality of users data.

Keywords: Fog computing, Cloud computing, Security, Encryption, Cyber-attacks.

I. INTRODUCTION

The cloud provides immense data storage and computation facility at low cost. Due to its on demand nature with low cost and zero maintenance cost features, organizations move their data and computation facilities to it. It consists of several servers and storage facility which are installed at huge data centers located at different places. It offers IT resources like storage, processing power, networking solutions, software, etc. It have many advantages like on demand, pay per use, rapid elasticity etc. While we are adopting cloud, the data is stored not in the local disk, but in the remote cloud datacenters.

However, day by day number of connected devices is increasing and they are using cloud computing for storing and managing their data. When technology and devices of internet of things are more occupied in peoples' life, present cloud technology cannot satisfy their needs like mobility support, low latency, intermittent network connectivity etc. It is also noted that cyber threats also increasing day by day. To fulfil these requirements, we need more intelligent distributed architecture like fog. It is an embryonic distributed architecture and it brings functions for computing, control, storage and networking closer to the end user devices. It chucks out the delay between the cloud and end devices connected to it. Usually fog computing is happening very near to the devices deployed. Data from these devices first pass to fog node and then to the cloud. The fog acts as a middle layer between things and the cloud. The system with fog nodes is considered as a three layer architecture as shown in the Fig. 1. Bottom layer consists of end devices and the things. Middle layer consists of fog nodes and cloud is considered as the top most layer.

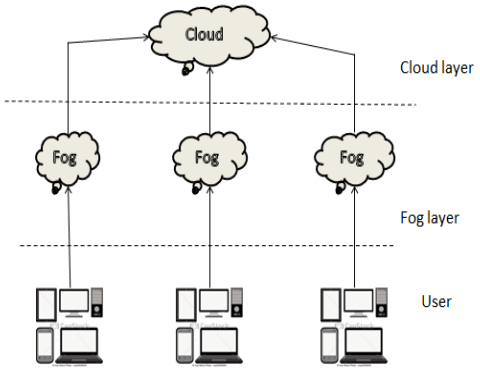

Fig.1. Three layer fog architecture

The fog [4][8][12]concept is a computing paradigm similar to cloud. A fog node can handle a large volume of data along with computing and management functions. Like cloud fog deals with heterogeneous services with different requirements. Hence, data can be store and processed at fog to avoid delay in computation. The data, device or application control functions for end user systems like control manufacturing systems, vehicles etc., can be handled by a fog node. Thus a fog node can act as an alternative of cloud nearest to the user rather than a remote cloud.

The cloud users are more concern about the data they stored at remote location. Fog can be used to enhance the security of data which is stored under cloud. It can also perform integrity checking when a user downloads the data from the cloud. In this paper a hybrid cloud-fog model is implemented to enhance the data security. It also enhances the number of data block handled at time to the cloud, since the computation is done at the fog node. The rest of this paper is organized as follows. Related works in this area is discussed in section II. Detailed system design is given section III and implementation details are given section IV. Analysis and conclusion are given section V and VI respectively.

II. RELATED WORKS

The vide adoption of cloud computing raises several new problems in this area. Data security is the most important issue in adopting a cloud platform for the end users. In this section, we will introduce these researches and analyses the advantages and weaknesses of them. Various security problems in adopting the cloud are discussed in [2]. There are several encryption methods available for data security in cloud, especially Advanced Encryption Standard (AES) [18]. Fog can apply to many fields like smart grids, connected vehicles, Internet of Things (IoT) and software defined networks. Fog forensics doesn't have a problem with bandwidth which is present in cloud forensics. The problems related to fog computing is mentioned in [5]. In order to simulate resource management scenarios and scheduling policies in fog computing various tools were invented like ifogSim [9]. Characteristics, applications, and security issues of fog computing are also discussed in paper [13][14].

The paper [3] proposes a third party auditing method to check the integrity of data. The users have to send a request to the third party auditor. The auditor is responsible for checking the integrity of data and he will prepare a detailed report and send to the user. But sometimes third party auditor may act as malicious. Another method discussed in [4] uses a trusted authentication, authorization, data encryption, hashing and key management technique. It makes use of both symmetric and asymmetric algorithms and One Time Password (OTP). But the problem is that OTP is not confidential at all. The paper [19] discusses a method to secure the data shared among social networks based on the cloud. User will encrypt and decrypt data using private and public keys. Then data first send to a proxy server. It will re-encrypt data using AES algorithm. Before send to another user it pre-decrypt data. Here group key manager is used to provide the public key, private key and symmetric key to the users and proxy server. Several authentication schemes for private cloud environments based on time stamp, one time secret password and nonce based approach are presented in [20]

A fog security mechanism in the healthcare system is tested with a decoy system [15]. In this a decoy medical big data is created at the fog layer to make attackers believe that it is the original data. But the original data is stored in cloud layer which can be only accessed by authenticated users after user profiling. Fog security mechanism is successfully used in IoT systems [16]. In this method fog layer is used to reduce latency. An authentication mechanism for fog-IoT computing using block chain technology is introduced in paper [17]. Here block chain is used for the authentication between fog and end users and also between fog nodes.

III. SYSTEM DESIGN

The proposed design is three-tier architecture as shown the figure 2. The bottom layer is device or things layer which consists of end devices and users. The data generated from this layer is transferred to middle layer. Middle layer consists of many fog nodes.

A. System Design

The problems with centralized cloud are data security and the transmission delay [1][11][18]. To tackle these problems, we propose a system which includes fog computing which have a several fog nodes between things and the centralized cloud. Here the data from the sensors are transferred to fog nodes. At fog nodes, there will be a series of security mechanisms to ensure the privacy and integrity of data. Fig. 2 shows the system design of the proposed approach. First, fog node accepts the data generated from the devices. At fog, the user data undergoes encryption. Here the AES [6][10] algorithm is used which is shown in Fig. 3.

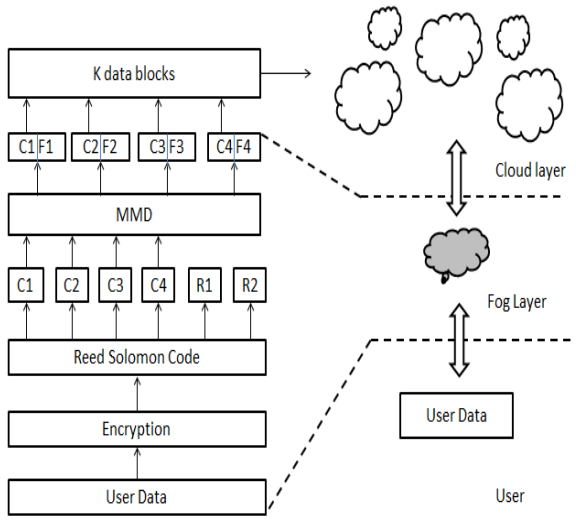

Fig. 2. System Design

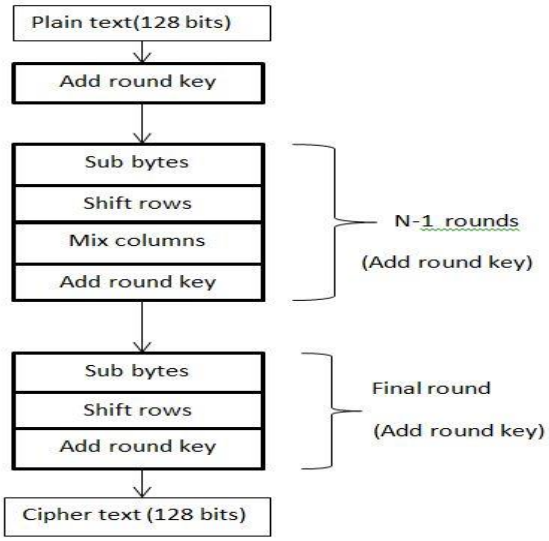

Fig. 3. AES encryption

Step 1	Generate an encoding matrix which have identity and vandermonde matrix.
Step 2	Multiply the user data with the encoding matrix. It generates $k+m$ data blocks.
Step 3	Upload or transfer data to the receiver.
Step 4	At the time of downloading, check whether it contains full data. If yes then exit,else go to step 5.
Step 5	To recover the full data, find the encoding matrix of remaining pieces of data. Let it be matrix X.
Step 6	Find the inverse of matrix X.
Step 7	Multiply the inverse of matrix X with remaining pieces of data to reconstruct the original data.

Fig. 4. Steps for reed Solomon code

After encryption, reed Solomon code [8] mechanism is applied to generate different data blocks. In this process, it generates $k+m$ data blocks, k is number of data blocks and m is the redundant data blocks. The steps are reed Solomon code is given Fig. 4. For experimental purpose, we have chosen k as 4 and m as 2. To this k data blocks, message digest 5 (MD5) [7] is applied to generate fingerprints to ensure the integrity of data. Redundant data blocks and fingerprints are then uploaded to fog and the remaining data blocks into different cloud servers. Usually, user's data is stored in only in one cloud location. But when that cloud service provider is under threat, entire data stored in it is also under threat. To avoid this problem this paper used a fog-cloud combination to store parts of data in a reasonable proportion. One of the advantages of this scheme is that, it can reduce the transmission delay. Because, fog situates very near to the end users. Cloud can't be used for the applications which need latency less than some milliseconds. This problem can be tackled with fog computing, since the transfer rate between fog computing layer and other layers is faster than the rate directly between cloud layer and the bottom layer.

Sometimes, attacker can modify the user's data. User and cloud service provider will be unaware of it. To address this issue we have used MD 5.

B. Uploading

If a user wants to upload files, the fog node takes it as an input and encrypts it using AES algorithm. After encryption, reed Solomon code mechanism is applied. It generates $k+m$ data blocks where k is the real data blocks and m is redundant data blocks. Then MD5 algorithm is applied on each data blocks to generate fingerprint. It is used for integrity checking of data. These fingerprints and redundant data are stored on fog and remaining data into different data blocks. The uploading process is shown in Fig. 5.

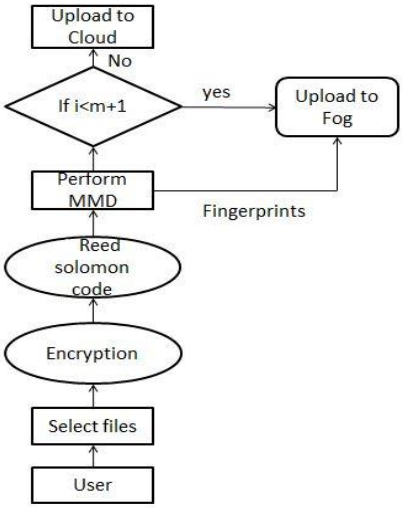

Fig. 5. Uploading

C. Downloading

When downloading a file, to ensure that there is no data change is happened, MD5 is applied for modification detection. Then a fingerprint is generated based on the downloaded data. This fingerprint and the already stored fingerprint at the time of uploading are compared with each other. If any change is found, we can recover the lost data through inverse reed Solomon code mechanisms. But as a worst case scenario, sometimes the amount of errors may be greater than the limit of error that can be recovered. In this case, the only way is to delete the data and give negative feedback about the cloud service provider. With this scheme,

we can improve the performance and the competition between cloud service providers. Fig. 6 shows the process of downloading.

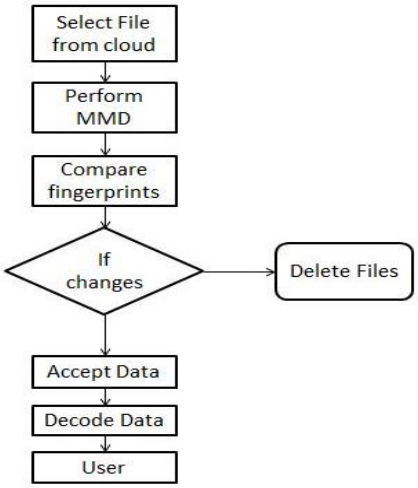

Fig. 6. Downloading

IV. IMPLEMENTATION

The proposed method is implemented using laptop as fog nodes and mobile phones as IoT devices. These devices are connected through Wi-Fi and Bluetooth. The data from a user reaches to the specific location of the laptop which can act as memory of fog Node. In this node security mechanisms like encryption, error detection and correction and integrity checking are carried out. Here Google drive is used as cloud and *k-1* data blocks uploaded to it and remaining redundant data blocks and data blocks stored in fog itself. At time of uploading, an identification number (ID) is generated for each data blocks. These ID and message digest of each data blocks are stored in the database for further checking. Encryption is applied to this file and this file will undergo reed Solomon code and generate 6 files, i.e., 4 data files and 2 redundant files. Output of the uploading process is shown in figure 7. From figure 6, we can see that file is divided into 6 parts and for each data block, MD5 checksum is generated and inserted the file name and its checksum in to the database. At the time of uploading, an ID is generated and this is also stored in the database. Here 3 blocks are uploaded with unique ID.

Next process is downloading of data stored in cloud. First we need to download these files into fog with the ID generated at the time of uploading which is stored in the database. From fog, the data undergo integrity checking with MD5 hash. After that, if there is no error, then data undergoes reed Solomon and AES decryption to decode and decrypt data. The change in data can be happen in two ways, one is from inside the cloud. Second one is at the time of transfer of data from cloud to fog. The change of data can be data loss or data modification. If data loss is happening at inside the cloud, data cannot be downloaded with the id generated at the time of uploading. Malicious modification also gives the same situation. In the next scenario, if the data lost at the time of transfer, lost data can be recovered with the reed Solomon code. Otherwise, if data is maliciously modified, it can be detected with MD5 comparison. Modified data is deleted and whole data is recovered with reed Solomon code. Figure 8 shows downloaded files from cloud and its MD5 hash also compared. New MD5 hash is generated for downloaded data. This hash is compared with the previously stored message digest of the corresponding data blocks which is stored in database.

```
wrote D:\drive\quickstart\text.txt2
MD5 checksum for file using Java :12ecdc9349462e89b2ed4ba3c9ceba09
Inserted records into the table...


wrote D:\drive\quickstart\text.txt3
MD5 checksum for file using Java :b70f02aeff84047f575b08fc8912fa59
Inserted records into the table...


wrote D:\drive\quickstart\text.txt4
MD5 checksum for file using Java :1ca172f85c9a98e3e467dd32fd0311f4
Inserted records into the table...


wrote D:\drive\quickstart\text.txt5
MD5 checksum for file using Java :aed6c9c7dd0eb51400206af8434585ef
Inserted records into the table...


Execution time in seconds: 5934.0
Jun 02, 2019 9:05:02 PM com.google.api.client.util.store.FileDataStoreFactory setPermissions
WARNING: unable to change permissions for everybody: D:\drive\quickstart\tokens
Jun 02, 2019 9:05:02 PM com.google.api.client.util.store.FileDataStoreFactory setPermissions
WARNING: unable to change permissions for owner: D:\drive\quickstart\tokens
Connecting to a selected database...
Sun Jun 02 21:05:02 PDT 2019 WARN: Establishing SSL connection without server's identity ve
Connected database successfully...
Inserting records into the table...
Uploaded file3  File ID: 13IrORRfFXK03OXJIsqaQzy6u3b9pHQ3A
Uploaded file4  File ID: 12rRLgEcwI0lIKe8G1nahjFHXJrlHLO0A
Uploaded file5  File ID: 19WIqPDdbxaCbC7J3FPjrXRGqSISaV8ts
```

Fig. 7. Output of encoding

```
download sucessfull text.txt3
download sucessfull text.txt4
download sucessfull text.txt5
Goodbye!
Execution time in seconds: 9456.0
MD5 checksum for file using Java :
Connecting to a selected database...
Sun Jun 02 21:15:40 PDT 2019 WARN: Establishing SSL connection
Connected database successfully...
Inserting records into the table...
check sum of the file is:b70f02aeff84047f575b08fc8912fa59
original file checksum:b70f02aeff84047f575b08fc8912fa59
no change in: text.txt3


check sum of the file is:1ca172f85c9a98e3e467dd32fd0311f4
original file checksum:1ca172f85c9a98e3e467dd32fd0311f4
no change in: text.txt4


check sum of the file is:aed6c9c7dd0eb51400206af8434585ef
original file checksum:aed6c9c7dd0eb51400206af8434585ef
no change in: text.txt5
```

Fig. 8. Output of downloading and decoding

V. ANALYSIS

Experimental evaluation and analysis consists of different parameters. First one is the performance of uploading and downloading, when the number of data blocks (*k*) increases.

Second one is the traffic analysis. It shows the amount of data needs to send to cloud with fog and without fog. Last one is the delay and it shows the time need to complete the process with fog and without fog.

A. Performance

Performance of the system is tested by varying the value data blocks (*k*). Time taken to upload and download is recorded. Here number of redundant data blocks fixed as 2. Table 1 show that, when number of data blocks increases, time taken to upload and download is also increases. In case of uploading, for bigger the value of *k*, time to upload is also increased. This is due to increased complexity of the security matrix. When the value of *k* increases, the complexity of encoding matrix is also increases. Thus, the security of data increases. In case of downloading, for larger value of *k*, the downloading time is high.

TABLE 1. PERFORMANCE

k	Upload time (ms)	Download time (ms)
4	16684	7846
5	17364	9348
6	18170	9516
7	19904	10549
8	23480	10874
9	23672	12480
10	27794	12984

B. Traffic Analysis

Table 2 compare the traffic to cloud with and without fog. For the experimental purpose the data blocks *(k*) is taken as 4 and redundant data block size (*m*) as 2. A fog node have substantial amount of data storage capacity. In this system, redundant data blocks remains in the fog and only *k-1* data blocks are uploaded to the cloud. Without fog entire data need to send to the cloud. For our experiments were conducted with small amount of data. But in real time, amount of data will be huge. It is also noted that in years, with the intervention of IoT, the data transmitted from end devices will increase drastically. At that time, cloud cannot afford this big data and it causes delay. Fog reduces the amount of data to be sent to the cloud which reduces traffic.

TABLE 2. TRAFFIC ANALYSIS

Data Size (KB)	With Fog (byte)	Without Fog(byte)
8	8192	6159
10	10240	7695
12	12288	9231
14	14336	10767
16	16384	12303
18	18432	13839
20	20480	15375

C. Delay

The table 3 and 4 shows that time taken to upload and download takes more time when fog is present but it is not much significant. This is justifiable due to the enhanced security mechanisms implemented at fog nodes. In this proposed work, data first pass to fog then only to the cloud. The fog takes a little time to process data i.e., to apply the proposed security mechanisms to data. The time taken at fog node is not much significant. Even though upload and download time is less for without fog implementation, but data traffic is more, which is to be further investigated.

TABLE 3. UPLOAD TIME - WITH AND WITHOUT FOG

Data Size (KB)	With Fog (ms)	Without Fog (ms)
8	16871	14955
10	16746	14223
12	16035	14854
14	17206	15833
16	16479	15900
18	16873	15472
20	16138	14011

TABLE 4. DOWNLOAD TIME - WITH AND WITHOUT FOG

Data Size (KB)	With fog (ms)	With fog (ms)
8	9657	8601
10	9340	8904
12	9204	8897
14	9851	9016
16	10218	9735
18	9695	8492
20	10735	9612

VI. CONCLUSION

Cloud computing is distributed and scalable architecture with massive storage capacity at low cost. But data loss and modifications are serious issue in adopting cloud as computation platform. The fog computing offers distributed computing, that officers control, data storage, and networking functions closer to end user devices. The proposed method provides security through cloud-fog integration with reed Solomon code and MD5.This enhanced method improves the security in cloud data storage. Here the Reed-Solomon code used to correct errors original data. It generates different data blocks and redundant data blocks. For each data blocks, MD5 is applied, which is used to generate fingerprints. These fingerprints and redundant data blocks are stored in fog and remaining data blocks are stored in to different cloud. With this cloud-fog hybrid storage technology, we can avoid cyber threats like data loss and malicious modification. By this way, the proposed technique can ensure the integrity, availability and confidentiality of data. As future scope, we can develop

more secured data encryption and error detection algorithms based on block chain technology to use in fog.

REFERENCES

[1] Tian Wang, Jiyuan Zhou, Minzhe Huang, MD Zakirul Alam Bhuiyan, Anfeng Liuc, Wenzheng Xud, Mande Xi, "Fog Based Storage Technology to Fight with Cyber Threat", Future Generation Computer Systems, Vol. 83, pp. 208-218, 2018.

[2] Tunisha Saxena, Vaishali Chourey, "A survey paper on cloud security issues and challenges", Conference on IT in Business, Industry and Government (CSIBIG), 2014. IEEE.

[3] T.Subha, S.Jayashri, "Efficient Privacy Preserving Integrity Checking Model for Cloud Data Storage Security", Conference on IT in Business, Industry and Government (CSIBIG), 2014. IEEE.

[4] Akshay Arora, Abhirup Khanna, Anmol Rastogi, Amit Agarwal, "Cloud security ecosystem for data security and privacy", 7th IEEE International Conference on Cloud Computing, Data Science & Engineering - Confluence, pp. 288-292, 2017.

[5] Mung Chiang, Tao Zhang, "Fog and IoT: An Overview of Research Opportunities", IEEE Internet of Things Journal, Vol. 3, No. 6, pp. 854 – 864, December 2016.

[6] Advanced Encryption Standard, "https://www.tutorialspoint.com/cryptography", Accessed: 3rd January 2019.

[7] MD5, "https://en.wikipedia.org/wiki/MD5", Accessed: 3rd January 2019.

[8] ReedSolomoncode, "https://www.cs.cmu.edu/~guyb/realworld/reedsolomon/reed_solomon_codes.html", Accessed: 5th January 2019.

[9] Harshit Gupta, Amir Vahid Dastjerdi, Soumya K. Ghosh, Rajkumar Buyya, "iFogSim: A toolkit for modelling and simulation of resource management techniques", Software: Practice and Experience, Special Issue: Cloud and Fog Computing, Vol. 47, Issue 9, pp. 1275-1296, September 2017.

[10] Akhilesh Vishwanath, Ramya Peruri, Jing (Selena) He, "Security in Fog Computing through Encryptions", Int. Journal of Information Technology and Computer Science, Vol. 5, pp. 28-36, 2016.

[11] Jiyuan Zhou, Tian Wang, Md Zakirul Alam Bhuiyan, Anfeng Liu, "A Hierarchic Secure Cloud Storage Scheme based on Fog Computing", IEEE 15th International Conf. on Dependable, Autonomic and Secure Computing, pp. 470-477, 2017.

[12] Maja Malenko, "Implementation of Reed-Solomon RS (255,239) Code", Proc. of the 2nd International Conference on Applied Innovations in IT, (ICAIIT), pp. 43-48, March 2014.

[13] Mithun Mukheerjee, Rakesh Matam, Lei Shu, Leandros Maglaras, Mohamed Amine Ferrag, Nikumani Choudhury, Vikas Kumar, "Security and Privacy in Fog Computing: Challenges", IEEE Access, Vol: 5, pp. 19293 – 19304, 2017.

[14] Yifan Wang, Tetsutaro Uehara, Ryoichi Sasaki, "Fog Computing: Issues and Challenges in Security and Forensics", IEEE 39th Annual International Computers, Software Applications Conference, pp. 53-59, 2015.

[15] H. A. Al Hamid, S. M. M. Rahman, M. S. Hossain, A. Almogren and A. Alamri, "A Security Model for Preserving the Privacy of Medical Big Data in a Healthcare Cloud Using a Fog Computing Facility With Pairing-Based Cryptography", IEEE Access, Vol. 5, pp. 22313-22328, 2017.

[16] S. Alharbi, P. Rodriguez, R. Maharaja, P. Iyer, N. Bose and Z. Ye, "FOCUS: A fog computing-based security system for the Internet of Things", 15th IEEE Annual Consumer Communications & Networking Conference (CCNC), pp. 1-5, 2018.

[17] Y. Imine, D. E. Kouicem, A. Bouabdallah and L. Ahmed, "MASFOG: An Efficient Mutual Authentication Scheme for Fog Computing Architecture", 17th IEEE International Conference On Trust, Security And Privacy In Computing And Communications/ 12th IEEE International Conference On Big Data Science And Engineering (TrustCom/BigDataSE), pp. 608-613, 2018.

[18] Babitha M P, K R Remesh Babu, "Secure cloud storage using AES encryption", IEEE International Conference on Automatic Control and Dynamic Optimization Techniques (ICACDOT), pp. 859-864, 2016.

[19] Praveena A, Smys S, "Ensuring data security in cloud based social networks", IEEE International conference of Electronics, Communication and Aerospace Technology (ICECA), Vol. 2, pp. 289-295, 2017.

[20] Sridhar S, Smys S, "A hybrid multilevel authentication scheme for private cloud environment", IEEE 10th International Conference on Intelligent Systems and Control (ISCO), pp. 1-5, 2016.

Proceedings of the Fourth International Conference on Communication and Electronics Systems (ICCES 2019)
IEEE Conference Record # 45898; IEEE Xplore ISBN: 978-1-7281-1261-9

Remote Controlled Car using Smartphone Accelerometer

Varsha Vishwa Kiran

Department of Computer Science and Engineering
Amrita School of Engineering, Bengaluru
Amrita Vishwa Vidyapeetham,India
varshakiranrpsit@gmail.com

S Santhanalakshmi

Department of Computer Science and Engineering
Amrita School of Engineering, Bengaluru
Amrita Vishwa Vidyapeetham,India
s_lakshmi@blr.amrita.edu

Abstract: **This thesis presents a development and implementation of a remote controlled car (RC) for surveillance purpose and the whole system is controlled from anyplace from the world by Smartphone accelerometer. The work was led by establishing Wi-Fi communication between RC car and Smartphone. After setting up the network connection between RC vehicle and Smartphone, the vehicle can be controlled by just tilting the Smartphone by using remote IMU application that is installed in android phone. This application uses accelerometer, gyrometer and magnetometer for linear and rotational movement of car. The values from this application are sent to the Raspberry Pi through UDP protocol. For the surveillance purpose and to navigate the area while controlling the car remotely we used pi camera that is joined to the vehicle. The test was carried on the RC vehicle with four directions. Directions are 1) Left 2) Right 3) Forward 4) Backward.**

Keyword: IMU, Accelerometer, RC car, Surveillance, Smartphone.

I. Introduction:

Research on mechanical autonomy has continued for a very long while. In spite of unique presence, robots offer a typical mechanical and movable structure. A robot utilizes sensors to see nature. Buyer robots will in general have microcontrollers along with restricted computational power and little measures of memory. Sensors for customer robots are additionally very expensive. In expansion, it takes micro controller assets to deal with these mounted sensors. With the progress of modern day Smartphone innovation, many regular sensors are officially implanted in a Smartphone [1]. The best preferred standpoint of utilizing a Smartphone is that it allows user to drive their vehicle away from their true location. Now days there are various accessible articles concentrating the advancement of correspondence models between a Smartphone and a machine. A modern Smartphone has numerous advantage (for example computerized compass, accelerometer, sound, mouthpiece and camera) and numerous helpful communication interfaces (for example Wifi, Bluetooth, etc.). There is no uncertainty that smartphone phone processors have higher processing power and large memory than the basic miniaturized scale controllers. This propels us to include a Smartphone into remote control vehicle in request to handle complicated tasks and progress the general execution. In this examination, we actualized a different directing agenda with Smartphone movement control. The general implementation of the proposed framework is assessed by activities that we planned. Our proposed work can be utilized in Surveillance purpose.

In light of the situations portrayed above, we present a versatile surveillance system that runs on raspberry pi. Raspberry pi drive the vehicle which is remotely connected with the client by means of the android application. A control board is additionally given through the remote IMU application introduced in the Smartphone that uses accelerometer and gyroscope to drive the car wirelessly by just tilting the Smartphone in the desired direction. Accelerometer are made up of multiple axes, two to determine most two dimensional movement with option of 3D positioning [2]. Most Smartphone typically make use of three axis model. We measures the values of 3 axes based on the phone movement. Figure1 shows the X, Y and

Z axis of Smartphone. X, Y and Z axis orientation relative to the device remain constant.

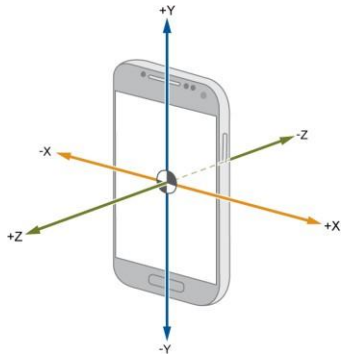

Figure1:Smartphone Accelerometer Axis

For rotation of car we use gyroscope. Rotation measured in rad/sec around the the X, Y, and Z axis of the gyroscope relative to the android device. For any positive axis on the device, clockwise rotation output negative value and vice versa. For example if we place the device up on table and spin it clockwise, then the block output is negative value for the z axis. Figure 2 shows the gyroscope axis orientation. Based on the sensed value of accelerometer and gyroscope movement of the vehicle is determined.

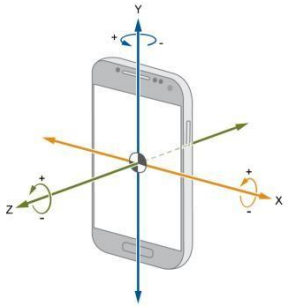

Figure 2: Gyroscope Axis Orientation

.

This paper proposed a prototype of remote controlled car which gets control of movement from Smartphone tilting position with greater control of car, while navigating the car from remote location. Steering of car using web interface key is not able to gives proper control of car, especially when one wants to slow down the speed or want to take slight turn of car they are not able to do. So our aim is to find proper solution to this context. The rest of this thesis is arranged as follows. Segment II describes the several work regarding the design and development of remote controlled car. Segment III describes the architecture of proposed work. Segment IV describes the working mechanism of the proposed work. Segment V talks about the result and segment VI presents the summary of this work.

II. Similar Work

There are various work has been done related to the remote controlled car for the various purposes. Paper [3-5] developed remote controlled car that is controlled by computer via a parallel port and controlling command is voice and facial expression. Computer convert this voice command/face image to the digital signal and then converted to radio signal and accordingly car takes decision for their movement . The Yuxinzing presents RC car using Arduino and Android communication for search mission. This system named AndroRC that require two separate Arduino Board (Mega and Uno) for RC unit. Due to the use of servo motors for turning, the speed is constrained for four directions [6]. A vision based obstacle avoidance algorithm for a low cost and off-the-shelf electronics has been implemented, where this algorithm is fast and works with very low resolution image. Ultrasonic sensor is widely used in mobile applications for measuring distance, which helps in detecting obstacles. A system was implemented using ultrasonic sensor and infrared sensor intended to help the elderly and people with vision impairment [7]. Another system proposed by R. Manduchi is a system based on stereo range measurements, for obstacle avoidance [8-10]. K. Dumbre presents a robotic vehicle for surveillance purpose that is embed with automatic arm that can be utilized to catch and shift things wherever required and it is controlled via keyboard [11]. G.Pavani and V. Kadiam presents Smartphone operated RC car using Raspberry Pi [12].

III. System Structural Design

In this work hardware that we used are connected as figure 1. These figure include Raspberry pi, picamera, L293D Dual H- bridge IC and RC car structure.

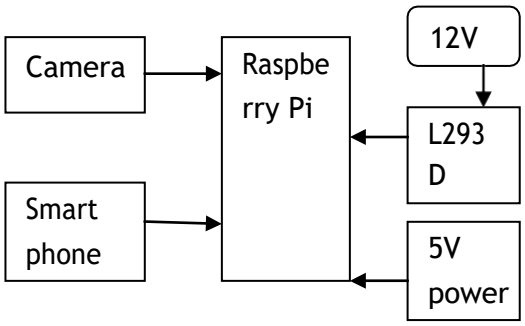

Figure 3: Block Diagram

A. Raspberry Pi B3

Raspberry pi is the heart of this system. Raspberry pi is used in this work because of its low cost, small size, compatible for most of the high language programming and that can be plug in to computer or TV. It is capable of doing many things like it acts as desktop computer, browsing the internet, game, word processing etc [13].

B. Motor control

Here we used L293d motor driver IC to control motor of rc car. Normal DC geared motor require current greater than 250 – 300 mA. ATMEGA16 microcontroller gets damage because they cannot supply this amount of current, so we need circuit that acts as a bridge between motor and microcontroller. Hence L293D IC acts as bridge between microcontroller and motor of RC car[14].

L293D IC is a dual H- bridge motor driver IC. Using this we can manage the direction of rotation of motor in both clockwise and anti-clockwise direction. Figure 2 shows the connection with DC motor.

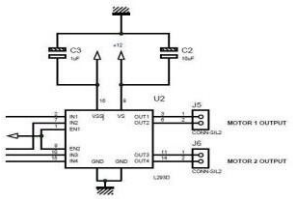

Fig 2: Circuit diagram of L293D and Motor connection

C. Drive Algorithm

RC car gets direction of movement according to the phone position with respect to the accelerometer axis. Accelerometer gives two outputs one for horizontal direction means left or right direction and other for vertical direction means forward and backward movement. Hence to drive the car according to the accelerometer value we need to set some range of rotation of phone with respect to accelerometer axis, for movement of car in these four directions. So for our work we set these values for x and y. Table 1 show the value of x and y relative to the position of phone.

Table1: X and Y coordinate Relative to accelerometer axis

Direction of movement	X – axis	Y – axis
Forward	X >= 3	-3 <Y< 3
Backward	X <= 3	-3 <Y< 3
Left	Y >= 3	-3 <X< 3
Right	Y <= -3	-3 <X< 3

Each output of accelerometer ranges from 1v to 2v. An ADC within the pi converts the outputs to digital signal and transmitted to the motor driver, there it decide direction of movement of car and accordingly car moves.

IV. Working Mechanism

This section describes how the work has been implemented. Whole work is divided into various phase.

A. Hardware Assembly

We connect Raspberry Pi with four geared motor using L293D module. For powering up the Raspberry pi we used power bank and to power geared motor we used 12v rechargeable battery. After assembling of wheels and geared motor into the chassis structure look like the figure I.

Figure I: RC car

L293D IC is used to drive the dc motor in any direction. It works on the principle of H-Bridge, that allows voltage to be flowing in any direction. It has four input which is trigged by raspberry pi. Connection of motor IC as below

GPIO7 – IN1

GPIO11 – IN2

GPIO13 – IN3

GPIO15 - IN4

GND Raspberry Pi – GND L293D

12 v of Raspberry pi - Enable pin

To make the car run forward pin 7 and pin 13 must be ON and other two pins are OFF, similarly to run backward pin 11 and pin 15 must be ON and other two are OFF. Now to run the car in left direction pin 13 is ON and other are OFF. To run the motor in right direction pin 7 is ON and other pins are OFF. For live video streaming we connect Pi camera to raspberry pi.

B. Setting Up the Raspberry Pi

To install the Raspberry pi several things are needed for proper functioning of Pi. Table 2 shows the needed device for the first time booting of Pi.

Devices	Details
SD Card: It is recommended to use at least 8GB class as the card will be installed with the Raspbian Image.	
HDMI/DV input : Work as a display for the pi.	
HDMI input will be the best result .	
Keyboard and Mouse: Any standard keyboard and mouse will work perfectly	
Power Supply: Pi is powered using USB micro power supply that gives at least 2A at 5v. Lower current like 700mA will work for basic usage. However pi will reboot if the power is drawing too much	

Table 2: Device needed for first time boot of Raspberry pi

First phase in setting up the Pi by placing the SD card with Raspbian(via NOOBS) into the micro SD card slot of the Raspberry Pi. Now plugged the keyboard and mouse into the USB port, and then turned on the monitor or TV. After that, plugged the HDMI wire to the monitor/TV, and then hooked the other end of the cable into the Raspberry Pi. Now it's time to give power supply to the raspberry pi, it turned on and boot up raspberry pi. A power indicator light now began to shine. Now downloaded and install the Raspbian operating system on the raspberry pi. When the warning window pops up, clicked yes to confirm. Once the installation process is finished, raspbian automatically began to reboot. Under the menu bar that is on the top left corner of screen, pick the preferences in the dropdown menu, then pick the raspberry pi configuration and in the configuration tab sat the location, time zone and keyboard language. Then again reboot the pi [15-16].

C. Wi-Fi Arrangement

Pi was configured to communicate automatically with the chosen network [17]. Two file that are network interface and wi-fi protected access (WPA) were edited using script editor to enable Wi-Fi. In this we have used a nano script editor which is easy to use. Pi has its own IP address. This prototype provides distinctive feature, where controller is allowed to control the vehicle by a remote controller that is placed at a distant far away from the vehicle location but remote controller should be connected with the network as the Pi connected. There are some techniques that can be use to activate this special feature. One of the techniques known as port forwarding can be used to access raspberry pi at a distant place from pi.

Port forwarding is a method that allows us to access a server or a device from anywhere. It can be initialize by setting up router as all incoming packets from the internet to the port of the specific local ip address of pi. Port forwarding has one drawback that it allows any device to connect with forwarded port, hence make slightly insecure so it must be handle cautiously.

D. Remote Control

For controlling the car we use accelerometer for linear movement and for rotational movement we used gyroscope. Accelerometer and gyroscope is inbuilt feature of android phone. To use this feature we use inertial measurement unit(IMU app) that was installed from google play. Now we established UDP connection between android phone and pi, then we create socket using python program for receiving the data from android app[18]. Python program wait for input from android app and process the data for movement of RC car. Now pi decodes the received data and sent command to the motor driver circuit. Direction of car depends upon the movement of android phone. After running the code and setting the IMU app with raspberry pi IP and port address we can tilt phone in that direction to which we want to drive the car. Figure 2 shows the IMU setup page where we filled ip address and port , then start the app. After running this app this app start to send output of accelerometer and gyroscope according to the phone position and accordingly RC car start to move.

Figure3: IMU setup page

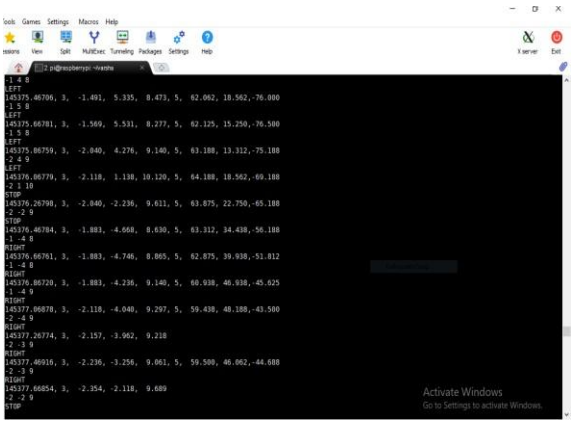

Figure 4: Navigation output

1. Live Video Streaming

Pi Camera is used as an eye of remote controller[19-20]. Following are the command to configure camera.

1. Run the " sudo apt – get update"
2. "sudo apt – get upgrade"
3. " sudo rasp – config"

After running this command, some option will pop up, among them, camera option is to select and enable it. Once all configurations have been established, write the script for video publishing. For this we created a new file called rpi_camera.py and saved it here. Under this write the code that is available in official picamera package documentation. After writing code, run this code, then go to web page and type the raspberry pi IP along with port 8080, now live video is streaming. Fig4 shows the live video streaming.

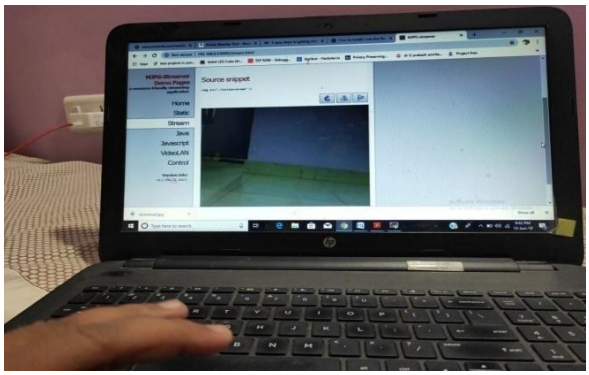

Figure 5: Live video streaming

V. Result and Discussion

The proposed work has been designed to run an RC car, and it gets direction of movement according to Smartphone tilt position and broadcasting network node was build for live video publishing that helps to navigate the area for controlling the car movement remotely. Raspberry pi drive the RC car and it has a Wi-Fi connection to communicate with Smartphone. For power supply pi is connected to 5v power bank and RC car is powered by 12v rechargeable battery. Figure 6 shows the fully functional prototype of this work.

For local access authentication, one can control RC car only by connecting both pi and Smartphone with the same Wi-Fi network as well as if pi is powered on.

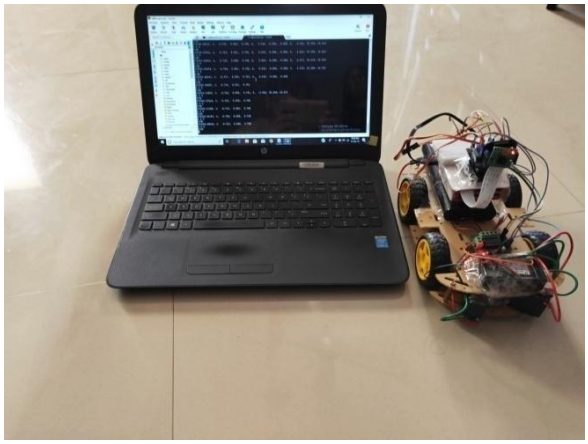

Figure 6: RC car and its control output

VI. Summary

This work prompts the prototype of Remote controlled car with the help of Smartphone Accelerometer. By means of a completely well-designed prototype this vehicle can be useful for surveillance purpose in dangerous area, industrial buildings, border and many more such areas with greater control of vehicle than the existing switch controlling mechanism. Several improvements are possible like one can use solar panel to give power of the motor so that charging problem of batteries will short out.

References:

[1] Yun Chan, c., Jae Wook, j.: Remote control system using mobile phone's DTMF. In: 6th International conference on Industrial Informatics, INDIN 2008, July 13-16, pp. 1441-1446(2008).

[2] [Sam Naghshineh, Golafsoun Ameri, Mazdak Zereshki, Dr. S. Krishnan & Dr. M. Abdoli-Eramaki. Human Motion capture using Tri-Axial accelerometers.

[3] C. Pornpanomchai, P. Sukklay, "Computer operated Radio-Controlled Cars", *IACSIT* International Journal of Engineering and Technology, vol. 3, no. 3, June 2011.

[4] Parichart Leechor; Chomtip Pornpanomchai; Phichate Sukklay 2010 2nd International Conference on Mechanical and Electronic Engineering.

[5] C. Pornpanomchai, P. Sukklay, "Operating Radio-Controlled Cars by a Computer", IACSIT International Journal of Engineering and Technology, Vol.3, No.3, June 2011. 2016 IEEE Conference on Systems, Process and Control (ICSPC 2016), 16–18 December 2016, Melaka, Malaysia 229.

[6] Yuxin Jing, "AndroRC : An Android remote control car unit for search missions", Integrated Medical Systems Laboratory, Dept. of Electrical and Computer Engineering New York Institute of Technology .

[7] Mohammad Hazzaz Mahmud, Rana Saha, Sayemul Islam ,"Smart walking stick - an electronic approach to assist visually disabled persons", International Journal of Scientific & Engineering Research, Volume 4, Issue 10, October-2013.

[8] Nara, S. Takahashi, S., "Obstacle Avoidance Control for Mobile Robots based on Vision",SICE-ICASE, 2006. International Joint Conference.

[9] Kalmegh, S.K.,Samra, D.H., Rasegaonkar, N.M., "Obstacle Avoidance For A Mobile Exploration Robot Using A Single Ultrasonic Range Sensor", Emerging Trends in Robotics and Communication Technologies (INTERACT), 2010 International Conference.

[10] R. Manduchi, "Obstacle Detection and Terrain Classification for Autonomous Off-Road Navigation"

,2005 Springer Science + Business Media, Inc. Manufactured in The Netherlands.

[11] "Robotic Vehicle Control using Internet via Webpage and Keyboard", K. Dumbre, S. Ganeshkar & A. Dhekne
International Journal of Computer Applications, Volume 114 – No. 17, March 2015.

[12] V. Kadiam and G. Pavani, "Smart Phone Controlled Two Axes Robot for Video Surveillance Using Wireless Internet & Raspberry Pi Processor", Hyderabad, India, 2014.

[13] “Raspberry Pi - Teach, Learn, and Make with Raspberry Pi", Raspberry Pi, 2016. at :http://www.raspberrypi.org.

[14].”L293D Motor Driver IC” at https://www.engineersgarage.com/electronic-components/l293d-motor-driver-ic.

[15] “Raspbian About - Raspbian", Raspbian.org, 2019 at https://www.raspbian.org/RaspbianAbout.

[16] ”configurations of raspberry pi – http://www.raspberrypi.org/documentation/configuration/raspi-config.md

[17] “Raspberry Pi access over the Internet - Raspberry Pi Documentation",Raspberrypi.org,

[18]“Python” –Available on http://docs.python.org/3/tutorial/index.htm.

[19] Will Hrudey, Ljiljana Trajkovid “Streaming Video Content Over IEEE 802.16/WiMAX Broadband Access”Simon Fraser University Vancouver, British Columbia.

[20]“RaspberryPi camera module”at http://www.geeetech.com/wiki/index.php/Raspberry Pi camera Module.

Proceedings of the Fourth International Conference on Communication and Electronics Systems (ICCES 2019)
IEEE Conference Record # 45898; IEEE Xplore ISBN: 978-1-7281-1261-9

Centralized System For Emergency Vehicle Passing With Authentication

L.Megalan Leo
Dept. of ETCE
Sathyabama Institute of Science and Technology
Chennai,Tamilnadu, India
megalanleo@gmail.com

Karthik Tummala
Dept. of ETCE
Sathyabama Institute of Science and Technology
Chennai,Tamilnadu, India
karthiktummala30@gmail.com

R.Pradeep Kumar Raju
Dept. of ETCE
Sathyabama Institute of Science and Technology
Chennai,Tamilnadu, India
pradeepraju33@gmail.com

Abstract- In recent times the growth of population has been increased very much, when compared to last 10 years. so there is a need to implement an effective traffic system to avoid congestion. In the present traffic situation the emergency vehicle is getting blocked in middle of traffic and not able to reach the destination in correct time. In this paper we suggested a centralized system for emergency vehicle passing with authentication where the driver he himself can control the traffic and can pass through from that signal with the use of authorized control system and the authorized control system will control all the traffic signals and only certified people can access the control system.

Keywords- Traffic Light, NRF, GSM, IOT, Emergency Vehicles, RTC.

I. INTRODUCTION

Transportation system is the prime service to provide peaceful life to the people. It is used to achieve the target of different audiences [7][8]. Main problem in the transportation system is the traffic congestion [1]. Traffic congestion is the problem which arises due to more number of vehicles than the road facility. Providing service without congestion demands huge investment. This problem is common among the different countries. Accident is occurred around the world due to poor management of traffic system [5]. Traffic congestion can be controlled by monitoring the traffic and makes a wise decision based on the situation[4]. But it is the toughest work to achieve. Mainly, in emergency condition, the ambulance and government vehicles should reach the desired location within the minimum time. So that human life can be saved as quickly. It involves data interpretation, authentication and also manpower. The above requirement can be satisfied with the help of recent technology. Data interpretation is the difficult task because it changes time to time and day to day. Sensors are placed in the vehicles. System can able to interpret the information about vehicles by reading sensor output[10]. Interpreted information can be analyzed with the help of suitable software tools, system can able to adjust the signal traffic time. Thus avoids long waiting of vehicles in queue [9]. Current system is failed to achieve the proposed outcome. It introduces delay and also it may be a reason for the loss of lives [2]. Recent survey says that death rate increases with poor traffic management system[6]. Researchers are proposing different ideas for solving the issues. One of the methods is the use of adaptive system based on various conditions. It uses internet of things and embedded technologies [8]. Other technology is in use was implemented the first based on RFID networking. Its main goals are minimizing travel time, improving safety and public transport service. Such improvements are beneficial to health and the environment, Traffic control system by using RFID technique. Compose of different RFID tags and other hardware peripheral components. Tags control the condition of real time. It can change the set times automatically. Sensors are used in the driver circuit to know the traffic jams [9]. The output can be demonstrated by LEDs. These are old techniques and also some of the technique are presently in use in different countries [4] [7] [9] and goal is to counteract the traffic control management system. This paper has three sections. Section II has the detail about the proposed system; Section III explains the result and its detail output. Conclusion and Future work is given in section IV. They are Control section, Traffic section, and Ambulance unit.

II. PROPOSED SYSTEM

Proposed consists of three sections. They are Control section, Traffic section, and Ambulance unit. In our work when the ambulance wants to go in a traffic area that ambulance driver should send a message to the control unit in which signal traffic he wants to clear. Message is sent through the GSM board. Then the control unit receives the message

using a GSM board. It sends the control message to the concerned traffic unit to change into green light using NRF. Power supply unit is available to provide the supply to the entire control unit. Arduino Uno board is used as central processor to control the various operations.LCD display is displaying the movement of the particular vehicle through GPS installed in the ambulance unit. IoT module is used for sharing the details globally. In traffic section receive this data using NRF. In this section it stops the normal loop of the traffic signal and the signal is switch on the green light. Using LCD and traffic signal it shows that the emergency vehicle is passing so that the people who are passing through that signal can understand the problem. Here using RTC it calculates the time duration. After some duration the traffic signal changed into normal loop. Then the next signal moved into green. This process will happen up to the destination of the ambulance. Finally, the ambulance sends the successfully reached message to the control unit. Here we are using an authorized control unit which will control all the traffic signals and only certified people can access the control system. And all the details will be updated in the web server for analysis purpose. LCD is used to display that emergency vehicle is passing. In this, we are using GSM where we can establish a wide range of network of more than a kilometer range.

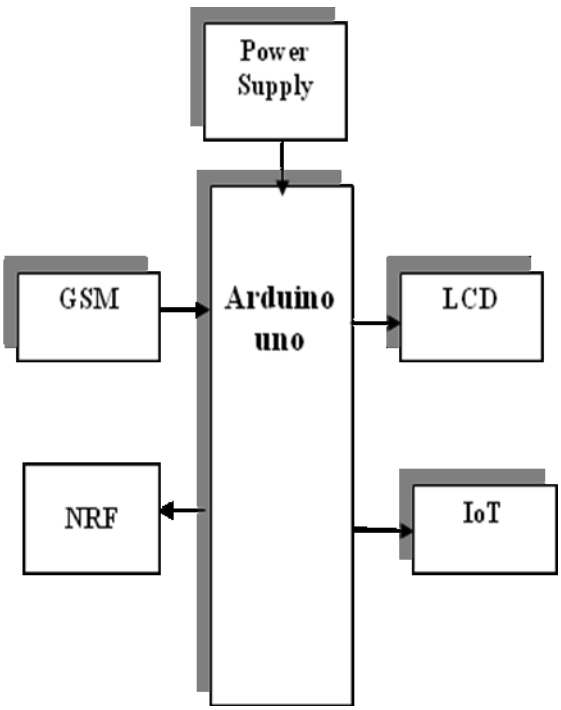

Figure 1. Control Unit

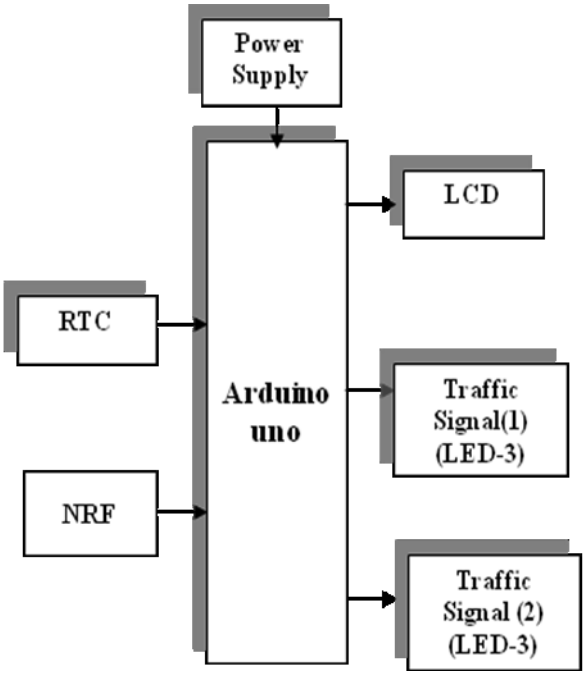

Figure 2. Traffic Unit

Figure 3. Ambulance Unit

In this project, we are using the following components like Arduino UNO, GSM modem, LCD, IOT, NRF, RTC, and LED. Here Arduino is an open-source microcontroller board based on ATmega328p and it has 14 digital input/output pins, 6 analog inputs, a USB connection, power jack, header and reset button. GSM is a wireless modem that works under GSM wireless network and it behaves like a dial-up modem that receives and sends data through radio waves. LCD is a liquid crystal display screen, it is an electronic display module with a wide range of applications. It has a 16*2 LCD display which is used in various devices and circuits. LCD has no limitations and it is

economical and easy to program. NRF is a highly integrated and ultra-low-power RF transceiver IC. It has advanced power management with a 1.9 to 3.6v supply range. The NRF24L01 has UPL solution which gives months to years of battery life to coin cell. The internet of things is a physical device network used in vehicles, buildings, electronics which uses the embedded system and it is the network connectivity that which enable these objects to collect and exchange the data. IOT sense the object and controls remotely across the existing network infrastructure. RTC is a real-time clock, it is low power and full binary coded decimal clock. The address and data are transferred serially. It is a timekeeping operation that works under time. LED is a light emitting diode(LED) is a semiconductor device that emits visible light when an electric current pass through it. LED's will have different colors in our project we are using 3 different colors like red, green and orange. At first, the Arduino board will take the coding and runs the circuit as per the code is given, then the message which was received in GSM modem will be sent to the LCD. There authenticates and verifies whether the message is sent by the certified user and the entry of the message will be stored in the IOT. From the control unit to traffic unit message will be sent through NRF. From there the traffic unit will change the red signal into the green signal by using RTC. After some time it will change to red and this process repeats whenever an emergency vehicle passes and all the data will be uploaded in IOT cloud.

III. RESULT AND DISCUSSION

Information will be received to centralized unit whenever accident happens. Centralized unit identify the nearest ambulance unit closer to the accident spot. Ambulance driver sends an acknowledgement signal to the centralized server once it ready. Movement of the ambulance vehicle can be monitored in the centralized section through GPS placed in the ambulance unit. After reaching the spot, ambulance unit sends an request message to centralized server to clear the traffic. Centralized unit verify the number and if it is authenticated then control message send to traffic unit. At first, the Arduino board will take the coding and runs the circuit as per the code is given, if a message is received in control unit by any emergency vehicle it will check whether the number is matching or not with the numbers given in the coding. If the number is matching then GSM modem will send message to LCD. There it will display that message received and number is matching message on LCD and the entry of the message will be stored in the IOT cloud. All this message will be stored for the authentication purpose and also to check that control unit is working according to the code given. From the control unit to traffic unit the message will be sent through NRF. Where NRF is a transceiver IC which can be used as short range signal transmitter and it acts as a communication device in between control unit and traffic unit . All the process and arrangement of components has shown in Figure 5.

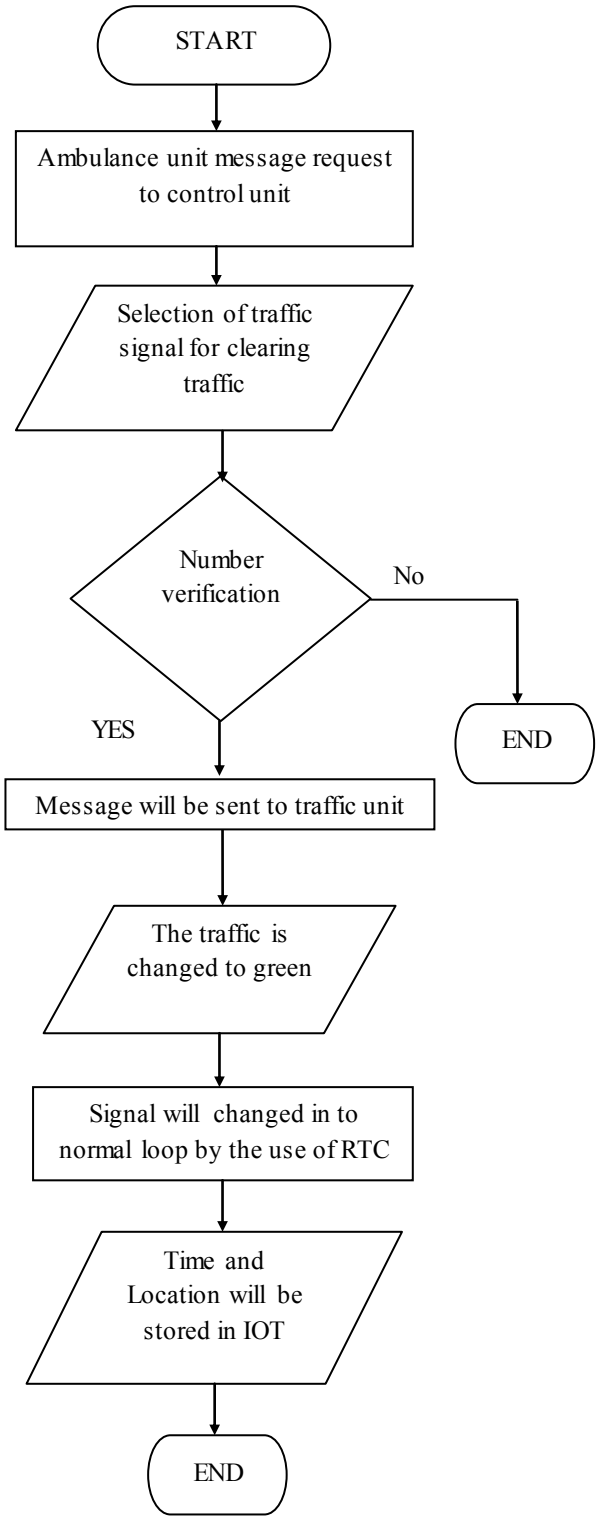

Figure 4. Flow Chart

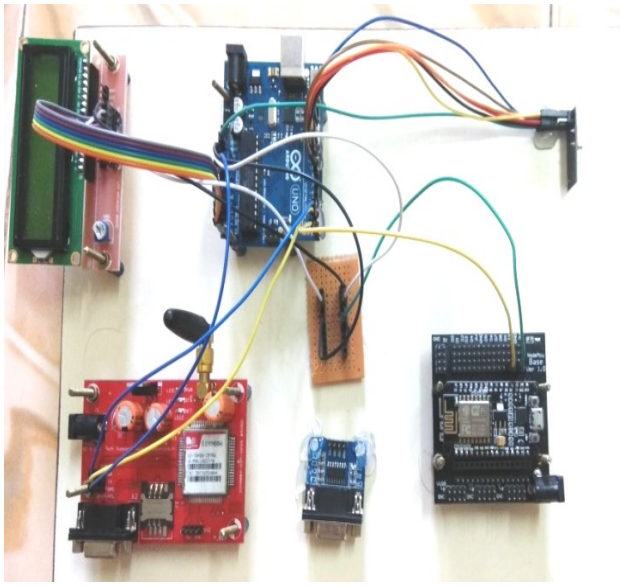

Figure 5. Control Unit

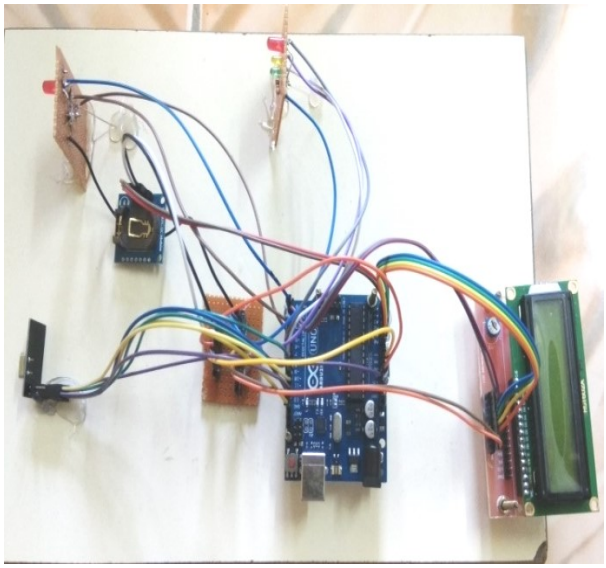

Figure 6. Traffic Unit

After receiving a message from the control unit the message will be sent to Arduino, as from there it will be transmitted to LCD there it will display the emergency vehicle is passing and the LED will change its color from red to green so that the driver can get a clear way to pass through from the traffic jam. Here we are using RTC, which acts as a clock. From the RTC after a period of time, it will change to red and this process repeats whenever an emergency vehicle passes and all the data will be uploaded in IOT cloud. It is the next unit, after receiving message from control unit as shown in Figure 6.

IOT web server will have all the access details of all the emergency vehicles which have been passed through the signal. Along with the time and the area of the traffic signal will be updated in the IOT cloud. It is shown in Table 1. And we can check all the details through this web-link:

http://www.iotclouddata.tech/506/

TABLE I. IOT MONITORING DATABASE

LogID	DATA	DATE_TIME
1	Sholinganallur_-_Karapakkam	20/1/2019_13:46:7
2	Sholinganallur_-_Karapakkam	20/1/2019_13:50:57
3	Sathyabama-Sholinganallur_request	20/1/2019_13:51:49
4	Sholinganallur_-_Karapakkam	20/1/2019_13:53:0
5	Sholinganallur_-_Karapakkam	20/1/2019_13:53:37
6	Sathyabama-Sholinganallur_request	20/1/2019_14:56:41
7	Success_mesage_receivedSuuccess_mesage_r	20/1/2019_14:58:18
8	Suuccess_mesage_receivedSuccess_mesage_r	20/1/2019_14:58:53

IV. CONCLUSION

We have designed a centralized system for the emergency vehicle passing with authentication where the driver he himself can control the traffic and can pass through from that signal with the use of authorized control system and it will control all the traffic signals and only certified people can access the control system. Request is given by a person who is in the location to the central station. Station assigns the jobs to the emergency vehicle based on their position to the spot. Emergency vehicle driver communicated to central office and central office send the control signals to the traffic signals which are available on the way. Centralized system can able to track the movement of vehicle. Based on the traffic it generates control signals and reduces the time delay .Thus the proposed system

can able to control the traffic effectively as well as saves people lives. In future the above system can expand by adding the identity number with the vehicle. Vehicle should have the capability to send information by own whenever accident happens. So that centralized system can able to receive the request about accident spot without receiving request from human.

V. ACKNOWLEDGMENT

The authors wish to thank ETCE department staff members of Sathyabama Institute of Science and technology, Chennai, India for their constant encouragement and motivation.

REFERENCES

[1]. S. Nagmode and S. M. Rajbhoj, "An IoT Platform for Vehicle Traffic Monitoring System and Controlling System Based on Priority," 2017 International Conference on Computing, Communication, Control and Automation (ICCUBEA), Pune, 2017, pp. 1-5.doi: 10.1109/ICCUBEA.2017.8463825

[2]. S. Ankitha, K. B. Nayana, S. R. Shravya and L. Jain, "Smart city initiative: Traffic and waste management," 2017 2nd IEEE International Conference on Recent Trends in Electronics, Information & Communication Technology, Bangalore, 2017, pp. 1227-1231.doi:10.1109/RTEICT.2017. 8256794.

[3]. A. A. Krishna, B. A. Kartha and V. S. Nair, "Dynamic traffic light system for unhindered passing of high priority vehicles: Wireless implementation of dynamic traffic light systems using modular hardware," 2017 IEEE Global Humanitarian Technology Conference (GHTC), San Jose, CA, 2017, pp. 1-5.doi: 10.1109/GHTC.2017.8239237.

[4]. Bi, Luzheng & Wang, Huikang & Teng, Teng & Guan, Cuntai. (2018). A Novel Method of Emergency Situation Detection for a Brain-Controlled Vehicle by Combining EEG Signals With Surrounding Information. IEEE Transactions on Neural Systems and Rehabilitation Engineering. PP. 1-1. 10.1109/TNSRE.2018.2868486.

[5]. L. Qi, M. Zhou and W. Luan, "A Two-level Traffic Light Control Strategy for Preventing Incident-Based Urban Traffic Congestion," in IEEE Transactions on Intelligent Transportation Systems, vol. 19, no. 1, pp. 13-24, Jan. 2018.doi: 10.1109/TITS.2016. 2625324.

[6]. S. Reeja and V. S. Jayaraj, "An embedded system for trafile rule violation and vehicle crash analysis using blaek box," 2017 International Conference on Innovations in Information, Embedded and Communication Systems (ICIIECS), Coimbatore, 2017, pp. 1-4.doi: 10.1109/ICIIECS.2017.8276143

[7]. C. Wright and P. Roberg, "The conceptual structure of traffic jams,"*Transp. Policy*, vol. 5,no.1,pp.23–5,1998,doi:org/10.1016/S0967- 70X(98)00006 -7.

[8]. H. Al-Deek, T. W. P. Lochrane, C. V. Srinivasa Ravi Chandra and A. Khattak, "Diversion during unexpected congestion on tollroads: the role of traffic information displayed on dynamic message signs," in IET Intelligent Transport Systems, vol. 6, no. 2, pp. 97-106, June 2012.doi: 10.1049/iet-its.2010.0163

[9]. P. Zhang, C.-X. Wu, and S. C. Wong, "A semi-discrete model and its approach to a solution for a wide moving jam in traffic flow," Phys. A,Statist. Mech. Appl., vol. 391, no. 3, pp. 456–463, 2012. Doi:10.1016/j.physa.2011.08.035.

[10]. V. Milanes, J. Godoy, J. Villagra and J. Perez, "Automated On-Ramp Merging System for Congested Traffic Situations," in IEEE Transactions on Intelligent Transportation Systems, vol. 12, no. 2, pp. 500-508, June 2011.doi: 10.1109/TITS.2010. 2096812

Proceedings of the Fourth International Conference on Communication and Electronics Systems (ICCES 2019)
IEEE Conference Record # 45898; IEEE Xplore ISBN: 978-1-7281-1261-9

IOT BASED PEST CONTROLLING SYSTEM FOR SMART AGRICULTURE

P.Uva Darshni,Student
Department of Computer Science and Technology
Kumaraguru College of Technology
Coimbatore,Tamilnaduuvadarshni.16cs@kct.ac.in

P.Uva Dharini,Student
Department of Computer Science and Technology
Kumaraguru College of Technology
Coimbatore,Tamilnadu
uva.16cs@kct.ac.in

S.Monisha,Student
Department of Computer Science and Technology
Kumaraguru College of Technology
Coimbatore,Tamilnadumonisha.16cs@kct.ac.in

K.Saranya, Assistant Professor
Department of Computer Science and Technology
Kumaraguru College of Technology
Coimbatore,Tamilnadu
saranya.k.cse@kct.ac.in

Abstract-In India, the agricultural economic loss is mainly due to insects and pests. Therefore, pesticides are widely used by farmers to control weeds, insects and plant diseases. Excess usage of pesticides is not only an adverse for the environment but also for human and economy of the nation. In this paper, we proposed a pest control system that makes use of IOT (Internet of Things) and image processing technologies to control pests, thereby reducing the use of pesticides. The proposed system uses infrared sensor (PIR) to detect the presence of insect by the heat radiated by their body. Image processing is used to capture images of the pest to confirm their presence in the field. After confirming the presence of insect by Image processing and PIR sensor, the ultrasonic generator is used to generate ultrasonic waves which are intolerable to insects and pests, drive them away from the agricultural field. The proposed system helps the farmers to improve the agricultural production and management in an eco friendly way.

I.INTRODUCTION

Pesticides are a major problem for Indian farmers compared to pests. There is always a bit of poison in the food we consume. Pesticides are agents used to destroy pests, which are detrimental to humans or human concerns like agriculture. Almost 30,000crores worthy of crops are destroyed by pests and insects in India every year, which make farmers to use pesticides. Experts believe that chronic low level pesticide exposure is associated with a broad range of nervous system symptoms such as headache, tension, dizziness, depression, anger.Agriculture scientists worldwide are working on biological alternatives to chemical pesticides with increasing consumer pressure on both farmers and supermarkets to minimise the use of chemical pesticides.

With the growth of organic market, people are taking much more interest on what farmers use to control pests. Nowadays farmers are encouraged for practicing organic farming. Organic farming produce good quality food but production costs are very higher, needed more workers and they cannot produce enough food that the world population need to survive. Both the approaches have their pros and cons. As Prevention is better than cure, the better solution for this problem could be preventing usage of pesticides rather than treating for its side effects.

One of the major problem in agriculture that limits the yield of crops is pest diseases which caused by pests including rodents. Farmer in spite of competing with pests for years, the Crop loss caused by pests has been increasing which threaten all around the world. It has been estimated that 70% of crops could be lost due to pests. These pests are controlled by applying either physical measures such as trapping or chemical measures such as usage of pesticides. Although pesticides benefits the crops and is most effective, it makes the crops toxic. In this paper, we provide an innovative solution to control pests by repelling it from the field instead of using pesticides. This is done by generating ultrasonic waves using ultrasonic sound generator.

The term ultrasonic or ultrasound refers to the sound with frequencies above 20,000 Hz or audible sound. The Ultrasonic sound generator uses various methods including piezoelectric method, magneto striction method to produce sound waves above 20,000 Hz. The demand for more food is increasing. Smart agriculture through use of IOT technologies will help the farmers to reduce generated wastes and enhance productivity. IOT helps the farmers to capture real time data regarding crops using sensors and to analyze the status of crop to make decisions earlier which increases the quality of production. It enables better monitoring of crops and avoids crop losses due to diseases or adverse weather.

In this paper, we proposed a pest controlling system which confirms the presence of pests in the field through PIR sensor and image processing technique and generates

ultrasound which is intolerable to rodents and insects. By doing this, we can prevent the pests feeding on the plants which results in the increase of crop's health and production thus increasing the economic level of farmers.In section II, the literature survey is discussed, in section III, the pest controlling system based on IOT is proposed and the implementation is described, in section IV, we conclude the whole work.

II. RELATED WORK

Dileep Kumar Tiwari, etal, [1] have proposed an electronic pest repellent that is capable of producing ultrasonic sound waves to repel rodents, insects and pests. The proposed system mainly aims to prevent pest in an eco-friendly and environment–friendly way. The proposed device can be used in both small and large scale. The system is alternative to chemical pesticides and repeller which have an adverse effect on human health.

Ibrahim, etal, [2] have discussed on the use of electronic pest control device, other measures, advantages and drawbacks of the device. Electronic pest control is an electronic device used for repelling pests. The advantage of this device is that, they are cheap, eco-friendly and not harmful to human beings. This device differs from other devices by targeting the hearing range of pest and work based on it. Thus this device is more efficient.

J.Mahalakshmi, etal,[3] has proposed an image processing algorithm for crop inspection and pest control. This work mainly focus on recognization of paddy plant diseases. Using this technique various paddy diseases are identified .

Johnny L. Miranda, etal, [4] has proposed a system that makes use of image processing techniques to detect pest in rice fields. Using the system the farmers can make monitoring process easier. The proposed system is simple and efficient and fully automated The experiment results shown by the prototype is reliable. As future work, neural network can be used to improve performance of the proposed system.

KanishkSisodiya and MandeepSingh ,[5] have designed a ultrasonic insect detector system that uses ultrasonic sensor and infrared sensor to detect the presence of insect and pest in the field. The system also makes use of GSM module to inform the farmers about the presence of pest in the field. This system is designed especially for oilseed crop. This prototype helps the farmers to increase agricultural management and production. In the future, some of the other sensors can be interfaced with the prototype system for more accurate results and image processing can also be used to take real time images of the pest.

KhapareNilima Kailas, etal ,[6] have proposed a system that uses electronic devices such as ultrasonic sound wave to repel the pest from the agricultural land. The drawbacks of chemical method, the use of bio-pesticides are also discussed in this paper. The main aim of the system is to control pest in an eco-friendly way.

Murali Krishnan, etal, [7]have proposed an image processing based, automatic pest control algorithm. This proposed algorithm aims to prevent coffee berry from insect and diseases. Rapid detection of insects can be achieved through this system.

Navin, etal, [8] have proposed a pest control system using wireless sensor network that uses acoustic device wireless sensor to detect the noise level of the pest and indicate farmers about the presence of pest through alarm. The proposed system is very low energy consuming and can cover maximum field area. The main focus of the system is to control and monitor pest for sugarcanes using wireless sensor network technology.

Nicholas Aflitto and Tom DeGomez ,[9] have discussed on sonic pest repellents which are devices that emit sound to repel insects, pests and rodents from the agricultural land. They briefly discussed on their working, advantages and drawbacks. The allure of sound for prevention of insects will be a successful approach in the future and will be safer for humans.

RichardW.Mankin, etal, [10] have discussed the structure of acoustic system for insect detection in plant stems, by attaching an accelerometer to the plant stem. The accelerometer system is used for detecting movement of insects.

Saeed Azfar, etal, [11] have discussed on a wireless sensor network for pest control and agricultural monitoring. Various pest control methods have been discussed in this paper. Agricultural areas will be using WSN technology in the future for beneficiary output. The designed system can be improved in the future to check the pest at early stage and convey the information to the farmers, thus reducing the manual burden of monitoring the field.

Simeon, etal, [12] have discussed on the performance of an electronic pest repeller. The main aim of the prototype is to emit ultrasonic energy of varied frequency. The experimental results show that the proposed system has the potential to repel rodents. The performance of the device is also more reliable. The prototype can be improved by using microcontroller and ultrasonic sensor. The proposed system is an alternative to chemical methods to repel pest.

III. PROPOSED SYSTEM AND RESULT

In India, the crops that require high usage of pesticides are paddy (17%), wheat (10%) and cotton (45%). So our proposed system mainly focuses on these crops. There are numerous pests such as beetles, bugs, moth and rodents including rats, squirrels, mouse, rabbits that feed on crops which causes a massive destruction to the yield of crops. In our proposal, these pests in the field are repelled by generating ultrasound instead of using pesticides. The proposed system comprises of

1. Passive Infrared(PIR) sensor
2. Image processing

3. Acoustic sensor
4. Microcontroller
5. Ultrasonic generator.

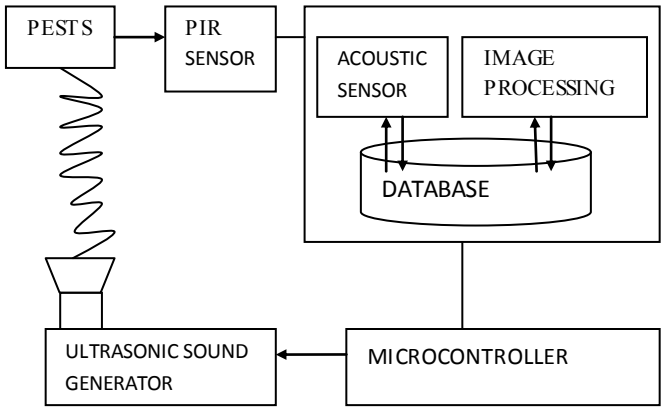

Figure1.The proposed system

1.Passive Infrared(PIR) sensor:

PIR sensor is used to detect the motion of pests around particular environment. All objects with temperature above absolute zero emit heat energy in the form of radiation. PIR sensor detects the motion by measuring the changes in the infrared levels emitted by the object, such as pests in the environment.PIR sensor covers a distance of up to 20 feet (6 m). They are small, inexpensive and easy to use.

2.Image processing:

Image processing is used to extract some useful information from images captured by performing some operations on it. It isused to detect the presence of pests in field by capturing images of pests and comparing it with stored images. The image processing includes the following steps:

- Capturing image and send it to the microcontroller.
- Processing the image to detect the object in microcontroller.

Image processing is classified into two types, analog and digital image processing. It enables to acquire a visual record of moving object.

3. Acoustic sensor:

Acoustic wave sensor is used to detect the noise level of the pests in the field. It also detects the invasion of pests on crops in early stage. Acoustic sensor detects sound by using microphone.

4. Microcontroller:

Microcontroller is an integrated circuit consisting of processor, memory and input/output peripherals to control actuators. It is used to process the data collected by the sensors and control the ultrasound generator to generate ultrasound of high frequency.

5. Ultrasonic Generator:

Ultrasonic sound refers to the sound with frequency greater than the 20,000 Hz or audible sound. Ultrasonic can be produced by different methods which includes mechanical method, piezoelectric method, magnetostriction method. In piezoelectric method, the ultrasonic waves are generated by a transducer which converts electric current to sound waves. In magnetostriction, iron or nickel is magnetised to produce ultrasound.

6. Working:

The proposed system shown in Figure1 produces a discomfort but not harmful, high frequency sound waves which is not audible to human beings. Every pest has sensory structures to produce and detect ultrasound. For example, cockroaches have sensory hairs, spiders, beetles, flies have tympanic membrane to sense ultrasound. The ultrasound sensors are present in the antennae or genetalia of the pests. Bats and rodents communicate through ultrasonic frequency. The ultrasonic sound being generated by the system will create a stress on the nervous system of the pests and jam their own ultrasound frequency. As a result, the pests get confused, scared and try to escape from the source of ultrasonic sound. Every pest has its own bearable decibel. Rodents respond to ultrasound with a frequency 60K Hz while fleas, mosquitoes, beetles respond to ultrasound with frequency 38-44K Hz.

In our proposed system, the presence of the pests is detected using PIR motion sensors which are deployed in the fields. The PIR sensor detects the pests by monitoring the changes in the amount of infrared radiation (heat) emitted by the pests. Heat is radiated from any object with temperature above absolute zero. The PIR sensor can cover a distance of 20 feet(6 m). Once the presence of pest is detected, the images of the pests are captured through the cameras in the field and then compared with the images of the pests in the database. An efficient image processing algorithm is used for the identification of the pests. The main aim of the image processing is to observe the pests that are not visible to human eyes. For more accuracy, in parallel, the sounds waves emanating by the pests during feeding, laying eggs are collected with the help of acoustic sensor and is analysed with the sounds in the database with which it is ensured that the eco-friendly pests will not get affected. This is done by using microphones which detects the sound signals and converts them into electrical signals. The outcome from both the process is combined to identify the pest type and their unbearable sound level is given as an input to the microcontroller. All these actions are done in microseconds.

Finally, the microcontroller automates the ultrasonic sound generator which is adjustable to produce powerful ultrasonic waves of different frequency. The output is coupled to the tweeter which repels away the pest in the

field. The Ultrasonic waves ranges up to 15 feet. The ultrasonic waves above 20K Hz is inaudible to humans and it also stimulates the plant growth. Therefore entire system will not cause any problem to the human beings as well as eco-friendly pests and crops. The beneficiary of the system is that it is automated so that there is no human intervention thus reducing labour and man power.

The purpose of the project is to design an ultrasonic pest repellent. Such a device can be very useful to counter the various problems caused by ants, insects, pests, rodents to the crops. This system is proposed aiming the target beneficial for farmers, consumers, crops and land. The farmers are benefited as it increases the possibility to have enhanced healthy plants and reduce the cost of input spent on buying fertilizers and pesticides. This promotes sound structure and healthy poison free plants for human consumption. The system aiming to reduce the environmental risks associated with pest management by encouraging the adoption of ecological practice.

The main goal of the proposal is to reduce the potential of air and ground water contamination and increase the yield. This can do a great positive effect on environment through decreasing the use of pesticide. The long term goal is helping the farmers to reduce the labours involved in pest management programs and also to eliminate pest residue issues. The qualitative outcome of this idea in is expected to encourage farmers as cultivators adopt and encourage non toxic pesticides farming. The inculcation of IOT in pest management supports for device to device communication without human intervention and reduce manpower and labour.

The proposed system has been tested within the bounds of pastureland and the outcomes are analysed. The presumed results are acquired with an accuracy of 87%.

IV.CONCLUSION AND FUTURE WORK

Agriculture is considered to be a backbone of India. Therefore, the development of villages mainly depends on the increase agricultural production and food security. The main objective of the system is, to aware the farmers about the pests and condition of the agricultural field. In the proposed system, for more accuracy image processing technology has been used and acoustic, PIR sensors are interfaced. The proposed system is a best alternative to chemical pesticides and can able to reduce the manual labour of monitoring the agricultural field. Therefore this proposal would help the farmers to increase their crop production by automated pest management at low costs and ensures a healthy food. Our proposed system mainly focuses on three crops (paddy, wheat and cotton). Hence our focus in future is to extend the implementation of system, which will be admissible to diversity of crops with varying heights and pest attacks. Our future goal is to provide the farmers an efficient pest control system with affordable cost to get rid of pests and thus increase their crop productivity.

V. REFERENCES

[1]Dileep Kumar, Tiwari MamtazAlam (March 2016), ‘Electronic Pest Repellent: A Review’ 2016, International Conference on Innovations in information Embedded and Communication Systems (ICIIECS’16).

[2]Ibrahim, A.G., Oyedum, O.D., Awojoyogbe, O.B., Okeke, ‘Electronic Pest Control Devices: A Review of their Necessity, Controversies and a submission of Design Considerations’, The International Journal Of Engineering And Science (IJES),Volume 2,Issue 9 (2013).

[3]J.Mahalakshmi1, G.Shanthakumari (March 2017), ‘Automated Crop Inspection and Pest Control Using Image Processing’ International Journal of Engineering Research and Development e-ISSN: 2278-067X, p-ISSN: 2278-800X, www.ijerd.com Volume 13, Issue 3, PP.25-35.

[4]Johnny L. Miranda, Bobby D. Gerardo, and Bartolome T. Tanguilig (May 2014), ‘Pest Detection and Extraction Using Image Processing Techniques’,International Journal of Computer and Communication Engineering, Vol. 3, No.3.

[5]KanishkSisodiya, Mandeep Singh (Oct - Dec 2016),’Design and Development of Ultrasonic and IR Insect Detector for Oilseeds Crop’,IJECT Vol. 7, Issue 4,ISSN : 2230-7109 (Online).

[6] KhapareNilima Kaila, BodkePranali S, Khapare Kailas Namdev (March-April, 2015),’ Development performance and evaluation of ultrasonic pest and insect repelling system’,International Journal of Engineering Research and General Science Volume 3, Issue 2, Part 2,ISSN 2091-2730.

[7]Murali Krishnan, Jabert.G (May.- Jun. 2013),’Pest Control in Agricultural Plantations Using Image Processing’,IOSR Journal of Electronics and Communication Engineering (IOSR-JECE) e-ISSN: 2278-2834,p- ISSN: 2278-8735. Volume 6, Issue 4, PP 68-74 www.iosrjournals.org.

[8] NavinSrivastava ,Gautam Chopra , Prateek Jain &BhavyaKhatter ,’Pest Monitor And Control System Using Wireless Sensor Network (With Special Reference To Acoustic Device Wireless Sensor)’,International Conference on Electrical and Electronics Engineering 27 Jan 2013, Goa, ISBN: 978-93-82208-58-7.

[9]Nicholas Aflitto and Tom DeGomez (2014),’Sonic Pest Repellents’, The University of Arizona College of Agriculture and Life Sciences Tucson, Arizona 85721.

[10] Richard W. Mankin, David K. Weaver, Matthew Grieshop, Barbra Larson, and Wendell L. Morrill (October 2004) ,‘Acoustic System for Insect Detection in Plant Stems: Comparisons of Cephuscinctus in Wheat and Metamasius 1,2 callizona in Bromeliads’ Center for Medical, Agricultural, and Veterinary Entomology, P.O. Box 14565, Gainesville, Florida 32604.

[11]Saeed Azfar, Adnan Nadeem, Abdul Basit S, ‘Pest detection and control techniques using wireless sensor network: A review’, Journal of Entomology and Zoology Studies 2015; 3 (2): 92-99.

[12]Simeon M. I, Mohammed A.S, Adebayo S. E (Jan -2013),’Development and preliminary testing of an electronic pest repeller with automatic frequency variation’,International Journal of Engineering Science Invention ISSN (Online): 2319 – 6734, ISSN (Print): 2319 – 6726 www.ijesi.org Volume 2 Issue 1, PP.14-20.

Proceedings of the Fourth International Conference on Communication and Electronics Systems (ICCES 2019)
IEEE Conference Record # 45898; IEEE Xplore ISBN: 978-1-7281-1261-9

Performance comparison of adaptive filters used for Acoustic Echo cancellation application under double talk scenario

S Radhika
Department of EEE
School of Electrical and Electronics Engineering
Sathyabama Institute of Science and Technology
Chennai. India
radhikachandru79@gmail.com

A Chandrasekar
Department of CSE
St.Joseph's College of Engineering
Chennai.India.
drchandrucse@gmail.com

***Abstract*—This paper compares the performance of Affine projection sign algorithm and Maximum Correntropy criteria based adaptive algorithm used for double talk scenario. The performance metric involves the speed of convergence, mean square error under steady state and complexity. Simulations were also performed to identify the best performing algorithm under different environmental conditions for double talk scenario. Finally it is concluded that Maximum Correntropy criteria based adaptive algorithm outperform the family of Affine projection sign algorithm under both sparse and non-sparse conditions.**

Keywords— Affine projection sign algorithm; Maximum Correntropy criteria ;convergence;mean square error;complexity.

I. INTRODUCTION

In all telecommunication systems, whether it is wireless or wired, the predominant problem is the presence of noise, which includes thermal noise, co-channel interference, echo signal etc. An echo signal is said to have delay and attenuation compared to the original signal with several reflections. It usually occurs in a room, mountain, under the sea or inside a cave. From [1], it is found that the effect of these echo signals is not considered when their delay is very small or the magnitude is below the threshold value. An acoustic echo is a type of echo signal that is generated whenever loudspeaker and the microphone are placed in a closed room such as teleconferencing system. These echoes are generated due to the reflections of acoustic signal between loudspeaker and microphone as well as from the walls, or through other objects present within the room etc.,

Under this condition, there is acoustic coupling between loudspeaker and microphone which is made up of direct path and echo paths which is not desirable. Hence echo cancellers are required to improve the quality of speech in telecommunication system. Therefore an adaptive filter that is capable of adjusting the filter coefficients according to the change of signal properties is required for Acoustic Echo Cancellation (AEC) application as the signal statistics are not known priory or it is time varying. The development of adaptive algorithms for AEC application is based the two scenarios that occur namely single talk and double talk. Under single talk scenario, the far end speech is assumed to be absent. If the far end signal is also present along with the near end signal, then the scenario is double talk. Hence the problem under consideration is an unknown system identification problem with impulsive noise along with background noise.

Traditionally Least Mean Square (LMS) adaptive filters and their variants have been used throughout because of its simple nature and easy implementation [2]. The main function of these algorithms is to estimate the echo in such a way that the Mean Square Error (MSE) is minimized. Since the echo path is said to be time varying and it requires a long length adaptive filter with hundreds of filter coefficients and a constant step-size parameter is used in the update recursion, there is performance trade-off and they perform poorly for speech signals. Affine Projection algorithm (APA) is better for echo cancellation application as it works faster convergence with lower steady state MSE especially for colored inputs, such as speech signal with the increase in computational complexity [3,4].Firstly variable step-size strategy have been developed. The next strategy is to exploit the sparse nature to improve the performance and hence sparsity aware adaptive filters have become very popular [5,6]. In the recent years, combinational approach has become very popular due its capability in obtaining better performance than the single filter approach but they are said to be more complex than the single filter approach [7].

Information theory criterion based adaptive filters and sign algorithms were the popular algorithms used for double talk scenario due to their robustness against impulse noise. Different variants were proposed under each category to improve the overall performance .Even though they serve the same purpose of robustness under impulsive noise, there is no previous study to the best of our knowledge that compares the performance of these two family of adaptive filters. Thus this paper focuses on the comparison of the family of APSA and MCC based adaptive filters. Convergence rate, MSE and complexity were used to identify the best performance algorithm suitable for double talk scenario.

The further sections are distributed as follows: Section 2 describes the problem formulation where the system under consideration is describes along with the notations. Section 3 and 4 are devoted to the review, description and comparison of the famous variants of APSA family and MCC family of adaptive filters respectively. The performance comparison among them is made in Section 5 in terms of speed, error and computational complexity and conclusions are drawn in Section 6.

II. PROBLEM FORMULATION

In order to formulate the problem, let us consider Fig 1 in which the Loudspeaker Enclosed Microphone (LEM) system is assumed to be an unknown, linear system with optimal filter weights w_o given by

$$\boldsymbol{w}_o = [w_o, w_1, w_2, \dots, w_{N-1}]^T \quad (1)$$

Let x(n) be the input to the system given by

$$\boldsymbol{x}(n) = [x(n), x(n-1), .., x(n-N+1)]^T \quad (2)$$

where n is discrete time and N is the input length and as well as weights. The desired response d(n),modeled as a linear regression model is as follows.

$$d(n) = w_o^T x(n) + v(n) + u(n) \quad (3)$$

where v(n) is the Gaussian background noise signal with variance σ_v^2 and u(n) be the interference signal which is the far end speech ($S_{Far\ end}$). Let w(n) be the estimated weights given by

$$\mathrm{w(n)} = [\mathrm{w(n)}, \mathrm{w(n-1)}, \dots., \mathrm{w(n-N+1)}]^{\mathrm{T}}. \quad (4)$$

The error signal $e(n)$ is given by

$$e(n) = d(n) - \boldsymbol{w}^T(n)\boldsymbol{x}(n) \quad (5)$$

Thus the aim is to update the filter coefficients such that error is minimized with increase in convergence speed with reduced complexity.

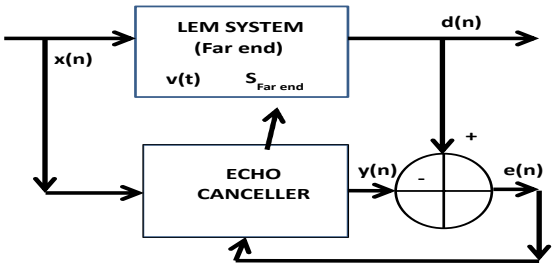

Fig 1. LEM system with echo canceller

III. .FAMILY OF AFFINE PROJECTION SIGN ALGORITHM

An Affine Projection Sign Algorithm is the combination of best feature of SA and APA [8] by providing robustness against impulse interference with lower computational complexity. The convergence and steady state MSE were considerably poor than APA. In [9], a general theoretical transient analysis of error non linearity adaptive filter using energy conservation relation is made. The validity of a priori error as Gaussian signal assumption is proved through simulations.

Two proportionate APSA was proposed by for AEC application [10]. Here proportionate type and APSA are combined to obtain Real Proportionate (RP-APSA) and Real Improved Proportionate APSA (RIP-APSA). Experiments were done to prove the performance improvement. Memory improved proportionate APSA in order to further improve the performance of proportionate APSA is proposed [11]. This is done by taking the past values of the input projection matrix. Thus improvement in steady state MSE is obtained at the cost of increase in memory requirement. A variable step size APSA is proposed to eliminate the performance tradeoff [12]. The ZA-APSA is proposed [13] by combining l_1 norm penalty and APSA. Improved performance is obtained under sparse environment. The update recursion of the general APSA [14] is

$$\boldsymbol{w}(n+1) = \boldsymbol{w}(n) - \frac{A(n)sgn(\boldsymbol{e}_p(n))}{\|A(n)sgn(\boldsymbol{e}_p(n))\|_2} \quad (6)$$

If l_1 norm is included, then ZA-APSA can be written as

$$\boldsymbol{w}(n+1) = \boldsymbol{w}(n) + \mu\frac{A(n)sgn(\boldsymbol{e}_p(n))}{\|A(n)sgn(\boldsymbol{e}_p(n))\|_2} - \rho sgn(\boldsymbol{w}(n+1)) \quad (7)$$

The update recursion of the proportionate family is given by

$$\boldsymbol{w}(n+1) = \boldsymbol{w}(n) + \mu\frac{A(n)sgn(\boldsymbol{e}_p(n))}{\|A(n)sgn(\boldsymbol{e}_p(n))\|_2} - proportionate\ term\ ) \quad (8)$$

Here μ is the step size. The strength of attraction of the zero coefficients is given by ρ called as the zero attractor controller which provides improved convergence when the system is sparse.

IV. INFORMATION THEORY CRITERION BASED ADAPTIVE FILTERS

The local similarity measure between two random variables based on the kernel width is called Correntropy [16]. If gradient descent approach along with Gaussian kernel for correntropy is used, the resulting algorithm is called MCC algorithm. Thus MCC has the advantages of robustness to outliers with appreciable performance for non-Gaussian data which is similar to MEE algorithm. Also the computational complexity involved in MCC is the same as that of the well-known LMS algorithm.

The steady state MSE of MCC algorithm and the tracking analysis has been made by [16,17] which indicates that MCC based algorithm is more suitable for non-Gaussian impulsive noises. Variable step size approach has been successfully used in LMS adaptive filters to remove the tradeoff. Therefore variable step size approach based on the instantaneous MSE for MCC adaptive filter is proposed [18]. The MCC adaptive filter with weights $W(n)$ and input $X(n)$ is defined as

$$W(n+1) = W(n) + \mu\, exp\left(\frac{-e^2(n)}{2\sigma^2}\right) e(n)X(n) \quad (9)$$

It should be noted that as kernel size tends to ∞ , the algorithm reduces to Stochastic Gradient LMS algorithm. A variable step size MCC algorithm update equation is given by

$$W(n+1) = W(n) + \mu(n) exp\left(\frac{-e^2(n)}{2\sigma^2}\right) e(n)X(n) \quad (10)$$

V. Performance Comparison

The different performance measures that are normally used by adaptive algorithm are discussed in this section.

A. Convergence Rate

One of the desirable characteristics of adaptive filter is faster convergence. It measures the rate at which the algorithm reaches to the final state. It is a dependent performance characteristic where, there is always a tradeoff in other performance criteria such as steady state MSE.

B. Mean Square Error

The Mean Square Error (MSE) is a second order statistical term that indicates the difference between ideal and actual values A small MSE is the desired one.

C. Computational Complexity

Computational complexity includes the number of arithmetic operations required to complete one full iteration of the algorithm, the amount of space required for data storage and the hardware requirement to implement the algorithm in real time applications. Therefore a less complex algorithm is the desirable feature because highly complex algorithm results in increase in cost, size, time , etc.

D. Robustness

Robustness is a measures the ability of the system to resist to noise . The robustness has a direct relationship with the estimated error. The disturbance can be either external or internal to the filter.

E. Misalignment

The Misalignment is another quantitative parameter measure which indicates the amount by which the final MSE differs from the minimum MSE produced by the Wiener filter.

VI. Results and Discussion

This section is devoted to the comparison of the recently proposed ZA-APSA along with recently proposed VSS-MCC algorithms with the list of algorithms designed for double talk scenario is made. The competing algorithms are APSA, RP-APSA, RIP-APSA,MIP-APSA, MCC and the traditional APA. The algorithms are evaluated through parameters namely a. MSE, b. Normalized Misalignment, c. Computational Complexity d. Convergence speed. In order to compare the two proposed algorithm for double talk scenario, a system with 512 unknown system coefficients are taken and two experiments were conducted. The first experiment consists of sparse system with sparseness level of 0.9375 and the second experiment is said to be dispersive with sparseness level of 0.0625.The experiments are conducted by considering the adaptive filter with the same length as the unknown system coefficient which is initialized as zero.

The first order system with pole at 0.8 is taken. The noise with variance σ_v^2 and zero mean is taken such that it has a particular signal to noise ratio (SNR). The interference signal u(n) is a Bernoulli-Gaussian (BG) signal with a particular signal to interference ratio (SIR). Here probability of success is represented as Pr. The results of simulations are obtained as follows: All the algorithms are made to run with 10,000 samples . An ensemble average is taken to obtain the figure of merit. The results in steady state are obtained by taking average of the last 2000 samples and averaged over 10 independent runs. All the algorithms are made to operate with a parameter selected in such a way that they has uniform convergence in the initial stage.

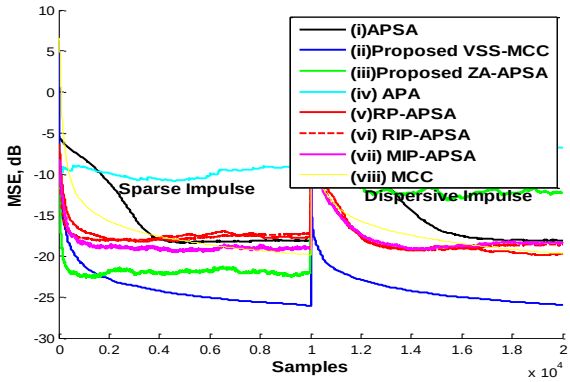

Fig 2.MSE analysis of the proposed algorithms with other algorithms at SNR=30dB, SIR=-10dB , pr=0.001 with colored input.

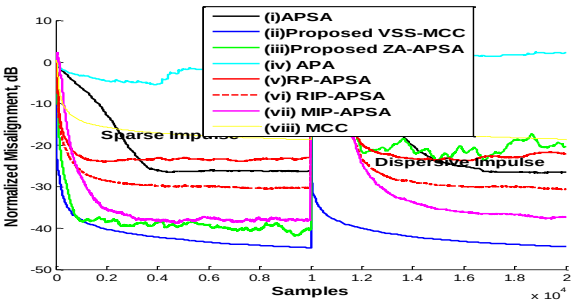

Fig 3. Normalized Misalignment analysis at SNR=30dB, SIR=-10dB , pr=0.001 with colored input

Table 1. Results of the proposed algorithms under steady state in double talk scenario at SNR=30db,SIR=-10dB,pr=0.001 with colored input.

	Experiment1		Experiment 2	
Algorithm	**MSE (dB)**	**Normalized misalignment (db)**	**MSE (db)**	**Normalized misalignment (db)**
APSA	-18.01	-26.26	-18.40	-26.65
RP-APSA	-17.43	-23.31	19.13	-22.63
RIP-APSA	-18.01	30.5	-19.29	-30.37
MIP-APSA	-19.41	-38	-19.51	-36.69
Proposed ZA-APSA	-21.67	-40.79	-12.33	-18.24
MCC	-18.12	-27.91	-18.32	-27.91
Proposed VSS-MCC	-25.17	-41.12	-25.67	--42.89

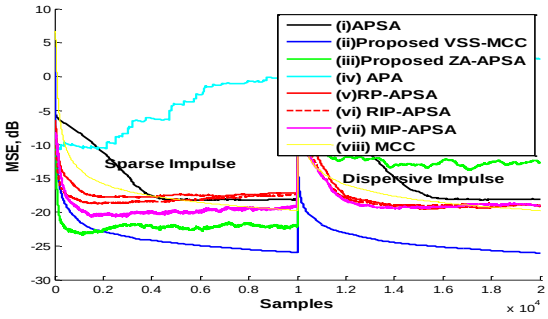

Fig 4.MSE analysis at SNR=30dB, SIR=-20dB , pr=0.001 with colored input.

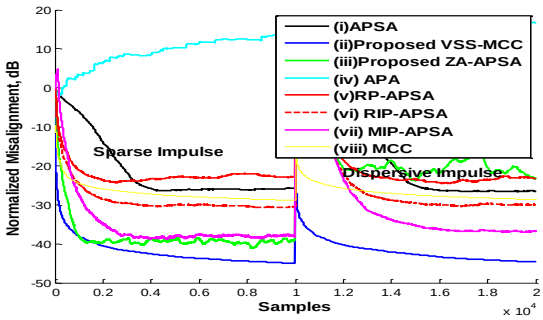

Fig 5.Normalized Misalignment analysis at SNR=30dB, SIR=-20dB , pr=0.001 with colored input.

Table 2. Results of the proposed algorithms under steady state in double talk scenario at SNR=30db,SIR=-20db,pr=0.001 with colored input.

	Experiment1		Experiment 2	
Algorithm	**MSE (db)**	**Normalized misalignment (db)**	**MSE (db)**	**Normalized misalignment (db)**
APSA	-18.00	-25.97	-18.09	-26.461
RP-APSA	-17.48	-23.01	-18.64	-22.91
RIP-APSA	-18.06	-30.12	-18.79	-29.83
MIP-APSA	-19.68	-37.68	-19.08	-36.65
Proposed ZA-APSA	-22.01	-38.24	-12.04	-21.23
MCC	-18.22	-27.8	-18.22	--27.68
Proposed VSS-MCC	-24.98	-42.86	-24.98	-42.70

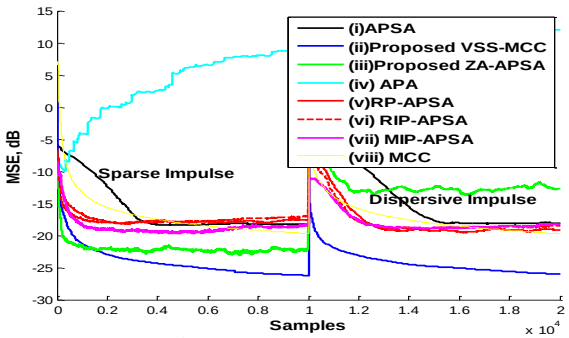

Fig 6.MSE analysis of the proposed algorithms with other algorithms at SNR=30dB, SIR=-30dB , pr=0.001 with colored input

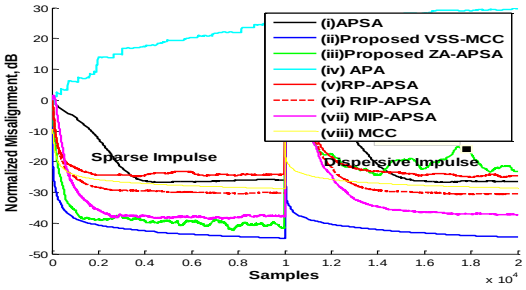

Fig 7.Normalized Misalignment analysis at SNR=30dB, SIR=-30dB , pr=0.001 with colored input

Table 3. Results of the proposed algorithms under steady state in double talk scenario at SNR=30db,SIR=-30db,pr=0.001 with colored input.

	Experiment1		Experiment 2	
Algorithm	**MSE (db)**	**Normalized misalignment (db)**	**MSE (db)**	**Normalized misalignment (db)**
APSA	-17.50	-26.52	-18.09	-26.36
RP-APSA	-18.02	-2383	-18.24	-24.85
RIP-APSA	-17.26	-29.69	-18.88	-30.46
MIP-APSA	-19.4	-37.82	-19.04	-36.56
Proposed ZA-APSA	-22.55	-38.40	-12.36	-22.1
MCC	-18.23	-27.42	-18.25	-27.5
Proposed VSS-MCC	-25.02	-42.59	-24.45	-42.89

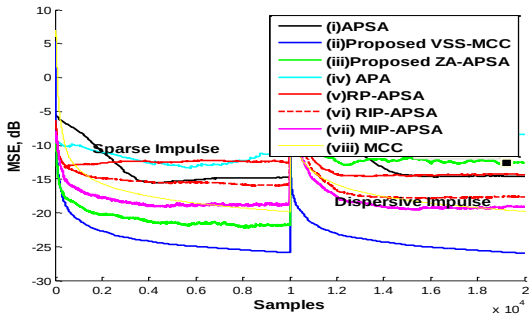

Fig 8.MSE analysis at SNR=20dB, SIR=-10dB , pr=0.001 with colored input.

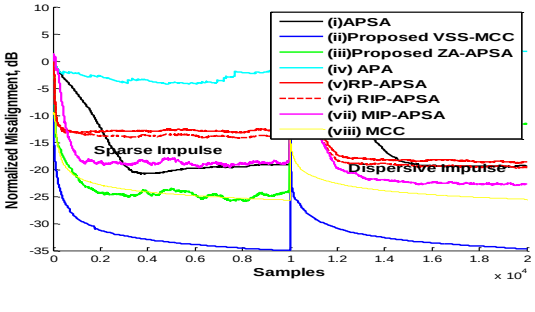

Fig 9.Normalized Misalignment analysis at SNR=20dB, SIR=-10dB , pr=0.001 with colored input.

Table 4. Results of the algorithms under steady state in double talk scenario at SNR=20db,SIR=-30db,pr=0.001 with colored input.

	Experiment1		Experiment 2	
Algorithm	**MSE (db)**	**Normalized misalignment (db)**	**MSE (db)**	**Normalized misalignment (db)**
APSA	-14.96	-20.69	-14.5	-18.85
RP-APSA	-12.5	-13.11	-14.4	-13.17
RIP-APSA	-15.31	-13.88	-17.64	-14.14
MIP-APSA	-18.77	-18.84	-19.08	-17.07
Proposed ZA-APSA	-21.18	-24.45	-12.68	-11.26
MCC	-17.59	-22.52	-25.59	-21.94
Proposed VSS-MCC	-25.28	-30.09	-17.59	-28.69

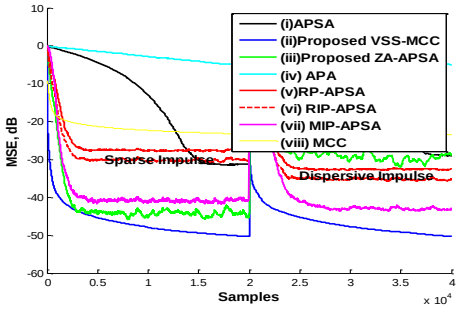

Fig 10. MSE analysis at SNR=20dB, SIR=-10dB , pr=0.001 for white input

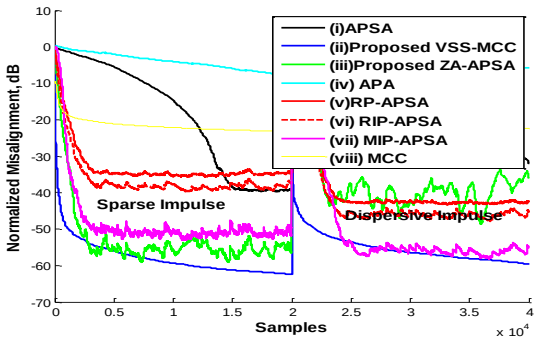

Fig 11. Normalized Misalignment analysis at SNR=30dB, SIR=-10dB , pr=0.001 for white input.

Table 5. Results of the proposed algorithms under steady state in double talk scenario at SNR=20db,SIR=-10db,pr=0.001 with colored input.

	Experiment1		Experiment 2	
Algorithm	**MSE (db)**	**Normalized misalignment (db)**	**MSE (db)**	**Normalized misalignment (db)**
APSA	-30.58	-39.48	-28.96	-39.18
RP-APSA	-27.56	-34.87	-32.7	-42.82
RIP-APSA	-30.21	-38.74	-35.35	-45.41
MIP-APSA	-19.41	-51.33	-42.16	-51.17
Proposed ZA-APSA	-40.83	-55.88	-30.96	-38.25
MCC	-22.49	-22.95	-23.13	-23.83
Proposed VSS-MCC	-22.49	-61.19	-48.96	-57.04

Table 6.Computational complexity analysis

Sl.No	Algorithm	Add	Mul	Div	Comp	Exp
1	APSA	NM	2N	1	-	-
2	RP-APSA	(M+1)N-1	5N	2	2N	-
3	RIP-APSA	(M+2)N	5N	2	-	-
4	MIP-APSA	(2M+3)N	(M+4)N	2	-	-
5	Proposed ZA-APSA	NM	2N+(N-Z)	1	-	-
6	MCC	2N+1	2N+2	-	-	1
7	Proposed VSS-MCC	2N+1	2N+3	2	-	2

The Figures 3-11 depicts the MSE and Normalized Misalignment of the above mentioned algorithms for a SNR of 30dB and 20dB ,SIR of -10 dB and -20 dB and pr as 0.001 and the results are tabulated in Tables 1-4. Table 1-3 summarizes the results obtained for different filter lengths, level of sparsity , SNR, pr values.

From the tabulated and simulation results shown in Tables 1-6, the following conclusions are obtained. Among the family of APSA ,the proposed ZA-APSA has the fastest convergence and lowest steady state MSE when the system is sparse and is the worst when the system changes to non sparse As far as ZA-APSA is considered,there is no matrix inversion and thus the computational complexity is lesser than ZA-APA and APA. When the number of multiplications is considered, we find that ZA-APSA requires only extra N multiplications more than APSA which is independent of M. Thus we find that the proposed ZA-APSA approach has lesser computational complexity when compared to the conventional APSA or the proportionate family of algorithms. The proposed VSS-MCC algorithm has the lowest value of steady state values of MSE and Normalized Misalignment thus it removes the steady state error and convergence tradeoff when compared to ZA-APSA under all conditions.

VII. CONCLUSIONS

A detailed performance comparison of APSA and MCC based adaptive filters is made. Both of them outperform their traditional counterparts. When compared among them, it is found that MCC based variable step size algorithm is found to be superior than ZA-APSA not only in convergence speed and steady state MSE but also in the computational complexity. Thus it can be concluded that variable step size MCC algorithm is a suitable candidate for double talk scenario. The future work is to find methods to choose the kernel width as it plays a key role in the final steady state mean square error.

REFERENCES

[1] Gay .S. L and Benesty .J. (Eds.). (2012), " Acoustic signal processing for telecommunication", Springer Science and Business Media , Vol. 551

[2] Paleologu .C et. al ., (2008), " A variable step-size affine projection algorithm designed for acoustic echo cancellation", IEEE Transactions on Audio, Speech, and Language Processing, Vol. 16, No. 8, pp. 1466-1478

[3] Haykin .S. S. (2008), "Adaptive filter theory", Pearson Education India.

[4] Radhika, S., and Sivabalan, A (2012). A Survey on the Different Adaptive Algorithms Used In Adaptive Filters. International Journal of Engineering Research and Technology, Vol. No: 1(9). ESRSA Publications.

[5] Radhika, S., and Sivabalan, A. (2016). Robust Adaptive Algorithm by an Adaptive Zero Attractor Controller of ZA-LMS Algorithm. Mathematical Problems in Engineering.

[6] Radhika, S., and Sivabalan, A. Robust variable zero attractor controller based za-lms algorithm for variable sparsity environment, National Academy Science letters,

[7] Radhika, S., and Sivabalan, A. (2015). Steady State Analysis of Convex Combination of Affine Projection Adaptive Filters. Research Journal of Applied Sciences, Engineering and Technology, Vol. No:10(1), pp. 56-62.

[8] Shao .T., et. al ., (2010), "An affine projection sign algorithm robust against impulsive interferences", IEEE Signal Processing Letters, Vol. 17, No. 4, pp. 327-330.

[9] Mathews .V .J and Cho .S .H (1987), "Improved convergence analysis of stochastic gradient adaptive filters using the sign algorithm", IEEE Transactions on Acoustics, Speech and Signal Processing, Vol. 35, No. 4, pp. 450-454.

[10] Al-Naffouri .T .Y and Sayed .A .H (2003), "Transient analysis of adaptive filters with error nonlinearities", IEEE Transactions on Signal Processing, Vol. 51, No.3, pp. 653-663.

[11] Yang .Z., et. al ., (2011), "Proportionate affine projection sign algorithms for network echo cancellation", IEEE Transactions on Audio, Speech, and Language Processing, Vol. 19, No. 8, pp. 2273-2284.

[12] Albu .F and Kwan .H. K (2012), "Memory improved proportionate affine projection sign algorithm", Electronics letters, Vol. 48, No. 20, pp.1279-1281.

[13] Shin .H .C et. al ., (2004), "Variable step-size NLMS and affine projection algorithms", IEEE signal processing letters, Vol. 11, No. 2, pp. 132-135.

[14] Radhika, S., and Sivabalan, A. (2016). Steady-State Analysis of Sparsity-Aware Affine Projection Sign Algorithm for Impulsive Environment. Circuits, Systems, and Signal Processing, pp.1-14.

[15] Shao .T., et. al ., (2010), "An affine projection sign algorithm robust against impulsive interferences", IEEE Signal Processing Letters, Vol. 17, No. 4, pp. 327-330.

[16] Liu .W et. al .,(2007), " Correntropy: properties and applications in non-Gaussian signal processing", IEEE Transactions on Signal Processing, Vol. 55, No. 11, pp. 5286-5298.

[17] Chen .B., et. al., (2014), " Steady-state mean-square error analysis for adaptive filtering under the maximum correntropy criterion, IEEE Signal Processing Letters, Vol. 21, No. 7, pp. 880-884.

[18] Khalili .A.,(2016), "Steady-State Tracking Analysis of Adaptive Filter With Maximum Correntropy Criterion", Circuits, Systems, and Signal Processing ,pp.1-10.

[19] Radhika, S., and Sivabalan, A. (2016). Variable Step Size Maximum Correntropy Criteria Based Adaptive Filtering Algorithm. Engineering, Technology and Applied Science Research, Vol. No:6(2), pp-923-926

Table 7.Performance comparison

Scenario		Algorithm	Sparse impulse			Dispersive impulse		
			Speed (Samples)	MSE(dB)	NMis .Align(dB)	Speed (Samples)	MSE(dB)	NMis .Align(dB)
SNR=30dB, SIR=-10dB, Pr=0.001, colored input	1	ZA-APSA	600	-21.67	-40.79	12000	-12.33	-18.24
	2	VSS-MCC	1000	-25.17	-41.12	1000	-25.67	-42.89
SNR=30dB, SIR=-20dB, Pr=0.001,colored input	1	ZA-APSA	400	-22.01	-38.24	10000	-12.04	-21.23
	2	VSS-MCC	1000	-24.98	-42.86	1000	-24.98	-42.70
SNR=30dB, SIR=-30dB, Pr=0.001, colored input	1	ZA-APSA	200	-22.55	-38.40	12000	-12.36	-22.1
	2	VSS-MCC	1000	-25.02	-42.59	1000	-24.45	-42.89
SNR=20dB, SIR=-10dB, Pr=0.001,colored input	1	ZA-APSA	400	-21.18	-24.45	13000	-12.68	-11.26
	2	VSS-MCC	1000	-25.28	-30.09	1000	-17.59	-28.69
SNR=30dB, SIR=-10dB, Pr=0.001,white input	1	ZA-APSA	2500	-40.83	-55.88	5000	-30.96	-38.25
	2	VSS-MCC	1000	-42.49	-61.19	1000	-48.96	-57.04

Proceedings of the Fourth International Conference on Communication and Electronics Systems (ICCES 2019)
IEEE Conference Record # 45898; IEEE Xplore ISBN: 978-1-7281-1261-9

Raspberry-Pi based Smart Power Monitoring system

Abhay Kshirsagar, Electronics Department, Vivekanand Education Society Institutet of Technology, abhay.kshirsagar@ves.ac.in
Narendra Walawalkar, Electronics Department, Vivekanand Education Society Institutet of Technology, 2015narendra.walawalkar@ves.ac.in
Harish Yadav, Electronics Department, Vivekanand Education Society Institutet of Technology, harish.yadav@ves.ac.in
Shrutisneha Prasad, Electronics Department, Vivekanand Education Society Institute of Technology, shrutisneha.prasad@ves.ac.in
Prajakta Paranjape, Electronics Department, Vivekanand Education Society Institute of Technology, 2015prajakta.paranjape@ves.ac.in

***Abstract*---This paper design a power monitoring system for household's plug-in loads which consumers use on a daily basis. This project once deployed in the field will sense the electrical quantities and upload it on the web server so that it will be accessible through the website as and when required. The output will show the graphical analysis of the analog electrical quantities which are easily analyzed by the non-technical person in the household. This system will help the user to have an analysis of power usage. On that basis, a detailed survey on power quality usage can be done by further developments and help us to have energy cut downs wherever necessary to save energy on industrial sites and distribution areas.**

Keywords—Analog voltage current sensing, Database, raspberry-pi, ADC.

I. INTRODUCTION

This system can be referred to as an Energy Management System (EMS). The main motive of the system is to reduce the power consumption by recording, monitoring, analyzing and comparing the load parameters. The system will draw energy consumption trends on a daily/weekly/monthly/yearly basis, so this will improve the energy budget corresponding to user requirement and it will also diagnose the specific area of wasted energy. In conventional energy meters, inaccuracies due to manual limitation and maintenance of log are quite tedious and time-consuming so the proposed system stores data at the server and can share the real-time data with electricity board and the user.

The paper presents the theoretical as well as experimental aspects related to the implementation of the power monitoring system. In the first section of the paper, the designed hardware is discussed with all the schematics and the waveform. After that, sensing and conversion of the sensed values using ADC are explained. The proposed method helps us to keep the database localize in order to be secure and reliable. The UI output of the monitoring system is also presented by running the prototype.

II. LITERATURE REVIEW

Nowadays on a global level, the main aim is to use electrical energy efficiently and to develop the usage system more profitably with less power consumption. Due to industrial growth and urbanization energy is the basic need of our life. Any vulnerability about its supply of energy can undermine the working of the whole economy. The production of electricity from utilities has increased from 11,67,584GWh during 2015-16 to 12,35,358 GWh during 2016-17, registering an annual growth rate of about 5.80%. Of the total consumption of electricity in 2016-17, industry sector accounted for the largest share (40.01%), followed by domestic (24.32%), agriculture (18.33%) and commercial sectors (9.22%) [1].

III. VOLTAGE AND CURRENT SENSING

A. Voltage Sensing

The voltage at the source needs to be sensed to be analyzed. The first step is using a Potential Transformer (PT) to reduce the AC mains voltage to a lower value in order to feed it to the low potential operating circuits. PT stepdown the 230 VAC voltage to 5 VAC. This voltage is then given to terminal IN_VLT1 and IN_VLT2. A reference voltage of 1.75V is fed to this signal which is generated by using a Precision Reference Generator. This is required so that the magnitude of the AC signal can be sampled by the ADC.

This project has deployed galvanic isolation for voltage sensing. The two main reasons for introducing isolation in the system [2].

1. To prevent passing high voltage to lower potential circuits such as Raspberry-pi and ADS1115 (ADC).
2. To break the ground loop, when there is more than one ground connection path between two pieces of equipment. The duplicate ground paths act as an equivalent loop antenna which easily picks up interference currents. Lead resistance transforms these currents into voltage fluctuations. As a consequence of a ground-loop induced voltages, the ground reference in the system is no longer a stable potential, so signals overlap and results as noise. This can cause interference in the ADC sampled values and can reduce the tolerance of the system conversion.

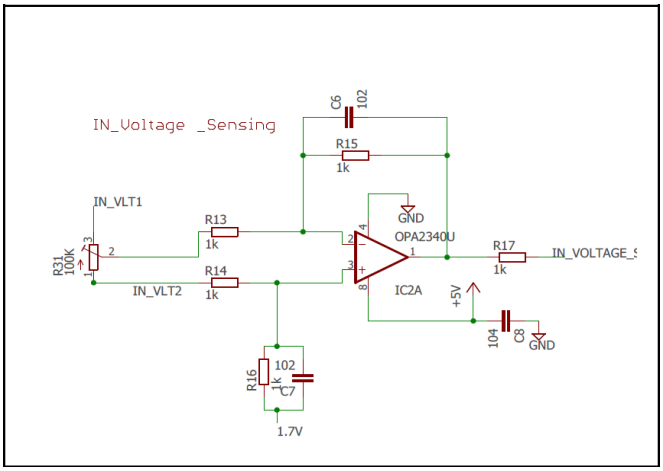

Fig. 1. AC voltage sensing circuit

B. Current Sensing

Normally current shunts were used for measuring the current flowing in the circuits. The shunt produces a voltage of 75mV per 10A of current. This voltage is sensed according to the requirement. A shunt resistor is frequency independent element (1>MHz) and it does not change the phase of the current with respect to voltage. The main drawback of the shunt resistor is that it does not provide galvanic isolation. This can cause damage to the lower potential sensing circuit during a fault condition [3]. To provide galvanic isolation with a direct method of measuring current ACS712 Hall sensor is used. The current flowing through the hall's crystal creates asymmetry in its internal structure that is reflected by the voltage potential. ACS712 provide electrical isolation up to 12.1kVrms and signal bandwidth of 80MHz. It is not appropriate to apply the ACS712 Module's analog output to ADC as input directly because the signal cannot be interpreted by the ADC, therefore, the supplementary circuit is shown in Fig. 2. that should be implemented for the purpose of signal conditioning.

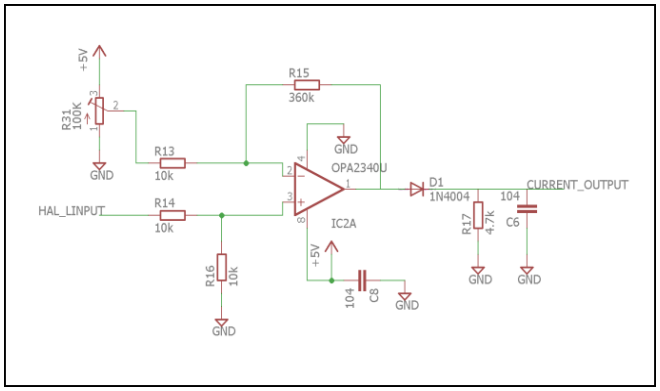

Fig. 2. AC Current Sensing Circuit for ACS712

Fig. 3. shows the resultant output waveform of the voltage and current sensing circuit. The yellow waveform shows the waveform that signifies the AC voltage across the load, and the cyan waveform signifies the current flowing through the load. There is a small lag between voltage and current waveform because the nature of the load is inductive. The output is tested on the load side using a digital signal oscilloscope (DSO) to check whether any spike or noise is present. The Fig. 3 shows the output of the analog voltage and current sensing circuits.

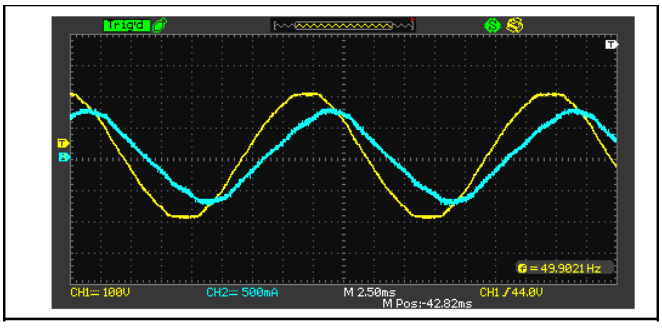

Fig. 3. Voltage and current output waveform on DSO

C. Reference Voltage Generator

Whenever the system encounters an AC signal, the negative magnitude is considered and is sampled by the ADC. The ADC will not be able to read values below the 0V level and hence this negative magnitude cannot be sampled. So we need to clamp this AC signal to a certain DC level. A simple Capacitor-Diode Clamper cannot be used because it does not have a fixed potential and varies according to the charging current of the capacitor that the input supplies. There is a need to generate a precise voltage at which the ADC signal can be clamped and the negative magnitude can be read as well. This is implemented by using a TL431 precision regulator which is operating at 2.5V as its reference voltage. Now, to clamp the signal we need to reduce it by a factor of 2/3rd which becomes 1.75V that is exactly Vdd/2 of the ADC (ADC works on 3.3V). This clamp voltage is buffered and fed wherever required. At the same time, it is sensed so that any deviation in the reference can be captured in real time.

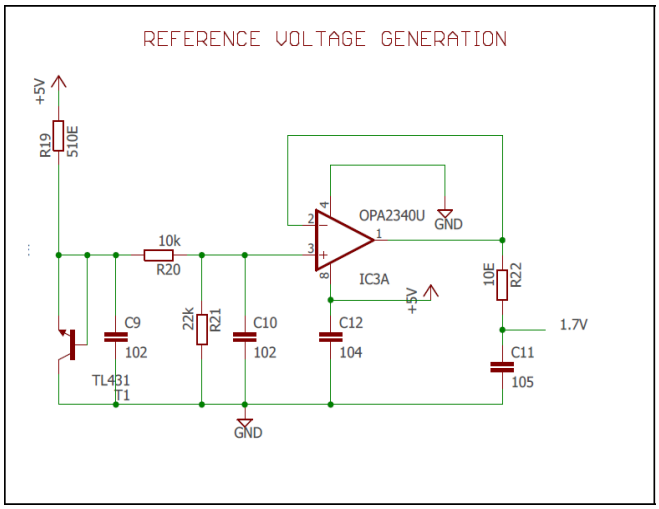

Fig. 4. Reference Voltage Generation

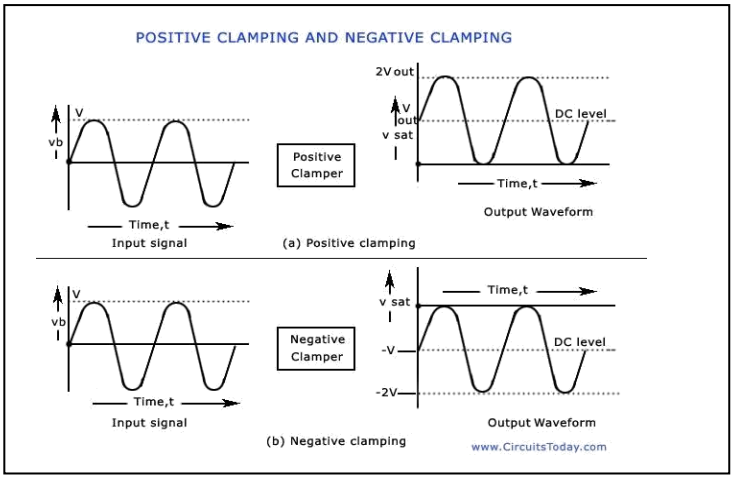

Fig. 5. Level sifted output

IV. ADC SAMPLING

A. *Analog to Digital conversion*

Now the analog values have been sensed by the above integration of circuits but at the output, there are analog values. The digital processing is simpler than analog sampling as the processing unit understands the digital samples. The digital values are generally in the binary format of 1's and 0's. The analog to digital conversion is necessary in order to have digital values. These discrete values are called as digital samples of analog quantity. This samples are further processed by the microprocessor and converted into the original analog values for reading purpose. The ease of processing is obtained because of ADC and the data transfer rate from ADC to the microprocessor depends upon the sampling rate and clock frequency of the microprocessor. The pre-processing of analog sinusoidal values takes place in this section. This is necessary in order to forward it to the Broadcom Processor which doesn't have onboard ADC.

B. *ADS1115 as ADC*

The ADS1115 is used for analog to digital conversion of the sensed values. ADS1115 devices (ADS111x) are precision, low-power, 16-bit, I2C-compatible, analog-to-digital converters (ADCs) offered in an ultra-small, leadless, X2QFN-10 package, and a VSSOP-10 package. The ADS111x devices incorporate a low-drift voltage reference and an oscillator. The ADS1115 also incorporate a Programmable Gain Amplifier (PGA) and a digital comparator [4]. The ADS1115 provides 16-bit precision at 860 samples/second over I2C. The Full-Scale Range of any analog quantity is been divided into 32676 discrete values. There are 4 different channels on ADC which can sense 4 analog quantities simultaneously or two differential inputs. The comparator is present inside the ADS1115 for those differential inputs. The data is transferred to the processor through SDA and SCL bus lines which are serial data and serial clock inputs to the processor.

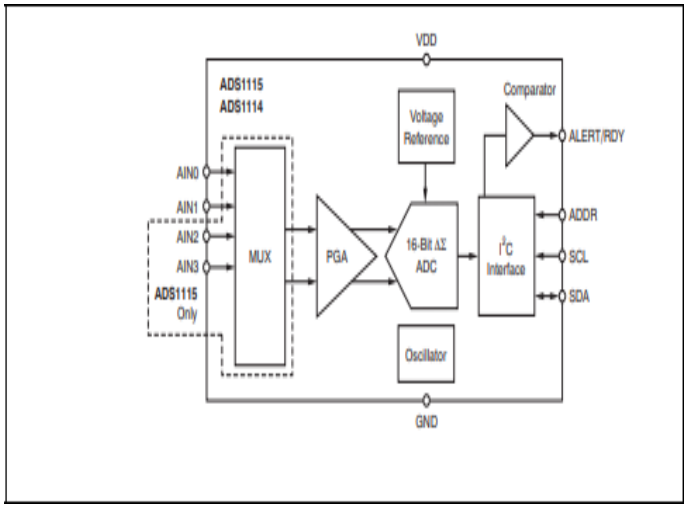

Fig.no 6. Internal block diagram of ADC ADS1115

C. *Digitizing the Analog values.*

Once the values are converted into digital samples the main task is to display them on the server but the user cannot decode this digital sample as the analog quantity. This is done by the Raspberry Pi's Broadcom processor. The block diagram for the ADC is as follows: Analog voltage and current are sensed and each of them is converted into digital values using two channels of ADC. This gives us a different set of digital values at the output. Hence, it is processed separately for voltage and current.

D. *Calculating the Analog values from processed digital values.*

The values for the analog voltage, current active power and reactive power are calculated using the digital values which are converted by ADC and is processed by Broadcom processor in Raspberry-pi. The ADC sampling rate is set at 860 SPS. It is better to maintain it at highest as to collect as many as samples in a second in order to get the accurate sinusoidal wave. Once we get the accurate sine wave, we can calculate its RMS value for voltage and current as well. We process the 860 samples each of voltage and current first to get the sinusoidal values and then processing it further to get the RMS values of each. The formula is as follows.

The threading method is used to calculate the RMS values of voltage and the current. Multithreading is a method of improving the execution performance of a process by the use of concurrency, that is allowing more than one thread to run independently of each other within that program. Since each thread could run on a different core at the same time, it is hoped that multithreading does not only improve the efficiency of both single and multi-core processors, but it could also increase the battery life of mobile systems [5]. Overall three threads are formed wherein first 2 are used for voltage and current samples calculation. The third thread is evolved to calculate the power using the earlier two. This way we process the accurate values of the voltage and current at the same instant and using those values in the third thread we calculate the active power. Now we need to find out the phase difference between the current and the voltage waveform to find the reactive power. Hence we have used zero-crossing detector code in python on Raspberry Pi to find the phase difference by calculating the difference between the two points at which the voltage and the current waveforms cross the time axis. Thus with that value, we calculate the phase difference and further the reactive power consumed. With the help of active and reactive power, we can calculate the real power consumed.

RMS Voltage:

$$V_{RMS} = K_v \sqrt{\frac{\sum_{n=1}^{Sample\ count} v^2(n)}{Sample\ count}} \quad (1)$$

RMS Current:

$$I_{RMS} = K_v \sqrt{\frac{\sum_{n=1}^{Sample\ count} i^2(n)}{Sample\ count}} \quad (2)$$

Active Power:

$$P_{ACT} = K_p \sqrt{\frac{\sum_{n=1}^{Sample\ count} v(n)*i(n)}{Sample\ count}} \quad (3)$$

Reactive Power:

$$P_{REACT} = K_p \sqrt{\frac{\sum_{n=1}^{Sample\ count} v_{90}(n)*i(n)}{Sample\ count}} \quad (4)$$

v(n)= Voltage sample at a sample instant 'n' i(n)= Current sample at a sample instant 'n' Sample count= Number of samples in 1 second K_v = Scaling factor for voltage K_I = Scaling factor for current
$v_{90}(n)$ = Voltage sample at a sample instant 'n' shifted by 90° K_p = Scaling factor for power

The quantity sensed and converted to the digital output can be plotted to sinusoidal by using the above calculations [6].

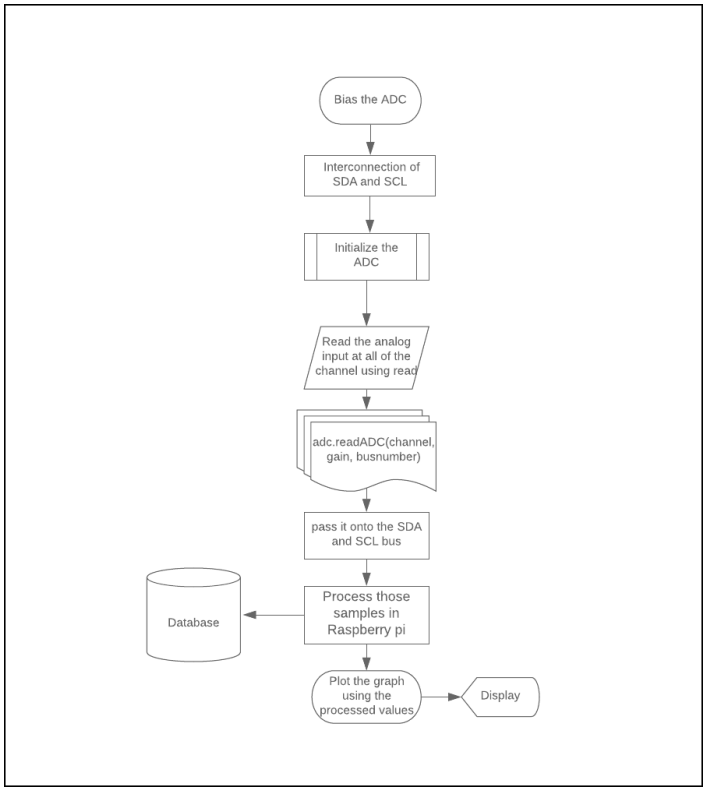

Fig. 7. Flowchart of ADC with the processor's operation

V. DATABASE CREATION AND HANDLING

HTTP is a set of protocols designed to enable communication between clients and servers. It works as a request-response protocol between a client and a server. The database is created so it can be accessed at anytime anywhere in the world and it should be well managed and the output should be directed to HTTP so that user can have an application layer over it to have a user interface.

A. Python Request library

Request is a Python HTTP library, released under the Apache2 License. The goal of the project is to make HTTP request simpler and more human- friendly. So user can direct all the outputs of power, voltage and current through the processor to the localhost server (standalone PC) which will record all the calculated output values and then plot them on the website with the help of PHP. It can customize as user want to have an interface. Here are some of the outputs which have been recorded while testing the system. here only active power is calculated as the load is resistive (200Watt) but the system can also calculate the reactive power if the load is inductive. The request library allows us not to have load on the Raspberry-Pi's Broadcom processor and thus all the load comes on the standalone computer. This method saves the power consumption of the processor as well as the memory bank. It has limitless advantage on the amount of information to be stored and the type of data to store in the database. The processor now acts as the bypass to the internet with the help of a local server.

VI. PROTOTYPE SYSTEM

The final prototype incorporates the onboard processor with the PCB of voltage and current sensing combined with the ADC along with voltage reference circuit and also onboard plugs and terminal. The final outlook of the system is shown in Fig.8.a. We just have to connect the load in between the plugs and connect the 230V power supply (line voltage) which will be sensed by the circuit. The Fig.8.b shows the connection of the Active load with the server setup. The Fig.10 is the final output on the website. Table I outlines the results obtained displaying the power, input voltage and the input current at the instant of time.

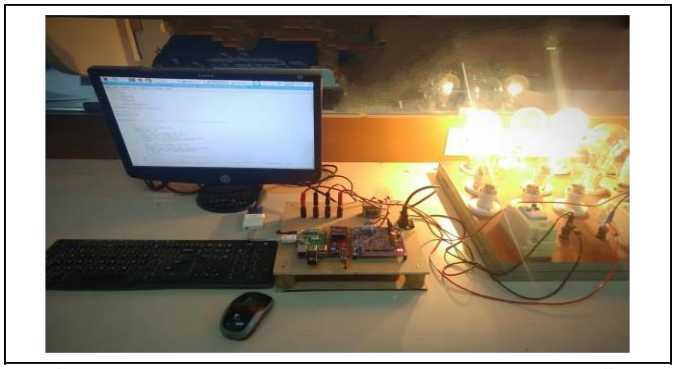

Fig. 8.a. Setup with Resistive Load and Server

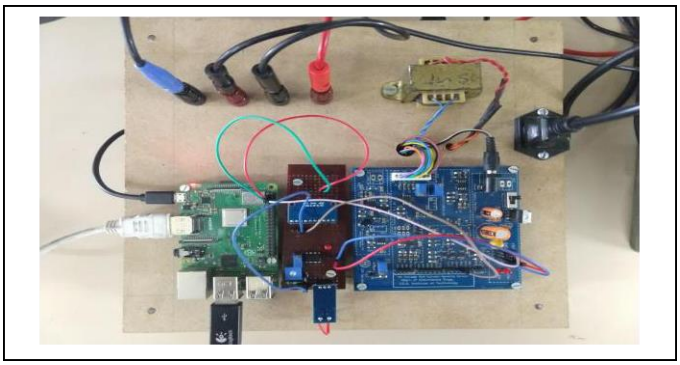

Fig. 8.b. Hardware Setup

TABLE I
DATALOG TABLE

TIME (HH:MM: SS)	OBSERVED POWER in watts	INPUT VOLTAGE in volts	INPUT CURRENT in Amps	ACTUAL POWER in watts
12:46:45	5.08	169.68	0.03	0
12:48:34	8.26	170.17	0.05	0
12:48:39	8.74	170.06	0.05	0
12:49:08	473.32	171.22	2.76	500
12:49:18	479.21	171.77	2.79	500
12:53:43	481.34	171.49	2.81	500
12:54:48	485.83	172.52	2.82	500
12:56:27	483.85	170.92	2.83	500
12:56:32	481.11	169.61	2.84	500
12:57:11	484.63	170.20	2.85	500
12:57:21	495.13	172.70	2.87	500
12:59:48	570.60	172.72	3.30	600
12:59:53	616.07	172.61	3.57	700
12:59:58	672.01	172.67	3.89	700
13:04:51	714.86	172.67	4.14	800
13:05:30	715.71	172.63	4.15	800
13:05:35	724.29	169.96	4.26	800
13:07:03	719.72	168.81	4.26	800
13:08:11	751.09	168.81	4.45	800

Fig. no.9 shown below is the terminal screen of the local host (RPI), thus getting the real-time data on the backend. This data is then transferred, using the python script in which the python request library is called, through the local network.

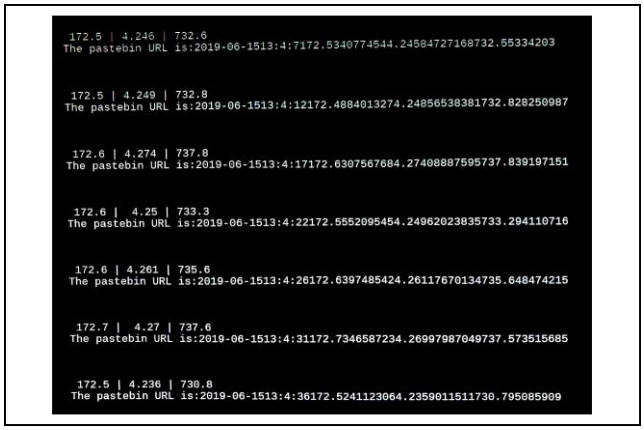

Fig. 9. The terminal screen of localhost

This data is then segregated on the server side and stored on the local database. Using PHP the graph is plotted and the website can be designed [7]. Rather than going into the complexity of designing the aim was to transfer data accurately and with minimum discrepancies. From the table that has been derived based on the calculations, we can calculate the efficiency by using (5).

$$Efficiency = \eta = ((output)/input) * 100\% \quad (5)$$

By measuring the maximum deviation of the output power from the actual load applied, the efficiency is calculated which comes nearly to 80%.Thus in order to increase the efficiency it needs to process more samples per unit time and bring the observed value close to the real value.

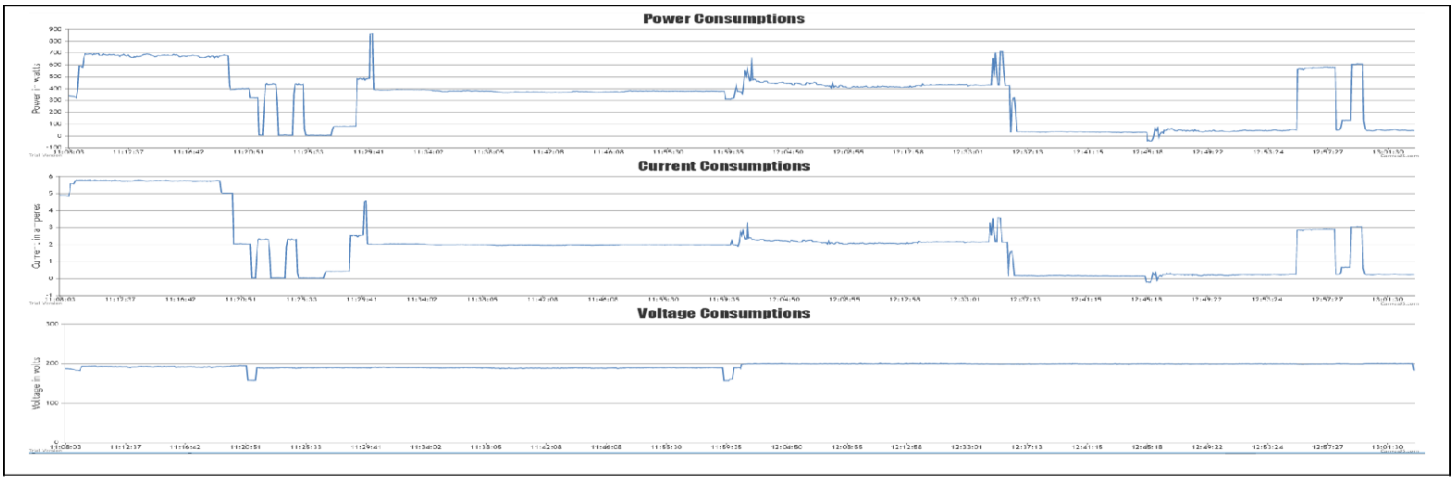

Fig. 9. Graphical output of voltage current and power

A. LIMITATIONS

1. The load cannot be increased beyond 2.1kW because of maximum isolation tolerance of Current sensor (ACS 712) is 2.1kW; this can be overcome by changing the higher rating current sensor.
2. The voltage across load cannot go beyond 240VAC because the potential transformer is customized to convert 230VAC to 5VAC.
3. Present setup is designed to monitor up to two household appliances. It can be increased by increasing the number of PTs and Current sensors.

B. FUTURE SCOPE

1. This system can be further developed for three phase supply and can be associated with industrial loads for their analysis.
2. The analysis can be brought to the app by designing it particularly for targeting the on-go customer.
3. The fault detection system can be implemented using the sensing system at a particular point of contact.
4. There can be a separate database for power calculations and fault detection storage so it will be better future analysis.
5. We can add solar PV system in order to reduce the grid consumption and we can analyse its power even. The environmental conditions can also be logged on to database for a solar system for detail analysis of it.

VII. CONCLUSION

As this system helps out to plot the data in real-time it is better to analyze the system malfunction and the usage of the electrical power. Power Quality is the major factor in the industry as well as in house plug-in loads performance. The power factor calculation aims at maximizing real power accuracy [8]. The calculations required for the cost of power consumed can be further added to the backend server so the bill is auto-generated. This can be a new method to calculate electricity expenses instead of currently available manual intervention method. By having a detailed analysis of the database, the points where more power is consumed unnecessarily can be detected and have a fault analysis, which directly helps to have energy cut downs in order to make the system consumption more efficient. The threading method involved will increase tolerance for errors in the output.

VIII. REFERENCE

[1] "Energy Statistics 2018" Ministry of statistics and Implementation.

[2] Michal Krbal, "High Voltage Current Analyzer with Galvanic Separation", Department of Electrical Power Engineering, Brno University of Technology, Brno, the Czech Republic.

[3] Acromag, "White Paper: The Importance of Isolation", Acromag, Incorporated 30765 S Wixom Rd, Wixom, MI 48393 USA,

[4] Texas Instruments, ADS1115 datasheet, ti.com.

[5] Power Efficiency Study of Multi-threading Applications for Multi-core Mobile Systems MARIUS MARCU, DACIAN TUDOR, SEBASTIAN FUICU, SILVIA COPIL-CRISAN, FLORIN MATICU, MIHAI MICEA

[6] Texas Instruments, "implementation of single-phase electronic watt-hour-meter using the MSP430F6736(A)", ti.com

[7] IOT Based Data Processing For Home And Industrial Monitoring Using Raspberry Pi, International Journal of Science, Engineering and Technology Research (IJSETR) Volume 6, Issue 9, September2017, ISSN: 2278 -7798

[8] Stealing Defense System Fei Wang, Fan Yang, Tianyu Liu, Xiaoguang HuSchool of Automation Science and Electrical Engineering Beihang University.

[9] I. S. Jacobs and C. P. Bean, "Fine particles, thin films and exchange anisotropy," in Magnetism, vol. III, G. T. Rado and H. Suhl, Eds. New York: Academic, 1963, pp. 271–350.

[10] IOT Based Smart Power Metering, International Journal of Scientific and Research Publications, Volume 6, Issue 9, September 2016 ISSN 2250-3153

[11] Measuring Energy Meter of Three-phase Electricity

[12] Design and Development of Embedded Energy Meter, International Journal of Engineering Research & Technology (IJERT) ISSN: 2278-0181 www.ijert.org Vol. 3 Issue 7, July – 2014

Proceedings of the Fourth International Conference on Communication and Electronics Systems (ICCES 2019)
IEEE Conference Record # 45898; IEEE Xplore ISBN: 978-1-7281-1261-9

Implementation of Non isolated DC DC Boost Converter based on Inductor for DC Microgrid Application

Vishwesh Anand Sahasrabudhe
Dept. of Electrical Engg
PVP Institute of technology,Budhgaon.
sahasrabudheva@gmail.com

S.Y.Gadgune
Dept. of Electrical Engg.
PVP Institute of technology,Budhgaon.
swapnilgadgune@gmail.com

Viraj Savakhande
Dept. of Electrical Engg.
PVP Institute of technology,Budhgaon
vrajsavakhande@gmail.com

***Abstract*:-This article introduces "A high voltage gain non - isolated DC DC converter based on inductors for Microgrid application." This converter presents high voltage gain without penalty of high duty ratio. The presented converter employs two single inductors, both are charging in parallel and discharging in series. The steady state analysis of proposed converter is shown in section IV. The simulation of proposed converter 17V/182V is developed in MATLAB Simulink to check the feasibility and performance of the converter.**

Keywords— DC DC converter, *microgrid, high voltage gain, two single inductors* .

I. INTRODUCTION

Demand for clean and sustainable energy sources has increased rapidly in past few years. DC microgrid is come forward with increase utilization in green energy. As DC power generator produces low output voltage hence it require high gain converter to meet the load conditions. [1-2]. Photovoltaic cell, batteries, fuel cells are commonly used as green energy sources for integration purpose.

A particular high gain converter is used for the individual solar panel. These converters are used for individual solar panel. These converters boost lower level input voltage to desirable higher output voltage[3]. Large duty ratio, compact size and high efficiency are main advantages of this system [4]. Large duty ratio contributes extended conduction losses, also it affects the operation of the switches as voltage stress increased on them.to overcome this the high rated switches are used[5]. Upcoming converters are consists of coupled inductor, switched mode capacitor, multiplier cell to get desired gain[6]. For getting high voltage gain and improved efficiency more converters have been invented by researchers.[7-9].

Various isolated and non isolated converters are invented by researchers in recent past years. The main goal for them is to get high voltage gain. In isolated converter main disadvantage is saturation of transformer core. Due to this researchers are moves towards non isolated type of converters such as cascaded boost[10], the quadratic boost[11], voltage lift[12-14] etc. the disadvantage of these are number of stages for capacitor and inductor. This increases complexity as well as cost of converter.

Some coupled inductor based converter system delivered high gain and considerable low stress on switche[15-17]. The elected duty ratio and turns ratio of inductors will produce high input ripple. So in addition eith converter filter circuit is implemented.[18]

In this paper, the solar PV panel with MPPT block is used as input source for the proposed topology. The converter is designed with three power switches which operate on 2 different duty ratios. Other than this following are some advantages of the proposed system.

1. Incremental conductance and integral regulator technique is used for maximum power point tracking algorithm.
2. The inductor is supplied with source directly without any additional coupling circuit. This stored energy is independent of other clamping circuits.
3. High voltage gain is the main advantage of proposed system.
4. The proposed system is independent of voltage multiplier cell[VMC] and switched capacitor technology.

The block diagram of the system is shown in figure (1).The proposed converter have solar panel as a input source. MPPT block is used to track maximum output for that particular time duration. This input source converts solar energy into electrical energy irrespective of irradiation and temperature. The maximum power for that particular time will be taken with the help of incremental conductance and integral regulator technique (MPPT). Due to maintenance batteries are removed from the circuit. The effective handling is the main concern. By economical point of view it is also advantageous to remove battery from input side..

Upcoming sections gives circuit details with parameters and steady state analysis. The next section gives simulation results for the both open loop as well as closed loop configuration of the proposed system.

The fig(1) shows block diagram of the proposed converter system. Solar PV panel is used as the input source for given system. The main converter block is used to convert lower level input voltage to desired higher level. To connect this system with MPPT some voltage and current sensing is required. This sense the voltage and current from the system

and passed to MPPT block where this sensed input is converter into required duty ratio of the operating switch. The PWM converter converts it into pulses and then it provided to the gate terminal of the operating switches.

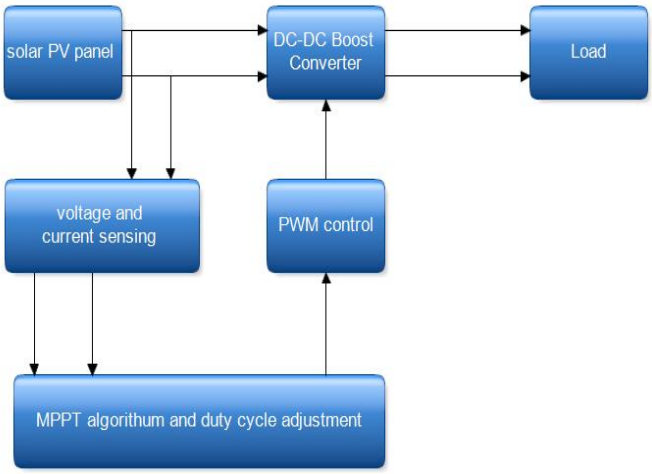

Fig.(1).Block diagram of DC-DC Boost converter.

II. CIRCUIT DETAILS:

Figure 2 shows the proposed system. It includes three switches P_1,P_2 ,P_3. It also consist of two inductor, 2 diode and one capacitor. The converter is operated in a Continuous Conduction mode. The duty ratio for P_1,and P_2 is D_1 and For P_3. It is D_2.

In steady state operation of the converter some assumption must be considered.

1) All the components should be in ideal condition.

2) Value of capacitor is considerably large so as to manitain constant output voltage.

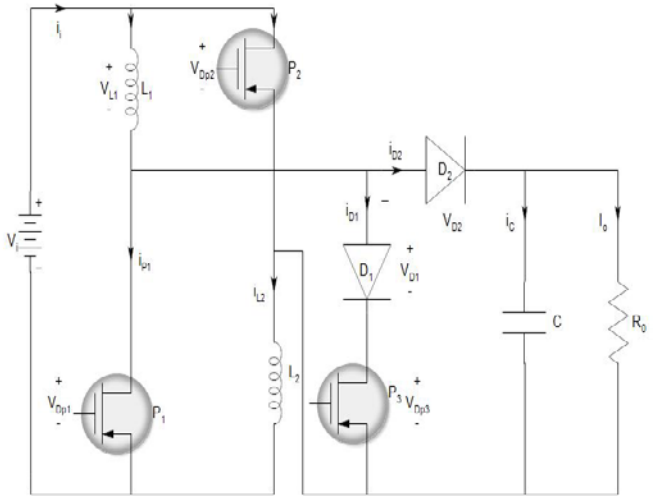

Fig.(2). Circuit Diagram for the proposed converter.

III. MAXIMUM POWER POINT TRACKING SYSTEM

Generally PV cell generates energy with respect of solar irradiation and temperature. The MPPT block is used to define a duty cycle for solar PV operation. In this incremental conductance methodology, dI/dV to work out the magnitude relation of dP/dV. Once dI/dV is equal and opposite to of I/V(where dP/dV=0) the concept is aware of that the maximum power point is reached and therefore it stop the loop and come back to the reference value of operational voltage. In this method rapidly changing irradiance sense exactly than P&O method. The basic working of the MPPT algorithm is as shown in fig (1)

IV. STEADY STATE OPERATION

In this section Continuous Conduction Mode is discussed. The proposed system is worked on three different modes of operation.[19]

Consider , the number of turns are same for both the inductors.

$$L_1 = L_2 = L \tag{1}$$

Voltage across inductors be,

$$V_{L1} = \mathrm{L}_1 \frac{di_{L1}}{dt} = \mathrm{L} \frac{di_{L1}}{dt} \tag{2}$$

$$V_{L2} = \mathrm{L}_2 \frac{di_{L2}}{dt} = \mathrm{L} \frac{di_{L2}}{dt} \tag{3}$$

Where $i_{L1}$and i_{l2} are current through L_1 And L_2.

As discussed earlier three modes of operation for the converter these are as follows.

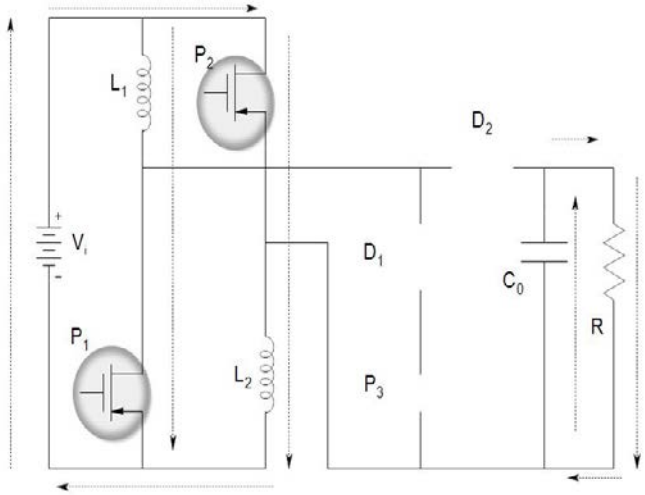

Fig.(3a). Mode I of operation.

CCM Mode- I

In this mode of operation Switch P_1 and P_2 are turned ON and P_3 is turned OFF. The flow of current is shown fig (3a) the current is pass through L_1,L_2 . Capacitor start discharging through the load as both diodes are in reverse biased. Due to this Inductors are parallel to the souse hence

input voltage will be equal to voltage across inductors, hence ,

$$V_{L1} = V_{L2} = V_i \quad (4)$$

Put equation 2 and 3 in equation 4

$$L\frac{di_{L1}}{dt} = L\frac{di_{L2}}{dt} = L\frac{di_L}{dt} = V_i, \quad t_0 \le t \le t_1 \quad (5)$$

$$\frac{di_{L1}}{dt} = \frac{di_{L2}}{dt} = \frac{di_L}{dt} = \frac{V_i}{L} \quad (6)$$

CCM Mode-II

In this mode P_1 and P_2 turned OFF and P_3 is turned ON. Due to this both inductor and source supply to load, And capacitor starts charging. This make diode D_2 forward biased. The direction of flow of current is as shown in fig (3b). Respective current and voltage equations are as follows,

$$i_{L1} = i_{L2} = i_L \quad (7)$$

$$V_{L1} + V_{L2} = V_i \quad (8)$$

Now substituting equation 2 and 3 in equation 8 we get,

$$\frac{di_L}{dt} = \frac{V_i}{2L}$$

$$t_1 \le t \le\le t_2 \quad (9)$$

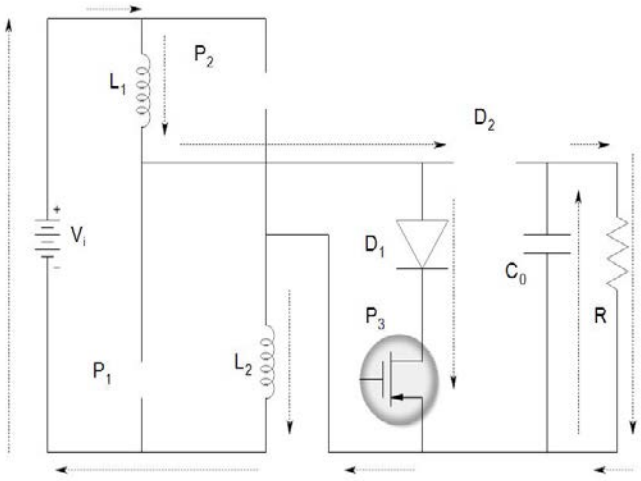

Fig.(3b). Mode II of operation.

CCM Mode-III

In this mode of operation aall the three switches turned OFF. Hence current will flow from L_1, D_2 ,C , load ,L_2 and back to the supply. Here D_2 is in forward biased while D_1 in reverse biased condition. As inductors are in series to the the average of input voltage is applied across the switches. The flow of current for this mode of operation is shown in fig (3c). the equations for voltage and current in this mode is as follows,

$$i_{L1} = i_{L2} = i_L \quad (10)$$

$$V_{L1} + V_{L2} = V_i - V_0 \quad (11)$$

Rearranging the above equation with equation 2 and equation 3 we get,

$$\frac{di_L}{dt} = \frac{V_i - V_o}{2L} \qquad t_2 \le t \le t_1 \quad (12)$$

Applying state space averaging method we get,

$$\int_0^{D_1 T_s} \left(\frac{di_L}{dt}\right)^I dt + \int_0^{D_2 T_s} \left(\frac{di_L}{dt}\right)^{II} dt + \int_0^{(1-D_1-D_2)T_s} \left(\frac{di_L}{dt}\right)^{III} dt = 0 \quad (13)$$

Where I, II, III, show mode of operation. Simplifying this equation (13) we get, final equation as follows,

$$\frac{V_o}{V_i} = \frac{(1+D_1)}{(1-D_1-D_2)} \quad (14)$$

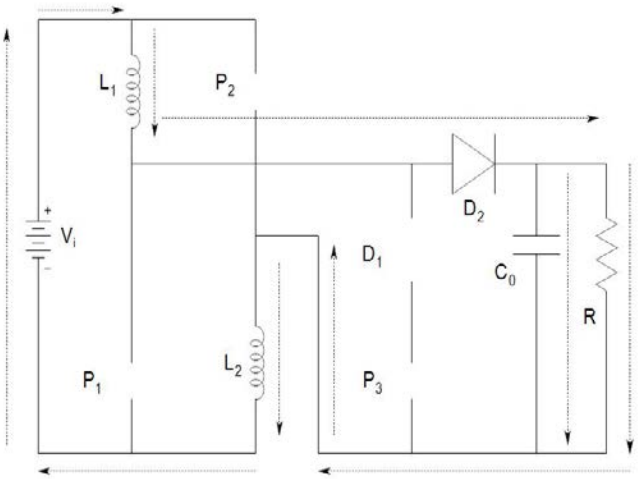

Fig.(3c). Mode III of operation.

V. SIMULATION RESULTS

To authenticate the performance of planed high gain boost converter is simulated in MATLAB Simulink software. The output voltage of planed converter is near about 182V. The input of the planed converter that is output voltage of the solar panel is around 17V.The duty cycle is set by MPPT algorithm with respect to irradiation and temperature of solar panel. After this the duty cycle is around '0.6' and '0.2' respectively to reduce conduction losses. The fig (04) shows the Simulink Model of the proposed converter and fig (05) shows the both values duty cycle. Output Voltage of the

converter is shown in fig.(06), PV Array Voltage fig (07), pulses of the both power switches is shown in fig (08). The table. I. shows all the feature details of the proposed system.

TABLE. I. FEATURES OF PROPOSED SYSTEM

Element	Parametric Quantity
P_{max}	100 W
V_{input}	17 V
V_{out}	182 V
Switching Hz	50 KHz
Duty Ratio	0.6, 0.2

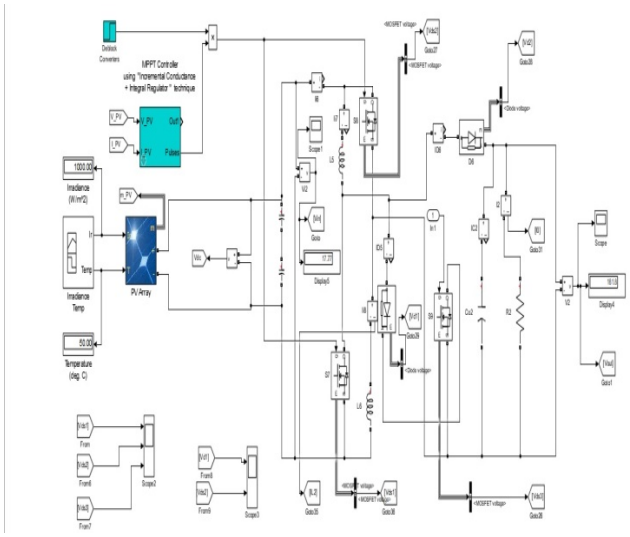

Fig.(04). MATLAB Model of proposed converter

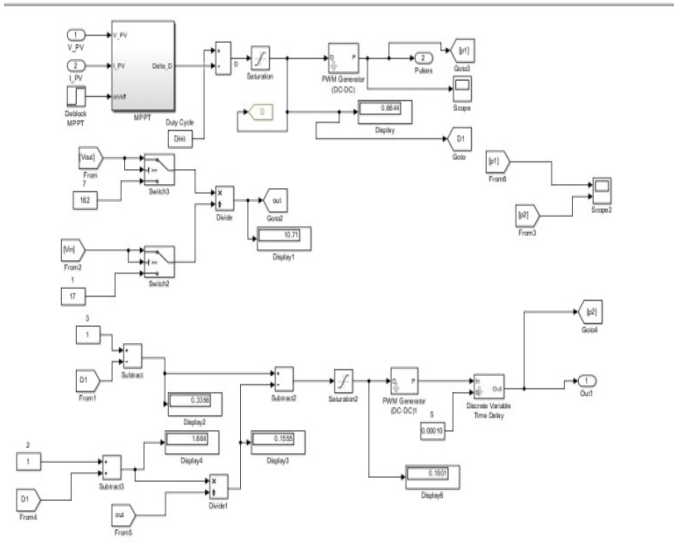

Fig.(05). MATLAB Model of proposed converter duty cycle

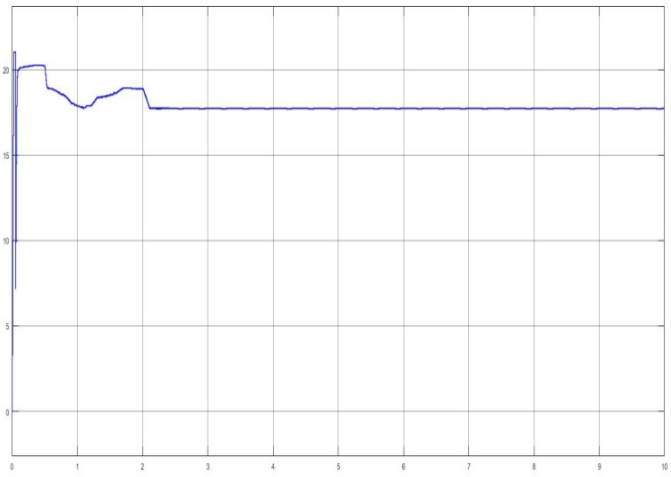

Fig.(07). PV Array output Voltage

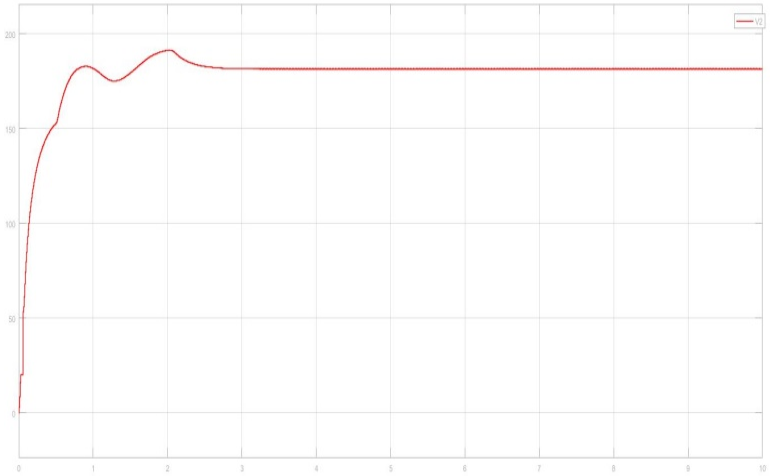

Fig.(06). Output voltage of the converter

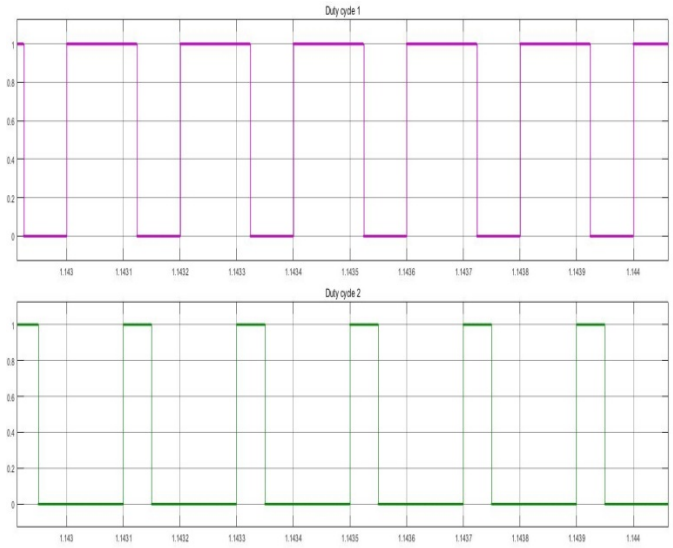

Fig.(08). Pulses for power switches

VI. CONCLUSION

In this paper new improved high gain DC-DC boost converter topology is discussed. The system deals with three switches with two different duty ratios results in higher efficiency and desirable high output voltage. Rather than this voltage gain of about 10 is achieved. Elimination of battery is also one of the advantages of this article. MPPT based solar panel sets autonomous duty ratio of DC-DC converter, which helps in providing constant output voltage even though fluctuating input voltage of the solar panel. This converter may be integrate with AC microgrid by developing the appropriate inverter circuit. By implementing ZVS and ZCS technique switching losses of converter will be reduced which may enhance efficiency of converter.

REFERENCES

[1] N. Eghtedarpour and E. Farjah, "Distributed charge/discharge control of energy storages in a renewable-energy-based DC micro-grid," IET Renew. Power Gen., vol. 8, no. 1, pp. 45-57, January 2014.

[2] J. M. Carrasco et al., "Power-Electronic Systems for the Grid Integration of Renewable Energy Sources: A Survey," IEEE Trans. Ind. Electron., vol. 53, no. 4, pp. 1002-1016, June 2006.

[3] Hsieh, Y.P., Chen, J.F., Liang, T.J. and Yang, L.S., "Analysis and implementation of a novel single-switch high step-up DC–DC converter." IET Power Electronics., Vol. 5, no. 1, 2012, pp. 11-21.

[4] Laird, Ian, and Dylan Dah-Chuan Lu.,"High step-up DC-DC topology and MPPT algorithm for use with a thermoelectric generator." IEEE Transactions on Power Electronics., Vol. 28, no. 7, 2013, pp. 31473157.

[5] Yilmaz, Murat, and Philip T. Krein., "Review of battery charger topologies, charging power levels, and infrastructure for plug-in electric and hybrid vehicles." IEEE Transactions on Power Electronics.,Vol. 28, no. 5, 2013, pp. 2151-2169.

[6] Chen SM, Lao ML, Hsieh YH, Liang TJ and Chen KH., "A novel switched-coupled-inductor DC–DC step-up converter and its derivatives." IEEE transactions on industry applications.,Vol. 51, no. 1, 2015, pp. 309-314.

[7] M. A. Chewale,V. B. Savakhande and H. T. Jadhav, "An interleaved flyback inverter for grid connected photovoltaic systems." International conference on circuit,power and cumputing technologies (ICCPCT), April 2017.

[8] V. B. Savakhande, C. L. Bhattar and P. L. Bhattar, "Voltage-lift DCDC Converters For Photovoltaic Application-A Review." International Conference of Data Management, Analytics and Innovation (ICDMAI), Feb.2017.

[9] Viraj Savakhande, C.L.Bhattar and Pctejasvi L. Bhattar, "A VoltageLift DC-DC Converter Using Modular Voltage Multiplier Cell For Photovoltaic Application." International conference on circuit, power and cumputing technologies(ICCPCT), April 2017.

[10] B. Singh, V. Bist, A. Chandra and K. Al-Haddad, "Power Factor Correction in Bridgeless-Luo Converter-Fed BLDC Motor Drive," IEEE Trans. Ind. Appl., vol. 51, no. 2, pp. 1179-1188, March-April 2015.

[11] L. H. S. C. Barreto, E. A. A. Coelho, V. J. Farias, J. C. de Oliveira, L. C. de Freitas and J. Joao Batista Vieira, "A quasi-resonant quadratic boost converter using a single resonant network," IEEE Trans. Ind. Electron., vol. 52, no. 2, pp. 552-557, April 2005.

[12] F. L. Tofoli, D. d. C. Pereira, W. Josias de Paula and D. d. S. Oliveira Júnior, "Survey on non-isolated high-voltage step-up dc–dc topologies based on the boost converter," IET Power Electron., vol. 8, no. 10, pp. 2044-2057, 10 2015.

[13] A. Elserougi, S. Ahmed and A. Massoud, "High voltage pulse generator based on DC-to-DC boost converter with capacitor-diode voltage multipliers for bacterial decontamination," 41st Annual Conf. of the IEEE Ind. Electron. Society, Yokohama, 2015, pp. 000322-000326.

[14] Y. Zhao, W. Li, Y. Deng and X. He, "High step-up boost converter with passive lossless clamp circuit for non-isolated high step-up applications," IET Power Electron., vol. 4, no. 8, pp. 851-859, September 2011.

[15] K. B. Park, G. W. Moon and M. J. Youn, "Non isolated High Step-up Boost Converter Integrated With Sepic Converter," IEEE Trans. Power Electron., vol. 25, no. 9, pp. 2266-2275, Sept. 2010.

[16] T. F. Wu, Y. S. Lai, J. C. Hung and Y. M. Chen, "Boost Converter With Coupled Inductors and Buck–Boost Type of Active Clamp," IEEE Trans. Ind. Electron., vol. 55, no. 1, pp. 154-162, Jan. 2008.

[17] W. Li and X. He, "A Family of Interleaved DC–DC Converters Deduced From a Basic Cell With Winding-Cross-Coupled Inductors (WCCIs) for High Step-Up or Step-Down Conversions," IEEE Trans. Power Electron., vol. 23, no. 4, pp. 1791-1801, July 2008.

[18] S. Dwari and L. Parsa, "An Efficient High-Step-Up Interleaved DC–DC Converter with a Common Active Clamp," IEEE Trans. Power Electron., vol. 26, no. 1, pp. 66-78, Jan. 2011.

[19] M.lakshmi S. hemamalini. "Non isolated High Gaib DC-DC converter for DC microgrid" , IEEE transection on industrial electronics, 2017.

Proceedings of the Fourth International Conference on Communication and Electronics Systems (ICCES 2019)
IEEE Conference Record # 45898; IEEE Xplore ISBN: 978-1-7281-1261-9

An Effective Content Based Image Retrieval Using Dot Diffusion Block Truncation Coding

Admile Nandkumar Sushen

Department of Electronics & Tele-communication Engineering

SVERI's College of Engineering,Pandharpur

nsadmile@coe.sveri.ac.in

Dr.Anup S.Vibhute

Department of Electronics & Telecommunication Engineering

SVERI's College of Engineering,Pandharpur

asvibhute@coe.sveri.ac.in

Abstract -- In the field of image processing application such as medical diagnosis, crime prevention, publishing or advertising, historical research a common image retrieval technique is used. Simple browsing can easily identify images in a small collection of images but for large and different collection of images identification of image becomes critical issue. In this paper for image retrieval four different features are extracted using DDBTC technique. The first two features such as Color Co-occurrence Features (CCF) and Color Histogram Features (CHF) are obtained using color quantizers, Bit Pattern Feature (BPF) and Bit Histogram Feature (BHF) are obtained using Bitmap image. In order to remove the false counter problem and blocking effect different error diffusion kernels are employed. The results shows better accuracy.

Keywords— Average Recall Rate Average Precision Rate, Bit pattern feature, color co-occurrence feature color histogram feature, Dot diffused block truncation coding.

I. INTRODUCTION

Content based Image Retrieval application of computer vision technique to minimize the problem of image retrieval.In annotated based method we have to annote every image based on information of metadata or keywords. In this process the system is not able to capture the exact keywords to represent The images and it becomes time consuming. In CBIR system search of images is based on visual contents rather than metadata. Here "content" is information of texture, shape, or color obtained from images. In 1979 [1] Mitchell and Delp introduces first Block Truncation Coding (BTC). Udpikar and Raina [2] describe the overhead statistical information using source encoding of a block truncation coding. (BTC). Author uses the vector quantization which reduces the bit up to 1.5 bit/ pixel. Yiyan Wu [3] derives Blo for image retrieval. BTC generates the vector quantized bitmap which are then decomposed into a set of vectors. It achieves the compression ratio up to 10:1. G. Qiu [4] uses BTC technique for feature extraction. N. Jhanwara [5] uses motif co-occurrence matrix (MCM) for content based image retrieval. The MCM is similar to the color co-occurrence matrix (CCM), but MCM performs the retrieval task better than the CCM. Experiment shows the MCM improves the retrieval performance as compared to CCM. In [7-10] author uses dot diffusion block truncation coding for image retrieval. To measure the performance of image retrieval various distance metrics are employed.

I.SYSTEM DESIGN

System design flow is mentioned in fig.1

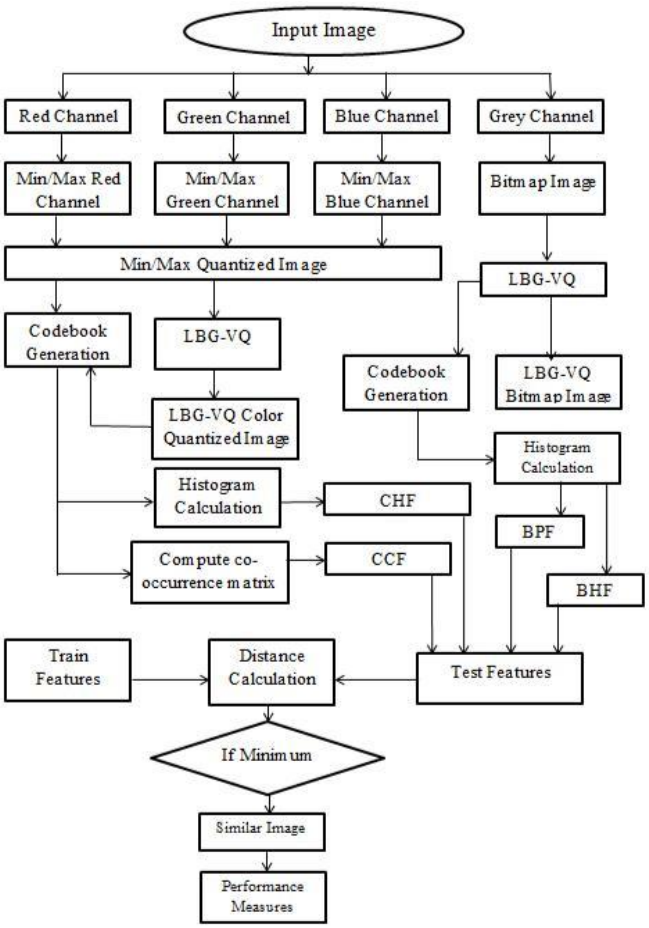

Fig. 1. System Design

A. *Dot Diffused Block Truncation Coding :*

A sample image is used to derive the minimum and maximum quantizers. In this assume at position (i, j) an f (i, j) be the image block. The color images are in RGB color space.

$$Q_{min} = \{\min f_R(x, y), \min f_G(x, y), \min f_B(x, y)\} \quad (1)$$

$$Q_{max} = \{\max f_R(x,y), \max f_G(x,y), \max f_B(x,y)\} \quad (2)$$

In this Red, Green and blue color are represented by R, G and B. The color image is converted into grey image using:

$$f\hat{}(x,y)=1/3[f_R(x,y)+f_G(x,y)+f_B(x,y)] \quad (3)$$

The Bitmap image is also computed using:

$$b_m=1; \text{ if, } f\hat{}(x, y) \ f(i, j) \quad (4)$$

$$0; \text{ if } f\hat{}(x, y) < f(i, j)$$

II.FEATURE EXTRACTION

1.Color Histogram Feature (CHF) :

The Process of CHF is shown in Fig 2.

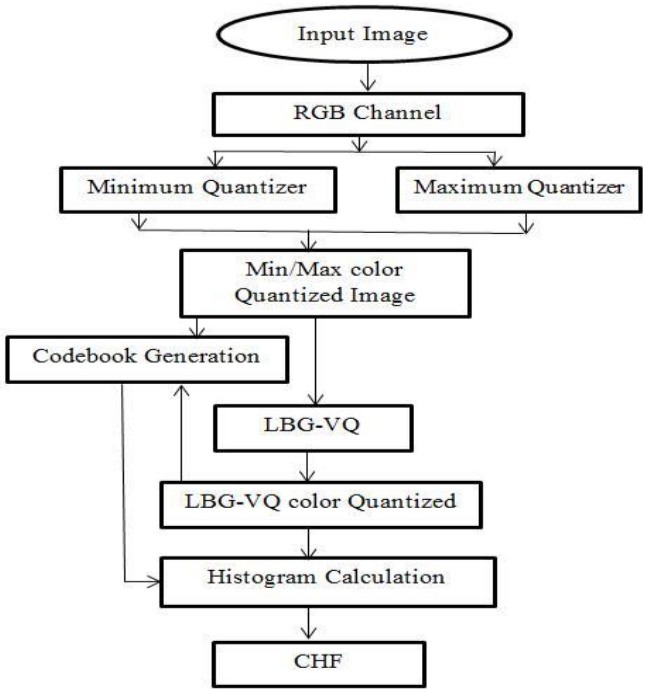

Fig. 2. Design flow of CHF

2. Color Co Occurrence Feature (CCF):

The Process of CCF is shown in Fig 3.

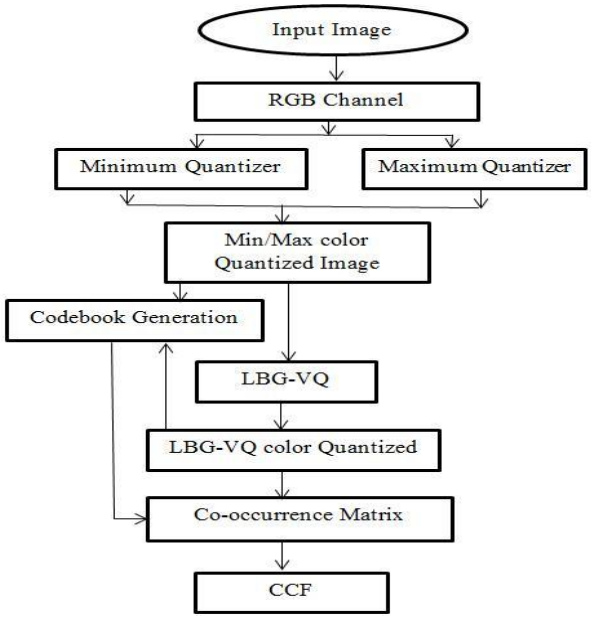

Fig. 3. Design flow of CCF

3. Bitmap Pattern Feature (BPF):

The Process of BPF is shown in Fig 4.

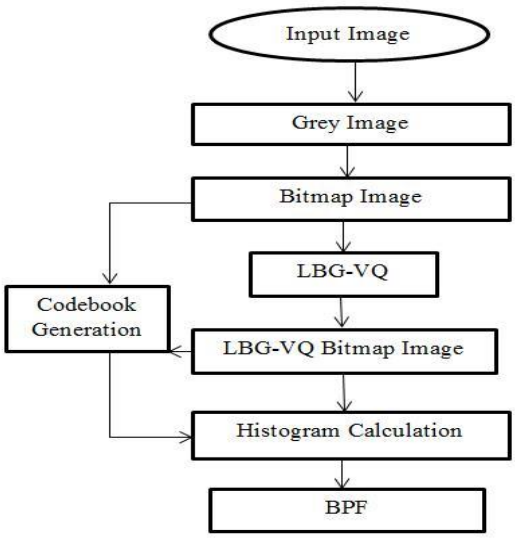

Fig. 4. Design flow of BPF

4. Bit Histogram Feature (BHF):

The Process of BHF is shown in Fig 5.

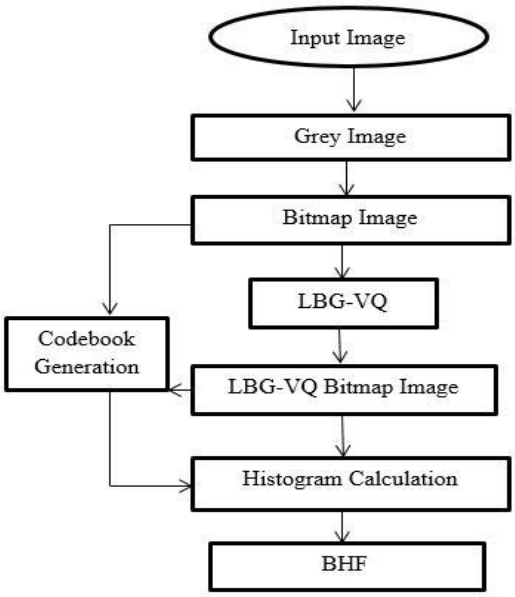

Fig. 5. Design flow of BHF

B. Distance Metrics :

The different distance metrics are given by:

1.L_1 distance

$$\delta(query, target) = a_1 \sum_{k=1}^{Nmin} | CHF_{min}^{query}(k) - CHF_{min}^{target}(k)| + a_2 \sum_{k=1}^{Nmax} | CHF_{min}^{query}(k)\, CHF_{min}^{target}(k)| + a_3 \sum_{k=1}^{Nb} | BPF^{query}(k) - BPF^{target}(k)| \quad (5)$$

2.L_2 distance

$$\delta(query, target) = [\, a_1 \sum_{k=1}^{Nmin} (CHF_{min}^{query}(k) - CHF_{min}^{target}(k))^2 + a_2 \sum_{k=1}^{Nmax} (CHF_{min}^{query}(k) - CHF_{min}^{target}(k))^2 + a_3 \sum_{k=1}^{Nb} (BPF^{query}(k) - BPF^{target}(k))^2]^{1/2} \quad (6)$$

3.x^2 Distance

$$\delta(query, target) = \alpha_1 \sum_{k=1}^{N_{min}} \left(\frac{CHF_{min}^{query}(k) - CHF_{min}^{target}(k)}{CHF_{min}^{query}(k) + CHF_{min}^{target}(k) + \varepsilon} \right)^2 + \alpha_2 \sum_{k=1}^{N_{max}} \left(\frac{CHF_{max}^{query}(k) - CHF_{max}^{target}(k)}{CHF_{max}^{query}(k) + CHF_{max}^{target}(k) + \varepsilon} \right)^2 + \alpha_3 \sum_{k=1}^{N_b} \left(\frac{BPF^{query}(k) - BPF^{target}(k)}{BPF^{query}(k) + BPF^{target}(k) + \varepsilon} \right)^2$$

4. Fu Distance:

$$\delta(query, target) = \frac{L_2 distance}{|CHF_{min}| + |CHF_{max}| + |BPF|}$$

5. Modified Canberra distance

$$\delta(query, target) = a_1 \sum_{k=1}^{Nmin} \frac{|CHF_{min}^{query}(k) - CHF_{min}^{target}(k)|}{CHF_{min}^{query}(k) + CHF_{min}^{target}(k) + \varepsilon} + a_2 \sum_{k=1}^{Nmax} \frac{|CHF_{max}^{query}(k) - CHF_{max}^{target}(k)|}{CHF_{max}^{query}(k) + CHF_{max}^{target}(k) + \varepsilon} + a_3 \sum_{k=1}^{Nb} \frac{|BPF^{query}(k) - BPF^{target}(k)|}{BPF^{query}(k) + BPF^{target}(k) + \varepsilon} \quad (7)$$

C. System Performance:

System performance determined using:

$$APR = \frac{1}{Nt\,L} \sum_{q=1}^{Nt} Nq(L) \quad (8)$$

$$ARR = \frac{1}{Nt\,Nr} \sum_{q=1}^{Nt} Nq(Nr) \quad (9)$$

D. Error Diffusion Kernels:

Here we can mention various Error Diffusion kernels in order to generate the Bitmap images. The advantage of Error diffusion kernels is that it can achieves better image quality as compared to Block Truncation Coding technique. The image compression using BTC and EDBTC and BTC also used in [3, 4, 6]. Here we mention the six different error diffusion kernels.

$$\left(\frac{1}{16}\right)\begin{bmatrix} & * & 7 \\ 3 & 5 & 1 \end{bmatrix} \quad \left(\frac{1}{42}\right)\begin{bmatrix} & & * & 8 & 4 \\ 2 & 4 & 8 & 4 & 2 \\ 1 & 2 & 4 & 2 & 1 \end{bmatrix} \quad \left(\frac{1}{32}\right)\begin{bmatrix} & & * & 5 & 3 \\ 2 & 4 & 5 & 4 & 2 \\ 0 & 2 & 3 & 2 & 0 \end{bmatrix}$$

(a) (b) (c)

$$\left(\frac{1}{32}\right)\begin{bmatrix} & & * & 8 & 4 \\ 2 & 4 & 8 & 4 & 2 \end{bmatrix} \quad \left(\frac{1}{48}\right)\begin{bmatrix} & & * & 7 & 5 \\ 3 & 5 & 7 & 5 & 3 \\ 1 & 3 & 5 & 3 & 1 \end{bmatrix} \quad \left(\frac{1}{200}\right)\begin{bmatrix} & & & * & & 32 & \\ 12 & & 26 & & 30 & & 16 \\ & 12 & & 26 & & 12 & \\ 5 & & 12 & & 12 & & 5 \end{bmatrix}$$

(d) (e) (f)

Error diffusion kernel: (a) Floyd-Steinberg (b) Stucki [62], (c) Sierra (d) Burkers (e) Jarvis and (f) Stevenson filter

Generally while using BTC technique many problems are occurred such as blocking effect and false counter problems. Due to this the image quality can be degraded. In order to overcome such problems various error diffusion kernels are employed

III. EXPERIMENTAL RESULTS

E. Experimental Setup:

Fig.6. Corel Image Dataset

The Fig.6.shows sample images from Corel 1000 Dataset. The Corel 1000 dataset having 10 different Classes. For our image retrieval task we can select 20 images from each class, so that the dataset.

Fig.7. Input color image

Input color image is selected as shown in Fig.7.The Fig.8. is obtained using quantization process From Gray color image Bitmap image obtained as shown in fig.9.

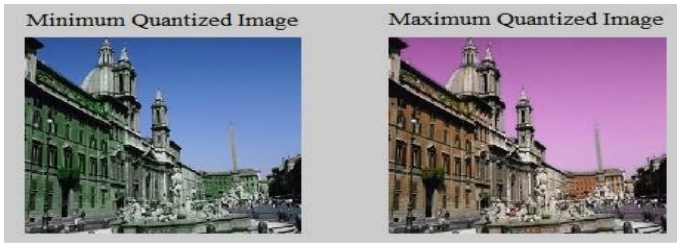

Fig. 8. Min. and Max. Quantized Image

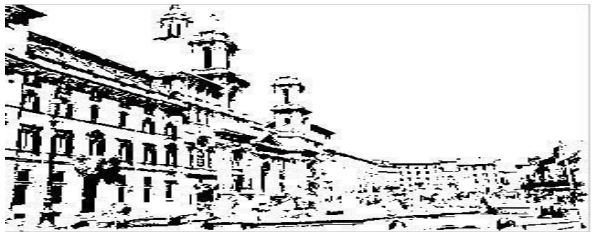

Fig.9. Bitmap Image

The fig.10 and fig. 11 are obtained Using color co-occurrence matrix the image can arrange with vertical, horizontal centered points and diagonally ordered centered points.

Fig.10.Ordered Matrix with centered Points

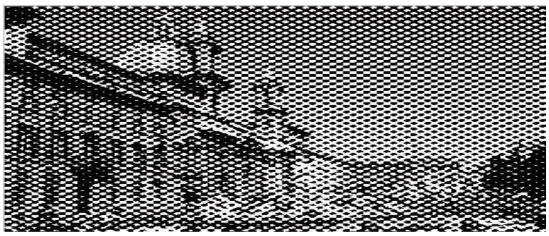

Fig.11.Diagonal Ordered Matrix with Balanced Centered Point

Fig.12.shows the Retrieved images using modified Canberra distance.

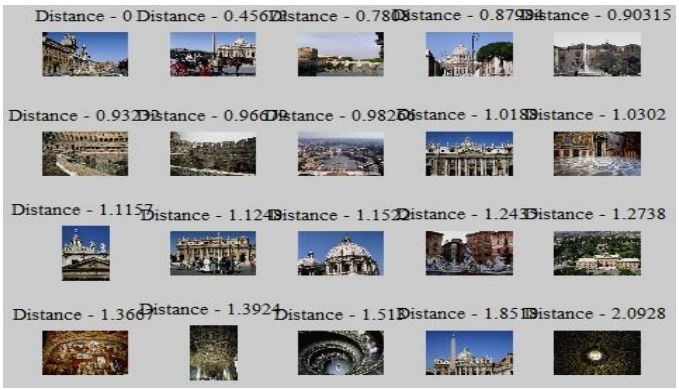

Fig.12. Retrieved Images

The image retrieval task can be performed by using five different distance metrics. The simulated results of L1 and L2 distance listed in Table I and X2 and Fu distance results are listed in Table II.The modified Canberra distance shows the better accuracy listed in Table. III.

Table.I

Class	L_1 distance	L_1 distance	L_2 distance	L_2 distance
	APR	ARR	APR	ARR
African	0.6875	60.19	0.6875	60.19
Beach	0.6875	65.19	0.6875	65.19
Building	0.6875	70.19	0.6875	70.19
Bus	0.8125	80.19	0.8125	80.19
Dinosaur	0.8750	90.19	0.8750	90.19
Elephant	0.5625	60.19	0.5625	60.19
Flower	0.8125	70.19	0.8125	70.19
Food	0.8750	65.19	0.8750	65.19
Horse	0.6875	65.19	0.6875	60.19
Mountain	0.9575	95.19	0.9375	95.19

Table.II

Class	X^2 distance	X^2 distance	Fu distance	Fu distance
	APR	ARR	APR	ARR
African	0.8750	90.19	0.6875	60.19
Beach	0.8750	90.19	0.6875	65.19
Building	0.8750	90.19	0.6875	70.19
Bus	0.9375	95.19	0.8125	80.19
Dinosaur	0.9375	35.19	0.8750	90.19
Elephant	0.9375	90.19	0.5625	60.19
Flower	0.8750	90.19	0.8125	70.19
Food	0.9375	90.19	0.8750	65.19
Horse	0.8750	90.19	0.6875	60.19
Mountain	0.9375	95.19	0.9375	75.19

Table.III

Class	Modified Can. Dist	Modified Can. Dist.
	APR	ARR
African	0.8750	90.19
Beach	0.8750	90.19
Building	0.8750	90.19
Bus	0.9375	95.19
Dinosaur	0.9375	95.19
Elephant	0.9375	90.19
Flower	0.9375	95.19
Food	0.9375	95.19
Horse	0.8750	90.19
Mountain	0.9375	95.19

Performance Image Retrieval is graphicallyshown in Fig.13. And Fig.14.

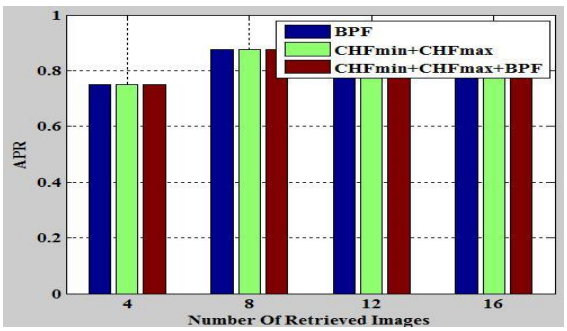

Fig.13. Performance Graph of APR

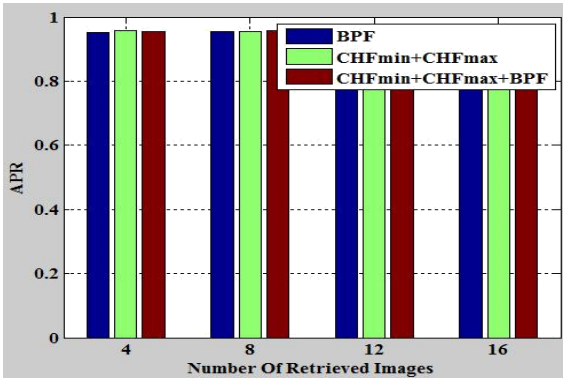

Fig.14.Performance Graph of ARR

COMPARISION OF RESULT WITH OTHER METHODS

In this experiment we measure performance of system and compare with the other retrieval methods.It shows that the proposed system shows the better retrieval accuracy. The Author N.Jhanwar in [4] uses modif co-occurance matrix for image retrieval which achieves 0.5268 accuracy.In our method the average precision rate is 0.9125.Table IV. Shows the comparison of APR with other techniques.

Table IV

Method→ Class ↓	Jhanwar [4]	Qui [5]	Yu [6]	ODBTC [7]	Proposed
People	0.453	0.495	0.849	0.847	0.8750
Beach	0.398	0.423	0.356	0.466	0.8750
Building	0.374	0.405	0.616	0.682	0.8750
Bus	0.741	0.909	0.818	0.885	0.9375
Dinosaur	0.915	0.955	1.000	0.992	0.9375
Elephant	0.304	0.498	0.591	0.733	0.9375
Flower	0.852	0.821	0.931	0.964	0.9375
Horse	0.568	0.689	0.928	0.939	0.9375
Mountain	0.293	0.313	0.404	0.474	0.8750
Food	0.370	0.443	0.682	0.806	0.9375
Average	**0.5268**	**0.5951**	**0.7175**	**0.7788**	**0.9125**

In paper [2] author uses the Error Diffusion Block Truncation Coding and derives the two features which achieves the Precision Rate as 0.797 under Corel 1000.

CONCLUSION

To perform the Experiment DDBTC method and four number of image features are used. The bit pattern feature (BPF) and Bit Histogram Feature (BPH) recognize the contents of image. The color co-occurrence feature (CCF) and color histogram feature (CHF) represents color distribution and image brightness. The simulated results shows better average recall rate and average precision rate. The Error diffusion kernels are employed to minimize the problem of blocking effect and false contour problem. The Modified Canberra distance shows better accuracy as compared to other similarity distance. In the future work, we can increase the size of dataset and computational time for image retrieval can also reduce.

REFERENCES

[1] E. J. Delp and O. R. Mitchell, “Image coding using block truncation Coding,” *IEEE Trans. Comm.*, vol. COM-27, no. 9, pp. 1335–1342, Sep. 1979.
[2] V. Udpikar and J. Raina, \BTC image coding using vector quantization," IEEE Trans.Commun., vol. 35, no. 3, pp. 352{356, Mar. 1987.
[3] Y. Wu and D. C. Coll, \BTC-VQ-DCT hybrid coding of digital images," IEEE Trans. Commun., vol. 39, no. 9, pp. 1283{1287, Sep. 1991.
[4] G. Qiu, “Color image indexing using BTC,” IEEE Trans. Image Process. vol. 12, no. 1, pp. 93–101, Jan. 2003.
[5] N. Jhanwar, S. Chaudhurib, G. Seetharamanc, and B. Zavidovique,\Content based image retrieval using motif co-occurrence matrix," Image Vis. Comput., vol. 22, pp. 1211{1220, Dec. 2004.
[6] Jing-Ming Guo,Heri Prasetyo , " Content-Based Image Retrieval Using Error DiffusionBlock Truncation Coding Features "IEEE Trans.on Image Processing, vol. 25, No. 3, pg.no.466-481 2015
[7] Nandkumar S. Admile and Prof. Rekha Dhawan, “Content Based Image Retrieval Using Feature Extracted from Dot Diffusion Block Truncation coding”, IEEE International conference on communication and Electronics Systems (ICCES-2016) Coimbatore, India,.**DOI:** 10.1109/CESYS.2016.7889864, 21-22 October 2016
[8] Nandkumar S. Admile “Image Retrieval Based on Block Truncation coding”, IEEE International conference on communication and Electronics Systems (ICCES-2018)Coimbatore, India, **DOI:** 10.1109/CESYS.2018.8724097, 15-16 October 2018
[9] Nandkumar S. Admile,Ajit Kanase and Rajesh Khiste ,”User Oriented Image Retrieval Using Feature Extracted by Dot diffusion Block Truncation coding”, IEEE International conference for convergence in Technology (I2CT-2019) Pune, India, 29-31 March 2019.
[10] Nandkumar S. Admile,”Performance Measure of image retrieval using different distance metrics”, IEEE International Conference on Intelligent Computing and Control Systems (ICICCS-2019) Madurai, India, 15-17 May 2019.
[11] Nandkumar S. Admile,”A survey on different image retrieval techniques”, International Research Journal of Engineering and Technology (IRJET-2018), Volume: 05 Issue: 10 | Oct 2018.
[12] Jing Ming Guo and Heri Prasetyo, “Effective Image Retrieval Using Feature Extracted Using Dot Diffused BTC,” IEEE Trans. Vol.24, no.3, pp 1010-1024.

Proceedings of the Fourth International Conference on Communication and Electronics Systems (ICCES 2019)
IEEE Conference Record # 45898; IEEE Xplore ISBN: 978-1-7281-1261-9

An Intelligent System for Phishing Attack Detection and Prevention

Megha N
Dept. of Technology
Government Engineering College,
Idukki, Kerala, India
Email: meghavineeth03@gmail.com

K R Remesh Babu
Dept. of Information Technology
Government Engineering College,
Idukki, Kerala, India
Email: remeshbabu@yahoo.com

Elizabeth Sherly
Indian Institute of Information
Technology and Management-Kerala
Thiruvananthapuram
Email: rsherly@iiitmk.ac.in

Abstract*—Cyber security is a most important trepidation in the widespread adoption of internet technologies in the everyday activities of human being. Even though more sophisticated technologies emerged on the Internet, but different kinds of attacks and threats are also increasing day by day. Cyber attacks causes loss of customer confidence in adopting internet based applications. Phishing attack is one of the common vulnerabilities in the cyber space. Most of the anti-phishing solutions proposed so are focused only on a single issue and needs improvement. For malicious web page detection and prevention, an intelligent multi agent solution is proposed in this paper with the help of machine learning methods. The proposed approach detects both phishing sites and websites with malicious content. This multi-agent system contains four autonomous intelligent agents, which communicate with each other using the Extensible Messaging and Presence Protocol (XMPP) for decision-making. The first is a monitoring agent, second and third is for decision-making (using the machine-learning classifiers) and the fourth is for action-performing. The first agent is responsible for extracting URLs. It passes the extracted URLs to the second agent for feature extraction and classification. If any phishing is detected, the second agent communicates with the fourth agent and the site is blocked. Otherwise, the second agent communicates with the third agent for malicious script detection. If any malicious script is detected then the fourth agent blocks the entire web page. We have tested the performance and accuracy of the proposed method and obtained results ensures its efficiency.

Keywords*—Phishing attack, machine learning, classifiers, intelligent agents, support vector machine.

I. INTRODUCTION

Cyber security is critical in adopting online services in today's world. Both academia and industry had given much attention in this field due to high threat rate. As the network becomes a more pervasive, all the cyber attacks have become a serious threat to the network users. Internet security is crucial, since most of the human business and social and financial activities occur through it. Even though more sophisticated technologies emerged for the internet, more focused attacks are also happening. Financial and personal information loss is the major hazard for a customer, while loss of trust and reputation is the resultant effect to the business owners due to security issues. Ultimately security threats will create lack of confidence in customers to adopt online services. The weak internet security, huge and quick economic benefit attracts criminals to this area. Since online services have become more popular, security risks on the internet is also grown exponentially. The attackers are more intelligent and they make newer and adaptable attacks that bypass existing security measures. Some of the attacks are DDOS, Man-in-Middle, Phishing, SQL injection, Cross-site scripting, etc.

One of the most common type of attack in cyber space is phishing. In phishing, a forged website is created by an attacker to mimic the original website so as to steal sensitive information or credentials of a user. In some cases, attackers may inject malicious scripts to the legitimate websites. The intruders adopt several methods to steal the information from the user. So it is difficult to provide security to the emerging new kind of attacks [3]. Phishing attack can be done in several forms. URL obfuscation, based on hyperlink and email are some of the common attacks. Many research proposals are offered to protect websites from this type of attack but the phishers are much smart, so that they try new methods to overcome the protection measures.

Recently phishing attacks became one of the serious issues due to the use of smart strategies for the creation of phishing websites. Phishing sites are actually a forged website created by an attacker that mimics the real website. Using these fake sites all the sensitive information are taken away by the attacker. First of all, an attacker creates phishing emails and sends it to the victim. For the receiver this email seems to be from an authentic person and request victim to update or validate their sensitive information related to bank account,

other personal information etc., by using the hyperlink provided in the email. This link will leads to a phishing website and when the user enters the details to this site all their confidential information or credentials will be captured by the hacker. To prevent these types of attacks anti phishing techniques are available [3], but still these attacks are evolving and bypassing all the countermeasures and most of these solutions are imprecise because of false positive rates. There are some existing machine learning technique for the detection of phishing attacks [8][9] and more, but it focus on single objective. To overcome, this paper presents a machine learning based method. For improving the accuracy and efficiency here we have incorporated another detection mechanism known as the Link Guard algorithm [6].

The objective of this work is the detection and prevention of phishing and malicious script attack using machine learning classifier and agent based intelligent system. The rest of this paper is organized as follows. Section 2 describes about the various literatures in this field. The detailed description of the proposed method is given in the section 3. Experimental setup and performance analysis of the proposed method is given in section 4. Finally this paper concludes in section 5.

II. RELATED WORKS

There are several methods adopted for ensuring phishing attack free website operations. These methods can be classified according to the mechanisms adopted in each one. Blacklisting, heuristic methods, visual similarity assessment methods and machine learning based methods. In the following paragraphs we have analyzed these methods.

Blacklist Methods

Blacklist is actually a database that stores all the previously detected phishing URLs or IP addresses. The paper [2] is an enhanced blacklist method that detects phishing by extracting the key features from source code. In this method already existing or the imitation of phishing websites or its variations are identified. Using the features these website are identified with a unique fingerprint. The unique fingerprint generation is based on the Simhash algorithm. The key features used are filename in the request URLs, path name and attribute values of tags used in the scripting language. Now a large number of toolkits are available for creating phishing websites. So detecting phishing using blacklist method like [16] has become inefficient. The white-listing method proposed in [17] that automatically updates a list of all familiar original websites.

Heuristic Methods

Blacklisted methods detect phishing sites, but still it has certain disadvantages such as new phishing attacks remain undetected. In order to address this issue heuristic methods are introduced. These are experience based techniques for solving a problem. These methods produce near optimal solutions. It finds solutions by learning the situation and then the discovery of solution to the problem under consideration. The solution obtained using these methods are not guaranteed to be optimal. The methods mentioned in [4][11] are heuristic approaches for phishing detection. The method in [10] called CANTINA is based on the term frequency and inverse document frequency of a word in the query.

Visual Similarity Based Methods

Another technique used by the phishers is visual similarity method. They create visually similar websites to the original ones. This similarity usually confuses the users and sometimes they think or feel that the mimicked website as original. Some research works are based on this similarity identification [5] [18]. The method proposed in [18] considers content and format of text in the website. It also considers images, tags, style sheets, etc., to detect the phishing. [5] is based on the image level, which matches the suspicious Web page snapshot image with the legitimate Web page snapshot image, and therefore can deal with the non-text tricks that make similar Web pages with various HTML contents. [5] uses local and global features of the snapshot images which can be used for phishing detection together.

Machine Learning Methods

Artificial Neural Network (ANN) is another method used to detect phishing attack [8]. The main aim of this machine learning based method is to model neural network to classify websites as legitimate or phishing. They have used one hidden layer for their experiments. They trained the neural network by changing the values of momentum and learning rate until a lower error rate is acquired. The papers [9][20] are also deals with machine learning methods for phishing detection. In [20] a wrapper-based features selection method was introduced. This method aid in the selection of most significant features. This selected features are subsequently used for the accurate phishing website prediction. But wrapper-based features selection method spends more time and need additional computational overhead than other methods.

The support vector machine achieved notable classification accuracy because it uses a labelled dataset. Web page source code characteristics can also be used for phishing detection [9]. There are certain features that differentiate phishing websites from original. Based on these characteristics, it finds the severity percentage. It considered characteristics like logos, suspicious URLs, short-lived, HTTPS, pop up window script, iframe and domain.

The paper [7] introduced multi-agents for phishing detection. In this paper, they try to detect a new type of phishing attack known as tab napping. They have used image retrieval method for detecting the website layout changes and

other reloads. Considering the above facts, an intelligent agent based method is proposed in this paper.

III. PROPOSED METHOD

In the proposed method, effective phishing detection and prevention mechanism using agent-based intelligent system is introduced. Here an agent-based intelligent system is used for the detection and prevention of phishing attacks. It also detects malicious scripts present in non-phishing sites. Agent technology is used to solve the critical problems with some sort of intelligence. Most of the existing methods used are based on single issue or agent. As the internet technology advances to horizon, new problem arises, so there is need for multi-agent based approach to prevent phishing attacks.

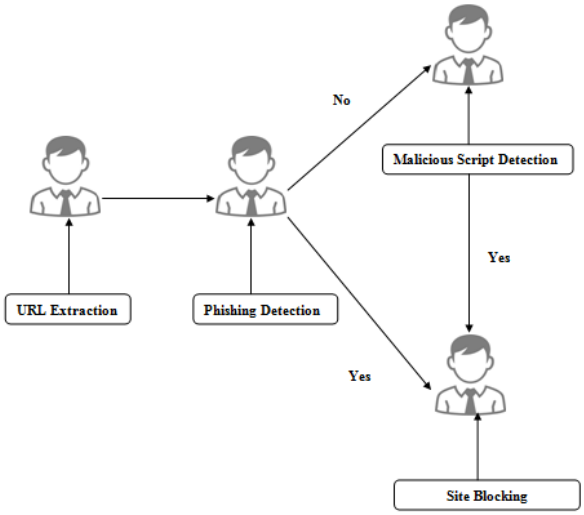

Fig.1. Overview of the Proposed Method

The overview of the proposed method is given in Fig. 1. The aim of this method is to use different intelligent agents for phishing detection. This multi-agent modular approach will increase the performance. The decomposition allows the agent to use the most appropriate technique for solving the problems. The multiple agents cooperate and coordinate with each other to solve the phishing issue continuously. These heterogeneous agents work autonomously. These agents communicate to each other using message passing mechanism.

Proposed system contains three tier software layers with four agents. These layers are named as lowest, middle and upper most layers. The first two layers contain one agent each while third layer contains two agents. The function of lowest layer is the extraction of URLs. The classification of phishing attacks are done at layer 2. The upper most layer contains two agents. One agent for blocking the phishing URLs and other for unauthorized malicious script detection. The proposed layered architecture is shown in the Fig. 2.

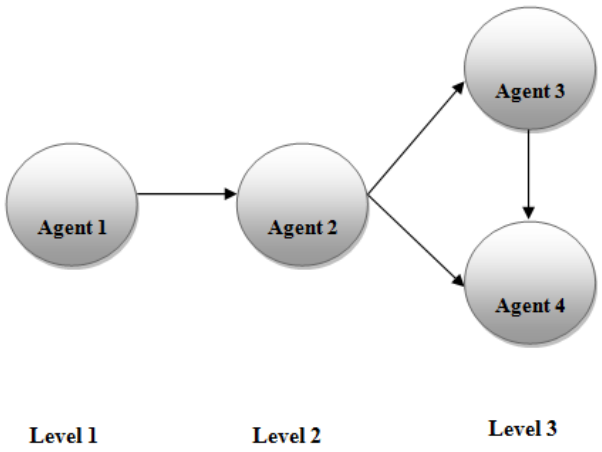

Fig.2. Layered Agent Architecture

In the proposed layered method the autonomous agents with high intelligence are distributed and they can cooperate each other. Here the task and responsibilities of each agent in the different layers are well defined. Each agent knows how to overcome a situation independently or collectively with the help of other agents. Thus, this multi-agent system has high learning capacity and it can easily adapt with the news changes in the system.

In the proposed architecture, the level 1 agent acts as a sensor module. It extracts the URL of web pages from email, browser or any other source. The results or the extracted URL information at this level is passed to agent at the next level i.e. level 2 in the hierarchy of the classification process. The detection of phishing is done at layer 2 with the help of agent at this level. Here webpage is classified as whether it is phishing or not. This is done using machine learning classifiers. In this level, we have used ANN and SVM for classification. At level 3 there are two agents. One agent for blocking the malicious website and another for script detection. After the script detection phase, if the URL is free from phishing attacks and scripts then it is marked allowable website. If any malicious script or phishing is detected then the URL is passed to blocking agent at this level and the webpage is finally blocked.

IV. EXPERIMENTAL SETUP AND RESULT ANALYSIS

The proposed method is experimented using data set from [12][13][14]. In order to confirm whether the data used is a phishing dataset, we have tested it with link guard algorithm. This algorithm is to analyze the difference between actual and visual links. The algorithm first extracts the DNS names. If the extracted names are not identical then it can be considered as a phishing. Next it checks is there is any dotted decimal IP address is directly used in the DNS. This is also considered as a phishing. Sometimes, actual and visual links are to be checked. For this encoded visual links are decoded and compare with the original link. If the method unable to obtain the destination information from this provided visual DNS

then it analyze the actual DNS. While analyzing the DNS the method checks whether actual DNS is present in black-list or white-list. If it is not present in any of the list then go for pattern matching. The pattern matching is invoked mainly to find unknown attacks. In pattern matching process, it checks whether the actual DNS name is different from the sender's DNS name. If it is similar then invoke similarity and calculate the minimal number of changes. If it is similar then the method concludes that two strings are identical. In the similarity check if number of changes are little, then there is high similarity rate. If two DNS names are similar but not exactly identical then they are also considered as phishing.

The proposed methodology is implemented using the Smart Python Agent Development Environment (SPADE) software framework [1]. The distributed multi-agents can communicate and cooperate with each other. For the agent communication the method used Extensible Messaging and Presence Protocol (XMPP). The XMPP is a protocol for streaming XML elements over a network in order to exchange messages. This protocol is mostly used in instant messaging applications. The agents are deployed at different levels to reduce the bad effect of a phishing attack and malicious scripts to a webpage.

Phishing and the malicious script are detected using a machine learning classifier. In the case of phishing detection, first system considers certain features from the URL. The features considered given in the Table 1. After feature extraction, the binary data is passed to the proposed model. This multi-layer multi-agent model first learns from the data set given. After that, we tests whether the model has learned properly or not. After the learning phase of the model, then a new URL are classified as phishing or non-phishing. In malicious script detection, a dataset is given to the model converted to vectors before learning and testing phase. Then the system classifies the inputs as malicious or not.

TABLE 1. FEATURES FOR PHISHING ATTACK DETECTION [12]

Features	Description
URL Length	Length of URL. Sometimes long URL names are used to hide the doubtful part in the phishing site.
IP Address	IP address is a substitute of URL names.
Shortening Service	Short URL can also be used direct to the requested webpage.
@ symbol	Ignore the rest of a URL after this @ symbol.
Double Slash Redirecting	The "//" symbol in a URL also used as redirection to another location.
Prefix or Suffix	Adding some prefix or suffix terms especially separated by (-) to the domain name is a phishing method.
Subdomain	If a URL have more than two dots (.), i.e., subdomains high chance of phishing.
Website Traffic	Websites can be classified according to traffic into it. Phishing website or suspicious websites has less traffic.
Favicon	Loading favicon from a domain is considered as phishing.
Port	Port opening is crucial. Anybody can access the data or attack through an open port.
HTTPS Token	Sometimes https token is used for phishing.
Request URL	Usually the all the contents such as images, videos, etc., are embedded in the page itself and shares same domain.
URL of Anchor	This is same as previous Request URL.
Links of Tags	Link tags are to be connected to the same domain.
Submitting to Email	Proper use of mail() and mailto() functions.
Abnormal or Nonstandard URLs	In this type URL doesn't contain the original host name.
iframe	Use of "iframe" tag and make it as invisible from the users.
Age of Domain	Phishing websites exists temporarily
DNSRecord	Entry in the DNSRecord is an attribute to find whether a website is original or not.
On Mouseover	Usually onMouseover() command is disabled in a phishing website. This is to prevent users from knowing the correct address shown in the address bar.
Right Click	Phishers also disable right click function. Since right click facility allows user to view and the page source code.
Pop up Window	An original website doesn't use any popup window to submit personal information.
Page Rank	Phishing website does not have a page rank.
Google Index	Usually Google index is created for each webpage. A Phishing site doesn't have any index.
Links Pointing to Page	Most of the phishing websites does not have hyperlinks points to them due to its volatile nature.

Performance Analysis

For the performance analysis and comparison, two different classifiers with five types of dataset are used to test the efficiency of the proposed technique. The proposed model uses support vector machine for classification and artificial neural network for the comparison. For the evaluation, the confusion matrix is considered. From the confusion matrix accuracy, precision, recall and specificity can be calculated. Table 2 and Table 3 show the accuracy, precision, recall, specificity, false positive and false negative of the proposed ANN and SVM classifiers in five different datasets with different sizes respectively. Accuracy is that the whether the proposed method correctly labelled a website from all the phishing websites. We have used 80 percentage data in the data set for training purpose and 20 percentage data for testing phase.

TABLE 2. ANALYSIS OF PROPOSED ANN CLASSIFIER (VALUES IN PERCENTAGE)

No. of Data	Accur-acy	Prec-ision	Recall	Speci-ficity	False Positive	False Negative
779	91.2	81.5	93.9	90	6	100
2456	59.6	25.2	76.5	56.4	23.4	43.5
8550	89	84.4	96	81.7	3.9	18.2
10000	87.8	83.5	93.7	82.1	6.2	17.8
11055	89.3	82.7	97.1	81.6	2.8	18.3

From the tables it is clear that accuracy of the proposed SVM method is high compared to ANN based method. This is

also true in the case of precision analysis. As the data increases the SVM shows good rate than ANN, i.e. it is correctly labelled phishing sites. Similarly recall and specificity value is high for the proposed method. False positive is the rate of incorrectly classified positive values and false negative is the incorrectly classified negative values.

TABLE 3 ANALYSIS OF PROPOSED SVM CLASSIFIER (VALUES IN PERCENTAGE)

No. of Data	Accur-acy	Prec-ision	Recall	Speci-ficity	False Positive	False Negative
779	92.3	79.4	100	89	0	10.9
2456	92.5	91.6	91.6	93.2	8.3	6.7
8550	97.4	98	97.4	97.3	2.5	2.6
10000	96.8	97.5	97	96.6	3.3	2.9
11055	97.1	97.7	97.1	97	2.8	2.9

From the table 3 it is clear that while comparing SVM and ANN, SVM shows better results for the every evaluation.

Next we have evaluated the script detection efficiency of the proposed SVM method with existing method in paper [15]. The obtained values are given in the Table 4. The experimental results shows that the proposed SVM have higher efficiency that the existing method. The comparison of evaluation parameters such as precision, recall, F-score and negative predictive power are better for the proposed method.

TABLE 4 SCRIPT DETECTION EFFICIENCY

Classifier	Precision	Recall	F-score	Negative predictive Power
Proposed SVM	95	99	97.43	99
SVM [15]	92	74.2	76.4	99.7

In the existing system, the malicious script detection is done based only on few features and in the proposed method the malicious script detection is done by directly converting the scripts into vectors. If the detection is completely based on few features it may limit the detection accuracy and sometimes all types of the script may not be able to detect. If certain condition fails detection process also fails. This is the one of the advantage of the proposed method. In future the proposed mechanism can be extended to block only the malicious script execution without interrupting the whole website.

V. CONCLUSION

In this proposed method an attempt is made for implementing an agent-based architecture and machine learning classifier for resisting different types of phishing attacks. The existing phishing methods are single agent mechanism. In the distributed internet we need a system that works using multiple agents that communicate in a peer-to-peer fashion by message passing. This paper presented a layered multi-agent framework for detecting and rectifying web phishing attacks. The multi-agents are used for URL extraction, phishing detection, script detection, and blocking. The method is capable to recognize and learn according to the environmental changes. The experimental result indicates that the proposed system is capable of achieving the objective. The experiment results also show that the proposed SVM method is an effective mechanism to detect phishing attacks and malicious scripts. The phishing detection is done using machine learning classifier SVM and ANN. From the results, it is clear that many functions can be incorporated in one method using multiple agents and these multi-agents can be triggered to find a solution for different complex problems.

REFERENCES

[1] Javi Palanca, SPADE 3.1.0 documentation, Release 3.0.0, https://buildmedia.readthedocs.org/media/pdf/spademas/feature-3.0/spade-mas.pdf, retrieved on Aug 17, 2018.

[2] Routhu Srinivasa Rao, Alwyn Roshan Pais, "An Enhanced Blacklist Method to Detect Phishing Websites", *Springer International Publishing AG*, ICISS 2017, LNCS 10717, pp. 323–333, 2017.

[3] Tenzin Dakpa, Peter Augustine, Study of Phishing Attacks and Preventions, *International Journal of Computer Applications*, Vol. 163 – No 2, April 2017.

[4] Jin-Lee Lee, Dong-Hyun Kim, Chang-Hoon Lee, "Heuristic-based Approach for Phishing Site Detection Using URL Features", *Proceedings of the 3rd International Conference on Advances in Computing, Electronics and Electrical Technology*, CEET-2015, pp. 131-135.

[5] Yu Zhou, Yongzheng Zhang, Jun Xiao, Yipeng Wang, Weiyao Lin, "Visual Similarity based Anti-Phishing with the Combination of Local and Global Features", *2014 IEEE 13th International Conference on Trust, Security and Privacy in Computing and Communications*, pp.189-196

[6] U.Naresh, U.V Sagar, C.V.M Reddy, "Intelligent Phishing Website Detection and Prevention System by Using Link Guard Algorithm", *IOSR Journal of Computer Engineering*, Vol. 14 (3), pp. 28-36, 2013.

[7] Sarika S, Varghese Paul, "Distributed Software agents for antiphishing", International Journal of Computer Science Issues, Vol. 10, Issue 3, No 2, pp. 125-130, 2013.

[8] R M. Mohammad, F Thabtah, Lee Mc Cluskey, "Predicting Phishing Websites using Neural Network trained with Back-Propagation", *Proceedings of the 2013 World Congress in Computer Science, Computer Engineering, and Applied Computing. WORLDCOMP 2013 and World Congress in Computer Science, Computer Engineering, and Applied Computing, Las Vegas, Nevada*, pp. 682-686.

[9] M G Alkhozae, O A Batarfi, "Phishing Websites Detection based on Phishing Characteristics in the Webpage Source Code", *International Journal of Information and Communication Technology Research*, Vol. 1 No. 6, , pp. 283-291, 2011.

[10] Yue Zhang, Jason Hong, Lorrie Cranor, "CANTINA: A Content-Based Approach to Detecting Phishing Web Sites". WWW '07 Proceedings of the 16th international conference on World Wide Web, pp. 639-648, 2007.

[11] Suman Bhattacharyya1 , Chetan kumar Pal2 , Praveen kumar Pandey3, "Detecting Phishing Websites, a Heuristic Approach", *International Journal of Latest Engineering Research and Applications (IJLERA) ISSN: 2455-7137*, Volume – 02, Issue – 03, March – 2017, PP – 120-129.

[12] "Detecting phishing websites/datasets", https://github.com/abhishekdid/detecting-phishing-websites/tree/ master/datasets retrieved on August 17, 2018.

[13] "Detecting phishing websites using machine learning", https:// github.com/abhishekdid/detecting-phishing-websites, retrieved on August 17, 2018.

[14] "Detecting phishing website using ML", https://github.com/rewanth1997/Detect-phishing-websites-using-ML, retrieved on August 17, 2018.

[15] P Likarish, E J I Jo, "Obfuscated Malicious Javascript Detection using Classification Techniques", IEEE *4th International Conference on Malicious and Unwanted Software (MALWARE)*, pp. 47-54, 2010.

[16] Sheng, S., Wardman, B., Warner, G., Cranor, L., Hong, J., Zhang, C., "An empirical analysis of phishing blacklists", In: Proceedings of the 6th Conference on Email and Anti-Spam, pp. 1-6, 2009.

[17] Ye Cao, Weili Han, Yueran Le, "Anti-phishing Based on Automated Individual White-List", Proceedings of the 4th ACM workshop on Digital identity management (DIM '08), pp. 51-60, 2018.

[18] Ankit Kumar Jain and B. B. Gupta, "Phishing Detection: Analysis of Visual Similarity Based Approaches," Security and Communication Networks, Vol. 2017, Article ID 5421046, 20 pages, 2017.

[19] Waleed Ali, "Phishing Website Detection based on Supervised Machine Learning with Wrapper Features Selection", *International Journal of Advanced Computer Science and Applications*, Vol. 8, No. 9, 2017, pp. 72-78.

[20] S Abu-Nimeh, D Nappa, Xinlei Wang, Suku Nair, "A Comparison of Machine Learning Techniques for Phishing Detection", Proceeding of the anti-phishing working groups - 2nd ACM annual eCrime researchers summit (eCrime '07), pp. 60-69, 2017.

Proceedings of the Fourth International Conference on Communication and Electronics Systems (ICCES 2019)
IEEE Conference Record # 45898; IEEE Xplore ISBN: 978-1-7281-1261-9

Deep Learning Based Classification Algorithm For Detection Of Diabetic Disease

Pavithra C M
Mtech, IE
Sri Jayachamarajendra College Of Engineering
jsstu, Mysuru, India
Pavithracm2@Gmail.Com

Dr Shankaraiah
Head Of Department
Sri Jayachamarajendra College Of Engineering,
Jssstu ,Mysuru, India
Shankaraiah@Sjce.ac.in

Dr Srikanth T
L&T Technolgy Service
Mysuru,India
Srikanthmysore@Gmail.Com

Abstract: Neural Networks And Deep Learning Currently Provide Best Sollutions To Many Problems In Image Recognition,Speech Recognition. Diabetic Is Diabetic Complication That Affects Eyes. Diabetic Can Easily Detect From Eye Image Of Person Optic Disk Detection And Segmentation Of Eye Is Very Difficult Due To Variation Of Size And Shape Of Optic Disk .In This Paper Deep Learning Network Applied To Train The Data .The Eye Images Collect From Public Database And Hospital . Train The Images By Using Neural Network. Store Features And Results From Trained Images. Then Upload Test Image To Get The Result Testing Image Procedure Include Preprocessing Feature Extraction, Then Random Forest Classifier Used To Extract Features And Classify The Image Based On Train Images Data Set .Accuracy Of The Model Is High.

Key Words: Deep Learning; Optic Disk Segmentation; Feature Extraction; Diabetic

Ⅰ.Introduction

Optic Disk Detection Is Key Step To Find Eye Diseases. In This Process, OD Detection Plays An Important Role [3] [2] Diabetic Retinopathy Can Be Detect In Different Ways, Like Eye Image, Blood Samples The Main Cause For Diabetic Is Sugar Level High In Blood Vessel. Increase In Sugar Mainly Damage Eye Vision .Main Symptoms Of Diabetic Retinopathy Blurred Or Double Vision, Difficult In Reading, Eye Pain, And And Eye Pressure. In The Eye Fundus Images OD Segmentation Can Be Categorized Into Three Categories [10] [11] Namely Template Based Methods, Deformable Model Based And Morphology Based Methods. Diabetic Disease Can Be Detects By Using Numerous Methods .Here Machine Learning And Deep Learning Methods Are Applied For Training And Classify Data. Preprocessing Of Eye Image And Feature Extraction [4] Optic Disk Segmentation Is Explained

Ⅱ. Related Work

There Are Several Methods Are There To Detect Diabetic Disease.Multiaproach Method To Segment The Optic Disk. A Machine Learning Graph Method Is .Used To Detect The Disease [1]

An Accurate And Efficient Optic Disc (Od) Detection 0d Segmentation Technique. A Circular Transformation Is Designed To Capture Both The Circular Shape Of The Od And The Image Variation Cross The Od Boundary Simultaneously [2] Structure Preserving Guided Image Filter For Analysis Of Optic Disk. In Preprocessing Stage This Filter Is Used. Then Detecting Eye Disease Procedure Take Place [3]

The New Algorithm Darwinian Particle Swarm Optimization Algorithm .This Algorithm Include Stages. Image Processing, Segmentation, Ellipse Fitting, And Od Localization. This Method Is Efficient Than Blood Vessel Based Method [4] Proposes Optic Disc And Optic Cup Segmentation Using Super Pixel Classification For Glaucoma Screening. This Paper Concatenates The Three Types Of Features From Different Sources. In Future Work, Multiple Kernel Learning Will Be Used For Enhancement [5]

New Method For Fast Optic Disc Segmentation In Retina Using Polar Transform. The Methodology Has Used Hierarchical Combination Of Morphological Operations And For The Optic Disc Localization. This Gives Better Results As Relying Only On The "Optic Disc As The Brightest Spot" Technique [6]

A Rule-Based Method Is Proposed To Segment Optic Disc. Firstly, We Apply Two Over-Segmentation Algorithms To Produce Super-Pixels. Taking Super-Pixels Instead Of Pixels As Basic Processing Units Greatly Improves The Efficiency But Still Defected Part Gives Inaccurate Segmentation [7]

Hybrid Approach Optic Disc Segmentation For Retinal Images. The Success Of The Hybrid Approach Was Evaluated According To Both Localization And Segmentation. Performance Of The Study Was Evaluated With 30 Images According To Dice And Jacquard Similarity. [8]Machine Learning Based Automatic Neovascularization Detection On Optic Disc Region Nv Particle Proves Indicator Proliferative Diabetic Retinopathy (Pdr) And It Is Featured By The Presence Of New Vessels In The Retina. The New Vessels Are Fragile And Pose A High Risk For Sudden Vision Loss [9]

Detection Of Diabetic By Using Multi Layer Perception Neural Network Classifier And Dct Transform Is Used To For Feature Extraction [10] Deep Learning Algorithm Method [11] Is Used To Detect Different Types Of Diabetics Like Type 1 Or 2. .Here Convolution Neural Network Method Is Using To Detect Automatic Detection Of Diabetic [12]

III. Proposed Method

There Are 2 Stages Shown In Figure 1

I Training Stage

2 Testing Stage.

Deep Learning Neural Network Applied To Train The Model .In Testing Stage First Performed Preprocessing Stage ,In Preprocessing Stage Following Procedures Are Done .Sharpening Image, To Remove Noise, Detect The Edges Of The Optic Disk, Calculating Gradient Magnitudes ..Here Dwt /Dct Feature Method Applied To Extract From Test Image. Extract Energy Contrast, Standard Deviation, Entropy By Using Random Forest Classifier Then Classify Based On The Trained Data Set. Drion Database There Are 110 Eye Images. In Hospital Database 125 Images Are There. We Use 125 Images For To Train The Model.110 Images For Testing .Deep Learning Network Gives High Accuracy,

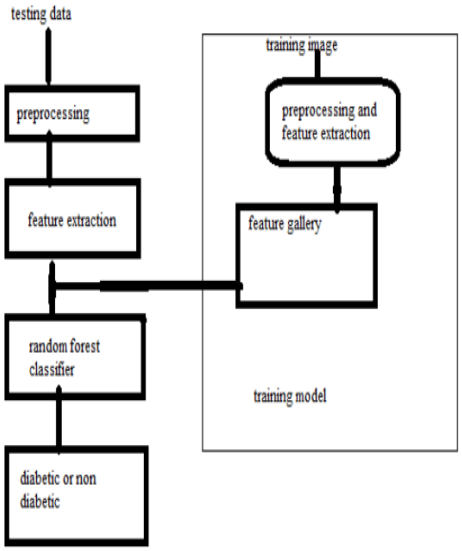

Fig 1.Shows Flow Diagram Of The Proposed System

IV .Implementation

Mat Lab Software Is Used To Implement The Proposed System. Mat Lab Is High Level Computing Language .Feasible And Easy To Work With Data. First Training Of The Image Is Done, After Completion Of Training, Upload The Test Image. Then Following Sections Are Performed

1 .Preprocessing Stage

First Crop The Eye Image To Get Optic Disk Portion. Then Detect The Optic Disk Of An Eye.[6][9] There Are Several Steps In Preprocessing Of Image .Like, Thresholding Circular, Hough Transform Finding Boundary Edges, Gradient Magnitude, Sharpening And Dct Of Image .Convert Color Image Into Gray Image. Gray Image Conversion Colors [7] [8] Displayed

On Retinal Images Are Usually Defined In Tri Colors As Red, Green And Blue Space Is Called As Rgb Color Space. There Are 2 Conversion Methods Are There

1, Average Method

2, Luminosity Method

Average Method Add All 3 Colors Of Image. Find Average 3 Colors.

Gray Scale Image = R+G+B/3

In Luminosity All Color Wavelength Is Change According To Intensity Of Wavelength, Grayscale Image Get From Below Equation

Gray Scale = ((0.3*R) + (0.59*G) + (0.11*B))

1.1 Canny Edge Detector

Canny Edge Detector Is Used To Detect Edges Of Optic Disk. It Contain Following Procedure. . Apply Gaussian Filter To Remove Noise .And Smoothening And Sharpening Of Image Find Intensity Of Gradient. Non Maximum Suppression Method. Apply Double Threshold To Get Edges .Upper And Lower Threshold. Then Track The Edges, Finally Get Boundary Of Optic Disk Haris Edge Detector Is Also Used To Get Perfect Boundary.[5] [14]

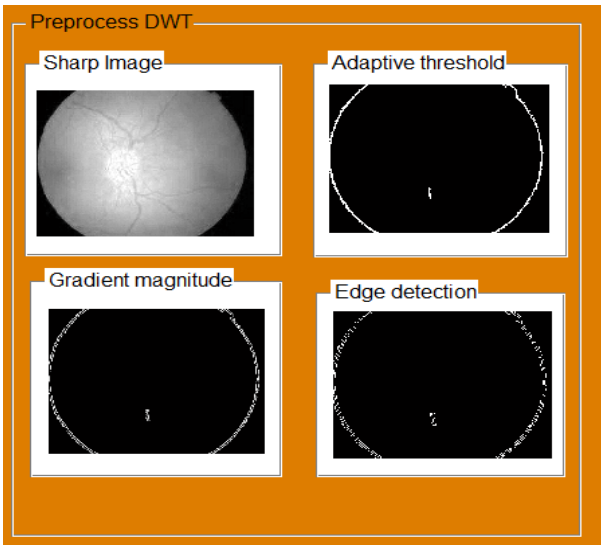

Fig 1.1 Shows Preprocessing Stage

1.2 Dct/Dwt Method For Feature Extraction

There Are Numerous Methods Are There To Extract Feature. In This Model Feature Extraction Is Done By Dct /Dwt Type. .Dct Decomposes The Signal Into Underlying Special Frequency. Allows Preprocessing Technique To Reduce Precision Of Dct Coefficients. Dct Coefficients Considered As Feature. And Ability To Represent Regularity, Complexity. Find Mean And Standard Deviation From Dct Coefficient Matrix .Dwt Generates Coefficient Matrix Horizontal, Vertical, Diagonal Components. For Example Dwt Generates 3 Horizontal, 3 Vertical, 3 Diagonal Matrix .Instead Of Using All Matrix Dwt Features Are Shown In Fig 1.2 And 1.3 Compute Mean And Standard Deviation Of Each Matrix. Store In Feature Vector .Dwt Is More Accurate And Efficient. Har Is Used As Mother Wavelet, By Comparing All Wavelet To, Mother Wavelet Finally Extract Dwt And Dct Features Segmented Images Are Shown In Figure 1.4 And 1.5

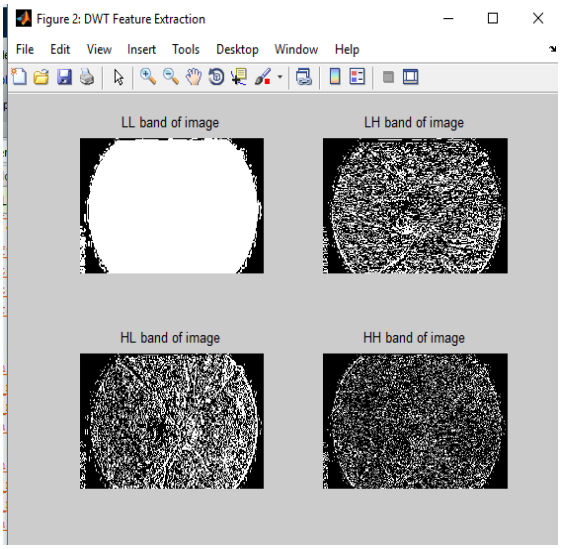

Fig 1.2 Shows Sub Bands of Dwt Features

Fig: 1.3shows segmented image

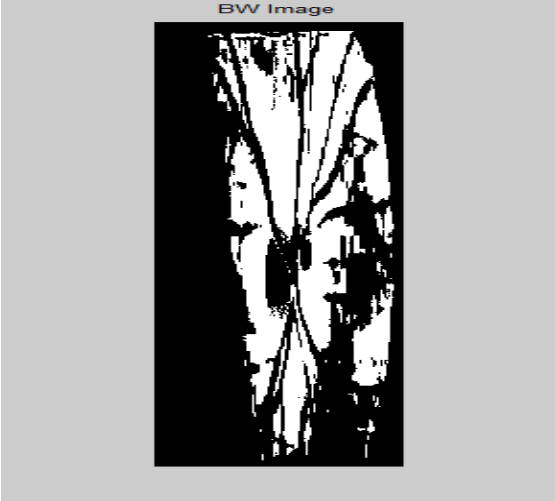

Fig 1.4 shows segmented BW image

1.3. Deep Learning

In Deep Learning Neural Network Play Important Role. Neural Network Have Multiple Hidden Layers Plus Mathematical Optimization .In Real Life Training Neural Network Is Not So Easy. Lot Of Procedure Must Be Done On Inputs To Make Them Learnable. Ann Work By Multiplying X Values (Weights) And Adding To Constant Called (Bias). Train The Model Until Model Learn Perfectly. Then Upload The Test Image. The Extracted Features Of Test Image Is Compared With Trained Image Data Set. Un Till Get Zero Error Or Best Result While Comparing With Trained Data Set, First Iteration Error Generated From The Model. Error Is Propagate Backward And Inputs Are Change Until Get The Correct Result, Or Zero Error. No Of Iteration Depends On Input Image [1] [8] That Zero Error Trained Eye Image Is Sent To Classifier .In This Model 125 Images Are Trained .In Dataset Diabetic Non Diabetic ,Mild ,Severe Type Diabetics Images Also There.[12] All The Images Are Well Trained Using Deep Learning Neural Network. And Results. Are Stored Trained Image Is Used As Target Image Neural Network Is Shown In Fig 2.1 And Neural Network Graphs Are Shown In Fig2.2 , 2.3 and 2.4

Random Forest Classifier Is Supervised Machine Learning Algorithm. .Decision Trees Are Generated Based On Nodes. This Algorithm Generates Forest With No Of Large Tress. More No Of Tress Give High Accuracy. In This Algorithm We Find Root Node And Splitting Feature Nodes Will Run Randomly. This Classifier Can Be Used For Both Classification And Regression Purpose [13] Test The Features Randomly Then Predict The Outcome. Again Start Predicts Until Get The Final Outcome. High Voted Predicted Target Is Final Outcome. By Using This Method Classification Is Too Easy No Missing Any Feature Or Value Over Fitting Problem Is Eliminated.

V.Experimental Result

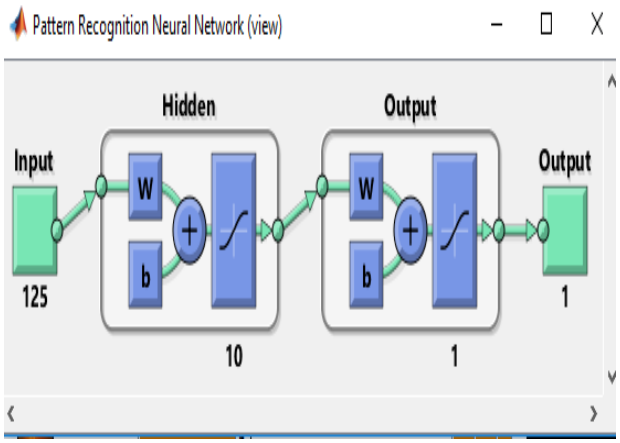

Fig2.1 .neural network

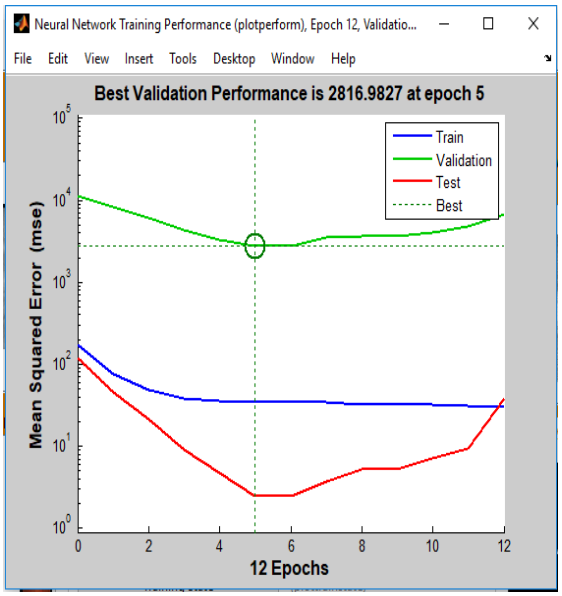

Fig 2.2 best validation performance

The Graph Shows Best Validation Occur At Epochs 6. For Given Test Image .The Plot Consist Three Lines In Fig 2, 2 Shows Trained, Test And Validation.

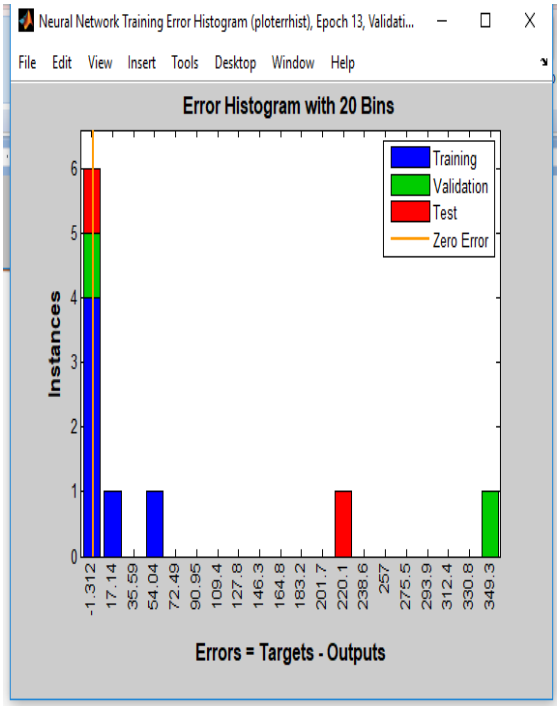

Fig 2.3 error histogram with 20 bins

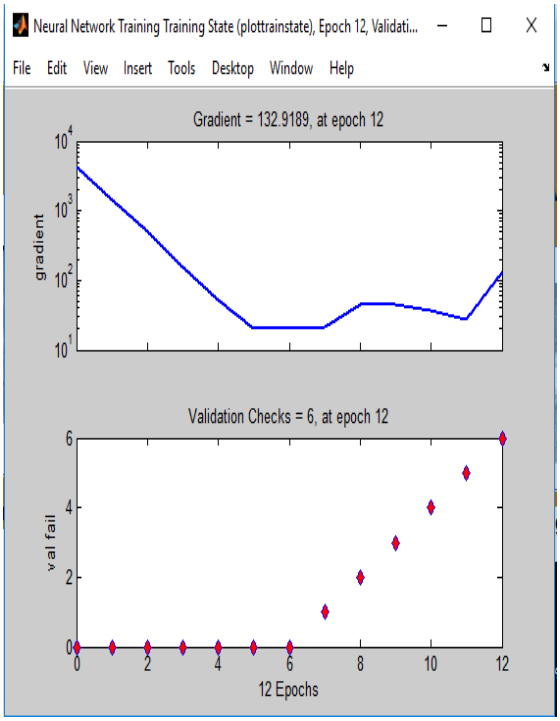

Fig 2.4 Shows States of Training Model

Zero Eror Is Shown In Fig 2.3 In Yellow Line.Validation Check Is Equal To 6 . .Errors Are Repeated 6 Times After Epoch 12. .Test Is Stopped At Epoch 12 Error Repeat Starts At 12 Epoch .Epoch 11 Is Base For The Given Test Image. And Its Value Is Final Output.

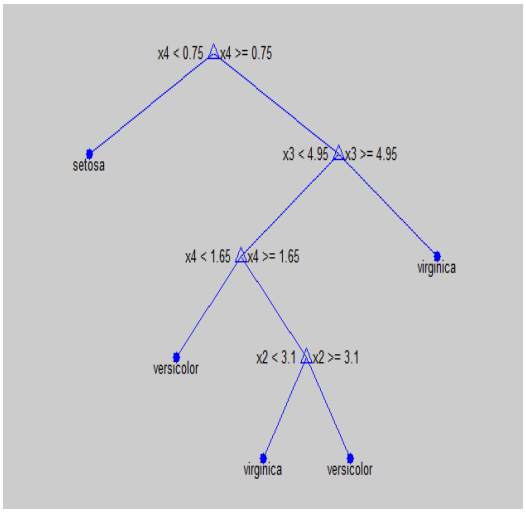

Fig 2.5 shows decision tree,no of grown tress

Fig 2.6 shows the result

```
performance =

  310.3798

  310.3798

     2

Detected
```

The Result Is Appeared In Command View

Mat Lab Software Used For This Model. The Preprocessing And Dwt Features

Results Are Shown. The Neural Network Graphs For Training Data Is Also Shown. The Result Is Too Accurate, And Over Fitting Data Problem Is Eliminated By Using Random Forest Classifier .Duration Of Time For Training The Data Is Also Less Random Forest Classifier Gives Correct Result. There Is Minimize In False Result. Accuracy Of The Model Is 100%

VI. Future Scope& Conclusion

This Model Can Be Extend To Distinct Type 1, Type 2 Diabetic. And Also % Of The Disease. It Is Easy To Train The High Rate Data Using This Model. .Mode L Can Be Extended To Train Large Number Of Data. It Can Be Implementing To Find All Disease, Its Easy To Predict Diabetic In Early Stage From The Trained Model .It Can Be Easy To Find Patient Condition Earlier Like Mild Or Serious Or Critical Or Normal. By Using This Classifier We Can Classify All The Eye Diseases Glucoma, It Gives 100% Accuracy. And Easy To Implement.

Acknowledgment

I would Like To Acknowledge The Guidance And Opinion Given By Shankaraiah ,Head Of Department , E&C, Jss Science And Technology University, Mysore. And, Dr Srikanth T, L&T Technology Service, Mysore Data Is Collected From Drion Database And Hospital.

References

[1] Faezehossadat Khademi" Predicting 28 Days Compressive Strength Of Concrete Using Artificial Neural Network "In I Manageris Journal On Civil Engineering ,Vol 6,May 2016 J. Clerk Maxwell, A Treatise On Electricity And Magnetism, 3rd Ed., Vol. 2. Oxford: Clarendon, 1892, Pp.68-73.

[2] S Lu "Accurate And Efficient Optic Disk Segmentation By Using Circular Transform" On Medical Image Ieee Transcation Vol 30 Pp 2126-2176,2011 Symponium Medical Image 2015,Pp 738-837

[3] H Li And Chutape " Automatic Loction Of Optic Disk In Retinal Image" In Proc Ieee Intrnatinal Conference 2011 Pp 837-840

[4] Jun Cheng Zhengguo Li, Zaiwang Gu, Huazhu Fu Damon Wing Kee Wong, Jiang Liu" Structure-Preserving Guided Retinal Image Filtering And Its Application For Optic Disc Analysis "In Ieee Transactions On Medical Imaging ,2018. Amuratha L Kabade"Canny Edge Detection Algorithm"In International Journal Advanced Research In Electronics And Communication Engineering,Vol 5,Issue 5,May 2016

[5] Kinjan Chauhan,Dr Ravi Gulati "Processing Of Retinal Image And Image Segmentation Using Otsu Histogram"In October 2015

[6] N Patton T M Aslam T Macgillivry I J Deary B Dhillon," Retinal Image Analysis ,Concept Application, Potential" 2006

[7] R Srivastva J Cheng D W K Wong J Liu Using Deep Learning For Robustness To Parellography Atropy In Optic Disk Segmentation" In Internatin Al Symposium On Biomedical Imaging H Li And Chutape " Automatic Loction Of Optic Disk In Retinal Image" In Proc Ieee Intrnatinal Conference 2011 Pp 837-840

[8] Xia Zheng, Dali Che,, Jia Zheng" Optic Disc Segmentation Based On Rules " In Ieee 978-1-5386-1243-9,2018

[9] Kinjan Chauhan,Dr Ravi Gulati "Processing Of Retinal Image And Image Segmentation Using Otsu Histogram"In October 2015

[10] A Singalavanja J. Supokavej, P, C. Sinthanayothin, S. Phoojaruenchanachai, And V. Kongbunkiat, "Feasibaly Study Of Computer Aided Screening For Diabetic Retinopathy"Vol 50 Pp 361-366,2006

[11] Segmentation And Optic Disk Detection"In International Journal Of Pure And Appled Mathematics Volume 119,No.7 2018,1053-1059

[12] Zhun Fana,Senior Member Yibiao Rongb, Xinye Caic Jiewei Lua Wenji Lia, Huibiao Lina And Xinjian Chenb" Optic Disk Detection In Fundus Image Based On Structured Learning" Biomedical And Health Informatics,Ieee Journal Of Biomedical And Health Informatics2168-3194, 2018,

[13] Ned Horning" Random Forests : An Algorithm For Image Classification And Generation Of Continuous Fields Data Sets"In International Conference On Geoinformatics For Spatial Infrastructure Development In Earth And Allied Sciences 2010

[14] Haixia Pan, Yanxiang Zhang, Chunlong Li, And Huafeng Wang" An Adaptive Harris Corner Detection Algorithm For Image Mosaic In S. Li Et Al. (Eds.): CCPR 2014, Part II, CCIS 484, Pp. 53–62, 2014. © Springer-Verlag Berlin Heidelberg 2014

Proceedings of the Fourth International Conference on Communication and Electronics Systems (ICCES 2019)
IEEE Conference Record # 45898; IEEE Xplore ISBN: 978-1-7281-1261-9

Implementation of IEEE 802.11p in Fixed Vehicle-to-Vehicle Communication System using NS3 Simulator

[1,2]Amanpreet Singh Saini, [1]Sarthak Agarwal*, [1]Snehal Agrawal*, [1]Srishti Agarwal*, [1]Umme Kulsum*

[1]*Department of Electronics and Communication Engineering, Galgotias College of Engineering and Technology, Greater Noida*
[2]*Department of Electronics Engineering, Indian Institute of Technology(ISM), Dhanbad*

**-Corresponding Author*

***Abstract*—V2V, also known as Vehicle-to-Vehicle communication system comprises of wireless networks where, the automobiles communicate with each other by sending message (which may include direction of travel, speed, location or loss of stability). In this paper, we are implementing IEEE 802.11p in a V2V communication system with mesh networking topology and Hybrid wireless routing protocol using NS3 Simulator. The vehicles (which here we symbolise as nodes) are stationary. Further, the paper presents performance analysis of proposed system on the basis of various parameters like Packet Size, Data Rate, Packet Delivery Function and Throughput etc.**

***Index Terms*—V2V, DSRC, WAVE, HWMP, NS3**

I. Introduction

The era of wireless communication has enabled the exchange of data between vehicles (V2V). The IEEE802.11p amendment has enabled the vehicles to communicate with each other through Dedicated Short Range Communication (DSRC). The Dedicated Short Range Communication (DSRC) and Long-Term Evolution for V2V (LTE-V2X) are two prior technologies used for V2V communication [1]. The broadband Internet and phone services to the mobile phones and other devices are spared by the Long-Term Evolution (LTE) network, a type of wireless communication network compatible with GSM and HSPA network [2] . Wireless Access in Vehicular Environment (WAVE) was added to the IEEE 802.11p protocol is an approved amendment to the IEEE 802.11 standard [3]. The half-duplex communication exists in DSRC by transmitting the data at rate of 3 to 27 Mbps. The modulation technique elaborated in DSRC [4] having communication range of up to 1000 meters is Orthogonal Frequency Division Multiplex (OFDM). DSRC has 7 channels in which for safety communication, the first channel is used, for critical safety communication- the second channel is used and for high power safety communication- the third channel is used, while the rest of the channels are used for either non-safety or safety communication [5]. While establishing the link between the two vehicles or in V2V communication system, the physical layer and the MAC layer are considered in implementation of the IEEE 802.11p. The physical layer is composed of two sub layers namely, the Physical Layer Convergence Protocol (PLCP) which is responsible for communicating with the MAC layer and the Physical Medium Access (PMA) which is the interface to the physical transmission medium, its task is to manage data encoding and perform modulation [3]. On the other hand, MAC layer provides flow control and the multiplexing for the transmission medium. Frame delimiting and recognition, addressing of designation stations, protection against errors, and control access to the physical transmission are the major functions of the MAC layer. In this paper, we present a V2V communication system using the mesh topology and as routing protocol we have considered the Hybrid Wireless Mesh Protocol(HWMP). To simulate the V2V communication system, here we have used the NS3 simulator as it provides substantial support for simulation of TCP, routing and multitask protocol over wired and wireless networks. The paper is divided as follows: Section1: Introduction provides a brief description of the V2V communication system using IEEE 802.11p and the considered topology. Section 2: Defines the parameters that we have considered for the proposed model. Section 3 defines the proposed methodology with its materials and methods and section 4 and 5 provides the result, conclusion and future direction.

II. System Description

Vehicle-to-vehicle communications is a system consisting of an inbuilt wireless network infrastructure in which the convertibles can send messages to each and every vehicle about the information of the real-time. These data may include speed, location of the vehicle, capacity of the vehicle and stability loss of the vehicle. In carrying out any simulation process, one needs a workflow via which the whole process is carried out. Below Fig1 is the workflow of the considered model.

According to Fig. 1, the first step is the topology definition. Generally, topology definition is used in defining the interre-

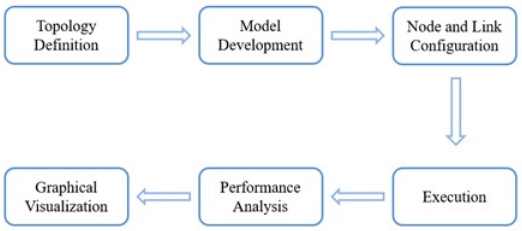

Fig. 1. Work Process

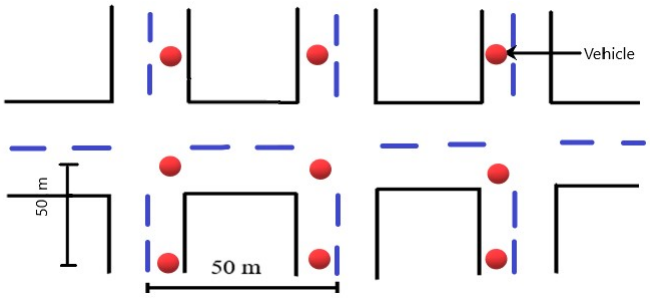

Fig. 2. V2V Communication Scenario

lationships and in providing easy creation of basic facilities. So, here we have considered the mesh topology to establish a link between the nodes. An extensible mesh networking framework has been defined to ensure a common standard that will synchronize all WLAN mesh network devices from all vendors.

In wireless mesh network, data packets travel over multi wireless hops [6]. The topology and routing information is shared by nodes in wireless mesh while communicating with other neighbouring nodes. The enlarged network capacity through various factors like spatial frequency reuse, shortened communication distance, automatic network configuration and better robustness has enabled high data transmission rate in WLAN mesh network [7]. Mesh stations are the devices that form mesh and forwards the frames wirelessly. The information about the mesh that helps other mesh stations to detect and join the mesh are carried by mesh station's beacon [6]. A single transceiver is used by mesh which operates in single frequency channel. If a larger channel precedence value is held by mesh station, it broadcasts its value and indicate different frequency channel [6]. Mesh network does not provide end-to end encryption as both mesh stations initiate together and both links are independently secured [6].

One of the benefits of mesh topology is its expanding nature as the new nodes can be added easily to self-adjusting network [7].The routing protocol that we have considered here is HWMP. It is a default routing protocol for wireless mesh network which is based on Ad hoc On-demand Distance Vector Routing (AODV). It has both reactive components and proactive components [8]. Proactive routing protocols periodically update its routing information and share the whole topology with other nodes. In reactive routing protocol, routing tables are constructed on the requirements of nodes, and the complete topology of the network is not shared with other nodes in a network [7]. In case of mesh networking these use MAC addresses for "routing", instead of IP addresses. Therefore, we call it as "path selection" instead of "routing". As per [8], HWMP has the lower average latency and the higher data transmission throughput .

As per Fig. 1 The next step is the model development which is shown in Fig. 2. In Fig. 2, we have considered the V2V communication model with 3 rows and 9 stationary nodes (3 in each row). All the adjacent nodes are 50m apart from each other. Here, a client-server type communication is considered. The server node can broadcast its information to other nodes (Client). The Client node can become the server node according to the need of the communication system. Again considering Fig. 1, the next process in the simulation workflow is the node and link configuration. To establish the node and link configuration we use the NS3 Simulator. NS3 is designed as a set of libraries that can be combined together. NS-3 is more modular as compared to other some simulation platforms. With NS3, one can easily use several external animators and data analysis and visualization tools. However, users should expect to work at the command line and with C++ and/or Python software development tools. NS3 has a work flow which needs to be followed while using the simulator.

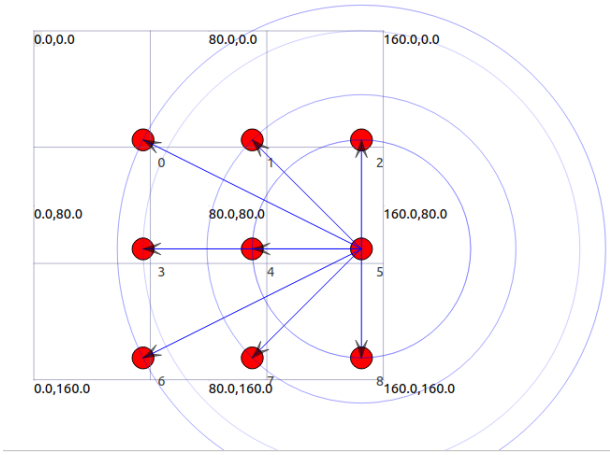

Fig. 3. Mesh Network Simulation

As per system description given in reference with Fig 2, the simulation is carried out in NS3 Simulator using NetAnim and the simulated result is shown in Fig. 3 and Fig. 4. Both the figures show a mesh network among the 9 nodes. All the adjacent nodes are placed at a constant distance of 50m. The total simulation time that is taken for simulation is 100s irrespective of the size of the packet.

III. Result and Discussions

The following results have been found from the extensive simulations from NS3 Simulator using Ne-

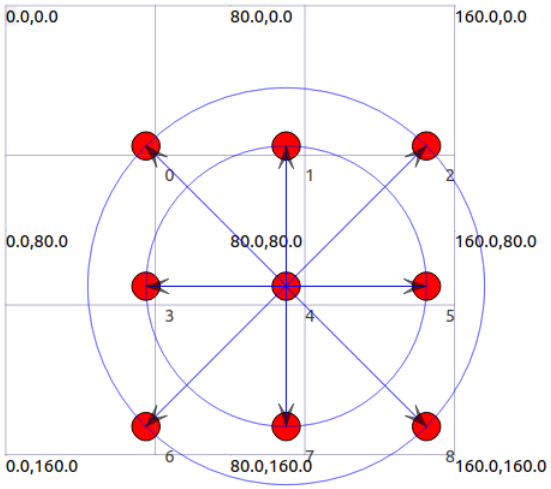

Fig. 4. Mesh Network Simulation

tAnim(Flowmonitor). In Fig. 5, a comparison is carried out

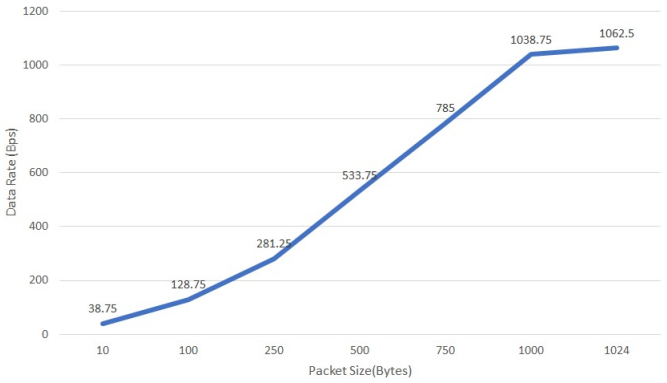

Fig. 5. Packet Size vs Data Rate

among Packet Size(kbits) and Data rate(kbits/sec). It is observed that, as we increase the amount of Packet size, the Data rate also increases. From the above observation, it is concluded that, the Packet Size is directly proportional to the Data Rate irrespective of the increase or decrease in the above two parameters.

PDF is defined as the ratio of the number of data packets delivered to the total number of packets. This gives the efficiency of data delivered to the destination.

In Fig. 6, a comparison is carried out among Packet Size and PDF. It is observed that, as we increase the amount of Packet size, the Packet Delivery Function(PDF) decreases. From the above observation, it is concluded that, the Packet Size is inversely proportional to the Packet Delivery Function.

In Fig. 7, a comparison is carried out among Packet Size and Throughput(bits/sec). It is observed that, as we increase the amount of Packet size, throughput also increases. From the above observation, it is concluded that, the Packet Size is directly proportional to the throughput, irrespective of the

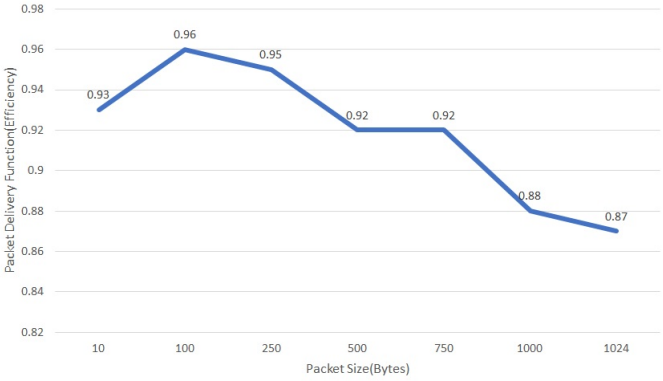

Fig. 6. Packet Size vs Packet Delivery Function(PDF)

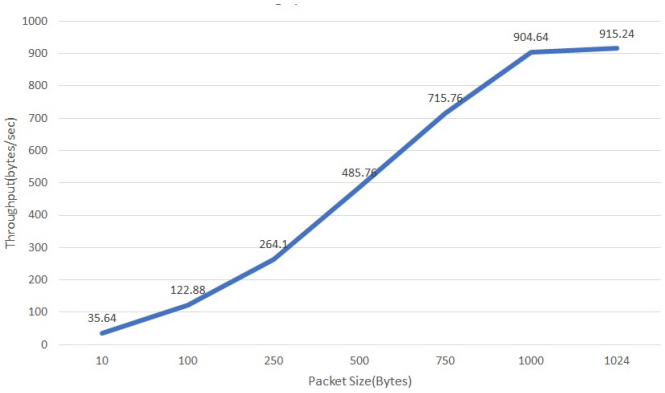

Fig. 7. Packet Size vs Throughput

increase or decrease in the above two parameters.

IV. Conclusion and Future Direction

The overall aim of this paper was to implement IEEE802.11p in V2V communication System for stationary vehicles using NS3 Simulator. In the beginning, we presented a brief description of the layers on which IEEE 802.11p is based upon and further discussed about DSRC. For establishing a link between the vehicles, mesh networking as the network topology and HWMP as the routing topology is considered. The results have been simulated using NS3 simulator and parameters are analysed based on the obtained result.

This paper consider stationary vehicle whereas in future mobility in vehicles can be added in comprehensive understanding of implementing IEEE802.11p in V2V communication system.

Acknowledgment

This research was supported by Galgotias College of Engineering and Technology, affiliated with Dr. A.P.J Abdul Kalam Technical University, Lucknow. We thank our faculties and staff who provided insight and expertise that greatly assisted the research.

We would also like to show our gratitude to Dr Pradeep Kumar TS, Deputy Director (Software Development Centre), VIT Vellore for sharing their pearls of wisdom with us during the course of this research.

REFERENCES

[1] Wang, J., Shao, Y., Ge, Y., and Yu, R. (2019). A survey of vehicle to everything (v2x) testing. Sensors, 19(2), 334.
[2] http://www.tec.gov.in/pdf/M2M/V2V
[3] Abdelgader, A. M., and Lenan, W. (2014, October). The physical layer of the IEEE 802.11 p WAVE communication standard: the specifications and challenges. In Proceedings of the world congress on engineering and computer science (Vol. 2, pp. 22-24).
[4] Cailean, A. M., Cagneau, B., Chassagne, L., Popa, V., and Dimian, M. (2014, November). A survey on the usage of DSRC and VLC in communication-based vehicle safety applications. In 2014 IEEE 21st Symposium on Communications and Vehicular Technology in the Benelux (SCVT) (pp. 69-74). IEEE.
[5] Bilgin, B. E., and Gungor, V. C. (2013). Performance comparison of IEEE 802.11 p and IEEE 802.11 b for vehicle-to-vehicle communications in highway, rural, and urban areas. International Journal of Vehicular Technology, 2013.
[6] Hiertz, G. R., Denteneer, D., Max, S., Taori, R., Cardona, J., Berlemann, L., and Walke, B. (2010). IEEE 802.11 s: the WLAN mesh standard. IEEE Wireless Communications, 17(1), 104-111.
[7] Ahmed, F., Khan, A. H., Mehmood, J., Sarwar, N., Ali, A., Mehboob, M., and Waqas, A. (2016). Wireless Mesh Network. International Journal of Computer Science and Information Security (IJCSIS), 14(12).
[8] Yang, K., Ma, J. F., and Miao, Z. H. (2009, December). Hybrid routing protocol for wireless mesh network. In 2009 international conference on computational intelligence and security (Vol. 1, pp. 547-551). IEEE.

Proceedings of the Fourth International Conference on Communication and Electronics Systems (ICCES 2019)
IEEE Conference Record # 45898; IEEE Xplore ISBN: 978-1-7281-1261-9

Augmenting Vehicular Network with Software Defined Internet-of Vehicles Paradigm

Sanjai Pathak, Ashish Mani, Mayank Sharma
Amity University, Uttar Pradesh Noida, UP, India
pathak.sanjai@gmail.com, {amani,
msharma22}@amity.edu

Amlan Chatterjee
California State University Dominguez Hills
Carson, CA, USA
achatterjee@csudh.edu

***Abstract* – The tightly coupled control plane and data plane in inbuilt hardware devices such as switches and routers are not suitable to meet the current needs of vehicular network requirements. The complexity to integrate moving devices with other high-speed moving devices and heterogeneous elements in the vehicular network is due to high-speed mobility where network topology changes dynamically and sometimes communication is also broken because of short network range of devices. The decentralized decisions of routing and switching in the traditional network architecture, where control plane and data plane are tightly coupled, demands an innovative approach for the routing and switching of network packets. Software-defined network (SDN) is a promising network architecture, which decouples the control plane from the inbuilt device. SDN can be a single or multiple controllers based network system. An SDN having multiple controllers with self-organization capability provides fault tolerance and handle heterogeneity and scalability with collaborative behaviour. In this paper, we propose to augment the traditional vehicular network architecture with SDN to embrace the required computational demand in networking with fault tolerance. The controller is a software program that can be programmed to address various issues of vehicular network intelligently by improving the performance of information exchange between the vehicles. OpenNet with POX controller is used to emulate the SDN on network topology and confirm its effectiveness.**

Keywords – Internet-of Vehicles, VANETs, SDN, IoV

I. Introduction

The Internet of the vehicle (IoV) is a vehicular ad hoc network in the wireless network environment and works on the concept of Mobile ad hoc network (MANETs). It supports creating the communication network spontaneously between vehicles with no pre-configured network infrastructure, which is unlike mobile ad hoc network [1]. The participating devices in the communication network rely on each other and are required to act as a router, to forward the network packets for all the devices including nodes that are not in range to keep connectivity. VANET creates an ad-hoc network spontaneously with communication capability for the high-speed moving devices and roadside units (RSUs). In VANETs, the moving devices communicate with no restrictions of energy unlike Mobile ad hoc Network (MANETs). The Internet of vehicles is engaging many researchers due to the potential it has to support connectivity with communication capable devices and provide network functionalities by improving safety and traffic such as Intelligent Transport System (ITS) [3]. ITS is not limited to road transport but includes all kind of transportation devices including inside vehicle, between the vehicles and also to rail, water and air transport. Therefore, ITS is a superset of the vehicular network [3].

The traditional network architecture is unable to meet the current trends in emerging communication technologies and innovation, this is due to the vendor-specific configuration where data plane and control plane are tightly coupled and prohibit the customization of routers and layer 3 switches as depicted in Fig.1. The current emerging computing technologies demands for the new communication network architecture, that is not vendor specific, open and flexible to adapt the recent changes in requirements [9]. SDN is a promising paradigm, implements the concept of decoupling of the control plane and data plane from tightly coupled devices in networking.

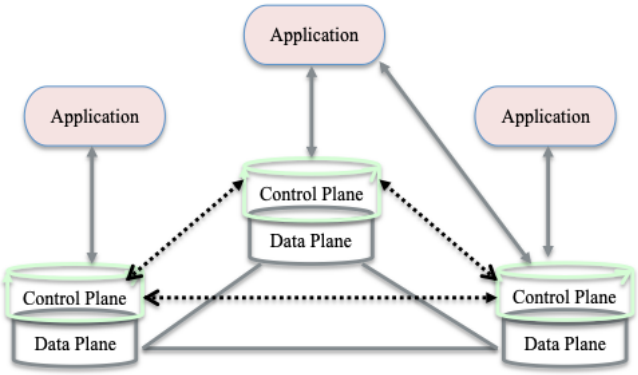

Fig.1. Distributed Control Plane

Software Defined Network (SDN) [3] envisioned and promotes innovation continuously by considering the vehicular network requirements, designed to work on the concept of flexible and customizable network configurations. SDN innovates continuously by providing an environment to program and customize according to the nature of change as in vehicular network [14]. It addresses the challenges of the vehicular network by increasing the efficiency of network services including resource management and network applications by the centralized SDN controller at the control plane. OpenFlow specification is developed to support the

programming interface (southbound interface) for the control plane to interact with data plane on the principle of communication technology [5, 6] protocol. The objective is to promote innovation by programmability, flexibility and simplify the network management operations for the network communication [4].

Augmenting vehicular network with a software-defined Internet of vehicles promotes innovation in communication network technology of vehicular network to meet the current computing demands. The separation mechanism of SDN decoupled the control plane from dedicated devices (refer to one or more switches) and leaves the switches to work only as a forwarding device. The OpenFlow foundation has developed the OpenFlow protocol to leverage the SDN principles using open source platforms. The protocol is developed based on the open architecture that can be programmed to modify the forwarding tables and used for the communication between the control plane and the data plane [3]. The main idea behind the SDN architecture is to decouple the control plane from the data plane. The control plane is used to manage and control the network traffic and the data plane is used for the data forwarding. The controller in the SDN is responsible to manage the flow control for the entire network. Fig.2 depicted the components of SDN.

The objectives of this research are to contribute in the area of software-defined Internet of vehicles by exploring the previous work and to augment the vehicular network with SDN for programmability and promote innovation [12]. There are following contributions made to increase the acceptance of an SDN approach into the existing vehicular network:

- Existing communication network architecture is reviewed and analyzed along with exploration on how SDN promotes innovation and programmability in the network and can be one of promising solution over the traditional approach.
- Simulate sample network topology on OpenNet with POX controller and evaluate its functions for common network operations.

The remaining work is organized as follows. In Section II, we discuss the related work on the architecture of the vehicular network and software-defined network. Section III presents the basic vehicular network model and its limitations. In Section IV, augmented software defined vehicular network is compared with existing network architecture. In section V, experiment and analysis of SDN on OpenNet with POX controller is discussed. In Section VI, conclusions and future work are discussed.

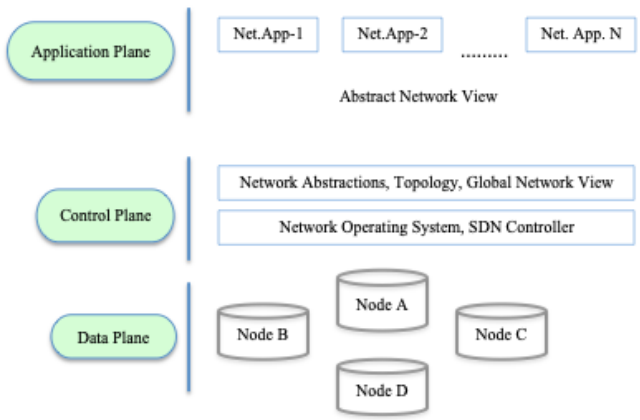

Fig.2. SDN Components

II. RELATED WORK

In this section, we reviewed the existing research work in vehicular network and adaptability of SDN for the network applications. Due to the emergence of network services in the vehicular network, the research organizations and industries are interested in improving on limitations of the traditional network, by proposing new network architecture in order to support services effectively.

I. Ku et al. [3] considered the services offered by VANETs as essential for the vehicles, which need to be improved, such as safety services, network management services and infotainment services. However, it lacks in flexibility and makes the deployment hard. They proposed software-defined based network architecture for the inter-vehicle ad-hoc communication in a vehicular network by introducing SDN controller in the network system. The simulated routing algorithms exploit the global view of the network and the results show its effectiveness. Jun Li [2] proposed an SDN controller based ARP for the network scalability that managed the network packets traffic effectively. Further, it considered some network application and fallback mechanism in vehicular network scenarios during the design of SDN for the deployment. The simulation and comparison of routing protocols in the traditional MANETs/VANETs were performed to highlight the benefits of using SDN in the network.

N.B Truong et al. [4] proposed the architecture of SDN with Fog computing in order to support the low latency services in network effectively. They considered the research in recent years on the offering of several network services by VANETs and the limitations during the deployment and management of traditional network, especially due to the poor connectivity, non-scalability, and less flexibility. The SDN based network architecture provides programmability in the network and makes the network to be more flexible, scalable and intelligent by the features of SDN controller, whereas the Fog computing managed to offer delay sensitive and location-based services to meet the demands of the future vehicular network. Further, they studied use cases of the data streaming

and lane change assistance with illustration benefits of the proposed architecture.

S. Wang et al. [7] proposed a novel architecture based on SDN to address the limitations by leveraging the decoupled mechanism of network control logic from the tightly coupled control plane and data plane in dedicated devices (refer to one or more switches). The proposed architecture provides a uniform way to configure heterogeneous switches. The tightly coupled devices in traditional networking are complex to configure and change, as it requires a lot of manual effort and physical presence for the network management activities. Further, it is observed that the network infrastructure cost is high to maintain. This novel architecture for Internet-of vehicles has the limitation on the size of flow tables and it impacts during the flow rule installation, hence it is required to build compact flow tables for OpenFlow enabled switches for the scalability of IoV [11].

III. Basic Vehicular Network Model

In this section, we describe the basic vehicular network components and communication model based on traditional network architecture.

The vehicular network comprises of high-speed moving devices that is vehicles, access points as roadside units (RSUs), mobile broadband (4G/LTE), and wireless broadband (WiFi/WiMax) to provide the network related application services. Vehicle-to vehicles communication performed by establishing a spontaneous communication network via RSUs and vehicles-to Internet communication by network broadband services. The interconnected network components and method for the communication in the traditional approach are depicted in Fig. 3 [3]. The network application related services in the VANETs includes safety of the vehicles, safety on the road, traffic management and infotainment-related services within vehicles. The vehicle and road safety services help in reducing accidents and loss of life of travellers. Traffic services network applications support in regulating the regular traffic on road by coordinating between vehicles and provides information from the local map. The infotainment-related services within vehicles include surrounding information on the road, music and multimedia by global Internet access.

The control plane and data plane are tightly coupled in inbuilt network devices such as switches and routers in the communication model of the traditional vehicular network, which is less flexible, less scalable, and less intelligent. To forward network packets from source to destination, there is a need to pre-configure the network communication elements that cannot be changed at the later stage of the communication. This method of communication prohibits supporting emerging networking technology in the communication network. The basic model of communication is depicted in Fig.1 in which switch's ports are pre-configured to accept and forward the packets in the connected network between source and destination. All the applications are required to be loaded with information about a pre-configured network and in case of any change in the network configuration, the inbuilt devices need to be reconfigured again, which is time-consuming and so is not practically feasible.

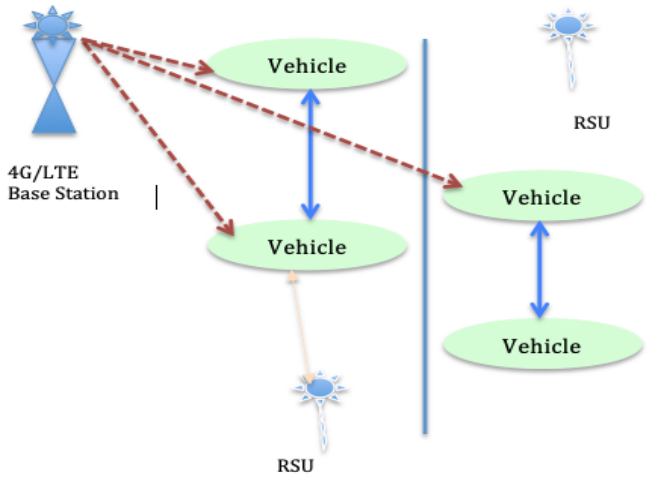

Fig.3 Vehicular Network Communication and Its Components

IV. Software Defined Vehicular Network

There have been several attempts made to resolve various issues of the traditional vehicular network in the era of the Internet-of vehicle, in which there are heterogeneous devices connected to work together in a collaborative and coordinative way for a common goal. These attempts are made mainly to meet the current network computing trends and improve the productivity of each network elements along with minimizing of various applications silos.

The proposed architecture embraces the dynamic nature of the vehicular network, i.e. it is a paradigm shift from traditional networking to software-defined networking, which enables programmability and intelligence in the network. Due to the centralized networking, SDN directly impacts the various issues in traditional IP networking such as improved resource utilization, better network management, avoiding redundant flow entries and collision. The software-defined network (SDN) is an emerging and promising paradigm shift in communication technology. It decouples the control plan from the tightly coupled devices and makes it work as a forwarding device only. The forwarding device works based on the instructions from the controller. The SDN controller is capable to monitor and control the entire network centrally with a global view [9].

The vehicular network architecture extends with SDN as it will be operated in wireless vehicular network environments that are expected in future VANETs and enable innovations [14]. According to the proposed architecture, different communication technology can be used in the control plane and data plane as depicted in Fig. 4, i.e. for control plane LTE/4G and for data plane WiFi/WiMax. There is a known problem in the vehicular network, that is all the network access points are not reachable via roadside units due to the network range and design of network infrastructure. The augmented software defined vehicular network with SDN

controller is depicted in Fig. 4 that includes the various access points and components of communication in the network. In this architecture, the inter-vehicle and intra-vehicle communications are efficient in data flow management, where the vehicles and roadside units are working as open flow enabled switches, and OpenFlow protocol is used for the communication between the control plane and the data plane.

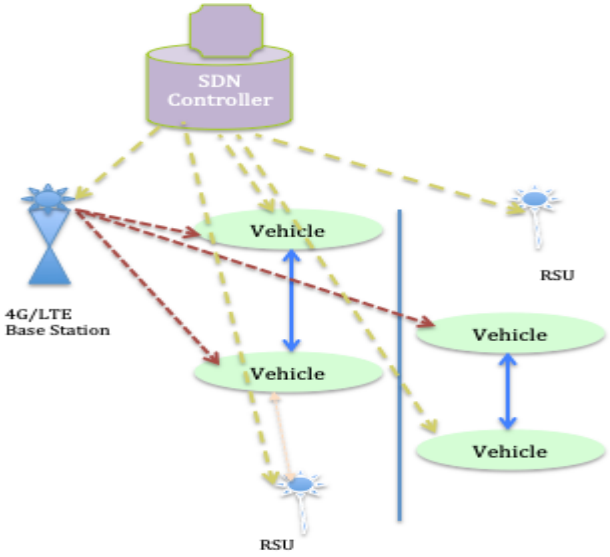

Fig.4 Software Defined Vehicular Network

The main idea behind augmenting the vehicular network with software-defined Internet-of vehicles paradigm is to bring flexibility, scalability and intelligence into the vehicular network. It is to meet the current computing demands in communication technology, where evolving requirements of user impacts the performance of the network badly. The existing communication system prohibits innovation due to tightly coupled control logic on inbuilt device and decision for a request is decentralized. This is to change the way the current vehicular network is adopting the changes in network technology. In this paper, we researched the functioning of the traditional vehicular network and analyzed how SDN can embrace the dynamic nature of vehicular network to meet the current developments in the communication network.

SDN promotes programmability and flexibility support in resolving the limitations of the vehicular network by providing a centralized control mechanism for the entire network. The centralized approach has the limitation to scale the network but can be addressed using the method of controller placement by placing multiple controllers in a network. Table-1 depicts the comparative benefits of the software-defined network over traditional networking.

TABLE-1 SDN ARCHITECTURE VS. TRADITIONAL NETWORK ARCHITECTURE

No.	*Parameters*	*Software Defined Network*	*Existing Network*
1	Network controlling and Monitoring	Control plane decoupled and function independently and make it easier	Complex due to the tightly coupled control plane in inbuilt device
2	The global view of Network	Centralized view due to SDN controller and an entire knowledge of network	Distributed view and limited knowledge of network
3	Maintenance cost	Lessor	Higher
4	Required time to update/error or resolve issues	Easy	Difficult and depends. Sometimes takes a month
5	The controller (s) utilization	Important	Not relevant
6	Network Consistency and Integrity	Important	Not Important
7	Network State and Forwarding tables	Important	Important
8	The capacity of the controller (s)	Important	Not relevant
9	Network resource utilization	High	Less

V. EXPERIMENT AND ANALYSIS OF SDN ON OPENNET

An emulator for SDN is OpenNet, which integrate MiniNet and NS3 to emulate the software-defined network [8][10]. It creates a virtual network environment in which network topology can be emulated as a real network. As shown in Fig. 5, it depicts an example of tree network topology with 7 open flow enabled switches, 1 SDN controller and 8 hosts. We simulated the two hosts h1 and h8, connected with switch s1 and s4 respectively to check the network connectivity. The OpenFlow enabled switches and SDN controllers are design to support the OpenFlow specification, the OpenFlow v.1.0 has been considered during this simulation. There are 7 OpenFlow enables switches in the tree topology depicted in Fig. 5, are interconnected to form the network and all switches are connected with an SDN controller (c0). When a packet arrives at OpenFlow enables switch, the switch has been programmed to connect with SDN controller using secure channel TCP connections and forwarding the packets based on the routing decisions and instructions installed into the forwarding table by the controller (c0). The programmed OpenFlow devices (s1-s7)

maintain a forwarding table, which SDN controller modifies by inserting or updating the flow rules as the installation process of the controller [8][10].

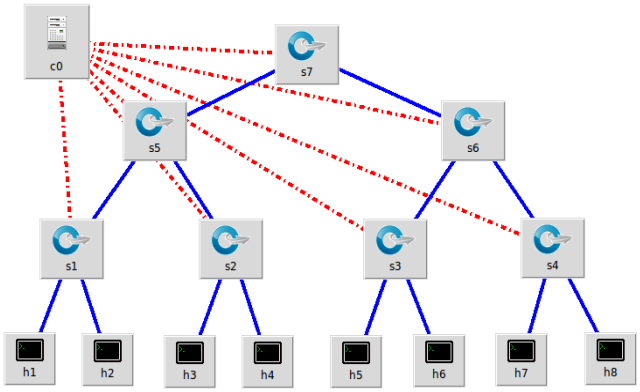

Fig.5 Network Tree Topology with 8 Hosts

MiniEdit along with POX controller is used to create the tree topology and simulate an instance of SDN. POX-controller supports OpenFlow protocol and installs the rules on the number of switches connected in the network. The controller is instantiated by running the python script of POX and is connected using port number 6633 as shown in Fig.6. An experiment has been performed to confirm the impact of the controller on the network i.e. when the POX controller is not instantiated, the network does not function and connected hosts are unreachable. It has confirmed that the SDN controller should be instantiated and functional for the network to function. The SDN controller has the control logic of the entire network, which is designed and programmed to initialize and modify the flow table contents of an OpenFlow enabled switch. Each entry of flow table consists of the field to match, request priority, required action, timeout, cookie and instructions. For an example, when a request of 64 bytes packet arrives on OpenFlow switch s1 then switch searches for the matching field in the table as per the programmed, on successful match the packet gets processed otherwise a table-miss occurs.

```
*** Starting CLI:
opennet> dump
<Host h3: h3-eth0:10.0.0.3 pid=7030>
<Host h6: h6-eth0:10.0.0.6 pid=7038>
<Host h2: h2-eth0:10.0.0.2 pid=7045>
<Host h8: h8-eth0:10.0.0.8 pid=7052>
<Host h5: h5-eth0:10.0.0.5 pid=7055>
<Host h7: h7-eth0:10.0.0.7 pid=7062>
<Host h4: h4-eth0:10.0.0.4 pid=7078>
<Host h1: h1-eth0:10.0.0.1 pid=7081>
<customOvs s2: lo:127.0.0.1,s2-eth1:None,s2-eth2:None,s2-eth3:None pid=7034>
<customOvs s6: lo:127.0.0.1,s6-eth1:None,s6-eth2:None,s6-eth3:None pid=7041>
<customOvs s1: lo:127.0.0.1,s1-eth1:None,s1-eth2:None,s1-eth3:None pid=7048>
<customOvs s3: lo:127.0.0.1,s3-eth1:None,s3-eth2:None,s3-eth3:None pid=7058>
<customOvs s7: lo:127.0.0.1,s7-eth1:None,s7-eth2:None pid=7065>
<customOvs s4: lo:127.0.0.1,s4-eth1:None,s4-eth2:None,s4-eth3:None pid=7069>
<customOvs s5: lo:127.0.0.1,s5-eth1:None,s5-eth2:None,s5-eth3:None pid=7084>
<RemoteController c0: 127.0.0.1:6633 pid=7073>
```

Fig.6 SDN Remote Controller C0 with 8 Hosts (Dump Information)

The created virtual hosts h1 to h8 on MiniEdit are connected in the network of 7 OpenFlow enabled switches s1 to s7 using Ethernet virtual links s1-eth1 through s7-eth2. For simulating the tree network topology and checking the consistency in connectivity in SDN, we measure the round trip time (RTTs) by ping operation between host h1 and h8 as it is on one of the longest path [13], as shown in Fig.7. When the ping command starts executing from h1 to h8, it first requests 64 bytes from h8. The connected switch s1 sends the request to SDN controller (c0), the controller then installs the required open flow rules after taking routing decision for packets into the forwarding table of switch s1 [12][13].

```
opennet> h1 ping h8
PING 10.0.0.8 (10.0.0.8) 56(84) bytes of data.
64 bytes from 10.0.0.8: icmp_seq=1 ttl=64 time=0.219 ms
64 bytes from 10.0.0.8: icmp_seq=2 ttl=64 time=0.078 ms
64 bytes from 10.0.0.8: icmp_seq=3 ttl=64 time=0.209 ms
64 bytes from 10.0.0.8: icmp_seq=4 ttl=64 time=0.095 ms
64 bytes from 10.0.0.8: icmp_seq=5 ttl=64 time=0.099 ms
64 bytes from 10.0.0.8: icmp_seq=6 ttl=64 time=0.118 ms
64 bytes from 10.0.0.8: icmp_seq=7 ttl=64 time=0.116 ms
64 bytes from 10.0.0.8: icmp_seq=8 ttl=64 time=0.103 ms
64 bytes from 10.0.0.8: icmp_seq=9 ttl=64 time=0.198 ms
```

Fig.7 Ping Command On Tree Topology from H1 to H8

The SDN network test has been conducted using ping and iperf command for 30 and 15 iterations respectively to check the reliability and consistency of the produced result on tree topology network on OpenNet. We recorded the results and plotted the trends for minimum, average and maximum RTTs along with TCP bandwidth in Fig. 8 and Fig.9 respectively. Where round trip time (RTTs) is an important metric to determine the health of connection and TCP bandwidth is to measure the quality of connection in a network. There are 10 packets of size 64 bytes used in the iteration of experiment and RTTs are recorded for the analysis. The minimum, average and maximum RTTs of the first request is higher as compared with rest of the RTTs, this is because OpenFlow switches (s1, s5, s7, s6, s4) are needs to initialize the forwarding tables in communication with SDN controller (c0).

SDN controller installs the forwarding rules in flow table considering the routing path in the network. In the measure of TCP bandwidth, the iperf command is executed 15 times to check the consistency (h1, h8) in performance of the network and recorded for the evaluation as trend depicted in Fig.9.

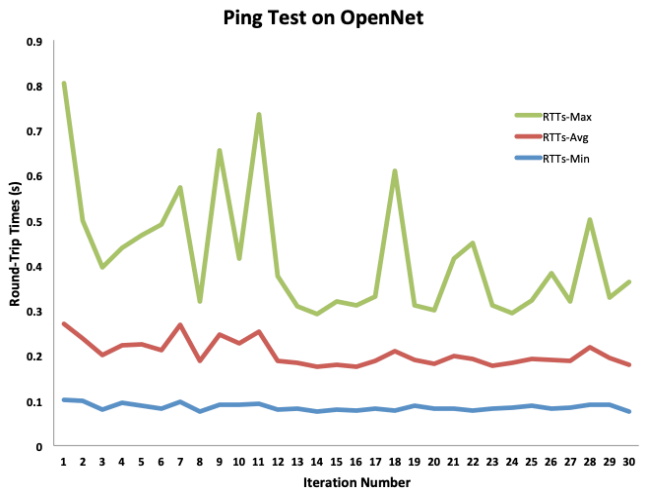

Fig. 8 RTTs of ping test on OpenNet (h1 to h8)

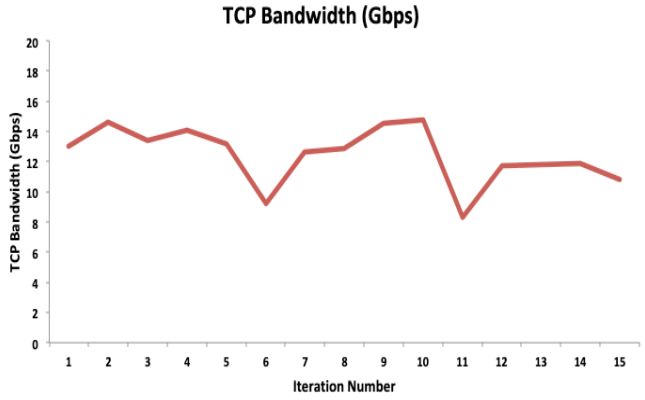

Fig. 9 TCP bandwidth between h1 and h8

VI. Conclusion and Future Work

The main idea to augment the vehicular network is to meet the current emerging computing technology's demands in communication. The augmented vehicular network with SDN can change the way of communication in a traditional network, this research work concluded that SDN could embrace the dynamic nature of the vehicular network and can be one of the promising solutions to suppress the limitations of a traditional network. We conducted an experiment on OpenNet with POX controller to emulate a sample tree topology, to confirm the effectiveness of SDN in the network. The augmented vehicular networks with SDN paradigm transform the traditional approach of communication and dynamically control the network packets flow by controlling the vehicles applications intelligently.

Most of the existing research work in the architecture of the vehicular network has considered the application in offline mode with global knowledge and centralized approach but there are cases where online approach is essential to consider such as works related to finding the route for a destination are required to consider the local knowledge and decentralized approach in online mode. The future work would consider the simulation of advanced network scenarios to validate the effectiveness of SDN in the vehicular network such as SDN connectivity strength or loss of connectivity with SDN controller, where isolated nodes are required to form the cluster network and connect with SDN controller.

References

[1] P.Ghosekar, G.Katkar, Dr. P.Ghorpade, “Mobile Ad hoc Networking: Imperatives and Challenges,” in International Journal of Computer Applications IJCA, vol. 1, pp. 153-158, 2010.

[2] Jun Li, Zeping Gu, Yongmao Ren, Haibo Wu, ShanShan Shi, "A Software-Defined Address Resolution Proxy," in IEEE Symposium on Computers and Communications (ISCC), pp. 404-410, Jul.2017.

[3] I. Ku, Y. Lu, M. Gerla, R. L. Gomes, F. Ongaro and E. Cerqueira, "Towards software-defined VANET: Architecture and services," in 13th Annual Mediterranean Ad Hoc Networking Workshop (MED-HOC-NET), Piran, pp. 103-110, 2014.

[4] N. B. Truong, G. M. Lee, Y. Ghamri-Doudane, "Software defined networking-based vehicular Adhoc Network with Fog Computing," in IFIP/IEEE International Symposium on Integrated Network Management (IM), pp. 1202-1207, May 2015.

[5] N. McKeown, T. Anderson, H. Balakrishnan, G. Parulkar, L. Peterson, J. Rexford, S. Shenker, and J. Turner, "OpenFlow: enabling innovation in campus networks," in SIGCOMM Comput. Commun. Rev., vol. 38, no. 2, pp. 69–74, 2008.

[6] OpenFlow Switch Specification, Version 1.4.0 (Wire Protocol 0x05). [Online]. Available: https://www.opennetworking.org/images/stories/downloads/sdn-resources/onf-specifications/openflow/openflow-spec-v1.4.0.pdf

[7] X. Wang, C. Wang, J. Zhang, M. Zhou, C. Jiang, "Improved Rule Installation for Real-Time Query Service in Software-Defined Internet of Vehicles," in IEEE Transactions on Intelligent Transportation Systems, vol. 18, no. 2, pp. 225-235, Feb. 2017.

[8] S. Pathak, A. Mani, A. Chatterjee and M. Sharma, "Software Defined Network Simulation Using OpenNet for Vehicular Network," in 3rd International Conference on Communication and Electronics Systems (ICCES), Coimbatore, India, pp. 170-175, Oct.2018.

[9] AK Singh, S Srivastava, ”A survey and classification of controller placement problem in SDN,” in International Journal of Network Management, vol. 28, Mar.2018.

[10] Bob Lantz, Brandon Heller, and Nick McKeown, “A Network in a Laptop: Rapid Prototyping for Software-Defined Networks” in ACM Hotnets 2010 Monterey, CA, USA, pp. 20-21, Oct.2010.

[11] X. Wang, C. Wang, J. Zhang, M. Zhou, C. Jiang, "Improved Rule Installation for Real-Time Query Service in Software-Defined Internet of Vehicles," in IEEE Transactions on Intelligent Transportation Systems, vol. 18, no. 2, pp. 225-235, Feb. 2017.

[12] S. Wang, C. Wu, C. Chou, "Constructing an optimal spanning tree over a hybrid network with SDN and legacy switches," in IEEE Symposium on Computers and Communication (ISCC), pp. 502-507, Jul.2015.

[13] C. Chen, Y. Chen, S. Tsai, M. Yang, "Forwarding path discovery with software defined networking," in 19th Asia-Pacific Network Operations and Management Symposium (APNOMS), pp. 299-302, Sept. 2017.

[14] M. Mendonca, K. Obraczka, T. Turletti, “The Case for Software–Defined Networking in Heterogeneous Networked Environments,” in ACM conference on CoNEXT student workshop, Dec.2012.

Proceedings of the Fourth International Conference on Communication and Electronics Systems (ICCES 2019)
IEEE Conference Record # 45898; IEEE Xplore ISBN: 978-1-7281-1261-9

Spike Correlations and Synchrony Affects the Information Encoding of Neurons

Manjusha Nair*, Richard Laji, Reshma Mohan
Department of Computer Science and Applications
Amrita Vishwa Vidyapeetham
Amritapuri, India
manjushanairm@gmail.com

***Abstract*— Coordination in neural activity is thought to be a key element in propagation of information. Coordinated spiking in neurons in an effective signaling mechanism and helps in self-organization of the network over time. Using computational techniques, this study investigates the parameters affecting the coordinated activity of a population of granular layer neurons of the cerebellum. This study investigates the spike train coordination using two basic measures: spike correlations and spike synchrony. The values were quantified from modeled granule neurons of the cerebellum under various excitatory and inhibitory synaptic balances and under induced plasticity states. Increased excitation from mossy fibers (MFs) increased the output correlation of granule neurons while increased inhibition from Golgi neuron reduced the output correlations. Synchronous firing of granular layer population under *in-vivo* like inputs was increased with the increase in excitation and inhibition. Synchrony was also estimated under different induced plasticity states of the modeled neurons. The firing was more synchronous under the long-term potentiation (LTP) state compared to control state and was more asynchronous under long-term depression (LTD) state compared to control. Since plasticity signifies the learning activity in the neurons and is affected by temporal coordination in spiking, these results have greater relevance in understanding the nature of neural code.**

Keywords*— *computational neuroscience; spike train analysis; correlation; synchrony;granule neuron

I. INTRODUCTION

A nerve cell (neuron) in the brain carries electrical impulses and fire signals to communicate with each other through the tiny gaps between them called synapses[1]. Depending on the nature of the neuron receptor present in the postsynaptic side, the postsynaptic membrane either becomes more electrically positive (excitatory) or become more electrically negative (inhibitory) and produce postsynaptic potentials (PSP) called Excitatory Postsynaptic Potential (EPSP) or Inhibitory Postsynaptic Potential (IPSP). PSPs thus formed are nonlinearly integrated across time (signals from the same pre synaptic neuron, one after the other) and space (signals from various presynaptic neurons, received at the same time) in the axon hillock and result in producing a signal called action potential.

Even though there are minor variations in the amplitude or shape of different such signals, these variations are assumed to be irrelevant. Neurons are assumed to use stereotyped and pulsed variants of such action potentials or spikes to communicate over long distances. A sequence of spikes from a neuron is represented as a spike train, consisting of a sequence of their spike times. Each spike typically lasts for 1-3 milliseconds approximately and are separated from other spikes by a few milliseconds[2]. These spike trains can be modeled as random processes since the same neuron produces a wide range of responses for the multiple invocation of identical stimuli. Neurophysiologists use multi electrode arrays to record simultaneous activity of several neurons within a particular brain region. Simultaneously recorded data from multiple neurons represent multidimensional point process time series.

Various coding schemes are used to study the transformation of information from one processing stage to another in a neural circuit. Rate coding assumes that the firing frequency of the neuron carries information. Since the shape of the action potential is not assumed to be significant in carrying information, the time of arrival of the action potential is used in many studies to measure the information content of the signal[3]. Hence time code considers the temporal patterns as information carriers. Inter spike interval based and first spike latency-based coding schemes also exist[4]. In frequency coding, neurons act as an analog to frequency converter while in latency code[5], neurons act as an analog to delay converter[6]. All these above-mentioned coding schemes study the neuron from a single neuron perspective and fail to represent the emergent properties of the joint activities of a group of neurons. Population level coding schemes are used to estimate the relationship between groups of neurons. For e.g., correlation coding studies suggest that correlations or synchrony between neurons could convey information in neuronal population level which is not contained in other coding schemes.

Correlation coding schemes are in practice from early 1960's [7] and several studies demonstrated the functional correlates of this measure with a multitude of parameters such as shared inputs, shared presynaptic partners, distance between neurons and receptive fields, intrinsic properties such as synaptic time constants etc.[8] It has been suggested that the neural responses are influenced not only by the firing rate of the inputs that it receives but also by the input correlations [9]. Spike train distance-based estimates also exist to measure the synchrony in neural firing[10].

This study investigates the correlation and synchrony between specific types of tiny neurons in the cerebellum, called granule neurons. The granular layer of the cerebellum, has more than 50% of the total number of the neurons in the brain. Granule neurons are present in the input layer of the cerebellum and receive inputs from various brain regions through long axons called mossy fibers. These mossy fiber inputs are excitatory in nature while the input connection that the granule neuron receive from another type of neurons called Golgi neurons, is inhibitory in nature. Each granule neuron, on an average receive one to four excitatory and inhibitory connections. Using computational models, this study investigates the coincident activity of multiple granule neurons under different synaptic conditions. The functional significance of these very tiny and densest neurons in the brain has greater relevance in computational modeling studies.

II. METHODS

A. Computational Modeling of Neurons

In computational modeling studies a neuron is abstracted as an RC circuit describing the electrical properties of the neuron [11].The RC circuit equivalent model is used to mathematically model the current flow in the circuit. In simulation studies, this mathematical framework is converted into a computational model. The biophysics of a single neuron is often abstracted as resistance-capacitance (RC) circuit with low-pass filtering properties wherein the lipid bi-layer of the neuronal membrane is modeled as capacitance (C), the voltage-gated ion channels in the membrane as electrical conductance (g) and the electrical gradient across the membrane as reversal potentials. Ohm's and Kirchhoff's laws are used to calculate the total current flowing and the voltage generated across the membrane of the neuron. The lipid bi-layer of the membrane acts as a capacitor by accumulating charges over its surface. The intracellular and extracellular solutions of the membrane act as the conducting plates separated by the non-conducting membrane. Total current flowing across the membrane is the sum of the capacitive and ionic currents:

$$I_{Total} = I_c + I_{ion} \quad (1)$$

When the capacitor is further charged with the input current I_{ext} which is applied into the cell, the current leaks through the membrane. Open membrane pores or channels in the membrane gives rise to more resistance components in parallel. Conductance of the channel increases with the increase in number of open ion channels in the membrane. Ionic current flow through a neuron with Sodium, Potassium and Leak channels can thus be modeled as,

[redacted] (2)

B. Multi compartmental modeling of granule neurons of the cerebellum

In multi-compartmental neuron modeling, each neuron is abstracted as a cylinder which is divided into different RC compartments. Each compartment is modeled with voltage gated ion channels and synaptic channels. The equations model close correspondence with the biophysical properties of neurons, ion channels and synapses. They also consider the propagation of membrane voltage change over axons and dendrites. Cable theory is used to model the variation of voltage across the axon. Every compartment is assumed to be iso-potential i.e., the voltage within each compartment is assumed to be constant and is modeled as an RC circuit. Multi-compartmental model of granule neuron used in this study contain 52 compartments[12] : N_A –No. of axonal compartments, N_D –No. of dendritic compartments, N_S –No. of somatic compartments, N_H –No. of hillock compartments (Figure 1: A). The membrane voltage V_m is estimated separately for each of the compartments separately.

$$\frac{dV}{dt} = \frac{1}{\tau_m}\left(\frac{\sum_i g_i(V-V_i)+\sum_{syn} g_{syn}(V-V_{syn})+\sum_{br} g_{br}(V-V_{br})}{g_{tot}}\right) \quad (3)$$

where the conductance of ion channel i is modeled as g , syn (synaptic dynamics), br representing the neighboring attached branch and $gtot$ (total) is the total conductance. The time constant is represented as $\tau_m = R_m C_m$ R_m is the membrane resistance and C_m is the membrane capacitance. The multi compartmental GrC model used included stochastic synapses where each synapse was constituted by few releasing sites comprising of pre-synaptic dynamics and release mechanisms. The granule cell model includes 1-4 excitatory and 1-4 inhibitory connections. Excitatory post-synaptic mechanisms were shown as AMPA and NMDA receptor components as seen in granule neurons [13]. AMPA receptor dynamics was modeled using a three-state scheme that was activated by a direct component of glutamate, modeled as pulse, and an indirect component representing the spillover of glutamate from nearby synapses in the glomerulus. Similarly, the NMDA receptors were modeled as five-state kinetic scheme, activated by the same direct and indirect glutamate components, and magnesium block was modeled by a Boltzmann equation [12]. The $GoC - GrC$ inhibitory synapses were modeled as in [13]. The granule neuron model was provided with 1-5 input spikes through each of the four MFs (Figure 1: B) and the simulations were performed in the presence and absence of inhibitory inputs to the neurons.

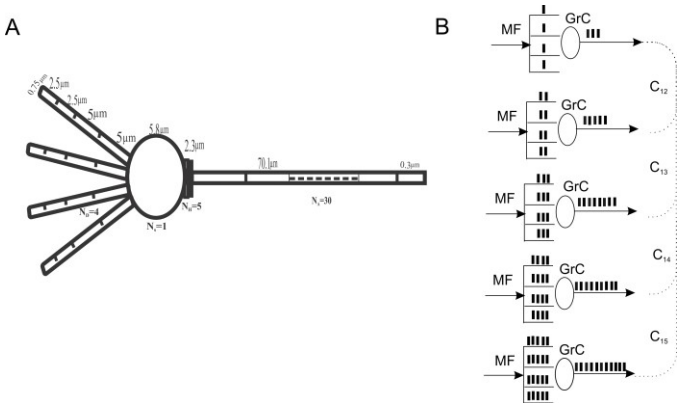

Figure 1: Computational modeling of neuron. A) The granule neuron model

used in this study included 52 compartments: 1 for the soma, 4 each for the four dendrites, 5 hillock compartments and 30 compartments for the axon. B) Input of varying spike rate was applied to the granule neuron model (GrC) through mossy fibers (MF). Cross correlation coefficients between paired neurons (C_{12}, C_{13}, C_{14}, C_{15}) was estimated as shown.

Plasticity states were also introduced in the neuron model. LTP and LTD were introduced by modifying the intrinsic excitability of the cell and also by modifying the release probability of the synapses[14].

C. Modeling the neural responses

Individual responses to the same stimulus are highly variable in the neurons. The process of action potential generation is a stochastic process. Poisson point processes on real line are used to model these spiking responses of neurons which are random spiking events in time. Point processes describe random events whose occurrence are timed. A Poisson point process is defined as a collection of random elements located on some mathematical space which can be used as mathematical models of some phenomena. The inter spike interval (ISI) of spike trains follows exponential distribution (Poisson distribution).

$$P(x) = \lambda e^{-\lambda t} \tag{4}$$

where λ is the inter-spike interval. Refractory periods modify this Poisson process to form Gamma distributions. Simultaneously recorded spike trains from multiple neurons are considered in our study as stochastic- dynamic multi-dimensional point process time series whose properties probabilistically change over time. Standard signal processing techniques used to analyze continuous valued data is not suitable to analyze such discrete datasets. The following sections describe the different techniques used in this study for spike train data analysis (Figure 2).

D. Measures of Spike Coordination

1) Cross correlation

Paired association between neurons (say a reference neuron and a target neuron) is tested traditionally using cross correlation measures. It shows the dependence of firing events of two neurons. The degree of correlation between neurons is quantified generally using various correlation measures. This study uses standard measures of correlation.

Given two time series,

$X = \{X_1, X_2, X_3 \ldots, X_n\}$ *and* $Y = \{Y_1, Y_2, Y_3, \ldots Y_n\}$

the correlation coefficient r measures the linear "similarity" between them.

$$r = \frac{\sum_{i-1}^{n}((X_i - \bar{X})(Y_i - \bar{Y}))}{\sqrt{\sum_{i-1}^{n}((X_i - \bar{X})^2}\sqrt{\sum_{i-1}^{n}((Y_i - \bar{Y})^2}} \tag{5}$$

Cross correlation measures the degree of similarity between spike trains as a function of its time shift. The values range between 0 and 1 where a 1 represents increased correlation strength.

2) Spike Train Synchrony

Since the standard measures of correlations work on a rate-based framework, neural coordination is also estimated by measuring relative timing in spiking events of two neurons.

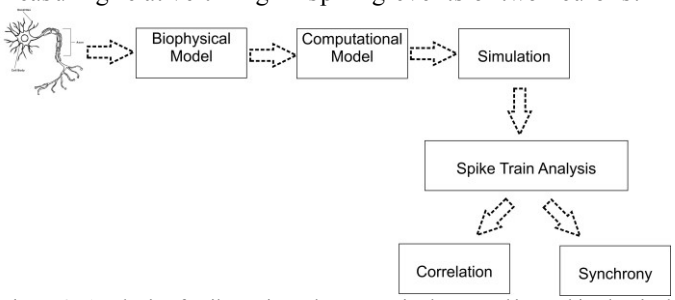

Figure 2: Analysis of spike trains. The neuron is abstracted into a biophysical model and is converted into computational model. The spike train responses of neural simulations are then used to quantify the coordination between neurons using the estimates of correlation and synchrony.

This study used a spike pattern distance measure called Victor-Purpura distance to estimate the synchrony in the neural responses [10][15].

Consider p and q as two spike trains with spike times $p_1, p_2 .. p_n$ and $q_1 q_2 .. q_n,$, . A measure of spike train synchrony maps the pair to a positive real number. A high value corresponds to two closely related spike trains and is expressed as $s(p,q)$ and a low value corresponds to very similar spike trains .In the case of dissimilarity measures expressed as the distance between spike trains $d(p,q)$, a measure of dissimilarity is a metric , so that $d(p,q) = 0$ implies $p = q$.

The Victor-Purpura distance measure

It is a measure of the amount of change required to transform one spike train into the other [15]. It uses a cost-based metric, measured while changing one spike train into another using three basic operations: spike insertion, spike deletion and spike shift. Spikes can be added or deleted at a cost of one for each operation, and spikes can be moved at a cost of $q|\delta t|$ for a cost per time unit q and a temporal distance δt.

Population measures were calculated in two ways in this study: those which measure the similarity (or dissimilarity) between a pair of responses and those that measure the over-all similarity of a set of responses and are calculated by averaging single-neuron measures.

III. RESULTS AND DISCUSSION

A. Neural correlation affected by synaptic excitation and inhibition

In order to estimate the effect of excitation and inhibition on coordination between neurons, two modeled neurons with differing synaptic balances were chosen and the paired correlation coefficient was estimated. In order to change the effect of input firing rate on correlation, MF inputs with 1 to 5 spikes through the four synapses was applied (Figure 1:B). Cross- correlograms were generated for paired spike trains.

It has been observed that cross-correlation was reduced as the neurons more differed in their firing frequency. The number of mossy fiber inputs were also changed from 2 to 4 and found that the correlation increased with the increase in mossy fiber inputs to the neuron (Figure 3: A). The granule neuron responses were also recorded in the presence of Golgi neuron inhibitory inputs and found that the correlation was high in the absence of inhibition and reduced with the introduction of more and more inhibition into the neurons (Figure 4: A). These correlation estimates suggested that the paired association between neurons is increased with more excitation and reduced with more inhibition into the neurons.

Correlation for time lags of ± 25 ms, centered on the first spike train was calculated and the peaks in the correlogram indicated the highest value of correlation between the spike trains. The correlation measures are the maximum values from the cross-correlograms of the spikes. Peaks in the cross correlograms represent the simultaneous firing events of target and reference neurons. The width of the correlogram increased with increase in excitation and the correlation peaks were more shifted towards the left (Figure 3: B, C, D). The width of correlogram was reduced with increase in inhibition and the correlation peaks were more shifted towards the center (Figure 4: B, C, D).

B. *Neural synchrony affected by synaptic excitation and inhibition*

The synchronous firing of granule neurons under different synaptic conditions were estimated using a spike distance measure. MF input spikes of 1 to 5 were applied to a granule neuron population and the multi-neuronal responses were recorded. Average spike distance between all pairs of responses (D_{Mean}) in the response set was estimated (Figure 5: A). This measure was observed to be decreased with the increase in MF excitatory inputs to the neuron, suggesting the increased synchronous firing with increased excitation.

D_{Mean} was also estimated with and without inhibition into the neurons in the population (Figure 5: B). Reduced distance measure with the increase in inhibition suggested the increased synchrony between firing responses.

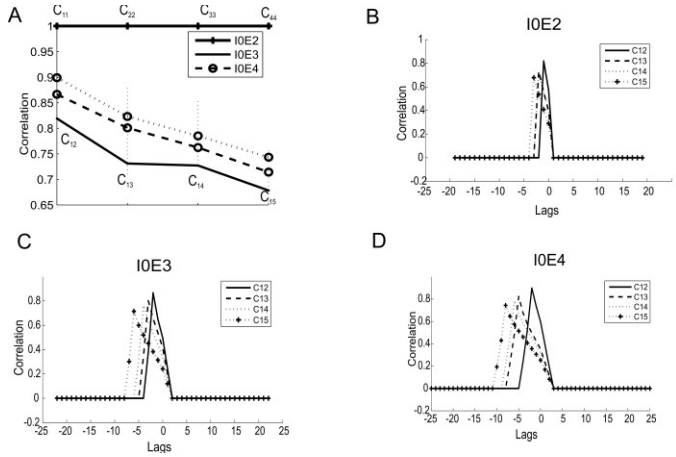

Figure 3: MF excitation and granule neuron response correlation. A) Cross correlation reduced with the increase in firing rate and increased with the increase in mossy fiber inputs. B, C, D) Cross correlograms plotted for three different synaptic conditions: I0E2 – Inhibition 0 excitation 2, I0E3 – Inhibition 0 excitation 3, I0E4 – Inhibition 0 excitation 4.

C. *Firing synchrony during induced plasticity states*

Simulations were performed under induced plasticity states of the neurons[16] .Long term potentiation (LTP) was introduced by increasing the intrinsic excitability of the neuron and by increasing the release probability of MF synapses above 0.41. Long term depression (LTD) was induced by reducing the
intrinsic excitability of the neuron and by decreasing the release probability of the MF synapses below 0.41. D_{Mean} was estimated for LTP, control and LTD conditions of the neuron and it was observed that D_{Mean} was decreased during LTP from control while D_{Mean} was increased during LTD from control (Figure 5:C). These results suggested that the neurons fired more synchronously in their LTP state compared to the control state and the firing was more asynchronous during LTD state compared to control state.

CONCLUSION

The observation from the study suggested how the inhibitory and excitatory synaptic balance modulates the post synaptic responses of a neuron. Also we propose that, coordinated activity is controlled in the neuronal level using such balances. Enhanced firing synchrony during plasticity conditions also reflect its influence on functional connectivity between neurons.

Due to the high dimensionality of the multi neuronal data, population coding studies are less advanced compared to studies on information coding in single neurons[17] . Even though cross correlation represents relationships that exist between the spiking activities of two neurons, this method assumes that the spike trains are stationary. The time varying adaptation of the spike trains in the time course of the stimulus, is not addressed in the method and it is assumed that the statistics of the spike trains are constant over time.

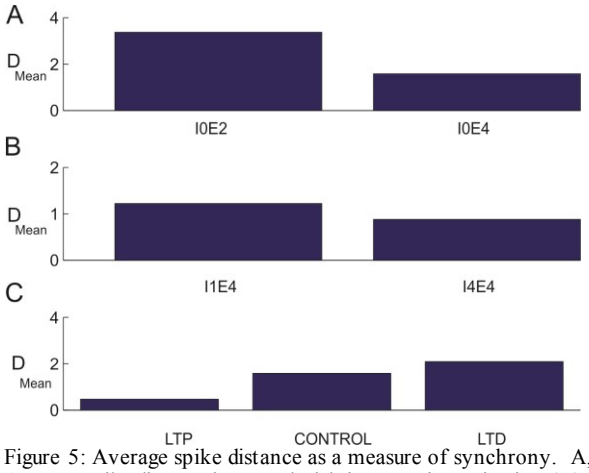

Figure 5: Average spike distance as a measure of synchrony. A, B) Average spike distance increased with increase in excitation (A) and inhibition (B). C) Average spike distance was decreased in LTP compared to control and increased in LTD compared to control.

Spike distance-based measures are able to capture the temporal structure and synchrony in the responses and is a powerful tool in mutual information-based studies[18] . Spike correlations and spike synchrony may function as an additional information transfer mechanism in neurons and further work is required in this direction to study the effect of such coordinated activities in the information encoding properties of the neurons.

ACKNOWLEDGMENT

This work derives direction and ideas from the Chancellor of Amrita University, Sri Mata Amritanandamayi Devi. The authors of this work also acknowledge the support received from Computational Neuroscience Lab, School of Biotechnology, Amrita Vishwa Vidyapeetham.

REFERENCES

[1] D. Purves, G. J. Augustine, D. Fitzpatrick, W. Hall, A.-S. LaMantia, and L. White, *Neurosciences*. De Boeck Supérieur, 2019.

[2] F. Rieke and D. Warland, *Spikes: exploring the neural code*. MIT press, 1999.

[3] T. Tateno and H. P. C. Robinson, "Rate coding and spike-time variability in cortical neurons with two types of threshold dynamics," *J. Neurophysiol.*, vol. 95, no. 4, pp. 2650–2663, 2006.

[4] A. Mita, H. Mushiake, K. Shima, Y. Matsuzaka, and J. Tanji, "Interval time coding by neurons in the presupplementary and supplementary motor areas," *Nat. Neurosci.*, vol. 12, no. 4, p. 502, 2009.

[5] P. Heil, "First-spike latency of auditory neurons revisited," *Curr. Opin. Neurobiol.*, vol. 14, no. 4, pp. 461–467, 2004.

[6] S. M. N. Woolley and J. H. Casseday, "Response properties of single neurons in the zebra finch auditory midbrain: response patterns, frequency coding, intensity coding, and spike latencies," *J. Neurophysiol.*, vol. 91, no. 1, pp. 136–151, 2004.

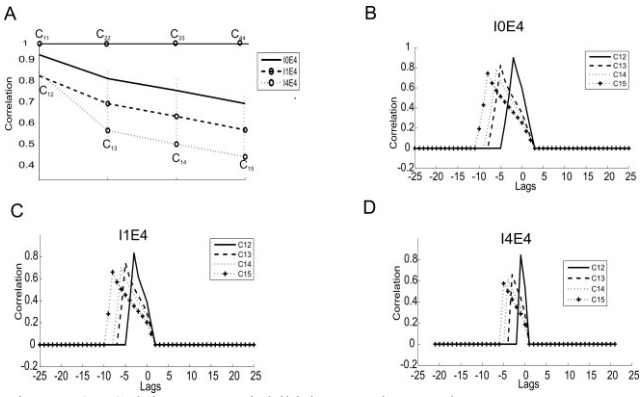

Figure 4: Golgi neuron inhibition and granule neuron response correlation. A) Cross correlation reduced with the increase in firing rate and with the increase in inhibitory inputs. B, C, D) Cross correlograms plotted for three different synaptic conditions: I0E4 – Inhibition 0 excitation 4, I1E4 – Inhibition 1 excitation 4, I4E4 – Inhibition 4 excitation 4.

[7] G. L. Gerstein and W. A. Clark, "Simultaneous studies of firing patterns in several neurons," *Science (80-.).*, vol. 143, no. 3612, pp. 1325–1327, 1964.

[8] A. Dettner, S. Münzberg, and T. Tchumatchenko, "Temporal pairwise spike correlations fully capture single-neuron information," *Nat. Commun.*, vol. 7, p. 13805, 2016.

[9] V. Budnik and P. C. Salinas, "Wnt signaling during synaptic development and plasticity," *Curr. Opin. Neurobiol.*, vol. 21, no. 1, pp. 151–159, 2011.

[10] T. Kreuz, "Measures of spike train synchrony," *Scholarpedia*, vol. 6, no. 10, p. 11934, 2011.

[11] K. M. Dabrowski, D. J. Castaño, and J. L. Tartar, "Basic Neuron Model Electrical Equivalent Circuit: An Undergraduate Laboratory Exercise," *J. Undergrad. Neurosci. Educ.*, vol. 12, no. 1, p. A49, 2013.

[12] S. Diwakar, J. Magistretti, M. Goldfarb, G. Naldi, and E. D'Angelo, "Axonal Na+ channels ensure fast spike activation and back-propagation in cerebellar granule cells," *J. Neurophysiol.*, vol. 101, no. 2, pp. 519–532, 2009.

[13] T. Nieus, E. Sola, J. Mapelli, E. Saftenku, P. Rossi, and E. D'angelo, "LTP regulates burst initiation and frequency at mossy fiber--granule cell synapses of rat cerebellum: experimental observations and theoretical predictions," *J. Neurophysiol.*, vol. 95, no. 2, pp. 686–699, 2006.

[14] L. Roggeri, B. Rivieccio, P. Rossi, and E. D'Angelo, "Tactile stimulation evokes long-term synaptic plasticity in the granular layer of cerebellum," *J. Neurosci.*, vol. 28, no. 25, pp. 6354–6359, 2008.

[15] C. Houghton, "Population measures of spike train synchrony," *Scholarpedia*, vol. 8, no. 10, p. 30635, 2013.

[16] M. Nair, N. Melethadathil, B. Nair, and S. Diwakar, "Information processing via post-synaptic EPSP-spike

complex and model-based predictions of induced changes during plasticity in cerebellar granular neuron," in *Proceedings of the 1st Amrita ACM-W Celebration on Women in Computing in India*, 2010, p. 5.

[17] S. Diwakar, C. Medini, M. Nair, H. Parasuram, A. Vijayan, and B. Nair, "Computational Neuroscience of Timing, Plasticity and Function in Cerebellum Microcircuits," in *Computational Neurology and Psychiatry*, Springer, 2017, pp. 343–371.

[18] M. Nair, P. Madhu, V. Mohan, A. G. Rajendran, B. Nair, and S. Diwakar, "GPGPU implementation of information theoretic algorithms for the analysis of granular layer neurons," in *2015 International Conference on Computing and Network Communications (CoCoNet)*, 2015, pp. 18–26.

Proceedings of the Fourth International Conference on Communication and Electronics Systems (ICCES 2019)
IEEE Conference Record # 45898; IEEE Xplore ISBN: 978-1-7281-1261-9

Real time Facial Expression Recognition using Grid of Local Binary Pattern and Histogram of Gradients and Genetic Algorithm on Raspberry Pi

ARISTON RODRIGUES
Sardar Patel Institute of Technology,
Mumbai-400058, India,
ariston.rodrigues@spit.ac.in

KIRAN TALELE
Sardar Patel Institute of Technology,
Mumbai-400058, India,
talelesir@gmail.com

***Abstract*—In this paper,real time Facial expression recognition on a raspberry pi using K Nearest Neighbors (KNN) classifier is proposed. Global shape features are extracted with Histogram Of Gradients (HOG) and Local texture features are extracted using Grid of Local Binary Patterns (GoLBP) and both the vectors are combined. Various block sizes for GoLBP feature vector extraction are evaluated. Genetic Algorithm is used for feature selection and optimisation, Change in efficiency of classification with number of iterations (Generations) is studied. The proposed method is tested using Japanese Female Facial Expression Database, Taiwanese Facial Expression Database and Cohn-Kanade Expression Database. The proposed technique is compared with some state of the art techniques. The proposed technique is trained with locally developed Indian facial expression dataset and deployed on raspberry pi Single Board Computer(SBC).**

Keywords: HOG, GoLBP, Genetic Algorithm, KNN.

I. Introduction

Facial Expression recognition is essential for human computer interaction and to build smarter systems. Today smart appliances and home automation work on the basis of interaction between the smart system and humans. According to Albert Mehrabian, a professor of psychology, In communication just 7% information is transmitted via verbal communication and 93% information is transmitted through non-verbal means [1]. These non-verbal modes range from Facial Expressions to body language and the tone of speech. Similar words said with different facial expressions often convey different emotions and give different meaning to the same message. Facial expressions are universal and dont vary over nationalities. Facial Expressions can be classified into seven categories, Happy, Surprise, Disgust, Unhappy, Fear, Anger and Neutral.

The above facial expression can be broadly classified into two emotional states. The facial expressions of Disgust, Unhappiness, Fear and Anger representing a persons negative emotional state. The facial expressions of Happy and Surprise representing and positive mood and a Positive state of mind. Classification of emotion is a binary classification problem, whereas facial expression classification is a multi-class classification problem. Apart from human computer interaction there are a lot of application areas where detection negative emotions can be applied. Few Such application areas are Crime-scene investigation from CCTV footage, Criminal Interrogation, It can be also applied to surveillance and preventing crimes. Other applications of Facial Expressions include medical sciences , E-learning and market research.

Genetic Algorithm is an algorithm which tries to mimic the process of natural evolution put forth by Charles Darwin. Genetic Algorithm is capable of extracting features from a given pool of features, which helps in reducing the total number of features and at the same time increase the accuracy of classification. Genetic Algorithm achieves this by selecting the fittest features from a pool of features. Our work is validated with help of widely used standard databases such as Japanese Female Facial Expression (JFED) [13] , Taiwanese Facial Expression Image Database (TFED) [12] and Cohn-Kanade Facial Expression Database(CKFED) [14].

II. Related Work

Viola and Jones proposed haar feature based face detection technique which used adaboost training and cascaded classifiers [3]. Zhe Sun et al. in [10] proposed a discriminative learning scheme for facial expression recognition. V-2DLDA was used to aid in classification tasks. The algorithm achieved accuracy of 91.87% on ck+ dataset, 82.24% on kdef dataset. Stefanos Eleftheriadis et al in [6] proposed a multi-view and view invariant classification of expressions using DS-GPLVM. The method achieved accuracy of 93.55% on Multi-pie database. Shojaeilangari et al in [7] proposed a model that can jointly learn dictionary and non-linear classification model. A spatio-temporal distinctive and pose invariant descriptor was proposed, the method also works on video data. The technique is computationally slow. Evangelos Sariyanidi et al. in [8] represented facial expression variation as localised basis functions. The technique utilizes svm for classification. Mengyi Liu et al. in [9] proposed method for video data. The technique extracts SIFT and HOG features. Universal Manifold model is learnt from low level features. S L Happy and Aurobinda Routray in [11] proposed method for low resolution images using SVM classifier. They proposed a novel framework by using appearance features of selected active facial patches. Khorsheed and Yurtkan in [16] used LBP for

feature extraction, a novel classifier was proposed, which used chi square distance metric. The technique has accuracy of 82%. The above methods have limitations such as illumination variations leading to misclassification, lack of global or local features

III. Facial Expression Recognition System

Facial expression recognition system comprises of 2 phases. The 1st stage is the training phase where the system is trained to recognize various facial expressions. In the training stage image samples for each facial expression are applied as input. The system learns from this input data. The input images to the system are first pre-processed. In pre-processing stage a face is extracted from the image. From the detected faces feature vectors are extracted. Best features are extracted from the feature vector in feature selection stage. The selected features are applied as input to learn a classification model. In testing face an unknown image is given to the system. The system pre-processes the image, extracts the features and then predicts the facial expression.

Face detection is the process of capturing a face of a person from an image frame. There are various methods for detecting faces, such as viola jones method [3] and various deep-learning based detectors. Due to better performance of deep learning techniques in real-time applications, in this proposed work deep learning based technique has been utilized. Andrew G. Howard et. al. proposed efficient convolutional neural network called MobileNet for mobile phones and embedded applications in [4]. Wei Liu et al. proposed a multi-box detector for detecting objects in images using single deep neural network in [5]. Googles tensorflow api provides an api which is combination of both the above works. The api is called ssdlite-mobilenet, and was designed for implementation on mobile-phones, embedded devices and single board computers such as raspberry pi. In the proposed work, tensor-flow object detection api is installed on the raspberry pi device. Tensorflows, ssdlite mobilenet model is transfer trained to detect faces in an image. The model is trained using 1200 images with different facial orientations and inclinations.

The tensor-flow model gives detection boxes, detection scores and detection classes as outputs. If the detection score is greater than 50%, it is assumed that the detected object is a human face. The detected face image is then pre-processed to make it robust for further processing. The face image is histogram equalized. Histogram equalization makes the face image invariant to illumination variations. To reduce the computation time, the image is converted to gray scale and resized.

Feature Extraction module is the most vital component of the entire system. The features extracted from each image provide vital information in identifying expressions. To extract features, a combination of Grid of Local Binary Pattern and Histogram of Gradients is used and a single feature vector is obtained. Feature extraction reduces dimensionality to a single dimension. The extracted features undergo feature selection, where the best features are selected from the pool of available features. After feature selection a feature vector of reduced length is obtained. The reduced features are used for further classification. A feature can be categorized either as a global or a local feature. Global features such as HOG try to capture the shape of structures in the image by capturing gradient information. In contrast Local descriptors such as LBP give information about textures in parts of the image. By applying feature extraction, the aim is to convert large quantity of pixel data into computationally efficient feature vector. The accuracy of classifications is directly impacted by the choice of feature descriptors.

The next step in Facial Expression Recognition System is Feature Selection. Feature selection has impact on both, the computational time required and the accuracy of classification. Feature Selection takes the feature vector as an input and selects the features which contribute most to describing an emotion. In doing so, redundant features are discarded and the length of feature vector is reduced. Reduction in feature vector length results in less computational time and also greater accuracy. Genetic Algorithm is used for feature selection. Genetic Algorithm is an Evolutionary Algorithm which follows the process of natural selection. Genetic Algorithm is ruled by the law of survival of the fittest.

The Final step in Facial Expression Recognition System is classifying the extracted features into predefined classes. Those classes are: Happy, Unhappy, Surprise, Disgust, Fear and Anger. Machine Learning is utilized for classification of these expressions. K- Nearest Neighbors (KNN) is a supervised learning Algorithm. KNN estimates output directly from the test data and training data, based on the classes of training data points surrounding the test data point. The entire system is deployed on raspberry pi for real time emotion classification.

A. Grid of Local Binary Pattern

Local Binary Patterns(LBP) are local texture descriptors proposed by Ojala et al [18]. LBP are simple yet powerful and robust features. LBP have been widely used for detection and recognition applications. LBPs illumination invariance make them highly suitable for face recognition and facial expression recognition applications. Ngoc introduced a modified version of LBP know as Grid of LBP (GoLBP) [19]. GoLBP provides better texture description as compared to original LBP [18]. LBP and its versions are applied on gray scale images. But it has also been extended to Colour images, videos and other volumetric data.

Fig 1 represents the GoLBP structure and the manner in which different pixel values are to be compared. Equation (1), shows that all the 8 neighbouring pixels contribute to the calculation of the GoLBP value. In calculating GoLBP, the difference between pixels according to GoLBP structure is calculated. If the difference between the numbers is non-negative, then 1 is assigned. If the difference between the pixels is negative than 0 is assigned.

$$A = d_{0,c} + d_{2,c}2^1 + d_{3,c}2^2 + d_{5,c}2^3 + d_{1,4}2^4 + d_{1,6}2^5 + d_{7,2}2^6 + d_{7,4}2^7 \quad (1)$$

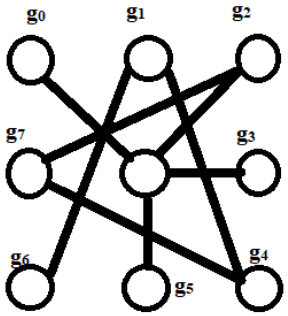

Fig. 1. GoLBP Structure [19]

$$d_{x,y} = s(x,y) = \begin{cases} 1, & \text{if } g_x \geq g_y. \\ 0, & \text{otherwise.} \end{cases} \quad (2)$$

If Fig 2 is the input image block, than by applying the grid structure and equation (1), the GoLBP code obtained is 111100012 . The decimal code equivalent is 241. Therefore a single decimal value is obtained for the entire block. The process is repeated over all the blocks in an image and an image feature vector is obtained. The biggest advantage of GoLBP and other LBP codes is that, it is invariant to illumination variation, as even after change in lightning conditions the difference between the pixels remain the same. Due to this GoLBP and other LBP variants are highly suitable for real time applications.

65	79	41
84	54	46
77	42	53

Fig. 2. Input Image Block

B. Histogram Of Gradients

Histogram of Gradients(HOG) are global features introduced by Dalal et. al. [17]. The aim of HOG is to extract shape information in an image. The shape information is obtained by extracting gradient and edge information. To calculate HOG, first gradients in x direction G_x and gradient in y direction G_y are computed. From the gradient information, the gradient magnitude and orientation are calculated.

$$M(x,y) = \sqrt{G_x(x,y)^2 + G_y(x,y)^2} \quad (3)$$

$$\theta(x,y) = \frac{G_x(x,y)}{G_y(x,y)} \quad (4)$$

The HOG features are extracted as follows: In a gray-scale or Colour image the gradients are calculated in horizontal and vertical direction. From horizontal and vertical gradients the magnitude is calculated according to equation(3) and orientations are calculated according to equation (4). The gradient histogram is divided into 9 bins from 0 to 180 degree. According to magnitude, each pixel is voted for its orientation.

C. Genetic Algorithm

K.F. Man et. al. proposed genetic algorithm as an evolutionary algorithm [20]. Genetic algorithm attempts to mimic the process of natural evolution. The algorithm is based on principle of survival of fittest, where the fittest features are selected to produce a next generation of features. The next generation inherits characteristics from parent features and are supposed to be fitter features. There are five phases in Genetic Algorithm:

- Obtaining Initial Population
- Evaluating Fitness using a fitness function.
- Feature Selection
- Cross-over
- Mutation

The Algorithm begins with a set of features called a population. Each point in a feature vector is called a gene. Each feature vector is called a chromosome. In genetic algorithm, the set of genes is represented as binary values. Thus chromosome is represented as a vector of 1s and 0s. Initially a random population is selected from the available features. Fitness score is calculated for each individual using a fitness function. Fitness function can be the classification score of a classifier. The individuals with higher fitness score are selected for further operation. Then the selected individuals will be used to create a new generation. A cross over point is selected and the genes of the two individuals are exchanged. The new generation created, inherits the fitness from both its parents. The new generation is now subjected to Mutation, where some genes are flipped from 0 to 1 or 1 to 0. After this again the fitness of new population is computed and the procedure of cross-over and mutation repeated.

Fig. 3. Population, Chromosomes, Genes

Fig 3 shows how each feature vector is represented as a chromosome, and each element of the vector is represented as a gene. In genetic algorithm the genes are represented as one and zeroes and during the crossover operation, according to crossover, certain number of genes of a chromosome

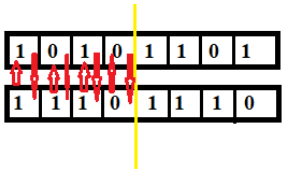

Fig. 4. Cross-Over Operation

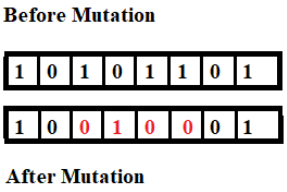

Fig. 5. Mutation Operation

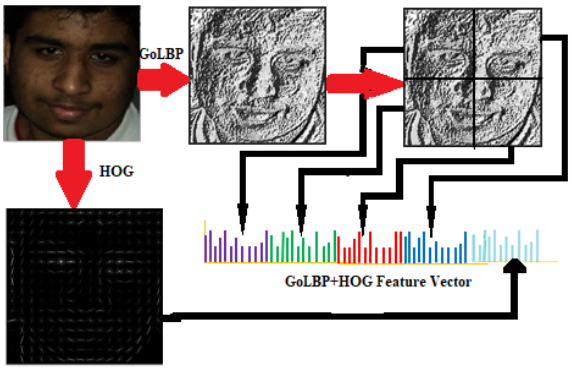

Fig. 6. Decomposition of Face Image into Feature Vector

TABLE I
OVERVIEW OF EXPERIMENTS PERFORMED WITHOUT GENETIC ALGORITHM

Block Size of GoLBP (Vector Length)	JFED	TFED	CKFED
256x256 (2020)	88.57	88.23	90.59
128x128(2788)	88.57	88.23	92.30
64x64 (5860)	92.85	90.19	93.16
32x32 (18148)	67.14	89.22	74.36

represented in binary form is exchanged with same number of genes of another chromosome as shown in fig 4. In mutation operation the genes are flipped as displayed in figure 5.

For application in image processing, a single feature vector will be considered as a chromosome and individual data points in the vector are genes. Initially fitness is calculated for all chromosomes and all the genes are considered. Then randomly for every chromosome some of the genes are neglected in computation. This genes can be represented by zero. The genes considered for evaluation are represented by 1. Fitness score is evaluated with this reduced number of genes. If greater fitness is obtained the cross-over and mutation operations are performed else a new population is generated.

IV. PROPOSED ALGORITHM

The proposed algorithm was developed to perform real time facial expression recognition on raspberry pi. In the proposed algorithm pyramid approach is used for feature extraction, the detected pre-processed face image is resized to 256x256 image. In pyramid approach a set of features are extracted and then image is resized to half its size and another set of features is extracted. The GoLBP image is calculated for 256x256 image. The image is then resized to 128x128 and HOG of the image is calculated. The GoLBP image is divided into blocks of equal size and histogram of each block is obtained as shown in fig 6. Histograms from various blocks are concatenated and at the end HOG vector is concatenated. The concatenated vector is the feature vector. Feature vectors from different images are obtained.

In the training phase, the genetic algorithm is applied to the extracted features. From the training images, 20 % images in the training set are used as validation images for the genetic algorithms fitness function. In the proposed work K-Nearest Neighbour(KNN) classifier is used as a fitness function. Higher KNN classification accuracy corresponds to higher fitness. Genetic Algorithm computes a solution which takes into account which element of the vector contributes how much information to the classification process. The best feature elements are selected, in doing so the length of feature vector is also reduced. The final result of genetic algorithm is a long integer number, which when represented in binary form, provides information about which Feature elements to be considered and which feature elements are redundant to the classification problem. With help of training set, and the validation set, a solution to genetic algorithm is obtained. This solution is used for feature selection in the test dataset and for real time execution on the raspberry pi.

V. EXPERIMENTATION AND RESULT ANALYSIS

The FER algorithm is developed to detect the basic emotions such as Happiness, Disgust, Fear, Surprise, Anger, Unhappy and Neutral. Different sets of images were used for training and testing the system. The Algorithm iteratively loads images from the datasets and features vector is calculated using combination of GoLBP and HOG. The image is divided into different block sizes and Histograms from different GoLBP image blocks and HOG are concatenated together to obtain the feature vector. KNN classifier then classifies the test images into one of the emotion depending on the trained image dataset.

Table I summarizes recognition rates at various block sizes leading to varying lengths of features vectors. It is observed that highest accuracy is obtained when the GoLBP image is divided into 16, 64x64 blocks. The histograms from the 16 blocks are concatenated into 4096 length vector. The HOG vector of length 1,764 obtained by resizing image to 128x128, using cell size of 16x16 and block size of 2x2 is concatenated at the end of the 4096 length vector. The HOG configuration is selected as it provides good balance between

HOG feature length and the amount of information captured. The confusion matrix for high accuracy recognition cases are tabulated further.

TABLE II
FER WITH GENETIC ALGORITHM ON COHN KANADE DATASET.

	Neutral	Happy	Surprise	Disgust	Unhappy	Fear	Angry	Accuracy
Neutral	21	1	0	0	1	1	0	87.5
Happy	0	21	0	0	0	0	0	100
Surprise	0	0	29	0	0	0	0	100
Disgust	0	0	0	8	0	0	0	100
Unhappy	1	0	0	0	7	1	0	77
Fear	0	0	0	0	0	10	0	100
Angry	0	0	0	0	0	0	16	100

Overall Accuracy (Test Set):95.72%

To optimize features using genetic algorithm, images from train set were used as validation set and optimized solution representing the features to select and features to discard was obtained. The solution is applied to test data set and optimized features are obtained from test data set too. This process was repeated for Cohn Kanade, Japanse Female and Taiwanese Facial Expression Datasets. Cohn Kanade train Dataset had 296 images out of which 60 images were included in validation set to calculate genetic algorithm solution. Using that solution, feature selection for test dataset is accomplished. Table II represents confusion matrix for Cohn Kanade dataset, where test set had 117 images and accuracy of 95.72% was obtained. Thus Genetic Algorithm increased accuracy from 93.16 to 95.72%.

TABLE III
FER WITH GENETIC ALGORITHM ON JFED.

	Neutral	Happy	Surprise	Disgust	Unhappy	Fear	Angry	Accuracy
Neutral	20	0	0	0	0	1	0	95
Happy	0	20	0	0	0	0	0	100
Surprise	0	0	14	0	0	0	0	100
Disgust	0	0	0	16	0	0	0	100
Unhappy	3	0	0	0	10	1	0	77
Fear	0	0	0	0	0	13	0	100
Angry	0	0	0	0	0	0	13	100

Overall Accuracy (Test Set):96.36%

Japanese Female train Dataset had 254 images out of which 60 images were included in validation set to calculate genetic algorithm solution. Using that solution, feature selection for test dataset is accomplished. Table III represents confusion matrix for Japanese Female dataset, where test set had 110 images and accuracy of 96.36% was obtained. Thus Genetic Algorithm increased accuracy from 92.85 to 96.36%.

Taiwanese train Dataset had 245 images out of which 60 images were included in validation set to calculate genetic algorithm solution. Using that solution, feature selection for test dataset is accomplished. Table IV represents confusion matrix for Taiwanese dataset, where test set had 102 images

TABLE IV
FER WITH GENETIC ALGORITHM ON TFED.

	Neutral	Happy	Surprise	Disgust	Contempt	Unhappy	Fear	Angry	Accuracy
Neutral	18	0	0	0	0	0	0	0	100
Happy	0	15	0	0	0	0	0	0	100
Surprise	0	0	11	0	0	0	0	0	100
Disgust	0	0	0	8	0	0	0	0	100
Contempt	1	0	0	0	23	0	0	0	96
Unhappy	2	0	0	0	0	7	0	0	78
Fear	0	0	0	0	0	0	8	0	100
Angry	1	0	0	0	0	0	0	7	78

Overall Accuracy (Test Set):95.09%

TABLE V
PERFORMANCE COMPARISON OF VARIOUS STATE OF THE ART TECHNIQUES WITH PROPOSED WORK

Database	SVM+ Bi-directional LBP [21]	SVM+ LBP + LDA +AFP [11]	BPN [22]	RBF [22]	LBP + GRNN [23]	Proposed work
JFED	96.91	92.22	69.82	85.71	95.48	96.36
TFED	94.66	-	83.85	92.85	94.25	95.09
CKFED	-	94.09	-	-	94.91	95.72

and accuracy of 95.09% was obtained. Thus Genetic Algorithm increased accuracy from 90.19 to 95.09%.

Fig 7 represents the number of generations Genetic algorithm is allowed to run for, and the accuracy corresponding to the number of generations. It can be seen that accuracy keeps on increasing to a certain point, after which the accuracy remains same, despite the number of generations the Genetic Algorithm runs.It is also seen that, genetic algorithm leads to 50% reduction in size of feature vector. On an average the feature vector length, for 64x64 GoLBP block was reduced to an average of 3000 from 5860. The Accuracy also varies with change in the size of initial population that is initiated, In our experiments, optimum results were obtained by considering an initial population of 50.

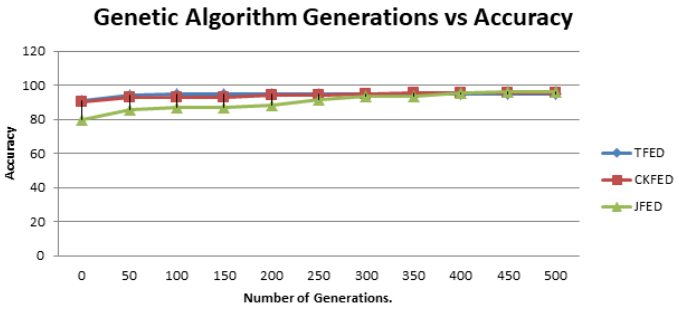

Fig. 7. Genetic Algorithm Training Generations vs Accuracy

It can be seen in table V, that the proposed work gives comparable results to state of the art techniques while at the same time providing optimized features.

For real-time implementation, a local database of Indian facial expression images was constructed and fed to the algorithm to be learnt. The dataset consisted of 78 images of angry expression, 126 images of disgust expression, 92 images of fear expression, 78 images of happy expression, 119 images of surprise expression and 151 images of unhappy facial expression. A validation set of 28 angry images, 26 disgust, 26 fear, 25 happy, 25 surprise and 25 unhappy images is constructed and Genetic Algorithm solution is evaluated. The solution is used for feature selection on the real time faces detected via tensor-flow model.

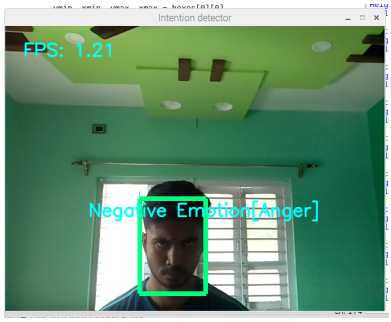

Fig. 8. Real time Angry Emotion detection

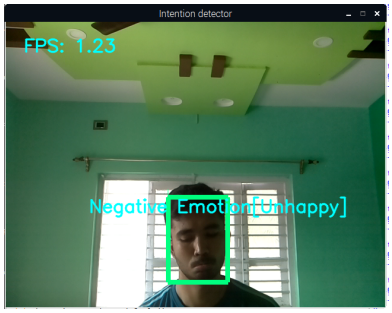

Fig. 9. Real time unhappy Emotion detection

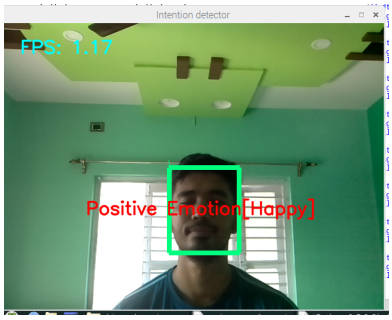

Fig. 10. Real time happy Emotion detection

Fig 8,9 and 10 show the real time detection results. The face is detected by raspberry pi using tensorflow model and marked with a green box. The face region is passed to the proposed algorithm to predict the facial expression. In fig 8, Unhappy emotion is predicted, in fig 9 anger is detected and in fig 10 Happy is detected. The FPS, in the figure represents the time required for entire process from, frame capture, face detection feature extraction and emotion prediction to complete. A FPS of greater than 1 represents computation time of less than 1 second, which is good enough for real time applications on a raspberry pi board.

VI. Conclusions

A new approach based on combination of global and local features has been proposed to encode shape and texture information. Genetic Algorithm is proposed for feature selection and optimization. The optimum block size for GoLBP image which generates a feature vector that gives highest accuracy, has been evaluated. The increase in accuracy with number of generations of Genetic Algorithm has been studied, It is seen that population of 50 and running the Algorithm for 300 generations gives the best optimized solution. The proposed work is tested on standard datasets, and the results are comparable to state of the art techniques. The algorithm operates at frame rate of more than 1fps, which is because of the light weight feature extraction algorithm, which still provides good accuracy. The future scope of the study can include applying Genetic Algorithm to other feature extraction techniques. Experimenting with Genetic Algorithm to use different mutation techniques and selection techniques such as roulette wheel, tournament and others. Creating a more robust dataset, for training the algorithm for real world application.

To deploy the system, for real time applications in real world scenarios, the system needs to be trained with a much robust dataset, where in the faces are inclined at certain angles or rotated in some direction.

References

[1] Mehrabian , ‘Communication without words’, *Psychology Today*1968 ,Vol 2 , pp 52-55.
[2] K.F. Man ; K.S. Tang ; S. Kwong, ‘Genetic algorithms: concepts and applications [in engineering design]’ , *IEEE Transactions on Industrial Electronics*,Vol 43 NO. 5, OCT 1996.
[3] Viola, Paul and Jones, Michael J., ‘Robust Real-Time Face Detection’, *International Journal of Computer Vision,* Vol 57 Issue 2, May 2004.
[4] Howard, Andrew G., Menglong Zhu, Bo Chen, Dmitry Kalenichenko, Weijun Wang, Tobias Weyand, Marco Andreetto and Hartwig Adam, ”MobileNets: Efficient Convolutional Neural Networks for Mobile Vision Applications” in *CoRR*, 2017.
[5] Liu, Wei, Dragomir Anguelov, Dumitru Erhan, Christian Szegedy, Scott E. Reed, Cheng-Yang Fu and Alexander C. Berg, ”SSD: Single Shot MultiBox Detector” in *European Conference on Computer Visionr*, 2016.
[6] Stefanos Eleftheriadis, Ognjen Rudovic and Maja Pantic, ‘Discriminative Sgared Gaussian Processes for Multi-view and View Invariant Facial Expression ’, *IEEE TRANSACTIONS ON IMAGE PROCESSING, 2015.*
[7] Seyedehsama neh ,Shojaeilangari, Wei-Yun ,Yau, Karthik Nandakumar, Li Jun, Eam Khwang Teoh,’Robust Representation and Recognition of Facial Emotions Using Extreme Sparse Learning’, *IEEE TRANSACTIONS ON IMAGE PROCESSING, 2015.*
[8] Evangelos Sariyanidi, Hatice Gunes and Andrea Cavallaro,’Learning Bases of Acticity for Facial Expression Recognition’, *IEEE TRANSACTIONS ON IMAGE PROCESSING, 2017.*
[9] Mengyi Liu, Shiguang Shan, Ruiping Wang, Xilin Chen,’Learning Expressionlets via Universal Manifold Model for Dynamic Facial Expression Recognition’, *IEEE TRANSACTIONS ON IMAGE PROCESSING, 2015.*
[10] Zhe Sun, Zheng-Peng Hu, Meng Wang, Shu-Huan Zhao, ‘Discriminative feature learning based pixel difference representation for facial expression recognition’, *IET Computer Vision 2017*,Vol 11 Issue 8.

[11] S L Happy and Aurobinda Routray, 'Automatic Facial Expression Recognition Using Features of Salient Facial Patches', *IEEE Transactions On Affective Computing, Sept. 2014*

[12] Li-Fen Chen and Yu-Shiuan Yen. , 'Taiwanese Facial Expression Image Database, Brain Mapping Laboratory, Institute of Brain Science', *National Yang-Ming University, Taipei, Taiwan* ,

[13] Fei Cheng, Jiangsheng Yu, and Huilin Xiong., 'Facial Expression Recognition in JAFFE Dataset Based on Gaussian Process Classification', *IEEE Transactions On Neural Networks, 2010.*

[14] Lucey, P., Cohn, J. F., Kanade, T., Saragih, J., Ambadar, Z., Matthews, 'The Extended Cohn-Kanade Dataset (CK+): A complete expression dataset for action unit and emotion-specified expression (2010). '

[15] Wan, 'Facial Expression Recognition based on MLP Neural Network ', *Springer 2014*

[16] Jeeman Ahmed Khorsheed and Kamil Yurtkan , 'Analysis of Local Binary Patterns for Face Recognition Under Varying Facial Expressions', *24th Signal Processing and Communication Application Conference (SIU),2016.*

[17] Navneet Dalal, Bill Triggs , 'Histograms of oriented gradients for human detection', *Proceedings of the IEEE Conference on Computer Vision and Pattern Recognition* vol 2, 886893 (2005).

[18] T. Ojala, M. Pietikainen and D. Harwood, 'A comparative study of texture measures with classification based on feature distributions', *ICAPR* (2001).

[19] Ngoc, T. N. , 'An efficient LBP-based descriptor for real-time object detection', *IEEE Symposium on Computational Intelligence for Security and Defense Applications (CISDA).* (2014).

[20] M. Mitchell, 'An Introduction to Genetic Algorithms', MA: MIT Press 1998

[21] Kiran, Talele, and Tuckley Kushal, 'Facial Expression Classification Using Support Vector Machine Based On Bidirectional Local Binary Pattern Histogram Feature Descriptor', *17th IEEE International Conference on Software Engineering, Artificial Intelligence, Networking and Parallel/Distributed Computing (SNPD),* (2016).

[22] Muttu, Yeshudas, and H. G. Virani, '"Effective face detection, feature extraction neural network based approaches for facial expression recognition', *IEEE International Conference on Information Processing,*(2015).

[23] Talele, K., Shirsat, A., Uplenchwar, T., Tuckley, K. (2016). , '"Facial expression recognition using general regression neural network', *IEEE Bombay Section Symposium (IBSS),*(2016).

Proceedings of the Fourth International Conference on Communication and Electronics Systems (ICCES 2019)
IEEE Conference Record # 45898; IEEE Xplore ISBN: 978-1-7281-1261-9

Conformal Reflector Backed Printed Dipole Antenna For Directional UAV Communications

Prashant Ravindra[**], Ravishankar B. N.[*], Samudra Dasgupta[*], Selvanayaki K[*]
[**]Research Associate, [*]Scientist
Aeronautical Development Establishment, DRDO
Bengaluru, India.
Email: selvanayaki@ade.drdo.in

***Abstract*— In this work, the design guidelines for conformal reflector backed printed dipole antenna for directional UAV applications is presented. Firstly, the concept of reflector backed printed dipole antenna for directional radiation is presented. Secondly, the concept of conforming the printed dipole antenna to the shape of a typical wing leading edge is studied by embedding the printed dipole antenna inside a Glass Fiber Reinforced Polymer (GFRP) structure for radiation transparency, backed with low dielectric constant foam with a thickness of λ/4 ending with a Carbon Fiber Reinforced Polymer (CFRP) ground plane to essentially produce directional radiation normal to the antenna plane. The conformal antenna is fabricated and tested for performance giving a gain of 5.22dB across a 1.66% measured bandwidth from 3.580 GHz to 3.638GHz. The 3dB beamwidth in the H-plane is around 70^0 and E-plane beamwidth is around 90^0. This idea readily satisfies the UAV conformal antenna requirements for high throughput directional communications.**

Keywords—printed dipole; conformal load bearing antenna structure; wing leading edge; unmanned aerial vehicles (UAVs)

I. INTRODUCTION

The recent advances in Unmanned Aerial Vehicle (UAV) technologies has led to an increasing demand for small, lightweight, directional and high gain antennas to be used for communication systems. UAVs are widely used in military, scientific and exploration missions. They are used routinely to collect data and send information back to a ground station that provides real-time information on the covered area. Through wireless links the data transmission from UAVs is done [1-2]. For transfer of data through RF link we require antennas. There are many antennas available in literature to meet these requirements with limited feasibility to use in case of UAVs. To meet these requirements for UAVs, the printed antenna is chosen as the candidate antenna to be embedded as it can meet the minimum gain required over ± 45^0angle [3-6].

In this paper, firstly, a bi-faced printed dipole antenna which is fed with a coaxial feed presented for low profile, conformal requirements of UAV applications [7-8]. The antenna radiates Omni directionally by nature. To have the directional radiation, secondly, the antenna is backed with a reflector spaced with a space of λ/4 in order to produce in phase reflected signal. The design optimization is carried out using FEKO's EM tool. Thirdly, the reflector backed dipole antenna is conformed to the wing leading edge of typical UAV, fabricated and tested for its performance.

II. DESIGN AND DEVELOPMENT OF REFLECTOR BACKED PRINTED DIPOLE ANTENNA

The configuration of the proposed printed dipole antenna (PDA) is shown in Fig. l. The physical parameters of the antenna are calculated by using formulae available in the literature [3-6] [9-11]. The antenna consists of two arms printed on both sides of the substrate in alternate configuration (each arm onto opposite sides).

First, the conventional printed dipole antenna (Antenna 1) is designed for 3.70GHz with FR4 dielectric substrate material of relative permittivity (εr) 4.4 and dielectric loss tangent (tanδ) 0.03036 with thickness of 0.2 mm. Secondly, the conventional antenna is backed by finite perfect electric conducting (PEC) ground plane (Antenna 2) with approximately quarter wavelength of gap (g). Thirdly, the aperture in the PEC ground plane exactly below the feed point with an aperture radius of 10mm is named as Antenna 3. The aperture is to accommodate the cable connection. The method of coaxial feed is used for 50Ω impedance. An impedance transformer is used for matching the input impedance to the feed impedance. All the physical dimensions are tabulated in Table 1. Altair's FEKO 17.1 EM Simulation tool is used for the modelling, simulation and optimization of doubled sided printed dipole antennas [12].

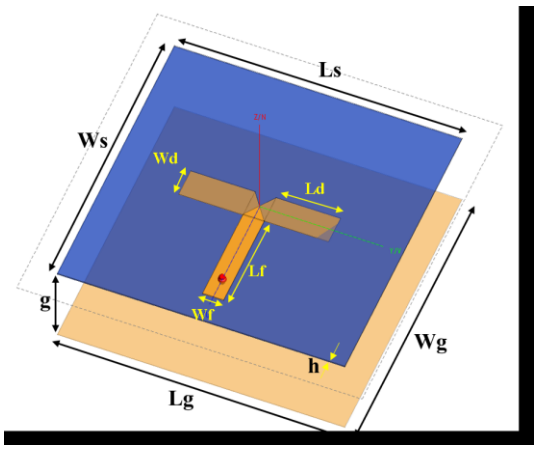

Fig. 1. Geometry of printed dipole antenna with ground

TABLE I. FINAL OPTIMAL PHYSICAL DIMENSIONS OF PROPOSED PRINTED DIPOLE ANTENNA

Sl. No.	Parameters	Value(mm)
1	Length of one arm of the dipole (Ld)	11.18
2	Width of the dipole (Wd)	5.13
3	Length of the feed (Lf)	17.33
4	Width of the feed (Wf)	3.68
5	Length of the substrate (Ls)	50
6	Width of the Substrate (Ws)	50
7	Length of the ground (Lg)	50
8	Width of the ground (Wg)	50
9	Gap between the patch and ground (g)	15
10	Thickness of the substrate (h)	0.2

III. DEVELOPMENT OF CONFORMAL LOAD-BEARING ANTENNA STRUCTURE (CLAS)

When the antenna has to be conformal to the surface of the UAV, it is required to have essential structural strength to endure the aerodynamic forces and still perform as an antenna with desired characteristics. The material design for embedding the dipole antenna at the leading edge of a typical UAV airframe for the development of Conformal Load-bearing Antenna Structure (CLAS) involved innovative employment of GFRP and CFRP composites and their foam sandwiches using combination of co-curing and co-bonding processes. The multi stage development process initially involved vacuum thermoforming (to conform to leading edge) of high performance rigid polymeric foam, which had dual (electrical and mechanical) functionalities in CLAS, viz., creating the necessary dielectric spacing (15mm) between the antenna and the conducting back plane / reflector as well as imparting the structural rigidity through the sandwich construction. The said dielectric spacer, carbon-epoxy back-plane and the glass-epoxy leading edge structure were then co-cured by out-of-autoclave processing of prepregs and the antenna was then conformed and bonded to the same on the dielectric spacer foam surface after creating necessary opening to pass the connector of the antenna to form an integral multi-functional structure. The process was completed after finally covering the mentioned structure with 0.5mm glass-epoxy skin acting as thin wall radome on the frontal foam side matching to the profile of the leading edge by co-bonding process. The schematic representation of the CLAS is given in the below Fig.2. The developed CLAS is shown in Fig. 8 (a) and (b).

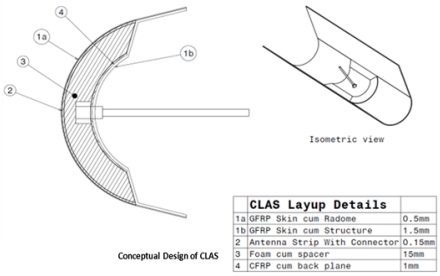

Fig. 2. Schematic representation of CLAS

IV. RESULTS AND DISCUSSION

A. Simulation studies

Fig. 3 shows the comparison of simulated VSWR versus frequency of Antennas. From the figure we can observe that the antenna with ground plane is tuning at lower side with 113MHz when compared to without ground plane.

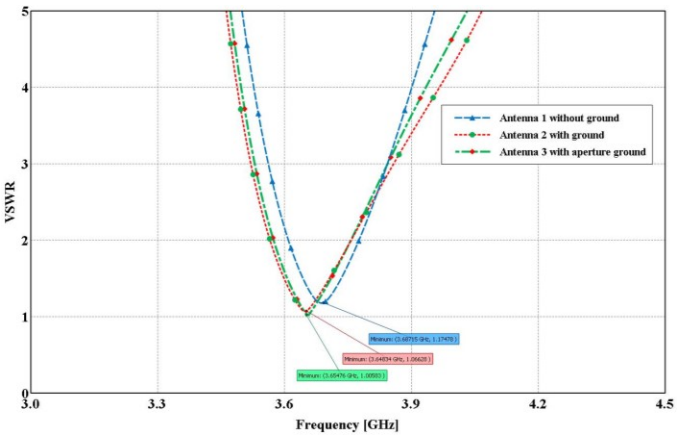

Fig. 3. Simulated VSWR versus frequency of Antenna 1, Antenna 2 and Antenna 3

Fig. 4(a) - (c) shows the simulated radiation patterns of antennas without ground and with ground plane. From these figures it is clear that the antenna with ground plane giving peak gain of 6.29 dBi with directional 3dB beamwidth of $\pm 67.75^0$ in H-plane and $\pm$ 92.59^0 in E-plane. But, the Antenna 3 with aperture giving peak gain of 4.84dBi with directional 3dB beamwidth of $\pm$ 70.80^0 in H-plane and $\pm$ 126.75^0 dBi in E-plane at its respective resonating frequency. This variation in pattern is due to the aperture in the ground pane.

Fig. 5(a)-(c) shows the simulated 3D far field radiation patterns of antennas without ground, with ground and with aperture in the ground plane respectively. Fig. 6 shows the simulated gain versus frequency of Antenna1, Antenna 2 and Antenna 3 from 3GHz to 4.5GHz.

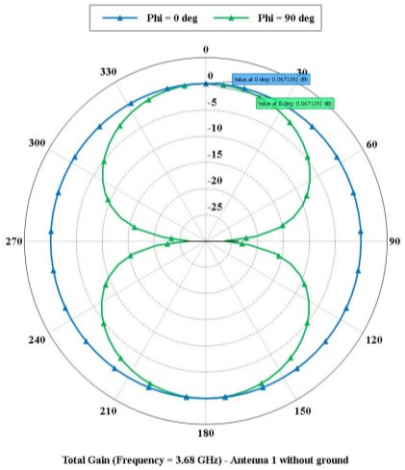

(a)

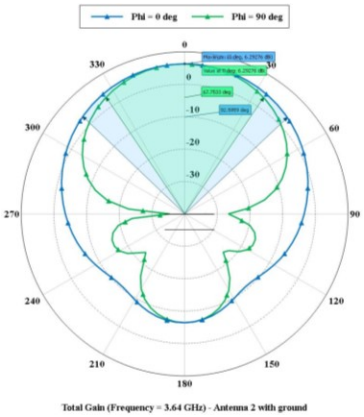

(b)

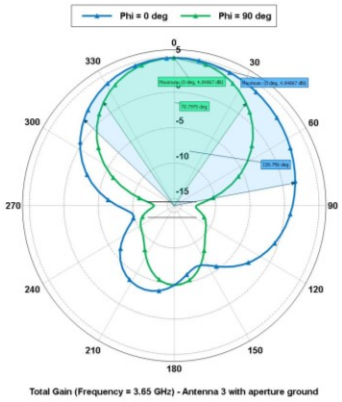

(c)

Fig. 4. Simulated far field radiation pattern of antennas, (a) without ground, (b) with ground and (c) with aperture ground

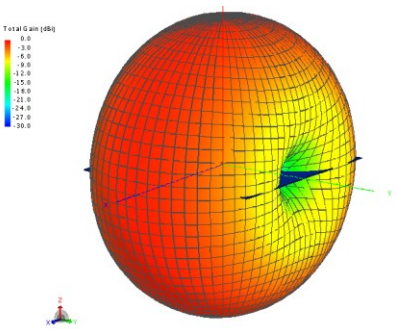

(a)

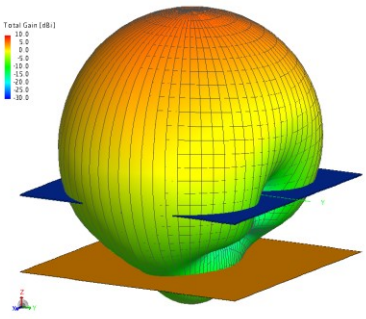

(b)

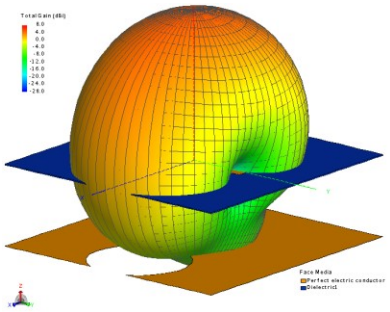

(c)

Fig. 5. Simulated 3D far field radiation patterns of antennas, (a) without ground, (b) with ground and (c) with aperture ground

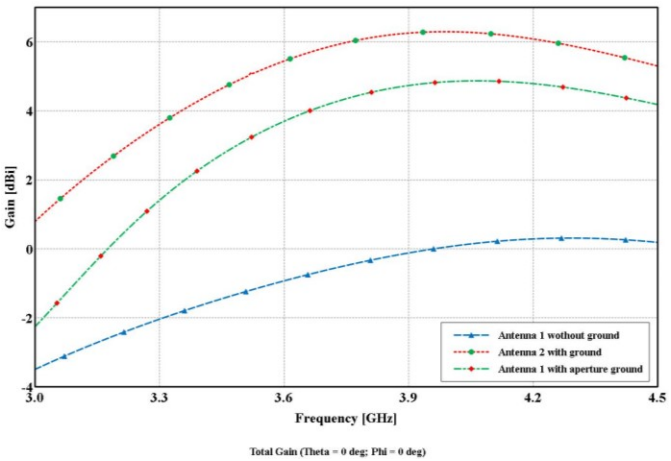

Fig. 6. Simulated gain versus frequency of Antenna1, Antenna 2 and Antenna 3

B. Measurement studies

In order to verify the validity of design method, the proposed fabricated antenna parameters are measured. A vector network analyzer is used to measure VSWR of the antenna and radiation pattern measurements are carried out in microwave anechoic chamber. Fig. 7 (a) shows the photograph of the fabricated reflector backed printed dipole antenna and corresponding measured VSWR versus frequency plot is shown in Fig. 7(b). The Measured Radiation characteristics of Antenna 3 is shown in Fig 7(c). Table 2 shows the comparison of results of simulated and measured results of printed dipole antenna without and with aperture in the ground plane.

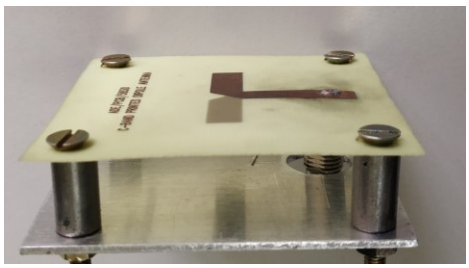

(a)

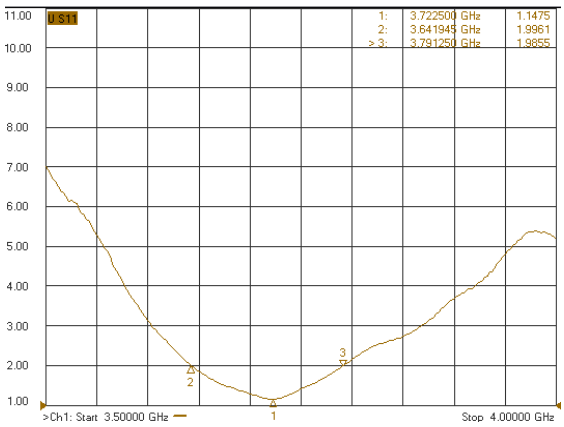

(b)

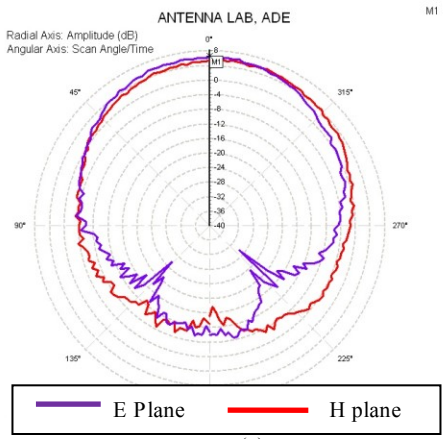

(c)

Fig 7. (a) Photograph of the fabricated reflector backed printed dipole antenna (Antenna 3), (b) Measured VSWR and (c) Measured Radiation characteristics

TABLE II. COMPARISON RESULTS OF SIMULATED AND MEASURED PRINTED DIPOLE ANTENNAS

Antenna	Resonating Frequency (GHz)		Bandwidth (MHz)		VSWR		Gain(dBi)	
	Sim	*Meas*	*Sim*	*Meas*	*Sim*	*Meas*	*Sim*	*Meas*
Antenna 1 (Without Ground)	3.68	3.75	156	143	1.17	1.12	0.06	0.68
Antenna 3 (With aperture Ground)	3.64	3.72	180	147	1.06	1.14	4.84	5.22

In next step, the measurements of fabricated reflector backed printed dipole antenna embedded in the leading edge of a typical UAV airframe is carried out (refer Fig. 2 for details). Fig. 8 (a) and (b) shows the photographs of CLAS – view 1 and CLAS – view 2 of the developed CLAS. Fig. 9(a) shows the measured VSWR versus frequency of Antenna 3 loaded inside wing. The frequency range in which VSWR is less than 2 is from 3.580 to 3.640GHz with a bandwidth of 60MHz, which is less than that of simulated antenna without loading inside the wing. This variation in result is due the 0.5mm glass-epoxy layer in front of the antenna.

Fig. 9(b) shows the measured radiation pattern of Antenna 3 i.e., printed dipole antenna embedded inside the typical wing leading edge of UAV. From the figure we observe that the perturbed radiation pattern is due to loading inside the wing and a peak gain of 5.22dB when normalised with respect to standard gain horn antenna. The asymmetry of about 4dB is observed in the H-plane is attributed to the asymmetric lossy wing surrounding the right hand side (RHS) of the antenna.

Fig. 10 shows the photograph of anechoic chamber setup for radiation pattern measurements.

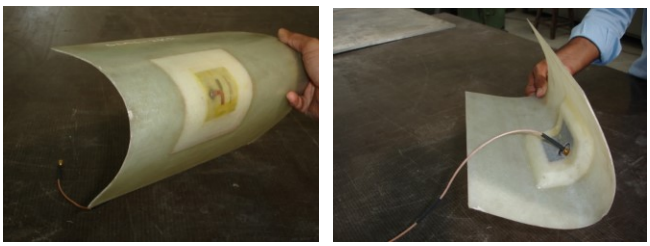

(a) (b)

Fig. 8. Photographs of (a) CLAS – View 1 and (b) CLAS – View 2

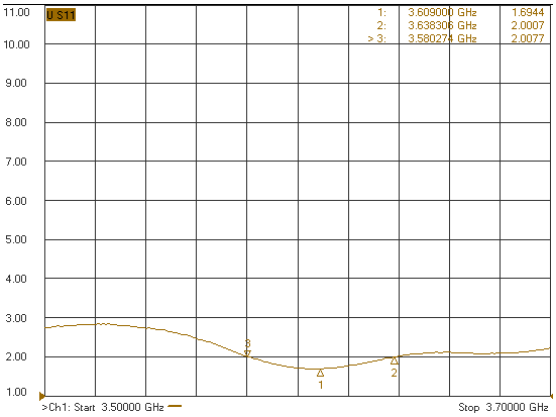

(a)

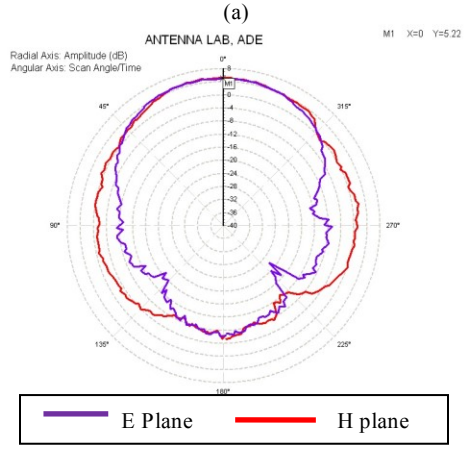

(b)

Fig. 9. (a) Measured VSWR and (b) radiation pattern of Antenna 3 embeded inside leading edge of a typical UAV airframe.

Fig. 10. Photograph of radiation pattern measurement setup in anechoic chamber

IV. CONCLUSION

The design and implementation of conformal reflector backed printed dipole antenna as a load bearing structure of a typical wing leading edge of a UAV is demonstrated and tested in anechoic chamber. The simulation and measurement results of the VSWR, radiation and gain patterns of antenna loaded wing structure are presented and compared to be in good agreement. The proposed concept will enable directional, high throughput communication link while occupying small space and volume. Such features will also reduce the power requirements of a transmitter to meet the given range compared to using on-board Omni directional antennas. Further study will be carried out to study the feasibility of such multi-functional CLAS with respect to the actual scale of UAV.

REFERENCES

[1] R. L. Cravey, "Structurally Integrated antenna concepts for Hale UAVs", NASA Langley Research Center, 2006, NASA/TM-2006-214513.

[2] Mohammad S. Sharawi, Daniel N. Aloi and Osamah A. Rawashdeh, "Design and Implementation of Embedded Printed Antenna Arrays in Small UAV Wing Structures", IEEE Transactions on Antennas and Propagation, vol. 58, No. 8, pp. 2531-2538, August 2010.

[3] C.A Balanis, "Antenna Theory Analysis and Design", John Wiley& Sons, Inc. 2nd Edition, New York, 1997.

[4] J. D. Kraus, "Antennas", Mc Graw Hill, Inc. 1950.

[5] G. Kumar and K. P. Ray, "Broadband microstrip antennas", London: Artech House, 2003.

[6] Z. G. Fan, S. Qiao, J. P. Huang fu and L. X. Ran, "A Miniaturized printed dipole antenna with V-shaped ground plane for 2.45GHz RF-ID readers", PIER 71, pp. 149-158, 2007.

[7] E. A. Vila-Navarro, C. Cayuelas and C. Reig, "Dual-band printed dipole antenna for Wi-Fi 802.11n applications", Electronics Letters, vol. 46, No. 2, 14th October 2010.

[8] He, Q.Q., Wang, B.Z., and He J., "Wideband and dual-band design of a printed dipole antenna", IEEE Antennas Wirel. Propag. Lett., 7, pp. 1–4, 2008.

[9] Chen H. M., Chen J. M., Cheng P. S, Lin Y.F, "Feed for dual band printed dipole antenna", Electronics Letters, vol. 40, Issue 21, pp. 1320 – 1322, 14 Oct. 2004.

[10] Duffley, B.G. Morni, G.A. Mikavica, M., Antar, Y.M.M. "A wide-band printed double-sided dipole array", IEEE Transactions on Antennas and Propagation, vol. 52, Feb. 2004.

[11] Thereza M. Macnamara, "Introduction to Antenna Placement and Installation", A John Wiley and Sons, Ltd., Publication.

[12] FEKO User Manual South Africa, EM Software and Systems Ltd. (EMSS), 2017.

AUTHOR BIODATA

Prashant Ravindra received his PhD in Microwave Antennas from Gulbarga University in 2017. Presently he is working as a Research Associate in Aeronautical Development Establishment, DRDO Bengaluru, India. His research interests include: Electromagnetic design, simulation and testing of airborne conformal antennas, antenna placements, Stealth Radomes, RCS analysis & measurements.

Ravishankar B N received his M.Sc. in Materials Science (Gold Medal) from Mangalore University & M.Tech in Materials Engineering from KREC, Surathkal. He is working as a Scientist in Composite Technology Centre of ADE, DRDO, Bengaluru since 2002. As in-charge of fabrication, he is responsible for the development of polymeric composite materials/processes and structures for unmanned aerial vehicles including for radome and stealth applications. He has the experience of working with cyanate ester based polymeric composites for high temperature microwave transparent applications. He has several technical papers to his credit, published/presented in various national and international journals/conferences and he holds multiple international patents on related inventions.

Samudra Dasgupta received his Bachelor of Metallurgical Engineering (Gold Medal) from Jadavpur University, Kolkata. He is working as a Scientist in DRDO since 2003 and is presently heading the Composite Technology Centre of Aeronautical Development Establishment (ADE), Bangalore, where he is responsible for the development and testing of various composite materials, processes and prototype structures for different unmanned air vehicles for the Indian defence forces. His domain expertise includes composite materials for various electromagnetic / electrical applications, including stealth and radome, and he holds multiple international patents on related inventions. He has several technical papers to his credit, published / presented in various national and international journals / conferences.

Selvanayaki K received her Master's in Engineering from CEG, Anna University. She joined ADE, DRDO in 2003 as a Scientist. Her research interests include conformal antennas, antenna arrays, Electromagnetic Near field analysis, Radar Cross Section analysis & measurements, engineered electromagnetic materials, material parameter extraction, mission modelling, aircraft survivability studies, UAV datalinks.

Proceedings of the Fourth International Conference on Communication and Electronics Systems (ICCES 2019)
IEEE Conference Record # 45898; IEEE Xplore ISBN: 978-1-7281-1261-9

An Ensemble-Based Feature Selection and Classification of Gene Expression using Support Vector Machine, K-Nearest Neighbor, Decision Tree

Anu J Nair: Department of Computer Science and Applications
Amrita Vishwa Vidyapeetham
Amritapuri, India
anu.j.nair022@gmail.com

Rizwana Rasheed: Department of Computer Science and Applications
Amrita Vishwa Vidyapeetham
Amritapuri, India
rizwanarasheed28@gmail.com

Maheeshma KM : Department of Computer Science and Applications
Amrita Vishwa Vidyapeetham
Amritapuri, India
maheeshmamadhu@gmail.com

Aiswarya LS: Department of Computer Science and Applications
Amrita Vishwa Vidyapeetham
Amritapuri, India
aiswaryalsaiswarya@gmail.com

Kavitha K R: Department of Computer Science and Applications
Amrita Vishwa Vidyapeetham
Amritapuri, India
kavithakr@am.amrita.edu

Abstract: **Analysis of microarray data for disease prediction is an arduous machine learning job. Due to its high proportions and low samples, the computational risk is high. To increase the efficiency of the classifier a Signal-to-Noise Ratio algorithm can be used to get the most relevant genes. Then to these selected gene datasets, an ensemble-based classification algorithm is applied to get an efficient classifier for future prediction. The ensemble-based algorithm is an optimal combination of a set of learner algorithms. Our research focuses on 3 main classification algorithms namely SVM, KNN and Decision Tree which increases the performance and give confidence to the result. The ensemble is done using majority voting method which outperforms the base classifier.**

Keywords—gene expression, SNR feature selection, SVM, KNN, Decision Tree.

I. INTRODUCTION

All organisms in the world excluding viruses consist of cells. Yeast has only a single cell, whereas human beings have trillions of cells. Humans have trillions of cells in them and each cell consists of a membrane, cytoplasm, and nucleus which provide structure for specialized functions. Nuclei contain most of the cell's genetic material organized as DNA molecules. Gene expression profiling has been proved to be a valuable resource for the classification of complex diseases such as cancer. By using feature selection methods on a large microarray Gene Expression data we can get the most probable cancer-associated genes. We use DNA microarray which consists of a collection of microscopic DNA. Proteins in genes are generated in two steps. First, DNA is converted to mRNA and the second, mRNA is translated into proteins. Gene expression can be defined as a protein which is the result of activations in genes and these proteins can be defined as the blueprints for the characteristics of each and every living organisms. A microarray is a particular arrangement of dots of DNA, proteins, or tissues aligned in an array for easy diagnosis. DNA microarray is a soul of the gene expression profiling that plays a vital role in classification purposes. Materials like glass, plastic or silicon chip are received as an end product of this process. Identification of genetic individuality, diagnosis of genetic and infectious diseases are the applications of the microarray.

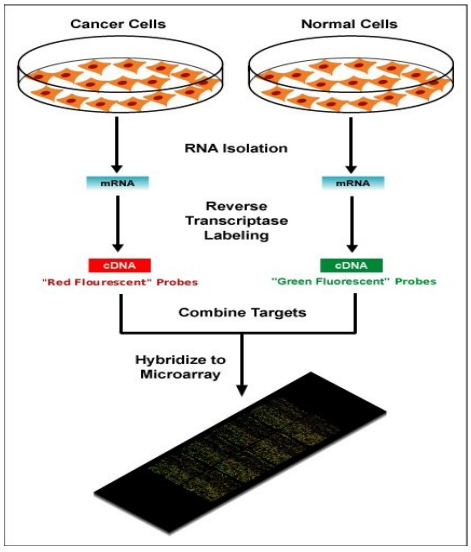

Fig 1: Conversion of cells to microarray

In general, abnormalities in the genetic material of the converted cell is referred to as being subjected to cancer. Cancer is known to be as a deadly disease, so there is a high scope for the research on these topics. We can predict the output of the data by using machine learning techniques like feature selection and classification.

The objective of the present work is to attain an enhanced classification accuracy by gene profile data comprising of a number of genes and samples of patients. These data are then used for cancer classification and prediction that if a person has colon tumor or not. For that, we are using feature selection methods to get the most probable and precise cancer-associated genes or features from large microarray gene expression profile, for that we use feature selection algorithms like SNR, Top Scoring and T-Statistics algorithms. Once we apply the feature selection methods we go for feature classification techniques like Decision Tree Induction, K-Nearest Neighbor (k-NN), Support Vector Machine (SVM), etc.

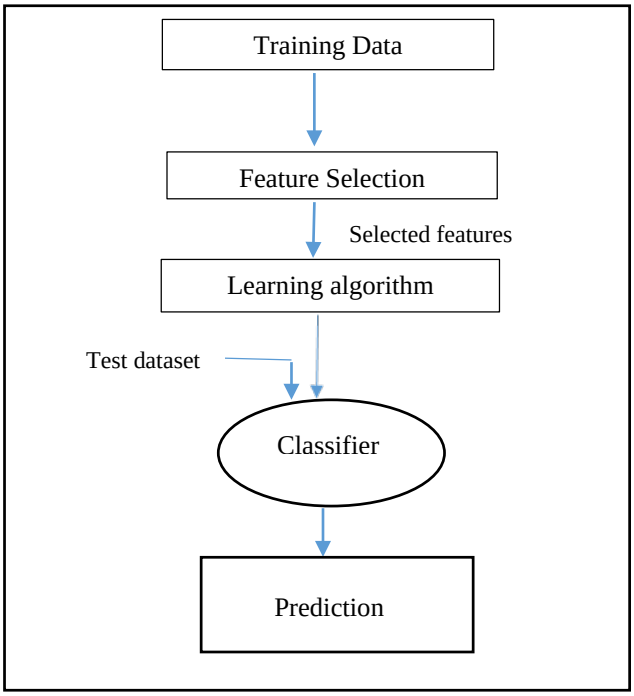

Fig 2: Feature Selection and Classification

The pinnacle of our paper is to make the study of gene expressions easier. That is techniques that can be used for finding the patterns or by doing the feature selection using SNR ranking and we apply a modification to the SNR by normalizing the equation and then applying the feature classification algorithm to analyze the result. The way in which we are going to normalize our data is by removing all the null values, remove all the space and making all the values unique. Then we can use this result to know which classification algorithm gives significant meaning to classify the genes using the SNR feature selection algorithm.

II. RELATED WORKS

Debahuti Mishra and Barnali Sahu. Feature Selection for Cancer Classification: A Signal-to-noise Ratio Approach, presents a comparative analysis of the SNR ranking applied with KNN before clustering and SNR ranking applied after clustering. We get all the top scored features from each of the clusters which will give as more accurate value as compared to that of the gene profile data without clustering i.e.; randomly selected features. In the second case, we are getting redundant features or unwanted noisy features with the same score and hence there is no chance of having any relevant information about our data and hence it will affect the performance of learning algorithm.

In Gene-Expression-Based Cancer Classification Through feature selection with KNN and SVM Classifiers by Sara Haddou Bouazza [6] presented a way of using filter approach of predicting the accuracy of the supervised classification in the field of medicine as a part of feature selection methods. In this, a comparative understanding of various feature selection algorithms like Fisher, T-Statistics, and SNR are applied out between different gene expression profiles and using two classifiers KNN and SVM intermediately. The pinpoint of the paper was to differentiate the entered data as Acute Lymphoblastic Leukemia or Acute Myeloid Leukemia.

In Feature Gene Selection and Classification with SVM for Microarray Data of Lung Tissue by Si-Hao [7] states that microarray analysis can be a widely used tool for detecting the diseases. They started the work by using SVM but as there continued they find it difficult for them to make use of SVM as the classifier so they go for finding an advanced version of SVM. It is better to classify the gene after epsilon-SVR analysis. This paper also says that SVM gives as the highest prediction with less number of original genes. And hence, writers say that it is better to use SVM as the classifier.

Jun Chin Ang, Andri Mirzal, Habibollah Haron and Haza Nuzly Abdul Hamed Supervised, Unsupervised and Semi-Supervised Feature Selection: A Review on Gene Selection", proposed the classification of the entire dataset to a set of three groups: supervised, unsupervised and semi-supervised. In this, they have done a comparative study between the top 5 gene expression and it shows that the accuracy of semi-supervised and unsupervised feature selection results is good enough as compared to that of the supervised feature selection algorithm result. As we have the output in supervised learning and we are training our dataset on the basis of this. So if we give new input to the supervised learning it will predict the output only on the basis of the data that we have trained but it is not in the case of the unsupervised or semi-supervised dataset.

Johannes Mohr [9] Automated Microarray Classification Based on P-SVM Gene Selection, presented a newly microarray gene selection and classification algorithm called P-SVM-GS. The method makes use of the P-SVM for getting the small subset of genes and a ν-SVM will give as a result which we can use as a classifier. It is said that the experiment conducted on two datasets gives the proof that a sparse set of the gene will give as a good prediction performance.

III. PROPOSED WORK

This part describes the proposed system. The modules are described here,

A. Feature Selection

The algorithm which can be used to reduce the overall features available in our gene expression profile. There are certain algorithms that can be considered as feature selection algorithms. Some of them are:

a. SNR (Normalized)
b. T-Score
c. Top Scoring

a. Signal to Noise Ratio

The collection of microarray data is known as a microarray gene expression profile. Here we have a microarray gene profile of colon tumor cancer which is given to modified SNR feature selection methods. In this method, we will find out all the mean and standard deviations of the class labels available. The means in this dataset refers to signal and the standard deviation refers to the noise. Then we apply mean and standard deviations to all the class labels for getting the ranks of each sample.

$$snr = (\mu 1 + /\mu 2)\ (\sigma 1 + \sigma 2)$$

Where μ denote the mean of the gene expression data and σ denotes the standard deviations of the entries in each class labels.

These ranks of the samples can be used to find out the number of columns to be taken for feature classification. Since the SNR we applied is good enough it is necessary for us to normalize it, so that we can increase the accuracy of the algorithm.

b. Normalized SNR

Data normalization means converting all the variables in the data to a specific range and its main purpose is to minimize the redundancy and remove null values, blank spaces. Data redundancy happens when the same data is held in two separate places. In order to reduce redundancy, we use a hash set. It contains unique elements only. The algorithm is normalized by removing a null value, removing blank space and also it stores unique details by using this hash set. By applying this our algorithm became more accurate and it gives most affected genes as the output thus feature selection become more efficient.

From the dataset we take the data and store it to an array list of an array, to store a dynamic collection of elements, then we convert that ArrayList to two-dimensional arrays. Finally, we will find mean (μ) value, standard deviation (σ) of each column of two-dimensional arrays then find the normalized SNR value.

Step 1: mean (μ) = $\sum X / n$
Step 2: standard deviation (σ) = $\sqrt{\sum (X-\mu)^2 / n-1}$
Step 3: to find the snr value
snr = μ / σ

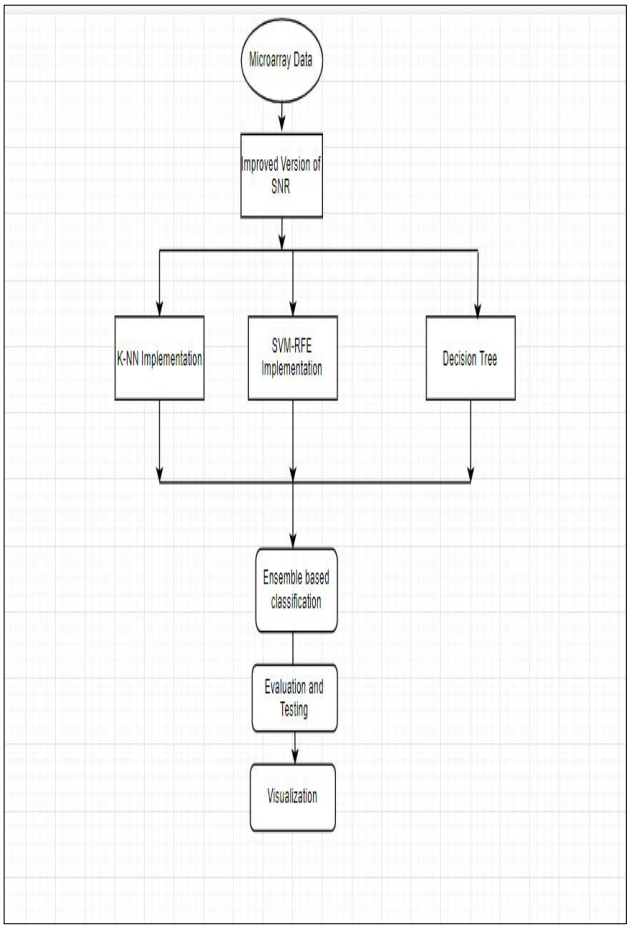

Fig 3: System Architecture

In parallel to this, we are going to apply SNR to the different feature classification algorithms like K-NN, SVM, and Decision Tree to get the comparative study of finding out which SNR is best suited with which of the above algorithms. We are then giving the result to an ensemble based classifier to group it into one. Then we are evaluating and testing our results to get a final output and this final output will be shown in the form of a graph.

B. K-Nearest Neighbor (K-NN)

In KNN for each training dataset values, we will be calculating the K nearest values of training data sets and then taking the most regularly occurring classes in the dataset and then assigning that class values to the test data. Therefore, K means the number of training data sets values falling in close to the test dataset point value which we are going to use for finding the class labels. If we don't have a separate testing dataset we can use the same training dataset as the testing dataset values.

Algorithm 2: K- Nearest Neighbor (KNN) [1]

Input: {r1,r2,r3,..,r_n} where r is each *row of a dataset.*
Output: the threshold of the features to remove
Output: The k nearest value of each row will be returned

1. Load testing and training dataset.
2. Pick a random the value for k.
3. For any data in the testing dataset:
   a. Find the Euclidean distance to all the training dataset.
   $$D = \sqrt{\sum_{i=1}^{k}(xi - yi)^2}$$
   b. Store these results in a list and sort it
   c. And then select the first k point
4. Return *the K nearest value.*

C. Support Vector Machine (SVM)

In machine learning, supervised learning models such as SVM is mainly implemented for pattern recognition and data analysis. SVM mainly is mainly known for classification and regression analysis. Its theory is mainly based on the structural risk minimization and is one of the best classification techniques which can best split the given data and discriminate between objects that belongs to one of the two categories(+ve or –ve). The distance between the support vectors (points) and the hyperplanes (lines) are as far as possible. SVM uses large margin and kernel function as a key concept to discriminate the data. The important factor in SVM is to select the appropriate kernel function as it is very important for higher dimensions. SVM is used in classification due to its high accuracy, ability to deal with high dimensions (gene expression) and its flexible technique in modeling the data. SVM technique is a very promising supervised learning tool in dealing with microarray gene expression data.
We are using Linear SVM for our data.

D. Decision Tree

Decision tree is one of the most successful classifications and decision tool that uses branching method to classify the example and each branch represents outcomes of the test.

In our work, we have used the J48 algorithm from Weka1, which is a library having a large number of machine learning methods. Weka J48 is a Java implementation of the well-known algorithm C4.5.

a. Apply decision tree on the input dataset
b. We have used the same dataset for both train and testing purposes.
c. Evaluate dataset and find correct and Incorrectly classified instances
d. Give the output for Ensembling.
e. Visualize the tree using a visualize function

IV. EXPERIMENTS AND RESULTS

The experiments and testing are conducted on two public available dataset Colon with 2000 genes and Leukemia with 3572 genes.

The initial experiment is conducted in order to decrease the dimensionality of the dataset by SNR based feature selection algorithm. The number of selected features after SNR is shown in the below table.

TABLE 1: AFTER APPLYING SNR BASED FEATURE SELECTION

Dataset	Total Number of genes	Number of Features Selected
Leukemia	3571	1534
Colon	2000	865

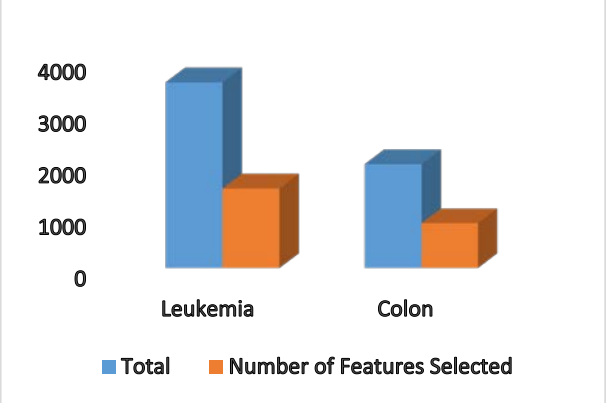

Fig 4: Number of genes after applying SNR algorithm

For evaluation purpose, we are initially ensemble all the feature classification algorithm that we have implemented. So, we go for a majority voting algorithm. Since each

algorithm makes a prediction that is voted for each instance of test and the final result is the prediction that receives votes more than half of its total votes. If any of the algorithms don't get any of the votes more than it's total votes, we can say that the particular algorithm doesn't have a consistent (stable) prediction for the particular instance. So the majority voting algorithm is mainly based on the majority of the voting, even if an instance doesn't have a majority of voting we go for the votes that have more number of prediction. This is also known as "plurality voting".

If we were using the nearest neighbor algorithm for evaluation purpose then the result will we the 100% accurate as we are using the same set of data, that is a dataset, for training and testing purposes. In general for evaluating any data mining algorithms with a testing dataset which is a subset of the training dataset results in the optimistic value generation which is not good. So in order to improve the evaluation pattern more accurate we use another algorithm which uses all the data of the dataset more efficiently and does the same process in an iterative manner and we can take the final value from the average of the resultant values from each iteration.

For the evaluation purpose, we are using a k-fold cross-validation method in which we are dividing the entire dataset to k packets each of which is having a set of values. We are taking the value of k as 10 hence we can say that we are using 10-fold cross-validation. In this we are dividing the entire dataset into 10 packets from which we are taking the first 9 datasets as the training dataset and the rest 1 dataset as the testing dataset in one iteration and in the next iteration the 9 testing dataset will change and as a result of this, the corresponding training dataset also changes. This will continue until the 10th iteration. The resulting value is added up to form the final result.

TABLE 2: EVALUATION OF EMBEDDED BASED CLASSIFIER

Dataset	Total Features	Accuracy	Error Rate
Lukemia	3572	98%	2%
Colon	2000	97%	3%

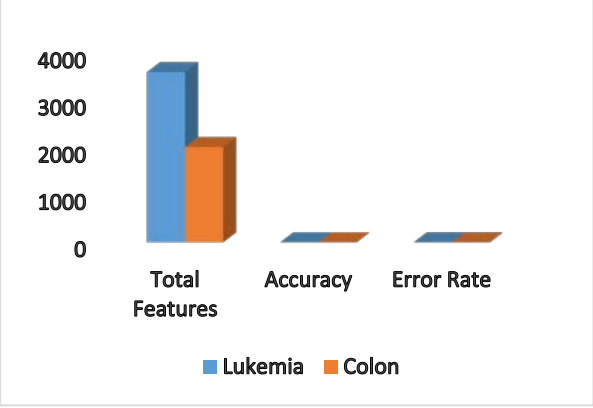

Fig 5: Accuracy and Error Rate of the Embedded Classifier

We can say that the 10-fold cross validation is an excellent choice because we are almost training 90% of the data. For example, if we have 2000 entries, we will train our classifier in 1999 of them and then test on 1 and repeat this process for 2000 times. We can increase the accuracy of our classifier by using the maximum amount of data that we possibly have for testing.

CONCLUSION

In our work we initially had a large dataset which is reduced to minimal size with all the necessary features that we want, for that purpose we used the Signal-to-Noise Ratio algorithm. Then to this reduced dataset, we apply feature classification algorithms like Support Vector Machine, K-Nearest Neighbor and Decision Tree. If we do these feature selection algorithm independently it will have more error rate and less accuracy as compared to that of the accuracy we get from an ensemble based system which has a combined effect of the above three algorithms. For ensemble, we have used the majority voting algorithm which is used to get the majority of the three algorithms. And finally, to this ensemble system apply 10-fold cross-validation to evaluate and test the dataset we get relatively high accuracy ie;98% for Leukaemia dataset and low error rate ie;2% for the same dataset. This work can be extended to include multiclass gene expression.

REFERENCES

[1] Rohith Gandhi," K Nearest Neighbours—Introduction to Machine Learning Algorithms",

[2] Kavitha K R, Ajith Gopinath, Midhun Gopi. "Applying Improved SVM Classifier for Leukemia Cancer Classification using FCBF." 978-1-5090-6367-3/17/$31.00 ©2017 IEEE

[3] Kavitha, K. R., G. SyamiliRajendran, and J. Varsha. "A correlation based SVM-recursive multiple feature elimination classifier for breast cancer disease using microarray." 2016 International Conference on Advances in Computing, Communications and Informatics (ICACCI). IEEE, 2016.

[4] Thushara, M. G., M. S. Krishnapriya, and Sangeetha S. Nair. "A model for auto-tagging of research papers based on keyphrase extraction methods." Advances in Computing, Communications, and Informatics (ICACCI), 2017 International Conference on. IEEE, 2017.

[5] Debahuti Mishra, Barnali Sahu. " Feature Selection for Cancer Classification: A Signal-to-noise Ratio Approach ".International Journal of Scientific & Engineering Research, Volume 2, Issue 4, April-2011 1 ISSN 2229-5518 IJSER © 2011 http://www.ijser.org

[6] Sara Haddou Bouazza, Nezha Hamid, Abdelouhad Zeroual, Khalid Auhmani. "Gene-Expression-Based Cancer Classification Through feature selection with KNN and SVM Classifiers".

[7] Si-Hao Du, Shun-Feng Su, Chih-Ching Hsiao, Jin-Tsong Jeng, "Feature Genes Selection and Classification with SVM for Microarray Data of Lung Tissues", SCIS&ISIS 2014, Kitakyushu, Japan, December 3-6, 2014.

[8] Jun Chin Ang, Andri Mirzal, Habibollah Haron and Haza Nuzly Abdul Hamed. "Supervised, Unsupervised and Semi-Supervised Feature Selection: A Review on Gene Selection", IEEE/ACM

Transactions On Computational Biology And Bioinformatics, Vol. 13.

[9] Johannes Mohr1, Sambu Seo1, Klaus Obermayer. "Automated Microarray Classification Based on P-SVM Gene Selection"2008 Seventh International Conference on Machine Learning and Applications.

[10] Ding, Chris, and Hanchuan Peng. "Minimum redundancy feature selection from microarray gene expression data." Journal of bioinformatics and computational biology 3.02 (2005): 185-205.

[11] Awada, Wael, et al. "A review of the stability of feature selection techniques for bioinformatics data." Information Reuse and Integration (IRI), 2012 IEEE 13th International Conference on. IEEE, 2012.

[12] Ang, Jun Chin, et al. "Supervised, unsupervised, and semi-supervised feature selection: a review on gene selection." IEEE/ACM transactions on computational biology and bioinformatics 13.5 (2016): 971-989.

[13] Yin, Jiapeng, et al. "Improving the performance of SVM-RFE on classification of pancreatic cancer data." 2016 IEEE International Conference on Industrial Technology (ICIT). IEEE, 2016.

[14] Zhang, Ying, et al. "An efficient feature selection strategy based on multiple support vector machine technology with gene expression data." BioMed research international 2018 (2018).

[15] Ani, R., et al. "Modified Rotation Forest Ensemble Classifier for Medical Diagnosis in Decision Support Systems." Progress in Advanced Computing and Intelligent Engineering. Springer, Singapore, 2018. 137-146.

[16] Li, Zifa, Weibo Xie, and Tao Liu. "Efficient feature selection and classification for microarray data." PloS one 13.8 (2018): e0202167.

[17] Sahu, Barnali, SatchidanandaDehuri, and AlokJagadev. "A Study on the Relevance of Feature Selection Methods in Microarray Data." The Open Bioinformatics Journal 11.1 (2018).

[18] Golub, Todd R., et al. "Molecular classification of cancer: class discovery and class prediction by gene expression monitoring." science 286.5439 (1999): 531-537.

[19] Dai, Jian J., Linh Lieu, and David Rocke. " Dimension reduction for classification with gene expression microarray data." Statistical applications in genetics and molecular biology 5.1 (2006).

Proceedings of the Fourth International Conference on Communication and Electronics Systems (ICCES 2019)
IEEE Conference Record # 45898; IEEE Xplore ISBN: 978-1-7281-1261-9

A Survey on IoT Based Agricultural Crop Growth Monitoring and Quality Control

Jayvant Devare
School of Computer Engineering and Technology
MIT Academy of Engineering
Pune, India
jhdevare@comp.mitaoe.ac.in

Neha Hajare
School of Computer Engineering and Technology
MIT Academy of Engineering
Pune, India
nphajare@comp.maepune.ac.in

***Abstract*—in the recent years, Internet of Things basically applied into smart city applications only, nowadays Internet of Things playing a vital role in changing the manual controlling and monitoring in agriculture towards automated and remotely controlled and monitored operations. Recent improvements to the Internet of Things help to increase efficiency in precision agriculture. Use of the Internet of Things is remodeling agriculture environment. By making farmers capable to face problems related to precision and sustainable agriculture. Internet of Things technology helps in remotely collecting information from various sensors placed in the field. Sensors are like soil pH, Moisture level, Humidity, temperature, the fertility of the soil, level of water, insect population, pest detection, crop growth. Farmers are remotely connected with his farm using IoT and Smartphones. By using wireless sensor network nodes collects crop and environmental related data from the field. Then transfer information through the ZigBee network to the server node. The main node performs processing on collected data. Microcontrollers are used to automatically monitor and control the processes on the farm. For visualizing farm conditions cameras are placed into fields. The use of smartphones keeps farmers updated regarding the changing condition in his farm automatically at anywhere and anytime. Due to the use of the Internet of Things in agriculture, it reduces farmer efforts, enhances productivity, save the cost and time and provides automated controlling and monitors agriculture remotely. Automated irrigation system, pest controlling, monitoring plant growth, analysis of pesticides, controlling the insect population, etc. are implemented through the Internet of Things which converts traditional farming into automated farming.**

Keywords—automated irrigation, pest control, crop productivity, precision agriculture

I. INTRODUCTION

Things on the earth connected to each other with the help Internet of Things for communicating with each other. Internet of Thing connects thing to thing, the thing to human and human to things for sharing information. The Main goal of the Internet of Things is to bring out the large network be connected. Combining and connecting various types of device to each other forms a large network. Cost saving, automation in everything and communication are major pillars of the Internet of Things. It allows users to remotely monitor and control routine activities. Using the internet and handheld devices like smartphones and IoT makes framers' life easy. It ultimately increases productivity and saves the cost and time of farmers. Remotely enables objects to be sensed and actuated with in-network using the Internet of Things.

Internet of Things plays a vital role in automated irrigation, smart farming, monitoring greenhouse, crop monitoring, crop growth monitoring, pest controlling and monitoring, insect population controlling and monitoring, etc. Collects real-time data from various sensors placed into the farms. The node contains sensors like temperature sensor, soil moisture, humidity sensor, ultrasonic sound, light intensity, atmospheric pressure sensor, and leaf wetness sensors. Cameras are used for capturing the images and videos of the farm. Zigbee protocol [16] takes care of all data collected from all sensor nodes. Also handles operations based on threshold values. ZigBee low powered device which helps in energy saving. Solar panels may be used for saving energy at wireless sensor network nodes. All information collected from sensors transferred to the main server (microcontroller/ Raspberry Pi, Arduino) node through the internet or local network for further analysis. Using moisture level and temperature sensor data converts manual irrigation system into automated irrigation [3] [5] system. Switching motor on/off sprinkling system results in the optimum use of water. With the help soil pH values and environmental conditions, soil condition is measured. According to results, required pesticides list is generated. Align with environmental conditions suitable solution is generated. The solution is provided to the farmers which result in over usage of pesticides into the farm. Also saves cost and time and increases the productivity of the crop. It's proved by science music helps to increase the growth ratio of crop and increases crop productivity. The major issue in the agricultural field is pest control [23]. Farmers make use of chemical for controlling pest in the farm. This harms crop growth as well as farmers health. An appropriate list of chemicals aligns with environment suggested to the farmers. Significantly proved, with various frequency ranges pets get affected. Various sound frequencies effects on pest brain and nerves system. This also effects on reproduction system of pets. Use of sound emitter will result in pets controlling. Making use of ultrasonic sound emitter into the fields helps in pest control. Generating various frequency farmers can control pest and saves cost. Also, it will increase the growth of the crop. Capturing real-time images from fields with insect [26] affected area and an environmental condition. Processing/server station informs farmers regarding the density of insect population through notification as SMS. Real-time data and historical data considered for monitoring and controlling the insect population in farms.

Using the latest low energy protocols like LoRaWAN, LoRa, ZigBee saves power consumption. Also secured data transfer from nodes to the main server [1] [2]. Challenges consider while a designing system using the Internet of things are security, key management, authentication and authorization, access control, routing protocol and data aggregation [8]. Farmers are notified regarding monitoring and controlling information via smartphones. With the help of the appropriate use of ICT [7] and various visualization tools. which result in ease of using. Farmers are remotely connected with their fields. Farmers can control and monitor their own

field operations through smartphones using GSM/ Cellular module [1] [2]. Making use of Internet of things enabled drones/ Agrobots get used in pesticide spraying. This will result in decreasing the death ratio of farmers.

II. LITERATURE SURVEY

The survey is based on the following points

a. Smart automation in irrigation.

b. Smart agriculture.

c. Plant/Crop growth monitoring and controlling.

d. Pest control.

e. Insect population controlling.

f. Use of latest technology, issues, and challenges in IoT based agriculture system.

A. Smart Automation in Irrigation

Vijay Kumar [1], Lin Zhang [2] work on automated water sprinkler irrigation system. Provide information regarding water usage, soil pH values using wireless sensor technology. WSN nodes formed with sensors like moisture sensor, temperature sensor, soil pH, atmospheric pressure sensor and leaf wetness sensor. All information collected from nodes and according to the soil moisture level sprinklers are controlled automatically and stopped when an adequate level of water is sprinkled. All information regarding water level and soil pH send to the farmer's mobile through the GSM module. Using this information farmer plans for fertilizers.

Joseph Haule [3] designed a system using a wireless sensor network for automation in irrigation. Based on moisture levels of soil optimum use of water distribution managed through automatic communication using wireless sensor technology in irrigation. A designed process which set parameters like time for water and the frequency of watering for proper water management and produce a high-quality crop. Build system using wireless sensor technology with making use Zigbee for battery life. The overall system is controlled with devices based on inputs received from various sensors with efficient manner.

G. Nisha [4] designed a system for automated irrigation using WSN and disease monitoring using Image processing technique. Images captured from the camera mounted in the field and send through WSN nodes for processing and inform to the farmers using GSM modules. An automated irrigation system designed for the adequate use of water in farming in dry areas using distributed nodes consisting of sensors like moisture, temperature, etc placed in the field. Automated irrigation system builds using WSN, Zigbee protocol, microcontroller, solar panels, and cellular network. Desired threshold values set for the proper functioning of the automated irrigation system.

R. Balamurali, K. kathiravan [5], Yunseop Kim [6] proposed a system considering parameters low power consumption, appropriate network topology, protocols with high reliability. Research major focuses on automatic irrigation monitoring and controlling. Using a wireless sensor network with network capabilities and sensor nodes deployed as Adhoc for monitoring and controlling the irrigation system. Operates based on data collected from sensor nodes which collect data from water level and motor movement. A system contains base stations place near to the residence which process all data and reduced farmers efforts, save the cost, minimal training required for installation of the system.

Manish Bhimarao Giri, Ravi Singh Pippal [43] designed system for smart irrigation system using Wireless Sensor Network and Linear Interpolation Programming. A system based on three parameters temperature, soil moisture, and light intensity. Based on readings timings are formulated for controlling water distribution using drip.

B. Smart Agriculture

K. A. Patil, N. R. Kale [7] designed a model for smart agriculture with the help of the Internet of Things and ICT. The system provides a real-time monitoring system for soil pH value, temperature, moisture and provides the advisory system for paste and diseases control and disease identification through SMS alerts system to the farmers. Also provides the facility to control various operations remotely with the help of smartphones.

Liu Dan, Cao Xin, Huang Chongwai, Ji Liang [8] experimented using Zig Bee technology on the greenhouse monitoring system. A system designed with low cost and minimizes human efforts and converted from wired technology to wireless technology. Provide good controlling and monitoring of greenhouse. The main motive behind research to provide an efficient system to manage the greenhouse environment and reduce farming cost with low energy. Make use of IoT technology with B-S structure and cc2530 as processing chip for coordinating wireless sensor nodes within the Linux environment.

Sivasankari S. Gandhimathi [9], Alan Main-Waring [10] reviewed a study of real-world agriculture operating through wireless sensor technology. Considered the set of design requirements and developed system with the help of Wireless sensor technology, accessing data remotely, processing at center places and monitoring based on data processing results. According to the above details implemented prototype which is tested at James San Jacinto Mountains in California reserved forest.

Zulhani Rasin [11], Wang Weighing, Cao Shuntian [12] presented a system based on Remote intelligent Monitoring System based on Zigbee and Wireless Sensor Network technology. A system designed using wireless mesh topology instead of wired connections.

K. Satish Kannan, G. Thilagavathi [13], Nguyen Tang Kha Duy [14] focuses on industrial household's shrimp farming. A designed system which provides a versatile solution to improving the accuracy monitoring environmental conditions and reducing human efforts. The proposed system is capable of collecting data, analyzing data and generating the graphical representation of data. A system designed in such a way that which reduces human efforts as well as electricity usage and result in helping small/medium scale farming.

Nelson Sales [15] making use of wireless sensor technology and cloud computing designed build system for monitoring and controlling agriculture. Smart objects interact with each and share environmental information and send to the main node for processing and analysis. Cloud computing provides high storage and processing capability for rapid processing and data analysis which defiantly make changes in agriculture computations.

C. Plant/Crop Growth Monitoring and Controlling

Arvind G. Athira, V. G. Haripriya, Akshaya Rani, Arvind S. [16] designed a system with advanced irrigation, paste control and seed germination with the help of Internet of Things, Artificial Intelligence and machine learning. With the help of moisture, humidity and temperature sensor data collected and send to the remote processing unit using an Arduino microcontroller and send via Zigbee to the database. Irrigation system gets controlled and monitored by the analysis performed on stored data during the lifecycle of the crop. Paste control is a major issue in agriculture. Basically, every farmer makes use of chemicals for controlling the population of paste. Researchers designed a system for paste control using ultrasonic sound emitters by placing emitters in the field. Which effect on pests brain and nerve a system. Research also focuses on plant growth by using sound emitters placing into the field. Scientifically it is proved that plan growth rate increased due to musical sounds.

Fu Bing [17], V. Sandeep, K. Lalith Gopal, S Naveen, A. Amudhan, L. S. Kumar [18] designed system in China making the transition from precision agriculture to modern agriculture. Research focuses on fruits production and controlling the quality of fruits. An experiment carried out on organic melons and fruit production and quality control. The system makes use of IoT and RFID and a sensor which results in to reduce farmers' efforts also reduce production cost by increasing fruit quality. Internet of Things plays a vital role in the transition to modern agriculture.

Sonal Verma [19], A. Sivasankari, S. Gandhimathi [9], Chen Xion Yi, Yang Xiong, Jin Zhi Gang[20] discussed the approach for crop growth monitoring using inexpensive camera system called crop phonology recording system. While estimating biophysical parameters camera based vegetation index helps. The design explores recorded header region of EXIF formatted JPEG files with RGB and proposed with vegetation indices like ev-NDVI, ev-SR and ev-CLgreen calculated using cDN and daytime exposure. With results en-VAR, I worked best for the maize and ev-CLgreen for soybean.

Meng Ji-Hua [21] designed a system for crop growth monitoring which satisfies the need for global crop growth monitoring. Research carried out on variations in growth trends of crop, status and crop seedlings. Design methods for crop real-time growing methods and crop growing status time by time through remote sensing techniques. Consider real-time data as well as historical data for processing information their result is prepared to show variations in crop growing levels with respect to the conditions. Used three scales based on geographical orientation like state level, country level and continent level for global crop growth and status of crop growing process.

So Yahata, Tetsu Onishi, Kanta Yamaguchi, Seiichi Ozawa, Jun Kitazono, Takenao Ohkhawa [22] research focuses on decision making for good yield for various agriculture condition. This paper focuses on soybean growth monitoring and controlling in real fields. Using image sensing methods observation are captured automatically of soybean flowers and seedpods. Appropriate cultivation of soybeans achieved through available bigdata on the growth status of agriculture and environment conditions. Research focus on flower detection and counting, Flower counting and seedpot detection which results in growth management of soybeans.

Santosh Warpe, Ravi Singh Pippal [44] research focuses on the appropriate distribution of fertilizers to increase the growth of corp and plants to increase yield. Soil with less amount of nutrients is nitrogen, phosphorus, and potassium. These nutrients should be applied to proper preparation to increase the crop yield. With the help of wireless sensor network, authors proposed a system for fertilizers distribution with proper proportion.

D. Pest Controlling

Archana Chougule, Vijay Kumar Jha, Debajyoti Mukhopadhyay [23] designed system using the Internet of Things for paste management with the use of algorithm ontology. The system works by considering data from Integrated Pest management generates ontology based on the text then performance relationship extraction, apply the pest description ranking algorithm and with help weather IPM appropriate conditions for calculated for applying pesticides.

Balaji Banu [24] designed system managing sensor node failures and energy efficiency. The system observes the conditions of the farming and increasing the crop yield and quality using a wireless sensor network. A system designed using various sensors like humidity, temperature, water level, etc. processor ATMEGA8535 and IC-S8817BS, analog to digital conversion, Zig bee protocol, and wireless sensor nodes.

Hemantkumar Wani, Nilima Ashtankar [25] research focuses on the prediction of pest/diseases of various crops using machine learning algorithms. Yield per hector is lesser in India than international standards. The main cause of lesser yield is planted diseases. Diseases are increased because of pest. Improper water management, the fewer number of soil nutrition which leads to increasing the pest. Using the Navie Bayes Kernel algorithm used to find out the patterns which control the flow of plant disease and flow of pest control.

E. Insect Population Controlling

N. A. Bhorgese, P. Tirelli [26] designed a system with visualizing insect population graph for predicting regions and monitoring and controlling insect populations with weekly span. Insect population affects crop production. The system captures images of insect population from different locations and forwarded to the main unit which will perform severity analysis and generate alarms to inform farmer regarding the insect intensity. Client nodes are mounted into fields which captures images and send to the master nodes for further processing which will generate graphs based on the insect population. A system based on wireless sensor network technology in a distributed manner which automatically captures images and performs the analysis.

Nikesh Gondchawar et al., [27] research based on smart agriculture using the Internet of Things. Designed and developed a robot for performing operations like spraying, weeding, and sensing. Spraying harms farmer's health. Spraying is done using robot will save farmer's life as well as proper spraying of pesticides. Systems designed with sensors, robot, ZigBee, microcontrollers, and raspberry pi. Provides information field condition. Irrigation issues detected and handled using remote based robots.

Tanmay Baranwal et. al., [28] this research proposed system on protection for field grains from various insects. PIR sensor used to identify heat and starts URD sensor and camera to

detect insects. Which provides security and protection of agricultural products from rodents and various insects.

G. Naveen Balaji et. Al., [29] proposed system provides a solution to protect the crop from animals using image processing techniques. Image processing using video surveillance detects animal intrusion into the agriculture land. Based on movement detection animal images will compare with stored data and animal is detected. Once the animal is detected will be identified and informed in the form if text message to the farmer through the GSM module.

F. Use of Latest Technology, Issues and Challenges

Danco Davcev, Kosta Mitreski, Nikola Koteli [30] designed a system for agriculture with the help of the Internet of Things with LoRaWAN and cloud computing. LoRaWAN network basically used to transfer data from nodes to backend cloud services.

Soumil Heble, Ajay Kumar, U. B. Desai [31] proposed system smart agriculture with the help of low power IoT network. Introduce solar-powered features sensors and nodes. For covering large agricultural area LoRA based gateways are used to solve line power problems. In future scope planning for drone-based remote controlling and monitoring precision agriculture.

Chen XianYi, Yang Xiong, JinZhi Gang [20], Rwan Mahmoud [32] research focuses on challenges and security issues in the Internet of Things. Focus on wide applications using IoT facing security issues. Paper starting with the basic architecture of IoT, Layered architecture of IoT and security issues and provides solutions to those issues. Discuss focuses on security, key management, routing protocol, access control and authentication with data fusion technology.

Fiona Edwards Murphy [33] research deals with monitoring honeybee colony and surrounding area using a wireless sensor network. Make use of a Wireless sensor network, Internet of things, cloud computing designed smart hive system. Cloud used to monitor data from a different colony collected from various sensor nodes with low power consumption. The system consists of smart hive communication, data aggregation, and visualization tools. Making system intelligent machine learning techniques adapted for extracting meaningful information for supervising and additional deployments of the system without the intervention of human efforts.

Ling-Ling [34], research major focus on software and hardware used for developing a system using Wireless Sensor Network nodes, topology, network, and Zigbee platform. The experimental result shows appropriate data capturing from various sensor nodes through network nodes from various sensors mounted into greenhouse like humidity, temperature, moisture, etc. system makes complex greenhouse monitoring automated and controlled inefficient manner. Provide good network stability to the system.

R. Balamurli [5], Chen XianYi, Yang Xiong, Jin Zi Gang [820, Narut Soontranon, Panwadee Tangpattarnakul, Panu Srestasatheirn [35] major focus on analyzing routing protocols like integrated MAC, DSR, AODV, AOMDV and routing protocols used in precision agriculture using wireless sensor network. For precision agriculture using wireless sensor network Integrated MAC and routing algorithm is suitable for multi-hop routing. Discussed regarding real-time precision agriculture based on soil pH sensor, moisture, humidity, etc. sends recorded data to the remote server for analysis and take appropriate action based on collected data.

Lei Xiao [36], Meng Ji-Hua, Wu Ning-fang, Li Qiang-is [21] designed system based on wireless sensor network which monitors agriculture conditions using real-time data collected from sensors like humidity, temperature, etc. Experimental setup handles all challenges regarding protocols, network topology, and data processing. Experimented on data collection and transmission ultimately improves production efficiency agriculture. The system builds with the appropriate framework, lightweight, good performance, and appropriate operations.

Elias Yaacoub [37], K. Satish Kannan, G. Thilagavathi [13] discussed system which monitors and analyze air quality in Doha based on wireless sensor technology. Using R programming performs analysis on stored data in a different form as per end user requirement.

Giuseppe Anastasi [38] designed a system for monitoring and controlling productivity in high-quality wine and deployed at Silicon winery. A system designed based on wireless sensor technology. Sensor nodes are placed in grapes fields as well as in the factory where wine is produced. A system designed with proper planning infield and in preservation workshops. WSN based Infrastructure controls distributed production chain nodes. All data collected the main unit which process information and monitors and controls the quality of graphs in the field and aging of produced wine in the workshop. Ensure good quality production of grapes and wine.

Dragos Mihai Ofrin [39], Zulhani Rasin, Shahrieel Mohd areas, Hizzi Hamzah Mohd [11] based on parameters like performance, efficiency, and flexibility designed system for controlling and monitoring environmental conditions. Parameters like accuracy, resolution, energy consumption and data acquisition system considered while designing. Low power Zigbee protocol is used in the system. The major disadvantage of the system is power consumption. The author predicts alternative for power consumptions, energy resources, traffic, alternative resources, etc. to monitor and control operations over long distance make use of Wi-Fi or GSM connectivity.

Duan Yan-e [40] enhancing agriculture production and utilizing all resources researcher explained Agriculture Information Technology used in every part of agriculture. Agriculture production efficiency gets affected by agriculture information management. MIS is designed with detailed agricultural data.

Rachel Cardell-Oliver [41] research more focuses on environmental drastically changing condition. Based on such conditions reactive event-driven network should build for controlling and monitoring environmental conditions. Reactive means as soon as condition changes system should predict and control. More focus is on dynamic responses and limits the useless data gathering as well as network lifetime and robustness. The researcher demonstrated on reactive sensor network gathering data in rainy and dry seasons based on soil moisture levels. Future scope provides improvement regarding the network, packet delivery, and event interest. The implemented system monitors the environment effectively based on moisture levels in the reactive driven model.

Mohanraj et. Al., [42] research uses ICT to provide help to farmers regarding agriculture yield. As farmers required guidance at different stages of plant/crop growth at the right time. Farmers facing various problems like weather condition, market analysis, irrigation planner, crop profit /loss analysis and water utilization. Using ICT authors connecting farmers to huge knowledge dataset which will increase productivity and yields by providing accurate information.

III. Discussion

With the above survey, we can provide a complete solution for smart farming using Wireless Sensor Network and Internet of Things. Smart Irrigation, Smart Agriculture - greenhouse monitoring, crop growth monitoring and controlling, pest controlling using various techniques mentioned above with the help Wireless Sensor Network and Internet of Things. With the help of Smartphones will make farmers life easy by maintaining and controlling of all agricultural activities on a single click.

Table I

Survey – Problem faced by farmers and their IoT based solutions

Reference Papers	Survey Parameters	Problem Faced by Farmers	IoT based Solution to the problems
1, 2, 3, 4, 5, 6, 43	Smart Irrigation	Adequate water levels, Improper usage of water Water distribution according to various plants	Proper utilization of water with the help WSN systems based on parameter like temperature, soil moisture, and leaf wetness sensors. Drip irrigation
7, 8, 9, 10, 11, 12, 13, 14, 15	Smart Agriculture	Facing problems in Greenhouse Management	Auto controlled greenhouse management
9 16, 17, 18, 19, 20, 21, 22, 44	Plant/Crop Growth and Monitoring	Selection of pesticides for different plant/crop The ratio of pesticides according to plant and environmental conditions Real-time monitoring of large scale farming Accuracy monitoring of environmental conditions Fertilizers distribution with the proportion Growth trends and growth methods of various crops according to geographical conditions	Fertilizer distribution with proportion to the available neutrinos with the help of soil testing. Easy to monitor large scale farming with the help WSN systems. Equal distribution of fertilizers and pesticides using remote control robots. With the help ICT tools, farmers get all information on their smartphones which leads to increased yield.
23, 24, 25	Pest Control	Controlling pest and Insect population without using pesticides Seed germination and Pest management Detection of various plant and crop diseases	Using Machine Learning techniques plant crop disease are predicted and appropriate solutions provided to farmers. Alternative options to control pest population using ultrasonic sound & save the life of farmers.
26, 27, 28, 29	Insect population Controlling	Controlling Insect population Protection of field storage grains and crop from animals	With the help of image processing density of insect population is calculated and informed to farmers. With the help video, surveillance technique plants and grains are protected from animals.
5, 13, 11, 21, 30, 31, 32, 33, 34, 35, 36, 37, 38, 39, 40, 41, 42	Used of Technology	Lack of technology usage	With the help ICT tools, farmers get all information on their smartphones which leads to increased yield.

IV. Conclusion

With the help of survey smart irrigation, smart agriculture, pest controlling, insect population controlling as well as plant growth management is improved with the help of Internet of Things. Death ration of farmers is minimized with such systems. Yield is increased with the help of technology. Using Wireless Sensor Networks technology nodes with various types of sensors placed into the farm. Node collects information regarding real-time environmental changes,

insect population, pest and crop conditions, etc. Then this information is processed and analyzed. Then the information is transmitted using the GSM network through smartphones. Actuators are controlling devices with corrective actions. Internet of Things profits the farmers by enabling manual operating into automated operating. Also makes crop monitoring easy. Pest monitoring and controlling and enhance crop productivity. Use of Internet of Things connects farmers remotely to their fields at any time. Predicting future conditions by using analytics on uncontrolled conditions like rainfall and drought enhance water usage and use of pesticides. Making use of cloud computing, Machine learning, Image processing makes smart farming much easier.

REFERENCES

[1] Meng ji-Hua, Wu Bing-Fang, Li Qiang-zi, "A Global Crop Growth Monitoring System Based on Remote Sensing", IEEE International Symposium on Geoscience and Remote Sensing.

[2] Zulhani Rasin, Hizzi Hamzah Mohd, Shahrieel Mohd Aras, "Application and Evaluation of High Power ZigBee Based Wireless Sensor Network in Water Irrigation Control Monitoring System", IEEE Symposium on Industrial Electronics and Application.

[3] R. Balamurali k. Kathiravan, "An Analysis of Various Routing Protocols for Precision agriculture using Wireless Sensor Network", IEEE International Conference on Technological Innovations in ICT for Agriculture and Rural Development (TIAR 2015).

[4] Alan Mainwaring, Joseph Polastre, Robert Szewczyk, David Culler, John Anderson, "Wireless Sensor Networks for Habitat monitoring", International Conference.

[5] Nguyen Tang Kha Duy, Nguyen Dinh Tu, Tra Hoang Son, Luong Hong Duy Khanh, "Automated Monitoring and Control System for Shrimp Farms Based on Embedded System and Wireless Sensor Network", Electrical Computer and Communication Technologies (ICECCT), IEEE International Conference.

[6] Chen XianYi, Jin Zhi Gang, Yang Xiong, "Design of Tropical crops Pests Monitoring System Based on Wireless Sensor Network", Consumer Electronics Communication and Networks, 2nd International Congress.

[7] Archana Choughule, Vijay Kumar Jha, Debajyoti Mukhopadhyay, "Using IoT for Integrated Pest Management", International Conference on Internet of Things and Applications (IOTA),2016, pp -17-22.

[8] Lin Zhang, Min Yuan, Deyi Tai, Xia Oweixu, Xiang Zhan, Yuanyuan Zhang, "Design and Implementation of Granary Monitoring System Based on Wireless Sensor Network Node", International Conference on Measuring Technology and Mechatronics Automation.

[9] Wang Weighing, Cao Shuntian, "Application Research on RemoteIntelligent Monitoring System of Greenhouse Based ZigBee WSN", 2nd International Congress.

[10] LIU Dan, Cao Xin, Huang Chongwei, JI Liang Liang, "Intelligent agent greenhouse environment monitoring system based on IoT technology", International Conference on Intelligent Transportation, Big Data and Smart City, 2015.

[11] Joseph Haule, Kisangiri Michael, "Deployment of Wireless Sensor Networks in Automated irrigation management and Scheduling Systems: A Review", Science, Computing and telecommunications, pan African Conference.

[12] Balaji Bhanu, Raghava Rao, J. V. N. Ramesh, Mohammed Ali Hussain, "Agriculture Field Monitoring and Analysis using Wireless Sensor Networks for Improving Crop Production", 11th International Conference on Wireless and Optical Communications Networks.

[13] Ling-Ling LI, Shi-Feng YANG, Li-yan WANG, Xiang-ming GAO, "The Greenhouse Environment Monitoring System Based on Wireless Sensor Network Technology", IEEE International Conference on Cyber Technology in Automation, Control and Intelligent systems.

[14] A. Sivasankari, S. Gandhimathi, "Wireless sensor-based Crop monitoring System for Agriculture using Wi-Fi Network Dissertation", International Journal of Computer Science and Information Technology Research, Vol 2, pp – 293-303.

[15] Rwan Mehmoud, Tasneem Yousuf, Fadi Aloul, "Internet of Things (IoT) Security: Current status, Challenges, and Prospective Measures", Internet Technology and Secured Transactions, 10th International conference.

[16] Yunsen Kim, Member, IEEE, Robert G. Evans, William M. Iversen, "Remote Sensing and Control of an Irrigation System Using Distributed Wireless Sensor Network", IEEE Transaction on Instrumentation and Measurement, Vol. 57,2 008.

[17] K. A. Patil, N. R. Kale, "A Model for Smart Agriculture Using IoT", International Conference on Global Trends in Signal processing, Information Computing and Communication, 2016, pp- 543-545.

[18] G. Nisha, J. Megala, "Wireless Sensor Network Based Automated Irrigation and Crop Field Monitoring System", 6th International Conference on Advanced Computing (IcoAC).

[19] Danco Davcev, Kosta Mitrski, Stefan Trajkovic, Viktor Nikolovski, Nikola Kotel, "IoT agriculture system based on LorWAN"

[20] Soumil Heble, Ajay Kumar, k.V.V Durga Prasad, Soumya Samirana, P. Rajalakshmi, U. B. Desai, "A Low Power IoT Network for Smart Agriculture"

[21] Fiona Edwards Murphy, Emanuel popovici, p. adraig Whelan, Michele Magno, "Development of Heterogeneous Wireless Sensor Network for Instrumentation and Analysis of BeeHives", IEEE International Conference on Instrumentations and Measurement Technology Conference (I2MTC), 2016.

[22] So Yahata, Tetsu Onishi, Kanta Yamaguchi, Seiichi Ozawa, Jun Kitazono, Takenao Ohkawa et. Al., "A Hybrid Machine Learning Approach to Automatic Plant Phenotyping for Smart Agriculture", IEEE, International Joint Conference on Neural Networks (IJCNN), 2017

[23] Nelson Sales, Orlando Remedios, Artur Arsenio, "Wireless Sensor and Actuator for Smart Irrigation on the Cloud", Internet of Things (WF-IoT), 2nd World Forum.

[24] Arvind G., V. G. Haripriya h., Akshay Rani R., Aravind S., "Automated irrigation with advanced seed germination and pest control", IEEE International Conference on Technological Innovations in ICT for Agriculture and Rural development (TIAR 2017), pp – 64-67

[25] Hemantkumar Wani, Nilima Ashtankar, "An Appropriate Model Predicting Pest/Diseases of Crops Using Machine Learning Algorithms", IEEE, International Conference on Advanced Computing and Communication Systems (ICACCS), 2017.

[26] S. Vijayakumar, J. Nelson Rosario, "Preliminary Design for Crop Monitoring Involving Water and Fertilizer Conservation Using Wireless Sensor Networks", Communication Software and Networks(ICCSN), IEEE 3rd International Conference.

[27] Nikesh Gondchawar, Prof. Dr. R.S. Kawitkar, "IoT Based Smart Agriculture", International Journal of Advanced Research in Computer and Communication Engineering, ISSN 2278-1021.

[28] Tanmay Baranwal, Nitika, Pushpendra Kumar Pateriya, "Development of IoT based Smart Security and Monitoring Devices for Agriculture", IEEE, 6th International Conference – Cloud Systems and Engineering.

[29] G. Naveen Balaji, V. Nandhini, S. Mithara, R. Naveena, N. Priya, "Advanced Crop Monitoring Using Internet of Things based Smart Intrusion & Prevention in Agriculture Land", International Journal Trend in Scientific Research and Development, ISSN No 2456-6470.

[30] K. Satish Knannan, G. Thilagavathi, "Online Farming Based on Embedded Systems and Wireless Sensor Technology", International Conference on Computation of Power, Energy Information and Communication (TCCPEIC).

[31] FuBing, "Research on the Agriculture Intelligent System Based on IOT", International Conference on Image Analysis and Signal Processing.

[32] V. Sandeep, k. lalith Gopal, S. Naveen, A. Amudhan, L. S. Kumar, "Globally Accessible Machine Automation Using raspberry pi based on Internet of Things" , Advances in Computing, Communications and Informatics, International Conference.

[33] Narut Soontranon, Panwadee Tangpattanakul, Panu srestasathiern, Preesan Rakwatin, "An Agricultural Monitoring System: Field Server Data Collection and Analysis on Paddy Field", International Symposium on Communications and Information Technologies.

[34] Lei Xiao, Lejiang Guo, "The Realization of Precision Agriculture Monitoring System based on Wireless Sensor Network", International Conference on Computer and Communication Technologies in Agriculture Engineering.

[35] N. A. Bhorgesse, P. Tirelli.

[36] Sonal Verma, Nokhil Chug, Dhananjay V. Gadre, "Wireless Sensor Network for Crop Field Monitoring", International Conference on Recent Trends in Information Telecommunication and Computing.

[37] Elias Yaacoub, Abdullah Kadri, Mohammed Mushtaha, Adnan Abu-Dayya, "Air Quality Monitoring and Analysis in Qatar using Wireless Sensor Network deployment", 9th International Wireless Communications and Mobile Computing Conference.

[38] Giuseppe Anastasi, Orazio Farruggia, Macro Ortolani, "Monitoring High-Quality Wine Production using Wireless Sensor Network", 42 Hawaii International Conference on system sciences.

[39] Dragos Mihai Ofrim, Bogdan Alexandru Ofrim, Dragos Ioan, "Improved environmental Monitor and Control using Wireless Intelligent Sensor Network", 3rd International Symposium.

[40] Duan Yan-e, "Design of Intelligent Agriculture Management Information system Based on IoT", 4th International Conference on Intelligent Computation Technology and Automation.

[41] Rachel Cardell-Oliver, Keith Smttem, Mark Kranz, Kevin Mayer, "Filed Testing a Wireless sensor Network fro Reactive Environmental Monitoring ", IEEE International Conference.

[42] Mohanraj I, Kirthika Ashokkumar, Naren J. "Field Monitoring and Automation Using IoT in Agricultural Domain", Elsevier, 6th International Conference on Advances in Computing and Communications, ICACC 2016.

[43] Santosh Warpe, Dr. Ravi Singh Pippal, "A Study of Fertilizer Distribution System for Agriculture using Wireless Sensor Network", International Journal of Computer Applications, 2016.

[44] Manish Bhimrao Giri, Dr. Ravi Singh Pippal, "Use of Linear Interpolation for automated Drip Irrigation System in agriculture using wireless sensor network", IEEE, International Conference on Energy, Communication, Data Analytics and Soft Computing (ICECDS), 2017.

Proceedings of the Fourth International Conference on Communication and Electronics Systems (ICCES 2019)
IEEE Conference Record # 45898; IEEE Xplore ISBN: 978-1-7281-1261-9

Simulink Model of Controlling Fuel Cell Powered Direct Current Motor with Comparative Performance Analysis

Md. Moontasir Rashid
Department of Electrical and Electronic Engineering
Leading University, Sylhet, Bangladesh
rashidmoontasir@gmail.com

Md. Niaz Morshedul Haque
Department of Electrical and Electronic Engineering
Leading University, Sylhet, Bangladesh
niaz.morshed@lus.ac.bd

Tasneema Akhtar
Department of Electrical and Electronic Engineering
American International University Bangladesh
Dhaka, Bangladesh
tasnee.akhtar@gmail.com

Md. Sayem Miah
Department of Electrical and Electronic Engineering
Leading University, Sylhet, Bangladesh
mdsayem.eee@gmail.com

***Abstract*— the paper focuses on a Simulink based model and design of the different control mechanisms of a DC motor powered via fuel cell. At first, fuel cell is used as the prime power source of the DC motor and a differential controller is used to achieve a uniform output. Then, the differential controller is replaced with Proportional Integral (PI) controller, Proportional Integral Differential (PID) controller and Fuzzy Logic Controller (FLC) subsequently to compare and demonstrate the variations that occur in the different characteristic curves with the change in various parameters. If Photovoltaic cell is used instead of fuel cell, the output operation of the DC motor may vary. So, in addition, a comparative performance analysis of both methods of power with regards to DC motor control is also presented.**

Keywords— DC motor; Fuel Cell; PI & PID controller; FLC controller; Simulink.

I. INTRODUCTION

Currently, there are finite source of conventional energy resources. Therefore, the only feasible solution for the future is to move towards the proper utilization of sustainable power sources. A Fuel cell derives energy from the reaction of two atoms of hydrogen with a molecule of oxygen producing water as by-product, hence converting chemical energy into electrical energy. It is considered a renewable source as it does not diminish with time. Fuel cells are used in applications such as in transportation systems and portable power backup systems. There are many different types of fuel cells like PEM (Polymer Electrolyte Membrane), AFC (Alkaline Fuel Cell), SAFC (Solid Acid Fuel Cell) and PAFC (Phosphoric acid fuel cell) [1]. On the other hand, the applications of DC motors are countless where optimization and fine-tuning is most desired. In order to calibrate DC motors at a proper level, controllers are necessary. Therefore, the prime objective of this paper is to design a DC motor control system which will be powered by PEM fuel cell and produce calibrated outputs with maximum performance targeting both efficiency and sustainability. A buck-boost DC to DC converter has been used for the purpose of switching the DC motor properly. It operates in discontinuous conduction mode and the duty cycles have been supplied to the converter using controllers which calculate and find the optimized performance factor of the DC motor.

II. LITERATURE REVIEW

There are many kinds of fuel cells currently available on market. PEM fuel cells need a common electrolyte called perfluorosulfonic acid. The operating temperature is below 120°, typical stack size is below 1 KW-100KW and electrical efficiency is around 60%. It is the most used fuel cell which has many advantages like how the solid electrolyte reduces corrosion, it works at low temperatures and it has quick start-up and load following. The only disadvantage of this cell is that it needs expensive catalysts and is sensitive to fuel impurities [2]. It has been observed that with increase rate of air flow, the maximum current increases in PEM fuel cell because of the decrease of the level of concentration polarization losses and also the voltage regulation for load increases. Maximum power generation in a PEM fuel cell is a logarithm function of rates of air flow [7]. Nevertheless, the Simulink model of fuel cell that is used in this paper is a generic model which represents most popular types of fuel cells operated with oxygen and hydrogen [3]. The simplified model represents a particular fuel cell stack operating at nominal conditions of temperature and pressure [2]. PEM fuel cells are the leading fuel cell technology which is used in material handling applications such as forklifts and for transportation applications [10]. Electric vehicle's main focus is DC motor. Robotic manipulators, guided vehicles, steel mills and electric traction are driven by DC motor which is highly controllable electrical drive [12]. Since our main focus is achieving optimized DC motoring outputs, this model was selected. For optimizing speed of DC motor, three different controllers have been used in this paper. Buck boost converter has the expertise to generate both step up and step down

output voltage [8]. Inductor's reluctance to allow rapid change in current is used to best understand the operation of a buck boost converter [9]. Proportional Integral controller is mainly used to eliminate the steady state error emerged from only proportional controller. The proportional parameter controls the reaction to the current error, the integral parameter controls the reaction established on the sum of previous errors and the derivative parameter controls the reaction based on the rate of changing error i.e. future error [11].

III. Methodology

Fig. 1 exhibits the basic block diagram of the Simulink model. A fuel cell with 48 Volt DC rating specially designed to meet the demands of a 10 HP DC motor has been used. The fuel cell supplies the Dc motor via a controller and a Buck-boost converter. The controller controls the duty cycle of the converter which in turn enhances the performance of the motor. A feedback loop consisting of a voltage sensor and a voltage feedback used to render reference voltage to the controller.

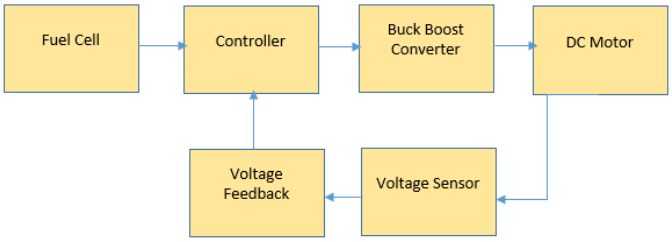

Fig. 1. Block Diagram of the Controlling System

IV. Modelling of Proposed System

Fig. 2 shows the overall Simulink model of the proposed system including Fuel cell, Converter and DC motor. Each component used are described below.

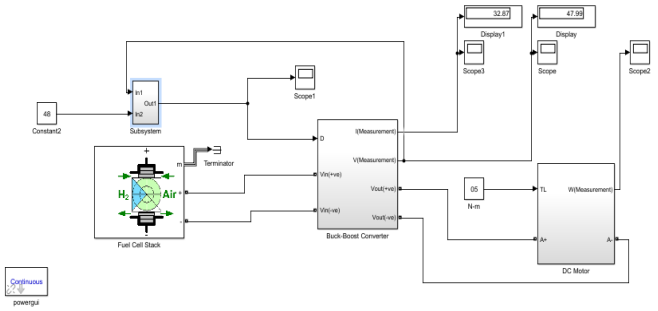

Fig. 2. Simulink Model of the System

A. Fuel Cell

The design utilizes a generic hydrogen fuel cell, a renewable source, of model PEM 50 KW 635V DC. Fig. 3 shows the VI (Voltage and Current) & PI (Power and Current) characteristics which is an inbuilt characteristics of the selected fuel cell. This is a simplified model appropriate for the system.

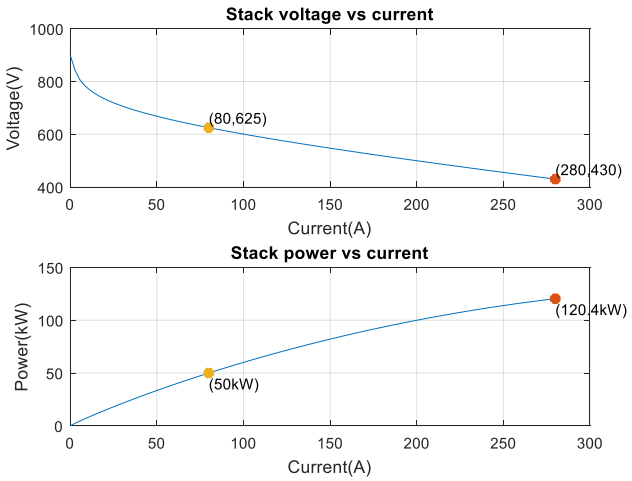

Fig. 3. VI & PI Characteristic Curve of Fuel Cell

B. Controller

Different types of controllers have been used in system for analysis. First, a differential controller was used and the outputs examined. Secondly, PI controller replaces the differential controller and the outputs are monitored again. Lastly, PID controller was used and the process is repeated and all of the observations are compared. All the converters are used in the discrete time domain.

1) Differential Controller

Fig. 4 illustrates the Simulink model of the differential controller with input 1 being the output voltage of the buck boost converter. Similarly, input 2 is the reference voltage of 48 V. The saturation and repeating sequence block used helps to generate proper duty cycles for the converter.

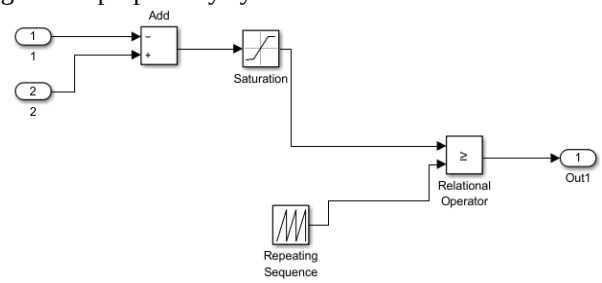

Fig. 4. Simulink Model of Differential Controller

2) PI Controller

Fig. 5 presents the Simulink model of the PI (Proportional Integral) controller situated between the rational operator and saturation block. It refines the system and provides improved outputs.

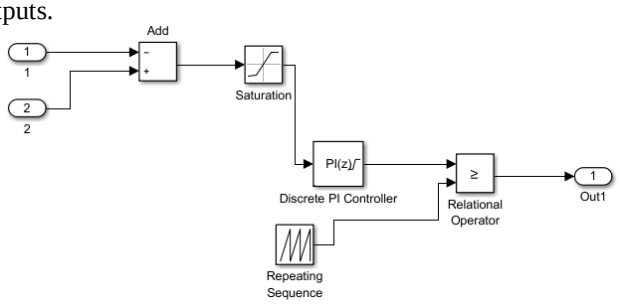

Fig. 5. Simulink Model of Proportional Integral (PI) Controller

3) PID Controller

Fig. 6 shows the Simulink model of PID (Proportional Integral Differential) controller. It further upgrades the design and provides smoother outputs.

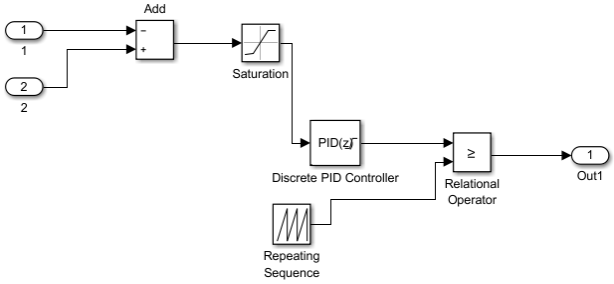

Fig. 6. Simulink Model of PID Controller

4) FLC Controller

A fuzzy controller with empirical rules are very useful in operator controlled plants [13]. Fig. **7** shows inclusion of Fuzzy logic controller between saturation and regional operator block. Fig. 8 shows fuzzy logic designer where input is taken from adder/comparator and output is going to out1 which is basically duty cycle for buck boost converter. In fuzzy logic designer, three membership function is taken which corresponds with three output functions. In fig. 9, the input rules have been arranged with the output functions. Input is taken from range 0 to 0.5 while output range is 0 to 1. For three MF(membership function), three parameters have been selected, first one is 0 to 0.1, second one is 0 to 0.5 and third one is 0.3 to 0.5. The output is taken corresponding to three input rules.

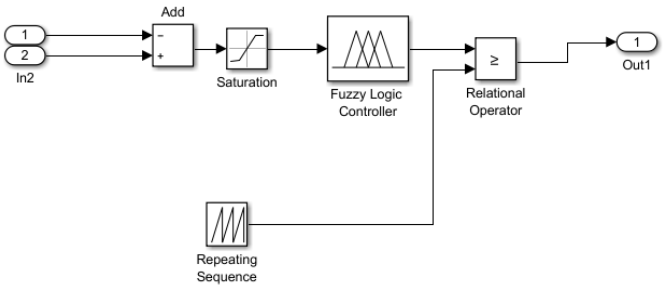

Fig. 7. Simulink model of FLC controller

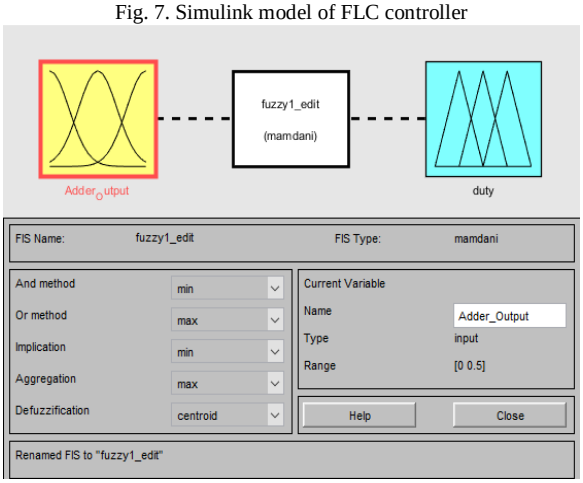

Fig. 8. Fuzzy Logic Designer

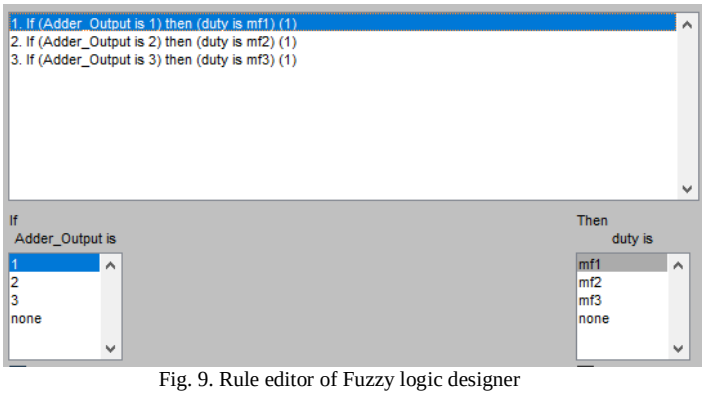

Fig. 9. Rule editor of Fuzzy logic designer

C. Buck Boost Converter

A DC to DC MOSFET switched buck-boost converter is used in the system as shown in Fig. 10. The inputs of the converter, V_{in} (+ve) and V_{in} (-ve), are outputs of the fuel cell. Port number 1 of the MOSFET serves the duty cycles supplied by the controller. Scopes have been used to obtain the curves of the switching elements. The outputs are connected to DC motor via ports. The inductor and capacitor values are chosen 4.5 mF and 15mH respectively for minimizing ripple effect of voltage and current.

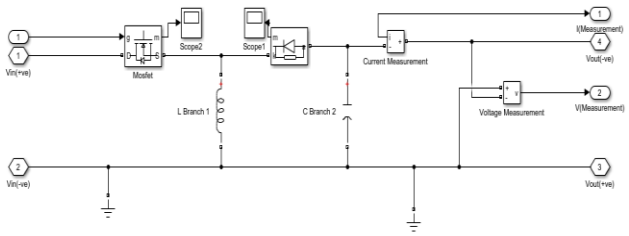

Fig. 10. Simulink Model of Buck Boost Converter

D. DC Motor

A PMDC motor is used in this system [4] as shown in Fig. 11 with ports 2(A+) and 1(A-) connected to V_{out} (+ve) and V_{out} (-ve) of buck boost converter. Port 1(TL) is connected to a constant torque of 5 N-m considering load torque. The given parameters are stated below [4]:

Power = 7776W
Voltage = 48 V
Full load current = 162 A
Break down torque = 21N-m
Constant torque = 0.13N-m
Motor speed = 367 rad/s

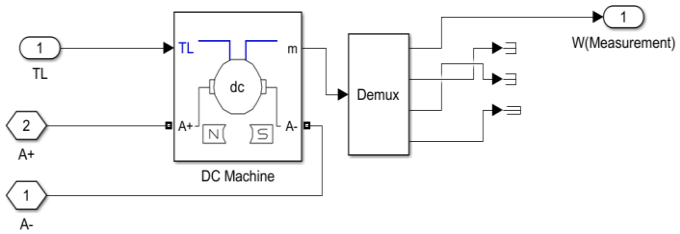

Fig. 11. Simulink model of the DC motor

V. Result Analysis of Output vs. Step Time Curve

A comparative analysis of the output characteristic curves of the DC motor and converter which varies with the use of different controllers has been conducted in this section. In some characteristics curve, spikes are generated because of turning on and off power or by increasing and decreasing the flow of power. It is caused by using buck-boost converter which operates on pre-determined duty cycle. Speed reference load torque and drive inertia are the quantities that can influence performance of a speed controller [12].

A. Differential Controller

From Fig. 12, it can be seen that the output voltage of the buck boost converter is 35.84 V and current is 1.7mA. A simulation step time of 20 is considered and varying voltage and current curves are generated as shown in Fig. 13 and Fig. 14 where small spikes are generated in range step 2 to step 3.5. At step 3.25, the spikes have high frequency and abruptly drop before reaching step 3.5. Voltage and current spikes are created due to improper generation of duty cycle which causes inefficient operation of buck boost converter.

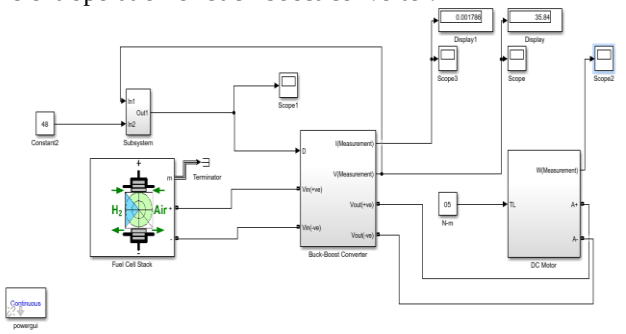

Fig. 12. Output obtained using Differential Controller

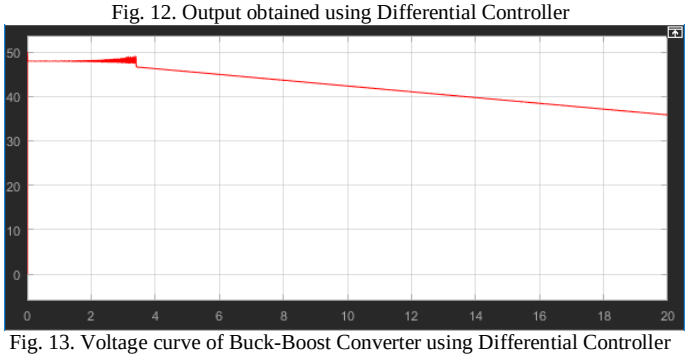

Fig. 13. Voltage curve of Buck-Boost Converter using Differential Controller

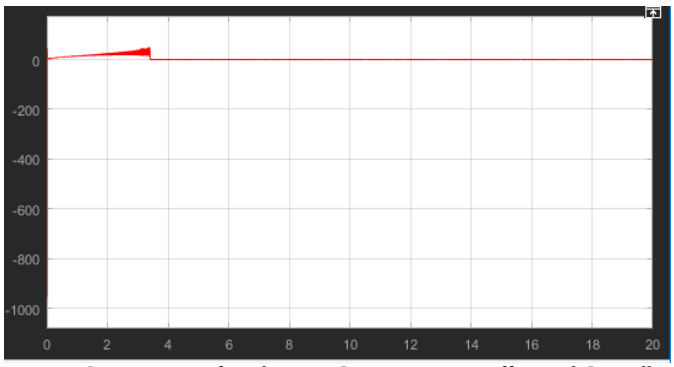

Fig. 14. Current curve of Buck-Boost Converter using Differential Controller

Fig. 15 shows the output speed curve of the DC motor. It can be seen that there is a change in gradient at point (3.45, 358) and the speed of the motor drastically decreases with steps number.

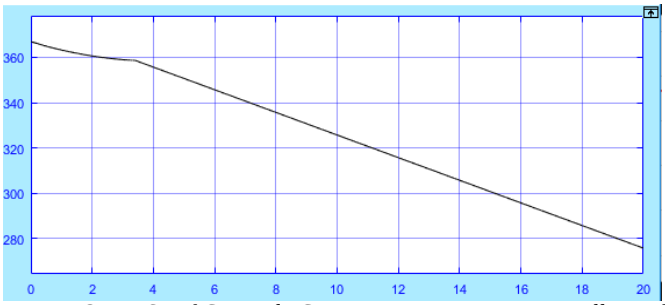

Fig. 15. Output Speed Curve of DC motor at 5 N-m torque using Differential Controller

B. PI Controller

In order to obtain smoother outputs, a PI controller is used the second time. From Fig. 16, it can be seen that the output voltage of the buck boost converter is 47.99 V and current is 32.87 A. A simulation step time of 20 is considered and varying voltage and current curves are generated as shown in Fig. 17 and Fig. 18 where there are small spikes at some intervals of curves. The curves are not completely smooth but compared to Fig. 10 and 12, they are improved and yield better results.

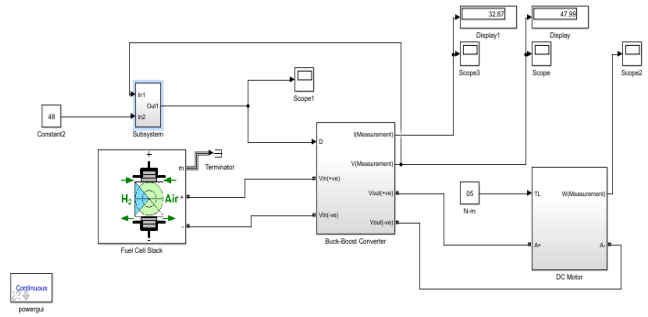

Fig. 16. Output Obtained using PI controller

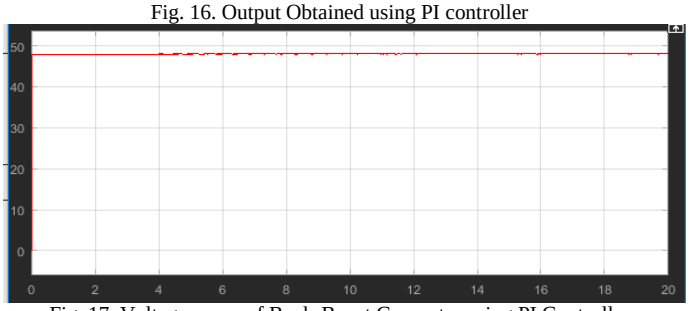

Fig. 17. Voltage curve of Buck-Boost Converter using PI Controller

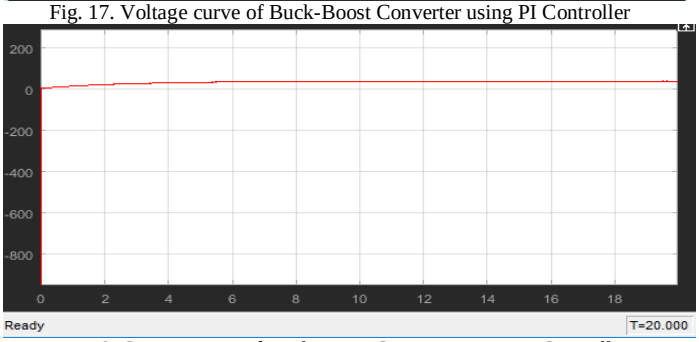

Fig. 18. Current curve of Buck-Boost Converter using PI Controller

Fig. 19 shows the output speed curve of the DC motor using PI controller. The speed curve is smoother compared to the one using differential controller shown in Fig. 13. This curve also contains small spikes from approximately step 4 to 14.

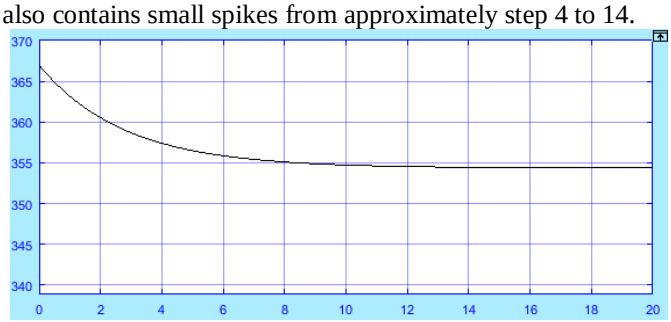

Fig. 19. Output Speed Curve of DC motor using PI Controller

C. PID Controller

A PID controller is used to further obtain smoother and stable characteristic curves. From Fig. 20, it can be seen that the output voltage and current of the buck boost converter is 48V and 38.66 A. A simulation step time of 20 is considered and varying voltage and current curves are generated as shown in Fig. 21 and Fig. 22 where there are no spikes and the curve is completely smooth and stable, yielding the most desirable and efficient results of the three controllers used.

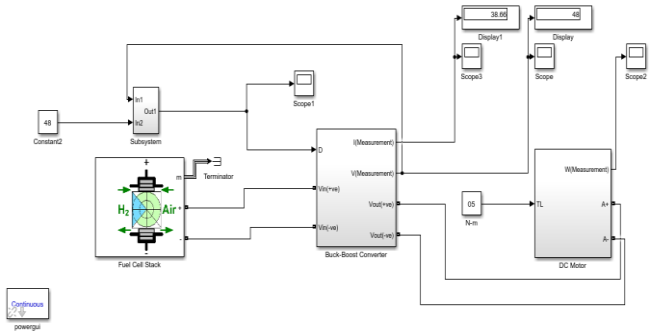

Fig. 20. Output Obtained using PID controller

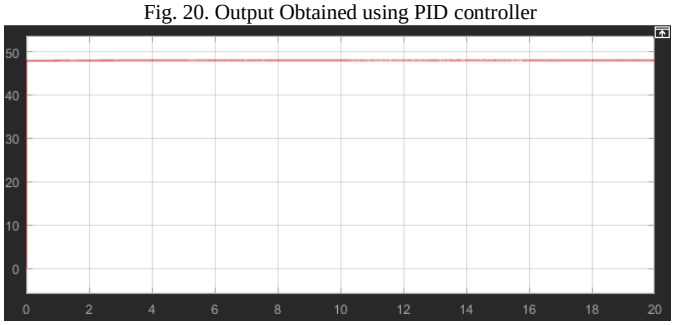

Fig. 21. Voltage curve of Buck-Boost Converter using PID controller

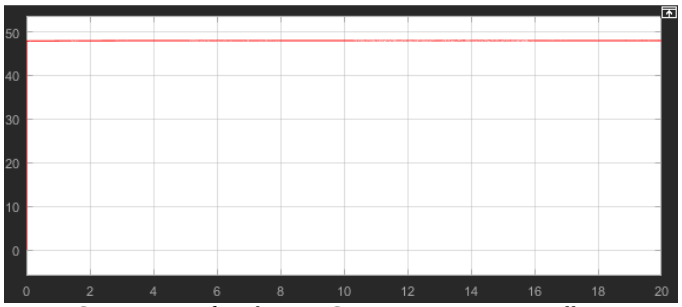

Fig. 22. Current curve of Buck-Boost Converter using PID controller

Fig. 23 shows the output speed curve of the DC motor using PID controller which is completely smooth with no spikes. The value of current is also better due to the stability and uniformity of the curve. Table. 1 presents a summary of the results obtained using all three controllers.

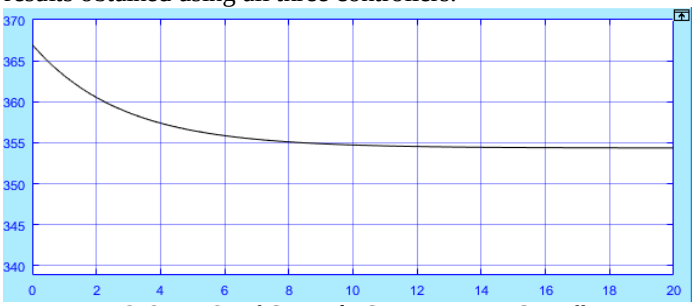

Fig. 23. Output Speed Curve of DC motor using PI Controller

D. Fuzzy Logic Controller

Finally, an FLC controller is used to obtain voltage and current output from buck boost converter. From Fig. 24, it can be seen that the output voltage and current of the buck boost converter is 48.53V and 45.78 A. A simulation step time of 20 is considered and varying voltage and current curves are generated as shown in Fig. 25 and Fig. 26. Small spikes are generated in current and voltage curves.

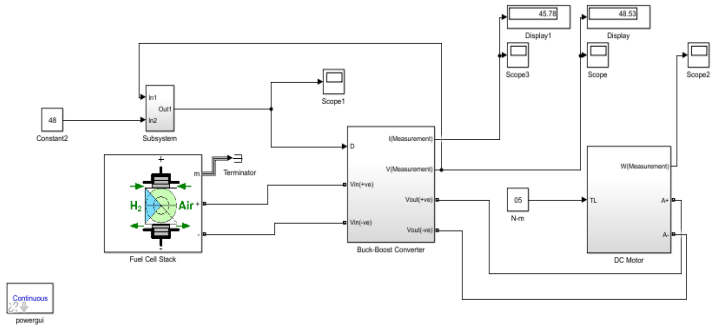

Fig. 24. Output obtained by using FLC

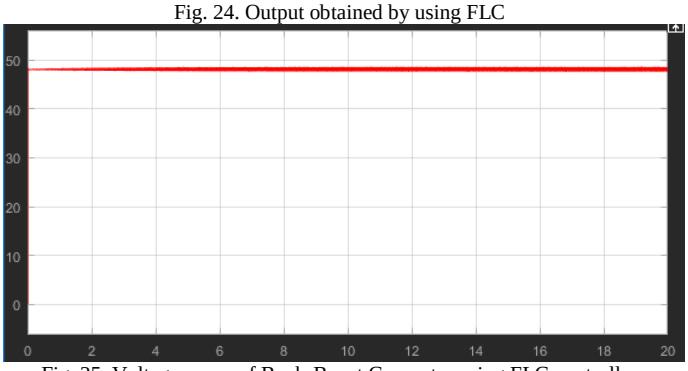

Fig. 25. Voltage curve of Buck-Boost Converter using FLC controller

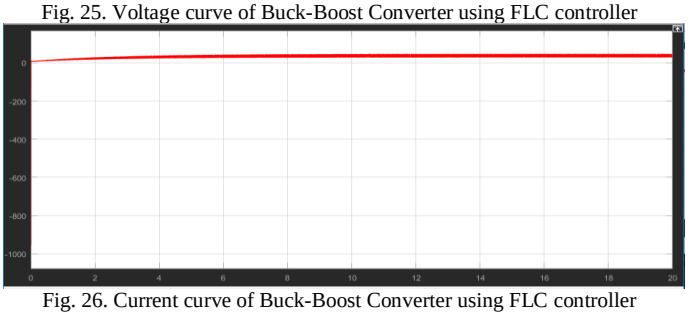

Fig. 26. Current curve of Buck-Boost Converter using FLC controller

Fig. 27 shows the output speed curve of the DC motor using FLC controller which is completely smooth with no spikes.

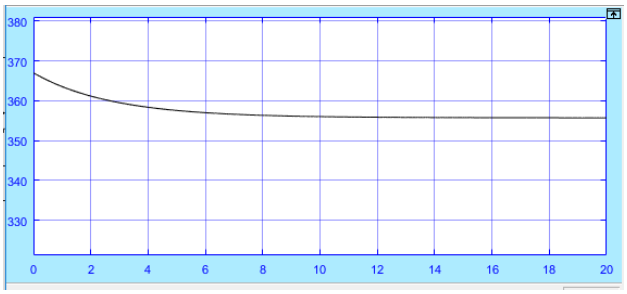

Fig. 27. Output Speed Curve of DC motor using FLC Controller

VI. Comparative Performance Analysis of DC Motored Powered by Fuel Cell and Solar PV

If solar PV is used instead of fuel cell, the performance of DC motor will be reduced to some extent. This can be observed by comparing the speed characteristic curves of both designs using PID controller. The output curves using solar PV power are shown in Fig. 28 and Fig. 29. It can be observed that the output of motor's speed is stable due to the use of PID controller but there are still a few spikes at. Hence, it is concluded that the motor will have steadier operation when powered using fuel cell compared PV cell.

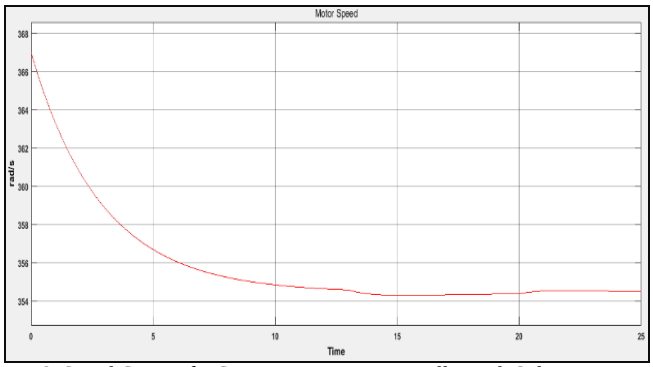

Fig. 28. Speed Curve of DC motor using PID controller with Solar PV as Power Source (System response of variable irradiance) [4]

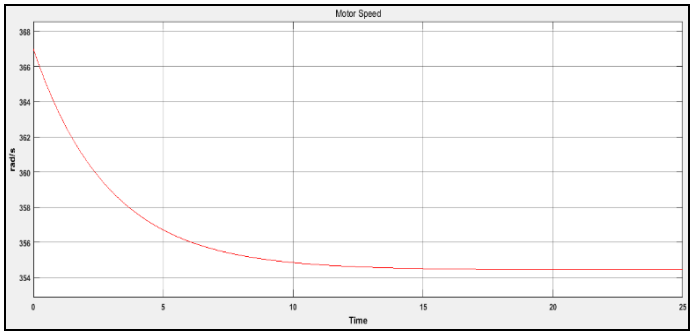

Fig. 29. Speed Curve of DC motor using PID controller with Solar PV as Power Source (System response of variable temperature) [4]

VII. Summary

In this paper, fuel cell powered DC motor system has been designed. For efficient output, converters and controllers have been used. Different controllers were used to compare and obtain the best result. It is finally observed that using PID controller yields the best output curves. PID always provides better results than FLC in such cases where uncertainty of characteristics (Current & Voltage) is bounded. Lastly, a comparison of using two different renewable sources is presented. It is concluded that fuel cell powered DC motors are more preferable in terms of efficiency and performance. Table. 1 presents a summary of the results obtained using all four controllers.

TABLE I. Summary of Output Range for Four Controller

Controller	Voltage (volts)	Current (Amps)	Speed(rad/s)
Differential	48-35.84	0-1.7*10^{-3}	275-367
PI	47-48	0-40	355-367
PID	48	0-40	354.5-367
FLC	48.53	0-45.78	357-367

VIII. Future Scope

In the proposed model, some changes can be brought for better performance. An ideal speed characteristics curve of DC motor can be obtained by continuously tuning different controllers. Adaptive neuro fuzzy inference system or fuzzy-PID can be used instead of PID or fuzzy logic controller for future research. Instead of buck boost converter, CUK converter or H-bridge buck boost converter can be used for swifter switching. Moreover, instead of DC motor, servo motor can be implemented.

IX. Conclusion

Fuel cells are increasingly becoming involved in vehicular, portable and stationary power generation systems [5]. Operating fuel cells in optimized conditions is very important in order to achieve optimum efficiency. In the design presented in this paper, a DC motor is provided power via a fuel cell. Optimizing the power efficiency is the main concern intention. By utilizing different converters, different optimization results have been analysed. PID controllers yielded the best output among all the controllers. The output of DC motor by using PID controller powered by solar PV is extracted from another research paper and compared with the outputs obtained in this paper using fuel cell. A DC motor is a machine with many applications therefore it is crucial to design systems of operation that are both sustainable and efficient and this paper presents exactly that. Overall, using a fuel cell has proven to be advantageous in terms of performance and sustainability. Future applications of this design in the field of electric vehicle which gained wide popularity because of the problem of increases in prices of fossil fuels in addition to lessening of this fuel [6]. The only

constraint is the expense of such systems but with the vast ongoing research in this field, this may be overcome as well.

REFERENCES

[1] "Types of Fuel Cell', Available: https://www.energy.gov/eere/fuelcells/types-fuel-cells (Accessed on: 28 February 2019).

[2] "Comparison of fuel cell technologies", Available: https://www.energy.gov/eere/fuelcells/ comparison-fuel-cell-technologies (Accessed on: 22 February 2019).

[3] "Fuel Cell Stack", Available: https://www.mathworks.com/help/physmod/sps/powersys/ref/ fuelcellstack.html (Accessed on: 22 February 2019).

[4] M.N..M. Haque, S.C. Sarker, M. Naeem-Ur-Rahman, M.S. Miah , I.Ahammad , M.A. Islam, "Design and Simulation of a Forcible Buck-Boost Controlling Solar Powered DC Motor," 2017 International Conference on Power, Control, Signals and Instrumentation Engineering (ICPCSI-2017).

[5] [5] S. Njoya, O. Tremblay, and L.A. Dessaint, "A Generic Fuel Cell Model for the Simulation of Fuel Cell Power Systems," Power & Energy Society General Meeting, 2009. PES '09. IEEE.

[6] Alnaib, Ahmed & Sultan, Nashwan & Mahmood, Omar, "Design a Fuel cell based drive DC motor for an electric vehicle applications," International Journal of Engineering & Technology, 7 (4) (2018) 2081-2087.

[7] O. Atlam and M.Kolhe, " Performance Analysis of PEM fuel cell with Varying Oxidant Supply rates', Journal of Energy Engineering, Vol 139, pp 60-63, 2013.

[8] J. Ejury, "Buck converter design," Infineon Technologies North America (TFNA) Corn Desion Note, vol. 1, 2013.

[9] D.C Hamill, et al, "Modeling of chaotic DC-DC converters by iterated non-linear mappings", IEEE transections on Power Electronics, vol 7, pp 25-36, 1992.

[10] GENCELL, Available: https://www.gencellenergy.com/news/comparing-fuel-cell-technologies/ (Accessed on: 30th April 2019)

[11] Smitha A B, Sachin C N Shetty, Bianca Baby, "PID controller Tuning and its case study", International Journal of Research in applied science & Engineering Technology (IJRASET), Volume 4 Issue VI, June 2016, ISSN: 2321-9653

[12] E. E. El-kholy, A. M. Dabroom , and Adel El-kholy, "PRINCIPLES OF FUZZY LOGIC CONTROLLERS FOR DC MOTOR DRIVES - PART 1", Available: https://www.researchgate.net/publication/228872642

[13] Essam Natsheh and Khalid A. Buragga, "Comparison between Conventional and Fuzzy Logic PID Controllers for Controlling DC Motors", IJCSI International Journal of Computer Science Issues, Vol. 7, Issue 5, September 2010.

Proceedings of the Fourth International Conference on Communication and Electronics Systems (ICCES 2019)
IEEE Conference Record # 45898; IEEE Xplore ISBN: 978-1-7281-1261-9

A Cloud Resource Scheduling Framework for big data stream and analytics in Cloud Environment

K. Manivannane
PG and Research Department of Computer Science
A.V.V.M Sri Pushpam College (Autonomous)
Poondi,Thanjavur, India

Dr. M. Chidambaram
PG and Research Department of Computer Science
Rajah Serfoji Govt. College (Autonomous)
Thanjavur, India

***Abstract*— The volume of data entering into cloud is rapidly increasing; therefore, on-demand cloud services should be provided to clients at any time, whereas providers must be able to preserve system availability as well as process a large volume of data. It is obligatory for cloud service providers to lessen large volumes of data; thereby they can reduce costs for maintaining large storage systems. Infrastructure level performance is an important problem which directly affects the overall working of cloud computing environment. The objective of our framework is enhancing the performance of cloud infrastructure. Our approach demonstrates high effective in cloud performance enhancement, as it displays enhancement in both the service providers as well as for cloud users.**

Keywords— Resource allocation; Cloud Computing; Fuzzy Scheduling; Hadoop

I. INTRODUCTION

Security issues and privacy are the main threats that threatens the field of cloud computing. This is due to the nature of multi-tenancy and the subcontracting infrastructures that are the reasons for the cloud computing challenges. Cloud computing are widely accepted in many fields, which includes several education institution, business organization and many other enterprise organization. Security is the main concern in the field of cloud services for the reliable and secured connection that helps the vendor with their computational needs and their business needs. Several malicious activities such as unusual software and application from the illegal users where they try to have an access with the confidential data that are typically used by the cloud handlers. Virtual environment is promoted in the cloud computing field. Important technologies that deal with the virtualization, networks, memory management, transaction management, load balancing, resource scheduling, operating system and finally the concurrency control face the security issues. These capacities deal with the security and hence special attention is required. Cyber-attacks are possible when necessary security frameworks and measures are not taken. A single malware could provide a pathway to several other attacks. Replication of confidential information could be done by these cyber-attacks. These challenges should necessarily be taken care in the industries and the academia. The storage enterprise that promotes the cloud services could be anonymous and several confidential data could be connected with the identical data that could lack in trust of an organization. Several linking attacks and identity theft could be overcome with the identity information technique known as the Anonymization. Further, the problem that arises due to the identity information and authentication should be necessarily addresses. Effective resource management can also benefit from authentication at least at its conceptual level. In cloud the amount of information is stored in the form of storage and computation.

II. CLOUD METRICS

In order to enhance cloud services, metrics must be taken into account since a metric delivers information about features of a cloud property by its parameters namely, unit, rules and expression and the values emerging from the observation of the property. For example, to estimate a particular response time property from one client to another, we can consider the customer response time metric employed in a cloud email service search feature. By considering the customer response time metric, we can drive indispensable information which can employed for verification of observations as well as analyzing the results.

Metrics for cloud computing services can be described employing the Cloud Service Metric model which states higher level perceptions about the abstract metric definitions employed for a precise cloud service property which maybe a service uptime. Definitions for abstract metrics contain parameters and rules to direct a formal understanding the property of interest. The CSM model entails concrete metric definitions that are based on abstract metric definitions.

Nevertheless cloud metrology has to be understood in a proper way. Frequent terminologies namely, definition of measurement, metric or groups of measurement artifacts, consists of have numerous definitions, these myriad terminologies becomes tedious for the cloud service customer to associate services or depend on third party tools to observe the health of the service. And cloud provider should be to analyze service whether it's operating correctly or to permit its service to arrive into an intricate cloud service federation. International organizations should construct a group of metrics which should be reliable, shareable and trustworthy .By defining the metrics; it not only increases the support of the decision-making process but enhances different phases of the cloud service lifecycle.

Cloud computing is regarded as a competent data management [15] which employs k-median clustering for managing data. Even though cloud computing entails high profitable technology for business value, it lacks certain security features. Hence it is obligatory to ensure that data and infrastructural resources in cloud are scheduled and data deduplication is carried out in an efficient way. Current frameworks have limitations and may not be resolving certain drawbacks encountered in cloud [16].

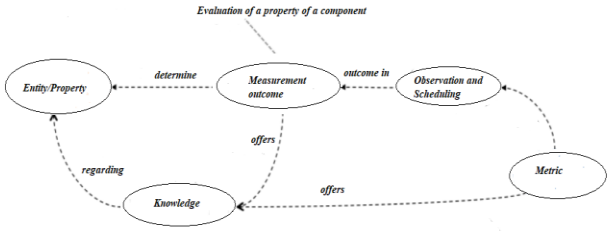

Fig. 1. Cloud Metrics

The volume of data entering into cloud is rapidly increasing; therefore, on-demand cloud services should be provided to clients at any time, whereas providers must be able to preserve system availability as well as process a large volume of data. It is obligatory for cloud service providers to lessen large volumes of data; thereby they can reduce costs for maintaining large storage systems. Cloud storage employs data deduplication technique to enhance performance of cloud storage. The technique of data deduplication employed for enhancement of efficiency in storage. In a normal deduplication system, duplicated data recognize as well as collect a single copy of data in storage. Generations of logical pointers are employed for supplementary replicas as a replacement for storing redundant data. The main advantage of employing deduplication is that it reduces storage space and network bandwidth. The drawback of employing this technique is that it will take a toll on system tolerance since files denote to the identical chunk of data, if it turns out to be unobtainable due to failure which will in turn lessen reliability. The static scheme is said to be a drawback that cannot grasp with the user's changing behavior and duplication of storage in the cloud services, which sufficiently requires a dynamic scheme that adapts several access patterns and the changing behavior.

A. Dependability Issues

In order to lessen storage space in cloud, we can employ data deduplication technique. This can be done by employing hash functions i.e. values to associate chunks of data with redundant data, thereby saving single copy and logical pointers to additional copies are created [17]. By employing deduplication technique, the following advantages are achieved:

- Amount of data residing in disk space is reduced
- Energy consumed by storage systems will be reduced.
- In cloud disaster recovery, deduplication plays a vital role by replicating data speeding up replication time and bandwidth cost savings.
- Data deduplication reduces physical capacity and network traffic which acts as a backup storage in clouds.

Important performance metrics which is obligatory to follow: overall data transmitted, service downtime and total migration time. Deduplication can overcome extensive downtime which leads to service failure. In virtual machines images, deduplication is employed to lessen storage of dynamic data. Balancing the trade-offs between storage space and performance plays an important factor in deduplication technique. Data chunks are required in groups while performing deduplication. Data chunks are assigned in the form of group of various files. Redundancy of data chunks are not required by the conventional deduplication methods. This reduces the reliability by eliminating certain data chunks from the storage system resulting in the loss of important files.

III. PROPOSED FRAMEWORK

Infrastructure level performance is an important problem which directly affects the overall working of cloud computing environment. The objective of our framework is enhancing the performance of cloud infrastructure. The cloud infrastructure deals with several nodes which eventually lead to queueing of systems, where huge amount of servers displays inconsistency in terms of processing arrival and service time. Considering the potentially high number of servers in a cloud system, we propose a fuzzy scheduling algorithm which is efficient and easy-to-implement solution. The proposed framework is integration of a fuzzy scheduling scheme to enhance infrastructure performance of cloud. Our approach demonstrates high effective in cloud performance enhancement, as it displays enhancement in both the service providers as well as for cloud users. By distributing resources as per business strategies and availability will benefit cloud service providers, at the same time enhancing services for cloud users. In nutshell, our proposed framework consists of following stages: Monitoring the data usage pattern and then cloud service provider allocating priority by cloud service provider according to our proposed fuzzy scheduling algorithm which in turn enhances infrastructure performance.

A. Fuzzy scheduling algorithm

The selection of parameters plays a vital role in providing effective scheduling. Considering real time tasks, three main scheduling parameters; computation time, arrival time, deadline and single output where the single output computes the order of task execution. In fuzzy scheduling system, these scheduling parameters are included with real-time tasks. The computation time is determined in terms of response time and utilization. S is said to be the fuzzy set of defined membership function on the universe of discourse P that is represented as a curve, which acts on every point of element of D in the space of input is diagrammed to a membership value amongst 0 and 1. The universe of disclosure is denoted as,

$$\mu_S: D \rightarrow [0, 1] \qquad (1)$$

Where value μ_S, denotes the membership that defines the membership grade of the element D in fuzzy set S. The various types of memberships are trapezoidal MF, Gaussian MF. We employ triangular MF because it is widely used in real-time implementations and effective computation.

$$\mu_D(d) = \begin{cases} 0, & d \leq n \\ \frac{d-n}{w-n}, & n < d \leq w \\ \frac{q-d}{q-w}, & w < d < q \\ 0, & d \geq q \end{cases} \quad (2)$$

Here, these three parameters {n, w, q} where n<w<q defines the triangle membership. The d coordinates of the underlying triangular MF in figure 2 were determined by n, w and q. In Fig. 2, the y axis signifies degrees of membership in the [0, 1] interval while x axis signifies the universe of discourse.

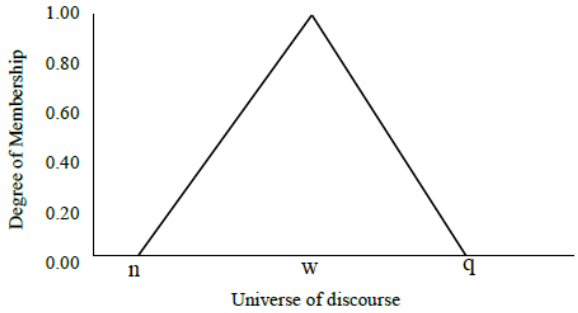

Fig. 2. Fuzzy inference model

Fig. 2 presents fuzzy inference model which consists of three main scheduling parameters, namely, computation time, arrival time, deadline and single output.

B. *Defining the Inputs/Output Membership Function*

The input parameters of the fuzzy along with their linguistic groups, namely, medium, long and short employed for arrival time, computation time and limit of the real-time tasks. Each and every task is allocated with the linguistic category for each parameter. The membership function distributions signifying the linguistic notion for fuzzy inputs and runtime priority were distinct. The fuzzy input parameters were defined by employing triangular membership functions as described as:

1) Arrival time:

TABLE I. REPRESENTS LINGUISTIC CATEGORIES DEFINED FOR THE ARRIVAL TIME OF ALL TASKS

Fuzzy Categories	Crisp input range
Early	0-5
Intermediate	0-10
Late	5-10

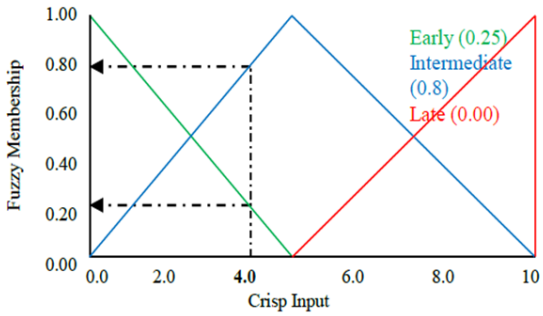

Fig. 3. Membership Function for Arrival Time

2) Computation Time:

TABLE II. REPRESENTS LINGUISTIC CATEGORIES DEFINED FOR THE COMPUTATION TIME OF ALL TASKS

Fuzzy Categories	Crisp input range
Short	1-10
Medium	1-20
Long	10-20

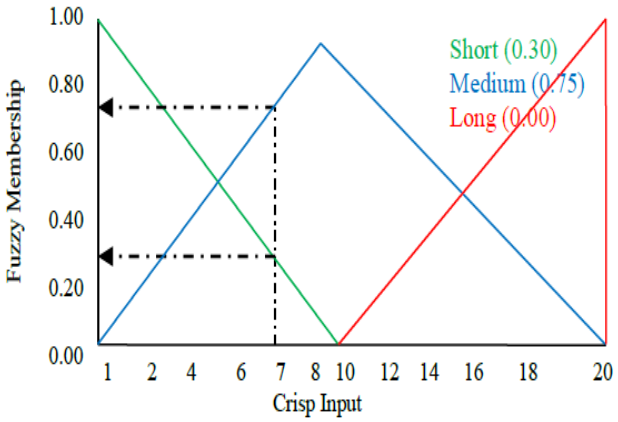

Fig. 4. Membership Function for Computation Time

3) Deadline:

TABLE III. REPRESENTS LINGUISTIC CATEGORIES DEFINED FOR THE DEADLINE OF ALL TASKS

Fuzzy Categories	Crisp input range
Critical	1-25
Normal	1-50
Sufficient	25-50

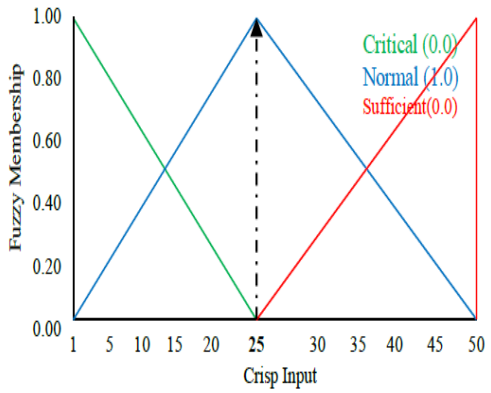

Fig. 5. Membership function for deadline of all tasks

4) Set-up Fuzzy Rule Base:

The set-up a fuzzy rule base on the foundation of the number of linguistic categories defined for each of the input parameter. Let q, w, n represent the number of linguistic categories defined for computation time, arrival time and deadline, then the fuzzy rule base will have 27 rules i.e. (3 × 3 × 3) rules of fuzzy logic.

TABLE IV: FUZZY RULES

S.No.	Arrival Time	Computation Time	Deadline
i.	Early	Short	Critical
ii.	Intermediate	Short	Sufficient
iii.	Late	Short	Critical
iv.	Early	Medium	Critical
v.	Late	Long	Sufficient

These fuzzy rules which have been created are attached with a standard fuzzy union in order to cumulate the membership functions of the three parameters attached with each task. Hence, we obtain 29 a crisp output value for each task. The crisp output value acts as a runtime priority for task allocation by virtual machines. When we apply these inputs with the membership function, we obtain the following values:

i. The crisp input for arrival time = 5.0,

The corresponding fuzzy outputs with membership values are; Early: 0.45 Intermediate: 0.56 Late: 0.78

ii. The crisp input Computation time =7.0,

The corresponding fuzzy outputs with membership values are;

Short: 0.30

Medium: 0.75

Long: 0.00

iii. When crisp input Deadline =25.0,

The corresponding fuzzy outputs with membership values are;

Critical: 0.00

Normal: 1.00

Sufficient: 0.00

The results generated only four from these rules:

i. If Arrival time is Early (5.0) AND Computation time is Short (0.45) AND Deadline is Normal (78.00), THEN Runtime priority is High.

ii. If Arrival time is Early (0.25) AND Computation time is Medium (0.75) AND Deadline is Normal (1.00), THEN Runtime priority is Normal.

iii. If Arrival time is Intermediate (0.8) AND Computation time is Short (0.30) AND Deadline is Normal (1.00), THEN Runtime priority is High.

iv. If Arrival time is Intermediate (0.80) AND Computation time is Medium (0.75) AND Deadline is Normal (1.00), THEN Runtime priority is Normal.

IV. EXPERIMENTAL RESULTS

We employed Java based toolkits, namely, CloudSim and HDFS Simulator that has the difference purposes for simulation. We employed CloudSim for testing the proposed allocation algorithm and simulating of cloud computing environments and infrastructure while HDFS simulator employed for replication. The evaluation of the proposed framework takes place through simulating cloud in terms of a performance and availability. The following components were created:

- The Namenode acts as metadata server.
- Datanodes which acts as file servers in XML format residing in the Namenode which stores instances of copies.

Various sizes of files employed are: 100 KB, 150 KB, 200 KB, 300 KB, 500 KB, 800, 1 MB, 2 MB, 250KB. Ten file are uploaded employing single data dedupilcators. We were able to reduce to 85.75% and 94.20% of the processing time taken by one data deduplicator. As the number of files increases, we created four deduplicators which lessen the processing time.

TABLE V : REPRESENTS LINGUISTIC CATEGORIES DEFINED FOR THE ARRIVAL TIME OF ALL TASKS

Fuzzy Categories	Five (upload)	Ten (upload)	Five (update)	Ten (update)
10	86.75	91.87	43.78	76.13
100	93.20	96.65	63.79	75.34
1000	91.30	95.58	64.78	83.90
10000	60.10	80.71	76.25	96.17

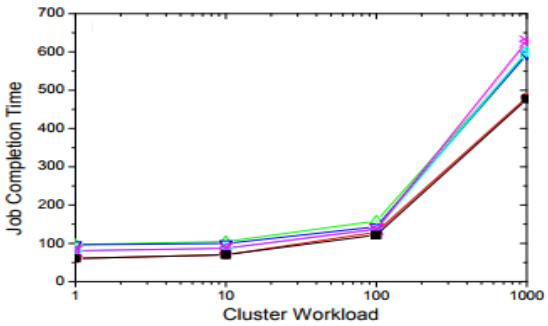

Fig. 6. Evaluation based on job completion time, where brown line signifies that the proposed algorithm completes faster

In order to evaluate the proposed algorithm, we compared with four task scheduling algorithms, namely, MaxCover-BalAssign(MB), Hadoop Default Scheduler(HDS), Delay Scheduling(DS). It is evident that the proposed scheduling has faster job completion time. It was detected that the response time varies when the system load, this proved that the proposed algorithm have better performance at higher system load..

V. CONCLUSION AND FUTURE WORK

The cloud infrastructure deals with several nodes which eventually lead to queueing of systems, where huge amount of servers displays inconsistency in terms of processing arrival and service time. Considering the potentially high number of servers in a cloud system, we propose a fuzzy scheduling algorithm which is efficient and easy-to-implement solution. The proposed framework is integration of a fuzzy scheduling scheme technique to enhance infrastructure performance of cloud. The technique of data deduplication employed for enhancement of efficiency in storage will be conferred in future work.

References

[1] I. Raicu, I. Foster, Y. Zhao. “Many-Task Computing for Grids and Supercomputers”, Invited Paper, IEEE MTAGS 2008.

[2] J. Dean and S. Ghemawat. MapReduce: simplified data processing on large clusters. In Proceedings of the 6th USENIX Symposium on Operating Systems Design and Implementation (OSDI), pages 137–150, 2004.

[3] M. Isard, M. Budiu, Y. Yu, A. Birrell, and D. Fetterly. Dryad: distributed data-parallel programs fromsequential building blocks. In Proceedings of the 2ndEuropean Conference on Coputer Systems (EuroSys), 2007.

[4] Apache Hadoop. http://hadoop.apache.org.

[5] Udendhran R, A Hybrid Approach to Enhance Data Security in Cloud Storage, ICC '17 Proceedings of the Second International Conference on Internet of things and Cloud Computing at Cambridge University, United Kingdom — March 22 - 23, 2017, ISBN: 978-1-4503-4774-7 doi>10.1145/3018

[6] Suresh, A., Udendhran, R., Balamurgan, M. et al. "A Novel Internet of Things Framework Integrated with Real Time Monitoring for Intelligent Healthcare Environment "Springer-Journal of Medical System (2019) 43: 165. https://doi.org/10.1007/s10916-019-1302-9

[7] Suresh, A., Udendhran, R. & Balamurgan, M. " Hybridized neural network and decision tree based classifier for prognostic decision making in breast cancers " Springer - Journal of Soft Computing (2019). https://doi.org/10.1007/s00500-019-04066-4

[8] K. Liu, H. Jin, J. Chen, X. Liu, D. Yuan, Y. Yang, A Compromised-Time-Cost Scheduling Algorithm in SwinDeWC for Instance-Intensive Cost-Constrained Workflows on a Cloud Computing Platform, Int. J. High Perform. Comput.Appl.

[9] K. Kaur, A. Chhabra, G. Singh, Heuristics based genetic algorithm for scheduling static tasks in homogeneousparallel system, Int. J. of Comp. Sci. and Sec.

[10] J. Kolodziej, F. Xhafa, Enhancing the genetic-based scheduling in computational grids by a structured hierarchical.

[11] P. Sempolinski, D. Thain, A Comparison and Critique of Eucalyptus, OpenNebula and Nimbus, in: Proceedings of the 2010 IEEE Second International Conference on Cloud Computing Technology and Science, CLOUDCOM ’10, IEEE Computer Society, Washington, DC, USA, ISBN 978-0-7695-4302-4, 417–426, doi: 10.1109/CloudCom.2010.42, URLhttp://dx.doi.org/10.1109/CloudCom.2010.42, 2010.population, Future Generation Computer Systems 27 (8) (2011) 1035–1046, ISSN 0167-739X, doi:10.1016/j.future.2011.04.011, URL http://dx.doi.org/10.1016/j.future.2011.04.011.

[12] B. Palanisamy, A. Singh, L. Liu, and B. Jain. Purlieus: locality-aware resource allocation for MapReduce in a cloud. In Proceedings of 2011 International Conference for High Performance Computing, Networking, Storage and Analysis (SC), 2011.

[13] J. Dean and S. Ghemawat, “Mapreduce: Simplified data processing on large clusters,” ACM Commun., vol. 51, Jan. 2008, pp. 107-113.

[14] M. Zaharia, D. Borthakur, J. Sen Sarma, K. Elmeleegy, S. Shenker, and I. Stoica. Delay scheduling: a simple technique for achieving locality and fairness in cluster scheduling. In Proceedings of the 5th European Conference on Computer systems (EuroSys), 2010.

[15] https://issues.apache.org/jira/browse/HIVE-396.

[16] S. L. Faraz Ahmad and T. V. Mithuna Thottethodi. MapReduce with communication overlap (marco). http://docs.lib.purdue.edu/cgi/viewcontent. cgi?article=1412&context=ecetr, 2007.

Proceedings of the Fourth International Conference on Communication and Electronics Systems (ICCES 2019)
IEEE Conference Record # 45898; IEEE Xplore ISBN: 978-1-7281-1261-9

Secondary User As An Opportunistic Relay Based Path Selection Network Using Fuzzy Logic In Cognitive Radio Network

Vasundhara, Avtar singh buttar- vasundharamimit@gmail.com, danshavtar@rediffmail.com

***Abstract*- Wireless spectrum is not properly utilized so for efficient usuage of the spectrum band and for mitigating the issue of spectrum scarcity cognitive radio network came into existence.For boosting the cooperative communication among the users cooperative relay network come into the picture.In that direct ,opportunistic relay based and partial relay based communication came into the picture.Here secondary user act as a relay for forwarding the information from source to destination.Two paths are taken one is direct path and the other one is indirect path .on the basis of some parameters like Throughput,distance between the nodes,degree of competence,power allocation best path should be choosen among the different paths.This all done through a fuzzy logic design and relay based algorithm is also usedfor taking the fuzzy decision**

Keywords—Cognitive radio network(CRN),relay based algorithm,parametrs based decision using fuzzy inference system(FIS).

I. INTRODUCTION

A smart wireless communication system which is well aware about its environment is none other than cognitive radio .According to the environment ,it changes its parameter like frequency range,modulation mode,and power at the transmitter etc.There are 4 functions of Cognitive radio

1.Spectrum sensing
2.Spectrum decision
3.Spectrum sharing
4.Spectrum mobility

Proper spectrum utilization is always a major concern in the wireless field .So for enhancing the spectrum utilization ,cooperative communication is now a days a hot topic for the wireless researchers .In earlier works of cooperative communication includes cooperative diversity on maximum ratio combining technique ,no. of cooperative protocols used at relay node like Amplitude &forward(AF) ,Decode and forward(DF) etc [1].To remove the noise at the intermediate stages DF protocol used .Cooperative communication used through the no. of relay node and we have to choose the best relay node out of them based on some parameters like throughput ,distance ,power and channel allocation [2].so by implementing the cooperative communication enhancing the SNR and also increase the efficiency of the system comparing the previous systems.study of basically three channels as Relay channel ,Direct channel ,Dual hop channel .when the spectrum range is present at all the cooperative nodes which are basically the relay nodes then the channel is called as a relay channel because it provides end to end communication also.if spectrum range is present at the source and destination node but absent at the relay then is known as a direct channel as here directly acheived end to end communication.if one spectrum range is present at the source and relay and one at the relay and destination node then it is known as a dual hop channel.

II. RELATED WORKS

Formulation of different power distribution schemes with the help of both Direct and relayed transmissions for the cognitive radio network [3]. Analysis of BER under Decode and Forward cognitive radio networks in the case of underlay. Cooperative relay channel are used to facilitate the end to end throughput in terms of Bandwidth and power parameters [4]. Using outdated channel state information(CSI),we visualize the secondary systems performance based upon a regression model.Consideration of the hybrid underlay and overlay model so that throughput of the primary users (PU's) increase by the use of idle Secondary users (SU's) as a relays. Here focusing that using relay selection scheme,cooperative network performance should be increased .from that point ,interest towards relay is going to a higher extent[5].

III.SYSTEM MODEL AND PROBLEM FORMULATION

Consider a base network having a primary transmitter and a primary receiver and a direct link is formed between a primary transmitter and a primary receiver and a no. of secondary users which behaves as a relay node for forwarding a signal data from the primary transmitter to primary receiver[6].From all the relay node ,choose the best relay node based on distance ,throughput etc.Various relay/cooperative protocols used in it like AF and DF[7].Considering the parameter of distance from transmitter to relay and from relay to receiver like in the diagram.

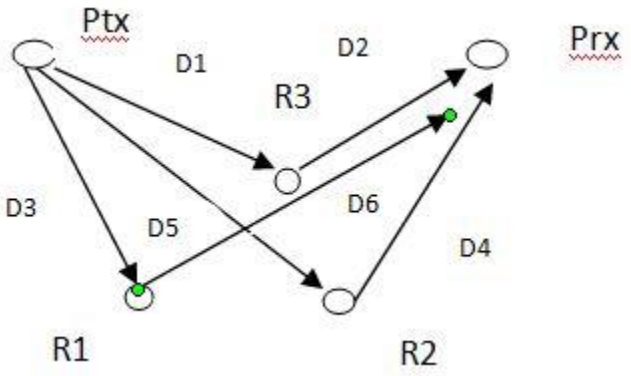

Fig1.Relay Model

Three distance path is considered
1.D1 D2[Ptx-R3-Prx]
2.D3 D6[Ptx-R1-Prx]
3.D5 D6[Ptx-R2-Prx]

Based on the reliable distance values from the receiver link that distance values would be considered using one of the fuzzy input .first of all a base network is designed in which all the three secondary users are shown which act as a relay .Three relays are there ,based on some parameters relay worked. Different distance are taken from Source to destination via relay. Decision are made based upon the different values of distance[8].

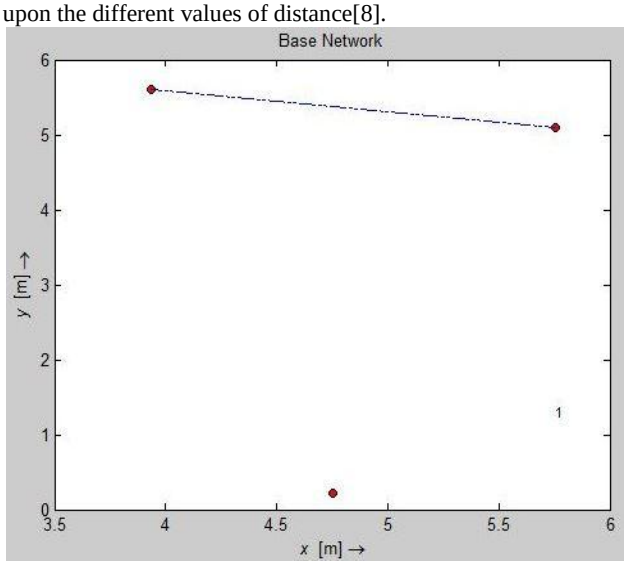

Fig2 is the base network consisting of the nodes location

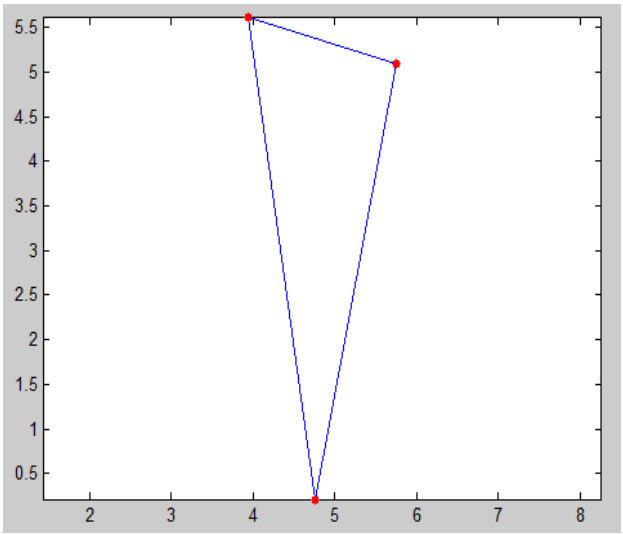

Fig3 is calculating the distance between the nodes

F ig2 shows the three secondary nodes ,it is the base network and fig3 shows the distance from the secondary nodes to each other[12].Now this distance parameter and degree of relevance which actually defines the strength of each rule are the two inputs in the fuzzy through fuzzy inference system(FIS) as shown below.

1. **SNR for direct path transmission as** [16]

$$\alpha_{s\text{-}D} = \frac{|h_{s\text{-}D}|}{N_D} \quad (1)$$

SNR for Ist hop for jth relay $SNR_{s\text{-}rj}$ and is

$$\alpha_{s\text{-}rj} = \frac{|h_{s\text{-}rj}|}{N_{rj}} \quad (2)$$

The decoded message /signal is forwarded to destination in 2nd hop.SNR at 2nd hop for jth relay is

$$\alpha_{rj\text{-}d} = \frac{\beta |h_{s\text{-}rj}|^2 |h_{rj\text{-}D}|^2}{N_{rj}(\beta^2 |h_{s\text{-}rj}|^2 + 1)} \quad (3)$$

SNR for Direct path is calculated that is from the source to the destination.Direct path SNR is then compared with the relayed path SNR value and on the basis of that best relay is selected.

β is the container of the decoded message .For ultimate relay selection ,the minimum SNR out of the two hop is used.

$$\alpha_i = \min(SNR_{s\text{-}rj}, SNR_{rj\text{-}d}) \quad (4)$$

2. **Relay selection with channel allocation** :As the cognitive radio source (CRS) don't have an initial knowledge that which relay is best one so depending on the channel allocation $CRR_{j(1\ N)}$-CRD links the best CRR(cognitive radio relay) is choosen .

$$R_{max}^{best\ CRR} = \max_{1 \le m \le N} |h_{rm}^{b}\, d|^2 \quad (5)$$

Where $R_{max}^{best\ CRR}$ designated as index of the selected best CRR.best CRRis selected from N relay (CRR's) and channel allocation is performed with this best CRR.basically there are 4 mode for channel allocation as:

Mode 1: Direct transmission from the source to the destination.

Mode 2: Dual-hop transmission from the source to the relay.

Mode3:Dual-hop transmission from the relay to the destination.

Mode 4: Relay diversity transmission by using all threelinks with cooperative relay protocols

3. **Power allocation:**Estimate which secondary node acquire more power allocated .Suppose ,a Node A having power

P1,and a Node B having power P2,so maximum power is formulated as

$$\max_{P1,P2} P_a(P1,P2) \qquad (6)$$

4.Interference power constraint :Interference power threshold is used with the objective to minimize the power consumption and channel estimation load. It is defined as interference temperature also denoted by T_c.

$$T_c = \frac{P_i(f_c,b_c)}{k * b_c} \qquad (7)$$

where k is the boltzman constant $=1.38*10^{-23}$ m^2 kg $s^{-2}k^{-1}$

In the next section consisting these 4 parameters as fuzzy parameters based on fuzzy logic design.

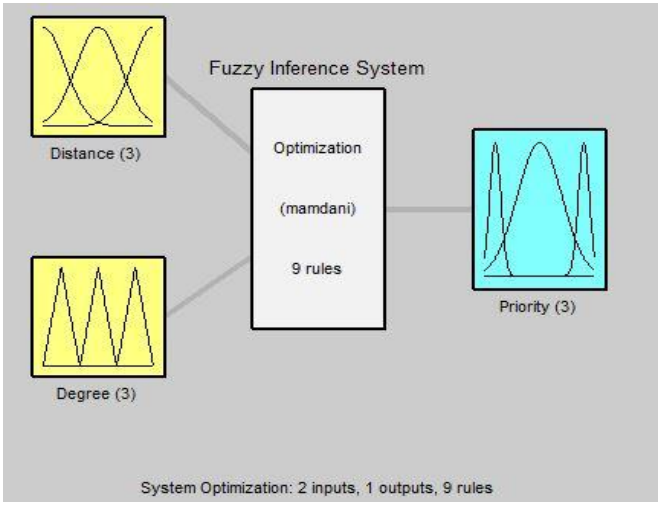

Fig4. Distance and Degree of Relevance as the two inputs in the fuzzy

Through this figure ,distance is being one of the parameter for depicting the priority at different values of distance through Fuzzy logic[13].So based on the values of distance,membership functions is designed of input 1.We formulated a Degree of Membership functions of input distance directing from low value to high ,by giving priority to the low value then to the medium value at last to the high values.

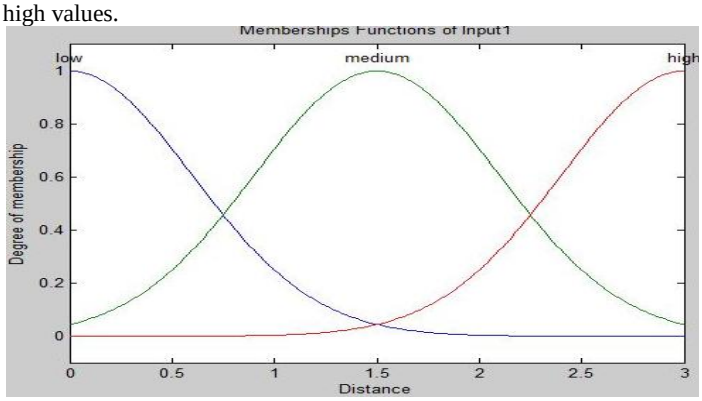

Fig5 Degree of Membership Function of Input 1

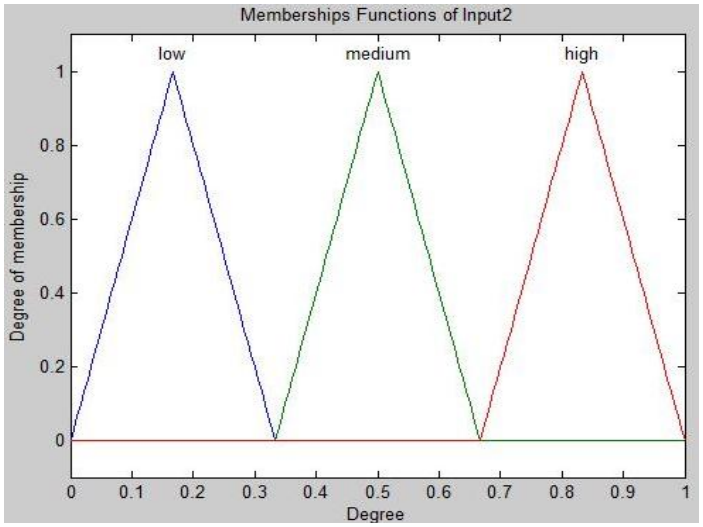

Fig6 Degree of membership function of input 2

This figure below shows the Degree of membership function basically defines a priority for the different inputs.

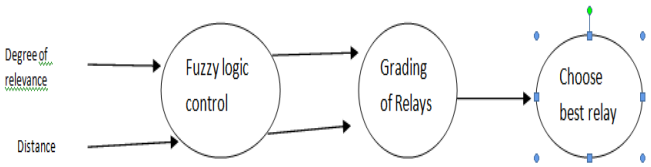

Fig7. Relay Grading Model using Fuzzy

On the basis of Fuzzy Logic Design selection of best relay is to be selected[9]. Degree of relevance and distance are the input parameter in the fuzzy logic controller on the basis of these two parameters Ranking /grading is provided to the relays and out of which best relay is selected,for this we have to use the algorithm also as stated below.

Step1.Start with k=0
Step2.Increment k=k+1
Step3.Design fuzzy parameter for the kth relay
Step4.Degree of relevance should be considered
Step5.If k=N then go to step 6 else go to step 2
Step6. Compare degree of relevance and select it having good degree of relevance.

IV.SIMULATION RESULTS

Random Deployment of nodes occur in which one is act as a source while the other one is act as a destination and rest of the nodes are the relay nodes [10].

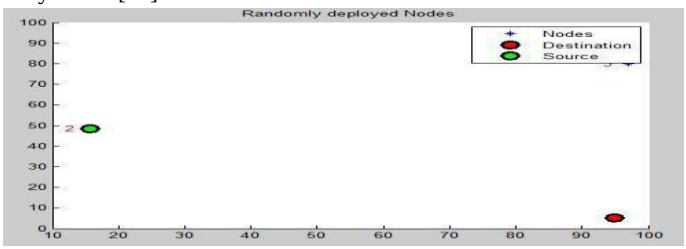

Fig 8.Random Deployment of nodes

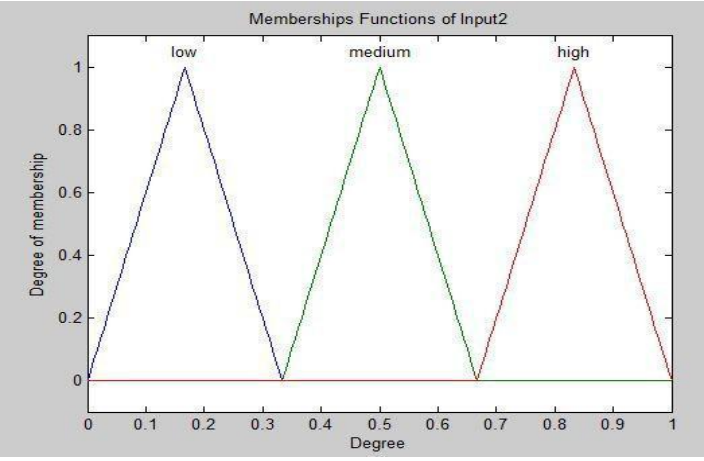

Fig 9. Degree of Membership Function of X2

This above figure shows that the Throughput is increasing with the power level by using Fuzzy logic design. This is what the end to end throughput from the source to a destination via relay. Rho is defined as the power spectral efficiency .It basically defined the spectrum efficiency of the nodes.

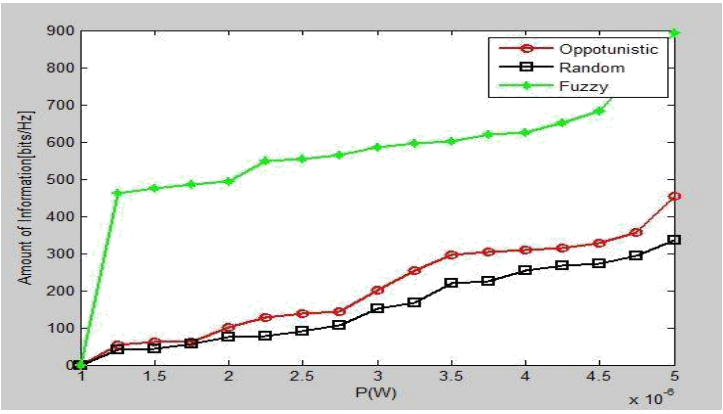

Fig 10 Amount of information bits verses power

Above figure shows that how the amount of information bits increase with power in case of fuzzy[11].Above figure shows that how the throughput is increasing with the increase of the power in case of fuzzy logic design as compared to opportunistic and random deployment of nodes. Green color line shows the amount of information bits is increasing means capacity of the relay nodes are increasing with the increase in the power level in case of using Fuzzy logic design.

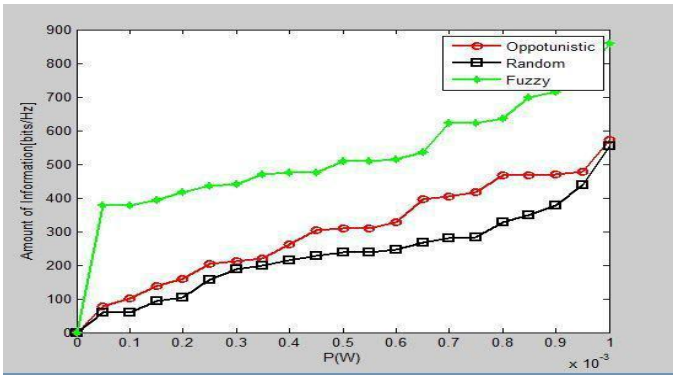

Fig 11 Steep Curve of amount of information varied with the power

This Figure depicts the Amount of information variation with the power .With the increase of power ,capacity of channel also varies linearly with the power variation.

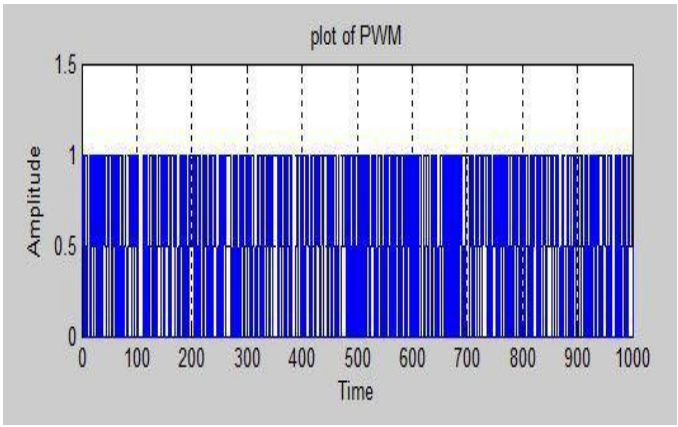

Fig 12 PWM output

This above figure depicts the PWM wave generation. This PWM wave generation basically tells about the switching mode of the application that when the relay is on and when it is off.

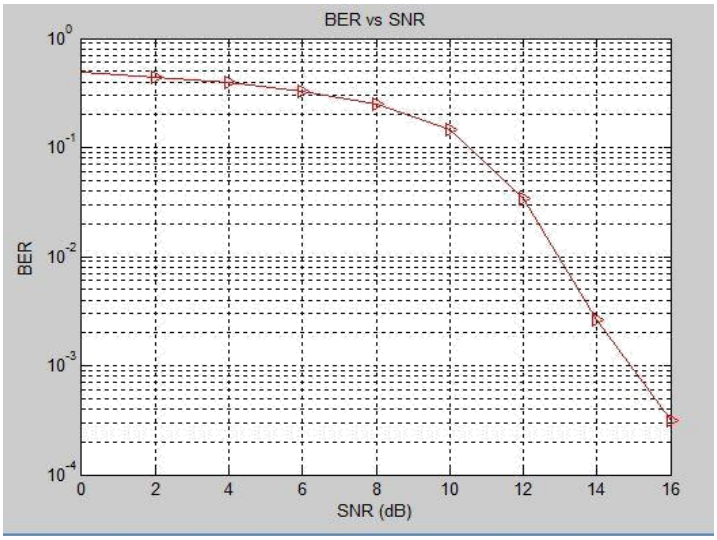

Fig 13 BER vs SNR

This figure depicts the BER verses SNR(dB).With increase in the SNR there is a decrease in the BER .Error probability decreases with the improvement in the SNR.

TABLE I. SIMULATION PARAMETERS

Parameters	Values
Source Transmit Power	1w
Relay Transmit Power	1w
Amplification Factor	Fixed
Modulation Scheme	B-PSK
Receiver Diversity	MRC
Number of Relays	5
Relaying Protocol	Amplify-and-Forward
Number of Bits	10^6
Receiver Noise	AWGN
Channel Model	Rayleigh, Nakagami, Rician

V. CONCLUSION AND FUTURE SCOPE

Simulation results that contain the Fuzzy logic based decision takes place based on some parameters Like Throughput, Amount of information bits ,Distance ,Power etc.On the basis of these parameters decision should be takes place and best relay path should be choosen among the N relay users. Meanwhile we compare the opportunistic, random and fuzzy distribution and analyze how the throughput ,amount of information bits varies in all the 3 cases. We generalize then BER vs SNR .we calculated the distance among the users. In fuzzy we built Rule set of X1 and X2 inputs and according to that labels have been assigned to the Y output. We generalize the 3D view also by analyzing the surface view structure .This surface view helps in giving the 3 D view when more than two inputs are given in the picture. For all this to occur we have taken the OFDM QPSK signal in the original and PWM (Pulse Width Modulation) signal as the input signal. We also analyze the network lifetime(LN) of the nodes which specify the increment in the nodes lifetime with the increase in power in case of random deployment of nodes[14].
In future, this work can be extended by determining the secrecy constraints parameters in proposed relay selection schemes.While Multihop with Multi user Cooperation with additional cooperation may enhance the performance of the system and Code rate is also expected to be increase[16].We can also make the secondary user as a relay in reconfigurable mode.We can also enhance the network by using multiple nodes as a relay in the network.Different channel models should be combined or collaborated in the fashion to increase the efficiency of the network.We can also implement threshold constraint on throughput parameter also[15].

V. REFERENCES

[1] M. McHenry ,D. McCloskey,and G.Lane –Roberts ,"New YorkCitySpectrumOccupancyMeasurementssep.2004,"Tech.Rep.,Dec.2004. (references)

[2] Shared spectrum occupancy ,"General survey of radio frequency bands - 30 Mhz to 3Ghz ",Tech.Rep.,Sep.2010.

[3] J. Mitola III, "Cognitive Radio: An Integrated Agent Architecture for Software Defined Radio," Ph.D. Thesis, KTH Royal Inst. Technology, Stockholm, Sweden, 2000.

[4] Mitola, J., Software Radio: WirelessA rchitecture for the 21" Centuv Mitola's STATISfaction ISBN 0-9671233-0-5) 1999.

[5] Mitola, J., Cognitive Radio - Model-based Competence for Software Radios, Licentiate Thesis (Stockholm: KTH) September 1999.

[6] &[7] J. Mitola, III, BCognitive radio,[Licentiate thesis, KTH, Royal Inst. of Technol., Stockholm, Sweden, Sep. 1999. & J. Mitola, III, BCognitive radio for flexible mobile multimedia communications,[in Proc. IEEE Mobile Multimedia Commun. Conf. (MoMuC), New York, Nov. 1999 .

[8] J. Mitola, III, Cognitive Radio Architecture. New York: Wiley, 2006.

[9] F. Fitzek and M. Katz, Cooperation in Wireless Networks. Dordrecht, The Netherlands: Springer, 2006 .

[10] Proc. IEEE Dyn. Spectrum (DySPAN) Conf. 2005 and 2007, New York.

[11] Proc. IEEE Cognitive Radio Oriented Wireless Netw. (CROWN) Conf., New York, 2007.

[12] Nan Zhao, Shuying Li, and Zhilu Wu, "Cognitive radio engine design based on ant colony optimization", Wireless Personal Communications, vol. 65, no. 1, pp. 15–24, 2011.

[13] Zhijin Zhao, Shiyu Xu, Shilian Zheng, and Junna Shang, "Cognitive radio adaptation using particle swarm optimization", Wireless Communications and Mobile Computing, vol. 9, no. 7, pp. 875–881, 2009.

[14] Amrutha.V, K.V. Karthikeyan, "Spectrum Sensing Methodologies in Cognitive Radio Networks: A Survey," IEEE International Conference on Innovations in Electrical, Electronics, Instrumentation and Media Technology ICIEEIMT 2017.

[15] M. T. Masonta, M. Mzyece, and N. Ntlatlapa, "Spectrum Decision in Cognitive Radio Networks: A Survey," IEEE Commun. Surv. Tutorials, vol. 15, no. 3, pp. 1088–1107, 2013.

[16] T. Zhang and X. Yu, "Spectrum sharing in cognitive radio using game theory–a survey," in Wireless Communications Networking and Mobile Computing (WiCOM), 2010 6th International Conference on, 2010, pp. 1 –5.

Proceedings of the Fourth International Conference on Communication and Electronics Systems (ICCES 2019)
IEEE Conference Record # 45898; IEEE Xplore ISBN: 978-1-7281-1261-9

Analysis of the Electric field of the 1200kv power transmission line using the Finite Element Method

Akibaehmad A. Arora
PG Student, Department of Electrical Engineering
Faculty of Technology & Engineering, MSU Baroda
Vadodara-Gujarat, India-390002
akibarora2907@gmail.com

Anuradha S. Deshpande
Assoc. Prof., Department of Electrical Engineering
Faculty of Technology & Engineering, MSU Baroda
Vadodara-Gujarat, India-390002
anuradhasdeshpande62@gmail.com

***Abstract*— With rapid industrial development and flourishing population, power demand is increasing rapidly. UHV power line is one of the ways to meet this increasing demand. 1200kv UHV transmission line, is India's forthcoming project to tackle this situation. Right Of Way (ROW) is one of the major concerns with transmission lines. An electric field is one parameter to define ROW. In this paper, electric field of three configurations of the 1200kv line is calculated by the Finite Element Method. FEM is used to solve partial differential equations. Calculations have been done by taking a case with the minimum ground distance of conductors of lines. Plotted results are compared with ICNIRP standards and safety limits defined. Biological effects of electric field on people, animals, and plants are also discussed.**

Keywords—Biological Effects, Electric field, Finite Element Method (FEM), International commission on non-ionizing radiation protection (ICNIRP), Right Of Way (ROW).

I. INTRODUCTION

To limit the Right Of Way with bulk amount of power transfer over long distances, countries need to incite the ultra-high voltage transmission system. Russia has 1200kv transmission line which operates at 1150kv up to few years since then it is operating at 500kv level. China has initiated the project of commissioning of 1000kv UHVAC transmission line [1].

In India major power transmission systems operates in 220kv and 400kv voltage level. To meet increasing power demand, India adopted 1200kv UHVAC transmission network which is under implementation. 1200kv test station is established at Bina, Madhya Pradesh. The first 1200kv test line is installed between Wardha to Aurangabad having length of 382km [2].

Many parameters need to be taken care with higher voltage level as its affects human beings. One of them is an electric field. ICNIRP is one of the standards which specify a limit of the electric field for occupational and general public, which helps to define ROW [3] [4].

In this paper, electric field produced due to the 1200kv transmission line is evaluated by Finite Element Method. An electric field is calculated at ground surface and above ground surface up to several meters of height. From these results right of way is defined for transmission line. Biological Effects of excess electric field on living beings, animals and plants also discussed [4] [6].

II. LINE PARAMETERS

A design specification of 1200kv transmission lines is given in table.1. In this paper, three configurations of a line have been discussed, which are single circuit horizontal configuration, single circuit delta configuration, and double circuit vertical configuration [5]. In table 1, R represents radius of bundle conductors. For evaluation of electric field bundle conductor can be represent as in single conductor with equivalent radius as given in (1).

TABLE I. LINE PARAMETERS

Description	Notation	Value	Units
Number of sub-conductors in a bundle	N	8	Nos.
Bundle Radius	R	0.60	m
Sub conductor spacing	B	0.46	m
Diameter of sub-conductor	d	4.63	cm
Conductor height above ground at a tower	H	37	m
Conductor height above ground at mid span	Hm	24.3	m
Phase spacing	S	27	m
Bundle conductor type	Bersimis/moose		

$$r_{eq} = R\left(\frac{Nr}{R}\right)^{\frac{1}{N}} = 0.518 \text{ m} \quad (1)$$

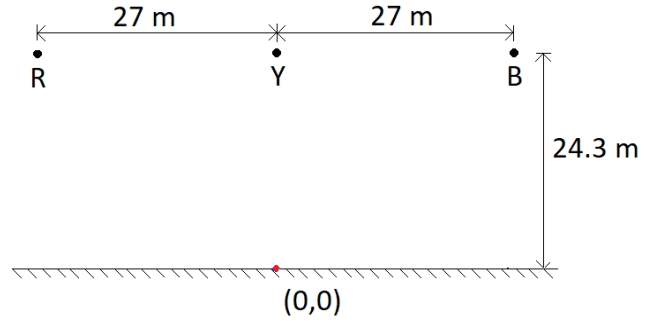

Fig.1. S/C horizontal configuration

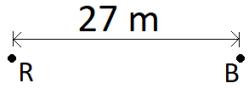

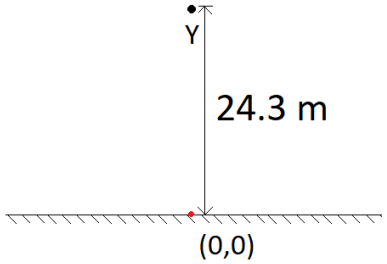

Fig.2. S/C delta configuration

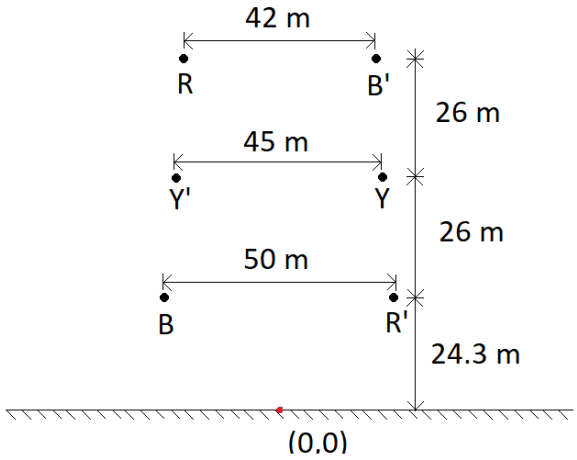

Fig.3. D/C vertical configuration

III. ELECTRIC FIELD CALCULATION

The Finite Element Method is used to calculate electric field distribution at the ground surface and above the ground surface up to 10-meter height [6]. In this study, one assumption is made that ground surface is flat. As per Gauss law relation between electric field and voltage is given as in (2) [7]-[8].

$$E = -\nabla V \tag{1}$$

Electric flux density correlates with charge density and electric flux density correlate with the electric field as given in (2) and (3) respectively.

$$\nabla \cdot D = Q \tag{2}$$

$$D = \varepsilon E \tag{3}$$

By substituting (1) and (2) in (3) final relation between voltage and charge density given as (4).

$$-\frac{\partial}{\partial x}\left(\varepsilon \frac{\partial V}{\partial x}\right) - \frac{\partial}{\partial y}\left(\varepsilon \frac{\partial V}{\partial y}\right) = Q \tag{4}$$

Here, E stands for Electric field intensity V/m
V stands for voltage Volt
D stands for electric flux density C/m^2
ε stands for permittivity of medium F/m
Q stands for volume charge density C/m^3

Overall procedure of Finite Element Analysis can be explained in four steps.

A. Domain Discretization

The first step of FEA is to divide the domain into a number of two-dimensional elements. In this problem, domain is divided into triangular elements with a quadratic shape. So each element has six nodes. A triangular element is shown in the fig.4 [7]-[8].

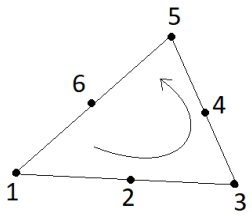

Fig.4. Quadratic type triangular element

Each node is associated with two label numbers, one local number which represents its location within that element and second number is called the global number to represent the location of a node in a domain. Voltage equation at a node can be given as in (5).

$$A_{(x_1,y_1)} = a + bx_1 + cy_1 + dx_1^2 + ex_1y_1 + fy_1^2 \tag{5}$$

In (5) a, b, c, d, e and f are unknown constants. Voltage at all six nodes can represent in same manner. One common

equation in matrix form can be represent. By simple matrix inversion, six constants can be representing in form of voltage and location point of node terms. Final equation for voltage at any (x, y) point in a particular element can be formed as (6).

$$V = \sum_{i=1}^{6} N_{i(x,y)} V_i \tag{6}$$

B. Formulation of a system of equations

Ritz method is used to formulate functional equations. Functional equations for eth element can be written as (7). It is a simple surface integration within the area of an element. V stands for voltage at nodes in an eth element. Q represents charge density in an eth element. Here, omega sign represents two dimensional problem [7]-[8].

$$\mathrm{F}^{\mathrm{e}}(V^e) = \frac{1}{2}\iint \left[\varepsilon \left(\frac{\partial V^e}{\partial x} \right)^2 + \varepsilon \left(\frac{\partial V^e}{\partial y} \right)^2 - 2QV^e \right] d\Omega \tag{7}$$

In (7) voltage is differentiating w.r.t. x and y. substituting (6) into (7), functional equation for eth element can be transformed into matrix form where the voltage at six nodes are used. Differentiation of functional equation w.r.t. a voltage at any node equals to zero. Expanding this differentiation with all node voltages. An expanded equation can be written as in (8). In (8) M is representing total numbers of nodes in domain of the system.

$$\frac{\partial F(V)}{\partial V_i} = \sum_{j=1}^{M} \iint \varepsilon \left(\left[\left(\frac{\partial N_i}{\partial x} \right) \left(\frac{\partial N_j}{\partial x} \right) + \left(\frac{\partial N_i}{\partial y} \right) \left(\frac{\partial N_j}{\partial y} \right) \right] V_j - QN_i \right) d\Omega = 0 \tag{8}$$

In a simplified manner, these equations can be represented in matrix form as in (9) [9].

$$[K]_{(M\times M)}[V]_{(M\times 1)} = [B]_{(M\times 1)} \tag{9}$$

Where K and B terms of matrices stand for,

$$K_{ij} = \iint \varepsilon \left[\left(\frac{\partial N_i}{\partial x} \right) \left(\frac{\partial N_j}{\partial x} \right) + \left(\frac{\partial N_i}{\partial y} \right) \left(\frac{\partial N_j}{\partial y} \right) \right] dxdy \tag{10}$$

$$B_i = \iint QN_i dxdy \tag{11}$$

In (9) terms of matrix V are unknown which can be found by matrices K and B.

C. Incorporation of boundary condition

Two types of boundary conditions have been used. One is Dirichlet condition and second is Neumann condition. At ground and conductor surfaces, Dirichlet condition is applied. Neumann condition is applied at an exterior boundary to bound air medium [7]-[8].

Dirichlet conditions:

$$V_g = 0V \tag{12}$$

$$V_r = 692.820323kV \tag{13}$$

$$V_y = 692.820323e^{-j\frac{2\pi}{3}}kV \tag{14}$$

$$V_b = 692.820323e^{j\frac{2\pi}{3}}kV \tag{15}$$

Neumann condition:

$$\left[\varepsilon \left(\frac{\partial V}{\partial x} \right) \hat{x} + \varepsilon \left(\frac{\partial V}{\partial y} \right) \hat{y} \right] \cdot \hat{n} = 0 \tag{16}$$

D. Continuity conditions

In the domain of 1200kv power line conductors and air medium have different permittivity value, so at conductor surface two different types of material are interfaced which produces discontinuity. So at boundary interface some continuity conditions needs to be satisfied [7]-[8].

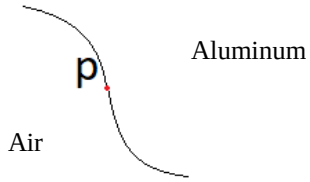

Fig.5. Two boundary interface

Fig.5 shows interface boundary interface of aluminum and air medium. So continuity conditions at interface given as in (19) and (20).

$$\left[\varepsilon_{air} \left(\frac{\partial V}{\partial x} \right) \hat{x} + \varepsilon_{air} \left(\frac{\partial V}{\partial y} \right) \hat{y} \right] \cdot \hat{n} = \left[\varepsilon_{con} \left(\frac{\partial V}{\partial x} \right) \hat{x} + \varepsilon_{con} \left(\frac{\partial V}{\partial y} \right) \hat{y} \right] \cdot \hat{n} \tag{16}$$

$$V_+^p = V_-^p \tag{17}$$

IV. IMPLEMENTATION IN COMSOL MULTIPHYSICS

For Analysis COMSOL Multiphysics software is used. First rectangle is drawn with 300 meter height and 600 meter width to represent air medium. Reason behind take that much long dimensions are to generate more practical case as in real case air medium cannot be bound in any dimension. In air medium three circles are drawn with radius of 0.518 meter, each circle is distanced with 27 meters. Three circles are representing R, Y and B phase cross sectional conductors respectively [10].

Electric field is to be calculated at ground surface and above ground surface with height 2m, 4m, 6m, 8m and 10m. For that 5 lines are drawn with 2 meter vertical distances. Final geometry in COMSOL Multiphysics is shown in fig.6. Aluminum material property is assign to three conductors and air medium property is assign to whole rectangular area except three conductors.

Ground surface representing as in red line in fig.6, has been applied Dirichlet condition as in (15). Conductor surfaces of R, Y and B phase also have been applied Dirichlet conditions as in (16), (17) and (18) respectively. At blue line boundaries representing in fig.6, Neumann condition is applied as in (19). Neumann condition represents that zero change in electric flux density in normal vector direction of boundary.

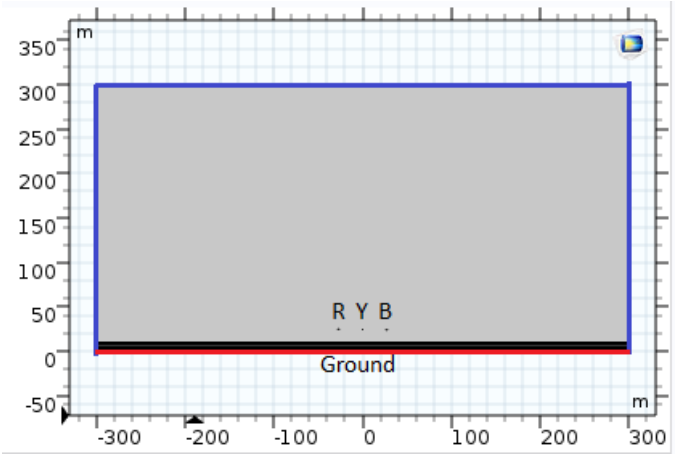

Fig.6. Geometry of S/C horizontal configuration 1200kV transmission line

COMSOL provides feature to decide element size as your analysis area to get higher accuracy with lesser computation time and less RAM of device The results are need to be obtained at ground surface and some meters above from ground surface up to 10 meters. Here, results are evaluated at six equidistance lines from ground surface to height of 10 meters from ground surface, so small sized elements are constructed with 1 meter maximum element size as shown in fig.7, element size within conductors is 20 mm and in remaining area coarser type elements are formed.

Final geometry with construction of elements in whole domain is called as mesh domain. Mesh domain of S/C horizontal configuration of 1200kV line is shown in fig.8. Similarly model of S/C delta configuration and D/C vertical configuration of 1200kV UHV transmission line can be implementing in COMSOL Multiphysics [10].

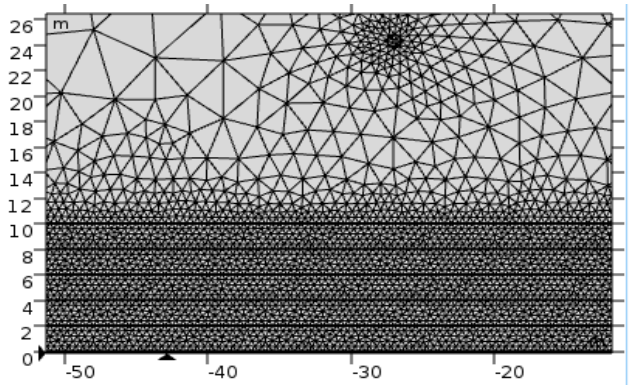

Fig. 7. Discretization of domain with different element sizes.

V. RESULTS

An electric field is calculated and plotted for three configurations of a 1200kV transmission line; electric field plot is carried out for up to some distance from reference point on ground surface. It is repeated for various heights from the ground, ground surface and 2m, 4m, 6m, 8m and 10m above from the ground surface. The analysis is performed by considering the minimum height of conductors in a span.

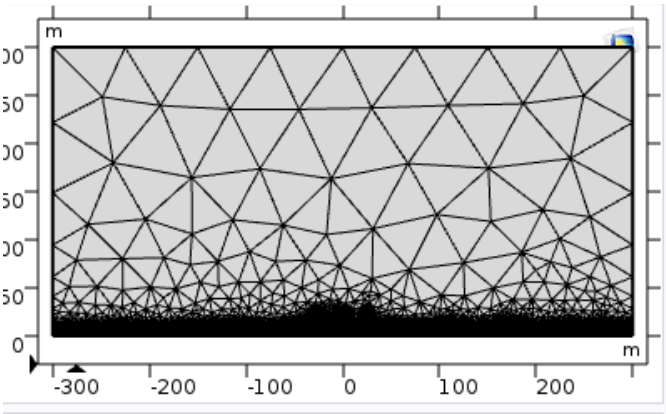

Fig.8. Mesh domain of S/C horizontal configuration

In fig.8. S/C horizontal configuration domain is discriminated into triangular elements. Similarly, fig.10. and

fig.12. shows mesh domain of D/C horizontal configuration and S/C delta configuration respectively. In fig.9. electric field is plotted for 70 meters from reference point in both directions. Maximum electric field for at 10 meter height above ground surface is 13,370 V/m at 27 meters from reference point. Within 52.25 meters from reference point electric field above 5000 V/m. So, ROW for S/C horizontal configuration is 104.5 meters.

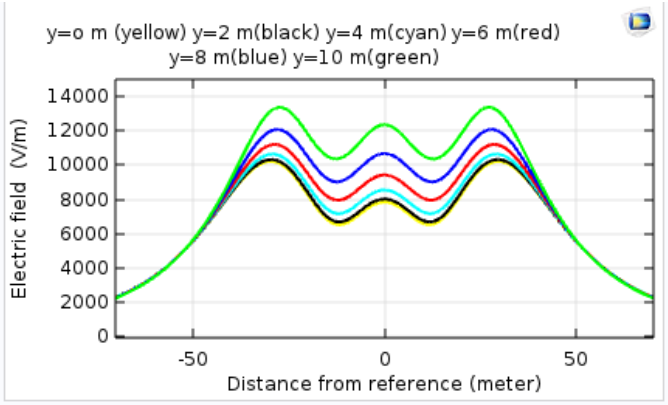

Fig.9. Electric field distribution for S/C horizontal configuration

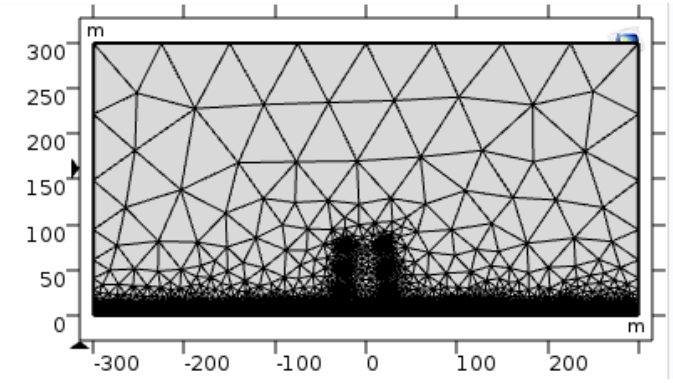

Fig.10. Mesh domain of D/C horizontal configuration

In fig.11. electric field is plotted for 50 meters from reference point in both directions. Maximum electric field for at 10 meter height above ground surface is 12,810.65 V/m at 25 meters from reference point. Within 46.04 meters from reference point electric field above 5000 V/m. So, ROW for S/C horizontal configuration is 92.1 meters. In fig.13. electric field is plotted for 50 meters from reference point in both directions. Maximum electric field for at 10 meter height above ground surface is 12,218.23 V/m at reference point. Within 19.45 meters from reference point electric field above 5000 V/m. So, ROW for S/C horizontal configuration is 39 meters. From fig.9. and fig. 11 it can show that, there is a dip in electric field at reference point due to partial cancellation of 3 phase fields [11].

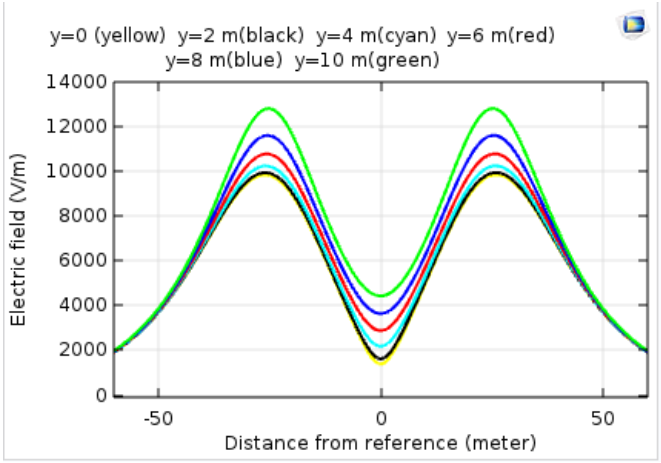

Fig.11. Electric field distribution for D/C vertical configuration

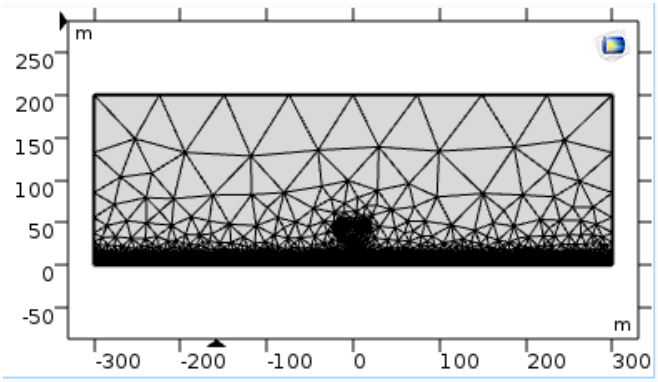

Fig.12. Mesh domain of S/C delta configuration

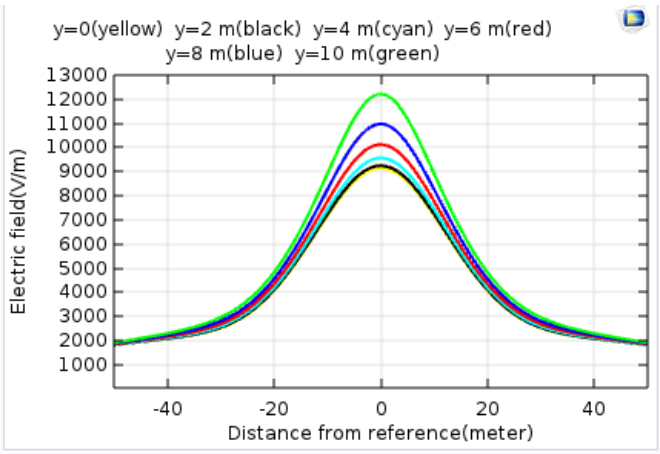

Fig.13. Electric field distribution for S/C delta configuration

VI. IMPORTANCE WITH ICNIRP GUIDELINES

International Commission on non-ionizing radiation protection had approved the exposure limit of 50Hz based on electric field is shown as in table 2 [4]-[12].

TABLE 2. ICNIRP GUIDELINES

Exposure type	**ICNIRP-2010**
Occupational	10kV/m
General public	5kV/m

From the results of three configurations, a region can be defined where electric field is excessing the safety limits. Due to excess electric field exposure many adverse effects may happens like cardiovascular disorders and neurodegenerative disorders [4].

VII. CONCLUSION

Application of Finite Element Method to evaluate an electric field of 1200kv transmission line is explained. From electric field of 1200kv transmission line, Right of way of line is defined. Here three configurations have been taken for analysis; results of lines are compared with international standards for safe limits of electric field for public. Calculation is taken at ground surface and several meters of height from ground surface like 2m, 4m 6m, 8m, and 10m. This paper highlights the application of FEM and COMSOL Multiphysics in analysis of electrical field.

REFERENCES

[1] “India to have world’s highest power transmission line”, THE HINDU Business Line Newspaper, December 04, 2013.

[2] “Power Grid to launch India’s first 1200-kv station” Business Standard, January 20 2013.

[3] R.D. Begamudre, “Extra High Voltage AC Transmission Engineering”, New Age, International Publication, 3rd Edition, 2006.

[4] “International Commission on Non-ionizing Radiation Protection Guidelines for limiting exposure to time varying electric and magnetic fields (1Hz to 100Hz)”, Health physics 99(6):818-836; 2010.

[5] H.K. Agarwal, K. Mukherjee, A.K. Pal and P.Barua, “Design and Development of 1200KV Transmission Line and Substation Insulation Hardware Fittings Clamps& Connectors”, CIGRE India journal Vol.1 issue 2, pp.10-18, 2012.

[6] M. Trlep, A. Hamler, M. Jesenik, and B. ˇStumberger, “Electric Field Distribution Under Transmission Lines Dependent on Ground Surface”, IEEE TRANSACTIONS ON MAGNETICS, VOL. 45, NO. 3, MARCH 2009.

[7] JIAN-MING JIN, “The Finite Element Method in electromagnetics”, Third Edition, IEEE Press, Willey Publication.

[8] Matthew N. O. Sadiku, “Numerical Techniques in Electromagnetics”, Second Edition, CRC Press.

[9] R. M. Radwan, M. M. Samy, S. Akef, "Calculations of Electric Fields Underneath Ultra High Voltage Transmission Lines", Proceeding of the 17th Middle-East Power Conference, 16-18 Dec. 2015.

[10] COMSOL Multiphysics User’s guide, May 2012.

[11] Mahadev G. Unde, Bansidhar E. Kushare, “Analysis of Electromagnetic Fields of 1200kV UHV-AC Transmission Lines”, 5th International Conference on Computational Intelligence and Communication Networks, 27-29 Sept. 2013.

[12] Aliyu Ozovehe, Maina Ibrahim, Ali Hamdallah, “Analysis of Electromagnetic Pollution due to High voltage Transmission Lines”, Journal of Energy Technologies and Policy, ISSN 2225-0573 (Online), Vol.2, No.7, 2012.

Proceedings of the Fourth International Conference on Communication and Electronics Systems (ICCES 2019)
IEEE Conference Record # 45898; IEEE Xplore ISBN: 978-1-7281-1261-9

Comparative analysis of Cuk converter with proportional integral controller & proportional resonant controller

Tejal Dinesh Patil
Department of Electrical Engg.
Walchand College Of Engineering
Sangli, India
tejalpatil012@gmail.com

D. S. More
Department of Electrical Engg.
Walchand College Of Engineering
Sangli, India
dsm.wce@gmail.com

***Abstract*—This study presents comparison between two different control techniques for PFC converters with less total harmonic distortion (THD). The PR current controller provides the gain at resonant frequency & eliminates steady state error. On other hand, PI controller has less disturbance rejection capability in high frequency range. Hence PR controllers can be applied to PFC converters to obtain extended DC-link voltage with enhanced power quality at input. Here, Cuk converter is introduced for power quality improvement and it's operation is described in three modes with corresponding waveforms. The simulation study of Cuk converter with PI controller & PR controller is carried out and comparative analysis of these two techniques is presented.**

***Index Terms*—power-factor correction, THD, power quality, PR controller, Cuk converter.**

I. Introduction

The rapid changes in world energy scenario encouraged design, development & control of power electronic converters with enhanced power factor. The PFC converters are often employed to obtain enhanced power factor and these can generate balanced DC-link voltage. The combination of buck & boost converters is selected, as operation in both modes can be obtained. The buck-boost converters is a combination of diode bridge rectifier with DC-DC converter [1], [2]. The Cuk converter is implemented here which is a single switch based converter & results in decreased torque & current ripple, approximately UPF and low harmonic distortion at AC mains.

Due to increased applications of AC-DC converters, they are evolved in single-stage with lower number of components & high efficiency to improve power quality & also considered as better option for flexible operation of system. The operation of PFC converters is studied in two modes, that is, continuous conduction mode (CCM) & discontinuous conduction mode (DCM). As switch suffers hard switching because of continuous inductor current, CCM is nominated for medium & high power applications while restricts DCM for low power applications. On control part, three sensors are required to operate in CCM while a DCM only requires single voltage sensor [3].

The selection of control scheme includes appropriate consideration between cost, complexity & waveform quality required to meet standards of power quality in low voltage applications. The simple proportional integral controllers have some limitations such as presence of steady-state error in stationary frame even though they are easy to implement [4]–[6]. Overcoming the drawbacks of PI controller & achieving equivalent frequency response characteristics as synchronous frame PI controller, PR controller is introduced to track reference current in stationary frame. This paper evaluates performance of PI controller, identifies limitation & presents PR controller as best selection to overcome the drawbacks of conventional PI controller [7]. The current controller put remarkable effect on quality of source current of converter & hence it has more importance to the fact that controller should provide best quality sinusoidal input source current with less distortion to neglect harmonics [8], [9].

To avoid adverse effect on power quality, several standards are made for THD and it is limited under permissible value by IEC 61000-3-2 standards. [10].

II. Overview of Operation of Cuk Converter

Cuk converter is a special type of DC-DC converter or it is a cascaded combination of boost converter followed by buck converter with capacitive energy transfer.

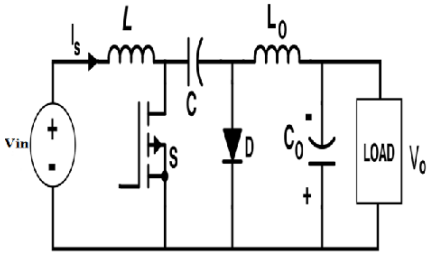

Fig. 1. Equivalent circuit diagram for Cuk converter

The Cuk converter works in both buck & boost mode. The operation of Cuk converter in DCM is studied in this section [11], [12].

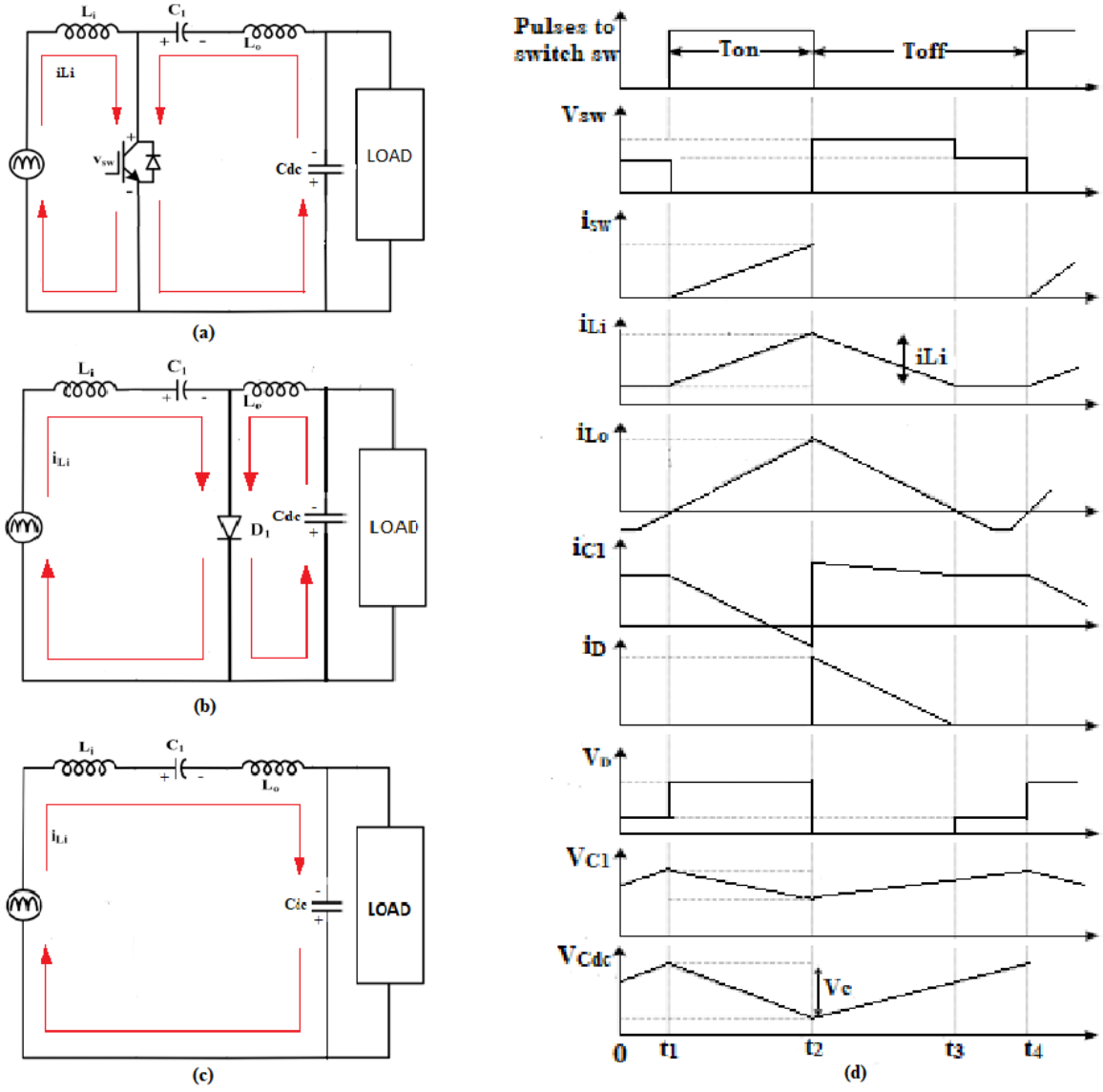

Fig. 2. Operation of Cuk converter when (a) Switch is on, (b) Switch is off, (c) Freewheeling period, (d) Related voltage & current waveforms

Fig. 1 shows equivalent Cuk converter which provides enhanced power quality at input side & precisely regulated DC output. It is known as ideal current shaper as input current shaping is inherent & DC output voltage controller decides duty cycle.

The complete switching cycle of converter is described in three different modes given in fig. 2 [13].

A. *Mode I* $(t_1 - t_2)$:

In this, switch is on (fig. 2a) in which energy from source (v_s) is transferred to input side inductor. The capacitor (C_1) discharges & energy is transferred to output side inductor (L_o). The input side inductor is used for continuous current conduction & short-circuit path is provided for capacitor current.

B. *Mode II* $(t_2 - t_3)$:

Fig. 2b shows second mode in which switch is turned-off & diode starts conducting. The intermediate capacitor absorbs the energy stored in input inductor (L_i) & output side inductor transfers it to output capacitor. The zero output inductor current is takes place at end of this mode.

C. *Mode III* $(t_3 - t_4)$:

The switch remains off in third mode as shown in fig. 2c and small current freewheels through output side inductor.

III. CONTROL IMPLEMENTATION

The closed-loop control of DC-DC converters is essential to maintain power quality at AC mains during transient in addition with steady-state operation. Here, two control schemes

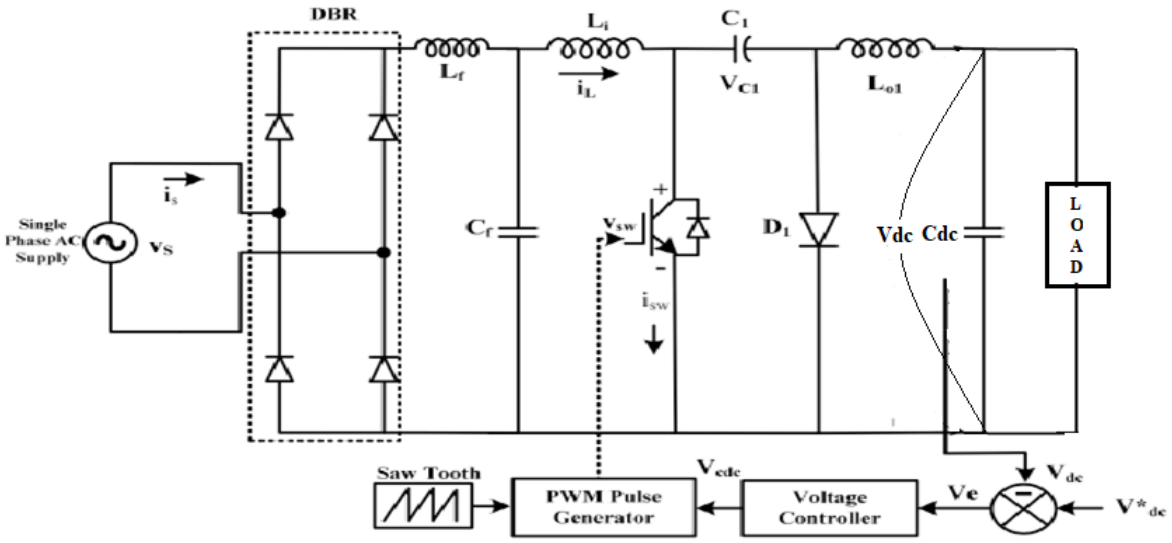

Fig. 3. Circuit diagram of PFC Cuk converter with conventional control scheme

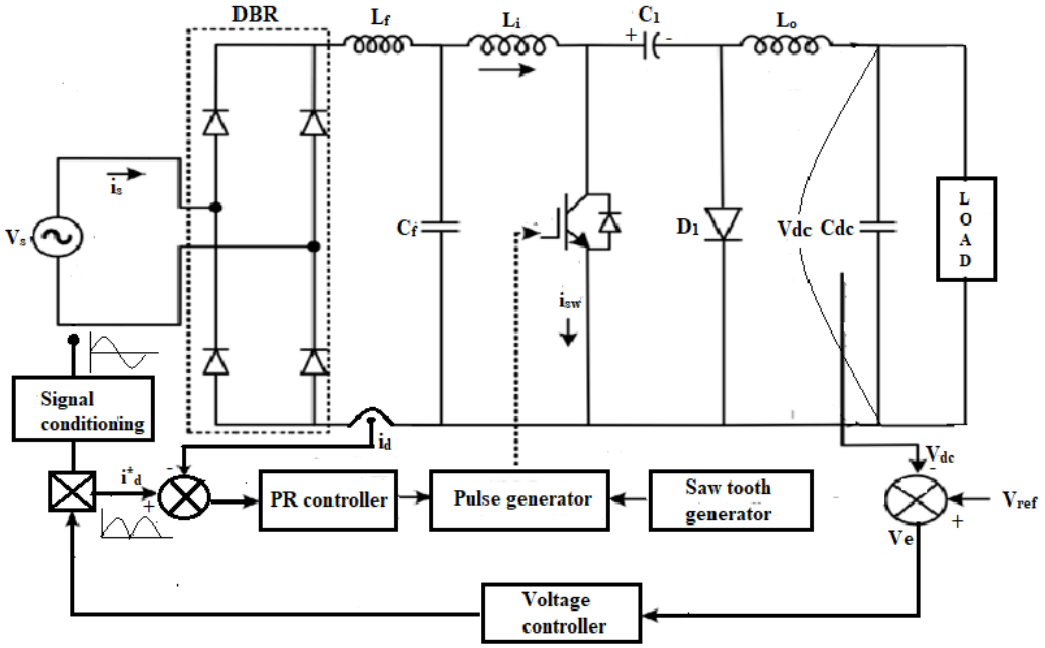

Fig. 4. Proposed control scheme for PFC Cuk converter

are reported to meet this requirement [14]. The proportional controller is chosen as inner loop controller to make system response faster. The implementation of conventional PI controller & proposed PR controller are discussed in this section. The PI controller does not track reference current in absence of steady-state error, hence proportional resonant controller is employed which introduces gain at resonant frequency & null gain at other frequencies.

A. PI implementation for Cuk converter

The Cuk converter with conventional PI implementation is as in fig. 3 in which DBR is used to provide rectified DC output as input to LC filter [15]. It keeps switching harmonics under control and puts limit on it from entering to system. The switching signal is generated by sinusoidal PWM method where DC-link output voltage is compared with reference voltage & obtained error signal provided to proportinal integral controller. The saw tooth carrier frequency of 20kHz is compared with PI controller output which generates PWM

signal. Both the signals are compared in PWM pulse generator to get switching pulses. This is most commonly used control method.

B. PR implementation for Cuk converter

Fig. 4 shows proposed control scheme of Cuk converter with PR controller. The principle of PR controller depends upon second order generalized integrator concept. The internal model control is applied to derive TF of PR controller, given as (1) for ideal PR controller in fundamental frequency. To avoid stability issues associated with this, the non-ideal PR controller is implemented as (2) by adding damping, where ω_c can be extended to control bandwidth. A value of ω_c is between 5-15 rad/s. The K_p is proportional gain to determine dynamics of system and tuned in conventional way while K_i is integral gain. The higher value of K_i is selected for the higher capability of PR controller to track the current reference [16].

$$G_{PR}(s) = K_p + \frac{2K_i s}{S^2 + \omega^2} \tag{1}$$

$$G_{PR}(s) = K_p + \frac{2K_i \omega_c s}{s^2 + 2\omega_c s + \omega^2} \tag{2}$$

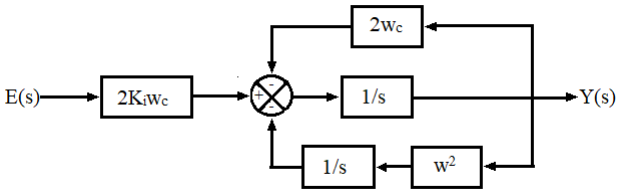

Fig. 5. PR controller implementation

The implementation of proportional resonant controller is shown in fig.5 where upper feedback path can be removed to obtain (2). Also, the system stability has great significance to make sure that controller is working within its stability region. The major part in stability analysis of controller having importance are gain margin & phase margin. The unstable point for gain margin is at 0dB while that for phase margin is at -180^0 [17].

The frequency response of (2) with Kp = 15, Ki = 400 and cut-off resonant frequency, ω_c = 10rad/s is given in fig. 6, where resonant peak has finite gain of 50 dB. The resonant term itself in proportional resonant controller exhibits an infinite gain at AC frequency & no phase shift for remaining frequencies. The study demonstrates that, higher the gain & phase margin better is the stability of system. The infinite gain margin means, the system at no time becomes unstable in future, even for the continuous increase in gain. This resonant peak can eliminate the voltage tracking error. The frequency response changes as the values of Kp, Ki or ω_c changes [18].

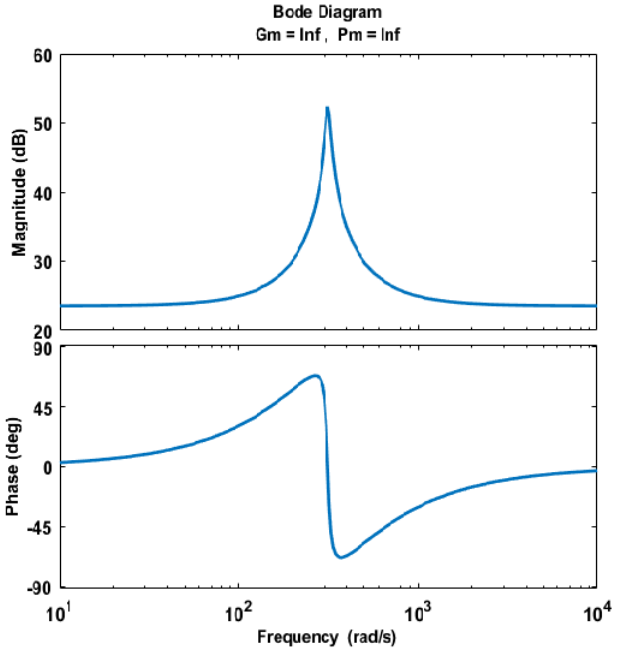

Fig. 6. Frequency response of non-ideal PR controller

IV. Simulation Results

The behaviour of both control schemes are investigated using MATLAB/Simulink with various system parameters. The selection of components for this converter is necessary to obtain enhanced power quality & DC output. The simulations are performed with 220 Volts, 50 Hz supply voltage having 100 ohm resistive load. The converter circuit & controller parameters are listed in Table-I.

TABLE I
SYSTEM PARAMETERS

Sr. No.	Symbol	Parameter	Value
1	v_s	Supply voltage	220V
2	L_f	Filter inductance	4mH
3	C_f	Filter capacitance	330nF
4	f_s	Switching frequency	20kHz
5	L_i	Input inductor	5mH
6	C_1	Inter-mediate capacitor	660nF
7	L_o	Output inductor	400μH
8	C_{d3}	DC-link capacitor	2200μF

The converter has been studied with both the controllers viz., PI controller & PR controller and results are presented in fig. 7 & fig. 8 for DC output voltage. It can be illustrated from fig. 7 that output voltage have some oscillations for some time for PI controller but it comes out to be smooth curve as in fig. 8 using PR controller. It is very clear from the above results that PR controller gives ripple free output voltage.

As per above discussion for power quality improvement, the THD should be under permissible limit given in IEC 61300-3-2 standards. Fig. 9 & fig. 10 shows, FFT analysis for source current THD of converter for both control implementation. The total harmonic distortion of converter source current is

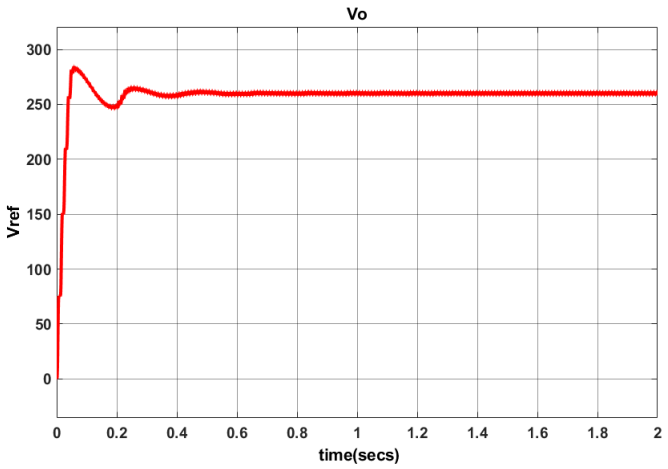

Fig. 7. Output voltage of controller with PI controller

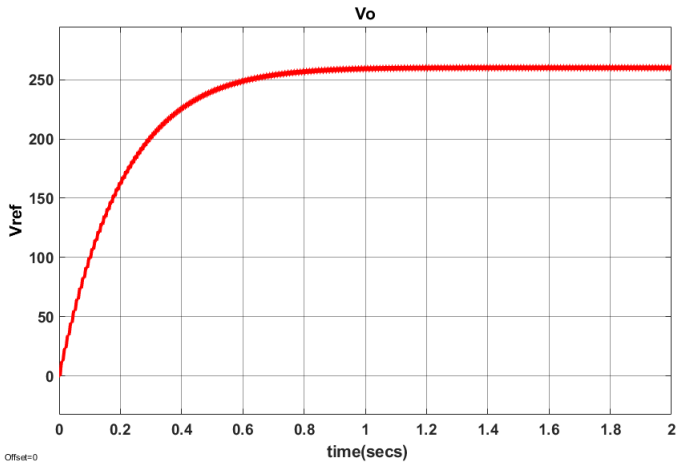

Fig. 8. Output voltage of controller with PR controller

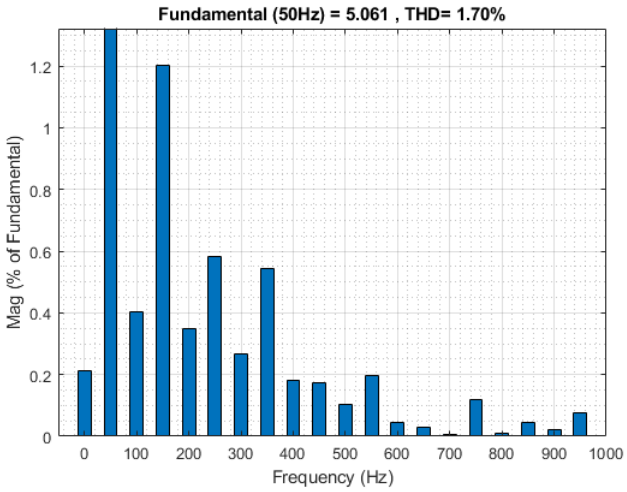

Fig. 9. FFT analysis of source current with PI controller

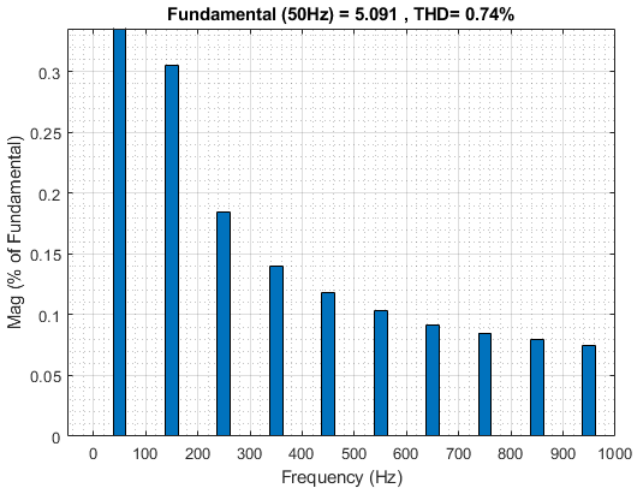

Fig. 10. FFT analysis of source current with PR controller

1.73% with conventional PI controller while it is 0.74% with PR controller. The results are graphically presented in fig. 11, PI controller curve shows that THD goes on decreasing upto the point where input voltage becomes equal to the reference voltage while for PR controller it decreases gradually for increasing reference voltage. Hence use of PR controller offers best power quality as compare to PI controller for Cuk converter.

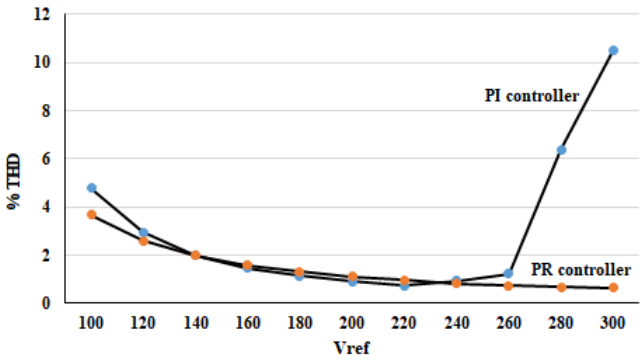

Fig. 11. Comparison for THD simulation results of Cuk converter with PI controller & PR controller

V. CONCLUSION

The suitability of PR controller for closed loop control of Cuk converter is discussed in this paper. The converter can be considered as suitable topology for many applications. The simplicity in implementing the current controller is advanced by use of PR controller and also current tracking capability is ensured. The theoretical analysis shows that proportional resonant controller has advantages as compared to proportional integral controller & it enables control system to adopt higher performance. It also shows that PR controller gives good transient response. The source current THD is less for PR controller as compared to PI controller.

REFERENCES

[1] R. Benedito Siqueira, E. M. S. Vieiro, and E. F. R. Romaneli, "Design and implementation of an ac-ac uk converter," in *2016 12th IEEE International Conference on Industry Applications (INDUSCON)*, Nov 2016, pp. 1–8.

[2] M. Brkovic and S. Cuk, "Input current shaper using cuk converter," in *[Proceedings] Fourteenth International Telecommunications Energy Conference-INTELEC'92*. IEEE, 1992, pp. 532–539.

[3] H. Wei and I. Batarseh, "Comparison of basic converter topologies for power factor correction," in *Proceedings IEEE Southeastcon'98'Engineering for a New Era'*. IEEE, 1998, pp. 348–353.

[4] A. Ayad, M. Hashem, C. Hackl, and R. Kennel, "Proportional-resonant controller design for quasi-z-source inverters with lc filters," in *IECON 2016-42nd Annual Conference of the IEEE Industrial Electronics Society*. IEEE, 2016, pp. 3558–3563.

[5] R. Teodorescu, F. Blaabjerg, M. Liserre, and P. C. Loh, "Proportional-resonant controllers and filters for grid-connected voltage-source converters," *IEE Proceedings-Electric Power Applications*, vol. 153, no. 5, pp. 750–762, 2006.

[6] N. F. Roslan, J. A. Suul, A. Luna, I. Candela, and P. Rodriguez, "A simulation study of proportional resonant controller based on the implementation of frequency-adaptive virtual flux estimation with the lcl filter," in *IECON 2015-41st Annual Conference of the IEEE Industrial Electronics Society*. IEEE, 2015, pp. 001 934–001 941.

[7] H. Cha, T.-K. Vu, and J.-E. Kim, "Design and control of proportional-resonant controller based photovoltaic power conditioning system," in *2009 IEEE Energy Conversion Congress and Exposition*. IEEE, 2009, pp. 2198–2205.

[8] C.-T. Pan and T.-Y. Chang, "An improved hysteresis current controller for reducing switching frequency," *IEEE Transactions on Power Electronics*, vol. 9, no. 1, pp. 97–104, 1994.

[9] S. Buso, L. Malesani, and P. Mattavelli, "Comparison of current control techniques for active filter applications," *IEEE transactions on industrial electronics*, vol. 45, no. 5, pp. 722–729, 1998.

[10] A. Prudenzi, U. Grasselli, and R. Lamedica, "Iec std. 61000-3-2 harmonic current emission limits in practical systems: need of considering loading level and attenuation effects," in *2001 Power Engineering Society Summer Meeting. Conference Proceedings (Cat. No. 01CH37262)*, vol. 1. IEEE, 2001, pp. 277–282.

[11] N. Zhang, H. Tang, and C. Yao, "A systematic method for designing a pr controller and active damping of the lcl filter for single-phase grid-connected pv inverters," *Energies*, vol. 7, no. 6, pp. 3934–3954, 2014.

[12] D. Zammit, C. S. Staines, and M. Apap, "Comparison between pi and pr current controllers in grid connected pv inverters," *WASET, International Journal of Electrical, Electronic Science and Engineering*, vol. 8, no. 2, 2014.

[13] A. Anand and B. Singh, "Design and implementation of pfc cuk converter fed srm drive," *IET Power Electronics*, vol. 10, no. 12, pp. 1539–1549, 2017.

[14] D. S. L. Simonetti, J. Sebastian, and J. Uceda, "The discontinuous conduction mode sepic and cuk power factor preregulators: analysis and design," *IEEE Transactions on Industrial Electronics*, vol. 44, no. 5, pp. 630–637, 1997.

[15] V. Vlatkovic, D. Borojevic, and F. C. Lee, "Input filter design for power factor correction circuits," *IEEE Transactions on Power Electronics*, vol. 11, no. 1, pp. 199–205, 1996.

[16] L. Herman, I. Papic, and B. Blazic, "A proportional-resonant current controller for selective harmonic compensation in a hybrid active power filter," *IEEE Transactions on Power Delivery*, vol. 29, no. 5, pp. 2055–2065, 2014.

[17] A. V. Timbus, M. Ciobotaru, R. Teodorescu, and F. Blaabjerg, "Adaptive resonant controller for grid-connected converters in distributed power generation systems," in *Twenty-First Annual IEEE Applied Power Electronics Conference and Exposition, 2006. APEC'06.* IEEE, 2006, pp. 6–pp.

[18] A. Vidal, F. D. Freijedo, A. G. Yepes, P. Fernandez-Comesana, J. Malvar, Ó. López, and J. Doval-Gandoy, "Assessment and optimization of the transient response of proportional-resonant current controllers for distributed power generation systems," *IEEE Transactions on Industrial Electronics*, vol. 60, no. 4, pp. 1367–1383, 2013.

Proceedings of the Fourth International Conference on Communication and Electronics Systems (ICCES 2019)
IEEE Conference Record # 45898; IEEE Xplore ISBN: 978-1-7281-1261-9

An Approach for Analysis and Prediction of CKD using Deep Learning Architecture

Navaneeth Bhaskar
Research Associate
VIT Chennai
navaneeth.bhaskar2015@vit.ac.in

Suchetha M
Associate Professor
VIT Chennai
suchetha.m@vit.ac.in

***Abstract*—This paper proposes an efficient and novel approach for non-invasive diagnosis of Chronic Kidney Disease (CKD). A novel sensing module for CKD diagnosis is designed and developed in the proposed work. The concentration of urea in the saliva sample is measured for detecting the disease. A Convolutional Neural Network-Support Vector Machine (CNN-SVM) hybrid deep learning model is implemented for making predictions by extracting and classifying the features from the sensor response. Experiments are conducted to test the proposed model with real-time samples and to compare its performance with conventional CNN. The experimental results indicate that the proposed model outperforms traditional data classification techniques. The proposed hybrid model achieved a prediction accuracy of 96.59%.**

***Index Terms*—Ammonia sensor, Chronic kidney disease, Convolutional neural network, Deep learning, Support vector machine.**

I. INTRODUCTION

Commonly, the blood test is used for the diagnosis of kidney disease. A blood test for CKD diagnosis will measure the urea or creatinine levels in the serum [1], [2]. Urea and creatinine levels in the serum will be elevated when the kidneys are not functioning adequately. Since blood extraction is an invasive technique, it will obviously cause pain and discomfort to the patients. Non-invasive and minimally invasive disease detection methods are gaining importance nowadays. Saliva is gaining popularity as an effective bio-fluid in the diagnosis of diseases. Recent studies have shown a positive correlation between urea and creatinine values in the saliva and serum [3], [4]. The results of these studies show that it is possible to detect CKD by monitoring the salivary urea or creatinine levels [5]. Saliva-based disease diagnosis is advantageous as it is easily available, and it can be collected non-invasively, using simple equipment.

In our pilot study, salivary urea is monitored to detect kidney disease. There are several methods available to measure salivary urea concentration clinically. However, for an end-to-end real-time detection application, the clinical detection techniques wont be suitable. In this work, we describe a novel method to monitor salivary urea levels. We have followed the enzymatic reaction which transforms the urea in saliva into ammonia gas. A sensing module is developed for carrying out this enzymatic reaction, and to measure the ammonia gas. The amount of ammonia gas produced will be proportional to the urea concentration.

Furthermore, in this work, we present a novel CNN-SVM hybrid network algorithm for automatically analyzing the sensor response to make predictions. The CNN network is commonly used in image and video recognition, language processing and in recommender systems [6]–[8]. The reason for choosing CNN network is because of its ability to extract the target features from the sensor response automatically. As SVM is more accurate in classifying the samples, it is used along with the CNN network in the proposed network [9], [10]. Although CNN is designed to process pixel data, it can also be used to process signals in 1-dimension (1-D). More recent works have attempted to use CNN for analyzing 1-D signals [11]–[14]. The 1-D CNN version of the CNN algorithm was first introduced for analyzing ECG signals by Kiranyaz et al. [11]. They have employed the CNN network for real-time classification of ECG signals. Recently Lekha et al. [12] developed a novel 1-D CNN architecture for detecting and classifying diabetes non-invasively. Ince et al. [13] have employed the 1-D CNN algorithm for detecting faults in the motors. Further, a study conducted by Acharya et al. [14] demonstrated the use of 1-D CNN for automated detection and classification of seizure using EEG signals. These papers in the literature suggest that the CNN network can be modified and applied for analyzing 1-D signals. As the sensor response in our study is a 1-D signal, the proposed hybrid model is designed to analyze 1-D signals.

The rest of this paper is structured as follows: Section II gives an overview of the proposed hybrid model. The methodology of the work is explained in section III. The experimental results and performance of the proposed approach is presented in section IV. Finally, the conclusion of the study is reported in section V.

II. CNN-SVM DEEP LEARNING MODEL

CNN network is a class of deep artificial neural network. The artificial neural network is derived from the design of the biological neural network. The key part of the artificial neural network is the artificial neurons. The neuron model involves multiplication, summation and activation functions. All inputs will be multiplied with the corresponding weight. The summation function sums up all the weighted input and bias, and the added inputs will be passed through an activation function to produce the output. A CNN deep learning network

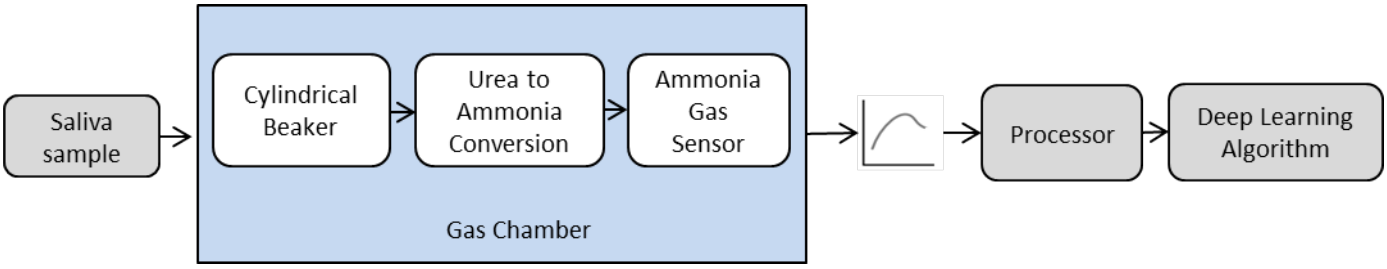

Fig. 1: Block representation of the overall system

consists of convolution layers and fully connected layers as in the multilayer neural network [15], [16]. The fully connected layer makes the final predictions.

The convolution layer performs convolution and subsampling operations. First, it convolves the kernel and the input signal. Then, it performs subsampling operation to reduce the signal dimension. These two operations are repeated for getting the reduced feature map from the signal. The convolution operation can be mathematically represented as:

$$F(n) = z(n) * k(n) \tag{1}$$

$$F_i(n) = z(n)k(1) + z(n-1)k(2) + ... + z(0)k(n) \tag{2}$$

where z and k represents the input signal and kernel filter.

After the convolution operation, a subsampling operation is performed on the convoluted signal. This will reduce the dimension of the feature set. A max-pooling subsampling operation is applied in the proposed work [17]. The max-pooling technique will divide the feature maps into multiple segments and will extract the maximum value from each segment. The maximum value is obtained as:

$$F_i = Max(F_i^*) \tag{3}$$

where F_i is the subsampled feature set.

The conventional CNN is incorporated with fully connected Multilayer Perceptron (MLP), which performs the classification task [18], [19]. In the proposed network, a more efficient SVM classifier is used instead of MLP. SVM is a better classifier compared to MLP, and it can provide better classification accuracy. The SVM classification function is given by:

$$F(x) = z_i w - b_i \tag{4}$$

where z_i represents the input to the classifier, w is the weight vector and b_i is the bias.

The input data is classified with respect to the defined maximum-margin hyper-plane based on the conditions:

$$z_i w + b_i > 0, C_i = 1 \tag{5}$$

$$z_i w + b_i < 0, C_i = -1 \tag{6}$$

where C_i represents the class label.

The margin is represented as:

$$margin = \frac{1}{\parallel w \parallel} \tag{7}$$

The training issue in the SVM classifier is considered as an optimization problem. For classifier optimization, the hyper-plane is estimated by reducing $\|\mathrm{w}\|$. Minimizing the value of $\|\mathrm{w}\|$ will increase the margin. For solving the optimization problem, the Lagrange multiplier is adopted. This is defined as:

$$L(w, b_i, \alpha) = \frac{w^2}{2} - \sum_{i=1}^{n} \alpha_i C_i z_i w + b_i \sum_{i=1}^{n} \alpha_i C_i + \sum_{i=1}^{n} \alpha_i \tag{8}$$

where α symbolizes the Lagrange multiplier.

Once the optimum Lagrange multiplier α_i^* is obtained, the optimal weight vector can be computed by:

$$w^* = \sum_{i=1}^{n} \alpha_i^* C_i z_i \tag{9}$$

The bias is updated as:

$$b^* = 1 - w^* z_i \tag{10}$$

The hyper-plane classification function in SVM classifier is:

$$F(x) = \sum_{i=1}^{n} \alpha_i C_i (z_i, z) - b_i \tag{11}$$

When the training data is not linearly separable, then the optimization problem will not have a solution. In this case, the slack variables are introduced which identifies the misclassification rate. The optimization problem, in this case, is defined as:

$$minimize\ Q(w, b_i, \xi) = \frac{1}{2} \parallel w \parallel^2 + C \sum_{i=1}^{n} \xi \tag{12}$$

Here C symbolizes the regularization parameter which decides the balance between the training error and the margin size. For classifying complex data set, appropriate kernel functions are applied for transforming the data set. The classification function with kernel function will be:

$$F(x) = \sum_{i=1}^{n} \alpha_i C_i K(z_i, z) + b_i \tag{13}$$

where K represents the kernel function.

III. MATERIALS AND METHODS

A. Saliva Collection and Testing

For experimentation, we have collected saliva samples from 98 participants. This includes 48 CKD patients with Glomerular filtration rate (GFR) less than 90 mL/min, and 50 healthy

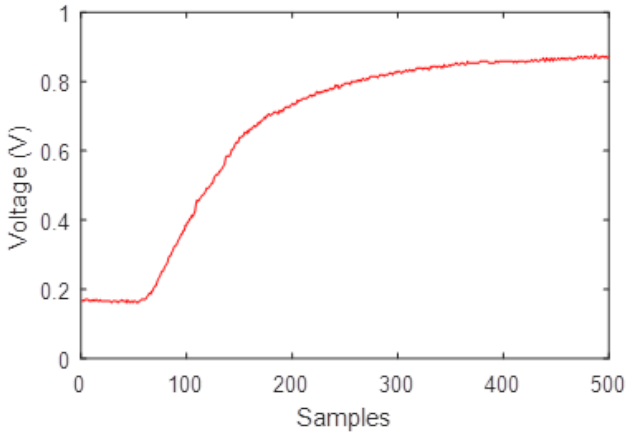

Fig. 2: Analog voltage response of the gas sensor for a test sample

individuals with GFR more than 90 mL/min [20]. We have collected 2ml of the sample in a sterile graduated test tube. The experimental analysis is carried out in accordance with the ethical guidelines of the Declaration of Helsinki.

The experimental testing is done with a novel detection method. The block representation of the overall system is illustrated in Fig. 1. The block diagram consists of a gas sensing apparatus chamber, an Arduino controller processor board and an MQ-137 ammonia gas sensor which is placed inside the gas chamber. Urea in the saliva sample is first transformed to ammonia using the traditional urea hydrolysis process [21], [22]. This conversion process involves urease enzyme which is responsible for urea conversion. Urease enzyme is placed inside the apparatus chamber in a small beaker. The saliva sample is dropped to this urease enzyme breaker through the inlet valve of the chamber. This enzymatic reaction produces ammonia gas. The MQ series ammonia sensor then measures the produced ammonia gas [23], [24]. The ammonia gas generated will be proportional to the urea concentration in the sample. In this conversion process, some amount of ammonia will be converted to ammonium ions as the testing sample here is a liquid. These ammonium ions can be converted to ammonia gas by increasing the pH of the solution. This can be done by adding a small amount of NaOH to the mixture. Output response from the gas sensor is received using the Arduino controller board. Sensor programming of the analysis is written in Matlab. The sensor reading is collected and recorded for 500 samples. Fig. 2 shows the analog voltage response of the gas sensor for a test sample in Matlab software. The snapshot of the sensing module is shown in Fig. 3.

B. Feature Extraction and Classification

The features are extracted and classified using the proposed CNN-SVM hybrid network. CNN performs the feature extraction operation and SVM performs the classification task. The analog voltage signal from the sensor is first convoluted with the kernel. A Gaussian kernel is used in our analysis [12]. The

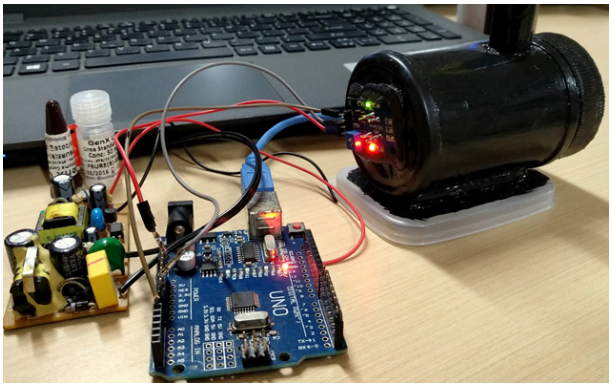

Fig. 3: Photograph of the sensing module

TABLE I: PERFORMANCE COMPARISON TABLE

Performance Parameters	Conventional CNN	Proposed Model
Accuracy (in %)	94.97	96.59
Sensitivity (in %)	93.33	94.59
Specificity (in %)	96.15	98.03
Precision	0.945	0.972
False Positive Rate (FPR)	0.038	0.019
False Negative Rate (FNR)	0.066	0.054
Negative Predictive Value (NPV)	0.952	0.961
False Discovery Rate (FDR)	0.054	0.027
F1 Score	0.939	0.958
Matthews Correlation Coefficient (MCC)	0.896	0.93

convolution of input and kernel will produce the convoluted signal:

$$F_i(n) = \sum_{i=-x}^{x} z(i+1)k(y-i+1) \tag{14}$$

where x represents the length of the input signal z and y represents the length of the kernel k.

The convolution operation is followed by max-pooling subsampling operation which reduces the size of the feature map. The proposed deep learning network has six convolution and sub-sampling layers. After repeating these two operations for six times, the reduced feature set is obtained.

The CNN network will extract the best features from the sensor signal. Further, these features are classified for predicting the output. For classification, we have employed an SVM classifier. We have implemented SVM with a Radial Basis Function (RBF) kernel [25]. The SVM classifier with RBF kernel has the classification function:

$$F(x) = \sum_{i=1}^{N} \alpha_i C_i \; exp \frac{(- \parallel z_i - z \parallel^2)}{2\sigma^2} + b_i \tag{15}$$

where σ is kernel width.

IV. RESULTS

Kidney disease is considered as a dangerous disease because once it is affected, it is impossible to overhaul the damage caused to the kidney. People die of CKD mainly due to limited medical facilities. In the proposed work, we have introduced an efficient method to detect CKD using simple hardware sensing module and deep learning technique.

In kidney patients, the urea concentration levels will be more. When the kidneys are affected, they fail to remove the urea levels out of the body. We have analyzed the sensor response by taking the samples from patients under different stages of kidney disease. In our analysis, we have observed higher voltage output values in CKD samples. This is because of the elevated urea levels in the CKD samples. As urea concentration is more in CKD samples, the ammonia gas produced inside the gas chamber will be high. This leads to a higher voltage output. We have observed a voltage level of 0.93V and above for CKD samples. The voltage values were below 0.93V for healthy samples.

A. *Performance Evaluation of the Hybrid Learning Model*

The output voltage signal from the sensing module is applied to the proposed hybrid learning algorithm for automatically predicting the output. The simulation results show that the proposed 1-D CNN-SVM hybrid algorithm can successfully classify the samples. The CNN network extracted the optimal features from the sensor output signal. These are then classified using SVM. For validation, a 10-fold validation approach is employed [26]. In this work, we have further implemented a conventional CNN network for comparing the performance of our proposed CNN-SVM hybrid network. The proposed CNN-SVM hybrid model and the conventional CNN network is analyzed with the same sensing module to detect kidney disease. The performance values obtained for both these networks are shown in Table I. The proposed CNN-SVM hybrid model achieved a prediction accuracy of 96.59%, which is more than the accuracy achieved by conventional CNN. The introduction of SVM classifier significantly improved the overall performance of the proposed network.

We have also evaluated the computational speed of the two algorithms. The total computational time includes the time consumption for extracting features and feature classification. Fig. 4 illustrates the computational time of the algorithms. The programming and simulations are carried out in an Intel Core i5-7200U 2.5 GHz base processor laptop with 4GB DDR4-2400 RAM. Conventional CNN has taken 1.196s for overall computation, whereas the proposed model has taken only 1.178s. The time consumed for feature extraction is almost the same for both the algorithms. However, the proposed hybrid model outperformed convention CNN in terms of classification speed. For feature classification, the conventional CNN algorithm has taken 0.783s, whereas the proposed algorithm has taken only 0.767s. The feature extraction speed is 0.4135s and 0.4113s for conventional CNN and proposed CNN-SVM deep learning algorithm respectively.

The performance of the model is also analyzed by evaluating the Area Under the Curve (AUC) value, which is obtained by plotting the Receiver Operating Characteristic (ROC) curve [27]. The ROC curve is the plot of sensitivity against 1-specificity, for different possible cutoff test values. The AUC value shows the ability of the model to classify the samples as 'healthy' or 'diseased'. The ROC plot is shown in Fig. 5. We have obtained the AUC values of 0.947 and 0.931 for the healthy and CKD samples.

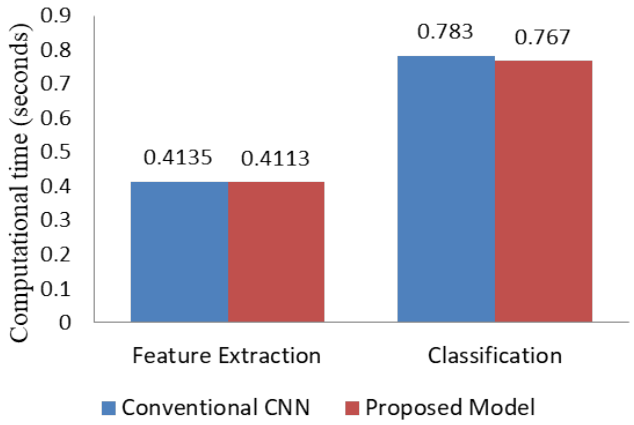

Fig. 4: Computational time comparison

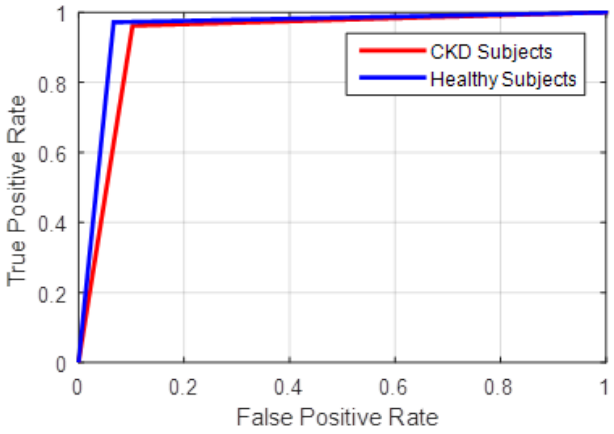

Fig. 5: ROC curve for the proposed model

B. *Clinical Validation*

The proposed sensing approach classified 45 samples as CKD patients and 53 samples as healthy subjects. To verify the results, we have carried out the clinical test to determine the GFR values of the participants. The GFR test is the gold standard used to identify kidney patients in clinical practice. The proposed model misclassified only three samples. The test results are validated by the medical professionals.

V. CONCLUSION

This paper proposes a novel approach for automated detection of CKD from saliva samples. A CNN-SVM hybrid deep learning network algorithm is developed for implementing the proposed sensing model. This network algorithm is computationally fast and efficient as the features are extracted automatically from the signal. The proposed model achieved remarkable results with a prediction accuracy of 96.59%. As the sensing approach we used in this work in new, we have validated and compared the output results with traditional clinical CKD detection method. The validation result and our experimental results are well correlated. This shows that the proposed approach can be used for monitoring and detecting CKD more effectively. In this study, we have focused on

enhancing the performance of the traditional CNN network by modifying the classification layer. We look forward to upgrading the performance of the proposed architecture by improving the feature selection and pooling part in the future. The proposed approach can be applied to further domains, by using appropriate sensors.

REFERENCES

[1] P. E. de Jong, N. Halbesma, and R. T. Gansevoort, "Screening for early chronic kidney diseasewhat method fits best?" *Nephrology Dialysis Transplantation*, vol. 21, no. 9, pp. 2358–2361, 2006.

[2] E. Skounakis, K. Banitsas, A. Badii, S. Tzoulakis, E. Maravelakis, and A. Konstantaras, "Atd: A multiplatform for semiautomatic 3-d detection of kidneys and their pathology in real time," *IEEE Transactions on Human-Machine Systems*, vol. 44, no. 1, pp. 146–153, 2013.

[3] M. A. Javaid, A. S. Ahmed, R. Durand, and S. D. Tran, "Saliva as a diagnostic tool for oral and systemic diseases," *Journal of oral biology and craniofacial research*, vol. 6, no. 1, pp. 67–76, 2016.

[4] P. Celec, L. Tóthová, K. Šebeková, L. Podracká, and P. Boor, "Salivary markers of kidney functionpotentials and limitations," *Clinica Chimica Acta*, vol. 453, pp. 28–37, 2016.

[5] B. S. Bagalad, K. Mohankumar, G. Madhushankari, M. Donoghue, and P. H. Kuberappa, "Diagnostic accuracy of salivary creatinine, urea, and potassium levels to assess dialysis need in renal failure patients," *Dental research journal*, vol. 14, no. 1, p. 13, 2017.

[6] X. Wang, L. Gao, J. Song, and H. Shen, "Beyond frame-level cnn: saliency-aware 3-d cnn with lstm for video action recognition," *IEEE Signal Processing Letters*, vol. 24, no. 4, pp. 510–514, 2017.

[7] H. Lee and H. Kwon, "Going deeper with contextual cnn for hyperspectral image classification," *IEEE Transactions on Image Processing*, vol. 26, no. 10, pp. 4843–4855, 2017.

[8] S. Banerjee and S. Das, "Mutual variation of information on transfer-cnn for face recognition with degraded probe samples," *Neurocomputing*, vol. 310, pp. 299–315, 2018.

[9] J. Wu and H. Yang, "Linear regression-based efficient svm learning for large-scale classification," *IEEE transactions on neural networks and learning systems*, vol. 26, no. 10, pp. 2357–2369, 2015.

[10] S. Raj and K. C. Ray, "Ecg signal analysis using dct-based dost and pso optimized svm," *IEEE Transactions on instrumentation and measurement*, vol. 66, no. 3, pp. 470–478, 2017.

[11] S. Kiranyaz, T. Ince, and M. Gabbouj, "Real-time patient-specific ecg classification by 1-d convolutional neural networks," *IEEE Transactions on Biomedical Engineering*, vol. 63, no. 3, pp. 664–675, 2015.

[12] S. Lekha and M. Suchetha, "Real-time non-invasive detection and classification of diabetes using modified convolution neural network," *IEEE journal of biomedical and health informatics*, vol. 22, no. 5, pp. 1630–1636, 2018.

[13] T. Ince, S. Kiranyaz, L. Eren, M. Askar, and M. Gabbouj, "Real-time motor fault detection by 1-d convolutional neural networks," *IEEE Transactions on Industrial Electronics*, vol. 63, no. 11, pp. 7067–7075, 2016.

[14] U. R. Acharya, S. L. Oh, Y. Hagiwara, J. H. Tan, and H. Adeli, "Deep convolutional neural network for the automated detection and diagnosis of seizure using eeg signals," *Computers in biology and medicine*, vol. 100, pp. 270–278, 2018.

[15] H.-C. Shin, H. R. Roth, M. Gao, L. Lu, Z. Xu, I. Nogues, J. Yao, D. Mollura, and R. M. Summers, "Deep convolutional neural networks for computer-aided detection: Cnn architectures, dataset characteristics and transfer learning," *IEEE transactions on medical imaging*, vol. 35, no. 5, pp. 1285–1298, 2016.

[16] S. Lekha and M. Suchetha, "A novel 1-d convolution neural network with svm architecture for real-time detection applications," *IEEE Sensors Journal*, vol. 18, no. 2, pp. 724–731, 2018.

[17] S. Lai, L. Jin, and W. Yang, "Toward high-performance online hccr: A cnn approach with dropdistortion, path signature and spatial stochastic max-pooling," *Pattern Recognition Letters*, vol. 89, pp. 60–66, 2017.

[18] F.-L. Chung, S. Wang, Z. Deng, and D. Hu, "Catsmlp: Toward a robust and interpretable multilayer perceptron with sigmoid activation functions," *IEEE Transactions on Systems, Man, and Cybernetics, Part B (Cybernetics)*, vol. 36, no. 6, pp. 1319–1331, 2006.

[19] D. Erdogmus, O. Fontenla-Romero, J. C. Principe, A. Alonso-Betanzos, and E. Castillo, "Linear-least-squares initialization of multilayer perceptrons through backpropagation of the desired response," *IEEE Transactions on Neural Networks*, vol. 16, no. 2, pp. 325–337, 2005.

[20] A. Shmarlouski, D. Schock-Kusch, Y. Shulhevich, V. Buschmann, T. Röhlicke, D. Herdt, M. Rädle, J. Hesser, and D. Stsepankou, "A novel analysis technique for transcutaneous measurement of glomerular filtration rate with ultralow dose marker concentrations," *IEEE Transactions on Biomedical Engineering*, vol. 63, no. 8, pp. 1742–1750, 2015.

[21] J. Georges, "Determination of ammonia and urea in urine and of urea in blood by use of an ammonia-selective electrode." *Clinical chemistry*, vol. 25, no. 11, pp. 1888–1890, 1979.

[22] B. Navaneeth and M. Suchetha, "Pso optimized 1-d cnn-svm architecture for real-time detection and classification applications," *Computers in Biology and Medicine*, 2019.

[23] T. Saidi, O. Zaim, M. Moufid, N. El Bari, R. Ionescu, and B. Bouchikhi, "Exhaled breath analysis using electronic nose and gas chromatography–mass spectrometry for non-invasive diagnosis of chronic kidney disease, diabetes mellitus and healthy subjects," *Sensors and Actuators B: Chemical*, vol. 257, pp. 178–188, 2018.

[24] T. Jayasree, M. Bobby, and S. Muttan, "Sensor data classification for renal dysfunction patients using support vector machine," *Journal of Medical and Biological Engineering*, vol. 35, no. 6, pp. 759–764, 2015.

[25] S. Jayasumana, R. Hartley, M. Salzmann, H. Li, and M. Harandi, "Kernel methods on riemannian manifolds with gaussian rbf kernels," *IEEE transactions on pattern analysis and machine intelligence*, vol. 37, no. 12, pp. 2464–2477, 2015.

[26] J. D. Rodriguez, A. Perez, and J. A. Lozano, "Sensitivity analysis of k-fold cross validation in prediction error estimation," *IEEE transactions on pattern analysis and machine intelligence*, vol. 32, no. 3, pp. 569–575, 2009.

[27] X. He, B. D. Gallas, and E. C. Frey, "Three-class roc analysistoward a general decision theoretic solution," *IEEE transactions on medical imaging*, vol. 29, no. 1, pp. 206–215, 2010.

Proceedings of the Fourth International Conference on Communication and Electronics Systems (ICCES 2019)
IEEE Conference Record # 45898; IEEE Xplore ISBN: 978-1-7281-1261-9

A Novel Approach to Aggregate and Secure Data in Wireless Sensor Networks

Harsha K.M
Department of Information Technology
Rajagiri School of Engineering and Technology
Kochi, India
Harsha.k.m84@gmail.com

Divya James
Department of Information Technology
Rajagiri School of Engineering and Technology
Kochi, India
Divyaj@rajagiritec.edu.in

***Abstract*-Wireless Sensor network has enhanced in extensive applications like sensing environment, area monitoring, threat detection. At the point when the node communicates with its neighboring nodes, it influences the system lifetime hence developed into huge utilization of energy. Data aggregation strategies have been used mainly to diminish the consumption of energy by curtailing the quantity of messages where it is migrated from the source node to the sink node. Since applications of wireless sensor network is increasing in a rapid speed it is essential to consider the security of the network. In a hostile environment, wireless sensor network is deployed the sensor nodes would be susceptible to security issues thus it would become critical. The data aggregation approach is used mainly used to protect the data, this is done by using like asymmetric protocol like RSA encryption. By using the various security issues has been preserved in data aggregation. Hence the proposed scheme secures and aggregates data in wireless sensor network there by improving the energy efficiency and communication overhead.**

Keywords: Data Aggregation, RSA, WSN,Energy Consumption

I. INTRODUCTION

Wireless Sensor Network is an extensive technology incorporated of immense quantity of sensor nodes which also includes the base station. The aspect of sensor node is to retrieve the information from the physical surroundings and accumulates and impart it to the base station. The applications in WSN which include hospital monitory, military surveillance which supervise the environmental conditions[1]. Because of the establishment of sensor nodes in an invulnerable circumstance, it is not easy for restore and compensating the batteries. The priority of WSN is to make the network lifetime to be enlarged[2].

The sensor network usually contains two types of nodes i.e. parent node and sensor node. Therefore can infuse inquiries in the network and also accumulate the outcome in the sink node, this should be possibly done in the event that anybody needs the data from the network. Data gathering is the process of assembling the recognized data from various sensor nodes that are dispersed to the main station for further handling. Hence, it is inadequate for the sensor network to impart the information straightforwardly to main hub due to these motes are resource constraint. In comprehensive network, the data created is commonly enormous for the base station. However, it is essential to consolidate and compress the information at the aggregator nodes which in the long run discard the abundance data that is sent to the main hub bringing about utilizing energy. This is adequately knowledgeable by Data aggregation. It is the coarse of collecting information from the network to remove the undesirable conveyance thus give grade data to the main hub.

WSNs are characterized into two kinds in terms of secure aggregation i.e End to End and Hop by Hop encryption. In former base station can only have the privilege to access the data and also privacy assures only in the sink node[3]. But the aggregator nodes does not have the privilege to gain proficiency with the keys that are shared among children and aggregator nodes (source and sink nodes).The type of encryption used in the proposed system is hop by hop encryption is utilized when all the sensor hubs are in the faith. Here the key imparting to the parent node arouse the complexity in the key management. It constitutes a model of data security than the former one[4].

II. RELATED WORKS

There are wide range of diverse techniques which makes to sure the preservation of the network. There are different techniques that has referenced in survey mostly used to secure protection of the source data.

PDKP [5] primarily depends on the data and key security in WSN. By utilizing this method it doesn't disclose the key and information to different nodes in the system. The aggregation function used is Sum which is also known as additive aggregation function. This Framework apply homomorphic encryption where it mainly accomplish confidentiality of data. The disclosure of data is less in this method. In proposed system time taken to process the data packets is less than compared to PDKP method.

PEPPDA[6] is an aggregation method which accomplishes non conceded data accumulation . Hence sensor nodes in the network attack recurrence would get decreased.The sink node obtain the result from its children nodes thereby diminishing the communication overhead. The principle aim is to provide a reserved data aggregation thereby guarantees security, validness and novelty of identified data and furthermore confidentiality of the gathered data by not showing a tremendous overhead. It uses slicing and mixing operation to ensure good accuracy, robust key and aggregating the data securely. The final aggregated result of integrity checking mechanism is missing in this scheme.

SEEDA[7] which is mainly used to curtail the messages that is transmitted to base station inorder to advance the network lifetime In order to achieve the data security it employs end to end type of encryption. It permits the aggregation on the ciphertext by employing homomorphic encryption. Thereby lessening the data packet that are transmitted because it does not include the data about the non acknowleged nodes. This scheme employs significant overhead where as in the proposed system the significant overhead is less.

H.S Annapurna et.al[8], it recommended a method called Fault Tolerance for systems that offers end to end privacy also adaptation to non-critical failure during data aggregation. Here the network is suffering from faults that may arise because of various motives along with communique communication failure, non functioning of hardware and software resources. It would result in a lessen the network lifetime and also hazardous effects in critical utility contexts. It proposes to apply shared cryptography to verify message correspondence. One of the most important codemn restoration method is the misuse of redundancy.

SDAP [9] employs hop by hop encryption and each group have one aggregate.It is primarily stationed by the concepts of divide-and-conquer and commit-and-attest. By using the latter method, aggregation is divided into association. The aggregates is confirmable by the main hub using commit and attest principle. The proposed method doesn't depend on the number of shares hence packet processing time is faster than SDAP.

III. BACKGROUND

Data aggregation which uses the consolidated information from various sensor nodes and its children nodes disseminate the gathered data to base station. Fig.1 shows the data aggregation process and its architecture. By using data aggregation algorithm such as centralized approach such as LEACH, TAG the aggregated data can be obtained. The type of data structure used in the proposed scheme is Tree based. This collected information is transmitted to the base station (sink node).

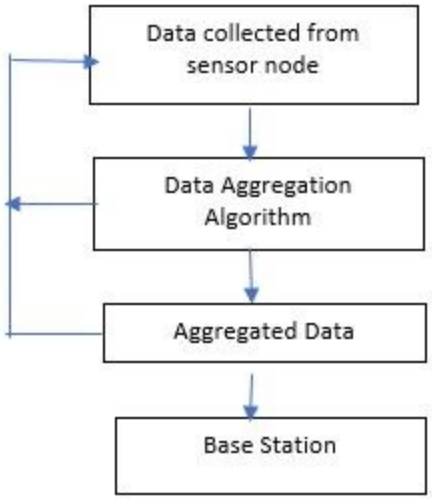

Figure 1 : Data Aggregation Process

There are different types of aggregation methods are employed,they are Centralised , In-Network aggregation, Tree Based Approach and Cluster Based Approach. In centralised approach.

In order to afford a secure communication in the sensor network it is necessary to satisfy few conditions. The necessities like availability, confidentiality, integrity and authentication. They provide guarantee to the data that is broadcasted in the network.

1) *Data Confidentiality*: When the data streams through many intermediate nodes the chances of data discharge is more. Hence it is necessary to implement data confidentiality when the encrypted content of data is utilized in such away that the data is decoded in different form.

2) *Data Integrity*: When the receiver receives the data for the first time it should not make attempt to alter the data. The assaulter changes the original content of the data mainly due to the physical environment conditions. At any point of time the assaulter can alter the data and send it to the receiver.

3) *Data Freshness*: When a message is broadcasted in the network each messages should be new and should not replay the old messages in the network. This is efficiently done by providing a time counter to each nodes to make sure that the data is new for each session.

4) *Data Availability:* Data Availability indicates even if there is assaults happens in the network, all the services should be available.

5) *Data Authentication:* It is the process in which the sink node should receive the correct data. Hence the

receiver node should do the verification process that it should receive the data from the authenticated node and should make sure should not receive the data from the malicious node.

IV. MODEL ARCHITECTURE

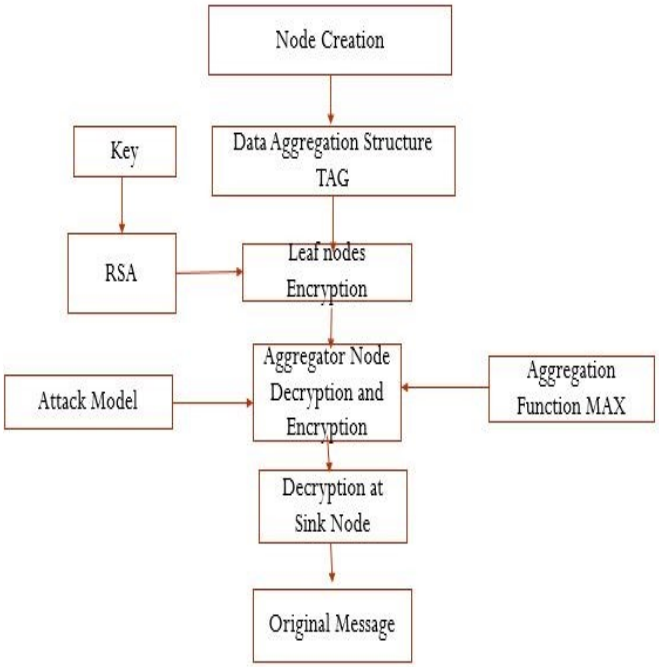

Figure 2 : System Architecture

The proposed system comprising of four modules which is shown in Fig.2 which is the proposed system architecture.

A. Network Module

The system comprises of countless compelled sensors, where as the base station is in a multi hop way. Three kinds of hubs are available in a WSNs; these are Base Station , Aggregator node and Sensor node. The children nodes is in charge of encoding the detected information and sending the aftermath to its intermediate node. Aggregator node is in charge of encoding the detected information and accumulating accepted information and forward its new outcome to its parent hub. Base Station receives the amassed outcome from various nodes.

B. Data Aggregation Structure

The data aggregation structure used is Tree Based approach[10]. This methodology characterizes from establishing the tree. Type of tree used is minimum traversing tree, central station grant as the root node and sensor hub grant as child nodes. The type of aggregation used is Tiny aggregation.

C. Secure Key Distribution and Encryption

The public key cryptography or asymmetric cryptography concocted an extreme difference in ideal models. Every sensor will figure its public/private key pair and communicate its public key to all hubs inside the system. In Key availability, the likelihood of one sensor hub finds a common key with its neighbor, is a significant factor to be considered in the key circulation plans. The type of encryption used is RSA strategy. In key generation, each node creates public key and its private key and provide two primes m and n and also prefer a integer k, gcd (k; Φ (n)) = 1. Thus node A public key is (n, k) and its private key is d. k and d are known as the encode operation and decode operation and n is modulus. For encryption B encrypts the A's message. It receive the node A's respective public key (n; k) and compute encryption and dispatch the result to A. For decoding it will get the plaintext by using the private key of the node A and does the decryption process.

D. Data Aggregation Approach

After the aggregation tree is constructed, the sink hub can spread keys to the hubs in the system. It comprises of various steps for aggregating the information, they are leaf hub encryption, encryption of intermediate node and sink node decryption. In request to aggregate the data, there are various sorts of data aggregation functions are used. The function used is max operation

E. Attack Module

Safeguarding considered as a basic worry of using the different utilizations in the network. The assailant will embrace different kinds of assault to crack the preservation of the information. The harm brought about by them fluctuates as indicated by the adversary model and system structure. There might be various potential assaults against a tree-based data aggregation protocol. One kind of assaults is behavior- based, in which the objective of an aggressor is to upset the ordinary task of the sensor organize. For instance, when a sensor hub in the tree is compromised, it can assault the fundamental routing convention, drop other hubs' readings deliberately, or cause refusal of message assaults to deny different hubs from getting communicate messages of the BS. The sort of assault that is utilized here is Blackhole assault which is executed in the aggregator hubs. An assault brought about by an outside foe on a subset of sensor hubs in a system is known as a black hole attack. The nodes are caught and re-customized by the adversary with the end goal that they don't transmit the data packets.

V. PROPOSED SYSTEM

The proposed framework utilized RSA encryption strategy is an public cryptosystem where the information are exchanged through powerful dynamic directing by time to time key esteem change securely and attack model is executed to check whether the data exchanged is verified or not.

A. Tree Construction

The type of structure used is Tiny aggregation which is a tree based structure. It is an information driven protocol, depends on a tree structure and explicitly intended for observing applications. The Fig.3 appeared above demonstrates that all motes are conveyed in the network. The base station send its id and level to the sensor motes as showed up in the figure. Right, when a center point D gets an impart notice first time from main hub S then F designates its level to be level of S plus one and allot its parent S. Then node F sends its level and id to all of its independent motes. Thus the path from children nodes to parent nodes have been constructed. This procedure is rehashed until every one of the motes have gotten the directive. The sink nodes sends question which it determines the amounts that it need to gather, and how there must be aggregated. After the tree development, the sink hub disperse the keys to every one of the hubs in the system.

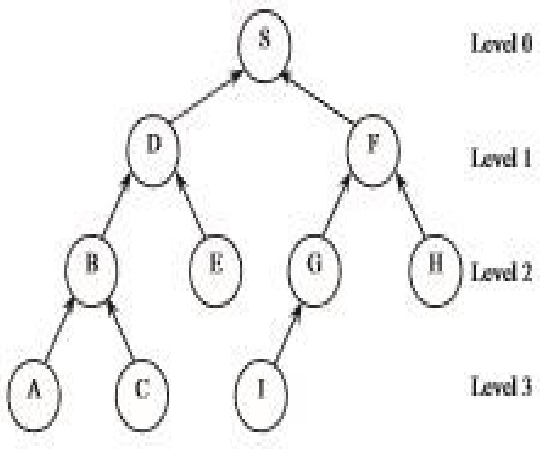

Figure 3: Structure of Tree using TAG

B. Encryption at Children nodes

The type of encryption used is RSA. Here the leaf node does only the encryption process. The children nodes broadcast the encode information to its intermediate mote even without gathering. When node A sends data to node B, the packet contains Identity of sensor node A and encryption process of node A.

$$c = m^e \bmod n$$

C. Aggregation at Aggregator node

The encrypted data in the leaf notes can be decoded uniquely by the central station. Aggregator node gets encoded information from children nodes which then decrypts and selects the max value by using aggregation function and send it to next aggregator node. This procedure proceeds for every one of the level in the tree till level 1.

D. Base Station Decryption

Base station gets the aggregated data which includes IDs of all the nodes. Committed sensor node is been identified by the base station.. To get original data it subtracts all nodes key in the system. The RSA decryption;

$$m = c^d \bmod n$$

IV. SIMULATION FRAMEWORK

It is carried out by employing Network Simulator-2 (NS-2). Ubuntu 16.04 is the Operating System. The framework where it is actualized is a 64 bit framework with Intel Pentium CPU and GB. The proposed technique has been implemented using different evaluation metrics like communication overhead and energy efficiency. The maximum packet size of the system is 100 bytes.

TABLE.1 SIMULATION PARAMETERS

Total Nodes	50
Total Frame Size	500 x 500 square meter
Transmission Range	200m
Time taken for Simulation	50 sec
Initial Energy	50J
Transmission Power	0.920J
Receiving Power	0.592J

V. PERFORMANCE ANALYSIS

A. Communication Overhead

Correspondence overhead is the quantity of information produced in the sensor network. The quantity of information expands corresponding to the quantity of motes in the network. Here one information in a sensor hub is encrypted and send to aggregator node and this encoded information are collected and send to the base station node. Communication overhead is plotted as time interval versus the number of messages. In this the number of messages is reduced by transferring the packet from low level nodes to high level nodes in the aggregation tree.

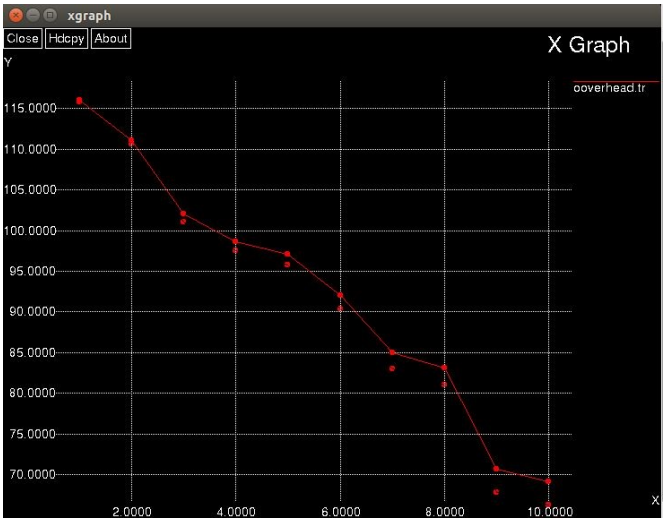

Figure 4 : Communication Overhead

B. Energy Efficiency

In this scheme the hop by hop encryption are employed. Here computational overload is less due to simple aggregation operations. The operation that is employed is Max operation. Here the information transmission and gathering requires more vitality of motes. Lessening the quantity of broadcasting fundamentally spare vitality of motes. From Fig. 5 energy efficiency of the motes increases after aggregation process.

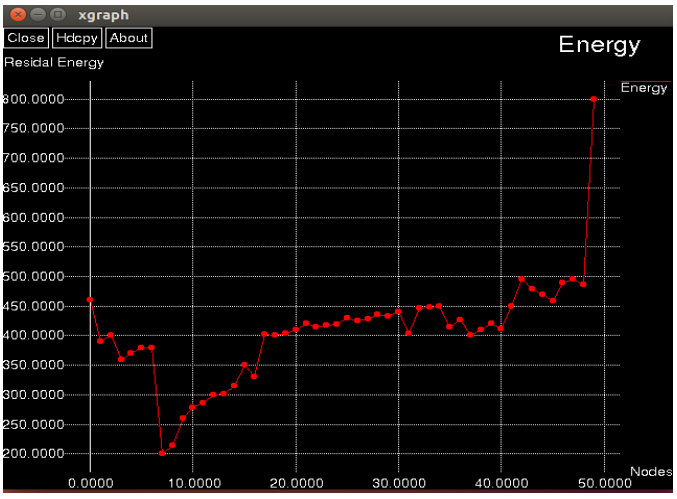

Figure 5: Energy Efficiency

C. Comparison Graph

The Fig.6 depicts the xgraph of data aggregation by using sum and max aggregation. From the pictorial representation it depicts that the time to process the data packets and complete the simulation is more in sum aggregation than max aggregation. Thus by using max processing time is efficient.

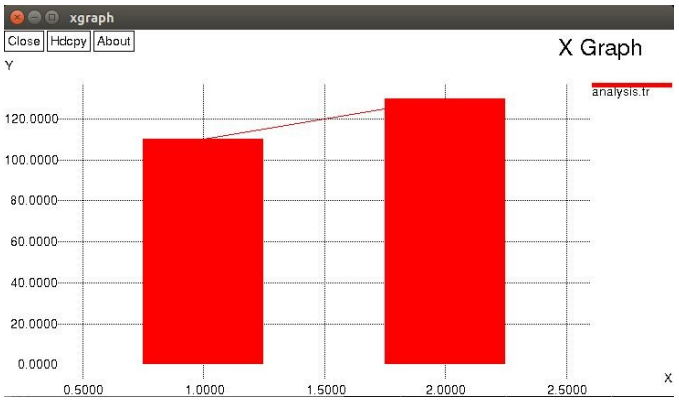

Figure 6: Comparison of MAX and SUM aggregation

VI.CONCLUSION

By utilizing data aggregation which brings about saving vitality and expands energy effectiveness, it additionally diminishes the quantity of transmissions in the system decreasing the data transfer capacity utilization and eliminating the superfluous energy utilization in the both transmissions and reception. Dependable and trustful information collection is required for every function in the network.

In this project, for securing the data there are key distribution and asymmetric encryption are employed. The kind of encryption utilized is RSA encryption. Hence time taken to process packets is less for max aggregation than sum aggregation. It additionally safeguards the different security issues, for example, data freshness, data trustworthiness, data secrecy in information total.

REFERENCE

[1] Taochun Wang, Xiaolin Qin, and Liang Liu, “An Energy-Efficient and Scalable Secure Data Aggregation for Wireless Sensor Networks”, International Journal of Distributed Sensor Networks, Hindawi, 2013.

[2] Shirshu Varma, Uma Shanker Tiwary, “Data Aggregation in Cluster based Wireless Sensor Networks”, Proceedings of the First International Conference on Intelligent Human Computer Interaction, Springer, 2009, pp 391-400.

[3] Priyanka B.Gaikwad, Manisha R.Dhage,”Survey on Secure Data Aggregation in Wireless Sensor Network”, International Conference on Computing Communication Control and Automation,2015.

[4] Adrian Perrig, Robert Szewczyk, Victor Wen, David Culler, J. D. Tygar, “SPINS: Security Protocols for Sensor Networks”, in ACM journal of Wireless Network.

[5] V.Akila , Dr T.Sheela , "Preserving Data and Key Privacy in Data Aggregation in Wireless Sensor Networks”, Second International Conference on Computing and Communication Technology,2017.

[6] Joyce Jose, M Prince and Josna Jose, “PEPPDA: Power Efficient Privacy Preserving Data Aggregation for Wireless Sensor Networks”, IEEE International Conference on Emerging Trends in Computing, Communication and Nanotechnology,2013.

[7] A.S Poornima , B.B Amberker “ SEEDA : Secure End-to End Data Aggregation in Wireless Sensor networks" IEEE Seventh International Conference on Wireless and Optical Communication Networks 2010.

[8] H.S Annapurna, M.Siddappa, "Secure Data Aggregation with Fault Tolerance in Wireless Sensor Networks", IEEE International Conference on Emerging, Research in Electronics and Computer science Technology 2015.
[9] Yi Yang, Xinran Wang, Sencun Zhu, Guohong Cao, "SDAP :A Secure Hop by Hop Data Aggregation Protocol for Sensor Networks", Proceedings of the ACM,2006.
[10] S. Madden et al., "TAG: a Tiny Aggregation Service for Adhoc Sensor Networks,OSDI 2002, Boston, MA,December 2015.
[11] Riker, André, Eduardo Cerqueira, Marilia Curado, and Edmundo Monteiro,"A two-tier adaptive data aggregation approach for M2M group communication", IEEE Sensor Journal 16,no.3(2016).
[12] Kiran Maraiya, Kamal Kant, Nitin Gupta," Wireless Sensor Network: A Review on Data Aggregation", International Journal of Scientific & Engineering Research, Volume 2, Issue 4, 2011.
[13] P.Raghu Vamsi,Krishna Kant,"Secure data aggregation and Instrution detection in Wireless Sensor Networks" ,IEEE International Conference on Signal Processing and Communication,2015.
[14] V.Vaidehi,R.Kayalvizhi,N.Chandra Sekar, "Secure Data Aggregation in Wireless Sensor Networks," IEEE International Conference on Computing Sustainable Global Development,2015.

Proceedings of the Fourth International Conference on Communication and Electronics Systems (ICCES 2019)
IEEE Conference Record # 45898; IEEE Xplore ISBN: 978-1-7281-1261-9

Analysing the learning style of an individual and suggesting field of study using Machine Learning techniques

Ananthu S Kuttattu[1], Gokul G S[2], Hari Prasad[3], Jijith Murali[4] Lekshmi S Nair[5]
Department of Computer Science and Engineering
Amrita Vishwa Vidyapeetham
Amritapuri, India
[1]anandhus.kuttattu@gmail.com, [2]gokulg35@gmail.com, [3]prasadhari905@gmail.com,
[4]jijith331@gmail.com, [5]lekshmiprabha.s@gmail.com

***Abstract*—The learning style can be referred to as the way a student prefers to acquire, process and retain information. The prominent learning style classification model is the VAK model. [1] According to this model visual, kinesthetic and auditory are the three major kinds of learning styles. Many research have shown that people prefer more than one way of learning, hence categorizing a person to just one of the above types as done in traditional methods is not accurate.[7] A method to identify our learning styles more accurately is required. Machine learning can be applied in this field to achieve our aim in the most efficient way. Once we have an accurate information about learning styles, we can use it to suggest career options. This research aims to predict the learning style combinations of students and suggest field of study using algorithms like k-means, SVM and decision tree.**

***Index Terms*—Machine Learning, auditory, visual, kinesthetic, Rule based system, k-means, SVM, Decision Tree**

I. Introduction

Choosing an appropriate field for higher studies is a complicated task. Most students require guidance in making the perfect choice. The domain of study of a student needs to suite not only the interest but also the learning style which will impart a way for career advancement. Even though there are many options that help in shortlisting career options, not many of them use learning style as one of the criteria for coming up with the choice.

Most of the traditional ways to identify the learning styles are predefined mathematical equations and patterns of questions that comes to a conclusion. It is not accurate because students prefer more than one mode of learning. The most widely accepted categories of learning styles are:

- Auditory
- Visual
- Kinesthetic

A student is said to be an auditory learner if he/she learns by listening. They tend to understand information in a better way when they hear it. These types of learners are comfortable with lectures, discussions and reading aloud. They get the idea after being told a couple of times since they are good listeners. They have a tendency to read aloud, this helps them in understanding the information in a better manner.

The main tool for a visual learner are their eyes, i.e they learn through vision. Visual learners benefit more from a live demonstration of how things are done. They require diagrams, flowcharts, presentations, etc for a better understanding of the information presented to them.

Kinesthetic learners are those who require hands-on experience to understand the concept. They like to be more involved in the processes that require their attention when compared to the other two types of learners. These learners require active learning methods like role-playing, hands-on workshops, practicals, etc for processing the information in a better manner.

Categorizing a student based on the above mentioned learning styles is not an easy task, because most students prefer more than one way of learning. For example, a visual learner might be interested in hands-on workshops. In such case a student can be considered as a kinesthetic learner too. In these type of situations, the traditional methods for identifying the learning style which are based on predefined equations and question patterns are less accurate. Thus it demands the possibility of the existence of combinations in learning styles. A student may exhibit more than one learning style. In order to find this combination of learning styles, we apply machine learning. We will be using the classification and the clustering to fit a learner into an appropriate class of learning style.

Clustering is an unsupervised machine learning technique. We used the k-Means clustering algorithm as it is an iterative algorithm, that tries to partition the dataset into k predefined distinct non overlapping subgroups where each data point belongs to only one group and inter cluster data points can be made. We do the classification which groups new data into known classes while clustering relies on underlying patterns to come up with the clusters. We have used two classification algorithms, Support vector machines (SVM) and Decision tree. We have used SVM to predict the individual learning style and decision tree to predict the learning style combination. All these algorithms were chosen in order to maximise the

accuracy and efficiency of our program.

Once we have acquired a student's learning style combination, we can compare it with the learning style combinations prevalent in existing field of study. Based on the degree of similarity we can suggest an area of study to that person. Career selection is a subjective process and depends on the interests of the individual too. With this work, we hope to suggest valid career options for prospective learners based on their learning style combination.

II. Background and related work

Much study was done in the field of identification or prediction of learning styles. For example, a survey was conducted in 2016 on 175 students studying MS programming in engineering. For this survey they have used the questions in Index of Learning Styles by Felder and Soloman [15]. According to this survey, there is a huge diversity in the learning styles among engineering students studying in different branches.[6]

A similar survey was conducted among medical students [3]. A questionnaire consisting thirty nine questions were used. Two-hundred and ninety students participated in the survey. Based on the results seventy three percent of the students who participated in the survey prefer only one learning style, twenty two percent prefer two learning styles and the rest prefer three learning styles. Most of the students who prefer single learning style prefer visual learning style followed by auditory and then kinesthetic. Among the students who prefer two learning style fifty four percent prefer visual and auditory, twenty six percent prefer visual and kinesthetic and the rest prefer auditory and kinesthetic.

An Indonesian translated version of Joy Reids (1984) Perceptual Learning Style Preference Questionnaire was used to conduct a survey among 3rd semester English Department students of Faculty of Cultural Studies at Universitas Brawijaya [2]. A total of hundred students participated in the survey, out of which sixty six were females and the rest were males. The study revealed that majority of the male students who took the survey prefers kinesthetic mode of learning while majority of female students preferred either kinesthetic or group study.

VARK questionnaire developed by Flemming and Miles (1992) was used to assess the learning style preferences of the engineering students at Atlm University [4]. The questionnaire was answered by 107 students out of which sixty one were from computer science, twenty two were from manufacturing engineering and twenty four were from mechatronics engineering. The study showed that around 25.2% of the students prefer more than one mode of learning style. 27.9% of the computer science students who took the survey prefers multiple modes of learning styles and among the students who prefer single learning style, the most preferred styles are auditory, kinesthetic and reading/writing. The most popular learning style among the manufacturing engineering students was found out to be auditory. 29.2% of mechatronics students prefer multiple learning style and among the rest of the students who prefer single learning style, the most preferred style was auditory.

One instance where machine learning was used to identify the learning style is the website 'First aid for you'. Here, machine learning was used to observe how the user interacts with the website and identify patterns in those interactions Those patters are then used to identify the best type of content for the next page. Here, they have used Felder & Solomon Index of Learning Style. Nave Bayes algorithm was used to identify the preferred learning style of the user and this information was used to customize the learning environment.[11]

In [5], the use of k-means in multi label classification is being discussed. The rule mining algorithm Apriori is a popular choice for rule generation, but when it comes to numerical data. With proper pre-processing, a lot of intricate rules can be derived form those numerical datasets. K-means algorithm can be used for this purpose. This helps in finding hidden patterns in huge numerical datasets.

A detailed study of the advantages and disadvantages of both traditional and modern techniques for learning style identification methods was done in [7]. Based on the result it was identified that most of the traditional methods which uses questionnaire and patters in questions lacks authenticity because they follow a general rule which cannot be applied in all individual cases. Modern techniques using machine learning are computationally expensive compared to the traditional ones but they tend to be more accurate.

Support vector machine (SVM) algorithm is widely used in classification and regression analysis. [8] does a detailed analysis on the implementation of SVM using both linear and Map-Reduce fashion. The performance of thus implemented algorithm is then compared.

A fuzzy inference system was used for predicting preferred learner style based on the features used for the VARK questionnaire. The system was tested on a group of students. The input data for the system was collected from a custom questionnaire that was designed specially to get the inputs for the fuzzy inference system. On comparing the output of the fuzzy system to that of the VARK system it was observed that 48% of the test cases were similarly classified.[10]

K-Means clustering encounters issues when it deals with text data. [12] focuses on eliminating this drawback by converting text data into a numerical value which results in more distinct clusters and accurate running times.

The use of tree augmented Bayes network was observed to have better classification accuracy when compared to naive Bayesian network. [13] Online learning environment was used as the platform for automatically detecting students learning style using tree augmented Bayesian network. The experimental results proved that the tree augmented naive Bayes network is capable of achieving higher detection accuracy when compared to the Bayesian network.

Decision trees are commonly used for representing data. In data mining, many different decision tree algorithms are used and each of those provide a unique decision tree from the input data. [14] focus on the comparison of different decision tree algorithms for data analysis.

A study was conducted among the dental students of King

Saud University to find their learning style pattern [16]. An arabic version of VARK questionnaire was used to conduct the survey. The results showed that most students (58.4%) preferred more than one learning style. Among the students who preferred single learning style, Kinesthetic and Auditory were the most prominent.

In [17] the authors have used supervised and unsupervised machine learning algorithms to predict the learners learning style. They have used the Felder and Silverman learning style model for categorizing learners. The unsupervised learning algorithm that they have used is K means and the supervised learning algorithm that they have used is Naive Bayes.

The learning style identification survey done among the architecture and interior design students reveal that there is no significant difference between the learning styles between students of architecture and interior design [18]. Here, the authors used Felder and Soloman's Index of Learning Styles questionnaire to conduct the survey.

III. Proposed Work

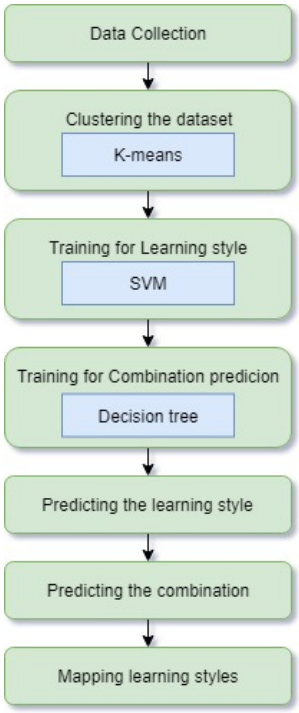

Fig. 1. Steps involved

A. Data Collection

A survey was conducted among the student community of Amrita Vishwa Vidyapeetam University. The survey consisted of fifteen questions. All the questions were multiple choice type and choices included "Strongly Disagree", "Disagree", "Neutral", "Agree" and "Strongly Agree". Each of the above value is mapped to a numerical value, with Strongly disagree as one and Strongly agree as five. The survey was conducted among people with age ranging from fifteen to twenty five. We were able to acquire one thousand one hundred and twenty three inputs. The obtained results was then stored in CSV format.

B. Data Clustering

Clustering of the data helps us to find underlying patterns and categorize them to different groups called clusters. Here we are using K-means clustering algorithm. k-means algorithm is computationally faster when compared to other clustering algorithms when the number of variables are more. According to this algorithm, the initial step is to assign k centroids randomly. Once we identify the centroids, Euclidean distance between each data point and the centroid is calculated. Each data points is then assigned to the centroid which is closest to it. The centroids are then re-positioned for optimization. These processes are iteratively repeated until the centroids doesn't change anymore i.e the centroids are at the center of the clusters that we wanted to create. Here, after applying the k-means algorithm we end up with fifty one clusters. Each and every data will have a cluster number associated with it. We add this cluster number as a feature in the dataset, so the total number of features will be sixteen after data clustering. Once the cluster number is also added to the dataset, we can divide the dataset into test set and train set. In this case we will be dividing the data set equally and one will be taken as test set and the other will be the train set.

C. Data Classification

Studies have shown that clustering the data before classification can increase the accuracy of the classification process. [9] Also the cluster number that we added after the clustering will play a vital role in classifying the data. Logistic regression is a simple and fast classification algorithm and we will be using it in our project. One of the simplest and highly preferred classification algorithm which produce significant accuracy with comparatively less computation power is the Support Vector Machines (SVM). Support Vector Machine is used for regression and classification. The objective of the support vector machine algorithm is to find a hyperplane in an N-dimensional space that distinctly classifies the data points. We apply this algorithm on the training set and trains the algorithm. Once the training is done we apply the same on the test set to predict the learning style. We compare the predicted value of learning style to the existing value and calculates the accuracy of our prediction. We obtained an accuracy of 92.87%.

D. Combination Prediction

We are at a stage where we could predict the learning style of a person but we are limited to a single learning style per person. Our next aim is then to find a combination of learning styles per person. For this we have used a statistical technique called Rand index. Rand index is used for finding the similarity between clusters. Combinations are obtained from clusters that are similar. If a data point that is in a cluster

that is predominantly auditory but if that cluster is similar to another cluster that is predominantly visual, we can trace that data point to visual learning style too, in such a way we find the combinations for all the data points present in training set.

Instead of calculating the combinations every time using adjusted rand index, we could use machine learning to predict the combinations. One of the most widely used predictive analytic algorithm is decision tree. Decision tree construct a tree of predictive decisions made based on actual values of attributes in the data. We create a training model using decision tree algorithm which takes the cluster value, the individual learning style and the combinations obtained using the rand index method as input. We pass the above said features of the training set as input to the training model. By doing so we are training the algorithm for prediction of combinations. Once we have trained the algorithm, we could pass the test set to the trained algorithm and obtain combinations as output.

E. Mapping

Now we are able to predict the learning style combination, in-order to suggest career options we require the information about the prevalent learning styles present in each career. The only way to acquire such information is through extensive survey. Once we have a database containing the most common career options and their prevalent learning style combinations, we could compare it with the learning style of a person and come up with valid suggestions. As of now, information in this regard is limited and based on some of the previous studies done in various parts of the world, we have acquired the following information:

- The prevalent learning styles present among **Computer Science** graduates are ***Auditory*** and ***Kinesthetic***.
- The prevalent learning style present among **Manufacturing Engineering** graduates is ***Auditory***.
- The prevalent learning style present among **Mechatronics Engineering** graduates is ***Auditory***.
- The prevalent learning style present among **Medical** graduates is ***Visual***.

Based on the learning style combination of a person we could suggest any one or more of the career options from the above list. We have used a rule based system for mapping the learning styles. The rules that we have created for the rule based system are as follows:

- ***Auditory***, ***Kinesthetic*** and ***Visual***: Computer Science, Manufacturing engineering, Mechatronics engineering and Medical
- ***Auditory*** and ***Kinesthetic***: Computer Science, Manufacturing engineering and Mechatronics engineering
- ***Kinesthetic*** and ***Visual***: Computer Science and Medical
- ***Auditory*** and ***Visual***: Computer Science, Manufacturing engineering, Mechatronics engineering and Medical
- ***Auditory***: Computer Science, Manufacturing engineering and Mechatronics engineering
- ***kinesthetic***: Computer Science
- ***Visual***: Medical

IV. RESULT

The initial distribution of learning styles in our database is as shown in Fig. 2.

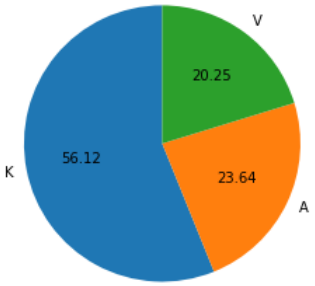

Fig. 2. Initial classification based on learning styles

Based on the rules that we have developed for mapping we can infer that fifty six percent of the students who took our survey can choose Computer Science related field as a career option and twenty three percent of the students can choose Computer science, Manufacturing engineering or Mechatronics engineering as a career option while the rest can choose medical field as their career choice. Using our proposed model we were able to efficiently predict the learning style combination of a student. After passing the same database to our program we obtained the result as depicted in Fig. 3.

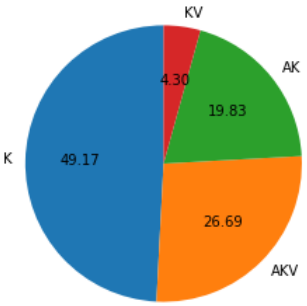

Fig. 3. classification based on learning styles after using our program

Here we observe the presence of combinations like Kinesthetic and Visual (KV), Auditory and Kinesthetic (AK) and Auditory, Kinesthetic and Visual (AKV) along with Kinesthetic. If we apply our mapping rules to the above result, we observe that around twenty six percent of the students who took our survey can choose any of the four career options, around twenty percent of the students can take Computer Science, Manufacturing engineering or Mechatronics engineering, nearly five percent of the students can take Computer Science or Medical as their choice while the rest can choose

Computer Science as their career option. Compared to the previous observation, learning style combinations have given us more accurate and specific results. Thus, identifying a student's learning style combination can help us in coming up with more precise and unique career suggestions.

V. Conclusion

We were able to learn in depth about student learning styles. Unlike the traditional methods, we are now able to predict the learning style combinations of a student using machine learning. The use of machine learning algorithms has provided a new perspective on the technique of finding learning styles. Using a rule-based system, we were able to map learning styles to certain fields of study and identifying the fields of study that suits a student's learning style can help the student in shortlisting career choices.

VI. Future Scope

As per the current implementation, we are able to suggest only four field of study. This is because of the lack of data regarding the prevalent learning styles in other fields of study. Much research can be done in this area and once we have enough information, we can suggest more and more options to students.

VII. Acknowledgement

We would like to express our sincere gratitude to the students of Amrita University who took part in our survey.

References

[1] MR. SREENIDHI S K and MS. TAY CHINYI HELENA, "Styles of Learning Based on the Research of Fernald, Keller, Orton, Gillingham, Stillman , Montessori and Neil D Fleming", INTERNATIONAL JOURNAL FOR INNOVATIVE RESEARCH IN MULTIDISCIPLINARY FIELD ISSN 2455-0620 Volume - 3, Issue - 4, Apr - 2017

[2] Peptia Asrining Tyas, Mega Safitri, "Kinesthetic Learning Style Preferences: A Survey of Indonesian EFL Learners by Gender", Journal of English Educators Society, (April 29, 2017).

[3] Alina-Mihaela Buan, "Learning Styles of Medical Students - Implications in Education", US National Library of Medicine National Institutes of Health, (April 2014)

[4] Burcu Devrim Ictenbas, Hande Eryilmaz, "Determining Learning Styles of Engineering Students to Improve the Design of a Service Course ", Procedia - Social and Behavioral Sciences (Volume 28 2011)

[5] H Haripriya, Prathibhamol Cp, Yashwant RPai and M Sai Sandeep, "Multi Label Prediction Using Association Rule Generation and Simple k-Means", 2016 International Conference on Computational Techniques in Information and Communication Technologies (ICCTICT)

[6] Tulsi PK; Poonia MP and Anu Priya, "Learning Styles of Engineering Students.", Journal of Engineering Education Transformations , Volume 30 , No. 2, October 2016

[7] Y. Helmy., A. Abdo. and R. Abdallah., "A Proposed Framework for Learning Style Prediction in Higher Education Environments.", International Journal of Advanced Research in Computer Science and Software Engineering (Volume 6, Issue 3, March 2016).

[8] M. V. Sukanya, Shiju Sathyadevan, and Sreeveni, U. B. Unmesha, Benchmarking support vector machines implementation using multiple techniques, in Advances in Intelligent Systems and Computing, 2015, vol. 320, pp. 227-238.

[9] Yaswanth Kumar Alapati, Korrapati Sindhu "Combining Clustering with Classification: A Technique to Improve Classification Accuracy", International Journal of Computer Science Engineering (IJCSE).

[10] Marwah Alian and Adnan Shaout, "Predicting learners styles based on fuzzy model", Springer Science + Business Media New York 2016

[11] Declan Kelly, Brendan Tangney, "First Aid for You: Getting to know your Learning Style using Machine Learning. In: Advanced Learning Technologies", 2005. ICALT 2005. Fifth IEEE International Conference (August 2005)

[12] Unnikrishnan, S.; Sreelakshmi, S.; Deepa, G.,"Enhancement of accuracy in K-means clustering" , International Journal of Control Theory and Applications Volume 9, Issue 15, 2016, Pages 7619-7626

[13] Ling Xiao Li and Siti Soraya Abdul Rahman, "Students learning style detection using tree augmented naive Bayes", Royal Society Open Science (June 21, 2018).

[14] Sathyadevan S., Nair R.R. (2015), "Comparative Analysis of Decision Tree Algorithms: ID3, C4.5 and Random Forest.", In: Jain L., Behera H., Mandal J., Mohapatra D. (eds) Computational Intelligence in Data Mining - Volume 1. Smart Innovation, Systems and Technologies, vol 31. Springer, New Delhi

[15] "Index of Learning Styles Questionnaire", https://www.webtools.ncsu.edu/learningstyles/

[16] Moshabab A. Asiry, "Learning styles of dental students", The Saudi Journal for Dental Research (2016) 7, 1317

[17] Ouafae EL AISSAOUI, Yasser EL ALAMI EL MADANI, Lahcen OUGHDIR and Youssouf EL ALLIOUI, "Combining supervised and unsupervised machine learning algorithms to predict the learners learning styles", Second International Conference on Intelligent Computing in Data Sciences (ICDS 2018)

[18] Wafa Labiba, Irene Pasinaa, Abdelhakim Abdelhadia, Goze Bayrama, Mohammad Nurunnabi, "Learning style preferences of architecture and interior design students in Saudi Arabia: A survey", MethodsX Volume 6, 2019, Pages 961-967

Proceedings of the Fourth International Conference on Communication and Electronics Systems (ICCES 2019)
IEEE Conference Record # 45898; IEEE Xplore ISBN: 978-1-7281-1261-9

Comparative Analysis of Texture Features and Deep Learning Method for Real-time Indoor Object Recognition

Jayakanth K
Computer Science and Engineering Department
Manipal Institute of Technology
Manipal Academy of Higher Education(MAHE)
Manipal, Karnataka, India
jayakanth.k.kunhoth@gmail.com

***Abstract*—Object recognition and classification are considered as major tasks in the field of computer vision. They are well suited for applications such as a real-time system for people counting, object recognition system for people with visual impairments, surveillance systems, etc. The deployment of computer vision, machine learning, and deep learning algorithms enable to recognize the objects from an image or video frame. This paper proposes a real-time system for indoor object recognition. Moreover, the proposed work mainly focuses on analyzing the performance of various texture features, machine learning classifiers and deep learning methodologies to recognize the objects in indoor areas. The proposed methodology is validated in a publically available indoor object dataset "MCindoor20000". The dataset consists of three categories of objects including doors, stairs, and sign. Our developed deep learning model using transfer learning approach yielded 100 % accuracy and texture features such as LPQ and BSIF have yielded an accuracy of more than 98% with SVM and KNN classifiers.**

Keywords—Indoor object recognition, LPQ, LBP, BSIF, Machine learning, SVM, KNN, NB, Transfer Learning

I. INTRODUCTION

Object recognition systems aid the user to classify the objects in indoor and outdoor areas into their respected categories. Object recognition is the important technology behind various systems such as driverless cars [1], robotic navigation systems [2], visual indoor navigation systems [3], etc. Indoor object recognition systems are developed to identify the objects commonly found in indoor areas such as door, tables, furniture, laptops, windows, food, medicines, etc. Indoor object recognition technology has various applications such as it can be extended to guide the people with visual impairments in complex buildings such as universities, shopping malls, museums. Moreover, indoor object recognition technology is leveraged in the development of robotic indoor navigation systems.

Considerable number of systems have been developed in the past decades to classify and recognize either indoor objects or outdoor objects or both indoor and outdoor objects. In addition, some of these systems are designed to recognize single objects while the rest of the systems can recognize multiple objects found in the single frame. In these systems, object recognition has been mostly performed by extracting various visual features of the images such as speeded up robust features (SURF) [4], color histograms [5], Histogram oriented gradients (HOG) descriptors [6] and utilizing machine learning methodologies such as SVM [7], artificial neural networks (ANN) [8] to do the classification task. Moreover artificial neural networks including deep convolutional neural networks [9] have been utilized in recent systems to recognize the objects.

Our work is mainly focused on the development of a fast and accurate system for the indoor object recognition task. The overview of the system is illustrated in figure 1. The main contribution of this work includes,

- Application of various image texture features such as LPQ [10], local binary pattern (LBP) [11] and BSIF [12] for indoor object recognition, where LPQ and BSIF have not been utilized for indoor object recognition in the past.
- Utilization of adequately large publically available indoor dataset for the validation experiments of proposed methods.
- Improving the recognition performance by utilizing the transfer learning approach with a pre-trained GoogleNet [13] model in the publically available indoor object dataset.

The rest of the paper is organized as follows. Section II reviews the related works briefly. The methodology of the proposed work is detailed in Section III. Section IV describes the details about the dataset. The evaluation results are provided in section V.Finally, in section VI we conclude the paper.

XXX-X-XXXX-XXXX-X/XX/$XX.00 ©20XX IEEE
978-1-7281-1261-9/19/$31.00 ©2019 IEEE

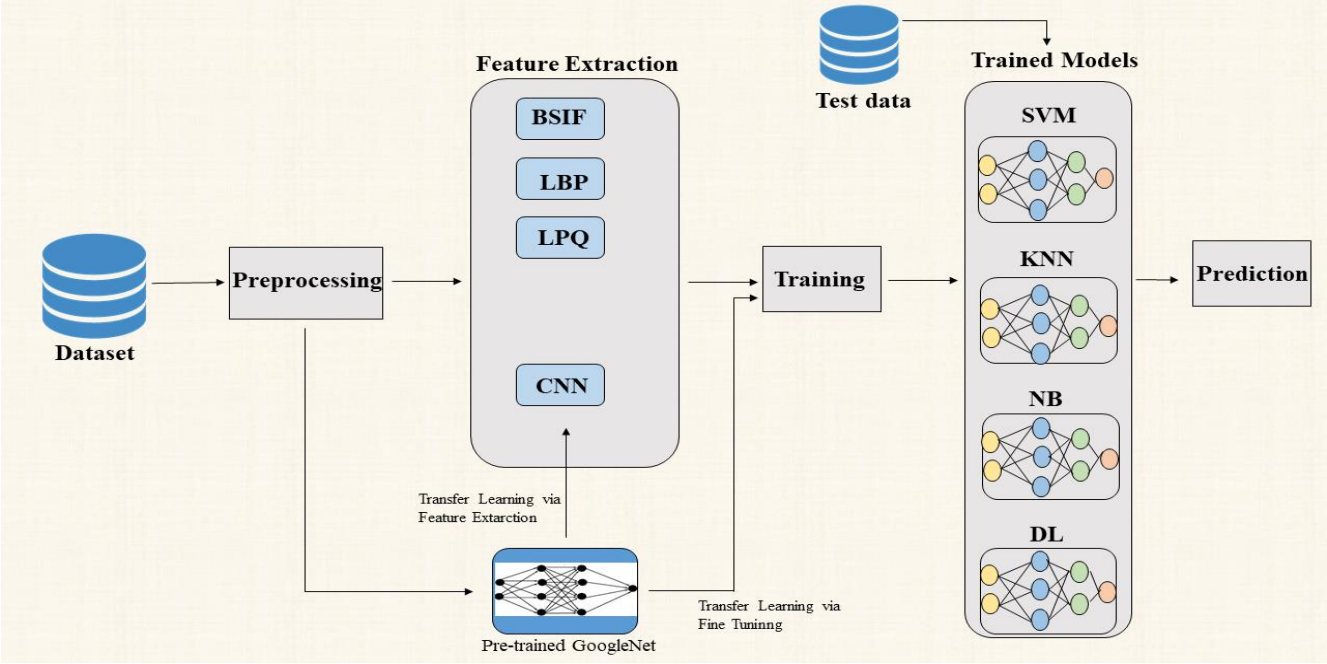

Fig. 1. System Overview

II. Related Works

Several indoor object recognition system has been proposed in the literature. Most of these systems are developed for a specific purpose such as to identify food [5] or currencies [14] or escalators [15] etc. There exist some systems developed especially for the people with visual impairments [16].In computer vision based systems, tag-based approaches are implemented in Badge3D [17], Shoptalk [18], Trinetra [19] to recognize objects. These systems make use of some visual tags or bar codes or visual marker embedded on the object to recognize them. A camera or smartphone will be available with the system to capture the tag and process it. In this section, we focused on the brief review of the systems which utilize handcrafted visual feature extraction techniques, machine learning algorithms and deep learning methodologies for the object recognition task.

Ramis et al. [20] proposed a SIFT features [21] based approach to recognize objects for mobile robots. The proposed method compares the sift keys of the query image with the sift keys of the images stored in the database. The nearest neighbor method using Euclidean distance metric was utilized for comparing the key points. Moreover, the Hough line transform is utilized to cluster the matching keys and thereby removing the outliers. The object recognition module of the LooKTel [22] utilized SIFT descriptor based bag - of- words features method to recognize the objects. The system is able to recognize packed goods, currencies, etc. To improve the recognition performance a tag-based approach was also combined with the SIFT feature based recognition system. Chincha et al. [23] proposed a system for people with visual impairments to recognize commonly found objects such as keys, wallets, mobile phones, etc. The proposed system utilized SURF feature descriptors of the query image and stored images to recognize the objects. Winlock et al. [24] proposed a system for the recognition of objects such as packaged items and other common objects found in grocery. The proposed system was specially designed for blinds. The system utilized SURF feature descriptor along with color histograms to recognize the objects.

Food cam [5] is designed for real-time food recognition using smartphones. The proposed system utilizes two machine learning models to fulfill the recognition task. The first model is an SVM classifier trained with color histogram and SURF features of the images. The second model is another SVM model trained with HOG patch and color descriptor. Lameira et al. [7] proposed an object recognition system using smartphones. The proposed system utilizes a trained SVM classifier model to recognize the objects in the captured images. The center-symmetric LBP features were extracted from the images to create the feature vectors for training the SVM classifier. Parkhi et al. [8] proposed a system to recognize objects such as coffee mugs, bags, laptops, containers, etc. An ANN trained with color and shape features of the objects is used for object recognition. The back-propagation algorithm was utilized to train the ANN and Sobel edge detector was used to extract the features. A smartphone-based currency recognition system was proposed in [14]. The proposed system analyzed the performance of different visual features of images such as SIFT, SURF, and ORB-FREAK for currency recognition. Obtained results displayed that SIFT feature descriptor improved the currency recognition accuracy compared to the other two feature descriptors. Bashiri et al. [25] proposed a system to assist the

visually impaired people in the indoor environment. The proposed system is able to recognize objects such as door, stairs, and signs. A deep convolutional neural network model was implemented for recognizing the indoor objects. Transfer learning approach was adopted for building the deep learning model using a pre-trained Alex Net model. The proposed system yielded a recognition accuracy of more than 98 %.

In brief, considerable number of systems have been developed for indoor object recognition. Various image features such as SIFT, SURF, HOG, and LBP are used in these systems. Deep learning models based on transfer learning approach was also adopted for object recognition. So we considered the usage of texture features such as LPQ, BSIF with SVM, KNN, NB classifiers and transfer learning approach using pre-trained GoogleNet model in our system.

III. METHODOLOGY

A. Feature Extraction

Local Binary Pattern(LBP) is a texture feature descriptor developed by Ojala et al. [26].LBP is a specific instance of the texture spectrum model. The LBP computation for an image consists of five steps. Figure 2 illustrates the steps involved in the calculation of the LBP feature of an RGB image.

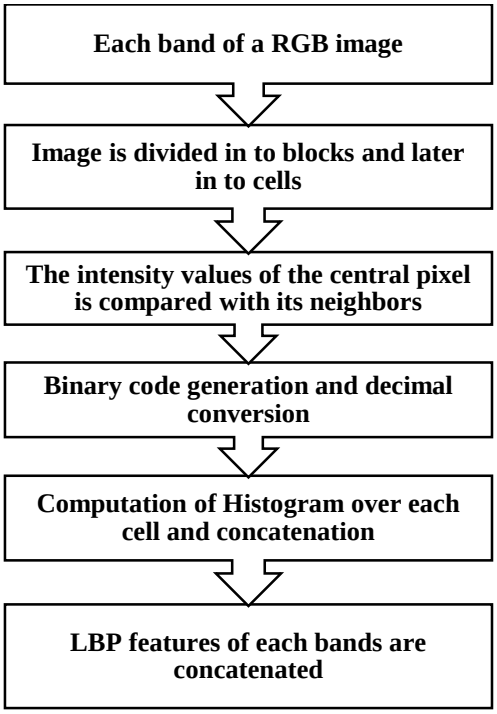

Fig. 2. LBP computation for a single RGB image

Binarized Statistical Image Features (BSIF) is similar to LPQ descriptor and LBP descriptor where pixel region or image patches are represented using binary strings. BSIF was proposed by Juho Kannala and Esa Rahtu [12]. Like LBP and LPQ, BSIF computation consists of two major steps; "Filtering the image with a set of linear filters" and "Quantization of filter responses". Instead of learning filters by utilizing hand-crafted or random filters, BSIF method utilizes the filters learned from natural images. In order to learn filter from natural images, a computational method namely independent component analysis is used to increase the statistical independence of the filter responses.

Consider an image patch P of size $l \times l$ pixels. F_i is the linear filter of size $l \times l$ pixels. Let R_i be the obtained filter response.

$$R_i = \sum_{x,y} F_i(x,y)P(x,y) = \mathrm{f}_i^{\mathrm{T}}\mathrm{p} \quad (1)$$

If there exist 'n' number of linear filters F_i, a matrix F is formed by stacking all F_i. Then all responses (R) are computed simultaneously.

$$\mathrm{R} = \mathrm{Wp} \quad (2)$$

For a random number of natural image patches, the filters F_i is determined in such a way that the elements R_i of R is maximum independent.

Let 'V' be the binary code string computed from the image patch P. Each element v_i of V is defined as;

$$v_i = \begin{cases} 1 & if\ R_i > 0 \\ 0 & otherwise \end{cases} \quad (3)$$

This method is repeated for each pixel to compute binary code and finally, the histogram is generated for image using pixels' binary code.

Local Phase Quantization (LPQ) is a texture descriptor proposed by Ojansivu and Heikkila [10]. This method depends on the quantized period of the discrete Fourier transform which is calculated in the local image window. The steps involved in the LPQ feature vector computation for a single RGB image is illustrated in figure 3.

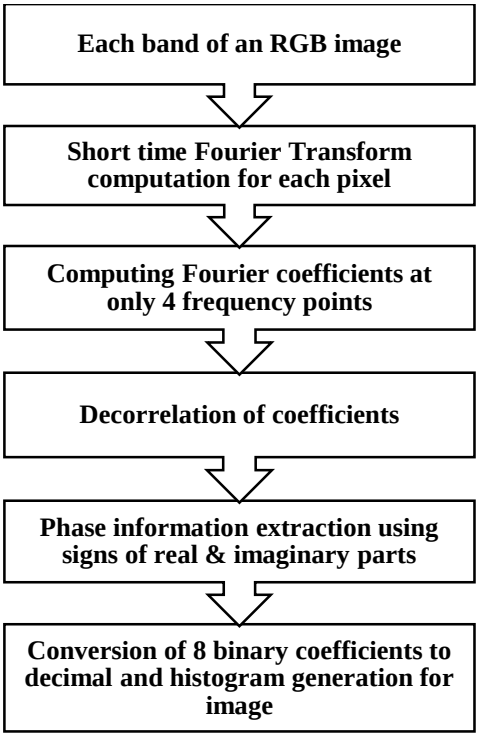

Fig. 3. LPQ computation for a single RGB image

B. Machine Learning Classifiers

After extracting the texture features (LBP, LBP, LPQ) from the images, the recognition performance was examined for three supervised learning algorithms: KNN, NB, and SVM. SVM algorithm was developed by Vladimir and Alexey in 1963.SVM is a classification and regression tool that utilizes machine learning methodology in order to improve the prediction results. SVM make use of one or more hyperplane to separate the classes on infinite dimensional space. To classify the new data (testing data), the SVM algorithm constructs an optimal hyperplane from the input labeled data [27].

KNN [28] is a non-parametric and simplest machine learning algorithm introduced by Fix and Hodges in 1951. The working principle of KNN is based on finding 'K'(k=1,2,3,4,….n) nearest neighbors in training samples from a specific query instance. In order to find the nearest neighbors, the distance between training samples and specific query instance are computed. KNN utilize different distance functions such as Euclidean distance, Manhattan distance, Minkowski distance and Hamming distance for distance calculation between data points.

NB [29] algorithm is a machine learning method based on Bayes' theorem. The prediction technique of NB classifier is based on the posterior probability calculation using Bayes' theorem. For a given query instance, the NB classifier computes the posterior probability for each class (training labels). The class which has the highest posterior probability is considered as the prediction result.

C. Transfer Learning

Transfer learning is a popular method in deep learning where a model created for a specific problem was reutilized for the development of the model for other related problems. In transfer learning, the pre-trained model is used as an initial point for training a new model with different input data. Usually, training a deep learning model from scratch requires a large amount of data. Transfer learning creates effective models even if the dataset is small. This is applicable only if the pre-trained model used in the transfer learning process was already trained with a large amount of data.

The transfer learning can be achieved in two ways: 1) Transfer learning via feature extraction and 2) Transfer learning via fine-tuning. In transfer. In the first approach, the existing pre-trained network is used as a feature extractor to obtain features from the input data. Later, the obtained features will be fed to supervised learning methods for training purpose. In fine-tuning approach, the pre-trained model will be used for training the new data. A small modification will be applied to the architecture of the existing pre-trained network.

GoogleNet is a well-accepted neural network model developed for image classification problem. The GoogleNet network is pre-trained in ImageNet [30] dataset. ImageNet is a large image dataset developed for object classification and recognition task. The images included in the ImageNet dataset fall under 1000 classes such as pen, pencil, laptop, various animals, etc. In this work, pre-trained GoogleNet model is used for transfer learning tasks.

IV. Dataset

The images used for the experiments are taken from MCindoor 20000 dataset [31]. The images of MCindoor 20000 dataset belongs to three classes: door, signs, and stairs. Figure 4 shows some sample images of the dataset. The dataset contains 2055 original images captured from indoor areas of Marshfield Clinic and different variations of the original images such as Gaussian noise models and Poisson noise models. The images were captured using a digital camera and a smartphone. We conducted the experiments using 2055 original images taken from this dataset.

Fig. 4. Sample images from Mcindoor20000 dataset

V. Evaluation and Results

All the evaluations were carried out in MATLAB. The libsvm toolbox is utilized to implement SVM classifier. Our SVM classifier is created using radial basis function kernel and a grid search method was utilized to compute the cost and gamma parameters. Statistics and Machine Learning Toolbox provided by MATLAB is used for KNN and NB implementation.

Accuracy is the major instinctive performance metric for image classification tasks and it is the ratio of correct prediction to the total observations. Accuracy can be considered as the best metric to rate the performance of a trained model only if the dataset is symmetric. In our case, the dataset is almost symmetric but not exact. However, we computed the precision, recall, and F1 scores along with the accuracy of the models to show the performance of our developed models.

The following equations are utilized to compute the above-mentioned performance metrics.

$$\text{Accuracy} = \frac{True\ Positive + True\ Negative}{True\ Positive + True\ Negative + False\ Positive + False\ Negative} \quad (4)$$

$$\text{Precision} = \frac{True\ Positive}{True\ Positive + False\ Positive} \quad (5)$$

$$\text{Recall} = \frac{True\ Positive}{True\ Positive + False\ Negative} \quad (6)$$

$$\text{F1 score} = 2 \times \frac{Precision \times Recall}{Precision + Recall} \quad (7)$$

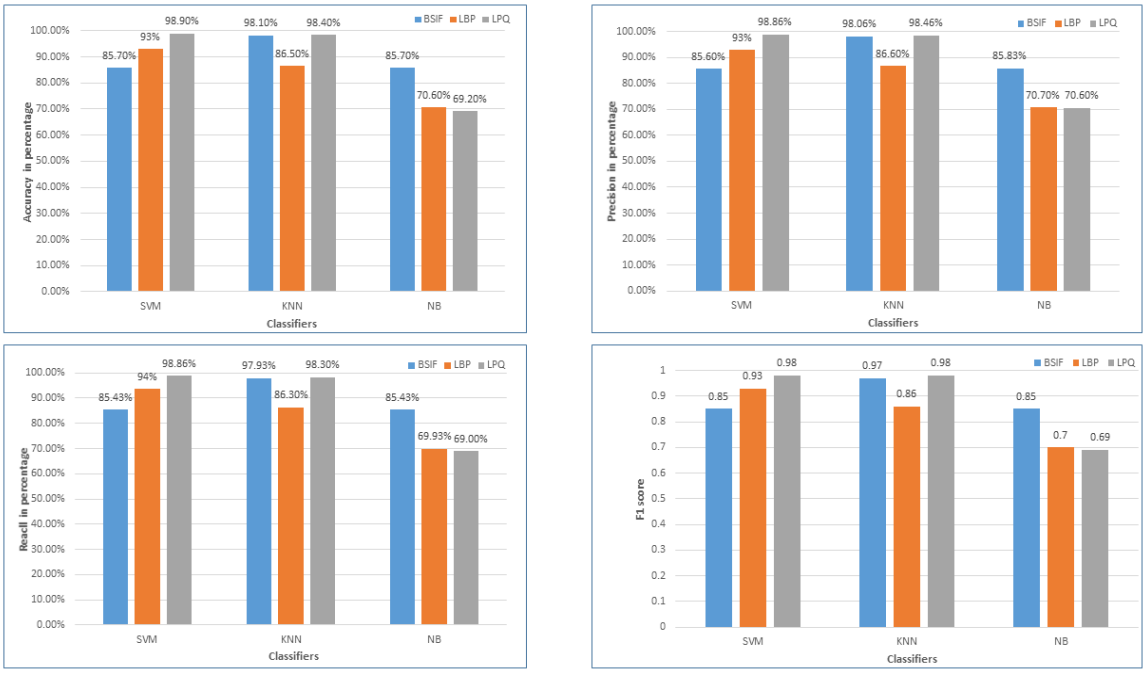

Fig. 5. Accuracy (Top left), Precision (Top right), Recall (Bottom left) and F1 score (Bottom right), of the developed object recognition models using texture features(BSIF, LPQ, LBP) with SVM, KNN and NB classifiers.

A. Texture Features with Machine Learning Classifiers

Many variants of LBP and LPQ features are available. We utilized uniform rotation invariant LBP with 8 neighborhood schema for extracting the LBP features. Rotation invariant LPQ with 8 neighborhood schema is used to extract LPQ features. A pre-computed filter is required for the LPQ feature extraction method. In our approach, we choose a filter with window size 7. In the case of BSIF features, we extracted the features in normalized histogram format. BSIF feature extraction method used a pre-learnt filter with size 7×7.

We partitioned the entire dataset into two portions. 70 % of the images are used for training the classifiers and 30 % for testing the performance of the trained classifiers. To extract LBP and LPQ features, the chosen image size is 640×480 pixels. The images are processed in RGB format itself and features were calculated for each band and later concatenated to form the final feature vector. In the case of BSIF implementation, during preprocessing the image was converted to grayscale, image size resized to 640×480 pixels.

The accuracy, precision, recall and F1 score of each trained model are displayed in figure 5.

The obtained results on the MCindoor 20000 dataset show superior performance of LPQ and BSIF for classifying indoor objects. While comparing with LBP features, LPQ and BSIF descriptors displayed substantial improvement in accuracy. LPQ features exhibited an accuracy of 98.9 % and 98.4 % with SVM and KNN classifiers respectively. BSIF features performed well with KNN classifier and provided an accuracy of 98.1%. Since the dataset is almost symmetric, the precision and recall values of each model are almost similar to their respective accuracy values. The precision and recall of the SVM classifier with LPQ feature are 98.86 % and 98.86 %. The KNN classifier with BSIF feature has 98.46 % precision and 98.30 % recall. The F1 score is the harmonic mean of precision and recall. The F1 score values of the SVM classifier with LPQ descriptor, KNN classifier with LPQ descriptor and KNN classifier with BSIF descriptor are 0.98, 0.98 and 0.97 respectively. The obtained F1 score values of above mentioned three models are almost near to 1, which shows the effectiveness of the developed model for classifying indoor objects such as doors, stairs, and signs. The performance results of the SVM classifier with LPQ descriptor, KNN classifier with LPQ descriptor and KNN classifier with BSIF descriptor were almost similar to the results obtained in [25] using transfer learning(pre-trained AlexNet model [32]) in the same dataset. This demonstrates the competitiveness of LPQ and BSIF features for indoor object recognition. SVM and KNN methods are well suited for classification tasks using texture features from images.

B. Transfer Learning

Deep learning toolbox provided by MATLAB is used to develop the deep learning model for indoor object recognition. The Deep learning toolbox contains various pre-trained model. We utilized the GoogleNet model trained in the ImageNet dataset as an initial point for training our model. The input images were resized to 224 × 224 pixels. In transfer learning via fine-tuning approach, the final two layers, 'loss3-classifier' and 'output', of the pre-trained model are replaced with new layers, according to the number of classes in our dataset. In order to speed up the training and prevent overfitting of data, the initial 10 layers of the pre-trained model were made frozen. In transfer learning via feature extraction approach, the activations on the fully connected layer ('loss3-classifier') were utilized to extract the features of the image. The extracted CNN features were utilized to train the SVM, KNN, NB classifiers.

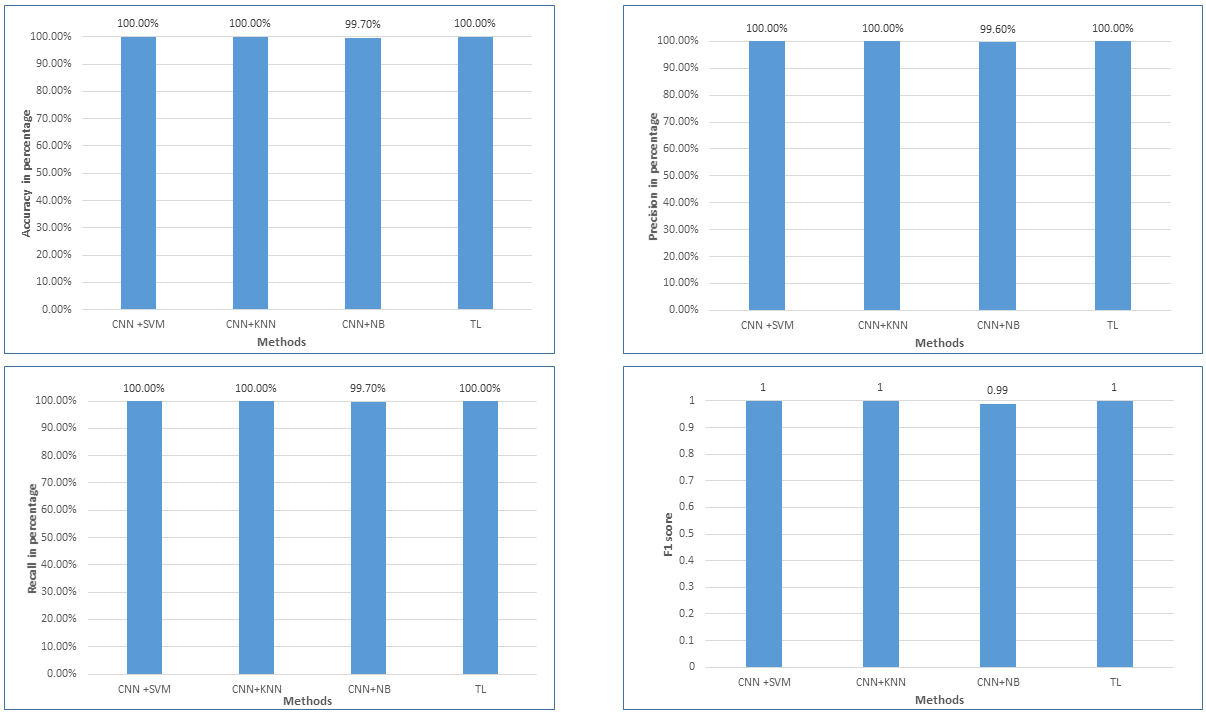

Fig. 6. Accuracy (Top left), Precision (Top right), Recall (Bottom left) and F1 score (Bottom right), of the developed object recognition models using Transfer learning(TL) approach, CNN features with SVM, KNN, and NB classifier.

The accuracy, precision, recall and F1 score of deep learning model, SVM, KNN, NB models trained with CNN features are displayed in figure 6.

The results displayed in figure 6 show the superior performance of our developed models using transfer learning approach. The four classification models including transfer learning (TL) model developed via fine-tuning and SVM, KNN and NB models trained with CNN features outperformed all other texture features in terms of accuracy, precision, recall, and F1 score.TL model, CNN features with SVM classifier, and CNN features with KNN classifier achieved a classification accuracy of 100 %. The CNN features with NB classifier showed 99.7 % accuracy. We extracted the CNN features from the final fully connected layer of the deep learning model. This approach gave us high-level features of the images to train the classifiers. Obviously, high-level features will perform better than low-level features with machine learning classifiers such as SVM, KNN, and NB. Since the dataset is almost symmetric, the precision, recall of the TL model, SVM, and KNN model are 100 %. The F1 score of the TL model, the SVM model, and KNN is model is 1 that is the maximum value a model can achieve.

In addition to accuracy, precision, recall, and F1 score we computed the average prediction time for each model to analyze its efficiency. The prediction time required by each developed model for a single image is shown in table 1.

We have already described the main applications of indoor scene recognition. During the implementation of a real-time system for object recognition, in addition to its accuracy and precision, the prediction time should be considered. Accuracy and precision of the developed models using TL, CNN with SVM, CNN with KNN, CNN with NB, LPQ with SVM, LPQ with KNN, BSIF with KNN are extremely good. But while considering the prediction time, LPQ with KNN and LPQ with SVM model takes more than 4 seconds for predicting the result for one image. The BSIF with KNN is very fast and took only 0.4 seconds which is similar to transfer learning models.

TABLE I. AVERAGE PREDICTION TIME FOR SINGLE IMAGE

Methods	Prediction time in seconds
BSIF+SVM	0.3276
BSIF+KNN	0.4569
BSIF+NB	0.6040
LBP+SVM	1.0204
LBP +KNN	1.0492
LBP +NB	1.1458
LPQ+SVM	4.6034
LPQ +KNN	4.8434
LPQ +NB	5.5722
CNN+SVM	0.4513
CNN+KNN	0.5906
CNN+NB	1.5038
TL	0.4908

[a.] TL means Transfer learning using pre-trained GoogleNet model

VI. Conclusion

In this work, we developed a computer vision-based system to recognize indoor objects. The proposed system was validated in a publically available dataset which contains images captured from indoor areas of a health clinic. SVM, KNN and NB classifiers were utilized to evaluate the performance of textures features such as BSIF, LPQ, and LBP. The indoor object recognition was very well performed with BSIF feature descriptor and LPQ feature descriptor.BSIF produced 98.1 % accuracy with KNN classifier. Moreover, LPQ yielded 98.9 % and 98.4 % accuracy with SVM and KNN classifiers respectively. Compared to NB classifier, SVM and KNN classifiers performed better with texture features. We performed the transfer learning via fine-tuning as well as feature extraction approaches. Our deep learning model developed using transfer learning approach yielded the highest accuracy of 100 % in the same dataset. The CNN features also delivered an accuracy of 100 % with SVM and KNN classifiers. Comparison with LPQ, BSIF feature descriptor, CNN features, and deep learning models took very less time for the prediction.

This work only considered the recognition of three indoor objects such as door, stairs, and sign. Recognition of multiple objects from a scene is not considered in this work. In the future, we will extend this system to recognize more common objects found in indoor areas including chairs, table, laptop, smartphone, etc. Moreover, we will consider the recognition of multiple objects found in a scene.

References

[1] H. Lipson and M. Kurman, Driverless: intelligent cars and the road ahead. Cambridge, MA: The MIT Press, 2017.

[2] M. Tomono and S. Yuta, "Mobile robot navigation in indoor environments using object and character recognition," in IEEE International Conference on Robotics and Automation (ICRA), vol. 1, 2000, pp. 313-320.

[3] Y. Tian, X. Yang, C. Yi, and A. Arditi, "Toward a Computer Vision-based Wayfinding Aid for Blind Persons to Access Unfamiliar Indoor Environments," Machine Vision and Applications, 2012, DOl: 10.1007/s00138-012-0431-7.

[4] H. Bay, A. Ess, T. Tuytelaars, and L. J. V. Gool. Speeded-up robust features (SURF). CVIU, 110(3), 2008.

[5] Y. Tawano, K. Yanai, "Foodcam: A real-time food recognition system on a smartphone", Multimedia Tools and Applications, pp. 1-25, 2014.

[6] W. Zhang, Q. Yu, B. Siddiquie, A. Divakaran, H. Sawhney, "Snap-n-Eat food recognition and nutrition estimation on a smartphone", Journal of Diabetes Science and Technology, vol. 9, no. 3, pp. 525-533, April 2015

[7] A. Lameira, R. Jesus and N. Correia, "Local object detection and recognition in mobile devices," 2012 19th International Conference on Systems, Signals and Image Processing (IWSSIP), Vienna, 2012, pp. 193-196

[8] Shruti Parkhi,S.S.Lokhande, N.D.Thombare,"Vocal Vision Android Application for Visually Impaired Person".International Journal of Science, Engineering and Technology Research (IJSETR) Volume 5, Issue 6, 2016

[9] T. Y. H. Chen, L. Ravindranath, S. Deng, P. Bahl, and H. Balakrishnan,"Glimpse: Continuous, real-time object recognition on mobile devices,"in Proceedings of the 13th ACM Conference on Embedded NetworkedSensor Systems. ACM, 2015, pp. 155–168.

[10] V. Ojansivu and J. Heikkila. Blur insensitive texture classification using local phase quantization. In ISP, 2008.

[11] M. Pietikäinen, A. Hadid, G. Zhao, T. Ahonen, "Local binary patterns for still images" in Computer Vision Using Local Binary Patterns, London, U.K.:Springer, vol. 40, pp. 13-47, 2011.

[12] J. Kannala, E. Rahtu, "BSIF: Binarized statistical image features", Proc. 21st Int. Conf. Pattern Recognit. (ICPR), pp. 1363-1366, Nov. 2012.

[13] C. Szegedy, W. Liu, Y. Jia, P. Sermanet, S. Reed, D. Anguelov, D. Erhan, V. Vanhoucke, and A. Rabinovich. Going deeper with convolutions. In CVPR, 2015.

[14] S. Singh, S. Choudhury, K. Vishal, C. V. Jawahar, "Currency Recognition on Mobile Phones", 22nd International Conference on Pattern Recognition (ICPR), pp. 2661-2666, 24 August 2014.

[15] D. Nakamura, H. Takizawa, M. Aoyagi, N. Ezaki, S. Mizuno, "Smartphone-based escalator recognition for the visually impaired", Sensors, vol. 17, no. 5, pp. 1057, 2017.

[16] S. Bagwan, S. Sankpal, "VisualPal: A mobile app for object recognition for the visually impaired", 2015 International Conference on Computer Communication and Control (IC4), pp. 1-6, Sept 2015

[17] G. Iannizzotto, C. Costanzo, P. Lanzafame, and F. L. Rosa, "Badge3D for visually impaired," Proceedings of IEEE Computer Society Conference on Computer Vision and Pattern recognition, San Diego, CA, USA, pp. 29, June 20-26, 2005.

[18] J. Nicholson, V. Kulyukin, D. Coster, "Shoptalk: Independent blind shopping through verbal route directions and barcode scans", Open Rehabil. J., vol. 2, pp. 11-23, 2009.

[19] P. Narasimhan, "Trinetra: Assistive Technologies for Grocery Shopping for the Blind", IEEE-BAIS Symp. Research on Assistive Technologies, 2007.

[20] A. Ramisa, S. Vasudevan, D. Aldavert, R. Toledo and R. L. Mantaras, "Evaluation of the SIFT Object Recognition Method in Mobile Robots," Proc. Int'l Conf. Catalan Association for Artificial Intelligence, 2009.

[21] T. Lindeberg, "Scale invariant feature transform", Scholarpedia, vol. 7, no. 5, pp. 10491, 2012.

[22] J. Sudol, O. Dialameh, C. Blanchard, T. Dorcey, "LookTel - A Comprehensive Platform for Computer-Aided Visual ssistance", CVPR, 2010.

[23] Ricardo Chincha, YingLi Tian, "Finding objects for blind people based on SURF features", Bioirformatics and Biomedicine Workshops (BIBMW) 2011 IEEE International Conference, pp. 526-527, 2011.

[24] T. Winlock, E. Christiansen, S. Belongie, "Toward realtime grocery detection for the visually impaired", CVPRW, 2010.

[25] F.S. Bashiri et al. "Object Detection to Assist Visually Impaired People: A Deep Neural Network Adventure." International Symposium on Visual Computing. Springer, Cham, 2018.

[26] T. Ojala, M. Pietikinen, D. Harwood, "A comparative study of texture measures with classification based on feature distributions", Pattern Recognition, vol. 29, no. 1, pp. 51-59, 1998.

[27] B. Scholkopf, A. J. Smola, Learning With Kernels, Cambridge, MA, USA:MIT Press, 2002.

[28] T. M. Cover, P. E. Hart, "Nearest neighbor pattern classification", IEEE Trans. Inf. Theory, vol. IT-13, no. 1, pp. 21-27, Jan. 1967.

[29] A. Y. Ng, M. I. Jordan, "On discriminative vs. generative classifiers: A comparison of logistic regression and naive bayes", Adv. Neural Inf. Process. Syst., vol. 14, 2002.

[30] J. Deng, W. Dong, R. Socher, L.-J. Li, K. Li and L. Fei-Fei, ImageNet: A Large-Scale Hierarchical Image Database. IEEE Computer Vision and Pattern Recognition (CVPR), 2009

[31] F. S. Bashiriab, E. LaRoseb, P. Peissigb, A. P. Taftib, Mcindoor20000: A fully-labeled image dataset to advance indoor objects detection, 2018, [online] Available: https://doi.org/10.1016/j.dib.2017.12.047.

[32] A. Krizhevsky, I. Sutskever, G. Hinton, "ImageNet Classification with Deep Convolutional Neural Networks", Proc. Neural Information and Processing Systems, 2012.

Proceedings of the Fourth International Conference on Communication and Electronics Systems (ICCES 2019)
IEEE Conference Record # 45898; IEEE Xplore ISBN: 978-1-7281-1261-9

Matlab And Arduino Based Real Time Face Detection And Tracking System

Mr. V. Prakasam[1],
Dept. of ECE
[1]Vignan Institute of Technology and Science,
Deshmukhi, India.
vprn2274@gmail.com

Mr. P. Sandeep[2],
Dept. of ECE
[2]Vignan Institute of Technology and Science,
Deshmukhi, India.
pingili.sandeep@gmail.com

***Abstract*— now a days, the real time detection and tracking of face is very mandatory. This is mainly used for recognition of movement, safety purpose and surveillance systems. In this paper, we are using two algorithms that is Viola-Jones Detection (VLJ) algorithm and KLT algorithm. KLT algorithm is used along with Arduino packages available in MATLAB. In this paper, the total progression is divided into two categories, that is first one is the human faces are detected by VLJ algorithm and another algorithm is used to track the feature evidences in the live video surround. Using webcam and servo motors, the human faces are detected and tracked. The perfect intention of this paper is to progress a faster algorithm in detecting, tracking and recognizing a face, which serves as a useful process in several Real time applications like security systems, video surveillance, video coding and Advanced Robotics etc.**

Keywords*— KLT, VLJ, Face tracking, Arduino, MATLAB, Face Recognition.

I. INTRODUCTION

In so many computer vision applications, the detection and tracking of object are very important and also including recognition of activity, surveillance and motorized safety. A face tracking system is very simple and mostly used system and which is established by separating the tracking problem into three distinct problems: Face detection in the frame, Initial facial features, which is used for tracking and Face Tracking. Face detection in MATLAB can be through using various dissimilar existing algorithms. These algorithms use different mechanisms to identify the facial features. Some use edge detection methods while some use contrast separation. Generally, it is used in object detection applications but, due to its capability of detecting facial features using Haar based feature filters, is extremely easy to use for the face detection applications. The main reason overdue using MATLAB for image processing is due to its features with inbuilt tools and provision for good choice of hardware parts like that Arduino and Raspberry Pi. In this project, Arduino Uno was used due to its simplicity and compatibility with the MATLAB. Arduino hardware support package can be added to MATLAB via Add-Ons. The main significance of this paper is to accentuate the use of Viola Jones object detection frame work on human faces in real-time.

For training, they used latent SVM which considers a classification which notches every example x with a function $f_\omega(x)$ = max $z\epsilon Z(x)$ ω . $\psi(H, z)$ where the fixed $Z(x)$ describes all conceivable hidden values for an example x. A binary brand for this instance x can be acquired by thresholding the notch. The model parameters ω can be trained from labeled examples (x_1, y_1), … , (x_m, y_m) by minimizing the objective function:

$$L(\omega) = \frac{1}{2}\|\omega\|^2 + C\sum_{i=1}^{m}\max(0, 1 - y_i f_\omega(x_i))$$

For detection, the response of the ith filter Fi in the lth level of H is calculated by $R_{i,l}(x, y) = Fi$.$\varphi a(H, (x, y, l))$ in a sub-window of H with topmost leftward corner at (x, y) and its size is defined by the size of the root filter. The updated response of the ith part filter in this optimum location $D_{i,l}$ and the corresponding optimal displacement $P_{i,l}$ are given respectively by:

$$D_{i,l}(x, y) = \max_{dx,dy}\ [R_{i,l}(x + dx, y + dy) - d_i \,.\varphi_d(dx, dy)]$$

$$P_{i,l}(x, y) = \operatorname{argmax}_{dx,dy}\ [R_{i,l}(x + dx, y + dy) - d_i \,.\varphi_d(dx, dy)]$$

II. METHODOLOGY

The proposed system used for detection of human face is designated under. This proposed system mainly categorized into four stages, they are briefly explained under.

A. Features of HAAR

Images are categorized primarily on feature constructed systems because in feature constructed systems the calculations essential is fewer. For face detection generally two rectangular dimensional features, three rectangular dimensional features and four rectangular dimensional features are used [2]. These features/structures are named as HAAR structures and are shown in below figure. The features are intended by simple adding and deduction operation. For any type of rectangular HAAR feature the features are intended in the above mentioned process. This process is frequent for dissimilar types of HAAR rectangular masks and also by fluctuating the dimension of the mask.

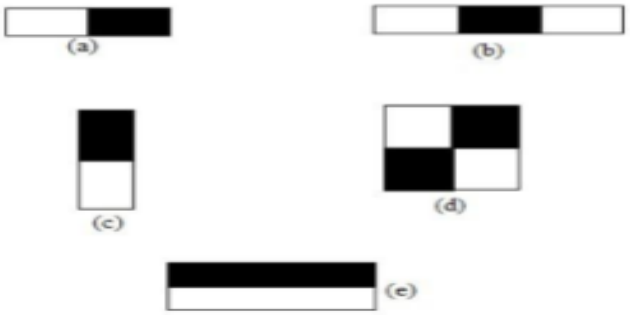

Fig 1: Features of HAAR

B. Image of Integral:

The image of integral is a rectangular structures of an image, which are greatly designated by its center. The equation calculation of integral form of an image is given by mathematically below and this can be described by captivating the below image [2].

$$qq(a,b) = \sum_{a' \le a, b' \le b} q(a', b')$$

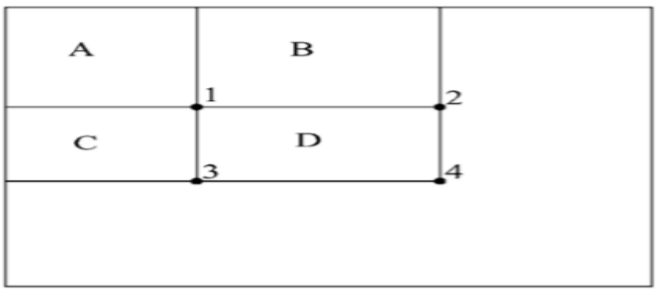

Fig 2: image of Integral

In the integral illustration, point1 designates the whole pixel sum which are existing in area A. the point2 indicates the area pixels sum. In the same way, point3 and point4 are area pixels sum (A, C) and (A, B, C, D) [3]. Where q(a,b) is an image of integral and q(a', b') is the original image.

$$P(a,b) = p(a,b-1) + q(a,b)$$
$$qq(a,b) = qq(a-1,b) + p(a,b)$$

C. AdaBoost Training (Adaptive Boost):

The integral image calculates a value at every pixel (A, B) that is the pixels sum values overhead and to the left side of (A, B) comprehensive [2]. The exercise set covers face and non-face examples with identical weight. For every round of boosting, it assesses every rectangular filter on every example and chooses the best threshold for every filter and then sets best threshold. After this, the weights are set again.

D. Cascading Classifiers:

After the exercise is completed, the integral images are coordinated with the filters and cascaded using the MATLAB objects. Using classifiers, the positive and negative portions of an image are separated, i.e., simple classifier. Weak classifiers are nothing but simple classifiers. Complex classifiers are sturdy classifiers in which it will yield the output from the preceding classifier and it will take as current input in which it may discard or accept that exact window.

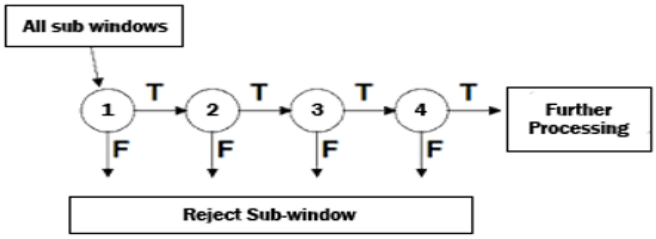

Fig 3: cascading

Cascade Objects in MATLAB:

- Cascading of the integral images is completed using the inherent cascade structures of MATLAB. vision.CascadeObjectDetector(); detects the distinct object from the video input.
- imaq.VideoDevice: This object allows MATLAB to interface camera to the system.
- vision.ShapeInserter: This object places the distinct outline at the position if recognized HAAR features.
- vision.VideoPlayer: This object shows the processing video with the recognized features.
- vision.HistogramBasedTracker: This object paths the actions in the HAAR features using the histogram information.

III. PROPOSED TECHNIQUE

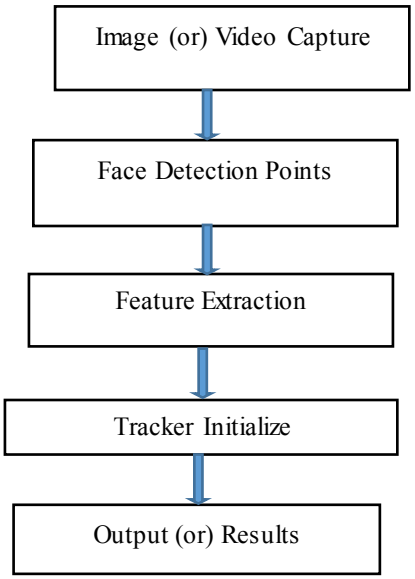

Fig 4: Proposed Model

The main purpose of the project work is to detect a human face in every frame of the video coming from a web camera and the captured image is processed using viola-jones algorithm using MATLAB and to detect the faces and send signals to the Arduino board to regulator the association of the camera using two servo motors. One of the servo motor is for horizontal variation and another servo motor is for vertical variation, face shall be tracked actively and maintained in the

frame. The MATLAB code may also include some of the built in functions for the effective face recognition and seamless tracking in real time environment [4]. Applications of this concept are wide spread from video coding to advanced robotics.

MATLAB Software: In this proposed method, MATLAB uses the built in vision objects to detect the faces from a live video feed [2]. For the first stage, a serial assembly to the Arduino hardware opens. Concurrently, the program recites the video feed from the webcam or external camera. For good efficiency, step is used for extracting frames from the continuous video feed. Using the Viola-Jones detection frame work, the frames extracted gets coordinated with the Haar features and faces are identified. Nose features gets matched after the faces. Then the boundary boxes will be placed at the identified face locations. Additional into the code, it computes the centroid of the boundary box and forms the portion of the frame it decreases in. As the frame of the video will be alienated into four quadrant, it computes the coldness from the center to the location of centroid of the bouncing box on both axes. These are fed to the Arduino serial input. MATLAB does this procedure constantly until the predetermined time after there is no face in the frame [4].

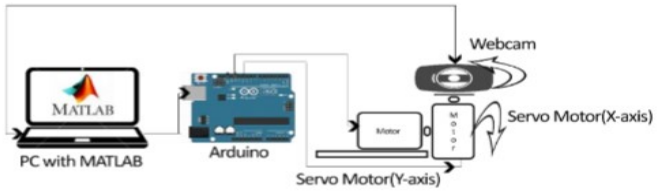

Fig 5: Block diagram

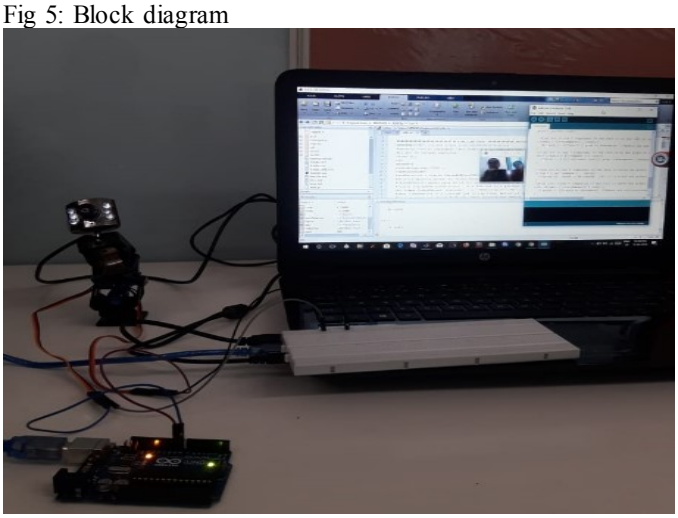

Fig 6: Hardware Setup.

Arduino IDE: In this paper, Arduino Uno is used which switch the tracking gesture for the camera on two servo motors (pan-motion & tilt-motion) [4]. We used Arduino platform for this model because of its simple interfacing and working with the MATLAB. Adding the hardware support package to the MATLAB through the add-ons is extremely convenient. As the procedure of face detection occurs, serial input at the Arduino obtains the detachments from the midpoint to that of the bounding box. With this input from the serial port, Arduino code is printed such that it associates the input co-ordinates to the conditions in the program and operates the servo motors accordingly.

Physical Connections: Components obligatory for this work comprises a web camera, Arduino Uno, a Computer with MATLAB (as well as Arduino hardware support packages) and Arduino IDE [4].

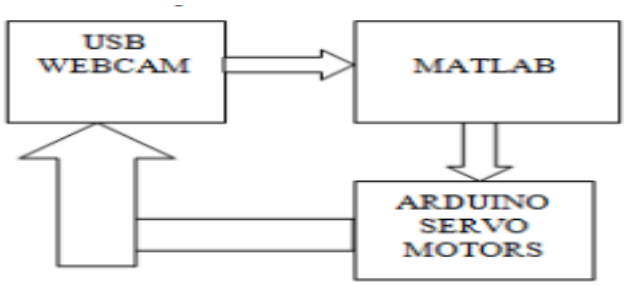

Fig 7: Connection between software and hardware

IV. SIMULATION AND RESULTS

In this paper, we are using Arduino Uno board, bread board, connecting wires and YUY2_160 x120 webcam. The below figures shows MATLAB section of the detection and tracking of the face.

Fig 8: Output for single face detection using Mat lab.

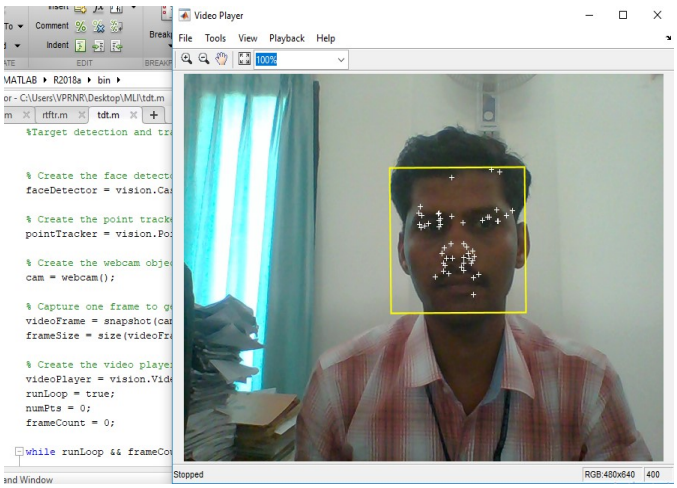

Fig 9: Output for single face detection using Mat lab.

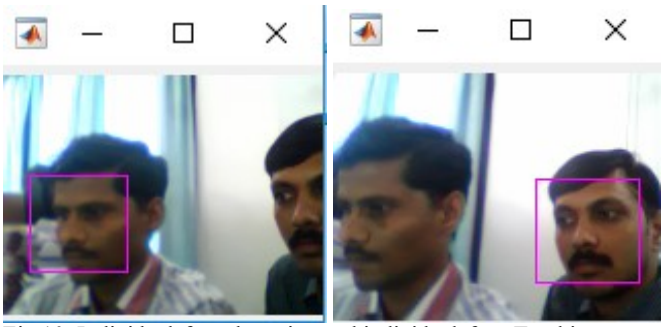

Fig 10: Individual face detection and individual face Tracking output.

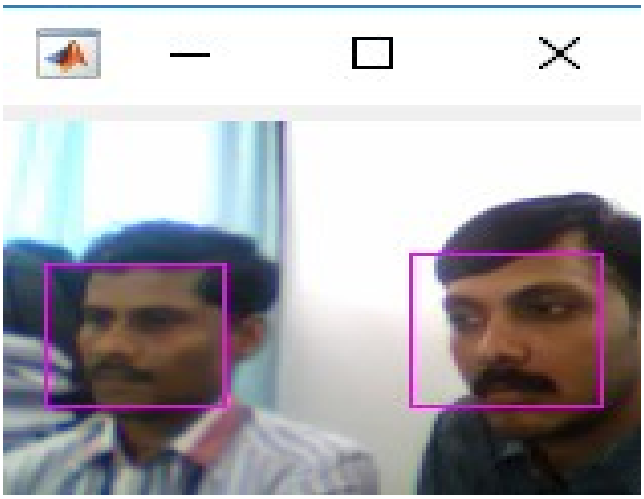

Fig 11: Output for Multiple face detection and Tracking.

The Individual face detection and individual face tracking output shown in figure 10 and multiple face detection and Tracking output as shown in figure 11. This output figures estimated from connection between MATLAB and Arduino setup. In this paper, C1, C2 represents centroid values, which are noted in below table.

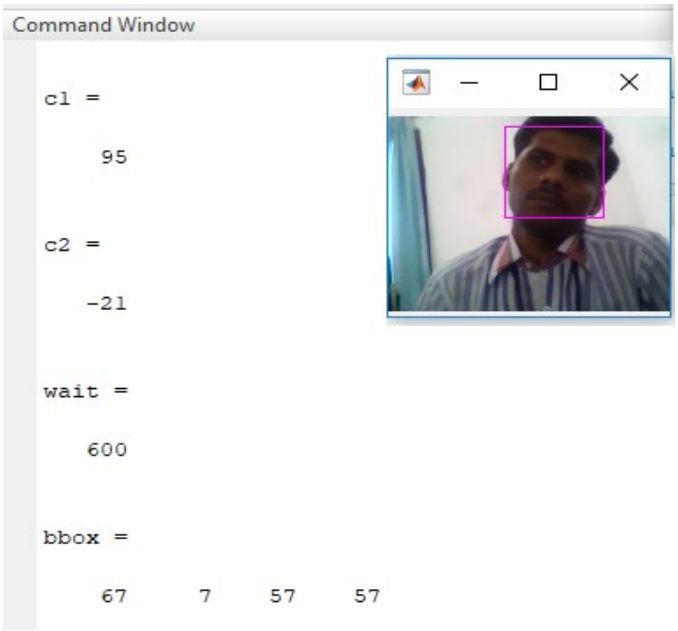

TABLE 1: Various wait time player's detection.

S. N	Wait time (in sec)	Output of video player	Calculation of centroid
1	287	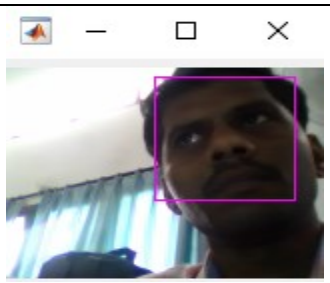	C1 = 94 C2 = -25
2	320	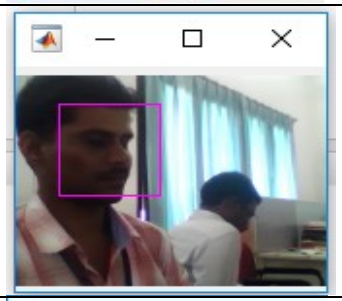	C1 = 52 C2 = -6
3	600	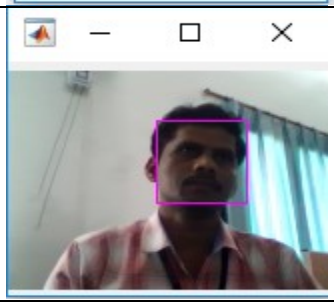	C1 = 100 C2 = 4

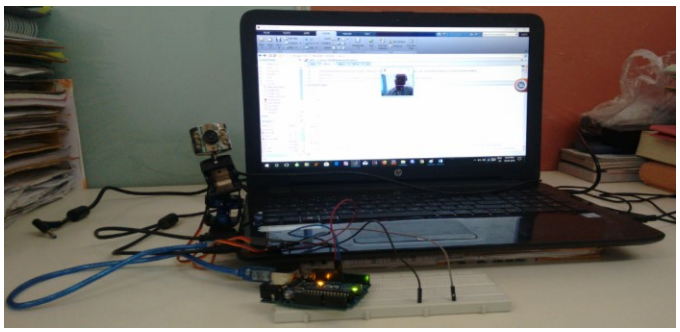

Fig 12: Hardware Setup

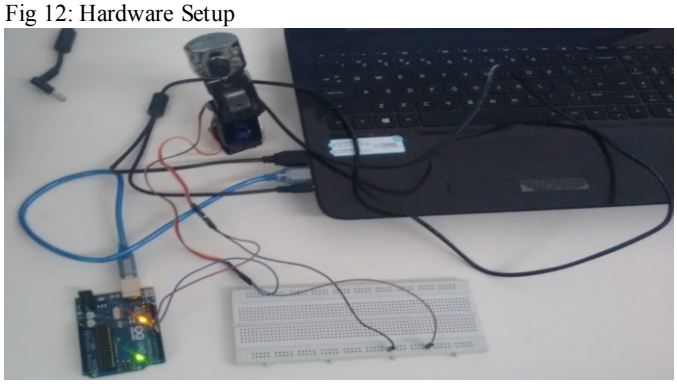

Fig 13: Servo Motor Setup

V. CONCLUSION

The planned system for tracking faces using Viola-Jones algorithm in MATLAB is better than the present methods. Usage of adaptive boosting for the algorithm helps in increasing the precision and efficiency of the proposed method. This kind of tracking can be used effectively in the surveillance field. Also, Computer Vision is the major field which holds a vast scope for robotics. It is an efficient and fast algorithm when compared to other algorithms. It is done by using MATLAB code, where Camera detects the face and tracking is done through the movement of camera using a Microcontroller called ARDUINO. We can implement this method in various places where security and video surveillance is highly essential. In this paper we are restricted with basic laboratory conditions where the application part can be done with high costs.

REFERENCES

[1] Pietroperona, JitendraMalik,"Scale-Space and edge Detection'',IEEE Transactions on Image processing,Vol 12 No 7,July 2010 .
[2] Maneesh Ayi1, Ajay Kamal Ganti2, Real-time Face Tracking using MATLAB and Arduino, FEB 2018 | IRE Journals | Volume 1 Issue 8, pp 59-61.
[3] Venkata Sasank Pamulapati, Yekula Sumith Rohan, Face Tracking and Recognition Using MATLAB and Arduino, IJRASET, Volume 5 Issue XII December 2017, pp 2398-2404.
[4] Maneesha K, Neha Sree, Pranava Datta R, Real Time Face Detection Robot, RTEICT, May 19-20, 2017, India, pp 58-63.
[5] Kiran R, M Lohith, Yogesh E, Sai Kumar A, Anitha, Interfacing of MATLAB with Arduino for Face Recognition, RATE-2017,
[6]. DhanarIntan Surya Saputra, Kamal Miftahul Amin, "Face Detection and Tracking Using Live Video Acquisition in Camera Closed Circuit Television and Webcam", 2016 1st International Conference on Information Technology, Information Systems and Electrical Engineering(ICITISEE),Yogyakarta, Indonesia
[7] AryuantoSoetedjo, I KomangSomawirata," Implementation of Face Detection and Tracking on A Low Cost Embedded System Using Fusion Technique", The 11th International Conference on Computer Science & Education (ICCSE 2016) August 23-25, 2016.
[8] RudrakshYagnik, Ashish Jangid, Sachin Jain "A Practical Implementation of Face Detection byusing Viola Jones Algorithm in MATLAB GUIDE", IJERT Vol. 3 Issue 9, September- 2014.
[9] Viola, P., Jones, M.J.: Robust Real-Time Face Detection. International Journal of Computer Vision 57(2), 137–154 (2004).
[10] Digital Image Processing, Third edition: Rafael C. Gonzalez, Richard E. Woods. Image Processing Algorithms.
[11] Book: Exploring Arduino, tools and techniques for engineering wizardry: Jeremy Blum
[12] Hoang minh Phuong "Extraction of Human Facial Features based on Haar Heature with Adaboost and Image Recognition Techniques" IEEE, 2012.
[13] P.Viola and M.Jones,"Rapid Object Detection using a Boosted Cascade of Simple Features",conf. on comp. vision and pattern recognition 2001.
[14] Jatin Chatrath, Pankaj Gupta, Puneet Ahuja, Aryan Goel and Shaifali M.Arora,"Real Time Human Face Detection and Tracking",International Conf. on Signal Processing and Integrated Networks
[15] Raquib Buksh, Soumyajit Routh, Parthib Mitra, Subhajit Banik, Abhishek Mallik, Sauvik Das Gupta, "Implementation of MATLAB based object detection technique on Arduino Board and iROBOT CREATE", IJSRP, Vol. 4, Issue 1, Jan 2014, ISSN: 2250-3153.

ABOUT THE AUTHORS

[1] V. Prakasam received B.Tech degree from JNTUA, M.Tech degree in VLSISD from JNTUK and pursuing p.hD. He is currently an Assistant Professor in the department of Electronics and Communication Engineering at vignan institute of technology and sciences, deshumuki. His research interests Signal processing, image processing, Microwave Engineering and RF Engineering.

[2] P.Sandeep received B.E degree from VTU, Belgaum, M.Tech degree in VLSID from Sathyabama University and pursuing p.hD. He is currently an Assistant Professor in the department of Electronics and Communication Engineering at Vignan institute of technology and sciences, deshumuki. His research interests Signal processing, image processing, Analog Electronics engineering, Low Power and High Speed Systems and VLSI Design.

Proceedings of the Fourth International Conference on Communication and Electronics Systems (ICCES 2019)
IEEE Conference Record # 45898; IEEE Xplore ISBN: 978-1-7281-1261-9

PERFORMANCE MEASURES FOR PASSBAND DIGITAL TRANSMISSION TECHNIQUES OVER AWGN CHANNEL

Parag Jain[1], Meha Shrivastava[2]

[1, 2] *Department of Electronics & Communication Engineering, Truba Institute of Engineering & Information Technology, Bhopal, India*

[1]jainparag11@gmail.com
[2]meha.shrivastava@trubainstitute.ac.in

Abstract— **Modulation plays a significant role in the field of electrical communication where different techniques are employed to achieve better performance and focusing in meeting the standards of various parameters such as BER, SNR, and MSE etc. In this paper we have analyzed BER for passband digital communication techniques on AWGN channel and results are verified using MATLAB.**

***Keywords*— Binary Phase Shift Keying (BPSK); Quaternary Phase Shift Keying (QPSK); Quadrature Amplitude Modulation (QAM); Bit Error Rate (BER); Signal to Noise Ratio (SNR); Additive White Gaussian Noise (AWGN); Mean Square Error (MSE)**

I. INTRODUCTION

The history of communication focuses the development of civilization and the way it influenced its impact on modern societies. Communication stands in simple words as sending or receiving of messages from one person to another. When the receiver interprets the exact message deliver by the transmitter then only effective communication is going to happen.

The communication systems broadly classified into three categories based on the nature of the input signal as well as the behaviour of the system. The system may be unidirectional or bidirectional, whether it uses as analog or digital signal, which type of transmission technique the system is going to opt. The above discussed classification is also shown in figure 1.

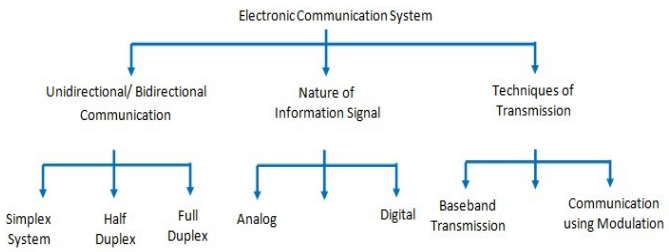

Figure 1 : Classification of Electronic Communication System

The current research majorly focusing on last category i.e. the techniques of transmission. We can also classify the transmission techniques in further two types namely baseband transmission and passband transmission (Communication systemusing modulation).

The message signals are directly transmitted in baseband transmission systems. The telephone networks are one of the common examples for these types of systems, where the input sound signal is going to convert into electrical signal and directly placed on the telephone lines and gets transmitted.

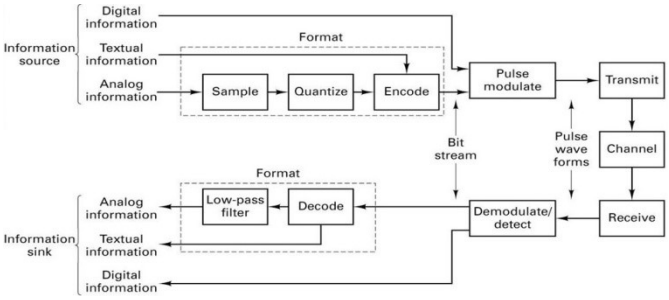

Figure 2 : Functional model of baseband data transmission system

The message signals are impresses onto a signal known as carrier in passband transmission systems. The space communications, terrestrial microwave communications and mobile communications are the areas which consider modulation where the modulated signal is shifted to an appropriate frequency band and then transmitted over large distance communication through antennas.

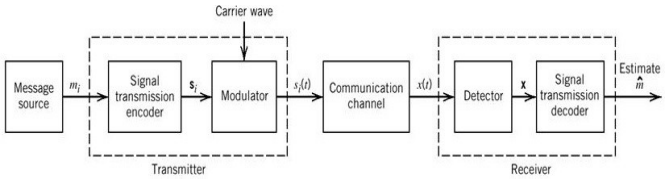

Figure 3 : Functional model of passband data transmission system

A. Literature Survey

Reference [1] presents different modulation schemes (BPSK, QPSK, and GMSK) and its performance evaluation in terms of BER in cellular mobile environment with GSM standard parameters. The main motive of this research is to identify the factors that go into consideration of the modulation schemes particularly in the wireless environment.

Reference [2] describes about BPSK, QPSK and QAM based OFDM system and performance comparison by employing different error correcting techniques (reed Solomon, convolution & concatenated coding) in wireless communication channel. The BER performance evaluated among each code and from these outcomes it is concluded that concatenated coding brings good results compare to other individual codes.

Reference [3] discusses the BER measurement for different modulation schemes over two different channel bandwidths of 1.25 MHz and 6 MHz respectively. The main objective of this research is to find out the best configuration between the modulation schemes and channel bandwidth, which helps to improve the system performance. The research has been performed by evaluation of BER and SNR for OFDM system models using MATLAB SIMULINK Tool.

Reference [4] analyses the BER, for different modulation techniques known to be BPSK, QPSK. After performing various simulations it is observed that performance can be enhance by selecting a proper modulation scheme and by employing suitable coding technique correspondingly. The performance is analyzed and compared by simulated results through Lab VIEW software.

B. Organization of the paper

The paper has been organized into six sections. Section I gives the brief introduction about the digital communication and some of the previous works related to this paper. Section II gives an idea about each scheme in digital communication. Section III focuses on details about the types of communication channel and its characteristics. Section IV is a more complex one deal with parameters to analyse various digital modulation techniques. Section V elaborates about the input signal specification. Section VI shown the simulated results in the form of graph and table. In section VII, based on the above observations, what can be inferred is described and conclusions drawn based on them.

II. DIGITAL TRANSMISSION SCHEMES

A. Introduction

The physical delivery of information (data) over a dedicated or distributed path (communication channel) is known as data transmission, digital transmission or digital communication. The digital transmission techniques basically classified into two types i.e. baseband transmission (Line Coding) and passband transmission (Digital Modulation)

B. Classification

The digital transmission is classified in into two major categories namely Baseband Transmission and Passband Transmission (communication using modulation). The layman classification of digital signals transmission is clearly depicted in below figure

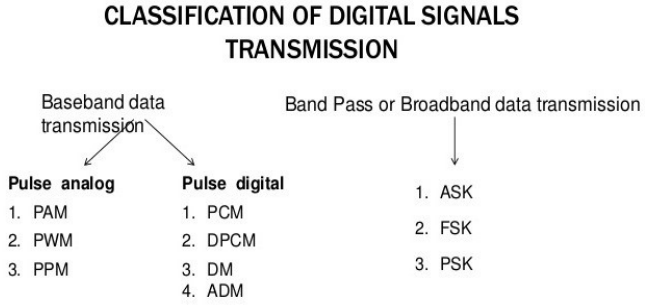

Figure 4 : Digital Modulation Classification Model

C. Passband digital modulation techniques

The main objective of passband digital modulation is to impresses the encoded digital information by varying the parameters of a sinusoidal waveform known as carrier signal, over an analog communication channel. There are 3 basic modulation techniques and based on parameters like amplitude, phase or frequency variations in the transmitted signals, the modulation is referred to as Amplitude Shift Keying (ASK), Frequency Shift Keying (FSK), and Phase Shift Keying (PSK).

D. Binary Phase Shift Keying (BPSK)

Binary Phase Shift Keying (BPSK) is also known by the name of Phase Reversal Keying (PRK) in some specific applications. In this modulation scheme two phases of the carrier signal represented either by 0° or by 180° depending on the sequence of binary message signal i.e. 0 or 1 accordingly.

The transmitted BPSK signal can also be represented mathematically shown in equation 1

$$s_n(t) = \sqrt{\frac{2E_b}{T_b}}\cos\big(2\pi f t + \pi(1-n)\big), \quad n = 0,1$$

Equation 1 : Transmitted Signal Expression for BPSK

The probability of error for BPSK under AWGN channel can be calculated from expression present in equation 2

$$P_b = Q\left(\sqrt{\frac{2E_b}{N_0}}\right) \quad or \quad P_e = \frac{1}{2}erfc\left(\sqrt{\frac{E_b}{N_0}}\right)$$

Equation 2 : BER Expression for BPSK

The output waveform representation of BPSK modulation corresponding to the input binary sequence is depicted in figure 5.

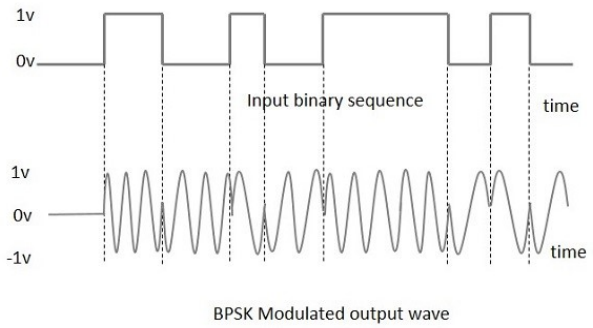

Figure 5 : Waveform Diagram of BPSK Modulation

E. Quaternary Phase Shift Keying (QPSK)

A four-level (4-ary) PSK is called Quaternary Phase Shift Keying (QPSK), and constellation points also chosen as four. As per the theoretical analysis, it is found that QPSK system and BPSK system having the same BER. The QPSK system can also be utilized to double the data rate compared with a BPSK system for some special applications.

The mathematical implementation of transmitted QPSK signal is clearly represented through equation 3

$$s_n(t) = \sqrt{\frac{2E_s}{T_s}}\cos\left(2\pi f_c t + (2n-1)\frac{\pi}{4}\right), n = 1to4$$

Equation 3 : Transmitted Signal Expression for QPSK

The QPSK using two independently modulated quadrature carriers known as in-phase component and quadrature-phase component. The BPSK is used on both carriers as they can be independently demodulated and therefore resulting BER for QPSK is like BPSK.

$$P_b = Q\left(\sqrt{\frac{2E_b}{N_0}}\right) \text{ or } P_e = \frac{1}{2}erfc\left(\sqrt{\frac{E_b}{N_0}}\right)$$

Equation 4 : BER Expression for QPSK

The QPSK can transmit 2 bits/symbol and shifts the phase of the signal to one of four states as clearly mentioned in figure 6.

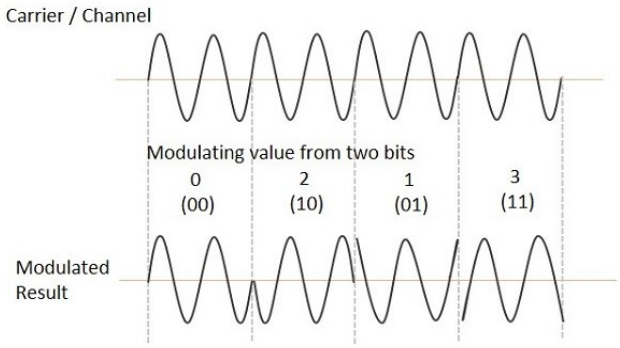

Figure 6 : Waveform Diagram of QPSK Modulation

F. Quadrature Amplitude Modulation (QAM)

QAM (Quadrature Amplitude Modulation) utilizes both amplitude and phase components of a carrier signal in order to achieve high levels of spectrum usage efficiency. This technique includes pulse amplitude modulation (PAM) in high speed data communication systems.

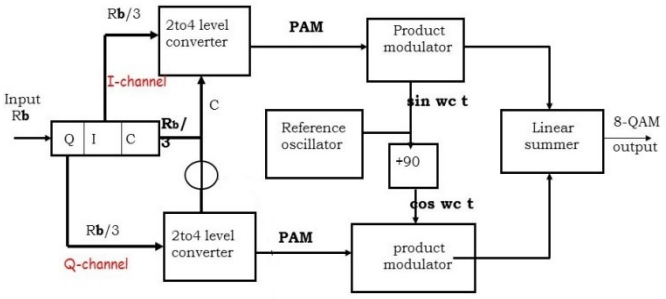

Figure 7 : Block Diagram of 8-QAM Modulator

M-QAM constellations involve two orthonormal basis functions and are two-dimensional. The transmitted QAM signal waveform can also be represented as

$$s_i(t) = \sqrt{E_i}\sqrt{\frac{2}{T_s}}\cos(2\pi f_c t - \theta_i)$$

$$where: E_i = \sqrt{A_{I,i}^2 + A_{Q,i}^2} \text{ and } \theta_i = \tan^{-1}\frac{A_{Q,i}}{A_{I,i}}$$

Equation 5 : Transmitted Signal Expression for M-QAM

M-QAM constellations involve two orthonormal basis functions and are two-dimensional. An important configuration of signal points is rectangular QAM, in each direction the signal points are spaced equally in amplitude and placed on a rectangular grid as clearly understood from the signal constellations diagram depicted in figure 8 for different values of M.

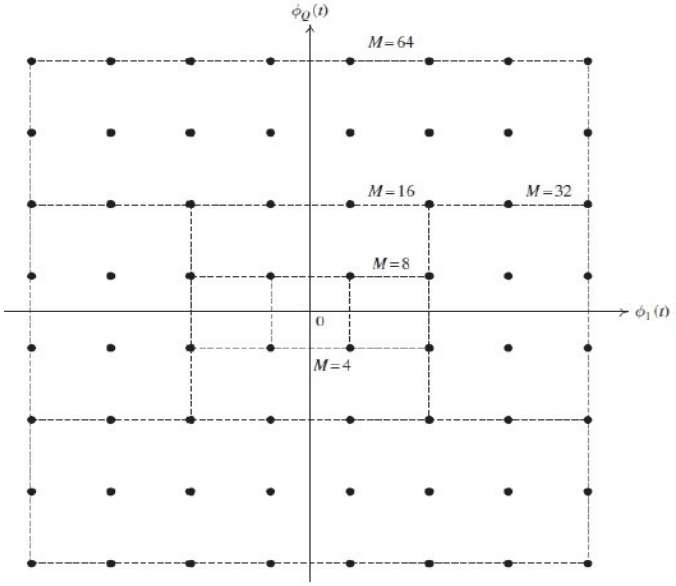

Figure 8 : Constellation Diagram of M-QAM Modulation

III. COMMUNICATION CHANNEL

Communication channels are basically of three types based on the classifications in terms of their characteristics as Noise model (AWGN), Radio frequency propagation model & Interference model. The detailed explanation about AWGN channel is given below based on the analysis.

A. Additive White Gaussian Noise Channel (AWGN)

The AWGN channel is mathematically represented by an output series *Yi* at different time index *i*. *Yi* is the summation of the input *Xi* and noise, *Zi*, where *Zi* is identically distributed and drawn independent from a zero-mean normal distribution with variance *N*.

$$Z_i \sim \mathcal{N}(0, N)$$
$$Y_i = X_i + Z_i$$

Equation 6 : Mathematical representation for AWGN Channel

The AWGN channel is often used for many satellite and deep space communication links. The major application of AWGN is to simulate background noise for channel under observation. This is not a good model for fading, frequency selectivity and does not account for terrain blocking, interference etc.

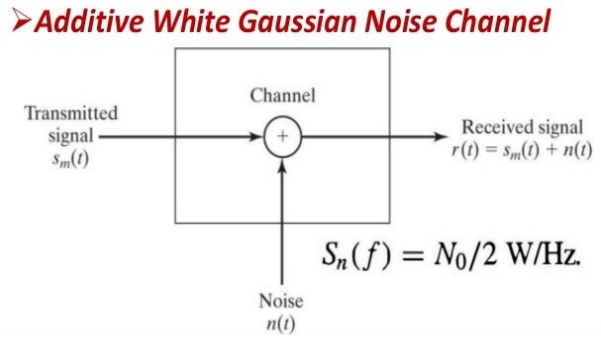

Figure 9 : AWGN Channel Model

IV. PERFORMANCE MEASURES

A. Bit Error Rate – BER

Bit errors are the number of bits corrupted or destroyed during the transmission of data from the source to destination. Bit error ratio is a unit less quantity and often measured in percentage.

$$BER = \frac{Number\ of\ bits\ in\ error\ (at\ receiver)}{Total\ number\ of\ bits\ (transmitted)}$$

Equation 7 : BER Formula

B. Signal To Noise Ratio - SNR

Signal-to-noise ratio is a measurement parameter that compares the level of signal power to a level of noise power and expressed its mathematical value in decibels. If the ratio is higher than 1:1, it shows that more signal than noise.

$$SNR = \frac{P_{Signal}}{P_{Noise}}$$

Equation 8 : SNR Formula

C. Mean Square Error – MSE

The mean squared deviation of an estimator measures the average squared difference between the estimated values and what is estimated. The MSE is the measure of quality of an estimator and the second moment of the error, therefore incorporates both bias and variance of an estimator.

$$MSE = \frac{1}{N}\sum_{i=0}^{N}(\hat{Y}_i - Y_i)^2$$

Equation 9 : MSE Formula

V. IMPLEMENTATION DETAILS

An input audio signal in .wav format having file size of 673 KB is fed as a common input to various modulation schemes and the same is analyzed by simulation through MATLAB. The resulted spectrum waveform of input audio is shown in Figure 10.

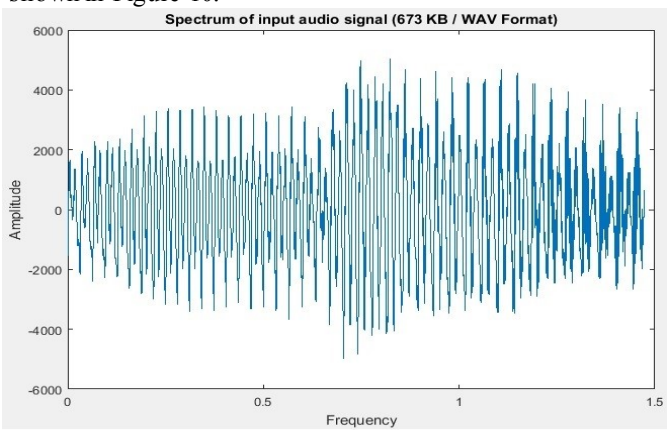

Figure 10 : Spectrum of input audio signal

Before processing to modulation, the real-time audio signal is converted to digital form and sampled at a rate of 44,100 Hz through MATLAB functions. In order to compare the digital modulation schemes performance, this digitize sequence is carrying through AWGN channel at different levels of SNR.

VI. EXPERIMENTAL EVALUATION

An audio signal whose spectrum as shown in figure 10 is fed as an input to obtain the results as mentioned below.

.

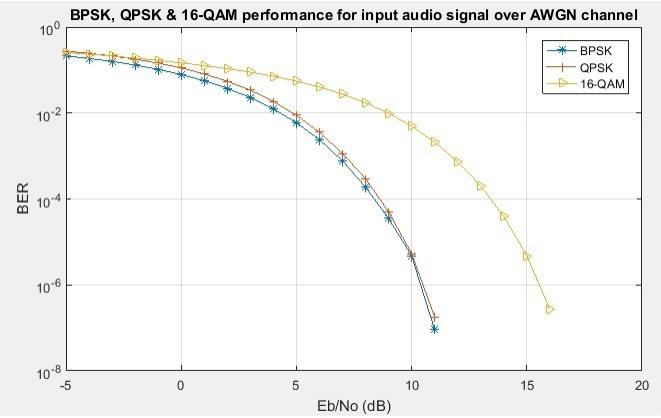

Figure 11 : BER curve for BPSK, QPSK & 16-QAM

From the obtained BER curve it is clear that the relation between SNR and BER quantities are inversely proportional. It is observed as SNR value increases the BER decreases.

In the table tabulated below, the observation made for different SNR levels on various techniques is mentioned.

MODULATION TECHNIQUES	BIT ERROR RATE
BPSK	0.0562
QPSK	0.1795
16-QAM	0.2557

Table 1 : BER value at SNR = 1dB

It is inferred that from the table 1 and table 2, at the lower SNR level say 1 dB the larger is amount of noise and at the medium SNR level say 5dB the amount of signal power is increased respectively.

MODULATION TECHNIQUES	BIT ERROR RATE
BPSK	0.0060
QPSK	0.0551
16-QAM	0.1678

Table 2 : BER value at SNR = 5dB

Considering the table 3 which says the SNR at 10dB there is a vast increase in the signal power and huge decrease in the BER values.

MODULATION TECHNIQUES	BIT ERROR RATE
BPSK	0.0000
QPSK	0.0012
16-QAM	0.0720

Table 3 : BER value at SNR = 10dB

From the above experimentation results we infer that when SNR is of high value the data rate techniques like 16-QAM shows better performance when compared to the lower data rate techniques.

VII. CONCLUSION

The respective conventional passband modulation schemes have been simulated in MATLAB software in terms of BER values as well as BER curve corresponding to different levels of SNR. The conclusion made from the above observation and discussions are as follows:

- Experimentally it is found that the minute difference of 1 dB (approx.) will occur among the BER curves of BPSK and QPSK as clearly shown in figure 11. Ideally the BER result of BPSK and QPSK are equal over AWGN channel.
- At low level SNR it is efficient to use low order modulation schemes such as BPSK or QPSK and at high level SNR it is better to use high order modulation schemes like 16-QAM as respective modulation schemes offer less amount of BER in respective levels of SNR.
- In future the research can also be proceed further while implementing these single carrier modulation schemes namely BPSK, QPSK & 16-QAM with multicarrier modulation schemes such as OFDM, FBMC, SEFDM etc in order to enhance the productivity of present communication system.

ACKNOWLEDGMENT

Our sincere thanks to all the associates & technical staff at Truba Institute of Engineering & Information Technology, Bhopal for rendering their valuable time & support in bringing this paper and also provided technical support for analyzing the results outcome. We would appreciate for more guidance and continuous support for all our future endeavours.

REFERENCES

[1] Hlwun Moe Aung, Win Zaw Hein, Hla Myo Tun, "Performance Evaluation of GSM Transmission over Different Modulation Schemes (BPSK, QPSK, GMSK)," International Journal of Scientific and Research Publications, Volume 4, Issue 4, April 2014 1 ISSN 2250-3153.

[2] Vineet Sharma, Anuraj Shrivastav, Anjana Jain, Alok Panday, "BER performance of OFDM-BPSK,-QPSK,- QAM over AWGN channel using forward Error correcting code," International Journal of Engineering Research and Applications (IJERA) ISSN: 2248-9622 Vol. 2, Issue 3, May-Jun 2012, pp.1619-1624.

[3] Charles U. Ndujiuba, Oluyinka Oni, Augustus E. Ibhaze, "Comparative Analysis of Digital Modulation Techniques in LTE 4G Systems," Journal of Wireless Networking and Communications 2015, 5(2): 60- 66 DOI: 10.5923/j.jwnc.20150502.02.

[4] Dixit Dutt Bohra1, Avnish Bora, "Bit Error Rate Analysis in Simulation of Digital Communication Systems with Different Modulation Schemes," International Journal of Innovative Science Engineering and Technology, ISSN 2348 – 7968.

[5] George Caşu, Mircea Nicolaescu, "A Comparative Performance Analysis of Digital Modulation Schemes used in Mobile Radio Systems," International journal of Advanced Research in Physical Science, Volume 2, Issue 5, May 2015, PP 7-13.

[6] Jaspal Bagga, Dr Neeta Tripathi, "Study and Comparison of Various Modulation Classification Techniques under Noisy Channel Conditions," International Journal of Emerging Technology and

Advanced Engineering, ISSN 2250-2459, Volume 2, Issue 4, April 2012.

[7] Jianfeng Feng, Digital Communications and Signal Processing– with Matlab Examples, Department of Computer science and Centre for Scientific Computing University of Warwick CV4 7AL,UK.

[8] S. O. Popescu, G. Budura, A. S. Gontean. "Review of PSK and QAM — Digital modulation techniques on FPGA", 2010 International Joint Conference on Computational Cybernetics and Technical Informatics, 2010.

[9] B Chirag, A Lohith, H S Prashantha. "Comparative performance analysis of various digital modulation schemes in AWGN channel", 2017 Innovations in Power and Advanced Computing Technologies (i-PACT), 2017.

[10] Md. Emdadul Haque, Md. Golam Rashed, M. Hasnat Kabir, "A Comprehensive Study and Performance Comparison of M-ary Modulation Schemes for an Efficient Wireless Mobile Communication," International Journal of Computer Science, Engineering and Application, Vol.1, No.3, June 2011.

[11] Jaipreet Kaur, Hardeep Kaur, Manjit Sandhu, "Comparison of BER for Various Digital Modulation Schemes in OFDM System," International Journal of Advanced Research in Electronics and Communication Engineering, Volume 5, Issue 4, April 2016.

[12] Umesh Sharma, "Comparative Study of Digital Modulation Techniques in WIMAX," International Journal of Engineering and Innovative Technology, Volume 2, Issue 2, August 2012.

[13] H.Hguyeu, E.Shwedyle, A first course in Digital Communications, Cambridge University Press, New York, 2009.

Proceedings of the Fourth International Conference on Communication and Electronics Systems (ICCES 2019)
IEEE Conference Record # 45898; IEEE Xplore ISBN: 978-1-7281-1261-9

Solving fuzzy clustering problem using fuzzy bacterial colony optimization

K.VIJAYAKUMARI
Department of Computer Science
Government Arts College
Karur, Tamilnadu, India
k.vijikumari@gmail.com

Dr. V. BABY DEEPA
Department of Computer Science
Government Arts College
Karur, Tamilnadu, India
deepamct@gmail.com

***Abstract*—Fuzzy clustering is a well-known data mining technique and it is used to solve some real world entity. In partitioned clustering, fuzzy c-means is one of the prominent techniques due to its straightforwardness and it produced least computational effort. Still, it falls into the problem of local optima. For solving this local optima problem, many swarms intelligent based optimization algorithm has been introduced and try to achieve a global optimum solution. Even though, some of the conventional optimization algorithms are failures to find global optimum because of premature convergence. In this research paper, a bacterial colony optimization algorithm is an integrated with fuzzy called fuzzy bacterial colony optimization has proposed and its purpose to solve both aforementioned shortcomings. The experimental outcomes are shows that the future new fuzzy clustering algorithm produced superior performance matched with previous fuzzy clustering methods.**

Keywords— Fuzzy Clustering Analysis; Fuzzy C-Means; Fuzzy Particle Swarm Optimization;Fuzzy Bacterial Colony Optimization

I. INTRODUCTION

The process of grouping a dataset based on their similar relationship is clustering. The low similar relationship data samples are handover to the one group and high similar relationship data samples are handover to other groups. The hard and fuzzy clustering are the two major types for solving the clustering problem. In both case, each data points are conveyed in different groups only in the hard clustering [1]. On the other hand, Fuzzy clustering techniques hosted a membership degree the dissimilar group of datasets [2].

The soft clustering is a famous data mining problem useful to solve many real world entities with effective manner. The fuzzy c-means is one of famous algorithm to solve the clustering problem[3]. But, it is falling into optima problems and could not achieve a global optimum. Several research works have been carried out in order to solve the shortcoming of conventional FCM. The problem of FCM noise sensitivity was excluded with the help of probabilistic Fuzzy c-Means [2]. Spatial information of the image can be effected the efficiency of the FCM and it does not completely used in FCM. Hence, a spatial functions is used with conventional FCM for extracting the spatial information of the images and it could be increased the accuracy of the image clustering [4]. However, the conventional and enhanced FCM has many weaknesses namely tend to local minima, arbitrary assignment of the cluster center values.

In the last decades, the clustering problem has been solved by using swarm intelligent based optimization techniques and it is more attention by the researchers. Such as ant colony optimization (ACO) based on the ants behavior [5], artificial bee colony optimization depends on bee performance (ABC) [6], particle swarm optimization (PSO) according to swarm activities [7], social spider optimization (SSO) [8], firefly algorithm (FA) [9] and bacterial foraging optimization algorithm(BFO)[10]. However, the traditional swarm intelligence based optimization clustering algorithms are failure due to lack of development aptitude that is simply to fall into premature convergence.

Hence, an advanced type of optimization algorithm is known as bacterial colony optimization (BCO) algorithm is combined with the fuzzy concept is referred as fuzzy bacterial colony optimization (FBCO) clustering proposed in this study work. The FBCO algorithm is scheduled through mimicking the behavior of bacterial colony and it has a positive evolutionary mechanism. It has given a modern implementation principle in swarm intelligence algorithms [11].

The robustness of the FBCO algorithm is applied to clustering problem and it compared with FCM and FPSO. The simulation effects are demonstrates that the proposed FBCO clustering algorithm produced significant classification accuracy. The document is structured as, a description of FCM is discussed in Section 2, FPSO is discussed in section 3, the behavior of BCO is discussed in Section 4, the proposed FBCO clustering algorithms is expressed in section 5, the experiment and outcome presented and discussed in Section 6. The conclusion of this research works conversed in the Section 7.

II. FUZZY C-MEANS (FCM)

In partition clustering, Bezdek et al developed FCM algorithm [3]. The iterative process of Fuuzy c-means is to discover meaningful patterns from obtained datasets and it apply the idea of soft membership as an alternative of conveying a pixel to a certain group, every pixel will include to dissimilar membership values on each group. In particular, unlabeled data set $O = \{O_1, O_2, \ldots\ldots O_n\}$ in R^d dimensional area, the Fuzzy c-Mean is to partitions the records into c ($1 < c < n$) fuzzy clusters with cluster centers $z = \{z_1, z_2, \ldots, z_n\}$ [12].

In fuzzy clustering, the data samples are expressed by a fuzzy matrix μ. It has with n rows and c columns. Where n is the number of data samples and the number of classes is denoted by c. The component μ_{ij} is in i^{th} row with j^{th} column. Them, μ specify the amount of association of the ith data samples with the jth cluster. The distinctiveness of μ is defined as follows:

$$\forall_i [0,\ 1]\ \forall_i = 1,\ 2 \ldots n\ \forall_j = 1,\ 2 \ldots c \quad (1)$$

$$\sum_{j=1}^{c} \mu_{ij} = 1\ \forall_{i=1,2,\ldots n} \quad (2)$$

$$o < \sum_{j=1}^{c} \mu_{ij} < n\ \forall_{j=1,2,\ldots,c} \quad (3)$$

The aim of minimization or maximization function is well-defined as follows,

$$J_m = \sum_{j=1}^{c} \sum_{i=1}^{n} \mu_{ij}^{m} d_{ij} \quad (4)$$

Where, $m(m > 1)$ is a values of scalar and is heavy exponents that regulating the fuzziness of the resultant clusters. Euclidian distance d_{ij} is denote the function from data point to the cluster center $z = \{z_1, z_2, \ldots, z_n\}$. The distance function d_{ij} is defined as follows,

$$d_{ij} = \left| o_i - z_j \right| \quad (5)$$

Where, the z_j centroids of the jth cluster and i^{th} data objects which is defined by using below equation

$$z_j \frac{\sum_{i=1}^{n} \mu_{ij}^{m} o_i}{\sum_{i=1}^{n} \mu_{ij}^{m}} \quad (6)$$

If convergence criteria does not met after completing every iteration, then the membership values is updated as follows,

$$\mu_{ij} = \frac{1}{\sum_{k=1}^{c} \left(\frac{d_{ij}}{d_{ik}}\right)^{\frac{2}{m-1}}} \quad (7)$$

III. FUZZY PSO

The PSO algorithm is a well-known optimization techniques which are applied to solve clustering problem to obtained efficient clustering accuracy[13]. The PSO mimics the bird flying behavior and fish schooling behavior. The PSO clustering searching the optimum cluster center on their search space which is moving toward an optimum solution which is produced efficient clustering members based on their similarity[14].

H. Izakian et al has proposed FPSO for solving clustering problem in fuzzy [15]. In Fuzzy PSO, the particle position and velocity are defined as a fuzzy relation between groups and objects that is each particle are represented membership degree μ and it should satisfy the condition of equations(1) and (2). Then , the position and velocity updating done are given as,

$$V(t+1) = \omega \times V(t) + (c_1 r_1) \times (pbest(t) - X(t)) + (c_2 r_2) \times (gbest(t) - X(t) \quad (8)$$

$$X(t+1) = X(t) \otimes V(t) \quad (9)$$

Where, *pbest* is the personal best values achieved from current particle and gbest is a global best value achieved by all particle from $c \times n$. However, the process of searching ability in the conventional PSO is an inefficient due to the search process not carried out completely. In this situation, the PSO algorithm can disturbed by a problem of premature convergence[16].

IV. THE FUNDAMENTAL BEHAVIOUR OF BACTERIA COLONY OPTMIZATION

The BCO was developed by Niu and Wang in 2012 followed by the behavior of E.Coli bacterial colony[11]. The behavior of BCO algorithm is a combination of two bacterial foraging algorithms such as bacterial foraging optimization[17] and bacterial chemotaxis algorithm[18]. The conventional bacterial based algorithm is considered only entity behaviors instead of social behavior of swarm intelligence algorithms. The bacterial colony is an autonomously searching the food in the search space by their personal knowledge.

However, the conventional bacterial based algorithm is a problem due to their features and it takes more computation time. To solve above revealed limitations, a innovative fuzzy clustering algorithm is proposed such as fuzzy bacterial colony optimization (FBCO). There are five types of main steps presents in the BCO namely chemotaxis, communication, elimination, reproduction and migration process. The following subsection are briefly explained the behavior of the conventional BCO and its steps [11].

A. Chemotaxis and communication model

The communication is major activities of the bacterial colonies that are accompanied with two processes such as runs and tumbles. It has performed three kinds of information exchanges during the process of communication such as random direction, group information, and personal information. The bacterial colonies are used for an exchange the information and guide to them in the behaviors of movement and its guidelines. The process of the communication can be accomplished either run or tumble which is expressed as follows,

$$Position_i(T) = Position_i(T-1) + R_i.(Run_{\inf o}) + R\Delta(i) \quad (10)$$

$$Position_i(T) = Position_i(T-1) + R_i.(Tumb_{\inf o}) + R\Delta(i) \quad (11)$$

The relationship between the individual and the group of the bacterial colonies are considered by the position updating process. The information on the each bacterial colony is shared with the help of communication process.

B. Elimination and Reproduction method

Each bacterial colony is noticeable with a degree of energy level based on the ability of searching in the exploration. The level of energy of every bacterial colony is defined by its probability. The energy level of each bacterial colony is sorted and analyzed, then decide the qualification of bacterial colony used as a criterion. The assessment of the elimination and reproduction process can be defined as follows,

$$\begin{aligned} &if\ L_i > L_{given}\ and\ i \in healthy,\ then\ i \in Candidate_{repr} \\ &if\ L_i < L_{given}\ and\ i \in healthy,\ then\ i \in Candidate_{eli} \\ &if\ i \in unhealthy,\qquad then\ i \in Candidate_{eli} \end{aligned} \quad (12)$$

Where, L_i -is the energy level of ith bacterial colony. All behavior of the bacterial colony was constrained surrounded by a reserved area. If bacterial colony moves left from reserving area, two schemes will be performed. Either, produce new entity to re-establish the outer one or modify the forward way to retains them effectively. In this stage, the boundary control is very important. The outer bacterial colony is considered as an unhealthy and it's ready to eliminate from the populations and then reproduce by the healthy bacterial colonies.

Algorithm 1 : Proposed FBCO clustering algorithms

Begin
- Step 1 : Initialize required parameters
- Step 2 : Each bacterial colony
- Step 3 : Chemotaxis and communication process in tumbling and swimming
- Step 4 : Calculate cluster center for each bacterial colony
- Step 4 : Performing an interactive exchange
  - Step 4.1 : If Individual Exchange
    - *if* Dynamic neighbor oriented
      - if found poorer fitness bacterial colony, then replace with random values
    - *else* Random oriented
      - Replace poorer colony after finding poor fitness value of bacterial colony from the given data chooses by randomly
  - Step 4.2 : Else if Group exchange
    - Replace the poorer after finding the best bacterial colony according to the fitness values
- Step 5 : Reproduction and elimination
  - Step 5.1 : Search the healthy bacterial colony using its fitness values
  - Step 5.2 : Perform the reproductions and elimination
- Step 7 : Migration process
- Step 8 : Update position for each bacterial colony
- Step 9: If terminating situation is not met, then go to step2.

End

C. Migration model

The migration is the process of constructing more nutrition and its performance is not followed by given probability. The bacterial colony would travel to a new random residence on the search space according to the given conditions satisfied. The BCO is performing the migration process in order to avoid the local minimum. It can be expressed as follows,

$$Position_i(T) = rand.(ub - lb) + lb \quad (13)$$

Where, lower and upper borders are lb and ub of the colony positions correspondingly. The random number generation is representing as *rand* that range between 0 and 1.

V. PROPOSED FUZZY BCO CLUSTERING ALGORITHM

The major purpose of the fuzzy clustering problem is to decrease the sum distance between samples which is defined as an objective function J_m as follows,

$$J_m = \sum_{j=1}^{c} \sum_{i=1}^{n} \mu_{ij}^{m} d_{ij} \quad (14)$$

Where, K is determine the number of clusters, D is the number of dimension in the data sets of x. The lowest values of J_m is considered as the best values. In the proposed FBCO, the fuzzy relation of the data sample X is defined as follows ,

$$X = \begin{bmatrix} \mu_{11} & \cdots & \mu_{1c} \\ \vdots & \ddots & \vdots \\ \mu_{n1} & \cdots & \mu_{nc} \end{bmatrix} \quad (15)$$

Where, μ_{ij} is the membership function value for i^{th} data samples and j^{th} cluster. It should be satisfied with the equation (1) and (2). Furthermore, the complete lives of the bacterial colonies are involved, two processes in the chemotaxis such as running and tumbling. Therefore, the updating the position of the each bacterial colony as follows,

$$\begin{aligned} Position_i(T) = {} & Position_i(T-1) + C(i) \\ & *[f_i.(G_{best} - Position_i(T-1)) + (1-f_i) \\ & *(P_{best_i} - Position_i(T-1)) + turb_i] \end{aligned} \quad (16)$$

$$\begin{aligned} Position_i(T) = {} & Position_i(T-1) + C(i) \\ & *[f_i.(G_{best} - Position_i(T-1)) + (1-f_i) \\ & *(P_{best_i} - Position_i(T-1))] \end{aligned} \quad (17)$$

$$C(i) = C_{\min} + \left(\frac{Iter_{\max} - Iter_j}{Iter_{\max}} \right).(C_{\max} - C_{\min}) \quad (18)$$

Where, $turb_i$ denotes the turbulent direction variance of the ith bacterial colony, $C(i)$- is the chemotaxis step size of the ith bacterial colony, $f_i \in (0,1)$, G_{best} is the global best and P_{best} is the personal best of the ith bacterial colony. $Iter_{\max}$, $Iter_j$ are the maximum iteration and current iteration respectively. In proposing FBCO, the n number of bacterial colonies of the position is defined as *Position* and that is produced $D \times K$ cluster centroid. Hence, $n \times K$ position will be moved for achieving minimum distance that move to the global minimum.

VI. Experimental Resulrs and Discussions

In this research works, the strength of the proposed model is evaluated using six types of benchmark data sets and it obtained from the UCI repository [19].

A. Dataset descriptions

- Fisher's iris consists of three different species of the iris flower, one fifty samples and four features were collected in each species.
- Glass datasets have 214 data objects with 6 types of glasses and it has nine different features in each type
- Wisconsin breast cancer (WBC) data set has 683 data samples with two categories and it categorized by 9 features.
- In wine data sets, it contains of 178 data objects with 3 different types of class and categorized by 13 features.
- Contraceptive Method Choice (CMC) dataset has 1473 data points with 3 types and 9 features
- Vowel data set contains 871 Indian vowels with three features and six overlapping classes.

B. Results analysis and discussions

The FCM clustering algorithm is set 100 iterations as maximum iterations, optimization based clustering techniques such as FPSO and FBCO are set 10 iterations as a maximum iteration. Other parameters are set as mentioned in [11]. Table 1 summarized the efficiency of the clustering algorithms such as FCM, FPSO and proposed method BCO based clustering. The objective function is used to estimates the efficiency of the clustering methods which is defined in (4). The final result is an obtained the average values of 10 independent runs on all compared clustering methods.

Three types of values are considered in this research work as results such as best, average, and worst. The best value is considered as a better performance and it decides according to problem in an optimization process. Here, a low value is considered as best performance because the major goal of this research work concentrates to reduce the objective values (distance) between the data sample with the help of the proposed FBCO clustering algorithm. From the experimental results, the objective value of the proposed model produced enhanced results other then compared clustering algorithms.

VII. Conclusions

Fuzzy clustering is a complicated NP-Hard problem to solve with efficient manner. Hence, the fuzzy bacterial colony optimization clustering algorithm has proposed to solve clustering problem in order to obtain the higher accuracy. The evaluation of the proposed model has conducted on four of kind's benchmark datasets. The experiment results demonstrate that the proposed fuzzy bacterial colony optimization based clustering model produced higher clustering efficiency.

TABLE I. Performance comparisons of the proposed model

Datasets	FCM			FPSO			FBCO		
	Best	Average	Worst	Best	Average	Worst	Best	Average	Worst
Iris	**74.68**	76.50	78.32	**65.33**	68.74	72.16	**63.22**	64.06	64.91
Glass	**75.78**	77.67	79.57	**69.16**	71.64	74.12	**67.96**	69.19	70.42
WBC	**2411.71**	2470.45	2529.20	**2126.20**	2278.63	2431.07	**1947.86**	1921.17	1894.49
Wine	**12128.65**	12778.83	13429.01	**11351.97**	11639.05	11926.19	**10498.32**	10724.79	10951.27
CMC	**3442.28**	3505.59	3568.91	**3321.94**	3356.43	3390.92	**3142.24**	3218.74	3295.25
Vowel	**73468.61**	74061.13	74653.65	**72721.95**	72851.48	72981.02	**71451.91**	71833.16	72214.41

REFERENCES

[1] S. Alam, G. Dobbie, Y. S. Koh, P. Riddle, and S. U. Rehman, "Research on particle swarm optimization based clustering: a systematic review of literature and techniques," *Swarm and Evolutionary Computation,* vol. 17, pp. 1-13, 2014.

[2] N. R. Pal, K. Pal, J. M. Keller, and J. C. Bezdek, "A possibilistic fuzzy c-means clustering algorithm," *IEEE transactions on fuzzy systems,* vol. 13, pp. 517-530, 2005.

[3] J. C. Bezdek, R. Ehrlich, and W. Full, "FCM: The fuzzy c-means clustering algorithm," *Computers & Geosciences,* vol. 10, pp. 191-203, 1984.

[4] K.-S. Chuang, H.-L. Tzeng, S. Chen, J. Wu, and T.-J. Chen, "Fuzzy c-means clustering with spatial information for image segmentation," *computerized medical imaging and graphics,* vol. 30, pp. 9-15, 2006.

[5] P. Shelokar, V. K. Jayaraman, and B. D. Kulkarni, "An ant colony approach for clustering," *Analytica Chimica Acta,* vol. 509, pp. 187-195, 2004.

[6] C. Zhang, D. Ouyang, and J. Ning, "An artificial bee colony approach for clustering," *Expert Systems with Applications,* vol. 37, pp. 4761-4767, 2010.

[7] X. Cui, T. E. Potok, and P. Palathingal, "Document clustering using particle swarm optimization," in *Swarm Intelligence Symposium, 2005. SIS 2005. Proceedings 2005 IEEE*, 2005, pp. 185-191.

[8] P. Padmavathi, V. Eswaramurthy, and J. Revathi, "Fuzzy Social Spider Optimization Algorithm for Fuzzy Clustering Analysis," in *2018 International Conference on Current Trends towards Converging Technologies (ICCTCT)*, 2018, pp. 1-6.

[9] J. Senthilnath, S. Omkar, and V. Mani, "Clustering using firefly algorithm: performance study," *Swarm and Evolutionary Computation,* vol. 1, pp. 164-171, 2011.

[10] M. Wan, L. Li, J. Xiao, C. Wang, and Y. Yang, "Data clustering using bacterial foraging optimization," *Journal of Intelligent Information Systems,* vol. 38, pp. 321-341, 2012.

[11] B. Niu, H. J. D. D. i. N. Wang, and Society, "Bacterial colony optimization," vol. 2012, 2012.

[12] K. Vijayakumari, M. Preetha, and K. Velusamy, "Performance Analysis of Clustering Based on Fuzzy System."

[13] T. Cura, "A particle swarm optimization approach to clustering," *Expert Systems with Applications,* vol. 39, pp. 1582-1588, 2012.

[14] K. Velusamy and R. Manavalan, "Performance Analysis of Unsupervised Classification based on Optimization," *International Journal of Computer Applications,* vol. 975, p. 8887, 2012.

[15] H. Izakian and A. Abraham, "Fuzzy C-means and fuzzy swarm for fuzzy clustering problem," *Expert Systems with Applications,* vol. 38, pp. 1835-1838, 2011.

[16] T. Niknam and B. Amiri, "An efficient hybrid approach based on PSO, ACO and k-means for cluster analysis," *Applied soft computing,* vol. 10, pp. 183-197, 2010.

[17] K. M. Passino, "Biomimicry of bacterial foraging for distributed optimization and control," *IEEE control systems magazine,* vol. 22, pp. 52-67, 2002.

[18] S. D. Muller, J. Marchetto, S. Airaghi, and P. Kournoutsakos, "Optimization based on bacterial chemotaxis," *IEEE Transactions on Evolutionary Computation,* vol. 6, pp. 16-29, 2002.

[19] Y. L. H. Z. L. Z. W. W. C. Zhang† and E. Z. M. Research, "MLBench: Benchmarking Machine Learning Services Against Human Experts," *Proceedings of the VLDB Endowment,* vol. Vol. 11, No. 10, 2018.

Proceedings of the Fourth International Conference on Communication and Electronics Systems (ICCES 2019)
IEEE Conference Record # 45898; IEEE Xplore ISBN: 978-1-7281-1261-9

Local Grid Connected Microgrid Musters with PV System along POC of BESS

Sandeep Verma

Department of Electrical Engineering

Rajasthan Technical University

Kota, INDIA

er.san.verma@gmail.com,

Dr. Annapurna Bhargava

Department of Electrical Engineering

Rajasthan Technical University

Kota, INDIA

Abrtu2006@gmail.com

Swati Bhasin

Department of Electrical Engineering

Rajasthan Technical University

Kota, INDIA

swatibhasin68@gmail.com

Vandana Chaudhary

Department of Electrical Engineering

Rajasthan Technical University

Kota, INDIA

v30chaudhary@gmail.com

Abstract **- Microgrid (MCG) musters of distribution system and distributed energy resources concurrently storage units and adjustable loads. Operating conditions for these systems are sovereign (Islanding mode) or depending (Grid connected mode). Various technologies are using now a days for making easeful the local generation using very small sources and the extendable (in time phrase)sources which are available in bulk and in the nature like wind, biomass, geothermal, sun radiation on earth etc. the planned accomplishment of local microgrid going through the view of study which contains residential type load whose nature may be critical or non-critical, a governed battery, pv system power by solar radiation as RES, distribution network of any grid which integrate an islanding MCG into grid through a pole mounted transformer. Different load conditions are examined over a 24-hour time phrase and the variation results on battery POC (Phrase of Charge) examined on MATLAB2018a software and relative imposition is examined for the time limit at various parameters of load for planned groundwork purpose.**

Keywords-Microgrid, BESS, SPV, Phrase of Charge, Battery Governer

I. INTRODUCTION

Microgrid is an incorporated plan for distributed Generation (micro-generation), energy storages, governable loads determine in local distributed grid with main grid. Various definitions are available for MCG on the basis of govern strategies and classified sources known as renewable energy resources integrate with in MCG; It is called MCG whenever it has governed abilities with in it. Microgrid able to govern both mode normal (grid- connected) and emergency (islanding) [1], [11]. In depending mode (grid-connected) the energy shortage is fulfilled by the main grid whereas the excessive generation by MCG is equipped to the grid at the distribution level. In the sovereign mode (islanding), the MCG generates itself both active (P) and reactive power (Q) and poise the demand of the load side which includes

the energy transfer micro-sources to storages and vice-versa [2], [10]. With the solar energy availability, SPV fed the power to the charge of battery which supply to the load which is insufficient because the availability of solar energy is intermittent. POC of battery is governed by governer. The planned accomplishment of the system brought out for diverse instance horizon for diverse phrase of time over 24-hour loads differed to examine whether battery governs the POC and POC with the resultant output power of battery is differing whenever the load is getting change in demand.

II. MICROGRID PLAN ON MATLAB

A local Microgrid plan taken for examination point of view, with single phase AC of 200 V, generation by solar (maximum capacity 5 KW) which is taken as RES. Three power sources are taken in this plan main grid power, SPV, BESS (150 V, 30 ah). The battery governer governs the BESS. If there is any excessive power in MCG system this power is imbibe by the battery governler and fed to the BESS or it also gives power to the MCG system whenever the power shortage conditions occur. For load purpose two type of loads are considered as captious (C) or non-captious (NC) load. Three basic home are taken as NC while a hospital is taken as C (captious load). Tripping circuit is implemented for every load if it is needed. Portion of a plan is from MathWorks example and forward alteration is done as per need.

The pole mounted supports the system in connecting the main grid with the MCG. The overview Fig. of plan is in Fig. A. For the main grid account, a three-phase alternating current 33kv voltage source, is linked to a transformer (33kv/3.3kv). This planned network again linked to pole mounted transformer (3.3kv/200v, 50hz).

The SPV and Battery are DC power sources in the nature that's why before connecting with MCG, convert into single phase AC. For the governing plan of MCG, there is assumption that power requirement dependability of MCG is not onto the grid, and all the required power is catered by SPV and BESS. Statistics of BESS carries POC and FOC of the BESS which is governed by battery governer with the voltage rating and current rating available by the source authority.

This planned network is examined the overall battery capacity throughout the POC and FOD. The define networks are considered on the basis of discharge current and temperature. In planned network of this paper standard values are considered for accomplished aim.

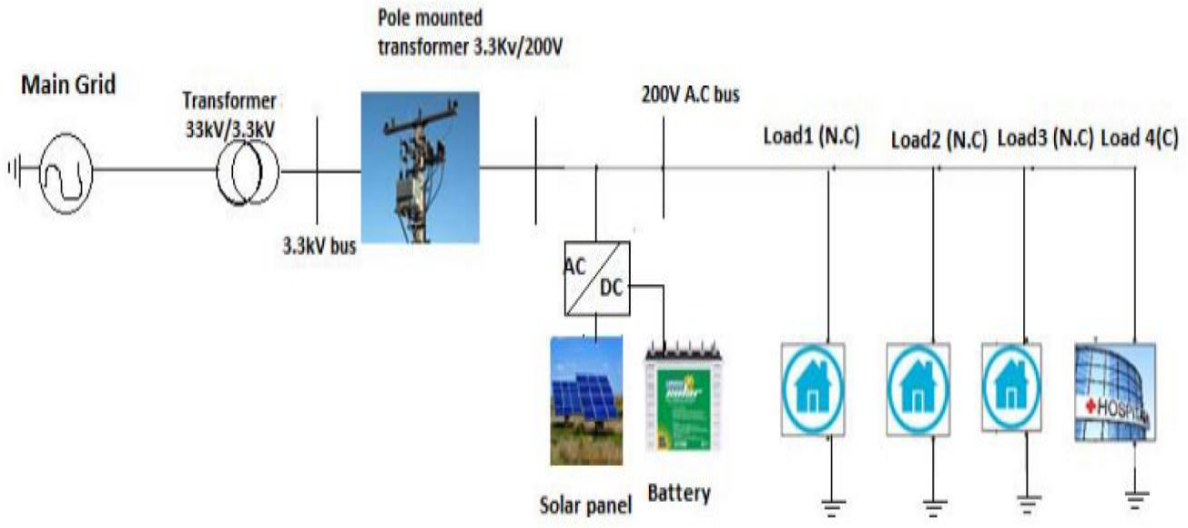

Fig. A. Planned MCG system musters with SPV, BESS, Four loads

III. POC PERFORMANCE DUE TO VARIATION IN LOAD VALUES

The fundamental for BESS strategies is totally turn up to the govern topologies which are implementing into charging or discharging mode of battery. For getting maximum output from the planned network on economy scale there is demand of accelerating the life cycle of BESS [3], [12]. Primary side current (I_{psc})/ voltage (V_{psc}) as it is secondary side current (I_{ssc})/ voltage (V_{ssc}) are two major measure aspects of primary and secondary side. I_{ssc} and V_{ssc} are account for the source as the authority for the SPV and battery at the battery end displayed on Fig. A. POC delineate as reference for the charge left with respect to the formal volume (capacity). In antecedent research FOD (Fall of discharging) defined the effect of POC on BESS life period, one cycle of battery [4], at this point cycle refers to the total process of battery including total charge and total discharge. The curve graph between FOD and life cycle shows in [5], resulting that at the lower FOD a raising many of formal cycles are demonstrating. In [6], [13] govern topologies for battery knowing FOD, the charging and discharge rate spans dealing with improvement into life of BESS. Optimal proportions and assigning methods are defining into [7] by economic analysis model that is given in the account for decrease the threat of energy import and export for BESS. Govern topologies applied for the keeping POC in the Range which are sets higher and lowering range for getting charged or discharged, defined in [8], [9], [14]. In this MCG plan, four cases accounts for check the result with the variation in the load. The Graph of time for all different arc is similar, displays in Fig. G, that is accounts for displays the POC in Fig. H, I and J. Time period is considered as 24-hour, one day for all the planning.

Case W: when all four loads are functioning

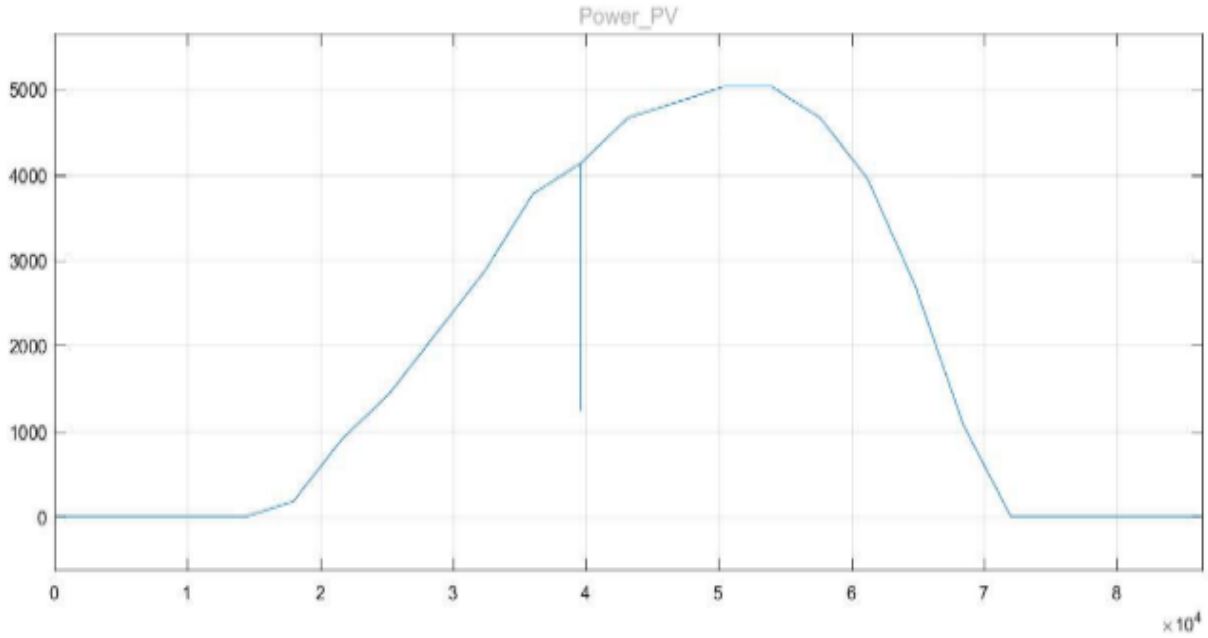

Fig. B. Power of SPV

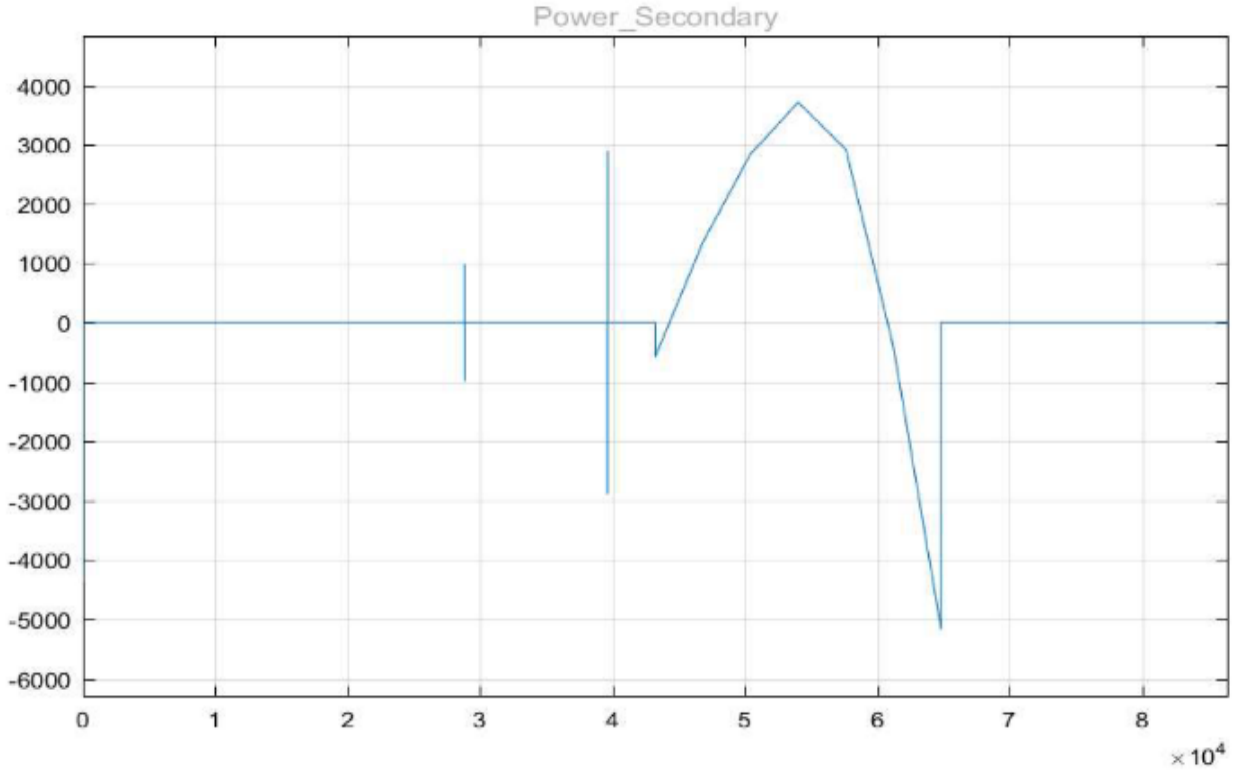

Fig. C. Power of Secondary side

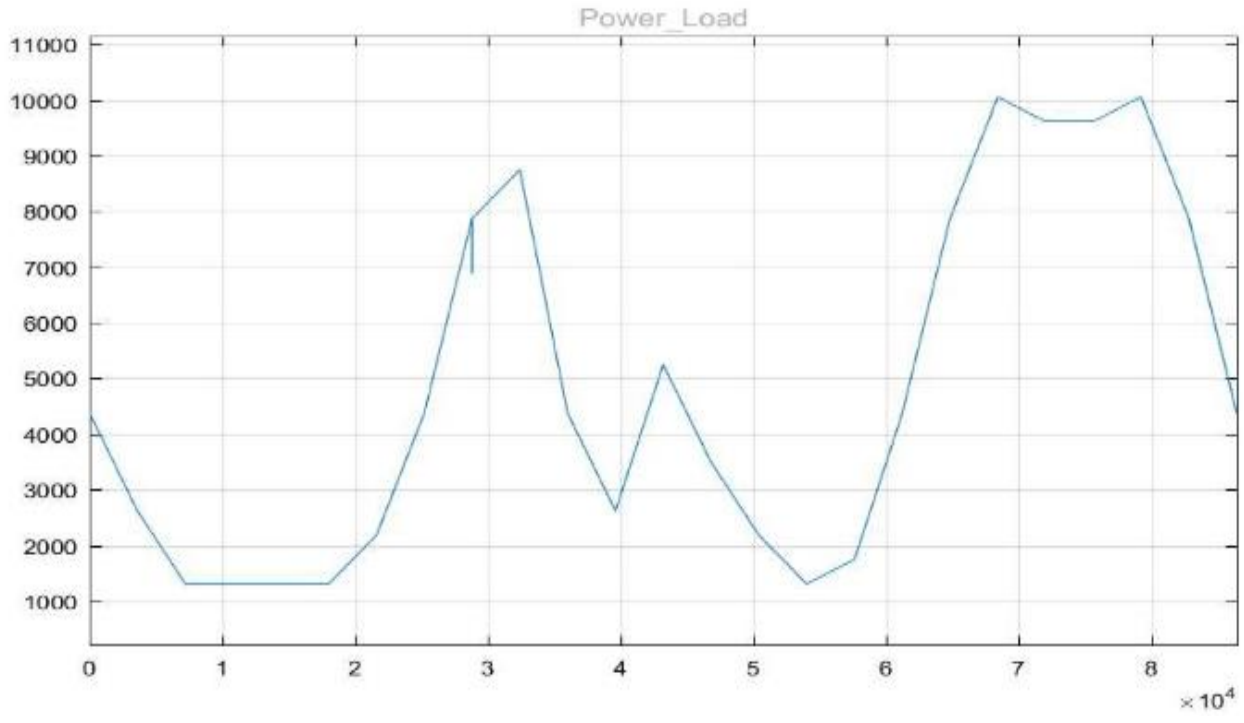

Fig. D. Power of Load side

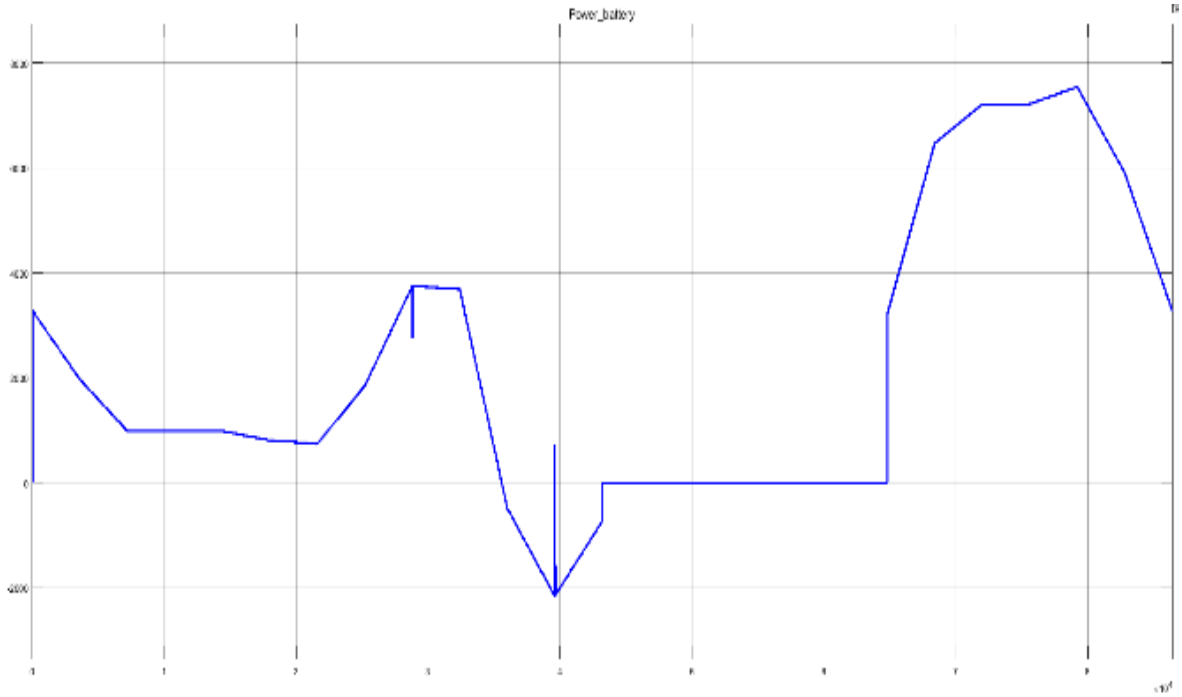

Fig. E. Power of Battery

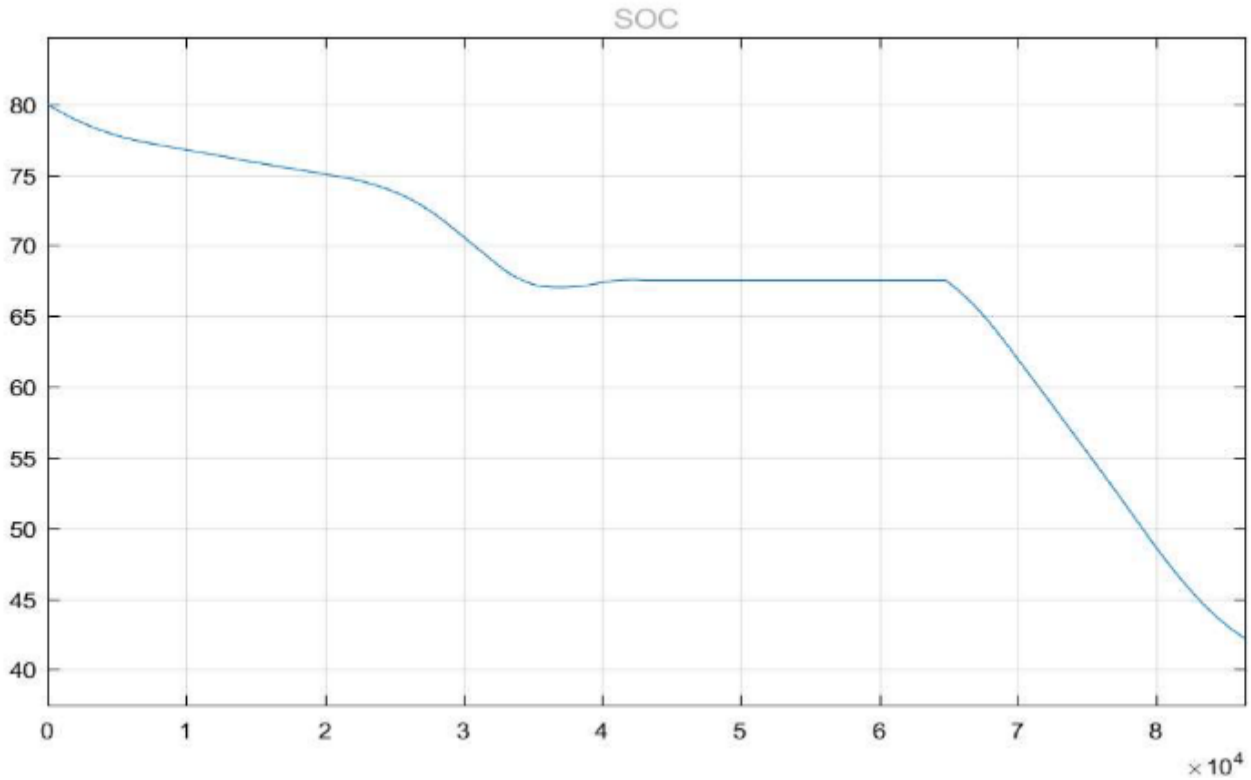

Fig. F. POC of BESS when all loads are functioning

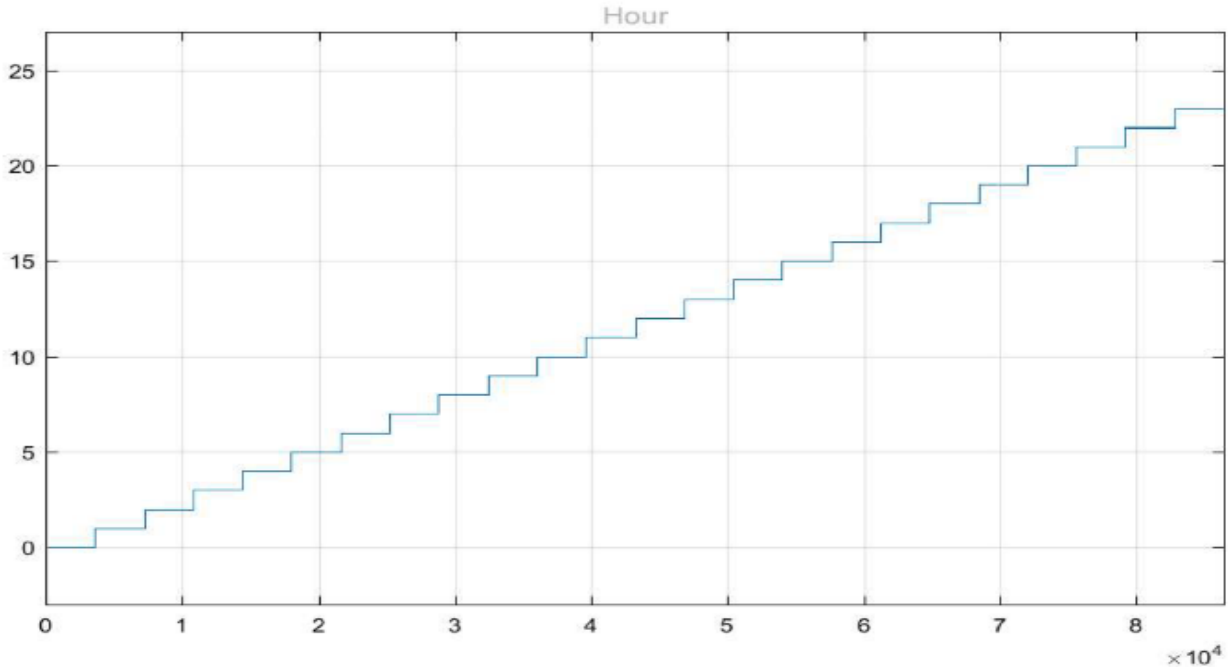

Fig. G. Days hour which are taken on various scale for calculation of planning.

Case X When all three loads are functioning.

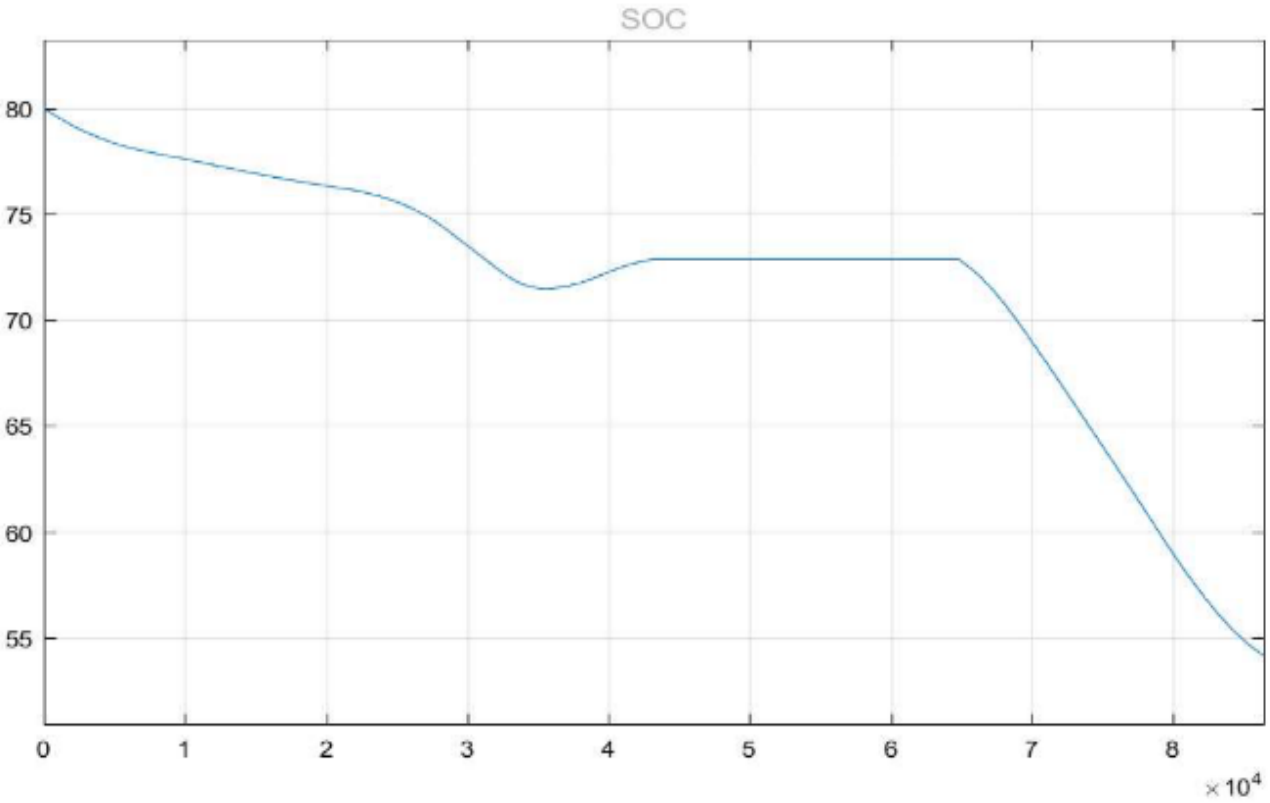

Fig. H. Battery POC for three load connecting network

Case Y: When two loads are functioning including critical one.

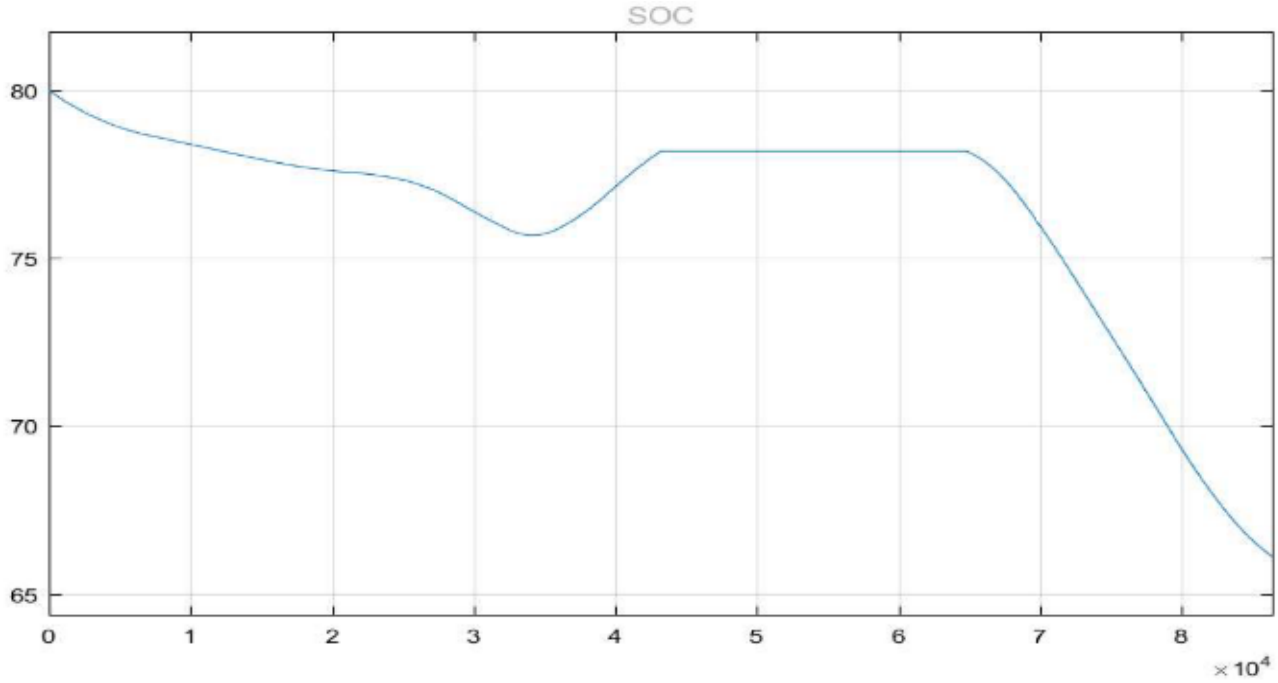

Fig. I. Battery POC for two load connecting network

Case Z: When only critical load is functioning.

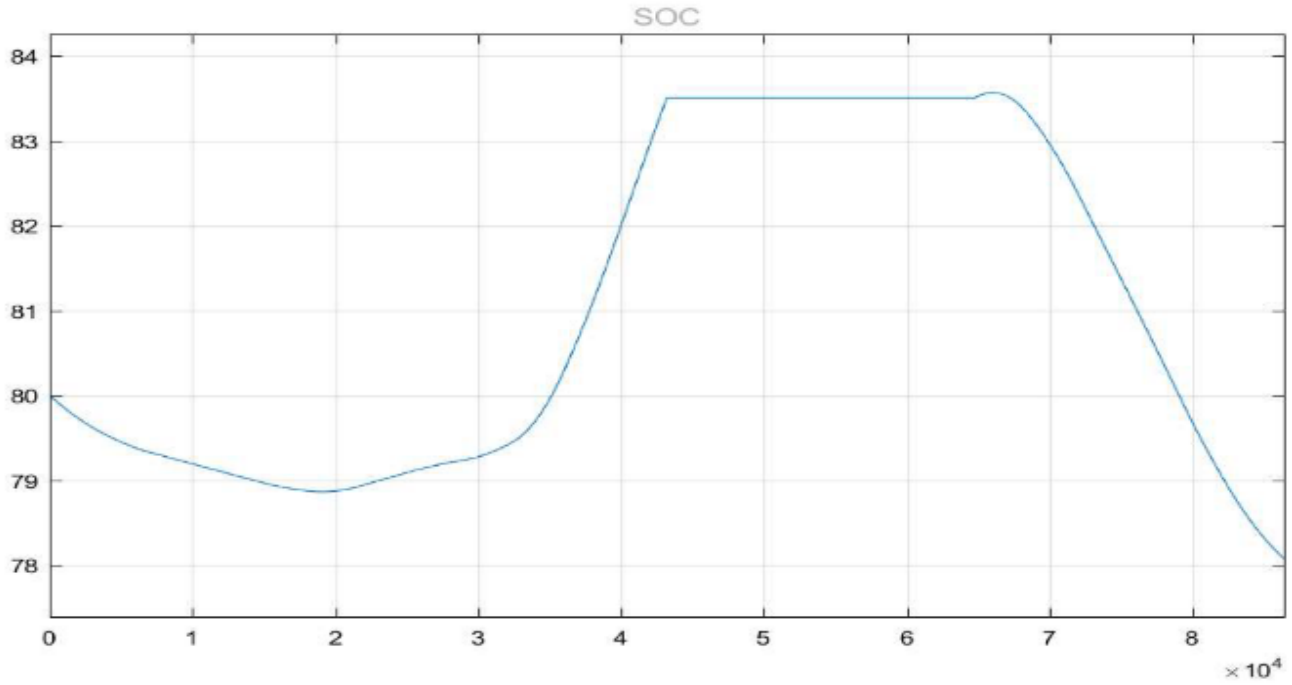

Fig. J. Battery POC for critical load

IV.RESULT ASSESMENT:

As shown cases i.e. case W, X, Y, Z, throughout the 20-hour to 4-hour, output of SPV is almost 0. A peak output (3 kW) is followed during 14 hour and 15 hour. Variation in nominal consumer load, the consumed power amount by load side get to the peak at 9 hour (2.1 kW), 19 hour and 22 hour (3.8 kW). The battery governer performs battery govern during 0 hour to 12 hour and 12 hour to 24 hour. govern of BESS contains the progressive tagging govern of the one of the parameters, current that's why true power flow towards the MCG, the power at MCG side of pole mounted transformer is fixed to zero. In case B three loads are working at a time which include one captious and other twos are non-captious, this decouple of one load accelerate the rate of POC with faster rate as compare to case- W. Hence in the planning of MCG load profile should be account for shaping aspects of overall network. Akin, in other two cases like case Y (Fig. I) and case D (Fig. J), a rapid variation in battery POC can be diagnose which displays the battery statistics and sizing of system. Battery ranges of POC governs by battery governer.

In case W, all loads are linked in system, power is fed by battery to the load, POC drop earlier. During 12h to 18h, no action performed by battery, load is directly supplied by system power. Later (after 18h) POC anew drop for the battery during the feeding of power to the load. Here SPV used as RES, it provides power for charging of battery during its maximum output hours and aid battery to conserve its POC. From case D, it is noticed that POC of battery is over 83% which is checked by battery governer.

V.CONCLUSION

It is observed that from the previous part of study that accomplishment of MCG is become more effective with size of BESS and POC which delivers a noticeable result that in the planning of MCG the battery type is the main consideration and also the govern topologies for battery govern.

It is suggested that for an intermittent load which vary with time i.e. works only for set of time and otherwise it is not active, in these conditions me must calculate the size of battery not the complete pv system. If load is not intermittent it works in uniform way then we must calculate PV system size not the size of battery. Plan for other MCG setups can also be executable with more RES or their fusion.

REFERENCES

[1] Nikos Hatziargyriou, Microgrids architecture and governs, John Wiley & Sons ISBN: 978-1-118-72068-4

[2] Matthew T. Lawder, Bharatkumar Suthar, Paul W. C. Northrop, Sumitava De, C. Michael Hoff, Olivia Leitermann, Member IEEE, Mariesa L. Crow, Fellow IEEE, Shriram Santhanagopalan, and Venkat R. Subramanian, "Battery Energy Storage System (BESS) and Battery Management System (BMS) for Grid-Scale Applications", Proceedings of the IEEE Vol. 102 , Issue: 6 , pp. 1014 – 1030, June 2014.

[3] Lei Chen , Hongkun Chen , Yanhong Li , Guocheng Li , Jun Yang , Xin Liu , Ying Xu , Li Ren ,Yuejin Tang, " SMES-Battery Energy Storage System for the Stabilization of a Photovoltaic-Based Microgrid", IEEE Transactions on Applied Superconductivity, vol. 28, no. 4, Article Sequence Number: 5700407, June 2018.

[4] Hao Qian, Jianhui Zhang, Jih-Sheng Lai, " A grid-tie battery energy storage system", IEEE Trans. on Power Electronics, Vol. 26, No. 3, pp. 886-896, March 2011.

[5] Hisham Mahmood , Dennis Michaelson , Jin Jiang, "Strategies for Independent Deployment and Autonomous Govern of PV and Battery Units in Islanded Microgrids", IEEE Journal of Emerging and Selected Topics in Power Electronics Vol. 3, Issue. 3, PP. 742-755, March 2015.

[6] Mostafa Farrokhabadi , Sebastian König , Claudio A. Cañizares , Kankar Bhattacharya , Thomas Leibfried," Battery Energy Storage System Models for Microgrid Stability Analysis and Dynamic Simulation", vol. 33, issue 2, pp. 2301 – 2312, March 2018.

[7] Valentin A. Boicea, " Energy Storage Technologies: The Past and the Present", Proceedings of the IEEE Vol. 102 , Issue 11, pp. 1777 – 1794, Nov. 2014.

[8] Ming-Hao Wang , Siew-Chong Tan , Chi-Kwan Lee , S. Y. Hui, "A Configuration of Storage System for DC Microgrids", Vol. 33 , Issue. 5, pp. 3722 – 3733, May 2018.

[9] Hisham Mahmood , Dennis Michaelson , Jin Jiang, "A Power Management Strategy for PV/Battery Hybrid Systems in Islanded Microgrids", IEEE Journal of Emerging and Selected Topics in Power Electronics Vol. 2 , Issue 4, pp. 870 – 882, Dec. 2014.

[10] S. Teleke, M. E. Baran, S. Bhattacharya, and S. Teleke, "Rule-based control of battery energy storage for dispatching intermittent renewable sources," IEEE Trans. Sustain. Energy, vol. 1, no. 3, pp. 117–124, Oct. 2010

[11] C. S. Hearn et al., "Utilization of optimal control law to size grid-level flywheel energy storage," IEEE Trans. Sustain. Energy, vol. 4, no. 3, pp. 611–618, Oct. 2013

[12] J. D. Dogger, B. Roossien, and D. J. Frans, "Characterization of Li-Ion batteries for intelligent management of distributed grid-connected storage," IEEE Trans. Energy Convers., vol. 26, no. 1, pp. 256–263, Mar. 2011.

[13] L. Xu, X. B. Ruan, C. X. Mao, and B. H. Zhang, "An improved optimal sizing method for wind-solar-battery hybrid power system," IEEE Trans. Sustain. Energy., vol. 4, no. 3, pp. 774–785, Jul. 2013

[14] Y. Zheng, Z. Y. Dong, F. J. Luo, K. Meng, J. Qiu, and K. P. Wong, "Optimal allocation of energy storage system for risk mitigation of DISCOs with high renewable penetrations," IEEE Trans. Power Syst., vol. 29, no. 1, pp. 212–220, Jan. 2014

Proceedings of the Fourth International Conference on Communication and Electronics Systems (ICCES 2019)
IEEE Conference Record # 45898; IEEE Xplore ISBN: 978-1-7281-1261-9

Modelling and Analysis of Gigahertz Transverse Electromagnetic Mode (GTEM) Cell

Prachi Kotwal
Electrical Power System
Dr. Babasaheb Ambedkar Technological University, lonere
Raigad, India
prachikotwal04@gmail.com

Gyanendra Verma
EMI/ EMC Division
SAMEER (R & D Lab of Ministry of Electronics and Information Technology, Government of India)
IIT Powai, Mumbai
gyanv@sameer.gov.in

Dr. P. K. Katti
Electrical Engineering
Dr. Babasaheb Ambedkar Technological University, lonere
Raigad, India
pkkatti@dbatu.ac.in

***Abstract*- In the fields of industry, communication, medical equipment and science that continuously emit electromagnetic radiation, the use of electronic and electrical equipment has risen dramatically over the past couple of decades. This electromagnetic radiation causes interference with other devices. To avoid the adverse effects of electromagnetic waves on equipment, the EMC compliance testing of electronic equipment is necessary. This paper introduces a Gigahertz Transverse Electromagnetic Mode Cell model for EMC testing over a DC to 1 GHz frequency range. The GTEM Cell is designed by adopting computer simulation technology (CST) microwave studio software. The performance of the cell has been examined. The measured results of the GTEM cell shows that the S11 is less than -10dB and VSWR is less than 1.7 during the 0.25 to 1 GHz of frequency band. The electric field uniformity and equipment testing volume below the septum is determined with the help of electric field probes which are placed at different heights.**

Keywords - Electromagnetic Compatibility (EMC), Gigahertz Transverse Electromagnetic Mode Cell (GTEM), EMC Compliance, Radio Frequency (RF) absorbers.

I. INTRODUCTION

In the modern age, technological development over the past years has been growing rapidly. The use of electrical and electronic devices is increased in day to day life. However, this equipment frequently generates electromagnetic signals. Consequently, these devices will act as a transmitter and receiver of electromagnetic energy. Therefore all electronics and electrical devices are tested with electromagnetic compatibility (EMC) test. The EMC test is classified in two types, emission and susceptibility (immunity). The emission is the generation of unwanted electromagnetic signals from the equipment under test (EUT) and susceptibility is the ability of electrical equipment to operate correctly in the presence of unwanted electromagnetic emission [1]. Different techniques are accessible for evaluating EMI / EMC readings. These depend on hypotheses like EUT size, frequency band, test limits, field types to be measured (electric or magnetic), field polarization, test signal electrical characteristics, etc.

Various EMC/EMI measuring techniques are used such as open area test sites, transverse electromagnetic cells, anechoic chamber and gigahertz transverse electromagnetic mode (GTEM) cell which depending on the size of the equipment. [2]. By considering all the above points a system designed with the help of CST MW software for EMC measurement equipment.

II. EMC MEASUREMENT METHODS

A. Open Area Test Sites (OATS)

One sort of EMC test technique is an open area test site. To perform the test in an open environment, some environmental conditions need to meet the standard requirements. For big systems such as railways, OATS is appropriate for performing both radiated emission and susceptibility tests. Most of the time all electronics and electrical equipment tested in shielded chamber. The shielded chamber could be transverse electromagnetic (TEM) cell, GTEM cell or anechoic chamber, etc. The only limitation in OATS is to establish a test without external interferences like radio frequency transmission from a civil communication system, satellites, radio transmitters, etc. [2, 3]

B. Anechoic Chamber

Anechoic chamber have been used for electromagnetic compatibility measurements in an electromagnetic isolated environment as per the international standards (e.g. IEC 61000-4-3). Anechoic chamber overcomes the restriction of the open area test site (OATS). It is often used to measure distinct EMC / EMI devices. The chamber is fully closed shielded room and the interior surfaces are covered with radiation absorbent material (RAM), i.e. RF absorbers and ferrite tiles. The most useful advantage of the anechoic chamber is that no external electromagnetic interference occurs, so EMC testing of equipment is more accurate. The limitations of this method are the high cost of a large amount of

RF absorbers and high input power required to establish the electric field [3, 4].

C. Transverse Electromagnetic Mode (TEM) Cell

The Transverse Electromagnetic Mode (TEM) cell, as shown in fig.1, was created in 1974. Its role is to produce normal electromagnetic (EM) fields in shielded environments over a frequency range of DC (0 Hz) to a few MHz [5]. The cell consists of a segment of rectangular coaxial transmission line tapered at each end to fit the normal coaxial connectors dimensionally. RF signal generator (input) linked to one end of the and 50Ω termination provided at the other end of the cell. In transverse electromagnetic mode, the EM waves produced in the cell propagate and therefore have the same features as plane waves. TEM cell's main limitation is that it cannot be used at a range of gigahertz. It is made up of three distinct components in shape. The length of the internal and outer conductors is distinct due to the bending of the transmission lines. Therefore, a wave traveling time along the outer conductor is longer. These field distortions result in higher mode propagation and thus affect the uniformity of the field inside the cell increasingly at higher frequencies. Another limitation is size of the cell, as the cell shows cavity effects, like resonances, at frequencies at which the dimensions of the cell are about half the wavelength. As the frequency of operation increases, its size decreases and the EUT size is restricted [6,7].

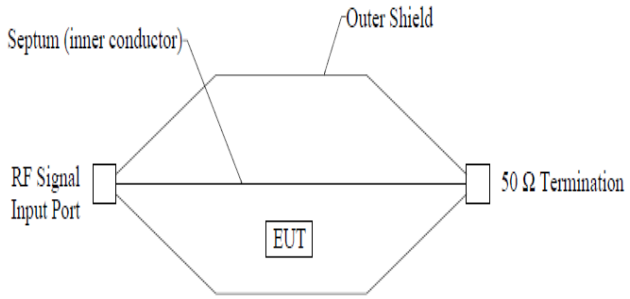

Fig. 1. Transverse Electromagnetic Mode (TEM) cell.

D. Gigahertz Transverse Electromagnetic Mode (GTEM) Cell

It is possible to use up to a gigahertz frequency range to overcome all of the above constraints by modifying the TEM cell, known as the GTEM cell. In 1987, D. Konigstein and D. Hansen launched the GTEM (Gigahertz Transverse Electromagnetic Mode) cell. It is the hybrid structure of TEM cell and anechoic chamber. Using a TEM cell strategy, the GTEM cell is a transmission line structure. Without the geometric distortion of the TEM wave, a spherical wave propagates from the RF source into a rectangular coaxial transmission line. Since the waveguide's opening angle is comparatively low, the undistorted spherical wave can be regarded as a plane wave. A tapered section of a rectangular transmission line is the structure of the GTEM cell. In the load termination section, RF absorbers utilize as absorbing material for EM wave termination and resistive load for current termination. The GTEM cell, therefore, needs less space and cost-effective relative to the anechoic chamber. Additionally, it is used for high frequency range. [8,9].

III. GTEM Cell Design and Construction

A. Design Guidelines

The Gigahertz Transverse Electromagnetic Chamber (GTEM) idea is focused on the transverse electromagnetic cell (TEM), which is essentially a coaxial rectangular transmission line operating in TEM mode. The necessary input power is obtained from the EUT position,

$$P = \frac{(E.h)^2}{Z} \quad (1)$$

And the field strength is given by,

$$E = \frac{\sqrt{P.Z}}{h} \quad (2)$$

From the equation (1) and (2) a small chamber of testing volume 10 cm^3 is defined. From equation (1) the intended intensity of electric field will be of 10 V/m, accounting for 0.2 W of input power within bottom of all and the septum. Accordingly, the exact location of the test volume is in the middle below the septum just in front of Radio Frequency (RF) absorbers. This is restricted to $\frac{1}{3}$ of height from the bottom to center conductor imposing the other restriction of boundary such as the height of absorbers i.e. 23 cm. A clearance about 5 cm is been considered to avoid the reflection on the body of chamber and the EUT. Thus, providing the cell length from the rule of thumb, the first estimate to the cell size is achieved as follows:

$$L = 3\ (T_V + D_{TA} + L_A) \quad (3)$$

Where,
T_V = testing volume
D_{TA}= safety distance between testing volume and absorbers
L_A= length of RF absorbers

The transition between N type connector and the cell body is very difficult for GTEM cell design. Design performs an significant part in determining the right size of an Apex.

GTEM cell output depends on the flared transmission line characteristic impedance. Therefore, for the construction of a cell, calculating the characteristic impedance is most essential. The electromagnetic wave is partially reflected back and high-order methods are stimulated due to the small volume and concentrated current in the transition part. To prevent these issues it is essential to match appropriate impedance [10].

The characteristic impedance of the lossless transmission line, according to the high frequency transmission line theory, is:

$$Z_0 = \sqrt{L/C} \quad (4)$$

Where, L and C are the inductance and capacitance of the transmission line per unit length, respectively. The speed of the electromagnetic wave in the lossless transmission line is determined by:

$$\upsilon = \frac{1}{\sqrt{\varepsilon_0 \mu_0}} = \frac{1}{\sqrt{LC}} = 3 \text{ X } 10^8 \text{ m/s} \quad (5)$$

Where,
ε_0 = permittivity of air or vacuum
μ_0 = magnetic permeability air or vacuum.

The equation (4) and (5) gives the characteristic impedance as follows,

$$Z_0 = \frac{1}{\upsilon C} \quad (6)$$

For standard transmission line, substitute $Z_0 = 50\ \Omega$ and $\upsilon = 3 \text{ X } 10^8$ m/sec in equation (6), per unit capacitance is found as C = 66.66pF. By adjusting the width of the septum for a given height to width ratio and height of septum above the center line (h) the desired capacitance and thus characteristic impedance can be achieved [11,12].

This paper introduces the structure of GTEM cells with a volume of 113 cm x 69 cm x 41.2 cm over a frequency range of DC to 1GHz by considering all of the above criteria. A test quantity of 10 cm x 10 cm x 10 cm is described because the chamber is supposed to operate only with small devices.

B. Simulation

GTEM cell evaluation designed by using the Finite Difference Time Domain (FDTD) method. The fig. 2 shows the simulated structure of GTEM Cell with load resistance and RF Absorbers for current termination and RF waves Absorption in CST MW.

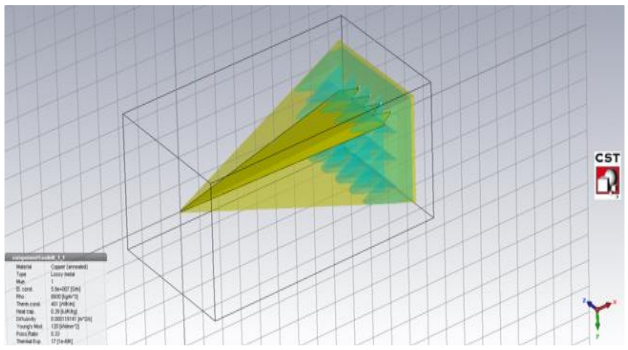

Fig. 2. A cross-Sectional view of GTEM Cell.

The fig. 3 and 4 show GTEM cell parameter S11 and VSWR. Over the frequency band, the results stated input reflection is below -15 dB. This implies impedance matching between source and load have been done very correct. The reflection loss for the frequency range 200 MHz to 400 MHz is below -20 dB and voltage standing wave ratio for GTEM Cell which is below 1.35.

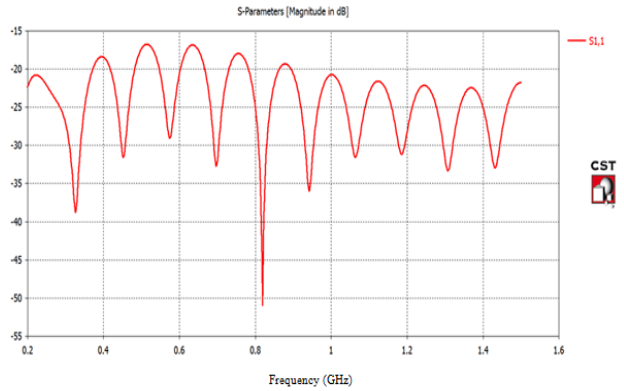

Fig. 3. Input Reflection vs. Frequency.

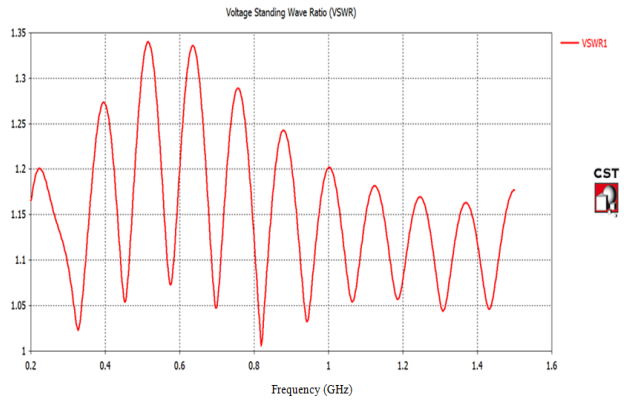

Fig. 4. VSWR vs. Frequency.

C. Fabrication

Aluminium 6082 sheet with 2 mm thickness used to fabricate GTEM cell. These sheets are joint together seam with the help of equal angles and aluminium rivet. All plates are assembled together with the help of nuts and bolts as shown in fig.5. For current termination 100 Ω carbon resistors are used. The combination of 2 X 100 Ω resistors in series connection mounted between the tip of septum and rear wall with the help of bolts as shown in fig.6. The pyramidal shape FUSU 9 RF absorbers of polyurethane material are used for RF wave absorption. The final fabricated GTEM cell with moving trolley is shown in fig.7.

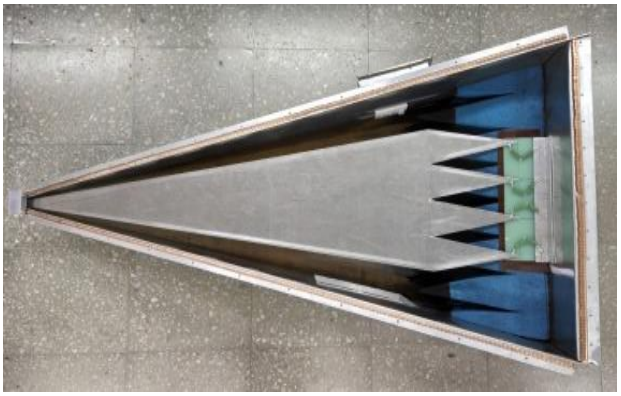

Fig. 5. Fabricated GTEM cell without top cover.

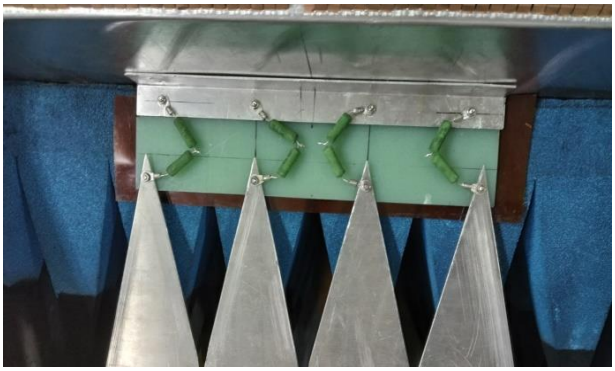

Fig. 6. Resistive load termination.

Fig. 7. Actual model of GTEM cell with trolley.

IV. MEASUREMENT AND TESTING

A. Input Reflection and VSWR

Following fig.8 and 9 show the input reflection and standing wave ratio of the GTEM Cell on vector network analyser respectively. Initially, frequency has set from 5 kHz to 2 GHz and fed radio frequency signals to the input (N type Connector) of GTEM Cell. The performance of the cell is observed from the graph of input reflection and frequency as well as standing wave ratio and frequency. The S11 and SWR parameter are measured at different frequency range by varying the marker position.

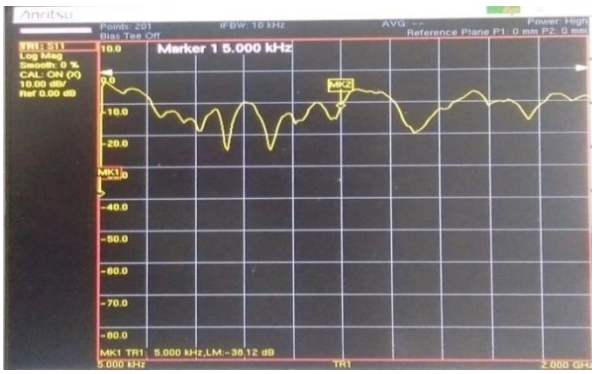

Fig. 8. Input Reflection vs Frequency.

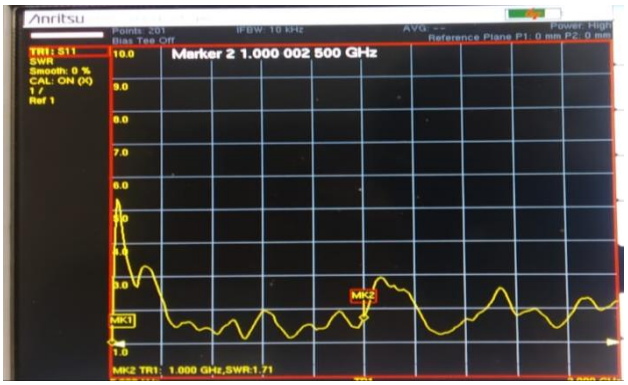

Fig. 9. Standing Wave Ratio vs Frequency.

The input reflection is found below – 10dB for the frequency range 250 MHz to 1 GHz. For frequency range 50 MHz to 250 MHz input reflection is below -8 dB. At frequency 600 MHz, it is -9.94 dB. Standing wave ratio is found to be 1.14 at the frequency of 700 MHz.

B. Electric Field Strength

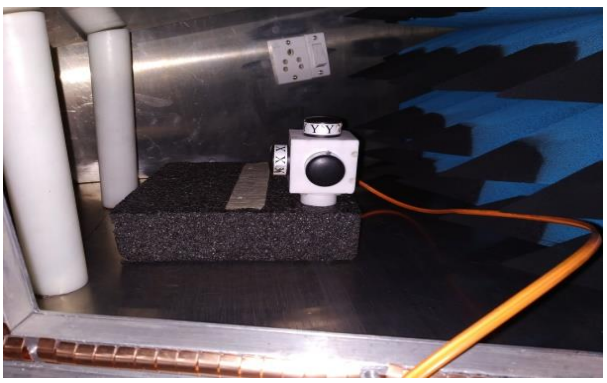

Fig. 10. Measured Electric field strength with isotropic field probe

The generated E-field below the septum is measured with the help of isotropic electric field probe, as shown in fig.10. It is found around 8 V/m at 4 cm height from bottom conductor. By changing the position of electric field probe the testing volume can be obtained below the center conductor. The maximum usable EUT height is recommended as 0.33h according to the IEC 61000-4-20 standard, with ' h ' being equal to the distance between the center conductor and the bottom conductor. By varying the position of E- Field probe, the obtained EUT size is 10 X 10 X 7 cm.

CONCLUSION

In this work a different EMC testing methods are discussed. It shows GTEM cell is one of the simple and easy techniques for EMC measurements. The Design and fabrication of GTEM cell are studied. The performance of the GTEM cell is observed with the help of vector network Analyzer. The maximum EUT size 10 X 10 X 7 cm is obtained below the septum. For the same electric field, it requires less input power as compared to anechoic chamber and open area test.

REFERENCE

[1] Prachi Kotwal, Gyanendra Verma and P. K. Katti, “Effect of Electromagnetic Compatibility and Interference on Electrical Gadgets”, International Journal of Management, Technology and Engineering, vol. 8, issue XII, pp. 1434-1440, Dec. 2018.

[2] Mark T. MA, Motohisa Kanda, Myron L. Crawford, “A review of electromagnetic compatibility/ Interference measurement methodologies”, Proceeding of IEEE, vol. 73, no.3, pp. 388-411, March 1985.

[3] M. L. Crawford, “Generation of standard electromagnetic fields using TEM transmission cells,” IEEE Transaction on Electromagnetic Compatibility, vol. EMC-16, pp. 189-195, Nov.1974.

[4] K. Shimada and K. Ishizuka, "A Study of RF Absorber for Anechoic Chambers Used in the Frequency Range for Power Line Communication System", Progress In Electromagnetics Research Symposium 2006, Cambridge, USA, and March 26-29.

[5] Kresimir Malaric, Juraj Bartolic, “ Dsign of a TEM-cell with increased usable test area” , Turk J Electrical Engineering, Vol. 11, pp. 143-154, 2003.

[6] Konigstein D.; and Hansen D, “A new family of TEM-cells with enlarged bandwidth and optimized working volume”, 7th International Zurich Symposium on Electromagnetic Compatibility, Zurich, Switzerland, pp. 127-132, 1987.

[7] Konigstein D.; and Hansen D,“A new family of TEM-cells withen larged bandwidth and optimized working volume”, 7th international Zurich Symposium on Electromagnetic Compatibility, Zurich Switzerland, pp. 127-132, 1987.

[8] C. Icheln, “The Construction and Application of a GTEM Cell”, Master’s Thesis, Technical University of Hamburg-Harburg / Helsinki University of Technology, November 1995.

[9] D.C. Pande, P. K. Bhatt, “ Characterization of a Gigahertz Transverse Electromagnetic Mode Cell”, proceedings of the International Conference on Electromagnetic Interference and Compatibility’97, pp. 31-38, 1997.

[10] H. X. Araujo, and L. C. Kretly, “Optimizing Impedance Matching between the Exciter – APEX and the GTEM Chamber”, Proc. IEEE Convention of Electrical and Electronics Engineers in Israel (IEEEI),

[11] Eliat, pp. 986 – 990, Nov. 2010.ZHANG Junru1, ZHU Wensi1, YU Mengxia1, WANG Yuanyuan, “Design of Ultra Wide band transition Connector for GTEM Cell”, Proc. IEEE International Conference Electronics Communication and Control (ICECC), Ningbo, pp. 3657-3660, Sept. 2011.

[12] Tinus Stander and Saurabh Sinha, “ Development, Simulation and Construction of cost effective GTEM cell”, 23th Conference Radioelectronika 2013, pp. 39-44, April 16-17.

Proceedings of the Fourth International Conference on Communication and Electronics Systems (ICCES 2019)
IEEE Conference Record # 45898; IEEE Xplore ISBN: 978-1-7281-1261-9

Credit Card Fraud Detection Using Various Classification and Sampling Techniques: A Comparative Study

J. V. V. Sriram Sasank, G. Ram sahith, K.Abhinav, Meena Belwal
Department of Computer Science and Engineering
Amrita School of Engineering, Bengaluru
Amrita Vishwa Vidyapeetham, India
sasankjayavarapu27@gmail.com, sahith.gorrepati@gmail.com
abhinavkavuri@gmail.com, b_meena@blr.amrita.edu

***Abstract*— with an ascent in the development of web-based business, the utilization of credit cards for internet shopping has expanded significantly. This, in turn, has brought about a great deal of credit card fakes. However, once in a while. Consequently, the execution of effective fraud detection frameworks has turned out to be fundamental for all banks to limit their misfortunes as far as credit card transactions are concerned. Numerous advanced systems have been created to monitor different credit card exchanges in literature. In this way, individuals have been attempting their best to identify the extortion in credit card exchanges as much as they can. Various machine learning techniques have been applied to predict whether a particular transaction is fraudulent or not. The biggest challenge with the techniques is the unavailability of the balanced dataset. Which is due to the nature of the transaction: the fraud transactions are too less when compared to genuine transactions. This work handles the challenge by balancing the dataset. Five machine learning techniques: Random forest, Naive Bayes, Support Vector Machine, K- Nearest Neighbor and Logistic regression were applied on the balanced dataset with different sampling techniques such as Oversampling, Undersampling, Both sampling, ROSE and SMOTE. The performance metric AUC – ROC suggests that logistic regression performs with an accuracy of 97.04% and precision of 99.99%.**

***Index Terms*— Credit Card fraud, online fraud, Sampling Techniques, Classification, Random Forest, Decision Trees, Precision, Recall, Receiver Operator Characteristics(ROC), Unbalanced Dataset, Undersampling, Oversampling, ROSE, SMOTE, Logistic Classifier, Support Vector Machine(SVM), Naive Bayes, K-Nearest Neighbor(KNN).**

I. INTRODUCTION

Classification is the problem of identifying to which set of categories a new sample belongs on the basis of training samples whose class variable is known. It is a supervised approach as the class variables for the training samples are already known. This is a binary Classification problem as the class variables are either Benign or Malicious. Classification techniques have been used in various domain such as text classification and speech recognition [1], Multi-label logistic regression [2-3], collaborative filtering [4]

In general, the level of each class assumes a significant job in model precision and accuracy performance measure. The information by and large accessible in such cases is largely skewed in light of the fact that out of every atomic exchange only a few of them might be actually fraudulent. Subsequently, it forces an issue of highly imbalanced information. Due to this class imbalance issue, many generic machine learning algorithms such as decision trees, random forest, and naive Bayes tend to overperform in terms of accuracy measure. In reality, these algorithms were successful in predicting the non-fraudulent transactions correctly rather than the fraudulent ones. The minority class of fraudulent exchanges is ignored as exchanges that are noise. The work effectively handles this misclassification by altering the raw data provided to the classification algorithms to precisely predict the minority class, not the majority class.

The next subsection describes the dataset and exploratory data analysis.

A. Dataset Description

The Dataset[5] used for training the model consists of 284,807 records in total, of which only 492 of them are fraudulent cases i.e. 0.172% of fraud cases resulting in high-class imbalance. Features V1 to V28 are numerical values obtained from Principal Component Analysis (PCA). The attributes which are not changed by PCA are Time and Amount. Attribute 'time' contains the seconds gone by between each trade and the essential trade in the dataset. The component 'amount' is the total exchange Amount. Feature 'Class' is the response variable and it takes a value of 1 if there is an occurrence of fraud and 0 generally.

B. Exploratory Data Analysis

All indicators in the dataset have been anonymized, consequently, the non-anonymized indicators 'time' and 'amount' of the transaction for Exploratory Data Analysis were considered. The dataset contains 284,807 transactions with a mean estimation of all records being $88.35, while the biggest transaction recorded in this collection adds up to $25,691.16. Conclusively, the distribution of the amount value of all records is heavily right-skewed. By far most of the exchanges are moderately little and just a fraction of transactions come even near the greatest transaction in the dataset.

The time is recorded in the number of seconds since the main exchange in the dataset. Hence, it can be presumed that this data incorporates all transactions recorded through a span of two days as shown in fig1, with time on x-axis and transactions on the y-axis. In the case of distribution of 'amount' feature shown in fig2, it is bimodal with amount and transactions on x & y-axes respectively. This shows that roughly 28 hours after the main exchange there was a huge drop in the volume of transactions. While the time of the primary transaction isn't given, it is sensible to expect that the drop-in volume happened amid the night.

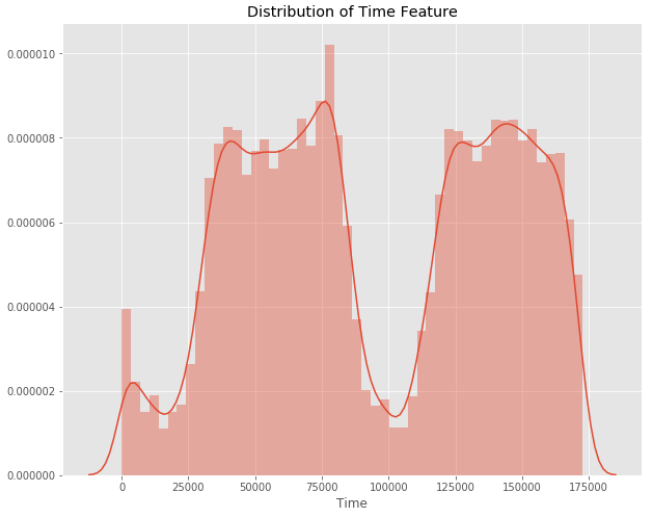

Fig. 1. Distribution of Time Feature

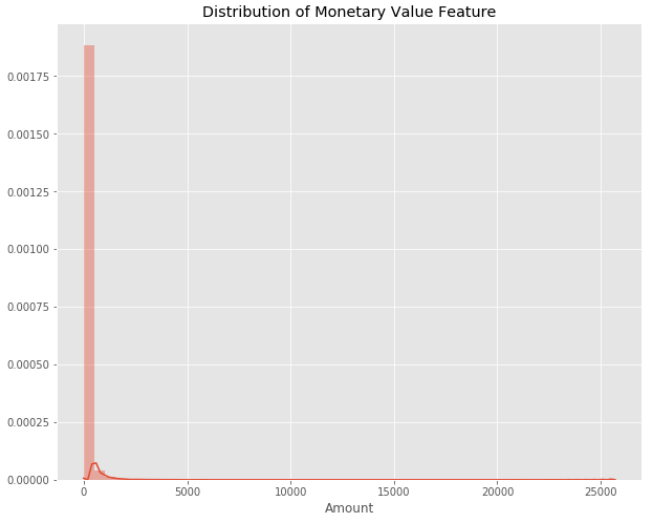

Fig. 2. Distribution of Monetary Value Feature

The remainder of this article is organized as follows: Section II speaks about the related work in the technology, Section III showcases the proposed system, Section IV describes the performance analysis of various classifications and sampling techniques, Section V showcases the experiment results; Section VI describes the conclusion and future work.

II. Literature Survey

A lot of work has been performed on classification techniques and handling class imbalance problem.

Samaneh Sorournejad et al. [6] work focuses on Statistical classification of occurrence of frauds in credit card, techniques for detection, difficulties which are majorly classified as fraud analysis (misuse detection) and user behavior analysis (anomaly detection) their work has also performed machine learning algorithms on many datasets of credit card transactions to detect the fraudulent transactions in that and figuring out the best one for overall credit card transactions.

The work by Lutao Zheng et al. [7] uses a method to construct behavior certificate. To begin with, they had modeled a lot of feature-based behavior highlights for every user from their card purchase records, and after that Behavior Certificate was built dependent on these highlights. Their work on fraud transaction detection is comprised of four characteristics: exchange type, hours of the transaction, sum, and area. After initial processing, they characterized a Behavior Feature Vector (BFV) utilizing 13 measurements to portray a card user's transaction conduct.

The work by V. Dheepa et .al [8] demonstrates the conduct of the client based on informational from the dataset, which are transaction amount, date, time, place, recurrence of procurement and charging Address. In this model, the Support Vector Machine (SVM) was used for classification. It will give great accuracy when fewer highlights are utilized. The other pressing issue is dealing with the class imbalance of information. To recuperate this issue viable component extraction technique is utilized, which is utilized for reducing the data. At that point, the model was trained with SVM classifier and they found the fraudulent transactions with lower error rates.

The work by Hien M. Nguyen et al. [9] presents an observational examination of over-sampling and under-sampling techniques. Test results demonstrate that under-sampling performs superior to over-sampling in the case of small datasets. All sampling techniques, be that as it may, are tantamount when the dataset size increases. All testing systems, be that as it may, are similar when the preparation set increases. This examination additionally proposes that a multiple random under-sampling (MRUS) method ought to be a decent decision for applications with imbalanced and spilling information on the grounds that MRUS is the best while as yet keeping a rapid accuracy.

The work by Arif syaripudin et al. [10] analyzes the strategies of handling imbalanced datasets with resampling and groups. From an alternate angle, this paper looks at how much impact the instances, number of traits, data types, the quantity of the objective class, and missing characteristic qualities influence the results with performance metric as f-measure. The test has come about that the criteria with respect to the number of characteristics, attribute information types, and the quantity of the objective class doesn't influence the order results. While the missing attributes with qualities have an influence on order result. For better high F-measure, the trial demonstrates that the best performing model is a blend of SMOTE 5000/0 and AdaBoostMl. The AdaBoostM1 method could be considered to address the imbalanced datasets. While in a couple of situations

SMOTE procedure can be used with duplication level of minority class (oversampling) of 500%. While in uncommon cases a blended procedure (a mix of SMOTE-500% and AdaBoostM1) has the best situation for dealing with imbalanced datasets. This is apparent from six of the sixteen datasets used to have high F-Measure esteem.

All of the above techniques try to either balance the dataset or apply different sampling methods. However, choosing the right sampling method and applying a valid classification technique plays an important role in credit card fraud detection. Therefore we propose a system that will compare different sampling methods such as over-sampling, under-sampling, Random Over-Sampling Examples (ROSE) and Synthetic Minority Over-sampling Technique (SMOTE), and apply the balanced data to the required classification algorithms, to obtain a high-performance model.

III. PROPOSED SYSTEM

The proposed framework for the model is shown below in figure 5. It clearly demonstrates the five important levels: Performing exploratory data analysis, Partitioning data, Building model on the training set, Applying sampling methods to balance dataset. The initial step of Exploratory data analysis consists of three sub-processing units: checking imbalance data, checking a number of transactions by the hour, checking mean using PCA variables.

EDA is done utilizing R to condense and envision huge qualities of the dataset. To discover the irregularity in the dependent variable, perform the accompanying, Gathering the information dependent on Class utilizing dplyr bundle containing "group by capacity", Use ggplot to demonstrate the level of class classification. To check the number of exchanges by day and hour, standardize the time by day and order them into four quarters as per the time. To discover anomalies, take mean of factors from V1 to V28 and check the variation.

In modeling, the information should be apportioned for preparing set (80% of records) and testing set (20% of records). Subsequent to apportioning the information, highlight scaling is connected to institutionalize the scope of free factors.

To build a model on the preparation set, perform the accompanying:

1) Apply model classifier on the preparation set.
2) Prediction of the test set.
3) Check the prediction yield on the imbalanced information.

Distinctive imbalance handling techniques are utilized to adjust the given information, apply the model on the balanced information, and check the quantity of good and extortion exchanges in the preparation set.

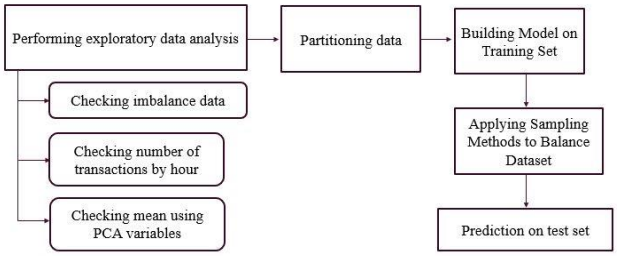

Fig. 5. Proposed System

IV. PERFORMANCES ANALYSIS OF VARIOUS CLASSIFICATION AND SAMPLING TECHNIQUES

The classification technique implemented in this work is explained below.

1) *Random Forest*: Random Forest is a managed supervised learning technique. It makes a collection of forests and makes it some way or another arbitrary [11]. The forest it constructs is an outfit of decision Trees, more often than not prepared with the "bagging" strategy. The general thought of the bagging strategy is a mix of learning models that expands the general outcome, it can be written as equation(1)

$$fi_i = \frac{\sum_{j:\, node\ j\ splits\ on\ feature\ i} ni_j}{\sum_{k \in\ all\ nodes} ni_k} \qquad (1)$$

where fi_i is the importance of feature i, ni_j is the importance of node j.

It is a supervised learning algorithm. It shapes different choice trees and consolidates them to show signs of improvement exactness and stable forecast. It has about the equivalent hyperparameters as a choice tree or a stowing classifier. Just an irregular subset of the highlights is thought about for part a hub. Trees can be made increasingly irregular, by also utilizing arbitrary limits for each component instead of looking for the most ideal edge.

2) *Naive Bayes:* Naive Bayes is a group of probabilistic calculations that exploit likelihood hypothesis and Bayes theorem to anticipate the tag of content [12]. They are probabilistic, which implies that they compute the likelihood of each tag for a given content and after that yield the tag with the most astounding one. The manner in which the model generates the probability is by utilizing Bayes theorem, which depicts the likelihood of a component, in view of earlier information of conditions that may be identified with that feature, as shown in equation(2)

$$p(A|B) = \frac{p(A)p(B|A)}{p(A)} \qquad (2)$$

3) *Support Vector Machines:* Support Vector Machines

is a model for classification and regression purposes [13]. In contrast to different models, it has an extraordinary choice limit and kernel components. The kernel is utilized to change the information vector into the ideal structure. kernels can utilize direct, nonlinear, polynomial, Radial Basis Function, and so forth. By utilizing kernels, Support Vector Machine at that point establishes the ideal limit which is called a choice limit that has the greatest separation from both the classes. Consequently, it in all respects viably characterizes the information as per limit.
Equations for SVM are shown below in equations(3-5)

Given some preparation vectors, i = 1,.....,n, in two classes and a vector, SVM classifier takes care of the accompanying base issue:

$$min\frac{1}{2}w^T + C\sum_{i=0}^{n}\zeta \quad (3)$$

subject to

$$yi\ (wT\varphi(xi)\ +\ b)\ \geq\ 1-\zeta i \quad (4)$$

$$yT\alpha\ =\ 0$$
$$0\ \ \leq\ \alpha i\ \leq\ C, i\ =\ 0,1,\ldots n \quad (5)$$

Figure 3 shows the hyperplane boundary created in SVM.

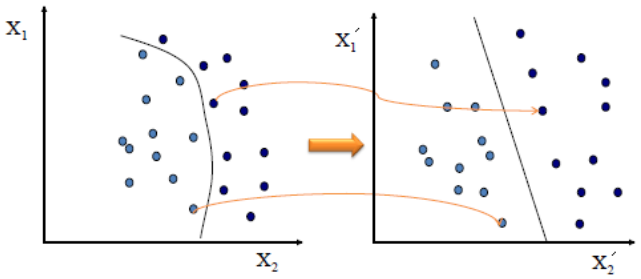

Fig. 3. Hyperplane in SVM

4) *K – Nearest Neighbors:* K nearest neighbors is a straightforward calculation that stores every single accessible case and characterizes new cases dependent on a closeness measure (e.g., remove capacities) [14]. KNN has been utilized in factual estimation and example acknowledgment as of now toward the start of the 1970s as a non-parametric system. A case is selected by a greater part vote of its neighbors, with the case being allocated to the class most regular among its K closest neighbors estimated by a separation work. On the off chance that K = 1, at that point the case is just allocated to the class of its closest neighbor. Various distance measures can be evaluated as explained in equation(6)

Euclidean Distance:

$$dist\big((x,y),(a,b)\big) = \sqrt{(x\ -\ a)^2} + (y\ -\ b)^2$$

Manhattan Distance:

$$dist\big((x,y),(a,b)\big) = |(x\ -\ a)\ +\ (y\ -\ b)\ | \quad (6)$$

Euclidean Distance:

$$dist((x,y),(a,b))\ =\ ((x\ -\ a)^{\mathrm{q}} + (y\ -\ b)^{\mathrm{q}})^{\frac{1}{q}}$$

5) *Logistic Regression*: Logistic regression is an arrangement calculation used to relegate perceptions to a discrete arrangement of classes [15]. Not at all like linear regression which yields nonstop number responses, logistic regression changes its yield utilizing the strategic sigmoid capacity value function to restore likelihood esteem which would then be able to be mapped to at least two discrete classes.

P ≥ 0.5, class=1
P < 0.5, class=0

The various sampling techniques implemented in this work are explained below:

6) *Oversampling*: This technique simply replicates the minority class records to perform class balancing. Firstly, the dataset has two lakh transaction records, this strategy is utilized to pattern replicate the minority class until it achieves balanced records. Finally, four lakh records are obtained. This can be achieved by setting up the strategy = "over".

7) *Undersampling:* These strategy capacities like the oversampling technique and is managed without substitution. In this technique, a non-fraudulent transaction is equivalent to fraudulent transactions. Henceforth, this method is not suitable for imbalance handling. This can be achieved by setting up the strategy = "under".

8) Both Sampling: Both samplings implements a blend of both oversampling and undersampling strategies. Utilizing this technique, the techniques simply undersampled the major class to half the size of the dataset and then increases the count of the minority class. This can be achieved by setting up the technique = "both".

9) Random Oversampling Examples (ROSE): 0ROSE is a class imbalance handling technique that generates data artificially, by providing a better estimate of original data.

10) Synthetic Minority Oversampling Technique (SMOTE): This strategy is utilized to prevent excess estimation while including careful copies of fraud transactions examples in principle dataset. For instance, a few fraud cases are taken. New manufactured comparable occurrences are made and added to the first dataset. One example of SMOTE instance shown in figure 4 shows how it synthetically maps the nearest rare case by assuming points on the path between them.

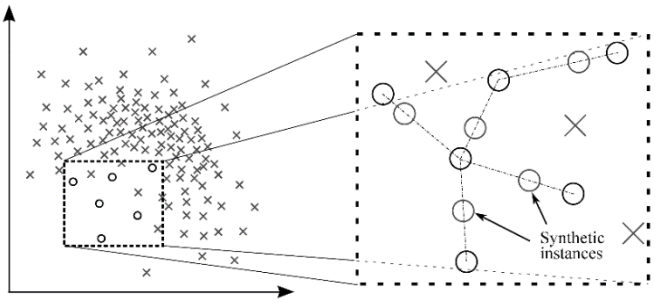

Fig. 4. SMOTE instances

V. EXPERIMENT

A. Experimental Setup

To abstain from building up a "naive" model, we should ensure the classes are generally adjusted. In this way, we will utilize a resampling (and, all the more correctly, oversampling) conspire called SMOTE. It works generally as pursues:
The calculation chooses at least 2 comparative examples of information.
It at that point irritates each example one component at any given moment by an irregular sum. This sum is inside the separation to the neighboring models.
The source code used is 'R' with required libraries such as mvtnorm, psych, pROC, ggplot, caTools and dplyr for data processing and various classification techniques.

B. Performance Evaluation Metric

AUC - ROC bend is estimation for the characterization issue at different limits settings. ROC is a likelihood bend and AUC speaks to the measure of dispersion. It compares whether the model is perfect for classification. A higher value of AUC indicates that the model is good at classification. By similarity, better the AUC score, better the model is at recognizing false and genuine.

The ROC is plotted with True Positive Rate against the False Positive Rate where the former is on the y-axis and the later on the x-axis.

Accuracy is the ratio is a ratio of correctly predicted observation to the total observations.

Precision is the ratio of correctly predicted positive observations of the total predicted positive observations.

The recall is the ratio of correctly predicted positive observations to all observations in actual class - yes.

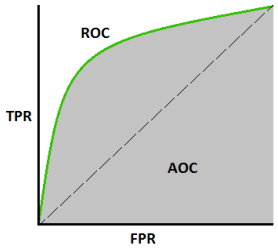

Fig. 5. ROC curve

VI. RESULTS

The results presented here are based on SMOTE as most astounding information exactness is acquired utilizing SMOTE strategy. The reason, SMOTE draws counterfeit examples by picking points that lie on hold interfacing the nearest neighbors to one of its closest neighbors in the component space. While different procedures produce better results that were inside and out unthinkable (negative Area sizes or rise).

Indisputably, logistic regression wins with an accuracy of **97.04%** and an amazing precision of **99.99%**. Logistic regression isn't actually a classifier. However, It is a likelihood/chance estimator. In contrast to different procedures, it takes into account and anticipates "near disasters". It will prompt an ideal solution since it doesn't attempt to trap the predictions into joining a utility capacity that is understood at whatever point the perceptions should be ordered. The objective of logistic regression is to utilize the most extreme probability estimation to give ideal appraisals of Probability.

	Accuracy	Precision	Recall	AUC
Naive Bayes	0.9693	0.0441	0.8163	0.9435
Random Forest	0.9871	0.1074	0.8877	0.9495
K-Nearest Neighbors	0.9689	0.0495	0.9387	0.9356
Support Vector Machines	0.9814	0.0750	0.8673	0.9257
Logistic regression	**0.9704**	**0.9999**	**0.9704**	**0.9704**

Table. 1. Performance results

The table displays the parameter results achieved. AUC-ROC values are displayed below.

AUC = **0.9495046**
False Positive Rate = **(1.000, 0.029, 0.000)**
True Positive Rate = **(1.00, 0.928, 0.000)**

VI. CONCLUSION AND FUTURE WORK

The proposed framework shows that balancing the dataset increases the chances of correctly classifying the fraudulent transactions. The SMOTE sampling performs

the best due to its method of synthetic sampling rather than the nearest values. Among the five techniques used, logistic regression performs well with an accuracy of **97.04%** and an amazing precision of **99.99%**. Therefore, SMOTE sampling along with logistic regression is suggested for credit card fraud detection

As future work, the framework is equipped for giving a large portion of the basic highlights required to avert fake and authentic exchanges. As innovation transforms, it winds up hard to follow the conduct and example of fake exchanges. Averting known and obscure extortion continuously isn't simple yet it is plausible. The proposed engineering is essentially intended to avoid credit card misrepresentation in online installments, and accentuation is made to give an extortion counteractive action framework to confirm an exchange as false or real.

REFERENCES

[1] Piyush Singh, P. K. Biju, Mani Shankar and Nalinadevi Kadiresan. “Multiclass Text Classification and Analytics for Improving Customer Support Response through different Classifiers.” 2018 International Conference on Advances in Computing, Communications and Informatics (ICACCI) (2018): 538-542.

[2] C. P. Prathibhamol, K. V. Jyothy and B. Noora, "Multi label classification based on logistic regression (MLC-LR)," 2016 International Conference on Advances in Computing, Communications and Informatics (ICACCI), Jaipur, 2016, pp. 2708-2712.

[3] R. Nair, T. Singh and R. Nayar, "Logistic regression for Mouth (orotracheal) or Nose (nasotracheal) endotracheal intubation," 2017 IEEE International Conference on Power, Control, Signals and Instrumentation Engineering (ICPCSI), Chennai, 2017, pp. 2026-2031

[4] S. Jaysri, Priyadharshini, J., Subathra P., and Dr. (Col.) Kumar P. N., “Analysis and Performance of Collaborative Filtering and Classification Algorithms”, International Journal of Applied Engineering Research, vol. 10, pp. 24529-24540, 2015

[5] Credit card fraud detection dataset: https://www.kaggle.com/mlg ulb/creditcardfraud

[6] Samaneh Sorournejad, Zahra Zojaji, Reza Ebrahimi Atani, Amir Hassan Monadjemi, “A Survey of Credit Card Fraud Detection Techniques: Data and Technique Oriented Perspective”, journal CoRR,volume 1611.06439,2016

[7] L. Zheng et al., "A new credit card fraud detecting method based on behavior certificate," 2018 IEEE 15th International Conference on Networking, Sensing and Control (ICNSC), Zhuhai, 2018, pp. 1-6.

[8] Dheepa, V., & Dhanapal, R. (2012). BEHAVIOR BASED CREDIT CARD FRAUD DETECTION USING SUPPORT VECTOR MACHINES. SOCO 2012.

[9] H. M. Nguyen, E. W. Cooper and K. Kamei, "A comparative study on sampling techniques for handling class imbalance in streaming data," The 6th International Conference on Soft Computing and Intelligent Systems, and The 13th International Symposium on Advanced Intelligence Systems, Kobe, 2012, pp. 1762-1767.

[10] A. Syaripudin and M. L. Khodra, "A comparison for handling imbalanced datasets," 2014 International Conference of Advanced Informatics: Concept, Theory and Application (ICAICTA), Bandung, 2014, pp. 293-298.

[11] Antonio Criminisi, Jamie Shotton and Ender Konukoglu (2012), "Decision Forests: A Unified Framework for Classification, Regression, Density Estimation, Manifold Learning and Semi-Supervised Learning", Foundations and Trends® in Computer Graphics and Vision: Vol. 7: No. 2–3, pp 81-227. http://dx.doi.org/10.1561/0600000035

[12] M. E. Maron. 1961, “Automatic Indexing: An Experimental Inquiry”. J. ACM 8, 3 (July 1961), 404-417. DOI=http://dx.doi.org/10.1145/321075.321084

[13] Cortes, Corinna; Vapnik, Vladimir N. (1995). "Support-vector networks". Machine Learning. 20 (3): 273–297. CiteSeerX 10.1.1.15.9362. doi:10.1007/BF00994018

[14] Altman, N. S. (1992). "An introduction to kernel and nearest-neighbor nonparametric regression". The American Statistician. 46 (3):*175*–185. doi:10.1080/00031305.1992.10475879. hdl:1813/31637

[15] Walker, SH; Duncan, DB (1967). "Estimation of the probability of an event as a function of several independent variables". Biometrika. 54 (1/2): 167–178. doi:10.2307/2333860

Proceedings of the Fourth International Conference on Communication and Electronics Systems (ICCES 2019)
IEEE Conference Record # 45898; IEEE Xplore ISBN: 978-1-7281-1261-9

Dynamic Load Shedding Management for Optimizing Power Distrubution

Karthik S, Devaraj BN,Keshav Kashyap A,
Avinash M, Department of ECE, Siddaganga Institute of Technology, Tumakuru, Karnataka, 572103, India.
1si16ec033@sit.ac.in,1si16ec019@sit.ac.in,1si16ec035@sit.ac.in,1si16ec011@sit.ac.in

B T Venkatesh Murthy
Assistant Professor, Department of ECE, Siddaganga Institute of Technology, Tumakuru, Karnataka, 572103, India,btv_murthy@sit.ac.in

***Abstract*—Load shedding refers to an intentional electrical power shutdown where electricity is cutoff for periods having not occupying parts of time over distinctdistribution region. This work aims at optimizing the power distribution during such cases using dynamic load shedding where the quantity of load shed is a defined variable based on the input signals. This process is programmed in the microcontroller and the circuits correspondingly switch the power to the prioritized plants and keep the system running. This is interfaced with an LCD to display the current status of production. The loads are implemented using Servos and LED. The rotation of load shedding is synchronized by real time clock (RTC). This circuit is powered with a transformer of 12V. The Load Shedding Module consists of microcontroller ATmega2560 which is used to control the overloading. Current Sensor is used to measure current reading from the load. Controlling is done with 'C' coding.**

Index Terms- Distributed generation, distributed control, optimum load shedding, system protection scheme.

I.INTRODUCTION

Load Shedding refers to instant removal of load from a grid to retain the remainder power as operational.Load shedding occurs when there is not enough electricity supply available to meet the demand.This works helps to optimize the power distribution during power outage, or low voltage cases. Using Arduino as microcontroller, a decision is taken whether to shed loads or not, based on the power drawn by the respective loads and consequently preventing sudden breakdown of the system and avoid blackouts.

This paper is organized as follows. Previously published related works are discussed in Section II. The proposed design of energy scrutinizing system is presented in section III.Section IV discusses the implementation of algorithm. Section V discusses the results of the work. In section VI work is concluded.

II. RELATED WORKS

Load Shedding is used when an imbalance of demand and supply due to weather occurs. In [1], the methods implemented for distributed under voltage load shedding are discussed. A new design is proposed based on load shedding against voltage instability. In [2], a new condensed, adaptive load shedding algorithm is proposed, the algorithm usesvoltage and frequency information provided by phasor measurement units (PMUs). The key contribution of this new method is the use of reactive power along with active power in the strategy of load shedding.Hence, this new method focuses the blending of voltage and frequency stability issue much better than in the independent approaches. In [3], the central contribution of the new method is the usage of reactive power together with active power in the load shedding strategy. In [4], the concept ofload shedding and Smart-direct load control (S-DLC) is proposed to reduce power outages in sudden grid load changes and to reduce the peak-to-average ratio. Forecasting and shedding method is used in the algorithm. To provide Real-time controlling of load this method also used stream analytics and Internet of Things (IoT). In [5],an uninterruptible-power-supply system powered using fuelcell is used. The grid interfacing inverter is connected by a fuel cell and a super capacitor through a 3-port bidirectional converter. The modes that a system can operate are stand-alone and grid connected mode.

III.PROPOSED DESIGN OF ENERGY SCRUTINIZING SYSTEM

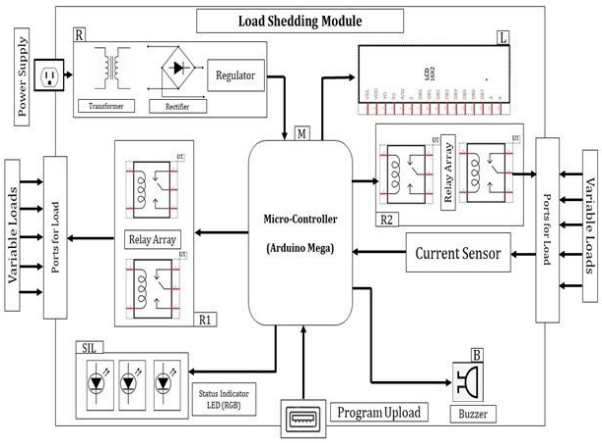

Fig.1. Block diagram of load shedding management module.

The block diagram consists of arduino microcontroller which is controller for the whole assembly as shown in Fig.1 and a rectifier unit to power the circuit. It has a current sensor to sense the current and based on those current values relay array switches off the non-prioritized load keeping only the prioritized loads on and it is displayed using an LCD[6-7].

A. Arduino Microcontroller (ATmega 2560)

Arduino Atmega2560 microcontroller is as shown in Fig.2.The Atmega2560 has 28 pins. It has 54 digital input-output pins, 16 analog inputs, some of the digital outputs acts as PWM outputs[8].

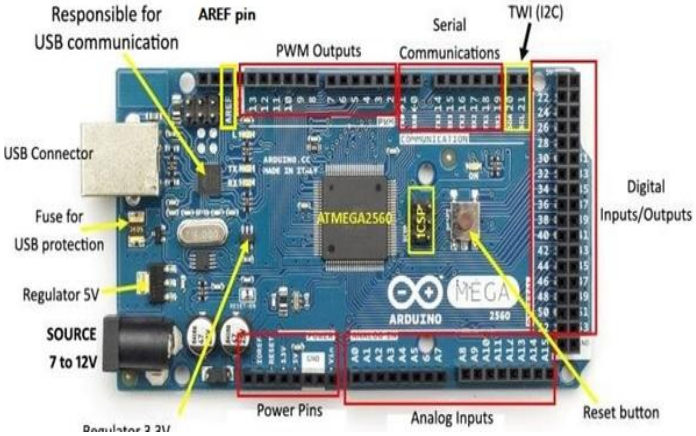

Fig.2. Architecture of Arduino Atmega2560 microcontroller.

B.LCD - Liquid Crystal Display

The picture of LCD is as shown in Fig. 3, which is used for displaying text, words and images having low information. Fig. 4 shows the interfacing of LCD with Atmega2560[9][10].

1. Pin VCC corresponds to +5Volts
2. Pin VEE is used for adjusting contrast
3. Pin VSS is Ground
4. The Pins from D0 – D7 corresponds to Data Lines
5. Pin R/W acts as Read when R/W is 1 and write when R/W is 0.
6. Pin RS is Register Select, acts as Instruction input when RS is 0 and Data input when RS is 1.
7. Pin EN corresponds to Enable Pin.

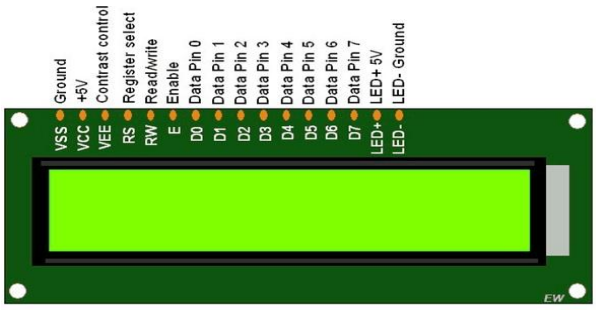

Fig. 3.

Fig.3. Liquid Control Display.

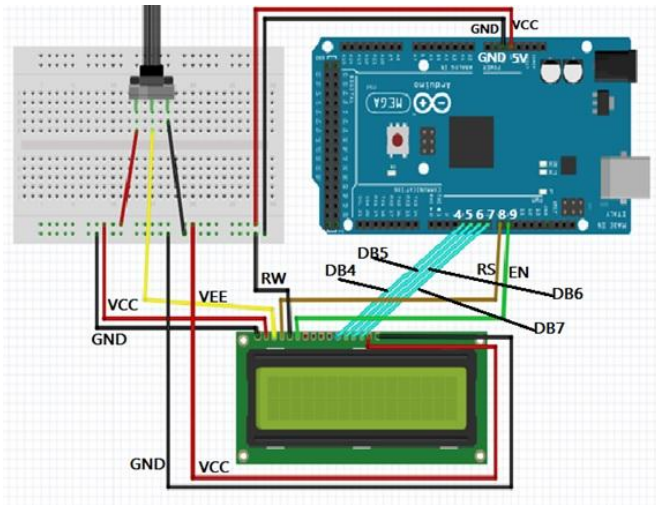

Fig.4.Interfacing LCD with atmega 2560.

C. Current Sensor

Fig. 5 shows the picture of Current Sensor ACS712 module. In Industries and communication systems where current sensing finds importance. ACS712 gives precise reading and solution for AC and DC currents. Customers finds easy because of its design package. Some of the applications like motor control, load detection and overcurrent fault protection use Current Sensor.

The basic principle of working of Current Sensor is Hall Effect. It says that when a current carrying conductor is placed in a magnetic field, a voltage will be generated perpendicular to the direction of the field and the flow of current[11].

Current passing through a semiconductor material causes potential difference and that potential difference will not be their ifzero magnetic field exists. The current flow is distorted when a perpendicular magnetic field exists. The potential difference across the output terminals will exists due to uneven distribution of electron density. The voltage due to this effect is called Hall Voltage. Hall voltage is directly proportional to the magnetic field's strength if input current is constant. Fig. 6 shows interfacing of ACS712 current sensor with ATmega 2560[12].

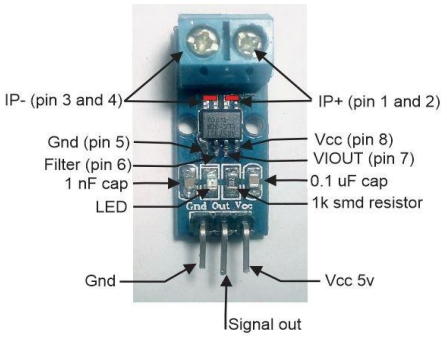

Fig.5. Current Sensor ACS712.

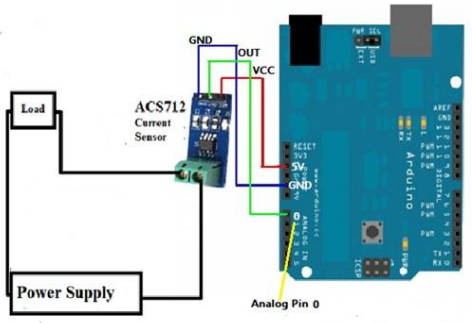

Fig.6. Interfacing current sensor with arduino.

D.Regulator Circuit

Regulator circuit consist of 12-0-12V transformer, rectifier and regulator is as shown in Fig. 7. The transformer lowers the voltage to the microcontroller working levels and the ac voltage is then rectified by using a bridge rectifier to get a pulsating dc which is then sent to a 7809 regulator which provides a constant 9V voltage to power up the arduino.

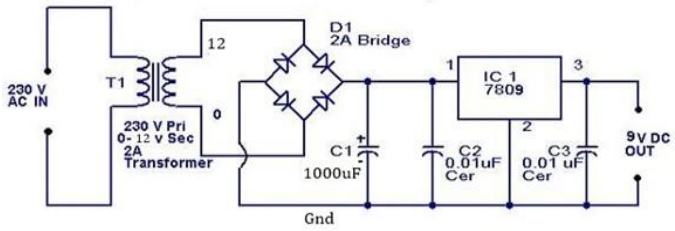

Fig.7. Rectifier Circuit.

E.Relay

A Relay is an electrical switch as shown in Fig. 8. Relay uses the concept of EM to act as switch and operating principle like solid-state relays are also used. They are used to control and switching of circuits when it is necessary. Nowadays Relays are found in most of the electrical circuits[13].

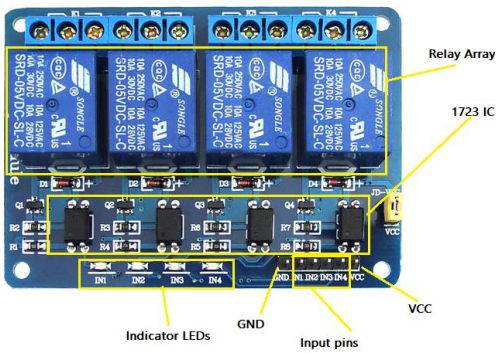

Fig. 8.5V Relay Array.

IV. IMPLEMENTATION OF ALGORITHM

The flow chart in Fig. 9 describes the control flow of the project model. The initial condition verified is the supply and demand imbalance. If the supply current is not able to satisfy the demand by loads then all the high power loads determined by the current sensor are shed. If power supply is able to provide current to additional loads after shedding then based on the priority the loads are reconnected. If an external supply like battery is available then cumulatively the power is supplied[14].

In the next conditional block the power capacity of the battery is monitored continuously along with the return of power in mains. If the battery capacity falls below 20% then the remaining loads are shed and only the basic necessities like light and fan that do not consume more power are retained. If power in the mains return, then all the loads are reset and the battery is connected for charging. Then the module starts checking for demand supply imbalance condition and this process goes on.

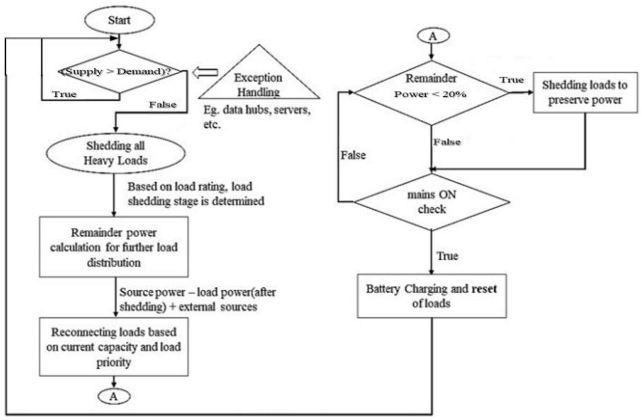

Fig.9. Flowchart of Energy Scrutinizing system.

V. RESULTS AND DISCUSSION

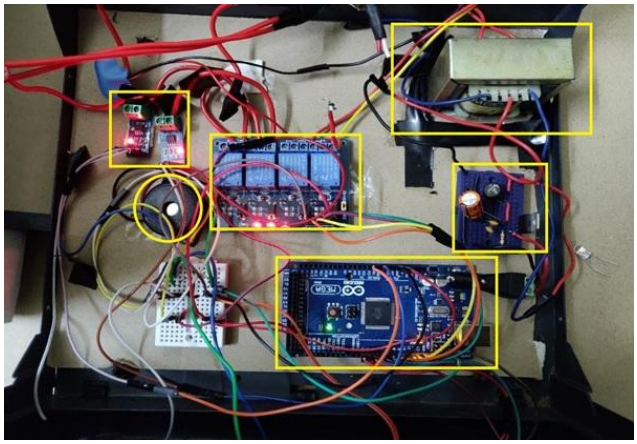

Fig.10.Model of the project with all connections.

Fig.11.Model with ports 1 and 2.

Fig.12. Output on LCD Displaying the Current reading values at Port 1 and 2.

Fig.13.Output at LCD display on overload.

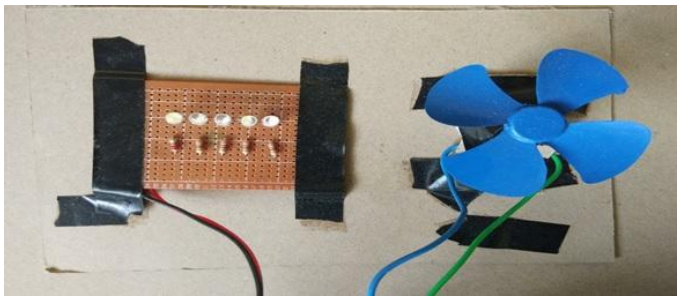

Fig.14.Loads at Port 3 and 4.

Fig. 10 shows the working model of the Load shedding system. At conditions where overload has not occurred, mains are kept ON and the loads at port 1 and 2 shown in Fig. 11are turned ON. Current readings from current sensor ACS712 connected at two ports monitor for current continuously. The LCD display in Fig. 12 displays the current values for user reference.

The microcontroller is programmed to detect current spikes above a defined threshold and take decisions accordingly. If the current in any of the connected ports exceed 1.4Amps, the microcontroller immediately disconnects that particular port and switches on the loads at ports 3 and 4 as in Fig. 14. These ports utilize power from the battery to run the loads. The port causing overload is displayed on the LCD screen as in Fig. 13 with the LED switching ON as an additional indicator.

VI. CONCLUSION

A microcontroller based energy scrutinizing system for dynamic load shedding management is designed and tested successfully. The loads which have high power rating tend to draw more current and cause overload condition and shuts down the whole grid. In such scenarios these modules detects such current spikes and based on a certain threshold, sheds all the high-power loads and reconnect prioritizedloads with low power consumption. In this way complete blackouts can be avoided and work can be continued even though at lower efficiency which is better than no work at all.

REFERENCES

[1] B. Otomega, M. Glavic and T. Van Cutsem, "Distributed Under voltage Load Shedding,"*IEEE Transactions on Power Systems*, vol. 22, no. 4, pp. 2283-2284, Nov. 2007.

[2] J. Tang, J. Liu, F. Ponci and A. Monti, "Adaptive load shedding based on combined frequency and voltage stability assessment using synchrophasor measurements,"*IEEE Transactions on Power Systems*, vol. 28, no. 2, pp. 2035-2047, May 2013.

[3] J. A. Laghari, H. Mokhlis, M. Karimi, A. H. Abu Bakar and H. Mohamad, "A New Under-Frequency Load Shedding Technique Based on Combination of Fixed and Random Priority of Loads for Smart Grid Applications", *IEEE Transactions on Power Systems*, vol. 30, no. 5, pp. 2507-2515, Sept. 2015.

[4] H. Mortaji, S. H. Ow, M. Moghavvemi and H. Abbas F. Almurib,"Load Shedding and Smart-Direct Load Control Using Internet of Things in Smart Grid Demand Response Management," *IEEE Transactions on Industry Applications*, vol.53,no. 6, pp. 1-9, Nov. /Dec. 2017.

[5] H. Tao, J. L. Duarte and M. A. M. Hendrix, "Line-Interactive UPS Using a Fuel Cell as the Primary Source," *IEEE Transactions on Industry Electronics*, vol. 55, no. 8, Aug. 2008.

[6] S.Kucuk, " Intelligent electrical load shedding in heavy loaded industrial establishments with a case study," *in IEEE International Conference on Electrical and Electronic Engineering*, 2018, pp. 463-467.

[7] H.J. Villamediana and A.C. Neira, "Dynamic stability improving at industrial electrical systems through the use of variable load shedding,"*in IEEE International Conference on transmission and distribution conference & exposition: Latin America*, 2006, pp. 1-5.

[8] L.Ye, Z. Baohui, T. Tingyue and G. Zhe, " Influence of load characteristic on system dynamics and load shedding

control effects in power grid," *in IEEE InternationalConference on Control and Decision,*2015, pp.5160-5163.

[9] T.N. Le, N.A. Nguyen and H.A. Quyen, "Emergency control of load shedding based on co-ordination of artificial neural network and analytic hierarchy process algorithm," *in IEEE International conference on system science and engineering (ICSSE),* 2017, pp. 57-60.

[10] Y. Lu, W.S. Kao and Y.T. Chen, " Study of applying load shedding scheme with dynamic D- factor values of various dynamic load models to Taiwan power systems," *IEEE Transaction on power systems,* vol. 20, no. 4, pp.1976-1984, 2005.

[11] M .H.A Hamid, H. Hashim, H A A Rashid, I Z Abdin, " Under voltage load shedding using voltage stability indices," *in IEEE International conference on innovative smart grid technologies,2014, pp. 732-736.*

[12] Y. Zhang, W.Wu, Q.Lu, S.Liu and Y. Zhu, " Security-based load shedding strategy considering the load frequency dependency in Island distribution system,"*in IEEE International conference on energy internet and energy system integration (EI2),* 2018, pp. 1-6.

[13]Gururaj P.M., Sharath Reddy, Punith C.M., B.T. Venkatesh Murthy, "IOT Based Mobile Charging With Solar Energy By Coin Insertion," *International Journal of Electrical, Electronics and Data Communication,*Vol.6, Iss.8, Aug.2018.

[14]Ranjitha B, Nikhitha M N, Aruna K, Afreen, B.T. Venkatesh Murthy, "Solar Powered Autonomous Multipurpose Agricultural Robot Using Bluetooth/AndroidApp," *in IEEE International Conference on Electronics and Communication and Aerospace Technology(ICECA 2019),*2019, pp. 1-5.

Proceedings of the Fourth International Conference on Communication and Electronics Systems (ICCES 2019)
IEEE Conference Record # 45898; IEEE Xplore ISBN: 978-1-7281-1261-9

An Efficient Reconfigurable FIR Filter for Dynamic Filter order variation

Bandreddi Ray Srinivasa Rao
Department of Electronics and Communication Engineering,
Amrita School of Engineering,Coimbatore.
Amrita Vishwa Vidyapeetham, India.
srinivassri551@gmail.com

Bala Tripura Sundari B
Department of Electronics and Communication Engineering,
Amrita School of Engineering,Coimbatore.
Amrita Vishwa Vidyapeetham, India
b_bala@cb.amrita.edu

Abstract— **FIR filter is main and important block in the digital signal processing applications. Even though several approaches for FIR filter designs proposed, because of increasing waste usage of digital applications and rapid growing in the VLSI industry still need and scope for to design a power and area efficient filter. In this paper proposed a novel scheme for the design of an area and power efficient digital finite impulse response (FIR) filter for future multi standard communications. The presented parallel architecture model supports run time variation of filter order and filter coefficients. In the design process discussed every block in detail mainly for faster computation time of the design selected faster multiplier and adder. To get the less hardware area and fast in computation time Vedic multiplier is used for the multiplication block and carry save adder is used for addition in the design. The proposed design can handle the length of 16-tap and 8-tap is and implemented in Verilog HDL. Implemented Verilog code for the design is verified by using simulation results and checked synthesis of the design in Vivado Xilinx IDE. The synthesizable code is compiled in Synopsys Design Compiler (DC) for Power and area calculations using SAED 90nm CMOS technology. The ASIC results shows the improvement in power 18.89% and 18.30% for 16-tap and 8-tap FIR filter respectively than the conventional method.**

Keywords— Digital signal processing, Reconfigurable FIR filter, Software defined radio, Vedic multiplier, Adder tree

I. INTRODUCTION

A filter is a device which passes the required frequencies and preventing the other frequencies based upon the application. Filter is essential and important block in most of the signal processing applications. Digital Filter applications are widely used for band selection, noise elimination, signal computation, estimating and analyzing the signal, and in many signal processing applications [1]. Based on the impulse response type filters are mainly categorized into two types namely, infinite impulse response (IIR) and finite impulse response (FIR) in those FIR Filters are widely used compared to IIR because if its ease to attain linear phase and inherent stability [5]. Due to rapid increasing in the usage of digital signal processing-based applications like multimedia, mobile communications in day to day life which demands highly efficient hardware and ultra-low power operations [1]. Similarly, as the growing in communication technology which requires of support multiple communication standards in a single hardware for this instead of designing different filters with different filter orders needed a single filter hardware design which can handle different filter orders based on the requirement. To handle this type of multiple filter orders in a single design reconfigurable filters came into picture whose filter order and coefficients could change dynamically during the run time. In advanced communication applications like software define radio, multichannel filters and up and down digital converters the need of reconfigurable filter is high to get low power and efficient hardware [2].

The input and output relation of a fir filter is given by the equation

$$y[n] = \sum_{k=0}^{N-1} h_k a[n-k]$$

Where h_k, for $0 \leq K \leq N-1$, implies the filter coefficients while $a[n-k]$ for $0 \leq K \leq N-1$ means the N recent input samples, and $y[n]$ is the current output of the filter. Reconfigurable FIR filters whose filter coefficients [h_k] and filter order [k] change during run time plays key role in future multiple communication standard systems to get the low power and high throughput. In latest years, a good deal of studies has been carried out to introduce effective reconfigurable FIR filters. In this work reconfigurable FIR filter designed with Verilog code in such a way that it to get the efficient in its performance, low power and effective usage of hardware. The suggested architecture includes a Serial in Parallel out Shift Register (SIPO), a multiplier and an addition tree. Serial in parallel out Shift Register designed with D-flip flops as synchronous manner. In general multiplications operation is performed with shift and add logic. Multiplier is the one of the major design blocks in the design which occupies larg silicon region and needs more energy several study works has been performed for this purpose and compared many multipliers like booth multiplier, sequential multiplier, Vedic multiplier and many [9]. Finally, selected Vedic multiplier to get the efficient and faster computation time in the design. Vedic multiplier is ancient multiplication method which eliminates the unnecessary computations in its logic [6]. Similarly, in place of addition carry save adder is used for better results with less computing time and less complexity. A hybrid design has been proposed for implementing Adder tree with half adders and full adders and this adder tree also designed with carry save adders to get the low power, less area occupancy and for best performance. In the design clock gating concept is used to select the filer order and to deselect the unused gates to make the reduction in power consumption dynamically [7]. The rest of the paper discuss with

architecture of reconfigurable FIR filter with each block design in section II, analyzed performance of 8-tap and 16-tap reconfigurable FIR filter in both FPGA and ASIC with results and compared with conventional approach in section III, and finally conclusion and future scope in section IV.

II. DESIGN OF RECONFIGURABLE FIR FILTER

The proposed reconfigurable design derived from direct form of FIR filter in which Serial in Parallel out Shift Register is used to shift the samples for every clock pulse, Vedic multiplier is used to multiply the shifted samples with coefficients with synchronize with clock and Adder tree is used to add the samples.

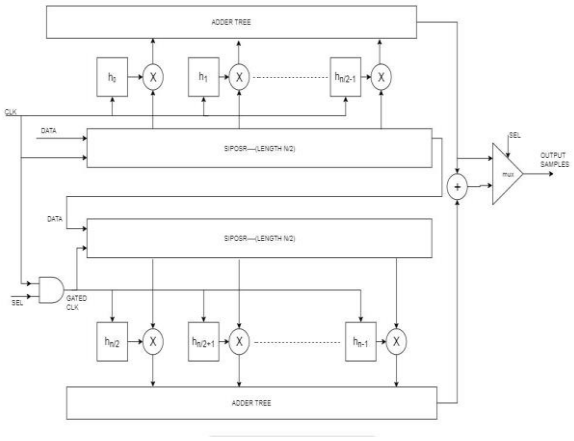

Fig.1.Archetecture Design of Reconfigurable FIR Filter

Here the Architecture contains two parts, depends upon the filter order the design works. During the function of the N/2 filter, the structure can decrease power consumption by using clock gating concept which disables the lower Serial in Parallel Out (SIPO) of length N/2. The registers used for storing the samples. The separation has been done with respect to clock the second part of the design contains gated clock derived from the main clock by using clock gating concept as represented in Fig.1. As shown in fig 1 architecture one clock is directly applied to registers, multiplier block and second clock is generated with AND gate logic and selection signal that's nothing but the gated clock signal. So, if the selection signal is logic high then only the elevated gated clock signal will trigger circuit. Generally, the notion of clock gating is used to decrease dynamic power dissipation and here in the design same clock gating concept is used to get the required length for filter order. The 2:1 MUX selects output of the upper adder tree if the selected filer length is N/2, the same MUX selects addition of upper adder tree and lower adder tree if the selected length of the filter is N. For MUX to produce the output based on the length of the filter SEL signal is used the signal which is used as input to produce the gated clock signal. By this if we need a filter in a single chip to work both for length N/2 and N in this case for filter order N the complete design is in on state and functionality is same but for N/2 length the half of the design is in on state and rest is in off state by using selection signal. For the length of N up to N/2 pulses, the half of the structure is in off state due to this unwanted switching power can decrease.

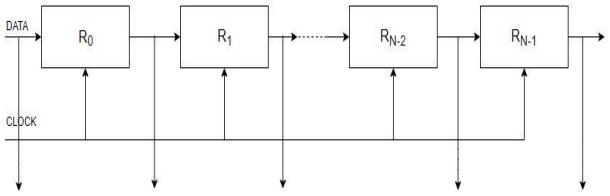

Fig.2.Serial in Parallel Out Shift Register (SIPO)of length N

The first block is serial-in-parallel-out (SIPO) shift register in which the samples are loaded with serial data as input one sample at a time and output is available in parallel form to the multiplier block. Multiplier block is designed with Vedic multiplier and the same clock which is applied for SIPO is applied for multiplier blocks also to get the maximum sync and to eliminate the timing checks between the coefficients and output of SIPO samples. Adder tree is designed with basic half and full adders as carry save adder type and this adder also in two separate parts for this designed one adder tree and is instantiated in two times for design. In the design based upon the filter length will get the sample output for this separation of adder tree output a multiplexer is used. with multiplexers by using selection line the output is procced and in case if the filter length is N/2 multiplexer selects direct first adder output as filter output in other case both adder trees output is added before procced as output. The detail information of multiplier and adder tree design is discussed as subsections.

A. Vedic Multiplier

Vedic multiplier is an ancient multiplication technique which is used mainly to reduce the complexity and unnecessary steps in the logic by this multiplication becomes faster and consumes less power compared to other multipliers.

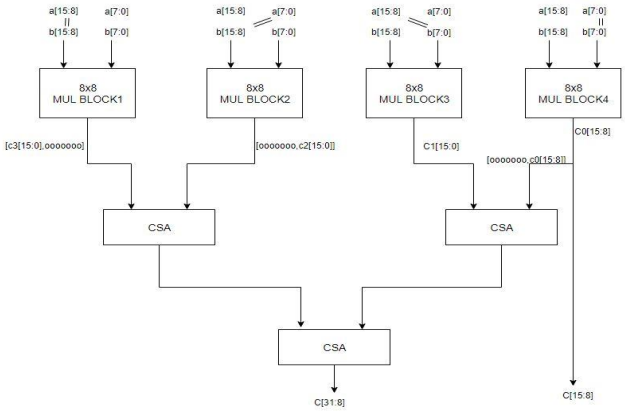

Fig.3.16-bit Vedic Multiplier

Vedic multiplier sutras and procedure in calculation is taken from research work from several papers. 16*16bit multiplier is needed in the present filter design and is designed by using bottom-up approach which is made up of by the 2*2bit, 4*4bit and 8*8bit multiplier. In every bit multiplier

partial product are added by using carry save adder. To get the equal weights before giving it to carry save adder padded extra zeros as mentioned in Vedic mathematics. At last least significant bits are directly produced from the multiplier block and remaining bits can produce by adding by using carry select adder.

C. Adder Tree

The output of multiplier block samples is addition, for this developed an adder tree with half adders and full adders with carry save addition. For this design first, full adder and half adder are implemented by instantiating the basic logic gates in the structure form. From half adder and full adder insanitation using for loop added single bit and result carry added by using carry save addition. As the maximum output of multiplier block is 32-bit number for this needed an adder tree which can add 32-bit number or less. Here in the design the eight outputs obtained from the multiplier block must add, for this designed eight samples adder tree and is instantiated in both lower and upper part of the design.

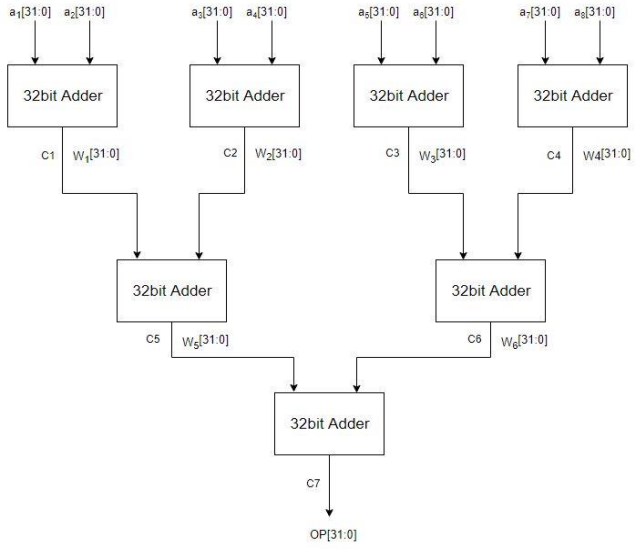

Fig.4. Adder Tree to add 32bit numbers

A 32-bit adder is required to add two 32-bit numbers. Here in the design eight 32-bit numbers must add for this designed an adder tree with four 32-bit adders at the stage-1 and the results are added in stage2 as same. In every 32bit adder output as 32bit number with carry. All the carry bits in every stage are added to get the MSB bits. For this full adder are used as represented in fig.5 by this full adder addition bit33, bit34, carry bit35. From Fig.4 and Fig.5 gives the complete adder tree to add eight 32bit numbers. By this adder tree to add eight 32bit numbers complete design is formed.

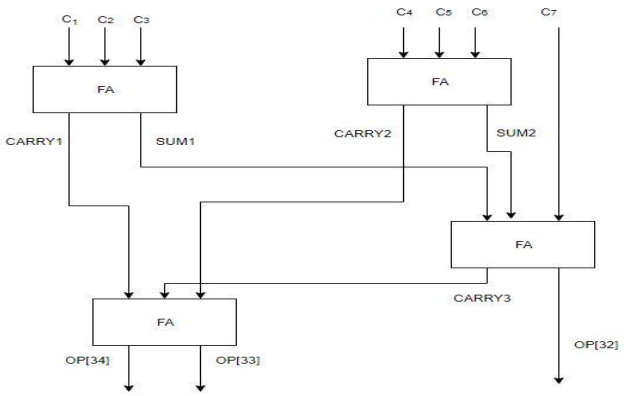

Fig.5.Adder Tree carry bits Addition for MSB bits

III. Results and Discussion

The proposed architecture design is implemented in Verilog HDL and simulated in Xilinx Vivado, the design is implemented with 16-tap reconfigurable FIR filter which also handle 8-tap with 16-bit as input. All the implementations are targeted FPGA is Artix-7. The coded Verilog module is successfully simulated and verified using Vivado. The simulations results are given in Fig.6 and Fig.7. Here gated clock used to reduce the switching times.

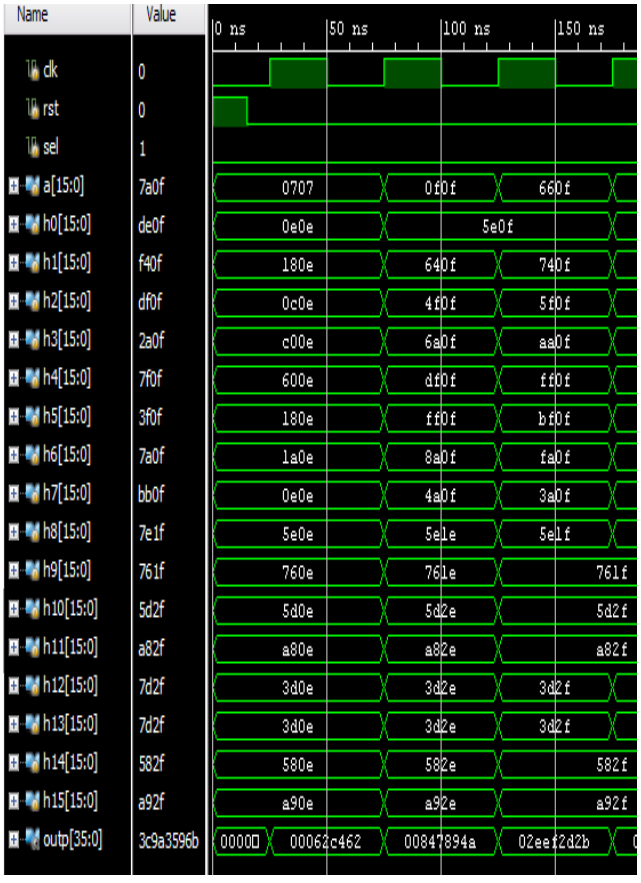

Fig.6.Reconfigrable 16-tap FIR Filter

For 16-tap, till the 8-clock pulses the lower part of the design is in off state as select signal is in logic-0 state by this switching power of lower registers and gates can abolish. This concept is same as clock gating which is used to reduce the dynamic power.

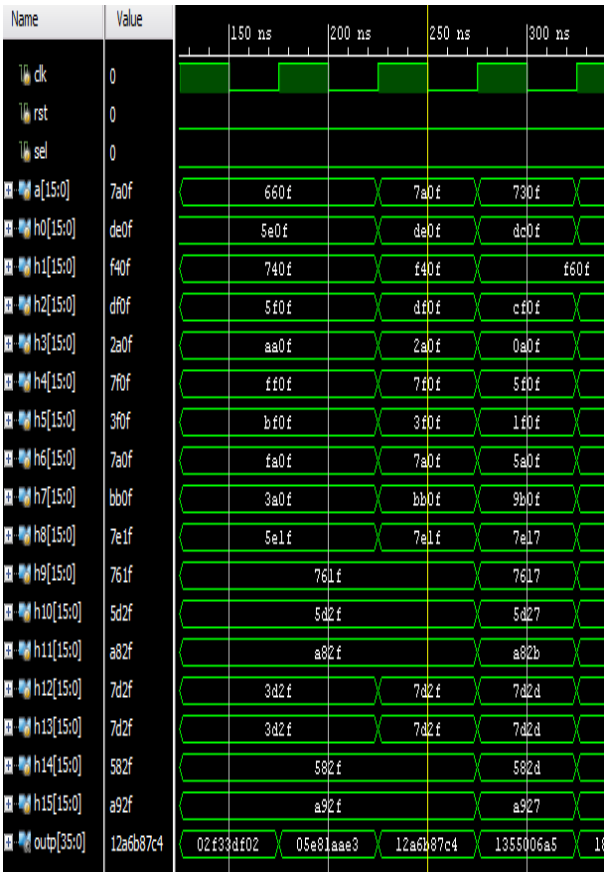

Fig.7.Reconfigrable 8-tap FIR Filter

For 8-tap FIR filter design has done in such a way that the lower shift registers completely in off state for this the selection signal always be in logic-0 state so that the gated clock is no more in active state. The same clock gating which is designed with selection signal is used to completely off the half of the design by which the 8-tap FIR filter is obtained in the same design of the chip.

Along with FPGA implementation, the proposed design Verilog code synthesized in 90nm CMOS technology using Synopsys Design Compiler (DC). In Fig,8, Fig.9 and Fig.10 represents comparison of power and area plots with proposed approach and conventional approach [2].

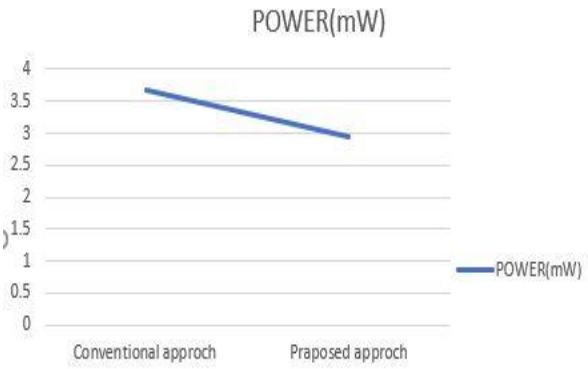

Fig.8. 16-tap FIR power comparison

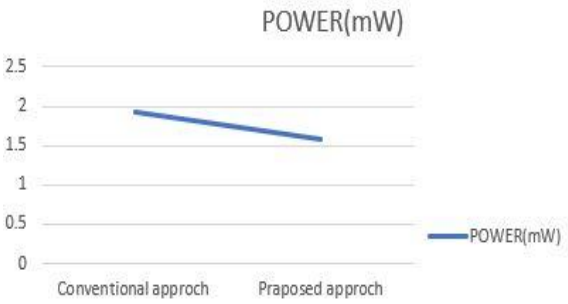

Fig.9. 8-tap FIR power comparison

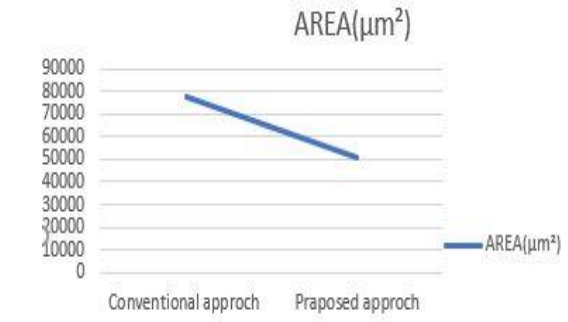

Fig.10. Area comparison

IV. CONCLUSION

The aim of this paper is to realize efficient digital FIR filter to work in multi-channel filter and for future communication systems. By using area and power graphs it is evident that the design meets improvement in power and occupancy of area. The proposed design achieves power reduction of 19.89% for 16-tap and 18.30% for 8-tap filter. Improvement also achieved in area from 77889 µm² to 50925 µm². Thus, proposed design of Reconfigurable FIR filter can be used in all type of DSP applications and advanced communication applications for improving the performance and speed.

In future, the work can be extended by using different types of gated clock designs and by using which the registers triggering to decrease the dynamic power and to select different filter orders in a single chip design.

REFERENCES

[1] Kumar,V.Nithish, Koteswara Rao Nalluri, and G. Lakshminarayanan. "Design of area and power efficient digital FIR filter using modified MAC unit." *2015 2nd International Conference on Electronics and Communication Systems (ICECS)*. IEEE,2015.

[2] Meher, Pramod Kumar, and Sang Yoon Park."Reconfigurable FIR Filter for Dynamic Variation of Filter Order and Filter Coefficients. "Journal of semiconductor technology and science" 16.3 (2016): 261-273.

[3] Lovina, P. A., and K. Aruna Manjusha. "SDR Applications using VLSI Design of Reconfigurable Devices." (2018).

[4] Kafi, Abdullah-Al, et al. "An efficient design of FSM based 32-bit unsigned high-speed pipelined multiplier using Verilog HDL." *8th* International Conference on Electrical and Computer Engineering. IEEE, 2014.

[5] Paul, Arnob, et al. "Reconfigurable architecture design of FIR and IIR in FPGA." *2015* 2nd International Conference on Signal Processing and Integrated Networks (SPIN). IEEE, 2015.

[6] Kumar, G. Ganesh, and V. Charishma. "Design of high speed vedic multiplier using vedic mathematics techniques." International Journal of Scientific and Research Publications2.3 (2012): 1.

[7] Srinivasan, N., Prakash, N. S., Shalakha, D., Sivaranjani, D., & Sundari, B. B. T. (2015). Power reduction by clock gating technique. *Procedia Technology*, *21*, 631-635.

[8] Pawar, Roshani, and S. S. Shriramwar. "Design & implementation of area efficient low power high speed MAC unit using FPGA." *2017 IEEE International Conference on Power, Control, Signals and Instrumentation Engineering (ICPCSI)*. IEEE, 2017.

[9] Chauhan, Aditya, and P. Sathish Kumar. "Implementation of FIR Filter & Mac Unit by Using Neural Networks in FPGA." 2018 International Conference on Advances in Computing, Communications and Informatics (ICACCI). IEEE, 2018.

Proceedings of the Fourth International Conference on Communication and Electronics Systems (ICCES 2019)
IEEE Conference Record # 45898; IEEE Xplore ISBN: 978-1-7281-1261-9

Sparse based Dimensionality Reduction for Big Data Management: SDN Perspective

Miss. Rajnandani Pawar
School of Electronics and Communication Science and Engineering,
Dr.Vishwanath Karad MIT World Peace University Pune, India
rajnandanipawar13@gmail.com

Prof. Vinod Jadhav
School of Electronics and Communication Science and Engineering,
Dr.Vishwanath Karad MIT World Peace University Pune, India
vinod.jadhav@mitcoe.edu.in

***Abstract*—Brainy Grid (BG) is a coordination of conventional power network with advanced data and communication framework for bidirectional vitality stream among grid together with end clients. An enormous measure of data is being created by different smart gadgets sent in BG frameworks. Such a gigantic information generation from different smart gadgets in BG frameworks may prompt different difficulties for the systems administration foundation conveyed among end clients and network. Consequently, an effective information transmission system is required for giving wanted QoS to clients in this condition. The high dimensions of information may influence the execution of majority of the designed solutions in this condition. Maximum of the current plans announced to have complex operation for the information dimensionality decrease issue which may decrement the execution of any actualized answer for this issue. To address these troubles, in this paper, Sparse-based dimensionality decrease for huge information is intended for dimensionality reduction issue of colossal data made from various smart Gadgets. First the Singular Value Decomposition (SVD) is applied to high-order tensors (utilized for information portrayal) to limit the remaking mistake of the decreased tensors. Then VLCP (Software-defined networks(SDN) Controller) is used to broadcast the compressed data. The adequacy of the proposed plan has been assessed utilizing simulations completed on the information follows using Python and various libraries. The outcomes got portray the viability of the proposed plan concerning the parameters, for example, dimensionality reduction ratio and approximation accuracy.**

Keywords—Brainy Grid, VLCP, SVD, Sparse, QoS, SDN

I. INTRODUCTON

A Low rank sparse approximation-based data administration scheme is designed for representation and dimensionality reduction of data acquired from enormous smart gadgets in BG network. Due to sparse estimation reconstruction error is reduced. To propose sparse based dimensionality reduction issue in brainy grid. Brainy grid (BG) is an agile power grid which backing a Two-way power stream among users and grid. It improves client's demand, power generated, and network availability to provide reliability and productivity using automated controls, sensors, metering devices, and distributed energy sources. It consist of components such as brainy meters and sensing devices linked to one another applying communication infrastructure. The delivery of numerous benefits such as energy, voltage, and frequency regulations to the ultimate consumer lean on the steady and real-time report about the data flow between consumers and utility providers (grid). For this goal, a reliable transmission framework is needed to conduct the flow of input among sources of data propagation and smart meters.

In the wake of examining the previously mentioned recommendations, it is deduced that an enormous measure of huge information is being produced by different smart gadgets in the BG. Be that as it may; taking care of this huge information in an effective way is one of the greatest difficulties in BG condition.

Different systems have been examined concerning these issues in the present proposals. Be that as it may, none of the present recommendations have concentrated on tremendous information examination in BG structures for a productive QoS provisioning. Additionally, the present proposal has not investigated any unified model for information portrayal.

VLCP is a modern SDN controller ready to be incorporated with Open Stack, Docker and other virtualization conditions. It is intended to be

exceptionally adaptable, exceedingly accessible and have extremely low overhead for virtual systems administration. As of now it is prepared for creation, and has been checked, tried and being used in bunches with around 10 physical servers. Tests demonstrate that the controller remains stable for over seven days under high weight as: 1000 endpoints for every server; 16+ Gbps traffic; 200 endpoint changes (manifestations and cancellations) every moment per server.

In straight variable based math, the SVD is a factorization of a genuine or complex network. It is the speculation of the Eigen decomposition of a positive semi certain ordinary grid (for instance, a symmetric framework with positive Eigen values) to any M*N matrix by means of an augmentation of the polar decay. It has numerous valuable applications in sign handling and insights.

II. Related Work

In paper [1], a tensor-established SDN demonstrate for size degradation issue for huge information procured from different SG gadgets is planned. As this reason, a F-HOSVD calculation is structured. The motivation behind the suggested plan is to speak to the mass information produced by BG gadgets in a tensor structure. After tensor portrayal, the sub-tensors are consolidated to shape a brought together tensor.

In article [2], SDN-established edge-cloud exchange is exhibited to manage stream planning among edge and cloud gadgets. In such manner, a various-objective transformative calculation utilizing Tchebycheff deterioration is intended for stream planning in SDN. The proposed plan is assessed as for two streamlining issues: 1. Exchange off between vitality productivity and idleness 2. Exchange off between vitality effectiveness and transmission capacity.

A MCE [3] gives the establishment to satisfy the requirements of end customers, be that as it may in order to conduct the gigantic proportion of framework information traffic, and the hashing limit is service to enlist the grim rundown to install, look, and eradicate an entry in a show. Regardless, there may rise an occasion of accident when a hash record can be remade. Along these lines, in such a condition, twofold hashing limit is used to enroll another hash record to decide the effect likewise; gainful propelled data managing philosophy is required. SDN advancement is a united building that settles on shrewd decisions for ground-breaking framework the board. Framework hypervisors expect a crucial activity for making virtual SDN controllers so as to make various shrewd resources for expanding the fulfillment of the benefits. In article, journalists have dismembered the fittingness of a Bloom-channel based response for improved stream table organization.

Web of Things (IoT), [4] a bit of Future Internet, contains countless Internet related Objects (ICOs) or 'things' where things may identify, bestow, register and likely cause similarly as information, various-particular intersection, physical/virtual characters and aspects. The IoT vision has starting late offered rise to creating IoT tremendous information operations for instance splendid essentialness systems, syndromic bio reconnaissance, regular checking, emergency condition care, propelled cultivating, and wise collecting that are fit for conveying lots of data stream from geographically scattered information sources.

The paper [5] examines the contemporary state of collateral GIS concerning collateral GIS models, parallel taking care of systems, and appropriate subjects. We present the regular headway of the GIS structure which fuses principal two parallel GIS models reliant on world class figuring pack and Hadoop gathering. By then they shorten the present spatial information package procedures, key systems to recognize parallel GIS in the point of view on data rot and headway of the unprecedented parallel GIS computations. They use the collateral treatment of GRASS as a logical examination.

Despite the gigantic theories happening in the exchanges establishment, this outstanding parts a bottleneck for the use of specific supplications.

Paper [6] gives a technique for lossy information weight in splendid movement structures utilizing the singular regard breaking down framework. The proposed methodology can do out and out diminishing the volume of information to be broadcast through the exchanges organize and correctly reproducing the principal information. These characteristics are appeared by outcomes from tests finished using certified information assembled from metering tools at a wide scope of substations.

In [7], organization engineering Macro Serv exhibited that plays out the constant course proposition for the evacuees at the period of a fiasco. The proposed organization utilizes the live information removed from the ITS and the road side sensors to find out favored clearing ways that have most outrageous traffic stream limit, least blockage, and travel cost.

One of the key factors that will choose the accomplishment of splendid meters is clever meter data examination which oversees data getting, transmission, planning, and interpretation that pass on points of scrutiny to all accomplices.

Paper [8] presents an intensive diagram of adroit power meters and their use concentrating on solution pieces of metering process, the assorted accomplice concerns and developments used to assure accomplice interests. Concentrating on versatility, extensibility, synchronization, and power, a scattered data examination stage is proposed in paper [9] to process broad volume, rapid dataset. An arrangement of progressing and non-nonstop synchrophasor data examination applications are encouraged by this stage. The estimation burden is bestowed to alter by different center points of the examination gathering, and colossal data examination instruments, for instance, Apache Spark are grasped to regulate considerable volume data and to help the data getting ready speed.
In [10], a SDN-based correspondence structure for micro grid is shown to overhaul micro grid adaptability. This plan has two outstanding characteristics: First, the control layer is self-governing of the apparatus systems, which facilitates fast utilization of varying applications. Second, the SDN controller fills in as a screen managing the whole status of the framework switches similarly as a controller handling framework issues, for instance, data obstruct, port down, and transmission limit task. Thusly, the correspondence organize is fit for giving strong and revamp organization to micro grid.

III. Proposed System

Sparse-based information administration plan is presented to get raw information and reduce it to lower magnitude thereby optimizing the reconstruction error. The acquisition of huge information in BG atmosphere associates numerous problems such as-absent values, unpredictability, duplex also avoidable values etc. However, the suggested scheme handles these provocations in a productive manner. The motive of this paper is, in ruler area huge electricity is generated at power plants and in urban cities the utilization of that electricity takes place. So the information of electricity utilization in brainy grid need to reach at the power plant which is located at ruler area, distance between BG and Power plant is a lot. Transmission of electricity data will take more time and bandwidth by using traditional network but if the data sending takes place by compressing data then the time to reach the information from one destination to other will become less.

Hence in proposed scheme firstly the manipulation of data takes place by using python library called a Tensor Flow. From the dataset, electricity and year information is taken for the data manipulation by using Tensor Flow the data is being converted into Tensor form. In Fig (1). The first block shows the data acquisition through the smart devices means the data generated by Brainy grid, the dataset carrying this information from which we take electricity and year information for compression and transmission.

Second block of system architecture consist of data storing in tensor model means converting the given information in tensor form. Numpy Python library is used to support large multidimensional arrays and Pandas library is used for data manipulation and analysis.

Third block shows unified tensor means electricity data tensor and year data tensors are merging to form unified tensor.

Forth block is dimensionality reduction of unified tensor applying SVD. For factorization and decomposition SVD is applied. By using traditional network it will take more time to transfer the data from Brainy grids to the power plant. SDN comes in picture; using VLCP Controller establishment of SDN is taken placed. For Transmission and reception VLCP Controller is programmed. Graphic User Interface is used for security purpose when analysis is taken place.

Fifth block represents communication using SDN. Last block is BG applications. So this is the system architecture. Fig.1 shows the flow chart of the proposed system. If the data is in reduced form then the time required to transmit it from one destination to other is less than the time required to transmit the original data.

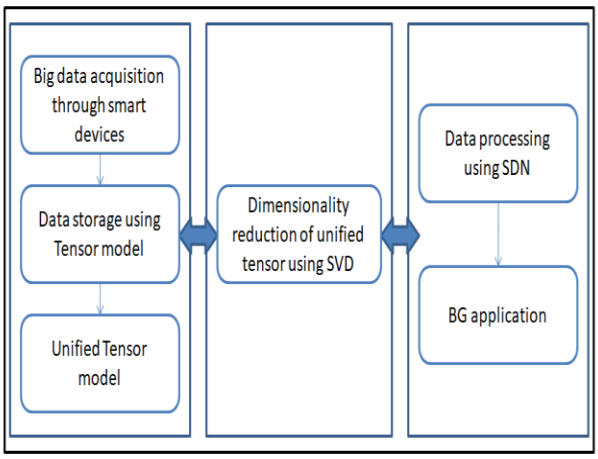

Fig 1.system architecture

IV. Result Analysis

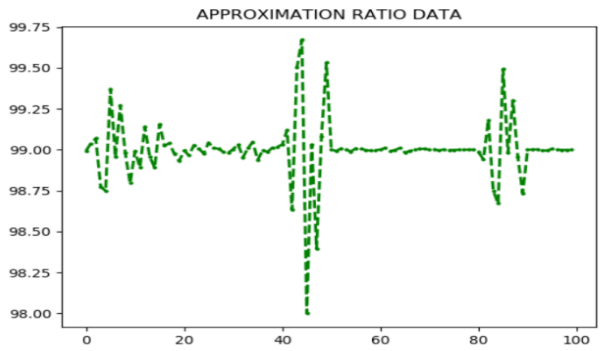

Fig 2.1 Approximation ratio of the data

The above graph is the outcome of the Subtraction of original data and reconstructed data. X axis indicates the 100 samples of the data and Y axis represents approximation ratio.

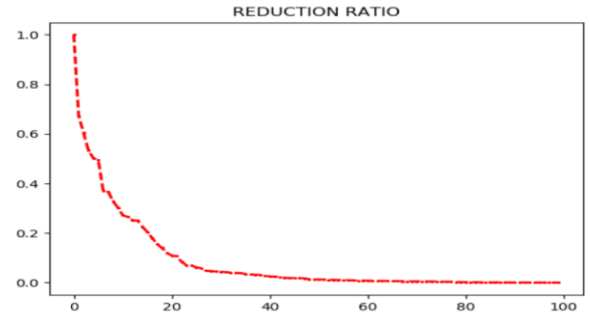

Fig (2.2). Reduction ratio

Above graph is obtained by subtracting reshaped data from reconstructed data. X axis indicates the 100 samples of data and Y axis indicates reduction ratio.

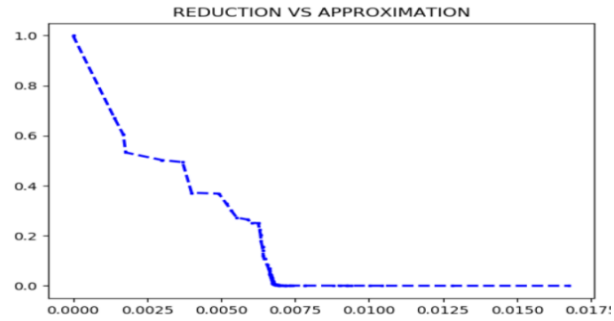

Fig (2.3). Reduction verses Approximation ratio

The graph present the comparison of reduction and approximation. The X axis is approximation ratio and Y axis is reduction ratio.

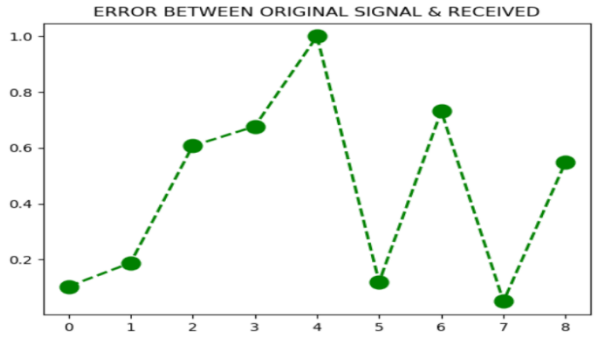

Fig (2.5). Error between Original Signal Verses Received signals

Above graph is a comparison of received data to the transmitted data to get to know the errors occurs between transmissions.

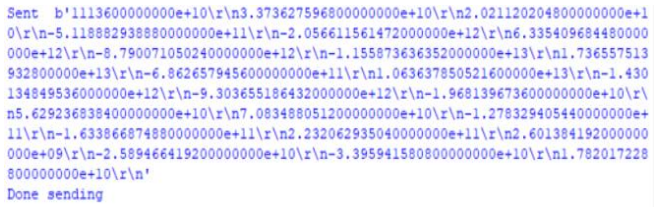

Fig (3). Sending of data to the Receiver

The manipulated data is sending it seems in this form because it's reconstructed data

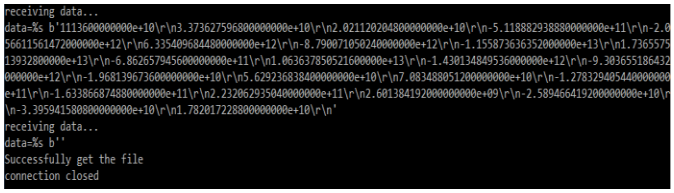

Fig (4). Reception of data.

The manipulated data is received to the port.

V. Conclusion

In this paper, Sparse based dimensionality reduction for big data is proposed. The purpose of proposed scheme is to reduce enormous data produced by the brainy grid. To manipulate data without losing the originality of the data is difficult task and finally to forward this data through the SDN network. Firstly to show the data in tensor form. Firstly enormous quantity of information is produced by smart devices

then by using TensorFlow in Python that data is converted into Tensor model. After that the data in the form of Sub Tensors, sub-tensors are adding together forming unified tensors then SVD is applied to unified tensors for decomposition of data. Analysis of the data is taken place and then using VLCP controller sending and reception of data taken place. VLCP controller is used as SDN controller. The outcomes show that dimensionality reduction in given data. Evaluation parameters in proposed scheme is approximation ratio means the differentiation of the actual data to the reconstructed data and reduction ratio means the amount of data reduced for the given samples, network performance and error between original data and received data means the error occurs in the send and received information, Sending of data to the receiver and reception of information is successfully done using VLCP controller. Hence, overall conclusion obtained from the suggested scheme is related to data administration and dimensionality contraction shows better performance.

VI. REFERENCES

[1] DevinderKaur , Gagangeet Singh Aujla , Neeraj Kumar , Albert Y. Zomaya , CharithPereraand Rajiv Ranjan, "Tensor-Based Big Data Management Scheme for Dimensionality Reduction Problem in Smart Grid Systems: SDN Perspective", IEEE Transactions On Knowledge And Data Engineering, Vol. 30, No. 10, October 2018

[2] K. Kaur, S. Garg, G. S. Aujla, N. Kumar, J. J. P. C. Rodrigues, and M. Guizani, "Edge computing in the industrial internet of things environment: Software-defined-networks-based edge-cloud interplay," IEEE Commun. Mag., vol. 56, no. 2, pp. 44–51, Feb. 2018.

[3] R. Chaudhary, G. S. Aujla, N. Kumar, and J. J. P. C. Rodrigues, "Optimized big data management across multi-cloud data centers: Software-defined-network-based analysis," IEEE Commun. Mag., vol. 56, no. 2, pp. 118–126, Feb. 2018.

[4] R. Ranjan, L. Wang, A. Y. Zomaya, J. Tao, P. P. Jayaraman, and D. Georgakopoulos, "Advances in methods and techniques for processing streaming big data in datacentre clouds," IEEE Trans. Emerging Top. Comput., vol. 4, no. 2, pp. 262–265, 2016.

[5] L. Zhao, L. Chen, R. Ranjan, K.-K. R. Choo, and J. He, "Geographical information system parallelization for spatial big data processing: A review," Cluster Comput, vol. 19, no. 1, pp. 139–152, 2016.

[6] J. C. S. de Souza, T. M. L. Assis, and B. C. Pal, "Data compression in smart distribution systems via singular value decomposition," IEEE Trans Smart Grid, vol. 8, no. 1, pp. 275–284, Jan. 2017.

[7] M. U. S. Khan, O. Khalid, Y. Huang, R. Ranjan, F. Zhang, J. Cao, B. Veeravalli, S. U. Khan, K. Li, and A. Y. Zomaya, "Macroserv: A route recommendation service for large-scale evacuations," IEEE Trans. ServComput, vol. 10, no. 4, pp. 589–602, 2017.

[8] D. Alahakoon and X. Yu, "Smart electricity meter data intelligence for future energy systems: A survey," IEEE Trans Ind. Informat., vol. 12, no. 1, pp. 425–436, Feb. 2016.

[9] D. Zhou, J. Guo, Y. Zhang, J. Chai, H. Liu, Y. Liu, C. Huang, X. Gui, and Y. Liu, "Distributed data analytics platform for wideareasynchrophasor measurement systems," IEEE Trans. Smart Grid, vol. 7, no. 5, pp. 2397–2405, Sep. 2016.

[10] L. Ren, Y. Qin, B. Wang, P. Zhang, P. B. Luh, and R. Jin, "Enabling resilient microgrid through programmable network," IEEE Trans. Smart Grid, vol. 8, no. 6, pp. 2826–2836, Nov. 2017.

[11] F. Li, J. Cao, X. Wang, and Y. Sun, "A SDN-based QoS guaranteed technique for cloud applications," *IEEE Access*, vol. 5, pp. 21229– 21241, Sep. 2017

[12] S. Agarwal, M. Kodialam, and T. Lakshman, "Traffic engineering in software defined networks," in *Proc. IEEE INFOCOM*, 2013, pp. 2211–2219.

Proceedings of the Fourth International Conference on Communication and Electronics Systems (ICCES 2019)
IEEE Conference Record # 45898; IEEE Xplore ISBN: 978-1-7281-1261-9

Hardware Implementation of VANET Communication based Collision Warning System

Rakesh.G
Department of Computer Science and Engineering
Amrita School of Engineering, Bengaluru
Amrita Vishwa Vidyapeetham, India
rakeshgovindan04@gmail.com

Meena Belwal
Department of Computer Science and Engineering
Amrita School of Engineering, Bengaluru
Amrita Vishwa Vidyapeetham, India
b_meena@blr.amrita.edu

***Abstract*—Vehicle and passenger safety is one of the key attributes in designing autonomous vehicles. Vehicles are equipped with several fast computing devices and sensors that will alert the driver in risk conditions, but there are events that cannot be identified by such sensors, such as road intersections. In such conditions, data collected from other devices or vehicles can help. Vehicular Networks ensure the safety of these by enabling the communication between the vehicles. The ideal scenario about Vehicular ad-hoc Network is, where the vehicles on the road are connected to each other and to RSU devices, details about their transit are transmitted to the manipulating devices. The objective of this work is to simulate such a condition via NS2 simulator and to implement the hardware prototype of such scenario to collect the data from various nodes and integrate it to the other nodes in the network. For Simulation, VANET environment is created with Vehicles and RSU units, shortest path routing algorithm is implemented for data communication between RSU units. The hardware prototype is created with two vehicles and one RSU unit, the data is collected from both the devices and emergency messages are transmitted to other vehicles. The setup is able to collect the data when collision occurs and this is transmitted to RSU for data processing.**

***Index Terms*—Autonomous vehicles, Navigation, computing device, collision avoidance, NS2, RSU range, data communication.**

I. Introduction

The next stage of vehicular safety is the evolution of unmanned vehicles or autonomous vehicles [1] , by far the development of these are started and taken the space in developed countries and are very soon visibly in the developing countries too. Autonomous vehicles brings us safety and also a doubt whether it can perform as theoretically mentioned or not. Figure 2 shows the overview of VANET system.

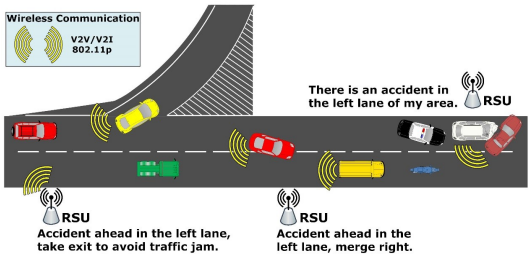

Fig. 1. Data Packet communication

In some cases only the data from sensors may not be sufficient to take a decision or it will lead to wrong decision making as in [2]. For example in a four way intersection road midpoint the sensors like camera cannot capture the obstacle on the other side of the road [3], in these cases the only solution is to collect information from the other vehicles that may cause as an obstacle.

Sensors are associated with special written algorithms [4] to process these data. Many states of these algorithms such as collision avoidance, stabilization of vehicle, lane tracking etc. are needed to be included in the system. Hence the controller prioritize these states according to the situation, such that the vehicle avoids big crash and provides smooth collision free navigation. Figure 2 shows the dependent of various sensors in a car.

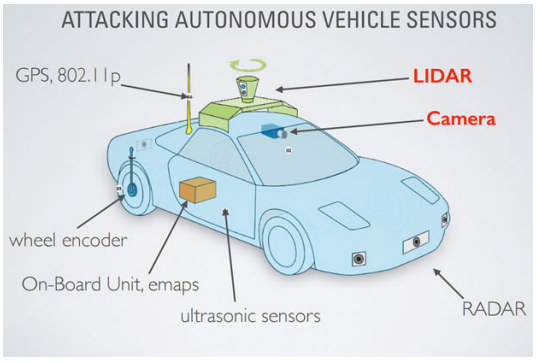

Fig. 2. Various Sensors in autonomous cars

Collision scenario can be understood earlier even before it is identified by the sensor, with the help of forming a network of vehicles known as Vehicular ad-hoc network.

Vehicular ad-hoc network is a kind of mobile ad-hoc network that forms network of vehicles based on the position of the vehicle. In VANET the vehicles are connected to each other and also connected to an infrastructure based computing device [5] called RSU (Road Side Units). These RSU's perform the possible manipulation of the data[6], the various RSU are interconnected to each other to share the details throughout the network. The vehicle in a network communicates with the RSU associated to it, and in some cases vehicle also

communicates to other vehicles in the network. RSU can also provide the details of the environment such as traffic status accidents in the route [7], speed limit, accident zone etc.

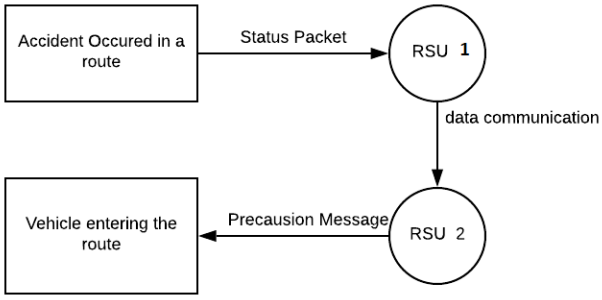

Fig. 3. Data Packet communication

The work proposes to develop a system as shown in Figure 3. The remainder of the paper is organised as follows: Section II speaks about the Literature Survey, Section III is about System Requirements,section IV discusses the proposed system and Section V showcase the Implementation and results.

II. Literature Survey

Various researches has been performed on VANET collision detection, collision avoidance and stabilization of autonomous vehicles.

A. Stabilization of autonomous vehicles

The authors J. Funke et al. in [8] discusses the need for stabilization in autonomous vehicles during certain emergency scenarios. The algorithm tries to stabilize the vehicle in some situations even though if it conflicts with collision avoidance. The control sequence is created by integrating vehicle stabilization, collision avoidance and path tracking. Model predictive controllers and feedback controllers are used to form the framework. In some scenarios collision avoidance is unavoidable therefore stabilization is performed. Prediction algorithm employs environment related parameters to predict the vehicles future dynamics.

B. QCP based Model Predictive Controller

Z. Wang et al. in [9] uses convex quadrature programming based MPC(model predictive controller) for navigation of Autonomous vehicles and collision avoidance, During trajectory generation the vehicle shape is considered as polygonal region. Cost function is created, that forms a model which navigates the vehicle through the environment, then the optimization of the cost function is performed for path planning. Simulations are done in MATLAB and CARSIM is used for better simulation of vehicle navigation. Model Predictive controller is formed in MATLAB.

C. Vehicle Risk Assessment

In [10] the work by H. Fahmy et al. perform simulations for different scenarios including the mechanical setup for controlling angle of trajectory. Vehicle risk is analysed by Vehicle communication and the optimal track is maintained by evaluation of cost of the various obstacle. The simulations are performed with a car and with different obstacle paths, obstacle avoidance and lane selection id for different scenarios. Several frameworks such as road model, driver model and vehicle mode are created by the numerical methods and are integrated to get the live vehicle model.

D. Vanet- Physical Model

In [11] D. Anadu et al. proposes the efficient algorithm for collision detection in a VANET environment. They address VANET security by implementing IFA(iterative filtering algorithm) that filters the wrong sensor reading. Various parameters of the vehicles such as position, speed and orientation are transmitted to the Vehicular network, from there the corresponding messages for the collision detection is created.

E. Numerical Methods

In [12], work by H. Fahmy et al. employ numerical methods to keep the track of the unmanned vehicles and prevent collision. The main theme of the work is that the road details are shared through Vehicular communication and hence the vehicles entering understand scenario well in advance, thereby preferring the exact lane, so that the obstacles are avoided in advance and necessary actions are taken as a prerequisite.

Various routing protocols [13], [14] for Vanet speaks about how quick the data packets can reach the destination with minimum hops required and with very less packet losses.

We summarize from the survey that collecting important data's and processing it plays vital role in collision detection/avoidance. Therefore we propose system that will collect data such as accidents occurence, traffic details and communicate this data to RSU through routing, which in turn makes decision for vehicles in its range.

III. System Requirements

The software and hardware used in the work is explained in this section

A. Software Requirements

For performing simulations, the following tools are used

1) NS2- Network Simulator 2
2) Arduino IDE

1) NS2: The network simulator 2 is used here to simulate network parameters. It is an open source simulator. The network simulation parameters includes routing protocol, topography, channel, link layer, MAC layer, initial energy, Antenna, etc. Scripts for simulating the network is written as TCL scripts.

OTCL is a scripting language that incorporates the object oriented properties of c++. The TCL script generates trace file that captures all the events that happen during the simulation

of the script. The algorithm for the project is written in AWK scripts, the awk script uses trace file to process the data. The output of the AWK script is written to another file, which is used in executing the NAM window in the TCL script.

2) Arduino IDE: It is a software which facilitates to write the code for Arduino and upload to the boards. The code for arduino boards are written in simple c language. This IDE also helps to serial monitor the arduino board.

B. Hardware Requirements

The hardware implementation of the system is done using the Arduino boards and nRF modules, for better understanding the system multiple nodes are created to imitate the real world like scenario. The components used in this project for prototyping the system are listed as below,

- Arduino uno boards- 3 units.
- nrf24L01 module- 3 units.
- LCD 16*2 module- 1 unit.
- GPS module- 1 unit.
- RC car- 3 units.
- joystick module- 2 units.
- IR sensor- 2 units.
- buzzer- 1 unit.
- lead acid battery- 2 units.

1) Arduino uno/ nano: Arduino Uno/nano is a microcontroller board containing ATmega328P as a Processor. It has 14 digital IO pins of which 6 pins can be used as PWM outputs, 6 analog inputs, a 16 MHz quartz crystal, a USB connection, a power jack, an ICSP header and a reset button. In this work we used arduino boards with nrf modules to create network out of it.

2) NRF24L01 module: NRF24L01 module is multi transceiver that can communicate with six other modules directly, by using routing this module can be used to communicate with large number of nodes by forming a network between nodes. Figure 4 shows the pinout of NRF24L01 module.

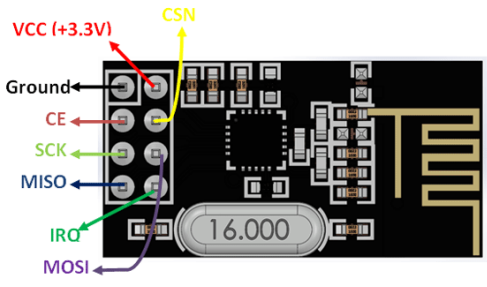

Fig. 4. nRF24L01 PINOUT

3) GPS module: Gps module is used to locate the vehicle with respect to the satellite positions, these data are then processed with arduino and the coordinates(x axis and y axis) are transmitted to the RSU unit.

4) Robot car: The robot car is developed with four geared motors and chassis, it is powered using 12v lead acid battery of capacity 1.3Ah. Some specifications of the robot car is mentioned below:

1) motors used: 12v geared DC motor.
2) Chassis: transparent plastic chassis.
3) battery: 12v 1.3 Ah Lead Acid battery.

IV. Proposed System

A. System Flow

A network is created with number of vehicle nodes and RSU nodes. When a vehicle enters in a range of RSU it gets connected to it. Vehicle shares its status and its destination to the RSU, whereas the RSU replies with the possible route and the status of this route. Shortest path routing algorithm (SPRA algorithm) is used to find the shortest path for data communication. The flow of the system is as shown in Figure 6.

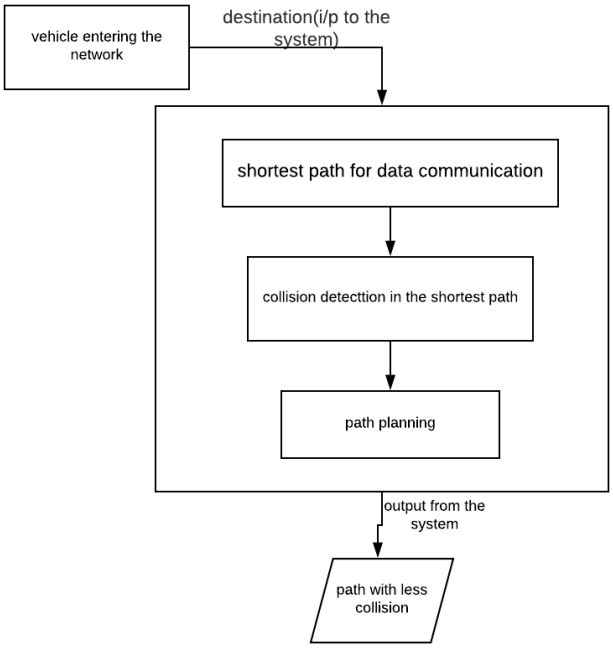

Fig. 5. System Flow Diagram

1) SPRA algorithm: The computing devices are placed apart with some distances to each other. When the vehicle triggers the system by giving a destination, the RSU with the vehicle's range compute the shortest path for which it can intimate the RSU near the destination. Shortest path routing algorithm based on Euclidean distance is employed to find the shortest path between source and destination. This path is used to share the data such as traffic status, accident occurrence in the route. Figure 7 shows the block diagram of SPRA algorithm.

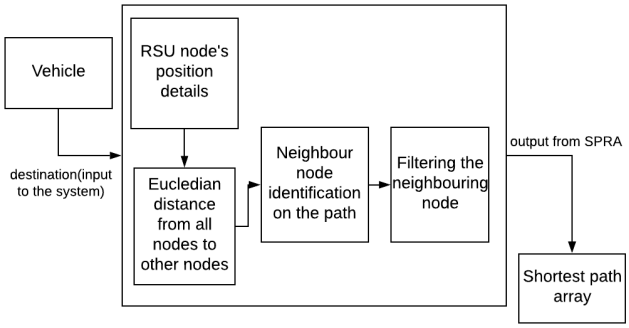

Fig. 6. SPRA block diagram

B. Hardware Prototype

To better understand the system a hardware prototype imitating the real world scenario of the system is implemented. A wireless network of three nodes are created with two vehicular node and 1 RSU node are created.

1) Vehicular node block diagram: Figure 8 shows the block diagram of the Vehicular node. GPS module is connected to the vehicles which records the GPS data and it is forwarded to the RSU in range to it.

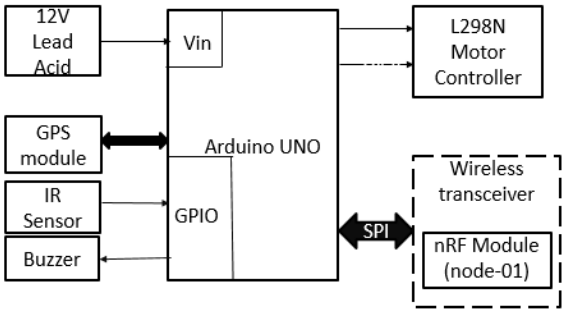

Fig. 7. Vehicular node block diagram

2) RSU node block diagram: Figure 9 shows the block diagram of the RSU node. It consist of Joystick module that imitates the control of vehicular node. The LCD module is used to display the messages received by the node from other nodes.

V. Implementation and Results Analysis

The prototype of the proposed system is implemented in NS2 simulator where vehicular ad-hoc network is created with various wireless nodes. To better understand the working, hardware implementation of the VANET is performed using microcontrollers, RC cars, NRF24L01 modules and other sensors.

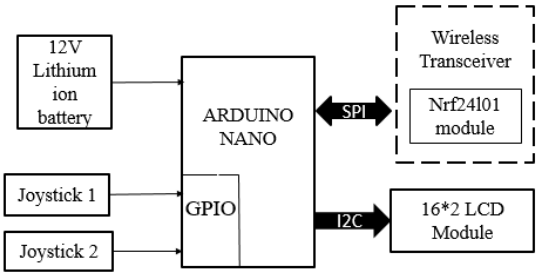

Fig. 8. RSU node block diagram

A. NS2 Simulation

For implementing the VANET in NS2, a network is created with number of wireless mobile nodes each having different functionality. The Figure 10 shows the created VANET environment in the Network Animator of the Network Simulator-2.

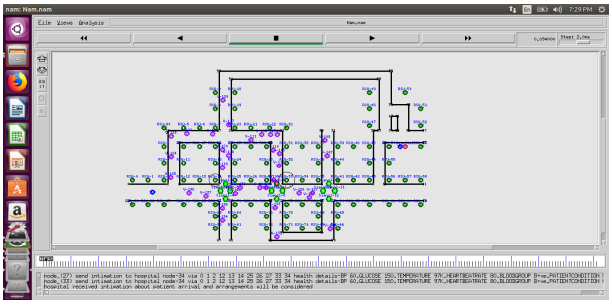

Fig. 9. Created Vanet Environment

B. Hardware Prototype

Physical Prototype consists of three nodes,

1) RSU node – which monitors the network and coordinates each of the vehicles within its range. Thereby it acts as server node.
2) Two vehicular node – which are the client nodes that perform some events based on the written code.

Figure 11 shows the server node that acts as RSU unit of the system, monitoring the network and sending crucial messages to the vehicles that enter the network. The two joystick is connected wirelessly to the two vehicles so that the vehicles are controlled for their forward and backward direction control.

Figure 12 shows the Vehicular node setup. The two wireless vehicles act as two clients for the server node of the network. These vehicles are controlled from the server node using the two joystick module. All the three nodes are wirelessly connected to each other by nRF24L01 wireless transceiver module.

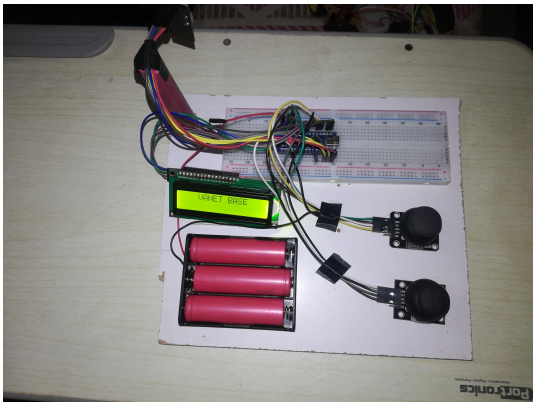

Fig. 10. RSU node setup

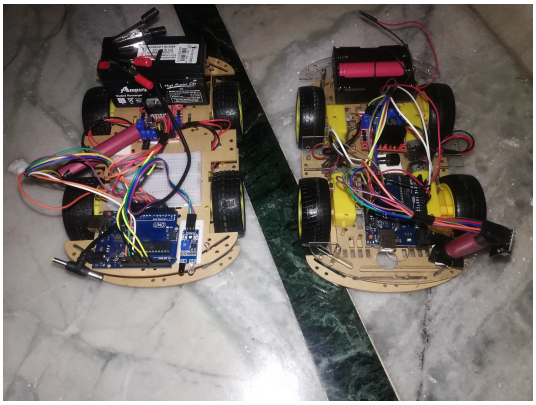

Fig. 11. Vehicular node setup

- 4 Wheel-Drive cars having four 12v BO geared motors are used, L298N motor driver is employed to control the motors via the arduino.
- One of the vehicles consist of IR sensor to detect any close obstacle within the vehicle, whenever this vehicle collapses with the obstacle the IR sensor creates a digital high which is transmitted to the network.
- Whenever this vehicles is guided to meet the obstacle the IR sensor present in it captures the event and transmits the data to the server node which acts as the coordinator of all the nodes in the network.
- The nRF24L01 module transmits the data to the node whose address is requested. Whenever this data is received in the server, the corresponding message is displayed in the LCD that is connected to the server node's Arduino via the I2C connector circuit.
- Then the server node transmits the data received to the vehicles that are entering in to the network (entering the range with the nRF24l01 module).

We tested the prototype by considering a vehicle in a route as an ambulance and another vehicle(v1) in the route. When vehicle v1 meets with collision in the route, the data is transmitted to the RSU, which identifies the entry of ambulance in the route and transmits the data to the ambulance. Thereby the ambulance is intimated with the incident.

VI. Conclusion and Future work

Vehicular ad-hoc networks in intelligent transport system help to improve the precision of decision making in autonomous vehicles by communication crucial data. In this work we simulated a system with VANET network created and SPRA algorithm implemented for data communication. The hardware prototype created by forming wireless network using sensors showed that the vehicle node can avoid accidents even before the sensor reads the scenario. Future work may include communication of parameters of the node like speed etc. so that other vehicle performs actions to avoid crashes.

References

[1] M. Jain and R. Saxena, "Overview of vanet: Requirements and its routing protocols," in *2017 International Conference on Communication and Signal Processing (ICCSP)*. IEEE, 2017, pp. 1957–1961.

[2] E. Pucher, A. Gruber, M. Innerkofler, and M. Buhmann, "Performance analysis of vehicle-specific methods and sensors for autonomous vehicles," in *The International Symposium for Production Research*. Springer, 2018, pp. 451–463.

[3] M. Akhil, N. Vasudevan, U. Ramanadhan, A. Devassy, D. Krishnaswamy, and A. Ramachandran, "Collision avoidance at intersections using vehicle detectors and smartphones," in *2015 International Conference on Connected Vehicles and Expo (ICCVE)*. IEEE, 2015, pp. 389–390.

[4] V. Athira, A. Mohandas, and A. Mukhopadhyay, "A survey on routing protocols used in vanets for telemedicine scenarios," in *2017 International Conference on Communication and Signal Processing (ICCSP)*, April 2017, pp. 0959–0963.

[5] G. M. N. Ali, P. H. J. Chong, S. K. Samantha, and E. Chan, "Efficient data dissemination in cooperative multi-rsu vehicular ad hoc networks (vanets)," *Journal of Systems and Software*, vol. 117, pp. 508–527, 2016.

[6] R. Murugesh, U. Ramanadhan, N. Vasudevan, A. Devassy, D. Krishnaswamy, and A. Ramachandran, "Smartphone based driver assistance system for coordinated lane change," in *2015 International conference on connected vehicles and expo (ICCVE)*. IEEE, 2015, pp. 385–386.

[7] H. Al Najada and I. Mahgoub, "Anticipation and alert system of congestion and accidents in vanet using big data analysis for intelligent transportation systems," in *2016 IEEE Symposium Series on Computational Intelligence (SSCI)*. IEEE, 2016, pp. 1–8.

[8] J. Funke, M. Brown, S. M. Erlien, and J. C. Gerdes, "Collision avoidance and stabilization for autonomous vehicles in emergency scenarios," *IEEE Transactions on Control Systems Technology*, vol. 25, no. 4, pp. 1204–1216, July 2017.

[9] Z. Wang, G. Li, H. Jiang, Q. Chen, and H. Zhang, "Collision-free navigation of autonomous vehicles using convex quadratic programming-based model predictive control," *IEEE/ASME Transactions on Mechatronics*, vol. 23, no. 3, pp. 1103–1113, June 2018.

[10] H. M. Fahmy, M. A. A. E. Ghany, and G. Baumann, "Vehicle risk assessment and control for lane-keeping and collision avoidance at low-speed and high-speed scenarios," *IEEE Transactions on Vehicular Technology*, vol. 67, no. 6, pp. 4806–4818, June 2018.

[11] D. Anadu, C. Mushagalusa, N. Alsbou, and A. S. A. Abuabed, "Internet of things: Vehicle collision detection and avoidance in a vanet environment," pp. 1–6, May 2018.

[12] H. M. Fahmy, G. Baumann, M. A. A. E. Ghany, and H. Mostafa, "V2v-based vehicle risk assessment and control for lane-keeping and collision avoidance," in *2017 29th International Conference on Microelectronics (ICM)*, Dec 2017, pp. 1–5.

[13] A. I. A. Ahmed, A. Gani, S. H. Ab Hamid, S. Khan, N. Guizani, and K. Ko, "Intersection-based distance and traffic-aware routing (idtar) protocol for smart vehicular communication," in *2017 13th International Wireless Communications and Mobile Computing Conference (IWCMC)*. IEEE, 2017, pp. 489–493.

[14] F. Cunha, L. Villas, A. Boukerche, G. Maia, A. Viana, R. A. Mini, and A. A. Loureiro, "Data communication in vanets: Protocols, applications and challenges," *Ad Hoc Networks*, vol. 44, pp. 90–103, 2016.

Proceedings of the Fourth International Conference on Communication and Electronics Systems (ICCES 2019)
IEEE Conference Record # 45898; IEEE Xplore ISBN: 978-1-7281-1261-9

FPGA Based Emulator Design of a DC Motor

Rama D.
Department of Electrical and Electronics Engineering,
Amrita School of Engineering, Coimbatore
Amrita Vishwa Vidyapeetham, India
rama.dinakaran@gmail.com

Ananthan T.
Department of Electrical and Electronics Engineering,
Amrita School of Engineering, Coimbatore
Amrita Vishwa Vidyapeetham, India

***Abstract*—Hardware emulator is a special purpose device which mirrors the operation of a software or dynamic system. Such devices can be implemented using Programmable Logic Devices, Field Programmable Gate Array (FPGA) and Application Specific Integrated Circuit(ASIC). Field Programmable Gate Array (FPGA) is one of the popular solutions to design an emulator due to its high speed, reduced power consumption, reconfigurability and reduced cost. It is more flexible than a PLD and has less development time when compared to ASIC. In this paper, hardware realization of DC motor emulator using FPGA is presented. The continuous-time transfer function model of an armature controlled DC shunt motor is determined by conducting suitable experiments. The discrete-time model of the DC motor is the emulator and it is realized as a second order digital Impulse Infinite Response (IIR) filter. The hardware of this filter is designed with adders, multipliers and delays using Verilog and mapped on a Spartan 6 FPGA. Speed and load characteristics of this emulator is compared with the actual motor characteristics. This model can be used in place of DC motor for testing speed estimators and for verifying the performance of motors with different ratings without using the actual motors.**

***Keywords*—DC shunt motor, Armature control, FPGA, Emulator.**

I. Introduction

An FPGA based hardware emulator is used to replicate the behaviour of a real-time system. It is used for debugging and verifying the functions of the dynamic system under consideration.For example, in automation industries, an emulator is created to verify the functioning of automation system in real time. It can be linked with the controllers that are developed to control the real system. These devices target hardware debugging and can emulate any system with different sizes and structures, unlike prototyping which focuses on achieving the speed of the specific design. Developing such a multi-purpose device with several number of FPGAs connected together is useful to emulate complex hardware systems. It can achieve execution speed of few Kilohertz to Megahertz. They provide better hardware and software integration for most complex designs along with reducing the designing cost. There are two main categories which are classified as low level and high level emulators. Low level emulators reproduce the operation of system under design with high accuracy. High Level devices create an abstract of the system and used mainly for emulating a software. FPGA based hardware emulators are used in various fields such as automation, computer and storage, defense, Renewable energy technologies and product test and measurement. For example, wind generation using a DC machine [1] , photo voltaic emulator [2] to reproduce the characteristics of commercial Photo voltaic panels, state space controller [3] to control fast dynamic systems and FPGA based monitoring of wind and solar generators [4] are used in Renewable energy field. They are also used in Computer Science domain such as using an ARM processor [5] to mirror a Intel 8080 processor, Prototyping a Parameter Random Access Memory (PRAM) [6] using FPGA. Digital Wireless Channel Emulator [7] to reproduce RF environment in military networks and emulate an aircraft based satellite [8] to test an antenna array in space are a few defense based applications. To emulate a system in FPGA, is to initiate with implementing design using Hardware Description Languages such as Verilog and VHDL. It can be also achieved by using model-based methods such as Xilinx System Generator in Simulink. Fixed point algorithm is used to represent the decimals, due to the simplicity compared to the Floating point algorithm. In this paper, hardware emulator for an armature controlled DC shunt motor is proposed. Armature resistance, inductance, motor constants, inertia and friction are estimated by conducting experiments on a 220V, 2HP motor. Proposed model is determined by substituting the estimated values in standard DC motor model. This model is discretized and realised as an IIR filter. Direct form I filter is designed using A Hardware Descriptive Language and mapped on a FPGA. Armature voltage is given as input and the speed characteristics are analysed.

An overview of similar works carried out using emulator is summarized in Section II. The proposed mathematical model of a DC motor and IIR filter is explained in Section III. Section IV shows the simulation result of intended model and architecture of the hardware implementation. Emulator results are evaluated and compared with simulation and actual motor results in Section V. Conclusion of the proposed work is mentioned briefly in Section VI.

II. Related Work

The numerical issues connected with the discrete time induction motor implementation is discussed in [9]. To implement and verify the simulation of control algorithms to the emulator for the motors. The designing is started

with continuous time system and shift algorithm is used to discretize the model. A Direct Torque Control algorithm is verified using this emulator. Implementation of brush-less DC motor speed controller is discussed in [10]. The design is mapped on FPGA for testing the different validation and verification methods . It is designed using Xilinx system Generator blockset from Xilinx in Simulink. A PI controller is implemented in FPGA to verify the performance. The discretization methods of an induction motor for implementing a real time emulator is investigated in [11]. Shift operator method, Tustin and Delta operator method are discussed and the simulation results are carried out using simulink. A hardware emulator design of DC motor is projected in [12] for emulating the system when designing controllers.This emulator is developed without taking losses into consideration. It is realized using VHDL and synthesized to Virtex II FPGA. A torque input is given and the output is measured from emulator. It is then connected with the hardware or software controller.

III. Mathematical Modelling of Proposed Work

DC motor speed can be varied by changing the armature voltage while keeping the flux constant. The speed is measured by changing the series resistance with armature winding.

$$T = K_t \Phi I_a$$

Since Flux is constant,

$$T = K_t I_a \tag{1}$$

$$E_b = K_b \omega \tag{2}$$

where, T = Torque)
I_a = Armature Current
K_t = Motor constant
E_b = Back emf
K_b = Back EMF constant
ω = Angular Velocity
R_a = Resistance
L_a = Inductance

If voltage and resistance in armature are kept constant, speed will be proportional to current. Differential equation for DC motor based on Kirchhoff's Voltage Law is derived as

$$V_a = I_a R_a + L_a \frac{dI_a}{dt} + E_b \tag{3}$$

The torque equation based on Inertia (J_m) and damping (B_m) is derived as

$$J_m \frac{d\omega}{dt} + B_m \omega = T$$

From (1),

$$J_m \frac{d\omega}{dt} + B_m \omega = K_t I_a \tag{4}$$

Laplace Transform of (3) & (4)

$$V_a(s) = R_a I_a(s) + s L_a I_a(s) + E_b(s) \tag{5}$$

$$J_m s\omega(s) + B_m \omega(s) = K_t I_a(s) \tag{6}$$

Rewriting (5) with (2),

$$V_a(s) = R_a I_a(s) + s L_a I_a(s) + K_b \omega(s)$$

$$I_a(s) = \left(\frac{V_a(s) - K_b \omega(s)}{L_a s + R_a} \right) \tag{7}$$

From (6) & (7),

$$G(s) = \frac{\omega(s)}{V_a(s)} = \frac{K_t}{(L_a s + R_a).(J_m s + B_m)} \tag{8}$$

Closed loop transfer function the DC motor with H(s)=K_b is given by,

$$\frac{\omega(s)}{V_a(s)} = \frac{K_t}{(L_a s + R_a).(J_m s + B_m) + K_t K_b} \tag{9}$$

On conducting suitable experiments on a DC motor, the following values are obtained.
R_a=2.715Ω,
L_a=36mH,
K_t=1.032 N.m/A,
K_b=1.2633 V/rad/sec,
J_m=0.039 Kg. m^2
B_m= 0.0116 N.m.s

By substituting these values in (9), the continuous time model becomes,

$$H(s) = \frac{Y(s)}{X(s)} = \frac{1.032}{0.001326s^2 + 0.1063s + 1.202} \tag{10}$$

Eqn. (10) is discretized using MATLAB and the transfer function becomes,

$$\frac{Y(z)}{X(z)} = \frac{0.03007z^{-1} + 0.2303z^{-2}}{1 - 1.38z^{-1} + 0.4487z^{-2}} \tag{11}$$

It can be implemented using a second order Impulse Infinite Response filter. This filter calculate new output using the current input along with past output. A digital IIR filter has better amplitude response, use minimal storage space and resemble analog filter output. The discrete tf of a filter is defined as,

$$\sum_{j=0}^{M} b_j z^{-j} Y(z) - \sum_{k=0}^{N} a_k z^{-j} X(z) \tag{12}$$

A second order filter from (12) is written as,

$$Y(z) = b_0 X(z) + b_1 z^{-1} X(z) + b_2 z^{-2} X(z) - a_1 z^{-1} Y(z) - a_2 z^{-2} Y(z) \tag{13}$$

where, b_0, b_1, b_2 - coefficients of zeros
a_0, a_1, a_2 - coefficients of poles.

X(z) - input signal
Y(z) - output signal.

From (11) the filter coefficients are estimated as
b_0=0; b_1=0.03007; b_2=0.02303 ;
a_0=1; a_1=1.38; a_2=-0.4487;

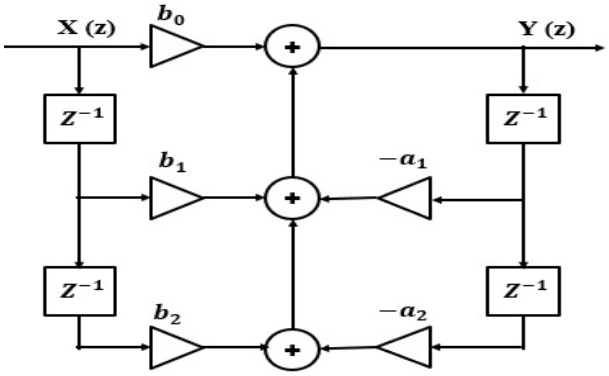

Fig. 1. Infinite Impulse Response Filter Direct Form 1

Replacing these coefficients in (11), it can be rewritten as,

$$Y(z) = 0.03007z^{-1}X(z) + 0.02303z^{-2}X(z) - 1.38z^{-1}Y(z) + 0.4487z^{-2}Y(z) \quad (14)$$

A Filter is designed in different methods. Direct form, canonical form and cascade form. Direct form I is often used to design filters of smaller order. The form I will execute the order of zeros initially followed by execution of poles in order. This helps to reduce errors occurring during run time.

IV. Emulator Design

A. Matlab Simulation Model

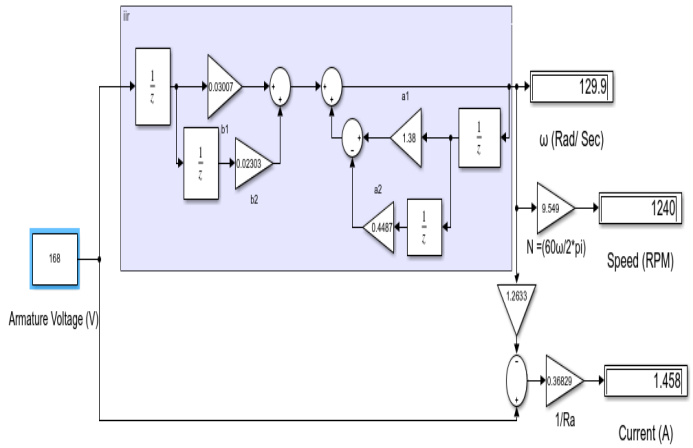

Fig. 2. Simulation of digital IIR filter using MATLAB Simulink

Fig. 2 shows the performance of digital IIR filter. model derived in (14) is simulated using using simulink. Input voltage, output speed and current values are shown in fig. 2.

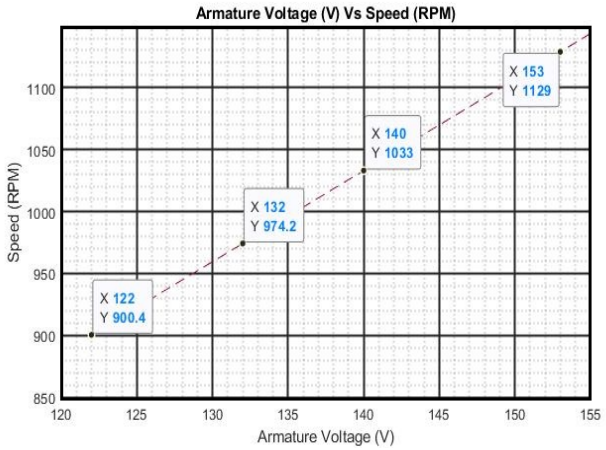

Fig. 3. DC motor Simulation Output for Speed in MATLAB Simulink

Simulation output of DC motor model is displayed in fig. 3. The input voltage Vs output speed characteristics of a motor is drawn using Matlab.

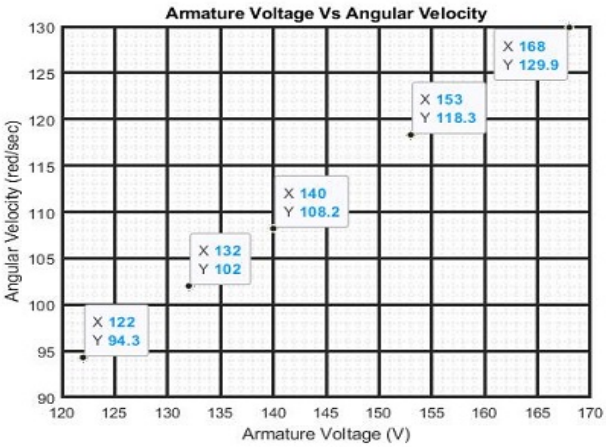

Fig. 4. DC motor Simulation Output for angular velocity in MATLAB Simulink

Simulation output of DC motor model for angular velocity is displayed in fig. 4.

B. Hardware Emulator Implementation

Eqn. (14) is used to design the DC motor emulator using IIR filter realization. Xilinx ISE software is used to design IIR filter in Verilog HDL. This IIR filter is implemented using multipliers, adders and delay units. The filter is synthesized and mapped on a Xilinx Spartan FPGA.

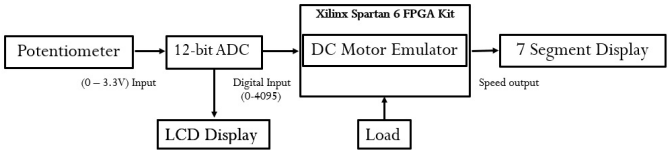

Fig. 5. FPGA Based Hardware Emulator Implementation Block Diagram

Fig. 5 represents the hardware implementation of the IIR filter emulator on a Xilinx Spartan 6 FPGA. A potentiometer is used to give input of 0-3.3V, which is discretized using a 12-bit ADC. The value is normalized according to the required 0-220 input and given to the emulator mapped on FPGA and the Speed output is shown using seven segment Display.

V. Results and Discussion

TABLE I
Comparison of Experiment, Simulation and FPGA output

Armature Voltage (V)	Experiment o/p		Simulation o/p		FPGA o/p	
	ω (Rad/Sec)	Speed (RPM)	ω (Rad/Sec)	Speed (RPM)	ω (Rad/Sec)	Speed (RPM)
122	95.82	914	94.3	900.4	93	887
132	102.6	980	102	974.2	101	964
140	108.5	1037	108.2	1033	107	1021
153	119.28	1139	118.3	1129	117	1116
168	131.69	1255	129.9	1240	128	1221

Table. 1 lists the comparison of experiment, simulation and FPGA emulator outputs to given armature voltage input and confirms that the emulator output is found closer to the actual motor speed.

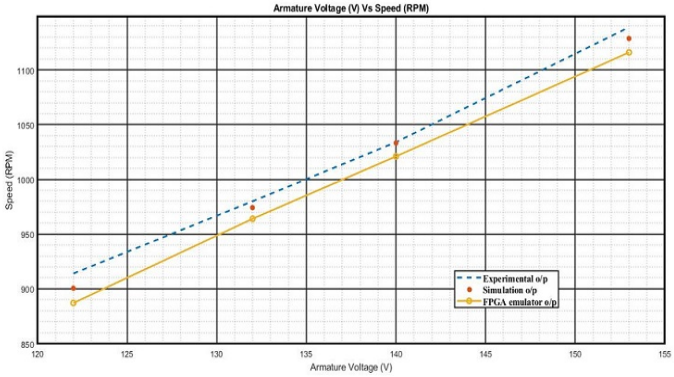

Fig. 6. Comparison among experiment, simulation and FPGA outputs

Fig. 6 shows the comparison of experiment, simulation and emulator outputs for given voltage input.

From table I, outcome of emulator with experimental and simulation outputs are found to be relatively similar. The hardware IIR filter is mapped and implemented on Xilinx Spartan 6 FPGA.

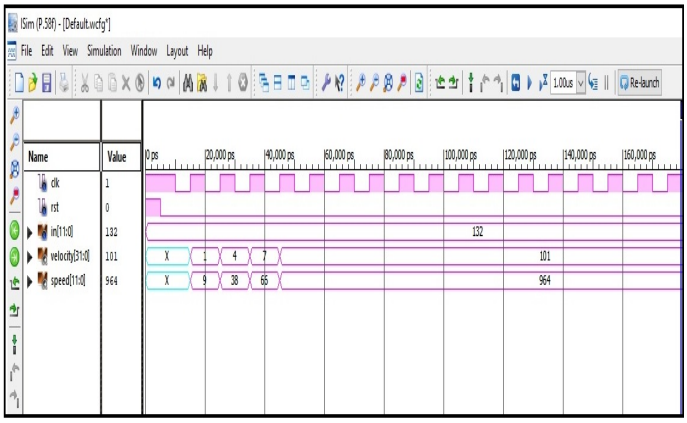

Fig. 7. IIR Filter Simulation for input=132 Using Xilinx ISE design suite

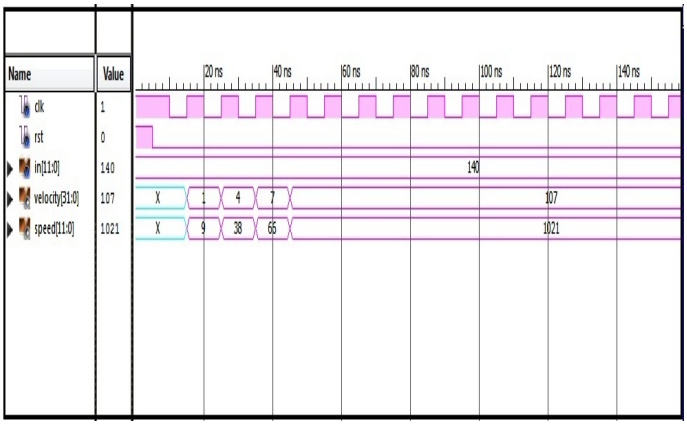

Fig. 8. IIR Filter Simulation Using Xilinx ISE design suite

Fig. 7 & Fig. 8 shows the IIR filter simulation output for various inputs in ISE software.

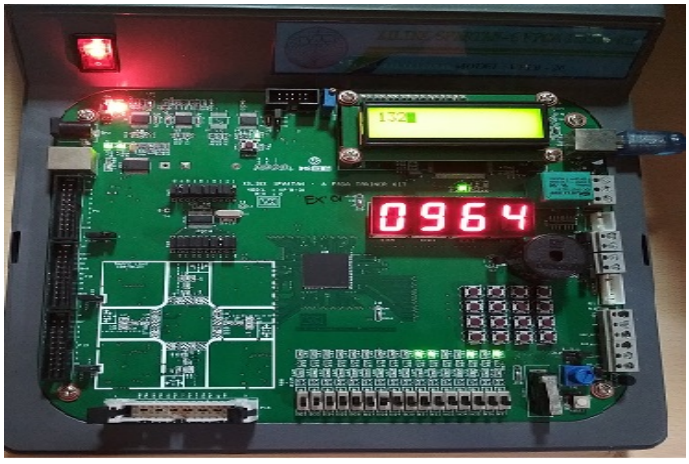

Fig. 9. Speed and ω output for armature voltage input=132V from emulator

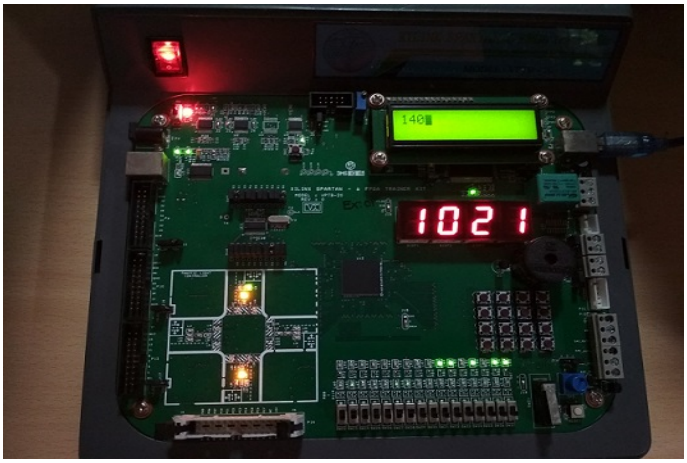

Fig. 10. Speed and ω output for armature voltage input=132V from emulator

The motor emulator results are shown in Fig 9 & Fig.10. Input armature voltage value is displayed in LCD, output velocity is shown using LED and output speed is shown using Seven Segment Display.

TABLE II
SYNTHESIS REPORT FOR THE EMULATOR DESIGN

Description	Used	Total
Number of Registers	191	18224
Number of LUTs	444	9112
Number of FFs	143	697
Minimum period	47.819ns	
Maximum Frequency	20.912MHz	

Table II specifies the utilization of resources to implement the emulator on an FPGA.

VI. CONCLUSION

Experiments are conducted on a 220V, 2HP, DC motor and its mathematical model is determined.The discrete function of the model is converted using Matlab Software. The obtained result is then realized as a second order IIR filter which is used for designing emulator. Hardware of this design is implemented in verilog and is mapped on Xilinx spartan-6 FPGA. The synthesis report is presented in Table II. The performance of the emulator is tested. Its speed and load characteristics are found to be same as the actual motor. In future, this FPGA based emulator may be used for the DC motor closed-loop speed control system.

REFERENCES

[1] Francisco Ar evalo, Pablo Estrada, Nataly Pozo, and Marcelo Pozo, "Wind Generation Emulator Using A DC Machine", IEEE Second Ecuador Technical Chapters Meeting (ETCM), 2017.
[2] Prabath J. Binduhewa and Mike Barnes., "Photovoltaic Emulator," IEEE 8th International Conference on Industrial and Information Systems , 2013.
[3] Ananthan, T., "A FPGA-based state space controller." International Journal of Automation and Control 13.1, 2019, 84-100.
[4] Prakash, N. K., Surjith, B., "FPGA Based Remote Monitoring System in Smart Grids", Indian Journal of Science and Technology, 10(5), 2017.
[5] Nariman Eskandari, Hatef Madani, and Mohsen Mahmoudi Aznaveh Armin Ahmadzadeh, and Saeid Gorgin, "A Fast Emulator for ARM-based Embedded Systems," Twelfth ACM/IEEE Conference on Formal Methods and Models for Codesign (MEMOCODE), 2014.
[6] Dongki Kim and Hyunsun Park Lee, Taemin and, Sungjoo Yoo, and Sunggu Lee, "Fpga Based Prototyping Systems for Emerging Memory Technologies," 25nd IEEE International Symposium on Rapid System Prototyping, 2014.
[7] Scott Buscemi, Will Kritikos, and Ron Sass., "A Range and Scaling Study of an FPGA Based Digital Wireless Channel Emulator", IEEE 21st Annual International Symposium on Field-Programmable Custom Computing Machines, 2013.
[8] Kruger, I., Wolhuter, R., "An aircraft based emulation platform for LEO satellite antenna beam steering", Fifth International Conference on Systems and Networks Communications (pp. 221-228).
[9] Charaabi, L., "FPGA-Based Fixed Point Implementation of a Real-Time Induction Motor Emulator," Advances in Power Electronics, 2012.
[10] Alecsa, Bogdan, and Alexandru Onea., "Design, Validation and FPGA Implementation of a Brushless DC Motor Speed Controller",17th IEEE International Conference on Electronics, Circuits and Systems, 2010.
[11] Dagbagi, M., Idkhajine, L., Monmasson, E., Charaabi, L., Slama-Belkhodja, I, " FPGA Implementation of a Synchronous Motor Real-time Emulator Based on Delta Operator", IEEE International Symposium on Industrial Electronics, 2011, (pp. 1581-1586).
[12] Rosa, V. S., Gervini, V. I., Gomes, S. C., Bampi, S., "A Hardware DC Motor Emulator",First IEEE Latin American Symposium on Circuits and Systems (LASCAS) , 2010, (pp. 45-48).

Proceedings of the Fourth International Conference on Communication and Electronics Systems (ICCES 2019)
IEEE Conference Record # 45898; IEEE Xplore ISBN: 978-1-7281-1261-9

A software Based Network simulation model For Internet Service Providers

Miss. Shrutika Mahale
School of Electronics and Communication
Science and Engineering,
Dr. Vishwanath Karad MIT World Peace
University Pune, India
shrutika.m.14@gmail.com

Prof. Vinod Jadhav
School of Electronics and Communication
Science and Engineering,
Dr. Vishwanath Karad MIT World Peace
University Pune, India
vinod.jadhav@mitcoe.edu.in

***Abstract* - Rise of Over the Top (OTT) administrations like Netflix, YouTube, VIU and Cloud Services like S3 (AWS), Cloud Storage (GCP), and Dropbox are possessing a large portion of the piece of transfer speed. These sorts of administrations have direct association with increment or diminishing income of web access suppliers. Since the majority of Internet Service Providers give boundless plans, the need of proficient utilization of data transfer capacity has turned out to be essential for both income and QoS/QoE. By considering these genuine situations this paper builds up a framework which will powerfully put client's solicitation on uncommon paths i.e., Fast Lane and Slow Lane. In this model fast track will be designated to spilling administrations and moderate path will be distributed to document move administrations. For an Internet Service Provider this is chance to build incomes by offering control to the Content Provider (CP) who solicitations for exceptional paths for their buyers. The above control will be spread by means of API to the Content Providers. This model is actualized in two sections. The First part portrays framework plan which will have connection between's Content Providers and Internet Service Provider and extreme reason for existing is to give better QoS to customers. Second part is to build up a re-enactment model of this framework utilizing python.**

Keywords: Over The Top (OTT), Software defined networking, Quality of Service, fast-lanes, and slow-lanes.

I. INTRODUCTION

Over the top (OTT) is a term used to allude to content suppliers that disperse streaming media as an independent item straight forwardly to watchers over the Internet, bypassing media communications, multichannel TV, and communicate TV stages that generally go about as a controller or wholesaler of such substance. The term is most synonymous with membership put together video with respect to request benefits that offer access to film and TV content (counting existing arrangement gained from different makers, just as unique substance created explicitly for the administration), including Amazon Video, Viu, Hulu, Netflix, Now TV, Sling TV, MercTV, and Sky Go just as a Suburban broadband consumption is spreading quickly, extending the hole between ISP costs and incomes. Proliferation of web empowered gadget is blocking access systems, deteriorating end-client presentation and influencing content suppliers adaptation.

The earlier frameworks has the following limitations:
Adaptation: An ISP has a restricted reason to send administration quality components except if there are a business return. Customers have to spend much more considered amount for improvement in a good Quality of service. CPs presumably have a higher capacity to pay be that as it may, a current "paid peering" modifications. Quality just for explicit shoppers or certain substance, and these decisions can differ powerfully (for example contingent upon time-of-day or misfortune/defer execution of the system).

Bandwidth Dominance: Considering todays network scenario the ISP has dominance over Bandwidth, who especially has an own framework and also contraption setups, conceivable by techniques for instruments (for example checking, protection, asset reservation, and linking) using Difference-Serve mechanism. Customers are completely unknown about what ISP is doing from their side and has the impact on their quality of service and customers felt helpless. At another side, CP's expecting a good quality of service from ISP's. Even some ISP have special bond with content providers that they will provide a good quality of service but because of they have rights of better quality of service And sometime because of any technical issues if ISP fails to provide the better quality of service it will have direct impact on content providers revenue generation.

SDN has numerous points of view:

1. A focal "mind" for the system makes it simpler for the ISP to recognize (for example by means of APIs) administration

quality controls required by an outside gathering,

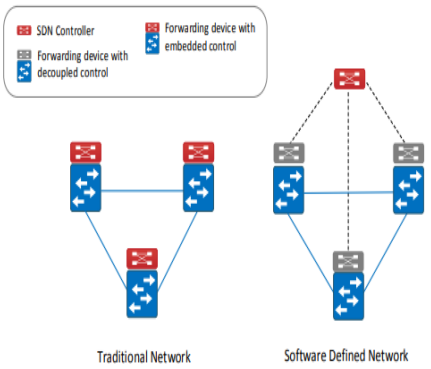

Fig.1 SDN vs. provision network architecture

for example the content providers we believe an API would be the outstanding way of data interchange instead of between associating existing conventions (for example RSVP) to outstanding gatherings.

2. The brought together cerebrum in SDN is progressively responsive for ideal Judgment making. Since the SDN controller has a worldwide perspective on assets, it can make educated decisions dependent on current accessibility and solicitations.
3. SDN gives the asset parceling which brought together programming over any sending component over any entrance innovation that underpins an institutionalized SDN interface, for example, Open Flow.

II. RELATED WORK

We first created four datasets of YouTube videos and two datasets of Netflix videos. The You Flash, YouHtml, YouHD, and YouMob dataset contain YouTube videos while the NetPC and the NetMob dataset contain Netflix videos [1] Based on data from a tier-1 European network, approximately 10 WhatsApp messages are sent and received per subscriber each day. Of these messages, 2.8% of all messages sent have a media file such as a photo or video attached. [2] Suppose that two adaptive HTTP streaming players share the same bottleneck. This can happen, for instance, when people in the same house watch two different movies - in that case the shared bottleneck is probably the residential broadband access link. [3]

Other work has proposed monitoring the user-perceived video quality, rather than just the network-level effects. A system to measure the user-perceived quality, taking into account the distortions in quality caused by losing particular packets, is discussed in this system [11] These Systems will provide quality of Service to end users. And data consumption by streaming services, what's app, HTTP requests. Whereas our contribution will work on the data consumption rate, quality of service and at network level.

III. USE-CASES AND OPPORTUNITIES

The course of action of employments that can benefit by unequivocal framework support for improved organization quality is tremendous and arranged: ongoing and spilling recordings can benefit by data transfer capacity affirmation, gaming applications, voice applications from low hardship, and so on.

IV. SYSTEM ARCHITECTURE

DNS Server: The system starts with the DNS Server. In this model the DNS server provide the functionality to other devices after receiving request from provider means Internet Service Provider the IP address is stored in the database of DNS Server.

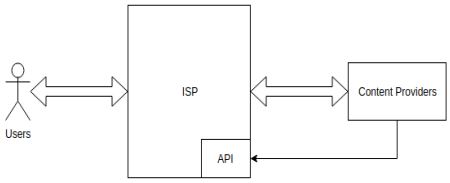

Fig 2. System Architecture

Internet Service Provider: The Internet service Provider will provide service to the customer by requesting them. Then Customers will give request according to their requirements. Then by serving the request the IP address will get stored in the database of DNS Server. System Architecture is shown diagrammatically in the Flow diagram.

SDN Controller: The SDN controller manages the flow control to improve network performance. The SDN controller uses TCP protocol to transfer data from source to destination. The Controller knows the source and destination address of the user. In the system model Socket-Server is used which is simpler form of writing a complex network server. And allows the request handler will allow that makes the file type of object that will lead to ease of communication. And provide a standard interface.

Controller-API: In this system REST API is used. API is Application Program Interface which use HTTP request to perform POST, PUSH, GET, DELETE operations. Significance of REST is

Representational State Transfer which is useful for web service development. API helps to visualize bandwidth of the data flow. According to given bandwidth the API will be called as API for Fast/Slow Lanes.

Client: Client will request for content, Request hit the API and data flow will start and simultaneously it will change the bandwidth.

While requesting special lanes. There is also possibility that the special lanes request cannot be fulfilled by the controller in that case minimum guaranteed bandwidth is allocated.

V. SIMULATION AND TRACE ANALYSIS

1. In this model we have a network switch and controller at ISP. Whenever request comes on network switch it enquires with the controller what to do about this flow. The controller installs default flow and the transfer of data packets begins.

2. The controller exposes REST API which the control provider can invoke. When any content provider invokes this REST API to request for special lanes, controller updates the switch flow table with modified flow. For Example host1 is requesting for www.netflix.com, the switch makes the connection and host get to see the content. Meanwhile Netflix also invokes the API provided by controller and request for fast lane.

3. Whenever the same host requests for video content their request is served using high bandwidth. The content provider is aware about the content length so they can also include time-out property

4. In this Model Long-Short-Term-Memory (LSTM) algorithm is used for storing bandwidth of users and Store it for some duration, So that it will be easy for controller to decide whom to assign how much bandwidth and ultimately it will be helpful in increasing quality of service to users and helps in increasing revenue of internet service providers and revenue generation of content providers

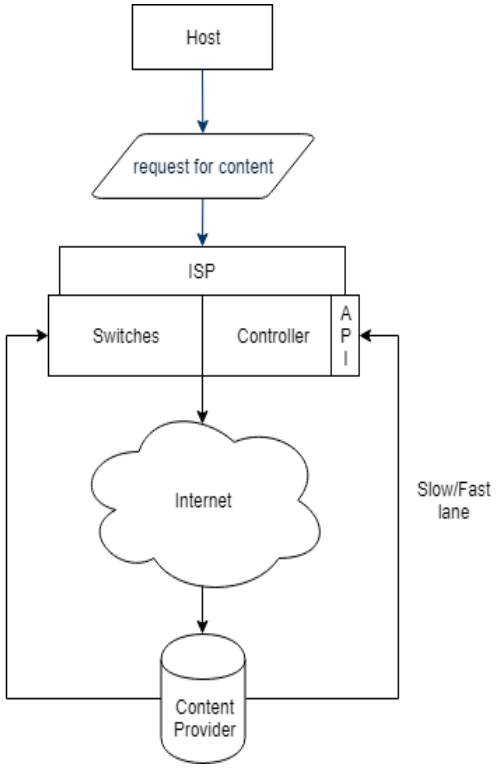

Fig. 3. Flow of typical residential broadband access network.

VI. EXPERIMENT RESULT

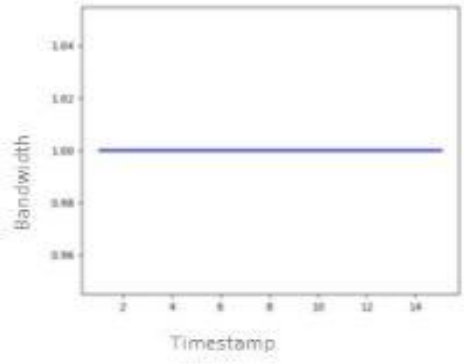

Fig. 4. Simulation result when bandwidth = 1

In the above figure we can see normal dataflow without reservations i.e., special lanes. Data is transferred using minimum guaranteed bandwidth. Here Y-axis represents bandwidth and X-axis represents timestamp.

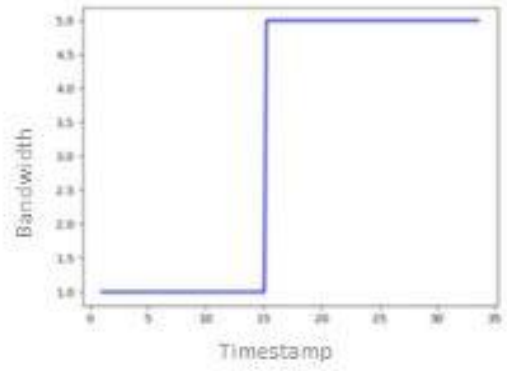

Fig.5. Simulation result when increase in bandwidth

Above figure demonstrates fast lane. When a host requests for content, the content provider immediately invokes controller API and reserves fast lane for the current dataflow. In above fig on X-axis the dataflow began with 1 Mbps and went up to 5 Mbps as per the provider's negotiation with

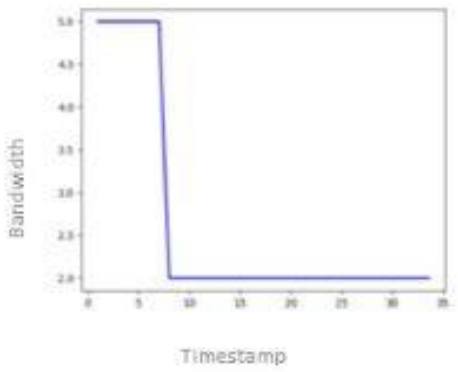

Fig.6. Simulation result when increase in bandwidth

Above figure demonstrates slow lane. Overall Procedure is same as compare with fast lane. Only difference is, when a host requests for content, the content provider immediately invokes controller API and reserves slow lane for the current dataflow. In above fig on X-axis the dataflow began with 5 Mbps and went down to 2 Mbps as per the provider's negotiation with the controller

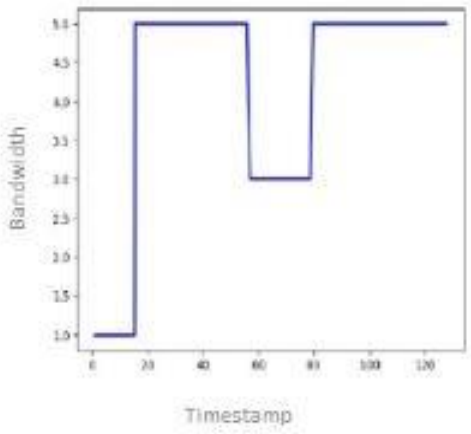

Fig.7.Simulation Result of Fast lane and slow lane.

In the above figure a request having fast lane reservation. When the switch gets new request and no bandwidth is available, controller temporarily modifies existing fast lanes with reduced bandwidth to accommodate the new requests and reverts the bandwidth to fast lane again

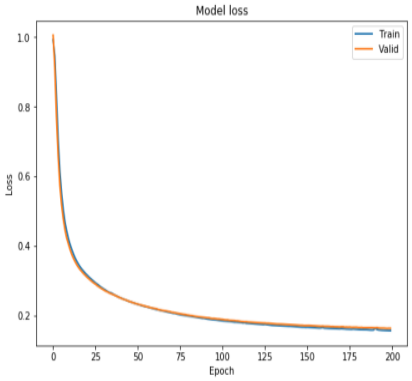

Fig.8. Model loss comparison between train data and test data.

Above diagram represents the model loss for train and test data. The LSTM has one data set where bandwidth of multiple users are stored. The model will run epoch for each user's bandwidth and it will calculate the loss according to it.

Fig.9 Reconstruction error with respect to threshold.

Above diagram represents the threshold which is nearly approx. 0.8. In the above graph the red line represents the threshold line and blue dots represent the true positive values and orange dots represents false positive values.
Below Table shows the Bandwidth (Mbps) according to user requirement.

Sr. No.	Title	Bandwidth
1.	Data Transfer Flow.	1 Mbps
2.	Fast Lane	1Mbps, 5 Mbps
3.	Slow Lane	5 Mbps, 2 Mbps
4.	Fast lane and Slow Lane Reservation.	(1 Mbps , 5 Mbps) And (5Mbps, 3Mbps)

Table 1. Simulation results of respective bandwidth variation.

VII. CONCLUSION

In This Paper we have effectively created Simulation model which shows Fast Lane and Slow Lane by hitting an API named as POSTMAN and Long Short Term Memory Algorithm which has Users Bandwidth Data set and distribute the Lanes to client as indicated by clients past transfer speed. The PUT request will be given to API where we have to enter the host at a server side then controller hits an API later as per customer demand information stream will begin. Depends upon This re-enactment model to comprehend the information which possesses more transfer speed for instance video records, And Creation of such paths will build the income of network access supplier. From the Body of an API source and destination IP address and Bandwidth. Will be set to accordingly. As soon as this request is sent the flow table will be updated. Simulation model runs in seven different terminal window where at First part registration of IP is done. After that controller will hit an API and according to client request the data transmission begins. This approach will be the initial move towards the consumer loyalty in light of the fact that by apportioning such paths will assist client with achieving such nature of administrations.

REFRENCES

[1] Network characteristics of video streaming traffic, A. Rao *et al.*, in *Proc. ACM CoNEXT*, Dec. 2011, Art. no. 25.

[2] Global Internet Phenomena Report. [Online]. Available: http://goo.gl/l7bU2 Sandvine. (2012).

[3] An experimental evaluation of rate-adaptation algorithms in adaptive streaming over HTTP, S. Akhshabi, A. Begen, and C. Dovrolis, in *Proc. ACM MMSys*, Feb. 2011, pp. 157–168.

[4] Trickle Rate limiting YouTube video streaming, M. Ghobadi, Y. Cheng, A. Jain, and M. Mathis in *Proc. USENIX ATC*, Jun. 2012, pp. 191–196.

[5] Enabling Fast and Slow Lanes for Content Providers Using Software Defined Networking Hassan Habibi Gharakheili, Vijay Sivaraman, *Member, IEEE*, Tim Moors, Arun Vishwanath, John Matthews, and Craig Russell June. 2017, pp. 31–42.

[6] Virtualizing the access network via open APIs, V. Sivaraman, T. Moors, H. H. Gharakheili, D. Ong, J. Matthews, and C. Russell, in *Proc. ACM Con NEXT*, Dec. 2013, pp. 31–42.

[7] Understanding the impact of video quality on user Engagement, F. Dobrian *et al.*, in *Proc. ACM SIGCOMM*, Aug. 2011, pp. 362–373.

[8] Address New Internet Ecosystem. [Online]. Available: http://goo.gl/VutcF ITRs Proposal to European Telecommunications Network Operators' Association. (2012).

[9] Rethinking flat rate pricing for broadband services, M. Nicosia *et al.*, Cisco Internet Business Solutions Group, White Paper, Jul. 2012. [Online]. Available: http://www.bradreese.com/blog/ciscobroadband - bottled-water.pdf

[10] Broadband Internet performance: A view from the gateway, in *Proc. ACM SIGCOMM*, Aug. 2011, pp. 134–145. S. Sundaresan *et al*

[11] Video stream quality impacts viewer behaviour: Inferring causality using quasi experimental designs, in *Proc. ACM IMC*, Nov. 2012, pp. 211–224.S. Krishnan and R. K. Sitaraman,

[12] IEEE Standard for Local and Metropolitan Area Networks—Bridges andBridged Networks, IEEE Standard 802.1Q-2014, 2014.

[13] H. Sugiyama, "Programmable network systems: Through the Junos SDK sand Junos space SDK," in *Proc. World Telecommun. Congr.*, 2012,
pp. 1–6.

Proceedings of the Fourth International Conference on Communication and Electronics Systems (ICCES 2019)
IEEE Conference Record # 45898; IEEE Xplore ISBN: 978-1-7281-1261-9

A Grid-Connected Single Step High Gain Buck-Boost Inverter Using Fuzzy Maximum Power Point Tracking

Saurabh Shripad Dixit
Department of Electrical Engg.
Walchand College Of Engineering
Sangli, India
saurabh.dixit@walchandsangli.ac.in

Dr. D. R. Patil
Department of Electrical Engg.
Walchand College Of Engineering
Sangli, India
dadgonda.patil@walchandsangli.ac.in

***Abstract*—In this paper, topology of Grid connected single step (GCSS) high gain buck-boost inverter with fuzzy maximum power point tracking (MPPT) controller is discussed. It can step up/down the output from PV & performs DC to AC conversion simultaneously in a single step with the help of fuzzy MPPT controller. This scheme has features such as high gain, less switching loss & with the help of fuzzy MPPT it tracks maximum power from PV very efficiently. Thus this scheme is conformable for PV applications with low voltage & varrying with time conditions. Design of proposed GCSS elements with derived equations & design of fuzzy MPPT is given in this paper. Presented topology is designed using MATLAB/SIMULINK. Detailed simulation of presented GCSS with fuzzy MPPT and it's results are given.**

***Index Terms*—Buck-Boost inverter, fuzzy MPPT, grid connected inverter, GCSS.**

I. Introduction

Non-renewable fuels are situated at selected places which are far away from load station. Hence, we need power transmission system to absolve power from generation stations to loads. The demand of power is increasing nowadays, which causes blackouts and also increases load above limit. Generation of electricity using solar PV can be an alternative to above problems [1]. As we know that solar voltage is variable due to atmospheric conditions like temperature, insolation, etc. We need a system which converts power from solar and used to deliver it to grid/load.

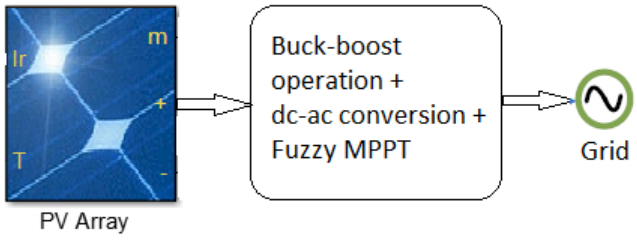

Fig. 1. GCSS PV system configuration

To deliver power to grid, conversion system has to buck/boost PV output voltage & convert it to ac. This type of conversion takes two steps hence called as two step conversion system.

Some of those two step grid connected system are represented in [2]. It has disadvantages like less certainty , more deprivations, broad size and costly [3]. In this case, we use power conversion system which does above two stage operation in one step along with fuzzy MPPT is required. Fuzzy MPPT is used to track maximum power from PV very efficiently. As single step conversion system is more certain, works at high efficiencies & less costly [4]. An ideal GCSS system with fuzzy MPPT controller is given in Figure. 1.

Related work

A GCSS boost dc-ac scheme is presented in [5], as given in Figure. 2.(i). This scheme has two boost converters are 180 degrees out of phase w.r.t each other & load is connected discriminatory across both converters. In this system, Operation of all switches are at high frequency in each half cycle of o/p voltage, which leads to more switching loss & EMI problems.

A half bridge buck-boost inverter conformation presented by kasa et al. [6]. shows that only two switches operating in half cycle. which has outcome of low conduction loss, less switching loss & low EMI problems. Only one PV source works for half time of operation is main disadvantage of this topology.

Hiren et al. presented double grounded GCSS in [7] as shown in Figure. 2.(ii). This system gives less gain. A GCSS which can step up, step down or step up/down to give ac output voltage is presented in [8] as given in Figure. 2.(iii). This scheme has some features like conciseness, low cost but this system can operate for less voltage gain conditions only. A system based on buck-boost operation with four active switches is given in [9], as shown in Figure.2.(iv). It has disadvantage of limited gain & more number of passive switches.

Some GCSS with large gain topologies are proposed in [10], [11] are given in Figure. 2. (v) and Figure. 2. (vi) respectively. Coupled inductor is used to get high gain. But there are baneful effects due to leakage inductance related with coupled inductor. Due to Leakage inductance there is

energy loss & voltage stress at switches. Topology presented in [12] is having high gain, minimum components & there is no need of capacitors to block leakage energy. Thus, this system is taken for grid connected applications with introduction of fuzzy MPPT controller to track maximum power efficiently.

The assistance of this paper are:

1) Presenting single step inverter system with large gain for connecting grid with PV system using fuzzy MPPT without any effect of leakage inductance.
2) Control of presented sytem to extract maximum power using fuzzy MPPT & deliver it to load/grid.

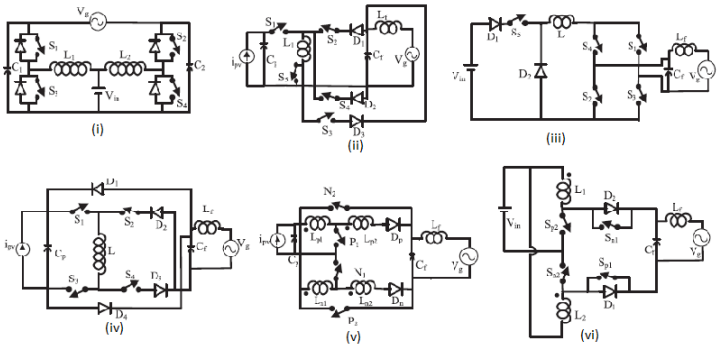

Fig. 2. Existing GCSS Systems

Presented GCSS with fuzzy MPPT controller block diagram is shown in Fig. 3.

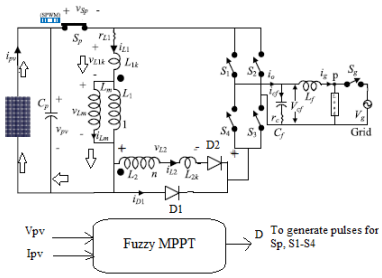

Fig. 3. Proposed GCSS with Fuzzy MPPT

Structure of paper is as follows. Section II gives description of GCSS operation. Section III gives components design. Tracking of MPP using fuzzy and GCSS control is given in section IV. Simulation &results in section V followed by conclusion in section VI.

II. Operation Of Single Step High Gain Inverter

Proposed GCSS consist of five active switches ($S_1 - S_4$, S_p) & two passive switches (D_1&D_2). Coupled inductors (L_1&L_2) is used to get high gain diode (D_1) is taken to avoid baneful effects caused because of leakage inductance of the coupled inductor. Filtering circuits at both input and output sides. The presented GCSS with fuzzy MPPT controller has following features.

1) It provides high gain with the use of coupled inductor.
2) Only one switch operates at high frequency & remaining operates at low frequency, hence it results in low switching loss.
3) Concise in size.
4) It requires simple sinusoidal PWM.
5) Maximum power from PV is tracked very efficiently with the help of fuzzy MPPT.

Let us assume duty cycle 'd' & T_s as switching period of S_p. In positive half cycle, switches (S_2&S_4) will be turned on & during negative half cycle switches (S_1&S_3) will be turned on. Converter topology works same & symmetrical in both half cycles of output voltage. It's working over a switching cycle is expounded as given.

A. Mode I ($t_0 - t_1$)

In this mode, L_m gets charged through S_p when switch S_p is on. Both diodes are reverse biased. Current in L_m increases in a linear way. Output capacitor (C_f) discharges through load as given in Figure. 4.

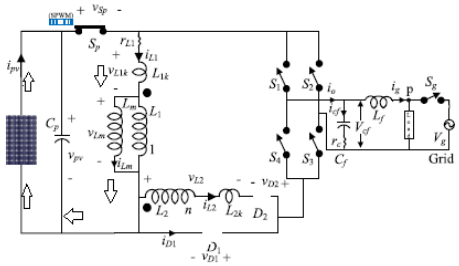

Fig. 4. Mode 1 working

B. Mode II ($t_1 - t_2$)

At S_p switched off diodes D_1&D_2 goes forward biased. Leakage energy related with inductance L_{1k} will be given to load through D_1. Current through L_1 decreases and at the same time current through L_2 increases. Remaining current from L_1 & L_2 will be taken by D_1. At the end of this mode, currents in both inductors become same, hence D_1 becomes reverse biased as given in Figure. 5.

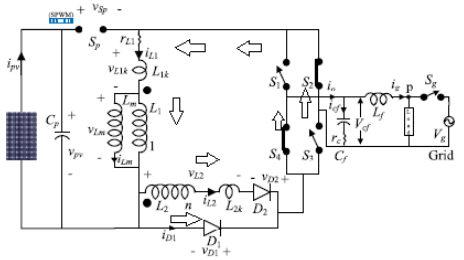

Fig. 5. Mode 2 working

C. Mode III ($t_2 - t_3$)

In this interval, D_2 is still forward biased, both inductors L_1&L_2 are series connected & feed power to load. Current in L_1&L_2 starts decaying. This interval ends when S_p is turned on again as shown in Figure. 6. As per number of turns of each inductor, output voltage is shown across both inductors.

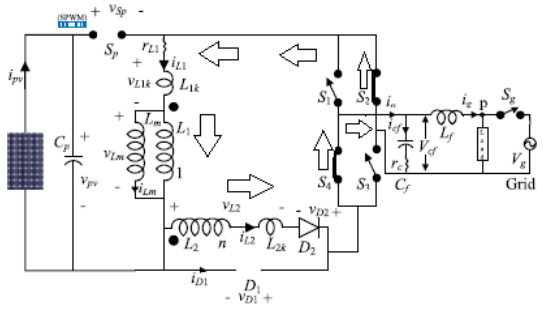

Fig. 6. Mode 3 working

D. Mode IV ($t_3 - t_0$)

When S_p is switched on, Diode D_2 still conducts due to very small current present in inductor L_2k & D_1 is still reverse biased. Negative voltage across L_2 resets current through it. Diode D_2 becomes reverse biased when current through L_2 becomes zero as shown in Figure. 7. & this mode ends. This Proposed scheme starts operating again from mode 1.

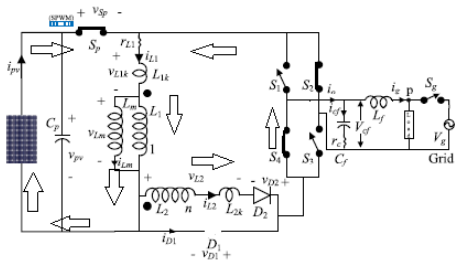

Fig. 7. Mode 4 working

mathematical waveforms of current through diodes D_1&D_2, L_1&L_2 inductors, voltage & current across C_f & gate pulse generation for a switching cycle are as given in Figure. 8.

In same topology, as switch S_p is turned on and operates with SPWM double the grid voltage frequency, a sinusoidal voltage across output capacitor C_f is developed. Mathematical waveforms of presented scheme for a full cycle of load voltage is as given in Figure. 9.

III. GCSS Input and Output Filter Design

A. Design of C_p

Maximum value of ripple in output voltage of PV is decided by input capacitor C_P. Maximum allowed value of PV voltage ripple & grid frequency is δVpv and f_g respectively. C_p value is given by [3].

$$C_p = \frac{2P}{4(2\pi f_g)\, V_{\text{pv}}\, \delta V_{\text{pv}}} \tag{1}$$

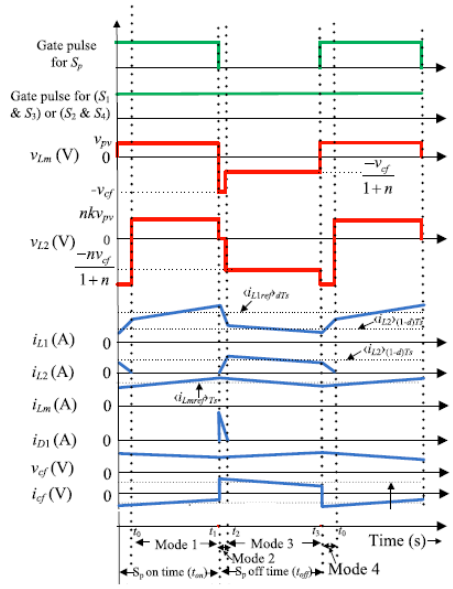

Fig. 8. GCSS working over a switching cycle

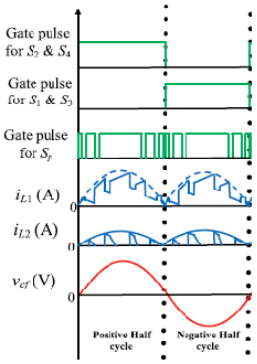

Fig. 9. GCSS working over a full cycle of output voltage

Where P = Tracked max. Power.

B. Design of L_f

Output inductor emaciate high frequency current which is given to the grid. Cut off frequency f_c should be taken as one tenth of switching frequency f_s for the design of output inductor [3]. Thus L_f is given by,

$$L_f = \frac{1}{(2\pi f_c)^2\, C_f}. \tag{2}$$

C. Design of C_f

The value of filter capacitance at output side is specified by the maximum energy through coupled inductor. By taking power factor of unity operation, transmitting power from i/p to o/p is high at grid voltage peak. By equating energy change in coupled inductor & filter capacitor C_f over switching cycle, result will be as given below.

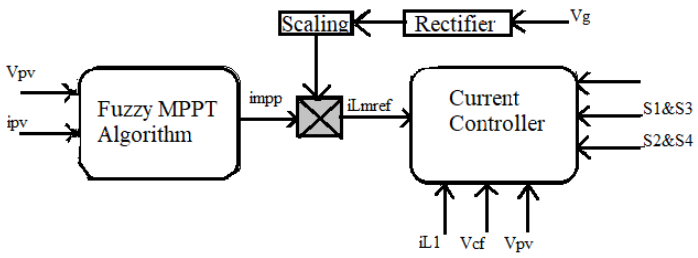

Fig. 10. Ref. current generation for mutual inductance current (i_{LM}).

$$\frac{1}{2}\times L_1\frac{(1+n^2+2n)}{1+n}\left[\left(I_{L1ref(\max)}+\frac{\Delta I_{L1}}{2}\right)^2 -\left(I_{L1ref(\max)}-\frac{\Delta I_{L1}}{2}\right)^2\right] = \frac{1}{2}\times C_f\left[\left(V_{g(\max)}+\frac{\Delta v}{2}\right)^2-\left(V_{g(\max)}-\frac{\Delta v}{2}\right)^2\right]. \quad (3$$

By rearranging the above equation we get capacitance value as,

$$C_f=\frac{L_1(1+n)I_{L1ref(\max)}\Delta I_{L1}}{V_{g(\max)}\Delta v}. \quad (4)$$

Where $I_{L1ref(\max)}$ is maximum primary inductor current w.r.t $P_{o/p}$ (rated) & Δv is maximum admissible ripple of output voltage (V_{cf}).

D. Design of Coupled inductor L_1 & L_2

Equation for coupled inductor L_1 & L_2 is designed using [4],

$$L_1=\frac{T_s\,V_{\rm pv}\,v_{g(\max)}}{\Delta I_{L1}[V_{\rm pv}(1+n)+v_{g(\max)}]}. \quad (5)$$

L_2 is calculated from

$$L_2=n^2L_1. \quad (6)$$

IV. Fuzzy MPPT and Control Techique

Fuzzy MPPT is a teachnique used to extract maximum power from PV under varrying irradiation and temperature conditions using converter system. Coordination between current control & MPPT is prescribed to feed maximum power to grid. MPPT is designed utilising Fuzzy logic controller[15]. Output of fuzzy MPPT is (i_mpp) multiplied with grid voltage V_g. Multiplied output further taken as reference current to track current in L_m by using current controller as given in Figure. 11. For practical purpose, initially proposed scheme must have to work in voltage control loop before linking it to grid as shown in Figure. 12. Hence, we conclude that both control loops are used for synchronization of given system with grid. Design and derivation of these control loops along with fuzzy MPPT algorithm will be presented in following subsections.

A. Current Control Loop Design

From Figure. 8, when switch S_p turned on, voltage is V_{pv} and during turned off time voltage is - v_{cf} /(1 + n). Average voltage over a switching cycle across L_m is given by,

$$\langle v_{\rm Lm}\rangle_{\rm Ts}=\langle v_{\rm pv}\rangle_{\rm Ts}d(t)-\frac{(1-d(t))\langle v_{\rm cf}(t)\rangle_{\rm Ts}}{1+n}. \quad (7)$$

By solving above equation duty cycle is,

$$d(t)=\frac{\langle v_{\rm Lm}(t)\rangle_{\rm Ts}(1+n)+\langle v_{\rm cf}(t)\rangle_{\rm Ts}}{\langle v_{\rm pv}(t)\rangle_{\rm Ts}(1+n)+\langle v_{\rm cf}(t)\rangle_{\rm Ts}}=B. \quad (8)$$

Where B is used to represent block in Fig.10. [14] Current through L_m is given by [4]

$$\langle i_{\rm Lm}(t)\rangle_{\rm Ts}=\langle i_{L1}(t)\rangle_{\rm Ts}\frac{(1+n)}{1+nd(t)}. \quad (9)$$

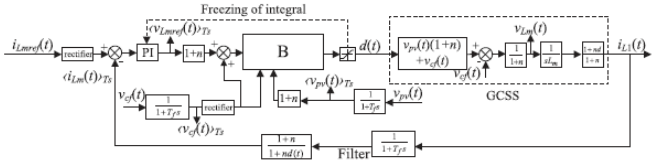

Fig. 11. Schematic of Current Control Loop

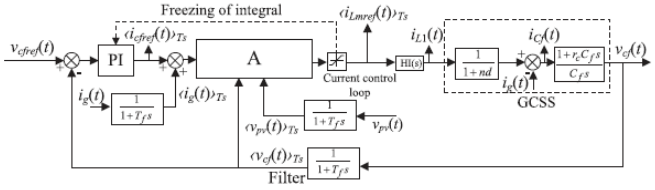

Fig. 12. Schematic of Voltage Control Loop

B. Voltage Control Loop Design

From Figure. 8, By considering contemptible leakage inductance & current ripple in inductors, Current i_{cf} for a switching cycle is given by,

$$\langle i_{\rm cf}(t)\rangle_{\rm Ts}=(1-d(t))\langle i_{L2}(t)\rangle_{(1-d)Ts}-\langle i_g(t)\rangle_{\rm Ts}. \quad (10)$$

From above equation i_{L2}(t)(1 - d)Ts can be written as,

$$\langle i_{L2}(t)\rangle_{(1-d)Ts}=\frac{\langle i_{\rm cf}(t)\rangle_{\rm Ts}+\langle i_g(t)\rangle_{\rm Ts}}{1-d(t)}. \quad (11)$$

From GCSS operation, i_{L1ref} and i_{Lmref} are equal during switch (S_p) on time [4]. Thus,

$$\langle i_{\rm Lmref}(t)\rangle_{dTs}=A= (\langle i_{\rm cf}(t)\rangle_{\rm Ts}+\langle i_g(t)\rangle_{\rm Ts})\left[\frac{\langle v_{\rm cf}(t)\rangle_{\rm Ts}+\langle v_{\rm pv}(t)\rangle_{\rm Ts}(1+n)}{\langle v_{\rm pv}(t)\rangle_{\rm Ts}}\right]. \quad (12)$$

Where, 'A' is exhibited as a block shown in Fig.12, Dual loop control presented in [14] is used to control voltage through C_f and current through L_m. Block diagram of voltage control is shown in Figure. 12. In that r_c is the equivalent series resistance related with C_f.

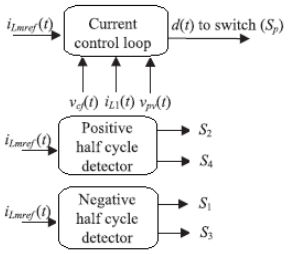

Fig. 13. Gate Pulse generation for Active switches

PI controller's gain are taken so as voltage and current loop are having bandwidth of 4000 Hz & phase margin of 60°. Gate pulse generation of all active switches is given in Figure. 13.

V. Simulation & Results

Presented scheme is designed using MATLAB/SIMULINK with parameters shown in Table I below. The topology is tested for different insolation level ($S = 1000W/m^2, S = 400W/m^2 and S = 600W/m^2$) at t = 0 sec, t = 1 sec, t = 2 sec respectively.

TABLE I
Simulation Parameters

Parameter	Value
Voltage ($V_{mpp}at1000W/m^2$)	38.6v
Current ($I_{mpp}at1000W/m^2$)	5.32A
Grid voltage (V_g)	110v(rms), 50Hz
Switching frequency (f_s)	50kHZ
Inductors (L_1 & L_2)	0.95mH & 1.90mH
Coupling Coeficient (k)	0.94
Output capacitor (C_f)	0.175 e-6
Filter inductor (Lf)	5.8 e-3
Filter capacitor (CP)	4.18 e-3

The Open loop simulation is carried out in the MATLAB/Simulink and the results are taken from that, Figure. 14. shows the open loop GCSS simulink model.

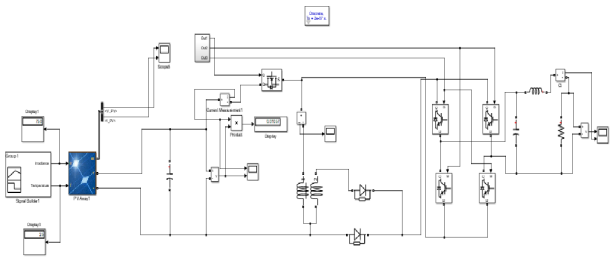

Fig. 14. Open Loop GCSS Simulink model

The voltage & current control loops are designed using derivations of voltage and current control loop in section IV, Figure. 15. shows the MATLAB/Simulink design for control loops,

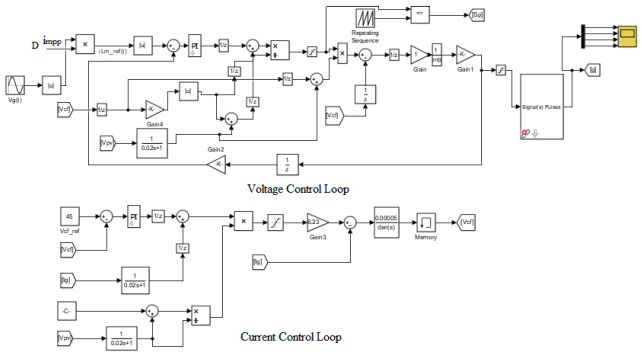

Fig. 15. Control Loop Diagrams for Proposed GCSS

Fuzzy logic controller block diagram is constructed with the help of MATLAB/Simulink and fuzzy logic design block diagram using mamdani fuzzy inference model is as given in Figure. 16 and Figure. 17 respectively [15]. There are two inputs fot fuzzy controller for buck and boost converters. The first input is error in the output voltage e and second is change in succesive errors ce. Output of fuzzy controller is change in duty cycle.Rule base or decision making are obtained from the analysis of system behaviour some of the control actions in the rule table are also obtained from trial and error.

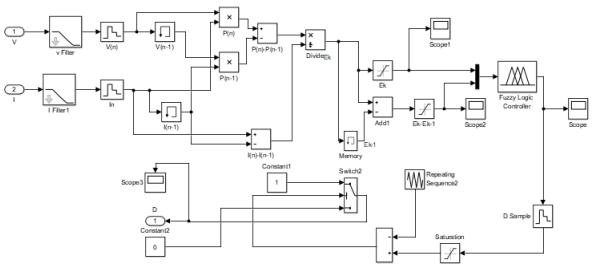

Fig. 16. Fuzzy Logic Controller simulation diagram

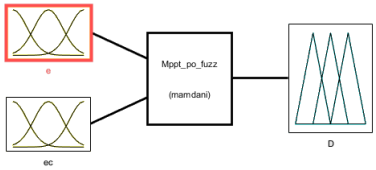

Fig. 17. Fuzzy Logic Design

Closed loop control technique of GCSS is discussed as follow. In this closed loop system, grid voltage is multiplied with duty cycle obtained from PV system Fuzzy MPPT controller. Multiplied output is given to current controller and then output of current controller is given to voltage controller. Gate pulse generation using current controller, positive and

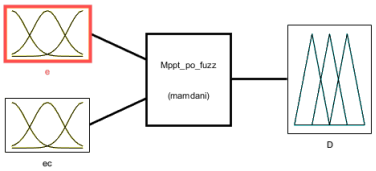

Fig. 18. Fuzzy Logic Design

negative half cycle detector is shown in Figure.13. The block diagram of the closed loop control as shown in Figure. 18.

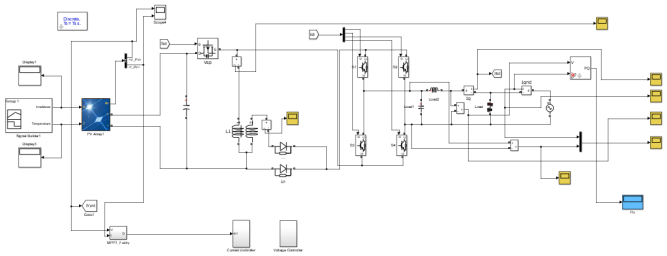

Fig. 19. Simulink model of Closed Loop GCSS with Fuzzy MPPT

Input side & Output side results are given in Figure. 19. & Figure. 20. respectively. In that, different Irradiation conditions are given with voltage across PV, current across PV. From the figure it is given that given topology is tracking MPP correctly.

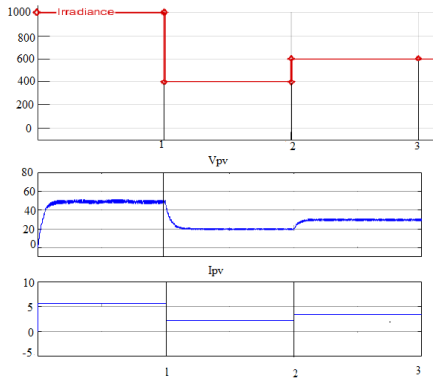

Fig. 20. Simulation results at PV side

Voltage across grid V_g, current across grid i_g and THD of current i_g is shown in Figure.19.

VI. Conclusion

Aim of this paper is to use fuzzy logic controller for grid connected single stage inveter system. This is done with help of the mamdani fuzzy model. Design of control loops along with fuzzy controller are given in brief. From the above results, the fuzzy logic controller can give the better results with less THD and it can deliver power from PV to load/grid efficiently with fuzzy MPPT. The open and closed loop system has been implemented in the MATLAB simulink. The implemented

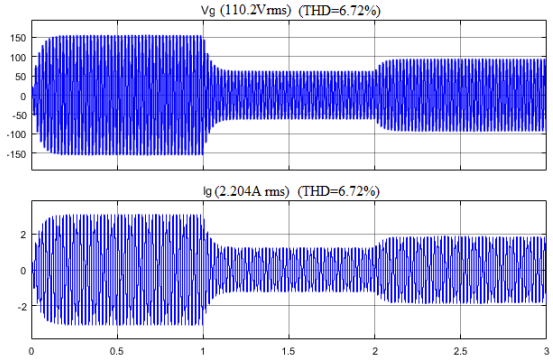

Fig. 21. Simulation results at Grid Side

circuit can work in the condition ($S = 1000W/m^2, S = 400W/m^2 and S = 600W/m^2$). Hence, this system can be used for PV applications with MPP tracking.

References

[1] J. Parikh and K. Parikh, "Growing pains: Meeting Indias energy needs in the face of limited fossil fuels", *IEEE Power Energy Mag.,* vol. 10, no. 3, pp. 5966, May 2012.

[2] D. Meneses, F. Blaabjerg, O. Garcia, and J. Cobos, "Review and comparison of step-up transformerless topologies for photovoltaic AC-module application," in *IEEE Trans. Power Electron.,* vol. 28, no. 6, pp. 2649-2663, Jun. 2013.

[3] S. Jain and V. Agarwal, "A single-stage grid connected inverter topology for solar PV systems with maximum power point tracking", *IEEE Trans. Power Electron.,*vol. 22, no. 5, pp. 1928-1940, Sep. 2007.

[4] T. Sreekanth, N. L. Narasamma, Mahesh K. Mishra "A Single-Stage Grid-Connected High Gain BuckBoost Inverter With Maximum Power Point Tracking," *IEEE Trans. on Energy Conversion.,* vol. 32, no. 1, march 2017

[5] S. Jain and V. Agarwal, "New current control based MPPT technique for single stage grid connected PV systems" *Energy Convers. Manage.,* vol. 48, no. 2, pp. 625-644, 2007.

[6] R. Caceres and I. Barbi, "A boost DC-AC converter: analysis, design, and experimentation," in *IEEE Trans. Power Electron.,* vol. 14, no. 1, pp. 134-141, Jan 1999.

[7] N. Kasa, T. Lida, and H. Iwamoto, "Maximum power point tracking with capacitor identifier for photovoltaic power system," in *Proc. IEE Electr. Power Appl. Conf.,* 2000, pp. 497-502.

[8] H. Patel and V. Agarwal, "A single-stage single-phase transformer-less doubly grounded grid-connected PV interface," *IEEE Trans. Energy Convers.,* vol. 24, no. 1, pp. 93-101, Mar. 2009.

[9] B. Prasad, S. Jain, and V. Agarwal, "Universal single-stage grid-connected inverter," *IEEE Trans. Energy Convers.,*vol. 23, no. 1, pp. 128-137, Mar. 2008.

[10] K. Shafeeque and P. Subadhra,"A novel single-phase single-stage inverter for solar applications," in Proc. *IEEE Adv. Comput. Commun.Conf.,*2013, pp. 343-346.

[11] J. Yris, H. Calleja, L. Hernandez, and J. Olmos, "Design and analysis of a grid-connected inverter without isolation for an AC module," in Proc. *IEEE Appl. Power Electron. Expo. Conf.,* 2012, pp. 2095-2099.

[12] T. Sreekanth, N. L. Narasamma, and M. K. Mishra, "A single stage high gain buck-boost inverter with coupled inductor," in Proc. *IEEE Power Electron., Drives Energy Syst. Conf.,* 2014, pp. 15.

[13] T. Sreekanth, N. L. Narasamma, M. K. Mishra, and S. Augustine, "A single stage coupled inductor based high gain DC-AC buck-boost inverter for photovoltaic (PV) applications," in *Proc. 2015 IEEE 42nd Photovoltaic Spec. Conf.,* Jun. 2015, pp. 1-5.

[14] E. G. P. Sanchis, A. Ursaea and L. Marroyo, "Boost dc-ac inverter: A new control strategy," *IEEE Trans. Power Electron.,* vol. 20, no. 2, pp. 343-353, Sep. 2005.

[15] Dr.T.Govindaraj, Rasila R, "Development of Fuzzy Logic Controller for DC DC Buck Converters," *Int J Engg Techsci.,* vol 2(2) 2011,192-198.

Proceedings of the Fourth International Conference on Communication and Electronics Systems (ICCES 2019)
IEEE Conference Record # 45898; IEEE Xplore ISBN: 978-1-7281-1261-9

PROFICIENT RESOURCE ALLOCATION TO SECONDARY USER USING NATURE INSPIRED TECHNIQUE IN COGNITIVE RADIO NETWORK

Ridhima

PG Student, ECE Department

I.K.G PTU Main Campus

Kapurthala,Punjab,India

ridzeeverma19@gmail.com

Avtar Singh Buttar

Professor, ECE Department

I.K.G PTU Main Campus

Kapurthala,Punjab,India

danshavtar@rediffmail.com

***Abstract*— In this paper, a new resource allocation paradigm is designed whereby a new SU is allowed to gain access to the spectrum of licensed PU. Appropriate bandwidth and power are the resources allocated to the SU during the inactivity of PU if the interference is below the maximum allowable IT limit of the channel. An efficient algorithm is developed for reconfiguration of SU's parameters using nature inspired computational intelligence technique named ADALINE i.e. Adaptive Linear Neuron. A demand supply based feedback mechanism is proposed to meet the data rate requirements of new unlicensed user. A scenario is considered wherein a single SU transmitter is able to initially coexist with the PU and then, is able to adapt its transmission parameters (bandwidth and signal strength) dynamically as per spectral availability and the demand of its receiving unit. The feedback system developed reduces difference from allowable IT limit and difference from the achievable capacity during each iteration, rendering efficient channel utilization and achieves user's data rate satisfaction.**

Keywords*— *Static Frequency Allocation (SFA), Federal Communications Commission (FCC), Cognitive Radio (CR), Interference Temperature (IT), Neural Network (NN), Quality of Service (QoS), Primary User (PU), Secondary User (SU).

I. INTRODUCTION

Wireless Communication is an emerging trend for the worldwide connectivity that has revolutionized the human lifestyle. Electromagnetic radio spectra ranging from 3 kHz to 300 GHz is a natural hub for the wireless connectivity in various fields as military, health, transportation, education, marketing etc. Static frequency allocation (SFA) of electromagnetic spectrum by the regulatory body FCC has exacerbated the problem of spectrum inefficiency [1]. Exponential growth of wireless users has resulted in spectral congestion. An opportunistic SU can alleviate the problem of spectrum scarcity and underutilization. For this purpose, Cognitive Radio (CR) is envisaged as a vital technology, a concept propounded by Dr. Joseph Mitola III at the Royal Institute of Technology in Stockholm which incorporates software based dynamic transceiver operability [2]. The key feature of CR technology is to firstly identify spectrum holes [3] i.e. which portion of spectrum is vacant (spectrum sensing) [4] and determine the suitable frequency band as per the requirement of the non-legitimate user (spectrum decision) [5], then to update the operating parameters to enable concurrent usage of the spectrum by multiple users (spectrum sharing) [6] and handoff its operation to other available vacant band upon the reclamation of PU activity in its licensed band (spectrum mobility) [7].

Considering the spectrum availability from PUs and the requirement of SUs; appropriate power, frequency, time slot and/or bandwidth are the resources of the primary network that can be allocated to SUs to sustain an interference free operation with maximal usage of underutilized PU spectrum [18]. Different resource allocation methods such as water filling concept [8], distributed power allocation algorithm [9], maximizing power for far SUs while minimal power allocation for nearby SUs are applicable, to allow SUs to transmit simultaneously with the PUs with minimal interference to the existing licensed users. The author in [20], used Deep Neural Network (DNN), for allocating transmit power to the SUs. Previous works have rendered bandwidth sharing via sum rate maximization in an underlay [6] or overlay [11] cognitive radio network but they have not considered the characteristics of receiving units. We have developed a new algorithm by which SU in underlay [21] can be dynamically allocated the resources using a receiver based feedback mechanism.

The paper describes the system model to be used and proposes a feedback based model for resource allocation to the SU. Then an ADALINE NN methodology is detailed with mathematical formulations used followed by the flowchart along with simulation results and comparative analysis.

II. SYSTEM MODEL

A Cognitive Radio Network (CRN) model involving a Primary and a Secondary network is considered. The primary network has P number of transmitters (PU-Tx.) with index i, $i \in I$ and $I = \{1,2\ldots P\}$ serving as routers for R

number of receiving units (PU-Rx.) index *i, i ∈ I and I*= {1,2…R}. The secondary network has S number of transmitters (SU-Tx.) with index *i, i ∈ I and I*= {1,2…S} accessing the spectrum resources of primary network to serve M number of receiving units (SU-RX.) with index *i, i ∈ I and I*= {1,2…M}. We will design how one SU as shown in Fig. 1 will be allocated the services of the legitimate user on an opportunistic basis to run new user applications in an unlicensed manner.

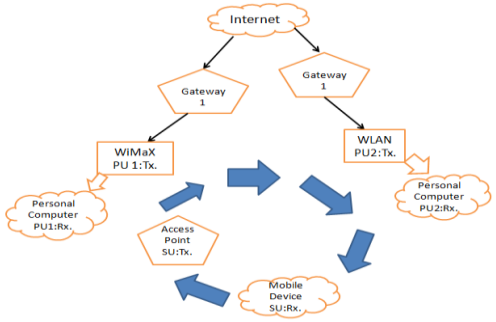

Fig. 1 System Model

III. PROPOSED FEEDBACK BASED MODEL

A system is designed to allocate bandwidth and appropriate strength to the SU in a manner that no hindrance is caused to existing PU services. The SU receiver unit in Fig. 2 will determine the availability of the spectrum of PU and will intimate the transmitter of the SU. The receiving unit (SU user) will specify its demands i.e. certain data rate and allowable interference level. Accordingly, the SU transmitter will be allocated certain set of bandwidth and power to achieve the user satisfaction. At each step, the SU transmission bandwidth and power will be updated based on the difference between achievable capacity and obtained data rate and the difference between allowable Interference Temperature [10] limit and achievable Interference Temperature caused by SU transmissions. Hence, the difference is reduced between the demand and supply.

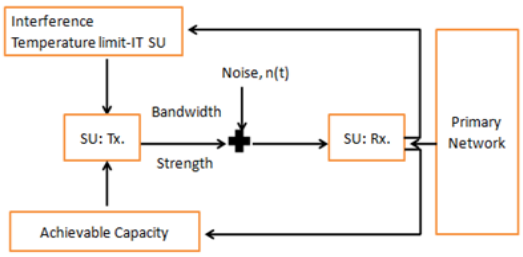

Fig. 2 Proposed Feedback Based Model

IV. MAPPING OF FEEDBACK BASED MODEL WITH NATURE INSPIRED NN TECHNIQUE

ADALINE is a single linear unit neuron which receives input from several units (x_i) and has one output unit (y). In the Fig. 3, ADALINE network is shown in which Bias (b) is a flexi-adjusting weight that enables best fit values for the network as required. The weights between the input and output units (w_i) can be adjusted to produce a desirable output with a learning parameter (α) that determines the step of updating.

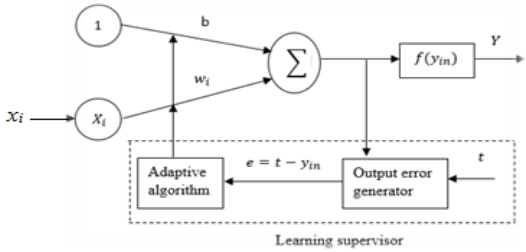

Fig. 3 ADALINE Neural Network [12]

The ADALINE network uses a Delta Rule or Widrow Hoff rule to update the weights between connections to reduce the difference (e) i.e. the error between net input to the output unit (y_{in}) and a desired target value (t) [12].

Mathematical formulas used:

Achievable Capacity for a user [13]

$$C^{i}_{av} = B*\log_2 (1+\frac{S}{N}) \text{ bits/s} \quad (1)$$

Data Rate achieved by each user [13]

$$R_i = \frac{Bi}{Ni} \log_2 (1+\frac{Pi(|h(i)|^2)}{No*\frac{Bi}{Ni}}) \text{ bits/s} \quad (2)$$

Interference Temperature Calculation [10]

$$T_c (f_c,bc) = \frac{pi(fc,bc)}{k*bc} \text{ dB Kelvin} \quad (3)$$

p_i is the signal power

f_c is the carrier frequency in GHz

b_c is the channel bandwidth in MHz

k= Boltzmann Constant =$1.38*10^{-23}$J/K

Weight updating formula [12]

$$w_i (new) = w_i (old) + \alpha(t\text{-}y_{in}) x_i \quad (4)$$

Objective

$$\min (IT_{av} - IT_i) \qquad \min (C^{i}_{av} - R_i) \quad (5)$$

We have used learning rate (α=0.5) for bandwidth and power reconfiguration by the Secondary User. At each step, difference between allowable IT_{av} limit for the channel and the IT_i due to individual user is found and also, and difference between capacity that could be achieved and the data rates achieved by current user transmission in the channel is calculated. Our strategy involves bandwidth adaptation by increasing number of subcarriers (N_i) per unit bandwidth using weight updating formula using different subcarrier spacing. Power is further increased step wise step using weight updating until the receiving unit gives the IT difference and capacity difference [19].

CASE: Single Secondary User accessing the Primary User spectral resource.

Primary device transmits in the licensed band but its transmission is not achieving the data rate demands of the user and the allowable IT limit of the system due to its fixed transmission parameters. Thus, the spectrum remains underutilized. So, it is possible to allocate certain bandwidth and signal strength to a new SU to coexist [14] with that PU such that SU transmission doesn't hampers the operation of existing PU. Then, we calculate the overall IT caused by both the PU and SU that is below the allowable IT limits. In case of PU inactivity, the IT falls and a sufficient gap from the allowable IT limit exists. Hence, an efficient resource allocation [16] mechanism is developed for adaptation and reconfiguration of the bandwidth and signal strength of the SU using NN to mitigate the gap between the receiver demands and the transmission done, so as to achieve the IT limit.

V. FLOWCHART

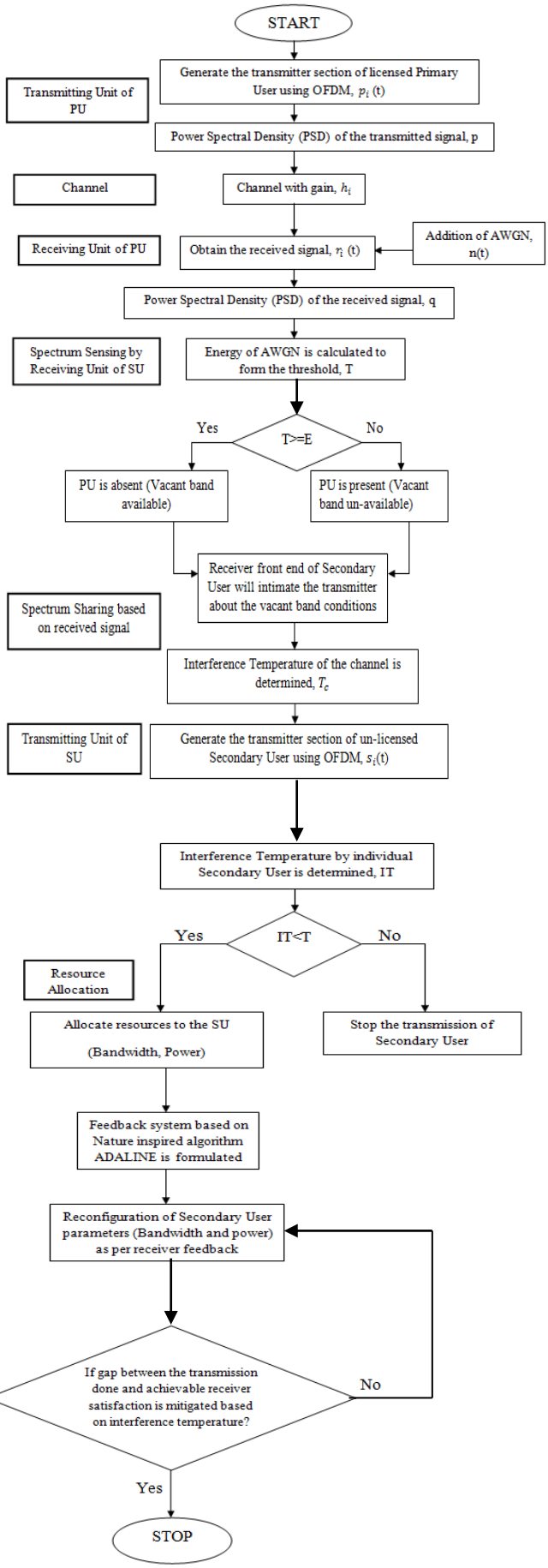

Fig. 4 Flowchart of Proposed Algorithm

The flowchart details the algorithm to be followed to enable resource allocation to the SU. Initially, an environment comprises of a PU transmitter, the signal of which is passed through an AWGN channel and the PSD of the received PU signal is obtained. To enable spectral access, the presence PU is firstly detected by SU receiver front end using Energy Detection based spectrum sensing method [4]. Comparison of PU signal energy (E) is made with that of the energy of noise (T). Absence of PU enables opportunistic transmission by SU. OFDM parameters are used to develop the signals of PU and SU. An allowable level of IT is fixed for the system. Transmission bandwidth and power is so allocated to the SU on an opportunistic manner that the interference caused by it does not cross the IT limit. At each step, the SU receiving unit provides feedback i.e. the difference from achievable capacity and gap from the IT limit. SU parameters are reconfigured using the NN until the data rate demands of the receiving unit within permissible limits of IT are achieved.

VI. SIMULATION AND RESULTS

The algorithm for the resource allocation is implemented in simulative form using MATLAB R2013b in which the code is written.

A. Primary User Simulation Parameters

An environment is created for simulation in which PU WLAN is allocated a frequency band from 1 GHz to 6.5 GHz. PU: WLAN transmits with 50dB power at centre frequency of 5.15 GHz. Table 1 details about the OFDM parameters [15] that are used to simulate the signal of PU.

TABLE I.
WLAN OFDM PARAMETERS

S. No.	OFDM PARAMETERS	SYMBOL	WLAN 802.11a
1.	FFT Size	N	64
2.	OFDM Bandwidth	BW	20 MHz
3.	Total No. of Subcarriers used	N_{ST}	52
4.	No. of Data Subcarriers	N_{SD}	48
5.	No. of Pilot Subcarriers	N_{SP}	4
6.	Subcarrier Frequency Spacing	F_{SP} = BW/N	312.5 kHz
7.	IFFT/FFT Period	T_{FFT} =1/F_{SP}	3.2 µs
8.	Guard Interval Time	T_{GI} = $T_{FFT/4}$	0.8µs
9.	Symbol Interval Time	T_{SYM} = T_{GI} + T_{FFT}	4µs
10.	Number of symbols allocated to Cyclic Prefix	N_{CP}= N*T_{GI} / T_{FFT}	16

B. Assumptions

We have assumed that the transmission of PU signal occurs over an AWGN channel with 10 dB noise SNR. Each OFDM user will have different subcarrier spacing. About 40000 samples are used with a sampling frequency of about 40 MHz.

C. Simulation Outputs

Fig. 5 illustrates the transmitted signal of the WLAN PU.

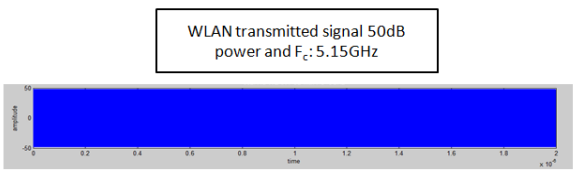

Fig. 5 Transmitted Signal of Primary User

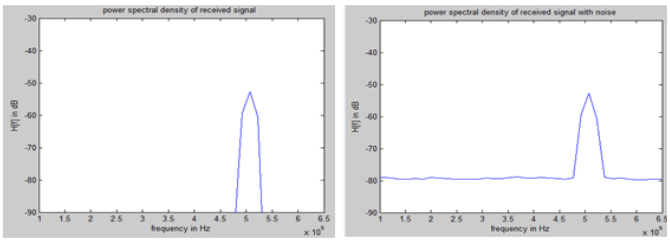

Fig. 6 Power Spectrum Density (PSD) of PU signal with and without noise

Fig. 6 illustrates the Power Spectral Density of the received PU WLAN signal at centre frequency of 5.15 GHz with and without noise.

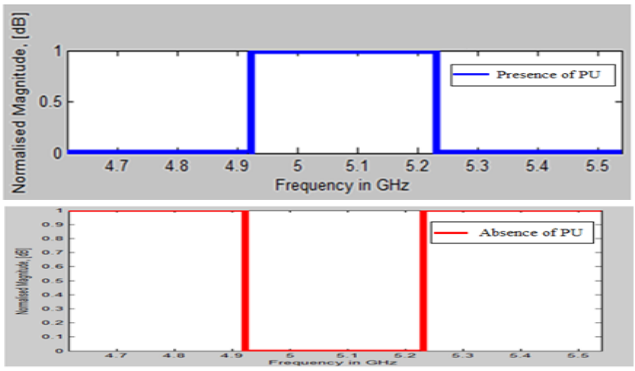

Fig. 7 Digital representation of PU signal and Vacant Band availability Using Energy Detection [4] based Spectrum Sensing

Fig. 7 demonstrates the detection of PU signal using Energy Detection based spectrum sensing [4]. In the digital representation binary 1 shows the presence of PU WLAN signal while binary 0 is indicative of absence of the PU.

TABLE II.

CALCULATION OF INTERFERENCE TEMPERATURE

Total allowable Interference Temperature limit	465 dB Kelvin
IT of PU in dB Kelvin	223.0641 dB Kelvin
IT difference	241.9359 dB Kelvin
Data Rate	54 Mbps
Achievable Bandwidth	20MHz
Achievable Strength	60dB
Achievable Capacity	87Mbps

Table II accounts that permissible IT limit of the system is 465 dB Kelvin which is not achieved by the PU transmission. Moreover, the data rate achieved by PU is also less due to less OFDM subcarrier density at a particular bandwidth. Also, allowed range of power for PU is 60 dB yet at certain time it is only transmitting at 50 dB power. Thus, the PU is inefficient in attaining complete spectrum utilization because of its fixed transmission parameters.

Due to spectrum underutilization by PU, gap of 241.9359 dB Kelvin from IT limit of 465 dB Kelvin persists. Thus, it becomes possible for the spectrum to be used for sustaining transmission by new opportunistic SU.

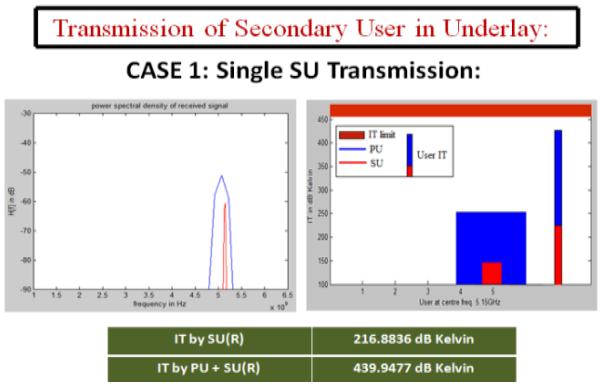

Fig. 8 Single SU Transmitting due to spectrum underutilization

Possible SU Wi-Fi transmission of 40 dB power and 5 MHz BW with OFDM subcarrier spacing (B/N_i) of 9.765625 KHz along with PU is indicated in Fig.8.

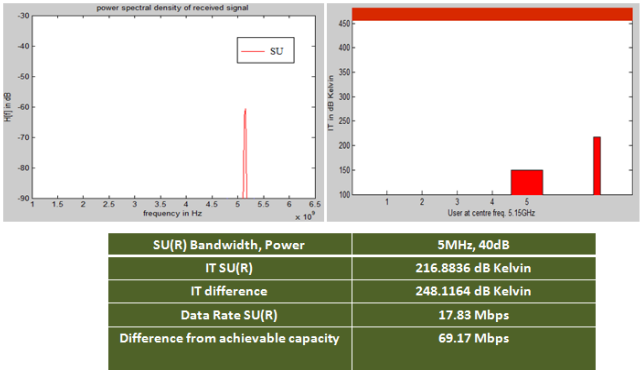

Fig. 9 Transmission of SU in case of PU inactivity

Fall in IT in caused during the case of inactivity of existing PU as indicated by Fig. 9. An oppurtunity is available for the SU to fully occupy the band and service in the underutilized spectrum.

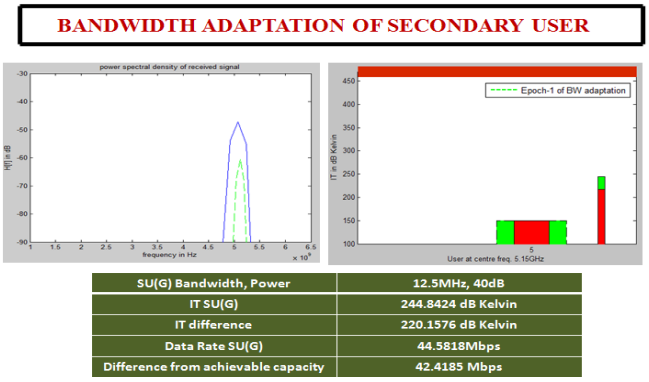

Fig. 10 Epoch-1 of the Bandwidth adaptation of SU

The SU enters into an adaptation mode once the PU gets inactive. At each epoch, the SU tries to readjust its bandwidth using the adaptive learing method until it covers the entire bandwidth of the PU that is available for it to access. Fig. 10 illustrates Epoch-1 of BW adaptation of SU in which it increases its subcarrier density at learning rate 0.5 attaining a BW of 12.5 MHz. The horizontal plot shows step increase in BW and column plot shows the rise in IT by SU BW adaptation.

Gap from achievable IT limit and achievable capacity leads to further epoches of BW adaptation based on difference given by the receiver.

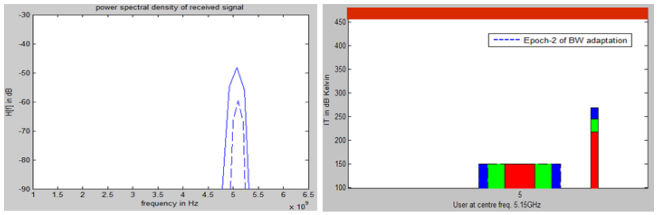

SU(B) Bandwidth, Power	16.25MHz, 40dB
IT SU(B)	268.1213 dB Kelvin
IT difference	196.8787dB Kelvin
Data Rate SU(B)	57.9553Mbps
Difference from achievable capacity	29.0447 Mbps

Fig. 11 Epoch-2 of the Bandwidth adaptation of SU

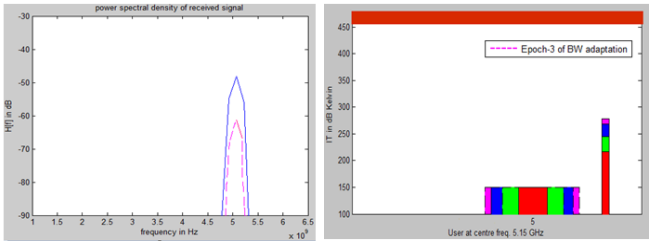

SU(M) Bandwidth, Power	18.1250 MHz, 40dB
IT SU(M)	279.0698 dB Kelvin
IT difference	185.9302 dB Kelvin
Data Rate SU(M)	64.6425 Mbps
Difference from achievable capacity	22.3575 Mbps

Fig. 12 Epoch-3 of the Bandwidth adaptation of SU

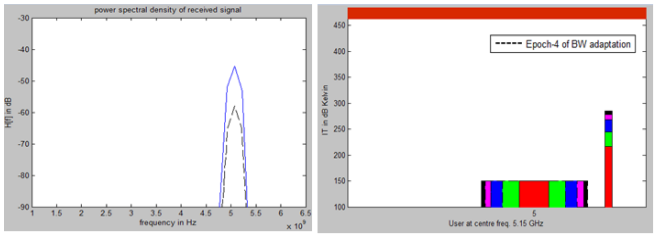

SU (BI) Bandwidth, Power	19.0625MHz, 40dB
IT SU (BI)	286.5078dB Kelvin
IT difference	178.4922 dB Kelvin
Data Rate SU (BI)	67.9861 Mbps
Difference from achievable capacity	19.0139 Mbps

Fig. 13 Epoch-4 of the Bandwidth adaptation of SU

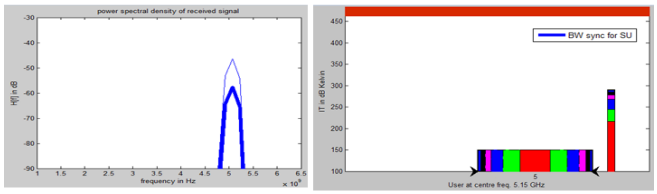

SU(B) Bandwidth, Power	20 MHz, 40dB
IT SU(B)	290.9248 dB Kelvin
IT difference	174.0752 dB Kelvin
Data Rate SU(B)	71.33 Mbps
Difference from achievable capacity	22.3575 Mbps

Fig. 14 Epoch-5 leads to the Bandwidth synchronization for SU

Fig. 14 shows at Epoch-5 the SU attains a bandwidth locking condition where by it occupies fully the available bandwidth of the legitimate PU and provides significant hike in data rate as compared to the PU due to improved subcarrier density. Fig. 15 shows increase in data rate with BW adaptation by the SU at each epoch.

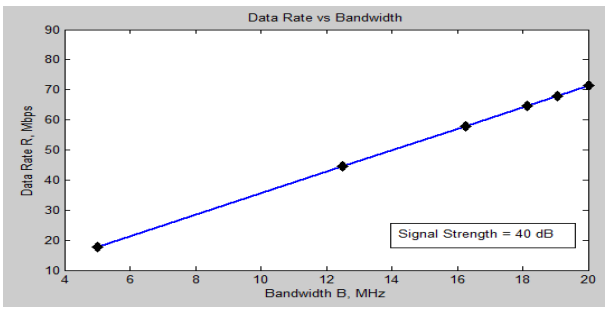

Fig. 15 Data Rate achieved after Bandwidth Adaptation

According to Shannon's Capacity curve [17], there is always a limit to increase the BW beyond which no significant increase in the data rate is achieved. Further, increase in the power is the alternative option to attain receiver satisfaction of data rates.

Presence of IT difference and gap from achievable capacity enables the SUs to increase their power. The receiving unit can change its position and thereby, demand of higher signal strength. For this, the SU transmitter follows power reconfiguration which is accomplished using the NN.

POWER RECONFIGURATION OF SECONDARY USER

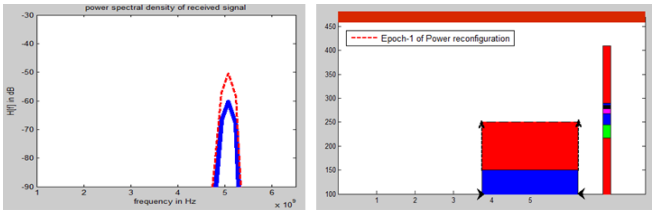

SU(R) Bandwidth, Power	20 MHz, 50dB
IT SU(R)	385.5076 dB Kelvin
IT difference	79.4924 dB Kelvin
Data Rate SU(R)	79.41 Mbps
Difference from achievable capacity	7.59Mbps

Fig. 16 Epoch-1 of the Power Reconfiguration of SU

Fig. 16 illustrates how the SU increases its transmission power from initial 40 dB to 50 dB. At each stage of power reconfiguration, the value of IT is increased significantly as shown by thin bar column.

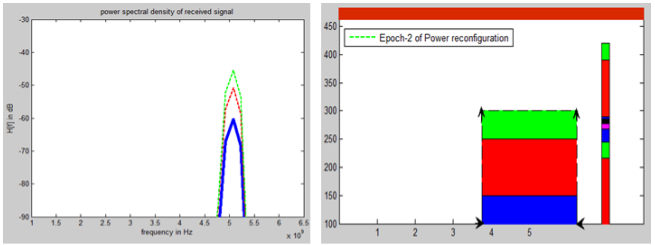

SU(G) Bandwidth, Power	20 MHz, 55.6dB
IT SU(G)	420.5078 dB Kelvin
IT difference	44.4922 dB Kelvin
Data Rate SU(G)	82.9575Mbps
Difference from achievable capacity	4.40425 Mbps

Fig. 17 Epoch-2 of the Power Reconfiguration of SU

This level of power reconfiguration is not possible in the case of PU as its operation is range constrictive due to fixed functionality and licensing by the government. Although the PU:WLAN in our case has been allowed a signal strength of about 60 dB but it is not fully transmitting using this signal strength at certain time. So, this range can be used for the dynamic SU transmission shown by different epoches until the levels of allowable IT are achieved.

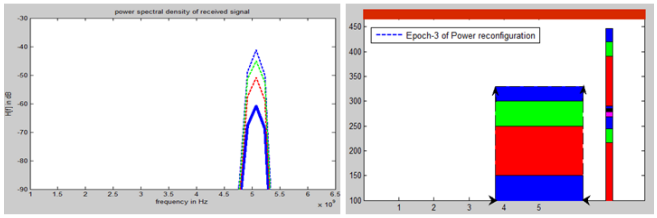

SU(B) Bandwidth, Power	20 MHz, 57.5dB
IT SU(B)	446.5078 dB Kelvin
IT difference	18.4922dB Kelvin
Data Rate SU(B)	84.6301 Mbps
Difference from achievable capacity	2.3699 Mbps

Fig. 18 Epoch-3 of the Power Reconfiguration of SU

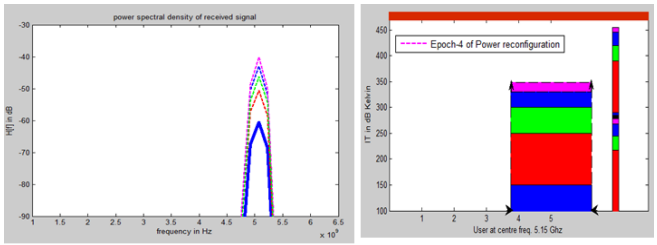

SU(M) Bandwidth, Power	20 MHz, 58.75dB
IT SU(M)	455.5078dB Kelvin
IT difference	9.4922 dB Kelvin
Data Rate SU(M)	85.4434 Mbps
Difference from achievable capacity	1.5566Mbps

Fig. 19 Epoch-4 of the Power Reconfiguration of SU

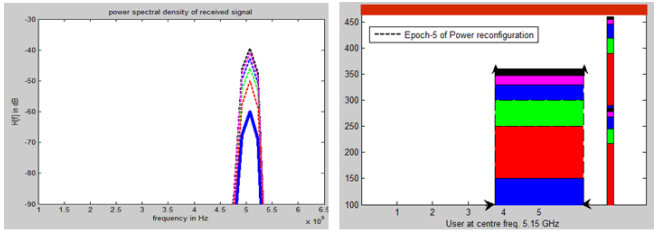

SU(B) Bandwidth, Power	20 MHz, 59.075dB
IT SU(B)	461.5078dB Kelvin
IT difference	3.4922 dB Kelvin
Data Rate SU(B)	85.6524 Mbps
Difference from achievable capacity	1.3476Mbps

Fig. 20 Epoch-5 of the Power Reconfiguration of SU

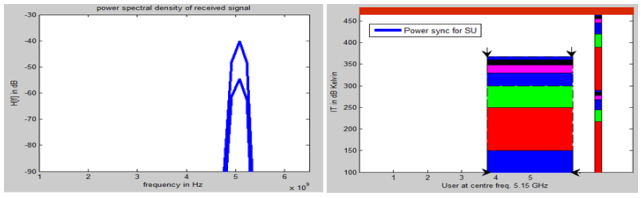

SU(B) Bandwidth, Power	20 MHz, 60dB
IT SU(B)	464.5078 Kelvin
IT difference	0.49 dB Kelvin
Data Rate SU(B)	86.2419 Mbps
Difference from achievable capacity	0.75Mbps

Fig. 21 Epoch-6 leads to Power synchronization for SU

Epoch-6 as illustrated by Fig. 21 accounts for the power locking condition for the SU at which IT limit is met and the receiver data rate requirement of 86.2419 Mbps is achieved. No further adaptaion is required as satisfactory levels of data rates for the receiver as shown by Fig. 22 are obtained by minimizing the objective function after significant epoches.

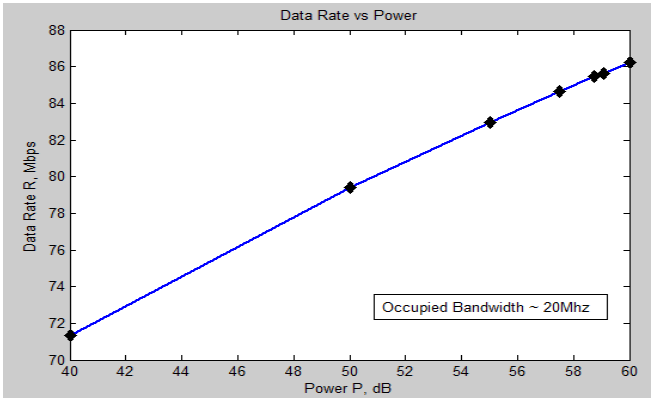

Fig. 22 Data Rate Achieved after Power Reconfiguration

VII. COMPARISON

Our proposed system provides channel utilization from 43% to 95% by proficient resource allocation to the Secondary User in contrast to existing systems without feedback as illustrated by Fig. 23.

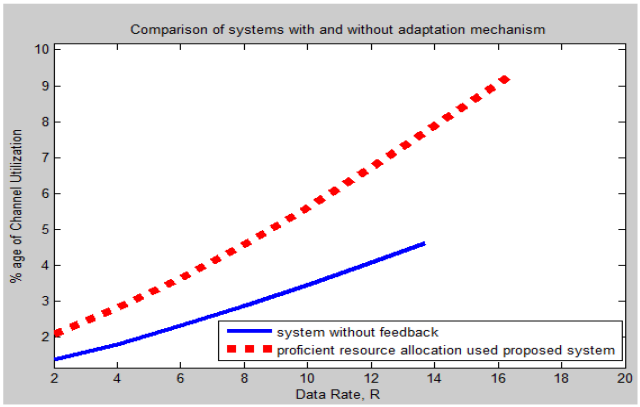

Fig. 23 Efficient channel utilization by our proposed feedback system

VIII. CONCLUSION AND FUTURE SCOPE

Cognitive Radio (CR) is envisioned as a promising technology to explore the underutilized portion of the electromagnetic spectrum and opportunistically gain an access to the vacant spectrum to service new wireless users. The paper focuses on how to provide appropriate resources to a new SU that can access the spectrum of the legitimate user. We propounded a feedback based resource allocation model to serve the SU. A reconfiguration algorithm was formulated to provide apt bandwidth and signal strength to the CR user during the inactivity of the PU. Significant iterations were carried out for SU bandwidth and power adaptation. The system IT constraints were met and the receiver data rate demands were satisfied upon the bandwidth and power locking conditions. Efficient channel utilization is attained based on the dynamic adaptation of

cognitive user using the nature inspired technique. The receiver feedback accounts for proficient resource allocation and improved spectrum utilization efficiency from 45% to 93% as compared to existing systems without feedback. Re-configuration of SU (bandwidth) achieves higher levels of data rates as per the user demands and re-configuration of SU (strength) achieves improved high range transmission for long distance communication.

In future work, hybrid computational intelligence techniques can be adopted using which multiple cognitive users would be able to adjust their transmission parameters to opportunistically access the spectrum of multiple PUs. Frequency Division Multiple Access (FDMA) and Time Division Multiple Access (TDMA) based transmission methods can be used for enhanced spectrum utilization based on feedback from the receiving units. Through FDMA multiple SUs can simultaneously be allocated the bandwidth and transmission power while TDMA may be expected to provide complete spectral access one at a time to the individual SUs. The feedback system of resource allocation can be used in FDMA and TDMA based Cognitive Radio Networks for improved spectral efficiency. Hardware and software implementation of cognitive modules can be developed for opportunistic services to new users. Improved methods of spectrum sensing apart from energy detection based sensing method which is vulnerable to noise uncertainties can be used.

REFERENCES

[1] Federal Communications Commission, “Spectrum Policy Task Force,” Rep. ET Docket no. 02-135, Nov. 2002..

[2] J. Mitola, "Cognitive Radios: Making Software Radios More Personal," IEEE Personal Communication, 6(4), 13-18, 1999.

[3] R. Tandra, S. M. Mishra and A. Sahai, "What is a Spectrum Hole and What Does it Take to Recognize One?," in Proceedings of the IEEE, vol. 97, no. 5, pp. 824-848, May 2009.

[4] M. Sansoy and A. S. Buttar, “Spectrum sensing algorithms in Cognitive Radio: A survey,” In 2015 IEEE International Conference on Electrical, Computer and Communication Technologies (ICECCT), pages 1–5, March 2015.

[5] Masonta, Moshe & Mzyece, Mjumo & Ntlatlapa, Ntsibane, “Spectrum Decision in Cognitive Radio Networks: A Survey,” 2013 IEEE Communications Surveys & Tutorials.

[6] R. Kaur, A. S. Buttar and J. Anand, “Spectrum Sharing Schemes in Cognitive Radio Network: A Survey,” 2018 Second International Conference on Electronics, Communication and Aerospace Technology (ICECA), Coimbatore, 2018, pp. 1279-1284.

[7] Krishan Kumar, Arun Prakash, Rajeev Tripathi, “Spectrum handoff in cognitive radio networks: A classification and comprehensive survey,” Journal of Network and Computer Applications, Vol. 61, 2016, pp. 161-188.

[8] Q. Qi, A. Minturn and Y. Yang, “An efficient water-filling algorithm for power allocation in OFDM-based cognitive radio systems,”*2012 International Conference on Systems and Informatics (ICSAI2012)*, Yantai, 2012, pp. 2069-2073.

[9] S. Bakşi and D. C. Popescu, “Distributed power allocation for rate maximization in cognitive radio networks with horizontal spectrum sharing,” *2015 IEEE Wireless Communications and Networking Conference (WCNC)*, New Orleans, LA, 2015, pp. 932-936.

[10] M. Sharma, A. Sahoo, K.D. Nayak, “Channel modeling based on interference temperature in underlay cognitive wireless networks,” *IEEE International Symposium on Wireless Communication Systems (ISWCS 2008)*, pp.224,228, 21-24 Oct. 2008.

[11] Z. Wei, D. Yang and L. Sang, “Dynamic system level frequency spectrum allocation scheme based on cognitive radio technology,” in *China Communications*, vol. 11, no. 7, pp. 84-91, July 2014.

[12] V. Pellakuri, D. Rajeswara Rao, J V R Murthy,“Modeling of supervised ADALINE neural network learning technique,” *2nd International Conference on Contemporary Computing and Informatics (IC3I)*, 2016.

[13] A. Vizzillo, R. Agusti, L. Favalli, P. Savazzi, “Cognitive Radio Resource Management exploiting Heterogeneous Primary Users,” *Proceedings of the 2011 IEEE GLOBECOM* 2011.

[14] M. El Tanab and W. Hamouda, "Resource Allocation for Underlay Cognitive Radio Networks: A Survey," *in* IEEE Communications Surveys & Tutorials, vol. 19, no. 2, pp. 1249-1276, Second quarter 2017.

[15] K. R. Chowdhury and I. F. Akyldiz, “OFDM-Based Common Control Channel Design for Cognitive Radio Ad Hoc Networks,” in *IEEE Transactions on Mobile Computing*, vol. 10, no. 2, pp. 228-238, Feb. 2011.

[16] G. I. Tsiropoulos, O. A. Dobre, M. H. Ahmed, and K. E. Baddour, “Radio resource allocation techniques for efficient spectrum access in cognitive radio networks,” *IEEE Communication Surveys& Tutorials*, vol. 18, no. 1, *FIRST QUARTER 2016.*

[17] L. Lovasz, "On the Shannon capacity of a graph," in *IEEE Transactions on Information Theory*, vol. 25, no. 1, pp. 1-7, January 1979.

[18] M. Devi, N. Sarma and S. K. Deka, “Allocation and Access Mechanisms for Spectrum Sharing in CRNs - A Brief Review,” 2016 *International Conference on Accessibility to Digital World (ICADW).*

[19] A. Nabil, A. V. Padaki, M. J. Abdel-Rahman, M. El Nainay, A. B. MacKenzie and J. H. Reed, “On Optimal Resource Allocation in Multi-RAT Wireless Networks With Receiver Characteristic Awareness,” in *IEEE Transactions on Cognitive Communications and Networking*, vol. 5, no. 1, pp. 103-118, March 2019.

[20] W. Lee, “Resource Allocation For Multi-Channel Underlay Cognitive radio Network based on Deep Neural network,” in *IEEE Communications Letters*, vol. 22, no. 9, pp. 1942-1945, Sept. 2018.

[21] Z. Zhou, Y. Jia, F. Chen, Kimfung Tsang, Guangyi Liu, and Zhu Han, “Unlicensed Spectrum Sharing: From Coexistence to Convergence,” *IEEE Wireless Communications*, vol. 24, pp.1536-1284, October 2017.

AUTHORS PROFILE

Ridhima

is a PG student in the Department of Electronics and Communication Engineering (Specialization in Wireless Communication) in I.K. Gujral Punjab Technical University, Main Campus, Jalandhar (Pb.) India. She pursued her Bachelor of Technology in Electronics and Communication Engineering from Atal Bihari Vajpayee Government Institute of Engineering and Technology, Shimla ***(University Medallist)***. She is an Associate Member of IEI. Her area of interest includes Cognitive Radio.

Avtar Singh Buttar

Avtar Singh Buttar is presently working as Associate Professor, I.K. Gujral Punjab Technical University, Main Campus, Jalandhar (Pb.) India. He obtained his B.E. in Electronics & Comm. Engg. from Punjab University in 1989. He qualified his Masters Degree in 1995 from National Institute of Tech., Kurukshetra. His research interests include Wireless Communication and Computational Intelligence

Proceedings of the Fourth International Conference on Communication and Electronics Systems (ICCES 2019)
IEEE Conference Record # 45898; IEEE Xplore ISBN: 978-1-7281-1261-9

Enhancement of UAV Performance Through Xbee Based Telemetry System Design

Chidura Bhanu Teja
Mechatronics Engineering
SRM Institute of Science and Technology
Chennai, Tamil Nadu
bhanutejachidura@gmail.com

Heena Sharma
Aerospace Engineering
SRM Institute of Science and Technology
Chennai, Tamil Nadu
bnmp12345@gmail.com

***Abstract*—The popularity of unmanned aerial vehicles is increased with advancing technology, usage of sensors and advanced control systems have made them more progressive and less expensive. Wireless Communication is the fastest growing and most vibrant technological areas of transmitting information from one point to other, without using any physical medium. Real-time data monitoring and analysis of the flight parameters can enhance the performance and the data is logged for further scrutiny of the aerial vehicle. In this pursuit, a telemetry system design for a Unmanned Aerial Vehicle is discussed in this paper with 915MHz XBee Pro S3B modules for a data communication from on-board to the ground station. The telemetry system is tested in actual flight, and the reliability and feasibility are evaluated.It has been found that the proposed design can enhance UAV performance .**

***Index Terms*—UAV, XBee, telemetry, communication, 915Mhz**

I. Introduction

An unmanned aerial vehicle is an aircraft without a human pilot on board and is controlled by autopilot or a remote station. Effective communication is the solution for more crucial problems in our current socioeconomic climate. By measuring the current parameters of UAV [2] [11] in flight, sending and logging the data elsewhere can make the performance of the vehicle more efficient. As the art of technology plays an increasingly important role in every aspect of communication, XBee-Pro S3B [1] is one of the effective module for transmission and receiving of data and information [12] from one place to another under the range (frequency) of 915 MHz. XBee's can operate in a transparent data mode or in a packet-based application-programming interface (API) mode. In the transparent mode, data-packets coming into the Data IN pin is legitimately transmitted over-the-air to the predetermined receiving radios with no alteration. Approaching parcels can either be straightforwardly routed to one target (point-to-point) or communicate to different targets[3] [9]. This mode is essentially utilized in occasions where a current convention can't endure changes to the data-packets format. AT directions are utilized to control the radio's settings. In API mode, the data packets are enveloped by a parcel structure that considers tending to, parameter setting and bundle feedback, including remote detecting and control of digital I/O and analogue I/O pins[5].

Section 1 delivers introduction of the telemetry system and comparison of 915 Mhz. with 2.4Ghz.
Section 2 describes the system overall architecture and design with the components and assembly.
Section 3 reports the experimental data and the data logging in the ground station display.
Section 4 presents the conclusion of the work.
Section 5 presents the future aspects of the telemetry system.

A. Merits of using 915 MHz over 2.4 GHz frequency

- 915 MHz recurrence fixed radio connection can travel practically 2.67 times more than a 2.4 GHz band.
- 915MHz suffered much less loss going through obstructions including trees, buildings, metal (poles).
- 915 MHz module has better Signal to Noise ratio than 2.4Ghz module.
- 915 MHz module does not require any line of sight.
- 915 MHz has 20-30% longer range between nodes (endpoints).
- Security cameras, Cell phones, Bluetooth all communicate in the 2.4 GHz domain and interfere with ZigBee mesh protocols.
- 915 MHz band is much more regulated than the 2.4 GHz band. While it has lower propagation loss than the 2.4 GHz band.

II. System Overall Architecture and Design

The proposed design have an open-source microcontroller that can programmed as per the required refresh rate and delay with respect to the requirements of the sensors. A ATmega328P [4] based arduino uno is used, that has a circuit board and user interface IDE to write to the circuit board. Various pins are determined for input and output data transfer. A XBee-PRO 900 HP RF module has been selected that is commanded by 802.15.4, multipoint and Digimesh protocols, these codes are characterized by low power consumption, extended range peer-to-peer mesh and maximum capacity of connection of nodes. The challenge on developing the telemetry system [6] is to keep the system compact and with nominal power consumption but with high flexibility to measure the parameters and transfer them to the ground station

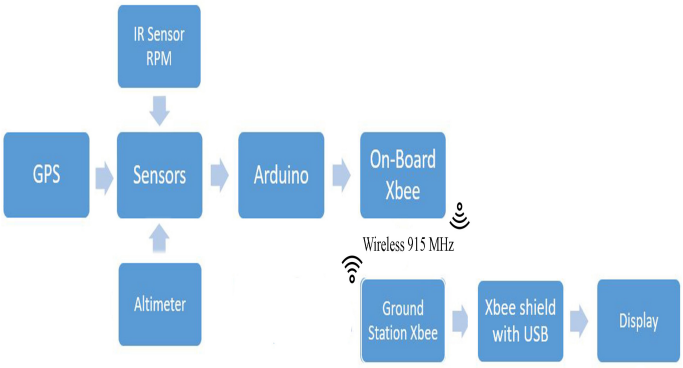

Fig. 1. Signal Flow of the Telemetry System

without losses. Figure 1 shows the signal flow in the telemetry system design.

For proper communication, both the XBees should have same parameters in settings and the transmitter should be set as coordinator and the receiver should be set as receiver. The coordinator will be placed with arduino setup on-board the UAV and receiver will be at ground station with XCTU software for receiving data and to display the data.

A. *On-board UAV : Sensors and signal conditioning*

The design architecture has the arrangement of sensors[7] required to measure the essential physical parameters on-board the UAV and a serial communication module for transmission of data through XBee PRO S3B module. The parameters that needs to be taken are current altitude, GPS location, Battery voltage, RPM of the motor and the temperature for the predictive maintenance that increases the efficiency of the actuator.

An XBee shield is used to connect the XBee S3B module to the arduino. The shields holds XBee pins to a solder pad. It provides digital 2 to 7 pins and the analogue inputs, which are given by the shield. With the jumpers in the USB position, the DOUT pin the XBee module is connected to the RX pin of the FTDI chip, and DIN on the XBee module is connected to the TX pin of the FTDI chip. This means that the XBee module can communicate directly with the computer.

The XBee-PRO S3B module allows wireless communication upto 6km range line of sight with 200 kbps RF data rate. It has a RPSMA connector dipole antenna with 2.1dB. The radio module equipment comprises of an Energy Micro EFM32G230F128 microcontroller, an Analog Devices ADF7023 radio handset, a RF power amplifier. A duck antenna is used to in the transmission[8].

Sensor converts the physical parameters into digital data. An MPL3115A2 employs a MEMS pressure sensor with an I^2C interface to provide accurate pressure data that is mapped to the altitude. Change in pressure vary the altitude with a 1.5 Pascal resolution and 0.3 meters altitude resolution. Its a low power module with the I^2C capability that uses SDA and SCL to transfer data. The sensor is connect to the microcontroller V+ and ground from its VDD and GND pins. As we employed a UNO, SCL to I2C clock analog pin 5 and SDA to I2C data analog pin 4. A MPL3115A2 library is installed to Arduino IDE to pull out the data from the sensor.

To locate the UAV current position in space a GPS sensor[10] is connected with the system, it provides real time latitude and longitude values with the heading direction . An Ublox NEO-M8N High Precision GPS Module with in-built compass module is used that includes an HMC5883L digital compass. This module have high level of sensitivity and features active circuitry for the ceramic patch antenna with the update rate of 5Hz and heading accuracy of 0.3 degrees.

To provide an efficient performance from the motor its working needs to be analyzed. A predictive maintenance setup is used in the UAV with implementation of sensors like temperature, RPM to log the performance of the motor in the flight.

A LM393 IR sensor is used in the setup to get the present RPM data of the power plant in the flight. The IR is connected to the power supply of the micro controller and to a digital pin that take in the data from the sensor. It works with detection of time difference between the same point in a propeller rotation. The RPM data is logged at the ground station for analysis.

The voltage of the battery is also determined with the voltage divider circuit from the UAV to the ground station. This help in increasing the performance and the endurance in the flight. It can also be used as the fail safe parameter once the battery voltage is below the limit it can give a warning to the ground station. Figure 2 shows the connection model of the on-board system and figure 3 shows the real model with sensors.

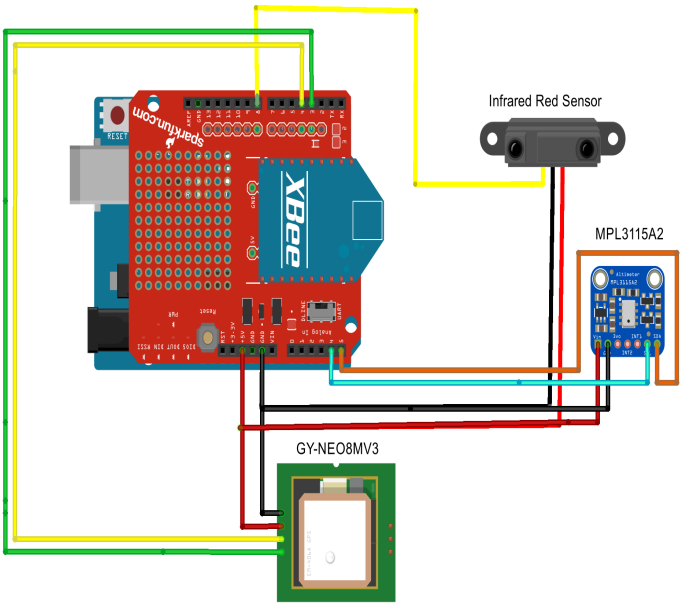

Fig. 2. Connection of the onboard system

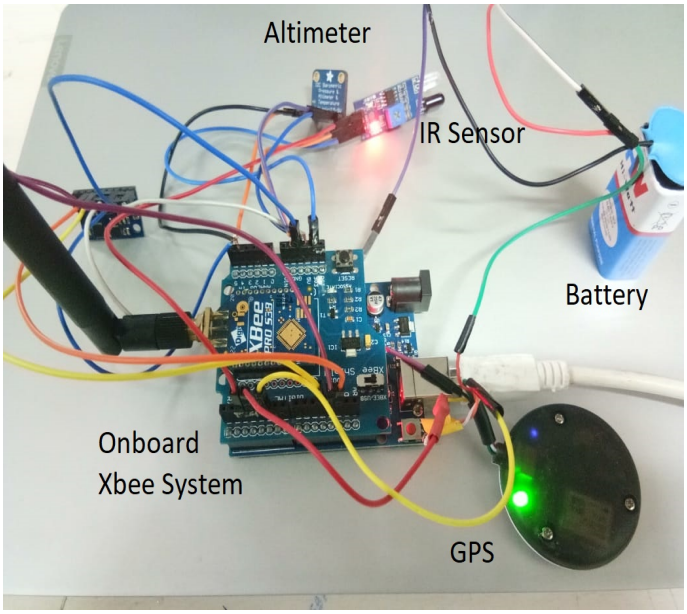

Fig. 3. Physical model of the on-board system

B. Ground Station Setup

The ground station setup has a receiver XBee mounted on a shield that is connected to computer through USB. Software like XCTU and Coolterm are used to display the data. The figure 4 shows the receiver setup.

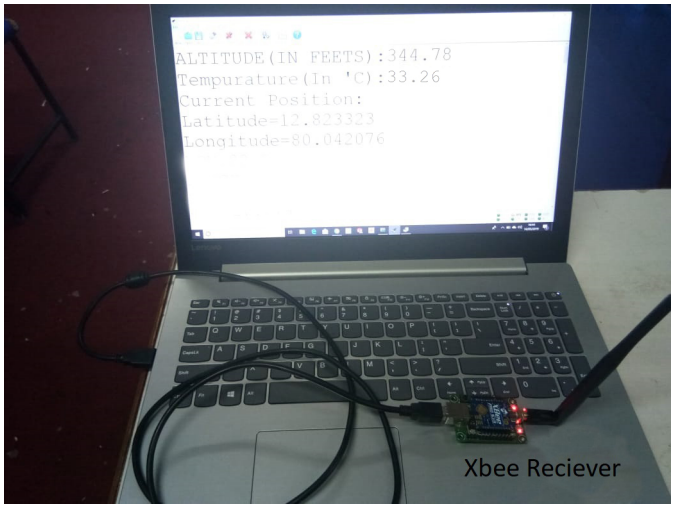

Fig. 4. Ground Station Setup.

1) XCTU software: XCTU is a free multi-stage application intended to empower developers to associate with Digi RF modules through an easy-to-utilize graphical interface. It incorporates new tools that makes it simple to set-up, configure and test XBee. XCTU incorporates the majority of the tools a builder needs to rapidly get ready for working with XBee. In XCTU we have to set up the default values in the module setting section. Accordingly we have used Transparent Mode in API Enable Mode. XCTU displays textual data and hexadecimal data.

2) Coolterm Software: CoolTerm simple serial port terminal application (no terminal emulation) with a need to exchange data with hardware connected to serial ports. The data received would be displayed on the software screen, it provides data logging and storage capability.

III. Experimental Results

The test results of all the instruments and components included in the setup at ground station and on-board responded effectively and the data is received is displayed on screen. The baud rate is 9600. Following figure 5 shows the required result received at ground station in XCTU software and figure 6 shows the result in Coolterm software.

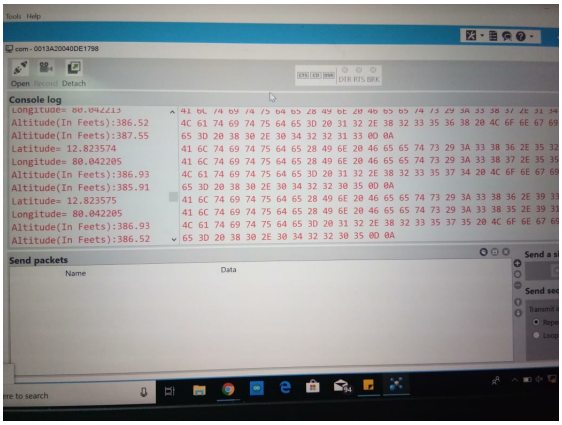

Fig. 5. Result in XCTU Software.

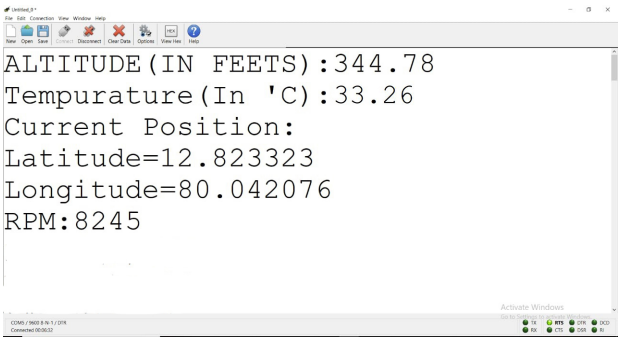

Fig. 6. Result in Coolterm Software.

Data logging is done by the Coolterm software. Maximum data rate that can be processed so that displaying visualization without pause is 20 data per second. The results of the data responses obtained can be seen in Table I.

The current altitude of the UAV is defined by the altimeter as the primary sensor and an altitude value is also available from the GPS. Comparing both the altitudes there was 97% accuracy of the data from both the sensors. By using the data the performance of the UAV can be altered as various parameters are available at the ground station by which the manoeuvring and motion of the UAV is controlled and monitored.

TABLE I
DATA LOGGING AT GROUND STATION

Altitude (feet)	Temperature (Celsius)	Latitude	Longitude	RPM
343.46	33.19	12.823723	80.042071	8245
343.45	33.19	12.828532	80.041532	8263
344.04	33.19	12.827523	80.045368	8245
344.68	33.26	12.823845	80.041556	8246
344.92	33.26	12.823789	80.049875	8255
344.98	33.26	12.823452	80.041256	8255
345.85	33.26	12.827856	80.046235	8236
345.23	33.26	12.825361	80.049235	8231
345.16	33.12	12.82842	80.042562	8231
344.98	33.12	12.828523	80.045626	8236
345.26	33.12	12.823875	80.048523	8246
345.99	33.12	12.827523	80.045626	8245
346.22	33.12	12.82132	80.045745	8249
346.25	33.12	12.82751	80.047423	8244
346.61	33.12	12.823752	80.047856	8244
346.87	33.12	12.82327	80.048563	8249
346.24	33.31	12.823512	80.0478	8244
345.25	33.31	12.823551	80.045674	8256

IV. CONCLUSIONS

From the tests performed, the system runs as determined. XBee Pro S3B on-board can communicate with other XBee module at ground station by receiving data obtained from senors with faster rate, minimal data loss and high range. From obtained results it can be concluded that the XBee-Pro S3b module can be used for telemetry efficiently and UAV parameters can be logged for flight path and the efficiency can be improved.

V. FUTURE WORKS

The telemetry data can to used in autopilot design to manoeuvre through various way-points in the space. Data can be used for payload drop in commercial applications.Predictive maintenance increase the efficiency and reduce the failure of the motor.

ACKNOWLEDGEMENT

This work was supported by Team SPARS, SRM Institute of Science and Technology.

REFERENCES

[1] L.Khriji, F.Touati and N.Hamzaon, “ZigBee-based telemetry system, ” The Journal odf Engineering Research , vol7, No2, 2010 pp.32–39
[2] Anil Kumar, Pinhas Ben-Tzvi and Murray Snyder, “UAV-based wireless telemetry system for the estimation of ship air wake patterns,” IEEE International Conference on Mechatronic and Embedded Systems and Applications (MESA) August 2-5, 2015.
[3] T H Nasution, I Siregar and M Yasir, “UAV telemetry communications using ZigBee protocol, ” International Conference on Materials Physics and Mechanics 2017.
[4] Wilton Lim, Hans Kaell Torres and Carlos M. Oppus “An agricultural telemetry system implemented using an arduino-android interface, ” IEEE International Conference Humanoid,Nanotechnology, Information Technology Communication and Control, Environment and Management,2014
[5] Li Bing,“Study on Modelling of Communication Channel of UAV, ”Procedia Computer Science, vol. 107, pp. 550-557, January 2017.
[6] K. L. Chen, Y. R. Chen, Y. P. Tsai, and N. Chen, ”A Novel Wireless Multifunctional Electronic Current Transformer Based on ZigBee-Based Communication,”IEEE Transactions on Smart Grid, vol. 8, no. 4, pp. 1888-1897, July 2017.
[7] T Muthuramalingam, M Mohamed Rabik, D Saravanakumar, K Jaswanth, ’Sensor integration based approach for automatic fork lift trucks,’ IEEE Sensors, 18(2), 736-740, 2018.
[8] M Mohamed Rabik, T Muthuramalingam, Tracking and locking system for shooter with sensory noise cancellation, IEEE Sensors, 18(2), 732-735, 2018.
[9] Ward, S., Hensler, J., Alsalam, B., Gonzalez, L. F. Autonomous UAVs wildlife detection using thermal imaging, predictive navigation and computer vision. 2016 IEEE Aerospace Conference.
[10] Puls, T., Kemper, M., Kuke, R., Hein, A. . GPS-based position control and waypoint navigation system for quadrocopters. 2009 IEEE/RSJ International Conference on Intelligent Robots and Systems.
[11] Mallick, T. C., Bhuyan, M. A. I., Munna, M. S. Design and implementation of an UAV (Drone) with flight data record. 2016 International Conference on Innovations in Science, Engineering and Technology (ICISET).
[12] Perez, D., Maza, I., Caballero, F., Scarlatti, D., Casado, E. Ollero, A. A Ground Control Station for a Multi-UAV Surveillance System. Journal of Intelligent and Robotic Systems 2012

Proceedings of the Fourth International Conference on Communication and Electronics Systems (ICCES 2019)
IEEE Conference Record # 45898; IEEE Xplore ISBN: 978-1-7281-1261-9

A Slotted Compact Antipodal Vivaldi Antenna(CAVA) for UWB Applications.

Harish Ravichandran [1], Jayakrishnan V M [2], Sethuraman N Rao [3]
[1,2,3] Amrita Center for Wireless Networks & Applications (AmritaWNA)
Amrita School of Engineering, Amritapuri, Amrita Vishwa Vidyapeetham, India
harishr@am.students.amrita.edu [1] jayakrishnanvm@am.amrita.edu [2] sethuramanrao@am.amrita.edu [3]

***Abstract*—A compact Antipodal Vivaldi Antenna(CAVA) with the dimension 60 x 65 x 1.6 mm3 is proposed in this paper. The structural modifications emanated from the original fan shaped fin structure have increased the electrical length of the antenna and has ensued in reduction in the lower operating frequency from 4.8 GHz to 3.7 GHz which is close to the desired lower operating band for an UWB covering antenna. The proposed antenna follows a simple structure but delivers good plot impedance characteristic. The antenna is designed on FR-4 substrate with dielectric constant 4.4 and height 1.6 mm. The antenna design and simulation has been carried out using ANSYS HFSS 17.0 software which uses Finite Element Method(FEM) for its working. The designed antenna offers higher gain and flat gain over the 3.1 to 10.6 GHz UWB operating spectrum with peak gain of 6.4dB which is high for any compact structure. The structure is simulated for its return loss, -10 dB impedance bandwidth, radiating power patterns and compared with earlier results in an iterative manner. The designed antenna is an eligible candidate for various wide band operating applications including medical imaging, Ground Penetrating Radar applications etc.**

Keywords*— Finite Element Method, Antipodal Vivaldi, Ultra Wideband, Exponential tapering.*

I. INTRODUCTION

NOwadays microwave imaging technique is finding a great demand in various fields including imaging targets buried under lossy earth surface, see through wall imaging, concrete wall imaging for detecting of cramps and cracks and understanding mixture of concrete based composite materials, non-destructive medical imaging to detect malignant tumors in human body and tissues. To do these microwave imaging, the system requires operation at relatively low frequency [1-18 GHz] as low frequency signal components can reach the target area in shorter time interval and also can offer good penetration depth [16]. Ultra wide-band technology here becomes a better option for imaging applications to get better resolution images by offering a higher gain over a wider operating bandwidth. In recent years, there is an immense interest in design of microwave imaging systems for various applications. But the critical part in the design of microwave imaging system is the antenna. Antenna becomes very crucial and important key element of any microwave imaging system. This antenna should necessarily have high gain, wide bandwidth and low profile. This low profile demand becomes important as most of the modern imaging systems are becoming handy and light weight. So a need for compact and miniaturized UWB antenna becomes mandatory to be employed in these imaging applications.

Conventionally, there are many effective UWB radiators that include Dual Ridged Horn Antenna, Classical TEM Horn, Log periodic antenna etc. still exist. These antennas also offer a very high gain and wide bandwidth over the entire operating band. However, these antennas are relatively large and heavy. The prominent option would be the Vivaldi Antennas that can provide satisfactory radiation performance with its planar and low profile structure. This relatively low profile structure can help in achieving low cost fabrication and integration with its simple design.

II. ANTIPODAL VIVALDI ANTENNA

Vivaldi antennas are a special family of UWB antennas that are often referred as Tapered Slot Antennas in the literature [15]. As originally proposed in [2], these vivaldi antennas are travelling wave antennas comprising of an exponentially tapered radiation element which leaves a way for a slot to support the travelling of incoming waves along the entire radiative slot till it leaves the antenna at its edges. The tapered slot edge [3] defined by the exponential curve is used to improve the lower end radiation characteristics. Various remarkable works and literatures have been presenting various design level variations. These original vivaldi antennas are called as coplanar vivaldi antennas that supports coupled feed using strip line cutting across the radiative aperture for some unit cross section. However, these coupled feeding techniques posed a limitation in attaining a desired bandwidth. To improve the bandwidth, an alternative vivaldi antenna was initially developed by [4] which is known as Antipodal Vivaldi Antenna(AVA). There is again one more improvement on these AVA to achieve further higher bandwidth and gain which resulted in creation of Balanced Antipodal Vivaldi Antenna (BAVA). However, this BAVA is lacking researches due to its two-layer design complexity. With conspicuous understanding about the tradeoff between higher gain and design complexity this paper focuses on Antipodal Vivaldi Antenna and its size reduction.

However, there are also some key challenges in designing this type of Vivaldi Antennas is that, the stability in the radiation

pattern over the frequencies. Only the lowest frequency is having hold in the design of these antennas and the upper

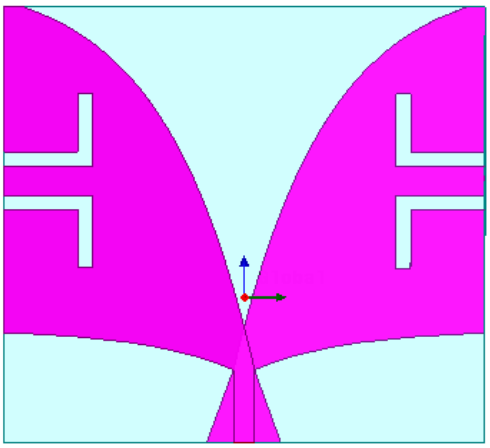

Figure 1a. Symmetric dual L-shaped slots etched on the outer edge of the fin.

operating frequency is not fixed. These antennas act as resonant antennas at lower frequencies and as a travelling wave radiator in the higher frequencies [5]. The waves travel along the inner edges of the flared aperture and couple to each other to produce required radiation [9]. For compact wireless systems it is essential to have a compact antenna geometry along with non-distorted radiation performance. The compact AVA means compactness with the fin body as well as with the feeding section of the antenna.

In couple of literatures [6] [7] [8], the compactness has been achieved by employing corrugations at the outer edge of the fins of the antenna. But this method brings additional design complexity.

In this paper, a compact Antipodal Vivaldi Antenna(CAVA) is designed without bothering the corrugations and the designed antenna covers 3.1 to 10.6 GHz allotted UWB band with notch behavior over 3.6-4.8 GHz which is the lowest band of UWB spectrum that is intended for the operation of Ground Penetrating Radar and several other imaging applications. Section III describes the evolution of the proposed antenna structure which doesn't suffer notch behavior but radiates from 3.7 GHz onwards in the complete UWB spectrum and section IV outlines the simulated results and its investigations. Section V is the conclusion of the letter.

III. PROPOSED ANTENNA STRUCTURE

Radiation characteristics of these type of Vivaldi antennas are decided by the exponential curves alongside the length of the aperture slots. Usually, compactness is brought by specific structural modifications such as etching specific slot geometry on the radiating fins to increase the electrical length in the space constraint applications without having need to modify the dimensions. Here, in this proposed structure the electrical length is increased by introduction of a rectangular cladding alongside the outer edge of the CAVA along with the introduction of the symmetric width slots on the outer edge of both the fins as shown in the Figure 1a and 1b. The current flow in the outer edge of the antenna is further reduced due to this additional structural combination. This way of increasing the electrical length wouldn't give rise to some additional radiation as in the case of the slotted fin antennas

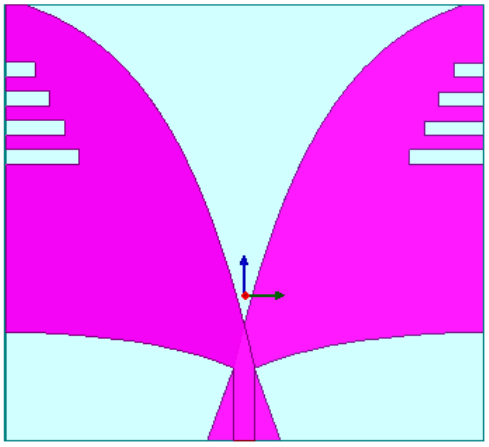

Figure 1b. Four equal width slots etched on the outer edge of the fin.

where the slots couple some amount of energy and adds to the total radiation which even worsen the radiation pattern by giving rise to unwanted side lobe level improvements. The proposed

antenna is carried out on the FR-04 substrate of dimensions of 60 x 65 x 1.6 mm^3. The substrate has dielectric constant of 4.4 and loss tangent of 0.01. Two symmetric shape fins are metallized on either side of the substrate (referred as upper and ground fin) responsible for the end-fire radiation, were created from two exponential curves with specific rate of bending. The exponential curve profile is defined by the following equations [1] - [3].

$$Y = C1e^{Rx} + C2 \quad \text{--(1)}$$

Where,

$$C1 = \frac{y_2 - y_1}{e^{Rx_2} - e^{Rx_1}} \quad \text{--(2)}$$

$$C2 = \frac{y1e^{Rx_2} - y2e^{Rx_1}}{e^{Rx_2} - e^{Rx_1}} \quad \text{–(3)}$$

Here, $C1, C2$ – Constants, R is the opening rate of the exponential curve and (x_1, y_1) , (x_2, y_2) are the start and end of the exponential curve respectively.

Table 1. Description of design parameters and its values.

Parameters	Values
Length of the substrate(Ls)	60 mm
Width of the substrate(Ws)	65 mm
Opening width of aperture(Wa)	60 mm
Length of Microstrip line(l)	10 mm
Width of Microstrip line(w)	3 mm
Width of ground plate head(Wg)	10 mm

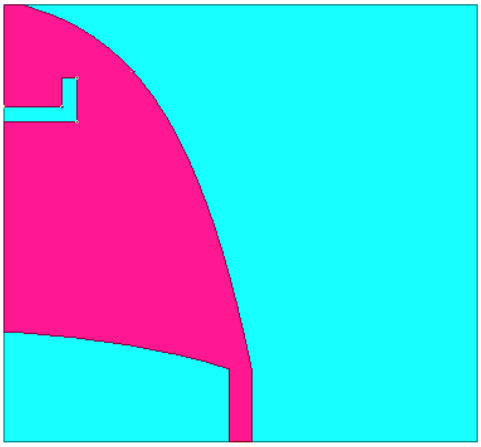

Figure 2a. Upper fin structure of the proposed antenna.

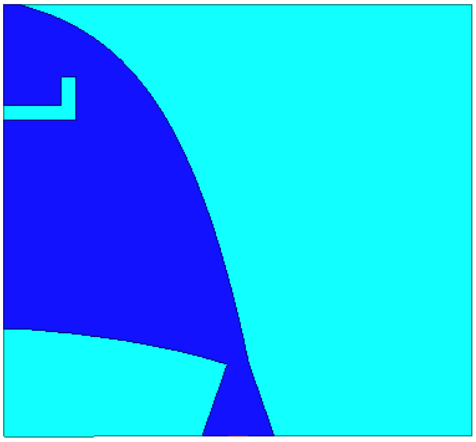

Figure 2b. Ground fin structure of the proposed antenna.

The proposed antenna design is shown in Figure 2a and 2b. The designed antenna is fed using Microstrip line feed having width 2.83mm and length 10mm to match the 50Ω impedance of that of the coaxial cable line. A transition plane as shown in Figure 2b is provided in the ground plane to convert the Microstrip feeding structure from unbalanced to balanced line. Triangular head is chosen for this purpose to provide a smooth transition from the feeding point to the fin structure. Smoother is the bending of the transition region, better is the obtained reflection coefficient and VSWR value. The values of each fixed design parameters are presented in Table 1.

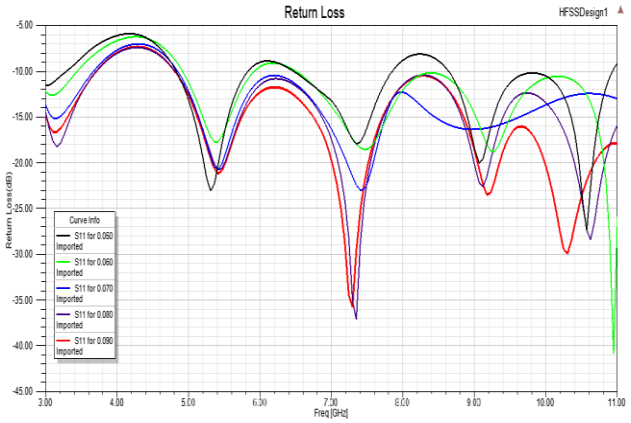

Figure 3a. S11 Performance characteristics of different rate parameters

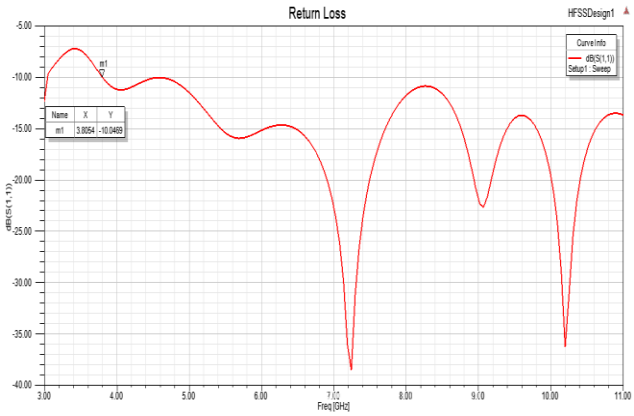

Figure 3b. Return Loss characteristics for proposed design

To reduce the overall form factor, the symmetric shape slots are opened on the outer edges of the fin structures which increases the electrical length and thereby pulling down the lowest operating frequency to some extent without the need to alter any other design dimension. According to the radiation theory of the tapered slot antennas, the flare is the main component of the radiation for the whole frequency band and the aperture opening width decides the lower cut-off frequency of the antenna which is described by the following equation [4].

$$W_a = \frac{c}{f_l}\sqrt{\frac{2}{\varepsilon_r+1}} \quad \text{--(4)}$$

Where, W_a – Aperture Opening width
c – Free space velocity
ε_r – Dielectric constant of the substrate
f_l – Lower frequency of operation

IV. Results and Discussion

The optimal dimensions of the proposed antenna structure are as follows: 60 x 65 x 1.6 mm^3 with la=10mm and w=3mm of that of the Microstrip line. The proposed antenna structure and its performance are optimized and analyzed using ANSYS HFSS 17.0 software. The computation is based on Finite Element Method(FEM). First of all, the variation with respect to the rate parameter is broadly investigated for different rates 0.050, 0.060, 0.070,0.080 and 0.090 in the chronological order. The comparison of S11 plots for different rate parameters are plotted in Figure 3a. An analysis on based on the resonance behavior over the wide spectrum is taken into consideration. It is understood that he antenna structure with highest rate parameter (0.090) performed well with good reflection coefficient. Secondly, the slot studies were carried out with equal width slots etched one on the upper fin and other on the ground fin in the symmetrical manner. Etching slots on the outer edge of the antenna increases the electrical length by some additional length of the slot. The number of slots were increased and the effect of these slots of different number are analyzed.

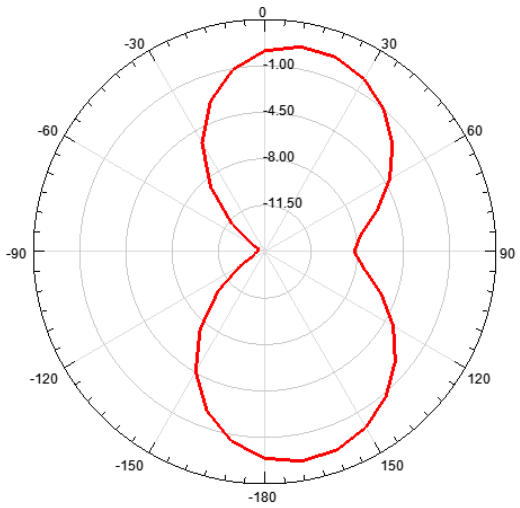

Figure 4a. E-plane radiation pattern for the proposed design

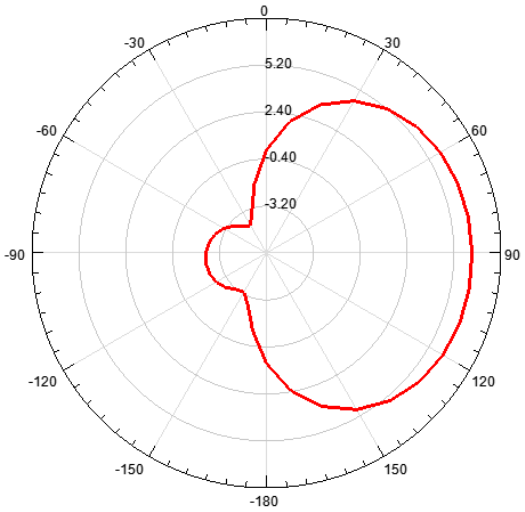

Figure 4b. H-plane radiation pattern for the proposed design.

Finally, the 3 slotted fin structure is fixed based on the return loss and radiation performance. The 3 slotted fin structure improved the overall gain of the antenna by nearly 3dB from its original structure. Similarly, two symmetric L shaped slots are also investigated. These dual L-shaped structure delivered higher radiation performance and the peak gain was nearly 6dB for the fixed dimension of the L-shaped slot. But however, the E-plane radiating pattern is changed as these Dual-L shaped slots couples some energy to radiate thus changing the end fire radiation and showing a perverse radiation characteristic.

Finally, a single L-shaped slot model for the both fin structures is proposed for which different dimensions of the L-shaped slot is studied and analyzed in an iterative way. The proposed fin structure here uses 16 mm x 2 mm as length and the width respectively. The s11 plot of the proposed model is presented in Figure 3b.

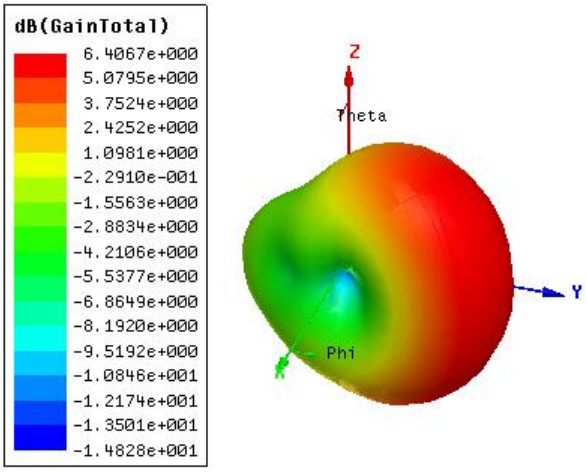

Figure 5. Gain performance of the proposed antenna.

The E-plane and the H-plane radiation pattern of this proposed antenna are depicted in Figure 4a and 4b respectively. The radiation performance in the term of gain is presented in Figure 5.

The peak gain of the proposed antenna structure is 6.4 dB. The slotted heads in the outer edges of the antenna has contributed to the additional radiations in the end-fire direction which has significantly improved the peak gain of the resonant structure.

V. CONCLUSION

In this paper, a compact Antipodal Vivaldi Antenna(CAVA) is presented with the dimension of 60 x 65 x 1.6 mm^3 keenly operating from 3.7 GHz to over 20 GHz. The L-shaped structural in the proposed antenna greatly reduced the lower operating frequency from 4.8 GHz to 3.7 GHz and achieved this without any alteration in the antenna's physical dimension. The antenna is studied for its tunability with the variation in the rate parameter of the inner edge and also the different slots and their performance are discussed. In future, the work will be furnishing the notions and effects of dielectric filling on these type of antennas. The proposed antenna shows a directional and stable radiation pattern which is highly desired for certain high resolution imaging applications. The proposed antenna delivers a peak gain upto 6.4 dB. The proposed antenna has eliminated the natural band limiting characteristic over 3.7 – 4.8 GHz in the earlier design. The design and simulation is performed using ANSYS HFSS 17.0 software. The various simulated results are presented in detail.

ACKNOWLEDGMENT

We are extremely grateful to our beloved Chancellor, Dr. Mata Amritanandamayi Devi, also known as Amma, for providing us the guidance, motivation and the support environment to work on this project.

REFERENCES

1. A Z. Hood, T. Karacolak, and E. Topsakal, "A small antipodal Vivaldi antenna for ultrawide-band applications," IEEE Antennas Wireless Propag. Lett., vol. 7, pp. 656–660, 2008.
2. P.J. Gibson. "The Vivaldi aerial." Proceedings of the 9th European Microwave Conference, pages 101–105, 1979.
3. P. Fei, Y. C. Jiao, W. Hu, and F. S. Zhang, "A miniaturized antipodal Vivaldi antenna with improved radiation characteristics," IEEE Antennas Wireless Propag. Lett., vol. 10, pp. 127–130, 2011.
4. Gazit.E. "Improved Design of the Vivaldi Antenna." Proc.IEE,1988,135H, pp.89-90.
5. Ibrahim T. Nassar, and and Thomas M. Weller,"A novel method for improving antipodal vivaldi antenna performance," IEEE Transactions on Antennas and Propagation, IEEE 2015.
6. Rajesh Natarajan, Jithila V George, Malathi Kanagasabai, and Arun Kumar Shrivastav, "A compact antipodal vivaldi antenna for uwb applications," IEEE Antennas and Wireless Propagation letters, vol. 14, 2015.
7. Hao Li, Lijia Chen, Jinghui Qiu, Caitian Yang, "A compact antipodal vivaldi antenna with improved radiation performance." Proceedings of ISAP2016, Okinawa, Japan.
8. Mahdi Moosazadeh, and Sergey Kharkovsky, "A Compact High-Gain and Front-to-Back Ratio Elliptically-Tapered Antipodal Vivaldi Antenna with Trapezoid-Shaped Dielectric Lens," IEEE Antennas and Wireless Propagation letters, 2015.
9. 1. A. K Reddy, Dr. Natarajamani S., and Behera, S. K., "Antipodal vivaldi antenna UWB antenna with 5.5 GHz band-notch characteristics", in International Conference on Computing, Electronics and Electrical Technologies [ICCEET], 2012.
10. Dr. Natarajamani S., Behera, S. K., and Patra, S. K., "A Compact planar diversity antenna for ultra-wideband application with band notched function", Microwave and optical technology letters (Willey Publication), vol. 55, 2013.
11. [15] G.K. Pandey, H. Verma, and M.K. Meshram, Compact antipodal Vivaldi antenna for UWB applications, Electron Lett 51 (2015), 308–310.
12. Dr. Natarajamani S., Behera, S. K., and Patra, S. K., "Planar ultrawideband antenna with 5.5GHz band dispensation characteristics", in 2010 Annual IEEE India Conference (INDICON), 2010.
13. Balanis, C. A., Antenna Theory Analysis and Design, 3rd edition, John Wiley & Sons, Inc., 2005.
14. D. M. Pozar, Microwave Engineering, John Wiley & Sons, 2009.
15. Prabhjot Kaur,and Karamjit Kaur, "Review paper on vivaldi antenna for UWB application," International Journal of Electronics & Communication Technology, IJECT Vol. 8, Issue 3, July - Sept 2017.
16. A. T. Mobashsher, K. S. Bialkowski, A. M. Abbosh, S. Crozier, "Design and Experimental Evaluation of a Non-Invasive Microwave Head Imaging System for Intracranial Haemorrhage Detection," International Journal of Biomedical Imaging,2013.

Proceedings of the Fourth International Conference on Communication and Electronics Systems (ICCES 2019)
IEEE Conference Record # 45898; IEEE Xplore ISBN: 978-1-7281-1261-9

K Medoids Based Clustering Algorithm with Minimum Spanning Tree in Wireless Sensor Network

Shaffali Jain
Dept. Computer Science
Shri Ram Group of College, Banmore
Gwalior, India
jainshaffali57@gmail.com

Prof. Nitesh Bharot
Dept. Computer Science
Shri Ram Group of College, Banmore
Gwalior, India
niteshbharot20@gmail.com

***Abstract*—Many Wireless Sensor Network named as (WSN) have the resource constrained sensor nodes, that are predictable to work autonomously for long-time, such as months / years. Because of there stricted accessibility of the power supply, the main worry in the WSN is energy preservation. Throughout previous phases of the development of WSN, the nodes were static & communication between any of 2 hubs was completed through utilizing the multi-hop pathway. Usually, the Minimum Spanning Tree named as (MST) utilized the optimum data aggregation tree for an energy-efficient routing. Earlier the consumption of energy condensed through the hop basis data transmission include the help of the Prim's Algorithm. In this article, K-Medoids clustering based algorithm utilized to create clusters & then tree creation to enhance the effectiveness of network. Simulation has been done on the tool of MATLAB & outcome display that the proposed work has better first dead node time.**

Keywords—Wireless Sensor Network, Energy, MST, Prim's Algorithm, Optimal Route.

I. INTRODUCTION

Developments in the integrated circuit technique have allowed large-scale production of small, the cost-effective, & the energy efficient wireless sensor named as(WS) tools with the processing abilities of on-board. Mobile & pervasive computing development has formed novel applications for them. The applications which is based on sensor extend an extensive range of the region, with the remote monitoring of the seismic events, the ecological aspects (example, water, air, wind, soil, chemicals), smart-spaces, the condition-based maintenance, the soldierly shadowing, the exactness farming, transport, the factory instrumentation, & the inventory tracing [1]. The WSNs has various small, lower cost hubs equipped with the sensor, microchips, wireless transceivers, memory, & battery-operated. They examine a physical, ecological condition & collect & transmit the data at one / more of the base-station. WSN consumes energy throughout the collection of data. Because of this there are various types of applications in different areas. The WSNs termed as (WSN) is a co-operative gathering of the sensor hubs, every has the dispensation capacity. The routing in the WSN is various as of the conservative fixed network routing through the numerous ways. The WSNs infrastructure is low, incredible wireless links, there are sensor hubs that can fail, & its routing protocols face the harsh energy reserves necessities.In contrast, the WSNs are wireless schemes with the incomplete power, are reserved in dynamism ingesting, & with dynamism have the actual time with the different sources [2].

The rest of the paper has various sections which have been described as: in section II, routing techniques of WSN are explained which has two techniques such as single & multi hop routing. In section III, Minimum Spanning Tree has been described with some detailed explanation and section IV described Prim's Algorithm. Section V discussed about some literature surveys to understand the concept. In section VI and VII, proposed work and result analysis has been described respectively.

II. ROUTING TECHNIQUES IN WSN

Routing is a procedure for structuring route amongst destination as well as destination to send information to request. This involves transmission of info after nodes, which assists as well as analyzes this info to BS to assist in decision-making process. There are numerous types of constructions to route information after nodes to BS, which are designated as surveys:

I. Single Hop Routing:

First & easiest method was an instant broadcast of data. Inside the given method every sensor hub will find & move its data directly to BS except the help of any middle hub. The form of BS is located on a distance as of sensor nodes named as (SN), this tell about the extended transmission expenditure of the info, because of which nodes energy reduces rapidly & thus the lifetime of SN's is small.

II. Multi-Hop Routing:

In it, every SN's conveys their data to their instant neighbor, & include the many hops data of neighboring nodes is moved to BS. In the multi-hop networks, each of the hub devours the fewer energy to transmit its data than the Single-hop. The Multi-hop WSN is most efficient then the single-hop types network. Inside the actual world annotations, the single-hop system is most effective if multi-hop network is in single-hop less package for future. This

architecture present the hubs located near the BS have higher load, so they expedite its dynamism faster than new nodes, that effect lifetime of network [3].

III. MINIMUM SPANNING TREE [MST]

Suppose indirect, associated graph. The spanning tree of particular graph will be sub-graph which joins altogether of vertices of tree. There may be several spanning trees in a single graph. If every weight is allocated some weight / numbers, then MST is a lower weight tree compared to the any other spanning tree in that particular graph.Figure 1 represent a graph. Each branch has been entrusted with weights. As has been seen, tinted tree is recognized spanning-tree. Several other spanning trees could too be made through joining vertices of this fig into various ways [4]. The edge-weighted graph is a diagram that we connect with weight as well as cost at every end. An MST of edge-weighted graph is a comprehensive tree whose weight (its weight besides its shaft joint) is no more than some other spanning tree.

- The graph is associated. Tree conditions in our definition show that graph must be connected to presence of MST. Uncertainty no graph is connected, then we can optimize our algo to calculate MST of each associated component, which is composed known as minimum spanning tree..
- Edge's weight is not far. Geometric awareness is sometimes valuable, nonetheless weight of side may be arbitrary
- Edge weight may be zero or negative, as well as if age weight is all positive, then subtract MST with minimum total weight connecting all verticals is enough.
- Edge Weight is dissimilar condition edges of ends are equal, then incomplete spanning trees are not single. Creation this assumption makes our evidence informal, nonetheless all of our algorithms work well in presence of equal weight.

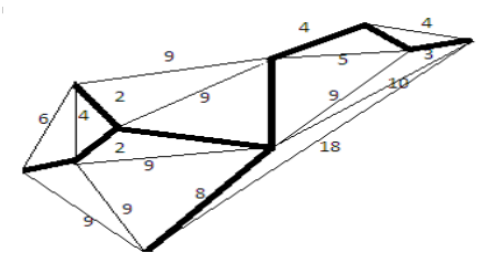

Fig 1. Edge weighted graph and it's MST

IV. PRIM'S ALGORITHM

Prim's algorithm is algo inside a theory of graph which looks aimed at minimum spanning tree toward an associated weight graph. Algo of prim's extends the minimum spanning tree named as (MSE) by increasing subtrees sequence. In this sequence, the primary sub-tree contains a solo vertex chosen randomly from set V of the vertices of graphs. Inside a following iterations, recent tree increases greedily, easily not connecting it to that tree with the adjacent vertex to the top. (Through adjacent vertex, the vertex not in tree associated to the vertex in tree through power of minimum weight.) Afterward being included in the creation of graph, the algorithm stops after adding vertices of all the graphs. However, algorithm extends a tree through just a vertex over its each iteration, overall numeral of their iterations is n-1, here n represent sum of vertices in graph. Tree created through algorithm is attained because edges set utilized to the development of tree. The algorithm of Prims nature create it required to offer each of the vertex not in recent tree include the info around a smallest edge joining vertex to the vertex of tree. Info is given through joining the 2-labels on the vertex: adjacent vertex of tree name & related edge length (weight). The vertices which aren't nearest to any vertices of tree could be provided ∞ tag indicative of its "infinite" distance to the vertices of tree & null tag to adjacent vertex of tree name. include these tags, verdict subsequent vertex to be added to recent tree represent as T = (VT, ET) turn out to be easy challenge of verdict the vertex includes minimum distance tag in set V – VT [5].

V. LITERATURE SURVEY

In given article [8], for WSN, the optimized routing protocol is implemented. We are attentive in building the effective routing spanning tree which reduces energy ingesting amongst all of the hubs in n/w & fit to WSN include decreased energy to attain the extended life-time. Keyconcept of such algorithm arises as of MST theory of graph. Such method attentions over minimum hop sum of every node to grasp target (basin-node) include the optimum pathway.

In [3] article, the protocol termed as Tier Based Minimum Spanning Tree Protocol also named as (TBMSTP) is implemented. This approach is on the basis of Tier idea that is dividing a n/w into the portions based on the hubs distance from a BS & MST building. We are utilized 2 level MST idea that is, a MST on the level of hub include the tier & the another on level of cluster-head among the various tiers to decrease load & intensification a WSN network life-time.

In [6] research paper, the algorithm based on networking-associated termed as local minimum spanning tree named as (LMST) working where as cooperating at the problems of energy balance, which is leading the network for brief life-

time, & implement the algorithm of energy-balance. The algorithm examines the energy usage completely to connect the remaining energy of data communiqué and communication nodes, to obtain balanced energy and to avoid complications related to excessive consumption of energy once intermediate node functions forwarding function, Like this. Expand the network life cycle. Simulated investigational results displayed the large capacity of the implemented algorithm which could capably extend the lifetime of the n/w & ensure a long-term performance of network, whereas another n/w's ensure act gauges, like the throughput & rate of delivery.

In[7] research paper, we join the routing features which is based on cluster for the cluster creation & the selection CH & the usage the (MST) for the communication of intra-cluster. The proposed method is based on optimizing MST using the Simulated Annealing named as (SA). In given research, mobility standards which is normalized, delay & residual energy are measured for discovering the optimum MST. The outcome which is given by simulation, determine the efficiency of implemented technique to improve package distribution proportion & reducing end-to-end delay.

VI. PROPOSED METHODOLOGY

The clustering of *k*-medoids is a dividing method which is usually utilized in the areas which need toughness to the outlier-data, metrics of arbitrary distance, / or for which there is no clear definition of mediod or median, requires strengthening.

This is same as to the *k*-means, & both approaches goal is to partition the measurements set / explanations in the *k*-subsets / clusters, so that sub-sets minimalize sum of the distances among the measurement & the center of measurement's cluster. In the algorithm of k-means, subset center is measurements mean into sub-set, frequently named the centroid. In the algorithm of *k*-medoids, sub-set center is a subset member, named as a medoid.

The algorithm of *k*-medoids returns the medoids that are real points of data in data-set. This permits you to usage the algorithm in the conditions wherever data mean doesn't occur include the data-set. This is key various among *k*-medoids & *k*-means algorithm where centroids give back through the k-means algorithm can't be include data-set. Hence forth the *k*-medoids algorithm is beneficial to cluster the definite data wherever the mean is dreadful to describe/understand.

The function k-medoids provides several iterative types algorithms which minimalize number of distances as of every item to its medoid of cluster, total clusters. Most of algorithms is called partitioning around medoids (PAM) which proceeds in two steps.

1. Build-step: Every *k* clusters is related include the possible medoid. Such task is done utilizing the method stated through 'Start' value name couple argument.
2. Swap-step: Inside each of the cluster, every point is examined the form of possible medoid through examination whether the sum of the distances of within-cluster becomes the lesser utilizing that particular point the form of medoid. If thus, point is definite the form of novel medoid. Each of the point is allocated to cluster include the the neighboring medoid.

The algo generates swap-steps and repeats until medoids are transformed or termination criteria are not completed. Consuming minimum control parameters of details, including early values of K-meridian, cluster meridian as well as maximum number of iterations. Through default, k-medoids usage k-mean ++ algorithm aimed at cluster medoids initiation, as well as a quadrangular Euclidean matrix.

In previous work, smallest spanning tree created with all the nodes in network. In this letter, we offer a customized route protocol aimed at wireless sensor nodes. We want to create a skilled routing tree that is compatible with low-power WSN, which reduces energy consumption and has longevity of all nodes in network. The main idea of this algo is as of minimum spanning tree (MST) graph theory. This method focuses on minimum hop calculation of every node to extent endpoint (sink node) within optimum pathway. After that data transmission performed among sink and the nodes. But this is very time consuming to create shortest route aimed at data transmission. So to overawed this problem as well as improve network competence, innovative method is introduced.

Consider the whole network in which the sink node is placed at (0, 0) coordinate and others are deployed randomly. Firstly, the network is divided into small groups known as clusters. This step is performed by K-Medoids algorithm to form optimal clusters. Now perform the minimum spanning tree formation using Prim's Algorithm by considering sink node as an input. Lastly, the data transmission performed through cluster heads of each clusters instead of each nodes which makes them more efficient then earlier.

Proposed Algorithm:
Step 1: Start
Step 2: Place sink node at (0, 0) coordinate
Step 3: Put all nodes randomly in two form i.e. 30 and 100 nodes
Step 4: Divide the network into clusters
Step 5: Apply K medoids algorithm
Step 6: Involve the network graph G(V, E), k is no. of clusters to be shaped, where V as well as E is the nodes also wireless links respectively
Step 7: Select k nodes arbitrarily as first cluster heads, also usage m to mean set of those k cluster heads
Step 8: CH performs by distance computation

Step 9: Formation of Minimum Spanning Tree
Step 10: Data transmission performed through cluster head
Step 11: Repeat step 10 until it reached destination node
Step 12: Stop

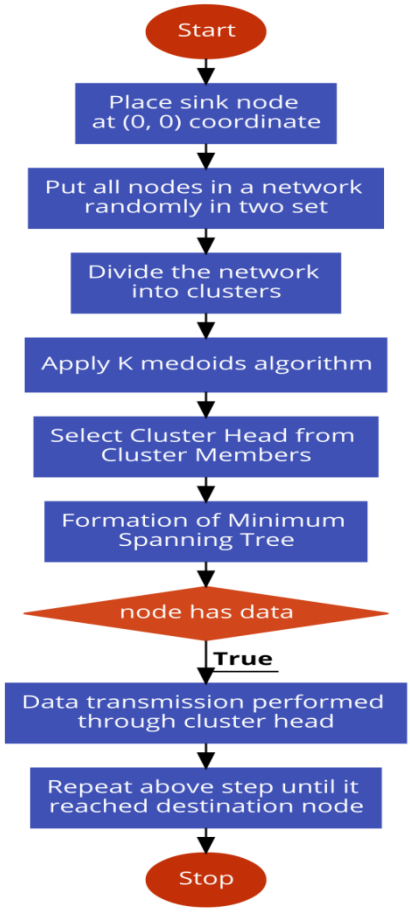

Fig.2. Proposed Algorithm Flowchart

VII. RESULT ANALYSIS

The simulation performed to illustrate the propose work by using MATLAB tool. We accept that confident measures of sensor nodes are consistently organized in a 100×100 square area. Initially 30 nodes are deployed in the network and then 100 nodes are deployed. Sensor nodes have following physiognomies: (1) in network, altogether protuberances are static after being organized; (2) altogether nodes are of same quantity of original power; (3) sink may be deployed at (0,0) in monitoring area; (4) altogether nodes have similar sensor radius, meant as *R*.

A. Scene1 (30 Nodes)

Here 30 nodes are deployed in the network and then the graph shows the variance of energy. The number of cluster heads formed is 15.

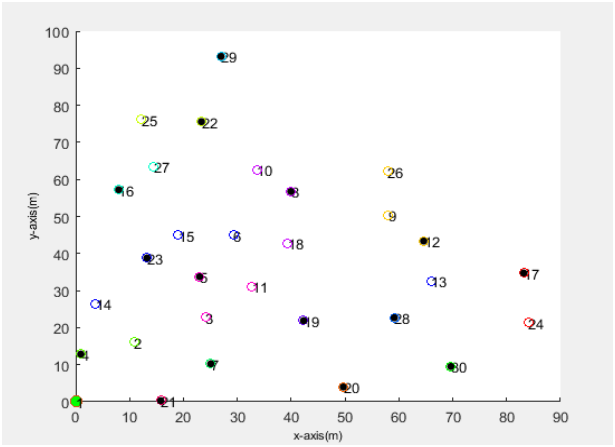

Fig.2. 30 Nodes deployment

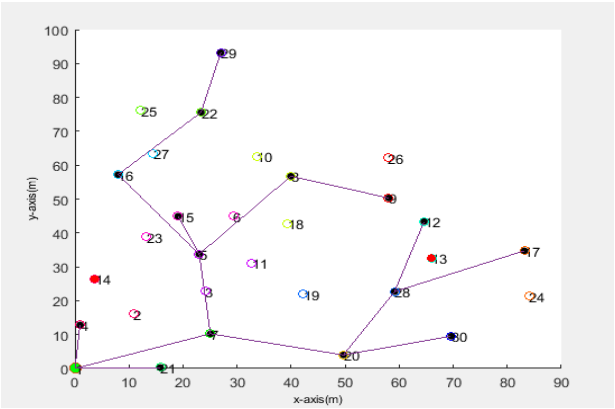

Fig.3. MST formed through K medoids

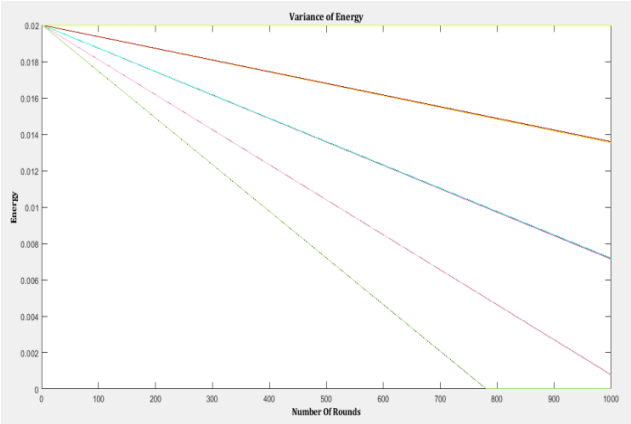

Fig.4. Variance of Energy at various rounds

B. Scene2 (100 Nodes)

Here 30 nodes are deployed in the network and then the graph shows the variance of energy. The number of cluster heads formed is 30.

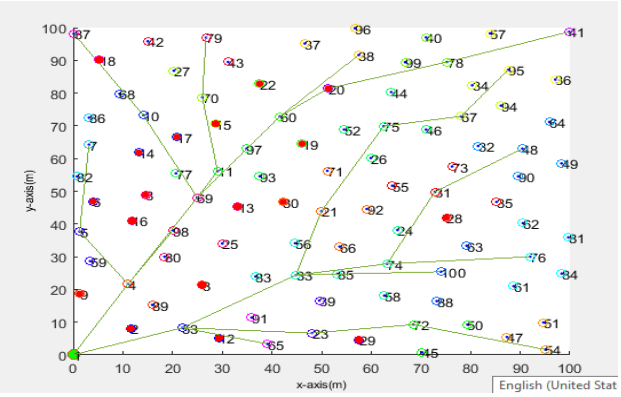

Fig.5. MST formed through K Medoids

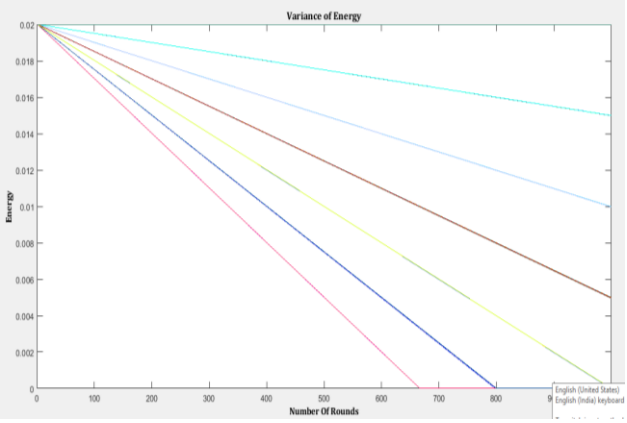

Fig.6. Variance of Energy at various rounds

C. *Scene3 (150 Nodes)*

Here 150 nodes are deployed in the network and then the graph shows the variance of energy. The number of cluster heads formed is 35.

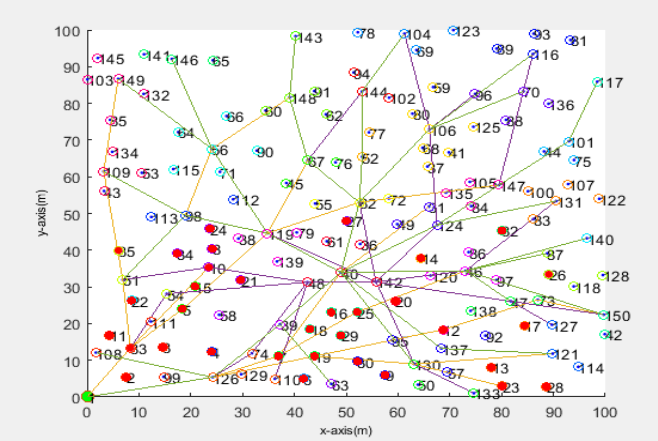

Fig.7. MST formed through K Medoids

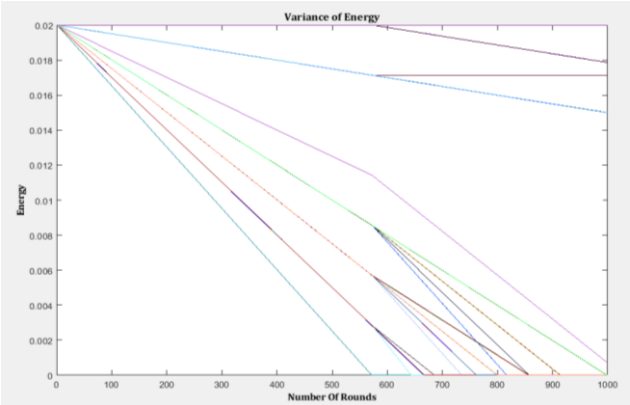

Fig.8. Variance of Energy at various rounds

D. *Scene4 (200 Nodes)*

Here 200 nodes are deployed in the network and then the graph shows the variance of energy. The number of cluster heads formed is 40. Then the table 1 shows the comparison of first dead node time of the base and proposed work.

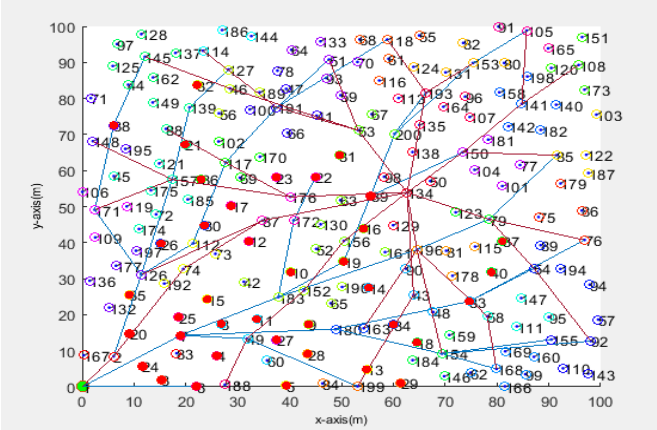

Fig.9. MST formed through K Medoids

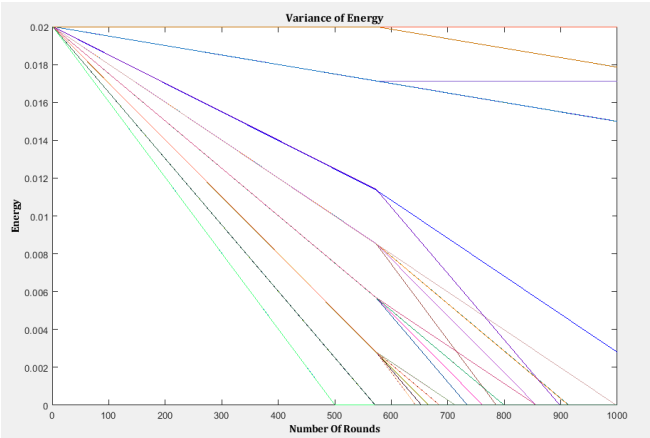

Fig.10. Variance of Energy at various rounds

Table 1 below shows the comparison among the previous work [10] with proposed work in terms of different scenes. There 4 different scenarios have taken into consideration i.e.

30 nodes, 100 nodes, 150 nodes and 200 nodes. Each scene has different number of nodes in the network and therefore we show that every scene has different dead time for the first node. Scene 1 has the maximum life time of the first dead node.

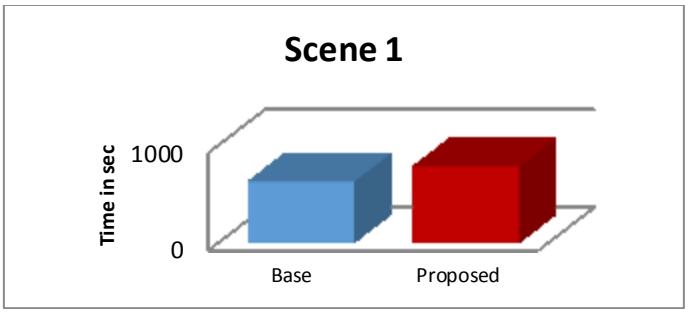

Fig.11. Comparison of Scene 1

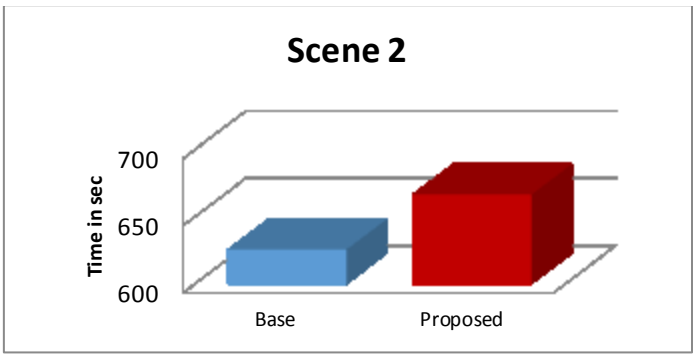

Fig.12. Comparison of Scene 2

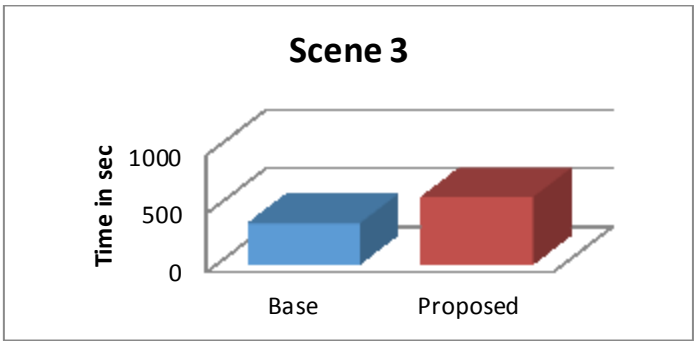

Fig.13. Comparison of Scene 3

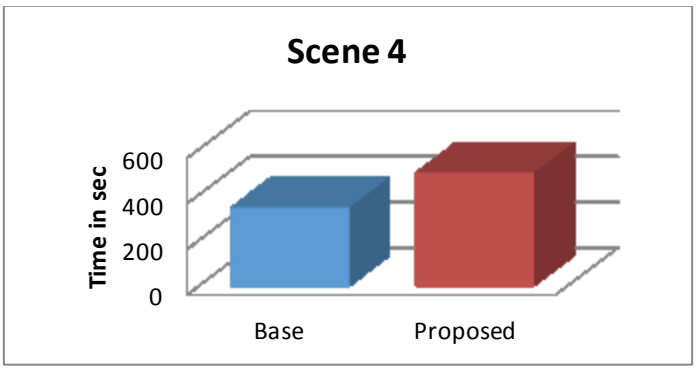

Fig.14. Comparison of Scene 4

TABLE 1: Time to first node death

	Time			
	Scene 1 (30 Nodes)	Scene 2 (100 Nodes)	Scene 3 (150 Nodes)	Scene 4 (200 Nodes)
Messous [8]	626	626	349	349
Our Proposed	781	667	573	501

Conclusion

Sensor nodes in a WSN are examples of resource constrained devices, because the processing power, The sensor nodes of memory as well as supply power distribution are limited. Wireless sensor networks, as a promising technology, are acceptance more as well as more interest from a wide range of applications for research communal. Detailed WSN applications comprise frequent distributed-deployed sensors as well as one or more base stations. Every sensor may understand, collect as well as transmission data aimed at sync in continuous or event-driven fashion. This paper improves network performance by generating clusters and then performed data transmission through the MST. From the result comparison, it can be demonstrated that 30 nodes has greater time for the node communication. In scene 4, the nodes become dead early with respect to the other scenes.

References

[1] Maleq Khan Gopal Pandurangan Bharat Bhargava, Energy-Efficient Routing Schemes for Wireless Sensor Networks, http://www.ee.oulu.fi/~carlos/WSNPapers/KH03.pdf.

[2] Bhat GeetalaxmiJayrama, D. V. Ashokab, Validation of multiple mobile elements based data gathering protocols for dynamic and static scenarios in Wireless Sensor Networks, 2nd International Conference on Intelligent Computing, Communication & Convergence(ICCC-2016), Procedia Computer Science 92 (2016) 260 – 266.

[3] Maninder Pal Kaur, Gaurav Bathla, Prolonging the Network Lifetime of Tier Based Minimum Spanning Tree Structured Wireless Sensor Network, International Journal of Innovative Research in Computer and Communication Engineering, Vol. 3, Issue 7, July 2015.

[4] RishaVashist, SunitiDutt, Minimum Spanning Tree based Improved Routing Protocol for Heterogeneous Wireless Sensor Network, International Journal of Computer Applications (0975 – 8887) Volume 103 – No.2, October 2014.

[5] Sudhakar, T. D., & Srinivas, K. N. (2011). Power system reconfiguration based on Prim's algorithm. 2011 1st International Conference on Electrical Energy Systems. doi:10.1109/icees.2011.5725295.

[6] Weiping Zhang1†, Yudong He1†, Ming Wan1, Mohit Kumar2 and Taorong Qiu1*, Research on the energy balance algorithm of WSN based on topology control, Zhang et al. EURASIP Journal on Wireless Communications and Networking (2018) 2018:292 https://doi.org/10.1186/s13638-018-1302-3.

[7] M. Saravanan, M. Madheswaran, A Spanning Tree for Enhanced Cluster Based Routing in Wireless Sensor Network, World Academy of Science, Engineering and Technology International Journal of Computer and Information Engineering Vol:9, No:9, 2015.

[8] Messous, S., Liouane, N., Pegatoquet, A., & Auguin, M. (2018). Hop-based routing protocol based on energy efficient Minimum Spanning Tree for wireless sensor network. 2018 International Conference on Advanced Systems and Electric Technologies(IC_ASET).doi:10.1109/aset.2018.8379893

Proceedings of the Fourth International Conference on Communication and Electronics Systems (ICCES 2019)
IEEE Conference Record # 45898; IEEE Xplore ISBN: 978-1-7281-1261-9

Detection of Zinc Mineralization in North India using Hyperspectral Image Processing

Aravinth J., Biplab Nath, Siva Subramanian M., Rohit V.S.S. Bulusu and Monish P.
Department of Electronics and Communication Engineering
Amrita School of Engineering, Coimbatore,
Amrita Vishwa Vidyapeetham, India
j_aravinth@cb.amrita.edu, biplabnath4jan1998@gmail.com

***Abstract*—This paper presents the use of hyperspectral image processing as an alternative to traditional mineral exploration techniques for identification of regions in the study area rich in zinc mineral. Zincian Dolomite is a known ore of zinc found in the study area. The Hyperion sensor dataset of a study area in Rajasthan, India is obtained from the USGS (United States Geological Survey) Earth explorer and pre-processed using ENVI (Environment for Visualizing Images) software to remove noise. The pre-processed data is later exported to a dedicated python program which uses machine learning algorithms to identify the regions rich in Zincian Dolomite. The proposed technique form mineral exploration is faster and cheaper than the traditional techniques and is also found to be very accurate in identification of the minerals.**

Keywords— ENVI (Environment for Visualizing Images), Hyperspectral remote sensing, Machine Learning, Mineral exploration, Hyperion, USGS Earth Explorer.

I. INTRODUCTION

Nearly 312 million Indians are at direct risk of zinc deficiency, which leads to stunted growth in children, diarrhea, impaired immune functions, reduced appetite and many other diseases. More than 50% of land under cultivation in India is zinc deficient, which is directly responsible for various crop related diseases.

Rajasthan is one of the most mineral abundant regions in India. It is also one of the largest Zinc exporting state in India. Proper identification of previously unidentified zinc rich regions can increase the production and export of zinc, not just for industrial use but also for producing zinc supplements and zinc rich fertilizer. The traditional identification methods involve manual soil sample collection from the region of interest and chemically analyzing each sample for finding traces of zinc, making it both costly as well as time consuming.

Remote sensing technology was developed in the late 1800s for covering more area in less time. Its application was mostly limited to the military until the 1970s, when its effectiveness for mapping was discovered. Grayscale imaging was used for the purpose of mapping and monitoring natural resources. Multi-spectral imaging, an upgrade of the grayscale imaging, was later found to be effective for mineral exploration. Multi-spectral remote sensing works on the principle of reflectance spectroscopy. Every chemical compound tends to absorb a few wavelengths and reflect the other wavelengths incident to it. Such absorption or reflection corresponds to the different chemical energies of the compound, such as bond energy, vibrational energy, etc., which can be used to identify the compound [2]. These absorptions and reflections are unique to every element/compound. Multi-spectral imaging gives us discrete information of very few wavelengths of the reflected spectrum. Hyperspectral Imaging is an advancement of multispectral imaging. It provides us with continuous data of hundreds of wavelengths. Continuous reflectance data can be used to identify major chemical properties of the region under study, which can be used to identify any/all the chemical compounds present in it [1].

Hyperion is a Hyperspectral sensor on board of the Earth Observing – 1 (EO-1) satellite launched by National Aeronautics and Space Administration (NASA) on 21st November 2000. The Hyperion sensor is capable of recording nearly 220 wavelengths ranging from 400 nanometers to 2500 nanometers, with a spatial resolution of 30 meters. The Hyperion dataset is one of the most widely used datasets in the field of hyperspectral imaging.

This study aims at identifying Zincian dolomite rich regions in the study area of Rajasthan, India using the data obtained from hyperspectral remote sensing.

The Hyperion sensor dataset is downloaded and then pre-processed using the ENVI tool to eliminate noise in the dataset. The Section II deals with the three machine learning algorithms, namely k-Means, Support Vector Machine and Random Forest which are used to independently identify the regions in the study area contain Zincian Dolomite. Finally, in section III the accuracy of the three algorithms are found by comparing their output to the actual ground truth and the Random Forest algorithm is found to be more accurate than the other two.

II. METHODOLOGY

The Hyperion sensor data for the study area is downloaded from the USGS Earth Explorer website in the L1R format. The dataset contains data of nearly 242 bands and represents 7.5-kilometer by 100-kilometer area on ground.

A. Sub-Setting

The raw data obtained needs to be properly pre-processed to remove noise and boost up the signal. The processing time

of the data is directly proportional on the size of the dataset. Unwanted regions and unwanted bands only increase the processing time; thus, it is imported to remove such data from the initial dataset for faster processing. Spatial and spectral sub-setting is the first step of pre-processing our data.

The dataset represents an area of 100 kilometer by 7.5 kilometer on ground and contains lot of cloud covered regions. Spatial sub-setting is done by selecting the area with the least cloud cover. Of the 242 bands in the dataset, bands (1-7), (57 - 77) and (225-242) are completely affected by noise. Spectral sub-setting is performed on the dataset to remove these bands. After the spatial and spectral sub-setting is completed, the resultant dataset represents a smaller area with each pixel containing information of 196 bands [3,4].

B. De-Stripping

Few bands in the dataset have almost no data present in them. Such bands are needed to be manually identified and their reflectance values are to be replaced by the average reflectance values of the two adjacent bands [3,4].

C. Radiometric calibration

Hyperspectral imaging works on the principle of reflectance spectroscopy. Sun is the source of energy used. Few of the incident wavelengths on the soil get absorbed and the remaining wavelengths are reflected back to the space. These reflected wavelengths travel 705 kilometers to reach the EO-1 Satellite with the Hyperion sensor. Cloud, water vapor, aerosols, pollutants, etc. may absorb some of these reflected wavelengths to further reduce the signal strength. Radiometric calibration is used to convert the sensor data into reflectance data by using gain and offset value for each wavelength [3,4].

D. FLAASH atmospheric correction

The components present in the atmosphere (water, aerosol, industrial soot, dust, etc.) not only suppress reflected wavelengths reaching the Hyperion sensor, but also add noise to some of the wavelengths. The noise is added during the propagation of the reflected wavelengths. The received signal is a mixture of the properties of the pixel under observation, the atmospheric components and also the effects of the surrounding pixel reflectance. FLAASH (Fast Line of sight Atmospheric Analysis of Spectral Hypercube) is an atmospheric correction algorithm developed by the Air Force Research Laboratory, Space Vehicles Directorate (AFRL/VS), Han-scom AFB and Spectral Sciences, Inc. (SSI) in order to properly analyze the reflectance data and remove any noise caused due to the environment. The algorithm makes use of the atmospheric data such as water content, temperature, aerosol content, etc. for each region and season and uses that to nullify the effects of the atmospheric noises [3,4].

E. K-Means

K-Means is a simple unsupervised learning algorithm used to group the previously uncategorized/ungrouped data. The algorithm divides the data into 'K' number of groups. It works iteratively and based on the features that are provided, it groups all the similar featured data points to one of the 'K' groups. The algorithm iterates between the Data Assignment step and the Centroid Update step. In the Data Assignment step, squared Euclidian distance is calculated between each data point and all the centroids, and the data point is assigned to the nearest centroid. In the Centroid Update step, the position of the centroid is changed to the mean position of all the data points assigned to the centroid. The algorithm iterates between both the steps until no data point changes clusters, or until the limit to the number of iterations is reached.

F. Support Vector Machine (SVM)

Support Vector Machine is a supervised machine learning model used for classification and regression analysis of data. Being a supervised model, it learns the classification parameters from a set of pre-classified training examples to build a hyperplane, which it then uses to classify unclassified data. A hyperplane is a plane which separate and classifies the data points. The accuracy of the hyperplane increases by increasing the number of training data. The shape of the hyperplane is decided by constructing it such that is farthest from the nearest points on either side of it [5].

G. Random forest

Random Forest is a supervised machine learning algorithm. As evident from its name, it creates a forest, consisting of random decision trees and gives the output the maximum no. of decision trees have given. By doing this, higher accuracy is achieved and the output is more stable. Random Forest grows the trees by searching the best feature among a subset of random features instead of searching for the most important feature. This algorithm uses only a random subset of features to split a node. Additionally, random thresholds for features can be used instead of using the best thresholds to grow more random trees. As this algorithm is supervised, the training data set is used to find out importance of each feature, which can then be used to give more preference to results which use those features [6].

III. RESULTS AND DISCUSSION

An area south of the city Ajmer, in Rajasthan state of India is chosen as our study area. The district of Ajmer is rich in minerals. It is known to host Dolomite (chemical formula Ca Mg $(CO_3)_2$). Metals like Zinc, Cobalt or Lead are known to be natural replacements to Magnesium in dolomite. Zinc rich dolomite (chemical formula Ca Zn $(CO_3)_2$) (see Fig. 1), commonly known as Zincian Dolomite is known to be found in our study area. Zincian Dolomite is the most popular source of Zinc in India and can be found in states of Rajasthan, Andhra Pradesh, Arunachal Pradesh and Uttarakhand. The Geological Survey of India (GSI) has manually sampled a few regions throughout India and located a few regions where zinc can be found. The GPS coordinates of these regions have been shared under the National Data Sharing and Accessibility Policy (NDSAP), and the study area has one of those coordinates.

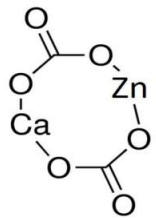

Fig. 1. Chemical Structure of Zincian Dolomite.

Traditional methods of identifying deposits are very accurate, but it is also time consuming and costly. Technological developments in the field of remote sensing have enabled us to accurately identify mineral deposits in a relatively cheaper and faster method. Hyperspectral image processing technique is used in this project for identifying dolomite mineralization. The Hyperion sensor of the EO-1 satellite gives us spectral information of 220 bands in the range of 400 nanometers to 2500 nanometers, with a spectral resolution of 10 nanometers and spatial resolution of 30 meters. As the sensor collected data from 705 kilometers from earth surface, the signal is weak in strength and contains noise. Hence, the data needs to be pre-processed to remove noise and boost up the signal. ENVI software is used for pre-processing the data.

Sub-setting is the first step used for pre-processing. As the sensor scans 100 kilometers by 7.5 kilometers on ground, and as each pixel contains data of 242 bands, it is important to reduce the size of the dataset to reduce processing time. The Hyperion sensor data is downloaded from the USGS earth explorer in L1R format. This data is imported in ENVI software, where spectral and spatial sub-setting is done on the data. The area with the least cloud cover is selected as the region of interest in the image for the spatial sub-setting part (see Fig.2). Bands (1-7), (55-77) and (225-242) are removed in the spectral sub-setting part, as these bands are known to be full of noise. After spatially and spectrally sub-setting the data, the number of pixels in the dataset decreases and the number of wavelengths is reduced to 196 bands for each pixel. This data is then saved in .hdr format.

Fig. 2. Study area after spatial sub-setting loaded in RGB bands.

Even after sub-setting, the data may contain bands with no information. These bands are identified by manually loading them in the ENVI classic software and identifying any black columns in the grey scale image. The black columns indicate that no data is present in them. That column's data is replaced by the average data of its two adjacent columns. This is done using the spatial pixel editor tool in ENVI classic. This step ensures continuity in the data.

After correcting the data using the spatial pixel editor tool, it is exported back to ENVI software for radiometric calibration. Radiometric calibration converts the sensor data (see Fig. 3) into reflectance data by multiplying a gain and adding an offset specific to each band. This step strengthens the signal and also converts the data from raw sensor data to proper reflectance data. The output of the radiometric calibrated data is in terms of percentage reflectance.

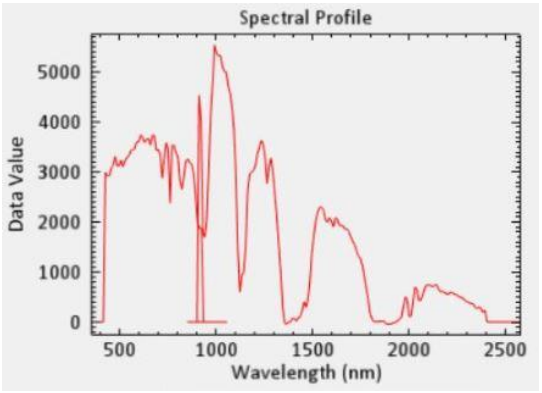

Fig. 3. Pixel data before radiometric calibration.

After converting the data in the 196 bands in terms of percentage reflectance, the next step is to apply FLAASH atmospheric correction to remove known noises from the signal. Water vapor, aerosols, industrial soot, and all the other particles in the atmosphere interfere with the wavelengths reflected from the study area, causing not only the signal strength to decrease, but also adds noise in a few bands. These atmospheric constituents also absorb sunlight and reflect a few wavelengths based on their chemical properties, which interferes with the reflected wavelengths from the area of interest. After manually configuring the FLAASH module based on the sensor used and the area of interest, the module uses known atmospheric data to effectively suppress most of the noise (see Fig. 4). In Fig. 4, red color is used to represent reflectance data before FLAASH correction and blue color is used to represent reflectance after FLAASH correction. The FLAASH corrected file is then saved in .hdr file format so that it can be exported for processing.

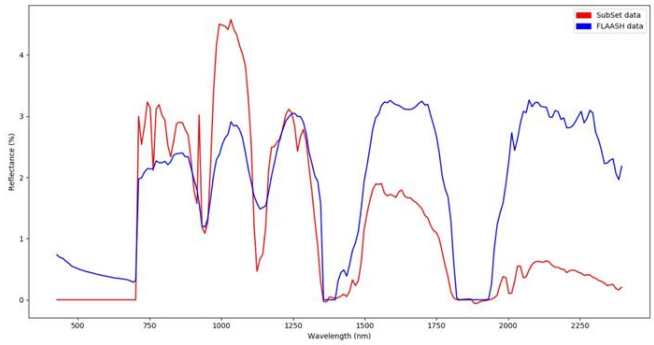

Fig. 4. Pixel reflectance data before and after FLAASH correction.

After pre-processing the data by sub-setting, de-stripping, radiometric calibration and FLAASH atmospheric correction, the data is fit for classification. The FLAASH corrected .hdr file is imported on the python code. The data is of the format (x, y, λ) where x and y denote the row no. ranging from (0-1330), and the column no. ranging from (0-255) and λ denotes the band number ranging from (0-195). Taking a look at the spectral signature of dolomite obtained from the ECOSTRESS spectral library [7- 9], 9 important wavelengths have been identified for the classification of dolomite. These wavelengths (in nanometers) are (1669.1, 1780.09, 1911.27, 2052.45, 2153.34, 2294.61, 2365.2, 2375.3 and 2395.5). A 3-dimensional array of size (x, y, 9), where x and y are the number of pixels in the x-axis and y-axis of the FLAASH corrected file, is initialized and the reflectance data of only the 9 bands out of 196 bands available is loaded into the array for each pixel.

The first algorithm used is k-means. The algorithm requires no training as it is unsupervised. k = 2 is selected and the algorithm segregates the data into two different clusters (Zinc cluster and Not Zinc Cluster). The GPS coordinate of the pixels containing dolomite in the study area was extracted from the Ministry of Mines database and the information of the 9 bands for one of the pixels was exported into a single dimension array of size 9. The k-means algorithm segregates pixels into one of the two clusters. The output of the k-means algorithm is a black and white image where black pixels represent the cluster having their cluster center nearest to the values saved in the single dimension array. Thus, the black pixels will denote pixels classified as dolomite and the white pixels will denote pixels not classified as dolomite (see Fig. 5(a)).

The second classification used is Support Vector Machine (SVM). It is a supervised machine learning model and requires a training dataset to build a hyper-plane. The pixels corresponding to GPS coordinate used in the k-means step (25˚46’00’’N, 75˚14’00’’E) is used to train the database for Zinc class. The Not Zinc class is assigned few pixels which are classified as not zinc by the k-means algorithm. Nearly 100 pixels each are used to train both the classes. Then, SVM algorithm uses the entire hyperspectral image as testing data and classifies each pixel individually. As nearly 200 pixels are used for training the hyperplane and each pixel is classified individually, the training: testing ratio is nearly 200:1. The output of the SVM module is also a black and white image where white pixels represent dolomite and black pixels represent region not having dolomite (see Fig. 5(b)).

The third classification used is Random Forest model. Being a supervised machine learning model like SVM, it also needs training dataset to configure the output of the decision trees. The same pixels used to train both the classes in SVM model are used here. As it is used for binary classification, its output is also a black and white image where the white pixels denote dolomite deposits and the black pixels denote regions not having dolomite (see Fig. 5(c)).

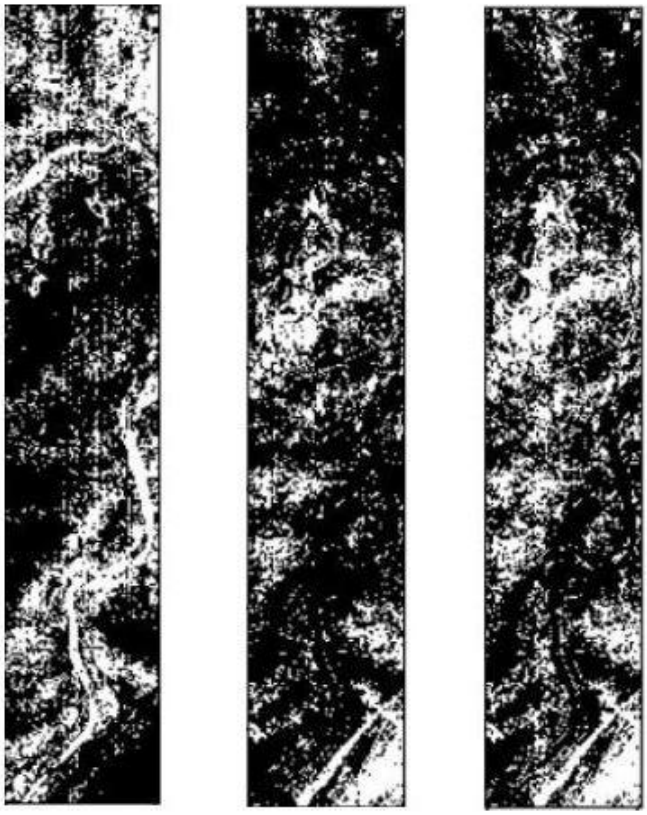

Fig. 5. Results of (a) k-means, (b) SVM and (c) Random Forest.

The region marked by Geological Survey of India as Zincian Dolomite deposit is also classified by the k-means, SVM and Random Forest modules as dolomite. Random Forest algorithm is known to be superior to the SVM and k-means models. As the ground information of each pixel in the study area is not available, finding the accuracy of the models directly is not possible. Instead, the Jasper Ridge dataset [10] is used to test the accuracy of the Random Forest model. After similarly pre-processing the dataset and classifying it using the Random Forest module, the output of the module is compared to the ground truth information available for the dataset and the confusion matrix is used to find the accuracy. The accuracy is found to be 99.27% (see Fig. 6). Thus, the output of the Random forest classification for our region of interest can be considered to be very accurate.

```
All Signatures Loded. Image Loaded
(4, 10000)
Random Forest Compared with Ground Truth.
Total Number of Pixels : 10000
Correctly Classified:  9927
Inorrectly Classified:  73
accuracy =  99.27
```

Fig. 6. Accuracy estimation of Random Forest algorithm implemented.

As the Random Forest algorithm is found to be 99.27% accurate, it's output can be used as ground truth to determine the accuracy of k-means and SVM models.

Fig. 7 (a) illustrates the confusion matrix to find the accuracy of k-means model. Fig. 7 (b) illustrates the confusion matrix to find the accuracy of SVM model.

```
Evaluating k-means
Total Number of pixels =  340736
Predicted Dolomite, Actually Dolomite :  114416
Predicted not Dolomite, Actually not Dolomite :  105960
Predicted Dolomite, Actually not Dolomite :  658
Predicted not Dolomite, Actually Dolomite :  119702
Correctly predicted pixels =  220376
Incorrectly predicted pixels =  120360
Accuracy of k-means is = 64.67646506386176
```

(a)

```
Evaluating SVM
Total Number of pixels =  340736
Predicted Dolomite, Actually Dolomite :  234046
Predicted not Dolomite, Actually not Dolomite :  76206
Predicted Dolomite, Actually not Dolomite :  30412
Predicted not Dolomite, Actually Dolomite :  72
Correctly predicted pixels =  310252
Incorrectly predicted pixels =  30484
Accuracy of SVM is = 91.05348422238919
```

(b)

Fig. 7. Accuracy estimation of (a) k-means and (b) SVM modules.

The GPS coordinates of the pixels classified as dolomite can be extracted and can be used to properly plan for mining the dolomite to extract zinc in an environment friendly way. The availability of spectral signature of Zincian Dolomite can make the classification even more accurate.

IV. Conclusion

Pre-processing the entire dataset using ENVI takes nearly 10 minutes and the three classifications implemented in python code takes one minute to execute. K-means being an unsupervised classification model gave only a 64.67% accurate output. Being a supervised model, SVM algorithm has an accuracy of 91.05% for our study area. Random Forest algorithm uses multiple decision trees for generating the output and has an accuracy of 99.27%. The Random Forest algorithm is found to be more accurate than other algorithms in the field of hyperspectral image processing and can be considered as a replacement to the existing mineral exploration techniques.

References

[1] Li Zhizhong et al., "A review on the geological applications of hyperspectral remote sensing technology," 2012 4th Workshop on Hyperspectral Image and Signal Processing: Evolution in Remote Sensing (WHISPERS), Shanghai, 2012, pp. 1-4.

[2] 2. Z. Ting-ting and L. Fei, "Application of hyperspectral remote sensing in mineral identification and mapping," Proceedings of 2012 2nd International Conference on Computer Science and Network Technology, Changchun, 2012, pp. 103-106.

[3] J. Aravinth and S. Roopa, "Identifying traces of copper in basavakote, Karnataka using hyperspectral remote sensing," 2017 International Conference on Technological Advancements in Power and Energy (TAP Energy), Kollam, 2017, pp. 1-6.

[4] S. Reshma and S. Veni, "Comparative analysis of classification techniques for crop classification using airborne hyperspectral data," 2017 International Conference on Wireless Communications, Signal Processing and Networking (WiSPNET), Chennai, 2017, pp. 2272-2276.

[5] Burges, C.J., "Data Mining and Knowledge Discovery (1998)" 2: 121. https://doi.org/10.1023/A:1009715923555.

[6] Mourya D., Bhatt A. (2018) "Classification of Hyperspectral Imagery Using Random Forest." In: Bhattacharyya P., Sastry H., Marriboyina V., Sharma R. (eds) Smart and Innovative Trends in Next Generation Computing Technologies. NGCT 2017. Communications in Computer and Information Science, vol 827. Springer, Singapore.

[7] Charlotte A. Bishop, Jian Guo Liu, Philippa J. Mason, "Hyperspecral Remote sensing for mineral exploration in Pulang, Yunnan Province China", International Journal of Remote Sensing, Vol. 32, No. 9, 10 May 2011, 2609-2426.

[8] Meerdink, S. K., Hook, S. J., Abbott, E.A., & Roberts, D.A. (in prep). The ECOSTRESS Spectral Library 1.0.

[9] Baldridge, A. M., S.J. Hook, C.I. Grove and G. Rivera, 2009. The ASTER Spectral Library Version 2.0. Remote Sensing of Environment, vol 113, pp. 711-715.

[10] Jasper Ridge dataset downloaded from http://lesun.weebly.com/hyperspectral-data-set.html.

Proceedings of the Fourth International Conference on Communication and Electronics Systems (ICCES 2019)
IEEE Conference Record # 45898; IEEE Xplore ISBN: 978-1-7281-1261-9

Analysis and Control of Hybrid Boost Converter with Simultaneous AC and DC Outputs

Akshay Laxman Pujari
Department of Electrical Engg.
Walchand College Of Engineering
Sangli, India
alpujari03@yahoo.in

D. S. More
Department of Electrical Engg.
Walchand College Of Engineering
Sangli, India
dsm.wce@gmail.com

***Abstract*—In this paper, a converter architecture which will provide a three-phase ac output and a boosted dc output simultaneously from a dc source in not more than one conversion stage is studied. This circuit known as 3-ϕ HBC (3-ϕ hybrid boost converter), is obtained from the traditional dc-dc converter operating in boost mode, where a three phase bridge circuit takes place of control switch. HBC shows immanent shoot-through protection proficiency. Such converter with better multi-output competency and authenticity is befitting the systems with both ac & dc loads in simultaneous mode e.g. PV charging stations, residential and industrial applications, etc. Independent regulation of Both the three-phase ac output and step-up dc output is attainable in case of HBC. For our intent to regulate dc as well as ac output, appropriate PWM control scheme is given in brief. To validate the converter operation, simulation results are demonstrated with resistive and inductive loads and the steady state performance analysis is done.**

***Index Terms*—Three-phase Hybrid Converter, pulse width modulation control, dc-dc boost converter, LCL filter.**

I. Introduction

Simultaneous ac and dc loads pervades most of the electric power distribution systems. Residential nano grids, electric vehicles, marinecraft power distribution are some of the typical examples of simultaneous ac and dc loads. So hybrid converter techniques are often used in all of these systems. Multiple voltage source inverters (VSI) and dc-dc converters are cascaded together to provide ac and dc outputs simultaneously, supposing that both ac and dc loads are simultaneously present. Multi-output dc-dc converters or many dc-ac inverters are used conventionally in above cases [1].

Using a hybrid-converter topology, a similar system can be obtained, which provide 3-ϕ AC and DC outputs concurrently with single circuitry. This architecture is named as a hybrid converter and is built from a boost converter where a 3-ϕ bridge network replaces the controlled switch [2]. The Hybrid converter when compared to traditional VSI, has built-in shoot-through protection capacity.

A dc-ac inverter and dc-dc converter are replaced by hybrid converter to minimize switching losses as conversion stages required are less. In the resulting hybrid converter, the essential number of switches is less to produce both 3-ϕ ac and dc outputs with enhanced reliability. Independent regulation of both the the three-phase ac and step-up dc output is possible in HBC [3]. A befitting PWM control technique [2] can be chosen to regulate both the outputs (dc and ac).

Section II presents development of hybrid boost converter. It gives insight to concept of HBC and its derivation from conventional boost converter. Section III presents the filter design both dc side output [4] and ac side output [5]. Section IV presents implementation of HBC in MATLAB simulink with experimental and graphical results for different types of load.

II. Development of Hybrid Boost Converter

As mentioned earlier, the HBC is used in marine-craft power distribution, residential Nanogrids [7], hybrid electric vehicle [8], airplanes etc.

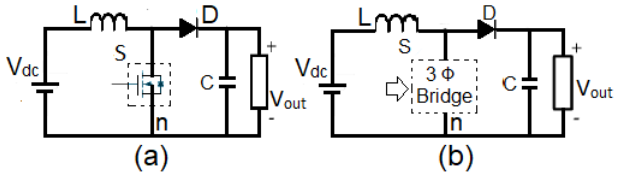

Fig. 1. Derivation of 3-ϕ HBC. (a) Traditional boost converter (b) Hybrid converter

The concept of HBC is as shown in figure 1. In Fig. 1(a), the traditional boost converter having a controlled switch S is shown.

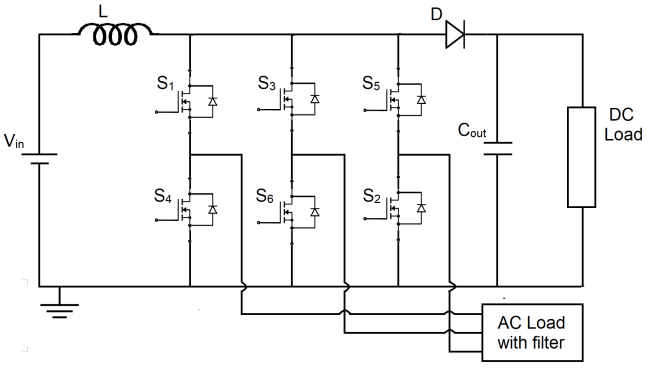

Fig. 2. Three phase hybrid converter

In case of 3ϕ HBC shown in Fig. 1(b), the three phase bridge circuit takes the place of controlled switch S. The resulting scheme shown in figure 2 is used to produce 3-ϕ ac and dc outputs.

A. Steady state operation

The regulation of both ac and the dc outputs is done by six switches of 3-ϕHBC. Converter operation can be explained through three operating intervals during its switching interval relied upon the switching states of all the six switches [2]. By turning ON both the switches of a particular limb of inverter simultaneously, the boost operation of HBC can be realized. This is similar to the condition of shoot-through, which is prohibited in traditional VSI.

The operating conditions and related intervals of the HBC are explained in this section and for entire analysis, the mode of operation assumed is continuous mode.

1) First interval : Shoot through (ST) $[(t_j - t_a)\&(t_e - t_f)]$*:* According to phase voltage magnitude, two switches of a specific leg are both turned on during this interval. The equivalent circuit diagram of hybrid converter during its first interval is shown in figure 3.

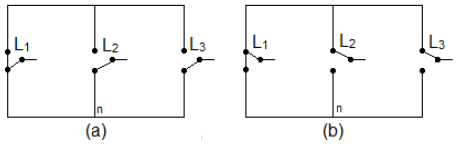

Fig. 3. Shoot through interval

Regulation the dc output is done by controlling the time duration of this interval, termed as D_{st}. This interval of HBC is analogous to the boost converter's diode 'D' being reverse biased while controlled switch being on [2]. In the first interval, the inverter output current circulates within the 3ϕ bridge circuitry. Therefore, the HBC enables an additional state that is prohibited in a VSI.

2) Second interval : Power (P) $[(t_b - t_d)\&(t_g - t_i)]$*:* In this interval any bottom or top switch of a leg and the opposite two switches of remaining legs is 'on' as shown in figure 4.

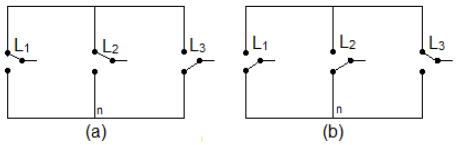

Fig. 4. Power Interval

During the second interval, the power is supplied from the source to the 3-Φ ac load. The diode D is conducting during the second interval, and 3ϕ ac current flows to the ac load [2].

3) Third interval : Zero (Z) $[(t_a - t_b), (t_d - t_e), (t_f - t_g)\&(t_i - t_j)]$*:* In the zero interval of HBC, either all the upper or all the lower switches of 3ϕ bridge network are kept 'on', as shown in figure 5.

The inductor which was charged during previous interval gets discharged during this interval. The diode D is conducting at this time and current is circulated. The third interval occurs when the inverter current gets circulated within switches of 3ϕ bridge network and does not supply any load. The key

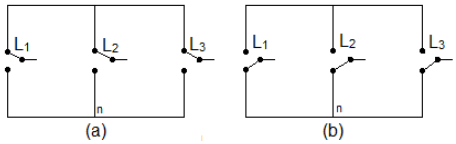

Fig. 5. Zero Interval

modification done in the states of switching is insertion of shoot-through period within the zero interval. Because of this alteration, there is no change or distortion in the magnitude or nature of ac outputs.

B. Modified pulse width modulation technique

For the purpose of regulation and control of HBC output a befitting PWM technique is described in this section and is shown in figure 6. For the 3ϕ HBC, a modification in

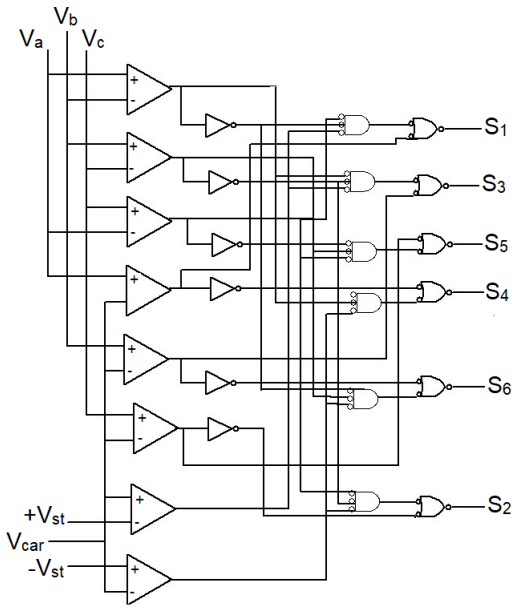

Fig. 6. Modified PWM control strategy based gate pulses for the 3-Φ HBC.

the traditional sinusoidal pulse width modulation scheme is given. This modified SPWM control strategy have a constant frequency shoot-through interval and is termed as CFST-SPWM technique [2].

In this modified PWM technique, the performed shoot-through period depends upon the relative voltage levels of the respective phases. Figure 7 shows the gate pulses obtained from the control logic where $v_a > v_b > v_c$ are the respective voltages of the three phases.

In the illustration shown in figure 7, switches S_1 & S_4 goes in shoot-through mode. To regulate and control both the 3ϕ

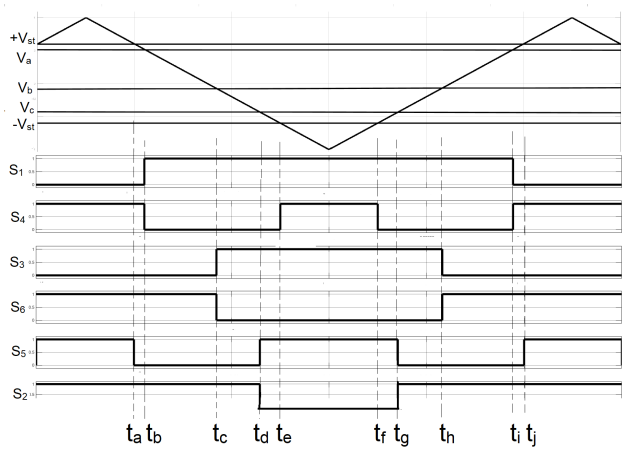

Fig. 7. Modified PWM control strategy for the 3-Φ HBC.

ac and dc outputs some references are required for generating gate pulses: v_a, v_b & v_c are the three reference ac signals which decides the modulation index and helps regulating the 3ϕ ac outputs. Magnitude of $+V_{ST}$, and $-V_{ST}$ are decided by the shoot-through duty cycle which controls the dc output.

III. Filter Design

Three phase voltage source inverters (VSI) are used widely In most of the grid connecting applications. The distorted grid current affects the performance of VSI. The use of power converter devices is very vital in enhancing power transmission from source to the utility grid. Harmonics are the main factors causing problems to apparatus and the loads connected to it, substantially for the applications above several KW, where the appraise of total harmonics distortion (THD) and filters is also an important regard in the systems designing. LCL filter has come into wide use in the grid connected inverter applications. What is the most difficult is that how to select the parameters and control the resonance [5].

A. DC-DC converter side

1) Boost Converter: A boost converter is used to step-up a dc voltage. The output voltage of boost converter is greater than the input voltage. The amplitude of the output voltage rely on duty cycle [4].

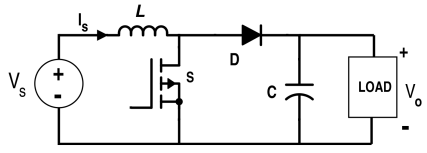

Fig. 8. Boost converter.

Figure 8 shows boost converter scheme. When 'S' is turned off, the inductor gets charged and energy is stored in it. If the switch opens, the energy stored in inductor is given to the load through diode 'D'.

The total power is conserved at the both ends, despite stepping up or stepping down of voltage level. The law of a conversion of energy can be expressed as,

$$Input\ \ power(P_{in}) = Output\ \ power(P_{out}) \tag{1}$$

The o/p voltage should be greater than i/p voltage ($V_{out} > V_{in}$) for the step up mode. Therefore the output current is less than the input current.

$$V_{in} < V_{out}\ \ and\ \ I_{in} > I_{out} \tag{2}$$

The voltage across inductor is,

$$V_L = L\frac{d_i}{d_t} \tag{3}$$

The ripple current in the inductor can be given as follows,

$$\Delta I = \frac{V_s}{L} \tag{4}$$

2) Necessary Parameters for the calculation: Following are the necessary parameters while calculating input inductor and output capacitor values [4]:

1) Input Voltage: V_{in}
2) Output Voltage: V_{out}
3) Max. Output Current: $I_{OUT(max)}$

After getting these parameters, calculation can be done as follows.

3) Determination the duty cycle: First it is essential to determine operating duty ratio D, for a particular level of input voltage.

$$D = 1 - \frac{V_{in} \times \eta}{V_{out}} \tag{5}$$

Where, $\eta =$ Converter efficiency, estimated value is 85 %

4) Input inductor selection: A fine estimate of the inductor ripple current is 20 % to 40 % of the obtained output current.

$$\Delta I_L = 1 - (0.2\ \ to\ \ 0.4) \times \frac{V_{out}}{V_{in}} \tag{6}$$

The calculation for the input inductor can be done as follows,

$$L = \frac{(V_{in} \times (V_{out} - V_{in})}{\Delta I_L \times f_s \times V_{out}} \tag{7}$$

Where, $f_s = Switching frequency$

5) Output capacitor selection: To calculate the appropriate output capacitor, following equation can be used [4].

$$C_{out} = \frac{(I_{out} \times D)}{f_s \times \Delta V_{out}} \tag{8}$$

Where, ΔV_{out} is the ripple in output voltage, we can take upto 1% of V_{out}

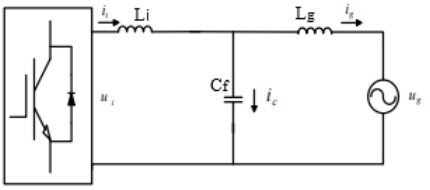

Fig. 9. LCL filter.

B. DC-AC converter side

Nowadays LCL filter is used replacing the traditional L-filter to get a ripple-free output current. The ability of LCL filter to lessen the amount of current distortion, makes it suitable for grid connected inverter systems [6].

A significant reduction in the total harmonic distortion (THD) can be obtained with the help of a LCL filter. Not only it lowers the current ripple across the inductor, but also it prevents direct coupling between filter and grid impedance. Hence, a suitable LCL filter is chosen for our application [5].

1) Essential Parameters for the calculation: Following are the essential parameters for calculating the filter parameters:

1) Inverter Output power: P_n
2) Expected inverter output voltage: E_n
3) Input voltage: V_{dc}
4) Switching frequency: f_{sw}
5) Operating frequency: f_n

2) Base values for inverter: While designing the LCL filter some base values are taken as reference and the LCL filter parameters will be determined in a percentage of it. The base capacitance and base impedance are calculated as follows. Thus,

Base impedance:

$$Z_b = \frac{E_n^2}{P_n} \tag{9}$$

Base capacitance:

$$C_b = \frac{1}{(w_n \times Z_b)} \tag{10}$$

3) Inverter side inductance: While designing the LCL filter components, first we will design the inverter side inductance. This inverter side inductor will suppress the current ripple by a significant percentage. It can be calculated as follows [6],

$$L_i = \frac{V_{dc}}{(16 f_s \times \Delta I_{Lmax})} \tag{11}$$

where, ΔI_{L_max} is the ac output current ripple which can be given as follows,

$$\Delta I_{L_max} = 0.1 \frac{\sqrt{2} \times P_n}{E_n} \tag{12}$$

4) Filter capacitance: To design the filter capacitance, the base capacitance value is taken as reference and value for filter capacitance is calculated as follows,

$$C_f = 0.05 \times C_b \tag{13}$$

Here, the estimated power factor variation seen is taken as 5%.

5) Load side inductance: Load side inductance is taken as r fraction of inverter side inductance and is calculated as follows,

$$L_g = r \times L_i \tag{14}$$

6) Resonant frequency: The calculation for resonant frequency for the L-C-L filter can be done as follows,

$$f_{reso} = \frac{1}{2\pi} \times \sqrt{\frac{L_i + L_g}{L_i \times L_g \times C_f}} \tag{15}$$

7) Damping resistance: To avoid resonance, the filter capacitor is kept with a damping resistor in series. It can be given by following equation [5],

$$R_d = \frac{1}{3\omega_{res} \times C_f} \tag{16}$$

Following are the system parameters obtained and used for implementation of HBC in MATLAB Simulink.

TABLE I
SYSTEM PARAMETERS

	Parameters		Parameters
DC	V_{in}=48V	AC	P_n=15W
	V_{out}=75V		E_n=21.72V
	$I_{OUT(max)}$=2A		f_{sw}=10KHz
	D=45%		f_n=50Hz
	$\Delta I_L = 625mA$		Z_b=31.45Ω
	L=2.764mH		C_b=101.2μF
	C_{out}=0.12 mF		L_i=3.073mH
			C_f=5.06μF
			L_g=1.84mH
			f_{res}=2.085KHz
			R_d=5.02Ω

IV. IMPLEMENTATION OF HBC IN MATLAB SIMULINK

Implementation of HBC is done in MATLAB Simulink along with the designed filter. The simulation results are taken for different types of loads. The effect of variation of modulation index and duty cycle are plotted in a graphical manner.

A. Load parameters of System

Following are the system load parameters used while developing and implementing the HBC.

TABLE II
LOAD PARAMETERS OF SYSTEM

	Parameters
DC load	R_{dc}=50ω
Resistive ac load	R_{ac}=50ω
Inductive load	R_{ac}=50ω ; L_{ac}=19.49mH

B. Simulation Results

By using the given system parameters, the simulation is done in MATLAB simulink for resistive load and inductive load. The simulation results are illustrated in fig 10, fig 11 and fig 12 for inductive load on HBC with filter. Fig 10 shows dc output current & dc output voltage for input voltage of 48V. The modulation index and the shoot through duty cycle taken for this particular simulation result are 0.55 and 0.4 respectively.

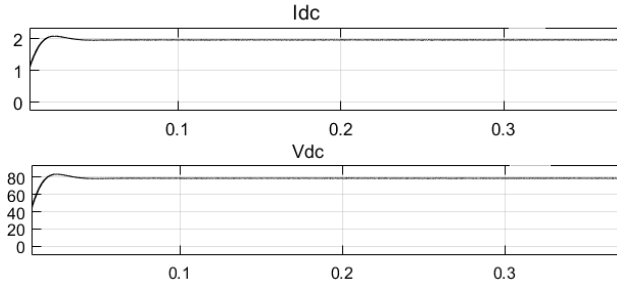

Fig. 10. DC Output of 3ϕ HBC.

Figure 11 illustrates the ac outputs i.e. phase current, phase voltage and line voltage where the dc input is 48V. In figure 12 FFT analysis window is displayed which gives THD in phase voltage which is approximately 1.55 %

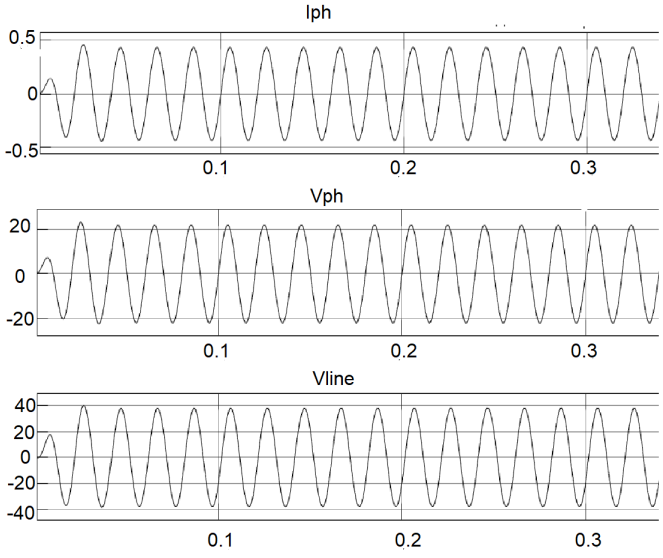

Fig. 11. AC Output of 3ϕ HBC.

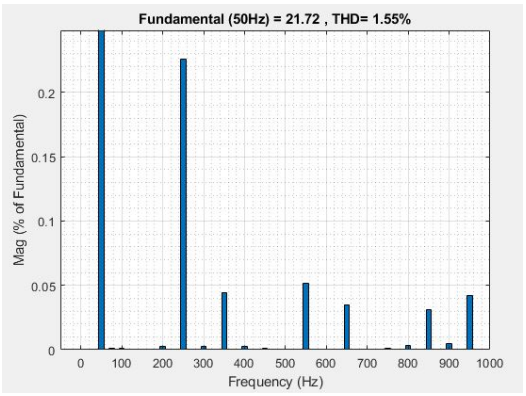

Fig. 12. THD in phase voltage of 3ϕ HBC

C. Graphical results

For different loadings, the observations are taken and results are plotted for the particular type of load. The objective is to see the effect of change in modulation index and change in shoot through duty ratio on both the outputs (dc output and ac output).

1) Resistive load without filter: First we vary the modulation index by keeping D_{st} constant and then we vary D_{st} by keeping the modulation index constant. By taking the observations as shown in above tables, we plot the graphs for THD V_s M, V_{dc} V_s M, and V_{ph} V_s M by varying modulation index as shown in fig 13(a) and THD V_s D_{st}, V_{dc} V_s D_{st}, and V_{ph} V_s D_{st} by varying shoot through duty cycle (D_{st}) as shown in fig 13(b).

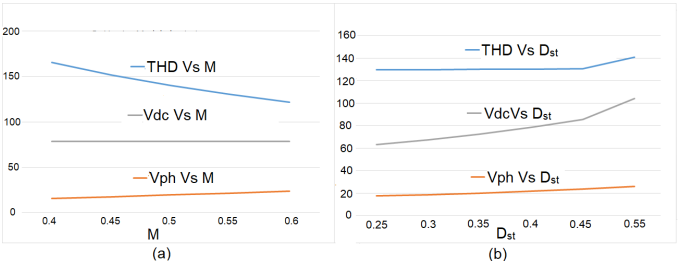

Fig. 13. Resistive load without filter (a) By varying M. (b) By varying D_{st}.

2) Resistive load with filter: After getting the observations for the simulation without using filter, the LCL filter designed in section III is used further. Here We plot the graphs for THD V_s M, V_{dc} V_s M, and V_{ph} V_s M by varying modulation index as shown in fig 14(a) and THD V_s D_{st}, V_{dc} V_s D_{st}, and V_{ph} V_s D_{st} by varying D_{st} as shown in fig 14(b).

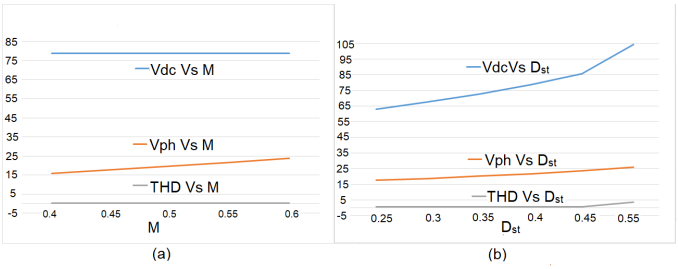

Fig. 14. Resistive load with filter (a) By varying M. (b) By varying D_{st}.

3) RL load with filter: First we vary the modulation index by keeping D_{st} constant and then we vary D_{st} by keeping the modulation index constant.We plot the graphs for THD V_s M, V_{dc} V_s M, and V_{ph} V_s M by varying modulation index as shown in fig 15(a) and THD V_s D_{st}, V_{dc} V_s D_{st}, and V_{ph} V_s D_{st} by varying D_{st} as shown in fig 15(b).

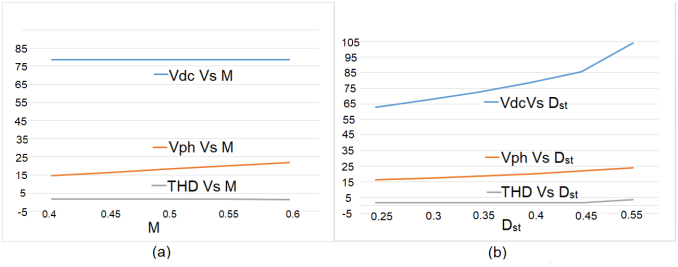

Fig. 15. RL load with filter (a) By varying M. (b) By varying D_{st}.

V. Steady State Analysis

For the purpose of steady state analysis of HBC, the mode of operation assumed is continuous conduction. The step-up dc output voltage is related to the dc input voltage as follows [2],

$$\frac{V_{dcout}}{V_{dcin}} = \frac{1}{1 - D_{st}} \tag{17}$$

For the modulation index 'M', relation between the ac output line voltage and dc input voltage can be given by following expression,

$$\frac{V_{acout}}{V_{dcin}} = 0.612 * \frac{M}{1 - D_{st}} \tag{18}$$

From the relations (17) and (18), it can be concluded that the shoot through duty cycle D_{st} regulates only the dc output and modulation index M regulates the ac output. Compared to the modulation index, if the variation of D_{st} is assumed to be small, then independent control of both the outputs can be achieved [2]. The magnitude of the input current of a HBC can be given by,

$$I_{dcin} = I_L = \frac{V_{dcout} I_{dcout} + 3 V_{ph} I_{ph} cos\phi}{V_{dcin}} \tag{19}$$

where, V_{ph}, I_{ph} and cosϕ are the ac output phase voltages, phase currents and load power factor respectively and V_{dcout}, I_{dcout} are the dc output voltage and output current respectively.

Expressions (20) and (21) show the expressions for dc and ac output power for the HBC [2]. Here, the loads at the dc and ac outputs are considered purely resistive, and equal to R_{dc} and R_{ac}.

$$P_{dc} = \frac{V_{dcin}^2}{R_{dc} * (1 - D_{st})^2} \tag{20}$$

$$P_{ac} = \frac{3 M^2 V_{dc_i n}^2}{4 R_{ac} * (1 - D_{st})^2} \tag{21}$$

In HBC, both the dc and ac outputs are regulated using two control variables within the same switching period. Hence, for independent control of each output, following relation must be satisfied [2].

$$M + D_{st} \leq 1 \tag{22}$$

VI. Conclusion

A three phase hybrid converter with ac and dc outputs in simultaneous manner is simulated. From the above observations and simulation results, it can be easily concluded that the HBC topology is advantageous over conventional multi-converter based topologies. It exhibits immanent shoot-through protection capability. In HBC switching loss is minimized by integrating a dc-ac converter and boost converter into a single converter architecture. The simulation results shows the potency of the modified PWM technique. DC output is regulated by D_{st} and is dependent only upon D_{st}. AC output is regulated by M and is dependent upon both M and D_{st}.

References

[1] O. Ray and S. Mishra, "Boost-derived hybrid converter with simultaneous DC and AC outputs," in IEEE Transactions on Industry Applications, vol. 50, no. 2, pp. 1082-1093, March-April 2014.
[2] O. Ray, V. Dharmarajan, S. Mishra, R. Adda and P. Enjeti, "Analysis and PWM control of three-phase boost-derived hybrid converter," 2014 IEEE Energy Conversion Congress and Exposition (ECCE), Pittsburgh, PA, 2014, pp. 402-408.
[3] Tazay and Z. Miao, "Control of a three-phase hybrid converter for a PV charging station," in IEEE Transactions on Energy Conversion, vol. 33, no. 3, pp. 1002-1014, Sept. 2018.
[4] Brigitte Hauke, Basic Calculation of a Boost Converter's Power Stage Texas Instruments SLVA372CNovember 2009Revised January 2014.
[5] A.E.W.H. Kahlane , L. Hassaine and M. Kherchi, LCL filter design for photo-voltaic grid connected systems, Revue des Energies Renouvelables SIENR14 Ghardaa (2014) 227 232.
[6] Vasconcelos Araujo, Samuel & Engler, Alfred Sahan, Benjamin & Antunes, F.L.M.. (2007). LCL filter design for grid-connected NPC inverters in offshore wind turbines. Fraunhofer IWES. 1133 - 1138. 10.1109/ICPE.2007.4692556.
[7] Santanu Mshra, Olive Ray, Advances in Nanogrid Technology and Its Integration into Rural Electrification in India The 2014 International Power Electronics Conference, 978-1-4799-2705-0/14/2014 IEEE.
[8] Murat Yilmaz, Philip T. Krein, Review of Battery Charger Topologies, Charging Power Levels, and Infrastructure for Plug-In Electric and Hybrid Vehicles IEEE Transactions On Power Electronics, Vol. 28, No. 5, May 2013.
[9] Mohan, Ned. Chapter 7 Dc-Dc Switch-Mode Converters. Power Electronics: Converters, Applications and Design, by Ned Mohan and Tore M. Undeland, John Wiley & Sons, 1995, pp. 161195.
[10] Bin Wu, High-Power Converters and AC Drives, IEEE press, A John Wiley & Sons,Inc., Publication.
[11] B. K. Bose, Modern Power Electronics and AC Drives, Prentice Hall PTR publications.

Proceedings of the Fourth International Conference on Communication and Electronics Systems (ICCES 2019)
IEEE Conference Record # 45898; IEEE Xplore ISBN: 978-1-7281-1261-9

An enhanced approach for movie review analysis using deep learning techniques

Aswathi Sajeevan
P.G Scholar, Department of Information Technology, Rajagiri School of Engineering and Technology, Kochi, Kerala, India

Lakshmi K S
Assistant Professor, Department of Information Technology, Rajagiri School of Engineering and Technology, Kochi, Kerala, India

***Abstract*—The principle thought behind the sentiment analysis is to predict the emotions or opinions of the general population towards a specific subject from organized, semi-organized or unstructured literary information. With the rapid growth of internet, people around the world are increasingly passionate about expressing their emotions and opinions on the internet. Most of the industries and organizations formulate significant decisions based on customer reviews available on social websites. Due to the fast advancement in text data processing, sentiment analysis has turned into a significant research direction in Natural language processing (NLP). In recent days, the popularity of the deep learning techniques is also gaining attention which in turn contributes to enhancements in existing sentiment analysis techniques. In this paper, we perform analysis of movie reviews using a combination of deep learning techniques, LSTM and CNN. CNN is a commonly used deep learning method used for feature learning. LSTM is a unique sort of RNN, which is equipped for adapting long term conditions. This model allows remembering of information over a much longer period. We apply two different deep learning models to classify IMDB movie reviews. The first model is a hybrid LSTM- CNN and second is hybrid CNN-LSTM. We found that LSTM-CNN model outperformed CNN-LSTM model with an overall accuracy of 79%.**

Keywords: CNN, Deep Learning, Machine Learning, LSTM, RNN

I. INTRODUCTION

Due to the popularity of internet and new technologies, the measure of data delivered by humanity is developing quickly every year. Big data refers to collection of large datasets that cannot be processed using traditional computing techniques. Huge information isn't simply information; rather it has turned into a total subject, which includes tools, techniques and frameworks. It utilizes predictive analytics, client behavior analytics, or certain other propelled data analytics techniques that extract valuable information from data. This is known as big data analytics. The essential objective of big data analytics is to help organizations settle on progressively educated business choices by empowering data scientists, predictive modelers and other analytics professionals to analyze huge volumes of data, just as other types of data that might be undiscovered by conventional business intelligence (BI) programs.

Analysis of sentiment has become an important research direction in the processing of natural language. The main idea behind the sentiment analysis is to predict people's emotions or opinions from structured, semi structured and unstructured textual data towards a particular topic [1]. The text data contains human more elevated level sentimental characteristics. With the quick development of internet, individuals around the world are progressively passionate about communicating their feelings and opinions on the web. Most companies and enterprises analyze customer satisfactions based on their reviews on various social internet sites. In most organizations, more than 75 percent of information is about how customers engage with the product. Tracking this relationship using text mining is essential when designing major tactics in any company. The large user-generated content requires the use of automated text mining and analysis technique as crowd sourced mining and analysis are often filled with errors, expensive and scale- free. In the early days people will seek opinions from colleagues, relatives and neighbors before purchasing an item or service. In recent days, people will get opinions from various social websites. For example, if a person wants to buy a new mobile manufactured by a particular company and he/she require the mobile with best camera clarity. Suppose he/she finds a review like, "The picture clarity of this mobile is very bad and doesn't provide zooming option properly", the user can opt for another mobile since the opinion is negative. In such situations, sentiment analysis plays a crucial role.

Sentiment analysis is done with the help of machine learning, which is an application of artificial intelligence (AI) that gives frameworks the capacity to automatically learn and improve from experience without being explicitly customized. The fundamental reason of machine learning is to construct algorithms that can take input information and utilize statistical analysis to foresee an output while refreshing output as new information becomes available. Deep learning is a data mining process [2]using deep neural network architecture, that are specific types of artificial intelligence and machine

learning algorithms that have become extremely important in recent years. Deep learning enables us to teach machines how to finish difficult tasks without coding them explicitly to do so. Machine learning methods detect the pattern available from given set of text data automatically. Deep learning is an advancement of machine learning.

This paper is to use deep learning techniques such as Convolutional Neural Network (CNN) and Long Short Term Memory (LSTM) network to analyze film reviews. Recently, deep learning methods have shown good results across different NLP tasks. We apply two different deep learning models to classify IMDB movie reviews. The first model is a hybrid LSTM- CNN and second is hybrid CNN-LSTM. We found that LSTM-CNN model outperformed CNN-LSTM model with an overall accuracy of 79%. Hybrid CNN-LSTM and LSTM-CNN architectures are implemented on the data set and results are compared.

II RELATED WORKS

Sentiment analysis method can be split into dictionary based and machine learning based. Two types of dictionary based methods are WordNet and Senti WordNet. WordNet is a lexical English language data base that combines English words with synonyms called synset. It distinguishes nouns, verbs, adjectives and adverbs. Next is the SentiWordNet is a WordNet extension. For each WordNet synset, Senti WordNet sets positive and negative sentiment scores. Using a positive and negative score, the object score can be calculated. We obtain object score as a summation of positive score and negative score subtracted from 1.Tokenization,speech tagging ,word sense disambiguation (WSD),Senti WordNet interpretation, sentiment orientation and tweet classification are used to perform dictionary based methods [3].Dictionary based approaches major downside is the inability to evaluate opinion words with domain and context.

Machine learning methods are categorized into two, supervised learning techniques and unsupervised learning techniques. Supervised learning uses labelled training documents. Training data includes a pool of training examples. Each example of supervised learning consists of an object of input and a value of output. Unsupervised methods of learning don't use the documents labelled. They create use of the statistical properties of the document for example, word co-occurrence, existing dictionaries with passionate words and natural language processing. Natural language or human objects such as photographs, news articles and audio recordings are unlabelled data, whereas each set of unlabelled data with meaningful tags is labelled data. For example, photo is an unlabelled data but that photo is an elephant that is labelled data.

Various machine learning methods [4] are used for classification of sentiments but are associated with certain disadvantages. For example commonly used machine learning methods are Support vector machine (SVM), Maximum entropy (ME) and Naive Bayes (NB) everyone has advantages and disadvantages. SVM and ME are complex models that take longer train. Naïve Bayes approach does not take the word order from the text input and therefore leads to a less accurate model. Another method of modeling is n-grams, but this has a fixed range and cannot be learned for long-term dependencies. Also, these approaches often refuse to categorize sentences with negation. Using deep learning methods, these problems are overcome.

A future where in machines will do many of the jobs right now being finished by people previously, we'd need to expressly program a PC well-ordered how to take care of an issue. A lot of if-then statements, loops, and logical operations were involved. Later on, machines will show themselves how to take care of issues; we simply need to give the information. Give us a chance to find out about the methods that enable profound figuring out how to take care of an assortment of issues. Deep learning is a data mining process using deep neural network architecture, that are specific types of artificial intelligence and machine learning algorithms that have become extremely important in recent years. Deep learning enables us to teach machines how to finish difficult tasks without coding them explicitly to do so. Machine learning methods detect the pattern available from given set of text data automatically. Deep learning is an advancement of machine learning.

By far most of studies have used SVM, Naïve bayes and other conventional strategies, which subject to physically labelling of a ton of energetic qualities, anyway paid a surprising expense. Hadi Pouransari et al [5] utilized the dataset given by Kaggle and connected the bag of words, and skip-gram word2vec models to represents words numerically. We at that point utilized a few classifiers, including random forest, SVM, and logistic regression to play out the binary classification task. The authors facing one of the difficulties is to aggregate word vectors into a solitary element vector for each review. We attempted vector averaging, and grouping to deliver the aggregated feature vectors. Be that as it may, these experience the ill effects of losing the order of words in sentences.

To improve this situation, Liu Yanmei et al [6] additionally examined deep learning and Micro-blog sentiment analysis, and introduce deep learning CNN with SVM classifier. This Framework maintains a strategic distance from issues because of the explicit feature extraction however numerous troubles are looked in emotional analysis utilizing deep learning. Creator doesn't discover great answer for this. This paper exhibits that, this structure is great to upgrade the exactness of sentiment analysis, anyway there are up till now various issues in the investigation of emotional analysis using deep learning, the accompanying stage will be to also think about the deep learning systems for finding a progressively sensible sentiment analysis.

Yaya Heryadi et al [7] use CNN, Stacked LSTM, and CNN-LSTM models to find fraudulent card transaction. In this paper obtain both short-term and long-term transaction pattern with the help of CNN and LSTM. Results of the experiment showed that CNN is more robust than SLSTM and CNN-LSTM as an imbalanced dataset classifier. It is further assumed that CNN layers contribute to the CNN-LSTM model's high performance.

Alec Yenter et al [8] This work utilize the benefits of both CNN and LSTM.CNN goes about as a good feature learner yet CNN doesn't catch long term dependencies .This issue defeat with the assistance of LSTM.LSTM layer is stacked above of convolutional layer. Output of the convolutional layer served as an input to the LSTM. While over fitting was a challenge for most forms of the model, appropriate layers and parameters had the option to decrease the disintegration and achieve new accuracy on the dataset.

III BACKGROUND

Basis of deep learning method is an Artificial Neural Network (ANN).An ANN is an information processing system that is simulated through biological nervous systems, meaning it contains lots of neurons, which are the key element of this paradigm and information about processes. An ANN is designed through a learning process for a particular application, e.g. hidden pattern recognition or data classification. Artificial neural network comprise of 3 layers named as input layer, hidden layer and output layer. Input layer, which connects to the input vector and output layer, which relates to the output vector. Moderate layer is called hidden layer, which play out some calculation with the assistance of some activation functions. Essential computational element of neural network is called activation function. Generally utilized activation functions [9] are sigmoid function, hyperbolic tangent function (tanh), or rectified linear function (ReLU). A line between two layer is indicates an association for the progression of data. Every association is related with an value is called weight, that controls the signal between two neurons. The common deep learning methods used for sentiment analysis are discussed here.

1) Convolutional Neural Network (CNN)

Convolutional neural networks [9] are deep neural networks that are utilized basically to classify pictures (for example name what they see), cluster them by similitude (photograph seek), and perform object recognition inside scenes. They are algorithms that can distinguish faces, people, road signs and many other different parts of visual information. The viability of convolutional net in image recognition is one of the principle reasons why the world has woken up to the adequacy of deep learning. Recently CNN can also be applied to text analysis.

CNN model comprises of one input layer, multiple hidden layers which are convolutional layers, pooling layers, fully connected layers, and one output layer. CNN contain some Convolutional layers that apply a convolution task to the input, and the outcome is going to the following layer. Convolutional layer contains different filters that do convolutional action. The filter is extremely an assortment of number or weights. After convolutional operation we get numerous number of feature maps. Next comes the pooling or down sampling layer, which comprises of applying some activity over regions in the input feature map and removing some delegate an incentive for every one of the examined regions. The pooling operation is utilized to consolidate the vectors coming about because of various convolution windows into a single dimensional vector. Finally the yield is goes to the fully connected layer of neural system for classifying.

2) Long Short-Term Memory (LSTM)

LSTM is a sort of Recurrent Neural Network (RNN)[8]. In conventional Neural Networks, all data sources are independent of each other. While this methodology is wasteful for certain assignments in NLP for this situation it is critical to realize the past word so as to foresee the following word in context. LSTM neurons have an association with the past neuron state notwithstanding the layer inputs. It's demonstrated extraordinary achievement in numerous NLP tasks. LSTM units have a memory which catches data in subjective, long sequences. The LSTM model comprises of memory cells to keep up information over extensive stretches of time with the assistance of gating units. The gating units are choosing what information to store and when to apply that information. Every memory cell isolated in to 3 gates named as input gate, forget gate and output gate.

Every one of the neural networks handles one time step. Rather than bolstering the information at every individual time step, you give information at all-time steps inside a window, or a context, to the neural network. The cell is in charge of monitoring the dependencies between the components in the input sequence.

IV PROPOSED WORK

In this area, we include the details of two proposed deep learning architecture hybrid CNN-LSTM and LSTM-CNN method. Proposed method comprises of pre-processing module, embedded module, feature extraction module and classification module.

A) Existing Method

Figure1 shows the architecture of CNN-LSTM method. Abdalraouf Hassan [10] et al introduces a deep convolutional and recurrent layer approach for sentiment classification. In this paper, Maxpool layer is replaced with recurrent layer in order to catch the long term dependencies. We are implementing CNN-LSTM framework without replacing the maxpool layer.

a) Text Reviews

System input consists of reviews of movies. Only English reviews are included, and there is a white space around punctuation such as period, bracket, and commas.

b) Pre-Processing
To improve the performance of our model we need to perform pre-processing steps. To begin with, we performed data pre-preparing steps on the dataset before bolstering them into the deep learning model. We expelled punctuations, stop words, brackets numbers and also perform stemming by using regular expressions. After cleaning the dataset next perform tokenization with the help of tokenize API. Tokenization is the process of converting words into a unique integer. Then we created a vocabulary to map these words into a integer.
c) Embedded Layer
Embedded layer takes the input text reviews as a sequence of words and embeds each word into a vector of a particular size

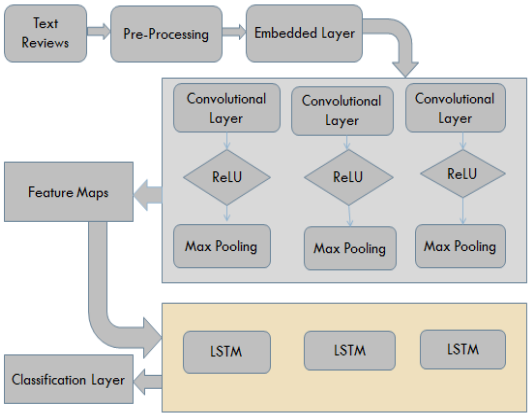

Figure 1 : Existing CNN - LSTM Architecture

d) Convolutional Layer
Convolutional layers can obtain feature horizontally from multiple words. For classification tasks, these characteristics are essential .Convolutional layer that will take word embedding as input. Numerous convolutional layers apply a convolutional operation to the input; the outcome is going to the following layer.
e) Max Pooling Layer
Pooling layer is likewise called sub sampling layer, which can minimize the number of features and the computational intricacy of the system. Sub sampling step retain most significant data.
f) LSTM Layer
Extracted features are classified with the help of LSTM layer. It is a special kind of RNN, which is equipped for adapting long term dependencies. LSTM's viability is its capacity to catch changing sentiments in a tweet. That has a memory that "remembers" previous data from the input and makes decisions based on that knowledge. The layer's steadiness permits learning of past info to impact subsequent input.
g) Classification Layer
Fully connected layer acts as a classification layer. The LSTM outputs are then fed to a Fully Connected Layer (FCL) which was built using Keras dense layer. A simple sigmoid activation function follows this layer to confirm the output somewhere in the range of 0 and 1.

B) Proposed Method
Proposed system used IMDB movie review dataset which contains positive movie reviews and negative movie reviews. The system is implemented in Anaconda(Python Distribution).Keras is used to implementing deep learning layers .It is an easy to use and powerful python library for deep learning. Tensor flow is set as a backend of Keras and Matplotlib is used to analyse the graph. Windows 8.1 is the Operating System. The system in which it is implemented is a 64 bit system with Intel Pentium CPU and 4 GB memory.

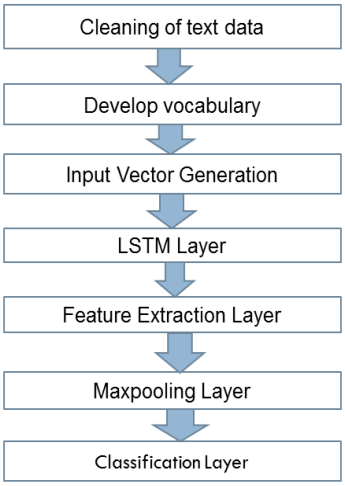

Figure 2 :Flow Diagram of LSTM-CNN Architecture

a) Cleaning of Text Data
Input of the system consists of text movie reviews. It is comprised only English reviews and there is a blank space around punctuation like period, bracket and full stop. This text data need a cleaning that implies remove punctuation from words, evacuate tokens that are simply accentuation, expelling tokens that contain numbers, expelling tokens that have one character and evacuate tokens that don't have much significance with the help of a regular expression.
b) Develop Vocabulary
We joined each review sentences as a string and split the sentences to make a list of all the individual words that appeared in the dataset. Then, we created vocabulary to map these words to integers. Each words in the vocabulary represented by a unique integer. We can keep track of the vocabulary in a Counter, which is a lexicon of words and their count with some additional convenience functions. Then needs to add every one of the tokens to counter and update count with the assistance of an update function. Then needs to add all the tokens to counter and update count with the help of an update function on the counter object.
c) Input Vector Generation
Input vector generation done with the help of an embedding layer [11]. the model will take as input an integer matrix of size (batch, input length).Embedding layer design with the help following function *" Model. Add (Embedding (vocab*

size, 100, input length))". Here, vocab_size indicate the magnitude of the vocabulary, 100 indicate the magnitude of embedding vector and input_length indicate length of input sequence.

d) LSTM Layer

LSTM is progressively viable to defeat the sequence data weakening issue when the text sequence data is somewhat long. Even though the input text sequence is long LSTM layer is able to capture long term dependencies efficiently. LSTM layer is designed with the help of LSTM function that contain 100 LSTM units represented as a *"model.add(LSTM(100,return_sequence=True)"*.Then,the LSTM output are fed to a convolutional layer

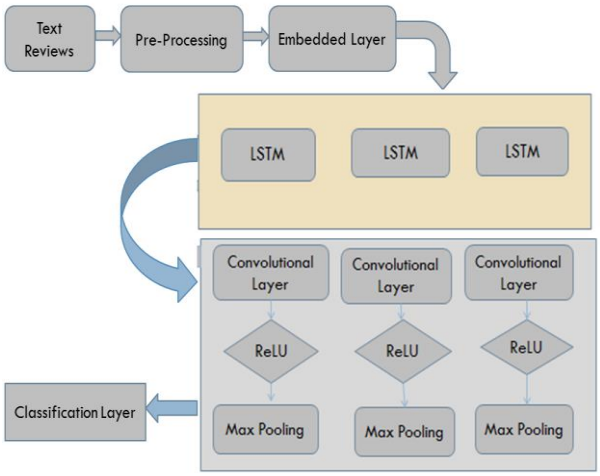

Figure 3 : Proposed LSTM-CNN Architecture

e) Feature Extraction

Convolutional layer acts as a feature extractor. Convolutional layer performs convolution operation with the help of filters. The filter is used to scan the input vector and get number of feature maps or activation map. Convolutional layer design with the help of following function *"model.add(Conv1D(filters=32, kernel size=8, activation='relu'))"*.Here filters indicate number of filters and kernel size represents size of the convolutional window. After convolutional task, applies a rectified linear unit (ReLU) activation function to the CNN layer's output. This layer substitute zero for any negative output. The output of this layer is a similar to input shape.

f)Maxpooling Layer

Subsampling layer is used to minimize the spatial size of the representation thus reduces the network computational complexity. Commonly used subsampling operation is maxpooling. Maxpooling layer retain most important feature maps or information and others are discarded. Maxpooling layer designed with the help of following function *"model. Add (MaxPooling1D (pool_size=2))"*

g) Dense Layer

Fully connected layer acts as a classification layer. The Pooled outputs are fed to a Fully Connected Layer (FCL) which was built using Kara's dense layer. A simple sigmoid activation function follows this layer to confirm the output somewhere in the range of 0 and 1.The final yield is a single output 0 which represents an adverse feeling and 1 represents positive feeling.

V RESULTS AND DISCUSSIONS

The proposed system uses IMDB movie review data set which contains 1000 positive reviews and 1000 negative reviews. For training and validation, we arbitrarily split the full training examples. Input dataset divided into two, training dataset and validation dataset. Keras provide two methods to evaluating deep learning model. First one is automatic verification of dataset and second is manual verification of dataset. Keras separate one portion of training data into validation data and then assess the performance of our model on that validation dataset on every epoch. Experiment used the following parameters which we fine-tuned through manual testing.

Embedding Dimension	100
Epoch	10
Filters	32
Kernel Size	8
Pool Size	2
Dropout	0.5

Table 1: Hyper parameters

A) Accuracy

The proposed LSTM-CNN network reached 79% accuracy in 10 epochs. Accuracy of the system is directly proportional to epochs.

	Epoch 10	Epoch 20	Epoch 30
	Average Accuracy	Average accuracy	Average Accuracy
LSTM-CNN	78%	79%	79.5%
CNN-LSTM	51%	51.5%	51.75%

Table 2: Comparison Table

From the Table 1 it is clear that LSTM–CNN model achieved a satisfactory accuracy score compared to CNN-LSTM model

B) Performance Analysis

Learning curves are widely used as performance analysis tool in case of deep learning. The model can be assessed on the training dataset and validation dataset. Graph that looks at the performance of a model on training and testing information over a fluctuating number of training instances. We should

generally observe performance improve as the number of training point's increments.

There are mainly two learning curves namely train learning curve and validation learning curve. If there should arise an occurrence of train learning curve, the learning curve is determined from the training dataset that gives a thought of how well the model is training. While if there should arise an occurrence of validation learning curve, the learning curve is determined from hold-out validation dataset that gives a thought of how well the model is generalizing. It is entirely expected to make double learning curves during training on both the training and validation dataset.

Here the horizontal axis denotes the Epochs while the vertical axis denotes the Accuracy and loss for the performance analysis of IMDB movie review dataset. Epochs represents the number of iteration taken by our project. Time taken by the method is directly proportional to epochs.

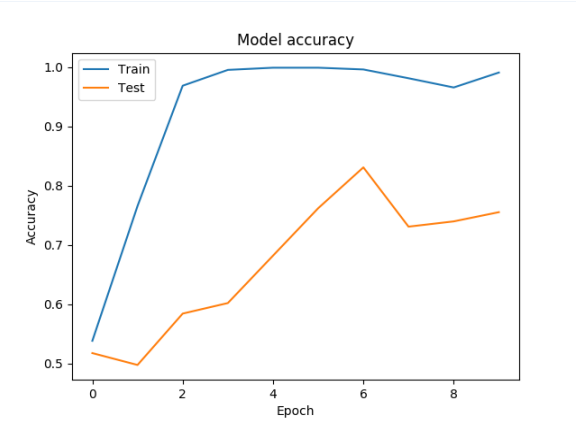

Figure 4: LSTM-CNN Accuracy

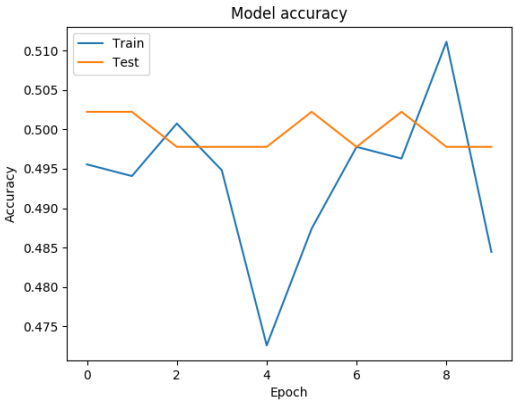

Figure 5: CNN-LSTM Accuracy

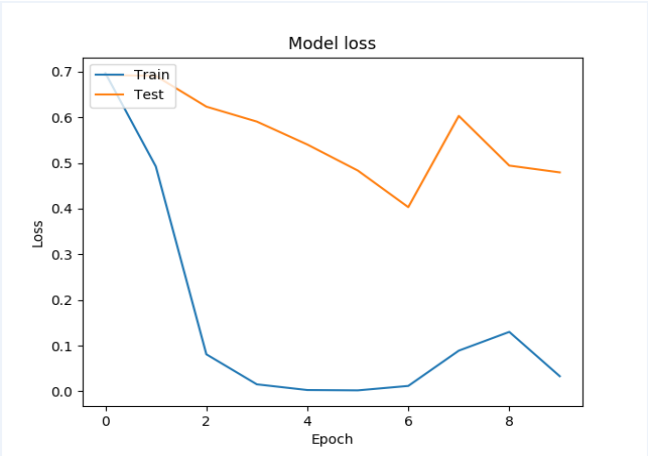

Figure 6: LSTM-CNN Loss

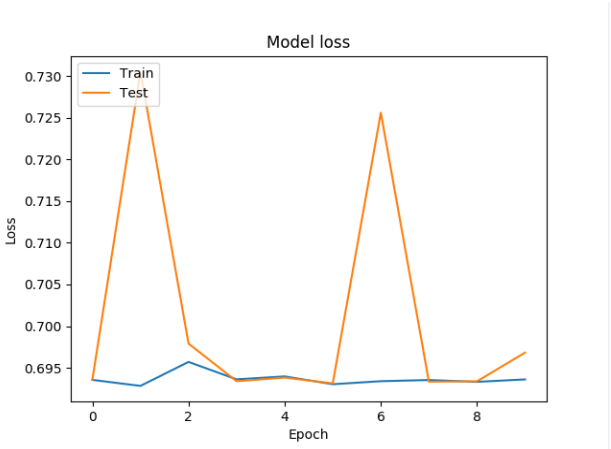

Figure 7: CNN-LSTM Loss

For each epochs during training, training accuracy and training loss as well as the validation accuracy and validation loss is calculated. Figure 4 and Figure 5 represents the LSTM-CNN and CNN-LSTM accuracy graph for IMDB reviews. LSTM-CNN accuracy graph shows great results in just 10 epochs compared with CNN-LSTM accuracy. In Figure 4, Curves indicate that the model is trained right. Figure 6 and Figure 7 represents the validation loss and training loss of both LSTM-CNN and CNN-LSTM model.

CONCLUSION

In day by day the velocity and volume of the text data increment rapidly. Sentiment analysis plays an important roles in our daily decision making process. Sentiment analysis is done with the help of various methods. In recent years deep learning methods provide better accuracy for sentiment classifications compared with traditional methods. Convolutional Neural Network acts as a good feature learner and extract features horizontally from various words. These characteristics are essential for classification tasks. Long Short Term Memory Network keeps long term dependencies in long sentences. LSTM's viability is its ability to catch changing sentiment in a tweet. That has a memory that "remembers"

past information from the input and takes decisions on that learning. Our framework utilizes the advantage of both CNN and LSTM.

In this project, we investigated two distinctive deep learning models for analyzing IMDB movie reviews. First is hybrid CNN-LSTM model and second is hybrid LSTM-CNN model. Our approach performed well on IMDB movie review dataset and achieved a better accuracy compared with other traditional models. In terms of future work, like to test other types of LSTMs (for example Bi-LSTMs) and CNN (for example multilayer CNN).In future this system implemented with a large datasets.

REFERENCES

[1] A.M.Abirami and V.Gayathri ***"A Survey on Sentiment Analysis Methods and Approach"*** 2016 IEEE Eighth International Conference on Advanced Computing (ICoAC).

[2] Qiongxia Huang, Xianghan Zheng, Riqing Chen, Riqing Chen ***"Deep Sentiment Representation Based on CNN and LSTM"*** International Conference on Green Informatics 2017.

[3] S. M. Vohra, J. B. Teraiya ***"A Comparative Study of Sentiment Analysis Techniques"*** Journal of Information, Knowledge and Research in Computer Engineering, 2016.

[4] Igor Santos, Nadia Nedjah , Luiza de Macedo Mourelle ***"Sentiment Analysis using Convolutional Neural Network with fast text embeddings"*** 2nd IEEE International Conference on Computational Intelligence and Applications 2017.

[5] HadiPouransari, SamanGhili ***"Deep learning for sentiment analysis of movie reviews"*** www.kaggle.com.

[6] Liu Yanmei , Chen Yuda***" Research on Chinese Micro-blog Sentiment Analysis Based on Deep Learning"*** 8th, IEEE International Symposium on Computational Intelligence and Design 2015.

[7] Yaya Heryadi, Harco Leslie Hendric Spits Warnars ***"Learning Temporal Representation of Transaction Amount for Fraudulent Transaction Recognition using CNN, Stacked LSTM, and CNN-LSTM"*** Journal of Electronics Vol.25, No.4, July 2016.

[8] Alec Yenter , Abhishek Verma ***"Deep CNN-LSTM with Combined Kernels from Multiple Branches for IMDb Review Sentiment Analysis"*** IEEE International Conference on Computer Communication and the Internet 2017.

[9] Aswathi Sajeevan, ***"A Survey on Review Analysis Using Deep Learning Techniques",*** International Journal of Latest Engineering and Management Research (IJLEMR), Volume 4, Issue 2, February 2019.

[10] Abdalraouf Hassan, Ausif Mahmood ***"Convolutional Recurrent Deep Learning Model for Sentence Classification"*** IEEE Access open access journal 2018.

[11] Xiaobo Zhang, Qingsong Yu ***" Hotel Reviews Sentiment Analysis Based on Word Vector Clustering" 2nd*** IEEE International Conference on Computational Intelligence and Applications 2017.

[12] Zhou, Yu, Ruifeng Xu, Lin Gui ***"A sequence level latent topic modeling method for sentiment analysis via CNN based diversified restrict boltzmann machine"*** Machine Learning and Cybernetics (ICMLC), 2016 International Conference on. Vol. 1. IEEE, 2016

Proceedings of the Fourth International Conference on Communication and Electronics Systems (ICCES 2019)
IEEE Conference Record # 45898; IEEE Xplore ISBN: 978-1-7281-1261-9

IMPROVING MEAN OPINION SCORE (MOS) OF VoIP IN WiMAX SYSTEM BY USING AN EFFICIENT TECHNIQUE

Misha
Department of Electronics and Communication Engineering
I.K Gujral Punjab Technical University
Jalandhar, India
mishaverma101993@gmail.com

Dalveer Kaur
Department of Electronics and Communication Engineering
I.K Gujral Punjab Technical University
Jalandhar, India
dn_dogra@rediffmail.com

***Abstract*—** VoIP is Voice over Internet Protocol which is a real time application which allows transmitting voice through internet protocol. It provides various services from which one of the important services is phone service over dedicated IP network. The important quality which is perceived by the users of VoIP telephony is speech quality. The quality of speech is degraded by various factors such as packet loss, delay, jitter, etc. This paper concentrate in making better speech quality and to improve the MOS score by using standard PESQ over WIMAX system. Tool used for this purpose is MATLAB R2013b.

Keywords—VoIP, Codecs , MOS

I. INTRODUCTON

VoIP is one of the applications which provide better quality of experience to the users. VoIP uses internet as a medium to transmit for telephone calls to send voice data as packets using IP network instead of PSTN. This is because the main benefit of IP network is that it can able to carry 5 to 10 times voice calls than circuit switch network. VoIP technology has various advantages which includes large savings and provide scalability [1]. The disadvantage of VoIP is that it requires Internet connection with large bandwidth. There are various codecs that VoIP uses (i.e. G.711, G.729, G.722, G.723.1, G.726, G.728 etc).The codecs have three basic tasks such as Encoding and Decoding, Compression and Decompression, Encryption and Decryption. There are two common codecs which are used such as G.711 and G.729. G.711 require higher bandwidth than G.729 (i.e. 64 kbps whereas G.729 requires 8 kbps).

Table.1 Audio Codecs [1]

ITU no.	Rate[kbps]	Algorithm
G.711	64	Pulse Code Modulation
G.723.1	5.3/6.4	Multipulse maximum likelihood quantization/algebraic-code-excited linear prediction
G.726	16/24/32/40	Adaptive differential PCM
G.728	16	Low-delay code-excited Linear prediction
G.729	8	Conjugate-structure algebraic-code-excited linear prediction

.

II. WIMAX

WIMAX is World Interoperability for Microwave Access. It is 4G promising technology which brought many different changes in industry now-a-day. WiMAX provides two different type of services such as line of sight (LOS) and non line of sight (NLOS). The radio coverage distance if WiMAX is 50 kilometers and data throughput is 70 Mbps. WiMAX is IEEE 802.16 standard which is considered as Broadband Wireless Access (BWA) because of high speed, worldwide and cost effective access. WiMAX is also considered as Metropolitan Area Network (MAN). The main purpose for designing WiMAX model using AWGN channel to make system compatible with atmospheric conditions. The WiMAX model with AWGN channel involves the following such as [2]:-

- Randomizer.
- Convolution encoder
- Quadrature Amplitude Modulator.
- AWGN channel.
- QAM demodulator
- Viterbi decoding.
- De-randomizer.

Randomizer is basically used to convert a large signal into bits (0's and 1's) so that the performance of coding can be improved. Convolution encoder is the forward error correcting code which is used to correct the error during the transmission of data. Hence, the output of convolution encoder removes the additional bit from the encoded streams and also remove bits depends upon the code rate.QAM modulator is used to map the incoming bit-stream onto the Constellation. AWGN channel is the channel which adds white Gaussian noise to input signal (real or complex signal). Viterbi decoding helps to

decrease the computational load. It basically involves calculation how to measure the similarities and distance.

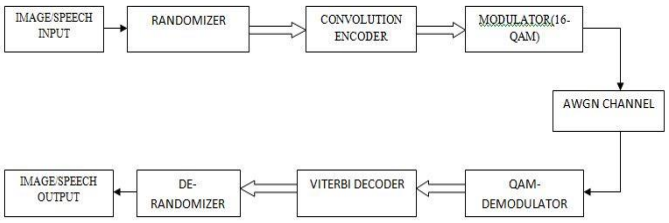

Figure 1.General Block Diagram of WiMAX

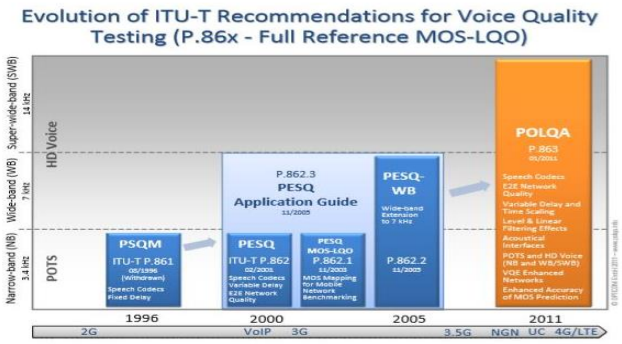

Figure 2. Perceptual Evaluation of speech quality [5]

III. PESQ AND MOS

MOS is considered as the most applicable test because it is person who uses voice network and whose opinion is counted. Basically, MOS is used to measure subject call quality for calls. The range for MOS score is 1 for unacceptable and 5 for excellent.

To calculate MOS value we have the following methods:

- PSQM.
- PESQ.
- POLQA.
- E-Model

The PSQM is Perceptual Speech Quality Measure which only assesses the speech codecs and does not have any proper account for filtering, variable delay and short localized distortions whereas PESQ uses this address with the equalization of transfer function alignment of time and new algorithm to average distortion over time [3]. PESQ is Perceptual Evaluation of Speech Quality. The PESQ speech quality uses 3.1 KHz. PESQ calculates the effect of one-way speech distortion and noise on speech quality. There are various effects such as loudness loss, delay, side tone, echo and so on , are considered as two-way communication which is not considered to calculate PESQ.

For PESQ, we consider an original signal x(t) and degraded signal y(t). Basically, PESQ compares the original signal with the degraded signal by passing the original signal over communication system. Hence, the PESQ output is the prediction of perceived quality given to the degraded signal by particular subjects in subjective listening test. The range of the P.862 score provided is -0.5 to 4.5. The mapping function from PESQ to MOS LQO is [4]:-

$$y = 0.999 + (4.999 - 0.999)/1 + e^{(-1.495x + 4.6607)}$$

Thus, the inverse function that allows the transformation to raw P.862score is given as:-

$$x = (4.6607 - \ln(4.999 - y)/(y - 0.999))/1.4945$$

IV. PROPOSED TECHNIQUE

FEC is the Forward Error Correcting technique which is used to correct and to detect the error i.e. there is continuous transmission of data, if errors are detected during the transmission and they must be corrected at receiver side. The work of FEC is to add the data at the transmitter side so that the one can receive the data without any error at the receiver side. The purpose of error correcting code is to improve the capacity of the data by the addition of some redundant nits while the data gets transmitted through the channel. It is very important in digital communication that data gets transmitted efficiently and reliably. There are various types of FEC codes such as:-

- Convolution code.
- Reed Solomon code.
- Linear Block code.
- Turbo code.
- Bose-Chaudhari-Hoequenghem code.

CONVOLUTION ENCODER

The work of encoding and decoding to translate the message that can be easily understood. Convolution code is the error correcting code which generates the parity symbol through the sliding application of Boolean polynomial function to stream of data.

VITERBI DECODING

Decoding is the inverse process of encoding i.e. encoded data is converted into the original state. The process of converting code to plain text or in any other format which is useful for further process is called decoding. The Viterbi algorithm is use for Viterbi decoding to decode the bit streams which are encoded using convolution encoding [6]. The Viterbi decoding

is consider as the most resource consuming. The constraint length that is used to decode the Convolution code is K<=10. But practically, the value that is used is K=15. There are three tasks for Viterbi decoder process are Branch Metric unit (BMU), Path Meteric Unit (PMU) and Trace back unit (TU).

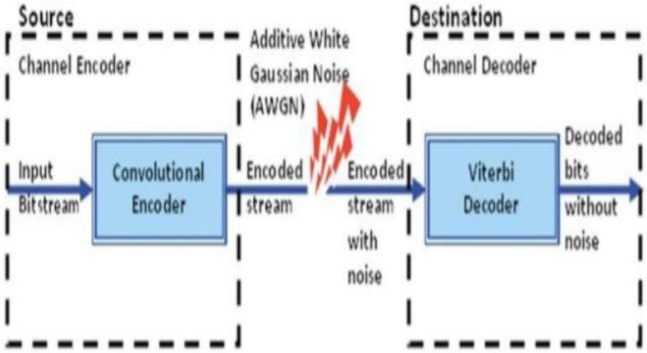

Figure 3. Convolution Encoder and Viterbi Decoder [6]

V. METHODOLOGY

1. At 8 bits per second, the audio signal (.wav) is processed.
2. At 8 KHz, sampling is done.
3. With the quantization level +0.5 and -0.5, the quantization is done.
4. Binary data (0's and 1's) is produced for the audio signal (Randomizer).
5. Convolution encoding is done on this binary data stream.
6. Then after the convolution encoding, the modulation is done and the signal is passed over AWGN channel.
7. At receiver side, demodulation and decoding is done to reconstruct the signal. For decoding, Viterbi decoder is used .
8. Once the decoding is done then signal is reconstructed.
9. Hence, PESQ is calculated and MOS value is obtained.

The following is the diagram of the methodology for transmitter section and receiver section [7] :-

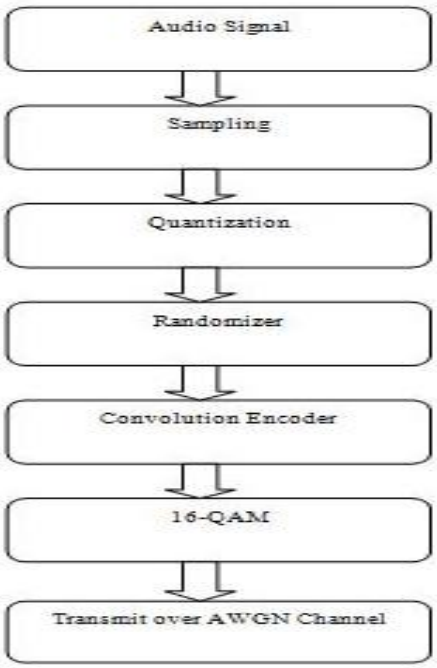

Figure 4. Transmitter Section

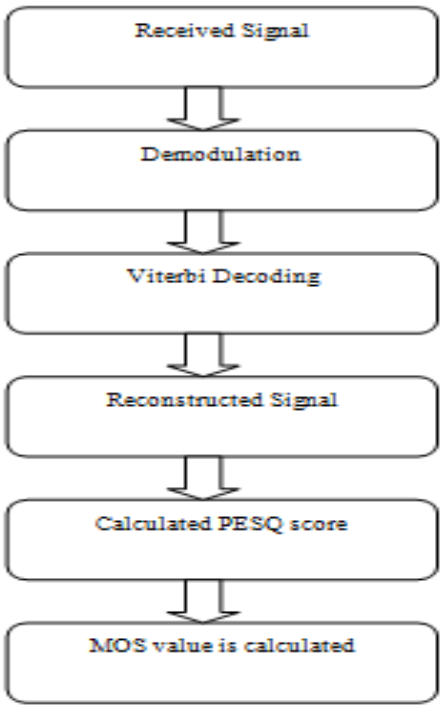

Figure 5. Receiver Section

VI. PERFORMANCE ANALYSIS

Here, the input parameters taken during the simulation process and the results are discussed below:-

A. Input Parameters

Table 2. Input Parameters

PARAMETERS	SPECIFICATION
n-bit PCM value	8
No. of samples/sec	8000
Max levels of Quantization	+0.5
Min levels of Quantization	-0.5
No. of Quantization levels	256
Modulation	16-QAM
Standard used to calculate MOS	PESQ

B. Results and Comparision

- Input Signal

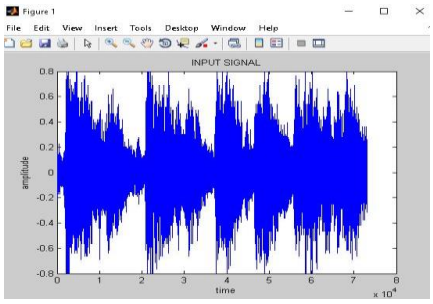

Figure 6. Input Signal

- Sampled Signal

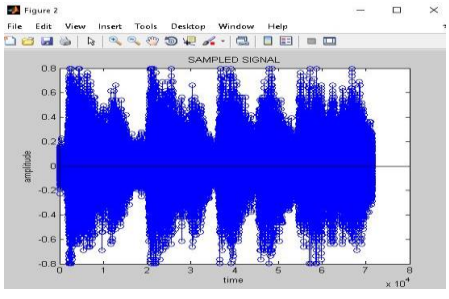

Figure 7. Sampled Signal

- Quantized Signal

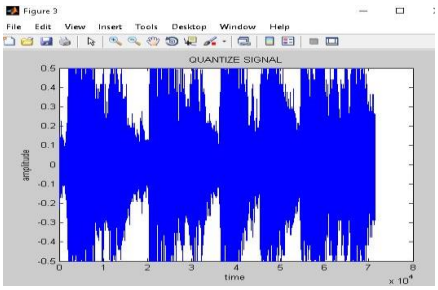

Figure 8. Quantized Signal

- Encoded Signal

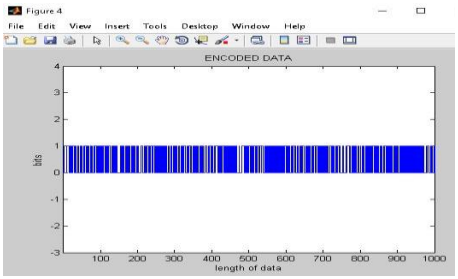

Figure 9. Encoded Signal

- AWGN Channel

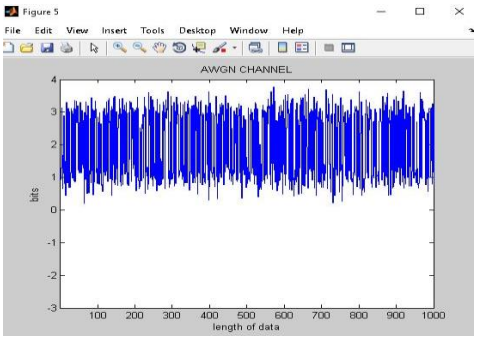

Figure 10. AWGN Channel

- Decoded Signal

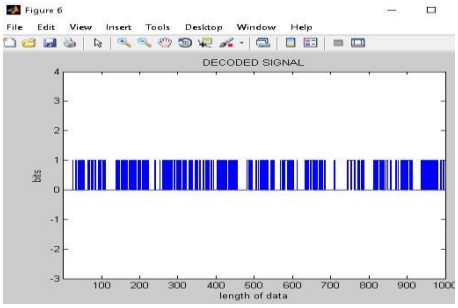

Figure 11. Decoded Signal

- Reconstructed Signal

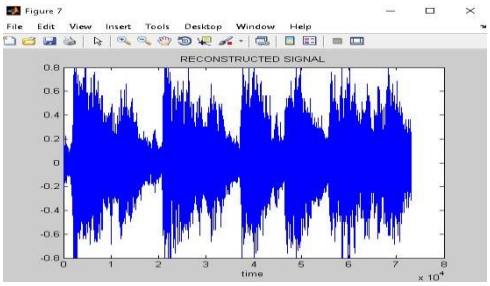

Figure 12. Reconstructed Signal

The simulation results of transmitting the signal using proposed algorithm over WiMAX system using AWGN channel in comparison with WIFI system (Rayleigh channel and Rician channel) are shown below:

Table 3. Comparison for AWGN and Different Fading Channels for proposed algorithm [7]

SYSTEM	PESQ	MOS
AWGN channel	4.500	4.548
Rayleigh channel	4.0498	4.2025
Rician channel	4.0118	4.1445

VII CONCLUSION

This paper is to provide better call quality at the output for VoIP. The same has been achieved using the proposed algorithm and there is an improvement in the voice quality at the receiver end which is determined by calculating the MOS. The MOS calculated for proposed algorithm is 4.548 which is compared which different fading channels and standard existing codecs. Hence, the proposed algorithm has been able to provide improved call quality at the receiving end using AWGN channel**.**

.

REFERENCES

[1] M A. Mohamed, F. W.Zaki, A. M.Elfeki, "*Implementation of VoIP over WiMAx Network*", International Journal of Electronics and Communication engineering & Technology (IJECET), Vol.**3,** Issue.**2**, pp.**310-320**, **2012**

[2] P. R Banswani , V.Tehre , "*Simulation Of WiMax Model Using AWGN Channel*", International Journal of Engineering Research and General Science Volume **3**, Issue **1**, January-February, **2015** .

[3] http://www.itu.int/rec/T-REC-P.862/en,ITU-Recommendation P.862:Preceptual Evaluation of Speech Quality assessment of narrow – band .

[4] http://www.itu.int/rec/T-REC-P.862/en,ITU-Recommendation P.862.1: Mapping Function for transforming P.862 raw score to MOS-LQO.

[5] www.polqa.info.(POLQA:*Perceptual Objective Listening Quality Analy sis* ,Technical White Paper,Udapted October 2011)\

[6] P.Saidulu, Md. Abdul Rawoof, "*Implementation of Convolution Encoder and Viterbi Decoder Using Verilog*", International Journal of Electronics and Communication Engineering, Vol.**11,** No.**1**, pp.**13-21**, **2018**.

[7] K. Kaur, D. Kaur, "*An Efficient Technique for Improving Mean Opinion Score (MOS) of VoIP in wireless system*", International Journal of Emerging Technology and Advanced Engineering , Vol **8**, Issue.**6**, **2018**.

[8] G.Samrat and B.Sudeept, "VoIP:Wireless, P2P and new Enterprise Voice over IP", John Wiley & Sons Ltd,, **2008**.

[9] A. Patil, P. Soni, V. Verma, "*Performance Evaluation of Physical Layer of 802.16e WiMAX Using Reed Solomon Code and Convolutional Code under Different Modulation Techniques and Communication Channels*," International Journal of Advanced Research in Electronics and Communication Engineering (IJARECE) Volume **3**, Issue **9**, September **2014.**

[10] T. Daengsi, N. Khitmosh, P.Wuttidittachotti."*VoIP quality measurement :subjective VoIP quality estimation model for G.7 11and G.729on native thai users* ," DOI 10.1007/s00530-0468-3.

[11] A.Banerjee, P. Das, Prof. S.Sen, "*A Mathematical Model to Enhance MOS for VoIP Application of WiMAX (IEEE 802.16e)*," International Conference on Computation and Communication Advancement (IC3A)-**2013.**

Proceedings of the Fourth International Conference on Communication and Electronics Systems (ICCES 2019)
IEEE Conference Record # 45898; IEEE Xplore ISBN: 978-1-7281-1261-9

Whale Optimization Algorithm Based Cognitive Radio System Design for Internet of Things

Kiranjot Kaur[1]
Department of Electronics & Communication Engineering
Punjabi University
Patiala, India
kiranjotdeo@yahoo.co.in

Munish Rattan[2]
Department of Electronics & Communication Engineering
Guru Nanak Dev Engineering College
Ludhiana, India
dr.munishrattan@gmail.com

Manjeet Singh Patterh[3]
Department of Electronics & Communication Engineering
Punjabi University,
Patiala, India
mspattar@yahoo.com

***Abstract*— Cognitive radio based internet of things is another new need of the hour as all the internet of things objects are not very expedient without holding cognitive capabilities. Cognitive radio is the only solution to the Issues like Spectrum scarcity and spectrum sharing, which are posing serious challenges to internet of things paradigm. This paper is a step forward in achieving the most optimal cognitive radio based internet of things system. For this, a recently developed optimization technique, named whale optimization algorithm is suggested for optimizing the transmission parameters of cognitive radio system by obtaining user defined QoS. The results obtained by whale optimization algorithm are compared with literature based biogeography based optimization, simulated annealing and genetic algorithm to ensure the utility and efficacy of whale optimization algorithm for cognitive radio system designing.**

Keywords—cognitive radio; internet of things; optimization whale optimization algorithm

I. INTRODUCTION (*HEADING 1*)

Internet of things (IoT) refers to a network of physical devices which are connected via internet for information exchange, bypassing any human interference. A complex network consisting of large number of physical devices requires a good amount of wireless spectrum to make communication possible [1]. Spectrum is limited. Advent of cognitive radio (CR) by joseph mitola [2] gave a ray of hope in solving spectrum problem by allowing the access of licensed band to even unlicensed user after avoiding interference. Hence a CR design is a handy tool for smooth implementation of IoT networks [3]. For generating the most efficient and effective CR enabled IoT, it becomes vital to begin with the optimality of CR system itself.

One of the ways of obtaining optimized design of CR system is to obtain the optimal values of its transmission parameters by aiming at certain objectives [4]. This is accomplished by using a number of optimization techniques available in literature. TR Newman first suggested this kind of work where he designed a cognitive engine using GA [5]. Later the same engine has been designed by many researchers using various techniques individually or in hybrid form [6-13]. Most of the CR systems discussed before have highlighted only two transmission parameters with an intention to fulfill three objectives. Present authors have suggested five transmission parameters and five objectives in a CR system design by using SA [14] and BBO [15], This paper focuses on use of another novel Whale optimization algorithm for CR system's optimal design that could blend with IoT.

Whale optimization algorithm (WOA) is another feather in the cap of mirjalili [16], who is parent to many other optimization techniques, including gray wolf optimization GWO [17], moth flame optimization MFO [18], ant lion optimization ALO [19], dragonfly optimization DF [20], SCA sine cosine algorithm [21], and SSA salp swarm algorithm [22]. WOA is inspired by humpback whales that create a bubble spring trap for their hunt. The provision of dedicating first few iterations to diversification and last few iterations to intensification makes it's a stable algorithm in terms of exploitation and exploration [16]. The successful implementation of WOA on many problems from diverse fields like economic dispatch [23], optimal power flow [24], image segmentation [25], neural network weights [26] etc. have persuaded the authors to design an optimal CR system using WOA.

Nest section of the paper illustrates WOA briefly, followed by CR problem definition in section 3. Simulation and results are discussed in section 4 with conclusion at the end.

II. WHALE OPTIMIZATION ALGORITHM (WOA)

Whales, the largest mammals on the earth are the smartest creatures after humans, even at par to humans. Whales have now inspired even an optimization algorithm too, named Whale optimization algorithm by mirjalili [16]. Out of their variant species, humpback whales are of interest to this algorithm. The bubble net feeding trap created by them during prey finding is the heart of WOA. After taking a deep dig in water, humpback whales suddenly follow a upward spiral path

forming bubble net around their target. WOA is mathematically modeling of this behavior.

Step by step procedure of WOA can be put in words as:

1. Algorithm Initialization: This algorithm begins with arbitrary initialization of the whales population (*N*), each whale has *n* dimensions within boundary constraints:

$$X_{i\ j} = X_{\min\ j} + rand\,(X_{\max\ j} - X_{\min\ j}) \quad (1)$$

for i= 1,2,3…*NP*; j= 1,2,3…*D*

Where X_{min} and X_{max} are lower and upper bounds for j^{th} component or decision variable.

2. Fitness Evaluation: Calculate the fitness for each possible solution (search agent) in population *N*.

3. Define the best search agent as (*X**), the fittest. This is assumed to be victim initially.

3. Until a termination criteria is reached (maximum iterations), repeat the steps 4 to 11.

4. Ensure all search agents are in the search space, otherwise alter them.

5. Variable initialization: Update all necessary variables, $\vec{a}$, $\vec{A}$, l, $\vec{C}$, p. Here $\vec{A}$ and $\vec{C}$ are coefficient vectors and are calculated form $\vec{a}$ and $\vec{r}$ as given below. $\vec{a}$ is gradually decreased from 2 to 0 as iterations falls from maximum to minimum and $\vec{r}$ is random vector.

$$\vec{A} = 2\vec{a}.\vec{r} - \vec{a} \quad (2)$$

$$\vec{C} = 2.\vec{r} \quad (3)$$

6. Encircling prey: Humpback whales use shrinking circling and spiral movement in upward direction to encircle their victim, both with 50% probability. These techniques are referred as bubble net attacking method and helps in exploitation of solution. A variable p is used to decide which movement will be selected by whales from these two using below equation;

$$\vec{X}(s+1) = \begin{cases} \overrightarrow{X^*}(s) - \vec{A}.\vec{D} & if\ p < 0.5 \\ \vec{D}'.e^{bl}.\cos(2\pi l) + \overrightarrow{X^*}(s) & if\ p \geq 0.5 \end{cases} \quad (4)$$

Where $\vec{D} = \left|\vec{C}.\overrightarrow{X^*}(s) - \vec{X}(s)\right|$ *and* $\vec{D}' = \left|\overrightarrow{X^*}(s) - \vec{X}(s)\right|$, b describes the shape of logarithmic spiral and l is random number [-1, 1]. S is number of iterations.

7. Searching prey: Instead of p, $\vec{A}$ (randomly selected values higher than 1) is deciding factor to use appropriate technique for searching agents, leading to exploration of solutions. Unlike exploitation, here position updating of agent is done on the basis of any randomly chosen search agent instead of best search agent.

$$\vec{X}(s+1) = \overrightarrow{X_{rand}} - \vec{A}.\vec{D} \quad (5)$$

$$\vec{D} = \left|\vec{C}.\overrightarrow{X_{rand}} - \vec{X}\right| \quad (6)$$

Where $\overrightarrow{X_{rand}}$ is randomly chosen whale (position) from current whales.

8. Solution found: Hence the better solution from a large search space is generated for the upcoming generation and the process continues until the termination criterion is met.

Complete algorithm can be understood better form its flowchart in figure 1.

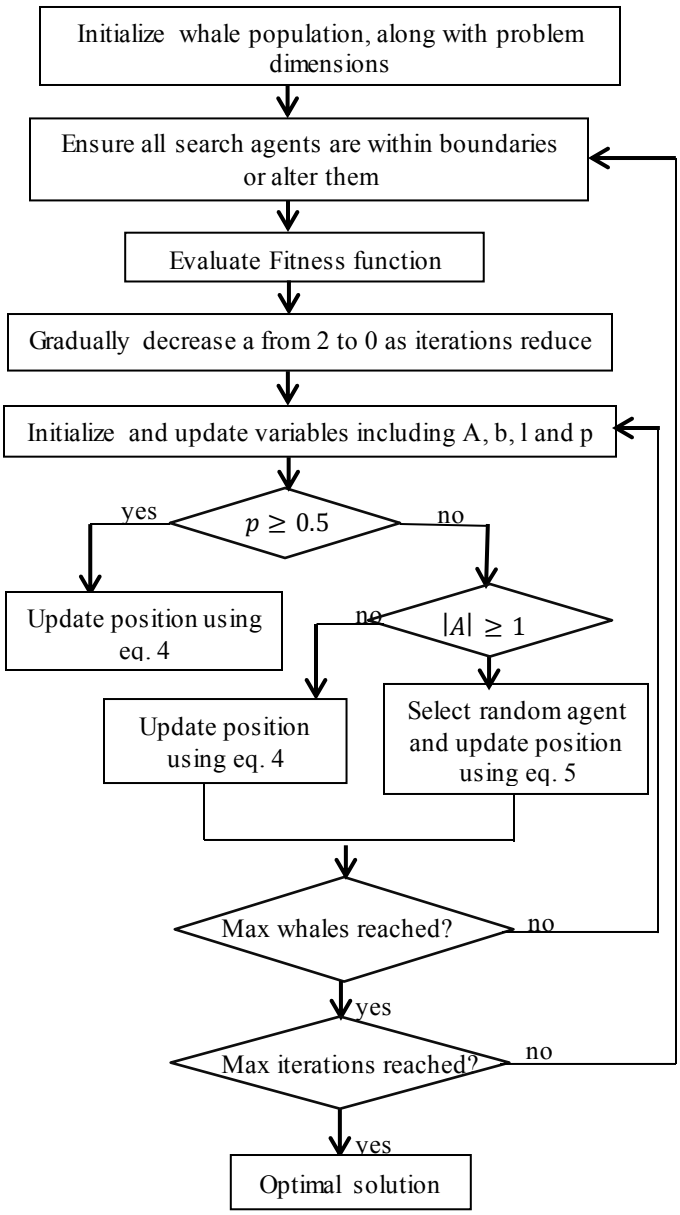

Fig. 1. Flow chart of WOA

III. COGNITIVE RADIO

A. Cognitive Radio System

For a cognitive radio system enabled IoT, a CR model consisting of a primary user (PU) and a secondary user (SU), is studied in this work. To design it in the most optimal way, its

transmission parameters are to be optimized with an intention to accomplish certain goals [5].

B. Cognitive Radio Parameters and Objectives

The adaptable transmission parameters optimized by WOA lists Transmitted Power (P), Modulation Type, Modulation Index (M), Bandwidth (B), Time Division Duplexing (TDD) and Symbol Rate (Rs). Bit-error-rate (BER), signal-to-noise ratio (SNR) and the noise power (N) are the considered environmental parameters in this work. Anticipated QoS goal of CR are met by establishing five objectives. Their fitness function are demarcated in the below section, in order to move the system towards an optimal region.

C. Formulation of Fitness Functions in Cognitive Radio System

Optimization the above enlisted transmission parameters of SUs is done to reach the preferred QoS, which is declared by five objectives.

1. Minimize power consumption: Shrink power to be consumed by the system.

$$f_{\min\ power} = \frac{P}{P_{max}} \tag{7}$$

where P is the average transmit power, and $P_{\max}$ is the maximum available transmit power.

2. Minimum BER: Decrease BER of the communication environment.

$$f_{\min\ ber} = \frac{log_{10}(0.5)}{log_{10}(P_{be})} \tag{8}$$

where P_{be} represents the BER of the modulation type being used, we have used QAM type. For M-ary QAM, the BER is defined as :

$$P_{be} = \frac{4}{log_2(M)}\left(1 - \frac{1}{\sqrt{M}}\right)Q\left(\sqrt{\frac{3log_2(M)P}{(M-1)N}}\right) \tag{9}$$

where P is the average transmitted power, M is the modulation index and N is the noise level equal to 0.1mW.

3. Maximum Throughput: Raise the throughput of radio transmission.

$$f_{\max\ throughput} = 1 - \frac{log_2(M)}{log_2(M_{max})} \tag{10}$$

where M is the modulation index of a single carrier, and $M_{\max}$ is the maximum modulation index.

4. Minimum Interference: Reduce the radio's interference contributions.

$$f_{\min\ interfernce} = \frac{(P+B+TDD)-(P_{min}+B_{min}+1)}{P_{max}+B_{max}+100} \tag{11}$$

where B is the bandwidth required for a single carrier, B_{min} and B_{max} is the minimum and maximum bandwidth available. TDD is time division duplexing, i.e. time taken for transmission and Rs is the symbol rate and Rs_{max} is the maximum symbol rate.

5. Maximum Spectral Efficiency: Maximize the proficient use of frequency spectrum.

$$f_{\max\ spectral\ eff} = 1 - \frac{(M \times B_{min} \times R_s)}{(B \times M_{max} \times Rs_{max})} \tag{12}$$

where M is the modulation index, B is the bandwidth used, Rs refers to the symbol rate.

Using weighted approach, these five multiple objectives are combined into one objective function. This conversion is exposed in equation (13).

Then the final combined objective is given as:

$$f_{five\text{-}objective} = w1 * (f_{min\text{-}power}) + w2 * (f_{min\text{-}ber}) + w3 * (f_{max\text{-}throughput}) + w4 * (f_{min\text{-}interference}) + w5 * (f_{max\text{-}spectraleff}) \tag{13}$$

In certain studies, only three objectives are considered, forming a combined three multi-objective function

$$F_{three\text{-}objective} = w1 * (f_{min\text{-}power}) + w2 * (f_{min\text{-}ber}) + w3 * (f_{max\text{-}throughput}) \tag{14}$$

w1 to w5 are the weights, multiples of each objective respectively. Five CR scenarios are created by these five weights. Table I carries the prerequisite weight values to accentuate the search on preferred path for a particular scenario [5].

IV. Simulations and Results

In this work, WOA is applied to CR system for optimizing its transmission parameters by achieving certain objectives. To make simulation results more clear and to ensure the satisfactory implementation of WOA for optimal CR design in comparison to its predecessor techniques [BBO [15], SA [14] and GA [5]], the simulation results are divided into two sections. With first section dealing with only three objectives and letting us optimize only two parameters, power (P) and modulation Index (M). Second section accomplishes five objectives and helps in obtaining optimal values of five transmission parameters.

A. Only three Objectives

In this subsection, only three objectives corresponding to eq. are optimized and two parameters, namely transmitted power and modulation index are worked upon. The range of transmitted power (P) varies between 0.1 mW and 2.4808 mW. QAM modulation scheme is used with number of symbols (M) ranging from 8 to 64 [5]. WOA related all parameters are tabulated below in table II.

The results obtained in terms of optimal values of transmission parameters, objective function value and the values of the objectives that are intended to be achieved are put up in table 3. They could be fairly compared with results those obtained by BBO [15], SA [14] and GA [5], cited in the same table. WOA is successful in achieving the targeted objective in that particular scenario (mode of operation). The results are

superior to SA and GA. But they are totally at par with BBO. Due to simplicity of problem same results have been produced by WOA and BBO while working on only three objectives. Picture is going to be clearer as problem density increases in next section.

B. Five objectives

Here, WOA is applied to CR system for optimizing its five transmission parameters by achieving five various five objectives. On the basis of these five objectives that are discussed in above section, five scenarios are created. Each scenario is mainly focusing on only one objective at a time. The range of five transmission parameters is predefined and is kept intact as available in literature [5, 14, 15] to ensure rational comparison. The transmitted power (P) varies between 0.158 mW and 251 mW. QAM modulation scheme is used with number of symbols (M) ranging from 2 to 256. Bandwidth (B) available is from 2 to 32 MHz. TDD percentage is taken between 25 and 100%. Symbol rate (Rs) is between 125 Ksps and 1 Msps. WOA related all parameters are tabulated in table III. Table IV hold all the values of optimized parameters, objectives, and fitness functions for all five scenarios for a CR systemobtained by applying WOA. Bold values illustrates that WOA has reached the intended objectives in all modes except interference mode. Interfernce is minimal in power mode whereas it is expected to be minimum in min interference mode. This happened because of interference's direct dependency on transmitted power. These results obtained by WOA are compared in table V with those obtained by BBO [15], SA [14] and GA [15]. As visible, for WOA, fitness values are best for all five modes. Talking about objectives, except in power and interference, WOA is performing best for other three objectives. SA managed to bag first position for power and interference.

Another feather in WOA's cap is least number iterations required to reach the optimal value. Fig.2 and Fig.3 are comparison characteristic curves for minimum power and maximum spectral efficiency mode respectively obtained by WOA, BBO, SA and GA for 300 iterations. These graphs narrate the story behind the search of the best value by every algorithm. WOA finds the best (minimum) form all in minimum iterations, making it superior than BBO, SA and GA for cognitive radio problem. Ability of WOA to assign some iterations in the beginning to exploration and then concentrate on exploitation in last iterations helps it in being fairly balanced algorithm.

V. CONCLUSION

An optimized cognitive radio system is designed for internet of things network using a newfound whale optimization algorithm. Internet of things, being a new and beneficial trend needs cognitive radio services for efficient use of spectrum, which is a limited resource with high demand. One of the ways of designing an optimal cognitive radio is by working on its transmission parameters. Here, five transmission parameters of cognitive radio system are optimized with an intention to achieve five objectives that are vital for user oriented quality s services. Whale optimization based results of optimal parameters, fitness functions, objectives are compared with those obtained earlier in literature using GA, SA and BBO. Convergence characteristics of all these techniques are also used a major performance metric. Owing to fine balance between intensification and diversification, superiority of WOA is established through simulation outcomes and graphs for optimal cognitive radio designing.

REFERENCES

[1] A. Alberti, D. Mazzer, M. Bontempo, L. de Oliveira, R. da Rosa Righi, and A.J. Sodr, "Cognitive radio in the context of internet of things using a novel future internet architecture called novagenesis," *Computers and Electrical Engineering*, vol. 57, pp. 147–161, 2017.

[2] J. Mitola and G. Q. Maguire, "Cognitive radio: making software radios more personal," *IEEE Personal Communications*, vol. 6, no. 4, pp. 13-18, 1999.

[3] A. Khan, M.H. Rehmani and A. Rachedi, "Cognitive-Radio-Based Internet of Things: Applications, Architectures, Spectrum Related Functionalities, and Future Research Directions," *IEEE Wireless Communications*, vol. 24, no. 3, pp. 17-25, 2017.

[4] T. R. Newman, "Multiple objective fitness functions for cognitive radio adaptation," Ph. D. Dissertation, Dept. Elect. Eng. & Comp. Sci. and the Faculty of the Graduate School, University of Kansas, 2008.

[5] T. R. Newman, B. A. Barker, A. M. Wyglinski, A. Agah, J. B. Evans and G. J. Minden, "Cognitive engine implementation for wireless multicarrier transceivers," *Wireless Communications and Mobile Computing*, vol. 7, no. 9, pp. 1129–1142, 2007.

[6] Z. Zhao, S. Xu, S. Zheng and J. Shang, "Cognitive radio adaptation using particle swarm optimization," *Wireless Commun. Mobile Comput*, vol. 9, no. 7, pp. 875-881, July 2009.

[7] X. You, X. He, X. Han, C. Wu, and H. Jiang, "A Novel Cognitive Radio Decision Engine Based on Chaotic Quantum Bee Colony Algorithm," *J. Inform. Compt. Sci.,* vol. 12, no. 6, pp. 2093-2106, 2015.

[8] N. Zhao, S. Li, and Z. Wu, "Cognitive Radio Engine Design Based on Ant Colony Optimization", *Wireless Pers. Commun.*, vol. 65, no. 1, pp. 15-24, July 2012.

[9] V. Rana and P.S. Mundra, "Simulation of QoS parameters in cognitive radio system using SMO algorithm," presented at ICICCT, Coimbatore, India, Mar. 10-11, 2017.

[10] X. You, X. He, and X. Han,"A Novel Solution to the Cognitive Radio Decision Engine Based on Improved Multi-Objective Artificial Bee Colony Algorithm and Fuzzy Reasoning," *Intell. Auto. Soft Compt.*, vol. 23, no. 4, pp. 643-651, 2017. DOI: 10.1080/10798587.2017.1316081

[11] W. Chen, T. Li, and T. Yang, "Intelligent control of cognitive radio parameter adaption: Using evolutionary multi-objective algorithm based on user preference," *Ad Hoc Networks*, vol. 26, pp. 3-16, Mar. 2015.

[12] A. Paraskevopoulos, P. I. Dallas, K. Siakavara, and S. K. Goudos, "Cognitive Radio Engine Design for IoT Using Real-Coded Biogeography-Based Optimization and Fuzzy Decision Making," *Wireless Pers. Commun.*, vol. 97, no. 2, pp. 1813-1833, Nov. 2017.

[13] G.Singh, M. Rattan, S.S. Gill, N. Mittal, "Hybridization of water wave optimization and sequential quadratic programming for cognitive radio system," *Soft Compt.,* pp. 1-21, 2018. https://doi.org/10.1007/s00500-018-3437-x,

[14] K. Kaur, M. Rattan, and M. S. Patterh, "Optimization of cognitive radio system using simulated annealing," *Wireless Pers. Commun.*, vol. 71, no. 2, pp. 1283-129, July 2013.

[15] K. Kaur, M. Rattan, and M. S. Patterh, "Biogeography based optimization of cognitive radio system," *Int. J. Electron*, vol 101, no. 1, pp. 24-36, 2014. https://doi.org/10.1080/00207217.2013.769183

[16] S. Mirjalili, A. Lewis, "The whale optimization algorithm." *Advances in Engineering Software*, vol. 95, pp. 51-67, 2016..

[17] S. Mirjalili, S. M. Mirjalili, A. Lewis, "Grey Wolf Optimizer," *Advances in Engineering Software*, vol. 69, pp. 46-61, 2014.

[18] S. Mirjalili, "Moth-flame optimization algorithm: A novel nature-inspired heuristic paradigm," *Knowledge-Based System*, vol. 89, pp. 228-249, 2015.

[19] S. Mirjalili, "The Ant Lion Optimizer," *Advances in Engineering Software*, vol. 83, pp. 80-98, 2015.

[20] S. Mirjalili, "Dragonfly algorithm: a new meta-heuristic optimization technique for solving single-objective, discrete, and multi-objective problems," *Neural Computing and Applications*, vol. 27, no. 4, pp. 1053-1073, 2016.

[21] S. Mirjalili, "SCA:A Sine Cosine Algorithm for solving optimization problems," *Know. Based Syst*., vol. 96, pp. 120-133, 2016.

[22] S. Mirjalili, A. H. Gandomi, S. Z. Mirjalili, S. Saremi, H. Faris, S. M. Mirjalili, "Salp Swarm Algorithm: A bio-inspired optimizer for engineering design problems," Advances in Engineering Software, vol. 114, pp. 163-191, 2017.

[23] H. J. Touma, "Study of The Economic Dispatch Problem on IEEE 30-Bus System using Whale Optimization Algorithm," International Journal of Engineering Technology and Sciences (IJETS), vol. 5, no. 1, pp. 11-18, 2016.

[24] B. Bentouati, L. Chaib and S. Chettih. "A hybrid whale algorithm and pattern search technique for optimal power flow problem," Modelling, Identification and Control (ICMIC), 2016 8th International Conference on. IEEE, 2016. DOI: 10.1109/ICMIC.2016.7804267

[25] M. A. El Aziz, A. A. Ewees and A. E. Hassanien. "Whale Optimization Algorithm and Moth-Flame Optimization for Multilevel Thresholding Image Segmentation," *Expert Systems with Applications*, vol. 83, pp. 242-256, 2017.

[26] I. Aljarah, H. Faris and S. Mirjalili, "Optimizing connection weights in neural networks using the whale optimization algorithm," *Soft Computing*, vol. 22, no. 1, pp. 1-15, 2018.

,

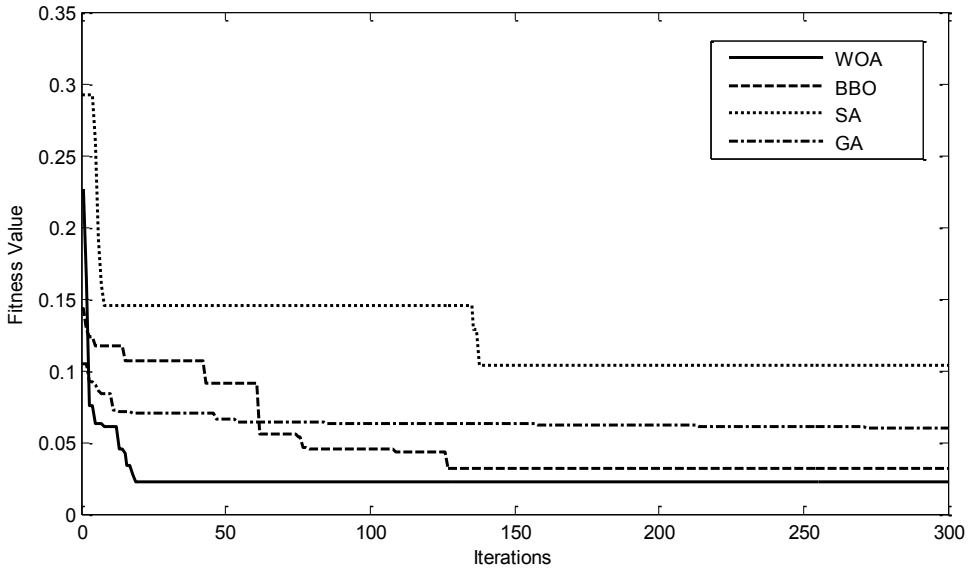

Fig. 2. Convergence characteristics for minimizing power

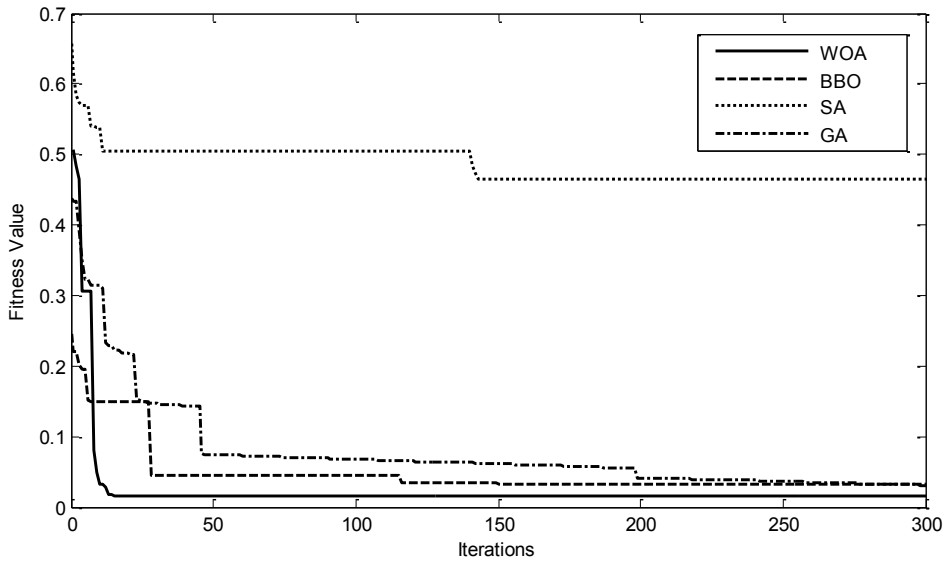

Fig. 3. Convergence characteristics for maximizing spectral efficiency

TABLE I. WEIGHTS ASSIGNED TO EACH MODE FOR FIVE AND THREE OBJECTIVES

Modes of Operation	**Weights for five modes**					**Weights for three modes**		
	***w*1**	***w*2**	***w*3**	***w*4**	***w*5**	***w*1**	***w*2**	***w*3**
Min. power mode	0.45	0.10	0.20	0.15	0.10	0.80	0.15	0.05
Min. BER mode	0.10	0.50	0.10	0.10	0.20	0.15	0.80	0.05
Max. throughput mode	0.10	0.15	0.50	0.15	0.10	0.05	0.15	0.80
Min. interference mode	0.10	0.10	0.20	0.50	0.10	-	-	-
Max. spec. eff. mode	0.10	0.15	0.15	0.10	0.50	-	-	-

TABLE II. WOA RELATED ALL PARAMETERS

Parameter Symbol	**Parameter Description**	**Value**
S	Maximum iterations	300
NP	Initial Population	10
a	Exploitation/exploration control variable	[0, 2]
b	Logarithmic spiral shape constant	1
l	Random variable	[-1, 1]

TABLE III. VALUES OF THE OPTIMIZED PARAMETERS, FITNESS SCORES AND OBJECTIVES FOR SCENARIOS USING WOA, BBO, SA AND GA

Optimization Technique	**Scenario** (Modes of Operation)	**Optimized Parameters**		**Fitness Score**	**Values of the Objectives Fulfilled**		
		P (mw)	M		Min. Power	Min. BER	Max. throughput
WOA	Min. power mode	0.1	64	0.0915	**0.0403**	0.3950	1
	Min. BER mode	0.8739	08	0.1474	0.3532	**0.0868**	0.5
	Max. throughput mode	0.7160	64	0.0478	0.2886	0.2227	**1**
BBO [15]	Min. power mode	0.1	64	0.0915	**0.0403**	0.3950	1
	Min. BER mode	0.8762	8	0.1474	0.3532	**0.0868**	0.5
	Max. throughput mode	0.7156	64	0.0478	0.2885	0.2228	**1**
SA [14]	Min. power mode	0.1	64	0.0915	**0.0403**	0.3950	1
	Min. BER mode	0.8480	8	0.1478	0.3418	0.0890	0.5
	Max. throughput mode	0.7620	64	0.0478	0.3072	0.2167	**1**
GA [5]	Min. power mode	0.1768	64	0.1097	0.0713	0.3515	1
	Min. BER mode	0.7400	08	0.1485	0.2893	0.0985	0.5

	Max. throughput mode	0.7144	64	0.0478	0.2880	0.2229	**1**

TABLE IV. VALUES OF OPTIMIZED PARAMETERS, OBJECTIVES, AND FITNESS FUNCTIONS FOR ALL FIVE SCENARIOS OF A CR SYSTEM OBTAINED BY APPLYING WOA.

Scenario (Modes of Operation)	**Optimized Parameters of WOA**					**Fitness Score**	**Values of the Objectives Fulfilled**				
	P (mw)	M	Rs (ksps)	B (Mhz)	TDD (%)		Min. P.	Min. BER	Max. Tp.	Min.Intr.	Max. Spec.Eff.
Min. Power Mode	04.418	256	1000	2.000	25.00	0.0229	**0.0176**	0.1495	1	**8.8808 e-010**	1
Min. BER Mode	36.215	256	1000	2.000	25.00	0.0313	0.1443	**0.0338**	1	1.8817 e-009	1
Max. Throughput Mode	17.530	256	1000	2.000	25.00	0.0161	0.0698	0.0609	**1**	1.2978 e-009	1
Min. Interference Mode	13.479	256	1000	2.000	25.00	0.0128	0.0537	0.0741	1	**1.1712 e-009**	1
Max. Spec. Eff Mode	17.530	256	1000	2.000	25.00	0.0161	0.0698	0.0609	1	1.2978 e-009	**1**

TABLE V. COMPARISON OF WOA, BBO, SA AND GA IN TERMS OF THE VALUES OF THE OBJECTIVES AND FITNESS OBTAINED IN EACH SCENARIO

Scenario	**Values**	**WOA**	**BBO** [15]	**SA** [14]	**GA** [15]
Min. Power Mode	Fitness Score	**0.0229**	0.0308	0.0366	0.0547
	Power	0.0176	0.0158	**0.0145**	0.0175
Min. BER Mode	Fitness Score	**0.0313**	0.0425	0.0700	0.0867
	BER	**0.0338**	0.0338	0.0448	0.06281
Max. Throughput Mode	Fitness Score	**0.0161**	0.0187	0.0238	0.0635
	Throughput	**1**	1	1	1
Min. Interference Mode	Fitness Score	**0.0128**	0.015	0.0492	0.0786
	Interference	1.1712e-009	0.0010	**4.5974e-10**	2.2643e-009
Max. Spec. Eff. Mode	Fitness Score	**0.0161**	0.0251	0.0194	0.0380
	Spec. Eff.	**1**	0.9823	0.9992	0.9577

Proceedings of the Fourth International Conference on Communication and Electronics Systems (ICCES 2019)
IEEE Conference Record # 45898; IEEE Xplore ISBN: 978-1-7281-1261-9

AUTOMATED MAPPING OF SERVICE LEVEL AGREEMENTS TO APPLICATION PROGRAMMING INTERFACES OF DIFFERENT CLOUD SERVICE PROVIDERS

Aishwarya S Pattar
Student, M.Tech (SE)
Dept. of Information Science and Engineering
RV College of Engineering
Bengaluru, India
aishwaryasp.sse17@rvce.edu.in

B K Srinivas
Assistant Professor
Dept. of Information Science and Engineering
RV College of Engineering
Bengaluru, India
bksrinivas@rvce.edu.in

***Abstract*— Most of the web (mobile) applications are using cloud computing technology. Developers who want to develop an application can make use of the provisions and services provided by a cloud service provider. There are a number cloud service providers (CSPs). Each of these cloud service providers offer a number of services. Going through all the services of all the CSPs and finding out what service matches the requirements in the SLA document, manually is time consuming, error prone and tedious. And opting for all the services will add extra charges for the owner. Hence it is important to have a system that can match the requirements in the SLA (Service Level Agreement) document with the APIs (Application Programming Interfaces) of the cloud service providers. This paper proposes a method to match the requirements of a businessman with the APIs of the CSPs. The requirements are written in a text document and the description of the APIs of CSPs are written in another text document. Then using text similarity in natural language processing, the APIs that satisfy the requirements in the text document are identified.**

Keywords*— *Cloud service providers, Service Level Agreement, Natural language processing, Application programming interface, text similarity

I. INTRODUCTION

Many web applications, mobile applications and internet businesses are using cloud computing environment. Small-scale businesses, technical giants and entrepreneurs opt for cloud computing for their applications. Cloud computing is delivery of IT services like data storage, computation, network resources, hardware and software resources which are provided by a third party vendor. The clients use these services and pay based on usage. The third party vendors who provide these services are called cloud service providers (CSP). These CSPs provide Application Programming Interfaces (APIs) that help to develop applications.

Many businessmen and entrepreneurs who wish to establish their online businesses opt for cloud computing. There are many cloud service providers. Each of these service providers have their own set of APIs to provide services. An application does not need all the services of a CSP for developing it. More over opting for all the services of the CSP makes the consumer to pay for the services which he does not need and use. Hence the developer of the application should know what services the application should provide and in turn what APIs of the CSPs are required to implement these services. Going through all the APIs of different CSPs manually is tedious, time consuming and error prone. In order, to overcome it, a method has been proposed that automatically matches the APIs of different CSPs with the requirements of the user. This method can be used as a recommender system that recommends the APIs to the developer of the application based on the requirements of the businessman.

The system is trained with the description of APIs of different CSPs. The businessman lists a set of requirements in the Service Level Agreement (SLA). The SLA is given as an input to the system. Both the APIs training set and the requirements list is pre-processed to extract the keywords individually. Using similarity measure, the APIs that match the requirements in SLA are fetched.

The paper is organized into five sections. Section I gives the introduction to the topic. In section II, relevant work has been surveyed. Section III gives the methodology of the proposed work and section IV gives the results of implementation of the proposed work. Section V includes the conclusion.

II. RELATED WORK

Many researchers are carrying out their studies to improve the text similarity and to improve the performance of the information retrieval systems.

[1] The authors use natural language processing techniques to extract knowledge from various cloud service providers to from knowledge base from text documents. [2] The authors discuss the existing methods for search operation such as inverted index, its limitations. They also propose a new method such as interval list to store and process indices that reduces the storage space.

Maake Benard Magara, Sunday O. Ojo , T. Zuva [3] try to find out what algorithms and what combinations of metrics of similarity can be used to optimize the search operation to recommend the relevant articles in a research paper recommender system. The authors used non-linear classification algorithms with text similarity metrics.

Marouane Birjali, Abderrahim Beni-hssane and M. Erritali in [4] propose an approach for measuring similarity between documents in a large corpus. The proposed approach was compared with other previous methods using MapReduce algorithm. It was found that the new MapReduce algorithm outperformed the previous ones with its running time and value of text similarity.

Chaobo He, Yong Tang, Feiyi Tang and Atiao Yang in [5] discuss the disadvantages of traditional approaches of document similarity and present a new structure of distributed inverted index, the algorithms based on MapReduce model and the architecture of cloud computing platform. Experiments have been carried out using the proposed approach and the results show that this approach is effective for computing similarity of large documents and is scalable also.

Yilin Feng, Jie Tang, Meilin Liu, Chongjun Wang and Junyuan Xie [6] propose a two step similarity measure of documents in on GPUs in CUDA environment. The results of the experiments show that the proposed approach solves the problem faster than the existing methods.

Sung-min Kim and Young-guk Ha in [7] present a method for finding similarity between movies with the help of movie scripts. The new method is about matching the documents using cosine similarity measure which overcomes the traditional matching keywords.

P. Vigneshvaran, E. Jayabalan and K. Vijaya in [8] developed a tool to calculate the similarity between key and source documents in a corpus. The experiments were done on the assignments submitted by the students to test the students' modesty. The tool can be used to find the similarity index of documents and remove the duplicate documents from the repository.

Ashraf S. Hussein [9] in his paper propose a content-based method to analyse document similarity and visualization.
Kishore Varma Indukuri, Anurag Anil Ambekar and Ashish Sureka [10] in their paper propose a method to find similarity analysis between two different patents using natural language processing techniques. The authors also built a GUI tool for the same.
Taeho Jo [11] in his paper propose a version of K Nearest Neighbour that considers similarity among attributes to compute similarity between feature vectors.
Qamar Mahmood, Muhammad Abdul Qadir and Muhammad Tanvir Afzal [12] in their paper propose a method to find document similarity by using semantic social network analysis techniques on RDF graphs of citations of research papers.
Sun Park, Dong Un An and Choi Im Cheon [13] in their paper propose a document clustering method which uses weighted semantic features and cluster similarity.
Xiaojie Yu, Xiaojun Chen and Jinqiao Shi in [14] present a vector based document similarity and a new protocol which uses latent semantic analysis.

III. METHODOLOGY

The methodology consists of two modules namely pre-processing and pattern matching. The APIs help file consists of the description of APIs of different CSPs that are available in their web pages.

Fig. 1. Shows the architecture diagram of the system. In this the system is trained with the APIs of different CSPs. The input to the system is the SLA document which consists of the requirements from the businessman. Both the documents are pre-processed to extract keywords from them. Then the common keywords from both these documents are identified in the pattern matching.

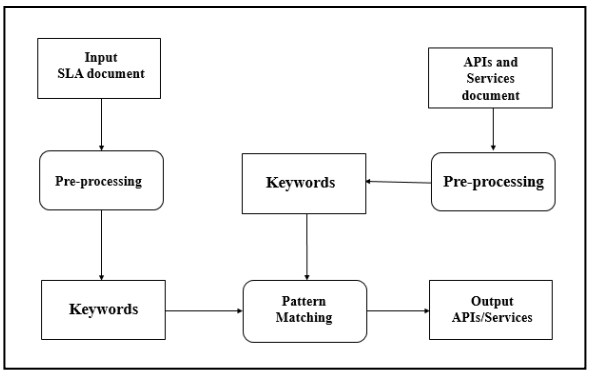

Fig. 1. System architecture of the system.

A. *Pre-processing module*

Fig. 2. Represents the pre-processing of training data. The input is the APIs help file. The content for this APIs help file is obtained from the description or documentation pages of the APIs of different CSPs. The steps performed in pre-processing are as follows:

a) Sentence tokenization:

The input document consists of a number of sentences. It is necessary to process each sentence in the document. So the content of the document is divided into its constituent sentences. The sentences are stored as keys of a dictionary like data structure.
For example, a document may contain 10 sentences, the number of keys in the dictionary data structure is 10 which are the same sentences in the document.

b) Word tokenization:

The sentences obtained from the previous step is given as input to this step. A sentence is usually made up of a number of words. In order to

find the list of common words between two documents, it is important to break the sentences into words. So each sentence is then split into its constituent words.

For example consider a sentence "A boy is playing with dogs". The result would be an entry in the dictionary where the key contains the sentence and its values will have the words – "A", "boy", "is", "playing", "with", "dogs".

c) Stopword removal:

Words like "a", "an", "the" and others which are frequent are not considered important. Such words are called stopwords. These words do not contribute for pattern matching as they do not carry any special meaning. Such words are removed from the document.

For the above example, this step will remove the words "A", "is", "with" from the value set of the dictionary.

*d) Lemmatization***:**

The words usually have prefixes, suffixes and will be in one of the eight different parts of speech.it will be easier to compare the documents if their constituent words are in the same form. So it is important to normalize the words. So each word in the document is converted into its root or base form. For the above example the words "boy", "playing", "dogs" are converted into "boy", "play", "dog".

The output of pre-processing is the keywords extracted from the APIs document. These keywords are stored as values of the dictionary whose keys are the sentences in the APIs help file. Similarly, the SLA document is given as input file which consists of the requirements needed to develop the application. The document consists of sentences where each sentence is a requirement. This is also pre-processed to obtain the keywords from each requirement. And the result is stored as another dictionary where the keys are the sentences (requirements) in the SLA document and the values are the keywords extracted from these sentences. These two dictionaries are then given as input to the pattern matching module.

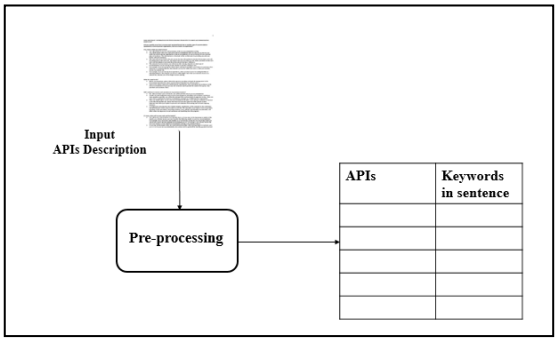

Fig. 2. Pre-processing of training data.

B. *Pattern matching module*

Fig. 3. Shows the pattern matching process where the keywords from both the input SLA document and the APIs help file are matched to fetch the required APIs.

The keywords obtained from the pre-processing of APIs help file is stored as a dictionary like data structure where the keys contain the APIs' names and the values contain the corresponding APIs' keywords. And the SLA document is stored in a different dictionary where the keys contain the sentences (requirements) and the values contain the keywords extracted from that sentence. The pattern matching technique involves finding the common keywords between the two dictionaries.

An intersection of the keywords in both the dictionaries is performed and stored in another dictionary. If a requirement in the SLA contains a threshold number of keywords that are present in the API dictionary's value set, then those corresponding APIs are the ones that match with the requirements of SLA. These APIs are fetched as the required APIs to the businessman. In the experiments conducted the threshold number of keywords that are matched is set to two.

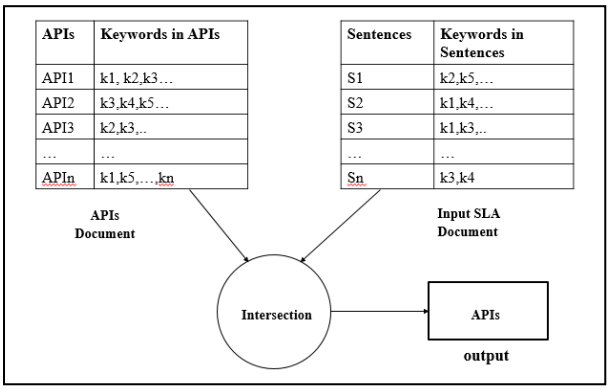

Fig. 3. Pattern matching

IV. RESULTS

APIs of Google Cloud were given as the APIs help file and a sample SLA document with ten requirements was given as input to the system. The system returned the APIs for five of the given requirements correctly. Figure 4 shows the result which shows a resultant dictionary which has the requirements that found matching APIs as keys and values as the respective APIs.

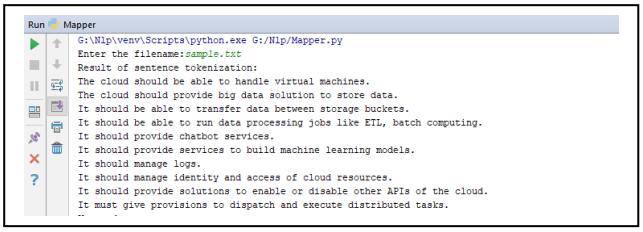

Fig. 4. Result of sentence tokenization.

Fig. 4. Shows the result of sentence tokenization where the content of input SLA document is split into sentences.

Fig. 5. Result of keyword tokenization.

Fig. 5. Shows the result of keyword tokenization where the sentences in the input SLA document is split into its constituent words.

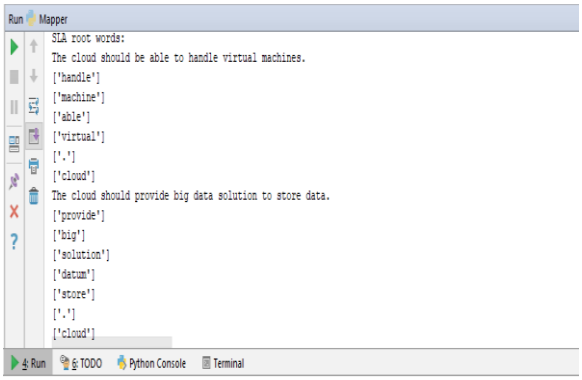

Fig. 6. Result of Lemmatization.

Fig. 6. Shows the result of lemmatization where the words in the input SLA document are converted into their root forms.

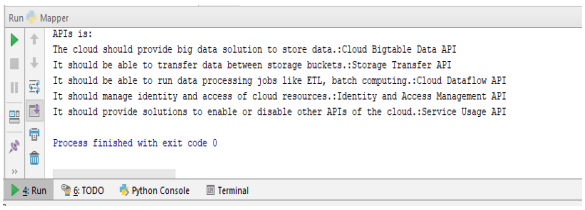

Fig. 7. Screenshot of APIs.

Fig. 7. Shows the APIs that matched with the requirements in the given input SLA document.

V. CONCLUSION AND FUTURE WORK

This paper proposes a method to match the requirements in an SLA document with the APIs of different CSPs. This system is useful to the developers who develop the application with cloud computing. It reduces the time taken to manually select the required APIs. It can be used as a recommender system by developers to match the requirements needed to develop an application with the APIs of different CSPs.

REFERENCES

[1] S. Mittal, K. P. Joshi, C. Pearce and A. Joshi, "Parallelizing natural language techniques for knowledge extraction from cloud service level agreements," *2015 IEEE International Conference on Big Data (Big Data)*, Santa Clara, CA, 2015, pp. 2831-2833.

[2] J. Giridharan and S. V. Vairavan, "Inverted index and interval lists for keyword search," *2014 International Conference on Green Computing Communication and Electrical Engineering (ICGCCEE)*, Coimbatore, 2014, pp. 1-4.

[3] M. Benard Magara, S. O. Ojo and T. Zuva, "A comparative analysis of text similarity measures and algorithms in research paper recommender systems," *2018 Conference on Information Communications Technology and Society (ICTAS)*, Durban, 2018, pp. 1-5.

[4] M. Birjali, A. Beni-Hssane and M. Erritali, "Measuring documents similarity in large corpus using MapReduce algorithm," *2016 5th International Conference on Multimedia Computing and Systems (ICMCS)*, Marrakech, 2016, pp. 24-28.

[5] Chaobo He, Yong Tang, Feiyi Tang and Atiao Yang, "Large-scale document similarity computation based on cloud computing platform," *2011 6th International Conference on Pervasive Computing and Applications*, Port Elizabeth, 2011, pp. 175-179.

[6] Feng, Yilin & Tang, Jie & Liu, Meilin & Wang, Chongjun & Xie, Junyuan. (2018), "Fast Document Cosine Similarity Self-Join on GPUs", 205-212. 10.1109/ICTAI.2018.00040.

[7] S. M. Kim and Y. G. Ha, "A New Method of Measuring Document Similarity for Movie Recommendation," *2014 Eighth International Conference on Innovative Mobile and Internet Services in Ubiquitous Computing*, Birmingham, 2014, pp. 41-44.

[8] P. Vigneshvaran, E. Jayabalan and K. Vijaya, "A predominant statistical approach to identify semantic similarity of textual documents," *2013 International Conference on Pattern Recognition, Informatics and Mobile Engineering*, Salem, 2013, pp. 496-499.

[9] A. S. Hussein, "Visualizing document similarity using n-grams and latent semantic analysis," *2016 SAI Computing Conference (SAI)*, London, 2016, pp. 269-279.

[10] K. V. Indukuri, A. A. Ambekar and A. Sureka, "Similarity Analysis of Patent Claims Using Natural Language Processing Techniques," *International Conference on Computational Intelligence and Multimedia Applications (ICCIMA 2007)*, Sivakasi, Tamil Nadu, 2007, pp. 169-175.

[11] T. Jo, "Using K Nearest Neighbors for text segmentation with feature similarity," *2017 International Conference on Communication, Control, Computing and Electronics Engineering (ICCCCEE)*, Khartoum, 2017, pp. 1-5.

[12] Q. Mahmood, M. A. Qadir and M. T. Afzal, "Document similarity detection using semantic social network analysis on RDF citation graph," *2013 IEEE 9th International Conference on Emerging Technologies (ICET)*, Islamabad, 2013, pp. 1-6.

[13] S. Park, D. U. An and C. I. Cheon, "Document Clustering Method Using Weighted Semantic Features and Cluster Similarity," *2010 Third IEEE International Conference on Digital Game and Intelligent Toy Enhanced Learning*, Kaohsiung, 2010, pp. 185-187.

[14] X. Yu, X. Chen and J. Shi, "Vector based privacy-preserving document similarity with LSA," 2017 IEEE 9th International Conference on Communication Software and Networks (ICCSN), Guangzhou, 2017, pp. 1383-1387.

Proceedings of the Fourth International Conference on Communication and Electronics Systems (ICCES 2019)
IEEE Conference Record # 45898; IEEE Xplore ISBN: 978-1-7281-1261-9

Control and Management of Autonomous Power between Standalone DC Microgrids

Prasad Subhash Kirtane
Post Graduate Student
G.H.Raisoni Institute of Engineering & Technology
Pune, India
prasadkirtane1991@gmail.com

Dr. A. D. Shendge
Associate Professor
G.H.Raisoni Institute of Engineering & Technology
Pune, India,
ashashendage@raisoni.net

***Abstract*—**
Electricity is fuel for today' s automated world, in near future scarcity of electricity will be major problem for all developing countries. Dependency on fossil fuel will not be feasible option and hence, people around world started deploying renewable energy sources on a larger content. The DC microgrids are serving the purpose by interconnecting the renewable sources to the power system. Proper management of renewable energy sources can be accomplished by using DC microgrid. But DC microgrid suffers from a disadvantage of energy efficiency. In the proposed method bus voltages are deployed for shifting modes thus does not require additional communication channel for controlling the grid voltage.

Keywords — Autonomous DC Micro grids, Power control, Bus signaling, Bus Management, Renewable sources, etc.

Introduction

Smart grid and microgrid will be the future of electricity distribution. Hence, researchers worldwide focus improving efficiency, performance and automated operation of these grids [1]. Pilot projects in few parts of world in been implemented for power generation, distribution and consumption in small area by forming microgrid [2][3]. There are various possibilities for operation of the microgrid either it can be part of the grid or standalone system. Stand alone systems may suffer from various disadvantages and frequent outages if energy demand is not met properly. Energy management systems will be a essential component for power sharing and maintaining voltage profile in microgrid. Traditional techniques use MPPT algorithms in case of wind and PV, in this case battery is treated as slack and leftover power is used for charging battery. However, overcharging of the batteries must be prevented to avoid damage to battery terminals. Normally, constant voltage – constant current charging is been used considering operational constraints of wind system. To regulate operations in this environment non linear control strategies with power curtail options may be deployed for controlling microgrid. Standalone DC microgrid are widely accepted as they possess few more advantages over other kinds of network e.g. no need of complicated control strategies and other AC electrical system parameter.

Centralized controller for controlling operation of the grid is better option for optimal operation of the various parameters. It suffers from the disadvantage of dependence on communication link. Moreover, in traditional grids droop control is implemented which gathers local information but doesn' t have capacity to utilize microgrid resources optimally. The mentioned drawback can be overcome by using DC bus signaling method (DCBSM) was tried but failed as it was not capable of considering battery status. Condition of state of charge is taken care by primary control on DCBSM. Secondary control is designated for adjustment of bus voltage. In case of DC microgrid battery is responsible for regulating the bus voltage, system reliability may deficit. Decentralizing operating regions is done through primary control DC bus voltage, along with coordination with secondary control midst various devices. In this case surplus generation is dealt using dump loads. In this paper various deploys different control strategy considering DC bus voltage variation to maintain voltage profile under continuously changing generation and storage condition. DC bus voltage is been used to read the DC microgrid status. Two different control loops are used for optimizing the system parameters and to improve efficiency.

I. . System Structure

DC microgrid stability is accessed by measuring DC bus voltage level [4]. Voltage source converters used in grid acts as slack terminals for regulating the voltage of microgrid. System shown in fig.1 is considered for simulation and developing hardware, system has two ADCMGs far from one another and has considerable line resistance between them.

Each ADCMG equipper two photovoltaic systems and batteries are used to represent any other equivalent renewable energy source and storage device. DC loads are generally

resistive in nature and also treated as constant power load (CPL), which are interconnected by using DC-DC converters. By using DC-DC converters we can ensure fixed output power irrespective of fluctuation in DC bus voltage. Photovoltaic systems are connected directly to DC bus by using boost converter. For connecting storage devices and batteries bi - directional devices are used. Interconnection of ADCMG is done with DABC for interfacing. DABC ensures isolation between two systems and also has high frequency feeding capacity in both the directions along with transformer (high frequency). The transformer uses the H-Bridge converters for producing the high frequency AC from DC. Ideal location of placing DABC would be near to low voltage DC system, so the losses can be avoided and communication can be made faster. Bus voltage data obtained from line between two ADCMG' s. If this line experiences open circuit fault voltage is measured at C_1 (i.e. V' a). In this case V' a is also utilized for BDC triggering at ADCMG1. If connection between both ADCMG is healthy then current flowing through the line is being measured to know the voltage drop (i.e. xp1 x R). To obtain the voltage at ADCMG1 V' a can be added to DABC high voltage side. This facilitates power exchange without any communication link.

II. Power Control and Management Strategy (PCMS)

The coordination of the grid is achieved by voltage as a signal to the coordination system. By Coulomb method of counting, the SoC is given by:

$$SoCi = SoCo - \frac{1}{CN}\int \delta\, ibat\, dt \quad \text{.....(1)}$$

Where
SoCi→ Instantaneous SoC
SoC0→ Initial Capacity
CN→ Nominal Capacity
ibat→ Battery current
δ → Loss coefficient (Range 0.98 – 1)

By controlling the charging and discharging current SoC can be limited.

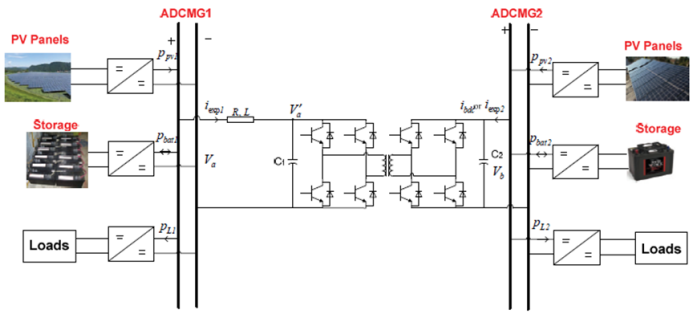

Figure1.Interconnection of two ADCMGs

Working of ADCMG is divided into five zones depending upon bus threshold voltage as shown in Fig. 2

Zone-1 (Balanced power mode):
In this zone power generated by photo voltaic systems is less or equal to load PL_1 in ADCMG1. Hence, batteries are any other storage device if any remains idle. Little fluctuations in load will not switch on storage units as a system is designed to sustain small fluctuations or load variations. Voltage regulation at a constant point is not possible in this case. As, reference voltage is missing, hence voltage varies between VaH1 and VaL1. Power exchange between two ADCMG is not done in this mode.
Status of various units in ADCMG1 are given by

$$P_{PV1} \cong P_{L1};\ P_{bat1} = 0;\ V_{aL1} < V_a < V_{aH1} \quad \text{..... (2)}$$

Where

Pbat1→ ADCMG1 Instantaneous battery power

Zone-2 (Battery discharging mode):
Power produced by photovoltaic systems cannot meet demand, bus voltage cannot be maintained. Once bus voltage falls below threshold voltage Val1, then power is derived from the storage systems to fulfill the demand. Battery power maintains the bus voltage in limit by using bus regulating mode. If ADCMG2 has excess power, ADCMG1 may absorb without reverse transfer of power.
ADCMG1 conditions is expressed as

$$P_{PV1} + P_{bat1} = P_{L1};\ V_a = V_{aL1} \quad \text{.....(3)}$$

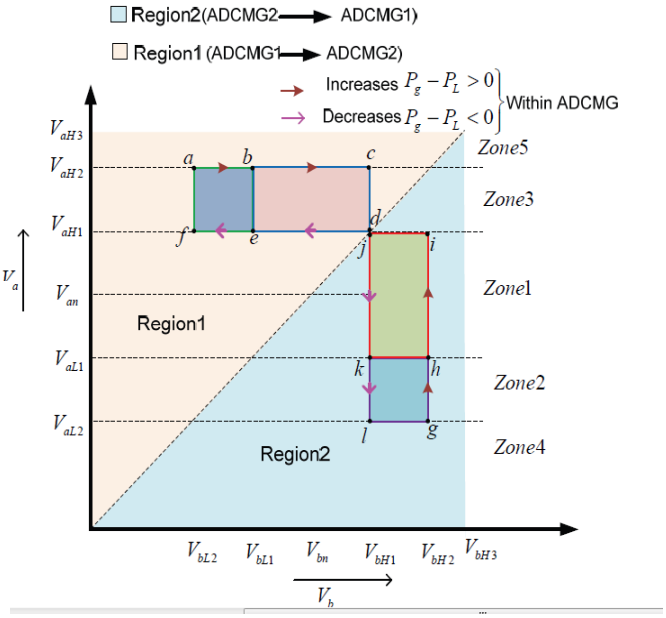

Figure2. Proposed PCMS between two ADCMGs

Zone-3 (Battery charging mode):
Power generated by photovoltaic is more than the demand, in this condition voltage Va increases due to availability of surplus power and reaches up to VaH1 this charges the battery. Battery is charged to maximum limit till it fully charged. In this case ADCMG1 will not exchange power with ADCMG2. At the same time it can absorb the power Vb and Vbh2 and battery in ADCMG1 is not fully charged.

$$P_{PV1} > P_{L1};\ P_{bat1} = -(P_{PV1} - P_{L1});\ V_a = V_{aH1} \quad \ldots\ldots\ldots(4)$$

Zone-4 (Power deficit mode):
If the demand is more than the battery charging rate, system is in zone-4 of operation. Battery has a capacity of draining the power when operated continuously. ADCMG1 can import proper from ADCMG2. In case 2, power is not taken from ADCMG2.
Case1:
ADCMG1 always check status ADCMG2 for availability of surplus power by measuring bus voltage Vb. In the same way voltage Va gives status of ADCMG1. If Vb=VbH2&Va≤VaH1, power flows from ADCMG2 to ADCMG1 by DABC.
Transferred power pushes the ADCMG1 for operation at various operating points dependent on imported power (pimp1) in region 2 as shown in fig. 3. Operating modes equations are explained further.

$$V_a = \begin{cases} V_{aL1} & ;if\ P_{PV1} + P_{bat1} + P_{imp1} = P_{L1} \\ V_{aL1} < V_a < V_{aH1}\ ;\ if\ P_{PV1} + P_{imp1} \cong P_{L1} & \\ V_{aH1}\ ;\ if\ P_{PV1} + P_{imp1} > P_{L1}, P_{bat1} = -(P_{PV1} + P_{imp1} - P_{L1}) & \end{cases} \quad \ldots\ldots (5)$$

Case2: Here, power transferred from ADCMG 2 to 1 is not sufficient or zero. It leads to load shedding in ADCMG1. The main cause is decrease in voltage beyond permissible limits.
The insertion of the voltage by means of renewable generation could help in this situation to restore the voltage level. The case is expressed as:

$$P_{PV1} + P_{bat1} + P_{imp1} < P_{L1}$$
$$P_{PV1} + P_{bat1} < P_{L1};\ P_{imp1} = 0 \quad \ldots. (6)$$

5) Zone-5 (Excess power mode):
Operation of this mode is further divided into two groups, depending upon ADCMG1 exporting excess power and without exporting excess power.

Case1:
There are ways to operate in this mode either excess generation or drop in load. If excess power remains in grid bus voltage will start rising. ADCMG status is been monitored by measuring its bus voltage. If ADCMG2 goes into excess power state (i.e. Vb≤VbH1), it causes the flow of power from ADCMG 1 to 2.

Case2:
This is similar to earlier case with little difference where ADCMG2 will not be capable to absorb the surplus power available at ADCMG1 which increases the bus voltage (Va). If the bus voltage Va above threshold voltage VaH2, control loop will change and all photovoltaic system will change operation from the MPP to bus voltage regulating mode which increases VaH3.

Mathematical equations of ADCMG1in zone5 is given by

$$V_a \begin{cases} V_{aH2}\ ;if\ P_{exp1} > 0 \\ V_{aH3}\ ;if\ P_{exp1} = 0;\ V_{PV\backslash ref} = V_{aH3} \end{cases} \quad \ldots\ldots(7)$$

Where
Pexp1→ power (instantaneous) exported from ADCMG 1 to 2.
VPV1→ PV voltage reference

III. SIMULATION RESULTS

Model of the implemented system is shown in fig.3. It is simulated on real time digital simulator (RTDS) for validating with PCMS. System is implementation is done on RSCAD/RTDS.

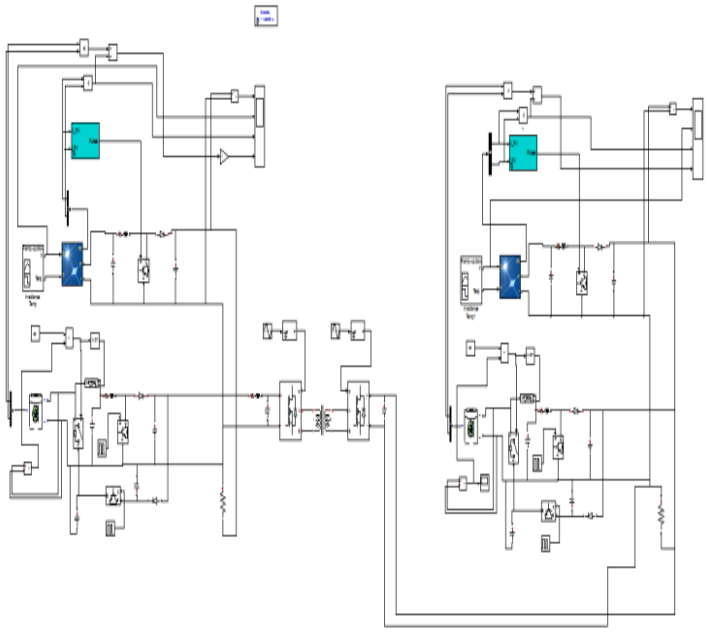

Figure3. Simulation Model

Representation of critical and non critical load is mentioned to the system. This discrimination is needed in order to shed non critical load in power crisis situation. Proposed PCMS is explored for different operating situations of ADCMG which also includes the extreme environmental situations of battery and grid.

A. Individual DC Micro grids
Different operating parameters of ADCMG 1 are depicted in fig.4. The batteries are having the voltage above cut off (lower) by small amount. Each zone has a voltage bandwidth

of 10V and tolerance limit of 5% of the nominal bus voltage. From the fig. 4 it is observed that generated power and demand is same in time period between 0 to t1 which is indicated as operating zone -1. In this mode bus voltage varies in upper and lower limit. At t1, power in grid is more than the demand, which charges the battery and it starts regulating bus voltage Va up to VaH1. Catastrophic change in load demand happened at 2t which impels the battery charging current to outstrips saturation limit, which causes rise of V since excess generated electrical power is not accepted by other ADCMG or any load. This causes PV mode to change in bus regulation mode and photovoltaic system changes state from MPP to bus regulation mode as shown in fig.5, typical zone -5 operations. Incorporated PV control bus voltage controls the regulated bus voltage up to time period 3t. At 3t bus voltage gets lesser than VaH2 due to fall of PV power with decay in irradiation. This causes zone-3 operation and same is visualized in time period 3 t to 4 t. At time 4 t, rapid increase in load causes the zone-2 to appear.

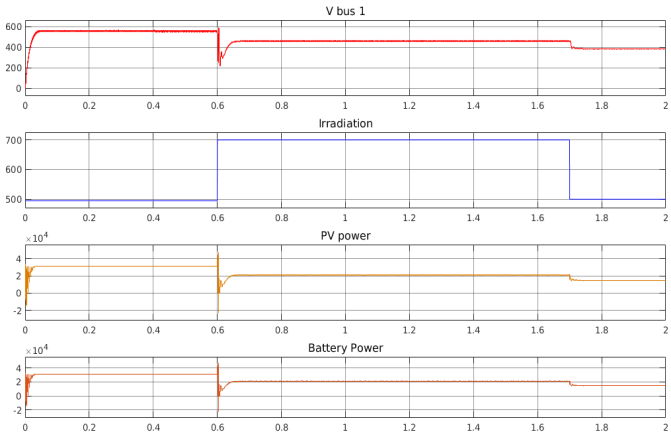

Figure4. Parameters of ADCMG1: (a) Bus voltage, (b) Irradiation, (c) PV output power, (d) Battery output power

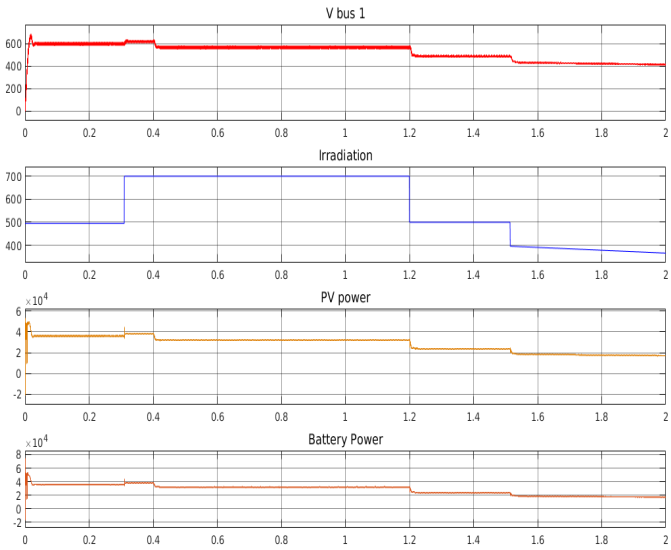

Figure5. Parameters of ADCMG2: (a) Bus voltage, (b) Irradiation, (c) PV output power, (d) Battery output power

TABLE I
SIMULATION PARAMETERS

Components	Parameters	ADCMG1	ADCMG2
PV Capacity	Maximum power@1000W/m2	4.5kW	750W
Battery	Capacity	10AH	10AH
	Nominal Voltage	90V	22V
Nominal grid voltage	Rated Voltage	380V	48V
Voltage Thresholds	V_{xH3}	410	54 V
	V_{xH2}	400	52 V
	V_{xH1}	390	50 V
	V_{xL1}	370	46 V
	V_{xL2}	360	44 V
DC Load	Fixed load	1kW	200W
	Variable load	2kW	300W
Line parameters	Resistance ®	0.15Ω	
	Inductance (L)	0.24mH	

In time period t4 to t5 demand is more than the generation excess needed power is provided by the batteries or any other storage devices in the system. The execution of load shedding is done at 6t as load is more than power in grid, shedding a load will bring ADCMG in normal condition. Time period 5 t to 6 t depicts the operating zone-4. Once load is shed, it is in zone-2. ADCMG2 operates in coordination with ADCMG1.

CONCLUSION

A well harmonized, multivariable continuously monitored NMPC control strategy is demonstrated in this paper for getting optimal EMS in microgrid. Bus signaling method is used for PCMS, implemented PCMS system is mainly used for DC grid power flow and between ADCMG' s. Two microgrids of 380V and 48V are considered for simulating the environment in real time simulator. Developed simulation is operated in normal and extreme conditions and simulated and same results are obtained on developed hardware. Developed system gives isolation and improves reliability of the system.

ACKNOWLEDGMENT

I Prasad Subhash Kirtane would like to thank the authorities of the G.H.Raisoni Institute of Engineering & Technology, Pune for providing us the facilities for completion of this paper.

REFERENCES

[1] Al-Sakkaf, Shehab, et al. "An Energy Management System for Residential Autonomous DC Microgrid Using Optimized Fuzzy Logic Controller Considering Economic Dispatch." Energies12.8 (2019): 1457.
[2] Han, Ying, et al. "Hierarchical energy management for PV/hydrogen/battery island DC microgrid." International Journal of Hydrogen Energy 44.11 (2019): 5507-5516.
[3] de Carvalho Neto, João T., Andrés O. Salazar, and Alberto S. Lock. "An analog based control scheme applied in stand-alone photovoltaic systems for DC power distribution." Renewable and Sustainable Energy Reviews 110 (2019): 236-246.

[4] Yang, Yun, et al. "Efficient Improvement of Photovoltaic-Battery Systems in Standalone DC Microgrids Using A Local Hierarchical Control for the Battery System." IEEE Transactions on Power Electronics (2019).
[5] Pu, Yuchen, et al. "Hierarchical energy management control for islanding DC microgrid with electric-hydrogen hybrid storage system." International Journal of Hydrogen Energy44.11 (2019): 5153-5161.
[6] Pu, Yuchen, et al. "Hierarchical energy management control for islanding DC microgrid with electric-hydrogen hybrid storage system." International Journal of Hydrogen Energy44.11 (2019): 5153-5161.
[7] Worku, Muhammed Y., Mohamed A. Hassan, and Mohamed A. Abido. "Real Time Energy Management and Control of Renewable Energy based Microgrid in Grid Connected and Island Modes." Energies 12.2 (2019): 276.
[8] Kumar, Shailendra, and Bhim Singh. "Self-Normalized Estimator Based Control for Power Management in Residential Grid Synchronized PV-BES Microgrid." IEEE Transactions on Industrial Informatics (2019).
[9] Nagaraja, Y., T. Devaraju, and M. Vijaykumar. "Optimal distributed control of renewable energy-based microgrid– an energy management approach." International Journal of Ambient Energy (2019): 1-8.
[10] Slouma, Safa, et al. "Frequency Separation Model Based on Infinite-Impulse Response Filter Applied To Hybrid Power Generation Intended For Residential Sector." International Journal of Renewable Energy Research (IJRER) 9.1 (2019): 118-127.
[11] Roslan, M. F., et al. "Microgrid control methods toward achieving sustainable energy management." Applied Energy240 (2019): 583-607.
[12] Roslan, M. F., et al. "Microgrid control methods toward achieving sustainable energy management." Applied Energy240 (2019): 583-607.

Proceedings of the Fourth International Conference on Communication and Electronics Systems (ICCES 2019)
IEEE Conference Record # 45898; IEEE Xplore ISBN: 978-1-7281-1261-9

Delay Minimization by Offloading in Fog Computing

1st Shahid Sultan Hajam
Department of Information Technology
National Institute of Technology, Srinagar
Hazratbal, India
shahid_02phd18@nitsri.net

2nd Dr. Shabir Ahmad Sofi
Department of Information Technology
National Institute of Technology, Srinagar
Hazratbal, India
shabir@nitsri.net

3rd Zahoor Ahmad Najar
Department of Information Technology
Central University of Kashmir
Ganderbal, India
zahoornajar@cukashmir.ac.in

***Abstract*—As technology is growing at fast rate, things are getting connected with each other through internet thus producing huge amount of data that need processing. Cloud computing provides the processing, storage and analysis of the collected data, but inspite of the fact that cloud usage is increasing rapidly still, there are various limitations such as unreliable latency, lack of mobility support and location awareness. High redundancy, high communication bandwidth and latency adds extra burden to process the data at the cloud. Fog devices located at the edge of the network solves these problems by processing the generated data locally closer to the end devices and hence avoiding the transmission latency and network bandwidth by not sending each and every bit of information to the cloud for processing. In this paper offloading policy at the Fog layer is proposed and it is also discussed how the Fog computing is efficient than Cloud computing in terms of latency.**

***Index Terms*—Priority, offloading, arrival rate, service rate, Queue.**

I. Introduction

The Internet of things is the interconnection of physical or virtual devices having sensing and networking capabilities and which can be accessed from anywhere through internet.IoT is increasing at a very rapid rate and thus sensing data from the environment that needs processing. The processing of the data can be either done in the IoT devices themselves or can be outsources to the cloud or the fog. The IoT devices as such are resource constraint devices, so to process the big data locally at the IoT devices is not an efficient way. The Cloud rich in resources provides the services from the pool of resources based on the demand of the users that can be easily accessed or released with the minimum effort [1]. But due to the various limitations like centralized approach, location unawareness, lack of mobility, multi hop distant from IoT node, huge bandwidth requirement cloud cannot be effectively used to process this big data generated by the IoT devices. So the need for another computational model arises, the Fog computing, which includes Fog devices like gateways, routers, access points etc was coined by Cisco [2]. It provides various services as like in cloud, but the Fog devices are resource constraint as compared to the cloud by having limited storage and processing capabilities. So the both cloud and the Fog cannot be used independently due to their limitations, they had to be used aggregately so as to maintain the quality of service. Kevin Ashton coined the term internet of things in 1999 [3]. Since then growth of IoT has increased in the exponential manner and is predicted by some major companies [4] [5] [6]. Offloading is the transfer of computational work from one device to another inorder to reduce the time of execution. Various work had been done by various authors, In [7], authors considered a three level architecture comprising of IoT level, Fog level and the cloud level. very level consists of multiple nodes and they are aggregated into various domains. The tasks can be either processed in IoT layer locally or can be send to the Fog or Cloud layer, internally Fog nodes can process requests or can forward the requests to other Fog nodes depending upon the estimated waiting time. They have considered centralised and distributed mode of interaction between Fog nodes. In centralised mode , a central Fog node controls ooading decision and interaction between Fog nodes. All the Fog nodes send their estimated waiting time to the centralised Fog node and the central node distributes that information to all the Fog nodes present in the domain, the estimated waiting time information is storing in the reachability table of every node. When the decision about the offloading has to be taken, the nodes looks into the reachability table and offloads to that node which has the least estimated waiting time listed in the table. In the distributed mode of interaction a distributed protocol is used to distribute the state information of nodes to each and every other neighbouring Fog node. A reachability table is maintained comprising the entries of estimated waiting time and round trip time. A best neighbour is selected which has the minimum estimated waiting time and half of round trip delay. When a task is submitted to the Fog node, if the estimated waiting time is smaller than the threshold, then the task is processed by that node otherwise the node offloads the task to its neighbouring nodes. If the ooad limit is greater than the number of times task is offloaded, the task will be forwarded to the cloud. In [8] transmission delay and power consumption are considered as parameters in fog cloud system. A tradeoff between these two parameters is proposed. It is shown that fog computing outperforms cloud computing by saving communication bandwidth and reducing service delay. GBD and Hungarian algorithm are used for solving optimization problem. In [9] a fog computing model and an offloading policy which effectively improves the

performance of the system is proposed. Offloading policy takes both energy and execution performance into consideration and they both need to be improved at the same time. In [10], Two layered architecture for Fog computing is considered, comprising of Fog nodes and Fog access points. Fog nodes are battery powered and are less computationally, storage and range powerful than Fog access points. Fog access points are connected to electrical supply and to the higher computational powers. Tasks submitted to the Fog nodes can be either processed locally on that Fog node or can be offloaded to the neighbour Fog nodes or can be offloaded to the Fog access points in range. The main of the paper is to select the amount of task or data that is to be offloaded to the candidate nodes in order to minimise the total energy consumption and the task processing delay. Firstly the Fog nodes are classified into low power and High power Fog nodes based on the amount of energy left within them. Secondly the low power Fog nodes offload their portion of task to either high power Fog nodes or to the Fog access points depending upon the coverage area. Thirdly the portion of task that is to be computed locally is calculated keeping node energy consumption and task processing delay into consideration. Lastly the portion of task that is offloaded is calculated by considering the data rate and the amount of data to be offloaded. In [11],main focus is on the communication between the Fog nodes. Fog nodes can communicate with each other within specific range, they have computational and storage capabilities and are battery powered. A cluster base offloading scheme is proposed, in which Fog nodes are classified as Fog cluster heads and Fog cluster members based upon the amount of energy left. Fog cluster heads have more left energy than Fog cluster members. There can be many clusters in a fog layer. Each cluster consists of one cluster head and many cluster members. Cluster members can offload their tasks to their cluster heads for computation. The fog nodes are classified into High power Fog nodes, Medium power Fog nodes and Low power Fog nodes using a quantile function based on the remained energy. Fog cluster heads can be selected from either High power Fog nodes only or from the high power Fog nodes first then from Medium power Fog nodes. Fog cluster members can be selected from either Low power Fog nodes only or from the Medium power Fog nodes then Low power Fog nodes. After selecting the Fog Cluster head, if there are no Fog cluster members remained then a cluster is formed with a single node performing local computation. The clusters are periodically updated because the Fog cluster heads will spend energy in computation of offloaded tasks and by updating Fog cluster head can be selected as the next Fog cluster member due to reduction in its energy. In [12], offloading in cloud and fog servers using hybrid policy is proposed. Tasks are allocated in such a manner so that total energy and processing delay is minimised. Offloading problem is solved by breaking the problem into four sub problems based on delay and energy efficiency. It is observed that the proposed policy performs better than conventional schemes. In this paper we study the delay minimisation in the Fog computing by formulating the offloading policy of centralised approach. Same offloading policy is applied for both Cloud, Fog and IoT layer and finally we will compare the delay obtained at different arrival rates. The remainder of the paper is organised as follows: section II will discuss the system model, in section III we will discuss the mathematical model concerned, section IV discusses the evaluation and results and finally in section V we will have the conclusion and future work.

II. Proposed Architectural Model

We are considering the three layered architecture consisting of lower IoT layer, middle Fog layer and top Cloud layer. The data generated by the sensors is collected at IoT layer and can be either processed or offloaded to the upper levels for processing. Each layer consists of multiple nodes, the data can be offloaded to any node depending upon the offloading policy. Each node has a queue associated with it. We are considering the centralised approach for offloading, from among n nodes a node is choosen as a coordinator depending upon which node receives receives request or the node which is at least distance from the data generating device. The rest n-1 nodes respond to the coordinator with their estimated waiting time. The waiting time in the queue plus the service time of the request forms the estimated waiting time. The coordinator will take the offloading decision depending upon the waiting time, the task is offloaded to the node with least waiting time. The work of the coordinator is only to take the offloading decision. If all nodes respond with the same waiting time, then any node is chosen as candidate for offloading. If all nodes are unreachable, then the task is offloaded to the cloud for processing. In case if the coordinator fails, the node with the least waiting time is chosen as coordinator. Tasks received by any node are forwarded to the coordinator for offloading decisions. In our offloading policy the tasks are offloaded based on the estimated waiting time and priority of the task. We divide the tasks in two types: type 1 of high priority tasks or class 1 tasks and type 2 of low priority tasks or class 2 tasks. Class 1 tasks has got priority over class 2 tasks. If the class 2 are are in processing stage and class 1 tasks arrive at the system, the class 2 tasks are pre-empted and class 1 tasks are processed first. The processing of class 2 tasks are never carried out when there are class 1 tasks in the system. System is implemented by the single server Markovain queuing system with infinite capacity. Requests generated by the devices are either processed locally within the micro controllers at the IoT layer like Arduino or the requests can be offloaded to the Fog or Cloud layer.

III. Mathematical Model

In our paper we are implementing same offloading policy for all the layers, so the equations to calculate the delay will be same for all the layers. Let N represents the set of nodes, all the nodes are assumed to be homogeneous:

$$N = n1, n2, n3, ...nN \tag{1}$$

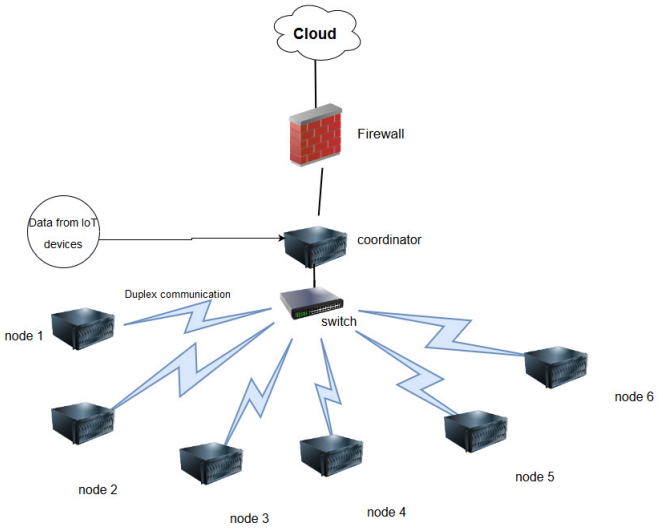

Fig. 1. Architectural Model.

We will choose among these N fog nodes a coordinator depending upon which node receives the request. All other nodes respond to the coordinator with their estimated waiting time. In order to model this we will consider a single server pre-emption priority queue model for the coordinator and rest of the nodes. We are classifying tasks or requests into two types, high and low priority tasks. Each request arrives according to the Poisson process having data rates $\lambda 1$ and $\lambda 2$ respectively. We have chosen the single queue for high and low priority requests. The service time for each class of requests are assumed to be independent with service rate μ. It is called M/M/1 because of memoryless property [13] [14].
The system is stable if:

$$\rho 1 + \rho 2 < 1 \tag{2}$$

$$\text{Where } \rho i = \frac{\lambda}{\mu}, i = 1, 2$$

The service of the class low priority requests is never carried out if there is a request belonging to the high priority class; means that class 1 request has absolute priority over class 2 requests. When class 2 requests are being processed and class 1 request arrives, the class 2 request is pre-empted and the system proceeds with the class 1 requests. The interrupted class 2 request is fed back to the system and is processed only when there are no class 1 requests in the system. Both class 1 and class 2 follows the first in first out queuing discipline. Average time class 1 requests are processed in the system is given as:

$$W_1 = \frac{1}{\mu - \lambda 1} \tag{3}$$

$$or \quad W_1 = \frac{\frac{1}{\mu}}{1 - \rho 1} \tag{4}$$

Where W_1 is the average time a request of class 1 spend in the system [11][12]. As class 2 requests are effected by the class 1 requests, so average time a request of class 2 spends in the system is given as:

$$W_2 = \frac{\frac{1}{\mu}}{(1 - \rho 1)(1 - \rho 1 - \rho 2)} \tag{5}$$

Where W_2 is the average time a request of class 2 spends in the system [3]. Total delay in coordinator is given as:

$$P_{cd} = W_1 + W_2 \tag{6}$$

Other n-1 are modelled same as the coordinator by single server markovanian queueing system. The total delay for each node is given as:

$$P = W_1 + W_2 \tag{7}$$

Total delay for a system is given as:

$$P_{total} = P_{cd} + \Sigma_1^{n-1} p_n \tag{8}$$

Average delay for the system is given as:

$$P_{average} = \frac{P_{cd} + \Sigma_1^{n-1} p_n}{n} \tag{9}$$

In case of Fog and Cloud computations, tasks need to be transmitted across the network so there is addition of the transmission delay.

$$RTT(ms) = 0.05 * distance + 5 \tag{10}$$

where RTT is round trip time

$$T_d = \frac{RTT}{2} \tag{11}$$

Therefore equation 10 can be written as:

$$P_{average} = \frac{P_{cd} + \Sigma_1^{n-1} p_n}{n} + T_d \tag{12}$$

IV. Results and Analysis

Simulation is performed in MATLAB and Simulink. System is analysed at different arrival rates and transmission delay for fog and cloud is taken as 0.5 seconds 2.5 seconds respectively [10].
We have considered a single queue for both types of tasks. It is observed that when the arrival rate of the tasks or the jobs from the IoT devices are lower, Fog layer processes the tasks in least period of time or with the minimum delay because the transmission delay for the Fog layer is lower than that of Cloud. No doubt Cloud had huge processing power but at the same time has got larger transmission delay. Processing the data at the IoT layer by IoT devices themselves is inefficient because they have got least processing power among the Fog and Cloud. When the arrival rate is increased beyond threshold, the cloud will efficiently handle the data because the Fog devices have got limited storage and processing capabilities, when the arrival rate is increased beyond threshold the queue length will get increased and hence will add to the delay which would be much larger than the transmission delay of the Cloud, hence Cloud performs better. So inorder to efficiently handle the data or to maintain the quality of

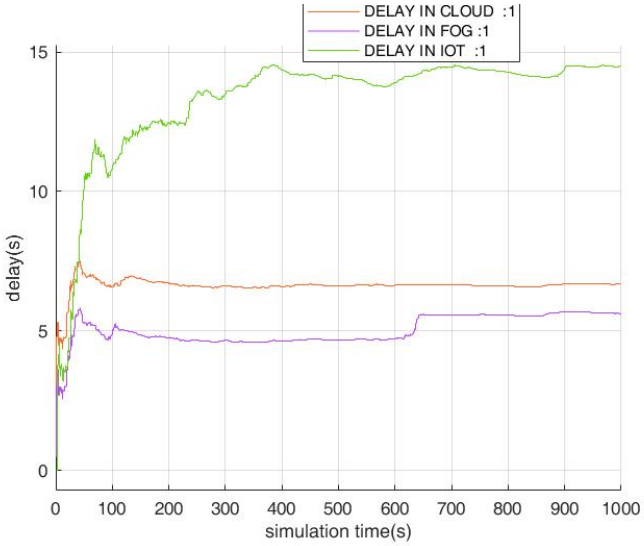

Fig. 2. when $\lambda 1$ =0.2 and $\lambda 2$ =0.4

service we have to make the use of both Cloud and Fog layers aggregately.

Case A: $when \lambda 1 = 0.2$ and $\lambda 2 = 0.4$

$\lambda 1$ and $\lambda 2$ are the arrival rates of the high priority and low priority tasks respectively. As we can see from the figure 2 that the fog computing outperforms cloud and IoT computing at this arrival rate.

Case B: when $\lambda 1$ =0.4 and $\lambda 2$ =0.2

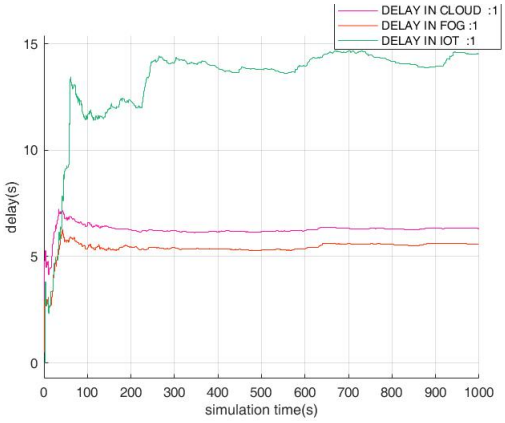

Fig. 3. when $\lambda 1$ =0.4 and $\lambda 2$ =0.2

Here we have taken arrival rate of high priority task greater than low priority tasks. Stop time for simulation is fixed as 1000 seconds and from the figure 3 it is observed that fog computing outperforms.

Case C: when $\lambda 1$ =0.3 and $\lambda 2$ =0.3

When the arrival rate of both the tasks are same, it is observed that the fog computing still outperforms the cloud computing and the computation at the IoT layer as shown in figure 4.

Case D: when $\lambda 1$ =0.3 and $\lambda 2$ =0.52

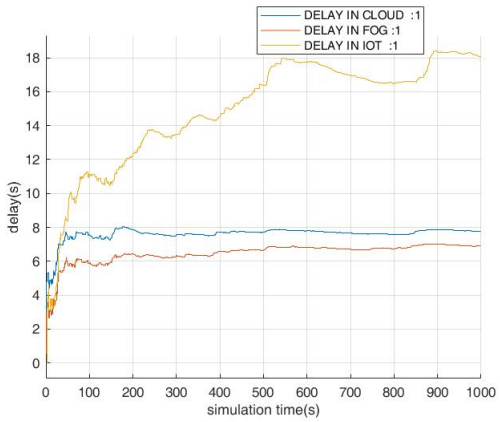

Fig. 4. $\lambda 1$ =0.3 and $\lambda 2$ =0.3

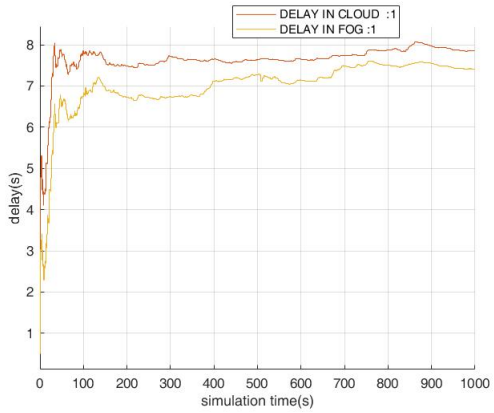

Fig. 5. $\lambda 1$ =0.3 and $\lambda 2$ =0.52

At this arrival rate fog computing outperforms as shown in figure 5.

Case E: when $\lambda 1$ =0.3 and $\lambda 2$ =0.53

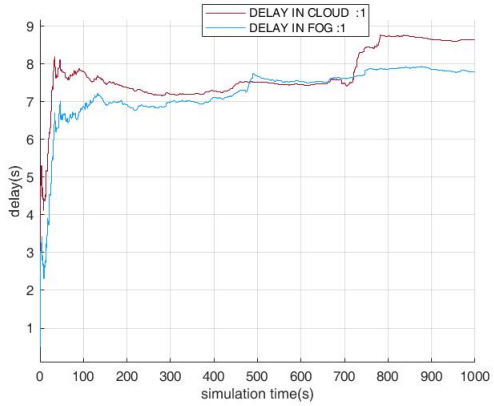

Fig. 6. $\lambda 1$ =0.3 and $\lambda 2$ =0.53

At this arrival rate there occurs small flactuations in the waiting time as shown in figure 6.

Case F: when $\lambda 1$ =0.3 and $\lambda 2$ =0.54

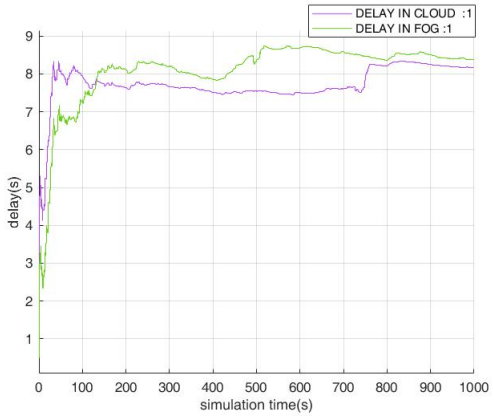

Fig. 7. $\lambda 1$ =0.3 and $\lambda 2$ =0.54

As we observe from the figure 7 that at this arrival rate, cloud computing outperforms the fog computing because the service rate of fog computing is lower than cloud computing. Cloud computing can easily handle the increased traffic rate due to its huge computational power. It is observed that upto arrival rate of 0.83 ($\lambda 1$+ $\lambda 2$), the fog computing outperforms and when the arrival rate is increased beyond 0.83, the cloud computing efficiently handles the traffic and outperforms. So 0.83 is the threshold up to which fog computing efficiently handles the traffic.

V. Conclusion

Fog computing has resulted in the making the system the system more efficient by minimizing the delay. We analyse the delay at different data arrival rates at three layers of IoT, fog and cloud. It is found that when the arrival rate is below certain threshold computation at fog layer produces minimum delay and when arrival rate overshoots limit or when number of tasks overshoots the threshold, the cloud computing efficiently handles the traffic and produces minimum delay. So to build an efficient system we need to have a mixture of both Cloud and Fog computing. In future one can compare this model with some existing model and compare the results, one can analyse the system.

References

[1] P. Mell, T. Grance *et al.*, "The nist definition of cloud computing," 2011.
[2] A. V. Dastjerdi, H. Gupta, R. N. Calheiros, S. K. Ghosh, and R. Buyya, "Fog computing: Principles, architectures, and applications," in *Internet of things*. Elsevier, 2016, pp. 61–75.
[3] H. Elazhary, "Internet of things (iot), mobile cloud, cloudlet, mobile iot, iot cloud, fog, mobile edge, and edge emerging computing paradigms: Disambiguation and research directions," *Journal of Network and Computer Applications*, 2018.
[4] Gartner. Gartner says 8.4 billion connected "things" will be in use in 2017, up 31 percent from 2016. [Online]. Available: https://www.gartner.com/en/newsroom/press-releases/2017-02-07-gartner-says-8-billion-connected-things-will-be-in-use-in-2017-up-31-percent-from-2016
[5] D. Evans, "The internet of things: How the next evolution of the internet is changing everything," *CISCO white paper*, vol. 1, no. 2011, pp. 1–11, 2011.
[6] M. Aazam, S. Zeadally, and K. A. Harras, "Fog computing architecture, evaluation, and future research directions," *IEEE Communications Magazine*, vol. 56, no. 5, pp. 46–52, May 2018.
[7] A. Yousefpour, G. Ishigaki, R. Gour, and J. P. Jue, "On reducing iot service delay via fog offloading," *IEEE Internet of Things Journal*, vol. 5, no. 2, pp. 998–1010, 2018.
[8] R. Deng, R. Lu, C. Lai, T. H. Luan, and H. Liang, "Optimal workload allocation in fog-cloud computing toward balanced delay and power consumption," *IEEE Internet of Things Journal*, vol. 3, no. 6, pp. 1171–1181, 2016.
[9] Q. Zhu, B. Si, F. Yang, and Y. Ma, "Task offloading decision in fog computing system," *China Communications*, vol. 14, no. 11, pp. 59–68, 2017.
[10] A. Bozorgchenani, D. Tarchi, and G. E. Corazza, "An energy and delay-efficient partial offloading technique for fog computing architectures," in *GLOBECOM 2017-2017 IEEE Global Communications Conference*. IEEE, 2017, pp. 1–6.
[11] ——, "An energy-aware offloading clustering approach (eaoca) in fog computing," in *2017 International Symposium on Wireless Communication Systems (ISWCS)*. IEEE, 2017, pp. 390–395.
[12] X. Meng, W. Wang, and Z. Zhang, "Delay-constrained hybrid computation offloading with cloud and fog computing," *IEEE Access*, vol. 5, pp. 21 355–21 367, 2017.
[13] S. M. Ross, "8 - queueing theory," in *Introduction to Probability Models (Twelfth Edition)*, twelfth edition ed., S. M. Ross, Ed. Academic Press, 2019, pp. 507 – 589. [Online]. Available: http://www.sciencedirect.com/science/article/pii/B9780128143469000135
[14] J. Sztrik, "Basic queueing theory," *University of Debrecen, Faculty of Informatics*, vol. 193, 2012.

Proceedings of the Fourth International Conference on Communication and Electronics Systems (ICCES 2019)
IEEE Conference Record # 45898; IEEE Xplore ISBN: 978-1-7281-1261-9

Designing a help system including website, mobile application along with secured locker as a communication medium for students

Dr.Thangam Palaniswamy[*], Ruba Al-Ghamdi[+], Ayshah Banabilah[+], Mawaddah Kuddah[+], Nesren Attiah[+]

[*]*Associate Professor, Department of ECE, Faculty of Engineering,*
King Abdulaziz University, Saudi Arabia
tswamy@kau.edu.sa
[+]*Senior Student, Department of ECE, Faculty of Engineering,*
King Abdulaziz University, Saudi Arabia

***Abstract*—This paper discusses a Help Spot System as a senior design project. Nowadays, the education organizations have become huge and divergent. Finding resources and tools that are related to the subjects is challenging for students. Therefore, a website work as a communication medium between students, alumni and faculties will help to solve the problem by letting them stay in touch whenever they need anything related to their major. To develop Help Spot system, we use latest technology and components such as, Beaglebone, Smart Door Latch, Logitech Webcam. This design was found to satisfy the project objectives and solve the problem in the shortest period of time. Based on the requirements three alternatives design were generated as a solution for the project problem. The first and second alternatives is about using three tier architecture and fortify. The 3rd alternative is the best solution which consists of a website, mobile application, and a locked locker to provide a self-delivery option. Moreover, the website is adaptable for different screen size. Automatic monitoring and guaranteed malware removal and open source programming languages are used. Along with several features such as chatbot.**

Keywords—help spot, QR code, website, mobile app, communication, lockers, web-based services.

I. INTRODUCTION

Each year and semester there is a batch of graduates and a new batch that come to the university. Each new batch used to struggle just to find college supplies related to their major. This is due to many factors like rarity of items, high cost textbooks, etc. Basically, students should have relatives or friends who have studied the same subjects as they will, so they can buy needed supplies as used products with much lower cost, or borrowing it for free, which is not always the case! Also, if a student wants to order books from Amazon or any other online stores, it may take long time to be delivered. So, there is a need for an effective communication medium between students and faculties to help them stay in touch whenever they need anything at any time. This problem is usually overcome by exchanging the needed resources within the college, communicate with older students through social media, and order the needed resources from abroad. All these solutions are temporary and inefficient. The most efficient and effective way is to automate the process of exchanging items to follow kingdom's 2030 vision and enhancing the progress of E-government by contributing in E-commerce . the problem can be tackled by implementing an online store that provide the ability of offering/selling items from one side and borrowing/buying items from other side. The organization of the paper is as follows: Section 1 introduces the problem, section 2 discussing the exiting technologies in the field, the next section describing the baseline design of the product, the following section is about the approach and the results of the project and the last section including the references.

II. LITERATURE REVIEW

A. Websites

Website is information and documents that can be stored and accessed through the Internet that help people to connect with large audience. The first website was created in 1991 by Tim Berners-Lee[1], Since then approximately one billion sites have been created for a huge variety of purposes. Every website has a unique (URL) to provide easy access to it. Websites are constructed using Hypertext Markup Language (HTML), a specialized language mixture of human language with computer-centric coding. Most sites contain of one page or more, depending on the website purpose. Designers create and develop websites with a vast array of features according to user requirements. Once a website is completed, it must be launched onto the World Wide Web to make it accessible to the public [2], [3] .

The first World Wide Web was conceived in 1989 by British physicist Tim Berners-Lee. Berners-Lee devised a method to allow the exchange of information with people via computer network. By 1991, he has created the first Website in history, which introduced his vision for a World Wide Web that would link information across the globe. Although this website was simple and pragmatic, it demonstrated the enormous potential of Berners-Lee's creation. Since then governments, businesses, schools, and individuals added their own sites to the network of publicly shared information, such as Yahoo, Google, Amazon, IMDb, and eBay [2].

The early 2000s brought with it an increase of support for CSS language, which allowed for the separation of content and design. Along with this, the ability to create a good website entailed far more than just knowing how to write the code. Accordingly, a science of website design has arisen. This gave greater creativity to web designers and developers. It made websites easier to maintain (less code and complexity), more flexible, and quicker to update.

Ultimately, the designer needs to study every design element in such a way and to bring the most relevant content to the user in the most efficient and effective way. People

want to access information to find what they need at any time, so any site that makes this job easier for a user, the user will be benefited [4].

By September 2014 one billion active websites could be found on the World Wide Web. After only two decades from the publication of first website, online shopping has established itself as an irreplaceable component of any good marketing strategy. Nowadays, websites help in performing various tasks like registration, purchase, payments, etc. In addition, websites provide an easier way for customer service. Websites can contribute to reduce customer service costs, saving time and money, and providing more information. Likewise, the education field, facilitate services between students, faculty, administrative staff and visitors, provide valuable academic information and services to its users without any difficulty [3]-[5].

The following Table is about implemented websites in real life that let people to lend their stuff for other people to borrow it by lower cost.

TABLE I
ADVANTAGES AND DISADVANTAGES OF EXISTING WEBSITES

Project	Peerby website [6]
Advantages	- Enables people to borrow from their neighborhood. - Save money. - People can borrow form Peerby anything they need.
Disadvantages	- Not supported by English language. - Delivery service is not available in the lending process

Ultimately, how websites started simply for the purpose of communication between people, to these days where one website can provide a lot of services that make life easier. A website is online and accessible 24 hours a day and can sell products at any time.

B. Mobile Applications

"Enterprise applications have the reputation for being business and educational tools. However, with the success of platforms such as iOS and Android, consumer expectations have raised the bar on what constitutes an acceptable user experience. Enterprise apps are now starting to feel the impact of this renewed focus on ease of use and visual design. Recent initiatives inside of IBM have launched IBM into a new world where it is no longer sufficient for an enterprise app to be merely functional. With our new focus, apps must also be easy to use, visually appealing, and engaging" [7].

The five major platforms in developing mobile applications are: Android, iOS, RIM (Blackberry), Symbian, and Windows [8]. For developing their apps, all these platforms use some C programming language and/or Java. Using their own developing environment and programming interface. The following Table 2 shows each platform with its core language and environment.

TABLE III
MOBILE OSPLATFORMS

Mobile Platform	Core Language	Environment
Android	Java or C++	Eclipse
iOS (Apple)	Objective-C	Xcode
RIM (Blackberry)	Java	Eclipse
Symbian	C++	Multiple choices
Windows	C#	Visual Studio

Recent market share information shows the number of apps available in leading app stores as of the 1st quarter of 2018 shown below in Figure 1. This alone shows that Android and iOS are the leaders platforms in mobile apps industry.

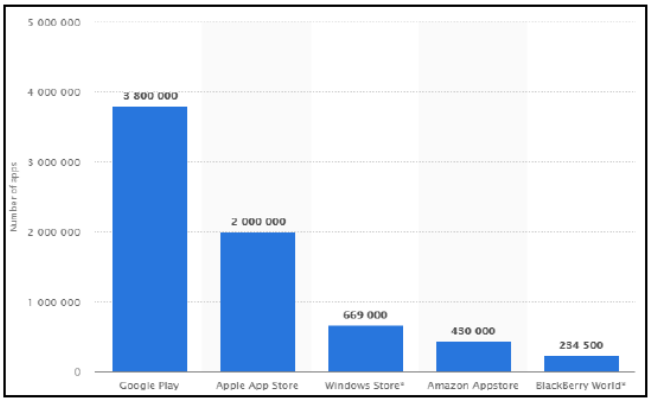

Fig. 1 Number of apps available in leading app stores as of 1st quarter 2018 [9]

To narrow the options more, Table 3 below shows a comparison between Android and iOS platforms.

TABLE IIIII
COMPARISON BETWEEN ANDROID AND IOS

	iOS	Android
Development Environment	Freely Available	Freely Available
Annual Fee	99$	Free
Technical Support	Paid	Free
Mobile Device Emulator	Available	Available

By means of this, all the elements pointed to Android platform as the most appropriate developing environment for students and beginners due to how affordable it is [10].

The following Table shows similar mobile applications related to universities, books, supplies, and education which are the scope of our project.

TABLE IVV
ADVANTAGES AND DISADVANTAGES OF EXISTING APPLICATIONS

Project	My college bookstore [11]	Marketplace [12]	Student desk [13]
Advantages	-Tracking the status of the bookstore orders. -Browsing articles about tips and advices for college. -Renting date reminders	-Variety of items to be traded. -Searching by community.	-Ability to rent or exchange books. -Availability of communities
Disadvantages	-No communication between the bookstore and students.	-No communication between the bookstore and students.	-No communication between the bookstore and students.

To solve lack of communication within universities, our project aims to be the medium of communication between students, which the previously mentioned mobile apps does not provide. Furthermore, all supplies can be can be offered, not only text books. In conclusion, our goal is to provide better services that previously implemented mobile applications and avoid their disadvantages.

C. Electronic Lock System

The most important thing to secure the self-delivery service's process is providing a secured place/locker for delivery and receive the items have been sold. Only a specific person must have access to the locker, so the best way to secure it, is an electronic lock system.

Electronic lock systems depend on controlling a small motor connected to the door bolt by an actuator. The motor is controlled by an electrical impulse, which may be triggered in many ways, such as a keypad, or a QR reader. This means that the electronic door lock will not start the motor-driven actuator until it has received the expected electronic input [14].

Keypad lock is an electronic lock for use with lockers assigned for transitory or permanent use, it has a keypad for entering a pre-selected sequence of digits. It has two modes: transitory mode and a longer term assigned locker mode. In the transitory mode, it is programmable for each use, the lock shifts a latch to the locked position on a first entry of a sequence chosen by the user and retracts the latch to unlocked position when the same sequence is re-entered by the user. A subsequent user of the locker (when unlocked) can enter any sequence of digits desired. In the mode of a longer-term assigned locker, the electronic lock is programmed by the user, and the same combination is retained as long as desired. In this mode, the selected sequence is used only to unlock, with the latch or mortise being spring-biased. The construction of the electronic lock is modular, easily fitting on nearly all contemporary locker designs, retained by only a few screws [15].

Many improvements have been made to keypad locks; one of the highly advanced locks is WIFI Smart Lock, as shown in Figure 2. It gives the user both wife-connected and no-internet lock control. But either way, the user should change the password each time manually, as he desires.

Fig. 2 WIFI Smart Lock [16]

A QR code (quick response code) is a type of 2D barcode that is used to provide easy access to information through a smartphone, using a barcode reader app. Figure 3 shows an example of a QR code.

There are two types of QR code: static and dynamic codes. Static codes have used to disseminate information to the public, as what often displayed in advertising materials everywhere, while the dynamic codes are more functionally and can be edited by the code owner [18].

Fig. 3 QR Code Example [17]

A great feature of QR codes is that they can be auto-generated, in contrast to keypad locks, which make the QR code reader lock more preferred to apply in the "Help Spot System". The QR code-based Door Lock System is a QR reader lock project. It used a simple web interface; approved users are added to the system via their email addresses. Once added, these users are sent a QR code via Email, that when held up to the system, allows them to unlock the door. After each scanning, the QR code will be expired and a new one will be auto-generated and sent to a specific person [19].

D. E-commerce

Electronic business or as it is known as E-business is "the process of buying and selling goods or services electronically rather than using conventional means" [20]. One of the functions of E-business is E-commerce, it involves commercial transactions done using an electronic

transmission medium and requires the use of a website. E-business is the broader concept including pre-sale and post-sale efforts, while E-commerce is the narrower concept and is restricted to buying and selling. In general, E-business is any electronic transactions, such as: information exchange which subsumes E-commerce. There are many applications of e-commerce, including online retailing, online banking, electronic markets, online auctions and others.

"Electronic commerce improves the efficiency and effectiveness of business, governments, and not-for-profit agencies" [21]. The ability to conduct business all over the world 24/7 is a major advantage of being online. "According to the U.S Department of Commerce, between December 1998 and August 2000, the share of American households with Internet access jumped from 26.2% to 41.5%. In 2000, more than half of U.S houses had PCs" [21]. All these factors have encouraged E-business and E-commerce in the last decade. For example, Nestle was one of the initiating companies in leading the E-commerce revolution. Peter Brabeck- Letmathe, CEO of Nestle, believes in this transformation and calls the process "E-revolution" [22].

E-commerce sites are either pure E-business, such as Amazon, or they have an E-commerce presence, such as Wal-Mart stores. The backbone of E-commerce is the Internet. Simply, it can be referred to as "network of networks" [21]. There are many popular services available on the Internet that support E-commerce program and enhance E-business, such as: E-mail, discussion groups, Internet Relay Chat (IRC), Instant messenger and others.

The popularity of e-commerce has increased due to the rapid development of the Internet which has motivated companies to enter the online market [23]. In the era of speed, E-commerce has impacted the community positively. There are many advantages of E-commerce which can be identified by three types. These include perceived economic, relationship-related, and strategic benefits. The speed and automation of the E-commerce applications help to improve the efficiency in the business process. Which directly affects the economy in a positive manner, including the reduction of transaction costs, administrative expenses, and time-saving from a faster trading cycle. Internet applications can increase and enhance trading partner's productivity and increase their capability to communicate globally [23], [24]. Despite the advantages of E-commerce, it may carry enormous risks for both retailers and customers. In fact, the travelling of information over the internet passing through many inter-mediating nodes before reaching the final destination is still a nightmare for many people.

III. Product Baseline Design

A. Block Diagram

The block diagram describes the process that happen to Help Spot system starting from developer and end with achieved goal of system.

First of all, the developer creates a database using SQL server store and retrieve information in a way that is accurate and effective. The Website is going to be programmed using Visual Studio and C# language. The website has Several features: Responsive which mean have one design but is adaptable with any screen size, Chatbot that answers all customer's doubts, Search engine optimization-friendly since it displays a search history for each user. GoDaddy is response about hosting and security of the website. The mobile app is connected to the same database for the website and is going to be programmed using Xamarin and C# language. Second stage the seller will register to website as seller then offer and item in the Website and select the payment method after getting approval from admin. In other side the buyer will register to website as buyer and then choose item, there will be contact between seller and buyer to decide the delivery method. Third stage is locker secured with QR code, the locker has a camera that scan QR code and translated into string and compared if it is identical the locker will be opened otherwise nothing will happen. When the item gets purchased and delivery method is selected to be self-service a QR code will be sent for seller and buyer, therefor seller will put the item in locker using that QR code, and buyer can take the item from locker by using same QR code after that QR code will be expired. By the end of this process the goal of Help Spot will achieved since we get Effective Communication.

B. System Description

The initial design of the circuit consists of beagle bone board powered by a 5V power supply, with a webcam connected to it through its USB port, in addition to an electric door strike connected to its pins. Also, there are two LEDs, green and red connected to the board pins with resistors. The user who owns the QR code will scan it using the webcam. If the QR code was valid, the green led will turn on and the electric door strike will turn on for few seconds, then it will turn off automatically. In case the QR code was invalid, the red led will turn on till the user scan the valid QR code. Figure 5 shows the circuit initial design.

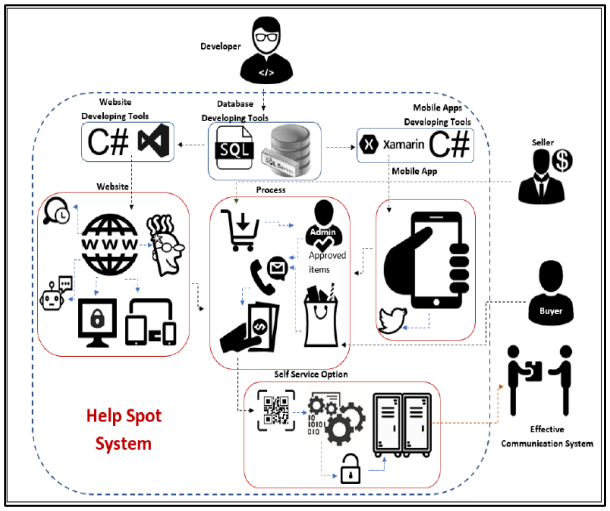

Fig. 4 The block diagram of the system

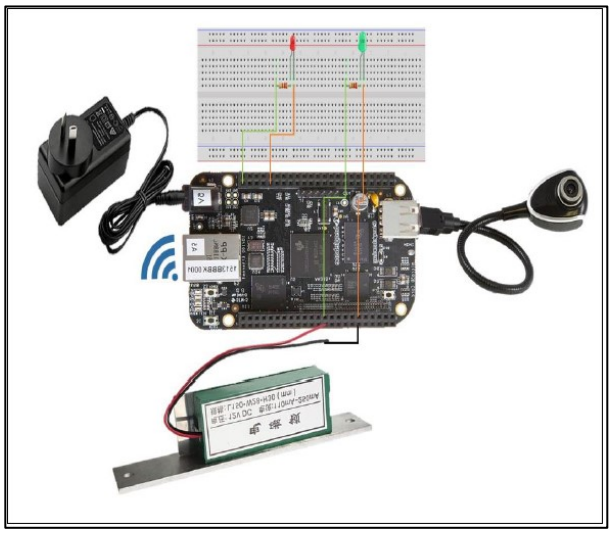

Fig. 5 The circuit schematic of the project.

The following flowcharts are explaining the flow of the system, and how the software and hardware parts are connected. The flowchart shown in Figure 6 can be applied on both website and mobile application, which starts by checking whether the user is registered or not. If registered, the user will be redirected to the home page, then for each role, an action can be taken. The admin can approve the offered items by the sellers, sellers can offer items for purchasing or borrowing in addition to selecting the payment method. Finally, buyers can search for an item according to certain categories, after selecting an item, the delivery method can be selected after coordinating with the seller. No need for coordinating with the seller about the delivery method if the method used is self service delivery, because a QR code will be generated and sent to both buyer and seller. After generating the QR code, it will be sent through WIFI to the beagle bone board to be compared with the scanned QR code by the camera after translating it to a string. Finally, once the scanned QR matches the one stored in the beagle bone board, the locker will open to put or pick up items. The hardware part process is shown in Figure 7.

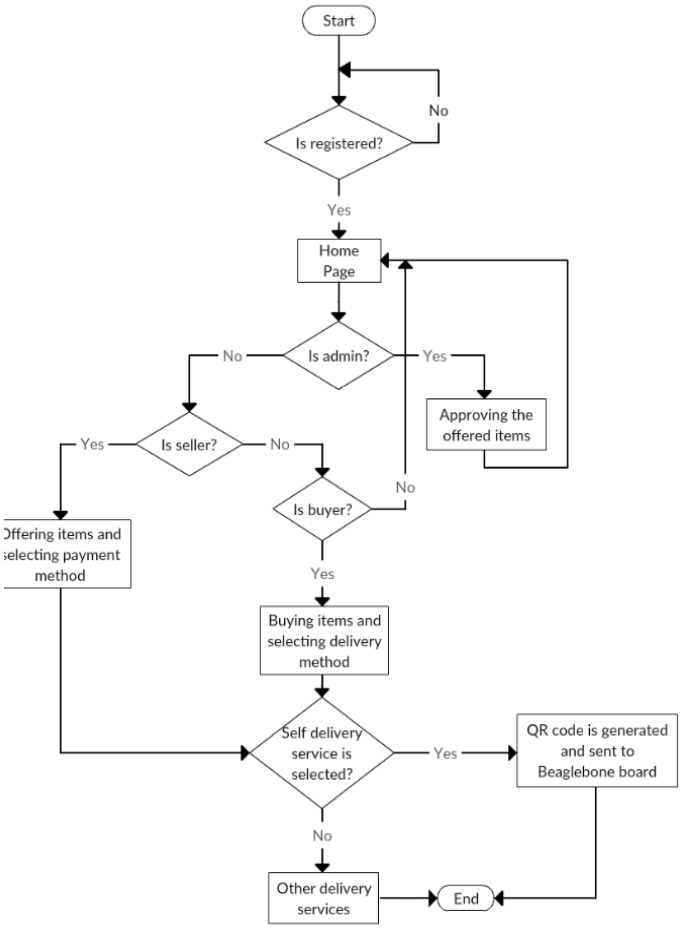

Fig. 6 Flowchart for QR code lock process

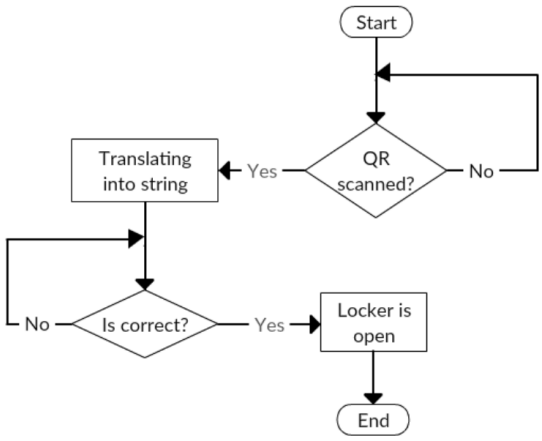

Fig. 7 Flowchart for website/mobile application process

C. *Impact of the Engineering Solutions*

Impact assessments are to assess impact of Help Spot system to ensure the system are economically viable, socially equitable and environmentally sustainable.

Implementing this system will provide effective communication between students in the campus to help them stay in touch whenever they need anything at any time.

The benefit of applying Help Spot system is more efficient in saving data from lost since all the data through the years are saved in database. Also, the website will save time, reduce effort since there is no need for more than one

admin responsible about all process in website, paper transactions will be canceled, so a lot of wastes will be reduced. Moreover, the delivery method will reduce pollution that come from transportation since the supplies can be received through campus.

IV. Approach And Results

This project is a system that consists of three main parts, website, mobile application, and secure locker. It aims to provide an appropriate medium to exchange, sell, and buy study resources for university students. The website and application allow the user to add items for sale and buy them; while the website provides a feature of self-delivery service, which is made through the locker after choosing the credit card as the payment method.

The idea of the locker is that it is locked by a QR code that is sent to the customer. This code will be valid for one scan only. After the scan, a new code is generated and becomes ready to be sent to the next customer. The one-scan validation makes the locker safe enough to send and receive items between customers

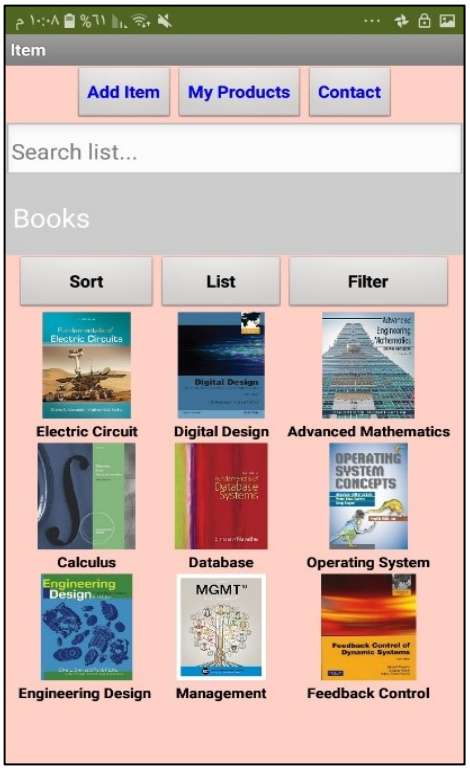

Fig. 9 Help Spot mobile application home page

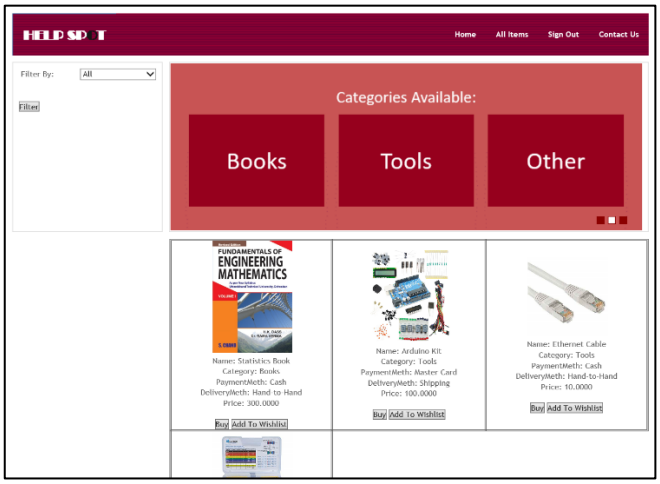

Fig. 8 Help Spot website home page

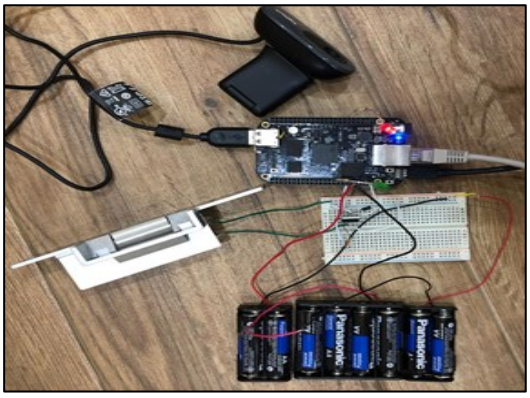

Fig. 10 Secured locker connection

V. Conclusion

The project aims to solve the student's problem of spending a lot of money on the needed supplies, from books, tools, to resources that are related to their field. Usually the students prefer to borrow these supplies from the older students within the university, but the lack of communication between the students will make this process harder. Hopefully, this system will help the students and faculties to find whatever they need whenever they want. There are many recommendations to improve the system in the future and make it capable to serve more customers efficiently. These suggestions are as follow: Targeting the educational bookstores as partners to provide books and sell them via Help Spot System. This will make the system's items rich with useful books for students, partnering with a delivery company to provide delivery service with revenues, making Help Spot System services available for other universities students.

References

[1] Berners-Lee, Sir Timothy John, Who's Who. 2015 (online Oxford University Press ed.). A & C Black, an imprint of Bloomsbury Publishing plc, ukwhoswho.com.

[2] Dziak, Mark. (2015) "website", Salem Press Encyclopedia of Science. pp.2.

[3] A.Ganiyu ,A.Mishra , J.Elijah3 and U.Gana." The Importance of Usability of a Website", IUP Journal of Information Technology; Sep2017, Vol. 13 Issue 3, p27-35.

[4] M. Kelly, "A Look Back at 20 Years of Website Design,"HubSpot Blog. [Online]. Available: https://blog.hubspot.com/marketing/look-back-20yearswebsite-design

[5] "Top 10 Benefits of Having a Website," Top 10 Benefits of Having a Website - Parachute. [Online]. Available: https://www.parachute.net/insights/top-10-benefits-of-having-a-website

[6] Welkom | Peerby. [Online]. Available: https://www.peerby.com/one

[7] R. Newhook, D. Jaramillo, J. Temple and K. Duke, "Evolution of the mobile enterprise app: A design perspective", in 6th International Conference on Applied Human Factors and Ergonomics (AHFE 2015) and the Affiliated Conferences, USA, 2015.

[8] "Mobile Application Developer", March 20, 2013, http://www.itcareerfinder.com/it-careers/mobileapplication-developer.html

[9] "App stores: number of apps in leading app stores 2018 | Statista", Statista, 2018, https://www.statista.com/statistics/276623/number-of-apps-available-in-leading-app-stores/

[10] M. Smith, "Developing Mobile Apps.", Journal of Management & Engineering Integration, vol. 6, no. 2, 79-85, 7, 2013.

[11] "Welcome to your Bookstore," Your Bookstore Mobile App. [Online]. Available: https://www.appbnc.com/

[12] Buy and Sell items from all categories in your city - Marketplace | Facebook, https://www.facebook.com/marketplace/

[13] "Student Desk - Exchange Books - Apps on Google Play," Google. [Online]. Available: https://play.google.com/store/apps/details?id=in.studentdesk&hl

[14] What Are Electric Door Locks and How Do They Work? (n.d.). [Online]. Available: https://www.safewise.com/home-security-faq/electric-door-locks

[15] Yucel. Keskin, K.; Asil Gokcebay, T.,"Programmable Digital Electronic Lock", U.S Patent 5 894 277, April 13, 1999.

[16] "RemoteLock 5i-B WiFi Lever Satin Nickel | RemoteLock", RemoteLock, 2019. [Online]. Available: https://shop.remotelock.com/product/remotelock-5i-b-lever-satin-nickel/

[17] "qrcode.react", npm, 2019. [Online]. Available: https://www.npmjs.com/package/qrcode.react

[18] What is QR code (quick response code)? - Definition from WhatIs.com. https://whatistechtarget.com/definition/QR-code-quick response-code/

[19] "LibeTech QR Code Door Lock," JeremyBlum.com, 27-Jul-2014. [Online]. Available: https://www.jeremyblum.com/portfolio/libetech/

[20] Wienclaw. Ruth A. (2017, Oct). "E-commerce." Research Starters: Business. https://kau.deepknowledge.io/edsDetails?An=89163657&dbId=ers

[21] H. Bidgoli, (2002). "Electronic commerce: principles and practice". [Online]. San Diego: Academic Press.

[22] P. Ratnasingam, (2003) "Inter-organizational trust in business-to-business e-commerce". [Online] Hershey, PA: IRM Press. [23] F. Loredana Dragomir, "Social Sciences: Economic theory, Ecnomic as a Science," Recommendation and Reputation in eCommerce, vol. 35, pp. 1–5, 2016.

[23] "The Risky Business of E-Commerce," BDO USA. [Online]. Available: https://www.bdo.com/blogs/consumer-business-compass/september-2017/the-risky-business-of-e-commerce

Proceedings of the Fourth International Conference on Communication and Electronics Systems (ICCES 2019)
IEEE Conference Record # 45898; IEEE Xplore ISBN: 978-1-7281-1261-9

Core Control System Of An Autonomous Electric Vehicle

Sponsored by: Tata Technologies Limited , Pune

Adeeba Fazal Pathan [1]
Department Of Electronics Engineering
Sanjay Ghodawat University
Kolhapur, India
adeebapathan007@gmail.com

Prof. Mahantesh P. Mattada [2]
Department Of Electronics Engineering
Sanjay Ghodawat University
Kolhapur, India
mattada.mp@sginstitute.in

***Abstract*—Keeping in mind the advancement of implementing the A-EVs on road, this project includes designing of a control system for a 4 wheeled autonomous electric vehicle using MATLAB/Simulink environment. The vehicle can travel to a predefined destination avoiding obstacles coming its way. The features and algorithms required to developed the robot is illustrated. MATLAB and Simulink environment is an ideal platform for developing such kind of projects. A typical scenario is shown to demonstrate the functionality of the robot. Autonomous electric vehicles come with their own procs and cons. Huge investment has been made by automobile companies to come over A-EV's limitations and make a breakthrough in the automobile industry.**

Keywords—Automation; four wheeled chassis; Arduino Mega 2560; rechargable battery; MATLAB/Simulink ; DC dual axis gare motor, SHARP IR sensor.

I. INTRODUCTION

Human life is dynamic. One of the greatest invention for the modern world is vehicle undoubtedly. The recent research of the transportation says that the main medium of travelling through the world is car and there are more than 900 million of passenger car moving on the track throughout the world. The self driving cars may be interpreted as the upgraded versions of our current vehicles that are competent enough of taking over control from the driver under certain situations. Robotic cars that are highly automated do not possess steering wheel or pedals that are installed for the driver. Fast development in electric vehicles has been leading to the need for the academic & industrial world. With hike in server environment problems around the globe, exploration of extraction of energy from undepletable has become a censorious topic. An essential part of transportation in the 21st century, vehicles are pervasive but also one of the main cause of pollution. Overall electric vehicles have an added advantage over the petroleum vehicles of being more hygienic, more energy efficient and environmentally friendly. Smart grid technology has become universal and is playing a major role in advancement of autonomous electric vehicles. Huge financial investment has been made by automobile manufactures around the world for research and abiding changing technology. The combination of an autonomous and battery powered vehicle has proven to be a breakthrough in automobile industry. Today thriving developers both hardware and software specialised are involved in sensors, plotting, machine learning, advanced assistance systems for drivers, car pool platforms & neural networks for transportation. Autonomous Electric Vehicles (A-EVs) use AI, next-generation batteries and other technologies and could transport passengers more efficiently, without the need for drivers or fossil-fuel-driven internal combustion engines (ICEs).Some of the autonomous electric cars in the industry today are: BMW Vision iNeXT, Volvo 360c, Renault Ez Ultimo, Chrysler Electric CARJAM TV, Mercedes Vision EQ etc. The thesis addresses developing an autonomous electric vehicle prototype. Keeping in mind the advancement of implementing the A-EVs on road , this project includes designing of a control system for a Four wheeled autonomous electric vehicle using MATLAB and Simulink environment that is capable of detecting obstacles and avoiding it in order to reach its destination. The core control mainly consists of controlling the motors speed and direction. Models to achieve the objective are developed in Simulink environment using Simulink tolls and packages.

A] POTENTIAL BENEFITS AND PROBLEMS OF AUTONOMOUS ELECTRIC VEHICLES

Automobile quality includes a set of benefits, like freedom of transportation for those that will afford to possess the automotive or perhaps shared automotive pools. Amusement technology like video screens, music etc. might be used by the driver without causing any hinderance in driving. Human drivers knowing or unknowingly tend to break rules and risk their lives, however autonomous cars can adapt each road rule and denote ordinance. Traffic jams and bottlenecks can reduce drastically in urban areas due to eminent coordination hence commute times will be reduced drastically. Poor navigation and driving fatigue would be things of the past. Those people who have difficulty driving such as the differently abled , elderly voters, and children would be able to travel alone safely. Along with efficient travelling comes benefits of cost cutting, lower fuel consumption else use of renewable resources like battery in electric vehicles and reduced negative impact on the environment.

A self-driving automobile would be unaffordable for many individuals accounting over $100,000 according to sources. There is a possibility that bus drivers, cab drivers like Uber or Lyft etc may tend to loose their posts as autonomous vehicles come into picture. Also minor crash in the computer like a glitch would simply cause a threatening accident than something human error may generally experience. Navigating crowds, pedestrians and deciding human intention on road baffles the vehicle under certain conditions and puts it in a position to take decisions that may be out of its scope. Snow interferes with cameras and heavy rain with roof mounted Laser sensors. Hence change in weather condition can hinders its smooth operation. The infrastructure and road system would doubtlessly need major customization for autonomous vehicles to collect data and run on them, for example Traffic lights ,caution light, street lights, would need upgrading. Hackers getting into the vehicle software, fetching the driver's location, personal detail and administrating and affecting the cars functioning would be a major concern and will violate the Data Protection and Privacy laws.

B] LEVELS OF AUTOMATION

SAE classifies automation in 6 levels, explained below:

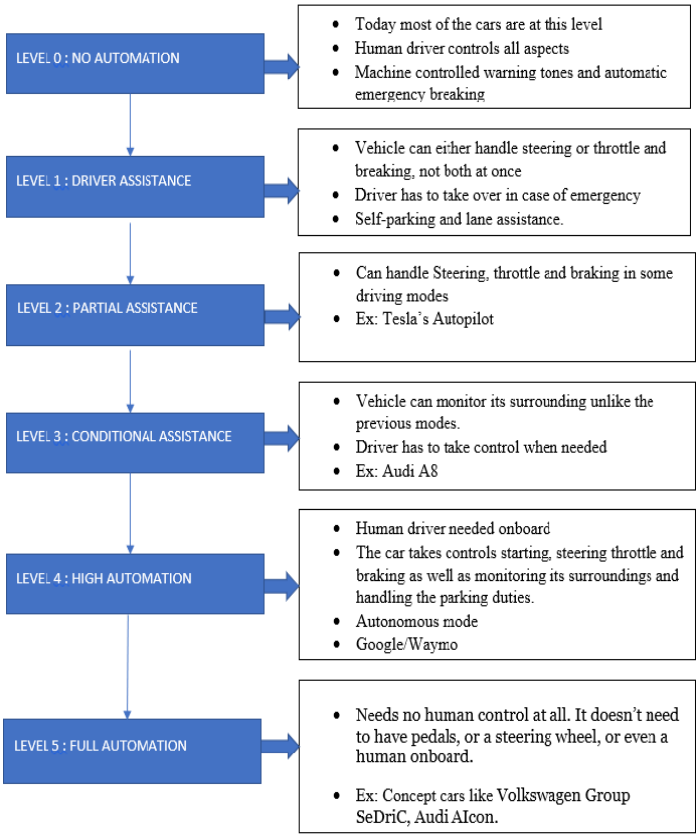

Figure 1 – Levels of automation flow chart

C] AUTONOMOUS VEHICLES IN VOGUE

Waymo has been acknowledged as a leader in the autonomous vehicle technology. It originated as a project of Google in December 2016 it become a subsidiary of Alphabet Inc. In April 2017, Waymo started a self-driving taxi service trial in Phoenix, Arizona. It uses LiDAR for navigation. Constant upgradation and transformation of the vehicle brought into picture new sensors and chips that are less expensive to manufacture, wipers to clear the LiDAR system and cameras that improve visibility. Waymor began designing its own LiDAR as a part of in house manufacturing of self-driving hardware. It eventually reduced its dependency on suppliers that lead to overall cost cutting. Sensors are used for 360°view, short range lasers are used to focus on the near objects approaching the car, long range Lasers can cover up to 300 meters. Radars are used to look around the car and detect moving objects. As of 2018, Waymo has driven more than 5 billion miles on road. But still waymo struggles to satisfy Level 5 expectations.

Tesla created a boom in the automotive industry by launching Model S, Model X, and the new Model 3. Tesla models do not come under completely autonomous or level 4 category. It provides a more advanced driver assistance system and is of Level 2. In recent times Tesla has started using its own custom chip for the Model S and Model X. Also a few days back they used it in Model 3. Two different advanced driver assistance packages offered by Tesla are: Autopilot and Full Self-Driving. The concept of Autopilot incudes an inline processing of better control on the steering and at the same time monitors the lane disciplines. This is now made available as a customized feature in new cars. Given that now this feature is included in the cars the price of car is also increased. The driverless cars, costs an additional $5,000 (And to be more specific, these cars are not completely self-driving).
Full Autonomous cars includes functions to command, uses wayfinding system on autopilot, uses an built-in guidance system which navigates a car on and off the highway ramp. Once the driver enters a destination for that trip into the navigation system, "Navigate on Autopilot" mode can be enabled.

Uber first announced its intentions of manufacturing automatic cars in February 2015. The cars were infused with around seven lasers, a Global Positioning System, radar detectors and LiDAR. Initially they started their research and service in Pittsburgh, where group of researchers were hired . They opened a Advanced Technologies Center. Uber couldn't find much luck in this sector as well as in march 2018, an Uber self-driving car in Arizona hit a lady who sadly died.
Companies like Volvo, BMW, Audi have taken keen interest and are in race for successfully manufacturing a fully autonomous vehicle.

II. LITERATURE SURVEY

The purpose of my project is to built up a car that can move without any driver. It just needs a command from the user and it will start moving towards the destination. I have researched

about my project and I found some equipment that I need to build my vehicle. Some of them are LiDAR, Radar, GPS, Sensors etc. RADAR and Ultrasonic sensors will work as the sense of the vehicle and provide a remarkable amount of information in the range of 750 MB/s, which is more than a human driver could even attain. I have referred the paper "LIDAR based Perception Solution for Autonomous Vehicles" by Domínguez R. to learn more about LiDAR sensing. A LiDAR can process a detailed 3D image and 360-degree map of the place. To know more about simulation in Simulink reference has been taken from "Electric vehicle drive simulation with MATLAB/Simulink" by David McDonald. Simulation is a tool that helps develop designs. It reduces the overall cost of product development. The design process includes constructing models that are capable of performing functions. Engineers can efficiently decrease the cost and time of the design both by integrating simulation within the design process thus companies can complete and validate the designed items. Jiajia Chen, University of science and Technology China Hefei, China, describes autonomous vehicle as a breakthrough in the automobile industry to decrease traffic accidents dramatically. The lane detection and changing for an autonomous vehicle is important for the system and also to generate a new way to pass the front vehicle without having any collision and maintaining safe distance. Geetinderkaur, Sourabh Joshi, Jaspreet Kaur, Samreet Kaur, Going Driverless with Sensors, International Journal of Science, Engineering and Technology, Volume 2 Issue 5 June 2014. This paper gives the information about the google driverless car. Google maps provides the information about the road, traffic signs etc. the second part is the different types of hardware sensors such as lidar, video camera, position estimator, distance sensor, aerial and computer these sensors are used for obstacle detection.

III. DESIGN AND SETUP

A] SCOPE OF WORK

To design a core control system that will autonomously drive a 4 wheeled vehicle which allows the vehicle to move to a predefined point or destination and avoid obstacles during the motion using the information got from sensors which are installed in the car. During navigation, if the car doesn't find enough space to pass through the obstacles it must stop there itself. The control system will be designed in Simulink environment. The vehicle will be battery powered. Core control mainly includes controlling the direction and speed of each wheel.

B] HARDWARE AND SOFTWARE USED

Hardware: Four wheeled chassis kit, Arduino Mega 2560, DC 3V - 6V Dual Axis Gear Motor, L298N Dual - H Bridge DC Stepper Motor Driver Module – Green, Micro Servo motor, Infrared sensor (IR sensor)- SHARP 2Y0A21 F 82 ,Short range (10 to 80 cm) and SHARP 2Y0A02 F 88, long range (20 to 150 cm), IR sensor module (10 cm), Rechargeable battery, wires.

Software: MATLAB/Simulink
MATLAB or Simulink environment software is used to model the functionality of automated driving cars and also develop algorithms of control development and computer vision. Most of the companies choose to go with MATLAB and Simulink as these platforms provide a better and an fused environment that makes it easy for engineers to model and validate perception algorithms that collect data from vision, Radar, and LiDAR . Sensor fusion technique helps create environment, vehicle, and driver models. Simulink, an bonus product to MATLAB, provides a synergistic, diagrammatic environment for designing, simulating, and scrutinizing of dynamic systems. It has a complete library of blocks whose function is predefined and utilized to build graphical designs of systems using select-and-place mouse operations. Sensor fusion is performed using a library of tracking and data association techniques including point and extended object trackers. To estimate vehicle position and orientation, simulate measurements from IMU/GPS sensors, and design fusion and localization algorithms. Hence, I have chosen to use Simulink environment to develop my model.

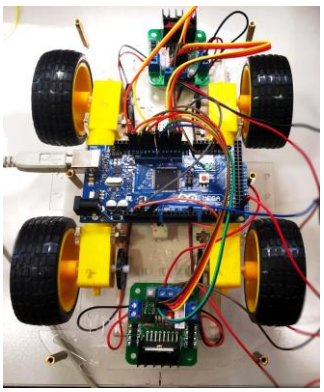

Figure 2- Four wheeled chassis kit along with Arduino Mega and L298N motor controller

C] SKID STEERING SYSTEM

Skid steering concept is used achieve the principle of driving at different speeds in forward and reverse course considering the wheels on each side. The main moto behind this is that the wheels on the same side should be driven at a similar rate. To achieve the zero radius turn in right that is clockwise direction the wheels on the DC motor at the left side drives the left wheel forward and the wheels on the right side are driven backwards as the DC motor spins in the opposite direction. The drawback is that moving in a straight path demands that wheels on each side to be should turn at the same RPM, which can be tricky to achieve. The advantage of this steering is increased grip of the car on the road.

D] PATH FINDER ROBOT EXPERIMENT

To configure the control system of the car we first need to develop an algorithm based on mathematical formulas and

sensor values. In the following experiment two obstacles are present at different distances from the car as shown in the figure 3.

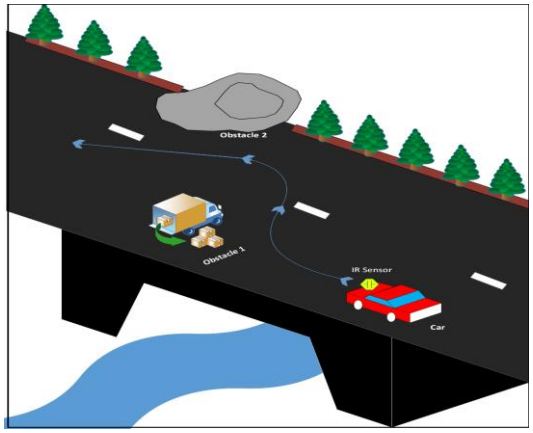

Figure 3-Senerio of an autonomous car overcoming obstacles

As the car moves forward it senses two obstacles. Using its artificial intelligence, it calculates the possibilities to pass through. The steps followed for the same are as per the flowchart below.

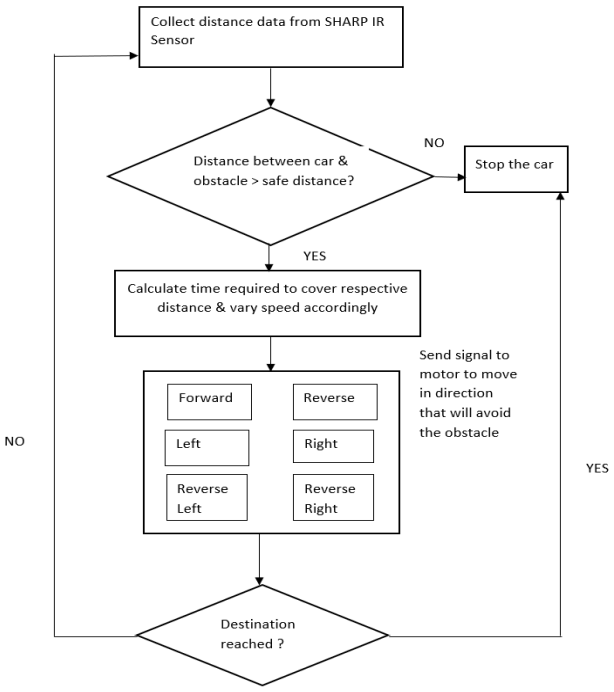

Figure 4 – Flow chart of the the motor algorithm

In figure 4, the following steps are executed in a series:

1. The car obtains the distance values from the short and long range Sharp IR Sensors that are fixed at different heights in the anterior section of the car. The IR sensor is placed on a servo motor that keeps rotating from 0°to 180°continuously.
2. Let distance between obstacle1 and the car be D1 and distance between obstacle2 and the car be D2. Using Pythagoras theorem and mathematical formulas distance between the two obstacles is calculated,D3.
3. An algorithm for the car to move forward, reverse, left, right, reverse left and reverse right is created.
4. Time can be calculated for the car, for example to move forward time is calculated using speed and distance relationship. In Simulink, time is used as a signal to trigger the direction of the vehicle.
    i. Time= Distance / Speed
5. With reference to the diagram, the car first moves forward. Based on what distance would be safe for the car to take a turn, signal is given to the motor to move right. Then maintaining a safe distance from obstacle2 and keeping D3 value in mind, the car turns slightly towards the left and then moves forward again.

IV. IMPLEMENTATION OF CORE CONTROL IN MATLAB/SIMULINK ENVIRONMENT

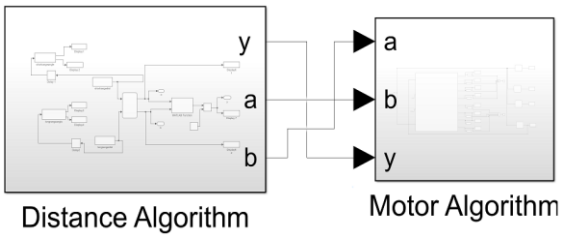

Figure 5- Integration of algorithms in Simulink

In figure 5, distance and motor algorithms are integrated. The motor algorithm consists of state flow diagrams, within it logic for the direction of the motor is implemented. It is time dependent for toggling from one state to another. Output of the state flow is connected to Digital Output block whose pin number is connected to the Arduino board.

A] ALGORITHM FOR CONTROLLING THE DIRECTION OF THE WHEEL

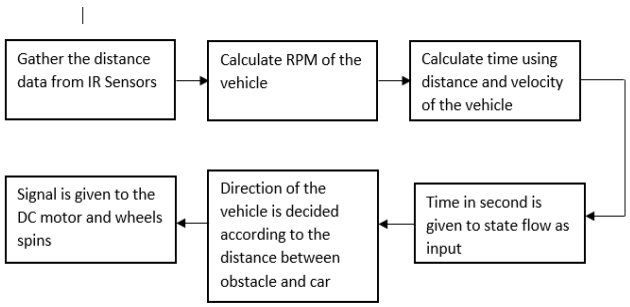

Figure 6- Direction control system of the vehicle

As shown in figure 6 ,distance coming from the short and long range IR Sensor is captured when an obstacle is detected from 0 to 180 degree. Based on the RPM of the vehicle and the distance data, time taken to more say foreward is calculated that is given as input to the state flow diagram. Within the state flow chart logic used for the car to turn in different directions is written . It is based on binary values. Transition from one state to another depends on input, time. Output of the state floe is given to the input of Digital output where the pin number is defined . The motor is connected to the arduino board via a motor controller-L298N. Hence each wheel has capability to turn in different directions.

B] ALGORITHM FOR CONTROLLING THE SPEED OF THE WHEEL

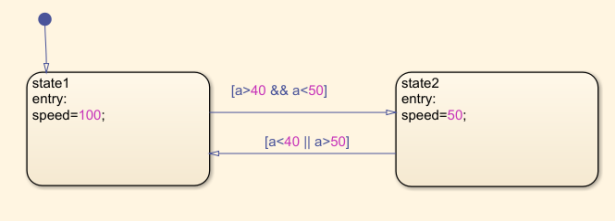

Figure 7- State flow diagram for speed control

In the above example, Figure 7, the speed of the motor is controlled. It is dependent on the distance coming from the short-range IR sensor (a). If the distance in between the car and obstacle is lesser than a predefined safer distance then the car must slow down its speed to say 50 meter/minute. If not speed of the vehicle will remain 100 meters/minute. Output of the state flow is given to the PWM (Pulse width modulation) block whose pin number is connected to the Arduino board. Hence Speed can be varied.

V. RESULTS

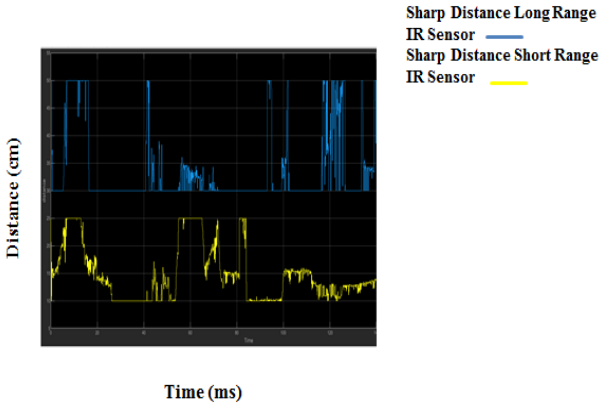

Figure 8- Distance v/s Time graph for SHARP IR sensors

figure 8 displays the distance of car from the obstacle while the IR sensor is moving from 0 to 180 degree. The steep changes that occur in the graph are when an obstacle is just detected or when the obstacle ends.

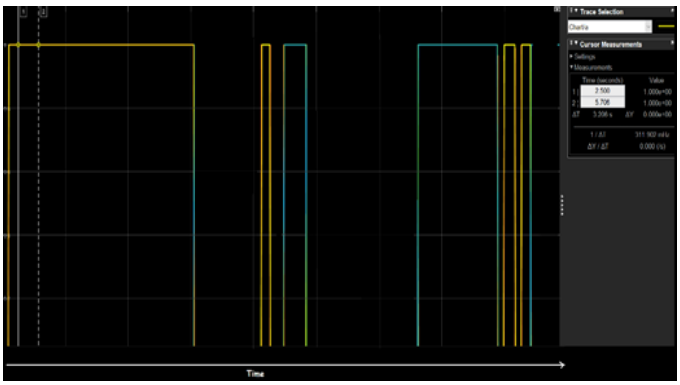

Figure 9- Motor control graph displayed on scope for two channel output

Output of the motor is displayed on the scope. If the car changes its direction the output waveform switches from high to low and vice versa. The time period for which the vehicle is in one direction, say forward can be easily calculated. In figure number 7, the speed of each wheel of the car can be changed by changing the RPM value. The PWM values used to control each wheel is first found out using open loop controller and LN393 (speed measuring sensor). These PWM values are used in Closed loop PID controller to control the overall speed of the car i.e. all wheels are capable of running at a same speed and in the same direction.

VI. FUTURE SCOPE

In order to archive more accuracy in detecting the distance values, LiDAR can be replace IR sensors. LiDAR's have high accuracy and quick response. Even a combination of camera and IR sensors can be used to effectively run an autonomous car. Image processing may be used to process the distance data.

VII. CONCLUSION

Building a obstacle avoidance robot that uses IR sensors & Arduino in Simulink environment is successfully completed. Programing the car to Level 2 automation for a prototype model is achieved. The car can now detect obstacles that comes it way and is able to reach its destination efficiently.

VIII. ACKNOWLEDGEMENT

I am pleased to present this paper. I feel blessed to be a part of such a wonderful college. I'm grateful to the entire staff. I would like to thank Tata Technologies,Pune for sponsoring my project and helping me expand my knowledge, I also express my deep sense of gratitude to my guides for their valuable guidance, encouragement and kind co-operation.

IX. REFERENCES

[1] R. Dominguez, E. Onieva, J. Alonso, J. Villagra and C. Gonzalez, "LIDAR based Perception Solution for Autonomous Vehicles," *11th International Conference on Intelligent Systems Design and Applications*, pp. 490-495, 2011.

[2] D. McDonald, "Electric Vehicle Drive Simulation with MATLAB/Simulink," *Proceedings of the 2012 North-Central Section Conference*, 2012.

[3] Geetinderkaur, S. Joshi, J. Kaur and S. Kaur, "Going Driverless with Sensors," *International Journal of Science, Engineering and Technology*, vol. Volume 2 , no. Issue 5,2014

[4] G. B. Pavithra, R. P. Shiva, A. Sharmila, S. Raja and S. J. Sushma, "Characteristics of different sensors used for Distance Measurement," *International Research Journal of Engineering and Technology (IRJET)*, vol. volume 4, no. Issue 12, pp. 698-702, Dec 2017.

[5] T. Mohammad, "Using Ultrasonic and Infrared Sensors for Distance Measurement," *World Academy of Science, Engineering and Technology*,273, 2009.

[6] Jaycil Z. Varghese, Professor Randy G. Boone. Overview of Autonomous Vehicle Sensors and Systems.*International Conference on Operations Excellence and Service Engineering Orlando, Florida, USA*, 178-179, 2015.

[7] William J. Fleming. Overview of Automotive Sensors. *IEEE Sensors Journal*, 01, 2001.

[8] R.Vairavan, S.Ajith Kumar, L.Shabin Ashiff, C.Godwin Jose. "Obstacle avoidance robotic vehicle using ultrasonic sensor, arduino controller,*"International Research Journal of Engineering and Technology (IRJET)*,2140-2142,2018.

[9] K.Vasavi, M.V.S.Praveen. "Obstacle Detection and Avoidance Autonomous Car," *International Journal of Engineering Trends and Technology (IJETT)*,783-788, 2014.

[10] Duan Jianmin, Zheng Kaihua , Shi Lixiao. "Road and Obstacle Detection Based on Multi-layer Laser Radar in Driverless Car," *34th Chinese Control Conference*, 8003, 2015.

[11] Thomas Stevens, Elliot Carlson, Ian Painter. "Autonomous Collision Avoidance". *1-12, 2013.*

[12] Sachin Modi, "Comparison of three obstacle avoidance methods for an autonomous guided vehicle". 5-9, 2002.

Proceedings of the Fourth International Conference on Communication and Electronics Systems (ICCES 2019)
IEEE Conference Record # 45898; IEEE Xplore ISBN: 978-1-7281-1261-9

Power Quality Improvement Using Unified Power Quality Conditioner with Distribution Generation

Sachin Baliram Shahapure
StudentDepartme of ElectricalEngg.
Walchand College of Engineering
Sangli, India
sachinshahapure186@gmail.com

Ramchandra P. Hasabe
Department of Electrical Engg.
Walchand College of Engineering
Sangli, India
ramchandra.hasabe@walchandsangli.ac.in

***Abstract*— In recent scenario Distributed Static Compensator (DSTATCOM) resolves the current related power quality problems and Dynamic Voltage Restorer resolves the voltage related power quality problems. The Unified Power Quality Conditioner is the integration of DSTATCOM and DVR with common DC link. Due to the major advancements in Solar PV systems and its availability in reasonable cost at consumer end the world is moving ahead for Solar PV system for renewable energy generation. Generally, the electrical power to the DC link is supplied from source side. This paper presents the UPQC with Solar PV system. In proposed system the electrical power is supplied to DC link of UPQC using Solar PV system. The proposed system is designed and implementation in MATLAB simulink environment. The performance of the proposed system is analyzed under various conditions of source voltage variation, load unbalanced condition. After MATLAB simulation the proposed system is implemented in OP4510 Real Time Digital Simulator.**

***Keywords*— DSTATCOM, DVR, DG, UPQC, MPPT**

I. INTRODUCTION

India is having rapidly growing economy with 1.3 billion peoples that facing an immense energy demand. India is the fifth in number on the basis of production and consumption of electricity. This country is having tremendous scope for the generation of solar energy and because of that central government of India has derived the solar energy policy that contains several guidelines and other aspects. There are several countries which are global leaders in solar energy generation such as United states, Germany, Japan, China. Solar power plants are installed in various regions in India and the performance of that solar PV systems is analyzed on the basis of various factors like temperature, humidity, wind speed, Rainfall and solar intensity in that particular sector [1] [2].

Solar power is discontinuous in nature. while connecting the solar PV system directly to the power grid without power grid management there may be power quality problems comes on that particular grid like voltage sag, voltage. For the management of solar PV generation in India there must be need to improvement of electricity grid codes for the satisfactory operation of power grid [3]. Solar PV systems is the combination of the various subsystems of solar PV panel, power conditioner/PWM inverters, Maximum power point tracker. This inverter is of various types like Micro inverters, String inverters. As the development in the computer technology and reduced in cost proportionally the use of software simulating tools rapidly increased. The widely used simulation software is MATLAB. For the real time performance analysis of the three phase residential solar PV system having control based on ANN is proposed in paper [4]. This papers explains solar PV generator reconfiguration for PV system which is formed by standalone and single central inverter driven by conventional MPPT algorithm. The effects on distribution transformer due to variable voltage of Solar PV system is presented in paper [5]. The Interharmonics are observed at the load end in the practical solar PV system and this journal presents analysis and modeling of the Interharmonics in this [6]. Introduction to power quality, power quality standards and monitoring, active and passive compensating devices, series and shunt compensating devices and loads that causes power quality problems are explained in paper [7]. The power electronics converter topologies used in various solar PV systems for increasing the reliability, cost effectiveness is proposed in paper [8]. Due to demand of clean power along with power quality improvement device the integrated photovoltaic dynamic voltage restorer system configuration is a good option. For the control of solar integrated DVR the synchronously rotating reference frame theory is proposed. Design control and operation of a DSTATCOM is explained in paper [9] [10]. The operation of shunt active filter based on synchronously rotating reference signal generation method is proposed in this journal [11].

A switching signal generation is the main function for control of DVR, DSTSTCOM and UPQC. The reference signal generation methods are broadly classified into time domain and frequency domain techniques. Time domain techniques are commonly used because of their lower evaluation time and faster operation. The commonly used time domain methods are IRP theory, SRF theory. The main concern with SRF theory is during load unbalanced condition second order harmonic is existing in the d axis of current [12] [13]. The IEEE prescribed standards for harmonic control in electric power system are proposed in [14] [15].

II. PROPOSED SYSTEM ARCHITECTURE

A. Distributed Generation System

In proposed work the solar photovoltaic system is used as the distributed generation. During darkness the solar PV system does not give rated voltage or current. Hence PV generators are neither be considered as constant voltage source or constant current source. If PV generators are connected to load it generates current which is called as diode current I_o and that diode determines the V-I

characteristics of the PV cell. The PV array is developed with the combination of the series and parallel solar cells. This solar cell equivalent circuit is represented in Fig. 1.

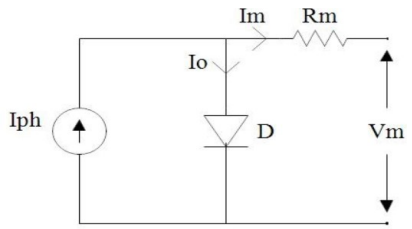

Fig. 1. Solar Photovoltaic cell circuit

The above circuit can be represented in equation

$$V_C = \frac{AKT_C}{e} ln\left(\frac{I_{ph} + I_D - I_M}{I_O}\right) - R_S I_M \quad (1)$$

Where the symbols are determined as fallows

V_C: output voltage V.
I_M: output current A.
I_O: diode current A.
R_M: resistance Ω.
T_C: Temperature C.
I_{ph}: photocurrent.
K: Boltzmann constant.
e: charge.

B. MPPT Circuit

MPPT system selects the output of the PV cell and implement the appropriate resistance for obtaining maximum power for particular environmental condition. In this paper incremental conductance method is implemented and this method design is based on observation of PV characteristics of solar cell. The output power from solar PV system is given as

$$P = V.I \quad (2)$$

When there is increasing change in voltage and current the improved power given in equation 3 and after neglecting the small terms, the equivalent equation is given in 4.

$$P+\Delta P = (I+\Delta I).(V+\Delta V) \quad (3)$$

$$\Delta P = \Delta V.I + \Delta I.V \quad (4)$$

`

At the peak point ΔP must be zero hence the hence the dynamic impedance of the source is given as

$$\frac{dV}{dI} = -\frac{V}{I} \quad (5)$$

The MPPT circuit consist converter having very high efficiency which selects optimal electrical load for the solar PV system.

C. Proposed System for UPQC

The UPQC is the integration of voltage quality improvement device connected in series and current quality improvement device connected in shunt with the system which contains nonlinear load. It is used in various combinations like right shunt and left shunt UPQC.

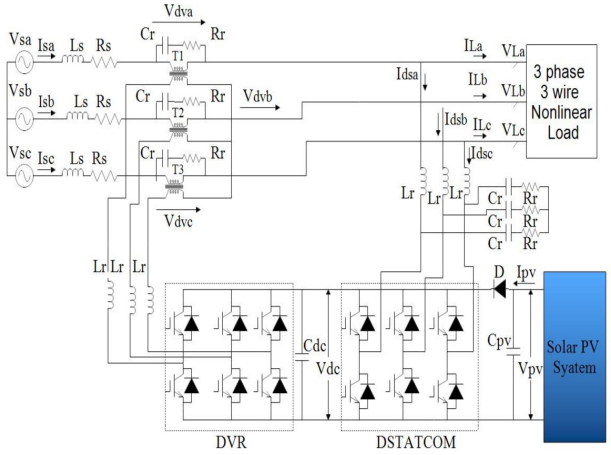

Fig. 2. Proposed UPQC system

The presented UPQC is right shunt UPQC. This system is having two inverters which are connected successively by a common dc link and power to that dc link is fed from the supply system through interfacing inductors. The series connected transformer is used to inject the voltage induced by the DVR into supply system. In the circuit nonlinear load is used as the diode bridge rectifier with RL load. Because of the switching action of the inverter switches the ripples are creating in to the system and to compensate this effect the ripple filters (RC filter) is used. The Fig.2. shows the proposed unified power quality conditioner circuit.

D. Design of proposed UPQC

Design of the three phase three wire UPQC consist of design of the shunt connected device and series connected device ripple filter dc link voltage interfacing inductors.

1) Design of shunt and series connected devices

a) 1.1 Dc Link voltage and bus capacitor rating

The capacitor is connected to common dc link of two inverters and acts as an energy barrier and set up the dc voltage for normal functioning of the UPQC. The least value for dc bus voltage across capacitor must be greater than two times of the maximum value of phase voltage of the system where the UPQC is connected.

$$V_{dc} = \frac{2V_{LL}\sqrt{2}}{m\sqrt{3}} \quad (6)$$

Where
m = modulation.
V_{LL} = line voltage for inverter.

For calculating the magnitude of the capacitance for the dc bus consider the principle of energy conservation.

$$C_{dc} = \frac{3KatI_{sh}V_{ph}}{0.5(V^2_{dc} - V^2_{dc1})} \quad (7)$$

Where

V_{dc} = nominal dc link voltage 700 volts.

V_{dc1} = least voltage level of the dc link 650.

O = overburden 1.2.

V_{ph} = voltage 239 volts.

I_{sh}= phase current 10 amp.

t = time required for dc voltage to come at rated value,20 msec.

K = constant 0.1.

Cdc = 10^{-3} farad.

b) Selection of series connected transformer for DVR

The voltage rating of transformer is determined by voltage to be added and the dc link voltage of the inverter. For compensating voltage difference and The turns ratio for the series connected transformer is calculated from equations.

$$V_{DVR} = X\ V_S = 95.84 \quad (8)$$

$$K_{DVR} = \frac{V_{VSC}}{V_{DVR}} = 3 \quad (9)$$

The voltage and current (VA) rating for series connected transformer has calculated 10 KVA.

c) Interfacing Inductors for DSTATCOM and DVR

The selection of interfacing inductor for DSTATCOM is depends upon various factors and some of the factors are Fs, dc link voltage (Vdcl). The equation 10 and 11 shows the interfacing inductors calculations for DVR and DSTATCOM

$$L_{rdstat} - \frac{mV_{dc}\sqrt{3}}{12af_{sh}I_{cr,pp}} - 2\text{mH} \quad (10)$$

$$L_{rdvr} = \frac{mV_{dc}K_{SE}\sqrt{3}}{12af_{SE}I_r} = 4\text{mH} \quad (11)$$

Where

m = modulation index = 1

a = overloading factor = 1.2

$I_{cr,pp}$ = current ripple = 15%

F_{sh}= switching frequency = 10 KHZ

d) Design of ripple filter

The switching frequency for the device is 10 KHz and because of that ripples are superimposed in to source voltage. To compensates this ripples in voltage the LC filter with appropriate time constant is used. The ripple filter Rating for DSTATCOM is R=0.2 ohm and C= 20 microfarad and ripple filter ratings for DVR is R=0.15ohm and C= 25 microfarad.

III. PROPOSED CONTROL ALGORITHEM

The control algorithms are mainly divided in to time zone algorithms and frequency zone algorithms. Some of the time zone algorithms are IRP theory, DQ theory, PB theory, ANN theory etc. some of the frequency zone algorithms are Fourier algorithm, DFT algorithm, FFT algorithm, wavelet transform algorithm etc. The frequency zone algorithms are accurate but sluggish and slow response. Hence these algorithms are used in power quality monitoring devices where the accuracy is constraints and operating time does not constrain.

For real time control the time domain algorithm is preferred because of faster dynamic response. Here the SRF control algorithm is used for control operation for UPQC.

A. Control structure for dynamic voltage restorer

The series compensator injects the active power in series with the system and this power is provided by solar system through dc bus of the UPQC. The PCC voltage and load voltage is sensed and converted into DQ reference frame theory. During the conversion the phase locked loop (PLL) block is used for calculating fundamental component of PCC voltage. Among the various classifications of UPQC UPQC-P is considered for in proposed system. The DVR is dealing with active power only therefore reference for Q axis component is set to be zero and reference for D axis is set as the peak value of the load voltage.

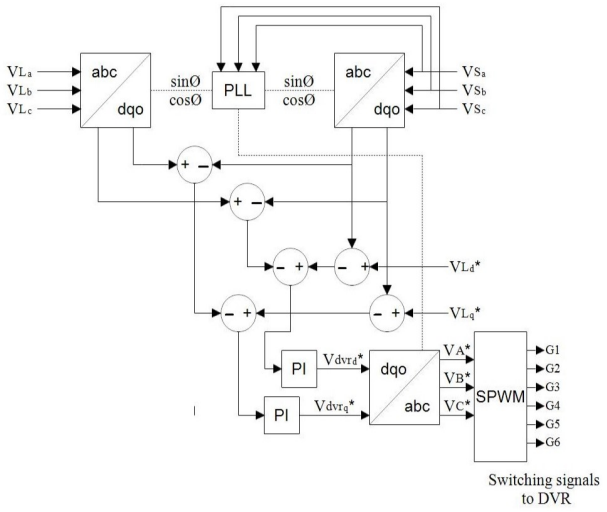

Fig. 3. Control structure for DVR

For calculating the reference voltage of the series compensator the subtraction of load reference voltage and PCC voltage is carried out. Again for calculating actual voltage to be compensated by series compensator the subtraction of load voltage and PCC voltage is carried out. To get appropriate reference signal from the control circuit the subtraction of reference voltage and actual voltage is estimated and output is passed through P-I controller. The switching pulse generation for inverter is obtained from reference signals passed through the pulse width modulation technique (SPWM) method.

B. *Control structure for distributed static compensator*

The solar PV system is connected to common bus of two inverters and voltage across that bus is maintained constant using PI controller. The load current is converted to dqo domain and low pass filter is used to estimate fundamental component of the load current. Estimated currents are then added to other currents which are getting from PI controller which are loss current and solar PV array current. Adding all the currents that generates fundamental reference current I sd*. In this control algorithm active power of the current is compensated hence I sq* is kept as zero and because of the three phase three wire circuit the I so* is also kept as zero. This above all the fundamental reference currents are converted into abc domain and passed through the hysteresis current controller. This PWM control algorithm compares the reference signals with the actual signals and gives appropriate pulses to the voltage source inverter.

$$I^*_{sq} = 0 \qquad (12)$$

$$I^*_{so} = 0 \qquad (13)$$

$$I^*_{sd} = I_{Ldf} + I_{Loss} - I_{Pvg} \qquad (14)$$

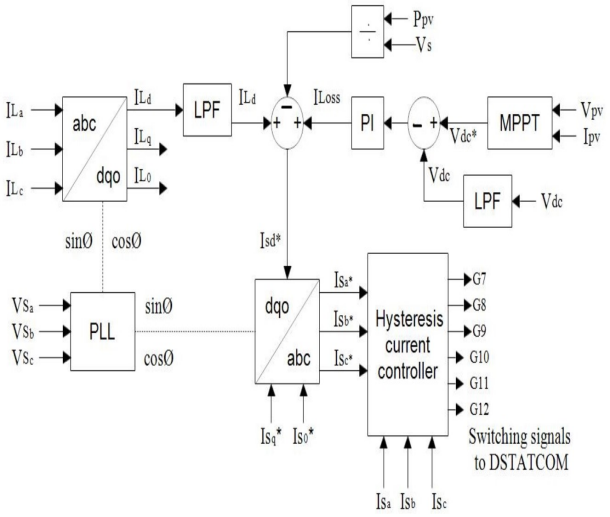

Fig. 4. Control structure for DSTATCOM

IV. MATLAB SIMULATION OF PROPOSED PV UPQC

In this study the solar integrated UPQC is designed in MATLAB Simulink environment. The result analysis is carried out under various conditions. That conditions are particularly of source voltage sag/swell condition and varying load unbalanced condition. The Matlab simulation for Solar PV system is given in Fig. 5. The temperature is considered at 30 degrees for the normal operation of the solar system. The Matlab simulation for UPQC with distributed generation is given in Fig. 6.

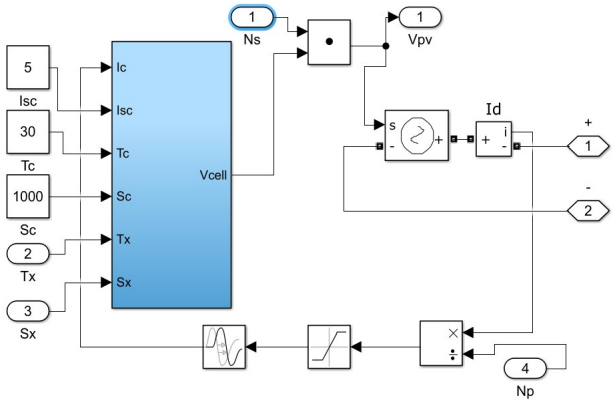

Fig. 5. Solar PV system in Matlab Simulink

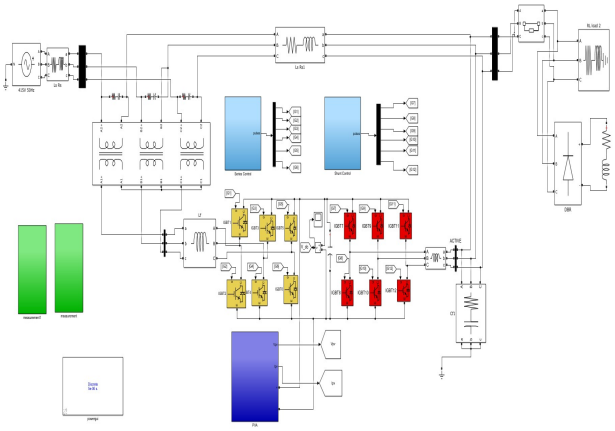

Fig. 6. UPQC with DG in Matlab Simulink

A. *Under source voltage sag and swell circumstances*

The performance of proposed UPQC with distributed generation under source voltage variations (swell and sag condition) is introduced in Fig. 7. The series compensator in the proposed UPQC with DG system settles the voltage across the load to a rated value under source voltage variations. The various observed waveforms are source voltage, shunt compensator current, load voltage, series compensator voltage, dc bus voltage, load current.

The voltage sag of 0.4 per unit and voltage swell of 0.4 per unit is considered in the source voltage. In source voltage sag condition the series compensator injects 0.4 per unit voltage in phase with source voltage and keeps load voltage constant at particular magnitude and in source voltage Swell condition the dynamic voltage restorer add the voltage into source voltage in such a way that the load voltage remains unchanged and settles at rated value which is 230-volt phase to phase. The source current takes some time in microsecond for stabilization. The load current nature does not get affected and changed when there is source voltage variation. In this condition it is clearly seen that there is no effect of voltage sag and swell on DC link voltage. The DC link current is increased in voltage sag condition and decreased in source voltage swell condition.

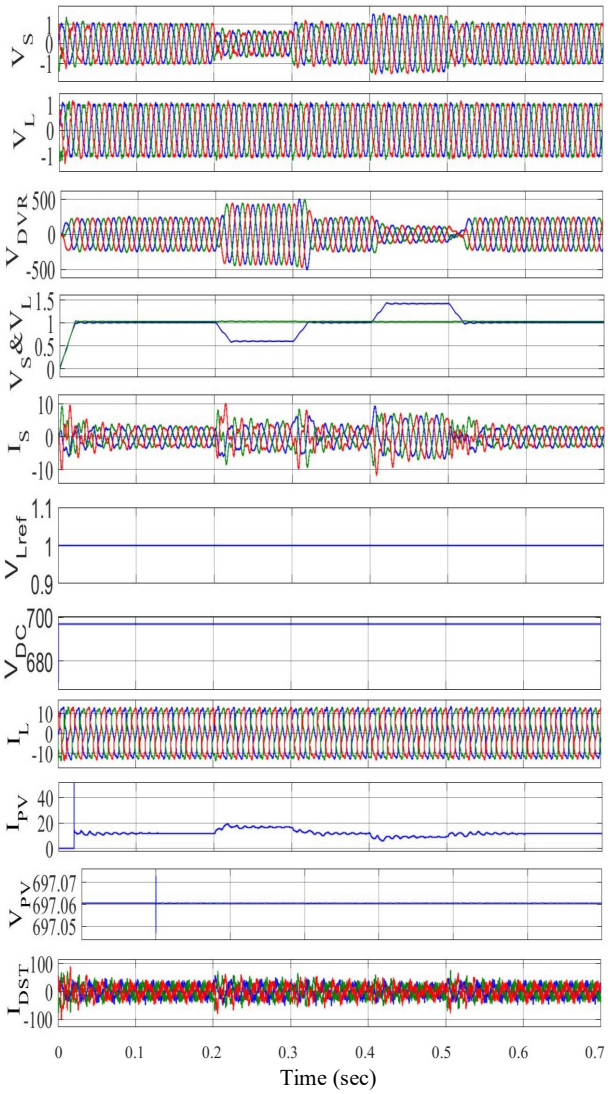

Fig. 7.MATLAB results of UPQC during source voltage variations

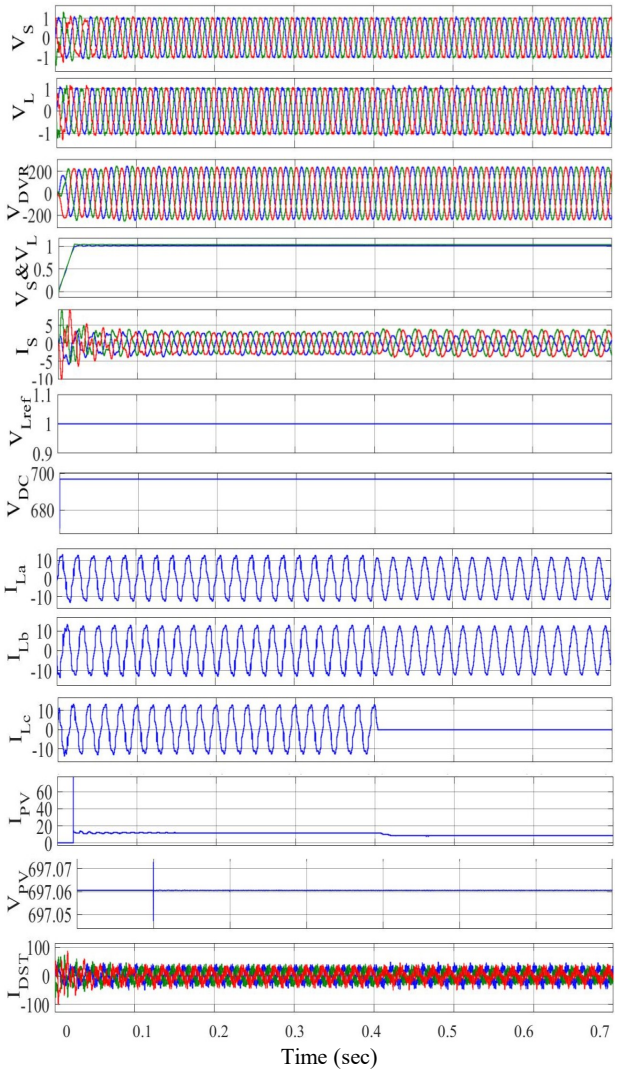

Fig.8. MATLAB results of UPQC during load unbalance condition

B. Under load unbalanced circumstance

The simulation results of proposed UPQC with distributed generation during load unbalance situation is presented in Fig.8. Load unbalance condition is generally observed in three phase system. During unbalanced condition the source current is sinusoidal with unity power factor and the effective source current is increased because of reduction in total effective load. For making the load unbalance the phase C of the load is deactivated at particular time. During load unbalanced circumstance the load voltage and source voltage remains sinusoidal in nature. These voltages do not get disturbed and remains at the constant rated value. The voltage generated in distributed generator and DC bus voltage is also not affected during load unbalanced condition. The DC bus voltage is remained constant at nearly 700 volts. Normally in load unbalanced condition the voltage rises but the Dynamic Voltage Restorer prevents this voltage rise. From Fig. 8 it can be observed that the control circuit for DVR works properly.

V. REAL TIME IMPLEMENTATION OF PROPOSED UPQC

In this study the real time digital simulator OP4510 is used for estimating and analyzing the performance of proposed solar integrated UPQC. The advantages of real time simulator are lowest cost required for hardware, increases test functionalities and reduces the personals risks. OP4510 has 4 cores with 3.5 GHz Intel processor and 4 i/o modules which are analog in (16channels), analog out (16 channels), digital in (32 channels) digital out (32 channels). It also has FPGA version kintex-7 along with the target computer having 16 GB RAM and 128 GB SSD. The hardware setup of OP4510 is shown in Fig. 9. For communication between host computer and target computer the communication protocol RS-232 (TCP IP4) is used. The software in loop (SIL) and hardware in loop (HIL) simulation is performed with the help of OP4510. Fig. 10. shows the MTLAB simulation file which made compatible with OP4510. In simulation file consist of two subsystems which are SM_MASTER and SC_CONSOLE runs at step time of 20 micro seconds.

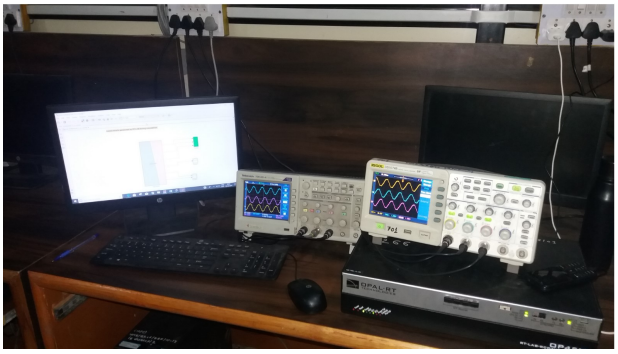

Fig. 9. Hardware Setup of OPAL-RT (OP4510)

For the communication of two subsystems the OPCOMM block is used. The analog signals in HIL simulation are taken out from OP4510 by using OPCONTROL block and ANALOG OUT block.

Fig. 10. Implementation of solar integrated UPQC on opal RT

The signals which are taken outside are source voltage without UPQC and source current without UPQC. These signal waveforms are shown in Fig. 11. Fig. 12. The THD analysis is carried and the THD comes for source voltage without UPQC is 24.58% and source current absence of UPQC is 27 % which is given in Fig. 13.

Fig. 11. Source voltage on digital oscilloscope

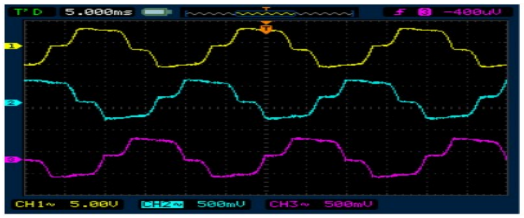

Fig. 12. Source current on digital oscilloscope

The other two signals are taken outside from OPAL-RT that are source voltage with UPQC and source current with UPQC shown in Fig. 14. and Fig. 15. THD analysis of this two signals are carried out and THD comes for source voltage Vs is 0.06% and for Is it comes as 5% which is shown in Fig. 16.

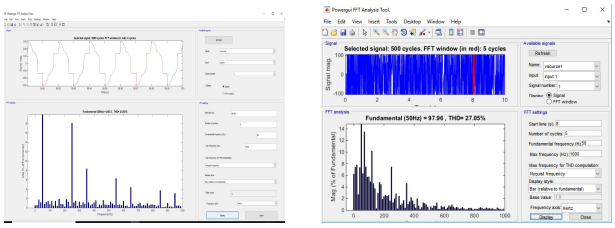

Fig. 13. THD analysis of Vs and Is

Fig. 14. Source voltage on digital oscilloscope

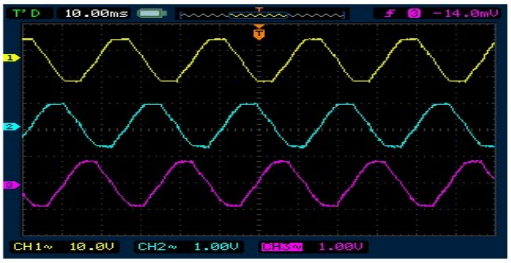

Fig. 15. Source current on digital oscilloscope

The total harmonic distortion for source voltage with UPQC and source current with UPQC is as per the standards of IEC61000-3. The THD analysis is carried out considering the Matlab generated window in Real Time Digital Simulator.

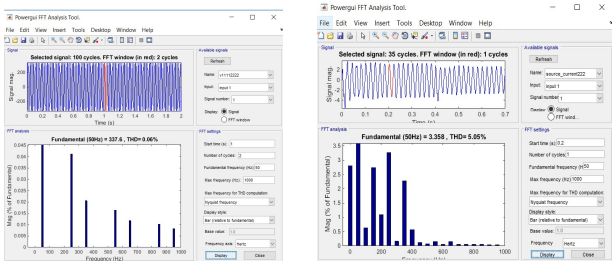

Fig. 16. THD analysis for Vs and Is after UPQC operation

VI. CONCLUSION AND FUTURE WORK

The UPQC with Distributed generation has been proposed in this paper. The proposed UPQC model with distributed generation has been designed and analyzed in Matlab Simulink environment. The various dynamic conditions for system are created at source side and load side. The response of proposed UPQC system has been analyzed during various system scenario. The proposed UPQC system is then implemented in OPAL RT OP4510 environment. The simulation results are discussed in detail and outcome of the simulation shows the proper operation of the controller and all the results comes as per the IEC61000 standards.

The future work for this solar integrated UPQC system is the replacement of the Solar system with wind generation system or BESS. The new time domain base control algorithms can also be applying to the above mentioned systems.

REFRENCES

[1] Om V. Bapat and Vishram Bapat, "An overview of Solar Energy Policy of India and Few Prominent Nations in the World," in 2016 *IEEE 1th International conference on power, electronics, inteligent control and Energy systems(ICPEICES 2016).* July 2016, PP. 1-6

[2] Madhuchandrika Chattopadhyay and R Rajavel, "A Comparative Study on Performance of a Grid Connected Solar PV System installed in the Urban, Rural and Coastal region of India," *2018 2nd International Conference on Inventive Systems and Control (ICISC).* January 2018, PP. 131-135

[3] Y. Yang, P. Enjeti, F. Blaabjerg, and H. Wang, "Wide-scale adoption of photovoltaic energy: Grid code modifications are explored in the distribution grid," *IEEE Ind. Appl. Mag.*, vol. 21, no. 5, pp. 21–31, Sept 2015.

[4] Yang Sun, Shuhui Li, Bo Lin, Xingang Fu, Malek Ramezani, and Ishan Jaithwa, "Artificial Neural Network for Control and Grid Integration of Residential Solar Photovoltaic Systems," *IEEE Transactions on Sustainable Energy,* Vol. 8, no.4, pp. 1484-1495, Oct. 2017.

[5] Abhineet Parchure, Stephen J. Tyler, MelissaA. Peskin, Kaveh Rahimi, Robert P. Broadwater and Murat Dilek, "Investigating PV Generation Induced Voltage Volatility for Customers Sharing a Distribution Service Transformer," *2016 IEEE Rural Electric Power Conference,* pp. 3-11, May 2016.

[6] Ariya Sangwongwanich, Yongheng Yang, Dezso Sera, Hamid Soltani and Frede Blaabjerg, "Analysis and Modeling of Interharmonics from Grid-Connected Photovoltaic Systems," *IEEE Transactions On Power Electronics*, Vol. 99, pp. 1-12, 2017

[7] B. Singh, A. Chandra and K. A. Haddad, *Power Quality: Problems and Mitigation Techniques*. London: Wiley, 2015.

[8] Mahinda Vilathgamuwa, Dulika Nayanasiri and Shantha Gamini, Power Electronics for Photovoltaic Power Systems. California: Morgan and Claypool, 2015

[9] Chandan Kumar and Mahesh K. Mishra, "An Improved Hybrid DSTATCOM Topology to Compensate Reactive and Nonlinear Loads," *IEEE Transactions On Industrial Electronics*, Vol. 61, No. 12, pp. 6517-6527, Dec 2014.

[10] Avik Bhattacharya, Chandan Chakraborty and Subhashish Bhattacharya, "Shunt Compensation: Reviewing Traditional Methods of Reference Current Generation," *IEEE Industrial Electronics Magazine,* Vol. 3, No. 3, pp. 38-49, Sep 2009.

[11] Bhim Singh and Jitendra Solanki, "A Comparison of Control Algorithms for DSTATCOM," *IEEE Transactions On Industrial Electronics*, VOL. 56, NO. 7, pp. 2738-2745, July 2009.

[12] "IEEE recommended practices and requirements for harmonic control in electrical power systems," *IEEE Std 519-1992*, pp. 1–112, April 1993.

[13] Lakshmi, Shubh, and Sanjib Ganguly. "Multi-objective planning for the allocation of PV-BESS integrated open UPQC for peak load shaving of radial distribution networks." *Journal of Energy Storage* 22 (2019): 208-218.

[14] Patel, Ashish, Hitesh Datt Mathur, and Surekha Bhanot. "A new SRF-based power angle control method for UPQC-DG to integrate solar PV into grid." *International Transactions on Electrical Energy Systems* 29.1 (2019): e2667.

[15] Ye, Jian, et al. "Two-Level Algorithm for UPQC Considering Power Electronic Converters and Transformers." *2019 IEEE Applied Power Electronics Conference and Exposition (APEC)*. IEEE, 2019.

Proceedings of the Fourth International Conference on Communication and Electronics Systems (ICCES 2019)
IEEE Conference Record # 45898; IEEE Xplore ISBN: 978-1-7281-1261-9

Security for IOT devices using Blockchain

Sri Harshini Popuri
Computer Science and Engineering
Institute of Aeronautical Engineering,
Hyderabad, India
sriharshini777@gmail.com

Y Mohana Roopa
Professor, CSE
Institute of Aeronautical Engineering,
Hyderabad, India
ymohanaroopa@gmail.com

Abstract:

IOT means internet of things. Here as the name suggests IOT has turned into a hugely developing technology in which billions of devices are interconnected by providing people with different services. Because of this huge connectivity among devices there may arise situations that will endanger the security and integrity of IOT systems and this threatens the security of data which is transmitted through those systems. In this paper, we will be discussing about the security problems of IOT and how they are caused. Then we would discuss how a widespread technology like block chain will provide security to IOT networks.

Keywords—IOT, Blockchain, Security

I. Introduction

IOT (Internet of Things) is a technology which is used to interconnect devices over a global network like internet. In this all the devices like computers, cameras, sensors etc. are considered as a thing and all these things are connected to each other and data transmission takes place between the systems. When data is transferred it also need to be stored. For that we would need a virtual infrastructure which will be provided by the cloud computing. The whole IOT thing is a mixture of sensor, networks, communication and computing technologies and the interconnectivity between them [1]. The whole IOT thing is a centralized model it means that these systems are identified individually, and they are provided with unique identity numbers, after that these devices are connected over internet, and services are provided using the cloud services. IOT made things simple to use and work with. IOT keeps the track about the devices, it reduces errors and showcase many complex systems into a simple structured network [2]. The structural part would be explained next.

II. IOT Architecture

IOT has four main levels [3].

Perception layer: The first one is perception layer. Here the objects or the things present in IOT environment are recognized.

Network Layer: After perception layers there will be a network layer. In network layer a network is formed between the objects.

Middle-ware Layer: The third layer is middleware layer where the data analysis is done by processing the information.

Application Layer: Then in application layer data is represented graphically and the data is used for creating smart applications using IOT. These smart applications are used for different purposes like system

management and business models can be created by using the applications.

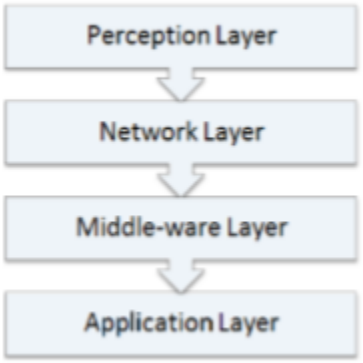

Fig 1: Structure of IOT

All the above-mentioned layer is important. The whole working of IOT is based on three major components i.e.

(1) hardware- These contributes the sensors, cameras and actuators.

(2) Middleware- These are the storage and computation section of the whole IOT systems which is basically cloud and analysis through big data.

(3) presentation- These are the application which give user interface to provide proper interpretation of the data [4].

III. Applications of IOT

IOT is an important area of technology which is grabbing attention from many industries [5]. The different domains of IOT and its applications are as below.

Despite of all these applications IOT has few challenges which will question the security and integrity of the services provided by the IOT systems.

IV. Challenges faced by IOT Devices

IOT is a centralized model connecting number of devices over a network. It is difficult to maintain those billions of devices; the maintenance cost will be high.

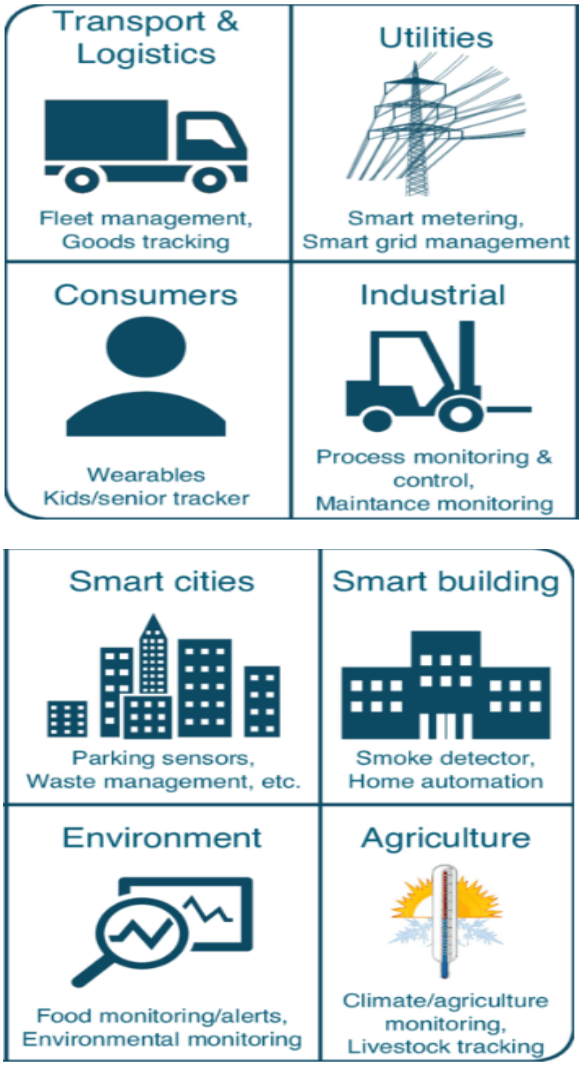

Fig 2: Applications of IOT

The major problems will be related to security of data that is transmitted through the network. During the IOT process data should pass through many devices, networks and frameworks[16]. All this would contribute to threaten the integrity of data. Few challenges faced by IOT are

A. Cost and capacity:

It will be challenging to maintain the devices. As there is exceptional growth in number of IOT devices.

Garter mentioned that by 2016, 5-6 million IOT devices are connected to each other every day over internet [6]. By 2020 the network will increase drastically.

B. Federated architecture:

The architecture of IOT does not have universal policies or standards that keeps the design in control to provide certain kind of security [7]. This scenario leads to denial of service attacks, data theft, hacking etc.

C. Inaccessibility to cloud Services:

Sometimes the cloud services are not available due to cyber-attacks, power, bugs and many other problems [8]. At that time the whole network shutdowns as the information is present in the cloud system.

D. Privacy issues:

The information present here in cloud is susceptible to be manipulated [9]. So that the information can be accessed and used for inappropriate uses.

All these problems can be solved by providing security to IOT devices using blockchain.

V. Blockchain Overview

A blockchain is a digital ledger in which blocks are connected and is used for transition [10]. Blockchain is a decentralized system. The basic concept of blockchain is that it is a tamperproof storage used for transaction.

The valid transactions are stored in blocks and each block is liked to previous block in the chain process. The first block is a genesis block and later all the new blocks have hash codes and change in hash code will take place if already existing block has changed information in it. The change in the hash code will be visible to all the users in that blockchain. This is the reason block chain is said to be secured. The structure of a block chain is like

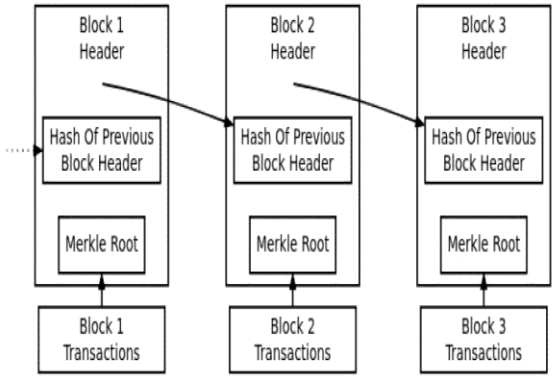

Fig 3: Block Diagram of Blockchain

The structured block chain has an ability to create, store and transmit different assets. It is tamperproof. Block chain was originally designed for transaction of ledger for bitcoin [11]. After bitcoin the scope of block chain was discovered in many other domains. IOT is one of the domains whose security issues can be solved by blockchain technology.

VI. Secured IOT devices using Blockchain

A. Some of the issues of IOT can be easily solved by blockchain technology. IOT is a centralized model. It will have huge infrastructure and the maintenance is also high. when it comes to block chain it is a decentralized model. This decentralized system will eliminate failure points and form a précised system of network.

B. Decentralization can provide a peer to peer networking [12]. As IOT

things are increasing every year decentralization is a better option.

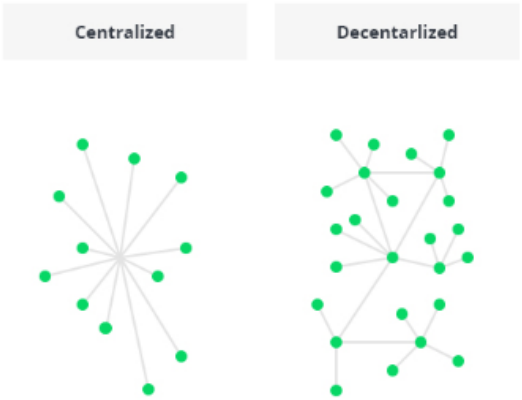

Fig 4: Differentiating Centralized and Decentralized model.

C. Like IOT the block chain does not have a deficient architecture. Here the data transaction between the devices is secured. The legitimacy of gadgets is checked, exchanges are marked, and they are cryptographically confirmed to know whether the inception of the message is from the sender itself.
D. Considering the server failure problems in cloud. We don't have any such issues in blockchain because the records or identical data are on different systems. So even one system is down we can retrieve data from other systems.
E. The control of information can be recognized and avoided in blockchain. The gadgets in blockchain are interlocked. On the off chance that one framework is refreshed. If any system is updated the changes will be rejected by the system with prior verification.
F. The cryptographic algorithms which are used in the block chain will provide proper security to the data which we accumulate from the IOT devices.

VII. Reference Work

There are different situations where there was a threat to smart home devices. Even basic devices like smart bulbs, smoke alarms are hacked [13]. In this smart home technology, the services are vulnerable to attacks even though the home gateway controls the exchange of packets [14]. The blockchain based architecture does performance evaluation. Here the actions of encryption and hashing takes place. Blockchain refers to a baseline method. Here IPv6 is used over WPAN as a communication protocol [15]. This whole thing will be suitable to provide security to smart homes.

VIII. Conclusion

Both IOT and blockchain are individually contributing a lot. IOT made everything so simple whereas block chain is providing a great security to financial modules like bitcoin. When we combine both technologies, the result will be a strong IOT system. Basically, IOT is a centralized module by decentralizing it the maintenance cost can be reduced and security issues are taken care of. Blockchain technology can be perfect solution for IOT security issues. So, IOT which is already a developed technology can be more security when it uses the Blockchain technology and its algorithms.

References

[1] Gigli, M. and Koo, S. "Internet of Things, Services and Applications Categorization. Advances in Internet of Things" 2011

[2] Ferguson, T. “Have Your Objects Call My Object”. 2002
[3] Hui Suo, Jiafu Wan, “Security in the Internet of Things” 2012.
[4] Somayya Madakam, R. Ramaswamy, Siddharth Tripathi. “Internet of Things (IOT): A Literature Review” 2015.
[5] Lee, I., & Lee, K.” The Internet of Things (IoT): Applications, investments, and challenges for enterprises” 2015.
[6] R. Van der Meulen, “Gartner Says 6.4 Billion Connected ‘Things’ Will Be in Use in 2016, Up 30 Percent From 2015
[7] Mahmoud, R., Yousuf, 2015.” Internet of things (IoT) security: Current status, challenges and prospective measures”. 2015.
[8] N. Kshetri, "Can Blockchain Strengthen the Internet of Things?" 2017.
[9] R. Hackett, “How Blockchains Could Save Us from Another Flint-Like Contamination Crisis,” Venturebeat, 25 Feb. 2017; bit.ly/2mx11zp.
[10] M. Samaniego and R. Deters, "Blockchain as a Service for IoT," 2016.
[11] Nakamoto, Satoshi. "Bitcoin: A peer-to-peer electronic cash system." 2008
[12] Wright, A., & De Filippi, P. “Decentralized Blockchain Technology and the Rise of Lex Cryptographia” 2015
[13] S. Notra, M. Siddiqi, and H. H. Gharakheili,, “An experimental study of security and privacy risks with emerging household appliances,” 2014.
[14] V. Sivaraman, D. Chan, D. Earl, and R. Boreli, “Smart-phones attacking smart-homes,” 2016.
[15] A. Dorri and P. Gauravaram, "Blockchain for IoT security and privacy: The case study of a smart home," 2017.
[16] Y. Mohana Roopa et.al ,”Middleware Architecture for the Internet of Things” Journal of Advanced Research in Dynamical and Control Systems, 2018

Proceedings of the Fourth International Conference on Communication and Electronics Systems (ICCES 2019)
IEEE Conference Record # 45898; IEEE Xplore ISBN: 978-1-7281-1261-9

GENETIC ALGORITHM BASED TUNING OF NONFRAGILE AND ROBUST PI CONTROLLER FOR PSFB DC-DC CONVERTER

Aswathi Divakar
Dept of Electrical Engineering
National Institute of Technology Calicut
Kerala, India
aswathidivakar13@gmail.com

Dr. Jeevamma Jacob
Dept of Electrical Engineering
National Institute of Technology Calicut
Kerala, India
jeeva@nitc.ac.in

***Abstract*—Phase shift full bridge (PSFB) DC-DC converters are used to convert high voltage to low voltage for medium and high power applications. In this paper a PSFB DC-DC converter is designed for converting 350 V DC supply to a constant output voltage of 12 V with a maximum load of 2 kW. It is desired to satisfy a stringent set of time domain specifications on settling time, steady state error and peak overshoot (to be less than 50 ms, 200 mV and 25% respectively) over a wide range of operating conditions. To obtain this objective, we propose a genetic algorithm (GA) based PI controller tuning for PSFB DC-DC converter. Simulation results show that K_p and K_i values that obtained using GA help to vary the load from 100 W to 2000 W, with steady state error, settling time and peak overshoot less than the specified limit. The system also supports an input voltage range from 300 V to 500 V and an output voltage from 8 V to 18 V. Fragility of the controller is analysed and the results show that controller is nonfragile.**

***Index Terms*—Phase shift full bridge (PSFB) DC-DC converter, Proportional integral(PI) controller, Genetic algorithm (GA), Fragility**

I. INTRODUCTION

PSFB DC-DC converters are widely used in high power applications because of their capability to handle higher power and zero voltage switching (ZVS) due to phase shift modulation technique. ZVS reduces the switching losses and improves the overall efficiency of the system [1]. High power handling capacity of MOSFET helps to achieve high power density [2] and it supports high switching frequency. Use of high frequency transformer in the PSFB DC-DC converter provides an isolation between high voltage input side and low voltage output side. Due to these advantages, they find applications in renewable energy systems, uninterruptible power supplies (UPS), hybrid electric vehicles (HEV) and telecommunications systems [3].

It is important to control the output voltage of PSFB DC-DC converter according to their applications. Different controllers are used for controlling the output voltage of DC-DC converter, namely sliding mode controller [4], PI controller, Linear quadratic regulator controllers [5], Adaptive controller [6] etc. By using these controllers, system has to satisfy certain time domain specifications such as maintain settling time, steady state error and peak overshoot with in certain limit. Most popular controller used in the industrial application is PI controller, due to its capability to achieve zero steady state error [7], better stability and reduced peak overshoot. Different types of tuning methods such as Ziegler-Nichols frequency domain method (ZNFDM), Damped oscillation method (DOM) and Good gain method (GGM) [8] are available for tuning the PI controller parameters for DC-DC converter. But these methods may not ensure minimum settling time, steady state error and peak overshoot. So an optimized tuning method is required to arrive at the PI controller parameters.

GA is used to find the optimum solution for different engineering problems [9]. The main advantage of this method is that it gives global optimum according to the type of solution required [10]. GA helps to find out the parameters that optimize the particular objective function. Tuning of PI controller parameters of DC-DC converter can be done by using GA method [11]. However most of the papers are dealing with the tuning of PI controller for single switch DC-DC converter with not much emphasis on the validation of time domain specification over the wide range of operating conditions. During controller design another aspect that must be taken into account is fragility analysis [12]. Fragility test helps to find out the robustness of controller against the model uncertainty.

In this paper a PSFB DC-DC converter is designed for a maximum load of 2 kW with a nominal output voltage of 12 V. The main aim of this paper is to find PI controller parameters, that maintain the settling time, steady state error and peak overshoot with in specified limit for all given operating conditions. Tuning of K_p and K_i value is done with the help of GA optimization method and Fragility of the controller is tested.

The rest of this paper is organized as follows: In section II a brief description about the working of PSFB DC-DC converter is given. Section III describes how GA can be used for tuning PI controller parameters for PSFB DC-DC converter. Simulation results are given in Section IV. Section V concludes the work of this paper.

II. PHASE SHIFTED FULL BRIDGE DC-DC CONVERTER

Full bridge DC-DC converter which uses the phase shift between gate signals as the output voltage control technique is known as PSFB DC-DC converter. Though Increased operating frequency offers reduction in the size of components and ripple in the output voltage, it causes an increase in the switching loss. One of the main advantages of phase shift modulation technique is that it allows ZVS. ZVS is achieved with the help of parasitic capacitance of MOSFET and leakage reactance of transformer. This soft switching technique helps to reduce the switching losses and improve the overall efficiency of the system.

Fig. 1 shows the circuit diagram of PSFB DC-DC converter. It consist of a full bridge inverter having four MOSFETs S1, S2, S3 & S4, a high frequency center tapped transformer is followed by a full bridge diode rectifier and an output LC filter. Each switch has a duty cycle of 50% as shown in Fig. 2. Two switches on the same leg are turned on complimentarily with each other. A phase delay is given to the gate signal of second leg (for S3 & S4) which is directly proportional to the required value of output voltage. Fig. 3 shows the primary transformer voltage and current corresponding to the gate signal shown in Fig. 2.

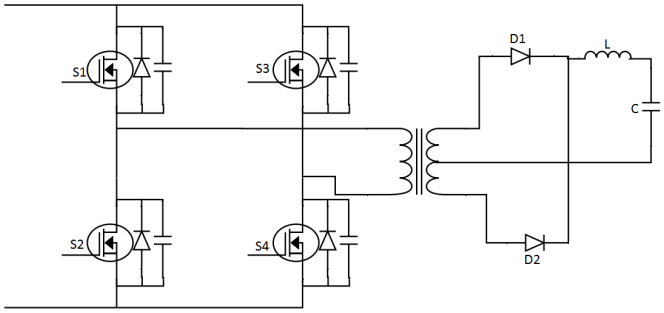

Fig. 1. Circuit diagram of PSFB DC-DC converter

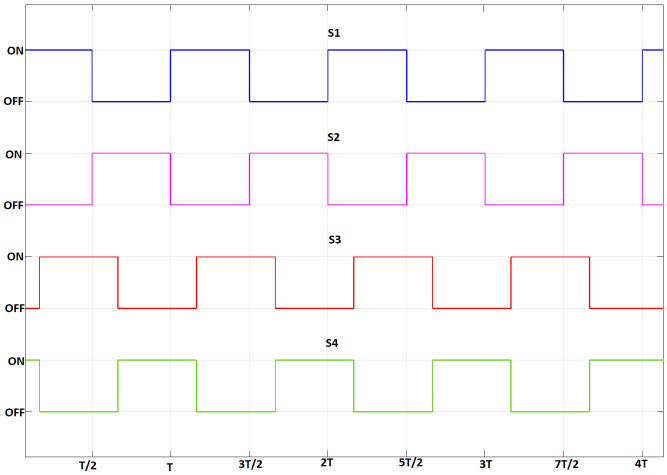

Fig. 2. Gate signals of PSFB dc-dc converter

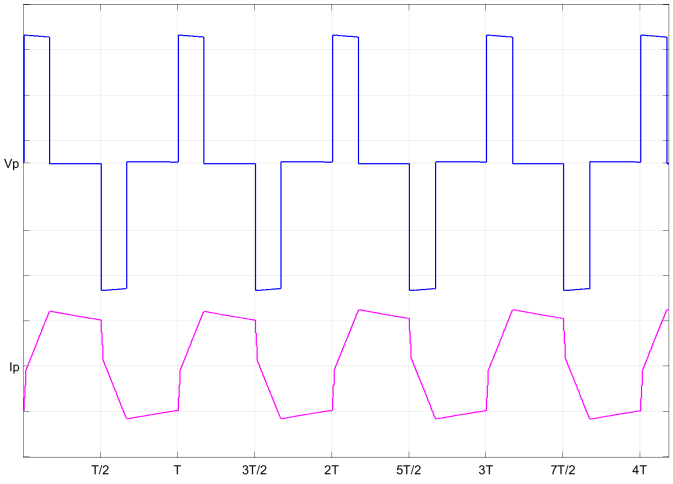

Fig. 3. Primary transformer voltage and current of PSFB DC-DC converter

III. PI CONTROLLER TUNING BY GA FOR PSFB DC-DC CONVERTER

In this paper output voltage of PSFB DC-DC converter is controlled by using PI controller, which is governed by equation (1). Our intention is to find out K_p and K_i values that minimize the steady state error, settling time and peak overshoot using a suitable optimization technique. GA can help to find out the global optimized value for PI controller parameters.

$$P_{out} = K_P e(t) + K_i \int_0^t e(t)dt \tag{1}$$

e(t) = setpoint - actual value
P_{out} = Controller output

A. OBJECTIVE FUNCTION

Most important step in the GA is the selection of the appropriate objective function. Actually objective function is an indicator for how well the individual is suited for the given application. For PI controller tuning the objective is to find out K_p and K_i values that minimize the difference between actual output and setpoint. Equation (2) shows the objective function used for tuning PI controller parameters, in this paper.

$$ITAE = \int_0^t t \mid e(t) \mid dt \tag{2}$$

Where ITAE is integral time absolute error.

B. FITNESS VALUE

PI controller is used to minimize the output error by minimizing the value of objective function. The fitness value can be defined as

$$\text{Fitness value} = \frac{1}{\text{Objective function}}$$

C. INITIAL POPULATION

First set a lower boundary and an upper boundary for the parameters to be determined. These boundaries are created in order to ensure that many of generated parameters do not lead to an unstable response. Initial population is created randomly within the boundaries.

Fig. 4 shows the the flow chart of GA optimization method used to tune PI controller parameters for PSFB DC-DC converter. At the beginning an initial population is generated randomly. Next step is the evaluation of generated population using the fitness function. After evaluation select the individual with highest fitness value. Selection process is followed by crossover and mutation. The above process will continue until it reaches the given number of maximum generation.

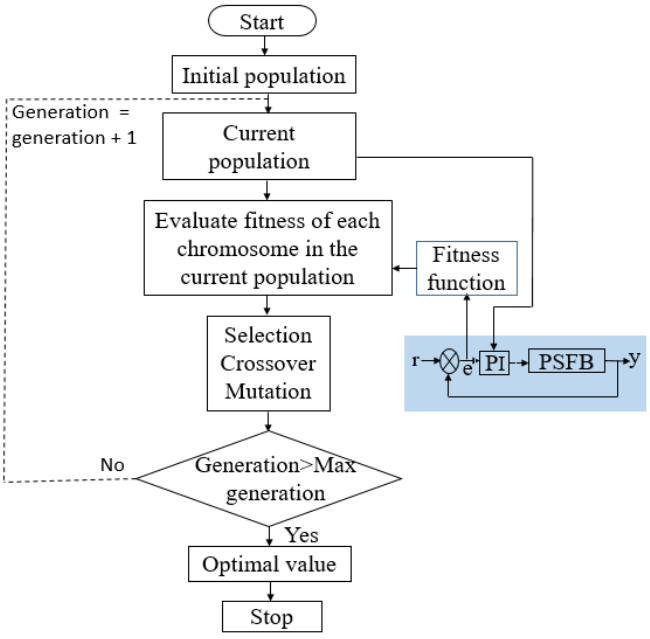

Fig. 4. Flow chart of GA optimization method

IV. SIMULATION RESULTS

Table I shows system parameters used for simulating a PSFB DC-DC converter in the MATLAB/Simulink. Output filter of the converter is designed for inductor ripple current of 10 % and 1 % ripple in the output voltage. GA parameters used for the tuning of DC-DC converter are shown in Table II.

TABLE I
SYSTEM PARAMETER OF PSFB DC-DC CONVERTER

Parameters	Values
Input voltage range	300 V-500 V
Nominal input voltage	350 V
Output voltage range	8 A-18 A
Nominal output voltage	12 V
Maximum load	2 kW
Switching frequency	100 kHz
Inductor	3.75 μH
Output capacitor	6.91 mF

Fig. 5 shows the block diagram of the complete system which includes PSFB DC-DC converter and control loop. Here output from the converter is compared with the setpoint voltage and the error is given to a PI controller.

Controller parameters are found with the help of GA through offline method. By using GA parameters in the Table II, K_p and K_i values are obtained as 4.9787 and 4661 respectively. Output of the controller will be a phase delay, required to reduce the error between actual output and the setpoint value. This phase delay is given as an input to the pulse generator.

Fig. 6 shows the output voltage during the load variation. The input voltage and setpoint voltage are kept as 350 V and 12 V respectively. Load is varied every 100 ms. Steady state error, settling time, overshoot and undershoot during each load variation given in Table III, show that the time domain specifications are satisfied.

TABLE II
PARAMETER OF GENETIC ALGORITHM

Parameters	Values
Population size	20
Maximum Generation	100
Mutation	.1 %
Upper and lower limit of K_p	[0 5]
Upper and lower limit of K_i	[0 5000]

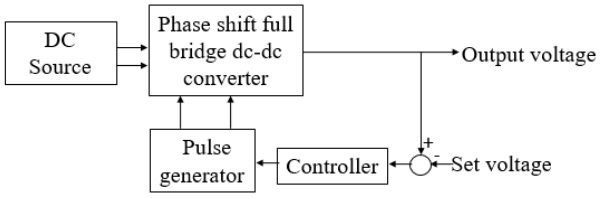

Fig. 5. Block diagram of complete PSFB DC-DC converter system

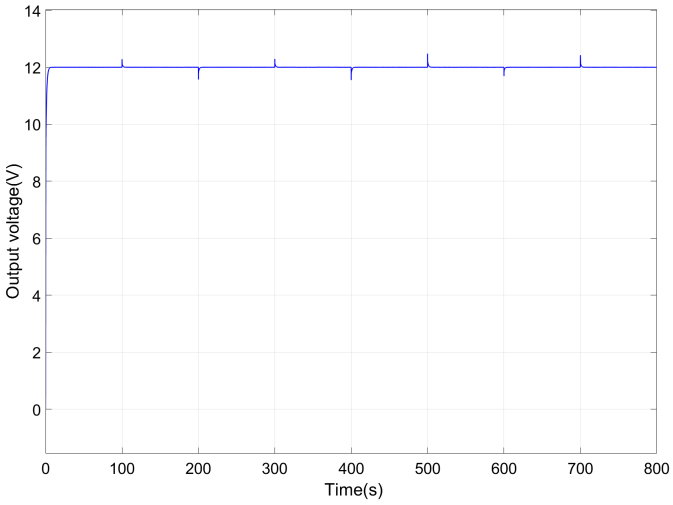

Fig. 6. Output voltage during load variation

TABLE III
STEADY STATE ERROR, SETTING TIME, OVERSHOOT AND UNDERSHOOT DURING EACH LOAD VARIATION

Load varition (W)	Time (ms)	steady state error (mV)	Settling time (ms)	Peak overshoot (V)	Under shoot (V)
1000	0-100	7	3.714	0	0
1000-100	100-200	6	.285	12.282	0
100-1500	200-300	5.58	.78	0	11.569
1500-500	300-400	6	.455	12.291	0
500-2000	400-500	6	.92	0	11.55
2000-500	500-600	6.5	.94	12.476	0
500-1500	600-700	6	.4	0	11.69
1500-500	700-800	7	.62	12.423	0

Fig. 7 shows the output voltage during different setpoint voltage conditions. Simulation is done for a load of 1500 W and input voltage of 350 V. In between the setpoint voltage from 8 V to 18 V, output voltage settles on their respective setpoint value satisfying all time domain specifications.

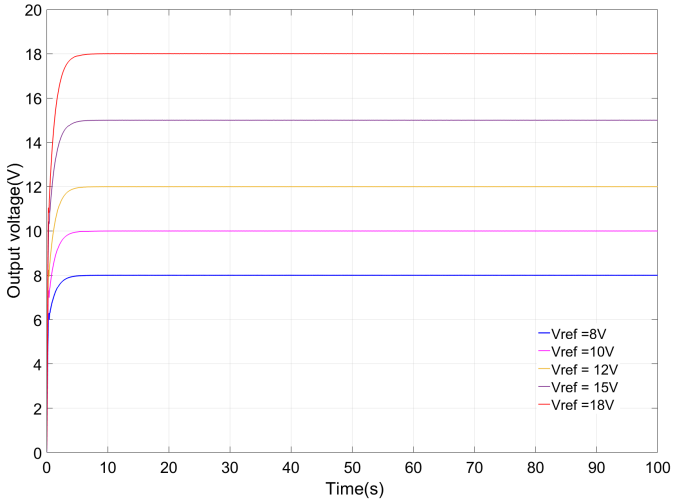

Fig. 7. Output voltage during different setpoint voltages

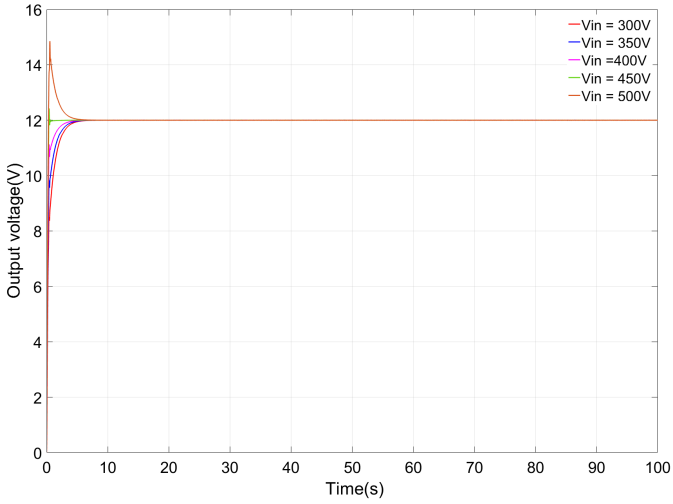

Fig. 8. Output voltage for different input voltages

Fig. 8 shows the output voltage for different input voltages. During simulation load and setpoint voltage are kept at 1500 W and 12 V respectively. In between 300 V to 500 V input voltage, settling time of the response is less than 5ms. For an input voltage of 300 V to 400 V there is no peak overshoot. If input voltage is 450 V then the peak overshoot is 12.425 V and if increased it up to 500 V then peak overshoot is 14.852 V. They are within the specified limits.

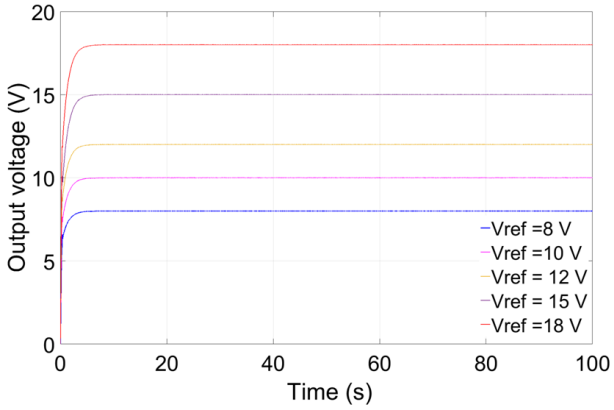

Fig. 9. Output voltage for different setpoint voltages with increased K_p,K_i

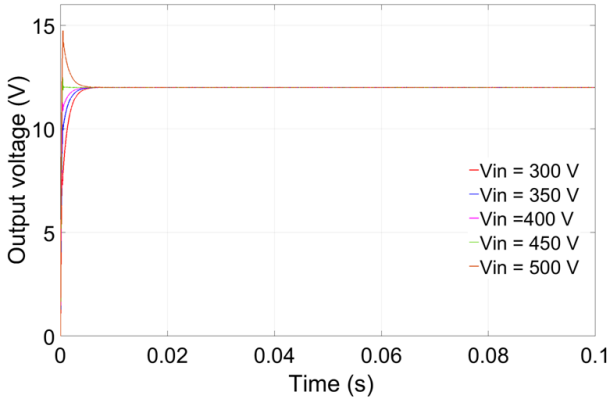

Fig. 10. Output voltage for different input voltages with increased K_p,K_i

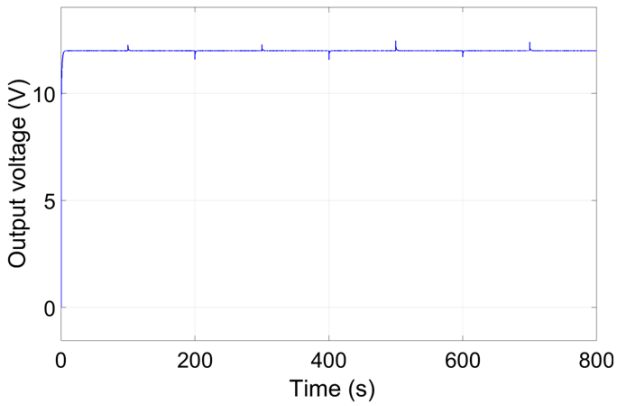

Fig. 11. Output voltage for different load with increased K_p,K_i

It may not be possible to realize the nominal PI controller parameters, 4.9787 and 4661. So fragility analysis of controller is carried out by varying the PI controller parameters with in $\pm 10\%$ of it's nominal value.

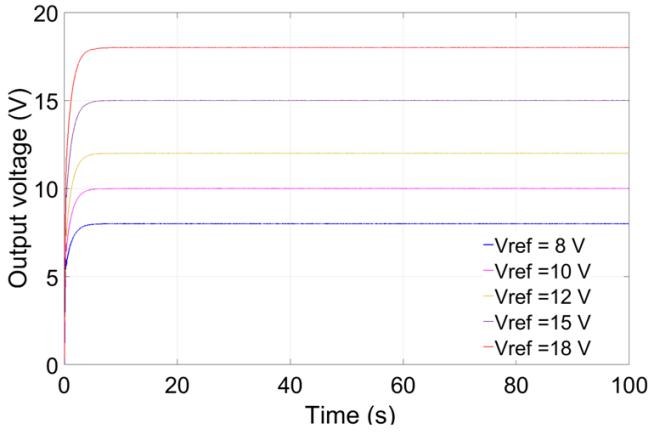

Fig. 12. Output voltage for different setpoint voltages with decreased K_p, K_i

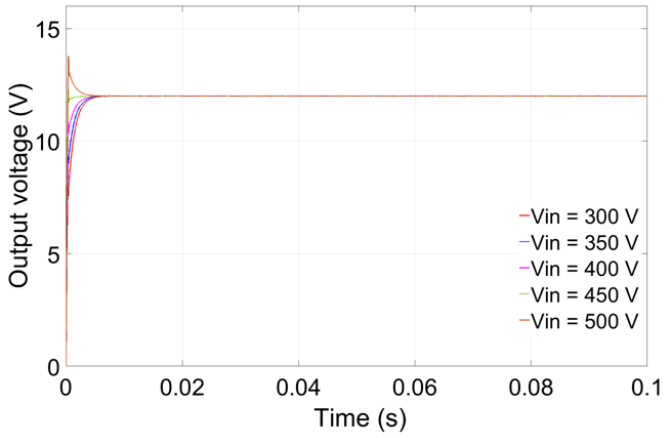

Fig. 13. Output voltage for different input voltages with decreased K_p, K_i

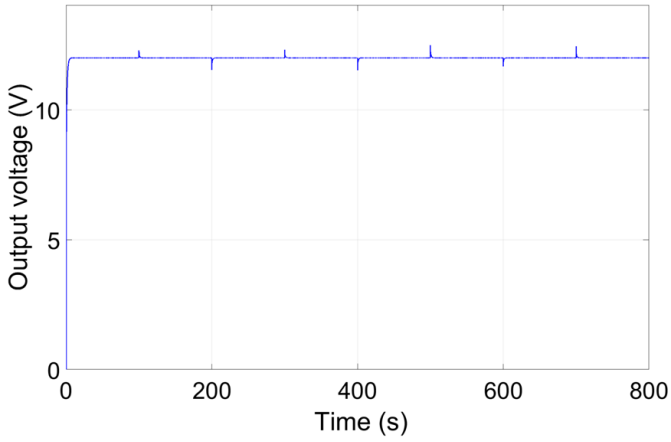

Fig. 14. Output voltage for different load with decreased K_p, K_i

Figures 9, 10 and 11 show the responses of the system for 10% increase in K_p and K_i values. For different load, setpoint and input voltage, this increased values of K_p and K_i satisfy all time domain specifications. Figures 12, 13 and 14 show the responses of the system for 10% decrease in K_p and K_i values. Here also all the time domain specifications are satisfied for all given operating conditions.

V. CONCLUSION

In this paper, a PSFB DC-DC converter is simulated using MATLAB/Simulink and its controller parameters K_p and K_i are found out using GA. By using a population size of 20 and a maximum generation of 200, K_p and K_i values are obtained as 4.9787 and 4661 respectively. With these controller parameters load can be varied from 100 W to 2000 W with steady state error, peak overshoot and settling time with in the specified limit. It also gives satisfactory performance for the variation of the input voltage from 300 V to 500 V and setpoint voltage from 8 V to 18 V. GA based PI controller parameter estimation gives a robust response. Fragility test is conducted by considering 10% increment and decrement in the nominal controller parameters and the result shows that controller is nonfragile.

REFERENCES

[1] H. Aksoy, T. Aydemir, Comparis on of Zero Voltage Switching Phase-Shifted PWM Full Bridge DC-DC Converter Topologies, *Intl Aegean Conference on Electrical Machines Power Electronics (ACEMP)*, 2015, pp. 818-824

[2] Oladimeji Ibrahim, Nor Zaihar Yahaya and Nordin Saad, "Phase-Shifted Full-Bridge Zero Voltage Switching DC-DC Converter Design with MATLAB/Simulink Implementation ", *International Journal of Electrical and Computer Engineering* , Pages 1488-1497 June 2018

[3] Tahsin Koroglu, M. Mustafa Savrun, Adnan Tan, Mehmet Ugras Cuma, Mehmet Ugras Cuma, Kamil cagatay Bayindir and Mehmet Tumay, "Design and Implementation of Full Bridge Bidirectional Isolated DC-DC Converter for High Power Applications ", *18th European Conference on Power Electronics and Applications* , 2016

[4] Wei Xiao, Lei Lei, Qihong Chen, Liyan Zhang and Shuhai Quan, "Sliding Mode Control of a Phase Shifted Full Bridge DC/DC Converter" *32nd Youth Academic Annual Conference of Chinese Association of Automation* ,May 2017

[5] M.A. Abdullah, C.W. Tan and .H.M. Yatim, "A Simulation Comparison of PI and Linear Quadratic Regulator Controllers in DC-DC Converter", *IEEE Conference on Energy Conversion*, Oct 2015

[6] Vasilica-Daniela Andries , Liviu Goras , Andi Buzo and Georg Pelz, "Automatic Tuning for a DC-DC Buck Converter with Adaptive Controller ", *International Symposium on Signals, Circuits and Systems* , July 2017

[7] Errouissi, A. Al-Durra, and S. M. Muyeen, Experimental validation of a novel PI speed controller for AC motor drives with improved transient performances, *IEEE Trans. Control Syst. Technol. , early access*, Jun. 2017, doi: 10.1109/TCST.2017.2707404 .

[8] O. Ibrahim, N. Z. Yahaya and N. Saad, "Comparative studies of PID controller tuning methods on a DC-DC boost converter," *2016 6th International Conference on Intelligent and Advanced Systems (ICIAS)*, Kuala Lumpur, 2016, pp. 1-5

[9] D. Xie, X. Sun, B. Bai, and S. Yang, Multiobjective optimization based on response surface model and its application to engineering shape design, *IEEE Trans. Magn.* , vol. 44, no. 6, pp. 10061009, Jun. 2008

[10] Vikrant Vishal, Vineet Kumar, K. P. S. Rana, Puneet Mishra and Jitendra Kumar , "Online PI controller tuning for a nonlinear plant using genetic algorithm ", *Innovative Applications of Computational Intelligence on Power, Energy and Controls with their impact on Humanity* , Nov 2014

[11] Subbiah Durgadevi and Mallapu Gopinath Umamaheswari, ”Analysis and design of single phase power factor correction with DCDC SEPIC Converter for fast dynamic response using genetic algorithm optimised PI controller ”, *IET Circuits, Devices Systems*,Volume: 12 , Issue: 2 , 3 2018

[12] V. M. Alfaro, R. Vilanova, O. Arrieta, ”Fragility analysis of PID controllers”, Proc. IEEE CCA ISIC, pp. 725-730.

Proceedings of the Fourth International Conference on Communication and Electronics Systems (ICCES 2019)
IEEE Conference Record # 45898; IEEE Xplore ISBN: 978-1-7281-1261-9

Adaptive Tracking Technique for Communication Cost Reduction in Wireless Sensor Network

Krishna Tulasi M.S
Department of Electronics and Communication Engineering
Amrita School of Engineering, Coimbatore
Amrita Vishwa Vidyapeetham, India
kt171194@gmail.com

Sudheesh .P
Department of Electronics and Communication Engineering
Amrita School of Engineering, Coimbatore
Amrita Vishwa Vidyapeetham, India
p_sudheesh@cb.amrita.edu

***Abstract*—Primary concern of Wireless Sensor Network(WSN) is energy efficiency. We need to increase the life span of the WSN. This work we uses the Unscented Kalman Filter (UKF) for reducing the communication energy cost of cluster based wireless sensor network. For transmission of data will require 1000 times more energy than computation. So for reducing this transmission UKF algorithm is used. The proposed UKF algorithm will run in the WSN and reduce the transmission of data. UKF algorithm run in the leaf node and head node to predict the value by computation, computation of the network will increase. But computation requires only less power than transmission. By using UKF technique, we can cut down the communication cost of cluster based wireless sensor network with a good data quality. Compare with the normal one to one communication we can save about 0.2Joule of energy, as we go for more number of transmission more amount energy can save. By using UKF technique we can achieve energy efficient system with increase in life span of the network.**

***Index Terms*—wireless sensor network(WSN), unscented Kalman filter(UKF), energy conservation**

I. Introduction

In cluster based WSN consist of large number of sensor nodes. Most of the WSN are not rechargeable they are battery driven. WSN is used to monitor the physical world for few months or even decades, energy utilization is the key problem. To decrease the energy utilization of the WSN and increase the life period of WSN, UKF technique is used [3].UKF algorithm will predict the present values using the past values. In this way transimmision between the head node and leaf node can reduce. Radio communication is the one of the most energy demanding process. It will consume large amount of energy [2]. One of the most energy-demanding process of WSN is the wireless communication. Transmission of data will consume 1000 more energy than computation [1].For transmission of data packets energy is needed to radio start up, accessing the channel, controlling the data packets, etc. Kalman filter (KF) based algorithm is used in WSN, because of its low complexity and accurate data quality. In kalman filter, UKF technique is used here. This technique will reduce the unnecessary tansmission between the head node and the leaf node.

In the cluster based WSN the sensor node will sense the data from the physical environment that data is transmitted to the head node [13]. Data process takes place in head node and send to sink node [4]. From the sink node the users can access the data. The sink node and the cluster head are some distance apart so continuously transmitting the data will require more energy. To reduce this transmission we are using the technique UKF. UKF algorithm is implemented in the head node and leaf node. The UKF will predict the next output with the help of the previous data. When the error between the predicted value and the original exceeds the threshold value the next transmission will takes place.

WSN is a collection of massive number of sensor nodes. Nodes are mostly placed in the environment to monitor the changes happening in the surrounding. Each node will rigged with memory, battery and transceiver [2]. The node will have processing, communication and sensing capabilities [8]. The nodes are placed in the environment where the humans have difficulty. Nodes are battery powered, we cannot recharge or replace the battery frequently, so we need to increase the life span of the battery [5]. Nodes will group together and form a cluster, each cluster will have head node. Node will sense the data from the surroundings and it is send to the head node. From the head node the data is transferred to the sink node. User can access the data from the sink node. In the cluster based wireless sensor network we can transfer data efficiently [7]. Cluster based WSN will minimize the energy utilization and reduces the data transference over the network this will improve the lifetime of the WSN.

Two-modal transmission is the one of the technique for reducing the energy consumption of the WSN. In this method they are using the predictive coding to reduce the transmissions. This is used for data compression and then transmissions can reduce in this way we can minimize the energy consumption. Each node will have the prediction based algorithm it will generate the next data with the help of past values. Information fusion is the another method used for reducing the communication cost of WSN.Information fusion is commonly used to detect events, target tracking, filter out the noise.WSN will considered as distributed database that can be accessed by the query language. These queries are computed with the help of information fusion. Clustering is the one of the method for improving the life span of WSN.

There are different clustering methods for increasing the life span of WSN. Mainly 3 types of clustering methods are discussed they are centralized, distributed and hybrid. After surveyed about the clustering technique they come to a conclusion that, by using unequal clustering life span of cluster head close to base station can increase in this way network life time also increase. Unequal clustering algorithms such as LEACH and HEED will give better performance [10]. Data compression is the one of the techniques For reducing the power consumption of WSN. Energy-efficient medium access control technique is used to reduce the communication between the inter-node. inter-node transmission will consume more power. By using this technique they analyse the performance and limitation of the WSN.Another method used for reducing the power consumption of WSN is Fuzzy approach. Fuzzy approach is used according to the battery level of network and sleeping time of the network is monitoring based on IEEE 802.15.4 protocol [7]. For real time monitoring of data is done and life time of WSN is increased with the help of fuzzy approach. They are taking the real time values so there will be certain limitations will be there and cannot achieve the better performance in the case of real time data monitoring case.

In this paper UKF is used in WSN to reduce the communication cost by reducing the transmission of data between the head node and the leaf node [10]. The UKF will predict the next value with the help of the pervious value. UKF is a prediction based technique for tracking the value with the help of the previous value. In the cluster based WSN, UKF algorithm is implemented in the cluster head and also in the sink node. In both the head node and in the leaf node the data will predict when the error increases a certain limit next transmission of data will takes place [11]. By using this technique we can reduce the transmission of data in that way we can cut down the communication cost of the wireless sensor network.

For non linear estimation UKF is used. UKF will overcome the resemblance problem of Kalman Filter(KF) and Extended Kalman Filter(EKF). UKF also called as the sigma point Kalman filter or linear regression Kalman filter [10]. UKF is used to linearize the nonlinear function. In UKF the state distribution is represented using the sigma points. UKF will contain 2 steps, model forecast and data assimilation. In the UKF the state distribution is characterised by Gaussian random variable (GRV), with the help of deterministically chosen sample points it is specified. True mean and covariance is captured by these sigma points. These sigma points transmitted through nonlinear system and take the posterior mean and covariance to 2nd order for any nonlinearity [9]. The process of estimating the mean and covariance with the sigma points is called unscented transform.

II. System Overview

The overview of the proposed system is explained in this section. The main idea behind this work is to reduce the energy utilized by the WSN, during the transmission of the data from leaf node to the cluster head. For reducing the energy consumed by the WSN we are using UKF technique.

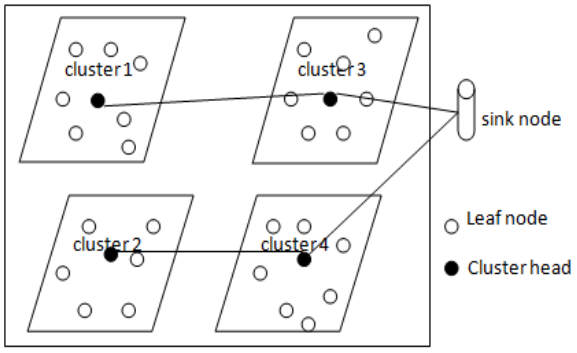

Fig. 1. Cluster based WSN.

First we need to form a cluster which consists of nodes and head node. The leaf node is the sensor and that will sense the environmental changes and transferred it to the cluster head. We need to reduce the communication between the nodes and the head nodes [10]. Transmission of data will require more energy than computation of data. So we use UKF algorithm to reduce the communication. The UKF algorithm will predict the future value with the help of present value. In UKF we will compute the sigma points, UKF algorithm will run with these sigma points. So we will get more accurate result than other KF. We will run the UKF in leaf node and cluster head. In leaf node the filter will filter out the noise from the sensor data. In the cluster head the UKF will predict the next value with the help of present value.

Wireless sensor network consist of the nodes and in center the head node. The leaf node will act as the sensor node and they will collect the information [17]. It is a self-configuring device it will communicate through radio signals. Nodes in the sensor network is called the mote [13]. The main application of the WSN include industry, science, transportation, civil infrastructure, and security [6]. The WSN is mostly of battery powered device. 802.15.4 and Zigbee are the 2 wireless standards used by WSN. These are low power protocols, because it will work on low duty cycles means most probably transceiver is in sleeping mode at the time of transmission and reception it will consume only the small amount of energy. Maximum distance the WSN can access is about 100m.

III. Methodology

Unscented kalman filter (UKF) technique is used in wireless sensor network for reducing the communication cost. UKF will predict the next value with the help of present value, so we can reduce the communication between the nodes and the head node. Transmission of data between the node to cluster head will consume more energy than computation. UFK will reduce this transmission by predicting the next value, for that there will be predict and update equations are used. Nodes

of the WSN will randomly arranged in the grid and form the cluster and cluster head is also selected [15]. Many clusters will together called as the cluster based WSN. The idea of the project is to reduce the transference between the head node and the nodes. The sensor node will sense the information from the surroundings and it is send to the head node. The head node will predict the current data by using the previous data with minimum error.

In the leaf node the KF run to filter out noise and produce the optimal value [14]. To reduce the energy consumed by WSN, UKF algorithm is run in the head node and also in the leaf nodes.Head node and in leaf node the UKF will runs and predict the value with the help of the past value [12]. If the prediction error exceed the given threshold value the transmission of the data from head node to the leaf nodes will takes place [18]. Next prediction will takes place by using the new transmitted data. By using this UKF technique we can reduce the transmission in this way we can reduce the tranmission cost and also the life span of the WSN.

For non linear estimation UKF is used. UKF will overcome the resemblance issues of KF and EKF. UKF also called as the sigma point kalman filter or linear regression kalman filter. UKF is used to linearize the nonlinear function.

There will be two state equations for all the adaptive filters

At time k the true state is emerge at time (k-1)

$$x_k = Ax_{k-1} + Bu_k + w_k \tag{1}$$

where A represents state transition matrix, B represents control input matrix, w_k represents the white Gaussian noise.

Observation equation of true state at time k is mapped to H.

$$z_k = Hx_k + v_k \tag{2}$$

where H represents observation matrix, v_k represents the white gaussian noise.

predict Phase

For generating the a priori estimate of present state, state estimate of the past sate is used.

$$\widehat{x}_k = A\widehat{x}_{k-1} + Bu_{k-1} \tag{3}$$

From equation 4 Uncertainity of the prediction is calculated uncertainity is calculated from covariance of error

$$\widehat{P}_k = AP_{k-1}A^T + Q_k \tag{4}$$

Update phase

In update phase the present measurement and a priori estimate will together form the improved a posteriori state estimate.

In the update phase we add average weight,it is called kalman gain

$$K_k = \widehat{P}_k.H^T.(H.\widehat{P}_k.H^T + R_k)^{-1} \tag{5}$$

Equation 6 is the update estimate of the system.

$$\widetilde{x}_k = \widehat{x}_k + K_k.(z_k - H.\widehat{x}_k) \tag{6}$$

Equation 7 is the final estimate of the system.

$$P_k = (I - K_k.H).\widehat{P}_k \tag{7}$$

After many iterations values become constant, where the covariance and kalman gain become constant value. after that the future value is predicted.

A. Unscented Kalman Filter

For non linear estimation UKF is used. UKF will overcome the resemblance problem of KF and EKF. UKF also called as the sigma point Kalman filter or linear regression Kalman filter. UKF is used to linearize the nonlinear function. In UKF the state distribution is represented using the sigma points. UKF will contain 2 steps, model forecast and data assimilation. True mean and covariance is captured by these sigma points. These sigma points transmitted through nonlinear system and take the posterior mean and covariance to 2nd order for any nonlinearity [11]. The process of estimating the mean and covariance with the sigma points is called unscented transform.

UKF will linearize the non linear functions. Compared to KF and EKF, UKF will improve the performance of the system. UKF will take bundle of points and we are approximating the Gaussian around that bundle of points, in this get we get improved approximation that traditional kalman filters [**?**]. The bundle points we choosen is called sigma points. From the source Gaussian we take some points and mapped to the destination Gaussian. These selected points pass through non linear function and then determine the new mean and variance of the Gaussian function. It is very challenging to reconstruct all state distribution through non linear function. But few points of state distribution, reconstruct very easily, that points are called sigma points. These sigma points are used for the UKF algorithm processing. We need to add weights to the sigma points so the sigma points are called weighted sigma points. Ukf transform Gaussian does not remain same as Gaussian function when it moves through the non linear system, but we relate from the resulting Gaussian figure. This process in UKF is called Unscented Transform.

IV. Result and Discussion

Random signal tracking using UKF is shown in Fig 2. From the figure we can see that the output signal exactly track the input signal path. The UKF algorithm is suitable for tracking the non linear signals. This UKF algorithm is used in the WSN nodes for reducing the communication cost.

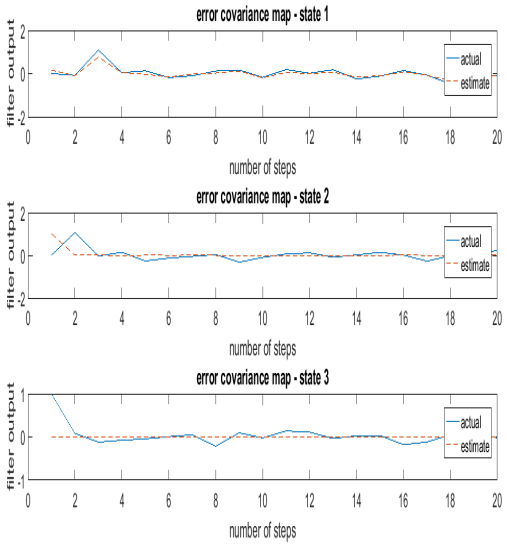

Fig. 2. Tracking of random signal using UKF.

Fig 3 is the tracking system of the UKF . In this the UKF track the true value with less error. This tracking system is implemented in the WSN and we can increase the life time of the network by reduce the energy consumption. We are giving some signal as input and UKF track the signal with minimum error.

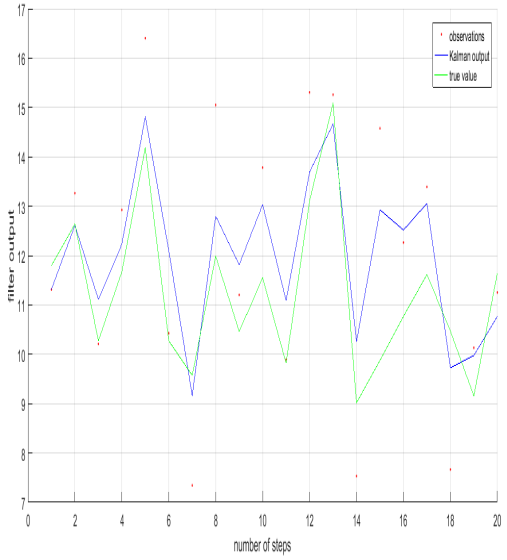

Fig. 3. Tracking system of UKF.

WSN cluster is shown in Fig 4 nodes are arranged randomly. One node which is closer to the center is selected as the cluster head and remaining nodes will be leaf nodes. The communication is done between the node and the head node.

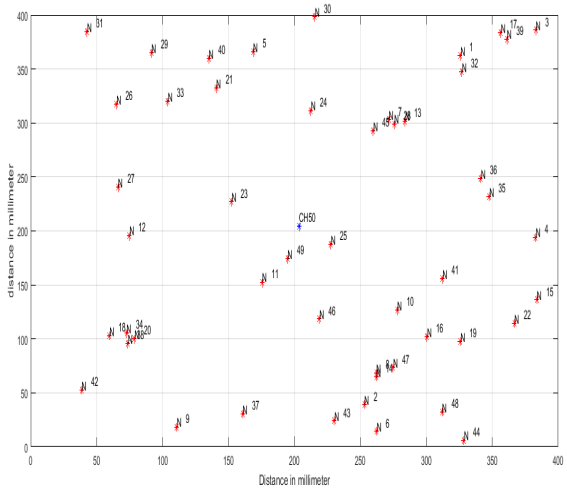

Fig. 4. Arrangement of nodes and cluster head as cluster.

Fig 5 is the comparison graph showing the energy efficiency of WSN with the normal communication and UKF after 10 communication. By using UKF method energy consumption is less compared to normal method. After 10 communications we can save about 0.3Joule of energy.

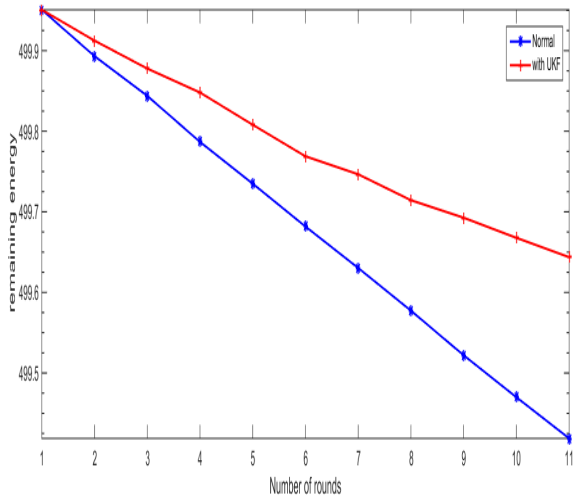

Fig. 5. Energy consumption after 10 communication.

Graph on the Fig 6 represents the energy comparison. This graph shows the remaining energy in the network after 25 communication. As number of communication increases we can save more amount of energy.after 25 communication we can save about 2Joule of energy. As number of communication increases we can save more energy.

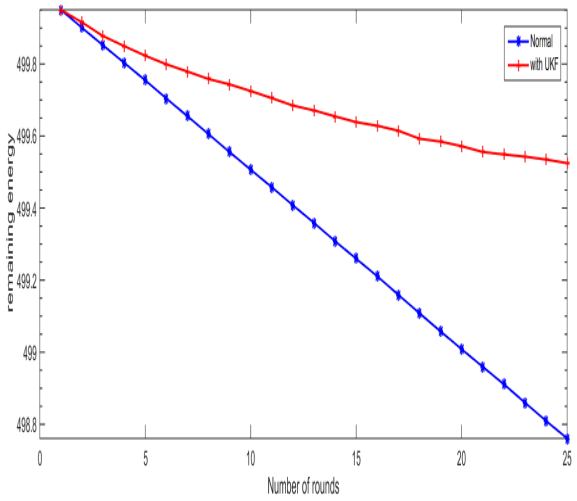

Fig. 6. Energy consumption after 25 communication.

Table I represents the remaining energy in the network after transmission. By using UKF method the energy utilization is less compared to the normal method. As the number of communications increases the energy consumption is more in the case of normal method. In UKF method energy consumption is comparatively less.

TABLE I
REMAINING ENERGY IN THE NETWORK

No.of communications	UKF method	Normal communication
10	499.6625	499.4333
25	499.4793	498.7211
50	499.3770	497.4625
75	499.2161	496.3032
100	499.1128	494.9663
150	498.7967	492.3048

Table II shows how much energy can be save for each number of communication. As number of communication increases, we can save more amount of energy. For 10 communication only 0.3Joule of energy is save but as we increase the number of communication we can save more energy

TABLE II
ENERGY SAVINGS IN UKF COMPARED TO NORMAL METHOD

No.of communication	Energy
10	0.3
25	0.7
50	1.9
75	2.9
100	4.1
150	6.4

V. CONCLUSION

UKF algorithm is used in the WSN for reducing the communication cost of network. UKF algorithm run in the leaf node and the head node of the wireless sensor network for reducing the communication cost. Initially the transmission will takes place, with this initial value further predicts will takes place in leaf node and head node, if the predicted value exceed the threshold value then next transmission will happen. UKF algorithm will give more accurate value than conventional kalman filtering technique. By using UKF method the energy consumption of WSN decreased when compared to the normal KF based technique. After 10 communications we can save about 0.3Joule of energy than the traditional method. As we are doing more communications we can save about more energy and the life time of the network can be increased. UKF method will save more energy in this way the life span of the sensor network will increase.

REFERENCES

[1] Y Huang, Wanli Yu, C Osewold, and A Garcia-Ortiz., Analysis of PKF: A Communication Cost Reduction Scheme for Wireless Sensor Networks, IEEE Transactions on Wireless Communication., Vol. 15, NO. 2, Feb 2016.

[2] Tao Wu , Yusong Yan, and Xi Chen., Reduction of Power Consumption in Wireless Sensor Networks for Railway Disaster Prevention and Safety Monitoring System., Intelligence Computation and Evolutionary Computation, AISC 180, pp. 983991.,2013.

[3] Vinod Gutta, KamalkanthToguruAnand, Tejasri Venkatasaidhar Movva, Bhargava Rama Korivi, Santosh Killamsetty, Sudheesh. P, Low Complexity Channel Estimation using Fuzzy - Kalman Filter for Fast Time Varying MIMO-OFDM Systems, 2015 International Conference on Advances in Computing, Communications and Informatics (ICACCI), pp.1771 -1774,2015.

[4] Shilpa M, and Pushpender Kumar D., Clustering in Wireless Sensor Networks: A Review., International Journal of Advanced Research in Computer Science, Volume 7, No. 3, May-June 2016.

[5] M Shuai, K Xie, G Chen, Xiuli Ma, and G Song., A Kalman Filter Based Approach for Outlier Detection in Sensor Networks., International Conference on Computer Science and Software Engineering 2008.

[6] G Anastasi , Marco Conti , Mario Di Francesco , and A Passarella., Energy conservation in wireless sensor networks: A survey., Elsevier, Ad Hoc Network : 537568, 2009.

[7] W. Heinzelman, A. Chandrakasan, and H. Balakrishnan, Energy efficient communication protocol for wireless microsensor networks. international Processing 33rd Annual. Hawaii International Conference Systems, p. 8020, 2000, .

[8] Meenakshi Sundaram and Ramanathan R, Performance optimization of RF energy harvesting wireless sensor networks, 7th International Conference On Advances In Computing Communications, ICACC 2017.

[9] Z Rezaei, and S Mobininejad., Energy Saving in Wireless Sensor Networks., International Journal of Computer Science and Engineering Survey (IJCSES), Vol.3, No.1, February 2012.

[10] A Pawar, and Divya K V., Secure and Efficient Data Transmission in Cluster based Wireless Sensor Network., International Journal of Computer Science and Mobile Computing, Vol. 4, Issue. 8, August 2015.

[11] G Xing, Chenyang Lu , Y Zhang, Q Huang, and R Pless., Minimum Power Configuration for Wireless Communication in Sensor Networks., ACM Transactions on Sensor Networks Vol. 3, No. 2, Article 11, June 2007.

[12] A Ribeiro, Ioannis D. Schizas, Stergios I. Roumeliotis,and Georgios B. Giannakis., Kalman Filtering in Wireless Sensor Networks., IEEE Control systems magazine, APRIL 2010.

[13] B Parbat, and R. K. Dhuware., Comparative Study of Classification Techniques with Labeled Data in Wireless Sensor Network., International Journal of Computer Applications, Volume 69 No.11, May 2013: 0975 8887.

[14] Giovanni Pau., Power Consumption Reduction for Wireless Sensor Networks Using A Fuzzy Approach., International Journal of Engineering and Technology Innovation, vol. 6, no. 1, pp. 55 - 67, 2016.

[15] J Singh, R kumar, A Mishra., Clustering Algorithms for Wireless Sensor Networks: A Review., 2nd International Conference on Computing for Sustainable Global Development (INDIACom), 2015.
[16] Rashmi Singh, R Mehra, L Sharma., Design of Kalman Filter for Wireless Sensor Network., International Conference on Internet of Things and Applications (IOTA), January 2016.
[17] Sergey Y. Yurish, Javier Caete, Francisco Puerta., Cost-effective Sensor Nodes for Wireless Sensor Networks., The Sixth International Conference on Sensor Technologies and Applications SENSORCOMM 2012.
[18] Mohammad Abdur Razzaque and Simon Dobson., Energy-Efficient Sensing in Wireless Sensor Networks Using Compressed Sensing., Sensors 2014.

Proceedings of the Fourth International Conference on Communication and Electronics Systems (ICCES 2019)
IEEE Conference Record # 45898; IEEE Xplore ISBN: 978-1-7281-1261-9

STAR – DELTA STARTER USING STATIC SWITCHES WITH ARDUINO MICROCONTROLLER AS A BASE DRIVE CIRCUIT

Shubham Sonawadekar

Student of KLS's Gogte Institute of technology Belgaum

EE department
Contact No. –9743258245
E-mail - ssonawadekar01@gmail.com

Shivprasad Desai

Student of KLS's Gogte Institute of technology Belgaum
EE department
Contact No. –8861517230
E-mail -shivprasaddesai96@gmail.com

ABSTRACT-

This paper represents automatic Star – Delta Starter of Three-Phase Induction Motors using soft switches, it overcomes all the disadvantages of conventional contactor based starters. This project is designed to provide low voltage start to induction motor. In this unit Arduino micro controller is used as base drive circuit and it makes the star delta conversion fully automatic. IGBT's are used as soft switches; each switch consists of two cascaded IGBT's. Now a day's automation is required in almost all industries, so this proposed unit can be effectively used. The Arduino is programmed in such a way that the starter operation automatically takes place based on the time delay provided. Since this unit uses soft switches, it will acquire less space with negligible maintenance. This system is more reliable than the conventional contactor based starter.

Keywords-

Arduino, Opto-isolator, Static Switch Module, Three - Phase Induction Motor

I. INTRODUCTION

Induction motors are popular due to their low cost, robust construction, low maintenance and good efficiency. An Induction Motor during start behaves like a short circuited transformer, when the supply is given to the stator windings; it draws high current. The starting current of Induction Motor is 6-7 times the full-load current. Starters are employed to reduce the starting current. [1]

The Star-Delta Starter is used to limit the starting current of induction motor. To limit starting current, the motor winding is connected in star configuration during starting and then in delta configuration. In star configuration

voltage across the winding will reduce by 0.57 times the line voltage thus the current will also reduce. To connect the windings in star and delta configuration static switches are used, each switch consist of two cascaded IGBT's. [2]

Arduino microcontroller is used as base drive circuit & it is programmed such that it will give gate signal to switches to connect the winding in star and delta configuration with certain delay. The gating signals from Arduino microcontroller are connected to each IGBT through an opto-isolator which provides the isolation of controlling circuit from power circuit. The Arduino controller is a sensitive device, so it is powered from a SMPS; which gives a constant DC voltage to the controller.[3]

II. EXISTING STAR DELTA STARTER BASED ON CONTACTOR-

Present star delta starters use three electromagnetic contactors, namely main, star& delta, and an electronic timer. At the first star and primary contactors are closed, after a short time interval the timer changes its switch positions such that star contactor gets opened and delta contactor gets closed for the remaining operating time of the motor.

At the time of starting the motor windings are star associated and each stator winding will receive $V_L/\sqrt{3}$, where V_L is the supply line voltage. Hence the line current drawn by the motor at starting is reduced to a safe limit.

Although these type of starter limit the starting current and start the motor safely but some drawbacks are associated with such starters those are- Coil may burn which would cause no magnetic field, hence the contactors won't close and the contactor wouldn't operate, Contacts may also weld shut which may cause the load to keep running even when there is no control voltage which may cause unsafe machine or damage to machine, The insects can get in the contacts which may cause the contactor failure which may ultimately cause the equipment failure. Since it uses three electromagnetic contactors which occupies relatively large space which is not suited for some application.

III. AUTOMATIC STAR-DELTA STARTER UNIT

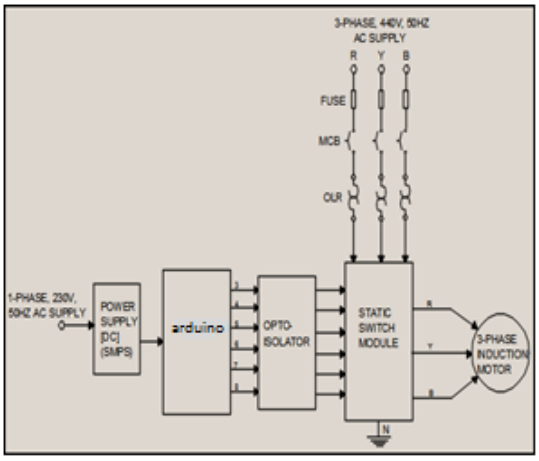

Fig. 1:Block diagram of Star-Delta Starter Unit

Figure (1) shows the block diagram of Star-Delta Starter Using Static switches. Single phase 230V supply is given to the SMPS which converts AC to DC. 5V DC supply is provided to the Arduino, when it is switched ON the Arduino starts executing the programs from its 1st instruction. This will give high output logic 1 to its pins 2, 4, 6 so the output of these pins is given to the Opto-isolator in order to give protection for the Arduino from the high voltage power circuit. From here it is connected to the Static Switch Module. It consists of 6 static devices IGBT's (IGBT/MOSFET/Power Transistor). Three static switches for Star connection and remaining three static switches for Delta connection.[4] When pin number 3, 4, 5 is at logic 1 the three Star connection static switches will turn on and three phase motor gets connected

in star fashion that is A2, B2, C2 winding terminals gets shorted through static switches. After few seconds delay (say 10 seconds according to the program) provided by Arduino pin number 3, 4, 5 will goes to logic 0 state and pin number 6, 7, 8 is at logic 1 at the same time star connection is converted into delta connection. And three phase motor gets connected in delta fashion that is A1-C2, B1-A2, C1-B2 winding terminals gets shorted.[5]

Hence with the help of this unit we are completely eliminating the use of contactors from the circuit operation of Star-Delta starters and making the operation easier and reliable. [6]

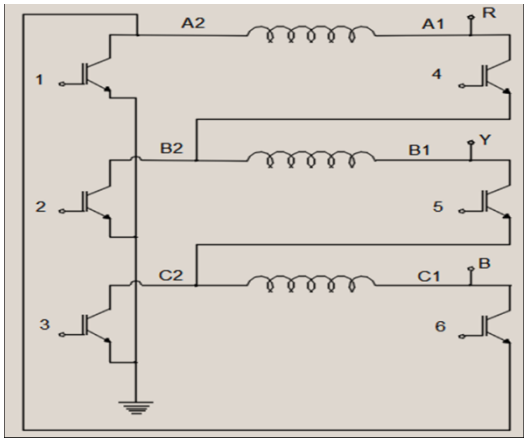

Fig.2 Static Switch Module

Figure (2) shows the static switch module which consists of 6 static switches used for Star-Delta Conversion. Switches 1, 2 & 3 for star connection and 4, 5 & 6 for delta connection respectively. These switches get the gate pulses from the Arduino.[7]

At the starting condition the motor is connected in star connection and switches 1, 2 & 3 are on and remaining switches are in off condition hence the current flows from A1-A2, B1-B2 and C1-C2 from RYB supply after the set delay in the arduino according to the time which motor takes to switch from starting condition to running condition. [8]

After the provided delay the motor switches from star to delta, in this state the switches 1, 2 & 3 are off and switches 4, 5 & 6 are gets turned on and hence switching to the delta condition from the star connection in this case the current flows from A1-B2, B1-C2 and C1-A2 from the RYB supply. [9]

IV. ADVANTAGES

- The motor can be controlled from any place with the help of GSM modem.
- The system is cost effective.
- The system is highly accurate & reliable & it requires less space.
- The effect of Gravity & Sparking can be eliminated.
- The system has a longer life.

V. DISADVATNTAGES

- If there is some malfunction in the Arduino, the system may misbehave. But chances of occurring such malfunction are almost nil.

VI. CONCLUSION

The automatic Star-Delta starter using Static Switches is having several advantages over the conventional methods. The system uses static switches instead of contactors which makes the proposed system more advantageous. This system uses Arduino microcontroller as a base drive circuit so it require less space.

VII. REFERRENCES

[1] B.L. Theraja A.K Theraja a textbook of electrical technology.

[2] AshfaqHussain, DhanpatRai& Co. (Pvt) Ltd., Electric Machines.

[3] Power Electronics circuits, devices and applications by M.H Rashid.

[4] I.J. Nagrath D.P kothari "Electrical machines 2nd ed.., Tata Mc Graw Hill, New Delhi.

[5] A guide of arduino.

[6] Implementation and Analysis of Microcontroller Based Soft Starters for Three-Phase Induction Motors
By Hamdy A Ashour;Rania. A Ibrahim
EUROCON 2007 – The International Conference on "Computer as a Tool"

[7] 2015 IEEE International electric machines & drives conference.
Fernado J.T.E.Ferreira.

[8] IEEE standard test procedure for polyphase induction motor and generators IEEE standard 112-1996 New York .

[9] Fernando J. T. E. Ferreira, André M. Silva, Sérgio M. A. Cruz, Aníbal T. De Almeida, "Comparison of losses in star- and delta-connected induction motors with saturated core", *Electric Machines and Drives Conference (IEMDC) 2017 IEEE International*, pp. 1-8, 2017.

Proceedings of the Fourth International Conference on Communication and Electronics Systems (ICCES 2019)
IEEE Conference Record # 45898; IEEE Xplore ISBN: 978-1-7281-1261-9

Performance Evaluation of Network Layer Routing Protocols on Wireless Sensor Networks

Amitkumar V. Jha, Bhargav Appasani and Abu Nasar Ghazali
School of Electronics Engineering, KIIT Deemed to be University
{bhargav.appasani, amit.jha and abu.ghazali}fet@kiit.ac.in

***Abstract*—The wireless sensor network is increasingly gaining attention due to the ubiquitous Internet of Thing (IoT). The wireless sensor network (WSN) basically consists of several nodes which are having the capability to communicate with each other over the wireless media. Further, in terms of network architecture, the most part of the WSN is infrastructure-less, however, the core of such network may comprise of the infrastructure including an access point (AP). The implementation of a particular routing protocol from the bunch of available, is of a great dilemma. Thus, this paper evaluates the effectiveness of different routing protocols for wireless sensor network applications. The effectiveness of the routing protocols is evaluated on the basis of different network performance matrices such as average End-to-End Delay (ETD) and Packet Delivery Ratio (PDR). To evaluate, the performance of WSN, QualNet 5.2, a network simulator is used which is accepted as one of the best network simulators to correctly represent the real-time scenario.**

Keywords—Wireless sensor networks, IoT, Ad-hoc network, Routing protocols, QualNet

I. INTRODUCTION

As a result of Internet of Things and its reach in the different area of applications, there have been tremendous amount of deployment of millions of intelligent devices embedded with technology to communicate with each other and to other network devices. The wireless sensor network is one of the major part of the implementation of IoT in which the devices are expected to communicate with each other over the wireless medium. The wireless network broadly classified in to two categories: 1) infrastructure Network and 2) Ad-Hoc Network. The WSN is always seen as the Ad hoc network as in this, every node is capable of sensing the information, gathering and forwarding the data, generating specific commands for communication, etc. Further, the ad-hoc network provides a high degree of freedom in terms of deployment as each of the participating node in this can behave as a router to forward the packets depending upon the routing algorithm. The higher degree of freedom and no requirement of infrastructure makes the WSN more pertinent for the communication, particularly, focusing the IoT applications.

Wireless sensor networks are expected to perform a numerous task ranging from environmental monitoring to battlefield surveillance, and it includes almost all the applications of IoT and paves an important role for the next generation of WSN [1]. There has been enormous amount of research on the performance WSN due to several routing protocols. X. Cai *et.al.,* in [2], reviews the literatures which shows the in-effectiveness of the certain routing protocols for large scale WSNs, and simultaneously, they propose AODV-RIRC (AODV-Route identification & RREP Capturing) routing protocol which is an amalgamation of Ad-hoc On-Demand Distance Vector (AODV) and AODV/Jr. with link layer feedback for large scale WSNs. The scalability analysis including, node mobility, node density and traffic load, is carried out by the authors in [3] in the context of WSN. A short and comprehensive analysis of a few most important routing protocols, DSR and AODV apart from TORA and LAR, in the context of infrastructure-less networks have been discussed by the authors in [4]. As the scalability of AODV is expected to be better as compared to its counterpart DSR [5], Xin Zhang et.al., in [3], evaluates the performance of infrastructure-less networks with AODV protocols.

In this article, we firstly overview different network layer routing protocols in the context of wireless sensor network prior to discussing the performance of some important protocols on the network performance. A wireless local-area-network (WLAN) is designed to study the behavior of the protocols within and outside the LAN [6]. To understand the effect of routing protocols on larger scale, the wide-area-network is designed which comprises of several local-area-networks [7]. The performance of the networks under consideration is analyzed by implementing the networks in QualNet 5.2 network simulator which is a discrete event simulation of communication network stack [8]. The reason of choosing the QualNet is that it is believed as a best network simulator to mimic the real world scenario.

The organization of rest of the paper is as follows: The Section II starts with an overview of routing protocols applicable in the context of WSNs. The complete modeling and design of WLAN and WAN under consideration is presented in a unique and the simplest way for understanding in section III. In Section III, the network is simulated using QualNet 5.2 to analyze the performance of different routing protocols under consideration. A detailed analysis on the simulation results are also described in this section. At the end, this paper includes Section IV, which concludes the research work and suggest some future work in this direction

II. OVERVIEW OF ROUTING PROTOCOLS IN WSN

In the last few decades many routing protocols have been proposed and tested in the literature [9] and few of the papers [10-12], also compares the performance of such protocols. For WSNs, the broad classifications of routing protocols are: flat routing protocols, hierarchical routing protocols, location-based routing protocols [13]. Among all, the routing protocols for ad-hoc networks are divided into two major categories- reactive (on-demand) and proactive (table driven). The destination sequenced distance vector protocol (DSDV) are selected as an example of proactive protocols, whereas, both AODV and DSR are selected as the examples of reactive protocols [14].

A brief overview some of the protocols for evaluating the network performance on the networks under consideration are presented in this section.

A. *Bellman-Ford*

The basic principle of DSDV is Bellman-Ford algorithm which works on the distributed approach. Each node stores the routing information and shares the information to its neighbor. DSDV effectively resolves the looping problem in routing. Further, it also eliminates the counting-to-infinity problem in routing. However, in terms of scalability, it does not provide the good outcomes.

B. *DSR*

Unlike, DSDV which uses hop-to-hop routing, it implements source routing. The route discovery and maintenance are the two important phases in DSR [15]. The necessity of flooding the network with update information as required in table-driven protocols, is eliminated in DSR, and thus, reduces the overhead in the network. However, this is achieved at the cost of higher connection set-up delay.

C. *AODV*

AODV works in the similar fashion as that of DSR [16]. The Route_Request message is used to establish a route from source to destination. The next node information is stored at the source as well as each intermediate nodes and the information is updated with respect to each flow. The routing information of a node is updated if and only of the destination sequence number (Des_Seq_Num) of the recent received packet is greater than that of the last stored packet at the corresponding node.

III. Network Design and Simulation

This section presents the simplified network design and simulation scenario of the network under consideration.

A. *WSN on the Perspective of Network Design*

To understand the network scenario under consideration, a simplest representation of the scenario is depicted in figure 1. A WSN consists of sensing devices and actuators represented by different symbols in the figure. A WSN along with the other end devices connected over a LAN, forms a WLAN which basically consists of routers, switches, end-devices, gateways, servers, sensors, actuators, etc. The devices over WLAN are connected through Wi-Fi technology using 2.4 GHz Channel represented by dotted line, and each WLAN are having an edge router which is used to establish the connection of WLAN to the rest of the IP networks.

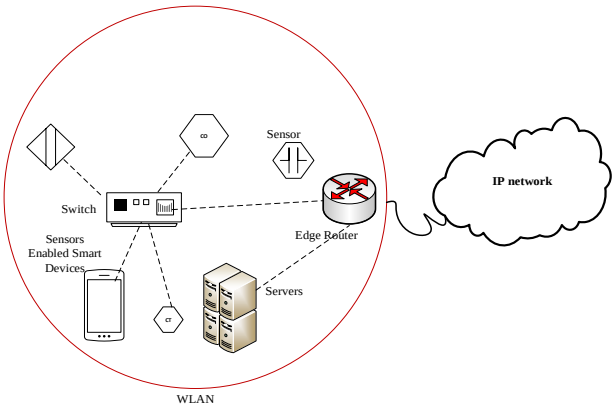

Fig.1: A Simplified Conceptual Representation of WSN

The different end devices communicate with each other over 2.4 GHz wireless channel. A wireless switch is utilized to interconnect several devices. The sensors and actuators work on the client-server based application layer protocols such as MQTT (Message Queuing Telemetry Transport) establishing a secure and low latency communication path for small amount of expected data in this application. The monitoring and controlling of the end devices can be achieved using any smart devices such as smart mobile phone, computer, laptop, etc., which are used to see the performance of the network in real-time. Despite of consisting many routers, all such WLAN will comprise of at least one edge routers, which is used to route the data from one WLAN to other WLAN. The figure 1 depicts all the necessary (but not exhaustive) components of the wireless sensor network under consideration. The other parts of the internet (named as '*IP Network*') are connected to the WSN under consideration using edge router.

B. *Network Design and Simulation Setup in QualNet*

The WSN under consideration is now designed in QualNet software to analyze the performance of this network for different routing protocols. The basics setups characteristics of the simulation is listed in the table 1 below.

Table 1: Simulation Setup in QualNet

Coordinate System	Latitude	SW Corner = 21.3022
		NE Corner = 29.422
	Longitude	SW Corner = 74.5784
		NE Corner = 93.4439
Altitude	1000 m	Above Sea level
Weather mobility		100 msec
Propagation Channel Frequency	2.4 GHz	
Propagation Path Loss Model	Two-Ray	

The WSN under consideration is designed and implemented in QualNet which is depicted in Figure 2. For the implementation of the WSNs, an area covering latitude of 21.3022 South-West corner, 29.422 North-East corner; and longitude of 74.5784 South-West corner, 93.4439 North-East corner is considered. This large geographic area is divided into a large number of small areas, where each small area is assumed to have a WSN of basic structure as shown in figure 1. Due to varying elevation profile at different coordinates, an average altitude of 1000 meter is considered above the mean sea level. This is worth noting that the effect of several weather related phenomenon viz., wind characteristics (e.g., direction and speed), temperature, rainfall, etc., cannot be ignored; and thus 'random' weather mobility pattern with interval of 100 msec is configured to replicate its effect in simulation. As a physical layer protocol, the IEEE 802.11 based on 2.4 GHz technology is utilized. The core (also referred to as backbone) of the network is designed by optical fiber to achieve maximum reliability with less communication failure probability. The backbone connection is shown in 'blue' color and the WSN is shown by the cloud symbol in figure 2. In figure 2, server at different location is also designed to collect and process the data. The 'green' color connection is used to represent an application layer protocol between source and destination node.

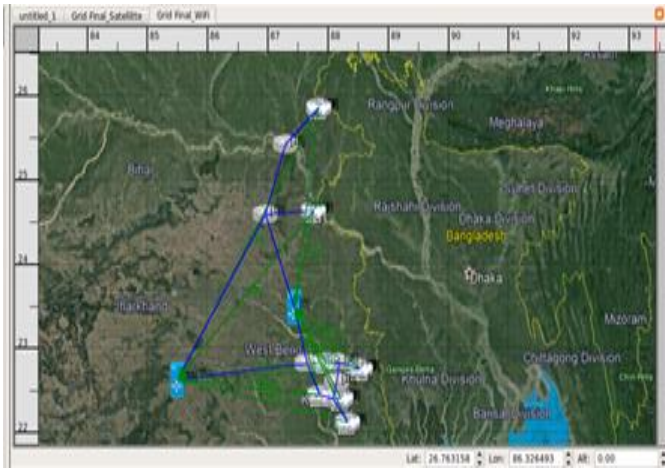

Fig.2: Implementation of WSN in QualNet

C. *Simulation Results and Analysis*

This section describes the simulation results and presents in-depth analysis on the result obtained. The simulation is run for 64 Kbps data rate using constant bit-rate (CBR) application layer properties in QualNet. Three different routing layer protocols are considered one-by-one: Bellman-Ford, DSR, and AODV to analyze the performance of the network.

The PDR metric is recorded for 300 sec simulation time and the plot of the same is shown in figure 3 below.

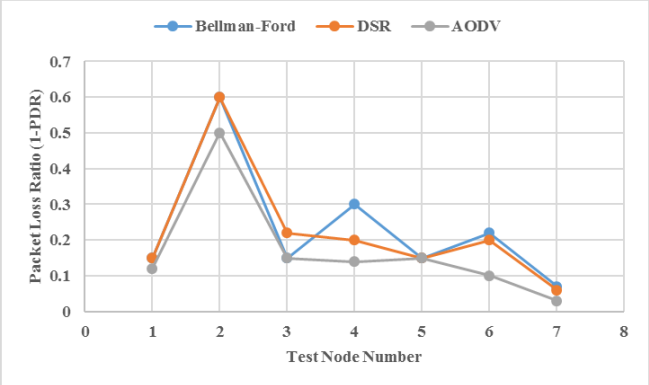

Fig.3: Effect of Routing Protocols on the Performance of WSN w.r.t PDR metric

The PDR indicates the network capability to tolerate the congestion and is calculated as the ratio of packet received successfully to the packet transmitted from the source. i.e.,

$$PDR = \frac{\text{Number of Received Packets}}{\text{Number of Transmitted Packets}} \quad (1)$$

The less value of PDR indicates that the network throughput is less as a result of discarding more packets on the network. Thus, a network with high PDR value gives maximum throughput and less packets will be discarded by the networks. The figure 3 indicates the percentage loss is less for AODV protocol as compared to Bellman-Ford and DSR protocols. As the less percentage loss indicates high PDR values and thus, WSNs with AODV as routing protocols performs better in terms of throughput. This is also worth noting that as there is less periodic update of the routing table information in AODV, which saves the bandwidth consumed significantly.

For a run time of 300 seconds, average end-to-end delay for the data to reach from source to destination is collected. These data are utilized to plot a graph of test node Vs ETD which is depicted in figure 4 below.

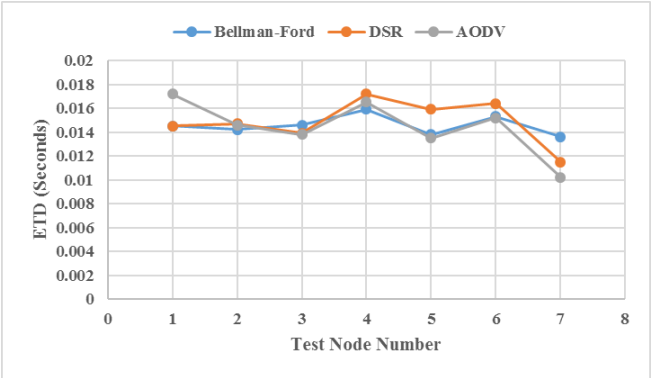

Fig.4: Effect of Routing Protocols on the Performance of WSN w.r.t ETD metric

The graph for average end-to-end delay plotted in figure 4. From the figure, it is observed that average end-to-end delay is more in DSR which is due to the connection set-up time as compared to that of AODV and Bellman-Ford protocols. The minimum delay is obtained for test node 7 for the ad-hoc on demand distance vector routing protocols and the maximum end-to-end delay is obtained for test node 4 for the DSR routing protocols. This is worth of mentioning that the values of ETD also depend upon the propagation time which is almost negligible in this case.

In depth analysis, thus, signifies that the AODV routing protocol performs better for wireless sensor networks as compared to the DSR and Bellman-Ford. However, this performance results are exclusively obtained for the two most important network parameters, average end-to-end delay and packet delivery ratio.

IV. Conclusion and Future Scope

The WSN is designed and implemented in QualNet which summarizes the effectiveness of several routing protocols in the following important conclusion. In wireless sensor network, AODV protocols gives maximum throughput, and consequently less packet loss as compared to DSR. However, DSR perform better than the Bellman-Ford in terms of PDR, but at the cost of higher end-to-end delay. On the other hand, AODV performs better in terms of PDR as well as ETD as compared to both Bellman-Ford and DSR. Even though, edges with negative weightage can be resolved using bellman-ford, AODV is shown to be performed better for wireless sensor networks in terms of PDR and ETD with a condition of non-existence of negative edges.

The performance analysis of these protocols with respect to scalability of dense WSN networks including MANET and VANET is the future work, which authors want to explore in the future.

REFERENCES

[1] F. Ren, J. Zhang, T. He, C. Lin and S. K. D. Ren, "EBRP: Energy-Balanced Routing Protocol for Data Gathering in Wireless Sensor Networks," in *IEEE Transactions on Parallel and Distributed Systems*, vol. 22, no. 12, pp. 2108-2125, Dec. 2011.

[2] Xuelian Cai, Jiandong Li and Lina Zhu, " Performance of Routing Protocols in Very Large Scale Wireless Sensor Networks," in *Journal of Networks*, vol. 7, no. 12, pp. 1996-2002, December 2012.

[3] X. Zhang and G. F. Riley, "Performance of routing protocols in very large-scale mobile wireless ad hoc networks," *13th IEEE International Symposium on Modeling, Analysis, and Simulation of Computer and Telecommunication Systems*, Atlanta, GA, 2005, pp. 115-122.

[4] l. Broustis, G. Jakllari, T. Repantis and M. Molle, "A Comprehensive Comparison of Routing Protocols for Large-Scale Wireless MANETs," *2006 3rd Annual IEEE Communications Society on Sensor and Ad Hoc Communications and Networks*, Reston, VA, 2006, pp. 951-956.

[5] D.B. Johnson, D.A. maltz, and Y.C. Hu, "The dynamic source routing protocol for mobile ad hoc networks (DSR)," *IETF Draft, draft-ieft-manet-dsr-09.txt,* Apr. 2003.

[6] N. I. Sarkar, "WLAN-Designer: a Web-based software tool to enhance teaching and learning wireless LAN design," *IEEE International Conference on Advanced Learning Technologies, 2004. Proceedings.*, Joensuu, 2004, pp. 624-628.

[7] IEEE Standard for Local Area Network/Wide Area Network (LAN/WAN) Node Communication Protocol to Complement the Utility Industry End Device Data Tables," in *IEEE Std 1703-2012* , vol., no., pp.1-239, 29 June 2012.

[8] Available at: https://www.scalable-networks.com/qualnet-network-simulation.

[9] V. Katiyar, N. Chand, Gopal Chand Gautam and A. Kumar, "Improvement in LEACH protocol for large-scale wireless sensor networks networks," *2011 International Conference on Emerging Trends in Electrical and Computer Technology*, Nagercoil, 2011, pp. 1070-10.

[10] C.E. Perkins, E.M. Belding-Royer, and S. Das, "Performance comparison of two on-demand routing protocols for ad hoc networks," IEEE Personal Communications, vol. 8, no. 1, pp. 16-28, 2001.

[11] networks," *2011 International Conference on Emerging Trends in Electrical and Computer Technology*, Nagercoil, 2011, pp. 1070-10.

[12] J. Broch, D.A. Maltz, D.B. Johnson, Y.C. Hu, and J. Jetcheva, "A performance comparison of multi-hop wireless ad hoc routing protocols," in Proc. 4th Annual ACM/IEEE International Conference on Mobile Computing and Networking (MOBICOM), 1998, pp. 85-97.

[13] P. Johansson, T. Larsson, N. Hedman, B. Mielczarek, and M. Degermark, "Scenario-based performance analysis of routing protocols for mobile ad-hoc networks," in Proc. 5th Annual ACM/IEEE International Conference on Mobile Computing and Networking (MOBICOM), 1999, pp. 195-206.

[14] M. Yassine and A. Ezzati, "Performance analysis of routing protocols for wireless sensor networks," *2014 Third IEEE International Colloquium in Information Science and Technology (CIST)*, Tetouan, 2014, pp. 420-424.

[15] Niansheng Liu, Huihuan Qian, Jingyu Yan and Yangsheng Xu, "Performance analysis of routing protocols for vehicle safety communications on the freeway," *2009 3rd International Conference on Anti-counterfeiting, Security, and Identification in Communication*, Hong Kong, 2009, pp. 85-88.

[16] D. Johnson, Y. hu, D. Maltz, The Dynamic Source Routing Protocol (DSR) for Mobile Ad Hoc Networks for IPv$. IETF MANET Working Group Internet draft (RFC4728). http://www.ietf.org/rfc/rfc4728.txt.

[17] C. Perkins, E. Belding-Royer, S. Das, Ad hoc On-Demand Distance Vector (AODV) Routing. IETF MANET Working Group Internet Draft (RFC3561). http://www.ietf.org/rfc/rfc3561.txt.

Proceedings of the Fourth International Conference on Communication and Electronics Systems (ICCES 2019)
IEEE Conference Record # 45898; IEEE Xplore ISBN: 978-1-7281-1261-9

The PI Controllers and its optimal tuning for Load Frequency Control (LFC) of Hybrid Hydro-thermal Power Systems

Amitkumar V. Jha[1] , Deepak Kumar Gupta[2] and Bhargav Appasani[3]
[{1,3}] School of Electronics Engineering, [2] School of Electrical Engineering, KIIT Deemed to be University
{ amit.jhafet, deepak.guptafel and bhargav.appasanifet}@kiit.ac.in

***Abstract*—The maintenance and controlling of certain parameters of large-scale hydrothermal power plant is of great challenge. In this paper, certain characteristics of the hydrothermal power plant are controlled using Proportional-Integral-Derivative (PID) controller. The PID controller is used to get the desired response of such power plant. The parameters of PID controllers are tuned to the optimum values using various available optimization methods such as Particle Swarm Optimization (PSO), Genetic Algorithm (GA) and Fire-Fly algorithm (FFA). All these algorithms evaluate controller parameter using different cost function such as Integral Time multiplied by Square Error (ITSE) and Integral-Time Absolute Error (ITAE). The hydrothermal power plant under consideration is implemented in MATLAB and simulation is carried out to get the optimum values of controller parameters. This paper also presents a comparative analysis of effect of different optimization algorithm under different cost function in the context of the power plant.**

Keywords—Hydrothermal Power Plant, PID Controller, Optimization Techniques and MATLAB

I. INTRODUCTION

The recent research in the area of hydrothermal power plants is focused on reducing the operational cost, particularly, the maintenance cost of the system. The power plants should be pro-active in the sense that it reduces the mismatch between demand at the load side and the generation at the generator side. Further, the mismatch cannot be reduced to zero, and therefore, variation in it should be limited to certain levels, precisely, as low as possible. In the real time, load (both real and reactive) from the demand side is always variable which is high in the day time and very low during the night time. However, the power generation at the generator side mostly remains constant. So, the variation in load causes the mismatch between total demand and total generation, which if not controlled, increases the loss and thus, the operational cost is further increased. A power system is viewed as multiple interconnected power generators, loads and tie-lines. The Automatic Generation Control (AGC) is viewed as the methodology by which the deviation in frequency of the system and tie-line power flow is maintained to the certain limits [1]. For a power system, the two variables: tie-line power and frequency of the system, are to be controlled and should be limited to certain deviation. The combination of these two variables are referred to as Area Control Error (ACE) [2].

The various research works have been carried out in the direction of modeling a hydro, thermal and their combinations in the liner fashion [3,4]. The problems of AGC and its implementation in the context of power system is also carried out in the literatures [5-8]. The different methods of controlling the characteristics of the power system is also discussed in the past such as, A.A.F.M Carniero, *et.al.*, in [9] proposes the fuzzy logic based controller for the operation of the hydrothermal power systems. Authors in [10], proposes the self-tuning of AGC using Proportional-Integral (PI) controller based on fuzzy logic for interconnected areas. A unique way for AGC technology based on Phase Measurement Unit (PMU) is proposed by the scholars in [11]. Apart from these, a numerous research finding on grid communications are also available in [12]. Further, the tuning of parameters of several controllers including PID is carried out in the literature [13]. Moreover, the various optimization algorithms such as PSO, GA, fuzzy logic control and firefly, are explored in the past for tuning of the parameters of the controllers to get its optimum values [14-18].

The linearized model of the hydro-thermal power system is presented in this paper. The paper addresses the challenges of maintaining the constant system frequency and tie-line power flow for the interconnected power stations. The deviation in the ACE which is combination of system frequency and tie-line power flow, is limited automatically using the PID controller. The parameter of such controller is optimized using algorithms such as PSO, GA and FFA based on ITSE and ITAE objective functions.

The proceedings of remainder of the paper are as follows: Section 2 starts with the linear modeling and design of hydrothermal power system and reviews the PID controller and the PSO optimization technique. In Section 3, the system is implemented in MATLAB for simulation to validate the design followed by the detailed analysis of the results. At last, Section 4 concludes the research work with a way forward.

II. MATHEMATICALLY MODELLING OF THE SYSTEM

This section focuses on the mathematical modeling of the system under consideration. A brief review of the controller and optimization techniques is also presented here.

A. Transfer Function of the Dynamic System

The PI controller is used to control the hydrothermal power plant system. The system under consideration is composed of thermal- a non-reheat turbine, in connection with hydro unit. The system transfer function is as shown in figure 1. For the analysis, step response of the system is considered using PI controller. To get the transfer function of the system is state space method is utilized which is given in equations below.

$$\dot{x} = Ax + Bu \tag{1}$$

$$y = Cx + Du \tag{2}$$

Here,

XXX-X-XXXX-XXXX-X/XX/$XX.00 ©20XX IEEE

x: State Vectors

u: Input Vectors

y: Output Vectors

Further, A, B, C and D are the system dependent real constant matrices.

$$x=\left[\Delta f_1,\Delta P_{mech1},\Delta P_{v1},\Delta f_2,\Delta P_{mech2},\Delta P_1,\Delta P_{v2},\Delta P_{12},\Delta P_{ref1},\Delta P_{ref2}\right]^T \tag{3}$$

$$u=\left[\Delta P_{L1},\Delta P_{L2}\right]^T \tag{4}$$

$$y=\left[\Delta f_1,\Delta f_2,\Delta P_{12}\right]^T \tag{5}$$

By using differential equations and analyzing the transfer function of each block independently, one can obtain the following equations necessary for the state matrix. Dynamic of power system is important because operating condition changes continuously such as load demand, output of the thermal and hydro plant.

$$\dot{x}_1=-\frac{1}{T_{p1}}x_1+\frac{K_{p1}}{T_{p1}}x_2-\frac{K_{p1}}{T_{p1}}x_8-\frac{K_{p1}}{T_{p1}}u_1 \tag{6}$$

$$\dot{x}_2=-\frac{1}{T_{t1}}x_2+\frac{1}{T_{t1}}x_3 \tag{7}$$

$$\dot{x}_3=-\frac{1}{R_1T_{g1}}x_1-\frac{1}{T_{g1}}x_3+\frac{1}{T_{g1}}x_9 \tag{8}$$

$$\dot{x}_4=-\frac{1}{T_{p2}}x_4+\frac{K_{p2}}{T_{p2}}x_5+\frac{K_{p2}}{T_{p2}}x_8-\frac{K_{p2}}{T_{p2}}u_2 \tag{9}$$

$$\dot{x}_5=-\frac{2T_2}{R_2T_1T_3}x_4-\frac{2}{T_w}x_5+\left(\frac{2}{T_w}+\frac{2}{T_3}\right)x_6+\left(\frac{2T_2}{T_1T_3}-\frac{2}{T_3}\right)x_7-\frac{2T_2}{T_1T_3}x_{10} \tag{10}$$

$$\dot{x}_6=-\frac{T_2}{R_2T_1T_3}x_4-\frac{1}{T_3}x_6+\left(\frac{1}{T_3}-\frac{T_2}{T_1T_3}\right)x_7+\frac{T_2}{T_1T_3}x_{10} \tag{11}$$

$$\dot{x}_7=-\frac{1}{R_2T_1}x_4-\frac{1}{T_1}x_7+\frac{1}{T_1}x_{10} \tag{12}$$

$$\dot{x}_8=T_sx_1-T_sx_4 \tag{13}$$

$$\dot{x}_9=\left(\frac{B_1K_{pr1}}{T_{p1}}-K_{pr1}T_s-K_{i1}B_1\right)x_1-\frac{B_1K_{pr1}K_{p1}}{T_{p1}}x_2+\ldots$$

$$\ldots K_{pr1}T_sx_4+\left(\frac{B_1K_{pr1}K_{p1}}{T_{p1}}-K_{i1}\right)x_8+\frac{B_1K_{pr1}K_{p1}}{T_{p1}}u_1 \tag{14}$$

$$\dot{x}_{10}=K_{pr2}T_sx_1+\left(\frac{B_2K_{pr2}}{T_{p2}}-K_{pr2}T_s-K_{i2}B_2\right)x_4-\ldots$$

$$\ldots\frac{B_2K_{pr2}K_{p2}}{T_{p2}}x_5+\left(-\frac{B_2K_{pr2}K_{p2}}{T_{p2}}+K_{i2}\right)x_8+\frac{B_2K_{pr2}K_{p2}}{T_{p2}}u_2 \tag{15}$$

After analyzing these equations, the real constant matrix obtained as follows:-

$$A=\begin{bmatrix}
-\frac{1}{T_{P1}} & \frac{K_{P1}}{T_{P1}} & 0 & 0 & 0 & 0 & 0 & -\frac{K_{P1}}{T_{P1}} & 0 & 0\\
0 & -\frac{1}{T_{t1}} & \frac{1}{T_{t1}} & 0 & 0 & 0 & 0 & 0 & 0 & 0\\
-\frac{1}{R_1T_{g1}} & 0 & \frac{1}{T_{g1}} & 0 & 0 & 0 & 0 & 0 & \frac{1}{T_{g1}} & 0\\
0 & 0 & 0 & -\frac{1}{T_{P2}} & \frac{K_{P2}}{T_{P2}} & 0 & 0 & \frac{K_{P2}}{T_{P2}} & 0 & 0\\
0 & 0 & 0 & \frac{2T_2}{R_2T_1T_2} & -\frac{2}{T_w} & (\frac{2}{T_w}+\frac{2}{T_3}) & (\frac{2T_2}{T_1T_3}-\frac{2}{T_3}) & 0 & 0 & -\frac{2T_2}{T_1T_3}\\
0 & 0 & 0 & -\frac{T_2}{R_2T_1T_2} & 0 & -\frac{1}{T_3} & (\frac{1}{T_3}-\frac{T_2}{T_1T_3}) & 0 & 0 & \frac{T_2}{T_1T_3}\\
0 & 0 & 0 & -\frac{1}{R_2T_1} & 0 & 0 & -\frac{1}{T_1} & 0 & 0 & \frac{1}{T_1}\\
T_s & 0 & 0 & -T & 0 & 0 & 0 & 0 & 0 & 0\\
A_{9,1} & -\frac{B_1K_{pr1}K_{P1}}{T_{P1}} & 0 & K_{pr1}T_s & 0 & 0 & 0 & (\frac{B_1K_{pr1}K_{P1}}{T_{P1}}-K_{i1}) & 0 & 0\\
K_{pr2}T_s & 0 & 0 & A_{10,4} & -\frac{B_2K_{pr2}K_{P2}}{T_{P2}} & 0 & 0 & (-\frac{B_2K_{pr2}K_{P2}}{T_{P2}}+K_{i2}) & 0 & 0
\end{bmatrix}$$

where , $A_{9,1}=(\frac{B_1K_{pr1}}{T_{P1}}-K_{pr1}T_s-K_{i1}B_1)$

$$A_{10,4}=(\frac{B_2K_{pr2}}{T_{P2}}-K_{pr2}T_s-K_{i2}B_2)$$

$$B=\begin{bmatrix}
-\frac{K_{P1}}{T_{P1}} & 0 & 0 & 0 & 0 & 0 & 0 & 0 & \frac{B_1K_{pr1}K_{P1}}{T_{P1}} & 0\\
0 & 0 & 0 & -\frac{K_{P2}}{T_{P2}} & 0 & 0 & 0 & 0 & 0 & \frac{B_2K_{pr2}K_{P2}}{T_{P2}}
\end{bmatrix}^T$$

$$C=\begin{bmatrix}1&0&0&0&0&0&0&0&0&0\\0&0&0&1&0&0&0&0&0&0\\0&0&0&0&0&0&0&1&0&0\end{bmatrix}$$ and

$$D=0;$$

The transfer function *H(S)* using state space model is given as:

$$H(s)=C[sI-A]^{-1}B+D$$

On analyzing the above matrices, transfer functions of the system can be evaluated as follows:

Transfer function $=C\left[SI-A\right]^{-1}B+D$

The order of transfer function is (3× 2) matrix.

$$\Delta f_1=\frac{\Delta f_1(s)}{\Delta P_{L1}(s)}\Delta P_{L1}+\frac{\Delta f_1(s)}{\Delta P_{L2}(s)}\Delta P_{L2} \tag{16}$$

$$\Delta f_2=\frac{\Delta f_2(s)}{\Delta P_{L1}(s)}\Delta P_{L1}+\frac{\Delta f_2(s)}{\Delta P_{L2}(s)}\Delta P_{L2} \tag{17}$$

$$\Delta P_{12}=\frac{\Delta P_{12}(s)}{\Delta P_{L1}(s)}\Delta P_{L1}+\frac{\Delta P_{12}(s)}{\Delta P_{L2}(s)}\Delta P_{L2} \tag{18}$$

B. PI Controller

The PI controller is used which includes advantages of proportional plus integral controller by mitigating the disadvantages of the individual. The transfer function of a typical PI controller is given by equation (19) where, K_p and K_i are the parameters of PI controller.

$$H(s)=\frac{U(s)}{E(s)}=K_p+\frac{K_i}{s} \tag{19}$$

The time domain representation of the PID controller is also shown by equation (20). Where, *u(t)* is the response due to the error input *e(t)*.

$$u(t)=K_p+K_i\int e(t)dt \tag{20}$$

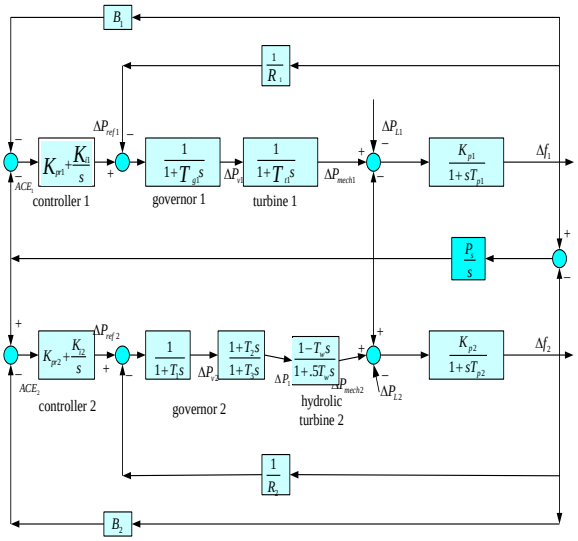

Fig.1: A Transfer Function Model of Interconnected Hydro-thermal Power System

C. Optimization Techniques

The optimization techniques viz., PSO, GA and FFA are used in order to tune the parameters of PI controller. Details of the particles swarm optimization can be understood in [18] whereas Genetic Algorithm (GA) and Firefly Algorithm (FFA) details are elaborated in [19] and [20] respectively. Since, the optimum values of controller parameters are unknown, initial values of these parameters are chosen randomly which are to be tuned using optimization algorithm. Since, all the optimization algorithm optimize the parameters based on the cost function, also referred to as objective function, we choose ITAE as one of the objective function. Further, to understand the effect of cost function in optimizing the parameters, ITSE as another objective function is chosen for comparison. The ITAE and ITSE objective functions are represented mathematically in equations (21) and (22).

$$ITAE=\int_o^\infty t\times|e(t)|dt \tag{21}$$

$$ITSE=\int_o^\infty |e(t)|^2\times t dt \tag{22}$$

III. Simulation Results and Discussion

This section presents the implementation of the system under consideration in the MATLAB to validate the results obtained.

A. CASE I : Performance using ITAE as Objective Function

Two area hybrid hydro-thermal power system has been considered as depicted in Fig. 1. Load has been changed in both areas to analyze the performance of Load Frequency Control (LFC). Tuning of the PI controller's parameters have been done by three well-known optimization techniques (GA, PSO and FA) and comparison have been made among all when ITAE performance indices is used as the objective function. (Pd1=0.2 pu. and Pd2=0.3 p.u.). Perturbation response of the frequency in each area and also the change in Tie-line power flow have been observed by varying the loading in respective area and comparison have been made among all the three optimization methods. Fig. 2 show the perturbed response for all the state variables and also Table I show the optimum parameters of PI controllers with different optimization techniques.

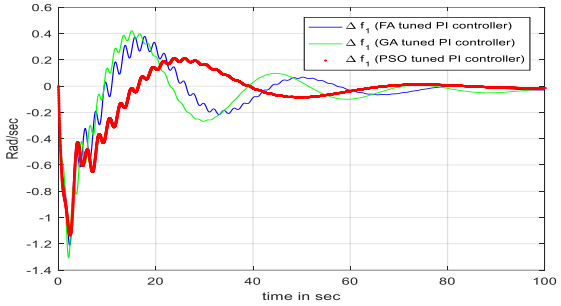

(a) Load Frequency of Area 1

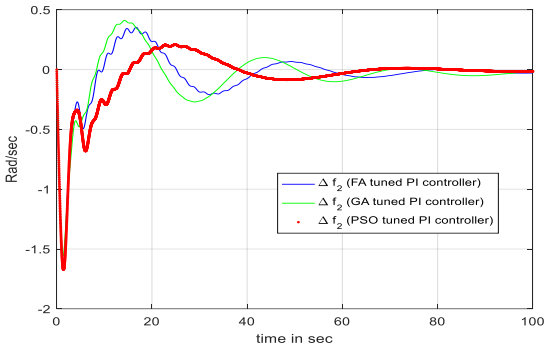

(b) Load Frequency of Area 2

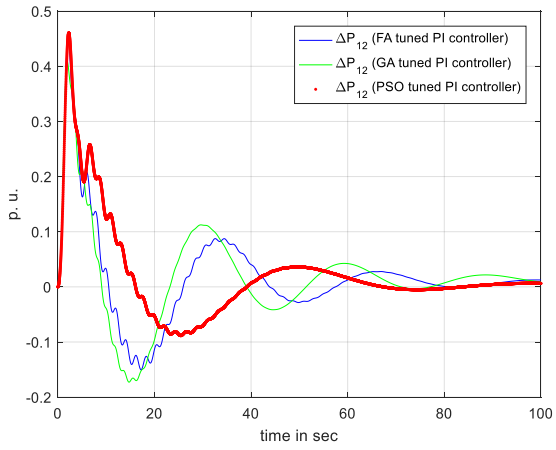

(c) Tie-line Power Flow

Fig. 2: Perturbed response of the system for Case 1

Table I: Tuned Parameters of PI Controllers with different optimization techniques for Case I

O.T	Time	K_{p1}	K_{p2}	K_{i1}	K_{i2}	ITAE
FA	260.718	0.289	8.531	0.999	0.041	$5.82x10^4$
GA	115.433	0.942	10.577	0.472	0.001	$7.13x10^4$
PSO	101.684	0	3.941	0.942	0.059	$4.77x10^4$

B. Performance using ITSE as Objective Function

Tuning of the PI controller's parameters have been done by three well-known optimization techniques (GA, PSO and FA) when load have been changed to 0.4 p.u. in area 1 and 0.2 p.u. in the area 2. Here ITSE has been considered as the objective function to be minimized by three optimization methods. (Pd1=0.4 pu. and Pd2=0.3 p.u.). Perturbation response of frequency effect in area 1 and area 2 as well as the change in Tie-line power flow for the case II have also been observed in respective area and comparison have been made among all the three optimization methods. Fig. 3 show the perturbed response for all the state variables and also Table II show the optimum parameters of PI controllers with different optimization techniques.

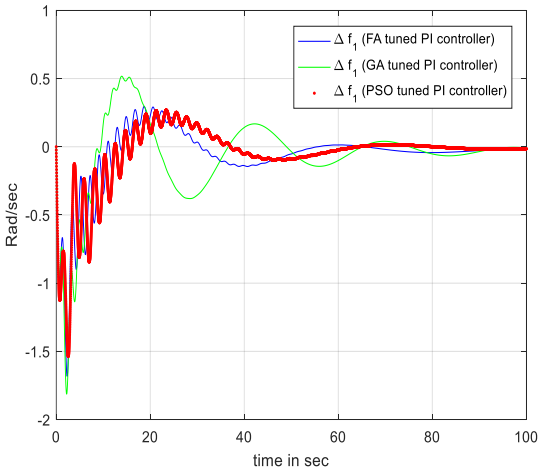

(a) Load Frequency of Area 1

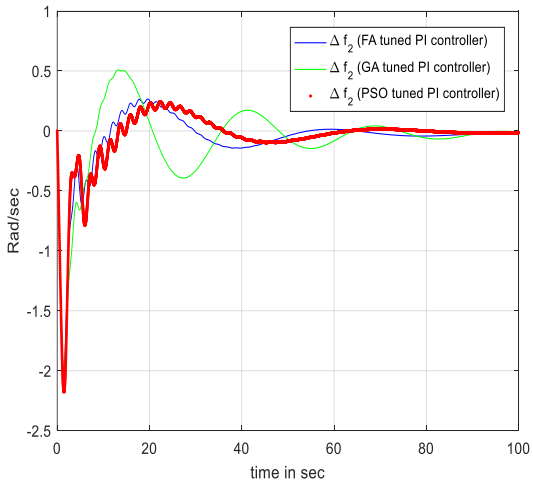

(b) Load Frequency of Area 2

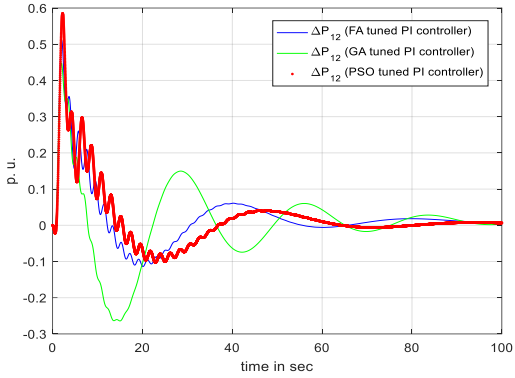

(c) Tie-line Power Flow

Fig. 3: Perturbed response of the system for Case II

Fig. 2 and 3 show the perturb response of all the state variables for both the hydro and thermal area subjected to any change in the loading in the demand side. Case I has been shown in the detail with Table I (optimum parameters of PI controller) and also the settling time and overshoot of all the state variables in Table III. Analysis of Case II is shown in Fig. 2 (perturbed response of state variables), Table II (optimum parameters of PI controller) and settling time and overshoot also in Table III. Eigenvalues for both the cases have been shown in Table IV. By observing the above responses, it can be concluded that among all three optimization methods used for the tuning the PI parameters through simulation, PSO shows the better response with respect to the settling time and overshoot. Also the ITAE performance indices is showing better capability of handling the system responses and bring them back to the stability as compared to ITSE performance indices.

Table II: Tuned Parameters of PI Controllers with different optimization techniques- Case II

O.T	Time	K_{p1}	K_{p2}	K_{i1}	K_{i2}	ITAE
FA	93.217	0.504	5.755	0.758	0.033	$8.46x10^3$
GA	95.67	0.766	11.853	0.177	0.001	$2.03x10^4$
PSO	92.474	0.9588	4.235	0.941	0.059	$8.14x10^3$

Table III: Settling time and Overshoot of the test system

		Case Study (ITAE)		Case Study (ITSE)	
O.T	**State Variables**	**Overshoot/ undershoot**	**Settling time (*msec*)**	**Overshoot/ undershoot**	**Settling Time (*msec*)**
FA	Δf_1	-1.2	80	-01.70	85
	Δf_2	-1.6	78	-02.00	82
	ΔP_{12}	0.42	81	0.52	87
GA	Δf_1	-1.3	85	-01.85	80
	Δf_2	-1.6	90	-02.00	83
	ΔP_{12}	0.42	95	0.45	90
PSO	Δf_1	-1.18	60	-01.50	63
	Δf_2	-1.70	61	-2.20	62
	ΔP_{12}	0.45	64	0.58	65

IV. Conclusion and Future Scope

The hydrothermal power plant is analyzed and implemented in MATLAB. The system parameter is

controlled using PI controller whose parameter is optimized using PSO, FA and GA algorithms. All these algorithms evaluate controller parameter using various cost function such as Integral Time multiplied by Square Error (ITSE) and Integral-Time Absolute Error (ITAE). By observing the above responses, it can be concluded that among all the three optimization techniques used to find the optimal parameters of PI controllers, PSO shows the better response with respect to the settling time and overshoot.

REFERENCES

[1] D. K. Gupta, R. Naresh and A. V. Jha, "Automatic Generation Control for Hybrid Hydro-Thermal System using Soft Computing Techniques," *2018 5th IEEE Uttar Pradesh Section International Conference on Electrical, Electronics and Computer Engineering (UPCON)*, Gorakhpur, 2018, pp. 1-6.

[2] M. R. I. Sheikh, S. M. Muyeen, R. Takahashi, T. Murata and J. Tamura, "Application of self-tuning FPIC to AGC for load frequency control in multi-area power system," *2009 IEEE Bucharest PowerTech*, Bucharest, 2009, pp. 1-7.

[3] I. C. Report, "Dynamic Models for Steam and Hydro Turbines in Power System Studies," in *IEEE Transactions on Power Apparatus and Systems*, vol. PAS-92, no. 6, pp. 1904-1915, Nov. 1973.

[4] F. P. Demello et al., "Hydraulic- turbine and turbine control- models for system dynamic studies", *IEEE Tran. on Power Systems*, vol. 7.1, pp. 167-179, 1992.

[5] J. Nanda, B. L. Kaul, "Automatic generation control of an interconnected power system", *Proc IEE*, vol. 125, no. 5, pp. 385-390, 1978.

[6] M. L. Kothari, B. L. Kaul, J. Nanda, "Automatic generation control of hydrothermal system", *J. Inst. Eng. India*, pp. 85-91, 1980

[7] M. L. Kothari, J. Nanda, P. S. Satsangi, "Automatic generation control of hydrothermal system considering generation rate constraint", *Journal of Inst. Eng. India*, vol. 63, pp. 289-297, June 1983.

[8] J. Nanda, M. L. Kothari, P. S. Satsangi, "Automatic generation control of an interconnected hydrothermal system in continuous and discrete modes considering generation rate constraints", *Proc. Inst. Elect. Eng.*, vol. 130, no. 1, pp. 17-27, 1983.

[9] A. A. F. M. Carneiro and D. Silva Filho, "Fuzzy logic applied to operation rules for large hydrothermal power systems," *POWERCON '98. 1998 International Conference on Power System Technology. Proceedings (Cat. No.98EX151)*, Beijing, China, 1998, pp. 918-922 vol.2.

[10] M. R. I. Sheikh, S. M. Muyeen, R. Takahashi, T. Murata and J. Tamura, "Application of self-tuning FPIC to AGC for load frequency control in multi-area power system," *2009 IEEE Bucharest PowerTech*, Bucharest, 2009, pp. 1-7.

[11] J. F. Villa Sierra, G. F. Paez Mendez and J. A. Perez Arenas, "Angle controlled power plants for PMU based AGC. A new AGC thecnology, based on the äV and äQ controlled nodes concept and PMU triggered load shedding," *2014 IEEE PES T&D Conference and Exposition*, Chicago, IL, 2014, pp. 1-1.

[12] B. Appasani and D. K. Mohanta, "Co-Optimal Placement of PMUs and Their Communication Infrastructure for Minimization of Propagation Delay in the WAMS," in *IEEE Transactions on Industrial Informatics*, vol. 14, no. 5, pp. 2120-2132, May 2018.

[13] A. Khodabakhshian, N. Golban, "Unified PID design for load frequency control", *proc. International Conference on control application*, vol. 2, pp. 1627-1632, 2004.

[14] K. S. S. Ramakrishna, T. S. Bhatti, "Load frequency control of interconnected hydro-thermal power systems", *Int. Conf. on Energy and Environment ICEE*, 2006

[15] S. Prakash, S K Sinha, "Artificial intelligenct and load frequency control of interconnected power system", *Int. Jour. of Computer Science & Emerging Technologies*, pp. 377-384, December 2010.

[16] Fini, M. Hajiakbari, G. R. Yousefi, H. H. Alhelou, "Comparative study on the performance of many-objective and single-objective optimisation algorithms in tuning load frequency controllers of multiarea power systems", *IET Generation Transmission & Distribution*, vol. 10, no. 12, pp. 2915-2923, 2016.

[17] Rajendra Khadanga, Amit Kumar, "A Novel Hybrid Adaptive gbest Guided Gravitational Search and Pattern Search Algorithm for Automatic Generation Control of Multi Area Power System", *IET Gen. Trans. & Distribution*, 2016.

[18] R.Eberhart, J. Kennedy, "Particle swarm optimization", *Proceedings of the IEEE Int. Conf. on Neural Networks*, December 1995.

[19] Davis, Lawrence. "Handbook of genetic algorithms." 1991.

[20] Yang, Xin-She. "Firefly algorithms for multimodal optimization." *International symposium on stochastic algorithms*. Springer, Berlin, Heidelberg, 2009.

Proceedings of the Fourth International Conference on Communication and Electronics Systems (ICCES 2019)
IEEE Conference Record # 45898; IEEE Xplore ISBN: 978-1-7281-1261-9

A SURVEY ON MESSAGE QUEUING TELEMETRY TRANSPORT (MQTT) PROTOCOL OF INTERNET OF THINGS (IOT)

Lokesh A R
PG student, Dept. of E and C
JSS Science and Technological University
Mysuru-06
arlokesh8@gmail.com

Shashidhar R
Assistant Professor, Dept. of E and C
JSS Science and Technological University
Mysuru-06
shashidhar.r@sjce.ac.in

Abstract— Fastest revolution among the region of information communication technology with digital things forcing fastest formation of IoT over the world. In IoT, communication is considered either by Pushing or Polling protocol. Push protocol is more suitable for IoT devices because of its light-weight and high productivity. There are many Push protocols available for IoT such as XMPP, MQTT and AMQP in which MQTT is most widely used. To ensure reliability of message transmission, MQTT supports three levels of QOS. The main feature of MQTT is its light-weight and bandwidth efficiency. MQTT can be designed by using many Brokers, with each broker has its own restriction. This paper provides necessary information about the MQTT architecture, brokers and issues related to MQTT.

Keywords— Internet of Things, Push Protocol, Message Queuing Telemetry Transport, Publish/Subscribe

1. INTRODUCTION

The network of smart devices approach was discussed in 1982, with a revised Coke machine at Carnegie Mellon University comely the first internet connected machine, in a position to report its catalogue and whether newly loaded drinks were cold. However the word "Internet of Things" is molded by British entrepreneur Kevin Ashton, executive director of Auto-ID centre in the year 1999. Nowadays, communicating between similar objects or dispatching instructions to home appliances is never thought anymore with evolution of wireless transmission mechanism, small-scale and less-potential appliances [2].

In IoT, transmission of data between different devices is important because an IoT appliance has to deliver an instruction to a further appliance to manage system [1]. Compared to polling protocol, Push protocol can be the best protocol for the communication of data for IoT appliances, since it is available in poor bandwidth network. MQTT, XMPP and CoAP protocol were implemented through these push message services [6]. These protocols are applicable according to different situations [5]. In particular, MQTT has been utilized as part of many IoT gadgets and instant message delivery systems because it was calculated to be working on little potentiality [2]. The rest of the article is analysing about introduction to MQTT protocol, architecture of MQTT protocol, utilization of MQTT protocol, brokers of MQTT and at last gives the termination of MQTT protocol.

II. MQTT PROTOCOL

Publish/Subscribe protocol is also called as MQTT protocol which was discovered in 1999 by IBM. MQTT was planned to send a data accurately under the long network delay and low-bandwidth network condition [34].

In MQTT, communication is based on changing of control packets in a specify manner [7]. There are fourteen control packets and each hold three section as shown in figure 1.

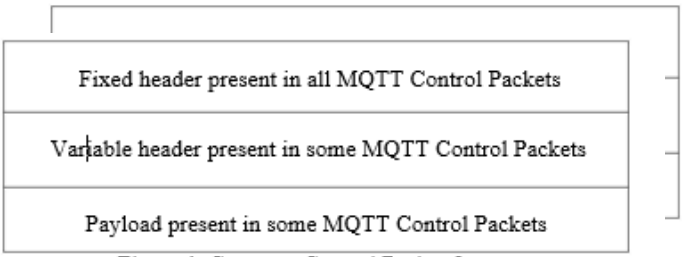

Figure 1. Common Control Packet format

A. MQTT concepts:

1) Publish/subscribe: In MQTT protocol, the client publishes messages to the subscribed topics and on other side the subscriber will be subscribed to those topics. Here, the topics can be used in order to differentiate the subscribers and this can be referred as Publish/Subscribe model [8].

2) Topics and subscriptions: In MQTT, the topics is used as a id for the subscriber and the client sends the data to that topic and the subscriber subscribes to that topics will receives the messages . The Subscriptions of topics can be express, that restricts the data which are collect to the particular topic [8]. Topics contain two wildcard level, to get data for a range of related

topics.

3) Quality of service levels: This protocol describes the Quality of Service (QoS) levels that are a deal within two parties of a message with respect to the assurance of distribution of data [2]. It supports three level of Quality of Services which are narrated beneath.

a) QoS0 (At most once): The message is sent at most once and it does not provide guarantee delivery of a message.

b) QoS1 (At least once): The data is sent at least once and it is possible to deliver a message more than once by setting the value of duplicate flag by 1.

c) QoS2 *(*Exactly once): The message is sent exactly once by using 4-way handshaking [9].

4) Retained messages: The information will be kept back in the broker after publishing it to all available clients. At the point, if a new subscriber gets subscribed to the same topic then the same information will be sent to the new customer [8].

5) Clean sessions and reliable connections: At the point when a subscriber associates with the broker, clean session association is considered as permanent, if its value is false. In this task, consecutive messages which come out conveying a highest QoS assignment are reserved for delivery when the association is resumed [10]. Use of these flag is optional.

6) Wills: A client tells the broker that it contains a will (message) which is need to be distributed to a particular topic or topics in case of a unantici-pated detach [8]. These will is especially valuable in the system such as security or alarm settings where managers instantly notified just as a sensor has extinct connection with the system.

III. MQTT ARCHITECTURE

The MQTT architecture splits into two main components as seen in figure 2. Each element is narrated beneath.

1) Client: The main work of the client , either can be a publisher or the subscriber to the broker and performs the following things as listed below[7]:

- ∑ Sends data to the broker.
- ∑ Subscribes to the broker in order to get the messages from the broker published by the client.
- ∑ Unsubscribe to extract within subscribed content..
- ∑ Can remove the connection with the broker.

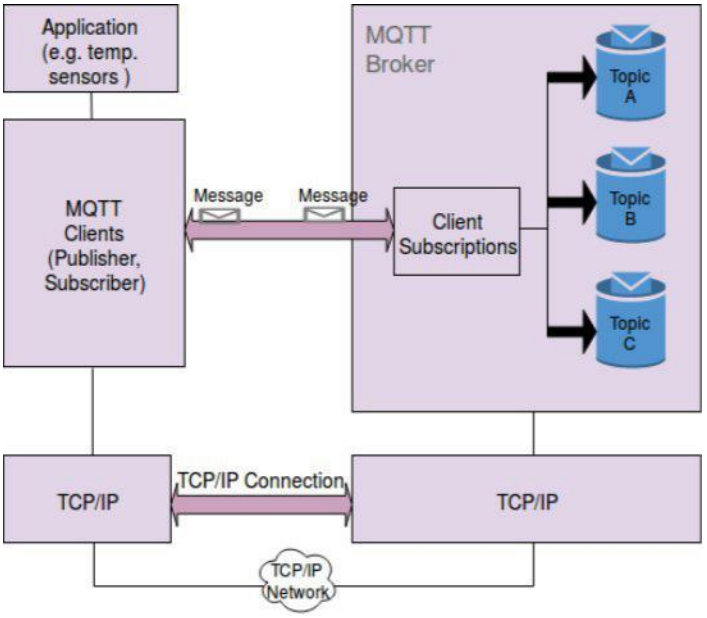

Figure 2. MQTT Architecture

2) Broker: Broker act as a server between the publisher and subscriber, where the client publishes the messages to the broker and the subscriber subscribes to the broker will receive the messages. The function of the broker is described below[7]:

- ∑ Broker will acquire the request from the client.
- ∑ Also receives the published messages from the users
- ∑ Broker also processes the requests like Subscribe and Unsubscribe within the users.
- ∑ The broker sends the messages to the interested subscribers after receiving the messages from the Publisher.

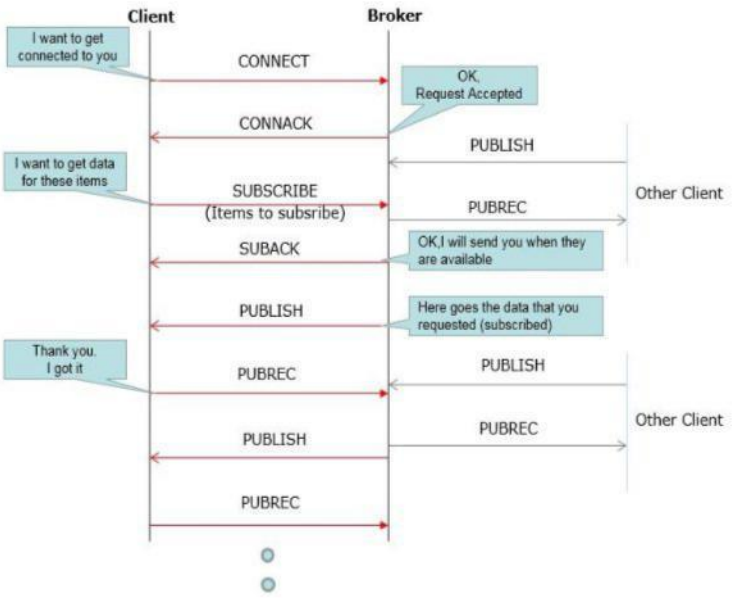

Figure 3. MQTT operation

IV. WHERE TO USE MQTT

MQTT can be used in many applications which are given in details below [8].

1) Healthcare*:* By using an MQTT, a healthcare association is required to create a flexible checking solution. Following are the arrangement expected to address of victim care:

- ∑ Keeping the track of victims besides they go away from the clinic.
- ∑ Upgrading the effectiveness of subsequent tests.
- ∑ Achieving advanced industry information catch principles.

The organization worked with IBM to make an answer in which an MQTT customer is inserted in a home observing machine that gathers diagnostics at whatever point the victim is in nearness to a base system. Then it forwards the indicative information through the web to the main domain, which is given to an application which analyses the measurements and aware the healthcare team if there are hints the victim perhaps carrying trouble. It spares cash for the association also its victims, as there is constrained requirement for victims to go hospital for regular check-ups if they are doing fine.

2) Energy and utilities: A service organization was confronted with increasing expenses to deliver power among with rising interest for electricity by their client root, which was not able, normally, to spend forever expanding amounts. Therefore instead of quickly carried out generation charges that their clients possibly couldn't spend, the organization first looked for an answer for decrease general request for power by putting smart meters in clients' apartments to remotely manage the application of definite power absorbing device. In any case, the arrangement expected to minimize utilization of accessible information network, for that the organization salaried according to the quantity of information transferred.

Making of Virtual power plant (VPP) was the arrangement which sits between the organization's producing origins and their clients. Smart meters gather use information for the different devices which are utilized there in-home apartment. At that point, apartment gateway examines, furnished with a progressed MQTT customer, distribute the utilization information to the VPP at normal interval throughout the nearby cell phone arrange.

3) Social Networking: A long range interpersonal communication organization experienced latency issues during transferring information. The strategy the organization utilized to deliver data was stable yet time-consuming, and if it remained to utilize the similar mechanism then the solutions were restricted [11]. Another structure for a constant association among the servers lacking absorbing more battery power was required, that is basic to clients of the organization's civic communication site.

Using MQTT protocol the organization's designers tackled the issue in social networking. With keeping up a MQTT association also directing data via MQTT's conversational channel (chat pipeline), the organization was capable to accomplish data distribution by speeds of 1×105 microseconds, instead of several minutes.

V. BROKERS OF MQTT

The MQTT broker is the heart of each MQTT arrangement. It provides connecting link between applications or physical devices and enterprise systems. Brokers are in charge of subscription, determined sessions, missed messages and general security, including authentication and authorization. The follow table describes mostly used brokers with their features and limitations [5].

Table 1:
Brokers with features and limitations

Broker	About	Features	Limitations
Mosquitto	It supports MQTT version 3.1 and it is an open source.	- All QoS - Authentica-tion - Bridge - Dynamic topics - Web sockets	- Clustering - Fewer Configuration Not allow simultaneous connection with using authenti-cation
RSMB (Really small message broker)	It is a tiny broker which supports V3 and V3.1.	- All QoS - Bridge - Dynamic topics	- Security - Web sockets - Cluster
MQTT.js	It is an MQTT broker among client/server API production recorded in JavaScript.	- All QoS - Dynamic topics - Web sockets - SSL	- Bridge - Authenti-cation - Cluster
HiveMQ	HiveMQ empowers organization to attach all devices and services with nominal effort by victimization the de-factor	- All QoS - Bridge - Dynamic topics - Web sockets - TLS/SSL - Cluster	- Open Standard - Performance degradation because of TLS

VI. MQTT DRAWBACKS

MQTT has its own restriction, which can be narrated as shown below:

1) Message Expiry: Right now in MQTT there is no message expiry, so in the event that you put a message in a broker and then forget to gather it or nobody ever comes to pick it up, it remains there forever. As a result, the broker is overloaded with messages and it degrades the overall performance.

2) Security: MQTT protocol provides username and password for authentication .So security in MQTT depends on the use case and selection of broker [19]. Mostly brokers provide security based on TLS, but TLS infect the improvement.

3) Ordering: The key challenges for a reliable data transmission organization in IoT environment are ordering messages and resending messages which lost during transmission. MQTT provides guaranteed delivery of messages, but maintain ordering of messages in MQTT is a challenging task.

4) Priority: MQTT does not support a feature called priority of messages. If any system has more important data then it must be immediately available to all the subscribers, for example the data which is gathered from fire alarm system is more important than temperature or pressure sensor data so it must be available first to all receivers. So for that priority of messages are required then sending data in order.

VII. CONCLUSION

IoT is assumed to provide advanced connectivity of services, devices and systems which is above machine-to-machine associations (M2M), which includes more number of applications, protocols and domains. The significance and evolution of MQTT in IoT, operation of MQTT, MQTT uses, different brokers used in MQTT and also discuss about the limitations of MQTT.MQTT can be used with minimum bandwidth along with less memory in IOT application.

REFERENCES

[1] Kraijak, S., & Tuwanut, P. (2015, October). A survey on internet of things architecture, protocols, possible applications, security, privacy, real-world implementation and future trends. In Communication Technology (ICCT), 2015 IEEE 16th International Conference on (pp. 26-31). IEEE.
.

[2]. Hwang, H. C., Park, J., & Shon, J. G. (2016). Design and implementation of a reliable message transmission system based on MQTT protocol in IoT. Wireless Personal Communications, 91(4), 1765-1777.

[3] Singh, Meena, et al. "Secure mqtt for internet of things (iot)." Communication Systems and Network Technologies (CSNT), 2015 Fifth International Conference on. IEEE, 2015

[4] Van Kranenburg, R., & Bassi, A. (2012). IoT challenges. Communications in Mobile Computing, 1(1), 9.

[5] Luzuriaga, J. E., Perez, M., Boronat, P., Cano, J. C., Calafate, C., & Manzoni, P. (2015, January). A comparative evaluation of AMQP and MQTT protocols over unstable and mobile networks. In Consumer Communications and Networking Conference (CCNC), 2015 12th Annual IEEE (pp. 931-936). IEEE.

[6] Banks, A. and Gupta, R,"MQTT version 3.1.1," OASIS Standard, 2014.

[7] Prada, A., & dkk, "Communication with resource-constrained devices through MQTT for control education," 11th IFAC Symposium on Advances in Control Education ACE, pp 150-155, Bratislava, Slovakia, 2016.

[8] ISACA Volunteer Member, "Cybersecurity Fundamentals Study Guide," ISACA, 2015.

[9] M. M. Hossain, M. Fotouhi and R. Hasan, "Towards an Analysis of Security Issues, Challenges, and Open Problems in the Internet of Things," *2015 IEEE World Congress on Services*, New York City, NY, 2015, pp. 21-28.

[10] M. Iqbal and M. Bayoumi, "Secure End-to-End key establishment protocol for resource-constrained healthcare sensors in the context of IoT," International Conference on High Performance Computing & Simulation (HPCS), pp. 523-530, 2016.

[11] W. Stallings, "Cryptography and Network Security Principles and Practice 7th Edition," Pearson, England, 2017.

[12] S. Alasmari and M. Anwar, "Security & Privacy Challenges in IoT-based Health Cloud,"

International Conference on Computational Science and Computational Intelligence, pp. 198-201, 2016.

[13] Caltum, E. and Segal, O, "Exploitation of IoT devices for Launching Mass-Scale Attack Campaigns," Akamai Threat Research, October 2016.

[14] C. Bormann, M. Ersue, and A. Keranen, " RFC 7228 Terminology for Constrained-Node Networks," IETF, May 2014.

[15] J. King and A. Ismail,"Distributed Security Mechanism for Resource Constrained IoT Device," Informatica 40, pp 133-143, 2016.

[16] Anonym. (2016, January 15). *Iot Security Awareness*. InfoSec Institute [Online]. Available: http://resources.infosecinstitute.com/iot-security-awareness/

[17] Anonym, "IoT Security: Protecting The Networked Society," Ericsson White Paper, February 2017.

[18] Ernst and Young, "Mobile device security: Understanding vulnerabilities and managing risks," Insight on governance, risk and compliance, January 2012.

[19] Bitdefender, "Security Awareness in the Age of Internet of Things," A Bitdefender Study White Paper, 2016.

[20] Anonym, "Internet of Things research study," Hewlett Packard Enterprise, 2015.

[21] F. Alisherov, and F. Sattarova, " Methodology for Penetration Testing", International journal of Grid and Distributed Computing, Vol 2 No 2, June 2009.

[22] L. Markowsky and G. Markowsky, "Scanning for Vulnerable Devices in the Internet of Things," The 8th IEEE International Conference on Intelligent Data Acquisition and Advanced Computing System: Technology and Applications, September 2015.

[23] L. Lundgren, "Light Weight Protocol Serious Equipment Critical Implications", Defcon 24, 2016.

[24] H. R. Zeidanloo and A. A. Manaf, "Botnet Command and Control Mechanisms," 2009 Second International Conference on Computer and Electrical Engineering, Dubai, 2009, pp. 564-568.

[25] M. Singh, M. A. Rajan, V. L. Shivraj and P. Balamuralidhar, "Secure MQTT for Internet of Things (IoT)," 2015 Fifth International Conference on Communication Systems and Network Technologies, Gwalior, 2015, pp. 746-751.

[26] A. Mektoubi, H. L. Hassani, H. Belhadaoui, M. Rifi and A. Zakari, "New approach for securing communication over MQTT protocol A comparison between RSA and Elliptic Curve," 2016 Third International Conference on Systems of Collaboration (SysCo), Casablanca, 2016, pp. 1-6.

[27] S.Katsikeas, "A lightweight and secure MQTT implementation for wireless sensor node", 2016 Technical University of Crete. Proc. EECSI 2017, Yogyakarta, Indonesia, 19-21 September 2017

[28] S. Nath, "Senseweb: An infrastructure for shared sensing," in US-Korea Conference on Science, Technology, and Entrepreneurship (UKC).

[29] C. Rodríguez-Domínguez, K. Benghazi, M. Noguera, J. L. Garrido, M. L. Rodríguez, and T. Ruiz-López, "A communication model to integrate the requestresponse and the publish-subscribe paradigms into ubiquitous systems," Sensors, vol. 12, no. 6, pp. 7648–7668, 2012.

[30] Swagger, "A framework for api definition," Available: https://swagger.io.

[31] S. Tarkoma, Publish/Subscribe Systems: Design and Principles. John Wiley& Sons, 2012, ch. 7. Distributed Publish/Subscribe.

[32] J. Taylor, H. S. Hossain, M. A. U. Alam, M. A. A. H. Khan, N. Roy, E. Galik, and A. Gangopadhyay, "Sensebox: A low-cost smart home system," in Pervasive Computing and Communications Workshops (PerCom Workshops), 2017 IEEE International Conference on. IEEE, 2017, pp. 60–62. References 48

[33] D. Thangavel, X. Ma, A. Valera, H.-X. Tan, and C. K.-Y. Tan, "Performance evaluation of mqtt and coap via a common middleware," in Intelligent Sensors, Sensor Networks and Information Processing (ISSNIP), 2014 IEEE Ninth International Conference on. IEEE, 2014, pp. 1–6.

[34] X. Tong and E. C. Ngai, "A ubiquitous publish/subscribe platform for wireless sensor networks with mobile mules," in Distributed Computing in Sensor Systems (DCOSS), 2012 IEEE 8th International Conference on. IEEE, 2012, pp. 99–108.

[35] M. Uehara, "A case study on developing cloud of things devices," in Complex, Intelligent, and Software Intensive Systems (CISIS), 2015 Ninth International Conference on. IEEE, 2015, pp. 44–49.

[36] B. Weiss, U. Hunkeler, A. Munari, W. Schott, and L. Truong, "A publish/subscribe messaging system for wireless sensor communication."

[37] A. Zigbee, "Zigbee specification," ZigBee document 053474r13, 2006

Proceedings of the Fourth International Conference on Communication and Electronics Systems (ICCES 2019)
IEEE Conference Record # 45898; IEEE Xplore ISBN: 978-1-7281-1261-9

A Review on tumor segmentation techniques for Magnetic Resonance Images

R. Sakthi prabha[1], Dr. M. Vadivel[2]

Research scholar, Sathyabama Institute of science and Technology, chennai[1]

Associate professor, Vidhya Jyothi Institute of Technology, Hyderabad[2]

ABSTRACT

Segmentation is defined as the process of splitting or dividing a digital image into multiple region. It plays a vital part in the field of medical image processing. At current scenario, tumor is represented as one of the most quite common dangerous disease found among the human beings. In general, tumor is defined to be an abnormal mass of tissue which can be either looks like a solid or fluid filled substance For detecting and fixing this kind of tumor different types of imaging methods are available, such as Computed Tomography (CT scan analysis), Positron Emission Tomography (PET scan analysis) and Magnetic Resonance Imaging (MRI scan analysis).. When a comparison is done between all these imaging modalities, each imaging modalities has its own individual specific mechanism in which the MRI imaging modality (scan detection) is considered to be one of the best defined system for its effective output. The target of the segmentation process is to define or to locate the tumor region and the extension of the tumor core, where it is said to be the active tumorous region. Even though several techniques has been implemented in image segmentation process, but still there is no accurate solution for image segmentation issue. Hence this survey explains briefly about various different types of image segmentation techniques which are used for MRI images.

Keywords- Segmentation, MRI image, Tumor FLAIR, SLIC

I. INTRODUCTION

Generally, segmentation process is classified into three different types such as manual segmentation, semi-automatic segmentation and fully automated segmentation. In manual segmentation as the name suggests, the entire work is done with the help of human intervention the work is done manually. Manual segmentation is considered to be one of the most easiest methods, whereas the accuracy level is less, with more time consumption Here the radiologist or the experts whoever does this work need not only have the present information from the image but also they need some more additional information related to the particular medical area. Whereas in semi – automatic segmentation, half of the work is done with the help of human intervention.

As we make a comparison between the previous methods the semi-automatic segmentation is considered to be the superior one, whereas the accuracy level is improved and the time consumption is also drastically reduced. And in fully automated segmentation method, the entire work is done with the absence of human intervention. So here we use some soft computing tools, human intelligence, etc., while a comparison is made between all these three various types of segmentation methods, fully automated segmentation is considered to be the superior one where it produces a high accuracy level, with drastically reduced time consumption and also thereby reducing the probability of error rate.

Even though several segmentation method has been implemented for tumor segmentation, but still there is no accurate solution for the segmentation problem. Hence the ultimate aim is to identify the tumorous core region at the same time to segment tumor core region with the extension of the tumorous core region namely the active tumorous core region. In addition to this we have various factors to be considered while performing the segmentation process such as removal of noise, spotting the specific region with less intensity boundaries, less prediction of tiny particles, etc., A wide variety of image segmentation techniques are available which produces more effective segmentation output. The remaining paper is organized as follows: In section II the literature survey with various techniques are discussed, which is followed by various Image segmentation techniques in section III and thereby section IV provides the overall conclusion about the related work.

978-1-7281-1261-9/19/$31.00 ©2019 IEEE

II. RELATED WORK

Kavitha A.R et.al [1] proposes a algorithm with the help of fuzzy initialization and seeded region growing(GFSMRG) method using neural network algorithm (BPNN). In this framework the problem addressed is to improve the level of accuracy in the identification of tumor thereby to improving the execution faster for performing the segmentation process. The methodology adopted here is, pre-processing as the initial step followed by the segmentation process and then the segmented output undergoes feature extraction and finally Classification is done. Hence in the proposed framework it's been found that it is proposed and thereby, the parameters like accuracy and time complexity is considerably improved and hence the achievement of the proposed work was verified by both quantitatively and qualitatively.

Bonte S et.al [2] defines a proposed framework in this paper with random forest model combined with the three dimensional co-ordinates and undesirable features analyzed and detected on the various relaxation times such as T1 and FLAIR Magnetic Resonance Imaging. Here, first the RF model determines and finds out the probability of the tumor class and the normal one. Similarly as a second step the algorithm is applied for the tumor segmentation process. This technique is suitable much for the high grade glioma. Here the propose method is trained on BRATS2017 database and validated. In this framework the T1 and FLAIR MRI image sequence are considered, since it provides much complementary information. The steps involved here is; first pre-processing is done wherein transforming brain scan into high dimensional feature vectors for every voxel. As a second step the obtained features (voxel) are now applied with Random Forest algorithm which determines and finds out the voxel based probabilities for the tumor tissue and the healthier one. And finally, the input is provided based on the Gaussian Mixture Model(GMM) probabilities. One of the parameter named dice score has been achieved of about 70%. Hence in this paper two types of features are extracted and analyzed they are advanced texture feature and abnormality feature

Jothi G. and Hannah Inbarani H [3] proposesa new framework algorithm, Hybrid Supervised algorithm namely Tolerance Rough Set Firefly based Quick Reduct (TRSFFQR) framework isproposed and much suitable and applicable for the MRI images. Hence two different types of hybridization techniques are applied in this work namely Tough Rough Set(TRS) and Firefly algorithm(FA). The steps involved are; First pre-processing is done. This step includes increasing the size of the image and thereby decrementing the noise without disturbing any of the relevant features. Once the preprocessing stage has been completed, the output image obtained from the above process is subjected for skull stripping process. Hence once skull stripping is done, the output hence carried is followed with various different types of segmentation techniques. And finally the feature extraction process is done for the segmented output image. The feature extraction process is done by using two methods. They are; Texture based feature and Intensity based feature. The proposed framework is also termed to be supervised features selection algorithm (TRS and FA). Finally a comparison is done with various algorithm and it's been concluded that Tolerance Rough Set (TRS) can be used as one of the real time medical image applications due to the various special features of it like its simplicity, consistency and Robustness.

Zaka Ur Rehmana et.al, [7] proposes a Random Forest (RF) algorithm based on regional classifier is considered. The Region based feature parameters considered is statistical, Textron histogram and fractal feature. In this proposed work the major parameter found is pixel level accuracy, Dice score, precision and specificity. The work flow is done in both training and testing phases. Hence the image is splitted into different square shaped patches named as super pixel of equal size with the help of the technique named Simple Linear Iterative Clustering (SLIC) and also finally feature extraction also can be done. The workflow for training phase of this paper includes, pre-processing as the initial stage and then feature extraction then feature selection and normalization. Then the output is fed for class balancing and further classifier training process is done. Similarly, in case of testing phase initially pre-processing is done followed up with feature extraction and the training mode is classified their by segmenting the tumor using super-pixel classification.

Chandan Singh and Anu Bala [4] addressed segmentation of MRI image has become a tedious job nowadays. It's mainly because of the Rician noise and intensity in homogeneities in the MRI images. The previous methodologies completely deals with these issues under spatial domain, and while dealing the case when the noise is removed from the sample image, some of the image data content is also lost, this must be rectified. As moment domain to be one of the factor is completely dealt in this proposed

978-1-7281-1261-9/19/$31.00 ©2019 IEEE

framework. So they have chosen Zernike moments which use the local and nonlocal information's, which discards the different types of noises from MRI images. Hence this algorithm can be applied to the various types of tissues available in brain such as Grey Matter (GM), white Matter (WM) and Cerebro Spinal Fluid (CSF).The proposed algorithm on the overall it's called to be intelligent knowledge driven approach. There is no human intervention during the segmentation process. Here, Local Zernike method (LZM) based on non-local means fuzzy C-means (LZM-UNLM-FCM) approach. The proposed work is compared with the existing work and thereby which gives improved segmentation accuracy level. LZM reduces the rician noise by holding the fine structure, edges and the other details available in the moment domain.

Kai Roman Laukamp et.al [5] defines that meningiomas is a kind of tumor that always are found on membranes, which covers the brain and spinal cord which is inside the skull. As stated by World Health Organization (WHO) the abnormal mass of tissue are categorized into different types of grades such as grade I, grade II, and grade III. In which grade II and grade III are considered to be at increased risk stage. Grade III are found often with irregular size and shape. The problem addressed in this paper is eventhough several type of techniques are available but still there is no radiological criteria for categorizing the grade I and grade II lesions. The proposed algorithm in the paper is an automatic detection and segmentation using deep learning mode is proposed. Angu lakshmi and Lakshmi priya [6] defines a newly proposed framework which is based on walshhadamard texture feature for using in multi modal brain tumor segmentation which is used for MRI images.

Mahmooda,b,A et.al [8] proposes a fully automated unsupervised segmentation framework method is implemented in MRI images. In this proposed frame work the technique provides high degree of accuracy level while performing the segmentation on both the synthetic and real T1 MRI image. The proposed method is validated for varying noise level aswell as spatial intensity level. The performance is also compared with various different types of segmentation toolboxes. The following are the steps involved. They are, pre-processing wherein brain extraction is done followed with bias field correction and the Bayesian AMS is applied. Nameirakpam Dhanachandra et.al, [9] proposes an algorithm that comprises of a group of techniques namely partial contrast stretching, subtractive clustering, etc., They observed that once the segmentation is done a comparison is made between the existing and proposed and it's been found that the quality level of the segmented output(proposed framework) seems to be higher than the existing one. It is also verified and checked with the help of various parameters such as RMS and PSNR.

Sangeetha K Siri, Mrityunjaya V Latte [10] applied neutrosophic set concept to image processing along with Chan -Vese model. The image is first read, noise is reduced using a median filter and a random section of liver is segmented for which a neutrosophic set is generated. They observed that the proposed algorithm is useful for the detection of tumor within the organ aswellas it is used for detecting the boundary of it. The important parameters such as its volume and area can be found which is used in diagnosis and liver transplantation. Hussain Alahmer, Amr Ahmed [11] proposed a new technique using multiple Region of Interest. Hence the liver is segmented with the help of fuzzy C-means clustering algorithm liver is segmented with the help of binary liver mask and divided into three classes. They observed whether the tumor is benign and malignant with the help of an proposed automated approach system and thereby the border area accuracy improved to 98%.

III. IMAGE SEGMENTATION TECHNIQUES

The main objective of image segmentation technique is, an image can be segmented based on the variation in intensity values, which is of discontinuity or similarity [8]. An image can be segmented wisely based on the sudden variations in the intensity levels or else an image can be segmented based on some of the segmentation methods which is widely used are classified as follows;

1. Threshold based segmentation method
2. Edge based segmentation method
3. Region based segmentation method and
4. Cluster based segmentation method

Generally all these method is done based on the following two types. They are;

1. Boundary based segmentation and
2. Region based segmentation.

3.1 Threshold based segmentation

Threshold based segmentation paves a major role in the image segmentation due to its simplicity of implementation, user friendly nature etc., The steps

978-1-7281-1261-9/19/$31.00 ©2019 IEEE

involved in this type of segmentation is pre-processing, followed by the segmentation process and as a final step the segmented output is given to the filtering process to get a clear segmented noise free output. Here the images can be divided into multiple numbers of regions based on the intensity values [12]. For example if a bright object is placed in front of a dark background, the object(region) can be extracted easily by identifying the intensity values. With the help of the provided technique, the given sample data which is to be performed. Hence the threshold based segmentation process is done successfully due to the intensity level of the pixel.

3.2 Edge based segmentation

In the given sample image an edge based segmentation is done with the help of sudden change either increase or decrease in the pixel intensity which is found closer to the edges. A binary image is obtained as an output for the edge based segmentation thereby edges of the each object in an image is detected and segmented accurately. The edge based segmentation is further classified into two types they are gray histogram and gradient based methods.

3.3 Region based segmentation

Segmentation is defined to be splitting or dividing a single image into multiple number of region. Such kind of splitting an image can be done either by finding out the boundaries between the regions based on the discontinuity in the intensity level between the regions or else the partition can be done with the help of certain criteria. One of the most commonly used segmentation method is Region growing method. The steps involved here is region splitting and region merging. The technique follows by choosing a set of seed points and thereby increasing the region by including neighborhood pixel, based on the value of the threshold, the process will be terminated once all the pixels under same threshold value are grouped together. Region growing technique is especially applied for simple images such as tumors etc.,

In case of region splitting and merging based on some of the properties and conditions an image is splitted into different types of regions. Once the region splitting process is done it is again further merged. At initial step the entire full image is described to be the single image wherein which the factor known as standard deviation is calculated for the internal similarity of the given image(sample data). Based on the variation range the image is divided into multiple number of regions, completely depending on the value of the threshold. The above process can be continued till there is no further splitting can be done. One of the most commonly used data structure for dividing the region is quad tree. The images which comes with contrast distribution of pixels or the images which comes with a great difficulty in differentiating both the foreground and background due to the variation in the intensity level can be used with watershed segmentation technique. In order to determine the weak edges in a given image watershed algorithm can also be used for better output.

3.4 Clustering based segmentation

One of the most commonly used technique in Magnetic Resonance Imaging (MRI) is the clustering method, here each pixels are splitted into multiple number of region[14]. The region is splitted based on the maximum probability range. In the cluster based segmentation the training process of the pixel is done with the help of analyzing the pixel characteristics and its properties.

a) K-means clustering algorithm

Based on the properties of pixel it's been concluded that this algorithm is one of the simplest of the existing algorithms. The clustering based segmentation involves the following steps; initially seed points are fixed for the objects that are grouped together and then assume the objects to a single group which possess the nearest centroid points. Once the objects are fixed again determine the value of the centroid. The K-means clustering algorithm can able to group multiple number of pixel together for a numerous region. Hence this technique is said to be hard clustering, moreover each clusters are separated by a long distance and each one of the pixel is allocated with a membership function, it is termed to be a hard clustering algorithm. Even though the clusters are located in distance all of them belongs to a single group of region

b) Fuzzy C means clustering algorithm

One of the unsupervised method for the analysis of the provided various input images are fuzzy c means clustering. Each and every pixel in an image is assigned a membership function based on the distance from the different cluster center by the clustering algorithm. Whereas the number of pixels which is placed nearer to the cluster head seems to possess higher membership function toward the given pixel. On the other side an algorithm groups various data objects available in an image to a groups of clusters, such algorithm is named as hierarchical

978-1-7281-1261-9/19/$31.00 ©2019 IEEE

algorithm. Whereas in hierarchical algorithm it is not needed to address the required number of clusters to be used in prior or in advance.

Different types of segmentation algorithm are available. They are as follows, fuzzy c-means algorithm, Region growing algorithm, Watershed segmentation and different types of clustering algorithm such as K means clustering algorithm, Fuzzy C means clustering algorithm, Region based segmentation and Threshold based segmentation, and so on. Based on all these segmentation process the following parameters can be analyzed. They are Global consistency error (GCE), peak signal to noise ratio (PSNR), Random Index (RI), variation of information(VOI), Boundary Displacement Error (BDE), Absolute Error (MAE) etc., For the better segmentation results the value of PSNR and RI must be higher and at the same time the parameters like GCE and VOI must be low

The paper presents an overall conclusion about the different types of available existing methodologies for image segmentation. Selection of a proper and exact segmentation technique mostly depends on the type of image used and to which application it's been used. Based on various obtained results it's been said that evaluating the obtained results of image segmentation is considered to be a tedious task. Also so many factors are taken into consideration while an image segmentation is performed, such as contrast, homogeneity, compactness, continuity, etc., there is no algorithm that is always the most accurate. Thereby generating a group of base learners which when combined provides high accuracy. The techniques such as fuzzy logic and Artificial Neural Network (ANN) is found to be the most suitable for image segmentation technique

In this paper, several existing techniques which is related to the brain tumor detection and segmentation is found and discussed for various brain MRI images. The various existing segmentation techniques like threshold based segmentation, region based segmentation, edge based segmentation and cluster based segmentation techniques are described for the removal of active tumorous core region from the MRI images. Some of the methods which gives better output results for intensity based thresholding techniques but gives very poor output for the high contrast images. Whereas for high contrast images region based segmentation is considered to be the best and superior one for providing the better output. When compared with all the other segmentation, edge based segmentation obtains an efficient output irrespective of noisy. If noise is of a major concern then clustering based segmentation is chosen to be one of the best, simple and highly efficient method for providing better output.

Table no.3.1: comparison between various image segmentation algorithm

S.NO	**YEAR**	AUTHOR NAME	TITLE	REMARKS
1	2017	Mina Esfandiarkarni Amir Hossein Foruzan	A generalised active shape model for segmentation of liver in low contrast CT volume	The proposed work resulted in failure in some of the cases as well as the interpolation resulted in large number of dubious points
2	Published by Springer 2016	Mohammadreza Soltaninejad, Guang Yang,tryphon Lambrou, Nigel Allinson	Automated Brain Tumor Detection And Segmentation Using Super-pixel Based Extremely Randomized Trees In FLAIR MRI	Features like intensity, fractal analysis, curvatures are calculated from each super pixel within the entire brain area
3	May 2016	Kavitha A R, et.al., Article in Imaging Science Journal	Brain Tumor Segmentation From MRI Image Using Genetic Algorithm With Fuzzy Initialization And Seeded Modified Region Growing Method	(i)A genetic based algorithm with back propagation neural network is proposed (ii) Accuracy and time complexity is considerably improved
4	Published by Elsevier 2016	Mohammad Havaei, Axel Davy, David Warde Farley, Antoine Biard,aaron Courville,yoshua Bengio	Brain Tumor Segmentation With Deep Neural Network	(i)As DNN being extremely efficient and highly flexible it can efficiently explore the shape, size and contrast of tumors in brain (ii) It reduces the time consumption
5	March 2019	Zaka Ur Rehmana, Syed S. Naqvi, Tariq M. Khana, Muhammad A. Khanb, Tariq	Fully automated multi-parametric brain tumor segmentation using Super-pixel based classification	(i)Random Forest (RF) algorithm based on regional classifier is considered (ii) Simple Linear Iterative Clustering (SLIC) technique is used (iii) Dice score, precision and specificity is determined

978-1-7281-1261-9/19/$31.00 ©2019 IEEE

6	Published by Elsevier 2016	Vasupradha vijay, Dr.A.R.kavitha, S.Roselene Rebecca	Automated Brain Tumor Segmentation and Detection in MRI using Enhanced Darwinian Particle Swarm Optimization	It overcomes the drawbacks of PSO It achieves a better quantitativerate
7	IEEE Transaction On Medical Imaging 2016	Fuyong Xing, Yuanpu Xie, Lin Yang	An Automatic Learning Based Framework For Robust Nucleus Segmentation	(i)The method is applicable to different histopathology images (ii) Efficiency is analyzed by means of the quality rate, sensitivity, specificity and the accuracy value
8	March 2019	Chandan Singh and Anu Bala	A Local Zernike moment based unbiased non local means Fuzzy C-means algorithm for segmentation of Brain MRI	i)Moment domain to be one of the factor is completely dealt in this proposed framework (ii)Zernike moments which uses the local and nonlocal information's, which discards the different types of noises from MRI images
9	July 2018	Bonte S, Goethals I, Holen R	Machine learning based brain tumor segmentation on limited data using local texture and abnormality	Random forest model calculates the probability of tumor and normal classes

IV CONCLUSION

Hence in case of image processing techniques segmentation process is considered to be one among the most important process. In this review work, various techniques of image segmentation has been discussed for Magnetic Resonance Imaging modalities. Various kinds of algorithms and methods which is used for image segmentation process has been discussed elobaratively. Image segmentation algorithms are mainly focused to improve the efficiency of the detected tumor region. Even though several techniques has been implemented but still there is no accurate solution for image segmentation problem. Hence in future work, it's been concluded to propose a novel technique where in which tumor segmentation process can be done efficiently and accurately irrespective of its location, shape and intensity when compared with the existing techniques, thereby will be helpful for the radiologist in evaluating the MRI to produce accurate results

V REFERENCES

[1]Kavitha A R, Chellamuthu C, "Brain tumor segmentation from MRI image using genetic algorithm with fuzzy initialization and seeded modified region growing method" pg: 285-297, March 2016.

[2]Bonte S, Goethals, Van Holen "Machine learning based brain tumor segmentation on limited data using local texture and abnormality" Comput Bio medical July 2018

[3]Jothi G A, Hannah Inbarani H, "Hybrid Tolerance rough set firefly based supervised feature selection for MRI brain tumor image classification", Applied soft computing pg no:639-651

[4] Chandan Singh, Anu Bala, "A Local Zernike moment based unbiased non local means Fuzzy C-means algorithm for segmentation of Brain MRI", Expert systems with Applications, vol: 118, March 2019, Page: 625-639

[5]Kai Roman Laukamp, Frank Thiele, Georgy Shakirin, David Zopfs, Andrea Faymonville, Marco Timmer, David Maintz, Michael Perkuhn, Jan Borggrefe, "Fully automated detection and segmentation of meningiomas using deep learning on routine multi parametric MRI"

[6]Angu lakhmi, Lakshmi priya, "Walsh hadamard kernel based texture feature for multimodal MRI brain tumor segmentation", Jan 2019

[7] Zaka Ur Rehmana, Syed S. Naqvi, Tariq M. Khana, Muhammad A. Khanb, Tariq Bashir, " Fully automated multi-parametric brain tumor segmentation using Super-pixel based classification", Expert systems with Applications, vol. 118, Page-598-613 March 2019

[8] Mahmooda,b,A. Chodorowskia,b,M. Persson,"Automated MRI brain tissue segmentation based on mean shift and fuzzy C means using a priori tissue probability maps" 2015

[9] Nameirakpam Dhanachandra, Khumanthem Manglem and Yambem Jina Chanu.,"Image

978-1-7281-1261-9/19/$31.00 ©2019 IEEE

Segmentation using K-means clustering algorithm and subtractive clustering algorithm", Eleventh International Multi-Conference on Information Processing IMCIP-2015.

[11] Hussein Alahmera, Amr Ahmeda, "Computer-Aided Classification of Liver Lesions from Images based on Multiple ROI.‖ MIUA", International Conference on Medical Imaging Understanding and Analysis 2016.

[12] G. Evelin Sujji, Y.V.S. Lakshmi, G. Wiselin Jiji, "MRI Brain Image Segmentation based on Thresholding", International Journal of Advanced Computer Research, vol. 3, no. 1, issue 8, pp. 2249-7277, March 2013.

[13] Tatiraju S, Mehta A, "Image Segmentation using k means clustering, EM and normalized Cuts", University Of California Irvine

[10] Sangeeta K Siri, Mrityunjaya V, "Latte Computer methods and programs in biomedicine. Combined endeavour of Neutrosophic Set and Chan-Vese model to extract accurate liver image from CT scan" 2016.

[13] Rafael C. Gonzalez, Richard E. Wood ,University of Tennessee Digital Image Processing Third Edition Pearson International Edition prepared by Pearson Education

[14] Harsimranjot Kaur, Dr. Reecha Sharma, "A Survey on Techniques for Brain Tumor Segmentation from MRI" IOSR Journal of Electronics and Communication Engineering, Vol 11, Issue 5,Oct 2016,PP01-05.

978-1-7281-1261-9/19/$31.00 ©2019 IEEE

Proceedings of the Fourth International Conference on Communication and Electronics Systems (ICCES 2019)
IEEE Conference Record # 45898; IEEE Xplore ISBN: 978-1-7281-1261-9

Load Frequency Control for Multi-Area Power System using Fuzzy Logic Controller

Himanshu Yadav
Department of Electrical Engineering
Rajasthan Technical University
Kota, India 324010
Email: himanshuyadav1151@gmail.com

D. K. Sambariya
Department of Electrical Engineering
Rajasthan Technical University
Kota, India 324010
Email: dsambariya_2003@gmail.com

Abstract—**In the contemporary power system, the load frequency control (LFC) of two area thermal power plant has broadly expended in frequency control suitable to having the quick replies. The fuzzy logic controller is considered for two area power plant. The pattern of system with fuzzy controller is imitation in MATLAB/SIMULINK. The dynamic replies of LFC with fuzzy and it equated through PID of frequency control for system. The success of the proposed fuzzy is better-quality the outcomes of power system in provisions of settling time and peak undershoot time**

Keywords- Load Frequency Control (LFC), Fuzzy logic controller, Proportional-Integral-Derivative (PID) controller, Frequency Deviation.

I. INTRODUCTION

In arrears to the status of the apportionment of electrical authority, the power establishments are accountable for stipulating, incessant, consistent, proficient and operative power source to their purchasers with an adequate superiority. Contemporary power organization system is completed active of numerous controlled expanses and for established process of power system components, the entire generation of individually controlled extent must competition with aggregate load strains favorable linked system losses and normalizes system frequency and conversations tie-line power consequently. This is entitled as automatic generation control (AGC) and LFC. Which performances an significant position in power system procedure and regulator [1]. For a consumption of Power system is important to remember the incessant source of electric authority to the purchaser without any commotion. For an steadiness, the power system is to continue a stability amongst load demand of the purchaser and power engendered of the power plant. Due to cumulative the complication in the world, the power petition is also intensifications. The load claim of the purchaser rises due to a frequency is renewed from its insignificant value. So, it is compulsory to keep the system frequency is to be continual. LFC is single of the rudimentary policies to reach complementary amongst the reactive power and real power. LFC is uninterruptedly supervising the system frequency and tie-line power. Estimate net variations of similar from their supposed standards (recognized as area control error, ACE). Consequently control the regulator settings of generators therefore as to retain ACE to its smallest worth. AGC initiatives ACE to zero and spontaneously together frequency and tie-line power will spontaneously transfer to zero [2,3]. The huge, composite and inter-linked power systems contribution with a massive number of nonlinear possessions consequently, fuzzy controller is single of the improved controller of these organizations. This article, the fuzzy controller is expended for LFC of the two areas system. The fuzzy is established on fuzzy set theory and being signified with the involvement and acquaintance of a anthropological operative of the system [4,5,6,7]. A power system contains of a generation, transmission and distribution of electrical supplies. Huge organized quantity of fundamentals consequences to a difficult power system which is generally associated via tie lines. In current periods, it is attractive a problematic duty to power engineer for sustaining the amplified power petition from the contemporary power system. The protected and consistent procedure of a huge organized multi-area power system necessitates the complementary amongst the producing load demand and power [8]. In [9], have proposed Grey wolf optimization (GWO) technique, Linear Quadratic Regulator (LQR) PSO-PID [10], BSA-PID [11], TLBO Optimization [12], chaotic optimization [13], Automatic Control Error (ACE) [14], LQR [15].

This paper performs a significance of lfc for two area power plant. The propositioned fuzzy logic is participate and significant part to get improved occurrences. This article, fuzzy controller has been pertained to accomplish the project features for power plant.

This paper is equipped in five sections. LFC for two area including mathematical modelling and state space equation are denoted in section 2. The fuzzy and PID controller denoted in section 3. The proposed fuzzy logic controller is compared by the PID controller. Frequency deviation in relations of settling time and peak undershoot of the is described in section 4. The conclusion of this paper is accessible in section 5 and involves of nomenclature, appendix and references.

II. MATHEMATICAL MODELLING FOR TWO AREA REHEAT-THERMAL POWER PLANT

The network frequency is contingent on active power and voltage enslavement on reactive power boundary. The network is divided into two autonomous complications. An significant responsibility of LFC is to reserve the frequency unconventionality constant in contradiction of due to incessant

discrepancy of loads. Which is correspondingly mentioned as un- known outside load interruption. Power conversation fault is an significant responsibility of LFC. Normally a power system involves of numerous generating elements associated composed. These generating constituents are inter-connected via tie-lines to developed fault accepting. This consumption of tie-line power produces contemporary fault in the control difficulty. Area controller error (ACE) is performance main character in interconnected network. Area 1 and area 2 are interconnected to separately previous by using a tie-line. The modification of tie-line power of each areas by transformation in restriction values. The elementary two area control block diagram is figure1.

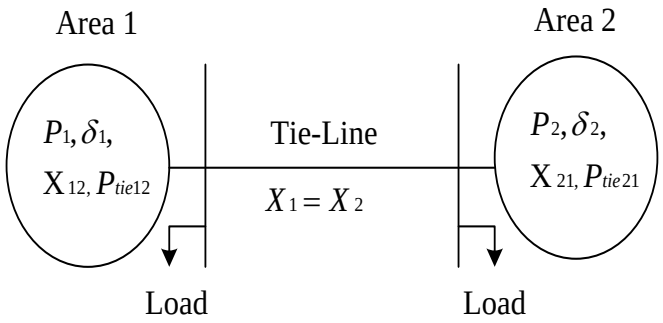

Figure 1. Basic control diagram of two-area power plant.

The basic control diagram of non-reheat thermal-thermal power plant is exposed in figure 2. Both areas have consumed a 2000MW rating and working on 1000MW nominal load. The speed governor, steam turbine and units of power system is consumed in both interconnected areas.

The power of area-1 is transfer to area-2 and its certain by equation (1)

$$P_{tie12} = \frac{|V_1||V_2|}{X_{12}} \tag{1}$$

In two areas the intend of load is depend on power angle. Both Δδ1 and Δδ2 is change incremental in configuration of δ1 and δ2. The power of change is specified by eq. (2) and eq. (3).

$$P_{tie12} + \Delta P_{tie12} = \frac{|V_1||V_2|}{X_{12}} \sin[(\delta_1 + \Delta\delta_1) - (\delta_2 + \Delta\delta_2) \tag{2}$$

$$P_{tie12} = \frac{|V_1||V_2|}{X_{12}} \cos(\delta_1 - \delta_2)(\Delta\delta_2 - \Delta\delta_2) \tag{3}$$

$$T_{12} = \frac{|V_1||V_2|}{X_{12} * P_1} \cos(\delta_1 - \delta_2) \tag{4}$$

$$\Delta P_{tie12}(p.u) = T_{12}(\Delta\delta_1 - \Delta\delta_2) \tag{5}$$

$$P_{\max 12} = \frac{|V_1||V_2|}{X_{12}} (\Delta\delta_1 - \Delta\delta_2) \tag{6}$$

$$T_{12} = \frac{P_{\max 12}}{P_1} \cos(\delta_1 - \delta_2) \tag{7}$$

$$2\Pi\Delta f = \frac{d\delta}{dt} \tag{8}$$

The incremental output power of tie-line of area1 is certain by eq. (9).

$$\Delta P_{tie12}(p.u) = 2\Pi T_{12}\left(\frac{\Delta f_1}{s} - \frac{\Delta f_2}{s}\right) \tag{9}$$

Applying the Laplace transform in both sides.

$$\Delta P_{tie21}(s) = \frac{2\Pi T_{12}}{s} (\Delta f_2(s) - \Delta f_1(s)) \tag{10}$$

Put T21=a12T12

$$\Delta P_{tie21}(s) = \frac{-2\Pi T_{21}}{s} (\Delta f_1(s) - \Delta f_2(s)) \tag{11}$$

Swing equation conferring to [4]. In area 1 the load is increase, the power is certain in eq. (12).

$$\Delta P_G - \Delta P_D = \frac{2H}{f^0} \frac{d}{dt} \Delta f + B\Delta f \tag{12}$$

Here in eq. (12).

H - Inertia constant, f0- Nominal frequency, Δf - Revolution in frequency, B - Parameter of area. Two area power is certain by eq. (13) and (14).

$$\Delta P_G - \Delta P_D = \frac{2H}{f^0} \frac{d}{dt} \Delta f + B\Delta f + \Delta P_{tie12} \tag{13}$$

$$\Delta P_G(s) - \Delta P_D(s) = \frac{2Hs}{f^0} \frac{d}{dt} \Delta f(s) + B\Delta f(s) + \Delta P_{tie12}(s) \tag{14}$$

$$\Delta f_1(s) = \frac{\Delta P_{G1}(s) - \Delta P_{D1}(s) - \Delta P_{tie12}(s)}{B_1\left(\frac{2H_1 s}{f^0 B_1} + 1\right)} \tag{15}$$

$$\Delta f_1(s) = \left[\Delta P_{G1}(s) - \Delta P_{D1}(s) - \Delta P_{tie12}(s)\right]\left[\frac{K_p s}{1 + sT_p s}\right] \tag{16}$$

Where

$$K_p s = \frac{1}{B_1} \text{ and } T_p s = \frac{2H}{B_1 f^0}$$

Similarly,

$$\Delta f_2(s) = [\Delta P_{G2}(s) - \Delta P_{D2}(s) - \Delta P_{tie21}(s)]\left[\frac{K_p s}{1 + sT_p s}\right] \tag{17}$$

In power network system, area control error is generated by a input of controller.

$$ACE_i = \sum_{j=1}^{N} \Delta P_{ij} + B_i \Delta \omega_i \quad (18)$$

Here,

N is total animated of consistent areas is depend on i. and P_{ij} is deviation of power and it is depending on both i and j areas.

In article, a two areas network have reserved. The power system involves of a governor, non-reheat turbine and power system load model in configuration of transfer function. Speed regulation are constant. The frequency of bias factor is contingent on reaction of output. The frequency deviation in power system is specified as Δf. Area-1 frequency deviation isΔf1 and area-2 frequency deviation is Δf2. The increment for area-1 is ΔPl1 and the augmentation for area-2 is ΔPl2. This power petition is specified in step load procedure. The fuzzy controller are expended for controlling the frequency. Power deviation in two area is controlling by proposed fuzzy. The block diagram of two area network shown in Fig. 2.

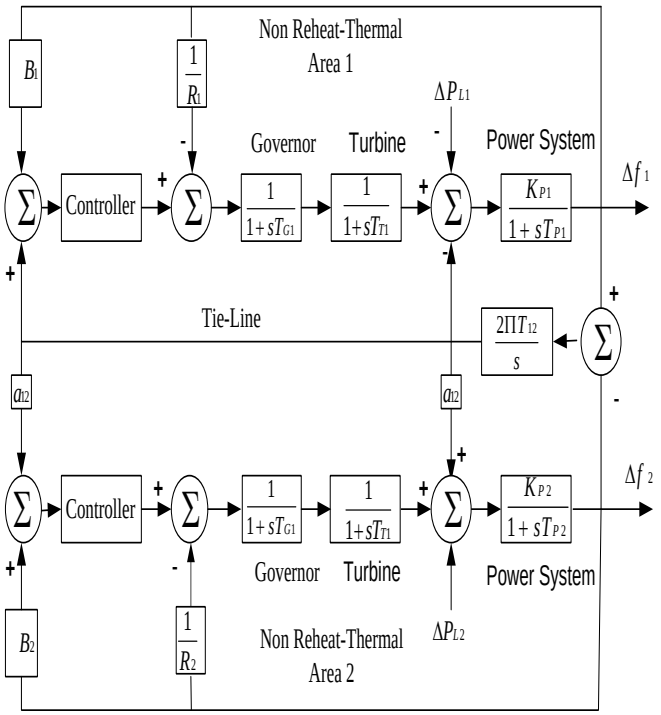

Figure 2. Block diagram of two area non re-heat thermal-thermal power plant with controller.

2.1 The state space equation of two area non-reheat thermal power plant.

This paper, the state space model is using for two area power system. System is continuous-time linear. The equivalent results for discrete-time systems, gained through division with continuous-time models. The state space network is continuous-time dynamic system. It terminate be resultant either from the network given in the time field. The illustration of differential equation or transfer function is giving equation form. The state space equation for two-area network is understand in this equation.

$$\frac{d}{dt}(\Delta f_1) = \frac{1}{\tau_{ps1}}\left[-\Delta f_1 + K_{ps1}\Delta P_{G1} - K_{ps1}\Delta P_{D1} - K_{ps1}\Delta P_{TL}\right] \quad (19)$$

$$\frac{d}{dt}(\Delta f_2) = \frac{1}{\tau_{ps2}}\left[-\Delta f_2 + K_{ps2}\Delta P_{G2} - K_{ps2}\Delta P_{D2} + K_{ps2}\Delta P_{TL1}\right] \quad (20)$$

$$\frac{d}{dt}(\Delta X_{E1}) = \frac{1}{\tau_{sg1}}\left[-\Delta X_{E1} + \Delta P_{C1} - \frac{\Delta f_1}{R_1}\right] \quad (21)$$

$$\frac{d}{dt}(\Delta X_{E2}) = \frac{1}{\tau_{sg2}}\left[-\Delta X_{E2} + \Delta P_{C2} - \frac{\Delta f_2}{R_2}\right] \quad (22)$$

$$\frac{d}{dt}(\Delta P_{G1}) = \frac{1}{\tau_{t1}}\left[-\Delta P_{G1} + \Delta X_{E1}\right] \quad (23)$$

$$\frac{d}{dt}(\Delta P_{G2}) = \frac{1}{\tau_{t2}}\left[-\Delta P_{G2} + \Delta X_{E2}\right] \quad (24)$$

$$\frac{d}{dt}(\Delta P_{TL1}) = 2\pi T_{12}^0\left[\Delta f_1 - \Delta f_2\right] \quad (25)$$

$$\begin{bmatrix}\Delta X_{E1}\\ \Delta X_{E2}\\ \Delta P_{G1}\\ \Delta P_{G2}\\ \Delta f_1\\ \Delta f_2\\ \Delta P_{TL1}\end{bmatrix} = \begin{bmatrix}\dot{x}_1\\ \dot{x}_2\\ \dot{x}_3\\ \dot{x}_4\\ \dot{x}_5\\ \dot{x}_6\\ \dot{x}_7\end{bmatrix} = \begin{bmatrix} -\frac{1}{\tau ps1} & 0 & 0 & 0 & \frac{Kps1}{\tau ps1} & 0 & -\frac{Kps1}{\tau ps1} \\ 0 & -\frac{1}{\tau ps2} & 0 & 0 & 0 & \frac{Kps1}{\tau ps1} & \frac{Kps1}{\tau ps1} \\ -\frac{1}{R1\tau sg1} & 0 & -\frac{1}{\tau sg1} & 0 & 0 & 0 & 0 \\ 0 & -\frac{1}{R2\tau sg2} & 0 & -\frac{1}{\tau sg2} & 0 & 0 & 0 \\ 0 & 0 & \frac{1}{\tau t1} & 0 & -\frac{1}{\tau t1} & 0 & 0 \\ 0 & 0 & 0 & \frac{1}{\tau t2} & 0 & -\frac{1}{\tau t2} & 0 \\ 2\Pi T_{12}^0 & -2\Pi T_{12}^0 & 0 & 0 & 0 & 0 & 0 \end{bmatrix} \begin{bmatrix}x1\\ x2\\ x3\\ x4\\ x5\\ x6\\ x7\end{bmatrix} + \begin{bmatrix}0 & 0\\ 0 & 0\\ \frac{1}{\tau sg1} & 0\\ 0 & \frac{1}{\tau sg2}\\ 0 & 0\\ 0 & 0\\ 0 & 0\end{bmatrix} \begin{bmatrix}u1\\ u2\end{bmatrix} + \begin{bmatrix} -\frac{Kps1}{\tau ps1} & 0 \\ 0 & -\frac{Kps2}{\tau ps2} \\ 0 & 0 \\ 0 & 0 \\ 0 & 0 \\ 0 & 0 \end{bmatrix} \begin{bmatrix}p1\\ p2\end{bmatrix} \quad (26)$$

III. CONTROLLER

3.1 Fuzzy Logic Controller

Fuzzy logic control is provides in artificial intelligence and control system engineering. Fuzzy controller is formed on a reasonable system called fuzzy logic. Fuzzy logic controller is developed a three components like as first is fuzzification (The breakable inputs are delineate with fuzzy parameters), second is rule base fuzzy (To implement the output for follow the each rule is giving for a fuzzy predecessor and to find out all collective outputs to follow a rules of fuzzy logic) and third is defuzzification (The breakable output are delineate by using a fuzzy parameters) is given in Fig (3).

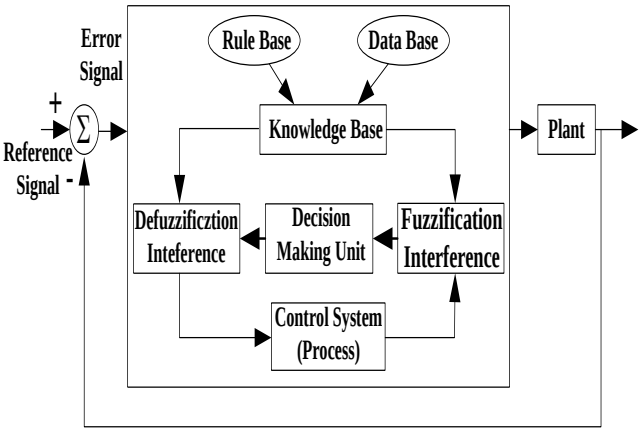

Figure 3. Block diagram of fuzzy logic controller

3.1.1 Fuzzification

Fuzzification is the method of changing a actual significance input indication into a syntactical parameter. Input signal is Knowledge base signal and it is a amalgamation of rule base and data base. Fuzzification is a work from two types, first accept the signal from knowledge base unit then send to decision making unit. And second is receive the signal from controlled system and send to decision making unit in fig (3). The actual significance inputs for a two areas thermal power plant is error and derivative of error. Mamdani configuration of fuzzy interface stage deliver amongst the inputs signal and the output signal. This paper a two kinds of input signal are used and included a five-linguistic parameter like as NB (negative base), NS (negative short), ZZ (zero), PS (positive short) and PB (positive base) is exposed in fig (4).

TABLE 1. RULE BASE TABLE FOR LFC.

Frequency Derivation error	Rate of change of frequency derivation error				
	NB	**NS**	**ZZ**	**PS**	**PB**
NB	S	S	M	M	B
NS	S	M	M	B	VB
ZZ	M	M	B	VB	VB
PS	M	B	VB	VB	VVB
PB	B	VB	VB	VVB	VVB

3.1.2 Rule Base Fuzzy

The rule base fuzzy includes of fuzzy if- then rules. The fuzzy rule could comprise fuzzy parameters and fuzzy subsection considered by member function. The fuzzy rule base as specified in Table 1. The rules are produced in this method: if the variable of error is NB (negative base) and the variable of derivative of error is NB (negative base) then the output control signal variable is S (small). Expending these member function and variable, the entire number of 49 rules are produced.

3.1.3 Defuzzification

Defuzzification converting the output fuzzy variable to a actual value indication. The centroid technique applied for defuzzification progression.

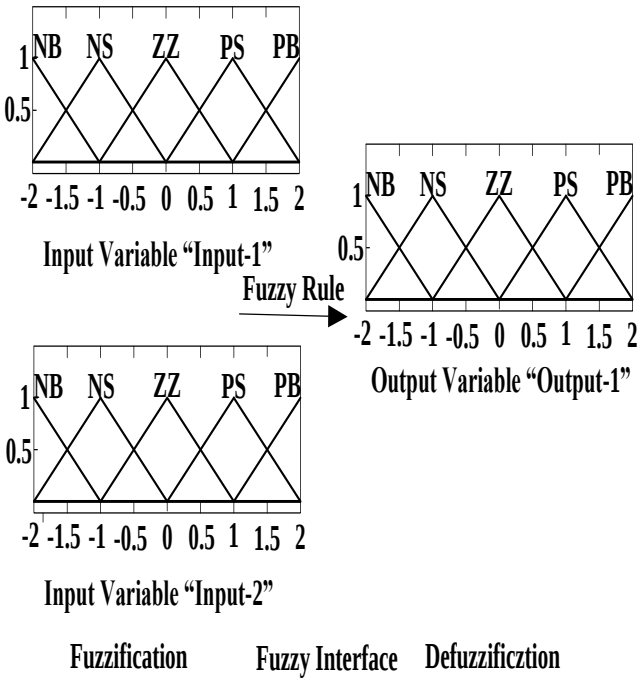

Figure 4. Inputs and outputs membership function for LFC.

IV. SIMULATION RESULTS AND DISCUSSION

In simulation research, we simulate power system with fuzzy logic controller. In this segment, we equated the presentations of thermal power plant with fuzzy logic controller through the PID controller. The reply of system parameters of PID controller is arranged in Table 2. Performance Comparison.

TABLE 2. PARAMETER VALUE OF PID CONTROLLER

S. No.	Method	Two Area PID Controller Parameter		
1.	PSO-PID Ragini, 2015 [11]	Area - 1	Kp1	0.6412
			Ki1	0.9459
			Kd1	0.4866
		Area - 2	Kp2	1.4907
			Ki2	2.0000
			Kd2	1.3564
2.	BSA-PID, Ragini 2015, [11]	Area - 1	Kp1	1.1154
			Ki1	0.9665
			Kd1	0.8358
		Area - 2	Kp2	1.1274
			Ki2	2.9687
			Kd2	1.3701
3.	A.Pritam 2017 [12]	Area - 1	Kp1	1.6301
			Ki1	1.9999
			Kd1	0.8038
		Area - 2	Kp2	1.2349
			Ki2	0.4976
			Kd2	1.5291
4.	Farahani M, 2012, [13]	Area - 1	Kp1	0.6003
			Ki1	0.6204
			Kd1	0.5224
		Area - 2	Kp2	0.3000
			Ki2	0.7319
			Kd2	0.3654

The two area non-reheat thermal power system is measured for load. We associated the replies of fuzzy controller with PID controller replies in relations of settling time, peak undershoot in confirmation in table 3

TABLE 3. COMPARISON ANALYSIS OF SETTLING TIME AND UNDERSHOOT TIME

S. No.	Method	Two Area Setting Time and Peak Overshoot Parameter		
		Areas	Setting Time (Seconds)	Undershoot
1.	Proposed Fuzzy	ΔF1	40.284	-1.583
		ΔF2	36.772	-1.564
		ΔP_{tie}	24.415	-0.300
2.	BSA-PID, Ragini 2015, [11]	ΔF1	45.688	-1.581
		ΔF2	40.781	-1.904
		ΔP_{tie}	32.434	-0.254
3.	PSO-PID, Ragini 2015, [11]	ΔF1	46.707	-1.793
		ΔF2	43.535	-2.219
		ΔP_{tie}	26.563	-0.290
4.	Pritam, 2017, [12]	ΔF1	52.164	-1.563
		ΔF2	52.822	-1.784
		ΔP_{tie}	42.850	-0.244
5.	Farahani M, 2012, [13]	ΔF1	75.682	-1.756
		ΔF2	88.494	-1.641
		ΔP_{tie}	20.691	-0.381

The proposed fuzzy has minimum settling time as associated to the PID controller and controller better the demonstrations of the system. The qualified investigative of settling time of proposed controller and PID controller for network is shown in Figure (5), (6) and (7).

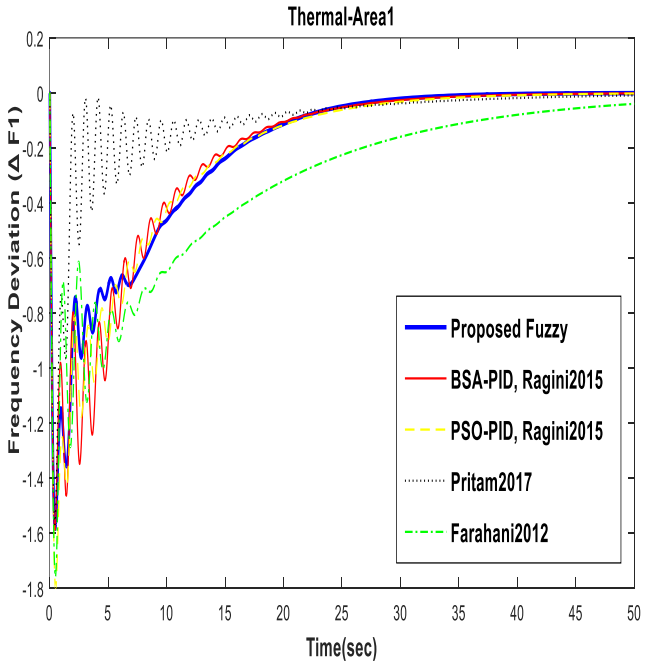

Figure 5. Comparison of thermal area-1 (frequency deviation Δf1) of proposed fuzzy with PID [10], [10],[11] and [12].

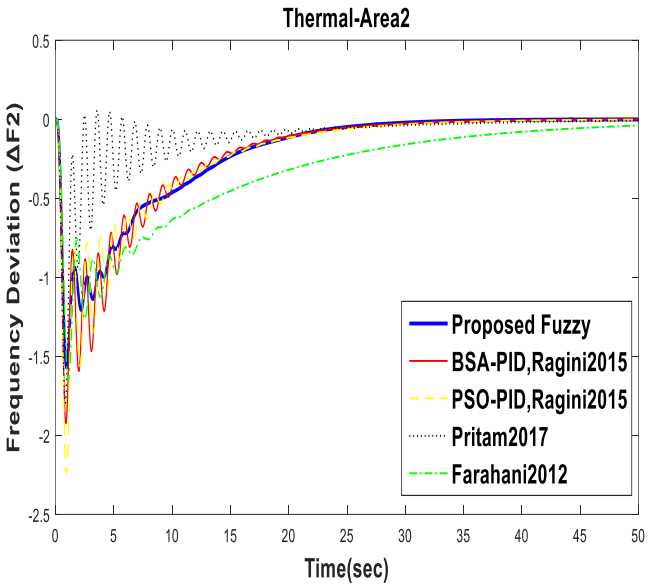

Figure 6. Comparison of thermal area-2 (frequency deviation Δf2) of proposed fuzzy with PID [11], [11], [12] and [13].

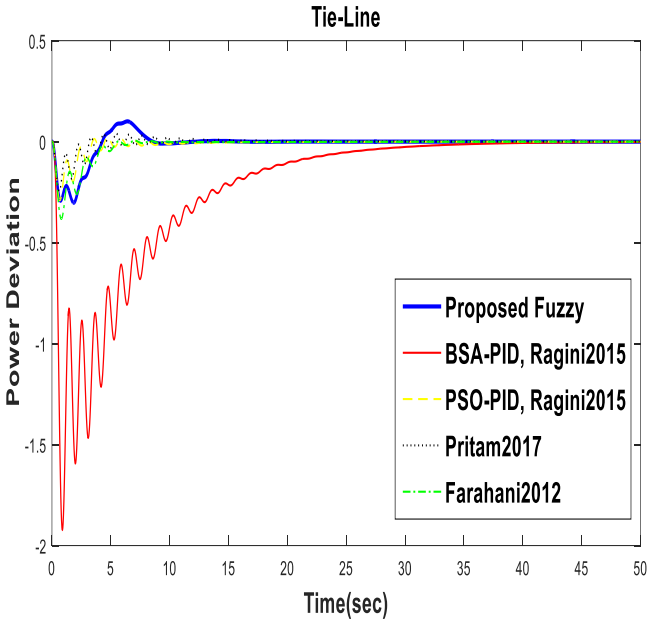

Figure 7. Comparison of tie-line of proposed fuzzy with PID [11], [11], [12] and [13].

V. CONCLUSION

In this article, the fuzzy logic controller are using for disentangling the load frequency predicament. A relative study was accessible using PID controller. Fuzzy logic controller and PID controller constraints are pertained to a two area non-reheat thermal power system. The core purpose of this paper is to better the dynamic implementations of the power plant. The condescension of proposed controller has been expressed for two area power plant. The simulation results countenance that the proposed fuzzy logic controller has superior carrying out

than the recommendation PID controller. The settling time and peak undershoot time of the two area non-reheat thermal power system measured by fuzzy logic controller gives superior result.

NOMENCLATURE

T_G : Stem governor time constant
T_T : Stem turbine time constant
K_{ps} : Power system gain constant for area.
T_{ps} : Power system time constant for area.
T_{12} : Co-efficient of synchronizing.
R_1, R_2 : Constant of speed regulation for area.
B_1, B_2 : Constant of frequency bias factor for area.
Δf_1, Δf_2 : Frequency deviation for area.

APPENDIX

Parameter of two area power plant.

Area-1
P_{r1} = 2000 MW, P_L = 1000 MW, T_{P1} = 20s, B_1 = 0.425 p.u. MW/Hz, R_1 = 2.4 Hz/p.u. MW, K_{P1} = 120, T_{t1} = 0.3s, T_{g1} = 0.08s.
Area-2
P_{r2} = 2000 MW, P_L = 1000 MW, T_{P2} = 20s, T_{12} = 0.545 s, a_{12} = -1, B_2 = 0.425 p.u. MW/Hz, R_2 =2.4 Hz/p.u. MW, K_{P2} = 120, T_{t2} = 0.3s, T_{g2} = 0.08s.

REFERENCES

[1] A. Khodabakhshian, M.E. Pour, R. Hooshmand, Design of arobust load frequency control using sequential quadratic programming approach, Int. J. Electr. Power Energy Syst.40(1)(2012)1–8.

[2] R.K. Sahu, S. Panda, G.T.C. Sekher, A novel hybrid PSO–PS optimized fuzzy PI controller for AGC in multi area inter connected power system, Int. J. Electr. Power Energy Syst. 64(2015) 880–893.

[3] R.K. Sahu, S. Panda, S. Padhan, A hybrid firefly algorithm and pattern search technique for automatic generation control of multi-area power systems, Int. J. Electr. Power Energy Syst. 64(2015) 9–23.

[4] Sambariya DK, Prasad R. Design of harmony search algorithm based tuned fuzzy logic power system stabilizer. International Review of Electrical Engineering (IREE). 2013;8(5):1594-1607.

[5] Sambariya DK. Power system stabilizer design using compressed rule base of fuzzy logic controller. Journal of Electrical and Electronic Engineering. 2015;3(3):52-64.

[6] Sambariya DK, Prasad R. Robust power system stabilizer design for single machine infinite bus system with different membership functions for fuzzy logic controller. In: 7th International Conference on Intelligent Systems and Control (ISCO, '13'). 2013;13-19.

[7] Sambariya DK, Gupta R. "Fuzzy applications in a multi-machine power system stabilizer," Journal of Electrical Engineering and Technology. 2010;5(3):503-510.

[8] Rajendra Fagna, Load Frequency Control of Single Area Thermal Power Plant Using Type 1 Fuzzy Logic Controller, Science Journal of Circuits, Systems and Signal Processing. Vol. 6, No. 6, 2017, pp. 50-56.

[9] D. Guha, Load frequency control of interconnected power system using grey wolf optimization vol. 27, 2015.

[10] M. Lokanatha, K. Vasu, 2014, Load Frequency Control of Two Area Power System using PID Controller, International Journal of Engineering Research & Technology (IJERT) Volume 03, Issue 11 (November 2014)

[11] S. K. Ragini, Akash, A. Nath, S. kumar Singh, Awanish, P. Das, A. Bhattacharya, "Automatic generation control for a two area power system using backtracking search algorithm," in 2015 International Conference on Energy, Power and Environment: Towards Sustainable Growth (ICEPE), 2015, pp. 1-6

[12] A. Pritam, S. Sahu, S. Dev Rout, S. Ganthia, and B. Ganthia, Automatic Generation Control Study in Two Area Reheat Thermal Power System vol. 225, 2017.

[13] Farahani M, Ganjefar S, Alizadeh M. PID controller adjustment using chaotic optimisation algorithm for multi-area load frequency control. IET- Control Theory Applications. 2012;6(13):1984-1992. DOI: 10.1049/iet cta.2011.0405

[14] D. K. Sambariya and V. Nath, "Load Frequency Control Using Fuzzy Logic Based Controller for Multi-area Power System," British Journal of Mathematics & Computer Science, vol. 13, pp. 1-19, 2016.

[15] Shah, Nilay & Kotwal, Chetan. (2012). The State Space Modeling of Single, Two and Three ALFC of Power System Using Integral Control and Optimal LQR Control Method. IOSR Journal of Engineering. 02. 10.9790/3021-0203501510.

Proceedings of the Fourth International Conference on Communication and Electronics Systems (ICCES 2019)
IEEE Conference Record # 45898; IEEE Xplore ISBN: 978-1-7281-1261-9

Analysis of Techniques for Correcting Power Factor of AC-DC Converters

Prerna Saxena
Department of Electrical Engineering
Rajasthan Technical University, Kota
Rajasthan, India
prernasaxena2@gmail.com

Lata Gidwani
Department of Electrical Engineering
Rajasthan Technical University, Kota
Rajasthan, India
lgidwani@rtu.ac.in

Ashok Kumar Sharma
Department of Electrical Engineering
Rajasthan Technical University, Kota
Rajasthan, India
aksharma@rtu.ac.in

Abstract— **With the advent of technology the use of power electronic devices rapidly increasing. Most of the power electronic devices require the rectifier i.e. AC- DC power converter for their working or charging purposes. Use of the power electronic converters introduces harmonics in the system thereby violating the limits of the international standard and also as the power level increases the harmonics of lower order which will deteriorates the power factor and thus affects the efficiency to a great extent. All these problems arises a great need of power factor correction. Here, in this paper analysis of different power factor correction topologies is done to understand their various techniques like passive and active and after that types of active power factor correction types are visualized and analyzed. The simulation result of the PFC buck and PFC boost converter communicate that both the techniques help to improvise the power factor .**

Keywords – Power factor, Passive PFC, Active PFC ,Buck converter,Boost converter

I. INTRODUCTION

Power factor is the measure of how effectively power is transferred from the source to load. Therefore, it is very important aspect of any power system but with the increasing use of power electronic devices in the power system for various purposes deteriorates the power factor as the power electronic converters introduce harmonics in the system. The leading and lagging power factor means there are transmission and distribution losses in the system due to which the power is not effectively utilized .A good power factor i.e. close to unity power factor implies effective utilization of power and low power factor implies that the power is not utilized properly. To overcome this problem many power factor correction techniques have been implemented so far. These PFC technologies help to meet the requirements of international standards, such as IEC 61000–3–2 and IEEE-519.

The need for the improvement of power factor arises from the fact that the rectification of alternating current is very ineffective process because it leads to the distortion of the waveform of current drawn from the input. This will give rise to large number of harmonics that will intervene with the working of other equipment. As the power level increases this intervention may become even worse as the harmonics enter in the power utility line this in turn increases the size of transformer and other equipment thereby increases the overall cost and decreasing the efficiency. All these problems greatly demand the requirement of the power factor correction. The various techniques of correcting the power factor of low power AC – DC converter [1],[8] evolved so far. Active PFC techniques using DC-DC converter is described in [2],[3].The performance evaluation of PFC boost converter given [7],[9] given. Power factor correction for switched mode power supplies presented in [4].Bridgeless power factor correction techniques [5] reduces the number of devices used. The research is done on single stage techniques of correcting the power factor [6].Some calculation for buck boost presents in [10].A voltage double circuit is represented in [12].[11] gives the correction of power factor by using switched inductor circuit.

This paper presents analysis of different techniques of power factor correction. The power factor technologies include both active and passive PFC techniques. Among the various types of active techniques here the PFC buck and boost techniques are visualized and simulated. The simulation result shows that the techniques help to obtain the power factor close too unity. Thereby, making the circuit cost effective and improves efficiency.

The section I of this paper includes the introduction of the power factor and different methods of its improvement. Section II represents the different techniques of improving power factor. The best techniques of power factor correction i.e. power factor boost converter is represented in section III. Finally, the simulation result and conclusion is presented in section IV and V.

II. TECHNIQUES OF CORRECTING THE POWER FACTOR

The PFC helps to obtain the maximum efficiency in the distribution of power. The power factor correction can be listed mainly into two groups:

- Passive PFC
- Active PFC

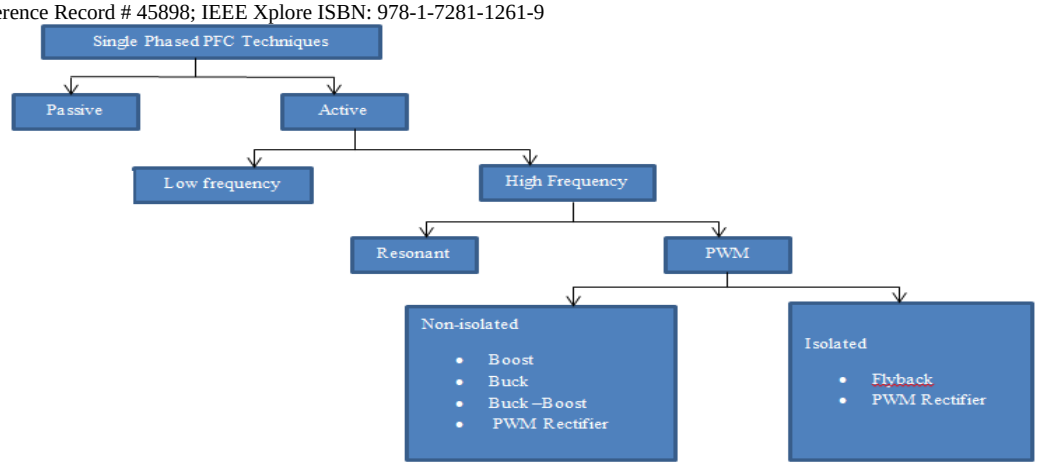

Fig 1. Power Factor Correction Techniques

The Various types of Power factor correction techniques are represented in Fig 1.

Passive Power Factor Correction

The passive power factor correction is the simplest way to remove the harmonics with the help of passive filters like capacitors, inductors, RC and LC filters .These filters allows the line current of a particular frequency (50 Hz-60 Hz) range only thus minimizing the total harmonic distortion (THD) and maintaining it with in the limited standard range. The disadvantage of this technique lies in the fact that the passive filter is bulky in size, thereby requiring the use of large value of inductors and capacitors. All this leads to increase in the cost of the circuit. Thus, generally another technique of PFC i.e. active PFC is preferred to passive PFC.

Active Power Factor Correction

The Active PFC technique utilizes the different power electronic devices to control the power travelling from source to load so that power factor close to unity can be easily achieved. These switching techniques consist of different types of switching regulators which consists of active elements like Field effect transistor, MOSFET, IGBT and diodes. Active power factor helps in increasing the power factor and lower the value of THD making the circuit cost effective. Active PFC techniques not only shape the input current but also lower the harmonics and regulate the voltage at the output with the help of feedback. Some examples of active PFC are boost converter, buck converter, dual boost converter, etc. Out of all these techniques the most preferred is boost one owing to its excellent current shaping ability.

III. THEORITICAL ANALYSIS OF ACTIVE PFC TECHNIQUES

A. PFC Buck Converter

Buck converter is DC to DC converter which is used to lower the value of voltage i.e. stepping down of voltage. This converter works only when the instantaneous voltage at the input is greater than the instantaneous value of the voltage at the output due to this reason the current at the input is distorted during some initial cycles. Fig 2 represents the basic PFC buck converter.

Working

- When the switch S_a is on the diode D_e is reverse biased and the inductor charges from the source.
- While when the switch S_a is turned off the diode is forward bias and the inductor discharges its energy to load.

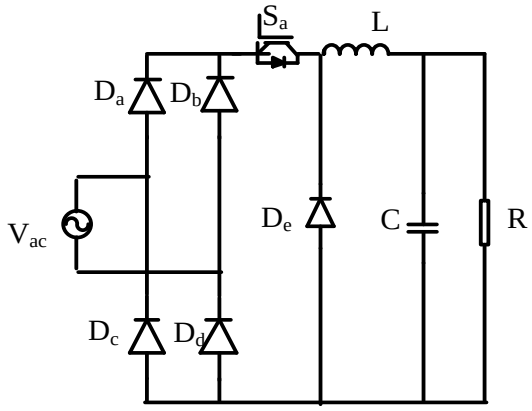

Fig 2. PFC Buck Converter

The duty cycle of buck converter is given by :

$$D = \frac{V_o}{V_{in}} \quad (1)$$

B. *PFC Boost Converter*

Boost converter is a DC to DC converter which is used to step up the voltage .PFC boost converter is the widely accepted technique of power factor correction because of its excellent current shaping ability and efficiency. Fig.3 displays the basic PFC boost converter.

Working

- When Switch S_a is on the DC energy converted from AC energy by rectifier charges the inductor during this time the voltage at the output is maintained by the capacitor by the previously stored energy in it.
- On the other hand when the switch is off the DC energy and the energy stored in the inductor is transferred to the load thereby boosting the voltage at the output. The voltage at the output can be controlled by controlling the duty cycle of the switch.

The value of different parameters of PFC boost converter can be calculated from the following equations:

$$D = \frac{V_o - V_{in}}{V_o} \quad (2)$$

$$L = \frac{R_L \times D \times (1 - D)}{2 f_s} \quad (3)$$

$$C = \frac{V_o \times D}{f_s \times \Delta V \times R_L} \quad (4)$$

where ,
R_L= Load resistance
f_s = switching frequency
ΔV = Output voltage ripple

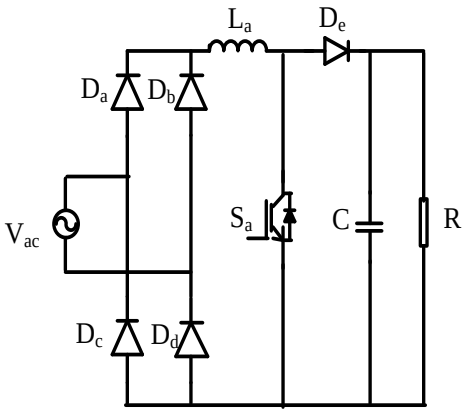

Fig 3. PFC Boost Converter

IV. SIMULATION AND VALIDATION OF THE PFC CONVERTER

Here MATLAB simulation result is presented. The input voltage V_{ac} = 220 V_{rms} and switching frequency f_s is taken as 20KHz.

Fig 4 displays the switching waveform of both the PFC buck and PFC boost converter. The switching waveform is essential to control the working of the circuit as by varying the duty cycle of the switching waveform the time of ON and OFF of the switch can be varied.

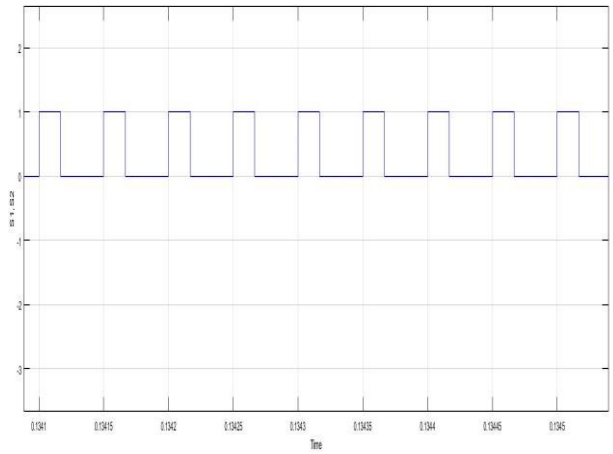

Fig 4. Switching Waveform

A. Simulaion Of PFC Buck Converter

- Fig 5. represents the Simulink model of the PFC buck converter.
- The waveform of the current at the input and voltage at the output of the PFC buck converter is being displayed in Fig 6.
- By observing the two waveforms it can be concluded that the two waveforms are in phase i.e. the voltage and current are in phase which represents that the unity power factor or the power factor is close to unity. Thus, power factor is improved by using the PFC buck converter.
- Fig 7. displays the output voltage waveform of the power factor correcting converter based on buck converter.

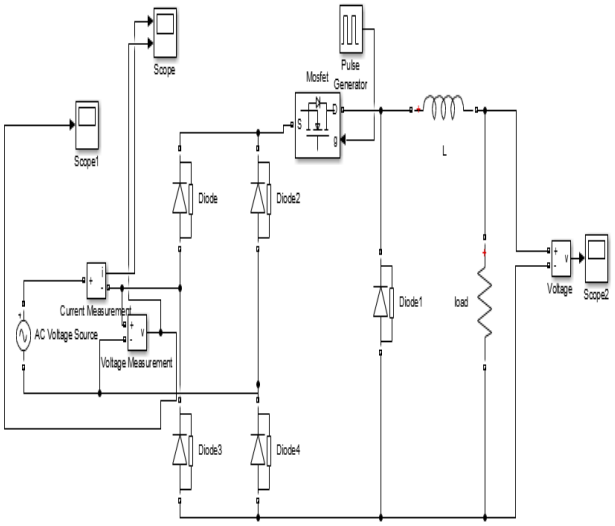

Fig 5. Simulink Model of PFC Buck Converter

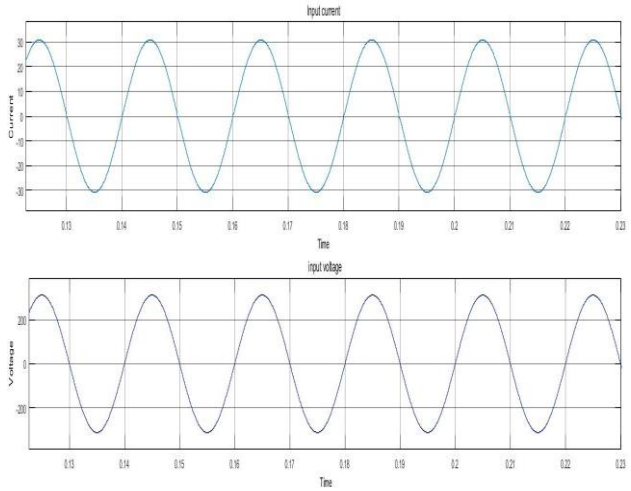

Fig 6. PFC Buck Converter Waveforms of Voltage and Current at the input

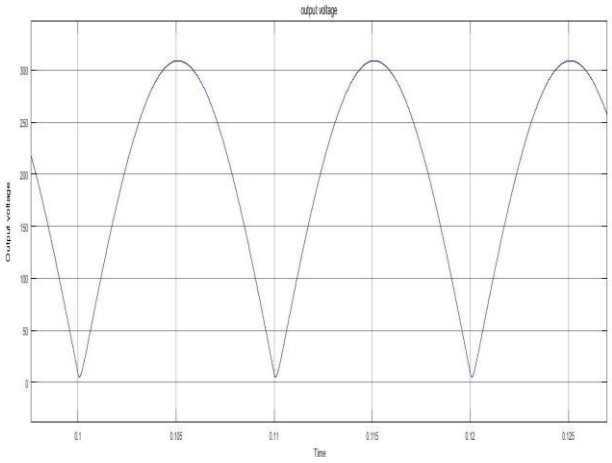

Fig 7. PFC Buck Converter Waveforms of Voltage at output

B. Simulaion Of PFC Boost Converter

- The Simulink model of the PFC boost converter is represented in Fig 8. The switching waveform of the switch of PFC boost converter is given by the pulse generator here.
- The waveform of the current at the input and voltage at the output of the PFC boost converter is being displayed in Fig 9.
- By observing the two waveforms it can be concluded that the two waveforms are in phase i.e. the voltage and current are in phase which represents that the unity power factor or the power factor is close to unity. Thus, power factor is improved by using the PFC boost converter.

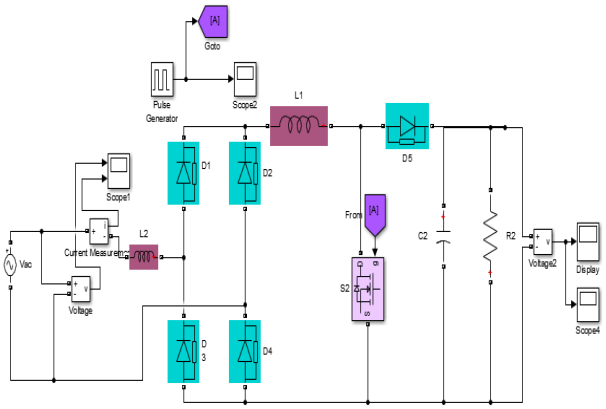

Fig.8. Simulink Model of PFC Boost Converter

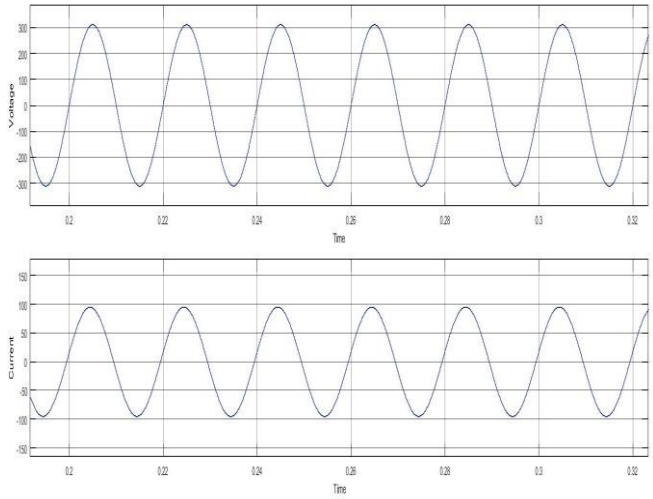

Fig 9 . PFC Boost Converter Waveforms of Voltage and Current at the input

- Fig.10. represents the voltage at output of the PFC boost converter which approximates to a constant value of 600 V.

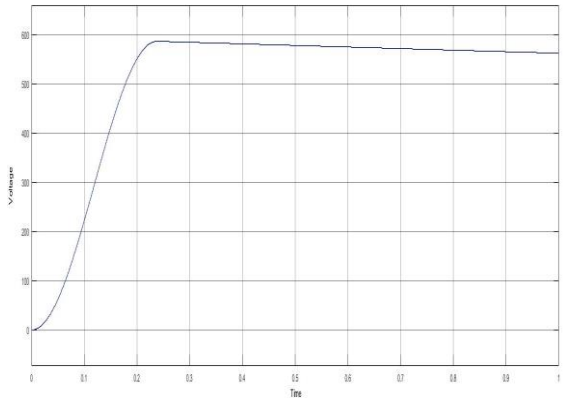

Fig 10. Output voltage of PFC boost Converter

V. CONCLUSION

Analysis of various techniques of correcting the power factor of the AC – DC converter is presented in this paper. The two types of active PFC methods based on PFC buck and boost converter is explained and simulated results of the two topology represents that the two converters obtain the power factor close to unity as the waveforms of the input voltage and the current is in phase ,thus the two converters correct the power factor to a great extent . Out of these topologies the PFC boost converter is the most preferred owing to its excellent current shaping ability and ability to remove harmonics. The future scope of the power factor topology includes the PFC converter based on SEPIC converter.

REFERENCES

[1] Azazi, H., & EL-Kholy, E. (2010). Review of passive and active circuits for power factor correction in single phase, low power AC-DC converters. *International Middle East Power Systems Conference*

[2] Journal, I., & Technology, A. (2014). Analysis of Different Topologies for Active Power Factor Correction Using Dc – Dc Converters. 4(1), 1–8.

[3] Asim, M., Parveen, H., M.A., M., & Siddiqui, A. (2015). Performance Evaluation of PFC Boost Converters. *Ijireeice*, *3*(11), 107–110. https://doi.org/10.17148/ijireeice.2015.31122

[4] Mathew, S., & Nayana, J. (n.d.). Review of DC-DC Converters for PFC in SMPS. *IOSR Journal of Electrical and Electronics Engineering (IOSR-JEEE)*, 35–43.

[5] Chen, Y., & Dai, W. (2013). Classification and Comparison of BPFC Techniques: A Review. *Przeglad Electrotechniczny*, *89*(2a), 179–186..

[6] Qiao, C., & Smedley, K. M. (2001). A topology survey of single-stage power factor corrector with a boost type input-current-shaper. *IEEE Transactions on Power Electronics*, *16*(3), 360–368. https://doi.org/10.1109/63.923768

[7] Mahalakshmi, R., & Seyezhai, R. (2016). Review of Integrated Power Factor Correction (PFC) Boost converter topologies for Telecommunication systems. *International Journal of Advanced Research in Basic Engineering Sciences and Technology (IJARBEST)*, *2*(11), 13–23.

[8] Kolte, N., & Wagh, N. B. (2014). Comparative Analysis of Power Factor Correction Techniques for AC / DC Converter at Various Loads. 1(2), 56–62.

[9] Figueiredo, J. P. M., Tofoli, F. L., & Silva, B. L. A. (2010). A review of single-phase PFC topologies based on the boost converter. *2010 9th IEEE/IAS International Conference on Industry Applications, INDUSCON 2010*. https://doi.org/10.1109/INDUSCON.2010.5740015

[10] Hagedom, J. (2018). *Basic Calculations of a 4 Switch Buck-Boost Power Stage*. (January), 1–13

[11] Lin, X., & Wang, F. (2018). High step-up voltage gain AC-DC rectifier based on transformerless switched-inductor converter for power factor correction. *Proceedings of the 13th IEEE Conference on Industrial Electronics and Applications, ICIEA 2018*, 2132–2136. https://doi.org/10.1109/ICIEA.2018.8398062

[12] Salmon, j. C. (1992). Topologies for single-phase voltage-doubler boost rectifiers john c. Salmon. 549–556.

Proceedings of the Fourth International Conference on Communication and Electronics Systems (ICCES 2019)
IEEE Conference Record # 45898; IEEE Xplore ISBN: 978-1-7281-1261-9

INTELLIGENT PUBLIC RATION DISTRIBUTION SYSTEM (IPRDS)

Vaisakh A.K, Ganesh K.V, Sooraj Suresh,
Linoy Vincent, Thobias P T
Department of Electrical and Electronics
College of Engineering Kidangoor
Kottayam, India
vaisakh248@gmail.com, ganeshkuttickattu@gmail.com

Dr.Indhu.P.Nair
Associate Professor
Department of Electrical and Electronics
College of Engineering, Kidangoor
Kottayam, India
indhunairp@gmail.com

***Abstract*— Public distribution scheme is a structure promoted by government and includes chain of shops. This scheme aims to provide food grains and commodities to people at affordable price. Public distribution scheme ails at many factors such as availability, overcharge, timing, undersupply illegal smuggling of goods and corruption. Intelligent Public Ration Distribution System (IPRDS) is similar to an Automated Vending Machine which allows customers to complete purchases and transactions of basic ration commodities with ease. The customer identification, distribution of commodities, billing and data updation etc. are automated. The customer identification is done by the finger print verification. The system was prototyped and tested to distribute three major commodities; rice, wheat and kerosene. The proposed scheme can be directly implemented in the existing ration shops and thereby reduce the labor works associated with distribution of commodities. Since all the activities will be monitored by the food supplies department, all activities takes place in accordance with the rules and regulations.**

Keywords*— *GSM Module, Finger Print Modue R307

I. INTRODUCTION

Govt. of India issues Ration Cards, with which families are able to buy commodities like Rice, sugar etc. at subsidized rates. The subsidized rates and the quantity of the materials are conditioned based on the family income and the number of members. This framework by the government aids several poor and needy families. However, this facility provided by the Government sometimes fails to reach the target group owing to human errors, inaccuracy in weighing machines, selling of leftover materials without the knowledge of the government and other forms of corruptions.

The propsed work attempts to bring out a system to eradicate the drawbacks in the chain of ration distribution and to ensure proper service of the system. The designed system is dubbed as "INTELLIGENT PUBLIC RATION DISTRIBUTION SYSTEM (IPRDS)" .With the implementation of IPRDS in all the existing ration shops, the data management becomes simpler and unfailing.

The major objective of this work is to automate the public ration distribution process. At present, ration distribution is carried out through ration shops which may neither work daily nor keep regular hours. This cause limited accessability and channelise the undisposed grain and other products to the open market. By this users do not get their rightful entitlement in terms of quantity. Moreover, the overcharging more than the mandated rate, and under-weighing of commodities are also widespread. These drawbacks of existing system can be reduced by the suggested IPRDS. Quality and quantity issues of supplied goods are also addressed in this work.

The IPRDS can be installed in existing ration shops or can be implemented even as a mobile ration shop. Since the user verification is done using fingerprint, chances of illegal transactions are minimized. The available quota of customers can be updated by the Central agencies through GSM. The details of every transaction can also be updated.

In the existing ration distribution system, the Ration Card brought by the customer is verified by the shopkeeper and thereby the materials are manually measured and supplied. Recently fingerprint system has also been introduced, which has reduced the rate of corruption occurrences. The present ration distribution system has categorized the people under 4 different categories and differentiates them by giving different colors to their Ration Cards. The yellow Ration Card is issued for the most economically backward section of society, pink for priority or Below Poverty Line (BPL) section of society, blue for non-priority subsidy or Above Poverty Line (APL) section of society and white for non-priority section of society.

Several attempts have been made in order to resolve the above discussed issues. An Automated Ration Distribution System using RFID and GSM module [1], Digitalized Ration Distribution System etc. Has already proposed.

K. Balakarthik proposed the "Cloud-Based Ration Card System using RFID and GSM Technology" [2], presents an efficient method for the user to buy the products in the ration shop by just flashing the card at the RFID reader.
A.N. Madur developed the "Automation in Rationing System using Arm 7" [3], Proposed the "Automatic Ration Material Distributions Based on GSM and RFID-Technology" Here each customer is provided with RFID cards.
In all these proposals the commodities are not weighed .

II. PROPOSED SYSTEM

The IPRDS is a microcontroller based system to control all the operations in the ration distribution system. It has a user interface with a keypad as input and LCD display as output. The customer has to provide his/her fingerprint to access the system. Once the fingerprint is authenticated, the system provides access to the customer's account. The quantity of commodities available to the specific customer is displayed on the LCD display. Now, the customer can enter the required amount of the commodities and the system will automatically distribute the commodities to the containers provided in the shortest possible time. A bill regarding the transaction is also generated and sent to the customer's mobile number.

After the process, the IPRDS will display the remaining quota available to the consumer and also update this data to the central agency by GSM method. The central agency can also control and modify the consumer allocation and data wirelessly.

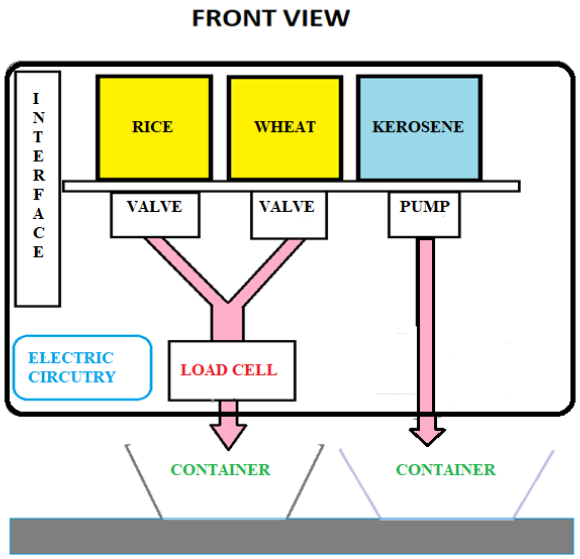

Fig 1: Structure of the proposed system.

A cross sectional view of the proposed system is shown in fig.1. There are storage cabins for wheat, rice and kerosene. These storage cabins are placed at the top and are operated using individual Servomotor valve mechanisms. The cabins are placed in such a way that the commodities in the cabin could easily flow towards the load cell by its own gravitational energy. The load cell is used to measure the quantity of grains such as wheat, rice, sugar. Whereas, the kerosene is supplied through a pre-calibrated submersible water pump. When the load cell reading is matched with the quantity entered by the user, the microcontroller provides a signal to close the valve mechanism and interrupts the grain flow. By this, the commodities can be effectively distributed to external containers. The block diagram of IPRDS is shown in fig.2. The microcontroller used is ATMEGA 2560. It controls the fingerprint sensor, load cell, pump and the valves.

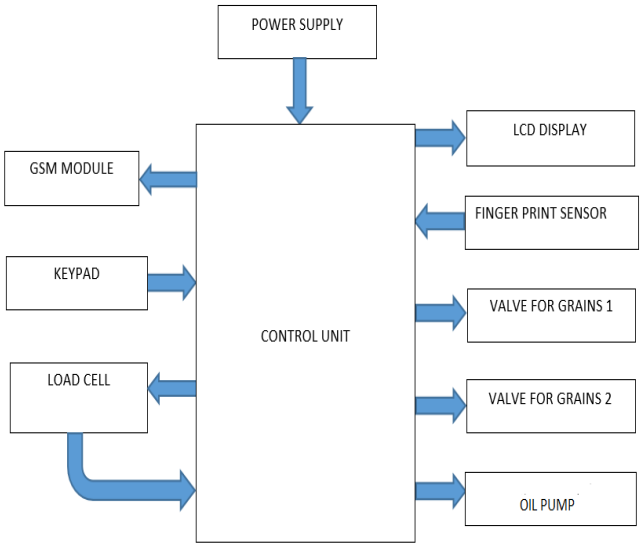

Fig 2: Block diagram of proposed system

III. WORKING

The system consists of mainly a valve mechanism, interface, electric circuitry, load cell and submersible pump. The interface acts as a medium between the customer and the system. Once the customer approaches the IPRDS, they are asked to verify their fingerprint. The fingerprint verification is done with R307 Module. The enrolment and deletion of customer fingerprints are done with the help of SFG Demo Software through a computer system.
Once the fingerprint of user matches with the stored data, the display shows the details of the Ration Card holder including the name, Ration Card number and their category. Then the display shows the available quantity of the materials allotted to the specified category from which the customer can select the needed commodity.
The user instructions are then verified by the microcontroller and control signals are given to the valve and pump mechanisms. The valve mechanism is designed with the help of a servomotor and used for the distribution of grains. Whereas the submersible pump is used to distribute the kerosene. Both valve and pump are operated till the necessary interrupt signal is received from the microcontroller.. The load cell weighs the distributed quantities from valve and pump and

continuously provides an output signal towards the microcontroller. Once the load cell reading is matched with the value entered by the user the microcontroller provides an interrupt signal to stop the operations of valve or pump. Once the process is finished the user can collect the commodities from the container provided externally.

A. Circuit Design

Arduino Mega is used as the prime controller. The Arduino first scans the fingerprint using R307 fingerprint module. R307 has an inbuilt memory having a capacity to store 1000 fingerprint modules. It takes less than 0.3 second to read the fingerprint image. Once the scanning process is done, the 20x4 LCD display shows the details of the corresponding person. The LCD display is controlled using I2C LCD controller. The conventional LCD display requires at least 6 pins for its functioning while I2C controller requires only 2 pins. The requirements are selected using a 4x3 Matrix Keypad. After the verification and the decision making process, the commodities are delivered. The grains are delivered via valves. The valves are operated using servomotors (SG90 Servo). The weight of the commodity is measured using Load cell. As the requirement is fulfilled, the servomotor operates to close the valve.

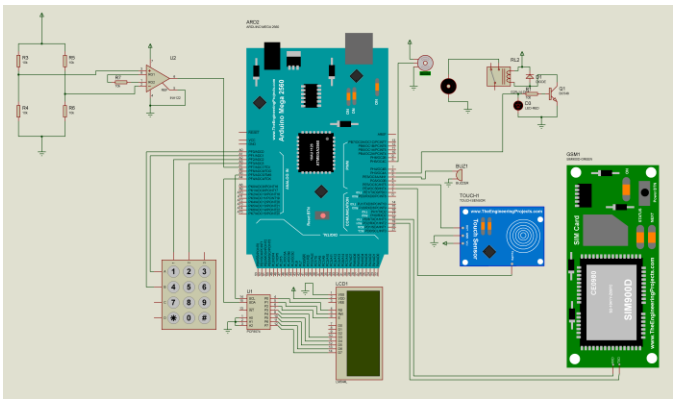

Fig 3: Circuit Diagram

The kerosene is supplied using Submersible Mini Water pump which is controlled by a relay circuit. As the grains are ready to be loaded, the consumer is alerted using a buzzer. This helps the person to ensure that the grains are collected properly. All these functions make way for reducing manual intervention.

A GSM module installed in the circuit ensures that the Ration Card Holder is informed about the collection of the commodities. It sends a message stating that the monthly Ration is dispersed and collected to the Registered Phone Number.

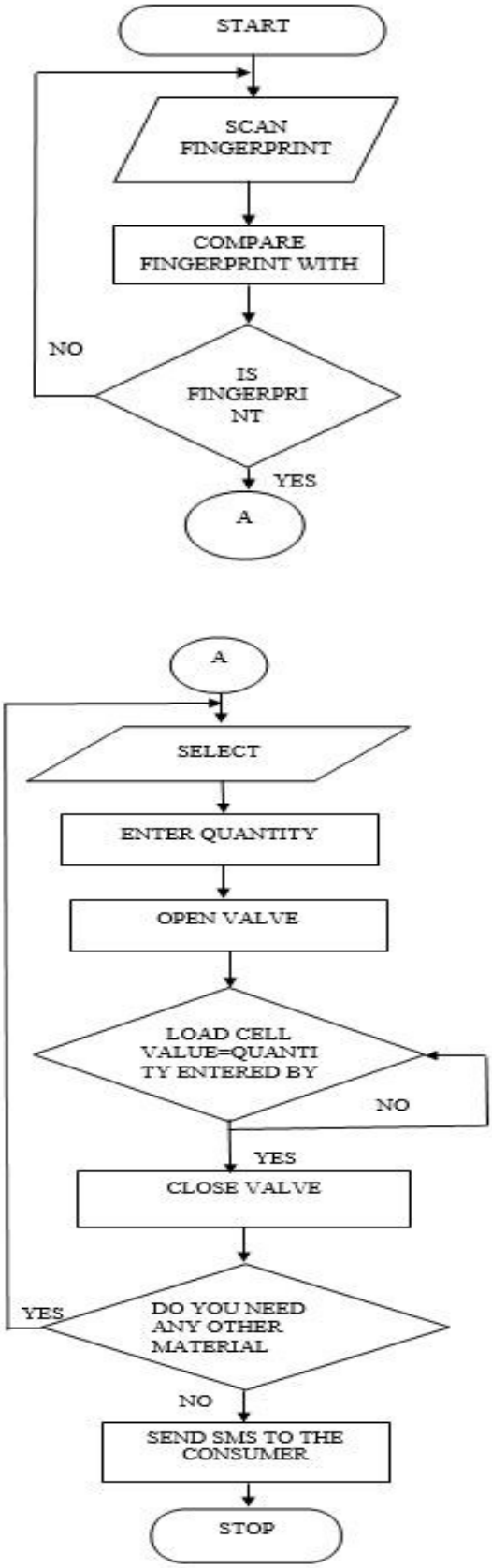

Fig 4: Flow Diagram

The program flow chart for the system is shown in fig.4. The consumer is granted the permission to access his requirements using the keypad.

IV. RESULT

The suggested IPRDS system was enacted as a prototype. The project model developed is shown in fig.5.

Fig 5: Project Model

V. CONCLUSION

This paper brings out a new venture to ensure full-fledged and transparent Ration Distribution system. Every user can collect their monthly ration and ensure its delivery via message sent to their registered phone number. The data updating and processing is made easy using the proposed system and hence saves a lot of paper work time. Any further extension to the existing model can be deployed by enabling IoT. More security aspects like face identification can be incorporated to secure the Ration Distribution system.

Though the system has to incur initial investment costs, the long term benefits overshadow it. Message will be sent to the government about the dispensing after each item being sold. Through transparency in all transactions, corruptions can be eliminated to an extent. For the completion and installation of this work in Ration Shops, the Government must ensure that the Ration Card is linked with the Adhar. If implemented in all the existing stores can revolutionize our public distribution system.

The systemcan be further developed to incorporate Online payment, which can reduce the time associated with the distribution and the use of paper currency.

With IOT the system can be made to work as a cloud based systemin which all the data regarding transactions, customers etc can be accessed from a single database.

VI. ACKNOWLEDGEMENT

This endeavour stands incomplete without expressing our gratitude to everyone who has contributed a lot towards the successful completion of this work. This project is funded by the Kerala State Council for Science Technology and Environment (KSCSTE).

VII. BIBLIOGRAPHY

[1] Mrs.Padmavathi.R, K.M Mohammed Azeezulla, “Digitalized Aadhar Enabled Ration Distribution Using Smart Card” , 2017 2nd IEEE International Conference On Recent Trends in Electronics Information & Communication Technology (RTEICT), May 19-20, 2017, India

[2] K.Balakarthik,”Closed-Based Ration Card System using RFID and GSM Technology,’’ vol.2, Issue 4, Apr 2013.

[3] A.N.Madur, Sham Nayse, ”Automation in RationingSystem Using Arm 7,” International journal of innovative research in electrical, electronics, instrumentation and control engineering ,vol.1, Issue 4, Jul 2013.

[4] Dr.M.Pallikonda Rajesekaran, D.Balaji, “Automatic Smart Ration Distribution System for Prevention of Civil Supplies Hoarding In India”, 2017 International Conference on Advanced Computing and Communication Systems (*ICACCS* -2017), Jan. 06 – 07, 2017, Coimbatore, INDIA

[5] Pranjal Pedwal, Ms. Shubhangi Borkar,“Real Time Automatic Ration Material Distribution System” Pranjal Pedwal *et al*, International Journal of Computer Science and Mobile Computing, Vol.5 Issue.3, March- 2016, pg. 734-7396966

[6] Aishwarya M, Ananya K Nayaka, “Automatic Ration Material Dispensing System” , International Conference on Trends in Electronics and Informatics ICEI 2017

[7] Balasubramani A, Sunil Kumar H U, “Cashless automatic rationing system by using GSM and RFID Technology”, Proceedings of the Second International conference on I-SMAC (IoT in Social, Mobile, Analytics and Cloud) (I-SMAC 2018) IEEE Xplore Part Number:CFP18OZV-ART; ISBN:978-1-5386-1442-6

[8] S. Valarmathy,R.Ramani “Automatic Ration Material Distributions Based On GSM and RFID Technology” I.J intelligent systems and applications,2013,11,47-54

[9] Parvathy A,VenkattaRohit Raj, Venumadhav, Manikantha, “RFID Based Exam Hall Maintenance System”, IJCA Special Issue on “Artificial Intelligence Techniques – Novel Approaches & Practical Applications” AIT, 2011

[10] Swapnil.R.Kurkute, Chetan medhe, Ashlesha Revgade, Ashwini.Kshirsagar "Automatic ration distribution system" 3rd International Conference on Computing for Sustainable Global Development (INDIACom), 2016, IEEE.

[11] Rajesh C Pinge, “Automatic Rationing for Public distribution system,” International Journal of Intelligent Systems and Applications, vol 5,pp.47-54, Oct 2013.

[12] S. Valarmathy,R.Ramani “Automatic Ration Material Distributions Based On GSM and RFID Technology” I.J intelligent systems and applications,2013,11,47-54.

Proceedings of the Fourth International Conference on Communication and Electronics Systems (ICCES 2019)
IEEE Conference Record # 45898; IEEE Xplore ISBN: 978-1-7281-1261-9

Reliable Constrained Application Protocol to Sense and Avoid attacks in WSN for IoT Devices

Divya.R
Research Scholar
Dept. of Master of Computer Applications
CMR Institute of Technology
Bengaluru, India
divya09chinnu@gmail.com

Dr.R.Chinnaiyan
Professor
Dept. of Information Science and Engineering
CMR Institute of Technology
Bengaluru, India
vijayachinns@gmail.com

Abstract- The application that are envisioned with IoT has a vital role played by the security. we make use of reliable Constrained Application protocol to sense the threat for the security purpose for any applications associated to IoT devices in a wireless sensor network environment. The task of Sensors sensing and the devices associated to it is, included with the end to end support system for the interior and exterior communication systems, which are always prone to all threats and attacks. Thus, we here propose a novel framework to sense and avoid the attacks in the framework of Internet-incorporated CoAP communication atmosphere. We here try to consequently estimate efficiency of reliable CoAP to sense and avoid attacks with respect to the DOS attacks in the communication protocol for IoT devices.
Keywords: IoT; reliable; DOS; CoAP; internet-incorporated

1.INTRODCTION

A Wireless sensor network with respect to IoT has many oblige comparable to energy, memory, performance and security. Talking of the Today's IoT security risk premeditated for typical IoT [1]. The pile being arranged with the protocols alike as 6LoWPAN, RPL and CoAP Constrained Application Protocol [2].We here divide the pattern for security sense and avoid attacks into two major section in this paper .First sector ,we identify the security encounters of reliable sense and avoid in the framework of IoT communication atmosphere , and view the present losses related to the solutions intended for Internet-incorporated CoAP and 6LoWPAN message atmosphere. In Second sector, we propose the design work for the reliable sense and avoid technique to employ the anomaly detect protocol by analysing the output from the experiment estimation. The Obtained results are purely based on the incongruity of the reliable the CoAP to sense and avoid attack in WSN's for IoT devices.

2. DETECT SECURITY AND RELIABLE THE IOT

2.1. Security in the Context of Internet-Incorporated Sensor Networks

The present pile of communication has enormous constrain, so we shift our interest on the CoAP [3], which is having standard reputation, to prove its potentials to perform a chief regulation in enabling the IoT. CoAP was intended in the force to put forth the Representational State Transfer, construction of the web to incorporate sensors and their devices. Here the CoAP protocol with respect to the security at application layer, share URL familiarity as well as the error codes which is alike to operations compared to the (ReST) with the Creating, Updating, Deleting and read only. At the transport layer the aim is to do safe communication between devices, CoAP envoys its provision to the Datagram Transport Layer Security protocol at the transport-layer. Here it also helps the devices to authenticate with the help of the DTLS by using the, public-keys, also the beforehand-shared keys or digital certificate X.509 .Thus ,its vital inspite of secured key sharing between the users in the system is already known , where it cannot guarantee the no-attack from various external and internal attacks in the culmination to culmination communication organization. Despite of this kind of attacks which has the cache manipulations, there exist a suspicion of DDoS amplified attack, man in the middle attack, which in turn has fooling(spoofing) and fractious(cross) layer attacks. Where these internal attacks will spoof the rules and regulations with the normal work of the CoAP protocol. Henceforth, endwise security devices could be accompanied by suitable sense and avoid methods positioned in this situation of the Internet-incorporated WSN, which is main moto of our work.

2.2. Reliable Detection methods on the Internet

It is importanat to know the role of the reliable detect are incorporated in techonologies with respect to the real systems and, . Host realted IDS incorparted are most rigourously given emphasis on one-to-one care and perceiving the detect action on the doubtful actions in hosts, which has the capacity to monitor every behaviour that is dynamic in nature and the system of with the dynamic state . today the IDS is the best solution to the internet which employed with the detect form in the classifications as: SO signature-oriented detect , anomaly-oriented detect and SPA State full protocol analysis[6].An anomaly is characterized to deviate from the traditional

(predictable) activity of network, to particularly built up form of activity of the network , which helps in the regular activity of the network.Here we can catogories to this into host-realted (HIDS), network-realted (NIDS) and wireless-realted (WIDS) [7]. By the analysis of the network jam ,here we capture the traffic rate of the network at tactical positions of communications organization. WIDS are way familiar to the NIDS,whereas in this case we concetrate more on the wireless communication state.

2.3. Detect Reliable the IoT

Here, we are known with the attack that are encountered while the devices are connected in the wireless state for communication, which are to be treated with suitable solutions. Hence this known attack is to be detected well in before. We take in to point that the attacks from the security, against the stable internet incorporated restricted sensing and associated devices. We may consider the varied layers of communication stack; hence we here consider to map up for application layer using the CoAP point of the IEEE 802.15.4[4]. In [4] the authors propose REATO, a regulations-oriented description with dynamism to detect and contract with DoS attacks. The structure here is premeditated to implement, with the evaluation for DoS attack in a numerous circumstance in directive to wedge unexpected communications circumstances. For example,the jamming and collisions attacks are encountered as expected DoS attacks in contradiction of IoT communication area, snooping whichever present at the route , application layers or link layer.Authors in [5], an fusion IDS attack to detect the contradiction of routing with RPL, which fuses the features of SO and AO reliable CoAP. Thus, suggestion is estimated with the concluded simulation for outcomes oriented with sinkhole attacks.

3. Reliable CoAP to sense Internet-Incorporated WSN

Here we extant the structure with framework of the reliable detection of DoS attacks for the applications layer in contradiction of the CoAP Protocol [6].

3.1. Considered Method

The method well thought-out in here could be considered from the taxonomy given in [7], which is given bellow:

• Network architecture of the existing system replace: Here a defend and detect the attacks on the CoAP with the help of the centralized method, which will destabilize the client serve model in the communication system.

•Method used to handle the web: familiar to other WSN's we consider hierarchical model, CoAP, 6LoWPAN and, RPL at the advanced layers and hop by hop communication support IEEE 802.15.4 at connection(link) layer [13].

•Collection of Data: data collection in centralized, here we target a particular node in the web to capture the data, known from the nature of traffic oriented web .Also the component to collect the data uses the .For traffic collection an agent IoT-LAB sniffer node used for specific locations or area.

•Type of the Data: the data type is pcap (Packet Capture) presentation for WSN's traffic.

•Detect Time: the off line implementation.

•Condition of being granular: intermittent (batch) method implemented for traffic capturing.

•Method to process: Detect attack and gather data makes use for processing a centralized method [4].

•Discipline to Detect: To restore the evaluation that is state-based with the discipline is used and, IDS intelligences if node is normal or negotiated state. We here recognize and mention the past as "NORMAL" through the paper and future as "RELIABLE".

•Method of Detection: as mentioned before in this paper, we in these circumstances of the projected framework, we deliberately analyze, instrument and estimate reliable CoAP to sense and avoid attack in WSNs.

3.2 structure Planning

To demonstrate the structure well-thought-out, the resolving of method to instrument and estimate reliable CoAP to sense and avoid attack in WSNs. in Figure 1. This structure planning is done deliberates to employ the 6LoWPAN edge routers (6LBR) arbitrating transport network, amid the internet devices in addition to WSN, here we use CoAP identifying(sense) and actuating(sensor)devices [10], also for the external (different WSN or internet devices) or internal (same WSN) for the hosts. Therefore, CoAP customers subordinate by means of CoAP attendants helps in directive to request, will stimulate otherwise perceive specific properties accessible at the application layers [7].

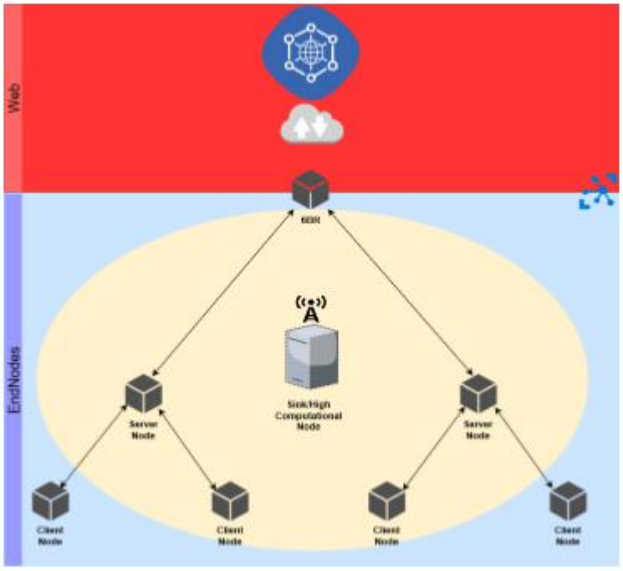

Figure 1. Structure for reliable CoAP sense framework of Internet-incorporated WSN's

As exemplified in Figure 1, Let us presume device employ to sustenance reliable CoAP sense processes. The device

possesses the properties essential for execution seizing of the transport network in the array within it, therefore substitute as a web sniffer in it. One more vital condition is that, this device employ for the anomaly detect through the machine learning language by supporting high level language. In this present employment of this architecture, this task is taken into the consideration by the 6LBR, and device is accountable for filtering (intermediating) between internet and WSN.As mentioned before, for the focus to employ ,anomaly-detect to experiment and implement by evaluating it, here uses the IoT LAB [4-8] stage, incorporated to provision a multi-hop topology. In place of a constraint to GET requests only for CoAP in this platform and enactment of numerous devices is completed by Contiki operating system, in specific by build above the basis (source)code intended for border router (6LBR), the implementations of the examples with respect to CoAP server and CoAP client [8].

4. Experimental Evaluation

We ensue by output analysis, attained from our evaluated experiment, for sense sense methods, begin with an analysis forwards through the experiments, till it is implemented and automate.

4.1. Automation and Implementation of Experiments

The first and foremost step to select the operating system to be employed, for implement and automate.It is necessary to provision, to gather the statistical data and component for reliable detection in architecture [9]. The OS working for persistence of supportive reliable CoAP to detect in the Contiki [10], because of its constancy, hardware affinity and attribute of credentials at indicator. According to this podium of OS, here working with the IoT-LAB to incorporate, a podium(platform) that enables the method of disposition in the ease way.

4.2. A problem for Multi class

The results obtained from the analysis of the pcap(packet capture) files are comprise to observe and consist of ,arrays of structures ordered as a rectangular matrix. These annotations are given in to data pre-processing, dimensionality reduce and classifier physical activity. The proportion of the number of NORMAL vs. inaccurate annotations (thus, result from the disobedient node) is of 2 to 1, thus for each two NORMAL observations we observe one inaccurate observation [11].In this process we employed the following SVM Kernels: Linear, RBF, polynomial and sigmoidal. The obtained results are illustrated in Figures 2

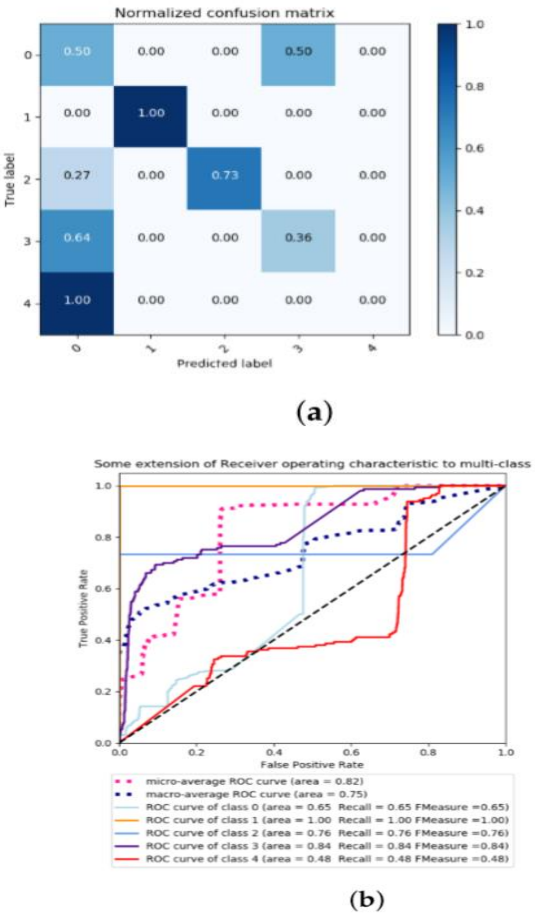

(a)

(b)

Figure 2: Problem Multi-session—Net Exploration SVM thru: RBF Kernel, purpose outline one against. Rest choice, 30 reiterations and keep score standard of exactness, Mix-up (confusion)Matrix (a) and ROC (Receiving Operator Characteristic) Curvature (b)[11-12].

4.3 Evaluation Strategy

The classification so for, on the reliable CoAP detect method are evaluate throughout the working out period, and in this context, take in count the basic metrics in the routine, specific Accurateness, the Recollection of True positive Proportion, Precision, False positive Proportion and F Degree, elucidate as beneath [12]:

$$Recall = \frac{TP}{TP + FN}$$

$$Accuracy = \frac{TP + TN}{n}$$

$$Precision = \frac{TP}{TP + FP}$$

$$False\ Positive\ Rate = \frac{FP}{FP + TP}$$

$$F\_Measure = 2 \times \frac{Precision * Recall}{Precision + Recall}$$

From the preceding precision in the count of numbers, TP means true positives, TN true negatives, FN false negatives, FP false positives and numeral explanations to consider [4-12]. Hence the particular metrics, estimated deliberate through the mix-up(confusion) matrices and ROC curvatures, in cooperation with binary classes as well as the, multiple classes methods for analysis.

5.Conclusion

In this paper, we partake projected a framework for the IDS, reliable CoAP to sense and avoid attacks in wireless sensor networks for IoT devices. The above framework used to evaluate efficiency required to employ the process of reliable CoAP by means of detect, as well in preventing the DoS attack, in contradiction of this communication atmospheres. As of a real perception with respect to the IDS structure, the Internet-incorporated CoAP detecting(sense) applications, it's vital in averting the extreme reliable a probable one. Whereas correspondingly, at times it assures for a truncated rate of FN, though there is unfluctuating cost of cumulative FP, we obtain the maximum output for managing the security. By identifying specific attack, the problem with respect to the multiple class method is suitable for, interior and Internet-originated attacks in contradiction of the security devices. Further consideration of additional reliability for the intrusions in future developments, predominantly concerning about the attack absorbed on disrupting the traditional rules and the protocol semantics of CoAP, either by interior or exterior attacks.

6.Refrence

1. Jorge Granjal * ID , João M. Silva ID and Nuno Lourenço ," Intrusion Detection and Prevention in CoAP Wireless Sensor Networks Using Anomaly Detection " mdpi ,Published: 27 July 2018
2. FITIOT-LAB.Iot Experimentation at a Large Scale. Available online: https://www.iot-lab.info/(accessedon 9 February 2018).
3. Atul Kahate, "cryptography and network security", Tata McGraw-Hill,2003
4. Montenegro, G.; Kushalnagar, N.; Hui, J.; Culler, D. Transmission of IPv6 Packets Over IEEE 802.15.4 Networks. Available online: https://tools.ietf.org/html/rfc4944 (accessed on 25 July 2018).
5. Eric Maiwald," Fundamental of network Security ", MCGraw-Hill,2003
6. Raj kamal," Internet of Things:Architecture and Design Principles" ,Mcgraw-Hill ,2017
7. Koblitz N, Introduction to Number Theory and cryptography, Springer verlag,1994
8. Dr.R.Chinnaiyan, Abishek Kumar (2017), Estimation of Optimal Path in Wireless Sensor Networks based on Adjancy List , 2017 IEEE International Conference on Telecommunication, Power Analysis and Computing Techniques (ICTPACT-2017) ,6,7,8th April 2017, IEEE 978-1-5090-3381-2.
9. **R.Divya*, Dr.R.Chinnaiyan, Dr.V.Ilango (2017),** RELIABILITY EVALUATION OF WIRELESS SENSOR NETWORKS- A Review, INTERNATIONAL JOURNAL OF ENGINEERING SCIENCES & RESEARCH TECHNOLOGY, Vol.5 Issue.No.12, December, 2016,pp ,598-604.
10. **R.Divya*, Dr.R.Chinnaiyan** " Reliability Evaluation of wireless sensor networks(REWSN - Reliability Evaluation of wireless sensor networks), International Conference on Intelligent Computing and Control Systems (ICICCS) ,IEEE, 2017, p:847-852.
11. R Chinnaiyan, S Somasundaram, An Experimental Study on Reliability Estimation of GNU Compiler Components–A Review, International Journal of Computer Applications (0975–8887)
12. **R.Divya*, Dr.R.Chinnaiyan** –"Reliability Evaluation of Wireless Sensor Networks-A Study "International conference on trends and innovation implying future technology 2017.

Proceedings of the Fourth International Conference on Communication and Electronics Systems (ICCES 2019)
IEEE Conference Record # 45898; IEEE Xplore ISBN: 978-1-7281-1261-9

Radiation Data Acquisition System Using Wireless Communication

Reshma Ramanan. M
Dept. of Electronics and Communication Engineering
Amrita Vishwa Vidyapeetham, Amritapuri, India
India
reshmaramanan94@gmail.com

G.Shekar
Dept. of Electronics and Communication Engineering
Amrita Vishwa Vidyapeetham, Amritapuri, India
India
geedimatlas@am.amrita.edu

Sreelatha. P
Scientist, AVN
VSSC, Thiruvanathapuram
p_pradeepkumar@vssc.gov.in

Pradeepkumar. P
Scientist, AVN
VSSC, Thiruvanathapuram
p_sreelatha@vssc.gov.in

***Abstract*—Radiation intensity which is measured in power per unit area is used to analyze the extent of effect of radiation and can be used for analytical studies. In this paper, a real time monitoring system is proposed to collect the intensity of sunlight and transmit the data using wireless communication for a suitable range with less transmission loss. Two radiation sensors are used to measure the intensity of light - one is to quantify intensity of directly incident light and other for reflected light from earth. It works on the basis that intensity of light is directly proportional to the voltage. This data acquired is transmitted using a powerful Sub-1GHz wireless microcontroller. The proposed system was tested at different intervals of time. The results showed stable voltage readings proportional to the light intensity. These radiation values were transmitted successfully in wireless mode for a range upto 250m without any transmission loss.**

Keywords—Solar radiation; Sensor networks; Data acquisition system; Wireless communication.

I. INTRODUCTION

Solar radiation is the major source of radiation affecting the entire universe as sun being the basic source of energy. The range of this radiation can be understood from the analysis of the amount and intensity of sunlight. The sunlight is a part of electromagnetic spectrum which includes infrared, visible and ultraviolet regions. The intensity of solar radiation is measured in power per unit area. This measurement is an integration of the solar irradiance and the solar insolation considered together. Solar irradiance is the amount of sunlight directly incident on the earth or the measuring equipment at any particular instant. This value ranges from 0 kW/m^2 at night to a maximum of 1kW/ m^2 throughout the day. Solar insolation is the amount of light that falls on the earth's surface and gets reflected to the atmosphere. This measurement is accurately made using a pyranometer and pyrheliometer for global radiation and direct radiation respectively. This knowledge of solar irradiance can be utilized for various analyses like predicting energy generation from solar power plants, and in weather forecasting and other climatological studies [1].

A Data Acquisition System (DAQ) functions to measure or control the physical signals of real world and convert it into digital values that can be manipulated using a computer. A DAQ system is generally comprised of sensors, DAQ device and a computer. Fig.1 shows the block diagram of a DAQ system. The sensor is used to convert the physical signals to voltage, resistance, current or any other electrical characteristics that varies over time. The physical signal can be temperature, pressure, light intensity, sound etc. The output from the sensor may have noise elements. The DAQ device mainly does signal conditioning, analog to digital conversion and transmission of the instructions and data measured using any proper bus. The commonly used bus for interfacing DAQ device to a computer are USB, PCI express and Ethernet. Recently, for wireless transmission 802.11 Wi-Fi, Bluetooth or other RF modules are used. The computer part includes driver software and application software. Driver software is for simplification of communication with DAQ device while application software is used for collecting, processing and presenting the data to user [2].

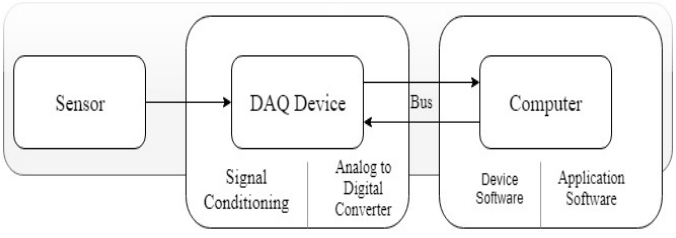

Fig. 1. Block diagram of a typical Data Acquisition System[2]..

Nowadays, wireless communication is being extensively used in various applications like medical [3], military, data communications, sensor networks [4], energy transfer, security [5] and many more. To collect data from remote areas like underground, underwater extreme hot and cold locations

wireless technologies are best in terms of energy efficiency and less transmission losses. Commonly, the wireless technologies use radio waves. Zigbee wireless technologies, Bluetooth, GPS, and Wi-Fi are also widely used .Wireless sensor networks transfer data collected via multiple nodes and gateways to networks like Ethernet. The wireless data transfer can be done between two microcontrollers also. In such a case any kind of wireless technology can be used as a bus to carry out the data transmission.

In this project, intensity of light from the sun is measured using sensors- one for the incident light and one for the reflected light. This data is collected and stored in a microcontroller which has its own radio to transmit the data. The transmitted data is received at a distant location using another microcontroller. The obtained data is processed understand the radiation intensity and proceed for further studies. The microcontroller used works in Sub-1 GHz radio frequency.

The related works are indicated in Section II and the proposed system is presented in Section III. The different components used in the project are explained in detail in Section IV. The experimental setup is familiarized and the performance evaluation is carried out in Section V. The work is concluded in Section VI.

II. Related Work

The remote data acquisitions system is of great importance in this era of unforeseen advancement in technology. The collaboration of sensor networks and or transmission modules makes it possible to collect the remote data and transmit over a large distance. As mentioned the data acquisition find its application in almost all fields. For example, the importance of a DAQ system in providing better mobile health care services is mentioned clearly by Chanhee Lee *et al.* [6] in their paper. The DAQ system is put in action by using USB, Ethernet or wireless means for testing, estimating and automation of data. Chanhee Lee introduce a data acquisition software using database querying facility along with mobile sensor networks to ease the process of filtering out of the unwanted overhead medical data [6].

The DAQ is also applied in recording signals from infrasound events. In the paper by José Chilo and Thomas Lindblad [7], the output signal from infrasound sensor is transformed into digital signal by a 16-bit ADC. It also employs an anti-aliasing filter for noise elimination. A multi-sensor DAQ system is used to analyze the thermo acoustic performance of refrigerator in the paper by Yuriy P. Kondratenko *et al.* [8]. The system uses an Ethernet and RS232 to communicate between sensors and end PC.

In the paper, Zhao Jinxiang and Sun Chuanwei [9] use a CC3200 MCU in remote data acquisition. Here, the data is accessed from cloud server by the use of the Wi-Fi module embedded in CC3200. Compared to all other methods of DAQ, this provides a low cost and less complex way of remote data sensing. The wireless data transmission is efficient as it makes the device simple and is cheaper in long range communication when compared to wired transmission. So, this paper presents the use of wireless sensor networks in data acquisition.

III. Proposed System

The system proposed is a combination of data acquisition system and wireless communication for acquiring the radiation intensity of sunlight in a particular area. It comprises of two radiation sensors and microcontroller used as transceiver. Power supply is also given to the microcontroller system and photodiodes. Fig. 2 shows the block diagram of the proposed system.

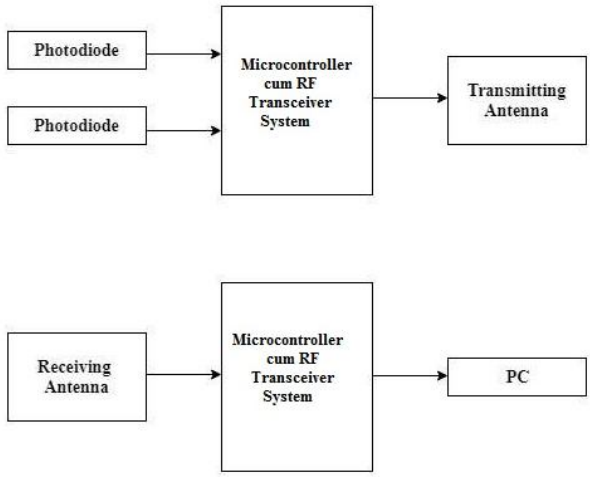

Fig. 2. Block diagram of the proposed system.

The photodiode shown in the block diagram is the radiation sensor. UDT-455UV is the photodiode used. It is a photodiode-amplifier hybrid. For the microcontroller system TI Launchpad Kit with CC1312 MCU is used is. The top microcontroller system is the transmitter and the bottom one act as receiver. The transmitting and receiving antennas are inbuilt within the transmitter and receiver MCUs. There is a PC (laptop or a desktop) connected to the receiver end to visualize the received data from MCU to the user.

IV. System Description

A. Radiation Sensor

The radiation sensor detects the incident light and converts the intensity of the incident light to voltage or related electrical parameters that varies over time. This conversion of light to electrical parameter is called photovoltaic. Photovoltaic detectors or photodiodes are usually employed to do this conversion due to its fast response, amplification, low noise, high sensitivity and wide dynamic range. The responsivity of a detector is the ratio of measured current and the input light power. It is an important characteristic feature.

Photodiode is a PN- junction diode that works in reverse bias condition [10]. The working is being explained as, when

light photon strikes the diode, an electron hole couple is generated. This is the inner photoelectric effect. If absorption occurs in depletion region, the holes move to anode and electrons move to cathode and photocurrent is generated. There are three modes of operation namely, photovoltaic (PV) mode, photoconductive (PC) mode and avalanche diode mode. PV mode is zero biased mode while the rest are mostly in reverse biased. An operational amplifier is connected to the photodiode to approximate to zero bias and to direct the signal to feedback resistor.The UDT 455-UV is a type of photodiode-amplifier hybrid that is used in this project as a radiation sensor. It is manufactured by UDT Sensors. Inc. This belongs to the Photops^{TM} series general purpose detectors and has a spectral range of 200nm to 1100 nm [11]. This series of photodiode has an operational amplifier connected internally to the detector.

UDT 455-UV has 8 pins arranged in a circular fashion. Pin numbers 1 and 5 are assigned as offset null. Pins 2 and 3 functions inverting input and non-inverting input respectively. V (+) and V (-) are assigned to pins 4 and 6 respectively. Output is taken from pin 6 while detector anode is connected to pin 8. It typically works for supply voltage of ±15 V and can withstand a maximum of ±18V. Fig. 3 shows the schematic diagram of the photodiode. In this the connection between pins 8 and 4 is avoided since only the PV mode is considered. A 0.1µF capacitor is connected in parallel to the 0.1µF to store more energy. Here, the light falls on the diode and is passed through RC circuit generating a voltage proportional to the intensity of light. The op-amp connected in the PV mode approximate the biasing to zero bias and directs the signal current via feedback resistor R_F.

$$V_{OUT} = I_D \times R_F$$

where V_{OUT} = output voltage,

I_D = intensity of light and

R_F = feedback resistance.

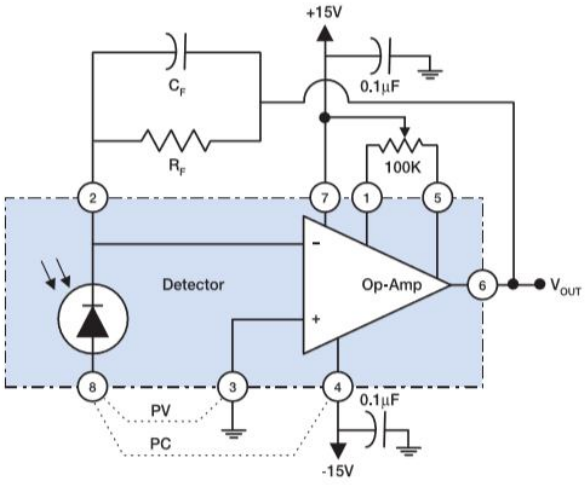

Fig. 3. Schematic diagram of UDT 455UV.

The feedback capacitor and resistor values are taken as 15.9pF and 100kΩ respectively to achieve operating frequency of 100 Hz.

B. Transceiver Unit

The radiation data collected by the sensor needs to be stored and transmitted to the receiver end. Transceiver is used to establish this wireless communication. In this project, TI Launchpad with CC1312 microcontroller unit is used as transceiver. The CC1312R device embedded in the Launchpad is a powerful wireless MCU that works in Sub-1 GHz frequency. The CC1312R is highly integrated single chip with an active RF core and inbuilt DC-DC converter. It has a 352 KB In-system programmable Flash, 256 kB of ROM and 8KB of cache SRAM. The compatible supply voltage range is 1.8 V to 3.8V [12].

The major parts in the functional block diagram of the device are system CPU, RF core, sensor interface and general peripheral devices and other modules. The device has three strong processors embedded in a single chip namely, ARM Cortex-M4F processor for system CPU, ARM Cortex-M0 processor for the RF core and another ARM processor for the sensor interface. The programming of these three processors is done using different soft wares like code composer studio, RF smart studio and sensor controller studio respectively. The CC1312R is 48 pin IC in which all the pins are general purpose input output pins. This IC along with a debugging portion presents the Launchpad. The Launchpad comes with 40 pins each with its own functions. Among the 40 pins, 8 numbers of pins are analog. Fig. 4 shows the Launchpad kit used as transceiver. It comes with a monopole antenna.

Fig. 4. TI Launchpad with CC1312 MCU.

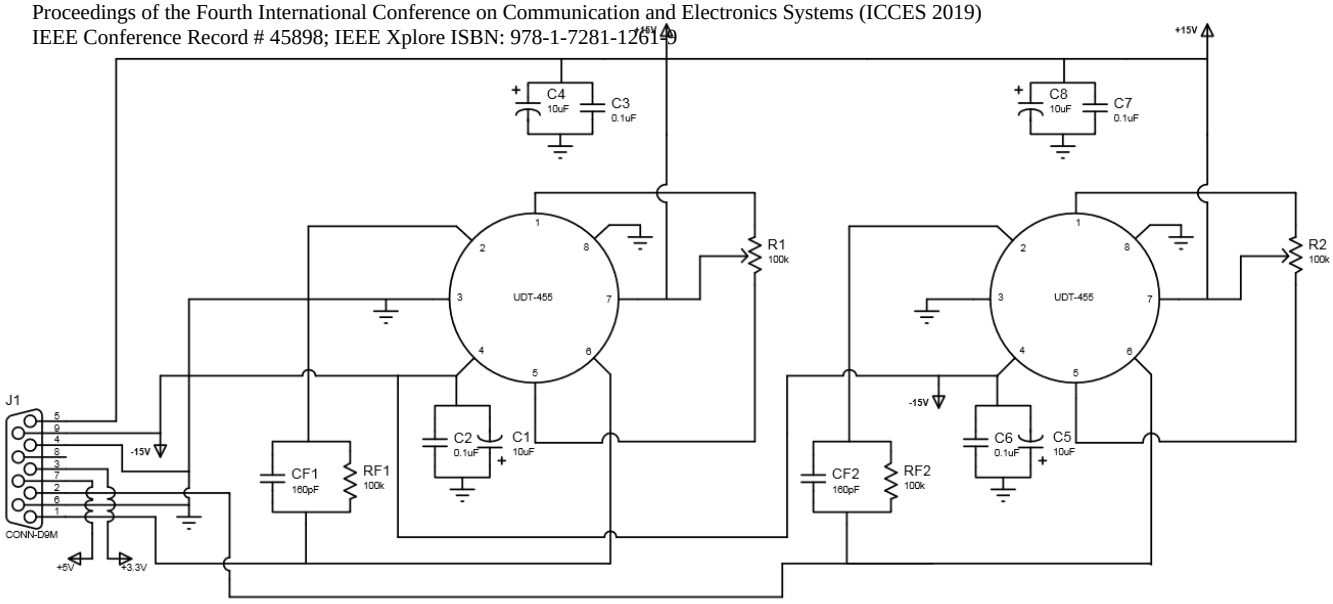

Fig. 4. Circuit diagram of radiation sensors drawn in Proteus software.

The sensor controller (SC) in the CC1312R is a core 16-bit. The SC is of ultra-low power and is not dependent on other parts of the system like Arm Cortex-M4F and RF core. It is user friendly and easily programmable. The code is executed from a dedicated memory of 4KB of RAM. SC has the right to program and execute analog and digital peripherals. If the MCU is in sleep mode, the SC will store the data to memory. Once the MCU is active, the SC will notify the main MCU. It has some additional perks like it can carry out advanced tasks like capacitive touch and inductive sensing.

The Arm Cortex M4F processor core of CC1312R has a 48 MHz RC oscillator and a 48 MHz crystal oscillator. When the device needs to work in low-power mode, the 32-kHz RC oscillator, 32-kHz crystal oscillator or 48 MHz crystal oscillator is used generate clock for timing maintenance. It also have Arm Cortex Sys Tick timer, an integrated system timer. Sys Tick supplies a basic, 24-bit, clear-on-write, decreasing, and wrap-on-zero counter with a varying control mechanism. The device also has Nested Vector Interrupt Controller (NVIC). It is deterministic and carries out robust processing of interrupts. The security core of CC1312R has Advanced Encryption Standard (AES) module. It also has 256-bit key support, DMA efficient and a local key storage. The device supports serial communication in both asynchronous and synchronous modes. It includes two UART modules, I2C module, I2S module and two SSI (SPI) modules.

V. Result Analysis

A. Experimental Setup

The hardware components used in the proposed system includes two UDT-455UV sensors, two CC1312R Launchpad kits. The schematic diagrams for each component are drawn in Proteus software. Fig. 6 shows the schematic diagram of two radiation sensors drawn in Proteus software. The connections

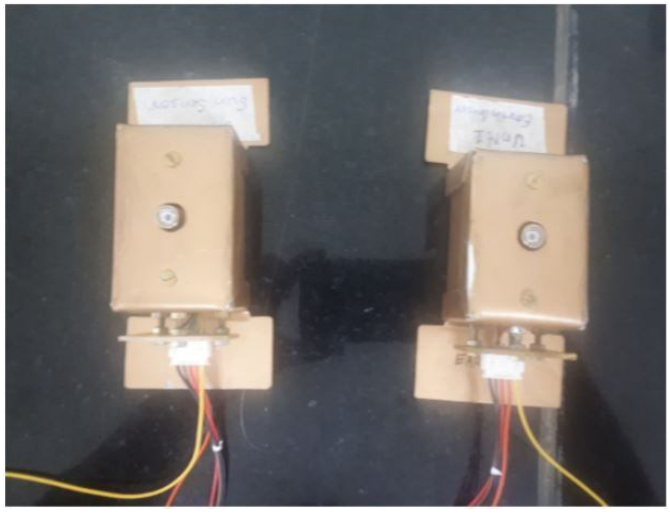

Fig. 5. Sensors enclosed in teflon casing.

are made according to the schematic diagram and each sensor is enclosed within a Teflon case. There are four connection wires V+, V-, ground and output from each sensor. One sensor is to measure the direct light and other is to measure the reflected light. These sensors and enclosed in Teflon case. Fig. 5 shows the sensors enclosed in the case.

Fig. 6. Experimental setup.

The experimental setup of the sensors is shown in Fig.6. In the figure brown coloured boxes are the radiation sensors and the white coloured device is a standard radiometer. The sensors were placed on a pole at a fixed height from the ground. One of the sensors (say, sun sensor) was placed upwards so that the direct sunlight falls on it. The other sensor was placed downwards to measure the intensity of light reflected from the earth's surface. Both are given a ±15V supply voltage using a dual DC power supply. Using a multimeter the output voltages for each instant of time at short intervals is taken and tabulated. Along with the sensors a standard radiometer was also placed and values were noted for comparison. Now, the output wires from both sensors are connected to the two analog pins in the TI Launchpad kit.

In the receiver part, another TI Launchpad kit is connected to a PC. Both the transmitter and receiver kits are supplied with a voltage of 5 V and are placed at non-line of sight path. The maximum distance up to which the data can be accurately transmitted is quantified. The software part of the system has SmartRF Studio 7. The transmitting and receiving packets specifications could be set in this software.

B. Results and Discussions

The experiment was carried out in two phases. In phase 1, the sensors were connected to the power supply and the output voltages from both the sensors were measured using a multimeter. The values were taken for different instants of time for a short interval of 5 minutes. Refer to Table.1. Whenever there is a change in the light intensity, the sensor gives a stable output voltage at each point. The voltage versus time graph obtained is shown in Fig. 7. When there is no light, multimeter shows zero voltage. The values obtained can be used to plot a graph of time versus radiation density graph.

TABLE I. RADIATION SENSOR TEST RESULTS

S. No.	Radiation Sensor Values		
	Time	*Sun Sensor (in V)*	*Earth Sensor (in V)*
1	15:00	2.297	0.567
2	15:05	2.2	0.579
3	15:10	2.199	0.619
4	15:15	2.174	0.589
5	15:20	2.128	0.58
6	15:25	2.617	0.537
7	15:30	2.065	0.515

The obtained graph is similar to that of Fig. 8. It shows the intensity of solar radiation throughout a day measured in the absence of clouds using existing method i.e., a standard radiometer. It shows a Gaussian curve. While testing the proposed system, only short duration of time is considered. It clearly shows that using two radiations sensors solar irradiance can be accurately measured. Hence, the proposed system may be used to replace the existing ones in future.

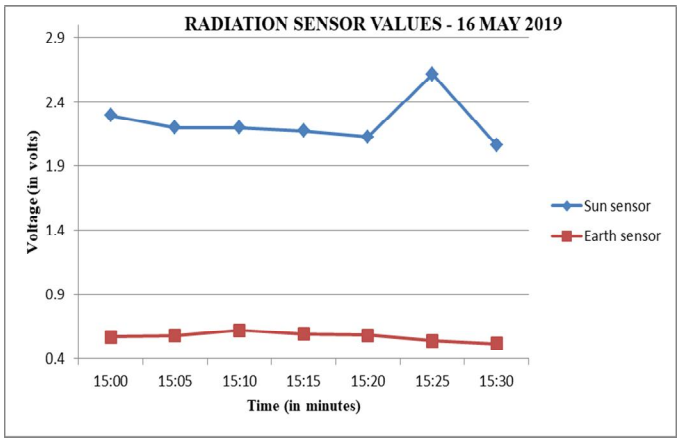

Fig. 7. Voltage versus time graph showing the radiation sensor values at different time intervals.

The phase 2 focuses in transmitting the obtained radiation data over wireless communication to a receiver located at distance. Receiver MCU is first placed at a near distance. The transmitter MCU was connected to the sensors. The output from the sensors was transmitted through it. Initially the receiver is kept in line of sight with the transmitter. At that point the data collected by sensors were transmitted accurately. Then, distance is increased. Finally the receiver is placed at non-line of sight path. The maximum distance up to which the transmitter data could reach the receiver MCU effectively in the non-line of sight path is found to be 250m. Beyond this distance, there were anomalies in the transmitted and received data. The system was tested taking the transmitter power as 14dBm. The antenna used in the MCUs was a monopole antenna. Hence, its alignment was also taken care of.

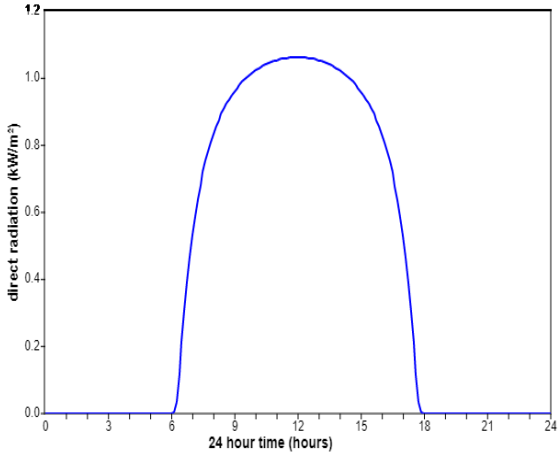

Fig. 8. Graph showing intensity of solar radiation in a day using existing method [13].

It was evident from the repeated tests that for transmitting power less than -100 dBm, the receiver showed varying results. So, the transmitting power of transmitter antenna needs to be more than -100dBm.

VI. CONCLUSION

The study of radiation effects on the atmosphere opens the door to manifold analysis. It is vital because by knowing the level of exposure to sunlight, photovoltaic systems could be designed with maximum efficiency. The use of sensor networks to acquire these data is efficient due to the high sensitivity, ultra-low power operating conditions of photodiode used. Data acquisition systems are useful to acquire data from remote places to make it easier for humans to monitor various types of data. This proposed system employs a wireless transceiver in combination with sensor networks to carryout data acquisition efficiently. Normally, to transmit data of sensor networks to a PC or user friendly device wireless modules could be used. In this system, by using a powerful microcontroller as transceiver the wireless communication is effectively done. It shows that by using the proposed system wireless communication can be used for data acquisition for a maximum distance of 250m. Here, only a photodiode is used to collect data. Since, a strong wireless MCU is employed as transmitter more sensors like temperature, humidity and pressure sensors could be incorporated to the existing system to collect more data from the area under observation.

ACKNOWLEDGEMENT

The authors would like to extend their gratitude to Rajiv Ranjan, Scientist, VSSC and other working members from Vikram Sarabhai Space Centre (VSSC) for providing space and help for the successful completion of this project.

REFERENCES

[1] A. Q. Jakhrani, A. K. Othman, A. R. H. Rigit and S. R. Samo, "A simple method for the estimation of global solar radiation from sunshine hours and other meteorological parameters," *2010 IEEE International Conference on Sustainable Energy Technologies (ICSET)*, Kandy, 2010, pp. 1-6.

[2] National Instruments, "What is Data Acquisition System, " *National Instruments*, 2019.[Online]. Available: http://www.ni.com [Accessed May 30, 2019].

[3] M. D. Hatagundi and G. Sadashivappa, "Wireless Communication in Medical Devices: Research Challenges," *2018 2nd International Conference on Trends in Electronics and Informatics (ICOEI)*, Tirunelveli, 2018, pp. 336-338.

[4] Rajesh Kannan Megalingam, Mohan V, Leons P, Shooja R, and Ajay M, "Smart traffic Controller Using Wireless Sensor Network for Dynamic Traffic Routing and OverSpeed Detection," *Proceedings-2011 IEEE Global Humanitarian Technology Conference, GHTC 2011, Seattle,WA*, 2011, pp. 528-533.

[5] Rajesh Kannan Megalingam, Nair, R.N,, Prakhya, S.M, and Mohan.M, "Low Power Intelligent Wireless Home Security System for the Elderly People," *ICECT 2011-2011 3rd International Conference on Electronics Computer Technology, Kanyakumari,2011*, vol. 4,pp.320-324.

[6] Chanhee Lee, Taehun Kim and S. J. Hyun, "A data acquisition architecture for healthcare services in mobile sensor networks," *2016 International Conference on Big Data and Smart Computing (BigComp)*, Hong Kong, 2016, pp. 439-442.

[7] Chilo, José & Lindblad, Thomas. (2007). A Low Cost Digital Data Acquisition System for Infrasonic Records. 35 - 37. 10.1109/IDAACS.2007.4488367.

[8] Kondratenko, Yuriy & V. Korobko, Volodymyr & Korobko, Oleksiy. (2011). Multisensor data acquisition system for thermoacoustic processes analysis. 54-58. 10.1109/IDAACS.2011.6072710.

[9] Jinxiang, Zhao & Chuanwei, Sun. (2017). Research and design of remote data acquisition system based on CC3200. 158-161. 10.1109/ICRAS.2017.8071936.

[10] Elprocus, " Photodiode Working Principle, Characterics and Applications,"*Elprocus*,2013.[Online]. Available:https://www.elprocus.com [Accessed May 30,2019]

[11] OSI Optoelectronics, " Photodiode –Amplifier Hybrids," UDT-455UV datasheet.

[12] Texas Instruments, "CC1312R SimpleLink™ High-performance Sub-1 GHz Wireless MCU, " *CC1312R datasheet*, Jan. 2018 [Revised Jan. 2019] .

[13] Christiana Honsberg , Stuart Bowden, "Homepage-," Feb. 2019. [Online]. Available: https://www.pveducation.org/ [Accessed May 24,2019].

Proceedings of the Fourth International Conference on Communication and Electronics Systems (ICCES 2019)
IEEE Conference Record # 45898; IEEE Xplore ISBN: 978-1-7281-1261-9

Integrated Cloud based Smart Home with Automation and Remote controllability

Aravind Hanumanthaiah[1], Arjun D[2], Liya M L[3], Chandni Arun[4], Athira Gopinath[5]
Amrita Center for Wireless Networks & Applications (AmritaWNA)
Amrita School of Engineering, Amritapuri
Amrita Vishwa Vidyapeetham
India
aravindh@am.amrita.edu[1], arjund@am.amrita.edu[2], liyaml@am.amrita.edu[3], chandniarun@am.amrita.edu[4], athirag@am.amrita.edu[5]

***Abstract*—IOT based smart home with cloud analytics are becoming popular, as it helps in analyzing the real time power consumption. Home Automation System [HAS] and remote control system in a smart home opens up many ways to control the loads in a smart home. But, there are a lot of challenges when all these features are combined together to make a low cost smart home system. Often in the design, the HAS and remote controllability can conflict with each other when trying to control the same load. This paper outlines the design of a low cost smart switch that incorporates HAS, remote controllability and IOT cloud platform. It also describes the challenges faced and a possible solution.**

Keywords—Smart Home, Home Automation System [HAS], IOT, Real time Monitoring, Cloud Analytics, Visualization

I. INTRODUCTION

The modern era is in the cusp of automation where most of the electrical systems are becoming automated in home, malls [1], industries [2] and hospitals [3].etc. Home automation is one among them, where the human effort and energy consumption can be reduced. Also, the remote controllability in smart home is becoming very popular as the cost of wireless solution is becoming cheaper. Implementation of both Home Automation System [4] and remote controllability [5] in smart home opens up more options to the user. But, there will be a conflict between them when HAS and remote user is trying to control the same load. There are various approaches to solve this issue. One could be to prioritize between these modes. But, prioritization is very subjective and differs from person to person. CISCO predicted that 50 Billion devices would be connected to IOT by 2020 [10]. This target can be reached comfortably if there is a smooth transition from a contemporary house to a smart home. Also, there is a large section in the society who would like to retain the manual controllability. But, because of mechanical switches, the signals have bouncing issues, which needs to be taken care of in the design.

In this paper we describe simple steps to build a smart switch for a smart home that can accommodate HAS, remote controllability and cloud analytics. The user shall be able to perform remote controllability when the system is in remote control mode. When the system is in HAS mode, the load will be automated to save energy. It also sends the power consumption data to the cloud-based server for the power analysis. This power consumption data can be accessed by the user while making decision to optimize the power consumption. This system also helps in not overloading the power grid at the peak usage time and avail lower tariffs if provided by the electricity board. All these features were implemented on an embedded system based on an Arduino UNO board, which tests the efficiency of the system.

In Section II, literature work of the existing home automation systems has been discussed. Section III elaborates the system architecture of the proposed work. Section IV highlights the methodologies used. Section V explains the detailed analysis and discussion. Finally, the conclusion and future work is discussed in Section VI.

II. RELATED WORKS

Kumar, Ramu, et.al., proposed a low cost IoT based home automation system by using Arduino board. An Android mobile application is developed to control the load. The proposed architecture is for indoor home automation using Bluetooth and the outdoor home automation using Ethernet [7].

The proper analysis of various sensor parameters and the data acquisition modules play a major role for building a Smart Home with Internet of Things [8]. The proposed framework utilizes Temperature and humidity sensors for continuously capturing the corresponding measurement parameters and to provide context aware services based on three-level context aware model with the help of Internet of Things.

Akorede, Fatigun, et.al., developed a remote control system for elder's safety [9]. A GSM modem and a Wi-Fi module are the major parts of the proposed model and can act as a client and server respectively. AT commands and SMS service in the GSM module and the STM32 microcontroller is integrated to control the state of the electrical switch based on the SMS and to turn ON/OFF the home appliances accordingly. They have segregated the commands in different zones (coded version), each command will perform the

functions accordingly. But the transmission can range from a short distance of 100-200 meters. This application does not store high memory status thus needs to erase the zones after reaching to certain limitations manually.

A proposed system of Husni Teja Sukmana, Muhammad Ghiyast Farisi, et.al., focused on three major process: home entertainment, remote monitoring and home automation [10]. Passive Infrared (PIR) sensor is used to detect the motion of the user and it is attached to an Arduino UNO microcontroller. After detecting the motion of the user, a lamp is turned ON through command from web application. There are chances of false alarms due to overheating due to the PIR sensor is kept ON for a long time, fluctuation in heat and temperature variations.

Ramlee, Othman, et.al., presented a paper that provides assistance and support for elderly and disabled persons in home. The proposed design is a Home Automation System with remote controllability and lower cost [11]. The system utilizes Bluetooth technology for providing remote accessibility of the smart home using Smartphone or Laptop. The traditional electrical switch is converted into a low voltage switch for giving safe environment to the user. The controller board is directly attached to the electrical switch. A relay is used to control the switch connections.

III. System Architecture

The overall system architecture shown in Fig. 1. can be classified into three main categories:

- Home Automation Systems [HAS]
- Remote control system.
- Cloud analytics in IOT

To eliminate the conflict between automation and remote controllability, the proposed system has two different modes and the selection of these mode is based on the position of the mechanical switch. When the mechanical switch is in the ON position, the microcontroller puts the system in home automation mode and when the switch is in the OFF position, the system will be in remote controllability mode. Generally, when users leave the house, the mechanical switch position will be in the OFF position.

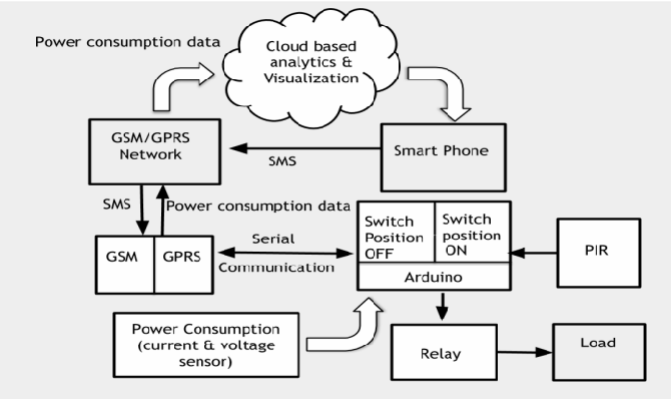

Fig. 1. Smart Home Architecture

A. Home Automation Systems [HAS]

In home automation system, the user will be able to control the load with the mechanical switch just like in traditional ways. But, with the addition of PIR sensor, unnecessary power wastage can be prevented when PIR senses the absence of users around it.

B. Remote Control System

In this mode, the user has to send an SMS request to the number associated with the Subscriber Identification Module (SIM) used in the GSM module [12]. The microcontroller then controls the load through the relay based on the received message.

C. Cloud Analytics in IOT

Power consumption of the smart home can be regularly monitored using current and voltage sensors and this data is sent to the cloud server through GPRS. User gets a notification from the cloud server, when the power consumption is more than the threshold value. Based on this a relevant action can be taken by the user. This cloud server supports analytic and visualization of the data.

IV. Methodology

Methodology has two sections: the hardware design and software implementation.

A. Hardware

The SIM-800 wireless module with an arduino enables remote controllability and the PIR sensor with an arduino enables home automation capability. The load is controlled through a relay and the switch SW1 position defines if the system is in HAS or remote control mode.

1) Wireless Module for Remote controllability and Cloud based IOT:

SIM-800 module has both GSM and GPRS features. As shown in the schematic (Fig. 2.), UART serial communication protocol is being used between the Arduino UNO and the SIM-800 module [13]. The SMS request over GSM network enables the remote controllability and TCP/IP protocol over GPRS enables the connection to the cloud server.

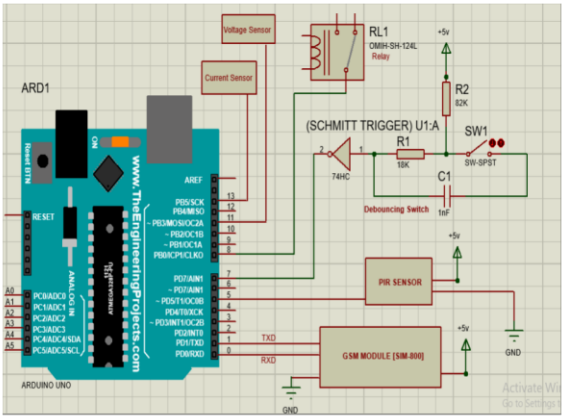

Fig. 2. Schematic of the smart switch

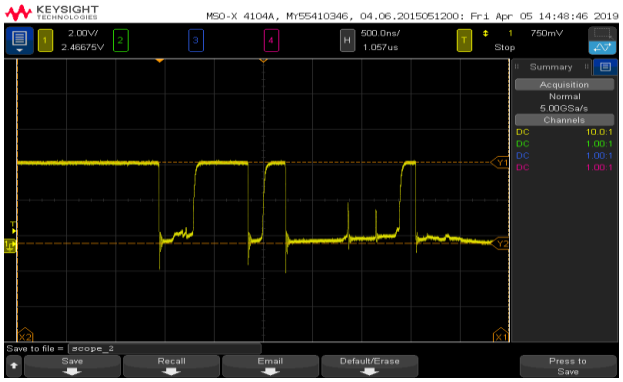

Fig. 3. Bouncing effect

2) Sensor for Home Automation.

PIR sensor detects the infrared light radiating from objects in its range. The presence of human beings near the sensor is depicted by an active high output signal from the PIR sensor. Once a human activity detected, the microcontroller starts counting the timer for 5 minutes and keeps the load in ON state for that duration. If there is no human activity detected in this duration, the load would be turned off [14] after 5 minutes.

3) Debouncing Circuit.

In order to read the status of the mechanical switch using a microcontroller, AC voltage is replaced with 5V DC at the input of the switch. Microcontroller controls the load through a relay, based on the mode selected by the user as explained previously. The inherent bouncing effect of mechanical switches creates issues in automation as shown in Fig. 3. Because of this problem, a single press of the mechanical switch is reflected as a multiple presses electrically. It can be solved by using a debouncing circuit as shown in Fig.4. The circuit consists of a schmitt trigger IC, resistors and capacitors which filters the ripple signals and give clean signals at its output.

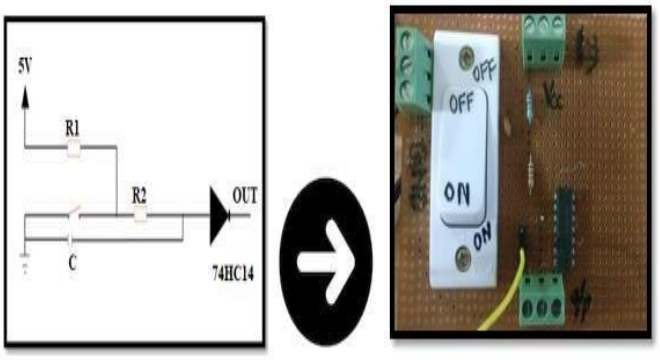

Fig. 4. Debouncing circuit and the hardware setup of the switch

B. Software Design

1) Home Automation and Remote Controllability:

The flowchart of the software for HAS and remote controllability is shown in Fig. 5. After initializing the GPIO pins of the Arduino UNO and GSM/GPRS SIM-800 module, the mechanical switch position is inspected. The switch is in the OFF position indicates the user is not in the home and the user will have privilege to control the load remotely by SMS.

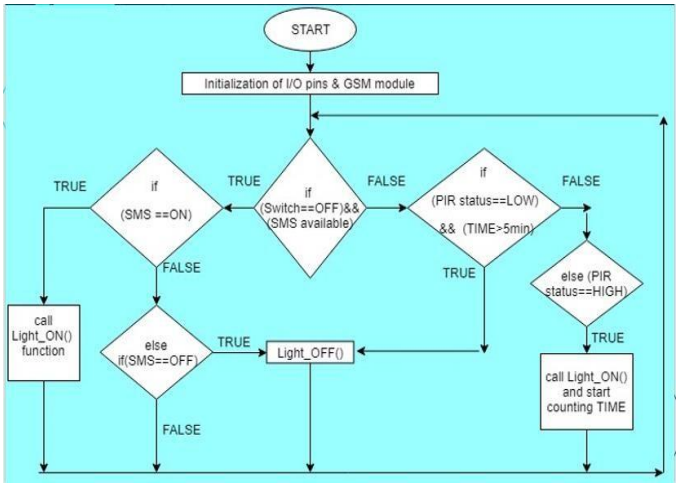

Fig. 5. Flow Chart for HAS and Remote control of the load

The user needs to send an SMS message to turn on the load (SMS==ON) or to turn off the load (SMS==OFF); the corresponding output pin of the microcontroller will control the load through the relay appropriately.

The mechanical switch in the ON position indicates the user is present in the room. As explained earlier, this mode works similar to manual mode. If the sensor detects human presence, its output will be a high pulse, which turns ON the load. But, then if the PIR sensor output continues to be low for more than 5 minutes, the load will be turned OFF. This process repeats as shown in the flowchart to control the load in smart home using a smart switch.

2) Communication and Data analytics:

The overall framework of the monitoring and visualization part is shown in Fig. 6. ThingSpeak is an open source Internet of Things (IoT) cloud platform service provides web services on the cloud to store and retrieve data. The power consumption data collected from the sensors are sent to the ThingSpeak over TCP protocol. User can view the real-time visualization of this data [16].

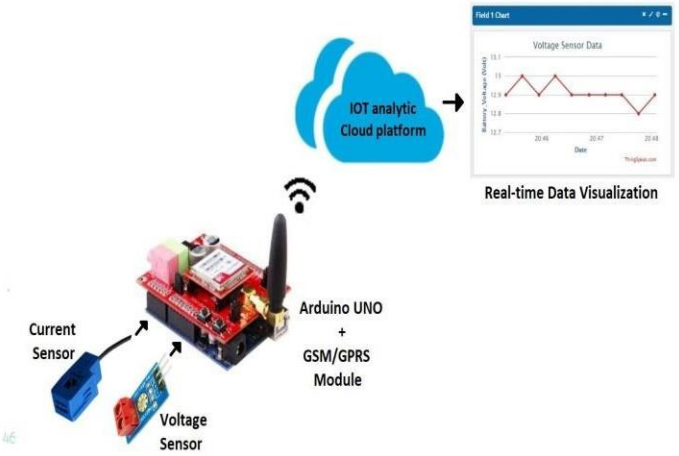

Fig. 6. Monitoring & Visualization

Steps to configure SIM-800 module to Communicate with ThingSpeak:

Step 1: Closing all the existing PDP context.
Step 2: Verifying the device is ready for communicating to the ThingSpeak application.
Step 3: Configure the device for single/multiple IP connection.
Step 4: Attach the device to packet domain service for - controlling load through SMS.
Step 5: Setup the APN with ISP name.
Step 6: Bring up the connection.
Step 7: Return the local IP address.
Step 8: Start a TCP connection.
Step 9: Send the data to ThingSpeak field using TCP - connection.
Step 10: Start the loop again.

V. Analyses and Results

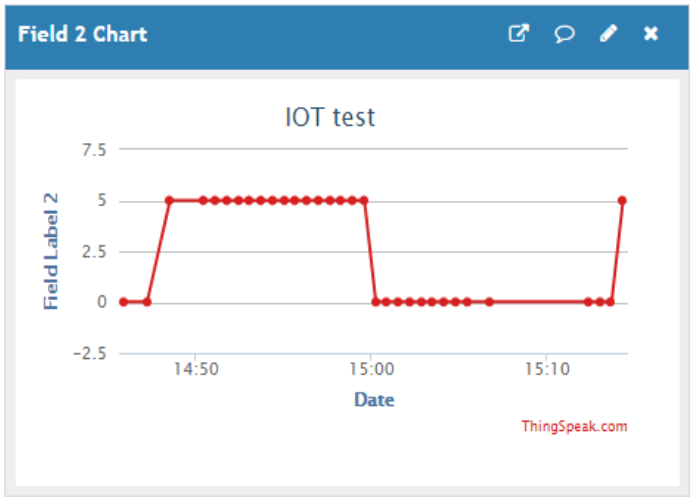

(a)

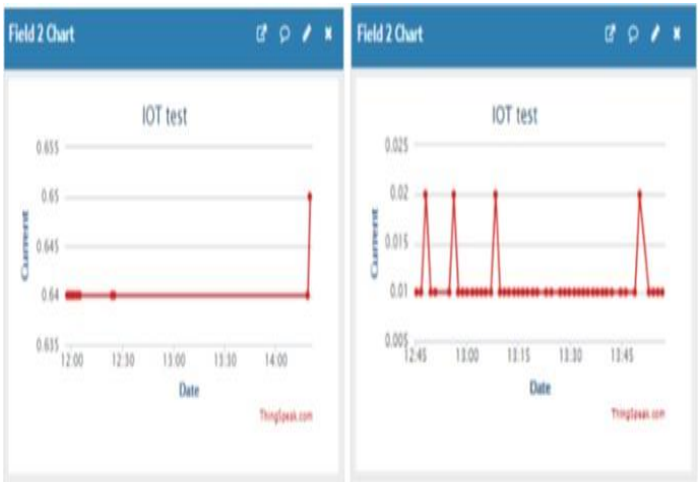

(b) (c)

Fig. 7. (a) Voltage reading & (b) Current consumption when the load is ON, (c) Current consumption when load is OFF

The Fig. 7. (a) represents the voltage values with respect to the switch position. When the voltage is at 5V, the switch is in the ON position and the corresponding current consumption of 0.64 Amps is shown in Fig. 7. (b). When the voltage is at 0V, the switch is in the OFF position and the corresponding current 0.01 Amps is shown in Fig. 7. (c).

As stated earlier the switch position configures the system in HAS or remote controllability mode. The sensors in HAS mode and the wireless module in remote controllability mode controlled the load successfully without any conflict. Implementation of cloud platform like ThingSpeak helped in analysing the real time data [15].

VI. Conclusion and Future Scope

The proposed work delivers the smart switch for Home Automation System [HAS] and remote controllability of the load. A complete functionality test was performed to validate the design of smart switch system and verified that the remote controllability and HAS does not have any collision while controlling the load. The debounce switch circuit is verified using the oscilloscope. The real time voltage and current values are sent to the cloud server to analyze the power consumption data. The user can access this real-time data to make decisions to optimize the usage. In future, we aim to build a Zigbee mesh communication network using multiple smart switches as nodes with Raspberry Pi as gateway and only the gateway can send the aggregated node data to the cloud server, which makes a better architecture. Also, Arduino UNO can be replaced with a low power consumption microcontroller with sleep mode [6]. ThingSpeak can give out warning twitter messages, which can be implemented to make quick decisions at crucial times.

Acknowledgment

We express our sincere gratitude to our beloved Chancellor and world-renowned humanitarian leader Sri. Mata Amritanandamayi Devi (Amma), for the inspiration and motivation in all our endeavors. We would like to thank our teammates and colleagues in the Amrita Center for Wireless Networks & Applications.

References

[1] Raimondi, Francesco Maria, Domenico Curto, Vicenzo Frazitta, and Daniele Milone. "Energy savings for indoor lighting in a shopping mall: a case of study." In 2018 Thirteenth International Conference on Ecological Vehicles and Renewable Energies (EVER), pp. 1-6. IEEE, 2018.

[2] Yang, Miao, Wei Liang, and Weijie Xu. "Design and implementation of industrial wireless network system based on WIA-PA." In 2010 8th World Congress on Intelligent Control and Automation, pp. 6799-6803. IEEE, 2010.

[3] Bhat, Amit, H. M. Jeevith, and B. Chirag. "Hospital power automation system using live gesture recognition." In 2016 International Conference on Wireless Communications, Signal Processing and Networking (WiSPNET), pp. 2279-2282. IEEE, 2016.

[4] Soumya, S., Malini Chavali, Shuchi Gupta, and Niharika Rao. "Internet of Things based home automation system." In 2016 IEEE International Conference on Recent Trends in Electronics, Information & Communication Technology (RTEICT), pp. 848-850. IEEE, 2016.

[5] Arjun D; Indukala P K; K A Unnikrishna Menon; “Border Surveillance and Intruder Detection Using Wireless Sensor Networks: A Brief Survey,” International Conference on Communication and Signal Processing, 2017, pp. 1125 - 1130.

[6] Murugesh, Remya, Aravind Hanumanthaiah, Ullas Ramanadhan, and Nirmala Vasudevan. "Designing a Wireless Solar Power Monitor for Wireless Sensor Network Applications." In 2018 IEEE 8th International Advance Computing Conference (IACC), pp. 79-84. IEEE, 2018.

[7] Mandula, Kumar, Ramu Parupalli, CH AS Murty, E. Magesh, and Rutul Lunagariya. "Mobile based home automation using Internet of Things (IoT)." In 2015 International Conference on Control, Instrumentation, Communication and Computational Technologies (ICCICCT), pp. 340-343. IEEE, 2015.

[8] Kang, Byeongkwan, Sunghoi Park, Tacklim Lee, and Sehyun Park. "IoT-based monitoring system using tri-level context making model for smart home services." In 2015 IEEE International Conference on Consumer Electronics (ICCE), pp. 198-199. IEEE, 2015.

[9] Akorede, M. F., J. J. Fatigun, J. A. Opaluwa, and E. Pouresmaeil. "Efficient remote control system using SMS and WiFi technology for outdoor security lighting applications." In 2017 IEEE PES PowerAfrica, pp. 512-517. IEEE, 2017.

[10] Sukmana, Husni Teja, Muhammad Ghiyast Farisi, and Dewi Khairani. "Prototype utilization of PIR motion sensor for real time surveillance system and web-enabled lamp automation." In 2015 IEEE Asia Pacific Conference on Wireless and Mobile (APWiMob), pp. 183-187. IEEE, 2015.

[11] Ramlee, Ridza A., Mohd A. Othman, M. H. Leong, Mohd M. Ismail, and S. S. S. Ranjit. "Smart home system using android application." In 2013 International Conference of Information and Communication Technology (ICoICT), pp. 277-280. IEEE, 2013.

[12] Teymourzadeh, Rozita, Salah Addin Ahmed, Kok Wai Chan, and Mok Vee Hoong. "Smart gsm based home automation system." In 2013 IEEE Conference on Systems, Process & Control (ICSPC), pp. 306-309. IEEE, 2013.

[13] Kim, Meesun, Kyoungsook Kim, Kyongduck Seo, Joosang Lee, Kyoungsik Park, and Kwanghoon Kim. "Modeling process-aware Internet of Things services over an ARDUINO community computing environment." In 2017 19th International Conference on Advanced Communication Technology (ICACT), pp. 163-166. IEEE, 2017.

[14] JeyaPadmini, J., and K. R. Kashwan. "Effective power utilization and conservation in smart homes using IoT." In 2015 International Conference on Computation of Power, Energy, Information and Communication (ICCPEIC), pp. 0195-0199. IEEE, 2015.

[15] https://spectrum.ieee.org/tech-talk/telecom/internet/popular-internet-of-things-forecast-of-50-billion-devices-by-2020-is-outdated

[16] Ramesh, Maneesha Vinodini, Renjith Mohan, and Soumya Menon. "Live-in-Labs: Rapid translational research and implementation-based program for rural development in India." In 2016 IEEE Global Humanitarian Technology Conference (GHTC), pp. 164-171. IEEE, 2016.

[17] Krishna, Savitha, Ullas Ramanathan, Manoj Pokkiyarath, and Renjith Mohan. "Real time monitoring of solar micro grid installations; discussion on three year performance analysis and system black out modelling." In 2017 International Conference on Technological Advancements in Power and Energy (TAP Energy), pp. 1-7. IEEE, 2017.

Proceedings of the Fourth International Conference on Communication and Electronics Systems (ICCES 2019)
IEEE Conference Record # 45898; IEEE Xplore ISBN: 978-1-7281-1261-9

Mutispectral brain Magnetic Resonance Imaging denoising using non-local means with statistical nearest neighbor

Utkarsha I. Jondhale
Department of Information Technology,
SGGS IE & T, Nanded.
Email: utkarshajondhale@gmail.com

Prof. Rachna S. Potpelwar,
Department of Information Technology,
SGGS IE & T, Nanded.
Email: rspotpelwar@sggs.ac.in

***Abstract*—The basic operation of computer vision is filtering. It is the overture process in applications of biomedical image processing. MRI denoising improves the diagnosis accuracy, quality of image with operations performed on it such as image segmentation and registration; and also parameter estimation. It has been observed that the noise in MRI follows gaussian and rician distribution. In this paper, algorithms are applied on multispectral brain MRI that are either T1-weighted or T2-weighted. The proposed method Multispectral non-local means with statistical nearest neighbor is applied and the results are compared with other NLM filters available. The experimental results show that proposed method provides better noise reduction than NLM with nearest neighbor and adaptive NLM.**

***Index Terms*—MRI, NLM, Multispectral, T1 and T2- weighted images.**

I. Introduction

THE radiology technology that uses radio waves, magnetism, and computer for producing images of different body structures are called Magnetic Resonance Imaging that is what we call MRI. When various tests fails to diagnose any disease, MRI comes into picture. Its an extremely accurate process for detection of disease throughout the body. The MRI gets affected by different parameters such as it gets affected by environment also due to equipment's and operators performance. These leads to the noisy images. So, we need appropriate techniques to get rid of noise from data. Removing the noise from the data becomes important because noisy image leads to improper diagnosis. The goal of any noise removal technique is to effectively get rid of noise without affecting the data available in the image.

The types of noise that are observed in MRI are Gaussian and Rician nosie. Gaussian noise is noises which have a probability density function (PDF) i.e. equal to the normal distribution, this is also known as the Gaussian distribution. We can also say that the values of noise are taken are Gaussian-distributed. Gaussian random variable z has probability density function p and is given by:

$$p_G(z) = \frac{1}{\sigma\sqrt{2\pi}} e^{-\frac{(z-\mu)^2}{2\sigma^2}} \quad (1)$$

where z defines the grey level, mean value is given as μ while Standard deviation defined as σ.

Major noise seen in MR images is Rician noise; this noise arose from complexity of Gaussian noise that are introduced in original frequency domain measurements. If x is the corrupted

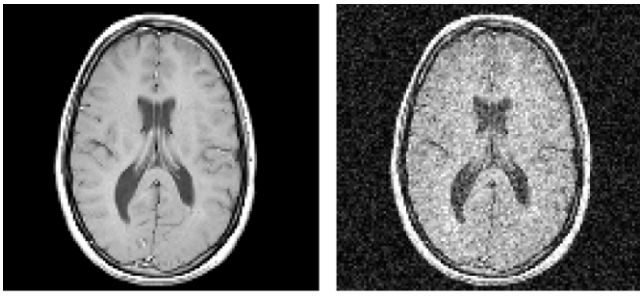

Fig. 1: Rician noise

intensity of image then, Rician probability density function will be given by:

$$p(x) = \frac{x^2}{\sigma^2} exp(-\frac{x^2 + A^2}{2\sigma^2}) I_0(\frac{xA}{\sigma^2}) \quad (2)$$

where A - amplitude of a noise-free image, σ^2- the Gaussian noise variance, I_0 - modified zero order Bessel function.

Diagnostic MRI frequently requires high SNR and high spatial resolution. SNR can be improved by applying image filtering during post acquisition. Different denoising techniques available are anisotropic diffusion filter(ADF)[1], [2],[3], [4]; bilateral filter [5], [6]; trilateral filter [7], [8]; wavelet domain transform, NLM [9]; discussed in Section III.

II. List of the Notations and Abbreviations:

NN	Nearest neighbor
SNN	Statistical nearest neighbor
NLM	Non-local means
NLM-NN	NLM with nearest neighbor
NLM-SNN	NLM with statistical nearest neighbor

MS-NLM-NN	Multispectral NLM-NN
MS-NLM-SNN	Multispectral NLM-SNN
A-NLM	Adaptive non-local means

III. Related Work

Some work done in this area are decribed below. The work is decribed in reference to the methods. The methods in which the work is decribed are:

- Anisotropic Diffusion Filter (ADF)
- Combination of range and domain filtering techniques:
  - Bilateral filter
  - Trilateral filter
- Wavelet domain transform
- Adaptive Non-local means

A. Anisotropic Diffusion Filter (ADF)

Perona and Malik [2] developed the schemes such as edge detection and also multiscale smoothing, and are called as anisotropic diffusion filter (ADF). This filter overcome spatial filtering drawback and it also significantly improved the quality of image i.e. by preserving boundaries of the object, efficient removal of noise from homogeneous regions and also sharpening of edges. This filter cast the problem in the heat equation form i.e based on 2nd order PDE (Partial differential equation). Diffusive process formulation is done for smoothening. The process is stopped at boundaries. This is done by selection of local gradient strengths over various directions. Here, image u is just convoluted in orthogonal way to that of image gradient. This ensures the edge preservation. The repetitive process of denoising for beginning image u_0 cab be given as:

$$\begin{cases} \frac{\partial u(x,t)}{\partial t} = div(c(x,t)\nabla u(x,t)) & u(x,0) = u_0(x) \end{cases} \quad (3)$$

In ∇u(x, t); x voxel's image gradient & t is the iteration, while ∂u(x, t)/∂t is u(x, t) 's partial temporal derivation and

$$c(x,t) = g||\nabla u(x,t)|| = e^{(-||\nabla u(x,t)||/K^2)} \quad (4)$$

K here consists of diffusivity parameter. For denoising MRI, Gerig et al. [3] has proposed the filter for 2D and 3D images. Although noise filter performance over images are excellent, the image model underlying has slow variance. A gray value constant slope is obtained due to edge sharpening. Here the noise of the image is considered to have zero means and also its Gaussian distributed. According to [4], adaptive anisotropic diffusion filter does not retain edge sharpening property. Here, level contours of local intensity orientation and its curvature is used to control the filter kernel and shape instead of local gradient strength. These ensured the preservation of edges and corners throughout the process.

B. Combination of range and domain filtering techniques

Bilateral filter:

An alternative for anisotropic diffusion filter i.e. bilateral filter was proposed by Manduchi and Tomasi [6]. These approaches smoothens the image and preserve the edges. Single iteration is enough for bilateral filter implementation. It does not involve PDE solution unlike anisotropic diffusion. Two Gaussian filters are combined to get this filter i.e. range and domain filter. The domain filter weights and geometric distance (i.e spatial) of a voxel/pixel are proportional around pixels neighborhood. Whereas, the range filter coefficients and intensity (photometric) distance are proportional around the pixel neighborhood. When average value replaces each pixel intensities in the image, we obtain filtered image. The average value is weighted with in a spatial window by the intensity and geometric similarities amongst the pixels.

[5] has proposed a filter named guided bilateral filter, which is a new way for deriving the joint/cross bilateral filter. Its for a particular case with more generic filter. Its generic, iterative and also inherits robustness properties of robust bilateral filter. It also uses a guide image.

Trilateral filter:

Trilateral filter was aimed by Wong et al. [7], [8] for reducing the noise within the MRI which works on the same line as bilateral filter.In addition to bilateral filter, trilateral takes local structures similarity into account for smoothening of the image. Using local structure's information, the non-homogeneous regions can be identified. In case of the homogeneous region, only the low pass filters are applied. In case of region that are non-homogeneous, each pixel intensity value is substituted by average value measured within a spatial window by three components i.e. photometric, geometric and local morphological similarities in amongst neighboring pixels. For edge prevention while smoothing narrow spatial window is used.

C. Wavelet domain transform

Robert D. Nowak [10] presented two methods on wavelet domain filtering for removal of noise from MRI. In case of high SNR, the MRI data governed by Rician distribution and is estimated as the Gaussian. The first algorithm is simple and also effective on noise removal for above mentioned cases. Gaussian is no longer valid at low sound-to-noise (SNR). Two degrading effects in Rician distribution are signal dependent bias and pixel value's random fluctuation. Due to which image contrast gets reduced. For such complications, wavelet domain filter was derived that would operate on squared magnitude image. The second algorithm works on the noise removal and bias removal from squared magnitude image.

D. Adaptive Non-Local means:

There are many filters which considers the noise is equally distributed throughout the image. If this consideration fails, the filter used gets suboptimal. This becomes the case with MR images which has spatially changing noise levels. These noises are obtained due to parallel imaging, surface coil-based acquisitions or intensity inhomogeneity-corrected images. In A-NLM, the information of local image and its noise level

are used for adjusting denoising strength amount of the filter. This data is automatically received from the images by using a new method explained in [11] and is named as a new local noise estimation method.

IV. Methodology

Defined on decrete grid I, lets consider multispectral images which are perfectly registered. These explains bounded spatial domain that are 3D and traversed by image, S = {S(i)| i ∈ I , S(i) ∈ R^K }. Here K is considered as number of frames that are of the multispectral data set. Spectral dimension is the a frame k taken as a peculiar image from the mutispectral dataset, obtained at peculiar value of a changing acquisition parameter. Measured signal intensity denoted by $S_k(i)$, obtained from frame k, voxel i which is calculated from conditional Rician probability $p(S_k(i)|A_k(i), \sigma_k(i))$, considering $A_k$as unknown underlying amplitude & $\sigma_k$as unknown noise std. deviation and is assumed spatially constant & set as σ.

A. NLM Filter with nearest neighbor:

Buades et al. [12], initially introduced NLM i.e the nonlocal-means filter. The voxel i intensity is approximated as the signal intensities' weighted mean that is computed over entire voxels j in R size large searching window that is centered across voxel i which is of interest [13], [14], [11], [12]. The weight w(i, j) measuring the resemblance between those two voxels i, j; in the frame k is estimated as

$$w_k(i,j) = \exp\left(-\frac{d_k(i,j)}{h^2}\right) \tag{5}$$

h is the smoothing parameter which paramaterize the GWED weighting. And in case of magnitude MRI, the estimate $\hat{A}_k(i)$ of amplitude $\hat{A}_k$ in kth frame and voxel i ,is given by

$$\hat{A}_k(i) = \sqrt{\max\left\{\frac{\sum_j^R w_k(i,j)\, S_k^2(j)}{\sum_j^R w_k(i,j)} - 2\hat{\sigma}^2, 0\right\}} \tag{6}$$

This is a modifiction to [15].

B. MS-NLM Filter with nearest neighbor:

Wiest-Daesslé et al. and Manjón et al. have expanded the NLM filter such that it includes data from MRI which are received with weightings various parameters in computation of w(i , j) [16], [17], [18], achieved by simply replacing GWED in Eq. 5 by its extension due to multispectral data by

$$w_k(i,j) = \exp\left(-\frac{\sum_{k=1}^K d_k(i,j)}{Kh^2}\right) \tag{7}$$

The estimate $\hat{A}_k(i)$ of the amplitude of kth frame and voxel i is calculated by

$$\hat{A}_k(i) = \sqrt{\max\left\{\frac{\sum_j^R w_k(i,j)\, S_k^2(j)}{\sum_j^R w_k(i,j)} - 2\hat{\sigma}^2, 0\right\}} \tag{8}$$

C. NLM filter with statistical nearest neighbor:

The noise free patch estimate's prediction error is reduced in Statistical NN (SNN). NN blurs low-contrast image with low SNR. But it is more in SNN.

An improvement in the quality of perceived image is observed due to SNN. It is assured by measuring over serveral metrics of quality; applied on some standard datasets of images. This improvement is observed in both white and colored Gaussian noise. It is also observed that, if SNN is applied with NLM that image quality enhances as compared to state-of-art with computational cost being much lower.[19]

Lets see how the neighbors are selected. NLM denoising [13], [20] averages similar patches in the image and in final stage averages are aggregated. Assume the representation in vector of S × S × C noisy reference patch is given as $\mu_r = [\mu_r^0, \mu_r^1, ..., \mu_r^{S^2C-1}]$, whereas for patch of noisy neighbor γ_k, the squared distance between $\mu_r$and γ_k is given by

$$d^2(\mu_r - \gamma_k) = \frac{1}{P} \cdot \sum_{i=0}^{P-1} \left(\mu_r^i - \gamma_k^i\right)^2 \tag{9}$$

where P=S^2C. If $\mu_r$and the neighbor $\gamma_k$are two noisy replica of the same patch; where $\mu_r$is the reference patch and $\gamma_k$is its neighbor; then what we get is

$$d^2(\mu_r - \gamma_k) = \frac{2\sigma^2}{P} \cdot \sum_{i=0}^{P-1} G(0,1)^2 \tag{10}$$

where $G\left(\mu, \sigma^2\right)$ means Gaussian random variable having mean $\mu$and σ^2variance. The summation of P squared normal variable have P degrees of freedom and χ_P^2distribution; therefore we can say that $d^2(\mu_r - \gamma_k) \sim \frac{2\sigma^2}{P} \cdot \chi_P^2$ and

$$E[d^2(\mu_r - \gamma_k)] = 2\sigma^2 \tag{11}$$

Hence we can conclude that the expected squared distance is not zero for two replicas of same patch.

Inspired by Eq. 11, an alternative to NN is collecting neighbors having squared distance close to expectation from the reference patch. SNN are the $\{\gamma_k\}_{k=1.....N_n}$ patches which minimize the following equation:

$$|d^2(\mu_r - \gamma_k) - o.2\sigma^2| \tag{12}$$

o is the additional offset parameter which helps to go from the traditional approach of nearest neighbor ($\sigma = 0$) to SNN approach($\sigma = 1$).[19]

V. Results

The results are analyzed on the basis of numerical as well as visually.

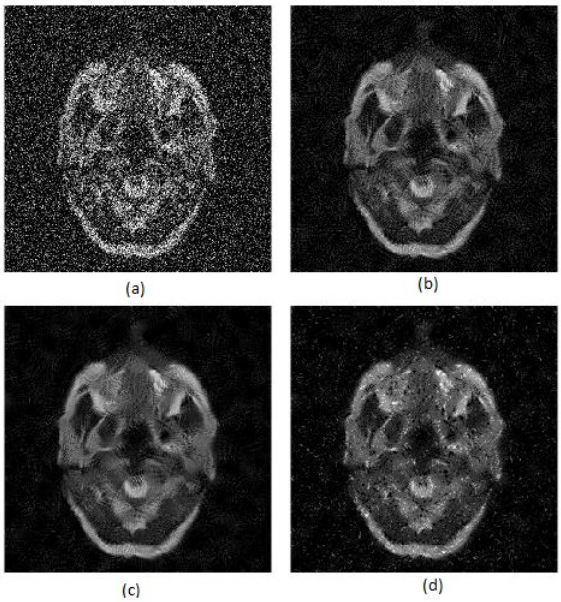

Fig. 2: Comparison of NLM-NN, NLM-SNN and ANL. (a) Noisy image (b) Output of Non-local means with nearest neighbor (c) Output of Non-local means with statistical nearest neighbor (d) Output of Adaptive non local means

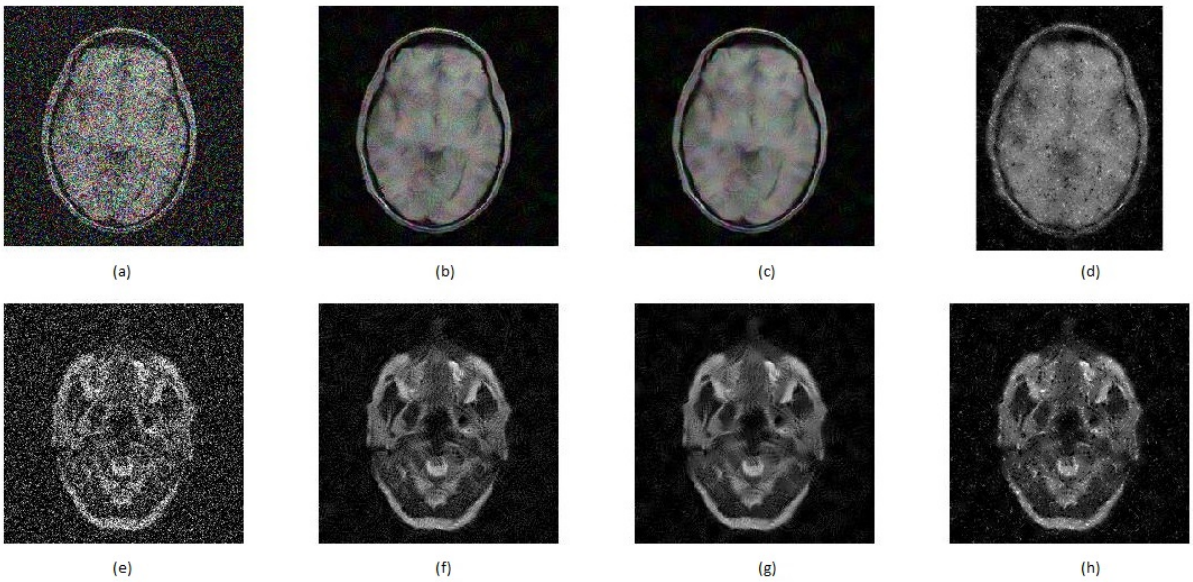

Fig. 3: Comparision of algorithms over T1 and T2 weighted barin MRI images (a) noisy T1 image (b) output of MS-NLM-NN over T1 (c) output of MS-NLM-SNN over T1 (d) output of A-NLM over T1 (e) noisy T2 image (f) output of MS-NLM-NN over T2 (g) output of MS-NLM-SNN over T2 (h) output of A-NLM over T2

	MS-NLM-NN			**MS-NLM-SNN**			**A-NLM**		
	PSNR	**SNR**	**MSE**	**PSNR**	**SNR**	**MSE**	**PSNR**	**SNR**	**MSE**
Image 1:	22.4492	11.4705	0.0056895	24.0454	13.0667	0.0039396	21.0835	11.3527	0.007792
Image 2:	22.3376	11.3592	0.0058376	23.9403	12.9618	0.0040362	21.0484	11.3176	0.0078553
Image 3:	22.4014	11.4218	0.0057526	23.967	12.9874	0.0040114	20.9999	11.2686	0.0079435

TABLE I: The calculation of PSNR, SNR and MSE for various T1-weighted MRI images

	MS-NLM-NN			MS-NLM-SNN			A-NLM		
	PSNR	**SNR**	**MSE**	**PSNR**	**SNR**	**MSE**	**PSNR**	**SNR**	**MSE**
Image 1:	20.3134	6.8448	0.0093039	22.7032	9.2346	0.0053664	20.8608	7.3923	0.008202
Image 2:	20.1951	7.1432	0.0095607	22.4819	9.43	0.0056469	20.7269	7.675	0.0084588
Image 3:	20.1899	7.589	0.0095721	22.3872	9.7863	0.0057714	20.7049	8.1041	0.0085017

TABLE II: The calculation of PSNR, SNR and MSE for various T2-weighted MRI images

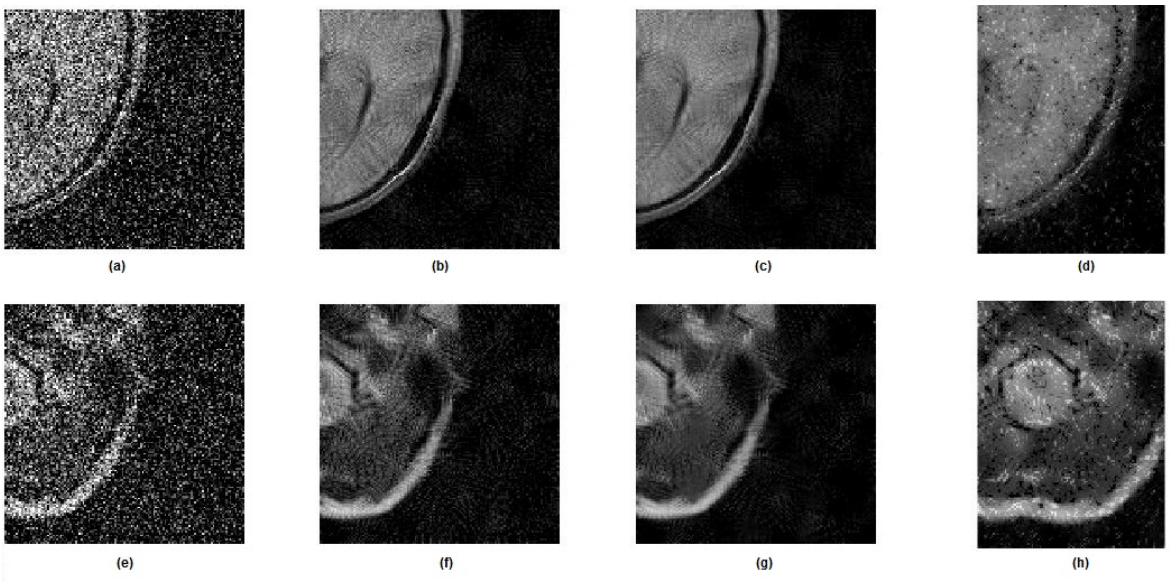

Fig. 4: Zoomed image Comparision of algorithms over T1 and T2 weighted barin MRI images (a) noisy T1 image (b) output of MS-NLM-NN over T1 (c) output of MS-NLM-SNN over T1 (d) output of A-NLM over T1 (e) noisy T2 image (f) output of MS-NLM-NN over T2 (g) output of MS-NLM-SNN over T2 (h) output of A-NLM over T2

The fig 2. shows the visual impact of the algorithms - NLM-NN, NLM-SNN and A-NLM over an MRI image. Fig 2. shows the output of the traditional methods developed. Whereas fig 3. shows the visual results for multispectral data over the various algorithm mentioned in Section IV. The first row shows the working of the multispectral algorithm over T1 image whereas the second row shows the working of the same methods over T2 image data. To get a better visual clarification, fig 4. shows the zoomed part of image.

Table I and II shows the numerical analysis of the algorithms mentioned in Section IV. The results are evaluated on the basis of mean square error, peak SNR and SNR.

VI. Conclusions

MRI images gets affected by external elements, the output images get inculcated with noise. Hence for better diagnosis this noise must be removed with any proper methodology. Hence we came up with a method. And this method is applied over different T1 and T2 weighted brain MRI images along with other methods. The conclusions are drawn based on the peak sound-to-noise ratio. The numerical analysis are shown in Table I and Table II. We can say that the peak SNR (PSNR) is high for MS-NLM-SNN for both T1 and T2 weighted brain images. Also we know if PSNR is high the quality of image is good. So, we can say that, this method is better than other two since it has high PSNR. Also we can observe that the mean square error for MS-NLM-SNN is less as compared to MS-NLM-NN and A-NLM. Fig. 2 and Fig. 3 shows the visual results.

References

[1] K. Liu, J. Tan, and B. Su, "Adaptive anisotropic diffusion for image denoising based on structure tensor," in *2014 5th International Conference on Digital Home*. IEEE, 2014, pp. 111–116.

[2] P. Perona and J. Malik, "Scale-space and edge detection using anisotropic diffusion," *IEEE Transactions on pattern analysis and machine intelligence*, vol. 12, no. 7, pp. 629–639, 1990.

[3] G. Gerig, O. Kubler, R. Kikinis, and F. A. Jolesz, "Nonlinear anisotropic filtering of MRI data," *IEEE Transactions on medical imaging*, vol. 11, no. 2, pp. 221–232, 1992.

[4] G.-Z. Yang, P. Burger, D. N. Firmin, and S. Underwood, "Structure adaptive anisotropic filtering for magnetic resonance image enhancement," in *International Conference on Computer Analysis of Images and Patterns*. Springer, 1995, pp. 384–391.

[5] L. Caraffa, J.-P. Tarel, and P. Charbonnier, "The guided bilateral filter: When the joint/cross bilateral filter becomes robust," *IEEE Transactions on Image Processing*, vol. 24, no. 4, pp. 1199–1208, 2015.

[6] C. Tomasi and R. Manduchi, "Bilateral filtering for gray and color images," in *Computer Vision, 1998. Sixth International Conference on*. IEEE, 1998, pp. 839–846.

[7] W. C. Wong and A. C. Chung, "A nonlinear and non-iterative noise reduction technique for medical images: concept and methods comparison," in *International Congress Series*, vol. 1268. Elsevier, 2004, pp. 171–176.

[8] W. C. Wong, A. C. Chung, and S. C. Yu, "Trilateral filtering for biomedical images," in *Biomedical Imaging: Nano to Macro, 2004. IEEE International Symposium on*. Citeseer, 2004, pp. 820–823.

[9] M. Bouhrara, J. M. Bonny, B. G. Ashinsky, M. C. Maring, and R. G. Spencer, "Noise Estimation and Reduction in Magnetic Resonance Imaging Using a New Multispectral Nonlocal Maximum-likelihood

Filter," *IEEE Transactions on Medical Imaging*, vol. 36, no. 1, pp. 181–193, 2017.

[10] R. D. Nowak, "Wavelet-based Rician noise removal for magnetic resonance imaging," *IEEE Transactions on Image Processing*, vol. 8, no. 10, pp. 1408–1419, 1999.

[11] J. V. Manjón, P. Coupé, L. Martí-Bonmatí, D. L. Collins, and M. Robles, "Adaptive non-local means denoising of mr images with spatially varying noise levels," *Journal of Magnetic Resonance Imaging*, vol. 31, no. 1, pp. 192–203, 2010.

[12] A. Buades, B. Coll, and J.-M. Morel, "A non-local algorithm for image denoising," in *2005 IEEE Computer Society Conference on Computer Vision and Pattern Recognition (CVPR'05)*, vol. 2. IEEE, 2005, pp. 60–65.

[13] ——, "A review of image denoising algorithms, with a new one," *Multiscale Modeling & Simulation*, vol. 4, no. 2, pp. 490–530, 2005.

[14] H. Liu, C. Yang, N. Pan, E. Song, and R. Green, "Denoising 3d mr images by the enhanced non-local means filter for rician noise," *Magnetic resonance imaging*, vol. 28, no. 10, pp. 1485–1496, 2010.

[15] N. Wiest-Daesslé, S. Prima, P. Coupé, S. P. Morrissey, and C. Barillot, "Rician noise removal by non-local means filtering for low signal-to-noise ratio mri: applications to dt-mri," in *International Conference on Medical Image Computing and Computer-assisted Intervention*. Springer, 2008, pp. 171–179.

[16] J. V. Manjón, N. A. Thacker, J. J. Lull, G. Garcia-Martí, L. Martí-Bonmatí, and M. Robles, "Multicomponent mr image denoising," *Journal of Biomedical Imaging*, vol. 2009, p. 18, 2009.

[17] N. Wiest-Daesslé, S. Prima, P. Coupé, S. P. Morrissey, and C. Barillot, "Non-local means variants for denoising of diffusion-weighted and diffusion tensor mri," in *International Conference on Medical Image Computing and Computer-Assisted Intervention*. Springer, 2007, pp. 344–351.

[18] M.-X. Zhou, X. Yan, H.-B. Xie, H. Zheng, D. Xu, and G. Yang, "Evaluation of non-local means based denoising filters for diffusion kurtosis imaging using a new phantom," *PloS one*, vol. 10, no. 2, p. e0116986, 2015.

[19] I. Frosio and J. Kautz, "Statistical nearest neighbors for image denoising," *IEEE Transactions on Image Processing*, vol. 28, no. 2, pp. 723–738, 2018.

[20] A. Buades, B. Coll, and J.-M. Morel, "Non-local means denoising," *Image Processing On Line*, vol. 1, pp. 208–212, 2011.

Proceedings of the Fourth International Conference on Communication and Electronics Systems (ICCES 2019)
IEEE Conference Record # 45898; IEEE Xplore ISBN: 978-1-7281-1261-9

Word Based Statistical Machine Translation

(*With Reference To Kashmiri Language)*

Neeha Ashraf
Dept. of Computer Science
University of Kashmir
Hazratbal, J&K, India
neehaashraf@gmail.com

Manzoor Ahmad
Dept. of Computer Science
University of Kashmir
Hazratbal, J&K, India
manzoor@kashmiruniversity.net

***Abstract*—Machine Translation is the programmed interpretation of one natural language to another natural language. Human languages can be processed by computers via grammars/rules or via statistics/data. There are many machine translation techniques which are either Rule-based or Knowledge-based. In this paper we will discuss the Statistical Machine Translation (SMT) techniques. The Statistical Machine Translation makes use of statistics or data to find the translation of a given source text. In word primarily based SMT, the simple unit of translation is a word. As a consequence words in an input sentence are translated phrase by phrase individually and these words are than sooner or later organized in a particular way to get the target sentence. The paper discusses numerous fashions for the word based Statistical Machine translation. The paper is written with reference to Kashmiri Language, as not much work has been done in this regard.**

Keywords—Machine Translation;Word based Statistical Machine Translation;Kashmiri,Kashur.

I. INTRODUCTION

One of the most successful approach to machine translation [1] is Statistical Machine Translation (SMT) [2]. Statistical system translation begins with a totally big facts set of right translations, that is, a corpus of texts which have already been translated into multiple languages, and then uses the ones texts to routinely infer a statistical version of translation. That statistical version is then implemented to new texts to make a guess as to a reasonable translation. The systems learns automatically how to translate text from source language to a target language using a large corpora of analogous translations .The corpora [3] used is a bilingual or parallel corpora. The notion of Statistical Machine Translation was conceived by IBM in early 1990's.The SMT was inspired by Shannon's Information Theory [4], but was not feasible with early computers.Inorder to use statistical models, we need to create many alternatives called hypothesis. Each hypothesis is then assigned a particular score. The best hypothesis is then searched using this score. The SMT can be word-based, phrase-based and hierarchical phrase–based system. The word –primarily based SMT method is relatively simple and green. The main downside of the system is that the oversimplified word by word translation of sentences, may additionally reduce the performance of the interpretation system.

II. LEXICAL TRANSLATION

The simple representation for statistical machine translation is defined using lexical translation, which is actually interpretation of each word without any regard to other words. In a Kashmiri-English dictionary we may find that most words have multiple translation E.g. Utensils, Dish **(**بانه), Mountain, Ball (بال) .Some translations for a particular word may be more likely, whereas others are used in certain circumstances. Statistical Machine Translation makes use of statistics. In case of the example given below, we can count how often (بانه) is translated to utensils and dish by looking at a corpus of Kashmiri [5],[6] to English translations.

Translation of بانه	Count
Dish	1600
Utensils	8000

Fig. 1.Different translations of Kashmiri word in English

These numbers can be used to calculate a lexical translation[7] probability distribution, which says that the function $\mathbf{P_f}$ should yield a maximum value if a given English word e is a most used interpretation or should give a low value if a given English word e is a infrequent interpretation. The function $\mathbf{P_f}$ is required to have two properties.

$$\sum_{e} Pf\ (e) = 1$$

Where e: $0 \leq Pf \leq 1$

II. MAXIMUM LIKELIHOOD ESTIMATION

The probability distribution may be given by calculated the ratio of counts. Consider an instance where we have 12000 incidences of the word بانه in the text and 8000 of these are translated as utensils and 4000 are translated as dish. If we

calculate the ratio for each translated word, we can get the probability for each translated word used. Therefore,

P (بانہ) (Utensils) = 8000/12000 =0.6

P (بانہ) (Dish) =4000/1200=0.3

Thus we end up with the following function.

P_f (e) = 0.6 if e = utensils

= 0.3 if e = dish

This estimation is called Maximum Likelihood Estimation [8]. For a Statistical Machine Translation system, we require a huge equivalent or bilingual corpus also known as bitext. This corpus consists of a document in source dialect and its translation in the target dialect. Using this corpus we can automatically find those sentences which are translations of one another. These word – aligned sentence pairs are used for automatic estimation of a statistical model. If a new text is given to translate, we apply this model to get most probable translation. Consider a Kashmiri sentence taken from Kashmiri-English corpora.

انسان چھٕ پنہ نہن کامین ہند پانہ ذمہ دار

We will use lexical translation probabilities for the above mentioned sentence. A lexical probability function say P (e l f) which denotes the probability of interpreting a Kashmiri word f into an English word e.

Following this word to word translation of the Kashmiri sentence **(**انسان چھٕ پنہ نہن کامین ہند پانہ ذمہدار**)**.The one possible translation is

"Man is responsible for his own deeds".

The next step is to align or map from English words to Kashmiri words.

ذ مہ دار	پانہ	ہند	کامین	پنہ نہن	چھ	انسان
7	6	5	4	3	2	1

Man	is	responsible	for	his	own	deeds
1	2	3	4	5	6	7

Fig.2.Depiction of Kashmiri Sentence and its English Translation

Alignment function **a** plots each output English word at location **j** to each given Kashmiri word at location **i.** Therefore alignment function can be denoted as.

a: j -> i

For the above example the alignment function can be determined as:

a**: {1->1,2->2,3->7,4->5,5->3,6->6,7->4}**

ذ مہ دار		پانہ		ہند		کامین		پنہ نہن		چھ		انسان	
e	**P(e|f)**	**e**	**P(e|f)**	**e**	**P(e|f)**	**e**	**P(e|f)**	**e**	**P(e|f)**	**e**	**P(e|f)**	**e**	**P(e|f)**
Responsible	0.7	Own	0.8	For	0.7	Deeds	0.8	His	0.8	Is	0.9	Man	0.7
Liable	0.15	Personal	0.16			Actions	0.5	Own	0.2			Human	0.4
Blamable	0.25	His	0.7			Conduct	0.2	Personal	0.15			Fellow	0.01
Accountable	0.5					Manner	0.05						

Fig.3.Depiction of Lexical Probability Distribution

We need to take care of certain things here.
1. It is possible that languages have different word order (sentence structure)
E.g. English has [SVO] word order whereas Kashmiri has [SOV] word order.
2. Languages also differ in number if words required to express the same concept.
E.g.

به چھس وقتك پابند
I am punctual

3. Words in one language say English may have no relative Kashmiri input word .To represent this a special symbol known as NULL is used.
E.g.

آب جھ وشن
The water is hot

a : {1->0,2->1,3->2,4->3}

III. MODELLING IN STATISTICAL MACHINE TRANSLATION

A. NOISY CHANNEL MODEL

If we wish to form a machine translation system for a given foreign sentence say "f" in Kashmiri language and produce its translation say "e" in English language by combining the interpretation model and the language model. To find the interpretation of sentence "f" in Kashmiri dialect, choose the English sentence "e" which maximizes **P (e|f). P(e|f)** is a sequence of words "**e"** in the translated dialect i.e. English is the translation of a sequence of words "**f** "in the source dialect i.e. Kashmiri. Modelling the probability distribution **P(e|f)** may be approached with Bayes Theorem.

$$P(e|f) \propto P(f|e)P(e)$$

- **P(f|e)** is the interpretation version ,that is the chance that the supply string "**f"** is the interpretation of the translated string "**e".** The translation version cares approximately selecting **e** phrases that were possibly used to generate **f (FAITHFULNESS**).
- **P(e)** is the Language version ,which gives the probability of on the grounds that translated language string or the form of sentences which are likely inside the goal language.
- The Language Model cares about picking **e** words that are likely to be said in English and that fit together (**FLUENCY)**.

We have to obtain the following.

$$\mathbf{argmax_e\ P(e|f)}$$

Thus we have to find an English sentence **e** that gives the highest value of **P(e|f).**Thus applying Bayes' Rule.

$$\mathbf{argmax_e\ P(e|f) = argmax_e\ P(f|e)\ P(e)\ /\ P(f)}$$

As P (f) is a constant we can drop it.

$$\mathbf{argmax_e\ P(e|f) = argmax_e\ P(f|e)\ P(e)}$$

B. IBM MODEL 1

IBM Model 1 produces varied interpretations for a sentence, each having diverse likelihoods .This model uses lexical translation probabilities. For each output word say **e** that is given by means of the version from an enter phrase **f**, we find translation probability **t(e|f)**. The interpretation probability for a overseas sentence in Kashmiri say **f=(f1,f2,…,flf)** of length **lf** to an English textual content **e=(e1,e2,…,ele)** of duration **le** with an alignment of every English word **ej** to a Kashmiri phrase **fi** as in step with the alignment function. **a:j-> i**

$$\mathbf{P(e,a|f)= Ɛ/(lf+1)^{le}}\ \prod_{j=1}^{le} t(\ ej|f\ a(j)\ )$$

Where,

- $\prod_{j=1}^{le} t(\ ej|f\ a(j)\ )$ is a product of all the lexical interpretation likelihoods for all generated English words e_j.
- **le** is no. of English words.
- $\mathbf{Ɛ/(lf+1)^{le}}$ is used for normalization.
- **Lf +1** is no. of input words .A special NULL token is also included.
- There are $\mathbf{(lf+1)^{le}}$ varied arrangements that plots **lf+1** into le output words.
- **Ɛ** is a normalization constant.

C. EXPECTATION MAXIMIZATION MODEL

The lexical translation models based on probability distribution can only be used if we have a word-aligned bilingual corpora. But we usually have sentence aligned bitext .We use Expectation Maximization (EM) Algorithm to look at interpretation opportunity distributions from a sentence-aligned matching textual content. Thus we have a sentence – aligned bitext corpus .We have to find the alignment between the words of the sentences. The EM model involves initializing the model parameters, assigning probabilities to the missing data, estimating parameters of model from completed data and the final step involves iteration over these previous steps. Consider the example of three Kashmiri sentences given below.

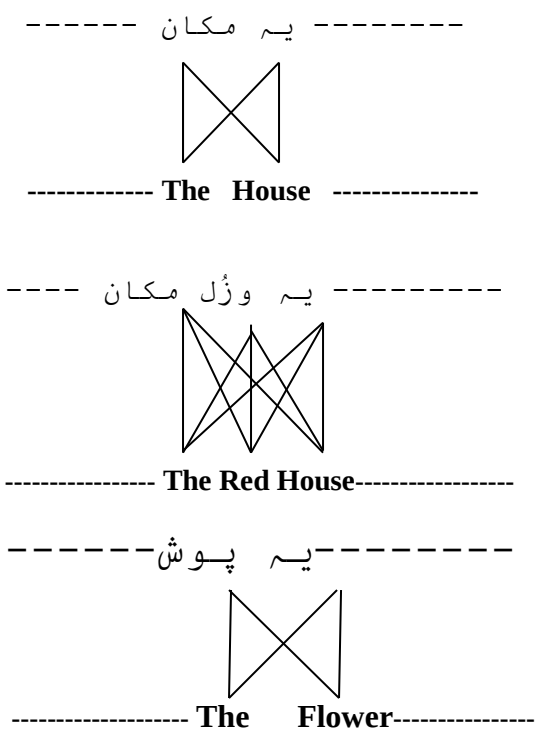

Fig.3. Depiction of alignments for first iteration

In the initial step all alignments are equally likely. The model learns here that یہ is often aligned with **The.** After first iteration the alignments between یہ and The are more likely.

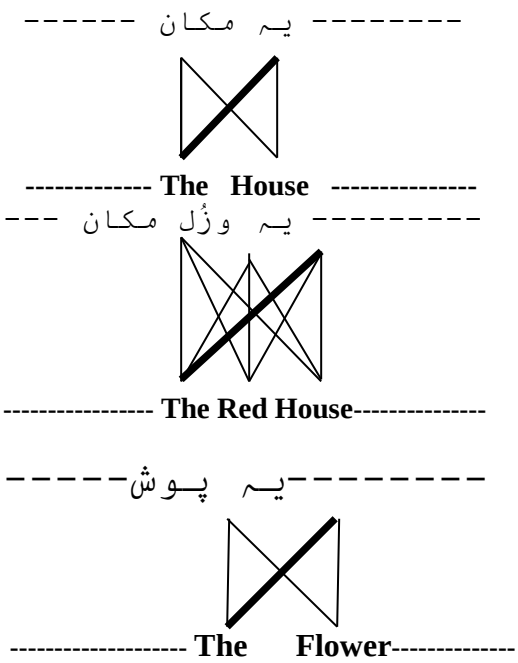

Fig.4. Depiction of alignments for second iteration

After another iteration it becomes clear that alignments between پوش and flower are more likely.

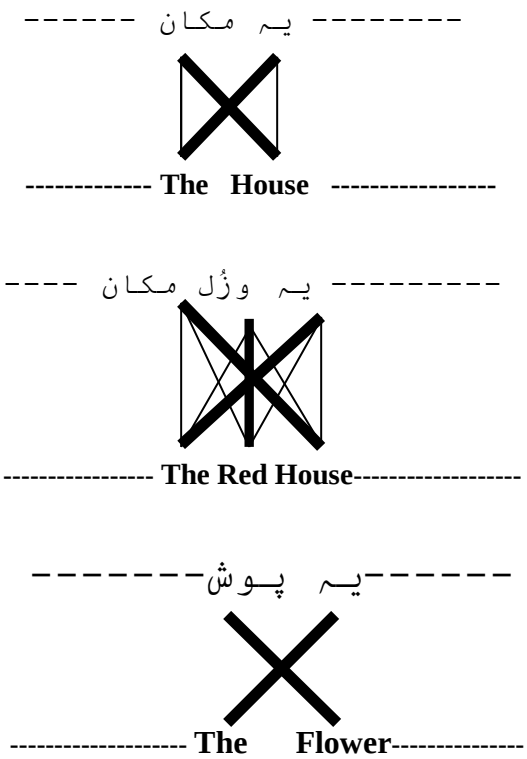

Fig.5.Depiction of alignments after many iterations.

After many iterations the following structure is revealed by Expectation Maximization Model.

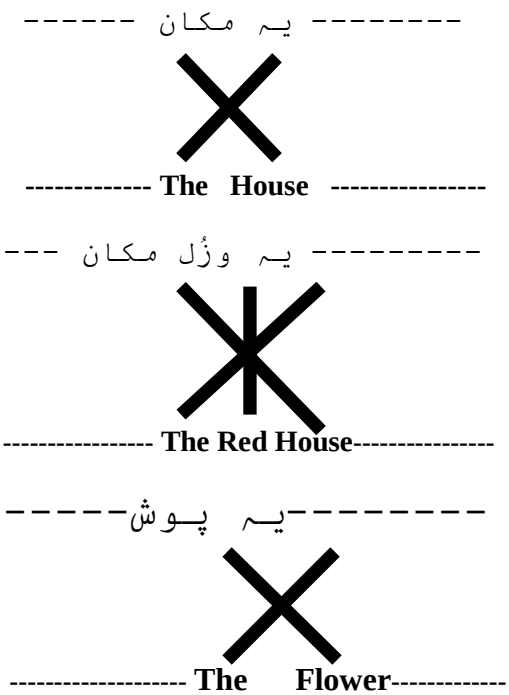

Fig.6. Depiction of alignments for final iteration

P (یہ **| the) = 0.534**

P (مکان **| house) = 0.443**

P (وزُل **| red) = 0.635**

IV. CONCLUSION

The Statistical Machine Translation [9] can be classified into word based, phrase-based and hierarchical-phrase based model. SMT systems are constructed by the usage of big collections of formerly translated texts (parallel textual content corpora), which can be instinctively aligned at the sentence and word ranges, that are saved as huge databases of terms, which can be translations of every other. The translations for new textual content are generated by way of wise search algorithms that recombine the segments from the database into a faithful and natural translation. SMT systems have quicker development cycle, are greater accurate in resolving ambiguities. Similarly, they require greater storage area and use greater computational power. The above paper discusses diverse models used for word-primarily based SMT .These models help us in finding the greater accurate translation of a given text by estimating the maximum likelihood probability .The Statistical Machine Translation system provides countless excellence when affluent and qualified corpora are available. The interpretation is accustomed and significant, if it uses well and qualified corpora .Formulating from huge parallel corpora is computerized and less expensive. Thus in any way, preparing on wide-ranging dialect corpora, importance content other than the preset space, is poor. Usually they run as web services on effective servers or computer clusters, which restrict their use for off-line cellular applications. At last Statistical Machine Translation requires huge equipment to assemble and oversee infinite interpretation models.

V. REFERENCES

[1] N. Ashraf and M. Ahmad, "Machine Translation Techniques and their Comparative Study," *International Journal of Computer Applications*, vol. 125, no. 7, pp. 25–31, Sep. 2015.

[2] K. B. Cohen and A. Dolbey, "Foundations of Statistical Natural Language Processing (review)," *Language*, vol. 78, no. 3, pp. 599–599, 2002.

[3] B. Maia, "Machine translation and human translation: Using machine translation engines and corpora for teaching and research", *in Current Trends in Contrastive Linguistics*, J. Benjamins ,Ed. Amsterdam , pp. 123–145,2008.

[4] E.M. Guizzo,"The Essential Message:Claude Shanon and the Making of Information Theory",PG dissertation, Dept. of Electrical Engineering, Massachusetts Institute of Technology, Cambridge, September 2003.

[5] R. M. Bhatt, "Kashmiri: A cognitive-descriptive grammar," Lingua, vol. 109, no. 4, pp. 311–314, Nov. 1999.

[6] F. Bukhari, Kashmiri Language Teacher. Kashmir: Medroo ,Tral ,1997.

[7] O.Etzioni, K. Reiter and etal," Lexical Translation with Application to Image Search on the Web" , Dept. of Computer Science and Engineering University of Washington, Seattle, WA 98195, USA

[8] S. Johansen and K. Juselius," Maximum Likelihood Estimation AndInference On Cointegration – With Applications To The Demand For Money", in Oxford Bulletin Of Economics And Statistics, 52,2(1990).

[9] B. Marie, R. Wang, A. Fujita, M. Utiyama and E. Sumita ,"NICT's Neural and Statistical Machine Translation Systems for the WMT18 News Translation Task", Presented at the Third Conference on Machine Translation ,Oct. 31 – Nov. 1 2018, Brussels, Belgium,2018.

Proceedings of the Fourth International Conference on Communication and Electronics Systems (ICCES 2019)
IEEE Conference Record # 45898; IEEE Xplore ISBN: 978-1-7281-1261-9

A Hybrid Approach to Improve Full Coverage in Wireless Sensor Networks

(Full Coverage Improving Hybrid Approach)

Amandeep Kaur Sohal
Department of CSE
GNDEC, Ludhiana
India
amandeepkaursohal@rediffmail.com

Dr. Ajay K. Sharma,
Vice-Chancellor, I K Gujral Punjab Technical University, Jalandhar,
India
vc@ptu.ac.in

Dr. Neetu Sood,
Department of ECE, Dr B R Ambedkar NIT, Jalandhar
India
soodn@nitj.ac.in

***Abstract*— In this paper, we propose a hybrid approach for wireless sensor networks which can reduce the total energy consumption of network operation therefore improving network lifetime along with complete coverage of remote monitoring field. The proposed method named as Hybrid Weight based Coverage Enhancing Protocol (H-WCEP) helps to select appropriate cluster heads and their respective cluster members by using weighted sum method and subsequent routing path by genetic algorithm. The network lifetime and coverage lifetime are computed by implementing this approach to achieve continuously monitoring of remote monitoring areas. The results of H-WCEP outperform as compared to other existing protocols. The network lifetime and full coverage lifetime of H-WCEP increase by 48 percentage and 42 percentage approximately respectively.**

Keywords—wireless sensor networkS; network lifetime; full coverage lifetime.

I. INTRODUCTION

Recently, remote sensing systems have received significant attention in electronic and computer science applications. In wireless Sensor Networks (WSNs), tiny component known as sensors are perform sensing and on-board processing, communication and storage facilities. The WSN provides remarkable benefits for a number of real world problems such as military surveillance, agricultural monitoring and oil pipelining monitoring [1] etc. The WSN has come to stay as one of the highly advanced technologies that can immediately respond against the rapid change in sensed data and send this to data analysis center in areas which could not be connected through cabling. Various applications of WSN are discussed in [2].

In order to tackle design challenges of WSNs, clustering algorithms play a very significant role. The clustering algorithms in WSN can greatly contribute to lifetime, energy efficiency and scalable issues of network [3]. The large number of sensors is deployed in remote monitoring field. In clustering, the sensor nodes are grouped into clusters. Each group/cluster of sensors is managed by a specific sensor called as Cluster Head (CH) and other group/cluster members in cluster are known as Cluster Members (CMs). The CMs monitor or sense the specific environment periodically. The CMs process the

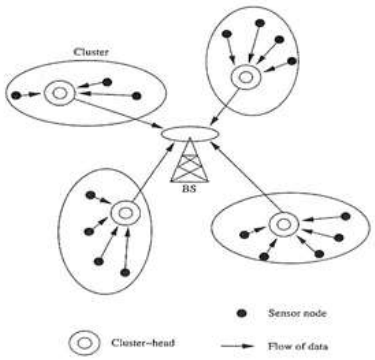

Fig. 1. Cluster based WSN

sensed data and transmit to their respective CH. The CHs aggregate data from their respective CMs and then transmits it to BS. In this way, clustering reduces the energy consumption and numbers of messages communicated to BS decreased. Moreover, data at BS can be encrypted in efficient manner before further transmission to any data centre[4].Thus, clustering achieves prolonged network lifetime [5].The measurements of various performance metrics viz. total energy consumption, network lifetime, number of CHs selected in each round, number of alive nodes in each round, and QoS support like coverage etc. are used to determines the performance of clustered based WSNs.Fig.1 indicates the clustered based network WSN architecture.

The prime objective of this paper is to present an energy efficient clustering protocol which is suitable for remote military area surveillance for achieving prolonged lifetime. Recently, proposed algorithm Weight based Coverage Enhancing Protocol (WCEP)[6] provides the full coverage for longer time as compared to existing clustering protocols. The WCEP works on the basis of weighted sum theory and it increases the lifetime and full coverage by minimizing the energy consumption during cluster formation. But, unable to minimize the energy consumption during inter cluster communication phase.

In this paper, Hybrid-WCEP (H-WCEP) is proposed to decrease energy consumption of the network by using Genetic Algorithm (GA) during data transmission of WCEP. A hybrid approach of weight based method for clusters formation and GA for data transmission is opted to achieve the objective of prolonged full coverage. The cluster head nodes (CHs) and cluster member nodes (CMs) are selected on the basis of coverage governing parameters. The coverage governing parameters taken for this selection procedure are; network remaining total energy, overlapping, node density and degree of sensor node. To conserve the energy consumption, weighted sum method is used. In this method, different weight values are assigned to governing parameters. The optimal set of CHs and alive nodes (as Cluster Member nodes CMs) are selected. Since simple evolutionary optimized algorithm GA has more capability to determine optimal path from CHs to Sink, this GA adopted in inter cluster communication of data transmission in order to conserve the energy consumption.

The rest of the paper is organized as follows. Section II discusses the literature review. Section III discusses the proposed H-WCEP. In Section IV, experimental results are discussed and finally in Section V, the paper is concluded.

II. LITERTURE REVIEW

In literature review, we studied different approaches to optimized energy usage to improve Quality of Service (QoS) in WSNs. The cluster based protocols mimic remote sensing in real time situations. Generally, these protocols are criticized for energy efficiency that involves limited QoS in WSNs. The brief description of related literature is as follows:

[7]proposed distributed cluster based routing protocol namely Low Energy Adaptive Clustering Hierarchy (LEACH) protocol for micro-sensor networks. LEACH improved the network life time, latency and application perceived quality in micro sensor network. However, the study does not investigate good distribution of CHs in the network and sink is assumed only one hop far away from other nodes/ CHs which is not feasible in geographically large network. The work had been extended further based on centralized approach, namely LEACH-C protocol. Still, it cannot solve the limitation of scalability in network. To extend network life time by uniformly CH distribution across the network and load balancing, the amalgamated concept for CH selection, [8] introduced a Hybrid Energy Efficient Distributed Clustering (HEED) protocol. The HEED incorporates two parameters: residual energy of node and node's proximity to its neighbors. However, the rise in iterations involved in cluster formation can lead to overhead cost.

[9] Proposed Distributed Weight-based Energy-efficient Hierarchical Clustering protocol (DWEHC) that designs multi-level structure in intra-cluster communication and limits a number of children of parent node. The author introduced the idea to select CH by calculating weight based on its residual energy and distance to its neighbors. This newly proposed technique improves HEED protocol by developing balanced size clusters and optimizes intra-cluster communication using location

In [10], the authors proposed a protocol incorporating residual energy and other metrics like distance to aggregation point, node reliability, and mobility for CH selection by using evolutionary computing method with purpose of maximizing network life time.

The CHs election techniques called as Coverage Preserving Clustering Protocol (CPCP) was proposed with aim of coverage preservation [11]. The CPCP is based on four coverage aware cost metrics which selects CH, active nodes and routing nodes from densely deployed sensors respectively. The CPCP integrates problem of coverage and energy consumption in network. But these cost metrics cause a large computational burden on sensor nodes. The CPCP is also unable to minimize redundantly covered area in each round.

In [12], the authors described a multi-function based on two factors i.e. choosing optimal CHs locations and minimizing transmission distance. In this protocol, topology of network is designed with three level hierarchical levels. Two CHs at level 2, One CH at level 1and sensor for collecting data placed at level 0. The BS knows the position of all nodes. Thus achieves the minimum distance for transmission.

A GA-based adaptive clustering protocol was proposed by [13] to achieve good performance in network life time in WSNs. Additional information was updates before beginning of first round. In this phase, role of node as sensor or CH, node identifications and geographical position are send to BSs. GA finds an optimal probability of nodes being CHs by minimizing the total energy consumption in one round. The optimal probability was determined by an evolutionary optimization process. This process incorporated non-deterministic rules in probabilistic transitions for prolonging the network life time.

The Distributed Energy Efficient Clustering Algorithm with Improved Coverage (DEECIC) was implemented to increase network lifetime and coverage using average number of clusters in scheme [14]. In this, CH is opted from a crowded area with more remaining energy and more degree of sensor.

Coverage aware Unequal Clustering Algorithm (CUCA) is distributed scheme to prevent hot spot issue and achieves energy efficient coverage preservation in WSNs [15]. The CUCA targets to obtain network load distribution uniformly. The CUCA necessitates overburden of control packets in routing purposes. As a result, unnecessary consumption of energy in each stage takes place that is unacceptable.

The WCEP is an energy efficient full coverage protocol [6]. The WCEP reduces computation burden of sensors and attains pro-longed full coverage with improvement in scalability. The WCEP incorporate the concept of clustering and sleep scheduling efficiently[16]. The WCEP is based on weight values which are assigned to certain governing parameters viz. network remaining total energy, overlapping degree, node density and degree of sensor node. These governing parameters affect the energy and coverage issues magnificently. However, main focus of WCEP is optimal selection of CHs and CMs, whereas energy consumption during data transmission is ignored.

The CPCP [11] and WCEP [6], both primarily focuses on cluster formation process but there is significantly less

importance given to energy consumption during data transmission phase of clustering. Therefore, motivation behind this proposes work is reduction in energy consumption during data transmission phase of WCEP. This has led to more conservation of residual energy and helps in more coverage.

III. PROPOSED WORK

The proposed work presents a hybrid approach using weighted sum method and evolutionary method to achieve coverage of remote and harsh environment for longer period of time. The proposed work is based on Weight based Coverage Enhancing Protocol (WCEP) for clustering and Genetic Algorithm (GA) for transmitting the data to end user controller. In clustering, CHs and CMs are selected in appropriate number for maintaining full coverage in each communication round. The process of clustering considers assigning weight merits to remaining total network energy, overlapping, node density and degree of sensor. The weighted sum method helps in conserving energy using different weight merits to respective governing parameters depending upon situational requirements. Further, GA based optimization procedure performed with each communication round to conserve the energy. The proposed hybrid approach is named as Hybrid -Weight-based Coverage Enhancing protocol using Genetic Algorithm (H-WCEP). The stepwise procedure of H-WCEP is discussed below:

A. *Information Update*

We assume that 'N' sensors are deployed in squared remote monitoring field in uniformly random manner. The deployment of sensors is such that they confirm the 100% coverage at the start of network procedure. The sensors are assumed stationary after deployment and each sensor is awared its own location and BS. The BS is placed at fixed point. The wireless communication channel is symmetric which means monitoring and communicating range is same. The range of sensor and transmission range is modeled as disk sensing model [8]. The transmission range is considered at least double the sensor's range. The network considered for proposed work is homogeneous i.e. all sensors have same computing and communication capacity.

B. *Network Model*

In this step, four coverage observing parameters are incorporated to assign a value to each sensor. These governing parameters are residual/remaining total network energy, overlapping, node density and degree of sensor. At each communication round, sensor dissipates part of their limited energy. As a result, remaining energy is called as residual energy of sensor need to be update periodically. The other governing parameters are node density, degree of sensor and overlapping degree are calculated only once at the start of network procedure. For each sensor, energy dissipation in transmitting and receiving 'L' bit information by each sensor is measured using simple radio model [6], [7], [11]. Equation (1) represents energy consumed by transmitter for performing transmits circuitry operation and Equation (2) indicates receiver's energy consumed due to receiver circuitry when it is receiving data.

$$E_{Tx}(L,d) = L\,E_{elec} + L \in d^{\alpha} \quad \text{where } \alpha=2 \text{ or } 4$$
$$\begin{cases} L\,E_{elec} + L\,\epsilon_{fs}\,d^2 & d < d_0 \\ L\,E_{elec} + L\,\epsilon_{fmp}\,d^4 & d \geq d_0 \end{cases} \quad (1)$$

And Equation [7] indicates formula for energy consumption in receiving L-bit packet.

$$E_{Rx}(L) = L\,E_{elec} \quad (2)$$

In equations (1) and (2),

L=Length of transmitted/ receiving packet,
d=Distance between transmitter and receiver,
d_0=Threshold distance (d_0) calculated from Equation (3):

$$do = \sqrt{\frac{\epsilon_{fs}}{\epsilon_{fmp}}} \quad (3)$$

The electronics energy E_{elec} controlled by digital coding, modulation of signal, filtering of packets, and spreading of the signal.

If $d < d_0$, then free space model is used. It means =2, and amplifier energy becomes $\epsilon_{fs}\,d^2$. Otherwise, $d \geq d_0$ multipath fading channel model is applied which means $\alpha = 4$ and amplifier energy becomes $\epsilon_{fs}\,d^4$.

With each communication round, residual energy is given by Equation (4):

$$E(residual) = E(initial) - E_{Tx} \text{ or } E_{Rx} \quad (4)$$

The other governing parameters such as node density can be calculated by obtaining number of sensors within its cluster range. The degree of sensor is determined by number of covered points in its range. The overlapping degree is number of sensors which produces overlapping area in the monitoring field. Higher the values of these governing parameters (residual energy ($E_{residual}$), overlapping degree ($O_{lapping}$) , node density (ND) and degree of sensor(D_s) for particular sensor make that eligible to become live sensor. The weight w_1, w_2, w_3 and w_4 are assigned to governing parameters using weighted sum method in order to calculate the weight value of each sensor. Equation (5) represents the formulation to compute sensor weight.

For a specific covered point, higher the weight of sensor, higher the chance to become live, otherwise idle or sleep.

$$Sensor.wt = E_{residual}.w_1 + O_{lapping}.w_2 + D_s.w_3 + ND.w_4 \quad (5)$$

Equation (6) is used to obtain CH role for a sensor in terms of CH weight.

$$CH.wt = Sensor.wt + (\text{distance between Sensor and Sink}) \quad (6)$$

C. Clustering Method

In the clustering method, set of sensor nodes are selected as CMs/ CHs which will be active and rest will be in sleep mode for a particular communication round. The proposed clustering algorithm comprises of two phases: cluster formation phase and data transmission phase.

- Cluster Formation Phase:

  The cluster formation phase of proposed algorithm uses a weight based method along with sleep scheduling mechanism to conserve energy while maintaining prolong full coverage of the monitoring field. The total weight of each sensor is calculated on the basis of governing parameters $E_{residual}$, $O_{lapping}$, ND and D_s. The selection of sensor as live sensor is based on maximum value of total weight of sensor for specific covered point. The total weight of sensor and distance from sink determines the CHs. These selected CHs find live sensor as part of cluster and termed as CMs within its cluster radius. These appropriate numbers of specific CMs and CHs are selected repeatedly that maintains the coverage in each communication round.

- Data Transmission Phase:

  In the data transmission phase, intra and inter cluster communication ensures that live sensors communicate to their respective CH directly using single hop method during intra cluster communication. The CHs transmits data to sink via multi hop method. The data transmission phase is optimized using energy and distance parameters using GA. The GA helps to determine path with minimum energy consumption to transfer all data from sensor CHs to sink. To find out an optimum path, the GA generates all possible paths for each of CH. Then, each path is evaluated to determine fitness value using fitness function of GA. The best chromosome is selected among number of generations by means of minimum energy consumption and minimum distance during data transmission. The data transmission phase of WCEGA is further elaborated in Algorithm 1, as follows:

  Algorithm 1: Data Transmission using GA

  D= cumulative distance between sensor and Sink
  w1=weight for residual energy
  w2= weight for distance

Data_transmission (CHs, live sensors, Eresidual, x, y)

```
{
   FOR i=1 to length(Cluster Head)
        FOR generation i=1 to 10
// Create the chromosomes
     FOR i=1 to 20
       Determine the path from each CH to sink
 // Compute the fitness of each chromosome
       Fitness=w1 * Eresidual + w2 * D
      END
// Select best-ranking individuals to reproduce using fitness value
        Min(fitness)  next generation
// Breed new generation using crossover and mutation
  Produce new offspring
  Evaluate the individual finesses of the offspring
  Exchange worst ranked part of population with off-spring
    END //end generation FOR loop
   Obtain the best route from specific cluster head to sink
    END //end Cluster Head FOR loop
    }
```

IV. RESULTS AND ANALYSIS

In this section, the impact of governing parameters on performance metrics for remote WSNs has been investigated. The results of WCEGA protocol is compared with common coverage aware clustering protocol (CPCP) and Weight based Coverage Enhancing Protocol (WCEP). The CPCP discussed four coverage aware cost metrics i.e. energy-aware (Cea), minimum-weight (Cmw), weighted sum (Cws) and coverage redundancy (Ccc). The CPCP (Cmw) focuses longer 100% coverage of monitoring field. Therefore, out of four CPCP cost metrics, CPCP (Cmw) is taken for comparison in these simulations. Generally, coverage related clustering protocols are compared with coverage, lifetime and energy consumption of the network.

In simulations 200 nodes, each with initial energy 1J are taken into monitoring field. The sensors are distributed randomly across 100x100 square units monitoring field. The implementation of WCEGA is iterated based on lifetime of network i.e. energy level of sensors become equal to threshold energy of sensor. The threshold level of energy is assumed zero in this paper. In all communication rounds of network operation, live sensors are selected to collect the sensing data and transmit them to their CHs using single hop communication. Once CH obtained data from its cluster then it transmits the data further to sink using multi-hop communication by GA method. The sink is located at (50,50) co-ordinates. The radius of each sensor is 15m and their communication radius is 30m. The parameters of proposed model are given Table I and parameters for GA approach are listed in Table II.

TABLE I. SIMULATION PARAMETERS

Parameters	***Value***
Initial Energy (E_{int})	1 J
Transmission/Receiving electronics circuitry constant [7]	50 10^{-9}J/bit
Amplifier circuitry constant [7]	10 $^{-12}$J/bit/m^2
Size of Data Packet [7]	240bits
Sensing Range (Rs) [7]	15m
Cluster Radius(Rc) [7]	30m
Transmission Range	40m

TABLE II. SIMULATION PARAMETERS

Parameters	***Value***
Population Size	20
Generation	10
Crossover	0.05
Mutation	0.01
Weight1 for distance factor	0.3
Weight 2 for energy factor	0.7

A. Coverage lifetime Energy Consumption Comparison

The H-WCEP outperforms in comparison to other similar protocols i.e. CPCP and WCEP. By decreasing the consumption of energy during data transmission, it increases the coverage of network. The Fig. 2 depicts comparison of coverage of network in H-WCEP with WCEP and CPCP (Cmw) with time.

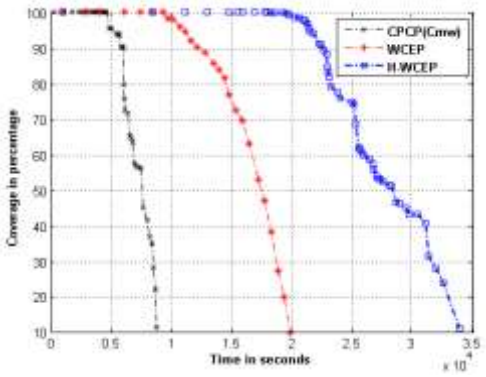

Fig. 2. Comparison of Coverage lifetime with Time for WCEP, CPCP (Cmw) and H-WCEP

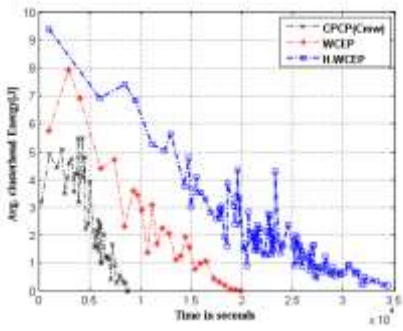

Fig. 3. Average CHs energy with Time for H-WCEP in comparison to CPCP (Cmw) and WCEP

The Fig. 3 indicates higher value of average residual energy of CHs in H-WCEP in comparison to WCEP and CPCP (Cmw) with time.

On the other hand, an important criterion to evaluate energy consumption of WSNs is the average number of CHs with time. If the Number of CHs are high, energy consumption increases. Fig. 4shows that H-WCEP has relatively low number of CHs as compared to CPCP(Cmw) and WCEP.

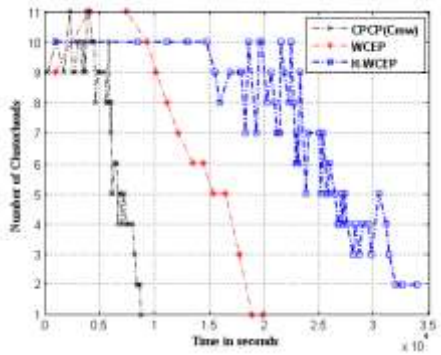

Fig. 4. Comparison of number of Cluster Heads Vs Time for H-WCEP, CPCP (Cmw) and WCEP

B. Lifetime comparison

Network lifetime is defined as start of specific WSNs to death of first sensor. Generally, lifetime of WSN is determined by time taken by First Node Dead (FND), Half Node Dead (HND), Last Node Dead (LND) and these are considered for evaluate performance of cluster based WSNs [11]. Further, FND indicates start of network operation to death of First sensor Node Died. The HND indicates start of network operation to death of Half sensor Node Died. The LND indicates start of network operation to death of Last sensor Node Died. The Fig. 5 represents that H-WCEP exhibits better results than other considered protocols.

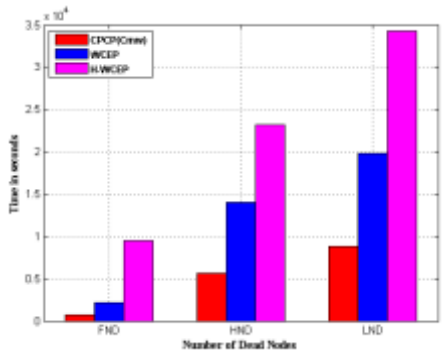

Fig. 5. Lifetime of WCEP, CPCP (Cmw) and H-WCEP in terms of FND, HND and LND

V. CONCULSION

In this paper, an evolutionary based method has proposed to improve longer full coverage in energy efficient clustering protocol. The proposed hybrid method helps in determining efficient optimal path for effective set of CHs and its members. The H-WCEP uses genetic algorithm based routing method that consider distance between cluster head and sink and sensor node's residual energy. Therefore H-WCEP achieves increase in network lifetime and full coverage lifetime. Thus, our hybrid approach uses network energy in effective manner for enhancing the full coverage lifetime in WSNs.

In our future work, we can extend this work by incorporating mobility of sink and pre-determined sensor deployment to enhance the coverage lifetime.

REFERENCES

[1] O. E. Elnaggar, R. A. Ramadan, and M. B. Fayek, "WSN in monitoring oil pipelines using ACO and GA," *Procedia Comput. Sci.*, vol. 52, no. 1, pp. 1198–1205, 2015.

[2] X. Liu, *A survey on clustering routing protocols in wireless sensor networks*, vol. 12, no. 8. 2012.

[3] J. N. Al-Karaki and A. E. Kamal, "Routing Techniques in Wireless Sensor Networks," vol. 2, no. 7, pp. 344–348, 2012.

[4] A. Praveena and S. Smys, "Efficient cryptographic approach for data security in wireless sensor networks using MES V-U," *Proc. 10th Int. Conf. Intell. Syst. Control. ISCO 2016*, 2016.

[5] B. Mamalis, D. Gavalas, C. Konstantopoulos, and G. Pantziou, "Clustering in Wireless Sensor Networks," in *RFID and Sensor Networks: Architectures, Protocols, Security, and Integrations*, Y. Zhang, L. T. Yang, and J. Chen, Eds. New York, USA: CRC Press, Taylor and Francis Group, 2009, pp. 323–354.

[6] A. K. Sohal, A. K. Sharma, and N. Sood, "Enhancing Coverage Using Weight Based Clustering in Wireless Sensor Networks," *Wirel. Pers. Commun.*, vol. 98, no. 4, pp. 3505–3526, 2017.

[7] W. B. Heinzelman, A. P. Chandrakasan, and H. Balakrishnan, "An Application-Specific Protocol Architecture for Wireless Microsensor Networks," *IEEE Trans. Wirel. Commun.*, vol. 1, no. 4, pp. 660–670, 2002.

[8] O. Younis and S. Fahmy, "HEED : A Hybrid , Energy-Efficient , Distributed Clustering Approach for Ad-hoc Sensor Networks," *IEEE Trans. Mob. Comput.*, vol. 3, no. 4, pp. 1–36, 2004.

[9] P. Ding, J. Holliday, and A. Celik, "Distributed Energy-Efficient Hierarchical Clustering for," pp. 322–339, 2005.

[10] G. Ahmed, N. M. Khan, and R. Ramer, "Cluster Head Selection Using Evolutionary Computing in Wireless Sensor Networks." pp. 9–12, 2008.

[11] S. Soro and W. B. Heinzelman, "Cluster head Election Techniques for Coverage Preservation in Wireless Sensor Networks," *Ad Hoc Networks, Elsevier*, vol. 7, no. 5, pp. 955–972, Jul. 2009.

[12] P.-C. Huruială, A. Urzică, and L. Gheorghe, "Hierarchical routing protocol based on evolutionary algorithms for Wireless Sensor Networks," *9th RoEduNet IEEE Int. Conf.*, pp. 387–392, 2010.

[13] J. Liu and C. V Ravishankar, "LEACH-GA : Genetic Algorithm-Based Energy-Efficient Adaptive Clustering Protocol for Wireless Sensor Networks," vol. 1, no. 1, pp. 79–85, 2011.

[14] Z. Liu, Q. Zheng, L. Xue, and X. Guan, "A Distributed Energy-Efficient Clustering Algorithm with Improved Coverage in Wireless Sensor Networks," *Futur. Gener. Comput. Syst. Elsevier*, vol. 28, no. 5, pp. 780–790, May 2012.

[15] N. Mazumdar and H. Om, "Coverage-aware Unequal Clustering Algorithm for Wireless Sensor Networks," *Procedia Comput. Sci.*, vol. 57, pp. 660–669, 2015.

[16] J. J. T. John and S. Ramson, "Energy-Aware Duty Cycle Scheduling for Efficient Data Collection in Wireless Sensor Networks," *Int. J. Adv. Res. Comput. Eng. Technol.*, vol. 2, no. 2, pp. 777–783, 2013.

Proceedings of the Fourth International Conference on Communication and Electronics Systems (ICCES 2019)
IEEE Conference Record # 45898; IEEE Xplore ISBN: 978-1-7281-1261-9

Performance Analysis of Switched-Boost DC to DC Converter for Distributed Generation system

Deepanshu Gautam
Kota, INDIA
gautam.gudiya11@gmail.com

Ashok kumar sharma
Kota, INDIA
aksharma_eck@hotmail.com

Jyoti shukla
Kota, INDIA
j.shukla111@gmail.com

Neeti Dubey
Kota, INDIA
neetidubey23@gmail.com

Priyanka Nehra
Kota, INDIA
priyankanehra769@gmail.com

Department of Electrical Engineering
Rajasthan Technical University, Kota

***Abstract*—This paper presents performance analysis of switched boost dc-dc converter for distributed generation system in CCM (continuous conduction mode) operation, which combine the conventional switched-boost circuit with the switched-capacitor and switched inductor switching structure. Compared with the conventional boost converter, which uses convenient duty ratio, the presented topology is utilized to uplifting in voltage gain. The proposed topology exhibits advantages of the continuous current at the input and boost voltage conversion ratio without use of high duty cycle (approx less than 1) and transformer. Proposed converter supports in producing high output voltage gain by operating in different modes. The simulation result brought out from MATLAB 2016 b.**

Keywords— ***DC-DC converter, Switched-boost network, Boost-ability, closed loop system, duty ratio, continuous conduction mode***

I. Introduction

Renewable energy sources based distributed generation (DG) system shows the trend of future generation system. [1-2]. In the distributed generation system, electrical power is generated and that have many benefits to renewable energy sources, which comprises wind power, photovoltaic (PV) cells and fuel cells. During this, the photovoltaic arrays are the new energy resources according to the utilization method, which have been take places in non-conventional energy resources. Block diagram of Power flow of the two-stage photovoltaic energy system is depicted in Fig. 1. PV stack has usually low output dc voltage. Thus, it is necessary to step-up the voltage by High step-up converter which has been included in the first stage of power flow diagram. This first stage is required to provide high gain of output voltage for DC/AC inverter. Thus, high gain of output voltage is provided by high step-up dc/dc converter. Then, second stage considers DC to AC power conversion and provides the desired power due to conversion of DC in AC. After conversion AC supply can be supplied to the utility grid and load as depicted in Fig. 1. Therefore, high step-up dc/dc converters are employed to interface the renewable energy source (PV stake) and inverters connected grid [3]. High step-up dc-dc converters have high voltage conversion ratio and have been utilized in numerous application such as uninterruptible power supply, power supply for electrical vehicle, medical x-ray appliance system and discharge headlamps of high-intensity etc. Renewable energy sources based on solar and wind are very much efficient and present in abundant amount as compared conventional energy sources and due to this reason demand of PV modules increases. To improve power quality, boost sustainability distributed generation technologies is more important and it also reduce energy costs. [12]

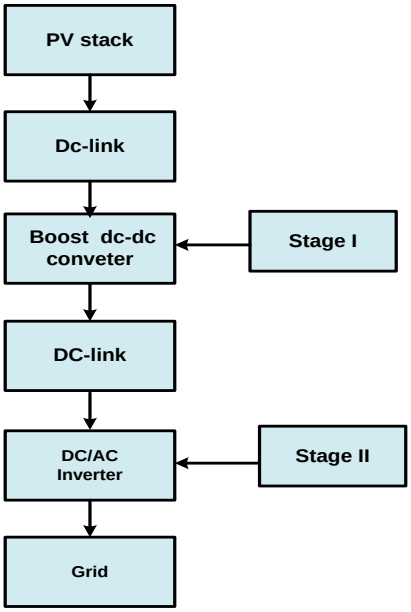

Fig. 1 Power flow diagram of two-stage PV Energy system

Diverse topologies of dc-dc converter have been evolved to increase a high voltage gain with low duty ratio. Converter's topologies like Isolated or non-isolated dc-dc converter [4-5], z-source impedance network have been utilized to achieve high voltage gain.

Isolated dc/dc converter can provide high conversion ratio with increasing turns ratio in transformer but it will lead to large leakage inductance due to high turns ratio. These converters can be create large voltage stress and spikes across switching devices. Further non-isolated can also be categorized as: coupled and non-coupled inductor. Couple inductor based dc to dc converters reduce current ripple of inductor and avoid the switching losses. However, these converter does not reduce the voltage spikes of switches (like IGBT and MOSFET) [4-7] and efficiency will be reduce.

However, these conventional converter topologies are not suitable and more reliable compare to proposed converter due to be less efficient and more expensive and manufacturing cost is also high. Transformer step-up dc-dc converter can be obtain high voltage gain with reduce the voltage and current stress which has been presented [10]. Same as z-source impedance network have been presented which has little number of passive components [14]. In addition, to achieve high step-up capability, switched capacitor-diode cells have been proposed in [9]. In that manner, techniques and topologies can also be employed in boost dc-dc converter are presented in [11]. Figure (3) shows the diagram of switched-capacitor dc-dc converter. The switched-capacitor converter has one switch (IGBT) and has different switching to proposed converter.

Key merits of these converter which have –

1) *No magnetic elements*
2) *Minimal electromagnetic interference*

But it has high inrush current at start up and inherent power loss which is disadvantages of switched-capacitor converter.

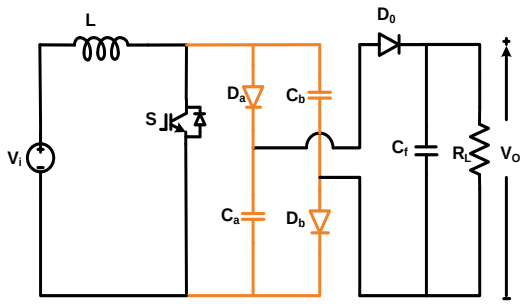

Fig. 3 Switched-capacitor converter (SC)

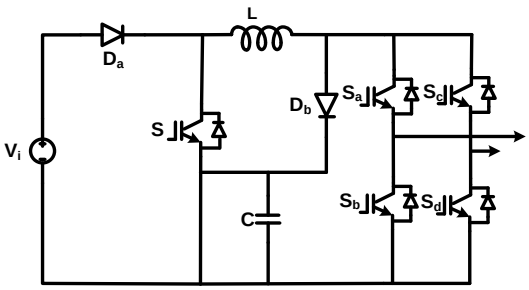

Fig. 4 switched-boost converter (SBC)

Switched-boost network has been presented and which is depicted in Fig. (4). However, output voltage gain of switched boost converter is not high enough in comparison with conventional Z-source converter [9]. This paper based on the conventional presents that topology is related with switched-boost converter, which is based on cells of SC/SL (switched-capacitor/switched-inductor) to boost the voltage at the output. The proposed topology has the advantage to nullify the voltage stress across the switches and diode [15].

II. Topology of Presesnted Converter

In the presented converter, switched capacitor combine with main network of switched boost converter as shown in figure. The basic circuit diagram of present converter SC-SBC is operating along with switched capacitor branch according to Fig 5(a) SC-SBC circuit of proposed converter have inductor L, diode D_0 and D_c, both switch S_a and S_b, is used IGBT in this circuit diagram and switched-capacitor cell is consisted of capacitor C_a, C_b with diode D_a, D_b.

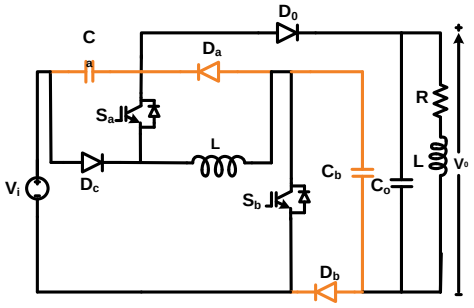

(a)

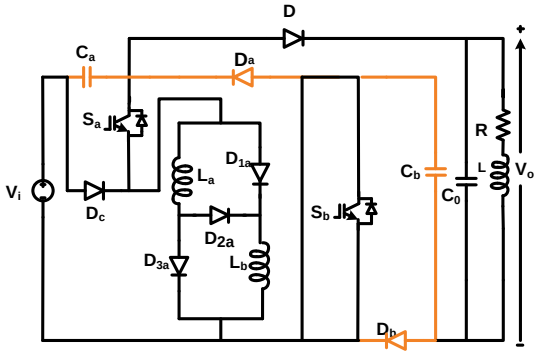

(b)

Fig. 5 circuit diagram of SBC (a) SC and (b) SC/SL

Combination of switched boost dc-dc converter, switched capacitor and switched inductor forms the proposed converter shown in fig. 5(b).This circuit diagram consist the different switching structure in compare Fig. 5(a) to obtain the high gain of voltage at the output. In Fig. 5(b) the switched boost converter consists inductor L is replaced with switched inductor cell which have the inductor L_a, L_b and diodes D_{1a}, D_{2a}, D_{3a}. SC/SL cell is combined with switched boost circuit S_a and S_b (power switches) are switched on, the input voltage charge the inductors and when S_a and S_b (power switches) are switched off inductor transfer the energy to charge the capacitors, SCs are conducted with series to supply the load. In consequence converter can generate a high voltage gain at output.

III. Operating Modes Of Presented Converter

To simplify the analysis, all the frequency independent, time invariant and linear components are assumed to be as passive components. These components are ideal resistor, capacitor and inductor.
The performance of the presented converter operated without any interruption in the power supply.

A. Operating Modes of the SBC with switched capacitor

Proposed converter of SC-SBC operates in two modes and equivalent circuit structure is depicted in Fig. 7(a). Waveforms of SC-SBC proposed converter operating without any interruption in CCM operation is depicted in Fig. 6

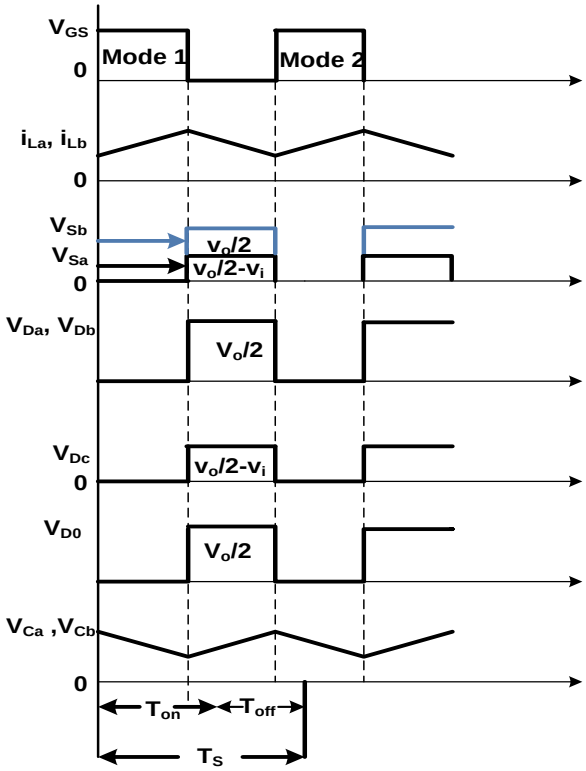

Fig. 6 Waveforms of the presented switched capacitor-switched-boost converter (SC-SBC

***1) Mode 1*:** In this mode of state, according with time interval, S_a, S_b (power switches) are switched on with the same control of switching and D_a, D_b and D_c (diode) are off which have reverse parallel connection with capacitors. In this state, circuit of proposed converter (SC-SBC) have two loops:

- In first loop of circuit, current is passing through the V_i (input voltage), C_a, S_a (switch), L (inductor), and S_b (switch). V_i and Capacitor C_a release the energy to inductor L.
- In second loop of this circuit current is passing through the V_i, C_a, D_o, C_o, *load(R, L)*, C_b and S_b.To supply of the load, capacitor C_a and C_b are in series with the input source *Vi* through S_b.

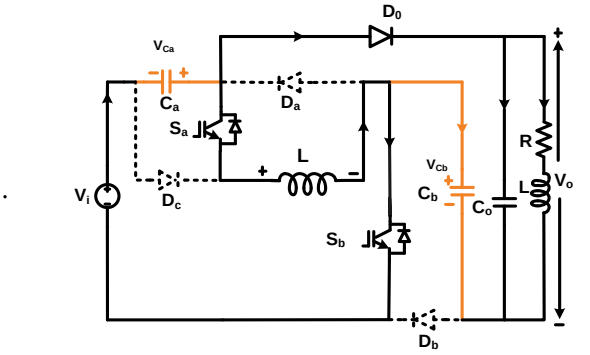

(a)

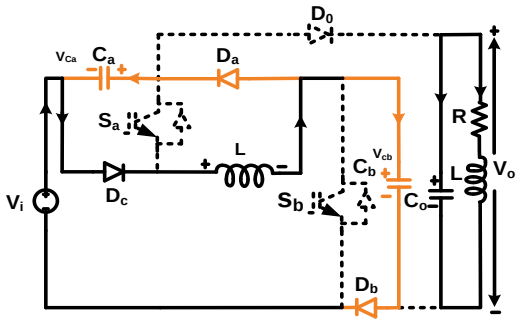

(b)

Fig. 7 Equivalent circuit structure of SC-SBC with step-up topologies

***2) Mode 2*:** in Fig. 7(b) S_a and S_b (switches) are switched off. In this state D_a, D_b, D_c (diodes) are on and D_O is reverse blocking. Three loops are considered in this state:

- In first loop, current is passing through L, D_a, C_a, and D_c. Capacitor is charged by the inductor L.
- In second loop, current is passing through V_i, D_c, L, C_b and D_b. V_i and L releases the energy to C_b
- In third loop, current is passing through C_o and R_L. The load is operated by capacitor C_o.

The duty ratio of S_a and S_b (power switches) which is defined as $d = Ton/T$. Switching period on-period of power switches represented as T_s, T_{ON} respectively.

$$u_L = V_i + V_a \quad (1)$$

$$u_L + V_{C_a} = 0 \quad (2)$$

$$V_{C_b} = V_i + V_{C_a} \quad (3)$$

$$V_{C_a} = \frac{d}{1-2d} V_i \quad (4)$$

$$V_{C_b} = \frac{1-d}{1-2d} V_i \quad (5)$$

$$V_O = \frac{2(1-d)}{1-2d} V_i \quad (6)$$

Eventually, the proposed converter of SC-SBC has output voltage gain which can be derived as:

$$G = \frac{V_0}{V_i} = \frac{2(1-d)}{1-2d} \quad (7)$$

B. Operating modes of SBC with switched capacitor/ switched inductor cell

The proposed converters have waveforms without any interruption which represents the CCM modes in Fig. 8. Further, the equivalent circuit diagram with boost topology is depicted in Fig. 9. It can be seperated in to two operating modes.

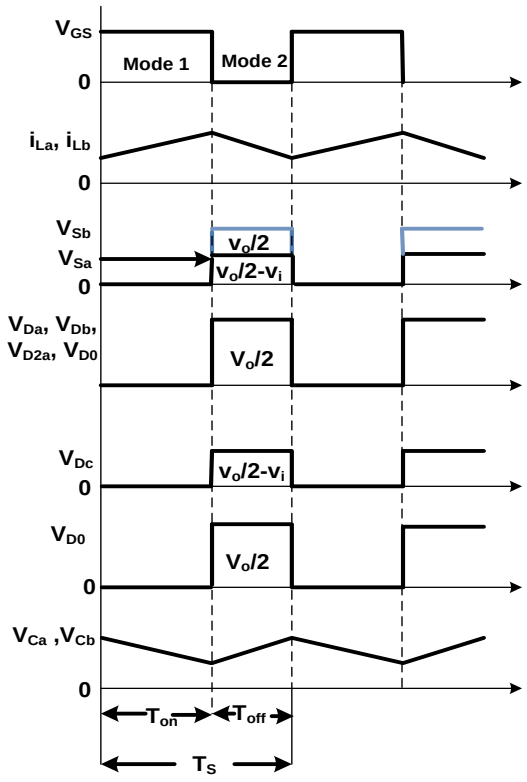

Fig. 8 Waveforms of the (SC/SL-SBC)

Mode 1: In this state, S_1 and S_2 are switched on with same switching control at same time which shown in Fig. 9(a). D_a (diode), D_b (diode), D_c (diode) and D_{2a} are off. V_i (input voltage), and C_a (capacitor) charge the two inductors L_1, L_2.

Meantime, Vi, C_a and C_b supply the load by S_b. Thus following equation is derived as

$$u_{L_a} = u_{L_b} = V_i + V_{C_a} \quad (8)$$

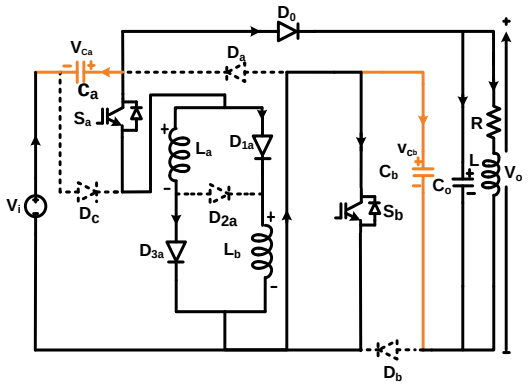

(a)

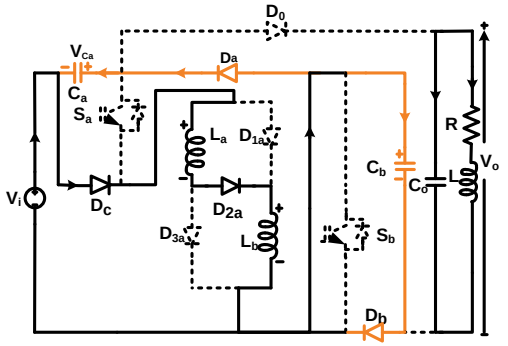

(b)

Fig. 9 Equivalent circuit structure of the proposed SC/SL-SBC with step-up topologies

2) Mode 2: $S_1$and S_2 are switched off, simultaneously shown in Fig. 9(b). Diodes D_a, D_b, D_c, and D_{2a} (diode) are on, D_{1a} *(diode)*, D_{3a} *(diode)*, and D_o (diode) are reverse biased. and L_a and L_b *(inductor)* release the energy to capacitor C_a in series.

Meantime, Series connected Inductors L_1 and *L2* with *Vi* charged the capacitor C_b and *load* is conducted by capacitor C_o

$$u_{L_a} + u_{L_b} + V_{C_a} = 0 \quad (9)$$

$$V_i = V_{C_b} - V_{C_a} \quad (10)$$

$$V_{C_a} = \frac{2d}{1-3d} V_i \quad (11)$$

$$V_{C_b} = \frac{1-d}{1-3d} V_i \quad (12)$$

Therefore, G represents the voltage gain ratio of SC/SL-SBC converter in equation 14

$$V_o = \frac{2(1-d)}{1-3d} V_i \qquad (13)$$

$$G = \frac{V_0}{V_i} = \frac{2(1-d)}{1-3d} \qquad (14)$$

Improved output voltage gain is achieved with SC/SL-SBC than that is obtained with SC-SBC, according to equation (7) and (14).

C. Voltage loop control

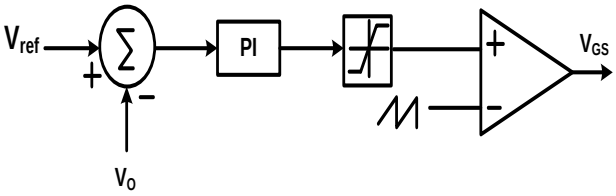

Fig.10 Control principle of proposed converter

Gate pulse can be controlled by the control principle .To obtain the ripple free step-up output voltage, the control strategy have been used in the proposed converter. That is shown in figure (8).

IV. Simulation Results

According to design parameters of simulation are selected: input voltage V_i=10V, switched inductors L_a=L_b=220uH, switched capacitors C_a=C_b=330uF, filter capacitor at output C_o=470uF, switching frequency f_s=30 kHz, and the load R_L=100Ω.

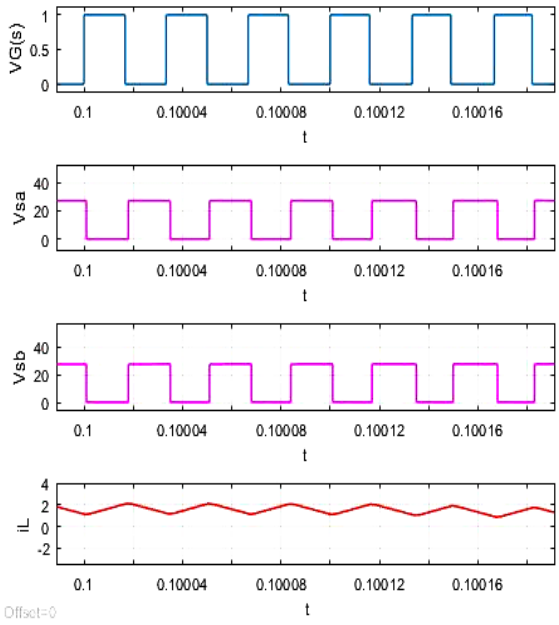

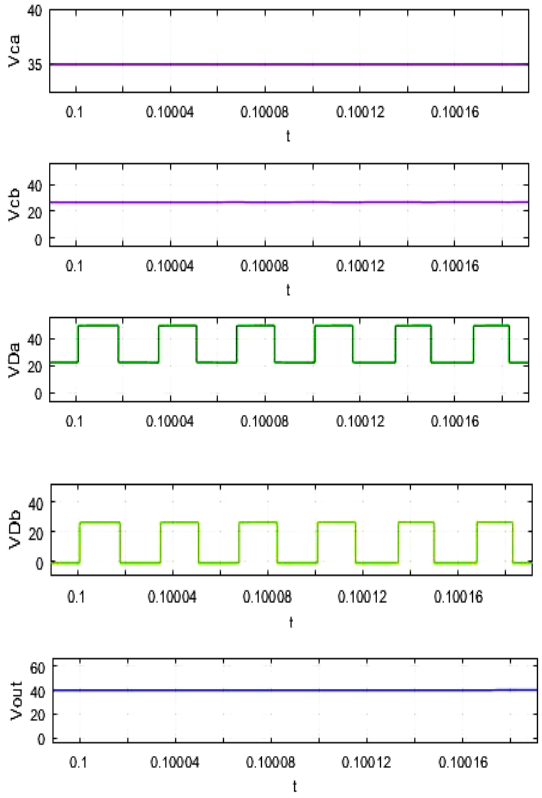

(a)

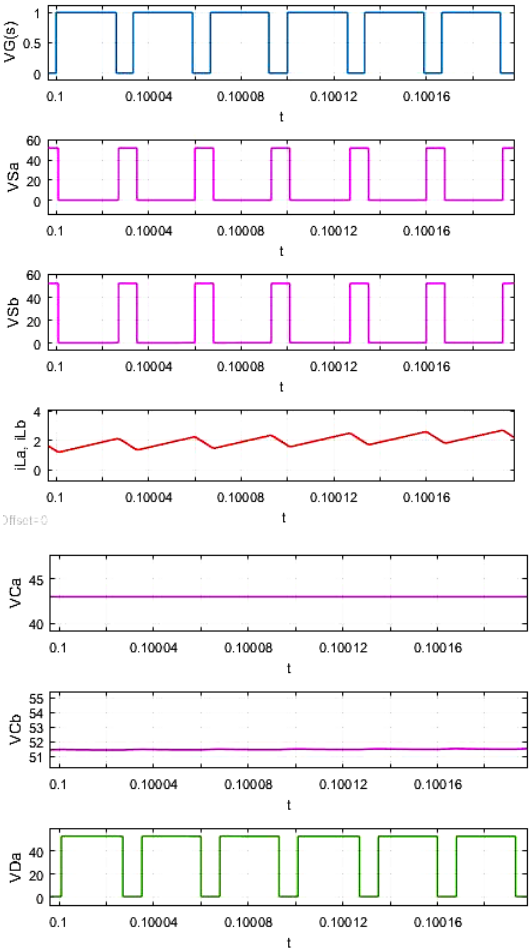

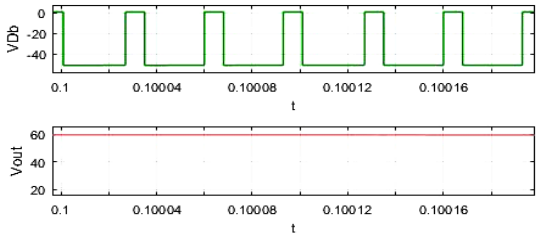

(b)

Fig.11 Simulation result for SBC with (a) SC (b) SC/SL

The simulation results of both type of converters are demonstrated in Fig.11. Fig. 11(a) shows the waveforms obtained with Switched-capacitor SBC. As can be observed that when d (duty ratio) is considered to be 0.5, the capacitor voltages V_{C1} and V_{C2} are magnified up to 25V and 35V, respectively, and the magnitude up to of obtained voltage gain V_o is 40V. While d (duty ratio) is considered to be 0.8, capacitor voltages V_{C1} and V_{C2} are 41V and 51V and thus, the output voltage V_o is 60V in fig11(b). This implies that with the same duty ratio, high voltage output is obtained with SC/SL SBC in comparison with that is obtained by SC SBC.

V. Conclusion

The combined switched boost converter has been presented in this paper. Presented converter is a combination of conventional dc-dc converter with switched capacitor and switching structure of switched inductor. These proposed converter large step-up capability with reducing voltage stress and spikes across active switched and output diodes than conventional switched-boost converter. Operating principle based on continuous conduction mode, combined switched boost topology and simulation results are presented. Thus presented structure enhances the performance for different applications with better achievements. Further, cascading cells can be propagated to obtain very high gain voltage at output.

References

[1] Y. Hsieh, J. Chen, T. Liang and L. Yang, "Novel High Step-Up DC–DC Converter for Distributed Generation System," in *IEEE Transactions on Industrial Electronics*, vol. 60, no. 4, pp. 1473-1482, April 2013.

[2] F. Blaabjerg, Zhe Chen and S. B. Kjaer, "Power electronics as efficient interface in dispersed power generation systems," in *IEEE Transactions on Power Electronics*, vol. 19, no. 5, pp. 1184-1194, Sept. 2004.

[3] J. M. Carrasco *et al*., "Power-Electronic Systems for the Grid Integration of Renewable Energy Sources: A Survey," in *IEEE Transactions on Industrial Electronics*, vol. 53, no. 4, pp. 1002-1016, June 2006.

[4] F. Sedaghati, M. Eskandarpour Azizkandi, S. H. L. Majareh and H. Shayeghi, "A High-Efficiency Non-Isolated High-Gain Interleaved DC-DC Converter with Reduced Voltage Stress on Devices," *2019 10th International Power Electronics, Drive Systems and Technologies Conference (PEDSTC)*, Shiraz, Iran, 2019, pp. 729-734

[5] M. Feng, K. Qu, J. Zhao, and M. Sun, "Non-isolated DC-DC converter with high voltage gain," *IEEE PES Innov. Smart Grid Technol. Conf. Eur.*, pp. 730–734, 2016.

[6] A. N. De Paula, D. De Castro Pereira, W. J. De Paula, and F. L. Tofoli, "An extensive review of nonisolated DC-DC boost-based converters," *2014 11th IEEE/IAS Int. Conf. Ind. Appl. IEEE INDUSCON 2014 - Electron. Proc.*, 2014.

[7] Kuldeep jayaswal, Dheeraj kumar palwalia, Gaurav jain, Prakash kumar, "Design-Oriented Analysis of Non-isolated DC-DC Buck Converter", Ciencia e Tecnica Vitivinicola journal, vol. 30, no. 2, pp. 177-213, February 2015.

[8] K. C. Wu, H. H. Wu, and C. L. Wei, "Analysis and Design of Mixed-Mode Operation for Noninverting Buck-Boost DC-DC Converters," *IEEE Trans. Circuits Syst. II Express Briefs*, vol. 62, no. 12, pp. 1194–1198, 2015.

[9] Y. Hu and A. Ioinovici, "High step-up, high power density boost converter integrated with switched capacitor-diode cell," *9th Int. Conf. Power Electron. - ECCE Asia "Green World with Power Electron. ICPE 2015-ECCE Asia*, pp. 2255–2260, 2015.

[10] L. S. Yang, T. J. Liang, and J. F. Chen, "Transformerless DC-DC converters with high step-up voltage gain," *IEEE Trans. Ind. Electron.*, vol. 56, no. 8, pp. 3144–3152, 2009.

[11] B. Axelrod, Y. Berkovich, and A. Ioinovici, "Structures for Getting Transformerless Hybrid DC – DC PWM Converters," *IEEE Trans. Circuits Syst. Pap.*, vol. 55, no. 2, pp. 687–696, 2008.

[12] Y. Tang, D. Fu, T. Wang, and Z. Xu, "Hybrid switched-inductor converters for high step-up conversion," *IEEE Trans. Ind. Electron.*, vol. 62, no. 3, pp. 1480–1490, 2015.

[13] Kuldeep jayaswal, DK Palwalia, "Performance Analysis of Non-Isolated DC-DC Buck Converter Using Resonant Approach", *Engineering, Technology & Applied Science Research*, Vol. 8, No. 5, pp. 3350-3354, October 2018.

[14] A. Gautam, A. K. Sharma, A. Pareek, and R. Singh, "Analysis of Combined Z-Source Boost DC-DC Converter for Distributed Generation Systems," *Proc. Int. Conf. Inven. Res. Comput. Appl. ICIRCA 2018*, no. Icirca, pp. 1162–1167, 2018.

[15] X. Zhu, B. Zhang, Z. Li, H. Li, and L. Ran, "Extended Switched-Boost DC-DC Converters Adopting Switched-Capacitor/Switched-Inductor Cells for High Step-up Conversion," *IEEE J. Emerg. Sel. Top. Power Electron.*, vol. 5, no. 3, pp. 1020–1030, 2017.

[16] A. Ravindranath, S. K. Mishra, and A. Joshi, "Analysis and PWM control of switched boost inverter," *IEEE Trans. Ind. Electron.*, vol. 60, no. 12, pp. 5593–5602, 2013.

[17] J. D. Navamani, K. Vijayakumar, R. Jegatheesan, and A. Lavanya, "High step-up DC-DC converter by switched inductor and voltage multiplier cell for automotive applications," *J. Electr. Eng. Technol.*, vol. 12, no. 1, pp. 189–197, 2016.

Proceedings of the Fourth International Conference on Communication and Electronics Systems (ICCES 2019)
IEEE Conference Record # 45898; IEEE Xplore ISBN: 978-1-7281-1261-9

Regenerative Model for Electric Vehicle Application

Aniket A. Manjare
School of Electrical Engineering
MIT Academy of Engineering, Alandi (D)
Pune, India
aniketmanjare96@gmail.com

Vishal M. Patil
School of Electrical Engineering
MIT Academy of Engineering, Alandi (D)
Pune, India
vishalmpatil8007@gmail.com

Mandar M. Bhalekar
School of Electrical Engineering
MIT Academy of Engineering, Alandi (D)
Pune, India
mmbhalekar@etx.maepune.ac.in

Promod R. Ubare
Department of Instrumentation and Control,
College of Engineering,
Pune, India
pramodubare@gmail.com

***Abstract* - Nowadays, Electric vehicles (EV's) have received much consideration as a substitute for conventional Internal Combustion Engine (ICE) vehicles for having exceptional highlights, for example, low emanation, high proficiency, calm activity, and so forth. But the major issues faced with EV (related with Control system) are Acceleration and Range (travelling distance). The use of the Regenerative Model in (EVs) offers regenerative of energy, battery protection, and improved vehicle increasing speed. The regenerative model for EVs driven by PMDC motor has three modes Normal vehicle mode, Regenerative mode and Battery charging mode. During Regenerative mode (No acceleration, vehicle is in motion) the PMDC works like a generator and this energy is harvested. Henceforth, by utilizing a suitable switching control, the DC voltage is enhanced and the energy is exchanged from the capacitor bank to the battery. The Regenerative Model improves the bank is used to develop vehicle battery security.**

Keywords — Electric Vehicle, Capacitor Bank.

I. INTRODUCTION

Electric Vehicles (EV's) have received much consideration as a substitute for conventional Internal Combustion Engine (ICE) vehicles. EV's uses battery framework which can be energized from standard electrical plugs. Since the demonstration qualities of EVs have become analogous to which is not better than, those of conventional ICE vehicles [1]. The chemical batteries have many deficiencies such as short cycle-life, less power density, as well as high cost, capacitors bank, offer numerous highlights like, high power, long life-cycle [2]. Although the capacitor bank offers better features in most of the characteristics, it cannot be used as principle component for storage since its energy capacity is generally low so the battery must be utilized as a principle energy storage unit. The converter is used to control the power stream between the battery and the capacitor bank. The converter is important to coordinate the power levels of the capacitor bank, so as to use the abilities of the capacitor bank, adequately.

The measure issues faced with EV (related with Control system) are Acceleration (pick-up), Range (Traveling distance), and Speed range (Maximum). The batteries have numerous inadequacies such as short life-cycle, less power capacity and high cost. Due to the limited capacity of a battery, it can travel up to a few kilometres only in one charge [9]. In this model, a structure of collaboration of battery and capacitor bank is suggested [8]. The designed regenerative model is made out of a capacitor bank, battery, buck/boost circuit, and diode. Different working modes of the suggested Regenerative model are:

1. Vehicle normal mode.
2. Regenerative mode.
3. Battery charging mode.

In this paper, different modes of Regenerative Model have experimented and they are as above mentioned. These modes of operation can give better performance Characteristics of EV's with ON – GO charging and increase the traveling distance. The remaining part of the paper is structured as follows: Section II describes the block diagram and detailed circuit diagram. Section III describes different modes of operation. Section IV discusses the results achieved. Section V concludes the paper.

II. BLOCK DIAGRAM

The block diagram presented in Figure (1), comprised of a capacitor bank to store the harvested energy, battery is the main storage, buck/boost converter is to convert voltage to appropriate battery level, and a diode. Diverse activity methods of the proposed regenerative model are advised in details. During Idle state, using a relevant switching control for the converter. Hence, the diode will be forward biased and the energy reproduced is collected by the capacitor bank without employing extra power converter. Voltage in the capacitor bank is balanced by PWM control through variation in duty cycle in converter. Consequently, when the capacitor bank is nearly charged, regenerative braking can be acknowledged by methods for the battery pack in the proposed strategy. Figure (2) represents the detailed circuit diagram of

the Regenerative Model which consist of 4 switches for operation of different modes.

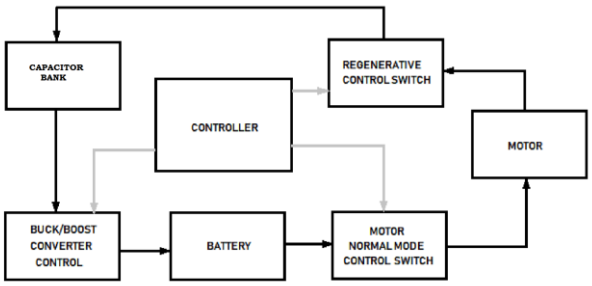

Figure 1: Block diagram of Regenerative Model

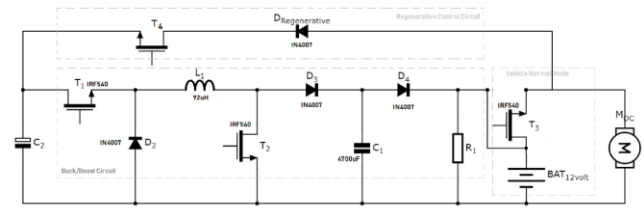

Figure 2: Circuit diagram in details

III. Functioning of Different Modes

The suggested Regenerative Model are categorized by its different modes of operation which are briefed as follows:

A. *Vehicle Normal Operation Mode*

The energy stream in the normal operation mode is shown in Figure (3). Here, the capacitor bank voltage is greater than the battery voltage hence, D1 is reverse biased. Furthermore, the capacitor bank module is idle as the buck converter is turned OFF. Hence, the battery exclusively supplies the energy to DC motor.

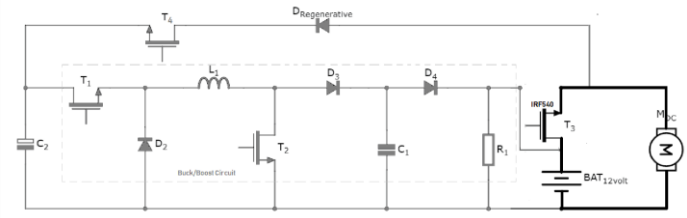

Figure 3: Vehicle Normal Mode operation

B. *Regenerative Operation Mode*

Figure (4) represents current flow during Regenerative mode with capacitor bank. It ought to be noted that the regenerative operation is initiated only if the vehicle in motion (no acceleration applied). High power capacity of the capacitor bank be able to be used to adequately collect the kinetic energy of vehicle (in motion) during this condition. Subsequently the regenerated energy could be efficiently saved, the driving scope of the vehicle can be impressively expanded. For Safety considerations and efficiency the Capacitor bank is proposed.

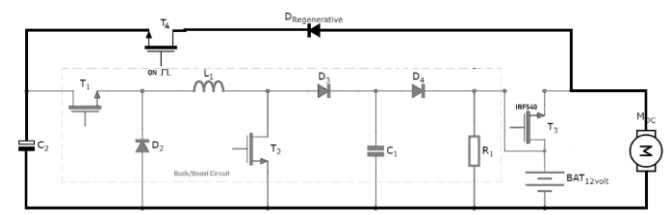

Figure 4: Regenerative operation with capacitor bank

C. *Battery Charging Operation Mode*

In this mode, energy is moved from the capacitor bank to battery through the buck-boost circuit and henceforth, regenerative braking energy is collected by the battery. Figure (5) indicates the current flow path during battery charging from capacitor bank through the Buck/Boost circuit. The DC voltage be able to boost/buck in the identical way and the energy is moved to battery through D3 and D4. Considering the changing aspects of the regenerative procedure, battery charging, and capacitor bank charging, it results that the impact of the capacitor bank is meaningfully greater than the battery for collecting the energy.

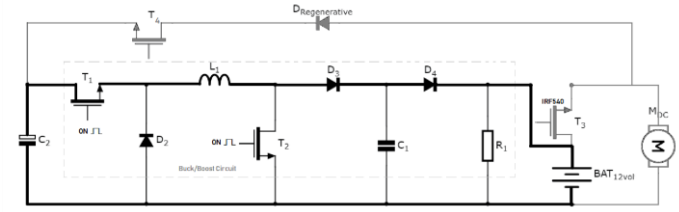

Figure 5: Battery charging from capacitor bank through Buck/Boost circuit

IV. Results & Discussion

Results are divided according to different modes of operation:

A. *Vehicle Normal Mode*

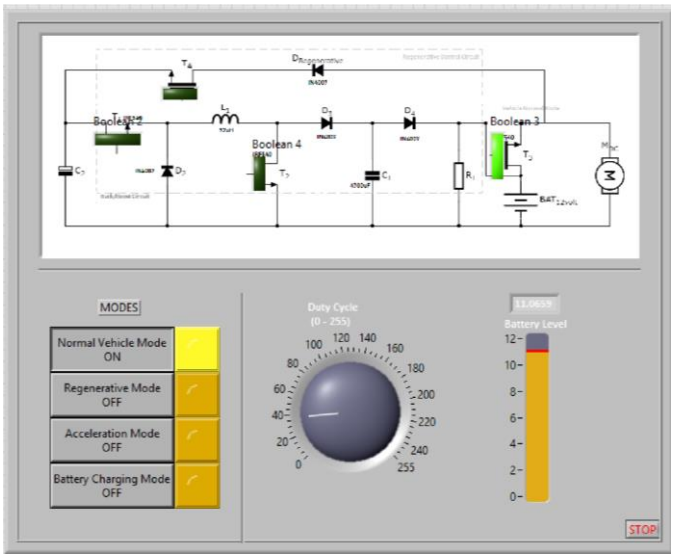

Figure 6: Vehicle Normal Mode Control

Table 1: Vehicle Normal Mode Working

Mode	T1	T2	T3	T4	$D_{Regenerative}$	Description
Normal Vehicle Mode	OFF	OFF	ON	OFF	OFF	T3 switch is made 'ON', Regenerative model operate the vehicle in a forward motoring shown in Figure (7)

Figure (6) shows the control panel for regenerative vehicle normal mode when the normal mode button is ON the motor starts rotating.

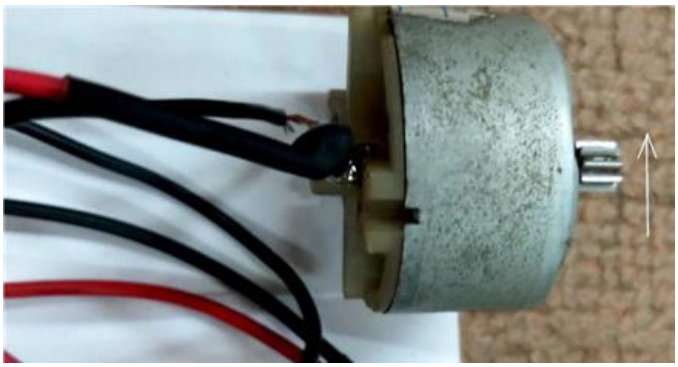

Figure 7: Motor rotating in a forward direction

Figure (7) shows the motor rotates in the forward direction when the regenerative model in Normal Vehicle Mode. Table (1) show the component which will be ON and OFF during this Mode.T1, T2, T4, and $D_{Regenerative}$ be OFF and T3 is ON.

B. *Regenerative Mode*

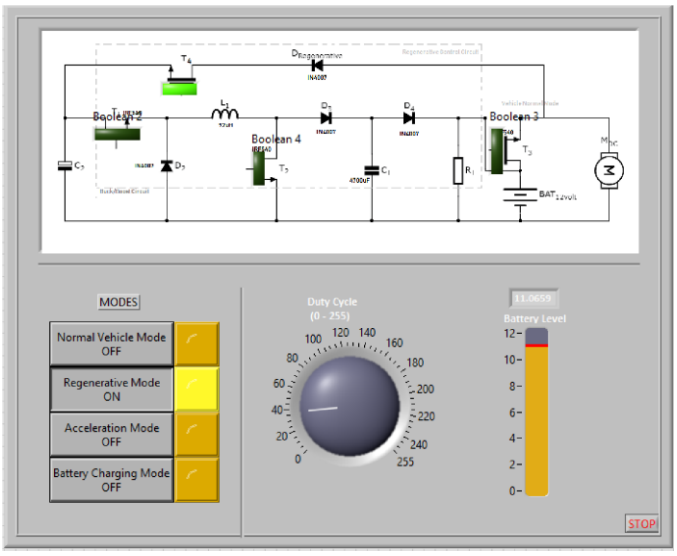

Figure 8: Regenerative Mode Control

Table 2: Regenerative Mode Working

Mode	T1	T2	T3	T4	$D_{Regenerative}$	Description
Regenerative Mode	OFF	OFF	OFF	ON	ON	$D_{Regenerative}$ Diode act as forward biased and the T_4 switch is 'ON', the energy is absorbed and stored using capacitor bank. The harvested voltage 2.21v by capacitor bank in shown in Figure 9.

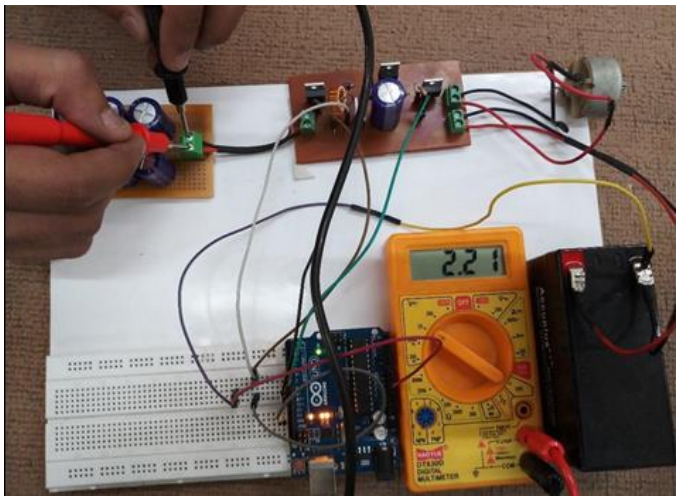

Figure 9: Voltage stored in the capacitor bank

In Regenerative mode, the energy generated by the motor is harvested and stores into the capacitor bank. Figure (8)

shows the control where Regenerative mode is ON. Table (2) shows the ON and OFF status of Components here T4 is ON and $D_{Regenerative}$ diode forward biased. Figure (9) shows the voltage stored in the capacitor bank during this mode.

C. *Battery Charging Mode*

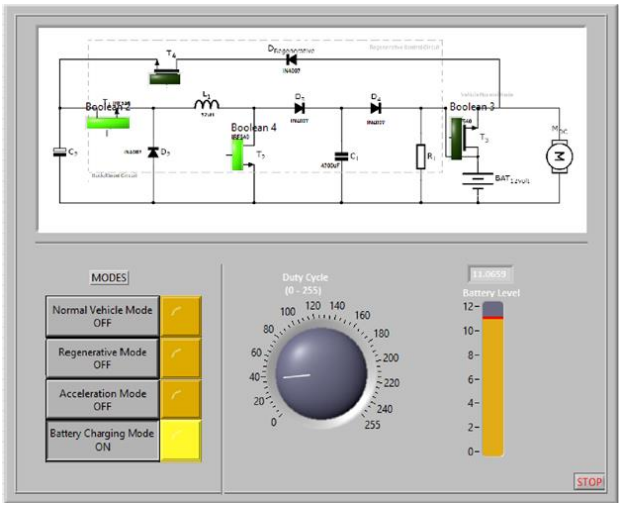

Figure 10: Battery Charging Mode Control

Table 3: Battery Charging Mode Working

Mode	T1	T2	T3	T4	$D_{Regenerative}$	Description
Battery Charging Mode	ON/ OFF	ON/ OFF	OFF	OFF	OFF	T1 and T2 switches are made 'ON/OFF' according to Buck and Boost Operation.

By using the applicable switching control, voltage is Boosted/Bucked by power converter. The voltage is tuned over variant of the duty-cycle of PWM. Hence, regenerative energy can be collected by means of the battery. Shown in Figure (11). Table (3) shows the Battery Charging Mode Operation.

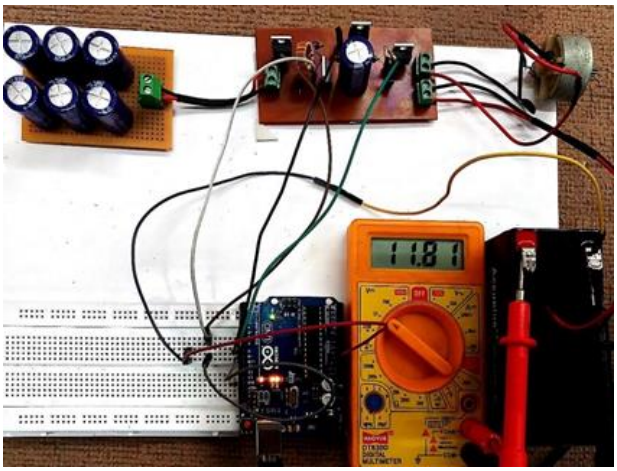

Figure 11: Battery voltage

V. CONCLUSION

Utilization of Regenerative model is suggested for EV's with PMDC motor. The Regenerative model circuit for EV's application is successfully designed and implemented. During this mode, kinetic energy of vehicle is harvested by capacitor bank.

The results are achieved for EV when the motor is driven in normal mode and in Regenerative mode. The Energy harvested is 16.66% of total battery capacity during the Battery Charging mode. The outcomes for Acceleration Mode are still under review.

In the future, the issues faced with Electric vehicle can be solved by employing an automatic control system for different modes of Regenerative model in appropriate conditions along with better acceleration, battery safety with ON-GO Charge.

REFERENCES

1. Xiaohong Nian, Fei Peng, Hang Zhang, "Regenerative Braking System of Electric Vehicle Driven by Brushless DC Motor" *IEEE Transactions on Industrial Electronics*, Vol. 61, No. 10, October 2014.
2. A. Emadi, "Transportation 2.0", *IEEE Power Energy Mag.*, vol. 9, no. 4, pp. 18-29, Aug 2011.
3. Jeongwoo Lee, Douglas J. Nelson, "Rotating Inertia Impact on Propulsion and Regenerative Braking for Electric Motor Driven Vehicles" *IEEE*, 2015.
4. Phaneendra Babu Bobba, K. R. Rajagopal, "Modeling and Analysis of Hybrid Energy Storage Systems Used in Electric Vehicles" *2012 IEEE International Conference on Power Electronics, Drives and Energy Systems*, December 16-19, 2012.
5. M. Ortuzar, J. Moreno, and J. Dixon, "Ultracapacitor-based auxiliary energy system for an electric vehicle: Implementation and evaluation," *IEEE Transactions on Industrial Electronics*, vol. 54, no. 4, pp. 2147–2156, August 2007.
6. J. Cao, and A. Emadi, ''A new battery/ultracapacitor hybrid energy storage system for electric, hybrid, and plug-in hybrid electric vehicles,'' *IEEE Trans. Power Electron.*, vol. 27, no. 1, pp. 122-132, May 2011.
7. Makena Coffman, Paul Bernstein Sherilyn Wee, "Factors Affecting EV Adoption", *University of Hawaii, Economic Research Organization.*
8. Farshid Naseri, Ebrahim Farjah, Teymoor Ghanbari, "An Efficient Regenerative Braking System Based on Battery/Supercapacitor for Electric, Hybrid, and Plug-In Hybrid Electric Vehicles With BLDC Motor", *IEEE Transactions on Vehicular Technology*, Volume: 66 , Issue: 5 , May 2017.
9. Sneha S. Bhurse , A.A. Bhole, "A Review of Regenerative Braking in Electric Vehicles", *2018 International Conference on Computation of Power, Energy, Information and Communication (ICCPEIC),* 08 November 2018.

Proceedings of the Fourth International Conference on Communication and Electronics Systems (ICCES 2019)
IEEE Conference Record # 45898; IEEE Xplore ISBN: 978-1-7281-1261-9

Design of smart Monitor for automobiles using FPGA based Data Logger

Merugu Bhavani
PG Research Scholar, Dept.of ECE
Sreenidhi Institute of Science & Technology,
Hyderabad, India
bhavanimerugu1995@gmail.com

Dharmavaram Asha Devi
Dept. of ECE
Sreenidhi Institute of Science & Technology,
Hyderabad, India
ashadevi@sreenidhi.edu.in

Abstract— **Data acquisition is a ubiquitous application for multiple fields and multiple environments. Till today, there is a vast demand and requirement of data loggers in automobiles to monitor and control several parameters. Therefore, data acquisition system for automobile application is discussed in this paper. While we are driving a vehicle, we sometimes take a left or right turn to overtake the other vehicle. While we are overtaking this there may be a chance of hitting the other vehicle or may be a chance of accidents. To avoid this, there should be an auto left or right indicator control with the help of accelerometer sensor. In addition to this, auto air conditioning in automobiles can be controlled by using temperature and humidity sensors. The proposed system is discussed about design and implementation of data acquisition system used for automobiles to perform above said applications. It is implemented using reconfigurable device, appropriate sensors and computer aided design tools. The communication of these sensors is performed with serial peripheral interface.**

Keywords—Analog to Digital Conversion, Data logger, Field Programmable Gate Array, Peripheral Module, Serial Peripheral Interface.

I. INTRODUCTION

Data acquisition system is the process of digitization of the data in a format that computer or a system can understand. High speed data acquisition system means sampling the data rate at high speed. Here, we are using a sampling rate of up to 1 million samples per second. Hence, proposed system is designed to acquire high speed data acquisition system for automobiles. As automobiles are increasing in day to day life, and driving with heavy speed, accidents are occurring.There are few ways to reduce that. one of the ways to reduce the risk of accidents is by keeping acceleration monitoring and controlling instrument.

In the proposed system, the monitoring is done by 3-axis accelerometer sensor [6], temperature and humidity sensors. 3-axis accelerometer sensor is used to measure static acceleration of gravity in tilt sensing and temperature and humidity sensors are used to monitor the AC temperature based on the sensor values.

Like any other data acquisition system, the automobile data acquisition system also consists of sensors, whose output signals are in analog form that has to be converted in to digital form to understand, process, and display the acquired results. The analog data from different sensors can be accessed by 4 channel or 8 channel multiplexers or data selectors. Between sensors and multiplexers, signal conditioning is required. The data access can be done by either serial or parallel manner depending on the required applications. If it is serial communication, we can use either Inter-Integrated Circuit I^2C or Serial Peripheral Interface SPI.

The main objective of this research work is to design high speed data acquisition system suitable for automobile applications. It is developed using Very High-Speed IC Hardware Description Language. Reconfigurable device, FPGA is used as the core of the data acquisition system, which collects, process and displays the data. FPGAs are the high-speed reconfigurable devices to process high-channel-density signals.

The organization of the paper is explained in XI sections including introduction. Section II is discussed about the history of the data acquisition system used in automobiles. Architecture design of the proposed system is explained in section III. Here, the interfacing of the sensors with the FPGA board is discussed in detail. Software Design Flow of Data Logger is explained in section IV. Section V shown about Results and Discussion of the proposed data logger system.

II. LITERATURE SURVEY

Prevention of accidents due to automobiles can be reduced by monitoring the vehicle velocity and acceleration using Raspberry Pi [1]. The communication used here is I2C protocol, the velocity and acceleration values are stored in SD card of Raspberry Pi, and there are some results of velocity and acceleration with respect to time.

The author in [2] explains about the acceleration data which is acquired from MEMS accelerometer and processed

through Spartan-6 FPGA. It was developed with VHDL and implemented in the Spartan-6 FPGA.

Tilting angle can be detected by using 3-axis accelerometer ADXL335 and Arduino Uno board was used to process the data. Tilt is measured towards its left or right direction[3].

To improve reliability and safety of automobile applications, real time embedded systems for automobiles that are used different sensors like MEMS Accelerometers, gyroscopes, pressure sensors, magnetic field sensors [4].

An efficient system has been designed in [5] for prevention of accidents in automobile systems. The main objective of the project is to design an app for car driver for safe driving of vehicles. The sensors are interfaced with Raspberry Pi, to monitor the required data.

The 3-axis MEMs accelerometer using AT89C52 microcontroller for the activation of airbag system for automobile applications discussed in [6]. They have used GPS and GSM SIM 900 to know the vehicle location exactly and it will drop a message.

The design of data acquisition system in [7] proposed a mechanism for patient monitoring in medical applications using FPGA. Here, they have used temperature and pulse rate sensor and produced some ECG waveform results.

Implementation of data transfer using Ethernet with a development board of Virtex-5 FPGA is discussed in [8]. Here, the results were displayed through SCD nothing but GUI and hyperterminal.

References [9], [10] and [11] are referred for the specification details of accelerometer, humidity and temperature sensors. The Zybo board architecture is referred from the references [12] and [13]. Finally, referred the software tool details from references [14] and [15].

III. Architecture design of the proposed system

In this design, we have used three sensors:accelerometer, temperature and humidity sensors. The ADC is used for converting the signals from analog to digital signals. The design is loaded in Artix 7 FPGA which consists of programmable logic, and interfacing of sensors are performed by processing system and ARM9 processor. The sensor interfacing with FPGA, which holds the automobile data acquisition system is illustrated in Fig.1.

A. Interfacing of Temperature Sensor

Temperature monitoring and measurement can be done with a temperature sensor LM35 in this proposed system. As it can measure the temperature range from −55°C to 150°C, and can have the calibrated value. It converts the voltage levels to temperature by using the relation as follows. VOUT = 10 mV/°C × T. Where, VOUT is the LM35, output voltage and T is the temperature in °C [10].

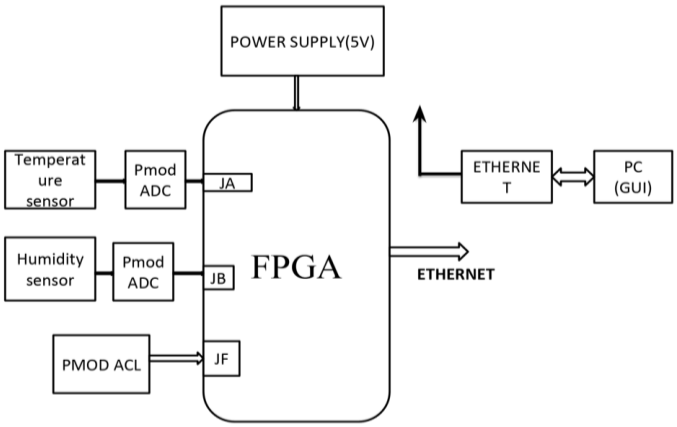

Fig.1 Interfacing of sensors with FPGA Board

The purpose of using this temperature sensor is used to know the exact temperature accumulated in the vehicle. Based on this temperature value, air conditioning (AC) can be maintained with a constant flow of conditioned air according to the passenger required option. The operating voltage of LM35's range is from 4V to 30V. It has 3 pins with naming VCC, GND and VOUT pins.VCC pin of LM35 is connected to VCC pin of ADC, GND pin of temperature sensor is connected to GND pin of ADC and VOUT pin of the sensor is connected to A0 pin of ADC peripheral module.

B. Interfacing of Humidity Sensor

In addition to temperature sensor, humidity sensor is also used to control the AC used in vehicles. The part number of humidity sensor used in the proposed work is SY-HS-220. Humidity is defined as the amount of water present in air. The operating range of humidity is 30-90% RH [11] and storable temperature range is from -30°C to 85°C and its current consumption will be less than 3mA. It consists of 3 pins namely VCC, GND, and VOUT as shown in Fig.2. VCC pin is connected to VCC pin of ADC peripheral module and GND pin of the sensor is connected to GND pin of PMOD ADC and output pin is connected to A1 pin of PMOD ADC.

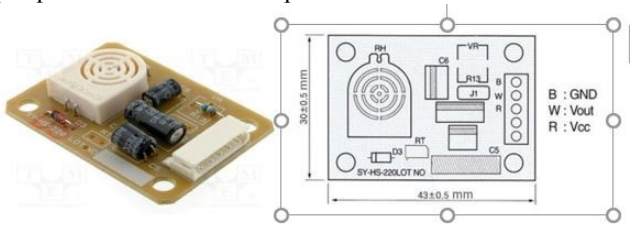

Fig.2 Humidity Sensor

In the proposed system, temperature and humidity sensors are connected to external ADC. It is 12 bit Analog to Digital Converter with part number AD7476A and the sampling rate of 1 million samples per second.

C. Interfacing of AccelerometerSensor

One of the most commonly used sensors in automobile system is accelerometer sensor. This sensor is used to measure the tilt angle in three dimensions. Based on the tilt angle, the indicator direction can be decided by the control unit used inthe automobile system.

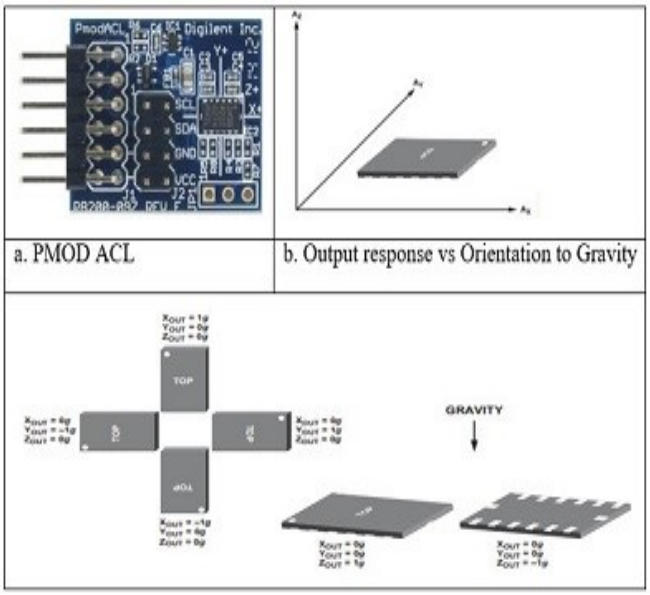

Fig. 3.Accelerometer sensor

Peripheral module for 3 axis accelerometer sensors used in the proposed work is ADXL345. It can measure the range up to ±16 g. It measures the gravity in tilt sensing applications. It gives the acceleration of gravity in x, y, and z axis respectively. It is interfaced with FPGA using serial peripheral interface (SPI). CS is the serial port chip select pin that is controlled by the serial peripheral interface. SCLK is the serial port clock. SDO and SDI is the serial data output and input respectively. It has 12 pin PMOD port with SPI interface [9].

The algorithm for single axis is illustrated in Fig.4. Raw angle is calculated by integrate the rate sensor output in real time. The accelerometer, ADXL345 is used to measure the direction of gravity and infer a tilt angle. The error signal can be calculated by calculating the difference between raw angle and gravity angle. Now, the stabilized angle can be calculated by mixing the raw signal with k times the error signal as shown in Fig.4. For example, if we get 0.1 G acceleration in the x-axis, then, it indicates a tilt of arcsine (0.4) = 23.57°. Once, if we could find the tilt angles, gravity of acceleration can be measured on x, y and z of accelerometer axes. Consider a rotation matrix with x, y and z axis aligned with the automobile, using pitch and roll, can rotate acceleration vector to the equivalent vector level with respect to earth as shown in Fig.5. In this system, gravity is completely vertical, therefore the level of x and y axes can measure motional acceleration, not gravity. The system discussed here can be implemented in real time, inexpensive system for vehicle motion testing.When these tilt value exceed the specified limit with respect to left or right then there will be auto indication of light.

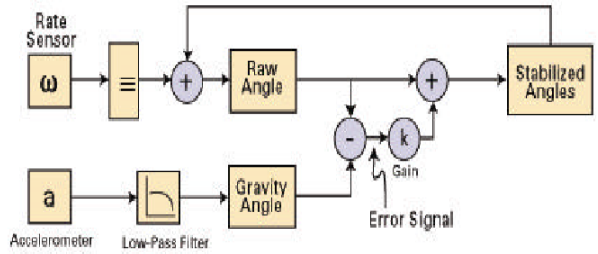

Fig.4 Stabilized angle calculation

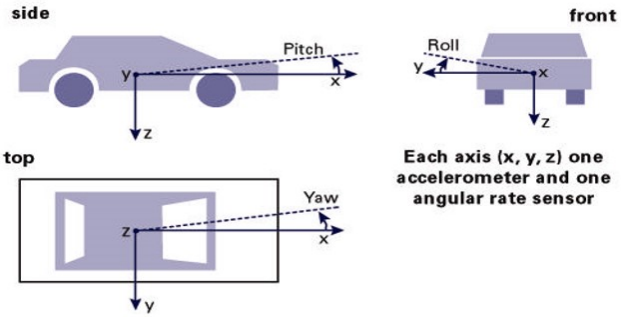

Fig.5 Sensor axis on automobiles

In the proposed system, the Zybo- FPGA development board which consists of Zynq processor and Artix 7 FPGA that are used to meet the specifications of high-speed data acquisition, high performance, with low power consumption. The Zynq-7000 SOC architecture consists of two major sections known as Processing Systems (PS) and Programming Logic (PL). FPGA comes under PL which holds the design logic and ARM Cortex-A9 Processor comes under PS which is used to control the peripheral interface. There are six PMOD connectors in this Zybo board. We connected temperature, humidity and accelerometer sensors to this FPGA board using PMOD connectors: JA, JB and JF respectively as shown in Fig.6.

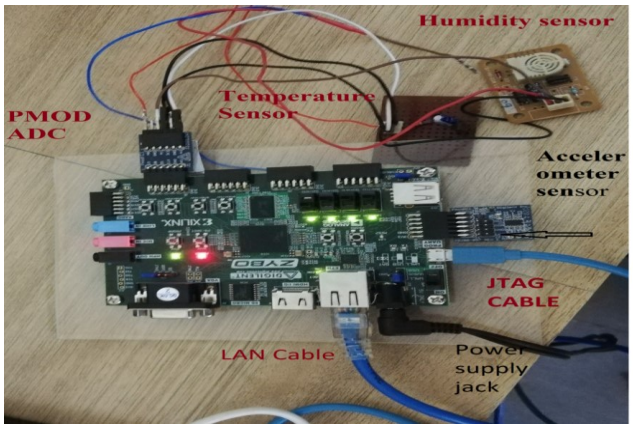

Fig. 6. Interfacing of three sensors with FPGA using Zybo development board

IV. Software Design Flow of Data Logger

To design data logger system, RTL design is created using hardware description language and XILINX 1SE 14.7 front end software tool. After verification, next step is we need to add required GPIO's in EDK (Embedded Development Kit). Then implement the design and generate bitstream for data logger design. After generating bitstream file, we need to export Hardware Design to software development kit (SDK) including the bitstream file. At SDK, we need to create application project along with application software developed in C and select as Light Weight Internet Protocol (lwIP) for Ethernet communication.

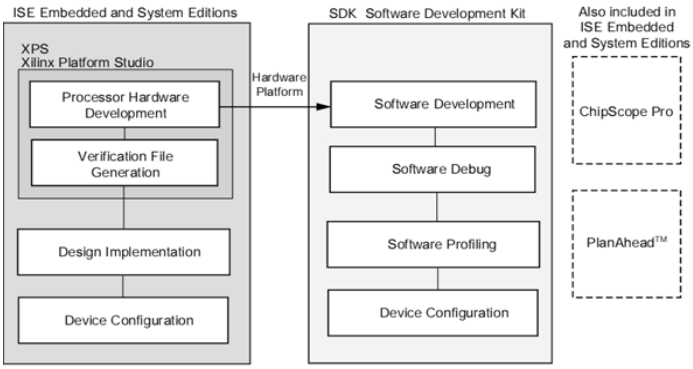

Fig. 7Embedded Design Process Flow

V. Results and Discussion

At SDK, board support package (BSP) is used to build the project. Once, the application project has built without errors and warnings, we can program the FPGA and then launch the hardware to verify the results. Make sure, the hardware setup has to be done and connected to a system where we can process all these steps. The Zybo board is connected to Ethernet cable using TCP/IP protocol. The communication between FPGA and PC is via Ethernet cable. The data is displayed using GUI. We need to assign IP address to PC which should be same as the board IP address. Now, Batch file need to be loaded into FPGA using JTAG cable. Now, we can ping the IP address. Then, after the establishment of proper link there will be a communication between board and system.

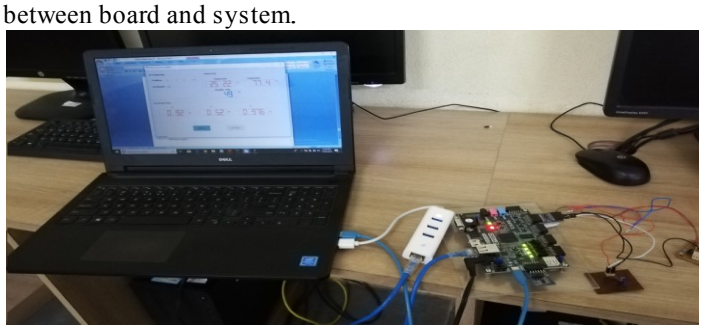

Fig.8 Experiment Setup for the data logger

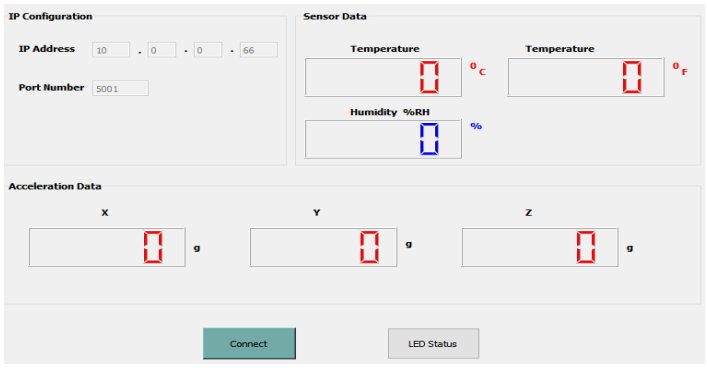

Fig.9 GUI display of data logger when no sensor is enabled

When no sensor is connected to proposed Data logger, then we can observe zero values at the GUI display as shown in the Fig.9.

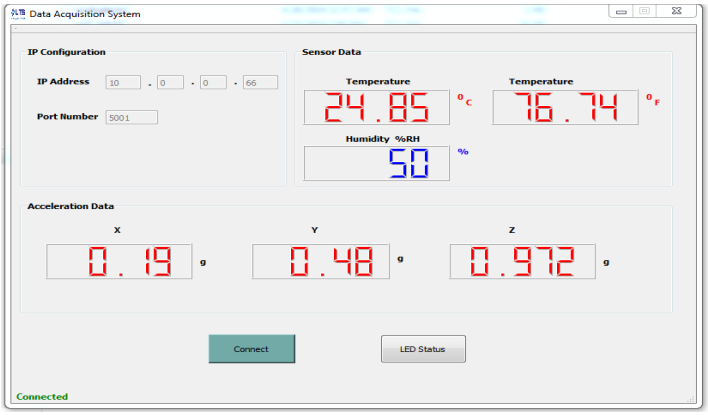

Fig:10 GUI display of data logger when sensors are enabled

When sensors are connected to proposed Data logger system, then we can observe respective measured parameters of the sensor values at the GUI display as shown in the Fig.10.

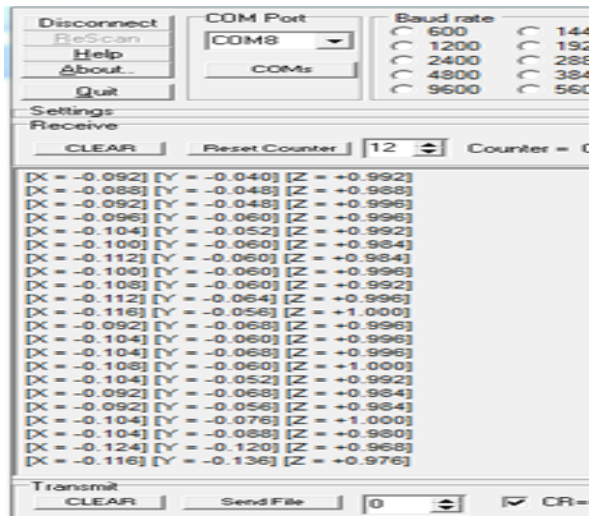

Fig. 11 Output results through terminal(acceleration tilting angle in x,y,z axis)

Terminal view for accelerometer sensor of x, y and z axis can monitor the gravity of acceleration in all x, y and z axis according to the movement of the vehicle. TeraTerm terminal is used when COM Port is connected.

VI. Conclusion

In the proposed data logger system, auto indicator options can be deployed based on the tilt angle of the accelerometer sensor. In addition to this, auto air conditioning feature also performed with reliable sensors and reconfigurable device. Based on the experiment results we can conclude that the proposed design gives accurate, high speed and reliable monitoring is possible in real time automobile applications.

Multiple sensors can be used for providing more comforts and security related features in automobiles like navigational system, tyre pressure monitoring, auto parking, telematics and alcoholic detection, back up collision sensors and many more.

Acknowledgements

We are thankful to our college management, Sreenidhi Institute of Science & Technology for providing the laboratory facilities in our department, Electronics and Communication Engineering to complete the project successfully.

References

[1] Catur Edi Widodo, Kusworo Adi, "Monitoring For Vehicle Velocity And Acceleration Using An Accelerometer", International Journal of Innovative Research in Advanced Engineering (IJIRAE) ISSN: 2349-2163 Issue 11, Volume 4, pp.20-23, 2017.

[2] N. LAVANYA , N. ARAVIND, "Spartan-6 FPGA Based MEMS Accelerometer Processing Electronics for Navigation", International Journal of VLSI System Design and Communication Systems, ISSN 2322-0929 Issue.04, Vol.05, pp.332-336, 2017.

[3] R. Rajesh, I. Baranilingesan, "Tilt Angle Detector Using 3-Axis Accelerometer", International Journal of Scientific Research in Science and Technology, Vol. 4, Issue 2, pp.784-791, 2018.

[4] UpeshMangalprasadPatel, Karishma Subhash Padole, "Overview of MEMS Sensors in Automotive Industry", International Journal of Engineering Research & Technology (IJERT), Issue 01, Vol. 7, pp.160-163, 2018.

[5] Arjun K, Prithviraj and Ashwitha, "Sensor Based Application For Smart Vehicles", International Journal of Latest Trends in Engineering and Technology, Issue 1, Vol 8 pp.526-532, 2017.

[6] Jaya Prakash Merepala, "Tri-axis MEMS Accelerometer for Vehicle Accident Monitoring", International Research Journal of Engineering and Technology (IRJET) Issue 10, Vol.8 pp.1068-1070, 2016.

[7] Vaishali Baste, D.K. Shende, S.K.More, Amol More, "FPGA based Data Acquisition System", International Journal of Engineering Science Invention Research & Development, Issue 4, Vol. 3, pp.262-268, 2016.

[8] Shruthi Sangani, K.Vikram, S.R. Pankaj Kumar, "Implementation Of Ethernet Based Data Transfer Using FPGA", International Journal of Electronics and Communication Engineering. ISSN 0974-2166 Vol. 8, pp.75-80, 2015.

[9] https://www.analog.com/media/en/technical-documentation/data-sheets/ADXL345.pdf.

[10] http://www.ti.com/lit/ds/symlink/lm35.pdf,Tempearature sensor.

[11] https://www.rhydolabz.com/documents/sensors/sy-hs-220.pdf.

[12] zybo_rm.pdf,zybo board reference manual, April 11, 2016.

[13] The_Zynq_Book_ebook%20.pdf.

[14] ISE_tutorial_14x7_schem.pdf.

[15] Tutorial-fpga-design-flow-based-xilinx-ise-and-isim.pdf.

Author Details

Merugu Bhavani, PG research Scholar, completed her M.Tech. in Digital Systems and Computer Electronics from the Department of ECE, Sreenidhi Institute of Science and Technology, Hyderabad. Her area of interest is to design low power circuits in VLSI Technology. Now she is working as a an Electronic Component Analyst in Unistring Tech solutions, Hyderabad.

Dharmavaram Asha Devi, Member IEEE, Fellow IETE. She is working as a Professor in the Department of Electronics & Communication Engineering, SNIST, Hyderabad. She became an Associate Member of IETE in Dec-2000 from the Institute of Electronics and Telecommunication Engineering, New Delhi, India. She awarded M.Tech. Degree in Digital Systems and Computer Electronics from JNTU Anantapur in 2005. She achieved a Doctorate Degree from Sri Krishnadevaraya University, Anantapur in Dec 2011, for her research contribution in Embedded System based Soil Analysis under the supervision of Prof. K. Malakondaiah, from SKU, Anantapur.

She has published more than 25 papers in International Journals and presented 40+ research papers in National and International level conferences on behalf of her research work

done in Embedded Systems and VLSI Designs.

Proceedings of the Fourth International Conference on Communication and Electronics Systems (ICCES 2019)
IEEE Conference Record # 45898; IEEE Xplore ISBN: 978-1-7281-1261-9

FPGA Implementation of segmented feature fusion in MRI images using wavelet

S.SREEKRISHNA YADAV
Electronics and Communication Engineering Department
National Institute of Technology, Kurukshetra-136119, India
s.sreekrishnayadav@gmail.com

VIKAS MITTAL
Electronics and Communication Engineering Department
National Institute of Technology, Kurukshetra-136119, India
vikasmittalkkr@gmail.com

Abstract— **Now-a-days, digital image processing in medical diagnosis is essential in almost all medical fields. Human eye is usually used to visually interpret a processed image as how well a particular technique used for its processing has worked. In medical diagnosis, two important techniques viz computed tomography (CT) offers less distortion with better information on denser tissues while magnetic resonance image (MRI) offers high distortion with best information on soft tissues. The multimodality of medical images in clinical applications has framed the idea of combining clinical images of distinct modality in medical applications. This knowledge of fusing clinical images has raised a new promising research field. The experiments on image fusion technique shows that it could extract useful information from distinct source images in fused images in order to obtain clear images. In this paper, an image fusion system with standalone hardware implementation framework is proposed. Xilinx platform studio (XPS), Visual Basic (VB) software's and FPGA Spartan 3 image processing kit is used for implementation. Firstly, input images are converted to .h files using MATLAB GUI. Then XPS is used to pick software and hardware components for fusing the images by incorporating source and .h files and converting them to bit streams for downloading them to FPGA Spartan3 kit. The fused image as obtained from FPGA can be seen using Visual Basic Graphic User Interface (GUI) on the monitor.**

Keywords— FPGA based implementation, SFTA, texture feature extraction, DWT.

I. INTRODUCTION

Recently, the huge advance in medical diagnostics methods has greatly improved the performance of assessment and reflection. The latest advances in magnetic resonance imaging (MRI), nuclear resonance instrumentation (NMRI) and Computed Tomography (CT) are used to picture the body's anatomy and physiological procedures. MRIs and CT's offer a 3D perspective and other high resolution features on distinct rates to detect any disease or abnormality.

This research focuses on the wavelet texture based function assessment of brain MR and CT pictures and their FPGA execution. Texture analysis (TA) has been demonstrated as an effective technique to detect any disease, such as brain tumor, etc. TA is the collection of matrices that offers the basis for the assessment of any specific picture and to check if the analyzed picture has texture similar to its sample.

Magnetic Resonance Image (MRI) offers high distortion with best information on soft tissues. The multi-modality of clinical images in medical applications has framed the to combing clinical images of distinct modality in medical applications

A. Brain MR and CT imaging

MRI is a clinical method for scanning inner nerves and tissues additional to X-ray and CT scans. The MRI of the brain system is made up of radio waves and magnetic field used to produce accurate brain pictures. It is capable of producing a three-dimensional brain perspective used to analyze any brain tumor diseases. The brain comprises of three main constituent groups of soft tissues like gray matter, white matter and cerebrospinal fluid. So, the quantity of GM, WM and CSF and their special allocation inside and chronological modifications need to be measured for the diagnosis of different brain diseases. The brain three tissue categories are shown in Figure 1. The three distinct planes i.e. axial plane, sagittal plane and coronal plane MRI are shown in Figure 2. This helps in study brain disorders such as various sclerosis, brain tumor Alzheimer's illness etc.

MRI and CT can identify various circumstances such as kysts, bleeding, Brest lesions, inflammation skeletal defects, ear diseases and blood vessel problems. Brain MRI and CT considers it useful to access the issues like dizziness, headaches, vulnerability and blurry. It can imagine the brain parts capably and at several resolution levels that X-ray and CAT scan cannot produce.

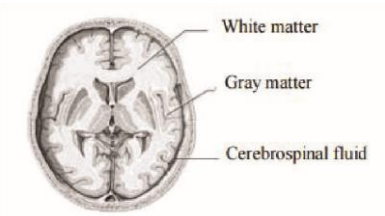

Figure 1. Brain MRI main tissue classes

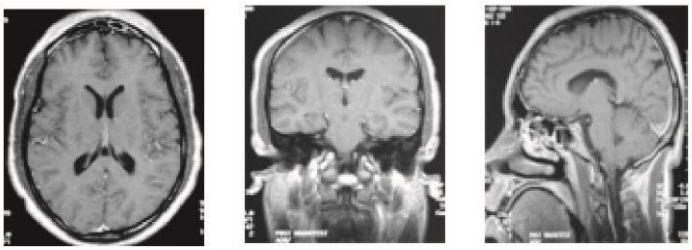

I. Axial View II. Coronal View III. Sagittal View

Figure 2: Different views for Brain MRI

TA plays a crucial role in diagnosing various diseases types and wavelet transformation along with gabor filter provides a framework for assessing the texture of brain MRI. TA includes extract, segment, classify and reconstruct features.

B. Discrete Wavelet Transform

Recently wavelet conversions that decompose a message into two parts, namely approximate and comprehensive part, are gaining more exposure. Freedom to choose the scale of decomposition is another advantage. So essentially this is a multiresolution analysis of brain MR images using three-dimensional resolution at different scales.

The discrete wavelet transformation (DWT) contains data about location information and frequency. The picture is decomposed into 4 sub parts LH1, LL1, HL1 as shown below in Figure 3 and Figure 4 for two different resolutions.

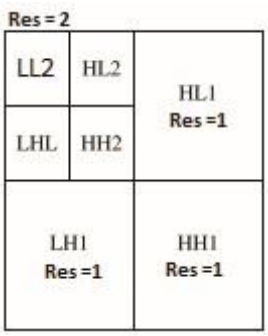

Figure 3: Single level Data/Image decomposition

Figure 4: Double level Data/imaged decomposition

The three parts of sub bands LL1, HL1, HH1, are called the numbers of estimation and element of LL1 is called precise index. The estimation ratio includes the peak sample data and can be used to divide the picture further in LL1. Figure 4 demonstrates the double-level picture regression using wavelet where the subbands are created again from LL1 as LL2 (ratio of estimation) and the comprehensive values are HL2, LH2, AND HH2. Similar to tier one decay, it is also possible to use LL2 subband to further decompose the message. LL subband is referred to as the crude point coefficient as it includes the highest data in all stages of decomposition. The converted indices are helpful for color assessment and discrimination at all subband concentrations. The numbers acquired in the pictures subband and/or their proportions portray the images texture distinctly.

C. Image fusion rule

Image fusion method is mostly performing a very fundamental operations such as pixel selection, addition, subtraction or averaging.

Simple Average: It is a fact that higher pixel intensity can be seen in the focused regions of the images. Hence, this method is a simplistic way of getting an output image with all regions that are in focus. Each image pixel value is taken and added. After this sum is divided by 2 to acquire the average value. Average value is allocated to the corresponding pixel of the output image. In the same way it is repeated for all pixel values.

Select Maximum: The pixels have greater values for more focused regions of the image. This rule suggests that it selects the in-focus areas from each input image by selecting the greater value for each pixel, resulting in highly focused output. Hence, each image pixel value is taken and compared to each other. The pixel having greater value is assigned to the corresponding pixel [22] [23].

Average of approximation coefficients is chosen in our Image fusion for both decomposed images so that low frequency information which is approximate information is not lost and high frequency information which is detail information is preserved. Therefore, corresponding vertical, horizontal and diagonal coefficients of both source images are compared and select maximum rule is applied to get maximum coefficient value that is assigned to corresponding coefficient in fused image.

D. Image fusion using DWT and inverse DWT.

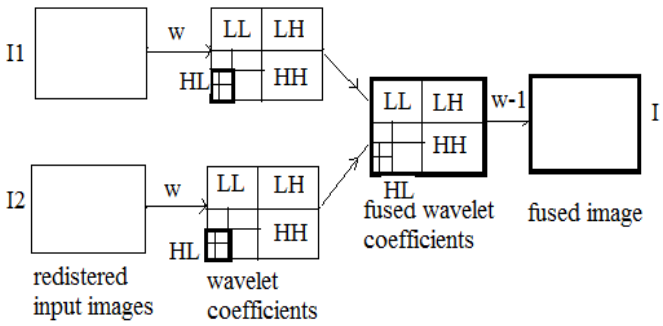

Figure 5. Process of fusing an image using DWT and Reverse DWT Methods

The development of DWT is used to apply the transformation technique to the digital information. The signal is disintegrated by the filter banks' low-pass and high pass filters. Image fusion steps are explained in detail based on WT in Figure 5.

- The input images I1 and I2 are first registered to arrange the equivalent pixels.
- DWT transformation is applied on the registered input images. The images are decomposed using wavelet bases. Here, wavelet transformation uses K-level decomposition on the registered images to obtain single low-frequency portion (LL band) and high-frequency 3K portions (HL bands, HH bands and LH bands).
- Different portions of the DWT image having with transform coefficients are achieved with an average of approximation fusion rule as explained in section I(C)
- The construction of fused image is done by performing inverse WT

Filter banks are used to decompose the signal into low and high-frequency components. Generally, most of the information of the signal lie at low frequency components. More details of the signal are available at high frequency components. Two-channel filter bank is used to implement wavelet decomposition technique. The decomposition of the image is done column by column and row by row. For illustration, the method to an M x N image as follows.

- The filter distinguishes each row and down-sample to obtain two M x (N/2) images to form H and L images.
- H and L images are formed using the formula

  H= odd-even = G1;

  L= round (G1/2) +even;
- Again, the filter combines each column and subsample of the filter to get output forming 4 (M/2) x (N/2) images. This is obtained using.

  LH= odd – even = G2;

  LL= round (G2/2) + even;

  HH= odd – even = G3;

  HL= round (G3/2) +even;
- G1, G2, G3 are reference parameters. The sub-image formed by low pass filtering is taken as LL image. in the same way using filtering other three sub bands formed are LH, HL and H. The sub images formed above can again be sub divided using filters and can form sub-sub bands and can be continued till desired filter images are obtained.
- Average of approximation fusion rule is applied on each pixel of the subbands of both the DWT images of the corresponding pixel to obtain a pixel with a single transform coefficient of the subband.
- The obtained sub bands of both images are having combined transformation coefficient. Using the combined transformation coefficient, the inverse or reverse DWT technique is applied to get fusion image. The fusion image obtained has the characteristics of both the DWT images that is useful for further observation.

E. Implementation tool:Field Programmable Gate Array (FPGA)

FPGA Procedure allows consumers or developers to develop logic circuits that could be reconfigured in real runtime, FPGA technology provides hundreds of combination of logic sets, a big range of entry output buttons and interconnections that are used depending on the provided logic.

The Zynq Evaluation and advanced board (ZedBoard) was used in this work to introduce the image handling scheme centered on extracted features. Xilinx ISE/Vivado HLS has been selected to program the FPGA board. The Xilinx ISE takes advantage of the concept of using intellectual property (IP'S) as section models and subsequently generates chip code for integrated layout. It includes the required features and can allow customization according to the chosen device by allowing creation of the custom computer logic. The board's expandability characteristics makes it perfect for rapid prototyping and proof-of-concept creation. Software portion can be coded using C, C++ and OpenCV for image processing tasks. Implementing the wavelet conversion on FPGA offers the advantage of reconfigurability at real runtime, simultaneous handling and execution of speed could be comparable to those achieved in software implementation.

II. BACKGROUND

There are basically two primary measures to follow for the diagnostic procedures in pathology. First procedure is that the tissue will be observed by a pathologist to recognize certain characteristics. The second step is to interpret and come up with a response. Several techniques to section and estimate the brain tumor have been suggested so far. Hall and Clark [1] suggested the picture mosaic as an assessment technique to assess the defects of the MRI scan. 57 Mosaic pictures were created by slicing ordinary fabric into different forms and sizes of defects. Using sophisticated diameter methods, Ibrahim and Khalid [2] suggested cancer identification using MRI information. Parra and Ifetekharuddin [3] suggested a scheme that automatically segments a tumor in the human brain's MRI. In [4], an improved application of the artificial neural net work software is used to block brain MRI information processing vector quantization and the findings achieved indicated great brain tissue segmentation.

Many algorithms for extraction of features are also used in this aspect. One among them is Texture Assessment (TA). TA performs a major part in the assessment of image segmentation. It has several applications like earth source mapping, medical processing, distant viewing, performance monitoring etc. Because TA is a sophisticated method and is linked to the local models of a picture, both picture removal and quantization are permitted. TA performs a major part in the assessment of image segmentation. It also out-performs the techniques of individual outcomes assessment and produces more precise diagnostic accuracy outcomes. Analysis of texture comprises essentially four steps [5]. Firstly, extraction of textual features, secondly, segmentation, thirdly, classification of texture

discrimination/classification, lastly, reconstruction of shape. Many algorithms are currently used to do so, but the most common of all current techniques to date are statistical methods and techniques appropriate for sophisticated medicinal imaging applications [6]. Most of the arithmetical methods are focused on temporal gray tier reliance model (TGTRM), gray point cooccurrence matrices [7], dominant cycle distance matrices (DCDM), statistical approaches centered on the use of textual assessment methods like Markov's test fields [10], fractal methods/models [11], and so many methods are appropriate for applications like textual characterization [8]. Since image analysis is conducted on a solitary scale, even though the visual cortex in a natural pictorial scheme is designed for depiction in a collection of autonomous streams with the specified direction and special frequency tuning [12] and it is a significant drawback. DWT's have a significant benefit by enhancing accuracy owing to multi-scale capacity and time-frequency localization relative to Gabor filter-based methods and TA Fourier transform [13], [14]. [15] and [16] uses two-dimensional wavelet extraction techniques for effective brain CT and MRI segmentation and texture analysis. These techniques are used alone in numerical methods.

Many DWT FPGA architectures were suggested to enhance time and resource consumption, primary focused on convolution [19], [20] and elating [21] schemes. Some of the parameters are not taken into account like group delay when calculating DWT and these delays have no effect in the processing of images or after the frame is processed by frame message, this architecture is considered. When the sample is processed by sample flow, the band errors of distinct filter routes cause the synchronization on problem s between the wavelet values at discrete scale concentrations, which is worsened by raising the scale value and therefore the structure of the image is modified by the wavelet numbers due to the accumulation of errors.

III.METHODOLOGY

The suggested scheme is implemented using the measures shown in Figure 6.

- Using MATLAB GUI feature, the registered MRI and CT scan images are converted into header files, where DWT and reverse DWT are going to apply on these images.
- Xilinx Platform Studio (XPS) is a tool used to select software and hardware components. In XPS all the header files, source codes etc. can be converted to bit stream and further going to download into FPGA
- Use Xilinx SDK and Xilinx Vivado to serially transfer the image matrix to FPGA through the JTAG cable.
- The input images. converted wavelet transform and reverse WT images are sent to the recipient facility via UART in FPGA. UART information was captured and seen through Visual Basic (VB) software in the monitor.

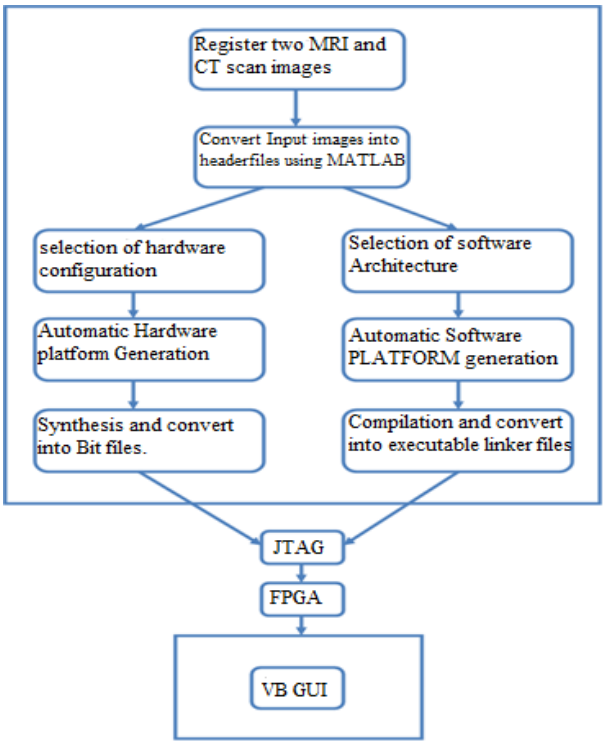

Figure 6: Proposed methodology

IV. RESULT AND DISCUSSION

Brain MRI and CT scan input images are registered for image fusion and converted into .h files using MATLAB. Hardware and software components for implementation are selected using Xilinx Platform Studio (XPS) tool which include RS232, MICOBLAZE software to access FPGA, SRAM, JTAG cable configuration, source codes, .h files etc. XPS converts all the source codes of DWT and inverse DWT and header files etc. into bitstreams. These source and .h files bit streams have .bit and .bmm extension, respectively. All these bit files are then exported to Software development kit (SDK) tool. SDK is part of Xilinx platform studio and it creates an Executable Linker File (ELF) to execute the program. Next step is to configure the JTAG settings with 500 kHz frequency and XILINX parallel IV cable type to LPT (Line Print Terminal) port. The bit stream codes are downloaded into a FPGA Spartan3 image processing Kit through JTAG serial transfer cable. Source codes, written in system c, contains DWT, Average approximation fusion rule and inverse DWT algorithms. The input, DWT's and inverse DWT images are stored in SRAM of the FPGA Spartan3 kit Board. The output from FPGA board can be configured through an UART cable into CPU COM port. All the input images, DWT MRI and CT scan images and output fused images are seen in Visual Basic GUI by executing ELF i.e. generated by XPS.

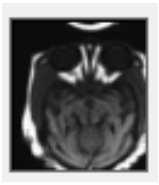

Figure 7: Input MRI image(I1)

Figure 8: Input CT scan image(I2)

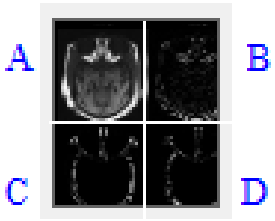

Figure 9: DWT MRI image

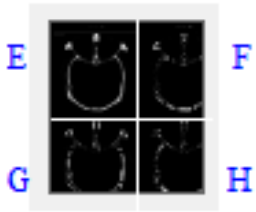

Figure 10: DWT CT scan image

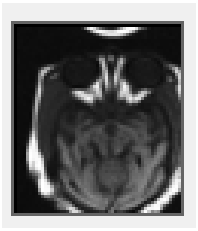

Figure.11: Output fused MRI and CT scan image using Inverse DWT

Figure 7 represents the MRI image having size of 64* 64 bits. More information is indicated by high intensity regions in the image. Decomposition is done using DWT algorithm. DWT is a technique used to convert the given information which contains mixed level of intensity of data into four subbands like low-low (LL) frequency band having high intensity of information, remaining frequency bands low-high (LH), high-low (HL) and high-high (HH) having less reliable information. Figure 9 represents DWT decomposition of the MRI image into four sub bands A, B, C, D. The subband A represents low-low (LL) frequency component which has more high intensity and hence more information from MRI image, the remaining subbands B represents the low-high (LH) frequency band, C represents the high-low (HL) frequency band and D (HH) represents the high-high frequency band. All these subbands viz. B, C and D contain less intensity regions of the image as we can see in the Figure 9. Figure 8 represents the CT scan image with size of 64*64 bits. The decomposition of the CT scan image is shown in Figure 10 with sub bands E, F, G, H. Here, it can be seen that E represents low-low (LL) frequency band having more intensity regions of the image and hence more information. The remaining subbands F represents low-high (LH) frequency band, G represents high-low (HL) frequency band, H represents high-high (HH) frequency band. Simple average approximation method of fusion rule is applied on MRI and CT scan LL images containing more intensity regions (more information) at low frequencies. The resultant image obtained after average approximation fusion is also like an DWT image which is having the combined coefficients of both MRI and CT scan image. The inverse DWT is applied on this combined/fused coefficient DWT image. Figure 11 represents the inverse DWT i.e. image fusion of MRI and CT scan images which contains more high intensity regions as compared to its constituent input images.

V. Conclusion

DWT method has been used in this paper for efficient feature transformation of the image using Average approximation Fusion rule. The suggested scheme has its own unique characteristics in the extraction of phase by enhancing the precision of identification. The application of FPGA Spartan3 image processing kit is used which demonstrates to be effective in the aspects of parallel processing and execution in real time. MRI and CT scan samples were gathered from the charts of the body. Using DWT and inverse DWT the fused image is obtained that has more precise information compared with original images. Average approximation fusion rule is used to fuse the images. So, the proposed scheme will help the physicians in making the ultimate choice for further therapy using a standalone hardware that is simpler and smaller. Future work will be focused on the enhancement of ranking precision by reducing redundant characteristics in DWT and its inverse.

References

[1] C. I. M. Cruz, J. P. Marasigan, A. P. G. Perez, J. E. V. Pillejera, N. P. Veron and A. R. dela Cruz, "A comparative study between DWT-ANFIS and DWT-SVM in ECG classification," *2016 IEEE Region 10 Conference (TENCON)*, Singapore, 2016, pp. 2052-2055

[2] Matthew C.Clark, Lawrence O.Hall , "Automatic tumor segmentation using Knowledge based techniques," IEEE transactions on medical imaging, vol 17, No 2, April 2018

[3] R. Karthikeyan and G. Hegde, "High performance VLSI architecture for 3-D DWT (discrete Wavelet Transform)," *2018 2nd International Conference on Inventive Systems and Control (ICISC)*, Coimbatore, 2018, pp. 892-897.

[4] Shafaf Ibrahim, Noor Elaiza Abdul Khalid, "Image Mosaicing for evalustion of MRI Brain Tissue abnormalities segmentation study", Int.J.Biology and Biomedical Engineering, issue 4, volume 5, 2016, pp 181-189

[5] Carlos A Parra, Khan Iftekharuddin, "Automated brain data segmentation and Pattern recognition using ANN" Proc. CIRAS, 2015

[6] L-K Soh and Costas Tsatsoulis. Textureanalysis of SAR sea ice imagery using gray level co-occurrence matrices. IEEE Transactions on Geoscience and Remote Sensing, 37(2):780–795, 2014.

[7] Trygve Randen and John Hakon Husoy. Filtering fortextureclassi¿cation tion:A comparative study. IEEE Transactions on Pattern Analysis and Machine Intelligence, 21(4):291–310, 2017.

[8] Yongyue Zhang, MichaelBrady, and Stephen Smith. Segmentation of brain MR images through a hidden markov random ¿eld model and the expectation-maximization algorithm. IEEE Transactions on Medical Imaging, 20(1):45–57, 2017.

[9] S.Karpagam, S.Gowri, "Detection of tumor growth by advanced diameter techni Que using MRI data", Proc.The world congress of Engineering 2015 Vol I WEC 2011, London, U.K

[10] Mohd Ali Balafar, Abdul Rahman Ramli, M Iqbal Saripan, and Syamsiah Mashohor. Review of brain MRI image segmentationmethods. Arti¿cialIntelligence Review, 33(3):261–274, 2014.

[11] Gholamreza Akbarizadeh. A new statistical-basedkurtosis wavelet energy feature for texture recognition of sarimages. IEEE Transactions on Geoscience and Remote Sensing, 50(11):4358–4368, 2012.

[12] GertVande Wouwer, Paul Scheunders, and Dirk Van Dyck. Statistical texture characterization from discrete wavelet representations. IEEE Transactions on Image Processing, 8(4):592–598, 2004.

[13] Tong Hau Lee, Mohammad Faizal Ahmad Fauzi, and Ryoichi Komiya. Segmentation of CT brain images using unsupervised clusterings. Journal of visualization, 12(2):131–138, 2009.

[14] Yi-hui Liu, Manita Muftah, Tilak Das, LiBai, Keith Robson, and Dorothee Auer. Classi¿cation of MR tumorimages based ongabor wavelet analysis. Journal of Medical and Biological Engineering, 32(1):22–28,2012.

[15] Stephane G Mallat. A theory for multiresolution signal decomposition: the wavelet representation. IEEE Transactions on Pattern Analysis and Machine Intelligence, 11(7):674–693, 2006.

[16] Sandeep Chaplot, LM Patnaik, and NR Jagannathan. Classi¿cationof magnetic resonance brain images using wavelets as input to support vector machine and neural network. Biomedical Signal Processing and Control, 1(1):86–92, 2006.

[17] A Padma Nanthagopal and R Sukanesh. Wavelet statistical texture features-based segmentation and classi¿cation of brain computed tomography images. Image Processing, IET, 7(1):25–32, 2013

[18] Anil Jain and Douglas Zongker. Feature selection: Evaluation, application, and small sample performance. IEEE Transactions on Pattern Analysis and Machine Intelligence, 19(2):153–158, 2017

[19] J-F Aujol, Gilles Aubert, and Laure Blanc-Fe´raud. Wavelet-based level set evolution for classi¿cation of textured images. IEEE Transactions on Image Processing, 12(12):1634–1641, 2003.

[20] A. Grzeszczak, M.K. Mandal, S. Panchanathan, VLSI implementation of discrete wavelet transform. IEEE Trans. Very Large Scale Integr. (VLSI) Syst. 4(4), 421–433 (1996)

[21] J. Chilo, T. Lindblad, Hardware implementation of 1D wavelet transform on an FPGA for infrasound signal classi¿cation. IEEE Trans. Nucl. Sci. 55(1), 9–13 (2008)

[22] WBCollis, PR White, and JK Hammond. Higher-order spectra: the bispectrum and trispectrum. Mechanical Systems and Signal Processing, 12(3):375–394,1998.

[23] K.G. Oweiss, A. Mason, Y. Suhail, A.M. Kamboh, K.E. Thomson, A scalable wavelet transform VLSI architecture for real-time signal processing in high-density intra-cortical implants. IEEE Trans. Circuits Syst. 54(6), 1266–1278 (2007)

[24] Shih-Gu Huang, "Wavelet for Image Fusion" Susmitha Vekkot, and Pancham Shukla "A Novel Architecture for Wavelet based Image Fusion". World Academy of Science, Engineering and Technology 57 2009

[25] Gonzalo Pajares , Jesus Manuel de la Cruz "A wavelet-based image fusion tutorial" 2004 Pattern Recognition Society.

Proceedings of the Fourth International Conference on Communication and Electronics Systems (ICCES 2019)
IEEE Conference Record # 45898; IEEE Xplore ISBN: 978-1-7281-1261-9

FDDS: An Integrated Conceptual FDDS Framework for DDS Based Middleware

Mukesh Kumar
Department of Computer Engineering
National Institute of Technology
Kurukshetra, India
mukeshgiran@gmail.com

Awadhesh Kumar Singh
Department of Computer Engineering
National Institute of Technology
Kurukshetra, India
aksingh@nitkkr.ac.in

***Abstract*— Data Distribution Services (DDS) has changed the way of the development process for complex distributed systems by tightly coupling QoS policies for achieving desired functionality at execution time. DDS middleware can be configured to handle edge-to-edge quality of service (QoS) policies. However, unpredictable environment imposes a greater challenge in the design and execution of these systems. The publish/subscribe middleware has improved the scalability and interoperability of the distributed systems. The stringent Quality of Services (QoS) standards imposes a greater challenge to developers. We propose a framework based approach for designing, development, and testing of distributed systems on top of Real-Time Innovations (RTI) and Open-Splice (OSPL) DDS middleware. The framework consists of ACGF Module which generates the code for application. DCF Module provides the abstraction from core functionality of DDS by using templates. Finally, ATF Module will help developer to test their application. This work will be beneficial for the development of different types of DDS applications rapidly.**

Keywords: Data Distribution Services (DDS); Object Management Group(OMG); Publisher/Subscriber Architecture; QoS; RTI; OSPL.

I. INTRODUCTION

DDS is an open standard for real-time distributed systems developed by Object Management Group (OMG) released in 2003 and revised in 2007. Real-time distributed systems can use DDS API's for Pub/Sub communication [2],[3]. DDS technology is used for the platform/target independent devices with secure data communication to all network devices (WSN, LAN, WAN). The environment is highly heterogeneous and requires dynamic pairing along with coordination of fast communicating entities. It is used as the integration technology for data sources and sinks. It provides an extremely high level abstraction along with a rock- solid infrastructure to build highly modular distributed systems [5]. It is like a universal glue that allows us to seal together highly heterogeneous environments while maintaining a single, elegant and efficient abstraction.

This paper proposed a framework based approach for designing, development and testing of distributed systems on top of Real-Time Innovations (RTI) and Open-Splice (OSPL) DDS middleware. The framework implementation is divided into three different modules named as Auto Code Generation Framework Module (ACGFM) generates source code for the application under develop; as per information provided by developer in the form of XML files as shown in Fig.2, DDS Communication Framework Module (DCFM) will provide the functionality related to DDS middleware to the application in the form of its own API's. Finally, Application Testing Framework Module (ATFM) will provide the interface to the developer for testing the application.

The remaining sections of the paper are as follows. Section II defines the evolution of DDS and its working model. Section III describes related work in the field by other researchers in design and modeling of DDS application. The design and implementation of framework is describes in section IV. Finally, in section V we conclude our paper with some future work.

II. BACKGROUND

Data Distribution Service (DDS) standards can be used for development of large scale computing machines as well as small IoT devices connected by network backbone (LAN/WAN). The DDS middleware provide flexibility to make an application scalable, location-independent as well as platform independent [12]. The QoS policies offered by DDS middleware provide the reliable communication for real-time computing devices [1],[3],[4]. The main functionality offered by DDS is Data-Centric Publisher Subscriber (DCPS) architecture. This architecture provides an interface to heterogeneous applications for reading/writing the data from Global Data Space (GDS). The software applications can exchange data in the form of Topics. The DCPS layer provides abstraction from the languages used for development [8]. The software application can exchange the information from other software applications after telling their intention to write the data as publisher by using Interface Description Language (IDL). In the same way software applications by telling their intention to read the data as an interested participant in the form of topic as subscriber [7].

The publish subscribe communication model as shown in Fig.1, enables real-time systems to exchange information by maintaining system performance, scalability and

interoperability [2],[9]. Publisher/ Subscriber model exchange information via central broker to avoid a single point failure. Interface Description Language (IDL) is used for defining the topics in .idl files.

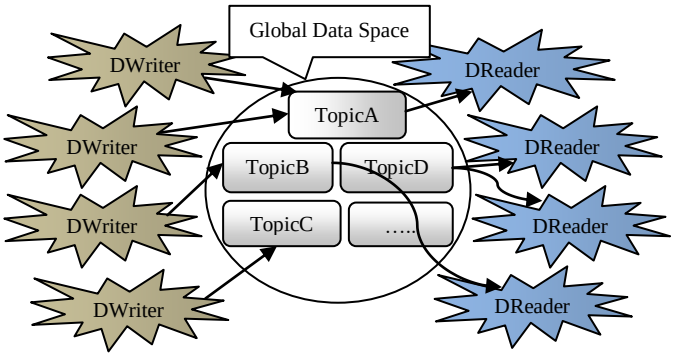

Fig.1. DDS Communication Overview

Architecture and key components of DDS are as follows [10]:

- **Global Data Space:** The software modules communicate with each other by writing and reading the data from Global Data Space(GDS).
- **Domain:** Domain is the main entry point for software modules. All modules are managed inside domain. Domain is a logical space inside the GDS for exchange of data. Software modules having same domain ID may only be able to communicate with each other in the form of topics.
- **Domain Participant:** This is the application that will be the member of Domain and it has right to manage DDS entities as an participient.
- **Publisher and Data Writer (DWriter):** The data writers has right to publish the domain specific data. Each publisher can have multiple data writers and the information about the data writer is maintained by the Publisher. The QoS policy defines the behavior of data writer and publisher.
- **Subscriber and Data Reader (DReader):** The data reader has right to subscribing the data from GDS. Each Subscriber can have multiple data readers and the information about the data reader is maintained by the Subscriber. The QoS policy defines the behavior of data reader and Subscriber. The data can be read from GDS with two approaches "listener-based (asynchronous)" or "waitset based(synchronous)".

III. LITERATURE SURVEY:

Many studies have been conducted regarding the challenges of the implementation of OMG DDS middleware in IoT objects. A lot of the investigations give varying insights into this area. However, what is common is the researchers' agreement on the pervasiveness of IoT and other distributed real-time systems (Alaerjan, Kim, & Al Kafaf, 2017) [1]. The increasing adoption of distributed real-time systems demands more support, with DDS being an example of publish-subscribe software that increases the communication and scalability aspects in IoT objects. The DDS has great significance in enhancing the quality of services (QoS) and promoting scalability; their absence means that these features will not be available. Consequently, according to Alaerjan, Kim, and Al Kafaf [1], one of the factors that hinder the implementation of the DDS middleware in the IoT objects and other distributed real-time systems has always been the absence of the DDS standard, which is required to offer the dynamic models for DDS.

The work on design and modeling aspects of OMG DDS is done by Inglés-Romero et al. [3]. He studies the QoS policies behavior of OMG DDS middleware for distributed systems. The selection and configuration of QoS is a great challenge for real-time systems. For system optimization, they have introduced the concept of communication templates for implementation of QoS in DDS middleware. These communication templates will give the flexibility to the designer and developer to enhance system performance by using adaptive QoS policies at run time. However, the work done by them has not covered any functional behaviour of DDS.

Corsaro et al. [4] talk about DDS and Java Message Service (JMS) standards for publish-subscribe systems, which aid in fully decoupling communication participants. According to Corsaro et al. [4], communication asynchrony is one of the challenges that the implementation of OMG DDS middleware faces.

Beckmann and Dedi [9] show how a lack of support for heterogeneous target platforms and limited interoperability are significant problems in the implementation of DDS middleware in IoT software. Although the OMG DDS is espoused as the breakthrough in addressing the issue brought about by the heterogeneous target platforms and interoperability, lack of DDS standards makes the implementation challenges persist. The problem of interoperability is not completely addressed by any off DDS vendor.

Hakiri et al. [11] propose an IoT network architecture that integrates Object Management Group's Data Distribution Services (OMG DDS) middleware and Software Defined Networking (SDN) as one of the solutions to the implementation problem.

The main problem is the lack of the DDS standards makes it difficult to understand DDS dynamic models and interoperability, which in turns not completely addressed by any vendors of DDS. The work offered in this research paper is a framework based development approach for software portability and reusability. By using the framework the developer can use the same piece of code written for one version of DDS to other version without rework. This work is more helpful in case of large number of heterogeneous IoT devices and coding is required for each and every IoT objects.

IV. FAST DDS IMPLEMENTATION FRAMEWORK

FDDS ("Fast DDS Implementation framework") is an approach by which software designer & developer can build DDS application easily for different type of DDS versions. This framework had provided the foundation classes to the software developers, so that they can use these classes for designing and building the DDS applications without worrying about the complex implementation of OMG DDS.

This framework systematizes the development process, by providing the rock solid infrastructure to the software developers for achieving the reusability of software application for different type of target environment. The framework functionality can be enhanced without effecting the implementation of application.

A. Brief Description of FDDS Framework

All communication of application being developed will be handled by FDDS framework. The functionality offered by framework is domain creation, registering topic, create publisher, create subscriber, create data reader, create data writer etc by re-implementing the DDS methods using class templates. The framework introduced here is a static library for reusability.

The application developer has to include the static library and header files in their project before calling the offered API's. The implementation of the framework is explained in the next section.

B. Implementation of FDDS Framework

The FDDS framework is divided into three modules:

1) Auto Code Generator Framework Module (ACGFM): This module generates the basic infrastructure for the application being developed; by generating the source code in the form of cpp and header files. DDS application development is completely dependent on the type of information exchanged between the publisher and subscriber in the form of topics.

The application developer has to write the topic information in the form of structure and data types in an .idl file. This .idl file is further used by rtiddsgen tool provided by the DDS vendor for compiling and generating the static library. Script for generating the library file is written in Listing. 1. The plug-in and support files generated in above process are carrying the send data, destroy data, print data, serialization and de-serialization methods as per the data structure provided in idl file. These files are used by the application and testing stub for further communication with DDS entities.

```
gcc -DUSE_IOSTREAM -I. -I. -I /opt/rti_connext_dds-5.3.0/include
-I/opt/rti_connext_dds-5.3.0/include/ndds  -DUSE_IOSTREAM -g -c
-DRTI_UNIX -o $f.o $f
```

Listing. 1. Script for generating the topics library

ACGFM is now ready for generating the application code by using the cpp and header files generated by the rtiddsgen. Firstly, this module collects the information about the list of publisher and subscriber with their data reader and data writer provided by the developer in the form of XML file as shown in Fig.1 and it stores the complete information in its local store. By using the file written C++ API's it will generate the cpp and header files carrying all methods and data types as per DDS requirement. The application raw source code is ready for further adding the functionality. In parallel it also generates the source files for the testing framework as per the topics selected by the developer. The application and tester generated in above steps are error free due to no human intervention for writing the code.

2) DDS Communication Framework Module (DCFM): This framework module is the heart for the application being developed. Applications by using this module can communicate with the DDS. The application has to register with DDS by providing the domain ID to which it intended to communicate. The threading and thread synchronization aspects of application is also handled by this module.

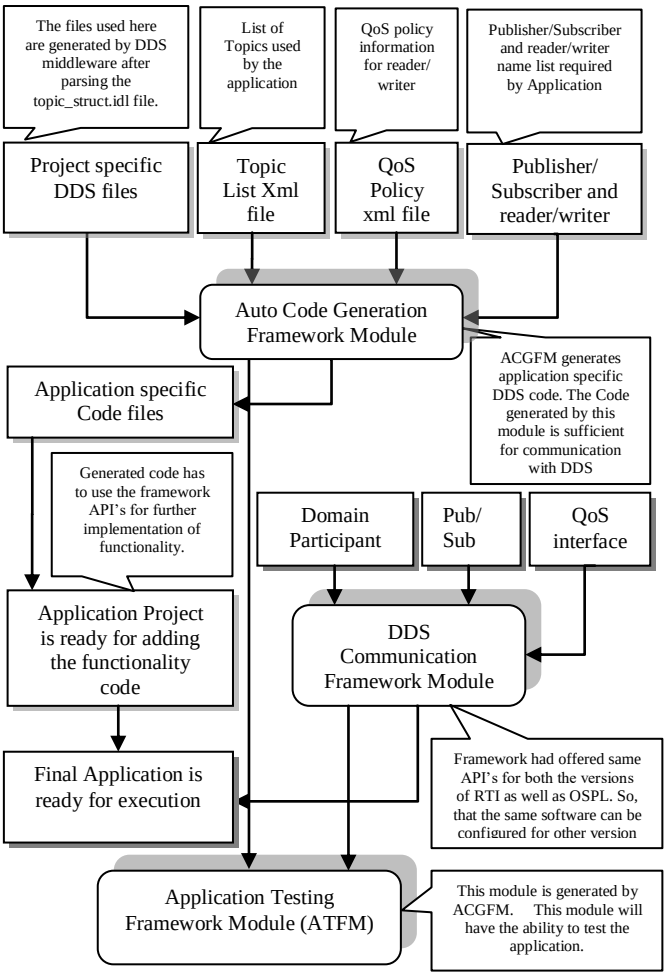

Fig. 2. Working Model of FDDS framework

The framework has re-implemented the DDS methods like

readData(), writeData(), TakeData(), LoanData(), disposeData() and many other methods for providing the simple interface to the DDS application developer.

The functionality of this module is divided into three interfaces. Each interface will provide the needed functionality to the application.

a) Domain Participant Interface: The Domain Participant Interface as shown in Fig.2 and Listing. 2, is the main entry point for the application for communication with DDS by extending its base class from the DomainParticipant class. The entities present in the same domain are only able to communicate with each other and not with other domain entities. The application developer has to enter the domain ID at the time of executing the application.

```
fDDSDomainParticipant::fDDSDomainParticipant(int fDDSdomainId) {
        ptrRtiparticipant = NULL;
        ptrRtiparticipant = DDSTheParticipantFactory-
        >create_participant(fDDSdomainId,
        DDS_PARTICIPANT_QOS_DEFAULT,NULL,
        DDS_STATUS_MASK_NONE);
    if (ptrRtiparticipant == NULL)
     {
        DEBUG_ERROR("create fDDS participant ->",ptrRtiparticipant);
     }
     DDS_SampleInfoSeq info_seq();
     ptrQosProviderRti = NULL;
}
```

Listing. 2. Domain Participant class Implementation

b) Publish/Subscribe Interface: The Publish/Subscribe Interface as shown in Fig.2, is providing the functionality related to publisher, subscriber, data-reader and data-writer to the application. This module is storing the information about the publisher and subscriber for further use by application. The application can request any of the publisher and subscriber by providing the string. The class templates implementation is used for achiving the abstraction from the core functionality of DDS.

c) QoS Interface: The Quality of services(QoS) controls the behavior of DDS systems by configuration a set of parameters, for Real-time Delivery, Redundancy, Persistence, Bandwidth as per system performance required to achieve. QoS Interface as shown in Fig.2 is responsible for attaching the QoS policies to publisher, subscriber, data-reader and data-writer. These QoS policies is decided by the system designer as per performance requirement of system under develop. A single QoS file is used for all the entities in the system. These QoS policies are provided by the designer in the form of XML file. Parsing of XML file is done by TinyXML parser.

sendData method implementation of framework	***sendData method implementation of application***
template <**class** T110,**class** T210> **inline int** sendData (T210 topic,std::string writerName) { DDSDataWriter* topicWriter= ptrRtiparticipant-	sendData<SEND_DATA_STRUCTDataWriter*, SEND_DATA_STRUCT*>(&obj,"DDSPublisher::system_Writer");

>lookup_datawriter_by_name(writerName.c_str());
if (topicWriter == NULL){
DEBUG_ERROR("lookup_datawriter>",writerName.c_str());
return -1;
}
DDS_InstanceHandle_t instance_handle = DDS_HANDLE_NIL;
T110 vDataWriter=(T110)(topicWriter);
DDS_ReturnCode_t retCode = vDataWriter->write(*topic,instance_handle);
if (retCode != DDS_RETCODE_OK){
DEBUG_ERROR("Write Error retCode->",retCode);
return -1;
}
return 1;
}	

Listing. 3. Framework snippet code of "sendData()"

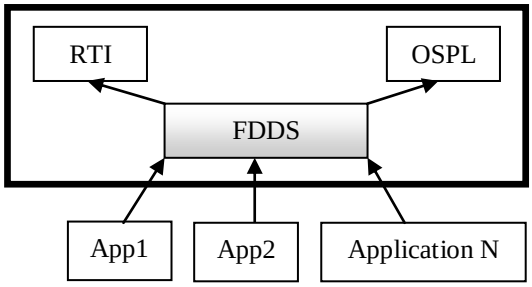

Fig. 3. FDDS framework overview

Fig.3 shows the framework based approach for implementation of RTI and OSPL DDS. The Application developed for RTI by adopting this framework need not required to be re-coded for OSPL because the framework has offered the same API's for both the versions to the developers. But Application developed without using the framework has to code the non functional requirement again for other DDS version. Listing. 3 Shows the implementation of send data method for framework as well as application. Application can write the data to GDS by making this API call. In the same way other API's are also designed and can be used by application.

3) Application Testing Framework Module (ATFM): This testing Module as shown in Fig.2, is auto generated by ACGFM and this module is using the DCF Module for communication with DDS. Only those features will be enabled in the testing framework which is selected as per the publisher, subscriber, data-reader and data-writer inputted in XML file. Developer can test his application by using this module and he did not required to build the testing stub for his application. ATFM is offering UI based manual interface to the developers.

C. Benefits of using framework in Software Development

The framework reduces, time to develop the application, by generating code for selected topics. This framework based approach has provided the infrastructure to the developers, so

that they did not require building the application from scratch. Some benefits of framework:

- **Reduction in Development Time:** The framework reduces the development time, by generating the code for the selected topics required to build the application. The code generated by the framework is able to communicate with DDS.
- **Less Domain Knowledge:** The developers only need to learn the basics of DDS. The complex functionality of DDS is abstracted by the framework by offering its own API's.
- **Reduction in Deployment Time:** The application developed using the framework reduces the time required to build and run the application on the target environment as half of code is auto generated.
- **Reduction in Testing Time:** The application developer only required to test the algorithmic aspects of the application.

V. Conclusion

In this research, an implementation of framework based approach; which provides its own API's for design and development of DDS application. By using the template based implementation application developer can achieve portability, reusability and get complete abstraction from the core functionality of DDS. The change in implementation of DDS will not affect the application and same application can be reused for other DDS version.

References

[1] Alaerjan, A., Kim, D. K., & Al Kafaf, D. (2017, August). "Modeling functional behaviors of DDS" In 2017 IEEE SmartWorld, Ubiquitous Intelligence & Computing, Advanced & Trusted Computed, Scalable Computing & Communications, Cloud & Big Data Computing, Internet of People and Smart City Innovation (SmartWorld/SCALCOM/UIC/ATC/CBDCom/IOP/SCI) (pp. 1-7). IEEE.

[2] Zu, X., Bai, Y., & Yao, X. (2016, August). "Data-centric publish-subscribe approach for Distributed Complex Event Processing deployment in smart grid Internet of Things". In Software Engineering and Service Science (ICSESS), 2016 7th IEEE International Conference on (pp. 710-713). IEEE.

[3] Inglés-Romero, J. F., Romero-Garcés, A., Vicente-Chicote, C., & Martínez, J. (2017). "A model-driven approach to enable adaptive qos in dds-based middleware". IEEE Transactions on Emerging Topics in Computational Intelligence, 1(3), 176-187.

[4] Corsaro, A., Querzoni, L., Scipioni, S., Piergiovanni, S. T., & Virgillito, A. (2006). "Quality of service in publish/subscribe middleware". Global Data Management, 19(20), 1-22.

[5] White, J., Dougherty, B., Schantz, R., Schmidt, D. C., Porter, A., & Corsaro, A. (2012). "R&D challenges and solutions for highly complex distributed systems: a middleware perspective". Journal of Internet Services and Applications, 3(1), 5-13.

[6] Atzori, L., Iera, A., & Morabito, G. (2010). "The internet of things: A survey". Computer networks, 54(15), 2787-2805.

[7] Pardo-Castellote, G., & Farabaugh, B. (2004). OMG Data Distribution Service (DDS): Architectural Update. In Proc. of IEEE Military Communications Conference. Orlando, USA: Is. n.

[8] Yuefeng, H. (2018, May). Study on Data Transmission of DCPS Publish-Subscribe Model. In 2018 2nd IEEE Advanced Information Management, Communicates, Electronic and Automation Control Conference (IMCEC) (pp. 1-2172). IEEE.

[9] Beckmann, K., & Dedi, O. (2015, October). sDDS: A portable data distribution service implementation for WSN and IoT platforms. In Intelligent Solutions in Embedded Systems (WISES), 2015 12th International Workshop on (pp. 115-120). IEEE.

[10] Wang, N., Schmidt, D. C., van't Hag, H., & Corsaro, A. (2008, November). Toward an adaptive data distribution service for dynamic large-scale network-centric operation and warfare (NCOW) systems. In Military Communications Conference, 2008. MILCOM 2008. IEEE (pp. 1-7). IEEE.

[11] Hakiri, A., Berthou, P., Gokhale, A., & Abdellatif, S. (2017). Publish/subscribe-enabled software defined networking for efficient and scalable IoT communications. arXiv preprint arXiv:1711.05036.

[12] Pardo-Castellote, G., Farabaugh, B., & Warren, R. (2005). An introduction to DDS and data-centric communications. RTI, Aug.

Proceedings of the Fourth International Conference on Communication and Electronics Systems (ICCES 2019)
IEEE Conference Record # 45898; IEEE Xplore ISBN: 978-1-7281-1261-9

Classification System for Lung Cancer Nodule Using Machine Learning Technique and CT Images

[1]S. Baskar, [2]P.Mohamed Shakeel, [3]K.P.Sridhar, [4]R.Kanimozhi
[1]Department Of ECE, Karpagam Academy of Higher Education, Coimbatore, India
[2]Faculty of Information and Communication Technology ,Universiti Teknikal Malaysia Melaka, Melaka, Malaysia
[3]Department Of ECE, Karpagam Academy of Higher Education Coimbatore, India
[4]Junior Research Fellow, Karpagam Academy of Higher Education, Coimbatore, India
[1]connectbaskar@gmail.com, [2]shakeelresearch@gmail.com, [3]capsridhar@gmail.com, [4]kanimozhiram2623@gmail.com

***Abstract*— Nowadays, Lung cancer is most common cancer for the people. According to statistics 4,30,000 people are affected by lung cancer. Computed Tomography is the popularly used diagnosis method for lung cancer. In contempt of accurate diagnosis at the early stages, there are some limitations for this method like time consumption and tumour boundaries are unclear. Delta Radiomics is another method used to analyze the image features with respect to time quantitatively for a region of interest and the extracted features are develop to improve the screening of lung cancer. In this paper the features of the cancer nodules are extracted by Delta Radiomics using the machine learning techniques. The Support Vector Machine (SVM) is used to predict the malignancy of the lung cancer nodules. The SVM is capable of analyzing compact features in a lung cancer nodule image and classification of an image is performed effectively for differentiating the various nodules. Therefore, SVM is suggested as the most suitable method for diagnosing and detecting the lung cancer.**

Keywords—SVM machine; lung cancer; diagnosing;Delta radiomics;

I. INTRODUCTION

Cancer is a genetic disorder that controls function of all the cells of a particular part of the human body as shown in fig 1.For a cancer affected person all the body cells are begin to divide continuously and spread to the surrounding tissues. When the cancer cell begins to develop it automatically stops the general new cell formation in a human body [1]. The cancer cells are become into a malignant tumour which can easily spread to the nearby tissues. Among various cancer types, Lung cancer is the second leading dangerous cancer that leads many death ratios [2].

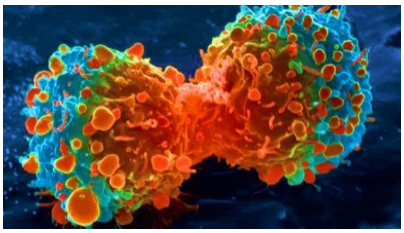

Fig 1: cancer cell

There are two types of lung cancer namely; non- small cell lung cancer and small cell lung cancer. According to the statistics of American Cancer Society, about 1,762,450 are newly affected by cancer and 6, 06,880 were died due to cancer in US. The Lung Cancer is generally detected using the Computed Tomography (CT) scan [3]. It is a medical imaging technology that produces 3D image structure of the internal body. It is most commonly used technique to do surveillance on a lung nodule. As it detected cancer early, It increases the survival rate of the cancer affected person. However, A medical specialist should screen large number of nodules for a proper diagnosis, It should a long time to have clarification. Thus, the CT method is highly time consuming and it is difficult to get a clear detail about the malignant tumour. Radionics is a medical process that helps to extract large set of features from a medical image using some algorithms. It gives quantitative feature extractions which are not visible through a naked eye [4]. The Delta Radiomics technique analyses the change in image feature over time so it is capable of examining the treatment response for the cancer affected person. As such delta radiomic analysis could be combined with the CT imaging for accurate and effective lung cancer screening [5]. In this study Support Vector Machine (SVM), a machine learning technique is being used as it can classify the interior and small features of an image data by reducing the dimensions. Along with reduction it can able to reconstruct the original input data. The classification is evaluated effectively for differentiating multiple nuclei as it can able to detect high level features [6]. Thus, in this process we utilized the CT images to generate screening and classified using SVM for

detecting lung malignant tumour cells [7]. The following sections are covered in this paper.

- The existing methodology of detecting lung cancer.
- A brief explanation about the proposed Methodology
- Experimental results and discussion
- Conclusion and future work.

II. RELATED WORKS

In [1] the author proposes a novel idea based on Structural Coherence Matrix (SCM) to classify the malignant and benign nodules of lungs and also their malignancy levels. SCM with four filters were applied on both grayscale Hounsfield unit images. In [2] the author analysed a performance by incorporating delta and non – delta features using machine learning methods to detect the lung nodule malignancy. They used two gene selection methods to extract lung cancer genes with the help of three machine learning methods namely, Multilayer perceptron, SM and Radial basis function neural network. In [3] the author presented a deep learning strategy called stacked sparse auto encoder (SSAE) for nuclei detection on high resolution [8] histopathological images of breast cancer.

III. LUNG CANCER CLASSIFICATION SYSTEM

The image dataset is used to locate the lung nodule by using the several steps such as Conversion to grey scale image, Image filtering and enhancement, Morphological operations, Feature Extraction and Classification. All the above-mentioned process is examined over the image dataset and the classification is done over the lung CT images. Figure 2 shows the lung cancer classification system structure.

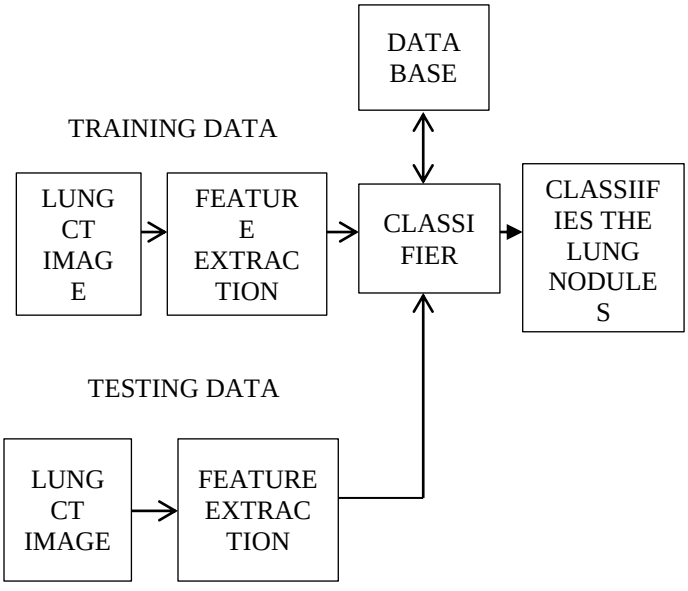

Figure 2: lung cancer classification system structure

A. Conversion To Gray Scale Image

The conversion of colour image to grayscale is simply converting the 3D pixel value (RGB) to 1D value. It is specially to reduce the complexity of processing and clear and accurate edge detection.

$$initial\ image = \ imread(lung\ CT); \quad (1)$$

The above eq (1) is to read lung CT image from the loaded dataset.

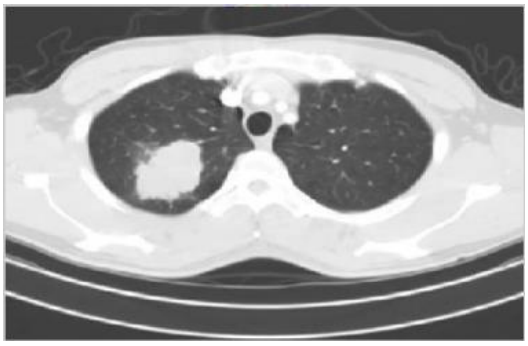

Fig 3: Input image

$$grayimage = rgb2gray(initial\ image); \quad (2)$$

Figure 3 shows the general input image. In general the gray scale pictures have a piixel values ranges from 0 to 255.It converts the RGB image to gray scale image indicates 24 bit image to 8 bit image. The eq (2) changes the given input lung CT image into 8 bit gray scale image. The color converted brain CT image is depicted in figure 4.

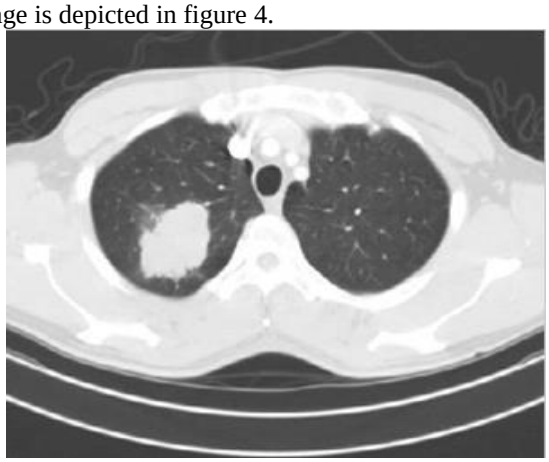

Fig 4: grayscale of the input image

B. Image Filtering And Enhancement

In many visual applications to get a clear analysis of image the image is being filtered and enhanced using some techniques. Filtering techniques are widely used to increase some special effects like brightness, contrast, tone, sharpness to the image under analysis [9]. Image enhancement is also to improve the image quality for further analysis especially both filtering and enhancement is to remove unwanted noise part in an image analysis.

$$adj = medfilt2(grayimage) \quad (3)$$

$$adj1 = hist\ eq(adj); \quad (4)$$

From the eq (3) and (4) we get the filtered (without noise) image of the given input. Here we used the median filter to remove the noise. Finally, we get the normalized histogram equalized image of the filtered lung CT image as shown in figure 5.

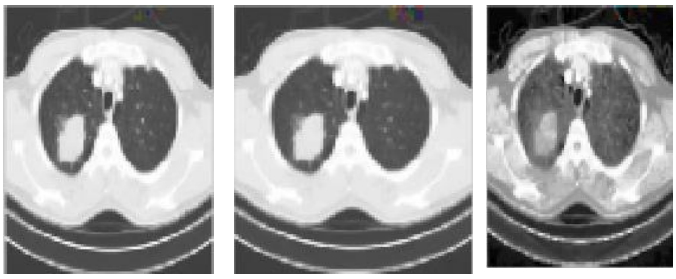

Fig 5: filtered output

IV. MORPHOLOGICAL OPERATIONS

In order to remove the non-tumour regions [10], we have to make use of morphological operators. All the edges of tumorous regions are mingled together with non-tumorous regions in dilation process the broken gaps at the edges are filled and there is a continuity at the boundaries.

$$mean = \frac{sum(C)}{sum(B)} \quad (5)$$

$$Var = \frac{sum(E)}{sum(B)} - mean * mea \quad (6)$$

$$std = (Var)^{\wedge 0.5} \quad (7)$$

$$where, C = A.* B; \quad (8)$$

$$D = A.* A; \quad (9)$$

$$E = B.*\mathrm{D} \quad (10)$$

The morphological operation is to done by doing dilation and erosion process consecutively.

$$\text{dilate=imdilate(bwimage,('arbitrary^',20);} \quad (11)$$

$$erode = erodeimerode(img_{dil}, ('arbitrary', 20); \quad (12)$$

The equation (11) & (12) indicates the dilation and erosion to obtain the morpholocal resulte image.We arbitrarilty set structuring element value of 20 to the black and white lung CT image for the morphologiacl alued image shown in figure 6.

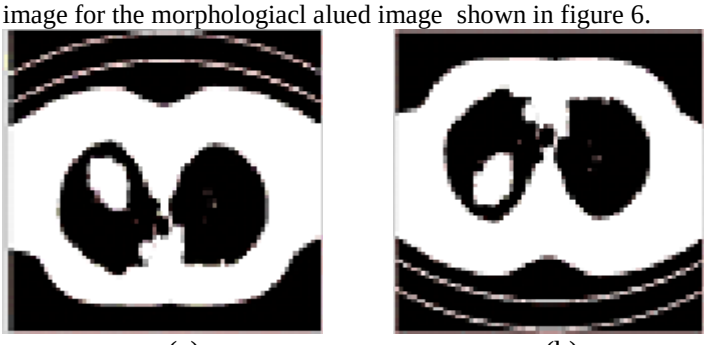

(a) (b)

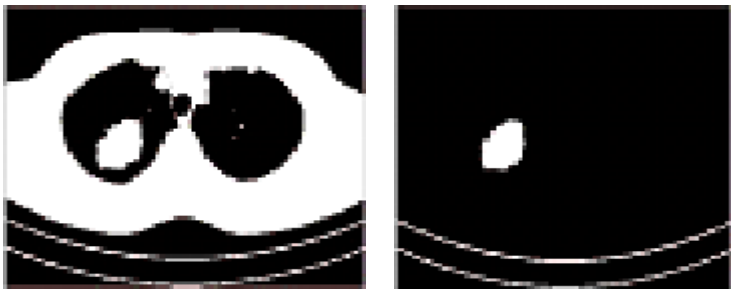

(c) (d)

Fig 6: morphological operation

A. Feature Extraction

Image recognition is obtained through extracting several features and stored in database. Gray Level Co-occurrence matrix is used to extract the normal and affected CT images. The feature extracted are listed as follows

$$contrast = \sum_{i,j=0}^{n-1} p(\mathrm{i,j}) * (i-j)^2 \quad (13)$$

$$inverse\ difference\ moment = \sum_{i,j=0}^{n-1} p(i,j)/1 + (i-j)^2 \quad (14)$$

The above equation of calculating the homogeneity is to examine the compact (bounded space) of the image pixels.

$$energy = \sum_{i,j=0}^{n-1} p(i,j)^2 \quad (15)$$

$$Dissimilarity = \sum_{i,j=0}^{n-1} p(\mathrm{i,i}) + |i-j| \quad (16)$$

The SVM classifier uses a hyper plane tow classify the given inputs. Generally, the hyper plane is expressed

$$W^T X=0 \quad (17)$$

$$f(x) = b0 + \Sigma\,(ai * (x, xi)) \quad (18)$$

The classification is done by the following expressions

$$\text{Class1: } W.a_i + b \geq 1 \quad (19)$$

$$\text{Class 2: } W.a_i + b \leq -1 \quad (20)$$

All the positive values come under the hyper plane 1 and the negative values comes under hyper plane 2.

In order to maximize the marginal distance of the hyper plane we need to have a change in weights

$$Yi\ (xi \bullet w) \geq 1 \quad (21)$$

As we know the input vector, we have to find the maxima of the hyper plane margin

$$w = \sum_{i=0}^{n} ai\ yixi \quad (22)$$

V. MACHINE LEARNING CLASSIFIER

Optimized machine learning techniques [11] like SVM are highly interconnected to large processing element the feature contrast of an image is to calculate the area of the image pixels into darkest and brightest no genetic or inverse difference moment

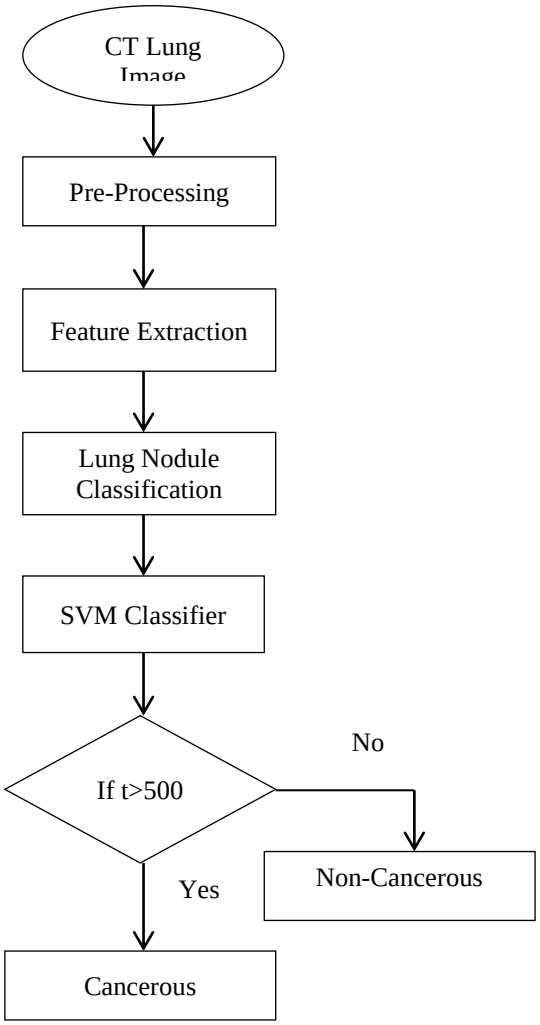

Fig 7: flow diagram of proposed model

Load the Input as Lung CT images.
STEP 1: read the input as CT lung image.
Init Image = imread (Filename);
Init Image= imresize (initImage,[300 300]);
[Rows, columns] = size (initImage);
STEP 2: Divide the data images into training image set and testing image set.
STEP 3: Pre-process the given image and get the grayscale, filtered and finally morphological output of the input image.
gray Image = rgb2gray (initImage);
Adj=medfilt2 (gray Image);
adj1=histeq (adj);
img_dil = imdilate (bwImage, strel ('arbitrary', 20));
BwImage = imerode (img_dil, strel ('arbitrary', 20));
SEP 4: Extract some features over the image such as contrast, homogeneity, dissimilarity, energy, correlation.
GLCM2 = graycomatrix (adj1,'Offset',[2 0;0 2]);
Stats=graycoprops
(GLCM2,{'contrast', 'homogeneity','energy','correlation'});
stats1=stats. Correlation (1);
stats2=stats. Contrast (1);
stats3=stats. Energy (1);
stats4=stats. Homogeneity (1);
STEP 5: Train the SVM classifier.
Step 6: Classify each input image as below.

Load the training, test and label data
Function class=svm(C)
Load train;
Load label;
% figure; title ('Train');
Data = svmtrain (round (train), label, 'show plot, true);
Class=sum classify (data, C,' show plot, true);
By using the kernel and RBF functions of the hyper plane
$W^TX=0$
The various group of class to be classified are
$W.a_i+b\geq 1$
$W.a_i+b\leq -1$
For proper classification by increasing the weights
$Y_i\ (x_i \bullet w) \geq 1$
The maximal marginal distance of the hyper plane kernel is calculated by $w = \sum_{i=0}^{n} ai\ yixi$

VI.RESULTS AND DISCUSSION

Lung CT images are taken as inputs. Different sample images are collected and given as input to the SVM training phase. Data base is categorized as 4 distinct classes [12]. For an automated disease detecting system it is necessary to compare the train sets with the healthy subjects. All the given images are examined for the presence, absence and condition of the disease. Figure 8 shows the sample lung CT image.

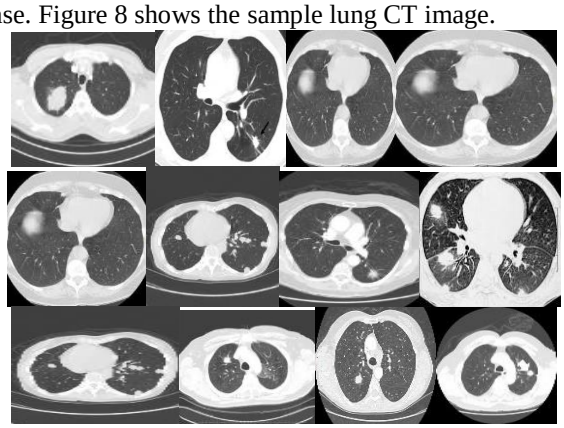

Fig 8: sample lung CT images

The table 1 represents the input image and the belonged class recognition sometimes there will be get the fault detection. In order to avoid the fault detection simulated for few times [13] and considers the result only when the minimum error is reached. The result which has appeared for maximum number of times can be taken as the class of input image. The sample dataset is classified with a good accuracy level where accuracy is a measure of capability to get maximum true results shown in eq(22)

$$Accuracy = \frac{TP+TN}{TP+TN+FP+FN} \quad (22)$$

Table1: extracted features

SI No.	IMAGE	CLASS
1	Image 1	Cancerous
2	Image 2	Cancerous
3	Image 3	Non-cancerous
4	Image 4	Cancerous
5	Image 5	Cancerous
6	Image 6	Cancerous
7	Image 7	Cancerous
8	Image 8	Non-cancerous
9	Image 9	Cancerous
10	Image 10	Cancerous

Table 2: classification results

Image	Contrast	Homogeneity	Correlation	Energy
1	0.9300	0.7753	0.0637	0.7940
2	0.9451	0.9852	0.0642	0.7856
3	0.9281	0.0601	0.6524	0.8056
4	0.8990	0.7421	0.6548	0.7412
5	0.5661	0.4587	0.5421	0.4521
6	0.9522	0.7741	0.8714	0.7821
7	0.9854	0.8541	0.9874	0.7894
8	0.6452	0.6589	0.5214	0.7458
9	0.9877	0.7753	0.5547	0.7845
10	0.9960	0.7745	0.8947	0.7578

The above table 2 represents the feature extracted from the CT lung image dataset. The features are obtained from the GLCM for the different images [14].

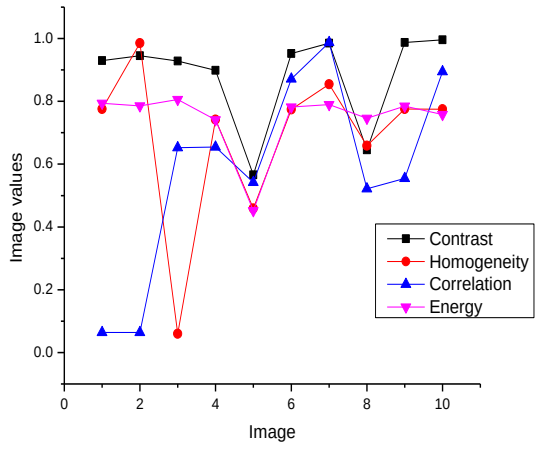

Fig 9: feature extraction

We obtained a accuracy level of 90.9% of given images. Sensitivity is the measure of maximum true positive values whereas the specificity is the measure of maximum true negative values shown in eq(23&24)

$$sensitivity = \frac{TP}{TP+FN} \quad (23)$$

$$specificity = \frac{TN}{TN+FP} \quad (24)$$

The percentage error is calculated for how much the values are accurate as follows in eq(25)

$$\%\ error = \left[\frac{FP-TP}{TP}\right] * 100 \quad (25)$$

The examined error rate is depicted in table 3.

Table 3: Error Rate

Image	MSE	RMSE	MAE
1	0.1293	0.17753	0.1637
2	0.1451	0.1852	0.1642
3	0.19281	0.1601	0.1524
4	0.1899	0.17421	0.1548
5	0.15661	0.14587	0.1421
6	0.19522	0.17741	0.1714
7	0.19854	0.18541	0.19874
8	0.16452	0.16589	0.15214
9	0.19877	0.17753	0.15547
10	0.1996	0.17745	0.18947

The table 3, depicted that the excellence of the error rate[15,16] and deviation of computed and predicted lung cancer results. From the analysis, system ensures MSE(0.177), RMSE(0.172) and MAE(0.164). Then resultant figure is depicted in figure 10.

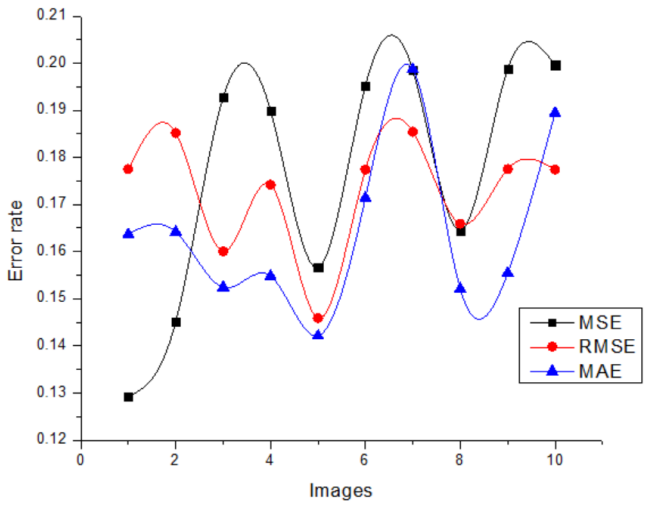

Fig 10: Error Rate

The above fig 10, depicted that the error rate of different images in which the introduced approach minimize deviation value from computing lung cancer effectively. In addition to this, the efficiency [17,18] of the system is depicted in fig 11.

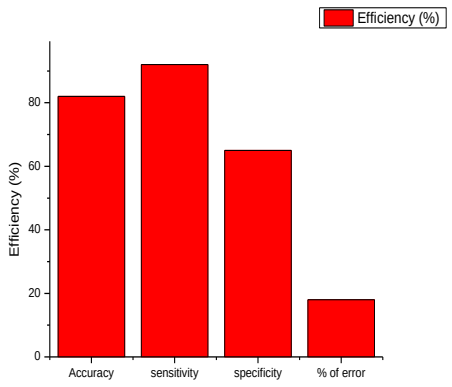

Fig 11: Efficiency

The above parameters are calculated from the obtained results [19,20]. From the above results it clearly depicted that introduced system successfully recognize the lung cancer from CT image effectively.

Reference

[1] Cruz, Joseph A., and David S. Wishart. "Applications of machine learning in cancer prediction and prognosis." *Cancer informatics* 2 (2006): 117693510600200030.

[2] Cruz, Joseph A., and David S. Wishart. "Applications of machine learning in cancer prediction and prognosis." *Cancer informatics* 2 (2006).

[3] Furey, Terrence S., et al. "Support vector machine classification and validation of cancer tissue samples using microarray expression data." *Bioinformatics* (2000): 906-914.

[4] Furey, Terrence S., Nello Cristianini, Nigel Duffy, David W. Bednarski, Michel Schummer, and David Haussler. "Support vector machine classification and validation of cancer tissue samples using microarray expression data." *Bioinformatics* 16, no. 10 (2000): 906-914.

[5] Furey TS, Cristianini N, Duffy N, Bednarski DW, Schummer M, Haussler D. Support vector machine classification and validation of cancer tissue samples using microarray expression data. Bioinformatics. 2000 Oct 1; 16(10):906-14.

[6] Akay, Mehmet Fatih. "Support vector machines combined with feature selection for breast cancer diagnosis." *Expert system900s with applications* 36.2 (2009): 3240-3247.

[7] Akay, M. F. (2009). Support vector machines combined with feature selection for breast cancer diagnosis. *Expert systems with applications*, *36*(2), 3240-3247.

[8] Akay, Mehmet Fatih. "Support vector machines combined with feature selection for breast cancer diagnosis." *Expert systems with applications* 36, no. 2 (2009): 3240-3247.

[9] Akay, M.F., 2009. Support vector machines combined with feature selection for breast cancer diagnosis. *Expert systems with applications*, *36*(2), pp.3240-3247.

[10] Akay MF. Support vector machines combined with feature selection for breast cancer diagnosis. Expert systems with applications. 2009 Mar 1;36(2):3240-7.

[11] P. Mohamed Shakeel; Tarek E. El. Tobely; Haytham Al-Feel; Gunasekaran Manogaran; S. Baskar., "Neural Network Based Brain Tumor Detection Using Wireless Infrared Imaging Sensor", IEEE Access, 2019, Page(s): 1. 10.1109/ACCESS.2018.2883957

[12]Shakeel, P.M., Tolba, A., Al-Makhadmeh, Zafer Al-Makhadmeh, Mustafa Musa Jaber, "Automatic detection of lung cancer from biomedical data set using discrete AdaBoost optimized ensemble learning generalized neural networks", Neural Computing and Applications,2019,pp1-14.https://doi.org/10.1007/s00521-018-03972-2

[13] Shakeel, P. M., Desa, M. I., & Burhanuddin, M. A. (2019). Improved watershed histogram thresholding with probabilistic neural networks for lung cancer diagnosis for CBMIR systems. Multimedia Tools and Applications, 1-19.https://doi.org/10.1007/s11042-019-7662-9

[14]Shakeel, P. M., Burhanuddin, M. A., & Desa, M. I. (2019). Lung Cancer Detection From CT Image Using Improved Profuse Clustering and Deep Learning Instantaneously Trained Neural Networks. Measurement, pp702-712. https://doi.org/10.1016/j.measurement.2019.05.027

[15] Baskar, S., Dhulipala, V.R.S., Shakeel, P.M., Sridhar, K. P., Kumar, R. Hybrid fuzzy based spearman rank correlation for cranial nerve palsy detection in MIoT environment. Health Technology. (2019). https://doi.org/10.1007/s12553-019-00294-8

[16] Kumar, R., Sakthidasan @ Sankaran, K., Sampath, R. et al. Analysis of regional atrophy and prolong adaptive exclusive atlas to detect the alzheimers neuro disorder using medical images, Multimed Tools Appl (2019). https://doi.org/10.1007/s11042-019-7213-4

[17] Gomathi, P., Baskar, S., Shakeel, P.M. et al. Identifying brain abnormalities from electroencephalogram using evolutionary gravitational neocognitron neural network, Multimed Tools Appl (2019). pp 1–20. https://doi.org/10.1007/s11042-019-7301-5

[18] Shakeel PM, Manogaran G., "Prostate cancer classification from prostate biomedical data using ant rough set algorithm with radial trained extreme learning neural network", Health and Technology, 2018:1-9.https://doi.org/10.1007/s12553-018-0279-6

[19] Manogaran G, Shakeel PM, Hassanein AS, Priyan MK, Gokulnath C. Machine-Learning Approach Based Gamma Distribution for Brain Abnormalities Detection and Data Sample Imbalance Analysis. IEEE Access. 2018 Nov 9.DOI 10.1109/ACCESS.2018.2878276.

[20] Sridhar KP, Baskar S, Shakeel PM, Dhulipala VS., "Developing brain abnormality recognize system using multi-objective pattern producing neural network", Journal of Ambient Intelligence and Humanized Computing, 2018:1-9. https://doi.org/10.1007/s12652-018-1058-y

Proceedings of the Fourth International Conference on Communication and Electronics Systems (ICCES 2019)
IEEE Conference Record # 45898; IEEE Xplore ISBN: 978-1-7281-1261-9

Analysis and Design of Precision Time Protocol System Based on IEEE1588 Standards

Priyanshu Pandey
School of VLSI and ESD
National Institute of Technology
Kurukshetra, India
priyanshupanday95@gmail.com

Bhanu Pratap
Electrical Engineering Department
National Institute of Technology
Kurukshetra, India
bhanumnnit@gmail.com

Radhey Shyam Pandey
System Software
Xilinx India Pvt. Ltd.
Hyderabad, India
radheys@xilinx.com

***Abstract*— With the development of the network control system, which is required for highly precise synchronizing of clocks, IEEE1588 protocol delivers an accurate clock synchronizing in the measurement and control devices. This system is precise at sub-microsecond level. In this paper, we have described a common approach with a brief examination of the synchronization principle. Here we described the state machine of the precision time protocol and the primary issues that affect the time precision. This paper also explains the achievement of time synchronization by implementing PTP and algorithm. In PTP, we implemented the best master clock algorithm (BMCA) for selecting a grandmaster in the networks. The IEEE1588 is for designing of software which consists PTP protocol engine, receipt and transmit controller. It is transplanted into Xilinx Zynq UltraScale+MPSoC devices and tested. This paper is based on designing for the requirement of a time synchronization of the networks.**

Keywords—IEEE1588; Clock synchronization; PTPd; reference design

I. INTRODUCTION

In recent years, the computer system had established various types application devices for networking environment. Along with development of the networking application, the demands have also increased for real time system and sharing information on the data. So, solve these issues the requirement of higher clock synchronization accuracy in the system. Right now, the SNTP is mostly used to clock synchronized as a system protocol in the network technology. SNTP is improved standard of the NTP [7]. These networks are precise up to millisecond (ms) level [2]. It can't meet the progressively strict necessity of the synchronizing in the trade.

To address problems in terms of accuracy while synchronizing of time in a measurement, control and communication between systems in industry, the IEEE1588 precision clock synchronization protocol had been proposed. The standard of IEEE 1588 got released in 2002, and the 2nd form released in 2008 [4]. The IEEE 1588 standard is "IEEE Standard for a Precision Clock Synchronization Protocol for Networked measurement and Control Systems", also known as Precision Timing Protocol (PTP) [7]. The IEEE 1588 standard defines precise clock synchronization in the highest distributed system. where could achieve sub-microsecond level (µs) precision. If we use hardware timestamp support for achieve nanosecond level (ns) [5]. It can totally fulfill prerequisites of time synchronizing of time in the control system such as local computing, network communication and distributed objects.

PTP application has minimum requirements of the processor performance and network bandwidth. It is also low administration effort and use via Ethernet networks but also via other networks. It uses for many applications like, automation, motion control, AVB, telecommunication etc.

II. OUTLINE OF THE IEEE1588

The PTP permits the clocks distributed across the standardized packet-based networks like Ethernet. The network is to be precisely synchronizing using a method wherever the distributed nodes exchanged timestamping packets.

In the synchronization, it is challenging to synchronize the networked computing devices to each other as far as clock. It's reported the measured values and provided that with a accurate device timestamp. the measured values can then be correlated to one another by these timestamps.

A. PTP Device Type

PTP device define 4 types clock are:

i. Ordinary clock works as a single port system. It may be only a Master or Slave clock.
ii. Boundary clock works as a multi-port system. It may be a Master and Slave clock.
iii. End to End transparent clock works as a multi-port system. It is used for a bridge between Master and Slave clock. It advances and adjusts all PTP messages by the bridge residence times accumulated in a distinct field, the correctionField inside the header of the PTP packets.
iv. Peer to Peer transparent clock works as a multi-port system. It is used for a bridge between Master and Slave clock. It advances and adjusts Sync and Follow_Up packets only. They are correcting accomplish by the bridge residence times and P2P delay are accumulated in special field, the correctionField inside the header of the PTP packets.

B. PTP Message Classes

Precision time protocol characterizes general and event message.
Event packets are timed packets in that precise timestamps are created at both transmit and receipt of the message. The arrangement of event message comprises of Sync, Delay_Req, PDelay_Req, Pdelay_Resp message.
General messages don't require accurate timestamp, yet it may comprise accurate timestamping for their related event message. The arrangement of the general message

comprises of Announce, Follow_Up, Delay_Resp, PDelay_Resp_Follow_Up, Management, Signaling message.

C. Clock Synchronization Principle

The IEEE1588 system clocks are equipped in a master-slave hierarchy. Firstly, the master clock is identified and after that, it's established two-way timing exchange. Where master state sends packets to slave state for start the synchronization. Each Slave state at that point reacts to master for synchronizing itself. This sequence is do again the specified networks.

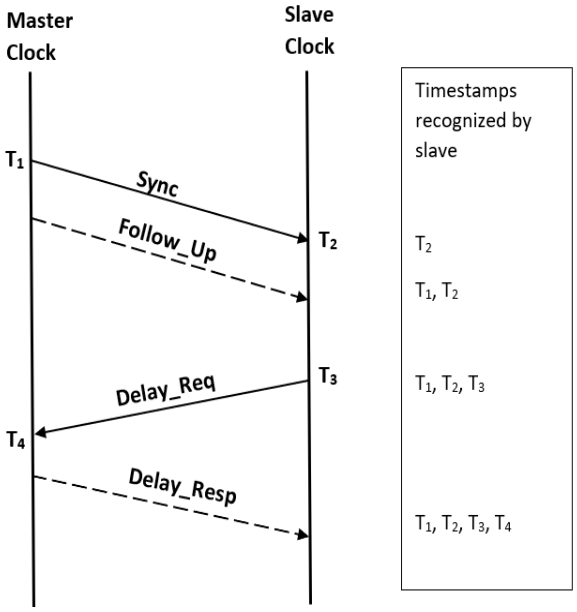

Fig. 1. IEEE 1588 synchronization message sequence

The message interchange procedure is as following:
a) The Grandmaster clock transmit a synchronization (Sync) packet to the Slave clock and registers the transmit timestamp T1.
b) Each Slave clocks accepts a Sync packet and registers the timestamp of response T2.
c) The master state carries to the slave state the timestamp T1 by:

i. Implanting the timestamp T1 in the Sync packet. This is one step clock for highest accuracy and precision.

ii. Implanting the timestamp T1 in a Follow_Up packet for two step clocks.

d) Each slave clock transmits a delay request (Delay_Req) packet to the Grandmaster state and registers the timestamping in t3 when a packet transmitted.
e) The Grandmaster Clock receives a Delay_Req packet from a Slave state and register the timestamp of response T4.
f) The Grandmaster takes to the given the slave a timestamp T4 by implanting the timestamp into a delay response (Delay_Resp) packet.
After completing this sequence, the slave has each of the four timestamps. The timestamps can be utilized to analyze the offset of the slave w.r.t. the master. The mean propagation delay of packets among the two clocks. PTP packet sequence example is shown in Fig. 2.

Delay & offset are calculated based on:
Delay = $[(T_2-T_1) + (T_4-T_3)]/2$
Offset = $[(T_2-T_1) - (T_4-T_3)]/2$

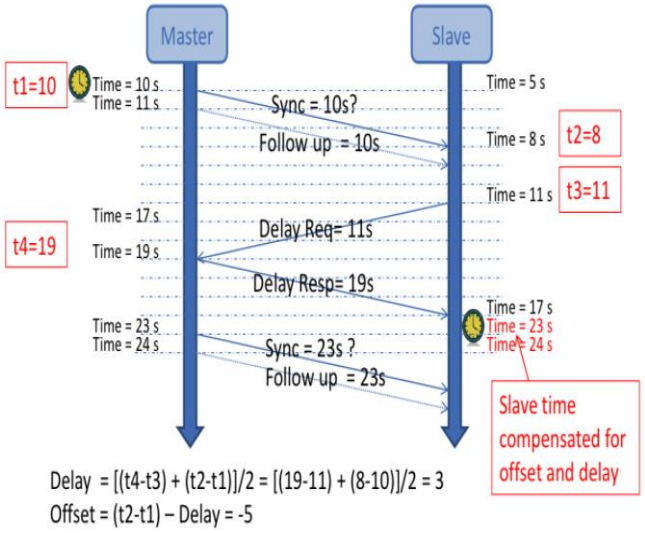

Fig. 2. Example of PTP packet sequence

Peer Delay hierarchy: It measures the port to port propagation time.

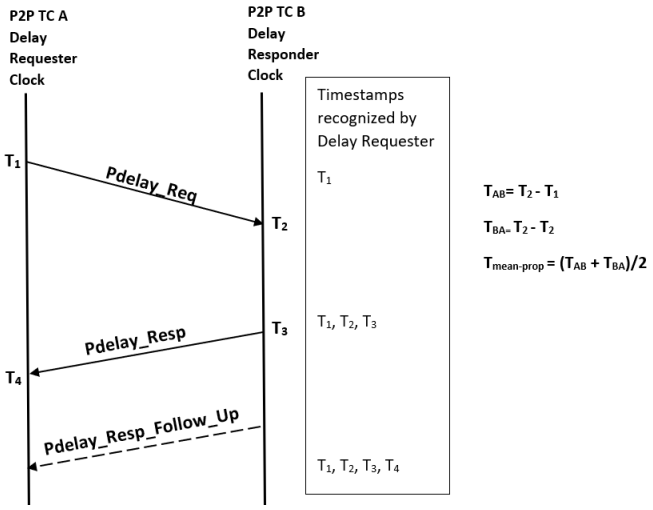

Fig. 3. P2P TC mechanism

In P2P TC operation the four big differences compared to E2E TC are:
1. Path Delay Request/Response messages are used
2. Sync packet is not required for delay calculation
3. The clock adds resident bridge delay + mean path delay to the correction field (instead of just the resident bridge delay)
4. Delay isn't necessarily measured between master and slave, it can be between any two devices hence the name peer to peer.

III. PTP State Machine

In the network, how clock master and slave clock is implemented can be shown as state machine as in the Fig. 4.

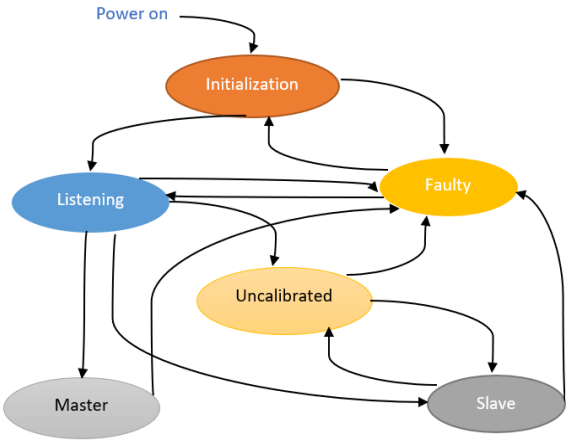

Fig. 4. State Machine

While the device is power on, the system should be initialized first so become enter the INITIALIZATION state. When initializing is finished then it will be going to the LISTENING state. Currently LISTENING state is listening to a system for gets Announce packets from different clock. After the timeout, in the event that it has not received one announce packet then at that point it assumes that the network has no grandmaster, so it will be entered MASTER state and take on the grandmaster role. At that point will send Sync, Follow_Up and Delay_Resp packets occasionally. It has received Delay_Req packets from slave states. Or if is receiving an Announce message from another network. It will choose an exact network as the grandmaster clock by BMCA. If a network is a grandmaster timer, it arrives the MASTER state. Else it will enter SLAVE state. Slave clock received Sync and Follow_Up packets from the master side. It's transmitted Delay_Req packet to the master side in random delay. While errors came, the state will be change to FAULTY state.

IV. Primary Issues That Affect the Clock Precision

a) Path Delay: In IEEE 1588, The path delay of precision time synchronization accept that communicate path delay shows symmetricity. In any case, it's difficult to fulfil the assumption absolutely in genuine system. Here few devices (e.g switches) which own their cache. When a system load is becoming serious, such devices can loss few messages. Likewise, the measuring of delay must not change. Such changes would result in delay jitter and delay asymmetry. It affects the directly synchronization precision. In a transmission would be decrease the variances of the delay. Here the finest way is to independently establish the test system.

b) System Time Drift and Jitter: Mostly the oscillators are crystal. Oscillators are subjected to mechanical, thermal, aging effects, and different factor. The phase and frequency of the master clock is work a input of the tracking control network. The slave clock is work for control object. Any variation in the performance of master clock, its affect a control network and bringing about the deviation together transient and steady state. In conclusion, the jitter and clock drift are lower, and accuracy is higher.

c) Location of the Timestamps: The timestamp accuracy is required for the accuracy of synchronizing of time in IEEE 1588. There are three positions P_1, P_2, P_3, which can be chosen as the timestamp, listed in the Fig. 5.

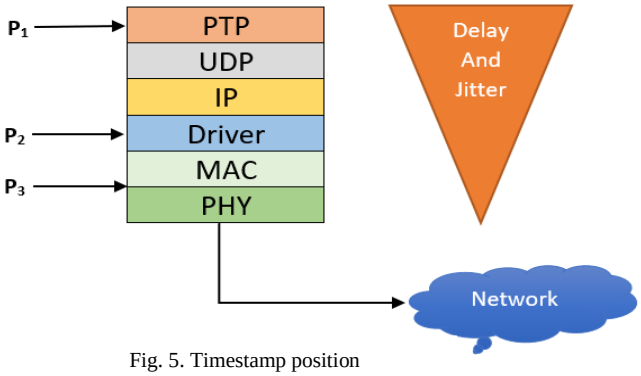

Fig. 5. Timestamp position

Here, the best point is P_3. Since its position is between the PHY and MAC layer. Its nearest to the base of Ethernet, so fault is the minimum. A point P_2 in driver layer is better than P_1 because its delay is within accepted range. But the point P_1 in the PTP application is the worst case because its delay is unpredictable. The specific implementation needs to consider about the propagation of timestamp to the application layer and other layers.

d) Clock Control: Addressing the deviation of the slave timer relies upon the control law. The constraints of control are set-up time, overshoot, adjust time and steady state deviation. These parameters will straight decide the performance of time synchronize of precision.

e) Others Factor: Apart from the above factors, there are few more factors which affect clock accuracy. For example, a delay created by transmit time of Sync, packet retransmitting in junction, time resolution, and otherwise [6]-[8].

V. PTP Analysis And Design Scheme

A model of precision time synchronization network module contains protocol engine, transmission and receipt control, port data sets and clock data sets. The complete architecture of the PTP network in describe in Fig. 6.

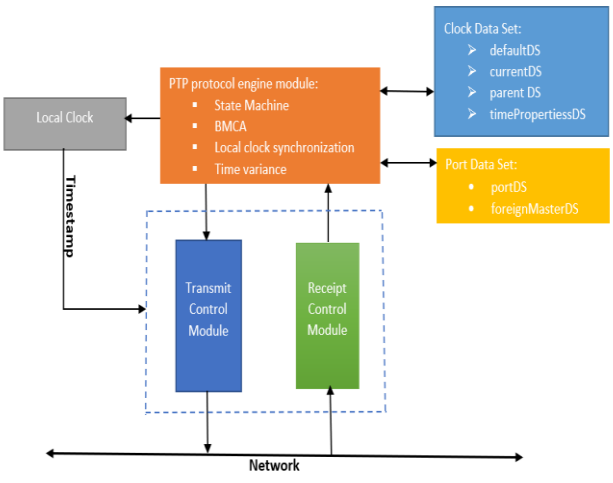

Fig. 6. Network model

A. The Protocol Engine Module

This is main part of precision time protocol network which includes packet calculation, state machine, maintains the data sets, and calculate time between network. It's also including and data interface between data sets, local clock and transmit and received segment. It can be divided into four parts: Best Master Clock (BMC), state machine, local time synchronization and time variance.

- The state machine is responsible for change between different states. Earlier one state arrives another, around for few works. Later a change, the device could start clocks for few packets. For example, Sync, Delay_Req packet periodically to transmit. In various states, the device will be handle relating packets, containing packed packet and unpacked packets. Its procedures forms synchronizing of time etc.
- The principle of local time synchronize procedure is to examine Sync packets from the peripheral master state. At that point when network is in SLAVE clock, it wants to decide that a present master state a best clock. Currently the slave state has accepted Follow_Up packet. At that point among master state and slave state. Here timestamping on four timestamps by three times handshakes. An Offset and Path Delay may be calculated.
- Whereas here might be many master clocks to an equivalent system. So, chosen as a best master clock from local clock by compared several key points by use a BMCA. The BMC contains of two parts: data set comparison DSC (data set comparison) and SD (state decision) process. In data set comparison algorithm, Compares the properties of two clocks, as indicated by their respective data sets and it's used to analyze state port on every timer.
- Time variance is a significant character of the local timer. By method for periodically gathering atomic clock and local clock values. Its deviations of the quartz oscillator rate could include in a local time. Regarding to Allan variance method, is measure the time deviations. It's store results in the timer registers.

B. PTP Transmit and Receipt Controller

The PTP characterize general and event messages. The General messages don't require a precise timestamp and Event message is generated accurate timestamp on both side transmission and receipt. In the delay request-response mechanism, the PTP messages are used to generating and communicating the timing info for time synchronization. This module is using UDP for receipt and transmits precision time protocol packets in multi-cast method. The timestamps will record by the physical layer of system stack. Then event packets are transmitted and receipt to rise the synchronizing of precision.

C. BMC Algorithm

The Best Master Clock Algorithm (BMCA) always runs on all boundary and ordinary clocks in the network. Being run constantly, the clock is able to adapt to dynamic changes in the network, e.g. in case of a grandmaster change or partial blackout in the network. BMCA uses data sets consisting of fields from two clocks to compare which clock is more eligible for being a grandmaster clock. Whenever a new potential grandmaster enters the network, all clocks will compare the data set from the old grandmaster with the new candidate. BMCA compares every field one by one, displayed below in decreasing precedence, only comparing the next field if the previous fields in the data set are identical [4].

Priority1 A field specified by the user ranging from 0 to 255, where a higher priority takes precedence in the BMCA.

Clock class The type of clock used by the device, ranging from an atomic calibrated clock to a slave only clock. A clock of the highest class shall never be used as anything other than a grandmaster clock [8].

Clock accuracy The accuracy of the clock specified in units of time, ranging from accuracy of 25 ns to an accuracy of less than 10 seconds.

Clock variance Static statistics of the variance and stability of the clock.

Priority2 Just like the priority one field, but with lower precedence.

Unique Port ID Often the physical MAC address of the port, this is only used in case of a tie and has no actual relation to the accuracy of the clock.

This way, two different devices comparing the same datasets (device A comparing itself to device B and vice versa) will always come to the same decision of which clock should be the grandmaster.

VI. PROPOSEL

In this paper, we have discussed and elaborate IEEE1588 protocol. We have reduced the offset and delay of PTP application based on IEEE1588v2 by using hardware timestamping between MAC and PHY (Physical) layer. IEEE1588v2 is revised version of IEEE1588. IEEE1588v2 defines shorter synchronization frames to save network bandwidth.

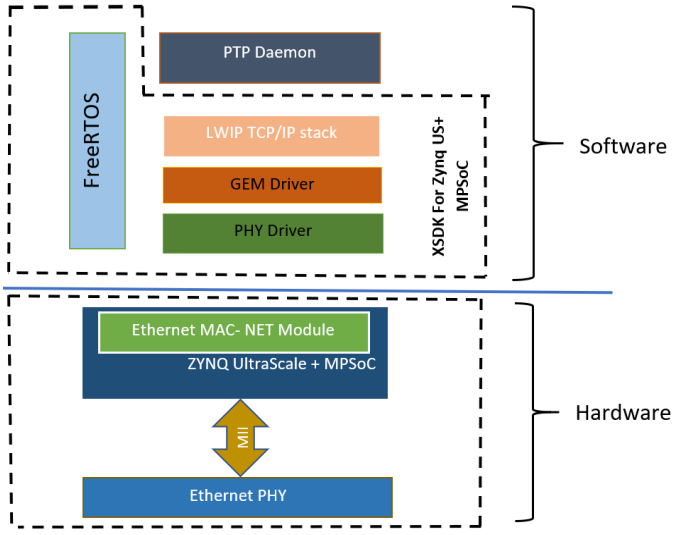

Fig. 7. PTP solution for Zynq US + MPSoC

Under FreeRTOS operating system, it works on peer delay mechanism. It will be creating a hardware timestamping between the PHY and MAC layer and running PTPd application on the hardware platform of Xilinx Zynq UltraScale Plus MPSoC board. We will be used lwip TCP/IP network stack for communication. After testing, the

deviation of time synchronization can be up to nanosecond (ns) level. The proposal shown in Fig. 7.

VII. CONCLUSION

Here, we have analyzed a principle of precision time protocol application, PTP state machine and issues affect of accuracy time synchronization. The design and implementation of IEEE1588 is elaborate. An improved design is used for hardware timestamp and a new method to synchronize clock of PTP application based FreeRTOS OS for Zynq UltraScale Plus MPSoC FPGA is proposed in this paper.

REFERENCES

[1] F.-Steinhauser, C.-Riesch, M.-Rudigier, "IEEE 1588 for time synchronization of devices in the electric power industry", in: Proceedings of International IEEE Symposium on Precision Clock Synchronization for Measurement Control and Communication, Klaus, Austria, pp.1-6, Oct. 2010.

[2] Y. Peng, Q.-H. Luo, and Z.-Q. Liu, “An automatic evaluation system for IEEE1588 synchronization clock unit,” in: Proceedings of the Ninth International Conference on Electronic Measurement and Instruments, Beijing, China, pp.408-413, Aug. 2009.

[3] IEEE1588, IEEE Standard for a Precision Clock Synchronization Protocol for Networked Measurement and Control Systems, IEEE Standard, Jul. 2008.

[4] X.-Q. Li, Y. Chen, and S. Liang, “Improvement of precise time synchronization algorithm based on IEEE1588,” in: Proceedings of International Conference on Computer, Mechatronics, Control and Electronic Engineering, Changchun, China, pp.70-73, Aug. 2010.

[5] W. Jiang, and P. Robert, “Synchronizing device clocks using IEEE 1588 and Blackfin embedded processors,” Analog Dialogue, vol. 43, no 11, pp.1-5, Nov. 2009.

[6] Zhaoqing Liu, Dongxing Zhao, Min Huang, Yigang Zhang, “A Universal Method for Implementing IEEE 1588 with the 1000M Ethernet Interface”, 2016 IEEE AUTOTESTCON Anaheim, CA, USA, 12-15 Sept. 2016.

[7] Zhao, Hongkun, X. Wang, and Z. Yang. "Design and implementation of precision time synchronization system based on IEEE1588." In *International Conference on Electric Utility Deregulation and Restructuring and Power Technologies*, 2011, Vol.47, pp, 610-613.

[8] Y. Peng, Q.-H. Luo, and Z.-Q. Liu, “An automatic evaluation system for IEEE1588 synchronization clock unit,” *in: Proceedings of the Ninth International Conference on Electronic Measurement and Instruments, Beijing, China*, pp.408-413, Aug. 2009.

[9] Zhaoqing Liu, Dongxing Zhao, “A Universal Method for Implementing IEEE 1588 with the 1000M Ethernet Interface,” *2016 IEEE AUTOTESTCON Anaheim, CA, USA*, 12-15 Sept. 2016.

[10] Meng Dong, Zhiliang Qiu, Weito Pan, Can Chen, Junxiang Zhang, Dong Zhang, “The Design and Implementation of IEEE 1588v2 Clock Synchronization System by Generating Hardware Timestamps in MAC Layer,” 2018 International Conference on Computer, Information and Telecommunication Systems (CITS), pp. 1-4, 2018.

[11] Mingzhu Qi, Xiaoli Wang, Zhiqiang Yang, "Design and implementation of IEEE1588 time synchronization messages timestamping based on FPGA," Electric Utility Deregulation and Restructuring and Power Technologies (DRPT) 2011 4th International Conference on, pp. 1566 1570, 6-9 July 2011.

[12] Zynq UltraScale+ Device Technical Reference Manual UG1085 (v1.8) August 3, 2018.

Proceedings of the Fourth International Conference on Communication and Electronics Systems (ICCES 2019)
IEEE Conference Record # 45898; IEEE Xplore ISBN: 978-1-7281-1261-9

Implementation of FreeRTOS based Precision Time Protocol (PTP) application as per IEEE1588v2 standards for Xilinx Zynq UltraScale Plus MPSoC devices

Priyanshu Pandey
School of VLSI and ESD
National Institute of Technology
Kurukshetra, India
priyanshupanday95@gmail.com

Bhanu Pratap
Electrical Engineering Department
National Institute of Technology
Kurukshetra, India
bhanumnnit@gmail.com

Radhey Shyam Pandey
System Software
Xilinx India Pvt. Ltd.
Hyderabad, India
radheys@xilinx.com

***Abstract*— This work proposes a method for the implementation of PTPd (Precision Time Protocol deamon) with the Gigabit Ethernet Module (GEM) Interface for test devices. The programmable real-time clock and timestamp unit was implemented in the programmable logic to achieve the synchronization accuracy of sub-microsecond. PTPd has been reconfigured and implanted into a FreeRTOS operating system to create a PTP state machine and the IEEE1588 IP core software driver has been created to give the application layer access to the precise timestamp in the link layer. This paper evaluates in detail the matter of the IEEE 1588 standard and provides a "Xilinx ZynqMP UltraScale plus SoC + MAC + PHY" technique, a hardware solution for stamping the arrival and departure period of PTP packets. Where packets are obtained between MAC and PHY layers from Media Independent Interface (MII). The result indicates that the solution can detect the messages transmit and receipt for synchronization accurately.**

Keywords*— *Xilinx ZynqMP UltraScale Plus SoC, IEEE1588v2, Time synchronization, Timestamping

I. INTRODUCTION

Nowadays, Time synchronization is alignment of time as well as advance of the over distributed network. it's critical in many applications such as real time application control system network or video applications and voice related applications [2]. there is frequency synchronization phase synchronization and timing synchronization. We can take a look at touch upon those along the way and it is important to coordinate action between distributed nodes or distributed computers and also, it's needing to trigger the measurement and then actually measure the same time over the different nodes also referenced events which can trigger all over distributed nodes.

In IEEE1588, it is about distributing the time reference time to the other nodes using the packet so it's the distribution of precise time over the packet-based system [3]. we can synchronize our frequency time or phase using IEEE1588 and it's providing high accuracy time over your network typically a sub microseconds range and it's based on hierarchical structure so master clock provides a time to your slave. the slave can synchronize the time of the master clock.

The objective of this paper is to develop a general system for IEEE1588 synchronization protocol in the GEM network, using Xilinx ZyncMP UltraScale Plus MPSoC as a platform for measuring synchronization performance parameters. For system synchronization, data synchronization and test data analysis, these parameters are essential. Based on the parameters, additional consideration is given to facts affecting synchronization and a optimized method is proposed and introduced the precise of sub-microsecond synchronization in test.

II. OUTLINE OF THE IEEE1588

The IEEE1588 system clocks are equipped in a master-slave hierarchy. Firstly, the master clock is identified and after that, it's established two-way timing exchange.

PTP message sequence with timestamp

In this figure 1, how PTP protocol message sequence actual works.

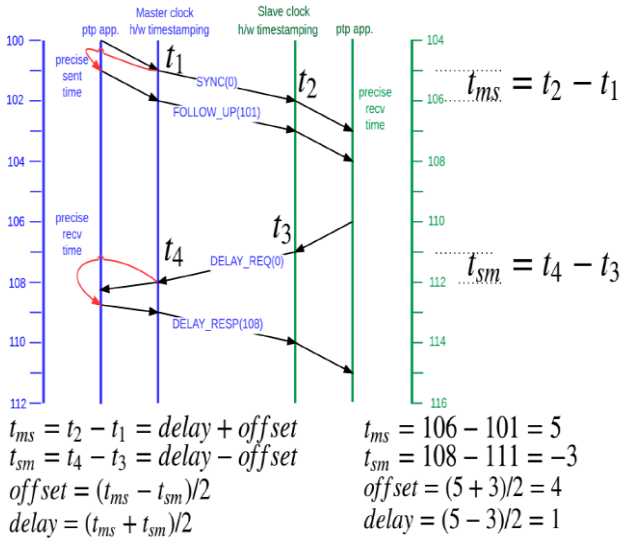

Figure 1. PTP message sequence

We put another line here that application and then this is the actual time stamping put it on a slave side as well master side. It is the hardware timestamping that reads the actual time. Master PTP application sends the packet out before we send the packet to the wire you don't know the time, so the sync that's the first message is called SYNC with no unknown time that's 0 here, but as soon as the packet is on the wire, your chipset says it's okay this packet sends t1 time. Using this t1 time put it in the next packet Follow_Up message sending. we sent previous packet at 101 second so at this point on a slave knows when it is sent the actual master says it sent and when it arrived here hardware says I receive this packet t2. The next sequence slave software

says send a packet as soon as Delay_Req packet is on the wire we know the t3 time sent it to master and then master received a packet. Then it received it knowns actual accurate timestamp t4 put it on to the next Delay_Resp packet. Which is the till they respond by the way this is still a request from the slave and then we send a delay response saying that after received your delay request packet. at this time so once sleep get all this packet collected then sleep can calculate that offset of between master and slave and then delay between two networks.

III. IEEE 1588 IMPLEMENTATION FOR XILINX ZYNQMP ULTRASCALE PLUS SOC

The zcu102 Evaluation Kit (for Xilinx ZynqMP UltraScale plus SoC) is used as the hardware platform for the hardware timestamp based IEEE1588v2 Precision Time Protocol. The solution uses the Xilinx SDK, which includes the GEM driver, the PHY driver, the ported FreeRTOS kernel, and the ported lwIP TCP/IP stack for the zcu102 board. The IEEE1588v2 Precision Time Protocol is implemented by the PTP daemon application. It's shown in fig.2.

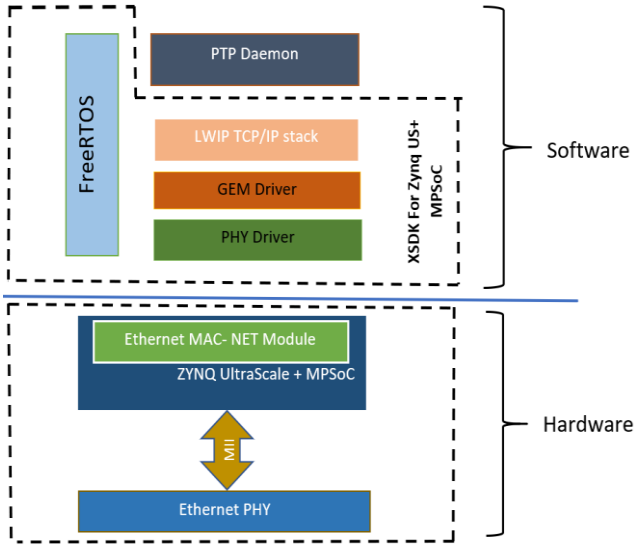

Fig. 2. PTP solution for Zynq US + MPSoC

i. Hardware components

Zynq UltraScale+ MPSoC is the Xilinx second-age Zynq platform, the combination of a processing system (PS) and user-programmable logic (PL) into the same board [8].

The PS includes the Arm® flagship Cortex®-A53 64-bit dual-core or quad-core processor and Cortex-R5 dual-core real-time processor. Apart from the earlier cost and integration benefits previously provided by the Xilinx Zynq-7000 devices, Xilinx Zynq UltraScale+ MPSoC and RFSoC boards also provide new benefits and features.

ii. Software components

The software of the IEEE 1588 usage incorporates the Xilinx SDK for the for Xilinx ZynqMP UltraScale plus SoC device hardware platform and the PTP daemon. The Xilinx SDK is a software structure for creating applications on the Xilinx MCUs, including GEM drivers, middleware, and FreeRTOS real time operating system.

a) lwIP TCP/IP stack

The lwIP implements a TCP / IP networking stack that is lightweight for embedded systems. lwIP is an open source available in C source code format providing under the Berkeley Software Distribution (BSD) style license. This stack is used to reduce the use of RAM through a full-scale TCP for use in embedded systems. The Xilinx SDK provides lwIP stack customized to run on different Xilinx installed frameworks [10]. It can be run on ARM-based Xilinx Zynq UltraScale+ MPSoC related all programmable SoC. The main stack is an IP implementation, on top of which you can choose to include the UDP, DHCP, IGMP, TCP and many other protocols according to your required and the memory size is available in the designed system.

b) FreeRTOS real-time operation system

FreeRTOS is an open source RTOS. It is real time operating system kernel or real time scheduler targeting embedded devices. It utilizes embedded application to fulfill its requirements in hard-real-time. The FreeRTOS features provided by the kernel are multithreading by tasks, queues, software timer, semaphore, mutexes and event groups. FreeRTOS kernel port is available for Xilinx Zynq UltraScale+ MPSoC, ZynqMP SoC and other Xilinx devices use FreeRTOS kernel 10.0 version.

c) *GEM hardware support for PTP*

The controller detects the transmission and receipt of PTP event packet Sync, Delay_Req, PDelay_Req, and PDelay_Resp. Master-slave clock synchronization is a two-stage method.

- The master will correct the offset between the master and the slave clocks by sending the slave a sync frame with a follow-up frame with the exact time the sync frame was sent. On the master hand, the GEM controller assists modules and the slave detects precisely when the master sent the sync frame and the slave got it. Then the slave adjusts his clock to suit the master clock.

- Correct the delay in transmission amongst the master and the slave. The slave sends the master a delay request frame that sends a response frame for delay reaction. On the master hand, the GEM controller assists modules and the slave detects precisely when the slave sent the delay request frame and the master got it. Then the slave has sufficient data to adjust his clock to account for the delay.

IV. TIMESTAMPING

A. Software Timestamping

Using a conventional Ethernet module, the PTP protocol can be fully implemented in the software shown in fig. 3. The delay variance implemented by the software stack operating on the master and slave systems implies that only a constrained accuracy can be obtained since the time stamp data is implemented at the application layer. As the Master has no hardware clock, both its own internal oscillator drift and the master's oscillator drift must be compensated for the

slave-running PTP daemon, degrading time synchronization precision.

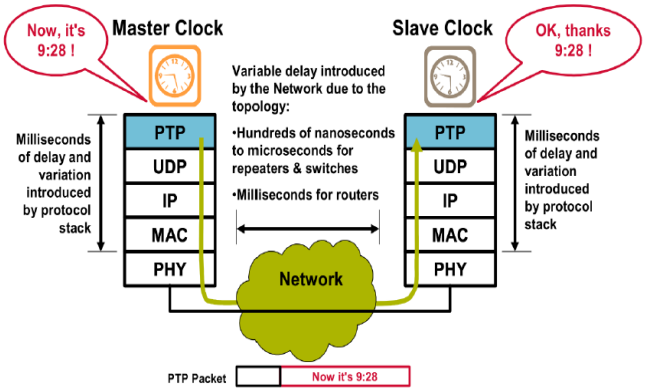

Fig. 3. Software Timestamping

B. *Hardware Timestamping*

Take timestamps nearer the physical interface, namely to the MAC or PHY layers to reduce the effect of the stack protocol delay shown in fig. 4. Master and Slaves with a Hardware time stamp then PTPd are providing time synchronizing accuracy less than 1 microsecond with independent of their operating system and network load.

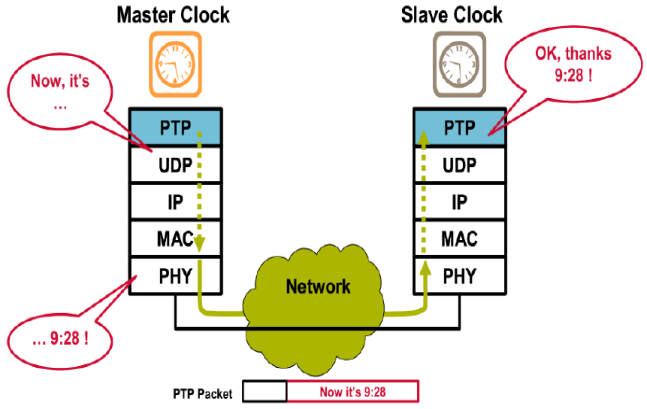

Fig. 4. Hardware Timestamping

In this proposed method, use hardware timestamping for reduce the stack protocol delay and make with FreeRTOS environment for board. It allows synchronization with significantly improved accuracy.

V. THE WHOLE PTPD DESIGN

The whole scheme is divided into three layers i.e. application, driver and hardware layer. The application layer understands the BMC algorithm, the packet processing and the PTP message transfer method based on the IEEE1588 protocol. We used PTPd is a open source software. It's achieved the software state machine. The original PTPd is established in the application layers by stacking the TCP / IP network protocol. This is a software timestamp which controls only with synchronization in milliseconds levels. We are need to solve the low precision of the software timestamp and to create an accurate hardware event trigger and improved the PTPd application.

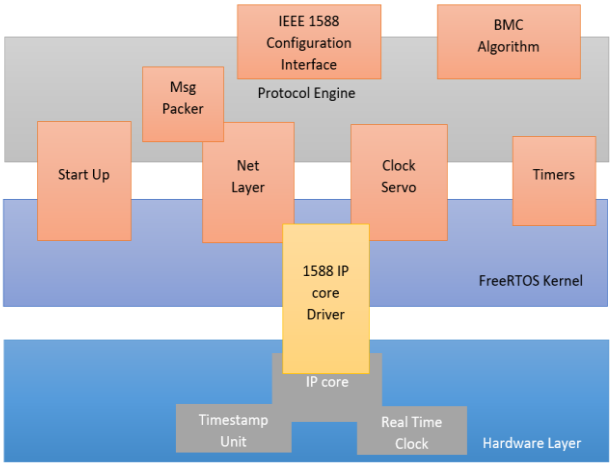

Fig. 5. The whole design of IEEE1588v2

The entire system after enhancement is shown in the Fig. 5. Here adding a scheduling process of IEEE1588 IP core for optimized the clock synchronization accuracy.

The core of the IEEE 1588 IP comprises primarily of three components: register module, timestamp module, real time clock module. The register module functions as an interface layer between the FPGA-based software and the IEEE1588 IP core.

A. *Timestamp Module*

The PTPd package format designed with ethernet based on IEEE 1588 standards, the specific standards of timestamp module are following:

a) 110bit timestamp (78bit time message, 32bit PTP packet recognition).

b) Support PTP packet format for two layers (Ethernet+PTP) and PTP packet format for four layers (Ethernet+IPv4/IPV6+UDP+PTP).

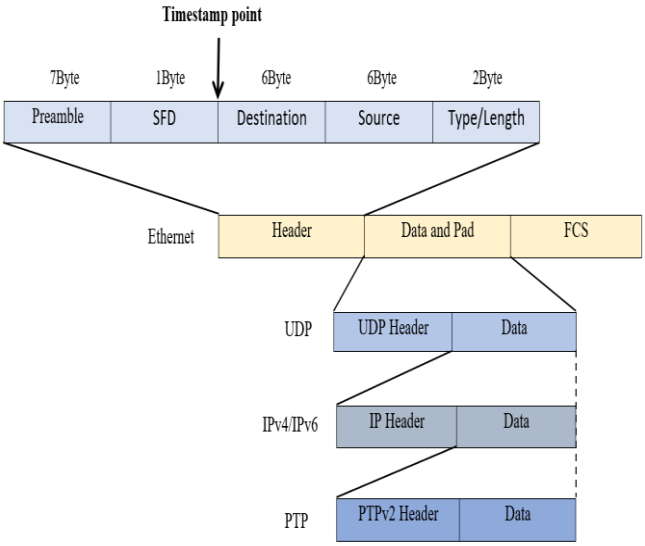

Fig. 6. IEEE1588 package format

The Timestamp module displays the data input stream consistently. PTP package format is shown in Fig. 6. Here two successive 1 at the end of the Ethernet packet SFD (start frame delimiter), this time characterize as timestamp point [6]. Currently, real-time clock time is being saved. Then we check the messages if the message is a PTP event message then the timestamp is store otherwise discard the timestamp.

B. PTP Packet Format

All PTP packets need a header, body, and suffix. This is a common header for all PTP messages [7]. IEEE1588v2 header format shown in Table 1. Here are two main points to define these messages.

Header 1588 V2									
Bits								Octets	Offset
7	6	5	4	3	2	1	0		
transportSpecific				messageType				1	0
reserved				versionPTP				1	1
messageLength								2	2
domainNumber								1	4
reserved								1	5
flagField								2	6
correctionField								8	8
reserved								4	16
sourcePortIdentity								10	20
sequenceId								2	30
controlField								1	32
logMessageInterval								1	33

Table 1. IEEE1588v2 header format

a) messageType

MessageType's value shall show the PTP message type as described in Table 1. Message type fields (1-4) for PTP event packets are accessible in the PTP header.

Message Type	Message class	Value(hex)
SYNC_MESSAGE	Event	0
DELAY_REQ_MESSAGE	Event	1
PATH_DELAY_REQ_MESSAGE	Event	2
PATH_DELAY_RESP_MESSAGE	Event	3
Reserved		4-7
FOLLOWUP_MESSAGE	General	8
DELAY_RESP_MESSAGE	General	9
PATH_DELAY_FOLLOWUP_MESSAGE	General	A
ANNOUNCE_MESSAGE	General	B
SIGNALING_MESSAGE	General	C
MANAGEMENT_MESSAGE	General	D
Reserved		E-F

Table 1. messageType

b) sequenceId

The sequenceId field value is allocated for Sync, Pdelay Req, and Announce packets by the originator of the packet. This field needs to be recorded to match packets.Real-time clocks modules

C. Real-time module

In the IEEE1588 protocol, this module supports the format and function are as follow:

i) 48-Bit seconds, 32-Bit nanoseconds and 32-Bit sub nanoseconds domain.
ii) In the real time clock can be used external clock oscillator for better stabilization.
iii) We designed clock setting and offset setting interfaces for the PM (phase modulation) function to adjust the clock value, the modify resolution is 2^{-8}ns.
iv) We have built FM and temporary FM interfaces for FM (frequency modulation), the period modulation resolution is 2^{-32}ns. 32bit counters are given to count temporary FM's efficient time.
v) For accurate measurement can be used hardware PPS output support.

D. Software And Driver Design

The specific access to the register address through the AXI bus completes the development. The IEEE1588 IP core is consistently configured by writing the control register. At this stage we read the status of the data registers for the real-time clock and timestamp values.

The IEEE1588 IP core requirement for multiple registers is being implemented. For the FreeRTOS software platform, the more information about driver supports implementation. The default PTPd source code exists for the Linux, NetBSD, FreeBSD, Mac OS X operating systems. So PTPd porting on FreeRTOS with lwIP and Xilinx SDK drivers for the Xilinx ZynqMP UltraScale plus SoC devices. The operation network related code, system related code, Hardware timestamp related code must be added or ported in the drivers. In the PTPd, the changes or ported work on the system time routines, software timer, system services, interact with network socket and some modification of the PTP protocol. These ported work covers under the FreeRTOS. The configuration FreeRTOS tasks with Xilinx ZynqMP UltraScale plus SoC board.

We are created three task threads using FreeRTOS in the PTPd application:

- *main_thread* task: It is created in the main function. This task initializes the lwIP TCP/IP stack, static IP address setting, netmask and gateway address configuration. It's also initializes MAC address configuration; Ethernet hardware initializes and starts the PTPd application task. After initializing the lwIP and PTPd tasks it's deleted itself by calling vTaskDelete function.
- *network_thread* task: In the TCP/IP initialization, it's created by main_thread task. This task run in the main lwIP task to access the lwIP core function.
- *ptpd_thread* task: this task runs the PTPd application and created this task denotes either the master or the slave clock.

In the lwIP driver, there are initializing the IEEE1588 timer, enabling the IEEE1588 timer, Setting the time function, getting the time function, adjust the IEEE1588 timer frequency, and getting the hardware timestamp for transmit/receive frames. These are the initialization function used in the IP core to initialize all the resisters.

Based on the above process, the improved PTPd mechanisms to achieve the scheduling of PTPd hardware resources.

VI. TEST AND RESULT

A. Hardware Setup

For the test hardware setup, used two ZCU102 board (Xilinx ZynqMP UltraScale plus SoC) and connected each other. The setup has a point to point configuration where using the Ethernet cable for connected two ZCU102 board. To prevent asymmetric transmission delay interference, master and slave ports are linked with the same switch. At this stage, a significant factor influencing synchronization efficiency is the difference between slave and master oscillator frequencies. A hardware setup shown in fig. 7. Specific jumper setting is not used in the test.

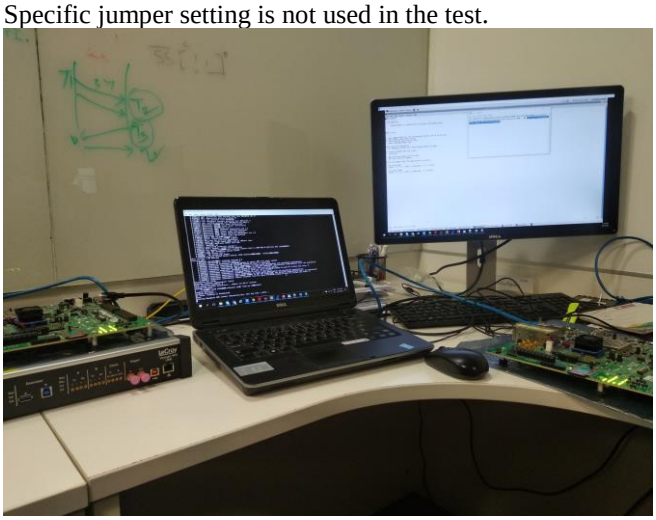

Fig. 7. Hardware Setup

B. Result

Under the FreeRTOS environment, this paper program implements the PTPd application's main function. The program runs on the psu cortexa53_0 hardware platform and used board support package (BSP) of Xilinx ZynqMP UltraScale plus SoC devices.

ptp4l Master clock output- Grandmaster:

We're going to start out listening to see if there's anybody else out there that's doing PTP. Since this is the only endpoint on the node right now, there's nobody else out there. So eventually, timeouts will start happening. You'll start realizing that, well, apparently there's nobody out there, so maybe I need to become the master. Since you're the only one out there, you'll probably get selected as the best master. And you'll become the master, and ultimately, you'll become the grandmaster it's shown in fig. 8.

```
xhdpunnaia40:~% sudo ptp4l -i eth2 -m
ptp4l[1231551.607]: selected /dev/ptp0 as PTP clock
ptp4l[1231551.608]: driver changed our HWTSTAMP options
ptp4l[1231551.608]: tx_type   1 not 1
ptp4l[1231551.608]: rx_filter 1 not 12
ptp4l[1231551.608]: port 1: INITIALIZING to LISTENING on INITIALIZE
ptp4l[1231551.608]: port 0: INITIALIZING to LISTENING on INITIALIZE
ptp4l[1231559.144]: port 1: LISTENING to MASTER on ANNOUNCE_RECEIPT_TIMEOUT_EXPIRES
ptp4l[1231559.144]: selected best master clock 64006a.fffe.71fde6
ptp4l[1231559.144]: assuming the grand master role
```

Fig. 8. Master clock output

Ptp4l slave clock output:

we become slave, we're going to start locking to that master. The strings s0, s1, s2 show the different state of the clock servo: s0 is unlocked, s1 is the phase of the clock and s2 is locked. The clock will not be jumped (only slowly adjusted) once the servo is in the locked condition. INITIALIZING, LISTENING, UNCALIBRATED and SLAVE are some possible port systems that modify in the events INITIALIZE, RS SLAVE, MASTER CLOCK SELECTED. The master offset value is the master's measured nanoseconds offset. This reduced from 1262284679078 to 970 showing successful synchronization with master change from UNCALIBRATED to SLAVE to port state. It's shown in fig. 9.

```
root@xilinx-zcu102-2018_3:~# ./ptp4l -i eth0 -m -s &
[1] 2603
ptp4l[3144.781]: selected /dev/ptp0 as PTP clock
ptp4l[3144.782]: port 1: INITIALIZING to LISTENING on INITIALIZE
ptp4l[3144.782]: port 0: INITIALIZING to LISTENING on INITIALIZE
root@xilinx-zcu102-2018_3:~# ptp4l[3152.039]: selected best master clock 000a35.fffe.00220
ptp4l[3157.137]: port 1: new foreign master 64006a.fffe.71fde6-1
ptp4l[3159.243]: selected best master clock 000a35.fffe.002201
ptp4l[3161.137]: selected best master clock 64006a.fffe.71fde6
ptp4l[3161.137]: port 1: LISTENING to UNCALIBRATED on RS_SLAVE
ptp4l[3162.136]: master offset 1262284969078 s0 freq      +0 path delay         0
ptp4l[3163.136]: master offset 1262284979028 s1 freq   +9949 path delay         0
ptp4l[3164.137]: master offset        970 s2 freq  +10919 path delay         0
ptp4l[3164.137]: port 1: UNCALIBRATED to SLAVE on MASTER_CLOCK_SELECTED
ptp4l[3165.137]: master offset       3288 s2 freq  +13528 path delay         0
ptp4l[3166.137]: master offset      -2120 s2 freq   +9107 path delay      3913
ptp4l[3167.137]: master offset        674 s2 freq  +11265 path delay      3466
ptp4l[3168.137]: master offset       3451 s2 freq  +14244 path delay      3019
ptp4l[3169.137]: master offset       1947 s2 freq  +13775 path delay      3019
ptp4l[3170.137]: master offset         88 s2 freq  +12500 path delay      3394
ptp4l[3171.137]: master offset      -1755 s2 freq  +10684 path delay      3770
ptp4l[3172.137]: master offset        963 s2 freq  +12875 path delay      3394
ptp4l[3173.137]: master offset       -909 s2 freq  +11292 path delay      3792
ptp4l[3174.137]: master offset       1422 s2 freq  +13350 path delay      3792
ptp4l[3175.137]: master offset        -87 s2 freq  +12268 path delay      3815
ptp4l[3176.137]: master offset      -1611 s2 freq  +10718 path delay      3833
ptp4l[3177.137]: master offset        777 s2 freq  +12623 path delay      3792
ptp4l[3178.137]: master offset       -734 s2 freq  +11345 path delay      3833
ptp4l[3179.138]: master offset       1601 s2 freq  +13459 path delay      3821
ptp4l[3180.138]: master offset         73 s2 freq  +12412 path delay      3872
ptp4l[3181.138]: master offset      -1552 s2 freq  +10809 path delay      3993
ptp4l[3182.138]: master offset        791 s2 freq  +12686 path delay      3993
ptp4l[3183.138]: master offset       -692 s2 freq  +11440 path delay      3993
ptp4l[3184.138]: master offset       1689 s2 freq  +13614 path delay      3942
ptp4l[3185.138]: master offset        411 s2 freq  +12842 path delay      3746
ptp4l[3186.138]: master offset      -1268 s2 freq  +11287 path delay      3942
ptp4l[3187.138]: master offset       1065 s2 freq  +13239 path delay      3942
ptp4l[3188.138]: master offset       -548 s2 freq  +11946 path delay      4060
ptp4l[3189.138]: master offset      -1927 s2 freq  +10402 path delay      3972
```

Fig. 9. Slave clock output

Over that hour, after we locked, we stayed within +/- 100 nanoseconds of the master offset. It's shown in figure. PTP application is precise clock synchronization in nanoseconds is successfully used hardware timestamping. It's shown in fig. 10.

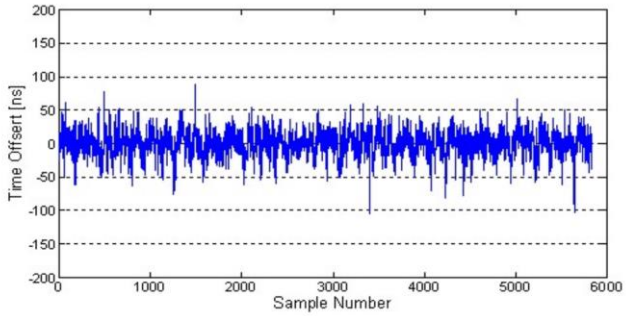

Fig. 10. Clock Synchronization test

VII. CONCLUSION

In this paper, we achieve under the FreeRTOS environment the hardware solution of GEM Ethernet in PTPd application based on IEEE1588v2 on the Xilinx ZynqMP UltraScale plus SoC platform, the program has high clock synchronized with high accuracy, excellent portability and scalability.

REFERENCES

[1] F.-Steinhauser, C.-Riesch, M.-Rudigier, "IEEE 1588 for time synchronization of devices in the electric power industry", in: Proceedings of International IEEE Symposium on Precision Clock Synchronization for Measurement Control and Communication, Klaus, Austria, pp.1-6, Oct. 2010.

[2] Y. Peng, Q.-H. Luo, and Z.-Q. Liu, “An automatic evaluation system for IEEE1588 synchronization clock unit,” in: Proceedings of the Ninth International Conference on Electronic Measurement and Instruments, Beijing, China, pp.408-413, Aug. 2009.

[3] IEEE1588, IEEE Standard for a Precision Clock Synchronization Protocol for Networked Measurement and Control Systems, IEEE Standard, Jul. 2008.

[4] X.-Q. Li, Y. Chen, and S. Liang, “Improvement of precise time synchronization algorithm based on IEEE1588,” in: Proceedings of International Conference on Computer, Mechatronics, Control and Electronic Engineering, Changchun, China, pp.70-73, Aug. 2010.

[5] W. Jiang, and P. Robert, “Synchronizing device clocks using IEEE 1588 and Blackfin embedded processors,” Analog Dialogue, vol. 43, no 11, pp.1-5, Nov. 2009.

[6] Zhaoqing Liu, Dongxing Zhao, Min Huang, Yigang Zhang, “A Universal Method for Implementing IEEE 1588 with the 1000M Ethernet Interface”, 2016 IEEE AUTOTESTCON Anaheim, CA, USA, 12-15 Sept. 2016.

[7] Zhao, Hongkun, X. Wang, and Z. Yang. "Design and implementation of precision time synchronization system based on IEEE1588." In International Conference on Electric Utility Deregulation and Restructuring and Power Technologies, 2011, Vol.47, pp, 610-613.

[8] Zynq UltraScale+ Device Technical Reference Manual UG1085 (v1.8) August 3, 2018.

[9] Gigabit Ethernet MAC (GEM) User Guide, ©2002 Cadence Design Systems, Inc. All rights reserved, Document Number: I-IPA01-0100-USR Rev 22 March 2010.

[10] Anirudha Sarangi, Stephen MacMahon and Upender Cherukupaly, “LightWeight IP (IwIP) Application Examples”, Xilinx, Vol. 5, No. 1, pp. 1-31, 2014.

[11] Cochran, R.; Marinescu, C.;, "Design and implementation of a PTP clock infrastructure for the Linux kernel," Precision Clock Synchronization for Measurement Control and Communication (ISPCS), 2010 International IEEE Symposium on, vol., no., pp.116-121, Sept. 27 2010-Oct. 1 2010.

[12] Meng Dong, Zhiliang Qiu, Weito Pan, Can Chen, Junxiang Zhang, Dong Zhang, “The Design and Implementation of IEEE 1588v2 Clock Synchronization System by Generating Hardware Timestamps in MAC Layer,” 2018 International Conference on Computer, Information and Telecommunication Systems (CITS), pp. 1-4, 2018.

[13] Priyanshu, Bhanu Pratap, and Radhey Shyam. “Analysis and Design of Precision Time Protocol System Based on IEEE1588 Standards” unpublised.

Proceedings of the Fourth International Conference on Communication and Electronics Systems (ICCES 2019)
IEEE Conference Record # 45898; IEEE Xplore ISBN: 978-1-7281-1261-9

Miniaturized Cupcake Fractal Patch Antenna for Biomedical Applications

Anita Garhwal
Amity University Rajasthan,
Jaipur, India.

Badrul Hisham Ahmad
Faculty of Electronic and Computer Engineering,
Universiti Teknikal Malaysia Melaka, Melaka, Malaysia.

Pushpendra Singh
Amity University Rajasthan, India.
Jaipur, India.

Anirban Bandyopadhyay
National Institute for Material Science, Japan.

Mohd Riduan Ahmad
Centre for Telecommunication Research and Innovation (CeTRI), Universiti Teknikal Malaysia Melaka (UTeM),
76100 Durian Tunggal, Melaka, Malaysia.

Sanyog Rawat
Manipal University Jaipur,
India.

Kanad Ray
Amity University Rajasthan, India.
Corresponding author: kanadray00@gmail.com

***Abstract*—Implantable antennas for biomedical applications are on leading edge of research for medical diagnosis such as glucose monitoring, tracking, pacemaker etc. Biomedical applications require antennas that are very small in size but can meet designated requirements. In this paper a 24mm x 34 mm cupcake shape fractal patch antenna is designed and simulated using CST software. The designed antenna operates in 2.45 GHz frequency band called industrial, scientific and medical band (ISM band). Designed antenna's reflection coefficient, VSWR, surface current, gain and far-field plot are simulated and observed. The designed antenna provides 670 MHz (27%) bandwidth in the band of 2.20 - 2.87 GHz. This antenna is miniaturized and compacted to be utilized as an implantable antenna for biomedical applications.**

Keywords—antenna; DGS; fractal;ISM band;patch;biomedical applications.

I. INTRODUCTION

There is a growing need of antenna design for efficient medical diagnosis and treatment. Implantable antennas are being used for glucose monitoring, endoscopy, pace maker etc [1]. For these applications there is need of small size, light weight and compact antennas. Antenna size can be miniaturized using fractal concept. The basic idea behind fractal design is that the same shape is repeated again and again but at different scales. Fractal patch antenna design results in smaller sizes and multiband frequencies. Octagonal and decagonal shaped fractal patch antennas are designed for S, C and X band applications [2]. Similar to octagon and decagon, a circular and elliptical shaped fractal patch antenna is fabricated and tested for multiple applications [3]. A 30mm x 40mm UWB antenna on Rogers's substrate is designed for lung cancer detection [4]. A wearable micro strip patch antenna of square shape spiral cut is simulated at 2.45 GHz frequency for body centric wireless communication. Three layer model using skin, fat and tissue is designed. PTFE (polytetrafluoroethylene) is used as a substrate [5]. A miniaturized dual-wideband circular patch antenna of radius 7mm is designed. The antenna radiates on 403.5 MHz MICS band, 433.9 MHz ISM band and 2.45 GHz ISM band. Single layer model is designed and simulated of volume 100 x 100 x 22 mm^3. A 600MHZ impedance bandwidth and maximum gain of -33.06 dB is achieved [6]. A review on implantable patch antennas for biomedical telemetry is given and challenges and solutions are discussed [7]. A hexagonal shape micro strip patch antenna is simulated for biomedical applications at 2.45 GHz [8]. Small size implantable micro strip antenna for MICS band is designed for body centric communication [9].

Defected ground structure (DGS) is simple design used for enhancement of antenna parameters. A double U shaped defected ground structure proposed on simple trapezoid monopole for bandwidth enhancement. Wider bandwidth is achieved from 790 MHz to 2060 MHz [10]. Many papers on DGS is reported in literature [11-13].

II. ANTENNA DESIGN

Antenna is designed on Fr-4 substrate with dielectric constant of 4.4 and thickness of 1.6mm. Fr-4 is considered because it has low dielectric losses and easy availability. The substrate size is 24mm x 34mm. Fr-4 substrate has PEC ground on bottom layer and PEC patch on top layer. Patch

design is cupcake shape [4]. The antenna design in this paper is of a fractal patch antenna in cupcake shape, inspired by [4]. The antenna design is shown in figure 1.

First of all, a circle of radius 9mm is selected, then a hexagon (circle radius=7.8mm) is drawn. To achieve half hexagon, a rectangle is subtracted and inserted into hexagon. Now half hexagon and circle is added and cupcake shape is obtained. To make this cupcake patch fractal, again same cupcake shape of smaller size is designed and then boolean subtracted from initial design. Initially antenna ground of size 24 x 8.6mm^2 is considered. Fractal cupcake upto iteration-3 is shown in figure 1. Cupcake shape is used because it has no sharp edges and can be used in implantable devices in biomedical applications.

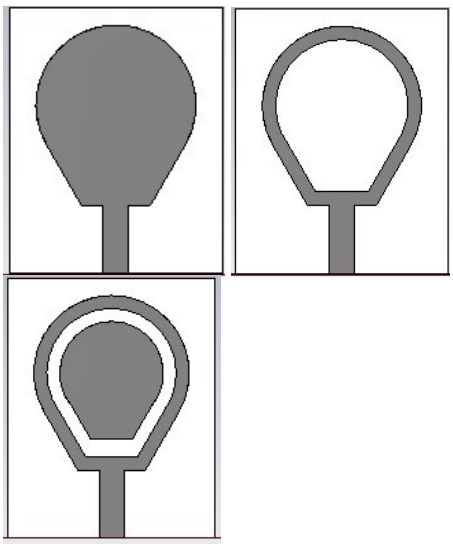

(a) Iteration-0 (b) Iteration-1 (c) Iteration-2

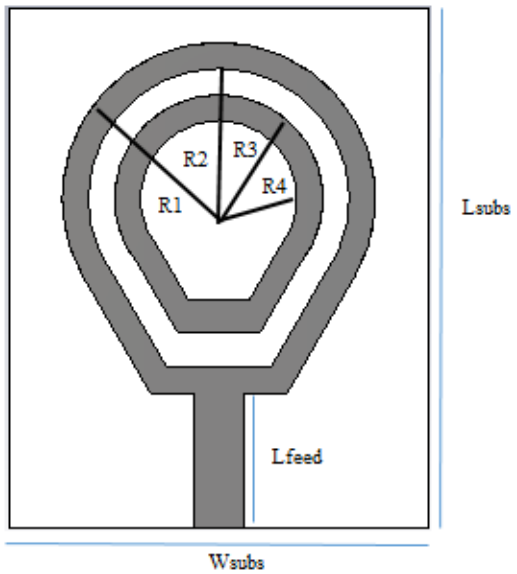

(d) Iteration-3

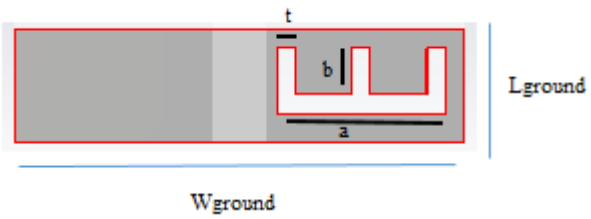

(e) Ground with DGS

Fig1. Cupcake fractal patch iterations and ground

For better resonance and bandwidth enhancement E shape slot (DGS) is inserted into ground as shown in fig 1 (e). The size of antenna ground is 8.6mm x 24mm. The designed antenna is simulated using CST software. Antenna is designed till itetaion-3. Optimized dimensions of proposed antenna is given in Table I.

TABLE I. FINAL ANTENNA DIMENSIONS

Dimension name	Size (mm)	Dimension name	Size (mm)
L_{subs}	34	L_{ground}	8.6
W_{subs}	24	W_{ground}	24
R1	9	a	9
R2	7.5	b	5.5
R3	6	t	1
R4	4.5	L_{feed}	12

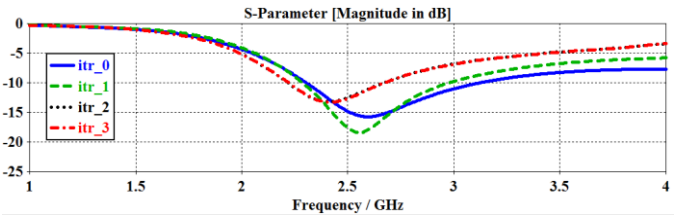

Fig 2. Compared S11 of different iterations without DGS

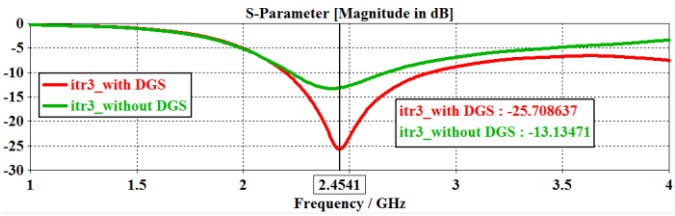

Fig 3. Iteration -3 reflection coefficient with and without DGS

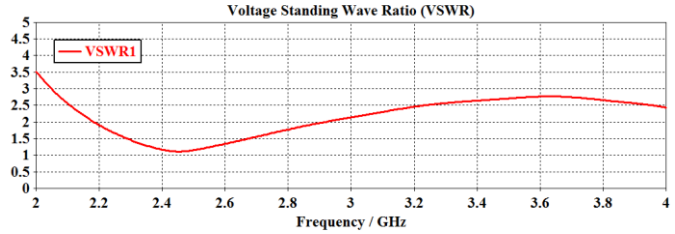

Fig 4. VSWR of iteration-3 with DGS

The compared reflection coefficients of all iterations are shown in fig 2. In iteration-0 antenna resonance frequency is 2.59 GHz (2.3-3.1 GHz), but this resonating frequency is not useful for medical applications. In next step, fractal concept is applied and iteration 1, 2 and 3 are designed. In iteration -3, resonating frequency of 2.45 GHz (2.20-2.87 GHz) is obtained. Reflection coefficient at ISM band centre frequency 2.45 GHz is -25.70 dB. Voltage standing wave ratio (VSWR) of iteration-3 is shown in fig 3. As a general rule the VSWR of under 2 is considered very good antenna design. It can be seen from fig 3 that for frequency range 2.20-2.87 GHz, VSWR is in between 1 and 2.

Iteration-3 results are summarized in table II. Here acceptable bandwidth and positive gain are achieved. The frequency band of 2.4GHz to 2.5GHz is reserved for industrial, scientific and medical (ISM) applications.

TABLE II. BANDWIDTH AND GAIN OF ITERATION-3

Iteration	Fr(GHz)	Fl(GHz)	Fh(GHz)	BW (MHz)	Gain (dB)
Itr-3	2.45	2.20	2.87	670	1.69

The centre of ISM band is 2.45 GHz. Current distribution in both patch and ground is shown in fig 4. Fig 5 shows gain at frequency 2.45 GHz, which is 1.69dB.

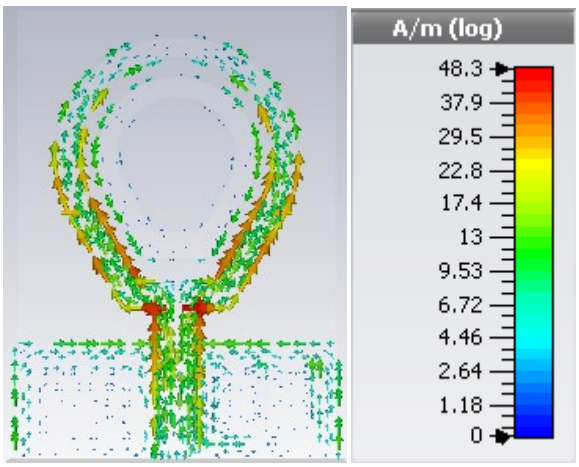

Fig 5. Surface current distribution at 2.45 GHz

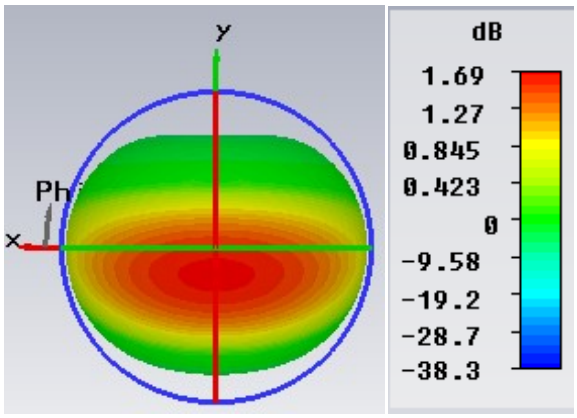

Fig 6. Gain at 2.45 GHz

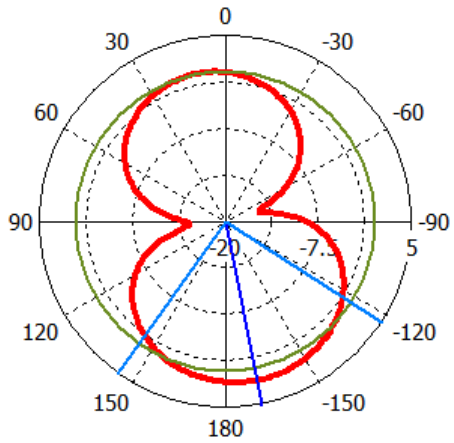

Fig 7. Far-field radiation pattern at 2.45 GHz

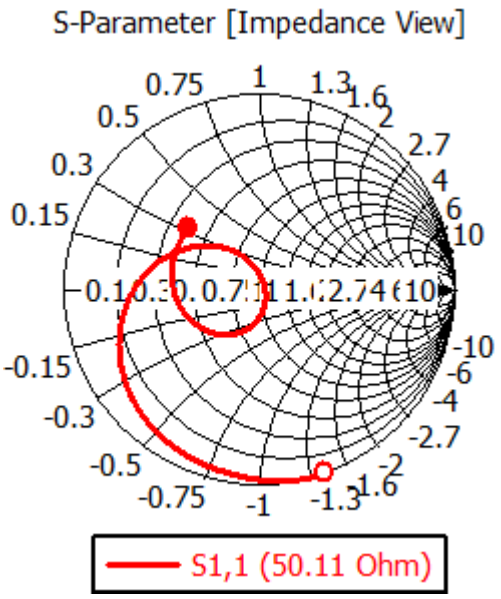

Fig 8. Smith chart of antenna

Simulated Far-field radiation pattern of antenna is shown in fig 7. The pattern is nearly omnidirectional as antenna size

is small. Figure 8 shows smith chart of antenna which gives 50.11ohm impedance, which clearly shows that there is good impedance matching.

Future applications of this antenna can be in the field of ambient computing. Further improvement will be designing of rectenna(rectifier antenna) for ambient energy harvesting. A hexagonal shaped fractal patch antenna for ambient computing is presented in [14]. The proposed antenna provides better impedance bandwidth and gain as compared to [6].

III. CONCLUSION

In this paper, a cupcake shaped fractal patch antenna with simple configuration, light weight and compact size is presented. This antenna is designed for implantable medical applications. Defected ground structure (DGS) are introduced in ground to achieve better impedance matching and bandwidth enhancement. The operating range frequency of this is 2.20-2.87 GHz. The ISM band of 2.4-2.5GHz falls within the operating range of this antenna.

REFERENCES

[1] Gurveer kaur, Amandeep Kaur, Gurpreet Kaur Toor, Balwinder S. Dhaliwal, Shyam Sundar Patnaik,: Antennas for Biomedical Applications" , Biomedical Engineering Letters , 2015, 5:203.

[2] Anita Garhwal, et al.,"Octagon and Decagon shaped Fractal Patch Antennas for S, C and X band Applications", International Journal of Recent Technology and Engineering (IJRTE), vol. 7, Issue 6, March 2019. https://www.ijrte.org/download/volume-7-issue-6/

[3] A Garhwal, M R Ahmad, B H Ahmad, S Rawat, P Singh, K Ray and A Bandyopadhyay, "Circular and Elliptical Shaped Fractal Patch Antennas for Multiple Applications", International Journal of Engineering and advanced Technology (IJEAT), volume-8 issue-5, June 2019

[4] May Mohamed Abdelhamid, Prof. Dr. Abdelmegid M. Allam, "Detection of Lung Cancer Using Ultra Wide Band Antenna", Loughborough Antennas & Propagation Conference (LAPC) , 2016.

[5] Raghvendra Singh, Pinki Kumari, Sanyog Rawat, Pushpendra Singh and Kanad Ray, "Design and Performance Analysis of Low Profile Miniaturized MSPAs for Body Centric Wireless Communication in ISM Band" , International Journal of Computer Information Systems and Industrial Management Applications, volume 9 (2017) pp. 153-161.

[6] AbdElrahman E. Mohamed and Mohammad S. Sharawi , "Miniaturized Dual-Wideband Circular Patch Antenna for Biomedical Telemetry", 11th European Conference on Antennas and Propagation (EUCAP), 2017.

[7] Asimina Kiourti and Konstantina S. Nikita, "A Review of Implantable Patch Antennas for Biomedical Telemetry: Challenges and Solutions", IEEE Antennas and Propagation Magazine,volume 54, No. 3, June 2012.

[8] Shashiketan Samal, Santanu Dwari, Ashudeb Dutta, S. Pradeep Reddy, "A Microstrip Patch Antenna for Biomedical Applications at 2.45 GHz", 5th International Conference on Computers and Devices for Communication (CODEC), 2012.

[9] Love Jain, Raghvendra Singh, Sanyog Rawat, Kanad Ray, "Stacked Arrangement of Meandered Patches for Biomedical Applications", International Journal of Systems Assurance Engineering and Management, 2015.

[10] Ka Hing Chiang and Kam Weng Tam, "Microstrip Monopole Antenna With Enhanced Bandwidth Using Defected Ground Structure", IEEE Antennas And Wireless Propagation Letters, vol. 7, 2008.

[11] Nasser Ojaroudi, "Compact Uwb Monopole Antenna With Enhanced Bandwidth Using Rotated L-Shaped Slots And Parasitic Structures", Microwave And Optical Technology Letters / Vol. 56, No. 1, January 2014.

[12] Mukesh Kumar Khandelwal, Binod Kumar Kanaujia, and Sachin Kumar, "Defected Ground Structure: Fundamentals, Analysis, and Applications in Modern Wireless Trends", International Journal of Antennas and Propagation, volume 2017.

[13] Poonam A. Kadam, Amit A. Deshmukh, "Multiband Microstrip Antenna Using Modified Pi-Shape Slot on Ground Plane", I.J. Wireless and Microwave Technologies, 2019.

[14] Anita Garhwal, M R Ahmad, B H Ahmad, Sanyog Rawat, Pushpendra Singh, Kanad Ray and Anirban Bandyopadhyay, et al, "Mechanically Reconfigurable Hexagonal Fractal Patch Antenna for Ambient Computing", International Journal of Innovative Technology and Exploring Engineering (IJITEE), volume-8 issue-6, April 2019.

Proceedings of the Fourth International Conference on Communication and Electronics Systems (ICCES 2019)
IEEE Conference Record # 44898; IEEE Xplore ISBN: 978-1-7281-1261-9

Bi-directional Methodology for Literature Extraction from PubMed Abstracts using Web Scrapper and Web Crawler

Koras. S
Phd.Research Scholar,
Dept. of Computer Applications,
Bharathiar University, Coimbatore-46
tokoras@gmail.com

Mannem.Venkatarao Rao
M.Sc Data Analytics,
Dept. of Computer Applications,
Bharathiar University, Coimbatore-46
venkatarao142165@gmail.com

V. Bhuvaneswari
Associate Professor,
Dept. of Computer Applications,
Bharathiar University, Coimbatore-46
bhuvanes_v@yahoo.com

***Abstract* - Searching of literaure is the prime processes in any research to gain insights on the progress carried out on specific probles. Literature search in biological science and bioinforamtics is more complex as the researchers has to find the relre vant articles specifi to the biological components like DNA, RNA, Gene, PROTEIN. Pubmed is a literature database which cosists of millions of articles submitted by researcher based on the experimerntal studies. Analysing Gene for the study is important for studies and experiments related to diseases. In this paper a bi-directional methdology is propsoed to extract literarure from pubmed abstracts using web scrapper and web crawler by providing gene names and map gene with Gene card Database. In the second approach a methdology is provided to analyse Gene expression profiles from GEO database using EDA and Map the significant gene reterived to the Pubmed and Gene Card database. The differentially expressed genes are grouped after performing PCA and clustered using k-means. Lung cancer is major cancer reported in WHO and hence in this study the Lung cancer is used as the usecase to test the methdology proposed. The experiemnts are implemented using Python. From the experimental results it is found that the propsoed approach reduce the time for searching the literature.**

Keywords - Clustering , K-means, PCA, Pubmed, GeneCards, EDA, Web Scrapper

I. INTRODUCTION

Lung cancer can be classified into "Non-small cell lung cancer (NSCLC) and Small-cell lung cancer (SMLC). Among lung cancer cases 85% of the reported cases are found to be NSCLC which spreads quickly [10]. The subtypes of Non-small lung cancer are Aqueous cell carcinoma, Adenocarcinoma, and Large cell. 5% of lung cancers are lung carcinoid tumors which are sometimes mentioned as neuroendocrine tumors. In this work lung cancer dataset is used for implementing the methodology.

Technological developments in the domain of genomic and proteomics helped to identify the causes of genetic variations at gene level which are reported in bioinformatics databases. Huge volumes of data are deposited at various repositories of NCBI, EMBL AND DDBJ. There are exists various classified databases which accumulate results reported by researchers in their experimental studies. Pubmed is a literature databases which accumulated millions of research findings submitted around the globe. Pubmed literature is used as an important research tool among various researchers to gain insight on different experiments and the association of biological entities. Cancer related to experimental analysis also requires integration and association of related entities such as mapping genomic sequences with structures, diseases gene, pathway and functionalities. Gene expression profiles are mainly used to analyze the variations of gene in various experimental conditions in diseases, diagnosis to understand their functionalities and pathways.

Researchers will search biomedical literature databases to study on the different experiments reported in articles with respect to disease and their genomic and proteomic entities. Manual searching of the database is time consuming and complex. The objective of this project is to download pubmed abstracts related to any specific diseases, gene name and other attribute for Literature search and extract the genes related to lung cancer to analyze the gene expressions using web scrappers.

In this paper a methodology is proposed to extract gene names from the pubmed abstract using web scrapper and map with diseases genes to group gene using clustering Remaining paper is organized as follows. Section 2 provides a brief view on computing techniques, followed by objective and methodology in section 3. The experimental results are discussed in section 4 followed by conclusion in section 5.

II. COMPUTING TECHNOLOGY

Web scraping software technique used for extracting information from websites. Web software access the World Wide Web directly using the hypertext transfer protocol, or through a web browser. Web scraping is scraping a web page fetching for information and extracting based on keywords and URIs. Web crawlers are also used to extract the data from websites [9]. Web scraping is used to scrape the web sites. It is not possible to scrape the specific data from websites or web pages, with web crawlers contents can be extracted from[3] multiple pages and also form specific parts using selectors like "css or Xpath", in a structure way. The components built in scrappers contain spiders, search engine, downloader, item pipeline, items and scheduler. The components of scrappy are shown in Fig.1

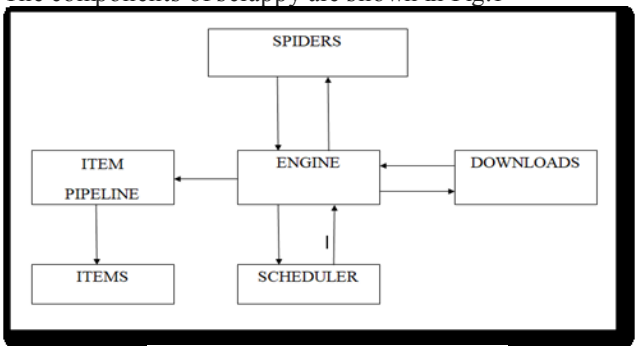

Fig. 1. Web Scrapper: Components

Web scrappers are used to extract pubmed abstracts related to small lung cancer genes. The detailed methodology is discussed in the methodology given below.

Principal Component Analysis

Principal component analysis is a statistical procedure used to reduce for dimensionality reduction based on orthogonal transformation where possible set of correlated observations are set into values of linearly uncorrelated variables called principal components. The main idea of the principal component analysis is reducing the dimensionality of the attributes by maintaining the variations by transforming the variables into a new set of variables as principal components. The principal components are represented using the mathematical representation as eigenvectors of a covariance matrix, and which are orthogonal. In this work dimensionality reduction is used as the Gene expression profile has high dimensions and there will be larger variance among same set of genes. PCA is used to identify the principal components in genes which help to improve the performance of the process.

K-Means Clustering

K-means clustering [2] algorithm is an unsupervised algorithm which is used to group items naturally based on the similarity patterns of the data. The similarity measures decide the grouping of items and various distance based similarity measures are used to group objects in the dataset.

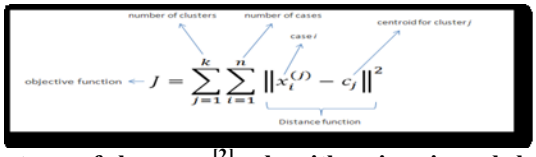

The steps of k-means[2] algorithm is given below as follows:

Input: - k i.e, the number of clusters and the set of points (x_1, x2…, x_n).

1. Choose the 'k' value i.e, k- determines [4] the number of groups the items in the dataset belong.
2. Initially randomly 'k' data points as chosen as centroids ($c_1, c_2,…,c_k$)from the vector space.
3. Repeat until convergence :
   i) For each data point is :
      a) Find the nearest centroid c_j using similarity metrics (i.e) Euclidian distance
      b) Assign x_i to that nearest cluster j
   ii) For each cluster find the new centroid which is the mean of all the x_i points assigned to that cluster j.
4. Terminate when none of the cluster assignment change.

The iteration can be terminated on specific criteria k-means clustering is used in this work to group similar genes related to lung cancer extracted from pubmed abstracts.

III. OBJECTIVE AND METHODOLOGY

The objective and Methodology of this work is to extract abstract from the Pubmed database related to Lung Cancer using Web crawler and map genes related to Lung cancer using gene expression profiles of small lung cancer in Phase I. Perform EDA to analyze the term associations of biological entities like Gene names, and analyze the variation of gene expression profiles of lung cancer types and group genes using clustering in Phase II to provide an insight on the most frequent genes used for analyzing lung cancer in literatures. The objective is implemented in two phases. The methodology for extracting and mapping gene's is given in Fig. 2 for Phase I and in Fig. 3 for Phase II.

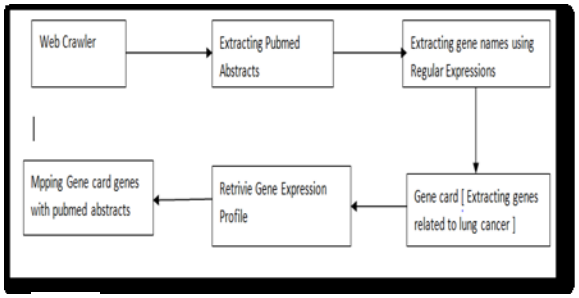

Fig. 2. Framework: Gene Expression Analysis

Phase I: Data Extraction Steps

1. As the first step the web crawler scrappy from python library is used to crawls the pubmed abstracts related to lung cancer.
2. The Gene names from the extracted abstracts are retrieved using regular expressions.
3. The Genes related to small lung cancer is extracted from the Gene card database with expression profiles to map the gene causing lung cancer presented in pubmed abstracts.

The gene expression profiles are analyzed in Phase II using extensive descriptive analytics.

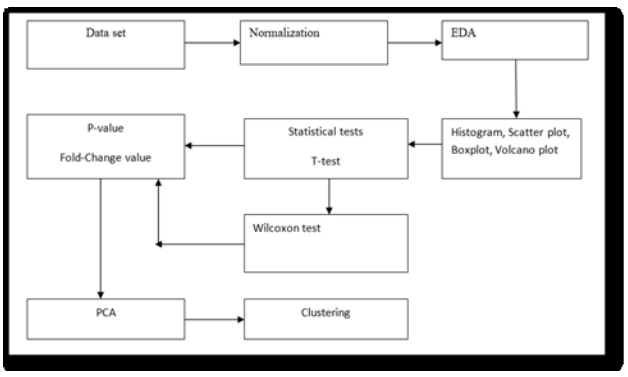

Fig. 3. Framework for EDA and Statistical Tests

Exploratory Data Analytics (EDA)

Exploratory data analysis[5] (EDA) is an approach to analyzing data set to summarize their main characteristics, with visual methods.EDA provides a clear insights for checking assumptions model fitting and hypothesis testing,

and handling missing values and make transformations. The EDA Visualization for Gene Expression Profile is given in Table 1.

Table 1: EDA[7] Visualization Vs. Gene Expression Profile

Visualization Vs. Gene Expression Profile	
Type of Visualization	***Gene Expression Profile***
Histogram is used to understand the deviation in the data set which provides a summary on discrete or continuous data.	Histogram is used to analyze the spread of the values. It is also used to identify the fold changes also to find the distribution of the data and plotted for p-values
Box plot is used to analyze the data distribution based on IQR, minimum and maximum.	Boxplot helps us to analyze the difference of variations of gene expressions
Scatter plot display relationship between two sets of attributes. It pairs up values of two quantitative variables in a dataset and displays them as geometric points.	Scatter plot is used to analyze the relationship between the different and similar genes.
Volcano plot is used to identify the variations in the large data sets.	Volcano plot helps us to analyze the significant changes with respect to fold values.

Gene Expression Analysis using EDA

The expression profiles are analyzed as given below

1. Normalize the data into logarathmic10
2. Perform the histogram, box plot, scatter plot, volcano plot analysis for gene expression profile.
3. Perform T-test and Wilcoxon[5] test to analyze significance of the gene and plot analyze histogram, boxplot, scatter plot, volcano plot with the p-value to find the fold change.
4. Group, identify and extract genes which are similarly expressed and differentially expressed

IV. RESULTS AND DISCUSSION

Phase I: Document Count

The web scrapper is implemented using Python library is used to search Pubmed database for abstracts groups related to lung cancer. The keywords such as Small Cell and Non small cell lung cancer are given as input to the scrappy. Around 4000 documents are downloaded from the pubmed database.

The pubmed abstracts downloaded are searched for gene causing lung cancer which is extracted from Gene Card Database. Around 30,000 gene were searched in the abstracts to find the frequency of occurrence which is given in Table 2

Table 2: Phase I: Document count

Document count		
S. No	***Pubmed***	***Frequency of genes***
1	Downloaded 4000 abstracts	300000 in Gene Card for Lung Cancer
2	Mapping of Gene card database genes for Abstracts	14000 [at least one time] 928 [more than 50 times]928 gene are at least one time

To analyze the functionalities of gene, expression profiles are downloaded from GEO database related to Lung cancer. The data adenocarcinoma and squamous cell carcinoma GDS3627 is downloaded for homospaiens which contains 58 samples and 54675 instances.

Phase II : Gene Expression Analysis

The limma and Bioconductor packages are used for analysing differential gene expression analysis using R and Python. Differentially gene expression were analysed using a double filtering approach based on fold change t-test and Wilcoxon test. The EDA is presented in the sections below.

A. Histogram

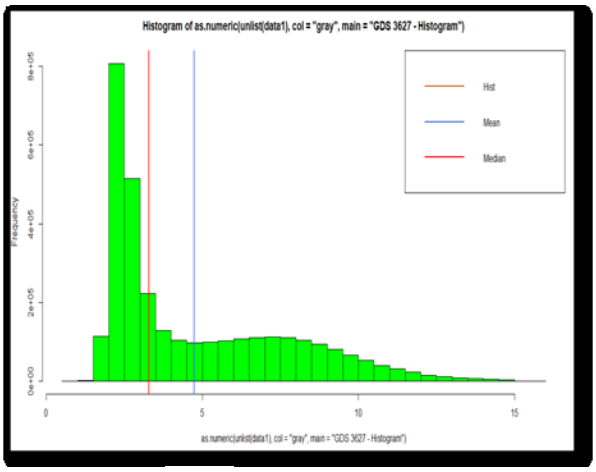

Fig. 4. Histogram for GDS3627

The histogram is shown in Fig. 4. is without normalization found to be right skewed and more genes have higher expression values greater than mean. Hence Histogram analysis after normalization is done which is show in Fig. 5.

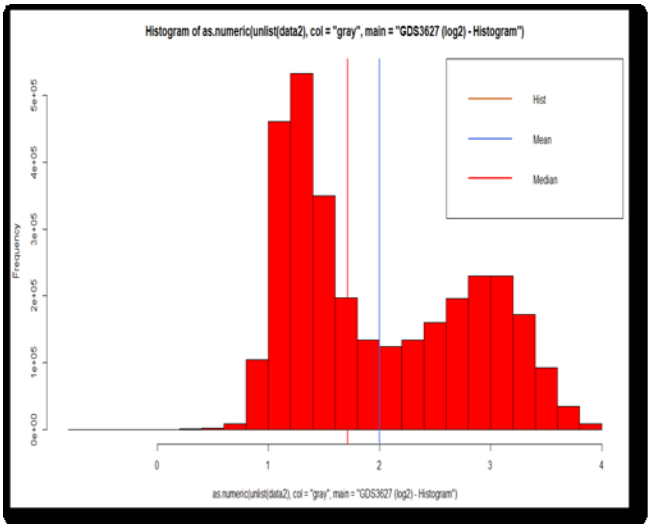

Fig. 5. Expression profile: Normalized – Log10

The distribution is found to be bi-modal distribution with two different groups. The first distribution belongs to adenocarcinomas and the other to squamous cell carcinoma. The data distribution can be further slice to review the expression values. After scaling the data the genes falls between 0 to 4 on x-axis. 60% genes are lies between 1 and 2. All the remaining genes fall between 2 to 4 on the x-axis.

Based on the inference the t-test is performed to compare the expression profile between two different groups in the same experiment for which the histogram fold difference is show in Fig. 8.

Parametric Test T-Test

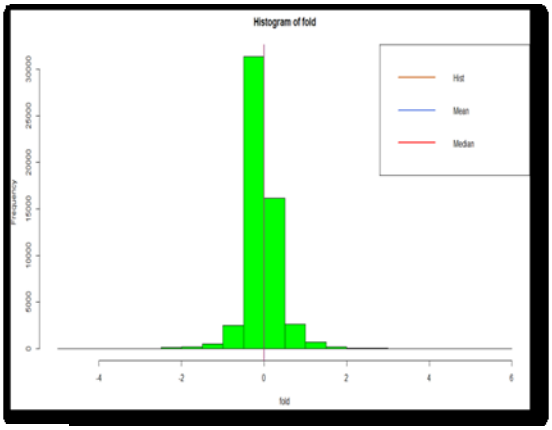

Fig. 6. Difference between the two means fold change

Fold change [5] is a biological significance difference between the means of the conditions. The histogram given in Fig. 6. refers to the fold values [the difference between the two mean's]. The fold value is between -2 and +2 with a fold value as 2.4 to measure the quantity of the attributes.

B. Scatter Plot

Scatter plot is a Bivariate plot used to find the relationship between two variables X and Y. It is normally used for analyzing the correlations among the variables. The scatter plot is drawn between the average mean of a type and the average mean of type b.

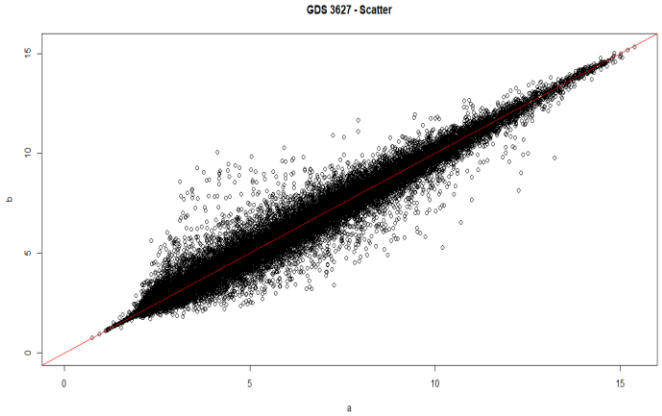

Fig. 7 Scatter plot: Adenocarcinomas vs Squamous cell carcinoma

In Fig. 7. Scatter plot line is drawn between to the cancer types Adenocarcinomas vs Squamous cell carcinoma. The relationship between these two groups are found to have a strongly correlation. The correlation value of the attributes is 0.98. That means of the attributes are positively correlated and the red line is connecting the mostly correlated attribute variables of the two groups.

C. Volcano plot

Volcano plot[7] given in Fig. 8 is used to plot the expression profiles for Fold_cutoff value (2) and p-value cutoff (0.05). The result is shown below.

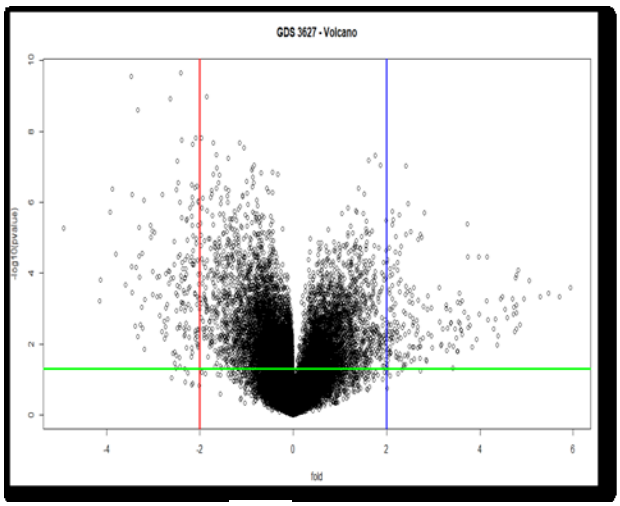

Fig. 8. Volcano Plot

The Volcano plot is shown in Fig.10. represent for the fold cutoff value 2 and the p-value is 0.05. The points found inside the boundaries are found to have similar expression profiles where the data points that are out of the boundaries red, blue and green show the genes expression profiles with are largely varying and differently expressed. Some outliers with are single, are also available which are out of boundaries. The x-axis has fold value (2) and the y-axis is logarithmic p-value. The word cloud for similarly expressed gene and differentially expressed gene is shown in Fig. 9. and Fig. 10

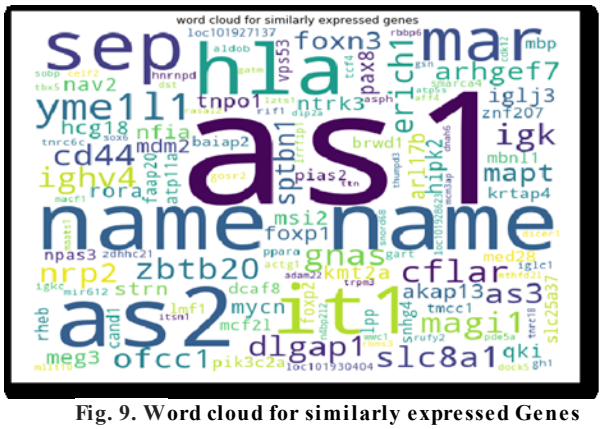

Fig. 9. Word cloud for similarly expressed Genes

Inference:

The Fig. 9. provides a word[12] cloud view of the similarly expressed genes. The 54389 genes are similarly expressed and the size of the gene names based on the frequency of the gene. Gene names as1, as2, is the highest frequency related to small lung cancer. The genes gsn, dst, ash2l are found to the have lowest occurrence.

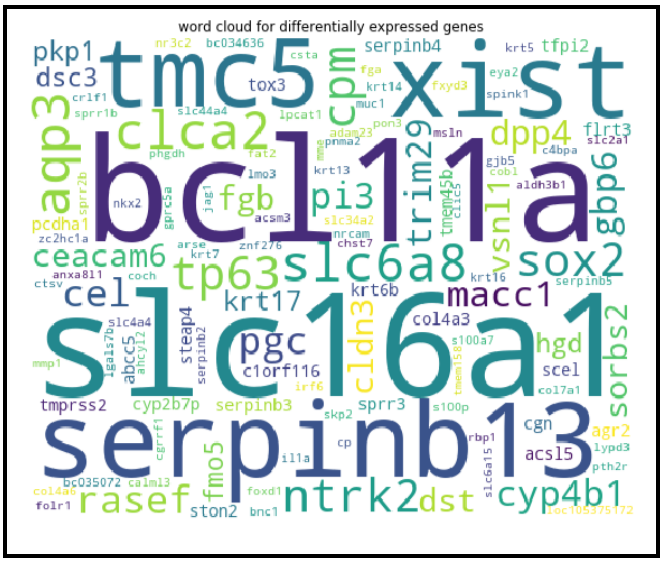

Fig. 10. Word cloud for differentially expressed Genes

Inference

The Fig.10 represents word-cloud of differentially expressed genes. 218b genes were found to be differentially expressed genes. The genes that have high frequency are XIST, BCI11a, serpinb13 and genes that are less frequency bnc1, nav1, muc1.., etc.

D. Mapping of Significant Gene: Pubmed and Gene Card

Based on the EDA expression profiles the gene which are within the fold and which satisfied the p-value condition >0.05 are filtered which is shown in Fig. 11.

	Name	Count
4	KRT5	1
7	HLA-DQA1	13
8	PI3	106
15	LMO3	5
16	DST	2

Fig. 11. Count of Filtered Genes > pvalue 0.05

115 genes satisfied the condition and verified for references in 4000 Pubmed abstracts downloaded. Out of 115 genes 29 genes are mentioned in pubmed abstracts atleast one time and 8 genes were found to be mentioned more than 100 times. The gene P13 is found to be mentioned 106 times PI3. This methodology will help the researchers to extract the relevant abstracts specific to gene for further analysis. The gene expression profile gene are also mapped with GeneCared genes and also verified for their occurrence in Pubmed abstracts which is shown in Fig.12.

	Name	Count
0	TP53	109
1	BRCA2	5
2	EGFR	998
3	PTEN	80
4	MLH1	16
5	BRCA1	13
6	KRAS	142
7	ERBB2	8
8	ATM	17
9	CDKN2A	9

Fig. 12. Count of occurrences

The gene EGFR has occurred in 998 pubmed abstracts and the 90% genes has not even mentioned in the abstract downloaded. 1200 genes are referred atleast in one abstract out of 30000 genes. The word cloud of Gene card genes extracted from Pudmed abstract is given in Fig. 13

Fig. 13. Word cloud for Gene card Genes

E. Clustering Of Differentially Expressed Genes

Based on the T-test statistics 115 genes were found to be similar and the remaining genes had wide variation in their expression .the genes with wider variation's are clustered using k-means clustering algorithm. As the sizes of the gene samples are more Principal Component Analysis [PCA] is performed to reduce the dimensionality.

a) PCA

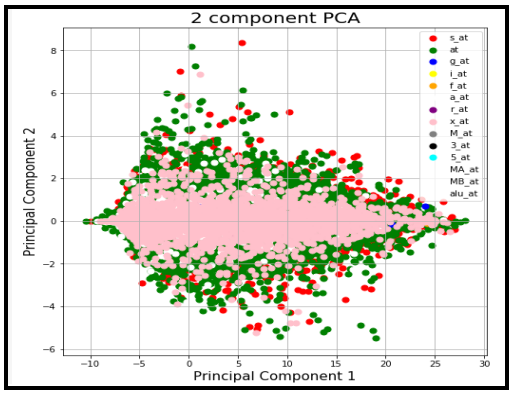

Fig. 14. PCA Results

The Fig.14. represents the principal components and subgroups of genes which are found to be overlapped based on their probe values. There are 14 different types of probe available for analyzing the gene expression. Among 14 types maximum number of genes are overlapped and can observe that 3% of genes that are not overlapped from the sub types of at, x_at, s_at sub types of genes.

b) Clustering: The genes are clustered [4] using the principal components. The differentially expressed genes are grouped in four clusters is shown in Fig. 15.

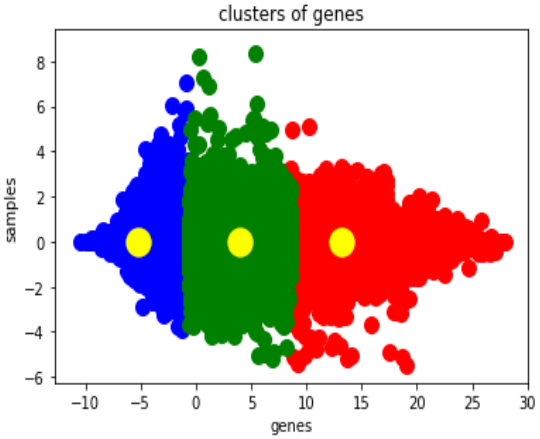

Fig. 15. Differentially Expressed Gene Clusters

- Cluster 1 represents the data 8827 genes are grouped in cluster 1.
- Cluster 2 represents the 32213 numbers of genes grouped.
- Cluster three represents 13063 numbers of human genes.

Out of three clusters the second cluster i.e green labeled cluster having the number of genes is very high compared two remaining two genes.

V. CONCLUSION

A methodology is proposed to extract abstracts from Pubmed databases using web crawler based on Keywords using regular expressions. The abstract are used to retrieve gene names and map with gene card to find the disease gene for lung cancer in Phase I. In second Phase a methodology is proposed to analyze Gene expression profiles with EDA and cluster differentially expressed genes after performing PCA. The Proposed methodology will help researchers to search literatures in an efficient way and Map gene to disease database with reduced time. Comparison of gene expression profiles are not done due to limitation of processing capability. In future the expression profile will be analyzed by applying MapReduce model using Machine Learning Algorithms.

REFERENCES

1. Cited at “global lung cancer statistics https://www.cancerresearchuk.org/health-professional/cancer-statistics/worldwide-cancer”
2. Cited at “https://www.datacamp.com/community/K-m eans-clustering-python ”
3. Cited at “https://jakevdp.github.io/PythonDataScienceHandbook/05 .11-k-means.html”
4. Cited at “https://www.sciencedirect.com/topics/medicine-and-density/cluster-analysis” , 2019
5. Cited at “statistical tests are https://www .researchgate.net/publication/323470574_Multivariate_Entropy_Characterizes_the_Gene_Expression_and_Protein-Protein_Networks_in_Four_Types_of Cancer” Angle Juarez-Flores, Marco V.jose. 28/02/2018
6. Cited at, “Limma packages https://f1000research .com/articles/5-1438 Aron A.T.L”
7. Cited at “http://bigdata-madesimple.com/ explora tory-data-analysis-in-python-using-pan das - matplotlib-and-numpy/”
8. Cited at “ https://www.cancer.gov/about-cancer /understanding/what-is-cancer”
9. Cited at “R & Bioconductor—Manuals. Available online:http://manuals.bioinformatics.ucr.edu/home/R_BioCondManual”
10. Cited at “www.sciencedirect.com Development of word cloud using python. A.DePaolo and Kelly Wilkinson, Indiana State University. https://www.researchgate.net/publication/272016699_Get_Your_Head_into_the_Clouds_Using_Word_Clouds_Using_Word_Clouds_for_Analyzing_Qualitative_Assessment_Data”
11. K Z akir Hussain, M durairaj and G.rabia jahanFarazana “application of Data mining Techniques for Analyzing Violent Criminal Behaviour by Simultation Model”, international journal of Computer Science and information Technology & Society, Vol .02, No. 01, ISSN:2249-9555,2012
12. De Bruin J.S.,cocx,T.K.Kosters, W.A., Laro,J. and kok,j.N(2006) Data Mining approaches to criminal carrer analysis Publisshed in proceeding of the sixth Inyernational Conference On Data mining(ICDM”06),pP. 171-177

Proceedings of the Fourth International Conference on Communication and Electronics Systems (ICCES 2019)
IEEE Conference Record # 45898; IEEE Xplore ISBN: 978-1-7281-1261-9

IoT Visibility Issues and securing using Deep Neural Networks

Moinak Bhattacharya
IEEE Member, SRM IST
Kattankulathur
moinakbhattacharya_utpal@srmuniv.edu.in

Dr. R. Annie Uthra
Associate Professor, SRM IST
Kattankulathur
annie.u@ktr.srmuniv.ac.in

Rounak Datta
SRM IST
Kattankulathur
rounakdatta_gautam@srmuniv.edu.in

Arindam Chakraborty
King Abdullah University of Science and Technology
Saudi Arabia
arindamx@gmail.com

***Abstract*— With exponential growth of IoT-based systems and the world being heavily dependent upon it, ensuring security in such systems becomes an issue of prime interest. With the advancement of technology, several security mechanism have been proposed, but securing the unknown threats is still not widely adopted. IoT visibility vulnerabilities propose a potential threat to the secured and highly sensitive data within the network. In this proposed work, deep neural networks have been trained to predict and secure some of the vulnerabilities which are still unknown to the authorized users. Our proposed ,mode achieves an accuracy of 95% over the predominant security measures with a precision of 87%.**

Keywords—IoT visibility, vulnerability, deep neural networks, security and privacy

I. INTRODUCTION

The last decade experienced a huge development in the automation and Smart architecture design. The quality of modernization received a boom with the advancement in the integration of the physical world with Wireless communication and sensor networks through applications (apps) and remote devices for quality infrastructure management design and environmental monitoring system. Smart Building Automation, Smart Housing, Smart City Management, Sustainable Energy management systems, etc are built on the top of IoT, hence it is one of the fastest emerging fields in the history of computing and is expected to grow to 10 billion by 2020 and 22 billion by 2025[52]. The data statistics of IoT devices is estimated up to 5 quintillion bytes of data per day[53]. The IoT technology is also being leveraged for highly secure applications like healthcare management, confidential information retrieval, etc. These high-end applications of IoT devices often experience malicious attacks, so these devices must be secured from all possible vulnerabilities.

IoT architectures are inherently complex and are designed with specific integrated features. Hence, the vulnerability may exist in a minimal-scale but a high consequential attack on the IoT system is still challenging. The potential solution is to identify the traits in the architecture and must contain specific considerations to meet the security demand. However, most of the vulnerabilities are not specifically visible and the malicious environment remains unattended. Hence, the adversary can exploit this environment to achieve physically access to sensitive data. The IoT network along with the private information in the communication channel remains exposed to the attacker. The IoT architecture cannot support complex security structures because of their limited computation power. Complex security structures of the IoT are due to not only limited computation, communication, and power resources but also trustworthy interaction with a physical domain, particularly the behavior of a physical environment in unanticipated and unpredictable modes, because the IoT system is also part of a cyber-physical system; autonomously, IoT systems must constantly adapt and survive in a precise and predictable manner with safety as a key priority, particularly in settings where threatening conditions, such as in health systems, might occur. Moreover, new attack surfaces are introduced by the IoT environment. Such attack surfaces are caused by the interdependent and interconnected environments of the IoT. Consequently, the security is at higher risk in IoT systems than in other computing systems, and the traditional solution may be ineffective for such systems.

II. Related works

Considerable amount of research has been done on (i) protocols and enabling technologies, (ii) application domains, (iii) context awareness, (iv) legal frameworks, (v) attacks against IoT, (vi) access models, (vii) security protocols, and (viii) intrusion detection techniques. Practical surveys on IoT security have not taken into account the ML/DL approaches for IoT security. Firstly, Surveys [1-7] demonstrated the challenges in network security, cryptographic encryption, authentication, access control and application security in IoT systems. Granjal, Monteiro and Silva [8] focussed on the IoT communication security. A survey was conducted on intrusion detection for IoT systems by Zarpelão et al. [9]. Weber [10] dealt with legal issues and regulatory approaches for determination of whether IoT frameworks satisfy the privacy and security requirements. Roman, Zhou and Lopez [11] analyzed security and privacy in the distributed IoT context. Survey [12] was particularly concerned of ransomware attacks. Xiao et al. [13] researched on various machine learning methods for protecting data privacy and security in the IoT context. Other survey papers [14, 15] shows how the uses of data mining and machine learning methods for cybersecurity can support intrusion detection. Surveys have also reviewed misuse and anomaly detections in cyberspace research [14, 15].

III. Introduction to IoT Security Architecture and Visibility Issues

Weber and Studer in [16] discussed available legal frameworks whereas, Zhang et al. [17] approached IoT security by analyzing results and reports in relation to IoT incidents. Data mining techniques were analyzed to design a capability which crawled Internet publications, including academic research, news, blogs, and cyber reports and through correlation of real IoT incidents with the available security solutions, the authors were able to unveil five seriously weak areas in the context of IoT security viz LAN and environmental mistrust, over-privileged applications, insufficient authentication and implementation flaws. With a plethora of research works discovery of botnet architectures and detection mechanisms in the context of traditional computing [18-21], Anagnostopoulos at al. [22] focussed on the mobile environment. Indeed, they also proposed two new commands and control (C&C) architectures which can be exploited by an attacker to test well-hidden botnet attacks with the minimal C&C cost. The IoT Visibility Vulnerability architecture is shown in Figure 1.

Burhan et al. [23] proposed a layered IoT architecture. These architectures typically have three-five layers and different functionality. Insecurities were identified and the authors went on to propose a six-layer architecture to patch these security challenges and took into context big data.

As an alternative work, Alaba et al. [24] analyzed IoT security by proposing various IoT deployment solutions, particularly distinguished between four classes, including, application, architecture, communication, and data. A major discussion came forward that heterogeneity of IoT devices along with resource limitations propose a serious issue, which prevents the development and scalability of standard security solutions. Gendreau and Moorman [25] reviewed intrusion detection techniques proposed for IoT and proposed that prevention of unauthorized access is a challenging goal due to the limited computation power of the IoT devices. Zarpelao et al. [9] also put in intrusion detection research efforts for IoT and differentiated them based on detection method, placement strategy, security threat, and validation strategy.

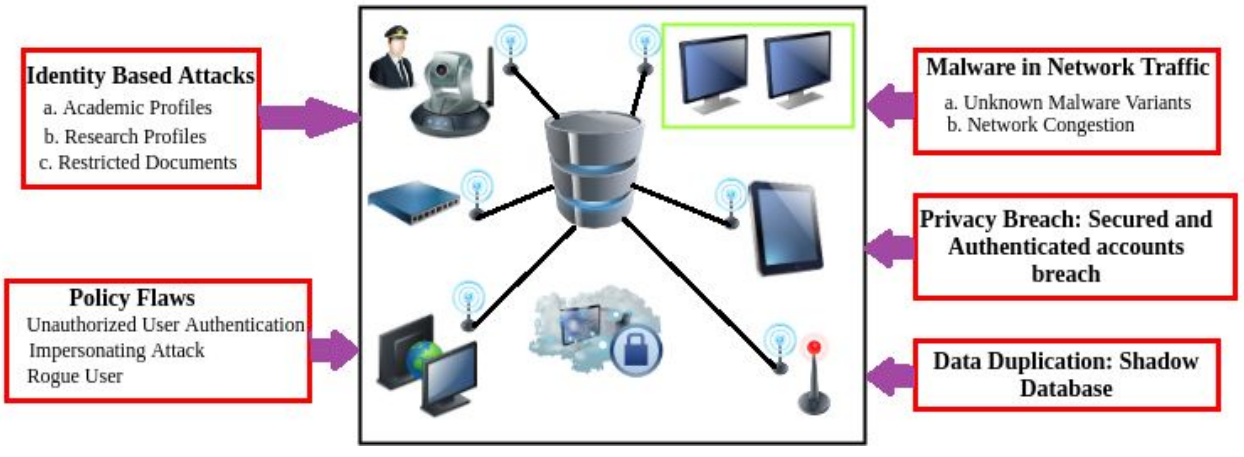

Figure 1: Architecture Diagram of IoT (Internet of Things) Visibility Vulnerabilities

IV. IoT Visibility Vulnerabilities

An exhaustive analysis of the research works related to the field of IoT security yielded nine classes of IoT vulnerabilities. It has been observed that the majority of IoT devices operate autonomously in unsolicited environments [26]. Often with an easy attempt, an adversary is able to obtain unauthorized physical access to these nodes and get control over them. Consequently, an attacker causes physical damage to the devices, unveiling deployed cryptographic schemes, duplicating their firmware using malicious node, or corrupting the control mechanism or the stored data. Representative research contributions in this context include [27-32]. An attacker might be able to drain the stored energy by creating a flood of legitimate or corrupted messages, rendering the devices unavailable for genuine processes or users. [33-36] have well covered this area of research. Alternatively, an attacker might exploit ineffective authentication approaches to add spoofed malicious nodes or violate the data integrity, thus intruding on IoT devices and network communications. Such cases can result in lost, destroyed, or corrupted public and private keys as shown in[37-42]. Data protection is of paramount importance in IoT realms, especially those operating in critical CPS (i.e., power utilities, manufacturing plants, building automation, etc). Although encryption gives considerable amount of confidence in securing, an attacker might be able to circumvent the deployed encryption techniques as shown in [43-48]. Open port vulnerabilities pose a plethora of vulnerabilities as shown in [49].

V. Analysis of Network Traffic Data

IoT Visibility specifies the knowledge of all of the activities being recorded on the network, all the modules running on the nodes, and data is being incrementally stored in the cloud databases. Naive methodologies of network visibility for example, tap or span port, might not be sufficiently useful for ensuring IoT security. To effectively manage the vulnerability present in the architecture, the proposed methodology implements knowledge-based identification of the visibility traits. Some of the vital points regarding this technique are elucidated below:

A. Public Policy Management

Policy Management is one of the background security measure of IoT systems. Data produced by IoT devices include sensitive and confidential data, such as medical, private and military data must be protected against unauthorised access [50] and must have stoing policy-based authorization. The solution to poor implementation of policy management involves finer-level access controls with layers of role-based authorization.

B. Intrusion Problem

In active threats, the attacker is not only skilful in eavesdropping on communication channels, but also in modifying IoT systems to change configurations, control communication, deny services and so on. Attacks may include a sequence of interventions, disruptions and modifications. For example, potential attacks on an IoT system may involve the following active attacks: impersonation[11], malicious inputs, data tampering and DoS.

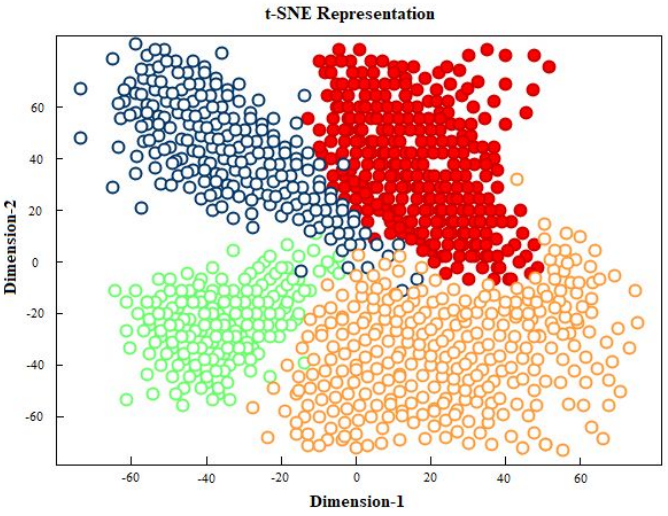

Figure 2: t-SNE Representation of the Malicious Attacks on the IoT systems

C. Security Awareness Issues

A potential passive threat is experienced due to lack of enough security over the communication channels of the network. Any attacker can get access to protected information from sensors, actuators, security and surveillance cameras. Health data, being private and sensitive is at central risk. Due to the lack of security awareness coupled with vulnerabilities present in the communication channels causes violation of privacy.

D. Vulnerability Assessment

An adversary can easily penetrate through networks layer as well as physical layer to discover finer vulnerabilities in the IoT system. This results in authentication breach of the centralized database and a shadow database is in performance which goes unnoticed.

E. Access and Authentication Issues

It is essential to identify the requirements of the authentication process as well as the security architecture of various IoT systems. The trade-off between security and safety in IoT medical devices is of utmost importance considering the privacy and sensitivity of information. Also, the trade-off can arise between an effective authentication system and battery-based devices or between security and privacy.

VI. IoT Visibility Testing using Deep Neural Networks (DNN)

In the present context, the applications of Deep Learning (DL) to IoT systems has been an impactful research domain [51]. The main advantage of DL over statistical Machine Learning algorithms, is its high performance while dealing with large

and non-parametric datasets. The proposed IoT system, as shown in Figure 3, produces a massive amount of both structured and unstructured data; thereby making DNNs most suitable for this system.

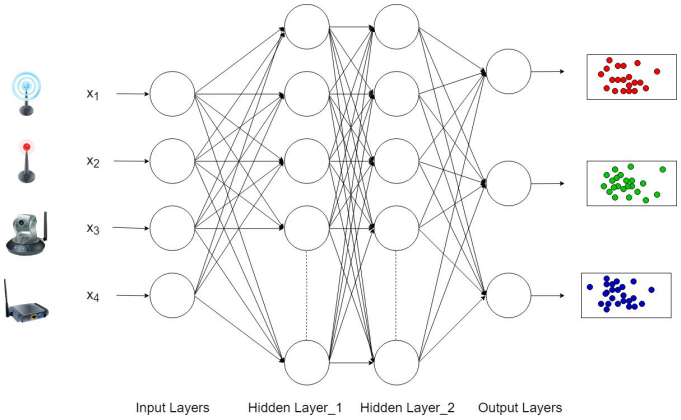

Figure 3: Deep Neural Network Architecture for visibility vulnerability prediction

VII. Experimental Analysis of IoT Visibility Vulnerabilities

This research experiment initially involved the study of various cases of breach of security in IoT devices, mostly in high performance systems, confidential organizations. We took into account various adversarial attacks, major as well as minor and came up with various techniques, both distributed as well as concentrated. We are able to demonstrate how deep neural networks have helped improve the accuracy upto 95% and 87% precision.

The Receiver Operating Characteristics curve (ROC curve) is plotted to visualize the ability of the proposed architecture and the simultaneous diagnostic analysis of the vulnerability prediction is made. Precision Recall curve is made to summarize the relationship between TPR (True Positive Rate) and the positive predictive value of the proposed model.

IoT visibility vulnerabilities	Prediction values		
	Existing	Accuracy	Usability
Identity-based attacks	30%	98%	Academic Accounts
Malwares	50%	95%	LAN
Privacy breach	20%	99%	Research accounts
Data Duplication	40%	96%	Public IoT data

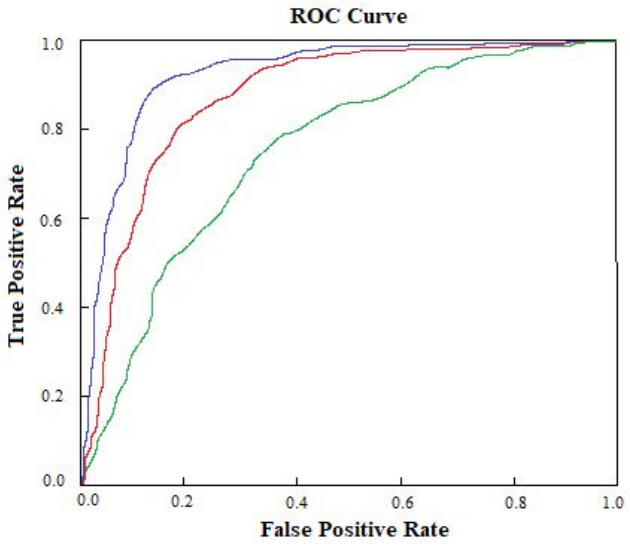

Figure 4: ROC Curve

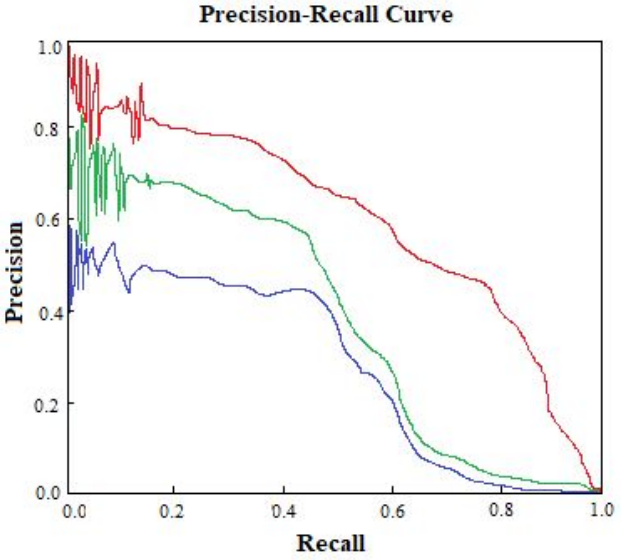

Figure 5: Precision-Recall Curve

VIII. Future Works

The future prospects of the research is to implement cognitive technologies for efficient understanding and to provide a potential solution eradicating the flaws in contextual deep learning methods. Further, quantum efficiency can also be studied to reach out the maximum level of proper identification of vulnerabilities.

IX. Acknowledgements

This work was supported by Department of Computer Science and Engineering, SRM Institute of Science and Technology, Kattankulathur. We would also like to thank the collaborative efforts of Next Tech Lab.

References

[1] [1] A. R. Sfar, E. Natalizio, Y. Challal, and Z. Chtourou, "A roadmap for security challenges in the Internet of Things," Digital Communications and Networks, 2017.

[2] [2] S. Sicari, A. Rizzardi, L. A. Grieco, and A. Coen-Porisini, "Security, privacy and trust in Internet of Things: The road ahead," Computer networks, vol. 76, pp. 146-164, 2015. [3] F. A. Alaba, M. Othman, I. A. T. Hashem, and F. Alotaibi, "Internet of Things security: A survey," Journal of Network and Computer Applications, vol. 88, pp. 10-28, 2017.

[3] [4] K. Zhao and L. Ge, "A survey on the internet of things security," in Computational Intelligence and Security (CIS), 2013 9th International Conference on, 2013, pp. 663-667: IEEE.

[4] [5] J. S. Kumar and D. R. Patel, "A survey on internet of things: Security and privacy issues," International Journal of Computer Applications, vol. 90, no. 11, 2014.

[5] [6] H. Suo, J. Wan, C. Zou, and J. Liu, "Security in the internet of things: a review," in Computer Science and Electronics Engineering (ICCSEE), 2012 international conference on, 2012, vol. 3, pp. 648-651: IEEE.

[6] [7] D. E. Kouicem, A. Bouabdallah, and H. Lakhlef, "Internet of Things Security: a top-down survey," Computer Networks, 2018.

[7] [8] J. Granjal, E. Monteiro, and J. S. Silva, "Security for the internet of things: a survey of existing protocols and open research issues," IEEE Communications Surveys & Tutorials, vol. 17, no. 3, pp. 1294-1312, 2015.

[8] [9] B. B. Zarpelão, R. S. Miani, C. T. Kawakani, and S. C. de Alvarenga, "A survey of intrusion detection in Internet of Things," Journal of Network and Computer Applications, vol. 84, pp. 25-37, 2017.

[9] [10] R. H. Weber, "Internet of Things–New security and privacy challenges," Computer law & security review, vol. 26, no. 1, pp. 23-30, 2010.

[10] [11] R. Roman, J. Zhou, and J. Lopez, "On the features and challenges of security and privacy in distributed internet of things," Computer Networks, vol. 57, no. 10, pp. 2266-2279, 2013.

[11] [12] I. Yaqoob et al., "The rise of ransomware and emerging security challenges in the Internet of Things," Computer Networks, vol. 129, pp. 444-458, 2017.

[12] [13] L. Xiao, X. Wan, X. Lu, Y. Zhang, and D. Wu, "IoT Security Techniques Based on Machine Learning," arXiv preprint arXiv:1801.06275, 2018.

[13] [14] A. L. Buczak and E. Guven, "A survey of data mining and machine learning methods for cyber security intrusion detection," IEEE Communications Surveys & Tutorials, vol. 18, no. 2, pp. 1153-1176, 2016.

[14] [15] P. Mishra, V. Varadharajan, U. Tupakula, and E. S. Pilli, "A Detailed Investigation and Analysis of using Machine Learning Techniques for Intrusion Detection," IEEE Communications Surveys & Tutorials, 2018.

[15] [16] R. H. Weber and E. Studer, "Cybersecurity in the internet of things: Legal aspects," Computer Law & Security Review, vol. 32, no. 5, pp. 715–728, 2016

[16] [17] N. Zhang, S. Demetriou, X. Mi, W. Diao, K. Yuan, P. Zong, F. Qian, X. Wang, K. Chen, Y. Tian et al., "Understanding iot security through the data crystal ball: Where we are now and where we are going to be," arXiv preprint arXiv:1703.09809, 2017

[17] [18] E. Bou-Harb, M. Debbabi, and C. Assi, "A novel cyber security capability: Inferring internet-scale infections by correlating malware and probing activities," Computer Networks, vol. 94, pp. 327–343, 2016.

[18] [19] E. Bou-Harb, C. Fachkha, M. Debbabi, and C. Assi, "Inferring internetscale infections by correlating malware and probing activities," in 2014 IEEE International Conference on Communications (ICC). IEEE, 2014, pp. 640–646.

[19] [20] ——, "Big data behavioral analytics meet graph theory: on effective botnet takedowns," IEEE Network, vol. 31, no. 1, pp. 18–26, 2017.

[20] [21] ——, "Behavioral analytics for inferring large-scale orchestrated probing events," in 2014 IEEE Conference on Computer Communications Workshops (INFOCOM WKSHPS). IEEE, 2014, pp. 506–511.

[21] [22] M. Anagnostopoulos, G. Kambourakis, and S. Gritzalis, "New facets of mobile botnet: architecture and evaluation," International Journal of Information Security, vol. 15, no. 5, pp. 455–473, 2016.

[22] [23] M. Burhan, R. Rehman, B. Khan, and B.-S. Kim, "IoT elements, layered architectures and security issues: A comprehensive survey," Sensors, vol. 18, no. 9, p. 2796, 2018.

[23] [24] F. A. Alaba, M. Othman, I. A. T. Hashem, and F. Alotaibi, "Internet of things security: A survey," Journal of Network and Computer Applications, 2017.

[24] [25] A. A. Gendreau and M. Moorman, "Survey of intrusion detection systems towards an end to end secure internet of things," in Future Internet of Things and Cloud (FiCloud), 2016 IEEE 4th International Conference on. IEEE, 2016, pp. 84–90.

[25] [26] R. Mahmoud, T. Yousuf, F. Aloul, and I. Zualkernan, "Internet of things (iot) security: Current status, challenges and prospective measures," in 2015 10th International Conference for Internet Technology and Secured Transactions (ICITST). IEEE, 2015, pp. 336–341.

[26] [27] J. Wurm, K. Hoang, O. Arias, A.-R. Sadeghi, and Y. Jin, "Security analysis on consumer and industrial iot devices," in Design Automation Conference (ASP-DAC), 2016 21st Asia and South Pacific. IEEE, 2016, pp. 519–524.

[27] [28] M. Smache, N. El Mrabet, J.-J. Gilquijano, A. Tria, E. Riou, and C. Gregory, "Modeling a node capture attack in a secure wireless sensor networks," in Internet of Things (WF-IoT), 2016 IEEE 3rd World Forum on. IEEE, 2016, pp. 188–193.

[28] [29] B. Ur, J. Jung, and S. Schechter, "The current state of access control for smart devices in homes," in Workshop on Home Usable Privacy and Security (HUPS). HUPS 2014, 2013.

[29] [30] M. Qabulio, Y. A. Malkani, and A. Keerio, "A framework for securing mobile wireless sensor networks against physical attacks," in Emerging Technologies (ICET), 2016 International Conference on. IEEE, 2016, pp. 1–6.

[30] [31] J. Zhao, "On resilience and connectivity of secure wireless sensor networks under node capture attacks," IEEE Transactions on Information Forensics and Security, vol. 12, no. 3, pp. 557–571, 2017.

[31] [32] C. Schuett, J. Butts, and S. Dunlap, "An evaluation of modification attacks on programmable logic controllers," International Journal of Critical Infrastructure Protection, vol. 7, no. 1, pp. 61–68, 2014.

[32] [33] W. Trappe, R. Howard, and R. S. Moore, "Low-energy security: Limits and opportunities in the internet of things," IEEE Security & Privacy, vol. 13, no. 1, pp. 14–21, 2015.

[33] [34] E. Y. Vasserman and N. Hopper, "Vampire attacks: draining life from wireless ad hoc sensor networks," IEEE transactions on mobile computing, vol. 12, no. 2, pp. 318–332, 2013.

[34] [35] A. A. Patel and S. J. Soni, "A novel proposal for defending against vampire attack in wsn," in Communication Systems and Network Technologies (CSNT), 2015 Fifth International Conference on. IEEE, 2015, pp. 624–627.

[35] [36] D. G. Costa, I. Silva, L. A. Guedes, F. Vasques, and P. Portugal, "Availability issues in wireless visual sensor networks," Sensors, vol. 14, no. 2, pp. 2795–2821, 2014.

[36] [37] N. Vidgren, K. Haataja, J. L. Patino-Andres, J. J. Ramirez-Sanchis, and P. Toivanen, "Security threats in zigbee-enabled systems: vulnerability evaluation, practical experiments, countermeasures, and

lessons learned," in System Sciences (HICSS), 2013 46th Hawaii International Conference on. IEEE, 2013, pp. 5132–5138.

[37] [38] P. Morgner, S. Mattejat, and Z. Benenson, "All your bulbs are belong to us: Investigating the current state of security in connected lighting systems," arXiv preprint arXiv:1608.03732, 2016.

[38] [39] T. Kothmayr, C. Schmitt, W. Hu, M. Brunig, and G. Carle, "Dtls based ¨ security and two-way authentication for the internet of things," Ad Hoc Networks, vol. 11, no. 8, pp. 2710–2723, 2013.

[39] [40] I. Hafeez, A. Y. Ding, L. Suomalainen, A. Kirichenko, and S. Tarkoma, "Securebox: Toward safer and smarter iot networks," in Proceedings of the 2016 ACM Workshop on Cloud-Assisted Networking. ACM, 2016, pp. 55–60.

[40] [41] P. Porambage, C. Schmitt, P. Kumar, A. Gurtov, and M. Ylianttila, "Pauthkey: A pervasive authentication protocol and key establishment scheme for wireless sensor networks in distributed iot applications," International Journal of Distributed Sensor Networks, 2014.

[41] [42] A. Furfaro, L. Argento, A. Parise, and A. Piccolo, "Using virtual environments for the assessment of cybersecurity issues in iot scenarios," Simulation Modelling Practice and Theory, vol. 73, pp. 43–54, 2017

[42] [43] E. Ronen and A. Shamir, "Extended functionality attacks on iot devices: The case of smart lights," in Security and Privacy (EuroS&P), 2016 IEEE European Symposium on. IEEE, 2016, pp. 3–12.

[43] [44] V. Sachidananda, S. Siboni, A. Shabtai, J. Toh, S. Bhairav, and Y. Elovici, "Let the cat out of the bag: A holistic approach towards security analysis of the internet of things," in Proceedings of the 3rd ACM International Workshop on IoT Privacy, Trust, and Security. ACM, 2017, pp. 3–10.

[44] [45] H. Shafagh, A. Hithnawi, A. Droscher, S. Duquennoy, and W. Hu, ¨ "Talos: Encrypted query processing for the internet of things," in Proceedings of the 13th ACM Conference on Embedded Networked Sensor Systems. ACM, 2015, pp. 197–210.

[45] [46] B. Wei, G. Liao, W. Li, and Z. Gong, "A practical one-time file encryption protocol for iot devices," in Computational Science and Engineering (CSE) and Embedded and Ubiquitous Computing (EUC), 2017 IEEE International Conference on, vol. 2. IEEE, 2017, pp. 114–119.

[46] [47] A. Biryukov, D. Dinu, and Y. Le Corre, "Side-channel attacks meet secure network protocols," in International Conference on Applied Cryptography and Network Security. Springer, 2017, pp. 435–454.

[47] [48] S. Siboni, A. Shabtai, N. O. Tippenhauer, J. Lee, and Y. Elovici, "Advanced security testbed framework for wearable iot devices," ACM Transactions on Internet Technology (TOIT), vol. 16, no. 4, p. 26, 2016

[48] [49] K. Angrishi, "Turning internet of things (iot) into internet of vulnerabilities (iov): Iot botnets," arXiv preprint arXiv:1702.03681, 2017

[49] [50] M. Abomhara, "Cyber security and the internet of things: vulnerabilities, threats, intruders and attacks," Journal of Cyber Security and Mobility, vol. 4, no. 1, pp. 65-88, 2015.

[50] [51] H. Li, K. Ota, and M. Dong, "Learning IoT in Edge: Deep Learning for the Internet of Things with Edge Computing," IEEE Network, vol. 32, no. 1, pp. 96-101, 2018

[51] [52] https://iot-analytics.com/state-of-the-iot-update-q1-q2-2018-number-of-iot-devices-now-7b/

[52] [53] https://blogs.cisco.com/datacenter/internet-of-things-iot-data-continues-to-explode-exponentially-who-is-using-that-data-and-how

Proceedings of the Fourth International Conference on Communication and Electronics Systems (ICCES 2019)
IEEE Conference Record # 45898; IEEE Xplore ISBN: 978-1-7281-1261-9

Autocorrelation based Chordiogram Image Descriptor for Image Retrieval

A.Saravanan
Division of Computer and Information Science
Annamalai University
Annamalai Nagar, India
sarancseau@gmail.com

*S.Sathiamoorthy**
Tamil Virtual Academy
Chennai,
India
ks_sathia@yahoo.com

Abstract—**This paper proposes an autocorrelation based chordiogram image descriptor (ACID) for image searching and retrieval. The standard 4D chordiogram image descriptor is a ordered collection of local edgel chordiogram (LEC) of all the patches of image and it encodes length of the line segment among the pair of edgels, orientation of each edgel and degree of angle among the line segment and horizontal plane for every pair of predominant edgels in a patch whereas proposed approach uses autocorrelation for computing the LEC and it exploits the spatial correlation and above mentioned features of standard LEC among the identical pair of edgels at distance d. The novelty of proposed CID is, it captures localized texture, spatial details besides to the geometric details offered by the standard CID except length of the line segment which is 1 in the proposed approach. The proposed ACID leads to better retrieval with resilient to illumination, scaling, translation, noise and small rotation. In our proposed approach, geometric details also more localized one. The experiments have been done for demonstrating the worth of proposed ACID on four different types datasets: (i). Gardens Point Walking, (ii) St. Lucia, (iii) UA Campus, (iv) Self photographed image. The results confirm the supremacy of proposed ACID approach by means of average retrieval precision and average retrieval rate over the state-of-the-art approaches**.

Keywords— Chordiogram image descriptor, Local edgel histogram,.Autocorrelation, Illumination, Orientation, Edgels.

I. INTRODUCTION

Shape information plays an imperative role in the computer vision and pattern recognition. Quality of image is stoutly coupled with the quality of shape. An outstanding shape descriptor must exhibit resilient to illumination, scaling, translation, rotation, appearance and noise [1]. Recently, various shape descriptors based on statistical, geometrical and topological approaches are reported. From the perspective of shape, there are 2 classes of shape descriptors: region and contour based approaches [2]. First one exploited the information of pixels within the shape. On the contrary, second one exploited the details from the edge pixels or contour. Since contour based approaches are very simple to process and can be viewed as long and regular structures instead of discontinuities [3] and is a significant component in object identification and image segmentation, lots of contour based approaches have been reported including distance among the random pair of pixels on contour [4], angle and length ratios among centroid and edge pixels [5]. The similarity among two shapes is computed using the shape context descriptor which is attached to each pixel and it exploits the histogram of residual pixels relative to it and results in global discriminative characterization then the similarity among two shapes is calculated using the differences in the sum of shape context among the corresponding pixels in two shapes [6].

The Border/interior pixel classification descriptor (BIC) considers both contour and region details and is reported by Stehling et al., [7]. In BIC, two different histograms are utilized for characterization and it counts the location and intensity of border/interior pixels. Color edge co-occurrence histogram is reported Jiebo et al., [8] and it computes distribution of separation between pairs of color edges. Histogram based on edge distribution at local level is suggested in [9] for retrieval using Sobel operator. But, due to its unsatisfactory retrieval results, [10] suggested an approach using the absolute location of edge and its global composition to improve the retrieval rate. Shim and Choi [11] proposed a method based on the color distribution of directional and non-directional edges and is combined with color histogram for image matching. A histogram of directions of keypoints is used in SIFT [12] and SURF [13], and are resilient to uniform scaling and illumination and partially resilient to affine distortion. Similar to SIFT, SURF and edge orientation histogram, the histograms (distribution) of directions (orientations) of gradients is reported in [14] and named as histogram of orientation gradients (HOG). Inspired by the discrimination power of HOG, HOG is represented in the form of pyramid in [15] for efficient computation and co-occurrence of HOG is presented in [16].

Based on the facts of series of edgels in the image and the dependencies among the edgels exhibit autocorrelation that characterizes texture in an image [17, 18], our contributions is autocorrelation based shape descriptor, is used for characterizing the repeating patterns in edgels over

consecutive non-overlapping regions of an image based on the correlation among identical edgels. In computer vision and pattern recognition, autocorrelation have been incorporated for more than a decade, but, only few works have been reported for contour based shape descriptors including edge orientation co-occurennce matrix [19] that exploits the spatial correlation for texture orientation which is extracted from the directional variation in the intensity; the correlation between neighboring edgels in accordance with the orientations is reported in [20] and coined a term Edge orientation autocorrelogram (EOAC) and it dig out rich shape, textures and spatial details in an image and the author proved that EOAC is appreciably better than edge histogram descriptor (EHD) [9, 21], and resilient to illumination, viewing position, translation and minute rotation. Along the way, Seetharaman and Sathiamoorthy advances EHD and EOAC [17, 18, 21] for both gray-scale and color images using Full Range Autoregressive (FRAR) model with Bayesian Approach which extracts incredibly minute and fine edgels and is confirmed that their edge based approaches significantly excellent than the conventional EHD [9] and EOAC [20] and the proposed approaches are also resilient to noise to some degree. In general, all edge detectors reported in the literature including Canny, Sobel, Roert, Laplacian and Prewitt are producing the output in gray-scale. Even for color images also, edge detectors change the image into gray-scale for identifying the edges [18, 21]. Thus, according to [17, 18, 21, 22], conventional edge detectors not succeed in identifying incredibly minute and fine edgels in color images owing to the variation in spectral and chromatic details. Moreover, [22] described that computing the edgels from H or S or V space alone also not succeed in computing incredibly minute and fine edgels owing to the variation in spectral and chromatic details and such a loss influences the accuracy of retrieval [22].

Though color edges are providing supplement details to content based image retrieval (CBIR), in this work, we are paying attention towards retrieval system for place recognition with illumination invariant based on edgels. In connection to this, several new approaches have been recommended in the past including chordiogram image descriptor (CID) based on the boundary pixels computed from the segmentation process [23], MROGH [24], LBP [25], BRIEF [26, 27] and CENTRIST [28], using deep descriptors in convolutional neural networks [29, 30]. Recently, CID [31] is presented by Wang et al., which is an accumulation of distribution of chord information of sub-images. That is the authors [31] divide the image into numbers of non-overlapping patches to decrease the influence of lightning. Since CID is robust to edge detector [31], the authors used one of the aforementioned edge detectors [31] to identify the edgels. Later on, for every pair of predominant edgels in each patch image, the distance among the edgels, orientations of each edgel and degree of angle between a line segment among pair edgels and horizontal axis is computed for every patch and the collection of aforesaid geometric details are called as local edgel chordiogram (LEC) [31]. The ordered collection of LECs of all patch images is called as CID. Though CID is well against illumination, translaton, in-plane rotation and scaling, it is significantly affected by the noise. Thus, the patches with noise are eliminated during the matching operation in [31] by avoiding the larger similarity results between the corresponding patches of query and target images.

The authors reported that the CID exploits the spatial structure from the image, independent of intensity and color details [32], well defined by local geometric elements, and thus it is an apt approach for place recognition with resilient to illumination. Accordingly, we are paying attention only in increasing the efficiency of shape descriptor called chordiogram image descriptor (CID) which is reported for appearance-based place recognition robust to illumination variant [31]. Since the autocorrelation assess the texture present in an image [17, 18] as aforementioned, the proposed chordiogram image descriptor is computed using autocorrelation function and it exploits the following

1. Spaial correlation among the edgels and find out the change of its correlation with distance d.
2. Orientation of edgels
3. Degree among line segment between a pair of edgels and horizontal axis

The experiments on standard dataset using the proposed four dimensional CID has better discrimination power then the state-of-art schemes based on edges.

The organization of paper is as follows. Section 2 discuss about chordiogram image descriptor. Sections 3 describe the CID based on autocorrelation function. Section 4 and Section 5 deal with experimental results and conclusion respectively.

II. CHORDIOGRAM IMAGE DESCRIPTOR

Given image is divided into number of non-overlapping rectangular patches, numbered from 1, 2, 3, . . . , N. Each patch is characterized using LEC. To compute LEC, salient edgels are identified for each patch then local geometric features are computed from the salient edgels. Later, the LECs of all patches are collected in an order to construct a CID. The chord details of an image patch are computed from each pair of salient edgels coordinated at p and q and is described as in [31] as follows

$$C_{i_{pq}} = (\ell_{pq}, \phi_{pq}, \theta_p, \theta_q) \quad (1)$$

Where $\ell_{pq}, \phi_{pq}, \theta_p$ and θ_q designates the distance among edgels p and q, angle between line and horizontal plane, degree of orientations of edgels p and q about normal directions respectively, and the values of ℓ_{pq} ranges from 0 to diameter of an image patch and ϕ_{pq}, θ_p and θ_q falls in range 0 and 2Π. The values of ℓ_{pq} is discretized in logarithmic space and are divided into η_d bins where d is the distance and is fix to 4 [31]. ϕ_{pq}, θ_p and θ_q are quantized into 8 bins of 50 degrees each [31]. Thus, CID is a 4D histogram and is normalized as in [31], and it encompasses chord details for every pair of salient edges in an image patch.

Since CID is not sensitive to edge detector, in the experiment, Sobel operator is incorporated to calculate the edges in each patch. After computing the edgels, response of each edgels are computed and are sorted. Then, proportion p of edgels having higher responses are chosen as in [31] to compute the LEC i.e. the salient edgels are chosen from the image patch with the intention of reducing the computation cost by means of considering the less numbers of salient edgels and the selected salient edgels must exploits the shape details of patch and it must provide robustness against illumination and small rotation. Thus, the set of chosen salient edgels has two information: one is response of edgels and another is proportion p which decide the dimension of set of salient edgels and is decided experimentally as in [31] using n=pm where m and n denotes number of edgels and chosen salient edgels respectively in image patch and p is constant for all patches. Finally, the computed LECs of all patches are collected in an order to form CID and is described as [31]

$$F = (C_1, C_2, ..., C_N) \tag{2}$$

Where $C_1, C_2, ..., C_N$ are the LEC of patches 1, 2, ..., N respectively.

III. AUTOCORRELATION BASED CID

This paper presented a novel characterization approach for an image using autocorrelation based CID, is just a step forward approach of [31]. The main objective is computing spatial correlation among the identified identical edgels and exploring the variation of its correlation with distance d then for each pair of the edgels at the centre of the sub-image and its identical edgels at distance d, we also compute the orientation of each edgel and degree of angle among line segment and horizontal plane for every pair of edgels in a sub-image of size 3x3 in a patch. The proposed approach recommends that the ACID has convinced discrimination power.

The identified edgels are depicted in a table and is indexed by value of *edgel* and distance. The entry in a table designate the probabilities of finding an edgel with value i at a correlation distance *d* from an edgel with value i. That is the proposed ACID considers spatial correlation among the identical edgels only and it fixes the correlation distance to 1 owing to least correlation distance offers the in depth local properties of an image. Table 1 depicts the proposed spatial correlation among identical edgels at distance 1 where the first and second columns depicts the edgel with value i and probability of finding an edgel with value i at correlation distance 1 from an edgel with value i. The autocorrelation among identical edgels are described as in [33] for as follows

Let *I* be an n x n image, an edgels in *I* are $e_1, e_2, ..., e_m$. For an edgel $E = (x, y) \in I$, let $I(E)$ represent its edge value. Let $I_e \overset{\Delta}{=} \{E | I(E) = e\}$. Hence, the notation $E \in I_e$ is synonymous with $E \in I, I(E) = e$. For convenience, [33] use the L_∞ norm to assess the distance among edgels that is for edgels $E_1 = (x_1, y_1), E_2 = (x_2, y_2)$, [33] define $|E_1 - E_2| \overset{\Delta}{=} \max\{|x_1 - x_2|, |y_1 - y_2|\}$. [33] denote the set $\{1,2,..., n\}$ by $|n|$.

Definitions. The histogram *h* of *I* is expressed for $i \in |m|$ by

$$h_{e_i}(I) \overset{\Delta}{=} n^2 \Pr_{E \in I} \left| E \in I_{e_i} \right| \tag{3}$$

For any edgel in the image, $h_{e_i}(I) \big/ n^2$ gives the probability that value of edgel is e_i.

Let a distance $d \in |n|$ be fixed a priori. Then, correlation of *I* is expressed for $i, j \in |m|, k \in |d|$ as

$$\gamma_{e_i, e_j}^{(k)} \overset{\Delta}{=} \Pr_{E_1 \in I_{e_i}, E_2 \in I} [E_2 \in I_{e_j} \ \| E_1 - E_2 | = k] \tag{4}$$

Given any edgel of value e_i in the image, $\gamma_{e_i, e_j}^{(k)}(I)$ gives the probability that an edgel at distance *k* away from the given edgel is of value e_j. The autocorrelation of *I* exploits spatial correlation among identical edgels only, and defined as in [33] by

$$\alpha_c^{(k)} \overset{\Delta}{=} \gamma_{e,e}^{(k)}(I) \tag{5}$$

In our work, the image is divided into numbers of patches and in each patch, to estimate the proposed ACID, we moved the 3x3 non-overlapping mask over an image from left to right afterwards from the topmost left corner of image for each identified edgel values. For instance, in Fig.1, when we move the 3x3 mask over an image for computing the autocorreltion value of an edgel with value 255, we found an identical edgel at the center of the first 3x3 sub-image and it has two identical edgels at distance 1. Thus, we estimate the probability as mentioned above in eq.(5) and we estimate the orientation of each edgel [17] in each pair of edgels and say θ_1 and θ_2 and the degree of angle of line segment between the each pair of edgel and horizontal axis is computed and say ϕ and is depicted in Fig.1(b). Now the 3x3 mask is moved in left direction and there is no edgel with the value 255 at the centre of the mask. Thus, the mask is moved further, in the 3rd 3x3 sub-image also there is no centre edgel with the value 255 but in the 4th one there is an edgel in the centre of sub-image with the value 255 and it has one identical edgel at distance 1. Therefore, for the 4th sub image we estimate the autocorrelation among the identical edgels as mentioned above in eq.(5) and the θ_1, θ_2 and ϕ are computed. This process continues for each identified edgel values in the patch. Finally, we obtained an autocorrelation of edgels as mentioned in Table. 1. and a set of θ_1, θ_2 and ϕ values and these values are represented using separate histograms and called as LEC. Similarly, the LEC for all the patches in an image is computed and the LEC of all the patches are collected in an order to

form a ACID. Thus, the proposed ACID approach is a 4D histogram.

TABLE. 1. The representation of proposed autocorrelation of edgels at d=1

Distance (d) / Edgel Value	d=1
255	0.019
254	0.075
253	0.102
.	.
.	.
.	.
.	.

228	218	0	0	0	0
0	255	196	189	0	0
0	255	255	198	202	0
0	0	225	190	168	255
0	225	184	0	255	206
0	244	0	162	192	188

Fig.1(a) Sample image of size 6 x 6

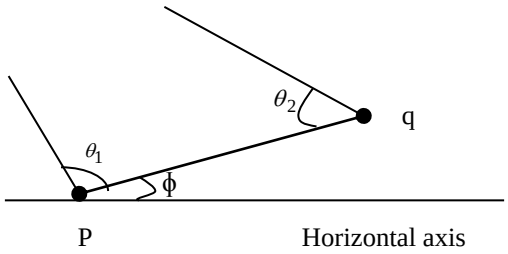

Fig.1(b). Computation of orientation of edgels p, q and angle between the horizontal axis and line segment of edgels p and q

As a result, we trust that proposed ACID is significantly superior in retrieval rate and considerably equivalent in computational cost to the CID approach [31] owing to the texture and spatial details exploited by autocorrelation function in addition to more localized geometric features among identical edgels. In the ACID approach, the 4D histogram is normalized to attain lighting variations to some more extent [31].

IV. EXPERIMENTAL RESULTS AND DISCUSSION

A. Datasets

In the experimental study, Gardens Point Walking [34], UA Campus [31], St. Lucia [31] databases and some self photographed images are incorporated. Few example images from the benchmark databases is shown in Fig.3. The Gardens Point Walking database contains of 3 classes of images namely day-left, day_right and night_right and each class consists of 200 images and are captured twice in day i.e., in a day and night and the dimension of the images are roughly 960 X 540. St. Lucia database contains images captured at five different times among early morning and late afternoon of a day and a day after two weeks and totally it has ten classes. We also utilized some self photographed images shooted at different time of a day in the experiments and it has 1140 images totally and size of images are roughly 1280 x 720 and 1040 x780. All the databases contains images captured at various times with sever and mild illumination changes.

B. Similarity Measuremnt

The dissimilarity among query and target image descriptors are evaluated by the dissimilarity measure derived from Pearson's correlation coefficient and is illustrated in [35] as

$$D(I,O) = 1 - |P| \tag{6}$$

where

$$|P| = \frac{n\sum_{i=1}^{n} I_i O_i - \left(\sum_{i=1}^{n} I_i\right)\left(\sum_{i=1}^{n} O_i\right)}{\sqrt{\left[n\sum_{i=1}^{n} I_i^2 - \left(\sum_{i=1}^{n} I_i\right)^2\right]\left[n\sum_{i=1}^{n} O_i^2 - \left(\sum_{i=1}^{n} O_i\right)^2\right]}} \tag{7}$$

where I_i designates query image descriptor vector, O_i is a target image descriptor vector and n designates the dimension of the descriptor vector. Higher |P| value represent query and target images are highly correlated.

In the proposed methodology, according to [31], dissimilarity measure between all corresponding patches in an image are computed and are ordered in descending manner and from the ordered distance values, higher distance values are removed with the assumption that either of those patches or both are affected by noise and it provides false matching [31]. Therefore, the sums of n least similarities are summed finally to find the best matching among query and target images.

C. Evaluation measures

The evaluation of proposed ACID is calculated in terms of precision, average retrieval precision (ARP), recall and average retrieval rate (ARR) [36]. For query image I_q, the precision ($P(I_q)$) and recall ($R(I_q)$) are described as follows:

$$Precision: P(I_q) = \frac{\text{Number of relevant images retrieved}}{\text{Total number of images retrieved}} \quad (8)$$

$$Recall: R(I_q) = \frac{\text{Number of relevant images retrieved}}{\text{Total number of relevant images in the database}} \quad (9)$$

$$ARP = \frac{1}{|DB|} \sum_{i=1}^{|DB|} P(I_i) \;\; |n \le 10 \quad (10)$$

$$ARR = \frac{1}{|DB|} \sum_{i=1}^{|DB|} R(I_i) \;\; |n \ge 10 \quad (11)$$

Where DB denotes total number of images in each class.

Fig.2.Few example images of experimental databases

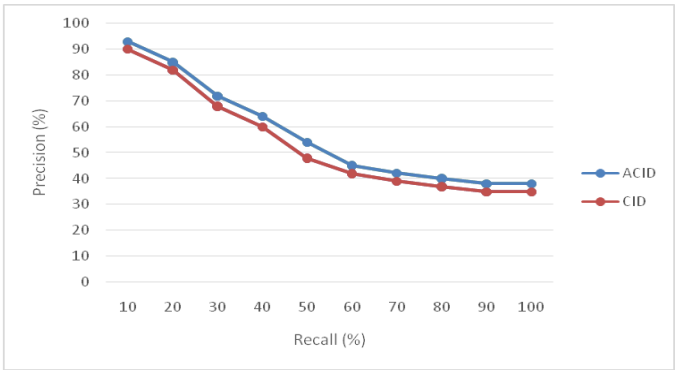

(a)

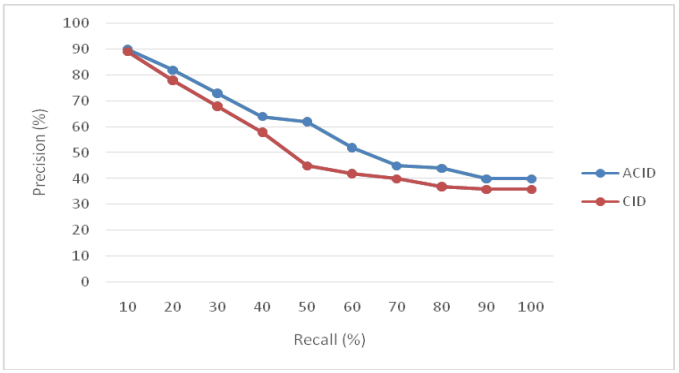

(b)

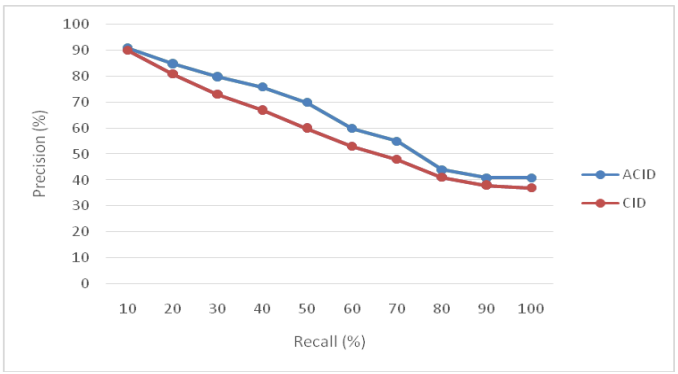

(c)

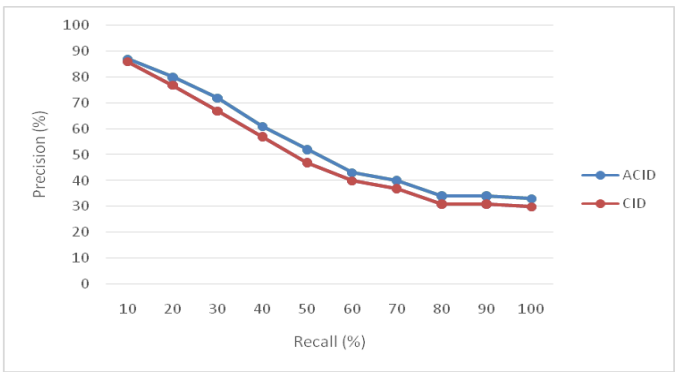

(d)

Fig.3.Precision Vs. Recall for the proposed ACID and the existing CID approaches for (a) Gardens Point Walking (b) UA Campus (c) St. Lucia (d) Self photographed image Datasets

D. Results and Discussion

The efficiency of suggested ACID is analyzed for image retrieval that robust to place recognition and illumination invariant by carrying out experiments on four databases. The results attained by the proposed ACID are examined as follows.

Each image in the benchmark database is selected as query image in all experiments. The proposed approach collects n target images $T=(T_1,T_2,...,T_n)$ from the database for each query utilizing the fusion of ACID and Pearson's correlation coefficient measure.

Table. 2 summarizes the time cost of ACID and CID approaches. Experiments are done on the images collected from the Gardens Point Walking database. The efficiency of the suggested ACID approach is estimated in terms of ARP and ARR is depicted in Fig.3 and Table 3. Fig.3 depicts the retrieval performance for top 100 matches of proposed ACID and CID by passing different query images from the Gardens Point Walking database. Table 3 summarize the performance proposed ACID in terms ARR. From Table 3 it is observed that ACID attains better performance over the CID approach.

Fig.3b and Table.3 illustrates the efficiency of suggested ACID approach and CID in terms of ARP and ARR on UA campus database. From Table.3 and Fig.3b, it is observed that proposed ACID showing better performance than the CID on UA campus database. Fig.3c shows the graphs depicting the efficiency of suggested ACID and CID in terms of ARP and APR on St.Lucia database. From Table.3 and Fig.3c, it is evident that proposed ACID outperforms the CID on St.Lucia database for image retrieval.

Finally, self photographed images are taken for evaluation of performance. The results of proposed ACID and CID in terms of ARP and ARR are depicted in Fig.3d and Table 3. Although the time cost of proposed ACID is slightly higher than CID owing to the computation of autocorrelation, it attains better retrieval performance due to the inclusion of textural and spatial details along with the geometric details and also more robust to place recognition, illumination, scaling, translation and small rotation.

The visual results of ACID descriptor for query image with top 5 matches in ascending order of distance among query and target images is illustrated in Fig 4 and Fig.5. From Fig.4 and Fig.5, it is visibly obvious that proposed ACID is illumination to invariant and for query image of day right class, the proposed ACID also retrieve images from the day left and night right. The experiments are done on core2 Quad computer with 2.66 GHz, 4GB of memory.

Table 2. Computational complexity of ACID and CID

Methods	Time in seconds
ACID	56
CID	45

Table 3. Precision. and Recall for proposed ACID and CID

.Datasets	**Performance**	**CID**	**ACID**
Gardens Point Walking	Precision (%)	57.78	60.21
	Recall (%)	8.25	7.41
UA Campus	Precision (%)	58.41	61.23
	Recall (%)	8.00	7.34
St. Lucia	Precision (%)	56.91	59.46
	Recall (%)	8.42	7.99
Self Photographed Images	Precision (%)	59.11	62.90
	Recall (%)	7.68	6.90

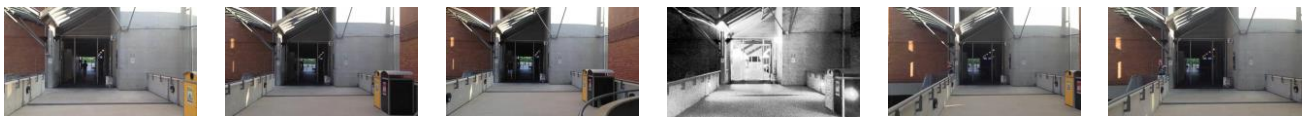

(a) (b) (c) (d) (e) (f)

Fig.4 (a). An example query image (b)-(f). Top 5 retrieval results for using proposed ACID

(a) (b) (c) (d) (e) (f)

Fig.5. (a). An example query image (b)-(f). Top 5 retrieval results for using proposed ACID

V. CONCLUSION

In this paper, a new descriptor named autocorrelation based chordiogram descriptor (ACID) is suggested for place recognition and illumination invariant images. The ACID calculates the spatial and textural details along with geometric details based on the autocorrelation function. The effectiveness and robustness of proposed ACID is tested by considering the results on 4 benchmark databases. The detailed examination of the results demonstrated a significant increase of proposed ACID in terms of ARP and ARR as compared to CID. In future experiments, the proposed ACID can be improved in terms of time cost.

References

[1] Zhang, D., Lu, G., 2004, Review of shape representation and description, *Pattern Recognition*. 37(1): 1-19..

[2] K. Seetharaman and S. Sathiamoorthy, "An improved edge direction histogram and edge orientation auto corrlogram for an efficient color image retrieval," *2013 International Conference on Advanced Computing and Communication Systems*, Coimbatore, 2013, pp. 1-4.

[3] Eric Van Reeth, Pascal Bertolino, Marina Nicolas, Jean-Marc Chassery. Adaptive edge orientation analysis. IS T/SPIE Electronic Imaging, Jan 2010, San Jose, United States. pp.CD. ffhal-00448948f.

[4] R. Osada, T. Funkhouser, B. Chazelle, D. Dobkin, Shape distributions, ACM Trans. Graph. 21 (2002) 807–832.

[5] J. Zhang, L. Wenyin, A pixel-level statistical structural descriptor for shape measure and recognition, Proceedings of the 10th International Conference on Document Analysis and Recognition, 2009, pp. 386–390.

[6] S. Belongie, J. Malik and J. Puzicha, "Shape matching and object recognition using shape contexts," in *IEEE Transactions on Pattern Analysis and Machine Intelligence*, vol. 24, no. 4, pp. 509-522, 2002.

[7] Stehling, R. de O., Nascimento, M.A., Falcão, A.X., 2002. A compact and efficient image retrieval approach based on border/interior pixel classification, in: *International Conference on Information and Knowledge Management*, pp. 102–109.

[8] Jiebo Luo and D. Crandall, "Color object detection using spatial-color joint probability functions," in *IEEE Transactions on Image Processing*, vol. 15, no. 6, pp. 1443-1453, June 2006.

[9] Cieplinski, L., Kim, M., Ohm, J.-R., Pickering, M., Yamada, A. (Editors), 2001. Text of ISO/IEC 15938-3/FCD Information Technology -Multimedia Content Description Interface-Part 3: Visual. Final Committee Draft, ISO/IEC/JTC1/SC29/WG11 (MPEG), document no. N4062.

[10] Chee Sun Won, Dong Kwon Park , Soo-Jun Park, Efficient Use of MPEG-7 Edge Histogram Descriptor, 2002, https://doi.org/10.4218/etrij.02.0102.0103.

[11] Seong-O Shim and Tae-Sun Choi, "Edge color histogram for image retrieval," *Proceedings. International Conference on Image Processing*, Rochester, NY, USA, 2002, pp. 957-960 vol.3. doi: 10.1109/ICIP.2002.1039133.

[12] Lowe, D.G., (2004). Distinctive image features from scale-invariant keypoints, *Int. J. of Comp. Vis*. 60 (2): 91–110.

[13] Ali N, Bajwa KB, Sablatnig R, Chatzichristofis SA, Iqbal Z, Rashid M, et al., (2016). A novel image retrieval based on visual words integration of SIFT and SURF. PLoS ONE 11(6):e0157428.

[14] Navneet Dalal, Bill Triggs. Histograms of Oriented Gradients for Human Detection. International Conference on Computer Vision Pattern Recognition (CVPR '05), Jun 2005, San Diego, United States. pp.886–893, ff10.1109/CVPR.2005.177ff. ffinria-00548512.

[15] V. Chandrasekhar, G. Takacs, D. Chen, S. Tsai, R. Grzeszczuk and B. Girod, "CHoG: Compressed histogram of gradients A low bit-rate feature descriptor," *2009 IEEE Conference on Computer Vision and Pattern Recognition*, Miami, FL, 2009, pp. 2504-2511.

[16] Watanabe T., Ito S., Yokoi K. (2009) Co-occurrence Histograms of Oriented Gradients for Pedestrian Detection. In: Wada T., Huang F., Lin S. (eds) Advances in Image and Video Technology. PSIVT 2009. Lecture Notes in Computer Science, vol 5414. Springer, Berlin, Heidelberg.

[17] Seetharaman. K., Sathiamoorthy. S., 2014. Color image retrieval using statistical model and radial basis function neural network. Egyptian Informatics Journal, 15, 59-68.

[18] K.Seetharaman, S.Sathiamoorthy, A Unified Learning Framework for Content Based Medical Image Retrieval Using a Statistical Model. Journal of King Saud University - Computer and Information Sciences, Vol. 28 (2016), No. 1, Dec 2015, pp. 110-124.

[19] F. Gholipour and H. Ebrahimnezhad, "An efficient content based image retrieval using edge orientation co-occurrence matrix," *2014 6th Conference on Information and Knowledge Technology (IKT)*, Shahrood, 2014, pp. 67-72.

[20] Mahmoudi, F., Shanbehzadeh, J., Eftekhari, A.M., and Soltanian-Zadeh, H, 2003. Image retrieval based on shape similarity by edge orientation autocorrelogram. Pattern Recognition, 36, 1725-1736.

[21] Seetharaman. K., Sathiamoorthy. S., December 2013. An Improved Edge Direction Histogram and Edge Orientation AutoCorrlogram for an Efficient Color Image Retrieval, International Conference on Advanced Computing Communication Systems (ISBN DVD 9781479935055), Coimbatore, India.

[22] Liu G.H., Li, Z.Y., Zhang, L., Xu. Y., 2011. Image retrieval based on micro-structure descriptor. Pattern Reco.. 44(9): 2123-2133.

[23] A. Toshev, B. Taskar, K. Daniilidis, Shape-based object detection via boundary structure segmentation, Int. J. Comput. Vision 99 (2) (2012) 123–146.

[24] B. Fan, F. Wu, Z. Hu, Rotationally invariant descriptors using intensity order pooling, IEEE Trans. Pattern Anal. Mach. Intell. 34 (10) (2012) 2031–2045.

[25] M. Heikkilä,et al., Description of interest regions with local binary patterns, Pattern Reco.. 42 (3) (2009) 425–436.

[26] M. Calonder, V. Lepetit, C. Strecha, P. Fua, Brief: Binary robust independent elementary features, in: European Conference on Computer Vision, Springer, 2010, pp. 778–792.

[27] N. Sünderhauf, P. Protzel, Brief-gist-closing the loop by simple means, in: 2011 IEEE/RSJ International Conference on Intelligent Robots and Systems (IROS), IEEE, 2011, pp. 1234–1241.

[28] J. Wu, J.M. Rehg, Centrist: A visual descriptor for scene categorization, IEEE Trans. Pattern Anal. Mach. Intell. 33 (8) (2011) 1489–1501.

[29] N. Sünderhauf, S. Shirazi, F. Dayoub, B. Upcroft, M. Milford, On the performance of convnet features for place recognition, in: 2015 IEEE/RSJ International Conference on Intelligent Robots and Systems (IROS), IEEE, 2015, pp. 4297–4304.

[30] Y. Hou, H. Zhang, S. Zhou, Convolutional neural network-based image representation for visual loop closure detection, in: 2015 IEEE International Conference on Information and Automation, IEEE, 2015, pp. 2238–2245.

[31] Xiaolong Wang, Hong Zhang, Guohua Peng, A chordiogram image descriptor using local edgels, J. Vis. Commun. Image R, 49 (2017) 129–140.

[32] M. Yang, K. Kpalma, J. Ronsin, A survey of shape feature extraction techniques, Pattern Recogn. (2008) 43–90.

[33] Chun, Y.D., Kim, N.C. and Jang, I.H., 2008. Content-Based Image Retrieval using Multiresolution Color and Texture Features, IEEE Transactions on Multimedia, 10(6):1073-1084.

[34] A. Glover, The gardens point walking dataset, (Feb 14, 2014).

[35] Liu.H., Song.D., Ruger.S., Hu.R., Uren.V, 2008. Comparing dissimilarity measures for content based image retrieval. Proceedings of the 4th Asia information retrieval conference on information retrieval technology (AIRS2008), pp. 44–50.

[36] S. Murala, W.Q. Jonathan, Local ternary co-occurrence patterns: a new feature descriptor for MRI and CT image retrieval, Neurocomputing 119 (7) (2013) 399–412.

Proceedings of the Fourth International Conference on Communication and Electronics Systems (ICCES 2019)
IEEE Conference Record # 45898; IEEE Xplore ISBN: 978-1-7281-1261-9

Multimodal Data Security Framework Using Steganography Approaches

Sarang Parikh [#1], Sanjay H A [#2], K. Aditya Shastry [#3], Amith K K [#4],

[#]Dept. of Information Science and Engineering, Nitte Meenakshi Institute of Technology
Yelahanka, Bangalore, India

[1] sarangparikh22@gmail.com

[2] sanjay.ha@nmit.ac.in

[3] adityashastry.k@nmit.ac.in

[4] amithkumaran@gmail.com

***Abstract*— Information or data is a very crucial resource. Hence securing the information becomes a critical task. Transfer and Communication mediums via which we send this information do not provide data security natively. Therefore, methods for data security have to be devised to protect the information from third party and unauthorized users. Information hiding strategies like steganography provide techniques for data encryption so that the unauthorized users cannot read it. This work is aimed at creating a novel method of Augmented Reality Steganography (ARSteg). ARSteg uses cloud for image and key storage that does not alter any attributes of an image such as size and colour scheme. Unlike, traditional algorithms such as Least Significant Bit (LSB) which changes the attributes of images, our approach uses well established encryption algorithm such as Advanced Encryption Standard (AES) for encryption and decryption. This system is further secured by many alternative means such as honey potting, tracking and heuristic intrusion detection that ensure that the transmitted messages are completely secure and no intrusions are allowed. The intrusions are prevented by detecting them immediately and neutralizing them.**

Keywords*— *Security; Multimodal; Framework; Steganography

I. INTRODUCTION

Steganography represents the mechanism of concealing secret and confidential data inside an image and the user can only decrypt it using a special password or application. Fig. 1 depicts the classical steganography model.

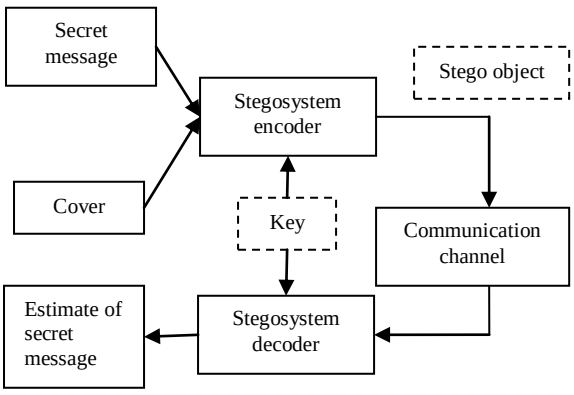

Fig.1. Classical Steganography Model

The problem statement calls for the creation of a steganography model where there is no modification of the target image and an additional authentication layer that is necessary before the secret message is retrieved. Additionally, it must be possible for any sort of data of any arbitrary size to be sent over the channel, including executable, documents and media like images and videos. The data must be actively protected end to end even when it is being transferred over the cloud. We are primarily driven by the lack of solutions to send steganography data attached to some object/image that would require the receiver to have both an image or physical copy of the steganographed image as well as a second point of authentication (the ARSteg app) which would let the user unmask image or document information hidden within the target image. Current solutions to this involve using algorithms like LSB alteration that requires modification of the source image and brings into the picture very miniscule file size limits and issues like loss of data and noise due to in-transit compression of the sent target image. We intend to solve the above issues using Augmented Reality Steganography, which would discard limitations such as file size limit and significantly improve the security implementation. A cloud security module ensures sandboxing of any received executable data, preventing it from causing any harm to the end user device.

The objectives of this works are as follows:

- To transfer encrypted data (text, images, videos, audios,3D Model) mapped to an image marker
- Implementing security mechanism such as pseudo authentication and fingerprint to secure the application from intruders and a backdoor system to self-destruct when app integrity is compromised
- To analyze the received message in a cloud sandbox environment and quarantine the malicious message
- Create a service based on cloud for Vulnerability Assessment and Penetration Testing using active Machine Learning

The devised framework considers a novel idea of steganography, using augmented reality. Unlike classical algorithms of steganography like LSB, ARsteg does not

modify the image size or colour which makes it difficult for the intruder to differentiate it from a normal image.

II. Related Work

This section describes the related works done regarding detectability of steganography methods and augmented reality. We've done a survey on the most popular steganography methods including LSB and found that there was significant literature that exposed its weaknesses, published in several reputed scientific journals.

In [1], the authors have developed a steganalytic method which is based on how pixel differences are distributed statistically. The technique detects the existence of steganography based on LSB matching embedded in natural images of high resolution. Chandramouli et al. [2] have performed detectability of steganography methods applied to text, images, audio/video information in a cover file.

We have also gone over improvements of existing methods by various techniques such as randomization and probability embedding. Karim et al. [3] have devised an innovative method for image steganography centred on LSB. The location of the hidden information is randomized to create the secret key.

Hence, the hidden information can be extracted by possessing knowledge about the retrieval methods. To overcome this challenge, our work stores the hidden information in diverse positions of the image LSB depending on the secret key. Therefore, the extraction of hidden information through the knowledge about the retrieval methods becomes difficult.

The probability of pixel change was reduced to one-third when one-third LSB embedding was performed by [4] without foregoing the embedded capacity, when compared to earlier methods of steganography based on LSB. This embedding resulted in a robust technique when compared with well-known LSB detectors.

III. Design of the Multimodal System

This section discusses the design of the multimodal system for transmission of the encrypted data. Fig.2 shows the transmission of the encrypted data.

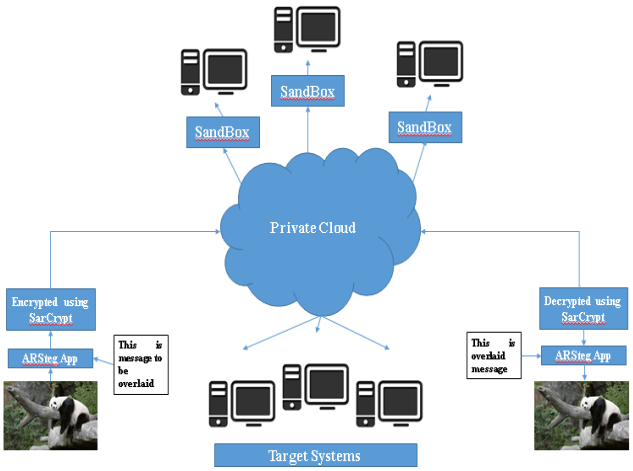

Fig.2. Transmission of encrypted data

The transmission of the Encrypted Data happens over a secure HTTPS channel to the server where the authenticity of the Message is checked using the Secure Hashing Algorithm (SHA256) to check if it valid or not.

Secure transmissions prevent the attacks such as loss of data and ARP spoofing. The information leak detection and prevention (ILP), Information Leak Prevention (ILP), Content Monitoring and Filtering (CMF) or Extrusion Prevention systems represents the hardware and software implementations that identifies and stops the unauthorized data transfer from an organizations computer to outside. These implementations ensure the secure data transmission.

Secure communications for internet related tasks like internet faxing, web browsing, instant messaging, e-mail, and additional data transfers are provided by the Transport Layer Security (TLS) and Secure Sockets Layer (SSL).

Fig.3 depicts the data transmission between sender and receiver.

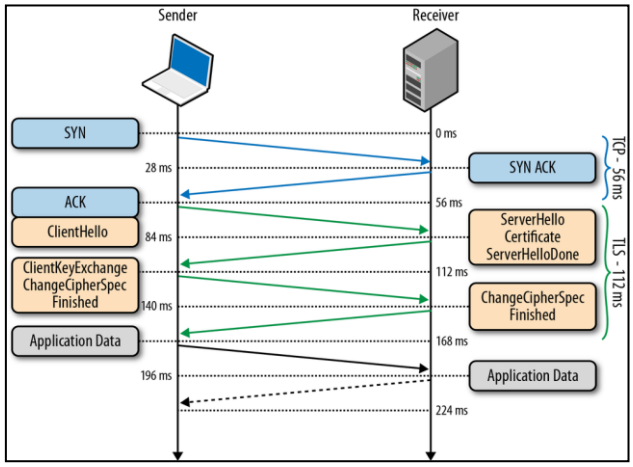

Fig.3. Data transmission between sender and receiver

In Fig.3, initially, the client transmits a Client Hello message to the server. The Client Hello includes the following information.

- **Client version:** The client transmits the different protocol versions of TLS/SSL where the preferred version which is usually the latest version is placed 1st on the list. For instance, TLS 1.2 possesses the client version 3.3 since TLS 1.0 is considered as a miner revision of SSL. Hence TLS 1.0 is 3.1; TLS 1.1 is 3.2 and so on.
- **Client Random:** It represents a random number of size 32 bytes. The key generation for the purpose of encryption is done by the client random and the server random.
- **Session ID:** It denotes the session id that will be utilized for the connection. If session_id is not empty, the server searches for earlier sessions that was cached and continues until that session match is found.
- **Compression methods:** These are utilized to compress the SSL packets. By utilizing compression

techniques we can attain lower bandwidth usage and hence achieve faster transfer speeds.

- **Cipher Suites:** These denote combinations of algorithms related to cryptography. Characteristically, the cipher suite is composed of one cryptographic algorithm related to each of the tasks like key exchange, encryption of bulk data, and authentication of messages. The cipher suites list is transmitted by the client in the order of preference. The connection is established by the client utilizing the first cipher suite sent.
    - Cipher suites are identified by strings. A sample cipher suite string is: TLS_ECDHE_ECDSA_WITH_AES_128_ GCM_SHA256. This string contains the following information:
    - TLS is the protocol being used
    - ECDHE is the key exchange algorithm (Elliptic curve Diffie–Hellman)
    - ECDSA is the authentication algorithm (Elliptic Curve Digital Signature Algorithm)
    - AES_128_GCM is the data encryption algorithm (Advanced Encryption Standard 128 bit Galois/Counter Mode)
    - SHA256 is the Message Authentication Code (MAC) algorithm (Secure Hash Algorithm 256 bit)

Fig.4 illustrates the mechanism of data transfer between the TLS client and the TLS server.

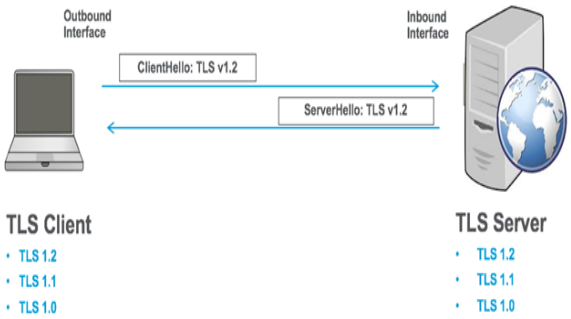

Fig.4. Data transmission between TLS Client and TLS Server

A secure SSL/TLS connection is established through various steps. The grouping of asymmetric and symmetric encryption is utilized by the SSL/TLS security protocols. The server and client negotiate the used algorithms and exchange the information related to key.

The TLS 1.2 connection is utilized with the objective of explaining this complex process. Handshake forms the most significant task of establishing a secure connection. Significant information is exchanged by the server and client during the TLS handshake.

A. Security Framework

With respect to computer security, the term “sandbox” represents a security mechanism for dividing programs which are running to reduce the spread of system failures or vulnerabilities in software. The sandbox is frequently utilized to implement programs which are not tested or trusted. These programs may come from third parties / suppliers / websites / users who are not verified and trusted. This mechanism ensures that the host machine or the operating system is not harmed. The utilities like scratch space on memory and disk is provided by the sandbox in order to ensure that the resources are tightly controlled. The sandbox restricts the network access which allows the inspection of host system or reading from the input devices.

The sandboxes can be perceived as a particular example of virtualization in which it provides an environment which is highly controlled. The sandboxes avoid the harm to host devices by testing unverified programs on virtual environments. Fig.5 depicts the app scenario with and without sandboxing technique.

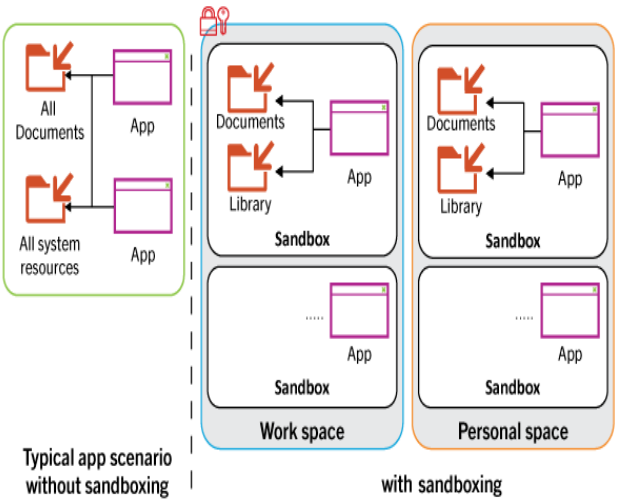

Fig.5. App scenario without sandboxing

The application would function normally without Sandboxing and the message received will be directly sent to Scanning and Identification. This would lead to a major Vulnerability in our system as the message received can be potentially dangerous and can harm the system.

IV. Results

The ARSteg framework consists of two components, the user app and the UMS Dashboard. The User App is our novel implementation of steganography using Augmented Reality scanning. The encryption used is Public-Private Key encryption. The application operates in following modes:

1) Add AR-User first enters the type of data (text, image, video, audio and 3D model) that needs to be sent, following which, user can choose a particular image from gallery or capture it with camera. On click of encrypt button, the image and the

corresponding overlaid information is uploaded on Cloud. The data is stored on the cloud with the sender's information and encrypted with our own algorithm.

2) Scan AR - On the other side, any other authorized user can scan the image using our application and view the hidden message overlaid on it.
3) It has various levels of authentication including generic username and password, finger print, face recognition, and OTP making it difficult to hack into data.
4) It has also a Honey Pot feature known as "Pseudo Authentication". Our database has some common username and password stored that hackers generally test on the login portal. Whenever a hacker uses them he gets into a pseudo application with wrong information. The hacker is fooled into thinking that he is using genuine information and does not think of other ways to hack into the application. Hence, our application becomes more secure.
5) We also have a User Management System that keeps track of the application activity on all the devices which works as an intrusion detection system. If the application gets installed to some unauthorized location (determination using fcm token), it will notify the UMS Admin and he can take control of the device. UMS admin can perform camera capture, location access and storage access, uninstall the application from the particular device and use self-app destruct option.
6) To safeguard the applications from hackers and de-compilation process we use Pseudo Authentication.
    a. Commonly used usernames and passwords will be added in the database and as soon as they match with the user input, the user will be redirected to a fake page with fake details.
    b. This is to engage the hacker from trying out other ways and making him believe he is having the correct data.
    c. Addition Security
    d. We would also have biometric authentication system such as Fingerprint, Face Recognition etc.
    e. Decompilation tested against apktool.

Fig.6 shows the User Login interface where the person who wants to log in can enter his User ID and Password.

Fig.6. Login screen

On entering an incorrect password, a flag is raised on the backend and the malicious actor is unaware that he is now pseudo-authenticated, making sure that brute force attacks are ineffective. Password attempts are limited by a time out. Our database has some common username and password stored that hackers generally test on the login portal.

Fig.7 illustrates the demo mode select screen where the user can either choose to create a new ARSteg message or scan for steganographed images using his phone camera.

Fig.7. AR interaction screen

Here, the user has the option to add a new AR image or scan an existing AR image. In ADD AR option, the user first enters the type of data (text, image, video, audio and 3D model) that needs to be sent, following which, user can choose a particular image from gallery or capture it with camera. On click of encrypt button, the image and the corresponding overlaid information is uploaded on Cloud. The data is stored on the cloud with the sender's information and encrypted with our own algorithm. On the other side, in the scan AR option any other authorized user can scan the image using our application and view the hidden message overlaid on it.

Fig.8 illustrates the process of sending a message.

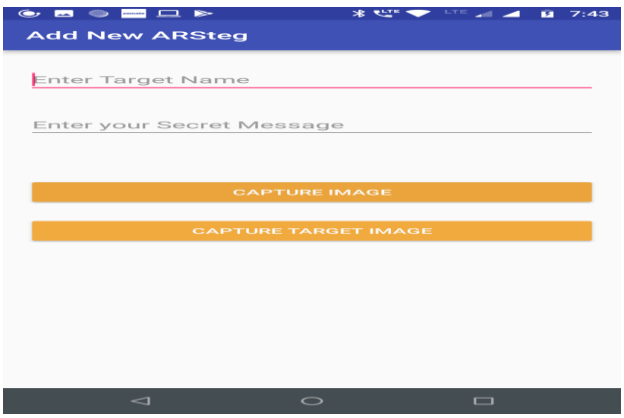

Fig.8. Sending a message

Fig.8 demonstrates the workflow for creating an ARSteg message, by selecting the name of the target, a secret message (metadata), the image/media that has to be embedded into the

steganographed image and finally the actual object/image that the steganography is to be performed on. The secure transmissions are done to stop attacks such as ARP spoofing and general data loss. The TLS and SSL cryptographic protocols are utilized to deliver secure communication over the internet.

Fig.9 shows the steganographed image viewfinder.

Fig.9. Steganographed Image Viewfinder

Fig.9 illustrates the screen used to capture the image/object that the steganography will be performed on. This is a viewfinder for the user's device camera.

Fig.10 demonstrates the metadata view for non-image data.

Fig.10 Metadata view for non-image data

Fig.10 illustrates a steganographed image / object being decoded and the metadata in addition to the associated encoded media being demonstrated on the user's viewfinder. Here, we send a JSON Object which has the following structure:

- "content-type": *"Image"/"text"/" video"/"3d"/" executable",*
- "data": "*Encrypted Data*",
- "signature": "*Signed Data Signature*"
- "hash": "*Hash of the data*"
- "sender": "*Public Key of the sender*"

The outcomes of the work are summarized below:

- We have managed to create a full stack solution backed by Vuforia [5] and Unity [7] to perform AR-Steganography
- App was bundled with remote self-destruct and tracking functionality.
- ML powered heuristics detection was used to find malicious activity and flag it.
- Pseudo Authentication used to deter potential malicious actors by honeypotting them into a false user account
- Backend with UMS (User Management System) allowing us to monitor and trigger events on the user apps as mentioned above
- Inbox functionality for temporarily storing received steganographed images
- Data received analyzed in a sandbox environment and checked for malicious intent
- All the network systems will be scanned for vulnerabilities based upon Open Ports, OS Information, Update patches etc.
- The entire service will be running on a Cloud Architecture [8].
- The network data can also be sent to the cloud server for detection for anomaly in the real time.
- This would highly reduce the false positive occurred during the scan.

We have contrasted and compared existing Augmented Reality platforms to determine a suitable framework for building our application. Our work was compared with the existing works by Santos et al. [5] and Zhang et al. [6]. These works have modified the source image and are constrained by file size limits. In our work, these drawbacks were successfully overcome by using the Augmented Reality Steganography. Furthermore, the harm to the end user device is avoided in our work by the usage of cloud security module with sandboxing technique.

V. Conclusion And Future Work

In this work, we have created a full stack solution backed by Vuforia and Unity to perform AR-Steganography. The App was bundled with remote self-destruct and tracking functionality. The ML powered heuristics detection was used to find malicious activity and flag it. Pseudo Authentication was used to deter potential malicious actors by honey-potting them into a false user account. The Backend with UMS (User Management System) allowed us to monitor and trigger events on the user apps as mentioned above. Inbox functionality for temporarily storing received steganographed images. The received data was analyzed in a sandbox environment and checked for malicious intent. All the network systems were scanned for vulnerabilities based upon Open Ports, OS Information, Update patches etc. The entire service was run on a Cloud Architecture. The network data can also be sent to the cloud server for detection for anomaly in the real time. This would highly reduce the false positive occurred during the scan.

We have hence created a robust system for securely transferring text, images, audio/video, executable data over a steganography image with support for a layer of authentication. A robust cloud sandbox and heuristic detection mechanism coupled with a UMS was developed to counter any intrusions into the system.

Future Prospects include the development of an active machine learning algorithm to detect and deal with threats posed by executable files sent over this system & Self-training of this model by automatically executing threat vectors on this system.

ACKNOWLEDGMENT

We are thankful to the Ministry of Human Resource Development (MHRD) for organising Smart India Hackathon 2018, which allowed us to showcase the potential of this product and to the Indian Space Research Organisation (ISRO) for sponsoring the work, taking this idea forward, guiding us throughout our work, and helping us to constantly improve our product.

We further thank the All India Council for Technical Education (AICTE) for enabling this sort of interaction between the institution and government organisations in order to create innovative products.

We are thankful to C Chandrasekhar Reddy for helping us and guiding us throughout the Project Timeline.

REFERENCES

[1] Tao Zhang, Wenxiang Li, Yan Zhang and Xijian Ping, "Detection of LSB matching steganography based on distribution of pixel differences in natural images," *2010 International Conference on Image Analysis and Signal Processing*, Zhejiang, 2010, pp. 548-552.doi: 10.1109/IASP.2010.5476056.

[2] R. Chandramouli and N. Memon, "Analysis of LSB based image steganography techniques," *Proceedings 2001 International Conference on Image Processing (Cat. No.01CH37205)*, Thessaloniki, Greece, 2001, pp. 1019-1022 vol.3. doi: 10.1109/ICIP.2001.958299.

[3] S. M. Masud Karim, M. S. Rahman and M. I. Hossain, "A new approach for LSB based image steganography using secret key," *14th International Conference on Computer and Information Technology* (ICCIT 2011), Dhaka, 2011, pp. 286-291. doi: 10.1109/ICCITechn.2011.6164800.

[4] S. Sarreshtedari, M. Ghotbi and S. Ghaemmaghami, "One-third probability embedding: Less detectable LSB steganography," *2009 IEEE International Conference on Multimedia and Expo*, New York, NY, 2009, pp. 1002-1005. doi: 10.1109/ICME.2009.5202666.

[5] AA. B. Dos Santos, J. B. Dourado and A. Bezerra, "ARToolkit and Qualcomm Vuforia: An Analytical Collation," *2016 XVIII Symposium on Virtual and Augmented Reality (SVR)*, Gramado, 2016, pp. 229-233. doi: 10.1109/SVR.2016.46

[6] Q. Zhang, W. Chu, C. Ji, C. Ke and Y. Li, "An implementation of generic augmented reality in mobile devices," *2014 IEEE 7th Joint International Information Technology and Artificial Intelligence Conference*, Chongqing, 2014, pp. 555-558. doi: 10.1109/ITAIC.2014.7065112

[7] Unity 3D development: https://unity.com/

[8] Amazon AWS: https://aws.amazon.com/

[9] H. Cao and K. C. Chang, "Nonintrusive Smartphone User Verification Using Anonymized Multimodal Data," *IEEE Transactions on Knowledge and Data Engineering*, vol. 31, no. 3, pp. 479-492, 1 March 2019. doi: 10.1109/TKDE.2018.2828309

[10] Mikhail I. Gofman, Sinjini Mitra, Tsu-Hsiang Kevin Cheng, Nicholas T, "Multimodal Biometrics For Enhanced Mobile Device Security", *Smith Communications of the ACM*, April 2016, Vol. 59 No. 4, Pages 58-65 10.1145/2818990.

[11] Shanthini B., Swamynathan S. (2011) A Secure Authentication System Using Multimodal Biometrics for High Security MANETs. In: Wyld D.C., Wozniak M., Chaki N., Meghanathan N., Nagamalai D. (eds) *Advances in Computing and Information Technology*, *ACITY* 2011. Communications in Computer and Information Science, vol 198. Springer, Berlin, Heidelberg

[12] Sui, Peipei & Li, Xianxian. (2017). A Privacy-preserving Approach for Multimodal Transaction Data Integrated Analysis. *Neurocomputing*. 253. 10.1016/j.neucom.2016.09.130.

Proceedings of the Fourth International Conference on Communication and Electronics Systems (ICCES 2019)
IEEE Conference Record # 45898; IEEE Xplore ISBN: 978-1-7281-1261-9

Investigations on Steel as Low Cost Substrate for Low Frequency Patch Antenna

Lakshmi K K[1], Sabarish Narayanan B[2]
Department of Electronics and Communication Engineering
Amrita School of Engineering, Coimbatore
Amrita Vishwa Vidyapeetham, India
Email: lakshmivylala@gmail.com[1], nb_sabarish@cb.amrita.edu[2]

***Abstract*— Industry uses different types of materials as microstrip substrates. This paper introduces steel, and thus explores its scope as a microstrip substrate. Its metallic nature creates a barrier, from using it as substrate. A low cost rectangular microstrip patch antenna using a multilayer substrate is proposed here. Martensitic steel of grade 440C and thermocol forms a layered substrate. The magnetic properties of steel and dielectric properties of thermocol helps for achieving good antenna parameters. Designed patch antenna has noticeable return loss of -24dB in 400MHz. Also directional radiation pattern with gain of 0.3dB has been obtained. It shows a narrow bandwidth of 3MHz which is due to the conductivity of steel. VSWR obtained is 1.13 which shows a tremendous matching with transmission line connected to it. The results shows that, newly introduced multilayer material can be used as microstrip substrate for low frequency structures. It can produce almost the same results, which a local substrate can. It can be used for wireless charging using low frequency and thus an application of RF energy harvesting.**

***Keywords*—Microstrip substrates, Martensitic steel, Thermocol, Patch antenna, wireless charging, RF energy harvesting**

I. INTRODUCTION

Rate of use of electronic devices like mobile phones, Wi-Fi modems, laptops etc are increasing year by year. By that, chances of harvesting radio frequency energies are becoming dominant. The harvested energy can be best used for wireless charging, and it provides a new dimension to mobile device manufacturing. Wireless charging method can be helpful in different situations. An electromagnetic harvester is implemented in South Korea, which can be used as a power requirement for ice removing device. These type of devices are used to remove ice and snow from power transmission lines[1]. Antennas are the main part of any Radio Frequency(RF) harvesting systems. The proper designing of antennas helps to build an efficient harvesting systems. Microstrip antennas are most common in RF circuits industry because of its countless advantages including low-profile, low-weight, and conformablity[2]. Microstrip antennas having a good bandwidth, better matching, and minimum reflection loss, acceptable radiation intensity, along with compact size can serve a good role in communication systems.

Materials used as substrates are predominantly dielectrics. Substrate properties heavily influence antenna parameters. Research on developing novel materials for substrates are going on. The applications is inherent to development of low profile communication systems for next generation technologies. Metamaterials are certain type, in which both ϵ_r and μ_r values are negative. They are used to build antenna arrays that helps for hyperthermia treatments[3]. Patch antennas with substrate as paper, coir, rubber are the outcomes of such experiments. These environmental friendly antennas can produce better results compared to GaAs antennas. This is one of the material which is available locally, and studies shows that it creates some environmental issues. Low cost patch antenna using cement as substrate can be used for indoor applications including WLAN, wireless sensors for IoT applications[4]. The introduction of non conducting magnetic substrates into the field adds the miniaturization capability to the existing structures[5]. They have ϵ_r, relative permeability $\mu_r$value, in between 10-15 range. Nickel-ferrites are such materials, which has both dielectric and magnetic properties. The mechanical, dielectric and magnetic properties for Nickel-ferrite composite materials are analyzed in[6]. Another flexible magnetic composite material having Z phase Co hexaferrite particles is used as substrate for making a quarter wavelength antenna in [7], the miniaturization capability was 2.4x with increased performance.

The existing wireless charging systems uses high frequency. 2.45GHz is the most, commonly available frequency used for any RF circuits or wireless charging circuits. It has some difficulties including heating effect, high voltage etc. Introduction of low frequency wireless charging can overcome these disadvantages. Conformable antennas at lower frequency helps to implement low cost wireless charging systems. Like other conventional substrate, here explores the possibility of development of antennas on a conducting material. A rectangular patch antenna at 400MHz is investigated employing steel as substrate. The return loss degradation due to steel conductivity is compensated by employing a multilayer substrate including commonly available thermocol. The radiation pattern for multilayer structure is analyzed.

Section II describes the properties of steel. Methodology and HFSS(High Frequency Structure Simulator) simulation results are included in section III and Section IV respectively. Section V gives the conclusion.

II. MATERIAL PROPERTIES

A. Steel

Iron and carbon are the main components of steel. Elements such as Nickel, Manganese, Phosphorous, Sulphur etc were introduced in it to form different grades having different properties. Carbon steel, Alloy steel, Stainless steel and Tool steel are the major types of steel. Stainless steels are commonly available in market. It has 10-20% chromium content, highly corrosion resistant. Austenitic steel, Martensitic steel, Ferritic steels are three types of stainless steel. In this, austenitic steels are nonmagnetic. Ferritic and martensitic steels are magnetic in nature. The model implemented here needs a magnetic steel. The available steel in market with comparatively low cost, and having appropriate properties is 440C grade steel. It is used for making knives, cutting tools, dental and surgical equipment. A study presents comparison of ten types of magnetic steels in terms of their magnetic properties[8]. The properties listed in Table I is taken from the same. Since steel can be considered as a metal the relative permittivity is taken as 1. The below mentioned values are used for steel in material development section of HFSS.

Parameters	Values
Relative permittivity	1
Relative permeability	160
Electric conductivity	$1.6X10^{6}$
Density	$7611Kg/m^{3}$
Dielectric loss tangent	$6.366X10^{-3}$
Magnetic loss tangent	$3.978X10^{-5}$

TABLE I
ELECTRICAL AND MAGNETIC PROPERTIES OF GRADE 440C STEEL

III. METHODOLOGY

As a first step, a rectangular patch antenna has been designed in HFSS, over the steel substrate. Since it is a magnetic material the length of patch has been computed by using[9][10]. The obtained value was too large. As a result, the length of patch has reduced by(1/128) times. Width of patch is calculated using equation (1)[11].

$$W = \frac{c}{2f_r}\left(\sqrt{\frac{2}{\mu_r + 1}}\right) \quad (1)$$

Where W is width of patch, c is velocity of light in vacuum $3*10^{8}$m/s, f_r is resonant frequency which is 400MHz, μ_r is relative permeability of steel which is 160. Obtained value was 4cm, that has increased by 3 times, for getting the required resonating frequency for a good return loss. Finally steel material having dimension 25cm x 25cm x 1.6cm has been fixed. Antenna has been designed at 400MHz frequency. Transmission line feed is opted in the design.

A. Feed Line Design

Fig. 1 shows the plot between width to height ratio vs characteristic impedance of transmission line for 1.6cm steel thickness. w is the width of transmission line and it is taken as 5mm from graph which corresponds to 38Ω.

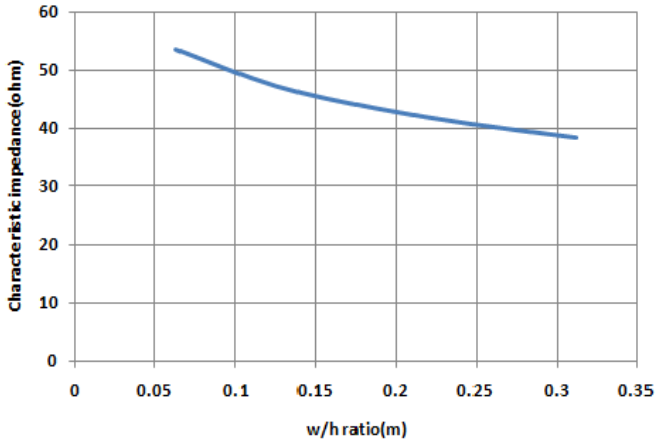

Fig. 1. (w/h) ratio Vs characteristic impedance of feed line

B. Patch Antenna Design on Steel Substrate

The mostly preferred is rectangular shape, because of its simpleness. The final dimension of antenna is listed in Table III. It is having rectangular shape with length of patch greater than width of patch. Fig. 2 shows the s11 Vs frequency plot of antenna. The s11 value is -0.27dB for 500-600MHz frequencies. It indicates a very high return loss.

Parameters	Values(in cm)
Length	21.3
Width	13
Feed line length	3
Feed line width	0.5

TABLE II
DIMENSIONS OF PATCH

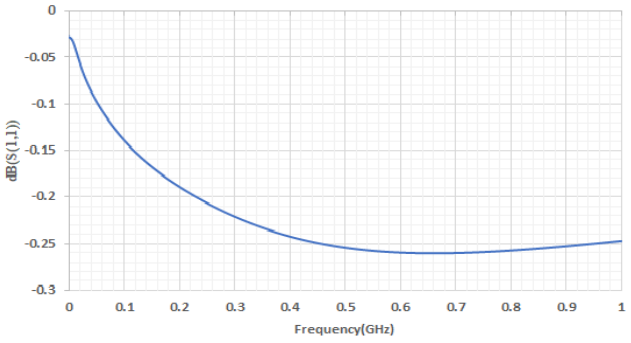

Fig. 2. Return loss of patch antenna on steel substrate

C. Antenna Design on Layered Substrate

Antennas having multilayer substrate posses advantages including antenna miniaturization. Periodically arranged magneto-dielectrics substartes are analysed for design of electromagnetic structures in VHF-UHF bands in[12]. A perfect dielectric on top of steel can compensate the conductivity of the same. A locally available material thermcol has been chosen for that. Thermocol is also called polystyrene, its a

hydrocarbon, derived from monomer styrene. Its ϵ_r is taken as 2.5. A thin layer having 4 mm thickness is used here. Fig. 3 shows the return loss Vs frequency graph of multilayer substrate antenna.

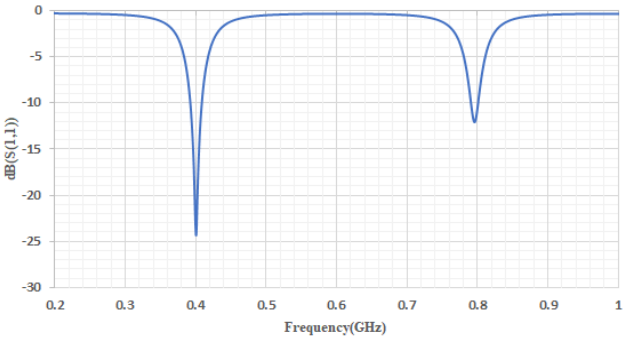

Fig. 3. Return loss of patch antenna

It shows that dielectric properties of thermocol layer helped to improve the return loss. Fig. 4 and Fig. 5 shows the E-plane and H-plane radiation pattern obtained after simulation. Fig. 6 shows Voltage Standing Wave Ratio(VSWR) Vs frequency plot. Antenna has a markable VSWR value 1.13.

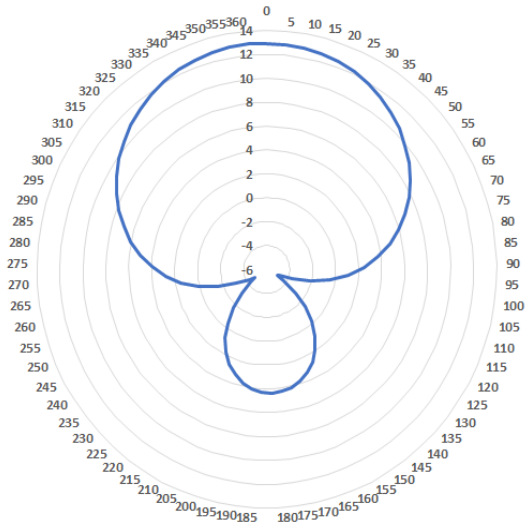

Fig. 4. E-plane radiation pattern

IV. RESULTS

Patch antenna on steel substrate is analysed first. Fig. 2 shows s11 Vs frequency plot for the same. The exponentially decaying graph shows that, antenna on steel substrate is less efficient to transmit or radiate electromagnetic waves. The reflection coefficient obtained is -0.27dB, which is very high, indicating that most of the power is reflecting back to feeding port. Then considering combined effect of magnetic and dielectric materials, commonly available thermocol layer is added to the design. Resulting return loss plot is shown in Fig. 3. Antenna achieves a noticeable return loss of -24dB

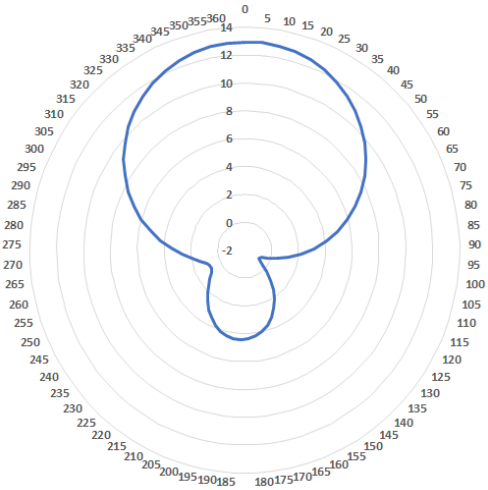

Fig. 5. H-plane radiation pattern

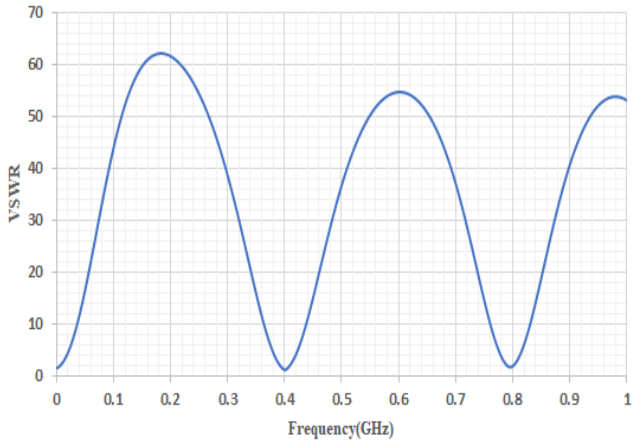

Fig. 6. VSWR Vs frequency plot

for 400MHz. -3dB bandwidth can be calculated from Fig. 3, and it is 3MHz. E-plane and H-plane radiation patterns in Fig. 4 and 5 shows that it can attain a directional pattern. The less gain of 0.3dB is attributed to conductivity of steel. VSWR is an important antenna parameter. It is a measure that numerically describes how well the antenna is impedance matched to the transmission line it is connected to. The value of VSWR obtained is 1.13, which indicates a good match.

As an analysis, microstrip antennas on other frequencies can be designed using the same substrate combination. For that design purpose, the following points can be best used. The increase in steel thickness further by 1mm, results a decrease in resonating frequency by 1MHz. When thermocol thickness is reduced by 1mm, frequency of operation reduces by 14MHz. When there is a slight air gap is introduced, return loss can be improved. It is found that increase in patch width by 10mm, improves the return loss by -5dB. 10mm increase in length of patch reduces resonating frequency by 35MHz. So keeping these points patch antenna on multilayer substrate can be designed for any frequency, respective to the applications. Also, further increase in relative permeability

can brought back many features including miniaturization.

V. CONCLUSIONS

A low cost microstrip patch antenna on multilayer substrate, formed by steel and thermocol has been designed in HFSS. The antenna is designed for low frequency 400MHz, which is in UHF spectrum. The antenna has a directional radiation pattern with 0.3dB gain. It can be used for charging applications in low frequency, and thus for RF energy harvesting systems. The simulated results shows that the combination of a conducting magnetic material and perfect dielectric can produce good results, which a microstrip antenna on a locally available substrate can.

REFERENCES

[1] Paul, Sarbajit, Sobia Bashir, and Junghwan Chang. "Design of a Novel Electromagnetic Energy Harvester With Dual Core for Deicing Device of Transmission Lines." *IEEE Transactions on Magnetics*, vol. 55, no. 2,pp: 1-4, June 2018.

[2] David M. Pozar, Microstrip antennas, *Proceedings of the IEEE*,vol. 80, no. 1, pp: 79-91, Jan. 1992.

[3] Vrba, David, Dario Rodrigues, and Paul R. Stauffer. "Metamaterial antenna arrays for improved uniformity of microwave hyperthermia treatments." *Progress In Electromagnetics Research*, vol. 156, pp: 1-12, 2016.

[4] Amrutha, M. V., and B. Sabarish Narayanan. "Low profile patch antenna on cement substrate for indoor applications".*International Conference on Wireless Communications, Signal Processing and Networking (WiSPNET)*. IEEE, 2017, pp:2508-2511

[5] Das, N., S. Chowdhury, and J. Chatterjee. "Circular microstrip antenna on ferrimagnetic substrate".*IEEE Transactions on Antennas and Propagation* vol. 31, no. 1, pp: 188-190, Jan 1983.

[6] Sankar S. Menon, Radhu Krishna, Lida Wilson, Sreedha Sambhudevan, B. Shankar, Anshida Mayeen, and Nandakumar Kalarikkal, Magnetic and dielectric properties of nickel-ferrite-embedded natural rubber composites, *Polymer Bulletin*, vol. 75, pp. 52175234, 2018.

[7] Martin, Lara J., et al. "Effect of permittivity and permeability of a flexible magnetic composite material on the performance and miniaturization capability of planar antennas for RFID and wearable wireless applications".*IEEE Transactions on Components and Packaging Technologies*, vol.32, no. 4, pp: 849-858, Dec 2009.

[8] Oxley, Paul, Jennifer Goodell, and Robert Molt. "Magnetic properties of stainless steels at room and cryogenic temperatures." *Journal of Magnetism and Magnetic Materials*, vol. 321, no. 14, pp: 2107-2114, Jan 2009.

[9] Das, Srin, and Santosh Chowdhury. "Rectangular microstrip antenna on a ferrite substrate." *IEEE Transactions on Antennas and Propagation*, vol. 30, no. 3, pp: 499-502, May 1982.

[10] Pucel, Robert A., and Daniel J. Mass. "Microstrip propagation on magnetic substrates-Part I: Design theory." *IEEE Transactions on Microwave Theory and Techniques*, vol. 20, no. 5, pp: 304-308, May 1972.

[11] Constantine A. Balanis, *Antenna theory: analysis and design*, Chapter 14, John Wiley Sons, 2016

[12] Mosallaei, Hossein, and Kamal Sarabandi. "Magneto-dielectrics in electromagnetics: Concept and applications." *IEEE Transactions on Antennas and Propagation*, vol. 52, no. 6, pp: 1558-1567, June 2004.

Proceedings of the Fourth International Conference on Communication and Electronics Systems (ICCES 2019)
IEEE Conference Record # 45898; IEEE Xplore ISBN: 978-1-7281-1261-9

Design and Implementation of Encoder and Decoder for Cyclic Redundancy Check

Arpita Sahu
M.Tech. Research Scholar of E & I Engg. Department
Shri G. S. Institute of Technology and Science
Indore (M.P.), India
arpita.sahu2802@gmail.com

Dr. R. S. Gamad
Prof. of E & I Engg. Department
Shri G. S. Institute of Technology and Science
Indore (M.P.), India
rsgamad@gmail.com

Dr. P. P. Bansod
Prof. of Biomedical Engg. Department
Shri G. S. Institute of Technology and Science
Indore (M.P.), India
pbansod@sgsits.ac.in

***Abstract*— Cyclic Redundancy Check (CRC) is one of the most important method to detect the errors occurred during the transmission of any data. Errors are detected in communication due to internal and external factors. This paper presents an implementation and analysis of encoder and checker of CRC8 which takes 16-bits of input data to create 24-bits code-word and can detect errors up to 8-bits. The proposed design is functionally synthesized with VHDL and verified using Xilinx ISE 14.7 Software. The hardware implementation of this design is done on Xilinx Artix-7 FPGA board. Simulation based results are reported in this paper.**

***Keywords*— CRC, Error detection, Communication, code-word, Encoder.**

I. INTRODUCTION

In a digital transmission system, error occurs when bits are changed in between the transmission and reception of data in a channel. Error takes place when binary 1 is transferred and binary 0 is there at the receiver or when binary 0 is transferred and binary 1 is there at the receiver. There are two types of errors: one is single bit error and the other one is burst error [1]. A single bit error is a sequenced error that modifies single bit and does not changes other bits. A burst error is an error in continuous sequence of bits which may have error in any number of bits [2]. A single-bit error occurs when white noise is present, because of slight arbitrary worsening of the signal-to-noise ratio, which is adequate to complicate the receiver's conclusion on a single bit. Burst error may occur due to impulse noise or waning in a mobile wireless environment. It occurs more as compared to single-bit error [3].

In optical links, the error is due to the presence of physical components like optical driver, connectors, optical fiber and optical receivers, etc. Errors may also occur because of optical dispersion and optical attenuation [4]. There are three types of Error detection techniques. First is Single parity check, second is Cyclic Redundancy Check, and the third one is Checksum technique. Cyclic Redundancy Code (CRC) is basically an error detecting code that is used to detect error in digital transmission system and storage devices [5]. The redundant word used in CRC is because it expands the input message without adding useful information to it. The detected error then can be corrected by using error correction codes which can identify and remove the errors present in transmission network [6]. CRC operates using binary 0 and 1. It's operation is based on modulo-2 addition (logical XOR) and multiplication (logical AND). Systematic codes is used for coding the scheme [7]. Let m(x) be polynomial of input message, g(x) be the generator polynomial and c(x) be the polynomial of code-word. We have c(x) = m(x)g(x) which can be represented as systematic form as $c(x)= m(x)x_{n-k} + r(x)$, where r(x) is the remainder occurring when $m(x)x_{n-k}$ is divided by g(x). The transmitted message c(x) contains k-information bits followed by 'n-k' CRC bits [8].

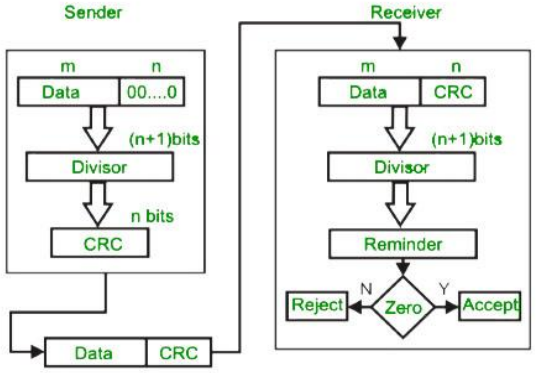

Figure 1: Basic structure of CRC

In figure 1, a simple structure of CRC is shown. It consist of two modules. One is Sender in which input message is given and another is Receiver in which the coded message is received. CRC is a process of encoding a data at sender and decoding it at receiver [9].

II. PRINCIPLE OF CRC

Cyclic Redundancy Check (CRC) is an error detecting method in which a transferred message is appended with a few redundant bits from the sender and then the code-word is plaid at the receiver using modulo-2 arithmetic for checking errors. The message is then communicated from the encoder and is received at the receiver where a CRC check is conceded out. This procedure supports to regulate any error in communication system over the channel. The total number of errors which a CRC may detect, depends on the generator polynomial. The degree of generator polynomial will decide the number of detected error. For example, CRC8 can detect errors up to 8-bit [10].

The most important step in the implementation of CRC algorithm is selecting a generator polynomial. The polynomial should be selected such that it maximizes the error-detecting capabilities and minimizes overall collision probabilities [11]. CRC can be divided into following types:

Table 1: Standard CRC and their polynomials

S. No.	CRC	Polynomial	Application
1.	CRC4	$x^4 + x^3 + 1$	Telephone
2.	CRC8 CCITT	$x^8 + x^7 + x^2 + x + 1$	1 wire bus
3.	CRC10	$x^{10} + x^9 + x^5 + x^4 + x + 1$	ATM AAL
4.	CRC16	$x^{16} + x^{15} + x^2 + 1$	HDLC/USB
5.	CRC16 CCITT	$x^{16} + x^{15} + x^5 + 1$	X.25/Modem
6.	CRC32	$x^{32} + x^{26} + x^{23} + x^{22} + x^{16} + x^{12} + x^{11} + x^{10} + x^8 + x^7 + x^5 + x^4 + x^2 + 1$	Ethernet

Table 1 shows different types of CRC based on generator polynomial and their application in communication system. The selection of generator polynomial should be done before the user computes the redundancy check of a communicated message. The generator polynomial must have a non-zero coefficient in the LSB and MSB positions and its degree should be greater than zero [12].

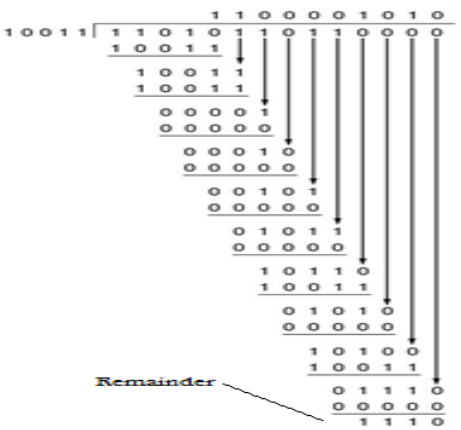

Figure 2: Division in CRC

Figure 2 shows the binary division in CRC. This is the basic operation in the implementation of CRC. In this, a 10-bit input is divided with 5-bit generator bits. As a result, CRC remainder is obtained [13].

III. PROPOSED DESIGN & SOLUTION

In this paper, Encoder and Checker are designed for CRC8 which uses $x^8 + x^7 + x^6 + x^4 + x^2 + 1$ as generator polynomial that is used in DVS-S2 (Digital Video Broadcasting – Satellite Second Generation). The input message given to Encoder is of 16-bits. This 16-bit message is binary divided with the given generator polynomial by which 8-bit CRC remainder is obtained. This remainder is then appended with the original input message which becomes the 24-bit input data for the checker. At checker, this 24-bit input data is again binary divided with the generator polynomial. The result of CRC Checker will show that how many bits are corrupted. The proposed design is synthesized using VHDL (VHSIC HDL) i.e. Very High Speed Integrated Circuit Hardware Description Language which describes the method for modelling and designing of Digital Circuits and Digital logic systems. It is verified using Xilinx ISE 14.7 software and for hardware implementation, Xilinx Artix-7 FPGA (Field Programmable Gate Array) board is used.

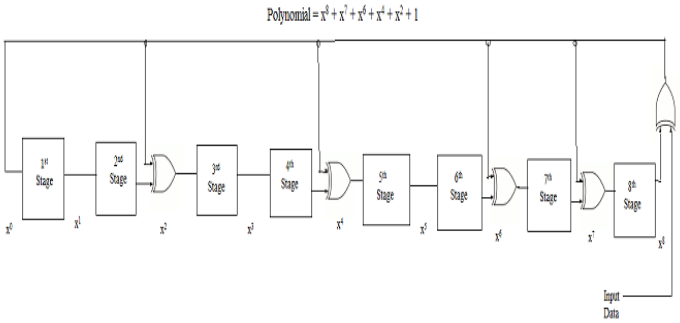

Figure 3: Designing of proposed CRC8

Division operation of CRC is based on modulo-2 operation. The divider circuit of CRC consist of shift registers and mod-2 adders. Figure 3 shows the hardware implementation of CRC8 by using $x^8 + x^7 + x^6 + x^4 + x^2 + 1$ as generator polynomial which consist of eight stages of shift registers and five EX-OR gates. Using this polynomial, we can detect error up to 8-bits.

Implementation of Encoder Algorithm

a. Read the message vector.
b. Take the generator polynomial order 'k'.
c. Shift the message vector 'k' times and store it order as 'n'. Compute (n-k).
d. Shift generator polynomial (n-k) times and store the result 'h'.
e. XOR the generator polynomial and message vector and store the result in 'x'.
f. Determine the highest polynomial index position of 'x' where 1 is occurred and take it as 'n'.
g. If n >=k go to step 4.
h. Concatenate the check bits with the message bits.

Implementation of Checker Algorithm

a. Read the received data and take its order as 'n' and store it in 'h'.
b. Take the order of generator polynomial as 'k'. Compute (n-k).
c. Shift the generator polynomial left (n-k) times and store the result in 'e'.
d. XOR the generator polynomial and received vector and store the results in 'x'.
e. Determine the highest index of 'x' where 1 is occurred and take it as a 'n'.
f. If n >= k go to step 3.
g. Store 'x' in rem.
h. If rem =0 then the received data is error free else data contains error.

IV. SIMULATION RESULTS & DISCUSSION

Authors have implemented the coding of proposed design and simulated using Xilinx ISE 14.7. Simulation based results are reported in this paper as shown in the figure 4 to figure 13.

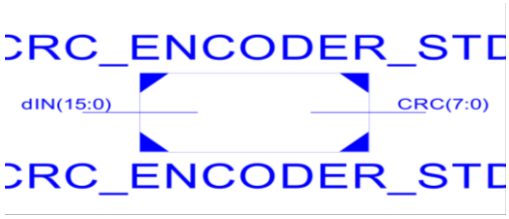

Figure 4: 1st level RTL of CRC Encoder

Figure 4 shows the symbol of CRC Encoder. This is the first level RTL of Encoder. It shows 16-bit input d_{IN} and 8-bit output CRC.

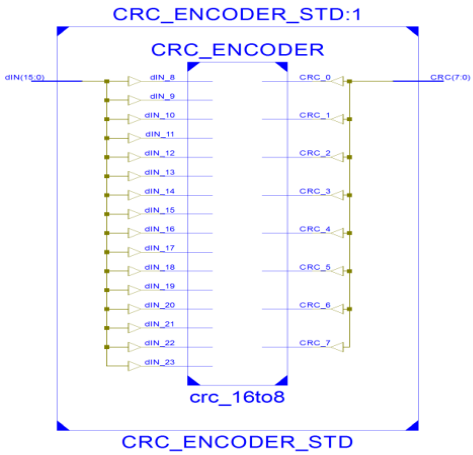

Figure 5: 2nd level RTL of CRC Encoder

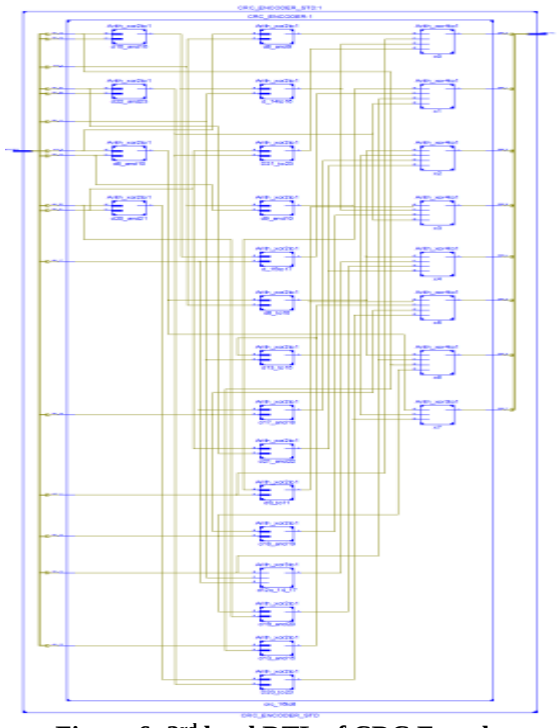

Figure 6: 3rd level RTL of CRC Encoder

Figure 5 and 6 shows the 2nd and 3rd level RTL Design of proposed CRC Encoder. In this, d_{IN} is the 16- bit input dataword and CRC is the 8-bit encoder output. This encoded output is appended with the input dataword which is being transmitted to the receiver.

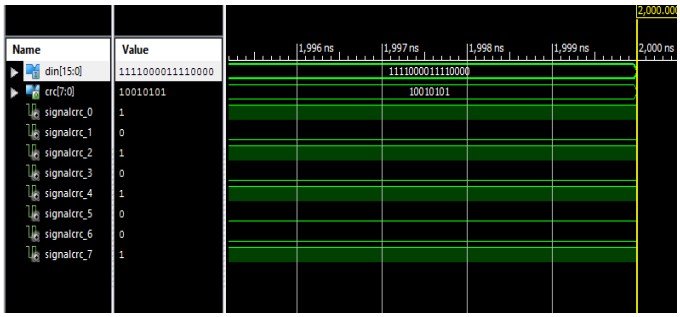

Figure 7: Output Waveform of CRC Encoder

Figure 7 shows the output waveform of CRC Encoder. In this, the given input is d_{IN} = 1111000011110000 for which the output obtained is CRC = 10010101. Now this value of CRC will be appended with the input data d_{IN} which will be the input of the CRC checker. Therefore, the input of CRC checker will be 24 bit code-word which is 111100001111000010010101.

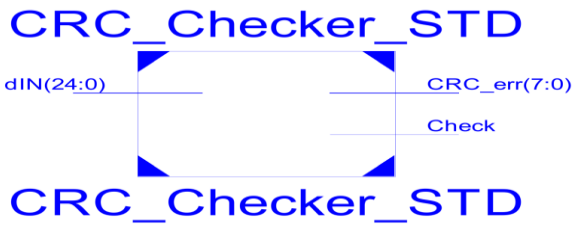

Figure 8: 1st level RTL of CRC Checker

Figure 8 shows the symbol of CRC Checker. This is the first level RTL design of Checker. It shows 24-bit input d_{IN} and two outputs. One is 8-bit CRC_err and other is check.

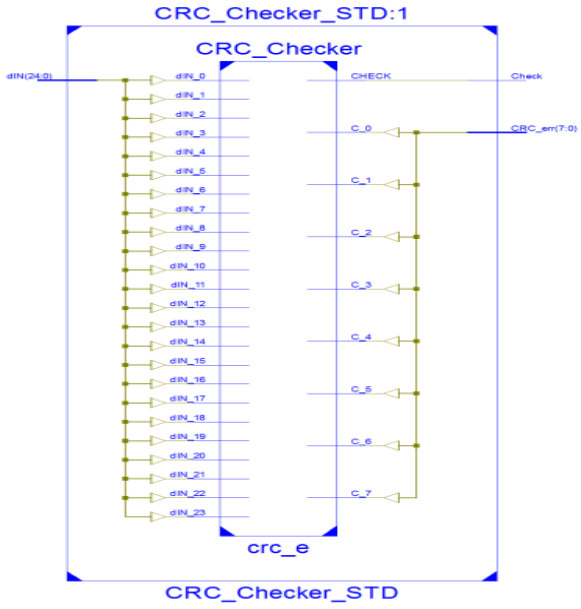

Figure 9: 2nd level RTL of CRC Checker

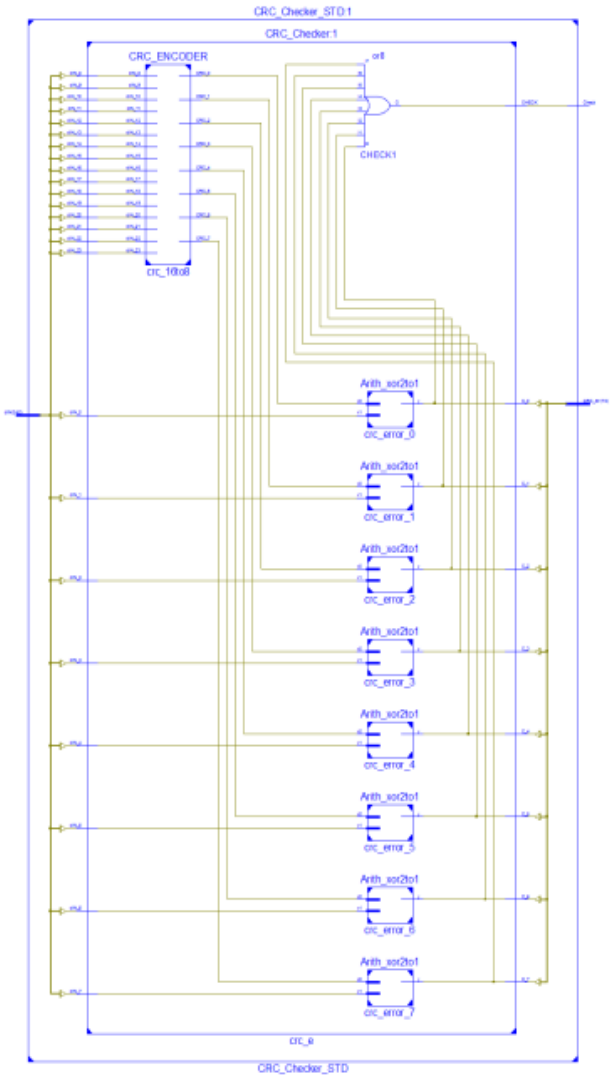

Figure 10: 3rd level RTL of CRC Checker

Figure 9 and 10 shows the 2nd and 3rd level RTL design of proposed CRC Checker. The input of CRC Checker is a 24-bit input d_{IN} [0, 24] and the output is 8-bit CRC_err and Check. The check=1 when the input is corrupted in between the encoder and checker i.e., when the input given to checker is other than the correct input.

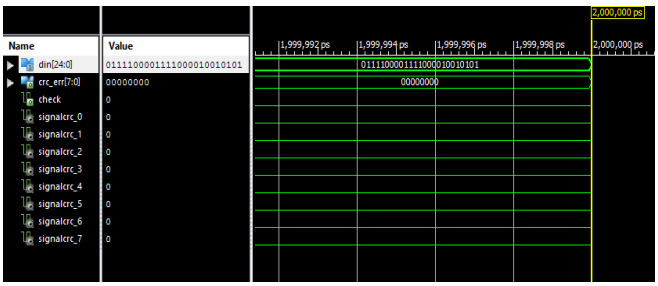

Figure 11: 1st Output waveform of CRC Checker

Figure 11 shows the output waveform of CRC Checker for input d_{IN} = 111100001111000010010101. For this input, output CRC_err = 00000000 that means no error since the input is same as the coded input i.e., 24 bit code-word. Here Check = 0 because no error is detected.

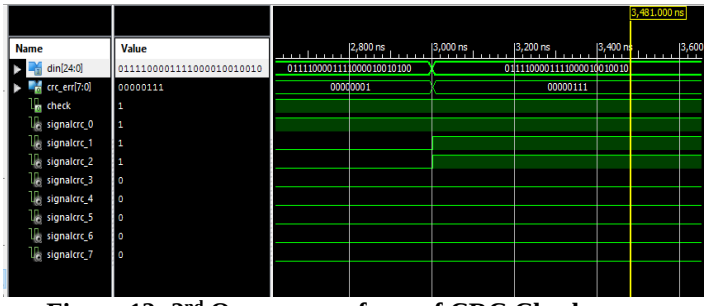

Figure 12: 2nd Output waveform of CRC Checker

Figure 12 shows the output waveform of CRC Checker for input d_{IN} = 111100001111000010010100 and d_{IN} = 111100001111000010010010. For the first input, output CRC_err = 00000001 that means 1-bit error is detected since the input differs from actual code-word by 1-bit. For the second input, output CRC_err = 00000111 i.e., 3-bit error is detected because this input varies from code-word upto 3-bits. Check=1 in both the cases since error is detected in each case.

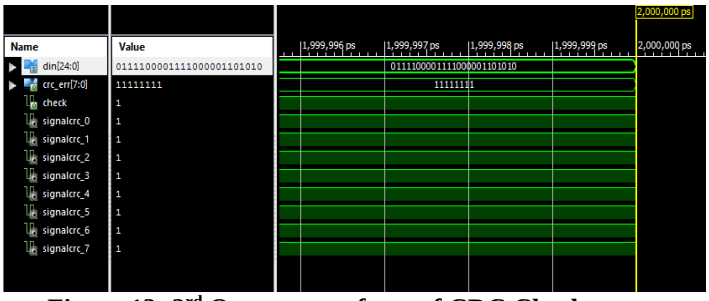

Figure 13: 3rd Output waveform of CRC Checker

Figure 13 shows the output waveform of CRC Checker for input d_{IN} = 111100001111000001101010. For this input, output CRC_err = 11111111 means all bits are corrupted. It represents 8-bit CRC error with check = 1. In this, the redundant bits which were appended with the input are all inverted with respect to the actual redundant bits.

These were the output waveforms of proposed CRC Checker/Decoder with different inputs and different CRC errors.

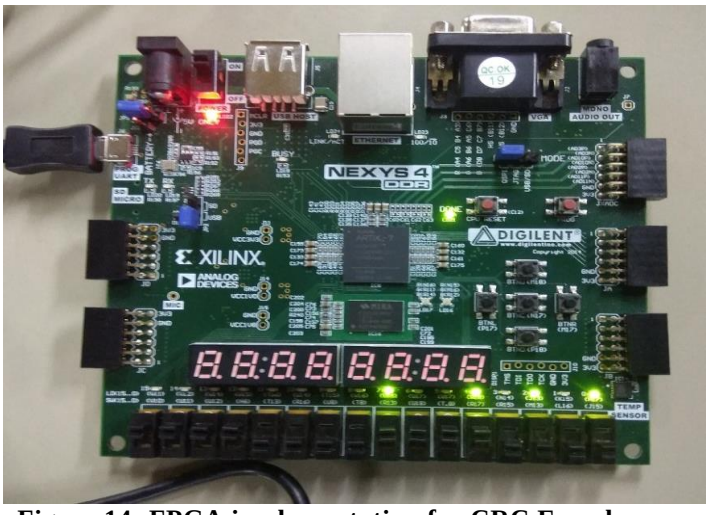

Figure 14: FPGA implementation for CRC Encoder

Figure 14 shows the FPGA implementation of CRC Encoder. The FPGA board used is Artix-7 with package CSG324. The input given to this encoder is d_{IN} = 1111000011110000 and the output obtained is CRC= 10010101. The input d_{IN} is given to the board through the switches shown in figure and the output CRC_err is shown from LED. For the LED blow, 1 is considered and 0 otherwise. Table 2 shows the details of Artix 7 FPGA board used for implementing CRC Encoder.

Table 2: Xilinx Tools used in proposed CRC

Family	Artix 7
Device	XC7A100T
Package	CSG324
Synthesis Tool	XST(Verilog/VHDL)
Simulator	ISim(Verilog/VHDL)
Language used	VHDL

Table 3 compares the results of proposed design with the previous design for CRC Decoder/Checker.

Table 3: Comparison of Proposed CRC

Slice Logic Utilization	Previous Design [8]	Proposed Design
Number of Slice LUTs	36	20
Number of bonded IOBs	41	33
Power (W)	1.064	0.042

Table 4 describes the logic utilization summary. Few parameters like LUT's, Power, Memory and Delay are obtained during the implementation of 16-bit Message polynomial and 8-bit CRC.

Table 4: Results of Proposed CRC

Slice Logic Utilization	Encoder	Checker
Number of Slice LUTs	13	20
Number of occupied Slices	5	8
Number of LUT Flip Flop pairs used	13	20
Number of bonded IOBs	24	33
Average Fanout of Non-Clock Nets	2.58	2.2
Delay (nsec)	1.481	2.737
Total memory usage (KB)	317684	316916
Power (W)	0.042	0.042

V. CONCLUSIONS

In this paper, the method of calculating the remainder for CRC and creating code-word for a given message is described. Figure 12 shows the output waveform of CRC checker and error received in code-word up to 8-bits. Table 4 shows the overall parameters obtained for CRC Encoder and Checker. The delay in the output for encoder is comparative lower than checker circuit. The overall result shows that low hardware usage which is required for implementation of any system.

REFERENCES

[1] T Stallings, William, "Data and computer communications", Upper Saddle River, N.J.: Pearson/Prentice Hall, 8th Edition, 2007.

[2] Palani Subbaiah, "Bit- Error Rate for High Speed Serial Data Communication", Data-communications Division, Cypress Semiconductor, November 2008.

[3] Peterson, W. & E. Weldon, "Error-Correcting Codes", Second Edition, MIT Press, 1972.

[4] Ulf Nordqvist, Thesis: "Protocol Processing in Network Terminals", Department of Electrical Engineering, Linkopings University, SE-581 83 Linkoping, Sweden 2004.

[5] U. Nordqvist, T. Henriksson, D. Liu, "CRC Generation for Protocol Processing", Norchip 2000, Turku, Finland, pp. 288-293.

[6] Ming-Der Shieh, Ming-Hwa Sheu, Chung-Ho Chen, Hsin-Fu Lo, "A Systematic Approach for Parallel CRC Computations", Journal of Information Science and Engineering, Vol. 17, 2001 pp. 445-461.

[7] Giuseppe Campobello, Giuseppe Patane, Marco Russo, "Parallel CRC Realization", IEEE Transactions On Computers, Vol. 52, No. 10, 2003, pp. 245-256.

[8] A. H. Saleh, K. M. Saleh and S. Al-Azawi, "Design and simulation of CRC encoder and decoder using VHDL", 1st International Scientific Conference of Engineering Sciences - 3rd Scientific Conference of Engineering Science (ISCES), IEEE 2018, pp. 221-225.

[9] A. K. Panda, S. Sarik and A. Awasthi, "FPGA Implementation of Encoder for (15, k) Binary BCH Code Using VHDL and Performance Comparison for Multiple Error Correction Control", International Conference on Communication Systems and Network Technologies, Rajkot, 2012, pp. 780-784.

[10] Bajarangbali P., Aparna Anand, "Design of High Speed CRC Algorithm for Ethernet on FPGA using reduced lookup table algorithm", IEEE Annual India Conference (INDICON) 2016.

[11] Zavodnik, T; Kekely, L.; and Pus, V., "CRC based hashing in FPGA using DSP blocks," in Design and Diagnostics of Electronic Circuits & Systems, 17th International Symposium on , vol., no., pp.179-182, 23-25 April 2014.

[12] Kounavis, M.E. and Berry, F.L. "Novel Table Lookup-Based Algorithms for High-Performance CRC Generation," in Computers, IEEE Transactions. pp. vol.57, no.11, pp.1550-1560, Nov. 2008.

[13] M.D. Shieh, M.H. Sheu, C.H. Chen, and H.F. Lo, "A Systematic Approach for Parallel CRC Computations," J. Information Science and Eng., vol. 17, pp. 445-461, 2001.

Proceedings of the Fourth International Conference on Communication and Electronics Systems (ICCES 2019)
IEEE Conference Record # 45898; IEEE Xplore ISBN: 978-1-7281-1261-9

Analysis of Various Security Techniques of Internet of Things

Chandni Krish (Research Scholar)
CSE Department
National Institute of Technical Teachers Training & Research, Chandigarh
India
chandnikrish705@gmail.com

Dr.Rakesh Kumar (Assistant Professor)
CSE Department
National Institute of Technical Teachers Training & Research, Chandigarh
India
raakeshdhiman@gmail.com

***Abstract*— The internet of things is the decentralized type of network in which various type of active and passive attacks are possible. The active attacks affect network performance in terms of certain parameters. The version number is the active type of attack it leads to denial of service in the network. The various methodologies are proposed by the authors for the isolation of version number attack in the network. In this work, the various methodologies for the detection of version number attack are reviewed in terms of various parameters. The novel approach can be designed for the isolation of version number attack which should be less complex and detect malicious nodes in least amount of time. In this paper, two scenarios are compared which are DODAG protocol scenario and version number attack scenario. It is analyzed that version number attack has low throughput and has high packet loss as compared to DODAG scenario.**

Keywords— Version number attack, IoT, Malicious nodes

I. INTRODUCTION

A technology in which several sensors, smart nodes, and objects are connected to each other in order to perform communication without using any human efforts is known as the Internet of Things (IoT). Depending upon the link amongst objects, the objects function autonomously. Analysis of collected data to make decisions, providing lightweight data and extracting the data by accessing and authorizing the cloud-based resources are some of the actions performed by IoT nodes. The users, services, sensors as well as objects are linked to each other very closely through IoT. The applications ranging from smart grid healthcare applications to intelligent transport systems deploy IoTs within them. The number of smart devices and intelligent services provided through IoT networks has been outgrowing due to the huge business opportunities provided in the IoT scenarios [1]. The cloud-based IoT networks have been developed due to the relativity of IoT devices on the cloud infrastructure such that the data can be transmitted across applications. There are mainly IP based web and IoT applications which provide transmission using TCP and UDP. However, among most of the IoT applications, there are few commonly used message distribution functions. Various applications implement these functions in interoperable standard ways [2]. Very similar to the client/server protocol, a publish/subscribe protocol architecture is designed which is called MQTT (Message Queue Telemetry Transport). Due to its simple structure and ability to avoid high CPU and memory utilization, MQTT protocol is known to be of huge important. Another protocol that is designed from the financial industry is the Advanced Message Queuing Protocol (AMQP). The TLS/SSL protocols are used here to manage the security. To ensure that less power and memory embedded devices are being used, CoAP is applied for communication. Various network layer protocols also have been designed. The most commonly known IoT standard for MAC is the IEEE 802.15.4 [3]. A frame format is defined in this protocol in which the source and destination addresses are defined in headers along with the manner in which nodes can communicate. Low power multi-hop networking is applied lately in IoT because it is not suitable to use frame formats applied previously in traditional networks since they cause overhead in these systems [4]. For ensuring high reliability, less cost and meeting the communication requirements of IoT, channel hoping and time synchronization are used. Another lighter version of original IEEE 802.11 wireless medium, access standard is the IEEE 802.11ah. The IoT requirements are met here by reducing the overhead. The most commonly used wireless standards are the IEEE 802.11 standards. For all the digital devices, these protocols have been used on large scale [5]. A category of Directed Acyclic Graph that is rooted at the sink and uses RPL routing protocol for organizing the routers is called Destination Oriented Directed Acyclic Graph (DODAG). The DODAG Information Object (DIO) messages are originated periodically by the DODAG root for initiating the formation of DODAG. The link-local multicast is used to advertise this generated DODAG. Information related to the root identity of DODAG, the used routing metrics, and the depth/ rank of originating router are included within the DIO messages. Depending on the information advertised by its neighbors within their DIOs, the router that joins the DODAG defines its own rank. A simple example of building process of DODAG is shown in figure 1. Node 3 is beyond the radio range of root node among all the three client nodes shown in the figure. The DIO control message is broadcasted with its rank and id is broadcasted to the client nodes when the root node initiates the generation of a network topology [5]. Here, DAO messages are sent in

response from the client node 1 and node 2 to the root for joining DODAG as they are in the radio range of the root. The Client node 3 waits for a period of time to hear from the root node but does not receive any response. Thus, the neighbor nodes start sending DIS message proactively to the solicit DIO. The DIO message that is received earlier to the client node 3 is forwarded if in any case this DIS message is received by client node 2. A DAO message is sent back to the client node 2 by the client node 3 when it receives the DIO message. This message will then be forwarded to the root node from client node 2. Thus, the construction process is completed when the client node 3 joins the DODAG at the end.

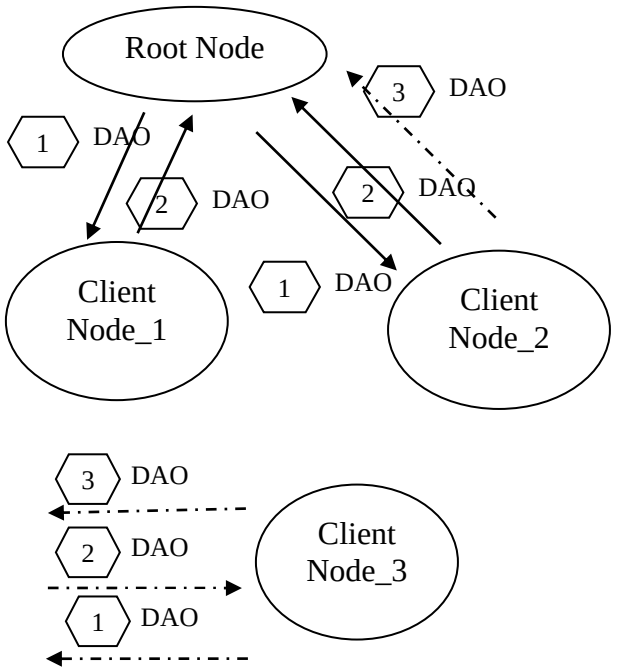

Fig. 1: DODAG construction process [10]

For ensuring that the global repair process of RPL is under control and all the nodes available in DODAG are updated as per the routing state, the root node uses version number [6]. The lifetime of IoT system is reduced due to the presence of version number attacks in it. Attacker can perform this attack with very less expense and the network can be overloaded by exploiting the global repair mechanism that is included as an immune system of protocol. With the presence of several inconsistencies in the network, a global repair is initiated by the root. The version number of DODAG is incremented for rebuilding the complete DODAG. DODAG Information Object (DIO) is the control message in which this version number is carried. Comparisons are made among the existing version number and the one received from its parent by every receiving node. In case of higher received version, the current rank information is ignored, the trickle timers are reset and a new procedure for joining the DODAG is initiated [7].

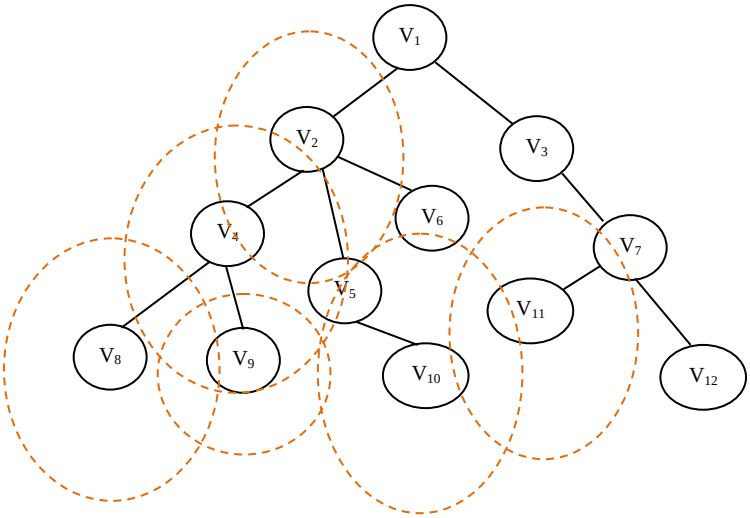

Fig. 2: Illustration of a version number attack

A loop free topology is guaranteed in this global repair although its cost is very high. It can be known that the node did not migrate to the new DODAG version if the previous value of version is being advertised in DIO messages. The other nodes must not select such a node as preferred parent. At the time of global repair, two versions of DODAG can exist at similar time. However, data packets that exist in old version can transit in new version for avoiding loops. The previous version is not considered as DODAG and there is no guarantee of availability of loop free topologies as the network is still beyond convergence state. Across DODAG, the version number must be propagated unchanged so that any possible inconsistencies of the network are avoided. For ensuring the integrity of version number available in received DIO messages, no technique has been provided in RPL [8]. The network can be harmed here when a malicious node might modify this value in its own DIO messages. The trickle timer is reset, the version is updated and the new version is advertised to the neighbors using DIO messages once a malicious DIO is received with a new version number.

This research work is based on the version number attack in the internet of things. In the introduction section, the introduction about the DODAG protocol is described in detail. The description about the version number attack is also given in the introduction section. In the second section is related work is described in detail. The problem formulation section illustrated the problems in the previous research work. The research methodology section describes the novel approach for the detection of malicious nodes in the network. In the last section, result and discussion is described in which two scenarios are compared which are DODAG protocol and version number attack in IoT.

II. REVIEW OF LITERATURE

Ahmet Arıs, et.al [9] proposed two simple alleviation approaches for the elimination of RPL version number attacks. The updates of the version number from the way of leaf nodes were eliminated by the first mitigation approach. The first approach gave information about the toughness of the locations for virtual numbers. The efficiency of the proposed approach was verified by using a number of topologies. In future, more experiments can be performed in the area of various virtual number invasions situation. The examination of the hybrid mitigation approach can also be performed in the near future.

Anthea Mayzaud, et.al [10] presented a novel classification approach for the categorization of the attacks found besides the RPL. For this approach, mainly three classes of attacks were considered. The lifespan of the network was reduced by the invasions against resources. The intruder node capture and the examined a wide part of the network in case of attacks. The researchers have proposed a lot of approaches for the prevention of these types of attacks based on different properties. The implementation and the management of the security modes were not mentioned by the RPL specification technique. Thus it was concluded that the transaction among different security levels was a major challenge for the accepted structure of RPL networks.

Amit Dvir, et.al [11] suggested the use of a new routing protocol for the elimination of the issues presented in the Low power and Lossy networks. This protocol was named as IPv6 routing protocol. The main objective of this routing protocol was to grant the functionality in the Low power and Lossy Networks. An updated version named DODAG was used for reconstructing the routing topology. It was also suggested that for the prevention of initial intruder, same approach should be used, for publishing the decreasing value of rank. In this method, a wider part of the DODAG was combined with the DODAG through the intruder for forwarding a long part of the network traffic. Thus with the use of this new security component, the illegal increase in the version number could be avoided.

Anthea Mayzaud, et.al [12] presented a novel classification approach for the categorization of the attacks found besides the RPL. For this approach, mainly three classes of attacks were considered. The lifespan of the network was reduced by the invasions against resources. The intruder node capture and the examined a wide part of the network in case of attacks. The researchers have proposed a lot of approaches for the prevention of these types of attacks based on different properties. The implementation and the management of the security modes were not mentioned by the RPL specification technique. Thus it was concluded that the transaction among different security levels was a major challenge for the accepted structure of RPL networks.

Zeeshan Ali Khan, et.al [13] proposes some new approaches for IDS which were very suitable for the tiny devices. For managing the status information about the neighbors, the proposed approach used the faith management technique. The proposed approach proved very successful for singling out nastily behaving units. After the recognition of attacker node, it was eliminated from the network. The presented approach was most suitable against the three types of RPL protocol attacks. The presented approach could also be used for other type of inclusions. For the validation of MATLAB simulations, a test bed involving Z1coponents will be developed in near future.

H. Abdo, et.al [14] proposed a novel approach for ensuring the security and safety in case of industrial threat investigation. For this purpose, a conventionally used safety investigating system named bowtie analysis was combined with the newly developed version of security analysis. A comprehensive demonstration of the risk scenario was presented by the combination of attack tree and bowtie analysis approach in terms of safety and security. For the evaluation of risk range relied on two term similar parts, a new mechanism was presented. The one part was for security while the other part was for safety. The tested results showed that the proposed approach performed well. In future, a more reliable and tough likelihood estimation technique will be developed by the researchers.

Ahmet Aris, et.al [15] presented a deep study of RPL version number attacks. The investigation of the attacks was also performed which was based on different scenarios. The investigation was performed on a practical network topology containing both mobile and stationary nodes. A probabilistic approach was used for calculating the attacks probabilities. The performance results were demonstrated according to the different valves of p. The outcomes of the simulation depicted that the mobile attackers and the distantly placed nodes had almost same effects on the network performance. In future, a study about the coming behavior of DIO information for the recognition of possible position of virtual number attack will be performed.

Hezam Akram Abdul-Ghani, et.al [16] proposed a new internet of things suggestion approach relied upon constructing blocks policy. This was basically a four layered reference model. An inclusive IOT invasion model was developed including four main phases. Firstly an IOT asset relied invasion plane comprising of four mechanism was presented. In the second phase, a pattern of IOT security aim was defined. The IOT invasion classification for every component was identified in the third phase. In the final phase, violation of security aims and the association among every attack was identified. A set of solution was also for protecting each asset was also identified in the last phase also. For the very first time, an IOT invasion model relied on building block reference model was developed. The tested results clearly depicted the effectiveness of the proposed model.

Anthea Mayzaud, et.al [17] proposed a recognition strategy for addressing the version number attack issues in RPL network. A solution based on distributed monitoring design was implemented for the conversation of node resources. After obtaining the recognition information from all monitoring nodes the intruder localization procedure was performed by the attacker. A lot of tests were conducted for the evaluation of the above approach. With the help of

strategic monitoring nodes placement, the false positive rate could be reduced. In future, many more complementary experiments based on real infrastructure with some other classes of components will be performed.

Seungyong yoon, et.al [18] proposed a novel well-implemented structural design of distant security handling server. This approach was proposed for ensuring the safety of IOT devices in an IOT handling scenario. A number of security constraints were managed and provided in an integrated and systematic manner by the remote security management server. The presented approach helped in the prevention of various unpleasant incidents in the IOT scenario in advance. With the identification of these attracts, the damage caused by these attacks could be minimized. In case of the occurrence of the attack, the prevented measures could be adopted. The various tested results indicated that the presented approach performed well on certain parameters like safety and security.

TABLE I. TABLE OF COMPARISON

Reference No. & Author's Name	Technique	Advantages/ Features	Disadvantages/ Improvements
[9] Ahmet Arıs, et.al	Two simple alleviation approaches for the elimination of RPL version number attacks are proposed.	The efficiency of the proposed approach was verified by using a number of topologies.	The analysis of the multiple VN attackers' situation was not performed in this study.
[10] Anthea Mayzaud, et.al	A novel classification approach for the categorization of the attacks found besides the RPL in which mainly three classes of attacks were considered.	The researchers have proposed a lot of approaches for the prevention of these types of attacks based on different properties.	This proposed technique is only able to secure the networks that include one malicious node and thus, the future work can be extended for making improvements in this technique to ensure that systems with multiple malicious nodes can be secured.
[11] Amit Dvir, et.al	The main objective of this routing protocol was to grant the functionality in the Low power and Lossy Networks.	In this method, a wider part of the DODAG was combined with the DODAG through the intruder for forwarding a long part of the network traffic.	The proposed technique was only implemented in standard systems for evaluations and the future work can be extended by implementing this technique in RPL and real wireless sensor deployments.
[12] Anthea Mayzaud, et.al	A novel classification approach was proposed for the categorization of the attacks found besides the RPL. For this approach, mainly three classes of attacks were considered.	It was concluded that the transaction among different security levels was a major challenge for the accepted structure of RPL networks.	The proposed work was not evaluated in real infrastructures that included additional classes of devices that were implemented in RPL protocol.
[13] Zeeshan Ali Khan, et.al	For managing the status information about the neighbors, the proposed approach used the faith management technique. The proposed approach proved very successful for singling out nastily behaving units.	For the validation of MATLAB simulations, a test bed involving Z1coponents will be developed in near future.	The proposed technique is not enough computing intensive due to which several issues are being faced.
[14] H. Abdo, et.al	A novel approach was proposed for ensuring the security and safety in case of industrial threat investigation. For this purpose, a conventionally used safety investigating system named bowtie analysis was combined with the newly developed version of security analysis.	The tested results showed that the proposed approach performed well.	The issue of uncertainty still exists after implementing the proposed approach which can be resolved by making improvements in this approach in future.

[15] Ahmet Aris, et.al	The investigation of the attacks was also performed which was based on different scenarios. The investigation was performed on a practical network topology containing both mobile and stationary nodes.	The outcomes of the simulation depicted that the mobile attackers and the distantly placed nodes had almost same effects on the network performance.	It is still easy to drain the resources and reduce the lifetime of networks if the malicious node is placed on mobile network identity.
[16] Hezam Akram Abdul-Ghani, et.al	A new internet of things was proposed suggestion approach relied upon constructing blocks policy.	For the very first time, an IOT invasion model relied on building block reference model was developed. The tested results clearly depicted the effectiveness of the proposed model.	No standard method has still been defined for securing the IoT systems.
[17] Anthea Mayzaud, et.al	A solution based on distributed monitoring design was implemented for the conversation of node resources. For the identification of the attacker in the proposed approach, the collaboration of observed nodes was exploited.	With the help of strategic monitoring nodes placement, the false positive rate could be reduced.	Only one certain parameter is emphasized here by the proposed technique which makes it possible for the technique to lack in accuracy and privacy aspects.
[18] Seungyong yoon, et.al	This approach was proposed for ensuring the safety of IOT devices in an IOT handling scenario. A number of security constraints were managed and provided in an integrated and systematic manner by the remote security management server.	The various tested results indicated that the presented approach performed well on certain parameters like safety and security.	The proposed approach is only tested on limited scenarios, which does not define its vulnerability to attacks in all other scenarios.

III. PROBLEM FORMULATION

The IoT network is much vulnerable to various type of security attacks. The DODAG is the routing protocol of IoT which establish path from source to destination based on the version number. The version number attack is trigger by the attacker and attacker increment version number which leads to establishment of path which have loop. The two version number attack mitigation techniques are proposed [18] in IoT. In the first technique, the virtual number attackers are mitigated based on the direction of leaf nodes. The version number attackers which are remained in the network will be mitigated with the second technique. In the second technique, the node will not update its virtual number until it has majority vote. The proposed technique [18] does not detect the multiple version number attack from the network. The mitigation scheme can be tested over the sensor devices which have low battery power and resources

IV. RESEARCH METHODOLOGY

The proposed methodology is based on the detection and isolation of version number attack in IoT. The proposed methodology is based on the trust based technique for the isolation of version number attack. The proposed approach isolates version number attack in DODAG attack. The implementation strategy will be based on the following steps:-

- Deployment of the Network: - The network will be deployed with the finite number of sensor devices and with the base station. The sensor devices are responsible to sense various types of conditions like temperature, pressure etc.
- Trigger of version number attack:- The malicious nodes will be formed in the network which are responsible to trigger version number attack. The malicious nodes will update the version number in the DODAG protocol.
- Trust Calculation:- The trust based scheme will be proposed in this research for the mitigation of version number attack. The trust based scheme will work, in the three phases which are pre-processing, trust calculation and trust updation.
- Analyze network performance: - In the last phase, the network performance will be analyzed in terms of certain parameters to check effectiveness of the proposed technique. The network performance will be analyzed in terms of throughput, packetloss and energy consumption.

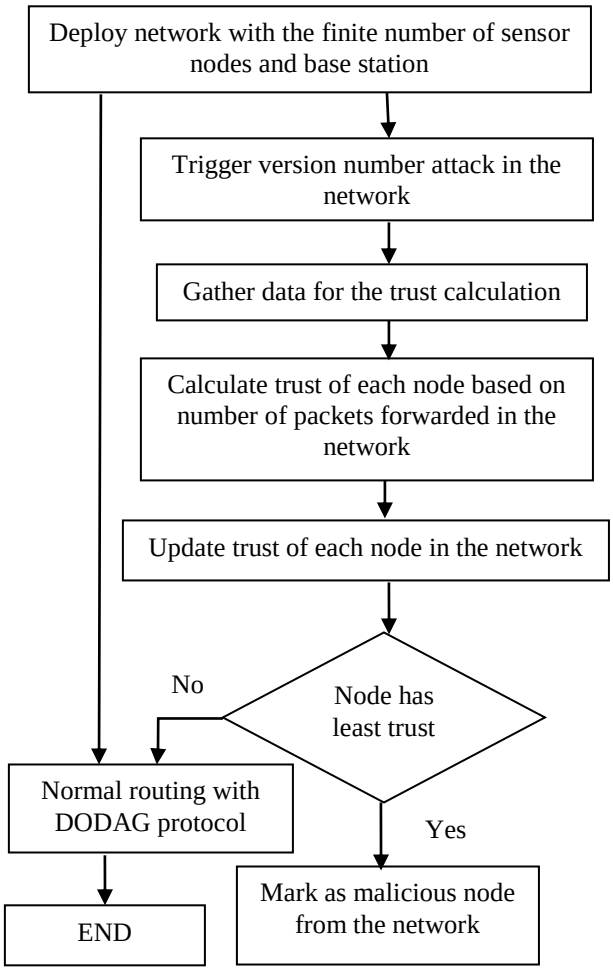

Fig. 3: Flowchart of Methodology

V. RESULTS AND DISCUSSION

This research work is related to isolation of version number attack in Internet of things. The version number attack is triggered in the DODAG protocol. In the result and discussion section, the two scenarios are compared which are DODAG protocol and impact of version number attack on performance of DODAG protocol in terms of throughput and packet loss.

TABLE II. SIMULATION PARAMETERS

Parameter	Values
Simulator	Ns2-2.35
Number of nodes	32
Area	800 * 800 meter
Antenna type	Omi-directional
Channel	Wireless channel
Propagation Model	Two ray

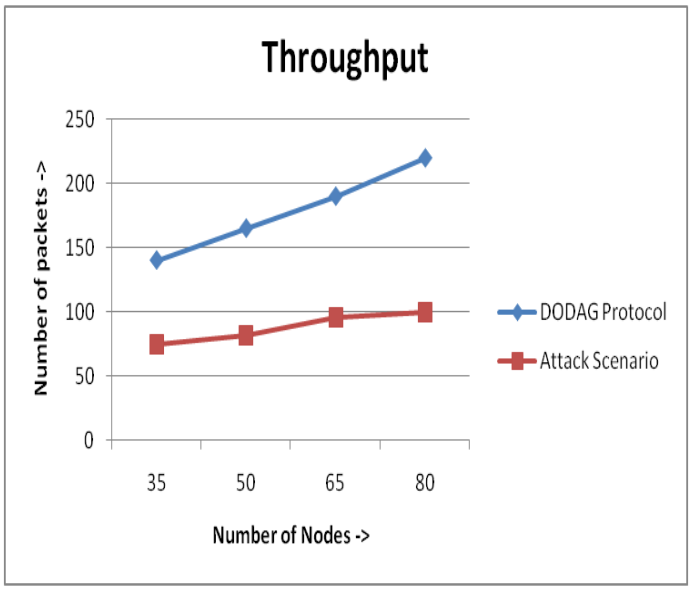

Fig. 4: Throughput Analysis

As shown in figure 4, the throughput of the DODAG protocol is compared with the attack scenario in which version number attack is triggered in the network. It is analyzed that when the attack is triggered in the network, throughput is reduced to certain extent as compared to attack scenario.

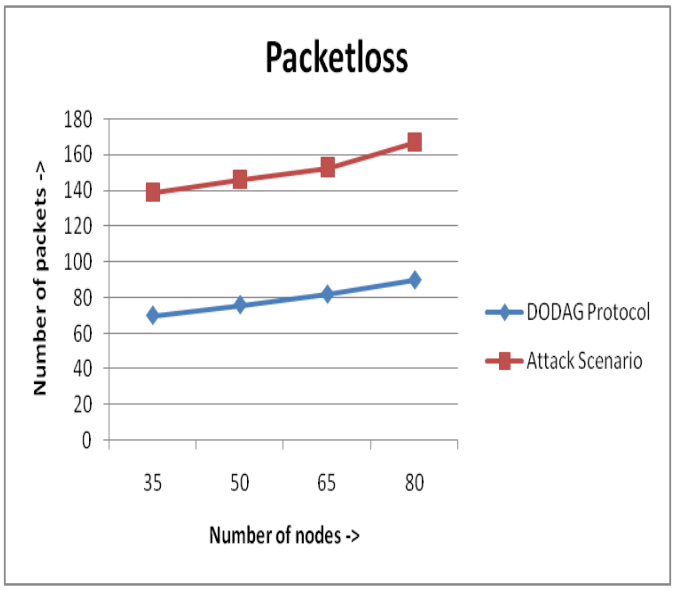

Fig. 5: Packet loss Analysis

As shown in figure 5, the packet loss of the DODAG and Attack scenarios are compared. It is analyzed that attack scenario has the greater packet loss as compared to DODAG scenario.

VI. CONCLUSION

In this paper, it is concluded that internet of things is much vulnerable towards various type of security attacks. The version number attack is the active type of attack which affects network performance. The various techniques which

already proposed are reviewed in this work. It is analyzed that some techniques are too complex and take much time for the isolation of malicious nodes. In future novel technique will be proposed for the detection of malicious nodes. The proposed technique will detect malicious nodes in least amount of time. In this paper, the DODAG protocol is compared with the attack scenario in which version number attack is triggered in IoT. The implementation results shows that throughput of the network is reduced when the version number attack in the network. The packetloss of the attack scenario is increased when the version number attack is triggered in the DODAG protocol. In future, proposed methodology will be implemented for the detection of malicious nodes in the network.

References

[1] Antar Shaddad Abdul-Qawy, Pramod P. J, E. Magesh, T. Srinivasulu, "The Internet of Things (IoT): An Overview", 2015, Int. Journal of Engineering Research and Applications, Vol. 5, Issue 12

[2] Debasis Bandyopadhyay, Jaydip Sen, "Internet of Things - Applications and Challenges in Technology and Standardization", Wireless Personal Communications, 2011, Volume 58, Issue 1, pp 49–69

[3] Dr. V. Bhuvaneswari, Dr. R Porkodi, "The Internet of Things (IoT) Applications and Communication Enabling Technology Standards: An Overview", 2014 International Conference on Intelligent Computing Applications

[4] Egemen Hopalı, Özalp Vayvay, "Internet of Things (IoT) and its Challenges for Usability in Developing Countries", 2018, International Journal of Innovation Engineering and Science Research, Volume 2 Issue 1

[5] Hui Suo, Jiafu Wan, Caifeng Zou, Jianqi Liu, "Security in the Internet of Things: A Review", 2012 International Conference on Computer Science and Electronics Engineering

[6] Emmanuel Baccelli, Matthias Philipp, "The P2P-RPL Routing Protocol for IPv6 Sensor Networks: Testbed Experiments", SoftCOM 2011, 19th International Conference on Software, Telecommunications and Computer Networks

[7] Tao Zhang, Xianfeng Li, "Evaluating and Analyzing the Performance of RPL in Contiki", 2014, Proceedings of the first international workshop on Mobile sensing, computing and communication, Pages 19-24

[8] Vera Suryani, Selo Sulistyo, Widyawan, "Trust-Based Privacy for Internet of Things", International Journal of Electrical and Computer Engineering (IJECE) Vol. 6, No. 5, October 2016, pp. 2396-2402

[9] Ahmet Arıs, Sıddıka Berna Ors Yal, Sema F. Oktug, "New Lightweight Mitigation Techniques for RPL Version Number Attacks", Ad Hoc Networks, Volume 85, 15 March 2019, Pages 81-91

[10] Anthea Mayzaud, Remi Badonnel, Isabelle Chrisment, "A Distributed Monitoring Strategy for Detecting Version Number Attacks in RPL-based Networks", IEEE Transactions on Network and Service Management, Volume: 14, Issue: 2, 2017

[11] Amit Dvir, Tamas Holczer, Levente Buttyan, "VeRA - Version Number and Rank Authentication in RPL", IEEE 8th International Conference on Mobile Adhoc and Sensor Systems

[12] Anthea Mayzaud, Remi Badonnel, Isabelle Chrisment, "Detecting Version Number Attacks in RPL-based Networks using a Distributed Monitoring Architecture", 2016 12th International Conference on Network and Service Management (CNSM)

[13] Zeeshan Ali Khan and Peter Herrmann, "A Trust Based Distributed Intrusion Detection Mechanism for Internet of Things", 2017 IEEE 31st International Conference on Advanced Information Networking and Applications

[14] H. Abdo, M. Kaouk, J-M. Flaus, F. Masse, "A safety/security risk analysis approach of Industrial Control Systems: A cyber bowtie - combining new version of attack tree with bowtie analysis", Computers & Security, Volume 72, January 2018, Pages 175-195

[15] Ahmet Aris, Sema F. Oktug, S. Berna Ors Yalcin, "RPL Version Number Attacks: In-depth Study", 2016 IEEE/IFIP Network Operations and Management Symposium (NOMS)

[16] Hezam Akram Abdul-Ghani, Dimitri Konstantas, Mohammed Mahyoub, "A Comprehensive IoT Attacks Survey based on a Building-blocked Reference Model", 2018, (IJACSA) International Journal of Advanced Computer Science and Applications, Vol. 9, No. 3

[17] Anthea Mayzaud, Remi Badonnel, and Isabelle Chrisment, "A Taxonomy of Attacks in RPL-based Internet of Things", International Journal of Network Security, Vol.18, No.3, PP.459-473, 2016

[18] Seungyong Yoon, Jeongnyeo Kim, "Remote security management server for IoT devices", 2017 International Conference on Information and Communication Technology Convergence (ICTC)

Proceedings of the Fourth International Conference on Communication and Electronics Systems (ICCES 2019)
IEEE Conference Record # 45898; IEEE Xplore ISBN: 978-1-7281-1261-9

Design and Development of IOT Based SMART water distribution network for Residential areas

Chetan S. Patel
Dept.of Instrumentation & Control Engg.
Vishwakarma Institute of Technology,
Pune, India.
chetan.patel18@vit.edu

Jitendra A. Gaikwad
Dept. of Instrumentation & Control Engg.
Vishwakarma Institute of Technology,
Pune, India.
jitendra.gaikwad@vit.edu

Abstract *– Water is most valuable in human beings but, now a day's water level in water resources are decreases fastly. Because of less rain fall the need of water is increases. Huge growth of residential areas have increases water demand to accomplish their daily needs. People use water for different ways and everyone use different amount of water as their needs. In this project, to focusing on real time monitoring of water supply in IOT based and also controlling a valve w.r.t. distributed same amount of water in all consumers, maintain a water quality and also maintain a water level in a main water tank. Basically this system is applicable for buildings/society.*

Raspberry pi is used for collected all sensor data (Flow sensor, Ultrasonic sensor, Turbidity sensor) and store it to cloud server. Thingspeak server is used as cloud for store a data and Firebase cloud server is used to showing real-time data in android application.

Keywords*: Raspberry pi, Stepper motor, IOT, Network Protocol – Wife Protocol, Application protocol- HTTP, Android app, Flow measurement, Automated Supply.*

1. INTRODUCTION

Water is basic need for all living beings. Now a days, Economic growth is increasing drastically and water demand of consumers are increasing. Therefore, in urban areas, we need to monitor a supply of water continuously and distributed equally. Here it focused to solve an issue of improper water supply and automatically maintaining water level of water in main water tank. Supply water in all consumers automatically.

In this research work, it is proposed to develop an IOT based remote water monitoring and controlling system by monitoring a flow rate at the consumer end and to control a water level in main supply tank is controlled using ultrasonic sensor and water pump. It also maintains a water quality by adding chlorine content in water. This web based system compatible with mobile phones to know the status of control room from remote locations. These recorded data is showing in real-time in mobile android application.

In this paper, solving a main issue for distributed equal amount of water, water quality and equal flow rate in all consumers. For maintaining equal flow rate to using stepper motor fitted manual control valve to change a position of valve with the help of rotation of stepper motor. This system is design on-line billing system for end- users. Therefore end-users are paying only for water used and thereby reducing the complaints.

1.1 EXISTING SYSTEM

The existing method provides a controlling electrical supply of motor to changing its speed for maintaining equality of flow rates to all consumers. Or another method is used a solenoid control valve of 4 direction to maintain equal flow rates. It will operate in manually/automatically.

1.2 PROPOSED SYSTEM

Before explaining the proposed system let us know about why we need to maintain a usage of water. Cities usually used source water from rivers, lakes, and ground reservoirs. A level of water quantity in these resources are decreasing rapidly because of less rainfall and increasing a use of water in cities. For providing water to all need to be control wastage of water. Our system focus on, Internet of Things which is a new concept to make city as a smart city with different application. Main objective to implement this project is to design and develop a low cost reliable and efficient technique to make proper water distribution and controlling its quality and flow rate to all so that we can solve water related problems. Proposed consist of Raspberry pi used as a mini computer, different sensor such as ultrasonic sensor, water flow sensor and turbidity sensor are used. Arduino collects the dada from sensors and send it to raspberry pi then raspberry pi is controlling a flow of water

with the help of changing a position of stepper motor which is fitted in shaft of manually operated control valve. Continuous monitoring is possible in central server and android application.

.

2. LITERATURE REVIEW

In [1] implemented an anti-theft control system for drinking water supply. Flow sensor is used for finding thieves.

In [2] the author is implemented an IOT based water supply monitoring and controlling system. In this system, to calculate a flow of water passes through flow sensor and also check a soil content in water and operated solenoid valve automatically fully ON/OFF.

In [3] the author is implemented an Automation in drinking water supply distributed system and testing of water. Author used a PLC and SCADA to check a water quality and added chlorine content in water.

In [6] Microcontroller Based Water Level Indicator and Controller system is developed for automatically control a level of water in tank using AT89C52 microcontroller and level sensor is used.

3. SYSTEM DESCRIPTION

3.1 Block Diagram :

Following figure 1 shows a block diagram of hardware used in system.

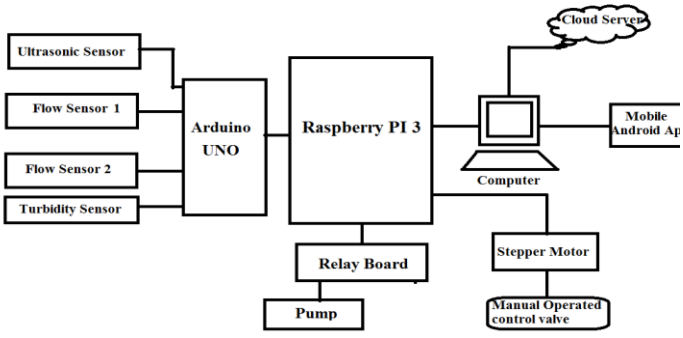

Fig. 1 Block Diagram of a system

System consists of Raspberry pi, Arduino UNO, Ultrasonic sensor, Flow sensor, Turbidity sensor, Water Pump, Stepper motor fitted Manual control valve.

3.2 Design and Implementation :

3.2.1 Flow Chart :

For this project, Arduino UNO and Raspberry pi are used to monitor a level of water in main water tank and control a water pump. Water is distributed equally and monitoring a flow rate and controlling a manual valve using stepper motor for changing its direction continuously. And turbidity sensor measures a quality of water and by adding chlorine in water to maintain a water quality.

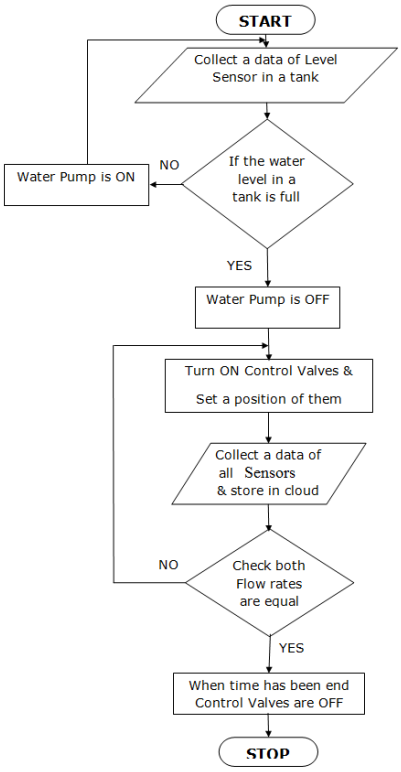

Fig.2 Flow chart of a system

In the above figure 2 shows, a process of our system. After starting a system firstly checks a level of water in tank and w.r.t. to water level pump should be ON/OFF automatically. Then turbidity sensor checks a water quality of water in tank and added chlorine w.r.t. turbidity, then control valves are open and flow sensors are starts recording a data and these recorded data sends to cloud. Using these flow rates controlling a stepper motor fitted manual control valves position for maintaining a equal flows. After time ends control valves are turns fully OFF.

3.2.2 Implementation :

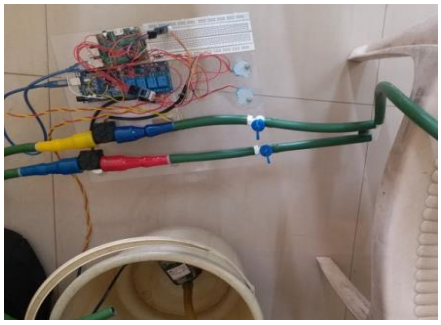

Fig. 3 Hardware of a system

Above figure 3 shows a hardware of a system, all modules can be implemented Raspberry pi and Arduino UNO. Automatically monitoring and controlling of

water supply can be well executed by all sensors data to the raspberry Pi module. Flow sensors are used for measuring a flow of water easily which passes through the consumer's pipeline. And turbidity sensors are check a quality of water.

Following components are used in system:

1. Ultrasonic Sensor:

HC-SR04 sensor is a ultrasonic module for non-contacting distance measurement. Ranges from 2cm to 400cm. this sensor uses sonar to measure distance with high accuracy and stable readings. This module consists of transmitter, receiver and control circuit. An ultrasonic sensor is fitted on the top of the main water tank. Ultrasonic sensor works on the transmitting and receiving a ultrasonic pulse at the speed of sound from the liquid surface. This sensor works on a time difference between transmission and reception of ultrasonic waves are calculated using formula of speed of sound, Speed=Distance/Time. Using this formula, easily measure a distance between the source and target. Distance= Speed*Time/2.

Installation of this sensor is easy on main water tank.

2. Flow Sensor:

This sensor is used for calculating a flow rate of water which passes in a pipeline of consumers. And also using this flow rate to calculate a total flow of water passes in a pipeline. For determining a liquid flow rate in such cases is Q= V * A. where Q is flow rate of water through pipe, V is average velocity of the flow and A is cross sectional area of the pipe. Equation –

Liters = Pulses / (7.5 * 60).

Flow sensors are mounted on every consumer's pipeline.

3. Turbidity sensor :

This sensor is used for checking a water quality in water tank. And using these recorded data to maintain a water quality by adding chlorine in water.

4. Control valves :

A manual control valve is used having fitted a stepper motor's shaft on the top of the control valve handle. This construction is used for maintaining an equal flow rate to all consumers. System checks all consumer's flow rate and compare these flow rates and if these are not equal then stepper motor is trying to control a equal flow passes in a pipelines to changing a stepper motor's shaft angle/direction. This controlling action is done through a raspberry pi. When consumer consumes its water quantity which are to be specified valves are closed. And if consumer needs more water then they should pay more for extra water.

5. Relay :

Relay is a switching device which is operated in a 5v/12v DC power supply. It is used for to switch ON /OFF a water pump. This relay is to be operated through a Raspberry Pi 3 controller.

6. Internet of Things :

The interconnection via the internet of computing devices embedded in everyday objects, enabling them to send and receive data. It has ability to transfer data over a network without requiring human to human or human to computer interaction.

In this project, Thingspeak and Firebase cloud servers are used to store a data.

Thigspeak server is a open IOT platform with MATLAB an analytics. It is used to store and retrieve data from things using a HTTP protocol over the internet. It provides apps that let you analyze and visualize your data. Firebase cloud server is used for store a real-time data continuously and showing a real-time data continuously in android mobile application which have developed.

Firebase is Google's mobile platform that helps you quickly develop high-quality apps.

In this project, all sensors data are recorded to Raspberry Pi through Arduino UNO and using Raspberry pi sent these data to both clouds Thingspeak and Firebase using IEEE 802.15-WiFi network protocol and used HTTP application protocol for sending and retrieving data to cloud.

3.3 Software :

The programming language is used in this project is PYTHON in Raspberry Pi and C in Arduino UNO. PYTHON 3.5 version is used for programming in Raspberry pi 3.

4. RESULT

After all connection are done, through putty login pi is start in laptop and run a command sudo python filename. Once a command executed project starts our execution in step wise which is mentions a flow of project in previous section. To store a recorded data used for Thingspeak and firebase. Thingspeak cloud server is displaying these data in a graph format. Following Figure 4 shows a Thingspeak web screen. Which is displaying a data of level of water in tank and both flow sensors recorded data in separate graphs. These graphs are used for monitoring and using these graphs further predication is easily done.

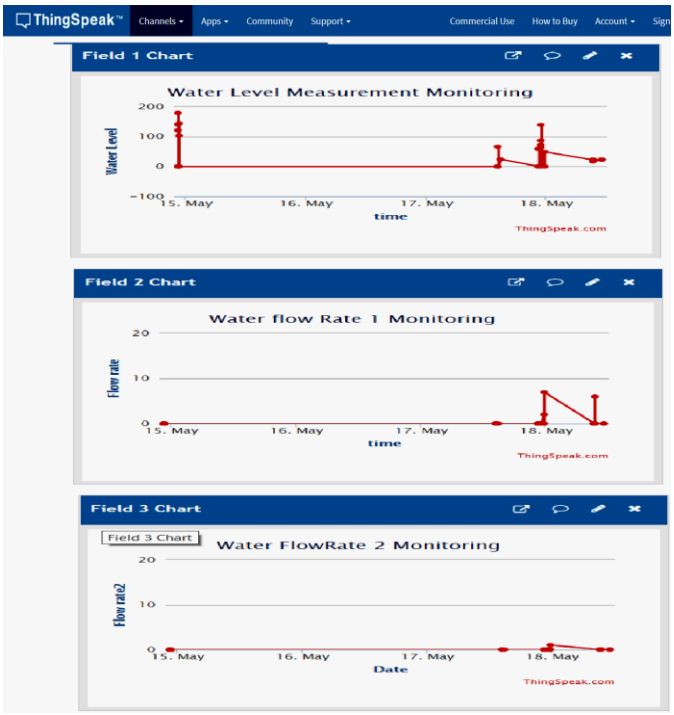

Fig.4 Thingspeak web monitor of a system

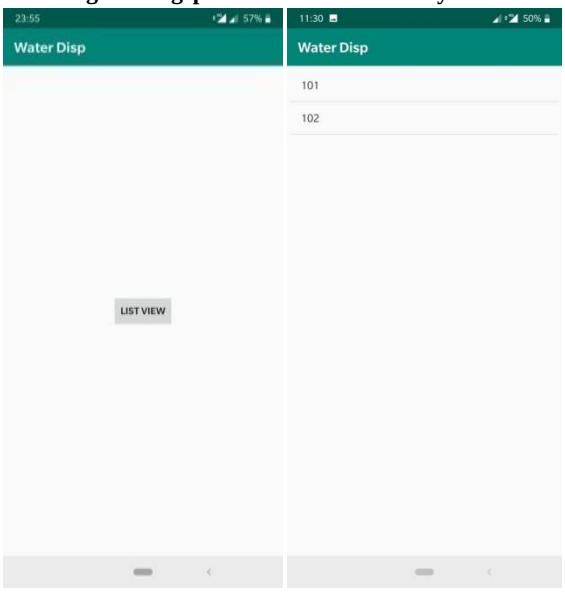

(a) (b)

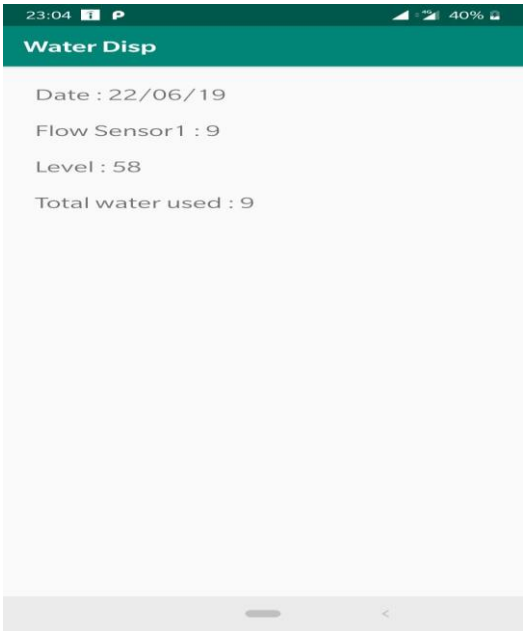

(c)

Fig.5 Android Application screens sequentially

The above fig. 5 shows an android mobile application screens. After opening an application 1st window is displayed, this is home screen of application. When click on button "LIST VIEW" different locations are listed in 2nd window. Then following figure 5(b) is displaying a list of flat numbers after clicking on any one in a list, a data of flow rate, level of main water tank and total water used in this flat consumer are displaying continuously with current date which are displaying in a figure 5(c). And on-line bill is generated for end-user for consuming its water.

5. CONCLUSION

Our proposed system is truly based on IOT. Using this system secure and continuous monitoring is possible No need to go on field for monitoring so manual work has been reduced it makes system more efficient, reliable, low cost and accurate. Data monitoring is easy from anywhere controlling is done automatically w.r.t. changing a flow rate. Flow rate is maintaining equally to changing a control valves position. Maintain a water quality by adding chlorine automatically. And also automatically maintain a water level in main water tank. Using this system, to reduce a water wastage. Water distribution as per Geographical survey and population density. Develop a web based and automatic Meter reading system. Therefore, 24*7 safe drinking water is provided.

In future this system is used for a specific area and city. Easily increase a number of connections and for using this system easily finding a theft of water and leakage of pipe.

6. REFERENCE

[1] REVANTH C.B," e-Water supply system using Python, Raspberry Pi and IOT", International Research Journal of Engineering and Technology (IRJET)- August 2017.

[2] Kusuma S S1, Anil G N2 "An IOT based Water Supply Monitoring and Controlling System", International Research Journal of Engineering and Technology (IRJET)-.Volume:05 issue: 02 feb.-2018.

[3] Mr. Prashant palkar1 , Prof. (Dr.) Shrinivas Patil2 Prof. Mrs. Pooja Belagali3, Mr. Ashish Chougule4, "Automation in drinking water supply distributed system and testing of water", IOSR Journal of Electronics & Communication Engineering (IOSR-ECE).

[4] E.Vinothini, N. (Suganya Department of Pervasive Computing Technology, Kings College of Engineering, Punalkulam, Tamilnadu)" Automated Water Distribution and Performance Monitoring System", International Journal of Engineering and Innovative Technology (IJEIT) Volume 3, Issue 8, February 2014.

[5] Debasis Bandyopadhyay · Jaydip Sen, "Internet of Things - Applications and Challenges in Technology and Standardization", May-2011.

[6] Ejiofor Virginia Ebere(PhD)"Microcontroller Based Water Level Control System", International journal of Innovative Research in computer and communication Research(IJIRCCR) Volume1,Issue6,August2013.

[7] A. J. Whittle, M. Allen, A. Preis and M. Iqbal "Sensor networks for monitoring and control of water distribution system" The 6th International Conference on Structural Health Monitoring of Intelligent Infrastructure Hong Kong 9---11 December 2013 Journal of Wireless Mobile Networks, Ubiquitous Computing, and Dependable Applications, volume: 6,number:1,pp.4-23.

[8] Mohammad Rizwan "Leak detection in pipeline system based on flow induced vibration methodology in pipeline International journal of science and research".

[9] Riasood, Manjitkaur, HemantLenka"Design and development of automatic water flow meter " International journal of computer science,engineering and applications vol 3 june 2013.

[10] DebasisBandyopadhyay · JaydipSen "Internet of Things - Applications and Challenges in Technology and Standardization".

[11] V.Rajeswari, Padma suresh, Y.Rajeswari: "Water Storage and Distribution System for Pharmaceuticals using PLC and SCADA", International conference on Circuits, Power and Computing Technologies, 2013.

[12] Panindra reddy, Eswaran: "Metro overhead tanks monitoring system using ZigBee based WSN", IEEE conference on Information and Communication Technologies, 2013.

Proceedings of the Fourth International Conference on Communication and Electronics Systems (ICCES 2019)
IEEE Conference Record # 45898; IEEE Xplore ISBN: 978-1-7281-1261-9

Standalone PV System Integrated with Hysteresis Current Controlled Inverter using MPPT Techniques

Saurav Sahoo
Department of Electrical Engineering
IIIT Bhubaneswar, Odisha, India
b315043@iiit-bh.ac

Saroj Kumar Mishra
Department of Electrical Engineering
IIIT Bhubaneswar, Odisha, India
saroj@iiit-bh.ac.in

Jayanta Kumar Sahu
Department of Electrical Engineering
IIIT Bhubaneswar, Odisha, India
jayanta@iiit-bh.ac.in

***Abstract* - PV System is one of the most clean and preferable source of energy. In this article, the PV System is used in special type of inverter known as Hysteresis Current Control (HCC) Inverter. The proposed system incorporates boost converter which uses tracking algorithm known as maximum power point tracking (MPPT). Various tracking mechanisms are available for extraction of maximum power, Two MPPT techniques used here are Perturb and Observe (P&O) method and Incremental Conductance (IC) method. The MPPT methods help the system to function more effectively. The output of the converter is given to a two level inverter. The inverter works on current control technique in which line current is forced to follow a reference current within a specific band. At last, the current output harmonics of the proposed system is compared with MPPT and without MPPT technique by using MATLAB simulation environment. Considering the THD values, it is found that MPPT optimized PV system gives better result.**

Keywords – Hysteresis Current Control (HCC), Incremental Conductance (IC), Perturb and Observe (P&O)

I. INTRODUCTION

For more than hundred years, we are dependent on the traditional source of energy like coal, oil, natural gas etc. But these fuels are increasingly depleting and there is a strong need of alternate source of energy. Also the problem with the conventional source of energy is that it creates atmospheric pollution and other health related problems in human beings. So there is a need of clean and sustainable source of energy. Due to these above reasons, it makes renewable source of energy as area of interest in research in recent times [1, 10]. There are variety of renewable source of energy such as solar, wind, hydro, geothermal energy etc. In this paper, the solar photovoltaic with the use of MPPT is the main focus of study [12].

Solar radiation is the virtually unlimited source of renewable energy. The solar PV converts light energy that is photon from the sun into electrical energy. A solar cell is the main building block of photovoltaic power generation. The PV panel output power varies inversely with temperature and directly with amount of solar radiation (irradiance).

It is important for the researchers to get maximum power from the solar cell. MPPT technique is used in order to get utmost performance from the solar panels. Two MPPT methods have been used here. P&O is a MPPT method in which the output power of solar panel is given a perturbation, and with the change in power, change in voltage is occurred according to which the duty ratio of the boost converter is varied for obtaining maximum power.

In IC method, the terminal voltage of array is as per MPP voltage. It works on basis of relationship between incremental and instantaneous conductance of PV array. The MPPT techniques are implemented by controlling the duty cycle of DC to DC boost converter. In order to get AC, another converter is used that is the inverter.

The inverter works on technique which follows the current within a specific band. Here inverter line current tracks a reference signal for obtaining switching optimization which leads to excellent effective response and high efficiency in steady state condition. In this paper, single band HCC inverter is used with RL load. Finally, the THD of inverter output current is compared with MPPT and without MPPT method.

II. PV ARRAY

A Photovoltaic system is a collection of solar panels built to exploit solar radiation by using solar cells. PV systems can be classified on basis of their functions, operations, configurations and how they are interconnected with the loads and sources. The two well-known classifications are Grid connected and Standalone system [4]. The PV modules are connected in series and parallel to form an array. The PV panels are generally rated by the maximum output power under standard operating conditions such as operating temperature of 25^0C / 298K, irradiance of 1000 watt per square meter and Air mass of 1.5 spectral distributions.

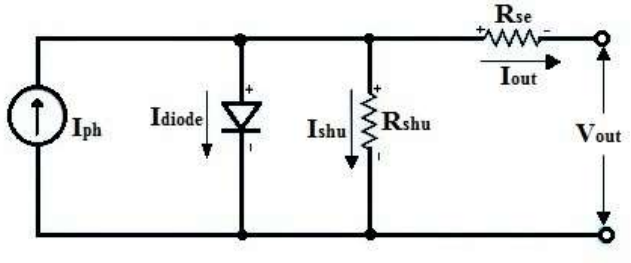

Fig. 1. Equivalent circuit of PV cell

From the above figure equations can be framed as [1]:

$$I_{out} = I_{ph} - I_{diode} - I_{shu}$$

$$I_{ph} = \left[I_{sc} + K_i \bullet (T - 298) \right] \times \left(\frac{G}{1000} \right)$$

$$I_{diode} = I_o \left\{ e^{\left(\frac{V_{diode}}{N \bullet V_T} \right)} - 1 \right\}$$

$$V_T = \frac{K \bullet T}{Q} \times N_{cell}$$

$$I_{shu} = \frac{V_{diode}}{R_{shu}} = \frac{V_{out} + I_{out} \bullet R_{se}}{R_{shu}}$$

$$I_{out} = I_{ph} - I_o \left\{ e^{\left(\frac{V_{diode}}{N \bullet V_T} \right)} - 1 \right\} - \left\{ \frac{V + I_{out} \bullet R_{se}}{R_{shu}} \right\}$$

Where I_0 is the reverse saturation current, I is the current through shunt resistor R_{shu}.

III. MAXIMUM POWER POINT TRACKING

Maximum Power Point Tracking is a technique used in PV System for deriving maximum power from solar module under all circumstances [11, 12]. Broadly, there are two types of MPPT techniques such as mechanical MPPT and electronics MPPT.

Mechanical MPPT is based on the solar angle incidence and mechanical moving of solar panel according to it. Electronic MPPT is based on the use of algorithm in order to extract maximum power from solar cell.

As the temperature and irradiance varies the load characteristics changes. This load characteristic is called MPP. The process of searching for optimum point & maintaining load characteristics there is called MPPT. In this paper, two types of MPPT algorithm are used that is P&O method and IC method.

1. PERTURB AND OBSERVE METHOD

P&O method is also denominated as hill climbing method. It is one of the most common forms of MPPT algorithm [11]. In this method, a small perturbation is given in the voltage of PV Module, like a small increment which results in change in power (ΔP). If ΔP increases or is positive, the operating point moves towards optimum point (V_{mpp}, I_{mpp}). Thus voltage is further changed in the same direction till it reaches optimum point (V_{mpp}, I_{mpp}). If ΔP decreases or is negative, the operating point moves away from optimum point (V_{mpp}, I_{mpp}). When stable condition arrives the algorithm oscillates around maximum power point. In this method if duty cycle taken is large value then there will be more oscillation around MPP and there will be power loss, to solve this problem we can reduce the value of duty cycle to a small value. But if the value of duty cycle is taken to be very low the time required to reach MPP will be more.

2. INCREMENTAL CONDUCTANCE METHOD

IC method works on adjustment of the PV Module terminal voltage. It is based on relationship between incremental and instantaneous conductance [10]. The system is assumed to reach the optimum point (V_{mpp}, I_{mpp}), when the change in the output conductance is equal to negative output instantaneous conductance. The mathematical formulation is given below.

P = V X I

Differentiating both sides w.r.t V

$$\Rightarrow \frac{\partial P}{\partial V} = I \times \left(\frac{\partial V}{\partial V} \right) + V \times \left(\frac{\partial I}{\partial V} \right)$$

$$\Rightarrow \frac{\partial P}{\partial V} = I + V \times \left(\frac{\partial I}{\partial V} \right)$$

For obtaining the maximum power, $\partial P/\partial V$ must be equal to 0

$$\Rightarrow \frac{\partial P}{\partial V} = 0$$

$$\Rightarrow V \times \left(\frac{\partial I}{\partial V} \right) = -I$$

$$\Rightarrow \left(\frac{\partial I}{\partial V} \right) = \frac{-I}{V}$$

$$\Rightarrow \left(\frac{\partial I}{\partial V} \right) + \left(\frac{I}{V} \right) = 0$$

If $\frac{\partial P}{\partial V} > 0$ or $\frac{\partial I}{\partial V} > \frac{-I}{V}$, left to MPP,

If $\frac{\partial P}{\partial V} < 0$ or $\frac{\partial I}{\partial V} < \frac{-I}{V}$, right to MPP

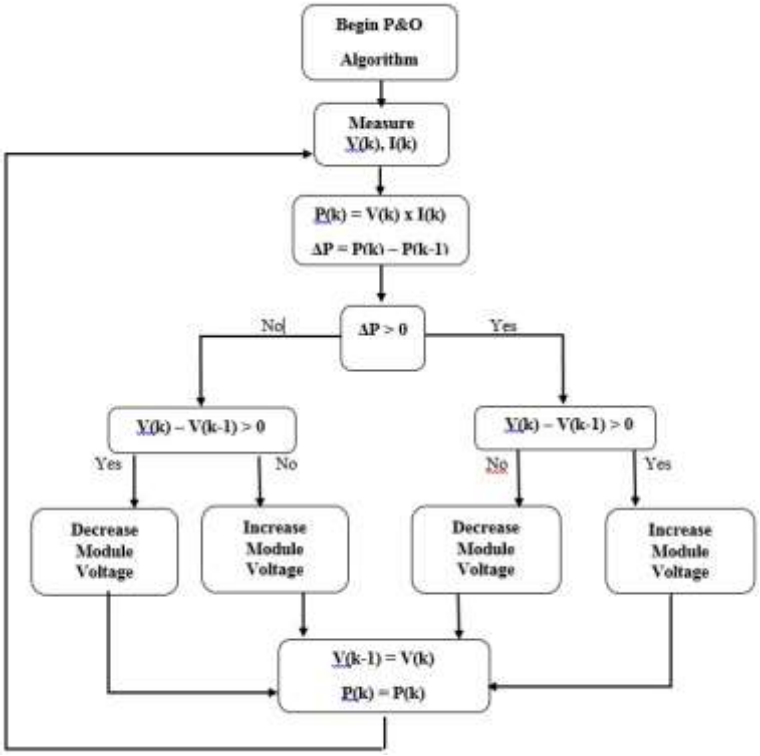

Fig. 2. P&O Algorithm Flowchart

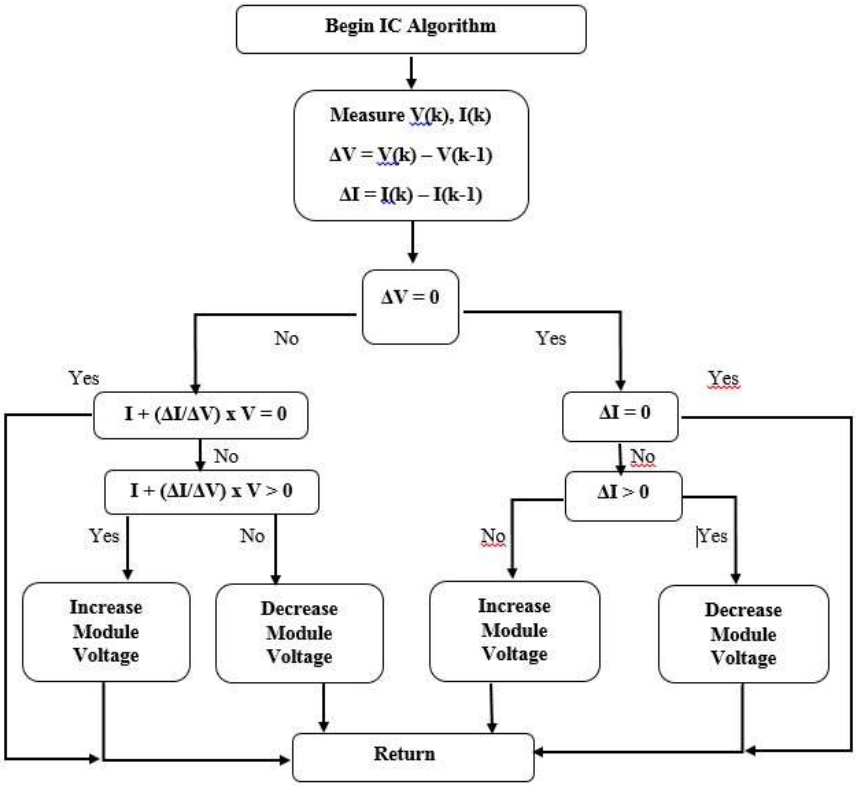

Fig. 3. IC Algorithm Flowchart

IV. BOOST CONVERTER

It acts as interface system between PV the module and the inverter. It is a type of dc-dc converter in which the average output dc voltage V_0 is greater than the input dc source voltage V_{exc} . When the converter is ON for a period of T_{on}, the inductor stores charge during this time. When the converter is OFF for a period of T_{off}, the current is forced to flow through the diode and the load. Due to which, the output load voltage is defined by $V_{out} = V_{exc} + L\left(\frac{di}{dt}\right)$ exceeds the source voltage V_s. The capacitor gives the stable voltage at the output. The equation governing the input and output voltage is given by [9]:

$V_{out} = \frac{V_{exc}}{(1-\alpha)}$, where α is the duty cycle and can be represented as:

$$\alpha = \frac{T_{on}}{T}$$

$$T = T_{on} + T_{off}$$

V. HYSTERESIS CURRENT CONTROL (HCC) INVERTER

HCC inverter is based on current control technique in which line current of inverter is forced to follow a reference current within a specific band known as Hysteresis Band [2, 6-8]. In HCC inverter switching pattern depend on feedback of inverter current which is different from PWM case where inverter current can be pre-detected.The tracking of inverter line current to reference current is done on an instantaneous basis. The difference of reference current and line current gives the error signal, which is then passed through a relay with a band or the Hysteresis band. The maximum and minimum value of this error signal is $e_{\max}$ and $e_{\min}$ respectively [3.5]. The output of the band is given as input as gated pulse to one pair of IGBT and the inverted signal to the other pair of IGBT using logical NOT gate. The produced output voltage is bipolar in nature and it switches from plus DC voltage to minus DC voltage, and vice versa, to control the output current so that it remains in the hysteresis band. The equations are given as:

$$e(t) = i_{inv}^{*} - i_{inv}$$

$$e_{\min} \le e(t) \le e_{\max}$$

If $e(t) = e_{\min}$, then $v_{inv}(t) = V$ and turn ON S1 and S4 else if

$e(t) = e_{\max}$, then $v_{inv}(t) = -V$ and turn ON S2 and S3

VI. THE PROPOSED SYSTEM

In the proposed system, the PV module is connected with a boost converter which boosts up the voltage and also gives stable voltage to the inverter. Here the simulation is done without MPPT in case 1. The simulation is done using P&O MPPT technique in case 2 and with IC MPPT technique method in case 3.

1. Without any MPPT Method
As the title suggest this part was done without the use of any MPPT technique. The PV array block is already present in MATLAB 2015a.

2. With P&O MPPT Method
All the specification remains same in all the blocks except pulse generator block which is replaced by P&O block. The P&O block takes the PV voltage and PV current as input and the output of the block is used to give pulse to the controlled switch of the boost converter.

3. With IC MPPT Method
All the specification remains same in all the blocks except pulse generator block which is replaced by IC block. The IC block takes the PV voltage and PV current as input and the output of the block is used to give pulse to the boost converter switch. It also has another input as step block to on and off the switch in the algorithm.

The proposed model is presented in fig.4.The reference current is taken as to be a sinusoidal current. The output of the relay block is kept '0', when off and '1' when on. The specification of PV array is declared at the beginning. The Model No. of the PV Module is Soltech 1STH-215-P. The switch of the boost converter is actuated by using pulse generator block of Simulink. The specification of the pulse generator block is given below:
Amplitude = 1
Time Period = 0.0001 sec
Pulse Width (% of Time Period) = 50%
Pulse Delay = 0

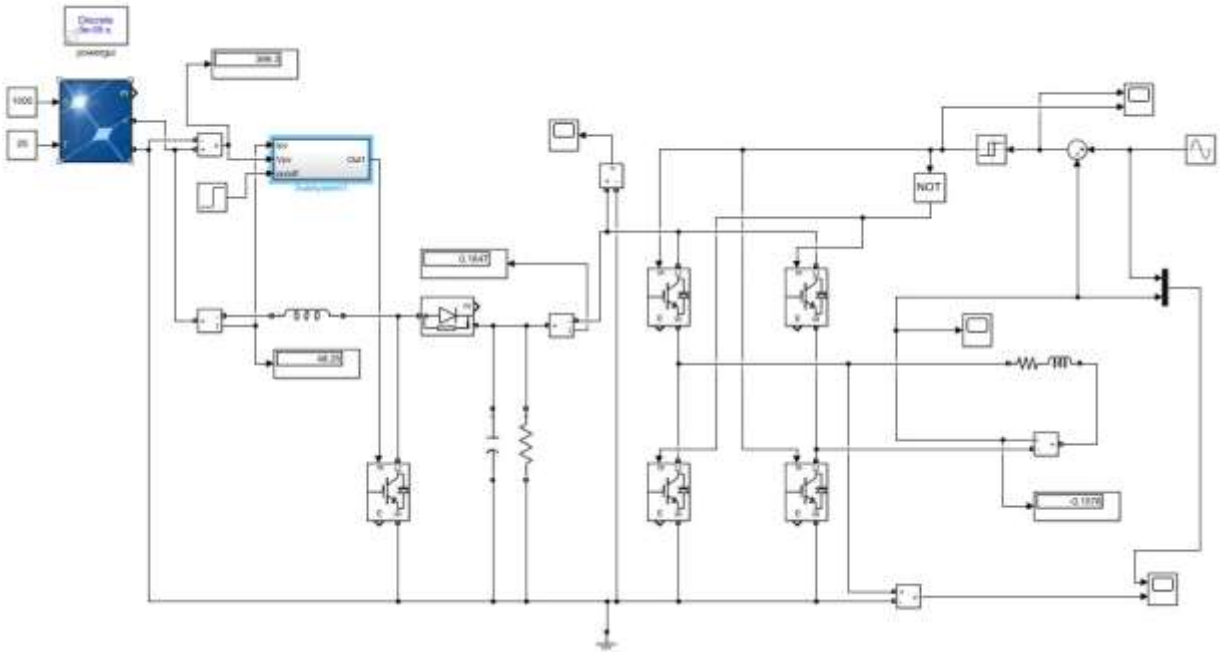

Fig. 4. Simulink model with IC Algorithm

VII. SIMULATION RESULTS

1. Without MPPT

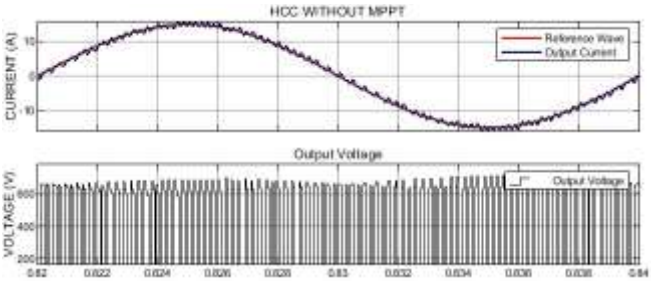

Fig. 5. Output current & voltage waveform

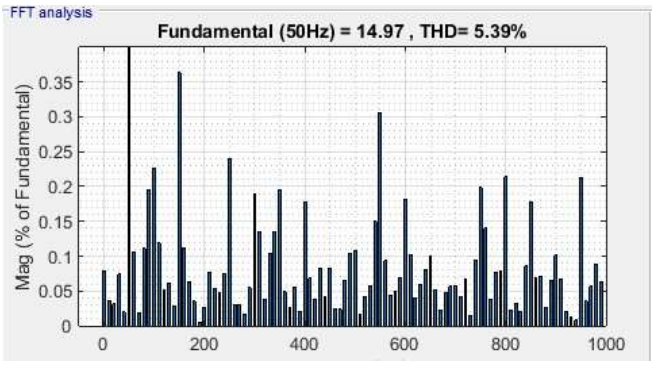

Fig. 6. THD Analysis

2. With P&O MPPT Algorithm

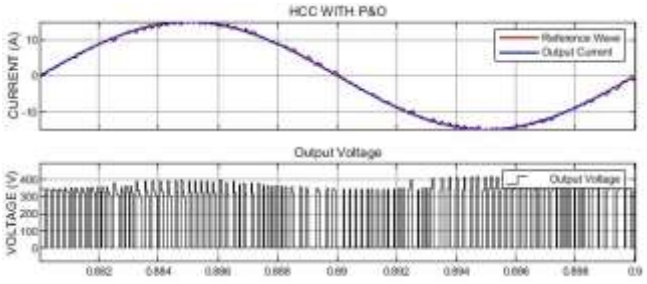

Fig. 7. Output current & voltage waveform

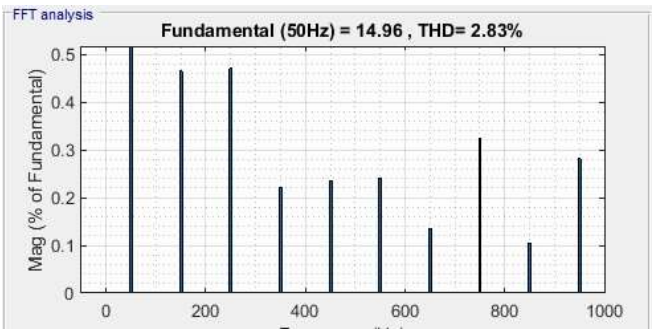

Fig. 8. THD Analysis

3. With IC MPPT Algorithm

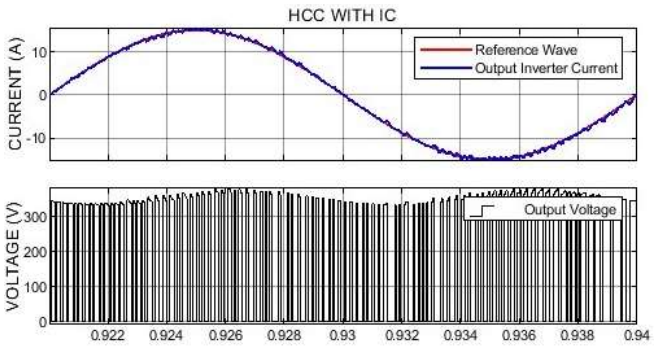

Fig. 9. Output current & voltage waveform

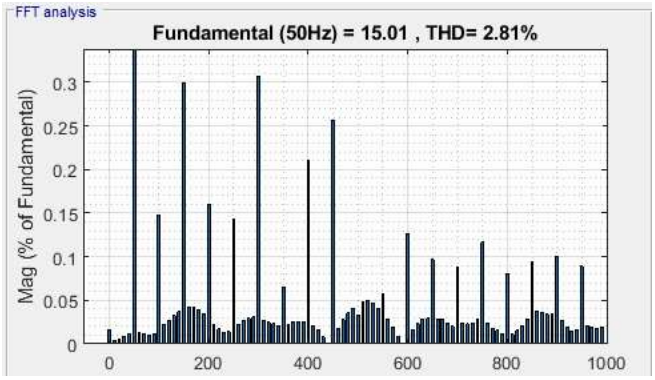

Fig. 10. THD Analysis

VIII. RESULT

Reference current Amplitude = 15A
Simulation time = 1 second
Frequency = 50 Hz
Start time = 0.5 second
No. of cycles = 5

Methods	*Without MPPT*	*With P&O MPPT*	*With IC MPPT*
THD	*5.39%*	*2.83%*	*2.81%*
Current Amplitude	*14.97*	*14.96*	*15.01*

IX. CONCLUSION

This paper presents about a Standalone solar PV integrated to the Hysteresis Current Control inverter. The solar PV is first connected to boost converter which is then connected to the inverter. At first the switching pulse of boost converter is controlled via pulse generator to generate appropriate duty cycle. The THD was calculated. The same process was repeated but this time the switching action of boost converter was controlled by P&O block which takes PV module voltage and current as input and in return controls the duty cycle of boost converter. The THD was found. The above process was again repeated by using IC block using voltage and current of PV array as input along with an on/off switch to control the pulses of boost converter. Considering the THD values, the method using MPPT techniques were better than the conventional method. The Implementation of IC MPPT technique was better than the P&O MPPT technique on the basis of harmonic analysis. The use of hysteresis current control inverter, which gives excellent effective response and high efficiency in steady state response, not only controls the current ripple within hysteresis band but also reduces overall harmonics.

REFERENCES

[1] Villalva M. G., Gazoli, J. R., & Filho E.R., "Comprehensive Approach to Modelling and Simulation of Photovoltaic Arrays", IEEE Trans. Power Elec., vol. 24, no. 5, pp: 1198–1208, 2009.

[2] Zhilei Yao & Lan Xiao, "Two-Switch Dual – Buck Grid – Connected Inverter With Hysteresis Current Control", IEEE Trans. on Power Elec., vol. 27, no. 7, July 2012.

[3] Ahmad Albanna, "Modelling & Simulation of Hysteresis Current Controlled Inverters Using MATLAB", Mississippi State University, General Motors Corporation, United States of America, *IntechOpen*, Sep. 2011.

[4] S. S. Pati, & S. K. Mishra, "A PSO Based Modified Multistage Controller for Automatic Generation Control with integrating Renewable Sources and FACT Device", International Journal of Renewable Energy Research, vol.9, no.2, pp.673-686, 2019.

[5] Pekik Argo Dahono & Iskandar Krisbiantoro, "A Hysteresis Current Controller for Single-phase Full-Bridge Inverters", *IEEE Conference*, pp. 415-419, 2001

[6] Fengjiang Wcu, Xiaoguang Li & Jiandong Duan, " Improved Elimination Scheme of Current Zero Crossing Distortion in Unipolar Hysteresis current control Grid –Connected Inverter ", IEEE Trans. on Industrial Informatics, vol. 11, no. 5, Oct. 2015

[7] D. Bini Sherlin & J. C. Paul Immanuel, "A PV Generation System Integrating a HCC Inverter for Stand-Alone Application". *IEEE ICCPCT*, pp. 668-673, 2014

[8] K. Punitha, D. Devaraj, S. Sakthivel, "Adaptive Hysteresis Current Controlled Multilevel Inverter for Solar PV Applications". *Springer*, June 2014.

[9] S. Sheik Mohammed & D. Devaraj, "Simulation and Analysis of Stand-alone Photovoltaic System with Boost Converter using MATLAB/Simulink". *IEEE ICCPCT*, pp. 814-821, 2014.

[10] S. K. Mishra, & S. S. Pati, "Modelling of Differential Evolution Based Automatic Generation Control for Two Area Interconnected Power Systems", Journal of Informatics and Mathematical Sciences, vol.11, no.1, pp.19-30, 2019.

[11] Subudhi Bidyadhar, Pradhan Raseswari, "A Comparative Study on Maximum Power Point Tracking Techniques for Photovoltaic Power Systems", IEEE Trans. on Sustainable Energy, vol. 4, no. 1, pp: 89-98, 2013

[12] Haithem Chaieb, & Sakly Anis. "A novel MPPT method for photovoltaic application under partial shaded conditions." *Solar Energy* , vol. 159, pp.291-299, 2018.

Proceedings of the Fourth International Conference on Communication and Electronics Systems (ICCES 2019)
IEEE Conference Record # 45898; IEEE Xplore ISBN: 978-1-7281-1261-9

IoT Enabled Smart Industrial Pollution Monitoring and Control System Using Raspberry Pi with BLYNK Server

S.Ramalingam, Research Scholar
Department of EEE
Alagappa Chettiar Government College of Engineering and Technology
Karaikudi, Tamilnadu, India
ramece74@gmail.com

Dr. K.Baskaran, Professor
Department of EEE
Alagappa Chettiar Government College of Engineering and Technology
Karaikudi, Tamilnadu, India
drbaskaran@gct.ac.in

D.Kalaiarasan, Assistant Professor
Department of ECE
Government College of Engineering,
Srirangam, Tamilnadu,
India
kalaiarasangct@gmail.com

***Abstract*— Now a day's environmental pollution becomes important issues in metropolitan cities and industries. The sudden growth of industries, infrastructure and transport vehicles have been producing environmental issues like greenhouse effect and diseases caused by harmful gases present in the environment which directly effect on human's health and thus needs a special monitoring system. To resolve have an effect on the environmental pollution issues, here we have a tendency to implement IoT based pollution monitoring and control system. Where it detects the deleterious gases present in the environment. The proposed IoT technology scrutinizes level of co gases released during industry process, temperature and humidity using sensor technology and Raspberry pi. Each process will have a separate data monitoring and controlling mechanism. The device are going to be put in through a BLYNK native server mobile application which is able to show the live updates of the environmental pollution level of the industries or remote space The thought of IOT helps to access knowledge from remote locations. The most plans behind the implementation work is to form a true time absolutely machine-controlled management mechanisms exploitation IoT.**

***Keywords*— *DHT11 Sensor, Gas Sensor, Internet of Thing, Ethernet, LCD, Raspberry pi 3*.**

I. INTRODUCTION

In Traditional methods for monitoring environmental pollution predominantly require high investment costs for laboratory analytical device and instruments, large maintenance, training and highly specialized human resource. The utilize of electronic equipment is authentic for measuring the secular trend of environmental pollutants, which is interconnected to the reactivity and transport on regional and local scale, but it is very expensive for the evaluation of the long-term toxicological risk on human health[1]. In fact, continuous equipments require high costs of maintenance and, since they are often hugely experienced they can be only used in a minimum number of sites.

It does not allow a detailed mapping of exposure in biggest areas. Furthermore, pollution parameter collected by automatic analyzers is not satisfactory for a swift exposition and except used to compare the data with pre-defined restraint or pollution level standards, it's not always practical [2].

Therefore, there is increasing insistence for the industrial environmental pollution monitoring and control systems. Environmental pollution has become biggest problems for each country; particularly it's developed country or developing country. Environmental pollution issue are increasing speedily particularly in metropolitan areas of developing countries wherever industrial enterprise and increasing range of vehicles results in liberate ton of environmental pollutants [3].

The projected IoT blynk server system senses the pollution level and transmits over thingSpeak webpage server mistreatment web. Once the gas, temperature and wetness level will increase higher than industries commonplace level, there's large quantity of harmful gases gift within the air like CO, smoke, LPG, alcohol, and NOx. The projected work can show the pollution level in PPM on the liquid show and thingSpeak website and blynk native server. It's obligatory to watch trade pollution and management for future and healthy living for all owing to flexibility and low value web of things (IoT) is obtaining utilized daily[4].

IoT is vital play major role in communication technology. it is an integrated communication technology in which all devices and any objects connected any remote location and any time. The IoT uses smart digital and analog interface to connect and interact with embedded devices, sensors and social contexts. These objects are having identities, virtual personalities operative in good environment. The IoT development provides numerous applications on different domains, such as consumer, home, industrial, manufacturing, utilities, energy resources, transportation, environment, safety, security, retail, healthcare, bio sciences automation, smart grid and many others [5].

Air Pollution has surfaced globally as a result of relating to industrial development. Transportation by road is also one of the major causes for air pollution, which contribute to weather change that has hazardous domestic and global consequences. These are increasingly emerging to reach the human needs. An efficient monitoring system is required to monitor and assess the conditions in case of increasing the prescribed gas level of parameter. The extent to which environment gets affected is observed and send to the user through the android app. Sensor devices are placed at remote industries to gather the information to predict the behavior of a Specific space of interest.

Objectives

Internet of things plays a major role in industries where large number of devices or objects interconnected through internet. These devices communicate with people and other things and provide the sensor data to webpage and blynk local server or cloud storage. The main challenge of the project is to detect and monitoring level of harmful gases released during industry process, temperature, humidity and other factors impact the environment. All data are monitored through thingspeak and blynk local server.

II. RELATED WORK

In existing work had introduced the wireless solution, based on GSM network for the monitoring and controlling of temperature and humidity in industrial environment [3].

In the previous system, pollution monitoring system implemented by using LABVIEW software and zigbee technology [8]. This method is to form a system for monitoring pollution parameters and to notify pollution control system when anyone of the factors crosses the threshold value declared by industry.

In the past, different methodologies and techniques which were used in some of the research works.WSN plays major role in intelligent environment monitoring in this work they are mainly focusing on making the city environment smart, by deploying WSN all across the city, public and private transportation systems [10]. By accessing all the dynamic global sensor networks, environmental behaviors are collected as a streaming data base to identify the environmental conditions.

The architecture and prototype of the IoT system was developed. An algorithm for air pollution source estimation using Mobile Sensor Networks. In industrialization, especially the workers have been suffering from some endangering situations, so monitoring and controlling the parameters which causes pollution is necessary in industrial environment.

III. PROPOSED WORK

The monitor and management of pollution parameter is risk challenges from deteriorates industries or remote space. The most intent of the research paper is to develop a value, accuracy and vigorous system to regulate the pollution parameters inflicting pollution and to diminish the impact of those parameters while not poignant the plant or natural atmosphere.

The implementation of current project is to design an IoT blynk server based mostly system to scan and monitor pollution parameters and send the information to pollution management authorized person. Once any of that parameter reaches on maximum of industries standards. A mechanism victimization Internet of things is introduced during this projected methodology, which is able to mechanically monitor once there's a disturbance moving the environments. The projected IoT technology scrutinizes level of co gases free throughout industries method, temperature and humidity victimization device technology and Raspberry pi.

Each method can have a separate knowledge observation and dominant mechanism. Internet of things provides operation interface and manipulation of information from remote industries or location and it's appropriate for interactive surroundings for transferring the information. The most plans behind the implementation work are to form machine-controlled management mechanisms exploitation IoT.

IV. SYSTEM SPECIFICATION

In proposed work use of Internet IoT to subscribe the industrial pollution presence of certain toxic gases pollutants. This system design represents the working flow based on IOT industrial pollution monitoring and controlling, which is shown in Fig. 1

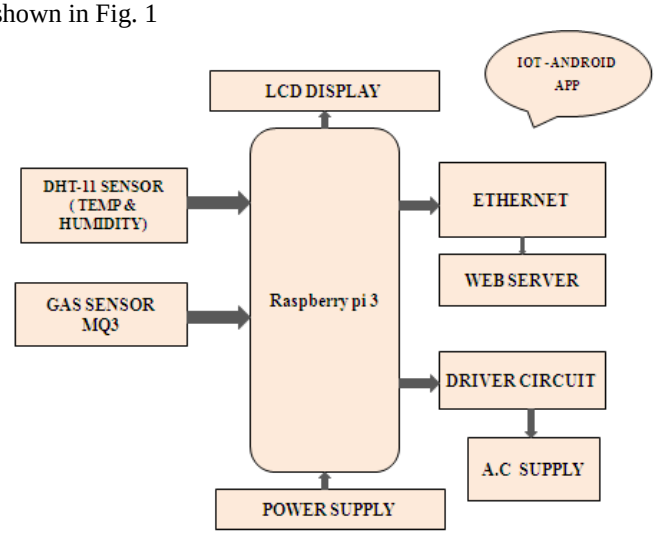

Fig.1 Block Diagram of Proposed Work

A. Working Principle:

This module proposes the use of a Raspberry pi board which collects the temperature and humidity parameter from the DHT-11Ssensor, ADC converter, CO2 concentration using MG-811 and the MQ-3 sensor senses smoke level in the atmosphere and amends output as a result in the form of an analog signal.

The pollutant parameters are updated into on-line information. Before data are passed to the Raspberry pi, it should be converted in to the digital value. The ADC0808 converts the detector analog values to corresponding digital values then raspberry pi will the additional process. this technique design represents the working flow supported IOT industrial pollution monitoring and dominant.

Fig 2 shows the circuit diagram of IoT based pollution monitoring system. A system will detect the hazardous gases that are emitted by industries across the particular area. It simultaneously provides data to authority and organization. The main goal of the planned work is to display the pollution level in WebPages based mostly harmful gas detective work and alerting system. The toxic gases like ammonia, nitric oxide, CO2 and various gases relating to the corresponding industries were sensed and processed by raspberry pi3 .it displayed each and every second on liquid crystal display and the level of pollution monitored online through blynk local server and thingspeak WebPages using MQTT protocol. The DHT 11parameters send in the online and blynk mobile app for every minute. By enable the Show Data button in the app, the numerical values and graphical data will be displayed.

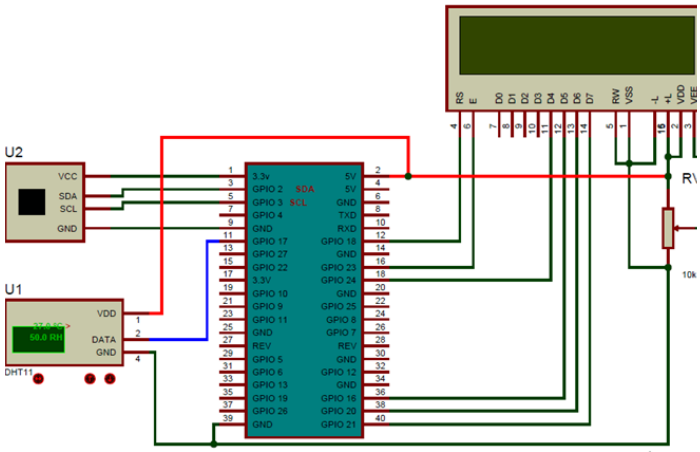

Fig.2 Interfacing DHT11 Sensor with Raspberry Pi

These mq3 and DHT 11sensors are popular for use in remote industrial pollution monitoring, soil monitors, and home automation systems. Only a single data line between an MCU like Raspberry Pi and the temperature Sensor is sufficient for exchange of information and it simultaneously provides data to authorized organization in turn leading swiftly diffusion of the unfavorable situation

V. HARDWARE DESCRIPTION

A. Co2 Sensor

Air pollutant sensor is a embedded sensor device used for detecting the pollutant in air. it is necessary to Measure the nitric oxide and carbon dioxide is important in monitoring factory air quality mq135 for measuring a different kind of gases. it detect Ammonia, Nitric oxide, alcohol , smoke and Carbon dioxide. it can be used in industries and environmental parameter measuring application. this sensor has low prize and particularly suitable for Air quality pollution monitoring application

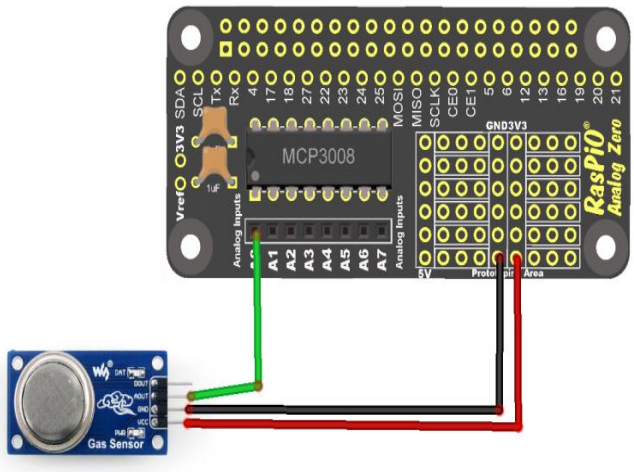

Fig. 3 Interfacing Mq3 Sensor with Raspberry Pi

B. DHT-11 Sensors

It is very effective sensor to sense and measure the environment temperature and humidity. The features of DHT11 sensor humidity ranges is 20 to 90% RH and temperature range is of 0 to 50°C in degree Celsius and supply voltage is +5 V.It has three pins such as Vcc, ground and analog output pin. It is interfaced with a high-performance raspberry pi microprocessor. This technology gives the high precision and long-term reliability. These sensors contain a resistive element and a sensor for negative temperature coefficient temperature measuring devices.

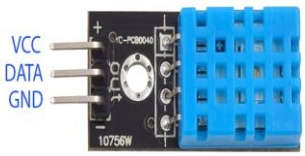

Fig. 4 DHT 11 Sensors

C. Driver Circuit

The relay driver circuit is interfaced with raspberry pi. If the pollution level is exceed maximum value, the Raspberry pi send signal to driver circuit. It automatically triggers Load or supply voltage.

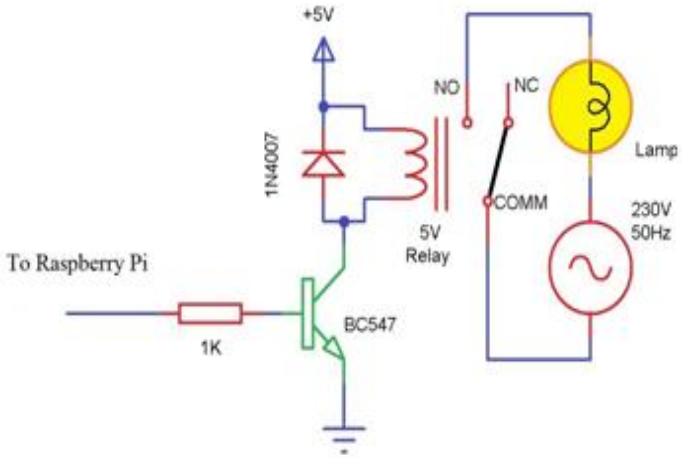

Fig 5 Interfacing relay with Raspberry pi

D. Raspberry pi

The Raspberry Pi is also called as a single printed circuit board micro computer. Raspberry Pi3 is a 1.2 GHz 64-bit quad core processor, on-board 802.11n Wi-Fi, Bluetooth and USB boot capabilities. The Raspbian operating system is stored in memory card. The DHT 11 and gas sensor is interfaced with raspberry pi GPIO pins. It process the measuring parameter and it transmit the data to web server and android BLYNK application

Fig. 6 Raspberry pi 3 board

V. RESULTS AND DISCUSSION

The implementation of proposed work is done by using raspberry pi, sensor and WIFI and blynk android application. Ethernet Shield is implemented by giving the A.C power supply and monitors by using the mobile controlled android applications. Connect the DHT11 sensor in pin A0. Ethernet shield is mounted on the Raspberry pi. .the industries environment parameters are monitored through blynk local server mobile application using internet of things via WIFI or Ethernet cable.

A. Thingspeak Webpage Result:

Fig.7 Shows Temperature and Humidity Using ThingSpeak Server

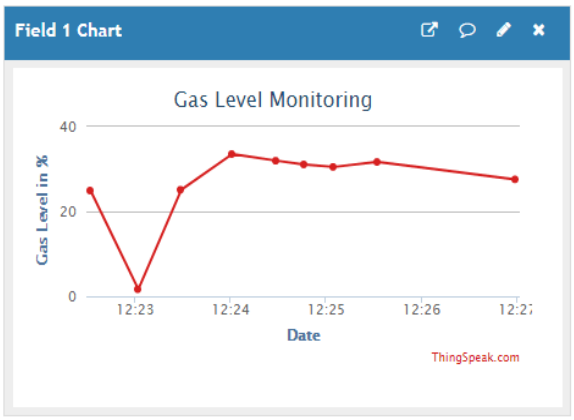

Fig.8 Shows Gas Level Monitoring Using ThingSpeak Server

Fig 7 and 8 shows the graphical wave form of industrial environment gas and temperature and humidity parameters. The Raspberry pi sends the sensor data to IoT thinkSPeak cloud server.

B. BLYNK – IoT APP Result

Address mistreatment the computer IP, we will explore the temperature and humidity value in browser in online Blynk IoT app platform was developed for the net of Things applications. This server doable to manage associate will show device info victimization raspberry pi hardware remotely from any location

This server operated regionally and it's chargeable for communication between golem devices and real time embedded devices .it will management the thousand of embedded devices and objects

A Blynk library is to activate communication with the server and processes all the incoming and out coming back commands from your Blynk app and Raspberry pi. This native server will store information and visualize it effectively. It give the superb preciseness and high performance.

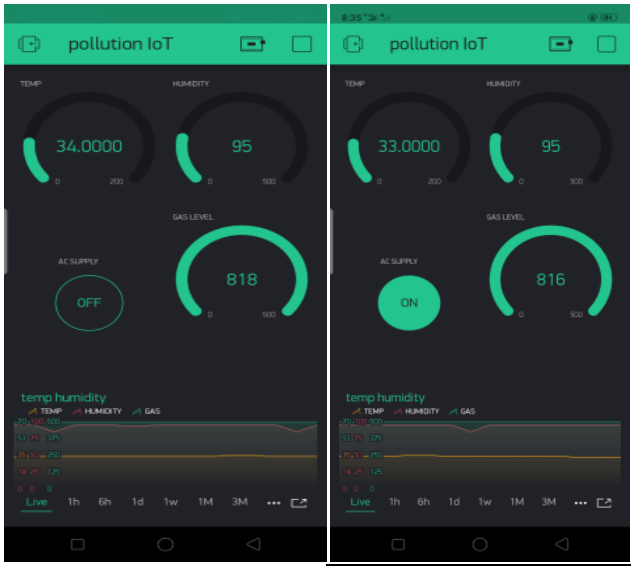

Fig.9 Result of IoT BLYNK ANDROID APP

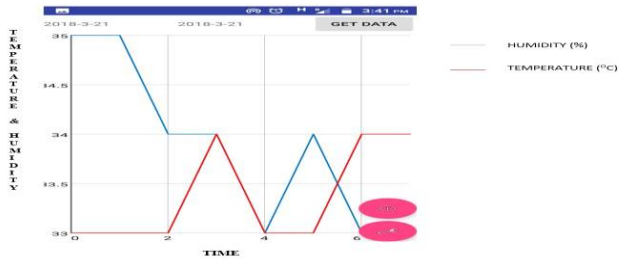

Fig.10 Final graphical output in android app

Fig 9 and 10 show the result of sensor data using IoT android Application Blynk Local server .All sensor information are transferred to android Mobile Blynk Application through Internet. The mobile application also display the data in graphical form

C. Applications

- Industrial application
- Environmental application
- Transport pollution control

VI. CONCLUSION

The most powerful technology IoT primarily based atmosphere observation pollution system was designed, implemented by mistreatment blynk local server and thingSpeak environment. The temperature gas, wetness level are monitored terribly glorious through net.

It's quite helpful as compared to manual observation and additionally it's reliable because it is not possible to watch continually the pollution, humidity and temperature parameter manually. to examine the temperature and wetness measure and so we will recover the system in less time and faults before any unsure failures so leading to important price saving in addition as up system reliableness. The performance between accuracy and price is achieved by creating use of single printed circuit board digital computer Raspberry pi and applicable sensors resulting in a well grounded system.

The attainment and robustious of the industrial pollution monitoring and control system can further be improved by implementing sensors for controlling pollution level thereby improving the industrial and natural environment. The blynk local server and android app contributes quick response rate and the diffusion of the critical situation can be made faster than the manual methods.

ACKNOWLEDGMENT

I, S.Ramalingam and Co-Author D. Kalaiarasan of this paper are thankful to Dr.K.Baskaran, Professor and HEAD EEE Dept. Alagappa Chettiar Government College of Engineering and technology, Karaikudi, Tamilnadu, India, for their valuable guidance and continuous support and for being a constant source of inspiration. And we are also thankful to our beloved friends for their huge motivation.

REFERENCES

[1]. Boubrima A, Benchuit W H, Rivano, Optimal WSN Deployment Models for Air Pollution Monitoring, IEEE Transactions on Wireless Communications.

[2]. Santosh G. Bhandarakawathe, Prof. S. B. Somani, Design and Development of Web based server for Monitoring Industrial Air Pollutants, International Journal of Electronics, Electrical and Computational System, Volume 6, Issue 8, August, (2017)

[3]. Jifeng Ding,Jiyin Zhao and Biao Ma, Remote monitoring system of Temperature and Humidity based on GSM, in proceedings of 2nd International Conference on Computational Intelligence and Industrial Application,pp.678-681(2008).

[4]. I. Korhonen, J. Parkka, and M. Van Gils, Health monitoring in the home of the future, IEEE Engineering in medicine and biology magazine22, no. 3 (2003): 66-73.

[5]. Mile Mrinal and Lakade Priyanka, Mashayak Saniya , Katkar Poonam and A.B. Gavali,, Smart Home – Automation and Security System Based on Sensing Mechanism (2013).

[6]. Zumyla Shanaz F1, Prem Kumar S R2, Rahul R, Rajesh Kumar M3, IoT based Industrial Pollution Monitoring System, International Research Journal of Engineering and Technology (IRJET) e-ISSN: 2395-0056, Volume: 06 Issue: 03 | Mar 2019

[7]. Nashwa El-Bendary, Mohamed Mostafa M.Fouad, Rabie Ramadan A,Soumya Banerjeee and Aboul Ella Hassanien, Smart Environmental Monitoring using Wireless Sensor Networks(2013).

[8]. Kunja Bihari Swain G. Santamanyu, Smart Industry Pollution Monitoring and Controlling using LabVIEW based IoT, International Conference on Sensing, Signal Processing and Security (ICSSS), 2017.

[9]. N.Xu, A Survey of the Sensor Network Applications, IEEE Communications Magazine, Volume 40,No.8,pp.102-1144,(2002).

[10]. J.Elson and A.Estrin, Sensor networks, a bridge to the physical world, Wireless Sensor Networks, Volume 9,pp.102-114,(2002).

[11]. Y. Zhao, and Z. Ye, A low cost GSM/GPRS based wireless home security system, IEEE Transactions on Consumer Electronics, 54.2, 567-572 (2008).

[12]. P. Harmo, T. Taipalus, J. Knuuttila, J. Vallet, and A. Halme. Needs and solutions-home automation and service robots for the elderly and disabled, In2005 IEEE/RSJ international conference on intelligent robots and systems, pp. 3201-3206. IEEE (2005).

[13]. Mallesham Yerragolla, Kamalakar pallela, Indira Priyadarshini Gera, Intelligent Security System for Residential and Industrial Automation, 2016 IEEE Uttar Pradesh Section International Conference on Electrical, Computer and Electronics Engineering (UPCON) Indian Institute of Technology (Banaras Hindu University) Varanasi, India, Dec 9-11(2016).

[14]. Devahema 1, P.V. Sai Surya Vamsi, IOT based Air Pollution Monitoring System, Journal of Network Communications and Emerging Technologies (JNCET) Volume 8, Issue 4, April (2018).

[15]. D.Arunkumar1,K.Ajaykanth, smart air pollution detection and monitoring using IoT, International Journal of Pure and Applied Mathematics, Volume 119 No. 15 ,935-941, (2018).

Proceedings of the Fourth International Conference on Communication and Electronics Systems (ICCES 2019)
IEEE Conference Record # 45898; IEEE Xplore ISBN: 978-1-7281-1261-9

ENHANCED RANKING OF WEBSITES BASED ON CREDIBILITY EVALUATION

Subbulakshmi. S
Department of Computer Science and Applications
Amrita Vishwa Vidyapeetham
Amritapuri, India
subbulakshmis@am.amrita.edu

Gopika. A
Department of Computer Science and Applications
Amrita Vishwa Vidyapeetham
Amritapuri, India
gopikakmvlk@gmail.com

Lincy Thomson
Department of Computer Science and Applications
Amrita Vishwa Vidyapeetham
Amritapuri, India
lincythomson10@gmail.com

***Abstract*—- In the current era of internet, with continuous flow of information to web, it is a difficult task for a user to choose the right information. Information belonging to analogous type is provided by diverse service providers and it is a challenging to diagnose the reliability of information. This paper implements a framework to determine the reliability by calculating credibility value of each web portal through analyzing information published, link details, spam details of information available and updation details of web portal. Credibility score is assessed by evaluating page rank value, black list web sites, average number of hits of different pages, two quality factor values trustworthiness and timeliness. Web crawler gives page link details of varied number of web sites based on the query given by user. Finally, web sites are ranked and listed based on the credibility of web portals, which ease the job of users in assessing reliability of information available in internet.**

Keywords*—Credibility, Web crawler, Content analysis, PR, Trustworthiness, Timeliness, Spamhaus, Blacklist.*

I. INTRODUCTION

Credibility is simply the capacity of belief. The credibility convinces users that they have reached Web site that provides useful information. Websites create an interesting challenge in evaluating credibility because no two websites are created the same way. There are many factors that lead to large volumes of non-credible and unreliable information which are published on the Web [2]. With the fast progress in technologies in the web services, there is an outflow of information to the web [4].

Internet plays a vital role in every field and it has become a part of every human beings life. Everyone depends on internet for information which helps them in different ways. In case of students, they rely on internet for education purpose, for their research, seminar and so on [9]. Internet has both advantages and disadvantages. One of the main disadvantages is that it sometimes provides low quality information, which user is not bothered about. There is a continuous flow of information to the web within minutes which can be both fake and real ones. As of now web size is bigger, hence most of the times we may not know which websites gives abstract reliable information [5]. For that we need to analyze the web links and the details provided by the service providers.

There are many research methods available in the present web-based search process to find the credibility of a web pages, which reveals the existence of real and valid information. Details of the web page like author's biodata, spelling and grammar mistakes, sites blocked by firewall, contents blocked and so on are considered as the main factors which the user can easily check to find out whether the web page is a credible one or not. But, still there are other quality factors such as consistency, trustworthiness, timeliness, completeness to find out whether a webpage is credible or not. So, here in our research work, we show the credibility value by considering few factors such as timeliness, trustworthiness, page rank value, and check whether a domain is blacklisted or not.

In this research work we focus on providing the best quality results to the user by assessing content credibility with quality factors of web sites since credibility is an important factor [1]. Initially, when a search request is given by the user [10], the set of web sites are identified based on the request. Web Crawlers are used to find web sites and the link details of the different pages in those web sites. The link details are used in the page rank calculation. The quality factor timeliness is assessed based on the last updated date and the trustworthiness of web site is assessed based on spam word count along with black listed web sites details. All the above calculated values are aggregated to get the credibility of the web sites which is used to rank web sites. Finally, web sites with highest rank are displayed as search results which provides a highly reliable information to end users.

The remaining section of this paper is defined as: Section II analyses the related work. Section III explains the proposed system methodologies. Section IV displays the results. Section V completes the paper with a brief conclusion.

II. RELATED WORKS

This section of the paper shows the researches and works that have been done relating to the assessment of web content credibility. In various surveys, different methodologies have been presented and compared several approaches towards the calculation of content credibility.

In the paper *Credibility Evaluation based on deep learning*, the assessment of credibility is based on Deep Learning Algorithm. Nowadays, Credibility of a recommendation system

is given prime importance. [7] Due to high recommendation system in the e-commerce platform, there are chances of false information getting added up in the system by the network intruders.

In 2014, Liu Shengzong and others proposed a new recommendation algorithm taking both the user credibility and similarity into account [7]. They analyzed the three main credibility factors, such as the adoption rate of the user's evaluation, the correctness of the scores and the number of scoring, and then established the relationship between the credibility and the three factors. The result obtained was that the analysis has limitations on assessment of user credibility and cannot evaluate effectively all around. Hence the traditional credibility assessment algorithm cannot assess the user credibility accurately.

This made to propose a new credibility algorithm based on Deep Learning Algorithm and the average user reliability value as a criterion, a second assessment of the credibility is applied to other users, the results of which are arranged in ascending order [7]. The result was that it removed suspicious user ranking and created a trustful adjacent group target user. The accuracy of the recommendation system was improved, and the risk coefficient of the recommendation system were also reduced in the later experiments.

The *PageRank algorithm using Markov Model and Hidden Markov Model* are used to rank websites in the google search engine. Markov Model gives a robust probability contraption to characterize sequential data. In this model, the user selects the webpage and based on the incoming and outgoing links of that webpage, ranks are determined. Hidden Markov Model is a simple way to model sequential data and finds its application within mapper/reducer. PageRank is one among the link analysis algorithm. In this algorithm, the probability distribution is between 0 and 1 [3]. It returns the importance of a webpage based on its rank whenever a search is performed by the user. Markov Model was also used to find the score of each site using the concept of Markov chain. It predicts the behavior of a state that transits from one state to another state and considers only the current state which contains all the future information.

Markov Model is a mathematical system model that predicts a probability distribution associated with the current state. [3] This model is defined by a Markov chain in which page *i* will be the probability in a stationary distribution on a Markov Model on all web pages. The transition states are considered as webpages and theoretically Markov chain means the certain fraction of time the surfer chooses a random page from the web. Hence Google search engine uses Markov chain to deal with random surfers by ranking the pages [3]. Hidden Markov Model deals with solving problems like encoding, decoding and training. The model has hidden and observed states where the observed states are given with the outputs and hidden states are to be determined. This model can also be used to find the score of each page for returning the page according to their importance. Therefore, the study has found out that the search engine uses Page rank algorithm and Markov model for determining the score of the page in web server and have implemented the HMM (Hidden Markov model) for map reduce function or for distributed sorting of data.

In the research *Understanding and Predicting Web Content Credibility using the Content Credibility Corpus*, they created a predictive model of Web content credibility evaluations, based on human evaluations. Based on a large dataset of Web content credibility evaluations, using text mining and crowdsourcing techniques, a comprehensive set of factors that affect credibility evaluations was derived and therefore it was used as labels in interfaces for rating web content credibility [2]. The impact of each factor was analyzed based on credibility evaluation scores. Based on the newly identified factors, a predictive model for Web content credibility was proposed. The model can be used to determine the significance and impact of discovered factors on credibility evaluations. These findings can guide future research on the design of automatic or semi-automatic systems for Web content credibility evaluation support.

In the paper *Websites and Webpages Credibility and Trust Evaluation*, the elements required to evaluate Websites and pages credibility are based on Website, Web pages, and authors credibility metrics are evaluated. This research aims to study the credibility of web pages by interpreting the credibility guidelines into several measurements [16]. The credibility is studied from three perspective, they are: - Domain or website will be measured in terms of domain age, number of indexed pages in various search engines such as Google, inlinks, outlinks, number of broken links, website size, number of authenticated pages, trust rank, and so on. Web page/file: each web page or file will be measured in terms of freshness, popularity, trust, inlinks, outlinks, and age. Author: the authors will be measured by number of citations and for example the number of indexed pages in Google.

Our work focuses on ranking of web sites based on credulity factor of web sites. It is calculated based on the link, content details and quality factor evaluation. Credibility assessment helps to enhance the search results by ranking the web sites to provide the list of reliable websites to the end users.

III. METHODOLOGIES

In the general search scenario, search results are based on the content matching of the text provided with the already existing web resources. Optimized text matching algorithms are used to select relevant resources, but it is highly essential to assess the reliability of the information provided. Otherwise, users will be misguided by the fake information provided by fraudulent web sites. So, calculating the credibility of a website is very important because it can produce huge benefits to end users.

The goal of our research work is to provide reliable information that can be both trustworthy and knowledgeable related to the users search [6]. In the search page implemented, whenever a user searches something, it will display results based

on the credibility score. To check credibility of a website, three important modules are implemented i) Site link extraction using web crawlers. ii) Predicting Page Rank value iii) Calculating two quality factors. Quality factors Timeliness and Trustworthiness are considered to determine the credibility of a website to produce better results.

PageRank algorithm is implemented with link and hit count details of the web pages. User can input a keyword and the crawler works in behind fetching webpages to show up in the search result. In the process of initial web site selection process, it considers only the exact text matching feature. Then, for each website, PageRank score is calculated based on the number of incoming and outgoing links, number of hits is calculated based on the clicks the user gives to a website. The two factors are calculated by checking the number of spam words in the content, identifying whether the website is blacklisted or not and checking the last updated date of the website. All these values will account to give the final credibility score of a website. The credibility score is displayed along with the search result, so that the user will have better understanding about the website content.

A. Site Link Extraction Using Web Crawler

Web crawling is a process of finding information from millions and trillions of webpages. The crawler browses the World Wide Web to retrieve webpages related to the search. From the fetched webpages we can determine the number of inbound and outbound links. The links which show up in the search results are stored in the database for further processing. The implementation details of the web crawler invoked when a search query is given by the user is explained as follows:

Algorithm for Web Crawling

Input: Data user wants to search for.
Output: Indexed Links crawled from Google.

i. Input a keyword to search.
ii. Using the source URL to crawl the web page
iii. Fetching content of the webpage for the corresponding search
iv. Extracting outgoing links from the page
v. Crawling the new pages
vi. Duplication of links are avoided
vii. URLs are maintained in a database

B. Predicting Page Rank value

PageRank algorithm was found by Lawrence Page and Sergey Brin which is used to rank webpages based on inbound and outbound links. Page links details stored in the database for a search results are retrieved, and page rank value is calculated. For each page a corresponding rank is obtained. Inbound links means the number of external links that point to the corresponding webpage. Outbound links can be defined as the number of links pointing to the external webpage. The value of inbound and outbound links of each domain is calculated and displayed distinctly. A transition matrix is simulated to output the final probability distribution. Adjacency matrix is given as input and can be calculated using a simple iterative algorithm. The importance of each page depends on the rank of the inbound page to it. The more inbound links, the more weightage the webpage have. This output is considered for further calculation.

Algorithm for Page Ranking Algorithm

Input: Details of webpage which user search for.
Output: Page Rank Value for corresponding webpages.

i. Identify the web domain for which page rank value is to be calculated.
ii. Identify the number of outgoing links and incoming links
iii. Apply the page ranking formula for the corresponding inbound and outbound links
iv. $PR(p) = (1-d) + d(PR(Ti) / C(Ti) + \ldots + PR(Tn) / C(Tn))$ where p is the page for which page rank is to be calculated, d takes value between 0 and 1, T_i represents the page directed to page p, PR( ) represents the page rank value, C( ) represents the number of outbound links.
v. Repeat the steps 1-4 for 'n' the number of pages.

Thus, page rank value for each web site is calculated which is used for final credibility calculation.

C. Calculating Quality Factors

Next, in order further improve our work we consider two quality factors such as trustworthiness and timeliness.

1. Trustworthiness: Trustworthiness of a web page basically means truthfulness of information provided in the web page. There are many alternatives to check whether a page is trustworthy or not. To calculate the trustworthiness value, we use two parameters- number of spam words and check whether the domain is blacklisted or not.

i). Find the Spam Count: Spam words are those words which are unsolicited and bulk words, for e.g.: - profit, discount and so on. The meta tag of each web page is parsed and the number of spam word is counted.

ii). Check whether a link is blacklisted or not: To check whether the link is blacklisted or not, we use the spamhaus.org. *Spamhaus* is an ISP (Internet Service Provider) which allows the distribution of the spam web pages. So, if a link is present in the sbl- xbl blocklist it means that the web page is blacklisted. Sbl-xbl is a database of IP address of the blocked list. Blocked list means those service providers are providing infected information or they are considered as spammers proving false information to misguide the end users. Thus, it is

easy to identify whether the web page is trustworthy or not. Untruthful pages could be omitted, and only valid reliable pages should be considered and given high credibility scores.

2. Timeliness: Timeliness is the second quality factor which means the last updated date. In this fast-developing era, 90% of people all over the world seek for latest information. So, it is necessary to bring the latest information is to them by providing the recently updated webpages related to their search. This can be done by finding out the date when the corresponding web domain was recently updated. There are different methods to figure out. One of the methods that we implemented is using the *Whois* API, where all the details of each webpage is stored. From this API, we can retrieve the last modified date of the webpage and the established date of that corresponding webpage. Later, the dates are ranked which helps user to identify the last modified webpage more easily.

D. Credibility Score Calculation

All the above parameters calculated in the above modules are considered for credibility score calculation. Page Rank values are considered and pages with higher values are given good ranks. The spam count is considered and if the spam count is in the minimum threshold range they are given rank 1 otherwise bad ranks are given. In the similar manner, recently updated web sites are given good ranks than other pages. Then, credibility score CS of web site i is calculated as:

$$CS(i) = PR(i) + D(i) + H(i) + S(i)$$

where PR is the page rank of the webpage, D is the rank based on the last updated date of a webpage, H is the number of hits of each webpage in the system and S is the output spam rank. The output credibility values $CS(i)$ is used for the final ranking of the web sites. The search results of the given query display the web sites only based on that ranking. Thus, the research work produces the list of web sites which provides only reliable information more valuable to the end users.

IV. RESULTS

Our work focuses on credibility score calculation after finding the value of page rank and quality factors. For computation of quality factors and page rank implementation, the dataset with the number of inbound links, outbound links of a specified set of web sites. Timeliness and Trustworthiness value of those web sites are also calculated using the predefined existing API's. Timeliness value is the output date rank which is ranked on basis of last modified date and the Trustworthiness value is the output spam rank which is ranked on basis of the total count of spam words present in different pages of the web site. Web sites with higher spam count is given worst rank as they provide unreliable and fake information. We consider the following websites for evaluation of credibility value: -

TABLE 1 : WEBSERVICES AND CORRESPONDING WEB PAGES

WEB SERVICE	*URL NAME*
ws1	Amritahospitals.org
ws2	Astermedcity.com
ws3	Astermims.com
ws4	Babymhospitals.com
ws5	Lourdeshospital.org
ws6	Kimsglobal.com
ws7	Rajagirihospitals.orgs

TABLE 2 : SAMPLE OUTPUT OF PAGERANK ALGORITHM AND QUALITY FACTORS CALCULATION

URL	Inbound Links	Outbound Links	Output Page Rank	Last Modified Date	Output Date Rank	Total Spam Count	Output Spam Rank
ws1	15	601	3.9	24/05/2019	1	62	1
ws2	16	526	3.2	24/05/2019	1	76	1
ws3	14	381	3.8	11/12/2018	2	82	2
ws4	14	174	4.20	28/02/2017	3	65	1
ws5	14	716	3.6	18/03/2016	4	73	1
ws6	13	631	2.4	20/05/2019	1	74	1
ws7	11	863	2.5	09/01/2019	1	90	2

Table 2 defines the rank for each web service based on factors that we have considered. To calculate the output page rank, number of inbound and outbound links are considered. The more inbound links, the more weightage the webpage has. Last modified date is extracted from the Whois API, and hence the output date rank is determined. The output spam rank is calculated based on the total spam count. If the spam count is between 0-80, rank will be initialized to 1, if the count is between 81-100, then the rank will be incremented by 1.

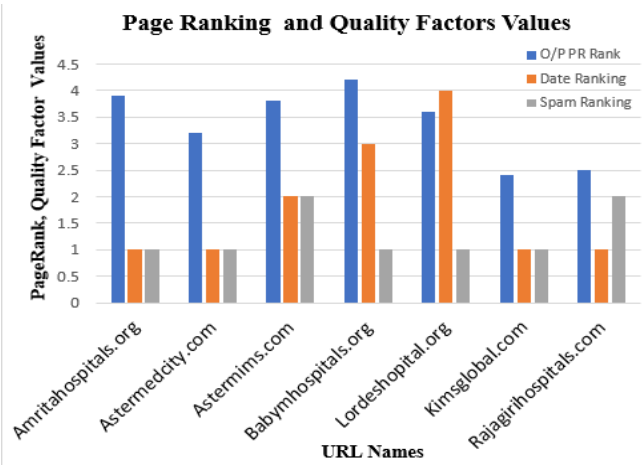

(Fig 2)

In Fig2, the graph represents the ranking of each web page depending on their output page rank, date rank, and the spam rank. Each ranking is done within a range, i.e. from 1-5.

TABLE 3 : INTERMEDIARY RESULTS USED FOR THE CREDIBILITY CALCULATION

URL	***OUTPUT PAGE RANK***	***OUTPUT DATE RANK***	***OUTPUT SPAM RANK***	***FINAL SCORE***
Amritahospitals.org	3.9	1	1	5.9
Astermedcity.com	3.2	1	1	5.2
Astermims.com	3.8	2	2	7.8
Babymhospitals.com	4.2	3	1	8.2
Lourdeshospital.org	3.6	4	1	5.6
Kimsglobal.com	2.4	1	1	4.4
Rajagirihospitals.org	2.5	1	2	5.5

Fig 3 shows the ranking of web sites based on the final credibility score of each web site in the increasing order. URL ID is considered along x-axis and the Credibility score is displayed along the y-axis. Web sites with high credibility score is given best ranking.

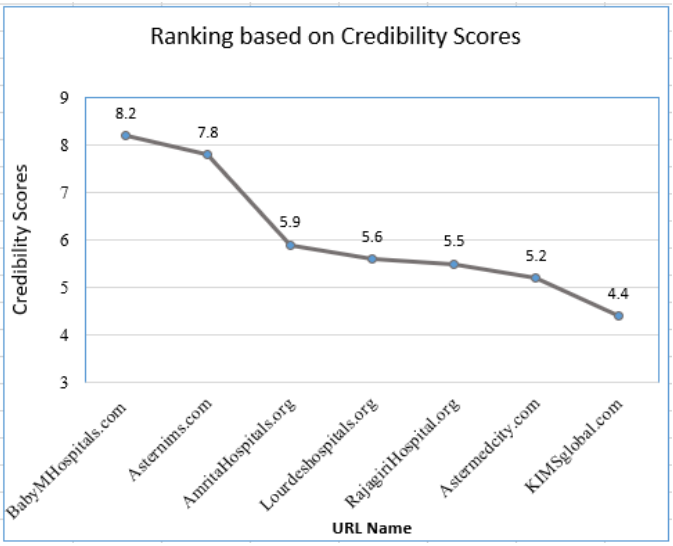

(Fig 3)

Thus, the research work is able to rank the web sites based on the credibility value and display them as the search results for query given by user. User is delivered with the links of web sites which provided reliable information as fradualent and fake site are removed and pages which are highly refered are given more weightage.

V. CONCLUSION

Present internet era demands for extensive research work to identify the best web site from among the huge amount of similar web sites to provide reliable information. Reliability is assessed through varied measures like trust worthiness of the service providers, quality aspects provided by services and so on. This paper describes the framework for calculation of credibility score with the following aspects of web sites: link details, spam details, black list, trustworthiness and timeliness of web sites. Web crawlers and page ranking algorithm is used for determining the rank of web sites. Trustworthiness and Timeliness of web sites are also calculated as users gives more importance for them. Then, credibility score is calculated using the aggregation of all the above factors, which helps users to identify the most reliable web site. In future the credibility assessment of other quality factors like completeness, durability and integrity could be done to further enhance the website ranking.

ACKNOWLEDGMENT

First, we thank the Chancellor of Amrita Vishwa Vidyapeetham, Sri Mata Amritanandamayi Devi, for her love and blessings. We are extremely thankful to Dr. Subbulakshmi S, Assistant Professor, Department of Computer Science and Applications, Amrita School of Engineering, Amritapuri for her primary support throughout the project. We also express our sincere gratitude to all the Faculty members of Department of Computer Science and Applications, Amrita Vishwa Vidyapeetham, Amritapuri for providing help and guidance.

REFERENCES

[1] Aleksander Wawer, Radoslow Nielek, Adam Weirzbicki, “Predicting web content credibility using linguistic features”, Proceedings of the 23rd International Conference on World Wide Web, Pages 1135-1140

[2] Michal Kakol, Radoslaw Nielek And Adam Wierzbicki, “Understanding and Predicting Web Content Credibility using the Content Credibility Corpus”, An International Journal,Information Processing and Management, Volume 53, issue 5, September 2017.

[3] Prerna Rai, Arvind Lal, “Google PageRank Algorithm: Markov Chain Model and Hidden Markov Model”, International Journal of Computer Applications, (0975–8887) Volume138 –, No.9 March 2016.

[4] S. Subbulakshmi, Ramar R, Shaji. A, Prakash. P, “Web Service Recommendation Based on Semantic Analysis of Web Service Specification and Enhanced Collaborative Filtering”, Intelligent Systems Technologies and Applications, January 2018.

[5] Chandresh Prathap Singh, Suman Saha, Suman Kumar Saurabh, “Link Analysis to Visualize a Web Graph”, International Journal of Computer Science, Volume 9, May 2012

[6] C. Carlos, M. Marcelo, P. Barbara,“PredictingInformation credibility in time-sensitive social media”, Internet Research, Volume: 23 Issue: 5, Pages: 560-588, 2013

[7] Liu Mengling,Li Zhendong, “Credibility Evaluation Algorithm Based on Deep Learning” , Applied and Computational Mathematics, Volume 6, Pages 208-214, 2017

[8] Michal Kakol, Adam Wierzbicki, Michele Castasta, Katarzyna Abramczuk, Michal Jankowski-Lorek, “On the

subjectivity and Bias of Web Content Credibility Evaluations", Proceedings of the 22rd International Conference on World Wide Web, Pages 1131-1136, 2013

[9] Fogg B.J., Sooho. C., Danielson D.R. Marable, L. Stanford J., Tauber E.R., "How do users evaluate the credibility of websites?", DUX'03 Proceedings of the 2003 Conference on designing for user experiences(2003), Pages. 1-15

[10] Y. Yamamoto, K.Tanaka, "Enhancing credibility judgment of web search results", Association for Computation Machinery (2011), Pages. 1235- 1244

[11] .Sondhi, V.V Vydisaran, C. Zhai, "Reliability Prediction Of webpages in the medical Domain", Springer (2012)

[12] Malarvizhi. P., Radhika. N., "Performance Evaluation by RM- MapReducer in web page categorization", Journal of Engineering and Applied Sciences, Medwell Journals, Volume 13, Number 23, Pages.10031-10038(2018)

[13] Ben Shneiderman, "Building trusted social media communities : A research roadmap for promoting credible content", University of maryland- college park, Sept 2013, Pages. 35-43

[14] Ping Zang, Gisela. M., Von Dran, "User expectations and ranking of quality factors in different website domains", International Journal Of Electronic Commerce(2014), Volume 6 issue 2, Number 2/winter 2001/02, Pages. 9-33

[15] Subbulakshmi S., K Ramar, Keerthana Krishna V C , Sandra Sanjeev, "Optimized Qos Prediction of web service using Genetic Algorithm and multiple Qos aspects",International Conference on advances in Computing,Communications&Informatics(ICACCI),2018

[16] Aisha Zaidan, Dr,Yahya Tashtoush, Dr. Izzat M Alsamdi, "Website and Webpage Credibility and Trust Evaluation",ISBN: 978-0-9853483-3-5 ©2013, The Society of Digital Information and Wireless Communications

Proceedings of the Fourth International Conference on Communication and Electronics Systems (ICCES 2019)
IEEE Conference Record # 45898; IEEE Xplore ISBN: 978-1-7281-1261-9

Design and Simulation of Two Stage Sample and Hold Circuit with Low Power using Current Controlled Conveyor

Vivek Kumar Jain
Dept. of Electronics & Instrumentaion
Shri G.S. Institute of Technology and Science
Indore, India
jainvivek158@gmail.com

Prof. D. S. Ajnar
Dept. of Electronics & Instrumentaion
Shri G.S. Institute of Technology and Science
Indore, India
ajnards@gmail.com

Prof. P. K. Jain
Dept. of Electronics & Instrumentaion
Shri G.S. Institute of Technology and Science
Indore, India
jainpramod1@gmail.com

***Abstract* — Two Stage Sample and Hold Circuit: In first stage, two-identical sample and hold circuits are connected in cascaded topology. In second stage, the output from first stage of sample and hold circuit is rectified again and the current conveyor is used as a switch which is controlled by the bias current pulses. Both the stages of sample and hold circuit are synched with each other and operate at same bias current with low power consumption. The features of proposed circuit has more accurate results with high linearity as well as more flatter output output waveform at the hold time. The proposed sample and hold circuit has been simulated using 0.18 µm complementary metal oxide (CMOS). The major interest is the simulation of an analog switch used in the circuit.**

Keywords* — *Sample & Hold Circuit, Current Conveyor, Low Power Consumption, Analog Switch.

I. INTRODUCTION

In electronics, all signals get processed in digital format as they are easy to store & transfer but in the physical world every single signal get processed in analog format and so comes the job of an electronic engineer who knows how to convert analog signal into digital signal with more efficiency in order to store and convey the information present in the signal from one place to another. For converting analog signal into digital signal, sample and hold circuit [1] is used. It create the samples of input voltage and hold these sample for definite time. Current conveyor [2] is used for its high frequency application and fast switching ability. Analog mixing stages and analog to digital converters are often needed between the antenna and the digital circuitry in various systems hence sample and hold circuit [3] is used in data conversion systems.

Sample and hold circuit is also used in the De-glitcher circuit to avoid the noise in signal and in analog de-multiplexer. Operational amplifiers do not perform adroitly when output current signal is required and therefore, application of current conveyor circuits comes into play as they operate without any global feedback, and also, they show different high frequency behavior results in comparison to operational amplifier circuits.

Proffered sample and hold circuit is controlled in two phases of clock. In first phase of clock, it tracks the input and in second phase, it holds the input. The circuit uses a square wave as a clock signal. Also, charge injection, pedestal error and aperture jitter etc. are some indubitable errors that are witnessed in a S/H circuit . Nowadays, sample and hold circuit is extensively used in biomedical systems. In this circuit, second generation current conveyor (CCII) [4] is used because it has one high and one low impedance input rather than the two low impedance inputs of first generation current conveyor. Current conveyor circuit is a three port network X, Y and Z. Second generation current conveyor can easily be used to process both current and voltage signals. CCII has two outputs Z+ and Z-. In Z+ pin, direction of current is same with X terminal and opposite with Z- pin. In the proposed circuit, current conveyor is used as a switch in sample and hold circuit. When CCII is used as a switch, a clock pulse is given, at low level of clock, voltage is transferred from Y terminal to X terminal and current is transferred from X terminal to Y terminal but at high level of clock, all pins go in the high impedance level. In two stage sample and hold circuit, output waveform is more accurate when compared with mono stage because in first stage, input is continuously varying which results in variation of output at the time of holding but in two stage, variation is less at the output of first stage which results in more flat output during holding time. Clock is given simultaneously for both the stages and synched with each other, hence both the stages operate simultaneously which in turn means they track and hold in same time.

Proposed circuit has highly efficient and desired results when compared with previous circuits in the data conversion system.

II. BASIC STRUCTURE OF CCII

Second generation current conveyor is different from the first generation conveyor in the manner that the There is no current flowing into Y terminal because terminal Y is a high impedance port while Z terminal is current output and X terminal is voltage input in CCII. So therefore unlike first generation current conveyor, CCII can easily be used for both current and voltage signal. Two type of conveyor present in CCII negative and positive. In positive conveyor, current direction of output terminal is same as that of input terminal but in negative conveyor, current direction of output terminal is opposite to that of input terminal. Both type of conveyor's symbol are shown in FIG 1.

The matrix representation of second generation current conveyor is

$$\begin{bmatrix} I_y \\ V_x \\ I_z \end{bmatrix} = \begin{bmatrix} 0 & 0 & 0 \\ 1 & 0 & 0 \\ 0 & \pm 1 & 0 \end{bmatrix} \begin{bmatrix} V_y \\ I_x \\ V_z \end{bmatrix}$$

In CCII voltage appear at terminal X is same as voltage appear at terminal Y act as a voltage follower and current

flowing in terminal Z is same as flowing in terminal X act as a current follower, connected together.

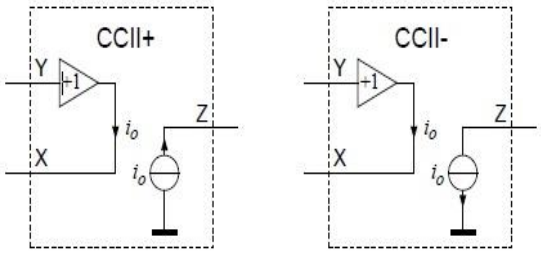

FIG 1: *Symbol representation of CCII+ and CCII-*

In sample and hold circuit, current conveyor is used as a switch which is administered by a current pulse. The operation of switch is to pass signal from one terminal to other terminal in a more methodical way without substantial signal loss. Hence, current conveyor passes the signal with minimum loss as well as it controls the signal when it passes through it.

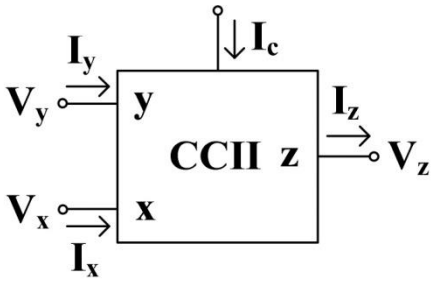

FIG 2: *Symbol of CCII with Bias current*

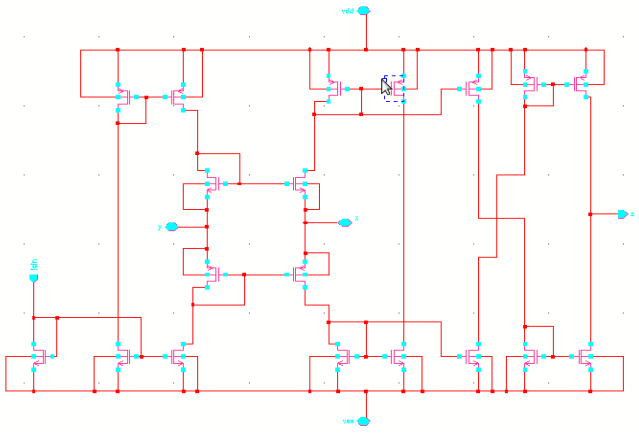

FIG 3: *schematic of CCII*

Current conveyor mainly depends on the current mirror circuit which plays a pivotal role in following the current as well as voltage between the terminals. Current mirror is used in this circuit due to which current will be identical in multiple branches and this current passes with same impedance of MOS. Hence voltage between the MOS terminals will also be same. Bias current is controlling the flow of current as it is controlling the MOS through which it is flowing. In FIG 2 Symbol of CCII with Bias current is shown and its schematic is shown in FIG 3 which is made up with NMOS and PMOS.

III. PROPOSED CIRCUIT

Sample and hold with two stages is simply cascaded two single stages where second stage rectifies the output of first stage. In single stage one CCII, one capacitor and one resister are used. Here, capacitor simply stores the charge at the time of holding and resister is used for timing constant along with the capacitor. CCII works as a switch which controls the switching for tracking and holding time. For switching timing, quiescent current is rendered in the form of current pulses.

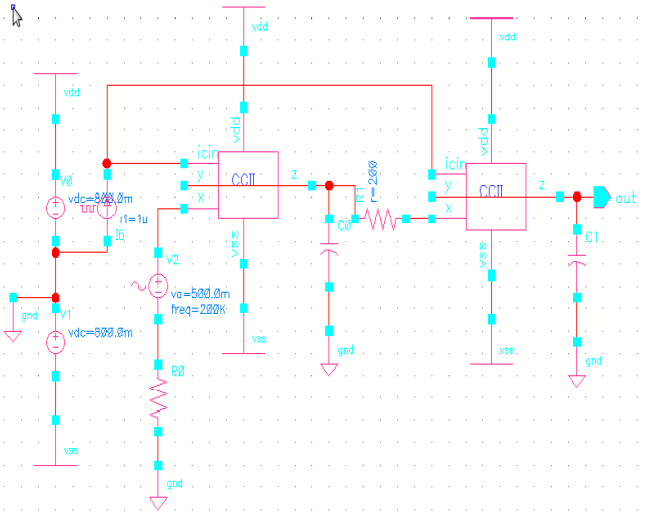

FIG 4: *Schematic of proposed circuit*

Same quiescent current is given for both CCII so that they can hold and track simultaneously. Schematic of proposed circuit is shown in FIG 4. Here, output of first stage is given to input of second stage which rectifies the output of first stage. Both stages are synched with same clock pulse because same input passes through both the stages. Hence, delay should be minimum for both the stages. Here, we cannot have high value capacitor because as we increase the value of capacitor, output of sample and hold circuit will decrease. If we again rectify that output from same circuit, output will be flatter compared to previous outputs. In first stage, more variations are present in the input at the time of holding the signal because of which output of first stage is not flat and capacitor discharges quickly. In second stage, at the holding time, less variations are present in the input hence, output is flatter compared to output of the first stage.

For more canonical results, we can increase the number of stages but the complication with the increment is that as the number of stages increases delay increases and because of increased delay, stages are not synched with the clock. For this reason, cascading of more stages is not possible but in two stages, results are more accurate. At the time tracking, gain of the CCII is approximately unity, so same voltage is transferred from X terminal to Z terminal. CCII is used as a voltage follower if we short terminal Y to terminal Z because voltage of X terminal is same as of Y

terminal and Z terminal has low impedance, so it is used for current driving.

Output of two stage sample and hold circuit is influenced by sampling frequency f_c (f_c=1/ t_c) where t_c is the time period of current pulses, where current pulses are used as a clock for CCII. Output of the circuit also depends on the time constant τ which is multiplication of the R and C (τ = RC) so, at the final output both the time constants are present.

Time constant for first stage is

$\tau_1 = R_1C_1$

Time constant for second stage is

$\tau_2 = R_2C_2$

So, time constant for final output is

$\tau = \tau_1 + \tau_2$

At the output of second stage, capacitor slowly discharges because time constant increases and output is more accurate compared to first stage output.

Then output voltage can be written as

$V_{out} = V_{in}(1- e^{1/\tau f})$

Output is dependent on time constant (τ=RC) and sampling frequency because the holding time change due to change in the sampling frequency.

IV. NON-IDEAL EFFECT

In previous circuit, all results are contingent on ideal parameters but parasitic is contemplated, all parameters will vary because every circuit has its own resistance and capacitance and at high frequencies, it will come in effect. Parameters of CCII also changes when changed parameters are taken into consideration and the matrix no longer contains unique zeroes and ones. Thus, new matrix representation will be

$$\begin{bmatrix} Iy \\ Vx \\ Iz \end{bmatrix} = \begin{bmatrix} Yy & Air & Gmr \\ Avf & Zx & Avr \\ Gmf & Aif & Yz \end{bmatrix} \begin{bmatrix} Vy \\ Ix \\ Vz \end{bmatrix}$$

Where A_{if} and A_{vf} are the current forward and conveyor voltage gains respectively, near to unity and A_{ir} and A_{vr} are the current reverse and conveyor voltage gains respectively, near to zero. Y_z, Z_x and Y_y are the limited terminal impedance and admittances. In certain applications, the trans-conductance G_{mf} from terminal Y to Z is significant, although the reverse trans-conductance G_{mr} seldom has any effect on the circuit behavior. If the current and voltage gains errors are taken into consideration, (3) can be rewritten as

$$V_{out} = V_{in}\ (1 - e^{1/\tau_n f})$$

Where $\tau_n = (R+R_x)(CC_x)$, R_x is the parasitic resistance and C_x is the parasitic capacitance.

In simulation result, we got resistance value as approx. 500KΩ and capacitance as 10fF. Here value of resistance is high so, it will be taken in to consideration. In ideal case, both should be less otherwise at the time of tracking, the circuit will be prone to errors.

V. POST LAYOUT SIMULATION

Two stage of sampled and hold circuit has been simulated on Cadence Virtuoso. QRC extraction has been also evaluated and compare results with the schematic results. Zero DRC error and zero LVS error with the comparison between results without QRC and with QRC have less variation. In post layout simulation utilize the minimum area with minimum parasitic effect. After post layout simulation GDS file has been generated with same output waveform in both the results. Area of the layout is 2269.6598 µm square.

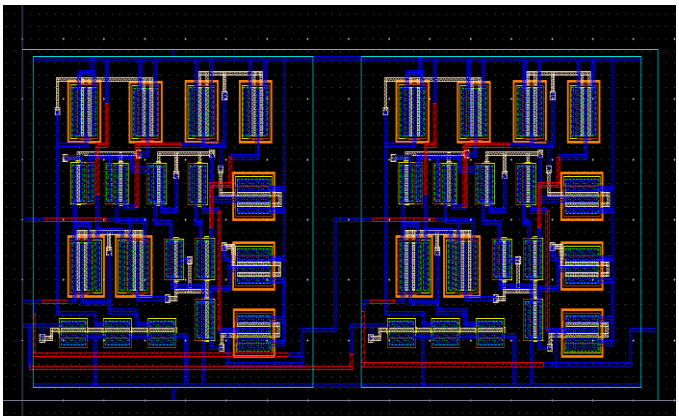

FIG 5: Layout of Proposed Circuit

VI. SIMULATION RESULTS

In this proposed circuit, all PSPICE simulation is carried out in cadence virtuoso and 180nm technology. All files are taken from gpdk180 library. The aspect ratio of NMOS is 300nm in length and 3µm in width and aspect ratio of PMOS is 300nm in length and 8µm in width. Power supply voltage is ±0.8 volt and peak to peak output voltage is 0.6 volt.

Value of biased current is 1µA and given in the pulses form with period of 1µs. This biased current, control the whole scenario as well as control the time of sample and hold period. When I_c is 0µA (Logic 0) then no transition of input to the output and this condition is called hold condition, at that time maximum resistance offering at the input by the circuit of 500KΩ. This condition is shown in FIG 7 where input is in sinusoidal form but out is straight line and output voltage is approximate zero. When I_c is 1µA (Logic 1) then transition of input to the output done without any loss because at that condition circuit offering low resistance approximate 1KΩ.

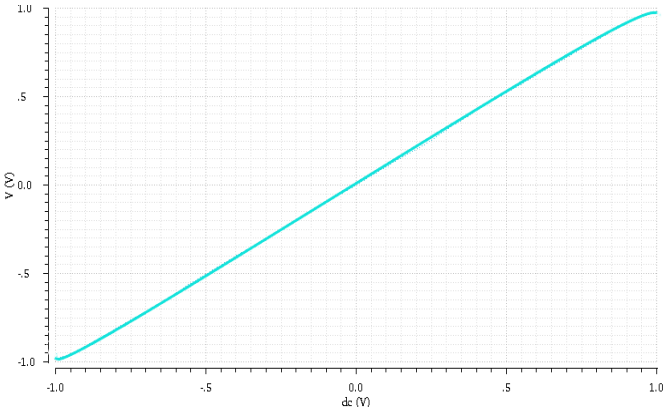

FIG 6: DC Transfer characteristics of CCII

DC transfer characteristic of CCII is shown in FIG 6. It shows the change in output voltage with respect to the change in input voltage which is depicted by the linear curve. Where input voltage is varied from -1V to 1V, output voltage varies from -0.98V to 0.98 V.

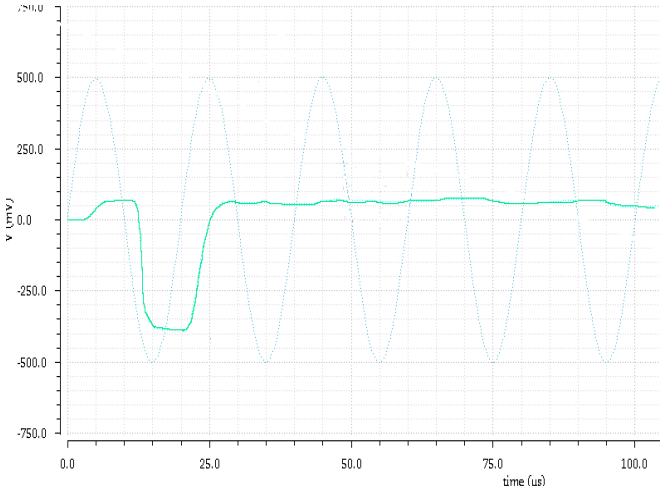

FIG 7: Output wave at hold condition

For sampling and holding the signal, sampling frequency of 1 MHz is applied to the circuit which is shown in the below FIG 8 , where, at high level of clock, it holds the signal and at low level, it tracks the input.

Output waveform is shown in FIG 8, where one is input wave and other two waves are output of the first stage and second stage. At the time of holding, output of first stage is not flat, at that time capacitor discharges quickly but in the second stage output is flatter and capacitor discharges slowly, time constant is 45µs which is calculated by external and parasitic capacitance and resistance.

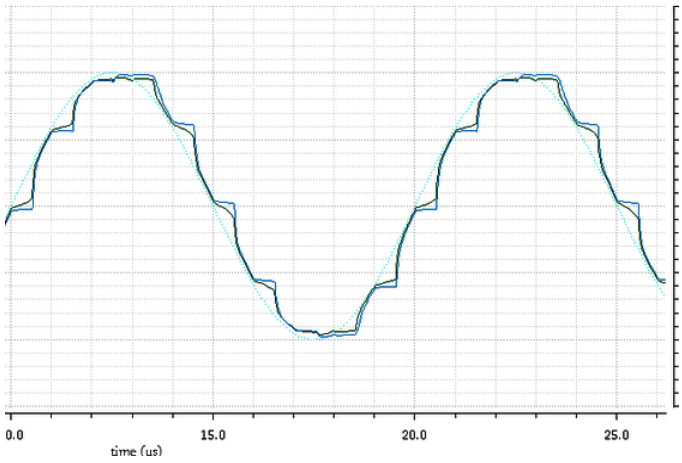

FIG 8: Output waveform

Total Harmonic Distorortion (THD) is -45 dB at clock frequency of 1MHz and V_{p-p} is ±0.8 V which is shown in FIG 9. All parameters are calculated at 100kHz input frequency.

TABLE I. COMPRASION TABLE BETWEEN PROPOSED CIRCUIT AND PREVIOUS CIRCUITS

Parameter	This work	M. Kumngern [4]	Chatterjee et al [5]	Ferreira et al [6]	Swigun et al. [7]
Technology (µm)	0.18	0.18	0.25	0.8	0.13
Supply voltage (V)	±0.8	±0.9	0.5	5	0.8
Bandwidh (MHz)	10	10	5	8	--
Sampling Rate (MS/s)	1	1	1	0.25	1
THD (dB)	-45	-60	--	--	--
Power consumption (mW)	0.010	0.014	0.3	1	1.84

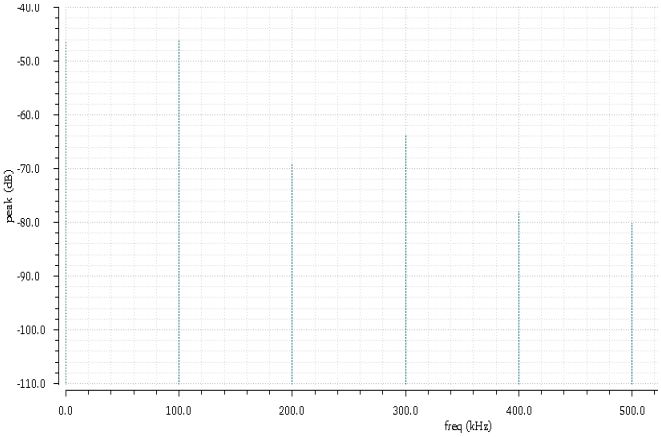

FIG 9: Total Harmonic Distortion

VII. CONCLUSION

Two stage sample and hold circuit is proposed in this paper where efficient and desired output is delivered by the current circuit compared to previous circuit. When two stage is used in the circuit it effects the output waveform at the time of holding. In this proposed circuit used the current conveyor as a switch and that circuit is offering the less power as well as increase the speed of the circuit. Main work of current conveyor is switch and minimize its effect on the circuit expect the switching. The circuit shows more flatter output at the hold time when compared to any other circuits which in turn increases accuracy in the digital form. Layout of that circuit also need the minimum area as well as effect of the parasitic is minimum so change in the results is minimum. The proposed S/H circuit offers high-speed, high linearity and is free of non-over lapping clock signal requirements.

VIII. REFERNCES

[1] Riewruja V., Sungkabunchoo T., Kamsri T., Mahatthumthanant P., Petchmaneelumka W.“A Current-mode CMOS Sample & Hold Ckt for ADC” IEEE International Joint Conference 2006, pp 57585761 .

[2] Koli K. “CMOS Current Amplifiers: Speed Vs Nonlinearity” Helsinki University of Tech, Electronic Ckt Design Laboratory 2000, pp 59-84.

[3] Chante J. P., Grisel R.., Abouchi N., Premont C. “A Current Conveyor Based High-Freq. Analog Switch” IEEE J., IEEE Transactions on Ckt & Systems I: Fundamental Theory and Applications (Volume: 45, Issue: 3 , Mar 1998), pp 298-300.

[4] Khateb F., Nonthaputha T., Kumngern M., “Low-power sample & hold ckt using current conveyor analogue switches” IEEE J., IET Ckt, (Volume: 12 , Issue: 4 , 7 2018), pp 398-402.

[5] Kinget, P.R., Chatterjee, S.: “A 0.5-V 1-Msps track & hold circuit with 60-dB SNDR”, IEEE Journal 2007, 42, pp. 722–729.

[6] Moreno, R.L. Ferreira, L.H.C.: “CMOS implementation of precise sample-and-hold circuit with self-correction of the offset voltage” IEE Proc. 2005, 152, pp. 451–455.

[7] Serdijn, W.A., Sawigun, C.: “Analysis and design of a low-voltage, low-power, high-precision, class-AB current-mode subthreshold CMOS sample and hold circuit”, IEEE, 2011, 58, pp. 1615– 1626.

[8] A Tonk, N Afzal: “Bulk Driven Second Generation Current Conveyor based All-Pass Section for Low Voltage Operation” IEEE, 2019, 2018 International Conference on Computing, Power and Communication Technologies (GUCON), pp 946-949.

[9] Yellampalli, Prakruthi T.G.: “Design and Implementation of Sample & Hold Circuit in 180nm CMOS Technology”, International Conference, Communications and Informatics (ICACCI), 2015, pp 1148-1151.

[10] Musil V., Prokop R. “Current Conveyor CCII as the Most Versatile Analog Circuit Building Block”, ANNUAL JOURNAL, pp 73-76

[11] Smith K., Sedra A.: “A 2nd generation current conveyor & its applications”, IEEE Trans. Circuit Theory, 1970, **17**, pp. 132–134.

[12] Razavi, B.: “Design of sample-and-hold amplifiers for high speed low-voltage A/D converters”. Proc. IEEE 1997, pp. 59–66.

[13] Monpapassorn, A.: “An analog switch using a current conveyor”, Int. J. Electron., 2002, 89, pp. 651–656.

[14] Sirinaovakul B., Chipipop B., Chaisricharoen R. “CMOS CCCII Structures, characteristics, and considerations” Int. J. Electron. Commun. 64 (2010) 540–557.

[15] Singh A.K., Bhaskar D. R., Senani R. “Current Conveyors: Variants, Applications and Hardware Implementations”, Springer.

[16] Anwar I., Yousuf R., Yasin M. Y., Mohammad U. “A novel square wave generator based on the translinear circuit scheme of second generation current controlled current conveyor-CCCII” Springer Nature Switzerland AG 2019.

[17] Sagbas, M., Minaei, S., Ayten, U.E.: ‘Component reduced current-mode fullwave rectifier circuits using single active component’, IET Circuits Dev. Syst., 2016, 10, pp. 1–11

[18] Monpapassorn, A.: ‘Programmable wide range voltage adder/subtractor and its application as an encoder’, IEE Proc. Circuits Dev. Syst., 2005, 152, pp. 697–702

Proceedings of the Fourth International Conference on Communication and Electronics Systems (ICCES 2019)
IEEE Conference Record # 45898; IEEE Xplore ISBN: 978-1-7281-1261-9

A Knowledge Interchange Format (KIF) for Robots in Cloud

Dhruba Ningombam
Computer Science and Engginerrng
Sikkim Manipal Institute of Technology
Majitar, Rangpo, India,
dningombam@gmail.com

Tejbanta Singh Chingtham
Computer Science and Engginerrng
Sikkim Manipal Institute of Technology
Majitar, Rangpo, India,
chingtham@gmail.com

Mrinal Kanti Ghose
Computer Science and Engginerrng
Sikkim Manipal Institute of Technology
Majitar, Rangpo, India,
mriinal.ghose1952@gmail.com

***Abstract*— The most important factor to increase knowledge is to share what is learned. This approach of sharing what is learned is incorporated in robotics so that the robots can solve day to day problems by learning when required. The proposed knowledge interchange format (KIF) deals with communication amongst heterogeneous robots through the cloud. Keeping in mind the size of data, the emphasis has given to generate a representation of the path for robots that can be processed parallelly and saved in the cloud, enabling the sharing of knowledge between robots. In order to achieve this compatibility, a path as a set of characters or a string is considered with a convention that is predefined so that no matter how much the robotics evolves, it can always interpret a string. The string is tested in a Hadoop map-reduce program to process the paths parallelly and provide the best path from the cloud.**

Keywords—knowledge interchange format, cloud ,heterogeneous robots, hadoop map-reduce.

I. INTRODUCTION

The impacts of automation technologies are already being felt throughout the economy [1]. The worldwide number of industrial robots has increased rapidly over the past few years [2] . The falling prices of robots, which can operate all day without interruption, make them cost-competitive with human workers. In the service sector, computer algorithms can execute stock trades in a fraction of a second, much faster than any human. As these technologies become cheaper [3] , more capable, and more widespread, they will find more applications in an economy driven society.

Over the years, internet has been providing many updates of the programs running in personal computers and servers. Internet had also enabled people to share and obtain certain information through the vast information stored in the World Wide Web (WWW) [4]. With the introduction of Distributed Computing, computers started expanding their resources like memory and processing power by pooling from many computers participating in the system. The cloud computing technology took a leap forward by facilitating devices to use storage and computing capability which are connected to use it [5]. As a result devices smaller and lighter with low power for its operation started depending on cloud. Cloud provides processing power to these devices thereby reducing the cost of processing power and decreases the time of execution for getting quick result [6]. The power consumption for these devices becomes lesser since it takes lesser time in processing.

Cloud facilitates connection of billion new devices to it [7] [8]. Due to rapid growth of electronic devices in recent time, there are also various mobile operating system (OS) developed to run those devices. Operating system like android OS (Google Inc.), bada (Samsung electronics), blackberry OS (Research In Motion), iphone OS/ iOS (Apple), palm OS (Garnet OS), symbian OS (Nokia), web OS (Palm/HP), windows mobile (Windows phone) are few mobile operating system commonly used for mobile devices [9]. Besides, with the evolution of internet of things (IOT) recently, small devices with different platform are also able to connect and talk to each other through cloud [10]. As cloud provides platform for devices likewise robots with less processing power will not only be able to communicate each other but also share knowledge base redundant data through cloud.

II. REALATED WORK

Since there exist a variety of robots with different types of hardware, robots use different robotic platforms. This is one of the main reasons why it is difficult to write software for robots and share the data when they are connected with cloud. With the motive to simplify the task of creating complex and robust robot software behavior across different platforms, robots operating system (ROS) an open source framework was developed [11]. Motive of ROS was to meet the set of challenges that where encountered while developing service robots as part of projects like Stanford AI Robot (STAIR) and the Personal Robots (PR) program [12] [13]. ROS being open source has contribution from different communities many new tools and libraries are updated. Still there are lots of people who are against the use of ROS [14] [15]. Reasons being, lack of support for some packages. Libraries are written and shared whenever there is a need for such libraries but failed to maintain bugs free, making it obsolete after a certain period of time ultimately. Still, the programs for robots are dependent highly on the hardware on which the robot is based. Hence reusing of program code across varied platforms is difficult [16] [17]. The lack of standard interfaces [18] [19] [20] [21] to robot hardware components also continues to be a great challenge in all areas of robotics.

With a well define knowledge interchange format (KIF), ontology can be used to develop a new generation information system [22] [23].Thus it may help merging and mapping of the information from different data source and preparing them in such a way that end user can use it. The same concept can be deploy in the field of cloud robotics where robots can interact with each other and enables robots to share and reuse their existing information/ knowledge [24] [21].

III. METHODOLGY

A Knowledge Interchange Format (KIF) [25] is designed for the interchange of knowledge among different computer programs. Typically, when a program reads a knowledge base in KIF, it converts the data into its own internal form of specialized pointer structures, arrays, etc..and all computations are done using these internal forms. When a program needs to communicate with another program, it maps its internal data structures into the common format viz; KIF through which the other computer communicates. Thus it can also be used for exchange of knowledge between the robots of different architectures. Hence a Knowledge Interchange Format (KIF) plays a vital in enabling the robots of different hardware to interpret a common format easily without much complexity, even in case of robots with lesser hardware configurations. Though there are several ways of representing knowledge interchange format for robots as mentioned in [27] [28], a parametric representation which deals with the low level representation is considered for masking the heterogeneity to an extent.

The knowledge is a 'map representation' in the form a continuous variable string representing a path taken by robot. Considering a robot takes only left, right, back or front, a representation of the path is discussed below.

The general format of the variable string considered in this study is:

[Distance/Angle] [Direction].....[Stop]

An Example: 30R90L45RS will cause the robot to move 53 cm distance on Right,, than take 90 cm Left, 45 cm Right and S is delimiter for stopping the robot as shown in figure 1.

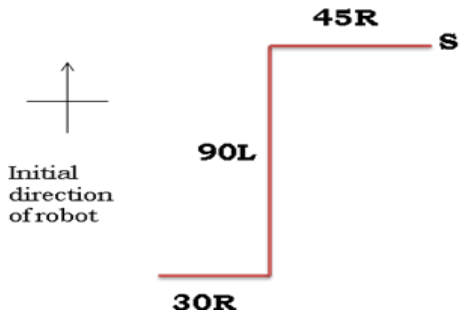

Fig. 1. Path map representation using continous variable string.

When the path gets stored in cloud, the destination and source gets added at the front of the string and all the intermediate nodes are added so that the string will look like

ab|50Lc60B40Rh30FS|

where,

ab= source destination pair

|= delimiter

A score/weight is added after the last delimiter '|'to assign or choose the likeability of paths. The integer value represents the distance.

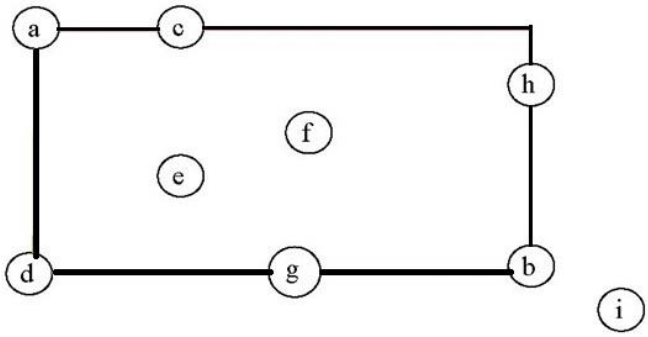

IV. IMPLIMENTATION

A. *Testing in Hadoop MapReduce*

To explain the environment with different stations and paths, an example with destination 'b' and source 'a' and two paths is shown in Figure 2, wherein the String 55Rc105F15Rh55FS represents one of the path from 'a' to 'b' marked by the thin line while the String 70Bd100Rg55FS represents the other path from 'a' to 'b' marked by the bold thick line.

In the bold thick line of Figure 4.1, the source is 'a' and the destination is 'b', and 'c' and 'h' are two intermediate nodes. There might be situations where robots need the path from 'c' to 'h', so it becomes necessary to list the intermediate nodes in the representation. The details of intermediate nodes in the representation have been provided by writing it in small letters to uniquely identify that it is an intermediate node. The representation of bold line will now be as ab|55Rc105F15Rh55FS| which implies that 'a' is source, 'b' is destination, after moving 55 cm right it reaches c and it moves 105 cm forward and then take right turn and move 15 cm to reach h and then finally reaches 'b' after moving forward for 55 cm and then stops.

Fig. 2. Representation of robots environment in graph.

For the simplicity of searching the paths from intermediate nodes after the first delimiter, the list of intermediate nodes are added to it and is represented as:

ab|ch|55Rc105F15Rh55FS|9.

In the above given string

- 'a' is the source.
- 'b' is the destination.
- 'c' and 'h' are the intermediate nodes.
- Robot starts from 'a' and moves 55 cms right to reach 'c'.
- Robot then moves 105 cms forward and then 15 cms right to reach h.
- From 'h' it moves 55 cms forward and then stops at 'b'.
- Number after the last delimiter is the score generated after processing.

B. *Processing of Paths*

Most often, the data gathered during traversing and finding paths by the robot is very large. As there will be collection of large no of paths, these data will eventually form big data and are usually stored in the Cloud. Since the traditional computing techniques cannot be used to process

these data sets, the parallel processing using Hadoop Map Reduce is commonly used to process the paths in parallel [29].

Map-reduce is a highly parallelized programming model that can be used for processing large data sets. The task of partitioning the input data, scheduling the programs execution in different clusters, making it fault tolerant, and managing inter machine communication is taken care by the run time system [29].

Hadoop is an Apache open source framework written in Java that allows distributed processing of large datasets across clusters of computers using simple programming models. The Hadoop framework application works in an environment that provides distributed storage and computation across clusters of computers. Hadoop [29] is designed to scale up from single server to thousands of machines, each offering local computation and storage. Hadoop has been setup in standalone mode on Ubuntu 14.04 system. The setup runs on a single Java Virtual Machine (jvm). It becomes easy to test and debug the map reduce programs. Less amount of sample sets are used so that the default properties are set for standalone mode to run the map reduce programs. 10 sample paths as shown below have been generated for the environment.

ab|10L5Rc20R50Fg50fS|0

ab|10L5R20Re70FS|0

ag|50L12Rf10Fh20BS|0

ab|10L5Rc20R50F25B20Rh50fS|0

vk|30L20Ru10Bw10RS|0

ab|30R10Lr25RS|0

ab|10L5Rc20Rd50Fe25Bf20Rg50fS|0

gk|5Rh10Li20BS|0

vk|20Rl10LS|0

ab|10L20Rd50FS|0

The last field is filled with zero which indicates that these paths has never been shared or processed. Once the request for any source destination pair is made, a Map Reduce program is executed to find all the strings that match the required source destination pair. There might be many intermediate nodes between the source and destination in the representation that forms a better path. Hence the entire string is checked to find the paths that might be intermediate nodes. To find all the paths matching some pattern there is no need to combine intermediate key-value pair and hence Reduce is not needed. Map takes path and outputs if it matches the pattern. This is not a good idea if there is a single large document, but works well if there are many documents. In a realistic scenario there might be many documents as there may be large number of robots. Therefore using of Map Reduce is justified.

C. Mapdriver Class

The task of map driver class is to control the entire job. It is the top level class and the main entry point. The main function in this class takes commands by an argument which is the input, output file and the source destination pair.

The job object gets instantiated, File input format and file output format describes the input and output specification for the job and creates path objects based on arguments variable. The output path gets created by Map Reduce job and output files are deposited there. The behavior for file input format is to read key value text separated by delimiter. WaitForCompletion method is called which launches the job and returns success or not. Now the mapper and reducer class are called. The flowchart for Mapdriver class is shown in Figure 3. The framework handles all the details all the numbers of mappers required and how to read distributed input file.

D. PathMapper

PathMapper extends the Mapper class to implement the map function. In a distributed computing model, data gets send from node to node via Remote Procedure Call and data must be serialized and desterilized as it goes. Hadoop built in data serialization format is called writable. Writable class exists as a wrapper for almost all Java primitive types.

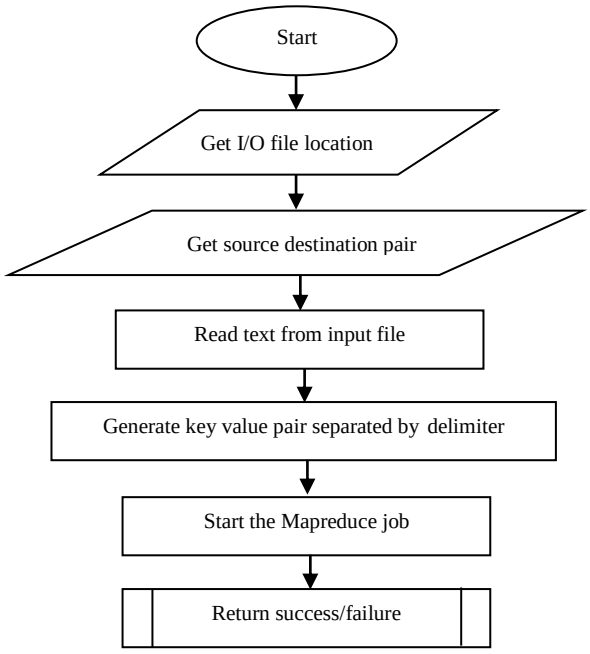

Fig. 3. Flowchart of MapDriver.

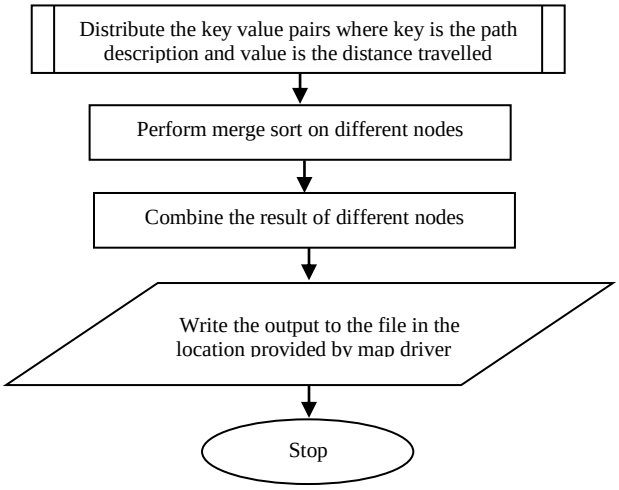

Fig. 4. Flowchart of PathReducer.

The declaration for the costumed Mapper class extends the class Mapper. The Mapper class uses parameterized types to define the types of key values for both input and output. The input key and input values are text, output keys are text and output values are integers. To implement map function, map method is overridden.

The map function searches if source and destination exists in the representation. If source and destination exists then the distance from source to destination is calculated by parsing the string and a list of key value pair where key is the string from source to destination and value is the distance to reach from source to destination. The flowchart for PathMapper is shown in Figure 6.

TABLE I. GENERATING SCORE FOR PATHS

Path	Penalty (p)	Reward (r)	Weight (r-p)
ab|a30R10Lr25RSb|0	*1*	*6*	*5*
ab|a10L20Rd50FSb|0	*2*	*5*	*3*
ab|a10L5Rc20R50Fg50fSb|0	*3*	*4*	*1*
ab|a10L5R20Re70FSb|0	*4*	*3*	*-1*
ab|a100L5R20Rg70FSb|0	*5*	*2*	*-3*
ab|a100L50R20Rh70FSb|0	*6*	*1*	*-5*

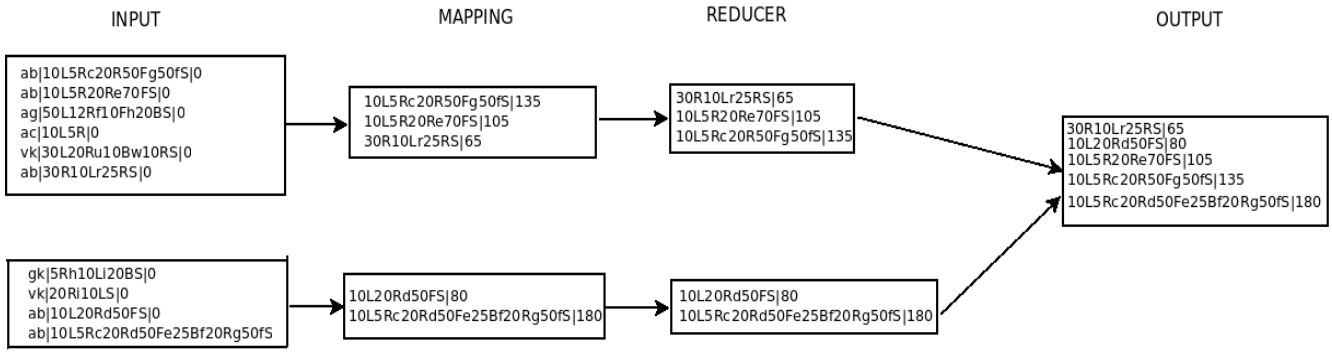

Fig. 5. Result of mapreduce programs.

The input and output key are text whereas the input and output values are integers. To implement the reduce function reduce method is overridden. The reduce function distributes the key value pairs to various node, where based on value the paths are sorted at each step. The sorting technique used is merge sort. At each node merge sort is done and later the results from each node are compared and combined. The sorted data from each node are checked with each other to finally output the sorted data. These data are stored in the output file at the location provided by MapDriver class. The flowchart for path reducer is shown in Figure 4.

E. Path Reducer Class

The PathReducer class extends the class reducer. Just like the Mapper the reducer class uses parameterized types to define the keys and values. The input and output key are text whereas the input and output values are integers. To implement the reduce function reduce method is overridden. The reduce function distributes the key value pairs to various node, where based on value the paths are sorted at each step. The sorting technique used is merge sort. At each node merge sort is done and later the results from each node are compared and combined. The sorted data from each node are checked with each other to finally output the sorted data. These data are stored in the output file at the location provided by MapDriver class. The flowchart for path reducer is shown in Figure 4.

F. Running Program on Hadoop Cluster

To run the program on Hadoop cluster, a jar file of the package PathFinder consisting of following classes is built.

- MapDriver
- PathMapper
- PathReducer

This jar file is copied to cluster where Hadoop job will run. MapReduce has a feature which lets the entire cluster to be Network File System (NFS) mounted which allows the cluster to be treated as any other disk and use native Linux commands to move data in and out. The input sample file is also copied to the Hadoop File System (HFS). The map-reduce program is run where the input location output location is provided as arguments. The output file is generated in Hadoop clusters which are copied to local file system, where a Java program to assign weights to the paths is run.

G. Assigning weights

The distance from source to destination is calculated by adding each integer value that exists in path representation. The distance is added at end of the string based on the distance the strings are sorted. Once the file contains sorted strings , weights are assigned to each strings , where w = r - p; r is the reward assigned to each string and p is the penalty, rewards are assigned in descending order, if there are n no of paths then p = n for n, p = n-1 for n-1 and the penalty is assigned in reverse order. ‘w’ is calculated and stored with the paths. Next time if the robot needs the path to same source destination pair then it can choose the path with highest weights and in case if there is some problem with the weight i.e. the path is broken or any obstacle is found then

robot can requests the path that has the next high weights. Table I shows the generation of weights for 6 different paths that exist from ‘a’ to ‘b’.

a) Input Samples

The input sample set is stored in a text file path.txt and copied to Hadoop file system.

ab|10L5Rc20R50Fg50fS|0

ab|10L5R20Re70FS|0

ag|50L12Rf10Fh20BS|0

ab|10L5Rc20R50F25B20Rh50fS|0

vk|30L20Ru10Bw10RS|0

ab|30R10Lr25RS|0

ab|10L5Rc20Rd50Fe25Bf20Rg50fS|0

gk|5Rh10Li20BS|0

vk|20Rl10LS|0

ab|10L20Rd50FS|0

V. RESULT AND DICUSSION

Reduce program is run on Hadoop clusters where the location of input file and output file is provided by arguments. The program is run to find the paths from source ‘a’ and destination ‘b’ the intermediate key value pair after finding distance from ‘a’ to ‘b.’ The reducer takes the key value pair generated by map function and sorts the value using merge sort which is combined to generate the required output. Figure 5 shows the input output and the intermediate key value pairs generated at each step of Map Reduce. The Mapper searches for all the paths from a to b and generates

The objective is to introduce a Knowledge Interchange Format (KIF) or variable length string for the heterogeneous robots to communicate on a generic cloud robotics platform. Emphasis has been given to generate a representation of path for robots (keeping in mind the size of data) that can be processed parallely and saved in cloud, enabling sharing of knowledge between robots. A variable length string data interchange format is considered for representing a path. Representation is made simple for compatibility across all microprocessors. The variable length string is tested in Hadoop MapReducee to simulate cloud processing.

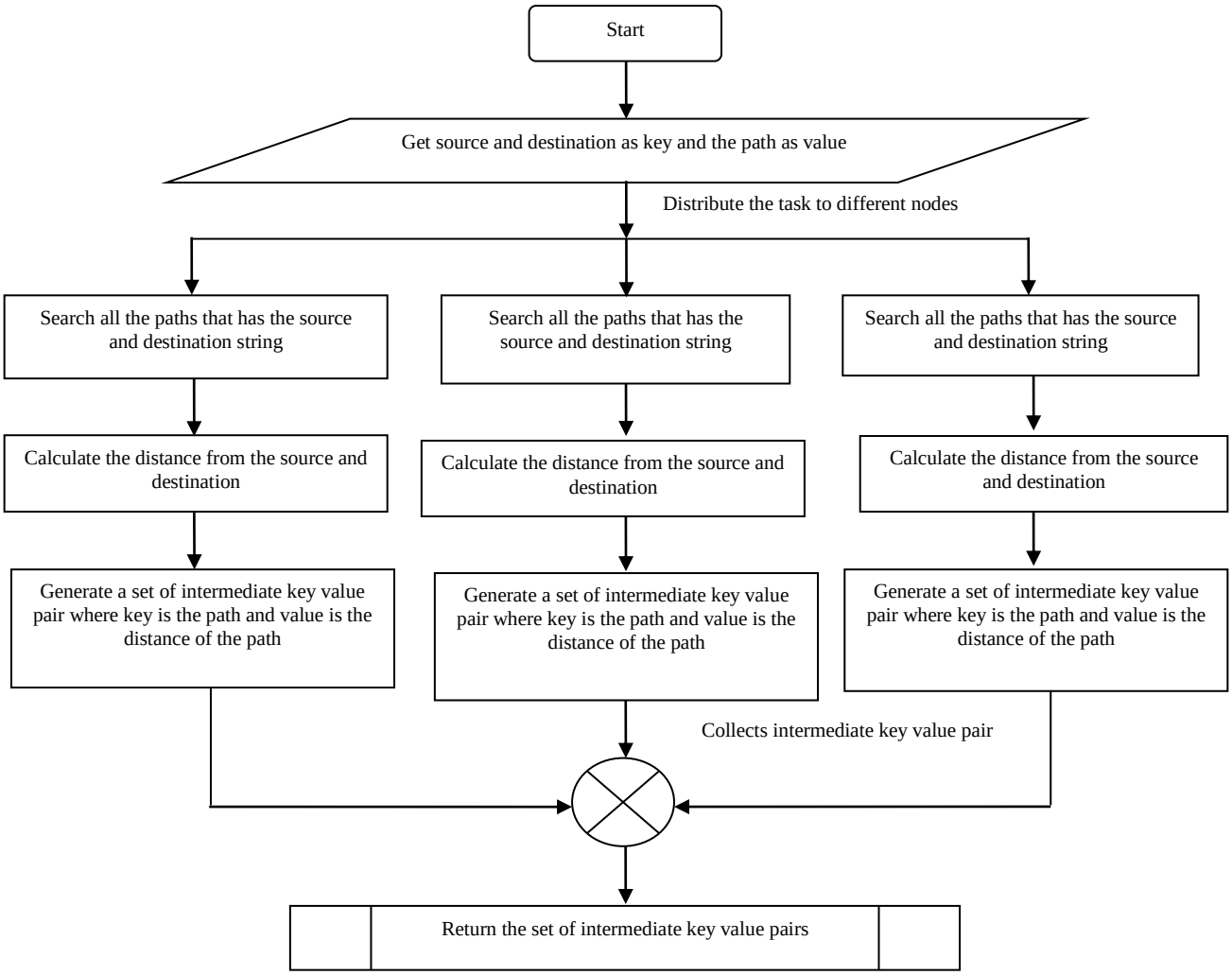

Fig. 6. Flowchart of PathMapper.

VI. LIMITATIONS

The Path map is designed with an ideal environment without considering obstacles and odometry error.

VII. FUTURE SCOPE

The Knowledge interchange can be extended to store other information such as object models, information about particular environment knowledge, than a path map.

Further, it can be implemented in educational robots like lego minstrom nxt and boebot through a thin middleware.

REFERENCES

[1] McKinsey, "A Future That Works: Automation, Employment And Productivity" A report from McKinsey Global Institute Research, January 2017.

[2] how robots could help elderly age in their homes, https://www.smithsonianmag.com/innovation/how-robots-could-help-elderly-age-in-their-homes-180964650/#GELZMmpW2ceLWJU2.99 Available online. Accessed on 2/1/2018.

[3] Paul Nunes and Larry Downes, "How Innovations Become Better And Cheaper", https://www.forbes.com/sites/bigbangdisruption /2013/05/09/welcome-to-the-world-of-better-and-cheaper/#77a61f6e5c83, Accessed on 18/5/2019.

[4] Barry M. Leiner, "A Brief History of the Internet", ACM SIGCOMM Computer Communication Review Volume 39, Number 5, October 2009.

[5] Padhy, Rabi & Patra, Manas, "Evolution of Cloud Computing and Enabling Technologies", International Journal of Cloud Computing and Services Science (IJ-CLOSER). 1. 10.11591/closer.v1i4, 1216. 2012

[6] Gurudatt Kulkarn, Rajnikant Palwe,Vikas Solanke ,Shrikant Belsare,Sangita Mohite," Mobile Cloud Computing - Bring Your Own Device", 2014 Fourth International Conference on Communication Systems and Network Technologies , INSPEC Accession Number: 14333764, IEEE, 7-9 April 2014.

[7] J. H. Hong, B.-C. Min, J. M. Taylor, V. Raskin, and E. T. Matson, "NL-based communication with firefighting robots," Systems, Man, and Cybernetics (SMC), 2012 IEEE International Conference on, pp. 1461-1466, 2012.

[8] S. Venkata Krishna Kumar , S.Padmapriya, "A Survey on Cloud Computing Security Threats and Vulnerabilities", International Journal Of Innovative Research In Electrical, Electronics, Instrumentation And Control Engineering Vol. 2, Issue 1, January 2014.

[9] Vangie Beal "Mobile Operating Systems (Mobile OS) Explained", available online: https://www.webopedia.com/DidYouKnow/Hardware_Software/mobile-operating- systems-mobile-os-explained.html, Accessed on 12/3/2019.

[10] Porkodi Dr.R,Bhuvaneswari VelumaniBhuvaneswari Velumani, "The Internet of Things (IoT) Applications and Communication Enabling Technology Standards: An Overview" International Conference on Intelligent Computing Applications, 2014.

[11] Adarsha Kharel, Dorjee Bhutia, Sunita Rai, Dhruba Ningombam" cloud robotics using ROS" IJCA Proceedings on National Conference cum Workshop on Bioinformatics and Computational Biology NCWBCB(3):18-21, May 2014.

[12] Rosjava, an implementation of ROS in pure Java with Android support, [Online]. Available: http://cloudrobotics.com, Accessed on 17/8/2014.

[13] Robot Operating System [online] Available: http://www.ros.org. Accessed on 17/8/2014.

[14] N. Mohamed, J. Al-Jaroodi, and I. Jawhar, "Middleware for robotics: A survey," in Proc. Int. Conf. Robotics, Automation and Mechatronics, , pp. 736–742, 2008.

[15] W. D. Smart, "Is a common middleware for robotics possible?" in Proc. Workshop Measures and Procedures for the Evaluation of Robot Architectures and Middleware at the Int. Conf. Intelligent Robots and Systems, 2007.

[16] E. Prassler, R. Bischoff, and H. Bruyninckx,, "It's a long way to useful standards," IEEE Robot. Automat. Mag., vol. 17, no. 3, pp. 18–19, 2010.

[17] Jeffrey L. Krichmar"Android™ Based Robotics: Powerful, Flexible and Inexpensive Robots for Hobbyists, Educators, Students and Researchers" University of California, Available: http://www.socsci.uci.edu/~jkrichma/ABR/, nov 26,2018.

[18] J.Srinivas, K.Venkata Subba Reddy, Dr.A.Moiz Qyser, "Cloud Computing Basics" ,International Journal of Advanced Research in Computer and Communication EngineeriangVol. 1, Issue 5, July 2012.

[19] Olimpiya Saha and Prithviraj Dasgupta, "A Comprehensive Survey of Recent Trends in Cloud Robotics ,Architectures and Applications",Robotics 2018, 7, 47; doi:10.3390/robotics7030047, 30 August 2018.

[20] Wuhui Chen, Yuichi Yaguchi ,Keitaro Naruse, Yutaka Watanobe, Keita Nakamura, Jun Ogawa, "A Study of Robotic Cooperation in Cloud Robotics: Architecture and Challenges", IEEE Access PP(99):1-1 DOI: 10.1109/ACCESS.2018. 285 – 295, July 2018.

[21] Leigh Duggan, James Dowzard, Jayantha Katupitiya, Ka C. Chan , "A Rapid Deployment Big Data Computing platform For Cloud Robotics", International Journal of Computer Networks & Communications (IJCNC) Vol.9, No.6, November 2017.

[22] K.Goldberg and B.Kehoe. "Cloud robotics and automation: A survey of related work," EECS Department, University of California, Berkeley, Tech. Rep. UCB/EECS-2013-5, Jan 2013 [Online] Available: http://www.eecs.berkeley.edu/Pubs/TechRpts/2013/EECS-2013-5.html. Accessed on 5/9/2018.

[23] Dipendra K Misra, Jaeyong Sung, Kevin Lee and Ashutosh Saxena, "Tell Me Dave: Context-Sensitive Grounding of Natural Language to Manipulation Instructions", International Journal of Robotics Research archive, Volume 35 Issue 1-3, Pages 281-300, 2016.

[24] Ben Kehoe Member, IEEE, Sachin Patil Member, IEEE, Pieter Abbeel Member, IEEE, Ken Goldberg Fellow, "A Survey of Research on Cloud Robotics and Automation", IEEE Transactions On Automation Science And Engineering, 12 Jan, 2014.

[25] Genesereth, M. R. 1990. Knowledge Interchange Format Version 2.0, Reference Manual. Report Logic-90-4, Computer Science Department, Stanford University. Available at http://logic.stanford.edu/kif/kif.html , Accessed on 14/2/2018.

[26] D. Hunziker, G. Mohanarajah, M. Waibel, and R. D'Andrea, "Rapyuta: The RoboEarth cloud engine," in Proc. IEEE International Conference on Robotics and Automation (ICRA), Karlsruhe, Germany, pp. 438–444, 2013.

[27] Craig Schlenoff, et. Al , "IEEE Standard Ontologies for Robotics and Automation", IEEE Std 1872™- ,2015.

[28] Craig Schlenoff, Gaithersburg, Stephen Balakirsky, "Performance evaluation of robotic knowledge representation (PERK)", Proceeding PerMIS '12 Proceedings of the Workshop on Performance Metrics for Intelligent Systems Pages 1-8 College Park, Maryland, ACM New York — March 20 - 22, 2012.

[29] Hadoop map reduce framework[online]. http://hadoop.apache.org/hdfs/ ,2015.hadoop, Accessed on 8/5/2018.

Proceedings of the Fourth International Conference on Communication and Electronics Systems (ICCES 2019)
IEEE Conference Record # 45898; IEEE Xplore ISBN: 978-1-7281-1261-9

Energy-Delay Based Route Request Scheme for Load Balanced Routing in Wireless Mesh Networks

Keerthi D S
Deparment of Electronics &Communication Engineering
Malnad College of Engineering
Hassan,India
keerthikumards@gmail.com`

Shobha Rani A
Department of Electronics and Communication Engineering
BMSIT
Bengaluru, India
shobharani@bmsit.nic.in

T G Basavaraju
Department of Computer Science & Engineering
Govt. SKSJTI
Bengaluru, India
tg.braju@gmail.com

***Abstract*—The tremendous growth in usage of internet technology has pawed way for advancement of diverse wireless networks. One of the wireless networks that have gathered a lot of attention is Wireless Mesh Network (WMN). WMN is being preferred because of its numerous advantages such as better coverage area, communication with other networks, cost effectiveness, increased network capacity and is compatible with all IEEE 802.11 standards. Low Capacity, management of the traffic and gateway nodes and end to end fairness problem are the major issues in the employment of WMNs. In order to reduce the existing challenges in WMNs load balancing plays a vital role. In our work we have proposed a load balancing protocol to overcome the problem of congestion using residual energy and delay. The simulation results are derived and they prove that our proposed protocol enhances the performance and life time of WMN compared to standard protocol with reference to residual energy, throughput, packets received jitter and delay.**

Keywords—WMN, Load balancing, Energy, Delay

I. INTRODUCTION

A wireless mesh network is an infrastured network which is based on mesh topology. The architecture of a WMN [1] consists of three major components which are clients, routers and gateways. The clients are often laptops, desktops, tablets, and mobile phones etc. which are end devices. The router performs the task of traffic management through gateways. In a mesh network, even when a single node fails to operate, the communication is not hampered as the rest of the nodes are still able to establish communication with each other either directly or via intermediate nodes. Thus this uniqueness of WMNs has made them highly reliable, resilient and offers a higher degree of redundancy. The integration of WMN [2] technology can also be implemented along technologies such as 802.11, 802.16, 802.15 standards in cellular technologies.

A WMN can be visualized as a distinctive wireless Ad-hoc network. However a WMN has a systematic i.e. configuration and delivers a dynamic and cost effective deployment of network over a specific geographical area. An Ad-hoc network is a unpremeditated network where communication can be established only when the wireless devices come in each other's communication range. WMN [3] can also be used for wide variety of applications such as transport systems, wireless sensor network, surveillance system, broadband home networking, building automation, health and medical system, community and neighborhood networking.

A mobile node consumes its battery energy not only when it actively sends or receives packets but also when it stays idle listening to the wireless medium for any possible communication requests from other nodes. Thus, energy efficient routing protocols minimize either the active communication energy required to transmit and receive data packets or the energy during inactive periods. In some protocols the active communication energy can be reduced to reach the receiving node by adjusting the node's radio power just enough to reach the receiving node. The optimal routing path that reduces the total transmission energy needed to send the data packets to the destination can be determined by using the transmission power control method. When there is no data to send or receive each node can retain the inactivity energy changing its mode of operation into sleep power down mode or simply turn it off like in other protocols. Considerable energy saving can be achieved here, if the network conditions is specified with low duty cycle of communication activities. But for guaranteed data transmission when many nodes are sleep and not forwarding packets for the next nodes it may require much well designed routing protocols. Load distribution approach in another powerful approach for optimizing active communication energy. It maximizes the new lifetime when selecting a routing path by avoiding over utilized nodes and also balances the energy usage among nodes. Though each protocol will have advantages and disadvantages and is convenient for certain situation, it is not clear that any one algorithm or a clan of algorithms is ideally suited for all situations. However, it is possible to offer a better energy saving routing mechanism by combining and integrating the existing solutions. Many efforts have been directed to develop energy aware-MAC and transport protocols to tackle energy efficiently in other network layers. In layered network architecture each layer is supposed to operate in isolation. But to maximize the energy performance some recent studies have recommended the cross layer design.

The paper is arranged in the following manner. The existing technology related to proposed work is discussed in second Section. The proposed routing scheme EBL-AODV is completely described in third section. The simulation results, performance comparison and analysis are presented in fourth section. The inference of the paper is in fifth section .

II. RELATED WORK

In this work we have proposed a modified AODV protocol called Energy-Delay Based Load Balancing Ad-hoc on Demand Protocol (EDBL-AODV), which considers residual energy and path delay as a routing metric during route discovery.

Aron et al. [4] have described a novel distributed topology control algorithm whose main objective is to reduce the consumption of energy by each node during transmission and extending lifetime of the network. It is a three phased topology control algorithm which involves establishing accessible neighborhood topology, constructing minimum energy local topology view and finally determining transmission power. Thus the above algorithm overcomes the topology control problem in hybrid WMNs equipped with heterogeneous wireless devices and altering transmission ranges by taking decisions based on information gathered locally and scaling it for large WMN.

Panagiotis et al. [5] have proposed a new energy efficient multi cost routing algorithm for WMN. According to the new routing algorithm, a vector of cost parameters are calculated at each link using appropriate operators for selecting an optimal path. The parameters are hop count, power required by the node to transmit and the remaining energy at each node. There are two models- Network evaluation model and dynamic one to one communication model under which the performance of the proposed protocol is evaluated. In the former evaluation model, the network aims to transmit maximum number of packets available preceding energy depletion. In the latter model, the data packets are generated uninterruptedly as the nodes are competent of periodically recharging their energy. This protocol is said to enhance the durability of the network.

Awad et al. 6] have proposed a cross layer optimization algorithm subject to a delay deadline constraint. The assumption is that all packets successfully received should have their end to end delay less than their corresponding delay deadline. The proposed algorithm optimizes network and physical layer by exploiting different control parameters viz. path selection parameter in the network layer, the transmission and modulation energy in the physical layer. The protocol is a little time consuming as for every path in the network, all cross layer parameters are calculated through all paths in the networks. The authors [7] have proposed a novel routing model called ERDB-AODV protocol in which remaining energy in the battery and energy draining rate are incorporated as additional metrics for an optimal path selection. Thus, the hop count, available energy at the node and the rate of energy consumption are considered as important factors of the path selection. The protocol avoids nodes with higher energy consumption and lesser energy levels to extend the lifetime of the network. However, this may affect the traffic to traverse a long path to reach destination despite successful transfer.

III. Energy-DELAY Based Load Balancing AODV Protocol

We have proposed a novel routing protocol Energy-Delay based load balancing EDBL-AODV which is improved form of DBL-AODV and which considers both energy and delay for path selection. EDBL-AODV has a modified routing table entry, route discovery and selection process. The additional constituents included in EDBL-AODV are expiration time field, hop count field and advertised hop court for achieving maximum possible paths. The operation of EDBL-AODV routing protocol can be described in Figure 1.

The source node broadcasts the RREQ packet. For immediate nodes with the help of RREQ packet computes the minimum unused energy depending on the incurred energy consumption and delay. The energy consumed can be obtained by the equation:

EC = Power Received or Transmitted * (8 * Packet size / Bandwidth).

$$EC = P * \left(8 * \frac{PS}{B_w}\right) \quad (1)$$

where, EC = Energy consumption.
P = Power Received/Transmitted.
PS = Packet size.
B_W = Bandwidth.

The relay nodes enter the delay and calculated energy consumption in RREQ message. They also check sequence number for a new route and update the same in routing table. The destination node replies to the source node via RREP message. During route selection, the same node chooses an optimal path possessing lesser delay and maximum residual energy.

The delay is calculated in the algorithm is as given below

Delay= (time at which RREQ received at current node) - (time at which RREQ sent from previous node) (2)

The average delay (D_a) is calculated by

$$D_a = \frac{\sum(Tpr - Tps)}{T} \quad (3)$$

where, T_{pr} = Packet received time
T_{ps} = Packet sent time.
T = Total data packets received.

The path selection (PA) process is performed by using

P_s = Max $[\sum\{(\frac{B1r}{B1f})\ (\frac{B2r}{B2f})\ \ldots\ldots\ldots(\frac{Bnr}{Bnf})\}]$ and Min$[\sum\{(D_1)\ (D_2)\ \ldots\ldots\ldots\ldots\ldots(D_n)\}]$ (4)

where, n = advertised hop count
B_r = remaining energy in node
B_f = full energy in node
D = time delay

IV. Performance Evaluation

The effectiveness of EDBL-AODV algorithm is verified by comparing it with the AODV protocol algorithm using Qualnet simulator. The parameters for all simulations are shown in Table 1. We change the number of nodes from16 to 120. For Each node density higher CBR is generated to create the congestion. We used five different quantitative measures to compare the performance of the proposed and existing protocol. In this comparative study, our proposed protocol 'EDBL-AODV' maintains network life time, higher throughput, and lesser delay unlike in AODV protocol.

We fix the packet size as 1024 bytes and change the number of node densities from 16 to 120 to observe the impact of load and node densities on the network performances. The performances of AODV and EDBL-AODV protocols are shown in Fig.1 to Fig.5.

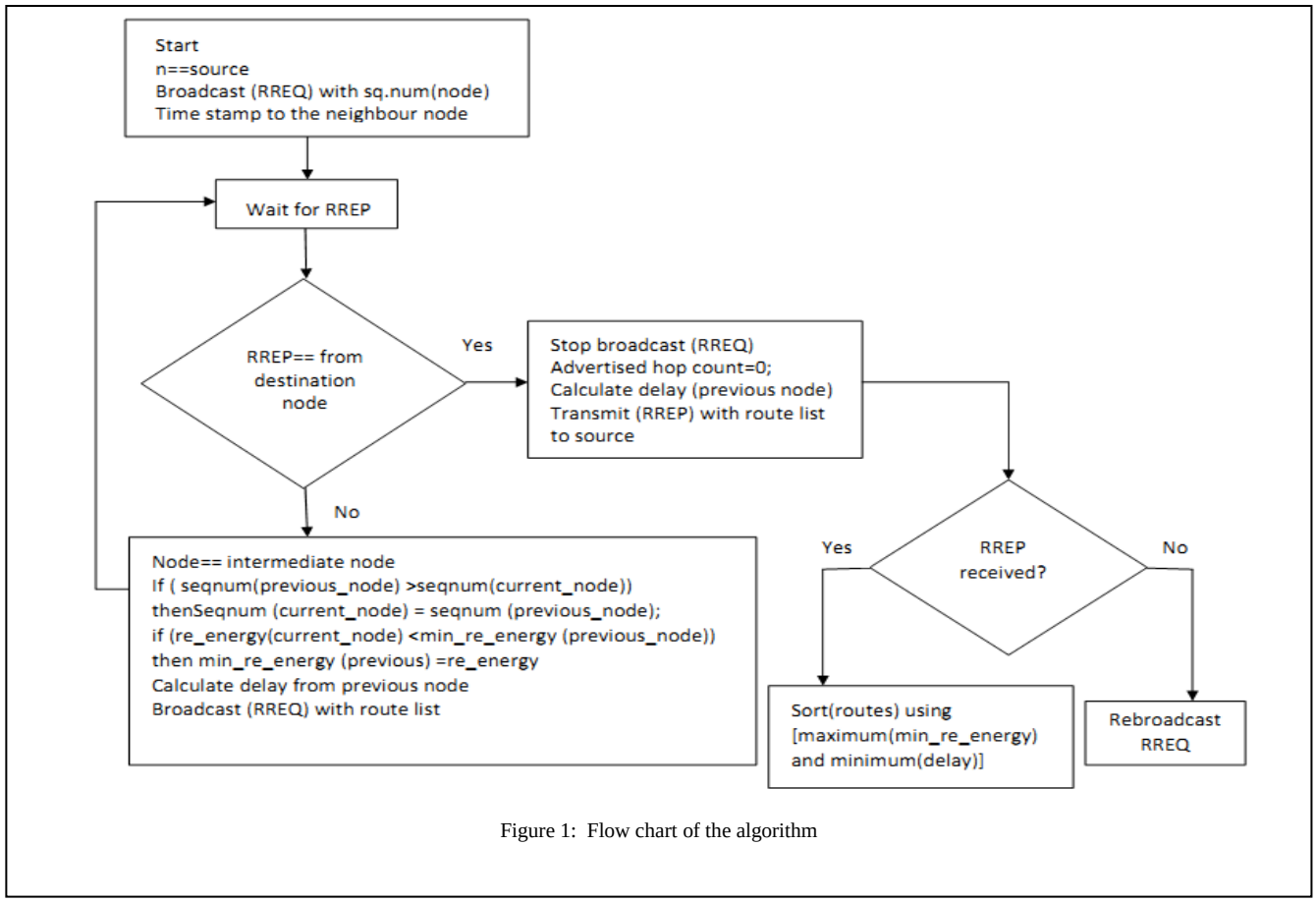

Figure 1: Flow chart of the algorithm

Table 1.Simulation Parameters

Parameter	Value
Protocols	AODV, EDBL-AODV
No. of Nodes	16, 25, 45, 70, 90, 120
Radio type	802.11b Radio
MAC Protocol	802.11s
Antenna Model	Omni-directional
Path Loss Model	Two ray propagation
Traffic Type	CBR

Fig.1 shows throughput comparison with respect to node density. As the number of nodes increases, the average network throughput of EDBL-AODV is always higher than AODV because data transmission is performed based on less delay, path having higher residual energy and minimum number in less time.

Fig. 2 shows that the total number of messages of nodes path. Due to less delay, more number of bits is transmitted received of EDBL-AODV remains higher than AODV with different number of node density since packet transmission is mainly based on less delay and minimum distance path. Due to this consideration, packets are transmitted evenly without any occurrence of node failure. Therefore, higher amount of packets is transmitted. As shown in Fig. 3, the average end-to-end delay of EBL-AODV is lower than that of AODV. Since AODV RREQ packet is modified by introducing delay parameter. Routing is performed using the delay parameter; less delay path is selected for packet transmission. Therefore, end-to-end delay is reduced. For the existing model, AODV packet transmission is performed based on minimum distance which increases congestion and leads to delay, which is even true for Jitter.

Fig. 5 shows that the residual energy of EDBL-AODV is higher than AODV for different node densities. This is because packets are transmitted based on higher residual energy, less delay and minimum distance path. Due to this consideration, packets are not queued at nodes which lead to less resource utilization and less energy consumption.

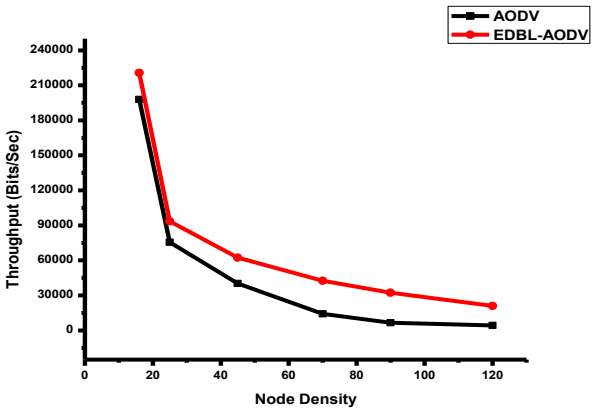

Figure 2: Variation of throughput v/s node densities

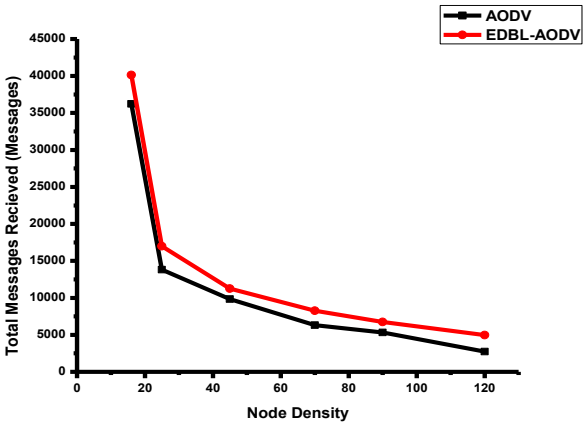

Figure3: Variation of total messages received v/s node densities

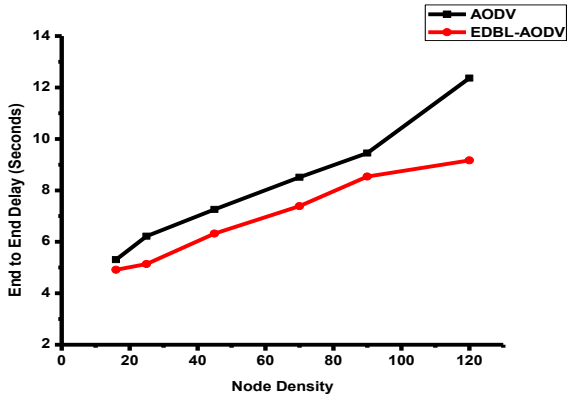

Figure 4: Variation of End to End Delay v/s node densities

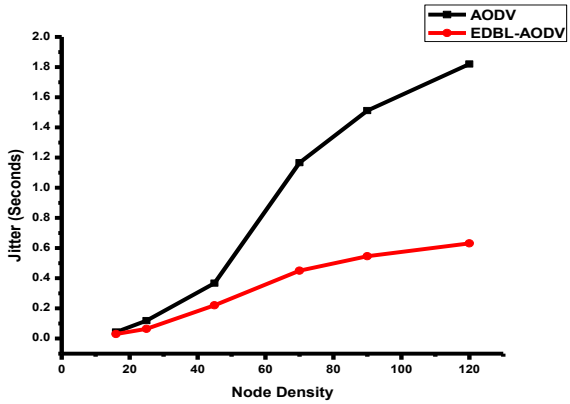

Figure 5: Variation of Jitter v/s node densities

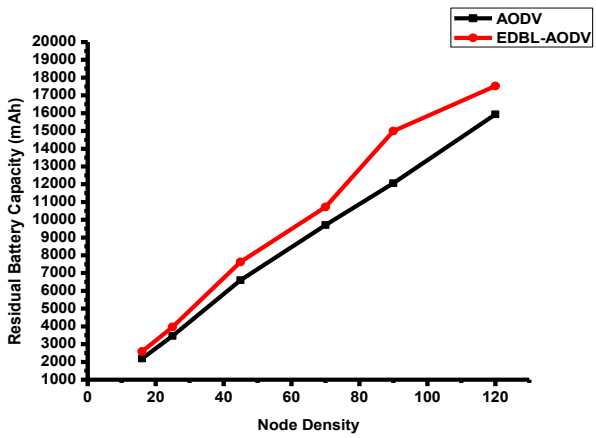

Figure 6: Residual Battery Power v/s node densities

V. Conclusion

In our proposed work energy efficiency is enhanced considerably by reducing routing overhead and delay. Comparative study has been carried out with existing routing protocol and the results are exhibited. Simulation results showed that the proposed protocol improves performance of the network and prolongs the lifetime of a WMN in comparison with the standard protocol. On an average, there is an overall increase in throughput of 12 to 14%, total number of messages received 15 to 18%, decrease in energy consumption of 4 to 6% and decrease in end-to-end delay of 6 to 8% when compared between proposed and existing algorithm.

Acknowledgment

This work is supported by the Technical Education Quality Improvement Program Phase III with the World Bank assistance. The authors would like to thank State Project Facilitation Unit, Directorate of Technical Education, Government of Karnataka, National Project Implementation Unit, MHRD, New Delhi for their support and encouragement.

References

[1] F. Akyildiz, X. Wang, and W. Wang "Wireless mesh networks: a survey", in Computer Networks Journal, vol.47, 2005,pp.445-487.

[2] Eslami, M, Karimi, O, Khodadadi T "A survey on wireless mesh networks: Architecture, specifications and challenges" Control and System Graduate Research Colloquium (ICSGRC), 2014, pp. 219 – 222.

[3] M. L. Sichitiu "Wireless mesh networks: Opportunities and challenge," in Proc. of the Wireless World Congress, (Palo Alto, Ca), May 2005.

[4] F. O. Aron, T. O. Olwal, A. Kurien, and M. O. Ohanga, "A distributed topology control algorithm to conserve energy in heterogeneous wireless mesh networks," *World Acad. Sci. Eng. Technol.*, vol. 40, 2009.

[5] P. Kokkinos, C. Papageorgiou, and E. Varvarigos, "Multi-cost routing for energy and capacity constrained wireless mesh networks," *Wirel. Commun. Mob. Comput.*, vol. 13, no. 4, pp. 424–438, Mar. 2013.

[6] A. Awad, O. A. Nasr, and M. M. Khairy, "Energy-aware routing for delay-sensitive applications over wireless multihop mesh networks," in *2011 7th International Wireless Communications and Mobile Computing Conference*, 2011, pp. 1075–1080.

[7] N. TN, "Energy Draining Rate Based-AODV Routing in Wireless Mesh Network, In 12th FRUCT conference, ISSN2305-7254." [Online]. Available: https://fruct.org/publications/abstract12/files/Nag.pdf. [Accessed: 10-Sep-2016].

[8] Kamal Mistry; Sanjay Srivastava; R. B. Lenin "Buffer aware routing in interplanetary Ad Hoc Network", First International Communication Systems and Networks and Workshops, 2009, pp. 1-10.

[9] JaniLakkakorpi, MikkoPitkänen and JörgOtt "Using buffer space advertisements to avoid congestion in mobile opportunistic DTNs" Proceedings of the 9th IFIP TC 6 international conference on Wired/wireless internet communications, 2011, pp. 386-397.

[10] Maroufi B.E., Rahmani M.D., Rziza M. (2016) Congestion Avoidance in AODV Routing Protocol Using Buffer Queue Occupancy and Hop Count. In: El Oualkadi A., Choubani F.

[11] El Moussati A. (eds) Proceedings of the Mediterranean Conference on Information & Communication Technologies 2015. Lecture Notes in Electrical Engineering, vol 381. Springer, Cham

[12] KrutiN. Kapadia. Dayanand D. Ambawade "Congestion aware load balancing for multi-radio Wireless Mesh Network" International Conference on Communication, Information & Computing Technology (ICCICT) 2015.

[13] Raffaele Bruno, Marco Conti, Antonio Pinizzotto "A Queuing Modeling Approach for Load-Aware Route Selection in Heterogeneous Mesh Networks", IEEE International Symposium on a World of Wireless, Mobile and Multimedia Networks & Workshops 2009.

[14] Sanjay Kumar Dhurandher, Isaac Woungang, Mohammad S. Obaidat "A Distributed Adaptive Admission Control Scheme for Multimedia Wireless Mesh Networks" IEEE Systems Journal Volume: 9, Issue: 2, June 2015, pp. 595 – 604.

[15] T. G. Basavaraju, S. K. Sarkar, C. Puttamadappa, and M. A. Gautham, "ECARP: an efficient congestion adaptive routing protocol for mobile Ad hoc networks," in Proceedings of the 6th International Conference on ITS Telecommunications Proceedings, pp. 715–718, Chengdu, China, June 2006.

[16] X. Chen, H.M. Jones, and A. D. S. Jayalath, "Congestion-aware routing protocol for mobile ad hoc networks," in Proceedings of IEEE Conference of Vehicular Technology, pp. 21–25,October 2007.

[17] Keerthi D S, T.G. Basavaraju "Load Balancing Routing Mechanisms For Wireless Mesh Networks: A Survey", in Fourth International Conference on "Emerging Research In Computing, Information, Communication And Applications (ERCICA)", 2016. (Published in Springer proceedings)

[18] Sooyeol Yang,Youngmi Baek,Junhyung Kim,Keuchul Cho and Kijun Han "A routing metric for load balance in wireless mesh networks", 11th Intrrnational Conference on Advanced Communication Technology (ICACT) Volume: 03,2009,pp.1560-1565.

[19] Ekram Hossain , Kin K. Leung "Wireless Mesh Networks: Architectures and Protocols", Springer, 2008.

.

Proceedings of the Fourth International Conference on Communication and Electronics Systems (ICCES 2019)
IEEE Conference Record # 45898; IEEE Xplore ISBN: 978-1-7281-1261-9

Driver Fatigue Detection Based On Eye State Recognition Using Convolutional Neural Network

Sharan S S
Dept. of ECE
College of Engineering Trivandrum
Thiruvananthapuram, Kerala, India
sharanss2001@gmail.com

Viji R
Assistant Professor, Dept. of ECE
College of Engineering Trivandrum
Thiruvananthapuram, Kerala, India
viji1804@gmail.com

Pradeep R
Associate Professor, Dept. of ECE
College of Engineering Trivandrum
Thiruvananthapuram, Kerala, India
pradeep@cet.ac.in

Sajith V
Associate Professor, Dept. of ECE
College of Engineering Trivandrum
Thiruvananthapuram, Kerala, India
sajithvijayaraghavan@gmail.com

***Abstract*—Fatigue driving is suspected to be a primary cause of vehicle related crashes. Driver fatigue resulting from lack of rest is a significant factor in the expanding number of the mishaps on roads. A warning system can possibly reduce the accidents related to drivers drowsiness. By putting the camera inside the vehicle, the system can read the expressions of the driver and search for the eye-developments which demonstrate that the driver is never again in condition to drive. In such a case, a warning sign ought to be issued. Our face contains a great deal of supportive data; we can utilize the condition of eyes to discover the tiredness. In this paper, a methodology has been proposed for the eye state recognition dependent on convolutional neural network (CNN), which eventually calculates the percentage of eyelid closure (PERCLOS), and blink frequency to figure out the level of the drowsiness. A real-time monitoring unit is additionally created to alert the closest control unit about the status of drowsiness of the driver. Google Cloud Platform is used for training CNN and the trained model is implemented on Raspberry Pi. The trial results demonstrate that the presented technique has reduced training time of CNN network model, high acknowledgment exactness of condition of eyes and can distinguish the drowsiness viably.**

Keywords - Fatigue Detection; CNN; Eye State recognition; Google Cloud; Raspberry pi

I. Introduction

With the increasing traffic collisions, it's carried genuine misfortunes to the country and public. Research demonstrates that the languid driving is one among the most reasons for traffic collisions. As of late, a few nations and governments as of now are giving more consideration to the driving well being issues. Researches for driver drowsiness detection have crucial importance.

Exhaustion and diversion are a piece of regular day to day existence for many individuals. They decrease response time, watchfulness, readiness and focus and as a result the the capacity of performing exercises, (for example, driving) is disabled. The causes leading to falling asleep behind the wheel are fatigue, alcohol intoxication, similar route, riding at night, driving after a heavy lunch, taking Medication.

The drowsiness detection techniques based on computer vision is a non-intrusive way. The features of the face can be determined by dissecting the progressions of facial appearance, for example, squinting (blinking), eye conclusion length, yawning, etc. Conventional image processing strategies for computing flickers which normally include a blend of Eye Localization, Threshold to discover the white portions of the eyes and deciding whether the "white" portion of the eyes vanishes for a time frame (demonstrating a squint or blink).

It is acknowledged that tiredness will appear as fast and consistent glinting, signaling or head swinging, and yawning constantly. PERCLOS [1] is seen as a reliable measure for predicting tiredness and has been melded in commercial things, for instance, Seeing Machines and Lexus. Other facial advancements, for instance, internal forehead rise, external temples rise, lip expand, jaw drop and eye flicker(blink) have additionally been known to be markers for tiredness. As of not long ago, Most vision-based detection relied on hand-created facial and head development checking characteristics. As a rule, hand-created features have demonstrated constrained adequacy in genuine situations which may incorporate drivers wearing shades and huge variety in light.

On the other hand, features of the face learned from an image in light of deep learning have been increasingly viable in genuine real-world situations. Choi et al. [2] built an algorithm for gaze zone detection depends on features learnt using a Convolutional Neural Network (CNN). Utilizing the learnt facial features, support vector machine (SVM) is used to anticipate drivers gaze looking zone. K. Dwivedi et al [3] utilized a 3-layered CNN to learn features of the face of distinguished face locale from the info picture. The yields of the last layer are considered as the extricated features. On the basis of the extricated features, the binary classifier was trained and utilized for drowsiness prediction. The strategy

based on this has higher acknowledgement accuracy. CNN [4] [5] can extract features adaptive and make the features to have a superior capacity of portray, CNN has better features expressive, keeping away the manual feature extrication.

In this paper, we have designed an image securing framework dependent on continuous(real time) pictures and propose a discovery technique about the state of eyes utilizing CNN. As appeared in Fig. 1, the method on a very basic level joins three segments: extricate the territory of eye, state of eye states, sleepiness or exhaustion recognition and alerting the driver and the nearest control room and there by the concerned authorities can take necessary actions like reaching the site in case of any adversaries or stop the vehicle to avoid any mishaps.

The remainder of the paper is created as pursues: Data set preparation, segment 2 demonstrates the proposed system. The Segment 3 demonstrates the training of the neural network.The condition of eyes acknowledgment(recognition) is appeared in segment 4. The Segment 5 demonstrates an alert framework. The Segment 6 shows the exploratory results for driver fatigue identification. The Conclusion is discussed in section 7.

II. Proposed System

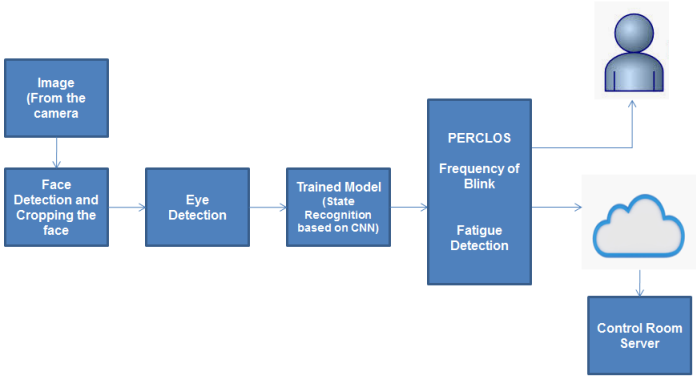

Fig. 1. Block Diagram of the Proposed System

A schematic of the proposed framework is appeared in Fig. 1 The framework comprises of two phases. First stage is to prepare and train the neural system and the second stage is the development of the detection system to test the condition of eye utilizing the neural network system which would be trained in the first stage.

Camera image is taken frame by frame and then input to the Haar Cascade classifier to detect the face.Different Haar Cascade classifier for the eye is then used to extract the eye portion which is then key in as input to the detection system to recognize the eye state.Based on PERCLOS [1] and blink frequency,determines the fatigue level and alert the driver and nearest control room in case of experiencing fatigue.

III. Training of the Neural Network

The various Steps associated with the training of CNN is indicated in Fig. 2

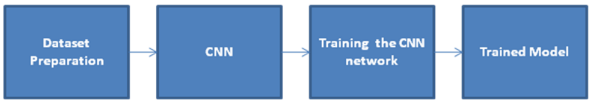

Fig. 2. Different steps in CNN training

A. Data set Preparation

Eye state recognition is a troublesome undertaking in the unconstrained true situation which is loaded with challenging varieties brought about by individuals and sorts of condition changes including darken, lighting, impediment, and mask. To distinguish the state of eye, need to train a binary classifier for open and closed eyes. To do this, we used a dataset to train our classifier. For open and closed eyes, we used cropped images of size 24x24 from the dataset. The complete dataset contains 4864 images and are then labelled as open and closed. Sample images are indicated in Fig. 3.

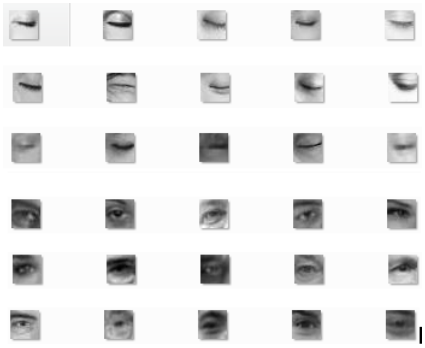

Fig. 3. Sample eye images

B. CNN Network

The architecture of CNN network is shown in Fig. 4.The CNN Architecture is similar to a binary classifier to identify whether the given image is a Dog or Cat. Input image(open and closed eye) of size [24*24*1] has the raw pixel values. The CNN network used in the system has three Convolutional filters. Each Convolutional filer has a ReLu initiation(activation). CONV layer computes the yield of neurons that are associated with neighborhood regions in the input, each registering a dot product between their weights and a small locale they are associated with in the input. First layer convolution results in volume [24x24x32] as we used 32 filters. RELU layer [6] does an element wise activation function, the max (0, x) thresholds at zero. First Relu activation layer results is such that the size of the volume ([24x24x32]) stays unaltered. Each Convolutional filter follows a Max-pooling layer. POOL layer down samples the operation along the spatial dimensions (width, height), resulting in volume of [16x16x12] in the first layer of Max Pooling.

Similar two operations performed with different filter size. Then a dropout layer to reduce the unwanted neurons which then followed by a fully connected layer with ReLu activation. Dropout randomly sets a fraction rate of 0.25 input units to

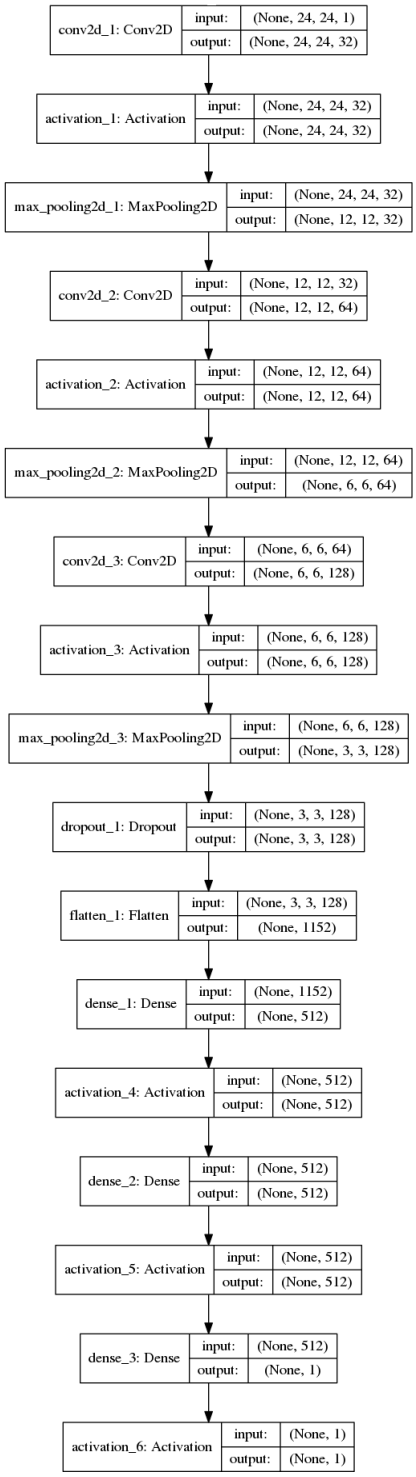

Fig. 4. Architecture of the CNN Network

0 at each update during training time as it helps prevent over fitting. Flatten layer is used to flatten the input. Three dense layers is induced to act as fully connected neural network layer so that each input node is connected to each output node. A single neuron is induced with Sigmoid activation for the binary classifier. Adam optimizer is used as it is an optimize algorithm to updated the weights in the network iterative in the training data set and for the loss function binary cross entropy is used to predict the losses.

C. Training of the CNN Network

Before loading the labeled images, CLAHE (Contrast Level Adaptive Histogram Equalization) is applied to evacuate the noise and to improve the picture. Then scaled the values of the images between 0 and 1 to makes the learning process faster. Finally trained the network for 50 epochs with batch size of 32 and 152 iterations. Epoch is the number of iteration related to each input samples in the data set. The network uses 50 epochs as large values of epochs could lead to train more times which gives better exactness. A complete data set is carried back and forth through the neural network only once is an EPOCH. The trained model is saved as a HDF5 (Hierarchical Data Format) file format. On Google Cloud training of the entire images took around 6 minutes. The recording of training metrics which includes the loss and the accuracy for each epoch at the end of the training in Google Cloud Platform is shown in the Fig. 5.

Each epoch took around 8 seconds and each step took around 52ms. So total time taken for training is 8 seconds x 50 Epochs, which is around 6 minutes.

As shown in the plot of accuracy Fig. 6, it is visible that the model reached almost same accuracy level at the end of the epochs.As shown in the plot of loss Fig. 7, it is visible that the model reached almost same loss level at the end of the epochs.

```
Epoch 42/50
152/151 [==============================] - 8s 50ms/step - loss: 0.0913 - acc: 0.9659
Epoch 43/50
152/151 [==============================] - 8s 51ms/step - loss: 0.0973 - acc: 0.9638
Epoch 44/50
152/151 [==============================] - 8s 52ms/step - loss: 0.1005 - acc: 0.9613
Epoch 45/50
152/151 [==============================] - 8s 51ms/step - loss: 0.0886 - acc: 0.9677
Epoch 46/50
152/151 [==============================] - 8s 51ms/step - loss: 0.1027 - acc: 0.9611
Epoch 47/50
152/151 [==============================] - 8s 51ms/step - loss: 0.1003 - acc: 0.9624
Epoch 48/50
152/151 [==============================] - 8s 52ms/step - loss: 0.0986 - acc: 0.9625
Epoch 49/50
152/151 [==============================] - 8s 51ms/step - loss: 0.0945 - acc: 0.9636
Epoch 50/50
152/151 [==============================] - 8s 51ms/step - loss: 0.0915 - acc: 0.9656
sharanss2001@instance-2:~$
```

Fig. 5. Training Summary in Google Cloud Platform

IV. EYE STATE RECOGNITION

The different steps involved in the eye state recognition is shown in Fig. 8

A. Image Capture and Preprocessing

Read each frame from the camera. The captured image which is an RGB image needs to convert to gray scale image with a depth of 1. This ensures the depth of the image is same as of the trained image.

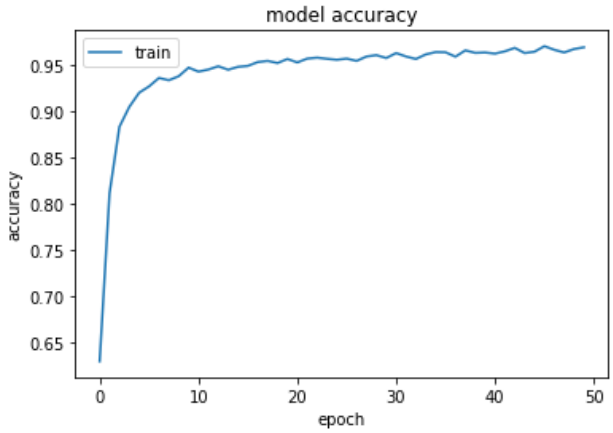

Fig. 6. Plot of Model Accuracy on Training Data

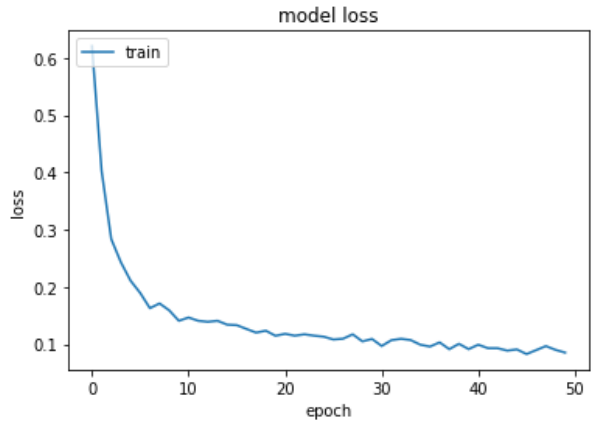

Fig. 7. Plot of Model Loss on Training Data

B. Image Enhancement

To enhance the image, CLAHE (contrast-limited adaptive histogram equalization) is applied. It enhances the contrast of the grayscale image by transforming the values. This contrast-limited adaptive histogram equalization (CLAHE) produces images that do not excessively enhance the noise content of an image, but provide sufficient contrast to visualize structures within the image. CLAHE processed images have a more natural appearance and make it easier to compare distinct regions of a picture.

C. Face and Eye detection

Object recognition is ordinarily characterized as technique for distinguishing the presence of objects of a specific class. In image processing, it is a strategy to discover an item or object from pictures. There are various approaches to characterize and discover objects in a frame. One way is depended on color identification. Be that as it may, it's anything but an effective technique to identify the article as a few diverse size objects of same shading might be available. Haar-like highlights, created by Viola and Jones [7] based on the proposition by Papageorgiou et. al in 1998 is a most efficient way to recognize items. Haar-like highlights are computerized picture highlights utilized in article identification or these are square shape molded dim and light regions having comparable sort of highlights like our face. The cascade classifier includes various stages, where each stage comprises of numerous frail highlights or features. The framework recognizes the subject by moving a window over the whole picture and by forming a solid classifier. The yield of each stage is marked as either positive or negative implying that an item was found and negative implies that the predetermined article was not found in the picture.

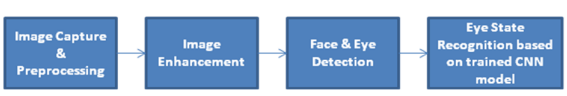

Fig. 8. Steps in Eye State Recognition

To detect the face and eye region, different haar cascade classifier is used to give better accuracy. Using Haar cascade classifier, face and eye region is cropped for various states. Fig. 9 shows the various states. A human region blinks both the eyes simultaneously. Hence one region is enough for the model to predict the state.

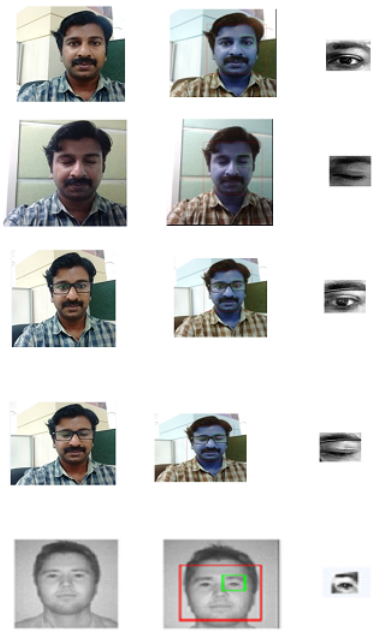

Fig. 9. Cropped Face and Eye
Source: Infrared Image is adapted from
http://www.scface.org/examples/001_cam8.jpg

D. Eye State Recognition Based on Trained CNN model

When the face and eyes are identified, the trimmed picture should be resized to 24X24.The resized picture is then sustained to prepared CNN model to make a prediction. The model has a binary classifier with a sigmoid neuron that gives

as yield as the likelihood of an eye to be open and on the off chance that the likelihood is more than 50 percentage, at that point the condition of eye is open and on the off chance that it is under 50 percentage, then condition of the eye is shut. The Fig. 10 shows that eye state recognized with a good accuracy.

Fig. 10. Prediction of Open and Closed State

V. Alert System

Once the eye states are identified and if the driver experiences drowsiness, then alert is send to driver in the form of sound.A buzzer is connected to Raspberry pi to raise alert in the form of sound.Initially the buzzer is set to low.Depends on eye states,alert is raised by applying high(Vcc) to the GPIO pin which is connected to the buzzer.Buzzer produces sound until the driver is alerted. In addition, a real-time alert system is established to send the alert to the nearest control unit to be monitored by the authorities concerned such as POLICE. The idea of such a system is to ensure that the authorities who are nearby will get the alert message and the vehicle details. The authority can take quick action either stopping the vehicle by calling the driver or reaching the location the site immediately in case of any accidents. However, the priority is to alert the driver.

The Fig. 11 illustrates the schematic diagram of the general MQTT system. The proposed system uses MQTT protocol to send the alert message from a vehicle (MQTT publisher) to the nearest control room (MQTT subscriber). MQTT is a standout amongst the most generally utilized conventions (protocols) in IoT world. It is a Message Queuing Telemetry Transport convention. A lightweight informing convention that utilizes operations to publish / subscribe to exchange information between customers and the server. Its small size, low power consumption, limited bundles of information and simplicity of execution make the convention perfect for the world of ”machine-to-machine” or ”Internet of Things” world. Each vehicle is being uniquely identified by the topic number and the alert message is then publish to a folder with that unique number to a server(Mosquitto Test Server) via internet. The subscriber (control room) subscribes the topics and continuously monitors the topic folder and in case of an alert received from any vehicle, it displays the details on a screen as indicated in Fig. 12 there by alerting the concerned authorities.

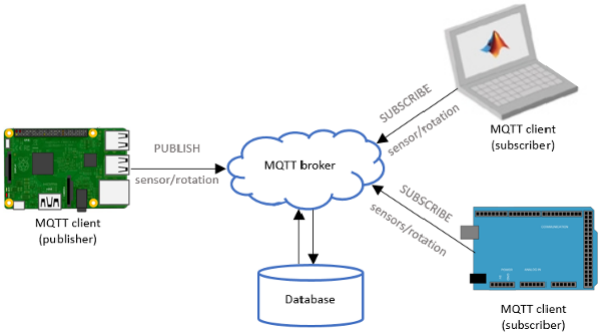

Fig. 11. MQTT System

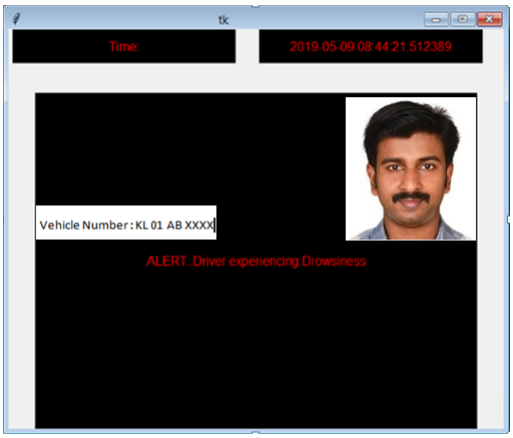

Fig. 12. An Alert Console in the Control Room

VI. Experiment and Results

A. Experimental Platform

Google Cloud Platform with Debian GNU/Linux9 Operating System,1 x NVIDIA Tesla K80(GPU) is used to train the CNN network. Raspberry Pi 3 Model B+ as shown in Fig. 13 is used to implement the detection system and to raise alert. The trained model is copied from Google Cloud Platform to Raspberry Pi and Logitech Camera is used to capture the real-time images. A buzzer is connected to Raspberry Pi to raise the alarm in case of drowsiness. MQTT and Mosquitto Test Server is used to send the alert to the Control Room. The whole application is build using Python 3.5.3, OpenCV 3.4.4, Keras 2.2.4 and Tensor Flow 1.11.0.

Fig. 13. Raspberry Pi Connected to Camera and Buzzer

B. Results

The driver drowsiness can be measured using PERCLOS and blink frequency. The PERCLOS [1] [8] (Percentage of eyelid closure). It is calculated as (1):

$$f_{PERCLOS} = \frac{n_{close}}{N_{total}} \times 100\% \quad (1)$$

Where n_{close} is the total number of eye closed frames and N_{total} is the total number of frames over a period. PERCLOS measurement gives alertness if drivers eye state is closed for a period of 5 to 6 seconds.

PERCLOS is used when driver closed his eyes for a period of 5 to 6 seconds as it indicates person is slept which can cause accident severely. Fig. 14 indicates that person is slept for a while in the beginning as the PERCLOS [1] [9] is more than 80%(n_{close} is around 30 of 35 total frames within a period of 5 to 6 seconds).

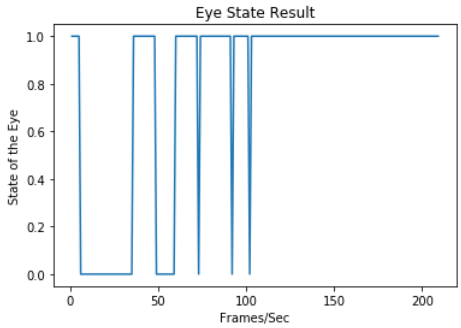

Fig. 14. Experiencing PERCLOS of 80% in the beginning

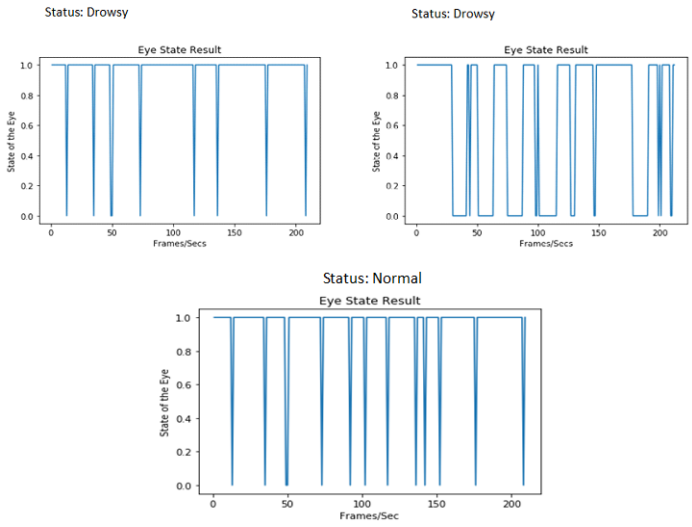

Fig. 15. Eye State Results

According to studies in [10] normal healthy person blinks eyes 10 to 15 times per minute and in case of drowsiness experiences blinks of more than 15 per minute. Driver may experience drowsiness as well if the blink frequency is less than 10 blinks per minute. The Fig. 15 depicts the status of the three different states obtained from the real-time image captured which shows that the system detects the blinks as per the expectation.Though the work done by [11] uses its own data set of around 7000 images, the Table I shows that the proposed system with 4864 images using Google Cloud platform fairs way better with training time than with the previous work.

TABLE I
COMPARISON OF WORKS

Reference	Network Structure	Training Time
[11]	Two Convolutional layers, Two Max Pooling layers with ReLu activation and one fully connected layer	42 Min
Proposed System	Three Convolutional layers, Three Max Pooling layers with ReLu activation and three dense layers	6 Min

VII. CONCLUSION

In this proposed system, we have developed a driver fatigue system based on eye states using CNN.Haar Cascade classifier is used to detect face and the eye from the image.The training system is implemented on Google Cloud Platform which reduces the time taken for training drastically compared to the previous works. The trained model file is implemented on Raspberry Pi to detect the eye states and raises an alarm in case the driver experiences drowsiness. Also developed a real-time monitoring system to send the driver fatigue alert to the nearest control unit to take necessary actions. Future work can be focused on attaching GPS to the system (vehicle) to send the location details as well to the control unit.

REFERENCES

[1] Zheng Pei, SONG ZHENG-He, ZHOU Yi-Ming, "PERCLOS-Based Recognition Algorithms of Motor Driver Fatigue", Journal of China Agricultural of China Agricultural University, 2002, 7(2).
[2] Choi, I. H., Hong, S. K., Kim, Y. G.: Real-time categorization of drivers gaze zone using the deep learning techniques. International Conference on Big Data and Smart Computing (BigComp), (2016) 143148.
[3] Dwivedi, K., Biswaranjan, K., Sethi, A.: Drowsy driver detection using representation learning. Advance Computing Conference (IACC), 2014 IEEE International, (2014) 99599913.
[4] Hossain, Lecun, Y., Boser, B., Denker, J. S., Henderson, D., Howard, R. E., and Hubbard, W., et al. (1989). Backpropagation applied to handwritten zip code recognition. Neural Computation, 1(4), 541-551.
[5] Dieleman, S., Willett, K. W., Dambre, J. (2015). Rotation-invariantconvolutional neural networks for galaxy morphology prediction.Monthly Notices of the Royal Astronomical Society, 450(2), 1441-1459.
[6] Nair, V., and Hinton, G. E. (2010). Rectified Linear Units Improve Restricted Boltzmann Machines Vinod Nair. International Conference on Machine Learning (pp.807-814).
[7] P. Viola and M. J. Jones, Robust real-time face detection, International Journal of ComputerVision, 57 (2004), pp. 137154.
[8] Wierwille, W. W., Ellsworth, L. A., Wreggit, S. S., Fairbanks, R. J., Kim, C. L. (1994). Research on vehicle-based driver status/performance monitoring:development, validation, and refinement of algorithms for detection of driver drowsiness. National Highway Traffic Safety Administration, Final Report: DOTHS 808 247.

[9] Knipling, R. R., Wierwille, W. W. (1994). Vehicle-based drowsy driver detection: Current status and future prospects. Moving Toward Deployment. Proceedings of the IVHS America Annual Meeting. 2 Volumes.

[10] BLEHM, C. et al. Computer Vision Syndrome: A Review. Survey of Ophthalmology. 2005, 50, 3, pages 253 262. ISSN 0039-6257. doi: 10.1016/j.survophthal.2005.02.008. Available from: http://www.sciencedirect.com/science/article/pii/S0039625705000093.

[11] Fang Zhang ; Jingjing Su ; Lei Geng ; Zhitao Xiao, 2017 International Conference on Machine Vision and Information Technology (CMVIT), Feb 2017

Proceedings of the Fourth International Conference on Communication and Electronics Systems (ICCES 2019)
IEEE Conference Record # 45898; IEEE Xplore ISBN: 978-1-7281-1261-9

Power quality enhancement using unified power flow controller in grid connected hybrid PV/Wind system

Vandana chaudhary*[1], Annapurna Bhargava[2] ,Sandeep Verma[3]

Department of Electrical engineering

Rajasthan technical university

Kota, INDIA

[1]V30chaudhary@gmail.com,[2]Abrtu2006@gmail.com,[3]er.san.verma@gmail.com

***Abstract*- This paper present amelioration power quality of hybrid power system integration with PV, wind and battery system by FACTS device .In transmission and distribution system power quality is major restraint . FACTS device have many merits in transmission like flexibility and high speed. Benefit of this system is the diverse sources can be connected to at one junction of power line, because of this these method are ascertaining to be an efficacious and ductile method for the development of the system. Harmonics produce when two diverse source connected to grid and it removed by using UPFC. The unified power flow control is the most promising device of fact family at which study in this paper is concentrated. In the study of this paper UPFC is modeled and interpretation of UPFC in a hybrid-grid connected system is examined. The extraordinary feature of the UPFC is such that it can control flow of real and reactive power as well as voltage amplitude at the same time at the UPFC nodes. The planned model is simulating in MATLAB/Simulink software.**

Keyword- MPPT, Voltage Regulator, UPFC,Hybrid system

I.INTRODUCTION

Now a days energy generation move towards the renewable sources because existing traditional energy sources are becoming more overpriced. In the some last some decades the renewable energy field is growing too fast in every aspects whether it is economical or environmental. The renewable energy sources are become essential need of power sector. At the time different sources like sun, wind, tidal etc. are utilized for generate electricity. Solar and wind energy acquiring more regarding generate electricity because it has insignificant impact of pollution on the environment.

This paper exhibit modeling and control of hybrid model which is comprise with PV, wind, battery. Output of the hybrid system is fluctuate according with solar irradiance, temp and wind speed and output characteristics is unstable. In grid associated system it is very crucial to supervise on electric power transfer. Diverse type of facts controller deliberate to raise capability of transmission line. UPFC is produce full control on electric network among different facts controller. This model made of PV array, wind turbine, battery storage, DC-DC converter, voltage controller & UPFC controller. To gain maximum power we are implementing MPPT technique for both energy sources and DC-DC converters are applying to boost the output voltage. Here Voltage regulator is integrated for control the pulse for inverter which is converting generated DC to AC. UPFC is utilizing to minimize voltage rise problem in output voltage of gird associated hybrid system, so improve power quality of system. MATLAB/Simulink is applied for PV/Wind simulation model.

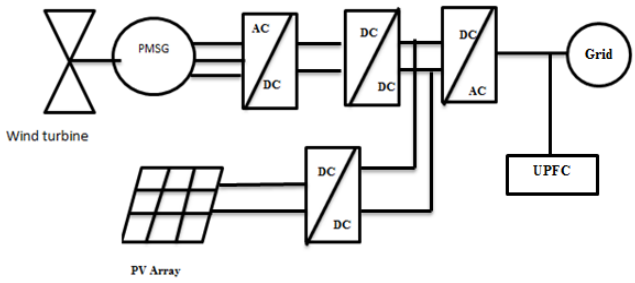

Fig.1 block diagram of grid connected hybrid system with facts controller

II.PROPOSED SYSTEM MODELING

A.PV SYSTEM

Photovoltaic system comprise PV array which is an set of series & parallel coupled PV cells. To produce high voltage, current, power PV cells coupled to one item, PV module. when the system come under sun radiation, which particle have the energy level more than the limiting gap energy of p-n

diode consumed and found electron hole pair corresponding to radiance, so spark light.

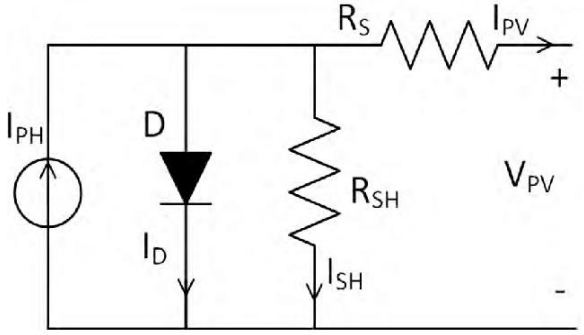

Fig.2 basic solar array diagram

The equation of current which supplied to load is given

$$Iop = Ipvi - Irev\left[\exp\left\{\frac{Vd + I1Rse}{qi\,Vtv}\right\} - 1\right] - \left[\frac{Vd + I1Rs}{Rpa}\right]$$

Ipv=PV current
Irev= reverse saturation current of diode
Vd= diode voltage
a_i=constant of ideality
Vth= thermal voltage
Rse=Resistance arrangement in series
Rpa= Resistance arrangement in parallel
Equation 2 show PV current of cell, in term of temp.& radiation

$$Ipvi = (Ipvi - stc + Kic\Delta Ti)\frac{Gi}{Gsitc}$$

Fig.3 show PV & IV aspect of PV module at 25^0 &45^0 temp. Given in fig

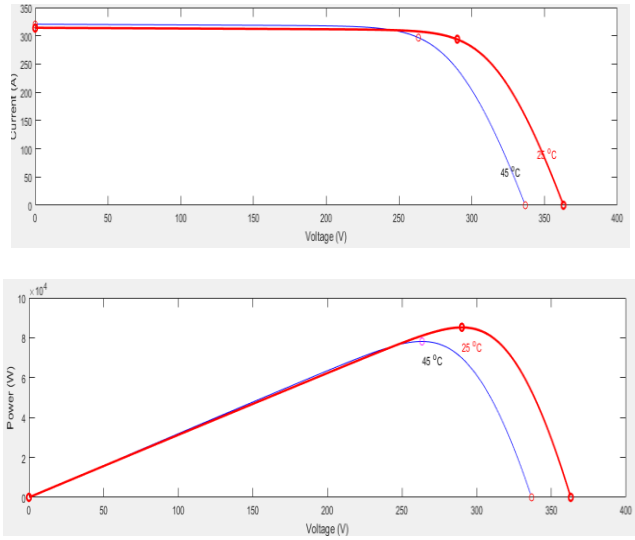

Fig.3 PV&IV characteristics

Max. Power= P_{max1}= $V_{max1}I_{max1}$

B.MPPT TECHNIQUE

We notice from attribute of PV module shown in fig 3 so we found that a maxima point exist there. To gain maxima power various technology applied .here P&O MPPT technique used for PV module

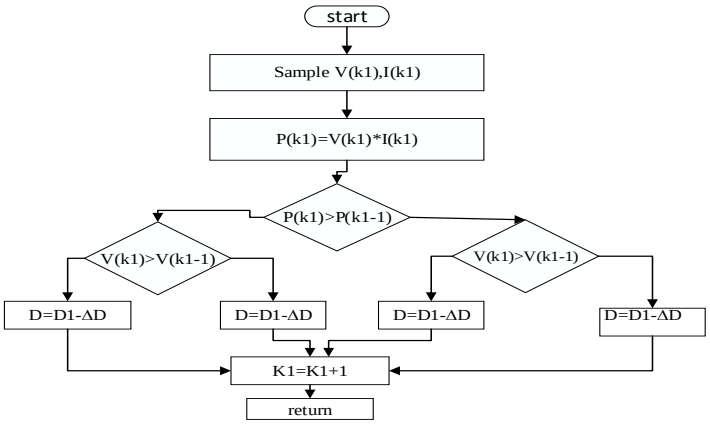

By changing the value of duty cycle, converter output voltage is maintain constant .the solar PV array output show

$$Vpv1 = (1 - De)Vout1 \qquad (2)$$

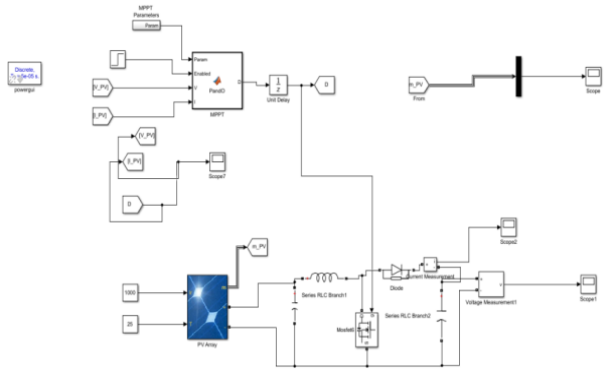

Fig.4 modeling of PV array with MPPT technique

C.WIND SYSTEM MODELING

Wind system is a device which convert wind energy to electricity form .it is comprise with wind turbine PMSG generator, uncontrolled rectifier which convert AC to DC form.Fig.5,6 show the governing mechanism for wind system which command the mechanical torque, wind speed, mechanical input and modeling of wind turbine respectively.

Expression for kinetic energy= ½ mv^2

The wind power produce by wind turbine based on aerodynamic characteristics can be expressed

$$Pi = \frac{1}{2}(p1(\gamma i, \beta i)p1\pi V^3 R^2)$$

Mechanical power for wind system is expressed as

$$Pmechp = Cpc(\alpha, \gamma)\rho A/2$$

Here ρ =1.225kg/m^3 which is denote air density,C_{pc} is represent power coefficient constant V_{wind} is wind speed in(m/s) area of rotor is shown by A. Cqs is torque coefficient and it is related with Cps as

$$Cqs = \frac{Cps}{\alpha}$$

$$\alpha = \frac{Rw * \omega s}{Vswind}$$

$$Tw = \frac{Psmech}{\omega s}$$

Cps = performance coefficient

ρ = air density

Vswind = speed of wind

A = swept area of turbine

Rs = wind turbine radius

Tw = wind turbine torque

ωs = angular freq.

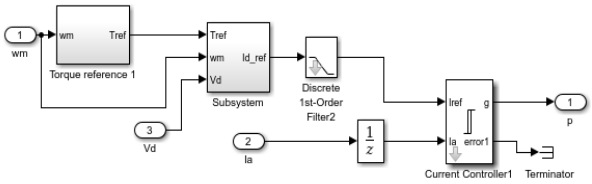

Fig.5 MPPT technique for wind turbine

.

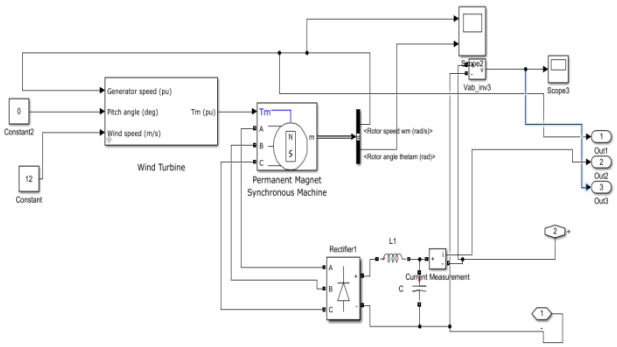

Fig.6 modeling of wind turbine

D.BATTERY SUBSYSTEM MODELING

Fig.7 introduces matlab battery subsystem which associated with hybrid system. This battery subsystem is stock the energy during usual power system operation & utilizes the energy, system run in abnormal condition where solar and wind energy is not available.

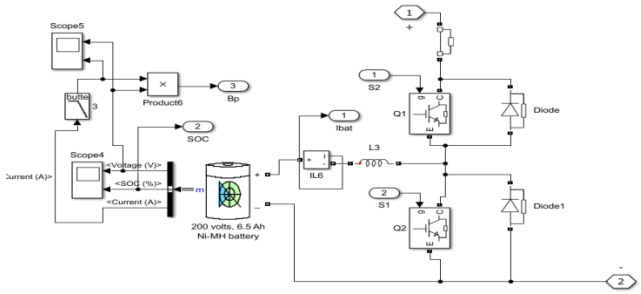

Fig.7 modeling of battery

E.LC FILTER

Fig.8display three phase LC filter circuit which removes harmonics & flicker in inverter output, then now harmonics free output attached with main power system.

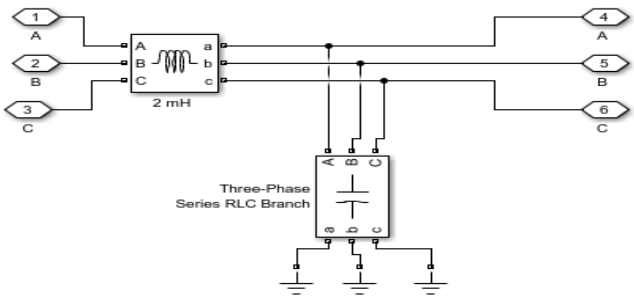

Fig.8 modeling of three phase LC filter

F.VOLTAGE REGULATOR

Voltage regulator is used for control the inverter by PWM signals at desired frequency. The PWM signals contain three phase sinusoidal signal with 120^0 phase difference. These signals compare with carrier signals and generate control pulse for inverter. Vph is phase voltage at fundamental frequency.

$$Vph = \frac{(2\sqrt{2})}{\pi}\cos\left(\frac{\pi}{6}\right)Vdcs1 \qquad (4)$$

Vdcs1=input voltage for inverter

To produce desired pulse for DC to AC converter PID control PWM technique used

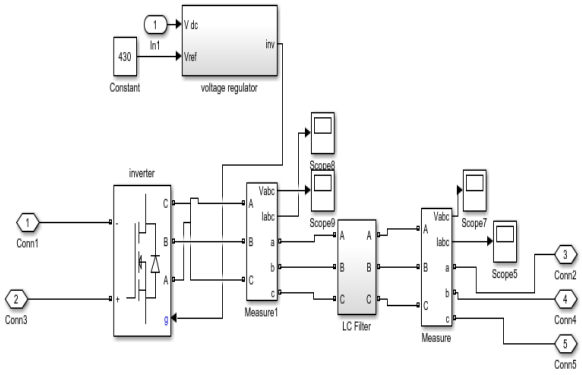

Fig.9 modeling of voltage regulator controlled inverter

G. UNIFIED POWER FLOW CONTROLLER

To control different parameters of transmission power system UPFC is used which is an ultimate facts device .the main characteristics of UPFC is control the active and reactive power. It is used for remove the impact of necessary disturbance on transmission system.it is connected to end of the transmission system.it is consist static shunt synchronous controller (STATCOM) and static series synchronous controller (SSSC) with DC link. UPFC output give to filter to eliminate the harmonics which is produce by IGBT & MOSFET device introduce in UPFC circuit.

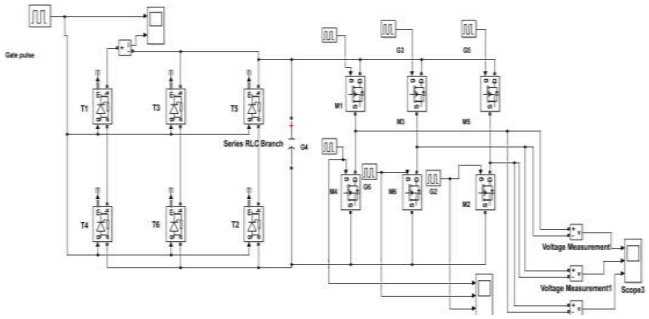

Fig.10 modeling of UPFC

By introduce fig.10 UPFC voltage dip profile improved at specified time and current flow continuous. Voltage spikes balanced and active & reactive power improved.

III.SIMULATION AND RESULT

Fig.10 is present simulation of grid connected hybrid system which is containing solar and wind energy sources and control by voltage regulator. To enhance power quality of grid connected hybrid system UPFC facts device is applied. Solar irradiance & wind speed is taken as input for simulation. Fig.10 indicates solar output and wind generation system. Grid connected Hybrid system is run for 1 sec in MATLAB/Simulink software. Fig.11, 12 present DC boost voltage after using converter which is increase PV array voltage to a DC high level voltage with MPPT (P&O) algorithm & output of wind turbine in which PMSG wind turbine generate AC voltage then convert to DC voltage by using rectifier, Fig.13 show coupling voltage after both PV/Wind subsystem connected to a common DC link. Fig.14 shows three phase output voltage after using converter. Fig 15, 16 show voltage and current interruption of grid connected hybrid system, grid side voltage without UPFC respectively.Fig.17 shows voltage and current with UPFC which improve the voltage spikes and recover the voltage interrupt problem.Fig.18 show grid side voltage with UPFC which remove the voltage spikes.

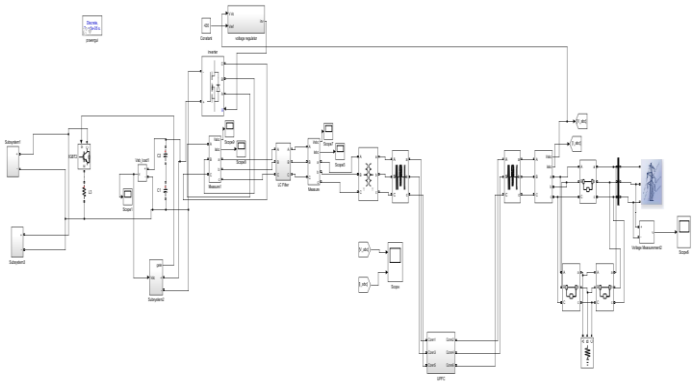

Fig.10 grid connected hybrid system with UPFC

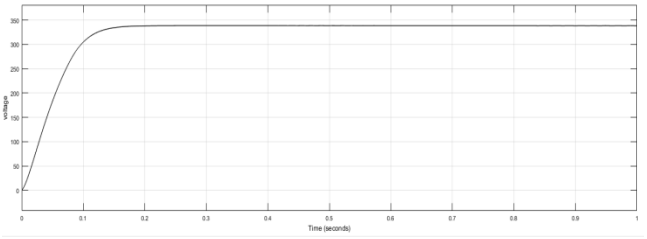

Fig.11 dc output voltage of PV array

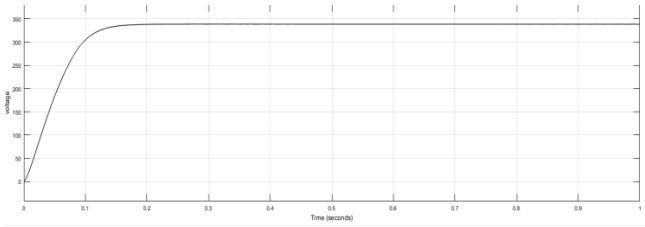

Fig.12 wind turbine output after rectifier

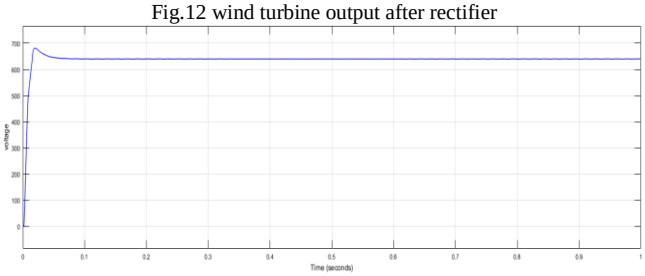

Fig.13 coupled output voltage of hybrid PV/Wind system

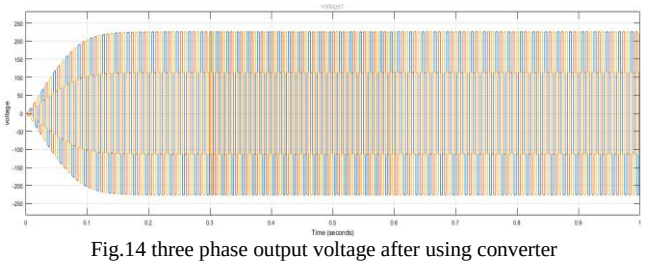

Fig.14 three phase output voltage after using converter

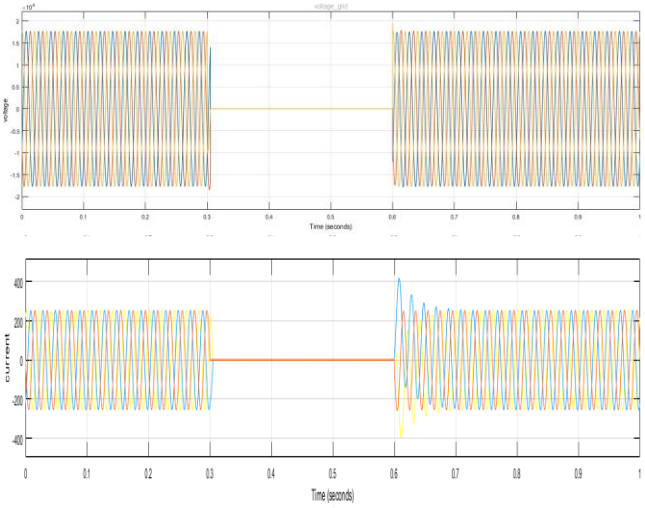

Fig.15voltage and current interruption of grid connected hybrid system without UPFC

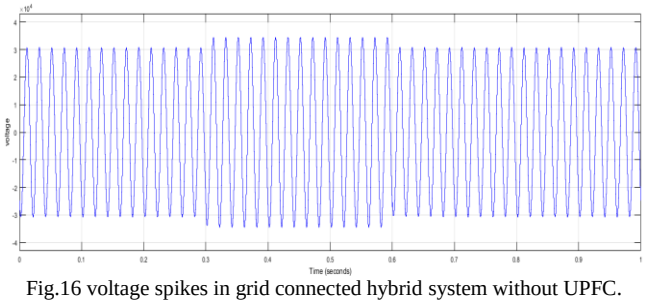

Fig.16 voltage spikes in grid connected hybrid system without UPFC.

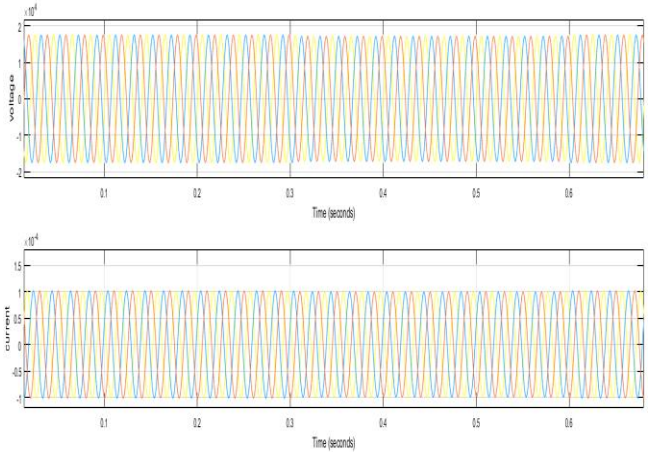

Fig.17voltage and current dip of grid connected hybrid system with UPFC

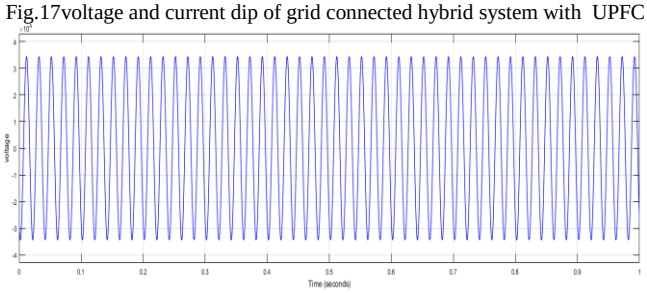

Fig.18 voltage spikes in grid connected hybrid system with UPFC.

IV.CONCLUSION

This paper present power quality improved by UPFC of a grid connected hybrid system which is contain solar and wind energy source, controlled by voltage regulator. Simulation of UPFC controlled hybrid system is carried out by MATLAB software. The operation of system is analyses at different wind speed and irradiance level. The introduce grid connected hybrid system is evaluation at wind speed at 12m/s and solar PV panel at irradiance 1000w/m^2 and temp 25^0 form t= 0 to t=1sec. is applied then coupled both DC voltage to DC link is controlled by voltage regulator and performance is estimate & refined. To accomplish the necessity of electricity in a remote area utilized grid connected hybrid system. The advanced system functioning is accomplished in MATLAB/Simulink software and results are shown.

REFERENCES

[1] J.Godson,M.Karthick,"Solar PV-Wind hybrid power generations system" Vol. 2, Issue 11, November 2013

[2] Kratika Yadav,Mehtab Fatima," performance analysis of grid connected hybrid PV/Wind power system" 978-1-5386-1887-5/17/2017 IEEE.

[3] Dr. Swapnil B. Mohod, Vikramsingh R. Parihar," Hybrid Power System with Integration of Wind Battery and Solar PV System" 978-1-5386-0814-2/17/2017 IEEE.

[4] Anjali Rana, Mohammand Ilyas" Implementation of WIND/PV Hybrid system using matlab"IJAREEIE Vol. 4, 10-15662 Issue 7, july 2015.

[5] Mubashar Yaqoob Zargar,Mairaj-ud-din Mufti,"Modelling and control of wind solar hybrid system using energy storage" 978-1-5090-1666-2/16/2016 IEEE.

[6] Kratika Jain,Annapurna Bhargava,"power enhancement using unified power flow controller in standalone grid connected solar PV system" 978-1-5386-2456-2/18/2018 IEEE.

[7] Prachi P.Chintawar,M.R.Bachwad,"Power quality imrovement Wind/PV hybrid system by using facts device" vol 4 issue 6,june 2015.

[8] N. Mendalek and K. Al-Haddad "Photovoltaic System Modeling and Simulation" vol 2. 978-1-5320-9 2017 IEEE.

[9] Oladimeji Ibrahim,Nor Zahir Yahaya, Bandar Seri Iskandar" Matlab/Simulink Model of Solar PV Array with Perturb and Observe MPPT for Maximising PV Array Efficiency" vol 3 issue Dec IEEE 2015.

[10] Mukesh Kumar, Mohit Kachhwaya, Bhavnesh Kumar" Development of MATLAB/Simulink based model of PV System with MPPT" 978-1-5090-4530-2016 IEEE.

[11] Rim ben ali, Horst schulte, Abdelkader mami "modeling and simulation of a small wind turbine system based on pmsg generator" in Evolving and Adaptive Intelligent Systems 978-1-5090-6444-1/17/$31.00 ©2017 IEEE

[12] Raghuvendra Kumar Tiwari, Krishna Kant Sharma" Simulation and Modeling of Wind Turbine using PMSG" In International Journal of Recent Research 2016.

[13] Ahmed Chaib,Djalloul Achour,Mohamed Kesraoui,"Control of a Solar PV/Wwind hybrid energy system", international scientific conference "Enviromental and climate Technologies"14-16 october 2015.

[14] Prajapati bhavna, Vaishali y. Patel, Madhusudan v. Gohil "simulation of a solar-wecs hybrid renewable energy conversion system using matlab/simulink" International Journal For Technological Research In Engineering Volume 2, Issue 8, April-2015..

[15] Neha Adhikari, Bhim Singh, A. L. Vyas, Ambrish Chandra, Kamal-Al-Haddad, "Analysis, Design and Control of a Standalone HybridRenewable Energy Conversion System" IEEE. .

[16] Partha Sarothi Sikder, Nitai Pal," Modeling of an intelligent battery controller for standalone solar-wind

hybrid distributed generation system 1018-3639/ 2019

[17] B.Kanagasakthivel ,Dr. D. Devaraj "Simulation and performance anyasis of solar PV-wind hybrid energy system using Matlab/Simulink" 978-1-4799-7633-2,2015 IEEE.

[18] Abeer A. M. EI-Hany,Shawky H.Arafa, Maged N.F.Nashed, "modeling and simulation for hybrid of PV-Wind system." In international Journal of Engineering Research volume No 4, issue No 4, pp: 178-183

Proceedings of the Fourth International Conference on Communication and Electronics Systems (ICCES 2019)
IEEE Conference Record # 45898; IEEE Xplore ISBN: 978-1-7281-1261-9

Speed Optimization of the AES Algorithm Using Pipeline Hardware Architecture

Dheeraj Punia
School of VLSI Design and Embedded Systems
NIT Kurukshetra
Kurukshetra, India
E-mail: dheerajpunia95@gmail.com

Dr. Brahmjit Singh
Department of ECE
NIT Kurukshetra
Kurukshetra, India
E-mail: brahmjit@nitkkr.ac.in

***Abstract*—Secure encryption algorithms with advanced key executive techniques constantly help to achieve privacy, verification, and security of the data and curtail the overheads of the system. Currently, the prominent cryptographic technique is the Advance Encryption Standard (AES). The 128-bit pipelined cipher AES components adopt the symmetric-block cipher algorithm for encryption of the data. Our application achieves a high-level of encryption of 25.6 Gbps with an effective inter-and-intra-round layout. This module is designed on Xilinx ISE® Design Suite 14.7 and optimized for faster conversion speeds as the module is based on the pipeline architecture to perform the repeated array of operations known as the round. The designed module is suitable for high-security data communication, image processing, and other embedded applications. Pipelined architecture reduces the time associated with each encryption process and decreases the total time it takes for a plaintext block to encrypt.**

Keywords*—Advanced Encryption Standard (AES), high throughput, pipeline architecture, cryptography, FPGA implementation

I. INTRODUCTION

The information is required to be secured and protected from any unauthorized access. The majorly accepted security enhancement solutions to prevent data theft to any third-party or unauthorized public access is the use of cryptography. Cryptography is the study and practice of technique s in the existence of third parties to secure the trans mission of data [1]. An encryption algorithm is an important component of the safety of the network. In recent times, cryptography has extended to algorithms based on demand. Modern cryptographic algorithms can offer safety services such as information privacy, data integrity, authentication, non-repudiation and control of access. Pipelining is a strategy to improve the AES encryption and decryption algorithm throughput. The amount of turns in the algorithm and the main generation depends on the AES encoding [2]. The Data Encryption Standard (DES), commonly accepted in safety products, is a well-known cryptographic algorithm. However, 56-bits key length is short and is not suitable for long-term security. The emergence of reconfigurable systems such as FPGAs made it simple to hardware the execution of complicated algorithms, which makes velocity improvements substantial.

The 10-round AES-128 bit includes a main module extension that produces 10 keys during the 10-round process. These keys are either produced, stored and subsequently used during the ten rounds or calculated per round on a fly. By using the iterative looping concept as well as the main extension module that calculates the keys on a fly, the proposals decrease the delay and the use of multistage pipeline ensures the best throughput possible. DES, AES, Triple-DES, RC4, etc. are the different symmetric-key algorithms types [3]. Elliptic-Curve cryptography, RSA, etc. are the various types of asymmetric-key algorithm.

Including ease of use, ease of upgrade, portability, and flexibility, all are the benefits of software application approach for AES. However, an application of software approach provides only restricted physical safety, particularly for important storage [13]. Conversely, the hardware implements cryptographic algorithms (and their associated keys), which can't be read or altered readily by an external attacker, are naturally more physically safe. An absence of flexibility regarding algorithms and parameter switching's is the downside of conventional Application Specific Integrated Circuits (ASIC) hardware applications. Reconfigurable hardware systems such as FPGAs are a promising option for block cipher execution.

II. BASIC ARCHITECTURE OF AES

Joan Daemen and Vicent Rijmen developed the algorithm for AES cipher. Group of bits forms a block and these blocks are used in the AES algorithm making it a block-cipher algorithm. Each block has a fixed-length. Encryption makes the information indecipherable as a cipher-text [4]. Decryption converts the cipher-text into the original

plain-text. AES symmetric cipher block can make use of 128, 192 and 256-bits of cipher-keys to operate the 128-bits of data. Each iteration is called round in the algorithm. 128-bits, 192-bits, and 256-bits of data require 10, 12 and 14 rounds respectively to process the original information into the cipher-text [5]. This paper presents the pipelined AES architecture which uses (AES-128) 128-bits as key-length for encryption 128-bits data. A matrix is formed known as the state by the arrangement of the 16-bytes grouped from the 128-bits data.

The size of the matrix is based upon the block size being utilized which is further composed of four rows and Number-of-bits (Nb) columns [5]. Each block is made up of 32-bits (4-bytes). The state matrix in the block design is a 4x4 matrix. Also, the cipher-key is composed in the same manner as of the state. The operational round in each iteration consists of quite a few procedural steps. Each step contains 4 similar but distinct phase, incorporating the step that is dependent on the encryption-key itself [6]. The different stages follow as,

- Sub Bytes
- Shift Rows
- Mix Column Transformation
- Add Round Key

AES algorithm data flow path is depicted in Fig. 1.

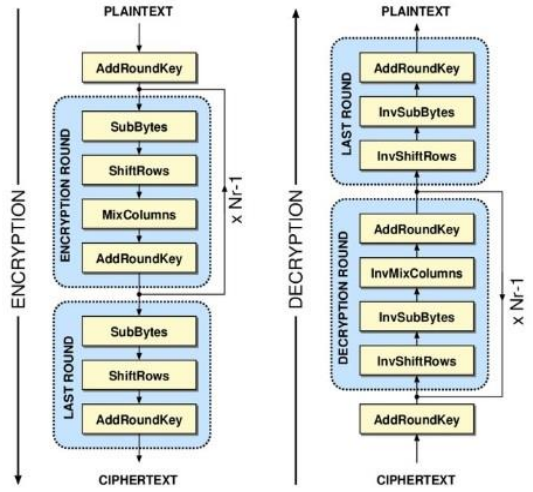

Fig. 1 AES algorithm architecture [16]

III. AES INTERNAL STRUCTURE

The initial key is combined with the input data at the first stage of the encryption phase, known as the preliminary round. Multiple repetitions succeed immediately after the initial round and follow up to an analogous modification for the final. The processes performed in each round are as follows:

A. Sub Bytes

The 16-bytes input is replaced (non-linear conversion) by referring to a predetermined Look-Up-Table (LUT) known as the Substitution-box (S-box). A 4x4 matrix is obtained as the result of the sub-byte conversion [7]. The Galois Field characteristics are fulfilled in the design.

B. Shift Rows

Each row in the 4x4 matrix is shifted to the left. The shift takes place as follow:
The data in the first row is not altered. Data is left-shifted by 1-byte, 2-bytes, and 3-bytes in the second, third and fourth row respectively [8]. A new matrix is obtained where the same 16-bytes are rearranged forming a new data matrix.

C. Mix-Column Transformation

The mix column conversion is governed by the Galois field multiplication. Herein each byte is replaced by a precise calculated value. Each multiplication data (r(x)) is determined by the formulae stated as below [9]. The mix columns theory is calculated using the below formula [18].

$$\begin{bmatrix} r_0 \\ r_1 \\ r_2 \\ r_3 \end{bmatrix} = \begin{bmatrix} 2 & 3 & 1 & 1 \\ 1 & 2 & 3 & 1 \\ 1 & 1 & 2 & 3 \\ 3 & 1 & 1 & 2 \end{bmatrix} \begin{bmatrix} a_0 \\ a_1 \\ a_2 \\ a_3 \end{bmatrix}$$

Where the conversion r0, r1, r2, and r3 are the outcomes. After the information undergoes a replacement in the S-boxes, a0 – a3 can be gathered from the matrix. It performs a linear operation on the columns of the matrix. This AES-architecture method needs more energy and a big chip area due to its complex circuitry.

D. Add Round key

The 128-bits of data is now present in the form of a 4x4 16-bytes matrix which is XOR-ed with the 128-bits round-key [10]. After the last round, the output is the Encrypted 128-bits data. The 128-bits data considering 16-bytes again goes for the related round if the current iteration is not the last one. The 10-cycle encryption is concluded with the achieved 128-bit data as output. The AES algorithm structure is as shown in Fig. 2.

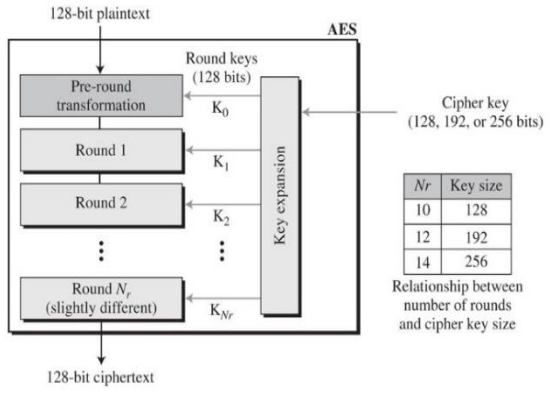

Fig. 2 AES algorithm Structure [17]

IV. Sequential And Parallel implementation

Sequential implementation of the AES method initially converts the plain text into a status array and then XORed with the entry cipher key for the add round key process. This is then done with the unit which consists of four subunits: Sub Bytes, Shift Rows, Mix Column and Add Round Key (round 1 to round N-1). This is followed by another unit with three sub units, Sub Bytes, Shift Rows and Add Round Key. The application covers a small area because it utilizes the same equipment from round 1 to round N-1. Fig. 3 shows the 3-stage AES implementation sequentially.

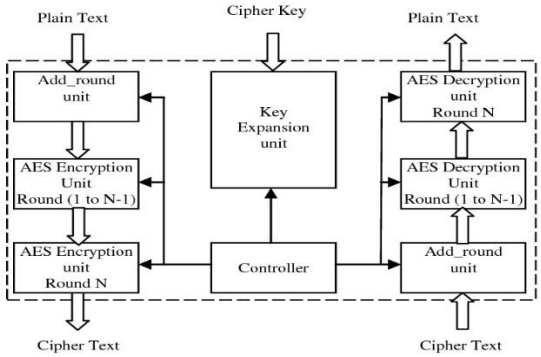

Fig. 3 Sequential 3-Stage AES implementation [13]

The combination method is used to reduce the delay and to boost the performance and the usage of the pipeline method, a further increase in the output can be achieved. In this method, after each rounding unit, a128-bit register is used to momentarily store the information. The highest frequency of operation is obtained from the 1-round delay [11]. High working velocity and frequency are the main benefits of the pipeline method. Fig. 4 shows the implementation of pipeline Rijndael and AES-128.

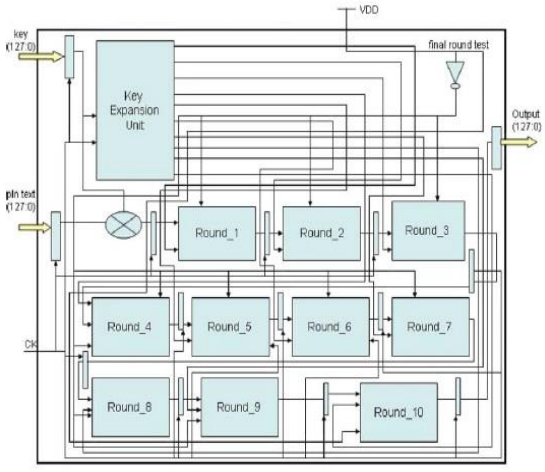

Fig. 4 Implementation of pipeline Rijndael and AES-128 [15]

V. Proposed Module And Verification

The aim of the AES implementation with pipeline architecture helps to achieve greater throughput with optimized delay. In the design, top module forms rounds relate key expansion with the use of pipeline architecture. Instantiate key expansion that feeds each round with round-key. According to the algorithm, the 1st cipher-key is XOR-ed with the plain-text [12]. Connect all the round with key-expansion and instantiate them. The final round consists of three stages only and so a delay register should be used with the key-expansion to balance the output. The module is designed on Xilinx ISE® Design Suite and this design can be tested and verified on hardware using Virtex®-6 FPGA. The first AES silicon implementation that delivers 2.29 Gbps of non-pipeline architectural performance. The T-Box was the first AES application to have more than 10 Gbps output, which included a mixture of sub-bytes, shift lines, and blended AES columns. With a 30-70 Gbit/s output, a fully piped AES processor works in a more difficult way. The conversion of the AES Mix Columns works in a four-column database and is separate for each column. In a single loop, 60% of the total latency results in the delays of execution of mix columns. Parallelism is therefore presented in the block of mixing columns. This increases the output of the execution of the mix columns.

The functional verification of the module is done with the help of the test-bench. The expected output and tested vectors are stored in the files. The top-end module (Top_PipelinedCipher_tb) for the test-bench covers 284 test patterns composed in AES validation suit document (AESVS). The compilation and simulation are optimized using do files for automation. For gate-level simulation, the first stage after synthesis and implementation is to place-and-route the simulation model and generate the Verilog net-list with the user-constraint file (ucf). The design hierarchy of the module at each level is shown in Fig. 5.

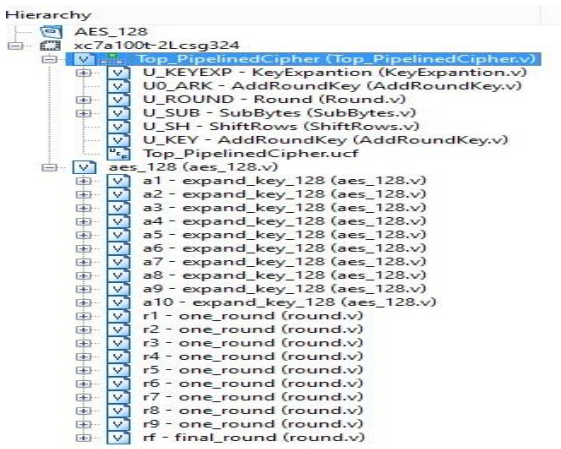

Fig. 5 Module hierarchy

VI. Experimental Results

The utilization of resources is less for the AES and the performance is high due to the pipelined approach. The AES processor based on S-box architecture provides a throughput of 1.5-2 times higher than that of the AES processor based on the common LUT S-box. As the S-box based on LUTs are faster, it is feasible to apply the LUT-based advance to S-box hardware approach as the starting point so as to further improve it through pipelining. Fig. 6 shows the top-level module which takes a 128-bit input and gives the output of 128-bit and Fig. 7 depicts the RTL expanded view of the module displaying the submodules and clock-gating implemented inside the module. The module operates at constraint frequency of 200 MHz and the clock time-period 5ns.

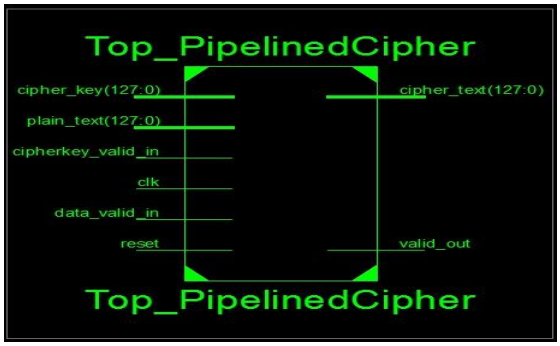

Fig. 6 Top-level view

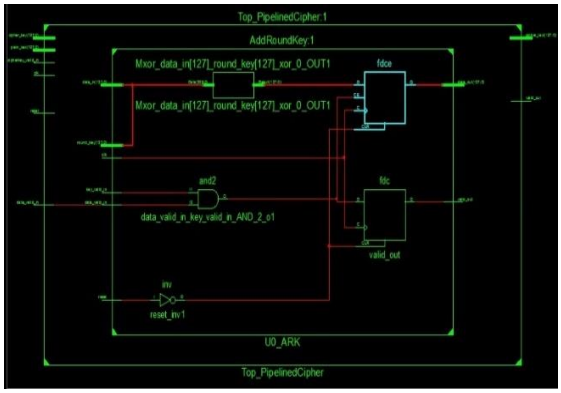

Fig. 7 Expanded RTL design

The simulation result of our designed module is shown in Fig. 8 i.e. AES encrypted output, where the input is taken from the test-bench (or manual input) and also the Encryption/Decryption modules are incorporated inside the Top-level module. The module's encrypted data and the simulation results are verified. The plain-text "2123233353addcc25213453125312534" it's AES encrypted output is as "d0b440f3b845ff73f542a095ba257798". To boost the output of AES encryption, the execution of both matrix components is done by implementing two parallel components simultaneously using the eight phase parallelism method. Parallel block performance is improved and their implemented area is reduced.

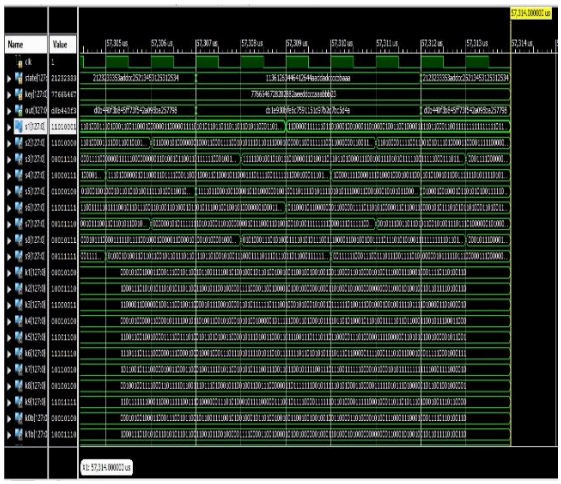

Fig. 9 AES Encryption module simulation waveforms

The latency and throughput are calculated as below:
Latency is the time delay from input to the required result.

- $Latency = constraint\ freq./period$

Latency = (41) clock-cycles*period (5ns)

$$41 \times 5 = 205ns$$

Throughput is the rate at which the information is processed by any system. It is measured in bits/sec.

- $Throughput = data/time$

$$Throughput = \frac{128}{5ns} = \frac{25.6bits}{ns} = \frac{25.6Gbits}{s}$$

VII. Conclusion

In our proposed work, we have designed a pipelined AES-architecture which has high throughput. Registers are inserted in the design at appropriate points to achieve the objective. For the proposed pipelined AES, the throughput achieved is 25.6Gbps with 200MHz of constraint frequency. We can use this architecture in many application-based designs such as voice-communication, video processing, banking systems, and image processing and mobile-network security. We can adopt this module in high-security data communication and prevent third-party attacks on our systems. The design can be included in many embedded applications to enhance the conversion speed and security of the system.

ACKNOWLEDGMENT

This work is carried out in the laboratory of School of VLSI Design and Embedded Systems at NIT Kurukshetra. The authors acknowledge the generous, technical and EDA tools support by the faculties and management of the department.

REFERENCES

[1] L. P. Kumar and A. K. Gupta, "Implementation of speech encryption and decryption using advanced encryption standard," *2016 IEEE International Conference on Recent Trends in Electronics, Information & Communication Technology (RTEICT)*, Bangalore, 2016, pp. 1497-1501.

[2] Thirer, N. (2013). A pipelined FPGA implementation of an encryption algorithm based on genetic algorithm. Machine Intelligence and Bio-inspired Computation: Theory and Applications VII. doi:10.1117/12.2014829

[3] M. Mohurle and V. V. Panchbhai, "Review on realization of AES encryption and decryption with power and area optimization," *2016 IEEE 1st International Conference on Power Electronics, Intelligent Control and Energy Systems (ICPEICES)*, Delhi, 2016, pp. 1-3.

[4] A. P. A. Naidu and P. K. Joshi, "FPGA implementation of fully pipelined Advanced Encryption Standard," *2015 International Conference on Communications and Signal Processing (ICCSP)*, Melmaruvathur, 2015, pp. 0649-0653.

[5] S. S. Chawla, S. Aggarwal, S. Kamal and N. Goel, "FPGA implementation of an optimized 8-bit AES architecture: A masked S-Box and pipelined approach," *2015 IEEE International Conference on Electronics, Computing and Communication Technologies (CONECCT)*, Bangalore, 2015, pp. 1-6.

[6] Jindal, P., & Singh, B. (2013). Performance Evaluation of Security-Throughput Tradeoff with Channel Adaptive Encryption. *International Journal of Computer Network and Information Security*,5(1), 49-55. doi:10.5815/ijcnis.2013.01.06

[7] D. Q. Huy, N. M. Duc, L. D. Khai and V. D. Lung, "Hardware Implementation of AES with S-Box Using Composite-Field for WLAN Systems," *2019 IEEE-RIVF International Conference on Computing and Communication Technologies (RIVF)*, Danang, Vietnam, 2019, pp. 1-6.

[8] Shreenivas Pai N, Raghuram S, Chennakrishna M and A. S. V. Karthik, "Logic optimization of AES S-Box," *2016 International Conference on Automatic Control and Dynamic Optimization Techniques (ICACDOT)*, Pune, 2016, pp. 1042-1046.

[9] S. Negi, P. Raj, S. K. Chauhan and P. Kumar, "Implementation of AES Employing Systolic Array and Pipelining Approach," *2018 3rd International Conference On Internet of Things: Smart Innovation and Usages (IoT-SIU)*, Bhimtal, 2018, pp. 1-5.,

[10] N. S. S. Srinivas and M. Akramuddin, "FPGA based hardware implementation of AES Rijndael algorithm for Encryption and Decryption," *2016 International Conference on Electrical, Electronics, and Optimization Techniques (ICEEOT)*, Chennai, 2016, pp. 1769-1776.

[11] Ritambhara, A. Gupta and M. Jaiswal, "An enhanced AES algorithm using cascading method on 400 bits key size used in enhancing the safety of next generation internet of things (IOT)," *2017 International Conference on Computing, Communication and Automation (ICCCA)*, Greater Noida, 2017, pp. 422-427.

[12] L. Kang and C. Wang, "The Design and Implementation of Multi-Precision Floating Point Arithmetic Unit Based on FPGA," *2018 International Conference on Intelligent Transportation, Big Data & Smart City (ICITBS)*, Xiamen, 2018, pp. 587-591.

[13] Gannot, G., & Ligthart, M. (n.d.). Verilog HDL based FPGA design. *International Verilog HDL Conference*. doi:10.1109/ivc.1994.323743

[14] Gupta, M., Mahto, S., & Patel, A. (2017). Implementation of 128, 192 & 256 bits Advanced Encryption Standard on Reconfigurable Logic. *International Journal of Engineering Trends and Technology*,*50*(6), 305-309. doi:10.14445/22315381/ijett-v50p251

[15] Babitha M.P. and K. R. R. Babu, "Secure cloud storage using AES encryption," *2016 International Conference on Automatic Control and Dynamic Optimization Techniques (ICACDOT)*, Pune, 2016, pp. 859-864.

[16] S. S. Chawla, S. Aggarwal, S. Kamal and N. Goel, "FPGA implementation of an optimized 8-bit AES architecture: A masked S-Box and pipelined approach," *2015 IEEE International Conference on Electronics, Computing and Communication Technologies (CONECCT)*, Bangalore, 2015, pp. 1-6.

[17] B. K. B. Raju, A. Krishna and G. Mishra, "Implementation of an efficient dynamic AES algorithm using ARM based SoC," *2017 4th IEEE Uttar Pradesh Section International Conference on Electrical, Computer and Electronics (UPCON)*, Mathura, 2017, pp. 39-43.

[18] Balamurugan, J., & Logashanmugam, E. (2013). Low power and high speed AES using mix column transformation. 2013 International Conference on Current Trends in Engineering and Technology (ICCTET). doi:10.1109/icctet.2013.6675950

Proceedings of the Fourth International Conference on Communication and Electronics Systems (ICCES 2019)
IEEE Conference Record # 45898; IEEE Xplore ISBN: 978-1-7281-1261-9

Analysis of Coupled Inductor Based Buck-Boost Single Phase PWM AC to AC Converter

Priyanka Nehra
priyankanehra769@gmail.com

Ashok Kumar Sharma
aksharma_eck@hotmail.com

Dolly Murodia
dolmurodia@gmail.com

Deepanshu Gautam
Gautam. gudiya11@gmail

Department of Electrical Engineering
Rajasthan Technical University, Kota
Kota, INDIA

***Abstract*—This paper introduces AC to AC converter for Single phase Pulse Width Modulation (PWM), which can solve the commutation issue by employing AC to AC converters without detecting the input voltage polarity. With a salient structure of SC and connected inductors. The PWM ac to ac converters replaced by the SC design and a coupled inductor by the standard leg hence the boost inductor buck and boost type suggested converter is developed. In this commended work the suggested converter has requirement of two coupled inductor and this coupled inductor is combined with the boost inductor. The input inductor of suggested converter could be much compact than that of standard Pulse Width Modulation (PWM) AC to AC converter. The MATLAB-2016 b setting presents the simulation-based buck-boost ac to ac converter.**

Keywords—AC-AC Converter, Pulse width modulation (PWM), Switching cell (SC), Coupled Inductor(CI), Boost Inductor,MATLAB.

I. INTRODUCTION

In power electronics, interleaving is a commonly used method. If more than one Pulse Width Modulation (PWM) converter is paralleled, each conversion carrier can be shifted in a phase and certain harmonics can be canceled at the output. The angle for phase change is generally 180 ° for two parallel cases, whereas other values can be determined to achieve certain design objectives [15]. In many applications, such as industrial heating & illumination the suggested regulator can upgrade or down output voltage to input voltage. The Phase Angle Control (PAC) control system is widely used in a variety of applications. In comparison with the standard Pulse Width Modulator (PWM) regulator, the suggested regulator also restricts more harmonic yield voltage [13]. A crossover technique reduces the output present ripples of coupled inductors [1]. The voltage control is needed in manufacturing systems, as it provides different benefits such as small-size, easy configuration, elevated effectiveness, low-cost and so on [9]. The greatest difficulty in the design of a boost converter is how to manage the large energy flow at the plant and high voltage [7]. The suggested converter inductor can have a much lower input than the standard PWM AC to AC converters [11].

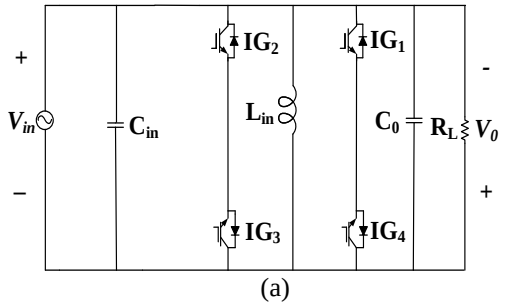

(a)

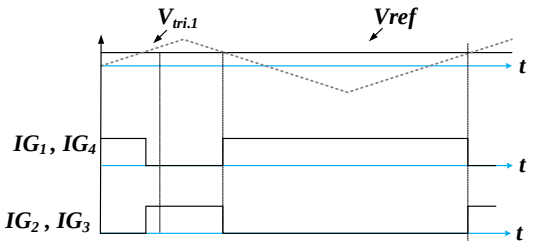

(b)

Fig.1 Standard direct pulse width modulation (PWM) AC to AC Converter (a) Type of Buck-Boost (b)Signals from the gate (optimal)

Fig1. Represents the Standard direct pulse width modulation (PWM) AC to AC Converter with type of buck-boost give signals from the gate (optimal) which can be implement with switching cell structure and boost inductor in this paper.

II. Composition Of Suggested Converter

The suggested converter consists of a fundamental switching cell, Boost inductor and coupled inductor. This fundamental SC structure is formed by employing a switching device and a diode that are connected to three terminals :(+), (-) & (→)/ (←). Figure.2. represents the suggested Single phase Buck Boost type Pulse Width Modulation (PWM) AC to AC converters.

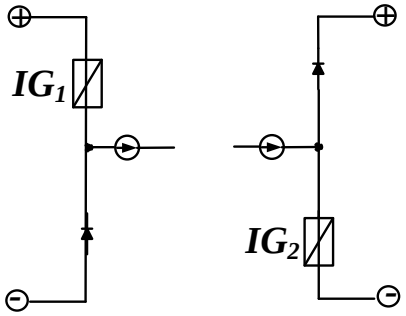

Fig.2 Fundamental SC structure

Fig.2 represents the fundamental switching scheme which is combination of any switching element and diode. Here S denoted in fig 2 any swiching element. The P-cell and N-cell two fundamental turning cells, and their electronic circuit-powered application[5].

The suggested converter consists upper side and lower side legs. The upper side leg has two switches [S1 & S2] ,two diodes [D1 & D2], a coupled inductor, a capacitor and a Boost inductor. Same as lower side can be formed. The two capacitors [C1 & C2] are added across each phase side to form a current path when S1 & S2 are both turned OFF. These capacitors are used as input or output filter. Furthermore serve as simple snubber capacitor to suppress switch voltage overshoot. energy factor and effectiveness and lower passive filters are better used, PWM ac choppers are preferred.[3].

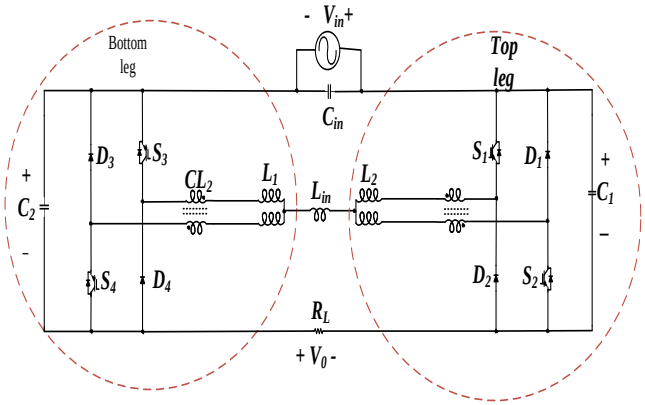

Fig 3. Suggested Buck-Boost single Phase PWM AC to AC converter

Fig.3. denoted suggested converter which is combination of SC structure, coupled inductor and boost inductor.

III. Analysis Of Ripple Current For Inductors

In this part of the paper the input inductor and two coupled inductors are investigated. The proposed converter is aimed at reducing the ripple without an increase in the inductor value. This is why the converter technology is interlinked.[6].

A. *INPUT INDUCTOR*

From the waveform fig.5 it is noticed that input inductor L_{in} is made smaller in the suggested converter for Buck Boost type than the input inductor in the standard Boost type AC to AC converter. Fig.4 represents input current of coupled inductor.

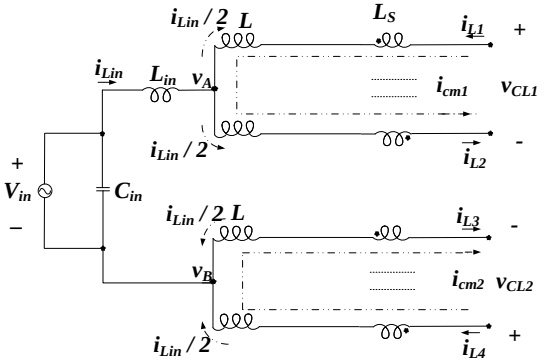

Fig.4. Boost inductor input current and mode of common

B. *INPUT INDUCTEOR DESIGH-* The calculation for current ripple in the L_{in} is mentioned as below

$$\Delta i_{L_{in}} = \frac{(0.5-D)D}{L_{in}} v_0 T_s \qquad (1)$$

Thus, when D = .25 with Vo = $Vo_{.max}$ then the occurring current ripple is maximum. Where T_s is the switching period of the converter.

C. *COUPLED INDUCTOR*

As coupled inductors have perfect coupling so the coupled inductor is assumed for the suggested converter to calculate the current ripple in the common mode.

D. *COUPLED INDUCTOR DESIGN-* The current ripple can be derived for the common mode as follows –

$$\Delta i_{cm1} = \frac{vc_1}{4L_s} DT_s \qquad (2)$$

$$\Delta i_{cm2} = \frac{vc_2}{4L_s} DT_s \qquad (3)$$

The ripple current equations can be calculated in each mode & maximum current ripple occurs when either Vc_1 or Vc_2 is which are explained as-

The winding currents equations of coupled inductor can be rewritten as –

$$\Delta i_{L_x.max} = \left[\frac{1}{L_S} + \frac{1-2D}{L_{in}}\right]\frac{v_0}{4} DT_s, x = 1,2,3,4. \quad (8)$$

Although a converter's output current ripples can decrease significantly due to the interleaving effect, even with the interleaving PWM method, the inductive current ripples cannot be decreased. A combined inductor is one way to fix this issue.[4].

$$\Delta i_{L_{in}.conv} = \frac{(1-D)\,D}{L_{in.conv}} v_0 T_s \quad (9)$$

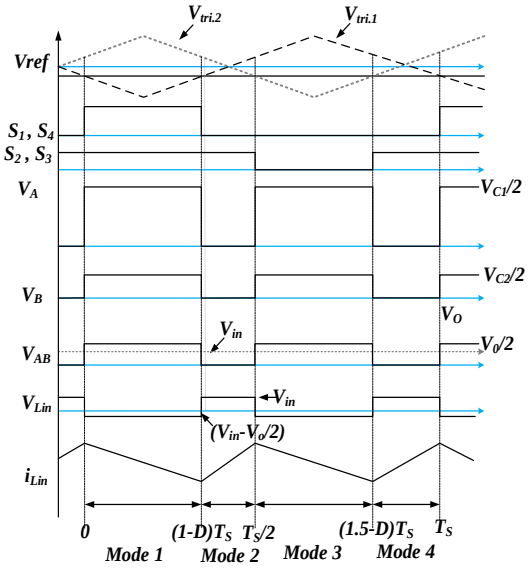

(a)

Fig.5. represents the comparison of key operational waveforms when duty ratio is less than 0.5 which is shown by waveform (a) and its opposite waveform (b) shows when duty ratio (D) value is greater than 0.5.

Where ideal gate switching is given for switching device and common mode current is also calculated for these input boost and coupled inductors which combine with switching cell structure.

In fig 5 represented switching of four converter which denoted by S1, S2, S3, S4 given by comparison of a triangular wave with reference or compare with duty cycle. Duty cycle is denoted by D. which is time interval of switch S2 and S4.

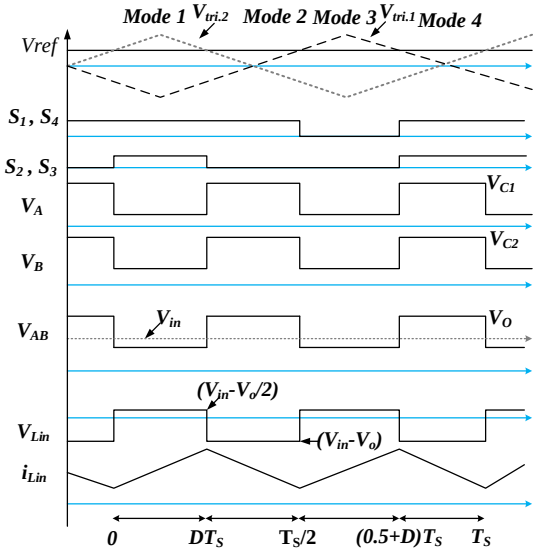

(b)

Fig.5. Key operational waveform analyzes if 0.5 < D > 0.5 for (a)&(b)

Fig.5 the effect on the common mode DC current element of switching turn ON and OFF delays when duty ratio is less than 0.5 which is shown by waveform (a) and its opposite waveform (b) shows when duty ratio (D) value is greater than 0.5.Small distinction mid of these four-switching devices can therefore fix the saturation issue by having adverse voltage drop across the boost and coupled inductors. Fig(b) Small distinction between S1 and S2 (or S3 and S4) can fix the saturation issue by having adverse voltage drop across the inductors.

With the converter elevated changing frequency procedure, the amount of the suggested converter magnetic parts can be further decreased as the diodes in the suggested system are internally chosen with very quick retrieval diodes. The necessary output inductance of the standard ac to ac converter (Lin.conv)is significantly higher than that of the converter suggested. For example, when D= 0.45, the Lin.conv is nearly 11 times Lin. Consequently, the total quantity of the suggested the standard ac–ac converter.

These types switching have four mode conduction period voltage input and output voltage waveform is shown in simulation model which leads to input inductor voltage in buck-boost ac to ac converter.in output current of inductor has some ripple current which highest on the 0.25 duty cycle and minimum in 0.5 duty cycle to finding ripple current using equations which expended in little ripple to compare issues and producing the switching frequency to reducing harmonic and power stages calculation in the process.

So, these types of key operational waveforms are shown above in two parts and represented effects of turn on and off delays also.

IV. Simulation Of Coupled Inductors Based Proposed Buck-Boost Converter

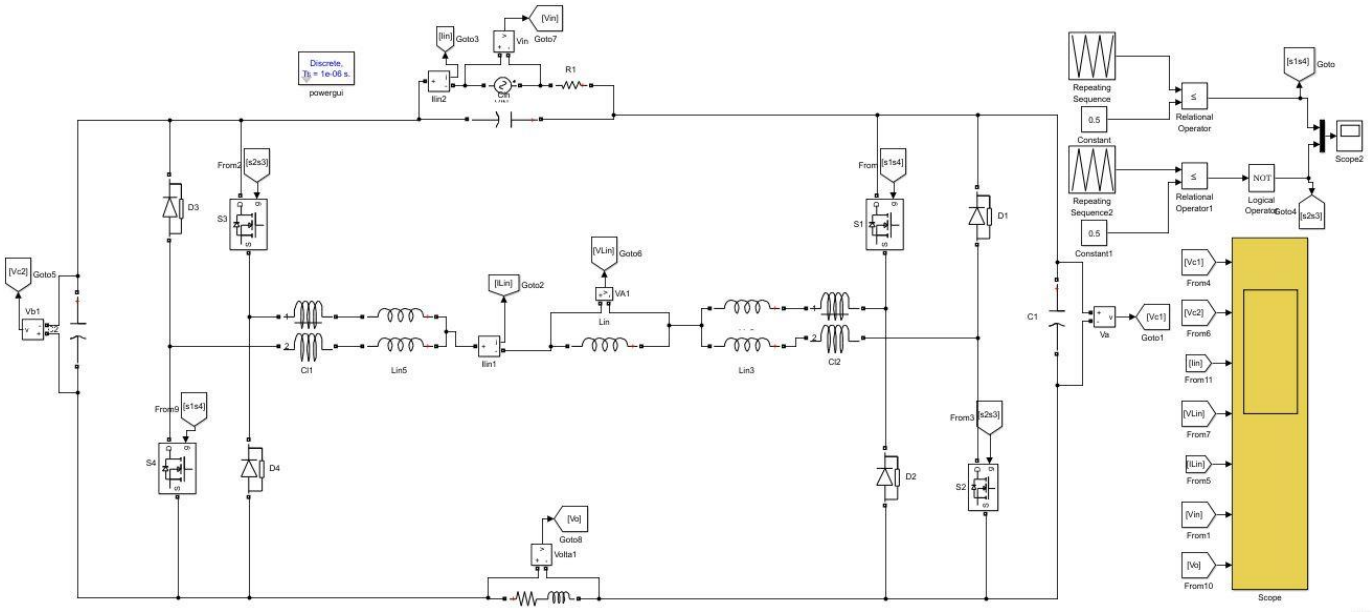

Fig.6.Matlab Simulation Model of Proposed Buck Boost Converter based on switching cell structure

V Simulation Results

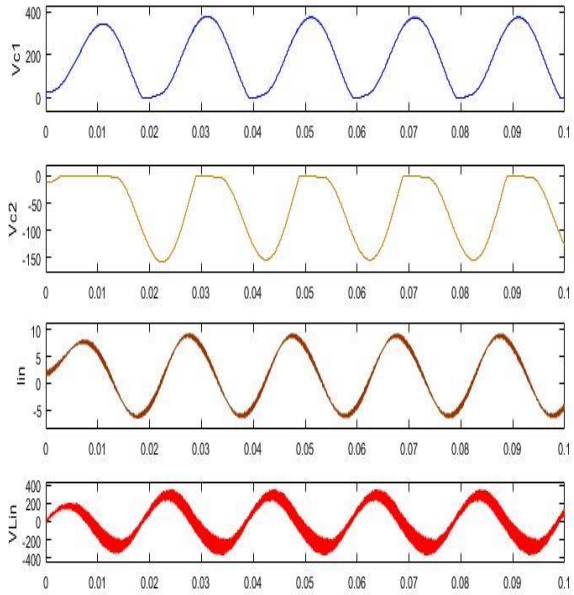

(a)

Fig.(a) shows voltage waveform of C1, C2,. Input current Iin and input inductor voltage V_{Lin} current .

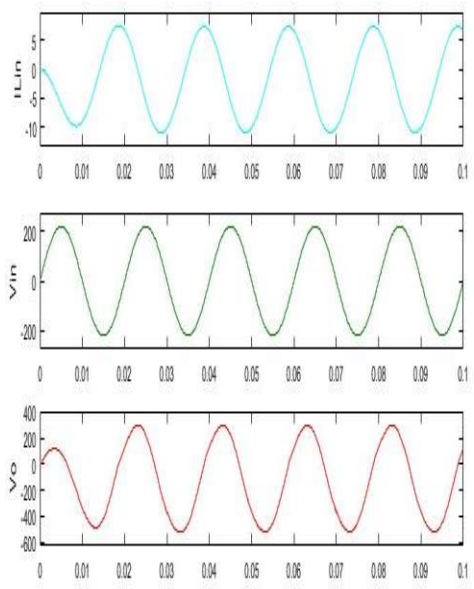

(b)

Fig.(b) shows input inductor current IL_{In}, input voltage V_{in}, output voltage V_0

Fig.7. MATLAB Simulation results

Fig.7 represents the simulation of the proposed converter. According to the parameter design simulation parameters are selected input voltage (v_{in}=110v_{rms}), output voltage (v_o=220v_{rms}), output power (p_o=200 w) and D =0.4.

V. Conclusion

In this paper the behavior of a coupled inductor is explained on the inductor and output current ripple in the brief. Since Single Phase Step up and down Buck Boost is suggested in this paper which can further implemented for the three-phase system in future point of view. Furthermore, this suggested grid technology is used for Wind Power Generation Scheme. Coupling inductor is applied as high frequency circuits because of high frequency circulating currents. Parallel inverters can be more stably operated in high present applications compared to non-coupled cases. With a coupling impact, the present filter inductor waves are decreased.

References

[1] S. T. Richard and R. G. Nirmala, “Design and Hardware implementation of Two Phase Coupled InductorInterleaved Boost Converter with Low Ripple Circuit,” vol. 8, no. 1, pp. 151–156, 2014.

[2] B. R. Lin, Y. C. Lee, and D. J. Chen, “Implementation of a single-phase AC/AC converter with neutral-point-clamped scheme,” *Proc. IEEE Int. Conf. Ind. Technol.*, vol. 2, pp. 780–785, 2002.

[3] M. Ganta, P. Nirupa, T. Akshitha, and R. Seyezhai, “Design and Simulation of PWM Fed Two-Phase Interleaved Boost Converter for Renewable Energy Source,” *Internantional J. Electr. Electron. Data Commun.*, vol. 1, no. 1, pp. 18–23, 2013.

[4] F. H. Khan, L. M. Tolbert, and F. Z. Peng, “Deriving new topologies of DC-DC converters featuring basic switching cells,” *Proc. IEEE Work. Comput. Power Electron. COMPEL*, pp. 328–332, 2006.

[5] D. Shin, J.-P. Lee, K.-J. Lee, D.-W. Yoo, H. Cha, and J.-Y. Yoo, “Analysis and Design of Coupled Inductors for Two-Phase Interleaved DC-DC Converters,” *J. Power Electron.*, vol. 13, no. 3, pp. 339–348, 2013.

[6] V. John and M. H. Hedayati, “Integrated common-mode inductor design for parallel interleaved converters,” *IET Power Electron.*, vol. 9, no. 10, pp. 2130–2138, 2016.

[7] A. A. Khan, H. Cha, and H. G. Kim, “Magnetic integration of discrete-coupled inductors in single-phase direct PWM AC-AC converters,” *IEEE Trans. Power Electron.*, vol. 31, no. 3, pp. 2129–2138, 2016.

[8] H. H. Shin, H. Cha, H. G. Kim, and D. W. Yoo, “Novel single-phase PWM AC-AC converters solving commutation problem using switching cell structure and coupled inductor,” *IEEE Trans. Power Electron.*, vol. 30, no. 4, pp. 2137–2147, 2015.

[9] F. Z. Peng, L. Chen, and F. Zhang, “Simple topologies of PWM AC-AC converters,” *IEEE Power Electron. Lett.*, vol. 1, no. 1, pp. 10–13, 2003.

[10] D. H. Jang and G. H. Choe, “Step-up/down AC voltage regulator using transformer with tap changer and PWM AC chopper,” *IEEE Trans. Ind. Electron.*, vol. 45, no. 6, pp. 905–911, 1998.

[11] H. F. Ahmed, H. Cha, S. H. Kim, and H. G. Kim, “Switched-Coupled-Inductor Quasi-Z-Source Inverter,” *IEEE Trans. Power Electron.*, vol. 31, no. 2, pp. 1241–1254, 2016.

[12] S. Ohn, X. Zhang, R. Burgos, and D. Boroyevich, “Two core implementation of coupled inductor for parallel three-phase power converters,” *Conf. Proc. - IEEE Appl. Power Electron. Conf. Expo. - APEC*, pp. 898–905, 2017.

[13] N. Selvaraju, P. Shanmugham, and S. Somkun, “Two-Phase Interleaved Boost Converter Using Coupled Inductor for Fuel Cell Applications,” *Energy Procedia*, vol. 138, pp. 199–204, 2017.

[14] D. Shin *et al.*, “1.5MVA grid-connected interleaved inverters using coupled inductors for wind power generation system,” *2013 IEEE Energy Convers. Congr. Expo. ECCE 2013*, no. September, pp. 4689–4696, 2013.

[15] H. F. Ahmed, H. Cha, A. A. Khan, and H. G. Kim, “A single-phase isolated high step-down ac-ac converter with no commutation problem using switching cell and coupled inductor,” *9th Int. Conf. Power Electron. - ECCE Asia "Green World with Power Electron. ICPE 2015-ECCE Asia*, pp. 2353–2358, 2015.

Proceedings of the Fourth International Conference on Communication and Electronics Systems (ICCES 2019)
IEEE Conference Record # 45898; IEEE Xplore ISBN: 978-1-7281-1261-9

Classification of Retinal Diseases Using Transfer Learning Approach

Amrit Das
Student
Department of ECE
SRM - IST, KTR Campus
Kancheepuram, India
amritdas1998@gmail.com

Rohan Giri
Student
Department of ECE
SRM - IST, KTR Campus
Kancheepuram, India
girirohan36@gmail.com

Gunjan Chourasia
Student
Department of CSE
SRM - IST, KTR Campus
Kancheepuram, India
gchourasia123@gmail.com

A. Anilet Bala
Assistant professor (O.G.)
Department of ECE
SRM - IST, KTR Campus
Kancheepuram, India
aniletbala.a@ktr.srmuniv.ac.in

Abstract*—Retinal disease classification of Color Fundus Images using Computational Imaging has been widely accepted. This paper proposes a transfer learning approach for Retinal Disease Classification using Deep Learning. Deep learning methods are widely used due to higher performance and accuracy but at the cost of time. A large amount of time and processing power is required to train a dataset and achieve considerable accuracy. Transfer learning reduces a load of using huge data-sets, thereby reducing the time complexity of the training data. We have selected VGG19 model to fine-tune the network for the extraction of knowledge. The VGG19 model is fine-tuned with a retinal database. The results contain accuracy the network on changing various hyper-parameters like learning rate, number of epochs, optimizer algorithm to find a suitable set of parameters for higher accuracy. The motivation for using Deep Neural network is the fact that it has multi-fold benefits like better performance compared to traditional machine learning techniques, higher accuracy, automated feature extraction and easier to design and process.

***Keywords*— Cognitive Intelligence, Deep Neural Networks, Eye, Knowledge Transfer, Medical Imaging**

I. INTRODUCTION

Retina is the photosensitive portion of our eyes which is delicate, crucial and responsible for the vision. Even minor damage to these tissues can result in symptoms like distorted vision, blurry vision and even loss of sight. These symptoms if left unattended can result in serious diseases like vision impairment or even temporary or permanent loss of sight. Hence it is very crucial to detect and attend to these diseases to the earliest. There are various different diseases that can be caused due to effects in the retina like Glaucoma, Diabetic Retinopathy, Retinal Tear, Retinal Detachment, Macular Degeneration etc., The rectification of these diseases is necessary as early as possible. In order to rectify the disease, it is necessary to figure out the type of disease. This paper provides a solution to this problem by detecting the disease through transfer learning, a deep learning method. Deep Learning requires a lot of data to train and it may require a lot of time and memory as well but this is an efficient method once the neural network model is trained of the data set completely. It effectively detects the retinal disease and even classifies them, making it easier to cure. The issue that usually occurs in traditional machine learning models and the neural network is the time and processing power which is required to compute the output. In order to improve the accuracy, new data should be fed to the system, but in case the system has a huge dataset, high processing power, and time commitment is required to get decent accuracy. In this paper we propose a system that transfers its knowledge from a relatively pre-trained model and implements this on our dataset, to update the weights and biases. This knowledge transfer between machine learning algorithms is known as Transfer Learning. The profit of using this methodology is it retains most of the neural architecture of the pre-trained model and tunes the architecture to minimize the loss for the un-trained model. Hence it requires less computing and is much faster as compared to the traditional CNN and Machine Learning algorithms.

II. LITERATURE REVIEW

In a very few decades, biomedical imaging and retinal image computing have gathered the attention of various researcher as the output of the computation system is considered better than verbal dictation of the system or other traditional methodologies. Prior works in this field are done by [1], [2] have used machine learning methods to generate an accuracy of 81-86%, [3] compared popular algorithms to produce and increase the accuracy in classification, while [4] uses simple image processing for detection of defects. This paper uses transfer learning as it is suitable for small scale data set [5]. The motivation of the proposed system was from [6], according to which VGG19 [7] model showed a decent accuracy as compared to other models.

III. SYSTEM SPECIFICATION AND OVERVIEW

A. Hardware Specification

When designing a prototype, the performance always depends upon the hardware specifications, the better the hardware, the less is the execution time and higher is the processing power there by increasing the overall performance. This section of the paper provides a detailed outline of the hardware specifications that we used to get to the result of this paper. The neural net model was designed and deployed on a system with the following specifications.

TABLE 1: HARDWARE SPECIFICATIONS

Sl. No.	Specifications	
	Name	***Value***
1.	Processor	Intel Core i5-8300H Processor
2.	RAM	8 GB DDR4 2666MHz
3.	GPU	NVIDIA GEFORCE GTX 1050 Ti (4GB GDDR5)

B. Software Specifications

PyTorch is a python based neural network computing frame work. We have used PyTorch to design and execute the neural network model. PyTorch is completely python based and hence it is preferred by us as it is very friendly with the native python based packages like Numpy, Scipy, Python Imaging Library (PIL) etc., VGG-19 is a pre-trained deep neural model which is 19 layers deep. We have preferred this model for fine-tuning our custom dataset and to transfer knowledge as it is faster and more efficient [8].

TABLE 2: SOFTWARE SPECIFICATIONS

Sl. No.	Specifications	
	Name	***Value***
1.	Language	Python 2.7
2.	Frame Work	Pytorch
3.	GPU	Cuda 9.0
4.	Pre-trained Model	VGG-19

The GPU used (Refer table 1) supports Cuda 9.0, which increases efficiency of the model [9].

C. Pre-trained Model – VGG19

VGG network was designed in [10], which proposed simple and effective network architecture for efficient accuracy and was trained on a million images.

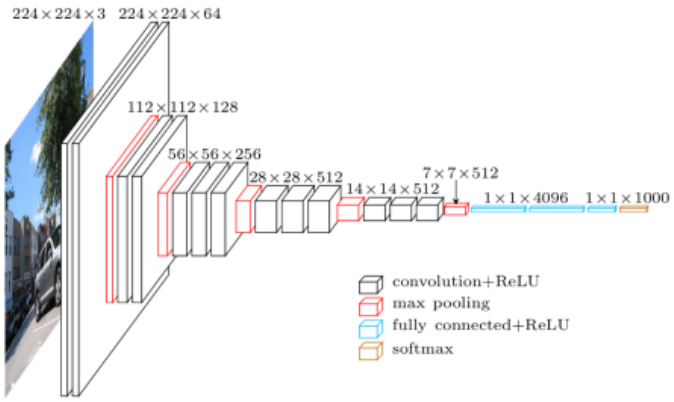

Fig.1. VGG Architecture

Source : (https://www.cs.toronto.edu/~frossard/post/vgg16/)

The proposed system involves 3x3 convolution layers planted one above another in respect of the increasing depth followed by two fully connected layers with 4096 nodes in each layer and one fully connected layer with 1000 nodes which is again followed by a soft-max layer for image classification.

ConvNet Configuration					
A	A-LRN	B	C	D	E
11 weight layers	11 weight layers	13 weight layers	16 weight layers	16 weight layers	19 weight layers
input (224 × 224 RGB image)					
conv3-64	conv3-64 **LRN**	conv3-64 **conv3-64**	conv3-64 conv3-64	conv3-64 conv3-64	conv3-64 conv3-64
maxpool					
conv3-128	conv3-128	conv3-128 **conv3-128**	conv3-128 conv3-128	conv3-128 conv3-128	conv3-128 conv3-128
maxpool					
conv3-256 conv3-256	conv3-256 conv3-256	conv3-256 conv3-256	conv3-256 conv3-256 **conv1-256**	conv3-256 conv3-256 **conv3-256**	conv3-256 conv3-256 conv3-256 **conv3-256**
maxpool					
conv3-512 conv3-512	conv3-512 conv3-512	conv3-512 conv3-512	conv3-512 conv3-512 **conv1-512**	conv3-512 conv3-512 **conv3-512**	conv3-512 conv3-512 conv3-512 **conv3-512**
maxpool					
conv3-512 conv3-512	conv3-512 conv3-512	conv3-512 conv3-512	conv3-512 conv3-512 **conv1-512**	conv3-512 conv3-512 **conv3-512**	conv3-512 conv3-512 conv3-512 **conv3-512**
maxpool					
FC-4096					
FC-4096					
FC-1000					
soft-max					

Fig.2. VGG Configuration (https://qph.fs.quoracdn.net/main-qimg-30abbdf1982c8cb049ac65f3cf9d5640)

IV. METHODOLOGY

This section of the paper explains the architecture of the proposed system and the method incorporated to reach to the conclusion.

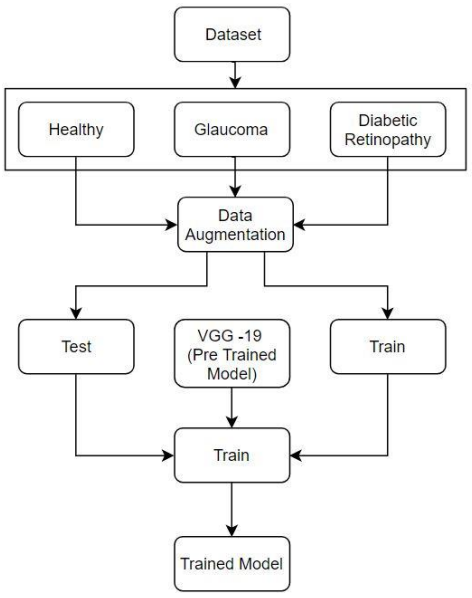

Fig.3. Model Representation

The dataset contains three types of images, healthy, glaucoma and diabetic (Refer to Fig. 5). These images are segregated into different folders. Here VGG network (Visual Geometric Group) [11] is used. First we go through preprocessing followed by extraction of features and then finally identification of images.

A. Preprocessing of images

Since the dataset [12] has less number of images, more images needs to be created because this helps in increasing accuracy of the model. We went through the process of data augmentation for this purpose. The process of data augmentation involves rotation, flipping and cropping of images. This helps in creating more number of images [13]. Not only does it just increase the number of images but also it increases the overall robustness of the model there by making it more accurate.

B. Extraction of features from image

This step involves extracting specific features from the images which later will be used in identifying and segregating the images into healthy, glaucoma and diabetic. For this processes VGG-19 [14] network is used, it was created by Oxford. VGG can contain 11-19 layers but here all 19 layers are used. This convolution network is built using layers having size of 3*3. The diagram below gives the description of layers in VGG [11].

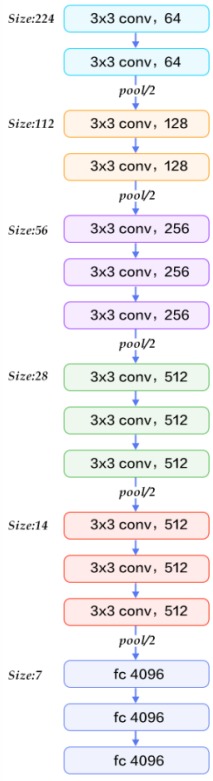

Fig.4 Layers of VGG (https://qph.fs.quoracdn.net/main-qimg-e657c195fc2696c7d5fc0b1e3682fde6)

C. Identifying the images

After getting the desired accuracy, we have saved the trained model into a dictionary format which we use for inference on the required data. In order to predict, we pass the retinal color fundus image through the model which identifies the features from the image and predicts the retinal disease. The results for the experimentations are discussed in the next section.

V. RESULTS AND DISCUSSION

In order to figure out the best preferred hyper parameters, or the optimum hyper parameters, we have used a brute force approach by plotting the epoch vs. accuracy curve at different frequently used learning rates. The accuracy of the model is changed by changing the number of epochs keeping a constant learning rate. It is observed that greater than 90% (Refer to Table 3) of the accuracy is reached in most cases. The model successfully classifies the images into healthy, glaucoma and diabetic (Refer to Fig.8).

TABLE 3: SOFTWARE SPECIFICATIONS

Epochs	Learning Rate	Accuracy (%)	Loss (%)
25	0.1	54.24	20.8
50	0.1	65.39	13
75	0.1	78.56	8
100	0.1	88.20	7
125	0.1	90.34	6.8
150	0.1	87.64	6.66

Epochs	Learning Rate	Accuracy (%)	Loss (%)
25	0.01	59.24	24.80
50	0.01	68.83	8
75	0.01	82.72	7.2
100	0.01	90.52	7.2
125	0.01	91.23	6.7
150	0.01	91.56	6.5

Epochs	Learning Rate	Accuracy (%)	Loss (%)
25	0.05	62.94	14.8
50	0.05	81.30	10
75	0.05	86.00	9
100	0.05	91.40	7
125	0.05	91.88	6.5
150	0.05	92.13	6.2

Epochs	Learning Rate	Accuracy (%)	Loss (%)
25	0.001	66.54	20.8
50	0.001	71.23	13
75	0.001	88.92	8
100	0.001	93.20	7
125	0.001	93.35	6.3
150	0.001	93.58	6.2

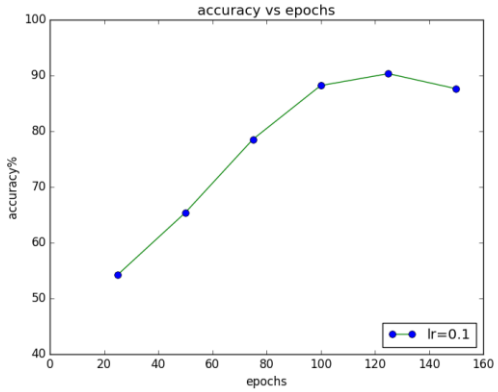

(a) Learning rate: 0.1

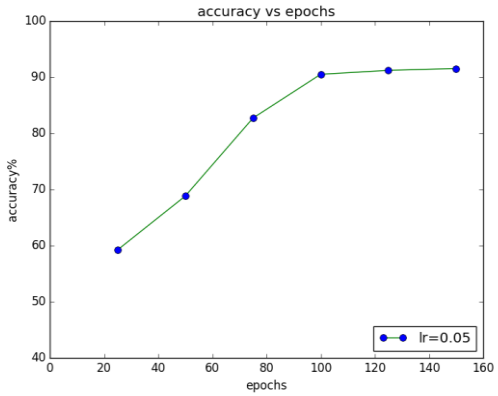

(b) Learning rate: 0.05

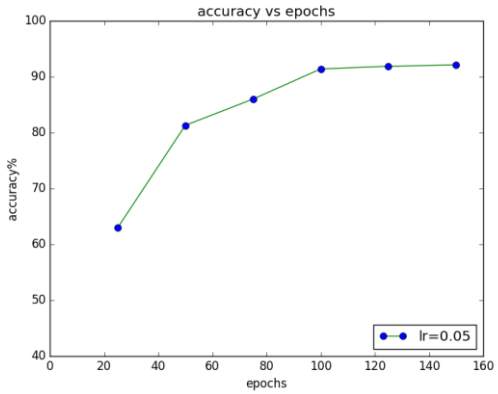

(c) Learning rate: 0.05

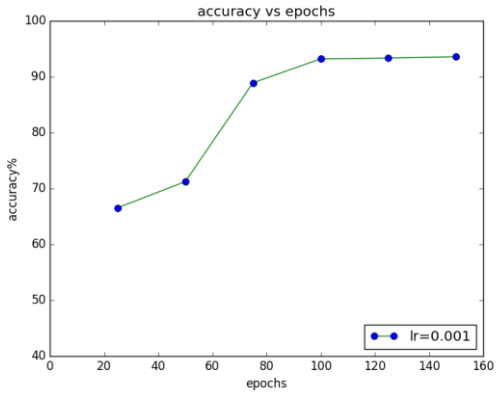

(d) Learning rate: 0.001

Fig . 5. Graphs depicting accuracy vs. epoch of various learning rates.

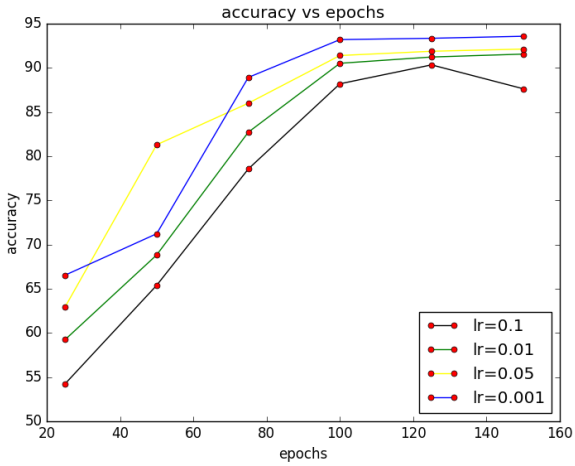

Fig. 6. Comparison Graph depicting the accuracy vs. epoch of experimented learning rates

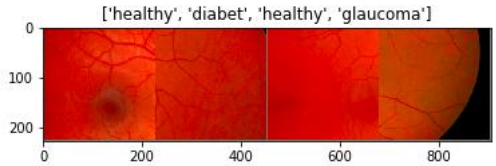

Fig.7 Training Set

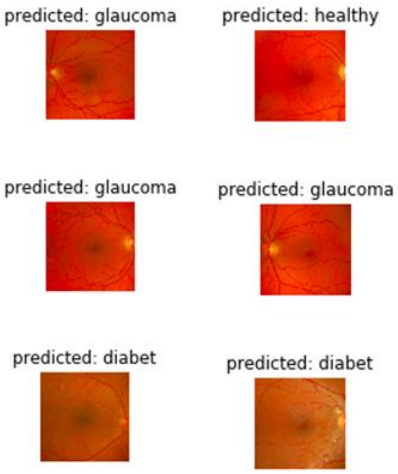

Fig.8 Classified retinal images

VI. CONCLUSION AND FUTURE SCOPE

It can be concluded that this method can be used for classifying and identifying various diseases in eyes and can prove to be helpful in medical purposes. The proposed method is accurate and can be used for mobile and early detection of retinal diseases. The number of classes used for this network is 3 (Healthy, Glaucoma, Diabetic) but number of retinal conditions can be included and a more accurate and variable network model can be created for better identification of retinal diseases using the proposed method.

REFERENCES

[1] Dong, Y., Zhang, Q., Qiao, Z., & Yang, J.-J. (2018). Classification of cataract fundus image based on deep learning. *2017 IEEE International Conference on Imaging Systems and Techniques (IST)*, 1–5. doi:10.1109/ist.2017.8261463

[2] Triwijoyo, B. K., Heryadi, Y., Lukas, Ahmad, A. S., Sabarguna, B. S., Budiharto, W., & Abdurachman, E. (2018). Retina disease classification based on colour fundus images using convolutional neural networks. *2017 International Conference on Innovative and Creative Information Technology (ICITech)*, 1–4. doi:10.1109/innocit.2017.8319141

[3] Khalaf, A. F., Yassine, I. A., & Fahmy, A. S. (2016). Convolutional neural networks for deep feature learning in retinal vessel segmentation. *2016 IEEE International Conference on Image Processing (ICIP)*, 385–388. doi:10.1109/icip.2016.7532384

[4] Raghu Raj P., Gurudatha Pai K., S. S. Shylaja. (2007). Algorithmic Approach for Prediction and Early Detection of Diseases Using Retinal Images. *Computer Graphics, Imaging and Visualisation (CGIV 2007)*, 501 - 505. DOI: 10.1109/CGIV.2007.16

[5] Ling Shao, Fan Zhu, Xuelong Li. (2015). Transfer Learning for Visual Categorization: A Survey. *IEEE Transactions on Neural Networks and Learning Systems*, 1019 - 1034. DOI: 10.1109/TNNLS.2014.2330900

[6] Zhang, Y., Wang, L., Wu, Z., Zeng, J., Chen, Y., Tian, R., … Zhang, G. (2018). Development of an Automated Screening System for Retinopathy of Prematurity Using a Deep Neural Network for Wide-angle Retinal Images. *IEEE Access*, 1–1. doi:10.1109/access.2018.2881042

[7] Manali Shaha, Meenakshi Pawar. (2018). Transfer Learning for Image Classification. *2018 Second International Conference on Electronics, Communication and Aerospace Technology (ICECA)*, 656 - 660. DOI: 10.1109/ICECA.2018.8474802

[8] Ananthakrishnan, A., Kanakiva, V., Ved, D., & Sharma, G. (2018). Automated Gait Generation for Simulated Bodies Using Deep Reinforcement Learning. *2018 Second International Conference on Inventive Communication and Computational Technologies (ICICCT)*, 90–95. doi:10.1109/icicct.2018.8473310

[9] Liang Deng, Hanli Bai, Dan Zhao, Fang Wang (2016). Evaluating Multi-core and Many-Core Architectures through Parallelizing a High-Order WENO Solver. *2016 IEEE Trustcom/BigDataSE/ISPA* , 2167 - 2174. DOI: 10.1109/TrustCom.2016.0333

[10] Liu, X., Chi, M., Zhang, Y., & Qin, Y. (2018). Classifying High Resolution Remote Sensing Images by Fine-Tuned VGG Deep Networks. *IGARSS 2018 - 2018 IEEE International Geoscience and Remote Sensing Symposium*, 7137–7140. doi:10.1109/igarss.2018.8518078

[11] Nistor, S. C., Marina, A.-C., Darabant, A. S., & Borza, D. (2017). Automatic gender recognition for “in the wild” facial images using convolutional neural networks. 2017 13th IEEE International Conference on Intelligent Computer Communication and Processing (ICCP). doi:10.1109/iccp.2017.8117018

[12] A.Budai, R. Bock, A. Maier, J. Hornegger, and G. Michelson, “Robust Vessel Segmentation in Fundus Images,” *International Journal of Biomedical Imaging*, *vol. 2013*, 2013.

[13] Sun, T., Wang, Y., Yang, J., & Hu, X. (2017). Convolution Neural Networks With Two Pathways for Image Style Recognition. IEEE Transactions on Image Processing, 26(9), 4102–4113. doi:10.1109/tip.2017.2710631

[14] Xu, M., Cheng, J., Li, A., Lee, J. A., Wong, D. W. K., Taruya, A., Wong, P. (2017). Fibroatheroma identification in Intravascular Optical Coherence Tomography images using deep features. 2017 39th Annual International Conference of the IEEE Engineering in Medicine and Biology Society (EMBC). doi:10.1109/embc.2017.8037120

Proceedings of the Fourth International Conference on Communication and Electronics Systems (ICCES 2019)
IEEE Conference Record # 45898; IEEE Xplore ISBN: 978-1-7281-1261-9

DESIGN AND IMPLEMENTATION OF VINCULUM BINARY CODED DECIMAL MULTIPLIERS USING VINCULUM BINARY CODED DECIMAL COMPRESSORS

G.Sreelakshmi,
Geethanjali College of Engineering and Technology,Hyderabad
gantisiriphd@gmail.com

Dr. Kaleem Fatima,
Muffakamjah College of Engineering and Technology,Hyderabad
kaleemfatima@mjcet.ac.in

Dr.B.K.Madhavi,
Sridevi Women's Engineering College,Hyderabad
bkmadhavi2009@gmail.com

Abstract:
Compressor logics are used to speed up the processing time. These structures are used for addition of Partial Products in multipliers. It reduces the complexity by reducing number of stages in addition. This paper speaks about addition of partial products using Vinculum BCD compressors under Vedic Mathematics. The proposed architecture reduces 7.04% of delay over VBCD and around 20% delay on conventional BCD multipliers when it was synthesized and simulated on vertex 6 platform using Xilinx 14.2i.

Keywords: Vinculum numbers, Compressors, multipliers

Introduction

In recent years nationally and internationally researches on Vedic mathematics is growing very much because of its efficiency, fast and ease of learning all algebraic and arithmetic operations. It was acknowledged by all over world that Vedic mathematics is faster than conventional methods.
Vedic mathematics is a part of Adharva Veda. It explains about the formulas pertaining to various Engineering branches, sculpture, Mathematics, and all other sciences which are an emerging field for research. These formulae are suitable for building digital circuits and can be implemented using binary and decimal number system. The work was focused on addition of partial products using compressor logic in Vedic Multiplier (Urdhav Triyakbhyam method)

The paper is organized as follows. Section I presents Vedic mathematics and its algorithm for an 8bit multiplication. Section II describes Compressor logic. Multiplier using Compressors is proposed in section III, Section IV shows simulation results and finally conclusion is provided in section V.

I. Vedic Mathematics:

1.1 8bit Vedic multiplier Line Diagram

Figure 1 shows step by step procedure of multiplication[15].

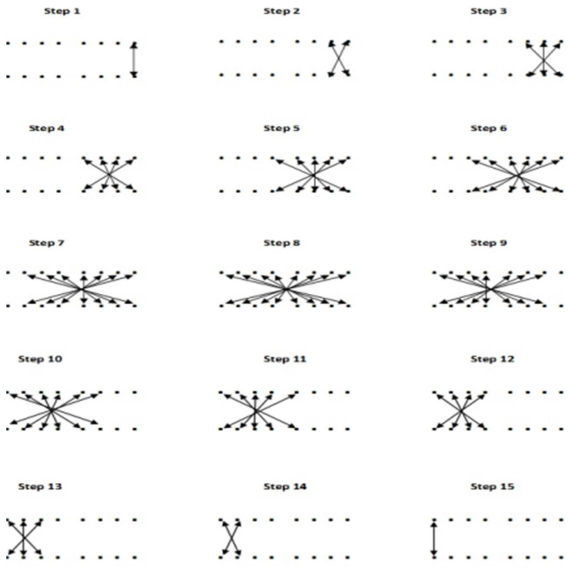

Fig 1: 8-bit Vedic Multiplier line diagram

Figure 1 describes step by step procedure of multiplication and final product is obtained by appending results from step 1(LSB) to step 15(MSB).

1.2. Conventional Multiplier Vs Vedic Multiplier

In Conventional Multipliers Final Product is obtained by shifting and addition. Considerable amount of time gets wasted in shifting bits. As number of bits increases, execution time increases which in turn increase hardware and power. Vedic Mathematics supports parallelism where large modules are separated into small modules. It has regularity and concurrency in structures. Complexity can be reduced by using small modules instead of large module.

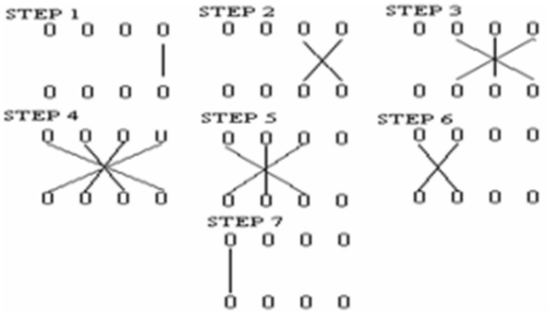

Fig2. 4x4 bit Vedic Multiplier Line diagram .

II. Adder Compressors

To achieve high speed and Low power digital or signal processing architectures we use different adder structures[8][18]. Compressors play a vital role in reducing delay and complexity. These are very useful in multipliers in adding partial products[19].Compressors with N-bit input provides Sum and Carry bits as outputs [8][5]. In literature there exist 3:2 compressors to 7:2 compressors. In our paper we used 3:2 compressors. 4:2 compressors have four inputs (a, b, c, d) with outputs sum and carry[8][15]. It receives an input C_{in} from the previous module and produces output C_{out} to the next compressor module as shown in figure 7.
Output C_{out} should be independent of input C_{in} to accelerate the carry save summation of the partial products.

VBCD Compressors

A decimal compressor consists of three operands a,b,c and Cin with Sum and Carry as outputs as shown in figure 4[18]. Algorithm is explained as below.

Algorithm for VBCD Compressor

$step\ 1$: $Read\ input\ operands\ as\ x, y, z\ of\ 4\ bit\ each\ in\ VBCD\ form$
$step2$: $Set\ output\ digits\ as\ Sum\ and\ Carry\ bits$
$step3$: $Add\ bit\ wise\ operands\ using\ Full\ Adders\ and\ check\ for\ Sum\ and\ Carry\ bits$
$case\ 1$: $If\ sum < 5\ or\ if\ sum < -4\ and\ carry = 1\ discard\ carry\ bit\ and\ take\ Final\ sum = sum$
$Case2$: $If\ sum > 5\ and\ carry = 0\ , Add + 6\ to\ the\ sum\ and\ set\ carry = 1$
$Case$: $3\ If\ sum > 5\ and\ carry = 1\ add - 6\ to\ the\ sum\ and\ set\ carry = -1$

Fig 3. Decimal 3:2 VBCD compressor

In the above example each bit of the operand is passed through full adders which results in intermediate sum and carry bits. It is added with carry bits to get final sum. If final sum is greater than 5 and carry bit '0' add 6 to it and take carry bit 1.The architecture of the compressor has been implemented through binary full adders, 2x1 multiplexer and adder/subtractor circuit. The architecture was shown in figure 5.

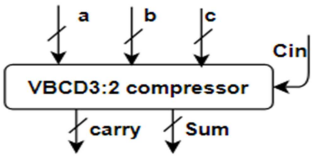

Fig 4. 3:2 VBCD Compressor

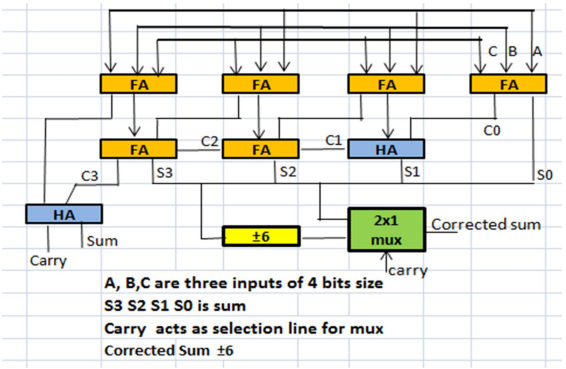

Fig 5. Basic Architecture of 3:2 Compressor

4:2 compressor consists of four operands and input carry as its inputs with two outputs Sum and carry along with intermediate carry C_{out} to the next stage as shown in the figure7 [4]. It is constructed using two 3:2 compressors where first three operands are given to 3:2 compressor1 and the output sum digit, fourth operand along with carry input is given to 2nd compressor 3:2. The output carry bit of first compressor is passed to next stage. This makes compressor faster than other adders. The weightage of the carry digit increases as the inputs increases. Same weight age of digits can be taken together for any digit compressor's inputs.

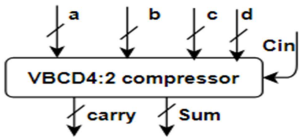

Fig 6. 4:2 VBCD Compressor

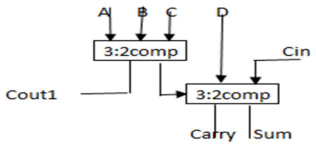

Fig 7. 4:2 Compressor using 3:2 Compressors

III. Proposed VBCD Multipliers:

3.1 Proposed Vinculum Number Representation

Vinculum is a term used in ancient (Vedas) mathematics which means bonding. It is used to represent decimal number system with less complex. Instead of using decimal digits from 0 to 9 it uses 0 to 5 to represent decimal 0 to 5 and -4 to -1 to represent digits 6 to 9 of decimal number system. Vinculum number set uses digits from $\{0, 1, 2, 3, 4, 5, \bar{4}, \bar{3}, \bar{2}, \bar{1}\}$ to represent 0 to 9[15].

3.2 Generation of Partial Products:

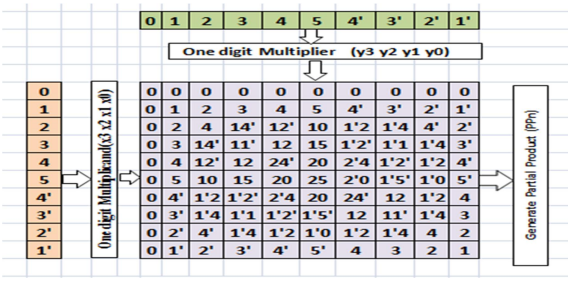

Fig 8. One digit VBCD Multiplier

LUT based one digit VBCD multiplier is implemented to reduce processing time, as shown in figure 8 where all partial products are saved in memory. The maximum value of the partial product generated by single digit is +25(5x5) where as in conventional BCD the maximum value generated is 81 (9x9).Very less combinations are available in proposed number system method which is simple and faster. This can be used as sub module while developing top module. [19]

3.3 Two Digit VBCD Multiplier:

Two digit multiplier uses vertical cross wire method (Urdhav Triyakbhyam) where it is divided in to two one bit multipliers to generate partial products as shown in example below. These partial products are added using VBCD compressors to generate partial product. Number of compressors required is equal to the number of bit multiplier.

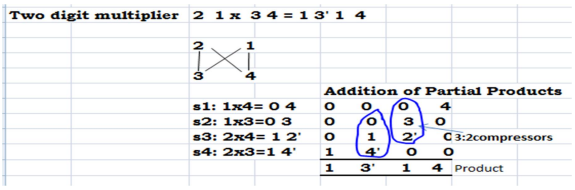

Fig 9: Example for 2 digit multiplication

Figure 9 shows the usage of Vedic multiplier, generation of partial products in terms of s1, s2, s3 and s4 and addition of partial products using 3:2 VBCD compressors. The output of these compressors provides final product. From the above example any two digit multiplier requires only two 3:2 compressors [18][19].

3.4 Four Digit Multiplication.

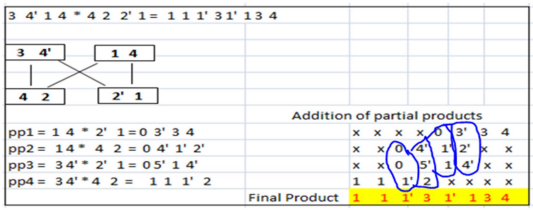

Fig 10: example for 4 digit multiplication

It is very simple to understand from figure 10 that four digits are divided into 2 halves, by using Urdhav Triyakbhyam method for generating partial products. Always for any digit number this method generates only four partial products (pp1, pp2, pp3 and pp4) and these partial products are added using

compressors as shown in figure10. In figure circle indicates compressor and for four digit multiplication we require four 3:2 compressors. Using this same logic multiplier architecture is developed which is as shown below.

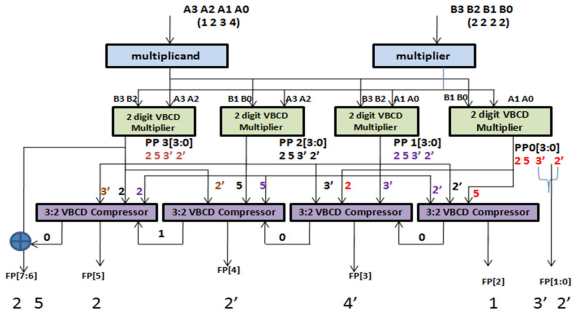

Fig 11. 4x4 digit Vedic VBCD multiplier using compressors

Using vertical and cross wire method these four digit multiplicand and multipliers are divided in to two, two digit numbers on which multiplication is performed. Two digit multipliers generates four partial products namely pp0, pp1, pp2 and pp3. Each partial product size is of 4 digit and these are given to VBCD compressors for performing addition. The output of these compressors gives final result as shown in figure 11.

3.4 Eight Digit Multiplier:

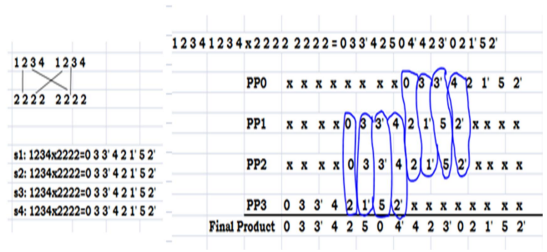

Fig 12: example for eight digit multiplication

The above example shows eight digit multiplication in which it is divided into two four digit multipliers. This Vedic method uses divide and conquer method where large module is divided into small modules for multiplication. This requires eight 3:2 compressors to get final product and all partial products can be added in parallel which is major advantage over conventional method. The maximum depth of the multiplier is only four always. For any multiplier it has only four partial products as shown in above examples. Therefore the basic 3:2 VBCD compressor is sufficient for adding partial products in Vedic method. For conventional multipliers as the number of bits increases partial products increases and depth of the column increases. So various sizes of compressors are required for conventional multiplication method.

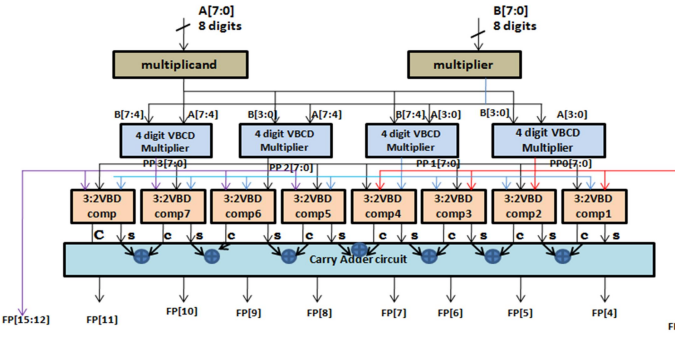

Fig 13. 8x8 digit Vedic VBCD multiplier using compressors

Figure 13 explains the hardware structure for eight digit multiplier using compressor logic. It uses four 4 digit multipliers, to generate partial products, eight 3:2 compressors and simple carry adder logic where i^{th} stage sum depends on i-1 carry. It has a delay of only one stage of carry always. The main advantage is there are no carry propagations in this method.

IV. Results:

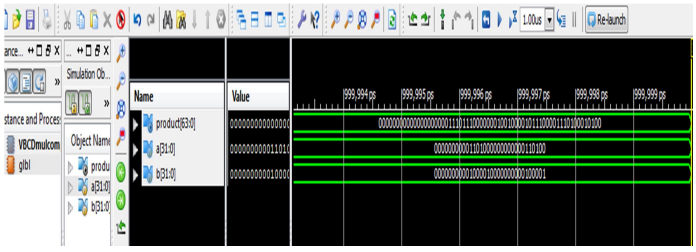

Fig 14. Simulation results for 16 digit VBCD multiplier

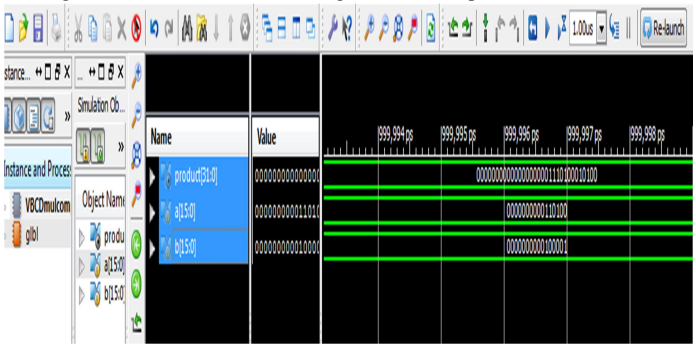

Fig 15. Simulation results for eight digit VBCD multiplier

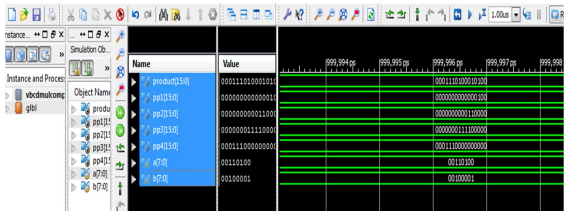

Fig 16. Simulation results for four digit VBCD multiplier

Figure 14,15 and 16 shows the simulation results of 16 digit, 8 digit and 4 digit multipliers.

Sl. No.	Type of Comp	Slice LUT's	IOB's	Delay (ns)
1	3:2	22	18	5.035
2	4:2	33	30	6.091
3	5:2	40	34	6.801
4.	8:2	58	69	7.210

Table 1. Synthesis report of VBCD compressors

Table 1 shows delay provided by each compressor and designed, simulated and synthesised from 3:2 compressors to 8:2 compressors.

	VBCD Multiplier Architectures			
	without compressor		with compressor	
	Delay(ns)	LUTs	Delay(ns)	LUTs
1 digit multiplier	1.654	27	1.654	27
2 digit multiplier	11.417	122	7.822	152
4 digit multiplier	16.69	816	10.92	869
8 digit multiplier	21.91	3405	14.87	3458

Table 2: Synthesis report of VBCD multipliers with and without compressor logic

Table 2 gives information related to various digit multipliers without compressor logic and with compressor logic in partial product generation. From table it is observed that around 7% of delay reduced with compressor logic for 8 digit (32 bit) multipliers.

Reference	Method Adopted	Delay (ns)
[4]	Conventional multiplier	58
[13]	Conventional multiplier	77
[14]	Vedic multiplier	12.42
[19]	VBCD multiplier	11.41
Proposed method	VBCD multiplier with compressor	7.822

Table 3:Comparision of Delay for 8 bit multiplier using various methods

The above table describes that multipliers with compressor logic are more efficient than normal structures for adding partial products.

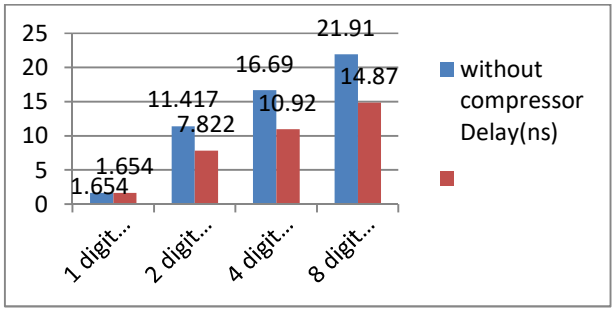

Fig. 17. Comparison of Delay with and without compressors in multipliers

From the above graph it was clear that the compressor based multipliers had less delay when compared to multiplier structures which without using compressor structures. One digit multiplier give same delay because we have chosen ROM based design and from two digit onwards delay reduces. We have checked almost for all cases and hence this architecture is efficient.

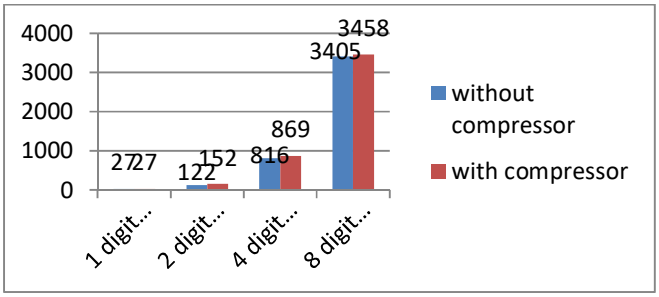

Fig 18. Comparison of LUTs between multipliers with and without compressor logic

This graph shows number of LUT's utilized for a given multiplier architecture and from this it was clear that less number of LUT's were used when compare to multipliers without compressor structures.

V. Conclusions and Future scope.

Hence we conclude that an efficient design of multipliers using VBCD compressors was designed and implemented using Xilinx 14.2i and is compared with other Vedic multipliers. It was observed that multiplier architectures using compressors are better than without compressor logic in terms of speed. In our previous work we have shown that VBCD multipliers are better than conventional multipliers. Hence in this paper we highlighted results only for VBCD architectures with and without compressor logics.

Researchers can work on decimal floating point multipliers using this concept for mantissa

multiplication and in Fused Multiply and Add Architectures.

References:

[1] M. F. Cowlishaw, "Decimal Floating-Point: Algorism for Computers", in Proc. 16th IEEE Symp. Computer Arithmetic, pp. 104-111, Jul. 2003.

[2] L. Dadda, "Multi operand Parallel Decimal Adder: A Mixed Binary and BCD Approach", IEEE Transactions on Computers, vol. 56, no. 10, pp. 1320-1328, Oct. 2007.

[3] M. A. Erle and M. J. Schulte, "Decimal Multiplication Via Carry-Save Addition", in Proc. IEEE Int. Conf. on Application-Specific Systems, Architectures, and Processors, pp. 348-358, Jun. 2003.

[4] M. A. Erle, E. M. Schwarz and M. J. Schulte, "Decimal Multiplication With Efficient Partial Product Generation", in Proc. 17th IEEE Symposium on Computer Arithmetic, pp. 21-28, Jun. 2005.

[5] G.Jaberipur, and A.Kaivani, "Improving the Speed of Parallel Decimal Multiplication", IEEE Transactions on Computers, vol. 58, no. 11, pp. 1539-1552, Nov. 2009.

[6] Vazquez, E. Antelo and P. Montuschi, "Improved Design of High-Performance Parallel Decimal Multipliers", IEEE Transactions on Computers, vol. 59, no. 5, pp. 679-693, May 2010.

[7] X.Cu, W. Lui, W.Dong and F.Lombardi, "A Parallel Decimal Multiplier using Hybrid Binary Coded Decimal(BCD) codes", in proc.23rd IEEE symp, computer Arithmetic,pp150-p155 Jul 2016.

[8] D. Castellanos and J. E. Stine. "Compressor Trees for Decimal Partial Product reduction," in Proc. 18th ACM Great Lakes Symp. VLSI, pp. 107-110, Jan. 2008.

[9] Vazquez and E. Antelo, "Multi-Operand Decimal Addition by Efficient Reuse of a Binary Carry-Save Adder Tree", in Proc. 44th ASILOMAR Conference on Signals, Systems and Computers, pp. 1685- 1689, Nov. 2010.

[10] R. D. Kenney and M. J. Schulte, "High-Speed Multi operand Decimal Adders", IEEE Transactions on Computers, vol. 54, no. 8, pp. 953-963, Aug. 2005.

[11] Shirazi, D. Y. Y. Yun, and C. N. Zhang, "RBCD: Redundant Binary Coded Decimal Adder", IEE Proceedings-Computers and Digital Techniques, vol. 136, pp. 156-160, Mar. 1989.

[12] Svoboda, "Decimal Adder with Signed Digit Arithmetic", IEEE Transactions on Computers, vol. C, pp. 212-215, Mar. 1969.

[13] Arvind Kumar Mehta,Mukesh Gupta,Vipin Jain, Sudhir Kumar,"High performance Vedic BCD multiplier and modified binary to BCD converter," Annual IEEE India Conference (INDICON), 2013.

[14] G.Sreelakshmi, Dr.Kaleem Fatima, Dr.B.K.Madhavi "Implementation of high speed Vedic BCD Multiplier using Vinculum method" Region 10 conference TENCON Nov 2016, Singapore .https://doi.org/10.1109/TENCON.2016.7847978

[15] Sri Bharati Krishna Tirthaji, "Vedic Mathematics", published by Motilal Banarsidass, 1965. ISBN 81208-0163-6.

[16] G.Sreelakshmi, Dr.Kaleem Fatima, Dr.B.K.Madhavi "A Novel Approach to the learning of Vinculum Numbers in two's compliment method for BCD Arithmetic Operations" IEEE Conference ICCMC 2018 ISBN:978-1-5386-3452-3, IEEE Xplore, IEEE conference record #42656

[17] G.Sreelakshmi, Mohamed Salman Ahmed, Dr.Kaleem Fatima, Dr.B.K.Madhavi "Efficient Signed Digit Decimal Adder" IEEE Conference ICDCS 2018 during 16th and 17th March 2018 , Coimbatore. ISBN: 978-1-5386-3476-9/18@IEEE 2018

[18] G.Sreelakshmi, Dr.Kaleem Fatima, Dr.B.K.Madhavi (2018)" Design of BCD compressors using vinculum code for efficient multiplication. IJAER , ISSN 0973- 4562, vol 13, 2018 pp 11901-904, RIP Publications.

[19] G.Sreelakshmi, Dr.Kaleem Fatima, Dr.B.K.Madhavi , Efficient realization of vinculum vedic BCD multipliers for High speed applications" Journal of circuits and systems ISSN 2153-1293, 2153-1285 2018, Vol9, July, Scientific Research Publication

Proceedings of the Fourth International Conference on Communication and Electronics Systems (ICCES 2019)
IEEE Conference Record # 45898; IEEE Xplore ISBN: 978-1-7281-1261-9

BVLCs and BDIPs in Covariance Descriptor with a Statistical Measure of Divergence for Image Retrieval

M. Bennet Rajesh
Research Scholar
Division of Computer and Information Science
Annamalai University, Annamalai Nagar, India
benraj@gmail.com

*S.Sathiamoorthy**
Tamil Virtual Academy
Chennai,
India
ks_sathia@yahoo.com

Abstract—**This paper proposes BVLC (block variation off local correlationcoefficients) and BDIP (block difference of inverse probabilities) into covariance descriptors for image recognition and retrieval. The images in RGB is partitioned to R,G and B then BVLCs and BDIPs are computed for each channel then BVLCs and BDIPs in covariance among R,G and B is computed. The proposed BVLCs and BDIPs in covariance descriptor is extremely precious to reflect the degree of linear association among identified textures, edges and valleys. Degree of similarity among query and target images is analyzed using statistical measures of divergence namely Chernoff and Bhattacharya and results shown that Chernoff is noticeably outperform Bhattacharya measure. Comprehensive experiments on Corel- 1k, Corel- 5k and Corel-10k databases illustrates that proposed BVLCs and BDIPs in covariance descriptor is satisfactory and can attains significantly enhanced retrieval accuracies than traditional techniques.**

Keywords— BDIP, BVLC, Covariance, Chernoff distance, Bhattacharya distance.

I. INTRODUCTION

Nowdays, with the progress of image acquisition, storage and display devices, massive collection of images is being produced and images are of immense importance for a variety of realistic applications like analysis and prediction of disease and weather, classification of land, crops, galaxies and stellar spectra, monitoring the deforestation, land use change, military surveillance, finger print and iris recognition and substitute for human vision in industries because of its clear and precise depiction of information and thus researchers give more attention to image analysis, classification and matching.

The effective retrieval of images from massive image database using the visual information is coined as content based image retrieval (CBIR). The CBIR is primarily depends on excellent description of image and it has been the topic of demanding study. Hence, numerous CBIR approaches were presented by the researchers over the decade like gray level co-occurrence matrix (GLCM) reported by Haralick [1] which is co-occurrence of pixels pairs, Co-occurrence of edgels is reported in [2] and it uses prewitt operator for edge detection [2], texture and color information is jointly computed by color co-occurrence (CCM) in [3, 4], Motif co-occurrence matrix (MCM) which is quite different from CCM by including 3rd order moments is reported in [5], 3D- histogram of gradient location and orientation named as SIFT and is suggested in [6] for matching of images, robustness of SIFT is improved in [7] by incorporating log-polar location grid and coined as Gradient location and orientation histogram (GLOH), speeded-up robust (SURF) is proposed by Herbert et al, and it uses Hessian matrix and Haar wavelet responses for its computation [8], local binary pattern (LBP) based on local intensity of pixel is reported in [9], Gabor filter for texture classification and matching is suggested in [10], histogram of oriented gradients (HOG) suggested in [11] counts the gradient orientation's occurrences in sub part of an image, edge histogram direction (EHD) for capturing global and local details of edgels based on its orientation is reported in [12, 13], center-symmetric local binary pattern (CS-LBP) based on intensity of centrosymmetric pixels is introduced in [14], local intensity order pattern (LIOP) is described by Wang et al, to compute order pattern between pixels located at a fixed radius [15], local contrast and ordering (LCO) descriptor for image matching is reported in [16] and exhaustive study on CBIR are revealed in [17,18].

On other side, owing to well performance of covariance descriptor, it is extensively used in various application including face recognition using covariance matrix is suggested in [19]; Gabor-LBP based region covariance descriptor (GLRCD) computed using RGB components, spatial coordinates, LBP decimal values and Gabor features is reported in [20]; identification of objects using covariance matrix is reported in [21]; compact form of LBP is derived using local binary covariance matrix (LBCM) is proposed in [22]; texture classification using covariance matrix is described in [23-26]; human detection using covariance matrix is introduced in [27,28]; mean riemannian covariance grid (MRCG) in [29] combines gradients magnitude and orientation of each RGB channel and fire and flame identification using covariance descriptor is suggested in [30] owing to its resilient behavior to scaling and rotation and considerably resilient to uniform luminance variation [31].

Therefore, in this paper, novel feature descriptor using mean and covariance of BVLC and BDIP in RGB color space is proposed.

II. RELATED WORK

Chun et al., [32] reported BVLC and BDIP of image for retrieval and are utilizing local probabilities and variations of local correlation coefficients correspondingly to assess local brightness variation and texture smoothness respectively. The authors computed low order moments for BVLC and BDIP and are combined with color autocorrelogram for retrieval of images. Later, low order moments for BVLC and BDIP are computed from multiresolution domain and is reported in [33]. In [33], authors converted images from RGB. to HSV space then each component of HSV space is decomposed using Haar wavelet transform and the level of decomposition is 2. From the decomposed V component, first order moments for BVLC and BDIP then from H and S images, color autocorrelogram is estimated for all sub-bands and in all level of decomposition.

Later on, both low and high order statistical moments for BVLC and BDIP is introduced in [34] for retrieval of images. Subsequently, since histogram representation is resilient to noise, scaling, translation and small rotation, histogram for BVLC and BDIP is computed [35] from quantized BVLC and BDIP values. The author fixed the level of quantization to 57. Thus, histogram for BVLC and BDIP has 57 bins [35] respectively. To encompasses spatial details of textures, edges and valleys, histogram of local spatial correlations among identical BVLC and identical BDIP values are computed and are combined with color autocorrelogram for retrieval [36].

Afterwards, in [37], retrieval of histology image is reported in which wavelet Packet and Daubechies-4 transforms are utilized together with orthogonal polynomial model coefficient for histology image decomposition then authors computed BVLC and BDIP from high frequency sub-bands, and dominant color descriptor and color autocorrelogram is computed from low frequency component. Recently, BVLC and BDIP is combined with color histogram for retrieval [38].

Inspired by the efficiency of BVLC and BDIP in exploiting texture, edges and valleys respectively, we introduced novel feature representation for image retrieval in which images in RGB space are separated into R,G and, B channels and BVLC and BDIP is computed for each channel image separately then mean and covariance matrix for BVLCs and BDIPs of R, Gand B channel images are computed individually. The covariance matrices of BVLC characterizes image using correlation between identified texture within the individual channel and between the channels respectively. Similarly, covariance matrices of BDIP characterizes image using correlation between edges and valleys within the individual channel and between the channels respectively. The diagonal values of covariance matrix specify correlation among BVLCs/ BDIPs of each channel image whereas non-diagonal values specify correlation between BVLCs/ BDIPs of each pair of channel image. Thus, proposed descriptor estimates directional relationship among identified texture, edges and valleys in R, Gand B channel images more powerfully. The proposed embedding of BVLC and BDIP in covariance matrix with statistical measure of divergence is assessed experimentally on different datasets and results recommended that proposed approach enhances compactness and descriptiveness of BVLC and BDIP descriptors at locally as well globally, produces better accuracy and resilient to scaling and rotation. The remainder of this work is explained as follows. Section 3 elucidates proposed technique and recalls, BVLC, BDIP and covariance computation. Section 4 explains experiments followed by conclusions in Section 6.

III. PROPOSED IMAGE RETRIEVAL TECHNIQUE

In this section, techniques that are used in proposed image retrieval i.e., descriptor computation, measure of divergence and measure of accuracy are discussed.

The basic idea behind the proposed BDIPs inclusion in covariance is capturing the spatial dependencies of textures and BVLCs inclusion in covariance is capturing the spatial dependencies of edges and valleys. The proposed algorithm consists of three steps. First, input image in RGB is separated into R, Gand B images. Later, BDIP and BVLC is computed separately for R,G and B respectively using eq. (1) and (3). Later on, covariance among BDIPs of R, Gand B images followed by covariance among BVLCs of R, Gand B images are computed using the eq. (4) and (5). Then mean for BVLCs and BDIPs of R,G and B images are computed. Therefore, proposed descriptor has two parts: first one has BDIPs in covariance and mean of BDIPs in R,G and B images respectively, and the second part has BVLCs in covariance and mean of BVLCs in R,G and B images respectively.

Since covariance is not lie on L1 and L2 norm [39], statistical measure of divergence namely Chernoff and Bhattacharya are employed. We compared the performance of Chernoff with Bhattacharya for proposed retrieval. In our approach, distance among proposed first part of descriptors (i.e based BDIPs) of input and target image is computed then distance among proposed second part (i.e. based on BVLCs) of descriptors of input image and the target image is computed. Later, average of distance results of first and second part of proposed descriptors is computed and is considered to measure the degree of similarity in the proposed CBIR. The results on standard Corel database [40] shown that proposed approach achieve noticeably better results than conventional techniques. It also noticed that Chernoff distance outperforms Bhattacharya for our approach. The proposed approach is illustrated in Fig.1. Computation of BVLC, BDIP and covariance is expressed as follows.

A. BDIP

BDIP [32], a sketch feature consisting of edges depicted by local intensity maxima and valleys depicted by local intensity minima and is given as [32]

$$BDIP^{d}(l) = \frac{\frac{1}{B_l^d}\Sigma_{(x,y)\in B_l^d}(\max_{(x,y)\in B_l^d} f(x,y) - f(x,y))}{\max_{(x,y)\in B_l^d} f(x,y)} \quad (1)$$

Where f(x,y) designates an intensity of pixel at position (x, y) in image block B_l^k of dimension (k+l)x(k+l), k denotes the utmost distance among pixels pairs and l denotes place index. Thus, $B_l^k = (k+1)^2$. In equation (1), numerator and denominator defines maximum intensity variation and representative value in a block respectively.

B. BVLC

BVLC [33], measures texture smoothness using difference among local correlation coefficients corresponding to $0^\circ, 90^\circ, 45^\circ, -45^\circ$ orientations and is given by [33]

$$\rho(k,l) = \frac{\frac{1}{M^2}\sum_{(x,y)\in B} f(x,y) f(x+k, y+l) - \mu_{0,0}\mu_{k,l}}{\sigma_{0,0}\sigma_{k,l}} \quad (2)$$

Where B denotes image block of dimension M x M and $\mu_{0,0}\mu_{k,l}$ and $\sigma_{0,0}\sigma_{k,l}$ are local mean and standard deviation. The (k,l) denotes a pair of horizontal and vertical shift connected with orientations $0^\circ, 90^\circ, 45^\circ, -45^\circ$. Subsequent to shifting of M x M mask in each of 4 directions, *p(0,1), p(1,0), p(1,1), p(1,-1)* is calculated. After that BVLC is calculated as follows

$$BVLC^d(l) = \max_{\Delta(k)\in O_4}[\rho^k(l,\Delta(k))] - \min_{\Delta(k)\in O_4}[\rho^k(l,\Delta(k))] \quad (3)$$

Where $\Delta(k) = (\Delta_x(k), \Delta_y(k))$ denotes shift in one four directions and $O_4 = \{(-k,0), (0,-k), (0,k), (k,0)\}$

C. Covariance matrix

Let *I* be a 3D color image in RGB color space. Let $\{K_f\}_{c\,f=1,2,...,n}$ and $\{L_f\}_{c\,f=1,2,...,n}$ be a set of BVLC/ BDIP descriptors of each individual color channel images, $\bar{K}$ and $\bar{L}$ are corresponding mean vectors, *c* is either R orG or B channel image then covariance [41] between BVLC/ BDIP descriptors of two individual color channel images is given as

$$\frac{1}{n}\left(\sum_{i=1}^{n}(K_f - \bar{K})(L_f - \bar{L})\right) \quad (4)$$

The mean of feature vector of R,G and B channel images is defined as follows

$$\mu = \begin{bmatrix} \mu_r \\ \mu_g \\ \mu_b \end{bmatrix} \quad (5)$$

The covariance measures [41] spatial relation among features of two images, is low dimensional one, removes noisy textures, edges and valleys by doing averaging in its computation. The covariance matrix for BVLC and BDIP descriptors of R,G and B channel images is expressed as follows

$$\Sigma = \begin{bmatrix} \sigma_{rr} & \sigma_{rg} & \sigma_{rb} \\ \sigma_{gr} & \sigma_{gg} & \sigma_{gb} \\ \sigma_{br} & \sigma_{bg} & \sigma_{bb} \end{bmatrix} \quad (6)$$

Where Σ and σ represents spatial relation among descriptors and variance among descriptors respectively.

D. Measure of Divergence

The retrieval performance is not only depends on discriminative power of feature descriptor, it is also depends on measure of divergence. Since proposed BVLCs and BDIPs in covariance not lie in the L1 and L2 norm, we selected Chernoff and Bhattacharya measures [42]. We analyzed the competence of both measure for the presented covariance of BVLCs and BDIPs. The Chernoff distance measure [42] is given by

$$D_{p,q}(s) = \frac{s(1-s)}{2}(\mu_2 - \mu_1)^T[s\Sigma_t + (1-s)\Sigma_2]^{-1}(\mu_2 - \mu_1) + \frac{1}{2}\ln\frac{|s\Sigma_1 + (1-s)\Sigma_2|}{|\Sigma_1|^{1-s}|\Sigma_2|} \quad (7)$$

Where $D_{p,q}(s)$ is the Chernoff distance, μ_q, μ_t, Σ_q and Σ_q denotes mean and covariance of query and the target descriptors, and the optimum *s* provides maximum value for Chernoff distance and is attained by using various *s* and it falls in range $0 \le s \le 1$.

The Bhattacharya distance measure [42] is expressed as

$$D(q,t) = \frac{1}{8}[\mu_q + \mu_t]^T\frac{[\Sigma_q + \Sigma_t]^{-1}}{2}[\mu_q - \mu_t] + \frac{1}{2}\ln\left(\frac{\frac{|\Sigma_q + \Sigma_t|}{2}}{\sqrt{|\Sigma_q||\Sigma_t|}}\right) \quad (8)$$

Where μ_q, μ_t, Σ_q and Σ_q denotes mean and covariance of query and target descriptors respectively.

E. Measure of Accuracy

Each database image is used as query in the experiments. The proposed approach is assessed by precision P(N) and recall R(N) for retrieving top matched N images and are expressed as in [33, 34]

$$P(N) = \frac{I_N}{N} \quad (9)$$

$$R(N) = \frac{I_N}{M} \quad (10)$$

Where I_N, *M* and *N* denotes number of related images, total number of retrieved images and total number of images in database.

IV. EXPERIMENTS

In this section, we assessed the performance of proposed BVLCs and BDIPs in covariance with Chernoff measure then proposed BVLCs and BDIPs in covariance with Bhattacharya measure to confirm the superiority of each using the Corel- 1k, Corel-5k and. Corel-10k databases[40]. Finally, we assessed computational and storage cost of BVLCs and BDIPs in covariance and mean.

Corel datasets are widely used to assess the performance of image descriptors. The Corel 1k [40] database

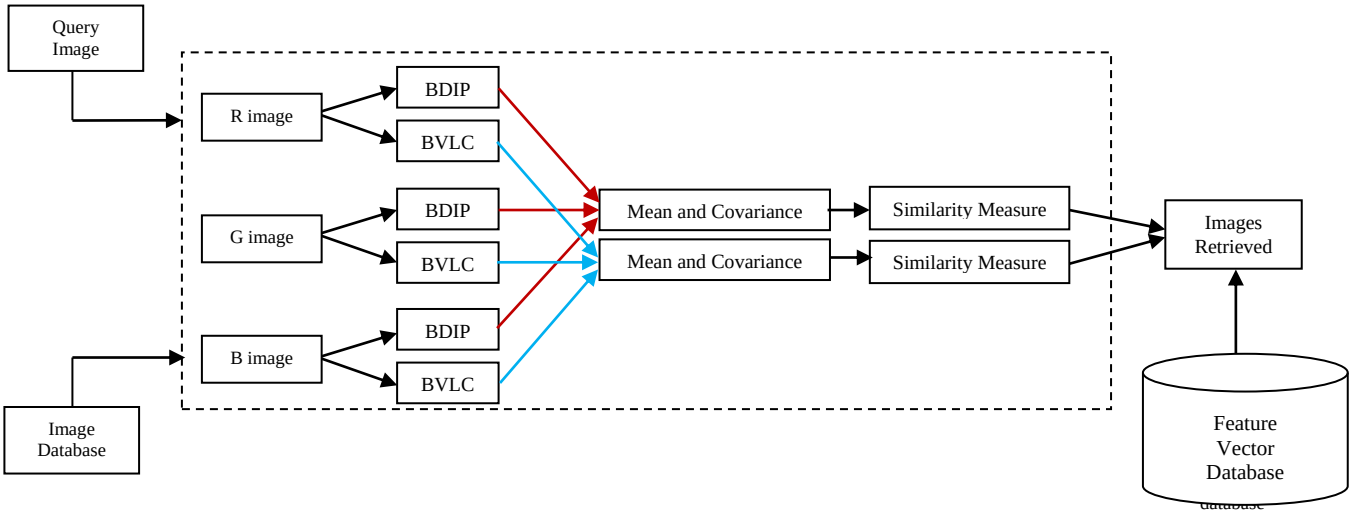

Fig.1. Proposed image matching technique using BVLCs and BDIPs in covariance and mean

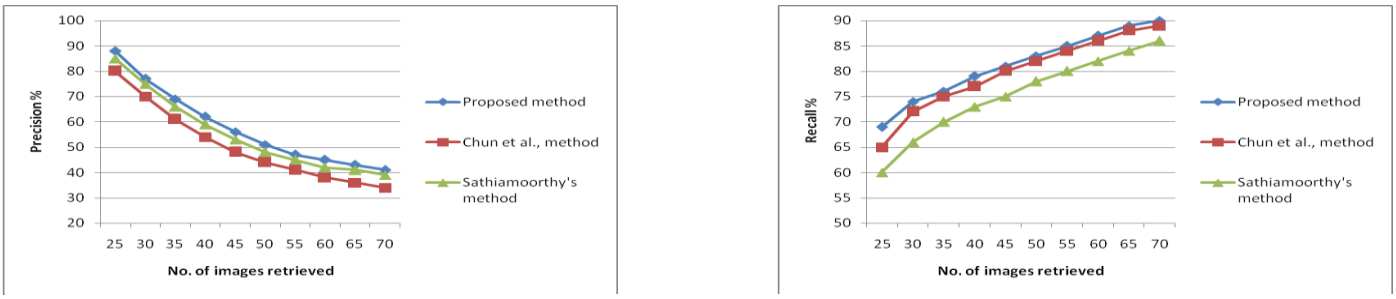

(a) (b)

Fig.3 Precision and recall with number of images retrieved for database 1.

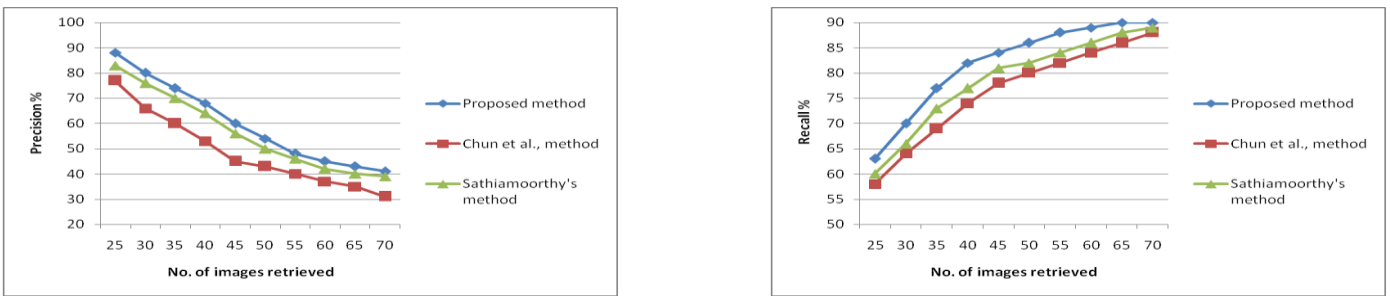

(a) (b)

Fig.4 Precision and recall with number of images retrieved for database 2

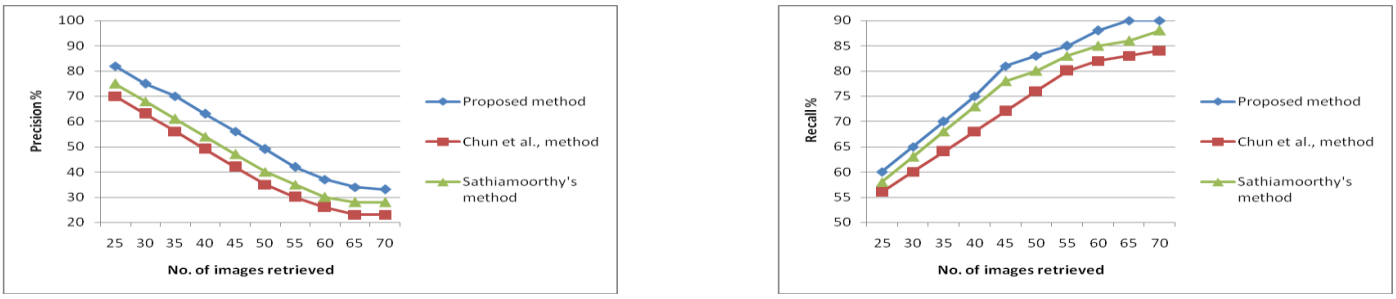

(a) (b)

Fig.5 Precision and recall with number of images retrieved for database 3

contains 10 classes of images whereas Corel 5k [40] and Corel 10k [40] databases consists of 50 and 100 classes of images like elephants, buses, horse, lion, ship, Africans, flowers, train, waves, forest, mountain, etc. and some samples are shown in Fig.2. The images in each database are categorized into five groups in which images in one group are utilized for training and others groups for testing process. The proposed system is developed such that all five groups of images are be included in both training and testing process. We compared proposed descriptors with the descriptors of [34] and [36].

A. Database 1

In the first experiment, Corel 1k database images are used. Each image is roughly of size 120x80 or 80x120. P(N) and P(R) for BVLCs and BDIPs in covariance and conventional techniques are computed and is illustrated through graphs. In Fig. 3, plots of P(N) and P(R) are shown. Fig. 3(a) illustrates variation in P(N) with number of images retrieved and Fig. 3(b) illustrates plots among R(N) and number of images retrieved. Both the plots evidently illustrates that presented approach is better to others by means of P(N) and P(R). Average retrieval rate (ARR) of presented approach with Bhattacharya and Chernoff distances have been augmented from first order moments of BVLC and BDIP [34] and histogram representation of BVLC and BDIP [36] by 13.23%, 3.89% and 13.96% and 5.03% respectively and are presented in Table.1 and Table. 2 respectively.

B. Database 2

In the second experiment, Corel 5k database have been taken and database have 100 images for each group and approximately the dimension are 120x80 or 80x120 and images are in jpg. The results of presented approach in the form of P(N) and P(R) are depicted in graphs. Graphs for P(N) and P(R) with number of images retrieved is exemplified in Fig.4. The presented approach is more agreeable than other approaches and is obviously visible in the plots. The ARR of presented approach with Bhattacharya and Chernoff distances increases from moments of BVLC and BDIP [34] and BVLC and BDIP representation of [36] by 12.11%, 3.79% and 12.88%, 4.06% respectively and are depicted in Table. 1 and 2 which entail that additional related images are retrieved by presented one when compare to conventional approaches.

C. Database 3

In the third experiment, Corel 10k database has been taken and has roughly 100 images for each group and sizes of images are 120x80 or 80x120. Outcome for Corel 10k database is presented in Fig.5. The yields from experiments obviously illustrates that presented approach is superior then others. The ARR of presented approach with Bhattacharya and Chernoff distances improved from [34] and [36] are 12.01%, 3.83% and 13.03%, 4.17% respectively and are depicted in Table.1 and Table 2. Thus, presented approach is promising then other techniques [34, 36] in terms of accuracy. Feature descriptor length of each technique is depicted in. Table 3. The feature descriptor of presented approach is comparatively less than [34] and [36]. Even BVLC and BDIP reported in [37] performs well than [36], its computational cost is very high. Thus, the approach presented in [37] is not considered in comparative study. From the results depicted in Table.1 and Table.2, it is obvious that combination of Chernoff with BDIP in covariance and BVLC in covariance approach outperforms when compare to fusion of Bhattacharya with proposed BDIPs in covariance and BVLCs in covariance approach. Fig.6 depicts retrieval outcome of query image and top 4 retrieved images from Corel database for proposed approach with Chernoff and Bhattacharya distance measure.

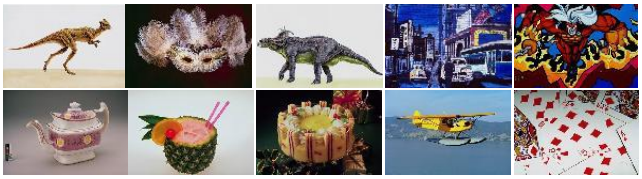

Fig.2 Example images from Corel database

Table 1. ARR of all databases using Bhattacharya Distance

Method	Corel 1k	Corel 5k	Corel 10k
Proposed method	67.23	66.32	64.56
Chun et al.,[34]	54.00	54.20	52.55
Sathiamoorthy [36]	62.23	62.53	60.73

Table 2. ARR of all databases using Chernoff Distance

Method	Corel 1k	Corel 5k	Corel 10k
Proposed method	68.74	67.99	66.18
Chun et al.,[34]	54.78	55.11	53.15
Sathiamoorthy [36]	63.11	63.93	61.01

Table 3. Dimension of feature descriptor of different methods

Method	Feature descriptor length
Proposed method	12
Chun et al.,[34]	32
Sathiamoorthy [36]	114

V. CONCLUSION

A novel approach, named BVLCs and BDIPs in covariance has been suggested in this paper. The presented method computes linear association among textures using BDIPs in covariance and linear association among edges and valleys using BVLCs in covariance. In this work, first we compute the BVLC and BDIP for R,G and B components of an image in RGB space then the mean for BDIPs in R,G and B components, mean for BVLCs in R,G and B components, covariance of BDIPs among R,G and B components and covariance of BVLCs among R,G and B components are computed. The presented descriptors are combined together and compared with wavelets based moments of BVLC and BDIP and histograms of BVLC and BDIP approaches. All the approaches are tested on Corel 1k, corel5k and Corel.10k databases. Precision and recall illustrates that proposed image descriptor is proficient and suitable for image retrieval, and dimension of descriptor is also more acceptable. Outcome of presented system also reveal that Chernoff outperforms Bhattacharya distance measure for retrieval. In future,

proposed descriptors can be combined with color information of an image to increase the retrieval rate of CBIR.

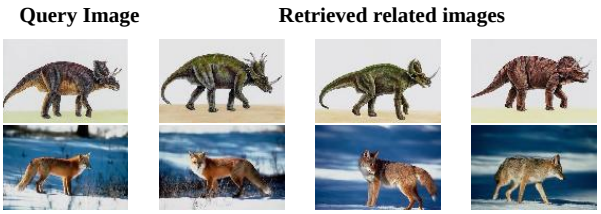

Fig.6 Query and top 4 retrieved images from Corel database for proposed approach with Chernoff (1st row) and Bhatacharya (2nd row) distance measure

References

[1]. R. M. Haralick, K. Shanmugam, and I. Dinstein, "Textural Features for Image Classification", IEEE Trans. on Systems, Man, and Cybernetics, Vol. SMC-3, No.6, November 1973, pp.610-621.
[2]. J. Zhang, G.l. Li, S.W. He, Texture-based image retrieval by edge detection matching GLCM, in: 10th IEEE International Conference on High Performance Computing and Communications, 2008, pp. 782–786.
[3]. Y Hendrawan1, M R Fauzi, N S Khoirunnisa, M Andreane, P O Hartianti, T D Halim and C Umam, 2019, Development of colour co-occurrence matrix (CCM) texture analysis for biosensing, IOP Conference Series: Earth and Environmental Science, Vol. 230.
[4]. F. Kong, "Image retrieval using both color and texture features," 2009 In. Conf. on Machine Learning and Cybernetics, Hebei, pp. 2228-2232
[5]. Jhanwar, N., Chaudhuri, S., Seetharaman, G. Zavidovique, B., 2004. Content based image retrieval using motif cooccurrence matrix, *Image and Vision Computing*, 22:1211–1220.
[6]. D.G. Lowe, Distinctive image features from scale-invariant keypoints, Int. J. Comput. Vis. 60 (2004) 91–110.
[7]. K. Mikolajczyk, C. Schmid, A performance evaluation of local descriptors, IEEE Trans. Pattern Anal. Mach. Intell. 27 (2005) 1615–30.
[8]. H. Bay, A. Ess, T. Tuytelaars, L. Van Gool, Speeded-up robust features (SURF), Comput. Vis. Image Underst. 110 (2008) 346–359.
[9]. T. Ojala, M. Pietikäinen, D. Harwood, A comparative study of texture measures with classification based on featured distributions, Pattern Recognit. 29 (1996) 51–59.
[10]. B.S. Manjunath, W.Y. Ma, (1996) Texture features for browsing and retrieval of image data, IEEE Trans. Pat Anal. Mach. Intel.18(8) 837–42.
[11]. Solmaz Abbasi, Farshad Tajeripour, Detection of brain tumor in 3D MRI images using local binary patterns and histogram orientation gradient, Neurocomputing, Volume 219, 2017, pp. 526-535.
[12]. Jain A. K. and A. Vailaya. 1996. Image retrieval using color and shape. *Pattern Recognition*. 29(8):1233–1244.
[13]. Cieplinski, L., Kim, M., Ohm, J.-R., Pickering, M., Yamada, A. 2001. Text of ISO/IEC 15938-3/FCD Information Technology -Multimedia Content Description Interface-Part 3: Visual. Final Committee Draft, ISO/IEC/JTC1/SC29/WG11 (MPEG), document no. N4062.
[14]. M. Heikkilä, M. Pietikäinen, C. Schmid, Description of interest regions with local binary patterns, Pattern Recognit. 42 (2009) 425–436.
[15]. Zhenhua Wang, B. Fan and F. Wu, "Local Intensity Order Pattern for feature description," *2011 International Conference on Computer Vision*, Barcelona, 2011, pp. 603-610.
[16]. Baochang Zhang, Yongsheng Gao, Sanqiang Zhao and Jianzhuang Liu, "Local Derivative Pattern Versus Local Binary Pattern: Face Recognition With High-Order Local Pattern Descriptor," in *IEEE Trans. on Image Processing*, vol. 19, no. 2, pp. 533-544, Feb. 2010.
[17]. Mohammed Suliman Haji; Mohammed Hazim Alkawaz; Amjad Rehman; Tanzila Saba, Content-based image retrieval: a deep look at features prospectus, Int. J. of Comp. V. and Robotics, 9(1) 2019.
[18]. Zhongyu Li, Xiaofan Zhang, Henning Müller, Shaoting Zhang, Large-scale retrieval for medical image analytics: A comprehensive review, Medical Image Analysis,Volume 43, 2018, Pages 66-84.
[19]. Y. Pang, Y. Yuan, X. Li, Gabor-based region covariance matrices for face recognition, IEEE Trans. Circ. Syst. Video Technol. 18 (7) (2008) 989–993.
[20]. Y. Zhang, S. Li, Gabor-LBP based region covariance descriptor for person re-identification, 2011 Sixth International Conference on Image and Graphics (ICIG), 2011, pp. 368–371.
[21]. O. Tuzel, F. Porikli, P. Meer, Region covariance: A fast descriptor for detection and classification, Comp. Vision–ECCV, 2006, pp. 589–600.
[22]. S. Guo, Q. Ruan, Facial expression recognition using local binary covariance matrices, 4th IET International Conference on Wireless, Mobile & Multimedia Networks (ICWMMN 2011), 2011, pp. 237–242.
[23]. J.Y. Tou, Y.H. Tay, P.Y. Lau, Gabor filters as feature images for covariance matrix on texture classification problem, Advances in Neuro-Information Processing, Springer, 2009, pp. 745–751.
[24]. P. Li, Q. Wang, Local log-Euclidean covariance matrix (L2ECM) for image representation and its applications, Computer Vision, ECCV Springer, 2012, pp. 469–482.
[25]. M.T. Harandi, C. Sanderson, A. Wiliem, B.C. Lovell, Kernel analysis over Riemannian manifolds for visual recognition of actions, pedestrians and textures, 2012 IEEE Workshop on Applications of Computer Vision (WACV), pp. 433–439.
[26]. S. Said, L. Bombrun, Y. Berthoumieu, Texture classification using Rao's distance on the space of covariance matrices, Geometric Science of Information, Springer, 2015, pp. 371–378.
[27]. O. Tuzel et al, 2008, Pedestrian detection via classification on Riemannian manifolds, IEEE Trans. Pat. Anal. Mach. Intell. 30(10) 1713–27.
[28]. J. Yao, J.-M. Odobez, Fast human detection from joint appearance and foreground feature subset covariances, Comput. Vision Image Understand. 115 (10) (2011) 1414–1426.
[29]. S. Bak et al., Boosted human re-identification using Riemannian manifolds, Image Vis. Comput. 30 (6) (2012) 443–452.
[30]. Y.H. Habiboğlu, O. Günay, Covariance matrix-based fire and flame detection method in video, Mach. Vis. Appl. 23 (6) (2012) 1103–1113.
[31]. S. Guo, Q. Ruan, Facial expression recognition using local binary covariance matrices, 4th IET International Conference on Wireless, Mobile & Multimedia Networks (ICWMMN 2011), 2011, pp. 237–242.
[32]. Y. D. Chun, S. Y. Seo, and N. C. Kim, "Image retrieval using BDIP and BVLC moments," IEEE Trans. Circuits Syst. Video Technol., vol. 13, pp. 951–957, Sep. 2003.
[33]. Chun, Y.D., Kim, N.C. and Jang, I.H., 2008. Content-Based Image Retrieval using Multiresolution Color and Texture Features, *IEEE Transactions on Multimedia*, 10(6):1073-1084.
[34]. S.Sathiamoorthy, M. Kamarasan, 2014, Content Based Image Retrieval Using the Low and Higher Order Moments of BDIP and BVLC, Int. J of Innovative Research in Sci, Engg and Technology, 3(1):8936-8941.
[35]. S.Sathiamoorthy, M. Kamarasan, 2014, A Novel Approach for Image Retrieval using BDIP and BVLC, Int. Journal of Innovative Research in Computer and Communication Engineering, 2(9):5897-5902.
[36]. S.Sathiamoorthy, 2014, Image Retrieval Using Texture and its Spatial Information, Int. J of Innovative Research in Sci, Engg and Technology, 3(10):17066-17075.
[37]. S.Sathiamoorthy, 2014, Color Image Retrieval Using Color, Texture and its Spatial Information, International Journal of Innovative Research in Computer and Communication Engineering, 2(11):7106-7114.
[38]. Singh, Chandan and Kanwal Preet Kaur. "A fast and efficient image retrieval system based on color and texture features." *J. Visual Communication and Image Representation* 41 (2016): 225-238.
[39]. Oncel Tuzel, Fatih Porikli , and Peter Meer, Region Covariance: A Fast Descriptor for Detection and Classification,
[40]. Guang-Hai Liu, Jing-Yu Yang, etc,. Content-based image retrieval using computational visual attention model, Pattern Recognition, 48(8) (2015) 2554-2566.
[41]. Michèle Gouiffès, Andres Romero Mier Terána , Lionel Lacassagne, Color enhanced local binary patterns in covariance matrices descriptors (ELBCM),Journal of Visual Communication and Image Representation 49 (2017) 447–458.
[42]. K. Fukunaga, Introduction to Statistical Pattern Recognition, Academic Press, London, 1990.

Proceedings of the Fourth International Conference on Communication and Electronics Systems (ICCES 2019)
IEEE Conference Record # 45898; IEEE Xplore ISBN: 978-1-7281-1261-9

Content Based Medical Image Retrieval Using Multi-Trend Structure Descriptor and Fuzzy k-NN Classifier

M.Natarajan
Division of Computer and Information Science
Annamalai University
Annamalai Nagar, India
mnind.2004@gmail.com

*S.Sathiamoorthy**
Tamil Virtual Academy
Chennai,
India
ks_sathia@yahoo.com

***Abstract*— In this work, Multi-trend structure descriptor is suggested for retrieving images from heterogeneous medical image dataset. The multi-trend structure descriptors acquires structures in the form of large, small and equal trends along four directions at both global and local level. For the retrieval of gray-scale medical images, only the structure information computed by Multi-trend structure descriptor from the texture and edge information of an image is used while for color medical images the color information acquired by Multi-trend structure descriptor is also taken in to consideration for attaining effective retrieval rate. The fuzzy k-NN approach is incorporated to classify the feature vectors and it enhances the retrieval accuracy as well it increases the speed of retrieval. The results obviously shown that the fusion of Multi-trend structure descriptor and fuzzy k-NN outperforms the state-of-the-art approaches.**

Keywords*— Multi-trend structure, fuzzy k-NN classifier, Euclidean measure, Precision, Recall.

I. INTRODUCTION

Nowadays, rapid growth in medical imaging modalities produces gigantic quantity of medical images in hospitals and most of the medical diagnostic approaches and health monitoring are completely depends on medical images. As a result , medical image repositories serve as a very important resource for physicians for making decisions by retrieving proper medical cases from extremely enormous medical image repositories. Day to day these data stores grow massively and diversely. Beside this, representing the rich and very subtle information is more difficult. Hence, extracting the relevant medical case images and annotating the vast and diversity of medical images turn out to be more complicated task and become a hot area of research. For this reason, number of new algorithms has been developed to aid physician and to tackle the massive collections of medical images.

Today, most of the hospitals use Picture archival and communication systems (PACS) which stores and searches images based on textual keywords and the textual keywords are plagued with many drawbacks like inadequate representation of medical images which results in difficulty of identifying and locating relevant images from the vast and diverse medical image collections and it necessitates the physicians to search the desired medical images manually and is wearisome and physicians get tired [1]. Further, Mustra et al., reported that medical images in DICOM format is error-prone [2]. Thus, the troubles with PACS led to the evolution of CBMIR system, where the contents of the medical images like shape, color and texture are exploited to access the related medical images from the massive repositories. Even though CBMIR has been studied broadly, most challenging problem remains in CBMIR systems is mapping the low level visual contents with high level semantics which is still more complex one because same semantics may represents different images and visual similar images may have different semantics [3, 4]. The gap among the semantics and low-level image descriptors is defined as semantic gap and it could affect the precision of retrieval by retrieving the irrelevant images. For example, the physician wants to retrieve a particular stage of breast cancer image from the collection of mammogram images, but the system may retrieve benign cases due to the less discrimination ability of the feature vector. Thus, the researchers attempted to reduce the gap by utilizing the machine and relevance feedback learning methods [5]. But, still the gap exists. Thus, it is really important ongoing issue and most vivid study area in the purview of multimedia and medicine.

In the CBMIR approaches, image representation is modeled using feature vector which is computed from the image itself by extracting the low level visual features. Subsequently, the similarity among input and the medical images in the enormous repository is estimated in the feature space using the similarity measures. Thus, image representation and similarity measure are the core component of CBMIR systems. Further, dimensionality reduction and classification techniques are adopted to diminish the dimension of computed image descriptor and to diminish the search space respectively.

Over the decade, researchers are working towards an effective CBMIR. ASSERT, a system for lung image retrieval in which shape and texture features of region of interest is used [6]. In [7], mean and covariance are computed for

representing the color information and grey-level co-occurrence matrice is computed to represent texture information for the retrieval of skin lesion images. In [8], retrieval system for dermoscopic medical images of pigmented lesions is performed by texture and color image descriptors. The scatter-plot of R Vs G, G Vs B and B Vs R color channels are employed as color feature, and co-occurrence distribution of color ratio and variance at local level image are utilized as texture descriptor. Lan et al., used bag of words for CT images which is computed from localized texture feature obtained by applying the Gabor and Schmid filters followed by uniform and non-overlapping partitions [9]. Wei et al., introduced a retrieval system for CT images of lung nodule in which both semantic and visual similarity measures are employed [10]. Quellec et al., extracted signatures from the wavelet transformed image and is used for image retrieval instead of domain specific features [11]. MedFMI-SiR system is presented in [12] that integrate the content and metadata-based queries for effective medical image searching. Murala and Wu [13] suggested local mesh patterns which capture the association between neighboring pixels instead of neighboring pixels and a pixel at the center of the mask and they verified the efficacy of local mesh patterns on MRI and CT image databases namely VIA/I-ELCAP, OASIS-MRI and NEMA-CT.

In [14], local binary patterns are computed from the binary wavelet transform applied binary bit planes of gray-scale images and is termed as directional binary wavelet patterns which reported more efficient for CT and MR image datasets. Murala and wu presented local ternary co-occurance patterns for effectively retrieving CT and MR images and it captures co-occurrence of akin ternary edgels from the gray-levels of center pixels and neighbors of it [15]. Center symmetric local binary patterns based on local wavelet is used with random forests in [16] for annotation of medical images and the annotated keywords are used for medical image retrieval and to enhance the retrieval accuracy, relevance feedback approach is used. Local wavelet patterns suggested by Dubey et al. in [17] for CT image searching and retrieval in which local neighboring information is computed using local wavelet decomposition then the authors utilized the decomposed gray-level values and wavelet transformed center gray-level values to compute local wavelet pattern. It is described in [18] that features from deep convolutional neural networks achieved better retrieval results and localized sensitive hashing based approaches also performs well for large image datasets. Jamil Ahmad et al., computed convolutional descriptors using deep learning method and by using fast Fourier transform, convolutional descriptors are compressed to binary codes and is utilized as a descriptor for searching and retrieving the radiology and endoscopy images [18].

Bag of visual words constructed from SIFT descriptor is described in [19] for brain MRI. Zhang et al., introduced scalable retrieval approach for histopathological medical images of breast tissues utilizing supervised kernel hashing method [20]. Nowaková et al., utilized vector quantization, fuzzy signatures and fuzzy S-trees for mammogram image retrieval [21]. In [22], bag of color is computed using SIFT for CBMIR. Haas et al., suggested bag of visual words, computed from the interest points resultant from super pixels using SIFT for medical image retrieval [23]. In sequence with this, many researchers presented CBMIR based on bag of visual words [24-27]. Seetharaman and Sathiamoorthy [28] suggested a system for retrieving images from heterogeneous medical image database using the fusion of color autocorrelogram, micro-textures and enhanced edge orientation autocorrelogram which are estimated from a framework based on Full range Autoregressive Model and outperforms the conventional methods due to the ability of capturing texture, color, shape and spatial details of them at both local and global level. In the past, many researchers presented the available literature for various technologies used for medical image retrieval [30-36] and described that the existing technologies presented for medical image retrieval are not proficient.

Lately, Zhao et al., [37] suggested Multi-Trend Structure Descriptor (MTSD) for image retrieval that captures structures in the form of equal, large and small trends for texture, color and shape details separately and extensive experiments are done to demonstrate the effectiveness of MTSD on benchmark datasets namely Corel image and Caltech datasets [37], and described that MTSD is superior in performance then the existing outstanding techniques namely MSD, TCM, SSH and MTH descriptors for retrieval of an image. According to the aforementioned revealing discussion, in this paper, fusion of Multi-trend structure descriptor [37] and fuzzy k-nearest neighborhood approach is proposed for medical image retrieval from heterogeneous image dataset.

This paper is drafted as follows: The proposed MTSD and fuzzy k-NN based CBMIR approach is defined in Section 2. In the 3rd Section, experimental results and discussion is described. Section 4 presented the conclusion.

II. Proposed Medical Image Retrieval System

Herein, the feature computation using MTSD, classification of computed feature vector using fuzzy k-NN classifier and the distance and evaluation measures employed in this study are discussed.

A. Feature Extraction

In this manuscript, we employed MTSD [37]. In order to compute MTSD, an image in RGB color space is transformed to HSV [37] color space then uniform quantization is done as in [37] which results in 12, 3 and 3 quantization levels for color i.e. totally 108; 20 is the level of quantization for texture which is estimated from the V component and 9 is the quantization level for edge information which is estimated from the edge detected image using the Sobel operator on V component of an image [37].

Subsequently, Zhao et al., partitioned the image into number of 3 x 3 non overlapping blocks in order to discover the structures on local level in the method of equal, small and long trends along 0°, 45°, 90° and 135° orientations [37]. For

each color quantized value, Zhao et al., route through bottom to top and left to right direction throught the entire image to discover the number of equal, small and long trends. According to Zhao et al., pixel values from small to large, pixel values from large to small and pixel values are same along 0°, 45°, 90°0and 135° orientations for each non overlapping blocks corresponds to large, small and equal trends respectively [37]. In the same manner, large, small and equal trends are identified for each texture and edge quantized values respectively. The color, edge and texture information estimated by MTSD are concatenated for histopathological images and color information is excluded for gray-scale medical images where the role of color is not significant in distinguishing the images. Thus, the feature vector is expressed as $(N_E^{Q_c}, N_S^{Q_c}, N_L^{Q_c})$, $(N_E^{Q_t}, N_S^{Q_t}, N_L^{Q_t})$, $(N_E^{Q_e}, N_S^{Q_e}, N_L^{Q_e})$ in which N, Q_c / Q_t / Q_e, E, S and L represents the number of trends, quantized color/texture/edge value, equal, small and large trends respectively. Therefore, MTSD is feature vector of quantized color/texture/edge values versus trends. The feature matrix computed by the MTSD for color is depicted in Fig.1 where number of equal, small and large trends for quantized color value 0 to 108 is depicted. Small and large trends along 0° and 45° and equal trends along 90° and 135° is illustrated in Fig.2.

	E	S	L
0	12	2	10
1	6	2	19
.	.	.	.
.	.	.	.
.	.	.	.
108	.	.	.

Fig.1. MTSD for color feature

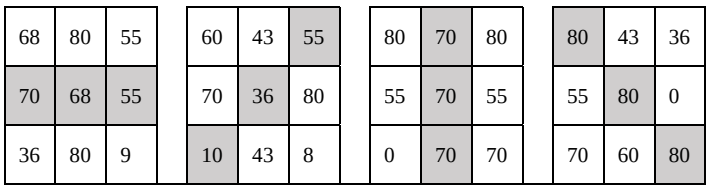

Fig.2. (a). Small trends along 0° (b). Large trend along 45° (c). Equal trends along 90° (d). Equal trend along 135°

B. Fuzzy k-NN classifier

Classification of images is successfully based on low-level features and is very difficult task in CBMIR and it significantly advances the performance of CBMIR by eliminating the images that are not relevant from the search space. Thus, more familiar fuzzy k-NN classifier is incorporated in this work due to its uncertainty in the results. The fuzzy k-NN is coming under supervised learning approach and deterministic form of k-NN [38] with the benefits of fuzzy set theory [38]. Though the computation time of fuzzy k-NN is significantly higher than the k-NN, due to the consideration of unbiased weighting of instances in the decision rule nevertheless of its distance to the pattern to be categorized, fuzzy k-NN attains better classification rate [38]. In the literature, fuzzy k-NN has been employed effectively by many researchers [39-41].

Let assume that the fuzzy k-NN classifies feature vectors $F = \{F_1, F_2, \ldots F_N\}$ into C classes where $1 < C < N$ and the fuzzy membership matrix D for N number of feature vectors and C number of classes is computed and D_{ij} is the degree of fuzzy membership of feature vector F_j where j=1,2,…N and i=1,2,…C. In fuzzy membership matrice, the degree D_{ij} lies within 0 to1 for all i and j. If $D_{ij} = 1$ for class i then the D_{ij} for other classes are 0. The summation of D_{ij} of all feature vectors must be greater than 0 for class i or else the class i does not exist. In fuzzy k-NN classifier, membership of feature vector F to class i is estimated by utilizing the feature vector's distances from their k-NNs membership [38], is expressed as

$$D_i(F) = \frac{\sum_{j=1}^{k}\left(\frac{D_{ij}}{\|F-F_j\|^{\frac{2}{(w-1)}}}\right)}{\sum_{j=1}^{k}\left(\frac{1}{\|F-F_j\|^{\frac{2}{(w-1)}}}\right)} \quad (1)$$

Where k is predefined and designates the numbers of nearest neighbor, $\|F - F_j\|$ designates the Euclidean distance among F and k nearest neighbor vector F_j, w is the weight parameter of the fuzzy distance function. D_{ij} is determined a-priori from the training data and is the degree of the fuzzy membership of jth neighbor to i^{th} class. The k is chosen through trail and error process.

We employed 5 fold cross validation for evading over-fitting and for attaining better generalization which occurs when the dataset is partitioned into training and testing is not adequate [28, 38]. That is, the dataset are randomly alienated into five folds without imposing any damage to the data. The size of each fold is approximately equal and for each run of five- folds cross validation, four data sub sets are utilized in training and the 5th one is utilized in testing like all 5 data sub-sets are utilized in both learning and testing phase.

C. Similarity Measuremnt

The relevancy is measured among input and the dataset images using distance measure which is an essential component of CBMIR system. In this work, Euclidean distance [42] is employed to discover the distance among input and the dataset images, and is expressed as follows

$$S(Q,T) = \sqrt{\sum_{i=0}^{N}(|Q_i - T_i|)^2} \quad (2)$$

Where T and Q designate the input image and target image feature vector and N designate the number of descriptors in an image feature vector.

D. Performance Assessment

The retrieval rate of proposed CBMIR approach is evaluated using the accuracy which is estimated based on most

frequently used precision (P) and recall (R) measures [28] and is described as

$$\text{Precision (P)} = \frac{\text{Number of relevant images retrieved}}{\text{Total number of images retrieved}} \quad (3)$$

$$\text{Recall (R)} = \frac{\text{Number of relevant images retrieved}}{\text{Total number of relevant images in the database}} \quad (4)$$

III. Experimental and Results

The proposed CBMIR approach is evaluated by utilizing the heterogeneous medical image dataset [28] which has 6400 images of 83 concepts of 1510, 592, 858, 580, 1708, 663 and 489 images captured using X-ray, CT, Mammogram, MRI, Microscopy, Ultrasound, and Endoscopy modalities respectively and are collected with ground truth from the RMMCH, Annamalai University, Annamalai Nagar, India. Fig.3 depicts some examples images from the dataset.

Table. 1. The dimension of proposed MDLDPTS and state-of-art techniques

Methods	Dimension	Accuracy rate
Seetharaman and Sathiamoorthy's approach	361	64.43
MTSD (for color medical images)	137	66.12
MTSD (only considering the texture and edge information for gray-scale medical images)	29	65.87

In this work, better image retrieval can be achieved with the fusion of high discriminate feature vector, MTSD [37] and efficient fuzzy k-NN classifier [38]. Since color information extracted by MTSD is not helpful for gray-scale images, the structure information estimated by the MTSD from the edge and texture information of an image is considered and its dimension is 29 whereas histopathological images requires color information also for significant differentiation. Thus, the dimension of MTSD for color medical images is 137. The MTSD is computed as discussed in section 2.1. To validate the performance of proposed mixture of MTSD and fuzzy k-NN approach, image database used in [28] is employed and the proposed results were evaluated with the results of [28] in experiments.

In the experiment, every image is utilized as input image and for every input image, the system reacts to the user with N number of relevant images that are having shortest distance matching with the input image and are displayed in the ascending order of distance matching value. The accuracy rate of responding a query is measured by utilzing average *P* and average *R*. We compared retrieval accuracy of MTSD with the approach described in [28] and the results are summarized in Table.1. Since the MTSD captures the structures in an image for color, texture and edges at both local and global level, better results is achieved. The experimentation was conducted with N number of retrieved images and is set as 10 to evaluate the *P* of each input image and we finally attain average *P* that is *P*/M where M designates number of images in a class. In addition, recall of each retrieved image and the average *R* is estimated. The average *P* and average *R* of retrieval results is depicted in Fig.4 and 5 and it depicts the variation of *P* and *R* with respect to number of images retrieved The experimental results obviously reveal that proposed approach is notably superior to an approach in [28]. In the experiment of average *R*, image retrieval *P* raises with the number N of returned images. Thus, the proposed approach is more superior to the approach of [28]. We also used MTSD for gray-scale medical images without excluding the color information that it captures. However, there is no significant raise in the accuracy rate instead computational cost is amplified owing to an enclosure of color information which is 108 in dimension.

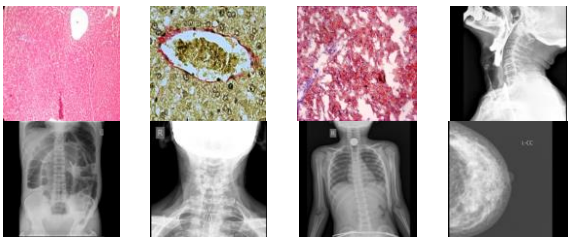

Fig.3.Some example images from the dataset

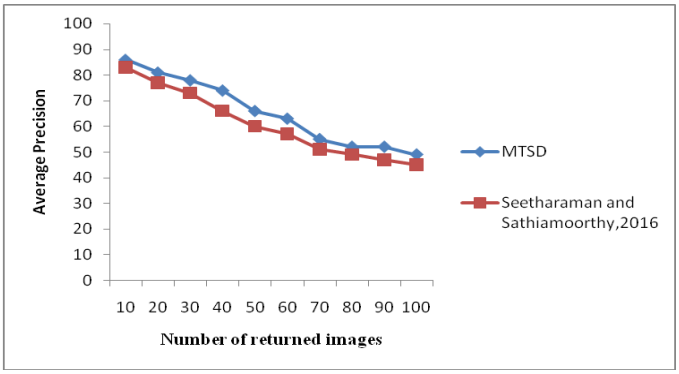

Fig.4.Average precision for proposed and existing approaches

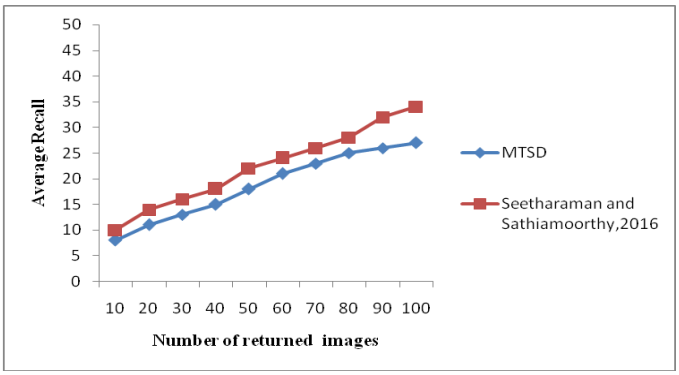

Fig.5.Average recall for proposed and existing approaches

The dimension and accuracy rate of the MTSD and the feature vector suggested in [28] is illustrated in Table.1. From the experimental results, it is obvious that fusion of MTSD and fuzzy k-NN not only attains better accuracy but can also reduced the time complexity of CBMIR. The

experiments are carried out in core i3 processor, 4 GB RAM and 64 bit Windows OS.

IV. Conclusion

We proposed a novel approach for heterogenous medical image retrieval system. Due to the diversity and very minute deformations in medical images, a feature vector with high discrimination ability is incorporated, MTSD which characterizes an image by using structures in the form of large, small and equal trends along 0°, 45°, 90° and 135° orientations. The MTSD captures texture, color and shape details at local as well global level. Fuzzy k-NN classifier is incorporated for classification task to avoid uncertainty in results. The experimental results reveal that fusion of MTSD, fuzzy k-NN classifier and Euclidean similarity measure is much better than the existing CBMIR methods. In future, proposed descriptor can be utilized in other domains

References

[1] Müller H., N. Michoux, D. Bandon, A. Geissbuhler. 2004. A review of content-based image retrieval systems in medical applications-clinical benefits and future directions. *Int. J. of Medical Informatics.* 73(1): 1-23.

[2] M. Mustra, K. Delac, M. Grgic, 2008. Overview of the DICOM standard, 50th Int Symp. ELMAR, 1: 10-12

[3] Dumitru Dan Burdescu, Cristian Gabriel Mihai, Liana Stanescu, Marius Brezovan, 2013. Automatic image annotation and semantic based image retrieval for medical domain, *Neurocomputing*. 109:33–48.

[4] Qing-Fang Zheng, October 2008. Constructing visual phrases for effective and efficient object-based image retrieval, *ACM Transactions on Multimedia Computing, Communications, and Applications (TOMCCAP)*, Vol 5(1).

[5] Hossein Nezamabadi-pour, Ehsanollah Kabir, 2009. Concept learning by fuzzy k-NN classification and relevance feedback for efficient image retrieval, *Expert Systems with Applications*. 36: 5948–5954.

[6] Shyu, C.R., Brodley, C.E., Kak, A.C., Kosaka, A., Aisen, A.M., Broderick, L.S., 1999. ASSERT: A physician-in-the-loop contentbased image retrieval system for HRCT image databases. Comput. Vis. Image Understand 75, 111–132.

[7] Lucia Ballerini, Xiang Li, Robert B. Fisher, Jonathan Rees, 2009.A Query-by-Example Content-Based Image Retrieval System of Non-melanoma Skin Lesions, Lecture Notes in Comp. Science, Vol. 5853.

[8] Alfonso Baldi, Raffaele Murace, Emanuele Dragonetti, Mario Manganaro, Oscar Guerra, Stefano Bizzi and Luca Galli, 2009. Definition of an automated Content-Based Image Retrieval (CBIR) system for the comparison of dermoscopic images of pigmented skin lesions, BioMedical Engineering, 8:18

[9] Lan, R., Zhong, S., Liu, Z. et al. Multimed Tools Appl (2018) 77: 10853. https://doi.org/10.1007/s11042-017-5341-2

[10] Wei, G., Cao, H., Ma, H. et al. J Med Syst (2018) 42: 13. https://doi.org/10.1007/s10916-017-0874-5.

[11] Quellec, Gwenole & Lamard, Mathieu & Cazuguel, Guy & Cochener, Béatrice & Roux, Christian. (2010). Wavelet optimization for content-based image retrieval in medical databases. Medical Image Analysis. 14. 227-241. 10.1016/j.media.2009.11.004.

[12] Kaster D.S. et al. (2011) MedFMI-SiR: A Powerful DBMS Solution for Large-Scale Medical Image Retrieval. In: Böhm C., Khuri S., Lhotská L., Pisanti N. (eds) Information Technology in Bio- and Medical Informatics. ITBAM 2011. Lecture Notes in Computer Science, vol 6865. Springer, Berlin, Heidelberg.

[13] S. Murala and Q. M. J. Wu, "Local Mesh Patterns Versus Local Binary Patterns: Biomedical Image Indexing and Retrieval," in *IEEE Journal of Biomedical and Health Informatics*, vol. 18, no. 3, pp. 929-938, May 2014.

[14] Murala S, Maheshwari RP, Balasubramanian R, Directional binary wavelet patterns for biomedical image indexing and retrieval, J Med Syst. 2012 Oct;36(5):2865-79.

[15] Subrahmanyam Murala, Q.M.Jonathan Wu, 2013, Local ternary co-occurrence patterns: A new feature descriptor for MRI and CT image retrieval, Neurocomputing, Volume 119, 7 November 2013, Pages 399-412.

[16] Ko, B.C., Lee, J. & Nam, JY. J Digit Imaging (2012) 25: 454. https://doi.org/10.1007/s10278-011-9443-5.

[17] S. R. Dubey, S. K. Singh and R. K. Singh, "Local Wavelet Pattern: A New Feature Descriptor for Image Retrieval in Medical CT Databases," in *IEEE Transactions on Image Processing*, vol. 24, no. 12, pp. 5892-5903, Dec. 2015.

[18] Ahmad J, Muhammad K, Baik SW, Medical Image Retrieval with Compact Binary Codes Generated in Frequency Domain Using Highly Reactive Convolutional Features, J Med Syst. 2017 Dec 19;42(2):24. doi: 10.1007/s10916-017-0875-4.

[19] M. Mizotin, J. Benois-Pineau, M. Allard, and G. Catheline, "Feature-based brain MRI retrieval for Alzheimer disease diagnosis," in 2012 19th IEEE International Conference on Image Processing, 2012, pp. 1241-1244.

[20] X. Zhang, W. Liu, M. Dundar, S. Badve and S. Zhang, "Towards Large-Scale Histopathological Image Analysis: Hashing-Based Image Retrieval," in *IEEE Transactions on Medical Imaging*, vol. 34, no. 2, pp. 496-506, Feb. 2015.

[21] Nowaková, J., Prílepok, M. & Snášel, V. J Med Syst (2017) 41: 18. https://doi.org/10.1007/s10916-016-0659-2

[22] García Seco de Herrera A., Markonis D., Müller H. (2013) Bag–of–Colors for Biomedical Document Image Classification. In: Greenspan H., Müller H., Syeda-Mahmood T. (eds) Medical Content-Based Retrieval for Clinical Decision Support. MCBR-CDS 2012. Lecture Notes in Computer Science, vol 7723. Springer, Berlin, Heidelberg

[23] Haas S., Donner R., Burner A., Holzer M., Langs G. (2012) Superpixel-Based Interest Points for Effective Bags of Visual Words Medical Image Retrieval. In: Müller H., Greenspan H., Syeda-Mahmood T. (eds) Medical Content-Based Retrieval for Clinical Decision Support. MCBR-CDS 2011. Lecture Notes in Computer Science, vol 7075. Springer, Berlin, Heidelberg

[24] Huang M, Yang W, Yu M, Lu Z, Feng Q, Chen W, Retrieval of brain tumors with region-specific bag-of-visual-words representations in contrast-enhanced MRI images, Comput Math Methods Med. 2012;2012:280538. doi: 10.1155/2012/280538. Epub 2012 Nov 25.

[25] Hwang S. Bag-of-Visual-Words Approach to Abnormal Image Detection in Wireless Capsule Endoscopy Videos. In: Bebis G. et al. (eds) Advances in Visual Computing. ISVC 2011. Lecture Notes in Computer Science, vol 6939. Springer, Berlin, Heidelberg

[26] M. Srinivas, R.R. Naidu, C.S. Sastry, C.K. Mohan, Content based medical image retrieval using dictionary learning, Neurocomputing, 168 (2015), pp. 880-895

[27] C.H. Cao, H.L. Cao, The research on medical image classification algorithm based on PLSA-BOW model Technol. Heal. Care, 24 (2016), pp. S665-S674, 10.3233/THC-161194.

[28] K.Seetharaman, S.Sathiamoorthy, A Unified Learning Framework for Content Based Medical Image Retrieval Using a Statistical Model. *Journal of King Saud University - Computer and Information Sciences*, Volume 28 (2016), Number 1, Dec 2015, pp. 110-124.

[29] A. García Seco de Herrera, H. Müller, Fusion techniques in biomedical information retrieval, Inf. Fusion Comput. Vis. Concept Recognit., 209–228 (2014), 10.1007/978-3-319-05696-8_9.

[30] Akgül, Ceyhun & Rubin, Daniel & Napel, Sandy & Beaulieu, Christopher & Greenspan, Hayit & Acar, Burak. 2010. Content-Based Image Retrieval in Radiology: Current Status and Future Directions. Journal of digital imaging. 24. 208-22. 10.1007/s10278-010-9290-9.

[31] A.Criminisi, 2016, Machine learning for medical images analysis, Medical Image Analysis, Volume 33, Pages 91-93.

[32] Geert Litjens, Thijs Kooi, Babak Ehteshami Bejnordi, Arnaud Arindra Adiyoso Setio, Francesco Ciompi, Mohsen Ghafoorian, Jeroen A.W.M.van der Laak, Bramvan Ginneken, Clara I.Sánchez, 2017, A survey on deep learning in medical image analysis Medical Image Analysis, Volume 42, Pages 60-88.

[33] Zhongyu Li, Xiaofan Zhang, Henning Müller, Shaoting Zhang, 2018, Large-scale retrieval for medical image analytics: A comprehensive review Medical Image Analysis, Volume 43, Pages 66-84.

[34] Ghosh, Payel & Antani, Sameer & Long, L & R. Thoma, George. (2011). Review of medical image retrieval systems and future directions. IEEE Int Symp Computer-Based Med Syst. 1-6. 10.1109/CBMS.2011.5999142.

[35] Shaoting Zhang, Dimitris Metaxas, 2016, Large-Scale medical image analytics: Recent methodologies, applications and Future directions, Medical Image Analysis, Volume 33, Pages 98-101.

[36] Rueckert , Ben Glocker, Bernhard Kainz, 2016, Learning clinically useful information from images: Past, present and future Daniel, Medical Image Analysis journal, Biomedical Image Analysis (BioMedIA) Group, Department of Computing, Imperial College London, UK.

[37] Meng Zhao, Huaxiang Zhang, Jiande Sun, (2016). A novel image retrieval method based on multi-trend structure descriptor, J. Vis. Commun. Image R., 38: 73–81.

[38] Mohammad Reza Nikoo, Reza Kerachian, Mohammad Reza Alizadeh, A fuzzy KNN-based model for significant wave height prediction in large lakes, Oceanologia, Volume 60, Issue 2, 2018, Pages 153-168

[39] N.M. Somari, M.F. Abdullah, M.K. Osman, A.M.I. Nazelan, K.A.Ahmad, S.P.R.S. Appanan, L.K. Hooi, Particles contaminations detection during plasma etching process by using *k*-nearest neighbors and Fuzzy *k*-nearest neighbors Computing and Engineering (ICCSCE), November 2016, 6th IEEE International Conference on Control System, IEEE (2016), pp. 512-516,

[40] I.B. Fredj, K. Ouni, Comparison of crisp and fuzzy kNN in phoneme recognition, 2017 International Conference on Advanced Systems and Electric Technologies (IC_ASET), 14–17 January 2017, Hammamet, Tunisia, IEEE(2017), pp. 118-122.

[41] P. Wang, X. Xiao, Predicting the risk type of human papillomaviruses based on sequence-derived features, iCBBE 5th International Conference on Bioinformatics and Biomedical Engineering, 10–12 May 2011, Wuhan, China, IEEE (2011), pp. 1-4.

[42] Fazal Malik, Baharum Baharudin, (2013). Analysis of distance metrics in content-based image retrieval using statistical quantized histogram texture features in the DCT domain, Journal of King Saud University - Computer and Information Sciences, 25(2):207-218.

Proceedings of the Fourth International Conference on Communication and Electronics Systems (ICCES 2019)
IEEE Conference Record # 45898; IEEE Xplore ISBN: 978-1-7281-1261-9

Co-occurrence of Edges and Valleys for Content Based Image retrieval

M. Bennet Rajesh
Research Scholar
Division of Computer and Information Science
Annamalai University, Annamalai Nagar, India
benraj@gmail.com

*S.Sathiamoorthy**
Tamil Virtual Academy
Chennai
India
ks_sathia@yahoo.com

Abstract—**Shape is prominent information in the image. Commonly shape analysis approaches based on edges for image retrieval simply consider the frequency of edgels or orientation of edgels which ignores local information and spatial relation among adjacent edgels. The BDIP (Block Difference of Inverse Probabilities) computes the edges with valleys instead of edges only and it gives more shape information. By computing the co-occurrences among the neighboring gray levels, GLCM (Gray level co-occurrence matrix) computes the spatial relations. Thus, in this paper, we addressed the above said issues with the characterization of edges using histogram by integrating the GLCM with BDIP, referred as co-occurrence matrix of BDIP (CMBDIP). The proposed CMBDIP considers valleys of edges also. After computing the edges and valleys, GLCM is applied over the BDIPs of the image along four directions. The results are four co-occurrence matrices of BDIPs and are integrated to form the proposed CMBDIP. The proposed CMBDIP is extensively tested on Holiday, Corel 10k and Caltech 101 datasets and results evident its efficiency by comparing low order moments of BDIP in multiresoultion domain and histogram of BDIP approaches.**

Keywords— BDIP, GLCM, Canberra distance, CMBDIP. Co-occurrence

I. INTRODUCTION

With significant progress in imaging technology, image datasets are rapidly increasing in numbers as well in size and these encouraged researchers to centre their attention on inventing novel methodologies for retrieving images in less time span and with high accuracy rate. Normally, content based image retrieval (CBIR) incorporates information that encompasses shape, texture or color or mixture of theses to typify the image and it facilitates image retrieving. Despite noticeable advances in CBIR, image retrieval remains challenging one, particularly with diversity of images and ever raising image data.

In real world, objects are characterized predominantly by their distinct shape information. Among the commonly utilized image descriptors, shape represents essential and prominent structure information, and is more important for human perception. Thus, over the decade, shape information of an image has been explored intensively in numbers and plays central role in image retrieval. In recent years, center of interest of many researchers are on local image characterization because easy differentiation from others and its resilient against occlusion, scaling, rotation, distortions and illumination variation. Thus, dozens of local level shape descriptors were reported based on different image characteristics [1-7]. Commonly, shape descriptors are of two types: 1. Contour based 2. Region based. The former one includes approaches like Fourier descriptor [8], elastic matching [9], contour point distribution histograms [10], curvature scale space [11], edge histogram direction [12, 13], MSD [14], Edge orientation autocorrelogram [15], etc and offers characteristics of image shape. The later one includes approaches like moment invariants [16], Zernike moment descriptor [17], generic Fourier descriptor [18], etc. and are coined as global shape descriptors.

Among the aforesaid shape techniques, BDIP [19] have come out as one of the prominent shape descriptor because of its outstanding performance. The BDIP operator is well-known method for shape analysis and it characterizes image using edges and valleys. Subsequently, many of its variants also been reported in [20-24]. The BDIP descriptor has been applied successfully with other characteristics of image for image retrieval [25]. Even if BDIP has gained success in image retrieval and most of the variants of BDIP have increased the performance of BDIP, it still suffers in accuracy.

On the other side, literature reports that histogram has been utilized widely for representing the most of local descriptors [1-7, 12, 13, 15, 22]. But [28, 29] reports that histogram ignores relationship among neighborhood gray levels and any correlation between gray levels, and it reduces the retrieval rate of histogram based descriptors. It is also reveled from literature that histogram based image descriptors are computationally cost and results in large dimensionality of descriptors [30]. Since descriptors based on edges [12-15], edges and valley [20] and textures [3, 4] has limitation with histogram representation, they are to be efficient to some extent only.

Thus the researchers turned their interest from histogram representation of descriptors. One among the ending of aforesaid weakness of histogram is gray level co-

occurrence matrix (GLCM) and is reported by Haralick [31] for gray levels and it measure the texture information of the image by computing the co-relation of neighborhood pixels and gives more spatial information. Thus it is incorporated in many applications [29, 32-36] and combined with other image descriptors including co-occurrence of adjacent local binary patterns (LBP) [28], co-occurrence of Center-Symmetric LBP [37], local ternary co-occurrence patterns [38], Gabor co-occurrence [39], co-occurrence of edges [40] and color edges [41] are reported for image retrieval..

Thus, in this manuscript, to address the weakness of BDIP as aforementioned, we propose simple, effective and yet robust approach by computing the co-occurrence of edges and valleys. Since edges and valleys are identified using BDIP, the proposed co-occurrence of BDIPs (i.e. identified edges and valleys) is referred as co-occurrence matrix of BDIP (CMBDIP) which captures spatial correlation among BDIP values i.e. edges and valleys Therefore, the approach presented by us takes the benefits of both co-occurrence matrix, and edges and valleys computed by BDIP and thus proposed method considerably improving the discriminative power of BDIP. Besides, to verify the accuracy of proposed CBDIP, a detailed comparative study using co-occurrences of adjacent edges and valleys, histogram of BDIP [22] and low order moments of BDIP in multiresolution doamin [20] is performed. The experimental outcome indicates that proposed CMBDIP approach offers high accuracy in image retrieval.

The remaining of this manuscript is given as: recall of conventional descriptors is précised in Section.2 and Section 3. Section 4 and 5 deals with proposed approach and experimental evaluations and conclusion are reveled in Section 5.

II. BDIP

BDIP [20], a sketch feature consisting of edges depicted by local intensity maxima and valleys depicted by local intensity minima and is given as [32]

$$BDIP^{d}(l)=\frac{\frac{1}{B_l^d}\sum_{(x,y)\in B_l^d}(\max_{(x,y)\in B_l^d} f(x,y)-f(x,y))}{\max_{(x,y)\in B_l^d} f(x,y)} \quad (1)$$

Where f(x,y) designates an intensity of pixel at position (x, y) in image block B_l^k of dimension (k+l)x(k+l), k denotes the utmost distance among pixels pairs and l denotes the place index. Thus, $B_l^k=(k+1)^2$. In equation (1), numerator and denominator defines the maximum intensity variation and representative value in a block respectively.

III. GRAY LEVEL CO-OCCURRENCE MATRIX

GLCM [31] is second order statistical method and is described over the image to be a distribution of co-occurring of gray-levels at a specified offset. The co-occurrences are computed according to specific distance and in a specific direction. The GLCM for an image is computed as

$$G_{(\Delta x,\Delta y)}(i,j)=\sum_{p=1}^{M}\sum_{q=1}^{N}1\{I(p,q)=i\}\text{ and }1\{I(p+\Delta x,q+\Delta y)=j\} \quad (2)$$

Where *I(p,q)* denotes gray level at *p* row and *q* column, i and j are gray levels for which co-occurrence is computed, Δx and Δy are positional offsets in x and y directions, 1{} is the indicator function, M and N denotes dimension of input image. For instance the GLCM calculation is given in. Fig.1

4	4	1	2
1	2	2	1
3	1	3	2
1	2	4	4
2	1	3	3
3	4	4	2

(a)

Gray Values	1	2	3	4
1	0	0	0	0
2	0	1	0	0
3	0	0	1	0
4	0	0	0	3

(b)

Fig.1. (a).Sample image pattern (b). GLCM of image (a) at $\theta=0^{\circ}$

Therefore, the proposed CMBDIP is an average of GLCMs of BDIPs along 0°, 45°, 90°, 135° directions and is:

$$=\frac{1}{4}\left([G_{d=1,\theta=0^{\circ}}]+[G_{d=1,\theta=45^{\circ}}]+[G_{d=1,\theta=90^{\circ}}]+[G_{d=1,\theta=135^{\circ}}]\right) \quad (3)$$

IV. PROPOSED CMBDIP

We proposed an approach based on the combination of more familiar GLCM and BDIP. In this work, we used BDIP to identify the edges and valleys and the GLCM is incorporated to get the frequency of co-occurrence of neighboring BDIPs and is used as descriptor for the proposed CBIR. In our work, the GLCM is computed at distance 1 andin 0°, 45°, 90°and 135° directions. Therefore, we attained four co-occurrence matrix and are integrated together to form the proposed CMBDIP which overcomes the pitfalls of histogram characterization of BDIPs by encompassing spatial relations among the edges and valleys. The reason for choosing distance as 1 in CMBDIP is, it captures details more locally. Fig.2 illustrates the computation of proposed descriptor. Fig.3 has shown the edges and valleys computed using the BDIP for bus and cat images of Corel dataset.

A. Measure of similarity

After computing the proposed descriptor for every image in the dataset, they are stored separately, called as feature vector dataset. The descriptor matching for input and target images is performed using similarity measures. The output of the similarity measure falls in range 0 to 1 and 0 stands for similar and 1 stands for dissimilar. In our approach, we incorporated Canberra distance [41] for measuring the similarity and is:

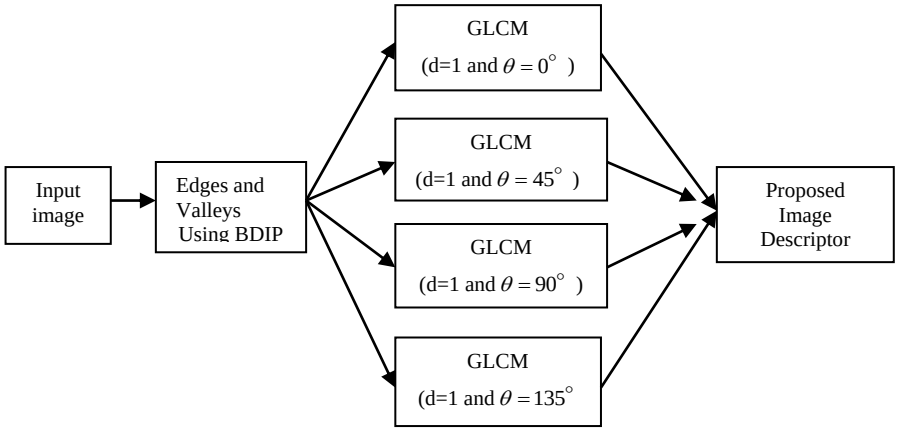

Fig.2. Proposed CMBDIP computation

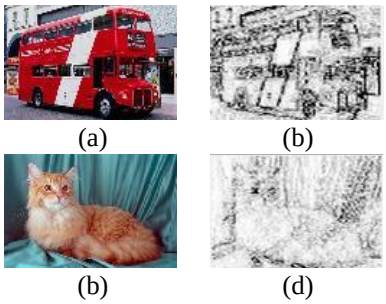

Fig.3.(a) and (b). Example image from Corel Dataset (c) and (d).BDIP of images of (a) and (b)

$$D_{Canbera}(Q,T) = \sum_{i=1}^{N} \left| \frac{T_i - Q_i}{T_i + Q} \right| \quad (4)$$

Where *Q and T* denotes input and target image descriptors and *N* denotes number of features. The computed distances among input and target image descriptors are sorted in ascending order using Bubble sort which is incredibly simple for sorting.

B. Measure of Accuracy

Each database image is used as query in the experiments. The proposed approach is assessed by precision P(N) and recall R(N) for retrieving the top matched N images and expressed as in [41]

$$\text{Precision} = \frac{I_N}{N} \quad (5)$$

$$\text{Recall} = \frac{I_N}{M} \quad (6)$$

Where I_N, *M* and *N* denotes number of relevant images, total number of retrieved images and total number of images. in database. The average P(N) and P(R) [41] for each class of images is as:

$$\text{Precision}(C_i) = \frac{1}{N_i} \sum_{k=1}^{N_i} \text{Precision}(I_k^i) \quad (7)$$

$$\text{Recall}(C_i) = \frac{1}{N_i} \sum_{k=1}^{N_i} \text{Recall}(I_k^i) \quad (8)$$

where *C* and *i* denotes the image class and number of images in each class, I_k^i is the k th image from class i. The average P(N) rate (APR) and average P(R) rate (ARR) are computed as in [41]:

$$APR = \frac{1}{N_n} \sum_{i=1}^{N_n} \text{Precision}(C_i) \quad (9)$$

$$ARR = \frac{1}{N_n} \sum_{i=1}^{N_n} \text{Recall}(C_i) \quad (10)$$

Where N_n denotes number of image classes in the dataset.

V. EXPERIMENTS

Holidays [42], Corel 10k [43] and Caltech 101[44] datasets are chosen for experiments. The Holidays dataset consists of 500 classes of images like water, natural, man-made, etc., and the numbers of images in each group differs and are in size 2448x3204. In our experiment, we resize it to 256x256. The Corel 10k dataset consist of approximately ten thousand images of 100 classes like African, cat, tiger, beach, sunset, door, waves, etc., and each class approximately has 100 images, the size of images are roughly 120 x 80 and 80 x 120 and images are in JPG format. Caltech dataset consists of 101 classes of 9,146 images and approximately image size is 300 x 200 and each class has roughly 40 to 800 images like ant, brain, chair, crab, cup, pizza, faces, panda, starfish, etc., and are in JPG format. Few example images from the experimental datasets are shown in Fig.4. In all the experiments, initially 10 images are retrieved later we increased it by 10 and it continues until number of images retrieved grows to be 100, and all the images of each class are used as query. Holidays dataset is taken in the experiment 1.The P(N) and P(R) curves for the CMBDIP [20] and [22] which obviously shown the variation in P(N) and P(R) with different number of retrieved images and shown in Fig.5 and it also obviously shown that CMBDIP is superior to the approaches presented in [20] and [22].

In Fig.8, 1st image belongs to query and remaining are the retrieved relevant images. The proposed CMBDIP has

the ARR of 57.12% for Holidays dataset and is significantly improved than others and is reported in Table.1.

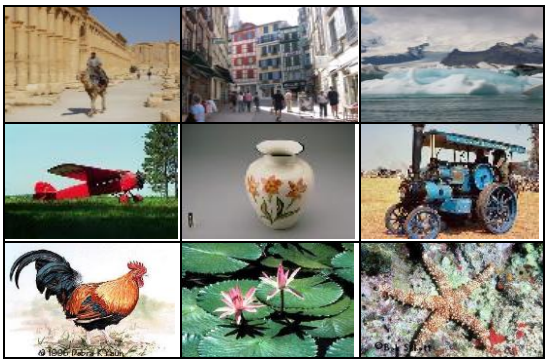

Fig. 4. Few example images of Holidays (Row 1 images), Corel 10k (Row 2 images) and Calitech 101 datasets (Row 3 images)

In the experiment 2, Corel 10k dataset is considered for evaluating proposed CMBDIP. The P(N) and P(R) is computed and performance of proposed CMBDIP is compared with histogram of BDIP [22] and low order moments of BDIP in multiresolution doamin [20]. Average P(N) Vs number of images retrieved and average P(R) Vs number of images retrieved for proposed CNBDIP, [20] and [22] is illustrated in Fig.6, which obviously reveals the dominance of proposed CMBDIP and the variations in P(N) and P(R) with respect to number of related images retrieved. The proposed CMBDIP has the ARR of 58.23% for Corel dataset and is higher than other approaches [20, 22] and is reported in Table.1. The query image and its top 4 retrieved relevant images are depicted in Fig.8.

Calitech 101 dataset is used in third experiment. The graphs for P(N) Vs P(R) of proposed CMBDIP, [20] and [22] with different number of retrieved images is illustrated in Fig.7 which obviously evident the supremacy of proposed CMBDIP and the variations in P(N) and P(R) with respect to number of related images retrieved. The proposed CMBDIP has the ARR of 61.81% for Calitech dataset and is noticeably superior to other methods [20, 22]. The query and retrieval of top 5 outcome of proposed CMBDIP for the dino, bus and sunflower images of Corel and Calitech dataset is depicted in Fig.8.

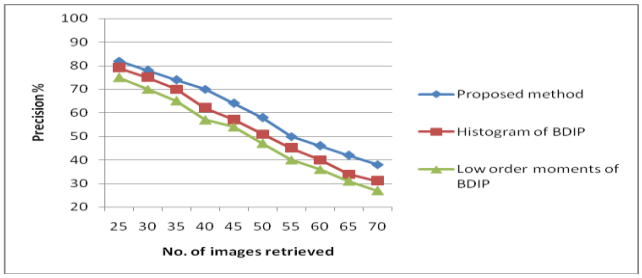

Fig.5 (a). Average precision of all the methods in Holiday dataset

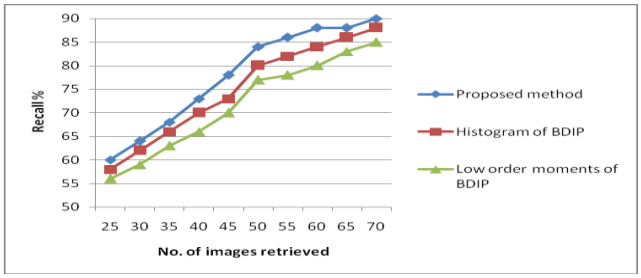

Fig.5 (b). Average recall of all the methods in Holiday dataset

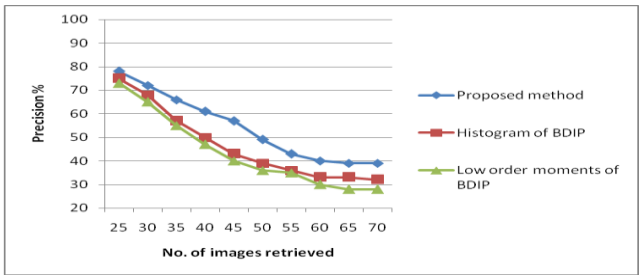

Fig.6 (a). Average precision of all the methods in Corel 10k dataset

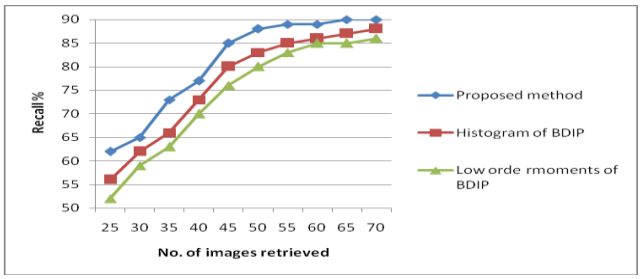

(b) Fig.6 (b). Average recall of all the methods in Corel 10k dataset

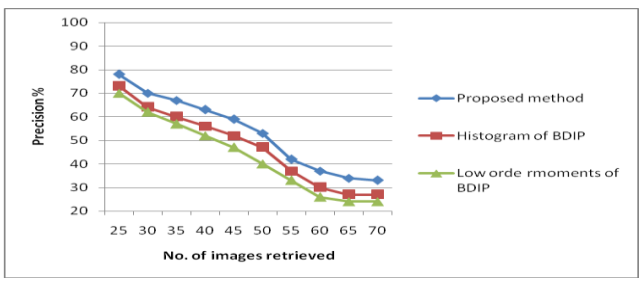

Fig.7 (a). Average precision of all the methods in Caltech dataset

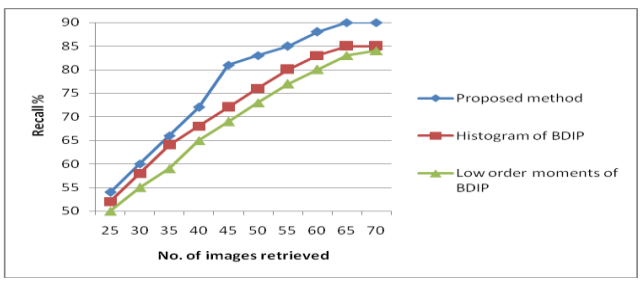

Fig.7 (b). Average recall of all the methods in Caltech dataset

Fig.8. First top 5 retrieval results for the dino, bus and sunflower images in Corel and Calitech database

Table.1. ARR for proposed and other approaches

Methods	Holiday Dataset	Corel 10k Dataset	Calitech 101 Dataset
Proposed	57.12%	58.23%	61.81%
Chun [20]	50.78%	49.23%	52.39%
Sathiamoorthy [22]	52.67%	51.45%	54.78%

In all the experiments, while we increase the number of related images retrieved above 200, the ARR remains stable and there is fluctuation in the plots of average P(N) and average P(R). The ARR values attained for proposed CMBDIP and others methods [20, 22] are reported in Table.1 and it is evidently understandable that proposed CMBDIP drastically outperforms for holiday, Corel and Calitech datasets than conventional approaches [20, 22]. In Fig.8, first two columns corresponds to the dino and bus images of Corel dataset and 3rd row had shown query and its related retrieved images for sunflower in Calitech dataset.

VI. CONCLUSION

In this paper, a novel edge based shape descriptor is proposed by combining BDIP with GLCM and named as co-occurrence matrix of BDIP (CMBDIP) which effectively computes local information and spatial information among adjacent edgels along 0°, 45°, 90°,135° directions and thus it overcomes the pitfalls of histogram of BDIP and integrates the gains of BDIP and GLCM. The proposed approach computes four CMBDIPs i.e. one for each direction and are joined together to construct the final CMBDIP. The proposed approach is verified on three image datasets namely Holiday, Corel10k and Caltech 101 and the results obviously demonstrate that proposed CMBDIP is significantly effective than conventional approaches. In future, proposed approach can be extended for various application domains.

References

[1]. Lowe, D.G., (2004). Distinctive image features from scale-invariant keypoints, *Int. J. of Comp. Vis*. 60 (2): 91–110.
[2]. H. Bay, A. Ess, T. Tuytelaars, L. Van Gool, Speeded-up robust features (SURF), Comput. Vis. Image Underst. 110 (2008) 346–359.
[3]. Heikkilä, M., Pietikäinen, M., Schmid, C., (2009). Description of interest regions with local binary patterns, Pattern Recognition 42, 425–436.
[4]. Murala S, Maheshwari RP, Balasubramanian R., (2012). Local tetra patterns: a new feature descriptor for content based image retrieval. IEEE Trans Image Process, 21(5):2874–86.
[5]. S.R. Dubey, S.K. Singh, R.K. Singh, 2015. Local diagonal extrema pattern: a new and efficient feature descriptor for CT image retrieval, IEEE Signal Process. Lett. 22 (9) 1215–1219.
[6]. S.R. Dubey, S.K. Singh, R.K. Singh, 2015. Local wavelet pattern: a new feature descriptor for image retrieval in medical CT databases, IEEE Trans. Image Process. 24 (12) 5892–5903.
[7]. Subrahmanyam Murala, Q.M. Jonathan Wu, (2013). Local ternary co-occurrence patterns: A new feature descriptor for MRI and CT image retrieval, *Neurocomputing*, 119: 399–412.
[8]. D. Zhang, G. Lu, A comparative study of curvature scale space and Fourier descriptors for shape based image retrieval, J. Vis. Commun. Image R 14 (2003) 41–60.
[9]. E. Attalla, P. Siy, Robust shape similarity retrieval based on contour segmentation polygonal multiresolution and elastic matching, Pattern Recoginit. 38 (2005) 2229–2241.
[10]. X. Shu, X.-J. Wu, A novel contour descriptor for 2D shape matching and its application to image retrieval, Image Vis. Comput. 29 (4) (2011) 286–294.
[11]. F. Mokhtarian, F. Abbasi, J. Kittler, Efficient and robust retrieval by shape content through curvature scale space, Int. workshop on Image Databases and Multi-Media Search (1997) 51–58.
[12]. Jain A. K. and A. Vailaya. 1996. Image retrieval using color and shape. *Pattern Recognition*. 29(8):1233–1244.
[13]. Cieplinski, L., Kim, M., Ohm, J.-R., Pickering, M., Yamada, A. (Editors), 2001. Text of ISO/IEC 15938-3/FCD Information Technology -Multimedia Content Description Interface-Part 3: Visual. Final Committee Draft, ISO/IEC/JTC1/SC29/WG11 (MPEG), document no. N4062.
[14]. Liu G.H., Li, Z.Y., Zhang, L., Xu. Y., (2011). Image retrieval based on micro-structure descriptor. *Pattern Recognition.* 44(9): 2123-2133.
[15]. K.Seetharaman, S.Sathiamoorthy, (2016), A Unified Learning Framework for Content Based Medical Image Retrieval Using a Statistical Model, *Journal of King Saud University - Computer and Information Sciences*, 28 (1): 110-124.
[16]. M.K. Hu, Visual pattern recognition by moment invariants, IRE Trans. Info. Theory 8 (1962) 179–187.
[17]. W.-Y. Kim, Y.-S. Kim, A region based shape descriptor using Zernike moments, Signal Process: Image Commun. 16 (2000) 95–102.
[18]. D. Zhang, G. Lu, Shape-based image retrieval using generic Fourier descriptor, Signal Process.: Image Commun. 17 (10) (2002) 825–848.
[1]. Y. D. Chun, S. Y. Seo, and N. C. Kim, "Image retrieval using BDIP and BVLC moments," IEEE Trans. Circuits Syst. Video Technol., vol. 13, pp. 951–957, Sep. 2003.
[19]. Chun, Y.D., Kim, N.C. and Jang, I.H., 2008. Content-Based Image Retrieval using Multiresolution Color and Texture Features, *IEEE Transactions on Multimedia*, 10(6):1073-1084.
[20]. S.Sathiamoorthy, M. Kamarasan, 2014, Content Based Image Retrieval Using the Low and Higher Order Moments of BDIP and BVLC, Int. J of Innovative Research in Sci, Engg and Technology, 3(1):8936-8941.

[21]. S.Sathiamoorthy, M. Kamarasan, 2014, A Novel Approach for Image Retrieval using BDIP and BVLC, Int. Journal of Innovative Research in Computer and Communication Engineering, 2(9):5897-5902.
[22]. S.Sathiamoorthy, 2014, Image Retrieval Using Texture and its Spatial Information, Int. J of Innovative Research in Sci, Engg and Technology, 3(10):17066-17075.
[23]. S.Sathiamoorthy, 2014, Color Image Retrieval Using Color, Texture and its Spatial Information, International Journal of Innovative Research in Computer and Communication Engineering, 2(11):7106-7114.
[24]. Singh, Chandan and Kanwal Preet Kaur. "A fast and efficient image retrieval system based on color and texture features." *J. Visual Communication and Image Representation* 41 (2016): 225-238.
[25]. Solmaz Abbasi, Farshad Tajeripour, Detection of brain tumor in 3D MRI images using local binary patterns and histogram orientation gradient, Neurocomputing, Volume 219, 2017, pp. 526-535.
[26]. K. Mikolajczyk, C. Schmid, A performance evaluation of local descriptors, IEEE Trans. Pattern Anal. Mach. Intell. 27 (2005) 1615–30.
[27]. Vahid Naghashi, Co-occurrence of adjacent sparse local ternary patterns: A feature descriptor for texture and face image retrieval, Optik 157 (2018) 877–889.
[28]. S. Pare , A.K. Bhandari , A. Kumar , G.K. Singh, An optimal Color Image Multilevel Thresholding Technique using Grey-Level Co-occurrence Matrix, Expert Systems With Applications (2017), doi: 10.1016/j.eswa.2017.06.021.
[29]. K. Mikolajczyk, C. Schmid, A performance evaluation of local descriptors, IEEE Trans. Pattern Anal. Mach. Intel. 27 (10) (2005) 1615–1630.
[30]. R.M. Haralick, K. Shanmugam, I. Dinstein, Textural features for image classification, IEEE Trans. Syst. Man. Cybern. 6 (1973) 610–621.
[31]. Yang, P. and Yang, G. (2016). Feature extraction using dual-tree complex wavelet transform and gray level cooccurrence matrix. Neurocomputing, 197, 212-220.
[32]. Gómez, W., Pereira, W. C. A., and Infantosi, A. F. C. (2012). Analysis of co-occurrence texture statistics as a function of gray-level quantization for classifying breast ultrasound. IEEE transactions on medical imaging, 31(10), 1889-1899.
[33]. Subrahmanyam, M., Wu, Q.J., Maheshwari, R.P. and Balasubramanian, R. (2013). Modified color motif cooccurrence matrix for image indexing and retrieval. Computers and Electrical Engineering, 39(3), 762-774.
[34]. Palm, C. (2004). Color texture classification by integrative co-occurrence matrices. Pattern recognition, 37(5), 965- 976.
[35]. Kandaswamy, U. etal.,.(2005). Efficient texture analysis of SAR imagery. IEEE Trans. on Geo. and Remote Sensing, 43(9), 2075-2083.
[36]. Manisha Verma, Balasubramanian Raman, Center symmetric local binary co-occurrence pattern for texture, face and bio-medical image retrieval, Journal of Visual Communication and Image Representation, Volume 32, October 2015, Pages 224-236.
[37]. Subrahmanyam Murala, Q.M. Jonathan Wu, (2013). Local ternary co-occurrence patterns: A new feature descriptor for MRI and CT image retrieval, *Neurocomputing*, 119: 399–412.
[38]. Cope J.S., Remagnino P., Barman S., Wilkin P. (2010) Plant Texture Classification Using Gabor Co-occurrences. In: Bebis G. et al. (eds) Advances in Visual Computing. ISVC 2010. Lecture Notes in Computer Science, vol 6454. Springer, Berlin, Heidelberg
[39]. Panda, R., Agrawal, S., and Bhuyan, S. (2013). Edge magnitude based multilevel thresholding using Cuckoo search technique. Expert Systems with Applications, 40(18), 7617-7628.
[40]. Charles YR, Ramraj R. A novel local mesh color texture pattern for image retrieval system. Int J Electron Commun (AEÜ) (2015), http://dx.doi.org/10.1016/j.aeue.2015.11.009.
[41]. http://lear.inrialpes.fr/people/jegou/data.php
[42]. Guang-Hai Liu, Jing-Yu Yang, etc,. Content-based image retrieval using computational visual attention model, Pattern Recognition, 48(8) (2015) 2554-2566.
[43]. http://www.vision.caltech.edu/Image_Datasets/Caltech101/

Proceedings of the Fourth International Conference on Communication and Electronics Systems (ICCES 2019)
IEEE Conference Record # 45898; IEEE Xplore ISBN: 978-1-7281-1261-9

Wavelet based Chordiogram Image Descriptor for Image Retrieval

A.Saravanan
Division of Computer and Information Science
Annamalai University
Annamalai Nagar, India
sarancseau@gmail.com

*S.Sathiamoorthy**
Tamil Virtual Academy
Chennai,
India
ks_sathia@yahoo.com

Abstract—**In this work, an efficient multiresolution approach based geometric details of localized edgels is proposed to represent an image, called wavelet based chordiogram image descriptor. The proposed approach mainly focuses on reducing the computational cost of retrieval system with the preservation of accuracy and resilient to illumination, scaling, noise and small rotations, and is performed by deriving the geometric features from the pyramid structure of an image using Discrete Haar Wavelet Transform. The proposed multiresolution approach based chordiogram image descriptor is comprehensively tested on benchmark datasets. The experimental results proved that proposed approach is considerably better in terms of time cost and retain the accuracy of existing approach.**

.

Keywords— Chordiogram image descriptor, L1 similarity measure, Haar wavelet, Multiresolution.

I. INTRODUCTION

Nowdays, most of the services and human communication in most of the domains rely heavily on digital images owing to ease of recognition for human as a consequence of rich amount of details available in digital images. With hasty increase of digital images, the size of digital image archives and libraries are expanding day by day and it leads to the core objective of retrieving system. Since the use of image retrieval has been flourishing in speed, researchers have much attention in the advancement of proper techniques to satisfy the users of all domains in image searching and retrieval from massive image archives and turns out to be most trendy subject in the domain of pattern recognition. Generally speaking, image retrieval approaches are categorized under three labels namely text, content and semantic based approaches.

Since 1970's, more numbers of research works contributed for image retrieval based on text. But, well annotation of digital images turns into inefficient and impractical owing to the massive digital image archives and its vast diverse image gathering, and it leads to the emerging of content based image retrieval (CBIR) in 1980's and numbers of CBIR approaches including QIBC [1], Virage [2], Web seek [3], and PicToSeek [4] have reported successfully. In CBIR approach, image representation is relying on feature vector which is formed using various low-level visual descriptors including color, shape and texture. In CBIR approach, according to similarity among the feature vectors of input image and dataset images, most pertinent images are retrieved by users. Commonly, feature descriptors falls into global and local categories. The first one focuses at whole image whereas the second concentrates on prominent key points and patches in an image and it has high discriminative ability then the global one. Since the semantic gap exists among the low level image descriptors and high level image concepts perceived by human, the retrieval performance of CBIR approaches are limited and to tackle this subject, approaches including dictionary learning and relevance feedback are introduced. Besides, researchers believe that optimized and locality preserving information is suitable for increasing the retrieval performance of CBIR approach because it characterize the image content accurately and viaduct the semantic gap as much as possible. [5] suggested that representing the image descriptors using histogram based feature representation is compact one and significantly decreases the noise and compact one.

Color-based clustering descriptor (CBC) and border/interior pixel classification descriptor (BIC) is described by Stehling et al., in [6]. In BIC, border and interior pixels are characterized by two separate histograms that count the intensity and locations of border/interior pixels. In [7], edge histogram descriptor is reported by Jain and Vailya, depicted based on edges computed by canny approach. It is also described in [7] that normalization of edges reduces the problem of resilient to scale and small rotation. Afterwards, EHD is developed by MPEG-7 [8] in which Sobel approach is incorporated for edge computation.

Along this way, Liu et al., [9, 10] defined that EHD is rich in texture, shape and spatial details of texture and shape, and thus extensively incorporated in numbers of CBIR approaches [11-18]. Edge orientation autocorrelogram (EOAC) is suggested by Mahmoudi et al. [19] and it exploits shape, textures and spatial details by utilizing the correlation among neighboring edgels based on its orientation and is demonstrated that performance of EOAC is noticeably better than EHD [8] and invariant to illumination, translation,

viewing position and minute rotation. Later, Liu et al., [16] suggested micro-structure descriptor (MSD) that exploits texture, color and shape particulars of an image by utilizing the orientation resemblance of edgels with an underlying color. Toshev et al. [20] suggested chordiogram which computes the geometric details of selected set of edgels found using segmentation. The exploited geometric details are distance and orientations of pair of edgels and also the degree of the vector connecting them. Thus, chordiogram is represented using a four dimensional histogram. But, boundaries attained through segmentation include fake edgels that affects the results. In [21], Kovalev and Volmer exploited the intensity and distance among the each pair of edgels and is characterized by utilizing a three dimensional histogram. Zitnick [22] presented a binary coherent edge descriptor, illustrated using a four-dimensional histogram which characterizes the coordinates and orientation of each edgels and length of an edge passing via the edgles.

Later on, Seetharaman and Sathiamoorthy presented an enhanced variety of EHD and EOAC [23-25] in HSV color space based on Full Range Autoregressive (FRAR) model with Bayesian Approach and it exploits incredibly minute and very fine edgels, also proved that their approach considerably best than the existing EHD [8] and EOAC [19] and owing to the behavior of the FRAR model their approaches also robust to noise to some extent. [16, 23, 25] reported that edge detectors including Sobel, Prewitt, Canny and Robert are developed for the images of gray-scale even they converts the color into gray-scale images for computing the edges and thus they failed in exploiting incredibly minute and very fine edgels owing to chromatic and spectral changes. Further, it is defined in [16] that finding edgels from H or S or V channels alone failed in exploiting incredibly minute and very fine edgels owing to spectral changes and such a loss play vital task in medical color image retrieval [24].

Afterward, a novel hybrid scheme is proposed in [26] which uses the statistical approaches namely color autocorrelogram (CA) and texture autocorrelogram (TA) together with the geometric approach namely chordiogram image descriptor (CID) for each region of a image for medical image retrieval. Since the localized geometric descriptors among edgels have been treated as resilient cauterization of shapes and images, Wang et al.,[27] proposed chordiogram image descriptor (CID), a histogram of chord details. The authors divided the image into number of patches then find the edges using the edge detectors [27] for each patch. Later geometric details including the distance among the pair of edgels, orientations of each edgel and degree of angle among line segment between a pair edgels and horizontal plane is exploited for every patch and they depicted it as local edgel chordiogram (LEC) [27]. The fusion of all LECs of image, named as CID. The authors demonstrated that CID exploits spatial structure in an image and is resilient to illumination.

It is affirmed by Zhang and Lu in [5] that contour extracted from spatial domain are sensitive to noise, and are not apt to be a separate descriptors, implementation and matching is also complex and cost. Thus, in this work, we proposed discrete Haar wavelet transformation based chordiogram image descriptor (CID) using for CBIR approach, called Wavelet based chordiogram image descriptor (WCID) which depicts the shape and exploits the localized geometric details from the locations of edgels computed from Haar wavelet transformations. The implementation and matching cost of proposed WCID approach is too less than the CID and the proposed WCID preserves an accuracy and robustness against illumination as that of CID.

The proposed work is expressed as follows. The proposed image feature is introduced in Section-2. Section-3 illustrates experimental results. Section-4 concludes the work.

II. DISCRETE HAAR WAVELET TRANSFORM

Over the decades, researchers are working in spectral domain including Fourier [28, 29] and wavelets [30], and the descriptors computed from wavelet domain is superior to Fourier, more number of researches carried out using wavelets [31-37]. Accordingly, in this paper, discrete Haar wavelet transform [38] is incorporated and it does the decomposition by calculating the approximations and details till the fine level and provide outcome in the form of wavelet pyramid image [38].

The discrete Haar wavelet transform is incorporated to attain the multi-resolution pyramid image as reported in [38] and is expressed as

$$\begin{bmatrix} a_0 \\ a_1 \\ a_2 \\ a_3 \\ w_0 \\ w_1 \\ w_2 \\ w_3 \end{bmatrix} \Leftarrow \begin{bmatrix} a_0 \\ w_0 \\ a_1 \\ w_1 \\ a_2 \\ w_2 \\ a_3 \\ w_3 \end{bmatrix} = \begin{bmatrix} 0.5 & 0.5 & 0.0 & 0.0 & 0.0 & 0.0 & 0.0 & 0.0 \\ 0.5 & 0.5 & 0.0 & 0.0 & 0.0 & 0.0 & 0.0 & 0.0 \\ 0.0 & 0.0 & 0.5 & 0.5 & 0.0 & 0.0 & 0.0 & 0.0 \\ 0.0 & 0.0 & 0.5 & 0.5 & 0.0 & 0.0 & 0.0 & 0.0 \\ 0.0 & 0.0 & 0.0 & 0.0 & 0.5 & 0.5 & 0.0 & 0.0 \\ 0.0 & 0.0 & 0.0 & 0.0 & 0.5 & 0.5 & 0.0 & 0.0 \\ 0.0 & 0.0 & 0.0 & 0.0 & 0.0 & 0.0 & 0.5 & 0.5 \\ 0.0 & 0.0 & 0.0 & 0.0 & 0.0 & 0.0 & 0.5 & 0.5 \end{bmatrix} \cdot \begin{bmatrix} I_0 \\ I_1 \\ I_2 \\ I_3 \\ I_4 \\ I_5 \\ I_6 \\ I_7 \end{bmatrix}$$

Where $I_{0,}, I_1, ..., I_k$ are the input images and contains k coefficients in which there are k/2 approximations and k/2 wavelet coefficients and are stored in the upper $\lfloor a_{0,}, a_1, .a_3 \rfloor$ and lower $\lfloor w_{0,}, w_1, .w_3 \rfloor$ arrays respectively and this method is repeated till fine level is attained and the fine level in this work is 3, is computed on the trial and error process. Multi-resolution pyramid image is constructed by utilizing a sub-sampling rate of 2 with no overlap method as described in [38]. Fig. 1 portrays the pyramid structure of a self photographed sample image upto the level 5. The dimension of self photographed sample image is 256 x 256 in level-0, 128 x 128 in level-1, 64 x 64 in level-2, 32 x 32 in level-3, 16 x 16 in level-4 and 8x8 in level-5. For each level of decomposition, the dimension of sample image is decreases to half of sample image at previous level and image at level 4 and 5 is not clear one. In the suggested approach, we fix the fine level experimentally.

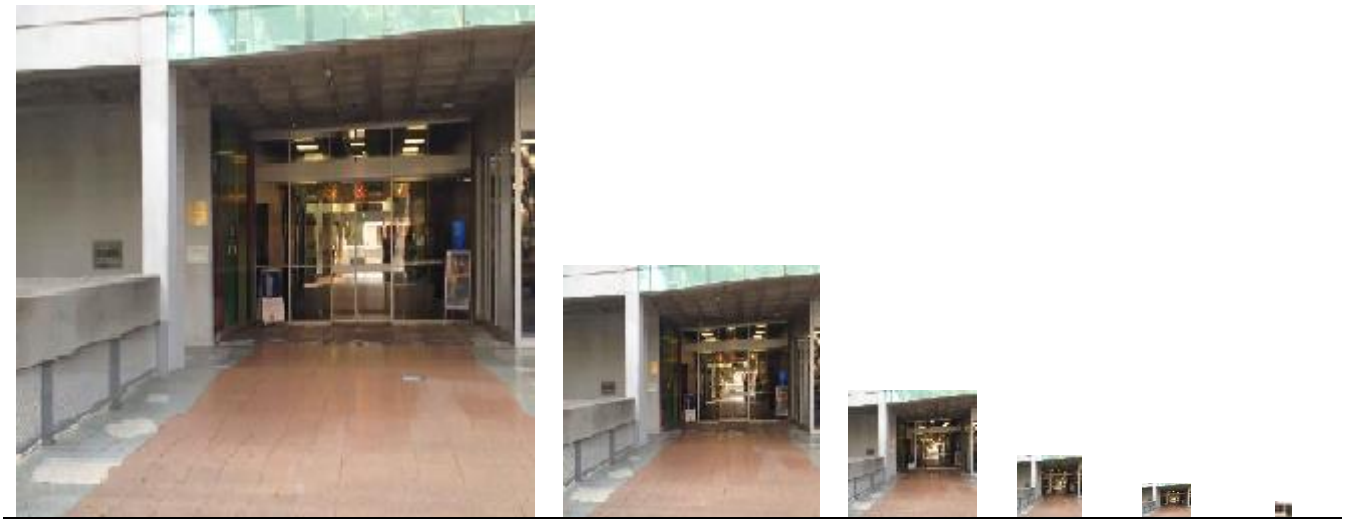

(a) (b) (c) (d) (e) (f)

Fig.1.Multi-resolution pyramid image from level-0 to 5 [(a)-(f)] using the discrete Haar wavelet transform. The input image at level 0 is of size 256 x 256 and images of succeeding level are of size 128x128, 64x64, 32x32, 16x16 and 8x8 respectively.

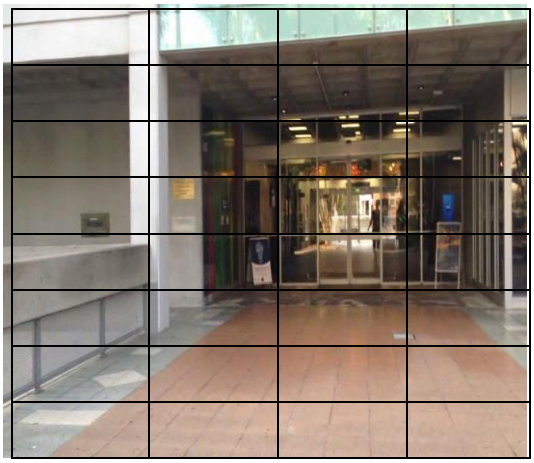

Fig.2. Image divided into 32 numbers of non-overlapping rectangular patches of size 8x8 for computing LEC

III. CHORDIOGRAM IMAGE DESCRIPTOR

Given image is partitioned into number of non-overlapping rectangular patches, numbered from 1, 2, 3, . . . , N. Each patch is characterized using LEC. In order to compute LEC, salient edgels are identified for each patch then local geometric features are computed from the salient edgels. Later, the LECs of all patches are collected in an order to construct a CID. The chord particulars of the patch image are computed from each pair of salient edgels coordinated at p and q and is described as in [27] as follows

$$C_{i_{pq}} = (\ell_{pq}, \phi_{pq}, \theta_p, \theta_q) \quad (1)$$

Where $\ell_{pq}, \phi_{pq}, \theta_p$ and θ_q designates the distance among edgels p and q, angle between line and horizontal plane, degree of orientations of edgels p and q about the normal directions respectively, and the values of ℓ_{pq} ranges from 0 to diameter of an image patch and ϕ_{pq}, θ_p and θ_q falls in between 0 and 2Π. The values of ℓ_{pq} are discretized in logarithmic space and are divided into η_d bins where d is the distance and is 4 in our work [27]. ϕ_{pq}, θ_p and θ_q are quantized into 8 bins of 50 degrees each [27]. Thus, CID is a 4D histogram and is normalized as in [27], and it encompasses chord details for every pair of salient edges in image patch.

Since CID is not sensitive to edge detector, in the experiment, Sobel operator is incorporated to compute the edges in each patch. After computing the edgels, response of each edgels are computed and are sorted. Then, proportion p of edgels having highest responses are preferred as in [27] to compute the LEC i.e. the salient edgels are preferred from the patch image with the intention of reducing the calculation cost by means of considering the less numbers of salient edgels and the selected salient edgels must exploits the shape details of patch and it must provide robustness against illumination and small rotation. Thus, the set of preferred salient edgels has two information: one is response of edgels and other is proportion p which decide the dimension of set of salient edgels and is decided experimentally as in [27] using n=pm where m and n are the amount of edgels in a patch and preferred salient edgels respectively and p is constant for all patches. Finally, the computed LECs of all patches are collected in an order to form a CID and is described as [27]

$$F = (C_1, C_2, ..., C_N) \quad (2)$$

Where $C_1, C_2, \ldots, C_N$ are the LEC of patches 1, 2, ..., N respectively.

IV. EXPERIMENTAL RESULTS AND DISCUSSION

A. Datasets

In the experimental study, Gardens Point Walking [39], UA Campus [27], St. Lucia [27] datasets and some self photographed images are utilized and some example images of

dataset consumed in the experiments are depicted in Fig.3. The Gardens Point Walking dataset has 3 folders namely day-left, day_right and night_right and each folder contains 200 images and are taken twice in day that is in a day and night and are roughly in 960x540 size and in JPG format. The datasets consists of images taken at varied times with sever and mild illumination changes. St. Lucia datasets consist of images taken at 5 varied times among early morning and late afternoon of a day and a day after two weeks. Thus, totally it has ten datasets. We have also used some self photographed images taken at varied time of a day in the experiments and it consists of 1140 images and are in JPG format and size of images are approximately 1280x720 and 1040 x780.

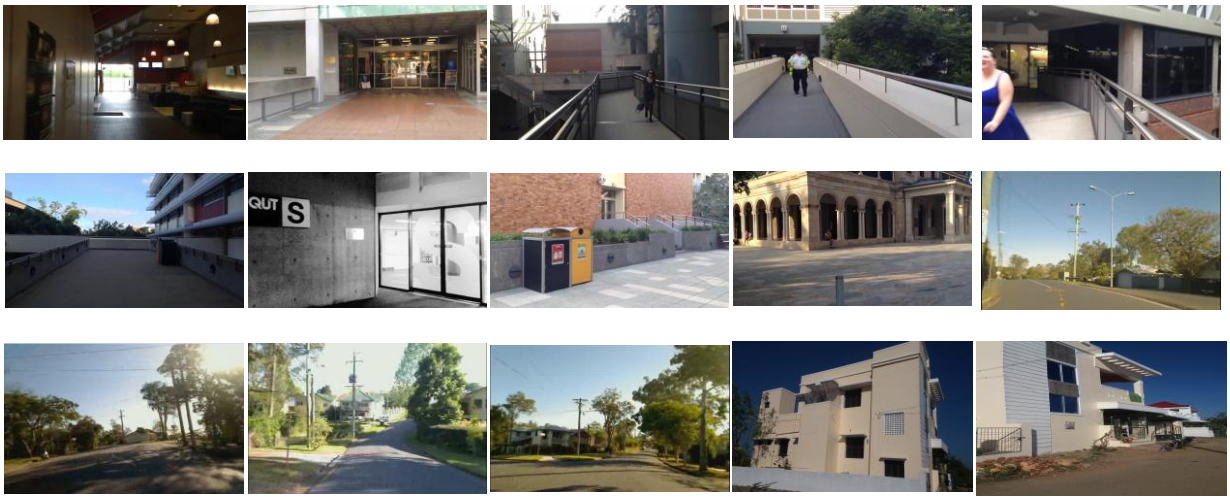

Fig.3.Few example. images of experimental datasets

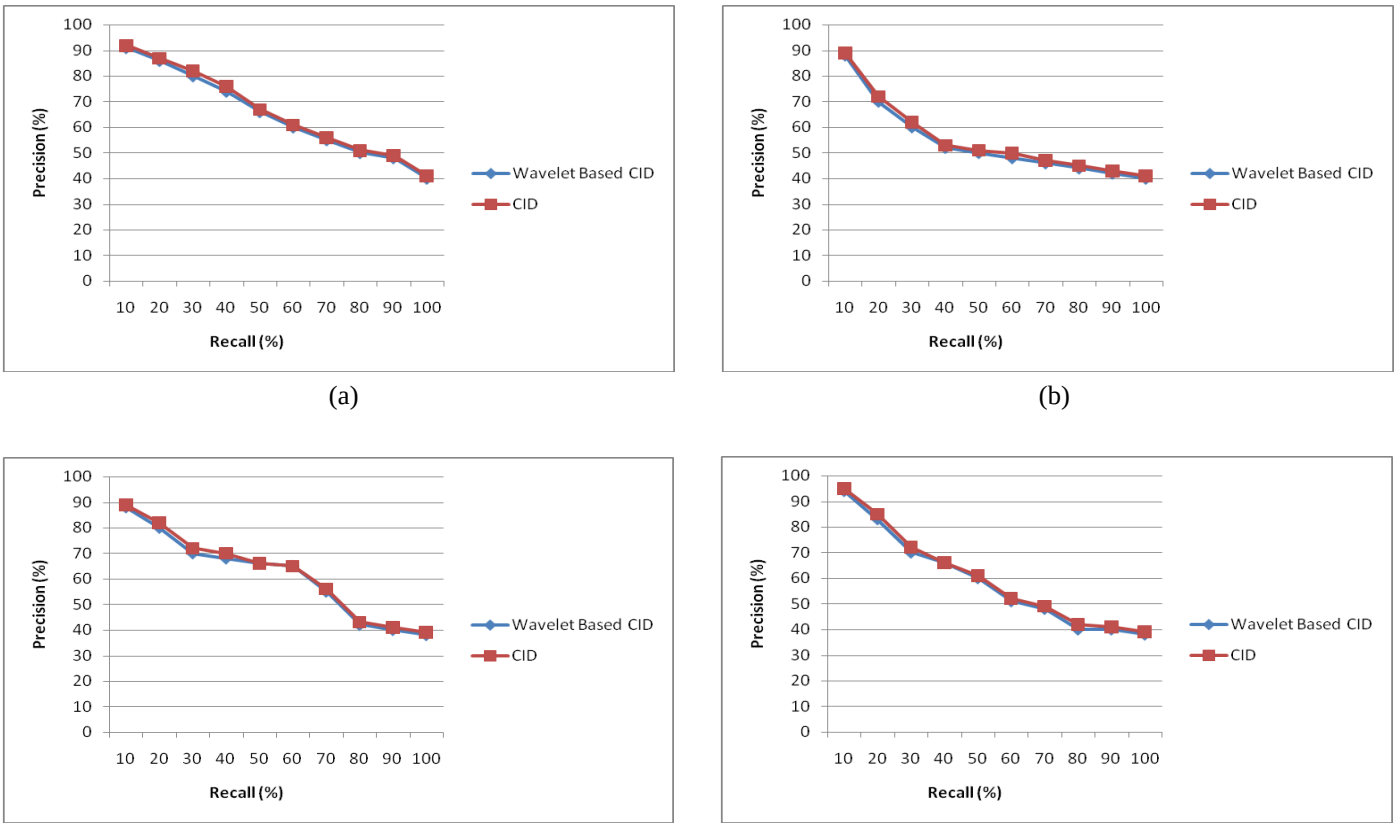

Fig.4.Precision Vs. Recall for the proposed Haar wavelet based CID and the conventional CID approaches for (a) Gardens Point Walking (b) UA Campus (c) St. Lucia (d) Self photographed image Datasets

B. Similarity Measuremnt

In the suggested work, L1 similarity measure is used and it computes sum of absolute differences of the variables [40] as a distance among 2 points in an Euclidean space with fixed Cartesian coordinate system [40]. The L1 distance among two images is given by

$$S\left(I^q, I^t\right) = \sum_{i=1}^{k}\left(I_i^q - I_i^t\right) \tag{3}$$

where, I_i^q and I_i^t are input and target image descriptor vectors respectively and k is size of the combined feature vector.

Instead of computing the similarity among query and target images based on the summation of similarity measures of all the corresponding patches, similarity measures of all the corresponding patches are computed and are ordered in ascending manner as in [27]. The higher similarity values between two images are eliminated to avoid impact of noise in the image which leads to false matching [27]. Thus, the summation of n smallest similarities computed from the corresponding patches of query and target images are summed finally to get the matching.

C. Performance Assessment

The capability of proposed wavelet based CID approach for image searching is illustrated on the basis of precision and recall. In the image retrieving process, for an input image, several images are retrieved and few of them are relevant to input image and remaining retrieved images are not relevant. The images satisfies the interest of user are known as relevant and total number of images retrieved for an input image is known as retrieved images. Precision (P) and recall (R) is calculated as [41,42]

$$P = \frac{(\text{Relevant images}) \bigcap (\text{Retrieved images})}{\text{Total number of images retrieved}} \tag{4}$$

$$R = \frac{(\text{Relevant images}) \bigcap (\text{Retrieved images})}{\text{Total number of releveant images in the database}} \tag{5}$$

The P and R associated with a class are computed as [41,42]

$$P_{avg}^{C} = \frac{1}{N}\sum_{i=1}^{N} P_i^C \tag{6}$$

$$R_{avg}^{C} = \frac{1}{N}\sum_{i=1}^{N} R_i^C \tag{7}$$

Where C designates the class number, N designates total number of images in each class. For complete dataset, the P and R is calculated as in [41,42]

$$P_{Tot}^{C} = \frac{1}{N}\sum_{s=1}^{N} P_{avg}^{C}(C) \tag{8}$$

$$R_{Tot}^{C} = \frac{1}{N}\sum_{s=1}^{N} R_{avg}^{C}(C) \tag{9}$$

Where N denotes number of classes available in the dataset. R, also named as average retrieval rate (ARR). In the suggested approach, each image in the dataset is used as query to the proposed retrieval system and for each of them, P and R is measured. For each class, P and R is measured.

D. Experimental setup

To prove the competence of the proposed WCID, input image is transformed into fine level using the discrete Haar wavelet and the level of fine is 3 which is decided experimentally. The images in the datasets are resized to 1028 x 512. The wavelet transformed image is partitioned in to number of patches of 8 x 8 sizes. Thus, for an image of size 1028 x 512, we obtained 512 x 256, 256 x 128, 128 x 64, 64 x 32 and 32 x 16 in level-1 to level-5 respectively and we have 32 numbers of 8x8 patches in the optimum level 3 and is depicted in Fig.2. According to [27], 15% of salient edgels are preferred from the patch for computing the LEC.

E. Results and Discussion

Gardens Point Walking dataset is considerd in the experiment1. P and R for the proposed WCID and conventional CID are computed and demonstrated via graphs. In Fig.4, plots for P and R are depicted. Fig.4a depicts variation in P with respect to R and very clearly it demonstrated that the suggested WCID approach is equalently performing with conventional CID and Table.1 depicts that the suggested scheme requires less time cost than the conventional CID. The P and R of presented WCID and conventional CID at level 0 and level 3 are 65.78%, 65.64% and 8.41%, 8.51% respectively. From the results it is obvious that the change in the values of precison and recall is very small from level 1 to level 3. But, from the level 4, there is drastic change in the values of both P and R.

In the second experiment, UA campus dataset have been used. The results of the proposed wavelet based CID and CID in the form of P and R is depicted in Fig.4b. The proposed approach is equally satisfying with the CID and is obviously visible in the graph. The P and R of presented and conventional techniques are 57.23%, 57.11% and 9.86%, 9.85% respectively. The outcome shown in Table 2 clearly depicted that after the 3rd level decomposition, the change in the P and R values are for above the normal.

Table 1. Computational complexity of WCID and CID

Methods	Time in seconds
Wavelet based CID	22
CID	45

In the third experiment, St.Lucia dataset has been taken for image retrieval. Results for St.Lucia dataset have been presented in Fig.4c. The results of performance measures clearly demonstrated that the proposed WCID equally outperforms the CID with leas computational time and preserves robustness capability of CID against illumination, noise scaling and small rotation. The P *and* R attain by

proposed and existing CID are 67.32%, 67.15% and 7.67% and 7.79% respectively.

In the fourth experiment, self photographed images are considered. The results of proposed WCID and CID in terms of P *and R* is depicted in Fig.4d. The precision and ARR for the WCID and CID are 66.23% and 66.05% and 6.68% and 6.79% respectively. Table 2 illustrates the average *P* and *R* for all the datasets used in the experimental study. In Fig.5 and 6, query image to the suggested system and its top five retrieval results are depicted which is similar to the results of CID. From Fig.5 and 6, it is obviously understood that the proposed WCID is illumination to invariant and for query image of day left category, the suggested system also retrieve images from day right and night right category as that of CID that is the results confirmed that proposed WCID is strongly invariant to illumination.

(a) (b) (c) (d) (e) (f)

Fig.5 (a). An example query image (b)-(f). Top 5 retrieval results using the WCID

(a) (b) (c) (d) (e) (f)

Fig.6. (a). An example query image (b)-(f). Top 5 retrieval results using the WCID

Table 2. Precision and Recall for proposed WCID and CID at various levels of decomposition by Haar wavelet transform

Level of Decomposition and Methods / Datasets	**Performance**	L_0 **CID**	L_1 **WCID**	L_2 **WCID**	L_3 **WCID**	L_4 **WCID**	L_5 **WCID**
Gardens Point Walking	Precision (%)	65.78	65.73	65.68	65.64	64.00	62.21
	Recall (%)	8.41	8.44	8.47	8.51	8.99	9.88
UA Campus	Precision (%)	57.23	57.19	57.15	57.11	56.01	54.10
	Recall (%)	9.76	9.78	9.81	9.85	10.88	11.90
St. Lucia	Precision (%)	67.32	67.26	67.18	67.15	65.09	63.22
	Recall (%)	7.67	7.70	7.76	7.79	8.82	9.85
Self Photographed Images	Precision (%)	66.23	66.16	66.10	66.05	64.00	62.16
	Recall (%)	6.68	6.71	6.75	6.79	7.82	8.86

V. CONCLUSION

A shape based image descriptor called chordiogram image descriptor is computed from the multi-resolution resolution domain which captures the local geometric descriptors rather than image intensities. The pyramid structure of an image is obtained using discrete Haar wavelet transform and is used for computation of chordiogram image descriptor which reduces computation time drastically for descriptor extraction and matching and preserves the same average retrieval rate as that of CID and also resilient to sever illumination, scaling, noise and small rotation. The presented approach is extensively tested on Gardens Point Walking, UA campus, St. Lucia datasets and the presented approach depicts a excellent tradeoff between interclass separability and interclass variance. In future, the proposed scheme can be combined with other visual details of image to further improve the accuracy of retrieval.

References

[1] Niblack, W., Barber, R., and *et al.*, Feb. 1994. The QBIC project: Querying images by content using color, texture and shape, in *Proc. SPIE Storage and Retrieval for Image and Video Databases.*

[2] Gupta, A and Jain, R, 1997. Visual information retrieval, *Communications of the ACM* 40(5).

[3] Smith, J. R., Chang, S.-F., 1997. Visually searching the web for content, *IEEE Multimedia Magazine* 4(3), 12–20.

[4] Theo Gevers and Arnold W. M. Smeulders, January 2000. PicToSeek: Combining Color and Shape Invariant Features for Image Retrieval, *IEEE Transactions on image processing*, 9(1).

[5] Zhang, D., Lu, G., 2004, Review of shape representation and description, *Pattern Recognition*. 37(1): 1-19.

[6] Stehling, R. de O., Nascimento, M.A., Falcão, A.X., 2002. A compact and efficient image retrieval approach based on border/interior pixel classification, in: *International Conference on Information and Knowledge Management*, pp. 102–109.

[7] Jain A. K. and A. Vailaya. 1996. Image retrieval using color and shape. *Pattern Recognition*. 29(8):1233–1244.

[8] Cieplinski, L., Kim, M., Ohm, J.-R., Pickering, M., Yamada, A. (Editors), 2001. Text of ISO/IEC 15938-3/FCD Information Technology -Multimedia Content Description Interface-Part 3: Visual. Final

Committee Draft, ISO/IEC/JTC1/SC29/WG11 (MPEG), document no. N4062.

[9] Liu, Y., Zhang, D., Lu, G., Ma, W.Y., 2007. A survey of content-based image retrieval with high-level semantics, *Pattern Recognition*. 40 (11): 262–282.

[10] Liu G, Zhang L, Hou Y, Li Z, Yang J., 2010. Image retrieval based on multi-texton histogram. *J. Pattern Recognit.* 43: 2380–2389.

[11] Mahmudur Rahman, Md., Prabir Bhattacharya, and Bipin C. Desai, 2007. A framework for medical image retrieval using machine learning and statistical similarity matching techniques with relevance feedback. *IEEE trans on infor technology in biomedicine*. 11(1), 58-69.

[12] Alefs, B., Eschemann, G., Ramoser, H., et al, 2007. Road sign detection from edge orientation histogramms. In: Proceedings of the IEEE Intelligent Vehicles Symposium, Istanbul, Turkey. pp. 993-998.

[13] Mahmudur Rahman, Md., Bipin C. Desai, Prabir Bhattacharya, 2008. Medical image retrieval with probabilistic multi-class support vector machine classifiers and adaptive similarity fusion. Computerized Medical Imaging and Graphics. 32, 95-108.

[14] Mahmudur Rahman, Md., Parbir Bhattacharya and Bipin C. Desai, 2009. A unified image retrieval framework on local visual and semantic concept based feature space. J. Vis. Commun. Image R. 20(7), 450-462.

[15] Chatzichristofis S.A., Zagoris, K., Boutalis Y. S., and Papamarkos. N., 2010. Accurate image retrieval based on compact composite descriptors and relevance feedback information. International Journal of Pattern Recognition and Artificial Intelligence. 24(2): 207-244.

[16] Liu G.H., Li, Z.Y., Zhang, L., Xu. Y., 2011. Image retrieval based on micro-structure descriptor. Pattern Recognition. 44(9): 2123-2133.

[17] Mahmudur Rahman, Md., Sameer K. Antani, and George R. Thoma, 2011. A learning-based similarity fusion and filtering approach for biomedical image retrieval using svm classification and relevance feedback. IEEE trans on information technology in biomedicine. 15(4), 640-646.

[18] Mahmudur Rahman, Md., Daekeun You, Matthew S. Simpson, Dina Demner-Fushman, Sameer K. Antani, and George R. Thoma, 2013. Multimodal biomedical image retrieval using hierarchical classification and modality fusion. Int J Multimed Info Retr. 2, 159-173.

[19] Mahmoudi, F., Shanbehzadeh, J., Eftekhari, A.M., and Soltanian-Zadeh, H, 2003. Image retrieval based on shape similarity by edge orientation autocorrelogram. Pattern Recognition, 36, 1725-1736.

[20] A. Toshev, B. Taskar, K. Daniilidis, Shape-based object detection via boundary structure segmentation, Int. J. Comput. Vision 99 (2) (2012) 123–146.

[21] V. Kovalev, S. Volmer, Color co-occurrence descriptors for querying-byexample, in: Multimedia Modeling, 1998. MMM'98. Proceedings. 1998, IEEE, 1998, pp. 32–38.

[22] C.L. Zitnick, Binary coherent edge descriptors, in: European Conference on Computer Vision, Springer, 2010, pp. 170–182.

[23] Seetharaman. K., Sathiamoorthy. S., December 2013. An Improved Edge Direction Histogram and Edge Orientation AutoCorrlogram for an Efficient Color Image Retrieval, International Conference on Advanced Computing Communication Systems (ISBN DVD 9781479935055), Coimbatore, India.

[24] Seetharaman. K., Sathiamoorthy. S., 2014. Color image retrieval using statistical model and radial basis function neural network. Egyptian Informatics Journal, 15, 59-68.

[25] K.Seetharaman, S.Sathiamoorthy, A Unified Learning Framework for Content Based Medical Image Retrieval Using a Statistical Model. Journal of King Saud University - Computer and Information Sciences, Vol. 28 (2016), No. 1, Dec 2015, pp. 110-124.

[26] A.Saravanan , M. Natarajan and S. Sathiamoorthy, A Novel Hybrid Framework for Medical Image Retrieval, Asian Journal of Engineering and Applied Technology, Vol. 7 No.1 Jan-June 2018 pp 37-41.

[27] Xiaolong Wang, Hong Zhang, Guohua Peng, A chordiogram image descriptor using local edgels, J. Vis. Commun. Image R, 49 (2017) 129–140.

[28] Otterloo, P.J. V, 1991. A Contour-OrientedApproach to Shape Analysis, Prentice-Hall International (UK) Ltd, Englewood Cliffs, NJ, pp. 90–108

[29] Arbter, K., Snyder, W.E., Burkhardt, H., Hirzinger, G., 1990. Application of affine-invariant Fourier descriptors to recognition of 3-D objects, IEEE Trans. Pattern Anal. Mach. Intell. 12 (7): 640–647.

[30] Ohm, J.R., Bunjamin, F.B., Liebsch, W., Makai, B., Muller, K., Somlic, A., Zier, D., 2000. A set of visual feature descriptors and their combination in a low-level description scheme, Signal Pro. Image Comm.16:157–179.

[31] He, Z., You, X., Yuan, Y., 2009. Texture image retrieval based on non-tensor product wavelet filter banks, Signal Processing. 89:1501–1510.

[32] Kokare, M., Biswas, P.K., Chatterji, B.N., 2005. Texture image retrieval using new rotated complex wavelet filters, IEEE Transactions on Systems, Man and Cybernetics – Part B. 35 (6):1168–1178.

[33] Selesnick, W.I., Baraniuk, R.G., Kingsbury, N.G., 2005. The dual-tree complex wavelet transform, IEEE Signal Proc. Mag.. 22 (6): 123–151.

[34] Muneeswaran, K., Ganesan, L., Arumugam, S., Ruba Sounder, K., 2005. Texture classification with combined rotation and scale invariant wavelet features, Pattern Recognition, 38 (10): 1495–1506.

[35] Srinivasa Rao, Ch., Srinivas kumar, S., Chatterji, B.N., 2007. Content based image retrieval using Contourlet Transform, ICGST-GVIP Journal. 7 (3): 9–15

[36] Krishnamoorthi, R., Sathiya devi, S., 2012. A multiresolution approach for rotation invariant texture image retrieval with orthogonal polynomials model, J. Vis. Commun. Image R. 23: 18–30.

[37] M. Kamarasan, S.Sathiamoorthy, 2014, Orthogonal Polynomial Model Based Image Retrieval using multiresolution Spatial-Temporal features, International Journal of Innovative Research in Science, Engineering and Technology, 3(12):17076-17083.

[38] K.Seetharaman, M.kamarasan, (2012), A smart color image retrieval method based on multiresolution features, IEEE International Conference on Computational Intelligence and Computing Research, pp.68-75.

[39] A. Glover, The gardens point walking dataset, (Feb 14, 2014).

[40] Fazal Malik, Baharum Baharudin, (2013). Analysis of distance metrics in content-based image retrieval using statistical quantized histogram texture features in the DCT domain, Journal of King Saud University - Computer and Information Sciences, 25(2):207-218.

[41] Chandan Singh , Ekta Walia , Kanwal Preet Kaur , Color Texture Description with Novel Local Binary Patterns for Effective Image Retrieval, Pattern Recognition (2017), doi: 10.1016/j.patcog.2017.10.021.

[42] Manisha Verma a, Balasubramanian Raman, Local tri-directional patterns: A new texture feature descriptor for image retrieval, Digital Signal Processing, 51(2016),62-72.

Proceedings of the Fourth International Conference on Communication and Electronics Systems (ICCES 2019)
IEEE Conference Record # 45898; IEEE Xplore ISBN: 978-1-7281-1261-9

Wavelet Based Multi-Trend Structure Descriptor for Effective Image Retrieval

M.Natarajan
Division of Computer and Information Science
Annamalai University
Annamalai Nagar, India
mnind.2004@gmail.com

*S.Sathiamoorthy**
Tamil Virtual Academy
Chennai,
India
ks_sathia@yahoo.com

Abstract— **We propose a novel descriptor for content based image retrieval called wavelet based multi-trend structure descriptor (WMTSD). The proposed WMTSD is an enhanced approach of multi-trend structure descriptor (MTSD). To diminish the computational cost of MTSD with the preservation of retrieval rate, WMTSD is derived. In order to diminish the time cost, an image is decomposed into optimum level using discrete Haar wavelet transform and it produces multi-resolution pyramid image. The multi-resolution pyramid image at optimum level is utilized to estimate the feature descriptor. The optimum level for the decomposition of an image is determined empirically. The proposed WMTSD is exhaustively tested on Corel 1k, Corel 5k, Corel 10k and Caltech benchmark datasets. The experimental study very clearly illustrated that the proposed WMTSD and MTSD attains almost similar retrieval accuracy. But, the time cost of WMTSD is too small then the MTSD which is required more in the era of big data. Euclidean distance measure is adopted to assess the similarity between the images. Precision and Recall are the measures used to assess the proposed approach.**

.

Keywords— Multi-Trend Structure descriptor, Euclidean similarity measure, Haar Wavelet, Wavelet based Multi-Trend Structure descriptor, Sobel operator.

I. INTRODUCTION

Today, in the domain of pattern recognition, content based image retrieval (CBIR) is an energetic area of research. Over more than three decades, more and more number of effective CBIR approaches has developed with reasonable retrieval rate and time. However, with an extensive uses of varieties of images like medical, biometric, historical archives, agriculture, media, etc over the web, the performance of existing systems for CBIR need to be enhanced.

Image retrieval system permits the end users to browse and access images more effectively from the datasets. The feature computation is the main component of retrieval system which entails an image to be characterized by high discriminative feature with high and small changes between the features of inter and intra class images, and the images are characterized either at global or local approach. The global approach disregard the local characteristics of pixels in an image and thus it endure issues related to scaling, translation, occlusion, illumination, noise etc and are overcome by the local approach which characterizes an image from local regions or partitions of an image.

It is reveled from the literature that more and more numbers of global approaches has suggested based on texture, shape and color details of an image including Tamura features [1], Gabor filtering [2], Markov random field model [3] and gray-level co-occurrence matrices [4] for texture details; contour features like circularity, eccentricity, convexity, major axis orientation [5, 6], shape signatures like curvature, cumulative angle, tangent angle, chord-length [7, 8], boundary moments [9, 10], edge histogram descriptor (EHD) [11-13] for shape details and color histogram (CH), dominant color descriptor (DCD), scalable color descriptor (SCD) and color layout descriptor (CLD) for color details [14].

Though global approach is the core of numbers of CBIR approaches, the aforesaid issues related with global approaches have required the characterization of images using local approaches including SIFT [15], SURF [16], LBP [17], HOG [18], local ternary co-occurrence patterns [19], local mesh pattern [20], multi-texton histogram [21], micro-structure descriptor [22], saliency structure histogram [23], structure element descriptor [24], texton co-occurrence matrices [25], multi-trend structure descriptor (MTSD) [26], etc. Among various local approaches MTSD has demonstrated to be the more efficient in state-of-art retrieval approaches and is successfully verified on benchmark datasets namely Corel and Caltech. The MTSD captures correlation of local structure in the form of trends for edge orientation, color and intensity details using the information variation of pixels along 0°, 45°, 90°and 135° orientations. It also found from literature that many of conventional local approaches characterizes an image using either texture or color or shape and very rare local approaches encompasses texture, color and shape and MTSD is one among them. But, we found that computational complexity of MTSD is significantly intensive. For example, consider an image of size 256 x 256 for which large, equal and small trends either for texture or color or shape details along 0°, 45°, 90° and135° orientations is computed from 7,281 non-overlapping windows of size 3 x 3. Thus, to compute texture, color and

shape details MTSD uses 21,843 non-overlapping windows of size 3 x 3. The major aim of this proposed work is developing a CBIR system that compromises between retrieval rate and computational cost. Hence, in this work., computational intensive issue of MTSD is addressed by computing the MTSD from the image which is decomposed into pyramid like multi-resolution structure utilizing discrete Haar wavelet transform [27] and the approach is named as Wavelet based multi-trend structure descriptor (WMTSD) in which an example image of size 256 x 256 is decomposed into optimum level i.e. 3, which is determined based on trial and error approach. Thus, we obtain 32 x 32 image at fine level from which we compute the MTSD. Large, equal and small trends either for texture or color or shape details along 0°, 45°, 90° and135° orientations is computed in the proposed approach (WMTSD) from 113 non-overlapping windows of size 3 x 3 and for encompassing all the three details mentioned above 339 non-overlapping windows of size 3 x 3 is used. Thus, in the proposed wavelet based approach, computational cost of MTSD is reduced without diminishing the discriminative power of MTSD and is demonstrated using the benchmark datasets.

	E	S	L
0	12	2	10
1	6	2	19
.	.	.	.
.	.	.	.
.	.	.	.
108	34	1.	9

Fig.1. MTSD for color feature

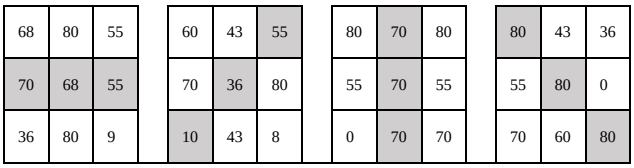

Fig.2. (a). Small trend along 0° (b). Large trend along 45° (c). Equal trend along 90° (d). Equal trend along 135°

This manuscript is structured as follows. In section II, overview of conventional MTSD is provided. The discrete Haar wavelet transform has been described in section III. Feature estimation is explained in section IV. Similarity and performance measures used in the proposed approach are explained in section.V and VI. Exhaustive experimental analysis based on retrieval rate and computational cost is reported in section VII. Conclusion is defined in section VIII.

II. MULTI-TREND STRUCTURE DESCRIPTOR

The MTSD [26] estimates the correlation of local structure in the type of trends for edge orientation, color and texture details using the information change of pixels along 0°, 45°, 90° and135° orientations. For estimating the MTSD, an image is alienated into 3 x 3 non overlapping windows. In [26], Zhao et al., defined large, small and equal trends based on quantized pixel values and are small to large, large to small and same along 0°, 45°, 90°and 135° orientations respectively.

The MTSD [26] is estimated from HSVcolor space. For estimating the local structure of color, texture and edge details based on trends, color quantization is carried out by separating the H, S andV channels into 12, 3 and 3 bins and it gives 108 colors; intensity details in V channel is quantized into 20; Sobel edge detection approach is applied on V channel image to extract edge details and the identified edges are quantized into 9 based on the orientations of edge pixels.

Accordingly, trends are estimated for quantized edge orientation, color and texture details and are integrated to form a feature vector. Fig.1 illustrates the image feature matrix estimated by the MTSD for color information where numbers of each trends for quantized colors 0 to 108 is described. Fig.2 illustrates an example for trends along 0°, 45°, 90°and 135° orientations.

III. DISCRETE HAAR WAVELET TRANSFORM

In recent years, researchers working in CBIR, employed wavelets due to its multi-resolution ability and attained better retrieval performance [27]. Subsequently, in the proposed work, discrete Haar wavelet transform [27] is employed which performs decomposition by estimating the approximations and details till the optimum level and results in wavelet pyramid image formation [27]. The multi-resolution pyramid image is obtained using discrete Haar wavelet transform as in [27] and is described as follows

$$\begin{bmatrix} a_0 \\ a_1 \\ a_2 \\ a_3 \\ w_0 \\ w_1 \\ w_2 \\ w_3 \end{bmatrix} \Leftarrow \begin{bmatrix} a_0 \\ w_0 \\ a_1 \\ w_1 \\ a_2 \\ w_2 \\ a_3 \\ w_3 \end{bmatrix} = \begin{bmatrix} 0.5 & 0.5 & 0.0 & 0.0 & 0.0 & 0.0 & 0.0 & 0.0 \\ 0.5 & 0.5 & 0.0 & 0.0 & 0.0 & 0.0 & 0.0 & 0.0 \\ 0.0 & 0.0 & 0.5 & 0.5 & 0.0 & 0.0 & 0.0 & 0.0 \\ 0.0 & 0.0 & 0.5 & 0.5 & 0.0 & 0.0 & 0.0 & 0.0 \\ 0.0 & 0.0 & 0.0 & 0.0 & 0.5 & 0.5 & 0.0 & 0.0 \\ 0.0 & 0.0 & 0.0 & 0.0 & 0.5 & 0.5 & 0.0 & 0.0 \\ 0.0 & 0.0 & 0.0 & 0.0 & 0.0 & 0.0 & 0.5 & 0.5 \\ 0.0 & 0.0 & 0.0 & 0.0 & 0.0 & 0.0 & 0.5 & 0.5 \end{bmatrix} \begin{bmatrix} I_0 \\ I_1 \\ I_2 \\ I_3 \\ I_4 \\ I_5 \\ I_6 \\ I_7 \end{bmatrix}$$

$I_{0,}, I_1, ..., I_k$ are the input images and contains k coefficients in which there are k/2 approximations and k/2 wavelet coefficients and are stored in the upper $[a_{0,}, a_1, .a_3]$ and lower $[w_{0,}, w_1, .w_3]$ arrays respectively and this procedure is repeated till optimum level is achieved. In this work, optimum level is 3 and is determined based on trial and error approach. Multi-resolution pyramid image is framed by a sub-sampling rate of 2 with no overlap approach as in [27]. Fig. 3 illustrates the pyramid structure of an example image for the optimum level i.e. 3. The size of an example image is 256 x 256 in the first level and is

decomposed up to optimum level i.e. 3. At each level of decomposition, the size of an example image is diminishing to half of an example image at previous level. Thus, we obtained 128 x 128, 64 x 64, 32 x 32 dimensions at levels 1st, 2nd and 3rd respectively.

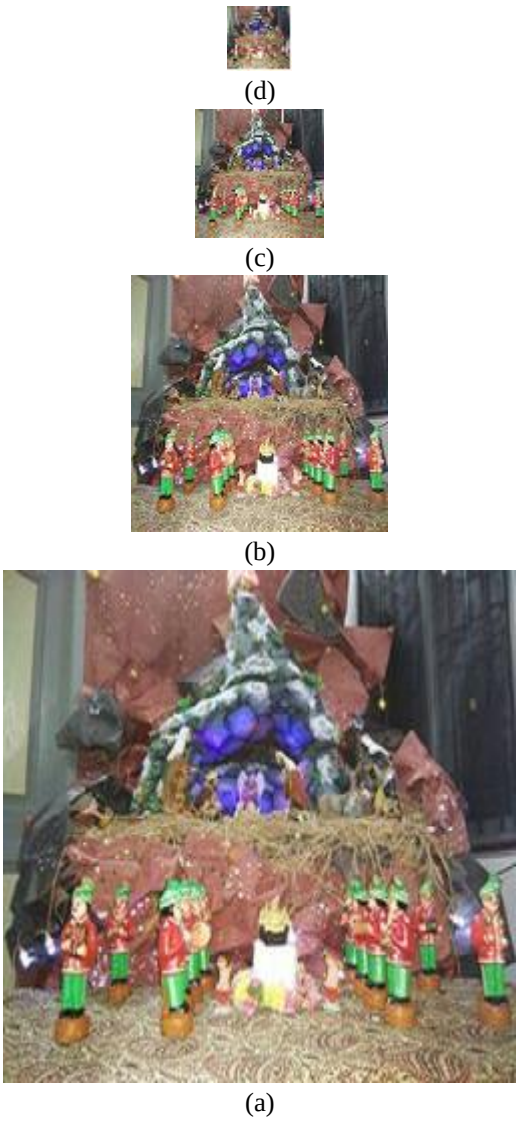

(d) (c) (b) (a)

Fig.3.Multi-resolution pyramid image from level-0 to level-3 [(a)-(d)] utilizing discrete Haar wavelet transform. The input image is of size 256 x 256 and images in the next level are of size 128 x 128, 64 x 64 and 32 x 32 respectively.

IV. PROPOSED WAVELET BASED MTSD ESTIMATION

The input images are in RGB color space, converted into HSV color space then for diminishing the time complexity without reducing the retrieval performance. The discrete Haar wavelet transform is utilized to form a multi-resolution pyramid image [27]. The level in which the numbers of details are very less without dropping the dominant details in an image is called fine or optimum level and is set to 4 in the proposed approach based on the trial and error process of retrieval. From the fine level of decomposed image, H, S and V channels are separated and color quantization is accomplished into 108 bins as in [26] and the WMTSD for color details are described as

$$\Gamma_c = \left(N_E^{Q_c}, N_S^{Q_c}, N_L^{Q_c}\right) \quad (1)$$

Texture details in the V channel are quantized into 20 bins as in [26] and the WMTSD for texture details are described as

$$\Gamma_t = \left(N_E^{Q_t}, N_S^{Q_t}, N_L^{Q_t}\right) \quad (2)$$

Using Sobel operator, edge information are identified and the detected edge pixels are quantized into 9 bins based on orientation details [26] and the WMTSD for edge orientation details are described as

$$\Gamma_e = \left(N_E^{Q_e}, N_S^{Q_e}, N_L^{Q_e}\right) \quad (3)$$

N, Q_c, Q_t, Q_e, E, S and L represents the number of trends, quantized color/texture/edge orientation details, equal, small and large trends respectively.

Finally, WMTSD for color, a texture and shape detail are integrated to form a combined feature vector and is defined as follows

$$\Gamma = \left(\Gamma_c, \Gamma_t, \Gamma_e\right) \quad (4)$$

The integrated WMTSD is employed for image classificaton and retrieval.

V. SIMILARITY MEASURE

Since the retrieval performance of CBIR approaches is also strongly associated with similarity measures and Euclidean distance [28] is more efficient and widely utilized in literature, we adopted it for estimating the similarity between input and the images in the benchmark dataset and is given as follows

$$S(I,T) = \sqrt{\sum_{i=0}^{N} \left(|I_i - T_i|\right)^2} \quad (5)$$

where I and T are the input and the target image feature vector and N is number of image features in image feature vector.

VI. PERFORMANCE MEASURE

In this work, each image in the benchmark dataset is utilized as an input to CBIR. The retrieval performance is estimated using precision *P(N)*, recall *P(R)*, mean average precision (*mAP*) and mean average recall (*mAR*) for top N retrieved images and are described as in [29] as follows

$$P(N) = \frac{I_N}{N} \quad (6)$$

$$R(N) = \frac{I_N}{M} \quad (7)$$

Where I_N designates number of top related images retrieved same as input image and M designates the total

number of related images in the benchmark dataset same as input image.

The average *P(N)* [29] for a given query image (*I*) is defined as an average of *P(N)* values of top N relevantly retrieved images and is given as follows

$$\mu_{P(I)} = \frac{1}{N} \sum_{i=1}^{N} P(N) \tag{8}$$

The *mAP* [29] is defined as average *P(N)* for all the input images and is expressed as follows

$$mAP = \frac{1}{N_I} \sum_{k=1}^{N_I} \mu_{P(I)} \tag{9}$$

Where N_I designates total number of input images.

VII. EXPERIMENTAL RESULTS AND DISCUSSIONS

A. Datasets

Corel dataset [22, 26, 30, 31]: Corel 10k dataset consists of 10800 natural and textural images of 80 concepts like dog, elephant, iceberg, ship, lion, flower, tier, mountain, car, ocean, fort, duck, train, fish, sunset, etc. and each concept consists of roughly 100 or more images. Corel 1k and Corel 5k datasets contains the 1st 1000 and 5000 images of Corel 10k dataset. The sizes of images are differ and are roughly in 384 x 256 or 256 x 384 or 126 x 187 or 187 x 126 or 192 x 128 or 128 x 192 sizes and the images are in JPEG format.

Caltech-101 dataset [26, 32]:

It contains 9,146 images of 101 concepts like octopus, crab, dolphin, rhino, pizza, panda, lamp, emu, cup, ant, etc and each concept consists of roughly 40 to 800 images. The size of the images is approximately 300 x 200 and are in JPG format.

B. Results and Discussions

In this section, experimental results are reported to reveal an effectiveness of proposed WMTSD and its results are compared with MTSD [26]. We carried out detailed experiments for each level of decomposition of images on benchmark datasets and the results are depicted in Table.1. From the results, it is obviously illustrated that WMTSD estimated from decomposed image at level 3 significantly provides better retrieval result than the decomposed image at level 4 and 5 despite the fact that its computational cost is less; and the retrieval results of decomposed image at level 3 and level. 0 to level. 2 are more or less similar nevertheless the computational cost of WMTSD from level 4 and 5 is too less and is shown in Table 1. As a result, in all our forgoing experiments we use optimum level as 3 for estimating the MTSD [26].

For example, in Fig.3, the size of an image at decomposed level 3 is 32 x 32 and the proposed approach estimates large, equal and small trends for texture, color and shape information along 0°, 45°, 90°and 135° orientations from 339 (i.e. 113+113+113) non-overlapping windows of size 3 x 3 as described in section 1. Whereas estimating the MTSD [26] from the level 1 image that is input image uses 21,843 non-overlapping windows of size 3 x 3. Thus, the proposed WMTSD approach preserves the accuracy of MTSD and demising the cost of computational complexity.

The retrieval performance of proposed WMTSD is compared with MTSD [26] using *mAP* and the *mAP* values attained by WMTSD and MTSD for top 10 images (*N*=10) on Corel 1k, 5k and 10k and Caltech-101 datasets are illustrated in Table 2. It is reveled from the Table 2 that proposed WMTSD maintains the *mAP* of MTSD on benchmark datasets and there is not much difference seen in between the *mAP* of MTSD and WMTSD. We also illustrated the *mAP* values for randomly selected 10 classes of Corel and Caltech datasets in Table 3 for *N*=10 which also reveal that proposed WMTSD and MTSD attains more similar results. Therefore, the proposed WMTSD maintains tradeoff between retrieval rate and computational cost. Thus, when compare to MTSD [26], WMTSD is the best choice.

Table 2. *mAP* for top 10 images retrieved by MTSD and WMTSD on Corel 1k, 5k, 10k and Caltech-101 datasets

Datasets	***mAP***	
	MTSD	**Proposed WMTSD**
Corel -1k	76.29	74.21
Corel- 5k	74.45	72.40
Corel -10k	70.19	70.11
Caltech-101	69.89	69.83

Table 3. Randomly selected class wise *mAP* for top 10 images retrieved by MTSD and WMTSD on Corel 1k, 5k, 10k and Caltech-101 datasets

Class	***mAP***	
	MTSD	**Proposed WMTSD**
Cat	82.34	82.30
Flower	75.45	75.42
Eagle	84.41	84.37
Deer	79.83	79.79
Lion	80.34	80.29
Elephant	86.71	86.66
Wolf	78.31	78.28
Sunset	74.34	74.30
Rhino	77.21	77.18
Bonsai	72.45	72.40

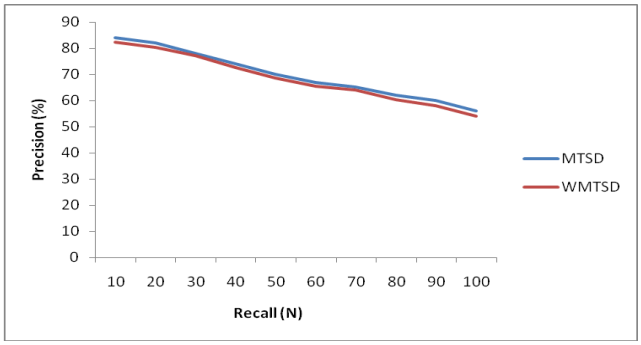

(a)

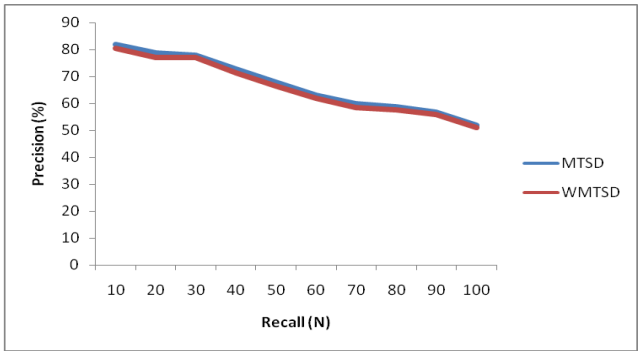

(b)

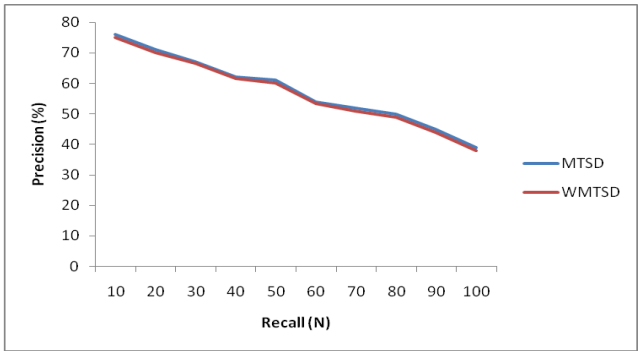

(c)

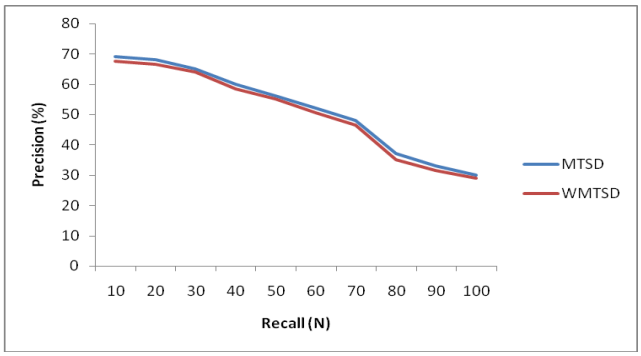

(d)

Fig.4.Precision Vs. Recall for the MTSD and the proposed WMTSD for (a) Corel 1k (b) Corel 5k (c) Corel 10k (d) Caltech Datasets

Table 4. Time taken (seconds) by the MTSD and the proposed WMTSD

Methods	**Time taken for feature computation**
MTSD	39
Proposed WMTSD	15

Fig.4 illustrates the plot of precision versus recall for both MTSD and WMTSD for Corel 1k, 5k, 10k and Caltech-101 datasets. It is reveled from the graph that the proposed WMTSD consistently provides retrieval performance which is more similar to MTSD. The retrieval performance of both MTSD and WMTSD with respect to the size of the Corel1k, Corel5k, Corel 10k and Caltech-101 datasets is consistent. While the size of dataset rises, there is a fall in the *mAP* values for both MTSD and WMTSD and the fall is almost similar.

Time complexity of any CBIR system encompasses feature estimation, similarity measure between input and database image and sorting of N related retrieved images based on the result of similarity measure. In this work, we employed very simple bubble sort. We integrated the times for feature estimation, similarity measure and sorting and is referred as retrieval time and is illustrated in Table 4. It is revealed from Table 4 that the proposed WMTSD takes least time for feature extraction then the MTSD and is because of decomposition of images upto level-3 utilized Haar wavelet transform. Since, similarity measure and sorting approaches are same for proposed and existing CBIR systems, the time taken for both of them are same. For quantitative analysis, we illustrate the time analysis of both MTSD and WMTSD in graphical form and is exposed in Fig 5.

Some sample images taken from the benchmark datasets are depicted in Fig.6. An example input image and its top 5 retrieval results are depicted in Fig.7 which is common for the MTSD and the proposed WMTSD.

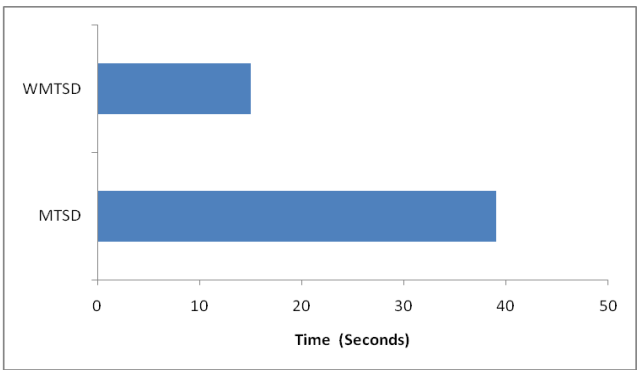

Fig.5. Time taken for MTSD and proposed WMTSD computation

VIII. CONCLUSION

The wavelet based multi-trend structure descriptor (WMTSD) is proposed in this work and is compared with multi-trend structure descriptor (MTSD). The WMTSD and MTSD provides almost similar retrieval results but the computational cost of WMTSD is too less. In the proposed work, to diminish the computational cost of MTSD, we decompose an image into level 3 utilizing discrete Haar wavelet transform, formed the multi-resolution pyramid image which in turn used to estimate the proposed WMTSD. Thus, the proposed WMTSD tradeoff between accuracy and time cost. In future, WMTSD representation may be combined with effective classifiers and implemented in the domain of medical to attain better results.

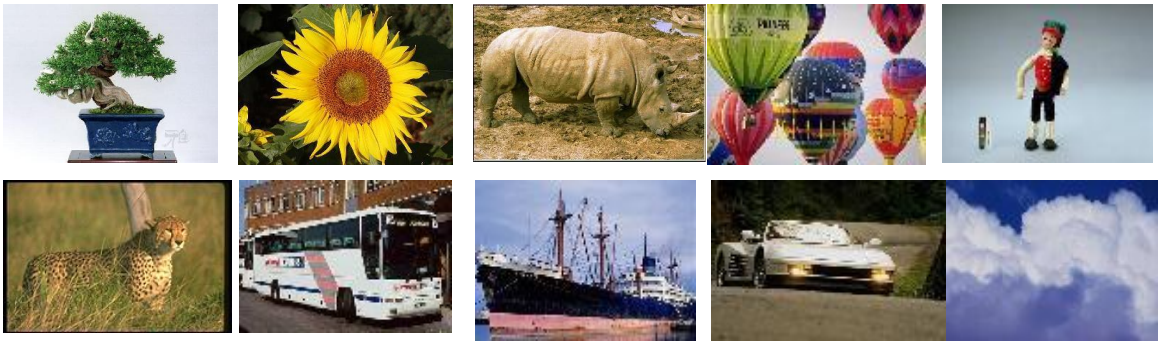

Fig.6. Example images from Corel 1k, Corel 5k, Corel 10k and Caltech Datasets

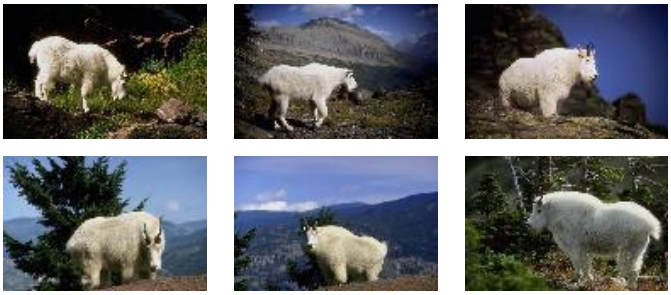

Fig.7. An example query image and its top 5 retrieval results for Corel dataset using the MTSD and proposed WMTSD

Table 1. Similarity values between input and the target image based on MTSD and WMTSD estimated at various level of decomposition using Haar wavelet transform

Level of Decomposition and Methods / **Concept and Image No.**	L_0 **MTSD**	L_1 **Proposed WMTSD**	L_2 **Proposed WMTSD**	L_3 **Proposed WMTSD**	L_4 **Proposed WMTSD**	L_5 **Proposed WMTSD**
Rhino: Image_0011 Vs Image_0022	0.5234	0.5259	0.5280	0.5294	0.5357	0.5579
Snoopy: Image_0011 Vs Image_0014	0.2451	0.2461	0.2485	0.2499	0.2589	0.2701
Wolf: 110022 Vs 110022	0.0000	0.0000	0.0000	0.0000	0.0000	0.0000
Bus: 581010 Vs 581111	0.4532	0.4544	0.4578	0.4589	0.4709	0.4987
Horse: 113089 Vs 113099	0.3812	0.3843	0.3868	0.3879	0.3955	0.4589

References

[1] H. Tamura, S. Mori, T. Yamawaki, Texture features corresponding to visual perception, IEEE Trans. Syst. Man Cybern. 8 (6) (1978) 460–473.

[2] L. Chen, G. Lu, D. Zhang, Effects of different Gabor filters parameters on image retrieval by texture, in: Proceedings of IEEE 10th International Multimedia Modelling Conference, 2004,pp. 273-278.

[3] G. Cross, A. Jain, Markov random field texture models, IEEE Trans. Pattern Anal. Mach. Intell. 5 (1) (1983) 25–39.

[4] R. M. Haralick, K. Shangmugam, Textural feature for image classification, IEEE Trans. Syst. Man Cybern. SMC-3 (6) (1973) 610–621.

[5] Yong, J. Walker, J. Bowie, 1974. An analysis technique for biological shape, *Comput. Graphics Image Process.* 25: 357–370.

[6] Peura, M., Iivarinen, J., May 1997. Efficiency of simple shape descriptors, in: *Proceedings of the Third Inter. Workshop on Visual Form*, Capri, Italy, pp. 443–451.

[7] Otterloo, P.J. V, 1991. A Contour-Oriented Approach to Shape Analysis, Prentice-Hall International (UK) Ltd, Englewood Cliffs, NJ, pp. 90–108.

[8] Zhang, D.S., Lu, G., January 22–25, 2002. A comparative study of Fourier descriptors for shape representation and retrieval, in: *Proceedings of the Fifth Asian Conference on Computer Vision (ACCV02)*, Melbourne, Australia, pp. 646–651.

[9] Sonka, M., Hlavac, V.,Boyle, R., 1993. Image Processing, Analysis and Machine Vision, Chapman & Hall, London, UK, NJ, pp. 193–242.

[10] R.C. Gonzalez, R.E. Woods, 1992. Digital Image Processing, Addison-Wesley, Reading, MA, pp. 502–503.

[11] K.Seetharaman, S.Sathiamoorthy, Mar 2014, "Color image retrieval using statistical model and radial basis function neural network.", *Egyptian Informatics Journal*, Vol. 15, No. 1, pp. 59-68.

[12] K.Seetharaman**,** S.Sathiamoorthy, ‘‘An Improved Edge Direction Histogram and Edge Orientation AutoCorrlogram for an Efficient Color Image Retrieval’’, *International Conference on Advanced Computing Communication Systems*, Dec 19-21, 2013, Shri Eshwar College of Engineering, Coimbatoore, pp. 1-4. DOI: 10.1109/ICACCS.2013.6938725.

[13] K.Seetharaman, S.Sathiamoorthy, A Unified Learning Framework for Content Based Medical Image Retrieval Using a Statistical Model. *Journal of King Saud University - Computer and Information Sciences (*ELSEVIER*)*, Vol. 28 (2016), No. 1, Dec 2015, pp. 110-124.

[14] Manjunath, B.S., Salembier, P., Sikora, T., 2002. Introduction to MPEG-7: Multimedia Content Description Interface, John Wiley & Sons Ltd.

[15] D.G. Lowe, Distinctive image features from scale-invariant keypoints, International Journal of Computer Vision (IJCV) 60 (2) (2004) 91–110.

[16] H. Bay, A. Ess, T. Tuytelaars, L.J.V. Gool, SURF: speeded-up robust features, Computer Vision and Image Understanding (CVIU), 110 (3)(2008) 346–359.

[17] T. Ojala, M. Pietik¨ainen, T. M¨enp¨a¨a, Multiresolution gray-scale and rotation invariant texture classification with local binary patterns, IEEE Transactions on Pattern Analysis and Machine Intelligence (PAMI) 24(7) (2002) 971–987.

[18] N. Dalal,B.Triggs, Histograms of oriented gradients for human detection, in: Proceedings of the IEEE Conference on Computer Vision and Pattern Recognition (CVPR),2005, pp 886–893.

[19] R. Gupta, H. Patil, A. Mittal, (2010). Robust order-based methods for feature description, in: Proc. IEEE Conf. Comput. Vis. Pattern Recognit., 334–341, doi:10.1109/CVPR.2010.5540195.

[20] Subrahmanyam Murala, Q.M. Jonathan Wu, (2013). Local ternary co-occurrence patterns: A new feature descriptor for MRI and CT image retrieval, *Neurocomputing*, 119: 399–412.

[21] Liu G, Zhang L, Hou Y, Li Z, Yang J., (2010). Image retrieval based on multi-texton histogram. *J. Pattern Recognit.* 43: 2380–2389.

[22] Liu G.H., Li, Z.Y., Zhang, L., Xu. Y., (2011). Image retrieval based on micro-structure descriptor. *Pattern Recognition.* 44(9): 2123-2133.

[23] G.H. Liu, J.Y. Yang, (2013). Content-based image retrieval using color difference histogram, Pattern Recogn. 46 (1) :188–198.

[24] Wang Xingyuan, Wang Zongyu, (2013). A novel method for image retrieval based on structure elements’ descriptor, *J. Vis. Commun. Image R.*, 24: 63–74.

[25] Liu, G.H., Yang, J.Y., (2008). Image retrieval based on the texton co-occurrence matrix, *Pattern Recognition*. 41 (12): 3521–3527.

[26] Meng Zhao, Huaxiang Zhang, Jiande Sun, (2016). A novel image retrieval method based on multi-trend structure descriptor , J. Vis. Commun. Image R., 38: 73–81.

[27] K.Seetharaman, M.kamarasan, (2012), A smart color image retrieval method based on multiresolution features, IEEE International Conference on Computational Intelligence and Computing Research, pp.68-75.

[28] Fazal Malik, Baharum Baharudin, (2013). Analysis of distance metrics in content-based image retrieval using statistical quantized histogram texture features in the DCT domain, Journal of King Saud University - Computer and Information Sciences, 25(2):207-218.

[29] Chandan Singh , Ekta Walia , Kanwal Preet Kaur , Color Texture Description with Novel Local Binary Patterns for Effective Image Retrieval, Pattern Recognition (2017), doi: 10.1016/j.patcog.2017.10.021.

[30] Guang-Hai Liu, Jing-Yu Yang, etc,. Content-based image retrieval using computational visual attention model, Pattern Recognition, 48(8) (2015) 2554-2566.

[31] D. Tao, X. Li, and S. J. Maybank, “Negative Samples Analysis in Relevance Feedback,” IEEE Transactions on Knowledge and Data Engineering (TKDE), vol. 19, no. 4, pp. 568-580, April 2007.

[32] http://www.vision.caltech.edu/Image_Datasets/Caltech101/

Proceedings of the Fourth International Conference on Communication and Electronics Systems (ICCES 2019)
IEEE Conference Record # 45898; IEEE Xplore ISBN: 978-1-7281-1261-9

Ambipolar suppression in L-shaped Tunnel Field Effect Transistor using dielectric pockets

Sonakshi Beniwal
School of VLSI Design and Embedded Systems
National Institute of Technology
Kurukshetra, INDIA
sonakshi_31705121@nitkkr.ac.in

Gaurav Saini
Department of Electronics and Communication Engineering,
National Institute of Technology
Kurukshetra, INDIA
gauravsaini@nitkkr.ac.in

Abstract—An L-shaped double gate tunnel field effect transistor (DG L-TFET) results in better ON-current (I_{on}) due to its wider tunnelling area. Hetero dielectric Box (HDB) helps in suppressing current conduction in ambipolar region. Hetero-gate dielectric is included to improve I_{on}. To suppress ambipolar conduction further, dielectric pockets are introduced at both the drain ends. It suppresses ambipolarity by 1.5×10^8 times compared to structure without dielectric pockets. However, I_{on} remains same for both the structures. For boosting I_{on}, Germanium (Ge) source is included instead of Silicon as source. Use of Ge-source not only enhances I_{on} but also OFF-current (I_{OFF}). It enhances I_{on} by almost a decade.

Keywords—Tunnel Field Effect Transistor (TFET), L-shape, hetero-gate dielectric, hetero dielectric box (HDB), ambipolarity, dielectric pocket

I INTRODUCTION

Semiconductor devices follow Moore's law for low power applications. Devices having low power dissipation and high switching speed are in trend and demanded world widely. The regime of down scaling is difficult to carry out in devices below 32 nm as it would result in very high power consumption and large leakage currents. Tunnel Field Effect Transistor (TFET) is considered to be a potential solution in state of low power and high frequency applications. TFET is discernible from Metal Oxide Semiconductor-Field Effect Transistor (MOS-FET) as its current conduction depends on Band-to-Band Tunneling (BTBT). Owing to BTBT mechanism, TFET is highly unsusceptible to short channel effects (SCEs). TFET crosses the thermal limit of MOS-FET and results in steeper subthreshold swing (SS) of <60mV/decade. However, TFET has some setbacks in the form of low current conduction in ON-state and heavy current conduction in ambipolar region [1]. Many solutions were proposed for enhancing performance matrices of TFETs.

Ritesh et al. [2] boosted electric field at the tunnel junction by inserting a source-pocket offering higher I_{on} and steepness in SS. Saurabh et al. [3] suppressed ambipolarity by introducing a pocket at drain with high drain doping (as high as source doping). Raad et al. [4] designed and simulated dopingless TFET with a metallic layer in the oxide region at source-gate interface. This proposed solution is helpful in achieving reduced barrier width of the source-channel tunneling junction, enabling higher tunneling rate of charge carriers at this interface. Virani et al. [5] investigated that increase in the gate dielectric in dual-k spacer underlap structure degrades the performance of the device. Mallikarjunarao et al. [6] proposed a symmetric double gate n-type TFET with underlap single-k spacer structure to improve the device performance.

Abdi et al. [7] proposed gate-drain overlap structure of a TFET which exhibits suppressed conduction in ambipolar region. Sahay et al. [8] proposed a hetero dielectric box (HDB) instead of SiO_2 box above a highly doped substrate. It controls the tunnelling barrier width at the drain-channel interface and thereby suppresses ambipolar current. Upasana et al. [9] incorporated dielectric pockets at source-channel and/or drain-channel tunnelling junction for improving device performance.

Yang [10] designed a TFET with L-shaped gate. The proposed device increases the ON-current (I_{on}) by enhancing the electric field. Li et al. [11] introduced L-shaped TFET (L-TFET) with hetero-gate dielectric and lower drain doping (LDD) for improving I_{on} and suppressing ambipolar current. The L-shaped channel of L-TFET has larger tunnelling area than conventional Tunnel FET.

In our previous work, performance of L-shaped DG-TFET with HDB and hetero-gate dielectric was analyzed. It was observed that this structure had improved I_{on}, SS but not I_{ambi} [12]. Addition of dielectric pockets in DG-TFET reduces amount of carriers tunneling at drain-channel interface in negative gate bias or ambipolar state [9].

In this work, a novel L-shaped DG-TFET with dielectric pockets at drain end is proposed to improve performance metrics.

II DEVICE STRUCTURE AND SIMULATION SETUP

TCAD tool (Version J.2018) of Sentaurus is used to perform all the device simulations [13]. All regions (Source, drain, channel and substrate) are uniformly doped. Tunnelling width between source region and gate dielectric is 5nm.

The simulation results are obtained using phonon assisted tunnelling and nonlocal BTBT model. Phonon assisted tunnelling is used for indirect bandgap semiconductors like Silicon (Si) and Germanium (Ge). Enormal model with default parameters is added because of high-k dielectrics. Philips unified Mobility (PhuMob) model is

incorporated. For heavily doped source and drain regions, OldSlotboom is added as Band gap narrowing (BGN) model. Use of WKB (Wentze Kramer Brillouin) method is done for calculating tunnelling probability and their numerical solution. Auger and Shockley-Read-Hall (SRH) are incorporated as recombination models [13].

Table 1: Design parameters of L-TFET

Parameters	Value
Drain doping [cm^{-3}] [n-type]	5×10^{18}
Source doping [cm^{-3}] [p-type]	1×10^{20}
Drain length [L_d] [nm]	40
Drain height [H_d] [nm]	16
Substrate doping [cm^{-3}] [p-type]	1×10^{18}
Source length [L_s] [nm]	33
Gate length [L_g] and height [H_g] [nm]	30
Channel doping [cm^{-3}] [n-type]	1×10^{17}
Gate oxide thickness [nm] [t_{ox}]	2
Gate metal work function [eV]	4.2
Gate oxide permittivity [HfO_2]	15
Gate oxide permittivity [SiO_2]	3.9
Height of HDB [nm]	25
Source height [L_s] [nm]	24
Length of DP [nm]	2

III RESULTS AND DISCUSSIONS

L-TFET has high I_{on} and steep subthreshold swing (SS) due to vast tunnelling area at source-channel junction. However, it exhibits heavy current flow in ambipolar region which draws attention and needs to be optimized. At gate, hetero dielectric is added to boost the device characteristics. Addition of high-k gate dielectric at source is to amplify I_{on} and low-k gate dielectric at drain end to reduce ambipolarity [12].

Hetero dielectric box reduces the current flow in ambipolar state. An HDB consists of HfO_2 under drain and SiO_2 under channel and source regions. It suppresses ambipolar current (I_{ambi}) to certain extent [8]. For further suppression, dielectric pockets (DP) are introduced at drain ends. Dielectric Pocket based L-TFETs are highly advantageous and efficient with the use of high-k gate dielectric material [9]. DP increases the tunnel barrier width at drain-channel interface in ambipolar state. I_{ambi} depends on the barrier width at drain-channel junction.

It is observed that the use of high-k gate dielectric increases the device leakage and ambipolar current [9]. The usage of DP results in negligible tunneling at drain-channel junction. It turns off DP Si L-TFET during ambipolar state or negative gate bias. Fig. 1 (a)-(b) shows the device structure of conventional Si L-TFET and DP Si L-TFET.

For this device, I_{on} is calculated at gate voltage (V_{gs}) =1V and drain voltage (V_{ds}) =1V. OFF-current (I_{OFF}) is the amount of current at V_{ds} =1V and V_{gs}=0V. I_{ambi} is observed at V_{gs}= −1V and V_{ds} =1V.

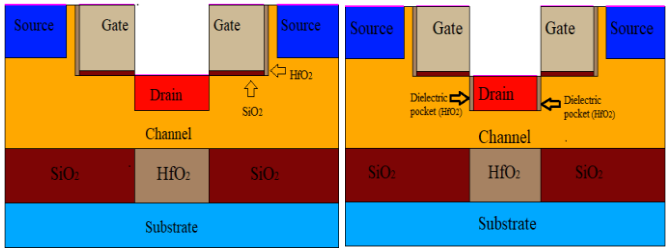

Fig.1. Schematic of (a) Conventional Si L-TFET (b) DP Si L-TFET

Calculation of threshold voltage (V_{th}) is done by constant current (CC) method assuming reference current to be 10^{-7} A/µm [14]. Average SS is the amount of V_{gs} applied to alter drain current (I_D) by a decade.

$$SS = \frac{V_{th} - V_{off}}{Log(I_{vth}) - Log(I_{Voff})} \quad (1)$$

V_{off} is the amount of applied V_{gs} at which I_D begins to take off, I_{Vth} is the I_D at $V_{gs} = V_{th}$ and I_{Voff} is the I_D when $V_{gs} = V_{off}$ [14].

The energy band diagram for conventional Si L-TFET and DP Si L-TFET in ambipolar state are shown in Fig. 2. The reduction in I_{ambi} for DP Si L-TFET is the result of increased barrier width at drain-channel junction. In ambipolar state, tunneling width for DP Si L-TFET is higher than conventional Si L-TFET structure.

Fig. 3 depicts the transfer characteristics for Conventional Si L-TFET and DP Si L-TFET. Characteristic curve plotted between I_D and V_{ds} is shown in Fig. 4.

The ON-state characteristic of DP Si L-TFET is very similar to Si L-TFET but the former has reduced I_{ambi} by a large amount. According to Fig.3, application of dielectric pockets at both drain ends in an L-TFET does not alter drive current and results in I_{on} of 6×10^{-6} A/µm. The ON-current for both L-TFETs is equal due to nearly equal amount of carrier generation rate. Ambipolar current in DP Si L-TFET is suppressed by 1.5×10^{8} compared to conventional structure. I_{OFF} and SS for Conventional Si L-TFET are 8.47×10^{-17} A/µm and 49.83 respectively whereas I_{OFF} and SS for DP Si L-TFET are 1.03×10^{-16}A/µm and 46.7 respectively.

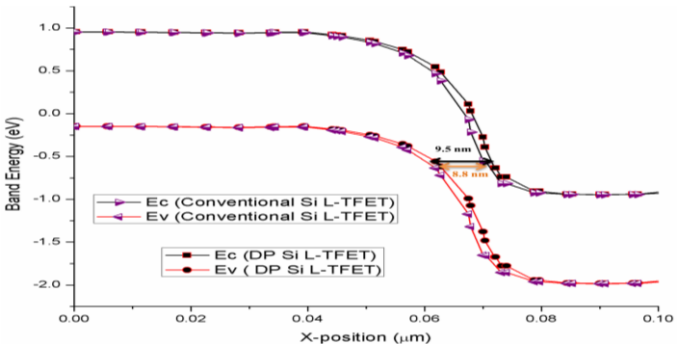

Fig.2. Conduction band (E_c) and valence band (E_v) diagrams for Conventional Si L-TFET and DP Si L-TFET in ambipolar state

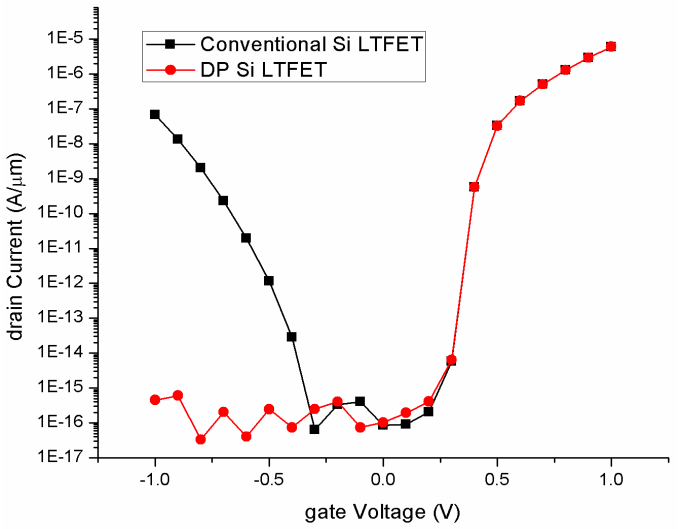

Fig.3. Plot between drain current and gate voltage (-1V≤V_{gs}≤1V) for Conventional Si L-TFET and DP Si L-TFET

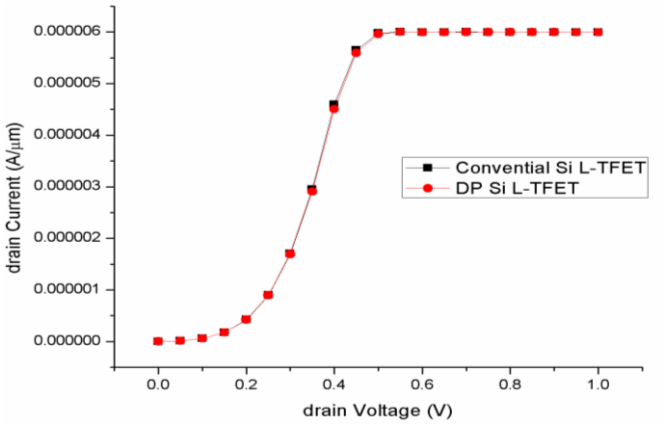

Fig.4. Plot between drain current and drain voltage (0V≤ V_{ds} ≤1V) for Conventional Si L-TFET and DP Si L-TFET

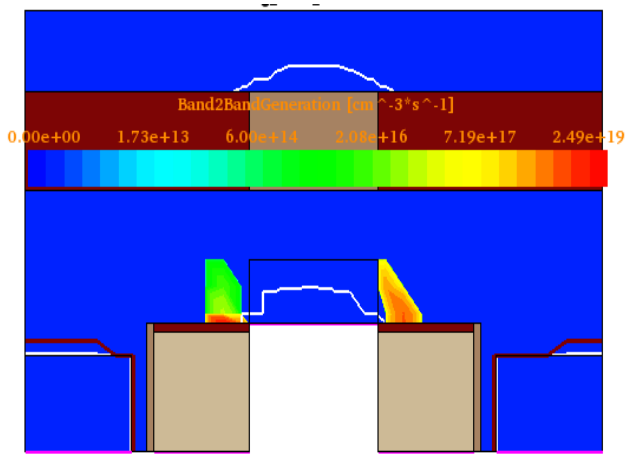

Fig.5. Band-to-band generation diagram for Conventional Si L-TFET in ambipolar state

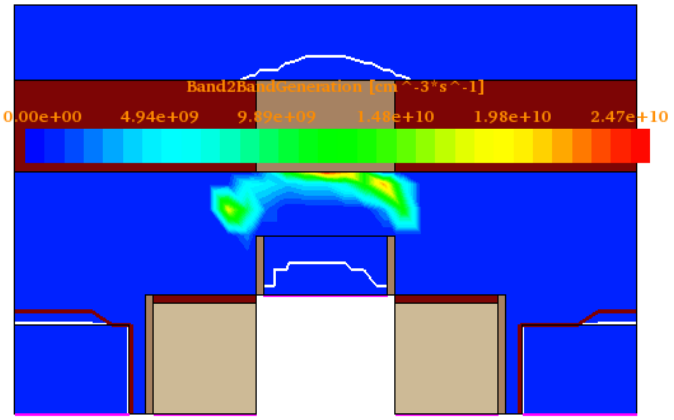

Fig.6. Band-to-band generation diagram for DP Si L-TFET in ambipolar state

Figs. 5-6 illustrate band-to-band (B2B) generation rate in ambipolar state for Conventional Si L-TFET and DP Si L-TFET. The B2B generation depicted is due to tunneling of carriers at drain-channel interface. The B2B generation is suppressed by almost 10^9 times in DP Si L-TFET resulting in reduction of I_{ambi}.

A. *BOOSTING Ion*

Current conduction in ambipolar state has been a serious concern in case of L-TFETs. DP Si L-TFETs show better characteristics in context of I_{ambi} compared to conventional L-TFETs. However, I_{on} in DP Si L-shaped TFET can be improved. Instead of Si as source material, usage of Ge-source helps in boosting I_{on} [15]. Use of low bandgap material like Ge, the tunnelling probability of carriers and I_{on} of the device are increased. However, Ge-source increases I_{on} as well as I_{OFF} as per Table. 2. Fig. 7 illustrates the DP Ge-source Si L-TFET structure.

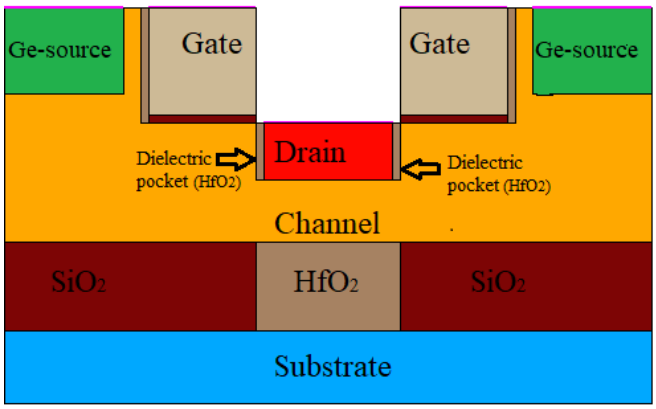

Fig.7. Schematic of DP Ge-source Si L-TFET

Owing to Ge-source, the tunneling width at source-channel interface is decreased resulting in higher I_{on} in ON-sate. ON-current in DP Ge-source Si L-TFET is incremented by a decade compared to DP Si L-TFET.

Table.2. Performance comparison between DP Si L-TFET and DP Ge-source Si L-TFET

Parameters	DP Si L-TFET	DP Ge-source Si L-TFET
I_{on} (A/μm)	6×10^{-6}	5.755×10^{-5}
I_{OFF} (A/μm)	1.027×10^{-16}	1.074×10^{-15}
I_{ambi}(A/μm)	4.52×10^{-16}	6.60×10^{-16}
V_{th} (V)	0.55	0.318
SS (mV/decade)	46.7	39

Band diagrams for DP Si L-TFET and DP Ge-source Si L-TFET in ON-state is shown in Fig.8. Ge deployed as source lowers energy bands at source region. The transfer characteristic for DP Si L-TFET and DP Ge-source Si L-TFET is depicted in Fig.9.

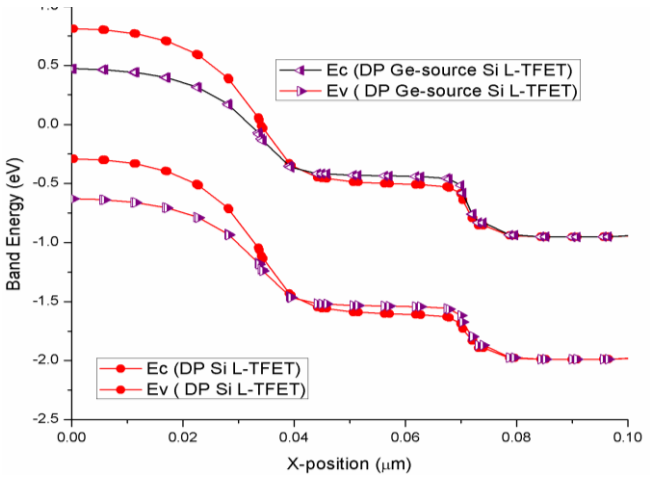

Fig.8. Conduction band (E_c) and valence band (E_v) energy diagrams for DP Si L-TFET and DP Ge-source Si L-TFET in ON-state

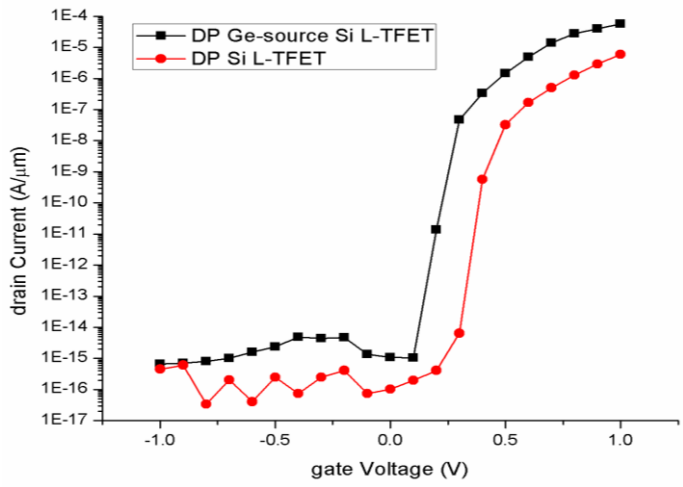

Fig.9. Plot between drain current and gate voltage (-1V ≤ V_{gs}≤ 1V) for DP Si L-TFET and DP Ge-source Si L-TFET

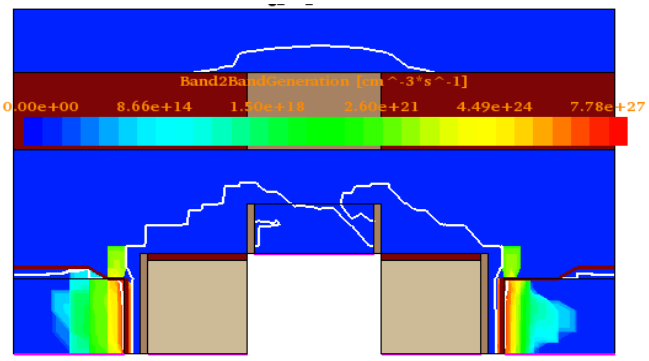

Fig.10. B2B Generation diagram for DP Si L-TFET in ON-state

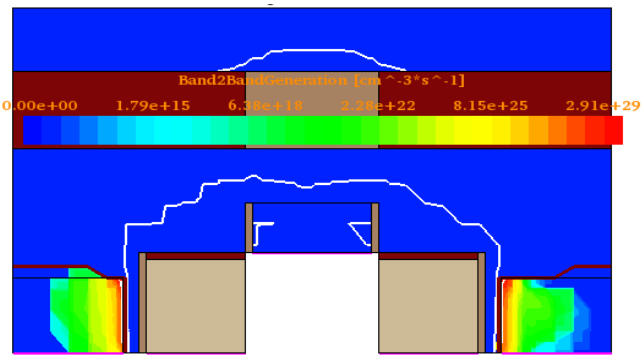

Fig.11. B2B Generation diagram for DP Ge-source Si L-TFET in ON-state

Figs. 10-11 illustrates B2B generation rate in ON-state for DP Si L-TFET and DP Ge-source Si L-TFET. The B2B generation depicted is due to tunneling of carriers at source-channel interface. The carrier generation rate is increased by 37.4 times and thus increasing I_{on}.

IV CONCLUSION

Simulation study shows that dielectric pocket Si L-shaped TFET has enhanced characteristics in context of ON-current, OFF-current, SS and ambipolar current. Dielectric pockets applied at both the drain ends help in improving ambipolar characteristics. In ambipolar-state, the carrier generation rate for dielectric pocket Si L-shaped TFET is suppressed by 10^9 times as compared to conventional Si L-shaped TFET. For boosting I_{on}, Si source is replaced by Ge. In ON-state, rate of generation of carriers for Ge-source L-TFET is improved. It enhances ON-current as well as OFF-current.

REFERENCES

[1] Sneh Saurabh, Mamidala Jagadesh Kumar, "Fundamentals of tunnel field-effect transistors", CRC Press, *Taylor & Francis Group*, p. no. 45-146, 2016.

[2] Ritesh Jhaveri, Venkatagirish Nagavarapu, and Jason C. S. Woo, "Effect of Pocket Doping and Annealing Schemes on the Source-Pocket Tunnel Field-Effect Transistor", *IEEE Transactions on electron devices*, vol. 58, no. 1, January 2011.

[3] S.Garg and S.Saurabh, "Suppression of ambipolar current in tunnel FETs using drain pocket: proposal and analysis" *Superlattices and Microstructures*, vol. 113, p.no. 261-270, 2018.

[4] Bhagwan Ram Raad, Sukeshni Tirkey, Dheeraj Sharma, and Pravin Kondeka, "A New Design Approach of Dopingless Tunnel FET for

Enhancement of Device Characteristics", *IEEE Transactions on electron devices*, vol. 64, no. 4, April 2017

[5] Virani, H.G., Adari, R.B.R., Kottantharayil, A., "Dual-k spacer device architecture for the improvement of performance of silicon n-channel tunnel FETs," IEEE Trans. Electron Devices 57(10), 2410–2417 (2010)

[6] Mallikarjunarao, Rajeev Ranjan, K.P.Pradhan, P.K.Sahu, "Dielectric engineered symmetric underlap double gate tunnel FET (TFET): An investigation towards variation of dielectric materials", Superlattices and Microstructures**,** vol. 96, p.no. 226-233, August 2016.

[7] Dawit B. Abdi and M. Jagadesh Kumar, "Controlling Ambipolar Current in Tunneling FETs Using Overlapping Gate-on-Drain", *Journal of the Electron Devices society*, vol.2, no.6, November 2014.

[8] Shubham Sahay and Mamidala Jagadesh Kumar, "Controlling the Drain Side Tunnelling Width to Reduce Ambipolar Current in Tunnel FETs Using Hetero-dielectric box" IEEE transactions on electron devices, vol. 62, no. 11, November 2015.

[9] Upasana, Rakhi Narang, Manoj Saxena, Mridula Gupta, "Exploring the applicability of well optimized dielectric pocket tunnel transistor for future low power applications", Superlattices and Microstructures, vol 126, p.no. 8-16 , February 2019

[10] Zhaonian Yang, "Tunnel Field-Effect Transistor With an L-Shaped Gate" IEEE electron device letters, vol. 37, no. 7, July 2016.

[11] Li, Cong, Zhao, Xiaolong,Zhuang, Yiqi, Yan, Zhirui, Guo, Jiaming Han, Ru, " Optimization of L-shaped tunnelling field-effect transistor for ambipolar current suppression and Analog/RF performance enhancement" Superlattices and Microstructures, vol.115, p. 154-167, March,2018.

[12] Sonakshi Beniwal, Gaurav Saini, "L-shaped Tunnelling FET with hetero-gate dielectric and hetero dielectric box" 3rd International Conference on Trends in Electronics and Informatics (ICOEI 2019), 23-25 March, 2019. (presented).

[13] Sentaurus TCAD User Guide, 2018 [online].Available: http://www.sentaurus.dsod.pl/index.html.

[14] Kathy Boucart, Adrian M. Ionescu, "Threshold voltage in Tunnel FETs: physical definition, extraction, scaling and impact on IC design", *Solid State Device Research Conference*, 2007

[15] N.Sharma, SS.Chauhan, "Dual metal drain Ge-source dopingless TFET with enhanced turn-ON steep subthreshold swing and high ON-current", IEEE Electronics Letters , vol 53 , p.no. 960 – 962, July 2017

Proceedings of the Fourth International Conference on Communication and Electronics Systems (ICCES 2019)
IEEE Conference Record # 45898; IEEE Xplore ISBN: 978-1-7281-1261-9

Use Of Electroencephalogram Signal and Screening Test For Detecting Cognitive Ability Of Person

Amruta Koli
MIT World Peace University, Pune, India
(amruta7.koli@gmail.com)

Prof. Shridevi Karande
MIT College of Engineering, Pune, India
(shridevi.karande@mitpune.edu.in)

***Abstract*— The term cognition is defined as how person understand the world, how person respond, how person react to particular situation. The basic definition of Cognitive Impairment is that person may not able to think properly, has some communication and language problem. There are lots of causes for having Cognitive Impairment such as infection, vitamin deficiency, dehydration, brain injury and many more. It is necessary to identify cognitive ability of person so that further treatment can be done on person for their better health. There are many ways to identify Cognitive ability. In this paper Electroencephalogram(EEG) signal and Screening test named as Mini Mental State Examination(MMSE) are used for knowing cognitive ability of person. Lot of previous work done on detecting Cognitive Impairment. In previous work they have used traditional Electrode system for capturing EEG of brain. In this non-invasive and portable device known as Emotiv Insight is used to capture brain activity. Real time data from different person of different age groups is collected by using combination of EEG signal and MMSE. Once Data is collected it has to go through different steps for knowing cognitive ability. Different techniques such as pre-processing, feature extraction, feature selection, classification which includes algorithm such as Linear Regression, Decision Tree, Support Vector Machine are applied on data.**

Keywords—Cognition; Cognitive Impairment; Mild Cognitive Impairment; Electroencephalogram; Mini Mental State Examination.

I INTRODUCTION

The term cognition is defined as something that is relating to different intellectual activities such thinking, logical reasoning, remembering things. Cognitive ability is known as person's ability of thinking i.e. how person think or even respond to some situation. In figure1[13] it shows how psychology of cognitive covers different areas such as language, thinking and problem solving, memory, attention. Perception, human Intelligence Cognitive Impairment in simple term defined as memory problem i.e. person with cognitive impairment may not able to perform their daily tasks, lack of communication problem, poor judgment, may not able to think properly as compared to normal healthy person. So there are different causes for this cognitive impairment such as brain injury, stroke, infections and many more.

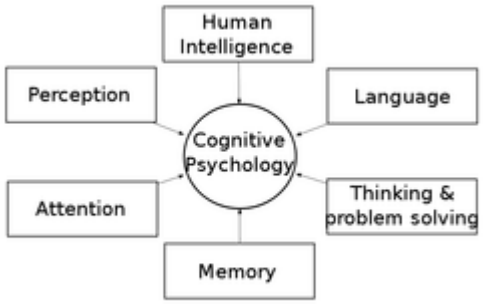

Fig. 1. Cognitive Level Of analysis

There are different stages of this cognitive impairment such as Mild, Severe and Medium. The person with mild cognitive impairment may begin with certain changes but they able to perform their daily tasks. The person having severe type of cognitive impairment include that they lose ability to talk, they can't go outside individually, understanding problem, lose the importance of something. Some of the major key facts regarding cognitive impairment are memory loss, frequently asking same questions, behaviour changes, mood

swings, difficulty in carrying out tasks, vision problem, not recognizing family members, friends, neighbours, problem in planning, taking decision.

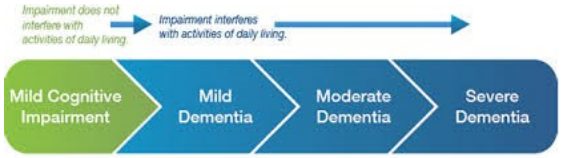

Fig. 2. MCI stages

Severe cause of Cognitive Impairment may lead to more higher type of disease such as Alzheimer's Disease(AD), Vascular Dementia(VD), Parkinson's dementia. The above figure 2[14] shows how mild cognitive impairment leads to different stages of dementia i.e. mild dementia, moderate dementia and severe dementia. Dementia is such kind of disease in which person loses memory. Such kind of disease mostly occurs at late ages i.e. may be at 60's. There are many symptoms of dementia which includes memory problem, communication and language problem i.e. problem while talking, not easily able to communicate with other person, have less ability in focus and attention, poor judgmental , short term memory, problem in performing daily activities like eating, dressing.

In hospital domain for identification of cognitive impairment lots of techniques carried out such as MRI, EEG, different blood tests. These several tests require large of amount of time and efforts. So there is need for such tools which ease in process of detection of cognitive ability. EEG and Screening Test are used for detection of cognitive ability. EEG (Electroencephalography) is used in capturing brain activity i.e. it helps in knowing functionality of brain. Screening test includes Mini Mental State Examination which helps in knowing cognitive ability of person. This test covers different areas of cognition such as language, attention and calculation, recall, orientation, memory, registration. It contains different questions which cover all above areas of cognition. It has total score of 30. Using combination of these two factors helps in giving good result for knowing cognitive ability of person.

II LITERATURE REVIEW

This section describes the previous work that has be done for detection of Cognitive Impairment of person using traditional method of collecting EEG signal of person and using device Emotiv Insight which is new and non-invasive technique to collect EEG signal of person.

In this paper[1] EEG signals and Screening test known as Montreal Cognitive Assessment(MOCA) were used in detection of Mild Cognitive Impairment(MCI). Different steps such as feature extraction, feature selection, classification and finally evaluation are used for detection of MCI. In classification different algorithms such as Support Vector Machine(SVM), Logistic Regression(LR) , Random Forest(RF) was used. At the end as a result it was proved that time frequency features are best among all other features. Classification accuracy got here was 87.9%.

In this paper[2] how EEG is used in detection of disease known as dementia is explained. EEG signal processing contains different steps such as pre-processing, features extraction, classification. Independent Component Analysis(ICA), Wavelet Transform(WT) methods was used for EEG signal processing. For classification different algorithms are used among which Support Vector Machine gives good result at detection of disease. So finally EEG is considered great biomarker for detection and classification of disease.

In this paper[3] EEG is used for detection of Alzheimer Disease(AD). Processing of EEG signal is explained in detail. EEG methodology includes Pre-processing, Feature extraction, feature selection, classification and finally Diagnosis. In classification, algorithms such as Linear Discriminant Analysis (LDA), Support Vector Machine (SVM) are used. Accuracy got with different algorithms in detection of Alzheimer Disease is compared with each other. Finally in conclusion EEG is found to be good technique in detection of Alzheimer Disease.

This paper[4] gives description about different frequencies of EEG signal which are helps in diagnosis of dementia. Different frequencies such as Dominant frequency, dominant frequency variability and dominant frequency prevalence was are used for detection and their corresponding performance is compared. The main goal is to distinguish MCI from healthy control. Finally conclusion is that EEG helps in finding dementia disease at early stage.

In this paper[5] screening test known as Mini Mental State Examination is used for

detection of Mild cognitive impairment. This MMSE test is used for knowing cognitive function which covers different areas such orientation, registration, attention and calculation, recall and language. Total MMSE score is 30. Individual score is given to each area. So as a result MMSE is good at detection of MCI and its different subtypes.

In [6][13] EEG is used in detection of dementia stage known as Mild Cognitive Impairment(MCI). Different spectral features are used and extracted for further processing. For classification k-nearest neighbour(KNN) is used. As a result it is found that EEG is great tool for detecting MCI stage.

In this paper[7] EEG signals are used in detecting Alzheimer disease(AD). EEG is great at early detection of disease. Relative Power(RP) feature of EEG signal is used in classifying healthy controls from MCI. For classification Deep Neural Network(DNN), Neural Network(NN) are used for early detection of disease. Accuracy got with these algorithm is compared for analysis purpose. Deep Neural Network(DNN) gives good result as compare to Neural Network(NN) for detection of Alzheimer Disease(AD).

In [8][12] EEG signals are used for detection of stroke related Mild Cognitive Impairment(MCI). Capturing of EEG signal is done when person performing some tasks. Wavelet Transform(WT) method is used for pre-processing of data i.e. removal of artifacts, noise. Approximation Entropy(ApEn) and permutation entropy(PerEn) features are used for detection. These feature shows less irregularity in EEG signal of MCI people as compare to normal healthy people. So in conclusion EEG is considered great technique at diagnosing MCI.

This paper[9] EEG is used for early detection of Alzheimer's Disease(AD). EEG is good at distinguishing AD from healthy control. In this EEG of Subjective Cognitive Impairment(SCI) patients, Mild Cognitive Impairment(MCI), Alzheimer's Disease(AD), and healthy control is captured. Features such as epoch based entropy and bump modelling are used for classification purpose. 91.6% accuracy is obtained while distinguishing SCI from AD patients. Sensitivity is 87.8% and specificity is 100%.

This paper[10] Mini Mental State Examination is used for knowing cognitive function. This test is very easy and takes only 5-10 minutes to complete. It covers all different areas of brain functioning. Standrad score of MMSE is 30. At conclusion it is said that MMSE is one of the great test at finding cognitive function.

In this paper[16] different EEG headset such as Emotiv Epoc, Emotiv Insight, InteraXon Muse and Imec EEG headset are explained. These device helps in knowing cognitive ability. Emotiv Insight device is used for capturing EEG of brain. Emotiv Insight helps in detecting stress or stress level of person as it helps in knowing brain functionality.

III METHODOLOGY

Use of EEG signal for detection of cognitive ability is considered one of the great technique to capture brain activity. In hospital region EEG is captured using electrodes which are placed on human brain with position specified by standard 10-20 International electrode position system. The basic flow for identification of cognitive ability contains different steps such as pre-processing, feature extraction, feature selection, classification and finally evaluation i.e. result of detection of cognitive ability. In this paper Emotiv Insight device is used to capture EEG of person of different age groups as EEG is one of the good factor for identifying cognitive impaired person. Emotiv Insight is non-invasive and portable device i.e. person need not go to hospital for recoding of EEG signal. Emotive device here used has 5 channels for capturing brain activity. When this device is connected on person head MMSE questions are asked. MMSE is used so that it covers functioning of all brain areas. Emotive pro software is used to capture this signal. Data is collecting from different people of different age groups using above two factors i.e. EEG and MMSE. After collection of data pre-processing need to perform as while capturing these signals person may perform some irrelevant movement such as eye moment or muscle moment so value may differ than original value while capturing these signal so pre-processing removes all this. After this, feature extraction is performed and then classification is performed which includes algorithms such Linear Regression(LR), Support Vector Machine(SVM), Decision Tree(DT), Naïve Bayes, K-nearest neighbour(KNN). Model is trained with these algorithms. These algorithms give different accuracy. Among this Decision Tree gives good result at detecting cognitive ability as compare to other algorithms.

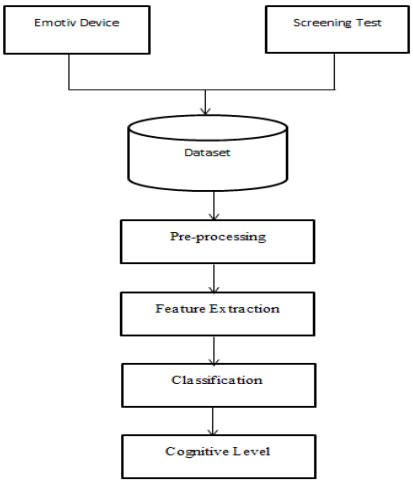

Fig. 3. System Architecture

Emotiv Device:

Fig. 4. Emotiv Insight Headset

The above figure [15] is an image of Emotiv Insight device. Emotiv Incorporation is one of the technical company which contribute in developing manufacturing wearable electroencephalography(EEG) products including other software, developing few mobile application regarding their software and some data products. Emotive Design of Emotive can be used for various purpose such as for brain-computer interface, and for research purpose also. EMOTIV device is available with different number of channel i.e. it is available with 5-channel and with 14-channel also. Emotiv basically used for producing clean, strong, robust signal of human brain irrespective of time and location of person i.e. location doesn't matter for producing signal of person brain. Emotiv is very user friendly device and its setup require hardly 2-3 minutes. Also it is wireless device and can be connected to computer. Its main goal is to produce EEG signal of human brain so that it helps in understanding brain activity of person while thinking or performing some tasks and finally it convert that EEG data into meaningful data that can be easily understood by user.

1. Pre-processing:

This is initial stage after collection of data from different people of different age groups. Pre-processing must be performed in order to remove irrelevant data. When data recording is performed there may be noise or person may perform some irrelevant tasks such as opening, closing eyes, muscle movement. So all this noisy data must be remove from original data in order to process further. For feature extraction phase data must be noise free which helps in giving good result. Method such as Independent Component Analysis(ICA) is used for pre-processing for removal of noise and artifacts.

2. Feature Extraction:

This is feature extraction phase where some of the features are extracted which are helpful in giving good result. EEG signal contains frequencies such as alpha, beta, gamma, theta and delta. When EEG test is performed on person as output of EEG signal these different waves are generated. These frequency have certain ranges. These all frequencies plays important role in detecting cognitive ability of person. So these features are extracted from original data. Techniques such as Fast Fourier Transform(FFT), is used for feature extraction.

3. Feature Selection:

This is third step of data processing. In this only some features are selected which contribute in giving cognitive ability of person. So these selected features are given to classification for further processing.

4. Classification:

This is the phase where actual model is going to build for detection by various algorithms. Features selected in earlier phase are going to use for applying algorithms. In this step algorithms such as Support Vector Machine(SVM), Linear Regression(LR), Decision Tree(DT), Naïve Bayes, K-nearest neighbour(KNN) are used in detection of cognitive ability of person.

5. Evaluation:

This is the final step where finally cognitive ability of person is detected. Accuracy obtained by various algorithms in earlier stage are going to compare for analysis purpose.

Decision Tree gives accuracy up to 90%.
Naïve Bayes gives accuracy up to 75%.
K-nearest neighbour gives accuracy up to 80%.

IV Result and Discussion

On real time dataset that I collected from different people of different age groups I applied some pre-processing techniques in order to remove noise, artifacts or any movements done by person while recording EEG of person. Pre-processing such as removal of blank fields, missing entry in some columns of CSV file i.e. data of people are removed.

Once pre-processing is done feature extraction is performed. Features such as Alpha, Theta are selected for further processing. After this Decision Tree, K-nearest neighbour, Support Vector Machine are applied on these features. Decision Tree gives highest accuracy of up to 90% among all algorithm.

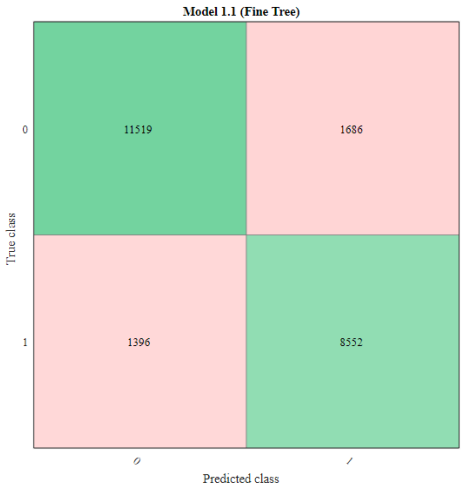

Fig. 5. Confusion Matrix For Fine Tree Algorithm

Above Figure 5 shows confusion matrix for Fine Tree Algorithm. It shows matrix of True class and Predicted class. Region in green colour should show highest value i.e. diagonal elements of matrix should contain highest value among all other values of matrix. Region in green colour shows True positive value and region in pink colour shows false negative value. True positive class contains value in which actual values and predicted values are matched. False negative class contains value in which actual values and predicted values are not matched.

Below figure 6 shows ROC curve for fine tree. ROC(Receiver Operating Characteristics) curve is a graphical plot which is used for checking performance of binary classification models. This curve plots two parameters such as true positive rate false positive rate. ROC represent probability curve.

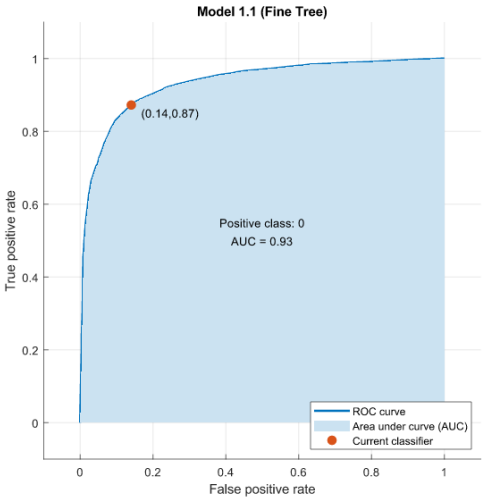

Fig. 6. ROC curve for Fine Tree

V Conclusion and Future Scope:

EEG with combination of Screening test can be consider as valid and very useful tool in finding Cognitive Ability. Use of Emotiv Insight device for capturing EEG signal helps in giving good result. Real time data from people of different age groups is collected. Data collection is done by using combination of EEG signal and MMSE test. Various abnormalities are found in data collected that are removed by pre-processing. Various feature extraction methods, classifiers helped in detection of cognitive ability. EEG and MMSE helps in identifying cognitive ability of person so that it helps in further better treatment if there any serious cause. Use of Decision Tree for classification gives accuracy up to 90%. Use of Naïve Bayes classifier gives accuracy of 75%. In this paper emotiv insight device used to capture brain activity has only 5 channels so if in future if we use 14-channel emotiv device then it may help in increasing accuracy of model as it covers more region of brain which helps in collecting very good brain activity and will give better result as compare to present result.

REFERENCES

[1] Saleha Khatun, Bashir I. Morshed, Gavin M. Bidlman, "Single Channel EEG Time-Frequency Features to Detect Mild Cognitive Impairment", IEEE, 2017.

[2] Noor Kamal Al-Qazzaz, Sawal Hamid Bin MD. Ali, Siti Anom Ahmad, Kalaivani Chellappan, Md. Shabiul Islam, and Javier Escudero, "Role of EEG as Biomarker in the Early Detection and Classification of Dementia", The Scientific World Journal, 2014.

[3] Nilesh Kulkarni, Prof. Dr. V. K. Bairagi, "Diagnosis of Alzheimer Disease using EEG Signals", International Journal of

engineering Research & Technology(IJERT), Vol. 3 Issue4, April-2014.

[4] G. Anuradha, Najumnissa Jamal and Syed Rafiammal, "Detection of Dementia in EEG Signal using Dominant Frequency Analysis", IEEE International Conference on Power, Control, Signals and Instrumentation Engineering, 2017.

[5] Breno S.O. Diniz, Monica S. Yassuda, Paula V. nunes, Marcia Radanovic and Orestes V. Forlenza, "Mini-mental State Examination performance in mild cognitive impairment subtypes", International Psychogeriatric Association, 2007.

[6] Masoud Kashefpoor, Hossein Rabbani, and Majid Barekatain "Automatic Diagnosis of Mild Cognitive Impairment Using Electroencephalogram Spectral Features", Journal Of Medical Signals and Sensors, Volume(6)1, Jan-Mar 2016.

[7] Donghyeon Kim, Student Member, IEEE, and Kiseon Kim, Senior Member, IEEE, "Detection of Early Stage Alzheimer's Disease using EEG Relative Power with Deep Neural Network", IEEE, 2018.

[8] Noor Kamal Al-Qazzaz ,Sawal Ali, Siti Anom Ahmad, Javier Escudero, "Stroke-related mild cognitive impairment detection during working memory tasks using EEG signal processing", International Conference on Advances in Biomedical Engineering (ICABME), 2017.

[9] Nesma Houmani, Franc ¸ois Vialatte, Esteve Gallego-Jutglà, Ge ´rard Dreyfus, Vi-Huong Nguyen-Michel, Jean Mariani, Kiyoka Kinugawa, "Diagnosis of Alzheimer's disease with Electroencephalography in a differential framework", PLOS, 2018.

[10] Marshal f. folstein, susan E. folstein and Paul R. Mchugh, "Mini-Mental State A Practical method for grading the cognitive state of patients for the clinician", J. Psychiat, 1975.

[11] Yonas E. Geda, "Mild Cognitive Impairment in Older Adults" Psychiatry Rep. Col. 14, August 2012.

[12] Eli s Neiman, "EEG in Dementia and encephalopathy", Medscape drugs and disease, 2013.

[13]http://psychtutor.weebly.com/cognitive-level-of-analysis.html.

[14]https://www.mccare.com/education/mcidementia.html.

[15] https://www.emotiv.com/product/emotiv-insight-5-channel-mobile-eeg/.

[16] Mohan Sai Ijjada ; Himanshu Thapliyal ; Allison Caban-Holt ; Hamid R Arabnia, "Evaluation of Wearable Head Set Devices in Older Adult Populations for Research", International Conference on Computational Science and Computational Intelligence (CSCI), 2015.

Proceedings of the Fourth International Conference on Communication and Electronics Systems (ICCES 2019)
IEEE Conference Record # 45898; IEEE Xplore ISBN: 978-1-7281-1261-9

Impact of Imperfect Channel State Information on Downlink Sum-Rate of Two user mmWave Non Orthogonal Multiple Access

Sumathi S., Arpita Thakre
Department of Electronics and Communication Engineering
Amrita School of Engineering, Bengaluru
Amrita Vishwa Vidyapeetham, India
ssumathi_me@yahoo.co.in, arpita.thakre@ieee.org

***Abstract*—Effect of imperfect channel state information on achievable data rates of a two user downlink non orthogonal multiple access scenario is considered in this paper. The optimum antenna array weight that steers the downlink beams towards the two users has been reported earlier based upon perfect knowledge of downlink channels at the base station. This antenna weight vector is no longer optimum as soon as the channel state information available with the base station becomes outdated. The effect of wrong angle of departure information and/or wrong channel gain information reduces the advantage of above access scheme over orthogonal multiple access scheme. How reduction in achievable data rate in a non orthogonal case depends on different transceiver parameters, such as the error in angle information, the absolute value of the angle of departure, number of antenna elements at the base station is shown in this paper.**

***Index Terms*—Non Orthogonal Multiple Access, Millimeter Wave communication, Beamforming, Imperfect CSI.**

I. Introduction

Next Generation Mobile broadband network is expected to support data rate of the order of Gigabits per second. An efficient radio access technology integrated with greater spectrum availability is vital to attain the above goal [1]. Huge bandwidth available in the wave band (20 GHz to 100 GHz) prompted engineers to look into transceiver techniques suitable for use in the this band [2].

Non Orthogonal Multiple Access (NOMA) is one of the key enablers that addresses the immense data rate requirement. Existing wireless communication standard employs orthogonal access techniques in which different users are assigned orthogonal resources such as time and/or frequency to minimize inter user interference [3]. Power domain NOMA uses same radio resource for more than one user but modulates individual user's data with different power levels.Power domain NOMA employs Superposition Coding (SC) allocates different powers to the two downlink users wherein the power distribution between the two users depends on the channel gains seen by the two users. The underlying assumption is that the two users see significantly different channel gains. The user which sees a weaker channel treats the other user's data as noise and decodes his data. The user which sees a stronger channel needs to perform Successive Interference Cancellation (SIC) to recover the data meant for him [4]. In a multiple antenna wireless communication scenario, number of radio frequency (RF) chains decides the number of users to be supported simultaneously. In fact number of users that can be supported by one time or frequency or code unit per RF chain is one. Increase in number of RF chains increases the hardware cost [5]- [8]. In such a case, NOMA can be used to effectively increase the number of users served in one resource block to two or more.

Beamforming is used in mmwave MIMO communication systems to generate highly directional beams to compensate for the losses incurred in mmwave band of frequencies.Various beamforming techniques in Rayleigh fading environment are discussed in [9]. The authors of [10] have considered a random beamforming approach to maximize the achievable sum rate of two downlink NOMA users. The users experience different channel gains but are at same azimuth angle or angle of departure (AoD) with respect to antenna array in [10]. Beam Sweeping is an approach where the base station radiates multiple beams in different directions assuming an uniform distribution for AoD. The handset reports the index of beam with highest received power to the base station. The number of beams used by the base station, i.e, the codebook size, depends on available number of antenna elements [11]. Given that codebook size cannot be chosen to be very large in a practical case, and the feedback link between the handset and base station introduces delay as well as error, we will not have perfect channel knowledge at the transmitter. No doubt, the deviation from correct value also depends on the speed at which the handset is moving and the channel propagation characteristics.

We consider a downlink NOMA scenarion in mmwave channel with two users where the base station has one RF chain and multiple antenna elements connected to the ouput of the RF chain via different weights. There are two users at different distances as well as at different azimuth angles with respect to the antenna array at the base station. The aim is to design the Antenna Weight Vector (AWV) as well as power allocated to the two users' data such that achievable sum data rate gets maximized. Xiao et. al in [12] have considered the above scenario but assumed that base station has perfect channel knowledge. We study the above downlink NOMA scenario where the base station does not have perfect CSI.

In this paper we show how an error, whether an error in azimuth angle information or an error in channel gain information causes a decrease in the achievable data rates for the two users. The reduction in achievable data rates is shown to depend on number of antenna elements, error in angle information, and the absolute value of AoD as well. Section II describes the system model. Simulation results are available in section III and we conclude the paper in section IV. Bold lower case letters denote vectors, $(.)^H$ denotes Hermitian operation, $(.)^T$ denotes Transpose, $|.|$ is for absolute operation, and $(.)^*$ is used for conjugation.

II. System Model

We consider downlink mmWave NOMA for two users with *multi-beamforming* which means that base station can form multiple narrow beams with different beam gains where the beams are steered towards multiple users that are spatially located at different azimuth angles. The transceiver at the base station is assumed to have one Radio Frequency chain whose output is connected to a Uniform Linear Array (ULA) of N antenna elements via N phase shifters and N Power Amplifiers (PA). The antenna elements are assumed to be $\lambda/2$ apart from each other where λ is carrier wavelength. Proper choice of the N phase shifts or AWV, **w**, will give rise to beams in the intended directions. All the power amplifiers are assumed to have same scaling factor. Throughout the paper it is assumed that the base station forms two narrow beams with different beam gains to serve two NOMA users as shown in Fig. 1.

The underlying assumption in NOMA is that the channel gains experienced by the two downlink users are significantly different. The base station uses superposition coding to send data to the two NOMA user equipment where relatively more power is assigned to the data that will pass through the weaker channel. The sum-rate achieved by the two user downlink system depends on the power allocated to the two bit streams. The authors in [12] came up with an AWV that would maximize the downlink sum-rate with the constraints that the AWV, **w** is constant modulus and the data rate

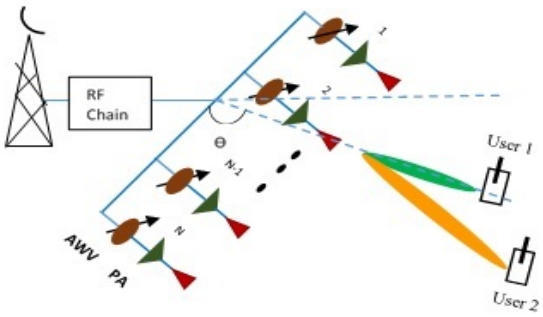

Fig. 1: Block Diagram of a two-user NOMA system with downlink beam-forming

achieved at the individual links is above a threshold value. The AWV calculation assumes that the base station knows the channel gains and the azimuth angles at which the two users are located accurately. The base station is assumed to steer the downlink beams towards the strongest multipath components of the respective users.

In a practical deployment scenario, the base station cannot have correct knowledge of channel gains and the azimuth angles of the users as explained in Introduction section. The present work aims at studying the effect of imperfect CSI on downlink user data rates. The mmWave channel between the base station and i-th user corresponding to the strongest multipath component is given by

$$\mathbf{h}_i = \lambda_i \mathbf{a}_i(N, \theta_i) \quad i = 1, 2. \tag{1}$$

where λ_i is the complex gain of the strongest multipath between base station and i-th user equipment, $\mathbf{a}_i(.)$ is antenna array response vector at the base station, and $\theta_i \in [0, \pi]$ is the azimuth angle of departure (AoD) of the strongest multipath component between base station and i-th user equipment. The antenna array response vector is given by

$$\mathbf{a}_i(N, \theta_i) = [1 \quad e^{j\pi\Omega_i} \quad e^{j\pi 2\Omega_i} \quad \ldots\ldots\ldots \quad e^{j\pi(N-1)\Omega_i}]^T \tag{2}$$

where $\Omega_i = cos(\theta_i)$.

λ_i is assumed to be Gaussian distributed and $\Omega_i \in [1, -1]$ as θ_i is uniformly distributed $\in [0, \pi]$. Throughout the paper it is assumed, without loss of generality, that $|\lambda_1| \geq |\lambda_2|$, which means that channel gain of user 1 is better than that of user 2. In mmWave frequency range of operation, the strongest multipath component is typically almost 20 dB stronger than the other multipath components. Therefore we stick to a single path model for the channel through out the paper.

Assuming s_i is the symbol meant for user i, and p_i is

the power assigned to user i, the baseband equivalent signal transmitted by the base station is given by

$$s = \sqrt{p_1}s_1 + \sqrt{p_2}s_2 \tag{3}$$

The baseband equations for the signals received by the users are respectively given by

$$\begin{aligned} y_1 &= \mathbf{h}_1^H \mathbf{w}(\sqrt{p_1}s_1 + \sqrt{p_2}s_2) + n_1 \\ y_2 &= \mathbf{h}_2^H \mathbf{w}(\sqrt{p_1}s_1 + \sqrt{p_2}s_2) + n_2 \end{aligned} \tag{4}$$

where $\mathbb{E}\{|s_i|^2\}$ = 1, n_1 and n_2 are additive noise with variance σ^2, $P = p_1 + p_2$ is the total transmit power, and P/σ^2 is the transmit Signal to Noise Ratio (tSNR). Noise is white and Gaussian distributed. The AWV, $\mathbf{w}$ should satisfy $|\mathbf{w}_k| = \frac{1}{\sqrt{N}}$ for $k = 1, 2, ..., N$.
With no loss of generality, we also assume that $|\mathbf{h}_1^H \mathbf{w}|^2 \geq |\mathbf{h}_2^H \mathbf{w}|^2$. This implies that user 1 decodes s_2 first, subtracts the signal component of s_2 from the received signal y_1 and then decodes s_1. The achievable rates of user i, for $i = 1, 2$, denoted by R_i, under the above assumption are given by

$$\begin{aligned} R_1 &= log_2\Big(1 + \frac{|\mathbf{h}_1^H \mathbf{w}|^2 p_1}{\sigma^2}\Big) \\ R_2 &= log_2\Big(1 + \frac{|\mathbf{h}_2^H \mathbf{w}|^2 p_2}{|\mathbf{h}_2^H \mathbf{w}|^2 p_1 + \sigma^2}\Big) \end{aligned} \tag{5}$$

The problem is to determine the vector $\mathbf{w}$ that makes the achievable sum rate of the two users maximum assuming that the downlink channels are known to the transmitter a priori. The constraints are that all the entries of AWV has to have same modulus and the individual data rates R_1 and R_2 should be above a predefined minimum value, say r.

$$\begin{aligned} \max_{p_1, p_2, \mathbf{w}} \ & (R_1 + R_2) \\ \text{subject to} \ & R_1, R_2 \geq r \\ & (p_1 + p_2) = P \\ |\mathbf{w}_k| = \frac{1}{\sqrt{N}}, \quad & k = 1, 2, ..., N \\ & |\mathbf{h}_1^H \mathbf{w}|^2 \geq |\mathbf{h}_2^H \mathbf{w}|^2 \end{aligned} \tag{6}$$

As described in [12] the solution to the above problem is found in three steps. In first step, the constant and equal modulus constraint on the vector $\mathbf{w}$ is relaxed. Powers p_1 and p_2 and beam gains $|\mathbf{h}_1^H \mathbf{w}|^2$ and $|\mathbf{h}_2^H \mathbf{w}|^2$ are determined that maximize the sum rate of two users while satisfying the total power avaialable and the minimum data rate requirement at the two users. In the second step, a constant modulus AWV, $\mathbf{w}$ that gives rise to beam gains equal to or more than the optimum beam gains obtained in first step is determined. In the third and final step, the $\mathbf{w}$ found in the second step is plugged into the expression for sum-rate of two users. Now the problem reduces to finding the power p_1/p_2 that makes the sum rate maximum under the minimum data rate requirements at the two users. Thereby after three steps, the optimum powers p_1, p_2, and AWV, $\mathbf{w}$ are obtained, i.e., solution to equation (6) is obtained. Please refer to [12] for further details.
In this paper we aim to study the effect on imperfect CSI on the sum-rate of two users. Imperfect CSI can be of two types. (i) The AoD θ_i can be wrong and/or (ii) the channel gain λ_i can be wrong. We first study the effect of wrong knowledge of AoD θ_i at the base station. Next we study the effect of incorrect knowledge of channel gain λ_i at the base station.

III. Impact of Imperfect AoD

We assume that $\tilde{\theta}_i$ is the correct AoD corresponding to the i-th user whereas the base station assumes θ_i to be the AoD corresponding to the i-th user equipment. We also assume that base station has correct knowledge of λ_i. In other words the channel knowledge that base station should have are given by

$$\begin{aligned} \tilde{\mathbf{h}}_1 &= \lambda_1[1 \quad e^{j\pi\tilde{\Omega}_1} \quad e^{j\pi 2\tilde{\Omega}_1} \ ..... \ e^{j\pi(N-1)\tilde{\Omega}_1}]^T \\ \tilde{\mathbf{h}}_2 &= \lambda_2[1 \quad e^{j\pi\tilde{\Omega}_2} \quad e^{j\pi 2\tilde{\Omega}_2} \ ..... \ e^{j\pi(N-1)\tilde{\Omega}_2}]^T \end{aligned} \tag{7}$$

Base station calculates optimum powers and AWV based on $\mathbf{h}_1$ and $\mathbf{h}_2$ following the three steps described in the previous section. Let us call these values as p_1, p_2 and $\mathbf{w}$. Therefore the actual downlink data rates $\tilde{R}_1$, $\tilde{R}_2$ obtained by the two users will be given by

$$\begin{aligned} \tilde{R}_1 &= log_2\Big(1 + \frac{|\tilde{\mathbf{h}}_1^H \mathbf{w}|^2 p_1}{\sigma^2}\Big) \\ \tilde{R}_2 &= log_2\Big(1 + \frac{|\tilde{\mathbf{h}}_2^H \mathbf{w}|^2 p_2}{|\tilde{\mathbf{h}}_2^H \mathbf{w}|^2 p_1 + \sigma^2}\Big) \end{aligned} \tag{8}$$

where,

$$\begin{aligned} \mathbf{h}_1 &= \lambda_1[1 \quad e^{j\pi\Omega_1} \quad e^{j\pi 2\Omega_1} \ ..... \ e^{j\pi(N-1)\Omega_1}]^T \\ \mathbf{h}_2 &= \lambda_2[1 \quad e^{j\pi\Omega_2} \quad e^{j\pi 2\Omega_2} \ ..... \ e^{j\pi(N-1)\Omega_2}]^T \end{aligned} \tag{9}$$

$$\mathbf{h}_1^H \mathbf{w} = \sum_{n=0}^{N-1} e^{-jn\pi\Omega_1} e^{j\mathbf{w}_n} = \sum_{n=0}^{N-1} \alpha_n \tag{10}$$

$$\tilde{\Omega}_1 = cos(\tilde{\theta}_1) = cos(\theta_1 + \Delta\theta_1) \approx \Omega_1 - \Delta\theta_1 sin(cos^{-1}\Omega_1) \tag{11}$$

$$\tilde{\mathbf{h}}_1^H \mathbf{w} = \sum_{n=0}^{N-1} e^{-jn\pi\tilde{\Omega}_1} e^{j\mathbf{w}_n} = \sum_{n=0}^{N-1} \alpha_n e^{jn\pi\Delta\theta_1 sin(cos^{-1}\Omega_1)} \tag{12}$$

$$|\mathbf{h}_1^H \mathbf{w}|^2 = \Big(\sum_{n=0}^{N-1} \alpha_n\Big)\Big(\sum_{k=0}^{N-1} \alpha_k^*\Big) \tag{13}$$

$$|\tilde{\mathbf{h}}_1^H \mathbf{w}|^2 = \Big(\sum_{n=0}^{N-1} \alpha_n e^{jnq}\Big)\Big(\sum_{k=0}^{N-1} \alpha_k^* e^{-jkq}\Big) \tag{14}$$

where $q = \Delta\theta_1 sin(cos^{-1}\Omega_1)$. It is clear from the above equations that for any arbitrary value of $\Delta\theta_1$ and Ω_1 $|\tilde{\mathbf{h}}_1^H \mathbf{w}|^2 < |\mathbf{h}_1^H \mathbf{w}|^2$. The sum-rate under perfect knowledge of channel gain and imperfect AoD knowledge are plotted in the paper.

IV. Impact of Imperfect Channel Gain

We assume $|\breve{\lambda}_i|$ to be the correct channel gain magnitude corresponding to the i-th user equipment. The base station, however, assumes $|\lambda_i|$ to be the channel gain magnitude. In other words the channel knowledge that base station should have are given by

$$\begin{aligned}\breve{\mathbf{h}}_1 &= \breve{\lambda}_1[1 \quad e^{j\pi\Omega_1} \quad e^{j\pi 2\Omega_1} \quad \ldots\ldots\ldots \quad e^{j\pi(N-1)\Omega_1}]^T \\ \breve{\mathbf{h}}_2 &= \breve{\lambda}_2[1 \quad e^{j\pi\Omega_2} \quad e^{j\pi 2\Omega_2} \quad \ldots\ldots\ldots \quad e^{j\pi(N-1)\Omega_2}]^T\end{aligned} \tag{15}$$

Base station calculates optimum powers and AWV based on $\mathbf{h}_1$ and $\mathbf{h}_2$. Let us call these values as p_1, p_2 and $\mathbf{w}$. However the actual downlink data rates $\breve{R}_1$, $\breve{R}_2$ obtained by the two users will be given by

$$\begin{aligned}\breve{R}_1 &= log_2\Big(1 + \frac{|\breve{\mathbf{h}}_1^H \mathbf{w}|^2 p_1}{\sigma^2}\Big) \\ \breve{R}_2 &= log_2\Big(1 + \frac{|\breve{\mathbf{h}}_2^H \mathbf{w}|^2 p_2}{|\breve{\mathbf{h}}_2^H \mathbf{w}|^2 p_1 + \sigma^2}\Big)\end{aligned} \tag{16}$$

V. Results And Discussion

Simulation has been done in matlab assuming P = 100 mW, σ^2 = 1 mW, $|\lambda_1|$ = 0.85, $|\lambda_2|$ = 0.4, $\theta_1 = 85^0$, $\theta_2 = 55^0$, N = 32. The data rates that have been plotted in the following figures are maximum achievable data rates.

Fig. 2 shows achievable sum rate vs. minimum supported data rate plot for perfect as well as imperfect AoD knowledge at the base station. The achievable sum rate decreases with increase in minimum data rate, r because data rate of near user decreases at a faster rate than the rate at which far user's data rate increases as evident from Fig. 3. The AWV, $\mathbf{w}$ changes so as to give higher data rate to far user at the expense of near user's data rate. The achievable sum rate in presence of wrong angle values available with the transmitter is always less than the perfect CSI case. The gap between sum rates for perfect and imperfect AoD increases as error in AoD increases. This behaviour is expected and explained in previous section. The power allocated to the two users' data by the base station while performing superposition coding is shown in Fig. 4. The base station transmits two users' signal with equal power at low supported data rate of 1 bps/Hz. However the gap between the powers allocated to the two users increases as the requirement for minimum supported data rate increases. Fig. 5 is a plot of beam gain as a function of angle of departure. The beam gain for near user becomes maximum at 85^0 because that is the direction along which the near user is placed. This plot also shows that as number of antenna elements at the transmitter increases, the beam becomes narrower, implying that (1) the total supported data rate would increase with number of antenna elements, N, and (2) an incorrect estimate of angle and/or channel gain at the transmitter would reduce the achievable data rates more, the higher the number of antenna elements , N. This observation is supported by simulation result shown in Fig. 6. Fig. 7 shows that incorrect knowledge of channel gain causes decrease in individual as well as sum data rate. It is to be noted that wrong channel gain information causes

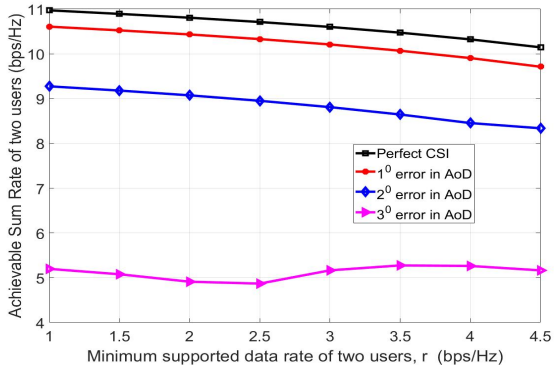

Fig. 2: Achievable sum rate vs minimum supported data rate with perfect and imperfect AoD estimates

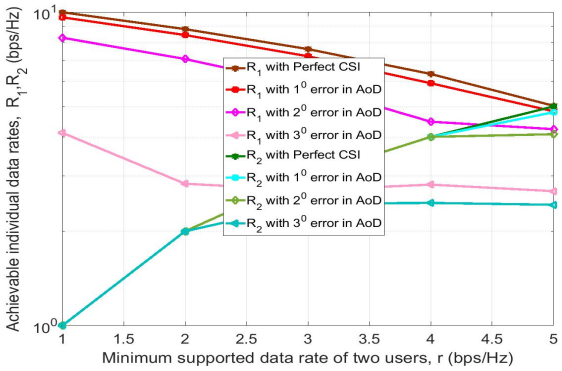

Fig. 3: Achievable data rates for Far and Near User vs minimum supported data rate with perfect and imperfect knowledge of AoD

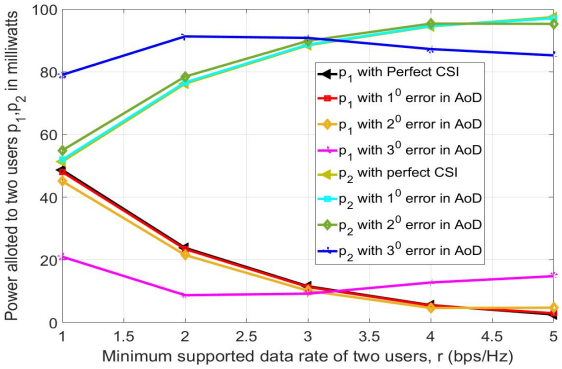

Fig. 4: Power allocated to the two users vs minimum supported data rate with perfect and imperfect AoD estimates at the base station

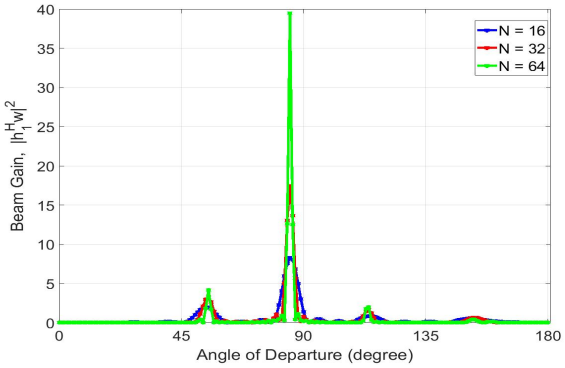

Fig. 5: Beam Gain of near user as a function of Angle of Departure for different no. of antenna elements

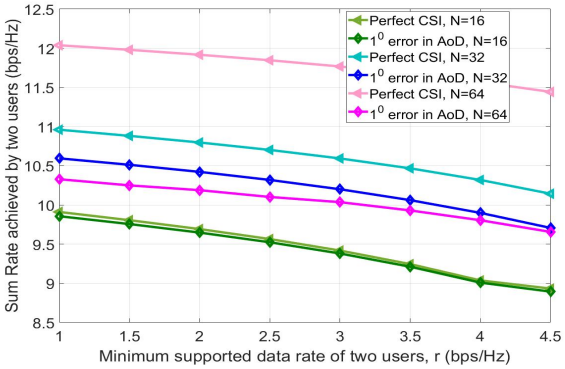

Fig. 6: Variation of achievable sum rate with number of antenna elements

a much less reduction in data rates compared to the reduction in data rate caused by imperfect knowledge of AoD. The best sum data rate achievable using TDMA with perfect CSI at transmitter has also been plotted here. The transmitter is assumed to allocate equal time to the two users. The AWV is chosen as $\mathbf{w} = \mathbf{h}_i/||\mathbf{h}_i||$ for $i = 1, 2$. Fig. 8 illustrates that absolute values of

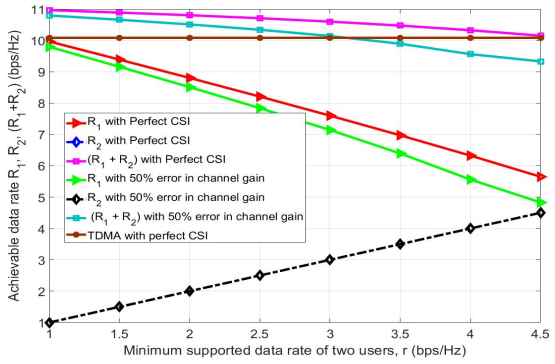

Fig. 7: Achievable data rates when the channel gain knowledge at the base station is erroneous

AoDs as well determine how much an error in AoD will affect the achievable data rates. We kept all the parameters same as before except $\theta_1 = 20^0$. Difference between Fig. 8 and Fig. 2 is clearly visible.

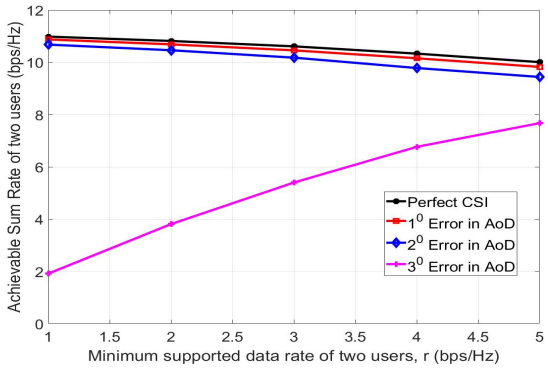

Fig. 8: Achievable sum rate vs minimum supported data rate with perfect and imperfect AoD estimates

VI. Conclusion

A two user NOMA supported on the downlink of a mmwave wireless communication system has been studied here wherein the users are assumed to be at different azimuth angles. Previous studies on NOMA assume that bases station has perfect channel state information. This paper shows how imperfect knowledge of angle of departure and/or channel gain at the base station reduces the achievable data rate for NOMA. Too much imperfection in channel knowledge may actually destroy the advantage of using non orthogonal multiple access technique compared to orthogonal multiple access techniques.

References

[1] T. S. Rappaport et al., "Millimeter wave mobile communications for 5G cellular: It will work!", IEEE Access, vol. 1, pp. 335–349, 2013.

[2] Y. Niu, Yong Li, Depeng Jin, Li Su and Athanasios V. Vasilakos, "A survey of millimeter wave communications (mmWave) for 5G: Opportunities and challenges", Wireless Netw., vol. 21, no. 8, pp. 2657–2676, 2015.

[3] Yuanwei Liu, Zhijin Qin, Maged Elkashlan, Zhiguo Ding, Arumugam Nallanathan and Lajos Hanzo,"Non-Orthogonal Multiple Access for 5G and Beyond", Proceedings of the IEEE, vol.105, no.12, pp. 2347 – 2381, Dec. 2017.

[4] Anass Benjebbour, Yuya Saito, Yoshihisa Kishiyama, Anxin Li, Atsushi Harada and Takehiro Nakamura, "Concept and practical considerations of non-orthogonal multiple access (NOMA) for future radio access", in International Symposium on Intelligent Signal Processing and Communication Systems, pp. 770–774, Nov. 2013.

[5] J. Wang et al., "Beam codebook based beamforming protocol for multi- Gbps millimeter-wave WPAN systems," IEEE J. Sel. Areas Commun.,vol. 27, no. 8, pp. 1390–1399, Oct. 2009.

[6] A. Alkhateeb, J. Mo, N. González-Prelcic and R. W. Heath Jr., "MIMO precoding and combining solutions for millimeter-wave systems," IEEE Commun. Mag., vol. 52, no. 12, pp. 122–131, Dec. 2014.

[7] W. Roh et al., “Millimeter-wave beamforming as an enabling technology for 5G cellular communications: Theoretical feasibility and prototype results,” IEEE Commun. Mag., vol. 52, no. 2, pp. 106–113, Feb. 2014.
[8] S. Sun, T. S. Rappaport, R. W. Heath Jr., A. Nix and S. Rangan, “MIMO for millimeter-wave wireless communications: Beamforming, spatial multiplexing, or both?” IEEE Commun. Mag., vol. 52, no. 12, pp. 110–121, Dec. 2014.
[9] Faezeh Alavi, Kanapathippillai Cumanan, Zhiguo Ding and Alister G. Burr, ”Beamforming Techniques for Non-Orthogonal Multiple Access in 5G Cellular Networks”, IEEE Transactions on Vehicular Technology, vol. 67, no. 10, pp. 9474–9487, Oct 2018.
[10] Z. Ding, P. Fan, and H. V. Poor, ”Random beamforming in millimeter-wave NOMA Networks”, IEEE Access, vol. 5, pp. 7667–7681, Feb. 2017.
[11] Marco Giordani, Michele Polese, Arnab Roy, Douglas Castor, Michele Zorzi ,” A Tutorial on Beam Management for 3GPP NR at mmWave Frequencies”, unpublished.
[12] Z. Xiao, L. Zhu, J. Choi, P. Xia, and X.-G. Xia, ”Joint power allocation and beamforming for non-orthogonal multiple access (NOMA) in 5G millimeter wave communications”, IEEE Transactions on Wireless Communications, vol. 17, no. 5, pp. 2961–2974, May 2018.

Proceedings of the Fourth International Conference on Communication and Electronics Systems (ICCES 2019)
IEEE Conference Record # 45898; IEEE Xplore ISBN: 978-1-7281-1261-9

Long-Short term Memory based Channel Prediction for SISO System

Draksham Madhubabu, Arpita Thakre
Department of Electronics and Communication Engineering
Amrita School of Engineering, Bengaluru,
Amrita Vishwa Vidyapeetham, India
madhubabu926@gmail.com, arpita.thakre@gmail.com

Learning the characteristics of a wireless channel is one of the most fundamental and challenging issues in the wireless communication. Many conventional signal processing techniques have been developed so far to estimate the channel state information. In this paper, we present a novel approach based on deep learning using long short term memory (LSTM) neural network to predict the fast-varying Rayleigh fading channel. Having known application of LSTM neural network in the field of time-series prediction problems, we have applied LSTM to predict the future state of the channel by providing the past channel state values. The predicted values of channel is used to recover the transmitted symbol from noisy signal received at the receiver end. We have optimized the configuration of LSTM network by correctly tuning the hyper-parameters so that we get a correct prediction of channel which is in turn used for reconstruction of signal at receiver end. The simulated Bit Error Rate vs. Signal-to-Noise ratio plot proves that LSTM based channel predictor works better than currently used interpolation based channel predictor.

Keywords— Deep Learning, Rayleigh fading channel, LSTM Neural Network, Wireless Communication, SISO system.

I. INTRODUCTION

Communication is a rich field consisting of domain knowledge regarding modelling different types of channels, signaling and detection techniques and different modulation schemes [1], [2] that ensure reliability of data transfer between transmitter and receiver [3]. Further to increase the efficiency in the performance of the wireless technologies. We need to be docile in adapting to the latest technologies, such as data-driven approaches by using machine learning and deep learning algorithms. There were different multiple access techniques like frequency division multiple access (FDMA) across frequency, time division multiple access (TDMA) across time and code division multiple access [4] schemes across different pseudo codes helped to increase the quality of service(QoS) and showed significant performance improvement but we cannot go any further with them. Now a days the data centric approach had gathered attention with huge success attained in fields as such realization of vision through computers, processing of human language and image classification [5], [6]. For a reliable data transmission to happen we need to model the channel correctly but accurate modelling of channel mathematically is almost impossible so we go for a probabilistic based approach. The core signal processing algorithms used in communications fails to improve in performance [7]. The deep learning based algorithms in the field of wireless communication [8] was used because it has the power to improve the performance in areas where it is impossible to generate mathematical models but by considering the deep learning model as a black-box we can tune hyper-parameters so that we can control the output of the system [9].

The next wave of wireless technology suffers with the problem of network latency as the number of connections over a network increases drastically in number the scope of deep learning is such that it has to automatically get tuned to the available network and increase or decrease power with respect to the corresponding receiver. In recent the machine learning which is a root class of deep learning had used in the field of communications for tasks such as recognition of modulation scheme, channel encoding techniques and decoding techniques, in estimation of channel and channel equalization [10], [11], [12], [13].

In the recent years the computing power has been drastically increased and the algorithms have been developed so far and fast that uses the data. In physical layer research, by considering the applications of deep learning we are not only trying to improve the performance of individual blocks but also we try to increase the performance of entire communication system by considering transmitter, channel and receiver as a deep learning model such type of arrangement is called as auto-encoder[14]. The channel estimation using least squares (LS) method and minimum mean square error (MMSE) method estimators have been utilized in many occasions [15]. Of that least squares estimator does not require any previous channel values. The MMSE estimator works better by considering the second order statistics of the channel. In a paper related to orthogonal frequency division multiple access (OFDM) [16] the application of deep learning which mainly focus on feed forward neural network have been studied it presents initial results in learning methods to deal with wireless channels and the removal of cyclic prefix in OFDM and usage of limited pilots and non-linear noise distortions has been discussed [17].

We, in this paper have opted for a single input single output system [18](SISO-system), modeled the channel as a fast fading channel with Rayleigh distribution and a moving receiver at 500kmph scenario is considered. Then at the receiver end we have built a LSTM neural network and trained it online using the data from the zero forcing estimation block after adding additive white Gaussian noise (AWGN). We optimized the data over the loss function between the true values of the channel and the values that were corrupted due to noise. The predicted values have been used for channel equalization and successful reconstruction of the signal at receiver end. We have fine-tuned the hyper-

parameters at a certain value of SNR and has been implemented for SNR of certain range. Finally, after the reconstruction of the transmitted bits the Bit Error Rate over different values of Signal to noise ratio has been plotted.

we will be describing about the wireless system model with the block diagram in Section II. In Section III we will be discussing about the Deep Learning basics and Deep Learning Architecture being used and how we have obtained the data and the corresponding performance metrics used in obtaining the results. That was followed by a discussion on the simulation results obtained in Section IV, Section V deals about conclusion of the topic and its future scope of the work done.

II. WIRELESS SYSTEM MODEL

We have assumed the problem of channel prediction as a supervised learning problem. Out of all the channel characteristics like attenuation, scattering, diversity, reflection and refraction we have been considering channel fading as the only phenomenon to tackle. The channel we have considered here is a Rayleigh fading channel. As *R* being its corresponding random variable and its probability density function is given by

$$f_R(r) = \frac{r}{\sigma^2} e^{\frac{-r}{2\sigma^2}}, \quad r \geq 0 \qquad (1)$$

we have been considering the case of moving receiver which introduces a Doppler shift in the receiving signal. We are considering the speed of the receiver as 500kmph in this problem. Here we have considered V as velocity and λ as wavelength and θ as the angle between the receiver and the incoming signal. The value of Doppler shift (ΔØ) affect the value of frequency of the received signal the change in frequency is calculated using Equation 2 and 3.

$$\Delta\emptyset = \frac{2\pi\Delta l}{\lambda} = \frac{2\pi v \Delta t}{\lambda} \cos\theta \qquad (2)$$

$$f_d = \frac{1}{2\pi}\frac{\Delta\emptyset}{\Delta t} = \frac{v}{\lambda}\cos\theta \qquad (3)$$

The problem we have taken is a complex optimization problem that address the time-series relationship in the data and we have modelled it as a supervised regression problem. The baseband equivalent of the bandpass SISO (single input single output) system for a faded channel of probability distribution as Rayleigh in the presence of noise will be

$$\mathbf{y = h\,x + n} \qquad (4)$$

Where y is the received complex baseband signal and h is a Rayleigh faded channel |h| is the magnitude of the fading and x is the input modulated signal to be transmitted and n is the Additive White Guassian Noise (AWGN). Where noise follows Guassian distribution. While solving the problem we have split the equations into real and imaginary parts shown in Equation 5 and 6.

$$y_{real} = h_{real} * x_{real} + n_{real} \qquad (5)$$

$$y_{img} = h_{img} * x_{img} + n_{img} \qquad (6)$$

From Fig.1, we have generated the 'N' bits where N ∈ (0, 1) and that bits has been sent to modulator block where the QPSK modulation happens on the input bits and the modulator block output symbols which are of complex in nature and they are of size N/2. Then those symbols are transmitted through wireless channel which in our case is a Rayleigh faded channel and the output of the channel is received by the receiver and adds an Additive White Gaussian Noise (AWGN) at the beginning of the receiver after the addition of noise we will consider the signal as y. 'y' is complex signal consisting of real part and imaginary part and The first 150 symbols were given as input to the zero-forcing estimator the output 150 symbols of the estimator are separated into real and imaginary values and are given to two LSTM blocks separately the LSTM block takes the input as first 150 values of h and predicts the next 600 values of h in both real and imaginary part. We call it as h' and then we collect h' and proceeds for channel equalization with the obtained values of h' and then after the channel equalization we will be demodulating the signal to reconstruct the originally transmitted information.

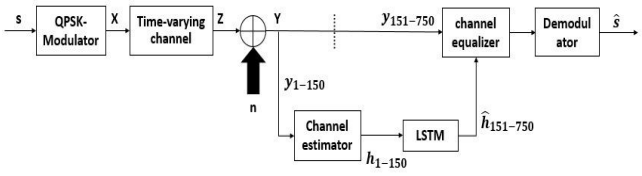

Fig.1: Signal-flow Diagram of the SISO system using LSTM neural network as channel predictor.

III. DATASET AND DEEP LEARNING ARCHITECTURE

A. Dataset

The dataset we used in this problem is a custom dataset it can be obtained by simulating the wireless communication system under specific channel conditions and the corresponding AWGN channel the data collected was the data before the noise being added to the wireless system and the data after the noise being added those two were collected and the data collected after the addition of noise is given as the input for the model to learn.

B. Deep Learning basics

Neural networks, an extension of machine learning has its own significance. Unlike, machine learning there is no need for doing feature extraction in neural networks the feature engineering is automatically done. The neural networks ideally consists of three layers. The first one is input layer, next one is hidden layer and the last one is output layer. Any neural network layer basically made up of nodes. Every node in one layer makes connection with every other node of the next layer by a weight and a bias at every node this forms the basic structure of feed-forward neural network.

Usually, the input and output nodes are common and the size of the network depends on the count of hidden layers. A neural network with one hidden layer can equally approximate any mathematical function. The Weights in the feed forward neural network are updated by an algorithm called back propagation as it updates the weights by minimizing the distance between the actual values and obtained values. The process of continuous update of weights continue until a global minima is attained on the error surface curve. The update of weights usually happen by a factor called learning rate. Generally, the output of a feed forward neural network is given by Equation 7.

C. Deep Learning Architeture

But, for our problem we need a neural network that

$$\mathbf{O} = \mathbf{Ø}\left(\sum_{i=1}^{m} \boldsymbol{W_i}.\boldsymbol{X_i} + \boldsymbol{b_i}\right) \qquad (7)$$

works a neural network that work well for time-series data. So, we have shifted our attention towards RNN (recurrent neural network). It has a same function similar to that of a feed forward neural network except for that each node in RNN consists of a feed-back which makes them efficient to deal with time-series data. RNN which is similar to feed forward net after unwrapping it in time. After unwrapping the RNN it appears like this

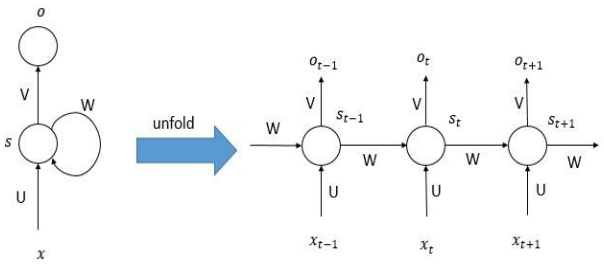

Fig.2: RNN neural network unwrapping in time.

RNN have a problem with length of time-series as the length of time-series goes on increasing the RNN suffers from a problem of disappearing gradient. The problem of disappearing gradient can be resolved by introducing a memory into RNN. This typical structure is named as LSTM (long short term memory) neural network which typically looks like this

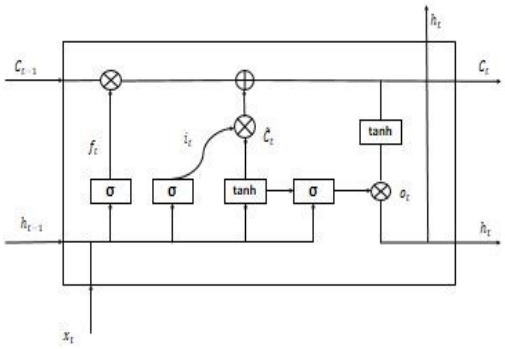

Fig. 3: LSTM memory unit structure

As in Fig.3, The LSTM memory unit consists of a three gates. These gates are responsible for the flow-control and storage of information. These functionality of these gates are used in naming them. The memory cell is responsible for the storage of current cell state which is to be applied for the future time-step. The input gate denoted by **i** responsible for the flow of fresh information into the memory cell. The forget gate which is denoted by **f** is responsible for the amount of information to be forget in the current state. The output gate which is taken as **o** is responsible for the control of amount of information to be flown into the rest of the network. The last layer in the LSTM neural network is connected to a fully connected neural network. The equations from 8 to 13 describe the functionality of LSTM.

$$\boldsymbol{i_t} = \boldsymbol{\sigma}(\boldsymbol{W_x^i}.\,\boldsymbol{x_t} + \boldsymbol{W_h^i}\,.\,\boldsymbol{h_{t-1}}) \qquad (8)$$

$$\boldsymbol{f_t} = \boldsymbol{\sigma}(\boldsymbol{W_x^f}.\,\boldsymbol{x_t} + \boldsymbol{W_h^f}\,.\,\boldsymbol{h_{t-1}}) \qquad (9)$$

$$\boldsymbol{o_t} = \boldsymbol{\sigma}(\boldsymbol{W_x^o}.\,\boldsymbol{x_t} + \boldsymbol{W_h^o}\,.\,\boldsymbol{h_{t-1}}) \qquad (10)$$

$$\tilde{\boldsymbol{C}}_t = \tanh(\boldsymbol{W_x^c}.\,\boldsymbol{x_t} + \boldsymbol{W_h^c}\,.\,\boldsymbol{h_{t-1}}) \qquad (11)$$

$$\boldsymbol{C_t} = \boldsymbol{i_t} \otimes \tilde{\boldsymbol{C}}_t + \boldsymbol{f_t} \otimes \boldsymbol{C_{t-1}} \qquad (12)$$

$$\boldsymbol{h_t} = \boldsymbol{o_t} \otimes \tanh(\boldsymbol{C_t}) \qquad (13)$$

D. Performance metrics

The predicted values of the channel are evaluated using a metric called root mean square error (RMSE) the error function upon which the weights are optimized. We will be dealing with the real component values and imaginary component values of the channel separately using two LSTM networks which are tuned differently and the result is combined to form a complex value prediction. The RMSE values are computed using a mathematical equation given by

$$\mathbf{RMSE} = \sqrt{\frac{1}{N}\sum_{i=1}^{N}\left(y_i^{pred} - y_i^{actual}\right)} \qquad (14)$$

the problem we are solving is a regression problem so we have taken the cost function as root mean square error. There are different cost functions for different types of problems we need to choose the cost function or loss function according to the problem in hand.

IV. Results and Discussion

Experiment was carried in a simulation based environment using MATLAB 2018b and to implement neural networks in MATLAB we used neural network toolbox. A SISO wireless system was simulated and the channel was modeled as a Rayleigh fading channel and we have considered a moving receiver scenario which is offering a Doppler shift of 0.0001534 as we are modeling the channel as a fast fading channel and we have been using a predefined function to simulate Rayleigh fading channel in MATLAB with carrier frequency 2.5GHz and signal bandwidth of 5MHz and with a sampling rate of twice the signal bandwidth and we are considering Jakes spectrum. The modulation scheme used at the transmitter side was QPSK-modulation and its counterpart QPSK demodulator was used at the receiver end.

Firstly, we have generated 1500 bits and then we have passed onto a QPSK modulator so that we may get 750 symbols which are complex numbers are obtained as the output of the modulator block and those symbols were transmitted through the channel with specifications as

mentioned above and at the beginning of receiver we are adding a AWGN noise which is a byproduct due to receiver components and that is termed as 'y'. Now y which is given as input to zero forcing channel estimator and the output of that is of dimension 750x1 is separated as 150 units for training is termed as h and the rest of the values are predicted using the trained neural network model that predicted values is denoted by h'. Here the neural network model consists of 2 LSTM layers with a fully-connected layer in the end and in the LSTM layer the activation function used at the gate level was sigmoid activation function and at the cell-state level we use tanh activation function. We use two separate models that were tuned separately one to predict the real values of h' and another to predict the imaginary values of h'. For the model which predicts the real values we have taken 50 hidden units that is 50 nodes and the we have considered certain parameters like Max.epochs 200 and Mini Batch size as 64 and an Initial Learning rate as 0.05 and Learning rate drop period as 125. And for the other model which predicts the imaginary values of h uses 50 hidden units and Max.epochs of 250 and a Mini Batch size of 64 and with an Initial rate of learning as 0.05 and a Rate of Learning drop period as 125. Then the predicted values are combined to form a complex value and this is used for channel equalization and after that we give the output of this block as an input to the demodulator block and after the demodulation we will get the transmitted bits while some are corrupted due to channel impairments and the receiver noise. The hyper-parameters that were considered separately for real and imaginary were indicated in Table. I and Table. II

Table. I: Hyper parameters tuned for real channel value prediction.

Number of hidden units	50
Max. epochs	200
optimizer	Adam
Initial learning rate	0.05
Learning rate drop of period	125
Learning rate drop of factor	0.2
Mini Batch size	64

Table. II: Hyper parameters tuned for imaginary channel value prediction.

Number of hidden units	50
Max. epochs	250
Optimizer	Adam
Initial learning rate	0.05
Learning rate drop of period	125
Learning rate drop of factor	0.2
Mini Batch size	64

Fig.4, demonstrates the predicted real values of the channel at 25dB SNR. Fig.5, demonstrates the predicted

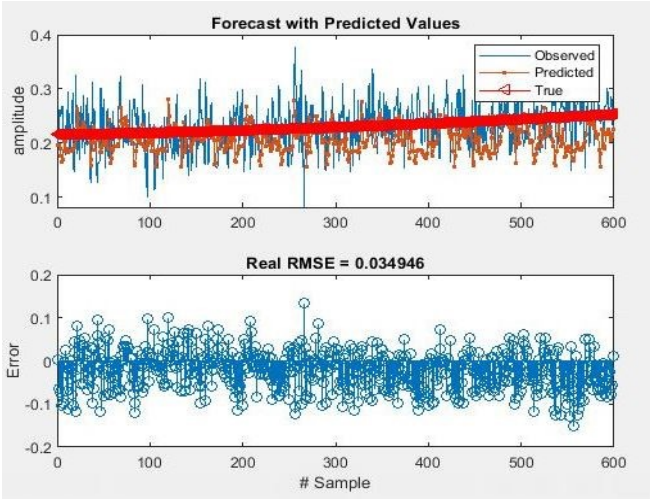

Fig. 4: predicted real values of LSTM block and Real RMSE value for sample.

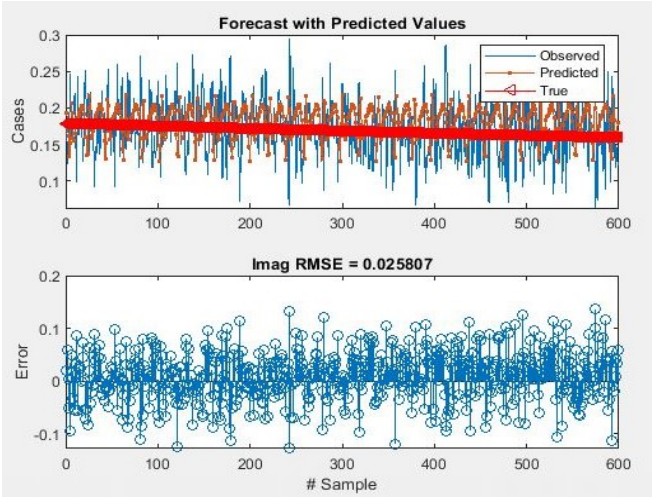

Fig. 5: predicted imaginary values of LSTM block and Imaginary RMSE value for sample.

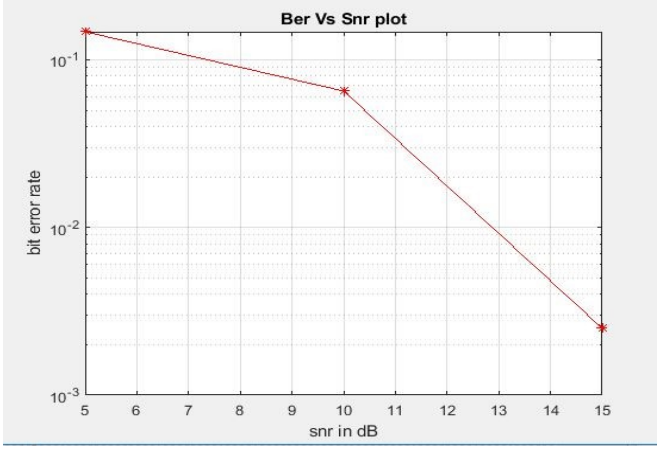

Fig. 6: BER versus SNR plot when N=1500.

imaginary values of the channel. Fig.6, indicates the Bit Error Rate (BER) versus Signal to Noise Ratio (SNR) curve for the number of bits equal to 1500. Now we will extend the concept further by extending the number of bits to 15000 and we will divide the entire 15000 bits into 10 blocks consisting of 1500 each. And then they are QPSK modulated. And these

symbols are transmitted through the channel modeled and AWGN noise was added at the beginning of receiver end. Then that symbols were collected. The symbols obtained may be represented like Fig. 7.

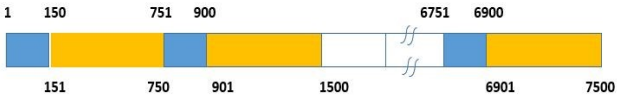

Fig .7: Representation of the symbols training and prediction.

Now the obtained symbols which have dimension of 7500x1 can be represented like the above shown figure. We consider 750 symbols as one set. Of that we will use 150 for training and the next 600 values will be predicted separately for real and imaginary values of the channel by using two different LSTM neural networks which have the hyper parameters as shown in Table. I and Table .II.

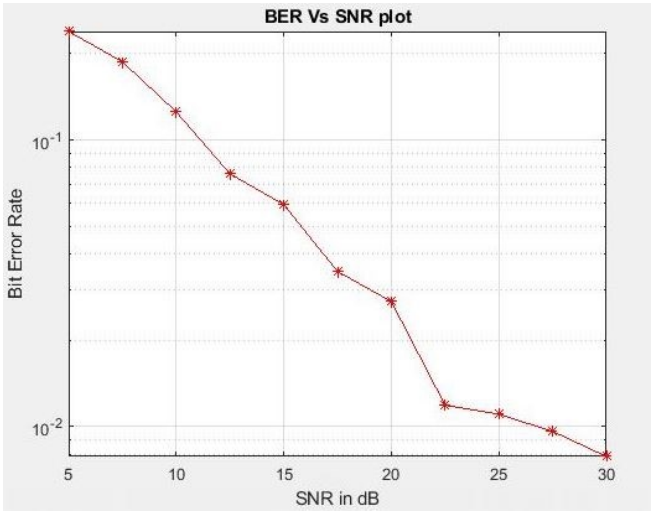

Fig. 8: BER versus SNR plot when N=15000.

We will train for every 150 symbols and predict the next 600 symbols and we will repeat this until 7500 symbols in sets of 750. The entire experiment is repeated for different values of SNR and the BER values were obtained. The BER Versus SNR plot is shown in Fig. 8. The activation function considered are for gate-level is sigmoid and cell-state level is tanh. The obtained Fig. 8, BER versus SNR plot indicates that LSTM are a good tools that can deal with time series data and can be used in application of wireless communication systems.

V. Conclusion and Future Scope

In this paper, we develop a system model that predicts the characteristics of a fast varying wireless fading channel in a moving/mobile receiver which is moving at a speed of 500kmph scenario by using a LSTM neural network and we have used that predicted channel values in order to reconstruct the message transmitted at the receiver end. For that we have tuned the hyper parameters of the LSTM neural network so that we will get a system performance better than the existing interpolation based systems. The experimental results suggested that LSTM's have the capability of predicting the time-series data i.e., getting insights from the historical data to predict the future state. we have modeled a SISO channel under the moving receiver case and trained the LSTM network online to predict the channel characteristics. LSTM's are helpful assets in building the next generation wireless technologies.

By considering this as a sub-channel in an OFDM system this concept with a little modification can be extended to multiple sub-channels in an OFDM system.

References

[1] T. S. Rappaport, Wireless communications: Principles and practice, 2nd ed. Prentice Hall, 2002.

[2] R. M. Gagliardi and S. Karp, Optical communications, 2nd ed. Wiley, 1995.

[3] J. Proakis and M. Salehi, Digital Communications, 5th ed. McGraw-Hill Education, 2007.

[4] K. Akkarajitsakul, E. Hossain, D. Niyato and D. I. Kim, "Game Theoretic Approaches for Multiple Access in Wireless Networks: A Survey," in IEEE Communications Surveys & Tutorials, vol. 13, no. 3, pp. 372-395, Third Quarter 2011.

[5] Y. LeCun et al., "Generalization and network design strategies," Connectionism in perspective, pp. 143–155, 1989.

[6] K. He, X. Zhang, S. Ren, and J. Sun, "Delving deep into rectifiers: Surpassing human-level performance on imagenet classification," in Proc. IEEE Int. Conf. Computer Vision, 2015, pp. 1026–1034.

[7] Tianqi Wang, Chao-Kai Wen, Hanqing Wang, Feifei Gao, Tao Jiang and Shi Jin, "Deep Learning for Wireless Physical Layer: Opportunities and Challenges", https://arxiv.org/pdf/1710.05312

[8] T. J. O'Shea and J. Hoydis, "An introduction to machine learning communications systems," arXiv preprint arXiv:1702.00832, 2017.

[9] T. O'Shea and J. Hoydis, "An Introduction to Deep Learning for the Physical Layer," in IEEE Transactions on Cognitive Communications and Networking, vol. 3, no. 4, pp. 563-575, Dec. 2017.doi: 10.1109/TCCN.2017.2758370

[10] E. E. Azzouz and A. K. Nandi, "Modulation recognition using artificial neural networks", in Proc. Automatic Modulation Recognition of Communication Signals, 1996, pp. 132176.

[11] J. Bruck and M. Blaum, "Neural networks, error-correcting codes, and polynomials over the binary n-cube", IEEE Trans. Inf. Theory, vol. 35, no. 5, pp. 976987, Sep. 1989.

[12] C. K. Wen, S. Jin, K. K. Wong, J. C. Chen, and P. Ting, "Channel Estimation for Massive MIMO Using Gaussian-Mixture Bayesian Learning", IEEE Trans. Wireless Commun., vol. 14, no. 3, pp. 13561368, Mar. 2015.

[13] J. Cid-Sueiro and A. R. Figueiras-Vidal, "Digital equalization using modular neural networks: an overview", in Proc. Signal Processing in Telecommunications. Springer, 1996, pp. 337345.

[14] T. J. OShea, K. Karra, and T. C. Clancy, "Learning to communicate: Channel auto-encoders, domain specific regularizers, and attention", IEEE Int. Symp. Signal Process. Inform. Tech. (ISSPIT), pp. 223228, 2016.

[15] Y. G. Li, L. J. Cimini, and N. R. Sollenberger, "Robust channel estimation for OFDM systems with rapid dispersive fading channels," IEEE Trans. Commun., vol. 46, no. 7, pp. 902–915, Jul. 1998.

[16] S. R. Hari, K. R. Kannan, N. Visagan, Latha and A. Thakre, "Performance of Dual mode OFDM-IM using Reduced Complexity Receiving Technique," 2018 International Conference on Advances in Computing, Communications and Informatics (ICACCI), Bangalore, 2018, pp. 2290-2294. doi: 10.1109/ICACCI.2018.8554370.

[17] H. Ye, G. Y. Li and B. Juang, "Power of Deep Learning for Channel Estimation and Signal Detection in OFDM Systems," in *IEEE Wireless Communications Letters*, vol. 7, no. 1, pp. 114-117, Feb. 2018.

[18] S. Ganesh, V. Sayee Sunder and A. Thakre, "Performance Improvement in Rayleigh Faded Channel using Deep Learning," 2018 International Conference on Advances in Computing, Communications and Informatics (ICACCI), Bangalore, 2018, pp. 1307-1312.

Proceedings of the Fourth International Conference on Communication and Electronics Systems (ICCES 2019)
IEEE Conference Record # 45898; IEEE Xplore ISBN: 978-1-7281-1261-9

CPW fed Antenna for Dual Band Applications with Loop Ground Plane

Anu Suresh and *Sreedevi K. Menon

Department of Electronics and Communication Engineering
Amrita Vishwa Vidyapeetham
Amritapuri, India
anusuresh@am.students.amrita.edu, *sreedevikmenon@am.amrita.edu

***Abstract*—A monopole antenna for multiband advanced wireless services is presented in this paper. Initially a single band antenna for 2.45 GHz is designed with Coplanar Waveguide (CPW) fed and loop ground plane. A peak gain of 3.55 dBi is observed for this configuration. Defects are introduced in the loop ground plane with the aim of obtaining dual frequency bands. Footprint of the antenna consumes same area for single and dual band configurations. The antenna characteristics – reflection and radiation properties are investigated and optimized using ANSYS HFSS. Prototype of the optimized antenna is analyzed using Vector Network Analyzer Keysight E 5080 A.**

Keywords — Coplanar waveguide (CPW), defected ground plane, dual band, Wi-Fi, WiMAX, wireless communication, monopole antenna.

I. INTRODUCTION

Wireless communication is rapidly emerging in the present day scenario. Compact gadgets which are highly efficient with large bandwidth operating in different frequency bands are preferred in the communication systems. There are variant categories of antennas that can provide these features applicable for wireless communication as they are of low profile, low price and light weight [1]. Wireless applications with multi-functional operations require multiband antennas. In recent past, multi-functionality has become a key component for many gadgets making design of compact multiband antenna need of the hour.

Different antenna configurations for dual band performance has been reported of which coplanar waveguide (CPW) fed antennas are more attractive as they can be implemented on a single plane and can easily mount active devices. A loop antenna energized with CPW can provide dual frequency band characteristics with enhanced gain [2]. Metamaterials can act as ground plane for monopole antennas providing good radiation characteristics [3]. CPW fed monopole antenna provides dual band when a planar patch with a cross slot generates two separate resonant modes [4]. A metallic strip which is of C shape etched in a rectangular slot is found to provide dual band and high bandwidth [5]. CPW fed dual-band circularly polarized antenna is discussed in [6]. CPW fed slot antenna operating for wireless applications having dual band is discussed in [7]. Small monopole antenna with inverted L-shaped and rectangular stubs can provide dual band characteristics [8]. Metamaterial-inspired antenna also provides dual frequency operation [9]. A multi-band antenna for tri-band applications using CPW is also reported [10].

A CPW fed monopole antenna which is designed at single frequency is presented in this paper, which is further modified to defected ground plane by adding stub in order to achieve dual bands. The proposed final antenna on measurement gave dual band response at 2.45 GHz and 4.59 GHz.

II. CONFIGURATION OF THE ANTENNA

The loop ground CPW fed monopole antenna is as shown in Fig. 1. To enable the antenna to radiate at 2.45 GHz, the parameters of the ground plane and monopole (Lp, Lg, Wg and d) (Fig.1) is optimized while 2g + Wp provides 50Ω impedance. The studies are carried out in a substrate with dielectric constant $\varepsilon_r = 4.4$ and a thickness h =1.6mm.

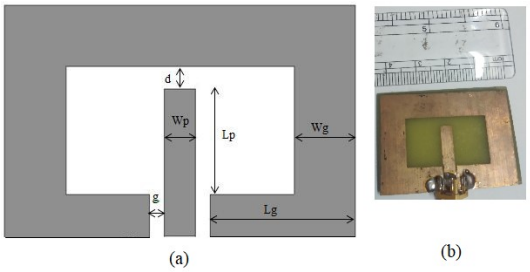

Fig. 1. Configuration of the proposed antenna
(a) Geometry (b) prototype fabricated in FR4

The antenna parameters are optimized as Lg = $\lambda_g/4$, Lp = $\lambda_g/6$, Wg = $\lambda_g/8$, Wp = $\lambda_g/14$ and d = $\lambda_g/16$, for any frequency of operation. Based on at 2.45 GHz, a prototype is fabricated and tested having a return loss as plotted in Fig.2. The antenna offers a bandwidth of 148 MHz at 2.46 GHz in simulation and 155 MHz at 2.48 GHz in measurement. The radiation performance of the antenna is studied in the bandwidth range and is presented in Fig.3. The antenna has a gain of 2 dBi in the entire bandwidth with omnidirectional characteristics.

This antenna is modified by including a stub in the ground plane to obtain dual band performance. This is discussed in the next section.

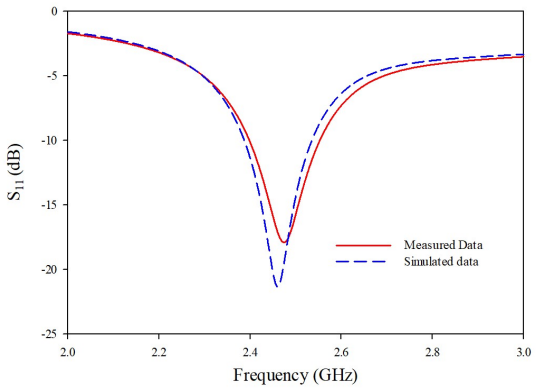

Fig. 2. Reflection Characteristics of the antenna
Lg = 19mm, Lp = 11.8mm, Wg = 8mm, d = 3.5mm
εr = 4.4, h =1.6mm.

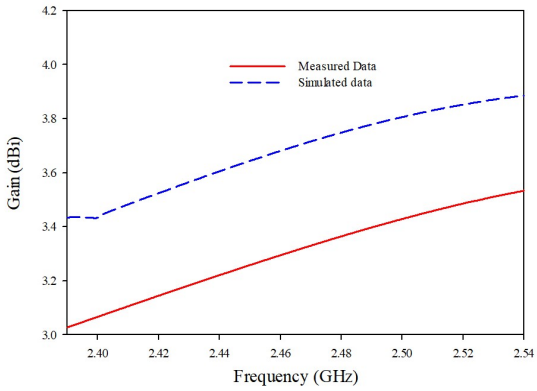

Fig. 3 (a). Gain of the antenna
Lg = 19mm, Lp = 11.8mm, Wg = 8mm, d = 3.5mm
εr = 4.4, h =1.6mm.

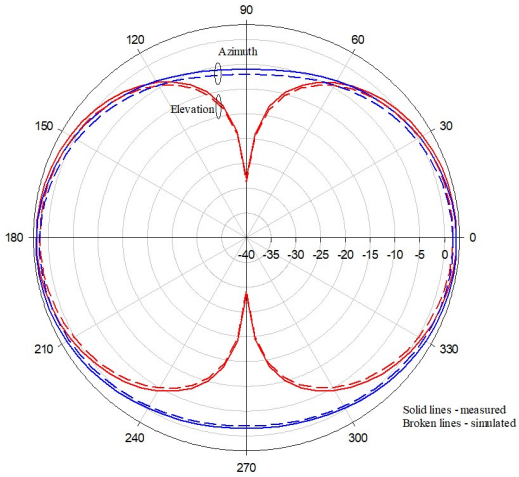

Fig. 3 (b). Radiation Pattern of the antenna at 2.46 GHz
Lg = 19mm, Lp = 11.8mm, Wg = 8mm, d = 3.5mm
εr = 4.4, h =1.6mm.

III. ANTENNA CONFIGURATION FOR DUAL BAND PERFORMANCE

The stub loaded CPW fed loop ground monopole antenna is as shown in Fig.4. The influence of the stub l1 × sw1 in the reflection and radiation characteristics is studied in detail. Initially, the position of the stub on the ground plane is optimized. For maximum gain the stub position is fixed at top middle as in the Fig.4.

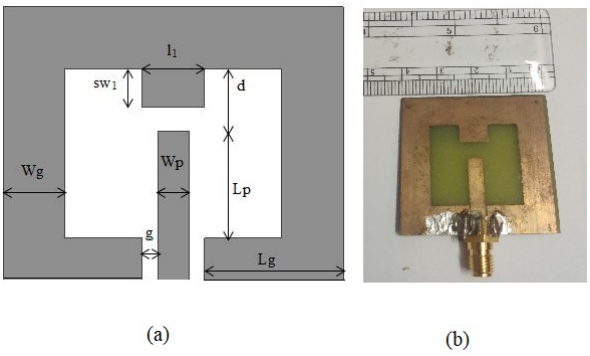

Fig. 4. Configuration of the proposed antenna for dual band performance
(a) Geometry (b) prototype fabricated in FR4

When width of the stub sw1 is increased, the first resonant frequency f1 decreases and second resonant f2 increases with decrease in gain. The stub parameters are varied in such a way that the maximum length l_1 of the stub can be varied up to 20mm ($\lambda_{g2}/2$) and width sw_1 can be varied up to 8.5mm ($\lambda_{g2}/4$) only, which gave single band response at 9.09 GHz. The stub dimension is optimized to get dual frequency bands. The frequencies f_1 and f_2 can be expressed as:

$$f_2/f_1 = \lambda_{g1}/\lambda_{g2}$$

For dual band response at 2.45 GHz and 4.59 GHz, it can be generalized as $f_2 = 1.8\ f_1$. With optimized parameters antenna is fabricated. The measured and simulated return loss is presented in Fig.5.

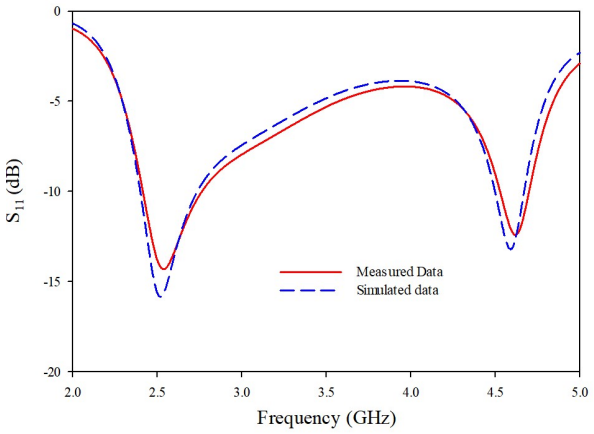

Fig. 5. Return loss characteristics of antenna with stub
Lg = 19mm, Lp = 11.8mm, Wg = 8mm, d = 3.5mm, sw1 = 5mm, l1 = 8mm, εr = 4.4, h =1.6mm.

In anechoic chamber, the gain of the antenna is measured by gain transfer method at both the bands. The obtained gain is as in Fig.6. The radiation pattern at both frequencies is measured and is as plotted in Fig.7.

The obtained results confirm the proposed antenna as a good radiator for dual band applications. The performance of the antenna with that found in the literature is compared and presented in Table.1.

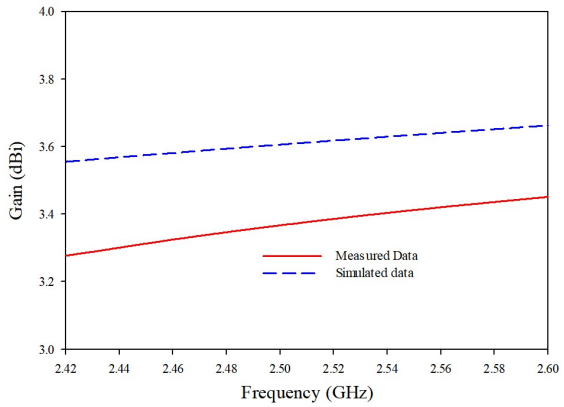

Fig. 6 (a). Gain of antenna in the first band
Lg = 19mm, Lp = 11.8mm, Wg = 8mm, d = 3.5mm, sw1 = 5mm, l1 = 8mm, εr = 4.4, h =1.6mm.

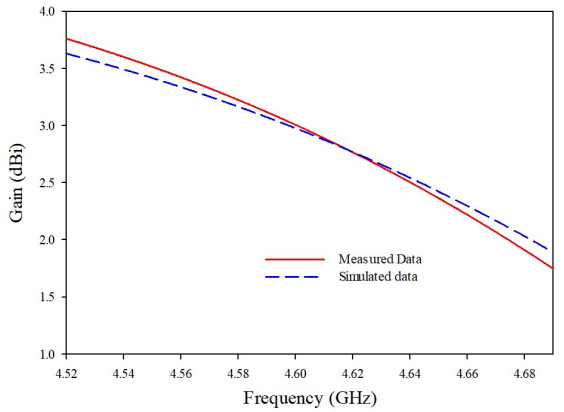

Fig. 6 (b). Gain of antenna in the second band
Lg = 19mm, Lp = 11.8mm, Wg = 8mm, d = 3.5mm, sw1 = 5mm, l1 = 8mm, εr = 4.4, h =1.6mm.

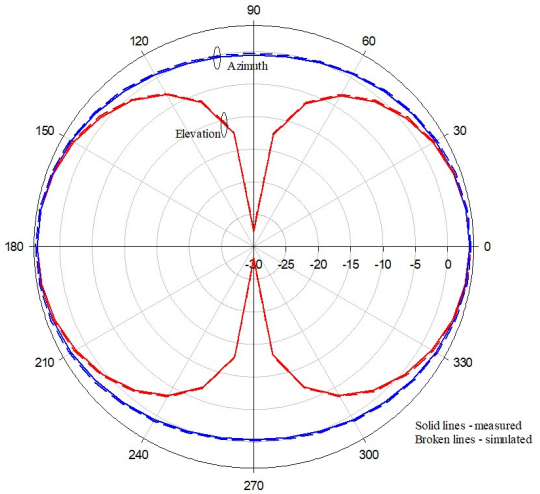

Fig. 7 (a). Radiation pattern at 2.45 GHz
Lg = 19mm, Lp = 11.8mm, Wg = 8mm, d = 3.5mm, sw1 = 5mm, l1 = 8mm, εr = 4.4, h =1.6mm.

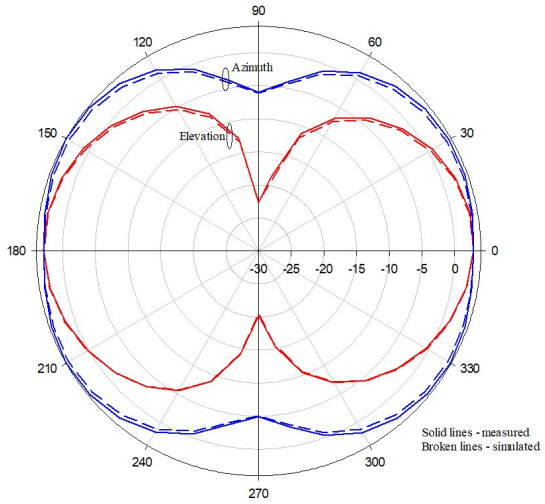

Fig. 7 (b). Radiation pattern at 4.59 GHz
Lg = 19mm, Lp = 11.8mm, Wg = 8mm, d = 3.5mm, sw1 = 5mm, l1 = 8mm, εr = 4.4, h =1.6mm.

TABLE I. COMPARISON - ANTENNA PERFORMANCE

Type of Antenna	Frequency (GHz)	Bandwidth (MHz)	Gain (dBi)	Size (mm × mm)
Proposed antenna	**2.45** **4.59**	**338** **210**	**3.41** **3.04**	**37.8 × 39.7**
Ref [4]	2.48 5.23	340 1280	3.17 3.23	51.55 × 42.06
Ref [5]	2.42 6.39	900 3220	3.68 3.33	60 × 61
Ref [6]	2.6 3.5	2002	2 0	63 × 75
Ref [7]	2.45 5.5	350 1470	4 6	70 × 70
Ref [8]	2.624 4.889	210 3591	Not mentioned	20 × 37
Ref [9]	2.802 3.713	59 1060	1 1.9	31.7 × 27
Ref [10]	3.31 5.3	780 1400	~ 0 ~ 2	17.5 × 17.5

IV. RESULTS AND DISCUSSION

A CPW fed dual band loop ground compact antenna is proposed. The antenna is simulated using Ansoft HFSS. Initial design gave response at 2.5 GHz with omnidirectional radiation pattern. The ground loop is modified by adding stub at the top of the loop, which gave dual band response at 2.45 GHz and 4.59 GHz. The stub is placed in such a position in order to obtain maximum gain.

V. CONCLUSION

Multiband antenna plays a major role in wireless communication. Multiband CPW fed monopole antenna working in Wi–Fi, WiMAX and other advanced wireless services is presented. The detailed steps of the design have been discussed in the above sections. The proposed antenna has been designed and optimized using HFSS and measurements are taken using Vector Network Analyzer (VNA). Dual bands are obtained by adding single stub to the ground loop. The stub dimension is tuned in such a way to get maximum gain at the resonant frequency. The simulated

result is validated by experiment. The effect of including more stubs to the ground plane is the work ahead.

REFERENCES

[1] Balanis, Constantine A. Antenna theory: analysis and design. John wiley & sons, 2016.

[2] L. Meenu, S. Aiswarya, Sreedevi K Menon, "Experimental Investigations on Monopole Loop Antenna with Dual Band Characteristics", *2017 International Conference on Wireless Communication, Signal Processing and Networking (WiSPNET), 22 - 24 March 2017.*

[3] L. Meenu, S. Aiswarya, Sreedevi K Menon, "Compact Monopole Antenna with Metamaterial Ground Plane", *2017 Progress In Electromagetics Research Symposium –Fall (PIER–FALL), Singapore, 19-22 November.*

[4] C.M.Wu, "Dual-band CPW-fed cross-slot monopole antenna for WLAN operation", *IET Microwaves, Antenna & Propagation, Volume: 1, Issue: 2, April 2007.*

[5] L.Hu, W.Hua, "Wide dual-band CPW-fed slot antenna", *Electronics Letters, Volume: 47, Issue: 14, July 7 2011.*

[6] Rohit Kumar Saini, Santanu Dwari, Mrinal Kanti Mandal, "CPW-Fed Dual-Band Dual-Sense Circularly Polarized Monopole Antenna", *IEEE Antennas And Wireless Propagation Letters, Vol. 16, 2017.*

[7] S. Ashok Kumar, T. Shanmuganantham, D. Dileepan, "Design and development of CPW fed monopole antenna at 2.45 GHz and 5.5 GHz for wireless applications", *Alexandria Engineering Journal (2017) 56, 231 - 234.*

[8] Ahmed Zakaria, Saida Ibnyaich, Abdelaziz EL Idrissi, Abdelilah Ghammaz, "A Compact Dual-Band CPW-Fed Planar Monopole Atenna for 2.62-2.73 GHz, Frequency Band, WiMAX and WLAN Applications", *Journal of Microwaves, Optoelectronics and Electromagnetic Applications, Vol. 16, No. 2,June 2017.*

[9] Li-Ming Si, Weiren Zhu, Hou-Jun Sun, "A Compact, Planar, and CPW-Fed Metmaterial-Inspired Dual-Band Antenna", *IEEE Antennas and Wireless Propagation Letters, Vol. 12, 2013.*

[10] Naidu, V. Praveen, Raj Kumar, "Design of Compact dual-band/tri-band CPW-Fed monopole antennas for WLAN/WiMAX applications", *Wireless Personal Communications 82.1 (2015): 267-282.*

Proceedings of the Fourth International Conference on Communication and Electronics Systems (ICCES 2019)
IEEE Conference Record # 45898; IEEE Xplore ISBN: 978-1-7281-1261-9

A unified Convolutional Neural Network framework for intelligent decision making related to navigation

Khyati Marwah
CSE Deptt, IKGPTU,Jullundar
Punjab,India

Dr. Jogeshwar Singh Sohal
Director,LCET,Ludhiana,
Punjab,India

***Abstract*—Prevalent intellective systems assist the driver in the navigation errands by taking a number of simple and intricate decisions based upon on available input information. Such decisions should be astute and prompt so as to provide realistic behaviour in real life navigation scenarios decisions. Proposed unified Convolutional Neural Network framework ensembles a powerful model that could augment the predictability of the system under construction.**

The suggested work is an extension to authors previous work in which best input features for decision making neural network were obtained by shortlisting eleven texture metrics out of thirty-six metrics using state of art algorithms: Boruta Algorithm and Earth Algorithm [1]. The above said texture metrics were obtained using Spatial Gray Level Dependence Matrices (SGLDM) , the Gray Level Difference Methods (GLDM) ,First order statistics(FOS), the Fourier Power Spectrum (FPS) , the Fractal Dimension Texture Analysis (FDTA),Statistical Feature Matrix(SFM),Laws Texture Energy Measures (TEM) .

In this paper, we have proposed a unification of Best Feature Selection Method (our previous work) and Principal Component Analysis Technique so as to consummate the most pertinent neural network inputs. CNN framework has been used here to provide simple decision that is either to move or stop at a particular instant on the basis of finalized inputs. It was found that unified model inputs (based on Best Feature Selection and PCA) yield better results in comparison to their standalone performance. Furthermore, it was observed that CNN framework can perform equally well with minimal training in comparison to high order training. It implies CNN's has remarkable ability to learn from imprecise data gives it an edge over others. In nutshell, the proposed model was able to decide promptly and astutely the next move of vehicle.

Keywords— SGLDM, GLDM, FOS, FPS, FDTA, SFM, TEM, CNN

I. INTRODUCTION

While driving, the driver mind takes choices in every move. The choice can be as easy as following the track correctly or it can be difficult like finding the correct way through the junction. These decisions are dependent upon some permanent components like roads, some semi-permanent components like traffic signs and some variable components like moving vehicles etc. For taking such decisions we need an Intelligent decision-making system that should possess full-fledged knowledge within a categorical domain just like the human mind and at the same time it should be able to acclimate themselves and thereby enhance performance in a transmuting environment. The system should be able to justify the steps being followed to take a particular action or decision.

Neural networks are a mimic to biological brain. Neural Networks just like human brain have the capability to cluster and classify the data. The unlabeled data is managed into groups on the basis of similarities. A mathematical or statistical function is applied to transform data into neural network inputs. The ability of deep learning algorithms to find correlations enable it to map inputs to outputs. Approximation of the unknown functions is also done using the same technique. These abilities of Neural Network have made them the most sought choice in a number of real-world applications. These networks have found a great usage in identifying patterns, classifying them and finding out the outcomes in previously unknown situations. Thus, they can be easily tamed to take decisions in typical situations of real life.

A variant of Neural Networks, Convolutional Neural Network is powerful enough to make strong assumptions in real life navigation scenarios. If we talk about images related to navigation, the pixels within are connected to each other even if they are far off. CNN's enable to focus on particular area and provides in depth screening of the same and helps in making strong decisions. To have a limit on the input search space, the most relevant dataset is selected and the outliers are removed. The network inputs are minimized using the techniques like Feature extraction, Principal components analysis etc.

The working speed and accuracy are the grey areas in the field of neural networks. So, more attention must be paid to performance issues apart working speed during the design

and testing phases. For this we need to work upon to find appropriate ratio of training and testing datasets. Moreover, we should go for proper selection of network architecture that is the appropriate no. of participating neurons should be find out as too less neurons will result in under training and too much will result into overtraining.

This paper presents a unified CNN framework to find out next decision for a moving vehicle that is either to stop or move with better accuracy and faster response time by overcoming the shortcomings of existing systems.

II. Literature Survey

Neural Networks in conjunction with navigation systems:

Navigation Systems have been actively utilizing Neural Networks. They learn through examples and create their own representation of information received during the learning time. Thus, it acts as expert that could be habituated to provide forecast in incipient situations of interest and can provide reasoning for the decisions taken. A control system based on Neural Networks was developed for intelligent planning of the path was made in [2]. It dealt with the movement of an autonomous robot in partially structured environment. The environment involved random number of obstacles of arbitrary shape. The "free" space was found by using ultrasound range finder and this sensor information was used for the robot movement. The study lagged to find the safe path in optimal time. A dynamic artificial neural network based mobile robot motion and path planning system was proposed in [3] to navigate a robot car on flat surface among static and moving obstacles. It used extended backpropagation through time algorithm. Their algorithm worked well only for slow moving vehicles as the computation speed of their proposed model was quite less. For navigation and control of a robot movement in a semi known environment, an integrated system was developed in [4]. A path-planning algorithm was proposed in it. Here a neural network was used to automatically build up the collision penalty function. The training procedure used the information of the environment to avoid obstacles but because of its gradient character this model meets the local minima problem and thus accuracy of this model was affected. On the basis of experiences shared by human drivers, a vehicle control system was developed in [5]. The proposed system used neural networks to learn from examples in order to identify navigable and non-navigable region. A neural network based sequential machine learning technique for autonomous spacecraft navigation was proposed in [6]. It fixated on the amendment of precision of the multiple inputs used. Neural networks in [7] were tried to control the robot to reach a particular target location in urban changing scenarios. The robot had to rely on GPS and compass sensor to navigate. It was showed that neural controller with separated hidden neurons connected to specific inputs only outperformed the fully connected input-hidden networks by providing a faster response there by laying stress on importance of selecting right architecture. An architecture based on a neural network named as QMDP-net was created in paper [8] for planning under partial observability. This network had the capability to combine the strengths of model-free learning and model-based planning. It involved a deep recurrent policy network that embeds POMDP structure priors for planning under partial observability. In general, neural networks inherit the capability to map the inputs to outputs. In contrast the QMDP-net is trained in two aspects related to modeling and solving planning task. This approach had problem in handling of huge state space representation and its counter effects on the working speed of the model. On the basis of uncalibrated spherical images, a lightweight robot navigation framework was proposed in [9]. It used Convolutional Neural Network to overcome the problems in conventional algorithms, such as intense computational complexity in the testing phase and difficulty in collecting high quality labels in the training phase. The robot navigation task is formulated as a series of classification problems based on uncalibrated spherical images. A practical system related to autonomous navigation of a quadcopter was proposed in [10]. It had the feature of indoor navigation which enabled it to find any kind of target. It used a deep learning model, Convolutional Neural Network (ConvNet), to learn a controller strategy so that it can reciprocate the driving of an expert pilot.

Literature Survey revealed that though the neural networks in conjunction with other methods have been used actively in navigation systems, still the working speed and accuracy of the models have lagged the attention of researchers and need to be worked upon .Moreover the input to the neural networks play a major role in the accurate predictability/decision of the system under construction so the correct choice of input dataset is of utmost importance

III. Materials and Methods:

Any automated motion planning and navigation system needs a data collection system, a decision-making system to depict the next action of driving vehicle in real time. Decision to navigate or not depends on topological, geometric and texture features of road. Based upon these features, the decision-making system is expected to take decisions just as a real human being. For this the processing capabilities of human brain should be inseminated into it. Neural Networks, a machine learning approach comes to rescue as it is inspired by the way in which the brain performs a particular learning task. The proposed algorithm presents a unified CNN framework to take intelligent and speedy decisions by overcoming the shortcomings of existing neural network-based navigation systems. Conv Net's were chosen over other neural networks as it uses variation of multilayer perceptions designed to require minimal pre-processing. It has capability to learn even without any prior knowledge or insufficient data. Without increasing complexity, it can look into all the possible

variations before taking any decision, thus its prediction can be sought as realistic one.

The Proposed algorithm comprises steps related to database acquisition and getting the best features using a best feature selection model and further the unification of this model with Principal Component Analysis technique.

A. Database Acquisition and Selection of Best Features from Navigation Images:

- The images related to motion planning like roads, buildings, vehicles, signs etc. were collected and detailed texture analysis of images was done. A database of thirty-six metrics for hundred images was created by using SGLDM, GLDM, FOS, FPS, FDTA, SFM, and Texture Energy Measures. The extracted attributes were taken into consideration to find the next action of moving vehicle that is either "Move" or "Stop". The search space is but obviously going to be very huge and needs to be cut short.
- To get rid of irrelevant features and thereby improve the response time and reducing the costs, A Best Feature Selection Model [1] was created. This model selects out the best features having direct impact on the navigation decisions and removes the outliers.
- The features being extracted from Best Feature Selection Model namely Correlation, Sum Entropy, Entropy, Difference Entropy, Information Measures of Correlation, Kurtosis, Contrast Measure, Average Texture Energy from LE and EL kernels, Average Texture Energy from LS and SL kernels, Fractal Dimension Texture Analysis Area () are fed as input to neural networks.

B. Unified Model

Unification of both Best Feature Selection Model [1] and principal component analysis technique (PCA) is done so as to finalize the most relevant neural network inputs to be feeded into CNN framework to achieve better accuracy. A Convolutional Neural Network is a Deep Learning algorithm. It is strong enough to take decisions by assigning importance like weights and biases to various features of the images present in the image database. Furthermore, it has ability to classify and cluster the patterns on the basis of its learning during the training duration. CNN's have remarkable ability to get in depth knowledge upon a focused area and thereby it can take strong decisions. To have a limit on the input search space, the most relevant dataset is selected and the outliers are removed. The network inputs are minimized using the techniques like Feature extraction, Principal components analysis etc. PCA improves our knowledge by providing intelligent insight into the information from input features by computing covariance among them. It gives independent and different combinations of features to describe data differently and thus helps to find out important features by revealing previously unsuspected relations and thus adding more uniqueness to the proposed system. Figure 1 shows the flowchart of proposed algorithm. Here, we have extracted five features from PCA technique. Three scenarios were created using different combination of input feature sets for the CNN framework. The corresponding neural network input set for three scenarios are as follows:

- Eleven features obtained through Best Feature Selection Method
- Five features obtained from PCA
- A combination of Best Feature Selection Method and Principal Component Analysis

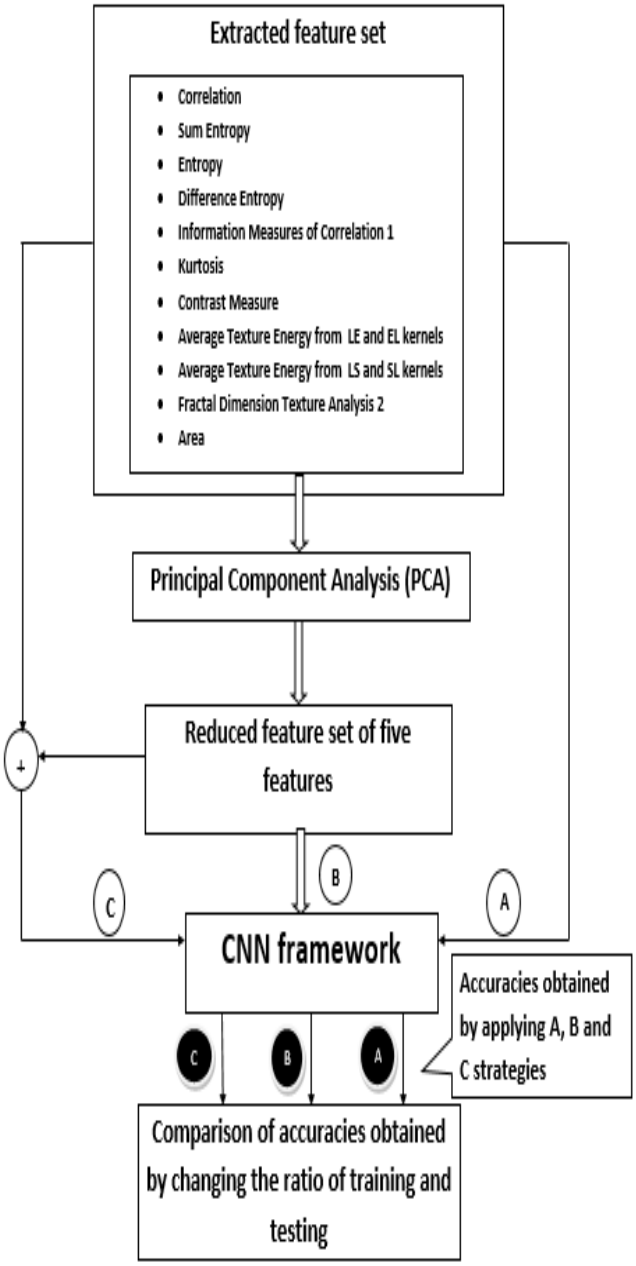

Figure 1: Flowchart of proposed Algorithm

Furthermore, we need to find the appropriate ratio of training and testing of neural networks.

Figure 1 clearly represents three approaches A, B and C to get accuracies for different ratios of training and testing for a dataset of eleven features, five features and sixteen features respectively.

The training time has direct impact on the speed of the any neural network system so we need to calculate minimum training time required by the network in such a way that it has no negative impact on accuracy of the model.

IV. Experimental Set up & Results

The algorithm was run in MATLAB for three different scenarios. Experimental Set up of CNN Framework in MATLAB tool is as follows in Figure:2. Here we have taken example of 16 input features whereas the outputs are limited to two in all the three cases. The number of hidden layers has been taken as 16 in all the scenarios. The performance metric being judged here is Mean Square Error.

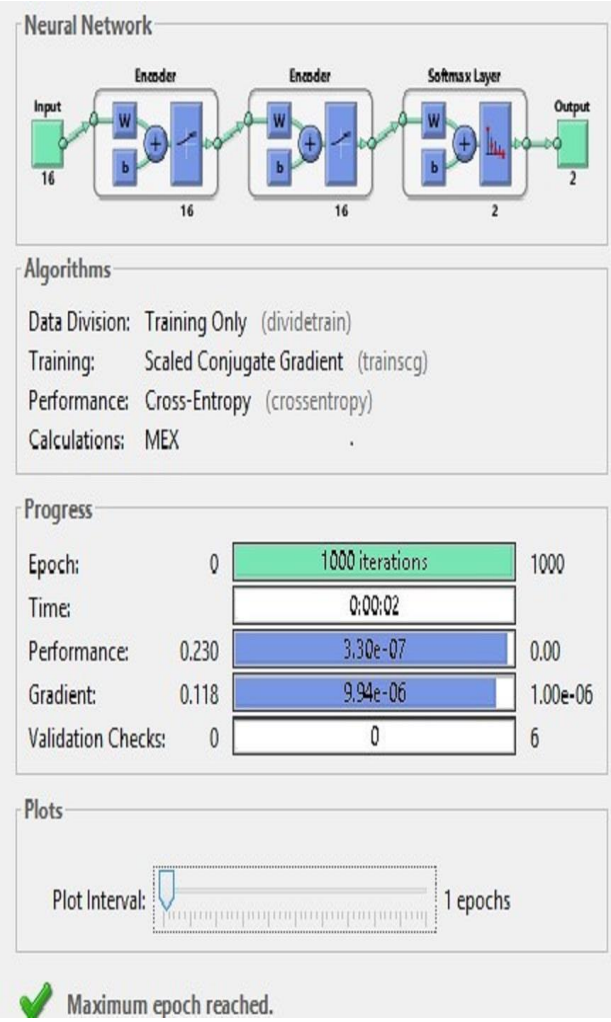

Figure 2: Experimental Set Up of CNN framework

As the training time has direct impact on processing speed so appropriate ration of training and testing needs to be calculated. Here we have assumed the training ration to be in the range of ten to seventy. Outside this range, the model will be under the effect of undertraining or overtraining.

We calculated accuracies of decision that is either to move or stop using different feature sets as inputs for convolution networks. Table 1 shows the accuracies by taking 11, 5 and 16 features as inputs for Convolutional Neural Networks. Figure 3 shows the graphical representation of change in accuracies with respect to training percentages.

Table 1: Accuracies in different scenarios

Accuracy Percentage obtained by using different input feature sets as Convolution Neural Network inputs			
Training Percentage	Case A: 11 features	Case B: 5 features	Case C: 16 features
70	66.6667	70	76.6667
60	67.5	72.5	77.53
50	68	68	80
40	73.3333	73.3333	75
30	68.5714	70	72.85
20	71.25	72.5	75
10	73.3333	73.3333	76.6667

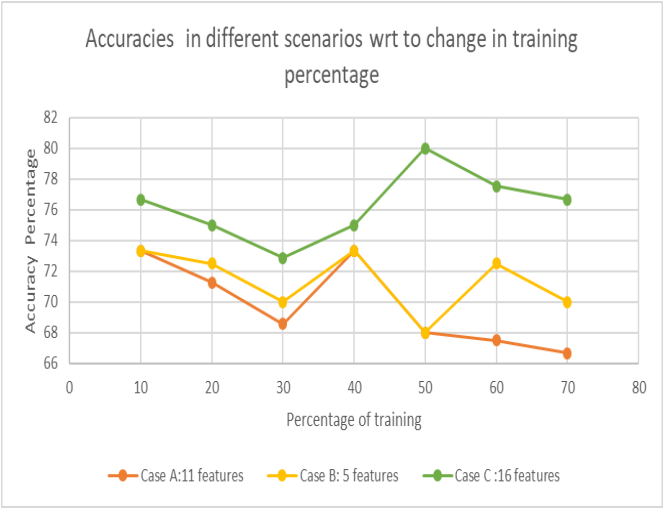

Figure 3:Accuracy graph

Furthermore, true positive rate (that is moves that are correctly identified) and false positive rate (that is moves of vehicle that were incorrectly identified) were calculated and the AUC (Area Under Curve) graphs were plotted for all the three cases

: 5 features,11 features and 16 features are shown in Figures 4, 5 and 6 respectively. The graphs further assert the previous accuracy graph and justifies that the results with sixteen features are more superior than standalone performance of CNN framework with five features and eleven features input datasets.

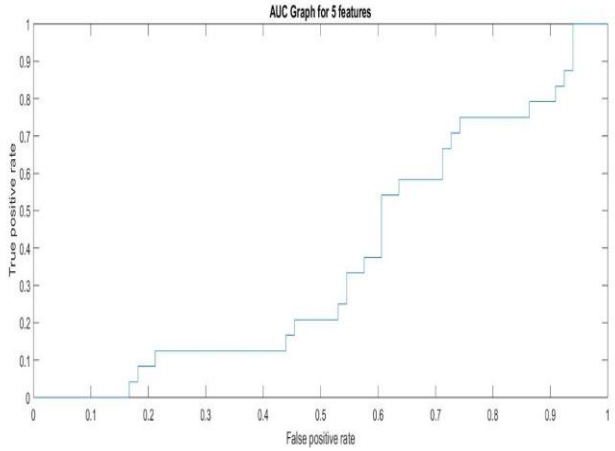

Figure 4: Area Under Curve(5 features)

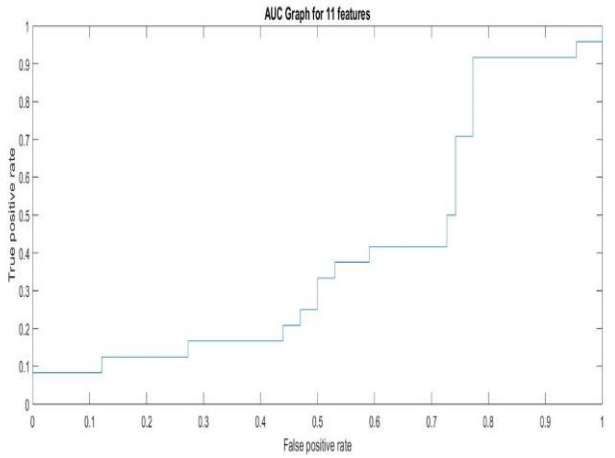

Figure 5: Area Under Curve(11 features)

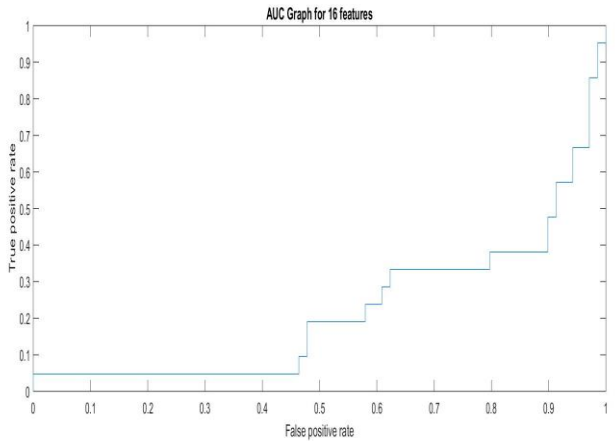

Figure 6 :Area Under Curve (16 features)

V. Discussions and Conclusions:

It was analysed that the combination of five features obtained from PCA and eleven features obtained previously from Best Feature Selection strategy have yielded better accuracies as compared to their standalone performance .This shows that PCA discovered previously unnoticed relations ,thus covering the dataset at full length .Its combination with inputs from Best Feature Selection Method provided improved information for the proposed model and paved way for better accuracies. Furthermore, it was noticed that the results for this feature set combination are same for ten percent and seventy percent training. This indicated that the ability of CNN to learn from imprecise data and finding out all variations before taking any decision makes it able to train itself well with ten percent training only. Thus, this model helps to achieve better accuracy rates even by training the model with only ten percent of dataset.

References

[1] Marwah,K. Sohal,J. (2018). “Improved Decision Making for Navigation Scenarios” In Advanced Computational and Communication Paradigms: Proceedings Volume 2, pages 717–726. Springer.

[2] Janglová, D. (2004). “Neural Networks in Mobile Robot Motion” In International Journal of Advanced Robotic Systems, Volume 1 Number 1, ISSN 1729-8806

[3] Engedy, I. and Horváth, G. (2009). “Artificial neural network based mobile robot navigation” In 2009 IEEE International Symposium on Intelligent Signal Processing, pages 241–246. IEEE.

[4] Diana D. Tsankova.(2010). “Neural Networks Based Navigation and Control of a Mobile Robot in a Partially Known Environment” In Mobile Robots Navigation, Alejandra Barrera (Ed.), ISBN: 978-953-307-076-6, InTech.

[5] Jefferson R Souza. (2011).“Vision-based Autonomous Navigation Using Neural Networks and Templates in Urban Environments” In SAC '11 Proceedings of the 2011 ACM Symposium on Applied Computing, Pages 1376-1381

[6] Matthew Wilkinson, M. C. and Meade Jr, A. J. (2014). “Neural-network-inspired machine learning for autonomous lunar targeting”. Journal of Aerospace Information Systems, 11(7):458–466.

[7] Capi, G., Kaneko, S., and Hua, B. (2015). Neural network-based guide robot navigation: an evolutionary approach. Procedia Computer Science, 76:74–79.

[8] Karkus, P., Hsu, D., and Lee, W. S. (2017). “Qmdp-net: Deep learning for planning under partial observability”. In Advances in Neural Information Processing Systems, pages 4694–4704.

[9] Ran, L., Zhang, Y., Zhang, Q., and Yang, T. (2017). Convolutional neural network-based robot navigation using uncalibrated spherical images. Sensors, 17(6):1341.

[10] Kim, D. K. and Chen, T. (2015). “Deep neural network for real-time autonomous indoor navigation”. arXiv preprint 14 arXiv:1511.04668.

Proceedings of the Fourth International Conference on Communication and Electronics Systems (ICCES 2019)
IEEE Conference Record # 45898; IEEE Xplore ISBN: 978-1-7281-1261-9

Speckle Noise Reduction Using Fuzzy Logic in Ultrasound Images

Azrah Rubanee, Harish Kumar Dogra
Department of Electronics and Communication Engineering
Sri Sai College of Engineering and Technology
Badhani, Pathankot, India

Giridhar Reddy Bojja
College of Business and Information Systems
Dakota State University
Madison, South Dakota, U.S.A

***Abstract*—Speckle alludes to the granular models that occur in ultrasound images because of wave impedance. Speckle expulsion can extraordinarily enhance the deceivability of the basic structures in an ultrasound image and upgrade resulting post-handling. A structure for speckle removal dependent on fuzzy logic algorithm. The noise present in the image can coat and diminish the visibility of specific attributes of the items present inside the images. Subsequently making it unfit for further upgrades. There has been an examination on the de-noising filters for long to expel the noise from images. In this research, we propose a unique method which beats outstanding techniques.**

Keywords—Image processing, Noise reduction, Fuzzy logic, Ultrasound images.

I. INTRODUCTION

Unique image de-noising techniques [1]–[4] using dissimilar channels recommended and executed in previous decade. A few straight and furthermore non-direct channels [5], [6] have been actualized for image de-noising reason utilized for various applications. Medicinal images [1], [7] are currently utilized for diagnosing the ailments in every single present-day clinic in regard to location of variations from the norm in human body with the help of a radiologist. Here, Medical images are accomplished using therapeutic imaging frameworks that give the data about the life systems, physical and metabolic exercises of different pieces of human body.

The discovery and expectation of imaging is getting simpler by the headway in the innovation. The snappy improvement is a result of the necessity for more quick, exact and less meddlesome treatment. Trend setting innovation in radiologic imaging rigging has also stimulated the utilization of imaging. The higher assurance comes at the expense of a consistently growing typical number of patients. The growing number and nature of the pictures cripples to overwhelm radiologist's capacities to interpret them. In various certifiable radiologic practices, automated and smart images examination and technique [8].

Ultrasound imaging is a standout amongst the most broadly utilized imaging advances in drug. This imaging methodology has accomplished incredible patient acknowledgment since it is sheltered, quick, effortless and generally modest when contrasted and the other imaging modalities. It has the extra favorable position of convey ability and might be utilized at bedside, which is exceptionally helpful for emergency unit. Ultrasound gives gritty imaging of delicate tissues that is normally clouded in X-beam images. Not at all like other tomographic methods, has ultrasound imaging offered intuitive representation of the basic life systems progressively [9]–[16].

A. Speckle Reduction Techniques

Filter has critical job in image de-noising process. Utilizing filter system, so as to choose specific estimation of pixel in yield image the neighbor pixels additionally take an interest. A few techniques have been utilized to decrease the speckle impact on ultrasound images. It comprises of a window moving over every pixel in the picture and applies a scientific count and substitutes for the estimation of the focal pixel under the window. The window moves along the picture one pixel at any given moment until it covers the whole image. The section below shows the different filtering techniques used widely in the literature.

- Mean Filter - It is a conventional technique for separating. A mean channel [14] follows up on an image by smoothing it. i.e., it decreases the variety as far as force between adjoining pixels. The mean filters are a key moving window moving filters, which replaces the middle an inspiration in the window with the common of all the neighboring pixel respects including that inside respect. It executed with a convolution shroud, which gives an outcome that is a weighted total of the estimations of a pixel and its neighbor pixels. It is known as a straight channel. The spread or bit is a square. Conventional channel approach is neighborhood average technique. The focal thought of this method is to supplant lessen scale estimation of the middle pixel by run of the mill estimation of neighborhood pixel diminish scale. It used to diminish AWGN, yet it can cause obscuring impact.
- Median Filter - The median filter is performed by taking the degree of most of the vectors inside a cloak and orchestrated by the degrees. The pixel with the center significance is then used to displace the pixel pondered the center channel is appointed an immediate channel. It works exceptionally to cover the Salt and pepper racket. A middle channel goes

under the class of nonlinear channel. It is like way looks for after the moving window standard, similar to mean channel. A 3× 3, 5× 5, or 7× 7 bit of pixels moved over the whole picture. First the focal point of the pixel respects in the window is taken care and a short time later within pixel of the window is superseded with the figured center regard. Check of Middle is done as first masterminding all the pixel regards from the incorporating neighborhood.

II. FUZZY RULES

The histogram adaptive fuzzy (HAF) filter is especially powerful to expel profoundly indiscreet noises while ensuring edge sharpness. This is rehearsed through a fluffy smoothing channel created from a ton of fluffiness In the event that made from a lot of fluffiness If rules, which substitute adaptively to control the yield mean squared goof as information histogram estimations change. A calculation is to use (debased) input histogram to pick parameters for the close-by impeccable comfortable intrigue limits. Advancement of the HAF channel incorporates three phases: (1) describe cushioned sets in the data space, (2) manufacture a ton of On the off chance that norms by combining input histogram experiences to outline the feathery support limits, and (3) assemble the channel subject to the course of action of standards. Not at all like various neuro-soft or fuzzy neuro channels, where a subjective strategy is used to pick starting enlistment capacities with respect to coming about extended getting ready, HAF can achieve close perfect execution with no preparation.

A. Technique

For the issue of excitement here, we expect an info dark image estimated 512×512 and a pixel power from 0 to 255. With flexible histogram approach for instance Histogram Versatile Channel (HAF), a fluffy method of reasoning-based procedure proposed to remove noise from innovative images. In this technique, we pick whether a pixel is disorderly or not established on the power of the pixels including the given pixel. For the said errand, we structure a fuzzy interface framework (FIS) that takes two wellsprings of information and produces one yield as showed up in Figure 1. The fundamental data taken by the FIS is qualification of within pixel and the pixel vertically on a dimension plane going before it. Second data within pixel and the pixel vertically on a dimension plane succeeding it. Figure 2. shows work publication supervisor for the FIS. Sugeno sort out is used to make the fuzzy measures.

Figure 2. demonstrates the rule editor for MATLAB tool. The pixel is viewed as an uproarious pixel whenever input 1 and information 2 i.e.; the distinctions of focus pixel with its neighboring pixels is higher. There are 49 rules executed in our work as appeared in the standard editorial manager.

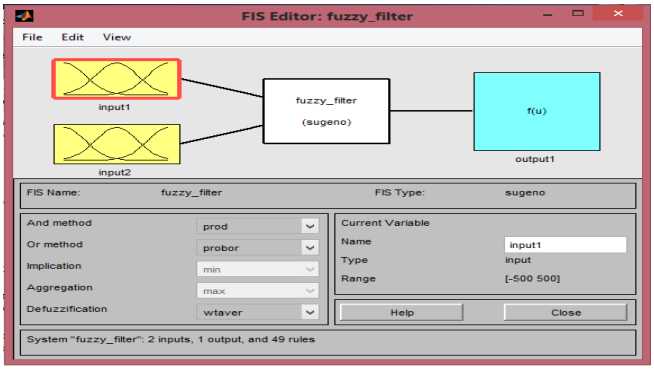

Figure 1. FIS with input and output

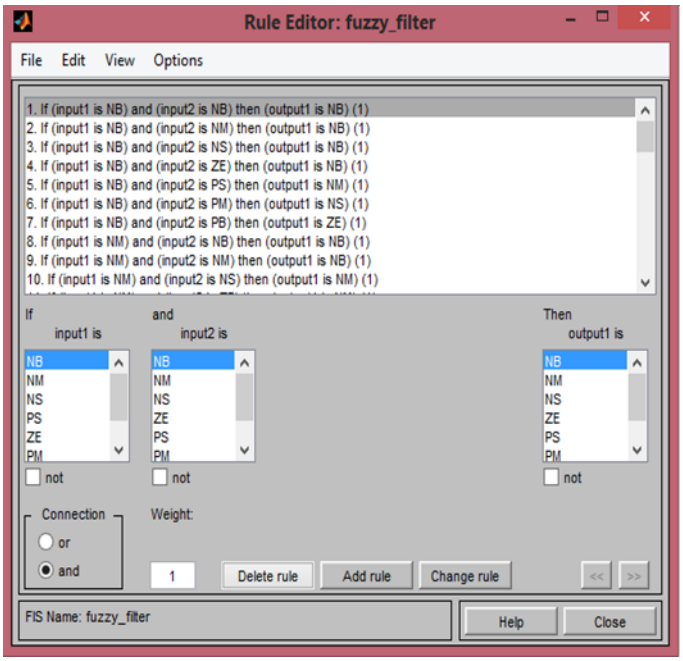

Figure 2. Rule Editor

III. PROPOSED WORK

The proposed work will give the effective filter, which expels the noises from dim scale image, and function admirably than other existing methods. To expel more than one noise from image, essential conventional that is established filters, mean filter and middle filter are joined. The proposed strategy fuses the fuzzy rationale procedures alongside the customary direct and nonlinear channels which makes it adaptable and thus ready to diminish more than one kind of noise.

The noise present in the image can coat and decrease the detectable quality of explicit characteristics of the articles present inside the image. Consequently, making it unfit for further updates. There has been an investigation on the de-noising channels for long to oust the noise from image. In our proposed the fuzzy set up channels which empties more than one kind of commotions from pictures. Traditional mean and center channels joined to empty more sorts of noises. Execution of the channel is differentiated, and various channels and the proposed technique beats existing methodologies. The

work proposed here related to the headway of a novel fluffy histogram versatile channel to diminish noise from automated images. The proposed procedure is better than other surely understood traditional strategies accessible for a similar reason. Fuzzy set is crisp sets calculated applying certain conditions corresponding to fuzzy set. This process known decussation. The field of the restorative image de-noising is extraordinary accentuation in different uses of ultrasound images. The aim of our proposed work are as follows:

- To remove the noise from an ultrasound image.
- To improve the accuracy.
- The algorithm used in proposed work are fuzzy logic alpha trim.

The proposed work is based on the fuzzy logic algorithm that works on the basis of fuzzy rules. They consist of two networks namely; mamdani and sugeno networks. With the help of these networks fuzzy rules are created. There are 49 rules IF-THEN that works based on various membership functions. The Mat lab codes works as initialize the screen and read the input image, if image is rgb convert that into gray scale and after add speckle noise to the input image. With the help of sugeno based network edges are weighted as linguistic variable and detect the resolution of the particular image. Update the mean and median values and also calculate the performance parameters. Thus, by PSNR values are compared with the existing system.

A. Step by Step Procedure

With the help of fuzzy logic algorithm, the following steps are followed:

Step-1: Input image and reads

Step-2: Adding noises in Input Image

Step-3: Create the fuzzy logic-based network

Step-4: Fuzzy Membership function is defined i.e. F(i, j)

Step-4: Calculate the weights of Edges in Image

Step-5: Restoration term for detected noise pixel is computed at Edges using Fuzzy Rules.

Step-6: Delete the d/2 largest and d/2 smallest grayscale values.

Step-7: Take Median for rest of grayscale values.

Step-8:Update the median values for every rows and columns.

Step-9: Reconstruct the de-noised Image

Step-10:Calculate the performance parameters like MSE,PSNR,SC,etc.

IV. EXPERIMENT

INPUT 1: a synthetic speckle noise model corrupts synthetic image input.

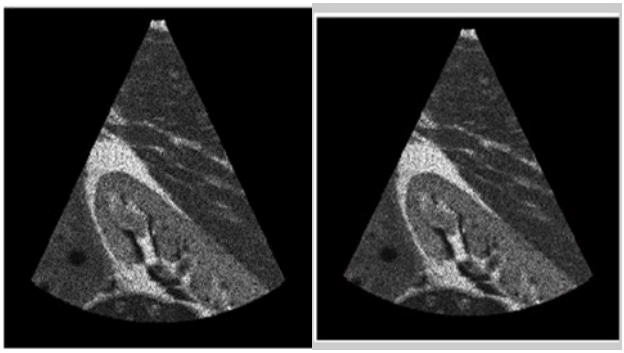

Figure 3. (a) input image (b) Noised image

INPUT 2: Despeckled results with fuzzy logic alpha trim

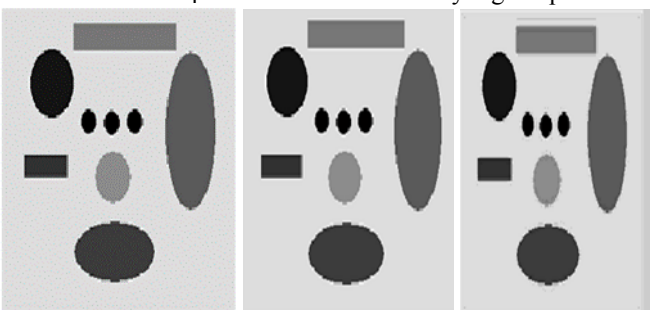

Figure 4. (a) Input image (b) Noised image (c) De-noised image

INPUT 3: Comparing on medical images

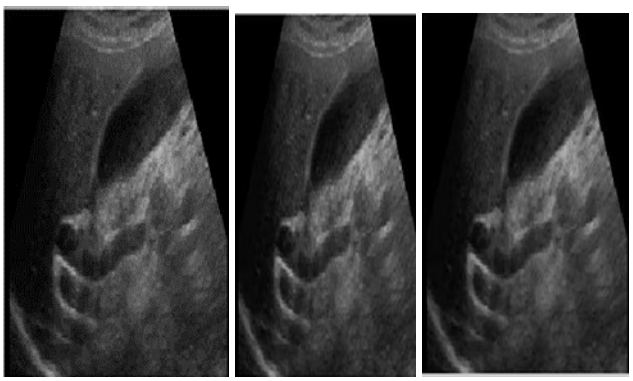

Figure 5. (a) input image (b) Noised image (c) De-noised image

INPUT 4: Comparing speckle reduction on the image with different methods. Here we are comparing performance parameters like PSNR, FOM ,SC UIQ etc with the existing system.

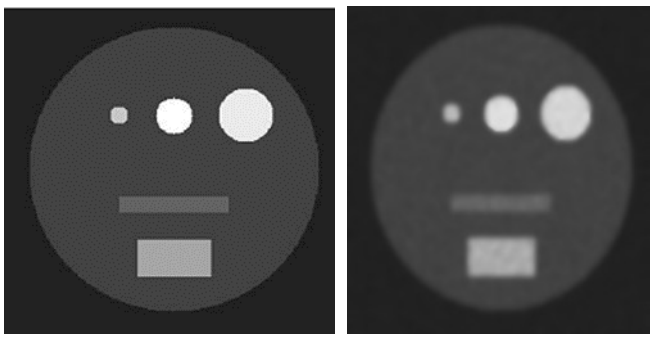

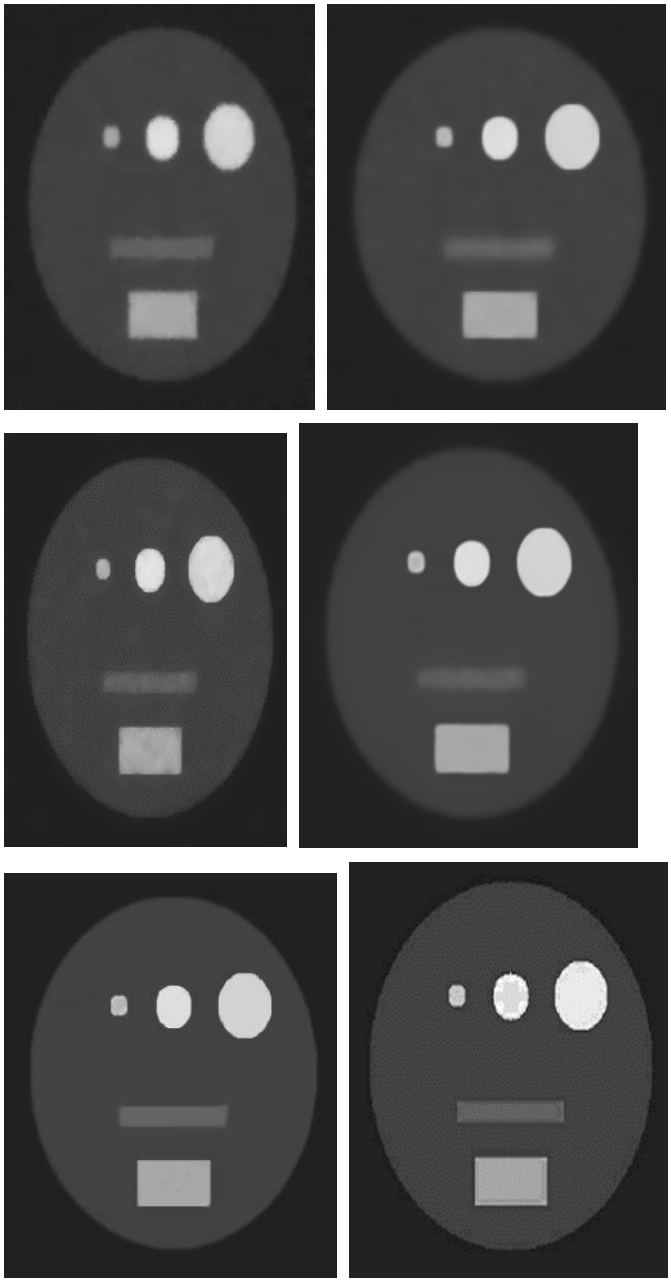

Figure 6. (a) input image (b) SRAD (c) SBF (d) OBNLM (e) ADLG (f) NLMSL (f) LR (g) proposed work

Table 1. Quantitative comparison for results at sigma value of our proposed work at 0.35

	PSNR	FOM	UQI	SSIM	VIF
SRAD	27.7	0.4581	0.0965	0.9237	0.2730
SBF	28.3	0.5238	0.1970	0.9455	0.3618
OBNLM	29.70	0.5207	0.1246	0.9484	0.3564
ADLG	30.05	0.7423	0.1318	0.9611	0.4138
NLMLS	30.315	0.7794	0.3951	0.9548	0.540.
LR	32.719	0.9242	0.6933	0.9812	0.6964
Proposed	**38.578**	**1.0163**	**0.95**	**0.9661**	**1.082**

GRAPH FIRST: Comparison between PSNR values with existing method and our method

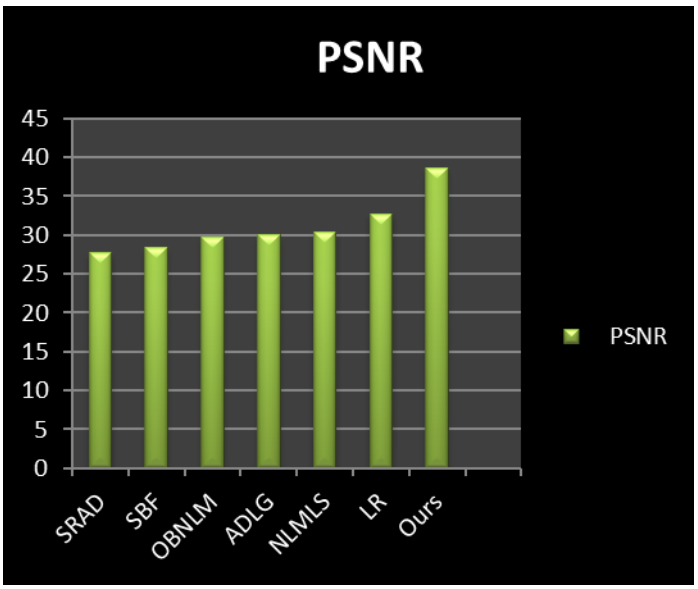

GRAPH SECOND: Comparison between FOM, UQI,SSIM and VIF values

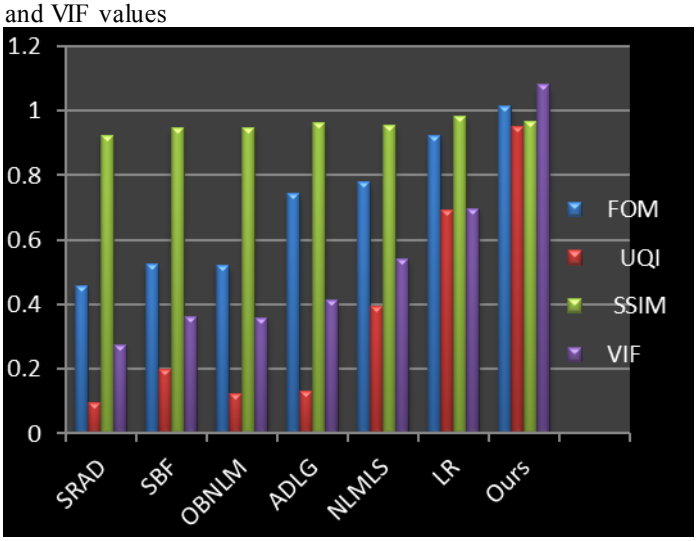

Table 2. Comparison of PSNR values for de-speckled results for results in figure at different noise levels.

	$s^2s = 0.15$	$s^2s = 0.2$	$s^2s = 0.25$	$s^2s = 0.3$
SRAD	27.64	25.56	25.08	23.75
SBF	27.75	26.04	25.65	23.89
OBNLM	28.68	26.27	25.90	24.11

ADLG	28.97	27.08	26.56	24.59
NLMLS	29.14	27.98	27.13	26.48
LR	30.77	29.60	28.42	27.61
Proposed	**38.6684**	**38.64**	**38.62**	**38.60**

GRAPH THIRD: Comparison of PSNR values of de- speckled results.

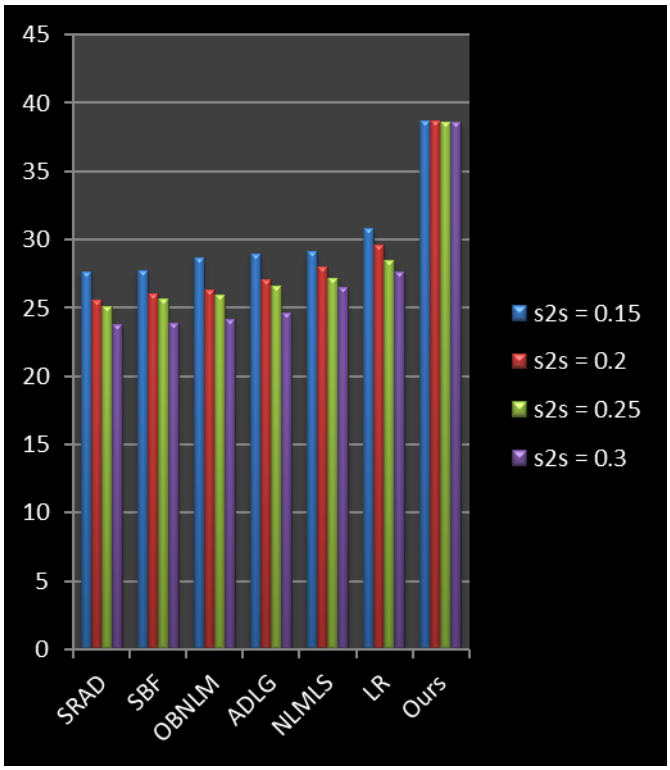

INPUT 5: Speckle decrease on a ultrasound with polycystic liver

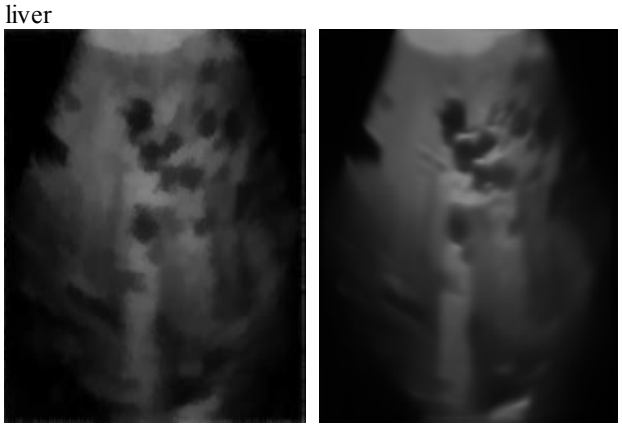

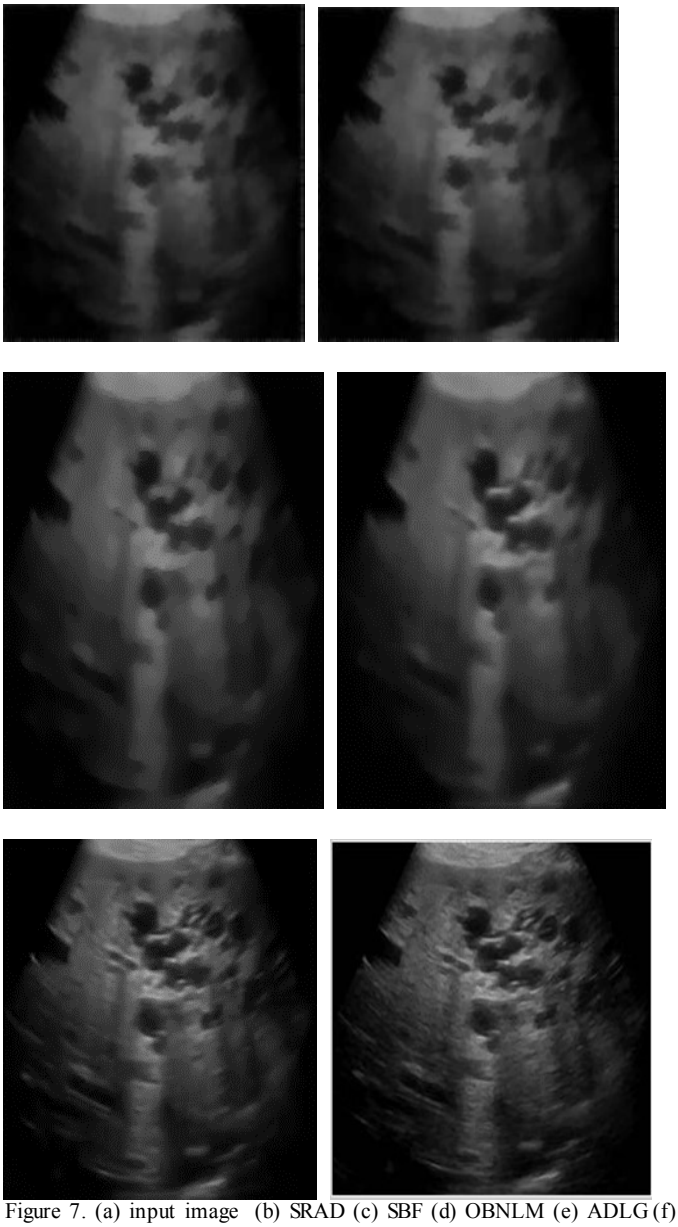

Figure 7. (a) input image (b) SRAD (c) SBF (d) OBNLM (e) ADLG (f) NLMSL (f) LR (g) proposed work

Table 3: Comparison of Performance parameters values for de-speckled results for results in figure at different noise levels.

	$s^2s = 0.15$	**$s^2s = 0.2$**	**$s^2s = 0.25$**	**$s^2s = 0.3$**
PSNR	41.1937	41.1713	41.148	41.12

GRAPH FOURTH: Examination of speckle decrease on a ultrasound picture with polycystic liver (PSNR) values.

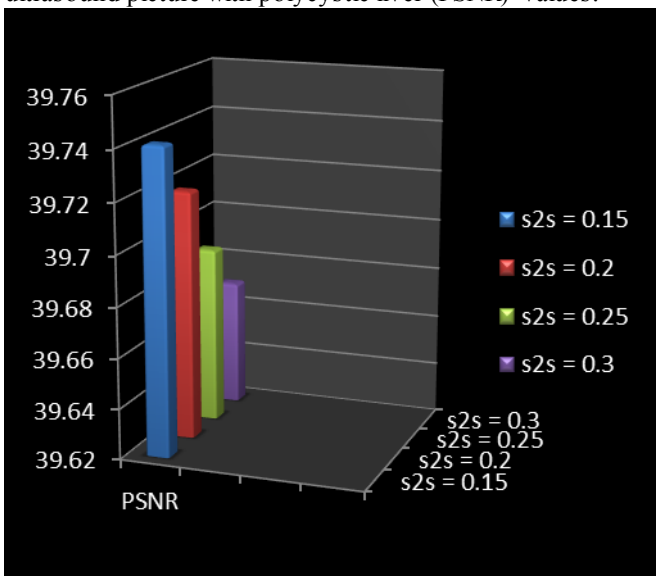

INPUT 6: Comparing speckle reduction on an ultrasound image with a malignant papil tumor in bile duct.

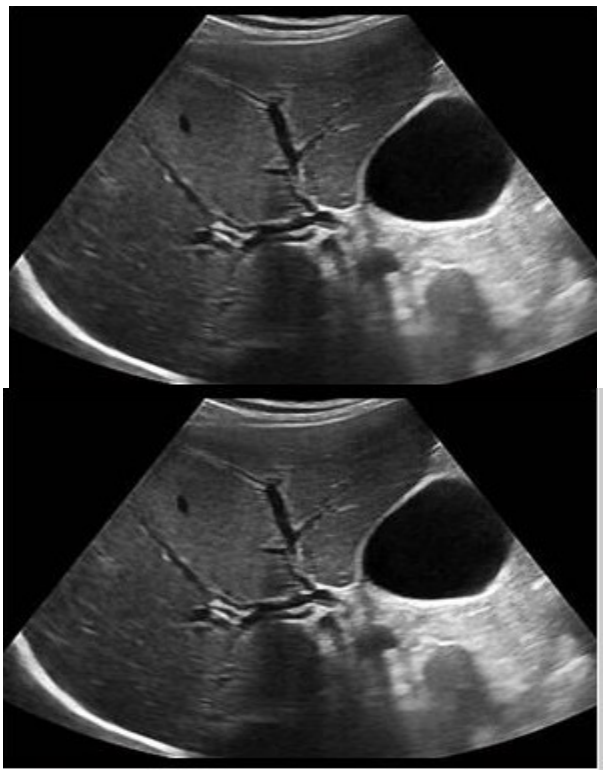

Figure 8. (a) input image (b) Noised Image

(c) Denoised Image

Table 4: Comparing speckle reduction on an ultrasound image with a malignant papil tumor in bile duct at different noise levels.

	$s^2s = 0.15$	$s^2s = 0.2$	$s^2s = 0.25$	$s^2s = 0.3$
PSNR	39.7411	39.7187	39.69	39.67

GRAPH FIFTH: Comparing speckle reduction on an ultrasound image with a malignant papil tumor in bile duct at different noise levels

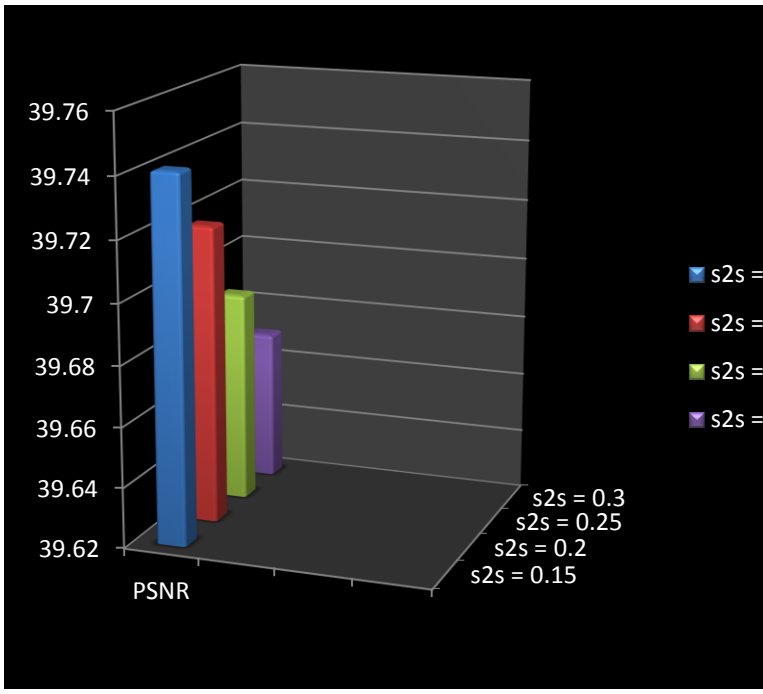

V. CONCLUSION

It is obvious from the outcomes area that the proposed procedure beats the outstanding de-noising channels called Mean channel and fuzzy channel. The proposed method, as it depends on fluffy rationale, is knowledgeable in dealing with the dubiousness of information contained in noisy digital images. Both quantitative and qualitative assessments on different manufactured and clinical images show that our strategy can adequately evacuate speckle and better save highlights contrasted and the cutting-edge de-spotting procedures. This procedure has improved the noises evacuation execution and reclamation systems. The proposed technique's performance is observed through computing de-noised images' PSNR value.

In future, segmentation comparison can be done different algorithm can be used to achieve better results. This work can be additionally improved to de-noise the other kind of images, too, as RGB, Indexed and Binary images.

VI. REFERENCES

[1] O. Magud, E. Tuba, and N. Bacanin, "Medical Ultrasound Image Speckle Noise Reduction by Adaptive Median Filter," vol. 14, p. 9, 2017.

[2] B. Mishra and A. Jain, "Reviews on Multiscale Transform Domain Image Denoising Methods," vol. Vol.8(6), Jun. 2017.

[3] C. Saxena and D. Kourav, Noises and Image Denoising Techniques: A Brief Survey. 2014.

[4] M. Sugeno, Industrial Applications of Fuzzy Control. New York, NY, USA: Elsevier Science Inc., 1985.

[5] Yongjian Yu and S. T. Acton, "Speckle reducing anisotropic diffusion," IEEE Trans. Image Process., vol. 11, no. 11, pp. 1260–1270, Nov. 2002.

[6] P. C. Tay, C. D. Garson, S. T. Acton, and J. A. Hossack, "Ultrasound Despeckling for Contrast Enhancement," IEEE Trans. Image Process., vol. 19, no. 7, pp. 1847–1860, Jul. 2010.

[7] P. Coupe, P. Hellier, C. Kervrann, and C. Barillot, "Nonlocal means-based speckle filtering for ultrasound images," IEEE Trans. Image Process., vol. 18, no. 10, pp. 2221–2229, Oct. 2009.

[8] P. Kaur, G. Singh, and P. Kaur, "A Review of Denoising Medical Images Using Machine Learning Approaches," Curr. Med. Imaging Rev., vol. 14, no. 5, pp. 675–685, Oct. 2018.

[9] U. Kamilov, E. Bostan, and M. Unser, "Wavelet Shrinkage With Consistent Cycle Spinning Generalizes Total Variation Denoising," IEEE Signal Process. Lett., vol. 19, no. 4, pp. 187–190, Apr. 2012.

[10] B. Wang, T. Cao, Y. Dai, and D. C. Liu, "Ultrasound Speckle Reduction via Super Resolution and Nonlinear Diffusion," in Computer Vision – ACCV 2009, 2010, pp. 130–139.

[11] W. Gómez Flores, W. C. de A. Pereira, and A. F. C. Infantosi, "Breast ultrasound despeckling using anisotropic diffusion guided by texture descriptors," Ultrasound Med. Biol., vol. 40, no. 11, pp. 2609–2621, Nov. 2014.

[12] K. K. V. Toh and N. A. M. Isa, "Noise Adaptive Fuzzy Switching Median Filter for Salt-and-Pepper Noise Reduction," IEEE Signal Process. Lett., vol. 17, no. 3, pp. 281–284, Mar. 2010.

[13] How-Lung Eng and Kai-Kuang Ma, "Noise adaptive soft-switching median filter," IEEE Trans. Image Process., vol. 10, no. 2, pp. 242–251, Feb. 2001.

[14] C. V. Cannistraci, F. M. Montevecchi, and M. Alessio, "Median-modified Wiener filter provides efficient denoising, preserving spot edge and morphology in 2-DE image processing," Proteomics, vol. 9, no. 21, pp. 4908–4919, Nov. 2009.

[15] L. Sendur and I. W. Selesnick, "Bivariate shrinkage with local variance estimation," IEEE Signal Process. Lett., vol. 9, no. 12, pp. 438–441, Dec. 2002.

[16] W. Zuo and Z. Lin, "A Generalized Accelerated Proximal Gradient Approach for Total-Variation-Based Image Restoration," IEEE Trans. Image Process., vol. 20, no. 10, pp. 2748–2759, Oct. 2011.

Proceedings of the Fourth International Conference on Communication and Electronics Systems (ICCES 2019)
IEEE Conference Record # 45898; IEEE Xplore ISBN: 978-1-7281-1261-9

Plants Leaf Segmentation using Bacterial Foraging Optimization algorithm

Siddharth Singh Chouhan[1,*]
[1] School of Computer Science and Engineering,
SMVDU, Katra, Jammu and Kashmir, 182320, India
*Corresponding author: siddharth.lnct@gmail.com

Ajay Kaul[2]
[2]School of Computer Science and Engineering,
Shri Mata Vaishno Devi University, Katra, Jammu and Kashmir, 182320, India
ajay.kaul@smvdu.ac.in

Uday Pratap Singh[3,*]
[3]School of Mathematics,
SMVDU, Katra, Jammu and Kashmir, 182320, India
*Corresponding author: usinghiitg@gmail.com

***Abstract*—Computer vision methodologies has been predominantly used for solving number of problems related with pattern recognition, machine vision, object detection, object classification and many more. This terminology along with soft computing approaches have proven to be a solution for various complex problems. But, in recent time it has been noticed that when conventional methods incorporated with optimization methods, the result achieves higher accuracy and also lessens the computational time. These Nature inspired algorithm (NIA) or Bio-inspired methods have been espoused in the number of applications for finding an accurate solution working with real-time or complex data. Image segmentation is one of them. It is the practice of separating an image into its constituent subparts in order to extract some meaningful information from it. There are number of methods used for performing segmentation. In this paper our aim is in studying one of the optimization method named as Bacterial Foraging Optimization Algorithm (BFOA). This method is then used for initializing the weights for Artificial Neural Network (ANN) that is deployed for image segmentation. Finally, when the results are compared with the other methods shows the efficiency BFO-ANN method.**

Keywords*—*Bacterial Foraging Optimization, Image segmentation, Image processing, Nature inspired algorithms.

I. INTRODUCTION

In image processing, image segmentation or object extrcation is the preprocessing and important step frequently used in the number of applications for partitioning an image in extracting a meaningful region of interest or object from given the images. It further helps in making an image easier to analyze and interpret useful information. This process of partitioning an image is carried out based on some homogeneous characteristics of an object. The level of segmentation is the process to be carried out until the desired object has been segmented. The application of segmentation can be found in medical images for the segmentation of tumor from magnetic resonance images, pedestrian segmentation from the real-time images, land-water segmentation from satellite images, disease segmentation from the agricultural images, handwritten digit or character recognition etc.[1]-[5].

Image thresholding is the most simple and commonly used process for separating an image into its consequent parts background and foreground (i.e. object or region of interest). This process is carried out for binary images depending on the thresholding parameter known to be T. Each pixel whose values are less than to threshold value T will be assigned to black pixel (background) and pixels greater than T value will be assigned to the white pixels (foreground or object). Finding an optimal thresholding value for partitioning an image is a complicated task to perform. This threshold value is varied until the desired region of interest has been segmented [2][4]. More importantly, it is a major concern when performing multilevel image thresholding. That is when segmentation has to be carried out for partitioning an image into different regions of interest or extracting multiple objects. In this case, optimal various threshold values have to be chosen for extracting multiple objects.

Generally, bi-level or multilevel segmentation is carried out with the help of Kapur or Otsu entropy functions. These functions are depended on the

evaluation of the histogram information and objective function for generating an effective optimal value. But this process results in enhancing the computational burden when opted for multilevel thresholding values generation. Nature-inspired algorithms have shown great efficiency in providing an optimal solution in solving the number of complex problems. The heuristic algorithms like Artificial Bee Colony, Cuckoo Search, Genetic Algorithm, Firefly Algorithm, Particle Swarm Optimization, Bacterial Foraging Optimization etc. has been effectively applied in solving the thresholding problems [2][4].

Some of the work includes in [6] Artificial Bee Colony (ABC) is used for searching optimum cluster centers for Fuzzy c means algorithm, in [7] for maximizing different objective functions of methods like Kapur's entropy, Tsallis entropy, Otsu's method, Shannon entropy, Renyi entropy the optimal thresholding value is calculated by using Bat Algorithm (BA), in [8] Crow Search optimization Algorithm (CSA) is used to find out the centroid of the clusters for the Fast Fuzzy C Means algorithm, in [9] the weight of the Feed Forward Neural Network is rationalized by Genetic algorithm (GA) for stated iterations, in [10] Spider Monkey Optimization (SMO) is used for the purpose of feature selection, in [11] RBF Network is optimized for the structure selection using the GA and Particle Swarm Optimization (PSO), in [12] have used bacterial foraging optimizing algorithm for assigning the weight to the feedforward neural network, in [13] PSO is used for the training of backpropagation network, in [14] Ant colony optimization is used for selecting best discriminant features improving results using support vector machine, in [15] used Firefly Algorithm (FFA) is used for the optimal number and center selection of the Radial basis function network, in [16] Whale Optimization Algorithm (WOA) is used for dividing the image into predefined cluster, and so on.

These optimization techniques result in improving the accuracy of the results and also reducing the computational efficiency of the proposed system. Therefore, this work aims in studying and presenting various applications of one such nature-inspired algorithm known as BFOA for the segmentation of images. Followed by introduction in section 1, section 2 presents the literature review with outcomes, in the next section 3, the concept and theory behind the BFO are introduced, section 4 presents the results, and section 5 concludes this article followed by the references.

II. RELATED WORK

The various studies related with the image segmentation or object extrcation incorporated using Bacterial foraging optimization algorithm are listed in Table I.

TABLE I. LITERATURE REVIEW

Authors	Applications of Bacterial Foraging Optimization Algorithm (BFOA)	Year
Mohammad Mahdi Dehshibi et al. in [1]	For improving the accuracy of the segmentation the optimum parameters of Otsu and Kapur functions are calculated.	2017
Nandita Sanyal et al. in [5]	In this work, the BFOA has been used for optimizing the fitness function of fuzzy entropy. During the foraging of bacteria in exploration or exploitation state the algorithm varies the run length unit parameter. This causes the movement of bacteria between exploration or exploitation state during the execution phase.	2011
Ismail Ahmed A. AL-Hadi et al. in [12]	BFO is used for the learning process of the Feedforward neural network to increase the convergence rate and accuracy. The best bacterium members representing the optimum weights are used with the testing of network for calculating the errors of the weights using different data patterns.	2011
Kezong Tang et al. in [17]	Authors have worked on improving the solution by enhancing global searching ability the convergence rate of the algorithm. So, in this work for obtaining the optimal values the Tsallis thresholding functions are maximized.	2017
Anitha Vishnuvarthanan et al. in [20]	The cluster center of the Modified Fuzzy K - Means algorithm is updated in identifying optimum threshold value using BFOA.	2017
Nandita Sanyal et al. in [21]	By limiting the population and varying the number of chemotactic steps BFO achieves optimal solution and also computational burden of the proposed method is reduced.	2014

Yongsheng Pan et al. in [22]	BFO is used to find the edges by tracking the movement of bacteria. In this the gradients of intensities are marked as the nutrient rich location and propel the bacteria to forage in that nutrient concentration by mimicking the behavior of E. Coli.	2017
Yang Liu et al. in [23]	The cell to cell conversation and self-adaptive foraging approach in BFO is used for finding the optimal thresholding values.	2015
Anitha Vishnuvarthanan et al. in [24]	The optimal threshold value generated by using BFO is used for re-clustering the cluster output from the modified Fuzzy C Means.	2018
P.D. Sathya et al. in [25]	The accuracy and the computational efficiency is improved by using BFO for performing multilevel thresholding with the help of Minimum Cross Entropy (MCE) method.	2011
Jyotika Pruthi et al. in [26]	The fitness function of the OTSU method is defined by using BFO for the segmentation of optic disc from retinal images.	2018
Anitha Narayanan et al. in [27]	The optimized cluster heads for the modified Fuzzy c means algorithm is obtained with the help of BFO.	2018
Mohamad Amin Bakhshali et al. in [28]	BFO is used for finding the optimal thresholding values for the Kapur and Otsu method in performing color lip segmentation.	2014
A. Sasithradevi et al. in [29]	Optimal thresholding value is obtained by using BFO for image segmentation.	2014
Hong Wang et al. in [30]	Best feature subset from the database with variable dimensionality has been selected with the help of BFOA .	2017
S. S. Chouhan et al. in [31]	Authors have presented the various studies for the theories of computer vision in plant pathology.	2019
U. P. Singh et al. in [32]	Convolutional neural network has been used for the classification of mango leaves among healthy and diseased ones.	2019

A. OUTCOMES

Bacterial Foraging Optimization (BFO) algorithm has been adopted in number of applications in image processing. This includes multilevel segmentation for color images, face recognition, lip segmentation, classification and identification of diseases from plant leaf images, segmentation of pedestrian and many more. It has been observed from the literature that optimizing the algorithm with the help of BFO results in better segmentation results. This confines the computational burden of the algorithm being used thus increases the efficiency of the algorithm when compared with the other optimization algorithms. Some of the features of optimization with BFO are given as under:

1. Finding the optimum parameters (thresholding values) for the functions like Otsu and Kapur results in improving segmentation performance.

2. Selection of optimum weights or initial weights helps the learning process of the neural networks, thus achieving higher convergence rates and accuracy.

3. With the help of optimization, the cluster heads or optimal cluster values are obtained for the methods like Fuzzy C Means or K-Means.

4. BFO has been used for finding the best feature subset from the database.

5. BFO has been used to find the edges of an object by the letting movement of bacteria placed at the rich nutrient location that is boundaries.

III. STANDARD BACTERIAL FORAGING OPTIMIZATION (BFO)

Animals when compared with a high sense of foraging, animals with a low sense of foraging behavior are having the high probability to extinct. *Echerichia coli* (*E.coli*) bacteria have one such imperative and captivating activity of food searching. They have the property of moving in the direction of food or nutrients without actually coming close to other cells and also avoiding the other noxious matters. Proposed by Kevin Passino (2002), BFO algorithm is a nature-inspired algorithm stimulated by the group foraging behavior of bacteria like *Echerichia coli*. The

bacteria searches for the nutrients in the search space taking small steps moving towards or away from the signal engendered. Initially, this method was developed for distributed optimization and control, but later it has confirmed to be an effective optimization solution in the number of real-time applications for improving convergence speed and accuracy [17]-[19]. BFO can be summarized in four basic steps given as [19]:

1. Search for the nutrient or food rich location.

2. Choosing whether to enter into the existing rational nutrient location or not.

3. If new nutrient location is entered then accomplishing thorough and careful foraging.

4. After consuming some nutrient or food then deciding, whether to enter into the new nutrient-rich location or continue in the same location.

These four basic steps are abridged into four stages known as 1. Chemotactic, 2. Swarming, 3. Reproduction, and 4. Elimination or Dispersal [17]-[19]. Following we will briefly describe the mentioned stages

1. Chemotaxis: This is the first phase of the algorithm. In this phase, the bacteria (*E. Coli*) starts tumbling to change its direction for period of time. After this initial step, the bacteria are moved to a step size. At this point if the bacteria finds rich nutrient location then it will keep swimming in the same direction otherwise it stops. Mathematically, if we consider that θ is the position of bacteria E.coli and $\theta^z(a,b,c)$= z^{th} bacterium in a^{th} chemotaxis, b^{th} = reproduction, c^{th} = elimination – dispersal method. Then the tumbling is given by the equation:

$$\varphi(z) = \frac{\Delta(z)}{\sqrt{\Delta(z)^T \Delta(z)}} \tag{1}$$

where $\Delta(z),\ z = 1, 2, \ldots S$ is a random vector. Each element $\Delta_m\,(z), m = 1,2, \ldots, p$ of $\Delta(z)$ is a random number between -1 to 1. S is the number of bacteria. The bacteria updating equation is given by

$$\theta^z(a+1,b,c) = \theta^z(a,b,c) + C(z)\,\Phi(z) \tag{2}$$

where $C(z), z = 1,2, \ldots, S$ is the moving step size in the swimming phase [17] [18].

2. Swarming: Swarming is the process of signaling or passing messages between cell to cell. This has two possible scenarios first if a bacteria founds nutrient rich location then it passes the signals or chemical substances attracting other bacteria and in the second case if no nutrient is found and bacteria starts dying the they release signal to repel from that bacteria or location. This behavior of the bacteria is given by the following equation.

$$J_{cc}\big(\theta,\ \theta^z(a,b,c)\big) = \sum_{z=1}^{s}\left[-d_{attract}\exp\left(-w_{attract}\sum_{f=1}^{p}(\theta_f-\theta_f^z)^2\right)\right] + \sum_{z=1}^{s}\left[h_{repellant}\exp\left(-w_{repellant}\sum_{f=1}^{p}(\theta_f-\theta_f^z)^2\right)\right] \tag{3}$$

where $\theta = [\theta_1, .., \theta_p]^T$ = bacterium optimization domain, θ_f^z = f^{th} component of the zth bacterium position θ^z. $J_{cc}\big(\theta,\ \theta^z(a,b,c)\big)$ = cell to cell communication value that is to be added to the result of the fitness function in the chemotaxis phase j. p = number of problem dimension, S = number of bacteria, $d_{attract}$, $w_{attract}$, $h_{repellant}$, and $w_{repellant}$ = the different coefficients which represents the strength of attraction or repulsion. Considering the swarming effect the fitness value of zth bacterium [17] [18] is given by

$$J\,(z,a,b,c) = J\,(z,a,b,c) + J_{cc}\big(\theta,\ \theta^z(a,b,c)\big) \tag{4}$$

3. Reproduction: After chemotactic steps (N_c), reproduction step is initialize. Let us assume that S be a positive even number, so S_r is the number of population that splits or reproduce into two having rich nutrient value. Given by

$$S_r = \frac{S}{2} \tag{5}$$

The accumulated cost of the bacteria is given by its health. When the accumulated cost is higher it means that the bacteria does not receive enough nutrients during its lifecycle of foraging. This means that the bacteria is unhealthy and will not get reproduce. The bacteria are then sorted according to their health in

descending order starting from the S_r least bacteria to S_r healthiest bacteria. In this process, the least bacteria dies and healthy bacteria splits into two and placed at the same location [17] [18].

4. Elimination or dispersal: Because of the abiotic factors like rise in temperature some bacteria tends to die. This process has been replicated by the elimination or dispersal of some bacteria with a probability of P_{ed}. On the other hand there is possibility of random generated bacteria for replacement [17] [18].

IV. RESULTS

The results were evaluated working on a system with 4GB RAM, i3 processor, 1TB HDD with the MATLAB 2017b environment. A real time dataset has been acquired for the images consist of about 240 images. First, the collected images has been preprocessed and divided among the training and testing dataset. Then for the segmentation work, we proposes an amalgamation of neural network with nature inspired algorithm for image segmentation. For this purpose a simple artificial neural is considered whose initial weight and training procedure has been optimized with the help of bacterial foraging algorithm. The plant leaf images are collected randomly for evaluating the performance of the proposed framework. Figure 1 shows the segmentation performance of the proposed work. The results are compared with k-means and ANN for two evaluation parameters known as Dice Similarity Coefficient (DSC) and Jaccard Coefficient (JC). Table II shows the segmentation results.

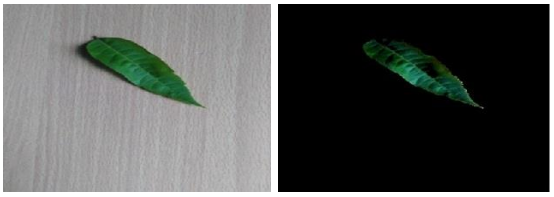

Image 1 (a) Original image (b) Segmented image

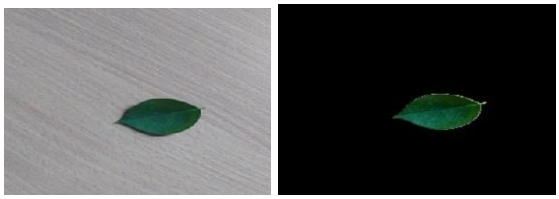

Image 2 (a) Original image (b) Segmented image

Figure 1. Segmentation results

TABLE II. RESULTS FOR DIFFERENT METHODS

Images	**Image 1**		**Image 2**	
Algorithms	DSC	JC	DSC	JC
k-means	0.7579	0.7614	0.7618	0.7520
ANN	0.8012	0.8111	0.8137	0.8145
BFO-ANN	0.8679	0.8596	0.8522	0.8539

V. CONCLUSION

This work presents, the importance of optimization technique for image segmentation. Bacterial Foraging Optimization is one of the best optimization methods belongs to the family of nature-inspired algorithms. This approach of finding an optimal solution has overcome the computational overhead and also improves the performance of the algorithms or methods. This hybridization of the bio-inspired algorithm also overcomes the problem of traditional approaches in dealing with complex data. Thus for attaining higher convergence rates and accuracy, it's been noticed that an optimization phase has to be espoused.

REFERENCES

[1] Mohammad Mahdi Dehshibi et al., "A hybrid bio-inspired learning algorithm for image segmentation using multilevel thresholding," Multimed Tools Appl, vol. 76, pp. 15951–15986, 2017, doi: 10.1007/s11042-016-3891-3.

[2] Siddharth Singh Chouhan et al., "Image Segmentation Using Computational Intelligence Techniques: Review," in *Archives of Computational Methods in Engineering*, 2018, doi: 10.1007/s11831-018-9257-4.

[3] Ashish Kumar Bhandari, "A novel beta differential evolution algorithm-based fast multilevel thresholding for color image segmentation," Neural Computing and Applications, doi: 10.1007/s00521-018-3771-z.

[4] Siddharth Singh Chouhan et al., "Soft computing approaches for image segmentation: A survey," in *Multimedia Tools Applications*, vol. 77 (21), pp. 28483–28537, 2018, doi: 10.1007/s11042-018-6005-6.

[5] Nandita Sanyal et al., "An adaptive bacterial foraging algorithm for fuzzy entropy based image segmentation," Expert Systems with Applications, vol. 38, pp. 15489–15498, 2011, doi: 10.1016/j.eswa.2011.06.011.

[6] Ankita Bose and Kalyani Mali, "Fuzzy-based artificial bee colony optimization for gray image segmentation," SIViP, vol. 10, pp. 1089–1096, 2016, doi: 10.1007/s11760-016-0863-z.

[7] Shashwati Mishra and Mrutyunjaya Panda, "Bat Algorithm for Multilevel Colour Image Segmentation Using Entropy-Based Thresholding," Arabian Journal for Science and Engineering, vol. 43, pp.7285–7314, 2018, doi: 10.1007/s13369-017-3017-x.

[8] Ahmed M. Anter et al., "An improved fast fuzzy c-means using crow search optimization algorithm for crop identification in agricultural," Expert Systems with

Applications, vol. 118, pp. 340–354, 2019, doi: 10.1016/j.eswa.2018.10.009.

[9] Kanthan Muthukannan and Pitchai Latha, "A GA_FFNN algorithm applied for classification in diseased plant leaf system," Multimed Tools Appl, vol. 77, pp. 24387–24403, 2018, doi: 10.1007/s11042-018-5710-5.

[10] Sandeep Kumar et al., "Plant leaf disease identification using exponential spider monkey optimization," Sustainable Computing: Informatics and Systems, doi: 10.1016/j.suscom.2018.10.004.

[11] Sultan Noman Qasem et al., "Multi-objective hybrid evolutionary algorithms for radial basis function neural network design," Knowledge-Based Systems, vol. 27, pp. 475–497, 2012, doi: 10.1016/j.knosys.2011.10.001.

[12] I. A. A. AL-Hadi, S. Z. M. Hashim and S. M. H. Shamsuddin, "Bacterial Foraging Optimization Algorithm for neural network learning enhancement," *2011 11th International Conference on Hybrid Intelligent Systems (HIS)*, Melacca, 2011, pp. 200-205, doi: 10.1109/HIS.2011.6122105.

[13] Shih-Wei Lin et al., "Parameter determination and feature selection for back-propagation network by particle swarm optimization," Knowl Inf Syst, vol. 21, pp. 249–266, 2009, doi: 10.1007/s10115-009-0242-y.

[14] Mohammad Ali Jan Ghasab et al., Feature decision-making ant colony optimization system for an automated recognition of plant species," Expert Systems with Applications, vol. 42, pp. 2361–2370, 2015, doi: 10.1016/j.eswa.2014.11.011.

[15] Vandana Agarwal and Surekha Bhanot, "Radial basis function neural network-based face recognition using firefly algorithm," Neural Comput & Applic, doi: 10.1007/s00521-017-2874-2.

[16] Abdalla Mostafa et al., "Liver segmentation in MRI images based on whale optimization algorithm," Multimed Tools Appl, vol. 76, pp. 24931–24954, doi: 10.1007/s11042-017-4638-5.

[17] Kezong Tang et al., "An improved multilevel thresholding approach based modified bacterial foraging optimization," Appl Intell, vol. 46, pp. 214–226, 2017, doi: 10.1007/s10489-016-0832-9.

[18] Siddharth Singh Chouhan et al., "Bacterial Foraging Optimization Based Radial Basis Function Neural Network (BRBFNN) for Identification and Classification of Plant Leaf Diseases: An Automatic Approach towards Plant Pathology," in *IEEE ACCESS*, 2018, doi: 10.1109/ACCESS. 2018.2800685.

[19] Betul Turanoglu and Gokay Akkaya, "A new hybrid heuristic algorithm based on bacterial foraging optimization for the dynamic facility layout problem," Expert Systems with Applications, vol. 98, pp. 93–104, 2018, doi: 10.1016/j.eswa. 2018.01.011.

[20] Anitha Vishnuvarthanan et al., "An automated hybrid approach using clustering and nature inspired optimization technique for improved tumor and tissue segmentation in magnetic resonance brain images," Applied Soft Computing, vol. 57, pp. 399–426, 2017, doi: 10.1016/j.asoc.2017.04.023.

[21] N. Sanyal, A. Chatterjee and S. Munshi, "Bacterial foraging optimization algorithm with varying population for entropy maximization based image segmentation," *Proceedings of The 2014 International Conference on Control, Instrumentation, Energy and Communication (CIEC)*, Calcutta, 2014, pp. 641-645, doi: 10.1109/CIEC.2014.6959168.

[22] Yongsheng Pan et al., "Cell image segmentation using bacterial foraging optimization," Applied Soft Computing, vol. 58, pp. 770–782, 2017, doi: 10.1016/j.asoc.2017.05.019.

[23] Y. Liu, K. Hu, Y. Zhu and H. Chen, "Color image segmentation using multilevel thresholding-cooperative bacterial foraging algorithm," *2015 IEEE International Conference on Cyber Technology in Automation, Control, and Intelligent Systems (CYBER)*, Shenyang, 2015, pp. 181-185. doi: 10.1109/CYBER.2015.7287931.

[24] Anitha Vishnuvarthanan et al., "Development of a combinational framework to concurrently perform tissue segmentation and tumor identification in T1 - W, T2 - W, FLAIR and MPR type magnetic resonance brain images," Expert Systems With Applications, vol. 95, pp. 280–311, 2018, doi: 10.1016/j.eswa.2017.11.040.

[25] P. D. Sathya and R. Kayalvizhi, "Image segmentation using minimum cross entropy and bacterial foraging optimization algorithm," *2011 International Conference on Emerging Trends in Electrical and Computer Technology*, Nagercoil, 2011, pp. 500-506, doi: 10.1109/ICETECT.2011.5760167.

[26] Jyotika Pruthi et al., "Metaheuristic Techniques for Detection of Optic Disc in Retinal Fundus Images," 3D Res, vol. 9 (47), 2018, doi: 10.1007/s13319-018-0198-3.

[27] Anitha Narayanan et al., "Multi-channeled MR brain image segmentation: A novel double optimization approach combined with clustering technique for tumor identification and tissue segmentation," Bio cybernetics and Bio medical Engineering, 2018, doi: 10.1016/j.bbe.2018.12.003.

[28] Mohamad Amin Bakhshali and Mousa Shamsi,, "Segmentation of color lip images by optimal thresholding using bacterial foraging optimization (BFO)," Journal of Computational Science, vol. 5, pp. 251–257, 2014, doi: 10.1016/j.jocs.2013.07.001.

[29] A. Sasithradevi and N. N. Singh, "Synergy of adaptive bacterial foraging algorithm and Particle Swarm Optimization algorithm for image segmentation," *2014 International Conference on Circuits, Power and Computing Technologies [ICCPCT-2014]*, Nagercoil, 2014, pp. 1503-1506, doi: 10.1109/ICCPCT.2014.7054778.

[30] Hong Wang and Ben Niu, "A novel bacterial algorithm with randomness control for feature selection in classification," Neurocomputing, vol. 228, pp. 176–186, 2017, doi: 10.1016/j.neucom.2016.09.078.

[31] Siddharth Singh Chouhan, U. P. Singh, & S. Jain, "Applications of Computer Vision in Plant Pathology: A Survey," Arch Computat Methods Eng (2019). doi:10.1007/s11831-019-09324-0.

[32] U. P. Singh, S. S. Chouhan, S. Jain and S. Jain, "Multilayer Convolution Neural Network for the Classification of Mango Leaves Infected by Anthracnose Disease," *IEEE Access*, vol. 7, pp. 43721-43729, 2019. doi: 10.1109/ACCESS. 2019.2907383.

Proceedings of the Fourth International Conference on Communication and Electronics Systems (ICCES 2019)
IEEE Conference Record # 45898; IEEE Xplore ISBN: 978-1-7281-1261-9

Optimization of Advanced Encryption Standard Algorithm (AES) on Field Programmable Gate Array (FPGA)

Mr. Neelesh Jain
Deptt. of Electronics and Instrumentation Engg.
Shri G.S. Institute of Technology & Science
Indore, India
Email : jainneelesh608@gmail.com

Associate Professor : Mr. D. S. Ajnar
Deptt. of Electronics and Instrumentation Engg.
Shri G.S. Institute of Technology & Science
Indore, India
Email : ajnards@gmail.com

Associate Professor : Mr. P. K. Jain
Deptt. of Electronics and Instrumentation Engg.
Shri G. S. Institute of Technology & Science
Indore, India
Email : jainpramod1@gmail.com

***Abstract*— In this paper, we have proposed high speed Advanced Encryption Standard (AES) hardware architecture by using parallelism in the process. National Institute of Standards and Technology (NIST) cases are predefined inside the module will be selected by test case bits, according to test case bit selection, the key and input will be selected, and module generate corresponding output and clock cycles reduces to 44 cycles. AES Algorithm synthesized using VHDL Code and targeted into FPGA. For Synthesis and Simulation Xilinx Design Suit Version 14.7 is used. The design has been Successfully tested on ARTIX-7 FPGA.**

Keywords*— NIST, AES, VHDL, FPGA, ARTIX-7.

I. INTRODUCTION

The Advanced Encryption Standard (AES) is an authorized cryptographic algorithm which can be used to secure delicate digital information that are sensitive. AES algorithm has used for Encryption and Decryption of information. The algorithm is designed to use 128, 192, 256-bit cryptographic keys to encryption and decryption information. Before AES, the Data Encryption Standard (DES) was standard for encryption [1]. The innovative way to implement algorithm on hardware speed and resource utilization has been main concern to researchers for implementing AES design. This structure includes a looping method with 128-bit block and key size. The AES algorithm implemented using VHDL coding in Xilinx 9.2 [2], throughput reaches in this implementation up to the value of 352 Mbit/sec for both encryption and decryption process with device XCV600 of Xilinx Virtex family. Another model has been coded in Verilog and synthesized on Quartus 9.0 (Model Sim) has latency of encryption and decryption process is 51 clock cycles each, throughput reaches to 1054 Mbit/sec and 615 Mbit/sec for respective process [3].

An implementation of high-speed algorithm based on FPGA; to improve the safety of data in transmission the design used parallel processing and pipelining approach, this design targeted on VIRTEX-5 FPGA [4]. The design shows the efficient use of inter-round and intra-round pipeline [5]. The architecture not store round keys and currently calculated accordance that AES algorithm used, this design is made to reduce hardware structure and used where low throughput is required [6]. A design has been implemented on Xilinx Spartan-3 FPGA and decrypts on PC, VHDL code synthesized by using Xilinx 8.2, uses 1403 slices and operates at 2059 Mbps (throughput) [7].

In proposed work, we are using Encryption block, Decryption block and clock generating block to simulate, synthesize and implement the architecture. Clock generation block generates limited number of clock cycle to operate overall architecture and it reduces latching problem in design. The architecture uses pipeline methodology and parallel processing to reduce time cycle.

The generic design and modified design are tested with NIST cases by comparing the result we can say that the design modification not affect the behavior of the architecture. This design is simulated and synthesized on Xilinx platform and implementation on Artix-7 platform.

II. PROPOSED DESIGN ARCHITECTURE

In proposed Design, Fig.1 shows the design of AES Block which contains 128-bit registers, Mux's, Flip-flop and counter, all these digital circuits have respective uses. The final output that of 8-bit LSB of 128 bits displaying in FPGA. Fig.2,3,4 and 5 are submodules of AES Block. Fig.2 describes the clock, how to generate in proposed design. Fig.3 is basis block of Encryption that have inputs and outputs have describes in submodules section. Fig. 4 shows Encryption process in AES, how these four operations (sub bytes, shift rows, mix column and add round key) performs in AES. Fig. 5 basic block of Decryption, encrypted output is decrypted. Fig. 7 shows decryption process.

The AES-128 module consists of clock generator circuit, encryption block, decryption block and key expansion block. The overall inputs to module are clock, reset, test cases (T2, T1, T0) and output are operation_done.

In this module NIST cases are predefined in registers and selected with the help of test cases (T2, T1, T0) through MUX logic. In a test case selection, accordingly data and key are selected and pass to the data and key register respectively. Data Register available to the Encryption block and Key Register available to Key Expansion block. Firstly, process start with reset pulse to reset the block and initial mode (00) is set after the AES_START is high which start clock generator to synchronize the module and with initial mode (00) key expansion process start, it expands key to ten unique key

which are used for encryption and decryption process. When the process has completed, it has indicated by OPERATION DONE pulse and mode change to 01 with the pulse. Encryption process start with mode (01), use data and key as input and process them for ten rounds to generate output (cipher data). When the process has completed, OPERATION DONE pulse is high and mode change to 10 with the pulse. Decryption process start with mode (10), encrypted data and key given as input and generate output. When the process has completed, OPERATION DONE pulse is high. At the last, decrypted last 8 bit shown in the FPGA LED's.

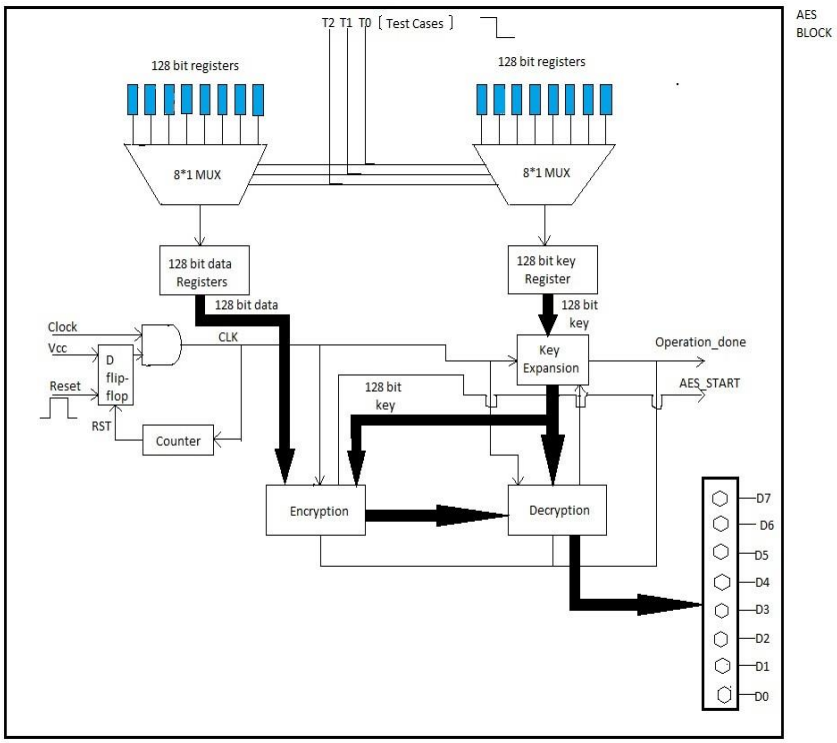

Fig. 1 – Design Architecture of Module

Above Designed Architecture to test the Encryption and Decryption module on one test bed with clock synchronization. After the modules perform Encryption and Decryption, the LSB bits (8 bits) of 128 plain text displayed on the FPGA board, to check authenticity of the architecture.

III. SUB MODULES OF ARCHITECTURE

1) *Clock Generator Circuit* :-

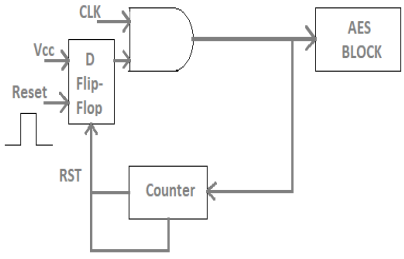

Fig.2 - Clock Generator

This circuit contains D flip-flop, AND gate and Counter. When RESET pulse high it works as Clock to D flip-flop and Set the output of flip-flop. The output of flip-flop is one of the inputs of AND gate and it allows to pass the Clock to AES Block and start the Counter. When the Counter reaches the set count it generates RESET pulse (RST) to reset the counter and flip-flop, it reset the output of flip-flop and clock to AES Block terminated.

2) *Encryption Block: -*

Number of rounds in AES process which depends on length of Key, for Key Length of 128 bit, rounds are to be 10. Key Length defined in Bytes. Using Rijndael's Key Schedule each round has separate key which is derived from Cipher Key.

In Encryption Block, Plain Text (data) and Key are given Inputs according to Control Signal. At time, when Key Load is active, Key Expansion block start processing the Key and generates Keys for 10 rounds of processing. Start

signal start the Encryption Process with synchronization of system clk

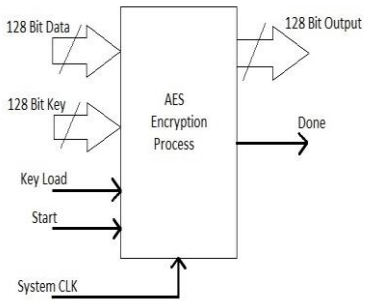

Fig.3 – Encryption Block

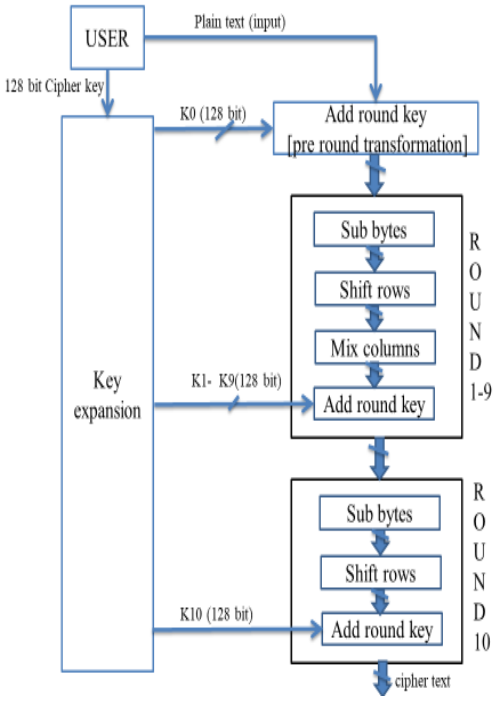

Fig.4 – Encryption Process

First Nine rounds of Encryption Algorithm consist of the following steps:

a) Add Round Key
b) Sub Byte
c) Shift Row
d) Mix Column

Tenth round of process does not have the Mix Column operation. According to Key Length Encryption Process performed by doing appropriate number of rounds.

Encryption Process run parallelly with Key Expansion block and Key Expansion block gives the current stage key to encryption block in synchronization with clk.

3) Decryption Block: -

In Decryption block, encrypted text and key are given as inputs according to control signal. When key load signal active, the Key Expansion block start processing the key and generate keys for 10 rounds of processing and start signal start the decryption process in synchronization with system clk.

There are four different operations are used in AES, out of these one is permutation and three are substitution.

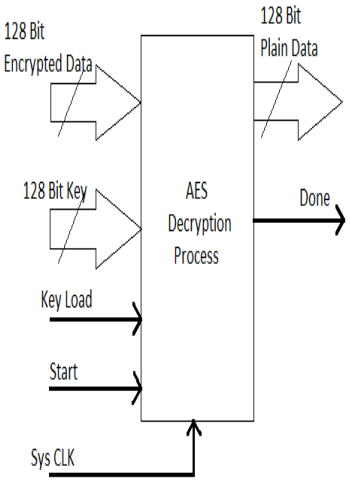

Fig.5 – Decryption Block

128-bit encrypted data and 128-bit key are inputs to decryption block, a part of that start and key load signals uses as inputs, system clock to run the overall process and timing utilization. 128-bit plain data are expected output and signal done uses as a output to complete the decryption. AES Decryption process block describes overall process in next section.

Decryption Process follows the same stages in reverse order.
The first nine rounds of Decryption Process consist of following steps:
a) Inverse Sub Bytes.
b) Inverse Shift Rows.
c) Inverse Mix Columns.
d) Inverse Add Round Key.

Tenth round does not have Inverse Mix Column Operation.

The Decryption Process run parallelly with Key Expansion block and key expansion block gives the current key to decryption block in synchronization with system clk.

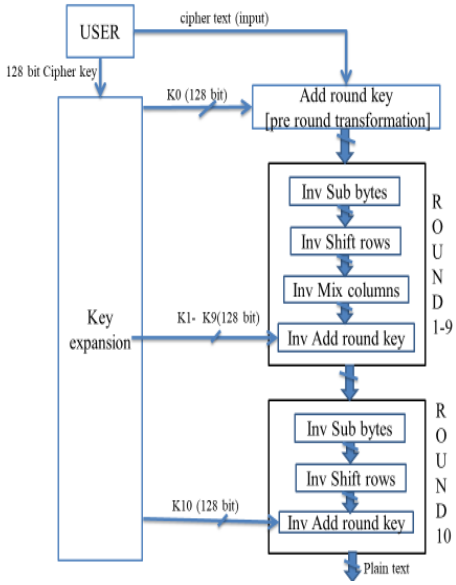

Fig.6 – Decryption Process

IV. RESULTS

FPGA Simulation results show the similarity between analysis and hardware representation. the details of Xilinx tools used tabulated below:

Family	Artix7
Device	XC7A100T
Package	CSG324
Synthesis Tool	XST (Verilog/VHDL)
Simulator	ISim (Verilog/VHDL)
Preferred Language	VHDL

Table 1 – Xilinx Tools Used

The Parallelism used in the architecture is such that the Key Expansion and Encryption block is operated in parallel with the delay of one clock cycle. Latency of Encryption and Decryption 51 clock cycle [3]. In new architecture, the latency comes down to 44 clock cycle

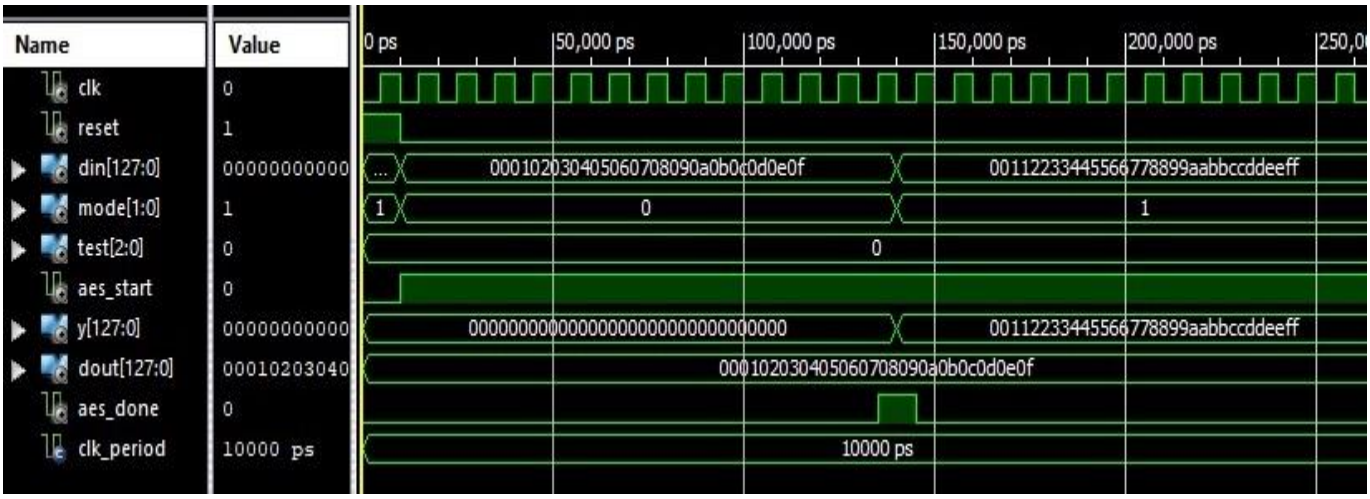

Fig.7 – Simulation Waveform of AES BLOCK

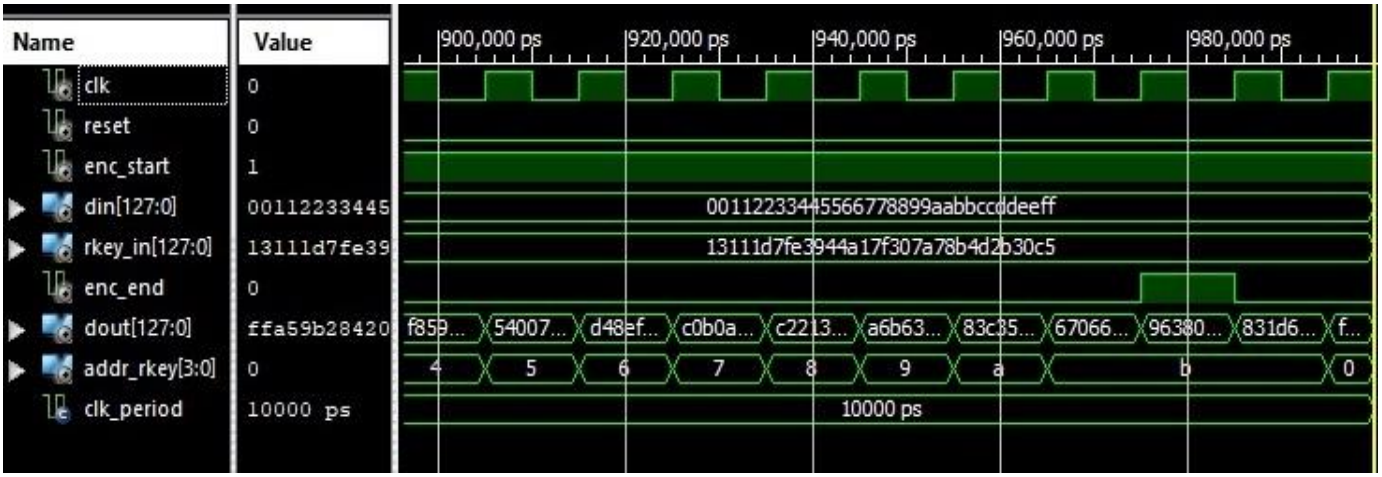

Fig.8 – Simulation Waveform of Encryption Block

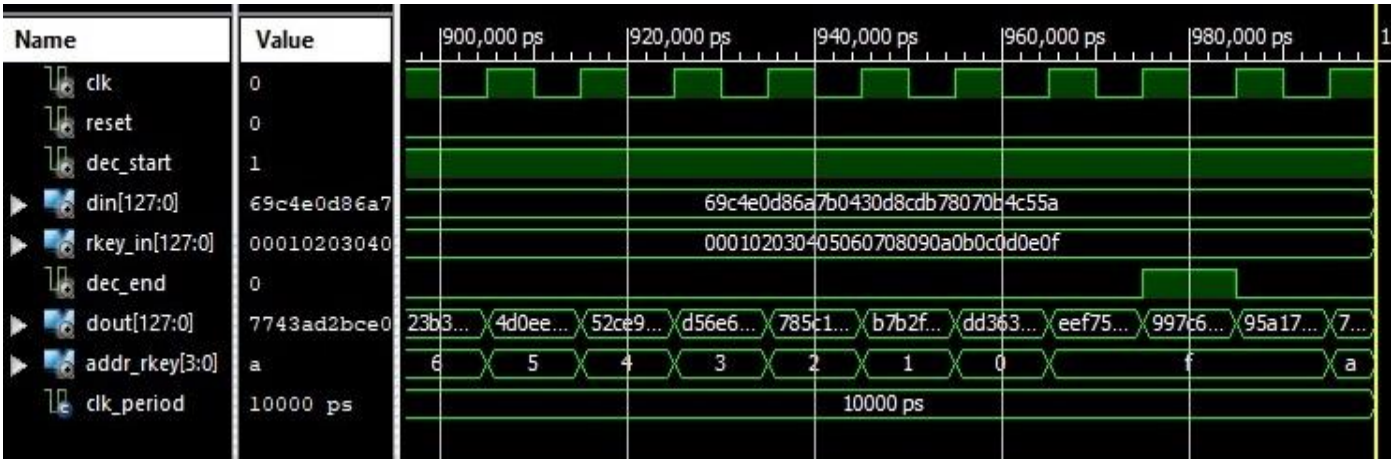

Fig.9 – Simulation Waveform of Decryption Block

Target Device: XC7A100T-3-CSG324 (ARTIX-7)
Timing Summary:

Speed Grade: -3

Minimum period: 3.659ns (Maximum Frequency: 273.289MHz)
Minimum input arrival time before clock: 4.431ns
Maximum output required time after clock: 0.668

Logic Utilization	Used Resources	Available Resources	Resource Utilization
Number of Slice Registers	811	126800	0%
Number of Slice LUT's	2814	63400	4%
Number of fully used LUT- FF pairs	718	2907	24%
Number of bonded IOB's	135	210	64%
Number of Block RAM/FIFO	2	135	1%
Number of BUFG/BUFGCTRLs	2	32	2%

Table.2 - Device utilization summary (ARTIX-7)

V. CONCLUSION

This design of AES – 128 Algorithm is Simulated and Synthesized by XILINX – ISE Software and got the expected results. This design is tested with ARTIX-7 board and device utilization summary shows maximum resources utilization, clock cycles reduces to 44, achievable frequency 273.289MHz. The main objective of paper is to reduces the clock cycles used by generic algorithm and efficient utilization of memory. In future, this algorithm can be further analyzed to make it faster by reducing clock cycles and make it more effective.

VI. REFERENCES

[1] National Institute of Standards and Technology (NIST), Data Encryption Standard (DES), National Technical Information Service, Sprinfgield, VA 22161, Oct. 1999.
[2] Atul M. Borkar, R.V. Kshirsagar, M.V. Vyawahare (2011) "FPGA Implementation of AES Algorithm", IEEE 978-1-4244-8679-3/11.
[3] Hong Tang and Nguyen van (2012), "An Efficient FPGA Implementation of Advanced Encryption Standard Algorithm" IEEE 978-1-4673-0309-5/12.
[4] WANG Wei, CHEN Jie, XU Fie (2012), "An Implementation of AES Algorithm based on FPGA", IEEE 978-1-4673-0024-7/10.
[5] Ankita Nampalliwar, Sheeja Suresh (2014), "Design and Implementation of AES Algorithm using FPGA', ISSN 2321-7782.
[6] Yang Jun, Ding Jun, Li Na, Guo Yixion (2010), "FPGA based Design and Implementation of reduced AES Algorithm", IEEE 978-0-7695-3972-0/10.
[7] Yewale Minal J, M.A. Sayyad (2014), "Implementation of AES on FPGA" IOSR Journal of VLSI and Signal Processing (IOSR-JVSP) Volume 4, Issue 5, Ver. II (Sep-Oct.2014), PP 65-69, e-ISSN:2319-4200, p-ISSN No.: 2319-4197.
[8] Advanced Encryption Standard (AES), Nov.26, 2001.
[9] FIPS 197, "Advanced Encryption Standard (AES)", http://csrc.nist.gov/publications.
[10] J. Daemen and V. Rijmen, "AES Proposal: Rijndael", AES Algorithm Submission, September3, 1999.
[11] Zabina Kouser, Manish Singhal, Amit M. Joshi (2016) "FPGA Implementation of Advanced Encryption Standard Algorithm", IEEE 978-1-5090-2807-8/16.
[12] Sumedh H. Nagdeve, Ujwala S. Ghodeswar (2015), "Synthesis of Advanced Encryption Standards Xilinx 13.4", IEEE 978-1-4799-8081-9/15.
[13] Amit Kumar, Manoj kumar, P. Balramudu (2017), "Implementation of AES algorithm using VHDL", IEEE 978-1-5090-4890-8/17.
[14] Soufiane Oukili, Seddik Bri (2017), "High speed efficient Advanced Encryption Standard implementation", IEEE 978-1-5090-4260-9/17.

Proceedings of the Fourth International Conference on Communication and Electronics Systems (ICCES 2019)
IEEE Conference Record # 45898; IEEE Xplore ISBN: 978-1-7281-1261-9

A Proposal of smart hospital management using hybrid Cloud, IoT, ML, and AI

Naveen Ananda Kumar J,
Institute of management,
Christ (Deemed to be University), Bengaluru,
India
jnaveens@icloud.com

Shivani Suresh,
Institute of management,
Christ (Deemed to be University), Bengaluru,
India
shivanisuresh109@gmail.com

***Abstract*- There has been a rapid shift in the medical industry from the service point of view. More importance is being given to patient care and customer satisfaction than ever before. The need to keep the customers happy with the hospital's service has increased rapidly and one way they can improve a patient's experience, even more is if they integrate cloud, IoT, ML, and AI into their system. This would help the medical sector to achieve customization which would enable them to address the needs of their customers more efficiently and offering personalized solutions. In this paper, we are proposing a novel model which focuses on a smart hospital information management system that runs by using hybrid cloud, IoT, ML, and AI. This system would be beneficial not only from the hospitals perspective but also from the patient's side as well. Patients and doctors unique ID would make the entire process a lot more efficient and easier. The advances happening in the field of AI and ML due to cloud-based computing is extremely beneficial for the medical industry. By integrating these components along with IoT it is possible for multi-specialty hospitals and super specialty hospital to be able to set up a smart hospital information management system.**

***Index Terms*-Hybrid cloud, Internet of things (IoT), machine learning (ML), Artificial Intelligence (AI).**

I. INTRODUCTION

The boom of the IT sector has revolutionized the face of the entire industry ranging from retail to even our homes. The focus of this paper is on the medical field which is one of the prime sectors that transformed immensely after the implementation. With the dynamic and complex changes happening in the field of medicine it is extremely difficult to operate a multi-specialty hospital and super specialty hospital without a proper management system. Most hospitals in today's era are equipped with a hospital information system or HIS which helps it to manage the functioning of the hospital. This web-based system helps them to make the whole process paperless by integrating the data regarding the patients, staff, doctors, administrative detail, etc to one software.[1]

At present there are several hospital information systems available in the market however most of them are focused on the day to day functionality of the hospital.[2] These systems need to be updated to be more streamlined, reduce duplicate tests or procedure and automate the manual process.[3] This can be achieved with the help of our proposed system where the hybrid cloud-based system would help to link the public cloud which contains information regarding their patients to the private cloud i.e. the hospitals on-premises cloud server. This system would help the patients to have their medical records available in unique ID and as a result, reduce time-lag in providing previous records to physicians and the physicians will also be able to identify the possible problem the patient is facing faster and appropriate treatment can be given.[4]

The aim of this paper is to propose a smart hospital management system which is self-sufficient and acts as an assistant to both the administration and the patients with the help of the hybrid cloud, IoT, ML, and AI.[5] This system would focus on personalization and systemizing the entire process with the help of smart assist and unique ID of both the patient and doctor. There have been numerous attempts at setting up cloud-based systems and is being used by several hospitals at present. However, most of these systems are not being used to its maximum potential mainly because they haven't integrated AI along with IoT and used ML for furthering its scope. With the help of AI and hybrid cloud, they would be able to automize the entire administrative and management side of the hospital.[6]

It has become quite common nowadays to see doctors with hand held display devices like tablets and iPad containing patient information and treatment.[7] The data collected on these handheld devices are scattered and as a result incompatible however if this vast amount of data is combined and collected through these devices data can be cleaned and processed with AI and hybrid cloud. The system would automatically be able to detect the cleaning and filtering to be done once algorithms for machine learning are applied as well.[8] This way hospitals would be able to have access to a large database which would help them and the patients in numerous ways.[9] Mainly it will help to detect prevalent diseases in the community, virology status, and treatments for the same by using the database for running various tests and experiments.[10]

II.PRESENT SCENARIO AND RESEARCH GAP

The present scenario of this sector only focuses on the secure exchange of health information between the hospital, insurance providers and the patient.[11]

Electronic health records are starting to be viewed as an effective tool to improve safety, quality and organized health delivery system.

- Without the help of a hybrid cloud system, it is hard to expand access to healthcare in an affordable manner. [12]
- By implementing this system hospitals will be able to reduce overall healthcare cost and increase administrative efficiency.
- With the penetration rate for clouds increasing in this sector the scope is widening. Telemedicine is catching up in the market soon and this proposed model would make it, even more, user-friendly.[13]
- The volumes of data generated would be useful to have real-time figures to identify the medical challenges faced by the country as a whole.[14]
- Public cloud would prove to be a major boon to the healthcare sector. Being able to combine data from hospitals, insurance providers and other sources would make national health data readily available to carry out various analysis. [15]
- The major benefit of this system is it would help to reduce the number of medical errors and increase accuracy and productivity with the help of the unique IDs of the patients and it would also facilities to reduce the overall procedural correctness. [16]
- The proposed model focuses on these problems which can be tackled with the help of effective integration of hybrid cloud, IoT, ML, and AI.

III.PROPOSED MODEL

The proposed model is equipped with the following features- patients would be able to schedule appointments with respect to the availability of the physician, view the physicians performance rating, read previous reviews, and the physician, in turn, would be able to prescribe medicines to their patients with the help of medical inventory management, use smart assistance for analyzing test results, go through the previous medical records of the patient for a more accurate problem detection, suggest treatment plans and prescription assistance. (Fig 1.1) This has been explained in detail below:

A. Patient unique Medical ID

Each patient will be assigned to his or her own unique medical ID. This ID would comprise of the patients sleeping patterns, workout schedule, and other basic health data which would be made available through the patient's smartphones and their smart wearable devices. This would also give insights into the patient's previous doctor's prescription, appointments, diagnosis, test results, allergies and also the updated changes get automatically stored into the ID.

B. Doctor ID

Just like how every patient is assigned with a unique ID the doctors would be assigned with the same as well. Each doctor would hold a unique ID based on which a time schedule can be made which would be in accordance with the appointments being scheduled. This helps to ensure that both the doctor and the patients time is utilized effectively. The doctor's ID would also comprise of the doctor's performance records, reviews by previous patients and ratings given on the bases of the performance by both the hospital and the patients. This would give enough information to the patient in order to make the booking.

C. Scheduling and appointments

The system would go through the patient's schedule in their smartphone to check for an available date/ time slot and for the doctor it would go through the system on the bases of this recommendations would be given. The most feasible solution for both the doctor and the patient would be scheduled finally. This would ensure that the doctor is available and the patient is also free as a result leading in no clashes of schedule.

Being able to schedule and book appointments would become an easy task for both the hospital and the patients. Patients would be able to view the doctor's schedule and based on a convenient time slot for both of them and will be able to book it accordingly. If the patient is coming for a follow-up or for continuing his treatment then the patient can book an appointment or the doctor can do the same on behalf of the patient. In case the patient is up for an ultrasound scan, X-ray or a simple procedure the patient or the doctor can book the required room in accordance with the availability and the doctor's preference.

If the patient has to be hospitalized then he can check for the availability of the beds and book it online. This can be achieved by computerizing the entire scheduling system. Al and ML will help to obtain the calendar or schedule data from the patient's smartphone and cross verify with the doctor's schedule. Once this is being done it would be able and identify a slot which is comfortable for both the patient and in sync with the availability of the doctor.

D. Medical Inventory management

Smart medicine dispensers are used to get the medication prescribed by the doctor. The patients can get the medicines by entering their unique ID into the dispenser which would then vend out the medicine by identifying the ID and linking it to the prescription given by the physician. Doctors would be able to check the availability in real time if it is not available AI would provide recommendation for alternate medications and would also notify the Inventory management team with respect to the shortage. On the bases of the operation or procedure scheduled, AI will check the inventory to ensure that the required supplies and medicines are available if not an alert will be given order can be placed accordingly. It would usually done on a particular time. This would help to reduce the inventory cost exponentially.

E. Smart assistance for test results

X-ray, scan, EEG, MRI and other tests or diagnosis results are automatically saved in the private hybrid cloud of the hospital and in the patient's unique medical ID. The saved X-rays, scanned copies are then analyzed by trained AI and ML algorithms and sent to the physicians to check. The thorough analysis done by both the machine and the

doctor reduces errors in problem detection. This acts as an assistant to the doctor and helps to diagnose and rectify the problem faster.

F. Treatment and Prescription assistance

On the bases of the analysis of the test, AI will assist in detecting the possible problem in the body. After identifying the problem, it will give recommendations for treatment and medicine prescription for the doctor. The doctor can then choose the best treatment to go ahead with based on the pros and cons. On the bases of option that the doctor selects from the recommendation being given by AI, the system with the help of ML will learn which recommendations should be made for a particular treatment and as a result will be able to give more accurate and precise treatment and prescriptions.

G. Working process

The smart hospital systems operations start from the patient using his or her medical ID to schedule an appointment. This step involves the doctor's unique ID and the patient's unique ID getting connected to the network. An appropriate time slot by checking the patient's calendar in his smartphone and the doctor's availability would be selected and the appointment booked. Figure 1.2 explains the working process.

The doctor would be able to access the patient's past medical records and his basic medical information through the patient's medical ID. This would be available through the hybrid cloud server which would contain the public cloud with AI and ML-based algorithms and the private cloud which is the hospital's database management.

After the patient meets the doctor the entire process of disease identification and treatment is made easy with the help of the diagnosis assistant. This would help the doctor in analyzing the results from the various test reports obtained. With the smart assistant, the doctor would be able to run problem diagnosis far more easily and be able to detect the cause and provide a cure to the patient in no time.

The inventory management system would let the doctor know more about the availability and suitability of the medicines and based on that would provide an apt treatment method or prescription. The availability of medicines gets updated in real-time with the help of IoT and in-built sensors. This would help to maintain the required levels of stock by the hospital.

- *Example*

John a 29-year-old male has been frequently experiencing sharp and sudden abdominal pains recently and decided to do a check-up with XYZ hospital. He booked an appointment with the hospitals app and registered in it by linking his medical ID which is available on his phone and contains basic information about his health and his past records.

After going to the hospital for his appointment he gets assigned to a particular doctor and is given a unique patient ID which gets linked to the doctor's unique ID. Once John meets the doctor, he lists out the various symptoms he has been feeling. When the John is informing the doctor, the issues being faced by him the handheld device by the doctor will record and take the voice note to analyze the problems by identifying the keywords with the help of AI and ML.

This would give the doctor a series of a checklist which would enable him to narrow down to a list of possibilities and schedule a series of tests to check if it could possibly be a kidney stone. An ultrasound is scheduled on the bases of Johns preference and AI along with ML will analyze and scan the results and update the system so that the doctor can finally confirm that it is a kidney stone.

The doctor would then analyze the data from Johns smartphone to find out that it was caused due to low consumption of water and food containing high levels of calcium. He checks with the medical inventory system to look for the medicines that can be prescribed and tells John he will book an appointment for a follow up check up to see if it is gone with the help of the medication if not a procedure can be done on the same day.

John gets the medication from the dispensers by entering his unique patient ID. Once he starts the dose, he starts feeling a lot of relief and goes for a follow-up to the doctor. The doctor informs him that

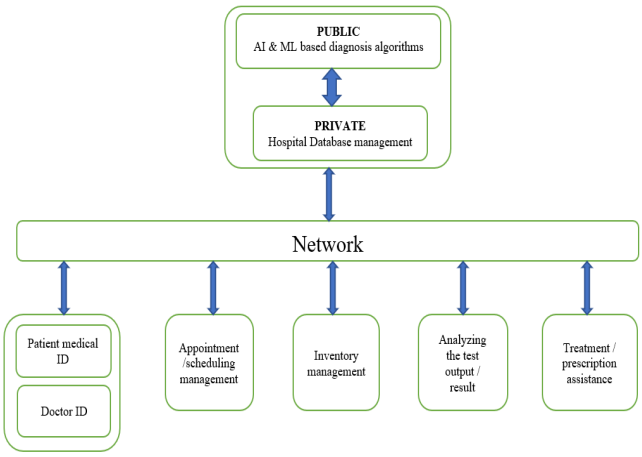

Fig 1.1 Architectural Block Diagram of Proposed system

the stone has dissolved due to the medication and he is much healthier now. After 5 years John is faced with stabbing pains again and this time he goes to a different hospital as he is out of the country. The new doctor uses Johns medical ID which was updated with the treatment he got in XYZ hospital for his kidney stone problem. The doctor is able to identify that the kidney stone has recurred and gives John the required treatment.

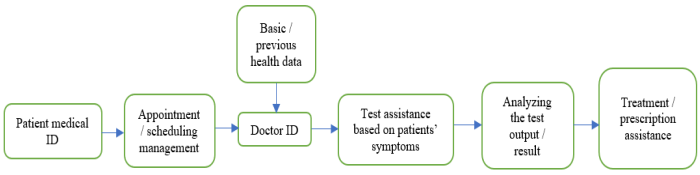

Fig 1.2 Process Flow Diagram

IV. FUTURE WORK

The implementation of this system would help to get access to large amounts of data with the help of this database AI would be able to develop an algorithm which would help to increase procedural correctness.[17] This would revolutionize the entire industry as it would help in the early detection of diseases and affordable and accurate treatment can be given. This system would help to reduce the waiting time for the test results of patients who would not have to wait for days to know the result of a particular test. It can be known just in few hours and as a result, very little time will be taken for providing a cure to the patients. In the long term this system would help to increase the efficiency of the hospital and its physicians, reduce manpower and time taken for various procedures as a result the operation cost would also decrease and would lead to automation of the entire hospital system.

V. CONCLUSION

The proposed model would change the face of healthcare IT by providing assistance to the entire hospital system by evolving its working by bringing in hybrid cloud, IoT, AI, and ML. These components when brought together would improve the entire working of hospitals. It would enable it to become more organized and efficient and focus on patient care and help to reduce the overall cost incurred by both hospitals and patients. By reducing the number of medical errors everyone would be benefited and this can be achieved with the help of this system. The diagnoses assistant would learn from the public pool made available through the hybrid cloud using ML. The system would reduce the waiting time for patients and as a result increase the number of patients treated per day. The system would eventually run on its own without manual support. In the long run, it is beneficial for both the hospital and the patient as well.

ACKNOWLEDGMENT

We thank our colleagues from the Institute of management, Christ (Deemed to be) University who provided us with insights which were a great assistance in shaping our research. We would like to express our gratitude to the faculties and colleagues of Institute of management, Christ (Deemed to be) University and Sunitha Devanand of KSMC Hospital, Riyadh for sharing their pearls of wisdom, reviewing our research and giving us key inputs.

REFERENCES

[1] Batalden, P. B., Davidoff, F., Aron, D., & Pogach, L. (n.d.). your houses ! ’’. https://doi.org/10.1136/qshc.2006.022046

[2] Archenaa, J., & Anita, E. A. M. (2015). A Survey Of Big Data Analytics in Healthcare and Government. *Procedia - Procedia Computer Science*, *50*, 408–413. https://doi.org/10.1016/j.procs.2015.04.021

[3] Raghupathi, W., & Raghupathi, V. (2014). Big data analytics in healthcare : promise and potential, 1–10.

[4] Thangaraj, M. (2015). Internet Of Things (IoT) Enabled Smart Autonomous Hospital Management System – A Real World Health Care Use Case with the Technology Drivers.

[5] Leijdekkers, P., Gay, V., & Barin, E. (2009). Trial Results of a Novel Cardiac Rhythm Management System using Smart Phones and wireless ECG Sensors.

[6] Gouaux, F., Adami, S., Arzi, M., Assanelli, D., Fayn, J., Forlini, M. C., … Erm, I. (n.d.). SMART DEVICES FOR THE EARLY DETECTION AND INTERPRETATION OF CARDIOLOGICAL SYNDROMES, 291–294.

[7] Sánchez, D., Tentori, M., & Favela, J. (n.d.). for the Smart Hospital.

[8] Huang, G. Q. (2011). No Room for Error: RFID-enabled Smart Point-of-Care Medication Process in Hospital Wards, 353–358.

[9] Of, N., & Of, N. (2010). W I R E L E S S T E C H N O L O G I E S F O R E-H E A LT H C A R E A COGNITIVE RADIO SYSTEM FOR E-H HEALTH APPLICATIONS IN A HOSPITAL E ENVIRONMENT D USIT N IYATO , N ANYANG T TECHNOLOGICAL UNIVERSITY, (February), 20–28.

[10] Alharbe, N., & Atkins, A. S. (2015). Use of Cloud Computing with Wireless Sensor Networks in an Internet of Things Environment for a Smart Hospital Network, (c), 52–58.

[11] Kim, S., Yoo, S. K., Kim, H., Bae, H., Park, J., Seo, K., & Chang, B. (2006). Smart Blood Bag Management System in a Hospital Environment, 506–517.

[12] Mauro, C., Sunyaev, A., Marco, J., Andreas, L., & Helmut, S. (2008). A Proposed Solution for Managing Doctor ’ s Smart Cards in Hospitals Using a Single Sign-On Central Architecture Health, 1–10.

[13] Abie, H. (2012). Risk-Based Adaptive Security for Smart IoT in eHealth, (SeTTIT), 269–275. https://doi.org/10.4108/icst.bodynets.2012.250235

[14] Chaczko, Z., & Singh, A. (2010). “ © 2010 IEEE. Personal use of this material is permitted. Permission from IEEE must be obtained for all other uses, in any current or future media, includingreprinting/republishing this material for advertising or promotional purposes, creating new collective works, for resale or redistribution to servers orlists, or reuse of any copyrighted component of this work in other works .” Smart Hospital Management System : An Integration of Enterprise Level Solutions Utilising Open Group Architecture Framework (TOGAF).

[15] Luschi, A., Belardinelli, A., Marzi, L., Frosini, F., Miniati, R., & Iadanza, E. (2014). Careggi Smart Hospital : a mobile app for patients, citizens and healthcare staff, 125–128.

[16] Catarinucci, L., Donno, D. De, Mainetti, L., Palano, L., Patrono, L., Laura, M., & Tarricone, L. (2015). An IoT - Aware Architecture for Smart Healthcare Systems, *4662*(c), 1–12. https://doi.org/10.1109/JIOT.2015.2417684

[17] Lymberis, A., & Olsson, S. (2003). ANDREAS LYMBERIS, Ph.D., and SILAS OLSSON, M.Sc., *9*(4).

Proceedings of the Fourth International Conference on Communication and Electronics Systems (ICCES 2019)
IEEE Conference Record # 45898; IEEE Xplore ISBN: 978-1-7281-1261-9

Dual Band Monopole Antenna with a Stepped Ground Plane

Sooraj Muralidharan and *Sreedevi K. Menon
Department of Electronics and Communication Engineering,
Amrita Vishwa Vidyapeetham, Amritapuri, India
*sreedevikmenon@am.amrita.edu

***Abstract*— The paper presents a dual band monopole antenna with a defected ground plane for Wi-Fi and WLAN applications. The defect is introduced as a step in the ground plane. Initially, a single band monopole antenna is designed. This is antenna is modified with the step defect to provide dual band characteristics. The depth and width of the defect decides the second band of operation for a given monopole length. The optimized antenna in ANSYS HFSS is fabricated and tested and are in concurrence with each other.**

Keywords*— *dual band, defected ground plane, step ground plane, monopole antenna.

I. INTRODUCTION

Today, the world demand small, compact and low cost wireless systems for effective usage and utilization of resources. Antenna forms the most important part of a wireless communication system and to be integrated in wireless modules antenna has to be as compact and light weight as possible. Different type of antennas has been proposed and studied in the recent past for communication applications [1-9]. Among these, planar monopole antenna can ensure omnidirectional characteristics with compact structure. So these antennas find use in portable systems as they are light weight and can be easily manufactured [3-5].

In recent literature, lot of work has been done to implement dual band characteristics in monopole antennas. In a microstrip circular patch antenna dual band characteristics with monopole radiation pattern is achieved by the usage of double layer substrate. In this both the frequency bands have a gain better than 5 dBi and multiple periodic structures is also used in this antenna [6]. Inclusion of U-shaped metamaterials in a coplanar wave guide fed monopole antenna has also contributed to dual band characteristics [7]. Together with dual band characteristics a circular polarization is achieved for a self-complimentary antenna at Wi-Fi frequencies. This antenna provides an axial ratio better than 3 dB at both the bands [8]. Using the principle of stacking a monopole patch antenna for dual broad band has been designed and both the bands have gain better than 5dBi [9]. For MIMO system a dual band antenna has been designed using micro-metal mesh of conductive film and this also works at both WLAN/ Wi Fi frequencies and is very compact and use coplanar waveguide as feeding technique [10]. For wireless body area networks a dual band operation has been implemented using microstrip patch antenna and this antenna is also energized by CPW with a parasitic patch on the other side of the coplanar wave guide [11]. In the experimental investigation done in [12], enhanced gain with dual frequency characteristics is found by optimizing the parameters of ground plane and loop of monopole loop antenna.

This paper describes the design and of a dual band monopole antenna with a stepped ground for dual band operations. Simulations are done to analyze the effect of the dimensions of the step defect on the antenna characteristics. Using ANSYS HFSS. The optimized antenna is fabricated and the results are verified using Keysight Vector Network Analyzer (VNA).

II. PLANAR MONOPOLE ANTENNA DESIGN

Initially a microstrip line fed planar monopole antenna is designed as illustrated in Fig 1.

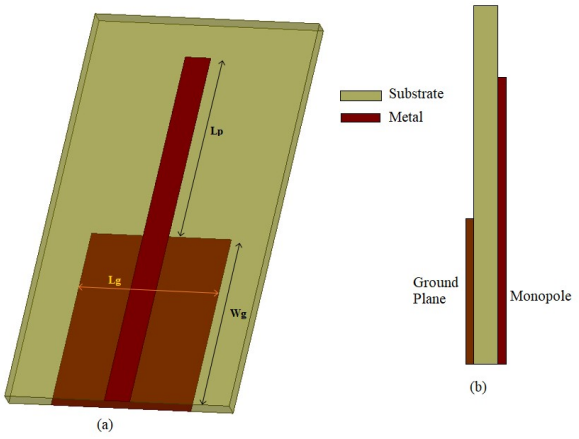

Fig.1. (a) Planar Monopole Antenna (b) cross-sectional view

When the dimensions of the antenna is taken such that the length (L_g) and width (W_g)of the ground plane is equal to the length of the monopole (L_p), the antenna offers a single band response and this is validated by simulation and the results are presented in Fig.2. The gain is found to ~ 2.4 dBi with more bandwidth at lower frequencies as presented in Table.1.

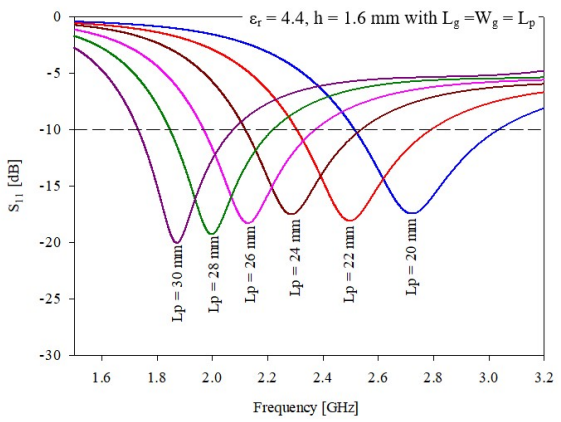

Fig.2. Variation of resonance frequency with monopole length, Lp

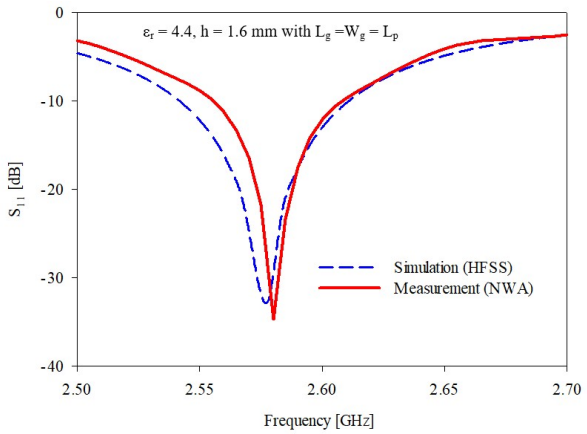

Fig.3 (a). Return Loss of the monopole antenna, Lp = 22mm

TABLE I. ANTENNA PERFORMANCE

Lp (mm)	$L_g = W_g = L_p$, $\varepsilon_r = 4.4$, h = 1.6 mm			
	Antenna Parameter			
	Frequency (GHz)	***Bandwidth (MHz)***	***Gain (dBi)***	***Radiation Pattern***
20	2.723	521	2.50	Omni – directional
22	2.503	491	2.45	
24	2.293	421	2.39	
26	2.132	411	2.41	
28	2.002	405	2.37	
30	1.872	341	2.36	

To aid the antenna to perform at Wi-Fi frequency length of the monopole L_p is taken as 22 mm for further studies. The reflection and radiation performance of this monopole is presented in Fig.3.

The ground plane of this monopole antenna is modified to provide the dual band operation by incorporating a step defect which is discussed in the next section.

III. DUAL BAND MONOPOLE ANTENNA

In the monopole operating at 2.5 GHz a step defect is introduced having a dimension, $Lg_2 \times Wg_2$. The geometry of the monopole with step defect is shown in Fig.4. In the design, Lg1 = Wg1 = Lp1 = 22mm to provide resonance at 2.5 GHz. Depending the defect dimension the second frequency can be tuned.

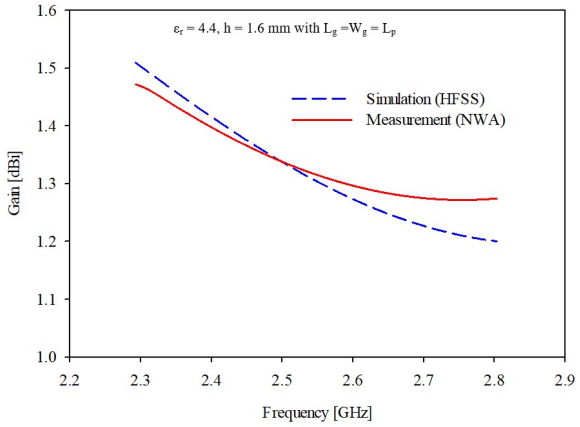

Fig.3 (b). Gain of the monopole antenna in the bandwidth of operation

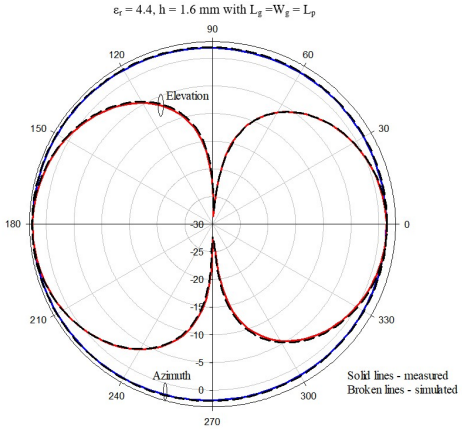

Fig.3 (c). Radiation Pattern of the monopole antenna at 2.503 GHz

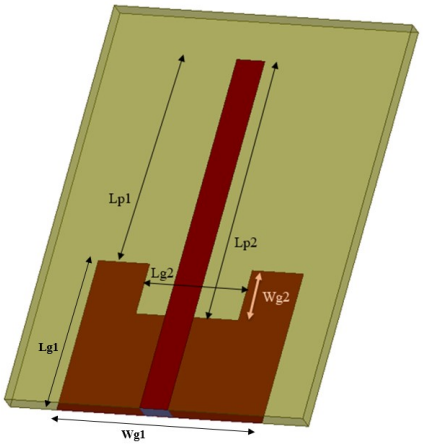

Fig.4 (a). Antenna with Defected ground plane

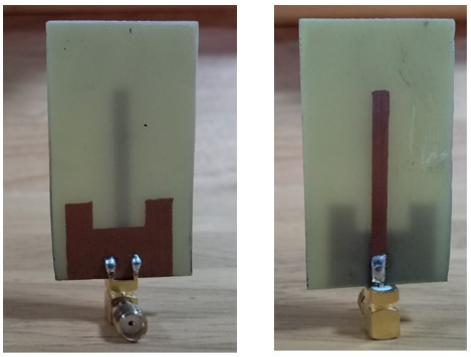

Fig.4 (b). Prototype of Planar Monopole Antenna with defected ground plane on FR4 epoxy

For the dual band performance, the defect dimension Lg2 × Wg2 is varied. The performance of the antenna based on this is presented in Fig.5.

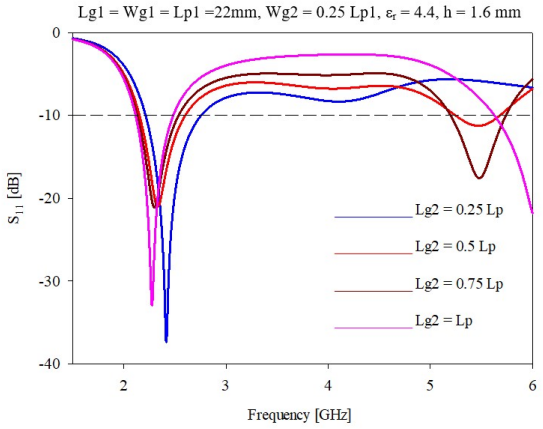

Fig.5 (a). Variation of return loss with length of the defect Lg2

For dual band performance, the defect dimension Lg2 has to be at least 0.5 Lp1 and when is same as Lp1 it is outside the band of interest. So the defect length lg2 is fixed as 0.75 Lp1. With this the depth of the defect Wg2 is optimized as 0.25Lp and the vibrational study is presented in Fig. 5(b).

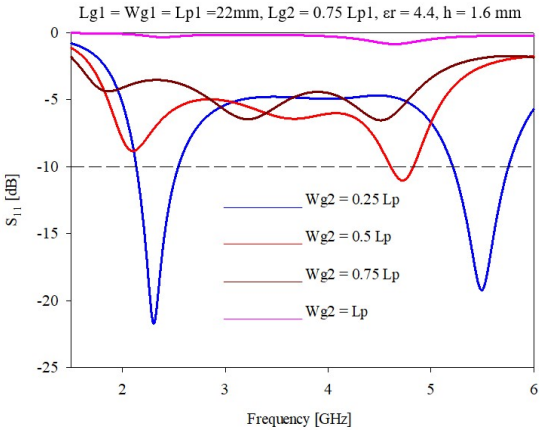

Fig.5 (b). Variation of return loss with length of the defect Wg2

The optimized defect dimension Lg2 × Wg2 is 0.75 Lp1 × 0.25 Lp1 for the dual band performance of the monopole antenna with Lp1 = 22mm. With these dimensions the antenna characteristics is analysed using ANSYS HFSS. A prototype of the optimised antenna is fabricated on FR4 epoxy as shown in Fig. 4 (b) and measured using Keysight E 5080 A Vector network Analyser. The simulated and measured results are presented as Fig.6. The defect shifts the first resonance to 2.36 GHz but 2.5 GHz is within the 2:1 VSWR bandwidth of the resonance.

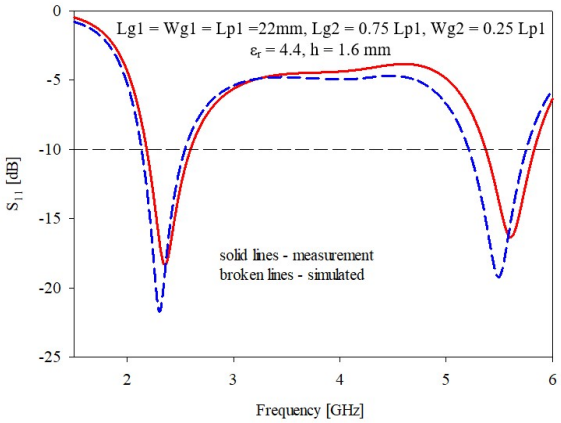

Fig.6. Variation of return loss with frequency

The simulated gain of the antenna is validated using two antenna method by measurement and is presented in Fig.7.

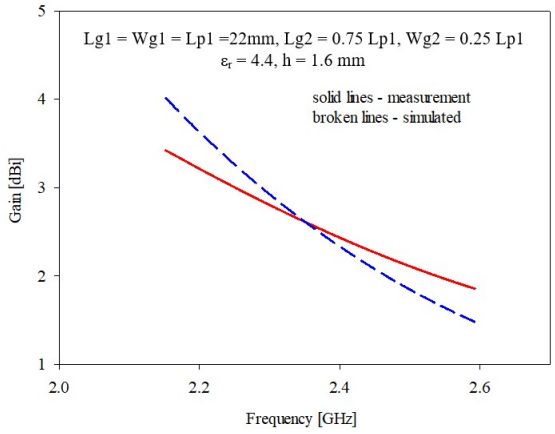

Fig.7 (a). Variation of gain with frequency at the first band

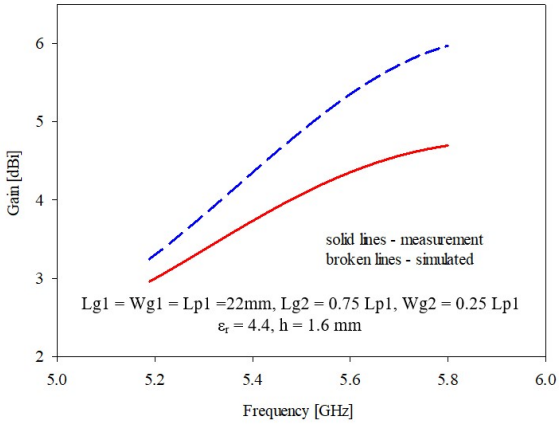

Fig.7 (b). Variation of gain with frequency at the second band

The measured and simulated radiation pattern of the antenna in the two principal planes is presented in Fig.8.

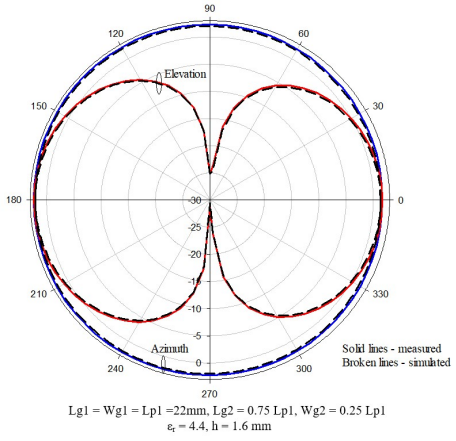

Fig.8 (a). Radiation Pattern at 2.36 GHz

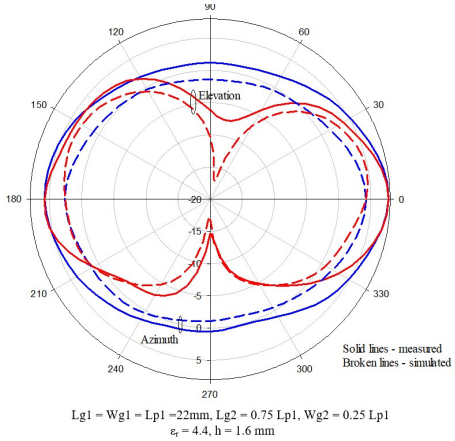

Fig.8 (b). Radiation Pattern at 5.6 GHz

The simulated and measured performance of the antenna is consolidated in Table.2. A comparison is done with the proposed antenna and that referred and is presented in Table.3.

TABLE II. DUAL BAND ANTENNA PERFORMANCE

Antenna Parameter	**Values obtained**	
	Measured	***Simulated***
First Frequency (GHz)	2.36	2.31
First Bandwidth (MHz)	410	400
Second Frequency (GHz)	5.6	5.51
Second Bandwidth (MHz)	450	520
Gain at 2.36 GHz (dBi)	2.54	2.56
Gain at 5.51 GHz (dBi)	4.13	4.97
Omni-directional in both bands		

TABLE III. PERFORMANCE OF DUAL BAND ANTENNAS COMPARED

Antenna	Frequency (GHz)	Gain (dBi)	Dimension (mm × mm × mm)
Proposed	**2.36** **5.6**	**2.54** **4.13**	**23 × 44.5 × 1.6**
Ref [4]	3.01 5.38	2.48 3.09	40 × 47 × 1.5
Ref [6]	4.01 5.24	5 5.5	84 × 84 × 1.5
Ref [7]	2.7 6.3	-1.8 -0.4	20 × 37 × 1.6
Ref [8]	2.4 5.4	Not mentioned	42 × 30 × 0.8
Ref [9]	2.415 5.525	5 6	130 × 130 × 3
Ref [10]	2.4 5.8	5 6	30 × 45 × 3.5

IV. CONCLUSION

The proposed monopole antenna exhibits dual band characteristics without the use of a dipole structure. The design is fully planar and consumes less area. The reduction in area further reduces the overall cost of the communication system. The antenna operates at the frequencies 2.45 GHz which is Wi-Fi operational frequency and at 5.45 GHz which is the WLAN operational frequency. The radiation pattern of the antenna is observed to be omnidirectional at both the frequencies making the antenna appropriate for wireless applications and portable systems.

REFERENCES

[1] M. V. Amrutha and Narayanan, B. S., “Low profile patch antenna on cement substrate for indoor applications”, in Proceedings of the 2017 International Conference on Wireless Communications, Signal Processing and Networking, WiSPNET 2017, 2018, vol. 2018-January, pp. 2508-2511.

[2] V. Arvind, Sowmiya, R., Vignesh, P., Kavin, S., and Jayakumar M., “Yagi Slot Antenna Based on Substrate Integrated Waveguide Cavity for Wider Bandwidth Applications”, Proceedings of 2016 International Conference on Advanced Communication Control and Computing Technologies, ICACCCT. pp. 303 - 307, 2017.

[3] Liu, Yu, et al. "A Planar Printed Nona-Band Loop-Monopole Reconfigurable Antenna for Mobile Handsets." IEEE Antennas and Wireless Propagation Letters 17.8 (2018): 1575-1579.

[4] Tan, Ming-Tao, and Bing-Zhong Wang. "A dual-band circularly polarized planar monopole antenna for WLAN/Wi-Fi applications." IEEE Antennas and Wireless Propagation Letters 15 (2016): 670-673.

[5] Abbasi, Muhammad Ali Babar, et al. "Compact EBG-backed planar monopole for BAN wearable applications." IEEE Transactions on Antennas and Propagation 65.2 (2017): 453-463.

[6] Xi-Wang Dai, Tao Zhou, and Guan-Feng Cui, “Dual-Band Microstrip Circular Patch Antenna with Monopolar Radiation Pattern,” IEEE Antennas and Wireless Propagation Letters, vol. 15, pp. 1004-1007, March 2016.

[7] Seyed Amir Hossein, and Zahra Atlasbaf, “Miniaturized Dual-Band CPW-Fed Antennas Loaded with U-shaped Metamaterials,” IEEE Antennas and Wireless Propagation Letters, vol. 14, pp. 658-661, March 2016.

[8] Weilong Liang, Yong-Chang Jiao, Yuchen Luan, and Chao Tian, “A Dual-Band Circularly Polarized Complementary Antenna,” IEEE Antennas and Wireless Propagation Letters, vol. 14, pp. 1153-1156, May 2015.

[9] Zhixi Liang, Juhua Liu, Yuanxin Li, and Yunliang Long, “A Dual-Frequency Broadband Design of Coupled-Fed Stacked Microstrip Monopolar Patch Antenna for WLAN Applications,” IEEE Antennas and Wireless Propagation Letters, vol. 15, pp. 1289-1292, April 2015.

[10] Jinpil Tak, Seungmin Woo, Jaekwang Kwon, and Jaehoon Choi, “Dual-Band Dual-Mode Patch Antenna for On-/Off-Body WBAN Communications,” IEEE Antennas and Wireless Propagation Letters, vol. 15, pp. 348-351, February 2016.

[11] L. Meenu, S. Aiswarya, and Sreedevi K. Menon, “Experimental Investigations on Monopole Loop Antenna with Dual-Band Characteristics,” IEEE WiSPNET Conference, pp. 636-639, 2017.

Proceedings of the Fourth International Conference on Communication and Electronics Systems (ICCES 2019)
IEEE Conference Record # 45898; IEEE Xplore ISBN: 978-1-7281-1261-9

Cooperative Hybrid Automatic Repeat Request Based on the Number of Retransmissions

Arpitha R, Chaithra B R and Usha Padma
Department of Telecommunication Engineering
RV College of Engineering
Bengaluru, India
arpithakotiyan@gmail.com

Abstract— **Cooperative communication has great potential to boost the wireless data rates by exploiting the antennas on wireless devices for spacial diversity. Since decode and forward (DF) approach eliminates noise accumulation problem, DF protocol is suitable for relay selection scheme. To improve the system performance turbo coding along with Hybrid Automatic Repeat Request (HARQ) technique is used where turbo coding adds redundant bits and HARQ minimizes the error rate in the system. The data is broadcasted over a Rayleigh fading channel. Maximal Ratio combining is used at the receiver to combine the information received from the source and the relay. If received data is found to be in error at the destination, then NACK is transmitted to the source. In this paper HARQ scheme for turbo coding is performed for different modulation order over Rayleigh channel in presence of Additive white Gaussian noise. The number of retransmissions required to clear total number of errors is calculated.**

Keywords— Cooperative communication, Decode and forward, Turbo coding, HARQ scheme, Maximal Ratio Combing.

I INTRODUCTION

The increasing number of users inspired intensive analysis in wireless communication. MIMO systems were introduced where multiple antennas were placed at the source and the destination. But usage of MIMO system in small nodes is proved to be a challenge and also it requires more number of resources.

In communication systems, wireless system is more often corrupted by the factors like fading and shadowing. In order to reduce the number of errors channel coding techniques are used. At the destination if the packet found to be in error, then retransmission is often requested by the destination. This scheme is termed as Automatic repeat request (ARQ) which ensures the low bit error rate [1]. But the efficiency of ARQ can be increased by reusing the data from the previous transmissions instead of simply discarding it. So, to improve efficiency of the system and also to reduce the number of errors, Hybrid automatic repeat request was introduced.

In order to address these challenges imposed by MIMO, Cooperative Communication concepts have been introduced. In this system relay node is introduced between source and the destination. In cooperative communication, one or multiple users can communicate with each other using relay networks [2]-[3].There are two relaying protocols in cooperative network i.e. Amplify & forward and decode & forward. At the relay, the AF protocol amplifies the data and forwards it to the destination [4]. In Decode and forward, the signal from the source is decoded and forwarded to the destination and these two protocols are commonly used [5]-[6]. But for relay selection scheme decode and forward protocol is better, since it eliminates noise accumulation problem. So DF protocol is used in this paper. The main aim of cooperative communicative is to improve the channel capacity of the wireless networks and it can be used in different applications like cellular networks, cognitive networks and also adhoc networks [7].

Adhoc network is formed by a group of communication devices where every device can communicate with each other without fixed infrastructure and without predefined organization [9].

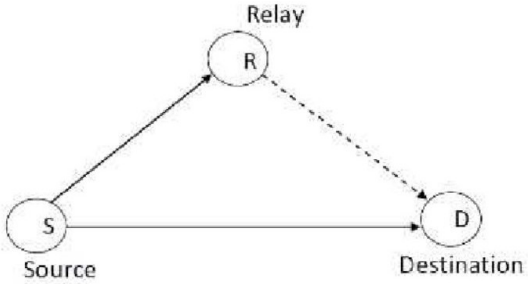

Fig 1: Scenario of Cooperative communication [8]

The channel coding techniques in a communication system can be used to reduce the number of errors. Turbo coding

plays a very important role in making the system more reliable and efficient [10].For cooperative communication, turbo codes were implemented in [16] using AWGN channel with QAM modulation.

In order to provide secure and reliable communication, error control mechanisms are essential. Hybrid automatic repeat request is the main error controlling process which is a combination of both automatic repeat request (ARQ) and forward error correction [11]. HARQ is mainly used in a communication systems like long term evolution (LTE) and High Speed Packet Access (HSPA) [12].There are mainly two types of HARQ found namely HARQ type-I and HARQ type-II. In HARQ type-I, the data packets which are broadcasted over a wireless Rayleigh channel are received at the destination. If the received data are found to be in error, then the data packets are discarded and a negative acknowledgement is sent to the transmitter. This process is continued till the maximum number of rounds is reached.

In type-II the data packets which is received at the reception is not discarded, it is stored in a buffer and combined with data of same packet which are received in the next rounds. The combined data are used in the decoding process. This process makes HARQ type-II more robust against fading and throughput will be increased [13]. There are mainly two schemes in HARQ type-II, namely HARQ with code combining (HARQ-CC) and HARQ with incremental redundancy (HARQ-IR) [14]. HARQ-IR performs better when the channel varies slowly and the retransmissions requests are responded quickly [15].

In this paper, Cooperative communication for a adhoc network is simulated with decode and forward approach. To reduce the number of errors in a system, turbo coding technique with HARQ-CC is used. To improve the performance of a system, QAM modulation technique is used. In HARQ process, if the received data bits are found to be in error then negative acknowledgement is sent to the source and SNR is for each transmission is varied till it reaches the maximum retransmissions. Multiple copies of the data bits which are received at the destination through multiple retransmissions are combined using maximal ratio combining (MRC) to obtain errorless information.

Rest of the paper is organized as follows: Section II describes the system model. Performance analysis and simulation results are explained in Section III. Section IV gives the conclusion and future scope of the proposed work.

II SYSTEM MODEL

Simulation of HARQ scheme using turbo coding technique in a cooperative adhoc network using QAM modulation is carried out in the proposed work.

Fig 2 represents the proposed work. In the above figure cooperative communication scenario is considered with a single relay. Turbo coder is used to minimize the number of errors using QAM modulation. The steps involved to implement a HARQ process is as follows:

At Source:

- The input data is encoded using turbo encoding technique**.**
- The encoded data is modulated using QAM modulation techniques and broadcasted over a Rayleigh fading channel.
- The data which is sent over Rayleigh fading channel forms two paths i.e. source to relay and source to destination.

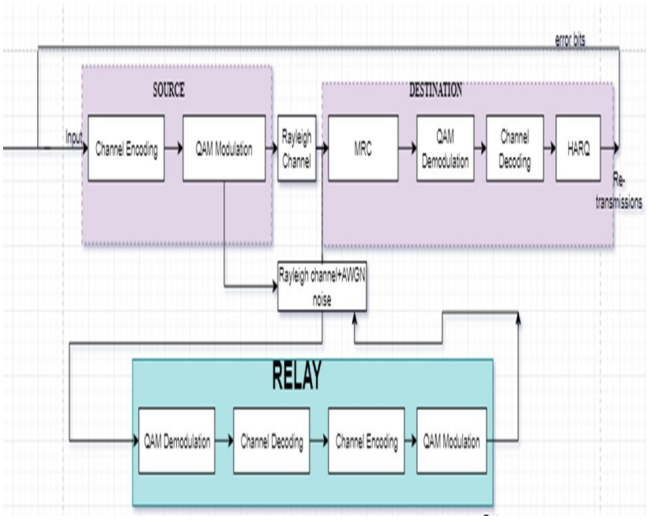

Fig 2: HARQ scheme in cooperative communication

At the relay:

- Relay is a helper node which is placed between source and the destination It uses decode and forward approach i.e. the received data is demodulated and decoded. Decoded data is again encoded and modulated.
- Then the modulated information is broadcasted over a Rayleigh channel with AWGN to the destination.

At Destination:

- The data from the source and the relay reaches the destination.
- The data received from the direct and the virtual paths are combined using maximal ratio combining (MRC).
- The combined data is demodulated and decoded using turbo decoder.
- If it found to be in error then negative acknowledgement is sent to the source.
- If the received data bits are erroneous, HARQ is used at the destination.
- To improve the performance of a system SNR is varied, and the data is combined at the destination using MRC.

Hybrid automatic repeat request (HARQ)

- Hybrid ARQ is a combination of automatic repeat request and forward error correction codes. Destination determines whether the received packet is correct or not by comparing it with the transmitted data. If the packet is correctly delivered, the destination broadcasts an acknowledge (ACK), Otherwise the destination broadcasts a NACK.
- The SNR of the system is varied, as the SNR increases, the noise spectral density (No) decreases.
- The data which is received by varying the SNR is combined using maximal ratio combining (MRC).
- If data received at the destination is erroneous, then retransmission request is sent to the source.
- For the next transmission, only the erroneous data bits are transmitted, this is continued till the data received is error free.
- Fig 3 represents the proposed work which performs HARQ mechanism.
- Channel encoding and decoding is performed using turbo coding, because in cooperative communication turbo coding scheme performs better and reduces number of errors.

III. PERFORMANCE ANALYSIS

A. Performance comparison of cooperative communication with QAM modulation with modulation order of 16 and 64.

In cooperative communication scenario, turbo coder is used to improve the performance of the system. Fig 4 shows the graph of BER vs Noise power spectral density using turbo coder. From the graph it can be noted that using turbo coding technique BER is around 33% for 16-QAM. For 64-QAM BER is almost reduced to 0.03%. By these results we can conclude that in cooperative communication scenario the performance of the network is better when turbo coding with 64-QAM is used.

B. Performance evaluation of Direct communication and decode and forward mechanism

Compared to direct communication, Cooperative Communication is better. Fig 5 shows the comparison of direct communication and decode and forward approach. When SNR increases then the number of errors decreases. 8900 bits has been transmitted from the source. In direct communication for 0db SNR, 6500 bits are found to be an error whereas in cooperative communication numbers of errors are almost reduced to 819 bits.

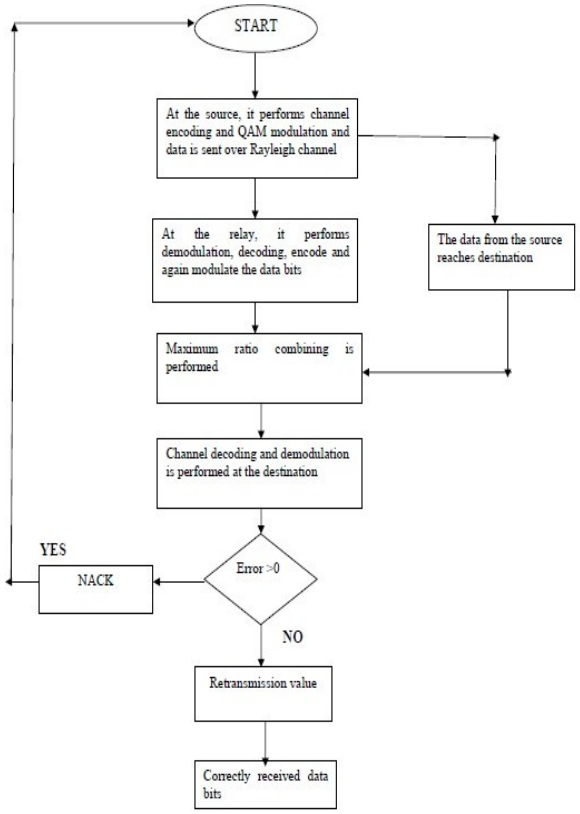

Figure 3: Flow chart of proposed work

C. Performance evaluation of Cooperative Communication when SNR is varied

The system with 64-QAM shows better performance, where BER is around 0.03% which is very less. Figure 6 shows the variation of BER vs SNR with turbo coder. This shows that when Signal to noise ratio increases then bit error rate of a system decreases.

D. Performance evaluation of HARQ scheme in decode and forward approach

With the transmission of 8900 bits for 16-QAM with cooperative HARQ, number of retransmissions required for reception of error free data are 1994. But for same number of transmitted bits, 64-QAM with cooperative HARQ provided error free data at the destination with only 165 retransmissions.

Table 1 provides the performance evaluation of HARQ scheme using QAM modulation technique.

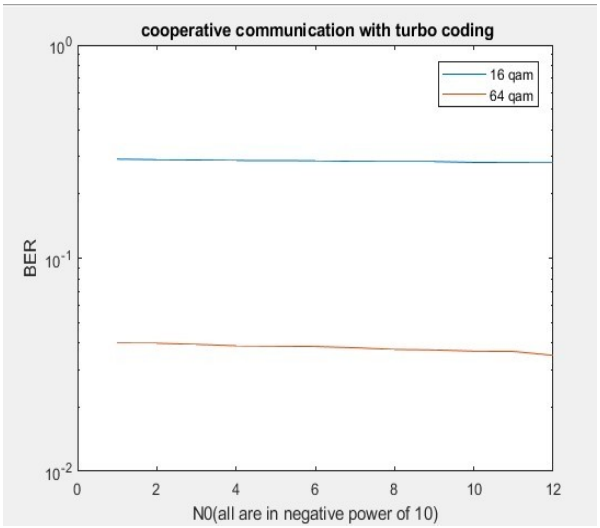

Fig 4: BER vs No using turbo coding technique for different modulation order.

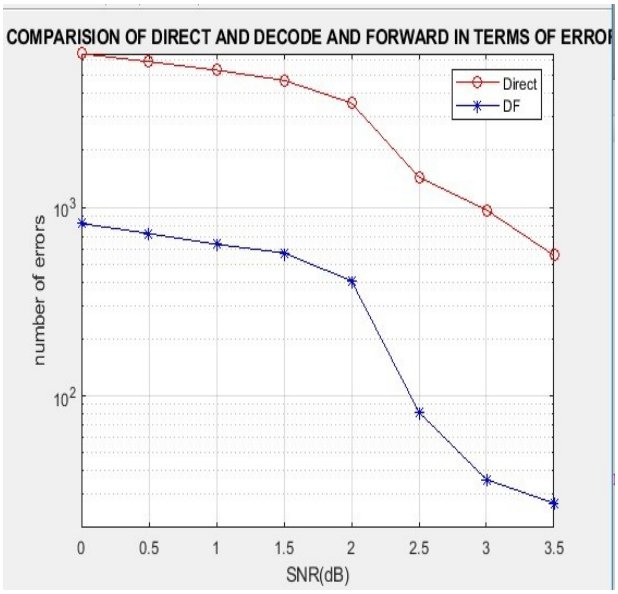

Fig 5: Performance comparisons of cooperative communication with decode and forward and direct communication

Table 1 : Performance evaluation of HARQ scheme using QAM modulation technique

Modulation order	BER	Number of errors	Number of retransmissions
16-QAM	0.3392	3019	1994
64-QAM	0.037	333	165

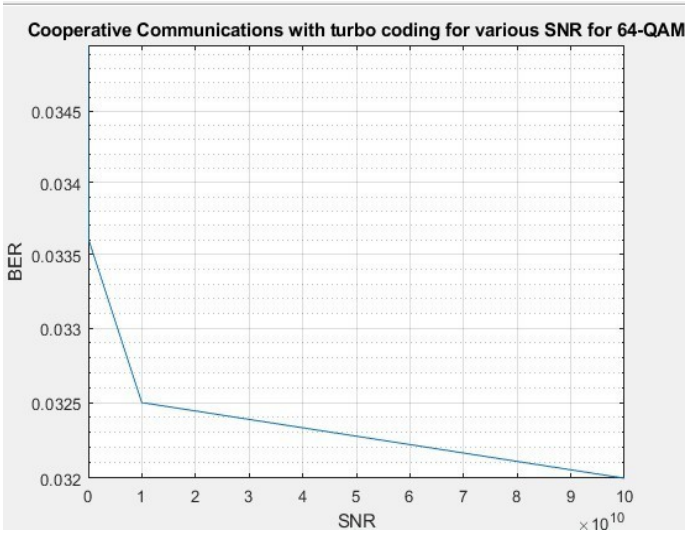

Fig 6: BER vs SNR for 64 QAM for various SNR

IV CONCLUSION

We have simulated Cooperative Adhoc Network with turbo coding technique and HARQ scheme. Performance analysis of cooperative adhoc network is carried out using 16 and 64 QAM modulation techniques. Decode and forward protocol is used at the relay to process the received data bits. Turbo coding technique is analyzed for different SNR values in cooperative adhoc network. It is shown that error rate decreases with increase in SNR. In Cooperative HARQ, 64-QAM showed better performance where only 165 retransmissions are required to correct the total number of errors, when 8900 bits are transmitted. HARQ-IR scheme can be used to reduce the total number retransmissions in future.

REFERENCES

[1] E. N. Onggosanusi, A. G. Dabak, Yan Hui and Gibong Jeong, "Hybrid ARQ transmission and combining for MIMO systems," *IEEE International Conference on Communications, 2003. ICC '03,* Anchorage, AK, pp. 3205-3209, 2003.

[2] A. Sendonaris, E. Erkip, B. Aazhang, "User cooperation diversity-part I: system description", *IEEE Trans. Commun.*, vol. 51, no. 11, pp. 1927-1938, Nov. 2003.

[3] Y. Jing, B. Hassibi, "Distributed space-time coding in wireless relay networks", *IEEE Trans. Wireless Commun.*, vol. 5, no. 12, pp. 3524-3536, Dec. 2006.

[4] B. Maham and A. Hjørungnes, "Opportunistic relaying for MIMO amplify-and-forward cooperative networks," *Springer: Wireless Pers. Commun.*, pp. 1067–1091, Jan. 2012.

[5] M. R. Bhatnagar and A. Hjørungnes, "ML decoder for decode-and-forward based cooperative communication system," *IEEE Trans. Wireless Comm.*, vol. 10, no. 12, pp. 4080–4090, 2011.

[6] M. R. Bhatnagar, "On the capacity of decode-and-forward relaying over Rician fading channels," *IEEE Commun. Lett.*, vol. 17, no. 6, pp. 1100– 1103, Jun. 2013.

[7] D. Yang, X. Fang and G. Xue, "Game theory in cooperative communications," in *IEEE Wireless Communications*, vol. 19, no. 2, pp. 44-49, April 2012.

[8] Shah, Pir Meher & Jan, Latif & Amin, Muhammad & Khan, Salman, Code Shifted Reference Based Cooperative Using Multiple Relays In Ultra Wide Band Communication System. VAWKUM Transactions on Computer Sciences, 2015.

[9] S. Sharmila and T. Shanthi, "A survey on wireless ad hoc network: Issues and implementation," *2016 International Conference on Emerging Trends in Engineering, Technology and Science (ICETETS)*, Pudukkottai, pp. 1-6, 2016

[10]G. Oletu and P. Rapajic, "The performance of turbo codes for wireless communication systems," *2011 3rd International Conference on Computer Research and Development*, Shanghai, pp. 346-349, 2011.

[11] D. J. Costello, J. Hagenauer, H. Imai and S. B. Wicker, "Applications of error-control coding," in *IEEE Transactions on Information Theory*, vol. 44, no. 6, pp. 2531-2560, Oct. 1998.

[12] E. Dahlman, S. Parkvall, J. Skold, and P. Beming, 3G Evolution: HSPA and LTE for Mobile Broadband. Academic Press, 2007.

[13] Chelli A, Zedini E, Alouini M-S, Patzold MU, Balasingham I, Throughput and Delay Analysis of HARQ with Code Combining over Double Rayleigh Fading Channels, *IEEE Transactions on VEHICULAR TECHNOLOGY,*2018.

[14] P. Frenger, S. Parkvall and E. Dahlman, "Performance comparison of HARQ with Chase combining and incremental redundancy for HSDPA," *IEEE 54th Vehicular Technology Conference. VTC Fall 2001. Proceedings (Cat. No.01CH37211)*, Atlantic City, NJ, USA, pp. 1829- 1833 vol.3,2001.

[15] Jung-Fu Cheng, "Coding performance of hybrid ARQ schemes," in *IEEE Transactions on Communications*, vol. 54, no. 6, pp. 1017-1029, June 2006.

[16]Y. Li, "Distributed coding for cooperative wireless networks: An overview and recent advances," in *IEEE Communications Magazine*, vol. 47, no. 8, pp. 71-77, August 2009.

.

Proceedings of the Fourth International Conference on Communication and Electronics Systems (ICCES 2019)
IEEE Conference Record # 45898; IEEE Xplore ISBN: 978-1-7281-1261-9

Symptom Based Health Prediction using Data Mining

Vijaya Shetty S
Department of Computer Science and Engineering
Nitte Meenakshi Institute Of Technology
Bengaluru,India
vijayashetty.s@nmit.ac.in

Karthik G A
Department of Computer Science and Engineering
Nitte Meenakshi Institute Of Technology
Bengaluru,India
karthikga124@gmail.com

M Ashwin
Department of Computer Science and Engineering
Nitte Meenakshi Institute Of Technology
Bengaluru,India
ashwin.m134@gmail.com

***Abstract*— The general day to day health of a person is vital for the efficient functioning of the human body. Taking certain prominent symptoms and their diseases to build a Machine learning model to predict common diseases based on real symptoms is the objective of this research. With the dataset of the most commonly exhibited diseases, we built a relation to predicting the possible disease based on the input of symptoms. The proposed model utilizes the capability of different Machine learning algorithms combined with text processing to achieve accurate prediction. Text processing has been implemented using Tokenization and, is combined with various algorithms to test the similarities and the outputs. In health industry, it provides several benefits such as pre-emptive detection of diseases, faster diagnosis, medical history for review of patients etc.**

Keywords—Tf-idf; Data Mining; Tokenize; Symptoms; diseases.

I. INTRODUCTION

The most common health issues among people often have some basic symptoms which are generally exhibited by a person. For example, an individual with headache may exhibit variety of other symptoms of other diseases. In such cases where we want to have instant diagnosis, we are dependent on physicians. A machine learning model can be built to predict the type of disease based on the symptoms. The model prediction can help early detection of diseases and faster diagnosis

For this purpose of our research, we used dataset which is available online to perform Machine learning based predictions to some test data. The aim of the study is to build a framework and a computational model for the prediction of diseases looking at various symptoms. For this purpose, we use a dataset which contains information about 150 most frequently occurring diseases and the associated symptoms with those diseases. The dataset used had a lot of cleaning and pre-processing needed to be done. The first step was to transpose the datasets into a form with diseases as the target column and each of the symptoms as dummy variables for the diseases, on which models were to be trained.

For the study, four different sets of algorithms were used for mapping symptoms into diseases. The first step was to split the dataset into training and testing sets, in order to effectively test the generality of the algorithms to be trained, we used 2/3rd of the dataset for training and the rest for testing purposes. However, for subsequent steps, it was seen that an over fitted model for the study was better suited and thus testing was done for the entire dataset.

II. RELATED WORK

There are several successful use cases which we come across in different predictions. Our plan was to survey various algorithms and select the most suitable one for prediction purpose.

N. Alshurafa et al.[1] used baseline questionnaires to gather labelled patient data along with real-time mobile data. The experiment revealed K-Nearest Neighbour is susceptible to noisy data. The heart disease prediction in [2] with symptoms uses a questionnaire to gather data from patients and pass it to a Support Vector Machine Algorithm. Prabakaran et al.[3] states that research shows a web system using Naïve Bayes to provide answers to complex queries to diagnose heart disease. Support Vector Machines (SVM) and Artificial Neural Networks (ANN) are the two most reused algorithms. Most commonly used methods to evaluate the classification methods accuracy are Leave-One Out and Cross-Validation. P. Chiang et al.[4] used data collected using health monitoring devices such as Fitbit and Omron for 8 people over a period of 1 month. Performed feature ranking based on RF feature selection. The study in [5] works on removing missing data and outliers using additive Least Square Support Vector Machine. The comparison between algorithms in [6] shows the use case scenarios for each algorithm with merits and demerits. An approach of sequential pattern mining is very feasible for the continuously emerging characteristics of stream data suggested in [7]. The dataset used in [8] shows how web-scraped data is useful for making predictions even without specific medical data. Open source repositories are utilized to gather updated datasets. They also implemented Naïve Bayes as one of their test algorithms. Feature engineering was done to remove outliers in the dataset such as bad data quality i.e. patients that appeared in the dataset with age less than 0 or greater than 120 and incident cases not “closed” properly. The survey in [9] provides comprehensive survey of algorithms and methods implemented in medical fields. They show Bayesian Network modelling to be one of the top used techniques in fields such as cancer and diabetes prediction.

Xin LI et al.[10] used a UCI dataset containing hospital records of diabetic patients. The records contain more than 10 years of data gathered from hospitals. It contains patient data with 50 different attributes and specifies if the patient has been re-admitted. They performed a collaborative filtering-enhanced deep learning algorithm (CFDL). For the End –User, Huang [11] proposed a health chatbot to provide recommendations such as diet and exercise , eating tips, nutrient intake and other features. The algorithms used in [12] and [13] shows implementation of Neural Networks, K-NN and Naïve Bayes. It also specifies the need to understand the importance of attributes and feature selection in the case of heart disease prediction i.e. attributes such as smoking and drinking habits.The application in [14] makes use of chatbot for medical data requests. This feature can be used for suggestive prediction with the help of NLP and integrated with general chatbot algorithms which also provide some added functionalities.

For the dataset purpose, we see [15] in which the National Health of Scotland (NHS) aided by the government provides A-Z symptom-disease data from which we manually web-scraped the dataset.

III. Data Summary And Processing

A. Dataset Preparation

The data we used was gathered from 2 sources- UMLS and NHS government websites. The web-scraped data of UMLS government database of diseases and symptoms. The Unified Medical Language System (UMLS) is a vocabulary based biomedical database of most common symptoms and disease pairs. This data was outdated, and prediction was not up to the expected outcomes. But, for the main testing and working model we curated a dataset using National Health of Scotland (NHS) data of A-Z diseases and its symptoms. This data proved to be more accurate for prediction since it was easy to gather list if most appropriate words which uniquely predict a disease or condition. We test this data with 3 main algorithms- Decision Trees, Random Forest and Naïve Bayes.

B. Text Processing

For the initial step, we consider the symptoms data and perform count-vectorization. This is done to sort the words in the corpus into a bag-of-words. The model is simple in that it ignores the order of words and relations rather focus on the occurrence of words the dataset.

For all the 3 algorithms, we use the tf-idf parameter which helps in keyword extraction to help in faster computation. The Term Frequency and Inverse Document Frequency play a major role in prediction and understanding the dispersion of symptoms. This shows how the dataset has keywords which vary in occurrences based on a certain disease.

Next, we use the above logic to perform bigram words classification of data. For example, we consider ‘abdominal pain’ as one word and check similar occurrences in dataset. This is sorted into a count vector matrix of binary matrix.

For the analysis for this data we use Term Frequency-Inverse Data Frequency (tf-idf) function which gives us the frequency of the word in each document in the corpus. It is the ratio of number of times the word appears compared to the total number of words present in the dataset. Using (1) and (2) we can get the required tf-idf mappings.

$$TF(t) = \frac{\text{(Number of word occurrences)}}{\text{(Total number of words in the dataset)}} \quad (1)$$

$$IDF(t) = \log_e \frac{\text{Total number of documents}}{\text{Number of documents with term t in it}} \quad (2)$$

IV. Methods

We test the data with 3 main classification algorithms- Decision Trees, Random Forest and Naïve Bayes. We make use of scikit-learn library and pandas data frames of the Python Programming language to process the data and implement the above algorithms.

A. Decision Trees

With the help of e Decision Tree classifier, we can derive the pairs of disease and generate a tree based on Gini index and weights of each symptom. The first step is to classify the data to fit the model of decision trees for the given dataset. We split the data into test data and training data for the model. Construct a node table to assign the different classifiers and Gini for splitting the nodes. Classify the model using Decision Tree Classifier. The value of target variable needs to be predicted using simple decision rules created using in the dataset and tf-idf features. The only extra advantage of using this is to apply it for both numerical and categorical dataset classification. This helps in reducing data cleaning based on what type of data is used for processing for each of the algorithm. Statistical testing is also easy compared to other methods. It uses 3 main criteria for determining the correct split. Gini Index, Information gain and Entropy. The Gini Index is subtracted sum of the squared probabilities of each class from one. Information Gain specifies the lowest entropy for each split and accordingly produces each node for lowest entropy calculated for each split. Figure 1 shows the section of the decision tree built with the count vector matrix after classification.

B. Random Forest

This is a more enhanced version of decision trees where we pick N random records from the dataset which contains symptoms. It is a supervised algorithm in which multiple decision trees are built with the help of bagging method. It does not rely on the most important features rather it uses random subset of features is considered while splitting a node. There is very low or no bias since it relies on the power of "the crowd". It follows 4 main steps:

1) Pick random samples from the dataset.
2) Produce decision tree using each sample and get a predicted result from each tree.
3) For each result, gain a vote to predict the result.
4) The final prediction with most overall votes gained by will be the result.

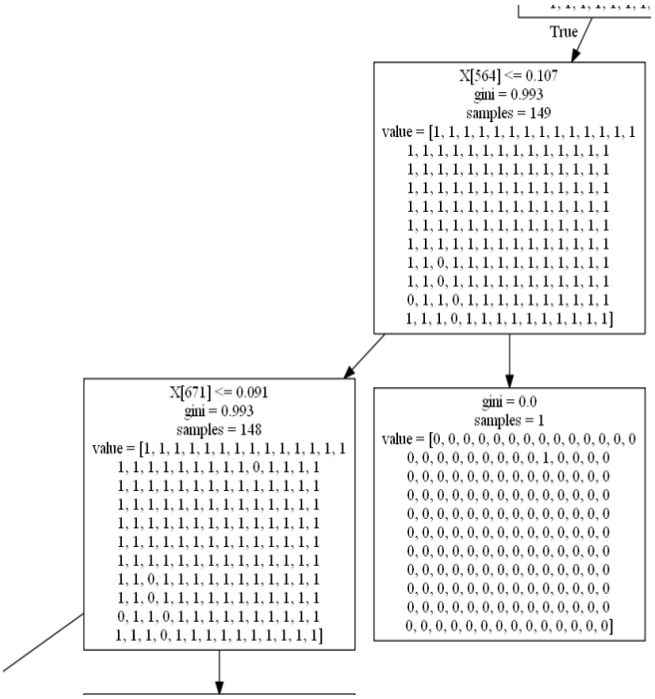

Figure 1: Section of the decision tree generated by count vector method

The general model for random forest selection and construction of tree is explained in Figure 2. The training set is randomly searched for a sample and the tree is constructed. Thus, it prevents overfitting of random subsets by creating trees on random subsets.

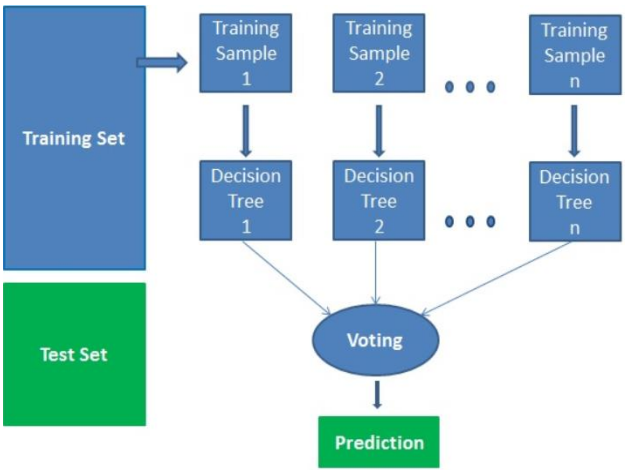

Figure 2: Random Forest Classifier Flow-chart

For our model, we use 300 n_estimators which specifies the number of trees and max_depth of 3 which specifies the maximum depth of each tree. There is an exponential increase in training time as we add more data to the existing dataset. Due to the branching and complexity it is not a viable option for future scaling, but it delivers more accurate results once it is trained compared to the other 2 algorithms.

C. Naïve Bayes

This is a conditional probability based algorithm. It is the most widely used and fastest algorithm since it uses less training data and strong independence assumptions. In our case, we use a built in function called MultinomialNaïveBayes which is mainly used for discrete features such as text classification. It requires a feature count parameter which helps in determining each class while fitting the sample with appropriate weights. For this we use the tf-idf count vector as the parameter.This experiment yielded around 99% accuracy. In text classification, the main aim is to find the best class for the given document. Figure 3 shows how text classification can be combined as a parameter to pass tf-idf vector which contains tokens and frequency data. We score the algorithm to obtain the results. It has 2 main functions. The first function is used to train the multinomial Naïve Bayes model based on the feature extraction and count vector. Each of the Count (C) of words and Document (D) can be done in a single pass through this training data. The conditional probability of Vector in each case is returned. The next step is to apply the algorithm to the tf-idf count vector (V) to assign score to each term collected as bag-of-words. The final score is obtained as the cumulative score for given document.

TRAINMULTINOMIALNB($\mathbb{C}, \mathbb{D}$)
1 $V \leftarrow$ EXTRACTVOCABULARY($\mathbb{D}$)
2 $N \leftarrow$ COUNTDOCS($\mathbb{D}$)
3 **for each** $c \in \mathbb{C}$
4 **do** $N_c \leftarrow$ COUNTDOCSINCLASS($\mathbb{D}, c$)
5 $prior[c] \leftarrow N_c / N$
6 $text_c \leftarrow$ CONCATENATETEXTOFALLDOCSINCLASS($\mathbb{D}, c$)
7 **for each** $t \in V$
8 **do** $T_{ct} \leftarrow$ COUNTTOKENSOFTERM($text_c, t$)
9 **for each** $t \in V$
10 **do** $condprob[t][c] \leftarrow \frac{T_{ct}+1}{\sum_{t'}(T_{ct'}+1)}$
11 **return** $V, prior, condprob$

APPLYMULTINOMIALNB($\mathbb{C}, V, prior, condprob, d$)
1 $W \leftarrow$ EXTRACTTOKENSFROMDOC(V, d)
2 **for each** $c \in \mathbb{C}$
3 **do** $score[c] \leftarrow \log prior[c]$
4 **for each** $t \in W$
5 **do** $score[c] \mathrel{+}= \log condprob[t][c]$
6 **return** $\arg\max_{c \in \mathbb{C}} score[c]$

Figure 3: Algorithm used for combining text classification with Multinomial Naïve Bayes

Test results shown in Table 1 imply that there is negligible difference between the 3 methods and the text processing plays a role in reducing the execution time. For more samples added to the same dataset, the model will function slower and the compilation time gap will increase due to variation in splitting methods and computational differences between probabilistic model and trees. As the comparison in [6] says, the tree model performs better with more data compared to Naïve Bayes.

TABLE I. TEST RESULTS

Algorithm	Accuracy
Decision Trees	98.18%
Random Forest	98.05%
Naïve Bayes	98.55%

V. RESULTS AND FUTURE WORK

Using the graphs and visualization, we can understand the trends in diseases. The prediction of diseases is also very accurate and yield fast results due to text pre-processing before any of the 3 algorithms is applied. This ensures faster execution and future scalability. The results obtained are very similar due to lack of large datasets in this field. There will be slight variations in result of each algorithm based on data processing. For the most part, they all yield the same results. The Token counts of each vector in word-count is mapped onto the graph in Figure 4 which reveals the most common disease symptom pairs which are found in any of the order as given in graph. The first 4 samples in graph represent dummy braces in the dataset.

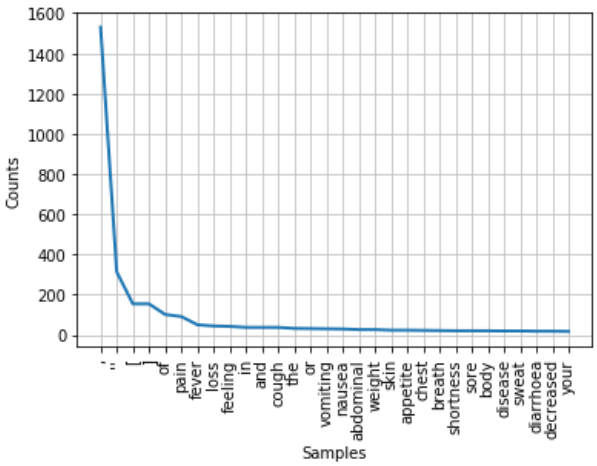

Figure 4: Counts of samples found for each disease

Figure 6 shows how words can be graphically represented from the dataset. The symptoms are arranged in accordance to font sizes i.e. the larger font size means higher frequency of occurrence and lower fonts mean the opposite. The input symptoms can be passed to get the predicted disease.Since there is only 154 most common diseases in the dataset, it is not possible to predict some diseases which may not be classified or present in dataset.It requires a minimum of 3 symptoms to predict a disease. The tests showed differences in predictions. In some cases, Naïve bayes was the only algorithm to predict the disease closest to the actual one when comparing with 3 or more of the same symptoms. In figure 6, 4 main terms stand out – pain, cough, fever and appetite loss. This helps us minimize the transaction time and predict diseases faster by adding parameters for recurring words in a corpus. All the above graphs have shown about the distribution on various symptoms which the most common irrespective of the disease and other symptoms which are occurring only for specific diseases. Figure 5 shows the T-distributed Stochastic Neighbor Embedding (t-SNE) plot which is used to visualize key data points in 3-dimensions. As specified in the graph, we show all the diseases classified as one single cluster of 154 data points. Each color represents a symptom.

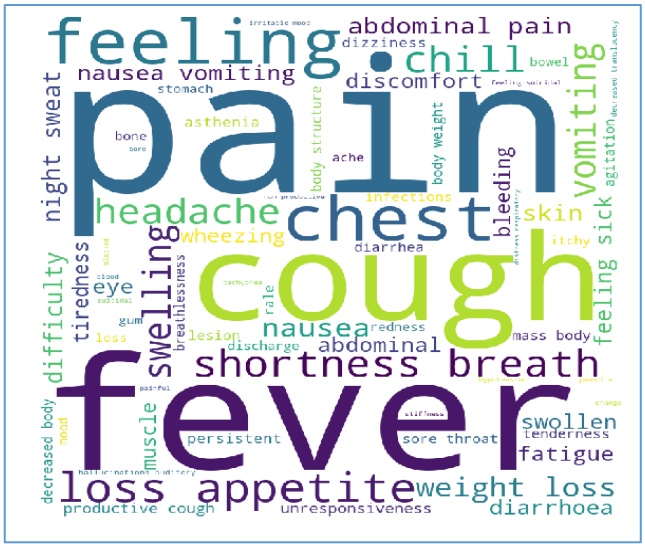

Figure 6: Visualization of words occurrence based on WordCloud

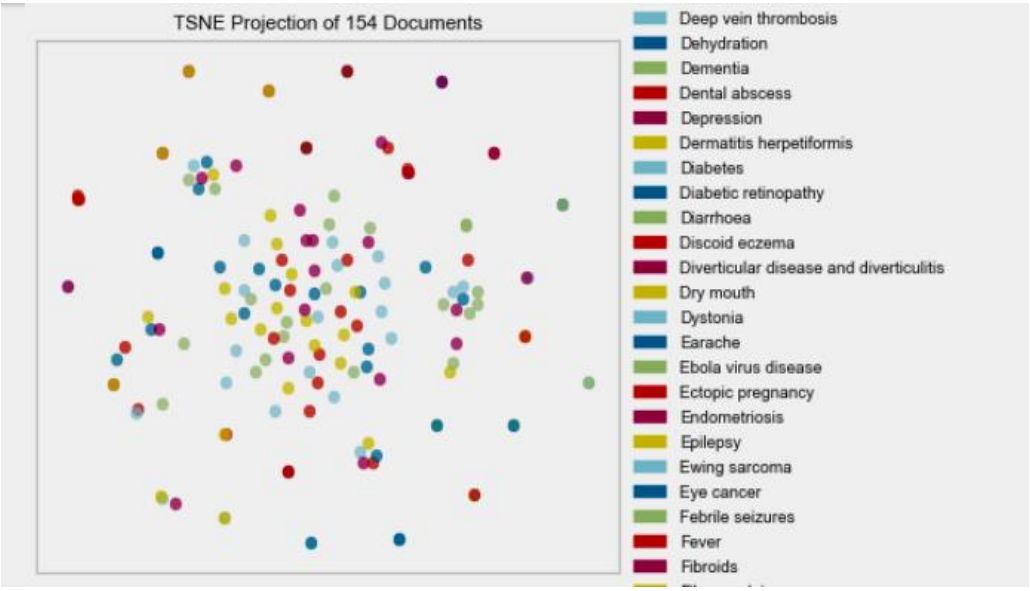

Figure 5: T-stochastic neighbor

We chose Naïve bayes model since it is the most favoured algorithm alongside text data and requires less pre-processing. It does not show all components of the Diagnosis system, but it focuses on the feature of classification. It shows how the data is web-scraped, analysed and is used to make prediction on the disease.

We propose the model in Figure 7 which uses crowd sourced and public data which can be collaborated with hospitals to feed the database of disease and symptoms, for example symptoms exhibited for new diseases like Zika Virus, help in getting data from patients such as heart rate, blood sugar etc.

The dataset can be dynamically updated for given set of attributes for better future prediction. The predictions can be linked to suggest ailments and possible causes of disease in future so the patients can understand the root causes of diseases based on symptoms. Since this model is efficient, we can parallelly add more data and run on multiple systems for faster processing. The future of data mining is more towards crowd sourced data which is gathered from wide variety of

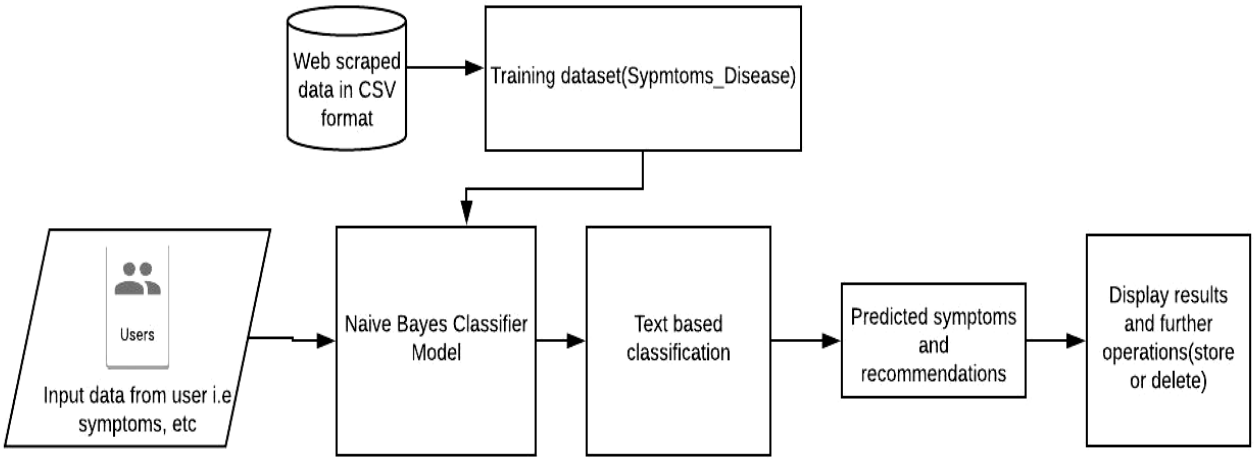

Figure 7: Proposed architecture diagram

etc.Due to lack to public data sources, we are unable to get more data. Collaborated data from hospitals can be curated accordingly for the model.

The block diagram that shows the major functional blocks that are part of the system being described, the outside entities (people and systems not part of the system being described), and the major interfaces between them. It does not show all components of the Diagnosis system, but it focuses on the feature of classification. It shows how the data is scanned, analysed and is used to make prediction on the disease.

VI. Discussion

The model trained for predicting diseases gives a very good result for the given dataset. The algorithms used are very efficient and accurate. The medical field has seen some new innovations in multi-platform availability such as smartphones and smart watch integration to predict and prevent some medical conditions. The power of Artificial Intelligence is also being integrated to Machine learning approaches to bring it closer to the human sentiment. This model can be integrated with chatbot models such as DialogFlow from Google to add some more interactions.

There is room for improving the method of delivering the results to the user by adding an intuitive UI for input of symptoms and prediction of disease. We can integrate the same code for processing on mobile devices for an easier access to healthcare. Various modern mobile sensors can also medical sources. This helps in directly integrating the models which are can process a variety of data based on the features and type of data appropriate for any specific algorithm. The dataset plays the most vital role in improving the model. The test set from UMLS open source dataset was found to be outdated. But it was a source of understanding how web-scraped data can be used to make predictions.

References

[1] N. Alshurafa, C. Sideris, M. Pourhomayoun, H. Kalantarian, M. Sarrafzadeh and J. Eastwood, "Remote Health Monitoring Outcome Success Prediction Using Baseline and First Month Intervention Data," in IEEE Journal of Biomedical and Health Informatics, vol. 21, no. 2, pp. 507-514, March 2017.

[2] P. Sudeshna, S. Bhanumathi, and M. A. Hamlin, “Identifying symptoms and treatment for heart disease from biomedical literature using text data mining,”2017 International Conference on Computation of Power, Energy Information and Commuincation (ICCPEIC), 2017.

[3] N. Prabakaran and R. Kannadasan, "Prediction of Cardiac Disease Based on Patient's Symptoms," 2018 Second International Conference on Inventive Communication and Computational Technologies (ICICCT), Coimbatore, 2018

[4] P. Chiang and S. Dey, "Personalized Effect of Health Behavior on Blood Pressure: Machine Learning Based Prediction and Recommendation," 2018 IEEE 20th International Conference on e-Health Networking, Applications and Services (Healthcom), Ostrava, 2018

[5] G. Wang, Z. Deng and K. Choi, "Tackling Missing Data in Community Health Studies Using Additive LS-SVM Classifier," in IEEE Journal of Biomedical and Health Informatics, vol. 22, no. 2, pp. 579-587, March 2018

[6] B. Nithya and V. Ilango, "Predictive analytics in health care using machine learning tools and techniques," 2017 International Conference on Intelligent Computing and Control Systems (ICICCS), Madurai, 2017

[7] M. Hassani and T. Seidl, "Towards a Mobile Health Context Prediction: Sequential Pattern Mining in Multiple Streams," 2011 IEEE 12th International Conference on Mobile Data Management, Lulea, 2011

[8] S. Pitoglou, Y. Koumpouros and A. Anastasiou, "Using Electronic Health Records and Machine Learning to Make Medical-Related Predictions from Non-Medical Data," 2018 International Conference on Machine Learning and Data Engineering (iCMLDE), Sydney, Australia, 2018

[9] Sohail M.N., Jiadong R., Uba M.M., Irshad M. (2019) A Comprehensive Looks at Data Mining Techniques Contributing to Medical Data Growth: A Survey of Researcher Reviews. In: Patnaik S., Jain V. (eds) Recent Developments in Intelligent Computing, Communication and Devices. Advances in Intelligent Systems and Computing, vol 752. Springer, Singapore

[10] X. Li and J. Li, "Health Risk Prediction Using Big Medical Data - a Collaborative Filtering-Enhanced Deep Learning Approach," *2018 IEEE 20th International Conference on e-Health Networking, Applications and Services (Healthcom)*, Ostrava, 2018, pp. 1-7.

[11] N. Albayrak, A. Özdemir and E. Zeydan, "An overview of artificial intelligence based chatbots and an example chatbot application," *2018 26th Signal Processing and Communications Applications Conference (SIU)*, Izmir, 2018, pp. 1-4.

[12] G. Shanmugasundaram, V. M. Selvam, R. Saravanan and S. Balaji, "An Investigation of Heart Disease Prediction Techniques," *2018 IEEE International Conference on System, Computation, Automation and Networking (ICSCA)*, Pondicherry, 2018, pp. 1-6.

[13] A. Aldallal and A. A. A. Al-Moosa, "Using Data Mining Techniques to Predict Diabetes and Heart Diseases," *2018 4th International Conference on Frontiers of Signal Processing (ICFSP)*, Poitiers, 2018, pp. 150-154.

[14] C. Huang, M. Yang, C. Huang, Y. Chen, M. Wu and K. Chen, "A Chatbot-supported Smart Wireless Interactive Healthcare System for Weight Control and Health Promotion," *2018 IEEE International Conference on Industrial Engineering and Engineering Management (IEEM)*, Bangkok, 2018, pp. 1791-1795.

[15] A to Z of symptoms | NHS inform. [Online]. Available: https://www.nhsinform.scot/symptoms-and-self-help/a-to-z. [Accessed: 15-Apr-2019].

Proceedings of the Fourth International Conference on Communication and Electronics Systems (ICCES 2019)
IEEE Conference Record # 45898; IEEE Xplore ISBN: 978-1-7281-1261-9

Design of Electrostatic Energy Harvesting Pre charge Circuit

Apoorva Raghunandan
Department of Electronics and Communication Enginerring
RV College of Engineering
Bengaluru, India
apoorva.rsi@gmail.com

Shilpa D R
Department of Electronics and Communication Enginerring
RV College of Engineering
Bengaluru, India
shilpadr@rvce.edu.in

***Abstract*—An energy harvesting system uses Pre charge circuits. The need for designing circuits that consume low power is the need of the day. In this paper a pre charge circuit has been designed in 45nm CMOS technology and the output energy and average power consumption of the circuit has been computed. The cascaded double tail comparator and the gate driver circuits are designed. The pre charge circuit is energy efficient and harvests more energy as compared to the invested energy. The capacitance value for designing the pre charge circuit has been obtained from the capacitive pressure sensor in COMSOL Multiphysics 5.3. A plot of capacitance versus pressure gives the equivalent capacitance for the applied pressure. A value of 1pF has been chosen for an applied pressure of 22.5 to 25 KPa. In the pre charge circuit, the energy consumption during charging of the capacitor was computed to be 4.5 µ W and during discharging it was computed to be 10 µW. The invested energy was 0.281 x 10^{-9} fJ and the obtained energy was 0.781 x 10^{-9} fJ. The net energy gain was 0.5 x 10^{-9} fJ and the percentage gain was 177.94%.**

Keywords— Pre charge circuit, Energy Harvesting, Low Power VLSI Design, Energy efficient circuits

I. INTRODUCTION

Energy harvesting systems use pre charge circuits to charge the capacitor to the applied voltage. Especially in Electrostatic Energy harvesting systems the capacitor is the most important element in the circuit. If the power flow into the device is rapid it will destroy it. Therefore, to prevent this a pre charge circuit is used. Electrostatic energy works on the principle of storing charge in the capacitor. As the distance between the parallel plates increase, the capacitance decreases. As charge is given by the product of capacitance and voltage, the voltage increases, and the capacitance decreases to keep the charge constant [1]. This leads to an increase in the energy.

In [1], an Electrostatic energy harvesting IC has been designed. At 30GHz, the IC harvested 1.27, 2.14, and 2.87 nJ/cycle. The power generated was 38.1, 64.2, and 86.1 nW, respectively. The proposed IC detects C_{MAX} during reset, pre charges CVAR, connects it to the battery, during harvest C_{MIN} is detected and disconnects C_{VAR} during reset. The IC has been designed using BiCMOS logic. A 1µF capacitor takes 35s to charge from 3.5 to 3.81V. In this work a pre charge circuit consisting of a pre charge comparator, pre charge de – energize comparator, bias current generator, harvest detection subsystem and pre charge detection subsystem are designed. Errick O Torres [2], presents a self- tuning electrostatic energy harvester IC. The inductor based pre charger adapts to a constantly changing supply voltage. The pre charger and its self-tuning reference, draw enough power but dissipate minimum energy. At battery voltages of 2.7, 3.5, and 4.2 V, the harvester generates, the IC generates 1.93, 2.43, and 3.89 nJ per vibration cycle, respectively. The operating frequency is 30GHz. The power for the respective voltages is computed as 57.89, 73.02, and 116.55 nW. A 1µF capacitor is charged from 2.7 to 4.2 V in 69s. The energy harvesting is demonstrated in three phases, the pre charge phase, the harvest phase and the reset phase. B Manoj Kumar [4] proposes a low power and high-speed double tail comparator. As compared to the other proposed comparator designs i.e the dynamic comparator, double tail comparator and modified double tail comparator, the one proposed in this paper is the fastest and consumes he least power. The proposed comparator has been designed in 180nm technology. The delay is computed to be 15.32ps and the average power consumption is 13.90 µW. In [3] and [5] the design of energy efficient electrostatic transducers has been discussed. SOI-based electro-mechanical transducer has been modelled and fabricated. The use of a capacitive pressure sensor to demonstrate the energy harvesting principle is discussed in [6], [7].

The literature survey provides evidence for the use of electrostatic energy for designing an energy efficient pre charge circuit.

II. BASICS OF ELECTROSTATIC ENERGY HARVESTING

Electrostatic energy harvesters use capacitors for storing and retrieving the charge. The conversion of vibration to charge can be considered as an electromechanical conversion process. The charge stored in a capacitor is given by equation 1. Q is the charge, V is the voltage and C is the capacitance.

$$Q = CV \tag{1}$$

The distance between the paralled plates d, the capacitance C, area A and the relative permittivity ε are given by equation 2.

$$C = \frac{\varepsilon A}{d} \tag{2}$$

The relationship between the Energy E, capacitance C and voltage V is given by equation 3.

$$E = \frac{1}{2}CV^2 \tag{3}$$

III. Implementation of Pre charge Circuit

The energy harvesting circuit contains a pre charge circuit used to reduce the rapidity of power flow into the device during charging. The pre charge circuit consists of the following sub circuits.

- Capacitor – The design value has been obtained from COMSOL. For a pressure of 20kPa, the equivalent capacitance is approximately equal to 1pF.
- Comparator – Based on Domino logic
- Gate driver circuit
- Inductor – The value is taken to be 10µH.

The voltage at the inductor is compared with the reference voltage. The capacitance value is assumed to be 1p F. The DC voltage amplitude given for Vpulse is 1V. The specifications for performing the transient analysis are shown in Table I.

TABLE I Specifications for Performing Transient Analysis

Analysis	Specification
Transient	Cap = 1pF Vpulse = 1V

Table I shows the Specifications for performing Transient Analysis. The capacitance value is chosen to be 1pF and the applied voltage to the Pre charge circuit is 1V. The Pre charge circuit is shown in Fig. 1.

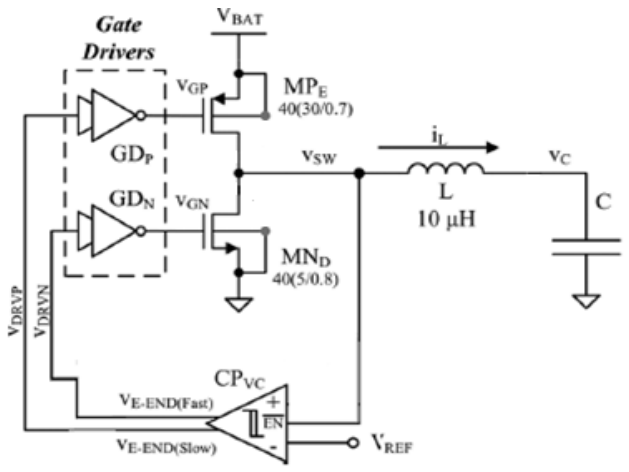

Fig. 1. Pre charge Circuit

Transistors MP_E and MN_D charge C to the supply voltage V_{BAT} by energizing and de-energizing inductor L. As L and C energize, comparator C_{PVC}

A. Obtaining the capacitance value from COMSOL

An electromechanical capacitive pressure sensor has been designed in COMSOL. The pressure from a range of 20 to 25KPa is applied. The equivalent of mechanical vibration is considered as pressure in this case. It is shown in Fig. 2. The legend on the right side of the figure indicates the displacement on the application of pressure. The displacement ranges from 0.2µm to 2µm. The pressure is maximum at the centre of the electromechanical pressure sensor i.e near the vacuum cavity. Near the vacuum cavity the displacement is around 2µm. Towards the surface of the pressure sensor is dradually decreases.

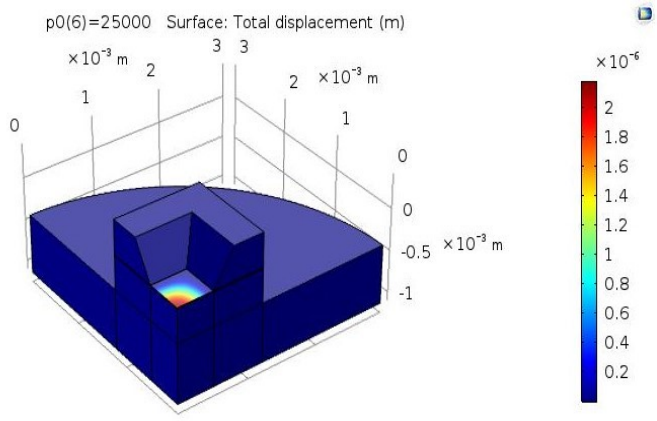

Fig. 2. Electromechanical capacitive pressure sensor

A plot of capacitance v/s pressure is shown in Fig. 3. The C value of 1pF has been considered for design for a pressure between 22.5 to 25KPa.

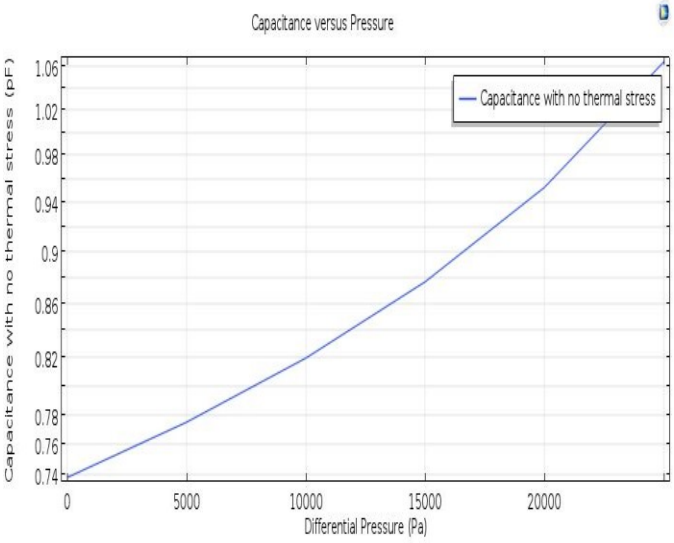

Fig. 3. Plot of capacitance v/s applied pressure.

B. Design of Gate Driver Circuit

The gate driver circuit consists of 14 transistors in total. Out of which, seven of them are PMOS and the other seven are NMOS transistors. The transistors are assigned the sizes as follows. MPP1, MPP2 and MPP3 are assigned W/L ratios of 12/0.7, 4(12/0.7) and 20(12/0.7) respectively [1]. MNP1, MNP2 and MNP3 are assigned W/L ratios of 3/0.8, 4(3/0.8) and 20(3/0.8) respectively. MNP1, MNP2 and MNP3 are assigned W/L ratios of 8/0.7, 4(8/0.7) and 20(8/0.7) respectively. MNN1, MNN2 and MNN3 are assigned W/L ratios of 2/0.8, 4(2/0.8) and 20(2/0.8) respectively. The transistors MPE and MND are

connected to GDP and GDN. The gate driver circuit is shown in Fig. 4.

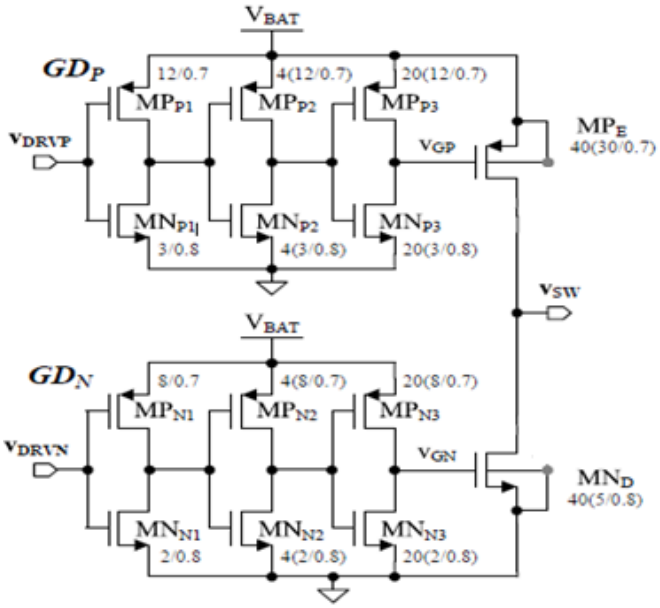

Fig. 4. Gate Driver Circuit [1]

C. *Design of Cascaded Double Tail Comparator*

Comparators form the basic building block in many Analog circuits such as Data converters and Signal Processing systems. A comparator also forms an important component of the Pre charge circuit.

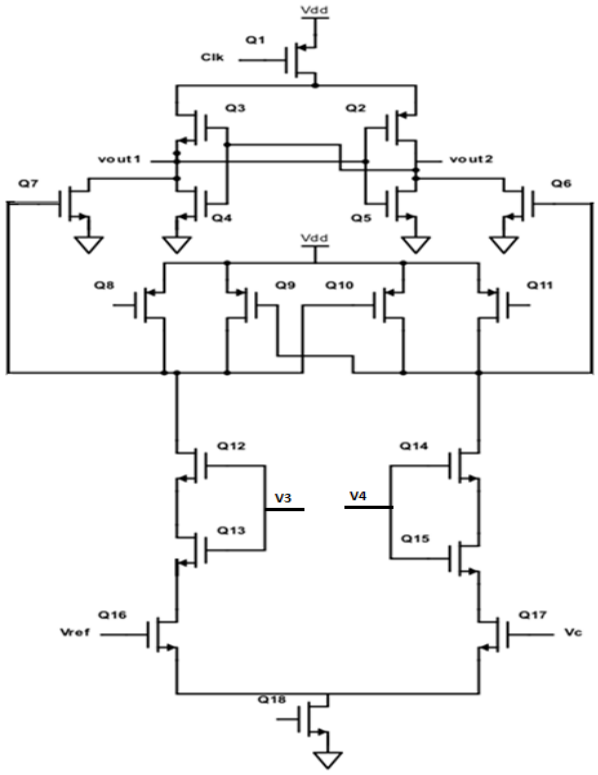

Fig. 5. Cascaded Double Tail Comparator [4]

The Cascaded Double Tail comparator is a high speed and a low power comparator and is most appropriate for the application.[4] It has been designed using the 45nm CMOS technology. The devices that are used are pmos1v and nmos1v which form a part of gpdk045. The pulse widths for V_c, V_{ref} and clk are specified. The voltages vpulse and vdc are a part of the library analogLib. The amplitude of 1V is applied to all. For V_c the period is 30ns, pulse width is 15ns and DC voltage is 0.8 V. For V_{ref} the period is 40ns, pulse width is 20ns and DC voltage is 1.1V. For clk the period is 20ns, pulse width is 10ns and DC voltage 1V. The supply voltage is 1V. The Double Tail comparator has been designed using Cadence Virtuoso Analog Design Environment and is shown in Fig. 5. The specifications for designing the pre charge circuit are shown in Table II.

TABLE II SPECIFICATIONS FOR DESIGNING COMPARATOR

Library	Model name	Pin Name	Specification
gpdk045	pmos1v, nmos1v	Vref, Vc	L = 45nm, VDD = 1V
analogLib	Vdd	Not applicable	1V
	vpulse	Not applicable	1.1 V
	gnd	Not applicable	-
analogLib	vpulse	Vref	Period = 40ns Pulse width = 20ns. DC Voltage = 1.1 V
		Vc	Period = 30ns Pulse width = 15ns DC Voltage = 0.8 V
		clk	Period = 20ns Pulse width = 10ns DC Voltage = 1V

The specification for performing transient analysis is shown in Table III. The transient analysis has been performed for the Cascaded Double tail comparator. The stop time is set to 200ns and the accuracy defaults are set to moderate.

.

TABLE III SPECIFICATIONS FOR PERFORMING TRANSIENT ANALYSIS OF THE COMPARATOR

Analysis	Specification
Transient	Analysis: tran Stop time: 200ns Accuracy defaults: Moderate

IV. RESULTS OF PRE CHARGE CIRCUIT

The pre charge circuit was designed with the Double tail comparator and a gate driver circuit. The output of the comparator was a constant DC voltage which verified it functionality and is shown in Fig. 6.

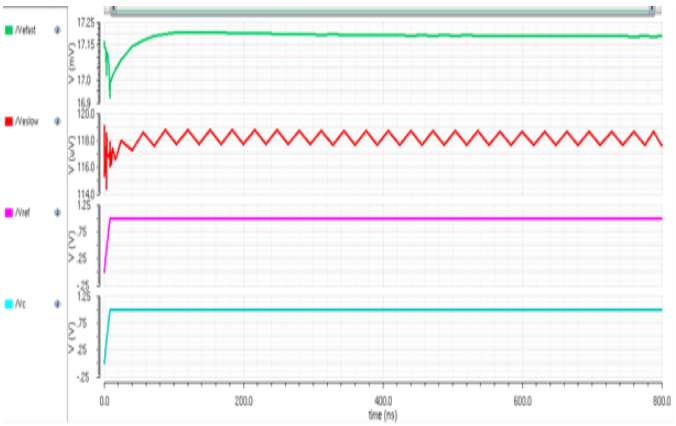

Fig. 6. Output of the comparator

The energizing and de-energizing of the capacitor is depicted in Fig. 7.

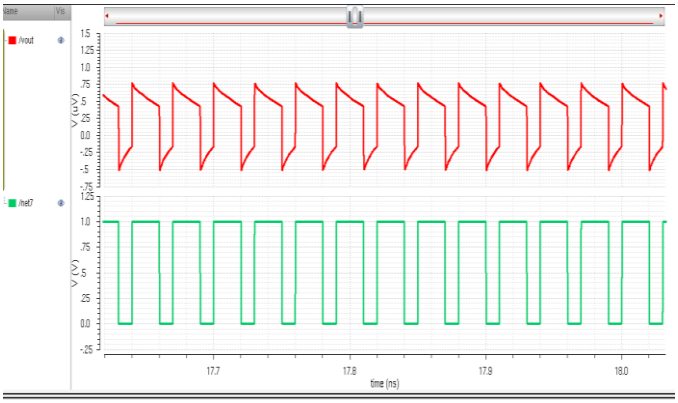

Fig. 7. Energizing and de energizing of the comparator

Vc and Vref were the two inputs and Vefast and Veslow were the two outputs. When the comparator output was 1, the gate driver sent the output to the capacitor, and it charged. When the output was 0, the capacitor de-energized. This happened when the comparator output was 0. The input voltage was 1V and the output voltage during charging was 0.75µV. This happened when the output of the comparator was high. When the output of the comparator was low, the capacitor discharged. This voltage was the difference between 0.75µV and -0.50 µV.

The energy during charging is given by

$$E = \frac{1}{2}CV^2$$
$$= \frac{1}{2} \text{x } 1\text{pF x } (0.75\mu V)^2$$
$$= 0.281 \text{ x } 10^{-9} \text{ f Joules}$$

The energy during discharging is given by

$$E = \frac{1}{2}C(V_{MAX} - V_{MIN})^2$$
$$= \frac{1}{2} \text{ X } 1\text{pF x } (0.75\mu V - (-0.50\ \mu V))^2$$
$$= 0.781 \text{ x } 10^{-9} \text{ f Joules}$$

The net energy increase by the capacitor is given by

= energy during discharging – energy during charging
= (0.781 x 10^{-9} f Joules - 0.281 x 10^{-9} f Joules)
= 0.5 x 10^{-9} f Joules

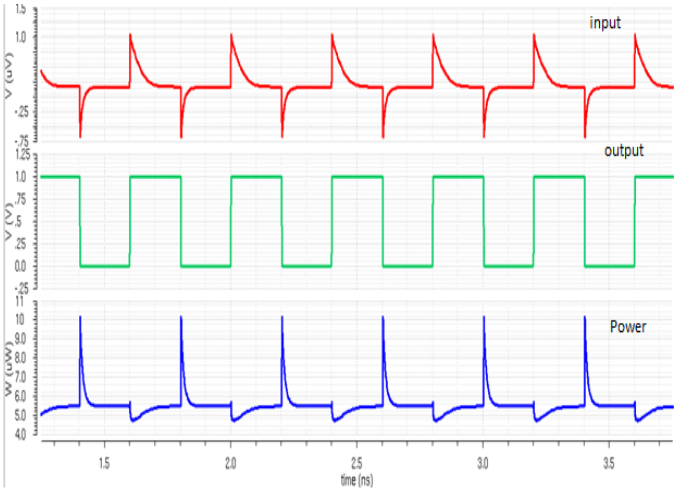

Fig. 6. Computation of power of pre charge circuit

Computation of power of the pre charge circuit is shown in Fig. 6. The applied input was 1V. During charging of the capacitor, the output peak power was 4.5µW. During discharging the power was higher which computed to 10µW. The energy consumption of the circuit is given by $E = \frac{1}{2}CV^2$. The energy and power consumption of the circuit is shown in Table IV.

TABLE IV ENERGY AND POWER CONSUMPTION OF PRE-CHARGE CIRCUIT

Power consumption		Energy consumed (fJ)	
Charging	**Discharging**	**Charging**	**Discharging**
4.5µW	10µW	0.281 x 10^{-9}	0.781 x 10^{-9}

A comparison was done with the previous works. The invested and obtained energies were compared. The energy during charging was 0.281 x 10^{-9} fJ and the energy during discharging was 0.781 x 10^{-9} fJ. Comparison of energy consumption with previous works is shown in Table V.

TABLE V ENERGY CONSUMPTION AND COMPARISON WITH PREVIOUS WORKS

Parameters	Invested Energy	Obtained Energy	Net Energy Gain	Gain in percentage
Previous work [1]	-5.629 nJ	-4.356nJ	1.273nJ	22.61%
Present work	0.281 x 10^{-9} fJ	0.781 x 10^{-9} fJ	0.5 x 10^{-9} f J	177.94%

In the previous work [1], the invested energy was -5.629 nJ and the obtained energy was -4.356nJ. The net energy gain per cycle was 1.273nJ. The gain in percentage was 22.61%. In the present design the invested energy was 0.281 x 10^{-9} fJ and the obtained energy was 0.781 x 10^{-9} fJ. The net energy gain was 0.5 x 10^{-9} f J. The net energy gain in percentage was 177.94%.

V. CONCLUSION

The capacitance value for designing the pre charge circuit has been obtained from the capacitive pressure sensor in COMSOL Multiphysics 5.3. A plot of capacitance versus pressure gave the equivalent capacitance for the applied pressure. A value of 1pF was chosen for an applied pressure of 22.5 to 25 KPa, to design the pre charge circuit. In the pre charge circuit, the energy consumption during charging of the capacitor was computed to be 4.5µW and during discharging it was computed to be 10 µW. The invested energy was 0.281 x 10^{-9} fJ and the obtained energy was 0.781 x 10^{-9} fJ. The net energy gain was 0.5 x 10^{-9} fJ and the percentage gain was 177.94%. In the previous work [1], the invested energy was -5.629 nJ and the obtained energy was -4.356nJ. The net energy gain per cycle was 1.273nJ. The gain in percentage was 22.61%.

REFERENCES

[1] E. O. Torres and G. A. Rincon-Mora, "A 0.7um BiCMOS Electrostatic Energy-Harvesting System IC," in *IEEE Journal of Solid-State Circuits*, vol. 45, no. 2, pp. 483-496, Feb. 2010.

[2] E. O. Torres and G. A. Rincon-Mora, "Self-Tuning Electrostatic Energy-Harvester IC," in *IEEE Transactions on Circuits and Systems II: Express Briefs*, vol. 57, no. 10, pp. 808-812, Oct. 2010.

[3] B. D. Truong, C. Phu Le and E. Halvorsen, "Analysis of Electrostatic Energy Harvesters Electrically Configured as Bennet's Doublers," in *IEEE Sensors Journal*, vol. 17, no. 16, pp. 5180-5191, 15 Aug.15, 2017.

[4] B.Manoj Kumar, Dr.N.Muthu Kumaran" Design of Low Power High Speed Cascaded Double Tail Comparator"in *International Journal of Advanced Research in Biology Engineering Science and Technology (IJARBEST)*, Vol. 2, Issue 6, pp. 18-22, , June 2016

[5] B. D. Truong, C. Phu Le and E. Halvorsen, "Analysis of Electrostatic Energy Harvesters Electrically Configured as Bennet's Doublers," in *IEEE Sensors Journal*, vol. 17, no. 16, pp. 5180-5191, 15 Aug.15, 2017.

[6] M. J. S. Smith, L. Bowman and J. D. Meindl, "Analysis, Design, and Performance of a Capacitive Pressure Sensor IC," in *IEEE Transactions on Biomedical Engineering*, vol. BME-33, no. 2, pp. 163-174, Feb. 1986.

[7] K. Ibrahim and G. Khanna, "Optimum design of a capacitive pressure sensor," *2016 3rd International Conference on Computing for Sustainable Global Development (INDIACom)*, New Delhi, 2016, pp. 1685-1688.

Proceedings of the Fourth International Conference on Communication and Electronics Systems (ICCES 2019)
IEEE Conference Record # 45893; IEEE Xplore ISBN: 978-1-7281-4261-4

DESIGN AND IMPLEMENTATION OF NOVEL ECG ACQUISITION SYSTEM

J.Dharneeshkar
Department of Electronics and Communication Engineering
Amrita Vishwa Vidyapeetham
Coimbatore, Tamilnadu, India.
dharneeshkar@gmail.com

Dr.V.Vanitha
Department of Computer Science and Engineering
Kumaraguru College of Technology
Coimbatore, Tamilnadu, India.
vanitha.v.cse@kct.ac.in

***Abstract*— The electrocardiogram (ECG) helps to read the electrical and muscular functions of the heart. The burdensome part in Electrocardiogram (ECG) acquisition is that the signal voltage levels are typically ranging between 0.1mV and 5mV but the noise levels are in few volts. This makes the signal too weak and extraction is done by amplification of the ECG signal, rejecting noise and interference signals. The amplification levels are fixed according to its compatibility with devices such as digital storage oscilloscope (DSO). This report deals with the design and implementation of an instrumentation amplifier with appropriate filtering circuits.9th order Butterworth lowpass and high pass filters are used to reject noise. The circuit is designed and simulated using Multisim. The circuit is hardware implemented and tested in real-time and analysis of the results are presented.**

Keywords*— *ECG, Butterworth filter, Instrumentation amplifier, sallen key topology, differential amplifier

I. INTRODUCTION

ECG signal records the electrical activity of the heart. One cycle of the ECG signal consists of the P wave, QRS complex along with T wave. Each has its own importance and value. Cardiovascular diseases account for more than a million deaths per year worldwide. Information about a wide range of cardiac disorders can be pulled out from an ECG signal. ECG can also detect the presence of any damage to the heart. The main objective of this paper is to acquire the ECG signal, display the signal on a DSO and to thus understand the system used in biomedical instrumentation. The circuit is divided into three parts namely,

- Instrumentation Amplifiers
- High pass filter
- Low pass filter

This paper explains the design and hardware implementation of the ECG acquisition system. Section 2 describes the various studies related to the ECG acquisition. Section 3 describes the proposed system with circuit design. Section 4 deals with the simulation and experimental results. Section 5 gives the conclusion of the work and future work.

II. RELATED WORKS

The authors in [1] use second order Butterworth low pass and high pass filters which don't exhibit higher roll off in filter response and removal of noise is not done to the expected levels. In [4] µa741 operational amplifier is used in the circuit which produces more internal noise and has higher offset values. The authors [5] implemented filtering circuits, that doesn't help in pulling out a clear ECG signal which contains high levels of noise. In [7] fifth-order Bessel filters were implemented. Higher order filters can be used to increase the precision of the circuit.

III. OBTAINING AN ECG SIGNAL

The block diagram of the ECG acquisition system is shown in Fig. 1. The Ag-AgCl electrodes are attached as shown to the human body and connected to the instrumentation amplifier (IA). The output of IA is given to filters and thus a clean ECG signal is obtained.

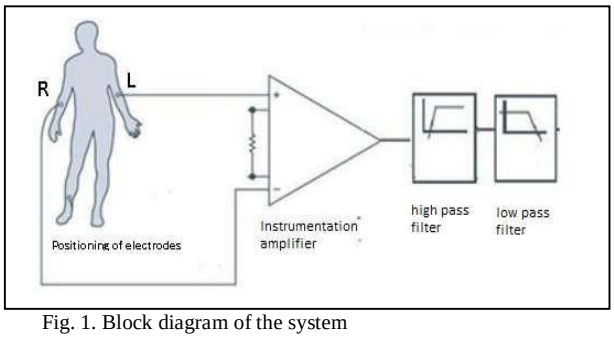

Fig. 1. Block diagram of the system

A. Instrumentation amplifier

An instrumentation amplifier (IA) as shown in Fig. 2 is a difference amplifier meeting the following specifications:

- Extremely high (ideally infinite) common-mode and differential mode input impedances.
- Very low (ideally zero) output impedance
- Accurate, stable gain and extremely high common-mode rejection ratio.

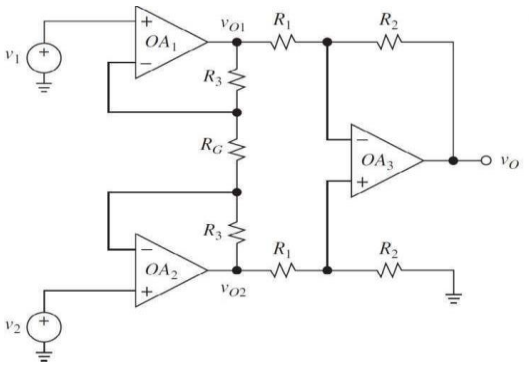

Fig. 2. Instrumentation Amplifier

The foremost function of the instrumentation amplifier is to reject common mode noise and amplify a low-level signal. This can be achieved by providing a good Common Mode Rejection Ratio (CMRR). Thus, from equation 1 it can be inferred that to increase CMRR, A_{cm} must be decreased.

$$CMRR=20*\log |A_{dm}/A_{cm}| \quad (1)$$

Normally the peak value of the ECG signal is 1mV. Thus, for further processing of the signal amplification is required. So, by using equation 2 gain is fixed.

$$gain= (1+2 R_3/R_G) *R_2/R_1 \quad (2)$$

Effect of resistance mismatches:

An instrumentation amplifier will be insensitive to common mode only as long as the resistors satisfy the balanced-bridge condition. In general, it can be said that if the bridge is unbalanced, the circuit will respond not only to differential mode but also to common mode signals. It is apparent that for high CMRRs the resistors must be very tightly matched, and this is achieved as shown in Fig. 3 by matching the values by adjusting the value of the Rpot until it is perfectly matched and lowest possible common mode gain is attained.

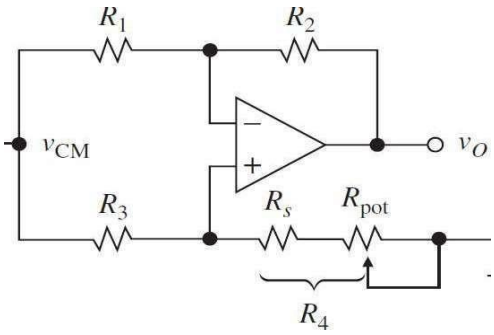

Fig. 3. CMRR Optimization

Another key aspect in IA is the choice of an operational amplifier. As the ECG signal is in very low amplitude levels an opamp with low offset voltage and low noise is required to accurately amplify the required signal. Thus, the op27 precision operational amplifier is suitable for this application.it has an offset voltage of 10 μ V and noise, en = 3.5 nV/ √ Hz, at 10 Hz. It also has Low drift: 0.2 μV/° C and High speed: 2.8 V/μs slew rate.

B. Filters

ECG signal lies in a frequency range of 0.5Hz to 40Hz. So, there is a need for a filter that allows only the ECG signal's frequency range and rejects all other frequencies. It is impossible to attain a brick wall response but the order of the filter plays an important role. Butterworth curve becomes somewhat rounded near cut off frequency and rolls off at an ultimate rate of −20 dB/Dec in the stopband.

The higher the order n, then the closer the response is to the brick-wall model. The cut off frequency is determined by equation 3.

$$fc=1/(2*\pi*R*C) \quad (3)$$

Fig. 4,5 depicts the Butterworth second order high pass and low pass filter. It serves as a building block for higher order filters. The operational amplifier used in the design is op07, which is cheap and has a low offset voltage.

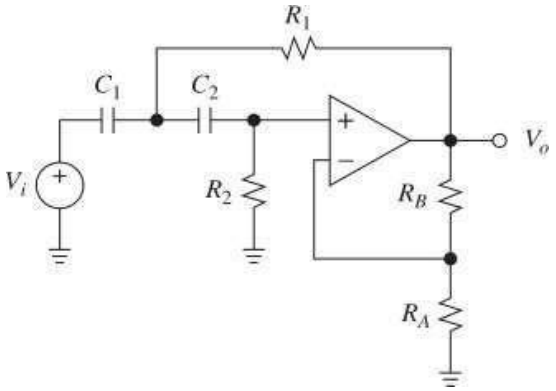

Fig. 4. Butterworth 2nd order High pass filter

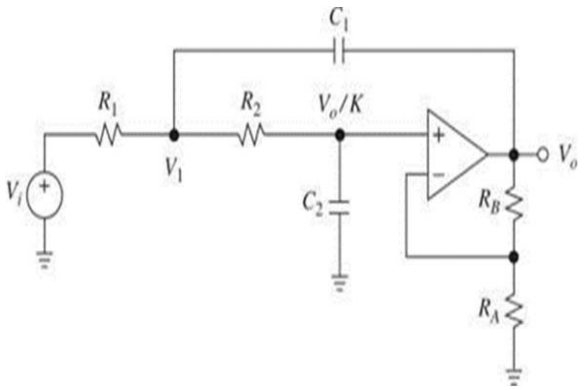

Fig. 5. Butterworth 2nd order Low pass filter

Imposing R1 = R2 = R and C1 =C2 =C we get the design equation,

$$RC=1/\omega, K=3-1/Q, RB=(K-1)RA \quad (4)$$

By using equation 4 we can design our desired nth order filter. In our case to get a 9th order filter, four 2nd order filters and one 1st order filter is cascaded. The Q values for each second order filter cascade is determined from the normalized Butterworth low pass filter table and substituted in equation 4 to get the required RA and RB values. Fig. 6 and 7 show the design for 9th order high pass and low pass filters respectively. The low pass and high pass designs are cascaded to get the desired response. Each operational amplifier circuit is a second order filter and thus four operational amplifier circuits constitute eighth order and finally, an RC is cascaded to get a desired ninth order.

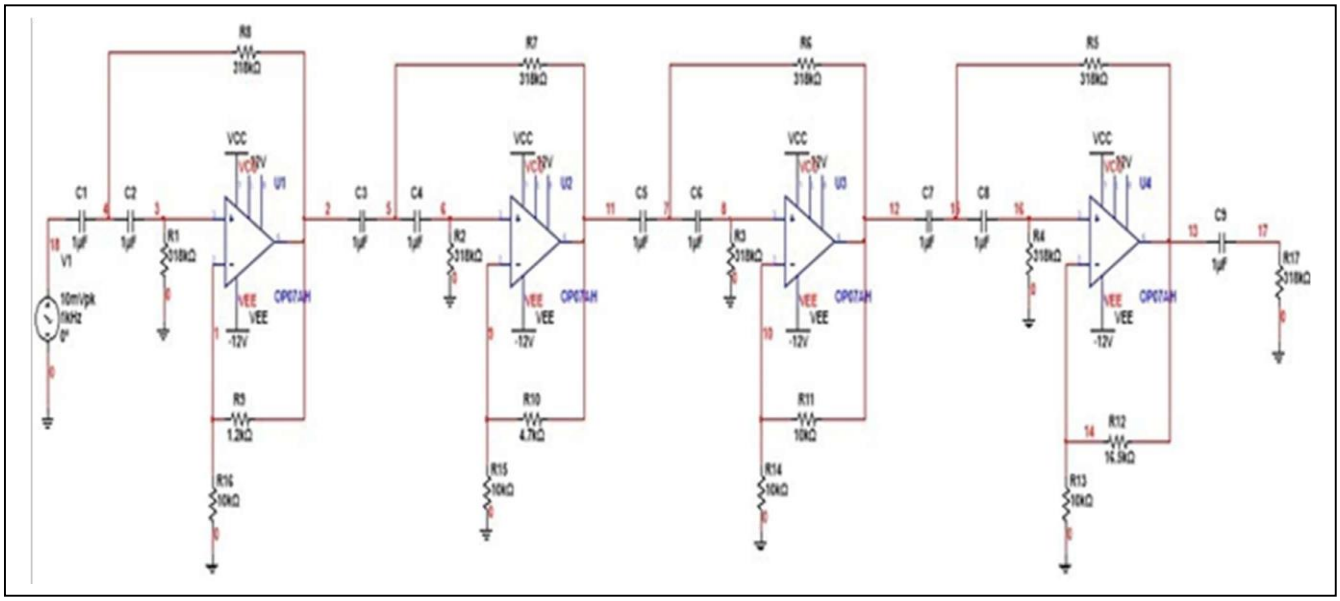

Fig. 6. Ninth order Butterworth High pass filter

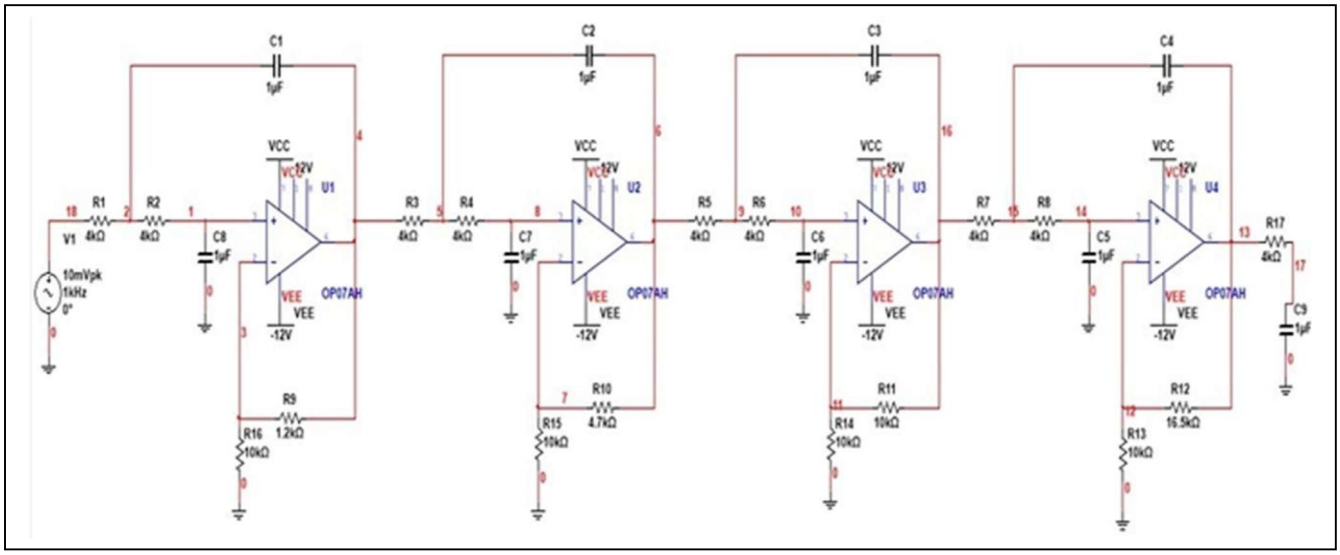

Fig. 7. Ninth order Butterworth Low pass filter

IV. RESULTS

The cascaded filter response is shown in fig. 8. The filter has a lower cutoff frequency as 0.5Hz and higher frequency cutoff of 40Hz. As it is a ninth order filter it has a roll off of -180dB/Dec. This higher roll off separates the noise and signal components. Simulations are carried out using Multisim tool and the results are verified. Fig. 9,10,11 shows the hardware implementation of the ECG acquisition system. Tolerance of the resistor plays a crucial role in our system, so 1% tolerance resistors are used throughout. Filters used in the circuit are active analog filters.

The cumulative gain of the high pass (Fig. 10) and low pass filter (Fig. 11) is 75. Thus, cascading instrumentation amplifier and the filter will yield a total gain of 750. Hence, the entire circuit amplifies the ECG signal 750 times and also filter of the noise.

Fig. 12 shows the final output of the proposed ECG acquisition system taken from a human volunteer. Thus, the system is able to reduce noise and amplify the ECG signal. It produces very efficient and continuous ECG signal that can be recorded.

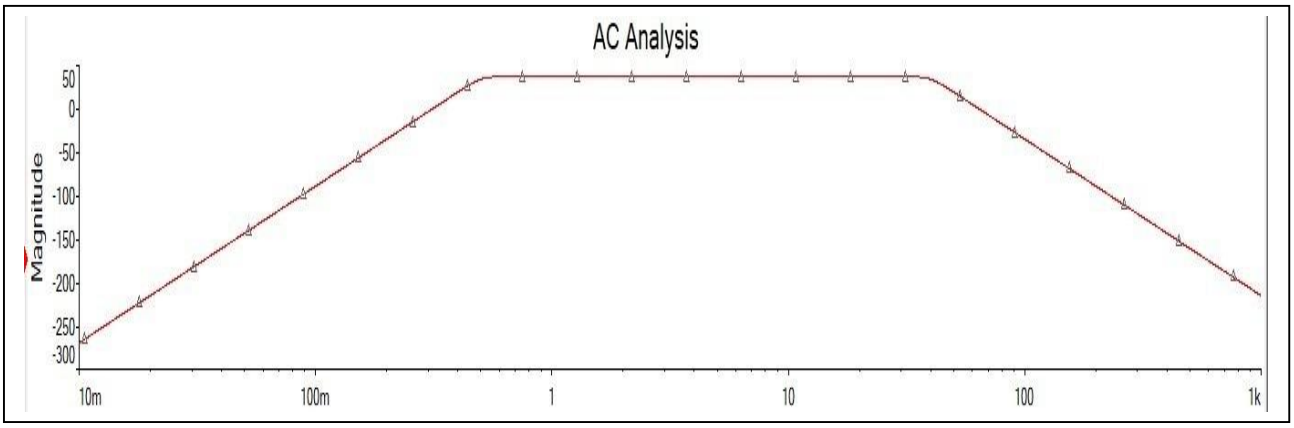

Fig. 8. Filter response

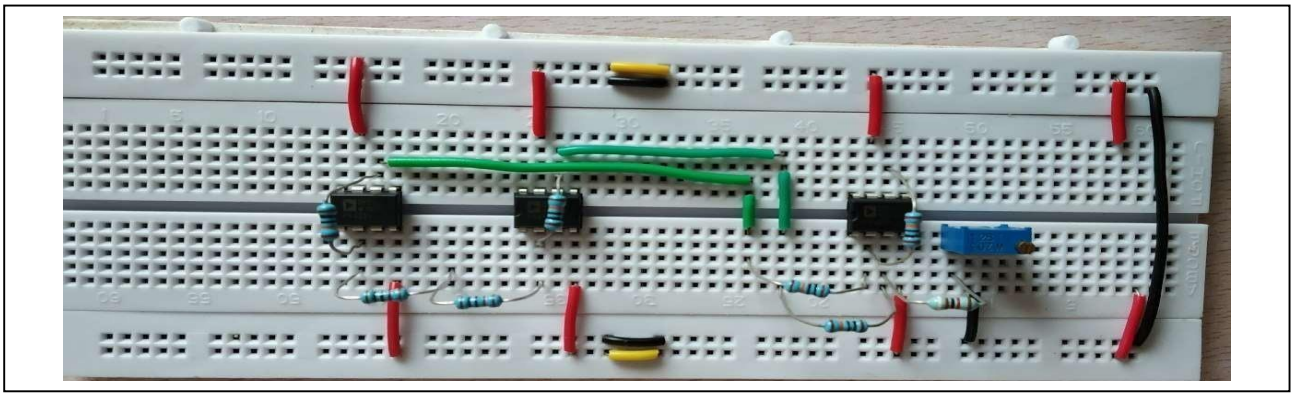

Fig. 9. Instrumentation amplifier

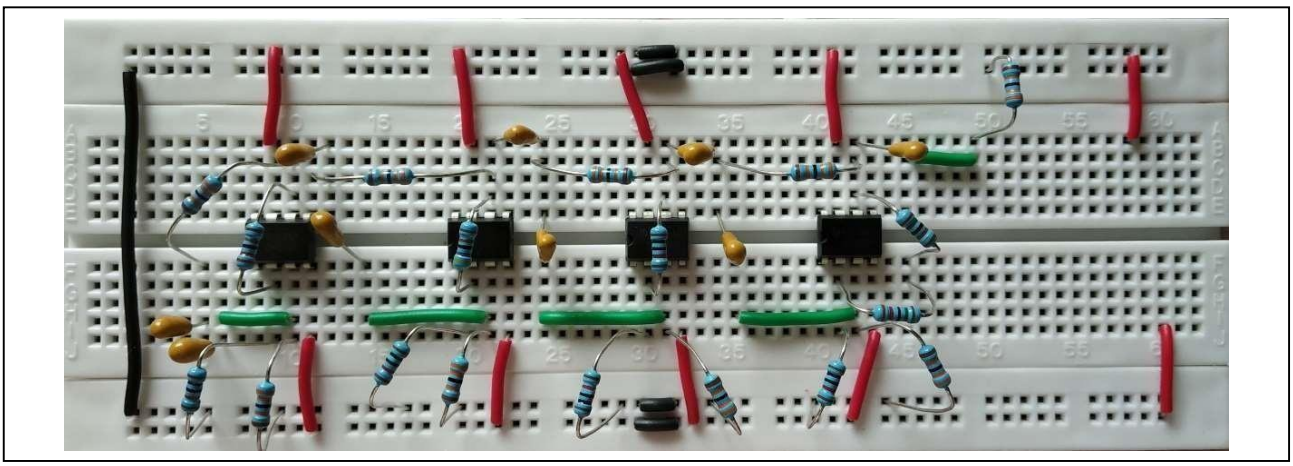

Fig. 10. Ninth order high pass filter

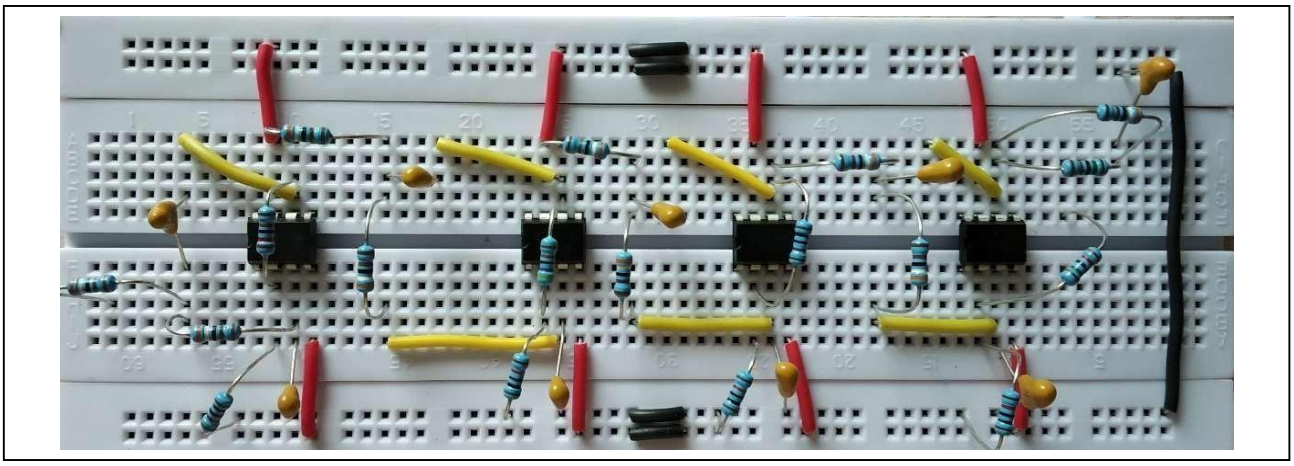

Fig. 11. Ninth order low pass filter

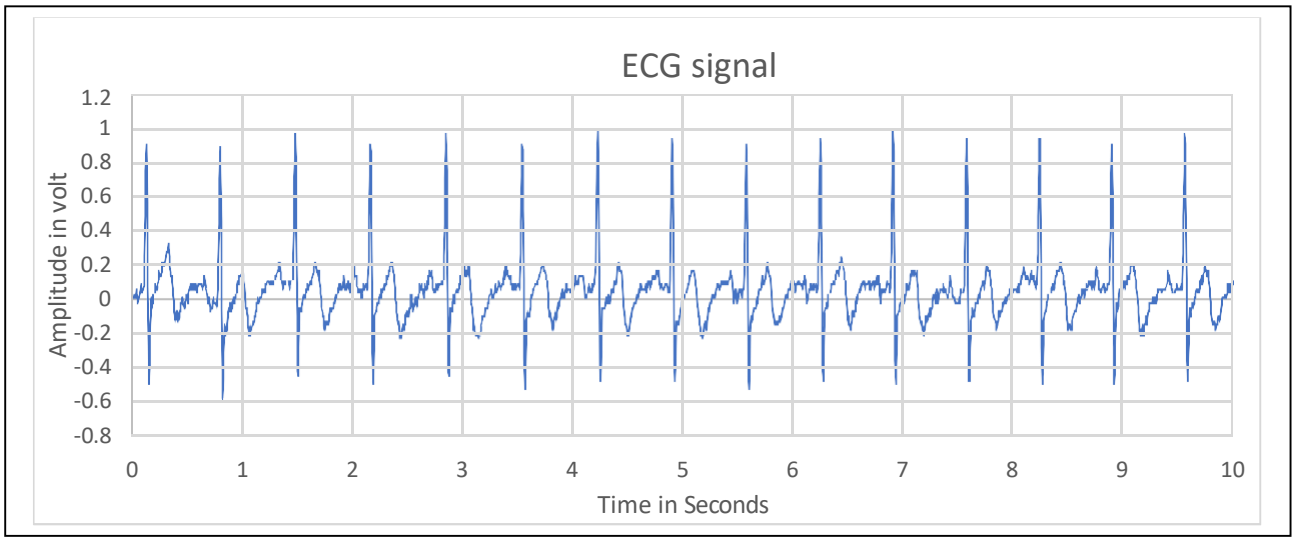

Fig. 12. The output of the system

CONCLUSION

A circuit that has a structure has been built on a breadboard. Conventional Ag/AgCl plated disposable ECG electrodes were used to get the ECG signals from the human volunteer. The output shows that successful conditioning of the raw ECG signal is performed. The system is able to remove artifacts and high-frequency noise. Ninth order filter plays a crucial role in the removal of the above-mentioned noises. Filter's sharp cutoff frequency removes the unwanted frequencies and thereby giving a smooth response of the output signal as seen in Fig. 12. Further, the system can be implemented in a printed circuit board to reduce noise to a greater extent. Also, using a Bessel filter instead of a Butterworth filter enhances the performance of the system.

REFERENCES

[1] Mr.Bhimasen G Tasaganva, Dr.Ganesh V Bhat, 2014, ECG Acquisition System, INTERNATIONAL JOURNAL OF ENGINEERING RESEARCH & TECHNOLOGY (IJERT) Volume 03, Issue 03 (March 2014).

[2] Sergio Franco. Design with operational amplifiers and analog integrated circuits. 4th ed. New York: McGraw-Hill Education,2015.

[3] J. Huang, T. Huang and F. Li, "Design of a low electrode offset and high CMRR instrumentation amplifier for ECG acquisition systems," 2018 14th IEEE International Conference on Solid-State and Integrated Circuit Technology (ICSICT), Qingdao, 2018, pp.1-3.

[4] Yadav, Uma & Pancholi, Utkarsh & Tugnawat, Aman & Patnaik, Ranjana. (2014). DESIGNING OF PORTABLE AND LOW COST ECG SIGNAL ACQUISITION SYSTEM. Journal of Biological Engineering Research and Review. 1.

[5] Z. Gao, J. Wu, J. Zhou, W. Jiang, and L. Feng, "Design of ECG Signal Acquisition and Processing System," 2012 International Conference on Biomedical Engineering and Biotechnology, Macao, 2012, pp. 762-764.

[6] S. Jain, S. Pathak and B. Kumar, "A robust design and analysis of analog front end for portable ECG acquisition system," 2016 IEEE Region 10 Humanitarian Technology Conference (R10-HTC), Agra, 2016, pp. 1-5.

[7] Du WY, Jose W. Design of an ECG sensor circuitry for cardiovascular disease diagnosis. Int J Biosen Bioelectron. 2017;2(4):120–1.

[8] M. A. Ahamed, M. K. Hasan, M. S. Alam, "Design and Implementation of Low Cost ECG Monitoring System for the Patient Using Smartphone," International Conference on Electrical & Electronic Engineering, 2015.

[9] U. Satija, B. Ramkumar and M. S. Manikandan, "Automated ECG Noise Detection and Classification System for Unsupervised Healthcare Monitoring," in *IEEE Journal of Biomedical and Health Informatics*, vol. 22, no. 3, pp. 722-732, May 2018.

[10] T. Tsai, J. Hong, L. Wang and S. Lee, "Low-Power Analog Integrated Circuits for Wireless ECG Acquisition Systems," in *IEEE Transactions on Information Technology in Biomedicine*, vol. 16, no. 5, pp. 907-917, Sept. 2012.

[11] J. Li, G. Deng, W. Wei, H. Wang and Z. Ming, "Design of a Real-Time ECG Filter for Portable Mobile Medical Systems," in *IEEE Access*, vol. 5, pp. 696-704, 2017.

[12] C. Sawigun and S. Thanapitak, "A 0.9-nW, 101-Hz, and 46.3-μVrmsIRN Low-Pass Filter for ECG Acquisition Using FVF Biquads," in *IEEE Transactions on Very Large Scale Integration (VLSI) Systems*, vol. 26, no. 11, pp. 2290-2298, Nov. 2018.

Proceedings of the Fourth International Conference on Communication and Electronics Systems (ICCES 2019)
IEEE Conference Record # 45898; IEEE Xplore ISBN: 978-1-7281-1261-9

Facial Expression Recognition using Convolutional Neural Network and SoftMax function on Captured Images

Ashish Deopa, Abhishek Sinha, Aditya Prakash, Rupesh Kumar Sinha
Electronics & Communication Engineering
Birla Institute of Technology, Mesra
Ranchi, India

***Abstract* - Facial Expression Recognition is an extremely interesting topic of research owing to the uniqueness attached to emotions of different humans. Deep Learning is a novel zone within the domain of machine learning which is exceedingly efficient in image classification problems. Methods of Deep Learning, (CNN) Convolutional Neural Networks in particular, have been used with great precision for the purpose of feature extraction. This paper categorizes each facial image into one of the seven human emotion classes by making use of a specially designed Convolutional Neural Network which employs four subsequent sets of layers and a loss function. The model has been trained and tested on the FER2013 data set from the *Kaggle Facial Expression Recognition Challenge*, which consists of 35,887, 48-by-48-pixel pictures of human faces, which are grayscale in nature, each with a label of one of the 7 emotion categories. The model gives an accuracy of about 64%.**

Keywords: Facial Emotion Recognition, Deep Learning, CNN, Convolutional Neural Network.

I. INTRODUCTION

Facial expression is a perceptible manifestation of the cerebral activity, physiology, psychology, temperament, intentions and state of mind of a person. Facial Expressions are vital for social interactions as they provide cues and guide conversations. It is also an essential mode of non-verbal communication, the study of which can make lives easier for all human beings. David Matsumoto declared that there are seven basic human emotions, namely sadness, happiness, anger, surprise, disgust, fear and neutral. and each term is a family of connected emotions. [1] It has also been seen that it is easier to differentiate between emotions which are genuine than among those that are unfelt. Facial Expression Recognition has continued to remain an inspiring and challenging problem in computer vision and continues to pique the interest of researchers because the way in which people show their expressions varies and this difference makes the objective of classification into categories exceptionally tedious. Facial Expression Recognition in computer vision because the difference in people's way of expressing Computer vision is a domain that provides computers with instincts and intelligence that is comparable to humans. It works towards training computers to perceive things in the same way as humans do, process that input and then provide the required output. However, this is a rather tedious task.

The edge between the physical and the digital world is continuously blurring. This has given rise to Human-Computer interaction. These new modes of interaction usually require the capture of the observable behaviour of the user for which artificial perception techniques like computer vision are useful. Vast strides in technology and artificial intelligence have made Human-Computer interaction very feasible and detection of human emptions by machines is one of the most trending subjects that is being researched. [2] Due to the vast applications of emotion recognition in areas of Human-Computer Interaction, various methods have been applied. Facial expression recognition usually utilizes a three-tier training involving Face Acquisition [3], Feature Extraction [4] and Classifier Construction [5,6]. In [7], the writers proposed four stages for recognition: face extraction, pre-processing, principle component analysis (PCA) and classification. Later, some works [8, 9] exhibited that combination of facial feature extraction stage and classifier construction stage can benefit the process of emotion recognition. A model to evaluate facial representation based on statistical local characteristics and binary patterns was devised in [10]. Lajevardi et al. used K-NN classifier to classify the selected features [11]. A different technique was proposed in [12], which made use of the 2-D discrete cosine transform, over the picture of the face, as a feature detector and a constructive feed forward neural network, with a concealed layer, as an emotion classifier.

However, due to a surge in the availability of computational power and increasingly huge training databases to train and test the models, the machine

learning technique has become the dominating force in the field of emotion detection in recent times. As times have evolved, Deep Learning, which is a subset of Machine Learning itself, has taken over; especially for cases which make use of image data. Deep Learning models not only work more efficiently with image datasets, but the algorithms can also self-determine whether a prediction is precise or not. Hong Wei NG et al. used a transfer learning approach for Deep CNN architectures. They pre-trained their network on the ImageNet dataset and fine-tuned their network in two stages using two different datasets. Their results verified that this cascading of fine-tuning yielded better results [13]. In [14], a face detection classification network was designed which was a collective of multiple deep CNNs. Again, the pre-trained networks were fine-tuned on SFEW 2.0 dataset and then combined to learn ensemble weights of individual networks. Heechul Jung et al. devised a double stage process. Firstly, the face was detected from image using Haar-like features. Secondly, the deep network was used for classifying the facial expression of the detected face. They also compared two types of deep networks, and the convolution neural network was found to trump the other neural network in performance [15]. In [16], Ma Xiaoxi et al. employed Deep Boltzmann Machine (DBM) and SVM (Support Vector Machine). Ali Mollahosseini et al. designed a network consisting of two convolutional layers each ensued by max pooling and then four Inception layers [17]. Abir Fathallah et al. offered a novel architecture based on CNN for facial expressions recognition. They used Visual Geometry Group model (VGG) to fine tune their architecture and acquired better results [18]. In [19], Neha Jain et al. proposed a hybrid Convolution-Recurrent Neural Network method. The architecture consisted of Convolution layers which extracted the relations and patterns in the images, subsequently followed by Recurrent Neural Network which considered the temporal dependencies in the images during classification. Bazrafkan in [20] showed that the accuracy in prediction of emotion was lower when different databases were used for training and testing.

By virtue of facial expression recognition, assistance can be lent to monitor patients in hospital or psychiatric wards. It can be used during sessions with therapists or psychiatrists. It is an excellent feedback tool whose services can be availed by banks, movie theatres, supermarkets etc. Another domain which can benefit greatly from facial expression detection is e learning where real time feedback can be supplied to online tutors or tutorial videos.

II. METHODOLOGY

The objective of this work is to correctly identify the emotion depicted on the human face by making diligent use of a Convolutional Neural Network. In this, network is configured in such a way that it has four convolutional layers, each followed by a down-sampling Pooling layer and a terminating fully connected layer as shown in fig. 1. In the Fully Connected Layer, SoftMax Activation function is used.

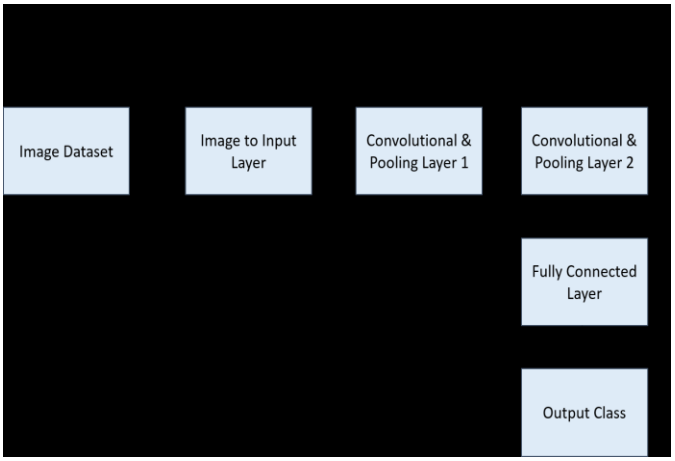

Fig 1. Flowchart

Convolutional Neural Networks fall under the domain of Deep Learning and the reasoning for choosing Deep Learning over Machine Learning is the fact that these algorithms can determine whether an estimate is accurate or not, on its own. Also, Deep Learning networks work better with large data than classical ML algorithms and image classification is one field where Deep Learning has shown immense hike in quality from Machine Learning. Convolutional Neural Networks, also known as ConvNets, aren't very different from ordinary Neural Networks. Their fundamental structure consists of neurons with weights and biases that possess the ability to learn themselves. Every neuron is provided with some input, a dot product with some weight is calculated and a non-linearity is optionally attached. From the raw input data input at one end, we get a class score at the other and this score is achieved by virtue of an activation function that succeeds the last fully connected layer. The difference from regular Neural Networks lies in the fact

that the layers of a CNN have neurons which are arranged in three dimensions: width, depth and height. This attribute is of utmost use when working with image or other visual data. We do not have to perform any operations on the images to extract features. Instead of features, the image themselves are provided as input to the network, unlike in the case of Artificial Neural Networks.

Generic Neural Networks do not scale properly to complete images. In FER2013, images are only of size 48*48*1, so a single fully connected neuron would have 48*48*1 = 2304 weights. This amount is still small enough to be managed but since the dataset has more than 35,000 images and we would most certainly be needing the use of several such neurons; the number of weights becomes unmanageable. Evidently, this full connectivity is futile, and the huge number of weights would easily cause overfitting.

The CNN layers used in the network are described below:

A. Convolutional Layer

This is the foremost layer which helps us to extract useful features from the input image. Convolution is the first layer to extract features from an image. Convolution conserves the relationship between pixels by learning features of the image using small squares of input data. This layer makes use of a set of filters which have learnable weights. The image is represented by its pixels in matrix form and a similar representation is used by the filters. The matrix extends across the three dimensions but since we have used grayscale images, the depth dimension is unity. Convolution takes place between the two matrices, where the filter slides across the height and width of the image matrix and calculates dot products, resulting in the formation of a convolved feature map. Stride is the value which tells the filter the number of pixels that need to be jumped for next convolution. When the stride is 1, every pixel is covered 1 by 1. Sometimes, padding the image with zeros around the edges helps to cover the entire image and prevent data loss. This is called zero padding.

B. Pooling Layer

Succeeding every convolutional layer is a Pooling Layer which helps us in decreasing the spatial volume of the samples, to lessen the quantity of parameters and to control computational load and overfitting. The Pooling Layer in the proposed network makes use of the MAX operation and operates independently on every depth slice of the input, ensuring that only the feature with the most prominence is protected. This results in down-sampling or resizing of the data.

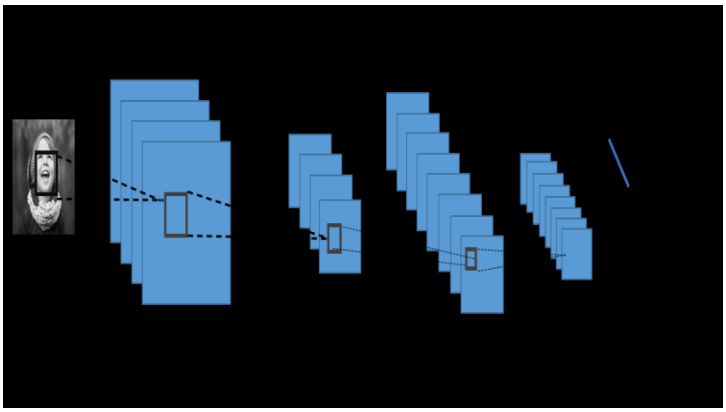

Fig 2. Representation of the network

C. Fully Connected Layer

After multiple convolutional and pooling layers, the final categorization of the images into emotion classes is performed by the Fully Connected Layer. The matrix is flattened to form a vector. All the neurons in this layer have connections to all outputs of the previous layer and the output of this can simply be calculated by matrix multiplication. The activation function used here is the SoftMax function. It is a type of sigmoid function, but it is of use when we are trying to classify data into several classes. In this work, the number of classes is 7. The SoftMax function squeezes the outputs for all these 7 classes between 0 and 1 and divides by the sum of the outputs.

III. DATASET

We have trained our model on the FER2013 data set from the *Kaggle Facial Expression Recognition Challenge*, which consists of 35,887, 48-by-48-pixel grayscale pictures of human faces, each with a label of one of the 7 emotion categories (table 2): **anger, disgust, fear, happiness, sadness, surprise, and neutral**. Training, cross validation and testing has been performed on the dataset in the ratio of 80: 10: 10.

Table 1. Model Configuration

Layer (type)	Output Shape	Param #
conv2d_1 (Conv2D)	(None, 48, 48, 64)	640
batch_normalization_1 (Batch	(None, 48, 48, 64)	256
activation_1 (Activation)	(None, 48, 48, 64)	0
max_pooling2d_1 (MaxPooling2	(None, 24, 24, 64)	0
dropout_1 (Dropout)	(None, 24, 24, 64)	0
conv2d_2 (Conv2D)	(None, 24, 24, 128)	204928
batch_normalization_2 (Batch	(None, 24, 24, 128)	512
activation_2 (Activation)	(None, 24, 24, 128)	0
max_pooling2d_2 (MaxPooling2	(None, 12, 12, 128)	0
dropout_2 (Dropout)	(None, 12, 12, 128)	0
conv2d_3 (Conv2D)	(None, 12, 12, 256)	295168
batch_normalization_3 (Batch	(None, 12, 12, 256)	1024
activation_3 (Activation)	(None, 12, 12, 256)	0
max_pooling2d_3 (MaxPooling2	(None, 6, 6, 256)	0
dropout_3 (Dropout)	(None, 6, 6, 256)	0
conv2d_4 (Conv2D)	(None, 6, 6, 512)	3277312
batch_normalization_4 (Batch	(None, 6, 6, 512)	2048
activation_4 (Activation)	(None, 6, 6, 512)	0
max_pooling2d_4 (MaxPooling2	(None, 3, 3, 512)	0
dropout_4 (Dropout)	(None, 3, 3, 512)	0
flatten_1 (Flatten)	(None, 4608)	0
dense_1 (Dense)	(None, 256)	1179904
batch_normalization_5 (Batch	(None, 256)	1024
activation_5 (Activation)	(None, 256)	0
dropout_5 (Dropout)	(None, 256)	0
dense_2 (Dense)	(None, 512)	131584
batch_normalization_6 (Batch	(None, 512)	2048
activation_6 (Activation)	(None, 512)	0
dropout_6 (Dropout)	(None, 512)	0
dense_3 (Dense)	(None, 7)	3591

Total params: 5,100,039
Trainable params: 5,096,583
Non-trainable params: 3,456

None
Accuracy on Test set : 0.6422401783226526

Table 2. Expressions

Anger	0
Disgust	1
Fear	2
Happiness	3
Sadness	4
Surprise	5
Neutral	6

IV. APPROACH

The CNN model that we have designed consists of three layers: 4 Convolutional, 4 Pooling and 1 Fully Connected Layer. The Convolutional Layer performs convolution of the features with the weights of the sliding filter.

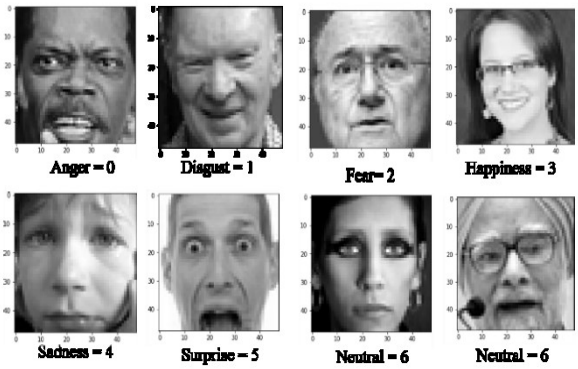

Fig 3. Sample Images from FER2013 dataset

A Batch Normalization Layer follows the convolutional layers to increase the learning rate of the network. After the Activation Layer introduces nonlinearity in the network, the Pooling Layer down samples the data. Post this, some random neurons are dropped out to prevent overfitting. The training of this model has been done on

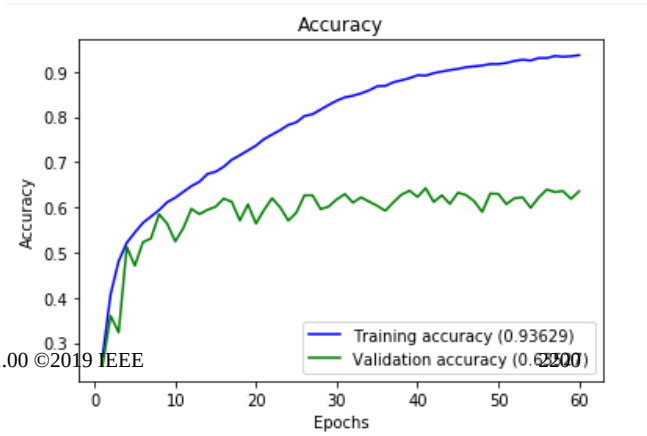

80% of the data of FER2013 dataset. The number of epochs for the training were finalised to be 60 from the following graph. Epoch is the number of iterations of the passing of the entire data through the model. Table 1 explains the model configuration of the proposed architecture. It gives the outputs of the different layers at different stages.

Fig 4. Accuracy vs Epochs graph

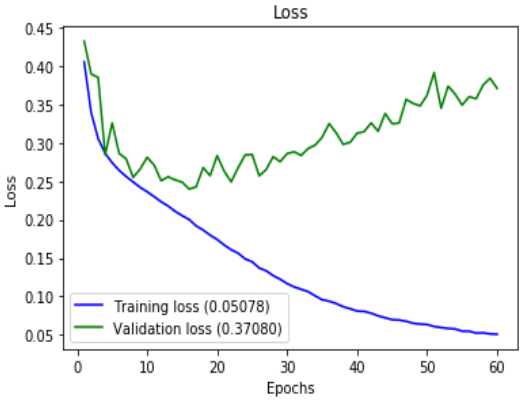

Fig 5. Normal Loss vs Epochs graph

It was observed that both the training and the validation i.e. cross-checking accuracy of the model does not increase beyond the employment of 60 epochs. After the model was trained, we tested it in two ways.

The first method of testing was the simple use of FER2013 dataset and its 10% images that had not been used for training or cross-validation. For the second method, we made use of OpenCV, a library of Python which deals with Computer Vision. By employing this, we were able to detect emotions on still images that were provided to the network as well as from images captured using a web camera.

To detect emotions on images from outside the dataset, either the image stream from our webcam or the images saved for testing, first the faces are detected using OpenCV and bounding boxes are added. Then the faces are converted to greyscale and resized so that the pre trained network can work on them. The predictions are received, and the label is added to the image. And finally, the original image stream is returned with the emotion label attached.

V. RESULTS

In our work, 28709 images from the FER2013 dataset, have been used for training and 3589 images have been used for validation and testing each. As shown in Fig. 4, the training accuracy reaches its peak at 0.93 whereas the validation accuracy comes out to be 0.64. Fig. 5 explains the normal loss. When the remaining 3589 images of the dataset are used for testing, the confusion matrix for all the seven emotions is generated. From Fig. 6, the overall accuracy for the testing images was found to be 0.6422.

The easiest emotions to detect on the dataset were Happy which had the accuracy of 0.79 and Surprise with an accuracy of 0.73. Meanwhile, Fear was a tough emotion

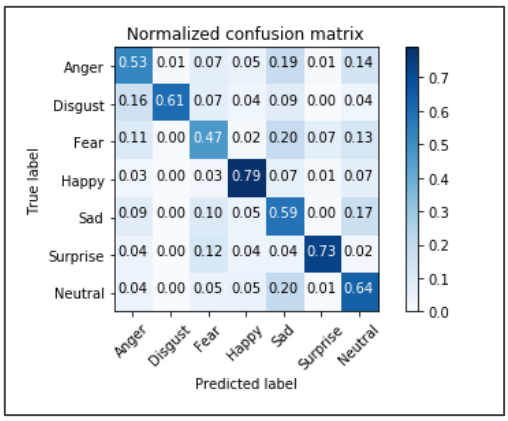

to

Fig 6. Confusion Matrix for FER2013 dataset

predict with the lowest accuracy of 0.47. The average of all the seven emotions is approximately 0.64.

In the case of live images (fig. 7), as has been previously mentioned, the emotion was returned as a label on top of the image.

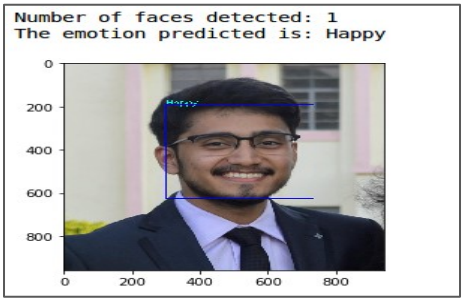

Fig 7. Emotion detection on a single stored image

The algorithm, for the extraction of faces from live or stored images, went so far as to detect multiple faces

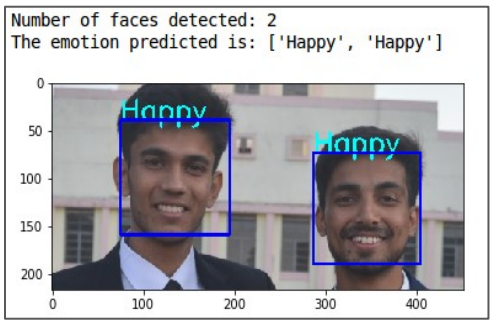

Fig 8. Stored image having multiple faces

(fig. 8) in a single image and return their respective emotions. There were also some cases where the emotions were wrongly predicted (fig. 9) and most of the confusion was centered around the emotions Neutral, Anger and Fear which were repeatedly confused for Sad.

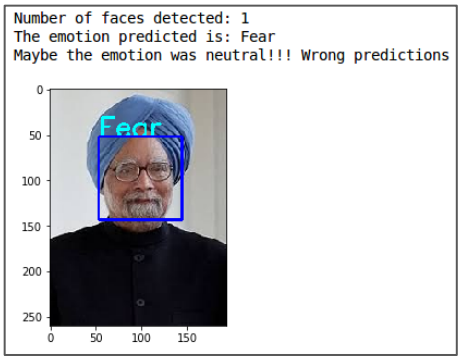

9. Wrong emotion detected

VI. CONCLUSION

Facial Emotion Recognition has been a vehemently researched topic and justifiably so owing to the innumerable applications that it allows to develop. Here, a neural network architecture is presented for the recognition of facial emotion on images. The proposed architecture consists of 4 convolutional, 4 pooling and 1 fully connected layer followed by the SoftMax activation function. After being trained on the FER2013 dataset, the model can be tested on both images from the dataset as well as on saved images or images captured from web cam. The model works for an image having a single person as well as multiple persons. The accuracy of the model turned out to be 0.64 and the emotions that were the most accurately predicted were Happy and Surprise while the emotions on the lower rungs of the accuracy leader were Fear and Anger. The proposed work can be extended for real time application by maximizing the accuracy.

REFERENCES

[1] *David Matsumoto "The Origin of Universal Human Emotions", Article prepared for National Geographic Science (Spain).*

[2] *Ali Mollahosseini, David Chan, and Mohammad H. Mahoor "Going Deeper in Facial Expression Recognition using Deep Neural Networks", IEEE Winter Conference on Applications of Computer, 2016.*

[3] *P. Viola and M. J. Jones, "Robust real-time face detection," International journal of computer vision, vol. 57, no. 2, pp. 137–154, 2004.*

[4] *S. M. Lajevardi and M. Lech, "Facial expression recognition from image sequences using optimized feature selection," in Image and Vision Computing New Zealand, 2008. IVCNZ 2008. 23rd International Conference, IEEE, 2008, pp. 1–6.*

[5] *A. Ben-Hur and J. Weston, "A users guide to support vector machines," Data mining techniques for the life sciences, pp. 223–239, 2010.*

[6] *R. Samad and H. Sawada, "Extraction of the minimum number of gabor wavelet parameters for the recognition of natural facial expressions," Artificial Life and Robotics, vol. 16, no. 1, pp. 21–31, 2011.*

[7] *Pushpaja V. Saudagare, D.S. Chaudhari, "Facial Expression Recognition using Neural Network –An Overview," International Journal of Soft Computing and Engineering (IJSCE), vol. 2, no. 1, 2012*

[8] *J. Susskind, V. Mnih, G. Hinton et al., "On deep generative models with applications to recognition," in Computer Vision and Pattern Recognition (CVPR), 2011 IEEE Conference on. IEEE, 2011, pp. 2857–2864.*

[9] *S. Rifai, Y. Bengio, A. Courville, P. Vincent, and M. Mirza, "Disentangling factors of variation for facial expression recognition," Computer Vision–ECCV 2012, pp. 808–822, 2012.*

[10] *Caifeng Shan, Shaogang Gong, Peter W. McOwan "Facial expression recognition based on Local Binary Patterns: A comprehensive study," Image and Vision Computing 27, 2009 pp. 803–816.*

[11] *S. M. Lajevardi and Z. M. Hussain, "Feature selection for facial expression recognition based on mutual information,"* 2009 5th IEEE GCC Conference & Exhibition, *Kuwait City, 2009, pp. 1-5.*

[12] *L. Ma and K. Khorasani, "Facial Expression Recognition Using Constructive Feedforward Neural Networks," IEEE Transactions on Systems, Man, and Cybernetics, Part B (Cybernetics), vol. 34, no. 3, 2004, pp. 1588 – 1595.*

[13] *Hong-Wei Ng, Viet Dung Nguyen, Vassilios Vonikakis, Stefan Winkler, "Deep Learning for Emotion Recognition on Small Datasets Using Transfer Learning," ICMI'15 Proceedings of the 2015 ACM on International Conference on Multimodal Interaction, 2005, pp. 443-449.*

[14] *Zhiding Yu and Cha Zhang, "Image based Static Facial Expression Recognition with Multiple Deep Network Learning", ICMI '15 Proceedings of the ACM on International Conference on Multimodal Interaction, 2015, pp. 435-442.*

[15] *Jung, Heechul & Lee, Sihaeng & Park, Sung Il & Kim, Byungju & Kim, Junmo & Lee, Injae & Ahn, Chunghyun, "Development of deep learning-based facial expression recognition system," 2015 21st Korea-Japan Joint Workshop on Frontiers of Computer Vision (FCV), Mokpo, 2015, pp. 1-4.*

[16] *M. Xiaoxi, L. Weisi, H. Dongyan, D. Minghui and H. Li, "Facial emotion recognition," 2017 IEEE 2nd International*

Conference on Signal and Image Processing (ICSIP), Singapore, 2017, pp. 77-81.

[17] *A. Mollahosseini, D. Chan and M. H. Mahoor, "Going deeper in facial expression recognition using deep neural networks," 2016 IEEE Winter Conference on Applications of Computer Vision (WACV), Lake Placid, NY, 2016, pp. 1-10.*

[18] *A. Fathallah, L. Abdi and A. Douik, "Facial Expression Recognition via Deep Learning," 2017 IEEE/ACS 14th International Conference on Computer Systems and Applications (AICCSA), Hammamet, 2017, pp. 745-750.*

[19] *Neha Jain, Shishir Kumar, Amit Kumar, Pourya Shamsolmoali, Masoumeh Zareapoor, "Hybrid deep neural networks for face emotion recognition," Pattern Recognition Letters, vol. 115, 2018, pp. 101-106.*

[20] *S. Bazrafkan, T. Nedelcu, P. Filipczuk and P. Corcoran, "Deep learning for facial expression recognition: A step closer to a smartphone that knows your moods," 2017 IEEE International Conference on Consumer Electronics (ICCE), 2017, pp. 217-220.*

Proceedings of the Fourth International Conference on Communication and Electronics Systems (ICCES 2019)
IEEE Conference Record # 45898; IEEE Xplore ISBN: 978-1-7281-1261-9

Analysis of Horizontal Grounding Electrode in Transmission Line Approach

Koppakula Nagarjuna
Department of Electrical Engineering
National Institute of Technology Raipur
Raipur, Chhattisgarh, INDIA
nagarjuna.koppakula@gmail.com

K Chandrasekaran
Department of Electrical Engineering
National Institute Of Technology Raipur
Raipur, Chhattisgarh, INDIA
Kchandrasekaran.ee@nitrr.ac.in

Abstract— **Understanding impulse response of a buried electrode helps for designing a better grounding system under the situations of surges. In this paper, the analysis of lightning impulse current has been carried on horizontal grounding electrode by varying its length. Present study has been performed using the approximate transmission line (TL) approach. In TL approach, space-time telegrapher's equation are reformed to Finite Difference Time Domain (FDTD) equations and the same are used for calculating induced voltage and current along the length of the grounding electrode. The aim of this work is to verify the applicability of this approach in the analysis of the horizontal grounding electrode excited by high impulsive currents. The effects of the ground conductivity (σ) on the induced over voltages and current on ground electrode is analyzed and results are reported.**

Keywords—finite difference time domain (FDTD), grounding, horizontal electrode, lightning, transmission line(TL)

I. INTRODUCTION

Grounding system main objective is to provide low path impedance for flow of surge and fault current, so that we can protect power system equipment. During lightning discharge large impulse current could flow in grounding systems and induces transients, these induced voltages will cause damage or mal function of sensitive devices. Transient electromagnetic field analysis which are coupled to horizontal grounding electrode is of continuous interest in electromagnetic compatibility (EMC) [1-3]. Analysis of transient response of grounding system excited by impulsive currents is given in [4-6]. Design of grounding system for protecting power system equipment including time dependent nonlinear soil ionization are reported in [7].

Basically there are two models to find voltage and currents in grounding conductor due to transient magnetic fields (i) antenna theory model and (ii) transmission line (TL) approximation [8]. Both models can be solved either in frequency or time domain. Antenna theory approach is more rigorous one and takes more computational time and cost. Transient analysis of simple ground by using wire AT is given in [9]. TL approach is a classical and sufficient approximation for long length lines with electrically small cross sections, but for high frequency excitations of finite length line it is not precise.

Standard TL approach restrictions can be overcome by using enhanced TL models [10]. Wire antenna theory model and modified transmission line model (MTLM) in frequency domain are used to find the transient response of horizontal grounding electrode is in [10].

Using Finite Difference Time Domain (FDTD) method induced voltages and currents at every node is calculated by using the approach developed by using Taylor MTL equations and the expressions representing localized networks [11]. Direct time domain analysis of electromagnetic fields coupling to buried thin wire by antenna theory approach and by TL approach are compared in [12].

By taking the soil ionization and coupling between elements in to consideration, the transient behavior of horizontal grounding electrode when excited with lightning currents [13]. The nature of impedance of horizontal grounding electrodes which is immersed in soil of various resistivity has been studied by applying the Transmission Line Method in [14].

Space time Pocklington integrodifferential equation used in AT model, and telegrapher's equation is used in TL model are compared and reported in [15]

In this paper transient currents due to lightning on horizontal grounding electrode is calculated by space time telegrapher's equations from transmission line approach. FDTD method is used to solve the telegrapher's equation to find current and voltages at each point along the length of the electrode.

II. HORIZONTAL GROUNDING ELECTRODE

The study of impulse currents and voltages on horizontal grounding electrode is helps for getting better knowledge of power system grounding and for proper operation of sensitive devices at load side.

A. transmission line model:

Approximate transmission line (TL) approach is using for transient analysis of a horizontal grounding electrode dunked

in ground for finding impulse current and voltages. In this study ground is considered as imperfect i.e. it is having finite value of ground conductivity (σ≠∞). The schematic diagram representing the study of impulse response of the grounding electrode is shown if Fig.1. In TL approach set of solution of telegrapher's equations will give voltage and current values at every space and instant of time. Finite Difference Time Domain (FDTD) method is used for simplifying and solving set of telegrapher's equations.

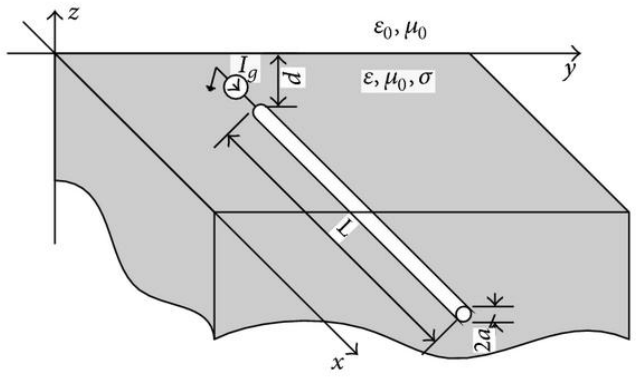

Fig. 1. Schematic diagram of horizontal grounding electrode

Lightning impulse current is the excitation or source for to examine transient behaviour of the horizontal grounding electrode buried at a certain depth of imperfect ground.

Exciting current can be theoretically represented using double exponential function (1) which is also a representation of lightning current [16]:

$$I_g(t) = I_0\left(e^{-\propto t} - e^{-\beta t}\right) \quad (1)$$

Where I_0 - is the amplitude of impulse current

$\propto$, β - constants for tail and front.

The numeric for above parameters considered in this study is as follows.

$$I_0 = 100 \times 10^3 A, \propto = 7.1622 \times 10^4 s^{-1}$$
$$\text{and} \beta = 2.0768 \times 10^7 s^{-1}.$$

The set of telegrapher's equations [17] used in this study for getting impulse voltages and current on grounding electrode is given in (2) and (3):

$$\frac{\partial v(x,t)}{\partial x} + Ri(x,t) + L\frac{\partial i(x,t)}{\partial t} = 0 \quad (2)$$

$$\frac{\partial i(x,t)}{\partial x} + Gv(x,t) + C\frac{\partial v(x,t)}{\partial t} = 0 \quad (3)$$

Consider ground electrode is a pure conductor, so resistance R=0, parameters L, G, C are calculated using (4) as follows.

$$L = \frac{\mu_0}{2\pi}\ln\left(\frac{2l}{\sqrt{2ad}} - 1\right),$$

$$G = \frac{2\pi\sigma}{\ln\left(\frac{2l}{\sqrt{2ad}} - 1\right)},$$

$$C = \frac{2\pi\varepsilon_0\varepsilon_r}{\ln\left(\frac{2l}{\sqrt{2ad}} - 1\right)}. \quad (4)$$

Here l is length, a is radius and d is depth of a horizontal electrode buried. μ_0 is permeability of air ε_0 is relative permittivity σ is conductivity of the ground.

B solution of telegrapher's equation using FDTD:

Telegrapher's equations numerical solution is done by using FDTD method [18-19]. FDTD method is proposed by YEE in 1966. It is popular numerical method for finding transient response of transmission line. The derivatives in the telegraph equations are discretized and approximated with various finite differences. In this method the position variable x is discretized to Δx and the time variable t is discretized to Δt.

FDTD method is originally used for solving the Maxwell's equation [20]. In this the differentiation is taken as difference of future and past values in time and difference of next and previous values in space differentiation. Maxwell's equations are having differentiation in terms of both time and space, and the values of magnetic field and electric fields are interdepend on each other. To find the next step electric field it is need to use present magnetic field values and similarly for finding next step magnetic needs present electric field values [21]. Fig.2. represents the Finite Difference Time Domain (FDTD) discretization used in the present study.

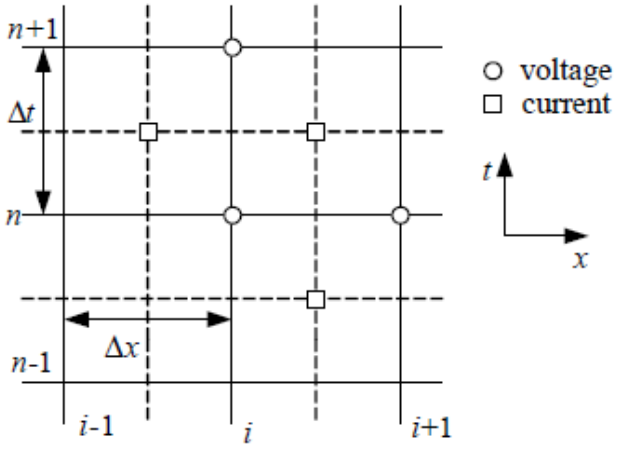

Fig. 2 Time and special discretization of line in FDTD method.

In Fig.2. shows the time and special discretization of horizontal conductor considered in this study. Taking finite differences for voltages and currents the following equation (5) is used as given in [22].

$$\frac{\partial v(x,t)}{\partial x} = \frac{v_{k+1}^{n} - v_{k}^{n}}{\Delta x}\,,$$

$$\frac{\partial i(x,t)}{\partial t} = \frac{i_{k+1/2}^{n+1/2} - i_{k+1/2}^{n-1/2}}{\Delta t} \qquad (5)$$

Substitute (5) in (2) and result is given in (6)

$$\frac{v_{k+1}^{n} - v_{k}^{n}}{\Delta x} + R\frac{i_{k+1/2}^{n+1/2} + i_{k+1/2}^{n-1/2}}{2} + L\frac{i_{k+1/2}^{n+1/2} - i_{k+1/2}^{n-1/2}}{\Delta t} = 0 \qquad (6)$$

By rearranging (6) gives (9) for finding current at every instant of time and space of conductor.

$$i_{k}^{n+\frac{3}{2}} = \left(\frac{\Delta x}{\Delta t}l + \Delta x\frac{r}{2}\right)^{-1} \cdot \left[\left(\frac{\Delta x}{\Delta t}l - \Delta x\frac{r}{2}\right)\cdot i_{k}^{n+\frac{1}{2}} - \left(v_{k+1}^{n+1} - v_{k}^{n+1}\right)\right] \text{ For k=1, 2…N} \qquad (7)$$

$$\frac{\partial i(x,t)}{\partial x} = \frac{i_{k+1/2}^{n+1/2} - i_{i-1/2}^{n+1/2}}{\Delta x}\,, \quad \frac{\partial v(x,t)}{\partial t} = \frac{v_{k}^{n+1} - v_{k}^{n}}{\Delta t} \qquad (8)$$

Substitute (8) in (3), and resultant is given in (9)

$$\frac{i_{k+1/2}^{n+1/2} - i_{i-1/2}^{n+1/2}}{\Delta x} + G\frac{v_{k}^{n+1} + v_{k}^{n}}{2} + C\frac{v_{k}^{n+1} - v_{k}^{n}}{\Delta t} = 0 \qquad (9)$$

By rearranging (9) gives (10) for finding voltage at every instant of time and space of conductor.

$$v_{k}^{n+1} = \left(\frac{\Delta x}{\Delta t}c + \Delta x\frac{g}{2}\right)^{-1} \cdot \left[\left(\frac{\Delta x}{\Delta t}c - \Delta x\frac{g}{2}\right)\cdot v_{k}^{n} - \left(i_{k}^{n+\frac{1}{2}} - i_{k-1}^{n+\frac{1}{2}}\right)\right] \text{ For k=2, 3…N} \qquad (10)$$

The following expressions are applied to evaluate the voltages at line terminations by using boundary conditions,

$$v_{1}^{n+1} = \left(\frac{\Delta x}{\Delta t}c + \Delta x\frac{g}{2}\right)^{-1} \cdot \left[\left(\frac{\Delta x}{\Delta t}c - \Delta x\frac{g}{2}\right)\cdot v_{1}^{n} - 2i_{1}^{n+\frac{1}{2}} + \left(i_{g}^{n+1} - i_{g}^{n}\right)\right] \qquad (11)$$

$$v_{nx+1}^{n+1} = \left(\frac{\Delta x}{\Delta t}c + \Delta x\frac{g}{2}\right)^{-1} \cdot \left[\left(\frac{\Delta x}{\Delta t}c - \Delta x\frac{g}{2}\right)\cdot v_{nx}^{n} + 2i_{nx}^{n+1/2}\right] \qquad (12)$$

The current excitation i_g^n at the time instant t=nΔt is given by (1). From (7) and (10) it is observed that, the current and voltages are interdependent on each other. Hence by coding (7), (10), and by taking voltage boundary condition (11), (12), results of voltage and current at each and every time instant at all spatial distances of conductor are evaluated. FDTD method gives best solution only when the spatial and temporal step are satisfying the stability condition as follows

$$\Delta t \cdot V_p < \Delta x$$

Where

$$V_p = \frac{1}{\sqrt{LC}}$$

III. RESULTS OF HORIZONTAL GROUNDING ELECTRODE

In this study a horizontal electrode which is having a length of L=10 m, and radius of a=5 mm, buried in a ground at a depth of d=0.5 m are considered. The relative permittivity of ground is ε_r =10. The source of excitation for the horizontal grounding electrode is simulated using a double exponential current function with I_0=100 kA. The numerical results are obtained by solving telegrapher's equations using FDTD method.

The excitation to the horizontal electrode for transient analysis is 0.1/1 μs pulse having parameter values are as follows,

$$\alpha = 9.4385 \cdot 10^{5} \text{ (1/s)}$$

$$\beta = 1.5 \cdot 10^{7} \text{ (1/s)}$$

Taking Δx=1 m and 10 m horizontal grounding electrode is divided into 10 equal parts. From the FDTD stability condition, the value of Δt should be less than $1 \cdot 10^{-8}$.

In this paper results shown are with

$$\Delta t = 0.4 \cdot 10^{-8}$$

Fig.3. represents the transient response at 2 m of 10 m long electrode, and Fig.4. represents the transient response at 5 m of electrode, and Fig.5. represents transient current at 8 m by taking ground conductivity of $\sigma_g = 1mS/m$.

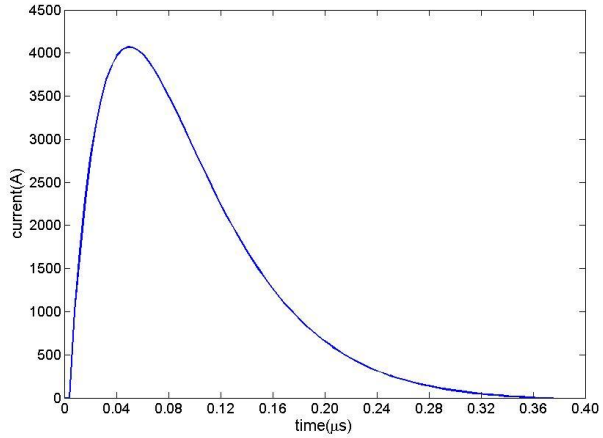

Fig. 3 current at 2 m of grounding electrode with ground conductivity of $\sigma_g = 1mS/m$

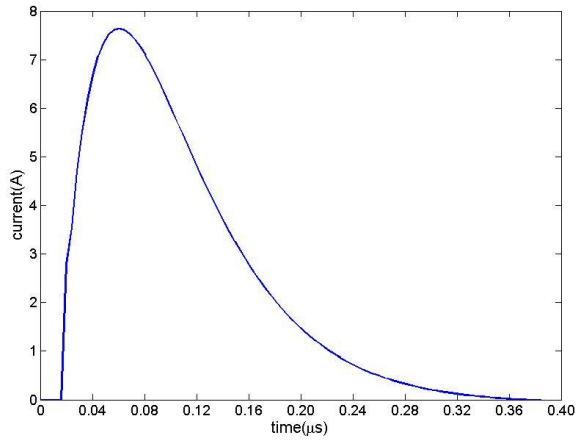

Fig. 4 current at 5 m of grounding electrode with ground conductivity of $\sigma_g = 1mS/m$

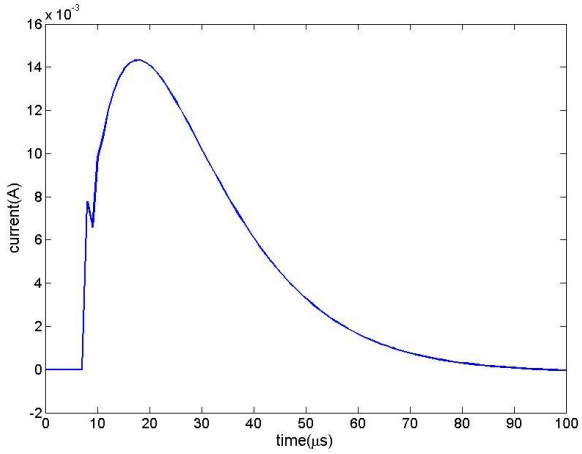

Fig. 5 current at 8 m of grounding electrode with conductivity of $\sigma_g = 1mS/m$

TABLE 1

Table.1: Peak value of impulse current at different observation point along 10 m length of horizontal electrode for different ground conductivities.

Conductivity of ground (σ_g) S/m	Peak of impulse current (A) from the injection point			
	2 m	5 m	8 m	10 m
0.0001	9186	18.15	0.03586	0.000501
0.0005	5622	10.85	0.02096	0.000288
0.001	4068	7.637	0.01432	0.000189
0.01	617	0.7851	0.001267	0.00001744

From Fig.3. and Fig.4. it observe that the peak of the impulse current at 2 m from injection point is in terms of kilo amperes. Whereas the impulse current peak is decreased to ampere at 5m and mille amperes at 8 m distance for the same injecting current.

For the same input with different conductivities of ground the peak and transient response of current changes at every observation point. Table 1 is provided peak values of current at 2 m, 5 m, 8 m and 10 m with different conductivities of ground. From the Table 1 we can observe that when the conductivity of ground is increasing peak of current is decreasing.

Impulse current at that injection point (0 m) in kA, but at the end of the conductor (10 m) is in mA. The impulse current reduces rapidly while it reaches to another end of conductor.

Fig.6, 7 and 8 shows the plots of the impulse current at the observation point 2 m, 5 m and 8 m distances from the origin, for the assumed ground conductivities varies from 0.0001S/m to 0.01S/m.

From the Fig.6. it can be observed that for a observation point close to the origin (2 m) the peak current is almost equal to 9 kA with 0.0001 S/m, were as same injecting current decreased to less than 1 kA with 0.01 S/m ground conductivity.

Hence, it can be that the ground conductivity plays as vital role to attenuate the current which is travelling on the horizontal grounding conductor.

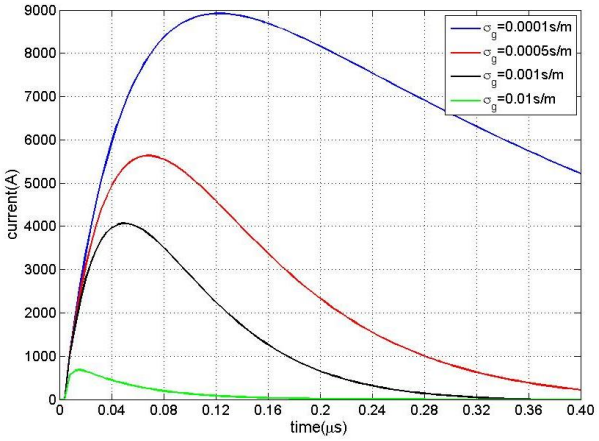

Fig. 6. impulse current at 2 m with different conductivities of ground.

In Fig.7. impulse current waveforms at 5 m distance from the starting of conductor with different conductivities of ground is given

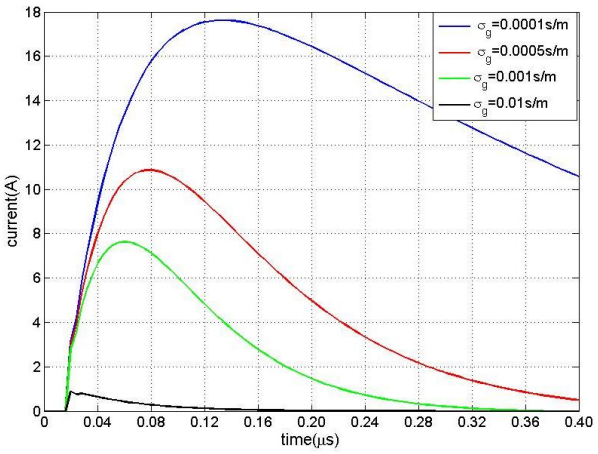

Fig.7. impulse current at 5m with different conductivities of ground.

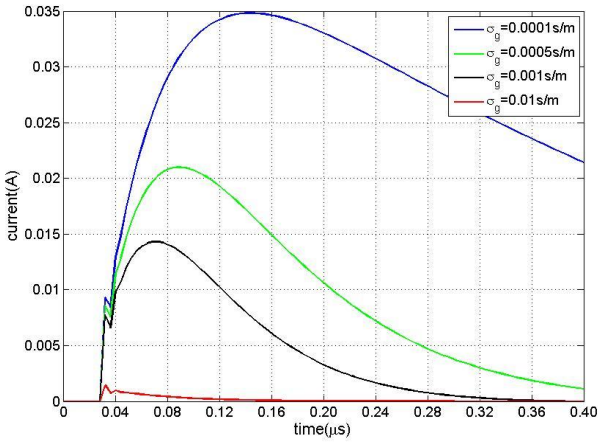

Fig. 8 impulse current at 8 m with different conductivities of ground.

From Fig.7. we can observe that impulse current having more peak value with low conductivity of ground than with the high conductivity of ground. In Fig.8 the same trend can be observe at 8 m distance from starting of the conductor. In Fig.6, 7 and 8 peak of current waveform with conductivity of 0.0001 is more than other conductivities, means the peak value is keep on reducing when conductivity of ground is increasing.

IV. CONCLUSION

The present study conducts investigation of impulse response in horizontal grounding electrode due to lightning surge. It can helps for efficient designing of grounding system under the aforementioned conditions. The transmission line (TL) model, telegrapher's equation solved by Finite Difference Time Domain (FDTD) is used for the transient analysis of the grounding system considered in in the study.

By applying double exponential impulse input to the horizontal grounding electrode we observe the transient current at 2 m and 6 m and 8 m from the source end. And from the graphs it can be observe that input impulse current magnitude is attenuating while it goes to another end of the electrode, from KA to mA. Also observe that the attenuation of the impulse is more if conductivity of earth is more.

REFERENCES

[1] Grcev, Leonid D., and Frank E. Menter. "Transient electromagnetic fields near large earthing systems." *IEEE Transactions on Magnetics* 32.3 (1996): 1525-1528.

[2] Liu, Yaqing, Mihael Zitnik, and Rajeev Thottappillil. "An improved transmission-line model of grounding system." *IEEE Transactions on Electromagnetic Compatibility* 43.3 (2001): 348-355.

[3] Ala, Guido, and Maria Luisa Di Silvestre. "A simulation model for electromagnetic transients in lightning protection systems." *IEEE Transactions on Electromagnetic Compatibility* 44.4 (2002): 539-554.

[4] Suflis, S. A., I. F. Gonos, F. V. Topalis, and I. A. Stathopulos. "Transient behaviour of a horizontal grounding rod under impulse current." *Recent Advances in Circuits and Systems, Word Scientific Publishing Company, Singapore* (1998): 61-64.

[5] Gonos, I. F., V. T. Kontargyri, F. V. Topalis, and I. A. Stathopulos. "Transient behaviour of a horizontal electrode under impulse current." In *XIIIth International Symposium on High Voltage Engineering*. 2003.

[6] Tsumura, Masanobu, Yoshihiro Baba, Naoto Nagaoka, and Akihiro Ametani. "FDTD simulation of a horizontal grounding electrode and modeling of its equivalent circuit." *IEEE transactions on electromagnetic compatibility* 48, no. 4 (2006): 817-825.

[7] Grcev, Leonid. "Modeling of grounding electrodes under lightning currents." *IEEE Transactions on Electromagnetic Compatibility* 51.3 (2009): 559-571.

[8] Tesche, Frederick M., et al. *EMC analysis methods and computational models*. John Wiley & Sons, 1997.

[9] Poljak, Dragan, Vicko Doric, Sinisa Antonijevic, Khalil El Khamlichi Drissi, and Kamal Kerroum. "Electromagnetic field coupling to overhead wires: comparison of wire antenna and transmission line model in the frequency and time domain." In *2007 19th International Conference on Applied Electromagnetics and Communications*, pp. 1-4. IEEE, 2007.

[10] Poljak, Dragan, Vicko Doric, Khalil El Khamlichi Drissi, Kamal Kerroum, and Ivan Medić. "Comparison of wire antenna and modified transmission line approach to the assessment of frequency response of horizontal grounding electrodes." *Engineering analysis with boundary elements* 32, no. 8 (2008): 676-681.

[11] Kaouche, Senaa, Bachir Nekhoul, Kamel Kerroum, and Khalil El Khamlichi Drissi. "Induced disturbance in power network by lightning." (2007): 52-58.

[12] Poljak, Dragan, Silvestar Sesnic, Khalil El Khamlichi Drissi, and Kamal Kerroum. "Transient response of a buried wire." In *ICECom 2013*, pp. 1-4. IEEE, 2013.

[13] Chiheb, Sofiane, Omar Kherif, Madjid Teguar, and Abdelouahab Mekhaldi. "Incorporation of soil ionization and mutual coupling in transient study of horizontal grounding electrode using TLM." In *2017 5th International Conference on Electrical Engineering-Boumerdes (ICEE-B)*, pp. 1-4. IEEE, 2017.

[14] Chiheb, Sofiane, Omar Kherif, Madjid Teguar, and Abdelouahab Mekhaldi. "Impedance nature of long horizontal grounding electrode employing TLM." In *2018 International Conference on Electrical Sciences and Technologies in Maghreb (CISTEM)*, pp. 1-4. IEEE, 2018.

[15] Poljak, Dragan, Silvestar Šesnić, Khalil El-Khamlichi Drissi, Kamal Kerroum, and Sergey Tkachenko. "Transient electromagnetic field coupling to buried thin wire configurations: antenna model versus transmission line approach in the time domain." *International Journal of Antennas and Propagation* 2016 (2016).

[16] Sunde, Erling Ditlef. *Earth conduction effects in transmission systems*. Dover Publications Inc., 1949.

[17] Paul, Clayton R. Analysis of multiconductor transmission lines. John Wiley & Sons, 2008.

[18] Song, Jianhui, Yanju Liu, and Yang Yu. "Numerical analysis of transmission line telegraph equation based on FDTD method." *JCIT* 7, no. 20 (2012): 258-265.

[19] Nagel, James R. "The Finite-Difference Time-Domain (FDTD) Algorithm." Department of Electrical And Computer Engineering, University of Utah. Dostupné z WWW: http://ece. utah. edu/~ ece3300/Labs/lab4/FDTD_Introduction. pdf.[cit. 2012-04-20] (2010).

[20] Gedney, Stephen D. "The application of the finite-difference time-domain method to EMC analysis." *Proceedings of Symposium on Electromagnetic Compatibility*. IEEE, 1996.

[21] Sullivan, Dennis M. Electromagnetic simulation using the FDTD method. John Wiley & Sons, 2013.

[22] Mimouni, Abdenbi, Zin E. Azzouz, and Boualem Ghemri. "Lightning-induced overvoltages on overhead lines: Modelling and experimental validation." *Journal of Electrical Engineering-Elektrotechnicky Casopis* 58.3 (2007): 146-151.

Proceedings of the Fourth International Conference on Communication and Electronics Systems (ICCES 2019)
IEEE Conference Record # 45898; IEEE Xplore ISBN: 978-1-7281-1261-9

Data Leakage Detection by Adaptive Weighted Graph Walk Model

Manoj kumar M N
Department of Computer Science and Engineering
Siddaganga Institute of Technology, Tumkur, India.
manojram261994@gmail.com

M B Nirmala
Department of Computer Science and Engineering
Siddaganga Institute of Technology, Tumkur, India.
mbnirmala@sit.ac.in

Abstract— In recent years data security rise into a prominent area of study as there are so many threats regarding maintenance of a sensitive data. Among these threats one of the most dangerous threats is insider attack [1] where an employee of an organization leaks data to an unauthorized third party. There are so many research activities going on in this area in recent times, but the accuracy of the data leakage detection needs more accuracy level. In this paper we are going to propose an Adaptive weighted graph model where instead of content we are going to consider the context of the sensitive terms and we are going to use graphical representation method for representing the contextual information of the sensitive words. The scalability of the fresh data is improved using the label propagation algorithm. Low complexity score walk method is used to improve accuracy in determining sensitivity of sensitive terms. Exploratory outcomes demonstrate that the proposed strategy can distinguish leakage with more exactness.

Keywords— data leakage, data security, weighted graph, label propagation.

I. INTRODUCTION

There is a saying in the business world "you have to work on the business first before it works for you", it indicates that before setting up a business or before starting a new organization one must work hard and understand the needs and success rate of the business. Data analytics assists organizations identify potential opportunities to streamline operations or maximize their business and increase their profit. Associations feel that they have to accumulate tremendous potential chances to streamline activities or expand their business and increment their benefit. Associations feel that they have to accumulate colossal volumes of information before performing examination so as to produce business experiences and improve basic leadership. As the importance of data increases, data security becomes our major concern. One of the most common threats in data security is Data leakage, which indicates depiction of unenviable exposures of data. Traditional security threats are caused by the outsiders but information leakage is for the most part brought about by the insider who may leak information to the outside unapproved elements accordingly it will be of real concern.

Seriousness of data leakage does not depend on the number of records compromised, but on how much risk or damage the leakage caused for organizations or the individuals. Data Transmission mainly comprises of two components Distributor and the agents. Distributor is owner of the data and agents are the third parties who request for the data based on their requirement from the distributor. For instance the SunTrust Bank information leakage happened in April 2018. SunTrust [3] announced a representative may have released the individual information of 1.5 million clients. It is trusted that the guilty party endeavored to duplicate the information and offer it with an unapproved outsider. Correspondingly, a Tesla representative endeavored leaking information to obscure outsiders and adjusted code in the Tesla Manufacturing Operating System in 2018. It is reputed the worker, a confided in client at the time, did it for the individual advantage. These unscrupulous improvements increment the need of a productive information leakage location technique.

To address the issue of information leakage detection, a lot of research work has been finished with the utilization of hash fingerprinting, n-gram, measurable strategies etc...Because of the fast advancement of Internet, numerous new correspondence innovations have developed. Subsequently, the size of the information develops significantly and the types of information become much confused. This prompts new difficulties for information leakage identification. Accordingly, new Data Leakage Detection strategy is required with better resistance of information change and higher proficiency to manage the lot of unstructured information in long examples. Existing methods mainly focuses on the content of the data leaving behind the context which is a major drawback. There may be an issue when a document is modified by adding some contents, which leads to transform the document into a no

sensitive document results in low accuracy in detecting data leakage.

In this paper, another model named Adaptive weighted Graph Walk model is proposed to identify changed information leakage. In this technique, every one of the reports is spoken to as graphs. The delicate setting weights are spoken to as node weights and edge weights, which improve the recognition precision of the changed information. In view of the setting around the catchphrases the setting weight can evaluate the affectability of the watchwords adaptively. The proposed strategy plans to distinguish transformed information leakage precisely and productively.

II. LITERATURE SURVEY

In this area principle center is around research approaches towards information leakage detection/prevention action. Wikileaks [2] a non-benefit worldwide distributing association established by Julian Assange known for uncovering atrocities, human rights misuses, and defilement released the Afghanistan war logs (July 2010), the Iraq war logs (October 2010) .This builds the need of the exploration take a shot at information leakage detection/prevention action. The ebb and flow explore chip away at information leakage recognition/aversion can be arranged into two classes which incorporates content analysis and context analysis.

1. Content analysis

The content analysis examines any piece of writing or occurrence of record communication. The content analysis is used in the field of information retrieval. The content analysis incorporates techniques like Rule based strategy, Fingerprinting technique, Statistical technique [6].In Rule based method the tested documents are scanned with respect to predefined regular expression. Sensitivity of the report relies upon the degree to which the tested archive matches with the predefined ordinary articulation. When there is leakage detection of new data accuracy level decrease in rule based method. Fingerprinting technique utilizes hashing strategy where hash estimation of the tested report is contrasted and the hash estimation of the prepared format archive. The recognition stage turns out to be quick and accurate when the tested archive is unique record. If the document is modified (or transformed) detection becomes difficult.

The statistical strategies for the most part center on the measurable highlights of the archive like term recurrence and opposite record recurrence. Term-frequency is the portrayal of how as often as possible an articulation (term or word) happens in an archive .Inverse document-frequency is the portrayal of delicate records as for non touchy archives. AI arrangement techniques like Naive Bayes [5] and support vector machines (SVM) are utilized where content is mapped into vector space and prepares the classifier with the highlights of terms and their highlights. In this technique Statistical highlights were featured however setting of the record is overlooked which prompts less exactness in recognition stage.

By and large content analysis techniques like rule based strategies and fingerprinting strategies are wrong to manage information change, since they for the most part center on the measurable highlights of the terms in an archive by overlooking the context weight of the terms. In present world as volume of the data increases various forms of data also increases. Content analysis methods are not appropriate methods to handle these transformed data.

2. Context Analysis

Context analysis analyzes macro environment of a business, which includes both internal and external environment of a business. The recent works on context analysis considers sensitive context of terms. The word N-gram based classification [4], [8] [9] of data leakage prevention is proposed where initially only statistical features of the sensitive key words are considered as the important component. To overcome the limitations context of the keywords are considered which resulted in a more accurate result. In spite of the fact that there is an improvement in the data leakage detection accuracy still there is a scope for improvement. To achieve the improvement to a greater level graphical representation is used. The graphical representation method [11] represents the sensitive terms and their contextual relations as hub loads and edge loads of the diagram. Context based model (COBAN) [10] is proposed contains mainly two stages learning stage and detection stage. Amid learning stage the sensitive terms and their contextual correlations are used to create graphs and clusters which represents the confidential document. During detection phase these graphs and clusters are used to check whether a document is sensitive or not. But only simple transformations are considered in all the above inventions so still there is a scope of improvement in data leakage detection.

III. PROBLEM STATEMENT

In the course of expanding a business, employer must share data among trusted third parties. Let’s consider an example of a hospital management system where patient records are shared among the researchers who help the

hospital management with new treatment measures. In the same way companies maintain their collaboration with different organizations that require sharing client information. As data plays a prominent role in present day business world data leakage became prominent area of interest. Among so many types of data leakage techniques insider attack is the major one, where human mistakes are the main causes of data loss. For this type of leakage solution is obtained by monitoring the storage and transmission and providing alert when for the organization mainstream whenever required. This approach must be carried out in secrecy otherwise it can get compromised.

Figure 1: Data leakage scenario

To address the issue of data leakage detection (DLD), a ton of research work has been done with the usage of hash fingerprinting, n-gram, quantifiable systems and whatnot. With the brisk improvement of Internet, various new correspondence progresses (e.g., Device-to-Device innovation) have risen. In like manner, the volume of data grows altogether and the sorts of data end up being very ensnared. This passes on new test to DLD. Thusly, new DLD method is required with better resistance of data change and higher capability to deal with the part of unstructured data in long precedents.

IV. PROPOSED METHOD

In this paper along with the content we also focus on context of the sensitive keyword or term. In the following proposed method we mainly have two stages learning stage and detection stage. Amid learning stage, we train using sensitive keywords and then use the correlation between them to indicate the context of the keyword. In detection phase we compare the test data with respect to trained data and find data leakage.

Weighted Graph Walk Model (AGW) is proposed to recognize changed information. In this model, every one of the archives is spoken to by graph. The sensitive setting weights as hub weights and edge weights are characterized in the chart to enhance the recognition precision towards the changed information. The setting weight can evaluate the affectability of the watchwords adaptively dependent on the setting around the catchphrases. The proposed arrangement plans to recognize a lot of recently created, widely changed information precisely and productively. The fundamental commitments are as per the following.

To all the more likely endure the since quite a while ago changed information, we characterize a versatile setting weight system to evaluate the affectability of the watchword dependent on its unique circumstance. The perplexing archives are additionally spoken to by weighted setting charts, containing both key terms and important information. To adjust for the limitation of the design and augmentation the versatility, we moreover consider the data semantics. An improved mark proliferation calculation label propagation algorithm (LPA) is used to name a comparable name on the significantly noteworthy terms of the attempted graphs.

Moreover join the diagram of each record into a general one - the template graph, to ensure more relationship information between key terms and overhaul the general delicate setting. To deal with a great deal of data, we propose estimation with low-unusualness. With a weight reward and discipline framework, the count assesses the affectability of the gave documents by one walk a shot their outlines, which empowers the acknowledgment to be realized continuously.

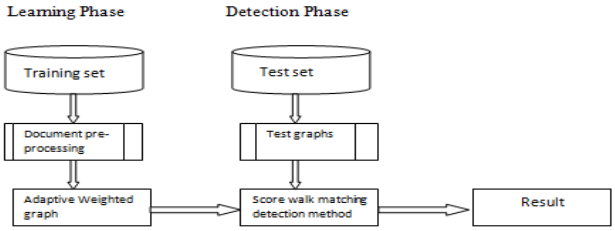

Figure 2: Overview of the model

A. Learning phase

Term frequency-inverse document frequency is utilized in the field of data recovery. Term frequency is utilized to locate the occasions an articulation (term, word) happens in a record. Inverse document frequency is the portrayal of the affectability of the report regarding non delicate archive. There TF-IDF (Term frequency-inverse document frequency) is utilized to speak to the heaviness of the delicate terms.

TF-IDF=tf(t,d) * idf (t,D) (1)

Where tf(t,d) is the term frequency and idf(t,D) is the inverse document frequency.

Term frequency can be evaluated using

$$\textbf{Term frequency (t, d)} = \frac{(n_t, d)}{\sum_{t' \epsilon d}(n_{t'}, d)} \quad (2)$$

Where $\sum_{t\prime\epsilon d}(n_{t\prime}, d)$ indicates the sum of all term in the document d.

Inverse document frequency

Idf(t,D)=log(Ds/1+{d'€Dn:t€d'}) (3)

Where Ds is the number of sensitive documents, {d'€Dn:t€d'} indicates the non sensitive documents where term t appears.

The calculated weight is used in the construction of adoptive weighted graph. Using threshold value specified for the sensitivity of the tem we are going to select N terms and those N terms are considered as the nodes and the correlation between them gives the edge weights using these Adaptive weight graph is constructed. These individual template graphs are merged to develop a generalized graph which increases detection accuracy. We cannot directly divide the graph into sub graphs which may result in incomplete or one sided graph. Therefore Label propagation method [12] [13] is used to partition the graph.

Algorithm: Pseudo Code for Sensitive Data Learning
Input: A set of documents
Output: The Adaptive Weighted graph developed for given sensitive keywords.

1. Input the sensitive keywords to be trained through a document or file.
2. Document pre-processing must be used to remove stop words.
3. Using the TF-IDF calculates the node weights and the edge weights and select the most significant N terms.
4. Using weight set of N terms, compute Weight matrix
5. N terms denote the N nodes and Using these and the weight matrix graph is constructed for each document.
6. Consolidate these individual diagrams and parcel the hubs into different classifications by utilizing label propagation algorithm.
7. Hub weights and edge weights are masked using hashing method to maintain privacy.
8. Stop

Amid Adaptive weighted graph learning phase administrator forms the touchy reports determined and extricates the delicate watchwords. As we are utilizing graphical portrayal for assessment of delicate reports, every touchy catchphrase is considered as the hub and their weight is gotten by utilizing term frequency (TF) and inverse document frequency (IDF). Considering all the touchy watchwords lead to haphazardness so an edge should be considered to constrain the quantity of delicate catchphrases. The relationship between's the touchy catchphrases is considered as edge weights and utilizing these qualities a versatile weighted graph is built for each report. Combining all these individual graphs prompts a solidified template graph which is built for assessment reason. Label propagation algorithm is utilized to order the hubs for better assessment. For safeguarding touchy catchphrases MD5 hashing technique is utilized for encryption.

B. Detection Phase

In this phase the user input the document the document is testified against the trained adaptive weighted graph if sensitive words weight exceeds the threshold the document is considered as the sensitive document. Alert message is sent to the user. It's up to user's choice to send the document or not.

Algorithm: Sensitive Data Detection Algorithm
Input: Document to be tested
Output: alert to the user if document is sensitive.

1. Input the file
2. Remove all unnecessary words, special characters from file and filter keywords from the file
3. Generate hash code for each keyword in file using MD5 Algorithm
4. Calculate weight and keyword ranking of each keyword in file
5. Calculate sensitive words data weight.
6. if sensitive weight of the words value increases threshold value, then that file is considered as sensitive file
7. Alert message is given to user whether file is sensitive or not
8. Stop

Amid detection phase the documents to be tested are pre-processed. The sensitive watchwords are removed by contrasting the substance of the record and regard to indicated touchy catchphrases. The weights of the touchy watchwords are determined utilizing TF-IDF (Term recurrence – Inverse report recurrence). The graph is built for sensitive watchwords present in the test document. Utilizing Depth first pursuit (DFS) the chart is navigated when the sensitive watchwords are experienced the weights are added. In the event that the absolute weight achieves the limit esteem, at that point the archive is proclaimed as sensitive documents.

C. Transformed Data Leakage Architecture

Information leakage happens when information is leaked or undermined by insider of an association to unapproved outsiders purposefully or coincidentally, which may make genuine harm the association. Thinking about a situation where a representative of an association releases delicate documents from authoritative neighborhood system to unapproved outsider. To maintain a strategic distance from information leakage, an identification operator must be conveyed at the outlet of the authoritative nearby system. The general design is appeared in figure 3

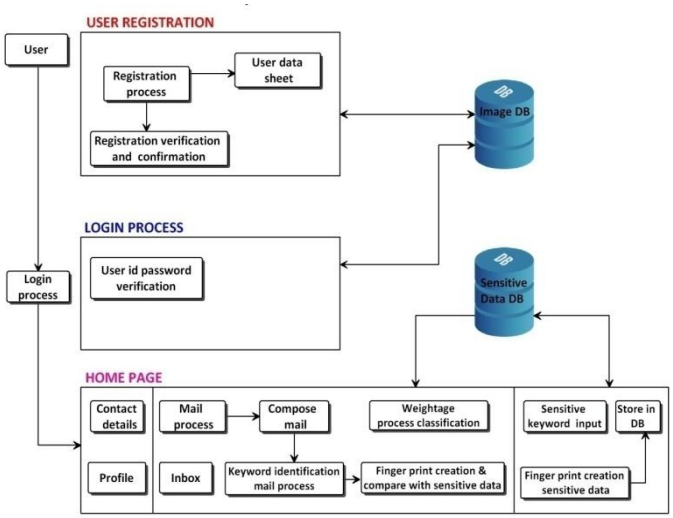

Figure 3: Transformed Data Leakage Architecture

If new user is registered, the user will be verified and confirmed then stored into the database. For User login, required credentials are username and password. Those credentials will be verified by accessing the database. User has multiple features such as Accessing inbox, composing mail, etc., Admin will manage sensitive keywords. If user composes mail, it will go through Keyword identification mail process and compares with sensitive data by accessing sensitive data DB.

V. RESULTS AND DISCUSSIONS

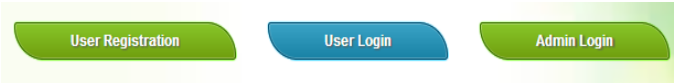

Figure 4: Home/Index page

Index page has three buttons labeled User Registration, User Login, and Admin Login. Admin has to login by submitting Admin name and Password to the application. After successful login of admin, admin can add keyword by submitting field sensitive keyword and sensitive keyword weight. Admin can see profile from view profile section. Admin can edit profile by giving valid details. To change password, admin has to input old password and then input new password and again by confirming password. Admin can see the user list by clicking user list. Admin can delete users by selecting the user admin wants to delete. Registration user has fields such as Username, UserId, UserPass, City, State, Contact No, Email then user has to submit to register.

Figure 8: Admin Login

This page allows the admin to login using their credentials. Admin has all the rights, like creating user, editing user details and deleting a user. Admin sets the roles and privacy settings. Privileges to use application will be set by admin. First time password will be set by admin, if the user forgets its username or password, they can request for reset of password or retrieve username. If the user is involved in any malicious activities admin have all the rights to take necessary actions and also admin will have access to all the data of the users and type of emails they compose and send.

Figure 9: Adding sensitive keywords using Admin credentials

User login process will take username and password as input and process the credentials provided. User will provide contact details in contact details section. In the inbox section, user will be able to view all the mails that received .User will be able to compose mail by clicking on compose

mail option. Compose mail will have fields such as to Address, Subject and Content (Body) of mail

Figure 5: User Login

Figure 6: Compose mail

While composing mail if user wants to attach file, can choose file by selecting choose file option then send the mail. After user clicks on Send, system will check for sensitive keywords in the composed mail and shows warning whether to send mail or cancel. If user still wants to send mail, can click on send option again to send mail. If cancelled, mail will not be sent and can modify the composed mail. User can view information about user by clicking on User profile option.

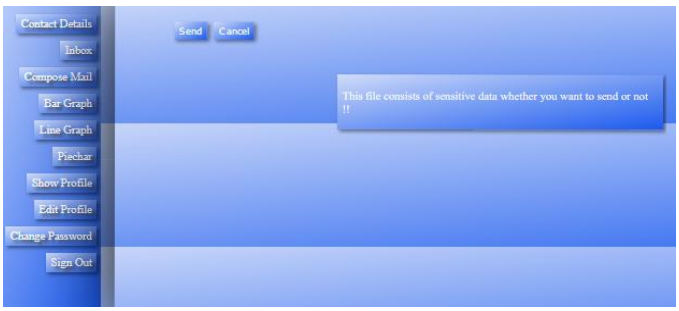

Figure 7: Alert to user regarding sensitive data in the document

If any information has to be edited, user can edit information by clicking on edit info option. User can change password by submitting current (Old) Password, then by giving new password and again confirming the password.

A. Test Cases

Test case Id	Test Input	Expected Result	Actual Result	Remarks
TC_01 User	Enter legitimate username and secret phrase click on login catch	User should be navigated to homepage with the following details as presented in figure 6 .	User should be navigated to homepage with the following details as presented in figure 6.	Pass
TC_02 Admin	Add Sensitive keyword and Sensitive keyword weight age.	Insert sensitive keyword and keyword weight age to the database.	Inserted sensitive keyword and keyword weight age to the database.	Pass
TC_03 User	View Inbox	View emails received by user.	View emails received by user.	Pass
TC_04 User	Compose Mail	Take input of To, Subject, and Body Content and if attached file and check with Fast Detection system.	Take input of To, Subject, and Body Content and if attached file and check with Fast Detection system.	Pass
TC_05 User	Fast Detection of Sensitive Keywords	Take input through Compose mail then check with Sensitive keywords from database. If found any Sensitive keywords, then Prompt	Take input through Compose mail then check with Sensitive keywords from Database. If found any Sensitive keywords, then Prompt	Pass

		user for correction.If Prompt was Yes, allow user to Edit mail.	user for correction.	
TC_06 User	Send Mail	If received prompt from Fast Detection system as No (No edit needed, proceed!) from the FD System then Send mail to Recipient.	If received prompt from Fast Detection system as No (No edit needed, proceed!) from the FD System then Send mail to Recipient.	Pass

Table 1: Test cases

CONCLUSION AND FUTURE ENHANCEMENT

In this venture, another model called Adaptive weighted graph walk model is proposed. This model comprises two stages, for example, learning stage and detection stage. Amid learning stage weighted setting charts are utilized to endure since a long time ago transformed information and to build the versatility to manage crisp arrived information improved mark engendering calculation is utilized. In detection stage weight reward and punishment system is utilized to improve the precision of information leakage detection.

REFERENCES

[1] InfoWatch. Global Data Leakages & Insider Threats Report: 2011 [Online]. Available: http://infowatch.com/sites/default/files/report/InfoWatch_global_data_leakage_report_2011.pdf

[2] P. Karhula, "What is the effect of WikiLeaks for Freedom of Information?," FAIFE Spotlight [online], vol. 19, 2011.

[3] x-SunTrust Employee May Have Tried Sharing 1.5 Million Customers' Data [online] Available: http://fortune.com/2018/04/20/suntrust-bank-security-breach/

[4] S. Alneyadi, E. Sithirasenan, and V. Muthukkumarasamy, "Word n-gram based classification for data leakage prevention," in Proc. 12th IEEE International Conference on Trust, Security and Privacy in Computing and Communications (TrustCom). IEEE, 2013, pp. 578–585.

[5] S. Xu, "Bayesian naïve bayes classifiers to text classification," Journal of Information Science, vol. 44, no. 1, pp. 48–59, 2016.

[6] M. Hart, P. Manadhata, and R. Johnson, "Text classification for data loss prevention," in Proc. International Symposium on Privacy Enhancing Technologies Symposium. Springer, 2011, pp. 18–37.

[7] G. Katz, Y. Elovici, and B. Shapira, "Coban: A context based model for data leakage prevention," Information sciences, vol. 262, pp. 137–158, 2014.

[8] S. Alneyadi, E. Sithirasenan, and V. Muthukkumarasamy, "Adaptable ngram classification model for data leakage prevention," in Proc. 7th International Conference on Signal Processing and Communication Systems (ICSPCS). IEEE, 2013, pp. 1–8.

[9] G. Giannakopoulos, V. Karkaletsis, G. Vouros, and P. Stamatopoulos, "Summarization system evaluation revisited: N-gram graphs," ACM Transactions on Speech and Language Processing (TSLP), vol. 5, no. 3, p. 5, 2008.

[10] Y. Lu, X. Huang, Y. Ma, and M. Ma, "A weighted context graph model for fast data leak detection," in Proc. IEEE International Conference on Communications (ICC). IEEE, 2018.

[11] D. Cai, X. He, J. Han, and T. S. Huang, "Graph regularized nonnegative matrix factorization for data representation," IEEE Transactions on Pattern Analysis and Machine Intelligence, vol. 33, no. 8, pp. 1548–1560, 2011.

[12] X. Zhu and Z. Ghahramani, "Learning from labeled and unlabeled data with label propagation," Technical Report CMU-CALD-02-107, Carnegie Mellon University, 2002.

[13] F.Wang and C. Zhang, "Label propagation through linear neighborhoods," IEEE Transactions on Knowledge and Data Engineering, vol. 20, no. 1, pp. 55–67, 2008.

A
Aarohi Vora,941
Abhander Chaudhary,91
Abhay Kshirsagar,1556
Abhilash D.S.H ,1146
Abhinav Jain,1453
Abhinav K,1708
Abhirami A ,1041
ABHISHEK M H,250
Abhishek Sinha,2197
Abu Nasar Ghazali,1857
Adeeba Fazal Pathan,1823
Aditya Prakash,2197
Aditya Shastry K,1992
Aditya V,1243
Admile Nandkumar Sushen,1116
Admile Nandkumar Sushen,1567
Adwitiya Mukhopadhyay,1348
Afzal Hussain Shahid,929
Aggarwal N,304
Aishwarya Lakshmi T,1280
Aishwarya Mishra,1134
Aishwarya S Pattar,1802
Aiswarya LS,1613
Ajay K. Sharma,1919
Ajay Kaul,1166
Ajay Kaul,2156
Ajay Khunteta,432
Ajay Kumar Sharma,1140
Ajeet Kumar,578
Ajey Gotkhindikar,952
Ajnar D S,2036
Ajnar D.S,2162
Akhil Chitreddy,156
Akhila E. M,563
Akhila S,404
Akibaehmad A. Arora,1643
Akshara Buchake,1110
Akshay Laxman Pujari,1777
Akshayaa Venkatesh,281
Akshita Saini,924
Akshya Reghunath,1402
Albin Mathew,368
Aleena Joseph,1478
Aman Jatain ,1212
Amandeep Kaur Sohal,1140
Amandeep Kaur Sohal,1919
Amanpreet Singh Saini,1585
Amarsinh V. Vidhate,637
Ameeta Seehra,449
Amit Abhishek,1464
Amit Kumar Singh,578
Amit Kumar Tyagi,1496
Amith K K,1992
Amitkumar Baburao Ranit,167
Amitkumar V. Jha,1857
Amitkumar V. Jha,1861
Amlan Chatterjee,1589
Amogh.M.Morey,650
Amrit Das,2075
Amrita Dutta,959
Amruta Koli,2123
Amulya Shivanath,1459
Ananthan T,1734
Ananthu S Kuttattu,1666
Anaswara Jayan ,1157
ANEESH K N,250
Aniket A. Manjare,1931
Anil Kumar G,1220
Anil Kumar.Kurra,1469
Anila Kuriakose,1093
Anilet Bala A,2075
Anirban Bandyopadhyay,1969
Anirudh V,896
Anirudh Vattikuti,156
Anisha P R,480
Anita Garhwal,1969
Anita J.P,428
Anitha S Prasad,975
Anitha Sarah Koshy,1023
Anjali,578
Anjaneyulu Katuru,1007
Ankur Bansal,1408
Ankur Utsav,1464
Ankush Mittal,757
Annapurna Bhargava,1312
Annapurna Bhargava,1694
Annapurna Bhargava,2059
Annie Uthra R,1979
Anshul Gautam,1317
Antonidoss A,345
Antony Thomas,428
Anu J Nair,1613
Anu Suresh,2140
Anup S.Vibhute,1116
Anup S.Vibhute,1567
Anuradha S. Deshpande,1643
Anuradha T,620
Aparna R,1429
Apoorv Kansal,1193
Apoorva Raghunandan,2187
Apoorva Raghunandan,553
Apte S.K,494
Aqsa Hashmi,729

Aravind Hanumanthaiah,1903
Aravinth J.,1772
Arbind Kumar Gupta,984
Arindam Chakraborty,1979
ARISTON RODRIGUES,1601
Aritro Roy Arko,678
Arivoli R,228
Arivukarasi M,345
Arjun D,1903
Arjun D,296
Arpita Sahu,2002
Arpita Thakre,2129
Arpita Thakre,2135
Arpitha R,2176
Arun Mani,1478
Arup Kr Nandi,335
Arya M Hari,281
Asha Vijayakumar,1478
Ashish Deopa,2197
Ashish Kumar Verma,410
Ashish Mani,1589
Ashish Mani,261
Ashish Sunil Thomas,1348
Ashok Kumar Sharma,1065
Ashok Kumar Sharma,1317
Ashok Kumar Sharma,1397
Ashok Kumar Sharma,1434
Ashok Kumar Sharma,1884
Ashok kumar sharma,1925
Ashok Kumar Sharma,2070
Ashok kumar Sharma,418
Ashutosh Sudam Shinde,807
Ashwin M,2181
Aswathi Divakar,1841
Aswathi Sajeevan,1783
Athira Gopinath,1903
Atul Ingale,1110
Atul Joshi,398
Avinav Joshi,1408
Avleen Kaur Malhi,269
Avtar singh buttar,1638
Avtar Singh Buttar,1750
Awadhesh Kumar Singh,1947
Awadhesh Kumar Singh,41
Ayshah Banabilah,1816
Ayushi Kandoi,795
Azrah Rubanee,2149

B

Bablu Kumar Das,516
BABY DEEPA V,1689
Badrul Hisham Ahmad,1969
Bala Tripura Sundari B,1719
Bala Tripura Sundari B,534
Bala Tripura Sundari B,848
Balaji Hariharan,1280
Baljeet Kaur,475
Banakar R.M,175
Bandreddi Ray Srinivasa Rao,1719
Bansod P.P,2002
Barsha Sharma ,443
Basavaraju T G,2047
Baskar.S,1952
Baskaran K,2025
Baskaran.K,1378
Bennet Rajesh M,2086
Bennet Rajesh M,2098
Bera T K,1243
Bera T.K ,304
Bhagyashri D.Kale,625
Bhagyshree Pawde,708
Bhanu Pratap,1958
Bhanu Pratap,1963
Bharat Sharma,1059
Bharathi Shetty,708
Bhargav Appasani,1857
Bhargav Appasani,1861
Bhavana Tiple,853
Bhavneet Sharma,310
Bhiwani R J,933
Bhogendra Rao P V R R,996
Bhowmick K,116
Bhubaneswar,1059
Bhumika Khetan,1018
Bhumika Narang,475
Bhupendra M,1243
Bhuvaneswari S,216
Bhuvaneswari V,1973
Bikash Sarma,1
Binoy B. Nair,1290
Biplab Nath,1772
Bishwabara Panda,181
Bishwajit Roy,455
Biswanath Dey,137
Brahmjit Singh,2065
Brumancia E,599
Budkuley,773

C

Chaithra B R,2176
Chakraborty S,116
Chandni Agarwal ,443
Chandni Arun,1903
Chandni Krish,2007
Chandra Shaker A,204
Chandrakala B M,984
Chandrakant Naikodi,110

Chandrakanth V,996
Chandrasekar A,1550
Cheryl Dsouza,1152
Chetan S. Patel,2014
Chetan Selwal,1337
Chethana N S,1249
Chetna Verma,1337
Chhavi Chaturvedi,1306
Chidambaram M,1633
Chidura Bhanu Teja,1757
Chinnaiyan R,1485
Chinnaiyan R,1893
Chintam Muni Kanaka Sri Shalini,910
Chirag Khandhar,1018
Chirag Paunwala,941
Cyril Prasanna Raj P,980
D
Dalveer Kaur,1162
Dalveer Kaur,1790
DARSHAN SINGH S,250
Dayananda R.B,489
Dayashankar Singh,1134
Debdutta Dey,41
Deep Shikha ,443
Deepa Palanisamy,329
Deepa,300
Deepak Kumar Gupta,1861
Deepak Rohilla,1518
Deepanshu Gautam,1925
Deepanshu Gautam,2070
Deepti Goyal,1496
Devaraj BN,1714
Devendra Kumar Sharma,558
Devi A,722
Devi.A,152
Devyani Gurjar,485
Dhanalakshmi Samiappan,281
Dhanalakshmi Samiappan,795
Dhananjay Borse,843
Dharani Devi,152
Dharmavaram Asha Devi,1935
Dharmendra Y,1243
Dharneeshkar J,2192
Dhaval Bagal,255
Dhaygude Akshay,1083
Dheeraj Kumar Sharma,1228
Dheeraj Punia,2065
Dhruba Ningombam,2041
Diksha Singh,589
Diksha Singh,594
Dinu V,210
Dipti Jadhav,12
Divakar Yadav,1511
Divya G,1157
Divya G,1478
Divya James,1660
Divya.R,1893
Dolly Murodia,1317
Dolly Murodia,1434
Dolly Murodia,2070
Dongre Y V,762
Dorairangaswamy M A,1478
Dr. Sathans,286
Drakhshan Jawaid,929
Draksham Madhubabu,2135
Duane Dsilva,510
Durgaprasad Gangodkar,757
Durge P V,167
Duvvaki Venkatesh,60
E
Ebha Koley,1128
Elizabeth Shelry,1528
Elizabeth Sherly,1573
Esther Rachel K,1237
F
Fariya Tamkeen,1249
Feni Patel,941
Fiza Firdose,1171
Flavia Leitao,510
Flavia Leitao,773
Freceena Francis,1013
G
G.Bhavani,193
Gadgune S.Y,1562
Gadicherla Sameer,244
Gajender Kumar,1
Gamad R S,2002
Ganapathi Hegde,1327
Ganapathi Raju N V,51
Ganaraj Borkar,773
Ganesh K.V,1889
Ganesh M. Magar,358
Garima Behl,1162
Gaurav Saini,2118
Gautam Nayan,129
Gayathri G,737
Geetha P,110
Geetika Aggarwal,199
Ghadge Tejraj,1083
Ghodeswar U.S,625
Giridhar Reddy Bojja,2149
Giridhar Reddy Bojja,801
Girish Kumar N. G.,886
Gloria Rodrigues,1152
Gogineni Manasa,244
Gokul G S,1666
Golam Sarowar,275
GOMATHY S,317
Gopala Krishna P,51
Gopala Krushna,1386
Gopika Rajan,1474
Gopika Rajan,900

Gopika. A,2030
Gopinath G,1001
Gourav Kanekar ,773
Gourav Saini,46
Gourav Shrivastava,410
Gunjan Chourasia,2075
Gupta B B,1300
Gupta B B,1306
Gupta B B,865
Gupta C.P,729
Gupta S,1122
Gurmohan Singh,881
Gurpurneet Kaur,767
Guru Prasath C,848
Guruprasad,187
Gururaj H L,643
Gyanendra Verma,1703
H
Haneesh K. M,1146
Happy Chapla,384
Hari Prasad,1666
Harish Kumar Dogra,2149
Harish Kumar Dogra,801
Harish Ravichandran ,1761
Harish Yadav,1556
Harminder Kaur,475
Harsha K.M,1660
Harshini R,1234
Harshith C H,210
Heena Sharma,1757
Hema dharani M,465
Hema M,1237
Hema Sekhar Reddy G,66
Hemanth Kumar N. G.,886
Hifza shaima,1342
Himanshi Babbar,85
Himanshu G,1243
Himanshu Yadav,1878
Himansu Das,181
Hogade B.G,1440
I
Immanuel Savio D,700
Imran Quadri,1053
Indhu.P.Nair,1889
Indrashis Das,1059
Indukala P K,296
Ingle R B,762
Ipsita Biswas Mahapatra,460
Iqbal Wani,1146
Ishrat jan,801
J
Jacob Savio,390
Jadhav Vasudev,1083
JaideepSai Narayan K,605
Jain M,304
Jain P ,304
Jain P K,2036
Jain P,1243
Jain P.K,2162
Jalpa Shah,1402
Jamal K,193
Janani MV,281
Jasdeep Singh,871
Jasmine Manandhar,1423
Jaswanth Marri,77
Jatin Talwar,881
Jayachitra J,1276
Jayachitra J,920
Jayakanth K,1671
Jayakrishnan V M,1761
Jayanta Kumar Sahu,2019
Jayvant Devare,1619
Jeevamma Jacob,1841
JENO PAUL,1358
Jeno Paul,743
Jeshmitha Reddy K,66
Jhanavi B S,737
Jianhua Zhang,684
Jijith Murali,1666
Jimmy Singla,222
Jitendra A. Gaikwad,2014
Jitendra Gaikwad,1110
Jogeshwar Singh Sohal,2144
Joshi P M,655
Joshi P.M,341
Junaid M Laskar,281
Justin Samuel S,599
Jyothi K,300
Jyothi Prakash K V,1249
Jyothi Prakash K.V,1386
Jyoti Parsola,757
Jyoti Shukla,1925
K
K Chandrasekaran,2204
Kailash Baindara,1264
Kailash Gogineni,156
Kala C S,1249
Kalaiarasan D,2025
Kalaivani S,1001
Kaleem Fatima,2080
Kalra M K,1199
Kalra Y,304
Kamalesh Tripathy,1122
Kamsala Ravi Theja,1386
Kanad Ray,1969
Kandi Suyash,1083
Kanimozhi R,1952
Karthik G A,2181
Karthik S,1714
Karthik Tummala,1541
Katapally Manognya,51
Katti P K,1703
Kaustubh Banninthaya K.,460
Kaustubh Pimparkar,896
Kavanashree N,975

Kavita Moholkar,807
Kavitha K R,1613
Kavya G,722
Kavya N R,1249
Keerthi D S,2047
Keshav Kashyap A,1714
Ketan Dessai,510
Ketzial Jebaseeli K,827
Kharade Mahesh,1083
Khevin Nair,848
Khyati Marwah,2144
Kiran Joseph,1146
Kiran Patil,1296
KIRAN TALELE,1601
Kiranjot Kaur,1795
Kirti S. Pande,632
Kishor Kumar Reddy C,480
Kodali Bhavana,60
Komal R Ahuja,1205
Koppakula Nagarjuna,2204
Koras. S,1973
Krishna Raju D R,1053
Krishna Tulasi M.S,1847
KRISHNAPRIYA VINOD,1358
Kritika Sharma,1177
Kuldeep Singh Rathode,969
Kulkarni S.M,171
Kumar D,1243
Kumar D,304
Kumar Debasis,695
Kumar R,1
Kumar R,281
Kumar R,795
Kumara Shama,187
Kumkum Dubey,578
Kumkum Dubey,584
Kunal R. Kumbhar,637
Kushal Gowda S,528

L

Lakshmanan M,216
Lakshmi K K,1998
Lakshmi K S,1783
Lakshmi V S,672
Lakshminarayanan Gopalakrishnan,162
Lakshmipriya K J,317
Lakshmipriya K J,743
Lata Gidwani,1065
Lata Gidwani,1884
Laxmi Khichadi,1088
Laxmi Khichadi,423
Lekshmi S Nair,1666
Likhith K,51
Limbasiya Mohit Dhirubhai,632
Lin Li,1391
Lincy Thomson,2030
Linoy Vincent,1889
Linu Shine,783
Liya M L,1903
Loganathan V,1105
Lokesh A R,1866
Love Kumar,881
Lovely Bansal,1258

M

Madhavi B.K,2080
Madhu M ,1276
Madhu M,920
Madhusmita Mishra,959
Mahadu A. Trimukhe,1440
Mahantesh P. Mattada,1823
Maheeshma KM,1613
Mahendra Kumar Murmu,1518
Mahendra Kumar Murmu,689
Mahendra Lalwani,1264
Mahesh Dronadula,1007
Maheshwari Prasad Singh,455
Maheshwari Prasad Singh,929
Maitreyee Dutta,1365
Makrand Samvatsar,876
Mallapareddi Sagar,1327
Malti Bansal ,589
Malti Bansal ,594
Manasi Gyanchandani,1447
Mandar M. Bhalekar,1931
MANISH PANDEY,778
Manisha J. Nene,1372
Manivannane K,1633
Manjeet Singh Patterh,1795
Manjula Shenoy K,1036
Manjunath T N,1423
Manjusha Nair,1595
Mannem.Venkatarao Rao,1973
Manoj kumar M N,2210
Manoj Kumar Mishra,181
Mantosh Biswas,612
Mantosh Biswas,924
Manzoor Ahmad,1914
Marshal Raj,162
Masood Ahmad Malik,102
Mawaddah Kuddah,1816
Maya Mohan,1013
Maya Mohan,368
Mayank Dave,310
Mayank Sharma,1589
Mayura N P,1412
Meena Belwal,1708
Meena Belwal,1729
Megalan Leo L,1541
Megha N,1573

Meha Shrivastava,1683
Mehtre B.M,665
Mehtre BM,818
Mekala Pranvitha nand,142
Mekaladevi V,465
Merugu Bhavani,1935
Minal Moharir,77
Misha,1790
Mohamed shakeel,1952
Mohammad Abir Hassan Sarker,275
Mohammad Dehan Rahman,275
Mohammad Yousuf Saifi,222
Mohammed Abdaldaim Ibrahim,1391
Mohana Priya P,379
Mohana Roopa Y,1836
Mohana Roopa Y,910
Mohana Roopa Y,916
Mohd Riduan Ahmad,1969
Mohini Naik,510
Mohit kumar,286
Mohit Sharma,1065
Mohit Sharma,1317
Moinak Bhattacharya,1979
Momin B.F,714
Monish P,1772
Monisha S,1546
Moontasir Rashid Md,1626
More D.S,1649
More D.S,1777
Mousumi Khanra,335
Mrinal Kanti Ghose,2041
Mukesh Kumar,1947
Munish Rattan,1795
Munish Rattan,871
Muqtadir Alam ,929
Muralishankar R,1269
Murkute S V,499
Mursal Siddique,1083
Murthy V S N A,996
Murty N.S,116
Mydhili K. Nair,437
Mythili P,18

N

Nadir N. Charniya,1205
Naga Raju G,605
Nagamani K.,1088
Nagamani K.,423
Nagaraj M J,650
Nahlah Aslam K.P.,946
Namboodiri E I Deepu,368
Nandan Andhare,1077
Nandhini P S,665
Narendra Walawalkar,1556
Natarajamani S,1234
Natarajan M,2092
Natarajan M,2111
Natarajan P,156
Navajyoti Nath,137
Navaneeth Bhaskar,1655
Naveen Ananda Kumar J,1031
Naveen Ananda Kumar J,1050
Naveen Ananda Kumar J,1443
Naveen Ananda Kumar J,2167
Naveen Ananda Kumar J,990
Naveen reddy B,465
Navin Baaskar E V,1234
Nazaf Rabbi Md,275
Neeha Ashraf,1914
Neelesh Jain,2162
Neeti Dubey,1925
Neeti Dubey,418
Neetu Sood,1140
Neetu Sood,1919
Neha Hajare,1619
Nemade S.B,837
Nesren Attiah,1816
Newton Rai,650
Niaz Morshedul Haque Md,1626
Nidhi,578
Nikita Pawar,853
Nikita,222
Niranjan N.,460
Nirmala M B,2210
Nirmala Mahawar,432
Nirupama Tiwari,1258
Nisha Rathore,374
Nitesh Bharot,1766
Nithin P S,1332
Nitin Borhade,1077
Nomitha Datla,620

O

Omer Elmukhtar,684

P

Pal Thethi H,350
Palakodeti Rohit,51
Palika Chopra,269
Pallavi Saindane,255
Panchade V.M,1354
Pankaj Kumar,1177
Parag Jain,1683
Parth Ghaware ,773
Patel ND,818
Patil C Y,1296
Patil D.R,1744
Pavithra C M,1579
Pavithra S,465
Phaneendra H D,859
Ping Wang,1391
Piriyyadarisani.V,152
Plasin Francis Dias,175
Ponugumati Pavani,60
Pooja C R,1027
Poorni R,216

Poornima T,1234
Prabal Gupta,350
Prachi Gharpure,234
Prachi Kotwal,1703
Pradeep Chandra T,1220
Pradeep Kumar Raju R,1541
Pradeep Kumar,1193
Pradeep R,2052
Pradeep R,750
Pradeep R,783
Pradeepkumar. P,1897
Pradyumna Hegade,795
Pragya Dwivedi,584
Prajakta Paranjape,1556
Prakasam V,1678
Pramesh,773
Pramod Shendge,522
Pranav Kumar M. P.,460
Pranesh,1490
Pranita Chavan,843
Prannoy Caeiro,773
Prasad Subhash Kirtane,1806
Prashant Ravindra,1608
Prateek Lakkar,1105
Prathima K R,528
Prathmesh N. Gunjgur,637
Pratik Rathod,896
Praveen Kaushik,410
Praveen Kumar Mishra,1199
Preeti Pannu,558
Prerana V,1423
Prerna Saxena,1065
Prerna Saxena,1317
Prerna Saxena,1884
Prince Rajpoot,578
Prince Rajpoot,584
Priti Sathe,843
Priya B. K,404
Priyanka Ahlawat,891
Priyanka D. Lanjewar,714
Priyanka Nehra,1397
Priyanka Nehra,1925
Priyanka Nehra,2070
Priyanshu Pandey,1958
Priyanshu Pandey,1963
Priyesh Kanungo,876
Promod R. Ubare,1931
Punyadeep K,1386
Purushotham Raju N,570
Purva Mohan Padmawar,807
Pushpa S K,1423
Pushpendra Singh,1969

R

Rachna S. Potpelwar,1908
Radha D,77
Radha Senthilkumar,329
Radhesyam Vaddi,142
Radhey Shyam Pandey,1958
Radhey Shyam Pandey,1963
Radhika S,1550
Raghavendra Prasad S G,97
Rahul Kumar Raj ,929
Rahul Lulla,896
Rahul Paknikar,234
Raj Kiran G S S,51
RAJALAKSHMI MENON,317
Rajalakshmi Menon,743
Rajashekar shastry,480
Rajashree R Menon,1093
Rajat Gupta,695
Rajat Kumar Maheshwari,24
Rajendra Chikkanagouda,980
Rajnandani Pawar,1724
RAJU G T,364
Rakesh Kumar,2007
Rakesh Kumar,91
Rakesh M D,528
Rakesh.G,1729
Rakshita Vishali V,848
Ram sahith G,1708
Rama D,1734
Ramakalyan Ayyagari,996
Ramalingam S,2025
Ramana Murthy B V,480
Ramaraju P V,605
Ramchandra P. Hasabe,1829
Ramesh R ,1157
Ramesh R,1478
Ramya T R,1027
Ranganatha Gowda S J,1053
Rani V.G,827
Ranjitha N,1023
Rashmi Jain,261
Rashmi Jha,1146
Rashmi M,97
Rashmi Suman,929
RATHIPRIYA R,35
Ratna Kanth E K,1342
Raveesh Hegde,1269
Ravishankar B. N. ,1608
Reaya Grewal,269
REJOICE THOMAS PAUL,1358
Rekha Bhandarkar,390
Rekha P,1280
Rekha Ramakrishna Hegde,1348
Remesh Babu K R,1528
Remesh Babu K R,1573
Renjith V. Ravi,1285
Renu Jose,1323
Reshma Mohan,1595

Reshma Ramanan. M,1897
Revathy S,323
Ria Benny,18
Richard Laji,1595
Riddhi Kotak,384
Ridhima,1750
Rima V G,672
Rishabh Kamal,891
Rishish Kumar Naik,1290
Risla Fathima P.,460
Ritesh Kr. Badhai,1464
Ritu Garg,516
Ritumbhra Uikey,1447
Rizwana Rasheed,1613
Rohan Giri,2075
Rohina khanam,146
Rohina khanam,6
Rohini N Khedkar,574
Rohit B. Chilwant,637
Rohit Kumar Arya,29
Rohit P,1053
Rohit V.S.S. Bulusu,1772
Rose K Johney,1528
Rosemary Varghese,1157
Roshwyn De Melo,510
Rosmy John,750
Rounak Datta,1979
Ruba Al-Ghamdi,1816
Rudramurthy V C,1429
Rukma Rekha N,1071
Ruksar Fatima,146
Ruksar Fatima,6
Rupesh Kumar
S
Sinha,2197
Saadat Hasan Khan,678
Sabarish Narayanan B,1998
Sabarmathi G,1485
Sabarrish S,848
Sachin Baliram Shahapure,1829
Safin Khan,1110
Sahana Y P,952
Sahil Desouza,510
Sahithi Samudrala,142
Sai Karan K,1522
Sai Shibu N B,1332
Sai Suhas L,886
Saif Kabir Md,275
Saiful Islam Md,678
Sajith V,2052
Sajith Vijayaraghavan,750
Sajith Vijayaraghavan,783
Sajmath P. K.,1285
Sakthi prabha R,1871
Sambariya D.K,1878
Sameeksha Munjal,767
Samidha Girish Vengurlekar,12
Samprita S,1023
Samudra Dasgupta ,1608
Sandeep HR,1188
Sandeep Jalui,124
Sandeep P,1678
Sandeep Singh Gill,767
Sandeep Verma,1694
Sandeep Verma,2059
Sandhiya.M,599
SANGITA PATIL,240
Sanjai Pathak,1589
Sanjay H A,1992
Sanjay Kumar C K,859
Sanjay Singh,261
Sanjeev Kumar,1228
SANJU B,1358
Sanoj Kumar Roy S.,904
Santhanalakshmi S,1534
Santhi Jabarani S,1418
Santhosh L Deshpande,1490
Santhosh T K,1423
Santosh Kr Sharma,969
Santosh Tuppad,210
Sanyog Rawat,1969
Sarang Parikh,1992
Saranya K,1546
Saravanan A,1985
Saravanan A,2104
Sarbjeet Kaur,1365
Sarika Jain,199
Saroj Kumar Mishra,2019
Sarthak Agarwal,1585
Sasamal T.N,24
Sasasmal T.N,469
Sasvanth Narayan R,1105
Sateesh Kumar T R,528
Satheeshkumar R,228
Sathiamoorthy S,1985
Sathiamoorthy S,2086
Sathiamoorthy S,2092
Sathiamoorthy S,2098
Sathiamoorthy S,2104
Sathiamoorthy S,2111
Sathya Durga V,609
Satish S. Kumbhar,485
Saurabh Shripad Dixit,1744
Saurav Sahoo,2019
Sawan Singh,1434
Sayem Miah Md,1626
Seema Agrawal,1177
Seema Agrawal,1264
Seema Gulam Shaikh,1036
Sehgal M,304
Selvanayaki K,1608
Seshaiah Ponnekanti,1332
Sethuraman N Rao,1761

Shabir Ahmad Sofi,1811
Shaffali Jain,1766
Shahid Sultan Hajam,1811
Shaifali Narayan,1300
Shaik humera tauseef,146
Shaik humera tauseef,6
Shaik Mohammed Faruk S.D,1276
Shaik Mohammed Faruk S.D,920
Shaikh Mohammad Aamir,341
Shaikh Mohammed Tauseef,171
Shailendra Kumar Tiwari,952
Shailendra Kumar,689
Shalini Bhaskar,1212
Shalini Vanaja Nair,1402
Shalli Rani,85
Shankaraiah,1171
Shankaraiah,1579
Shanmukha Swamy M N,71
Shano Solanki,1453
Shantha V,650
Shanthakumara A H,1098
Sharan S S,2052
Sharma R.K,21
Sharma R.K,46
Sharon Mathew,1418
Shashank Gupta,1511
Shashank Sinha,543
Shashidhar R,1866
Sheetal Shivagunde,612
Shehan P Rajendran,783
Shekar G,1897
Shendge A D,1806
Shetty B.S,538
Shilpa D R,2187
Shilpa D R,553
Shiny G,904
Shirin Bellary,1152
Shivani Suresh,1050
Shivani Suresh,2167
Shivprasad Desai,1853
Shloka Bhalgat,1018
Shobha Rani A,2047
Shraddha S. Deshpande,290
Shravan G. S,886
SHREEKANTH T,250
Shrey Shah,234
Shreyas Aigal,510
Shreyas S Bagi,210
Shridevi Karande,2123
Shrinidhi K.R.,437
Shrivijay Phadke,522
Shriya Nithyan,404
Shrutika Mahale,1739
Shrutisneha Prasad,1556
Shubashree S,1031
Shubashree S,1443
Shubham Jain ,1212
Shubham Kalidas Shinde,807
Shubham Sonawadekar,1853
Shubhneet Kaur,449
Shusmita M. Rathod,494
Shwetali Joshi,1023
Siddharth S. Rautaray,1059
Siddharth Singh Chouhan,1166
Siddharth Singh Chouhan,2156
Sinchana C,643
Sinchana K,643
Sindhuja Banu.S,1378
Singh M.P,374
Singh M.P,695
Singh R,304
Sirisha Devi J,910
Siva Ganesh Kumar,423
Siva Subramanian M.,1772
SIVABALAN S,35
Sivapradhayni A,465
Sivasangari A,599
Smita anil sonawale,655
Sneha Sivaramakrishnan ,534
Sneha V.,437
Snehal Agrawal,1585
Somani R.K,1177
Sonakshi Beniwal,2118
Sonali Agrawal,1522
Sonali Agrawal,29
Sonam V Maju,1157
Sonavane S.P,812
Sonavane S.P,837
SONU SAHU,778
Sooraj Muralidharan,2171
Sooraj Suresh,1889
Soumes Ghosh,124
Soumya Saha,1372
Sowjanya,660
Sowmya C,404
Sowmya Sri Kilaru,620
Sree Lakshmi S,1332
Sree Vasulu,1504
Sreedevi K. Menon,2140
Sreedevi K. Menon,2171
Sreedevi Nair,1152
SREEHARI S,1358
SREEKRISHNA YADAV S,1941
Sreelakshmi G,2080
Sreelatha. P,1897
Sreeshma A,1418
Sri Harshini Popuri,1836
Sridhar K.P,1952
Srija Chimmani,990
Srikantaswamy R,210

Srikanth N,1522
Srikanth T,1579
Srinivas B K,1802
Srinivas B,1071
Sriram Sasank J V V,1708
Srishti Agarwal,1585
Sruthi Ravindran,1323
Subbarao Y.V,1071
Subbulakshmi. S,2030
Subhabrata Banerjee,959
Subramanya G. Nayak,965
Suchetha M,1655
Sudha Yadav,1220
Sudha Yadav,570
Sudheesh .P,1847
Sudheesh P,1041
Sudip Mondal,21
Suganthan B,1105
Suganthi Evangeline C,398
Suhail Mohammad,142
Suhara E. M,563
Suja Palaniswamy,1182
Sujata Bhairnallykar,574
Sujata Dhumal,538
Sujit Barhate,1296
Sultana Najeeb,1093
Sumana M,1459
Sumathi S.,2129
Sumathi.B,833
Sumit Kumar,790
Sunder Manishankar,77
Suneetha Manne,60
Sunil Dhar,1199
Sunil Kumar B R,643
Sunilkumar,1098
Sunitha Cheepurishetti,916
Sunitha Lasrado,660
Sunitha R. S.,437
Supriya Naik,1128
Supriya P. Diwan,290
Suraj P,1464
Surbhi Shringi,969
Suresh Chandra Moharana,181
Suresh L,110
Suruchi G Dedgaonkar,896
Sushant Chaudhari,522
Sushil S. Karvekar,504
Sushmitha. R,984
Swapnil Shinde,12
Swaraj Ahire,1110
Swaraj K.P,946
Swarnali Dey,959
Swathika Shanmugam,534
Swati Bhasin,1312
Swati Bhasin,1694
Swati RajeshKumar Maurya,358
Swetha Amit,1023
Swetha Amit,1027
Swetha N Prabhu,1093
Syed Noorul Faraz,499

T

Talat Zakirhusen Sayyed,807
Tanushree Samaria,1264
Tanya Keshari,1182
Taraka Sai Srinatha Reddy V,66
Taral S. Sarvagod,637
Tarandeep Singh,871
Tarun P,1220
Tasneema Akhtar,1626
Tejal Dinesh Patil,1649
Tejashree S. Bhave,1372
Tejashri S .Wable,1354
Tejaswi Kumar K M T,1386
Tejaswini S,1423
Tejbanta Singh Chingtham,2041
Thangakumar Jeyaprakash,609
Thangam Palaniswamy,1816
Thangam S,1188
Themrichon Tuithung,1
Theresa Anitta Jaison,1418
Thobias P T,1889
Tiwari S,543
Tiwari S,548
Treesa Angel George,1093
Tulika Hathi ,124
Tushar Agarwal,1018
Tushar Hait ,124
Tushar Khanke,522

U

Uday Pratap Singh,1166
Uday Pratap Singh,2156
Udit Kr. Chakraborty,443
Udit Kr. Chakraborty,700
Uma Hombal,489
Umayia Mushtaq,105
Umesha G B,71
Umme Kulsum,1585
Unnikrishna Menon K A,296
Unnikrishnan K N,1478
Usha Padma,2176
Usha Padma,737
Usha Rani.Nelakuditi,1469
Utkarsh Goel,795
Utkarsha I. Jondhale,1908
Uva Darshni P,1546
Uva Dharini P,1546

V
Vadivel M,1871
Vadivu.T,833
Vaibhav R. Pandit,933
Vaibhav S. Virkar,504
Vaisakh A.K,1889
Vaishali Jadhav,574
Vandana Chaudhary,1312
Vandana Chaudhary,1694
Vandana Chaudhary,2059
Vandana Jirafe,1077
Vandana S,1027
VANITA NAKADE,240
Vanitha V,2192
Varsha Pradeep,1418
Varsha Vishwa Kiran,1534
Varun Kumar Mahawar,548
Varun Prajapati,865
Vasundhara,1638
Veera Reddy B,193
Velliza Gonsalves,1152
Veni S,1412
Venita Babu,1253
Venkata Harshavardhan Reddy Allu,795
Venkatesh Chakravartula,281
Venkatesh Murthy B T,1714
Venkatesh U,570
Vidhya D.S,773
VIDHYA E,35
Vijay Kumar Sharma,102
Vijay Kumar Sharma,105
Vijay Kunjir,1077
Vijaya Shetty S,2181
VIJAYAKUMARI K,1689
Viji D,323
Viji R,2052
VIKAS MITTAL,1941
Vikram A,1001
Vinay Prasad M S,1053
Vinay S.,886
Vinod Jadhav,1724
Vinod Jadhav,1739
Vinodhini M,66
Vinoth Babu Kumaravelu,398
Vinoth Ramalingam,1474
Vinoth Ramalingam,900
VINUTHA D C,364
Viraj Savakhande,1562
Vishal M. Patil,1931
Vishnu Rajan,1253
Vishwanthi Suvetha.R,599
Vishwesh Anand Sahasrabudhe,1562
Vivek Kumar Jain,2036
Vuppu Padmakar,480
Y
Yamini Katta,620
Yash Pal,790
Yashaswini L,528
Yashvir Singh Chauhan,469
Yashwanth S D,1342
Yathin Sai T,737
Yelure B.S,812
Z
Zahoor Ahmad Najar,1811

4th ICCES

17-19, July 2019

ISBN(IEEE Xplore): 978-1-7281-1261-9
ISBN(DVD): 978-1-7281-1260-2

http://icoecs.org/icoecs2019/